P.O.Box 2345, Beijing 100023,China
Fax: +86-10-85381893
E-mail: wjg@wjgnet.com www.wjgnet.com

World J Gastroenterol 2003;9(7):1385-1389
World Journal of Gastroenterology
 ISSN 1007-9327

• REVIEW •

Diverticular disease of the colon: New perspectives in symptom development and treatment

Antonio Colecchia, Lorenza Sandri, Simona Capodicasa, Amanda Vestito, Giuseppe Mazzella, Tommaso Staniscia, Enrico Roda, Davide Festi

Antonio Colecchia, Lorenza Sandri, Giuseppe Mazzella, Enrico Roda, Davide Festi, Department of Internal Medicine and Gastroenterology, University of Bologna, Italy
Simona Capodicasa, AmandaVestito, Tommaso Staniscia, Department of Medicine and Aging, University G. d' Annunzio, Chieti, Italy
Correspondence to: Davide Festi, M.D., Department of Internal Medicine and Gastroenterology, Policlinico S. Orsola-Malpighi, Via Massarenti 9, 40100 Bologna, Italy. festi@med.unibo.it
Telephone: +39-051-6364123 **Fax**: +39-051-63641223
Received: 2003-02-25 **Accepted:** 2003-03-15

Abstract

Diverticular disease of the colon is a common disease worldwide. Although the disease is asymptomatic in about 70-80 % of patients, it represents, at least in Western countries, one of the most important gastrointestinal diseases in terms of direct and indirect health costs. Pathogenesis of the disease is still unknown. However, it is the result of complex interactions between colonic structure, intestinal motility, diet and genetic factors. Whilst efficacious preventive strategies remain to be identified, fibre supplementation in the diet is recommended. Why symptoms develop is still unclear. Results of recent experimental studies on irritable bowel syndrome speculated that low grade inflammation of colonic mucosa, induced by changes in bacterial microflora, could affect the enteric nervous system, which is crucial for normal gut function, thus favouring symptom development. This hypothesis could be extrapolated also for diverticular disease, since bacterial overgrowth is present, at least in a subgroup of patients. These perspectives on symptom development are reviewed and new therapeutic approaches are hypothesized.

Colecchia A, Sandri L, Capodicasa S, Vestito A, Mazzella G, Staniscia T, Roda E, Festi D. Diverticular disease of the colon: New perspectives in symptom development and treatment. *World J Gastroenterol* 2003; 9(7): 1385-1389
http://www.wjgnet.com/1007-9327/9/1385.asp

INTRODUCTION

Diverticular disease (DD) of the colon is very common especially in the elderly[1]. Although DD is present worldwide, a higher incidence has been reported in developed countries, compared to underdeveloped countries[2]. DD has important socioeconomic implications on the health system, due not only to its worldwide distribution, but also to the lack of knowledge concerning its natural history and the risk factors involved in development of symptoms. As a consequence, it is difficult to define efficacious preventive strategies.

According to a recent report by the American Gastroenterological Association on the burden of digestive diseases in the United States[3], DD represents, in terms of direct and indirect costs, the 5th most important gastrointestinal disease, with a mortality-rate of 2.5 per 100 000 per year.

DD is a manifestation of an acquired deformity of the colon wall and is characterized by the development of pseudodiverticula, i.e., protrusions of the mucosa and submucosa through the muscular wall. These protrusions occur in weak areas of the wall where blood vessels penetrate due to the high pressure inside the colon[4].

No uniform definition of DD exists as yet. However, according to a recent Consensus Development Conference[5], colonic DD can be defined as a condition involving primarily the sigmoid region of the colon. This condition may be either asymptomatic, and is referred to as "diverticulosis", or associated with symptoms, and termed "diverticular disease", which may, in turn, be either complicated or non-complicated. The term diverticulitis is used to indicate inflammation of the bowel wall.

A brief review is made herein of the epidemiology, pathogenesis and treatment of DD, and in accordance with recent experimental results, some hypotheses on pathogenesis of symptom development are advanced, which may be usefully taken into consideration in defining more effective preventive strategies.

EPIDEMIOLOGY

Epidemiological studies have demonstrated that the prevalence rates differ considerably from one country to another. Indeed, the disease is very common in Western developed countries, with a much higher frequency (30-40 %) than that in Eastern and developing countries (1-4 %)[2, 6-8].

Furthermore, in Western countries, about 90 % of the patients have diverticula in the sigmoid segment, while in Asian populations the caecum and the right colon are most frequently involved[9-12].

Recent studies, however, indicate an increase in the prevalence rate of DD also in Eastern populations, possibly due to increasing globalization and the fact that lifestyle has become increasingly similar in various parts of the world[11-13].

No definitive data have emerged, so far, on the prevalence rate of DD, mainly because the majority of patients are asymptomatic, and are hence difficult to identify. The most important risk factor appears to be aging, the prevalence rate increases with age and varies from <10 % in subjects <40 years old to an estimated 50-66 % in patients >85 years[1, 14, 15].

Some studies have reported a slightly higher frequency in females, however, no sex-related predominance has been demonstrated[16, 17].

PATHOGENESIS

The pathogenetic mechanisms of DD are still poorly understood, however it is generally recognized that these are probably related to complex interactions between colon structure, intestinal motility, diet as well as genetic features[18].

DD has been correlated with "a low residue diet"[2], and furthermore, the prevalence of diverticulosis is higher with a reduced dietary intake of raw fibres[19] and lower in vegetarians[20]. These data are supported by studies both in

animals[21, 22] and humans[23-28]. However, although the fibre deficiency hypothesis has been widely quoted, conflicting evidence and much controversy still exist[29, 30]. The exact mechanism involved remains to be defined, even if prolonged colonic transit time and decreased stool volume in subjects on a low residue diet, seem to induce an increase in intraluminal pressure, which in turn, predisposes to diverticular herniation[31, 32]. Furthermore, the lower faecal bile acid output in patients with DD suggests a pathogenetic role of these compounds which stimulate colon motor activity and as a result reduce colonic transit time[33]. Albeit, these hypotheses have not been confirmed by controlled clinical studies comparing healthy subjects with DD patients[1].

As far as colonic structure is concerned, early surgical and autopsy studies demonstrated an association between muscular hypertrophy of the colon and presence of DD[34, 35], thus suggesting that increased muscle bulk plays a role in enhancing intraluminal pressure.

Furthermore, electron microscopy evidence of a two-fold increase in elastin content in the taenia coli[36] suggests a further pathogenetic mechanism. The elastin content in the taenia results in contraction and bunching of the circular muscle, giving the appearance of a hypertrophic muscle with narrowing of the bowel lumen.

The increased prevalence of DD with aging could be due to a progressive, age-related accumulation of elastin in the taenia coli[36, 37]. In fact, in the elderly, the bowel wall is invariably increased in thickness with reduced elasticity[1] and thus, intraluminal pressure increases and, according to Laplace' s law, formation of diverticula is more likely.

The tendency to elastin accumulation in the taenia coli could be resulted from a low residue diet that extends the bowel intermittently and incompletely, thus favouring prolin (an elastin precursor) uptake[1].

Whilst several pathogenetic hypotheses have been advanced to explain the development of colon diverticula, the fact remains that the pathologic aspects of the disease are resulted from lifelong exposure to a low residue diet and a complex interaction between colonic structure, intestinal motility and genetic factors[18].

CLINICAL ASPECTS OF DIVERTICULAR DISEASE

Clinical classification

Current classifications of DD are based on localization, distribution, symptoms, clinical presentation and pathology[1, 5, 38-40]. Two different types of classification have been proposed: a clinical classification and the Hinchey classification[41], which is used to describe the stages of perforated DD. For the purposes of the present article, the clinical classification is taken into consideration here (Table 1).

Table 1 Classification of diverticular diseases of the colon

Clinical classification (modified from ref. 5)
· Symptomatic uncomplicated disease
· Recurrent symptomatic disease
· Complicated disease (haemorrhage, abscess, phlegmon, perforation, purulent and faecal peritonitis, stricture, fistula, small-bowel obstruction due to post-inflammatory adhesions)
Modified Hinchey classification (modified from refs. 41, 71)
· Stage I: pericolic abscess
· Stage IIa: distant abscess amenable to percutaneous drainage
· Stage IIb: complex abscess associated with / without fistula
· Stage III: generalized purulent peritonitis
· Stage IV: faecal peritonitis

However, the hallmark of painful DD is abdominal pain in the absence of any indications of inflammation. Pain is usually colicky, but may also be steady. It is exacerbated by eating, and is typically relieved by flatus or bowel movements. Associated symptoms vary considerably: diarrhoea, constipation, flatulence, heartburn, nausea and vomiting, palpable abdominal mass, abdominal distension[1, 5, 38].

Natural history

The natural history of DD remains to be elucidated and the few prospective studies carried out so far[9, 42-44] indicate that 80-85 % of patients with DD remain asymptomatic. Of the 15-20 % of patients presenting abdominal pain, approximately 75 % have a painful DD whilst the remainder have diverticulitis, as well as complications of diverticulitis and haemorrhage[1]. Furthermore, about 1-2 % will require hospitalisation and 0.5 % will require surgery[1, 45, 46]. Unfortunately, due to the lack of prospective studies, factors predicting the development of symptoms remain to be identified. However, it has been suggested[47] that evaluation of the colonic motility index (pressure amplitude exceeding 120 mmHg), together with a brief history of left lower quadrant pain, a short segment of involved colon and a relatively younger age (about 50 years), may be useful in recognizing a group of patients at risk of developing symptoms.

Moreover, investigations[48, 49] have suggested that lack of physical activity is independently associated with an increased risk of symptomatic DD, while smoking, caffeine and alcohol intake are not associated with a substantially increased risk of asymptomatic disease. Furthermore, a significant inverse association has been found between insoluble dietary fibre intake (especially fruit and vegetables, e.g. cellulose fibre) and the risk of subsequently developing symptomatic DD[24]. In contrast, a study on the efficacy of fibre supplementation in symptomatic patients with DD did not lead to an improvement in symptoms[50].

Since few data exist on risk factors, preventive measures for the development of diverticula are only speculative, and can be aimed only at preventing development of symptoms. Despite controversial data, fibre supplementation is recommended[1, 38].

Symptom development

The causes of symptom development, in some patients, are still unclear. Since it has been observed that DD patients who have a history of diverticulitis have more episodes of recurrent abdominal pain and impaired bowel function[6, 51, 52], a possible role of previous episodes of intestinal inflammation may be hypothesised. This finding is not unlike that which has been recently demonstrated in other gastrointestinal diseases such as infectious enteritis and inflammatory bowel disease[53, 54] and, as also speculated[55] in irritable bowel syndrome (IBS). In these patients, the presence of a chronic, low-grade intestinal inflammation would induce a sensory-motor dysfunction, leading to symptom development and/or persistence[53-56].

Changes in intestinal microflora could be one of the putative mechanisms responsible for low grade inflammation, at least in IBS[55]. In patients with DD, bacterial overgrowth may be present[57]. This bacterial overgrowth aided by the faecal stasis inside the diverticula, could contribute to chronic low-grade inflammation which sensitises both intrinsic primary efferent and extrinsic primary afferent neurons. These alterations could lead to smooth muscle hypertrophy, and increased sensitivity to abdominal distension[56,58], and finally, to symptom development. This hypothesis is based mainly on experimental studies, investigation in man, being limited at present. However, an increased level of the neuropeptide substance P, which may be related to impaired visceral sensation, has been

demonstrated in patients with DD with abdominal pain but without inflammation[59]. This finding is not unlike that observed by Di Sebastiano *et al*[60] who documented a role of neuroproliferation within the appendix, associated with an increased concentration of substance P and vasoactive intestinal polypeptide, in the pathophysiology of right iliac fossa pain in the absence of inflammation. Moreover, in patients with diverticulitis, abnormal nerves with axonal sprouting have been observed[61], suggesting previous injury. These findings would appear to be compatible with post-inflammatory neural and muscle dysfunction, probably induced also by intestinal bacterial overgrowth, which would contribute to symptom development.

Further studies, both experimental and in man, are obviously needed to confirm the pathogenetic role (which is summarized in Figure 1) of intestinal infection and low grade inflammation, in the development of symptoms in patients with DD.

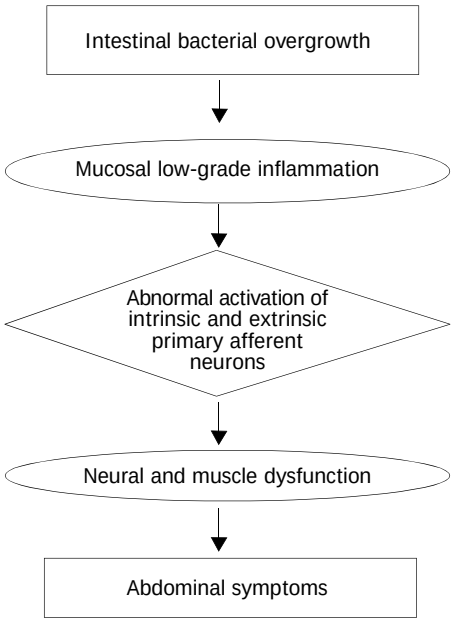

Figure 1 Diverticular disease: putative role of intestinal bacterial overgrowth in symptom development. Altered intestinal microflora could contribute to chronic low-grade inflammation (supported by both immunocytes and mast cells) which abnormally sensitised both intrinsic primary efferent and extrinsic primary afferent neurons. This condition could lead to neural and muscle dysfunction (i.e. altered intestinal motility and visceral sensitivity) and, finally, to symptom development.

Non-surgical treatment

There is a general consensus that conservative treatment is indicated in cases with newly onset uncomplicated diverticulitis[5, 38, 62, 63]. The rationale for this strategy is that about 50-70 % of patients treated for a first episode of acute diverticulitis will recover and have no further clinical problems. Furthermore, only about 20 % of these patients will develop symptoms whilst those with recurrent symptoms have a 60 % risk of developing disease complications[5, 44].

In patients with uncomplicated diverticulosis, a diet with abundant fruit and vegetables is recommended since it seems that this protective effect reduces symptom development and prevents major complications as demonstrated in uncontrolled studies. Nevertheless, recent guidelines[38] advise the use of a high fibre diet, which should be prescribed also for the well-known potential health benefits.

Anticholinergic and antispasmodic agents may be effective in some cases of uncomplicated DD. However, their use remains to be confirmed by controlled studies.

Although the role of antibiotics in uncomplicated DD is still debated[38], recent clinical studies[64-66] have demonstrated that cyclic administration of rifaximin (Normix®, Alfa Wassermann S.p.A., Alanno Scalo, Chieti, Italy) (a broad-spectrum poorly absorbable antibiotic) is more effective in reducing symptoms than fibre supplementation alone (Table 2).

Latella *et al*[66] performed a large, multicentre, prospective, randomized study, enrolling 968 outpatients with symptomatic diverticulosis. Among them, 595 patients received fibre supplement (glucomannan 4 g/day) plus rifaximin 400 mg bid for 7 days, per month, and 373 patients received glucomannan alone. After 12 months, a significant reduction in the occurrence rate of symptoms was documented in the group treated with rifaximin and fibre. 56.5 % of the patients were asymptomatic as compared to 29.2 % of the fibre group. Moreover, the incidence of major complications was lower in the rifaximin plus fibre group *vs* the group treated with fibre alone. The mechanism of of rifaximin in reducing the frequency of symptoms and the rate of complications of DD is only speculative. It has been suggested that rifaximin reduces the metabolic activity of intestinal bacterial flora, the degradation of dietary fibres, and the production of gas. The latter effect is important since an increased production of intestinal gas and of gas-related symptoms such as pain and bloating have recently been documented, in patients with IBS[67]. Furthermore, treatment with non-absorbable antibiotics was shown to reduce symptoms frequency and intensity in these patients. Similar results were obtained by others[68] who documented an association between small intestinal overgrowth and functional intestinal disorders. Moreover, eradication of bacterial overgrowth seems to be related to a reduction in intestinal symptoms.

In conclusion, if low grade mucosal inflammation is confirmed in DD patients, and if such inflammation is provoked and maintained by changes in bacterial microflora as in IBD (change IBD with IBS), then these impairments likely play a role in the pathogenesis and symptom development of both diseases, and thus, new preventive approaches could be identified. According to this hypothesis, cyclic administrations of antibiotics, and in particular of non-absorbable antibiotics such as rifaximin, could reverse the process, i.e., intestinal bacterial overgrowth which is held to trigger the cascade of events which starts from intestinal low grade inflammation to reach symptom generation. In fact, rifaximin, which is highly

Table 2 Effects of rifaximin (R) administration on symptoms in patients with diverticular disease

First author (year, ref)	Pts (*n*)	Treatment (type)	Duration (months)	Reduction in symptoms (%)	*P*
Papi (1992, 64)	217	R (400 mg daily) + glucomannan (2 g daily) *vs* glucomannan	12	63.9 *vs* 47.6	<0.001
Papi (1995, 65)	168	R (400 mg daily) + glucomannan (2 g daily) *vs* placebo +glucomannan	12	68.9 *vs* 38.5	<0.001
Latella (2003, 66)	968	R (400 mg daily) + glucomannan (4 g daily) *vs* glucomannan	12	56.5 *vs* 29.2	<0.001

effective against anaerobic bacteria[69], is effective also in intestinal bacterial overgrowth[70,71].

It is important, at this stage, to identify and characterize those DD patients with intestinal bacterial overgrowth and, then, to perform controlled clinical trials to evaluate the effects of antibiotic administration on symptom and complication frequency, i.e., on the natural history of this disease.

REFERENCES

1 **Farrell RJ**, Farrell JJ, Morrin MM. Diverticular disease in the elderly. *Gastroenterol Clin North Am* 2001; **30**: 475-496
2 **Painter NS**, Burkitt DP. Diverticular disease of the colon: a deficiency disease of Western civilization. *Br Med J* 1971; **2**: 450-454
3 **Sandler RS**, Everhart JE, Donowitz M, Adams E, Cronin K, Goodman C, Jemmen E, Shahs A, Avdic A, Rubin R. The burden of selected digestive diseases in the United States. *Gastroenterology* 2002; **122**: 1500-1511
4 **Truelove SC**. Movements of the large intestine. *Physiol Rev* 1966; **46**: 457-412
5 **Kohler L**, Sauerland S, Neugebauer E. For the scientific committeee of the european association for endoscopic surgery (EAES). diagnosis and treatment of diverticular disease. Results of a consensus development conference. *Surg Endosc* 1999; **13**: 430-436
6 **Cheskin LJ**, Lamport RD. Diverticular disease. Epidemiology and pharmacological treatment. *Drugs Aging* 1995; **6**: 55-58
7 **Kim EH**. Hiatus hernia and diverticulum of colon: their low incidence in Korea. *N Engl J Med* 1964; **271**: 764-768
8 **Vajrabukka T**, Saksornchai K, Jimakorn P. Diverticular disease of the colon in a Far-Eastern community. *Dis Colon Rectum* 1980; **23**: 151-154
9 **Parks TG**. Natural history of diverticular disease of the colon. *Clin Gastroenterol* 1975; **4**: 53-79
10 **Perry PM**, Morson BC. Right-sided diverticulosis of the colon. *Br J Surg* 1971; **58**: 902-904
11 **Chia JG**, Wilde CC, Ngoi SS, Goh PM, Ong CL. Trends of diverticular disease of the large bowel in a newly developed country. *Dis Colon Rectum* 1991; **34**: 498-501
12 **Lee YS**. Diverticular disease of the large bowel in singapore: an autopsy study. *Dis Colon Rectum* 1986; **29**: 330-335
13 **Ihekwaba FN**. Diverticular disease of the colon in black africa. *J R Coll Surg Edin* 1992; **37**: 107-109
14 **Young-Fadok TM**, Roberts PL, Spencer MP, Wolff BG. Colonic diverticular disease. *Curr Prob Surg* 2000; **37**: 459-464
15 **Larsson PA**. Diverticulitis is increasing among the elderly: significant cause of morbidity and mortality. *Lakartididningen* 1997; **94**: 3837-3840
16 **Eide TJ**, Stalsberg H. Diverticular disease of the large intestine in northern norway. *Gut* 1979; **20**: 609-615
17 **Kohler R**. The incidence of colonic diverticulosis in Finland and Sweden. *Acta Chir Scand* 1963; **126**: 148-155
18 **Simpson J**, Scholefield JH, Spiller RC. Pathogenesis of colonic diverticula. *Br J Surg* 2002; **89**: 546-554
19 **Heller SN**, Hackler LR. Changes in the crude fiber content of the American diet. *Am J Clin Nutr* 1978; **31**: 1510-1514
20 **Gear JSS**, Furdson P, Nolan DJ. Symptomless diverticular disease and intake of dietary fibre. *Lancet* 1979; **11**: 511-514
21 **Hodgson WJB**. An interim report on the production of colonic diverticula in the rabbit. *Gut* 1972; **13**: 802-804
22 **Fisher N**, Berry CS, Feam T, Gregory JA, Hardy J. Cereal dietary fiber consumption and diverticular disease: a lifespan study in rats. *Am J Clin Nutr* 1985; **42**: 788-804
23 **Brodribb AJM**, Humphreys DM. Diverticular disease: Three studies. I. Relation to other disorders and fibre intake. *Br Med J* 1976; **1**: 424-430
24 **Aldoori WH**, Giovannucci EL, Rimm EB, Wing AL, Trichopoulos, Willet WC. A prospective study of dietary fiber types and symptomatic diverticular disease in men. *Am J Clin Nutr* 1994; **60**: 757-764
25 **Brodribb AJM**. Treatment of symptomatic diverticular disease with high-fibre diet. *Lancet* 1977; **1**: 664-666
26 **Painter NS**, Burkitt DP. Diverticular disease of the colon a 20th century problem. *Clin Gastroenterol* 1975; **4**: 3-21
27 **Leahy A**, Ellis RM, Quill DS, Peel ALG. High fiber diet in symptomatic diverticular disease of the colon. *Ann R Coll Surg Engl* 1985; **67**: 173-174
28 **Miettinen TA**, Tarpila S. Fecal beta-sitosterol in patients with diverticular disease of the colon and in vegetarians. *Scand J Gastroenterol* 1978; **13**: 573-576
29 **Davey WW**. Diet and diverticulosis. *Br Med J* 1968; **1**: 118-120
30 **Mendeloff AI**. A critique of "fibre deficiency". *Am J Dig Dis* 1976; **21**: 109-112
31 **Painter NS**, Truelove SC. The intraluminal pressure patterns in diverticulosis of the colon. Part I and II. *Gut* 1964; **5**: 201-213
32 **Painter NS**, Truelove SC. The intraluminal pressure patterns in diverticulosis of the colon. Part III and IV. *Gut* 1964; **5**: 365-373
33 **Tarpila S**, Miettinen TA, Metsaranta L. Effects of bran on serum cholesterol, fecal mass, fats, bile acids and neutral sterols and biliary lipids in patients with diverticular disease of the colon. *Gut* 1978; **19**: 137-145
34 **Arfwidsson S**. Pathogenesis of multiple diverticula of the sigmoid colon in diverticular disease. *Acta Chir Scand* 1964; **342**: 1-68
35 **Slack WW**. Bowel muscle in diverticular disease. *Gut* 1966; **7**: 668-670
36 **Whiteway J**, Morson BC. Elastosis in diverticular disease of the sigmoid colon. *Gut* 1985; **26**: 258-266
37 **Smith AN**. Colonic muscle in diverticular disease. *Clin Gastroenterol* 1986; **15**: 917-935
38 **Stollman NH**, Raskin JB. Practice guidelines. Diagnosis and management of diverticular disease of the colon in adults. *Am J Gastroenterol* 1999; **94**: 3110-3120
39 **Torsoli A**, Inoue M, Manousos O, Smith A, Van Steensel CJ. Diverticular disease of the colon: data relevant to management. *Gastroenterol Int* 1991; **4**: 3-20
40 **Wong WD**, Wexner SD, Lowry A. Practice parameters for the treatment of sigmoid diverticulitis: Supporting documentation. The standards task force. The american society of colon and rectal surgeons. *Dis Colon Rectum* 2000; **43**: 290-297
41 **Hinchey EJ**, Schaal PH, Richards MB. Treatment of perforated diverticular disease of the colon. *Adv Surg* 1978; **12**: 85-109
42 **Haglund U**, Hellberg R, Johnsen C, Hulten L. Complicated diverticular disease of the sigmoid colon. An analysis of short and long term outcome in 392 patients. *Ann Chir Gynaecol* 1979; **68**: 41-46
43 **Ambrosetti P**, Robert JH, Witzig JA, Mirescu D, Mathey P, Borst F, Rohner A. Acute left colonic diverticulitis in young patients. *J Am Coll Surg* 1994; **179**: 156-160
44 **Farmakis N**, Tudor RG, Keighley MR. The 5-year natural history of complicated diverticular disease. *Br J Surg* 1994; **81**; 733-735
45 **Almy TP**, Howell DA. Diverticular disease of the colon. *N Engl J Med* 1980; **302**: 324-331
46 **Simmang CL**, Shires GT. Diverticular disease of the colon. In: Feldman M, Sleisenger MH, Scharschmidt BF, Eds, sleisinger & fordtran's gastrointestinal and liver disease, 6th Edition, Philadelphia, WB. *Saunders Company* 1998: 1788-1798
47 **Cortesini C**, Pantalone D. Usefulness of colonic motility study in identifying patients at risk for complicated diverticular disease. *Dis Colon Rectum* 1991; **34**: 339-342
48 **Aldoori WH**, Giovannucci EL, Rimm EB. Prospective study of physical activity and the risk of symptomatic diverticular disease in men. *Gut* 1995; **36**: 276-282
49 **Aldoori WH**, Giovannucci EL, Rimm EB. A prospective study of alcohol, smoking, caffeine, and the risk of symptomatic diverticular disease in man. *Ann Epidemiol* 1995; **5**: 221-228
50 **Ornstein MH**, Littlewood ER, Baird IM, Fowler J, Cox AG. Are fiber supplements really necessary in diverticular disease of the colon? A controlled clinical trial. *Br Med J* 1981; **282**: 1353-1356
51 **Simpson J**, Neal KR, Scholefield JH, Spiller RC. Relation between inflammatory and non inflammatory pain in diverticular disease. *Gut* 2000; **46** (Suppl II): A80
52 **Simpson J**, Neal KR, Scholefield JH, Spiller RC. Symptomatology following acute diverticulitis. *Neurogastroenterol Mot* 2001; **13**: 43
53 **Neal KR**, Hebden J, Spiller R. Prevalence of gastrointestinal symptoms six months after bacterial gastroenteritis and risk factors for development of the irritable bowel syndrome: postal survey of patients. *Br Med J* 1997; **314**: 779-782

54 **Isgar B**, Harman M, Kaye MD, Whorwell PJ. Symptoms of irritable bowel syndrome in ulcerative colitis in remission. *Gut* 1983; **24**: 190-192

55 **Barbara G**, De Giorgio R, Stanghellini V, Cremon C, Corinaldesi R. A role for inflammation in irritable bowel syndrome? *Gut* 2002; **51** (Suppl 1): i41-i44

56 **Collins SM**, Vallance B, Barbara G, Borgaonkar M. Putative inflammatory and immunological mechanism in functional bowel disorders. *Bailleres Best Pract Res Clin Gastroenterol* 1999; **13**: 429-436

57 **Ventrucci M**, Ferrieri A, Bergami R, Roda E. Evaluation of the effect of rifaximin in colon diverticular disease by means of lactulose hydrogen breath test. *Curr Med Res Opin* 1994; **13**: 202-206

58 **Sanovic S**, Lamb DP, Blennerhasset MG. Damage to the enteric nervous system in experimental colitis. *Am J Pathol* 1999; **155**: 1051-1057

59 **Watanabe T**, Kubota Y, Muto T. Substance P containing nerve fibers in rectal mucosa of ulcerative colitis. *Dis Colon Rectum* 1997; **40**: 718-725

60 **Di Sebastiano P**, Fink T, di Mola FF. Neuroimmune appendicitis. *Lancet* 1999; **354**: 461-466

61 **Brewer DB**, Thompson H, Haynes IG, Alexander-Williams J. Axonal damage in Crohn's disease is frequent but not specific. *J Pathol* 1990; **161**: 301-311

62 **Larson DM**, Masters SM, Spiro HM. Medical and surgical therapy in diverticular disease. A comparative study. *Gastroenterology* 1976; **71**: 734-737

63 **Ferzoco LB**, Raptopoulos V, Silen W. Acute diverticulitis. *N Engl J Med* 1998; **338**: 1521-1526

64 **Papi C**, Ciaco A, Koch M, Capurso L. And diverticular disease study group. Efficacy of rifaximin of uncomplicated diverticular disease of the colon. A pilot multicentre open trial. *Ital J Gastroenterol* 1992; **24**: 452-456

65 **Papi C**, Ciaco A, Koch M, Capurso L. Efficacy of rifaximin in the treatment of symptomatic diverticular disease of the colon. A multicenter double-blind placebo-controlled trial. *Aliment Pharmacol Ther* 1995; **9**: 33-39

66 **Latella G**, Pimpo MT, Sottili S, Zippi M, Viscido A, Chiaramonte M, Frieri G. Rifaximin improves symptoms of acquired uncomplicated diverticular disease of the colon. *Int J Colorectal Dis* 2003; **18**: 55-62

67 **Di Stefano M**, Strocchi A, Malservisi S, Veneto G. Ferrieri A, Corazza GR. Non absorbable antibiotics for managing intestinal gas production and gas-related symptoms. *Aliment Pharmacol Ther* 2000; **14**: 1001-1008

68 **Pimentel M**, Chow EJ, Lin CL. Eradication of small intestinal overgrowth reduces symptoms in irritable bowel syndrome. *Am J Gastroenterol* 2000; **95**: 3505-3506

69 **Gillis JC**, Brogden RN. Rifaximin. *Drugs* 1995; **49**: 468-484

70 **Di Stefano M**, Malservisi S, Veneto G. Ferrieri A, Corazza GR. Rifaximin versus chlortetracycline in the short-term treatment of small intestine bacterial overgrowth. *Aliment Pharmacol Ther* 2000; **14**: 551-556

71 **Sher ME**, Agachan F, Bortul M, Nogueras JJ, Weiss EG, Wexner SD. Laparoscopic surgery for diverticulitis. *Surg Endosc* 1997; **11**: 264-267

Edited by Xu XQ and Wang XL

P.O.Box 2345, Beijing 100023,China
Fax: +86-10-85381893
E-mail: wjg@wjgnet.com www.wjgnet.com

World J Gastroenterol 2003;9(7):1390-1393
World Journal of Gastroenterology
 ISSN 1007-9327

• ESOPHAGEAL CANCER •

NQO1 C609T polymorphism associated with esophageal cancer and gastric cardiac carcinoma in North China

Jian-Hui Zhang, Yan Li, Rui Wang, Helen Geddert, Wei Guo, Deng-Gui Wen, Zhi-Feng Chen, Li-Zhen Wei, Gang Kuang, Ming He, Li-Wei Zhang, Ming-Li Wu, Shi-Jie Wang

Jian-Hui Zhang, Yan Li, Rui Wang, Wei Guo, Deng-Gui Wen, Zhi-Feng Chen, Li-Zhen Wei, Gang Kuang, Ming He, Li-Wei Zhang, Ming-Li Wu, Shi-Jie Wang, Hebei Cancer Institute and the Fourth Affiliated Hospital of Hebei Medical University, Shijiazhuang 050011, Hebei Province, China
Helen Geddert, Institute of Pathology, University of Duesseldorf, Moorenstr.5 40225 Duesseldorf, Germany
Supported by the "Stiftung für Altersforschung" of Germany (grant number: 701800167) and Scientific Grant of Educational Department of Hebei Province, China (grant number: 2001150)
Correspondence to: Professor Shi-Jie Wang, The Fourth Affiliated Hospital of Hebei Medical University, Jiankanglu 12, Shijiazhuang 050011, China. wang.sj@hbmu.edu
Telephone: +86-311-6085231 **Fax:** +86-311-6077634
Received: 2002-12-24 **Accepted:** 2003-02-11

Abstract

AIM: To investigate the association of the *NQO1* (C609T) polymorphism with susceptibility to esophageal squamous cell carcinoma (ESCC) and gastric cardiac adenocarcinoma (GCA) in North China.

METHODS: The *NQO1* C609T genotypes were determined by polymerase chain reaction-restriction fragment length polymorphism (PCR-RFLP) analysis in 317 cancer patients (193 ESCC and 124 GCA) and 165 unrelated healthy controls.

RESULTS: The *NQO1* C609T C/C, C/T and T/T genotype frequency among healthy controls was 31.5 %, 52.1 % and 16.4 % respectively. The *NQO1* T/T genotype frequency among ESCC patients (25.9 %) was significantly higher than that among healthy controls (χ^2=4.79, *P*=0.028). The *NQO1* T/T genotype significantly increased the risk for developing ESCC compared with the combination of C/C and C/T genotypes, with an age, sex and smoking status adjusted odds ratio (OR) of 1.78 (1.04-2.98). This increased susceptibility was pronounced in ESCC patients with family histories of upper gastrointestinal cancers (UGIC) (adjusted OR=2.20, 95 % CI=1.18-3.98). Similarly, the susceptibility of the *NQO1* T/T genotype to GCA development was also observed among patients with family histories of UGIC, with an adjusted odds ratio of 2.55 (95 % CI=1.21-5.23), whereas no difference in *NQO1* genotype distribution was shown among patients without family histories of UGIC.

CONCLUSION: Determination of the *NQO1* C609T genotype may be used as a stratification marker to predicate the individuals at high risk for developing ESCC and GCA in North China.

Zhang JH, Li Y, Wang R, Geddert H, Guo W, Wen DG, Chen ZF, Wei LZ, Kuang G, He M, Zhang LW, Wu ML, Wang SJ. *NQO1* C609T polymorphism associated with esophageal cancer and gastric cardiac carcinoma in North China. *World J Gastroenterol* 2003; 9(7):1390-1393
http://www.wjgnet.com/1007-9327/9/1390.asp

INTRODUCTION

China is a country with high incidence regions of esophageal squamous cell cancer (ESCC) and gastric cardiac adenocarcinoma (GCA). Chemical carcinogenesis existed in consumed alcohol and tobacco or ingested food[1,2], nutrition deficiency[3], unhealthy living habits[2] and pathogenic infections[4-6] are in general considered as the risk factors for developing these two cancers. However, not all individuals exposed to the above exogenous risk factors will develop ESCC or GCA, indicating that the host susceptibility factors may play an important role in the cancer development. The role of a genetic background in developing these cancers was also strongly suggested by the familial clustering of upper gastrointestinal cancer (UGIC) patients in high incidence regions[7,8].

In recent years, many polymorphic genes encoded carcinogen metabolic enzymes have been found to be associated with susceptibility to chemically induced cancers such as esophageal cancer and gastric cancer[9-13]. NAD(P)H: quinone oxidoreductase 1 (NQO1) is a cytosolic enzyme which catalyzes the two-electron reduction of quinone compounds and prevents the generation of semiquinone free radicals and reactive oxygen species, thus protecting cells from oxydative damage[14]. On the other hand, NQO1 catalyzes the reductive activation of quinoid chemotherapeutic agents and of environmental carcinogens such as nitrosamines, heterocyclic amines and cigarette smoke condensate[15]. The activity of the NQO1 enzyme may be influenced by a single C to T substitution at nucleotide 609 of exon 6 of the *NQO1* cDNA that causes the Pro187Ser amino acid change[16]. The homozygous wild-type (C/C) encodes NQO1 protein with complete enzyme activity, whereas the protein encoded by the heterozygous phenotype (C/T) has approximately three-fold decreased activity and the homozygous mutant (T/T) phenotype has a complete lack of enzyme activity[15-18]. The *NQO1* C609T polymorphism is correlated with the susceptibility to several chemical carcinogen induced tumors such as lung cancer[19,20] and leukemia[21,22]. The association of *NQO1* C609T polymorphism with the susceptibility to ESCC and GCA has not been reported so far. Therefore, the current study investigated the *NQO1* C609T genotype distribution in ESCC and GCA patients and healthy controls from North China.

MATERIALS AND METHODS

Subjects

This case-control study recruited 317 patients with histologically confirmed cancers (193 esophageal cancer and 124 gastric cardiac cancer) and 165 unrelated healthy controls. The cancer patients were hospitalized for tumor resection in the Fourth Affiliated Hospital of Hebei Medical University between 2001 and 2002. The histological pattern of the resected samples was determined by pathologists of the same hospital according to the international standard[23]. The healthy controls were unrelated blood donors or voluntary staff of Hebei Cancer

Institute. All of the patients and controls were from Shijiazhuang city or its surrounding regions. The information about sex, age, smoking habits and family history was obtained from the cancer patients by their hospital recordings and from the healthy controls by interview directly after bleeding. The smokers were defined as ex- or current smoking 5 cigarettes per day for at least two years. The individuals with at least one first-degree relative or at least two second-degree relatives having esophageal/cardiac/gastric cancer were defined as having family histories of upper gastrointestinal cancers (UGIC). The informed consent was obtained from all the recruited subjects. The study was approved by the Ethics Committee of the Hebei Cancer Institute. The demographic data of the cancer patients and healthy controls are presented in Table 1.

DNA extraction

Five ml of venous blood from each subject was drawn in vacutainer tubes containing EDTA. The genomic DNA was extracted within one week after bleeding using proteinase K digestion followed by a salting out procedure.

NQO1 genotyping

NQO1 genotyping of healthy controls and ESCC patients was performed at the Molecular Laboratory of the Institute of Pathology, Heinrich-Heine University, Duesseldorf. The genotyping of the GCA patients was performed at the Molecular Biology Laboratory of the Hebei Cancer Institute with the same reagents and the same methods. The base change (C to T) at nucleotide 609 of *NQO1* cDNA created a *Hinf I* restriction site. Therefore, the *NQO1* C609T genotyping was performed by PCR and subsequent restriction fragment analysis. PCR was performed in a 25 μl volume containing 100 ng DNA template, 2.5 μl 10×PCR-buffer, 1 U Hotstar Taq-DNA-polymerase (Qiagen, Hilden, Germany), 200 μmol dNTPs and 10 pmol sense primer (5' AAGCCCAGACCAACTTCT-3') and antisense primer (5' -ATTTGAATTCGGGCGTCTGCTG-3'). Initial denaturation for 14 min at 94 ℃ was followed by 40 cycles at 94 ℃ for 1 min, at 56 ℃ for 1 min, and at 72 ℃ for 2 min. The PCR products were subsequently digested with 20 units of *Hinf* I (Boehringer, Mannheim, Germany) for 3 h at 37 ℃ and separated on a 2 % agarose gel (Figure 1). The *NQO1* wild-type allele showed a 172-bp PCR product resistant to enzyme digestion, whereas the null allele showed a 131-bp and a 41-bp band. For quality control, each PCR reaction used distilled water instead of DNA as a negative control, and 10 % of the samples were analyzed twice.

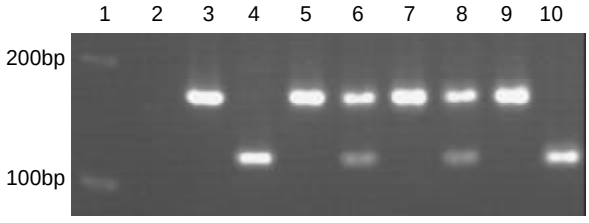

Figure 1 Genotype patterns for *NAD(P)H: quinone oxidoreductase 1 (NQO1)* C609T polymorphism analyzed by PCR-*Hinf I* digestion. Lane 1, 100bp molecular marker; lane 2, negative control; lane 3, PCR fragment containing *NQO1* C609T polymorphism; lanes 4,10, homozygous null genotype (T/T); lanes 5,7,9, homozygous wild genotype (C/C); lanes 6,8, heterozygous genotype (C/T).

Statistical analysis

The comparison of *NQO1* genotype distribution in the study groups was performed by means of two-sided contingency tables using Chi-square test. Hardy-Weinberg analysis was performed to compare the observed and expected genotype frequencies using Chi-square test. A probability level of 5 % was made as statistically significant. The odds ratio (OR) and 95 % confidence interval (CI) were calculated and adjusted for age, sex and smoking status with the unconditional logistic regression model. Statistical analysis was made using SPSS software package (10.0 version).

RESULTS

As shown in Table 1, the composition of gender, age and the proportion of smokers in ESCC and GCA patients were compared with the healthy controls. Eighty-six (44.6 %) of the ESCC and 45 (36.3 %) of the GCA patients had family histories of UGIC. The proportion of age, sex and smoking status in ESCC and GCA patients with and without family histories of UGIC was also not significantly different (data not shown). None of the healthy controls had a family history of UGIC.

The *NQO1* C609T genotyping was successfully performed in all study subjects. The observed *NQO1* genotype frequencies were not significantly deviated from those expected from Hardy-Weinberg equilibrium in the healthy controls (χ^2=0.061; *P*=0.970), ESCC patients (χ^2=0.166; *P*=0.920) and GCA patients (χ^2=0.832; *P*=0.660). The *NQO1* C609T genotype distribution among healthy controls was 31.5 % (C/C), 52.1 % (C/T), and 16.4 % (T/T) respectively (Table 1). The genotype distribution was not correlated with gender, age and smoking status in each study group (data not shown).

Table 1 Demographic characteristics and *NQO1* polymorphism among ESCC, GCA patients and controls

Groups	Control *n* (%)	ESCC *n* (%)	GCA *n* (%)
Sex			
Male	109(66.1)	124(64.3)	92(74.2)
Female	56(33.9)	69(35.7)	32(25.8)
Mean age ±SD (yrs)	52±7.16	59±8.73	60±8.24
Smoking status			
Smoker	82(49.7)	104(53.9)	68(59.8)
Non-smoker	83(50.3)	89(46.1)	46(40.2)
Family history of UGIC			
Positive	0	86(44.6)	45(36.3)
Negative	165(100)	107(55.4)	79(63.7)
Genotype			
C/C	52(31.5)	51(26.4)	40(32.3)
C/T	86(52.1)	92(47.7)	55(44.3)
T/T	27(16.4)	50(25.9)[a]	29(23.4)
Allele type			
C	190(57.6)	194(50.3)	135(54.4)
T	140(42.4)	192(49.7)[b]	113(45.6)

Note. ESCC: esophageal squamous cell carcinoma; GCA: gastric cardiac adenocarcinoma; *NQO1: NAD(P)H: quinone oxidoreductase 1;* UGIC: upper gastrointestinal cancer; a. The genotype frequency was significantly higher than that in healthy controls (χ^2=4.79, *P*=0.028); b. The allele frequency was marginaly higher than that in healthy controls (χ^2=3.83, *P*=0.05).

The overall *NQO1* null-allele frequency among ESCC patients (49.7 %) was marginally higher than that among healthy controls (42.4 %) (χ^2=3.83, *P*=0.05). There was no difference in allele distribution between GCA patients and healthy controls (χ^2=0.567, *P*=0.451) (Table 1). The distribution of *NQO1* C/C and C/T genotypes among ESCC and GCA

patients was not significantly different from that among healthy controls (P>0.05) (Table 1).

Interestingly, in ESCC patients, the *NQO1* T/T genotype was significantly more frequent (25.9 %) than that among healthy controls (χ^2=4.79, P=0.028) (Table 2). The relative risk of the T/T genotype for the ESCC development was increased by about 1.8 fold compared with the combination of the C/C or C/T genotypes, with an age, sex and smoking status adjusted odds ratio of 1.78 (95 % CI=1.04-2.98). When stratified for the family history of UGIC, the *NQO1* T/T genotype was significantly more common among patients with family histories of UGIC (30.2 %) than that among healthy controls (χ^2=6.53, P=0.011). The T/T genotype significantly increased the risk for developing ESCC among patients with family histories of UGIC, compared with the C/C and C/T genotypes (adjusted OR=2.20, 95 % CI=1.18-3.98). In contrast, the *NQO1* T/T genotype frequency was not significantly different between ESCC patients without family history of UGIC (22.4 %) and healthy controls (χ^2=1.49, P=0.223) (Table 2).

In line with the result of ESCC, the *NQO1* T/T genotype significantly increased the risk for developing GCA compared with the C/C and C/T genotypes. However, this increased risk was only demonstrated when stratified for the family history. Thus, among GCA patients with family histories of UGIC, the T/T frequency (33.3 %) was significantly higher than that among healthy controls (χ^2=6.36, P=0.012). In this patient group, the relative risk of the T/T genotype for developing GCA was more than two-fold higher compared with the combination of C/C and C/T genotypes (adjusted OR=2.55, 95 % CI=1.21-5.23), whereas the *NQO1* T/T genotype frequency among the overall GCA patients (23.4 %) and GCA patients without family histories of UGIC (17.7 %) remained similar to that of the healthy controls (P>0.05) (Table 2).

Table 2 Relative risk of the *NQO1* C609T homogenous null for ESCC and GCA development

Groups	*NQO1* genotype		aOR (95%CI)[d]
	C/C+C/T *n* (%)	T/T *n* (%)	
Healthy controls	138(83.6)	27(16.4)	
ESCC patient	143(74.1)	50(25.9)[a]	1.78 (1.04-2.98)
Family history of UGIC			
Positive	60(69.8)	26(30.2)[b]	2.20 (1.18-3.98)
Negative	83(77.6)	24(22.4)	1.46 (0.79-2.63)
GCA patient	95(76.6)	29(23.4)	1.44 (0.86-2.30)
Family history of UGIC			
Positive	30(66.7)	15(33.3)[c]	2.55 (1.21-5.23)
Negative	65(82.3)	14(17.7)	1.10 (0.80-1.34)

Note. ESCC: esophageal squamous cell carcinoma; *NQO1:NAD (P)H: quinone oxidoreductase 1*; UGIC: upper gastrointestinal cancer; a,b,c. The genotype frequency was significantly higher than that in healthy controls (a. χ^2=4.79, P=0.028; b. χ^2=6.53, P=0.011; c. χ^2=6.36, P=0.012); d. The age, sex and smoking status adjusted relative risk of the *NQO1* C609T homogenous null genotype (T/T) against the combination of the heterozygote (C/T) and homozygous wild type (C/C).

To observe the different influence of the *NQO1* C609T polymorphism on the ESCC or GCA development among smokers and non-smokers, the genotype distribution was also stratified according to the smoking habits. No difference in *NQO1* genotype distribution among smoking or non-smoking ESCC and GCA patients was observed as compared with that of the healthy controls (data not shown).

DISCUSSION

Both of ESCC and GCA are characterized by a particularly poor prognosis since most of patients are diagnosed at advanced stages. Endoscopic examination is the only feasible way to detect ESCC and GCA at early and/or precancerous stages. However, the wide application of this method is limited by the high cost and painfulness of the examination. The laboratory identification of high-risk individuals, in combination with the clinical detection, will provide a promising way to detect the early tumors.

The present hospital based case control study suggests that *NQO1* C609T homozygous null genotype may increase the susceptibility to ESCC and GCA in the northern Chinese population. This result is consistent with the previous investigations, which showed that the *NQO1* homozygous null genotype increased the susceptibility to other tumor types such as lung cancer[19], leukemia[21,22] and cutaneous cancers[24]. The underlying mechanism of the correlation of *NQO1* C609T polymorphism with increased risk for developing various tumors may be related to the different enzyme activities encoded by the different *NQO1* genotypes. Thus, lack of NQO1 activity encoded by the homozygous null genotype results in a reduced detoxification of exogenous carcinogens and leads cells to be easily damaged by oxidation, and thereby increasing the susceptibility to chemically induced cancers such as ESCC and GCA. In addition, the recessive effect of the *NQO1* C609T null allele on the development of ESCC and GCA was suggested by the current study, since the heterozygous genotype frequency among tumor patients was similar to that among healthy controls. The result indicates that although the *NQO1* heterozygous genotype results in a three-fold decrease of the NQO1 enzyme activity, it may be sufficient for protecting cells from damage by exogenous carcinogens.

In this study, the increased risk of the *NQO1* C609T homozygous null genotype for developing both of ESCC and GCA was only evident in patients with family histories of UGIC, indicating that in families aggregated with UGIC patients, a predisposition to ESCC and GCA may be inherited by lack of *NQO1* enzyme activity. A strong association of increased risk for esophageal cancer with a positive family history of UGIC in the first-degree relatives has been reported in the high incidence regions of China[7,8]. The segregation analysis on the high-risk nuclear families suggested that the ESCC occurrence was best fit to the autosomal recessive Mendelian inheritance[8]. However, the underlying molecular mechanisms for the familial clustering of UGIC patients have not been elucidated so far. Our results suggested, that the *NQO1* C609T polymorphic gene, together with other possible susceptible genes, might give an opportunity to challenge the genetic mechanisms of cancer development in the UGIC clustered families and provide a chance to predict high-risk individuals in the high-incidence regions. In addition, the consistent association of *NQO1* C609T polymorphism with the susceptibility to ESCC and GCA, as shown in this study, supports that there might be a common genetic background in the development of these two tumor types. However, the result should be interpreted cautiously, since the number of cases, especially in the subgroup analyses, was probably too small to draw a final conclusion.

In summary, our preliminary data suggest that the *NQO1* C609T gene polymorphism may influence the susceptibility to ESCC and CAC in a northern Chinese population. Determination of *NQO1* C609T genotype may provide a useful genetic marker in predicating high-risk individuals for the development of ESCC and CAC. It is worthwhile conducting additional population-based studies including enlarged subjects before its clinical application.

ACKNOWLEDGEMENTS

We greatly acknowledge the expert technical assistance of Mrs. C. Pawlik, Mrs. H. Huss and Mrs. B. Maruhn-Debowski. We also thank Mrs. Heyu Tong, Mr. Fanshu Meng, and Mr. Baoshan Zhao for their assistance in recruiting study subjects.

REFERENCES

1 **Launoy G,** Milan CH, Faivre J, Pienkowski P, Milan CI, Gignoux M. Alcohol, tobacco and oesophageal cancer: effects of the duration of consumption, mean intake and current and former consumption. *Br J Cancer* 1997; **75**: 1389-1396

2 **Yokokawa Y,** Ohta S, Hou J, Zhang XL, Li SS, Ping YM, Nakajima T. Ecological study on the risks of esophageal cancer in Ci-Xian, China: the importance of nutritional status and the use of well water. *Int J Cancer* 1999; **83**: 620-624

3 **Yang CS.** Vitamin nutrition and gastroesophageal cancer. *J Nutr* 2000; **130**(Suppl 2S): 338S-339S

4 **Cai L,** Yu SZ, Zhang ZF. *Helicobacter pylori* infection and risk of gastric cancer in Changle County, Fujian Province, China. *World J Gastroenterol* 2000; **6**: 374-376

5 **Matsha T,** Erasmus R, Kafuko AB, Mugwanya D, Stepien A, Parker MI. CANSA / MRC Oesophageal Cancer Research Group. Human papillomavirus associated with oesophageal cancer. *J Clin Pathol* 2002; **55**: 587-590

6 **Lavergne D**, de Villiers EM. Papillomavirus in esophageal papillomas and carcinomas. *Int J Cancer* 1999; **80**: 681-684

7 **Chang-Claude J,** Becher H, Blettner M, Qiu S, Yang G, Wahrendorf J. Familial aggregation of oesophageal cancer in a high incidence area in China. *Int J Epidemiol* 1997; **26**: 1159-1165

8 **Zhang W,** Bailey-Wilson JE, Li W, Wang X, Zhang C, Mao X, Liu Z, Zhou C, Wu M. Segregation analysis of esophageal cancer in a moderately high-incidence area of northern China. *Am J Hum Genet* 2000; **67**: 110-119

9 **Matsuo K,** Hamajima N, Shinoda M, Hatooka S, Inoue M, Takezaki T, Tajima K. Gene-environment interaction between an aldehyde dehydrogenase-2 (ALDH2) polymorphism and alcohol consumption for the risk of esophageal cancer. *Carcinogenesis* 2001; **22**: 913-916

10 **Song C,** Xing D, Tan W, Wei Q, Lin D. Methylenetetrahydrofolate reductase polymorphisms increase risk of esophageal squamous cell carcinoma in a Chinese population. *Cancer Res* 2001; **61**: 3272-3275

11 **Tan W,** Song N, Wang GQ, Liu Q, Tang HJ, Kadlubar FF, Lin DX. Impact of genetic polymorphisms in cytochrome P450 2E1 and glutathione S-transferases M1, T1, and P1 on susceptibility to esophageal cancer among high-risk individuals in China. *Cancer Epidemiol Biomarkevs Prev* 2000; **9**: 551-556

12 **Cai L,** Yu SZ, Zhang ZF. Glutathione S-transferases M1, T1 genotypes and the risk of gastric cancer: a case-control study. *World J Gastroenterol* 2001; **7**: 506-509

13 **Cai L,** Yu SZ, Zhan ZF. Cytochrome P450 2E1 genetic polymorphism and gastric cancer in Changle, Fujian Province. *World J Gastroenterol* 2001; **7**: 792-795

14 **Winski SL,** Koutalos Y, Bentley DL, Ross D. Subcellular localization of NAD(P)H: quinone oxidoreductase 1 inhuman cancer cells. *Cancer Res* 2002; **62**: 1420-1424

15 **Larson RA,** Wang Y, Banerjee M, Wiemels J, Hartford C, Lebeau MM, Smith MT. Prevalence of the inactivating 609C→T polymorphism in the NAD(P)H: quinone oxidoreductase (NQO1) gene in patients with primary and therapy-related myeloid leukemia. *Blood* 1999; **94**: 803-807

16 **Kuehl BL,** Paterson JW, Peacock JW, Paterson MC, Rauth AM. Presence of a heterozygous substitution and its relationship to DT-diaphorase activity. *Br J Cancer* 1995; **72**: 555-561

17 **Moran JL,** Siegel D, Ross D. A potential mechanism underlying the increased: susceptibility of individuals with a polymorphism in NAD(P)H: quinone oxidoreductase 1 (NQO1) to benzene toxicity. *Proc Natl Acad Sci USA* 1999; **96**: 8150-8155

18 **Smith M**. Benzene, NQO1, and genetic susceptibility to cancer. *Proc Natl Acad Sci USA* 1999; **96**: 7624-7626

19 **Chen H,** Lum A, Seifried A, Wilkens LR, Le Marchand L. Association of the NAD(P) H: quinone oxidoreductase 609C→T polymorphism with a decreased lung cancer risk. *Cancer Res* 1999; **59**: 3045-3048

20 **Xu LL**, Wain JC, Miller DP, Thurston SW, Su L, Lynch TJ, Christiani DC. The NAD(P)H: quinone oxidoreductase 1 gene polymorphism and lung cancer: differential susceptibility based on smoking behavior. *Cancer Epidemiol Biomarkers Prev* 2001; **10**: 303-309

21 **Wiemels JL,** Pagnamenta A, Taylor GM, Eden OB, Alexander FE, Greaves MF. A lack of a functional NAD(P)H: quinone oxidoreductase allele is selectively associated with pediatric leukemias that have MLL fusions. United kingdom childhood cancer study inv estigators. *Cancer Res* 1999; **59**: 4095-4099

22 **Smith MT,** Wang Y, Kane E, Rollinson S, Wiemels JL, Roman E, Roddam P, Cartwright R, Morgan G. Low NAD(P)H: quinone oxidoreductase 1 activity is associated with increased risk of acute leukemia in adults. *Blood* 2001; **97**: 1422-1426

23 **Gabbert HE**, Shimoda T, Hainaut P, Nakamura Y, Field JK, Inoue H. Squamous cell carcinoma of the oesophagus. *Lyon IARCP Press* 2000: 11-32

24 **Clairmont A,** Sies H, Ramachandran S, Lear JT, SmithAG, Bowers B, Jones PW, Fryer AA, Strange RC. Association of NAD(P) H: quinone oxidoreductase (NQO1) null with numbers of basal cell carcinomas: use of a multivariate model to rank the relative importance of this polymorphism and those at other relevant loci. *Carcinogenesis* 1999; **20**: 1235-1240

Edited by Ma JY

P.O.Box 2345, Beijing 100023,China
Fax: +86-10-85381893
E-mail: wjg@wjgnet.com www.wjgnet.com

World J Gastroenterol 2003;9(7):1394-1397
World Journal of Gastroenterology
 ISSN 1007-9327

• ESOPHAGEAL CANCER •

CYP1A1, GSTs and mEH polymorphisms and susceptibility to esophageal carcinoma: Study of population from a high- incidence area in north China

Li-Dong Wang, Shu Zheng, Bin Liu, Jian-Xiang Zhou, Yan-Jie Li, Ji-Xue Li

Li-Dong Wang, Cancer Institute, Zhejiang University, Hangzhou, 310009, Zhejiang Province, China and Laboratory for Cancer Research, College of Medicine, Zhengzhou University, Zhengzhou, 450052, Henan Province, China
Shu Zheng, Cancer Institute, Zhejiang University, Hangzhou, 310009, Zhejiang Province, China
Jian-Xiang Zhou, Yan-Jie Li, Ji-Xue Li, Laboratory for Cancer Research, College of Medicine, Zhengzhou University, Zhengzhou, 450052, Henan Province, China
Bin Liu, Department of Gastroenterology, Tongren Hospital, Capital Medical University, Beijing 100013, China
Supported by National Outstanding Young Scientist Award of China 30025016 (China), State Key Project for Basic Research G1998051206 (China), Foundation of Henan Education Committee 1999125 and the U.S. NIH Grant CA65871
Correspondence to: Li-Dong Wang, M.D., Professor of Pathology and Oncology, Invited Professor of Henan Province, Director of Laboratory for Cancer Research, College of Medicine, Zhengzhou University, Zhengzhou, 450052, Henan Province, China. lidong0823@sina.com
Telephone: +86-11-371-6970165 **Fax**: +86-11-371-6970165
Received: 2003-03-12 **Accepted:** 2003-05-11

Abstract

AIM: To characterize cytochrome P4501A1 (CYP1A1), glutathione S-transferases (GSTs) and microsomal epoxide hydrolase (mEH) polymorphisms in Chinese esophageal cancer patients.

METHODS: Multiplex polymerase chain reaction (PCR) and PCR based restriction fragment length polymorphisms (PCR-RFLP) were used to detect polymorphism changes of CYP, GSTs and mEH on esophageal cancerous and precancerous lesions as well as in case control group. All the examination samples were obtained from Linzhou (formerly Linxian), Henan Province, the highest incidence area for esophageal cancer.

RESULTS: The frequency of CYP1A1 3' polymorphism in case control group (26/38, 68 %) was significantly higher than in esophageal squamous cell carcinoma group (ESCC) (29/62, 47 %) ($P<0.05$). A significant difference in the incidence of mEH slow allele variant was observed between case control group (15/38, 39 %) and esophageal dysplasia group (22/32, 69 %) or ESCC group (39/62, 63 %) ($P<0.05$). However, no significant difference was observed among different groups in the polymorphisms of CYP1A1 exon 7, GSTM1, GSTT1, GSTP1 and mEH fast allele.

CONCLUSION: The present results suggest that CYP1A1 3' polymorphism may be one of the promising protective factors and its wild gene type may be an indicator for higher susceptibility to esophageal cancer. mEH slow allele variant, associated with the progression of esophageal precancerous lesions, may contribute to the high susceptibility to esophageal carcinoma.

Wang LD, Zheng S, Liu B, Zhou JX, Li YJ, Li JX. CYP1A1, GSTs and mEH polymorphisms and susceptibility to esophageal carcinoma: Study of population from a high- incidence area in north China. *World J Gastroenterol* 2003; 9(7):1394-1397
http://www.wjgnet.com/1007-9327/9/1394.asp

INTRODUCTION

It has been revealed that carcinogenesis may be resulted from mutations or deletions in cancer-related genes. Meanwhile, a large proportion of human cancers is associated with diet, tobacco smoking and other environmental factors[1], suggesting that a combination of endogenous and exogenous factors is responsible for human carcinogenesis. In recent years, a relatively new field of cancer research has focused on the interaction between genes and enrironment to understand the aetiology of cancer[2]. Primary candidates for gene-environment interaction studies are those which encode enzymes related to the metabolism of established cancer risk factors. It has been known that most carcinogens require metabolic activation in the human body for the carcinogenic effects. There are two major enzyme systems that metabolize potential carcinogens, either synthetic or naturally occurring in the body, which have been classified as phase I and phase II. Generally, phase I enzymes can activate the carcinogen directly and produce more active metabolites. Phase II enzymes can detoxify and process the activated metabolites for final breakdown or excretion. Therefore, the genotypes with high phase I enzyme activity and low phase II enzyme level are considered to pose a high risk to cancer development[3].

Cytochrome P450 (CYP) isoenzymes are one major kind of phase I enzymes and play an important role in the oxidation of chemical compounds, such as polycyclic aromatic hydrocarbons (PAH), often resulting in the formation of highly reactive compounds that are the ultimate carcinogens[4]. Glutathione S-transferases (GSTs) are phase II enzymes and responsible for catalyzing the biotransformation of a variety of electrophiles, and have a central role in the detoxification of activated metabolites of procarcinogens produced by phase I reactions. GSTP1 is the main GST isoform expressed in esophageal mucosa[5,6]. Microsomal epoxide hydrolase (mEH) plays a dual role both in detoxication and activation of procarcinogens because it is not only involved in detoxication reaction but also generates some trans-dihydrodiols that could be metabolized to highly toxic, mutagenic and carcinogenic polycyclic hydrocarbon diol epoxides[7].

Esophageal cancer is one of the most common malignant diseases worldwide with a sharp variation in its geographic distribution[8]. The ratio in incidence between high- and low-risk areas could be as great as 500:1. The high incidence in special areas indicates the importance of environmental factors in esophageal carcinogenesis. However, only a small part of individuals in the high-risk area for esophageal cancer develop into esophageal cancer, although all the residents in that area share very similar environment-related risk factors and lifestyle,

suggesting that host susceptibility factors, such as the polymorphisms of phase I and phase II enzymes, may play an important role in increased risk for esophageal cancer. Thus, the present study was undertaken to assess the genetic polymorphisms of CYP1A1, GSTM1, GSTT1, GSTP1 and mEH in esophageal precancerous and cancerous lesions as well as in case control group from the subjects in high-incidence area for esophageal cancer in Henan to correlate these genetic polymorphisms and susceptibility to esophageal cancer.

MATERIALS AND METHODS

Patients and controls

Sixty-two cases of esophageal squamous cell carcinoma (ESCC), including 32 males with a mean age of 55 (55±9.8) and 30 females with a mean age of 60 (66±10.5) were recruited from Yaocun Esophageal Cancer Hospital in Linzhou, who were histopathologically confirmed in 1999. All the cases were from Linzhou district and were interviewed to exclude other simultaneous malignancies. Thirty-eight subjects with matched age and sex frequencies were randomly selected as control group from the same region during the field surveys between 1998 and 1999. Thirty cases of esophageal basal cell hyperplasia (BCH), including 20 males with a mean age of 52 (52±8) and 10 females with a mean age of 54 (54±7) and thirty-two cases of esophageal dysplasia (DYS), including 18 males with a mean age of 54 (54±8) and 14 females with a mean age of 55 (55±7) were also randomly recruited from the same region during the field surveys between 1997 and 1999.

PCR analysis of CYP1A1 gene polymorphism

Genomic DNA was extracted from surgically resected ESCC specimen, BCH and DYS biopsies and buccal smear (for control group). The PCR was performed in a total volume of 25 μL with GeneAmp 9700 (Perkin-Elmer Corp., Norwalk. CT) in this study. The concentration of primers for GSTT1 was 0.3 μM, and others were 1.0 μM. The A to G transition polymorphism in exon 7 of the CYP1A1 gene was analyzed by primers 5' GAAAGGCTGGGTCCACCCTCT and 5' CCAGGAAGAAA GACCTCCCAGCGGGCCA. Briefly, 100 ng of the DNA sample was amplified in buffer (10 mM Tris-HCl, 50 mM KCl, 1.5 mM MgCl2 pH 8.4) with 0.1 mM of each dNTP (Pharmacia, Piscatoway, NJ) and 1.25 U Taq polymerase (Perkin Elmer Corp., Norwalk. CT). Pre-heated at 80 ℃ for 3 sec, then initial denaturation was performed at 95 ℃ for 10 min, followed by 35 cycles of annealing for 1 min at 55 ℃, extention for 1 min at 72 ℃ and denaturation for 1 min at 95 ℃, finally extention for 5 min at 72 ℃. The PCR products were digested with NcoI (New England Biolabs, Inc., Beverly, MA) at 37 ℃ overnight, subjected to electrophoresis in an ethidium-bromide-stained 3 % agarose gel (Nusieve 3: 1; American Bioanalytical, Natick, MA) in TBE buffer (89 mM Tris-HCl, 0.89 mM boric acid and 2 mM EDTA, pH 8.0). PCR-RFLP analysis resulted in the following genotype classification: A predominant homozygote (Ile/Ile), a heterozygote (Ile/Val) and a rare homozygote (Val/Val).

For 3'-flank region polymorphism of CYP1A1, PCR was performed using the primers 5' CAGTCAACAGGTGTAGC and 5' GAGGCAGGTGGATCACTTGAGCTC. After preheated for 3 sec at 80 ℃, initial denaturation was performed at 94 ℃ for 1 min, followed by 37 thermal cycles consisting of denaturation for 25 sec at 94 ℃, annealing for 25 sec at 62 ℃, extention for 25 sec at 72 ℃ and a final extention for 5 min at 72 ℃. The PCR products were digested with MspI (New England Biolabs, Inc., Beverly, MA) at 37 ℃ overnight and subjected to electrophoresis on a 3 % agarose gel. The genotypes of CYP1A1 3' were classified as follows: Wild-type, heterozygous variant and homozygous variant.

GSTM1 and GSTT1 genotyping

GSTM1 and GSTT1 genotyping for gene deletion was carried out by a multiplex PCR using primers 5' GAACTCCCT GAAAAGCTAAAGC and 5' GTTGGGCTCAAATATACG GTGG for GSTM1, which produced a 219 bp product, primers 5' TTCCTTACTGGTCCTCACATCTC and 5' TCACCGGATCATGGCCAGCA for GSTT1, which produced a 480 bp product. At the same time, amplification of the b-globin gene (5' ACACAACTGTGTTCAC TAGC and 5' CTCAAAGAACCTCTGGGTCC) was used as an internal control and produced a 299 bp product. PCR was performed in a 25 μL mixture consisting of 100 ng sample DNA, 10 mM Tris-HCl, 50 mM KCl, 1.5 mM $MgCl_2$ pH 8.4, 0.1 mM of each dNTP and 1.25 U Taq polymerase. After initial denaturation for 3 min at 94 ℃, 35 cycles were performed at 94 ℃ for 1 min (denaturation), at 62 ℃ for 2 min (annealing) and at 72 ℃ for 2 min (extention), followed by a final step for 5 min at 72 ℃. The amplified products were visualized by electrophoresis in ethidium-bromide-stained 3 % agarose gel in TBE buffer. For null deletions of GSTM1 and GSTT1, no amplified product could be observed.

PCR-RFLP analysis of GSTP1 gene polymorphism

The primers 5' GTATTTTGCCCAAGGTCAAG and 5' AGCCACCTGAGGGGTAAG were used to amplify exon 5 of GSTP1 gene that includes the BsmAI enzyme recognition site. The same reaction mixture as above was used, after digestion with BsmAI at 55 ℃ overnight, the following genotypes could be shown: Wild type (one restriction site yielded two fragments of 329 bp and 113 bp), variant with 2 restriction sites, heterozygous variant yielded 3 fragments (329, 216, 113 bp), homozygous one yielded 2 fragments (216, 113 bp).

Analysis of mEH gene polymorphism

Primers 5' GATCGATAAGTTCCGTTTCACC and 5' ATCCTTAGTCTTGAAGTGAGGAT were used to amplify mEH slow allele (113 code). Primers 5' ACATCCAC TTCATCCACGTT and 5' ATGCCTCTGAGAAGCCAT were used to amplify mEH fast allele (139 code). After two separate PCR reactions, the varant, correlated with decreased mEH activity (His 113) was identified through the presence of EcoR V restriction site, and the allele correlated with increased activity (Arg 139) was identified through the presence of RsaI site.

Statistical analysis

The χ^2 test was used to examine the differences in genotype distribution between patients and controls. The difference was considered significant in case of a two-tailed *P* value less than 0.05.

RESULTS

CYP1A1 genetic polymorphism (Table 1)

DNA samples subjected to PCR and enzymatic digestion with MspI revealed the expected fragment lengths and resulted in three genotypes of CYP1A1 3' noncoding area (Figure 1). The frequency of combined heterozygous and homozygous variant genotype detected in the groups of control, BCH, DYS and ESCC was 68 %, 63 %, 62 %, 47 %, respectively (Table 1), the difference was significant between control group and ESCC group ($P<0.05$). However, no significant difference was observed for heterozygous and homozygous variant incidence among the different groups ($P>0.05$). CYP1A1 exon 7 polymorphisms in the groups of control, BCH, DYS and ESCC were observed with an incidence of 47 %, 53 %, 50 % and 52 %, respectively, but there was no significant difference

among these groups (P>0.05). The corresponding heterozygous and homozygous variant frequency did not show a significant difference among these groups.

Table 1 Distribution of CYP1A1 genetic polymorphism in controls and subjects with cancer and different severity of lesions *n*(%)

	Control (*n*=38)	BCH (*n*=30)	DYS (*n*=32)	ESCC (*n*=62)
CYP1A1 3'				
Wild type	12(32)	8(27)	9(28)	33(53)
Heterozygous	22(58)	16(53)	17(53)	25(40)
Homozygous variant	4(10)	3(10)	3(9)	4(6)
Heterozygous+ Homozygous	26(68)	19(63)	20(62)	29(47)[a]
CYP1A1 exon 7				
Ile/Ile	20(53)	14(47)	16(50)	30(48)
Val/Ile	16(42)	14(47)	15(47)	28(45)
Val/Val	2(5)	2(7)	1(3)	4(6)
Val/Ile + Val/Val	18(47)	16(53)	16(50)	32(52)

[a]P<0.05, *vs* case control group.

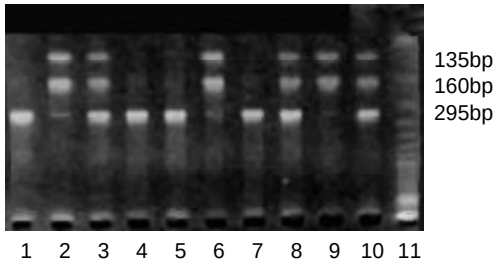

Figure 1 Examples of CYP1A1 3' polymorphism. The RFLPs of PCR-amplified fragments obtained using MspI and subjected to agarose gel electrophoresis. Wild type without MspI restriction site shows a 295 bp band (lanes 1, 4, 5, 7), variant with MspI restriction site results in two bands of 135 and 160 bp (homozygous variant, lanes 2, 6, 9) or all three bands (heterozygous variant, lanes 3, 8, 10).

GSTs genetic polymorphism (Table 2)

Table 2 shows the homozygous deletion of GSTM1 and GSTT1. A similar percentage (around 50 %) for GSTM1 and T1 homozygous deletion in the groups of control, BCH, DYS and ESCC was observed. GSTP1 polymorphism incidence in control group (37 %) was a little lower than that in other groups (about 50 %), but the difference was not significant (P>0.05). There was also no apparent difference for their corresponding heterozygous and homozygous variant distribution in all groups.

Table 2 Genotypes of GSTM1, GSTT1 and GSTP1 in controls and subjects with different severity of lesions and cancer *n*(%)

	Control (*n*=38)	BCH (*n*=30)	DYS (*n*=32)	ESCC (*n*=62)
GSTM1				
+	19(50)	16(53)	18(56)	35(56)
-	19(50)	14(47)	14(44)	27(44)
GSTT1				
+	18(47)	17(57)	15(47)	28(45)
-	20(53)	13(43)	17(53)	34(55)
GSTP1				
Ile/Ile	24(63)	15(50)	15(47)	29(47)
Val/Ile	13(34)	15(50)	16(50)	30(48)
Val/Val	1(3)	0(0)	1(3)	3(5)
Val/Ile + Val/Val	14(37)	15(50)	17(53)	33(53)

mEH genetic polymorphism (Table 3)

mEH polymorphism was observed occurring frequently in exons 3 and 4, which resulted in substitution of amino acid histidine to tyrosine at residue 113 (slow allele) and arginine to histidine at residue 139 (fast allele), respectively. The variant of mEH fast allele was observed with a relatively low frequency in all groups. The homozygous and heterozygous variant for mEH was also detected with a low incidence and no significant difference was observed among different groups (Table 3, P>0.05). However, the different distribution of mEH slow allele variant was observed in the present study. The frequency for mEH slow allele variant (39 %) was the lowest in the control group and increased in BCH (53 %), DYS (69 %) and ECSS (63 %), the difference was significant between control group and BCH, or DYS and ESCC (P<0.05). Figure 2 shows slow allele polymorphism for mEH.

Another interesting result was that none of polymorphic variants of all detected genes was found to be associated with ESCC differentiation in this study.

Table 3 Slow and fast allele polymorphism of mEH in controls and subjects with different severity of lesions and cancer *n*(%)

	Control (*n*=38)	BCH (*n*=30)	DYS (*n*=32)	ESCC (*n*=62)
mEH slow allele				
Tyr/Tyr	23(61)	14(47)	10(31)	23(37)
His/Tyr	10(26)	13(43)	15(47)	22(35)
His/His	5(13)	2(7)	7(22)	17(27)
His/Tyr+His/His	15(39)	16(53)	22(69)[a]	39(63)[a]
mEH fast allele				
His/His	32(84)	22(73)	23(72)	50(81)
Arg/His	5(13)	6(20)	7(22)	11(18)
Arg/Arg	1(3)	2(7)	2(6)	1(2)
Arg/His + Arg/Arg	6(16)	8(27)	9(28)	12(19)

[a]P<0.05, *vs* case control group.

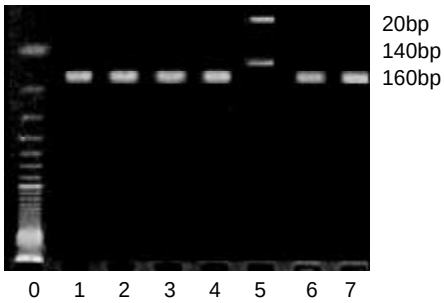

Figure 2 Example of mEH slow allele polymorphism. The RFLPs of PCR-amplified fragments obtained using EcoR V and subjected to agarose gel electrophoresis. Lane 5 is homozygote, lanes 1, 2, 3, 4, 6, 7 wild type.

DISCUSSION

In this study, a similar frequency of CYP1A1 exon 7 polymorphism was observed in the groups of control, ESCC and precancerous lesions, but the CYP1A1 3' flank polymorphic variants most frequently occurred in control group, 1.4 times that in ESCC group (68 % *vs* 47 %), indicating that CYP1A1 3' variants could be a protective factor for ESCC in this population. Two major relevant genetic polymorphisms have been demonstrated in the CYP1A1 gene: One is a T to C substitution in the 3' flanking region altering protein folding, whereas an Ile to Val substitution may occur in exon 7. Both substitutions were considered to result in the enhancement of

enzyme activity[9], but polymorphism in the noncoding region of CYP1A1 was unlikely to have direct functional consequences on CYP1A1 activity[10], even the variant of CYP1A1 exon 7 was not sure to induce an increased enzyme activity[11]. These controversial reports suggest that the effect of CYP1A1 polymorphism on cancer development remains to be characterized.

The second interesting observation in the present study was that a high rate of GSTM1 and GSTT1 null genotype and GSTP1 polymorphic variant occurred not only in the control group but also in ESCC patients and the subjects with different precancerous lesions (BCH and DYS), suggesting that GSTs polymorphism may be responsible for the higher-risk for esophageal cancer in this population. GSTM1 and GSTT1 null genotypes have been reported to enhance the risk of developing gastric, colorectal, and lung cancers[12,13], although other studies did not show such a genetic predisposition[14]. Again, in normal esophageal epithelium, GSTP1 was the mean isoform for GST[5]. An Ile to Val substitution in the GSTP1 gene has been found more often in patients with bladder and testicular cancer[5].

The third interesting observation was that mEH sequence alteration from tyrosine to histidine at residue 113 (slow allele), but not polymorphism at residue 139, was associated with progression of esophageal lesions from normal to BCH to DYS and ESCC, and might contribute to a high susceptibility to esophageal carcinoma. mEH is involved in the metabolism of carcinogens found in cigarette smoke and cooked meat, such as PAH. Expression studies of cDNA *in vitro* indicated that mEH enzymatic activities were decreased by exon 3 polymorphism and increased by exon 4 polymorphism. Reactive and toxic epoxides are frequently generated during PAH oxidative metabolism. Epoxides can be detoxicated partly by mEH, which catalyzes their hydrolysis, thereby yielding the corresponding trans-dihydrolysis. Although hydrolysis is generally considered to represent a detoxication reaction, some trans-dihydrodiols are substrates for additional metabolic changes to highly toxic polycyclic hydrocarbon diol epoxides[7]. It has been suggested that mEH gene His113 variant allele increases the risk of hepatocarcinoma[15] and lung cancer[16] but decreases the risk of ovarian cancer[17]. Further characterization of mEH polymorphism in a larger scale population will be needed to clarify the significance of mEH in high-risk area for esophageal cancer.

Finally, it is noteworthy that the genetic variants of all detected genes in this study were not associated with ESCC differentiation, suggesting that genetic polymorphism may represent susceptibility to ESCC.

ACKNOWLEDGEMENTS

We acknowledge the help given by graduate students in Laboratory for Cancer Research, College of Medicine, Zhengzhou University (Drs. Ya-Nan Jiang, Ran Wang) in preparation of the manuscript.

REFERENCES

1 **Doll R**, Peto R. The causes of cancer: quantitative estimates of avoidable risks of cancer in the united states today. *J Natl Cancer Inst* 1981; **66**: 1191-1308

2 **Mucci LA**, Wedren S, Tamimi RM, Trichopoulos D, Adami HO. The role of gene-environment interaction in the aetiology of human cancer: examples from cancers of the large bowel, lung and breast. *J Intern Med* 2001; **249**: 477-493

3 **Kihara M**, Kihara M, Noda K. Risk of smoking for squamous and small cell carcinomas of the lung modulated by combinations of CYP1A1 and GSTM1 gene polymorphisms in a Japanese population. *Carcinogenesis* 1995; **16**: 2331-2336

4 **Guengerich FP**. Roles of cytochrome P-450 enzymes in chemical carcinogenesis and cancer chemotherapy. *Cancer Res* 1988; **48**: 2946-2954

5 **Peters WH**, Roelofs HM, Hectors MP, Nagengast FM, Jansen JB. Glutathione and glutathione S-transferases in Barrett's epithelium. *Br J Cancer* 1993; **67**: 1413-1417

6 **Nakajima T**, Wang RS, Nimura Y, Pin YM, HE M, Vinio H, Murayama N, Aoyama T, Iida F. Expresssison Of cytochrome P450s and glutathione S-transferases in human esophagus with squamous-cell carcinomas. *Carcinogenesis* 1996; **17**: 1477-1481

7 **Sims P**, Grover PL, Swaisland A, Pal K, Hewer A. Metabolic activation of benzo (a) pyrene proceeds by a diol-epoxide. *Nature* 1974; **252**: 326-328

8 **Wang LD,** Zhou Q, Feng CW, Liu B, Qi YJ, Zhang YR, Gao SS, Fan ZM, Zhou Y, Yang CS, Wei JP, Zheng S. Intervention and follow-up on human esophageal precancerous lesions in Henan, northern China, a high-incidence area for esophageal cancer. *Jpn J Cancer Chemother* 2002; **29**: 159-172

9 **Landi MT**, Bertazzi PA, Shields PG, Clark G, Lucier GW, GarteSJ, Cosma G, Caporaso NE. Association between CYP1A1 genotype, mRNA expression and enzymatic activity in humans. *Pharmacogenetics* 1994; **4**: 242-246

10 **Bailey LR**, Roodi N, Verrier CS, Yee CJ, Dupont WD, Parl FF. Breast cancer and CYPIA1, GSTM1, and GSTT1 polymorphisms: evidence of a lack of association in Caucasians and African Americans. *Cancer Res* 1998; **58**: 65-70

11 **Zhang ZY**, Fasco MJ, Huang L,Guengerich FP, Kaminsky LS. Characterization of purified human recombinant cytochrome P4501A1-Ile462 and -Val462: assessment of a role for the rare allele in carcinogenesis. *Cancer Res* 1996; **56**: 3926-3933

12 **Chenevix-Trench G**, Young J, Coggan M, Board P. Glutathione S-transferase M1 and T1 polymorphisms: susceptibility to colon cancer and age of onset. *Carcinogenesis* 1995; **16**: 1655-1657

13 **Deakin M**, Elder J, Hendrickse C, Peckham D, Baldwin D, Pantin C, Wild N, Leopard P, Bell DA, Jones P, Duncan H, Brannigan K, Alldersea J, Fryer AA, Strange RC. Glutathione S-transferase GSTT1 genotypes and susceptibility to cancer: studies of interactionswith GSTM1 in lung, oral, gastric and colorectal cancers. *Carcinogenesis* 1996; **17**: 881-884

14 **Katoh T**, Nagata N, Kuroda Y, Itoh H, Kawahara A, Kuroki N, Ookuma R, Bell DA. Glutathione S-transferase M1 (GSTM1) and T1 (GSTT1) genetic polymorphism and susceptibility to gastric and colorectal adenocarcinoma. *Carcinogenesis* 1996; **17**: 1855-1859

15 **Mcglynn KA**, Rosvold EA, Lustbader ED, Hu Y**,** Clapper ML, Zhou T, Wild CP, Xia XL, Baffoe-Bonnie A, Ofori-Adjei D, Chen G, London WT, Shen F, Buetow KH. Susceptibility to hepatocellular carcinoma is associated with genetic variation in the enzymatic detoxification of aflatoxin B1. *Prol Natl Acad Sci USA* 1995; **92**: 2384-2387

16 **Benhamou S**, Reinikainen M, Bouchardy C, Dayer P, Hirvonen A. Association between lung cancer and microsomal epoxide hydrolase genotypes. *Cancer Res* 1998; **58**: 5291-5293

17 **Lancaster JM**, Brownlee HA, Bell DA, Futreal PA, Marks JR, Berchuck A, Wiseman RW**,** Taylor JA**.** Microsomal epoxide hydrolase polymorphism as a risk factor for ovarian cancer. *Mol Carcinog* 1996; **17**: 160-162

Edited by Zhu L and Wang XL

P.O.Box 2345, Beijing 100023,China
Fax: +86-10-85381893
E-mail: wjg@wjgnet.com www.wjgnet.com

World J Gastroenterol 2003;9(7):1398-1403
World Journal of Gastroenterology
 ISSN 1007-9327

• GASTRIC CANCER •

Carbonic anhydrase isozymes IX and XII in gastric tumors

Mari Leppilampi, Juha Saarnio, Tuomo J. Karttunen, Jyrki Kivelä, Silvia Pastoreková, Jaromir Pastorek, Abdul Waheed, William S. Sly, Seppo Parkkila

Mari Leppilampi, Department of Clinical Chemistry, University of Oulu, Oulu, Finland
Juha Saarnio, Department of Surgery, University of Oulu, Oulu, Finland
Tuomo J. Karttunen, Department of Pathology, University of Oulu, Oulu, Finland
Jyrki Kivelä, Department of Anatomy and Cell Biology, University of Oulu, Oulu, Finland. Institute of Dentistry, University of Helsinki, Helsinki, Finland. Research Institute of Military Medicine, Central Military Hospital, Helsinki, Finland
Silvia Pastoreková, Jaromir Pastorek, Institute of Virology, Slovak Academy of Sciences, Bratislava, Slovak Republic
Abdul Waheed, William S. Sly, Edward A. Doisy Department of Biochemistry and Molecular Biology, School of Medicine, Saint Louis University, St. Louis, Missouri, USA
Seppo Parkkila, Departments of Clinical Chemistry and Anatomy and Cell Biology, University of Oulu, Oulu, Finland. Institute of Medical Technology, University of Tampere and Tampere University Hospital, Tampere, Finland
Supported by the grants from Sigrid Juselius Foundation, from Finnish Cultural Foundation and Finnish Dental Society, from the National Institutes of Health (DK40163, GM34182, and GM53405), from Slovak Grant Agency (2/7152/20), and from Bayer Corporation
Correspondence to: Mari Leppilampi, M.Sc, Department of Clinical Chemistry, P.O.Box 5000, FIN-90014 University of Oulu, Finland.
mari.leppilampi@oulu.fi
Telephone: +358-40-5164790 **Fax:** +358-8-3154494
Received: 2003-03-19 **Accepted:** 2003-04-03

Abstract

AIM: To systematically study the expression of carbonic anhydrase (CA) isozymes IX and XII in gastric tumors.

METHODS: We analyzed a representative series of specimens from non-neoplastic gastric mucosa and from various dysplastic and neoplastic gastric lesions for the expression of CA IX and XII. Immunohistochemical staining was performed using isozyme-specific antibodies and biotin-streptavidin complex method.

RESULTS: CA IX was highly expressed in the normal gastric mucosa and remained positive in many gastric tumors. In adenomas, CA IX expression significantly decreased towards the high grade dysplasia. However, the expression resumed back to the normal level in well differentiated adenocarcinomas, while it again declined in carcinomas with less differentiation. In comparison, CA XII showed no or weak immunoreaction in the normal gastric mucosa and was slightly increased in tumors.

CONCLUSION: These results demonstrate that CA IX expression is sustained in several types of gastric tumors. The variations observed in the CA IX levels support the concept that gastric adenomas and carcinomas are distinct entities and do not represent progressive steps of a single pathway.

Leppilampi M, Saarnio J, Karttunen TJ, Kivelä J, Pastoreková S, Pastorek J, Waheed A, Sly WS, Parkkila S. Carbonic anhydrase isozymes IX and XII in gastric tumors. *World J Gastroenterol* 2003; 9(7):1398-1403
http://www.wjgnet.com/1007-9327/9/1398.asp

INTRODUCTION

The carbonic anhydrases (CAs) catalyze the reversible hydration of carbon dioxide, $CO_2 + H_2O \Leftrightarrow HCO_3^- + H^+$, and participate in various physiological processes, including respiration, bone resorption, renal acidification, gluconeogenesis, and formation of cerebrospinal fluid and gastric acid. At present, 11 functionally active CA isozymes, differing in their tissue distribution and enzymatic activity, have been identified in mammals[1-3].

CA IX was initially described as a tumor-associated integral plasma membrane antigen (MN)[4]. It has been reported to contain an extracellular domain with the essential structural features and high activity of CAs[5-7]. CA IX has been detected in the normal gastric, intestinal, and biliary mucosa[8]. Because CA IX is more strongly expressed in the proliferating cryptal epithelium than in the upper part of the mucosa, it may play a role in the control of proliferation and differentiation of intestinal epithelial cells[9]. Cell proliferation is abnormally increased in premalignant and malignant lesions, and therefore CA IX has been considered as a potential biomarker for tumor progression[10]. Previous studies have shown that CA IX is expressed in a high percentage of human epithelial tumors, including carcinomas of uterine cervix, lung, kidney, biliary tract, colon, and breast[11-20]. Most of these tumors arise from tissues with no or low CA IX expression. On the other hand, it has been proposed that CA IX is absent or reduced in most tumors originating from CA IX-positive tissues[8].

CA XII is another transmembrane CA isozyme, whose expression has been demonstrated in normal human kidney, colon, prostate, pancreas, ovary, testis, lung, and brain[21, 22]. By immunohistochemistry, CA XII has been detected at the basolateral plasma membrane of the superficial epithelial cells of the colon and rectum, while the small intestine has remained negative[23]. CA XII protein has also been located in the epithelial cells of endometrium[24], renal tubules[25], and efferent ducts[26]. CA XII shows a clear association with some tumors, which was first reported by Türeci *et al.*[27]. They showed that in 10 % of patients with renal cell cancer, the CA XII transcript was expressed at much higher levels in the tumor than in the surrounding normal kidney tissue. These results have been recently confirmed by immunohistochemical staining showing CA XII expression in most cases of clear cell carcinomas and oncocytomas[25]. In addition to renal tumors, CA XII is expressed in a number of colorectal tumors[23] and in ductal carcinomas of the breast[19].

CA IX and XII seem to be regulated by similar mechanisms. First, Ivanov *et al.*[21] identified the *CA9* and *CA12* genes as von Hippel-Lindau (VHL) target genes. They observed that the wild-type VHL protein down-regulated the transcription of CA IX and XII mRNA, indicating that these isozymes may have a potential role in VHL-mediated carcinogenesis. Second, both isozymes have been induced under hypoxic conditions in tumors and cultured tumor cells[22,28]. Hypoxia activates transcription through hypoxia inducible factor-1 (HIF-1), which is composed of two subunits (HIF-1α and HIF-1α)[29]. It is also known that VHL gene product (pVHL) interacts with HIF-1α and is required for the destruction of HIF-1α under normoxic conditions[30]. Taken together, it seems plausible that

CA IX and XII are functionally connected to neoplastic processes controlled by HIF-1 and pVHL[22]. Furthermore, high expression of CA IX and XII in tumors has suggested that they may functionally participate in the invasion process, which is facilitated by acidification of extracellular space. In favor of this hypothesis, it has been shown *in vitro* that CA inhibitors can reduce the invasion capacity and/or proliferation of cancer cells[31-34].

The present study was designed to examine the expression of CA IX and XII in gastric tumors. Even though gastric mucosa is known to be the predominant site of CA IX expression, tumors originating from this area have not been comprehensively studied for the expression of these isozymes.

MATERIALS AND METHODS

Antibodies

The polyclonal rabbit antibodies against human CA XII have been produced earlier[24]. The monoclonal antibody M75 against human CA IX has also been described earlier[4]. Both antibodies have been characterized for specificity and they have shown no cross-reactivity with other CAs[9,24].

Immunocytochemistry

The tissue samples from the non-neoplastic gastric mucosa and the corresponding benign and/or malignant neoplastic samples were obtained alongside routine histopathological specimens collected at Oulu University Hospital (Oulu, Finland). The numbers of samples in each histological category are shown in Table 1. The study was approved by the Ethics Committee of Oulu University Hospital and performed according to the guidelines of the Declaration of Helsinki.

Table 1 Number of gastric specimens analyzed for CA IX and XII expression

Diagnosis	CA IX (*n*)	CA XII (*n*)
Nonneoplastic cardia	7	5
Nonneoplastic corpus	21	15
Nonneoplastic antrum	26	17
Hyperplasia	13	3
Adenoma, slight dysplasia	11	4
Adenoma, moderate dysplasia	8	3
Adenoma, severe dysplasia	3	1
Adenocarcinoma, grade I	11	8
Adenocarcinoma, grade II	16	15
Adenocarcinoma, grade III	16	15
Diffuse carcinoma	18	15
Metastasis of gastric carcinoma	13	13
Intestinal metaplasia	33	20

The specimens were fixed in 4 % neutral-buffered formaldehyde for 24-48 h. Then they were dehydrated, embedded in paraffin in a vacuum oven at 58 ℃, and 5 μm sections were placed on Superfrostä microscope slides (Menzel Gläser, Braunschweig, Germany). The CA isozymes were immunostained by the biotin-steptavidin complex method, employing the following steps: (a) Pretreatment of sections with undiluted cow colostrum (Biotop Ltd, Oulu, Finland) for 30 min and rinsing in phosphate-buffered saline (PBS). (b) Incubation for 1 h with anti-CA XII serum (1:100), normal rabbit serum (1:100) or hybridoma medium with M75 antibody (1:10) in 1 % BSA-PBS. (c) Incubation for 1 h with biotinylated swine anti-rabbit IgG (Dakoplatts, Glostrup, Denmark) or goat anti-mouse IgG (Dakopatts) diluted 1:300 in 1 % BSA-PBS. (d) Incubation for 30 min with peroxidase-conjugated steptavidin (Dakoplatts) diluted 1:500 in PBS and (e) incubation for 2 min in DAB solution containing 9 mg 3,3'-diaminobenzidine tetrahydrochloride (Fluka, Buchs, Switzerland) in 15 ml PBS and 5 μl 30 % H_2O_2. The sections were washed 3 times for 10 min in PBS after incubation steps b and c, and 4 times for 5 min after step d. All the incubations and washings were carried out at room temperature. After the immunostaining, the tumor sections were counterstained with hematoxylin. The stained sections were examined and photographed with Zeiss Axioplan 2 microscope (Zeiss, Göttingen, Germany).

The immunohistochemical results were semiquantitative based on the percentage of the positive cells and on the intensity of the epithelial staining evaluated in a total field of a single section. The extent of staining (EXT) was scored by four investigators (M.L., J.S., T.J.K., and S.Par.) as 1 when 1-10 % of the cells stained, 2 when 11-50 % of the cells stained, and 3 when 51-100 % of the cells stained. A negative score (0) was given to tissue sections which had no evidence of specific immunostaining. The intensity of staining (INT) was scored on a scale of 0 to 3 as follows: 0, no reaction; 1, weak reaction; 2, moderate reaction; 3, strong reaction. In the normal and hyperplastic gastric mucosa, the scores were first counted in the luminal surface, proliferative zone and glands, and relative staining indices (on the scale 0-3) were calculated separately for each histological layer using the following formula: $\sqrt{(EXT \times INT)}$. In the adenomas and metaplasias, the EXT and INT scores were counted separately in the deep and superficial parts of the mucosa, and the relative staining indices were calculated accordingly for both regions. Finally, the staining indices obtained in each region were used to calculate the mean values for each normal sample or lesion. The principle of these calculations is shown in Figure 1.

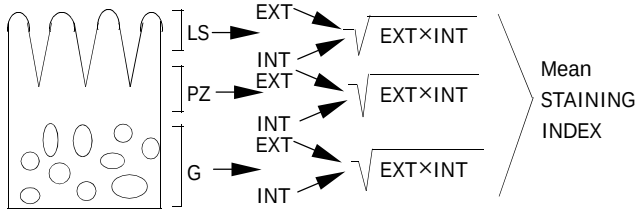

Figure 1 The principle for calculation of the relative staining index in one normal gastric sample (LS=luminal surface, PZ=proliferative zone, G=gastric glands).

Statistical analysis

Statistical analysis of the results was performed using SPSS for Windows software (SPSS Inc.). One-way analysis of variance was used to compare the staining for CA isozymes in different lesions. The pairwise comparisons between group means were performed using multiple comparison tests: Bonferroni, Tukey's honestly significant difference test, Sidak, Gabriel, Hochberg, and LSD (least significant difference).

RESULTS

Expression of CA IX

One intriguing finding of the present study was that the CA IX expression was sustained at relatively high level in many gastric tumors. Figure 2 shows some examples of CA IX immunostaining in the normal gastric mucosa (A) and different

gastric lesions (B-F). In the normal mucosa, CA IX was localized in all major cell types including parietal cells, chief cells, and mucus producing surface epithelial cells as described previously by Pastoreková *et al*.[8]. The positive staining covered all epithelial types of the gastric mucosa including glands, proliferative zone and the superficial epithelium of the mucosa. The staining was observed to be slightly weaker in the proliferative zone (data not shown) that contrasted with previous staining results in intestine where CA IX was mainly confined to the proliferative enterocytes[9]. Figure 2B demonstrates a typical distribution pattern of CA IX in intestinal metaplasia. It was notable that it was expressed in the crypts of metaplastic epithelium which was in line with its high expression in Lieberkühn crypts of the normal gut. Figure 3 demonstrates the mean staining indices for CA IX in the samples of normal gastric mucosa, hyperplasia, adenoma, adenocarcinoma, diffuse carcinoma, metastasis of gastric cancer, and metaplasia. The results demonstrated that the average staining reactions were quite similar in normal and hyperplastic gastric mucosa, while they became significantly weaker in dysplastic and malignant lesions. Figure 4 shows CA IX staining indices in gastric lesions grouped according to the stages of dysplasia and grades of malignancy. This analysis surprisingly revealed that adenomas and carcinomas formed two distinct entities based on the CA IX immunostaining. In adenomas, CA IX staining indices declined from 1.3-1.4 in lesions with slight or moderate dysplasia to 0.3 in those with severe dysplasia. In grade I adenocarcinomas, the staining index remained at the same level with normal and hyperplastic mucosa, while it again declined in carcinomas with higher malignancy grades.

Expression of CA XII

Figure 5 shows examples of CA XII immunostaining in the normal gastric mucosa and different lesions. Figures 6 and 7 show the staining indices for CA XII. In the non-neoplastic gastric mucosa, CA XII showed no or weak immunoreactions. The staining indices appeared to be significantly increased in hyperplastic and adenomatous lesions as well as in grades I and II adenocarcinomas and metastases, although they did not reach the values observed with CA IX. The indices were only very slightly increased in grade III adenocarcinomas and diffuse carcinomas, but the difference was not statistically significant.

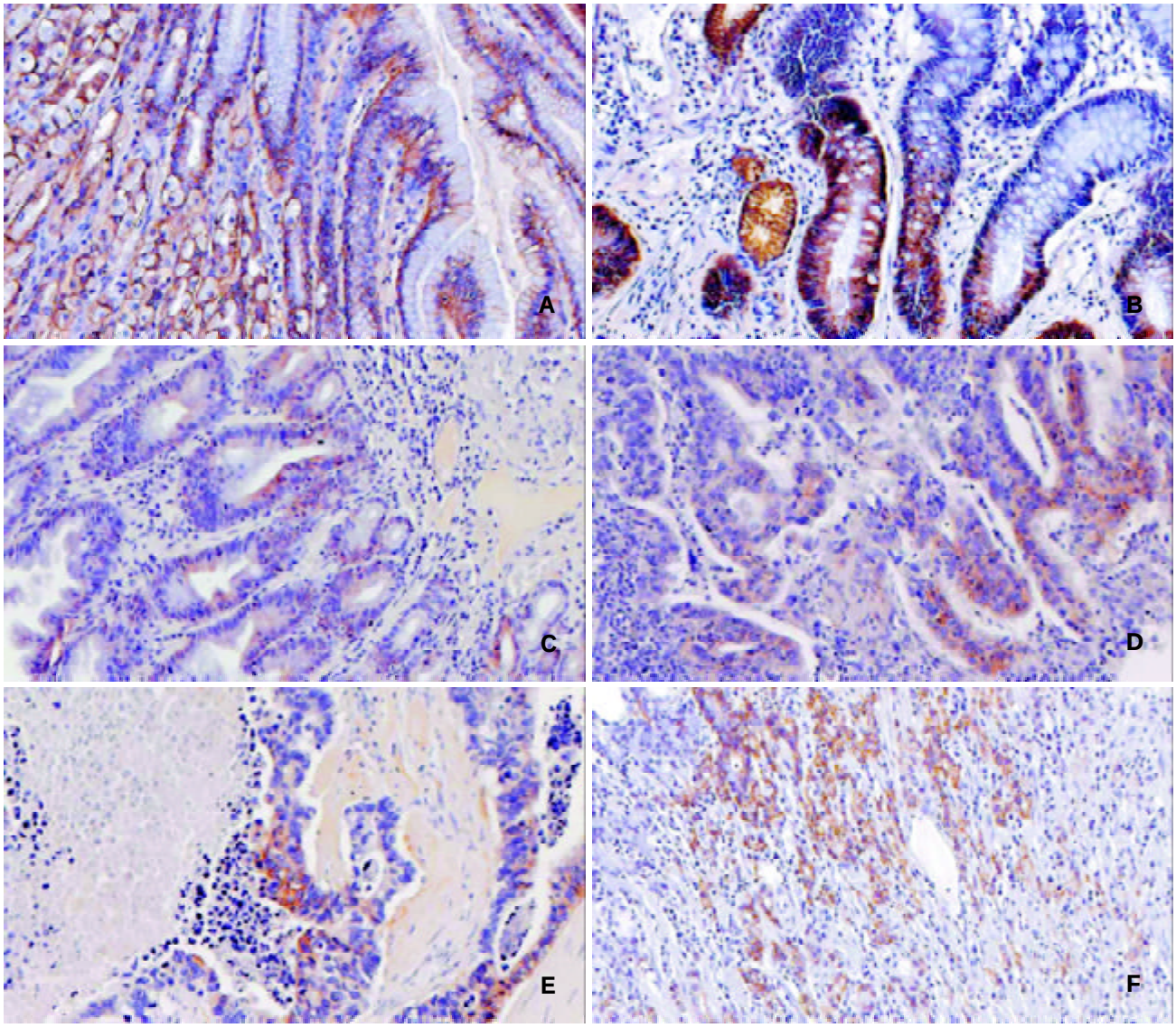

Figure 2 Immunohistochemical staining of CA IX in normal gastric mucosa (A), metaplasia (B), adenoma with moderate dysplasia (C), adenocarcinoma grade II (D), adenocarcinoma grade III (E), and diffuse carcinoma (F). In the normal mucosa, CA IX was expressed in all histological layers covering the luminal surface (LS), proliferative zone (PZ), and gastric glands (G). It was notable that CA IX was confined to deep crypts in metaplastic epithelium. The adenoma sample and all malignant lesions shown in this figure were positive for CA IX. (Original magnifications ×200).

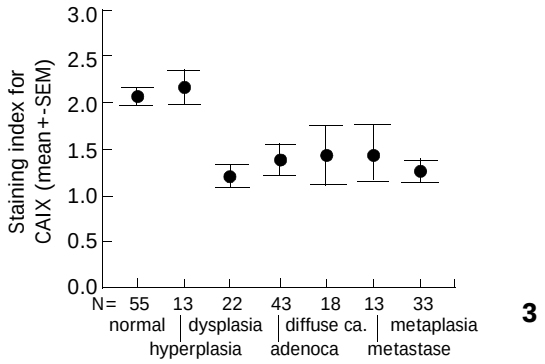

3

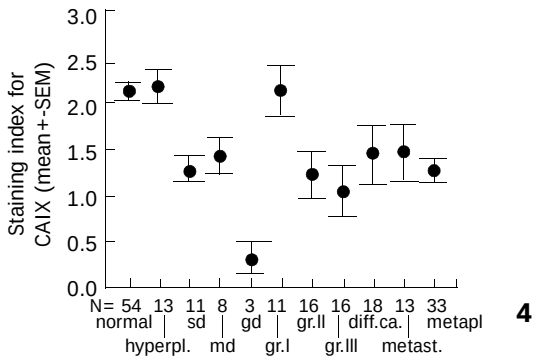

4

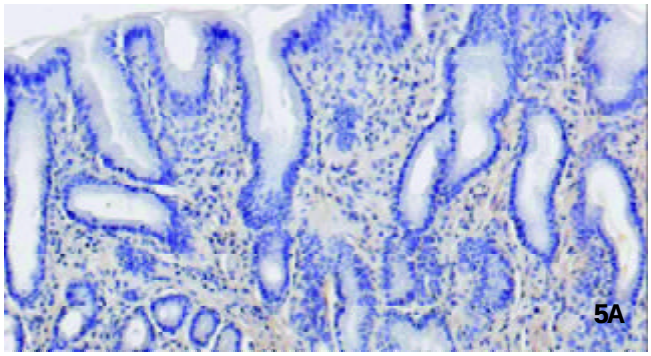

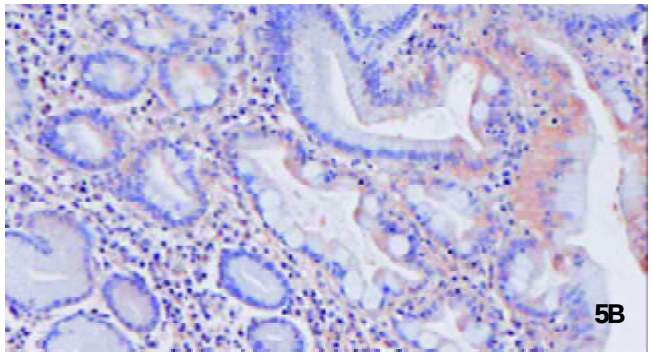

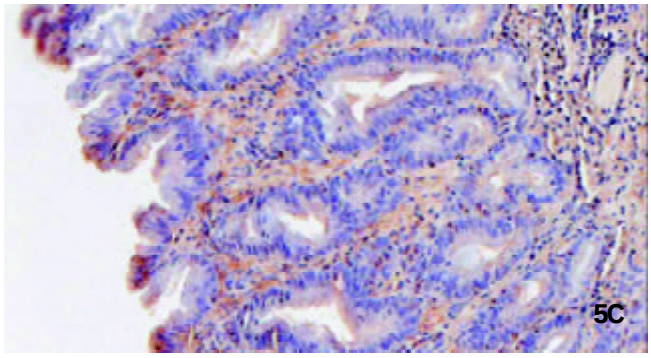

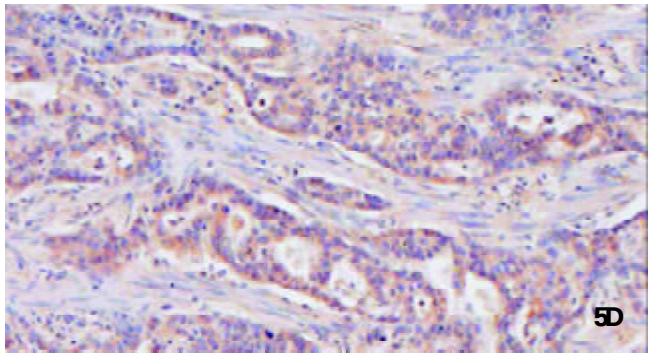

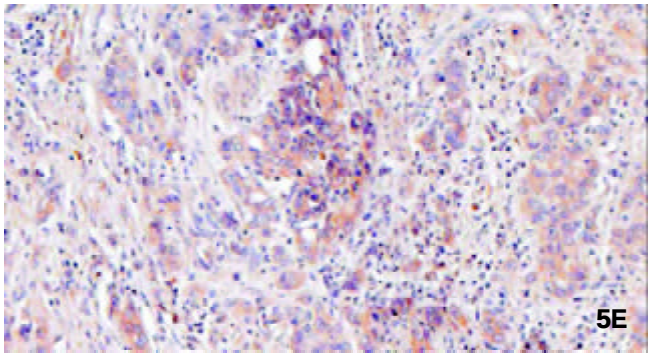

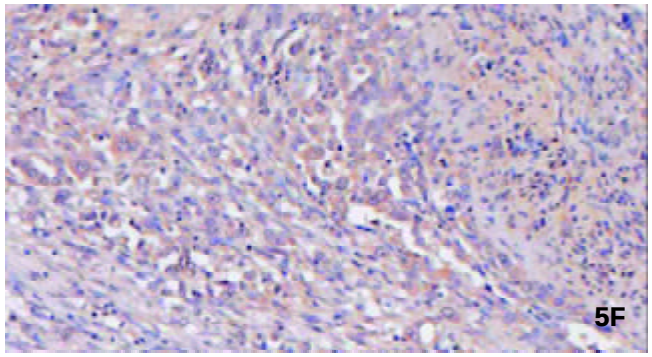

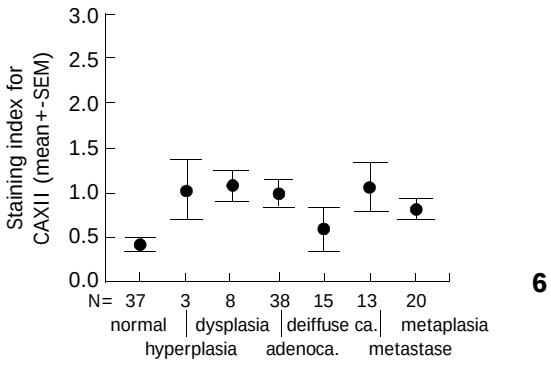

6

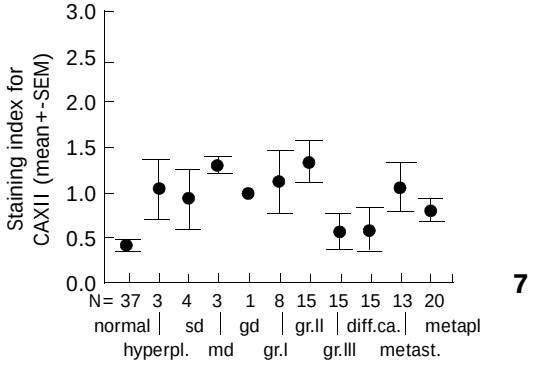

7

Figure 3 The mean staining indices for CA IX in the normal gastric mucosa and different gastric lesions (P=0.002, normal *vs* dysplasia, adenocarcinoma, and metaplasia).

Figure 4 The mean staining indices for CA IX in the normal gastric mucosa and lesions grouped according to the stages of dysplasia and grades of malignancy (P<0.05, normal *vs* gd, gr. II and gr. III).

Figure 5 Immunohistochemical staining of CA XII in normal gastric mucosa (A), metaplasia (B), adenoma with moderate dysplasia (C), adenocarcinoma grade II (D), adenocarcinoma grade III (E), and diffuse carcinoma (F). From these samples, CA XII was

not expressed in the normal epithelium and showed weak expression in metaplastic epithelium and diffuse carcinoma. The signal was stronger in adenoma and adenocarcinoma samples.

Figure 6 The mean staining indices for CA XII in the normal gastric mucosa and different gastric lesions ($P<0.05$, normal *vs* adenocarcinoma).

Figure 7 The mean staining indices for CA XII in the normal gastric mucosa and lesions grouped according to the stages of dysplasia and grades of malignancy ($P=0.003$, normal *vs* gr. II).

DISCUSSION

CA IX is present in several types of human tumors, whereas it is usually absent in the normal tissues from which these tumors originate. For example, it is expressed in neoplasias of uterine cervix and renal cell carcinomas, but not in the normal cervix or kidney[12,13,15,35]. On the other hand, there are only a few non-cancerous tissues expressing MN/CA IX, including epithelia of stomach, intestine, and gallbladder[8]. The present study was focused on the tumors arising from the gastric mucosa, which is normally the predominant site of CA IX expression. One interesting finding of the present study was that CA IX expression was sustained in most cases of gastric neoplasias, even though the expression indices declined compared to the normal and hyperplastic gastric mucosa.

The exact molecular mechanisms of gastric tumorigenesis are still under discussion. Some investigators have postulated that differentiated adenocarcinoma may arise from pre-existing adenoma, following a similar adenoma-carcinoma sequential axis as described for colorectal tumors[36]. However, when gastric adenomas and adenocarcinomas were examined for loss of heterozygosity using microsatellite markers or *MUC* gene expression, the results suggested that the adenoma-carcinoma sequence was not a major pathway in gastric carcinogenesis[37-41]. Since CA IX expression levels seemed to be very low in adenomas with severe dysplasia and normal in grade I adenocarcinoma, the present findings could support the concept that these tumor types are usually distinct entities and do not represent progressive steps from one to the other. In this respect, CA XII did not show any prominent changes in different tumor categories, although its expression was slightly increased in all pathological lesions compared to the nonneoplastic gastric mucosa.

CA IX differs from the other CA isozymes in that it has a proposed dual function as an efficient enzyme[7] and as an adhesion molecule[42,43]. This dual function appears to be related to the structure of CA IX molecule that consists of an extracellularly exposed N-terminal proteoglycan-like region and a CA domain. The CA domain may contribute to the regulation of acid-base homeostasis on the basolateral surfaces of the gastrointestinal epithelial cells. In tumors, CA activity has been suggested to participate in acidification of an extracellular microenvironment facilitating tumor invasion[21]. On the other hand, the adhesion properties of CA IX may be involved in the maintenance of mucosal integrity contributing to proper intercellular contacts and communication[42,43]. Recent studies in *CA9* knockout mice have indicated that CA IX is, indeed, an important factor in gastric morphogenesis and homeostasis of the gastric epithelium possibly acting through the control of cell differentiation and proliferation[44]. The proposed involvement of CA IX in cell differentiation agrees with our observation that high expression of CA IX was associated with a differentiated phenotype of gastric epithelial cells. However, this fact is in contrast to data from other types of tumors, e.g. breast carcinomas, where CA IX expression is increased in tumors with less differentiation, while the opposite is true for CA XII[19].

Even though the present results indicated that CA IX and XII were not specific biomarkers for any categories of gastric tumors, and thus their clinical significance may be limited in this area, they have already revolutionized the field of the CA research in terms of the proposed functions. CA IX and XII are not only enzymatically active isoforms, but also play several important roles in biological processes such as malignant cell invasion[31], cell adhesion[42,43], and cell proliferation[9,10]. These "cancer-associated CAs" are also considered as potential targets in cancer therapy[21,35,45] and a number of promising anticancer therapeutic agents directed to inhibition of CA activity have already been developed and await further evaluation[32-34].

ACKNOWLEDGMENT

The technical assistance of Lissu Hukkanen is gratefully acknowledged.

REFERENCES

1 **Sly WS,** Hu PY. Human carbonic anhydrases and carbonic anhydrase deficiencies. *Annu Rev Biochem* 1995; **64:** 375-401

2 **Hewett-Emmett D,** Tashian RE. Functional diversity, conversation, and convergence in the evolution of the α-, β-, and γ-carbonic anhydrase gene families. *Mol Phylogenet Evol* 1996; **5:** 50-77

3 **Hewett-Emmett D.** Evolution and distribution of the carbonic anhydrase gene families. In: Chegwidden WR, Carter ND, Edwards YH, eds. The carbonic anhydrases. New Horizons. *Basel: Birkhäuser Verlag* 2000: 29-76

4 **Pastoreková S,** Závadová Z, Kost'ál M, Babusiková O, Závada J. A novel quasi-viral agent, MaTu, is a two-component system. *Virology* 1992; **187:** 620-626

5 **Pastorek J,** Pastorekovà S, Callebaut I, Mornon JP, Zelnìk V, Opavský R, Zatòvilovà M, Liao S, Portetelle D, Stanbridge EJ, Zàvada J, Burny A, Kettman R. Cloning and characterization of MN, a human tumor-associated protein with a domain homologous to carbonic anhydrase and a putative helix-loop-helix DNA binding segment. *Oncogene* 1994; **9:** 2877-2888

6 **Opavský R,** Pastorekovà S, Zelník V, Gibadulinovà A, Stanbridge EJ, Zàvada J, Kettman R, Pastorek J. MN/CA9 gene, a novel member of the carbonic anhydrase family: structure and exon to protein domain relationships. *Genomics* 1996; **33:** 480-487

7 **Wingo T,** Tu C, Laipis PJ, Silverman DN. The catalytic properties of human carbonic anhydrase IX. *Biochem Biophys Res Commun* 2001; **288:** 666-669

8 **Pastoreková S,** Parkkila S, Parkkila AK, Opavský R, Zelnik V, Saarnio J, Pastorek J. Carbonic anhydrase IX, MN/CA IX: analysis of stomach complementary DNA sequence and expression in human and rat alimentary tracts. *Gastroenterology* 1997; **112:** 398-408

9 **Saarnio J,** Parkkila S, Parkkila AK, Waheed A, Casey MC, Zhou ZY, Pastoreková S, Pastorek J, Karttunen T, Haukipuro K, Kairaluoma MI, Sly WS. Immunohistochemistry of carbonic anhydrase isozyme IX (MN/CA IX) in human gut reveals polarized expression in the epithelial cells with the highest proliferative capacity. *J Histochem Cytochem* 1998; **46:** 497-504

10 **Saarnio J,** Parkkila S, Parkkila AK, Haukipuro K, Pastoreková S, Pastorek J, Kairaluoma MI, Karttunen TJ. Immunohistochemical study of colorectal tumors for expression of a novel transmembrane carbonic anhydrase, MN/CA IX, with potential value as a marker of cell proliferation. *Am J Pathol* 1998; **153:** 279-285

11 **Závada J,** Závadová Z, Pastoreková S, Ciampor F, Pastorek J, Zelník V. Expression of MaTu-MN protein in human tumor cultures and in clinical specimens. *Int J Cancer* 1993; **54:** 268-274

12 **Liao SY,** Brewer C, Zàvada J, Pastorek J, Pastorekovà S, Manetta A, Bermann ML, DiSaia PJ, Stanbridge EJ. Identification of the MN antigen as a diagnostic biomarker of cervical intraepithelial squamous and glandular neoplasia and cervical carcinomas. *Am J Pathol* 1994; **145:** 598-609

13 **McKiernan JM,** Buttyan R, Bander NH, Stifelman MD, Katz AE,

Chen MW, Olsson CA, Sawczuk IS. Expression of the tumor-associated gene MN: a potential biomarker for human renal cell carcinoma. *Cancer Res* 1997; **57:** 2362-2365

14 **Vermylen P,** Roufosse C, Burny A, Verhest A, Bosschaerts T, Pastorekova S, Ninane V, Sculier JP. Carbonic anhydrase IX antigen differentiates between preneoplastic malignant lesions in non-small cell lung carcinoma. *Eur Respir J* 1999; **14:** 806-811

15 **Liao SY,** Stanbridge EJ. Expression of the MN antigen in cervical papanicolau smears is a diagnostic biomarker of cervical dysplasia. *Cancer Epidemiol Biomarkers Prev* 1996; **5:** 549-555

16 **Saarnio J,** Parkkila S, Parkkila AK, Pastoreková S, Haukipuro K, Pastorek J, Juvonen T, Karttunen TJ. Transmembrane carbonic anhydrase, MN/CA IX, is a potential biomarker for biliary tumours. *J Hepatol* 2001; **35:** 643-649

17 **Giatromanolaki A,** Koukourakis MI, Sivridis E, Pastorek J, Wykoff CC, Gatter KC, Harris AL. Expression of hypoxia-inducible carbonic anhydrase-9 relates to angiogenic pathways and independently to poor outcome in non-small cell lung cancer. *Cancer Res* 2001; **61:** 7992-7998

18 **Chia SK,** Wykoff CC, Watson PH, Han C, Leek RD, Pastorek J, Gatter KC, Ratcliffe P, Harris AL. Prognostic significance of a novel hypoxia-regulated marker, carbonic anhydrase IX, in invasive breast carcinoma. *J Clin Oncol* 2001; **19:** 3660-3668

19 **Wykoff CC,** Beasley N, Watson PH, Campo L, Chia SK, English R, Pastorek J, Sly WS, Ratcliffe P, Harris AL. Expression of the hypoxia-inducible and tumor-associated carbonic anhydrases in ductal carcinoma *in situ* of the breast. *Am J Pathol* 2001; **158:** 1011-1019

20 **Bartošová M,** Parkkila S, Pohlodek K, Karttunen TJ, Galbavý S, Mucha V, Harris AL, Pastorek J, Pastoreková S. Expression of carbonic anhydrase IX in breast is associated with malignant tissues and related to overexpression of c-erbB2. *J Pathol* 2002; **197:** 314-321

21 **Ivanov SV,** Kuzmin I, Wei MH, Pack S, Geil L, Johnson BE, Stanbridge EJ, Lerman MI. Down regulation of transmembrane carbonic anhydrases in renal cell carcinoma cell lines by wild-type von Hippel-Lindau transgenes. *Proc Natl Acad Sci USA* 1998; **95**: 12596-12601

22 **Ivanov S,** Liao SY, Ivanova A, Danilkovitch-Miagkova A, Tarasova N, Weirich G, Merrill MJ, Proescholdt MA, Oldfield EH, Lee J, Zavada J, Waheed A, Sly W, Lerman MI, Stanbridge EJ. Expression of hypoxia-inducible cell-surface transmembrane carbonic anhydrases in human cancer. *Am J Pathol* 2001; **158:** 905-919

23 **Kivelä A,** Parkkila S, Saarnio J, Karttunen TJ, Kivelä J, Parkkila AK, Waheed A, Sly WS, Grubb JH, Shah G, Türeci Ö, Rajaniemi H. Expression of a novel transmembrane carbonic anhydrase isozyme XII in normal human gut and colorectal tumors. *Am J Pathol* 2000; **156**: 577-584

24 **Karhumaa P,** Parkkila S, Türeci Ö, Waheed A, Grubb JH, Shah G, Parkkila AK, Kaunisto K, Tapanainen J, Sly WS, Rajaniemi H. Identification of carbonic anhydrase XII as the membrane isozyme expressed in the normal human endometrial epithelium. *Mol Hum Reprod* 2000; **6:** 68-74

25 **Parkkila S,** Parkkila AK, Saarnio J, Kivelä J, Karttunen TJ, Kaunisto K, Waheed A, Sly WS, Türeci Ö, Virtanen I, Rajaniemi H. Expression of the membrane-associated carbonic anhydrase isozyme XII in the human kidney and renal tumors. *J Histochem Cytochem* 2000; **48:** 1601-1608

26 **Karhumaa P,** Kaunisto K, Parkkila S, Waheed A, Pastoreková S, Pastorek J, Sly WS, Rajaniemi H. Expression of the transmembrane carbonic anhydrases, CA IX and CA XII, in the human male excurrent ducts. *Mol Hum Reprod* 2001; **7:** 611-616

27 **Türeci Ô,** Sahin U, Vollmar E, Siemer S, Göttert E, Seitz G, Parkkila AK, Shah GN, Grubb JH, Pfreundschuh M, Sly WS. Human carbonic anhydrase XII, cDNA cloning, expression, and chromosomal localization of a carbonic anhydrase gene that is overexpressed in some renal cell cancers. *Proc Natl Acad Sci USA* 1998; **95:** 7608-7613

28 **Wykoff CC,** Beasley N, Watson PH, Turner KJ, Pastorek J, Sibtain A, Wilson GD, Turley H, Talks K, Maxwell PH, Pugh CW, Ratcliffe PJ, Harris AL. Hypoxia inducible expression of tumor associated carbonic anhydrases. *Cancer Res* 2000; **60:** 7075-7083

29 **Semenza GL.** Hypoxia, clonal selection, and the role of HIF-1 in tumor progression. *Crit Rev Biochem Mol Biol* 2000; **35:** 71-103

30 **Maxwell PH,** Wiesener MS, Chang GW, Clifford SC, Vaux EC, Cockman ME, Wykoff CC, Pugh CW, Maher ER, Ratcliffe PJ. The tumour suppressor protein VHL targets hypoxia-inducible factors for oxygen-dependent proteolysis. *Nature* 1999; **399:** 271-275

31 **Parkkila S,** Rajaniemi H, Parkkila AK, Kivelä J, Waheed A, Pastoreková S, Pastorek J, Sly W. Carbonic anhydrase inhibitor suppresses invasion of renal cancer cells *in vitro*. *Proc Natl Acad Sci USA* 2000; **97:** 2220-2224

32 **Supuran CT,** Scozzafava A. Carbonic anhydrase inhibitors. *Curr Med Chem* 2001; **1:** 61-97

33 **Supuran CT,** Briganti F, Tilli S, Chegwidden WR, Scozzafava A. Carbonic anhydrase inhibitors: Sulfonamides as antitumor agents? *Bioorg Med Chem* 2001; **9:** 703-714

34 **Supuran CT,** Scozzafava A. Applications of carbonic anhydrase inhibitors and activators in therapy. *Expert Opin Ther Patents* 2002; **12:** 217-242

35 **Uemura H,** Nakagawa Y, Yoshida K, Saga S, Yoshikawa K, Hirao Y, Oosterwijk E. MN/CA IX/G250 as a potential target for immunotherapy of renal cell carcinomas. *Br J Cancer* 1999; **81:** 741-746

36 **Uchino S,** Noguchi M, Ochiai A, Saito T, Kobayashi M, Hirohashi S. p53 mutation in gastric cancer: a genetic model for carcinogenesis is common to gastric and colorectal cancer. *Int J Cancer* 1993; **54:** 759-764

37 **Maesawa C,** Tamura G, Suzuki Y, Ogasawara S, Sakata K, Kashiwaba M, Satodate R. The sequential accumulation of genetic alterations characteristic of the colorectal adenoma-carcinoma sequence does not occur between gastric adenoma and adenocarcinoma. *J Pathol* 1995; **176:** 249-258

38 **Tamura G,** Sakata K, Maesawa C, Suzuki Y, Terashima M, Satoh K, Sekiyama S, Suzuki A, Eda Y, Satodate R. Microsatellite alterations in adenoma and differentiated adenocarcinoma of the stomach. *Cancer Res* 1995; **55:** 1933-1936

39 **Tamura G.** Molecular pathogenesis of adenoma and differentiated adenocarcinoma of the stomach. *Pathol Int* 1996; **46:** 834-841

40 **Semba S,** Yokozaki H, Yamamoto S, Yasui W, Tahara E. Microsatellite instability in precancerous lesions and adenocarcinomas of the stomach. *Cancer* 1996; **77:** 1620-1627

41 **Tsukashita S,** Kushima R, Bamba M, Sugihara H, Hattori T. MUC gene expression and histogenesis of adenocarcinoma of the stomach. *Int J Cancer* 2001; **94:** 166-170

42 **Závada J,** Závadová Z, Machon O, Kutinova L, Nemeckova S, Opavský R, Pastorek J. Transient transformation of mammalian cells by MN protein, a tumor-associated cell adhesion molecule with carbonic anhydrase activity. *Int J Oncol* 1997; **10:** 857-863

43 **Závada J,** Závadová Z, Pastorek J, Biesová Z, Jezek J, Velek J. Human tumor-associated cell adhesion protein MN/CA IX: identification of M75 epitope and of the region mediating cell adhesion. *Br J Cancer* 2000; **82:** 1808-1813

44 **Gut MO,** Parkkila S, Vernerová Z, Rohde E, Závada J, Höcker M, Pastorek J, Karttunen T, Gibadulinová A, Závadová Z, Knobeloch KP, Wiedenmann B, Svoboda J, Horak I, Pastoreková S. Gastric hyperplasia in mice with targeted disruption of the carbonic anhydrase gene *Car9*. *Gastroenterology* 2002; **123:** 1889-1903

45 **Uemura H,** Kitagawa H, Hirao Y, Okajima E, Debruyne FMJ, Oosterwijk E. Expression of tumor-associated antigen MN/G250 in urologic carcinoma: potential therapeutic target. *J Urol Suppl* 1997; **157:** 377

Edited by Xu XQ

P.O.Box 2345, Beijing 100023,China
Fax: +86-10-85381893
E-mail: wjg@wjgnet.com www.wjgnet.com

World J Gastroenterol 2003;9(7):1404-1408
World Journal of Gastroenterology
 ISSN 1007-9327

• GASTRIC CANCER •

Spiral CT in gastric carcinoma: Comparison with barium study, fiberoptic gastroscopy and histopathology

Feng Chen, Yi-Cheng Ni, Kai-Er Zheng, Sheng-Hong Ju, Jun Sun, Xi-Long Ou, Man-Hua Xu, Hao Zhang, Guy Marchal

Feng Chen, Kai-Er Zheng, Sheng-Hong Ju, Jun Sun, Department of Radiology, Zhongda Hospital, 87 Dingjiaqiao Road, Nanjing 210009, Jiangsu Province, China
Xi-Long Ou, Man-Hua Xu, Department of Digestive Diseases, Zhongda Hospital, 87 Dingjiaqiao Road, Nanjing 210009, Jiangsu Province, China
Feng Chen, Yi-Cheng Ni, Hao Zhang, Guy Marchal, Department of Radiology, University Hospital, Herestraat 49, B-3000 Leuven, Belgium
Supported by ECR 2000-EAR-ECR Research & Education Fund Fellowship Grant
Correspondence to: Professor Yi-Cheng Ni, Department of Radiology, University Hospital, Herestraat 49, B-3000 Leuven, Belgium. yicheng.ni@med.kuleuven.ac.be
Telephone: +32-16-345940 **Fax:** +32-16-343765
Received: 2003-03-12 **Accepted:** 2003-04-11

Abstract

AIM: To evaluate spiral computed tomography (CT) including virtual gastroscopy for diagnosis of gastric carcinoma in comparison with upper gastrointestinal series (UGI), fiberoptic gastroscopy (FG) and histopathology.

METHODS: Sixty patients with histologically proven gastric carcinoma (54 advanced and 6 early) were included in this study. The results of spiral CT were compared with those of UGI and FG. Two observers blindly evaluated images of spiral CT and UGI and video recording of FG with consensus in terms of diagnostic confidence with a five-point scale. Sensitivities of lesion detection, Borrmann's classification of spiral CT, UGI and FG, as well as the accuracy of TNM staging of spiral CT were determined by comparing them to surgical and histological findings.

RESULTS: The lesion detection rate was 98 % (59/60), 95 % (57/60) and 98 % (59/60) for spiral CT, UGI and FG, respectively. There were no statistical differences in the detection sensitivity among the three techniques ($P>0.05$). For the sensitivity in Borrmann's classification, spiral CT was higher than that of UGI ($P=0.025$) and similar to that of FG ($P>0.05$). The accuracy of spiral CT in staging the gastric carcinoma was 76.7 %. Six cases of early gastric carcinoma were all detected by spiral CT as well as FG.

CONCLUSION: Spiral CT is equivalent to UGI and FG in the detection of gastric carcinoma, and superior to UGI but similar to FG in the Borrmann's classification of advanced gastric carcinoma. Spiral CT is more valuable than FG in the staging of gastric carcinoma.

Chen F, Ni YC, Zheng KE, Ju SH, Sun J, Ou XL, Xu MH, Zhang H, Marchal G. Spiral CT in gastric carcinoma: Comparison with barium study, fiberoptic gastroscopy and histopathology. *World J Gastroenterol* 2003; 9(7): 1404-1408
http://www.wjgnet.com/1007-9327/9/1404.asp

INTRODUCTION

Fiberoptic gastroscopy (FG) is generally regarded as a standard test for detection of gastric cancer. Upper gastrointestinal series (UGI), however, still represents a routine or survey examination for imaging gastric abnormalities although it has certain limitations in clinical use. Even though the application of conventional computed tomography (CT) in staging gastric carcinoma has been introduced, the results are unsatisfactory[1-3]. Recently, spiral CT, including various three-dimensional (3D) reconstructions such as virtual endoscopy and axial source images (2D) has been used in imaging the alimentary tract[2-16]. While most reports in literature laid emphasis on colon polyps[11-12, 14-15], there have been a few studies investigating gastric carcinoma with spiral CT[4-10]. In clinical practice, advanced gastric carcinoma is defined using Borrmann's classification, which is the pathological basis for UGI diagnosis, and the resectability of the tumor and prognosis of the patients are evaluated presurgically using TNM staging[17], which is one of the suggested applications of spiral CT.

In this study, 2D and 3D display techniques after spiral CT scan were cross-referenced. The role of this combined spiral CT technique was compared with that of UGI and FG in the detection and Borrmann's classification of gastric carcinoma, which, to our knowledge, has not been reported in literature. The staging of gastric carcinoma with spiral CT was also correlated with histopathology.

MATERIALS AND METHODS

Patients

During a 12-month period, 60 consecutive patients (36 males, 24 females) ranging from 27 to 79 years old (mean=62 a.), who were diagnosed of gastric carcinoma with FG and subsequent biopsy were recruited. Among the 60 gastric carcinoma patients, 43 were undertaken gastrectomy or subtotal gastrectomy, 17 were undertaken surgical exploration only because of severe adhesion between tumor and surrounding tissues. This study was approved by the administrative authority of the university hospital and fully informed consent was obtained from each patient. Within one week after FG procedure, UGI was performed prior to spiral CT scanning on each patient.

Imaging acquisition

Spiral CT was performed with a Hispeed CT/i scanner (General Electric Medical Systems, Milwaukee, WI). All patients were fasted for 12 hours. Before the CT scanning, 20 mg raceanisodamine hydrochloride was intramuscularly administered and two packs (6 g) of effervescent granules were taken orally. Usually patients were immediately placed on the scanning table in an oblique supine position. A scout projection was made to confirm the stomach to be distended by gas. If insufficient distention of stomach was found, half to one pack of effervescent granules was added and a scout projection was scanned again. Then, spiral CT was performed with a 3-mm collimation and a pitch of 1.2-1.5 mm during a single breath-hold of 22-33 seconds, which produced a 3D-volume

acquisition that included the entire stomach. Tube current was 200-280 mA, voltage was 120 kVp and scan time was 1 second per rotation.

Barium double contrast technique with standard projection was used for UGI studies by an experienced radiologist. Standard FG examination was performed by an experienced gastrologist and the biopsy samples were processed as a clinical routine of pathology department.

Image reconstruction

3D-postprocessing modes including CT virtual gastroscopy (CTVG), surface shaded display (SSD) and "Raysum" Display (virtual double contrast barium study) were performed by a built-in workstation (Advantage Window 2.0, General Electric Medical Systems, Milwaukee, WI) after raw data reconstruction with 1 mm interval. For intraluminal views of the stomach, a default level of -525 (Hounsfield unit, HU) provided by the Navigator (GE Company) was chosen. SSD and "Raysum" display were obtained with a threshold of -311HU.

Image analysis

Sixty sets of hard copy of grayscale spiral CT images (including axial source images, CTVG, SSD, and "Raysum" display) and UGI radiograms from 60 patients were obtained by one radiologist and were randomly reviewed and scored with consensus by two other experienced radiologists who were blinded to clinical data, pathology, and the information of other imaging techniques. Video recording of FG examinations was reviewed and scored with consensus by two experienced gastrologists.

The diagnostic confidence, appearance, location, and size of suspected lesions on images of spiral CT, UGI and FG were recorded. For spiral CT, the observers made the final judgments after referring to all 4 techniques including CTVG, SSD, "Raysum" and axial source images. The lesions were then classified as early and advanced gastric carcinoma according to Borrmann's classification[2]. Based on spiral CT, TNM staging[16] of gastric carcinoma of each case was also noted. Diagnostic confidence for detecting a lesion was rated as 1, definitely no lesion; 2, probably not a lesion; 3, possible lesion; 4, probable lesion; 5, definite lesion[18]. Any image artifacts that degraded diagnostic confidence were also noted.

All findings of lesions with spiral CT, UGI and FG were further verified with the results of surgical exploration, dissected specimen and histology, which were used as the gold standard for detection, Borrmann's classification and spiral CT staging of gastric carcinoma.

Statistical analysis

Data entry procedures and statistical analysis were performed with a statistical software package (SAS for windows, version 6.12, SAS Institute, Cary, NC). By using only those lesions allocated with confidence rate of 3 or higher, the sensitivity of detection and classification of gastric carcinomas of each technique was assessed[18] (Chi-square test). Significant differences were considered when the *P* value was less than or equal to 0.05.

RESULTS

The classification, size and location of the gastric cancer in this study are summarized in Table 1. A complete set of image data of a patient is exemplified in Figure 1.

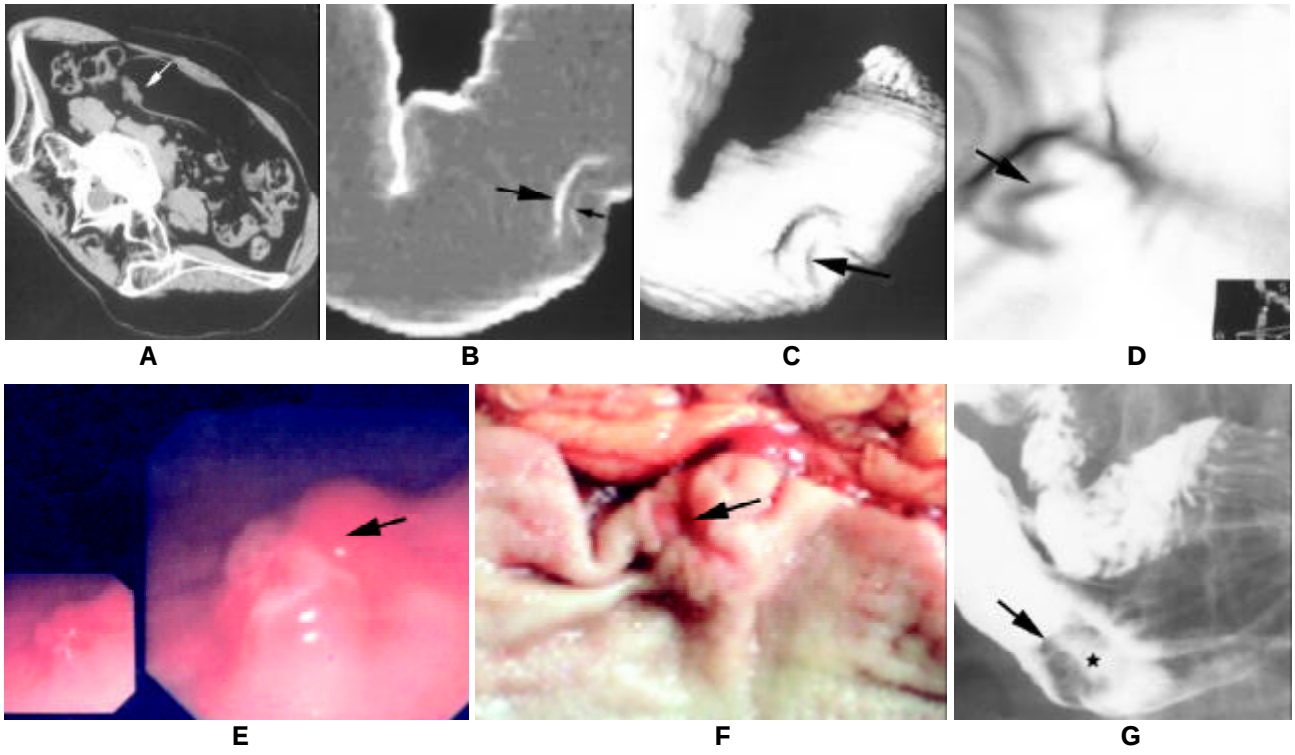

Figure 1 A complete set of image data of a patient. Spiral CT images (A-D), fiberoptic gastroscopy (E), surgical specimen (F) and corresponding barium study (G) from a patient (female, 48 a.) of Borrmann's type 2 and TNM stage 1 of advanced gastric carcinoma. (A), axial image (supine position with right side elevated) showed a focal irregular protruding (arrow) from the posterior wall of antrum. (B), "Raysum" display (virtual double contrast barium study) stressed double-margin changes at the greater curvature of antrum: tumor (large arrow) and ulcer (small arrow) margins. (C), SSD image showed depression at the antrum with a central ulcer (arrow). (D), CTVG image depicted an intraluminal irregular mass with a flat ulcer (arrow). The view angle was illustrated by the 2D image at lower right corner. (E), fiberoptic gastroscopic view showed a lobulated mass. (F), surgical specimen demon stratad a mass with a small central ulcer (arrow). (G), barium study revealed an intraluminal filling defect (arrows) with a flat ulcer (asterisk) at the greater curvature of antrum.

Table 1 Classification, size and location of gastric carcinoma (n=60)

Gastric cancer classification						Size of the tumor		
Early			Advanced*			<1 cm	1-3 cm	>3 cm
Type 2c	Type 3	Type 1	Type 2	Type 3	Type 4			
4 (6.7%)	2 (3.3%)	10(16.7%)	25 (41.7%)	14 (23.3%)	5 (8.3%)	6	24	30
Location of the tumor								
		Cardia area	Antrum	Great curv	Lesser curv	Antrum and body		
		29	18	5	5	3		

Notes: Numbers were patients. Curv.=curvature. *Borrmann's type of classification.

Lesion detection

In advanced gastric carcinoma, the lesion detection (with diagnostic confidence of 3 or higher) sensitivity of spiral CT was similar to that of UGI and FG (P>0.05). In early gastric carcinoma, it was higher than that of UGI (P=0.031) and similar to that of FG (Table 2). One false positive lesion (due to peristalsic wave at the lesser curvature) and one false negative lesion (with diagnostic confidence rate of 3 or lower) were noted in spiral CT. 3 and one false negative lesion was noted in UGI and FG, respectively (Table 3).

Table 2 Comparison of sensitivities on gastric carcinoma between different techniques

	Detection		Classification
	Early	Advanced	Advanced
SCT	100%	98%	77%
UGI	33%	95%	47%
FG	100%	98%	80%
	Chi-Square test		
SCT *vs* UGI	P=0.031	P>0.05	P=0.025
SCT *vs* FG	P>0.05	P>0.05	P>0.05

Notes: SCT=spiral CT, UGI=upper gastrointestinal series, FG=fiberoptic gastroscopy.

Table 3 Comparison of different techniques in erroneously interpreted lesions

	n	False positive	False negative	Bormann's classification	
				Can not be classified	Erroneously classified
SCT	60	1	1	2	12
UGI	60	0	3	9	23
FG	60	0	1	0	12

Notes: Data were the number of lesions. SCT=spiral CT, UGI=upper gastrointestinal series, FG=fiberoptic gastroscopy.

Borrmann's classification

The ability of spiral CT to correctly classify the lesions according to Borrmann's classification was statistically higher than that of UGI (P=0.025) and similar to that of FG (P>0.05) (Table 2).

For spiral CT, 12/60 lesions were erroneously classified and 2/60 could not be classified which were attributed to image artifacts of respiration movement and fluid retention in stomach. For UGI, 23/60 lesions were erroneously classified and 9/60 could not be classified. For FG, 12/60 lesions were erroneously classified (Table 3). So, a total of 47 lesions were erroneously classified from spiral CT, UGI and FG. The rates of erroneously classified lesions in Borrmann's types 1, 2, 3, and early gastric carcinoma were 6.4 % (3/47), 61.7 % (29/47), 25.5 % (12/47), and 6.4 % (3/47), respectively. The majority of erroneously classified lesions occurred in Borrmann's type 2 (61.7 %) and type 3 (25.5 %). No erroneously classified lesion was found in Borrmann's type 4.

TNM staging of spiral CT

43 of 60 patients were included in the TNM staging. Of the 43 cases, stage I was found in 12, 6 of which were early gastric carcinoma, stage II in 7, stage III in 19 and stage IV in 5. The accuracy of spiral CT in TNM staging was 76.7 % (33/43). 5 cases of overestimation and underestimation were noted respectively in spiral CT staging (Table 4).

Table 4 Comparison of TNM staging of gastric carcinoma between spiral CT and pathology

Pathological staging	Spiral CT staging				Total
	1	2	3	4	
1	10	2	0	0	12
2	0	4	3	0	7
3	0	7	12	0	19
4	0	0	2	3	5
Total	10	13	17	3	43

DISCUSSION

The evaluation of gastric carcinoma by conventional barium studies is hampered by the following limitations: (1) the impossibility to produce endoscopic views, (2) the projective nature of the technique, (3) the quality of barium coating and the examiner's technique and skills. The disadvantage of FG examination is that it cannot evaluate the tumor involvement of gastric wall and surrounding tissues and therefore it has inability of TNM staging. Spiral CT has brought about additional possibilities for the evaluation of gastric tumors. Since the assessment of endoluminal morphology of gastric tumors is limited when only source images are used, 3D visualization techniques have been advocated[4-10]. In a recently published paper, the SSD and virtual double contrast imaging were compared with conventional barium studies and CTVG was compared with gastroscopy in various types of gastric pathologies respectively[6]. The present report represents a comprehensive clinical study that covers all three different 3D techniques of spiral CT (CTVG, SSD and virtual double contrast), as well as axial source images in comparison with UGI and FG focusing on the detection, classification and staging of gastric carcinoma.

We used two reconstruction algorithms for the 3D visualization of the stomach. One was SSD display, which provided outside opaque images of inner surface of the gastric

wall generated with a thresholding technique and could be interpreted similarly as in single-contrast barium study[12]. The other was volume rendering technique including CTVG and virtual double contrast imaging as described elsewhere[12,13]. CTVG with perspective volume rendering technique produced intraluminal view similar to those obtained from fiberoptic gastroscopy. Virtual double contrast imaging displayed somewhat translucent images similar to those of double contrast barium study.

As different 3D techniques, the advantage of SSD and virtual double contrast display was to demonstrate the overall aspect and the contour changes of the stomach, but with poor mucosal information[6] (Figure1 B, C), and CTVG offered the overview of the intraluminal tumors but with indiscernible surface coloration and extraluminal tumor invading (Figure1D). Therefore, it is important to realize that information from 3D CT displays should be combined with that of source images in interpreting the gastric carcinoma clinically (Figure 1 A-D).

In our study, tumor detection sensitivities among spiral CT, UGI and FG were similar (P>0.05). However, the sensitivity was higher with spiral CT than that with UGI (P=0.031) and similar between SCG and FG (P>0.05) in early gastric carcinoma. Only a few studies on the detection of early gastric carcinoma with spiral CT were reported, the results so far have been controversial[10]. The detection rate of early gastric carcinoma was 93.5 % reported by Lee[10] with contrast enhanced SSD technique, and it was only 26 % by spiral CT according to Fukuya[19]. Moreover, it was even lower with 3D CT than that of UGI according to Ogata[6]. In our study, spiral CT correctly detected all 6 cases of early gastric carcinomas, the detection rate (100 %) was much higher than that of UGI (33.3 %). However, the very limited number of cases with early gastric carcinoma in this series did not allow any conclusion in this regard.

The distribution and prevalence rate of gastric tumor according to Borrmann' s classification in this study was slightly different from that reported, in which the most prevalent type was Borrmann' s 3 and the most common site of tumor was the posterior wall of the antrum[8]. In our investigation, the most prevalent type was Borrmann' s 2 and the most common site of tumor was the cardia and fundus. It has been reported that accurate classification of gastric tumor based on Borrmann' s classification is possible with 3D CT[7,8]. Our study indicated that Borrmann' s classification with spiral CT was better than that with UGI (P=0.025), and similar to that of FG (P>0.05). In this study, the majority of misclassification occurred in Borrmann' s types 2 and 3, in which UGI accounted for a highest proportion of the misclassification rate. The main reasons were most likely due to the following: (1) in the present study, cardia or fundus carcinoma was found in the highest percentage of the patients (48.3 %, 29/60), therefore Borrmann' s type 2 or 3 tumors at cardia tended to be misclassified as type 1, because of the poor visualization of some small and flat ulcers within the tumor. (2) The limited capability of UGI in visualizing the ulcer and the infiltrating nature of tumors at the cardia was also a reason for the difficult differentiation between Borrmann' s types 2 and 3. (3) On the contrary, Borrmann' s type 2 or 3 at the antrum tended to be erroneously classified as type 4, because these tumors were poorly visualized by spiral CT[8].

The rational work out of treatment scheme and accurate evaluation of gastric carcinoma are mainly dependent on TNM staging before surgery. Spiral CT is a practical approach in TNM staging because it can visualize the gastric wall, surrounding tissue and organs. Many studies on gastric carcinoma staging with conventional CT have been reported so far. The results in the literature were various due to the different CT scanner and materials and methods used[20]. Using a spiral CT technique of thin slice thickness (3 mm) and plain scanning, staging accuracy of gastric carcinoma in this study reached 76.7 %. This result was higher than that (72.0 %) obtained by conventional CT scanning with contrast enhancement[21], and was lower than that (81 %) obtained by triphase contrast enhancement of spiral CT[22]. Certainly, multiphase contrast enhanced spiral CT scan may further improve the staging of gastric carcinoma, the method we used, however, was simple, practical and more acceptable by the patients.

Some limitations of this study should be mentioned: (1) Since the size of more than half of the lesions in this group was large (>3 cm), the conclusions drawn from the results might not be applicable to small or flat gastric lesions. (2) Because all the CT examinations were performed in patients with known gastric carcinoma, the specificity of different imaging techniques was not investigated in our study.

In summary, the present clinical study demonstrates that spiral CT is equal to UGI and FG in the detection of gastric carcinoma. For Borrmann' s classification of gastric carcinoma, spiral CT scores better than UGI and similar to FG. Spiral CT is also of value in TNM staging of gastric carcinoma. It is suggested that spiral CT is an alternative to UGI and supplement to FG in gastric carcinoma diagnosis. However, further investigations on a larger scale are necessary to confirm the role of spiral CT in the evaluation of gastric carcinoma.

REFERENCES

1 **Sussman SK,** Halvorsen RA Jr, Illescas FF, Cohan RH, Saeed M, Silverman PM, Thompson WM, Meyers WC. Gastric adenocarcinoma: CT versus surgical staging. *Radiology* 1988; **167:** 335-340

2 **Fishman EK,** Urban BA, Hruban RyH. CT of the stomach: spectrum of disease. *RadioGraphics* 1996; **16:** 1035-1054

3 **Balthazar EJ,** Siegel SE, Megibow AJ, Scholes J, Gordon R. CT in patients with scirrhous carcinoma of the GI tract: imaging findings and value for tumor detection and staging. *AJR* 1995; **164:** 839-845

4 **Lee DH,** Ko YT. Gastric lesions: evaluation with three-dimensional images using helical CT. *AJR* 1997; **169:** 787-789

5 **Wood BJ,** O'Malley ME, Hahn PF, Mueller PR. Virtual endoscopy of the gastrointestinal system outside the colon. *AJR* 1998; **171:** 1367-1372

6 **Ogata I,** Komohara Y, Yamashita Y, Mitsuzaki K, Takahashi M, Ogawa M. CT evaluation of gastric lesions with three-dimensional display and interactive virtual endoscopy: comparison with conventional barium study and endoscopy. *AJR* 1999; **172:** 1263-1270

7 **Lee DH,** Ko YT. Advanced gastric carcinoma: the role of three-dimensional and axial imaging by spiral CT. *Abdom Imaging* 1999; **24:** 111-116

8 **Lee DH.** Two-dimensional and three-dimensional imaging of gastric tumors using spiral CT. *Abdom Imaging* 2000; **25:** 1-6

9 **Lee DH.** Three-dimensional imaging of the stomach by spiral CT. *J Comput Assist Tomogr* 1998; **22:** 52-58

10 **Zheng KE,** Feng C, Ju SH, Sun J, Liu WH. CT virtual endoscopy: a preliminary clinical study in gastrointestinal tract. *World Chinese J Digestol* 1999; **7:** 629-631

11 **Springer P,** Stohr B, Giacomuzzi SM, Bodner G, Klingler A, Jaschke W, Zur-Nedden D. Virtual computed tomography colonoscopy: artifacts, image quality and radiation dose load in a cadaver study. *Eur Radiol* 2000; **10:** 183-187

12 **Rogalla P,** Bender A, Bick U, Huitema A, Terwisscha-van-Scheltinga J, Hamm B. Tissue transition projection (TTP) of the intestines. *Eur Radiol* 2000; **10:** 806-810

13 **Rogalla P,** Werner R, Huitema A, van-Est A, Meiri N, Hamm B. Virtual endoscopy of the small bowel: phantom study and preliminary clinical results. *Eur Radiol* 1998; **8:** 563-567

14 **Fletcher JG,** Luboldt W. CT colonography and MR colonography: current status, research directions and comparison. *Eur Radiol* 2000; **10:** 786-801

15 **Hara AK,** Johnson CD, Reed JE, Ehman RL, Ilstrup DM. Colorectal

polyp detection with colography: two-versus three-dimensional techniques. Work in progress. *Radiology* 1996; **200:**49-54

16 **Wu LF,** Wang BZ, Feng JL, Cheng WR, Liu GR, Xu XH, Zheng ZC. Preoperative TN staging of esophageal cancer: Comparison of miniprobe ultrasonography, spiral CT and MRI. *World J Gastroenterol* 2003; **9:** 219-224

17 **Moss AA,** Schnyder P, Marks W, Margulis AR. Gastric adenocarcinoma: a comparison of the accuracy and economics of staging by computed tomography and surgery. *Gastroenterology* 1981; **80:** 45-50

18 **Ward J,** Chen F, Guthrie JA, Wilson D, Lodge JP, Wyatt JI, Robinson PJ. Hepatic lesion detection after superparamagnetic iron oxide enhancement: Comparison of five T2-weighted sequences at 1.0 T by using alternative-free response receiver operating characteristic analysis. *Radiology* 2000; **214:** 159-162

19 **Fukuya T,** Honda H, Kaneko K, Kuroiwa T, Yoshimitsu K, Irie H, Maehara Y, Masuda K. Efficacy of helical CT in T-staging of gastric cancer. *J Comput Assist Tomogr* 1997; **21:** 73-81

20 **Miller FH,** Kochman ML, Talamonti MS, Ghahremani GG, Gore RM. Gastric cancer: Radiologic staging. *Radiol Clin North Am* 1997; **35:** 331-349

21 **Minami M,** Kawauchi N, Itai Y, Niki T, Sasaki Y. Gastric tumors: radiologic-pathologic correlation and accuracy of T staging with dynamic CT. *Radiology* 1992; **185:** 173-178

22 **Takao M,** Fukuda T, Iwanaga S, Hayashi K, Kusano H, Okudaira S. Gastric cancer: evaluation of triphasic spiral CT and radiologic-pathologic correlation. *J Comput Assist Tomogr* 1998; **22:** 288-294

Edited by Xu XQ and Wang XL

P.O.Box 2345, Beijing 100023,China
Fax: +86-10-85381893
E-mail: wjg@wjgnet.com www.wjgnet.com

World J Gastroenterol 2003;9(7):1409-1414
World Journal of Gastroenterology
 ISSN 1007-9327

• GASTRIC CANCER •

Association of VCAM-1 overexpression with oncogenesis, tumor angiogenesis and metastasis of gastric carcinoma

Yong-Bin Ding, Guo-Yu Chen, Jian-Guo Xia, Xi-Wei Zang, Hong-Yu Yang, Li Yang

Yong-Bin Ding, Guo-Yu Chen, Jian-Guo Xia, Xi-Wei Zang, Hong-Yu Yang, Li Yang, Department of General Surgery, the First Affiliated Hospital of Nanjing Medical University, Nanjing 210029, Jiangsu Province, China
Supported by the Science Fund of Department of Science and Technology of Jiangsu Province, No.Bj 99064
Correspondence to: Yong-Bin Ding, Department of General Surgery, The First Affiliated Hospital of Nanjing Medical University, Nanjing 210029, Jiangsu Province, China. njdyb@sina.com
Telephone: +86-25-6796006
Received: 2002-12-10 **Accepted:** 2003-02-13

Abstract

AIM: To investigate the relationship between the expression of vascular cell adhesion molecule-1 (VCAM-1) and oncogenesis, tumor angiogenesis and metastasis in gastric carcinoma, and to evaluate the clinical significance of serum VCAM-1 levels in gastric cancer.

METHODS: Specimens from 41 patients with gastric cancer, 8 patients with benign gastric ulcer, and 10 healthy subjects were detected for the expression of VCAM-1 by immunohistochemistry. Microvessel density (MVD) was measured by counting the endothelial cells immunostained with the monoclonal antibody CD34 at x200 magnification. Serum VCAM-1 concentrations were measured by an enzyme linked immunosorbent assay in the 41 gastric cancer patients before surgery, and at 7 days after surgery as well as in 25 healthy controls. The association between preoperative serum VCAM-1 levels and clinicopathological features, and their changes following surgery was evaluated. In addition, serum carcinoembryonic antigen (CEA) was also examined.

RESULTS: Of the 41 gastric cancer tissues, 31 (75.6 %) were VCAM-1 positive. The VCAM-1 positive gastric cancers were more invasive and classified in the more advanced stage than the VCAM-1 negative ones. The VCAM-1 positive cancers were associated with more lymph node metastases than VCAM-1-negative ones ($P<0.05$). The expression of VCAM-1 was detected in tissues of two of the eight patients with gastric ulcer and two of the 10 healthy controls. The expression of VCAM-1 in gastric cancer patients was significantly more frequent than that in the healthy controls and ulcer group (both $P<0.05$). MVD in VCAM-1 expressing tissues was higher than that in VCAM-1 negative tissues ($t=2.13$,$P<0.05$). Serum VCAM-1 levels in gastric cancer patients were significantly higher than those in controls ($t=3.4$, $P<0.05$). There was a significant association between serum VCAM-1 levels and disease stage, as well as invasion depth of the tumor and the presence of distant metastases. The concentrations of serum CEA in gastric cancer were higher than normal controls. Both serum VCAM-1 and CEA levels decreased significantly after radical resection of the primary tumor ($P<0.05$). Furthermore, the serum levels of VCAM-1 were positively correlated with the expression of VCAM-1 in the tumor tissue ($r=0.85$, $P<0.05$).

CONCLUSION: The expression of VCAM-1 is closely related to oncogenesis, tumor angiogenesis and metastasis in gastric carcinoma. Serum VCAM-1 level in gastric cancer patients is significantly increased compared with normal controls, which decreases significantly after radical resection of the primary tumor. The serum concentration of VCAM-1 may be considered as an effective marker of tumor burden of gastric cancer. Moreover, overexpression of VCAM-1 in gastric cancer tissue is likely a major source of serum VCAM-1.

Ding YB, Chen GY, Xia JG, Zang XW, Yang HY, Yang L. Association of VCAM-1 overexpression with oncogenesis, tumor angiogenesis and metastasis of gastric carcinoma. *World J Gastroenterol* 2003; 9(7):1409-1414
http://www.wjgnet.com/1007-9327/9/1409.asp

INTRODUCTION

Solid tumors are composed of two distinct but interdependent compartments, malignant cells themselves and the vascular and connective tissue stroma induced by malignant cells where malignant cells are dispersed. Stroma provides the vascular supply that tumors require for obtaining nutrients, gas exchange, and waste disposal. Thus, any increase in tumor mass, either primary or metastatic, must be accompanied by angiogenesis formation[1,2]. The mechanism by which tumors induce stroma has caused considerable attention in recent years. Emphasis is increasingly placed on tumor angiogenesis. Tumor angiogenesis has been linked to tumor progression and metastasis. Many reports have suggested that cell adhesion molecules (CAM) not only play key roles in various stages of tumor angiogenesis, but also are involved in tumor progression and metastasis[3-5].

CAMs are cell-surface glycoproteins which are critical for cell- to-cell interactions. Intercellular adhesion mediated by CAMs directly influences differentiation, and disruption of normal cell-cell contacts has been noted in neoplastic transformation and in metastasis. CAMs expressed on lymphocytes and vascular endothelial cells are thought to play an important role in lymphocyte trafficking for immune anti-infection response. There is evidence that vascular cell adhesion molecule-1 (VCAM-1) may be involved in tumor progression and metastasis[5,6].

VCAM-1 belongs to the immunoglobulin super family group of adhesion molecules, and is one of the most important adhesion molecules which plays a crucial role in this process. VCAM-1 is an 110 KDa glycoprotein that is constitutively expressed on tissue macrophage, dentric cells and epithelial cells, as well as on the surface of stimulated endothelial cells. Thus, VCAM-1 is a widely distributed protein. It is possible that VCAM-1 is a candidate for mediating tumor cell adhesion to vascular endothelial cells and promoting the metastatic process. Recent reports have shown that angiogenesis favors tumor growth and facilitates entry of cells into the circulation[7,8].

It has recently been reported that the microvessel density (MVD) in a tumor correlates with tumor progression, hematogenous metastasis and recurrence of gastric carcinoma.

MVD also reflects tumor angiogenesis[2-4,9]. In the present study, the expression of VCAM-1 and the density of microvessels were examined by immunohistochemistry in patients with gastric cancer. The association between the expression of VCAM-1 and oncogenesis, tumor angiogenesis and metastasis of gastric carcinoma was evaluated. Meanwhile we also detected the concentration of soluble forms of VCAM-1 and serum levels of carcinoembryonic antigen (CEA) in patients with gastric cancer and investigated its relation to clinical and pathological features.

MATERIALS AND METHODS

Patients

A total of 41 patients with histologically confirmed gastric cancer who had undergone curative gastrectomy at our department from March 1999 to March 2000 were included in this study. They consisted of 26 male and 15 female patients ranging in age from 35 to 74 years (mean, 58.4 years). The clinicopathologic findings were determined according to the principles set by the Japaneese Society Committee on Histologial Classifiation of Gastric Cancer. Of the 41 patients, 28 had lymph node metastasis. The patients had not received either chemotherapy or radiation therapy before operation. A tumor sample and a normal part of the stomach were obtained during surgical resection. The samples were each divided into two pieces, which were subjected to fixation in 10 % formalin for histological examination and immunohistological test. All patients had been performed distal partial gastrectomy, proximal partial gastrectomy, or total gastrectomy with regional lymph node dissection to group 1(D1), group 2(D2), group 3 (D3) with a curative intention. Gastric specimens from eight patients with gastric ulcer and 10 patients with normal gastric tissues were obtained by fiber gastroscope.

Both the expression of VCAM-1 and the density of microvessels were examined by immunohistochemical staining. Meanwhile, blood samples from the 41 gastric cancer patients were obtained before any treatment and at 7 days after surgery. There were no infections in all these patients. Additionally, blood samples were also obtained from 25 healthy subjects as controls. The mean age of these subjects was 39.1 years (age range 20-55 years), with a ratio of male to female of 12:8.

Immunohistochemistry

Specimens were fixed in a 40 g· L^{-1} formaldehyde solution and embedded in paraffin. Four-micrometer thick sections were cut and mounted on glass slides. Immunohistochemistry was performed using the avidin-biotin complex (ABC) method. Sections were dewaxed in xylene, dehydrated in ethanol, washed by phosphate-buffered saline solution (PBS, pH=7.4) and then heated in a microwave oven for 10 minutes to retrieve the antigens. Endogenous peroxidase activity was blocked by incubation of samples with 3 % hydrogen peroxide in methanol for 30 minutes. After being washed with PBS, 50 μl 10 % normal goat serum was added to glass slides for 10 minutes to reduce nonspecific antibody binding. Specimens were then incubated with a 1:250 dilution of anti-VCAM-1 antibody overnight at 4 ℃, followed by three washes with PBS. Sections were then incubated with biotinylated goat antimouse immunoglobulin G (Nanjing Sangon Biotechnology Co.) at a dilution of 1:50 for 2 hours followed by three washes. Slides were then treated with the complex of reagent A and reagent B (ABC kit, Nanjing Sangon Biotechnology Co.) for 2 hours at a dilution of 1:50 and were washed with PBS three times. Finally, slides were incubated in PBS containing diaminobenzidine and 300 mL· L^{-1} hydrogen peroxide for 10 minutes. Normal mouse immunoglobulin-G was substituted for primary antibody as the negative control. Immunoreactivity was graded as follows: +, more than 10 % of carcinoma cells were stained; -, no detectable expression or fewer than 10 % of carcinoma cells were stained.

Microvessel detection and counting

A detection procedure for microvessels was performed using anti-CD34 monoclonal antibody (Nanjing Sangon Biotechnology Co.). Envision-labeled polymer reagent was applied for immunoreaction. A single microvessel was defined as any brown immunostained endothelial cells, and other connective tissue elements. The stained sections were screened at ×100 magnification under a light microscope to identify the five regions of the section with the highest number of microvessels. The image was visualized on a computer display through a color video camera module and color image freezer. Microvessels were counted in this area at ×200 magnification, and the average number of microvessels in these five regions was recorded, and defined as MVD. The visualized area on the display was determined to be 0.075 mm^2.

Assay of soluble VCAM-1

For assay of soluble adhesion molecules venous blood samples. were collected into plain tubes, allowed to clot for up to 1 hour and centrifuged at 5 000 g for 5 min. The serum was removed, aliquoted and stored at -70 ℃ until assayed. Concenrations of soluble VCAM-1were measured with commercially available sandwich ELISA kits based on dual monoclonal antibodies. CEA test, a routine test in our department, was also performed.

Statistical analysis

The data were presented as $\bar{x}\pm s$. Differences in categorical variables between groups were determined by chi-square test, and differences in enumeration data between groups were determined by *t* test or by analysis of variance. Correlations between the levels of soluble adhesion molecules and the clinical and pathological variables were determined by Spearman rank correlation method.

RESULTS

Expression of VCAM-1 in gastric cancer, gastric ulcer and normal gastric tissue

VCAM-1 was positively stained in the cytoplasm or the membrane of vascular endothelial cells in brown or yellow in gastric cancer tissue. VCAM-1 was expressed not only in vascular endothelial cells, but also in the majority of gastric cancer cells. Generally, VCAM-1 expression was intense throughout the tumor, especially in keratin pearl of gastric cancer. VCAM-1positive vessels were preferentially found in vascular-rich tumor areas. VCAM-1 expression was present in 31 (75.6 %) out of 41gastric cancer tissues and in 5 (12.2 %) adjacent normal gastric tissue. The rate of expression of VCAM-1 in gastric caner tissue was significantly higher than that in adjacent normal gastric tissue (χ^2=52.1, P<0.05).

VCAM-1 expression was present in 25 % (2/8) of gastric ulcer tissue, and in 20 % (2/10) of healthy subjects (χ^2=0.1,P> 0.05). However, The rate of VCAM-1 expression in gastric cancer was remarkably higher than that in gastric ulcer and healthy subjects (both P<0.05).

CD34 was positively stained mainly in the cytoplasm of vascular endothelial cells as brown or yellow granules. MVD ranged from 21.5 to 71.2, with a mean value of 30.2 in gastric cancer tissues, and ranged from 2 to 14, with a mean value of

11.5 in normal gastric tissues. MVD in tumor tissue was significantly higher than that in normal tissues (t=3.1, P<0.05).

Association of the expressions of VCAM-1 and MVD with pathological features of gastric carcinoma

As shown in Table 1, VCAM-1 expression was present in 26 (92.9 %) of the 28 gastric cancer patients with lymph node metastasis, but in only 5 (34.5 %) of the 13 gastric cancer patients without lymph node metastasis. The rate of VCAM-1 in patients with lymph node metastasis was significantly higher than that in patients without lymph node metastasis (χ^2=11.4, P<0.05). Meanwhile VCAM-1 expression in the gastric cancer patients was also associated with clinicopathological stage and depth of infiltration (both P<0.05).

Furthermore, microvessel count in patients with gastric cancer was related to clinicopathological stage, depth of infiltration and lymph node metastasis (all P<0.05,). The rate of expression of VCAM-1 and MVD in gastric carcinoma tissue had no significant differences among the size, location, age and gender (data not shown).

Table 1 Association of expressions of VCAM-1 and MVD with pathological features of gastric carcinoma

Pathological chacteristics	*n*	Positive VCAM-1(%)	MVD($\bar{x}$+*s*)
Size of tumor			
<3 cm	10	6	37.1±12.1
3 cm	31	25	39.5±12.7
Location			
Lower third	10	7	39.4±7.3
Middle third	20	17	36.2±11.3
Upper third	11	7	41.4±13.3
Depth of invasion			
Mucosa and submucosa	11	5	28.4±8.1
Muscle and subserosa	12	9	36.9±10.7
Serosa	18	17[a]	49.6±15.1[b]
Clinicopathologic stage			
I	7	3	29.3±3.54
II	12	7	33.9±9.3
III	16	15	46.3±10.3
IV	6	6[c]	55.4±8.1[d]
Lymph node metastasis			
Present	28	26	45±9.8
Absent	13	5[e]	28.5±5.5[f]

MVD and expression of VCAM-1 had no significant difference in the size, location. The rate of positive VCAM-1 expression and MVD were positively correlated with depth of invasion ([a]P<0.05, [b]P<0.05 respectively). There was a significant difference between the rate of positive VCAM-1 expression, MVD and clinic pathological stage ([c]P<0.05, [d]P<0.05). The rate of positive VCAM-1 expression and MVD were significantly higher than that in those without lymph node metastasis ([e]P<0.05, [f]P<0.05 respectively).

Correlation between expression of VCAM-1 and MVD

MVD was 46.5±11.3 in VCAM-1 positive tissue in gastric cancer, while it was 31.2±8.4 in negative VCAM-1 tissue. MVD in VCAM-1-positive tumors was significantly higher than that in VCAM-1-negative tumors (t=2.13, P<0.05).

Association of soluble VCAM-1 with gastric cancer

In gastric cancer patients, soluble VCAM-1 was significantly elevated in comparison with that in healthy subjects (878±46 μg/lm *vs* 297±35 μg/ml, P<0.05, Table 2). The difference in serum concentration of soluble VCAM-1 was also significant between patients with stage I-II and those with stage III-IV gastric cancer, indicating that soluble VCAM-1 concentration correlated well with the staging of gastric cancer. No significant difference was found between ulcer group and controls (P>0.05). Concentrations of serum CEA in gastric cancer patients were higher than those in control group and ulcer group (both P<0.05). But no significant difference was found between stage I-II and stage III-IV gastric cancer.

Table 2 Soluble levels of VCAM-1, CEA in gastric cancer patients, ulcer patients and control group

	n	Soluble VCAM-1(μg / ml) ($\bar{x}$±*s*)	CEA
Gastric cancer	41	878±46[a]	4.7±0.43
I-II	17	764±24[b]	4.1±0.23
III-IV	24	1006±78[c]	4.9±0.31
Ulcer	8	301±21	4.5±0.41
Control	25	297±35	2.3±0.28

[a]P<0.05, [b]P<0.05, [c]P<0.05, (*vs* control group).

The concentration of soluble VCAM-1 was higher in the patients with lymph node metastasis than that in those without lymph node metastasis (P<0.05). Positive correlation was found between concentration of soluble VCAM-1 and depth of invasion of gastric cancer. In contrast, no significant association was found between concentration of soluble VCAM-1 and location, size, age and gender (data not shown).

Levels of postoperative soluble VCAM-1 in gastric cancer patients were reduced significantly compared to preoperative levels (578±39 μg/lm *vs* 878±46 μg/ml, P<0.05, Table 3). It was noteworthy that concentration of soluble VCAM-1 was positively correlated with expression of VCAM-1 in the tumor tissue (r=0.85, P<0.05). The level of serum CEA was also decreased significantly after radical resection of the primary tumor (P<0.05).

Table 3 Concentrations of soluble VCAM-1 and CEA at pre-operative and postoperative stages

	$\bar{x}$±*s* (ng / L)	*P*
sVCAM-1		
preoperative	878±46	
postoperative	578±39	0.0001
CEA		
preoperative	10.3±18.4	
postoperative	6.3±11.5	0.0031

Serum VCAM-1 and CEA levels decreased significantly after radical resection of the primary tumor (P<0.05).

DISCUSSION

Gastric carcinoma, as one of the most common human malignant tumors, ranks worldwide the first leading cause of gastrointestinal cancer-related mortality. In China, it now ranks the second among all malignant tumors. Recent important advance in oncology is the finding that tumor angiogenesis plays an important role in tumor genesis, growth and metastasis, and an increasing number of studies have proven that vascular targeting therapy is very effective[9-11]. Many factors are involved in tumor angiogenesis, one of the most important factors is VCAM-1, Which is capable of promoting and maintaining the establishment of tumor vascular system[12]. Thus it can directly stimulate tumor growth and metastasis. Generation of new blood vessels, or angiogenesis, plays a key role in the growth

of malignant disease and has drawn great interest in developing agents that inhibit angiogenesis. Angiogenesis is characterized by invasion, migration, and proliferation of endothelial cells, processes that depend on cell interactions with extracellular matrix components[12-14]. Our current study has shown VCAM-1 is a key player by providing a vasculature-specific target for antiangiogenic treatment strategies.

Expression of VCAM-1 may facilitate oncogenesis

Recent advances in molecular biology and genetic technology studies on adhesion molecules have demonstrated that cell-cell and cell-extracellular matrix interactions play an important role in cancer metastasis. In addition to activation of oncogenes and inactivation of tumor suppressor genes, alteration of adhesion molecules seems to be critical for the development of gastric cancer[15]. Tumour development is a multi-step process during which genetic and epigenetic events determine the transition from a normal to a malignant cellular state. In the past decade, extensive effort has been made not only to define the molecular mechanisms underlying progression to malignancy but also to predict the development of the disease and to identify possible molecular targets for therapy. Common to most tumours, several regulatory circuits are altered during multistage tumour progression of gastric cancer, which includes control of proliferation, balance between cell survival and programmed cell death (apoptosis), communication with neighbouring cells and extracellular matrix, induction of tumour neovascularization (angiogenesis) and tumour cell migration, invasion and metastatic dissemination. De-regulation of each of these processes represents a rate-limiting step for tumour development and, hence, has to be achieved by tumour cells in a highly selective manner during tumour progression. In this complex process, more attention has been placed on adhesion molecules, because adhesion molecules are necessary to mediate cell-matrix and cell-cell interactions, metabolism, and differentiation. Moreever, adhesive interactions between tumor cell surface receptors and endothelial cell adhesion molecules are thought to contribute to tumor cell arrest and extravasation during hematogenous metastasis[14-17]. Changes in expression and function of adhesion molecules are important characteristics in the development of gastrointestinal malignancies and might be used in future as prognostic factors or as new targets in diagnosis and therapy. VCAM-1, one of the adhesion molecules involved in malignant tumor, is found to be expressed mainly in activated endothelial cells, and dentric cells.

Maurer *et al*. confirmed that VCAM-1 protein was over-expressed in colorectal cancers at the mRNA level by Northern blotting, In comparison to normal controls, the expression of VCAM-1 mRNA was increased by 3.4 fold in colorectal cancers. Our study found that the expression of VCAM-1 in gastric tumor tissue was higher than that in adjacent-cancer tissue, and the ratio of positive VCAM-1 in gastric cancer tissue was higher than that in gastric ulcer and normal mucosa, suggesting that VCAM-1 may play a key role in the growth of gastric cancer.

However, we noteed that VCAM-1 expression was positive in one healthy subject, and in two patients with gastric ulcer, indicating that there are other factors involved in the expression of VCAM-1. Some studies believed that *Helicobacter pylori* infection of gastric mucosa was one of the causes responsible for VCAM-1 expression[18,19].

VCAM-1 expression stimulates tumor angiogenesis

Angiogenesis is of key importance in the process of tumour progression in a number of tumour types. Angiogenesis is a biological process by which new capillaries are formed from pre-existing vessels. It occurs in physiological conditions such as embryo development, and cyclically in wound repair of female genital system, and during pathological conditions, such as arthritis, diabetic retinopathy and tumors. In the both physiological conditions, angiogenesis is mediated accurately by feedback system. However, in solid tumor growth, a specific ally critical turning point is the transition from the vascular to the vascular phase. Having developed an intrinsic vascular network, the neoplastic mass is able to grow indefinitely (unlike other forms of cell growth, tumor angiogenesis is not limited in time) both *in situ* and at distant sites (metastasis). Thus, tumor angiogenesis cannot be controlled by feedback. Angiogenesis is capable of providing continuous nutrients, gas exchange, and waste disposal for tumors growth. Any increase in tumor mass, either primary or metastatic, must be accompanied by vascular formation. Therefore, tumor angiogenesis is a very complex process. At present, an increasing number of studies have shown that abnormal adhesion molecules contribute to tumor angiogenesis by stimulating neoplastic cells to produce growth factors specific for endothelial cells and able to stimulate growth of the host' s blood vessels[6,8,13,15]. Recent studies have demonstrated that VCAM-1 may contribute to tumor angiogenesis. MVD, a reliable index of tumor angiogenesis, has been confirmed to be linked to tumor progression, hematogenous metastasis, and tumor recurrence.

Our study indicated that MVD of gastric cancer tissues with VCAM-1 expression was significantly higher than that in tissues negative for VCAM-1, suggesting that VCAM-1 expression may be one of the factors mediating the activation of angiogenesis. Several reports have observed that gastric cancer cells are capable of activating vessel endothelial cells, which leads to expression of VCAM-1, and thus the induction of tumour neovascularization. Maeds *et al*. proposed that VCAM-1 binding to its ligand VLA4 not only results in activation of vessel endothelial cells, but also leads to shedding of tumor cells and invasion of adjacent tissue[20,21]. Byrne *et al*. suggested that VCAM-1 was expressed on endothelial cells as a result of stimulation by vascular endothelial growth factor (VEGF). In general, these findings suggest that VCAM-1 may be used for sustained angiogenesis and tissue invasion and metastasis via autocrine/paracrine manners[7].

Howerever, in some tumors, high MVD VCAM-1 expression was not detected, which suggests that other factors such as extracellular matrix, and metabolic and mechanical factors also contribute to tumor angiogenesis. Hence anti-angiogenesis therapy should utilize multiantiangiogenesis tactics[23,24].

MVD may be different according to the observer, and cut-off values are also different. In addition, it has been reported that different MVD could be obtained with different antibodies used in different studies. Therefore, MVD that was observed in this study may be different from those previously reported.

VCAM-1 favors lymph node metastasis of gastric cancer

It is generally accepted that the presence or absence of regional lymph node involvement is one of the important factors influencing survival in respectable gastric cancer. Lymph node metastasis occurs even in some patients with early gastric cancer. Recently, studies have confirmed that prognosis of gastric cancer patients with lymph node metastasis is very poor. Gastric caner patients with lymph node metastasis have been commonly reported to have poorly differentiated adenocarcinoma, and deeper invasion, in comparison with gastric cancer patients without lymph node metastasis. In our present study, we observed that VCAM-1 expression in 26 of 28 cases with lymph node metastasis, whereas in only 5 of 13 gastric cancer patients without lymph node metastasis. There

was a significant difference between the two groups ($P<0.05$), indicating that expression of VCAM-1 may be associated with lymph node metastasis of gastric cancer. VCAM-1 is predominantly expressed on gastric carcinoma cells, giving these tumor cells the ability to perform lymph-node metastasis. Meanwhile, expression of VCAM-1 significantly alters malignant transformation[11,20,21].

Tumor metastasis involves the release of cells from primary tumor due to a firmly formed cluster of tumor cells probably by detaching from the tumor nests with unstable adhesiveness, followed by their migration in extracellular matrix, adhesion to vessel walls, arrest in microcirculation of distant organs, and subsequent extravasation. Extravasation of metastatic tumor cells from bloodstream of the tissue space in a secondary organ is related specific binding to determinants on endothelial cell surface. Each step requires cell adhesive interactions involving specific adhesion molecules and receptors. Several families of adhesion molecules have now been identified, some of which are promising candidates for a role in neoplasia. So tumor metastasis is a very complex process, Colette *et al*. thought that VCAM-1 overexpression stimulated tumour neovascularization, and angiogenesis was necessary for tumor growth and metastasis, VCAM-1 expression was linked to lymph node metastasis[2,3,21-24].

We observed that VCAM-1 expression was present in 5 of the 13 cases without lymph node metastasis, which may be related to lymph node micrometastasis. It has been demonstrated that micrometastases consisting of one to a few cells in lymph nodes resected during gastrectomy are difficult to identify using conventional hematoxylin and eosin (H&E) stains[25,26].

Concentration of soluble VCAM-1 may be one of the important markers for gastric carcinoma

Our study demonstrated that serum concentration of VCAM-1 was elevated in patients with gastric cancer before treatment in comparison with the healthy group; hence, the concentration of soluble VCAM-1 may be of significance in diagnosis of gastric carcinoma. In addition, a positive correlation was observed between levels of soluble VCAM-1 and tumor stage, and invasion depth. More important was that the concentration of soluble VCAM-1 in patients with lymph node metastasis was significantly higher than that in patients without lymph node matastasis. These findings suggest that the levels of soluble VCAM-1 are linked to tumor growth and metastasis. Our results are consistent with the findings by Velikova *et al*, who also reported elevated serum levels of VCAM-1 in gastric cancer, and proposed that patients with elevated serum VCAM-1 have a poorer survival rate. Measurement of circulating VCAM-1 may bring additional prognostic information for patients with gastric cancer in relation to different stages and tumor pathology, and it should be included in future large multivariate analyses of prognostic factors should be performed whenever possible[27,28]. Animal experiments have confirmed that soluble VCAM-1 promotes angiogenesis in rat cornea, which is supported by our findings[29,30].

Additionally, It was first observed that postoperative concentrations of soluble VCAM-1 decreased significantly in patients with gastric cancer in comparison with preoperative concentrations ($P<0.05$). This finding suggests that measurement of circulating VCAM-1 may play a critical role in prognosis of gastric cancer patient. It is likely that tumor burden in patients with gastric cancer is decreased after operation, so the concentration of soluble VCAM-1 is reduced. If the levels of soluble VCAM-1 increase again after operation, we should pay great attention to tumor recurrence. Therefore, soluble VCAM-1 may be considered as a marker for tumor burden. Some investigators have reported a positive correlation between serum concentration of VCAM-1 and age of patients, but no such a correlation was found in healthy subjects. Our study did not confirm this although we noted that the median age in healthy group was lower than that of gastric cancer patients. Therefore, the effect of age on serum levels of VCAM-1 can not be excluded, and future studies should take it into account[31].

In our department, CEA is one of the routine tests in gastric cancer. It is well accepted that CEA is one of the most important marks of gastrointestinal carcinoma, and preoperative positivity for CEA is an independent risk factor for hematogenous recurrence of gastric carcinoma. Our finding on CEA is consistent with those previously reported[32,33].

Expression of VCAM-1 in tumor tissue is one of the sources of soluble VCAM-1 in gastric cancer

The source of soluble VCAM-1 is not yet known. VCAM-1 is known to be expressed predominantly on activated endothelial cells, dendritic cells and renal proximal tuble cells. We found that strong VCAM-1 expression occurred in gastric cancer cells and endothelial cells in tumor tissues, especially in vessel abundant regions. Some studies have reported that VCAM-1 has been found in malignant epithelial tissue, including metastasis gastric cancer cells, melanoma cell lines and hepatocellular cells. In our study, a strong correlation was found between expression of VCAM-1 in gastric cancer tissue and serum concentration of soluble VCAM-1 ($r=0.85$, $P<0.05$). Increased expression of VCAM-1 in gastric cancer cells and their shedding into circulation may be the factor accounting for the significantly elevated serum levels of VCAM-1. Other studies have reported that soluble VCAM-1 may be related to the white cell count. To eliminate this possibility, blood tests were performed, and gastric cancer patients with normal blood tests were included. We observed that expression of VCAM-1 in gastric carcinoma tissue was positively correlated with concentration of soluble VCAM-1, indicating that expression of VCAM-1 in gastric cancer tissue is a major source of soluble VCAM-1. VCAM-1 is expressed on endothelial cells as a result of vascular endothelial growth factor (VEGF) stimulation[4,6,19-21,34,35].

In conclusion, VCAM-1 may be involved in the progression of human gastric carcinoma, particularly via lymphangiogenesis. VCAM-1 expression at invading edge of gastric carcinoma may be a sensitive marker for metastasis to lymph nodes. Differentially expressed vascular molecules may influence the functional characteristics of extravasating leukocytes and represent new targets in anti-gastric cancer therapy. In general, an increasing number of studies on a variety of malignant diseases have suggested that VCAM-1 may play a role in the process of adhesion of tumor cells to endothelial cells and neovascularization. Expression of VCAM-1 is associated with oncogenesis, tumor angiogenesis and metastasis in gastric carcinoma. MVD in gastric carcinoma tissue is closely associated with lymph node metastasis, clinical stage and depth of invasion. Expression of VCAM-1 is closely related to MVD in gastric cancer, and thus VCAM-1 can act as an important index reflecting the biological behaviors of gastric carcinoma. VCAM-1 may be used as a metastasis marker and/or a target for antiangiogenic therapy. VCAM-1 has been shown to be a key player by providing a vasculature-specific target for antiangiogenic treatment strategies. Concentration of soluble VCAM-1 correlates well with tumor growth and metastasis. Expression of VCAM-1 in gastric cancer tissue is positively correlated with concentration of soluble VCAM-1. Elevated soluble VCAM-1 is decreased significantly in gastric caner patients after operation, and thus soluble VCAM-1 may be one of the markers for gastric carcinoma tumor burden, and

serum VCAM-1 may be considered as an effective diagnostic and prognostic factor.

REFERENCES

1 **Ghossein RA**, Bhattacharya S, Rosai J. Molecular detection of micrometastases and circulating tumor cells in solid tumors. *Clin Cancer Res* 1999; **5**: 1950-60

2 **Liu DH**, Zhang XY, Fan DM, Huang YX, Zhang JS, Huang WQ, Zhang YQ, Huang QS, Ma WY, Chai YB, Jin M. Expression of vascular endothelial growth factor and its role in oncogenesis of human gastric carcinoma. *World J Gastroenterol* 2001; **7**: 500-505

3 **Saito H,** Tsujitani S, Kondo A, Ikeguchi M, Maeta M, Kaibara N. Expression of vascular endothelial growth factor correlates with hematogenous recurrence in gastric carcinoma. *Surgery* 1999; **125**: 195-201

4 **Ren J,** Dong L, Xu CB, Pan BR. The role of KDR in the interactions between human gastric carcinoma cell and vascular endothelial cell. *World J Gastroenterol* 2002; **8**: 596-601

5 **Alexiou D,** Karayiannakis AJ, Syrigos KN, Zbar A, Kremmyda A, Bramis I, Tsigris C. Serum levels of E-selectin, ICAM-1 and VCAM-1 in colorectal cancer patients: correlations with clinicopathological features, patient survival and tumour surgery. *Eur J Cancer* 2001; **37**: 2392-2397

6 **Maurer CA,** Friess H, Kretschmann B, Wildi S, Muller C, Graber H, Schilling M, Buchler MW. Over-expression of ICAM-1, VCAM-1 and ELAM-1 might influence tumor progression in colorectal cancer. *Int J Cancer* 1998; **79**: 76-81

7 **Byrne GJ**, Bundred NJ. Surrogate markers of tumoral angiogenesis. *Int J Biol Markers* 2000; **15**: 334-339

8 **Li DY,** Sorensen LK, Brooke BS, Urness LD, Davis EC, Taylor DG, Boak BB, Wendel DP. Defective angiogenesis in mice lacking endoglin. *Science* 1999; **284**: 1534-1537

9 **Kakeji Y,** Koga T, Sumiyoshi Y, Shibahara K, Oda S, Maehara Y, Sugimachi K. Clinical significance of vascular endothelial growth factor expression in gastric cancer. *J Exp Clin Cancer Res* 2002; **21**: 125-129

10 **Tao HQ,** Lin YZ, Wang RN. Significance of vascular endothelial growth factor messenger RNA expression in gastric cancer. *World J Gastroenterol* 1998; **4**: 10-13

11 **Takahashi N,** Haba A, Matsuno F, Seon BK. Antiangiogenic therapy of established tumors in human skin / severe combined immunodeficiency mouse chimeras by anti-endoglin (CD105) monoclonal antibodies, and synergy between anti-endoglin antibody and cyclophosphamide. *Cancer Res* 2001; **61**: 7846-7854

12 **Muller AM,** Weichert A, Muller KM. E-cadherin, E-selectin and vascular cell adhesion molecule: immunohistochemical markers for differentiation between mesothelioma and metastatic pulmonary adenocarcinoma? *Virchows Arch* 2002; **441**: 41-46

13 **Brandvold KA,** Neiman P, Ruddell A. Angiogenesis is an early event in the generation of myc-induced lymphomas. *Oncogene* 2000; **19**: 2780-2785

14 **Langley RR,** Carlisle R, Ma L, Specian RD, Gerriten ME, Granger DN. Endothelial expression of vascular cell adhesion molecule-1 correlates with metastatic pattern in spontaneous melanoma. *Microcirculation* 2001; **8**: 335-345

15 **Maehara Y,** Kabashima A, Koga T, Tokunaga E, Takeuchi H, Kakeji Y, Sugimachi K. Vascular invasion and potential for tumor angiogenesis and metastasis in gastric carcinoma. *Surgery* 2000; **128**: 408-416

16 **Park HJ,** Lee YW, Hennig B, Toborek M. Linoleic acid-induced VCAM-1 expression in human microvascular endothelial cells is mediated by the NF-kappa B-dependent pathway. *Nutr Cancer* 2001; **41**: 126-134

17 **Seon BK,** Takahashi N, Haba A, Matsuno F, Haruta Y, She XW, Harada N, Tsai H. Angiogenesis and metastasis marker of human tumors. *Rinsho Byori* 2001; **49:** 1005-1013

18 **Ohnita K,** Isomoto H, Mizuta Y, Maeda T, Haraguchi M, Miyazaki M, Murase K, Murata I, Tomonaga M, Kohno S. *Helicobacter pylori* infection in patients with gastric involvement by adult T-cell leukemia / lymphoma. *Cancer* 2002; **94**: 1507-1516

19 **Mori N,** Wada A, Hirayama T, Parks TP, Stratowa C, Yamamoto N. Activation of intercellular adhesion molecule 1 expression by Helicobacter pylori is regulated by NF-kappaB in gastric epithelial cancer cells. *Infect Immun* 2000; **68**: 1806-1814

20 **Kwon S,** Kim GS. Prognoatic significance of lymph node metastasis in advanced carcinoma of the stomach. *Br J Surg* 1996; **83**: 1600-1603

21 **Gulubova MV.** Expression of cell adhesion molecules, their ligands and tumour necrosis factor alpha in the liver of patients with metastatic gastrointestinal carcinomas. *Histochem J* 2002; **34**: 67-77

22 **Charpin C,** Garcia S, Andrac L, Horschowski N, Choux R, Lavaut MN. VCAM (IGSF) adhesion molecule expression in breast carcinoma detected by automated and quantitative immunocytochemical assays. *Hum Pathol* 1998; **29:** 896-903

23 **Hemmerlein B,** Scherbening J, Kugler A, Radzun HJ. Expression of VCAM-1, ICAM-1, E- and P-selectin and tumour-associated macrophages in renal cell carcinoma. *Histopathology* 2000; **37**: 78-83

24 **Lode HN**, Moehler T, Xiang R, Jonczyk A, Gillies SD, Cheresh DA, Reisfeld RA. Synergy between an antiangiogenic integrin alphav antagonist and an antibody-cytokine fusion protein eradicates spontaneous tumor metastases. *Proc Natl Acad Sci USA* 1999; **96**: 1591-1596

25 **Vlems FA,** Diepstra JH, Cornelissen IM, Ruers TJ, Ligtenberg MJ, Punt CJ, van Krieken JH, Wobbes T, van Muijen GN. Limitations of cytokeratin 20 RT-PCR to detect disseminated tumour cells in blood and bone marrow of patients with colorectal cancer: expression in controls and downregulation in tumour tissue. *Mol Pathol* 2002; **55**: 156-163

26 **Lee E**, Chae Y, Kim I, Choi J, Yeom B, Leong AS. Prognostic relevance of immunohistochemically detected lymph node micrometastasis in patients with gastric carcinoma. *Cancer* 2002; **94**: 2867-2873

27 **Alexiou D,** Karayiannakis AJ, Syrigos KN, Zbar A, Sekara E, Michail P, Rosenberg T, Diamantis T. Clinical significance of serum levels of E-selectin, intercellular adhesion molecule-1, and vascular cell adhesion molecule-1 in gastric cancer patients. *Am J Gastroenterol* 2003; **98**: 478-485

28 **Karayiannakis AJ,** Syrigos KN, Polychronidis A, Zbar A, Kouraklis G, Simopoulos C, Karatzas G. Circulating VEGF levels in the serum of gastric cancer patients: correlation with pathological variables, patient survival, and tumor surgery. *Ann Surg* 2002; **236**: 37-42

29 **Velikova G,** Banks RE, Gearing A, Hemingway I, Forbes MA, Preston SR, Hall NR, Jones M, Wyatt J, Miller K, Ward U, Al-Maskatti J, Singh SM, Finan PJ, Ambrose NS, Primrose JN, Selby PJ. Serum concentrations of soluble adhesion molecules in patients with colorectal cancer. *Br J Cancer* 1998; **77**: 1857-1863

30 **Yoo NC,** Chung HC, Chung HC, Park JO, Rha SY, Kim JH, Roh JK, Min JS, Kim BS, Noh SH. Synchronous elevation of soluble intercellular adhesion molecule-1 (ICAM-1) and vascular cell adhesion molecule-1 (VCAM-1) correlates with gastric cancer progression. *Yonsei Med J* 1998; **39**: 27-36

31 **Locker GJ,** Stoiser B, Losert H, Wenzel C, Ohler L, Kabrna E, Geissler K. Decrease of circulating hematopoietic progenitor cells During interleukin-2 treatment is associated with an increase of vascular cell adhesion molecule-1, a critical molecule for progenitor cell adhesion. *Leuk Lymphoma* 2000; **39**: 355-364

32 **Marrelli D,** Pinto E, De Stefano A, Farnetani M, Garosi L, Roviello F. Clinical utility of CEA, CA 19-9, and CA 72-4 in the follow-up of patients with resectable gastric cancer. *Am J Surg* 2001; **181**: 16-19

33 **Kinugasa T,** Kuroki M, Takeo H, Matsuo Y, Ohshima K, Yamashita Y, Shirakusa T, Matsuoka Y. Expression of four CEA family antigens (CEA, NCA, BGP and CGM2) in normal and cancerous gastric epithelial cells: up-regulation of BGP and CGM2 in carcinomas. *Int J Cancer* 1998; **76**: 148-153

34 **Kaptur S,** Riedel F, Erhardt T, Hormann K. Serum concentrations of soluble adhesion molecules sICAM-1 and sVCAM-1 in patients with malignant ENT tumors. *HNO* 2001; **49**: 910-913

35 **Ikeda M,** Furukawa H, Imamura H, Shimizu J, Ishida H, Masutani S, Tatsuta M, Kawasaki T, Satomi T. Surgery for gastric cancer increases plasma levels of vascular endothelial growth factor and von Willebrand factor. *Gastric Cancer* 2002; **5**: 137-141

Edited by Xia HHX and Wang XL

P.O.Box 2345, Beijing 100023,China
Fax: +86-10-85381893
E-mail: wjg@wjgnet.com www.wjgnet.com

World J Gastroenterol 2003;9(7):1415-1420
World Journal of Gastroenterology
 ISSN 1007-9327

• GASTRIC CANCER •

Expression of Fas ligand and Caspase-3 contributes to formation of immune escape in gastric cancer

Hua-Chuan Zheng, Jin-Min Sun, Zheng-Li Wei, Xue-Fei Yang, Yin-Chang Zhang, Yan Xin

Hua-Chuan Zheng, Jin-Min Sun, Xue-Fei Yang, Yin-Chang Zhang, Yan Xin, The Fourth Lab. Cancer Institute, the First Affiliated Hospital of China Medical University, Shenyang 110001, Liaoning Province, China
Zheng-Li Wei, Department of Oncology, Affiliated Hospital of China Medical University, Shenyang 110001, Liaoning Province, China
Correspondence to: Dr. Hua-Chuan Zheng, the Fourth Lab. Cancer Institute, The First Affiliated Hospital of China Medical University, Shenyang 110001, Liaoning Province, China. zheng_huachuan@hotmail.com
Telephone: +86-24-23256666 Ext. 6351 **Fax:** +86-24-23253443
Received: 2002-12-22 **Accepted:** 2003-01-18

Abstract

AIM: To study the role of Fas ligand (FasL) and Caspase-3 expression in carcinogenesis and progression of gastric cancer and molecular mechanisms of relevant immune escape.

METHODS: FasL and Caspase-3 expression was studied in adjacent epithelial cells, cancer cells and lymphocytes of primary foci, and cancer cells of metastatic foci from 113 cases of gastric cancer by streptavidin-biotin-peroxidase (S-P) immunohistochemistry. Expression of both proteins in cancer cells of primary foci was compared with clinicopathological features of gastric cancer. The relationship between FasL expression in cancer cells and Caspase-3 expression in cancer cells or infiltrating lymphocytes of primary foci was investigated.

RESULTS: Cancer cells of primary foci expressed FasL in 53.98 % (61/113) of gastric cancers, more than their adjacent epithelial cells (34.51 %, 39/113) (P=0.003, χ^2=8.681), while the expression of Caspase-3 in cancer cells of primary foci was detected in 32.74 % (37/113) of gastric cancers, less than in the adjacent epithelial cells (50.44 %, 57/113) (P=0.007, χ^2=7.286). Infiltrating lymphocytes of the primary foci showed positive immunoreactivity to Caspase-3 in 70.80 % (80/113) of gastric cancers, more than their corresponding adjacent epithelial cells (P=0.001, χ^2=10.635) or cancer cells of primary foci (P=0.000, χ^2=32.767). FasL was less expressed in cancer cells of metastases (51.16 %, 22/43) than in those of the corresponding primary foci (81.58 %, 31/38) (P=0.003, χ^2=9.907). Conversely, Caspase-3 was more expressed in cancer cells of metastases (58.14 %, 25/43) than in those of the corresponding primary foci (34.21 %, 13/38) (P=0.031, χ^2=4.638). FasL expression was significantly correlated with tumor size (P=0.035, rs=0.276), invasive depth (P=0.039, rs=0.195), metastasis (P=0.039, rs=0.195), differentiation (P=0.015, rs=0.228) and Lauren's classification (P=0.038, rs=0.196), but not with age or gender of patients, growth pattern or TNM staging of gastric cancer (P>0.05). In contrast, Caspase-3 expression showed no correlation with any clinicopathological parameters described above in cancer cells of the primary foci (P>0.05). Interestingly, FasL expression in primary gastric cancer cells paralleled to Caspase-3 expression in infiltrating lymphocytes of the primary foci (P=0.016, χ^2=5.825).

CONCLUSION: Up-regulated expression of FasL and down-regulated expression of Caspase-3 in cancer cells of primary foci play an important role in gastric carcinogenesis. As an effective marker to reveal the biological behaviors, FasL is implicated in differentiation, growth, invasion and metastasis of gastric cancer by inducing apoptosis of infiltrating lymphocytes. Chemical substances derived from the primary foci and metastatic microenvironment can inhibit the growth of metastatic cells by enhancing Caspase-3 expression and diminishing FasL expression.

Zheng HC, Sun JM, Wei ZL, Yang XF, Zhang YC, Xin Y. Expression of Fas ligand and Caspase-3 contributes to formation of immune escape in gastric cancer. *World J Gastroenterol* 2003; 9(7): 1415-1420
http://www.wjgnet.com/1007-9327/9/1415.asp

INTRODUCTION

Gastric cancer is one of the commonest malignancies in China, and even in the world[1-7]. Although early diagnosis and treatment have somewhat improved the patients' outcome, gastric cancer still remains the major killer among Chinese[8,9]. The stepwise transitions during gastric carcinogenesis and progression show that growth-limited gastric epithelial cells become immortalized and in turn exhibit malignant phenotypes[10,11]. It is obvious that the intrinsic regulatory systems for normal cell survival and death are perturbed in these sequential changes of gastric carcinogenesis and progression, so a further understanding of aberrant apoptosis of gastric epithelial cells and cancer cell will be of great significance in the prevention, diagnosis and treatment of gastric cancer.

Fas ligand (FasL) is a family member of tumor necrosis factor (TNF) and nerve growth factor (NGF), which maps to human chromosome 1[12]. When membrane FasL (mFasL) crosslinks with membrane Fas (mFas), cellular apoptosis is induced. However, soluble Fas is released into tumor microenvironment to neutralize FasL on tumor infiltrating lymphocytes and consequently blocks their apoptotic induction, leading to tumor immune escape[13]. Some matrix metalloproteinases can hydrolyze the mFasL into impotent soluble FasL, which can resist apoptosis-induced effect by lymphocytes[14]. In Fas/FasL pathway, association of Fas with FasL can activate the Fas-associated death domain (FADD) and make mitochondrion release cytochrome C[15], which eventually initiates the key Caspase-3 in catalyzing the specific cleavage of many important cellular proteins during apoptosis[16,17].

Capase-3/CPP32 is a member of the interleukin-1β-converting enzyme (ICE) family, which specifically cleaves substrates at the C-terminal of aspartic acid residues. Capase-3 includes two types of CPP32α and CPP32β with cysteine protease activity, and shows a high homology to the pro-apoptotic ced-3 of C elegans[18,19]. Several members of the Caspase family have been implicated in apoptosis, among

which Caspase-3 is thought to act as a central mediator of programmed cell death (PCD) in mammalian cells[20]. Caspase-3 is synthesized as an inactive 32 kd proenzyme and processed during apoptosis into its active form that is composed of two subunits, p17-20 and p10-12. Activated Capase-3 is responsible for the cleavage of poly (ADP-ribose) polymerase (PARP), actin and sterol regulatory element binding protein (SREBP), which relate to apoptosis[19,21-23]. Inhibition of the CPP32-induced proteolytic breakdown of PARP has been demonstrated to result in the attenuation of apoptosis[15].

Previous study suggested that high expression of Fas and FasL was involved in gastrocarcinogenesis[24]. In the current study, we aimed to evaluate the expression of FasL and Caspase-3 in adjacent epithelial cells, cancer cells and lymphocytes of the primary foci, and cancer cells of the metastatic foci of gastric cancer and to find out if there is any relationship between their expressions in cancer cells of the primary foci and clinicopathological features of gastric cancer, as well as between FasL expression in cancer cells of the primary foci and Caspase-3 expression in cancer cells or its infiltrating lymphocytes of the primary foci in order to clarify the role of FasL and Caspase-3 expression in carcinogenesis and progression of gastric cancer and the molecular mechanism of relevant immune escape.

MATERIALS AND METHODS

Subjects

Surgical specimens of 113 gastric cancers were studied from the Second Affiliated Hospital of China Medical University from Sep. 1997 to Feb. 2001. None of the patients underwent radiotherapy or chemotherapy before operation. Adjacent mucosa and primary tumors of all the cases, as well as 43 metastases from 38 cases were fixed in 4 % formaldehyde solution, embedded in paraffin and cut into 4 μm sections.

Evaluation of clinicopathological features

Hematoxylin-and-eosin-stained sections were examined by two pathologists to confirm the histological diagnosis and other microscopic characteristics. These cancers were histologically classified into differentiated and undifferentiated cancers. Their growth pattern was classified into mass, nest, or diffuse types, as reported previously[6]. Penetration of gastric wall, lymph node and distal metastases were routinely described in each patient. Tumor staging was assessed according to TNM classification system.

Immunohistochemistry

The representative and consecutive sections from each adjacent mucosa, primary and secondary tumor were immunostained with streptavidin-peroxidase technique (S-P kit, Zhongshan Biotech.). Anti-FasL antibody (Boster Biotech.) and anti-Caspase-3 antibody (DAKO Biotech.) were diluted in phosphate-buffered saline (PBS, 0.01 mol/L, pH7.4) at the dilution ratio of 1:50 and 1:100 respectively. All procedures were implemented according to the product illustration. For negative controls, sections were processed as the above but with PBS instead of the primary antibodies.

Evaluation of FasL and Caspase-3 staining

The immunoreactivity to FasL or Caspase-3 was localized in the cytoplasm. From 5 randomly selected representative fields of each section, one hundred cells were counted by two independent observers, who did not know the clinicopathological features of these gastric cancers. According to proportion of positive cells, the degree of staining achieved with their antibodies was graded as follows: negative (-), $\leqslant$5 %; weakly positive (+), 5-25 %; moderately positive (++), 25-50 %; and strongly positive (+++), $\geqslant$50 %.

Statistical analysis

Statistical evaluation was performed using *chi*-square to differentiate the rates of different groups and using Spearman's test to analyze ranking correlation. $P<0.05$ was considered statistically significant. SPSS 10.0 software for Windows was employed to analyze all data.

RESULTS

FasL and Capase-3 expression in adjacent epithelial cells, cancer cells and lymphocytes of the primary foci, and cancer cells of the metastatic foci of gastric cancer

Cancer cells of the primary foci expressed FasL in 53.98 % (61/113) of gastric cancers, more than the adjacent epithelial cells (34.51 %, 39/113) (P=0.003, χ^2=8.681), while Caspase-3 in cancer cells of primary foci was expressed in 32.74 % (37/113) of gastric cancers, less than in the adjacent epithelial cells (50.44 %, 57/113) (P=0.007, χ^2=7.286). Infiltrating lymphocytes in the primary foci showed strong immunoreactivity to Caspase-3 in 70.80 % (80/113) of gastric cancers, more than that in the corresponding adjacent epithelium (P=0.001, χ^2=10.635) or cancer cells of the primary foci (P=0.000, χ^2=32.767). FasL was less expressed in cancer cells of metastases (51.16 %, 22/43) than in those of the corresponding primary foci (81.58 %, 31/38) (P=0.003, χ^2=9.907). Conversely, Caspase-3 was more positively expressed in cancer cells of metastases (58.14 %, 25/43) than in those of the corresponding primary foci (34.21 %, 13/38) (P=0.031,χ^2=4.638) (Table 1, Figures 1-4).

Relationship between FasL and Caspase-3 expression in cancer cells of the primary foci and the clinicopathological features of gastric cancer

FasL expression was significantly correlated with tumor size (P=0.035, rs=0.276), invasive depth (P=0.039, rs=0.195), metastasis (P=0.039, rs=0.195), histological classification (P=0.015, rs=0.228) and Lauren's classification (P=0.038,

Table 1 Expression of FasL and Caspase-3 in adjacent epithelial cells, cancer cells of primary and metastatic foci of gastric cancer

	n	FasL expression			Caspase-3 expression		
		-	+~+++	PR(%)	-	+~+++	PR(%)
Adjacent epithelial cells	113	74	39	34.51	56	57	50.44
Cancer cells of primary foci	113	52	61	53.98[a]	76	37	32.74[b]
Cancer cells of metastatic foci	43	21	22	51.16[c]	18	25	58.14[d]

[a]P=0.003 (χ^2=8.681, Pearson' R=0.176), *vs* adjacent epithelial cells; [b]P=0.007 (χ^2=7.286, Pearson' R=0.180) , *vs* adjacent epithelial cells; [c]P=0.003 (χ^2=9.907, Pearson' R=0.245), *vs* cancer cells of the corresponding primary foci; [d]P=0.031 (χ^2=4.638, Pearson' R=0.239), *vs* cancer cells of the corresponding primary foci; PR,positive rate.

rs=0.196) of gastric cancer in cancer cells of the primary foci, whereas not with growth pattern or TNM staging of gastric cancer, gender or age of patients (P>0.05). Comparatively, Caspase-3 expression showed no significant correlation with tumor size, invasive depth, metastasis, histological classification, TNM staging, age and gender of patients in cancer cells of the primary foci (P>0.05) (Table 2).

Relationship between FasL and Caspase-3 expression in gastric cancer

Interestingly, our results showed FasL expression in cancer cells of the primary foci was positively associated with Caspase-3 expression in their infiltrating lymphocytes (P=0.016, χ^2=5.825), not with Caspase-3 expression in cancer cells of the primary foci (P>0.05) (Table 3).

Table 2 Relationship between the expression of FasL , Caspase-3 in cancer cells of primary foci and clinicopathological features of gastric cancer

Clinicopathological features	*n*	FasL expression						Caspase-3 expression					
		-	+	++	+++	PR(%)	*P* value	-	+	++	+++	PR(%)	*P* value
Age							0.318						0.414
<50 years	33	13	7	6	7	60.61		21	3	3	6	36.36	
⩾50 years	80	39	17	14	10	51.25		55	13	4	8	31.25	
Gender							0.548						0.514
Male	83	37	16	16	14	55.42		57	12	5	9	31.32	
Female	30	15	5	7	3	50.00		19	4	2	5	36.37	
Tumor size							0.035						0.802
<4 cm	47	27	8	7	5	42.55		33	3	5	6	29.79	
⩾4 cm	66	25	13	16	12	62.12		43	13	2	8	34.84	
Invasive depth							0.039						0.987
Above submucosa	26	16	4	4	2	38.46		18	3	3	2	30.76	
Muscularis propria	34	16	6	8	4	52.94		22	6	0	6	32.35	
Below subserosa	53	20	11	11	11	62.26		36	7	4	6	33.96	
Metastasis							0.039						0.913
-	75	40	12	15	8	46.67		51	9	3	12	32.00	
+	38	12	9	8	9	68.42		25	7	4	2	34.21	
TNM staging							0.312						0.506
O	18	10	3	3	2	44.44		12	3	1	2	33.33	
I	28	13	4	8	3	53.57		18	3	2	5	35.71	
II	40	19	8	8	5	52.50		26	7	2	5	35.00	
III	17	7	2	2	6	58.82		13	1	1	2	23.53	
IV	10	3	4	2	1	70.00		7	2	1	0	30.00	
Growth pattern							0.338						0.735
Mass	23	8	5	10	0	65.22		17	3	1	2	26.09	
Nest	30	12	4	5	9	60.00		18	5	1	6	40.00	
Diffuse	34	18	7	3	6	47.06		23	5	2	4	32.35	
Lauren's classification							0.038						0.333
Intestinal type	36	12	7	13	4	66.67		27	3	1	5	25.00	
Diffuse type	57	32	10	8	7	43.86		36	9	5	7	36.84	
Mixed type	20	8	4	2	6	60.00		13	4	1	2	35.00	
Histological classification							0.015						0.754
Differentiated	53	19	9	14	11	64.15		37	6	2	8	30.18	
Undifferentiated	60	33	12	9	6	45.00		39	10	5	6	35.00	

PR, positive rate.

Table 3 Relationship between FasL and Caspase-3 expression in gastric cancer

FasL expression In CC of PF	*n*	Caspase-3 expression in CC of PF			Caspase-3 expression in ILC of PF		
		-	+~+++	PR(%)	-	+~+++	PR(%)
-	52	39	13	26.92	21	31	65.38
+~+++	61	37	24	37.70	12	49	75.41[a]
Total	113	76	37	32.74	33	80	70.80

[a]P=0.016 (χ^2=5.825, Pearson'R=0.227), *vs* FasL-negative cases; CC, cancer cells; PF, primary foci; ILC, infiltrating lymphocytes; PR, positive rate.

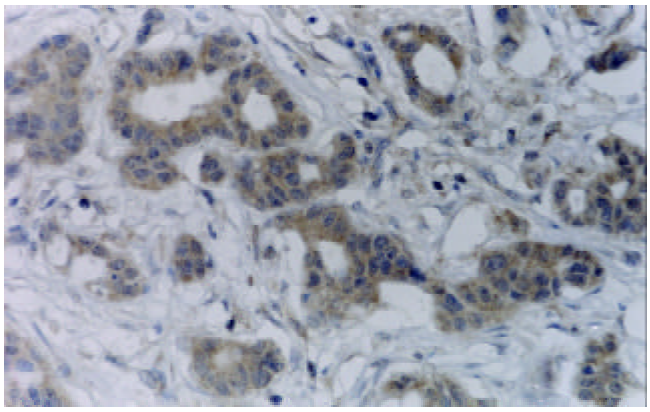

Figure 1 FasL was strongly expressed in moderately differentiated adenocarcinoma of stomach (+++). S-P×400.

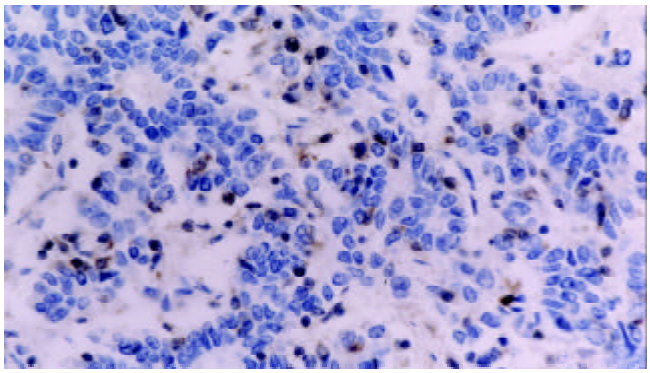

Figure 2 Caspase-3 was negatively expressed in poorly differentiated adenocarcinoma of stomach (-), while strongly positive in tumor infiltrating lymphocytes (+++). S-P×400.

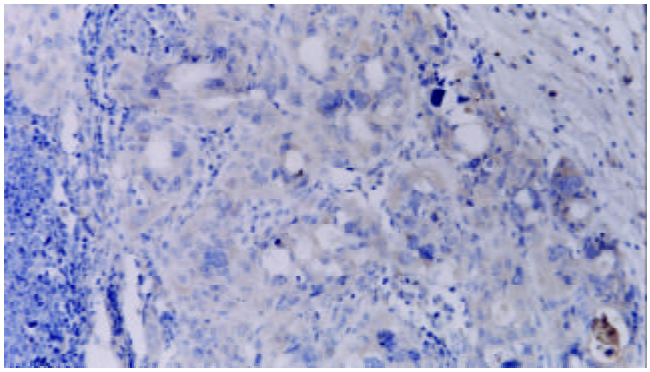

Figure 3 FasL was strongly expressed in gastric cancer cells of lymph node metastasis (+++). S-P×400.

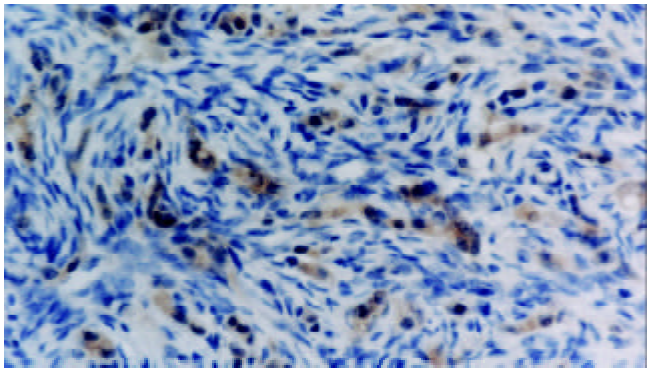

Figure 4 Caspase-3 was strongly expressed in gastric cancer cells of ovary metastasis (+++). S-P×400.

DISCUSSION

As a transmembrane type II protein, FasL initiates PCD through activating FADD when coupled with mFas, so FasL greatly contributes to apoptotic induction in most cells[25]. During the course, Caspase-3 will be activated by a series of cascade reactions, and eventually DNase (CAD, CPAN, or DEF40) is activated, which belongs to the Mg^{2+}-dependent endonuclease and acts as a killer in apoptosis. Some previous studies demonstrated that esophageal and colon cancers highly expressed FasL at the levels of mRNA and protein. Furthermore, increased FasL can bind to mFas in infiltrating lymphocytes, which is eliminated by inducing their apoptosis[26,27]. Therefore, cancer cells can form an immune escape.

In this study, we found that FasL and Caspase-3 were expressed in 34.51 % (39/113) and 50.44 % (57/113) of adjacent epithelial of gastric cancer respectively, most of which exhibited inflammation, regeneration, or intestinal metaplasia. Li *et al*.[24] detected FasL expression in normal gastric mucosa and atrophic gastritis. It was previously documented that most cells from human organs showed positive immunoreactivity to Caspase-3, including cryptal cells of gastric pit. These data indicate that FasL and Caspase-3 play an important role in regulating the balance of cellular proliferation and apoptosis in gastric mucosa by inducing apoptosis.

Moreover, FasL is more frequently expressed in cancer cells of primary foci than in their adjacent epithelial cells ($P<0.05$). Belluco *et al*.[28] found that FasL was overexpressed in adenoma-adenocarcinoma of colorectum and FasL expression paralleled to malignant degrees. These results suggest that up-regulated expression of FasL contributes to gastric carcinogenesis. On the other hand, Capase-3 expression was less frequently detected in cancer cells of the primary foci, than in the adjacent epithelial cells ($P<0.05$), as described previously[29]. Hoshi *et al*.[30] also found the positive rate of Caspase-3 expression was lower in gastric cancers than in their adjacent mucosa and gastric adenoma, and was correlated negatively with proliferative index of Ki-67, as well as positively with apoptotic index labeled by TUNEL. These studies reveal that down-regulated expression of Capase-3 is implicated in gastric carcinogenesis.

Additionally, our results also indicated that Caspase-3 expression in infiltrating lymphocytes was found in 70.80 % of gastric cancers, significantly more than in cancer cells and adjacent epithelial cells of their primary foci ($P<0.05$). So most of primary gastric cancers showed strong expression of Capase-3 in infiltrating lymphocytes, whereas weak or no expression of Caspase-3 in primary cancer cells. Interestingly, we found that FasL expression in primary cancer cells was closely correlated with Caspase-3 expression in filtrating lymphocytes of the primary cancer ($P<0.05$). Although FasL-positive gastric cancer expressed more Caspase-3 than FasL-negative one, the positive rates of Caspase-3 expression in FasL-positive and FasL-negative carcinomas were of no significant difference ($P>0.05$). The more FasL was expressed in cancer cells, the more Caspase-3 was expressed in lymphocytes in the primary foci. Some investigators found that FasL-positive cancer showed increased apoptosis in its infiltrating lymphocytes and decreased apoptosis in cancer cells[31]. Our study showed that more expression of Caspase-3 in infiltrating lymphocytes of gastric cancer demonstrated its critical contribution to Fas-mediated immune escape. However, FasL-positive gastric cancer also showed high expression of Caspase-3, suggesting there were other mechanisms that played an important role in Fas-Caspase apoptotic pathway of gastric cancer cells.

In our study, FasL expression in cancer cells of primary foci was not correlated with gender or age of patients with gastric cancer ($P>0.05$), suggesting that FasL expression in

the primary cancer cells genetically did not depend on the gender or age of patients, and they therefore had no effect on relationship between FasL expression and patho-biological behaviors of gastric cancer. Our results showed that FasL expression in cancer cells of primary foci was closely associated with tumor size, invasive depth, metastasis, histological differentiation and Lauren' s classification (P<0.05), but not with growth pattern or TNM staging of gastric cancer (P>0.05). Tsutsumi *et al*[32] found serum content of soluble FasL (sFasL) was correlated with invasive depth, lymph node and distal metastasis. These indicate that FasL is implicated in progression of gastric cancer by forming immune counterattack. Although FasL expression in primary cancer cells was not significantly associated with growth pattern of gastric cancer, higher expression of FasL in mass-type than in nest-type or diffuse-type gastric cancer revealed that increased FasL expression in cancer cells responsed to elevated infiltrating lymphocytes in gastric cancer with mass growth. Notably, FasL was expressed more in intestinal-type gastric cancers than in diffuse-type ones (P<0.05), indicating that both types of gastric cancer have different histogenetic pathways. Furthermore, this study showed no relationship between down-regulated expression of Caspase-3 and clinicopathological features of gastric cancer described above (P>0.05), suggesting that Caspase-3 expression is genetically independent of gender or age and is not implicated in progression.

FasL was significantly expressed in cancer cells of the primary foci than in corresponding metastatic foci (P<0.05), while Caspase-3 was less expressed in cancer cells of primary foci than in corresponding metastatic foci of gastric cancer (P<0.05), demonstrating that decreased ability of metastatic cancer cells to induce apoptosis of lymphocytes and increased apoptosis in metastatic cancer cells, might be influenced by tumor microenvironment. It was documented that metastases grew rapidly after the primary foci of tumor were removed, and a kind of substance from the primary foci could inhibit growth of metastases[33]. If so, another reason for this phenomenon might be that primary foci regulate the expression of Caspase-3 and FasL of metastatic cancer cells so as to suppress their ability to proliferate.

In conclusion, up-regulation of FasL expression and down-regulation of Caspase-3 expression in cancer cells of primary carcinoma are involved in gastric carcinogenesis. As an effective marker to reveal the patho-biological behaviors, FasL contributes to differentiation, growth, invasion and metastasis of gastric cancer by inducing apoptosis of infiltrating lymphocytes. Chemical substances from primary foci and metastatic microenvironment can induce apoptosis of metastatic cancer cells or weaken ability of metastatic cancer cells to counterattack adjacent lymphocytes by decreasing FasL expression and increasing Caspase-3 expression of metastastic cancer cells, eventually resulting in the inhibition of their growth.

ACKNOWLEDGEMENT

We thank Mrs Zhao Yuhong and Mrs Huang Yaming for their contribution to the preparation of this manuscript.

REFERENCES

1 **Zhou YN**, Xu CP, Han B, Li M, Qiao L, Fang DC, Yang JM. Expression of E-cadherin and beta-catenin in gastric carcinoma and its correlation with the clinicopathological features and patient survival. *World J Gastroenterol* 2002; **8**: 987-993
2 **Fang DC**, Luo YH, Yang SM, Li XA, Ling XL, Fang L. Mutation analysis of APC gene in gastric cancer with microsatellite instability. *World J Gastroenterol* 2002; **8**: 787-791
3 **Song ZJ,** Gong P, Wu YE. Relationship between the expression of iNOS,VEGF, tumor angiogenesis and gastric cancer. *World J Gastroenterol* 2002; **8**: 591-595
4 **Yao XX,** Yin L, Sun ZC. The expression of hTERT mRNA and cellular immunity in gastric cancer and precancerosis. *World J Gastroenterol* 2002; **8**: 586-590
5 **Niu WX**, Qin XY, Liu H, Wang CP. Clinicopathological analysis of patients with gastric cancer in 1200 cases. *World J Gastroenterol* 2001; **7**: 281-284
6 **Xin Y,** Li XL, Wang YP, Zhang SM, Zheng HC, Wu DY, Zhang YC. Relationship between phenotypes of cell-function differentiation and pathobiological behavior of gastric carcinomas. *World J Gastroenterol* 2001; **7**: 53-59
7 **Jiang BJ**, Sun RX, Lin H, Gao YF. Study on the risk factors of lymphatic metastasis and the indications of less invasive operations in early gastric cancer. *World J Gastroenterol* 2000; **6**: 553-556
8 **Jemal A**, Thomas A, Murray T, Thun M. R.Cancer statistics, 2002. *CA Cancer J Clin* 2002; **52**: 23-47
9 **Theuer CP**. Asian gastric cancer patients at a southern California comprehensive cancer center are diagnosed with less advanced disease and have superior stage-stratified survival. *Am Surg* 2000; **66**: 821-826
10 **Schmidt PH**, Lee JR, Joshi V, Playford RJ, Poulsom R, Wright NA, Goldenring JR. Identification of a metaplastic cell lineage associated with human gastric adenocarcinoma. *Lab Invest* 1999; **79**: 639-646
11 **Bajtai A**, Hidvegi J. The role of gastric mucosal dysplasia in the development of gastric carcinoma.*Pathol Oncol Res* 1998; **4**: 297-300
12 **Sakata K**, Sakata A, Kong L, Dang H, Talal N. Role of Fas/FasL interaction in physiology and pathology: the good and the bad. *Clin Immunol Immunopathol* 1998; **87**: 1-7
13 **O'Connell J**, Bennett MW, O'Sullivan GC, Roche D, Kelly J, Collins JK, Shanahan F. Fas ligand expression in primary colon adenocarcinomas: evidence that the Fas counterattack is a prevalent mechanism of immune evasion in human colon cancer. *J Pathol* 1998; **186**: 240-246
14 **Mitsiades N**, Yu WH, Poulaki V, Tsokos M, Stamenkovic I. Matrix metalloproteinase-7-mediated cleavage of Fas ligand protects tumor cells from chemotherapeutic drug cytotoxicity. *Cancer Res* 2001; **61**: 577-581
15 **Wilson MR**. Apoptosis: unmasking the executioner. *Cell Death Differ* 1998; **5**: 646-652
16 **Slee EA**, Adrain C, Martin SJ. Serial killers: ordering caspase activation events in apoptosis.*Cell Death Differ* 1999; **6**: 1067-1074
17 **Porter AG**, Janicke RU. Emerging roles of caspase-3 in apoptosis. *Cell Death Differ* 1999; **6**: 99-104
18 **Shaham S,** Reddien PW, Davies B, Horvitz HR. Mutational analysis of the Caenorhabditis elegans cell-death gene ced-3. *Genetics* 1999; **153**: 1655-1671
19 **Tian R,** Zhang GY, Yan CH, Dai YR. Involvement of poly (ADP-ribose) polymerase and activation of caspase-3-like protease in heat shock-induced apoptosis in tobacco suspension cells. *FEBS Lett* 2000; **474**: 11-15
20 **Kutsyi MP,** Kuznetsova EA, Gaziev AI. Involvement of proteases in apoptosis. *Biochemistry (Mosc)* 1999; **64**: 115-126
21 **Truong-Tran AQ,** Carter J, Ruffin RE, Zalewski PD. The role of zinc in caspase activation and apoptotic cell death. *Biometals* 2001; **14**: 315-330
22 **Fujii Y**, Matsura T, Kai M, Matsui H, Kawasaki H, Yamada K. Mitochondrial cytochrome c release and caspase-3-like protease activation during indomethacin-induced apoptosis in rat gastric mucosal cells. *Proc Soc Exp Biol Med* 2000; **224**: 102-108
23 **Umeda T,** Kouchi Z, Kawahara H, Tomioka S, Sasagawa N, Maeda T, Sorimachi H, Ishiura S, Suzuki K. Limited proteolysis of filamin is catalyzed by caspase-3 in U937 and Jurkat cells. *J Biochem (Tokyo)* 2001; **130**: 535-542
24 **Li H**, Liu N, Guo L, Li JW, Liu JR. Frequent expression of soluble Fas and Fas ligand in Chinese stomach cancer and its preneoplastic lesions. *Int J Mol Med* 2000; **5**: 473-476
25 **Chang HY,** Yang X. Proteases for cell suicide: functions and regulation of caspases. *Microbiol Mol Biol Rev* 2000; **64**: 821-846
26 **O'Connell J**, Bennett MW, Nally K, Houston A, O'Sullivan GC, Shanahan F. Altered mechanisms of apoptosis in colon cancer: Fas resistance and counterattack in the tumor-immune conflict. *Ann N Y Acad Sci* 2000; **910**: 178-192

27 **Izban KF**, Wrone-Smith T, Hsi ED, Schnitzer B, Quevedo ME, Alkan S. Characterization of the interleukin-1beta-converting enzyme/ced-3-family protease, caspase-3/CPP32, in Hodgkin's disease: lack of caspase-3 expression in nodular lymphocyte predominance Hodgkin's disease. *Am J Pathol* 1999; **154**: 1439-1447

28 **Belluco C**, Esposito G, Bertorelle R, Alaggio R, Giacomelli L, Bianchi LC, Nitti D, Lise M. Fas ligand is up-regulated during the colorectal adenoma-carcinoma sequence .*Eur J Surg Oncol* 2002; **28**: 120-125

29 **Bennett MW,** O'Connell J, Houston A, Kelly J, O'Sullivan GC, Collins JK, Shanahan F. Fas ligand upregulation is an early event in colonic carcinogenesis. *J Clin Pathol* 2001; **54**: 598-604

30 **Hoshi T**, Sasano H, Kato K, Yabuki N, Ohara S, Konno R, Asaki S, Toyota T, Tateno H, Nagura H. Immunohistochemistry of Caspase3/CPP32 in human stomach and its correlation with cell proliferation and apoptosis. *Anticancer Res* 1998; **18**: 4347-4353

31 **Bennett MW**, O'Connell J, O'Sullivan GC, Brady C, Roche D, Collins JK, Shanahan F. The Fas counterattack *in vivo*: apoptotic depletion of tumor-infiltrating lymphocytes associated with Fas ligand expression by human esophageal carcinoma. *J Immunol* 1998; **160**: 5669-5675

32 **Tsutsumi S**, Kuwano H, Shimura T, Morinaga N, Mochiki E, Asao T. Circulating soluble Fas ligand in patients with gastric carcinoma. *Cancer* 2000; **89**: 2560-2564

33 **Torosian MH,** Bartlett DL. Inhibition of tumor metastasis by a circulating suppressor factor. *J Surg Res* 1993; **55**: 74-79

Edited by Zhang JZ

P.O.Box 2345, Beijing 100023,China
Fax: +86-10-85381893
E-mail: wjg@wjgnet.com www.wjgnet.com

World J Gastroenterol 2003;9(7):1421-1426
World Journal of Gastroenterology
 ISSN 1007-9327

• GASTRIC CANCER •

Prognostic significance of expression of cyclooxygenase-2 and vascular endothelial growth factor in human gastric carcinoma

Hai Shi, Jian-Ming Xu, Nai-Zhong Hu, Hui-Jun Xie

Hai Shi, Jian-Ming Xu, Nai-Zhong Hu, Hui-Jun Xie, Department of Gastroenterology, the First Affiliated Hospital, Anhui Medical University, Hefei 23022, Anhui Province, China
Correspondence to: Dr. Hai Shi, Department of Gastroenterology, the First Affiliated Hospital, Anhui Medical University, Hefei 23022, Anhui Province, China. shmdah@hotmail.com
Telephone: +86-551-2922039
Received: 2002-12-28 **Accepted:** 2003-02-18

Abstract

AIM: To investigate the role of cyclooxygenase-2(COX-2) and vascular endothelial growth factor (VEGF) in the development of gastric carcinoma and correlation between expression of COX-2 and VEGF and clinicopathologic features in tissues from patients with gastric carcinoma.

METHODS: 281 patients with gastric carcinoma who underwent surgical resection between 1990 and 1999 at the First Affiliated Hospital, Anhui Medical University, PRC, were followed up. Expression of COX-2 and VEGF was investigated retrospectively in 232 gastric carcinoma tissues and 60 noncancerous specimens by using immunohistochemistry.

RESULTS: The 5-year survival rates of early gastric carcinoma (EGC) and advanced gastric carcinoma (AGC) were 93.4 % and 59.0 %, respectively. Survival time was highly correlated with lymph node metastasis, vascular invasion, depth of invasion and treatment with chemotherapy. Compared with paired noncancerous tissues, expression of COX-2 and VEGF and microvessel density (MVD) value in carcinoma tissue were significantly higher. The MVD value was much higher in COX-2-positive group and VEGF-positive group than that in COX-2-negative group and VEGF-negative group. Expression of COX-2 and VEGF, as well as MVD value were highly correlated with lymph node metastasis and vascular invasion. The 5-year survival rate of patients with expression of COX-2 or VEGF was significantly lower than that of patients without COX-2 or VEGF expression. Multivariate analysis revealed that VEGF overexpression, lymph node metastasis, COX-2 overexpression, depth of invasion and vascular invasion were all independent prognostic factors of gastric carcinoma.

CONCLUSION: Overexpression of COX-2 and VEGF in patients with gastric carcinoma can enhance the possibility of invasion and metastasis, implicating a poor prognosis. They may serve as the fairly good prognostic factors to indicate biologic behaviors of gastric carcinoma.

Shi H, Xu JM, Hu NZ, Xie HJ. Prognostic significance of expression of cyclooxygenase-2 and vascular endothelial growth factor in human gastric carcinoma. *World J Gastroenterol* 2003; 9(7):1421-1426
http://www.wjgnet.com/1007-9327/9/1421.asp

INTRODUCTION

Gastric carcinoma is one of the most common malignancies worldwide. Carcinogenesis and progression of carcinoma are believed to be from multi-stage processes involving the activation of oncogenes and/or the loss of suppressor genes. Epidemiologic studies have shown that nonsteroidal anti-inflammatory drugs (NSAIDs) can reduce the incidence rate and mortality of digestive tract carcinomas, including esophageal, gastric, colon, and rectal lesions[1,2]. The prostaglandin synthetic enzyme cyclooxygenase (COX) is a target for NSAIDs therapy, and a key enzyme in the conversion of arachidonic acid to prostaglandins. Recent studies have confirmed the presence of two forms of COX, constitutively produced COX-1 and inducible COX-2[3]. COX-1 is a constitutively expressed gene in many tissues, and levels of this protein do not fluctuate in response to stimuli[4]. COX-2 is induced by pathologic stimuli, such as inflammation, various growth factors, and cytokines produced by tumor cells[5]. Human gastric mucosa, however, normally expresses barely detectable levels of COX-2 protein[6]. To date, whether COX-2 is involved in the growth of gastric carcinoma remains to be clarified, although COX-2 overexpression has recently been reported in human gastric adenocarcinoma[7].

Recently, many studies have reported on the relation between the malignant potential of neoplasms and tumor angiogenesis[8-10]. Vascular endothelial growth factor (VEGF) is one of these angiogenic factors, and is known to play a crucial role in the formation of neovasculature[11]. VEGF expression is correlated significantly with tumor vascularity and a marker for tumor angiogenesis[12,13]. In the current study, we examined COX-2 and VEGF expression in primary gastric carcinoma tissues at various stages to investigate the relations between COX-2 and VEGF expression and clinicopathologic features of these tumors. We also investigated the prognostic value of these two biologic factors in gastric carcinoma and compared them with the conventional clinicopathologic factors.

MATERIALS AND METHODS

Clinical materials

Totally 281 patients with gastric carcinoma who received gastrectomy without preoperative chemotherapy between 1990 and 1999 at our university hospital were followed up. Among the 281 patients, there were 110 patients with early gastric carcinoma (EGC) in which carcinoma invasion was confined to the mucosa or submucosa and 171 patients with advanced gastric carcinoma (AGC) that invaded beyond the submucosal layer (but not to serosa in our study) according to the criteria of the Japanese Research Society for Gastric Cancer[14]. The patients were comprised of 198 men and 83 women with an average age of 55.6 years (range, 22 to 80 years). Of these 281 patients, 66 had lymph node metastasis and 39 had vascular invasion. Patients who died of other disease were excluded from the study. 60 paired control samples (including 30 cases of chronic atrophic gastritis (CAG) and 30 cases of gastric epithelial dysplasia) were obtained from the antrum.

Immunohistochemical techniques

In brief, archival paraffin-embedded tissue specimens and controls were sectioned at a thickness of 4 μm, deparaffinized,

and rehydrated. The slides were incubated with 3 % hydrogen peroxide in methanol for 10 minutes to block endogenous peroxidase activity, and then washed in phosphate-buffered saline (PBS) and incubated in 10 % normal rabbit serum for 5 minutes to reduce nonspecific antibody binding. Rabbit polyclonal antibody specific for human COX-2 (H-62; Santa Cruz Biotechnology, Inc. Santa Cruz, CA) was applied as the primary antibody at a dilution of 1:100. Mouse monoclonal antibody against VEGF(A-20, Santa Cruz Biotechnology, Inc. Santa Cruz, CA) or Factor VIII related antigen (PC-10, Maxim Biotech, Inc.) was also applied as the primary antibody. These slides were incubated with primary antibody for 60 minutes at room temperature, followed by 3 washes with PBS. Sections then were incubated with biotinylated IgG for 20 minutes followed by 3 washes. Slides then were treated with streptoavidin-peroxidase reagent for 20 minutes and washed with PBS 3 times. Finally, slides were incubated in PBS containing diaminobenzidine and 1 % hydrogen peroxide for 5-10 minutes, counterstained with Mayer hematoxylin, and mounted. PBS was substituted for primary antibody as the negative control.

Staining analysis

COX-2 staining The expression of COX-2 was semiquantified. The degree of immunostaining for COX-2 was considered positive when unequivocal staining of the cytoplasm was observed in tumor cells[7].

VEGF staining Immunoreactivity was graded as follows[12]: Positive, unequivocal staining of the membrane or the cytoplasm was seen in more than 5 % of carcinoma cells, negative, no detectable expression or less than 5 % of tumor cells were stained.

Microvessel staining and counting Intratumoral microvessels were highlighted by immunostaining with anti-Factor VIII related antigen monoclonal antibody. Any single brownly-stained cell or cluster of endothelial cells that was clearly separated from adjacent microvessels, tumor cells, and other connective tissue elements were considered a vessel[12]. Branching structures were counted as a single vessel unless there was a discontinuity in the structure. The stained sections were screened at ×100 magnification under a light microscope to identify the 5 regions of the section with the highest vascular density. Vessels were counted in the 5 regions at ×200 magnification, and the average numbers of microvessels were recorded[12]. Two observers did the counting, and the mean value was used for the analysis.

Statistical analysis

Data were analyzed using the chi-square test for categoric variables and Student' s *t* test for continuous variables. Five-year survival was compared using the Kaplan-Meier method and analyzed by the log rank test. Factors affecting survival were analyzed by Cox proportional hazards model using the SPSS statistic package Version 10.0. Differences with *P* values <0.05 were considered statistically significant.

RESULTS

The detection rates of EGC between 1990 and 1999 fluctuated between 1.1 % and 6.6 %. The average detection rate was 4.3 % (110/2533). In patients with EGC, cardia gastric tumors more frequently occurred than corpus and antrum gastric carcinoma in 60-69 age group (50.0 % *vs* 28.9 %, 21.3 %, *P*<0.05).

Five-year survival rate

The follow-up rates of EGC and AGC were 88.2 % (97/110) and 84.8 % (145/171), respectively. The overall disease-specific 5-year survival rates for patients with EGC and AGC were 93.4 % and 59.0 %, respectively. The 5-year survival rates for patients with EGC with different tumor location were as follows: cardia, 90.9 %; corpus, 91.3 %; and antrum, 96.3 %. The 5-year survival rate for patients with EGC with different depth of invasion was 96.7 % for mucosa invasion and 90.3 % for submucosa invasion. The 5-year survival rates for patients with AGC with different tumor location were as follows: cardia, 45.0 %; corpus, 69.6 %; and antrum, 60.0 %.

Correlation between postoperative survival time and clinicopathologic factors

Table1 shows the clinicopathologic data of 106 patients who survived for ⩾5 years and 47 patients who died within 5 years. There were no differences with respect to gender, age, location of the tumor, or histology between patients with long and short survival time. But survival time was highly correlated with depth of invasion, lymph node metastasis, vascular invasion, and treatment with chemotherapy (*P*<0.05-0.01).

Table 1 Correlation between clinicopathologic factors and survival time

Variables	Alive more than 5 years *n*=106	Died within 5 years *n*=47	*P* value
Gender			
Male	76(71.7)	33(70.2)	NS
Female	30(28.3)	14(29.8)	
Age(years)			
<60	28(26.4)	18(38.3)	NS
⩾60	78(73.6)	29(61.7)	
Location of tumor			
Cardia	19(17.9)	11(23.4)	NS
Corpus	37(34.9)	17(31.9)	
Antrum	50(47.2)	21(44.7)	
Depth of invasion			
Mucosa or submucosa	57(53.8)	6(12.8)	<0.01
Muscularis propria	49(46.2)	41(87.2)	
Histology			
Differentiated	41(38.7)	19(40.4)	NS
Undifferentiated	65(61.3)	28(59.6)	
Lymph node metastasis			
Present	21(19.8)	38(80.9)	<0.01
Absent	85(80.2)	9(19.1)	
Vascular invasion			
Present	9(8.5)	26(55.3)	<0.01
Absent	97(91.5)	21(44.7)	
Chemotherapy			
Yes	69(65.1)	20(42.6)	<0.05
No	37(34.9)	27(57.4)	

Note: NS, not significant.

Immunohistochemical analysis

Correlation between expression of COX-2 and clinicopathologic factors Immunoreactivity for COX-2 protein was present in the cytoplasm of tumor cells, smooth muscle cells, and surrounding glands, but not in the surrounding stroma (Figure 1). Positive immunostaining for COX-2 was also seen in some CAG (23.3 %) and mucosal atypical hyperplasia (60.0 %) specimens (Figure 2). However, it was observed more frequently in tumor cells (Table 2), which showed that the expression of COX-2 was significantly higher in mucosal atypical hyperplasia than that in CAG (*P*<0.01).

Compared with paired noncancerous specimens, COX-2 levels in carcinoma tissue were significantly higher (P<0.05-0.01). There was no significant association between COX-2 expression and gender, age, location of the tumor, or depth of invasion. However, significant difference was noted with respect to histologic type, lymph node metastasis, and vascular invasion. The COX-2-positive rate was significantly higher in patients with lymph node metastasis or vascular invasion than that in those without such metastasis or invasion (P<0.05-0.01). Similar results were obtained in relationship between the histologic type and the COX-2-positive rate (P<0.01, Table 2).

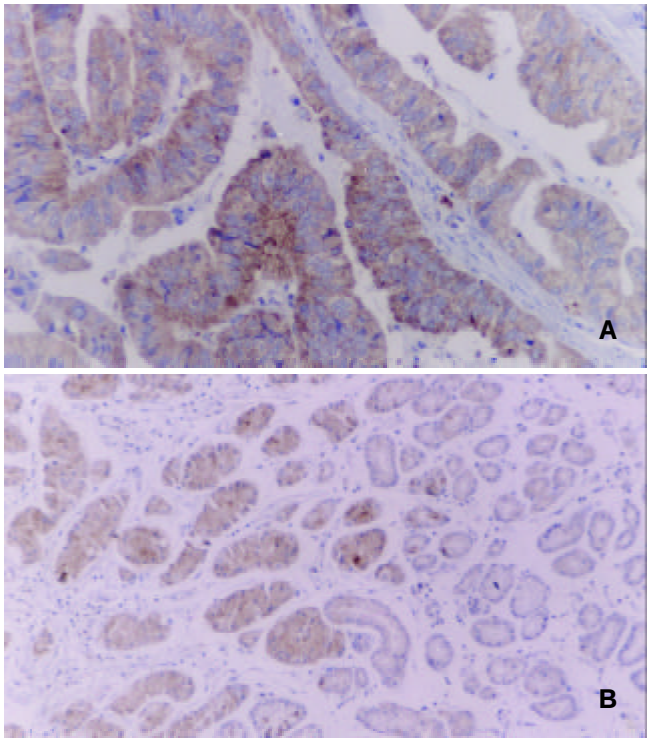

Figure 1 Immunohistochemical staining of COX-2 protein in gastric carcinoma. Immunoreactivity for COX-2 protein was present in the cytoplasm of tumor cells, smooth muscle cells (A, ×200), and surrounding glands (B, ×100).

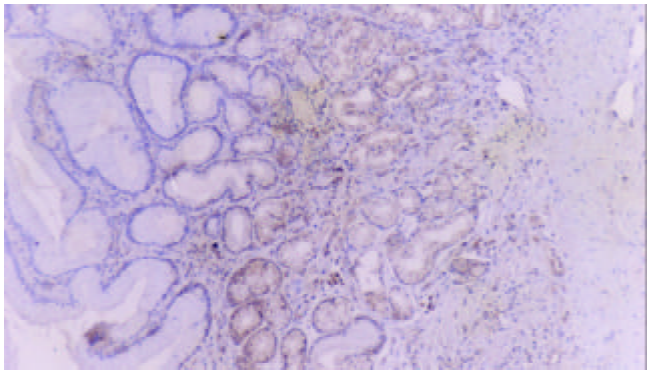

Figure 2 Positive immunostaining for COX-2 was observed in some CAG specimens (×100).

Correlations between expression of VEGF, microvessel counting and clinicopathologic factors VEGF was mainly localized in the cytoplasm or on the membrane of carcinoma cells (Figure 3). Tumor cells that were strongly immunopositive for VEGF were observed more often in the invasive front than that in the center of the tumors. Weakly positive VEGF staining was seen in some endothelial cells and noncancerous specimens. VEGF expression was detected in 122 (52.6 %) tumors and significantly higher (P<0.01) than that in noncancerous specimens (13.3 %). Correlations between VEGF expression, MVD and different clinicopathologic variables are shown in Table 3. VEGF-positive rate and MVD value were significantly correlated with depth of invasion, lymph node metastasis, and invasion of blood vessels (P<0.01). There was no significant association among VEGF expression, MVD value and histologic type. The microvessel count in COX-2-positive or VEGF-positive tumors (28.76±8.58 and 26.23±8.47, respectively) was significantly higher than that in COX-2-negative or VEGF-negative tumors (19.27±8.36 and 18.91±8.12, respectively), P<0.01.

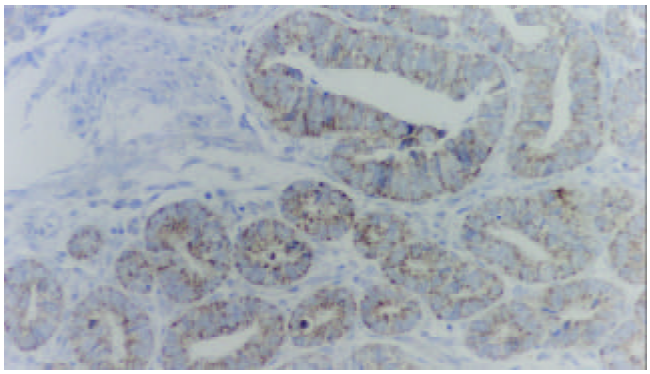

Figure 3 Immunohistochemical staining for VEGF in gastric carcinoma. VEGF was mainly localized on the membrane of the carcinoma cells or in the cytoplasm (×200).

Table 2 Correlation between COX-2 expression and clinicopathologic factors

Variables	*n*	COX-2 *n*(%)		*P* value
		Positive	Negative	
Gender				
Male	168	30(17.9)	138(82.1)	NS
Female	64	12(18.7)	52(81.3)	
Age(years)				
<60	145	25(17.2)	120(82.8)	NS
⩾60	87	17(19.5)	70(80.5)	
Location of tumor				
Cardia	61	7(11.5)	54(88.5)	NS
Corpus	77	19(24.7)	58(75.3)	
Antrum	94	16(17.1)	78(82.9)	
Histology				
Differentiated	129	7(5.4)	122(94.6)	<0.01
Undifferentiated	103	35(33.9)	68(66.1)	
Lymph node metastasis				
Present	64	2(3.1)	62(96.9)	<0.01
Absent	168	40(23.8)	128(76.2)	
Vascular invasion				
Present	39	2(5.1)	37(94.9)	<0.05
Absent	193	40(20.7)	153(79.3)	
Depth of invasion				
Mucosa or submucosa	94	19(20.2)	75(79.8)	NS
Muscularis propria	138	23(16.7)	115(83.3)	
Noncancerous tissue				
CAG	30	23(76.7)	7(23.3)	<0.01
Atypical hyperplasia	30	12(40.0)	18(60.0)	

Notes: NS, not significant; CAG, chronic atrophic gastritis.

Table 3 Correlation between VEGF, MVD and clinicopathologic factors

Variables	*n*	VEGF *n* (%)		MVD	
		Positive	*P* value	$\bar{x}\pm s$	*P* value
Gender					
Male	168	88(52.4)	NS	22.11±9.14	NS
Female	64	34(53.1)		24.21±8.85	
Tumor size (cm)					
<5 cm	163	87(53.4)	NS	23.17±9.53	NS
⩾5 cm	69	35(50.7)		23.69±8.26	
Depth of invasion					
Mucosa or submucosa	94	26(27.7)	<0.01	18.08±8.32	<0.01
Muscularis propria	138	96(69.6)		26.41±8.44	
Histology					
Differentiated	129	70(54.3)	NS	23.48±9.01	NS
Undifferentiated	103	52(50.5)		23.25±9.06	
Lymph node metastasis					
Present	64	47(73.4)	<0.01	28.52±4.39	<0.01
Absent	168	75(44.6)		19.73±8.47	
Vascular invasion					
Present	39	29(74.4)	<0.01	28.94±5.03	<0.01
Absent	193	93(48.2)		21.67±9.12	
Noncancerous tissue					
CAG	30	3(10.0)	NS	10.43±4.22	NS
Atypical hyperplasia	30	5(16.7)		11.56±6.17	

Notes: NS, not significant; CAG, chronic atrophic gastritis

Correlations between postoperative survival time and expression of COX-2 and VEGF COX-2 or VEGF positive rate was significantly higher in patients who died within 5 years (93.6 % and 78.7 %, respectively) than that in those survived ⩾5 years (69.8 % and 49.1 %, respectively, $P<0.01$). Expression of COX-2 or VEGF was highly correlated with postoperative survival time. The 5-year survival rate was 67.9 % in patients with COX-2-positive tumors and 91.4 % in patients with COX-2-negative tumors. Accordingly, the prognosis for patients with a COX-2-negative tumor was significantly better than that for patients with a COX-2-positive tumor (Figure 4, $P<0.01$). The survival curves subdivided according to VEGF expression are shown in Figure 5. The 5-year survival rate was 61.2 % in patients with VEGF-positive tumors, which was significantly lower than the rate in those patients with VEGF-negative tumors (91.5 %, $P<0.01$).

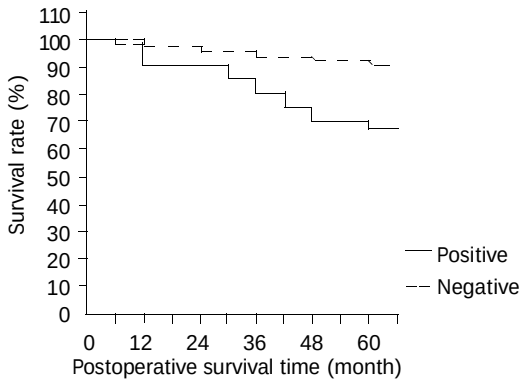

Figure 4 Kaplan-Meier survival curves of patients with gastric carcinoma with regard to COX-2 expression (positive and negative), $\chi^2=7.56$, $P<0.01$.

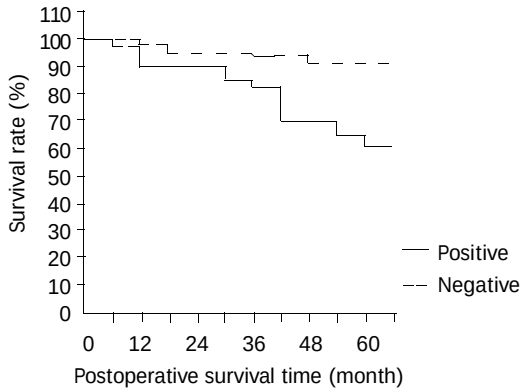

Figure 5 Kaplan-Meier survival curves of patients with gastric carcinoma with regard to VEGF expression (positive and negative), $\chi^2=16.51$, $P<0.01$.

Multivariate analysis

The effects of variables presumably associated with prognosis were studied by multivariate analysis using the Cox model. As a result, the depth of wall invasion, lymph node metastasis, vascular invasion, COX-2 expression, and VEGF expression emerged as independent prognostic factors (Table 4). Among these parameters, VEGF expression was the most important factor for predicting overall survival, followed by lymph node metastasis and COX-2 expression.

Table 4 Risk factors affecting survival determined by multivariate analysis using the Cox proportional hazards model

Variables	Regression coefficient	Standard error	Odds ratio (95% confidence interval)	*P* value
Histology (differentiated / undifferentiated)	0.564	0.337	1.758 (1.583-2.147)	NS
Depth of invasion (EGC / muscularis propria)	0.524	0.248	1.688 (1.638-1.714)	<0.05
Lymph node metastasis (present / absent)	0.796	0.1934	2.220 (1.518-3.239)	<0.01
Vascular invasion (present / absent)	0.413	0.213	2.003 (1.499-2.460)	<0.01
COX-2 expression (positive / negative)	0.776	0.194	2.173 (1.486-3.178)	<0.01
VEGF expression (positive / negative)	1.071	0.254	2.917 (1.774-4.796)	<0.01

Note: NS, not significant.

DISCUSSION

Recently, detection of gastric cancer at an early stage has been widely used in diagnostic procedures such radiography and endoscopy with targeted biopsy. In Japan, more than 50 % patients with gastric carcinoma were EGC[15]. However, in U.S., the proportion of EGC was approximately 20 %[16]. In the current study, our detection rate of EGC (4.3 %) was lower than that in above reports. This indicates the need to upgrade diagnostic efforts in the future. The incidence of adenocarcinoma of the gastric cardia has increased gradually in the West[17]. In our study, carcinoma of the gastric cardia accounted for 16.4 % of EGC and 30.4 % of AGC. The absolute number and the rates of cardia carcinoma have been increasing significantly and this increase may be derived from advances in endoscopic techniques and equipment. Our data also showed that carcinoma of the gastric cardia more frequently occurred in 60-69 age group than distal gastric cancer. Thus, we should pay attention to those patients who are older than 60 years in

the diagnosis of early carcinoma of the gastric cardia during an endoscopic examination.

The prognosis for EGC is universally excellent. Almost all Western and Japanese authors reported 5-year survival rates were over 90 % for EGC if relative survival or deaths from gastric carcinoma alone were considered. The results of the current study indicat that prognosis of patients with AGC was poorer than that with EGC and that prognosis of patients with submucosa invasion was poorer than that with mucosa invasion. The survival of patients with tumors in the upper third of the stomach was significantly worse compared with that of patients with tumors in the middle third and lower third of the stomach[16,18]. Our study disclosed that the 5-year survival rate of patients with tumors in the upper third of the stomach was lower than that of patients with tumors in the middle third and lower third of the stomach, especially in patients with AGC. However, there were no statistically significant differences among them (data not shown).

The depth of wall invasion, lymph node metastasis, and vascular invasion were reported to be the most important prognostic parameters in gastric carcinoma[19]. The current study demonstrated that long or short survival time was highly correlated not only with depth of invasion, lymph node metastasis, and vascular invasion, but also with adjuvant chemotherapy. The results were in agreement with other reports.

However, preoperative diagnosis of the extent of wall invasion or the presence of lymph node metastasis and vascular invasion is difficult in some cases. Therefore, not only conventional clinicopathologic factors but also biologic factors should be examined for the prediction of clinical outcome. Recently, some studies[20,21] found an increase in COX-2 protein levels in gastric carcinoma beyond the levels in paired normal gastric mucosa samples. The present study demonstrated that expression of COX-2 was significantly higher in mucosal atypical hyperplasia than that in CAG and that its expression was significantly higher in carcinoma tissue compared with noncancerous specimens. These indicate that COX-2 is involved in the growth of gastric carcinoma and that COX-2 promotes malignant transformation in human gastric carcinoma.

Recent studies have found that overexpression of COX-2 protein is associated significantly with lymph node metastasis[22,23] and depth of invasion[24,25] and that there is no correlation between the hisologic types of gastric carcinoma and the expression of COX-2 protein[24,26]. We found that COX-2 expression was associated with lymph node metastasis, vascular invasion, and the degree of tumor cell differentiation and did not connect to depth of invasion. The results suggest that COX-2 might enhance the metastatic potential as well as tumorigenicity and might be mainly involved in the progression of well-differentiated gastric carcinoma. The different conclusions of our study and above reports might have two explanations. First, differences in the methods employed (COX-2 mRNA level or protein immunoreactivity) and subjects may well influence the results of these studies. Second, there may have been discrepancies in the histologic type distribution among different areas.

Solid tumors need angiogenesis for growth and metastasis. Tumor angiogenesis may be regulated by angiogenic factors that are secreted by tumor cells, and VEGF is thought to be such a factor[27,28].VEGF is a selective mitogen for endothelial cells and may directly stimulate the growth of new blood vessels[27]. Numerous studies have demonstrated that the expression of VEGF is a significant predictor of an increased risk of metastatic disease and overall survival by stimulating angiogenesis in gastric carcinoma[9,28] and other carcinomas[29]. In this study, we found that VEGF expression and microvessel count were significantly associated with lymph node metastasis, depth of invasion, and vascular invasion. The finding that the microvessel count in VEGF-positive or COX-2-positive tumors was significantly higher than that in VEGF-negative or COX-2-negative tumors suggests that COX-2 as well as VEGF may faciliate tumor progression by promoting tumor angiogenesis[9,30].

With regard to prognosis, many studies have shownd that expression of VEGF is an independent prognostic indicator[12,31]. However, there have been few studies on the association of COX-2 expression and the postoperative survival rate of patients with gastric carcinoma[32]. The current study demonstrated that the 5-year survival rate in patients with COX-2-positive or VEGF-positive tumors was significantly lower than that in patients with COX-2-negative or VEGF-negative tumors. The results suggest that the presence of COX-2 or VEGF expression, as well as conventional clinicopathologic factors, are prognostic indicators in patients with gastric carcinoma. Multivariate analysis revealed five independent prognostic factors. Combination analysis of these pathologic and biologic features of gastric carcinoma will give aid to the improvement of the prognosis of some patients. If these assessments of COX-2 and VEGF expression are confirmed in long term follow-up of a larger group of patients, COX-2 and VEGF staining using endoscopically biopsied specimens prior to surgery could be used for the prediction of clinical outcome and in the preoperative selection of treatment for patients with gastric carcinoma. Accordingly, the inhibition of COX-2 activity may have an important therapeutic benefit in the control of gastric carcinoma[33].

ACKNOWLEDGMENTS

We thank Drs. Li-Xing Zhu, Ji-Fong Wu, Hong-Fu Zhang and Xi-Yu Gong for their excellent technical support.

REFERENCES

1 **Thun MJ,** Namboodiri MM, Calle EE, Flanders WD, Health CW Jr. Aspirin use and risk of fatal cancer. *Cancer Res* 1993; **53**: 1322-1327

2 **Boolbol SK,** Dannenberg AJ, Cadburn A, Martucci C, Guo XJ, Ramovetti JT, Abreu-Goris M, Newmark HL, Lipkin ML, Decosse JJ, Bertagnolli MM. Cyclooxygenase-2 overexpression and tumor formation are blocked by sulindac in a murine model of familial adenomatous polyposis. *Cancer Res* 1996; **56:** 2556-2560

3 **Smith WL,** Garavito RM, DeWitt DL. Prostaglandin endoperoxide H synthases (cyclooxygenase) -1 and -2. *J Biol Chem* 1996; **271:** 33157-33160

4 **Vane J.** Towards a better aspirin. *Nature* 1994; **367**: 215-216

5 **Eberhart CE,** Dubois RN. Eicosanoids and the gastrointestinal tract. *Gastroenterology* 1995; **109**: 285-301

6 **Mizuno H,** Sakamoto C, Matsuda K, Wada K, Uchida T, Noguchi H, Akamatsu T, Kasuga M. Induction of cyclooxygenase-2 in gastric mucosal lesions and its inhibition by the specific antagonist delays healing in mice. *Gastroenterology* 1997; **112:** 387-397

7 **Ristimaki A,** Honkanen N, Jankala H, Sipponen P, Harkonen M. Expression of cyclooxygenase-2 in human gastric carcinoma. *Cancer Res* 1997; **57**: 1276-1280

8 **Weidner N,** Folkman J, Pozza F, Bevilacqua P, Allred EN, Moore DH, Meli S, Gasparini G. Tumor angiogenesis: a new significant and independnet prognostic indicator in early-stage breast carcinoma. *J Natl Cancer Inst* 1992; **84**: 1875-1887

9 **Song ZJ,** Gong P, Wu YE. Relationship between the expression of iNOS, VEGF, tumor angiogenesis and gastric cancer. *World J Gastroenterol* 2002; **8**: 591-595

10 **Dvorak HF,** Brown LF, Detmar M, Dvorak AM. Vascular permeability factor/vascular endothelial growth factor, microvascular hyperpermeability, and angiogenesis. *Am J Pathol* 1995; **146:** 1029-1039

11 **Folkman J.** What is the evidence that tumors are angiogenesis dependent? *J Natl Cancer Inst* 1990; **82**: 4-6

12 **Maeda K**, Chung YS, Ogawa Y, Takatsuka S, Kang SM, Ogawa M, Sawada T, Sowa M. Prognostic value of vascular endothelial growth factor expression in gastric carcinoma. *Cancer* 1996; **77**:858-863

13 **Tao HQ,** Lin YZ, Wang RN. Significance of vascular endothelial growth factor messenger RNA expression in gastric cancer. *World J Gastroenterol* 1998; **4**: 10-13

14 **Japanese Research Society for Gastric Cancer**. Japanese classification of gastric carcinoma. First English edition. Tokyo: Kanehara & Co., Ltd., 1993

15 **Maehara Y**, Kakeji Y, Oda S, Takahashi I, Akazawa K, Sugimachi K. Time trends of surgical treatment and the prognosis for Japanese patients with gastric cancer. *Br J Cancer* 2000; **83**: 986-991

16 **Noguchi Y**, Yoshikawa T, Tsuburaya A, Motohashi H, Karpeh MS, Brennan MF. Is gastric carcinoma different between Japan and the United States? *Cancer* 2000; **89**: 2237-2246

17 **Ekstrom AM**, Signorello LB, Hansson LE, Bergstrom R, Lindgren A, Nyren O. Evaluating gastric cancer misclassification: a potential explanation for the rise in cardia cancer incidence. *J Natl Cancer Inst* 1999; **91**: 786-790

18 **Okabayashi T**, Gotoda T, Kondo H, Inui T, Ono H, Saito D, Yoshida S, Sasako M, Shimoda T. Early carcinoma of the gastric cardia in Japan: Is it different from that in the West? *Cancer* 2000; **89:** 2555-2559

19 **Adachi Y,** Yasuda K, Inomata M, Sato K, Shiraishi N, Kitano S. Pathology and prognosis of gastric carcinoma: well versus poorly differentiated type. *Cancer* 2000; **89**: 1418-1424

20 **Uefuji K**, Ichikura T, Mochizuki H, Shinomiya N. Expression of cyclooxygenase 2 protein in gastric adenocarcinoma. *J Surg Oncol* 1998; **69:** 168-172

21 **Guo XL**, Wang LE, Du SY, Fan CL, Li L, Wang P, Yuan Y. Association of cyclooxygenase-2 expression with HP-cagA infection in gastric cancer. *World J Gastroenterol* 2003; **9:** 246-249

22 **Murata H**, Kawano S, Tsuji S, Tsujii M, Sawaoka H, Kimura Y, Shiozaki H, Hori M. Cyclooxygenase, 2 overexpression enhances lymphatic invasion and metastasis in human gastric carcinoma. *Am J Gastroenterol* 1999; **94**: 451-455

23 **Xue YW,** Zhang QF, Zhu ZB, Wang Q, Fu SB. Expression of cyclooxygenase-2 and clinicopathologic features in human gastric adenocarcinoma. *World J Gastroenterol* 2003; **9**: 250-253

24 **Ohno R,** Yoshinaga K, Fujita T, Hasegawa K, Iseki H, Tasunozaki H, Ichikawa W, Nihei Z, Sugihara K. Depth of invasion parallels increased cyclooxygenase-2 levels in patients with gastric carcinoma. *Cancer* 2001; **91**: 1876-1881

25 **Gao HJ**, Yu LZ, Sun L, Miao K, Bai JF, Zhang XY, Lu XZ, Zhao ZQ. Expression of cyclooxygenase-2 oncogene proteins in gastric cancer and paracancerous tissues. *Shijie Huaren Xiaohua Zazhi* 2000; **8:** 578-579

26 **Yamamoto H,** Itoh F, Fukushima H, Hinoda Y, Imai K. Overexpression of cyclooxygenase-2 protein is less frequent in gastric cancers with microsatellite instability. *Int J Cancer* 1999; **84:** 400-403

27 **Leung DW,** Cachianes G, Kuang WJ, Goedel DV, Ferrara N. Vascular endothelial growth factor is a secreted angiogenic mitogen. *Science* 1989; **246**: 1306-1309

28 **Liu DH**, Zhang XY, Fan DM, Huang YX, Zhang JS, Huang WQ, Zhang YQ, Huang QS, Ma WY, Chai YB, Jin M. Expression of vascular endothelial growth factor and its role in oncogenesis of human gastric carcinoma. *World J Gastroenterol* 2001; **7:** 500-505

29 **Fontanini G,** Vignati S, Boldrini L, Chine S, Silvestri V, Lucchi M, Mussi A, Angeletti CA, Bevilacqua G. Vascular endothelial growth factor is associated with neovascularization and influences progression of non-small cell lung carcinoma. *Clin Cancer Res* 1997; **3**: 861-865

30 **Fosslien E.** Molecular pathology of cyclooxygenase-2 in cancer-induced angiogenesis. *Ann Clin Lab Sci* 2001; **31**: 325-348

31 **Maeda K**, Kang SM, Onoda N, Ogawa M, Kato Y, Sawada T, Chung KH. Vascular endothelial growth factor expression in preoperative biopsy specimens correlate with disease recurrence in patients with early gastric carcinoma. *Cancer* 1999; **86**: 566-571

32 **Chen CN,** Sung CT, Lin MT, Lee PH, Chang KJ. Clinicopathologic association of cyclooxygenase 1 and cyclooxygenase 2 expression in gastric adenocarcinoma. *Ann Surg* 2001; **233:** 183-188

33 **Fosslien E.** Biochemistry of cyclooxygenase (COX)-2 inhibitors and molecular pathology of COX-2 in neoplasia. *Crit Rev Clin Lab Sci* 2000; **37:** 431-502

Edited by Xu XQ

P.O.Box 2345, Beijing 100023,China
Fax: +86-10-85381893
E-mail: wjg@wjgnet.com www.wjgnet.com

World J Gastroenterol 2003;9(7):1427-1430
World Journal of Gastroenterology
 ISSN 1007-9327

• GASTRIC CANCER •

Preventive effect of hydrotalcite on gastric mucosal injury in rats induced by taurocholate

Bao-Ping Yu, Jun Sun, Mu-Qi Li, He-Sheng Luo, Jie-Ping Yu

Bao-Ping Yu, Jun Sun, Mu-Qi Li, He-Sheng Luo, Jie-Ping Yu, Department of Gastroenterology, Renmin Hospital of Wuhan University, Wuhan 430060, Hubei Province, China
Correspondence to: Professor Bao-Ping Yu, Department of Gastroenterology, Renmin Hospital of Wuhan University, Wuhan 430060, Hubei Province, China. yubaoping62@yahoo.com.cn
Telephone: +86-27-88041911-2135
Received: 2002-05-13 **Accepted:** 2002-06-12

Abstract

AIM: To study the preventive effect of hydrotalcite on gastric mucosal injury in rat induced by taurocholate, and to investigate the relationship between the protective mechanism of hydrotalcite and the expression of trefoil factor family 2 (TFF2) mRNA and c-fos protein.

METHODS: Forty five male Wistar rats were randomly divided into hydrotalcite group, ranitidine group and control group. Gastric mucosal injury was induced by introgastric acidified taurocholate. OD value of TFF2 mRNA expression in gastric mucous cells was determined by hybridization and computer image analysis system. OD value of c-fos protein expression in gastric mucous cells was measured by immunohistochemistry and computer image analysis system.

RESULTS: The gross mucosal injury index in hydrotalcite group was significantly lower than that in ranitidine group and control group (8.60±2.20 *vs* 16.32±4.27, 29.53±5.39; $P<0.05$, $P<0.01$). The expression level of TFF2 mRNA in hydrotalcite group was markedly higher than that in ranitidine group and control group (0.56±0.09 *vs* 0.30±0.05, 0.28±0.03, $P<0.05$). The OD value of c-fos protein in hydrotalcite group was higher than that in ranitidine group and control group (0.52±0.07 *vs* 0.31±0.04, 0.32±0.05, $P<0.05$).

CONCLUSION: Hydrotalcite can protect gastric mucosal injury in rats induced by taurocholate, which may be related to the increased expression of TFF2 and c-fos protein.

Yu BP, Sun J, Li MQ, Luo HS, Yu JP. Preventive effect of hydrotalcite on gastric mucosal injury in rats induced by taurocholate. *World J Gastroenterol* 2003; 9(7): 1427-1430
http://www.wjgnet.com/1007-9327/9/1427.asp

INTRODUCTION

Hydrotalcite is one kind of protective agents for gastric mucosal[1,2], it neutralizes the gastric acid[29], stimulates the synthesis of prostaglandin and the release of epidermal growth factor[3] from gastric mucosa[4]. Because hydrotalcite binds to cholalic acid in the stomach[5,6], it is effective on bile reflux gastritis. Trefoil factor family 2 (TFF2)[7-9] is one of the members in the trefoil peptide factor family[10-13] mainly produced by mucus-secreting cells in the gastrointestinal tract[1,14,15]. It involves restitution of epithelial lining after epithelial cell injury[16,17], mucosal defense[18,19] and healing of ulcer[20-23]. c-fos gene[24,25] is one of the earlier expressed genes after gastric mucosa injury. c-fos protein relates to mucosal repair after mucosal injury[26]. In the present study, we aimed to study the preventive effect of hydrotalcite on gastric mucosal injury in rat induced by taurocholate and the relationship between the protective mechanism of hydrotalcite and the expression of TFF2 mRNA and c-fos protein.

MATERIALS AND METHODS

Methods

Animals model Forty-five adult male Wistar rats weighing 200-250 g were divided into three groups randomly: hydrotalcite group, ranitidine group and control group, 15 rats in each group. The animals were housed at the Experimental Animal Center of Wuhan University. Taurocholate was dissolved in normal saline and HCl was added to a final concentration of 0.2 mol/L with pH value of 1.4[27]. The rats in hydrotalcite group were given 100 mg/kg hydrotalcite. The rats in control group were given 1.5 ml normal saline at the same time. The rats in ranitidine group were given 30 mg/kg ranitidine twice 12 hrs the day before. After one hour of hydrotalcite administration, gastric mucosal damage in three groups was induced by introgastric administration of 1.5 ml taurocholate[1] at 15 mmol/L. Two hours later, the animals were killed by cervical dislocation. The abdomen was opened, and the stomach was removed and incised along the greater curvature. The mucosal surface was gently washed with normal saline. Gastric lesions were scored by a previously described scoring system[28] as follows: one point, point erosion; two point, <1 mm of erosion; three point, 1-2 mm of erosion; four point, 3-4 mm of erosion; five point, >4 mm of erosion. The mucosa injury index was calculated on the totally accumulated points. After scored, the mucosa was obtained and prepared for histological examination and other tests.

TFF2 mRNA *in situ* hybridization Gastric mucosa tissue immersion-fixed in neutral buffered formaldehyde was dehydrated, oriented in cross section and embedded in wax. Four micrometer sections were cut, dewaxed, and rehydated to PBS. Sections were permeabilized with proteinase K, postfixed in 4 % paraformaldyhyde in PBS, and acetylated with acetic anhydrated in 0.1 mol/L triethanolamine. The tissues were then dehydrated for hybridization. Hybridization was performed according to the instructions of text kit (Sigma Co). Oligo-nucleo tides probe sequence was 5'-GTAGTGACAAATCTTCCACAGA. The optic density (OD) value of the hybridization signals was assessed by image analysis system.

Immunohistochemistry of c-fos protein Sections of gastric mucosa tissues were incubated with monoclonal antibody against human c-fos protein for four hours at 37 ℃. Immunostaining of c-fos protein was revealed using a commercially available peroxidase-based method (SP vectastain, Zhongshan Co.) according to the instructions of the manufacturer. The optic density of immunosignals was determined by image analysis system.

RESULTS

Gross inspection showed that there were obvious hyperemia, edema, sheet or strip of necrosis and spot hemorrhage in the gastric mucosa of control groups. There were milder lesions after hydrotalcite pretreatment, and microscopic examination confirmed marked protection against taurocholate-induced gastric injury. The degree of lesion in ranitidine group fell in-between the two groups. The gastric mucosa injury index was 8.60±2.20, 16.32±4.27, 29.53±5.39 in hydrotalcite, ranitidine and control groups, respectively. The gastric mucosa index in hydrotalcite group was significantly lower than that in ranitidine group ($P<0.05$) and control group ($P<0.01$).

In all three groups TFF2 mRNA was expressed in the atrium of stomach as revealed by *in situ* hybridization. TFF2 mRNA was mainly confined in gastric epithelial cells and gastric gland mucous neck cells, especially in the margin of the injury region (Figure 1-2).

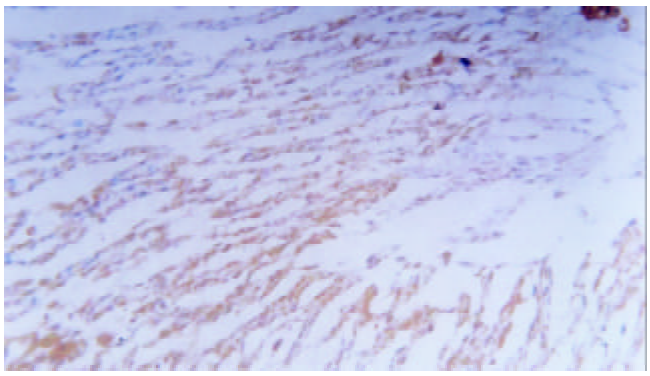

Figure 1 TFF2 mRNA in situ hybridization in hydrotalcite group Positive cells were stained brown-yellow ×200.

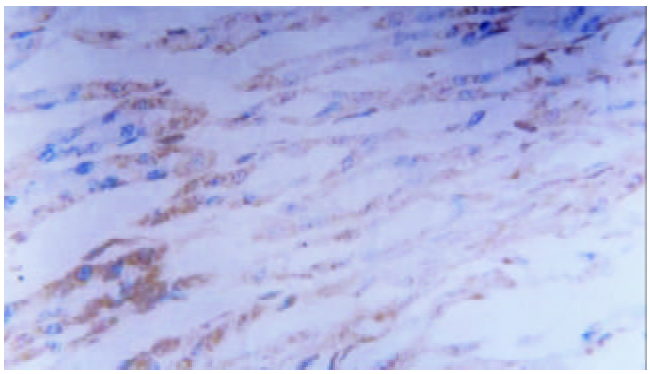

Figure 2 TFF2 mRNA in situ hybridization in hydrotalcite group Positive cells were stained brown-yellow ×400.

Immunochemistry showed that c-fos protein localized in nuclei of positively stained cells, which were mainly gastric gland mucous neck cells (Figure 3-4). The OD values of TFF2 mRNA and c-fos protein in the three groups are shown in Table 1.

Table 1 OD values of TFF2 mRNA staining and c-fos protein staining

Group	Animal number	TFF2 mRNA	c-fos protein
Hydrotalcite	15	0.56±0.09[a]	0.52±0.07[a]
Ranitidine	15	0.30±0.05[b]	0.31±0.04[b]
Control	15	0.28±0.03	0.32±0.05

[a]$P<0.05$ *vs* control, [b]$P>0.05$ *vs* control.

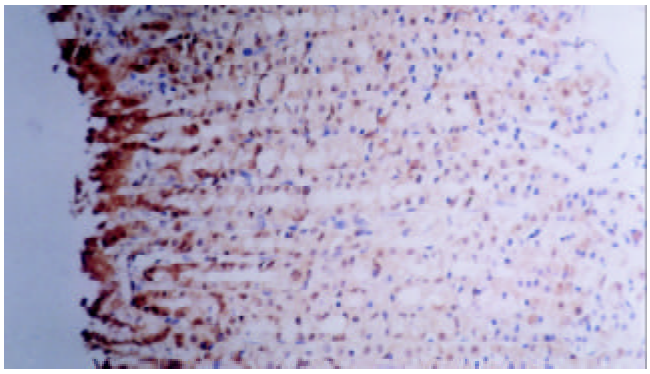

Figure 3 c-fos protein Immunostaining in hydrotalcite group Nuclei of positive cells were stained brown-yellow ×200.

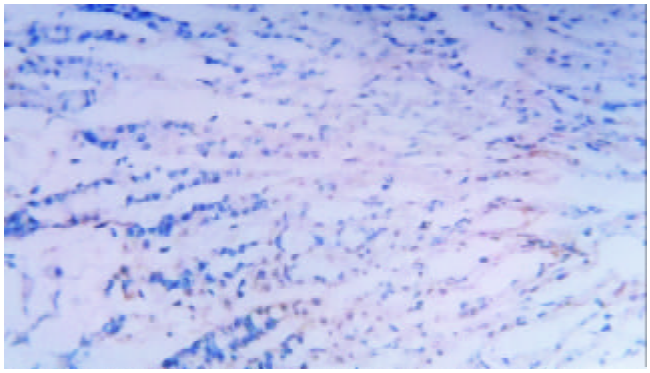

Figure 4 c-fos protein Immunostaining in ranitidine group Nuclei of positive cells w ere stained buff ×200.

DISCUSSION

Hydrotalcite is a complex comprised of aluminum hydroxide, magnesium hydroxide, carbonate and H_2O, which neutralizes gastric acid[29], binds pepsin[30,31] and choliac acid[5,31], *etc*. Our study showed that hydrotalcite could markedly protect gastric mucosa against taurocholate-induced lesions. The mucosal injury index in hydrotalcite group was significantly lower than that in ranitidine and control groups. Choliac acid has been thought to elicit gastric injury by degrading the difference of potential in gastric mucosa, increasing inversed diffusion of acid, and stimulating mast cell to release histamine. Recent researches indicated that transforming growth factor was related to the recovery of gastric mucosal injury induced by taurocholate[27,32,33]. Hydrotalcite has been shown to enhance the synthesis and release of prostaglandin and to increase the amount of epidermal growth factor in mucosal blood[4].

The mechanism of the protective and healing effect of TFF2 on gastric mucosa is still not fully elucidated. *In vitro* studies, TFF2 was shown to stimulate cell migration[34]. Recently hTFF was shown to decrease proton permeation through interacting with mucus in both *in vivo* and *in vitro* studies[35]. Orally-administrated TFF2 was found to bind to the mucus layer of the stomach[36,37], which accelerates the healing of gastric ulcer in the rat[38-41]. In this study, we have shown that hydrotalcite reduces gastric injury induced by taurocholate in rats, and it also increases expression of TFF2 mRNA in margin of the injury region, suggesting that the protective effect of hydrotalcite on gastric mucosa is related to the increase of TFF2 expression. The reason why hydrotalcite increases expression of TFF2 is not yet fully understood. Previous studies indicate that TFF expression and secretion are regulated by neuropeptides and acetylcholine[42], and hydrotalcite increases the amount of epidermal growth factor in gastric mucosa[4]. It is presumed

that hydrotalcite regulates TFF2 mRNA expression through the increase of epidermal growth factor.

C-fos gene is one of the immediate early genes which are involved in the control of cell proliferation in a variety of cell types[43-46]. Change of c-fos mRNA expression is found as early as two hours in the healing of gastric mucosal stress ulcer[26,47]. In this study, the expression of c-fos protein was found two hours later in gastric mucosal damage induced by taurocholate. The amount of c-fos protein in hydrotalcite was higher than that in ranitidine and control groups, suggesting that c-fos protein participates in the mechanism of the protective effect of hydrotalcite in gastric mucosa. It has been shown that EGF[48,49] stimulates the proliferation[50] of cells derived from gastric fundus and induces the expression of c-fos and c-myc, and hydrotalcite increases the amount of epidermal growth factor in gastric mucosa. It may be presumed that hydrotalcite increases c-fos protein through the increase of the amount of epidermal growth factor in gastric mucosa.

REFERENCES

1 **Rankin BJ**, Zhu H, Webb M, Roberts NB. The development and in-vitro evaluation of novel mixed metal hydroxy-carbonate compounds as phosphate binders. *J Pharm Pharmacol* 2001; **53**: 361-369

2 **Holtermuller KH**, Liszkay M, Bernard I, Haase W. [Therapy of stomach ulcer-a comparison between the low dosage antacid hydrotalcite and ranitidine-results of a randomized multicenter double-blind study. Talcivent Study Group]. *Z Gastroenterol* 1992; **30**: 717-721

3 **Lambrecht N**, Trautmann M, Korolkiewicz R, Liszkay M, Peskar BM. Role of eicosanoids, nitric oxide, and afferent neurons in antacid induced protection in the rat stomach. *Gut* 1993; **34**: 329-337

4 **Schmassmann A**, Tarnawski A, Gerber HA, Flogerzi B, Sanner M, Varga L, Halter F. Antacid provides better restoration of glandular structures within the gastric ulcer scar than omeprazole. *Gut* 1994; **35**: 896-904

5 **Tarnawski AS**, Tomikawa M, Ohta M, Sarfeh IJ. Antacid talcid activates in gastric mucosa genes encoding for EGF and its receptor. The molecular basis for its ulcer healing action. *J Physiol Paris* 2000; **94**: 93-98

6 **Dreyer M**, Marwinski D, Wolf N, Dammann HG. [Acidity profile in humans after multiple oral administration of hydrotalcite]. *Arzneimittel Forschung* 1991; **41**: 738-741

7 **Vatier J**, Ramdani A, Vitre MT, Mignon M. Antacid activity of calcium carbonate and hydrotalcite tablets. Comparison between in vitro evaluation using the "artificial stomach-duodenum" model and in vivo pH-metry in healthy volunteers. *Arzneimittel Forschung* 1994; **44**: 514-518

8 **Simoneau G**. Absence of rebound effect with calcium carbonate. *Eur J Drug Metab Pharmacokinet* 1996; **21**: 351-357

9 **Watters KJ**, Murphy GM, Tomkin GH, Ashford JJ. An evaluation of the bile acid binding and antacid properties of hydrotalcite in hiatus hernia and peptic ulceration. *Curr Med Res Opin* 1979; **6**: 85-87

10 **Mendelsohn D**, Mendelsohn L. Hydrogen ion, pepsin and bile acid binding properties of hydrotalcite. *S Afr Med J* 1975; **49**: 1011-1014

11 **Poulsom R**. Trefoil peptides.*Baillieres Clin Gastroenterol* 1996; **10**: 113-134

12 **Podolsky DK**. Mechanisms of regulatory peptide action in the gastrointestinal tract: trefoil peptides. *J Gastroenterol* 2000;**35** (Suppl 12): 69-74

13 **Taupin D**, Wu DC, Jeon WK, Devaney K, Wang TC, Podolsky DK. The trefoil gene family are coordinately expressed immediate-early genes: EGF receptor- and MAP kinase-dependent interregulation. *J Clin Invest* 1999; **103**: R31-R38

14 **Dignass A**, Lynch-Devaney K, Kindon H, Thim L, Podolsky DK. Trefoil peptides promote epithelial migration through a transforming growth factor beta-independent pathway. *J Clin Invest* 1994; **94**: 376-383

15 **Al-azzeh ED**, Fegert P, Blin N, Gott P. Transcription factor GATA-6 activates expression of gastroprotective trefoil genes TFF1 and TFF2. *Biochim Biophys Acta* 2000; **1490**: 324-332

16 **Sommer P**, Blin N, Gott P. Tracing the evolutionary origin of the TFF-domain, an ancient motif at mucous surfaces. *Gene* 1999; **236**: 133-136

17 **McKenzie C**, Thim L, Parsons ME. Topical and intravenous administration of trefoil factors protect the gastric mucosa from ethanol-induced injury in the rat. *Aliment Pharmacol Ther* 2000; **14**: 1033-1040

18 **Farrell JJ**, Taupin D, Koh TJ, Chen D, Zhao CM, Podolsky DK, Wang TC. TFF2/SP-deficient mice show decreased gastric proliferation, increased acid secretion, and increased susceptibility to NSAID injury. *J Clin Invest* 2002; **109**: 193-204

19 **Tran CP**, Cook GA, Yeomans ND, Thim L, Giraud AS. Trefoil peptide TFF2 (spasmolytic polypeptide) potently accelerates healing and reduces inflammation in a rat model of colitis. *Gut* 1999; **44**: 636-642

20 **Taupin D**, Pedersen J, Familari M, Cook G, Yeomans N, Giraud AS. Augmented intestinal trefoil factor (TFF3) and loss of pS2 (TFF1) expression precedes metaplastic differentiation of gastric epithelium. *Lab Invest* 2001; **81**: 397-408

21 **Kawanaka H**, Tomikawa M, Baatar D, Jones MK, Pai R, Szabo IL, Sugimachi K, Sarfeh IJ, Tarnawski AS. Despite activation of EGF-receptor-ERK signaling pathway, epithelial proliferation is impaired in portal hypertensive gastric mucosa: relevance of MKP-1, c-fos, c-myc, and cyclin D1 expression. *Life Sci* 2001; **69**: 3019-3033

22 **Fu X**, Gu X, Sun T. [mRNA and protein expression of three growth-related factors and their possible signal transduction pathways in wound healing] *Zhonghua Waike Zazhi* 2001; **39**: 714-717

23 **Schuligoi R**, Herzeg G, Wachter C, Jocic M, Holzer P. Differential expression of c-fos messenger RNA in the rat spinal cord after mucosal and serosal irritation of the stomach. *Neuroscience* 1996; **72**: 535-544

24 **Polk WH Jr**, Dempsey PJ, Russell WE, Brown PI, Beauchamp RD, Barnard JA, Coffey RJ Jr. Increased production of transforming growth factor alpha following acute gastric injury. *Gastroenterology* 1992; **102**: 1467-1474

25 **Lanza FL**, Royer GL Jr, Nelson RS. Endoscopic evaluation of the effects of aspirin, buffered aspirin, and enteric-coated aspirin on gastric and duodenal mucosa. *N Engl J Med* 1980; **303**: 136-138

26 **Vatier J**, Vitre MT, Lionnet F, Poitevin C, Mignon M. Assessment of antacid characteristics of drugs containing a combination of aluminium and magnesium salts using the "artificial stomach" model. *Arzneimittel Forschung* 1990; **40**: 42-48

27 **Kokot ZJ**. Effect of pepsin on the kinetics of HCl neutralization by dihydroxyaluminum sodium carbonate, hydrotalcite and dihydroxyaluminum aminoacetate. *Acta Pol Pharm* 1991; **48**: 27-31

28 **Murphy MS**. Growth factors and the gastrointestinal tract. *Nutrition* 1998; **14**: 771-774

29 **Jones MK**, Tomikawa M, Mohajer B, Tarnawski AS. Gastrointestinal mucosal regeneration: role of growth factors. *Front Biosci* 1999; **4**: D303-D309

30 **Hahm KB**, Lee KM, Kim YB, Hong WS, Lee WH, Han SU, Kim MW, Ahn BO, Oh TY, Lee MH, Green J, Kim SJ. Conditional loss of TGF-beta signalling leads to increased susceptibility to gastrointestinal carcinogenesis in mice. *Aliment Pharmacol Ther* 2002; **16**(Suppl 2): 115-127

31 **Fukuda M**, Ikuta K, Yanagihara K, Tajima M, Kuratsune H, Kurata T, Sairenji T. Effect of transforming growth factor-beta1 on the cell growth and Epstein-Barr virus reactivation in EBV-infected epithelial cell lines. *Virology* 2001; **288**: 109-118

32 **Kanai M**, Konda Y, Nakajima T, Izumi Y, Takeuchi T, Chiba T. TGF-alpha inhibits apoptosis of murine gastric pit cells through an NF-kappaB-dependent pathway. *Gastroenterology* 2001; **121**: 56-67

33 **Ebert MP**, Yu J, Miehlke S, Fei G, Lendeckel U, Ridwelski K, Stolte M, Bayerdorffer E, Malfertheiner P. Expression of transforming growth factor beta-1 in gastric cancer and in the gastric mucosa of first-degree relatives of patients with gastric cancer. *Br J Cancer* 2000; **82**: 1795-1800

34 **Kang B**, Alderman BM, Nicoll AJ, Cook GA, Giraud AS. Effect of omeprazole-induced achlorhydria on trefoil peptide expression in the rat stomach. *J Gastroenterol Hepatol* 2001; **16**: 1222-1227

35 **Dignass A**, Lynch-Devaney K, Kindon H, Thim L, Podolsky DK. Trefoil peptides promote epithelial migration through a transforming growth factor beta-independent pathway. *J Clin Invest* 1994; **94**: 376-383
36 **Playford RJ**, Marchbank T, Chinery R, Evison R, Pignatelli M, Boulton RA, Thim L, Hanby AM. Human spasmolytic polypeptide is a cytoprotective agent that stimulates cell migration. *Gastroenterology* 1995; **108**: 108-116
37 **Kato K**, Chen MC, Nguyen M, Lehmann FS, Podolsky DK, Soll AH. Effects of growth factors and trefoil peptides on migration and replication in primary oxyntic cultures. *Am J Physiol* 1999; **276**: G1105-G1116
38 **Goke MN**, Cook JR, Kunert KS, Fini ME, Gipson IK, Podolsky DK. Trefoil peptides promote restitution of wounded corneal epithelial cells. *Exp Cell Res* 2001; **264**: 337-344
39 **Langer G**, Walter S, Behrens-Baumann W, Hoffmann W. [TFF peptides. New mucus-associated secretory products of the conjunctiva]. *Ophthalmologe* 2001; **98**: 976-979
40 **Wright NA**. Aspects of the biology of regeneration and repair in the human gastrointestinal tract. *Philos Trans R Soc Lond B Biol Sci* 1998; **353**: 925-933
41 **Poulsen SS**, Thulesen J, Christensen L, Nexo E, Thim L. Metabolism of oral trefoil factor 2 (TFF2) and the effect of oral and parenteral TFF2 on gastric and duodenal ulcer healing in the rat. *Gut* 1999; **45**: 516-522
42 **Ogata H**, Podolsky DK. Trefoil peptide expression and secretion is regulated by neuropeptides and acetylcholine. *Am J Physiol* 1997; **273**: G348-354
43 **Chen L**, Tong A, Yu D. [Effects of fluoride on the expression of c-fos and c-jun genes and cell proliferation of rat osteoblasts] *Zhonghua Yufang Yixue Zazhi* 2000; **34**: 327-329
44 **Di Toro R**, Campana G, Murari G, Spampinato S. Effects of specific bile acids on c-fos messenger RNA levels in human colon carcinoma Caco-2 cells. *Eur J Pharm Sci* 2000; **11**: 291-298
45 **Osaki M**, Tsukazaki T, Yonekura A, Miyazaki Y, Iwasaki K, Shindo H, Yamashita S. Regulation of c-fos gene induction and mitogenic effect of transforming growth factor-beta1 in rat articular chondrocyte. *Endocr J* 1999; **46**: 253-261
46 **Li G**, Wu D, Xiao B, Li J. Effect of lead on the expression of immediate early genes in different regions of rat brain. *Weisheng Yanjiu* 1999; **28**: 65-69
47 **Fu X**, Jiang L, Sun T. The significance and characteristics of the gene expressions of c-fos and c-jun in hypertrophic scar and chronic ulcer tissues] *Zhonghua Shaoshang Zazhi* 2000; **16**: 300-302
48 **Tarnawski AS**, Pai R, Wang H, Tomikawa M. Translocation of MAP (Erk-1 and -2) kinases to cell nuclei and activation of c-fos gene during healing of experimental gastric ulcers. *J Physiol Pharmacol* 1998; **49**: 479-488
49 **Yanaka A**, Suzuki H, Shibahara T, Matsui H, Nakahara A, Tanaka N. EGF promotes gastric mucosal restitution by activating Na (+) / H(+) exchange of epithelial cells. *Am J Physiol Gastrointest Liver Physiol* 2002; **282**: G866-G876
50 **Wong BC**, Wang WP, So WH, Shin VY, Wong WM, Fung FM, Liu ES, Hiu WM, Lam SK, Cho CH. Epidermal growth factor and its receptor in chronic active gastritis and gastroduodenal ulcer before and after Helicobacter pylori eradication. *Aliment Pharmacol Ther* 2001; **15**: 1459-1465
51 **Hsieh JS**, Wang JY, Huang TJ. The role of epidermal growth factor in gastric epithelial proliferation in portal hypertensive rats exposed to stress. *Hepatogastroenterology* 1999; **46**: 2807-2811
52 **Miyazaki Y**, Hiraoka S, Tsutsui S, Kitamura S, Shinomura Y, Matsuzawa Y. Epidermal growth factor receptor mediates stress-induced expression of its ligands in rat gastric epithelial cells. *Gastroenterology* 2001; **120**: 108-116

Edited by Bo XN

P.O.Box 2345, Beijing 100023,China
Fax: +86-10-85381893
E-mail: wjg@wjgnet.com www.wjgnet.com

World J Gastroenterol 2003;9(7):1431-1434
World Journal of Gastroenterology
 ISSN 1007-9327

• GASTRIC CANCER •

Expression of NGF family and their receptors in gastric carcinoma: A cDNA microarray study

Jian-Jun Du, Ke-Feng Dou, Shu-You Peng, Bing-Zhi Qian, Hua-Sheng Xiao, Feng Liu, Wei-Zhong Wang, Wen-Xian Guan, Zhi-Qing Gao, Ying-Bin Liu, Ze-Guang Han

Jian-Jun Du, Ke-Feng Dou, Wei-Zhong Wang, Wen-Xian Guan, Zhi-Qing Gao, Department of General Surgery, Xijing Hospital, The Fourth Military Medical University, Xi' an 710032, Shanxi Province, China
Shu-You Peng, Ying-Bin Liu, Department of General Surgery, the Second Affiliated Hospital, Medical College, Zhejiang University, Hangzhou 310009, Zhejiang Province, China
Bing-Zhi Qian, Hua-Sheng Xiao, Feng Liu, Ze-Guang Han, China Human Genome Center at Shanghai, Shanghai 201203, China
Correspondence to: Dr. Ze-Guang Han**,** China Human Genome Center at Shanghai, 351 Guo Shou Jing Road, Zhangjiang High-Tech Park, Shanghai 201203, China. hanzg@chgc.sh.cn
Telephone: +86-29-3375256
Received: 2003-02-26 **Accepted:** 2003-03-28

Abstract

AIM: To investigate the expression of NGF family and their receptors in gastric carcinoma and normal gastric mucosa, and to elucidate their effects on gastric carcinoma.

METHODS: RNA of gastric cancer tissues and normal gastric tissues was respectively isolated and mRNA was purified. Probes of both mRNA reverse transcription product cDNAs labled with α-^{33}P dATP were respectively hybridized with Atlas Array membrane where NGF and their family genes were spotted on. Hybridized signal images were scanned on phosphor screen with ImageQuant 5.1 software after hybridization. Normalized values on spots were analyzed with ArrayVersion 5.0 software. Differential expression of NGF family and their receptors mRNA was confirmed between hybridized Atlas Array membranes of gastric cancer tissues and normal gastric mucosa, then their effects on gastric carcinoma were investigated.

RESULTS: Hybridization signal images on Atlas Array membrane appeared in a lower level of nonspecific hybridization. Both of NGF family and their receptors Trk family mRNA were expressed in gastric cancer and normal gastric mucosa. But adversely up-regulated expression in other tissues and organs. NGF, BDGF, NT-3, NT-4/5, NT-6 and TrkA, B and C were down-regulated simultaneously in gastric carcinoma in comparison with normal gastric mucosa. Degrees of down-regulation in NGF family were greater than those in their receptors Trk family. Down-regulation of NT-3 and BDGF was the most significant, and TrkC down-regulation level was the lowest in receptors Trk family.

CONCLUSION: Down-regulated expression of NGF family and their receptors Trk family mRNA in gastric cancer is confirmed. NGF family and their receptors Trk family probably play a unique role in gastric cancer cell apoptosis by a novel Ras or Raf signal transduction pathway. Their synchronous effects are closely associated with occurrence and development of gastric carcinoma induced by reduction of signal transduction of programmed cell death.

Du JJ, Dou KF, Peng SY, Qian BZ, Xiao HS, Liu F, Wang WZ, Guan WX, Gao ZQ, Liu YB, Han ZG. Expression of NGF family and their receptors in gastric carcinoma: A cDNA microarray study. *World J Gastroenterol* 2003; 9(7): 1431-1434
http://www.wjgnet.com/1007-9327/9/1431.asp

INTRODUCTION

Recently, NGF family and their receptors family have been found in other non-neural tissues of the body, and more and more attentions are being paid to their effects on these tissues, especially on tumor tissues. Gene expression of NGF and Trk families in gastric tissue and gastric carcinoma has been seldom documented. Simultaneous detection of NGF family and their receptors family expression has become possible since cDNA microarray was developed[1]. As abnormal expression of many genes is involved in gastric carcinogenesis[2-11], it contributes to a better understanding of their roles in the occurrence and development of gastric cancer and helps reveal mRNA expression of the family genes in gastric tissue and gastric carcinoma.

MATERIALS AND METHODS

RNA extraction and mRNA purification

RNA of gastric cancer tissues and normal gastric mucosa was respectively isolated with Trizol (Gibco) in five cases of gastric cancer from Xijing Hospital, Fourth Military Medical University. To ensure good total RNA quality 28S/18S $\geqslant$1.5, samples were immediately placed into liquid nitrogen after being removed intraoperatively, and trituration of the samples was performed in liquid nitrogen. Then, mRNA was purified in Oligotex mRNA Kit (Qiagen). An equal mRNA mixture of gastric cancer tissues and normal gastric mucosa from five patients respectively constituted gastric cancer group and normal gastric mucosa group. At last, reverse transcription product (the first stranded cDNAs) of mRNA mixture was electrophoresed to evaluate its size and quality.

Probe labeling

One μg of mRNA mixture of gastric cancer tissue and normal gastric mucosa from five patients was respectively transcripted into cDNAs as a probe labeled with 3.5 μl α-^{33}P dATP (>2, 500 kCi· mol^{-1}, 10 Ci· L^{-1}, Dupont) and 1 μl CDS primer 1 (Clontech) in a mixture containing 1 μl MMLV, 1 μl 10× dNTP Mix (for dATP label), 0.5 μl DTT (100 mM), and 2 μl 5× reaction buffer in a final volume of 10 μl was incubated for 0.25 h at 50 ℃ using an unregulated heat block (Eppendorf). Labeled reaction was stopped by adding 1 μl 10×Termination Mix. To purify the labeled cDNA from unincorporated ^{33}P-labeled nucleotides and small (<0.1 kb) cDNA fragments, the above probe synthetic reactions were diluted to 200 μl total volume with Buffer NT2 included in Atlas cDNA Expression Arrays (Clontech), then transferred to a NucleoSpin Extraction Spin Column. 400 μl Buffer NT3 was added into the column after centrifugation at 14 000 rpm for 1 min and the flowthrough

was discarded. The procedure was repeated twice. To elute the labeled probe, 100NE was added into the column, centrifuged at 14 000 rpm for 1 min. The flowthrough was obtained as the labeled probe.

Prehybridization and hybridization

Prehybridization of Atlas Array membrane was carried out in 0.5 mg heat-denatured sheared salmon DNA, and 5 ml prewarmed ExpressHyb solution (Clontech) in a hybridization bottle was incubated for 0.5 h at 68 ℃. Then, heat-denatured cDNA probes were added into the above prehybridization bottle together with 5 μl heat-denatured C_0t-1 DNA. The hybridization reactions were performed at 68 ℃ overnight. The next day, the Atlas Array membrane was washed three times in prewarmed wash solution 1 (2×SSC, 1 % SDS) with continuous agitation at 68 ℃ for 0.5 h, and in prewarmed wash solution 2 (0.1×SSC, 0.5 % SDS) at 68 ℃ for 0.5 h. The damp Atlas Array membrane was wrapped in a plastic wrap after the last washing in 2×SSC at room temperature for 5 min.

Exposure of hybridization signals to phosphorimager and result analyses

Atlas Array hybridization membrane was exposed to phosphor screen at room temperature overnight. The hybridization signals were analyzed with ArrayVersion 5.0 software (MD) after the phosphor screen was scanned with ImageQuant 5.1 software (MD). Quantitative data of each hybridization signals were obtained.

RESULTS

Identification of mRNA quality

Good total RNA quality was confirmed by 28S/18S ⩾1.5. Size range of reverse transcription product cDNAs represented a smear from 0.2-4kb both in gastric cancer and normal gastric mucosa (Figure 1).

Image of scan on hybridization signals of phosphor screen

Hybridization signal images on Atlas Array membrane appeared in lower levels of nonspecific hybridization (Figure 2).

Expression of NGF family and their receptors Trk family mRNA

To quantify hybridization signals, signal intensity was detected after hybridized signal normalization of two hybridization Atlas Array membranes between gastric cancer and the normal mucosa. Signal intensity of NGF family and their receptors Trk family on Atlas Array membranes represented their mRNA expression level. NGF, BDGF, NT-3, NT-4/5, NT-6 and TrkA, B and C were down-regulated in gastric carcinoma in comparision with normal gastric mucosa. Degrees of down-regulation in NGF family were greater than those in their receptors Trk family. Down-regulation of NT-3 and BDGF was the most significant, and TrkC down-regulation level was the lowest in receptors Trk family (Table 1).

Table 1 Signal intensity of NGF family and their receptors Trk family

Dot	Gene	CAVOL	NORnVOL	NORnVOL/CAnVOL
D07n	NT-3,BDGF	0.031	0.311	10.128
D11n	NGF	0.045	0.272	6.036
D08n	NT-4/5, NT-6	0.06	0.352	5.822
D02i	TrkC	0.029	0.119	4.172
D03k	Trk	0.038	0.157	4.093
D14h	TrkA	0.043	0.141	3.252
D01i	TrkB	0.026	0.051	1.926

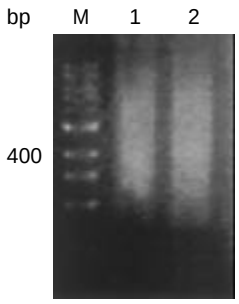

Figure 1 Size range of mRNA on 2 % agarose gel electrophoresis. Normal gastric mucosa mRNA(lane1) and gastric carcinoma mRNA (lane 2). 100 bp size marker (lane M).

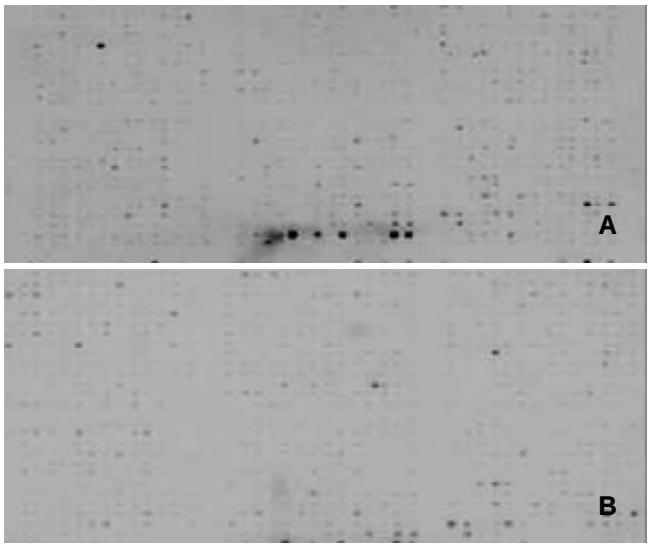

Figure 2 Hybridization signals of reverse transcription products cDNAs hybridized with Atlas Array membrane. A: hybridization signals of reverse transcription products cDNAs of normal gastric mucosa mRNA hybridized with Atlas Array membrane. B: hybridization signals of reverse transcription products cDNAs of gastric cancer mRNA hybridized with Atlas Array membrane.

DISCUSSION

Gene microarray has been rapidly and extensively used in detecting expression of genes, DNA sequence, novel genes and gene mutants, DNA polymorphism, and in screening drugs, diagnosing diseases and mapping gene library since Schena reported it in 1995[12-28]. Profiling of differentially expressed genes in human gastric carcinoma by cDNA expression array was also reported[29]. The study detected expression of NGF family and their receptors Trk family mRNA by using cDNA microarray. The Atlas Array membranes were provided by Clontech. A set of housekeeping genes was included on the Atlas Array membranes to normalize mRNA expression levels. Our good total RNA and mRNA quality, as well as successful synthesis and labeling of a cDNA probe with highly specific activity ensured the best possible results. ExpressHybTM hybridization solution was used in our hybridization experiments, a low-viscosity hybridization solution that significantly enhances the sensitivity of detection and reduces background.

NGF is composed of three subunit proteins (α, β and γ) among which β subunit represents an active form. NGF produced by targets of sympathetic neuron, sensory central neuron exerts an important effect on growth, development, differentiation of these neurons. Brain-derived nerve growth factor (BDNF), NT-3, NT-4/5 and NT-6 are members of the

NGF family, and NGF has 50 % of homology with BDNF. Difference between members of the family comes from the distribution of tissues, the early and/or later expression, and different receptors. NGF family receptors are subdivided into three types: Trk A, TrkB and TrkC. The structure of the three receptors consists of cellular external region, transcellular membrane region and cellular internal region. The receptors all are tyrosine kinase, and there is 66-68 % of homology between them. NGF binds TrkA, and BDNF, NT-3, NT-4/5 and NT-6 bind TrkB, in which binding of NT-3 is weaker and mainly with TrkC. As the functions of NGF family, TrkA, TrkB and TrkC can regulate growth, development and differentiation of corresponding neurons while receiving signals of NGF, BDNF, NT-3, NT-4/5 and NT-6. NT-3 and its receptor TrkC play a role in early growth, development and differentiation of neural systems.

Recently NGF family and their receptors family were found in other non-neural tissues of the body, and more and more attentions are being paid to their effects. It was reported that dermal pigment cells expressed NGF and Trk[30], hepatic cells expressed BDNF, NT-3, NT-4/5 as well as TrkA, which were related to liver pathophysiology. Hepatic stellate cells expressed BDNF, NT-3, NT-4/5, TrkB and TrkC that were involved in liver remodeling[31]. NT-3, NT-4/5, TrkB and TrkC expressed by microphages played a role in tissue inflammatory reaction and repair[32]. Cardiac myocytes expressed TrkC and NT-3, and early growth and development of the heart were retarded when blockage of TrkC was used[33]. Schneider *et al*[34] demonstrated TrkA and TrkC expression in pancreatic ducts and pancreatic islets, TrkB in apha-cells of islets, NGF in pancreatic ducts and pancreatic acinar cells, NT-3 and NT-4 respectively in capillary endothelia and ductule cells. Additionally, TrkB and TrkC were found in endocrine cells of gut epithelium and neural tissues in fish[35,36], and TrkA, TrkB and TrkC were all expressed in testis of rats. A current study also indicated NGF family and their receptors played an essential role in the development of tubulogenesis in embryonic kidney, spermatogenesis, hair follicle, heart and vascular differentiation and maintenance of blood and immune cells[37].

Similarly, more attentions are being paid to their effects on tumors. Antagonists of NGF family and their receptors are being applied to kill tumor cells experimentally. It was noted that NGF family and their receptors were not expressed in some normal tissues, but expressed in their corresponding tumors. For example, up-regulated expression of Trk was present in tumors originating from thyroid and ovary while absent in the normal tissues. When chromosomal translocation occurred, a fusion protein of Trk-T1 composed of carboxyl terminal tyrosine kinase domain of NTRK1 and amino terminal portion of TPR (translocated promoter region) was formed. Trk-T1 was oncogenic *in vivo* and contributed to the papillary neoplastic transformation of the thyroid[38]. These results suggest that NGF family and their receptors are involved in tumorigenicity. A recent study showed that pancreatic carcinoma cells could express NGF, TrkA and TrkC[34]. It is interesting that Trk was highly expressed in esophageal carcinoma, thyroid carcinoma and prostate carcinoma, and adversely Trk expression revealed significantly lower in gastric carcinoma and colon carcinoma[39,40]. Difference between NGF and Trk expression in various tumors suggests that NGF family and their receptors may play a different role or have directly reverse effects on various carcinoma originating from different tissues. Some studies verified the assumption that ocurrence of apoptosis could be inhibited and/or enhanced while cascade effect was brought out by intracellular signal transduction pathway blocking or inducing programmed cell death[41,42]. Its signal transduction pathways include Ras, the Cdc42/Rac/RhoG protein family, MAPK, PI3K and PLC-gamma. Adversely, other novel Ras and/or Raf pathways participate in signal transduction paths mediating programmed cell death. For example, prostate growth depends on autocrine NGF interaction with Trk expressed by itself, otherwise, apoptosis occurred in medulloblastoma when NGF was bound to Trk[43]. Therefore, inhibition or enhancement of apoptosis induced by Trk depended on cellular types and development periods of cells[44].

The study showed that expression of NGF family and their receptors were simultaneously down-regulated in gastric cancer tissues. NT-3 and BDGF down-regulation was the lowest in NGF family, Trk C down-regulation was the lowest in Trk family. The evidences support that NGF family and their receptors Trk family may play a unique apoptotic role in gastric cancer by a new Ras or Raf signal transduction pathway. These further substantiate that NGF family and Trk family have synchronous effects on the occurrence and development of gastric carcinoma induced by reduction in signal transduction of programmed cell death brought out by simultaneously down-regulated expression of NGF family and Trk family. It remains unclear that which cells in gastric mucosa secret NGF family, and whether NGF plays a role in the occurrence and development of gastric carcinoma in autocrine or paracrine way.

REFERENCES

1 **Schena M**, Shalon D, Davis RM, Brown PO. Quantitative monitoring of gene expression patterns with a complementary DNA microarray. *Science* 1995; **270**: 467-470

2 **Liu HF**, Liu WW, Fang DC, Men RP. Expression and significance of proapoptotic gene Bax in gastric carcinoma. *World J Gastroenterol* 1999; **5**: 15-17

3 **To KF**, Leung WK, Lee TL, Yu J, Tong JH, Chan MW, Ng EK, Chung SC, Sung JJ. Promoter hypermethylation of tumor-related genes in gastric intestinal metaplasia of patients with and without gastric cancer. *Int J Cancer* 2002; **102**: 623-628

4 **Gao HJ**, Yu LZ, Bai JF, Peng YS, Sun G, Zhao HL, Miu K, Lü XZ, Zhang XY, Zhao ZQ. Multiple genetic alterations and behavior of cellular biology in gastric cancer and other gastric mucosal lesions: *H. pylori* infection, histological types and staging. *World J Gastroenterol* 2000; **6**: 848-854

5 **Liu DH**, Zhang XY, Fan DM, Huang YX, Zhang JS, Huang WQ, Zhang YQ, Huang QS, Ma WY, Chai YB, Jin M. Expression of vascular endothelial growth factor and its role in oncogenesis of human gastric carcinoma. *World J Gastroenterol* 2001; **7**: 500-505

6 **He XS**, Su Q, Chen ZC, He XT, Long ZF, Ling H, Zhang LR. Expression, deleton was deleton and mutation of p16 gene in human gastric cancer. *World J Gastroenterol* 2001; **7**: 515-521

7 **Kaneda A**, Kaminishi M, Yanagihara K, Sugimura T, Ushijima T. Identification of silencing of nine genes in human gastric cancers. *Cancer Res* 2002; **62**: 6645-6650

8 **Ficorella C**, Cannita K, Ricevuto E, Toniato E, Fusco C, Sinopoli NT, De Galitiis F, Di Rocco ZC, Porzio G, Frati L, Gulino A, Martinotti S, Marchetti P. P16 hypermethylation contributes to the characterization of gene inactivation profiles in primary gastric cancer. *Oncol Rep* 2003; **10**: 169-173

9 **Li HL**, Chen DD, Li XH, Zhang HW, Lu YQ, Ye CL, Ren XD. Changes of NF-kB, p53, Bcl-2 and caspase in apoptosis induced by JTE-522 in human gastric adenocarcinoma cell line AGS cells: role of reactive oxygen species. *World J Gastroenterol* 2002; **8**: 431-435

10 **Xia L**, Yuan YZ, Xu CD, Zhang YP, Qiao MM, Xu JX. Effects of epidermal growth factor on the growth of human gastric cancer cell and the implanted tumor of nude mice. *World J Gastroenterol* 2002; **8**: 455-458

11 **Fang DC**, Luo YH, Yang SM, Li XA, Ling XL, Fang L. Mutation analysis of APC gene in gastric cancer with microsatellite instability. *World J Gastroenterol* 2002;**8**:787-791

12 **Eisen MB**, Brown PO. DNA arrays for analysis of gene expression. *Methods Enzymol* 1999; **303**: 179-205

13 **Brown PO**, Botstein D. Exploring the new world of the genome with DNA microarrays. *Nat Genet* 1999; **21**(Suppl): 33-37

14 **Hannon MF**, Rao S. Transcription: of chips and ChIPs. *Science* 2002; **296**: 666-669

15 **Duggan DJ,** Bittner M, Chen Y, Meltzer P, Trent JM. Expression profiling using cDNA microarrays. *Nat Genet* 1999; **21** (Suppl): 10-14

16 **Iyer VR**, Eisen MB, Ross DT, Schuler G, Moore T, Lee JC, Trent JM, Staudt LM, Hudson J Jr, Boguski MS, Lashkari D, Shalon D, Botstein D, Brown PO. The transcriptional program in the response of human fibroblasts to serum. *Science* 1999; **283**: 83-87

17 **Favis R**, Barany F. Mutation detection in K-ras, BRCA1, BRCA2, and p53 using PCR/LDR and a universal DNA microarray. *Ann N Y Acad Sci* 2000; **906**: 39-43

18 **Wang K**, Gan L, Jeffery E, Gayle M, Gown AM, Skelly M, Nelson PS, Ng WV, Schummer M, Hood L, Mulligan J. Monitoring gene expression profile changes in ovarian carcinomas using cDNA microarray. *Gene* 1999; **229**: 101-108

19 **Xu S**, Mou H, Lu G, Zhu C, Yang Z, Gao Y, Lou H, Liu X, Cheng Y, Yang W. Gene expression profile differences in high and low metastatic human ovarian cancer cell lines by gene chip. *Chin Med J (Engl)* 2002; **115**: 36-41

20 **Wellmann A**, Thieblemont C, Pittaluga S, Sakai A, Jaffe ES, Siebert P, Raffeld M. Detection of differentially expressed genes in lymphomas using cDNA arrays:identification of clusterin as a new diagnostic marker for anaplastic large-cell lymphomas. *Blood* 2000; **96**: 398-404

21 **Golub TR**, Slonim DK, Tamayo P, Huard C, Gaasenbeek M, Mesirov JP, Coller H, Loh ML, Downing JR, Caligiuri MA, Bloomfield CD, Lander ES. Molecular classification of cancer: Class discovery and class prediction by gene expression monitoring. *Science* 1999; **286**: 531-537

22 **Alizadeh AA**, Eisen MB, Davis RE, Ma C, Lossos IS, Rosenwald A, Boldrick JC, Sabet H, Tran T, Yu X, Powell JI, Yang L, Marti GE, Moore T, Hudson J Jr, Lu L, Lewis DB, Tibshirani R, Sherlock G, Chan WC, Greiner TC, Weisenburger DD, Armitage JO, Warnke R, Staudt LM. Distinct type of diffuse large B-cell lymphoma identified by gene expression profiling. *Nature* 2000; **403**: 503-511

23 **Assersohn L**, Gangi L, Zhao Y, Dowsett M, Simon R, Powles TJ, Liu ET. The feasibility of using fine needle aspiration from primary breast cancers for cDNA microarray analyses. *Clin Cancer Res* 2002; **8**: 794-801

24 **Hippo Y,** Yashiro M, Ishii M, Taniguchi H, Tsutsumi S, Hirakawa K, Kodama T, Aburatani H. Differential gene expression profiles of scirrhous gastric cancer cells with high metastatic potential to peritoneum or lymph nodes. *Cancer Res* 2001; **61**: 889–895

25 **Tiwari G,** Sakaue H, Pollack JR, Roth RA. Gene expression profiling in prostate cancer cells with akt activation reveals fra-1 as an akt-inducible gene. *Mol Cancer Res* 2003; **1**: 475-484

26 **Mycko MP,** Papoian R, Boschert U, Raine CS, Selmaj KW. cDNA microarray analysis in multiple sclerosis lesions: detection of genes associated with disease activity. *Brain* 2003; **126**: 1048-1057

27 **Man K,** Lo CM, Lee TK, Li XL, Ng IO, Fan ST. Intragraft gene expression profiles by cDNA microarray in small-for-size liver grafts. *Liver Transpl* 2003; **9**: 425-432

28 **Kawaguchi K,** Kaneko S, Honda M, Kawai HF, Shirota Y, Kobayashi K. Detection of hepatitis B virus DNA in sera from patients with chronic hepatitis B virus infection by DNA microarray method. *J Clin Microbiol* 2003; **41**: 1701-1704

29 **Liu LX**, Liu ZH, Jiang HC, Qu X, Zhang WH, Wu LF, Zhu AL, Wang XQ, Wu M. Profiling of differentially expressed genes in human gastric carcinoma by cDNA expression array. *World J Gastroenterol* 2002; **8**: 580-585

30 **Innominato PF**, Libbrecht L, van den Oord JJ. Expression of neurotrophins and their receptors in pigment cell lesions of the skin. *J Pathol* 2001; **194**: 95-100

31 **Cassiman D**, Denef C, Desmet VJ, Roskams T. Human and rat hepatic stellate cells express neurotrophins and neurotrophin receptors. *Hepatology* 2001; **33**: 148-158

32 **Barouch R**, Appel E, Kazimirsky G, Brodie C. Macrophages express neurotrophins and neurotrophin receptors. Regulation of nitric oxide production by NT-3. *J Neuroimmunol* 2001; **112**: 72-77

33 **Lin MI**, Das I, Schwartz GM, Tsoulfas P, Mikawa T, Hempstead BL. Trk C receptor signaling regulates cardiac myocyte proliferation during early heart development *in vivo*. *Dev Biol* 2000; **226**: 180-191

34 **Schneider MB,** Standop J, Ulrich A, Wittel U, Friess H, Andren-Sandberg A, Pour PM. Expression of nerve growth factors in pancreatic neural tissue and pancreatic cancer. *J Histochem Cytochem* 2001; **49**: 1205-1210

35 **Radaelli G**, Domeneghini C, Arrighi S, Castaldo L, Lucini C, Mascarello F. Neurotransmitters, neuromodulators, and neurotrophin receptors in the gut of pantex, a hybrid sparid fish (Pagrus major x Dentex dentex). Localizations in the enteric nervous and endocrine systems. *Histol Histopathol* 2001; **16**: 845-853

36 **De Girolamo P**, Lucini C, Vega JA, Andreozzi G, Coppola L, Castaldo L. Co-localization of Trk neurotrophin receptors and regulatory peptides in the endocrine cells of the teleostean stomach. *Anat Rec* 1999; **256**: 219-226

37 **Sariola H**. The neurotrophic factors in non-neuronal tissues. *Cell Mol Life Sci* 2001; **58**: 1061-1066

38 **Russell JP,** Powell DJ, Cunnane M, Greco A, Portella G, Santoro M, Fusco A, Rothstein JL. The TRK-T1 fusion protein induces neoplastic transformation of thyroid epithelium. *Oncogene* 2000; **19**: 5729-5735

39 **Koizumi H**, Morita M, Mikami S, Shibayama E, Uchikoshi T. Immunohistochemical analysis of TrkA neurotrophin receptor expression in human non-neuronal carcinomas. *Pathol Int* 1998; **48**: 93-101

40 **Weeraratna AT**, Arnold JT, George DJ, DeMarzo A, Isaacs JT. Rational basis for Trk inhibition therapy for prostate cancer. *Prostate* 2000; **45**: 140-148

41 **Patapoutian A**, Reichardt LF. Trk receptors: mediators of neurotrophin action. *Curr Opin Neurobiol* 2001; **11**: 272-280

42 **Chou TT,** Trojanowski JQ, Lee VM. A novel apoptotic pathway induced by nerve growth factor-mediated TrkA activation in medulloblastoma. *J Biol Chem* 2000; **275**: 565-570

43 **Muragaki Y**, Chou TT, Kaplan DR, Trojanowski JQ, Lee VM. Nerve growth factor induces apoptosis in human medulloblastoma cell lines that express TrkA receptors. *J Neurosci* 1997; **17**: 530-542

44 **Nakagawara A**. Trk receptor tyrosine kinases: a bridge between cancer and neural development. *Cancer Lett* 2001; **169**: 107-114

Edited by Zhang JZ and Wang XL

P.O.Box 2345, Beijing 100023,China
Fax: +86-10-85381893
E-mail: wjg@wjgnet.com www.wjgnet.com

World J Gastroenterol 2003;9(7):1435-1438
World Journal of Gastroenterology
 ISSN 1007-9327

• GASTRIC CANCER •

Expression of survivin in human gastric carcinoma and gastric carcinoma model of rats

Xiao-Dong Zhu, Geng-Jin Lin, Li-Ping Qian, Zhong-Qing Chen

Xiao-Dong Zhu, Geng-Jin Lin, Li-Ping Qian, Department of Gastroenterology, Huashan Hospital, Fudan University, Shanghai, 200040, China
Zhong-Qing Chen, Department of Pathology, Huashan Hospital, Fudan University, Shanghai, 200040, China
Correspondence to: Dr. Geng-Jin Lin, Department of Gastroenterology, Huashan Hospital, Fudan University, NO.12 wulumuqi Road, Shanghai, 200040, China. xddr@netease.com
Telephone: +86-021-62489999
Received: 2003-01-04 **Accepted:** 2003-02-18

Abstract

AIM: To study the expression of survivin, an inhibitor of apoptosis protein, in human gastric carcinomas and gastric carcinoma models of rats.

METHODS: With the method of immunohistochemical staining, we studied the expression of survivin in 20 cases of chronic gastritis and 56 cases of gastric carcinomas. We used N-methyl-N'-nitro-N-nitrosoguanidine (MNNG) and high dose sodium-chloride diet to induce rat gastric carcinomas. Survivin expression was studied in glandular stomachs of normal rats, adenocarcinomas and tissues adjacent to the tumor, as well as in rats during the induction period.

RESULTS: Survivin was expressed in 27 of 56 (48.2 %) cases of human gastric carcinoma tissues and 1 of 20 (5 %) cases of chronic gastritis. It was found that the expression of survivin had no relation with the elements of age, tumor depth, tumor size, and disease stage, but was significantly related to histological type. The positive rate of survivin expression in cases of intestinal type was significantly higher than that in cases of diffuse type ($P<0.05$). In animal experiments, survivin expression in glandular stomachs of normal rats, of rats in middle induction period, in adenocarcinomas and tissues adjacent to tumor were 0, 40.0 %, 78.3 % and 38.9 %, respectively. Compared with the survivin expression in normal rats, the differences were significant.

CONCLUSION: These data imply that survivin plays an important role in the onset of gastric carcinoma and that high survivin expression is an early event of gastric carcinoma.

Zhu XD, Lin GJ, Qian LP, Chen ZQ. Expression of survivin in human gastric carcinoma and gastric carcinoma model of rats. *World J Gastroenterol* 2003; 9(7): 1435-1438
http://www.wjgnet.com/1007-9327/9/1435.asp

INTRODUCTION

Survivin, a member of the inhibitors of apoptosis protein (IAP) family, is a mitotic spindle-associated protein involved in linking mitotic spindle function to the activation of apoptosis in mammalian cells. The structure of full-length human survivin determined by X-ray crystallography is 2.7 A°. The structure forms a very unusual bow tie-shaped dimer. The unusual shape and dimensions of survivin suggest that it serves as an adaptor through its alpha-helical extensions[1]. Just like other IAP members, survivin can suppress apoptosis through combination with Caspase3, Caspase7 by baculoviral IAP repeat (BIR)[2,3]. The common pathway of apoptosis is the activation of Caspase3, Caspase7 or Caspase 6, hence high expression of survivin may protect cells from many apoptosis signals and help cells survive[4,5]. Now, substantial data have shown that inhibition of apoptosis plays a great role in carcinogenesis[6-10], so survivin may be an important factor in the development of cancer. It has reported that survivin is undetectable in terminally differentiated adult tissues and becomes prominently expressed in transformed cell lines and in most common human cancers of lung, colon, pancreas, prostate and breast[2]. Some data indicate that high expression of survivin is correlated with poor prognosis and chemotherapy resistance[11-13]. In this study, we investigated the expression of survivin in human gastric carcinoma and its relationship with clinicopathological factors, as well as the expression of survivin in gastric carcinoma models of rats.

MATERIALS AND METHODS

Patients and samples

A total of fifty-six cases of gastric carcinoma were involved in this study including 46 males and 10 females. The age range was 26-79 years, mean age was 59.8 years. The patients with gastric carcinoma, having undergone potentially curative tumor resection at Huashan Hospital from 2000 to 2001, had received neither chemotherapy nor radiation therapy before surgery. The histological types of tumors were classified according to Lauren as intestinal type and diffuse type, and the disease stage was defined in accordance with the tumor-node-metastasis (TNM) classification[14]. There were 32 cases of intestinal type and 24 cases of diffuse type. Materials were composed of 19 cases of stage I, 8 cases of stage II, and 29 cases of stage III. The tissues containing principal tumor were selected and fixed with formalin, embedded in paraffin routinely. Serial sections of 4 μm were prepared for immunohistochemical examination and histopathological study. The expression of survivin was investigated in these 56 gastric carcinoma patients and 20 cases of chronic gastritis by immunohistochemical examination.

Animal experiment

Forty-six male 6-week-old Wistar rats were divided into 2 groups. Thirty rats in group A were fed with a diet supplemented with 8 % NaCl for 20 weeks and simultaneously given N-methyl-N'-nitro-N-nitrosoguanidine (MNNG) in drinking water at a concentration of 100 ug/ml for the first 17 weeks. From week 18, these rats were given normal water. From week 21, these rats were fed with normal diet for 15 weeks. The other sixteen rats in group B were fed with normal diet for 35 weeks and served as the control. At week 20, 10 rats in group A were killed and all the rest animals were killed

at the end of week 35. The whole stomach and a part of duodenum were sampled and cut open along the greater curvature. The number of tumors with their locations and sizes were recorded in details. All the specimens were histopathologically investigated and the expression of survivin was examined with immunohistochemical analysis as they were done in human specimens.

Immunohistochemical staining for survivin and assessment of its expression

Anti-survivin polyclonal antibody was purchased from Santa Cruz Company. Immunohistochemical analysis was carried out with the standard streptavidin-biotin-peroxidase (SP) complex technique using the Ultra sensitive™ S-P kit (Maixin-Bio Company). One case of stage III gastric carcinoma intensively and reproducibly stained for survivin expression in more than 50 % of tumor cells served as positive control. Negative control slides were stained without primary antibody. To assess the expression of survivin in various samples examined, a 4-grade-method was established according to the mean percentage of positive tumor cells and their intensity. Moderately stained slides with a mean percentage of positive tumor cells no less than 30 % were scored as positive (+). Moderately or intensively stained slides with a mean percentage of positive tumor cells more than 70 % were scored as intensely positive (+++). Slightly or moderately stained slides with a mean percentage of positive tumor cells between 30 % and 70 % were scored as moderately positive (++). Slightly or moderately stained slides with a mean percentage of positive tumor cells less than 30 % were scored as negative (-).

Statistical analysis

Software Stata (version 6.0, STATA Corp, College Station) was applied to compare the rates.

RESULTS

Correlation between expression of survivin and clinicopathological factors in human gastric carcinomas

Positive staining for survivin was located in cytoplasm of tumor cells (Figure 1). A clinicopathological analysis of survivin-positive cases is shown in Table 1. The expression of survivin was positive in 27 of 56 (48.2 %) cases of gastric carcinoma tissues and 1 of 20 (5 %) cases of chronic gastritis. Expression of survivin had no relation with age, tumor depth, tumor size, and disease stage (P>0.05), but it was significantly related to histological type. The positive rate of survivin expression in cases of intestinal type was significantly higher than that in cases of diffuse type (P<0.05).

Table 1 Correlation between expression of survivin and clinicopathological factors in human gastric carcinomas

Variables	Cases	Survivin expression *n* (%)	*P*
Chronic gastritis	20	1(5%)	<0.001
Gastric carcinoma	56	27(48.2%)	
Age			
<55	18	11(61.1%)	0.184
>55	38	16(42.1%)	
Invasion size			
<12.3 cm^2	31	16(51.6%)	0.571
>12.3 cm^2	25	11(44.0%)	
Invasion depth			
Muscular layer unaffected	14	5(35.7%)	0.280
Muscular layer affected	42	22(52.4%)	
Lymph node metastasis			
Regional lymph Node unaffected	20	9(45.0%)	0.720
Regional lymph Node affected	36	18(50%)	
Histological type (Lauren) intestinal	32	20(62.5%)	0.013
Diffuse	24	7(29.2%)	
Disease stage(TMN)			
I	19	8(42.1%)	0.873
II	8	4(50.0%)	
III	29	15(51.7%)	

Notes: The disease stage of each tumor was defined in accordance with the tumor-node-metastasis (TNM) classification, the histological type was classified according to Lauren, and other pathological variables were defined in accordance with the Gastric Carcinoma[14].

The expression of survivin in gastric carcinoma models of rats

By the end of week 35, neoplastic foci were found in antral mucosa in 18 rats of group A which were histologically determined to be adenocarcinomas. Of these 18 rats, the total number of adenocarcinomas was 23, and 22 were very well differentiated, which could be classified as intestinal type according to Lauren classification. Just like human gastric carcinoma, positive staining for survivin was located in cytoplasm of tumor cells (Figure 2). No survivin expression was detected in antral mucosa of normal rats (group B). As shown in Table 2, in antral mucosa of those rats at week 20, survivin expression was positive in 4 of 10 rats. In adenocarcinomas and tissues adjacent to the tumor, the ratio was 78.3 % and 38.9 %, respectively. Compared to normal tissue, the difference was significant (Table 2).

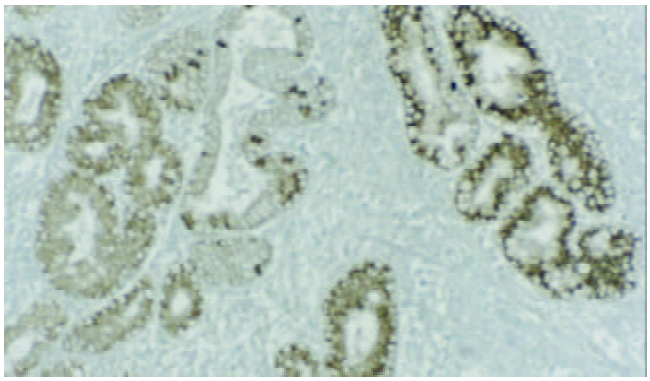

Figure 1 Immunohistochemical staining for the expression of survivin in human gastric carcinoma. Positive staining for survivin was located in cytoplasm (×50).

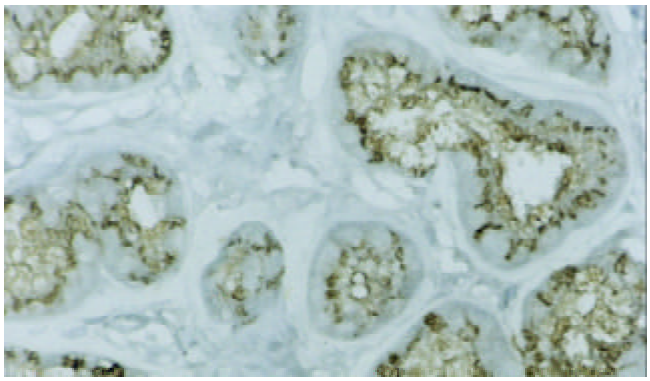

Figure 2 Immunohistochemical staining for the expression of survivin in gastric carcinoma of rat model. Positive staining for survivin was also located in cytoplasm. (×100).

Table 2 Survivin expression in experimental gastric carcinoma

	Cases	Survivin expression	Positive rate(%)
Control (group B)	16	0	0
Group A			
Antral mucosa of rats at week 20	10	4	40%[a]
Adenocarcinomas	23	18	78.3%[b]
Tissues adjacent to tumor	18	7	38.9%[c]

Ten rats of group A were killed at week 20, and the antral mucosa were examined. At week 35, all rats in both group A and B were killed and investigated. Tissues adjacent to tumor were defined as the tissues 5 mm away from the edge of tumor. [a]$P<0.05$ *vs* control group, [b]$P<0.001$ *vs* control group, [c]$P<0.01$ *vs* control group.

DISCUSSION

Survivin is expressed in a series of human cancers, and it has been widely accepted that survivin is highly related to the onset and development of cancer. In this study, we adopted human gastric carcinoma specimens and experimental gastric carcinoma models to discuss the effect of survivin on gastric cancer.

Survivin was expressed in 27 of 56 (48.2 %) cases of human gastric carcinoma tissues and only 1 of 20 (5 %) cases of chronic gastritis. In experimental gastric carcinoma, the positive rate rose to 78.3 %. These data suggest that high expression of survivin is a common phenomenon in gastric cancer and inhibition of apoptosis resulted from survivin expression may play an important role in carcinogenesis.

Our data on human gastric carcinoma proved that the expression of survivin in intestinal type cases is significantly higher than that in diffuse type cases and the expression of survivin is correlated with intestinal histological type. This result is consistent with Lu[15]. The Lauren histological classification has a specific epidemiological significance because the epidemiological study has determined that intestinal type cases are dominant in high risk areas while diffuse type cases are dominant in low risk areas. Substantial data suggest that intestinal type cases are highly related to circumstances and diffuse type cases are related to heredity. At present, Correa' s theory of an atrophy-metaplasia-dysplasia-carcinoma sequence in the development of intestinal type gastric carcinoma has been widely accepted[16-22]. The fact that the expression of survivin in intestinal type was higher than that in diffuse type suggests that survivin plays a more important role in the former and indicate that survivin may be an important factor contributing to the conversion from atrophy to carcinoma. Our animal experiment provided further evidences.

In our animal experiment, 95.7 % of the induced gastric carcinomas were intestinal type, and we did find atrophy and dysplasia lesions during the induction period. These data suggest that our rat model could simulate the development of human gastric carcinoma (intestinal type). We dynamically investigated the expression of survivivn during the induction period and found 4 cases were positive in 10 rats at week 20, and 78.3% was positive in gastric carcinoma. These data indicate a rising trend of survivin expression during the development of gastric cancer, and suggest an important role of survivin expression in tumor formation.

Some scholars concluded that survivin could only be found in tumor[15], but others thought it could be found in precancerous lesions[23,24]. Our results supported the latter. In our experiment, the expression of survivin was positive in some gastritis patients, and in some rats during the induction period, as well as in some tissues adjacent to tumor. Hence, we may conclude that survivin is not only expressed in cancer tissues but also in damaged tissues. The expression of survivin occurs before the formation of adenocarcinomas, and is an early event in carcinoma development.

Recently, some studies have partly explained why survivin was highly expressed in cancer. According to the study of Hoffman *et al*[25], the anti-apoptotic gene, survivin, is a p53-repressed gene. Chromatin immunoprecipitations indicate that wild type p53 binds survivin promoter *in vivo*, which results in transcriptional repression. Mirza *et al*[26] study implicated that wild-type p53 suppresses survivin expression at both mRNA and protein levels. It is widely accepted that mutated p53 loses its function as a tumor inhibitor and this may contribute to the loss of inhibition to survivin. Due to the high incidence of p53 mutation in gastric cancer, we put forward the hypothesis that long term effect of carcinogen should lead to p53 or other important gene damage, which results in survivin expression and apoptosis inhibition. Abnormal apoptosis leads to carcinogenesis.

According to our clinical data, age and prognostic factors such as different tumor size, tumor depth, lymph node metastasis or disease stage have no significant correlation with survivin expression, which indicates that survivin has little impact on tumor biological behavior.

Survivin plays an important role in gastric carcinoma and is a key molecule of cell cycle, mitosis and apoptosis[27]. Moreover, inhibition of survivin function will result in cell apoptosis[28-30]. The antisense oligonucleotide targeting survivin expression sensitizes lung cancer cells to chemotherapy[30]. All these data suggest that survivin may be an attractive target for gastric cancer therapy.

REFERENCES

1 **Chantalat L**, Skoufias DA, Kleman JP, Jung B, Dideberg O, Margolis RL. Crystal structure of human survivin reveals a bow tie-shaped dimer with two unusual alpha-helical extensions. *Mol Cell* 2000; **6**: 183-189

2 **Ambrosini G**, Adida C, Altieri DC. A novel anti-apoptosis gene, survivin, expressed in cancer and lymphoma. *Nat Med* 1997; **3**: 917-921

3 **Johnson AL**, Langer JS, Bridgham JT. Survivin as a cell cycle-related and antiapoptotic protein in granulosa cells. *Endocrinology* 2002; **143**: 3405-3413

4 **Tamm I,** Wang Y, Sausville E, Scudiero DA, Vigna N, Oltersdorf T, Reed JC. IAP-family protein survivin inhibits caspase activity and apoptosis induced by Fas (CD95), Bax, caspases, and anticancer drugs. *Cancer Res* 1998; **58**: 5315-5320

5 **Conway EM**, Pollefeyt S, Steiner-Mosonyi M, Luo W, Devriese A, Lupu F, Bono F, Leducq N, Dol F, Schaeffer P, Collen D, Herbert JM. Deficiency of survivin in transgenic mice exacerbates Fas-induced apoptosis via mitochondrial pathways. *Gastroenterology* 2002; **123**: 619-631

6 **Xu AG**, Li SG, Liu JH, Gan AH. Function of apoptosis and expression of the proteins Bcl-2, p53 and C-myc in the development of gastric cancer. *World J Gastroenterol* 2001; **7**: 403-406

7 **Wu MY**, Liang YR, Wu XY, Zhuang CX. Relationship between Egr-1 gene expression and apoptosis in esophageal carcinoma and precancerous lesions. *World J Gastroenterol* 2002; **8**: 971-975

8 **Shan CM**, Li J. Study of apoptosis in human liver cancers. *World J Gastroenterol* 2002; **8**: 247-252

9 **Zhang Z**, Yuan Y, Gao H, Dong M, Wang L, Gong YH. Apoptosis, proliferation and p53 gene expression of *H. pylori* associated gastric epithelial lesions. *World J Gastroenterol* 2001; **7**: 779-782

10 **Xu HY**, Yang YL, Guan XL, Song G, Jiang AM, Shi LJ. Expression of regulating apoptosis gene and apoptosis index in primary liver cancer. *World J Gastroenterol* 2000; **6**: 721-724

11 **Ikeguchi M**, Kaibara N. Survivin messenger RNA expression is a good prognostic biomarker for oesophageal carcinoma. *Br J Cancer* 2002; **87**: 883-887

12 **Chakravarti A**, Noll E, Black PM, Finkelstein DF, Finkelstein DM,

Dyson NJ, Loeffler JS. Quantitatively determined survivin expression levels are of prognostic value in human gliomas. *J Clin Oncol* 2002; **20**: 1063-1068

13 **Zaffaroni N**, Pennati M, Colella G, Perego P, Supino R, Gatti L, Pilotti S, Zunino F, Daidone MG. Expression of the anti-apoptotic gene survivin correlates with taxol resistance in human ovarian cancer. *Cell Mol Life Sci* 2002; **59**: 1406-1412

14 **Chen B,** Wang SB. The clinical manifestation and disease stage of gastric cancer In: Zhang WF, Zhang YC, Chen JQ, eds. Gastric cancer. 2nd ed. Shanghai: Shanghai Science and Technology Publishing Company 2001: 249-255

15 **Lu CD**, Altieri DC, Tanigawa N. Expression of a novel antiapoptosis gene, survivin, correlated with tumor cell apoptosis and p53 accumulation in gastric carcinomas. *Cancer Res* 1998; **58**:1808-1812

16 **Su Q**, Luo ZY, Teng H, Yun WD, Li YQ, He XE. Effect of garlic and garlic-green tea mixture on serum lipids in MNNG-induced experimental gastric carcinoma and precancerous lesion. *World J Gastroenterol* 1998; **4**: 29

17 **Cui RT**, Cai G, Yin ZB, Cheng Y, Yang QH, Tian T. Transretinoic acid inhibits rats gastric epithelial dysplasia induced by N-methyl-N-nitro-N-nitrosoguanidine: influences on cell apoptosis and expression of its regulatory genes. *World J Gastroenterol* 2001; **7**:394-398

18 **Zhou HP**, Wang X, Zhang NZ. Early apoptosis in intestinal and diffuse gastric carcinomas. *World J Gastroenterol* 2000; **6**: 898-901

19 **Goldstein NS**, Lewin KJ. Gastric epithelial dysplasia and adenoma: historical review and histological criteria for grading. *Hum Pathol* 1997; **28**: 127-133

20 **Walker MM.** Is intestinal metaplasia of the stomach reversible? *Gut* 2003; **52**: 1-4

21 **Ming SC**. Cellular and molecular pathology of gastric carcinoma and precursor lesions: A critical review. *Gastric Cancer* 1998; **1**:31-50

22 **Lauwers GY**, Riddell RH. Gastric epithelial dysplasia. *Gut* 1999; **45**: 784-790

23 **Grossman D**, McNiff JM, Li F, Altieri DC. Expression of the apoptosis inhibitor, survivin, in nonmelanoma skin cancer and gene targeting in a keratinocyte cell line. *Lab Invest* 1999; **79**: 1121-1126

24 **Kawasaki H,** Toyoda M, Shinohara H, Okuda J, Watanabe I, Yamamoto T, Tanaka K, Tenjo T, Tanigawa N. Expression of survivin correlates with apoptosis, proliferation, and angiogenesis during human colorectal tumorigenesis. *Cancer* 2001; **91**: 2026-2032

25 **Hoffman WH**, Biade S, Zilfou JT, Chen J, Murphy M. Transcriptional repression of the anti-apoptotic survivin gene by wild type p53. *J Biol Chem* 2002; **277**: 3247-3257

26 **Mirza A**, McGuirk M, Hockenberry TN, Wu Q, Ashar H, Black S, Wen SF, Wang L, Kirschmeier P, Bishop WR, Nielsen LL, Pickett CB, Liu S. Human survivin is negatively regulated by wild-type p53 and participates in p53-dependent apoptotic pathway. *Oncogene* 2002; **21**: 2613-2622

27 **Li F**, Ambrosini G, Chu EY, Plescia J, Tognin S, Marchisio PC, Altieri DC. Control of apoptosis and mitotic spindle checkpoint by survivin. *Nature* 1998; **396**: 580-584

28 **Xia C**, Xu Z, Yuan X, Uematsu K, You L, Li K, Li L, McCormick F, Jablons DM. Induction of apoptosis in mesothelioma cells by antisurvivin oligonucleotides. *Mol Cancer Ther* 2002; **1**: 687-694

29 **Grossman D,** Kim PJ, Schechner JS, Altieri DC. Inhibition of melanoma tumor growth in vivo by survivin targeting. *Proc Natl Acad Sci U S A* 2001; **98**: 635-640

30 **Olie RA**, Simoes-Wust AP, Baumann B, Leech SH, Fabbro D, Stahel RA, Zangemeister-Wittke U. A novel antisense oligonucleotide targeting survivin expression induces apoptosis and sensitizes lung cancer cells to chemotherapy. *Cancer Res* 2000; **60**: 2805-2809

Edited by Xu XQ and Wang XL

P.O.Box 2345, Beijing 100023,China
Fax: +86-10-85381893
E-mail: wjg@wjgnet.com www.wjgnet.com

World J Gastroenterol 2003;9(7):1439-1443
World Journal of Gastroenterology
 ISSN 1007-9327

• GASTRIC CANCER •

cDNA suppression subtraction library for screening down-regulated genes in gastric carcinoma

Jian-Jun Du, Ke-Feng Dou, Shu-You Peng, Hua-Sheng Xiao, Wei-Zhong Wang, Wen-Xian Guan, Zhong-Hua Wang, Zhi-Qing Gao, Ying-Bin Liu

Jian-Jun Du, Ke-Feng Dou, Wei-Zhong Wang, Wen-Xian Guan, Zhong-Hua Wang, Zhi-Qing Gao, Department of General Surgery, Xijing Hospital, The Fourth Military Medical University, Xian 710032, Shaanxi Province, China
Hua-Sheng Xiao, Department of Neurobiology, The Fourth Military Medical University, Xi an 710032, Shaanxi Province, China
Shu-You Peng, Ying-Bin Liu, Department of General Surgery, the Second Affiliated Hospital, Medical College, Zhejiang University, Hangzhou 310009, Zhejiang Province, China
Correspondence to: Dr. Ke-Feng Dou, Department of General Surgery, Xijing Hospital, The Fourth Military Medical University, Xian 710032, Shaanxi Province, China. zhongmrh@yahoo.com
Telephone: +86-029-3375256
Received: 2003-01-04 **Accepted:** 2003-02-16

Abstract

AIM: To establish cDNA suppression subtraction library with a high subtraction efficiency by counterpart normal gastric mucosa mixture mRNA subtracting gastric cancer cells mixture mRNA for screening down-regulated genes in gastric carcinoma.

METHODS: RNA of gastric cancer tissues and counterpart normal gastric mucosa were respectively isolated in five patients with gastric cancer, and their mRNA was purified. cDNA suppression subtraction library was established by counterpart normal gastric mucosa mixture mRNA (tester) subtracting gastric cancer tissues mixture mRNA (driver) of five patients with gastric carcinoma. The library plasmids were transformed into competent bacteria DH5a after ligation of the library cDNA fragments with T vectors. Library plasmids were extracted after picking colonies and shaking bacteria overnight. Its subtraction efficiency was confirmed by PCR and reverse hybridization of a nylon filter onto which the colonies of bacteria were transfered with probes of reverse transcription products cDNA of gastric cancer tissues mRNA and counterpart normal gastric mucosa mRNA labeled with α-^{32}P dCTP.

RESULTS: mRNA purified from total RNA of gastric cancer tissues and counterpart normal gastric mucosa in five patients with gastric carcinoma revealed a good quality. cDNA suppression subtraction library constructed for screening down-regulated genes in gastric carcinoma represented a high subtraction efficiency. 86 % of differential expression in down-regulated genes between counterpart normal gastric mucosa and gastric carcinoma was confirmed.

CONCLUSION: cDNA suppression subtraction library with a high subtraction efficiency for screening down-regulated genes in gastric carcinoma is successfully established.

Du JJ, Dou KF, Peng SY, Xiao HS, Wang WZ, Guan WX, Wang ZH, Gao ZQ, Liu YB. cDNA suppression subtraction library for screening down-regulated genes in gastric carcinoma. *World J Gastroenterol* 2003; 9(7): 1439-1443
http://www.wjgnet.com/1007-9327/9/1439.asp

INTRODUCTION

High incidence of 50-80 % LOH (loss of hybridization) in gastric carcinoma cells reveals obvious chromosome fragments loss[1,2], e.g 8p, 18q12.2, 21q22, 1p35-pter of regions of LOH were currently found[2-8]. These suggest the novel tumor suppressor genes in the regions of LOH are involved in gastric tumorigenicity[9]. But these novel tumor suppressor gene candidates have not been cloned. To reach the targets, we screened down-regulated genes in a suppression subtraction cDNA library established by counterpart normal gastric mucous membrane mixture mRNA (tester) subtracting gastric cancer cells mixture mRNA (driver) of five patients with gastric cancer based on the suppression subtractive hybridization (SSH) technique[10]. These down-regulated genes obtained from the library probably are tumor suppressor gene candidates. Up to now, down-regulated genes in gastric cancer cloned from gastric tissues have been seldom documented except CA11, LDOC1[11-13].

MATERIALS AND METHODS

RNA extraction and mRNA purification

RNA of gastric cancer tissues and counterpart normal gastric mucosa was respectively isolated with Trizol (Gibco) in five patients with gastric cancer from Xijing Hospital, Fourth Military Medical University. To ensure good total RNA quality 28S/18S $\geqslant$1.5, samples were immediately placed into liquid nitrogen after being removed intraoperatively, and trituration of the samples must be performed in liquid nitrogen. Then, mRNA was purified in Oligotex mRNA Kit (Qiagen). An equal mRNA mixture of gastric cancer tissues and counterpart normal gastric mucosa in five patients with gastric cancer contributed to driver group (gastric cancer tissues) and tester group (counterpart normal gastric mucosa) respectively. At last, reverse transcription products (the first stranded cDNAs) of mRNA mixture were electrophoresed to evaluate their size range and quality.

Suppression substraction library construction

First-strand was synthesized with 1 μl cDNA synthesis primer (10 μmol· L^{-1}, Clontech) in a mixture containing 2 μg mRNA mixture, 20U AMV, 2 μl 5×first-strand buffer in a final volume of 10 μl at 42 ℃ for 1.5 h. Then, second-strand synthesis was carried out in 10 μl first strand react volume, 4.0 μl 20× second-strand enzyme cocktail, 48.4 μl of sterile H_2O, 1.6 μl dNTP Mix (10 mM· L^{-1}), 16.0 μl 5×second-strand buffer solution for 2 h at 16 ℃. Polymeric reaction was performed at 16 ℃ for 0.5 h after 2 μl (6 units) of T4 DNA polymerase was added into the above reaction volume. The second-strand synthesis was terminated by adding 4 μl of 20×EDTA/Glycogen Mix (Clontech). After phenol:chloroform: isoamyl alcohol (25:24:1) and chloroform: isoamyl alcohol (24:1) extraction twice respectively, and 4 M NH4OAc and 95 % ethanol precipitation of the second stranded cDNAs, the pellet was dissolved in 50 μl of sterile H_2O when precipitate was washed in 80 % ethanol and residual ethanol was evaporated after the supertant was removed.

The second double-stranded cDNA was digested with 15U RsaI in a final volume of 50 μl at 37 ℃ for 1.5 h. Enzyme digestion was terminated by adding 2.5 μl 20×EDTA/Glycogen Mix. After extraction and precipitation of digested second-strand cDNAs, the pellet was dissolved in 5.5 μl of sterile H_2O when precipitate was washed in 80 % ethanol and residual ethanol was evaporated after the supertant was removed.

One μl of digested first-strand cDNAs of normal gastric mucosa was diluted with 5 μl of sterile H_2O. Each 2 μl of the cDNA was acted as tester1-1 and tester1-2 that were respectively mixed with adaptor1 and adaptor 2, and 1 μl T4 DNA ligase (400 $kU \cdot L^{-1}$) in a final volume of 10 μl, while mixture of 2 μl of each tester1-1 and tester1-2 was taken as control (Tester C). Ligation to adaptors completed at 16 ℃ overnight.

Then, 1.5 μl of tester1-1 with adaptor 1 and tester1-2 with adaptor 2 was respectively hybridized with 1.5 μl digested first-stranded driver cDNA of gastric cancer in 1.0 μl 4×hybridization buffer solution at 68 ℃ for 10 h. Tester1-2 hybridization sample was drawn into the pipette tip. Afterwards, 1 μl denatured mixture from 1 μl digested second-stranded driver cDNA, 2 μl H_2O, 1 μl 4×hybridization buffer solution at 98 ℃ was drawn into the pipette tip with a slight air space below the droplet of the above tester1-2 hybridization sample. Sequentially, the entire mixture of pipette tip was transferred to a tube containing the above tester1-1 hybridization sample overnight at 68 ℃. After second hybridization, 200 μl dilution buffer was added into the tube. One μl of tester C was diluted with 1 000 μl of sterile H_2O. 1 μl of diluted tester C and the secondary hybridization sample were amplified with PCR primer 1 and 50×advantage cDNA polymerase mix in a final volume of 25 μl respectively after adaptors were extended at 75 ℃. 3 μl of primary PCR product was diluted with 27 μl of sterile H_2O. 1 μl of diluted primary PCR products was again amplified with nested PCR primer 1, 2R and 50×advantage cDNA polymerase mix in a final volume of 25 μl for 12 cycles.

Analyses of adaptor ligation efficiency and subtraction efficiency by PCR

One 1 μl of tester1-1 and tester1-2 with adaptors was diluted with 200 μl of sterile H_2O respectively. 1 μl of diluted tester1-1 and tester1-2 was repeatedly amplified respectively using G3PDH 3' primer, PCR primer 1 as well as G3PDH 3' primer, G3PDH 5' primer after adaptors were extended at 75 ℃. 1 μl of subtraction cDNA and secondary PCR product of tester C was diluted with 9 μl of sterile H_2O. 1 μl of diluted subtraction cDNA and secondary PCR product of tester C was respectively amplified with G3PDH 3' primer, G3PDH 5' primer. 5 μl of PCR products collected at 18, 23, 28, and 33 cycles was electrophoresed on 2 % agarose gel respectively.

Identification of suppression substraction library

Six μl of secondary PCR product of subtraction cDNA was ligated to T vectors in a mixture containing 2 μl T vectors, 1 μl T4DNA ligase in a final volume of 10 μl at 16 ℃ for 36 h. Then, 5 μl of ligated product was transformed into 100 μl of competent DH5a (stratgene) for electroporation. Competent DH5a transformed by ligated product was grown on LB medium plates. White colonies were placed into LB medium and shaken overnight at 37 ℃. In a large scale, fragments inserted into library plasmids were identified by PCR amplification with SP6 and T7 primers after library plasmids were extracted. Each colony of plasmids with inserted fragments was inoculated twice on a LB medium plate (100 colonies per plate, and one pair of positive and negative controls per plate) and grown until colony diameter reached to 3 mm. At time, colonies were transfered onto a nylon filter (NEN), then the nylon filter was cross-linked by using an UV stratalinker (CL-1000, Upland). Each 200 ng mRNA of the normal mucosa and gastric carcinoma was reverseiy transcripted with 1 μg Oligo $(dT)_{15}$ and super transcriptase II as a probe labeled with α-^{32}PdCTP, hybridized respectively with filters. The filters were exposed to phosphore screen and analyzed.

RESULTS

Identification of mRNA quality

Good total RNA quality was confirmed by 28S/18S ⩾1.5. Size range of reverse transcription product cDNAs was represented in a smear from 0.2-4kb both in gastric cancer and normal mucosa (Figure 1).

RsaI enzyme digestion

Size range of double-strand cDNA without digestion showed a normal size as expected. By comparison, RsaI enzyme digested double-strand cDNA on electrophoresis represented a smear from 0.2-2kb caused by complete digestion (Figure 2).

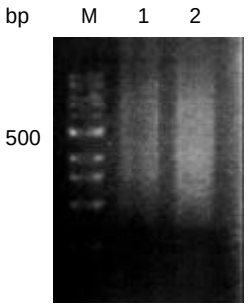

Figure 1 Size range of mRNA on 2 % agarose gel electrophorsis. Normal gastric mucosa mRNA (lane1) and gastric carcinoma mRNA (lane 2). 100 bp size marker (lane M).

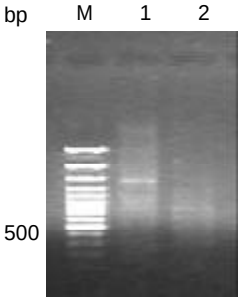

Figure 2 Digested and undigested double strands cDNA products. Undigested double strands cDNA products (lane 1) and RsaI digested double strands cDNA products (lane 2). 100bp size marker (lane M).

Detection of adaptor ligation efficiency and analyses of PCR products

A 0.75 kb band of tester1-1 and tester1-2 PCR product accorded with the theoretic size as expected when they were amplified with G3PDH3' primer and PCR1 primer respectively. The 0.75 kb band intensity of tester1-1 and tester1-2 PCR product also was as same as the band of tester1-1 and tester1-2 PCR product amplified with G3PDH3' and G3PDH5' primers (Figure 3). Secondary PCR product of subtraction sample exhibited a smear from 0.2-2 kb with some distinct bands that were greatly different from that appeared in unsubtraction samples (Figure 4).

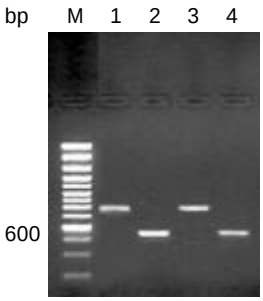

Figure 3 Detection of adaptors ligation efficiency. Tester1-1 was amplified with G3PDH3' primer, PCR primer1 (lane 1) and tester1-1 with G3PDH3', 5' primers (lane 2). Tester1-2 was amplified with G3PDH3' primer, PCR primer1 (lane 3) and tester1-2 with G3PDH3', 5' primers (lane 4). 100 bp size marker (lane M).

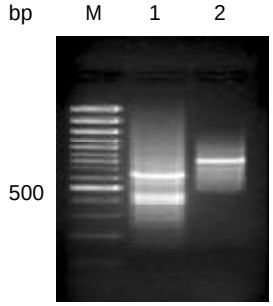

Figure 4 Analyses of PCR products. Secondary PCR products of subtraction samples (lane 1) and unsubtraction samples (lane 2). 100 bp size marker (lane M).

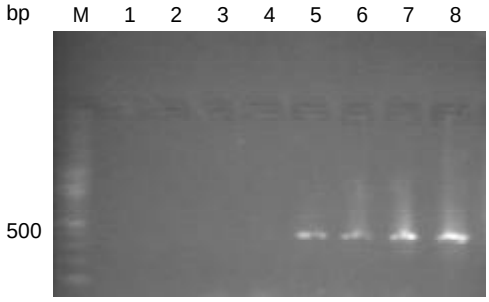

Figure 5 Identification of subtraction efficiency by PCR. G3PDH PCR products of subtracted samples at 18, 23, 28 and 33 cycles (lanes1, 2, 3 and 4) respectively and G3PDH PCR products of unsubtracted samples respectively at 18, 23, 28 and 33 cycles (lanes 5, 6, 7 and 8). 100 bp size marker (lane M).

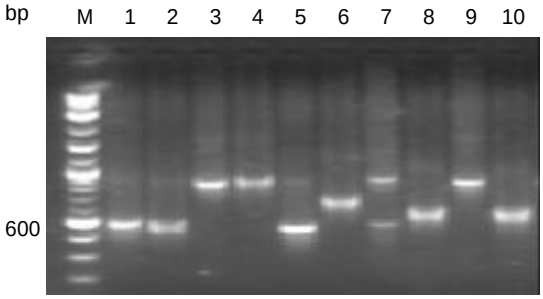

Figure 6 Identification of inserted fragments in plasmids of library by PCR. Inserted fragments in plasmids of library (lanes 1-10). 100 bp size marker (lane M).

Analyses of subtraction efficiency by PCR

G3PDH persistently was expressed at 18, 23, 28 and 33 cycles of PCR and the bands exhibited greater and greater intensity with increasing cycle numbers in unsubtraction control group, but not expressed in subtraction group (Figure 5).

Identification of inserted fragments in plasmids of library by PCR and positive clone by reverse hybridization

PCR products of library plasmids amplified with SP6 and T7 primers on a larger scale showed that each plasmid included one inserted fragment ranging from 300-700 bp (Figure 6). 86 % of down-regulated genes between normal gastric mucosa and gastric carcinoma were confirmed by hybridization of a transferred filter with probes of reverse transcription product cDNAs.

DISCUSSION

Many genes involves in gastric tumorigenicity and tumor metastasis[14-24]. Occurrence and development of gastric carcinoma are closely associated with loss or lower expression of suppressor genes[25,26]. It contributes to a better understanding of the molecular mechanism of gastric tumorigenicity, and the expression profiles of down-regulated genes in gastric carcinoma, as well as cloning of novel genes , especially human stomach-specific gene. The novel genes usually express in lower abundance, and play an important role in cell differentiation and development. We have successfully established the cDNA suppression subtraction library to screen down-regulated genes in gastric carcinoma.

It is an important step to guarantee mRNA quality in constructing cDNA suppression subtraction library with a high subtraction efficiency because it is directly relatd to subtraction efficiency. Good mRNA quality depends on total RNA quality except for mRNA purification. To ensure good total RNA quality of 28S/18S $\geqslant$1.5, samples must be immediately placed into liquid nitrogen after removed intraoperatively, and trituration of samples must be performed also in liquid nitrogen. At last, reverse transcription products (the first stranded cDNAs) of mRNA were electrophoresed to evaluate its size and quality. The mRNA size range should accord with its theoretic value.

Each step for establishing cDNA suppression subtraction library was verified by corresponding methods provided by Clontech to ensure suppression subtraction efficiency. Many reports have shown that the suppression subtractive technique has successfully constructed a lots of cDNA suppression subtraction library with high efficiency, and cloned many novel genes[27-45]. Our experiments were carried out strictly according to the rule. Identifications of experimental results step by step revealed complete enzyme cutting, and enzyme digested size of double-strand cDNA accorded with theoretic size range, enough ligation of the digested fragments of double-strand cDNA and adaptors. It demonstrated that, in cDNA suppression subtraction library with high subtractive efficiency, G3PDH was persistently expressed at 18, 23, 28 and 33 cycles of PCR and the bands exhibited greater and greater intensity with increasing cycles in unsubtraction control group, but not expressed in subtraction group.

After establishment of the cDNA suppression subtraction library with a high efficiency, maximum cloning of novel down-regulated genes in gastric cancer depends on highly efficient plasmid transformation method and competent bacteria cells. Lower abundance of gene fragments will be likely cloned if commercially availiable high concentration competent cells are used ($1\times10^{12}\cdot L^{-1}$) for transformation with a high transformation rate ($1\text{-}2\times10^{8}$/μg PUC19).Use of electroporation method can greatly enhance library plamids transformation rate by obtaining 10^{8}/μg PUC19. Additionally, it especially fits transformation of the small fragments produced in cDNA suppression subtraction library.

Several identified methods for cDNA suppression subtraction library were described below. The expression pattern of individual clones could be confirmed by Northern blot analysis. 10-20 clones were randomly picked from the subtracted library as probes on Northern blots. If less than two clones were confirmed as differentially expressed genes, the differential screening procedure should be performed to eliminate false positives. Dot or Southern blot analysis was performed. Secondary PCR products of the unsubtracted tester cDNA, the unsubtracted driver cDNA, and the subtracted cDNA were electrophoresed on a 1.5 % agarose gel, transferred onto nylon filters and hybridized respectively with differential expressing genes as probes labeled with α-^{32}PdCTP. But more background bands of unpredicted sizes often appeared. Nylon filters onto which the library colonies of bacteria were transferred and hybridized with reverse transcript product cDNA of gastric cancer tissues mRNA and normal gastric mucosa mRNA were used as probes labeled with α-^{32}PdCTP respectively. This method has been extensively used. The disadvantage is that only a high abundance of mRNA can be detected. Another approach can bypass the problem of losing a low-abundance of sequences. By this method, the subtracted library was hybridized with forward- and reversely-subtracted cDNA probes. To make reversely-subtracted probes, subtractive hybridization was performed with the original tester cDNA as a driver and the driver cDNA as a tester. Plasmids colonies that are truly differentially expressed will hybridize only with the forward-subtracted probe. Plasmids colonies that hybridize with the reversely-subtracted probe may be considered as the background. This approach requires one additional step: before it can be used as probes, the forward- and reversely-subtracted probes must undergo restriction enzyme digestion to remove the adaptor sequences. Despite their small size, these adaptors can cause a very high background when the subtracted probes are hybridized to the subtracted cDNA library.

REFERENCES

1 **Park WS,** Oh RR, Park JY, Yoo NJ, Lee SH, Shin MS, Kim SY, Kim YS, Lee JH, Kim HS, An WG, Lee JY. Mapping of a new target region of allelic loss at 21q22 in primary gastric cancers. *Cancer Lett* 2000; **159**: 15-21

2 **Kim HS**, Woo DK, Bae SI, Kim YI, Kim WH. Allelotype of the adenoma-carcinoma sequence of the stomach. *Cancer Detect Prev* 2001; **25**: 237-244

3 **Baffa R**, Santoro R, Bullrich F, Mandes B, Ishii H, Croce CM. Definition and refinement of chromosome 8p regions of loss of heterozygosity in gastric cancer. *Clin Cancer Res* 2000; **6**: 1372-1377

4 **Igarashi J**, Nimura Y, Fujimori M, Mihara M, Adachi W, Kageyama H, Nakagawara A. Allelic loss of the region of chromosome 1p35-pter is associated with progression of human gastric carcinoma. *Jpn J Cancer Res* 2000; **91**: 797-801

5 **Wang Q**, Chen H, Bai J, Wang B, Wang K, Gao H, Wang Z, Wang S, Zhang Q, Fu S. Analysis of loss of heterozygosity on 19p in primary gastric cancer. *Zhonghua Yixue Yichuanxue Zazhi* 2001; **18**: 459-461

6 **Sud R**, Wells D, Talbot IC, Delhanty JD. Genetic alterations in gastric cancers from British patients. *Cancer Genet Cytogenet* 2001; **126**: 111-119

7 **Chung YJ**, Choi JR, Park SW, Kim KM, Rhyu MG. Evidence for two modes of allelic loss: Multifocal analysis on both early and advanced gastric carcinomas. *Virchows Arch* 2001; **438**: 31-38

8 **Han HS**, Kim HS, Woo DK, Kim WH, Kim YI. Loss of heterozygosity in gastric neuroendocrine tumor. *Anticancer Res* 2000; **20**: 2849-2854

9 **Nishioka N**, Yashiro M, Inoue T, Matsuoka T, Ohira M, Chung KH. A candidate tumor suppressor locus for scirrhous gastric cancer at chromosome 18q 12.2. *Int J Oncol* 2001; **18**: 317-322

10 **Diatchenko L**, Lau YF, Campbell AP, Chenchik A, Moqadam F, Huang B, Lukyanov S, Lukyanov K, Gurskaya N, Sverdlov ED, Siebert PD. Suppression subtractive hybridization: A method for generating differatially regulated or tissue-specific cDNA probes and libraries. *Proc Natl Acad Sci USA* 1996; **93**: 6025-6030

11 **Yoshikawa Y**, Mukai H, Hino F, Asada K, Kato I. Isolation of two novel genes, down-regulated in gastric cancer. *Jpn J Cancer Res* 2000; **91**: 459-463

12 **Nagasaki K**, Manabe T, Hanzawa H, Maass N, Tsukada T, Yamaguchi K. Identification of a novel gene, LDOC1, down-regulated in cancer cell lines. *Cancer Lett* 1999; **140**: 227-234

13 **Jung MH**, Kim SC, Jeon GA, Kim SH, Kim Y, Choi KS, Park SI, Joe MK, Kimm K. Identification of differentially expressed genes in normal and tumor human gastric tissue. *Genomics* 2000; **69**: 281-286

14 **Wang B**, Shi LC, Zhang WB, Xiao CM, Wu JF, Dong YM. Expression and significance of P16 gene in gastric cancer and its precancerous lesions. *Shijie Huaren Xiaohua Zazhi* 2001; **9**: 39-42

15 **Wang RQ**, Fang DC, Liu WW. MUC2 gene expression in gastric cancer and preneoplastic lesion tissues. *Shijie Huaren Xiaohua Zazhi* 2000; **8**: 285-288

16 **Machado JC**, Oliveira C, Carvalho R, Soares P, Berx G, Caldas C, Seruca R, Carneiro F, Sobrinho-Simoes M. E-cadherin gene (CDH1) promoter methylation as the second hit in sporadic diffuse gastric carcinoma. *Oncogene* 2001; **20**: 1525-1528

17 **Liu HF**, Liu WW, Fang DC, Yang SM, Wang RQ. Bax gene expression and its relationship with apoptosis in human gastric carcinoma and precancerous lesions. *Shijie Huaren Xiaohua Zazhi* 2000; **8**: 665-668

18 **He XS**, Su Q, Chen ZC, He XT, Long ZF, Ling H, Zhang LR. Expression, deletion [was deleton] and mutation of p16 gene in human gastric cancer. *World J Gastroenterol* 2001; **7**: 515-521

19 **Liu DH**, Zhang XY, Fan DM, Huang YX, Zhang JS, Huang WQ, Zhang YQ, Huang QS, Ma WY, Chai YB, Jin M. Expression of vascular endothelial growth factor and its role in oncogenesis of human gastric carcinoma. *World J Gastroenterol* 2001; **7**: 500-505

20 **Gu HP**, Ni CR, Zhan RZ. Relationship between CD_{15} mRNA and its protein expression and gastric carcinoma invasion. *Shijie Huaren Xiaohua Zazhi* 2000; **8**: 851-854

21 **Endo K**, Maejara U, Baba H, Tokunaga E, Koga T, Ikeda Y, Toh Y, Kohnoe S, Okamura T, Nakajima M, Sugimachi K. Heparanase gene expression and metastatic potential in human gastric cancer. *Anticancer Res* 2001; **21**: 3365-3369

22 **Nesi G**, Palli D, Pernice LM, Saieva C, Paglierani M, Kroning KC, Catarzi S, Rubio CA, Amorosi A. Expression of nm23 gene in gastric cancer is associated with a poor 5-year survival. *Anticancer Res* 2001; **21**: 3643-3549

23 **Murahashi K**, Yashiro M, Takenaka C, Matsuoka T, Ohira M, Chung KH. Establishment of a new scirrhous gastric cancer cell line with loss of heterozygosity at E-cadherin locus. *Int J Oncol* 2001; **19**: 1029-1033

24 **Wang CD**, Chen YL, Wu T, Liu YR. Association between lower expression of somatostatin receptor II gene and lymphoid metastasis in patients with gastric cancer. *Shijie Huaren Xiaohua Zazhi* 1999; **7**: 864-866

25 **Yamamoto M**, Tsukamoto T, Sakai H, Shirai N, Ohgaki H, Furihata C, Donehower LA, Yoshida K, Tatematsu M. p53 knockout mice (-/-) are more susceptible than (+/-) or (+/+) mice to N-methyl-N-nitrosourea stomach carcinogenesis. *Carcinogenesis* 2000; **21**: 1891-1897

26 **Xu X**, Brodie SG, Yang X, Im YH, Parks WT, Chen L, Zhou YX, Weinstein M, Kim SJ, Deng CX. Haploid loss of the tumor suppressor Smad4/Dpc4 initiates gastric polyposis and cancer in mice. *Oncogene* 2000; **19**: 1868-1874

27 **Osherov N**, Mathew J, Romans A, May GS. Identification of conidial-enriched transcripts in Aspergillus nidulans using suppression subtractive hybridization. *Fungal Genet Biol* 2002; **37**: 197-204

28 **Petersen S**, Petersen I. Expression profiling of lung cancer based on suppression subtraction hybridization (SSH). *Methods Mol Med* 2003; **75**: 189-207

29 **Liu ZW**, Zhao MJ, Li ZP. Identification of Up-regulated genes in rat regenerating liver tissue by suppression subtractive hybridization. *Shenwu Huaxue Yu Shengwu Wuli Xuebao* (Shanghai) 2001; **33**: 191-197

30 **Ji W**, Wright MB, Cai L, Flament A, Lindpaintner K. Efficacy of SSH PCR in isolating differentially expressed genes. *BMC Genomics* 2002; **3**: 12-14

31 **Shridhar V**, Sen A, Chien J, Staub J, Avula R, Kovats S, Lee J, Lillie J, Smith DI. Identification of underexpressed genes in early- and late-stage primary ovarian tumors by suppression subtraction hybridization. *Cancer Res* 2002; **62**: 262-270
32 **Tanaka F**, Hori N, Sato K. Identification of differentially expressed genes in rat hepatoma cell lines using subtraction and microarray. *J Biochem* (Tokyo) 2002; **131**: 39-44
33 **Lin S**, Chugh S, Pan X, Wallner EI, Wada J, Kanwar YS. Identification of up-regulated Ras-like GTPase, Rap1b, by suppression subtractive hybridization. *Kidney Int* 2001; **60**: 2129-2141
34 **Majda BT**, Meloni BP, Rixon N, Knuckey NW. Suppression subtraction hybridization and northern analysis reveal upregulation of heat shock, trkB, and sodium calcium exchanger genes following global cerebral ischemia in the rat. *Brain Res Mol Brain Res* 2001; **93**: 173-179
35 **Shi J**, Cai W, Chen X, Ying K, Zhang K, Xie Y. Identification of dopamine responsive mRNAs in glial cells by suppression subtractive hybridization. *Brain Res* 2001; **910**: 29-37
36 **Wang X**, Feuerstein GZ. Suppression subtractive hybridisation: Application in the discovery of novel pharmacological targets. *Pharmacogenomics* 2000; **1**: 101-108
37 **Dey R**, Son HH, Cho MI. Isolation and partial sequencing of potentially odontoblast-specific / enriched rat cDNA clones obtained by suppression subtractive hybridization. *Arch Oral Biol* 2001; **46**: 249-260
38 **Ye Z**, Connor JR. Identification of iron responsive genes by screening cDNA libraries from suppression subtractive hybridization with antisense probes from three iron conditions. *Nucleic Acids Res* 2000; **28**: 1802-1807
39 **Kim JY**, Chung YS, Paek KH, Park YI, Kim JK, Yu SN, Oh BJ, Shin JS. Isolation and characterization of a cDNA encoding the cysteine proteinase inhibitor, induced upon flower maturation in carnation using suppression subtractive hybridization. *Mol Cells* 1999; **9**: 392-397
40 **Diatchenko L**, Lukyanov S, Lau YF, Siebert PD. Suppression subtractive hybridization: A versatile method for identifying differentially expressed genes. *Methods Enzymol* 1999; **303**: 349-380
41 **Fang J**, Shi GP, Vaghy PL. Identification of the increased expression of monocyte chemoattractant protein-1, cathepsin S, UPIX-1, and other genes in dystrophin-deficient mouse muscles by suppression subtractive hybridization. *J Cell Biochem* 2000; **79**: 164-172
42 **Zhang L**, Cilley RE, Chinoy MR. Suppression subtractive hybridization to identify gene expressions in variant and classic small cell lung cancer cell lines. *J Surg Res* 2000; **93**: 108-119
43 **Chim SS**, Cheung SS, Tsui SK. Differential gene expression of rat neonatal heart analyzed by suppression subtractive hybridization and expressed sequence tag sequencing. *J Cell Biochem* 2000; **80**: 24-36
44 **Porkka KP**, Visakorpi T. Detection of differentially expressed genes in prostate cancer by combining suppression subtractive hybridization and cDNA library array. *J Pathol* 2001; **193**: 73-79
45 **Villalva C**, Trempat P, Zenou RC, Delsol G, Brousset P. Gene expression profiling by suppression subtractive hybridization (SSH): A example for its application to the study of lymphomas. *Bull Cancer* 2001; **88**: 315-319

Edited by Zhang JZ

P.O.Box 2345, Beijing 100023,China
Fax: +86-10-85381893
E-mail: wjg@wjgnet.com www.wjgnet.com

World J Gastroenterol 2003;9(7):1450-1454
World Journal of Gastroenterology
 ISSN 1007-9327

• LIVER CANCER •

Observation of DNA damage of human hepatoma cells irradiated by heavy ions using comet assay

Li-Mei Qiu, Wen-Jian Li, Xin-Yue Pang, Qing-Xiang Gao, Yan Feng, Li-Bin Zhou, Gao-Hua Zhang

Li-Mei Qiu, Wen-Jian Li, Yan Feng, Li-Bin Zhou, Gao-Hua Zhang, Institute of Modern Physics, the Chinese Academy of Sciences, Lanzhou 730000, Gansu Province, China
Xin-Yue Pang, Qing-Xiang Gao, School of Life Science, Lanzhou University, Lanzhou 730000, Gansu Province, China
Supported by President Special Foundation of Chinese Academy of Sciences, grant No. TB990601
Correspondence to: Li-Mei Qiu, Institute of Modern Physics, the Chinese Academy of Sciences, Lanzhou 730000,Gansu Province, China. qiuqiu69@sina.com
Telephone: +86-931-4969338 **Fax:** +86-931-4969201
Received: 2002-10-22 **Accepted:** 2002-11-28

Abstract

AIM: Now many countries have developed cancer therapy with heavy ions, especially in GSI (Gesellschaft für Schwerionenforschung mbH, Darmstadt, Germany), remarkable results have obtained, but due to the complexity of particle track structure, the basic theory still needs further researching. In this paper, the genotoxic effects of heavy ions irradiation on SMMC-7721 cells were measured using the single cell gel electrophoresis (comet assay). The information about the DNA damage made by other radiations such as X-ray, γ-ray, UV and fast neutron irradiation is very plentiful, while little work have been done on the heavy ions so far. Hereby we tried to detect the reaction of liver cancer cells to heavy ion using comet assay, meanwhile to establish a database for clinic therapy of cancer with the heavy ions.

METHODS: The human hepatoma cells were chosen as the test cell line irradiated by 80Mev/u $^{20}Ne^{10+}$ on HIRFL (China), the radiation-doses were 0, 0.5, 1, 2, 4 and 8 Gy, and then comet assay was used immediately to detect the DNA damages, 100-150 cells per dose-sample (30-50 cells were randomly observed at constant depth of the gel). The tail length and the quantity of the cells with the tail were put down. EXCEL was used for statistical analysis.

RESULTS: We obtained clear images by comet assay and found that SMMC-7721 cells were all damaged apparently from the dose 0.5Gy to 8Gy (*t*-test: $P<0.001$, *vs* control). The tail length and tail moment increased as the doses increased, and the number of cells with tails increased with increasing doses. When doses were higher than 2Gy, nearly 100 % cells were damaged. Furthermore, both tail length and tail moment, showed linear equation.

CONCLUSION: From the clear comet assay images, our experiment proves comet assay can be used to measure DNA damages by heavy ions. Meanwhile DNA damages have a positive correlation with the dose changes of heavy ions and SMMC-7721 cells have a great radiosensitivity to $^{20}Ne^{10+}$. Different reactions to the change of doses indicate that comet assay is a useful tool to detect DNA damage induced by heavy ions.

Qiu LM, Li WJ, Pang XY, Gao QX, Feng Y, Zhou LB, Zhang GH. Observation of DNA damage of human hepatoma cells irradiated by heavy ions using comet assay. *World J Gastroenterol* 2003; 9(7): 1450-1454
http://www.wjgnet.com/1007-9327/9/1450.asp

INTRODUCTION

During the past few decades, radiation research has developed into specialized sub-disciplines, from basic physics and chemistry to tumor biology and experimental radiation therapy[1]. Although the radiobiological effects are extensively investigated for X-ray and γ-ray, little work has been directed towards heavy ion beams. With the exploration of the outer space, the research of high linear energy transfer (LET) has attracted more and more attention. Since heavy ions were first applied in the mid-1970s to cure cancer at Bevalac of Lawrence Berkeley Laboratory (LBL), United States, promising results have been reported when compared with the conventional radiotherapy for soft tissue sarcoma, bone sarcoma and prostate cancer[2]. Now scientists in many countries (GSI in Germany, HIMAC in Japan[25,26], HIRFL in China) have designed accelerators to deliver beams of ions for the treatment and started basic researches of cancer therapy with heavy ions such as carbon, neon, oxygen and argon.

The aim of our present study was to investigate DNA damages induced by heavy ions by comet assay. The theoretical value was then compared to responses to external X-ray or γ-ray and other irradiations, so that we could establish the data base for clinical therapy.

Comet assay, the alkaline version in particular, has become a very popular method for the analysis of DNA damage caused by various chemical and physical agents because of its simplicity and rapidity[4-10]. DNA damages consisted of DNA strand breakage, alkali-labile sites and incomplete excision repair sites[11]. Although the direct DNA-breaking capacity can be estimated by alkaline elution, nick translation and alkaline single cell gel electrophoresis (SCGE), SCGE has been shown to be more sensitive than the former two. It had been proved that the sensitivity of SCGE is significantly higher than that of cytokinesis-blocked micronucleus (CBMN) test[12]. The most important point is that comet assay is an electrophoretic technique, which allows measurements of DNA damages as well as DNA repair rates on an individual cell. Therefore its contribution to DNA damages by irradiating cells with heavy ions at once or after a while can be reflected as initial damages or residual DNA damages, if time is allowed for enzymatic repairs of initial DNA strand break. In our lab, we focused on the radiobiological effects of heavyions on tumor cells. Previous experiments were mainly on cell survival measurements and could not explain the underlying radiosensitization mechanism at molecular level[2]. To verify the radiobiological effects of heavy ions on cellular DNA, SCGE also called comet assay was used to directly measure DNA damages in cells.

MATERIALS AND METHODS

Cells and cell culture

Human hepatoma cells SMMC-7721, purchased from Second Military Medical University in Shanghai, were cultivated in

RMIP-1640 medium (Gibco product) supplemented with 15 % calf serum in a standard incubator at 37 ℃. One passage of cells every 2-3 days and change of the medium everyday were performed, to ensure the cells growth in good conditions. Two days before the irradiation, the cells were shifted to Φ 35 mm petri-dishes, each had 2 ml cell suspension, and the density of the cells was 5×10^4 cells/ml. Each dose had 5 petri-dishes. Before irradiation, cells in each petri-dish were examined under the inverted light microscope to select materials good in growth and even in density, and medium 1640 in petri-dishes was removed, only Dulbecc' s phosphate -buffered saline medium (PBS) was left to keep the moisture of the cells when irradiated.

Selection of ion beams

Irradiation was performed using $^{20}Ne^{10+}$ with energy of 80 Mev/u and intensity of 0.00136nA (2.1×10^6p/s). The cells were irradiated at the doses of 0, 0.5, 1, 2, 4, 8Gy. The doses of cells were measured by an air ionization chamber.

Preparation of single cell suspension and comet assay

As soon as irradiation ended, the cells were washed and collected, the final concentration of cells was adjusted to $(5\text{-}10)\times10^6$ by adding Dulbecc' s phosphate -buffered saline medium (PBS) to the single cell suspension.

The alkaline version of comet assay was carried out based on the work of Ostling and Johansson with some minor modifications as followings: On the day of electrophoresis, an aliquot of 10 μl freshly prepared suspension of cells was mixed with 30 μl 0.5 % low- melting-agarose in Dulbecc' s PBS (pH 7.4). The mixture was layered on top of an ordinary microscope slide precoated with 0.5 % normal-melting -agorose, which was allowed to dry at room temperature protected from dust and other particles. After low-melting-agarose was solidified in a refrigerator for 10 minutes, the coverslip was carefully removed and the slide was gently immersed in a freshly prepared lysing solution (2.5MNaCl, 10mM Tris, 1 % sodium lauryl sarcosinate, 100mM Na_2EDTA, with 1 % Triton-100 and 10 % DMSO added just before use). From this moment until the end of neutralization, all steps needed to avoid the sunlight.

After lysis for 1-1.5 h, the microscopy slides were transferred to electrophoresis session, 18 microscopy slides from 6 samples (3 slides/each sample) were randomly placed in a electrophoretic unit.

After 20-30 minutes of DNA unwinding in electrophoresis buffer (1 mM EDTA-Na_2, 300 mM NaOH, pH>13), single cell gel electrophoresis was performed in the same buffer (20 min, 20 V, 300 nA). After electrophoresis the slides were neutralized with 0.4 M Tris buffer (pH7.5).

Evaluation of DNA damage

The microscopy slides were stained with ethidium bromide in water (40 μg/ml, 50 μl/slide). After application of a coverslip was removed, each slide was examined at 10×20 magnification in a fluorescence microscope (excitation filter: 400nm, barrier filter: 590nm). 100-150 cells per dose-sample (30-50 cell were randomly observed at constant depth of the gel, avoiding the edges of the gel on each of three replicate slides). The tail length and the quantity of the cells with the tail were put down, at the same time, photos were taken with 135# black and white film (ISO 400). Then analysis was done using EXCEL.

RESULTS AND DISCUSSION

Formation of comet assay images-DNA loops and alkaline unwinding

The comet assay is attractive for many reasons. Apart from being a quick, simple, sensitive, reliable and fairly inexpensive way of measuring, it also produces appealing images.

There are two explanations about what the comet tails consist of. One is that it is a fragment DNA, the other is that the length of such a fragment is about 1 mm, but the length of the tail of a comet is a few percentages of it[13-16], as to our experiment the longest mean length of tail was no more than 200 μm. Nuclear DNA is not a tangle of string, even after treatment with detergents and a strong salt solution, as in the SCGE procedure, the nuclear (or nucleoid) had a structure, the DNA was organized as loops, which retained the super coils that were contained in the nucleosome. Cook *et al*[17] deduced the presence of supercoiled loops and then they observed that, when DNA was broken by irradiation, supercoiling was relaxed and loops spilled out into a ' halo' around the nucleoid. By analogy, it is assumed that the Comet tail is made up of relaxed loops, and that the number of loops in the tail indicates the number of DNA breaks.

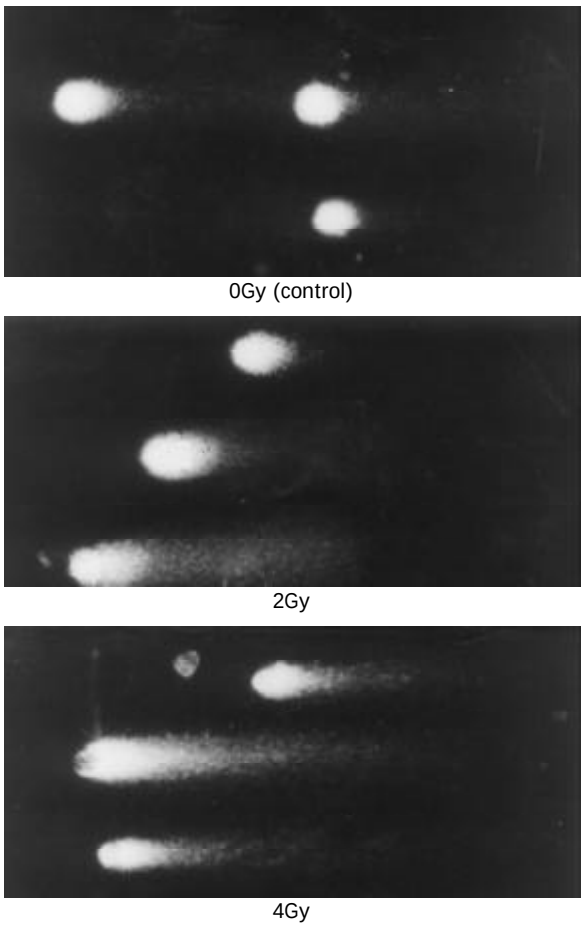

Figure 1 Comet assay image at different doses.

The alkaline comet assay can detect DNA breaks including single and double DNA strand breaks, and AP sites, which are alkali-labile and probably converted to breaks while DNA is in the electrophoretic solution at high pH[14-16]. The present comet assay is generally practiced including incubation of DNA at high pH before and during electrophoresis, different from the original work of Ostling and Johansson who employed near-neutral pH. Collins AR[13] proved that both the neutral and alkaline methods could detect low levels of DNA damage, however, the breaks by higher levels of damage were more clearly resolved from the head under alkaline conditions[18]. Thus in our experiment, the alkaline version was used.

Furthermore, breaks will be transiently present when cells repair lesions via base excision or nucleotide excision so that

a high level of breaks in the Comet assay may indicate either severe damage or efficient repair[13]. In fact, much useful information can be obtained by exploiting cellular repair to produce DNA breaks and thus to reveal or amplify the effect of radiation that otherwise may not show positive effects by the comet assay. This will be discussed in our later work on the repair effects of heavy ions.

DNA damage caused by heavy ions

The SCGE test or comet assay is a straightforward visual method for the detection of DNA damage of cells in interphase. This technique is especially sensitive in detecting DNA single-strand breaks, alkali-labile damage and excision repair sites in individual cells[13-16]. The Comet assay has been widely applied in the following fields: radiation biology[5-6,9-12,19], excisable DNA damage, DNA cross-links[20], oxidative damage[21,22], genetic toxicology and apoptosis[23,24].

Ionizing radiation is a ubiquitous environmental agent. Its physiochemical interaction with cellular DNA produces a variety of primary lesions, such as single-strand breaks (SSB), double-strand breaks (DSB), DNA-DNA and DNA-protein crosslinks, and damage to purine and pyrimidine bases. And using ionizing radiation may avoid complications of drug metabolism, intracellar distribution, membrane permeability and drug efflux. Although the technique of SCGE is very sensitive to ionizing radiation, information about DNA damage made by other radiations such as X-ray[10,12], γ-ray[8,9], UV[9] and fast neutron[19] irradiation is very plentiful, little work has been done on heavy ions so far.

Microdosimetric considerations suggest that, in a given type of radiation, the yield DNA damage must be proportional to dose, so that besides the influence of changing repair efficiency, the magnitude of the dose might not be expected to be critical in comparison of the results. Heavy ion is a kind of high LET (Linear Energy Transfer) irradiation, as emphasized long ago by Lea, high-LET radiation could, through the increased frequency of DSB in close proximity, cause interactive damages and misrepair[27-28]. We anticipated that heavy ions probably had strong effects on the cellular DNA, but we wonder if it can make the linear equation after irradiation by heavy ions.

In our experiment, the data for DNA damages induced by heavy ions at the doses of 0-8Gy are presented in Table 1. The dose-response curves for tail length and tail moment (the fraction of DNA in the tail multiplied by tail length) are shown in Figure 2. We could see tail length and tail moment showed linear equation. It proved that SMMC-7721 cells have high radiosensitivity to heavy ions and comet assay is very useful to detect DNA damages induced by heavy ions.

Figure 3 shows the change of tail DNA as the dose increased. It was found that almost 100 % cells were damaged when the dose reached at 2Gy. But the details were unknown about how badly DNA was damaged when the dose was higher than 2Gy. To completely evaluate DNA damages by different doses, comets of every dose-sample were sorted visually into classes 0-4, representing increasing amount of damage. Figure 4, result shows that with increase of the dose, slighter damage of DNA tail (class 0-2) converted to more severe change of DNA (DNA migrated from the head to form longer and longer tail).

We should pay more attention to the dose of 2Gy, which is the conventional choice of γ-ray radiotherapy. At the dose of 2 Gy, 100 % cells were damaged, with different grade of DNA damage (classes 1-4). Among them nearly 25 % cells were badly damaged. It is known that a central phenomenon in radiobiology is the efficiency of densely ionizing radiation for cellular effects. As in our experiment, chromosomal aberrations or cell killing occurred on these badly damaged cells[27-30, 33-35]. Additionally, we noticed that nearly 80 % cells were most severely damaged (class 4) at the dose of 8Gy. It showed that 8Gy might be or near the highest dose that the cells could withstand.

Table 1 Values of damages detected by Comet assay after 80Mev/u $^{20}Ne^{10+}$ irradiation

Dose Gy	Tail length mean ±S.E. μm	Tail DNA mean ±S.E %	Tail moment mean ±S.E.	*t*-test *P*
0	29.44±1.46	38.50±3.50	11.53±1.45	
0.5	54.18±11.74	59.21±9.21	33.02±11.80	2.06227E-07
1	90.16±6.66	85.54±2.21	76.96±3.44	8.7291E-21
2	115.09±3.26	100.00±0.00	115.09±3.25	6.97944E-31
4	134.17±8.18	98.86±1.07	134.17±8.10	4.48617E-68
8	194.08±15.58	100.00±0.00	194.08±15.58	6.4087E-104

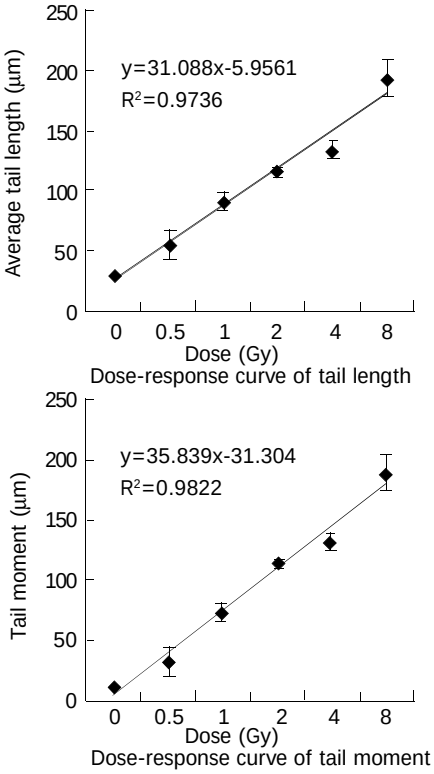

Figure 2 Curve of tail length and tail moment.

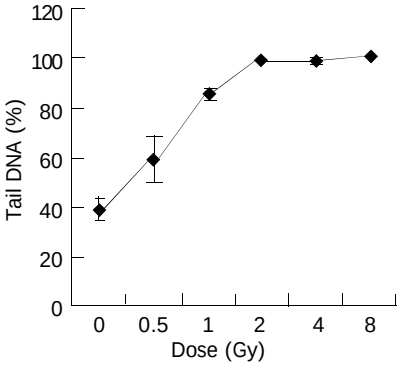

Figure 3 Dose-response curve of tail DNA.

One thing to be mentioned here is that the relative biological effectiveness (RBE) tends to increase with linear energy transfer (LET). For very heavy ions with LET in excess of about 100-200 kev/μm, a more complex dependence on particle track structure emerges[31,32]. Therefore, the study on particle track structure is very important for further research.

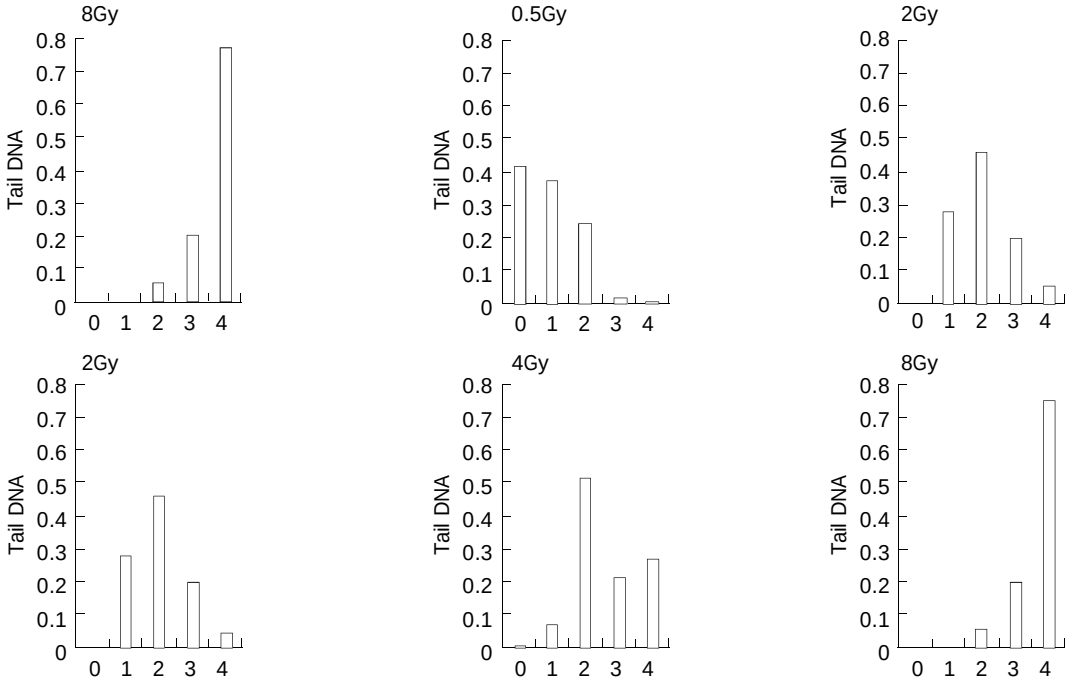

Figure 4 Comet class at the dose of 0-8Gy of heavy ions irradiation.

REFERENCES

1 **Dorr W**, Dorschel B, Sprinz H. Report on the third annual meeting of the Society for Biological Radiation Research, GBS '99. *Radiat Environ Biophys* 2000; **39**: 147-152

2 **Li WJ**, Gao QX, Zhou GM, Wei ZQ. Micronuclei and cell survival in human liver cancer cells irradiated by 25MeV / u $^{40}Ar^{14+}$. *World J Gastroenterol* 1999; **5**: 365-368

3 **Zhou GM**, Chen WQ, Gao QX, Li WJ, Li Q, Wei ZQ. Biological effects of hepatoma cells irradiated by 25MeV / u ^{40}Ar14+. *World J Gastroenterol* 1998; **4**: 271-272

4 **Wojewodzka M**, Kruszewski M, Iwanenko T, Collins AR, Szumiel I. Application of the comet assay for monitoring DNA damage in workers exposed to chronic low-dose irradiation. I. Strand breakage. *Mutat Res* 1998; **416**: 21-35

5 **Kruszewski M**, Wojewodzka M, Iwanenko T, Collins AR, Szumiel I. Application of the comet assay for monitoring DNA damage in workers exposed to chronic low-dose irradiation. II. Base damage. *Mutat Res* 1998; **416**: 37-57

6 **Muller WU**, Bauch T, Stuben G, Sack H, Streffer C. Radiation sensitivity of lymphocytes from healthy individuals and cancer patients as measured by the comet assay. *Radiat Environ Biophys* 2001; **40**: 83-89

7 **Wojewodzka M**, Kruszewski M, Iwanenko T, Collins AR, Szumiel I. Lack of adverse effect of smoking habit on DNA strand breakage and base damage, as revealed by the alkaline comet assay. *Mutat Res* 1999; **440**: 19-25

8 **Mayer C**, Popanda O, Zelezny O, von Brevern MC, Bach A, Bartsch H, Schmezer P. DNA repair capacity after gamma-irradiation and expression profiles of DNA repair genes in resting and proliferating human peripheral blood lymphocytes. *DNA Repair (Amst)* 2002; **1**: 237-250

9 **Mohankumar MN**, Paul SF, Venkatachalam P, Jeevanram RK. Influence of in vitro low-level gamma-radiation on the UV-induced DNA repair capacity of human lymphocytes-analysed by unscheduled DNA synthesis (UDS) and comet assay. *Radiat Environ Biophys* 1998; **37**: 267-275

10 **Koppen G**, Angelis KJ. Repair of X-ray induced DNA damage measured by the comet assay in roots of Vicia faba. *Environ Mol Mutagen* 1998; **32**: 281-285

11 **Cebulska-Wasilewska A**, Nowak D, Niedzwied ZW, Anderson D. Correlations between DNA and cytogenetic damage induced after chemical treatment and radiation. *Mut Res* 1998; **421**: 83-91

12 **He JL**, Chen WL, Jin LF, Jin HY. Comparative evaluation of the *in vitro* micronucleus test and the comet assay for the detection of genotoxic effects of X-ray radiation. *Mut Res* 2000; **469**: 223-231

13 **Collins AR**, Dobson VL, Dusinska M, Kennedy G, Stetina R. The comet assay: what can it really tell us? *Mutat Res* 1997; **375**: 183-193

14 **McNamee JP**, McLean JR, Ferrarotto CL, Bellier PV. Comet assay: rapid processing of multiple samples. *Mutat Res* 2000; **466**: 63-69

15 **Godard T**, Gauduchon P, Debout C. A first step in visual identification of different cell populations by a modified alkaline comet assay. *Mutat Res* 2002; **520**: 207-211

16 **Mariano Ruiz de Almodovar J**, Guirado D, Isabel Nunez M, Lopez E, Guerrero R, Teresa Valenzuela M, Villalobos M, del Moral R. Individualization of radiotherapy in breast cancer patients: possible usefulness of a DNA damage assay to measure normal cell radiosensitivity. *Radiother Oncol* 2002; **62**: 327-333

17 **Cook PR**, Brazell IA, Jost E. Characterization of nuclear structures containing superhelical DNA. *J Cell Sci* 1976; **22**: 303-324

18 **Hartmann A**, Agurell E, Beevers C, Brendler-Schwaab S, Burlinson B, Clay P, Collins A, Smith A, Speit G, Thybaud V, Tice RR. Recommendations for conducting the *in vivo* alkaline Comet assay. *Mutagenesis* 2003; **18**: 45-51

19 **Gajendiran N**, Tanaka K, Kamada N. Comet assay to sense neutron 'fingerprint'. *Mutat Res* 2000; **452**: 179-187

20 **Merk O**, Reiser K, Speit G. Analysis of chromate-induced DNA-protein crosslinks with the comet assay. *Mutat Res* 2000; **471**: 71-80

21 **Guetens G,** De Boeck G, Highley M, van Oosterom AT, de Bruijn EA. Oxidative DNA damage: biological significance and methods of analysis. *Crit Rev Clin Lab Sci* 2002; **39**: 331-457

22 **Godard T**, Deslandes E, Sichel F, Poul JM, Gauduchon P. Detection of topoisomerase inhibitor-induced DNA strand breaks and apoptosis by the alkaline comet assay. *Mutat Res* 2002; **520**: 47-56

23 **Heng Z**, Li R, Zhang Z. Distinguishing apoptotic cells from DNA strand-broken cells by comet assay. *Weisheng Yanjiu* 2001; **30**: 149-151

24 **Roser S**, Pool-Zobel BL, Rechkemmer G. Contribution of apoptosis to responses in the comet assay. *Mutat Res* 2001; **497**: 169-175

25 **Ando K**. High LET radiobiology at NIRS-current status and future plan. *Phys Med* 2001; **17**(Suppl): 292-295

26 **Imamura M**, Murata T, Akagi K, Tanaka Y, Imamura M, Inoue K, Mizuma N, Kobayashi Y, Watanabe H, Hachiya M, Akashi M, Furusawa Y, Yamanaka H, Takahashi S, Nakano T, Nagaoka S, Ohnishi T, Obiya Y, Harada K. Relationship between LET and

RBE values for Escherichia coli determined using carbon ion beams from the TIARA cyclotron and HIMAC synchrotron. *J Gen Appl Microbiol* 1997; **43**: 175-177

27 **Sutherland BM,** Bennett PV, Schenk H, Sidorkina O, Laval J, Trunk J, Monteleone D, Sutherland J. Clustered DNA damages induced by high and low LET radiation, including heavy ions. *Phys Med* 2001; **17**(Suppl): 202-204

28 **Goodwin EH**, Blakely EA. Heavy ion-induced chromosomal damage and repair. *Adv Space Res* 1992; **12**: 81-89

29 **Blakely EA**. New measurements for hadrontherapy and space radiation: biology. *Phys Med* 2001; **17**(Suppl): 50-58

30 **Suzuki M**, Kase Y, Yamaguchi H, Kanai T, Ando K. Relative biological effectiveness for cell-killing effect on various human cell lines irradiated with heavy-ion medical accelerator in Chiba (HIMAC) carbon-ion beams. *Int Radiat Oncol Biol Phys* 2000; **48**: 241-250

31 **Katz R**, Cucinotta FA. Tracks to therapy. *Radiat Meas* 1999; **31**: 379-388

32 **Kraxenberger F,** Weber KJ, Friedl AA, Eckardt-Schupp F, Flentje M, Quicken P, Kellerer AM. DNA double-strand breaks in mammalian cells exposed to gamma rays and very heavy ions. Fragment-size distributions determined by pulsed-field gel electrophoresis. *Radiat Environ Biophys* 1998; **37**: 107-115

33 **Edwards AA**. RBE of radiations in space and the implications for space travel. *Phys Med* 2001; **17**(Suppl)**:** 147-152

34 **Rydberg B**, Lobrich M, Cooper PK. Repair of clustered DNA damage caused by high LET radiation in human fibroblasts. *Phys Med* 1998; **14**(Suppl): 24-28

35 **Belli M**. An overview of recent charged-particle radiation biology in Italy. *Phys Med* 2001; **17**(Suppl): 278-282

Edited by Zhao P, Zhu LH and Wang XL

P.O.Box 2345, Beijing 100023,China
Fax: +86-10-85381893
E-mail: wjg@wjgnet.com www.wjgnet.com

World J Gastroenterol 2003;9(7):1455-1459
World Journal of Gastroenterology
 ISSN 1007-9327

• LIVER CANCER •

Preparation and characterization of polyclonal antibodies against ARL-1 protein

Jun-Fei Jin, Liu-Di Yuan, Li Liu, Zhu-Jiang Zhao, Wei Xie

Jun-Fei Jin, Liu-Di Yuan, Li Liu, Zhu-Jiang Zhao, Wei Xie, Genetics Research Center, Medical School, Southeast University, Nanjing 210009, Jiangsu Province, China
Supported by Health Department Grant of Jiang Su Province (H9925) and National Award for Excellent Research and Teaching from the Ministry of Education (2001/182)
Correspondence to: Dr. Wei Xie, Genetics Research Center, Medical School, Southeast University, Nanjing 210009, Jiangsu Province, China. wei.xie@seu.edu.cn
Telephone: +86-25-3220761 **Fax:** +86-25-3220761
Received: 2002-11-19 **Accepted:** 2002-12-18

Abstract

AIM: To prepare and characterize polyclonal antibodies against aldose reductase-like (ARL-1) protein.

METHODS: ARL-1 gene was inserted into the *E. coli* expression vector pGEX-4T-1$(His)_6$C and vector pQE-30. Recombinant ARL-1 proteins named ARL-$(His)_6$ and ARL-GST were expressed. They were purified by affinity chromatography. Sera from domestic rabbits immunized with ARL-$(His)_6$ were purified by CNBr-activated sepharose 4B coupled ARL-GST. Polyclonal antibodies were detected by Western blotting.

RESULTS: Recombinant proteins of ARL-$(His)_6$ with molecular weight of 35.7 KD and ARL-GST with molecular weight of 60.8 KD were highly expressed. The expression levels of ARL-GST and ARL-$(His)_6$ were 15.1 % and 27.7 % among total bacteria proteins, respectively. They were soluble, predominantly in supernatant. After purification by non-denatured way, SDS-PAGE showed one band. In the course of polyclonal antibodies purification, only one elution peak could be seen. Western blotting showed positive signals in the two purified proteins and the bacteria transformed with pGEX-4T-1$(His)_6$C-ARL and pQE-30-ARL individually.

CONCLUSION: Polyclonal antibodies are purified and highly specific against ARL-1 protein. ARL-GST and ARL-$(His)_6$ are highly expressed and purified.

Jin JF, Yuan LD, Liu L, Zhao ZJ, Xie W. Preparation and characterization of polyclonal antibodies against ARL-1 protein. *World J Gastroenterol* 2003; 9(7): 1455-1459
http://www.wjgnet.com/1007-9327/9/1455.asp

INTRODUCTION

Aldose reductase (AR) is a NADPH-dependent enzyme that is involved in diabetic complications[1-17]. Some reports showed that AR was induced in rat hepatoma, suggesting that it may be essential for detoxifying harmful metabolites produced by fast growing cancer cells[18-27]. Partial sequence determination of a protein induced in rat hepatoma called Spot 17 showed that it was highly homologous to the rat AR[28,29]. Cao *et al*.[22] found about 29 % of liver cancers over-expressed AR. Moreover, they identified a novel human protein that was highly homologous to AR, then submitted it to GenBank™ (HARL U37100). This protein, known as ARL-1, consists of 316 amino acids, the same size as AR, and its amino acid sequence is 71 % identical to that of AR. About 54 % of hepatocellular carcinoma (HCC) over-express ARL-1 gene. These suggest ARL-1 might be related to liver cancers.

ARL-1 is a novel gene, its function and exact relationship with liver cancers are unclear. In order to clarify the role of ARL-1 in HCC, two recombinant proteins of ARL-$(His)_6$ and ARL-GST were expressed, and highly specific polyclonal antibodies against ARL-1 protein were prepared.

MATERIALS AND METHODS

Restrictive endonuclease and T4 DNA polymerase enzymes were purchased from TaKaRa Biotech Corp. Glutathione sepharose 4B, CNBr-activated sepharose 4B and pGEX-4T-1 $(His)_6$C were obtained from Pharmacia Biotech. Rainbow markers and mid-range protein molecular weight markers were obtained from Amersham Pharmacia Biotech and Promega, respectively. PVDF membrane was from Schleicher & Schüll. T4 DNA ligase and GeneRuler™ 100 bp DNA ladder plus were products of MBI Fermentas. TALON^R metal affinity resin was obtained from Clontech. Freund' s adjuvant incomplete and Freund' s adjuvant complete were purchased from Sigma. *E.coli* strains were from Stratagene. Horseradish peroxidase (HRP)-conjugated anti-rabbit secondary antibody was from New England Biolabs Inc.

The following primers used in this study were made by HaoJia Corp: cg gaa ttc atg gcc acg ttt gtg gag c, cg ctc gag tca ata ttc tgc atc gaa ggg according to GenBank™ (accession number HARLU37100).

RT-PCR to subclone cDNA of ARL-1

According to the reference[22], cDNA of ARL-1 was obtained by RT-PCR (data not shown).

Expression of ARL-1 in E. coli

ARL-1 polymerase chain reaction-amplified products were inserted into the *E. coli* expression vector pGEX-4T-1$(His)_6$C, and their proteins would be translated in-frame from the vector' s start codon. The plasmid DNA was then transformed into bacteria host BL21. Induction of expression of ARL-1 inserts and purification of the recombinant proteins named ARL-GST were done according to the manufacturer' s manual. Briefly, bacteria growing to A_{600}=0.4 were induced by 0.05 mM isopropyl-1-thio-β-D-galactopyranoside at 30 ℃ overnight. Cells were harvested and lysed by sonication. After centrifugation to remove debris, the supernatant was mixed with a 50 % slurry of glutathione sepharose 4B, which bound to the glutathione S-transferase (GST) at the amino terminus of the recombinant protein. The slurry was then loaded onto a column and eluted with 5 bed volumes of elution buffer (10 mM reduced glutathione in 50 mM Tris-HCL, pH 8.0). Fractions of 500 μL were collected, and samples from the column were analyzed in 15 % SDS-polyacrylamide gel electrophoresis. Fractions containing the recombinant protein ARL-GST were stored at -20 ℃.

We subcloned ARL-1 gene into another *E. coli* expression vector pQE-30 (Qiagen), expressed another recombinant protein named ARL-$(His)_6$. According to the user manual, ARL-$(His)_6$ was purified with TALON^R metal affinity resin whose cobaltions bound to the 6-histidine residues at the amino terminus of the recombinant protein. Briefly, TALON^R metal affinity resin was saturated with a bacterial polyhistidine-tagged GFPuv lysate in extraction buffer (pH 8.0). The resin was then washed twice with 5 mL of wash buffer (pH 7.0). At last, bound protein was eluted by washing three times with 1 mL elution buffer (pH 7.0), a sample of each eluate was analyzed by electrophoresis on a 15 % SDS-polyacrylamide gel to verify the purity of elution protein. The purified ARL-$(His)_6$ was stored at -20 ℃.

Preparation of polyclonal antibodies against ARL-1 protein

Domestic rabbits were injected with 0.4 mg recombinant protein ARL-$(His)_6$ with Freund' s complete adjuvant. Three weeks later, they were injected with 0.16 mg ARL-$(His)_6$ with Freund' s incomplete adjuvant, which was repeated four times at 2-week intervals. After a little serum was collected from rabbit ear and proved positive by double agar diffusion test, rabbit sera were taken by carotid intubation and stored in 0.1 % sodium azide at -20 ℃.

According to the manufacturer' s manual, polyclonal antibodies against ARL-1 protein were purified with CNBr-activated sepharose 4B. Firstly, rabbit sera were filtered through a 0.22 μM filter and diluted one to four times with phosphate-buffered saline (PBS, pH 7.4). Secondly, the gel was prepared with 1mM HCL. The purified recombinant protein ARL-GST was then coupled with the prepared gel in coupling buffer (0.1M $NaHCO_3$, pH 8.3, containing 0.5M NaCL). Finally, the prepared rabbit sera were mixed with the sepharose coupled ARL-GST in a stopped vessel. The mixture was rotated end-over-end overnight at 4 ℃ and subsequently stood at room temperature for hours. The gel was washed with 1×PBS (pH 7.4), 2M NaCL in 1×PBS (pH 7.4) and 1×PBS (pH 4.5) till the OD_{280} of washed solution was zero, respectively. At last, it was eluted with 0.1M glycine (pH 2.8). The polyclonal antibodies were collected in 0.05 mM Tris-base (pH 9.5) and stored in 0.1 % sodium azide at -20 ℃.

Western blotting

All plasmids including pGEX-4T-1(His)$_6$C-ARL, pGEX, pQE-30-ARL and pET-CTF that encoded protein ARL-GST, GST, ARL-$(His)_6$ and CTF-$(His)_6$, were transformed to BL21, respectively. After bacteria grew to A_{600}=0.4, they were induced by 0.05 mM isopropyl-1-thio-β-D-galactopyranoside at 37 ℃ for 3 h. A 1/4 volume of SDS sample buffer containing Tris-HCl 0.33 mol· L^{-1}, 10 % SDS (w/v), 40 % glycerol (v/v), and 0.4 % bromophenol blue was added to cell lysates above and purified ARL-$(His)_6$ and ARL-GST. After being boiled for 5-10 min, 10 μg protein was electrophoresed on 15 % SDS-polyacrylamide gel. The protein was transferred to PVDF membrane, which was then blocked for 1 h at room temperature with 5 % BSA in TBST (100 mmol/L Tris-HCl and 0.9 % NaCl containing 0.05 % Tween-20). The blots were incubated with the primary polyclonal antibodies against ARL-1 protein (1:2 000 in TBST) and subsequently with HRP-labeled second antibody (1:5 000 in TBST) at room temperature for 1 h, respectively. At last, immunoreactive signals were visualized by DAB in 0.03% H_2O_2.

RESULTS

Construction of pGEX-4T-1(His)$_6$C-ARL and pQE-30-ARL

The recombinant plasmids were identified by restrictive endonuclease and/or polymerase chain reaction. All products of pGEX-4T-1(His)$_6$C-ARL amplified by polymerase chain reaction and digested by *EcoR*I only or *EcoR*I and *Xho*I in combination, underwent 1.5 % agarose electrophoresis. The expected 950 bp could be seen, which was ARL-1 gene (Figure 1). In the same way, pQE-30-ARL was identified by restrictive endonuclease. All fragments were expected including 4.5kb fragment of pQE-30-ARL which was digested by *HindIII* alone, 0.7kb and 3.8kb fragments of pQE-30-ARL digested by *BamH*I only, and 3.4kb, 0.7kb and 0. 3kb fragments of pQE-30-ARL digested by *BamH*I and *HindIII* in combination (Figure 2).

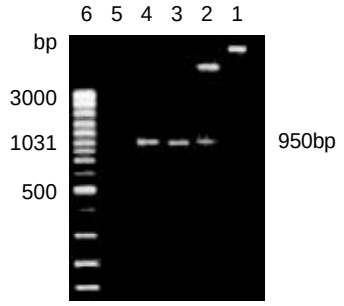

Figure 1 Recombinant plasmid pGEX-4T-1(His)$_6$C-ARL was identified by restrictive endonuclease and polymerase chain reaction (1.5 % agarose electrophoresis). Lane 1: The recombinant plasmid pGEX-4T-1(His)$_6$C-ARL digested by *EcoR*I only, about 5.9 kb fragment could be seen; Lane 2: The recombinant plasmid pGEX-4T-1(His)$_6$C-ARL digested by *EcoR*I and XhoI, two fragments of 5.0 kb and 950 bp could be seen; Lane 3: pGEX-4T-1(His)$_6$C-ARL being template, 950 bp was amplified by polymerase chain reaction; Lane 4: positive control of PCR; Lane 5: negative control of PCR; Lane 6: GeneRuler™ 100 bp DNA ladder plus.

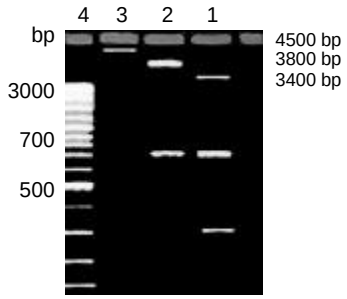

Figure 2 Recombinant plasmid pQE-30-ARL was identified by restrictive endonuclease (1.5 % agarose electrophoresis). Lane 1: 3.4 kb and 0.7 kb and 0.3 kb fragments of pQE-30-ARL digested by *BamH*I and *HindIII* together; Lane 2: 0.7 kb and 3.8 kb fragments of pQE-30-ARL digested by *BamH*I only; Lane 3: 4.5 kb fragment of pQE-30-ARL digested by *HindIII* alone; Lane 4: GeneRuler™ 100 bp DNA ladder plus.

Expression of recombinant proteins ARL-GST and ARL-$(His)_6$

The transformed pGEX-4T-1(His)$_6$C-ARL BL21 induced by 0.05 mM isopropyl-1-thio-β-D-galactopyranoside could express the protein with molecular weight of 60.8 KD, which was recombinant protein ARL-GST. Its expression level was 15.1 % of total bacteria proteins. Under the same conditions, the transformed pQE-30-ARL BL21 expressed recombinant protein ARL-$(His)_6$ with molecular weight of 35.7 KD. Among total bacteria proteins, ARL-$(His)_6$ expression level was 27.7 %. Two recombinant proteins were purified by non-denatured method because they were soluble, predominantly in supernatant. After purification, only one band could be seen,

indicating that ARL-GST and ARL-$(His)_6$ were highly purified (Figures 3 and 4).

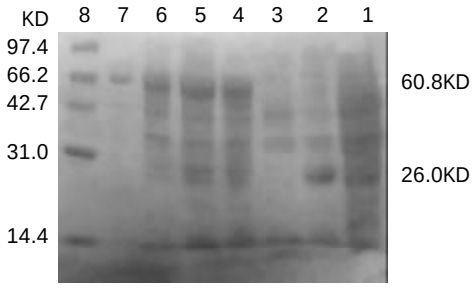

Figure 3 The transformed pGEX-4T-1$(His)_6$C-ARL BL21 induced by 0.05 mM isopropyl-1-thio-β-D-galactopyranoside. Lane 1: BL21 transformed with pGEX-4T-1$(His)_6$C, no IPTG induced; Lane 2: BL21 transformed with pGEX-4T-1$(His)_6$C, IPTG induced, GST (26KD) was expressed; Lane 3: BL21 transformed with pGEX-4T-1$(His)_6$C-ARL, no IPTG induced; Lane 4: BL21 transformed with pGEX-4T-1$(His)_6$ C-ARL, IPTG induced, recombinant protein ARL-GST (about 60.8 KD) was expressed; Lane 5: supernatant; Lane 6: pellet; Lane 7: purified ARL-GST; Lane 8: mid-range protein molecular weight markers.

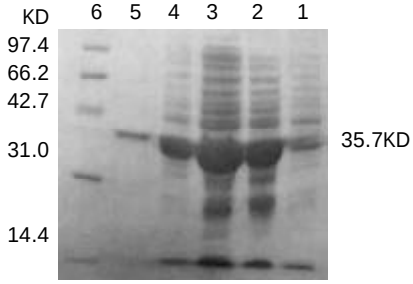

Figure 4 The transformed pQE-30-ARL BL21 induced by 0.05 mM isopropyl-1-thio-β-D-galactopyranoside. Lane 1: BL21 transformed with pQE-30-ARL, no IPTG induced; Lane 2: BL21 transformed with pQE-30-ARL, IPTG induced, ARL-$(His)_6$ (35.7KD) could express; Lane 3: supernatant; Lane 4: pellet; Lane 5: purified ARL-$(His)_6$; Lane 6: mid-range protein molecular weight markers.

Preparation of polyclonal antibodies against ARL-1 protein

Purification of polyclonal antibodies against ARL-1 protein: The rabbit sera immunized with ARL-$(His)_6$ were purified by CNBr-activated sepharose 4B coupled ARL-GST. After mixed with sera, washed with solution as described above, the gel was eluted with 0.1 M glycine (pH 2.8), only one elution peak could be seen in the elution curve (Figure 5), suggesting that polyclonal antibodies against ARL-1 protein were highly purified.

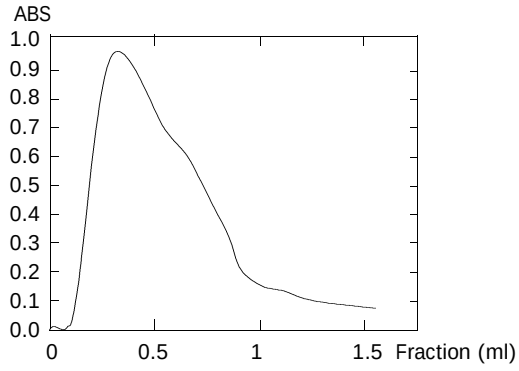

Figure 5 The gel eluted with 0.1 M glycine (pH 2.8).

Specification of polyclonal antibodies against ARL-1 protein: Proteins of all bacteria described were tested by Western blotting using polyclonal antibodies against ARL-1. Figure 6 displays that positive signals could be seen in the two purified proteins and the bacteria transformed with pGEX-4T-1$(His)_6$C-ARL and pQE-30-ARL individually.

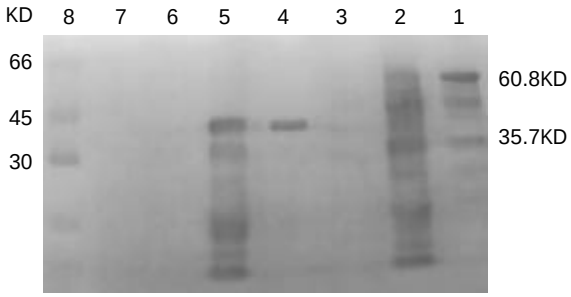

Figure 6 Proteins of all bacteria described were tested by Western blotting using polyclonal antibodies against ARL-1. Lane 1: purified ARL-GST; Lane 2: BL21 transformed with pGEX-4T-1$(His)_6$C-ARL; Lane 3: BL21 transformed with pGEX-4T-1$(His)_6$C; Lane 4: purified ARL-$(His)_6$; Lane 5: BL21 transformed with pQE-30-ARL; Lane 6: BL21 transformed with pET-CTF; Lane 7: BL21; Lane 8: Rainbow markers.

DISCUSSION

The cDNA of ARL-1 gene was cloned and identified by Cao *et al*. The amino acid sequence of this protein called ARL-1 was 71 % identical to that of AR. It is more homologous to a group of AR-like proteins. Its amino acid sequence was 80 %, 82 %, 83 %, and 94 % identical to that of the mouse vas deferens protein (MVDP), the mouse fibroblast growth factor-regulated protein (FR-1), the Chinese hamster ovary (CHO) reductase, and Spot 17 in rat hepatoma, respectively[22].

ARL-1 is a new member of AKR1B group of aldoketo reductases including AR, MVDP, FR-1, CHO reductase, Spot 17, etc. The gene expression spectrum is not the same. MVDP gene was primarily expressed in the vas deferens and the adrenal gland[30-37]. AR, was different. In adults, AR message was most abundant in the prostate, testis, skeletal muscle, and the heart. Substantial amounts were found in the ovary, small intestines, colon, thymus, spleen, kidney, and the placenta. Lower levels were found in the brain, lung, leukocytes, and the pancreas. Of the four fetal tissues tested, AR mRNA was most abundant in the kidneys, a substantial amount was found in the brain, and a low level in the lung and liver[38,39]. FR-1 was expressed quite strongly in the small intestines, and it was expressed in testis, ovary, brain, heart, liver, kidney, and muscle, but FR-1 expression has not been screened in urinary bladder and jejunum[40-44]. CHO reductase mRNA was quite abundant in the urinary bladder and the jejunum, this gene was also expressed in the testis and the ovary. However, CHO reductase mRNA was not detectable in brain, heart, liver, kidney, and muscle[45-47]. ARL-1 was not expressed in many tissues. Its message was most abundant in the small intestines and colon, and a low level of its mRNA was found in the liver, thymus, prostate, testis, and skeletal muscle. No ARL-1 mRNA was detected in the four fetal tissues tested including the kidney, brain, lung and liver. Moreover, ARL-1 mRNA was not present in human vas deferens. Although many functions of all these AR-like genes are not known, different expression spectrums indicate that their physiological functions are quite different[22].

Not only 71 % of ARL-1 amino acid sequence was identical to that of AR, but also all of the key amino acids being responsible for AR' s enzymatic activities were conserved in

this protein. They included Ser[159], Asn[160], Gln[183], and Lys[262] for cofactor NADPH binding, Tyr[48] and His[110] as potential hydrogen donors, and active site residues Lys[77], Tyr[209], and Cys[298]. The enzymatic activity of ARL-1 was similar to that of the well-characterized human AR. In terms of pH optimum, salt requirement, and kinetics in reducing some substrates, these two proteins were different. For example, the activity of ARL-1 was not affected by 0.3 M sulfate ion, which was the optimum concentration for stimulating AR activity[22]. In the present project, two recombinant ARL-1 proteins were expressed and highly purified, polyclonal antibodies against ARL-1 were prepared and characterized. Polyclonal antibodies prepared by us were only against ARL-1 protein, the yeast and fly tissues were detected by Western blotting using our antibodies, no signals were visualized (data not shown), suggesting that these polyclonal antibodies were highly specific. Other characters of ARL-1 protein should be studied, as well as the relation between ARL-1 and human diseases.

AR is thought to be involved in diabetic complications such as cataract, retinopathy, neuropathy, and nephropathy. It is not clear if ARL-1 also contributes to these diabetic complications. So two recombinant ARL-1 proteins and polyclonal antibodies against ARL-1 prepared in our research would help determine the relationship between ARL-1 and diabetes. AR and an AR-like protein called Spot 17 were induced in rat hepatomas, suggesting that these proteins may be needed to detoxify methylglyoxal or other metabolites generated by fast growing cancer cells. About 29 % of individual human HCCs over-expressed AR and 54 % of them over-expressed ARL-1. The deduced protein sequence of ARL-1 was 94 % identical to that of Spot 17, indicating that it is most likely the human homologue of that protein[22]. In our studies, ARL-1 protein was detected in 94.4 % (17/18) liver cancer tissues, but only in 82.4 % (14/17) surrounding nontumorous tissues. Moreover, in all normal liver tissues (5 cases), ARL-1 protein was negative, ARL-1 expression in all detected liver cancer tissues was up-regulated (data not shown). All these studies suggest that ARL-1 is closely related to liver cancers.

In conclusion, two recombinant ARL-1 proteins and polyclonal antibodies against ARL-1 protein were prepared. As a basic research, these would help us identify the function of ARL-1, the exact relationship between ARL-1 and liver cancers. The life expectancy of HCC patients is hard to predict because of the high possibility of postoperative recurrence. Many factors, such as patients' general conditions, macroscopic tumor morphology, as well as tumor histopathological features, have been proven of prognostic significance[48-58]. With the progress in ARL-1 studies, the early diagnosis rate and the therapy level of liver cancers might be elevated, which will improve the prognosis of patients with liver cancer in the future.

REFERENCES

1 **Fanelli A**, Hadjadj S, Gallois Y, Fumeron F, Betoule D, Grandchamp B, Marre M. Polymorphism of aldose reductase gene and susceptibility to retinopathy and nephropathy in Caucasians with type 1 diabetes. *Arch Mal Coeur Vaiss* 2002; **95:** 701-708

2 **Cisarik-Fredenburg P.** Discoveries in research on diabetic keratopathy. *Optometry* 2001; **72:** 691-704

3 **Chandra D,** Jackson EB, Ramana KV, Kelley R, Srivastava SK, Bhatnagar A. Nitric oxide prevents aldose reductase activation and sorbitol accumulation during diabetes. *Diabetes* 2002; **51:** 3095-3101

4 **Naya Y,** Soh J, Ochiai A, Mizutani Y, Kawauchi A, Fujito A, Ushijima S, Ono T, Iwamoto N, Aoki T, Imada N, Nakamura N, Yabe-Nishimura C, Miki T. Erythrocyte aldose reductase correlates with erectile dysfunction in diabetic patients. *Int J Impot Res* 2002; **14:** 213-216

5 **Jung SH,** Lee YS, Lee S, Lim SS, Kim YS, Shin KH. Isoflavonoids from the rhizomes of Belamcanda chinensis and their effects on aldose reductase and sorbitol accumulation in streptozotocin induced diabetic rat tissues. *Arch Pharm Res* 2002; **25:** 306-312

6 **Kryvko IuIa,** Kozyts'kyi ZIa, Serhiienko OO, Kuchmerovs'ka TM, Velykyi MM. Diabetic neuropathies. Metabolism of sorbitol in sciatic nerve tissue in streptozotocin diabetes. *Ukr Biokhim Zh* 2001; **73:** 69-74

7 **Chang KC,** Paek KS, Kim HJ, Lee YS, Yabe-Nishimura C, Seo HG. Substrate-induced up-regulation of aldose reductase by methylglyoxal, a reactive oxoaldehyde elevated in diabetes. *Mol Pharmacol* 2002; **61:** 1184-1191

8 **Aukunuru JV,** Sunkara G, Ayalasomayajula SP, DeRuiter J, Clark RC, Kompella UB. A biodegradable injectable implant sustains systemic and ocular delivery of an aldose reductase inhibitor and ameliorates biochemical changes in a galactose-fed rat model for diabetic complications. *Pharm Res* 2002; **19:** 278-285

9 **Park HK,** Ahn CW, Lee GT, Kim SJ, Song YD, Lim SK, Kim KR, Huh KB, Lee HC. (AC)(n) polymorphism of aldose reductase gene and diabetic microvascular complications in type 2 diabetes mellitus. *Diabetes Res Clin Pract* 2002; **55:** 151-157

10 **Kaul CL,** Ramarao P. The role of aldose reductase inhibitors in diabetic complications: recent trends. *Methods Find Exp Clin Pharmacol* 2001; **23:** 465-475

11 **Colciago A,** Negri-Cesi P, Celotti F. Pathogenesis of diabetic neuropathy-do hyperglycemia and aldose reductase inhibitors affect neuroactive steroid formation in the rat sciatic nerves? *Exp Clin Endocrinol Diabetes* 2002; **110:** 22-26

12 **Hansen SH.** The role of taurine in diabetes and the development of diabetic complications. *Diabetes Metab Res Rev* 2001; **17:** 330-346

13 **Raptis AE,** Viberti G. Pathogenesis of diabetic nephropathy. *Exp Clin Endocrinol Diabetes* 2001; **109**(Suppl)**:** 424-437

14 **Hotta N,** Toyota T, Matsuoka K, Shigeta Y, Kikkawa R, Kaneko T, Takahashi A, Sugimura K, Koike Y, Ishii J, Sakamoto N. Clinical efficacy of fidarestat, a novel aldose reductase inhibitor, for diabetic peripheral neuropathy: a 52-week multicenter placebo-controlled double-blind parallel group study. *Diabetes Care* 2001; **24:** 1776-1782

15 **Rippin JD,** Patel A, Bain SC. Genetics of diabetic nephropathy. *Best Pract Res Clin Endocrinol Metab* 2001; **15:** 345-358

16 **Kubo E,** Maekawa K, Tanimoto T, Fujisawa S, Akagi Y. Biochemical and morphological changes during development of sugar cataract in otsuka long-evans tokushima fatty (OLETF) rat. *Exp Eye Res* 2001; **73:** 375-381

17 **Wallner EI,** Wada J, Tramonti G, Lin S, Srivastava SK, Kanwar YS. Relevance of aldo-keto reductase family members to the pathobiology of diabetic nephropathy and renal development. *Ren Fail* 2001; **23:** 311-320

18 **Zeindl-Eberhart E,** Klugbauer S, Dimitrijevic N, Jungblut PR, Lamer S, Rabes HM. Proteome analysis of rat hepatomas: carcinogen-dependent tumor-associated protein variants. *Electrophoresis* 2001; **22:** 3009-3018

19 **Lee KW,** Ko BC, Jiang Z, Cao D, Chung SS. Overexpression of aldose reductase in liver cancers may contribute to drug resistance. *Anticancer Drugs* 2001; **12:** 129-132

20 **Kelly VP,** Ireland LS, Ellis EM, Hayes JD. Purification from rat liver of a novel constitutively expressed member of the aldo-keto reductase 7 family that is widely distributed in extrahepatic tissues. *Biochem J* 2000; **348:** 389-400

21 **Muzio G,** Salvo RA, Taniguchi N, Maggiora M, Canuto RA. 4-Hydroxynonenal metabolism by aldo/keto reductase in hepatoma cells. *Adv Exp Med Biol* 1999; **463:** 445-452

22 **Cao D,** Fan ST, Chung SS. Identification and characterization of a novel human aldose reductase-like gene. *J Biol Chem* 1998; **273:** 11429-11435

23 **Scuric Z,** Stain SC, Anderson WF, Hwang JJ. New member of aldose reductase family proteins overexpressed in human hepatocellular carcinoma. *Hepatology* 1998; **27:** 943-950

24 **Zeindl-Eberhart E,** Jungblut PR, Otto A, Kerler R, Rabes HM. Further characterization of a rat hepatoma-derived aldose-reductase-like protein-organ distribution and modulation *in vitro*. *Eur J Biochem* 1997; **247:** 792-800

25 **Takahashi M,** Hoshi A, Fujii J, Miyoshi E, Kasahara T, Suzuki K,

Aozasa K, Taniguchi N. Induction of aldose reductase gene expression in LEC rats during the development of the hereditary hepatitis and hepatoma. *Jpn J Cancer Res* 1996; **87:** 337-341

26 **Takahashi M,** Fujii J, Miyoshi E, Hoshi A, Taniguchi N. Elevation of aldose reductase gene expression in rat primary hepatoma and hepatoma cell lines: implication in detoxification of cytotoxic aldehydes. *Int J Cancer* 1995; **62:** 749-754

27 **Canuto RA,** Ferro M, Muzio G, Bassi AM, Leonarduzzi G, Maggiora M, Adamo D, Poli G, Lindahl R. Role of aldehyde metabolizing enzymes in mediating effects of aldehyde products of lipid peroxidation in liver cells. *Carcinogenesis* 1994; **15:** 1359-1364

28 **Zeindl-Eberhart E,** Jungblut PR, Otto A, Rabes HM. Identification of tumor-associated protein variants during rat hepatocarcinogenesis. Aldose reductase. *J Biol Chem* 1994; **269:** 14589-14594

29 **Zeindl-Eberhart E,** Jungblut P, Rabes HM. Expression of tumor-associated protein variants in chemically induced rat hepatomas and transformed rat liver cell lines determined by two-dimensional electrophoresis. *Electrophoresis* 1994; **15:** 372-381

30 **Martinez A,** Aigueperse C, Val P, Dussault M, Tournaire C, Berger M, Veyssiere G, Jean C, Lefrancois Martinez A. Physiological functions and hormonal regulation of mouse vas deferens protein (AKR1B7) in steroidogenic tissues. *Chem Biol Interact* 2001; **130-132:** 903-917

31 **Ho HT,** Jenkins NA, Copeland NG, Gilbert DJ, Winkles JA, Louie HW, Lee FK, Chung SS, Chung SK. Comparisons of genomic structures and chromosomal locations of the mouse aldose reductase and aldose reductase-like genes. *Eur J Biochem* 1999; **259:** 726-730

32 **Fabre S,** Darne C, Veyssiere G, Jean C. Protein kinase C pathway potentiates androgen-mediated gene expression of the mouse vas deferens specific aldose reductase-like protein (MVDP). *Mol Cell Endocrinol* 1996; **124:** 79-86

33 **Lau ET,** Cao D, Lin C, Chung SK, Chung SS. Tissue-specific expression of two aldose reductase-like genes in mice: abundant expression of mouse vas deferens protein and fibroblast growth factor-regulated protein in the adrenal gland. *Biochem J* 1995; **312:** 609-615

34 **Gui T,** Tanimoto T, Kokai Y, Nishimura C. Presence of a closely related subgroup in the aldo-ketoreductase family of the mouse. *Eur J Biochem* 1995; **227:** 448-453

35 **Fabre S,** Manin M, Pailhoux E, Veyssiere G, Jean C. Identification of a functional androgen response element in the promoter of the gene for the androgen-regulated aldose reductase-like protein specific to the mouse vas deferens. *J Biol Chem* 1994; **269:** 5857-5864

36 **Pailhoux E,** Martinez A, Veyssiere G, Tournaire C, Berger M, Jean C. Characterization of cDNA and of the gene corresponding to androgen-dependent protein of the vas deferens in mice. *Ann Endocrinol (Paris)* 1991; **52:** 437-440

37 **Pailhoux EA,** Martinez A, Veyssiere GM, Jean CG. Androgen-dependent protein from mouse vas deferens. cDNA cloning and protein homology with the aldo-keto reductase superfamily. *J Biol Chem* 1990; **265:** 19932-19936

38 **Moczulski DK,** Scott L, Antonellis A, Rogus JJ, Rich SS, Warram JH, Krolewski AS. Aldose reductase gene polymorphisms and susceptibility to diabetic nephropathy in Type 1 diabetes mellitus. *Diabet Med* 2000; **17:** 111-118

39 **Bain SC,** Chowdhury TA. Genetics of diabetic nephropathy and microalbuminuria. *J R Soc Med* 2000; **93:** 62-66

40 **Glickman M,** Malek RL, Kwitek-Black AE, Jacob HJ, Lee NH. Molecular cloning, tissue-specific expression, and chromosomal localization of a novel nerve growth factor-regulated G-protein-coupled receptor, nrg-1. *Mol Cell Neurosci* 1999; **14:** 141-152

41 **Winkles JA.** Serum- and polypeptide growth factor-inducible gene expression in mouse fibroblasts. *Prog Nucleic Acid Res Mol Biol* 1998; **58:** 41-78

42 **Frank S,** Werner S. The human homologue of the yeast CHL1 gene is a novel keratinocyte growth factor-regulated gene. *J Biol Chem* 1996; **271:** 24337-24340

43 **De Boer WI,** Schuller AG, Vermey M, van der Kwast TH. Expression of growth factors and receptors during specific phases in regenerating urothelium after acute injury *in vivo*. *Am J Pathol* 1994; **145:** 1199-1207

44 **Quelle DE,** Ashmun RA, Shurtleff SA, Kato JY, Bar-Sagi D, Roussel MF, Sherr CJ. Overexpression of mouse D-type cyclins accelerates G1 phase in rodent fibroblasts. *Genes Dev* 1993; **7:** 1559-1571

45 **Kaneko M,** Carper D, Nishimura C, Millen J, Bock M, Hohman TC. Induction of aldose reductase expression in rat kidney mesangial cells and Chinese hamster ovary cells under hypertonic conditions. *Exp Cell Res* 1990; **188:** 135-140

46 **Li H,** Nobukuni Y, Gui T, Yabe-Nishimura C. Characterization of genomic regions directing the cell-specific expression of the mouse aldose reductase gene. *Biochem Biophys Res Commun* 1999; **255:** 759-764

47 **Ye Q,** Hyndman D, Li X, Flynn TG, Jia Z. Crystal structure of CHO reductase, a member of the aldo-keto reductase superfamily. *Proteins* 2000; **38:** 41-48

48 **Qin LX,**Tang ZY. The prognostic significance of clinical and pathological features in hepatocellular carcinoma. *World J Gastroenterol* 2002; **8:** 193-199

49 **Tang ZY.** Hepatocellular carcinoma-Cause, treatment and metastasis. *World J Gastroenterol* 2001; **7:** 445-454

50 **Wu MC,** Shen F. Progress in research of liver surgery in China. *World J Gastroenterol* 2000; **6:** 773-776

51 **Rabe C,** Pilz T, Klostermann C, Berna M, Schild HH, Sauerbruch T, Caselmann WH. Clinical characteristics and outcome of a cohort of 101 patients with hepatocellular carcinoma. *World J Gastroenterol* 2001; **7:** 208-215

52 **Yip D,** Findlay M, Boyer M, Tattersall MH. Hepatocellular carcinoma in central Sydney: a 10 year review of patients seen in a medical oncology department. *World J Gastroenterol* 1999; **5:** 483-487

53 **Sithinamsuwan P,** Piratvisuth T, Tanomkiat W, Apakupakul N, Tongyoo S. Review of 336 patients with hepatocellular carcinoma at Songklanagarind Hospital. *World J Gastroenterol* 2000; **6:** 339-343

54 **Niu Q,** Tang ZY, Ma ZC, Qin LX, Zhang LH. Serum vascular endothelial growth factor is a potential biomarker of metastatic recurrence after curative resection of hepatocellular carcinoma. *World J Gastroenterol* 2000; **6:** 565-568

55 **Jiang YF,** Yang ZH, Hu JQ. Recurrence or metastasis of HCC: predictors, early detection and experimental antiangiogenic therapy. *World J Gastroenterol* 2000; **6:** 61-65

56 **He P,** Tang ZY, Ye SL, Liu BB. Relationship between expression of α-fetoprotein messenger RNA and some clinical parameters of human hepatocellular carcinoma. *World J Gastroenterol* 1999; **5:** 111-115

57 **Parks RW,** Garden OJ. Liver resection for cancer. *World J Gastroenterol* 2001; **7:** 766-771

58 **Wu ZQ,** Fan J, Qiu SJ, Zhou J, Tang ZY. The value of postoperative hepatic regional chemotherapy in prevention of recurrence after radical resection of primary liver cancer. *World J Gastroenterol* 2000; **6:** 131-133

Edited by Ma JY

P.O.Box 2345, Beijing 100023,China
Fax: +86-10-85381893
E-mail: wjg@wjgnet.com www.wjgnet.com

World J Gastroenterol 2003;9(7):1460-1464
World Journal of Gastroenterology
 ISSN 1007-9327

• LIVER CANCER •

Characteristics and application of established luciferase hepatoma cell line that responds to dioxin-like chemicals

Zhi-Ren Zhang, Shun-Qing Xu, Xi Sun, Yong-Jun Xu, Xiao-Kun Cai, Zhi-Wei Liu, Xiang-Lin Tan, Yi-Kai Zhou, Jun-Yue Zhang, Hong Yan

Zhi-Ren Zhang, Shun-Qing Xu, Xi Sun, Yong-Jun Xu, Xiao-Kun Cai, Zhi-Wei Liu, Xiang-Lin Tan, Yi-Kai Zhou, Jun-Yue Zhang, Hong Yan, Institute of Environmental Medicine, Tongji Medical College, Huazhong University of Science and Technology, Wuhan, 430030, Hubei Province, China
Supported by the National Natural Science Foundation of China, No. 29877020 and 20107002
Correspondence to: Dr. Shun-Qing Xu, Institute of Environmental Medicine, Tongji Medical College, Huazhong University of Science and Technology, Wuhan, 430030, Hubei Province, China. shunqing@public.wh.hb.cn
Telephone: +86-27-83693417 **Fax:** +86-27-83657705
Received: 2002-01-28 **Accepted:** 2002-05-11

Abstract

AIM: To establish a luciferase reporter cell line that responds dioxin-like chemicals (DLCs) and on this basis to evaluate its characteristics and application in the determination of DLCs.

METHODS: A recombinant luciferase reporter plasmid was constructed by inserting dioxin-responsive element (DREs) and MMTV promoter segments into the pGL_3-promoter plasmid immediately upstream of the luciferase gene, which was structurally demonstrated by fragment mapping analysis in gel electrophoresis and transfected into the human hepatoma cell line $HepG_2$, both transiently and stably, to identify the inducible expression of luciferase by 2, 3, 7, 8-tetrachlorodibenzo-*p*-dioxin (TCDD). The time course, responsive period, sensitivity, structure-inducibility and dose-effect relationships of inducible luciferase expression to DLCs was dynamically observed in $HepG_2$ cells stably transfected by the recombinant vector ($HepG_2$-Luc) and compared with that assayed by ethoxyresorufin-*O*-deethylase (EROD) in non-transfected $HepG_2$ cells ($HepG_2$-wt).

RESULTS: The inducible luciferase expression of $HepG_2$-Luc cells was noted in a time-, dose-, and AhR-dependent manner, which peaked at 4 h and then decreased to a stable level at 14 h after TCDD treatment. The responsiveness of $HepG_2$-Luc cells to TCDD induction was decreased with culture time and became undetectable at 10th month of $HepG_2$-Luc cell formation. The fact that luciferase activity induced by 3, 3', 4, 4'-PCB in $HepG_2$-Luc cells was much less than that induced by TCDD suggests a structure-inducibility relationship existing among DLCs. Within the concentrations from 3.5×10^{-12} to 5×10^{-9} mol/L, significant correlations between TCDD doses and EROD activities were observed in both $HepG_2$-luc and $HepG_2$-wt cells. The correlation between TCDD doses from 1.1×10^{-13} to 1×10^{-8} mol/L and luciferase activities was also found to be significant in $HepG_2$-luc cells ($r=0.997$, $P<0.001$), but not in their $HepG_2$-wt counterparts. For the comparison of the enzyme responsiveness between cell lines to TCDD, the luciferase sensitivity and reproducibility in $HepG_2$-luc cells were both better than that of EROD in $HepG_2$-wt cells, the former was at 1.1×10^{-13} mol/L and 3.5×10^{-12} mol/L, and the coefficients of variation (CV) of the latter was 15-30 % and 22-38 %, respectively.

CONCLUSION: The luciferase expression of $HepG_2$-luc cells established in the present study could sensitively respond to the DLCs stimulation and might be a prospective tool for the determination of DLCs.

Zhang ZR, Xu SQ, Sun X, Xu YJ, Cai XK, Liu ZW, Tan XL, Zhuo YK, Zhang JY, Yan H. Characteristics and application of established luciferase hepatoma cell line that responds to dioxin-like chemicals. *World J Gastroenterol* 2003; 9(7): 1460-1464
http://www.wjgnet.com/1007-9327/9/1460.asp

INTRODUCTION

It has been well known in recent years that dioxin-like chemicals (DLCs) such as 2,3,7,8- tetrachlorodibenzo-*p*-dioxin (TCDD) can produce a wide variety of species- and tissue-specific toxic and biological effects, such as epidermal lesion, wasting syndrome, birth defect, hepatotoxicity, lethality, alteration in endocrine homeostasis, tumor promotion, myelotoxicity, immunotoxicity and induction of numerous enzymes (e.g. cytochrome P4501A1)[1-4]. Many of these responses are mediated by the cytosolic aryl hydrocarbon receptor (AhR) and modulated by the interaction of DLCs: AhR complex with its DNA recognition sequence [the dioxin-responsive element (DRE)][5-9]. Generally, the combination of DLCs with cytoplasmic AhR is the initial step of DLCs-triggered cell signaling pathway. After that, two molecules of hsp90 dissociate from DLCs: AhR complex, and the latter enters the nucleus to form a new complex with AhR nuclear translocator protein (ARNT), which further binds to the DRE, leading to the transcriptional activation of adjacent genes and toxic effects[10,11]. Therefore, AhR and its related signal pathway have been usually taken as the useful targets to be investigated for the determination of DLCs in different situations. Till now, the DLCs-responsive receptor assays have been established in mammalian cell lines[12] and in mice[13].

However, not all of these assays have been considered to be satisfactory yet. For example, the ethoxyresorufin-*O*-deethylase (EROD) induced as a common and rapid response to DLCs under DREs control has been widely used to evaluate the relatively toxicological potency of a complex mixture containing DLCs[14-16] except that higher concentrations appear when the enzyme activity is inhibited. Some detecting methods are time-consuming, expensive and inadequate to be used for screening and diagnosing dioxin and dioxin-like compounds in large numbers of samples[17-19]. Even if the chemical-activated luciferase expression (CALUX) bioassay method based on the pGL_2 vector[20] is to a certain extent lack of sensitivity and needs to be improved.

We therefore conducted the present study in an attempt to establish a more effective luciferase reporter cell line that responds to the alteration of DLCs concentrations and to evaluate its characteristics and applications in measurement of DLCs.

MATERIALS AND METHODS

Materials

Plasmids pHAV and pMcat were generously provided by Dr. James P. Whitlock Jr., Stanford University. Restriction endonuclease and other reagents used for molecular cloning were from Huamei Ltd. (China, Shanghai) or Promega Corporation. 2,3,7,8-TCDD and 3',4,4' - polychlorinated biphenyl (PCB) were purchased from Accustanfards Inc. (New Haven, CT). Dimethylsulphoxide (DMSO) was from BIB Corporation. Luciferase assay reagents came from Promega Corporation.

Construction of inducible luciferase expression vector

Plasmid pHAV containing DREs was cleaved with *HindIII*. Following purification by agarose gel electrophoresis, the smaller *Hin*d*III* fragment was further digested by *BamHI* and *EcoRV* to produce a 630-bp segment containing DREs, which was then ligased with *BglII* linkers and cleaved with *BglII* to create cohesive ends. To get the MMTV promoter, plasmid pMCat was cleaved with *Hin*d*III* and the smaller *Hin*d*III* fragment was then cleaved with *BglII* to produce cohesive 5' *BglII* and 3' *Hin*d*III* termini. The two segments containing DREs and MMTV promoter were connected with T_4 DNA ligase to form a 1 020 bp fragment with cohesive 5' *BglII* and 3' *Hin*d*III* termini, which was further subcloned into the *Bgl*II-*Hin*d*III* site immediately upstream of the luciferase gene in the pGL_3-promoter plasmid (Promega). As such, the luciferase' s expression was under the control of DREs. The recombinant vector was identified structurally with restriction endonuclease analysis.

Inducible expression of recombinant vector

$HepG_2$ cells were seeded in a 60 mm culture dish at a density of 3×10^5 cells in 5 ml of RPMI1640 supplemented with 10 % heat-inactivated fetal calf serum at 37 ℃ with saturated humidity and a 5 % (v/v) CO_2 atmosphere[21]. After cultured for 24 h, the cells were transiently or stably transfected by 15 μg of recombinant vector with calcium phosphate mediated method[22]. For transient transfection, the cells were allowed to grow for 48 h, followed by adding 0.5 % DMSO or 0.1-1 nmol/L TCDD dissolved in DMSO. After cultivated for another 24 h[22], cells were harvested to determine luciferase expression.

For the establishment of stable transfection, $HepG_2$ cells were cotransfected with the selective plasmid PTK-Hyg and the recombinant vector simultaneously. Following 24 h of cultivation in nonselective medium, the transfected cells were transferred into a selective medium containing hygromycin and cultured for 4 weeks when TCDD-induced luciferase expression was conducted. The clone with the largest ratio of inducible to constitutive expression of luciferase was selected for further study[23]. To identify the time course of inducible luciferase expression, the stably transfected cells ($HepG_2$-Luc) were cultured with exposure to 0.5 % DMSO or 1 nmol/L TCDD and the induced luciferase activities were determined at every 2 h up to 28 h post-exposure. For determination of the responsive period of luciferase induction, the $HepG_2$-Luc cells were treated with the same kinds of inducers for 24 h and their luciferase activity was assayed, which was performed at every month up to 12 months. The structure-inducibility and dose-effect relationships of different inducers that might represent their ability to bind AhR were also analyzed in $HepG_2$-Luc cells with the indicated concentrations of 3, 3' , 4, 4' -PCB, another member of DLCs, and TCDD.

Luciferase assay was performed by the routine procedures. Briefly, after removal of the culture medium, the incubated cells were washed twice with phosphate buffered saline (PBS) and lysed using luciferase lysis reagent for 15 min at room temperature. Following centrifugation, 20 μl of supernatant was added into 100 μl luciferase assay reagent, the resulting bioluminescence was quantified immediately with Lumate LB 9570 luminometer over 3 s. The concentration of the sample protein was determined with Bio-Rad method[24]. The luciferase activity was finally expressed as relative light unit (RLU) per microgram protein[21, 25].

Comparative study with EROD determination

EROD activity was employed as a variable to evaluate the effectiveness of $HepG_2$-luc cells in response to TCDD and to compare with luciferase. $HepG_2$ ($HepG_2$-wt) and $HepG_2$-luc cells were seeded in 6-well dishes at a density of 2×10^5 cells in 3 ml of medium and cultivated for 24 h, then they were exposed to the indicated concentrations of TCDD in DMSO and further incubated for 72 h. Following removal of the culture medium, the cells were washed twice with PBS and stored at -80 ℃. EROD activity was assayed using fluorescent method. The concentrations of sample protein were determined with Bio-Rad method[24]. EROD activity was finally expressed as pmol resorufin production per microgram protein per minute[26, 27].

Statistical analysis

Data values in the present study were presented as the mean for each independent determination of four replicates. The detection limit was expressed as the average value plus three times of standard deviations (SD). Coefficients of variation (CV) were calculated by SD/mean ×100 %. Correlation coefficients (r) were obtained using least-squares linear regression analysis.

RESULTS

Identification of inducible expression of recombinant vector

Structurally, segment analysis by restriction endonuclease digestion confirmed that the inserted fragment sequences containing DREs and MMTV promoter in the constructed plasmids were completely consistent with that of the theoretical calculations as shown in Figure 1.

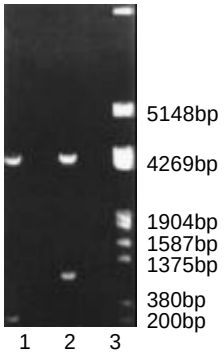

Figure 1 Fragment mapping analysis of recombinant plasmid digested with *Bgl*II and *Hin*dIII in gel electrophoresis. Lane 1: pGL_3 plasmid was cleaved into two fragments, which showed about 5 000 bp and 200 bp respectively. Lane 2: Recombinant plasmid was cut into a fragment of about 5 000 bp and the one of about 1 000 bp. Lane 3: DNA marker.

Inducible expression of luciferase by the recombinant plasmid was identified in transiently transfected $HepG_2$ cells, which produced a significantly higher induction of luciferase activity (80-fold, data not shown) compared with that of their non-transfected counterparts when exposed to TCDD. Dynamically, TCDD-induced luciferase activity in $HepG_2$-Luc cells peaked at 4 h and then decreased to a stable level at about

14 h after TCDD treatment (Figure 2). Responsiveness of $HepG_2$-Luc cells to the TCDD induction was decreased with culture time and became undetectable at 10th month of $HepG_2$-Luc cell formation (Figure 3), which indicats that the recombinant plasmid could not integrate stably with $HepG_2$ chromosome. The structure-inducibility relationship of different DLCs inducers was demonstrated by the fact that the luciferase activity induced by 3, 3', 4, 4' -PCB was much less than that induced by TCDD and a dose-dependent increase of luciferase activity was evoked by both of the DLCs inducers as shown in Figure 4.

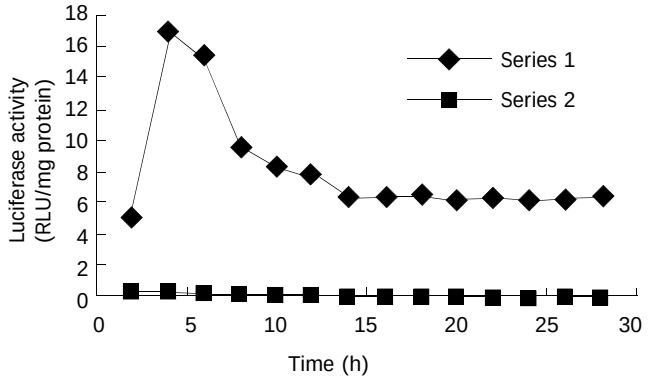

Figure 2 The time course of luciferase activities induced by TCDD and DMSO in stably transfected cells. The TCDD-induced luciferase activity in $HepG_2$-Luc cells peaked at about 4 h, and then decreased to a stable level at about 14 h after TCDD treatment.

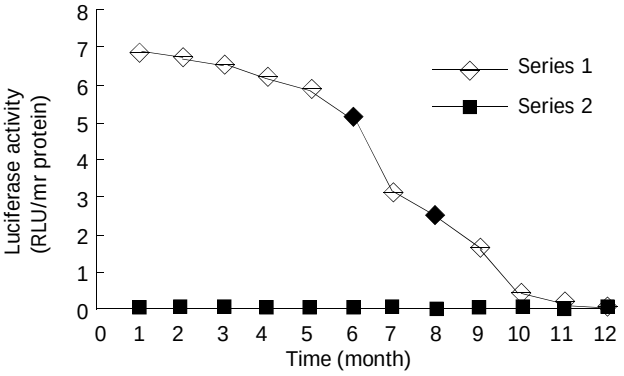

Figure 3 Responsive period of $HepG_2$-Luc cells to TCDD induction. The responsiveness of $HepG_2$-Luc cells to TCDD induction was decreased with culture time and became undetectable at about 10th month.

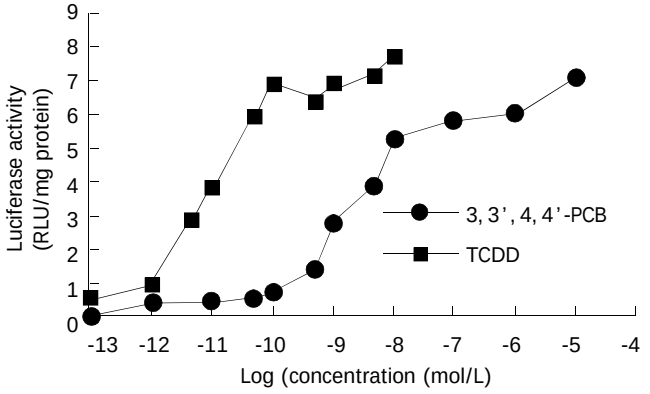

Figure 4 Comparison of luciferase activity induced by TCDD and 3, 3', 4, 4'-PCB in $HepG_2$-Luc cells. The luciferase activity induced by indicated concentrations of 3, 3', 4, 4'-PCB was much less than that induced by TCDD.

Comparative study

Within concentrations from 3.5×10^{-12} to 5×10^{-9} mol/L, significant correlations between TCDD doses and EROD activities were observed in both $HepG_2$-luc and $HepG_2$-wt cells. The correlation between TCDD doses from 1.1×10^{-13} to 1×10^{-8} mol/L and luciferase activities was also found to be significant in $HepG_2$-luc cells (r=0.997, P<0.001), but not in their $HepG_2$-wt counterparts. For comparison of the enzyme responsiveness between cell lines to TCDD, the luciferase sensitivity and reproducibility in $HepG_2$-luc cells were better than those of EROD in $HepG_2$-wt cells, which were 1.1×10^{-13} mol/L and 3.5×10^{-12} mol/L, whose CV was 15-30 % and 22-38 % (data not shown), respectively.

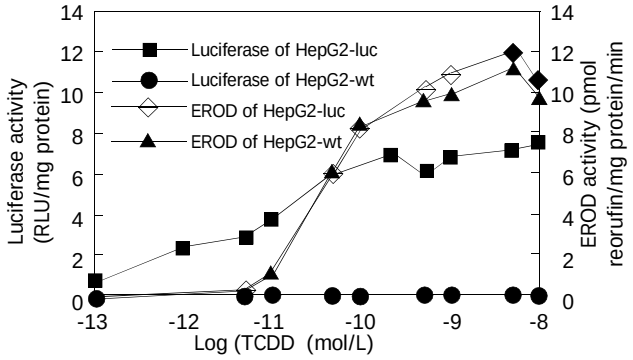

Figure 5 Comparison of EROD and luciferase responsiveness to the induction of TCDD in both $HepG_2$-luc and $HepG_2$-wt cells.

DISCUSSION

Few environmental compounds have generated much interest within the scientific community and in the lay public as polychlorinated dibenzo-p-dioxins (PCDDs) and polychlorinated dibenzofurans (PCDFs). Their ubiquitous presence in the environment and the risk of accidental exposure have raised concern over a possible threat of PCDDs or PCDFs to human health. The most extensively studied potent isomer is TCDD or dioxin, which is known to induce a wide range of toxic and biochemical responses in laboratory animals and humans[8, 11]. Therefore, monitoring the levels of DLCs in environmental pollutants is important for assessing and maintaining the safety of food and the health of environment. Exploring new biodetectors such as bioassays, biomarkers, enzyme immunoassays (EIAs), or other bioanalytical tools has been a continuously growing area in recent years[15]; in which, however, establishing luciferase reporter cell lines for bioassays has been considered as the rapid, sensitive and inexpensive methods for the screening and diagnosis of dioxin and dioxin-like compounds[20, 28].

In the present study, we constructed a recombinant expression plasmid that contained the luciferase gene under TCDD-inducible control of several DREs and responded to DLCs with the induction of firefly luciferase, which has been identified by both transient and stable transfection of this vector into $HepG_2$ cells. Our results indicate that this established $HepG_2$-luc cell bioassay reporter system can respond sensitively to DLCs with the induction of luciferase in a time-, dose-, and AhR-dependent manner and harbors lots of better features. Firstly, it bears higher level of sensitivity and can detect TCDD within the linear range from 1.1×10^{-13} to 1×10^{-8} mol/L, which is 10-fold more sensitive than that of previously similar studies and 30-fold more sensitive than the EROD assay. This is partially because the vector plasmid employed in the study is pGL_3, whose expression efficiency of luciferase is 10-100 times more than that of pGL_2. In addition, no post- transcriptional procedures are needed to regulate the expression of prokaryotic

luciferase, thus its linear relationship is better than that of endogenous gene. Secondly, its pronounced accuracy has been demonstrated by the significant correlation between inducible luciferase activities and TCDD doses (r=0.997, P<0.001), and by the satisfactory reproducibility of TCDD determination with $HepG_2$-luc cells (CV=15-30 %). Finally, the simplicity and facility of $HepG_2$-luc cells in analytical methodology make it possible to perform a rapid screening and semi-quantitation of DLCs[29, 30] and to deal with lots of samples in a short period of time.

Besides the detection of DLCs described above, $HepG_2$-luc cells can also be applied to many other DLCs-related research fields. Since ARNT is required to exert biological effects by some TCDD and related ligands, interactions between AhR and hypoxia signaling pathways can be studied by using luciferase transfected cell line[31]. In accordance with the fact that the toxic factor of 3,3' ,4, 4' -PCB equivalent to TCDD is 0.01[32], our results showed that the ability of 3, 3' , 4, 4' -PCB to induce luciferase expression was much less than that of TCDD, suggesting that the structure-inducibility relationship existing in some DLCs could be reflected by $HepG_2$-luc cells, and the latter can be used alone or with chromatographer to evaluate the relative toxicity of DLCs[19, 33, 34]. In addition, this kind of recombinant cell lines can also be used for the detection and relative quantitation of AhR agonists/ antagonists in complex mixtures of environmental and biological samples, for identification and characterization of novel AhR agonists, and for examination of species differences in DLCs responsiveness[12].

One limitation of the present study is the relatively short duration of responsiveness to DLCs by established $HepG_2$-luc cells, although it is in accordance with that reported by most of the other studies. Up to the present, many established luciferase reporter cell lines such as MLE/BV, H4IIE, GPC16 and HGL1.1c3 responding to DLCs maintain their stable TCDD responsiveness for 6-12 months, except for Hepa1 which maintains its sensitivity for over 3 years[27]. Therefore, our further study has been designed aiming at improving and maintaining the sensitivity of $HepG_2$-luc cells to DLCs for a longer time.

ACKNOWLDGEMENTS

We thank Dr. James P. Whitlock Jr. (Stanford University) for his kind gift of plasmids pHAV and pMcat.

REFERENCES

1 **Couture LA,** Abbott BD, Birnbaum LS. A critical review of the developmental toxicity and teratogenicity of 2,3,7,8-tetrachlorodibenzo-*p*-dioxin: advances toward understanding the mechanism. *Teratology* 1990; **42:** 619-627

2 **Martinez JM,** Afshari CA, Bushel PR, Masuda A, Takahashi T, Walker NJ. Differential toxicogenomic responses to 2, 3, 7, 8-tetrachlorodibenzo-p-dioxin in malignant and nonmalignant human airway epithelial cells. *Toxicol Sci* 2002; **69:** 409-423

3 **Dong W,** Teraoka H, Yamazaki K, Tsukiyama S, Imani S, Imagawa T, Stegeman JJ, Peterson RE, Hiraga T. 2, 3, 7, 8-tetrachlorodibenzo-p-dioxin toxicity in the zebrafish embryo: local circulation failure in the dorsal midbrain is associated with increased apoptosis. *Toxicol Sci* 2002; **69:** 191-201

4 **Kerkvliet NI.** Recent advances in understanding the mechanisms of TCDD immunotoxicity. *Int Immunopharmacol* 2002; **2:** 277-291

5 **Lindstrom G,** Hooper K, Petreas M, Stephens R, Gilman A. Workshop on perinatal exposure to dioxin-like compounds. I. Summary. *Environ Health Perspect* 1995; **103**(Suppl): S135-S142

6 **Legare ME,** Hanneman WH, Barhoumi R, Burghardt RC, Tiffany-Castiglioni E. 2, 3, 7, 8- Tetrachlorodibenzo-p-dioxin alters hippocampal astroglia-neuronal gap junctional communication. *Neurotoxicology* 2000; **21:** 1109-1116

7 **Hankinson O.** The aryl hydrocarbon receptor complex. *Annu Rev Pharmacol Toxicol* 1995; **35:** 307-340

8 **Wilson CL,** Safe S. Mechanisms of ligand-induced aryl hydrocarbon receptor-mediated biochemical and toxic responses. *Toxicol Pathol* 1998; **26:** 657-671

9 **Unkila M,** Pohjanvirta R, Tuomisto J. Biochemical effects of 2, 3, 7, 8-tetrachlorodibenzo-p-dioxin (TCDD) and related compounds on the central nervous system. *Int J Biochem Cell Biol* 1995; **27:** 443-455

10 **Dragan YP,** Schrenk D. Animal studies addressing the carcinogenicity of TCDD (or related compounds) with an emphasis on tumor promotion. *Food Addit Contam* 2000; **17:** 289-302

11 **Vanden Heuvel JP,** Lucier G. Environmental toxicology of polychlorinated dibenzo-p-dioxins and polychlorinated dibenzofurans. *Environmental Health Perspectives* 1993; **100:** 189-200

12 **Garrison PM,** Tullis K, Aarts JM, Brouwer A, Giesy JP, Denison MS. Species-specific recombinant cell lines as bioassay systems for the detection of 2, 3, 7, 8-tetrachlorodibenzo-p-dioxin-like chemicals. *Fundamental and Applied Toxicology* 1996; **30:** 194-203

13 **Willey JJ,** Stripp BR, Baggs RB, Gasiewicz TA. Aryl hydrocarbon receptor activation in genital tubercle, palate and other embryonic tissues in 2, 3, 7, 8-tetrachlorodibenzo-p-dioxin-responsive lacZ mice. *Toxicol Appl Pharmacol* 1998; **151:** 33-44

14 **Whyte JJ,** Jung RE, Schmitt CJ, Tillitt DE. Ethoxyresorufin-O-deethylase (EROD) activity in fish as a biomarker of chemical exposure. *Crit Rev Toxicol* 2000; **30:** 347-570

15 **Behnisch PA,** Hosoe K, Sakai S. Bioanalytical screening methods for dioxins and dioxin-like compounds: a review of bioassay / biomarker technology. *Environ Int* 2001; **27:** 413-439

16 **Whitlock JP.** Induction of cytochrome P4501A1. *Annu Rev Pharmacol Toxicol* 1999; **39:** 103-125

17 **Diehl-Jones WL,** Bols NC. Use of response biomarkers in milk for assessing exposure to environmental contaminants: the case for dioxin-like compounds. *J Toxicol Environ Health B Crit Rev* 2000; **3:** 79-107

18 **Schwirzer SM,** Hofmaier AM, Kettrup A, Nerdinger PE, Schramm KW, Thoma H, Wegenke M, Wiebel FJ. Establishment of a simple cleanup procedure and bioassay for determining 2,3, 7,8- tetrachlorodibenzo-p-dioxin toxicity equivalents of environmental samples. *Ecotoxicol Environ Saf* 1998; **41:** 77-82

19 **Behnisch PA,** Hosoe K, Brouwer A, Sakai S. Screening of dioxin-like toxicity equivalents for various matrices with wildtype and recombinant rat hepatoma H4IIE cells. *Toxicol Sci* 2002; **69:** 125-130

20 **Sanderson JT,** Aarts JM, Brouwer A, Froese KL, Denison MS, Giesy JP. Comparison of Ah receptor-mediated luciferase and ethoxyresorufin-O-deethylase induction in H4IIE cells: implications for their use as bioanalytical tools for the detection of polyhalogenated aromatic hydrocarbons. *Toxicol Appl Pharmacol* 1996; **137:** 316-325

21 **Chen CA,** Okayama H. Calcium phosphate-mediated gene transfer: a highly efficient transfection system for stably trans formiong cells with plasmid DNA. *Bio Techniques* 1988; **6:** 632-639

22 **Zhang ZR,** Xu SQ, Zhou YK, Ren S, Lu B. Construction of luciferase reporter plasmid which is under the control of dioxin-responsive enhancers. *Shengwu Gongcheng Xuebao* 2001; **17:** 170-174

23 **Chen C,** Okayama H. High-efficiency transformation of mammalian cells by plasmid DNA. *Mol Cell Biol* 1987; **7:** 2745-2752

24 **Bradford MM.** A rapid and sensitive method for the quantitation of microgram quantities of protein utilizing the principle of protein-dye binding. *Anal Biochem* 1976; **72:** 248-254

25 **Murk AJ,** Legler J, Denison MS, Giesy JP, Van De Guchte C, Brouwer A. Chemical-activated luciferase gene expression (CALUX): a novel in vitro bioassay for Ah receptor active compounds in sediments and pore water. *Fundam Appl Toxicol* 1996; **33:** 149-160

26 **Li W,** Wu WZ, Xu Y, Li L, Schramm KW, Kettrup A. Measuring TCDD equivalents in environmental samples with the micro-EROD assay: comparison with HRGC / HRMS data. *Bull Environ Contam Toxicol* 2002; **68:** 111-117

27 **Postlind H,** Vu TP, Tukey RH, Quattrochi LC. Response of hu-

man CYP1-luciferase plasmids to 2, 3, 7, 8-tetrachlorodibenzo-p-dioxin and polycyclic aromatic hydrocarbons. *Toxicol Appl Pharmacol* 1993; **118:** 255-262

28 **Hahn ME.** Biomarkers and bioassays for detecting dioxin-like compounds in the marine environment. *Sci Total Environ* 2002; **289:** 49-69

29 **Allen SW,** Mueller L, Williams SN, Quattrochi LC, Raucy J. The use of a high-volume screening procedure to assess the effects of dietary flavonoids on human cyp1a1 expression. *Drug Metab Dispos* 2001; **29:** 1074-1079

30 **Khim JS,** Lee KT, Villeneuve DL, Kannan K, Giesy JP, Koh CH. In vitro bioassay determination of dioxin-like and estrogenic activity in sediment and water from Ulsan Bay and its vicinity, Korea. *Arch Environ Contam Toxicol* 2001; **40:** 151-160

31 **Nie M,** Blankenship AL, Giesy JP. Interactions between aryl hydrocarbon receptor (AhR) and hypoxia signaling pathways. *Environ Toxicol Pharmacol* 2001; **10:** 17-27

32 **Safe SH.** Polychlorinated biphenyls (PCBs): environmental impact, biochemical and toxic responses, and implications for risk assessment. *Crit Rev Toxicol* 1994; **24:** 87-149

33 **Machala M,** Vondracek J, Blaha L, Ciganek M, Neca JV. Aryl hydrocarbon receptor-mediated activity of mutagenic polycyclic aromatic hydrocarbons determined using in vitro reporter gene assay. *Mutat Res* 2001; **497:** 49-62

34 **Hamers T,** van Schaardenburg, Felzel EC, Murk AJ, Koeman JH. The application of reporter gene assays for the determination of the toxic potency of diffuse air pollution. *Sci Total Environ* 2000; **262:** 159-174

Edited by Zhu L

P.O.Box 2345, Beijing 100023,China
Fax: +86-10-85381893
E-mail: wjg@wjgnet.com www.wjgnet.com

World J Gastroenterol 2003;9(7):1465-1468
World Journal of Gastroenterology
 ISSN 1007-9327

• LIVER CANCER •

Construction and expression of recombined human AFP eukaryotic expression vector

Li-Wang Zhang, Jun Ren, Liang Zhang, Hong-Mei Zhang, Bin Jin, Bo-Rong Pan, Xiao-Ming Si, Yan-Jun Zhang, Zhong-Hua Wang, Yang-Lin Pan, Stephen M Festein

Li-Wang Zhang, Jun Ren, Liang Zhang, Hong-Mei Zhang, Bin Jin, Bo-Rong Pan, Xiao-Ming Si, Yan-Jun Zhang, Department of Oncology, Xijing Hospital, Fourth Military Medical University, Xi' an 710032, Shaanxi Province, China
Zhong-Hua Wang, Department of Hepatobiliary Surgery, Xijing Hospital, Fourth Military Medical University, Xi' an 710032, Shaanxi Province, China
Yang-Lin Pan, Department of Gastroenterology, Xijing Hospital, Fourth Military Medical University, Xi' an 710032, Shaanxi Province, China
Stephen M Festein, Department of Biology, Hamiliton College, 198 College Hill Road Clinton, New York 13323, USA
Supported by Teaching and Research Award Program for Outstanding Young Teacher in Higher Education Institutes, No. TRAPOYT99-016, and the Fund for Distinguished Young Scholars of Chinese PLA, No.01J016
Correspondence to: Dr. Jun Ren, Department of Oncology, Xijing Hospital, Fourth Military Medical University, Xi' an 710032, Shaanxi Province, China. renjun@fmmu.edu.cn
Telephone: +86-29-3375407
Received: 2003-01-11 **Accepted:** 2003-03-05

Abstract

AIM: To construct a recombined human AFP eukaryotic expression vector for the purpose of gene therapy and target therapy of hepatocellular carcinoma (HCC).

METHODS: The full length AFP-cDNA of prokaryotic vector was digested, and subcloned to the multi-clony sites of the eukaryotic vector. The constructed vector was confirmed by enzymes digestion and electrophoresis, and the product expressed was detected by electrochemiluminescence and immunofluorescence methods.

RESULTS: The full length AFP-cDNA successfully cloned to the eukaryotic vector through electrophoresis, 0.9723 IU/ml AFP antigen was detected in the supernatant of AFP-CHO by electrochemiluminescence method. Compared with the control groups, the differences were significant ($P<0.05$). AFP antigen molecule was observed in the plasma of AFP-CHO by immunofluorescence staining.

CONCLUSION: The recombined human AFP eukaryotic expression vector can express in CHO cell line. It provides experimental data for gene therapy and target therapy of hepatocellular carcinoma.

Zhang LW, Ren J, Zhang L, Zhang HM, Jin B, Pan BR, Si XM, Zhang YJ, Wang ZH, Pan YL, Festein SM. Construction and expression of recombined human AFP eukaryotic expression vector. *World J Gastroenterol* 2003; 9(7): 1465-1468
http://www.wjgnet.com/1007-9327/9/1465.asp

INTRODUCTION

Hepatocellular carcinoma (HCC) is a very common malignancy in China[1-5], and it has a very poor prognosis[6-9]. Only a minority of patients are eligible for surgical therapies due to advanced tumors or extrahepatic diseases at primary diagnosis[10,11]. Therefore, it is urgent to find a novel strategy to prevent the proliferation of malignant cells. It is a hot spot at present to study prophylactic vaccination targeting the tumor-associated antigen (TAA) or tumor-specific antigen (TSA). This approach has been successful in mouse models, such as the tyrosinase-related protein (TRP)-2 in murine melanoma[12,13]. A colon cancer specific DNA vaccination directed against the carcinoembryonic antigen (CEA) is in phase I clinical trial[14].

The oncofetal alpha-fetoprotein (AFP) may be a possible target for an HCC-specific vaccination. It is a 70-ku to 80-ku secretory protein that is heterogeneously glycosylated. AFP is usually expressed at high concentrations in fetal liver, gastrointestinal tract, and the yolk sack. It is transcriptionally down-regulated after birth, and frequently re-expressed in HCC and therefore, used as a diagnostic marker for this tumor[15-21]. Serum AFP is useful not only for diagnosis, but also a prognostic indicator for HCC patients[22,23]. AFP mRNA has been proposed as a predictive marker of HCC cells disseminated into the circulation and for metastatic recurrence[24-27]. Some experiments *in vitro* have also demonstrated that AFP promotes cell proliferation of hepatoma cell lines[28,29].

AFP may be used as a target molecule for immunotherapy or prophylaxis against HCC. For this purpose, we constructed the recombined human AFP eukaryotic expression vector, and hope that it will provide experimental data for the treatment of HCC.

MATERIALS AND METHODS

Cell line and culture condition

CHO cell line was provided by the Department of Biochemistry, Fourth Military Medical University. Cells were maintained in RPMI 1640 medium, supplemented with 10 mL/L FCS, 1 mmol/L glutamine, and 100 kU/L penicillin.

Plasmids

The prokaryotic expression vector pRESTA-AFP containing human full-length AFP-cDNA was presented by Dr. Stephen M Festein, Hamiliton College, USA. The eukaryotic vector pCEFL was provided by Dr. Pan YL, Fourth Military Medical University.

Amplification of pRESTA-AFP

Transformation of competent bacterial DH5-α was carried out with pRESTA-AFP. The transformed cell DH5-α was transferred onto LB medium which was anti-aminobenzyl penicillin, cultured overnight in an incubator at 37 ℃. Four-five clones were selected and maintained in LB medium, and shaken overnight at 37 ℃.

Evaluation of pRESTA-AFP

Five mL bacterial medium was picked up, and the plasmid

DNA was extracted following the procedures of EZNA plasmid miniprep kit (Omega). The extracted DNA was digested by *Bam*H I and *Eco*R I (TaKaRa). The digested products were evaluated with 10 g/L agarose gel electrophoresis.

Construction of recombined human AFP eukaryotic expression vector

The human full-length AFP-cDNA was retrieved following the procedures of UNIQ-10 centrifugation column type gel retrieve kit (Sangon, Shanghai) and ligated to the multi-clony sites of pCEFL that was digested by *Bam*H I and *Eco*R I at a ratio of 10:1 with T4 DNA ligase (TaKaRa). Amplification, extraction, digestion and evaluation were performed according to the above-mentioned methods. It demonstrated that the full-length AFP-cDNA was inserted into pCEFL successfully, and named pCEFL-AFP.

Transfections of CHO cells

CHO cells were transiently transfected with pCEFL-AFP by liposome, Lipofectamine™ 2000 (Gibco). All the procedures were performed according to the guidance of the reagent. CHO cells were also transfected with pCEFL as control group, CHO cells not being transfected also served as control.

Detection of AFP expression by electrochemiluminescence

The supernatants of the cells from the three groups were collected, and detected by electrochemiluminescence method with Elecsys 1010 (Roche) and AFP electrochemiluminescence detection kit (Roche).

Detection of AFP expression by immunofluorescence

The transfected cells were stabilized with 10 g/L formaldehydum polymerisatum for 30 minutes at 4 ℃, and blocked with 100 g/L bovine serum albumin (BSA) for 1 hour at room temperature, then coated with rabbit anti-human AFP antibody (Dako) for 45 minutes at 37 ℃, followed by goat anti-rabbit IgG-FITC (Boster, Wuhan) for 30 minutes at 37 ℃. The antibody-coated cells were observed under fluorescence microscope (Optiphot XIF, Nicon, Japan) within 24 hours.

Statistical analysis

Student' s *t* test was used to compare the difference of AFP molecule in the supernatants between control groups and transfected pCEFL-AFP group. *P* value less than 0.05 was considered statistically significant.

RESULTS

Evaluation of pRESTA-AFP

pRESTA-AFP was digested by *Bam*H I and *Eco*R I and evaluated with electrophoresis. Figure 1 shows that pRESTA-AFP contained the full-length human AFP-cDNA.

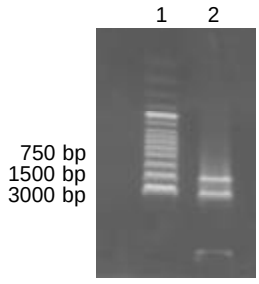

Figure 1 Electrophoresis of pRESTA-AFP. 1. Marker, 2. Full length AFP-cDNA in the upper, pRESTA in the lower.

Evaluation of pCEFL-AFP

To demonstrate that the full-length human AFP-cDNA was inserted into the multi-clony sites of pCEFL correctly, pCEFL-AFP was digested by *Bam*H I and *Eco*R I and evaluated with electrophoresis. Figure 2 shows that AFP-cDNA was inserted into pCEFL successfully.

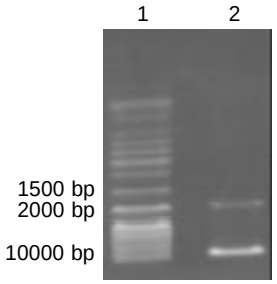

Figure 2 Electrophoresis of pCEFL-AFP. 1. Marker, 2. Full length AFP-cDNA in the upper, pCEFL in the lower.

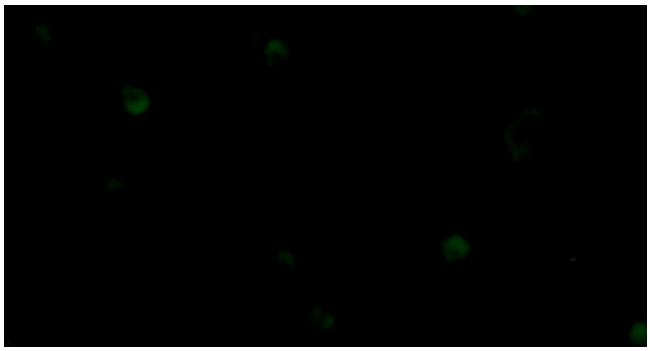

Figure 3 CHO transfected with pCEFL-AFP. The fluorescence staining in the cytoplasm was positive. ×400.

Figure 4 CHO transfected with pCEFL. The fluorescence staining in the cytoplasm was negative. ×400.

Figure 5 Non-transfected CHO. The fluorescence staining in the cytoplasm was negative. ×400.

AFP molecule expression in the supernatant

CHO cells were transfected with pCEFL-AFP. To demonstrate that the transfection was successful, the supernatant of CHO cells was detected by electrochemiluminescence method. The results showed that AFP molecule expression in the supernatant of CHO cells transfected with pCEFL-AFP was higher (972.3±69.9 IU/L) than that transfected with pCEFL (556.3±60.2 IU/L, $P<0.05$) and also higher than that not being transfected (582.3±58.0 IU/L, $P<0.05$). The differences were significant.

Immunofluorescence staining of transfected cells

The transfected cells were coated with AFP antibody and fluorescent antibody. Under fluorescence microscope, it could be observed that the fluorescence staining was positive in the cytoplasm of CHO cells transfected with pCEFL-AFP and negative in the controls (Figures 3-5).

DISCUSSION

In China, the incidence of HCC is very high, and surgical operation, chemotherapy, and interventional therapy are the common therapies. But only a few patients of earlier stage without extrahepatic malignancy are indicated for operation, and for the advanced cases, chemotherapy and interventional therapy usually cannot achieve a satisfactory effect. AFP is a TAA of HCC, which may be used as a target for treatment.

Vollmer *et al*[30] firstly showed a prophylactic effect of an AFP-specific DNA vaccination on the growth of AFP-positive tumor cells in C57BL/6 mice. In their experiments, only 7.4 % of mice were fully protected from tumor growth. In the remaining animals, a prolonged time until tumors reached diameters of 10 mm was observed. Wang *et al*[31] found that antisense S-ODNs targeting AFP gene treatment led to reduced AFP gene expression. Specific antisense S-ODNs, but not control S-ODNs, inhibited the growth of hepatoma cells *in vitro*. *In vitro*, only antisense S-ODNs exhibited obvious antitumor activities. Guo *et al*[32] found that the dendritic cells (DCs) based vaccine with HLA-A2 restricted peptide epitope derived from hAFP have marked cytotoxicity against AFP positive primary HCC. In their experiments, after stimulated by DCs loaded with CTL epitope based peptide derived from hAFP, lymphocytes showed good characteristics and the culture medium of activated lymphocytes contained a high level of Th1 type cytokines of IL-12 and TNF. Activated lymphocytes not only specifically lysed HLA-A2 (+) HepG2 line but also had the cytotoxicity against T2 target cells loaded with peptide of hAFP. Hanke *et al*[33] demonstrated that DNA vaccination with AFP-encoding plasmid DNA could prevent the growth of subcutaneous AFP-expressing tumors and not interfere with liver regeneration in mice. Grimm *et al*[34] achieved similar outcomes.

Since immunotherapy or gene therapy targeting TAA or TSA is a direction of tumor therapy, AFP as a TAA of HCC, has shown its profound effect on HCC treatment in animal models. In our experiment, we constructed the recombined human AFP eukaryotic expression vector successfully. This, we believe, provides experimental data for gene therapy and immunotherapy of HCC. It may be used as a treatment target of human HCC.

REFERENCES

1 **Wu W**, Lin XB, Qian JM, Ji ZL, Jiang Z. Ultrasonic aspiration hepatectomy. For 136 patients with hepatocellular carcinoma. *World J Gastroenterol* 2002; **8**: 763-765

2 **Jiang HC**, Liu LX, Piao DX, Xu J, Zheng M, Zhu AL, Qi SY, Zhang WH, Wu LF. Clinical short-term results of radiofrequency ablation in liver cancers. *World J Gastroenterol* 2002; **8**: 624-630

3 **Zhang G**, Long M, Wu ZZ, Yu WQ. Mechanical properties of hepatocellular carcinoma cells. *World J Gastroenterol* 2002; **8**: 243-246

4 **Tang ZY**. Hepatocellular carcinoma-cause, treatment and metastasis. *World J Gastroenterol* 2001; **7**: 445-454

5 **Rabe C**, Pilz T, Klostermann C, Berna M, Schild HH, Sauerbruch T, Caselmann WH. Clinical characteristics and outcome of a cohort of 101 patients with hepatocellular carcinoma. *World J Gastroenterol* 2001; **7**: 208-215

6 **Jiang YF**, Yang ZH, Hu JQ. Recurrence or metastasis of HCC: predictors, early detection and experimental antiangiogenic therapy. *World J Gastroenterol* 2000; **6**: 61-65

7 **Zhao WH**, Ma ZM, Zhou XR, Feng YZ, Fang BS. Prediction of recurrence and prognosis in patients with hepatocellular carcinoma after resection by use of CLIP score. *World J Gastroenterol* 2002; **8**: 237-242

8 **Qin LX**, Tang ZY. The prognostic molecular markers in hepatocellular carcinoma. *World J Gastroenterol* 2002; **8**: 385-392

9 **Zeng WJ**, Liu GY, Xu J, Zhou XD, Zhang YE, Zhang N. Pathological characteristics, PCNA labeling index and DNA index in prognostic evaluation of patients with moderately differentiated hepatocellular carcinoma. *World J Gastroenterol* 2002; **8**: 1040-1044

10 **Durr R**, Caselmann WH. Carcinogenesis of primary liver malignancies. *Langenbecks Arch Surg* 2000; **385**: 154-161

11 **Caselmann WH**, Blum HE, Fleig WE, Huppert PE, Ramadori G, Schirmacher P, Sauerbruch T. Guidances of the german society of digestive and metabolic diseases for diagnosis and therapy of hepatocellular carcinoma. German society of digestive and metabolic diseases. *Z Gastroenterol* 1999; **37**: 353-365

12 **Bronte V**, Apolloni E, Ronca R, Zamboni P, Overwijk WW, Surman DR, Restifo NP, Zanovello P. Genetic vaccination with "self' tyrosinase-related protein 2 causes melanoma eradication but not vitiligo. *Cancer Res* 2000; **60**: 253-258

13 **Tuting V**, Gambotto A, DeLeo A, Lotze MT, Robbins PD, Storkus WJ. Induction of tumor antigen-specific immunity using plasmid DNA immunization in mice. *Cancer Gene Ther* 1999; **6**: 73-80

14 **Conry RM**, LoBuglio AF, Loechel F, Moore SE, Sumerel LA, Barlow DL, Pike J, Curiel DT. A carcinoembryonic antigen polynucleotide vaccine for human clinical use. *Cancer Gene Ther* 1995; **2**: 33-38

15 **Shen LJ**, Zhang ZJ, Ou YM, Zhang HX, Huang R, He Y, Wang MJ, Xu GS. Computed morphometric analysis and expression of alpha-fetoprotein in hepatocellular carcinoma and its related lesion. *World J Gastroenterol* 2000; **6**: 415-416

16 **Sithinamsuwan P**, Piratvisuth T, Tanomkiat W, Apakupakul N, Tongyoo S. Review of 336 patients with hepatocellular carcinoma at Songklanagarind Hospital. *World J Gastroenterol* 2000; **6**: 339-343

17 **Wawrzynowicz-Syczewska M**, Leonciuk A, Jurczyk K, Karpinska E, Boron-Kaczmarska A. Increased incidence of hepatocellular carcinoma. *Pol Merkuriusz Lek* 2002; **13**: 100-102

18 **Chou SF**, Hsu WL, Hwang JM, Chen CY. Production of monoclonal and polyclonal antibodies against human alpha-fetoprotein, a hepatocellular tumor marker. *Hybrid Hybridomics* 2002; **21**: 301-305

19 **Chu PG**, Ishizawa S, Wu E, Weiss LM. Hepatocyte antigen as a marker of hepatocellular carcinoma: an immunohistochemical comparison to carcinoembryonic antigen, CD10, and alpha-fetoprotein. *Am J Surg Pathol* 2002; **26**: 978-988

20 **Nguyen MH**, Garcia RT, Simpson PW, Wright TL, Keeffe EB. Racial differences in effectiveness of alpha-fetoprotein for diagnosis of hepatocellular carcinoma in hepatitis C virus cirrhosis. *Hepatology* 2002; **36**: 410-417

21 **Ma J**, Gong Q, Lin M. Combined five tumor markers in detecting primary hepatic carcinoma. *Zhonghua Waike Zazhi* 2000; **38**: 14-16

22 **Qin LX**, Tang ZY. The prognostic significance of clinical and pathological features in hepatocellular carcinoma. *World J Gastroenterol* 2002; **8**: 193-199

23 **Song BC**, Suh DJ, Yang SH, Lee HC, Chung YH, Sung KB, Lee YS. Lens culinaris agglutinin-reactive alpha-fetoprotein as a prognostic marker in patients with hepatocellular carcinoma undergoing transcatheter arterial chemoembolization. *J Clin Gastroenterol* 2002; **35**: 398-402

24 **Witzigmann H**, Geissler F, Benedix F, Thiery J, Uhlmann D, Tannapfel A, Wittekind C, Hauss J. Prospective evaluation of circulating hepatocytes by alpha-fetoprotein messenger RNA in patients with hepatocellular carcinoma. *Surgery* 2002; **131**: 34-43
25 **Ijichi M**, Takayama T, Matsumura M, Shiratori Y, Omata M, Makuuchi M. Alpha-Fetoprotein mRNA in the circulation as a predictor of postsurgical recurrence of hepatocellular carcinoma: a prospective study. *Hepatology* 2002; **35**: 853-860
26 **Wu X**, Lin Z, Fan J, Lu J, Wang L, Tang Z. Quantitation of alpha-fetoprotein messenger RNA in peripheral blood of nude mice and its relationship with tumor recurrence and metastasis after curative resection of hepatocellular carcinoma. *Zhonghua Ganzangbing Zazhi* 2002; **10**: 189-191
27 **He P**, Tang ZY, Ye SL, Liu BB. Relationship between expression of alpha-fetoprotein messenger RNA and some clinical parameters of human hepatocellular carcinoma. *World J Gastroenterol* 1999; **5**: 111-115
28 **Li MS**, Li PF, He SP, Du GG, Li G. The promoting molecular mechanism of alpha-fetoprotein on the growth of human hepatoma Bel7402 cell line. *World J Gastroenterol* 2002; **8**: 469-475
29 **Li MS**, Li PF, Li G, Du GG. Enhancement of Proliferation of HeLa Cells by the alpha-Fetoprotein. *Shengwuhuaxue Yu Shengwuwuli Xuebao* 2002; **34**: 769-774
30 **Vollmer CM Jr**, Eliber FC, Butterfield LH, Ribas A, Dissette VB, Koh A, Montejo LD, Lee MC, Andrews KJ, McBride WH, Glaspy JA, Economou JS. Alpha-fetoprotein-specific genetic immunotherapy for hepatocellular carcinoma. *Cancer Res* 1999; **59**: 3064-3069
31 **Wang XW**, Yuan JH, Zhang RG, Guo LX, Xie Y, Xie H. Antihepatoma effect of alpha-fetoprotein antisense phosphorothioate oligodeoxyribonucleotides *in vitro* and in mice. *World J Gastroenterol* 2001; **7**: 345-351
32 **Guo J**, Cai M, Wei D, Qin L, Huang J, Wang X. Immune responses of dendritic cells after loaded with cytotoxicity T lymphocyte epitope based peptide of human alpha-fetoprotein (hAFP). *Zhonghua Ganzangbing Zazhi* 2002; **10**: 178-180
33 **Hanke P**, Serwe M, Dombrowski F, Sauerbruch T, Caselmann WH. DNA vaccination with AFP-encoding plasmid DNA prevents growth of subcutaneous AFP-expressing tumors and does not interfere with liver regeneration in mice. *Cancer Gene Ther* 2002; **9**: 346-355
34 **Grimm CF**, Ortmann D, Mohr L, Michalak S, Krohne TU, Meckel S, Eisele S, Encke J, Blum HE, Geissler M. Mouse alpha-fetoprotein-specific DNA-based immunotherapy of hepatocellular carcinoma leads to tumor regression in mice. *Gastroenterology* 2000; **119**: 1104-1112

Edited by Ma JY

P.O.Box 2345, Beijing 100023,China
Fax: +86-10-85381893
E-mail: wjg@wjgnet.com www.wjgnet.com

World J Gastroenterol 2003;9(7):1469-1473
World Journal of Gastroenterology
 ISSN 1007-9327

Mast cells and human hepatocellular carcinoma

Fabio Grizzi, Barbara Franceschini, Maurizio Chiriva-Internati, Young Liu, Paul L. Hermonat, Nicola Dioguardi

Fabio Grizzi, Barbara Franceschini, Nicola Dioguardi, Scientific Direction, Istituto Clinico Humanitas, Rozzano, Milan, Italy. Fondazione "M. Rodriguez", Istituto Scientifico per le Misure Quantitative in Medicina, Milan, Italy
Maurizio Chiriva-Internati, Health Sciences Center, Texas Tech University, Amarillo, Texas, USA
Young Liu, Paul L. Hermonat, Department of Obstetrics and Gynecology, Division of Gynecologic Oncology, University of Arkansas, Little Rock, Arkansas, USA
Supported by the grants from the Foundation "Michele Rodriguez". Istituto Scientifico per le Misure Quantitative in Medicina, Milan, Italy
Correspondence to: Fabio Grizzi, Ph.D., Scientific Direction, Istituto Clinico Humanitas, Via Manzoni, 56 20089 Rozzano, Milano, Italy. fabio.grizzi@humanitas.it
Telephone: +390282244548 **Fax:** +390282244590
Received: 2002-11-30 **Accepted:** 2002-12-22

Abstract

AIM: To investigate the density of mast cells (MCs) in human hepatocellular carcinoma (HCC), and to determine whether the MCs density has any correlations with histopathological grading, staging or some baseline patient characteristics.

METHODS: Tissue sections of 22 primary HCCs were histochemically stained with toluidine blue, in order to be able to quantify the MCs in and around the neoplasm using a computer-assisted image analysis system. HCC was staged and graded by two independent pathologists. To identify the sinusoidal capillarisation of each specimen 3 μm thick sections were histochemically stained with sirius red, and semi-quantitatively evaluated by two independent observers. The data were statistically analysed using Spearman's correlation and Student's *t*-test when appropriate.

RESULTS: MCs density did not correlate with the age or sex of the patients, the serum alanine aminotransferase (ALT) or aspartate aminotransferase (AST) levels, or the stage or grade of the HCC. No significant differences were found between the MCs density of the patients with and without hepatitis C virus infection, but they were significantly higher in the specimens showing marked sinusoidal capillarisation.

CONCLUSION: The lack of any significant correlation between MCs density and the stage or grade of the neoplastic lesions suggests that there is no causal relationship between MCs recruitment and HCC. However, as capillarisation proceeds concurrently with arterial blood supply during hepatocarcinogenesis, MCs may be considered of primary importance in the transition from sinusoidal to capillary-type endothelial cells and the HCC growth.

Grizzi F, Franceschini B, Chiriva-Internati M, Liu Y, Hermonat PL, Dioguardi N. Mast cells and human hepatocellular carcinoma. *World J Gastroenterol* 2003; 9(7): 1469-1473
http://www.wjgnet.com/1007-9327/9/1469.asp

INTRODUCTION

Mast cells (MCs) have fascinated the biomedical sciences ever since they were first recognised by Paul Ehrlich in the late 1800s' [1]. MCs originate from haematopoietic stem cells in bone marrow[2, 3]. MCs circulate in the blood only as progenitors, and it is not until they enter the tissues that they undergo their terminal differentiation into mature cells. MCs provide granule and membrane mediators as well as different cytokines during the course of many human and experimental diseases[4-8]. It has recently been shown that MCs play an important role in antigen presentation to T cells, and that there is a direct interaction between them and the B cells signalling immunoglobulin E (lgE) production. Although a number of studies have shown that MCs play different roles in human tumours[9-26], the exact nature of the relationship between them and HCC has still to be established. The aim of the present study was to investigate MCs density in HCC and compare it with stage and grade of the neoplasia, and some clinical and histopathological characteristics of the patients.

MATERIALS AND METHODS

Patient profiles and surgical specimens

The study was conducted in accordance with the guidelines of the Ethics Committee of the hospital treating the patients (Istituto Clinico Humanitas, Rozzano, Milan, Italy), all of whom were informed of the possible discomforts and risks of surgical treatment.

The study involved 22 primary HCC patients (15 men and 7 women, mean age: 68.22 years, range 48-80 years) who were surgically treated between 1997 and 2001 (Table 1). Tumours were independently graded and staged by two experienced histopathologists. The study was performed on surgical specimens fixed in formalin and embedded in paraffin.

Histochemical detection of MCs and capillarisation

Sections of 3 μm were cut, mounted on glass slides, de-waxed in xylene and re-hydrated using graded alcohol/water baths. They were then rinsed in distilled water for 5 minutes and incubated for 30 minutes at room temperature with a freshly made staining aqueous solution consisting of 0.1 % toluidine blue (Sigma Chem. Co., MO, USA) and 0.005 % acetic acid. The number of MCs detectable on the whole surface of the available liver sections at a magnification of 200× was quantified using a computer-assisted image analysis system consisting of an Axiophot light microscope (Zeiss, Germany), a 3-CCD camera (JVC KY-F55BE, Italy), a Pentium 600 computer (Hewlett-Packard, Italy) with an incorporated frame-grabber board (Imascan, USA), and Image-Pro Plus image analysis software (Immaginie Computer, Rho, Italy). The digitized image, which was composed of a variable number of fields tiled together to form a unique final image, represent all of the histological materials available for examination (>30 mm^2 for each slide). The Image Pro-Plus software automatically selected stained MCs as single objects on the basis of similarities in the color of adjacent pixels, the image intensity was the same throughout the study. MCs density (d) was automatically calculated using the formula: d=(number of

MCs)/(sample surface), where the sample surface was expressed in μm^2.

In order to evaluate the hepatic sinusoid capillarisation of each specimen, a 3 μm section was stained with Direct-red 80 (Sigma Chem. Co., MO, USA; 0.1 % in saturated picric acid). The sections were subsequently washed in running tap water for 30 minutes to remove excess staining, counter-stained in Mayer's hemallum solution, dehydrated, and mounted in Eukitt (Bio-Optica, Milan, Italy). Sinusoid capillarisation was independently scored as strong (+++), moderate (++), weak (+) or absent (0) by two experienced histopathologists.

Statistical analysis

Linear regression analysis was used to assess the statistical correlation between MCs density and the other histopathological and clinical data. The relationships were determined using Spearman's correlation and Student's *t*-test when appropriate. Statistical analysis was performed using Statistica software (StatSoft Inc., Tulsa, OK, USA). $P<0.05$ was considered statistically significant.

RESULTS

Table 1 shows the baseline characteristics of the 22 patients involved in the study. MCs were strongly identified in 18 cases (82 %). They were found in and around the neoplastic tissue. MCs density did not correlate with the patients' age ($r=0.1698$). It correlated non-significantly with disease stage (Figure 1A) and disease grade (Figure 1B), nor with serum alanine aminotransferase (ALT, $r=0.20765$) or aspartate aminotransferase (AST, $r=-0.0439$) (Figure 2). There was no significant difference in the density of MCs between the patients with and without chronic hepatitis C virus disease (Figure 3), but a semi-quantitative evaluation showed that MCs density did correlate significantly with the capillarisation process (Table 2). MCs were found abundantly in tissues showing a higher capillarisation phenomenon (Figure 4).

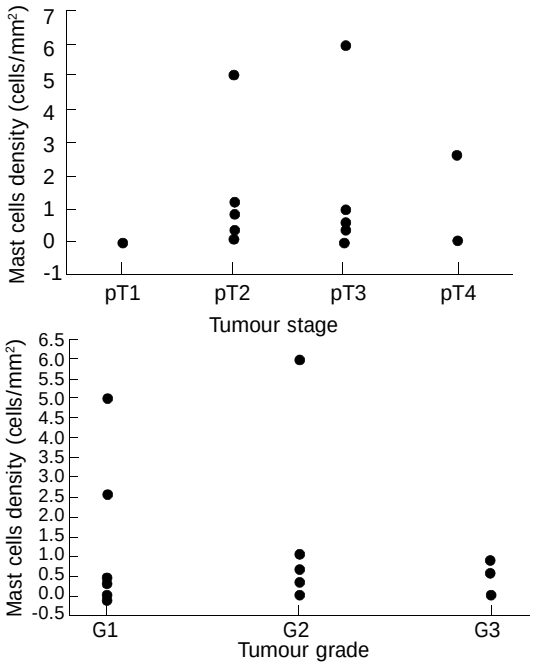

Figure 1 Relationship between MCs density and tumour stage (A) and tumour grade (B).

Table 2 Semi-quantitative evaluation of sinusoidal capillarisation related to MCs density (cells / mm^2)

MC density	Presence of capillarisation			
	Absent	Weak	Moderate	Strong
0-0.01	3	2	0	0
0.01-0.1	3	0	0	0
0.1-1	1	5	1	0
>1	0	0	2	3[a]

[a]$P<0.005$ *vs* the other categories.

Table 1 Baseline characteristics of the patients involved in the study

n	Age	Sex	ALT(UI / l)	AST	Histology	Stage	Grade	Angioinvasivity	HCV-Ab	MCs density(cells / mm^2)
1	73	m	98	37	TR	G1	pT2	absent	_	0
2	70	m	61	37	PS	G2	pT2	peritumoural	_	0
3	76	f	97	94	TR	G2	pT3	peritumoural	+	0
4	59	m	169	48	TR	G3	pT4	peritumoural	+	0
5	72	f	40	29	TR	G1	pT3	peritumoural	nd	0.0053
6	51	f	20	32	TR	G3	pT3	peritumoural	_	0.0061
7	70	f	62	66	C	G1	pT1	absent	+	0.0062
8	67	m	108	82	TR	G3	pT3	peritumoural	+	0.0483
9	71	m	48	64	PS	G1	pT2	peritumoural	_	0.0625
10	78	m	75	116	TR	G3	pT2	absent	+	0.0726
11	71	m	199	110	C	G1	pT4	peritumoural	+	0.253
12	74	m	40	25	TR	G1	pT2	absent	nd	0.3846
13	76	f	75	94	TR	G2	pT3	intratumoural	+	0.446
14	77	m	286	95	TR	G3	pT3	absent	+	0.55
15	63	m	97	78	TR	G2	pT3	peritumoural	+	0.625
16	69	m	55	74	C	G3	pT3	absent	+	0.894
17	80	f	58	64	TR	G3	pT3	peritumoural	+	0.9422
18	51	m	103	153	C	G2	pT2	absent	+	1.1
19	68	f	79	113	TR	G1	pT2	absent	+	1.15
20	48	f	149	76	TR	G1	pT2	absent	_	2.58
21	73	m	116	45	TR	G1	pT3	absent	_	5.041
22	64	m	131	70	C	G2	pT3	absent	+	6.006

TR=trabecular, PS=pseudoglandular, C= combined.

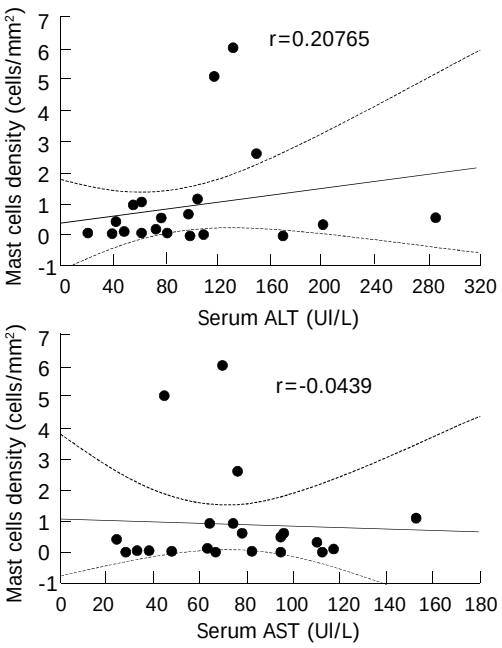

Figure 2 Correlation between MCs densities and serum ALT (A) and AST (B).

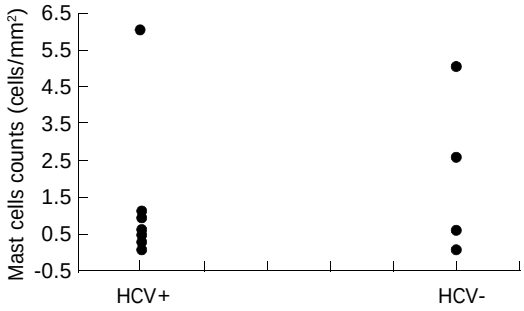

Figure 3 MCs densities in patients with and without hepatitis C virus (HCV) infection.

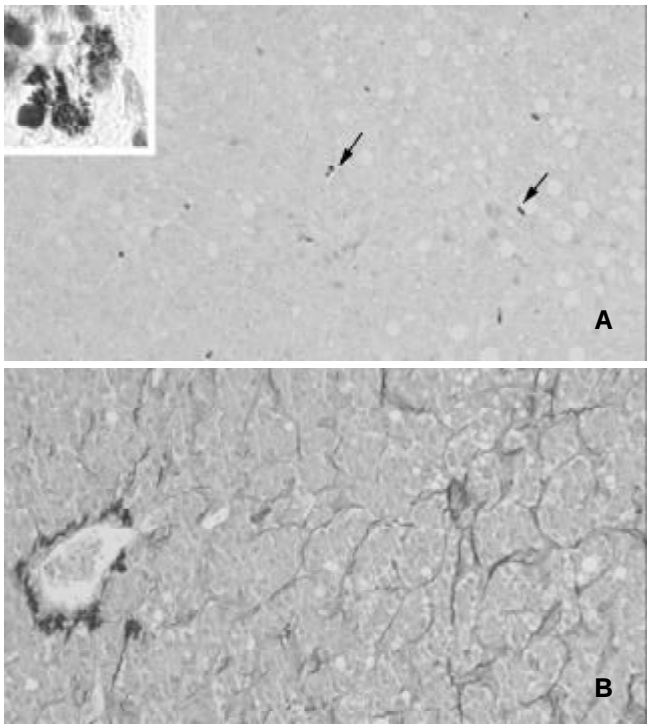

Figure 4 MCs were found abundantly in tissues showing a higher capillarisation phenomenon. (a) High densities of stained MCs (arrows) in human HCC tissues (toluidine blue, objective magnification 5×; insert, objective magnification, 100×). (b) Sinusoidal capillarisation in HCC tissue (sirius red, objective magnification 20×).

DISCUSSION

MCs are a group of long-living cells of bone marrow origin that are commonly found in the skin and the gastrointestinal and respiratory systems. These cells produce, store and release a high number of bioactive mediators, such as TNF-α, IL-1, IL-4, IL-5, IL-6, IL-8, IL-13, NGF, β-FGF and TGF-β, histamine, and the serine proteases, tryptase and chymase[3, 4, 27].

MCs are known to be present in normal and pathological livers. In normal human livers, there are a few resident MCs located near the portal tracts which are more densely distributed around the biliary tree. Large amounts of MCs have been detected in the fibrotic septa and portal regions in cirrhotic human livers. A number of studies have indicated that MCs are associated with hepatic fibrosis as they promote fibroblast growth, collagen synthesis and may inhibit extracellular matrix degradation by means of inhibitors of metalloproteases (TIMPs)[6, 27-32]. MCs density is a valid index of acute liver inflammation[7, 8].

MCs were recognized in various human tumours[8, 26]. The accumulation of MCs around the neoplasia is a well-known phenomenon in basal cell carcinoma, melanoma, lung, prostate and breast cancer.

Although the functions of intra-tumour MCs are yet unclear (some MCs have been evidenced in close apposition to tumour cells, suggesting the existence of direct cell-to-cell interactions), two main hypotheses have been proposed: The first is that MCs may accelerate tumour growth, invasion and neovascularity. Contrarily, the second is that MCs have cytotoxic activity for some tumours (especially those sensitive to TNF-α), as a result of cytotoxic products or the enhancement of the cytotoxic activation of mainly peri-tumoural eosinophils and macrophages[33-36].

Experimental studies have shown that an increase in MCs density is stimulated by IL-3 and IL-4, thus suggesting that their defensive role against tumour growth may be particularly associated with T cells[37-39]. IL-4 is essential for the triggering of Th2 lymphocytes that they themselves produce to initiate inflammatory cell accumulation and B lymphocyte immunoglobulin class switching to IgE[40].

However, the well documented relationship between MCs and angiogenesis makes the first hypothesis more persuasive[23,27]. Secreting MCs are able to induce and enhance angiogenesis via multiple in part interacting pathways[27]. The supporting evidence includes: (a) The fact that tumour cells produce agents promoting MC chemotaxis. Moreover, most of the tumour-infiltrating MCs exhibit anaphylactic or piecemeal degranulation, indicating that the MCs are activated *in situ*. (b) MCs degranulation facilitates the endothelial cell invasion in connective tissue. (c) MC heparin stimulates the endothelial cell motility essential for the angiogenic process. (d) The *metachromasia* that is determined by the presence of highly sulphated proteoglycans in the secretory granules of MCs, is commonly found at the tumour periphery, suggesting the release of vasoactive substances around the tumour. (e) Histamine, VEGF, and certain lipid-derived mediators that induce microvascular hyperpermeability having pro-angiogenic effects.

In the present paper, we showed that HCC contained a higher density of toluidine blue stained MCs, thus suggesting that the recruitment of MCs increases during the development of HCC. However, the results obtained from 22 HCC patients

did not indicate any significant correlation between MCs density and disease stage. We hypothesize that the lower density observed in the most severe stage may be due to the massive degranulation of a large number of MCs.

Moreover, the obtained results allow the following conclusions to be drawn: (a) MCs density did not significantly correlate with disease grade, but there was a trend towards a decrease in MCs number as the grade increased. (b) There was no correlation between MCs density and some baseline characteristics of the patients, such as the sex or age of the patients, since the tumour evolves more slowly in older patients, we expected to find a higher density in younger cases. This hypothesis was partially substantiated by an albeit statistically non-significant negative correlation between MCs density and age. This behaviour was in line with theoretical models showing that a large number of biological events were age-dependent [7]. (c) MCs density did not correlate with serum ALT or AST levels. HCV, cirrhosis and HCC were associated with persistent or fluctuating elevations in ALT levels, but did not distinguish among these conditions. (d) There was no significant difference in the density of MCs between patients with and without HCV disease. As it is known that there is a close relationship between HCC and hepatitis C virus infection, it is not surprising that we had more HCV-positive than HCV-negative cases. Nevertheless, MCs density was similar in both groups, suggesting that HCV infection did not increase MC recruitment. (e) The close proximity of MCs and surrounding tumour cells suggested the existence of roles of MCs in the development of HCC, including tumour growth as well as host immunity and stromal reaction. (f) The density of MCs was higher in the specimens showing a greater capillarisation of sinusoidal endothelial cells.

A number of studies have indicated that the sinusoidal endothelial cells tend to show phenotypic changes in the early stage of hepatocarcinogenesis. In HCC, endothelial fenestrae are diminished and basement membrane become thick: due to the fact that as the arterial blood supply for HCC increases, the sinusoidal endothelial cells may form basement membranes, mainly consisting of type IV collagen and laminin, and take on the morphological appearance of capillaries[41-44].

Capillarisation of sinusoids has also constant features such as the appearance of new junctions between endothelial cells, deposition of fibrillary material in Disse' s spaces, and flattening of hepatocyte microvilli. Capillarisation of the sinusoid may also cause a disturbance in exchanges of many bioactive substances between the sinusoidal blood and liver cells across the Disse space. Capillarisation, resulting in impairment of microcirculation, subsequently, affecting the exchange of the oxygen and substance of the liver cell seriously, thus brings about or aggravates the damage of liver cell[45]. Capillarisation may contribute to the HCC metastatic process. The angiogenesis of liver metastases may progress stepwise as the metastases enlarge, and capillarisation of sinusoidal endothelium around the liver metastases may occur. A number of papers have suggested that (a) tumour vessels in metastatic liver cancers consist of endothelium, collagenic basement membrane and pericytes, (b) the sinusoids adjacent to tumours undergo capillarisation, and (c) VEGF, a well-demonstrated mediator secreted by MCs may contribute to angiogenesis in metastatic HCC.

It is well documented that heparin, combined to a range of heparin-binding factors such as b-FGF or TGF-β, or other potent factors, such as IL-8 and VEGF, are able to promote neovascularity, and that MC proteases cause loss of the extracellular matrix integrity[27].

All these comments suggest that MCs accumulation at the tumour site may lead to increased rates of tumour vascularity and, consequently, increased rates of tumour growth and metastasis.

In conclusion, since capillarisation proceeds concurrently with arterial blood supply during hepatocarcinogenesis, MCs may be considered as a key element in the process of transition from sinusoidal endothelial cells into capillary-type endothelial cells and concurrently in the development of collagen' s basement membrane. MCs mediated capillarisation may thus be of pathogenic significance in tumor growth.

ACKNOWLEDGMENTS

The authors are grateful to prof. Massimo Roncalli and Dr Piergiuseppe Colombo for supplying the HCC specimens, and for their grading and staging classification. They would also like to thank Giorgia Ceva-Grimaidi for her precious technical support.

REFERENCES

1 **Ehrlich P.** Beitrage zur kenntniss der quilinfarbunger und ihrer verivendung in der mickroskopischen technik. *Alch Mikros Anat* 1877; **13:** 263-267
2 **Welle M.** Development, significance, and heterogeneity of mast cells with particular regard to the mast cell-specific proteases, chymase and tryptase. *J Leukoc Biol* 1997; **61:** 233-245
3 **Fodiger M**, Fritsch G, Winkler K, Emminger W, Mitterbauer G, Gadner H, Valent P, Mannhalter C. Origin of human mast cells: development from transplanted hematopoietic stem cells after allogenic bone marrow transplantation. *Blood* 1994; **84:** 2954-2959
4 **Galli SJ**. Mast cells and basophils. *Curr Opinion Haematol* 2000; **7:** 32-39
5 **Metcalfe DD**, Baram D, Mekori YA. Mast cells. *Physiol Rev* 1997; **77:** 1033-1079
6 **Farrell DJ**, Hines JE, Walls AF, Kelly PJ, Bennett MK, Burt AD. Intrahepatic mast cells in chronic liver diseases. *Hepatology* 1995; **22:** 1175-1181
7 **Grizzi F**, Franceschini B, Gagliano N, Barbieri B, Arosio B, Annoni G, Chiriva-Internati M, Dioguardi N. Mast cell density: a quantitative index of liver acute inflammation. *Anal Quant Cytol Histol* 2002; **24:** 63-69
8 **Grizzi F,** Franceschini B, Gagliano N, Moscheni C, Annoni G, Vergani C, Hermonat PL, Chiriva-Internati M, Dioguardi N. Mast cell density, hepatic stellate cell activation and TGF-β_1 trascript in aging Sprague-Dowely rat during the early acute liver injury. *Toxicol Pathol* 2003; **31:** 173-178
9 **Sari A**, Serri TA, Candir O, Ozturk A, Kosar A. Mast cell variations in tumour tissue and with histopathological grading in specimens of prostatic adenocarcinoma. *BJU International* 1999; **84:** 851-853
10 **Imada A**, Shijubo N, Kojima H, Abe S. Mast cells correlate with angiogenesis and poor outcome in stage lung adenocarcinoma. *Eur Respir J* 2000; **15:** 1087-1093
11 **Tomita M**, Matsuzaki Y, Onitsuka T. Effect of mast cells on tumor angiogenesis in lung cancer. *Ann Thorac Surg* 2000; **69:** 1686-1690
12 **Simak R**, Capodieci P, Cohen DW, Fair WR, Scher H, Melamed J, Drobnjak M, Heston WD, Stix U, Steiner G, Cordon-Cardo C. Expression of c-kit and kit-ligand in benign and malignant prostatic tissues. *Histol Histopathol* 2000; **15:** 365-374
13 **Toth-Jakatics R**, Jimi S, Takebayashi S, Kawamoto N. Cutaneous malignant melanoma: correlation between neovascularization and peritumor accumulation of mast cells overexpressing vascular endothelial growth factor. *Hum Pathol* 2000; **31:** 955-960
14 **Terada T**, Matsunaga Y. Increased mast cells in hepatocellular carcinoma and intrahepatic cholangiocarcinoma. *J Hepatol* 2000; **33:** 961-966
15 **Demitsu T**, Inoue T, Kakurai M, Kiyosawa T, Yoneda K, Manabe M. Activation of mast cells within a tumor of angiosarcoma: ultrastructural study of five cases. *J Dermatol* 2002; **29:** 280-289
16 **Yano H**, Kinuta M, Tateishi H, Nakano Y, Matsui S, Monden T, Okamura J, Sakai M, Okamoto S. Mast cell infiltration around gastric cancer cells correlates with tumor angiogenesis and metastasis. *Gastric Cancer* 1999; **2:** 26-32

17 **Cabanillas-Saez A**, Schalper JA, Nicovani SM, Rudolph MI. Characterization of mast cells according to their content of tryptase and chymase in normal and neoplastic human uterine cervix. *Int J Gynecol Cancer* 2002; **12:** 92-98

18 **Yavuz E**, Gulluoglu MG, Akbas N, Tuzlali S, Ilhan R, Iplikci A, Akhan SE. The values of intratumoral mast cell count and Ki-67 immunoreactivity index in differential diagnosis of uterine smooth muscle neoplasms. *Pathol Int* 2001; **51:** 938-941

19 **Elpek GO**, Gelen T, Aksoy NH, Erdogan A, Dertsiz L, Demircan A, Keles N. The prognostic relevance of angiogenesis and mast cells in squamous cell carcinoma of the oesophagus. *J Clin Pathol* 2001; **54:** 940-944

20 **Fukushima N**, Satoh T, Sano M, Tokunaga O. Angiogenesis and mast cells in non-Hodgkin's lymphoma: a strong correlation in angioimmunoblastic T-cell lymphoma. *Leuk Lymphoma* 2001; **42:** 709-720

21 **Tomita M**, Matsuzaki Y, Edagawa M, Shimizu T, Hara M, Sekiya R, Onitsuka T. Association of mast cells with tumor angiogenesis in esophageal squamous cell carcinoma. *Dis Esophagus* 2001; **14:** 135-138

22 **Erkilic S**, Erbagci Z. The significance of mast cells associated with basal cell carcinoma. *J Dermatol* 2001; **28:** 312-315

23 **Ribatti D**, Vacca A, Nico B, Crivellato E, Roncali L, Dammacco F. The role of mast cells in tumour angiogenesis. *Br J Haematol* 2001; **115:** 514-521

24 **Nielsen HJ**, Hansen U, Christensen IJ, Reimert CM, Brunner N, Moesgaard F. Independent prognostic value of eosinophil and mast cell infiltration in colorectal cancer tissue. *J Pathol* 1999; **189:** 487-495

25 **Reynolds JL**, Akhter JA, Magarey CJ, Schwartz P, Adams WJ, Morris DL. Histamine in human breast cancer. *Br J Surg* 1998; **85:** 538-541

26 **Kankkunen JP**, Harvima IT, Naukkarinen A. Quantitative analysis of tryptase and chymase containing mast cells in benign and malignant breast lesions. *Int J Cancer* 1997; **72:** 385-388

27 **Norrby K**. Mast cells and angiogenesis. *APMIS* 2002; **110:** 355-371

28 **Cairms JA**, Walls AF. Mast cell tryptase stimulates the synthesis of type 1 collagen in human lung fibroblast. *J Clin Invest* 1997; **99:** 1313-1321

29 **Inoue Y**, King TE Jr, Barker E, Daniloff E, Newman LS. Basic fibroblast growth factor and its receptors in idiopathic pulmonary fibrosis and lymphangioleiomyomatosis. *Am J Respir Crit Care Med* 2002; **166:** 765-773

30 **Armbrust T**, Batusic D, Burkhardt R, Ramadori G. Mast cells distribution in human liver disease and experimental rat liver fibrosis. Indications for mast cell participation in development of liver fibrosis. *J Hepatol* 1997; **26:** 1042-1054

31 **Yamashiro M**, Kouda W, Kono N, Tsuneyama K, Matsui O, Nakanuma Y. Distribution of intrahepatic mast cells in various hepatobiliary disorders. An immunohistochemical study. *Virchows Arch* 1998; **433:** 471-479

32 **Neubauer K**, Saile B, Ramadori G. Liver fibrosis and altered matrix synthesis. *Can J Gastroenterol* 2001; **15:** 187-193

33 **Tani K**, Ogushi F, Shimizu T, Sone S. Protease-induced leukocyte chemotaxis and activation: roles in host defense and inflammation. *J Med Invest* 2001; **48:** 133-141

34 **Coussens LM**, Werb Z. Inflammatory cells and cancer: think different. *J Exp Med* 2001; **193:** F23-F26

35 **Montemurro P**, Nishioka H, Dundon WG, de Bernard M, Del Giudice G, Rappuoli R, Montecucco C. The neutrophil-activating protein (HP-NAP) of Helicobacter pylori is a potent stimulant of mast cells. *Eur J Immunol* 2002; **32:** 671-676

36 **Dimitriadou V**, Koutsilieris M. Mast cell-tumor cell interactions: for or against tumour growth and metastasis? *Anticancer Res* 1997; **17:** 1541-1549

37 **Bradding P**, Feather IH, Wilson S, Bardin PG, Heusser CH, Holgate ST, Howarth PH. Immunolocalization of cytokines in the nasal mucosa of normal and perennial rhinitic subjects. The mast cell as a source of IL-4, IL-5, and IL-6 in human allergic mucosal inflammation. *J Immunol* 1993; **151:** 3853-3865

38 **Bradding P**, Roberts JA, Britten KM, Montefort S, Djukanovic R, Mueller R, Heusser CH, Howarth PH, Holgate ST. Interleukin-4, -5, and -6 and tumor necrosis factor-alpha in normal and asthmatic airways: evidence for the human mast cell as a source of these cytokines. *Am J Respir Cell Mol Biol* 1994; **10:** 471-480

39 **Okayama Y**, Petit-Frere C, Kassel O, Semper A, Quint D, Tunon-de-Lara MJ, Bradding P, Holgate ST, Church MK. IgE-dependent expression of mRNA for IL-4 and IL-5 in human lung mast cells. *J Immunol* 1995; **155:** 1796-1808

40 **Wilson SJ**, Shute JK, Holgate ST, Howarth PH, Bradding P. Localization of interleukin (IL) -4 but not IL-5 to human mast cell secretory granules by immunoelectron microscopy. *Clin Exp Allergy* 2000; **30:** 493-500

41 **Kin M**, Torimura T, Ueno T, Inuzuka S, Tanikawa K. Sinusoidal capillarization in small hepatocellular carcinoma. *Pathol Int* 1994; **44:** 771-778

42 **Yamamoto T**, Kaneda K, Hirohashi K, Kinoshita H, Sakurai M. Sinusoidal capillarization and arterial blood supply continuously proceed with the advance of the stages of hepatocarcinogenesis in the rat. *Jpn J Cancer Res* 1996; **87:** 442-450

43 **Zimmernann A**, Zhao D, Reichen J. Myofibroblast in the cirrhotic rat liver reflects hepatic remodelling and correlates with fibrosis and sinusoidal capillarization. *J Hepatol* 1999; **30:** 646-652

44 **Park YN**, Yang CP, Fernandez GJ, Cubukcu O, Thung SN, Theise ND. Neoangiogenesis and sinusoidal "capillarization" in dysplastic nodules of the liver. *Am J Surg Pathol* 1998; **22:** 656-662

45 **Huang GW**, Yang LY. Metallothionein expression in hepatocellular carcinoma. *World J Gastroenterol* 2002; **8:** 650-653

Edited by Xu XQ and Wang XL

P.O.Box 2345, Beijing 100023,China
Fax: +86-10-85381893
E-mail: wjg@wjgnet.com www.wjgnet.com

World J Gastroenterol 2003;9(7):1474-1476
World Journal of Gastroenterology
 ISSN 1007-9327

• LIVER CANCER •

Antitumor and immunomodulatory activity of resveratrol on experimentally implanted tumor of H22 in Balb/c mice

Hong-Shan Liu, Cheng-En Pan, Wei Yang, Xue-Min Liu

Hong-Shan Liu, Cheng-En Pan, Wei Yang, Xue-Min Liu, Department of Hepatobiliary Surgery, First Affiliated Hospital, Xi' an Jiaotong University, Xi' an 710061, Shaanxi Province, China
Correspondence to: Dr. Hong-Shan Liu, Department of Hepatobiliary Surgery, First Affiliated Hospital, Xi' an Jiaotong University, Xi' an 710061, Shaanxi Province, China. doctorliuqi@ yahoo.com.cn
Telephone: +86-29-5324009 **Fax:** +86-29-5324009
Received: 2002-10-17 **Accepted:** 2002-12-07

Abstract

AIM: To study the antitumor and immunomodulatory activity of resveratrol on experimentally implanted tumor of H22 in Balb/c mice

METHODS: The cytotoxicity of peritoneal macrophages (M ϕ) against H22 cells was measured by the radioactivity of [^{3}H]TdR assay, mice with H22 tumor were injected with different concentrations of resveratrol, and the inhibitory rates were calculated and IgG contents were determined by single immunodiffusion method. the plaque forming cell (PFC) was measured by improved Cunningham method, the levels of serum tumor necrosis factor-α (TNF-α) were measured by cytotoxic assay against L929 cells.

RESULTS: Resveratrol 2.5 mg·L^{-1}, 5.0 mg·L^{-1}, 10.0 mg·L^{-1}, 20.0 mg·L^{-1} (E:T=10:1, 20:1) promoted the cytotoxicity of M ϕ against H22 cells. Resveratrol ip 500 mg·kg^{-1}, 1 000 mg·kg^{-1} and 1 500 mg·kg^{-1} could curb the growth of the implanted tumor of H22 in mice. The inhibitory rates were 31.5 %, 45.6 % and 48.7 %, respectively (P<0.05), which could raise the level of serum IgG and PFC response to sheep red blood cell. Resveratrol 1 000 mg·kg^{-1} and 1 500 mg·kg^{-1} and BCG 200 mg·kg^{-1} ip could increase the production of serum TNF-α in mice H22 tumor. However, the effect of resveratrol was insignificant (P >0.05).

CONCLUSION: Resveratrol could inhibit the growth of H22 tumor in Balb/c mice. The antitumor effect of resveratrol might be related to directly inhibiting the growth of H22 cells and indirectly inhibiting its potential effect on nonspecific host immunomodulatory activity.

Liu HS, Pan CE, Yang W, Liu XM. Antitumor and immunomodulatory activity of resveratrol on experimentally implanted tumor of H22 in Balb/c mice. *World J Gastroenterol* 2003; 9(7): 1474-1476
http://www.wjgnet.com/1007-9327/9/1474.asp

INTRODUCTION

Recently, considerable attention has been focused on identifying naturally occurring chemopreventive substances capable of inhibiting, retarding, or reversing the multi-stage carcinogenesis. Resveratrol (3,5,4' -trihydroxy-trans-stilbene), a phytoalexin found in grapes and other dietary and medicinal plants, has been shown to have anti-inflammatory, antioxidant and antitumor activities[1-7]. Many of these beneficial effects of resveratrol require participation of the cells of the immune system. However, the effect of resveratrol on the development of immuological responses remains unknown.

In the present study, the antitumor activity and immunomodulatory actions of resveratrol, including M ϕ against H22 cells, serum IgG and the plaque forming cells and tumor necrosis factor (TNF-α) content in Balb/C mice with experimentally implanted tumor of H22 were investigated.

MATERIALS AND METHODS

Materials

Resveratrol, MTT, IPS and dimethylsulfoxide (DMSO) were purchased from SGMA Co. Mouse hepatocellular carcinoma cells H22, L929 and sheep red blood cell (SRBC) were kindly supplied by Cheng Wei (Center of Molecular Biology, First Affiliated Hospital, Xi' an Jiaotong University). Cells were subcultured in RPMI 1640 (Gibco) which was supplemented with 10 % fetal bovine serum, penicillin (100 IU·ml^{-1}) and streptomycin (100 mg·l^{-1}). Stock solution of resveratrol was made in dimethylsulfoxide (DMSO) at a concentration of 10 g·L^{-1}. Working dilutions were directly made in the tissue culture medium. [^{3}H]TdR was purchased from Shanghai Nuclear Research Institute. IL test kit and LPS were purchased from Gibco Co. Balb/C mice, 2.5 month old, weighing 20±2 g, were purchased from the Animal Center, Xi' an Jiaotong University.

Methods

Effect of resveratrol on cytotoxicity of peritoneal macrophages (M ϕ) against H22 cells M ϕ was collected from the peritoneal cavity of Balb/c mice 3 days after ip 10 % sheep red blood cells (SRBC,1 ml/mouse). The cells were washed twice and resuspended in RPMI 1640 culture medium. H22 cells were cultured for 12 h, and 100 μl M ϕ suspension and different concentrations of resveratrol were added to each well of 96-well plates at a ratio of effectors: target (E:T) cell 10:1 or 25:1. After cultured for 24 h, each well was added with [^{3}H]TdR (9. 3 kBq/well), and then was incubated for another 6 h. Cells were placed onto the glass fiber filter and [^{3}H]TdR incorporation was determined by liquid scintillation. The cytotoxicity was calculated with the following formula: the cytotoxicity of M ϕ =(control-treatment)/control×100 % (dpm).
Anti-tumor activity of resveratrol and its effect on serum antibody IgG, plaque forming cells (PFC) in Balb/C mice with implanted tumor of H22 Mouse ascites (including 2×10^5 cells) were injected into the right axilla of 40 Balb/c mice. On the second day, 40 Balb/c mice were divided into 4 groups randomly, and then were injected with resveratrol at a dose of 500 mg·kg^{-1},1000 mg·kg^{-1}, 1 500 mg·kg^{-1} and normal saline for 10 d. Mice were sensitized to ip SRBC (3×10^7 cells). After 4 d, the mice were bled to obtain serum for IgG investigation. At the same time, spleens were excised for PFC counting. IgG contents were determined by single immunodiffusion method. PFC was measured by modified Cunningham method.
Effect of resveratrol on serum tumor necrosis factor alpha

(TNF-α) production induced by LPS in Balb/c mice Ascites cells of 2×10^5 were injected into the Balb/c mice. Resveratrol at a dose a 500 mg· kg^{-1}, 1 000 mg· kg^{-1} and 1 500 mg· kg^{-1} was injected for 10 d, and BCG of 200 mg· kg^{-1} as a positive control agent was injected ip on d 1.On d 11, 90 minutes after ip LPS of 0.1 mg· kg^{-1}, the mice were exsanguinated. Blood was centrifuged (400×g,10 min). The levels of serum TNF-α were measured by cytotoxic assay against L929 cells as described previously. The TNF-α activity was calculated with the following formula: cytotoxicity=$(A_{control}-A_{test})/A_{control}\times100$ %.

RESULTS

Effect of resveratrol on cytotoxicity of peritoneal macrophages (M φ) against H22 cells

Resveratrol at 2.5 mg· l^{-1} could decrease the cytotoxicity of M φ against H22 cells (P>0.05). Resveratrol at l2.5 mg· l^{-1}, 5.0 mg· l^{-1}, 10.0 mg· l^{-1} could enhance insignificantly the cytotoxicity of M φ against H22 cells (P>0.05) concentration-dependently, However, resveratrol at 20.0 mg· l^{-1} could raise significantly the cytotoxicity of M φ against H22 cells (P<0.05) (Table 1).

Table 1 Effect of resveratrol on cytotoxicity of peritoneal macrophages (M φ) against H22 cells *in vitro* (n=3)

Resveratrol (mg·l^{-1})	Cytotoxicity of M φ: H22 (10:1)	φ(%) M φ: H22 (25:1)
Control	12.6±7.9	15.6±6.0
1.25	10.9±2.9[a]	10.6±5.4[a]
2.50	12.5±3.2[a]	16.4±1.8[a]
5.0	13.4±2.8[a]	27.6±2.6[a]
10.0	14.6±3.7[a]	18.3±4.2[a]
20.0	16.7±4.7[b]	20.2±3.1[b]

[a]P>0.05, [b]P<0.05 *vs* control.

Anti-tumor activity of resveratrol and its effect on serum antibody IgG, plaque forming cells(PFC) in Balb/c mice with implanted tumor of H22

Resveratrol ip at a dose 500 mg· kg^{-1}, 1 000 mg· kg^{-1} and 1 500 mg· kg^{-1} could significantly curb the growth of implanted tumor of H22 in mice. The inhibitory rates were 31.5 %, 45.6 % and 48.7 %,respectively (P<0.05, Table 2).

Table 2 Inhibitory rates of resveratrol on H22 in mice *in vivo*

Group	Dose mg.kg^{-1}	Route	Mice begin/end	Tumor weight (x±s) (g)	Inhibitory rate (%)	P value
Control		ip	10/9[b]	1.81±0.62		
Resveratrol 1	500	ip	10/8[b]	1.24±0.40	31.5	<0.05[a]
Resveratrol 2	1000	ip	10/9[b]	0.99±0.35	45.6	<0.05[a]
Resveratrol 3	1500	ip	10/10	0.93±0.25	48.7	<0.05[a]

[a]P<0.05 *vs* control; [b]killed by other mice.

The result also showed that the immunity of mice with tumor could be more significantly inhibited than that of normal mice, and resveratrol ip could raise the level of serum LgG and number of PFC in Balb/c mice with implanted tumor of H22 *in vivo*. Resveratrol, however, could insignificantly increase the immunity of mice with tumor (P>0.05, Table 3).

Effect of resveratrol on serum tumor necrosis factor alpha (TNF-α) production induced by LPS in Balb/c mice

The ability of TNF-α production of mice with H22 tumor was significantly stronger than that of normal mice. Furthermore, the group of control and BCG at 200 mg· kg^{-1} ip had an increase in the at production of serum TNF-α in mice with H22 tumor (P<0.05), but resveratrol at a dose of 500 mg· kg^{-1}, 1 000 mg· kg^{-1} and 1 500 mg· kg^{-1} had less effect on mice with H22 tumor (P>0.05, Table 4).

Table 3 Effects of resveratrol on serum antibody IgG, plaque forming cells (PFC) in Balb/c mice with implanted tumor of H22 *in vivo*

Group	Dose mg.kg^{-1}	Route	IgG/g·L^{-1}	PFC/10^6 cells
Normal mice	NS	ip	27±8	441±32
Control	NS	ip	19±6[a]	297±57[a]
Resveratrol 1	500	ip	20±8[a]	305±53[a]
Resveratrol 2	1000	ip	23±6[a]	328±49[a]
Resveratrol 3	1500	ip	24±5[a]	348±46[a]

[a]P>0.05 *vs* normal mice or control.

Table 4 Effect of resveratrol on TNF-α production induced by LPS in Balb/c mice

Group	Dose (mg· kg^{-1})	Route	TNF-α activity specific lysis
Normal mice	NS	ip	7.1±3.2
Control	NS	ip	16.3±2.3[a]
Resveratrol 1	500	ip	15.8±2.0[ab]
Resveratrol 2	1000	ip	17.7±2.9[ab]
Resveratrol 3	1500	ip	19.5±3.1[ab]
Control+BCG	200	ip	29.8±3.7[ab]

[a]P<0.05 *vs* normal mice; [b]P>0.05 *vs* control.

DISCUSSION

Resveratrol is a phytopolyphenol isolated from the seeds and skin of grapes. Recent studies have indicated that resveratrol can block the process of multistage carcinogenesis, namely, tumor initiation, promotion and progression. Resveratrol can also reduce the risk of cardiovascular diseases in man. These activities have been identified by some authors[8-13]. Roberto *et al*[14] have shown that PBMC exposure to resveratrol produced a biphasic effect on the anti-CD3/anti-CD28-induced development of both IFN-y-IL-2 and IL4-producing CD8+ and CD4$^+$T cells, with stimulation at low resveratrol concentrations and suppression at high concentrations. Similarly, the compound was found to induce a significant enhancement at low concentrations and suppression at high concentrations of both CTL and NK cell cytotoxic activity. Gao *et al*[15] found that mitogen-, IL-2- or alloantigen-induced proliferation of splenic lymphocytes, induction of cytotoxic T lymphocytes (CTLs) and lymphokine activated killer (LAK) cells, and production of the cytokine interferon (IFN)-y, interleukin (IL)-2, tumor necrosis factor(TNF)-α were significantly suppressed at 25-50 μM resveratrol, but in some cases mitogen/IL-2-induced production and CTL generation were enhanced following pretreatment of cells with resveratrol. The effects of resveratrol on immune function of mice *in vivo* have not been reported yet.

Our results indicate that resveratrol of 2.5 mg· l^{-1} could decrease the cytotoxicity of M φ against H22 cells (P>0.05). Resveratrol of 2.5 mg· l^{-1}, 5.0 mg· l^{-1} and 10.0 mg· l^{-1} could insignificantly enhance the cytotoxicity of M φ against H22 cells concentration-dependently (P>0.05). However, resveratrol of 20.0 mg· l^{-1} could raise significantly the cytotoxicity of M φ against H22 cells (P<0.05). So, resveratrol could alone affect the [^{3}H]TDR uptake by H22 cells *in vitro*,

suggesting that the antitumor action of resveratrol had a direct cytotoxic effect. This result is coincident with the previous studies[16-18]. Resveratrol ip could insignificantly increase the host nonspecific immunological defense of mice with H22 tumor, by raising the level of serum IgG and TNF-α and the number of PFC (P>0.05). *In vivo* resveratrol could also augment the cytotoxicity of peritoneal macrophages against H22 cells, and there was an insignificant difference compared with the control group (P>0.05). Therefore, resveratrol could inhibit the growth of H22 cells *in vivo*, but it could not significantly enhance the host immune defense against tumor. Based on the results of the present study, it can be suggested that the antitumor activity of resveratrol might be due to direct cytotoxic/antiproliferative activity against tumor cells, but not to the augmentation of immune response against tumors. It has demonstrated that resveratrol inhibits cell proliferation, cell-mediated cytotoxicity, and cytokine production, at least in part through the inhibition of NF-kappa B activation. But the molecular mechanism by which resveratrol imparts cancer chemopreventive effects has not been clearly defined and further studies are needed.

REFERENCES

1 **Kris-Etherton PM,** Hecker KD, Bonanome A, Coval SM, Binkoski AE, Hilpert KF, Griel AE, Etherton TD. Bioactive compounds in foods: their role in the prevention of cardiovascular disease and cancer. *Am J Med* 2002; **30:** 71S-88S

2 **Park EJ,** Pezzuto JM. Botanicals in cancer chemoprevention. *Cancer Metastasis Rev* 2002; **21:** 231-255

3 **Olas B,** Wachowicz B, Saluk-Juszczak J, Zielinski T. Effect of resveratrol, a natural polyphenolic compound, on platelet activation induced by endotoxin or thrombin. *Thromb Res* 2002; **107:** 141-145

4 **Martinez J,** Moreno JJ. Effect of resveratrol, a natural polyphenolic compound, on reactive oxygen species and prostaglandin production. *Biochem Pharmacol* 2000; **59:** 865-870

5 **Latruffe N,** Delmas D, Jannin B, Malki MC, Passilly-Degrace P, Berlot JP. Molecular analysis on the chemopreventive properties of resveratrol, a plant polyphenol microcomponent. *Int J Mol Med* 2002; **10:** 755-760

6 **Ding XZ,** Adrian TE. Resveratrol inhibits proliferation and induces apoptosis in human pancreatic cancer cells. *Pancreas* 2002; **25:** 71-76

7 **Cal C,** Garban H, Jazirehi A, Yeh C, Mizutani Y, Bonavida B. Resveratrol and Cancer: Chemoprevention, Apoptosis, and Chemo-immunosensitizing Activities. *Curr Med Chem Anti-Canc Agents* 2003; **3:** 77-93

8 **Asensi M,** Medina I, Ortega A, Carretero J, Bano MC, Obrador E, Estrela JM. Inhibition of cancer growth by resveratrol is related to its low bioavailability. *Free Radic Biol Med* 2002; **33:** 387-398

9 **De-Ledinghen V,** Monvoisin A, Neaud V, Krisa, S, Payrastre B, Bedin C, Desmouliere A, Bioulac-Sage P, Rosenbaum J. Trans-resveratrol, a grapevine- derived polyphenol, blocks hepatocyte growth factor-induced invasion of hepatocellular carcinoma cells. *Int J Oncol* 2001; **19:** 83-88

10 **Tian XM,** Zhang ZX. The anticancer activity of resveratrol on implanted tumor of HepG2 in nude mice. *Shijie Huaren Xiaohua Zazhi* 2001; **9:** 161-164

11 **Liu HS,** Pan CE, Qi Y, Liu QG, Liu XM. Effect of resveratrol with 5-FU on growth of implanted H22 tumor in mice. *Shijie Huaren Xiaohua Zazhi* 2002; **10:** 32-35

12 **Sun ZJ,** Pan CE, Liu HS, Wang GJ. Anti-hepatoma activity of resveratrol *in vitro*. *World Gastroenterol* 2002; **8**: 79-81

13 **Zhou HB,** Yan Y, Sun YN, Zhu JR. Resveratrol induces apoptosis in human esophageal carcinoma cells. *World J Gastroenterol* 2003; **9:** 408-411

14 **Falchetti R,** Fuggetta MP, Lanzilli G, Tricarico M, Ravagnan G. Effects of resveratrol on human immune cell function. Effect of resveratrol on human immune cell function. *Life Sciences* 2001; **70:** 81-96

15 **Gao X**, Xu YX, Janakiraman N, Chapman RA, Gautam SC. Immunomodulatory activity of resveratrol: suppression of lymphocyte proliferation, development of cell-mediated cytotoxicity, and cytokine production. *Biochemical Pharmacol* 2001; **62:** 1299-1308

16 **Delmas D,** Jannin B, Malki MC, Latruffe N. Inhibitory effect of resveratrol on the proliferation of human and rat hepatic derived cell lines. *Oncol Rep* 2000; **7:** 847-352

17 **Brakenhielm E,** Cao R, Cao Y. Suppression of angiogenesis, tumor growth, and wound healing by resveratrol, a natural compound in red wine and grapes. *FASEB J* 2001; **15:** 1798-1800

18 **Dong Z.** Molecular mechanism of the chemopreventive effect of resveratrol. *Mutat Res* 2003; **523-524:** 145-150

Edited by Ma JY

P.O.Box 2345, Beijing 100023,China
Fax: +86-10-85381893
E-mail: wjg@wjgnet.com www.wjgnet.com

World J Gastroenterol 2003;9(7):1477-1481
World Journal of Gastroenterology
 ISSN 1007-9327

• COLORECTAL CANCER •

Laparoscopic total mesorectal excision of low rectal cancer with preservation of anal sphincter: A report of 82 cases

Zong-Guang Zhou, Zhao Wang, Yong-Yang Yu, Ye Shu, Zhong Cheng, Li Li, Wen-Zhang Lei, Tian-Cai Wang

Zong-Guang Zhou, Zhao Wang, Yong-Yang Yu, Ye Shu, Zhong Cheng, Li Li, Wen-Zhang Lei, Tian-Cai Wang, Department of General Surgery and Institute of Digestive Surgery, West China Hospital, Sichuan University, Chengdu 610041, Sichuan Province, China
Supported by the Key Project of National Outstanding Youth Foundation of China, No. 39925032
Correspondence to: Zong-Guang Zhou, Department of General Surgery and Institute of Digestive Surgery, West China Hospital, Sichuan University, Chengdu 610041, Sichuan Province, China. zhou767@21cn.com
Telephone: +86-28-85422484
Received: 2002-06-14 **Accepted:** 2002-07-19

Abstract

AIM: To assess the feasibility and efficacy of laparoscopic total mesorectal excision (LTME) of low rectal cancer with preservation of anal sphincter.

METHODS: From June 2001 to June 2003, 82 patients with low rectal cancer underwent laparoscopic total mesorectal excision with preservation of anal sphincter. The lowest edge of tumors was below peritoneal reflection and 1.5-7 cm from the dentate line (1.5-5 cm in 48 cases, 5-7 cm in 34 cases).

RESULTS: LTME with anal sphincter preservation was performed on 82 randomized patients with low rectal cancer, and 100 % sphincter preservation rate was achieved. There were 30 patients with laparoscopic low anterior resection (LLAR) at the level of the anastomosis below peritoneal reflection and 2 cm above from the dentate line; 27 patients with laparoscopic ultralow anterior resection (LULAR) at the level of anastomoses 2 cm below from the dentate line; and 25 patients with laparoscopic coloanal anastomoses (LCAA) at the level of the anastomoses at or below the dentate line. No defunctioning ileostomy was created in any case. The mean operating time was 120 minutes (ranged from 110-220 min), and the mean operative blood loss was 20 mL (ranged from 5-120 mL). Bowel function was restored and diet was resumed on day 1 or 2 after operation. The mean hospital stay was 8 days (ranged from 5-14). Postoperative analgesics were used in 45 patients. After surgery, 2 patients had urinary retention, one had anastomotic leakage, and another 2 patients had local recurrence one year later. No interoperative complication was observed.

CONCLUSION: LTME with preservation of anal sphincter is a feasible, safe and minimally invasive technique with less postoperative pain and rapid recovery, and importantly, it has preserved the function of the sphincter.

Zhou ZG, Wang Z, Yu YY, Shu Y, Cheng Z, Li L, Lei WZ, Wang TC. Laparoscopic total mesorectal excision of low rectal cancer with preservation of anal sphincter: A report of 82 cases. *World J Gastroenterol* 2003; 9(7): 1477-1481
http://www.wjgnet.com/1007-9327/9/1477.asp

INTRODUCTION

The optimal operation for rectal cancer still remains controversial. Surgical management of rectal cancer has undergone a significant change during the past two decades, a new concept of total mesorectal excision (TME) was introduced[1], and its feasibility and efficacy had been confirmed by a series of clinical trials[2-5]. Compared with conventional procedure, TME markedly improved both oncological and functional outcomes of rectal cancer[6-9], therefore, this procedure has been used as a golden standard for rectal cancer.

Laparoscopic approach has been employed in colorectal surgery for ten years, and its feasibility has been shown in a variety of colorectal operations[10-14]. However, for inadequate operative vision and limitation of the narrow pelvis, total laparoscopic TME with construction of colo-anal anastomosis for low rectal cancer has been regarded as being difficult and time-consuming, and mainly used for upper rectal cancer for a long time[15,16]. Few cases about laparoscopic TME with anal sphincter preservation (SP) for low rectal cancer were reported[17]. The current study was performed to assess the feasibility and efficacy of laparoscopic total mesorectal excision (LTME) for low rectal cancer with preservation of anal sphincter.

MATERIALS AND METHODS

Patients

Between June 2001 and June 2003, randomized 82 patients with low rectal cancer underwent laparoscopic total mesorectal excision with anal sphincter preservation at Department of General Surgery of West China Hospital. The lowest edges of tumors were below peritoneal reflection and 1.5-7 cm from the dentate line (1.5-5 cm in 46 cases, and 5-7 cm in 36 cases). Patients with previous abdominal surgery, obese body, and other surgical benign diseases were not excluded from the laparoscopic procedure. Clinical and demographic data including age, sex, tumor diameter, distances of tumor from the dentate line, concomitant diseases are shown in Table 1.

Table 1 Clinical and demographic data

Parameters	Data
Age, mean (years)	26-85, 44
Sex (No. of patients)	
Male	46
Female	36
Tumor diameter, mean (cm)	1.5-13, 5.6
Distance of the tumor from the dentate line (cm)	1.5-7
1.5-5 cm from lowest edge of tumors to the dentate line (No. of patients)	48
5-7 cm from lowest edge of tumors to the dentate line (No. of patients)	34
Concomitant diseases (No. of patients)	
Chronic cholecystitis, cholecystolithiasis, torsion of ovarian cyst and diabetes	2
Chronic cholecystitis and cholecystolithiasis	6
Previous lower abdominal operation	7

Preoperative examinations including flexible endoscopes, biopsy, ultrasonography, CT scan, radiography of the chest were performed routinely. All patients underwent preoperative bowel preparation (1L 10 % mannite electrolyte solution). Prophylactic antibiotics (ciprofloxacin and metronidazole) were given three days before operation routinely. A urinary catheter and a nasogastric tube were used.

Operative techniques

Under general anesthesia, 82 patients were operated in lithotomic position with 15° head-down tilt by the same surgeon (ZZ ZHOU) with two assistants (YY. YU and Y. SHU). Pneumoperitoneum was introduced through subumbilical incision to maintain pressure at 12-14 mmHg (1 mmHg=0.133 Kpa). A camera port was created in subumbilical zone with trocar, then an operative port in the right midclavicular line at the level of umbilicus, and an other two operative ports in the left and right McBurney point were created.

Laparoscope was inserted at 25° or 30° into abdominal cavity via the camera port. Routine intra-abdominal exploration was performed. All sharp dissections and divisions on peritoneum, fascia, and connective tissue in retroperitoneal space were performed with a harmonic scalpel. Left lateral peritoneal was divided first, and then sigmoid and descending colon were mobilized completely to ensure the subsequent colo-anal anastomosis free of tension. Then the bowel and its mesentery by a cotton tape at the level 8-10 cm above the upper margin of the tumor were tied, lymph nodes around inferior mesenteric vessels were dissected, and inferior mesenteric vessels were ligated at the high level.

With the operation proceeding of total mesorectal excision, division was moved downward into the pelvis along the anatomic space between visceral and parietal endopelvic fascia. Lateral ligaments of the rectum containing the middle rectal artery or its branches (Figure 1) were gradually divided with the harmonic scalpel from the inner limit of the inferior hypogastric nerve fibers (Figure 2). The pelvic splanchnic nerves were preserved intact as far as possible. Anteriorly, Denonvilliers' fascia was dissected and the seminal vesicles and prostate or the posterior wall of the vagina were exposed (Figure 3). At posterior, the rectosacral ligament, anococcygeal ligament, and pubococcygeus muscle were divided, and S_2, S_3, and S_4 sacral splanchnic nerves were identified and protected carefully. The mesorectum, especially the distal mesorectum (DMR), was excised completely till levator ani. Thus, longitudinal muscle layer of the distal precutting rectum and levator ani could be clearly visualized under laparoscopic view, so-called ' denudation' and ' muscularization' . For low bulky tumor, the ' denudation' should be performed under intra-anal finger-guidance to avoid inadvertent damage of adjacent structures. The rectal cross clamping was performed 1.5-3.5 cm below the tumor with endo-cutter (Figure 4).

To extract the bowel loop of the tumor, the port incision was extended at the left McBurney' s point to about 3.5 cm long, and isolated the tumor routinely by inserting in a sheath-shaped plastic bag through the incision. The tumor and the proximal colon was extracted through the bag, and then transected the bowel at the level of 10-15 cm above upper margin of the tumor. After inserting the anvil of 29 or 30 mm-sized circular stapler into the end of proximal bowel and securing with 2/0 prolene purse-string suture, the proximal bowel was internalized and the extended incision was closed. Pneumoperitoneum was induced again. Laparoscopic colo-anal or colo-rectal anastomosis was done with CDH 29 circular stapler. After the circular stapler was inserted into the anus, its puncturing cone was pricked through the midpoint of the distal occluding line of the rectum (Figure 5), and fitted into the anvil of the stapler in the pelvic cavity. The stapler was then closed slowly with extreme cautions to avoid inadvertent stapling of adjacent important structures. In this way, the low/ultralow/ colo-anal anastomoses were accomplished smoothly. A 10 mm-sized latex tube was routinely put into pelvic cavity through the port at the right McBurney point. No defunctioning ileostomy was created in any case. Distal clearance measurements were taken in an unfixed and unpinned status of surgical specimen in the operating room. The specimen was routinely checked if the visceral endopelvic fascia was dissected completely, and then sent for pathologic examination (Figure 6).

Laparoscopic cholecystectomy and ovariectomy could be performed simultaneously for patients with cholecystolithiasis, chronic cholecystitis, ovarian cyst, and torsion of the ovary.

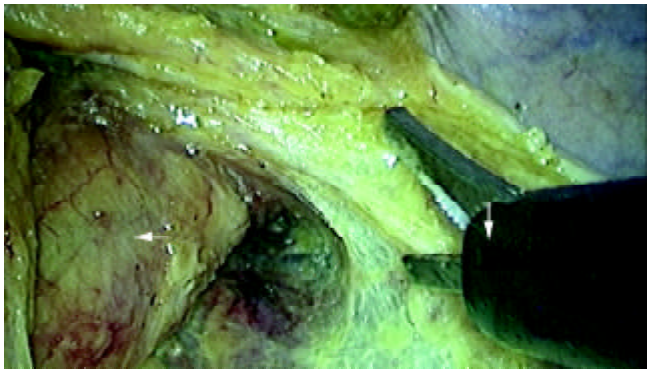

Figure 1 The "lateral ligaments" (→) of rectum containing middle rectal artery or its branches, and mesorectum (←) were dissected completely with a harmonic scalpel (↓).

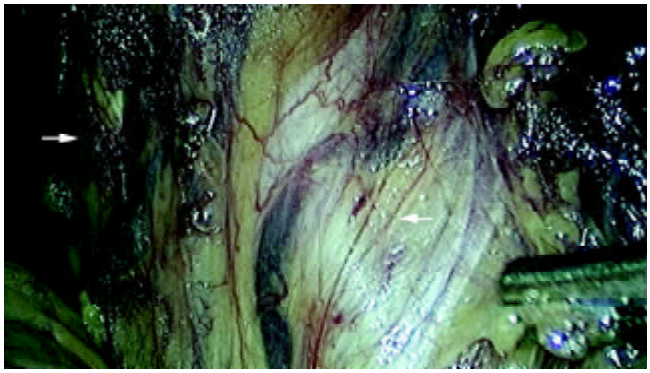

Figure 2 The left pelvic splanchnic nerves were preserved intact as far as possible. Inset shows the inferior hypogastric nerve nerve fibers (←) and the ureter (→).

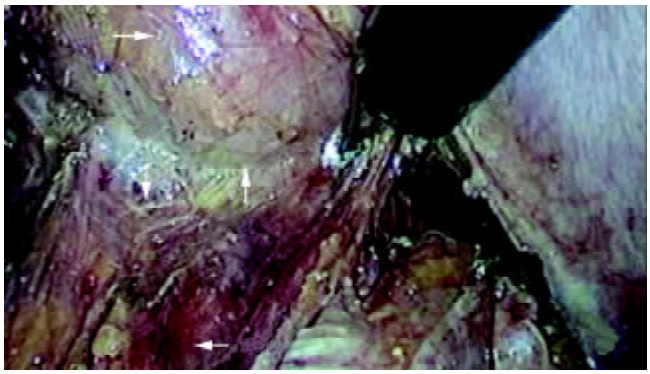

Figure 3 Denonvilliers' fascia (↓)was dissected along the space (↑) between the posterior wall of vagina (→) and the rectum (¡ û).

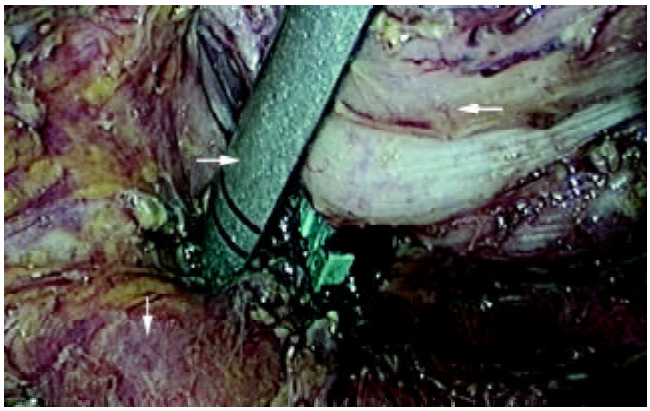

Figure 4 The cross clamping of the rectum (←) was performed 1.5~3.5cm below the tumor with endo-cutter (→). Pelvic floor 'muscularization' was shown (↓).

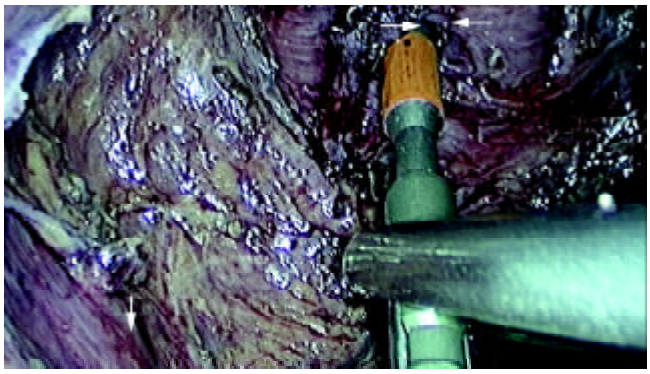

Figure 5 The puncturing cone (→) of the circular stapler pricked through the midpoint of occluding line of the distal rectum(←). Levator ani muscles were exposed (↓).

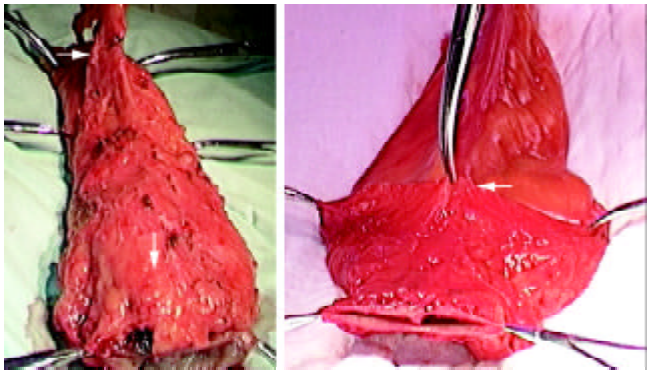

Figure 6 The dorsal mesorectum (→) and distal mesorectum (↓) of the rectal specimen were shown (6a). The anterior side of the specimen and distal margin (←) were shown (6b).

RESULTS

TME with anal sphincter preservation was accomplished with laparoscope in 82 randomized patients with low rectal cancer, and 100 % sphincter preservation rate was achieved. There were 30 patients by laparoscopic low anterior resection (LLAR) at the level of the anastomosis below peritoneal reflection and 2 cm above the dentate line; 27 patients by laparoscopic ultralow anterior resection (LULAR) at the level of the anastomosis 2 cm below the dentate line; and 25 patients by laparoscopic coloanal anastomoses (LCAA) at the level of the anastomosis at/below the dentate line (Figure 7). No defunctioning ileostomy was created in any case. The mean operating time was 120 minutes (ranged from 110-220 min), and the mean operative blood loss was 20 mL (ranged from 5-120 mL). Both bowel function recovery and diet resumption occurred within 1-2 days after surgery, and the mean hospital stay were 8 days (ranged from 5-14). Postoperative analgesics were used in 45 patients. One patient was converted to open surgery due to dysfunction of coagulation. After operation, 2 patients had urinary retention, one had anastomotic leakage, 2 patients had local recurrence one year later, and no interoperative complication was observed. Clinical and surgical details in this study including tumor and anastomotic levels from anal verge, stage of disease, duration of surgery, length of specimen removed, duration of parenteral analgesia, time to passage of flatus, time to resumption of liquids and solids, and length of post-operative stay are shown in Tables 2,3 and 4.

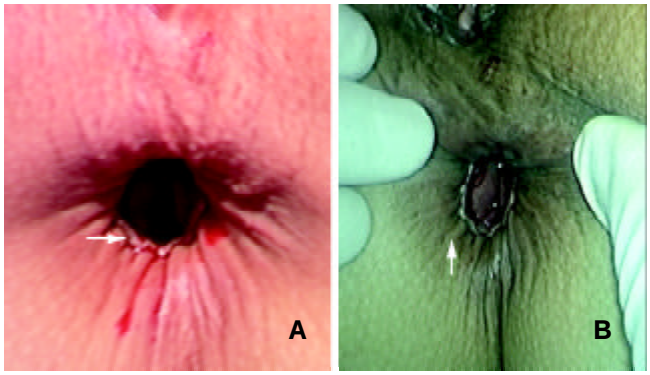

Figure 7 The anastomotic ring (→) could be shown easily in the patient receiving colo-anal anastomosis (a). Satisfactory contractive function of the saved anus (↑) was achieved in the patients receiving laparoscopic TME with anal sphincter preservation at the first day after operation (b).

Table 2 Clinical parameters for patients with LTME and SP

Parameters	Data
Dukes stage (No. of patients)	
A	5
B	10
C1	33
C2	30
D	4
Pathologic types (No. of patients)	
High differentiated adenocarcinoma	24
Moderately differentiated adenocarcinoma	37
Low differentiated adenocarcinoma	21
Multiple primary carcinomas on the bowel wall	3
Distance of the tumor from the section edge (cm)	1.5-4
Cancer cell found in the cut margins (No. of patients)	1
Colo-rectal / anal anastomotic height (cm) (No. of patients)	
LLAR, below peritoneal reflection and 2 cm above the dentate line	30
LULAR, 2 cm below the dentate line	27
LCAA, at / below the dentate line	25

Table 3 Early results for laparoscopic TME and SP

Parameters	Data
Operation time (min)	120(110-220)
Operative bleeding (ml)	20(5-120)
Time for bowel function recovery (d)	1-2
Time to resume normal diet (d)	1-2
Post-operative analgesic requirement (No. Of patients)	45
Total hospital stay (d)	8 (5-14)
Sphincter preservation rate (%)	100 %
Mortality (%)	0

Table 4 Complications of laparoscopic TME and SP

Complications	No. of patients
Total number of patients	82
Perforation of rectum	0
Urethra damage	0
Intra-abdominal bleeding	0
Pelvic abscess	0
Urinary retention	2
Anastomotic Leakage	1
Local recurrence	2

The patients were mobilized two days after operation. Oral intake was gradually increased with the recovery of intestinal function. Most of the patients with low anastomosis as well as about 1/2 of the patients with ultralow or colo-anal anastomosis experienced a quick recovery in anal sphincter' s function and controlling of defecation, while 50 % of patients with ultralow anastomosis or colo-anal anastomosis suffered from urgent defecation about 5-10 times per day, and their defecation was controlled gradually by proper medication and functional exercise of anal sphincter and levator ani around half a year.

There were no portal site recurrence and mortality observed during follow-up, which ranged from 1 to 24 months.

DISCUSSION

Study on the management of rectal cancer has progressed greatly in both clinical practice[18-23] and basic research[24-27] in recent years. Multiple clinical studies have demonstrated the correlation of high pelvic recurrence with the degree of mesorectal excision[28]. Residual mesorectum, especially inadequate excision of distal mesorectum (DMR), contributed to poor oncologic outcomes. Regarding DMR, histopathological evidence revealed a high metastasis rate in this region, and it was also found that patients with metastasis in this region would experience a poor prognosis. This is why the principle of TME should be followed in the treatment of rectal cancer[29-31]. Since clinical application of TME, the local recurrence rate of the cancer has decreased dramatically to 5-7.1 %[7,32,33], while that of conventional operative procedure remains 18.5 %.

Up to now, there are only a few reports on laparoscopic procedure for low rectal cancer in the literatures, which was mainly due to inadequate surgical vision and limitation of the narrow pelvis. The area 5-8 cm from anal verge and below peritoneal reflection has ever been considered as a blind zone and that within 5 cm from anal verge as a forbidden zone. The current study revealed that the so-called blind and forbidden zones could be broken through, and minimally invasive TME with anal sphincter preservation could be performed safely for patients with rectal cancer based on our success of the large number of open TME and low/ultralow/colo-anal anastomosis and proficient laparoscopic skill. This study is concerned with our experience in colorectal surgery and deals with special laparoscopic colorectal techniques including LLAR, LULAR and LCAA.

Based on our clinical experiences, laparoscopic TME and SP have the following advantages: (1) it helps surgeons identify accurately the interspace of loose connective tissue between visceral and parietal pelvic fascia, and select operative access by amplifying inner image on the monitors. (2) 25° or 30° laparoscope, the third eye of the surgeon, can reach the narrow lesser pelvis and magnify the local vision; (3) it is more definite to identify and protect the pelvic autonomic nerve fiber and plexus due to its magnifying function. (4) hemostatic benefit was owed to minimally invasive sharp dissection with minimal blood loss under laparoscopic view.

However, the laparoscopic technique has its disadvantages, such as long operative time, short of direct hand feeling, technical constraints of the narrow pelvis, difficulty in assessing adequate surgical margins and in ultralow rectal cross clamping, and a long learning course for surgeons.

Good experience with laparoscopic surgery leads to shorter operating time and encouraging results. A bulky tumor or a thickening mesentery usually occupies the most space of narrow pelvic cavity and often influence the operation. To avoid this impact, the camera operator should try his best to adjust laparoscope constantly by 25-30°, which keeps the operator at a correct position. Crack sight and smog are other troublesome problems. Crack sight often occurs after the operation moving into lesser pelvis and it can be solved by adjusting the angle of laparoscope properly. Smog results from the operation of using the harmonic scalpel or cautery, which often distracts operator' s vision, even breaks the operative process. The camera operator should withdraw the laparoscope and disperse the smog in time when smog is too heavy or obscures the lens of laparoscope. Therefore, the role of the camera operator is so important that his skill can directly influence the operative processes and results.

The anastomosis is a critical step for the success of this minimally invasive technique with anal sphincter preservation[28]. Double stapling technique (DST) is the remarkable progress in the anastomosis for the operation of low rectal cancer in recent years. Research showed that local recurrence rate was much lower in patients treated with DST than those treated with conventional anastomosis[34]. Low/ultralow/colo-anal anastomoses in all cases of laparoscopic procedure were achieved with DST at this hospital. Based on our experience, there are two special points regarding the anastomosis with DST: (1) denudation of the distal rectal tube, and (2) selection of the pricking point on the occluding line. By denuding the pre-cutting part of the rectal tube, the fat and lymphatic tissue within the mesorectum of distal rectum could be thoroughly excised, the denuded rectal longitudinal muscle could be visualized, and the distal rectum could easily be divided and occluded with endo-stapler. The pricking point of the cone on the stapler should locate at midpoint of the occluding line, because too much displacement of the pricking point may result in ischemia and leakage of the anastomosis, or stapling of adjacent important structures. These two steps can effectively prevent rectal wall from damage and dehiscence of the anastomosis, reduce the use of endo-staplers, and decrease local recurrence.

Special training on TME technique is necessary for surgeons to have enough experience of TME and SP[35]. Proficient skills of laparoscopic operation in pelvis and plentiful experience of open TME are important factors for the success of LTME and SP.

REFERENCES

1 **Heald RJ**, Husband EM, Ryall RDH. The mesorectum in rectal cancer surgery - the clue to pelvic recurrence? *Br J Surg* 1982; **69**: 613-616
2 **Goldberg S**, Klas JV. Total mesorectal excision in the treatment of rectal cancer: a view from the USA. *Semin Surg Oncol* 1998; **15**: 87-90
3 **MacFarlane JK**, Ryall RD, Heald RJ. Mesorectal excision for rectal cancer. *Lancet* 1993; **341**: 457-460
4 **Ceelen W**, Pattyn P. Total mesorectal excision in the treatment of rectal cancer: a review. *Acta Chir Belg* 2000; **100**: 94-99
5 **Kapipeijn E**, van De Velde CJ. European trials with total mesorectal excision. *Semin Surg Oncol* 2000; **19**: 350-357
6 **Lazuskas T**, Lelcuk S, Michowitz M, Rabau M. Anterior resection with colo-anal anastomosis for low rectal cancer. *Harefuah* 1994; **126**: 505-506
7 **Killingback M**, Barron P, Dent OF. Local recurrence after curative resection of cancer of the rectum without total mesorectal excision. *Dis Colon Rectum* 2001; **44**: 473-483

8 **Bolognese A**, Cardi M, Muttillo IA, Barbarosos A, Bocchetti T, Valabrega S. Total mesorectal excision for surgical treatment of rectal cancer. *J Surg Oncol* 2000; **74**: 21-23

9 **Kapiteijn E**, Putter H, van de Velde CJ. Impact of the introduction and training of total mesorectal excision on recurrence and survival in rectal cancer in The Netherlands. *Br J Surg* 2002; **89**: 1142-1149

10 **Monson JR**, Darzi A, Carey PD, Guillou PJ. Prospective evaluation of laparoscopic-assisted colectomy in an unselected group of patients. *Lancet* 1992; **340**: 831-833

11 **Huscher C**, Silecchia G, Croce E, Farello GA, Lezoche E, Morino M, Azzola M, Feliciotti F, Rosato P, Tarantini M, Basso N. Laparoscopic colorectal resection. A multicenter Italian study. *Surg Endosc* 1996; **10**: 875-879

12 **Kwok SP**, Lau WY, Carey PD, Kelly SB, Leung KL, Li AK. Prospective evaluation of laparoscopic-assisted large bowel excision for cancer. *Ann Surg* 1996; **223**: 170-176

13 **Barlehner E**, Decker T, Anders S, Heukrodt B. Laparoscopic surgery of rectal carcinoma. Radical oncology and late results. *Zentralbl Chir* 2001; **126**: 302-306

14 **Watanabe M**, Teramoto T, Hasegawa H, Kitajima M. Laparoscopic ultralow anterior resection combined with per anum intersphincteric rectal dissection for lower rectal cancer. *Dis Colon Rectum* 2000; **43**(Suppl): S94-S97

15 **Hartley JE**, Mehigan BJ, Qureshi AE, Duthie GS, Lee PW, Monson JR. Total mesorectal excision: assessment of the laparoscopic approach. *Dis Colon Rectum* 2001; **44**: 315-321

16 **Weiser MR**, Milsom JW. Laparoscopic total mesorectal excision with autonomic nerve preservation. *Semin Surg Oncol* 2000; **19**: 396-403

17 **Chung CC**, Ha JP, Tsang WW, Li MK. Laparoscopic-assisted total mesorectal excision and colonic J pouch reconstruction in the treatment of rectal cancer. *Surg Endosc* 2001; **15**: 1098-1101

18 **Cao GW**, Qi ZT, Pan X, Zhang XQ, Miao XH, Feng Y, Lu XH, Kuriyama S, Du P. Gene therapy for human colorectal carcinoma using human CEA promoter controled bacterial ADP-ribosylating toxin genes human CEA: PEA & DTA gene transfer. *World J Gastroenterol* 1998; **4**: 388-391

19 **Mao AW**, Gao ZD, Xu JY, Yang RJ, Xiao XS, Jiang TH, Jiang WJ. Treatment of malignant digestive tract obstruction by combined intraluminal stent installation and intraarterial drug infusion. *World J Gastroenterol* 2001; **7**: 587-592

20 **Makin GB**, Breen DJ, Monson JR. The impact of new technology on surg ery for colorectal cancer. *World J Gastroenterol* 2001; **7**: 612-621

21 **Deng YC**, Zhen YS, Zheng S, Xue YC. Activity of boanmycin against colorectal cancer. *World J Gastroenterol* 2001; **7**: 93-97

22 **Wang SH**, Zheng YQ. A clinicopathologic analysis of 354 cases of large intestinal cancer in western. *Hunan Xin Xiaohuabingxue Zazhi* 1996; **4**: 325-326

23 **Kapiteijn E**, Marijnen CA, Nagtegaal ID, Putter H, Steup WH, Wiggers T, Rutten HJ, Pahlman L, Glimelius B, van Krieken JH, Leer JW, van de Velde CJ. Preoperative radiotherapy combined with total mesorectal excision for resectable rectal cancer. *N Engl J Med* 2001; **345**: 638-646

24 **Yuan HY**, Li Y, Yang GL, Bei DJ, Wang K. Study on the causes of local recurrence of rectal cancer after curative resection: analysis of 213 cases. *World J Gastroenterol* 1998; **4**: 527-529

25 **Qing SH**, Jiang HY, Qi DL, Zhou ZD, Huang XC, Zhang FM, Sheng QG. Relationship between related factors with lymph node metastasis of colorectal cancer. *Shijie Huaren Xiaohua Zazhi* 2000; **8**:654-657

26 **Gao ZS**, Yin CH, Song DY, Liu FZ, Gu YZ, Liu YP. Clinical significance of pedicled greater omentum transplantation in radical resection of rectal cancer. *Huaren Xiaohua Zazhi* 1998; **6**: 875-876

27 **Yang JH**, Rao BQ, Wang Y, Tu XH, Zhang LY, Chen SH, Ou Yang XN, Dai XH. Clinical significance of detecting the circulating cancer cells in peripheral blood from colorectal cancer. *Shijie Huaren Xiaohua Zazhi* 2000; **8**: 187-189

28 **Wexner SD**, Rotholtz NA. Surgeon influenced variables in resectional rectal cancer surgery. *Dis Colon Rectum* 2000; **43**: 1606-1627

29 **Choi JS**, Kim SJ, Kim YI, Min JS. Nodal metastasis in the distal mesorectum: need for total mesorectal excision of rectal cancer. *Yonsei Med J* 1996; **37**: 243-250

30 **Tocchi A**, Mazzoni G, Lepre L, Liotta G, Costa G, Agostini N, Miccini M, Scucchi L, Frati G, Tagliacozzo S. Total mesorectal excision and low rectal anastomosis for the treatment of rectal cancer and prevention of pelvic recurrences. *Arch Surg* 2001; **136**: 216-220

31 **Scott N**, Jackson P, al-Jaberi T, Dixon MF, Quirke P, Finan PJ. Total mesorectal excision and local recurrence: a study of tumour spread in the mesorectum distal to rectal cancer. *Br J Surg* 1995; **82**: 1031-1033

32 **Heald RJ**. Total mesorectal exsicion (TME). *Acta Chir Iugosl* 2000; **47**(4 Suppl 1): 17-18

33 **McCall JL**, Cox MR, Wattchow DA. Analysis of local recurrence rates after surgery alone for rectal cancer. *Int J Colorectal Dis* 1995; **10**: 126-132

34 **Law WL**, Chu KW. Impact of total mesorectal excision on the results of surgery of distal rectal cancer. *Br J Surg* 2001; 88: 1607-1612

35 **Heald RJ**. Total mesorectal excision is optimal surgery for rectal cancer: a scandinavian consensus. *Br J Surg* 1995; **82**: 1297-1299

Edited by Ren SY

P.O.Box 2345, Beijing 100023,China
Fax: +86-10-85381893
E-mail: wjg@wjgnet.com www.wjgnet.com

World J Gastroenterol 2003;9(7):1482-1486
World Journal of Gastroenterology
 ISSN 1007-9327

• COLORECTAL CANCER •

Expression of proliferating cell nuclear antigen and CD44 variant exon 6 in primary tumors and corresponding lymph node metastases of colorectal carcinoma with Dukes' stage C or D

Ji-Cheng Zhang, Zuo-Ren Wang, Yan-Juan Cheng, Ding-Zhong Yang, Jing-Sen Shi, Ai-Lin Liang, Ning-Na Liu, Xiao-Min Wang

Ji-Cheng Zhang, Zuo-Ren Wang, Ding-Zhong Yang, Jing-Sen Shi, Department of Hepatobiliary Surgery, First Hospital of Xi' an Jiaotong University, Xi' an 710061, Shannxi Province, China
Yan-Juan Cheng, Department of Medical Education, Shannxi Provincial Cancer Hospital, Xi' an 710061, Shannxi Province, China
Ai-Lin Liang, Ning-Na Liu, Xiao-Min Wang, Department of Pathology, Shannxi Provincial Cancer Hospital, Xi' an 710061, Shannxi Province, China
Correspondence to: Professor Zuo-Ren Wang, Department of Hepatobiliary Surgery, First Hospital of Xi' an Jiaotong University, Xi' an 710061, Shannxi Province, China. zjc1986@hotmail.com
Telephone: +86-29-5324009
Received: 2002-10-09 **Accepted:** 2002-11-12

Abstract

AIM: To study changes in characteristics of colorectal carcinoma during the metastatic process and to investigate the correlation between cell proliferation activity and metastatic ability of patients with Dukes' stage C or D.

METHODS: Formalin fixed and paraffin embedded materials of primary tumors and corresponding lymph node metastases resected from 56 patients with Dukes' stage C or D of colorectal carcinoma were stained immunohistochemically with proliferating cell nuclear antigen (PCNA) and CD44 variant exon 6 (CD44v6).

RESULTS: Thirty-one of 56 patients (55.4 %) expressed PCNA in the primary sites and 36 of 56 patients (64.3 %) expressed PCNA in the metastatic lymph nodes. A significant relation in PCNA expression was observed between the primary site and the metastatic lymph node ($0.010<P<0.025$). Forty-one of 56 patients (73.2 %) expressed CD44v6 in the primary site and 39 of 56 patients (69.6 %) expressed CD44v6 in the metastatic lymph node. There was also an significant relationship of CD44v6 between the primary site and the metastatic lymph node ($0.005<P<0.010$). No difference was observed between expression of CD44v6 and PCNA in the primary site ($0.250<P<0.500$).

CONCLUSION: This study partially demonstrates that tumor cells in metastatic lymph node of colorectal carcinoma still possess cell proliferation activity and metastatic ability of tumor cells in primary site. There may be no association between cell proliferation activity and metastatic ability in colorectal carcinoma.

Zhang JC, Wang ZR, Cheng YJ, Yang DZ, Shi JS, Liang AL, Liu NN, Wang XM. Expression of proliferating cell nuclear antigen and CD44 variant exon 6 in primary tumors and corresponding lymph node metastases of colorectal carcinoma with Dukes' stage C or D. *World J Gastroenterol* 2003; 9(7): 1482-1486
http://www.wjgnet.com/1007-9327/9/1482.asp

INTRODUCTION

Colorectal carcinoma appears to be increasing in Chinese populations and is characterised by an aggressive course and frequent metastases resulting in death. To reduce morbidity and mortality, identification of those patients with a high propensity to develop distant metastases is of great importance, since they might benefit from adjuvant chemotherapy and/or radiotherapy[1,2]. Although Dukes' classification is still considered as the most accurate predictor of prognosis after resection, even within a group of tumors of a specified stage, tumor behaviour and prognosis of the disease is not uniform[3-5]. For this reason, additional markers that predict tumor metastatic behaviour are needed[6-9]. At present, PCNA has been described as a significant factor in the prognosis of colorectal carcinoma in several studies[10-12]. On the other hand, many studies demonstrated that expression of CD44v6 correlated with poor survival and was an independent prognosticator in patients who underwent radical surgery[13-17]. However, to our knowledge questions concerning metastases, characteristic changes that occur during the metastatic process, and the correlation between tumor characteristics have to be clarified in detail[18-20]. To our knowledge, there has been neither any study regarding patients with Dukes' stage C or D analyzing both primary sites and corresponding metastatic lymph nodes genetically or immunohistologically nor a study assessing their relationship.

We examined the expression of these two factors in both primary sites and metastatic lymph nodes to elucidate the characteristic changes of the tumor during metastases and to evaluate the correlation between cell proliferation activity and metastatic ability of the tumor in patients with Dukes' stage C or D of colorectal carcinoma.

MATERIALS AND METHODS

Materials

175 consecutive patients with colorectal carcinoma admitted to our department underwent resection between 1989 and 1996. The total rate of lymph node metastasis was 33.7 %, 77.2 %, of which lymph node metastasis next to the colorectum was, 17.9 % and 4.9 % mesentery and mesenteric artery ligation point respectively. Of these 175 patients, 62 (35.8 %) were diagnosed with Dukes' stage C or D. Among these 62 patients, 56 whose primary site and metastatic node tissues were immunohistochemically evaluable were enrolled in the study. They were comprised of 30 males and 26 females with a mean age of 51.3±14.2 years. Forty nine patients with Dukes' stage C underwent a complete tumor resection with lymph node dissectioned and 7 patients with Dukes' stage D underwent a palliative tumor resection with lymph node dissectioned in the Department of Gastroenterology, Shannxi Provincial Cancer Hospital in Xi' an, China. The patients had not been treated before. Their respective clinical data were collected through the review of their medical records. Histologic typing revealed 12 papillary adenocarcinomas, 27 tubular adenocarcinomas, 10 mucinous adenocarcinomas, 5 signet-ring cell carcinomas

and 2 undifferentiated carcinomas. Of these patients, there were 49 patients with Dukes' stage C, whose average number of metastatic lymph nodes was 5.3±2.1 and 7 patients with Dukes' stage D, whose average number of metastatic sites including lymph node, liver, greater omentum and peritoneum was 8.7±2.6. The paraffin-embedded blocks and histological slides were taken from the Department of Pathology, Shaanxi Provincial Cancer Hospital (Table 1).

Table 1 Characteristics of patients with Dukes' stage C or D colorectal carcinoma

Gender	Male	30
	Female	26
Age(yrs) (mean±SD)	51.3±14.2	
Histology	Papillary adenocarcinoma	12
	Tubular adenocarcinoma	27
	Mucinous adenocarcinoma	10
	Signet-ring cell carcinoma	5
	Undifferentiated carcinoma	2
Dukes' classification	Stage C	49
	Stage D	7

Methods

Formalin fixed, paraffin embedded sections of samples were stained immunohistochemically with labeled streptavidin-biotin (LSAB) using a LSAB Kit (Doctor Biotechnology Company, Wuhan, Hubei Province, China). The samples were thinly sectioned (4 μm thick). After deparaffinization, the sections were hydrolyzed with ethanol and endogenous peroxidase activity was inhibited with 0.3 % hydrogen peroxide-containing methanol at room temperature for 15 minutes. For antigen retrieval, the sections were mounted in 300 mL 0.01 M sodium citrate buffer (pH 6.0) in a container and microwaved for 15 minutes at maximum power in a Sharp microwave oven (850 W). Nonspecific binding sites were blocked with 10 % nonimmune goat serum. For PCNA, PC10 (Zymed Laboratories, California) whose optimal dilution was 1:150 was used for the first antibody and allowed to react at 4 ℃ for 12 hours. For CD44v6, CD44 variant exon 6 (VFF-18; Bender Co.) whose optimal dilution was 1:100 was used for the first antibody and allowed to react at 4 ℃ for 12 hours. After the second antibody was made to react, peroxidase-labeled streptoavidin was finally allowed to react as an enzyme reagent. Diaminobenzidine was used for coloring. Sections of human tonsils and submucosal lymphoid follicles were used as positive control for PCNA. Positive control of CD44v6 was normal human stratified squamous epithelium which could be strongly stained by anti-CD44v6 antibodies[15]. Sections stained by omitting the primary antibody were used as their negative controls. At least 5 visual fields of the immunohistochemically stained sample were observed at random at ×100 or ×400 magnification. More than 1000 tumor cells were counted by two investigators who were blinded to the clinical outcome. The number of positive cells was counted and expressed as percentage. For PCNA, when the percentage of positive cells was ≤50 %, the specimen was diagnosed as negative, and when >50 %, the specimen was diagnosed as positive. We also determined the percentage of cells positively stained for CD44v6, as well as the intensity of this staining. Negative, ≤ 10 % of cells were positively stained, and positive, >10 % cells were positively stained[21]. The data were analyzed using χ^2 text and a P value <0.05 was considered significant.

RESULTS

Immunohistochemical staining with PCNA showed a selective nuclear pattern (Figures 1,2). Thirty-one of 56 patients (55.4 %) expressed PCNA in the primary site and 36 of 56 patients (64.3 %) expressed PCNA in the metastatic lymph node. Among these 56 patients, twenty-four expressed PCNA in both the primary site and metastatic lymph node, seven patients expressed PCNA in the primary site but did not express it in the metastatic lymph node, whereas twelve patients did not express PCNA in the primary site but expressed it in the metastatic lymph node, thirteen patients expressed PCNA in neither the primary site nor metastatic lymph node (Table 2). For expression of PCNA in these 56 patients, a significant relation was observed between the primary site and the metastatic lymph node ($0.010< P<0.025$).

Table 2 Expression of PCNA in colorectal carcinoma at primary sites and metastatic lymph nodes

Metastatic lymph nodes	Primary sites	
	-	+
-	13	7
+	12	24

Note: $\chi^2=5.21$, $0.010<P<0.025$.

Intensely positive staining with CD44v6 mainly occurred on the cell membrane surface of tumor cells (Figure 3). Forty-one of 56 patients (73.2 %) expressed CD44v6 in the primary site and 39 of 56 patients (69.6 %) expressed CD44v6 in the metastatic lymph node (Figure 4). Among these 56 patients, thirty-three expressed CD44v6 in both the primary site and metastatic lymph node, eight expressed CD44v6 in the primary site but did not express it in the metastatic lymph node, whereas six did not express CD44v6 in the primary site but expressed it in the metastatic lymph node, nine expressed CD44v6 in neither primary site nor metastatic lymph node (Table 3). For expression of CD44v6 in these 56 patients, there was also an significant relationship between the primary site and the metastatic lymph node ($0.005< P<0.010$).

Table 3 Expression of CD44v6 in colorectal carcinoma at primary sites and metastatic lymph nodes

Metastatic lymph nodes	Primary sites	
	-	+
-	9	8
+	6	33

Note: $\chi^2=6.71$, $0.005<P<0.010$.

Table 4 Expression of PCNA and CD44v6 in colorectal carcinoma at primary sites

PCNA	CD44v6	
	-	+
-	5	20
+	10	21

Note: $\chi^2=1.06$, $0.250<P<0.500$

To evaluate the correlation between cell proliferation activity and metastatic ability, we studied expression of PCNA and CD44v6 in the primary site. Among these 56 patients, twenty-one expressed both PCNA and CD44v6 and 5 expressed neither PCNA nor CD44v6 in the primary site, twenty expressed CD44v6 but did not express PCNA, whereas ten did not express CD44v6 but expressed PCNA in the primary site (Table 4).

No difference was observed between expression of CD44v6 and PCNA in the primary site($0.250< P<0.500$).

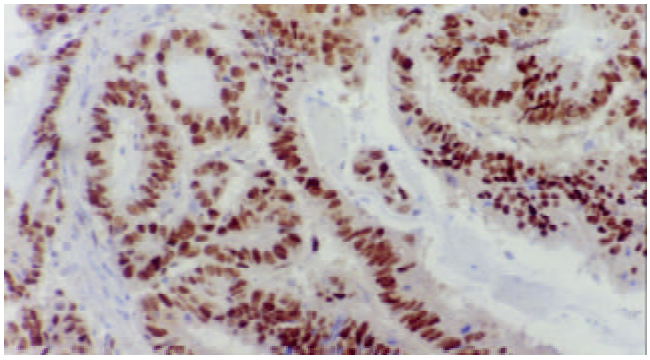

Figure 1 Positive expression of PCNA in primary colorectal carcinoma tissue (LSAB×100).

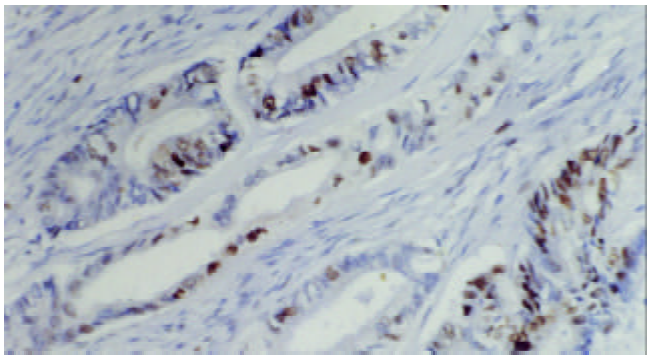

Figure 2 Negative expression of PCNA in primary site (LSAB×100).

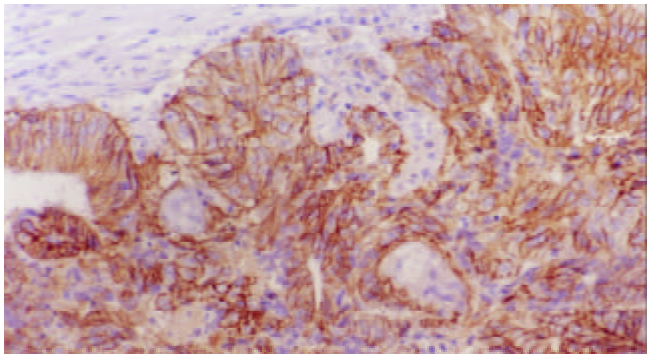

Figure 3 CD44v6 was observed on the cell membrane of tumor cells (LSAB×100).

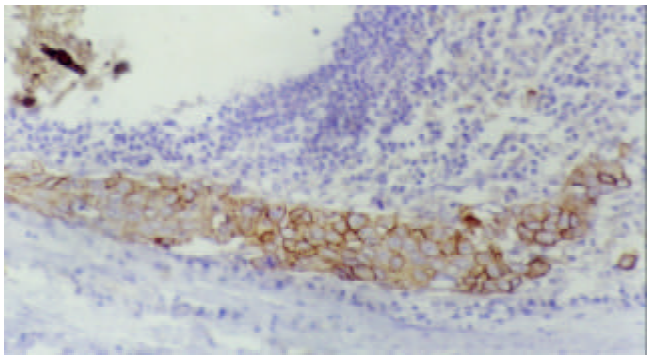

Figure 4 Expression of CD44v6 in corresponding metastatic lymph node, showing that tumor cells were invading lymph node from periphery. (LSAB×100).

Cell morphology

Immunohistochemical staining with PCNA showed a selective nuclear pattern (Figures 1,2). Intensely positive staining with CD44v6 mainly occurred on the cell membrane surface of tumor cells (Figure 3). Expression of CD44v6 in corresponding metastatic lymph node showed that tumor cells were invading lymph node from periphery (Figure 4).

DISCUSSION

One of the first steps in multistage colonic carcinogenesis is increased cell proliferation. PCNA, which is a nonhistone nuclear protein of 36 kilodaltons, also is known as cyclin and an auxiliary factor in DNA polymerase, plays a very important role in DNA replication[22]. Because of this direct relation with cell proliferation, PCNA is considered to be an important factor in prognosis. In fact, it has been described as a significant factor in the prognosis of colorectal carcinoma in several studies[10-12]. CD44, a glycoprotein of the membrane penetration type, functions as an extracellular matrix glycan receptor and a hyaluronate receptor[23]. As a consequence of studies in rats showed that CD44v6 could confer metastatic potential to rat pancreatic carcinoma cell lines[24], studies addressing the prognostic and biological significance of CD44 variant expression in human cancer have largely been focused on CD44v6. Overexpression of CD44v6 has been demonstrated in colorectal neoplasia by immunohistochemistry, RT-PCR and *in situ* hybridization. Their expression was found to correlate with tumor stage[13-17]. As for prognosis, it was shown that expression of CD44v6 correlate with poor survival rate and was an independent prognosticator in patients who underwent radical surgery. Hence, it identifies individuals with a high propensity to develop metastases. These patients might benefit from adjuvant therapy[16].

Despite intensive research in recent years, very little is known about the characteristic changes of malignant colorectal tumor cells during the process of metastases. We examined expression of these two factors in both primary site and metastatic lymph node. Among these 56 patients, twenty-four expressed PCNA in both the primary site and metastatic lymph node and thirteen expressed PCNA in neither the primary site nor metastatic lymph node. The concordence rate of PCNA expression in the primary site and in the metastatic lymph node was 66.1 % ($0.010< P<0.025$). That is to say, compared with primary site, PCNA expression in metastatic lymph node had no significant change. This suggests that cell proliferation activity revealed by PCNA still exists in the tumor cells of metastatic lymph nodes. Similarly, the concordence rate of CD44v6 expression in the primary site and in the metastatic lymph node was 75.0 % ($0.005<P<0.010$). This also means that metaststic ability revealed by CD44v6 still exists in the tumor cells of metastatic lymph nodes.

Although cell proliferation and metastasis are a very complicated problem involving many molecular mechanisms and biologic factors, our study partially showed that tumor cells in metastatic lymph node of colorectal carcinoma still possessed cell proliferation activity and metastatic ability of tumor cells in primary site. However, Kimball *et al*[25] isolated a cellular subpopulation from a human colonic carcinoma cell line and Brattain *et al*[26] reported that malignant cells from a human colonic carcinoma possessed heterogeneity. A question rises: do tumor cells of colorectal carcinoma not possess heterogeneity between the primary site and the metastatic lymph node? It is well known that cancer cell population, either as a solid tumor mass *in vivo* or as a continuous cell line *in vitro*, is an ever-changing entity due to their genetic instability and selective environmental pressure. A tumor mass consists of different cell clones, a phenomenon known as tumor

heterogeneity[27,28]. Based on this phenomenon, tumor cell clones with different biological properties have been isolated from a number of human and animal tumor cell lines. The differences included a variety of biological characteristics such as tumor cell morphology, karyotypes, *in vitro* and *in vivo* growth patterns[29,30], DNA ploidy[31] tumorigenicity, metastatic patterns and metastatic potentials[32]. Cancer metastasis is the ultimate display of complex interactions between the malignant cells and the host defense mechanism. The process of metastasis consists of selection and sequential steps that include angiogenesis, detachment,motility, invasion of the extracellular matrix, intravasation, circulation, adhesion, extravasation into the organ parenchyma and growth[28]. The ability of cancer cells to form metastasis depends on a set of unique biological properties that enable the malignant cells to complete all those steps of metastatic cascade. But this basically biological theory is not in contradiction with our present study, because our results are a clinicopathologic outcome depending upon experiment.

Our study showed that there was no significant association between expression of CD44v6 and PCNA in the primary site ($0.250< P<0.500$). This result partially indicated that there existed no absolute association between cell proliferation activity and metastatic ability in colorectal carcinoma. At present, whether tumor cell growth rate is directly related to metastasis is not clear yet. Yasoshima *et at*[33] using metastatic gastric cancer cell line, and Samiei *et al*[34] using metastatic mammary clones found that metastasis was independent of tumor cell growth, while other works[35-37] showed a close association between tumor cell growth rate and metastasis. Further study of the correlation between cell proliferation activity and metastatic ability in colorectal carcinoma is therefore needed.

In conclusion, we have partially demonstrated in the present study that tumor cells in metastatic lymph node of colorectal carcinoma still possess cell proliferation activity and metastatic ability in primary site. There may be no association between cell proliferation activity and metastatic ability in colorectal carcinoma.

REFERENCES

1 **Mayer RJ,** O'Connell MJ, Tepper JE, Wolmark N. Status of adjuvant therapy for colorectal cancer. *J Natl Cancer Inst* 1989; **81**: 1359-1364

2 **Moertel CG.** Chemotherapy for colorectal cancer. *N Engl J Med* 1994; **330**: 1136-1142

3 **Steele G Jr.** Advances in the treatment of early- to late-stage colorectal cancer: 20 years of progress. *Ann Surg Oncol* 1995; **2**: 77-88

4 **Greene FL,** Stewart AK, Norton HJ. A new TNM staging strategy for node-positive (stage III) colon cancer: an analysis of 50, 042 patients. *Ann Surg* 2002; **236**: 416-421

5 **Fisher ER,** Sass R, Palekar A, Fisher B, Wolmark N. Dukes' classification revisited. Findings from the National Surgical Adjuvant Breast and Bowel Projects (Protocol R-01). *Cancer* 1989; **64**: 2354-2360

6 **Douglass HO Jr,** Moertel CG, Mayer RJ, Thomas PR, Lindblad AS, Mittleman A, Stablein DM, Bruckner HW. Survival after postoperative combination treatment of rectal cancer. *N Engl J Med* 1986; **315**: 1294-1295

7 **Laurie JA,** Moertel CG, Fleming TR, Wieand HS, Leigh JE, Rubin J, McCormack GW, Gerstner JB, Krook JE, Malliard J. Surgical adjuvant therapy of large-bowel carcinoma: an evaluation of levamisole and the combination of levamisole and fluorouracil. The North Central Cancer Treatment Group and the Mayo Clinic. *J Clin Oncol* 1989; **7**: 1447-1456

8 **Krook JE,** Moertel CG, Gunderson LL, Wieand HS, Collins RT, Beart RW, Kubista TP, Poon MA, Meyers WC, Mailliard JA. Effective surgical adjuvant therapy for high-risk rectal carcinoma. *N Engl J Med* 1991; **324**: 709-715

9 **Harris GJ,** Church JM, Senagore AJ, Lavery IC, Hull TL, Strong SA, Fazio VW. Factors affecting local recurrence of colonic adenocarcinoma. *Dis Colon Rectum* 2002; **45**: 1029-1034

10 **Kanazawa Y,** Onda M, Tanaka N, Seya T. Proliferating cell nuclear antigen and p53 protein expression in submucosal invasive colorectal carcinoma. *J Nippon Med Sch* 2000; **67**: 242-249

11 **Onodera H,** Maetani S, Kawamoto K, Kan S, Kondo S, Imamura M. Pathologic significance of tumor progression in locally recurrent rectal cancer: different nature from primary cancer. *Dis Colon Rectum* 2000; **43**: 775-781

12 **Seong J,** Chung EJ, Kim H, Kim GE, Kim NK, Sohn SK, Min JS, Suh CO. Assessment of biomarkers in paired primary and recurrent colorectal adenocarcinomas. *Int J Radiat Oncol Biol Phys* 1999; **45**: 1167-1173

13 **Wielenga VJ,** Heider KH, Offerhaus GJ, Adolf GR, van den Berg FM, Ponta H, Herrlich P, Pals ST. Expression of CD44 variant proteins in human colorectal cancer is related to tumor progression. *Cancer Res* 1993; **53**: 4754-4756

14 **Finn L,** Dougherty G, Finley G, Meisler A, Becich M, Cooper DL. Alternative splicing of CD44 pre-mRNA in human colorectal tumors. *Biochem Biophys Res Commun* 1994; **200**: 1015-1022

15 **Fox SB,** Fawcett J, Jackson DG, Collins I, Gatter KC, Harris AL, Gearing A, Simmons DL. Normal human tissues, in addition to some tumors, express multiple different CD44 isoforms. *Cancer Res* 1994; **54**: 4539-4546

16 **Mulder JW,** Kruyt PM, Sewnath M, Oosting J, Seldenrijk CA, Weidema WF, Offerhaus GJ, Pals ST. Colorectal cancer prognosis and expression of exon-v6-containing CD44 proteins. *Lancet* 1994; **344**: 1470-1472

17 **Gotley DC,** Fawcett J, Walsh MD, Reeder JA, Simmons DL, Antalis TM. Alternatively spliced variants of the cell adhesion molecule CD44 and tumour progression in colorectal cancer. *Br J Cancer* 1996; **74**: 342-351

18 **Fukuse T,** Hirata T, Tanaka F, Yanagihara K, Hitomi S, Wada H. Prognosis of ipsilateral intrapulmonary metastases in resected nonsmall cell lung cancer. *Eur J Cardiothorac Surg* 1997; **12**: 218-223

19 **Ichinose Y,** Hara N, Ohta M. Synchronous lung cancers defined by deoxyribonucleic acid flow cytometry. *J Thorac Cardiovasc Surg* 1991; **102**: 418-424

20 **Martini N,** Melamed MR. Multiple primary lung cancers. *J Thorac Cardiovasc Surg* 1975; **70**: 606-612

21 **Nanashima A,** Yamaguchi H, Sawai T, Yasutake T, Tsuji T, Jibiki M, Yamaguchi E, Nakagoe T, Ayabe H. Expression of adhesion molecules in hepatic metastases of colorectal carcinoma: relationship to primary tumours and prognosis after hepatic resection. *J Gastroenterol Hepatol* 1999; **14**: 1004-1009

22 **Bravo R,** Frank R, Blundell PA, Macdonald-Bravo H. Cyclin/PCNA is the auxiliary protein of DNA polymerase-delta. *Nature* 1987; **326**: 515-517

23 **Aruffo A,** Stamenkovic I, Melnick M, Underhill CB, Seed B. CD44 is the principal cell surface receptor for hyaluronate. *Cell* 1990; **61**: 1303-1313

24 **Gunthert U,** Hofmann M, Rudy W, Reber S, Zoller M, Haussmann I, Matzku S, Wenzel A, Ponta H, Herrlich P. A new variant of glycoprotein CD44 confers metastatic potential to rat carcinoma cells. *Cell* 1991; **65**: 13-24

25 **Kimball PM,** Brattain MG. Isolation of a cellular subpopulation from a human colonic carcinoma cell line. *Cancer Res* 1980; **40**: 1574-1579

26 **Brattain MG,** Fine WD, Khaled FM, Thompson J, Brattain DE. Heterogeneity of malignant cells from a human colonic carcinoma. *Cancer Res* 1981; **41**: 1751-1756

27 **Fidler IJ.** Tumor heterogeneity and the biology of cancer invasion and metastasis. *Cancer Res* 1978; **38**: 2651-2660

28 **Fidler IJ.** Critical factors in the biology of human cancer metastasis: twenty-eighth G.H.A. Clowes memorial award lecture. *Cancer Res* 1990; **50**: 6130-6138

29 **Dexter DL,** Spremulli EN, Fligiel Z, Barbosa JA, Vogel R, VanVoorhees A, Calabresi P. Heterogeneity of cancer cells from a single human colon carcinoma. *Am J Med* 1981; **71**: 949-956

30 **Dexter DL,** Kowalski HM, Blazar BA, Fligiel Z, Vogel R, Heppner GH. Heterogeneity of tumor cells from a single mouse mammary

tumor. *Cancer Res* 1978; **38**: 3174-3181

31 **Bonsing BA,** Corver WE, Fleuren GJ, Cleton-Jansen AM, Devilee P, Cornelisse CJ. Allelotype analysis of flow-sorted breast cancer cells demonstrates genetically related diploid and aneuploid subpopulations in primary tumors and lymph node metastases. *Genes Chromosomes Cancer* 2000; **28**: 173-183

32 **Solimene AC,** Carneiro CR, Melati I, Lopes JD. Functional differences between two morphologically distinct cell subpopulations within a human colorectal carcinoma cell line. *Braz J Med Biol Res* 2001; **34**: 653-661

33 **Yasoshima T,** Denno R, Kawaguchi S, Sato N, Okada Y, Ura H, Kikuchi K, Hirata K. Establishment and characterization of human gastric carcinoma lines with high metastatic potential in the liver: changes in integrin expression associated with the ability to metastasize in the liver of nude mice. *Jpn J Cancer Res* 1996; **87**: 153-160

34 **Samiei M,** Waghorne CG. Clonal selection within metastatic SP1 mouse mammary tumors is independent of metastatic potential. *Int J Cancer* 1991; **47**: 771-775

35 **Li Y,** Tang ZY, Ye SL, Liu YK, Chen J, Xue Q, Chen J, Gao DM, Bao WH. Establishment of cell clones with different metastatic potential from the metastatic hepatocellular carcinoma cell line MHCC97. *World J Gastroenterol* 2001; **7**: 630-636

36 **Price JE,** Bell C, Frost P. The use of a genotypic marker to demonstrate clonal dominance during the growth and metastasis of a human breast carcinoma in nude mice. *Int J Cancer* 1990; **45**: 968-971

37 **Suzuki N,** Frapart M, Grdina DJ, Meistrich ML, Withers HR. Cell cycle dependency of metastatic lung colony formation. *Cancer Res* 1977; **37**: 3690-3693

Edited by Zhao M and Wang XL

P.O.Box 2345, Beijing 100023,China
Fax: +86-10-85381893
E-mail: wjg@wjgnet.com www.wjgnet.com

World J Gastroenterol 2003;9(7):1487-1490
World Journal of Gastroenterology
 ISSN 1007-9327

• VIRAL HEPATITIS •

Gastric autoimmune disorders in patients with chronic hepatitis C before, during and after interferon-alpha therapy

Carlo Fabbri, M. Francesca Jaboli, Silvia Giovanelli, Francesco Azzaroli, Alessandro Pezzoli, Esterita Accogli, Stefania Liva, Giovanni Nigro, Anna Miracolo, Davide Festi, Antonio Colecchia, Marco Montagnani, Enrico Roda, Giuseppe Mazzella

Carlo Fabbri, M. Francesca Jaboli, Silvia Giovanelli, Francesco Azzaroli, Alessandro Pezzoli, Esterita Accogli, Stefania Liva, Giovanni Nigro, Anna Miracolo, Antonio Colecchia, Marco Montagnani, Enrico Roda, Giuseppe Mazzella, Department of Internal Medicine and Gastroenterology, University of Bologna, Bologna, Italy
Davide Festi, Department of Medicine and Aging, University "G D' Annunzio" Chieti, Italy
Correspondence to: Professor Giuseppe Mazzella, Department of Internal Medicine and Gastroenterology, University of Bologna, Ospedale S. Orsola- Malpighi, via Massarenti 9, I-40138 Bologna, Italy. mazzella@med.unibo.it
Telephone: +39-51-6363276 **Fax:** +39-51-343398
Received: 2003-02-25 **Accepted:** 2003-03-16

Abstract

AIM: To explore the prevalence of autoimmune gastritis in chronic hepatitis C virus (HCV) patients and the influence of α-interferon (IFN) treatment on autoimmune gastritis.

METHODS: We performed a prospective study on 189 patients with positive anti-HCV and viral RNA enrolled in a 12-month IFN protocol. We evaluated: a) the baseline prevalence of autoimmune gastritis, b) the impact of IFN treatment on development of biochemical signs of autoimmune gastritis (at 3, 6 and 12 months), c) the evolution after IFN withdrawal (12 months) in terms of anti-gastric-parietal-cell antibodies (APCA), gastrin, anti-thyroid, and anti-non-organ-specific antibodies.

RESULTS: APCA positivity and 3-fold gastrin levels were detected in 3 (1.6 %) and 9 (5 %) patients, respectively, at baseline, in 25 (13 %) and 31 (16 %) patients at the end of treatment (both $P<0.001$, *vs* baseline), and in 7 (4 %) and 14 (7 %) patients 12 months after withdrawal ($P=0.002$ and $P=0.01$ respectively, *vs* baseline; P=not significant *vs* end of treatment). The development of autoimmune gastritis was strictly associated with the presence of autoimmune thyroiditis ($P=0.0001$), no relationship was found with other markers of autoimmunity.

CONCLUSION: In HCV patients, IFN frequently precipitates latent autoimmune gastritis, particularly in females. Following our 12-month protocol, the phenomenon generally regressed. Since APCA positivity and high gastrin levels are associated with the presence of antithyroid antibodies, development of autoimmune thyroiditis during IFN treatment may provide a surrogate preliminary indicator of possible autoimmune gastritis to limit the need for invasive examinations.

Fabbri C, Jaboli MF, Giovanelli S, Azzaroli F, Pezzoli A, Accogli E, Liva S, Nigro G, Miracolo A, Festi D, Colecchia A, Montagnani M, Roda E, Mazzella G. Gastric autoimmune disorders in patients with chronic hepatitis C before, during and after interferon-alpha therapy. *World J Gastroenterol* 2003; 9(7): 1487-1490
http://www.wjgnet.com/1007-9327/9/1487.asp

INTRODUCTION

Chronic hepatitis C virus (HCV) infection can lead to the development of chronic liver disease, cirrhosis and hepatocellular carcinoma (HCC)[1]. Chronic HCV patients frequently have a broad spectrum of autoantibodies and/or concurrent autoimmune disease[2-4], apparently not closely associated with the HCV genotype[5] or to the severity of liver disease[6]. Several studies have indicated that immunological abnormalities are sometimes unmasked by interferon-α (IFN) therapy[7-12]. Although autoimmune thyroiditis is one of the most common immunological side effects of IFN treatment, with very close monitoring, its presence is not an absolute contraindication for the therapy. A close association has been reported between autoimmune thyroiditis and autoimmune (i. e. type A) gastritis[13]. Autoimmune gastritis involves the fundus and the body of the stomach while sparing the antrum. It is associated with pernicious anemia, autoantibodies to gastric parietal cells, achlorhydria, low serum pepsinogen I with normal serum pepsinogen II concentrations[14] and high serum gastrin concentration, the latter is resulted from hyperplasia of gastrin-producing cells. It is thought that *Helicobacter pylori* (*H.pylori*) could be implicated in the development of autoimmune gastritis[15,16], since it induces antigenic mimicry[17] and antibodies against *H. pylori* can cross-react with both antral mucosal and gastrin-producing cells.

The frequencies of thyroiditis manifestations during IFN treatment of chronic hepatitis C infection are well documented[7,9,10]. However, the impact of IFN therapy on the development of autoimmune and other types of gastric disease is unknown. To address this issue, we designed a prospective study on 189 chronic HCV patients treated with IFN. In particular, we investigated: a) the baseline prevalence of autoimmune gastritis, b) the impact of IFN on the development of biochemical signs of autoimmune gastritis, c) the outcome of twelve months after withdrawal of IFN. We also examined the presence of antithyroid, antigastric parietal-cell and anti-non-organ-specific (anti-NOS) antibodies. Finally, we investigated whether the presence of *H. pylori* affected the development of autoimmune gastritis.

MATERIALS AND METHODS

Patients and study design

We prospectively studied a group of 189 consecutive IFN-treated chronic hepatitis C patients (95 males, 94 females, mean age 58±18 years) who entered an IFN therapeutic program at our institution from September 1996 to July 1998 (Table 1). Criteria for the diagnosis of chronic HCV infection were: 1) presence of anti-HCV antibodies and polymerase chain reaction (PCR) positivity for HCV-RNA, 2) histological confirmation of chronic hepatitis C, 3) exclusion of other causes of chronic liver diseases (alcoholism, Wilson's disease, drugs, hemochromatosis, a1 antitrypsin deficiency, autoimmune hepatitis, PBC). Criteria for inclusion in the IFN treatment program were the generally recognized ones (transaminase levels over two times the upper limit, age between 18 and 70

years, absence of pregnancy and psychiatric history or other chronic severely invalidating conditions). None of the patients had received immunosuppressive or immunostimulatory therapy before entry into the study. All the patients were negative for human immunodeficiency virus (HIV) antibodies and hepatitis B surface antigen (HBsAg). Disease activity and stage were evaluated according to Scheuer' s histological score. None of the patients were receiving proton pump inhibitors or anti-H_2 antagonist drugs. Informed consent was obtained from each patient and approval for the study protocol was granted by the Ethical Committee of our institution.

Table 1 Baseline characteristics of patients

Patients (*n*)	189	
Age (*year*) ± SD	58±18	
Sex (M / F)	95 / 94	
ALT (U / L) ± SE	142±8	
AST (U / L) ± SE	103±7	
Genotype 1-4 *vs* others	115 *vs* 74	61 *vs* 39%
Anti-*Hp* positive antibody	60	31.8%
Gastrin (pg / ml)(median±SE)	52.0±10.4	
TSH (UI / ml)	2.2±0.15	
ANA positive (*n*)	34	18%
AMA positive (*n*)	-	
ASMA positive (*n*)	57	30%
LKM positive (*n*)	1	0.5%
APCA positive (*n*)	3	1.6%
ATM positive (*n*)	15	7.8 %
Liver histology (*n*)		
CAH without cirrhosis (*n*)	138	73 %
CAH with cirrhosis (*n*)	51	27 %

All the patients received 6 MU of recombinant IFN daily for the first month, followed by 6 MU each alternate day for 5 months and then 3 MU each alternate day for a further 6 months. In the event of side-effects, the dosage was decreased. If side effects were severe or sustained, IFN treatment was suspended.

Serum samples were analyzed in all the patients for presence of gastric parietal cell autoantibodies and gastrin at the following time points: baseline, after 3 and 6 months of treatment, the end of IFN treatment (i.e. at 12 months, or at the time of suspension, if earlier), 12 months after suspension of IFN. Multiple endoscopic gastric biopsies were always performed when positive anti-gastric parietal cell autoantibodies and/or serum levels of gastrin were found to be over 3 times the normal upper limit, presence of gastrinoma was excluded by the secretin stimulation test. In all patients, *Helicobacter pylori* status was serologically tested before the start of treatment. Criteria for diagnosis of autoimmune gastritis were according to Sidney classification system[18,19].

Biochemical and virological assays

Serum samples were analyzed for routine biochemical liver function tests with a multichannel autoanalyzer. HBsAg and anti-HBs and anti-hepatitis B core (HBc) antibodies were tested using a commercial solid-phase radioimmunoassay (Abbott Laboratories, North Chicago, IL). HIV determination was done according to a standard enzyme-linked immunosorbent assay (ELISA) procedure (HIV ELISA, Abbott Laboratories, North Chicago, IL). Anti-HCV antibodies were tested using a second-generation ELISA procedure (ELISA-2, Ortho Diagnostic Test Systems, Raritan, NJ). HCV RNA was detected by nested PCR analysis using primers from the highly conserved 5' non-coding region of the HCV genome (Shindo *et al*, 1991). HCV genotype was determined by InnoLipa.

Immunoserological evaluation

Anti-nuclear, anti-mitochondrial, smooth-muscle and liver-kidney microsome-1 auto-antibodies (ANA, AMA, SMA and LKM-1) were determined using indirect immunofluorescence assays on unfixed cryostat frozen sections of mouse liver, kidney and stomach. Sera were screened for anti-parietal cell autoantibodies (APCA) by immunofluorescence reactivity with paraffin-embedded sections of mouse stomach and for H^+/K^+-ATPase autoantibodies by ELISA. A positive result required a titer of at least 1/40. Basal serum gastrin and thyroid serum hormone (TSH) concentration were measured by radioimmunological assay (RIA), which detects sulfated and non-sulfated human heptadecapeptide (hG-17), as well as human big gastrin (hG-34). Gastrin results were expressed as pg/ml. Thyroid microsomal and thyroglobulin autoantibodies (TMA and TGA) were analyzed using hemagglutination tests (Ames, Elkhart, IN, USA). The cut-off points for both TMA and TGA were 1:100.

H. pylori investigation

Serum immunoglobulin G (IgG) response to *H. pylori* purified antigens was measured by ELISA, the cut-off value used was an optical density ratio >1.0. The presence or absence of *H. pylori* was also defined by histological examination of multiple gastric biopsy specimens from the antrum, fundus, or cardia in all the patients with positive APCA and/or elevated levels of gastrin. All biopsy specimens were fixed in Hollande' s fixative and stained with H&E and Giemsa.

Statistical analysis

Intent-to-treat analysis was adopted. To analyze associations among groups the Fisher' s exact test and the χ^2 test with Yates' correction were used. A two-tailed *P* value less than 0.05 was considered significant.

RESULTS

Treatment outcome

The entire 12-month treatment schedule was completed by 168/189 (89 %) of patients. In 21 patients, the IFN dose was reduced due to the severity of side effects (severe thrombocytopenia and/or severe leukopenia with neutrophil count <800/mm^3, continuous fever unresponsive to paracetamol, or severe myalgia). At least three months of treatment were completed by all but two of the patients (one suspended due to severe depression and suicidal tendency, the other due to side effects coupled with lack of motivation). None of the patients who discontinued therapy was positive for APCA.

Abdominal symptoms

In 164/189 (87 %) patients, no abdominal symptoms were reported. The most frequently reported symptoms were epigastric pain and/or abdominal discomfort. Presence of abdominal symptoms was not affected by positivity/negativity for *H. pylori*.

APCA and hypergastrinemia outcome (Tables 2, 3)

At the start of treatment, APCA positivity was detected in 3 (1.6 %) patients, and hypergastrinemia (i.e. serum gastrin levels over three times the normal upper limit) was found in a further 9 (5 %). At the end of treatment, these incidences rose to 25 (13 %) and 31 (16 %) patients, respectively (both $P<0.001$ *vs* baseline values). Thus, 22 patients developed both APCA and hypergastrinemia, mostly by the third month of therapy. Twelve

months after suspension of IFN, APCA and hypergastrinemia were still present in 7 (4 %) and 14 (7 %) patients, respectively (P=0.002 and P=0.01, respectively, *vs* end of IFN treatment; both P=not significant *vs* baseline). During IFN treatment, females were more prone to have increased APCA (P=0.017) or increased serum gastrin levels (P=0.011) than males.

Serum gastrin levels (defined as median ± Standard Error) increased during administration of IFN (from 52±10.4 pg/ml to 57±17.2 pg/ml, P=0.001). Twelve months after withdrawal of therapy, serum gastrin levels (56±12.6 pg/ml) were still higher than those at baseline (P=0.001), although they were significantly lower than those at the end of treatment (P=0.001). Serum TSH levels increased during administration of IFN (from 2.6±0.13 MCU/ml to 3.2±0.17 MCU/ml, P=0.02), and subsequently remained higher than the baseline values at 12 months from withdrawal of therapy (3.2±0.3 MCU/ml, P=0.02 *vs* baseline, P =not significant *vs* withdrawal). As can be seen from Tables 2 and 3, the behavior of the antithyroid autoantibodies TPO was very similar to that of APCA. By contrast, IFN did not affect the non-organ-specific antibodies ANA, SMA and AMA.

Table 2 Variations of APCA positivity and hypergastrinemia in IFN treated patients

	Before IFN *n* (%)	IFN withdrawal *n* (%)	12 months after withdrawal *n* (%)
APCA positivity	3 (1.6%)	25 (13%)[a]	7 (4%)[b,d]
Hypergastrinemia	9 (5%)	31(16%)[a]	14 (7%)[c,d]

[a]P<0.001 *vs* before IFN; [b]P<0.002 *vs* IFN withdrawal; [c]P<0.01 *vs* IFN withdrawal; [d]P=not significant *vs* before IFN.

Table 3 Organ-specific and non-organ-specific autoantibodies

	Before IFN + (%)	IFN withdrawal + (%)	12 months after withdrawal+(%)
Organ-specific antibodies			
TPO	14 (8.0%)	39 (20.6%)[a]	23 (12.2%)
Non-organ-specific antibodies			
ANA	34 (18.0%)	45 (24.0%)	41 (22.0%)
SMA	56 (30.0%)	62 (33.0%)	60 (31.0%)
AMA	-	1 (0.5%)	1 (0.5%)
LMK 1	1 (0.5%)	3 (1.6%)	2 (1.1%)

[a]P<0.001 *vs* before IFN; P=0.036 *vs* 12 months after IFN withdrawal.

H. pylori status

At baseline, 61/189 (32.3 %) patients had a positive serum IgG response to *H. pylori* whole-cell antigen. These included 3 of the 9 (33.3 %) patients with autoimmune gastritis and 12 of the 31 (38.7 %) who developed biochemical signs of autoimmune gastritis during treatment.

Histology

Multiple endoscopic gastric biopsies were performed when positive APCA and/or serum levels of gastrin were found to be over 3 times the normal upper limit. At biopsy, all the patients with either baseline APCA positivity (n=3) or hypergastrinemia (n=9) showed a histological picture consistent with autoimmune gastritis. Among the 22 patients who developed both APCA positivity and hypergastrinemia during IFN therapy, the histology of the fundus was consistent with autoimmune gastric atrophy in 13 (59 %). Four other patients who were persistently consistent with presence of gastric atrophy maintained histological lesions at 12 months from IFN withdrawal.

Outcome of HCV infection

At baseline, 115/189 (61.0 %) patients were found to be infected with HCV genotype 1 or 4, while the remaining 74 (39.0 %) were infected with more IFN-responsive strains. Overall, 37/189 (19.5 %) patients showed a long-term virological response to IFN (at 12 months from withdrawal). In particular, long-term response was observed in 8/109 (7.3 %) patients with genotype 1, 21/39 (35 %) with genotype 2, 7/14 (50 %) with genotype 3, and 1/6 (16 %) with genotype 4, respectively. No difference in responsive rate was observed among the patients who developed hypothyroidism and/or hypergastrinemia and those who did not. No relationships were observed between HCV genotype and the development of autoimmune gastritis.

DISCUSSION

The prevalence of autoimmune gastritis in chronic HCV patients is currently unknown. Autoimmune gastritis can be associated with thyroid autoimmune abnormalities. The hypothesis that IFN therapy encourages the development of autoimmune gastritis in these patients has never been tested.

In this prospective study, we investigated the occurrence of autoimmune gastritis in 189 chronic HCV patients treated with IFN. The baseline prevalence of biochemical signs and histological features of autoimmune gastritis was similar to that found in the general population. However, the number of patients who displayed biochemical and/or histological signs of autoimmune gastritis significantly increased during IFN treatment. By 12 months after interruption of IFN, the number of patients showing these signs had partially regressed, although it still remained higher than the baseline value. Seven more patients continued to have elevated APCA and gastrinemia, all with histological evidence of autoimmune gastritis. These findings are in line with the hypothesis that IFN can unmask patients with latent autoimmune gastritis and sometimes may even induce permanent alterations consistent with autoimmune gastritis. Our findings also support the concept that these abnormalities are more frequent in females.

Patients with autoimmune gastritis have a 3-fold increased risk of gastric carcinoma and a 13-fold higher risk of gastric carcinoid tumours[20]. However, it is not known whether hypergastrinemia or mucosal damage plays a dominant etiologic role[21]. Evidence exists that endogenous hypergastrinemia is associated with stimulation of rectal[21] and liver cell proliferation[22,23], as also occurs in conditions that are known to raise the risk of colon cancer and HCC. HCV patients are at increased risk of developing HCC anyway[1] but IFN treatment seems to prevent or delay its onset[24]. Hence, the implications of the occurrence of hypergastrinemia followed by autoimmune gastritis during IFN treatment of HCV infection require careful consideration.

Although 13/22 of our patients developed histological signs of autoimmune gastritis during the 12-month period of therapy, in the majority of cases, these signs regressed in the following year. Persistent histological and biochemical hallmarks of autoimmune gastritis were only eventually found in 4 % (7 of 189) of our patients. The relatively short duration of immunostimulation by IFN may explain why the autoimmune gastritis regressed in most cases. Therefore, our findings may only be applicable to the effects of short-term treatment.

The presence of antithyroid antibodies does not absolutely contraindicate the use of IFN[25], even though it has to be remembered that IFN leads to permanent thyroid alterations in more than one-fifth patients[26,27]. Likewise, although the presence of autoimmune gastritis does not contraindicate IFN treatment, it has to be considered that some patients may develop permanent gastric alterations.

In the present study, we also investigated the possibility that *H. pylori* infection might play a pathogenetic role in the onset of autoimmune gastritis in IFN-treated chronic HCV patients[15,16]. Our data provided no support for this hypothesis. Indeed, in our series of patients, there was no observable difference in the frequencies of autoimmune gastritis between chronic HCV patients with and without *H. pylori* infection, either before, during or after IFN treatment.

Furthermore, we were unable to find any association between the presence of non-organ specific antibodies and that of antithyroid antibodies or APCA. This finding is of clinical interest because positivity for antithyroid antibodies or APCA reveals autoimmune thyroid or gastric disease, whereas the presence of anti-NOS antibodies may only refer to an autoimmune epiphenomenon. This underlines the importance of testing antithyroid antibodies and APCA as well as the anti-NOS ones.

In conclusion, IFN treatment for chronic hepatitis C does appear to be associated with frequent occurrence of autoimmune gastritis, particularly in female patients. In the majority of cases, autoimmune gastritis in the wake of our protocol appeared to be a transient phenomenon. However, this may depend on the limited (12 month) duration of treatment, and this point requires further investigation, especially in regard to the effects of long-term treatment. Autoimmune gastritis is an asymptomatic disease, but in the long run increases the risk for developing a variety of tumors especially in the stomach. Our experience underlines the importance of measuring APCA and/or gastrin levels in chronic HCV patients treated with IFN, and especially those who develop thyroid dysfunction. Development of autoimmune thyroiditis during IFN treatment might provide a surrogate indicator of possible autoimmune gastritis, limiting the need for invasive gastric procedures.

ACKNOWLEDGMENT

We thank Robin MT Cooke' s help for working up the manuscript.

REFERENCES

1 **Fattovich G,** Giustina G, Degos F, Tremolada F, Diodati G, Almasio P, Nevens F, Solinas A, Mura D, Brouwer JT, Thomas H, Njapoum C, Casarin C, Bonetti P, Fuschi P, Basho J, Tocco A, Bhalla A, Galassini R, Noventa F, Schalm SW, Realdi G. Morbidity and mortality in compensated cirrhosis type C: a retrospective follow-up study of 284 patients. *Gastroenterology* 1997; **112:** 463-472

2 **Meyer zum Buschenfelde KH,** Loshse AW, Gerken G, Treichel U, Lohr HF, Mohr H, Grosse A, Dienes HP. The role of autoimmunity in hepatitis C infection. *J Hepatol* 1995; **22**(Suppl 1): 93-96

3 **Hadziyannis SJ.** Non hepatic manifestations and combined diseases in HCV infection. *Dig Dis Sci* 1996; **41:** 63S-74S

4 **Eddleston AL.** Hepatitis C infection and autoimmunity. *J Hepatol* 1996; **24**(Suppl 2): 55-60

5 **Pawlotsky JM,** Roudot-Thoraval F, Simmonds P, Mellor J, Ben Yahia MB, Andre C, Voisin MC, Intrator L, Zafrani ES, Duval J, Dhumeaux D. Extrahepatic immunologic manifestations in chronic hepatitis C and Hepatitis C serotypes. *Ann Int Med* 1995; **122:** 169-173

6 **Czaja AJ,** Carpenter HA, Santrach PJ, Moore SB. DR human leukocyte antigens and disease severity in chronic hepatitis C. *J Hepatol* 1996; **24:** 666-673

7 **Nagayama Y,** Ohta K, Tsuruta M, Takeshita A, Kimura H, Hamasaki K, Ashizawa K, Nakata K, Yokoyama N, Nagataki S. Exacerbation of thyroid autoimmunity by interferon alpha treatment in patients with chronic viral hepatitis: our studies and review of the literature. *Endocr J* 1994; **41:** 565-572

8 **Chakrabarti D,** Hultgren B, Steward TA. IFN-alpha induces autoimmune T cells through the induction of intracellular adhesion molecule-1 and B7.2. *J Immunol* 1996; **157:** 522-528

9 **Marcellin P,** Pouteau M, Messian O, Bok B, Erlinger S, Benhamou. Hepatitis C virus, interferon alpha, and dysthyroidism. *Gastroenterol Clin Biol* 1993; **17:** 887-891

10 **Lisker-Melman M,** Di Bisceglie AM, Usala SJ, Weintraub B, Murray LM, Hoofnagle JH. Development of thyroid disease during therapy of chronic viral hepatitis with interferon alfa. *Gastroenterology* 1992; **102:** 2155-2160

11 **Ronnblom LE,** Alm GV, Oberg KE. Autoimmunity after alpha-interferon therapy for malignant carcinoid tumors. *Ann Int Med* 1991; **115:** 178-183

12 **Mazzella G,** Salzetta A, Casanova S, Morelli MC, Villanova N, Miniero R, Sottili S, Novelli V, Cipolla A, Festi D, Roda E. Treatment of chronic sporadic-type non-A, non-B hepatitis with lymphoblastoid interferon: gamma GT levels predictive for response. *Dig Dis Sci* 1994; **39:** 866-870

13 **Centanni M,** Marignani M, Gargano L, Corleto VD, Casini A, Delle Fave G, Andreoli M, Annibale B. Atrophic body gastritis in patients with autoimmune thyroid disease: an underdiagnosed association. *Arch Intern Med* 1999; **159:** 1726-1730

14 **Samloff IM,** Varis K, Ihamaki T, Siurala M, Rotter JI. Relationships among serum pepsinogen I, serum pepsinogen II, and gastric mucosal histology. A study in relatives of patients with pernicious anemia. *Gastroenterology* 1982; **83:** 204-209

15 **Faller G**, Steininger H, Kranzlein J, Maul H, Kerkau T, Hensen J, Hahn EG, Kirchner T. Antigastric autoantibodies in *Helicobacter pylori* infection: implications of histological and clinical parameters of gastritis. *Gut* 1997; **41**: 619-623

16 **Negrini R,** Savio A, Appelmelk BJ. Autoantibodies to gastric mucosa in *Helicobacter pylori* infection. *Helicobacter* 1997; **2:** S13-S16

17 **Ierardi E,** Francavilla R, Balzano T, Negrini R, Francavilla A. Autoantibodies reacting with gastric antigens in *Helicobacter pylori* associated body gastritis of dyspeptic children. *Ital J Gastroenterol Hepatol* 1998; **30:** 478-480

18 **Price AB.** The Sidney system: histological division. *J Gastroenterol Hepatol* 1991; **6:** 209-222

19 **Dixon MF,** Genta RM, Yardley JH, Correa P. The participants in the international workshop on the histopathology of gastritits, houston 1994. *Am J Surg Pathol* 1996; **20:** 1161-1181

20 **Toh BH,** van Driel IR, Gleeson PA. Pernicious anemia. *New Engl J Med* 1997; **337:** 1441-1448

21 **Penston J,** Wormsley KG. Achlorhydria: hypergastrinemia: carcinoids-a flawed hypothesis ? *Gut* 1987; **28:** 488

22 **Renga M,** Brandi G, Paganelli GM, Calabrese C, Papa S, Tosti A, Tomassetti P, Miglioli M, Biasco G. Rectal cell proliferation and colon cancer risk in patients with hypergastrinemia. *Gut* 1997; **41:** 330-332

23 **Rasmussen TN,** Jorgensen PE, Almdal T, Poulsen SS, Olsen PS. Effect of gastrin on liver rigeneration after partial hepatectomy in rats. *Gut* 1990; **31:** 92-95

24 **Caplin M,** Khan K, Savage K, Rode J, Varro A, Michaeli D, Grimes S, Brett B, Pounder R, Dhillon A. Expression and processing of gastrin in hepatocellular carcinoma, fibrolamellar carcinoma and cholangiocarcinoma. *J Hepatol* 1999; **30:** 519-526

25 **Mazzella G,** Accogli E, Sottili S, Festi D, Orsini M, Salzetta A, Novelli V, Cipolla A, Fabbri C, Pezzoli A, Roda E. Alpha interferon treatment may prevent hepatocellular carcinoma in HCV-related liver cirrhosis. *J Hepatol* 1996; **24:** 141-147

26 **Saracco G,** Touscoz A, Durazzo M, Rosina F, Donegani E, Chiandussi L, Gallo V, Petrino R, De Micheli AG, Solinas A. Autoantibodies and response to α-interferon in patients with chronic viral hepatitis. *J Hepatol* 1990; **11:** 339-343

27 **Ganne-Carrie N,** Medini A, Coderc E, Seror O, Christidis C, Grimbert S, Trinchet JC, Beaugrand M. Latent autoimmune thyroiditis in untreated patients with HCV chronic hepatitis: a case-control study. *J Autoimmun* 2000; **14:** 189-193

Edited by Xu XQ and Wang XL

P.O.Box 2345, Beijing 100023,China
Fax: +86-10-85381893
E-mail: wjg@wjgnet.com www.wjgnet.com

World J Gastroenterol 2003;9(7):1491-1495
World Journal of Gastroenterology
 ISSN 1007-9327

• VIRAL HEPATITIS •

Long-term alpha interferon and lamivudine combination therapy in non-responder patients with anti-HBe-positive chronic hepatitis B: Results of an open, controlled trial

M. Francesca Jaboli, Carlo Fabbri, Stefania Liva, Francesco Azzaroli, Giovanni Nigro, Silvia Giovanelli, Francesco Ferrara, Anna Miracolo, Sabrina Marchetto, Marco Montagnani, Antonio Colecchia, Davide Festi, Letizia Bacchi Reggiani, Enrico Roda, Giuseppe Mazzella

M. Francesca Jaboli, Stefania Liva, Francesco Azzaroli, Giovanni Nigro, Silvia Giovanelli, Francesco Ferrara, Anna Miracolo, Sabrina Marchetto, Marco Montagnani, Antonio Colecchia, Enrico Roda, Mazzella Giuseppe, Department of Internal Medicine and Gastroenterology, University of Bologna, Italy
Carlo Fabbri, Department of Gastroenterology and Gastrointestinal Endoscopy, Bellaria Hospital, Bologna, Italy
Davide Festi, Department of Medicine and Aging, University of Chieti, Italy
Letizia Bacchi Reggiani, Department of Cardiology, University of Bologna, Italy
Correspondence to: Professor Giuseppe Mazzella, Department of Internal Medicine and Gastroenterology, University of Bologna, Ospedale S. Orsola- Malpighi, via Massarenti 9, 40138 Bologna, Italy. mazzella@med.unibo.it
Telephone: +39-51-6363276 **Fax:** +39-51-300700
Received: 2003-02-25 **Accepted:** 2003-03-16

Abstract

AIM: To investigate the safety and efficacy of long-term combination therapy with alpha interferon and lamivudine in non-responsive patients with anti-HBe-positive chronic hepatitis B.

METHODS: 34 patients received combination treatment (1 month lamivudine, 12 month lamivudine+interferon, 6 month lamivudine), 24 received lamivudine (12 months), 24 received interferon (12 months). Interferon was administered at 6 MU tiw and lamivudine at 100 mg orally once daily. Patients were followed up for 6 months after treatment.

RESULTS: At the end of treatment, HBV DNA negativity rates were 88 % with lamivudine+interferon, 99 % with lamivudine and 55 % with interferon, (P=0.004, combination therapy *vs.* interferon, and P=0.001 lamivudine *vs.* interferon), and serum transaminase normalization rates were 84 %, 91 % and 53 % (P=0.01 combination therapy *vs.* interferon, and P=0.012 lamivudine *vs.* interferon). Six months later, HBV DNA negativity rates were 44 % with lamivudine+interferon, 33 % with lamivudine and 25 % with interferon, and serum transaminase normalization rates were 61 %, 42 % and 45 %, respectively, without statistical significance. No YMDD variants were observed with lamivudine+interferon (*vs.* 12 % with lamivudine). The combination therapy appeared to be safe.

CONCLUSION: Although viral clearance and transaminase normalization are slower with long-term lamivudine+interferon than that with lamivudine alone, the combination regimen seems to provide more lasting benefits and to protect against the appearance of YMDD variants. Studies with other regimens regarding sequence and duration are needed.

Jaboli MF, Fabbri C, Liva S, Azzaroli F, Nigro G, Giovanelli S, Ferrara F, Miracolo A, Marchetto S, Montagnani M, Colecchia A, Festi D, Reggiani LB, Roda E, Mazzella G. Long-term alpha interferon and lamivudine combination therapy in non-responder patients with anti-HBe-positive chronic hepatitis B: Results of an open, controlled trial. *World J Gastroenterol* 2003; 9(7): 1491-1495
http://www.wjgnet.com/1007-9327/9/1491.asp

INTRODUCTION

Chronic hepatitis B virus (HBV) infection remains a major worldwide public health problem. Over 300 million people are affected by the disease[1], which is associated with high mortality and morbidity due to the associated risk of cirrhosis and hepatocellular carcinoma[2]. In addition, HBV infection is becoming an increasingly relevant problem for transplanted and immunodeficient patients, who are prone to develop more severe, accelerated liver disease[3].

Until recently, interferon-α (IFN) was the only drug approved throughout the world for chronic HBV infection[4,5]. Unfortunately, relapse with return of viremia and hepatitis occurs in up to 50 % of cases[6]. The hepatitis B s antigen (HBsAg) may become negative in months to years after the end of treatment, suggesting total viral clearance[7]. IFN is less effective in the presence of HBeAg negativity[8], or in patients who have already developed cirrhosis or have had recurrence of HBV after a hepatic allograft.

Lamivudine (3TC) is the first potentially non-cytotoxic[9,10] oral nucleoside analogue approved for the treatment of chronic hepatitis B. It suppresses viral DNA replication by means of chain termination, and competitively inhibits viral polymerase, but does not act on supercoiled DNA. For these reasons, lamivudine rapidly reduces serum HBV DNA, enhances transaminase normalization, and improves the histological picture[11-13]. But only 16 % achieve full HBeAg seroconversion, and after suspension of therapy serum HBV DNA levels and transaminases generally return to pretreatment values[14]. Furthermore, after clearance of HBV DNA, mutations in the sequence of the YMDD locus of the HBV RNA-dependent DNA polymerase appear in 15 % of cases after one year of therapy, leading to recurrence of viremia[15]. Onset of resistance generally occurs after six months to several years of lamivudine therapy[16].

Combination therapy with IFN and lamivudine is being investigated in order to take advantage of the drugs' different mechanisms of action[17-21]. However, the results of short-term treatment studies have been not altogether encouraging[18]. The aim of the present study was to investigate whether long-term combination therapy was safe and well tolerated, and whether it could provide additional therapeutic benefits with respect to either of the single drug regimens. In particular, we set out to evaluate efficacy in terms of primary and sustained viremia and transaminase responses. We also assessed histological response, incidence of YMDD-variant HBV, and safety.

MATERIALS AND METHODS

Patients

This open trial concerned 82 adult Italian patients with chronic anti-HBe positive hepatitis B (68 males, 14 females) enrolled between February 1997 and February 1999 who had either not responded to or had relapsed after previous interferon treatment. The experimental protocol was carried out in accordance with the Helsinki Declaration, and was approved by the Ethics Review Committee, and all patients gave written informed consent to participate in a trial involving long-term treatment either with interferon plus lamivudine or with lamivudine or interferon alone.

Inclusion criteria for the study were: age between 18 and 70 years, detectable hepatitis B surface antigen (HBsAg) in serum at the time of screening and for at least six months before the start of the study, serum HBV DNA levels of at least 5 pg/ml at screening, raised alanine transaminase values within three months before the start of therapy. Exclusion criteria were: presence of co-infection with hepatitis C and D virus or HIV, signs of hepatic decompensation or hepatocellular carcinoma, other possible causes of chronic liver damage (i.e. alcohol abuse, hemochromatosis, Wilson' s disease, a1-antitrypsin deficiency, autoimmune diseases, drug-induced hepatotoxicity and congestive heart failure), assumption of immunosuppressive or antiviral therapy within six months before the study. Needle biopsy performed in all cases within 2 years of the study, showed that 33 patients had a Scheuer score for fibrosis >3.

The patients were divided into three groups: group A (n=34) for combination treatment, group B (n=24) for treatment with lamivudine alone, group C (n=24) for treatment with interferon alone.

Treatment protocols and study design

Patients in group A received 100 mg/day of lamivudine (Glaxo-Wellcome Inc, Research Triangle Park, NC, USA) orally for one month, followed by lamivudine (100 mg/day) in association with six million units three times per week of natural interferon (Wellferon, Glaxo-Wellcome Inc, Research Triangle Park, NC, USA) for twelve months, and then lamivudine (100 mg/day) alone for six months. Patients in group B received lamivudine (100 mg/day) orally for twelve months. Patients in group C received six million units three times per week of natural interferon for twelve months. Interferon was administered subcutaneously by the patients after adequate training. Patients were followed up after the end treatment for twenty-four weeks. All patients had a liver biopsy within 2 years of entering the study, and were requested to have another at the end of treatment. Hepatitis flare up was defined as an increase in serum ALT during therapy and classified as mild, moderate or severe (>1.5, 5, 10 times respectively) according to the preceding ALT value.

The main end point of the study was to evaluate the end-of-treatment and sustained response, defined as HBV DNA loss and serum ALT normalization at the end of therapy and follow-up, respectively. Secondary variables included histological response, incidence of YMDD-variant HBV, and safety.

Laboratory methods

Blood samples were obtained immediately before therapy, after 15 days, and then every month during treatment and follow-up. Routine biochemical tests and blood cell counts were performed. HBsAg, HBeAg, and anti-HBs and anti-HBe antibodies were determined by enzyme immunoassay. Serum HBV DNA was measured quantitatively by a solution-hybridization assay (Abbott, Chicago, USA) with a lower limit of 3.0 pg/ml of serum.

Presence of the YMDD variant was evaluated by a restriction fragment length polymorphism assay in all ends of treatment samples and in cases where initial loss of HBV DNA was followed by a return to positivity, regardless of transaminase values. The biopsy specimens were scored according to the Scheuer histological activity index[22].

Statistical analysis

Baseline characteristics of the patients were presented as mean values ± standard error (SE). Statistical evaluations were conducted according to the intention-to-treat procedure. The Chi-square test or the Fisher' s exact test was used to compare differences in proportion between treatment groups. Continuous data were analyzed using Kruskall-Wallis test and Mann-Whitney test. A two-tailed P value of less than 0.05 was considered to be statistically significant.

RESULTS

Study population

All treatment arms were well matched with regard to baseline characteristics (Table 1). Of the 82 patients, 79 completed the treatment schedule, while the remaining 3 dropped out of the study: one group A patient withdrew, one group B patient and one group C patient experienced depression.

Table 1 Baseline characteristics of patients

Characteristics	Lamivudine+ interferon (n=34)	Lamivudine alone (n=24)	Interferon alone (n=24)
Age (year)	44.0±2.0	48.7±2.4	44.4±2.5
Sex (m / f)	30 / 4	18 / 6	20 / 4
ALT (U / l)	151±21	160±39	130±17
AST (U / l)	81±10	111±37	66±10
GT (U / l)	48±3	57±6	47±3
Albumin (gr / dl)	3.94±0.04	3.97±0.04	4.01±0.03
HBV DNA (pg / ml)	60±25	85±43	73±36
Histology:			
Cirrhosis	13 (38%)	10 (42%)	10 (42%)
Severe activity	10 (29%)	7 (29%)	9 (37%)

P value was not significant for all comparisons.

Virological response (Figure 1)

End-of-treatment response HBV DNA negativity was observed at the end of treatment in 30 (88 %) patients who received combination therapy (i.e. group A), 23 (99 %) who had lamivudine alone (i.e. group B), and 13 (55 %) who had interferon alone (i.e. group C). HBV DNA negativity was achieved in week 12, 4 and 32, respectively, in the three groups. Two differences in primary response among the three groups were highly significant [combination *vs.* interferon: *OR* 6.34 (95 % CI: 1.7-23 %), P=0.004; lamivudine *vs.* interferon: *OR* 19.46 (95 % CI: 3.3-113 %), P=0.001].

Sustained response A total of 15 (44 %) patients in group A, 8 (33 %) in group B and 6 (25 %) in group C were HBV DNA negative at the end of the follow-up. None of the differences in sustained virological response among the three groups reached statistical significance.

Biochemical response (Figure 2)

End-of-treatment response Serum transaminases became normal at the end of treatment in 29 (84 %) patients in group A, 21 (91 %) in group B and 13 (53 %) in group C [combination *vs.* interferon: *OR* 4.9 (95 % CI: 1.4-17 %), P=0.01; lamivudine *vs.* interferon: *OR* 5.92 (95 % CI: 1.28-25.3 %), P=0.012]. Normalization was achieved in week 20, 8 and 38, respectively,

in the three groups. A mild flare-up without bilirubin alteration was observed only in 8 group A patients. In all cases, serum transaminase normalization was preceded by a rise of HBV DNA at 2-8 months of therapy. The flare-up was always followed 1-2 months later by serum HBV DNA negativization and transaminase normalization. None of these patients had a YMDD variant.

Sustained response Sustained serum transaminase normalization was observed in 21 (61 %) patients in group A, 10 (42 %) in group B and 11 (45 %) in group C. None of the differences in sustained transaminase response among the three groups had statistical significance. Only 4 of the 8 patients who experienced a flare-up during combined therapy mantained their primary response.

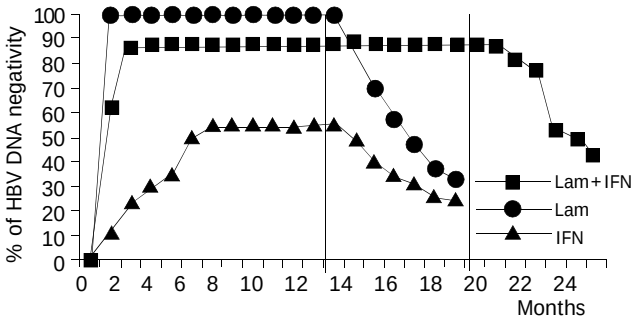

Figure 1 Virological response. Percentages of patients with HBV DNA negativity related either to the treatment or to the follow-up times. The vertical lines were drawn at the end of each treatment (19 months for interferon and lamivudine in combination, and 12 months for lamivudine and interferon monotherapy).

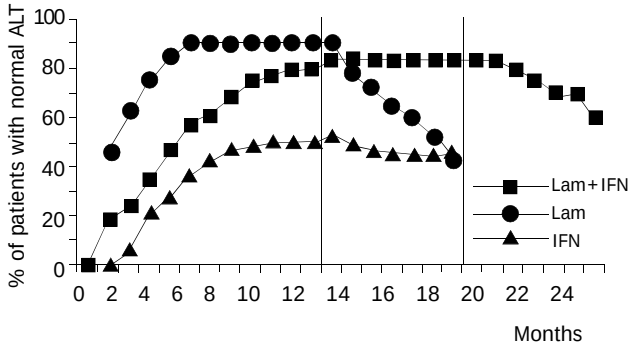

Figure 2 Biochemical response. Percentages of patients with normal ALT levels related either to the treatment or to the follow-up times. The vertical lines were drawn at the end of each treatment (19 months for interferon and lamivudine in combination, and 12 months for lamivudine and interferon monotherapy).

Secondary criteria of efficacy

Histological findings Paired pre- and post-treatment liver biopsies were available for 22 (65 %), 15 (62 %) and 14 (58 %) patients in groups A, B and C, respectively. None of the post-treatment biopsies showed a worsening or unchanged histological picture. Significant improvements in necro-inflammatory activity in parenchyma ($P<0.01$) and portal space ($P<0.01$) were observed in each group. Significant improvements in fibrosis were found in groups A and B ($P<0.05$), but not in group C.

Incidence of YMDD variant HBV YMDD variants of HBV were not detected in any of the patients who received combination or IFN therapy. 3 of the 24 (12 %) patients treated with lamivudine alone had a YMDD variant after 6-9 months of therapy. In particular, two had a YVDD variant and the other had a YIDD variant. They continued lamivudine therapy and were monitored weekly. After a progressive rise of serum HBV DNA, two of the patients showed 5 times of elevation of transaminases (with respect to the upper limit) and another showed 1.5 times of elevation. However, after the emergence of the variant, the HBV DNA and transaminase levels always remained lower than the baseline.

Safety

The whole treatment program was completed by 33 (98 %), 23 (96 %) and 23 (94 %) patients in groups A, B and C, respectively. No patient received reduced dosage but we directly stopped treatment. The side effects of the combination regimen were generally similar to those of interferon treatment. In addition, among the 34 patients in group A, symptomatic and reversible rises in serum levels of amylase, lipase and creatinine phosphokinase were recorded in 9 (28 %), 2 (5 %) and 1 (3 %) cases, respectively. Worsening of pre-existing hypertriglyceridemia was recorded in 2 (7 %) cases. By comparison, among the 24 patients in group B, lamivudine therapy was associated with an asymptomatic and reversible rise in amylase, lipase or creatinine phosphokinase in 6 (25 %), 1 (4 %) and 1 (4 %), respectively. No case of hepatocellular carcinoma, liver decompensation or death was recorded, and no patient requested orthotopic liver transplantation (Table 2).

Table 2 Adverse events documented during treatment

Adverse events	Lamivudine+ interferon (n=34), n (%)	Lamivudine alone (n =24), n (%)	Interferon alone (n =24), n (%)
Influenza-like symptoms	24 (70%)	none	19 (79%)
Hair loss	8 (23%)	none	9 (38%)
Weight loss	5 (16%)	none	4 (15%)
Depression	none	1 (4%)	1 (6%)
Low white-cell count	19 (56%)	none	14 (59%)
Low platelet count	14 (42%)	none	10 (44%)
Amylase rise	9 (28%)	6 (25%)	none
Lipase rise	2 (5%)	1 (4%)	none
CPK rise	1 (3%)	1 (4%)	none
Hypertriglyceridemia	2 (7%)	none	none

DISCUSSION

The development of effective treatment strategies for patients with HBV remains a major clinical challenge. We investigated the possible benefits of a long-term interferon/lamivudine combination treatment regimen in a cohort of patients who had already received unsuccessful treatment with interferon alone. The effects of this long-term combination regimen were compared with single-agent treatment with either interferon or lamivudine in three similar groups of patients. In regard to virological response, we found that at the end of therapy, HBV DNA had become undetectable in 88 % of the patients receiving combination treatment, as compared with 99 % and 55 % of those who had single-line therapy with lamivudine or interferon, respectively. These differences in end-of-treatment response were statistically significant in comparison of the combination therapy and lamivudine monotherapy with interferon monotherapy. The analysis of sustained response showed that 44 % patients in the combination therapy group maintained DNA clearance as compared with only 33 % in the lamivudine group and 25 % in the interferon group. Although these differences did not have statistical significance, there was a trend in favor of the combination regimen. Similarly, although the end-of-treatment transaminase normalization rate was significantly higher in the combination

treatment (84 %) group and in the lamivudine group of patients (91 %) than that in interferon (53 %) group, the sustained response showed a non-significant trend in favor of the combination regimen (61 % in the combination group *vs.* 42 % and 45 % with lamivudine or interferon alone, respectively).

As has been reported for short-term treatment[23], during our long-term combination therapy regimen there was a progressive viral decline, whereas with single-line lamivudine therapy the HBV DNA levels leveled off. Our data are in keeping with the concept that lamivudine therapy is more rapid and effective on virological and biochemical response than interferon alone or even in combination with lamivudine. However, after discontinuation of therapy, virological and biochemical relapses were considerably more common with lamivudine alone than those with the combination regimen (even though this difference did not actually reach statistical significance). Moreover, there was a trend suggesting that combination therapy delays relapse. The non-significant status of these trends could be due to the relatively small cohort sizes.

Among the two monotherapy options, interferon appeared less effective than lamivudine. In our study, interferon provided less end-of-treatment responses than lamivudine, and no advantages in terms of sustained response. The relatively poor capacity of interferon monotherapy to promote viral clearance may be explained by an inability to induce an efficient immune response.

After about 5 months of combination therapy, we observed a mild flare-up in 8 patients following a rise in serum HBV DNA. The flare-up was always followed, after a further one to two months of therapy by a return to serum HBV DNA negativity and normalization of transaminases. They may have been caused by enhanced immune responses prompted by increased mutant viral replication other than YMDD, which however were unable to permanently eradicate the virus.

As regards the secondary criteria of response, all the patients who underwent a post-treatment biopsy derived histological benefit in terms of necro-inflammatory activity in parenchyma and in portal space, regardless of their serological response. However, in keeping with other reports[24], interferon monotherapy provided no improvement in fibrosis.

YMDD HBV variants were not detected in any of the patients who received combination therapy or interferon alone. After 6-9 months of lamivudine monotherapy, 3 (12 %) patients had YMDD, a rate similar to that reported in Asian patients. Interferon therapy seemed to exert a protective effect against the emergence of variants, probably because it lowers viral replication and enhances immunological response. In any case, in the three affected patients, the serum HBV DNA levels did not return completely to pretreatment levels. Thus, the mutant strains of HBV DNA that break through during prolonged therapy with lamivudine may not be as replicative-efficient or as pathogenic as wild-type strains. As in other reports[25], we found that 3 to 4 months after lamivudine treatment was stopped, there was disappearance of this HBV mutant and re-emergence of the wild type virus. Honkoop *et al.*[26] observed acute exacerbation of chronic HBV infection after withdrawal of lamivudine therapy and concluded that the relationship between the development of "lamivudine-withdrawal hepatitis" and the lamivudine-resistant mutant virus was currently unclear, since both the emergence of a lamivudine resistant viral mutant and the resurgence of wild-type virus after withdrawal of therapy were able to induce severe hepatitis exacerbations. Studies of rechallenge with lamivudine have yet to be reported, and the significance of YMDD variant is being evaluated in the ongoing follow-up clinical trials.

As regards safety, the combination therapy was well tolerated and no serious side effects were observed. The side effects observed during the course of the long-term combination regimen were those that were commonly associated with the two drugs. As expected, in the two monotherapy groups, the incidence of drug-related adverse events was much lower with lamivudine than that with interferon.

In conclusion, these results suggest that for patients who have already been unsuccessfully treated with interferon, long-term combination therapy may have some advantages over single-line treatment with lamivudine or interferon[27]. Other studies with other regimens regarding dose, sequence and duration of interferon and lamivudine are needed. Finally, correct staging of patients according to the particular phases in the natural history of chronic hepatitis B appears to be important to personalise patients' management. It is possible that combinations of two[28,29] or more nucleoside analogs may reduce the development of viral resistance, increase overall response rates, decrease adverse events. In general, multi-drug therapies[30] that take advantage of different modes of action concurrently may provide a more appropriate approach for particular subgroups of patients.

ACKNOWLEDGMENT

We are grateful to Robin MT Cooke for editing.

REFERENCES

1 **Maynard JE**. Hepatitis B: global importance and need for control. *Vaccine* 1990; **8**: (Suppl): S18-S20
2 **De Jongh FE**, Jansen HL, de Man RA, Hop WC, Schalm SW, van Blankenstein M. Survival and prognostic indicators of hepatitis B surface antigen-positive cirrhosis of the liver. *Gastroenterology* 1992; **103**: 1630-1635
3 **Davies SE**, Portmann BC, O'Grady JG, Aldis PM, Chaggar K, Alexander GJ, Williams R. Hepatic histological findings after transplantation for chronic hepatitis B virus infection, including a unique pattern of fibrosing cholestatic hepatitis. *Hepatology* 1991; **13**: 150-157
4 **Dusheiko GM**. Treatment and prevention of chronic viral hepatitis. *Pharmacol Ther* 1995; **65**: 47-73
5 **Korenman J**, Baker B, Waggoner J, Everhart JE, Di Bisceglie AM, Hoofnagle JH. Long term remission of chronic hepatitis B after interferon therapy. *Ann Inter Med* 1991; **114**: 629-634
6 **Hoofnagle JH**, Lau D. Chronic viral hepatitis-benefits of current therapies. *N Eng J Med* 1996; **334**: 1470-1471
7 **Mazzella G**, Saracco G, Festi D, Rosina F, Marchetto S, Jaboli F, Sostegni R, Pezzoli A, Azzaroli F, Cancellieri C, Montagnani M, Roda E, Rizzetto M. Long term results with interferon therapy in chronic type B hepatitis: a prospective randomized trial. *Am J Gastroenterol* 1999; **94**: 2246-2250
8 **Hadziyannis SJ**. Hepatitis B e antigen negative chronic hepatitis B: from clinical recognition to pathogenesis and treatment. *Viral Hepatitis Rev* 1995; **1**: 7-15
9 **Cui L**, Yoon S, Schinazi RF, Sommadossi JP. Cellular and molecular events leading to mitochondrial toxicity of 1-(2-de-oxy-2-fluoro-1-beta-D-arabinofuranosyl)-5-iodouracil in human liver cells. *J Clin Invest* 1995; **95**: 555-563
10 **Nicoll A**, Locarini S. Review: present and future directions in the treatment of chronic hepatitis B infection. *J Gastroenterol Hepatol* 1997; **12**: 843-854
11 **Dienstag JL**, Perrillo RP, Schiff ER, Bartholomew M, Vicary C, Rubin M. A preliminary trial of lamivudine for chronic hepatitis B infection. *N Eng J Med* 1995; **333**: 1657-1661
12 **Lai CL**, Chien RN, Leung NWY, eta Chang TT, Guan R, Tai DI, Ng KY, Wu PC, Dent JC, Barber J, Stephenson SL, Gray DF. A one year trial of lamivudine for chronic hepatitis B. *N Eng J Med* 1998; **339**: 61-68
13 **Kweon YO**, Goodman ZD, Dienstang JL. Lamivudine decreases fibrogenesis in chronic hepatitis B: an immunohistochemical study of paired liver biopsies. *Hepatology* 2000; **32**: 870P
14 **Honkoop P**, de Man RA, Heitjtink RA, Schalm SW. Hepatitis B reactivation after lamivudine. *Lancet* 1995; **346**: 1156-1157

15 **Dienstag JL**, Schiff ER, Mitchell M, Casey DE Jr, Gitlin N, Lissoos T, Gelb LD, Condreay L, Crowther L, Rubin M, Brown N. Extended lamivudine re-treatment for chronic hepatitis B: : maintenance of viral suppression after discontinuation of therapy. *Hepatology* 1999; **30**: 1082-1087
16 **Hoofnagle J**. Therapy of viral hepatitis. *Digestion* 1998; **59**: 563-578
17 **Schiff E**, Karayalcin S, Grimm I, Grimm IS, Perrillo RP, Husa P, de Man RA, Goodman Z, Condreay LD, Crowther LM, Woessner MA, McPhillips PJ, Brown NA. Lamivudine and 24 weeks of lamivudine/interferon combination therapy for hepatitis B e antigen-positive chronic hepatitis B in interferon nonresponders. *J Hepatol* 2003; **38**: 818-826
18 **Mutimer D**, Naoumov N, Honkoop P, Marinos G, Ahmed M, de Man R, McPhillips P, Johnson M, Williams R, Elias E, Schalm S. Combination alpha-interferon and lamivudine therapy for alpha-interferon-resistant chronic hepatitis B infection: results of a pilot study. *J Hepatol* 1998; **28**: 923-929
19 **Heathcote J**, Schalm SW, Cianciara J, G Farrell, V Feinmann, M Shermann, AP Dhillon, AE Moorat and DF Gray. Lamivudine and Intron A combination treatment in patients with chronic hepatitis B infection. *EASL* April, 1998, Lisbon
20 **Schalm SW**, Heathcote J, Cianciara J, Farrell G, Sherman M, Willems B, Dhillon A, Moorat A, Barber J, Gray DF. Lamivudine and alpha interferon combination treatment of patients with chronic hepatitis B infection: a randomised trial. *Gut* 2000; **46**: 562-568
21 **Farrell G**. Hepatitis B e antigen seroconversion: effects of lamivudine alone or in combination with interferon alpha. *J Med Virol* 2000; **61**: 374-379
22 **Scheuer P**. Classification of chronic viral hepatitis: a need for reassessment. *J Hepatology* 1991; **13**: 372-374
23 **van Nunen AB**, Hansen BE, Mutimer DJ. Viral kinetics during 16 weeks of interferon and lamivudine monotherapy versus interferon-lamivudine combination therapy in chronic hepatitis B patients. *Hepatology* 2000; **32**: 878
24 **Brook MG**, Petrovic L, McDonald JA, Scheuer PJ, Thomas HC. Histological improvement after anti-viral treatment for chronic hepatits B virus infection. *J Hepatol* 1989; **8**: 218-225
25 **Chayama K**, Suzuki Y, Kobayashi M, Kobayashi M, Tsubota A, Hashimoto M, Miyano Y, Koike H, Kobayashi M, Koida I, Arase Y, Saitoh S, Murashima N, Ikeda K, Kumada H. Emergence and takeover of YMDD motif mutant hepatitis B viru during long-term lamivudine therapy and re-takeover by wild type after cessation of therapy. *Hepatology* 1998; **27**: 1711-1716
26 **Honkoop P**, de Man RA, Niesters HGM, Zondervan PE, Schalm SW. Acute exacerbation of chronic hepatitis B virus infection after withdrawal of lamivudine therapy. *Hepatology* 2000; **32**: 635-639
27 **Janssen HLA**, Schalm SW, Berk L, de Man RA, Heijtink RA. Repeated courses of alpha-interferon for treatment of chronic hepatitis B. *J Hepatol* 1993; **17**(Suppl 3): S47-51
28 **Perrillo R**, Schiff E, Yoshida E, Statler A, Hirsch K, Wright T, Gutfreund K, Lamy P, Murray A. Adefovir dipivoxil for the treatment of lamivudine-resistant hepatitis B mutants. *Hepatology* 2000; **32**: 129-134
29 **Lau GK**, Tsiang M, Hou J, Yuen S, Carman WF, Zhang L, Gibbs CS, Lam S. Combination therapy with lamivudine and famciclovir for chronic hepatitis B-infected Chinese patients: a viral dynamics study. *Hepatology* 2000; **32**: 394-399
30 **Marques AR**, Lau DT, McKenzie R, Straus SE, Hoofnagle JH. Combination therapy with famciclovir and a-interferon for the treatment of chronic hepatitis B. *The J Infect Dis* 1998; **178**: 1483-1487

Edited by Xu XQ

P.O.Box 2345, Beijing 100023,China
Fax: +86-10-85381893
E-mail: wjg@wjgnet.com www.wjgnet.com

World J Gastroenterol 2003;9(7):1496-1500
World Journal of Gastroenterology
 ISSN 1007-9327

Acute hepatitis C in a chronically HIV-infected patient: Evolution of different viral genomic regions

Diego Flichman, Veronica Kott, Silvia Sookoian, Rodolfo Campos

Diego Flichman, Veronica Kott, Rodolfo Campos, Catedra de Virologia, Facultad de Farmacia y Bioquimica, Universidad de Buenos Aires, Argentina
Silvia Sookoian, Unidad de Higado, Hospital "Dr.Cosme Argerich", Argentina
Supported by the grants from the Universidad de Buenos Aires (SECyT-UBA, TB14), Consejo Nacional de Investigaciones Cientí ficas y Técnicas (CONICET, PIP723), Agencia Nacional de Promoción Cientí fica y Tecnológica (ANPCyT, PICT 01610) and Ministerio de Salud Pública de la Nación (Beca Carrillo-Oñativia)
Correspondence to: Dr. Rodolfo Campos, Facultad de Farmacia y Bioquimica, Junin 956, 4th floor, (1113), Capital Federal, Argentina. rcampos@ffyb.uba.ar
Telephone: +5411-49648264 **Fax:** +5411-45083645
Received: 2003-02-26 **Accepted:** 2003-03-16

Abstract

AIM: To analyze the molecular evolution of different viral genomic regions of HCV in an acute HCV infected patient chronically infected with HIV through a 42-month follow-up.

METHODS: Serum samples of a chronically HIV infected patient that seroconverted to anti HCV antibodies were sequenced, from the event of superinfection through a period of 17 months and in a late sample (42nd month). Hypervariable genomic regions of HIV (V3 loop of the gp120) and HCV (HVR-1 on the E2 glycoprotein gene) were studied. In order to analyze genomic regions involved in different biological functions and with the cellular immune response, HCV core and NS5A were also chosen to be sequenced. Amplification of the different regions was done by RT-PCR and directly sequenced. Confirmation of sequences was done on reamplified material. Nucleotide sequences of the different time points were aligned with CLUSTAL W 1.5, and the corresponding amino acid ones were deduced.

RESULTS: Hypervariable genomic regions of both viruses (HVR1 and gp120 V3 loop) presented several nonsynonymous changes but, while in the gp120 V3 loop mutations were detected in the sample obtained right after HCV superinfection and maintained throughout, they occurred following a sequential and cumulative pattern in the HVR1. In the NS5A region of HCV, two amino acid changes were detected during the follow-up period, whereas the core region presented several amino acid replacements, once the HCV chronic infection had been established.

CONCLUSION: During the HIV-HCV superinfection, each genomic region analyzed shows a different evolutionary pattern. Most of the nucleotide substitutions observed are non-synonymous and clustered in previously described epitopes, thus suggesting an immune-driven evolutionary process.

Flichman D, Kott V, Sookoian S, Campos R. Acute hepatitis C in a chronically HIV-infected patient: Evolution of different viral genomic regions. *World J Gastroenterol* 2003; 9(7): 1496-1500
http://www.wjgnet.com/1007-9327/9/1496.asp

INTRODUCTION

It has been proven that patients with HIV infection are frequently coinfected with other viruses, including that of HCV. Both HIV and HCV share the same route of transmission, and thus, coinfection with these two viruses is rather common among intravenous drug users or transfused patients[1, 2]. HCV infection is considered as an HIV opportunistic disease[3].

The clinical impact of HIV-HCV coinfection has been widely studied[4]. However, the viral molecular interaction during the establishment of HCV superinfection is not yet well understood as the acute phase is frequently a subclinical event.

HCV, an RNA virus, shows a marked variability but nucleotide substitutions are unevenly distributed along the entire genome[5]. HCV diversity is the greatest in the envelope proteins E1 and E2, especially in a 27 amino-acid segment at the N-terminus of E2 designated hypervariable region 1 (HVR1). The variation of this region is thought to be related to the maintenance of persistent infection by emerging escape variants[6] and it is considered as the main target for humoral immunity as well as an immunologic decoy[7].

A similar degree of heterogeneity is found within the gp120 V3 loop region of HIV, an RNA virus that also causes persistent infections in the host. This region has been found to elicit neutralizing antibodies as well as cytotoxic and Th-cell responses, properties that are also ascribed to the HVR1[8].

NS5A is an HCV nonstructural protein that is associated with several functions such as being an *in vitro* transcriptional repressor[9] and tightly associated via the "interferon sensitivity determining region" (ISDR), with the subversion of the IFN activity. ISDR inhibits the cellular double-stranded RNA-activated protein kinase R[10], an effector of the IFN antiviral activity. There is also evidence that the C-terminal domain of NS5A including the ISDR contains transcriptional activity[11], suggesting that NS5A might function as a viral transactivator. The core gene is located in the 5' end of the HCV genome and its primary function is to form the viral nucleocapsid. The core protein has many effects on host-cell signalling pathways that includes the host-cell gene expression[12], apoptosis by interaction with the cytoplasmic tail of the lymphotoxin receptor and with TNF receptor[13, 14], transforming activity[15], modulation of lipid metabolism[16, 17]. Several studies have shown that the region contains multiple and highly immunogenic humoral[18, 19] and cellular [19, 20] epitopes.

In a previous report we described the *in vivo* down regulation of HIV replication in an HIV-infected patient after HCV superinfection[21]. Herein we presented a further study of this patient through the analysis of hypervariable regions of both viruses, and the less variable core and NS5A regions of HCV.

MATERIALS AND METHODS

Patient

A 16 year-old HIV patient was referred to the Liver Unit because of an acute hepatitis-like illness with the manifestations of jaundice, nausea, abdominal pain, fever, diarrhea, itching and elevated ALT and AST levels. She was in the 30th week of gestation and her prenatal course had been uneventful until this episode. Diagnosis of acute hepatitis C was established by

seroconversion of HCV antibodies by an EIA test (HCV EIA 2.0; Ortho Diagnostics) and confirmed with a strip immunoblot assay (RIBA HCV 2.0; Chiron Corporation). HIV and HCV were thought to be acquired by intravenous drug use. Serum HCV and HIV RNAs were detected by RT-PCR using primers for the 5NC and the gag regions, respectively[21] (Table 1).

Thereafter, the patient was followed up for 42 months and serum samples were taken monthly during the first 17 months of the analyzed period and in the 42nd month as a late specimen. Serum samples before HCV superinfection were also available. Liver function tests (AST, ALT, γ-glutamyl-transferase, alkaline phosphatase, albumin, gamma globulin, bilirubin and prothrombin time) were routinely performed using automatic standard procedures.

A liver biopsy was obtained at the 15th month of follow-up showing a histological picture of chronic hepatitis (Knodell score 5) without fibrosis.

No antiviral therapy was implemented during the study period because of the patient's refusal. This study followed the ethical standards of the World Medical Association Helsinki Declaration adopted in 1964 and amended in 1996 and was approved by the local Ethics Committee. At all times, written consents were obtained from the woman.

Methods

RNA extraction RNA was recovered from 150 µl aliquots as described by Chomczynski and Sacchi[22] using components from a commercially available RNA extraction kit (Trizol®, Life Technologies) and resuspended in 20 µl dH_2O.

cDNA synthesis and PCRs RNA was used as templates in randomly primed reverse transcription reactions to produce cDNA in the following conditions: 50 mM TrisHCl (pH 8.3), 25 mM KCl, 3 mM $MgCl_2$, 0.1 mM DTT, 1.0 mM dNTPs, 18 U RNasin ribonuclease inhibitor (Promega) and 100 U Moloney murine leukemia virus RT (Life Technologies). The reactions were performed for 90 min at 37 ℃. After heat inactivation at 95 ℃ for 5 min and chilling on ice, the cDNA was amplified.

Different genomic viral regions -gp120 V3 loop region of HIV and the HVR1, core and NS5A regions of HCV- were amplified and directly sequenced. The PCR reaction (50 µl) contained 20 mM TrisHCl, 50 mM KCl, 50 pmol of each primer and 1.25 U *Taq* DNA polymerase (Promega). Nested PCR was performed with 2 µl PCR product as a template, using internal primers under the same conditions as the first round. The first and second round primers and cycling parameters for each region are shown in Table 1 and were made according to Kwok and Higuchi's recommendations[23].

Nucleotide sequencing Each DNA was purified and directly sequenced with a Thermo Sequenase radiolabeled-terminator-cycle sequencing kit (U.S. Biochemical Corporation) using the same cycling parameters of the second PCR round. Confirmatory sequencing was performed on reamplified DNA.

RESULTS

The genomic regions of HCV: HVR1, core and NS5A and the gp120 V3 loop of HIV were sequenced during a 42 month follow-up of a chronically HIV patient acutely infected with HCV. Phylogenetic analysis of core and NS5A grouped the HCV sequences into genotype 1a (data not shown).

After alignment and comparison of genomic sequences obtained before and after HCV superinfection, the nucleotide sequence of HIV gp120 V3 loop showed three nonsynonymous mutations (I309L, T317A and E320D) that appeared in the sample obtained 2 months after HCV superinfection and

Table 1 Oligonucleotide primers used to amplify various HIV and HCV regions

Viral region	Nucleotide position	Primer sequence (5'→3')	PCR cycling parameters
HIV			5 min at 94 ℃, 40 cycles of
gag			30 s at 94℃, 30 s at 55℃ and
OS	4653 – 4675	CCCTACAATCCCCAAAGTCAAGG	45 s at 72℃ and a final
OA	4956 – 4976	TACTGCCCCTTCACCTTTCCA	extension of 7 min at 72 ℃
V3 loop			
OS	6957 - 6976	GTACAATGTACACATGGAAT	
OA	7357 - 7376	GTAGAAAAATTCCCCTCCAC	Idem HIV-gag PCR
IS	7010 - 7029	TGGCAGTCTAGCAGAAGAAG	
IA	7319 - 7339	ACAATTTCTGGGTCCCCTCCT	
HCV			
5UT			
OS	44 - 69	CCTGTGAGGAACTACTGTCTTCACGC	Idem HIV-gag PCR
OA	321 - 341	GGTGCACGGTCTACGAGACCT	
HVR1			
OS	1273 – 1296	GCCATATAACGGGTCACCGCATGG	
OA	1681 – 1704	TCTCAGGACAGCCTGAAGMGTTGA	Idem HIV-gag PCR
IS	1296 – 1379	GCATGGGATATGATGATGAACTGG	
IA	1623 – 1646	GGTGTTGAGGCTATCATTGCARTT	
core			5 min at 94 ℃, 30 cycles of
OS	272 - 291	CGAAAGGCCTTGTGGTACTG	1 min at 94 ℃, 1 min at 50 ℃
OA	1020 - 1037	CTCGCGRACGCAAGGGAC	and 2 min at 72 ℃ and a final
IS	281 - 302	TTGTGGTACTGCCTGATAGGGT	extension of 10 min at 72 ℃
IA	956 - 976	ATACTCGAGTTAGGGCAATCA	
NS5A			
OS	6716 - 6739	TAGATGGGGTGCGCCTGCAYAGGTT	
OA	7310 - 7332	GCTTCTTCCGRGGCGGAGGCACWG	Idem HCV core PCR
IS	6734 – 6753	TAGGTTTGCGCCCCCCTGMA	
IA	7287 – 7306	GGGGACYKTGGAGGTGGAAG	

Notes: OS: outer sense primer; OA: outer antisense; IS: inner sense; IA: inner antisense. Nucleotide positions were according to HIVHXB2 (K03455) for the HIV region and to HCV-1 (M62321) for HCV regions. Degenerate bases were indicated with standard codes of the International Union of Pure and Applied Chemistry.

A

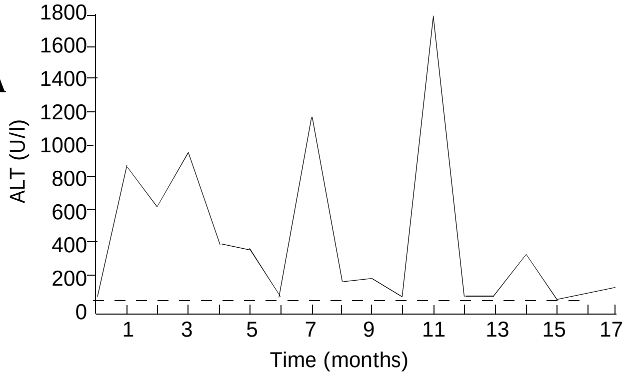

B V3 loop

```
   296                                 309                     317       320                   326
0. C T S P N N N T R K S I Q I G P G R A F Y T T G E I I G D I R
2. - - - - - - - - - - - - - L - - - - - - - A - - D - - - - - -
17.- - - - - - - - - - - - - L - - - - - - - A - - D - - - - - -
42.- - - - - - - - - - - - - L - - - - - - - A - - D - - - - - -
```

C HVR1

```
   384               393     397 398 399                    410
0. E T H V T G G T A G R A A A G F A S L F T P G A K Q N
1. - - - - - - - - - - - - - - - - - - - - - - - - - - -
3. - - - - - - - - - - - - - - - - - - - - - - - - - - -
6. - - - - - - - - - - - - - - - L - - - - - - - - - - -
7. - - - - - - - - - - - - - - - L - - - - - - - - - - -
8. - - - - - - - - - S - - - - - L - - - - - - - - - - -
9. - - - - - - - - - S - - - - - L - - - - - - - - - - -
12.- - - - - - - - - S - - - S - L - - - - - - - - - - -
13.- - - - - - - - - S - - - S - L - - - - - - - - - - -
15.- - - - - - - - - S - - - S - L - - - - - - - - - - -
17.- - - - - - - - - S - - - S - L - - - - - - - - - - -
42.- - - - - - - - - S - - - S A - - - - - - - - - - - -
```

Figure 1 (A) Biochemical profile of the HIV / HCV superinfected patient during the first 17 months of follow-up. Amino acid sequences of consecutive samples corresponding to V3 loop (B) and HVR1 (C). V3 loop sequence was obtained in the initial sample (0) and after 2, 17 and 42 months of follow-up. HVR1 sequences in samples were obtained from 0 to the 17th month of follow-up and in the 42th month of follow-up. The number at the left of each sequence corresponded to the month of the follow-up when the samples were sequenced. Nucleotide sequences at the different time points were aligned with CLUSTAL W 1.5, and the corresponding amino acid ones were deduced.

A NS5A

```
                 2220       2230       2240       2250       2260       2270
 0 KATCTTNHDS PDAELIEANL LWRGEMGGNI TRVESENKVV VLDSFDPLVA EEDEREISVP
 6 ---------- ------Q--- ---------- ---------- ---------- ----------
10 ---------- ------Q--- ---------- ---------- ---------- ----------
17 ---------- ------Q--- ---------- ---------- ---------- ----------
42 ---------- ------Q--- ---------- ---------- I--------- ----------
```

B Core

```
                   70         80         90        100        110        120
 0 RRQPIPKAHR PEGRTWAQPG YPWPLYGNEG CGWAGWLLSP RGSRPSWGPT DPRRRSRNLG
 6 ---------- ---------- ---------- ---------- ---------- ----------
10 ---------- ---------- ---------- ---------- ---------- ----------
17 --P-----R- ---G------ ---------- ---------- ---------- ----------
42 -------VR- ---------- ---------- ---------- ---------- ----------

                  130        140        150        160        170        180
 0 KVIDTLTCGF ADLMGYIPLV GAPLGGAARA LGHGVRVLED GVNYATGNLP GCSFSIFLLA
 6 ---------- ---------- ---------- ---------- ---------- ----------
10 ---------- ---------- ---------- ---------- ---------- ----------
17 ---------- ---------- ---------- ---------- ---------- ----------
42 ---------- ---------- ---------- -A-------- ---------- ----------
```

Figure 2 Amino acid sequences of consecutive samples corresponding to HCV NS5A (A) and core (B). The number at the left of each one corresponded to the month of the follow-up when the sequences were done. The black bar indicated the ISDR. Amino acid positions were according to the HCV-1 (M62321).

maintained thereafter for the rest of the period (Figure 1).

As far as HCV sequences were concerned, in the HVR1 three nonsynonymous mutations were observed (F399L, G393S and A397S) in the acute phase of the infection, conversely, the mutation dynamics followed a sequential and cumulative pattern, occurring at the 6th, 8th and 12th follow-up months. Each mutation was associated with an ALT flare-up (Figure 1). In the last sample, 42 months after HCV superinfection, two more amino acid changes were selected (G398A and L399F).

Different patterns of substitutions were observed in the HCV core and NS5A regions. In the core, three nonsynonymous substitutions (Q63P, H69R and R74G) appeared at the 17th month of the follow-up (Figure 2), once chronic hepatitis was fully established. Late on the follow-up, four mutations were selected: P63Q, A68V, G74R and G152A. The amino acids that were resulted from the modifications in positions 63 and 74 were the same as that which was present in the earliest samples.

In the portion of NS5A sequenced (nt 6632-7077), one amino acid substitution was observed in the acute phase (E2227Q) and remained thereafter, and another one was selected at the end of the follow-up (V2251I).

The sequences were submitted to GenBank and assigned accession numbers: AF361170 through AF361176 and AF359345 through AF359354.

DISCUSSION

In this study, we analyzed the evolution of different viral genomic regions during HCV superinfection of a chronically HIV infected patient.

Most of the nucleotide substitutions fixed during the HCV superinfection process were nonsynonymous and located at described epitopes, suggesting a positive immune selection mechanism driving their molecular evolution.

We found that hypervariable regions of both HCV and HIV had several amino acid modifications during the acute phase of superinfection. However, these changes occurred simultaneously on the gp120 V3 loop whereas they were sequentially selected and showed a cumulative pattern in the HVR1.

The selection of an HIV viral population with three amino acid modifications in the V3 loop region right after HCV superinfection maybe resulted from the overgrowth of markedly different but minor HIV quasispecies from the initial sample.

In contrast, the HVR1 evolved showed a cumulative pattern of mutations during the 17 month period. Each time of sequential incorporation of a nonsynonymous mutation was associated with an ALT flare up and resulted from the selection process, also exerted by the evolving host immune response[24].

It has been proposed that the evolution of hypervariable regions may be caused by the successive accumulation of point substitutions as we have seen in the HVR1-HCV or, alternatively from the selection of a pre-existing minor subpopulations, which was different from the previous one, as observed in V3 loop of HIV[25].

Once the chronic infection was established, two extra amino acid mutations were observed in the HVR1, the first one was at position 398 (G→A), and the second one was at position 399 (L→F). F or L occupied the last position alternatively in most of the HVR sequences published elsewhere[26] and may be considered as a return to a previous state of the quasispecies equilibrium.

The timing of the substitutions observed in the core region, which were late (after 17 months and 42 months of infection), implied its involvement in the infection once persistence had been established. Non-synonymous changes clustered in HCV epitopes that stimulated the humoral and cellular response and were previously described[18, 20, 27], suggesting an active participation of these epitopes in the persistence of HCV infection. Moreover, the sample at the end of the follow-up showed two modifications (aa 63 and 74 of the core protein) that recovered the early amino acid sequences. As far as the HVR sequences concerned, this effect that might be due to the return to a quasispecies equilibrium state favored the outgrowth of the fittest quasispecies for that particular host conditions, as a consequence from the interplaying of virus populations in every situation.

Two substitutions were selected in the NS5A region. One of them occurred at the early phase of the infection whereas the second appeared at the end of the follow-up. The first mutation selected (E2227Q) was located in the ISDR, described as related to the IFN resistance of some HCV genotypes by means of its interactions with the cellular PKR and in a cellular epitope, as previously described[19].

In conclusion, during the HCV superinfection process, each genomic region analyzed presents a different pattern of evolution, and is probably related to their functions in the viral life cycle. The localization of mutations at described epitopes suggests the participation of the host immune system drives the balance of the viral subpopulations towards escape and better fitness ones. In order to study this hypothesis, a quasispecies analysis is worth to be done to address the changes showed during the coinfection by means of the population equilibriums.

REFERENCES

1 **Waldrep TW,** Summers KK, Chiliade PA. Coinfection with HIV and HCV: more questions than answers? *Pharmacotherapy* 2000; **20:** 1499-1507

2 **Laskus T**, Radkowski M, Piasek A, Nowicki M, Horban A, Cianciara J, Rakela J. Hepatitis C virus in lymphoid cells of patients coinfected with human immunodeficiency virus type 1: evidence of active replication in monocytes/macrophages and lymphocytes. *J Infecti Dis* 2000; **181**: 442-448

3 **Centers for Disease Control and Prevention**. 1999 USPHS/IDSA guidelines for the prevention of oppotunistic infections in persons infected with human immunodeficiency virus: disease-specific recommendations. USPHS/IDSA Prevention of Opportunistic Infections Working Group: U.S: Public Health Services/Infectious Diseases Society of America. *Morbility and Mortality Weekly Report* 1999; **48:** 1-82

4 **Rockstroh JK,** Woitas RP, Spengler U. Human immunodeficiency virus and hepatitis C virus coinfection. *Europ J Med Res* 1998; **3:** 269-277

5 **Rispeter K,** Lu M, Behrens SE, Fumiko C, Yoshida T, Roggendorf M. Hepatitis C virus variability: sequence analysis of an isolate after 10 years of chronic infection. *Virus Genes* 2000; **21:** 179-188

6 **Smith DB.** Evolution of the hypervariable region of hepatitis C virus. *J Viral Hepatitis* 1999; **6**(Suppl 1): 41-46

7 **Ray SC,** Wang YM, Laeyendecker O, Ticehurst JR, Villano SA, Thomas DL. Acute hepatitis C virus structural gene sequences as predictors of persistent viremia: hypervariable region 1 as a decoy. *J Virol* 1999; **73:** 2938-2946

8 **Hwang SS**, Boyle TJ, Lyerly HK, Cullen BR. Identification of the envelope V3 loop as the primary determinant of cell tropism in HIV-1. *Science* 1991; **253**: 71-74

9 **Ghosh AK**, Steele R, Meyer K, Ray R, Ray RB. Hepatitis C virus NS5A protein modulates cell cycle regulatory genes and promotes cell growth. *J General Virol* 1999; **80**: 1179-1183

10 **Gale MJ Jr**, Korth MJ, Tang NM, Tan SL, Hopkins DA, Dever TE, Polyak SJ, Gretch DR, Katze MG. Evidence that hepatitis C virus resistance to interferon is mediated through repression of the PKR protein kinase by the nonstructural 5A protein. *Virology* 1997; **230**: 217-227

11 **Kato N,** Lan KH, Ono-Nita SK, Shiratori Y, Omata M. Hepatitis C virus nonstructural region 5A protein is a potent transcriptional activator. *J Virol* 1997; **71:** 8856-8859

12 **McLauchlan J**. Properties of the hepatitis C virus core protein: a structural protein that modulates cellular processes. *J Viral Hepat* 2000; **7**: 2-14
13 **Matsumoto M**, Hsieh TY, Zhu N, VanArsdale T, Hwang SB, Jeng KS, Gorbalenya AE, Lo SY, Ou JH, Ware CF, Lai MM. Hepatitis C virus core protein interacts with the cytoplasmic tail of lymphotoxin-beta receptor. *J Virol* 1997; **71**: 1301-1309
14 **Zhu N**, Khoshnan A, Schneider R, Matsumoto M, Dennert G, Ware C, Lai MM. Hepatitis C virus core protein binds to the cytoplasmic domain of tumor necrosis factor (TNF) receptor 1 and enhances TNF-induced apoptosis. *J Virol* 1998; 72: 3691-3697
15 **Jin DY**, Wang HL, Zhou Y, Chun AC, Kibler KV, Hou YD, Kung H, Jeang KT. Hepatitis C virus core protein-induced loss of LZIP function correlates with cellular transformation. *EMBO J* 2000; **19**: 729-740
16 **Barba G**, Harper F, Harada T, Kohara M, Goulinet S, Matsuura Y, Eder G, Schaff Z, Chapman MJ, Miyamura T, Brechot C. Hepatitis C virus core protein shows a cytoplasmic localization and associates to cellular lipid storage droplets. *Proceed Nati Acad Sci USA* 1997; **94**: 1200-1205
17 **Sabile A**, Perlemuter G, Bono F, Kohara K, Demaugre F, Kohara M, Matsuura Y, Miyamura T, Brechot C, Barba G. Hepatitis C virus core protein binds to apolipoprotein AII and its secretion is modulated by fibrates. *Hepatology* 1999; **30**: 1064-1076
18 **Akatsuka T**, Donets M, Scaglione L, Ching WM, Shih JW, Di Bisceglie AM, Feinstone SM. B-cell epitopes on the hepatitis C virus nucleocapsid protein determined by human monospecific antibodies. *Hepatology* 1993; **18**: 503-510
19 **Ward S**, Lauer G, Isba R, Walker B, Klenerman P. Cellular immune responses against hepatitis C virus: the evidence base 2002. *Clin Experimental Immunol* 2002; **128**: 195-203
20 **Koziel MJ**, Dudley D, Afdhal N, Choo QL, Houghton M, Ralston R, Walker BD. Hepatitis C virus (HCV)-specific cytotoxic T lymphocytes recognize epitopes in the core and envelope proteins of HCV. *J Virol* 1993; **67**: 7522-7532
21 **Flichman D**, Cello J, Castano G, Campos R, Sookoian S. *In vivo* down regulation of HIV replication after hepatitis C superinfection. *Medicina* 1999; **59**: 364-366
22 **Chomczynski P**, Sacchi N. Single-step method of RNA isolation by acid guanidinium thiocyanate-phenol-chloroform extraction. *Analytical Biochemistry* 1987; **162**: 156-159
23 **Kwok S**, Higuchi R. Avoiding false positives with PCR. *Nature* 1989; **339**: 237-238
24 **Hjalmarsson S**, Blomberg J, Grillner L, Pipkorn R, Allander T. Sequence evolution and cross-reactive antibody responses to hypervariable region 1 in acute hepatitis C virus infection. *J Med Virol* 2001; **64**: 117-124
25 **Lu L**, Nakano T, Orito E, Mizokami M, Robertson BH. Evaluation of accumulation of hepatitis C virus mutations in a chronically infected chimpanzee: comparison of the core, E1, HVR1, and NS5b regions. *J Virol* 2001; **75**: 3004-3009
26 **Penin F**, Combet C, Germanidis G, Frainais PO, Deleage G, Pawlotsky JM. Conservation of the conformation and positive charges of hepatitis C virus E2 envelope glycoprotein hypervariable region 1 points to a role in cell attachment. *J Virol* 2001; **75**: 5703-5710
27 **Beld M**, Penning M, van Putten M, Lukashov V, van den Hoek A, McMorrow M, Goudsmit J. Quantitative antibody responses to structural (Core) and nonstructural (NS3, NS4, and NS5) hepatitis C virus proteins among seroconverting injecting drug users: impact of epitope variation and relationship to detection of HCV RNA in blood. *Hepatology* 1999; **29**: 1288-1298

Edited by Xu XQ and Wang XL

P.O.Box 2345, Beijing 100023,China
Fax: +86-10-85381893
E-mail: wjg@wjgnet.com www.wjgnet.com

World J Gastroenterol 2003;9(7):1501-1503
World Journal of Gastroenterology
 ISSN 1007-9327

• VIRAL HEPATITIS •

Interruption of HBV intrauterine transmission: A clinical study

Xiao-Mao Li, Yue-Bo Yang, Hong-Ying Hou, Zhong-Jie Shi, Hui-Min Shen, Ben-Qi Teng, Ai-Min Li, Min-Feng Shi, Ling Zou

Xiao-Mao Li, Yue-Bo Yang, Hong-Ying Hou, Zhong-Jie Shi, Hui-Min Shen, Ben-Qi Teng, Ai-Min Li, Ling Zou, Department of Obstetrics and Gynecology, The Third Affiliated Hospital, Sun Yat-Sen University, Guangzhou 510630, Guangdong Province, China
Min-Feng Shi, Maternity Hospital, School of Medicine, Zhejiang University, Hangzhou 310006, Zhejiang Province, China
Supported by the Science and Research Foundations of Sun Yat-Sen University and Guangzhou Science Committee, No.1999-J-005-01
Correspondence to: Xiao-Mao Li, Department of Obstetrics and Gynecology, The Third Affiliated Hospital, Sun Yat-Sen University, Guangzhou 510630, Guangdong Province, China. tigerli777@163.com
Telephone: +86-20-85515609 **Fax**: +86-20-87565575
Received: 2003-03-13 **Accepted:** 2003-04-11

Abstract

AIM: To investigate the effect of hepatitis B virus (HBV) specific immunoglobin (HBIG) and lamivudine on HBV intrauterine transmission in HBsAg positive pregnant women.

METHODS: Each subject in the HBIG group (56 cases) was given 200 IU HBIG intramuscularly (im.) every 4 weeks from 28-week (wk) of gestation, while each subject in the lamivudine group (43 cases) received 100 mg lamivudine orally (po.) every day from 28-wk of gestation until the 30th day after labor. Subjects in the control group (52 cases) received no specific treatment. Blood specimens were tested for HBsAg, HBeAg, and HBV-DNA in all maternities at 28-wk of gestation, before delivery, and in their newborns 24 hours before the administration of immune prophylaxis.

RESULTS: Reductions of HBV DNA in both treatments were significant ($P<0.05$). The rate of neonatal intrauterine HBV infection was significantly lower in HBIG group (16.1 %) and lamivudine group (16.3 %) compared with control group (32.7 %) ($P<0.05$), but there was no significant difference between HBIG group and lamivudine group ($P>0.05$). No side effects were found in all the pregnant women or their newborns.

CONCLUSION: The risk of HBV intrauterine infection can be effectively reduced by administration of HBIG or Lamivudine in the 3rd trimester of HBsAg positive pregnant women.

Li XM, Yang YB, Hou HY, Shi ZJ, Shen HM, Teng BQ, Li AM, Shi MF, Zou L. Interruption of HBV intrauterine transmission: A clinical study. *World J Gastroenterol* 2003; 9(7): 1501-1503
http://www.wjgnet.com/1007-9327/9/1501.asp

INTRODUCTION

It is of vital importance to interrupt the transmission of viral hepatitis B from mother to fetus in control of its prevalence[1-3], including HBV intrauterine infection[4-7]. This study investigated the effect of administration of HBIG (im.) and lamivudine (po.) on the interruption of HBV intrauterine infection from the 3rd trimester of gestation.

MATERIALS AND METHODS

Subjects

One hundred and fifty one pairs of women and their newborns who followed the antepartum care were selected and admitted for labor in our hospital from January of 1999 to December of 2001. These pregnant women were HBsAg positive, with normal liver and kidney function. Serial tests were negative for HAV, HCV, HDV and HEV in these women and no other severe complications were found and no other drugs, including the ones that were studied, anti-virus, cytotoxic, steroid hormones, or immune regulating drugs were administrated. The patients were randomly allocated into 3 groups. There were 56 patients in the HBIG group (22 were both HBsAg and HBeAg positive) and 43 in the lamivudine group (33 were both HBsAg and HBeAg positive). There were 52 patients in the control group (17 were both HBsAg and HBeAg positive). No significant differences were found in age, race, time of gestation and parturition, gestational age, way of delivery, and incidence of threatened abortion, threatened labor or pregnancy-induced hypertension syndrome (PIH). The 151 pregnant women delivered 151 newborns.

Methods

Patients in the HBIG group were administered HBIG 200IU intramuscularly (im.) from 28-wk of gestation, once every 4 weeks till labor. Patients in the lamivudine group were administered 100 mg (po.) lamivudine orally daily till the 30th day after labor. Patients in the control group were given no specific treatment. Blood specimens were tested for HBsAg, HBeAg, and HBV-DNA in all the subjects at 28-wk and before delivery, and their newborns (blood from the femoral vein) 24 hours before administration of immune prophylaxis.

HBsAg and HBeAg were assessed by ELISA, the assay kits were produced by Zhongshan Biological and Engineering Co. Ltd. HBV-DNA was assessed by fluorogenic quantitative polymerase chain reaction (FQ-PCR), and the assay kits were produced by Da'an Gene Diagnosis Center, Sun Yat-Sen University.

Before the administration of positive and/or active prophylaxis at 24 hours after delivery, intrauterine HBV infection would be considered if HBsAg and/or HBeAg were tested positive in neonatal peripheral blood.

Statistics

The *t*-test and χ^2 test were used to analyze our data using Excel software. Statistical significance was set at $P<0.05$. HBV DNA values were expressed as $\bar{x}\pm s$, and neonatal intrauterine HBV infection rates were expressed as percentage of total cases in each group.

RESULTS

Changes of HBsAg, HBeAg and HBV DNA

HBsAg turned negative in 1 case of the HBIG group, but HBeAg turned negative in no case. HBsAg and HBeAg turned negative in 1 case of the lamivudine group. No cases turned negative of HBsAg or HBeAg in the control group.

Before administration of agents, there was no significant difference in the values of HBV DNA among 3 groups

(P>0.05). But there was significant difference between the values of HBV DNA in HBIG group and lamivudine group after administration of either reagent respectively (both values reduced, P<0.05). The reduction of value before and after administration of the reagents was significantly different between the administered groups and control group (P<0.05). (Table 1).

Table 1 Comparison of HBV DNA values before and after administration of the reagents

Group	*n*	Log10 HBV DNA before administration of drugs (copies / ml)	Log10 HBV DNA before labor (copies / ml)	Minus value of log10 HBV DNA before and after administration of agents (copies / ml)
HBIG	56	7.38±1.17[a]	5.28±2.77[bd]	2.09±2.28[b]
Lamivudine	43	7.49±0.54[a]	5.33±1.34[bd]	2.16±1.27[b]
Conrol	52	7.05±1.29[a]	6.23±3.66[c]	0.82±2.73[c]

[a]P>0.05 *vs* other groups; [b]P>0.05 between HBIG group and lamivudine group; [c]P<0.05 *vs* HBIG group or lamivudine group; [d]P<0.05 (before *vs* after administration).

Incidence of HBV intrauterine infection

Three newborns were HBsAg positive, and 7 cases were HBeAg positive, one of them was doubly positive for HBsAg and HBeAg in HBIG group. Corresponding cases in lamivudine group and control group were 1, 7, and 1, or 8, 11, and 2 respectively. The infection rates of HBIG, lamivudine, and control groups were 16.1 %, 16.3 %, and 32.7 %, respectively. There were significant differences between the incidence of HBV intrauterine infection in either reagent administrated group and control group (P<0.05), while there was no significant difference between HBIG group and lamivudine group (P>0.05). (Table 2).

Table 2 Incidence of neonatal intrauterine infection in 3 groups

Group	*n*	HBsAg(+) *n*	HBeAg(+) *n*	Intrauterine infection	
				n	%
HBIG	56	3	7	9	16.1[a]
Lamivudine	43	1	7	7	16.3[a]
Control	52	8	11	17	32.7[b]

[a]P>0.05 between HBIG group and lamivudine group; [b]P<0.05 *vs* HBIG group or lamivudine group.

Safety

There were no incidences of fever, rigor, rash, or other complaints and dysfunction of the liver and kidney in subjects throughout administration and follow-ups. There were no significant differences in gestational age, severity of postpartum hemorrhage, rate of cesarean section, neonatal weight, neonatal height, circumference of neonatal head and Apgar score (P>0.05).

DISCUSSION

There are several thoughts about the mechanisms of HBV intrauterine transmission, including placental infection[8], placental exudation and transudation[9-11], peripheral blood monocyte (PBMC)[12] infection, fraternal transmission, etc. Infection through placenta is the most active pathway in maternity-fetus transmission. It is suggested that infection mainly occurs in the 3rd trimester. This might be resulted from the fact that the layer of trophoblastic cells becomes thinner and turns into chorion-vessel membrane, which makes it easier for HBV to pass the placental barrier[13]. The organs of fetus during this period have already developed, therefore, it is safe for the administration of reagents. So we chose this period to begin the interruption of infection. Lamivudine (po.) or HBIG (im.) was administered from 28-wk of gestation.

Barrier-destroying factors, such as threatened abortion, threatened premature labor and TORCH (toxoplasmosis, others, rubella, cytomegalovirus, herpes) infection, were the highly risk factors for HBV intrauterine infection[14]. It is generally considered that intrauterine infection might be the general effect of maternity and virus. In this study, there were no significant differences among the 3 groups in the highly risk factors (threatened abortion, threatened premature labor) or age, time of gestation and delivery, pregnant complication, medical or surgical complication, gestational age at labor or way of delivery.

It has been clinically accepted to administer joint immune reagents (HBIG together with HBV vaccine) to neonates with high risks, but the immune failure rate is still about 10-20 %[15,16], the main reason is intrauterine infection. So, it is important to study the mechanism of HBV intrauterine infection, and we further investigated the intrauterine prevention and interruption of HBV infection.

HBIG is a highly effective immune globulin[17], which is purified from highly effective plasma or serum taken from healthy individuals after the use of HBV vaccine. HBs antibody can bind HBsAg, activate the complimentary system at the same time and strengthen humoral immune, clear HBV, and reduce the number of virus in the maternal blood. It can prevent and decrease the incidence of normal cell infection and might reduce HBV copy in the body. Placenta has the function of transmitting antibody in the form of IgG to the fetus. It is suggested that after maternal administration of HBIG (im.), HBsAb can be transmitted to fetus, which makes it possible for the fetus to obtain the protection of intrauterine passive immunization and to prevent intrauterine infection[18]. The results of this study suggest that regular administration of HBIG (im.) to HBV positive pregnant women might reduce the amount of HBV DNA in blood, and neonatal intrauterine infection rate also reduced significantly when compared with control group. DNA polymerase of HBV has many functions in the process of virus replication. After infection of liver cells by HBV, the incomplete double strand DNA integrates into a complete one, enters the nuclei, forming super helix covalent closed circular DNA (cccDNA). cccDNA is extremely stable, and is the resource of viral DNA and directs the formation of viral protein. The whole mRNA replicated from cccDNA model can form a single strand minus-DNA by reverse-transcription of the HBV DNA polymerase. This DNA can form incomplete double strand DNA through DNA polymerase. The latter can also integrate with antigen proteins in the endoplast, forming new, contagious mature viral particles and be released into blood, or migrate into the nuclei to supply cccDNA there. The multiple functions of HBV polymerase enable it to become one of the most prosperous anti-virus targets.

Lamivudine is a potent anti-virus nucleotide analogue to HBV and HIV. Through competitive inhibition of HBV DNA polymerase and formation of new HBV DNA strand, it can terminate the synthesis of new strand[19,20]. After several days of the administration of lamivudine, the level of HBV DNA drops dramatically, and throughout the treatment, HBV DNA will be suppressed continuously. It can reduce the necrosis and inflammation of the liver and bring ALT level to normal without significant side effects or malformation-causing effects[21-31]. We found the amount of HBV DNA in blood and the rate of neonatal intrauterine infection after administration of lamivudine in the 3rd trimester were significantly lower than that in control group. This suggests that administration of lamivudine of HBV positive pregnant women in the 3rd trimester can effectively decrease the rate of intrauterine HBV infection.

As a passive antibody, the main effect of HBIG is to neutralize HBV in the body, prevent and decrease infection of normal cells[32]; while lamivudine is a potent anti-virus agent, which can suppress the replication of HBV actively, decrease HBV level during pregnancy. Our data showed that the neonatal infection rates, after these two reagents were used in the 3rd trimester to interrupt intrauterine HBV infection, were 16.1 % and 16.3 %, respectively, with no significant difference between these 2 groups (P>0.05). But compared with control group, the infection rates of both groups were significantly lower. These data indicate that both of them are safe and effective in the interruption of intrauterine HBV infection.

We found in our previous studies that HBV DNA level in maternal serum was an important factor for intrauterine infection[1]. Especially when HBV DNA is $\geqslant 10^8$ copies/ml, it has significant correlation with neonatal HBV infection[33]. Administration of HBIG in combination with lamivudine in these patients might decrease the neonatal HBV infection rate more effectively. Further studies are required to improve our understanding about this problem.

REFERENCES

1 **Li XM**, Liu SL, Li X, Huang HJ, Lu JX, Gao ZL. The level of HBV DNA in peripheral, umbilical, and milk of maternal and its correlation. *Zhongshan Yike Daxue Xuebao* 2000; **21**: 233-235

2 **Merle P**, Trepo C, Zoulim F. Current management strategies for hepatitis B in the elderly. *Drugs Aging* 2001; **18**: 725-735

3 **Hamdani-Belghiti S**, Bouazzaou NL. Mother-child transmission of hepatitis B virus. State of the problem and prevention. *Arch Pediatr* 2000; **7**: 879-882

4 **Zhang SL**, Han XB, Yue YF. Relationship between HBV viremia level of pregnant women and intrauterine infection: neated PCR for detection of HBV DNA. *World J Gastroenterol* 1998; **4**: 61-63

5 **Shiraki K**. Perinatal transmission of hepatitis B virus and its prevention. *J Gastroenterol Hepatol* 2000; **15** (Suppl): E11-15

6 **Michielsen PP**, Van Damme P. Viral hepatitis and pregnancy. *Acta Gastroenterol Belg* 1999; **62**: 21-29

7 **Tang JR**, Hsu HY, Lin HH, Ni YH, Chang MH. Hepatitis B surface antigenemia at birth: a long-term follow-up study. *J Pediatr* 1998; **133**: 374-377

8 **Xu DZ**, Yan YP, Zou S, Choi BC, Wang S, Liu P, Bai G, Wang X, Shi M, Wang X. Role of placental tissues in the intrauterine transmission of hepatitis B virus. *Am J Obstet Gynecol* 2001; **185**: 981-987

9 **Kroes AC**, Quint WG, Heijtink RA. Significance of isolated hepatitis B core antibodies detected by enzyme immunoassay in a high risk population. *J Med Virol* 1991; **35**: 96-100

10 **Suga M**, Shibata K, Kodama T, Arima K, Yamada S, Yachi A. A case of HBs antigen negative fulminant hepatitis with IgM antibody to hepatitis B core antigen persisting more than seven years. *Gastroenterol Jpn* 1991; **26**: 661-665

11 **Wang JS**, Zhu QR. Infection of the fetus with hepatitis B e antigen via the placenta. *Lancet* 2000; **355**: 989

12 **Leung NW**, Tam JS, Lau GT, Leung TW, Lau WY, Li AK. Hepatitis B virus DNA in peripheral blood leukocytes. A comparison between hepatal cellulo carcinoma and other hepatitis B virus-related chronic liver diseases. *Cancer* 1994; **73**: 1143-1148

13 **Yan YP**, Xu DZ, Wang WL, Liu B, Liu ZH, Men K, Zhang JX, Xu JQ. The relation between HBV placenta infection and intrauterine transmission. *Zhonghua Fuchanke Zazhi* 1999; **34**: 392-395

14 **Del Canho R**, Grosheide PM, Schalm SW, de Vries RR, Heijtink RA. Failure of neonatal hepatitis B vaccination: the role of HBV-DNA levels in hepatitis B carrier mothers and HLA antigens in neonates. *J Hepatol* 1994; **20**: 483-486

15 **Zhu Q**, Lu Q, Gu X, Xu H, Duan S. A preliminary study on interruption of HBV transmission in uterus. *Chin Medl J (Engl)* 1997; **110**: 145-147

16 **Xu DZ**, Yan YP, Choi BC, Xu JQ, Men K, Zhang JX, Liu ZH, Wang FS. Risk factors and mechanism of transplacental transmission of hepatitis B virus:A case-control study. *J Med Virol* 2002; **67**: 20-26

17 **Ghendon Y**. Perinatal transmission of hepatitis B virus in high-incidence countries. *J Virol Methods* 1987; **17**: 69-79

18 **Yue YF**, Yang XJ, Zhang SL, Han XB. Clinical research of the effect of intramuscular administration of HBIG on HbsAg positive pregnant women to prevent vertical transmission. *Zhongguo Shiyong Fuke Yu Chanke Zazhi* 1999; **15**: 547-548

19 **Yao GB**, Wang SB, Cui ZY, Yao JL, Zeng MD. A multi-center random double-blind case-control study of the treatment of chronic hepatitis B by Lamivudine. *Zhongguo Xinyao Yu Linchuang Zazhi* 1999; **18**: 131-135

20 **Johnson MA**, Moore KH, Yuen GJ, Bye A, Pakes GE. Clinical pharmacokinetics of lamivudine. *Clin Pharmacokinet* 1999; **36**: 41-66

21 **Rizzetto M**. Efficacy of lamivudine in HBeAg-negative chronic hepatitis B. *J Med Virol* 2002; **66**: 435-451

22 **Ricceri L**, Venerosi A, Valanzano A, Sorace A, Alleva E. Prenatal AZT or 3TC and mouse development of locomotor activity and hot-plate responding upon administration of the GABA(A) receptor agonist muscimol. *Psychopharmacology (Berl)* 2001; **153**: 434-442

23 **Calamandrei G**, Venerosi A, Branchi I, Valanzano A, Alleva E. Prenatal exposure to anti-HIV drugs. long-term neurobehavioral effects of lamivudine (3TC) in CD-1 mice. *Neurotoxicol Teratol* 2000; **22**: 369-379

24 **Culnane M**, Fowler M, Lee SS, McSherry G, Brady M, O'Donnell K, Mofenson L, Gortmaker SL, Shapiro DE, Scott G, Jimenez E, Moore EC, Diaz C, Flynn PM, Cunningham B, Oleske J. Lack of long-term effects of in utero exposure to zidovudine among uninfected children born to HIV-infected women. *JAMA* 1999; **281**: 151-157

25 **Conner EM**, Sperling RS, Gelber R Kiselev P, Scott G, O'Sullivan MJ, VanDyke R, Bey M, Shearer W, Jacobson RL. Reduction of maternal-infant transmission of human immunodeficiency virus type-1 with zidovudine. *N Engl J Med* 1994; **331**: 1173-1180

26 **Vuthipongse R**, Bhadrakom C, Roongpisuthipong P. Administration of Zidovudine during late pregnancy and delivery to prevent perinatal HIV transmission-Thailand 1996-1998. *MMWR* 1998; **47**: 151-154 / / *JAMA* 1998; **279**: 1061-1062

27 **Moodley J**, Moodley D, Pillay K, Coovadia H, Saba J, van Leeuwen R, Goodwin C, Harrigan PR, Moore KH, Stone C, Plumb R, Johnson MA. Pharmacokinetics and antiretroviral activity of lamivudine alone or when coadministered with zidovudine in human immunodeficiency virus type 1-Infected pregnant women and their offspring. *J Infect Dis* 1998; **178**: 1327-1333

28 **van Leeuwen R**, Lange JM, Nijhuis M, Schuurman R, Reiss P, Danner SA, Boucher CA. Results of long-term follow-up of HIV-infected patients treated with lamivudine monotherapy, followed by a combination of lamivudine and zidovudine. *Antivir Ther* 1997; **2**: 79-90

29 **Dienstag JL**, Perillo RP, Schiff ER, Bartholomew M, Vicary C, Rubin M. A preliminary trial of lamivudine for chronic hepatitis B infection. *N Engl J Med* 1995; **333**: 1657-1661

30 **Liaw YF.** Current therapeutic trends in therapy for chronic viral hepatitis. *J Gastroenterol Hepatol* 1997; **12**: S346-353

31 **Lai CL**, Ching CK, Tung AK, Li E, Young J, Hill A, Wong BC, Dent J, Wu PC. Lamivudine is effective in suppressing hepatitis B virus DNA in Chinese hepatitis B surface antigen carriers: a placebo-control trial. *Hepatology* 1997; **25**: 241-244

32 **Yue Y**, Yang X, Zhang S. Prevention of intrauterine infection by hepatitis B virus with hepatitis B immuneglobulin: efficacy and mechanism. *Chin Med J (Engl)* 1999; **112**: 37-39

33 **Ngui SL**, Andrews NJ, Underhill GS, Heptonstall J, Teo CG. Failed postnatal immunoprophylaxis for hepatitis B: characteristics of maternal hepatitis B virus as risk factors. *Clinical Infectious Diseases* 1998; **27**: 100-106

Edited by Yuan HT and Wang XL

P.O.Box 2345, Beijing 100023,China
Fax: +86-10-85381893
E-mail: wjg@wjgnet.com www.wjgnet.com

World J Gastroenterol 2003;9(7):1504-1507
World Journal of Gastroenterology
 ISSN 1007-9327

Inhibition of HBV targeted ribonuclease enhanced by introduction of linker

Wei-Dong Gong, Jun Liu, Jin Ding, Ya Zhao, Ying-Hui Li, Cai-Fang Xue

Wei-Dong Gong, Jun Liu, Jin Ding, Ya Zhao, Ying-Hui Li, Cai-Fang Xue, Department of Pathogenic Organisms, Fourth Military Medical University, Xi' an 710033, Shaanxi Province, China
Supported by National Natural Scientific Foundation of China, No. 30100157 and Innovation Project of FMMU, No.CX99005
Correspondence to: Professor Cai-Fang Xue or Dr. Jun Liu, Department of Pathogenic Organisms, Fourth Military Medical University, Xi' an 710033, Shaanxi Province, China. etiology@fmmu.edu.cn
Received: 2003-03-05 **Accepted:** 2003-04-01

Abstract

AIM: To construct human eosinophil-derived neurotoxin (hEDN) and HBV core protein (HBVc) eukaryotic fusion expression vector with a linker $(Gly_4Ser)_3$ between them to optimize the molecule folding, which will be used to inhibit HBV replication *in vitro*.

METHODS: Previously constructed pcDNA3.1(-)/TR was used as a template. Linker sequence was synthesized and annealed to form dslinker, and cloned into pcDNA3.1(-)/TR to produce plasmid pcDNA3.1(-)/HBc-linker. Then the hEDN fragment was PCR amplified and inserted into pcDNA3.1(-)/HBc-linker to form pcDNA3.1(-)/TNL in which the effector molecule and the target molecule were separated by a linker sequence. pcDNA3.1(-)/TNL expression was identified by indirect immunofluorescence staining. Radioimmunoassay was used to analyse anti-HBV activity of pcDNA3.1(-)/TNL. Meanwhile, metabolism of cells was evaluated by MTT colorimetry.

RESULTS: hEDN and HBVc eukaryotic fusion expression vector with a linker $(Gly_4Ser)_3$ between them was successfully constructed. pcDNA3.1(-)/TNL was expressed in HepG2.2.15 cells efficiently. A significant decrease of HBsAg concentration from pcDNA3.1(-)/TNL transfectant was observed compared to pcDNA3.1(-)/TR (P=0.036, P<0.05). MTT assay suggested that there were no significant differences between groups (P=0.08, P>0.05).

CONCLUSION: Linker introduction enhances the inhibitory effect of HBV targeted ribonuclease significantly.

Gong WD, Liu J, Ding J, Zhao Y, Li YH, Xue CF. Inhibition of HBV targeted ribonuclease enhanced by introduction of linker. *World J Gastroenterol* 2003; 9(7): 1504-1507
http://www.wjgnet.com/1007-9327/9/1504.asp

INTRODUCTION

Hepatitis B virus (HBV) remains a major public health problem worldwide[1-6] and causes transient and chronic infection of liver[7-9]. Transient infection may produce serious illness, and chronic infection may also have serious consequences: nearly 25 % of chronic HBV infected patients terminate in untreatable liver cancer of 350 million chronic HBV infected patients. The available treatments are of limited efficacy, such as interferon-α (INF-α)[10-12], nucleoside analogues[13-15] and gene therapy strategy[16,17]. Alternative approaches to inhibit HBV replication are urged. Capsid-targeted viral inactivation (CTVI, also called virion-targeted viral inactivation) was established by Natsoulis and Boeke in 1991, in which a viral capsid protein or other virion associated protein as a carrier guides a degradative enzyme into virus particles specifically to inhibit virus replication or kill it[18]. CTVI has been thoroughly investigated in experimental treatment for retrovirus, such as Moloney murine leukemia virus (MMLV) and HIV, showing a promising prospect as an antiviral treatment[19,20]. Previously we fused HBV core protein (HBVc) to human eosinophil-derived neurotoxin (hEDN), and after transfection of the fusion protein encoding plasmid into HepG2.2.15 cells HBV replication was inhibited, due to the fact that HBV pregenome RNA (pgRNA) was degraded by the effector molecule, hEDN, *via* the guiding of the target molecule, HBVc[21,22]. Here we reported the further enhancement of the degradative effect by introduction of a linker sequence $(Gly_4Ser)_3$ to separate the effector molecule and the target one.

MATERIALS AND METHODS

Reagents and equipments

pcDNA3.1(-)/TR was constructed in our laboratory[21]. HepG2.2.15 cells were kindly provided by Dr. Hao (Tangdu Hospital, Fourth Military Medical University). Restriction enzymes, alkaline dephosphoratase, *TaKaRa Ex Taq*™, DNA marker-DL2000 and T_4 DNA ligase (*TaKaRa* Biotechnology Co., Ltd., Dalian), Plasmid Miniprep Kit, Agarose Gel Extraction kit (Watson Biotechnology, Shanghai), LipofectinMine2000 (GIBCO), mouse anti-HA and rabbit anti-mouse IgG labeled with FITC (Sino-American Biotechnology Company), Radioimmunoassay Kit (Beijing Bei Mian Dongya Biotech Institute), GeneAmp PCR System 9600 (Perkin Elmer).

Linker and primers

All the oligomers were synthesized by Sangon (Shanghai).
LinkerF 5' -gcg cgg atc cgg tgg cgg tgg ctc ggg cgg tgg tgg gtc ggg tgg cgg cgg atc tga tga gct cgc gc- 3' (*Bam*HI, *Sac*I)
LinkerR 5' -gcg cga gctc aga tcc gcc gcc acc cga ccc acc acc gcc cga gcc acc gcc acc gga tcc gcg c- 3' (*Sac*I, *Bam*HI)
P1: 5' - gcg ggatcc acc atg aaa cct cca cag tt- 3' (*Bam*HI)
P2: 5' - gcg agatct gat gat tct atc cag gtg aa- 3' (*Bgl*II)

Cell culture

HepG2.2.15 cells integrated full-length HBV genome were cultured in DMEM medium containing 150 mL/L fetal bovine serum at 37 ℃, in 50 mL/L CO_2. G418 was added to screen cells at the final concentration of 100 g/L. The media were freshed once every two days and the cells were passaged every six days.

Introduction of linker

To prepare double stranded linker, linkerF and linkerR were annealed by heating at 100 ℃ for 5 min and then slowly cooling to room temperature, and dissolved at a concentration of 0.1 g/L.

Dslinker bearing *Bam*HI and *Sac*I restriction sites was digested and cloned into pcDNA3.1(-)/TR digested by the same restrictions, to produce plasmid pcDNA3.1(-)/HBc-linker.

hEDN fragment acquired from pcDNA3.1(-)/TR was PCR amplified by using primers and taking pcDNA3.1(-)/TR as a template. The PCR products digested by *Bam*HI/*Bgl*II were inserted into pcDNA3.1(-)/HBc-linker which was restricted by *Bam*HI and dephosphorated, and the direction of hEDN was identified by enzyme restriction. The constructed plasmid was called pcDNA3.1(-)/TNL in which the effector molecule and the target molecule were separated by a linker sequence. The linker sequence and the PCR products were confirmed by sequencing by gencore (Shanghai).

Transfection and indirect immunofluorescence

Transfections were performed as described by the provider of LipofectinMine2000 and the transfecting condition had already been optimized by our laboratory[21]. The cell density of 4×10^8 /L was added by 500 μL/well in 24-well plate in which the cover glasses were put in advance. Transfecting work was performed when cells were adhered, usually after 24 hours[18]. The experiment was divided into 3 groups: test group in which pcDNA3.1(-)/TNL was used, and two control groups in which blank vector pcDNA3.1(-) was used in the second group and the third was taken for mock transfection. Tri-wells were contained in each group. 48 hours post-transfection cells were quickly washed with 1mL sterile PBS (pH8.0) for 5 minutes, fixed in 1 g/L TritonX-100 diluted with 20 g/L paraformaldehyde and put on ice for 30 minutes. The fixed cells were washed three times with cold PBS, incubated with mouse anti-HA (1:100) for 15 minutes at 4 ℃, and then washed three times in cold PBS, followed by incubation in rabbit anti-mouse IgG labeled with FITC (1:100) for 10 minutes at 4 ℃. After rinsed with PBS for 1 hour, the slides were mounted with cover ships by using 500 g/L glycerol/PBS. The results were observed by fluoroscopy and pictures were taken.

Analysis of anti-HBV activity for pcDNA3.1(-)/TNL

24 hours before transfection, HepG2.2.15 cells were plated into a 96 well-plate with of 4×10^4 cells per well. Transfections were performed as described above. To determine HBsAg concentration, transfection experiment was divided into 7 groups, they were pcDNA3.1(-)/TNL, pcDNA3.1(-)/TR, pcDNA3.1(-)/hEDN$_{mut}$-HBVc, pcDNA3.1(-)/HBVc, pcDNA3.1(-)/hEDN, pcDNA3.1(-) and mock transfection, named as A to G respectively. Each transfection was performed in triplicate. After 48 hours of transfection the cell suspension was taken and HBsAg concentration was determined by RIA kit (completed by Nuclear Medicine Department of Xijing Hospital). Meanwhile the transfected cells were used to analyze the metabolic activity in order to analyze the effect of expressing protein on host cells. The data obtained were analyzed by SPSS software.

MTT assay

Metabolism of cells was evaluated by MTT colorimetry. 48 hours following transfections, 20 μL of MTT solution (5 g/L) was added into each well and incubated at 37 ℃ for another 4 h. 150 μL DMSO was added and surged for 10 min to dissolve the crystal completely. Absorbance values were identified at 490 nm wavelength by ELISA reader.

RESULTS

Linker introduction

To separate HBc and hEDN, a linker was introduced. Both the linker sequence cloned into plasmid pcDNA3.1(-)/HBc-linker and hEDN fragment from PCR products, were subsequently inserted into pcDNA3.1(-)/TNL, and confirmed by sequencing. plasmid pcDNA3.1(-)/TNL was identified by restrictions of *BamH*I/*Sac*I and *Sac*I/*Hind*III, the results suggested the construction was successful (Figure 1).

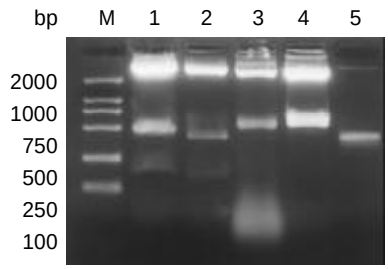

Figure 1 Identifications of plasmids in construction of pcDNA3.1(-)/TNL. 1: pcDNA3.1(-)/TNL digested by *Sac*I/*Hind*III; 2: pcDNA3.1(-)/TR by *Bam*HI/*Sac*I; 3: pcDNA3.1(-)/TR by *Sac*I/*Hind*III; 4: pcDNA3.1(-)/TNL by *Bam*HI/*Sac*I; 5: PCR products of hEDN.

Indirect immunofluorescence

To observe the expression of linker-separated fusion protein of pcDNA3.1(-)/TNL, indirect immunofluorescence was performed after 48 h of transfection (Figure 2).

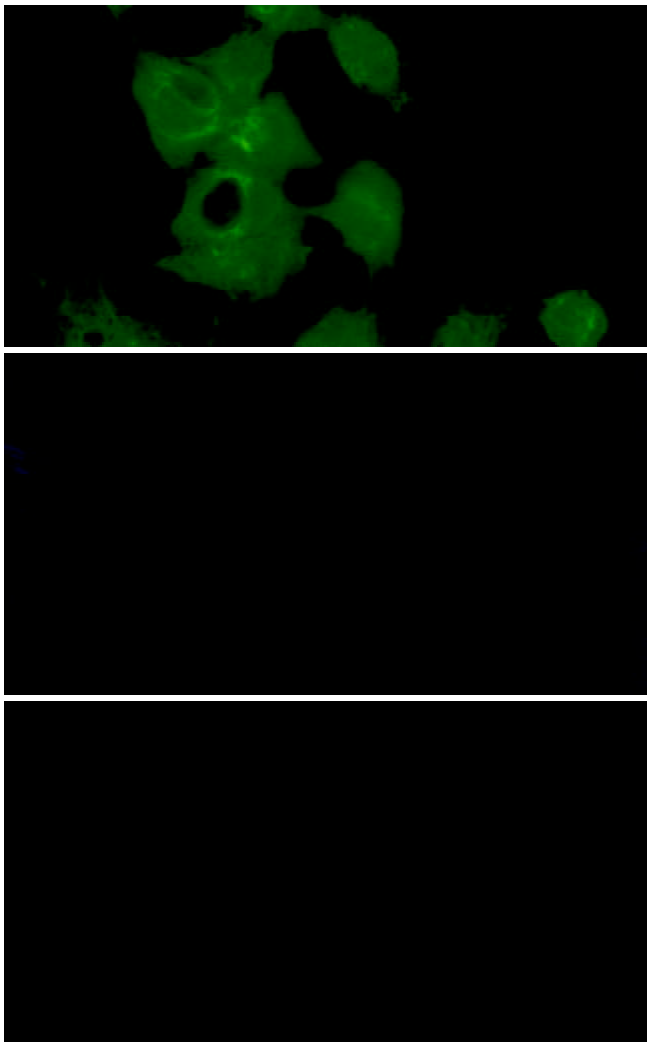

Figure 2 Detection of fusion protein by indirect immunofluorescence. 1: Green fluorescence in cells transfected by pcDNA3.1(-)/TNL; 2, 3: No fluorescence was observed in pcDNA3.1(-) transfectant and mock transfection.

Linker effect

To analyze the digestion effect of hEDN separated by a linker with HBVc. HBsAg concentration was determined by RIA after transfection. The significant decrease of HBsAg concentration in pcDNA3.1(-)/TNL transfectant, compared to pcDNA3.1(-)/TR(P=0.036, P<0.05, Figure 3), suggested that linker introduction enhanced hEDN digestion effect, which may be due to optimization of the folding of both hEDN and HBVc molecules. Also there were significant differences between groups A, B and groups C, D, E, F, G (P=0.0054, P<0.01), and no significant difference was found between groups C, D, E, F and group G (P=0.085, P>0.05).

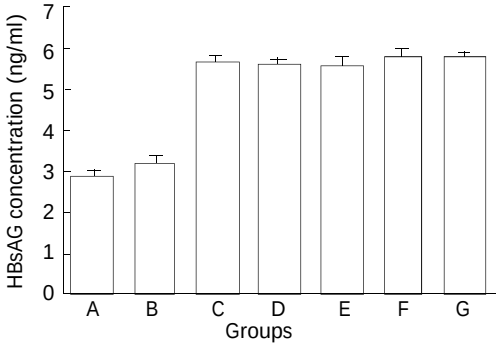

Figure 3 Comparision of HBsAg concentration in transfection groups.

Cell toxicity effect

48 hours post-transfection cell growth was observed and cell toxic effect of linker-separated fusion protein on host hepatocytes was detected by MTT assay. The A_{490} value of HepG2.2.15 cells transfected with pcDNA3.1(-)/TNL, pcDNA3.1(-)/TR, pcDNA3.1(-)/hEDN$_{mut}$-HBVc, pcDNA3.1(-)/HBVc, pcDNA3.1(-)/hEDN, pcDNA3.1(-) and mock transfection was 0.62±0.16, 0.69±0.10, 0.70±0.05, 0.64±0.04, 0.75±0.08, 0.78±0.04, 0.54±0.16, respectively ($\bar{x}$±s, n=3). The results suggested that there were no significant differences between groups (P=0.08, P>0.05).

DISCUSSION

HBV infection is an important health problem worldwide. Int-erferons and nucleosides analogues are effective drugs for chronic HBV infection, but only 20-30 % of treated patients maintain a long-lasting response to anti-viral drugs[23]. The expense of prolonged treatment makes these therapies poorly suitable for people in developing countries, where the prevalence of chronic HBV infection is often high. Therefore, new therapy strategy for HBV infection is urgent.

A new strategy called CTVI was established to guide effector molecule to target molecule and inhibit virus replication[18]. Previously we fused HBVc to hEDN, and after transfection of the fusion protein encoding plasmid into HepG2.2.15 cells, HBV replication was inhibited due to the fact that HBV pregenome RNA (pgRNA) was degraded by the effector molecule, hEDN, by guiding the target molecule, HBVc[21,22]. To further enhance the degradative effect of targeted ribonuclease, the classic linker $(Gly_4Ser)_3$ was introduced to separate the effector molecule and the target one. In our investigation, HBsAg concentration decreased significantly in pcDNA3.1(-)/TNL transfectant compared to pcDNA3.1(-)/TR transfectant due to linker introduction which may augment the digestion effect of hEDN significantly (P=0.036, P<0.05) via optimizing the protein folding.

Linker introduction, one of the gene fusion techniques, has become an increasingly useful tool in a variety of biomedical researches[24]. Many naturally occurring enzymes are composed of two or more distinct modules that are joined into a single macromole by stretches of amino acids referred to as linkers[25]. In structural biology, construction of recombinant fusion proteins has been used as a means to increase the expression of soluble proteins and to facilitate protein purification[26-28]. In recent years, a wide range of applications of gene fusion techniques has been reported in the fields of biotechnology. These applications include selection and prodution of antibodies and proteins with specialized functions, such as proteins that target specific genes[29-31]. Recent studies have provided examples of linkers that are important in establishing the structural and functional assembly of multi-domain proteins[32]. These interdomain linkers are relatively long and probably flexible in order to allow the two modules to perform independent functions. Recombinant production of chimeric enzymes requires stable linkers to join fusion partners without interfering with their function. The use of long linkers may result in low yield of active fusion protein since unprotected and flexible regions are often susceptible to proteolytic cleavage during recombinant protein production. A shorter linker might overcome problems associated with protease degradation. On the other hand, there is a risk that a shorter linker brings the modules too close to each other, resulting in a loss of function[25]. In many studies functional single-chain antibodies (scFvs) were engineered by linking immunoglobulin heavy and light chain variable domains (V_H and V_L) *via* $(G1y_4Ser)_3$, which satisfies the needs above. Further enhancement of hEDN digestion and inhibitory effect may be completed by further linker design and screening, and the work involved in this field is in progress in our lab.

REFERENCES

1 **Fleming J**. Current treatments for hepatitis. *J Infus Nurs* 2002; **25**: 379-382
2 **elSaadany S**, Tepper M, Mao Y, Semenciw R, Giulivi A. An epidemiologic study of hepatocellular carcinoma in Canada. *Can J Public Health* 2002; **93**: 443-446
3 **Hassan MM**, Hwang LY, Hatten CJ, Swaim M, Li D, Abbruzzese JL, Beasley P, Patt YZ. Risk factors for hepatocellular carcinoma: synergism of alcohol with viral hepatitis and diabetes mellitus. *Hepatology* 2002; **36**: 1206-1213
4 **Torbenson M**, Thomas DL. Occult hepatitis B. *Lancet Infect Dis* 2002; **2**: 479-486
5 **Lok AS**. Hepatitis B infection: Pathogenesis and management. *J Hepatol* 2000; **32**(Suppl 1): 89-97
6 **Mazumdar TN**. Management of chronic hepatitis B infection: an update. *J Indian Med Assoc* 2001; **99**: 306-308, 310
7 **Chen N**, Zhu C, Hu D, Zeng F. The clinical significance of negative serological markers of hepatitis B infection in hepatitis B virus carriers with chronic hepatic disease. *Zhonghua Neike Zazhi* 2002; **41**: 653-655
8 **Hino O**, Kajino K, Umeda T, Arakawa Y. Understanding the hypercarcinogenic state in chronic hepatitis: a clue to the prevention of human hepatocellular carcinoma. *J Gastroenterol* 2002; **37**: 883-887
9 **Esteban R**. Management of chronic hepatitis B: an overview. *Semin Liver Dis* 2002; **22**(Suppl 1): 1-6
10 **Wai CT**, Chu CJ, Hussain M, Lok AS. HBV genotype B is associated with better response to interferon therapy in HBeAg(+) chronic hepatitis than genotype C. *Hepatology* 2002; **36**: 1425-1430
11 **Manns MP**. Current state of interferon therapy in the treatment of chronic hepatitis B. *Semin Liver Dis* 2002; **22**(Suppl 1): 7-14
12 **Shindo M**, Hamada K, Koya S, Sokawa Y, Okuno T. The clinical significance of core promoter and precore mutations during the natural course and interferon therapy in patients with chronic hepatitis B. *Am J Gastroenterol* 1999; **94**: 2237-2245
13 **Liaw YF**. Therapy of chronic hepatitis B: current challenges and opportunities. *J Viral Hepat* 2002; **9**: 393-399
14 **Wolters LM**, Hansen BE, Niesters HG, de Man RA.Viral dynamics in chronic hepatitis B patients treated with lamivudine,

lamivudine-famciclovir or lamivudine-ganciclovir. *Eur J Gastroenterol Hepatol* 2002; **14**: 1007-1011
15 **Santantonio T**, Mazzola M, Iacovazzi T, Miglietta A, Guastadisegni A, Pastore G. Long-term follow-up of patients with anti-HBe / HBV DNA-positive chronic hepatitis B treated for 12 months with lamivudine. *J Hepatol* 2000; **32**: 300-306
16 **Song YH**, Lin JS, Liu NZ, Kong XJ, Xie N, Wang NX, Jin YX, Liang KH. Anti-HBV hairpin ribozyme-mediated cleavage of target RNA *in vitro*. *World J Gastroenterol* 2002; **8**: 91-94
17 **Chiou HC**, Lucas MA, Coffin CC, Banaszczyk MG, Ill CR, Lollo CP. Gene therapy strategies for the treatment of chronic viral hepatitis. *Expert Opin Biol Ther* 2001; **1**: 629-639
18 **Natsoulis G**, Boeke JD. New antiviral strategy using capsid-nuclease fusion proteins. *Nature* 1991; **352**: 632-635
19 **VanBrocklin M**, Federspiel MJ. Capsid-targeted viral inactivation can eliminate the production of infectious murine leukemia virus *in vitro*. *Virology* 2000; **267**: 111-123
20 **Wu X**, Liu H, Xiao H, Kim J, Seshaiah P, Natsoulis G, Boeke JD, Hahn BH, Kappes JC. Tageting foreign proteins to human immunodeficiency virus particles via fution with Vpr and Vpx. *J Virol* 1995; **69**: 3389-3398
21 **Li YH**, Liu J, Xue CF. Construction of HBV targeted ribonuclease and its expression in 2.2.15 cell line. *Xibao yu Fenzi Mianyixue Zazhi* 2002; **18**: 217
22 **Ding J**, Liu J, Xue CF, Li YH, Gong WD. Construction and expression of prokaryotic expression vector for pTAT-HBV targeted ribonuclease. fusion protein. *Xibao yu Fenzi Mianyixue Zazhi* 2003; **19**: 49-51
23 **Raj V**. Treatment of hepatitis B. *Clin Cornerstone* 2001; **3**: 24-36
24 **Arai R**, Ueda H, Kitayama A, Kamiya N, Nagamune T. Design of linkers which effectively separate domains of a bifunctional fusion protein. *Protein Eng* 2001; **14**: 529-532
25 **Gustavsson M**, Lehtio J, Denman S, Teeri TT, Hult K, Martinelle M. Stable linker peptides for a cellulose-binding domain-lipase fusion protein expressed in *Pichia pastoris*. *Protein Eng* 2001; **14**: 711-715
26 **Stein A**, Dalal Y, Fleury TJ. Circle ligation of in vitro assembled chromatin indicates a highly flexible structure. *Nucleic Acids Res* 2002; **30**: 5103-5109
27 **Kiczak L**, Kasztura M, Koscielska-Kasprzak K, Dadlez M, Otlewski J. Selection of potent chymotrypsin and elastase inhibitors from M13 phage library of basic pancreatic trypsin inhibitor (BPTI). *Biochim Biophys Acta* 2001; **1550**: 153-163
28 **Reiter Y**, Schuck P, Boyd LF, Plaksin D. An antibody single-domain phage display library of a native heavy chain variable region: isolation of functional single-domain VH molecules with a unique interface. *J Mol Biol* 1999; **290**: 685-698
29 **Rojas G**, Almagro JC, Acevedo B, Gavilondo JV. Phage antibody fragments library combining a single human light chain variable region with immune mouse heavy chain variable regions. *J Biotechnol* 2002; **94**: 287-298
30 **Klug A**. Zinc finger peptides for the regulation of gene expression. *J Mol Biol* 1999; **293**: 215-218
31 **Tang L**, Li J, Katz DS, Feng JA. Determining the DNA bending angle induced by non-specific high mobility group-1 (HMG-1) proteins: a novel method. *Biochemistry* 2000; **39**: 3052-3060
32 **Gokhale RS**, Khosla C. Role of linkers in communication between protein modules. *Curr Opin Chem Biol* 2000; **4**: 22-27

Edited by Ren SY and Wang XL

P.O.Box 2345, Beijing 100023,China
Fax: +86-10-85381893
E-mail: wjg@wjgnet.com www.wjgnet.com

World J Gastroenterol 2003;9(7):1508-1511
World Journal of Gastroenterology
 ISSN 1007-9327

• VIRAL HEPATITIS •

Detection of anti-HAV antibody with dot immunogold filtration assay

Zhong-Jun Shao, De-Zhong Xu, Yong-Ping Yan, Jing-Hua Li, Jing-Xia Zhang, Zhi-Ying Zhang, Bo-Rong Pan

Zhong-Jun Shao, De-Zhong Xu, Yong-Ping Yan, Jing-Hua Li, Jing-Xia Zhang, Zhi-Ying Zhang, Department of Epidemiology, Fourth Military Medical University, Xi' an 710032, Shaanxi Province, China
Jing-Hua Li, Department of Traditional Chinese Medicine, Xijing Hospital, Fourth Military Medical University, Xi' an 710032, Shaanxi Province, China
Bo-Rong Pan, Oncology Center, Xijing Hospital, Fourth Military Medical University, Xi' an 710032, Shaanxi Province, China
Supported by National Natural Science Foundation of China, No 30230320
Correspondence to: De-Zhong Xu, Department of Epidemiology, Fourth Military Medical University, 169 Changle West Road, Xi' an 710032,China. xudezh@fmmu.edu.cn
Telephone: +86-29-3374871 **Fax:** +86-29-3374868
Received: 2003-03-04 **Accepted:** 2003-04-03

Abstract

AIM: To establish a rapid, sensitive and specific immunogold assay for detection of hepatitis A virus infection.

METHODS: Rabbit monoclonal antibodies to anti-human IgM and IgG (Dako) were dotted on a nitrocellulose membrane (NCM) respectively to capture the human sera IgM and IgG. Then the captured antibodies would conjugate to HAV antigen, which was revealed by mouse anti-HAV IgG conjugated to gold particles. Final results were assessed by blind method.

RESULTS: Sera from 96 patients with acute hepatitis were used for our study. Compared with well-recognized standard (Abbott Laboratory, USA), the sensitivity and specificity of IgM-DIGFA (self-made) were 91.3 % (42/46) and 96.0 % (48/50), and those of IgM-ELISA (Kehua, Shanghai) were 97.8 % (45/46) and 100.0 % (50/50). The identical results were produced from the study with reagents at different conditions, and the study was repeated in 15 negative sera and 10 positive sera. The serum anti-HAV IgG was tested with DIGFA at the same time. In comparison with ELISA, the sensitivity and specificity of DIGFA for IgG anti-HAV were 87.2 % (41/47) and 91.8 % (45/49), respectively.

CONCLUSION: This assay can detect anti-HAV IgM and IgG simultaneously, and be done within 3 minutes. The simplicity, rapidity and specificity of the assay were useful for screening and epidemiological study.

Shao ZJ, Xu DZ, Yan YP, Li JH, Zhang JX, Zhang ZY, Pan BR. Detection of anti-HAV antibody with dot immunogold filtration assay. *World J Gastroenterol* 2003; 9(7): 1508-1511
http://www.wjgnet.com/1007-9327/9/1508.asp

INTRODUCTION

Hepatitis A is a self-limiting disease and often a subclinical disorder[1,2]. Since symptomatic hepatitis A infection can be clinically undistinguished from hepatitis B, C or E, serological testing is an important tool in its diagnosis[3-6]. Diagnosis of HAV infection depends mainly on the detection of specific antibody[3,4]. Although enzyme linked immunosorbent assay (ELISA) and RT-PCR are currently used for the detection of HAV infection and meet most of the clinical requirements[7-11], the two methods provide little information on prevention of diseases[12-15]. Dot immunogold filtration assay for the detection of anti-HAV IgM was established[16,17]. In our study a dot immunogold filtration assay was established to detect both anti-HAV IgM and IgG simultaneously.

MATERIALS AND METHODS

Sera

Blood samples were continuously collected from acute hepatitis inpatients in Xi' an Infectious Disease Hospital from March to October 2000 with permission of both the hospital and patients. Five milliliters of blood were drawn from each patient and the specimen was centrifuged at 3 000 r/min for 15 minutes to separate the serum. Ninety-six sera specimens were collected by the end of study. Anti-HAV IgM was detected as positive in 46, anti-HBc IgM in 31, anti-hepatitis C in 15, transmission-transmitted virus (TTV) in 3 by RT-PCR[18]. No hepatitis virus markers were found in 6 specimens, and positive anti-HAV and HBV were detected simultaneously in 2 sera.

Preparation of probe

Colloidal gold was produced by citromalic acid trisodium recovery method. The colloidal gold solution was scanned between 400 nm and 700 nm by using a spectrophotometer. The batch with λmax between 519 and 520 was used subsequently for conjugating with mouse anti-HAV IgG (CAPM). The pH was adjusted to 8.0 with 0.2 mol/L K_2CO_3. Then mouse anti-HAV IgG (1 μg per milliliter) was added into the colloidal gold solution and mixed for 30 minutes, then stored at 4 ℃ overnight. The pellet was collected by centrifugation at 15 000 r/min for 60 minutes, and the absorbance (A) was regulated by 0.02 mol/L PBS to the value of 1.5.

ELISA test for anti-HAV IgM and IgG

ELISA test was performed strictly according to instructions of the kit (anti-IgM kit from Kehua Biotech Co. and anti-IgG kit from Huaguang Biotech Co). Diluted sera (1:1 000) were incubated at 37 ℃ for one hour in a reactive well, and after washed, HAV Ag and anti-HAV peroxidase conjugates were added and incubated at 37 ℃ for 10 minutes, and followed by washing. Then the substrate was added, and the reaction was stopped by diluted sulfuric acid 10 minutes later. The absorbance was measured at 540 nm. An absorbance of 2.1 times the negative control value was considered as positive. The detecting procedures for HAV IgG were the same as for IgM except for serum dilution (1:50).

AXSYM HAVAB-M (Abbott Laboratory) was based on microparticle enzyme immunoassay technology[19-21]. Samples and all AXSYM HAVAb-M reagents required for one test were pipetted with the sampling probe into wells in reactive vessel in the sampling center. The reaction vessel was immediately

transferred into the processing center. Further pipetting was done in the processing center by the processing probe. All steps were completed automatically and the diagnostic results were reported immediately.

DIGFA

There were 4 components in the kit: solid phase reaction board (SPRD, self-made), HAV Ag, color-developing reagents and lotion. Anti-human IgM and IgG antibodies (Dako, USA) were blotted onto small round nitrocellulose membranes (Hyclone, USA) separately, air-dried at room temperature, and then incubated in 20 g/L bovine serum albumin (BSA) overnight, and finally washed and air dried. These nitrocellulose membranes prepared were fitted in SPRD with coated side facing exteriorly. Then SPRD was filled with water-absorbed stuff. One drop of lotion (PBS-T, pH8.0 containing 05 g/L Tween20 and 20 g/L BSA) was added to prepare SPRD. 100 μL of serum with dilution of 1:100 was added to each reaction well, and then washed with one drop of lotion. Then one drop of HAV Ag was added, and then was washed. Finally two drops of anti-HAV IgG colloidal gold conjugates were added, and then washed with one drop of lotion. A reddish dot with sharp margin was considered as positive.

Statistical analysis

The following definitions and formulae were used in this study. A true positive (a) sample was both reactive by DIGFA/ELISA and ABBOTT. A true negative (d) sample was nonreactive by both DIGFA/ELISA and ABBOTT. A false positive (b) sample was reactive by DIGFA/ELISA but negative by ABBOTT and a false negative (c) sample was negative by DIGFA/ELISA but positive by ABBOTT. The sensitivity of DIGFA was defined as the probability that a sample containing anti-HAV antibodies would be positive in DIGFA/ELISA. The specificity of DIGFA/ELISA was defined as the probability that a sample without anti-HAV antibodies would be negative in DIGFA/ELISA. Chi-square test was used.

RESULTS

Preparation of probe

Transmission electron microscopic studies revealed that the average diameter of the gold particle was 15 nm (15±0.7 nm). The maximum absorbing wavelength was 519 nm, indicating that the colloid gold met the experimental requirements. After purification of labeling anti-HAV IgG to gold particle, one drop of probe was added to SPRD coated by goat anti-mouse IgG and a pink dot appeared 30 seconds later, indicating effectiveness of the probe.

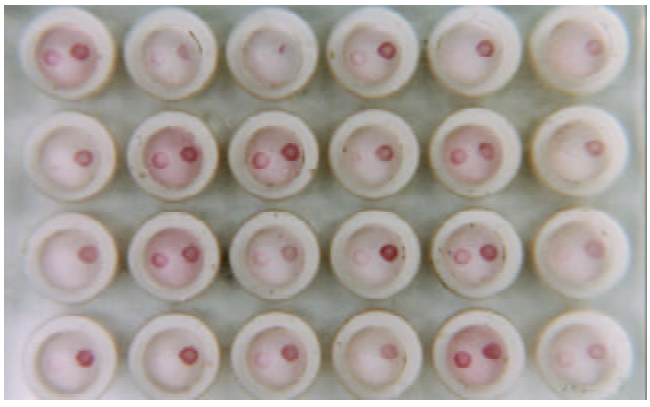

Figure 1 Detection of 24 sera from acute hepatitis inpatients by DIGFA. Red dot: positive; Left: anti-human IgG; Right: anti-human IgM.

Comparison of three diagnostic methods (Tables 1, 2 and 3)

Abbott kit has been widely recognized in the world, but its usage was limited in China due to the relatively high cost. The comparative analysis of 96 serum specimens showed that the sensitivity and specificity of IgM-ELISA were higher than those of IgM-DIGFA (Table 1). Statistical analysis (two tailed binomial probability test) showed no significant differences in sensitivity and specificity (Figure 1). Cross-reaction was found in DIGFA for anti-HAV IgM in a serum specimen, which was diagnosed as anti-HBV positive by ELISA.

Table 1 Comparison of DIGFA, ELISA and AXSYM HAVAb-M

IgM		HAVAB-M (Abbott laboratory)		Total
		+	-	
DIGFA	+	42	2	44
	-	4	48	52
ELISA	+	45	0	45
	-	1	50	51

Sensitivity of IgM-DIGFA was 91.3 % (42/46) and specificity was 96.0 % (48/50). Sensitivity of IgM-ELISA was 97.8 % (45/46) and specificity was 100.0 % (50/50). There were no significant differences in sensitivity (P=0.36) and specificity (P=0.49).

Anti-HAV IgG and IgM were detected in all sera. ELISA kit was purchased from Huaguang Biotech Co, Xi' an, China. Forty-one of 96 sera specimens were detected as positive with both methods and 86 were diagnosed coincidentally. The sensitivity and specificity were 87.2 % (41/47) and 91.8 % (45/49), respectively (Table 2).

Table 2 Comparison of IgG-DIGFA with IgG-ELISA

IgG-DIGFA	IgG-ELISA		Total
	+	-	
+	41	4	45
-	6	45	51
Total	47	49	96

In this study, twenty-three sera specimens were detected as positive for IgG, and 30 as negative for both IgM and IgG, which indicated that some individuals in general population were possibly susceptible to HAV infection (Table 3).

Table 3 Analysis of anti-HAV IgG and IgM by DIGFA method

Anti-HAV IgG	Anti-HAV IgM		Total
	+	-	
+	23	22	45
-	21	30	51
Total	44	52	96

Repeatability and stability

All reagents could be stored effectively at 4 ℃ for 3 months, at room temperature for 15 days and at 48 ℃ for 2 days. Fifteen negative and ten positive sera samples were selected randomly and detected with reliable results.

DISCUSSION

Detection of antibody against hepatitis A virus

DIGFA is a new technique of solid phase labeled immunoassay,

in which NCM is used as a support and colloidal gold as the label, and the principle of filtration is adapted for the rapid reaction of antigen and antibody[22,23]. The use of visible gold-conjugated monoclonal antibody instead of enzyme in ELISA makes the test simple[24]. The sensitivity of DIGFA is lower than that of ELISA. This method can detect two kinds of anti-HAV antibodies simultaneously that are similar to protein biochip, but the cost is much lower than that of biochip[25]. It is very suitable for screening and vaccination program[26-29]. IgM antibody persists for 3 to 6 months afterwards, and is seldom found after vaccination. Patients with asymptomatic hepatitis A may have detectable anti-HAV IgM for a shorter period than patients with symptomatic diseases[30]. Although anti-HAV IgG may be present at early stage of infection, it is always accompanied by anti-HAV IgM at the onset of illness. Anti-HAV IgG alone indicates a past infection and persists for decades after acute HAV infection, reflecting recovery and resistance to reinfection[31,32]. However, detection of anti-HAV IgG is often ignored due to its limited clinical value, but it can show whether a person is susceptible to HAV and offer a good instruction to health workers. Twenty-two sera were detected as negative for both anti-HAV IgM and IgG, which indicated that these people need to be vaccinated.

Comparison with ELISA

The sensitivity and specificity of IgM-DIGFA for HAV in these sera were lower than those of IgM-ELISA. However, there was no significant difference in specificity of both assays. IgM-DIGFA can be used as an eligible assay to screen HAV infection for its rapidity and specificity. It takes a few minutes to complete the whole process by DIGFA, and the detection of 30 sera specimens can be done within 30 minutes. Shortened reaction time gives a proper explanation to the lower sensitivity of IgM-DIGFA. A cost-analysis of DIGFA and ELISA was done, and found that pure reagents cost of DIGFA was 0.75 Yuan (RMB) and that of anti-HAV IgM ELISA was 1.20 Yuan (RMB). It was not as expensive as expected and two kinds of antibodies were detected at one time[33]. All the reagents leaked through NCM and took a full reaction with antibodies attached to NCM. This was due to the effect of immunoconcentration [34]. It is easy to tell the results without the help of extra apparatus. Therefore, it can be widely used in an epidemiological survey.

REFERENCES

1 **De Paula VS**, Saback FL, Gaspar AM, Niel C. Mixed infection of a child care provider with hepatitis A virus isolates from subgenotypes IA and IB revealed by heteroduplex mobility assay. *J Virol Methods* 2003; **107**: 223-228

2 **Sedyaningsih-Mamahit ER**, Larasati RP, Laras K, Sidemen A, Sukri N, Sabaruddin N, Didi S, Saragih JM, Myint KS, Endy TP, Sulaiman A, Campbell JR, Corwin AL. First documented outbreak of hepatitis E virus transmission in Java Indonesia. *Trans R Soc Trop Med Hyg* 2002; **96**: 398-404

3 **Yayli G**, Kilic S, Ormeci AR. Hepatitis agents with enteric transmission an epidemiological analysis. *Infection* 2002; **30**: 334-337

4 **Koff RS**. Prevention of Viral Hepatitis.*Curr Treat Options Gastroenterol* 2002; **5**: 451-463

5 **Han LH**, Sun WS, Ma CH, Zhang LN, Liu SX, Zhang Q, Gao LF, Chen YH. Detection of soluble TRAIL in HBV infected patients and its clinical implications. *World J Gastroenterol* 2002; **8**: 1077-1080

6 **Jiang YG**, Wang YM, Li QF. Expression and significance of HLA-DR antigen and heat shock protein 70 in chronic hepatitis B. *Shijie Huaren Xiaohua Zazhi* 2001; **9**: 907-910

7 **Jean J**, Blais B, Darveau A, Fliss I.Simultaneous detection and identification of hepatitis A virus and rotavirus by multiplex nucleic acid sequence-based amplification (NASBA) and microtiter plate hybridization system. *J Virol Methods* 2002; **105**: 123-132

8 **Li JW**, Wang XW, Yuan CQ, Zheng JL, Jin M, Song N, Shi XQ, Chao FH. Detection of enteroviruses and hepatitis A virus in water by consensus primer multiplex RT-PCR. *World J Gastroenterol* 2002; **8**: 699-702

9 **Vernozy-Rozand C**, Feng P, Montet MP, Ray-Gueniot S, Villard L, Bavai C, Meyrand A, Mazuy C, Atrache V. Detection of Escherichia coli O157:H7 in heifers' faecal samples using an automated immunoconcentration system. *Lett Appl Microbio* 2000; **30**: 217-222

10 **Rood JC**, Lovejoy JC, Tulley RT. Comparison of a radioimmunoassay with a microparticle enzyme I mmunoassay of insulin for use with the minimal model method of determining whole-body insulin sensitivity. *Diabetes Technol Ther* 1999; **1**: 463-468

11 **Koraka P**, Zeller H, Niedrig M, Osterhaus AD, Groen J. Reactivity of serum samples from patients with a flavivirus infection measured by immunofluorescence assay and ELISA. *Microbes Infect* 2002; **4**: 1209-1215

12 **Nikolova M**, Liubomirova M, Iliev A, Krasteva R, Andreev E, Radenkova J, Minkova V, Djerassi R, Kiperova B, Vlahov ID. Clinical significance of antinuclear antibodies, anti-neutrophil cytoplasmic antibodies and anticardiolipin antibodies in heroin abusers. *Isr Med Assoc J* 2002; **4**: 908-910

13 **Nikolaeva LI**, Blokhina NP, Tsurikova NN, Voronkova NV, Miminoshvili MI, Braginsky DM, Yastrebova ON, Booynitskaya OB, Isaeva OV, Michailov MI, Archakov AI. Virus-specific antibody titres in different phases of hepatitis C virus infection. *J Viral Hepat* 2002; **9**: 429-437

14 **Zhao YL**, Meng ZD, Xu ZY, Guo JJ, Chai SA, Duo CG, Wang XY, Yao JF, Liu HB, Qi SX, Zhu HB. H2 strain attenuated live hepatitis A vaccines: Protective efficacy in a hepatitis A outbreak. *World J Gastroenterol* 2000; **6**: 829-832

15 **Santos DC**, Souto FJ, Santos DR, Vitral CL, Gaspar AM. Seroepidemiological markers of enterically transmitted viral hepatitis A and E in individuals living in a community located in the North Area of Rio de Janeiro, RJ. *Brazil Mem Inst Oswaldo Cruz* 2002; **97**: 637-640

16 **Han FC**, Hou Y, Yan XJ, Xiao LY, Guo YH. Dot immunogold filtration assay for rapid detection of anti-HAV IgM in Chinese. *World J Gastroenterol* 2000; **6**: 400-401

17 **Wu W**, Xu DZ, Yan YP, Zhang JX, Liu Y, Li RL. Evaluation of dot immunogold filtration assay for anti-HAV IgM antibody. *World J Gastroenterol* 1999; **5**: 132-134

18 **Hu ZJ**, Lang ZW, Zhou YS, Yan HP, Huang DZ, Chen WR, Luo ZX. Clinicopathological study on TTV infection in hepatitis of unknown etiology. *World J Gastroenterol* 2002; **8**: 288-293

19 **el Saadany S**, Gully P, Giulivi A. Hepatitis A, B, and C in Canada. Results from the national sentinel health unit surveillance system, 1993-1995. *Can J Public Health* 2002; **93**: 435-438

20 **Keevil BG**, McCann SJ, Cooper DP, Morris MR. Evaluation of a rapid micro-scale assay for tacrolimus by liquid chromatography-tandem mass spectrometry. *Ann Clin Biochem* 2002; **39**: 487-492

21 **Dietemann J**, Berthoux P, Gay-Montchamp JP, Batie M, Berthoux F.Comparison of ELISA method versus MEIA method for daily practice in the therapeutic monitoring of tacrolimus. *Nephrol Dial Transplant* 2001; **16**: 2246-2249

22 **Hirota WK**, Duncan MB, Hirota WK, Tsuchida A.The utility of prescreening for hepatitis A in military recruits prior to vaccination. *Mil Med* 2002; **167**: 907-910

23 **Yang SS**, Wu CH, Chen TH, Huang YY, Huang CS. TT viral infection through blood transfusion: retrospective investigation on patients in a prospective study of post-transfusion hepatitis. *World J Gastroenterol* 2000; **6**: 70-73

24 **Lu J**, Xu WX, Zhan YQ, Cui XL, Cai WM, He FC, Yang XM. Identification and characterization of a novel isoform of hepatopoietin. *World J Gastroenterol* 2002; **8**: 353-356

25 **Moreno-Bondi MC**, Alarie JP, Vo-Dinh T. Multi-analyte analysis system using an antibody-based biochip. *Anal Bioanal Chem* 2003; **375**: 120-124

26 **Acharya SK**, Batra Y, Saraya A, Hazari S, Dixit R, Kaur K, Bhatkal B, Ojha B, Panda SK.Vaccination for hepatitis A virus is not re-

quired for patients with chronic liver disease in India. *Natl Med J India* 2002; **15**: 267-268
27 **Wang KX**, Li CP, Wang J, Tian Y. Cyclospore cayetanensis in Anhui, China. *World J Gastroenterol* 2002; **8**: 1144-1148
28 **Ohto H**, Ujiie N, Takeuchi C, Sato A, Hayashi A, Ishiko H, Nishizawa T, Okamoto H. Verticl transmission of hepatitis viruses collaborative study group. TT virus infection during childhood. *Transfusion* 2002; **42**: 892-898
29 **Fleming J**. Current treatments for hepatitis. *J Infus Nur* 2002; **25**: 379-382
30 **Jarvis B**, Figgitt DP. Combined Two-Dose Hepatitis A and B Vaccine (AmBirix trade mark). *Drugs* 2003; **63**: 207-213
31 **Hu NZ**, Hu YZ, Shi HJ, Liu GD, Qu S. Mutational characteristics in consecutive passage of rapidly replicating variants of hepatitis A virus strain H2 during cell culture adaptation. *World J Gastroenterol* 2002; **8**: 872-878
32 **Edoute Y,** Malberger E, Tibon-Fishe O, Assy N. Non-imaging-guided fine-needle aspiration of liver lesions: a retrospective study of 279 patients. *World J Gastroenterol* 1999; **5**: 98-102
33 **Shyu RH**, Shyu HF, Liu HW, Tang SS. Colloidal gold-based immunochromatographic assay for detection of ricin. *Toxicon* 2002; **40**: 255-258
34 **Vernozy-Rozand C**, Ray-Gueniot S, Ragot C, Bavai C, Mazuy C, Montet MP, Bouvet J, Richard Y. Prevalence of Escherichia coli O157:H7 in industrial minced beef. *Lett Appl Microbiol* 2002; **35**: 7-11

Edited by Ren SY and Wang XL

P.O.Box 2345, Beijing 100023,China
Fax: +86-10-85381893
E-mail: wjg@wjgnet.com www.wjgnet.com

World J Gastroenterol 2003;9(7):1512-1515
World Journal of Gastroenterology
 ISSN 1007-9327

• VIRAL HEPATITIS •

Generation of cytotoxic T cell against HBcAg using retrovirally transduced dendritic cells

Chuan-Lin Ding, Kun Yao, Tian-Tai Zhang, Feng Zhou, Lin Xu, Jiang-Ying Xu

Chuan-Lin Ding, Kun Yao, Feng Zhou, Department of Microbiology and Immunology, Nanjing Medical University, Nanjing 210029, Jiangsu Province, China
Tian-Tai Zhang, Department of Medicine, Affiliated Hospital of Lanzhou Medical College, Lanzhou 730000, Gansu Province, China
Lin Xu, Jiang-Ying Xu, Gene Center of Nanjing Military Medical College, Nanjing 210099, Jiangsu Province, China
Supported by a grant from Key Lab Programs of Jiangsu Province, No. k2030
Correspondence to: Professor Kun Yao, Department of Microbiology and Immunology, Nanjing Medical University, Nanjing 210029, Jiangsu Province, China. yaokun@njmu.edu.cn
Telephone: +86-25-6662901 **Fax:**+86-25-6508960
Received: 2003-01-14 **Accepted:** 2003-03-05

Abstract

AIM: Cytotoxic T lymphocytes (CTLs) play an important role in resolving HBV infection. In the present study, we attempted to evaluate the efficiency of bone marrow-derived dendritic cells (DCs) transduced with recombinant retroviral vector bearing hepatitis B virus (HBV) core gene and the capability of generating CTLs against HBcAg by genetically modified DCs *in vivo*.

METHODS: A retroviral vector containing HBV core gene was constructed. Replicating DC progenitor of C57BL/6 mice was transduced by retroviral vector and continually cultured in the presence of recombinant mouse granulocyte-macrophage colony-stimulating factor (rmGM-CSF) and interleukin-4(IL-4) for 6 days. LPS was added and cultured for additional two days. The efficiency of gene transfer was determined by PCR, Western blot and FACS. Transduced DCs immunized C57BL/6 mice subcutaneously 2 times at an one-week interval. Intracellular IFN-γ and IL-4 of immunized mice lymphocytes were analyzed. Generation of CTLs in lymphocytes stimulated with mitomycin C-treated EL4-C cell which stably expresses HBcAg was determined by LDH release assays.

RESULTS: Recombinant retroviral expression vector (pLCSN) was positively detected by PCR as well as enzyme digestion with *EcoR*I and *BamH* I. Retroviruses were generated by pLCSN transfection packing cell and the virus titer was 3×10^5 CFU/ml. Indirect immunofluorescence and FACS showed that HBV core gene was expressed in murine fibroblasts. Transduced bone marrow cells had capability of differentiating into DCs *in vitro* in the presence of rmGM-CSF and rmIL-4. The result of PCR showed that HBV core gene was integrated into the genome of transduced DCs. Western blot analysis showed that HBV core gene was expressed in DCs. The transduction rate was 28 % determined by FACS. Retroviral transduction had no influence on DCs expressions of CD80 and MHC class II. HBcAg specific CTLs and Th1 type immune responses could be generated in the mice by using transduced DCs as antigen presenting cells (APCs).

CONCLUSION: Retroviral transduction of myeloid DCs progenitors expresses efficiently HBcAg, and genetically modified DCs evoke a higher CTLs response than HBcAg *in vivo*.

Ding CL, Yao K, Zhang TT, Zhou F, Xu L, Xu JY. Generation of cytotoxic T cell against HBcAg using retrovirally transduced dendritic cells. *World J Gastroenterol* 2003; 9(7): 1512-1515
http://www.wjgnet.com/1007-9327/9/1512.asp

INTRODUCTION

Individuals with chronic hepatitis B virus(HBV) infection have a high risk of developing liver cirrhosis and primary hepatocellular carcinoma. Current treatments for chronic HBV infection are poorly efficacious[1-3].

Cytotoxic T lymphocytes (CTLs) are thought to contribute to HBV clearance by killing infected hepatocytes and secreting antiviral cytokines. Acutely infected patients characteristically produce a vigorous, polyclonal, and multispecific CTLs response that is usually sufficient to clear the infection, while persistently infected patients produce a weak or undetectable HBV-specific CTLs response. The cumulated data suggest that CTLs activity may play an important role in resolving HBV infection[4-13]. Based on these observations, therapeutic enhancement of T cell responsiveness to HBV has the potential to terminate chronic HBV infection.

Dendritic cells (DCs) are highly specialized antigen presenting cells (APCs) that possess unique immunostimulatory properties and function as the principal activators of naï ve T cells[14,15]. DCs are distributed throughout the body and can be expanded with granulocyte-macrophage CSF (GM-CSF) and IL-4. When DCs are pulsed with antigen protein or peptide, they can induce specific antibody and CTLs responses both *in vitro* and *in vivo*. Since activated DCs express a high level of costimulatory molecules and secrete inflammatory cytokines, they have the potential to activate anergic T cells.

In the present study, we attempted to induce CTLs response using retrovirally transduced DCs. The results demonstrated that administration of retrovirally transduced DCs could evoke HBcAg-specific CTLs responses in mice.

MATERIALS AND METHODS

Generating expression vector

The full-length HBV core gene was generated by PCR amplification from pADR(kindly provided by Prof. Zheng-Hong Yuan) which contains complement nucleotide sequence of HBV subtype adr with a pair of primers (5'-TGTGAATTCTGGCTTTGGGGCATGGACATTG-3', corresponding to the nucleotide sequence 1891-1912 of HBV genome with an additional *EcoR*I restriction site, and 5'-GCTGGATCCAGTTTCCCACCTTATGAGTCCA-3', corresponding to the nucleotide sequence 2462- 2483 of HBV genome with an additional *BamH*I restriction site). After digestion with *EcoR*I and *BamH* I, PCR products were inserted downstream of LTR of retroviral vector pLXSN (Clontech,USA) to obtain a recombinant retroviral expression vector pLCSN.

Virus production

To produce retroviral virus, packing cell (PT67, Clontech, USA) was cultured in a 24 well culture plate with D-MEM containing 10 % heat-inactivated FBS and transfected with 1 μg of retroviral vector plasmid pLCSN by lipofectAMINE2000 (GIBCO,USA). Colonies were isolated by neomycin selectin (G418, Amresco, USA) and expanded. Supernatants of cloned packing cells were harvested, filtered (0.45 μm pore size), and tested for the presence of virus. Viral titration was performed on NIH3T3 according to the instructions of the manufacturer yielding a titer of 3×10^5 infectious particles/ml.

DC culture, transduction and immunization

Bone marrow cells were collected from femurs of C57BL/6 mouse and depleted of red cells with ammonium chloride. After extensively washed with RPMI1640, cells (5×10^5 cells/ml) in RPMI1640 supplemented with 10 % FBS, 500 U/ml rmGM-CSF and 250 U/ml rmIL-4 were plated in a 24 well culture plate, incubated at 37 ℃ in 5 % CO_2-atmosphere. After 24-h incubation, the cells were transducted with retroviral supernatants and polybrene (Sigma,USA) at a final concentration of 8 μg/ml. The cells were incubated at 37 ℃, in 5 % CO_2 atmosphere for 2-3 h. The supernatant was replaced with RPMI1640 supplemented with 10 % FBS, 500 U/ml rmGM-CSF and 250 U/ml rmIL-4 overnight. The transduction procedure was repeated 3 times. After 6 days, LPS (1 μg/ml) was added and mature DC was obtained after additional culture for 2 days. The cells were washed three times, and 5×10^5 DCs suspended in 0.5 ml of PBS were injected subcutaneously. The immunization was repeated after 7 days.

Polymerase chain reaction

DNA from retrovirally transduced and untransduced DCs was isolated according to the manufacturer' s protocol (Boehringer, Germany). DNA was isolated from the G418 resistant PT67 cell line as positive control. Primers used for amplification of HBcAg were mentioned above. PCR was performed for 1 min at 94 ℃, for 1 min at 54 ℃, and for 1 min at 72 ℃ for 30 cycles, followed by a final extension time of 6 min at 72 ℃. The PCR product was resolved on a 1.5 % agarose gel.

Western blot analysis of HBcAg

Cell lysates were made from retrovirally transduced and untransduced DCs. Protein samples were separated by SDS-PAGE and transferred to nitrocellulose. HBcAg protein was identified using the anti-HBc positive serum as primary Ab and goat anti-human IgG peroxidase-conjugate (1:500, volume ratio) as secondary Ab. The blots were developed using substrate solution containing DAB and H_2O_2.

Intracellular cytokine analysis

Spleen lymphocytes were stimulated with Con A at 20 μg/ml, and 1 μl GolgiPlugTM was added for every 1 ml of cell culture to inhibit cytokine secretion. Lymphocytes were incubated for 6 hours, then harvested and washed with staining buffer. Cells were thoroughly resuspended and 100 μl of cytofix/cytoperm solution was added into each well for 20 min at 4 ℃. Cells were washed and stained with FITC-labled anti-mouse IFN-γ and PE-labled anti-mouse IL-4, incubated at 4 ℃ for 30 min in the dark, then washed twice and analyzed with a flow cytometer.

CTL_S assay

The tumor cell line EL4 ($H\text{-}2^b$) was transduced with recombinant retrovirus and then selected in the presence of 400 ug/ml G418. The G418-resistant clones (EL4-C) were screened for HBcAg expression by PCR and indirect immunofluorescence. Spleen cells obtained from individual mice were stimulated with EL4-C treated by 25 μg/ml mitomycin C at effector:stimulator ratio of 20. The specific CTLs were expanded by adding 50 IU/ml of IL-2 for 7 days. The CTLs activity in the cultures was measured in triplicate in a standard four-hour LDH release assay using EL4-C cells as target cells according to the manufacturer' s instructions(Roche, Switzerland).

RESULTS

Generation of retroviral expression vector and retrovirus

The HBV core gene fragment generated by PCR amplification and digested with *EcoR*I and *BamH* I was successfully cloned into downstream of LTR of pLXSN to obtain recombinant retroviral expression vector pLCSN (Figure 1). Recombinant retroviral vector was positively detected by PCR as well as enzyme digestion with *EcoR*I and *BamH*I. To produce retroviral virus, packing cells were transfected with retroviral expression vector pLCSN. Colonies were isolated by neomycin selectin and expanded. Supernatants of G418 resistant cells were harvested. The virus titer was 3×10^5 infectious particles/ml. It was found that retroviruses could infect a number of eukaryotic cells, such as NIH3T3, EL4, and SP2/0(data not shown).

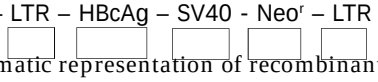

Figure 1 Schematic representation of recombinant retroviral vector pLCSN.

Retroviral transduction of bone marrow cells and differentiation into DCs

To assess the expression of HBcAg in DCs, we transduced bone marrow cells from C57BL/6 mice in packing cell supernatants. The transduced cells were then cultured in the presence of rmGM-CSF, rmIL-4 and LPS for the purpose of differentiation into mature DCs. After cultured for 8 days, the majority of cells displayed distinct DC morphology with many fine dendrites. Retroviral transduction had no influence on DCs expressions of CD80 and class II molecule of MHC (72.94 % *versus* 73.43 %, 86.54 % *versus* 91.75 %, respectively). T-cell stimulatory activity of DCs in MLR was expressed as stimulation index (SI) value, at a T cell:DC ratio of 80:1, 40:1, 20:1 and 10:1. The SI values were 3.16, 7.26, 23.99, 31.70, respectively. The HBV core gene in transduced DCs was demonstrated by PCR (Figure 2). Approximately 28 % of the bone marrow derived cells could express HBcAg determined by flow cytometric analysis. Finally, Western blot analysis demonstrated that HBcAg was expressed in transduced DCs (Figure 3).

Induction of CTLs responses in vivo

Next we evaluated the capability of retrovirally transduced DCs to induce CTLs responses *in vivo*. C56BL/6 mice were immunized subcutaneously with 5×10^5 DCs transduced with HBcAg. The immunization was repeated after one week. 7 days after the last immunization, the mice were sacrificed and splenocytes were collected. Splenocytes were restimulated *in vitro* for 7 days in the presence of mitomycin C-treated EL4-C cell and IL-2, and then cocultivated with different target cells at varied E:T ratios to measure target cell lysis with LDH release cytotoxic assay. As shown in Figure 4, splenocytes from mice immunized with transduced DCs demonstrated significantly higher cytotoxicity than those from controlled mice. To determine the type of Th responses, we measured the lymphocyte which could secret IFN-γ or IL-4 with intracellular cytokine analysis. After immunization of retrovirally transduced DCs in mice, lymphocyte producing IFN-γ was significantly higher than that from mice injected

only with untransduced DCs (1.15 % *versus* 0.28 %). At the same time, lymphocyte producing IL-4 in both mice with injections of transduced and untransduced DCs was similar (0.74 % *versus* 0.47 %).

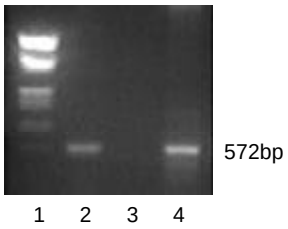

Figure 2 PCR analysis of HBV core gene in retrovirally transduced DCs. 1. Marker; 2. Transduced DCs; 3. Untransduced DCs; 4.G418 resistant PT67 cell.

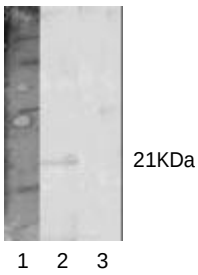

Figure 3 Western blot analysis of HBcAg expression in retrovirally transduced DCs. 1. Marker; 2. Transduced DCs; 2. Untransduced DCs.

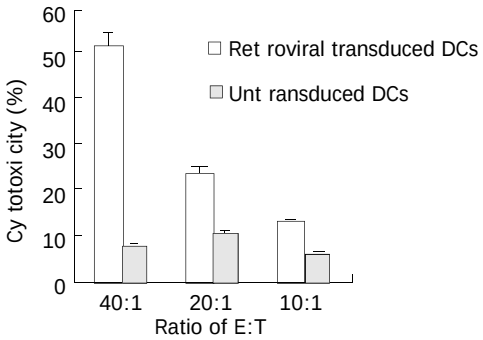

Figure 4 Induction of CTLs against HBcAg responses *in vivo*.

DISCUSSION

Chronic HBV infection has a significant association with liver cirrhosis and hepatocellular carcinoma. Studies on immunological mechanisms have demonstrated that CTLs play a critical role in the control and termination of HBV infection. CTLs are thought to contribute to HBV clearance by killing infected hepatocytes and secreting antiviral cytokines. Acutely infected patients characteristically produce a vigorous, polyclonal, and multispecific CTLs response that is usually sufficient to clear the infection, while persistently infected patients produce weak or undetectable HBV-specific CTLs responses[4-13]. Based on these observations, therapeutic enhancement of T cell responsiveness to HBV has the potential to terminate chronic HBV infection.

A number of experimental reports showed that CTLs responses could be induced. Vaccination with HBsAg-anti-HBs immune complex could affect HBeAg seroconversion and clearance of serum HBV DNA in patients[16]. Sallberg *et al*[17] observed a marked decrease of HBV DNA level and seroconversion of HBeAg to anti-HBe in sera of experimental chimpanzees after immunization of HBV core gene using retrovirus. Plasmid DNA immunization has been shown to induce specific antibody and CTLs responses in normal mice and rhesus monkeys[18-20]. ISCOMS-based hepatitis B polypeptide vaccine could also induce a higher CTLs response *in vivo*[21].

DCs play a central role in humoral and cellular immunity because they can take up and process antigen in peripheral tissues and present the antigen to T cells in secondary lymphoid tissues, such as lymph nodes. The mature DCs screen for passing antigen-specific naï ve T cell, and induce primary T cell-mediated immune response. Mature DCs are thought to be functionally competent and have been used in clinical studies to induce antigen-specific T cells[14,15,22,23]. In this study, we used DCs as an attractive approach for immunotherapy of chronic HBV infection. In developing strategies to optimize the use of DCs in immunotherapy, viral transduction of DCs with antigen genes may offer more advantages over peptide-pulsed DCs. The efficacy of peptide-pulsed DCs might be limited *in vivo*, because peptides pulsed onto DCs stay bound to MHC molecules only transiently. Additionally, use of peptide-pulsed DCs is dependent on the knowledge of the HLA haplotype of patients. Transduction of DCs by viral vectors can produce a high level of antigen expression, and endogenous protein synthesis may allow presentation of antigens by class I molecules of MHC, resulting in induction of $CD8^+$ CTLs responses. Several viruses have the potential for use in immunotherapy, such as vaccina virus, adenovirus, and retrovirus[24]. Retroviral transduction of DCs may allow constitutive expression of protein leading to prolonged antigen presentation *in vivo*, and presentation of multiple or unidentified antigen epitopes in the context of class I and II molecules of MHC. But as nonreplicating, mature DCs are poor candidates for retroviral gene modification. However, dividing bone marrow progenitor cells can be efficiently transduced with retroviral vectors[25-29]. In this study, rapidly dividing bone marrow progenitor cells were used as targets for retroviral transduction and cultured in the presence of GM-CSF and IL-4 plus LPS. Our results showed that retrovirally transduced progenitor cells could differentiate into mature DCs *in vitro*, transduced or untransduced dendritic cells expressed comparable levels of CD80 and class II of MHC, the transduction efficiency was about 28%. Retrovirally transduced DCs could be used to induce strong CTLs responses in C57BL/6 mice *in vivo*.

Previous studies showed that Th1 type response was beneficial for the clearance of chronically infected viruses[30,31]. The profiles of cytokine production were indicators of helper T cell responses. IFN-γ and IL-4 were observed in the present experiment as Th1 and Th2 type cytokines, respectively. After immunization of retroviral transduced DCs, lymphocyte producing IFN-γ was significantly higher than that from mice injected only with untransduced DCs, indicating Th1 type immune responses occurred in mice immunized with retroviral transduced DCs.

These results together with other studies support the ongoing efforts to develop genetically modified DCs for immunotherapy of chronic HBV infection. Further study is underway to determine whether this genetically modified DCs can break the immune tolerance in the HBV transgenic mouse model.

REFERENCES

1 **Gow PJ,** Mutimer D. Treatment of chronic hepatitis. *BMJ* 2001; **323**: 1164-1167

2 **Malik AH,** Lee WM. Chronic hepatitis B virus infection: treatment strategies for the next millennium. *Ann Intern Med* 2000; **132**: 723-731

3 **Locarnini SA,** Bartholomeusz A, Delaney WE. Evolving therapies for the treatment of chronic hepatitis B virus infection. *Expert Opin Investig Drugs* 2002; **11**: 169-187

4 **Sette AD,** Oseroff C, Sidney J, Alexander J, Chesnut RW, Kakimi K, Guidotti LG, Chisari FV. Overcoming T cell tolerance to the hepatitis B virus surface antigen in hepatitis B virus-transgenic mice. *J Immunol* 2001; **166**: 1389-1397

5 **Maini MK,** Bertoletti A. How can the cellular immune response control hepatitis B virus replication? *J Viral Hepat* 2000; **7**: 321-326

6 **Guidotti LG,** Chisari FV. Noncytolytic control of viral infections by the innate and adaptive immune response. *Annu Rev Immunol* 2001; **19**: 65-91

7 **Sing GK,** Ladhams A, Arnold S, Parmar H, Chen X, Cooper J, Butterworth L, Stuart K, D'Arcy D, Cooksley WG. A longitudinal analysis of cytotoxic T lymphocyte precursor frequencies to the hepatitis B virus in chronically infected patients. *J Viral Hepat* 2001; **8**: 19-29

8 **Thimme R,** Wieland S, Steiger C, Ghrayeb J, Reimann KA, Purcell RH, Chisari FV. CD8(+) T cells mediate viral clearance and disease pathogenesis during acute hepatitis B virus infection. *J Virol* 2003; **77**: 68-76

9 **Cao T,** Desombere I, Vanlandschoot P, Sällberg M, Leroux-Roels G. Characterization of HLA DR13-restricted $CD4^+$ T cell epitopes of hepatitis B core antigen associated with self-limited, acute hepatitis B. *J Gen Virol* 2002; **83**: 3023-3033

10 **Kimura K,** Kakimi K, Wieland S, Guidotti LG, Chisari FV. Activated intrahepatic antigen-presenting cells inhibit hepatitis B virus replication in the liver of transgenic mice. *J Immunol* 2002; **169**: 5188-5195

11 **Guidotti LG.** The role of cytotoxic T cells and cytokines in the control of hepatitis B virus infection.*Vaccine* 2002; **20**(Suppl 4): A80-82

12 **Kakimi K,** Isogawa M, Chung J, Sette A, Chisari FV. Immunogenicity and tolerogenicity of hepatitis B virus structural and nonstructural proteins: implications for immunotherapy of persistent viral infections. *J Virol* 2002; **76**: 8609-8620

13 **Maini MK,** Boni C, Lee CK, Larrubia JR, Reignat S, Ogg GS, King AS, Herberg J, Gilson R, Alisa A, Williams R, Vergani D, Naoumov NV, Ferrari C, Bertoletti A. The role of virus-specific CD8(+) cells in liver damage and viral control during persistent hepatitis B virus infection. *J Exp Med* 2000; **191**: 1269-1280

14 **Banchereau J**, Schuler-Thurner B, Palucka AK, Schuler G. Dendritic cells as vectors for therapy. *Cell* 2001; **106**: 271-274

15 **Guermonprez P,** Valladeau J, Zitvogel L, Thery C, Amigorena S. Antigen presentation and T cell stimulation by dendritic cells. *Annu Rev Immunol* 2002; **20**: 621-667

16 **Wen YM,** Qu D, Zhou SH. Antigen-antibody complex as therapeutic vaccine for viral hepatitis B. *Int Rev Immunol* 1999; **18**: 251-258

17 **Sallberg M,** Hughes J, Javadian A, Ronlov G, Hultgren C, Townsend K, Anderson CG, O'Dea J, Alfonso J, Eason R, Murthy KK, Jolly DJ, Chang SM, Mento SJ, Milich D, Lee WT. Genetic immunization of chimpanzees chronically infected with the hepatitis B virus, using a recombinant retroviral vector encoding the hepatitis B virus core antigen. *Hum Gene Ther* 1998; **9**: 1719-1729

18 **Huang ZH,** Zhuang H, Lu S, Guo RH, Xu GM, Cai J, Zhu WF. Humoral and cellular immunogenecity of DNA vaccine based on hepatitis B core gene in rhesus monkeys. *World J Gastroenterol* 2001; **7**: 102-106

19 **Thermet A,** Rollier C, Zoulim F, Trepo C, Cova L. Progress in DNA vaccine for prophylaxis and therapy of hepatitis B. *Vaccine* 2003; **21**: 659-662

20 **Michel ML,** Loirat D. DNA vaccines for prophylactic or therapeutic immunization against hepatitis B. *Intervirology* 2001; **44**: 78-87

21 **Guan XJ,** Guan XJ ,Wu YZ, Jia ZC, Shi TD, Tang Y. Construction and characterization of an experimental ISCOMS-based hepatitis B polypeptide vaccine. *World J Gastroenterol* 2002; **8**: 294-297

22 **You Z,** Huang XF, Hester J, Rollins L, Rooney C, Chen SY. Induction of vigorous helper and cytotoxic T cell as well as B cell responses by dendritic cells expressing a modified antigen targeting receptor-mediated internalization pathway. *J Immunol* 2000; **165**: 4581-4591

23 **Stober D,** Trobonjaca Z, Reimann J, Schirmbeck R. Dendritic cells pulsed with exogenous hepatitis B surface antigen particles efficiently present epitopes to MHC class I-restricted cytotoxic T cells. *Eur J Immunol* 2002; **32**: 1099-1108

24 **Jenne L,** Schuler G, Steinkasserer A. Viral vectors for dendritic cell-based immunotherapy. *Trends Immunol* 2001; **22**: 102-107

25 **Nakamura Y,** Suda T, Nagata T, Aoshi T, Uchijima M, Yoshida A, Chida K, Koide Y, Nakamura H. Induction of protective immunity to listeria monocytogenes with dendritic cells retrovirally transduced with a cytotoxic t lymphocyte epitope minigene. *Infect Immun* 2003; **71**: 1748-1754

26 **Lapointe R,** Royal RE, Reeves ME, Altomare I, Robbins PF, Hwu P. Retrovirally transduced human dendritic cells can generate T cells recognizing multiple MHC class I and class II epitopes from the melanoma antigen glycoprotein 100. *J Immunol* 2001; **167**: 4758-4764

27 **Meyer zum Buschenfelde C,** Nicklisch N, Rose-John S, Peschel C, Bernhard H. Generation of tumor-reactive CTL against the tumor-associated antigen HER2 using retrovirally transduced dendritic cells derived from CD34+ hemopoietic progenitor cells. *J Immunol* 2000; **165**: 4133-4140

28 **Takayama T,** Kaneko K, Morelli AE, Li W, Tahara H, Thomson AW. Retroviral delivery of transforming growth factor-beta1 to myeloid dendritic cells: inhibition of T-cell priming ability and influence on allograft survival. *Transplantation* 2002; **74**: 112-119

29 **Akiyama Y,** Maruyama K, Watanabe M, Yamaguchi K. Retroviral-mediated IL-12 gene transduction into human CD34+ cell-derived dendritic cells. *Int J Oncol* 2002; **21**: 509-514

30 **Wang FS,** Xing LH, Liu MX, Zhu CL, Liu HG, Wang HF, Lei ZY. Dysfunction of peripheral blood dendritic cells from patients with chronic hepatitis B virus infection. *World J Gastroenterol* 2001; **7**: 537-541

31 **Livingston BD,** Alexander J, Crimi C, Oseroff C, Celis E, Daly K, Guidotti LG, Chisari FV, Fikes J, Chesnut RW, Sette A. Altered helper T lymphocyte function associated with chronic hepatitis B virus infection and its role in response to therapeutic vaccination in humans. *J Immunol* 1999; **162**: 3088-3095

Edited by Ren SY and Wang XL

P.O.Box 2345, Beijing 100023,China
Fax: +86-10-85381893
E-mail: wjg@wjgnet.com www.wjgnet.com

World J Gastroenterol 2003;9(7):1516-1520
World Journal of Gastroenterology
 ISSN 1007-9327

• VIRAL HEPATITIS •

A novel stop codon mutation in HBsAg gene identified in a hepatitis B virus strain associated with cryptogenic cirrhosis

Xu Yang, Xiao-Peng Tang, Jian-Hua Lei, Hong-Yu Luo, Yong-Hong Zhang

Xu Yang, Xiao-Peng Tang, Jian-Hua Lei, Hong-Yu Luo, Yong-Hong Zhang, Liver Disease Research Center, The Second Xiangya Hospital, Central South University, Changsha 410011, Hunan Province, China
Correspondence to: Dr Xu Yang, Liver Disease Research Center, The Second Xiangya Hospital, Central South University, 86 Ren Min Avenue, Changsha 410011, Hunan Province, China yangxu@vip.163.com
Telephone: +86-731-5524222-2263 **Fax:** +86-731-5533525
Received: 2003-03-04 **Accepted:** 2003-04-01

Abstract

AIM: HBsAg is the most important serological marker for acute or chronic hepatitis B. Nevertheless, there were reports of HBsAg-negative infection caused by hepatitis B virus in recent years. We had a patient with crytogenic cirrhosis who was negative for HBsAg, positive for anti-HBs and HBeAg. This paper was to explore the pathogenic and molecular basis of the unusual serological pattern.

METHODS: HBV serologic markers were qualitatively and quantitatively determined. HBV DNA in serum was qualitatively tested using routine Polymerase chain reaction (PCR), and the viral level was determined with real-time fluorescence quantitative PCR. HBsAg gene was amplified and cloned. Four clones were sequenced. The new genomic sequences were compared with GenBank on the DNA level as well as the protein level.

RESULTS: The qualitative results of serological markers were HBsAg(-), anti-HBs(+), HBeAg(+), anti-HBe(-) and anti-HBc(+). The quantitative results of serological marker were HBsAg (S/N): 0.77 (cut off of S/N: $\geqslant$2.00), HBeAg (S/N): 56.43 (cut off S/N: $\geqslant$2.10), anti-HBc (S/C_O): 2.03 (cut off of S/C_O: $\leqslant$1.00). The viral level was as high as 1.54×10^9 copies/ml. Sequencing of the HBsAg gene clones revealed a unique point mutation at nucleotide 336 (C to A), which resulted in a novel stop codon at aa 61. The novel HBsAg gene stop mutation had not been described.

CONCLUSION: The lack of detection of HBsAg in the presence of high viral levels of replication may be caused by the existence of viral genomes harboring point mutations which resulted in stop codon upstream of the "a" determinant in HBsAg gene.

Yang X, Tang XP, Lei JH, Luo HY, Zhang YH. A novel stop codon mutation in HBsAg gene identified in a hepatitis B virus strain associated with cryptogenic cirrhosis. *World J Gastroenterol* 2003; 9(7): 1516-1520
http://www.wjgnet.com/1007-9327/9/1516.asp

INTRODUCTION

Hepatitis B virus (HBV) is a small DNA-containing virus with 4 overlapping open reading frames. The four genes are core, surface, X and polymerase. The surface antigen open reading frame is divided into three regions, pre-S1, pre-S2 and S, which encode three envelope proteins respectively termed large, middle and major protein. All the three envelope proteins contain the major protein, HBsAg, which consists of 226 amino acids and is the predominant protein of the 20 nm small spherical particles representing circulation excess surface protein[1,2].

Serological evidence for acute or chronic hepatitis B is provided most commonly by assays detecting the HBsAg. Its detection is believed to prove the presence of hepatitis B virus in the liver and the peripheral blood. Both the clearance of HBsAg from serum and the appearance of antibodies to HBsAg (anti-HBs) are associated with a resolution of hepatitis in acute or chronic hepatitis B infection[3]. However, the development of polymerase chain reaction (PCR) technique has permitted the detection of very low levels of HBV in patients. There are a number of reports of HBsAg-negative virus carriers[4,5]. Moreover, even cases of anti-HBs-positive carriers have been described although antibodies against the viral envelope usually neutralize the virus and confer protection from infection[6]. China is a highly endemic area for HBV infection, some studies suggested that 30 % to 40 % of HBsAg-negative patients with cryptogenic cirrhosis, chronic active hepatitis, or chronic persistent hepatitis had HBV-DNA in serum or liver tissue[7]. A well-characterized explanation for the latter pattern is surface mutation. Over the past decade many kinds of surface mutations have been described. We present here a patient with cirrhosis and active viral replication in the presence of anti-HBs. Sequencing of the HBV DNA from the patient revealed a point mutation at nucleotide 336 (C to A) in HBs-gene. This mutation led to a stop codon at 61 amino acids of HBsAg and a premature translation stop, which has not been described elsewhere up to now.

MATERIALS AND METHODS

Case report

The patient was a 56-year-old man. He was positive for HBsAg but asymptomatic in 1988. In 1990 his alanine aminotransferase (ALT) level was slightly elevated. In 1992 he developed a very severe disease which was diagnosed as severe type hepatitis B. He recovered 3 months later. He felt well from 1992 to 1998, no data about HBV serology and liver function were available during that period. However, he began to feel fatigue, weakness, abdominal distension from the beginning of 1999. His WBC and platelet were markedly decreased, but negative for HBsAg, and positive for anti-HBs. Abdominal ultrasound examination showed splenomegaly. Cryptogenic cirrhosis was diagnosed. Cirrhosis caused by HCV, alcohol, drugs, Wilson' s diease and schistosomiasis was excluded. In order to find the cause of the cirrhosis, he came to our hospital in August 2000. Serum was collected at the time and stored at -70 ℃ until analysis.

HBV serological markers detection

HBsAg, anti-HBs, HBeAg, anti-Hbe, anti-HBc-IgG and anti-HBc-IgM were tested using commercially available standard enzyme immunoassay kit (Kehua Bio-Engineering Co. LTD, Shanghai, China). HBsAg, HbeAg and anti-HBc-IgG were

quantitatively determined using Abbott reagent with IMX automatic immunoassay analyzer (Abbott Laboratories, North Chicago, IL), according to the manufacturer' s instructions.

Serum HBV DNA detection

HBV DNA detection was carried out using commercially available PCR kit (Liver Research Institute, Beijing Medical University, Beijing, China), according to the manufacturer' s instructions. Serum samples (200 μl) were digested with 1 g/L proteinase K and 0.5 % sodium dodecyl sulfate (at 37 ℃ **for** 2 hours), followed by phenol-chloroform extractions and ethanol precipitation. After centrifugation, the pellet was dissolved in 10 μl distilled water. Five μl elute was used for PCR. Thermal cycling conditions were as follows: 35 cycles of amplification were performed at 94 ℃ for 30 s and at 60℃ for 45 s. The PCR products were investigated by staining with ethidium bromide on ultraviolet transilluminatior after electrophoresis in 1.5 % agarose gel.

HBV DNA quantification

HBV DNA in serum was quantified using a commercially available real-time fluorescence quantitative PCR (FQ-PCR) kit (Da An Gene Diagnostic Center, Sun Yet-Sen Medical University, Guangzhou, China), in accordance with the manufacturer' s instructions. Briefly, 40 μl of serum was mixed with 40 μl of DNA-extracting solution (provided by the kit). The mixture was vortexed and placed in a 100 ℃ heating block for 10 min, then overnight at 4 ℃. The mixture was centrifuged for 5 min at 10 000 rpm. Two μl of supernatant was added to the tube containing FQ-PCR core reagent (provided by the kit). FQ-PCR was performed using a GeneAmp 5700 sequence detection system (Perkin Elmer, Foster City, CA). Thermal cycling conditions were as follows: at 93 ℃ for 2 min for initial denaturation, followed by 40 cycles of at 93 ℃ for 30 s, at 55 ℃ for 60 s. Analysis of raw data was done with the GeneAmp 5700 SDS Software (PE Biosystems). Data were collected at the annealing step of each cycle, and the threshold cycle (C_T) for each sample was calculated by determining the point at which the fluorescence exceeded the threshold limit. The standard curve was calculated automatically by plotting the C_T value against each standard of known concentration and calculation of the linear regression line of this curve. Calculation of the correlation coefficient was done for each run, and the minimal value was 0. 98. Sample copy numbers were calculated by interpolation of the experimentally determined standard curve.

Amplification of HBsAg gene

The primers were designed by ourselves according to the sequences published[8,10], which could amplify whole HBsAg gene (from nt 155 to 833). The procedures for HBV DNA extraction were the same as routine PCR described above. The reaction conditions were: the total volume was 30 μl, containing 50 mmol/L KCl , 10 mmol/L tris-HCl (pH9.0), 0.1 % triton 100, 0.2 mmol/L dNT, 1.5 mmol/L $MgCl_2$, 15 pmol primer 1 and primer 2, TaqDNA polymerase 2.5U, a drip of paraffin oil was added on the top of the solution. PCR conditions were as follows: at 94 ℃ for 5 min for initial denaturation, followed by 30 cycles at 94 ℃ for 1 min, at 56 ℃ for 50 s, at 72 ℃ for 10 s, at 72 ℃ for 10 min for extension. The PCR products were investigated by staining with ethidium bromide on ultraviolet transilluminatior after electrophoresis in 1.5 % agarose gel or used for HBsAg gene cloning.

Forward primer: 5' GGGAAGCTTATGGAGAACATCACATCAGGATTC3'

Reverse primer: 5' CGCGGATCCTTAAATGTATACCCAGAGACAAAA3' .

Cloning and sequencing of HBsAg gene

The amplified products of HBsAg gene were cloned using pGEM-T easy vectors system kit (Promega Co., Madison, WI.), according to the manufacture' s instructions. To detect the vectors containing the PCR products, white/blue colony selection was used. The inserted products were analyzed by electrophoresis in 1 % agarose gel after EcoR 1 digestion and PCR (as amplification of HBsAg gene described above). Four clones were sequenced. The sequence of the complete HBsAg gene was obtained by forward and reverse reading of overlapping fragments using ABI PRISM BigDye terminator cycle sequencing ready reaction kit (Perkin Elemer, Foster City, CA). To identify mutations, the new genomic sequences were compared with GenBank on the DNA level as well as the protein level.

RESULTS

All HBV serologic markers were tested repeatedly. HBsAg, HBeAg and anti HBc were tested again using Abbott reagent. The results confirmed that the patient was HBsAg-negative, anti-HBs-positive and HBeAg-positive. It was estimated that the patient had cirrhosis caused by HBV. To confirm the diagnosis, the presence of HBV DNA in serum of the patient was tested using routine PCR and HBV DNA was detected. The quantity of HBV DNA in serum was determined using real-time fluorescent quantitative PCR, which was unexpectedly as high as 1.54×109/ml (Tables 1 and 2).

Table 1 Viral and clinical examination results of the patient

Item	Jan. 1999	Apr. 1999	Oct. 1999	Aug. 2000	Nov. 2000	Mar. 2001
HBsAg	-	-	-	-	-	-
Anti-HBs	+	+	+	+	+	+
HbeAg	+	+	+	+	+	+
Anti-Hbe	-	-	-	-	-	-
Anti-HBc-IgG	+	+	+	+	+	+
Anti-HBc-IgM	+	-	-	-	-	-
HBV DNA	Nd	Nd	Nd	Nd	+	+
HBV DNA copies/ml	Nd	Nd	Nd	Nd	1.02×10^8	1.54×10^9
ALT (U/L)	49.0	56.9	67.1	74.4	69.0	68.6
Albumin (g/L)	42.3	40.4	38.5	40.3	41.5	40.8
Globulin (g/L)	28.6	30.7	28.5	34.4	31.9	32.6
Bilirubin (μmol/L)	18.9	23.2	28.6	25.8	27.7	28.4
Hemoglobin (g/L)	Nd	Nd	Nd	111	115	110
WBC (10^9/L)	Nd	Nd	Nd	2.1	2.8	2.6
Platelet (10^9/L)	Nd	Nd	Nd	26	58	40

Nd, not determiined; +, positive; -, negative. ALT, alanine aminotransferase; WBC, white blood cell.

Table 2 HBsAg, HBeAg and anti-HBc level determined using Abbott reagent

Item	Results	Cut off
HBsAg	0.77	≥2.00(S/N)
HbeAg	56.433	≥2.10(S/N)
Anti-HBc	2.033	≤1.0(S/Co)

Due to the massive production of viral particles in the absence of HBsAg and presence of anti-HBs, HBsAg gene mutation, possibly in the "a" determinant, was suspected. Therefore, HBV DNA was extracted from the serum of the patient, HBsAg gene was amplified. After electrophoresis of the PCR products corresponding to the complete HBsAg gene amplified from serum and ethidium bromide staining of the gel, a PCR fragment about 700 bp was detected (the figure was not shown). Then the PCR products of HBsAg gene were cloned, 4 clones were sequenced. The complete sequence of

the HBsAg gene was obtained by forward and reverse reading of overlapping fragments (Table 3). All of the 4 clones had the same sequence. The nucleotide and amino acid sequences of the HBsAg gene were compared with GenBank. There were no nucleotide insertions or deletions in the HBsAg gene. Surprisingly, sequencing of the HBsAg gene clones revealed a unique point mutation at nucleotide 336 (C to A), which resulted in a novel stop codon at aa 61. Thus, only a truncated version of HBsAg containing 21 amino acids could be synthesized from this gene, which lacked the entire "a" determinant. The novel HBsAg gene stop codon caused by a point substitution mutation upstream of the "a" determinant of HBsAg gene has not been described up to now.

The isolate belonged to subtype adw2 according to the amino acid sequence deduced from the nucleotide sequence of the HBsAg gene. The patient's nucleotide sequence and amino acid sequence were compared with a published sequence of the same subtype reported by Ono *et al*[9] and a Chinese consensus sequence of the same subtype (China J Microbiol Immunol, 1999; 19: 197-200). A two by two analysis of the three nucleotide and amino acid sequences demonstrated a relatively high degree of homogeneity. The nucleotide and amino acid difference was 5.28 % and 8.37 % between the patient's and Ono's sequences, and was 4.84 % and 7.92 % between the patient's and the Chinese consensus sequences, respectively. The "a" determinant of the patient's sequence differed from the Ono's sequence by only 2 amino acids and differed from the Chinese consensus sequence by another 2 amino acids, which might reflect the genetic heterogeneity of the same subtype and could not be the mutation (Table 4).

Table 3 The complete nucleotide sequence of the HBsAg gene from the patient

nt															Codon
155	ATG	GAG	AAC	ATC	ACA	TCA	GGA	TTC	CCA	GGA	CCC	CTG	CTC	GTA	TTA	15
200	CAG	GCG	GGG	TTT	TTC	TTG	TTG	ACA	AAA	ATC	CTC	ACA	ATA	CCA	CAG	30
245	AGT	CTA	GAC	TCG	TGG	TGG	ACT	TCT	CTC	AAT	TTT	CTA	GGG	GGA	ACA	45
290	CCC	GTG	TGT	CTT	GGC	CAA	AAT	TCG	CAG	TCC	CAA	ATC	TCC	AGT	CAC	60
335	**TAA**	CCA	ACC	TGC	TGT	CCT	CCA	ATT	TGT	CCT	GGT	TAT	CGC	TGG	ATG	75
380	TGT	CTG	CGG	CGT	TTT	ATC	ATC	TGC	CTC	TGC	ATC	CTG	CTG	CTA	TGC	90
425	CTC	ATC	TTC	TTG	TTG	GTT	CTT	CTG	GAC	TAT	CAA	GGT	ATG	TTG	CCC	105
470	GTT	TGT	CCT	CTA	CTT	CCA	GGA	TCA	ACA	ACA	ACC	AGC	ACC	GGA	CCA	120
515	TGC	AAA	ACC	TGC	ACG	ACT	CCT	GCT	CAA	GGC	AAC	TCT	AAG	TTT	CCC	135
560	TCT	TGT	TGC	TGT	ACA	AAA	CCT	ACG	GAC	GGA	AAC	TGC	ACC	TGT	ATT	150
605	CCC	ATC	CCA	TCA	TCT	TGG	GCT	TTC	GCA	AAA	TAC	CTA	TGG	GAG	TGG	165
650	GCC	TCA	GTC	CGT	TTC	TCT	TGG	CTC	AGT	TTA	CTA	GTG	CCA	TTT	GTT	180
695	CAG	TGG	TTC	GTA	GGG	CTT	TCC	CCC	ACT	GTC	TGG	CTT	TCA	GTT	ATA	195
740	TGG	ATG	ATG	TGG	TTT	TGG	GGG	CCA	AGT	CTG	TAC	AAC	ATC	GTG	AGT	210
785	CCC	TTT	ATG	CCG	CTG	TTA	CCA	ATT	TTC	TTT	TGT	CTC	TGG	GTA	TAC	225
830	ATT	TAA														227

Table 4 Comparison of nucleotide sequences and amino acid sequences of HBsAg gene among the 3 adw subtypes

Codon	4	9	14	24	29	45	47
Sequence(1)	ATC Ile	CTA Leu	GTG Val	AGA Arg	CCG pro	TCA Ser	CTA Leu
Sequence(2)	ATC Ile	CCA Pro	GTA Val	A**A**A Lys	CCA Pro	TCA Ser	GTA Val
Sequence(3)	ACA Thr	CTA Leu	GTG Val	AGA Arg	CCA Pro	GCT Ala	GTA Val
Codon	49	56	57	59	61	64	71
Sequence(1)	CCT pro	CCA His	ACC Thr	AAT Asn	TCA Ser	TCC Ser	GGT Gly
Sequence(2)	CTT Leu	C**A**A Glu	ATC Ile	A**G**T Ser	**TAA** stop	T**G**T Cys	GGT Gly
Sequence(3)	CTT Leu	CCA His	ACC Thr	AAT Asn	TCA Ser	TCT Ser	GGC Gly
Codon	82	83	85	94	99	100	110
Sequence(1)	ATA Ile	TTC Phe	TTC Phe	TTA Leu	GAT Asp	TAT Tyr	ATT Ile
Sequence(2)	AT**C** Ile	T**G**C Cys	T**G**C Cys	TTG Leu	GAC Asp	TAT tyr	CTT Leu
Sequence(3)	ATA Ile	TTC Phe	TTC Phe	TTG Leu	GAC Asp	TAC Tyr	CTT Leu
Codon	113	114	115	117	118	122	126
Sequence(1)	TCA Ser	ACA Thr	ACA Thr	AGT Ser	ACG Thr	AAA Lys	ACT Thr
Sequence(2)	TCA ser	TCA Ser	ACA Thr	AGC Ser	AC**C** Thr	AAC Lys	ACT Thr
Sequence(3)	ACA Thr	TCA Ser	ACT Thr	AGC Ser	ACG Thr	AAG Lys	ATT Ile
Codon	130	131	132	136	143	144	146
Sequence(1)	GGC Gly	AAC Asn	AAG Lys	TCA Ser	ACG Thr	GAT Asp	AAT Asn
Sequence(2)	GGA gly	ACC Thr	ATG Met	TCA Ser	ACG Thr	GAC Asp	AAC Asn
Sequence(3)	GGA Gly	ACC Thr	ATG Met	TCT Ser	TCG Ser	GAC Asp	AAC Asn
Codon	148	154	155	160	161	171	190
Sequence(1)	ACC Thr	TCG Ser	TCC Ser	AAA Lys	TAC Thr	TCT Ser	GTT Val
Sequence(2)	ACC Thr	TCA Ser	TCT Ser	AAA Lys	TAC Thr	TCT Ser	GT**C** Val
Sequence(3)	ACT Thr	TCA Ser	TCT Ser	AGA Agr	TTC Phe	TCC ser	GTT val
Codon	194	200	207	209	213	214	215
Sequence(1)	GCT Ala	TAT Thr	AGC Ser	GTG Val	ATA Ile	CCG Pro	CTC Leu
Sequence(2)	GTT Val	T**T**T Phe	AAC Asn	TTG Leu	ATG met	CCG Pro	CTG Leu
Sequence(3)	GTT val	TAT Thr	AAC Asn	TTG Leu	TTA Leu	CCT Pro	CTA Leu
Codon	222						
Sequence(1)	CTC Leu						
Sequence(2)	CTC Leu						
Sequence(3)	CTT Leu						

Sequence (1): adw subtype reported by Ono *et al*. Sequence (2): The patient's sequence. Sequence (3): The Chinese consensus sequence of adw subtype.

DISCUSSION

Hepatitis B virus replicates via an RNA intermediate, using a reverse transcriptase that appears to lack a proofreading function. Therefore, HBV exhibits a mutation rate more than 10-fold higher than other DNA virus[10-12]. Mutations in all 4 genes have been described. Surface gene mutation were initially noted as vaccine escape mutants, detected in 2-3 % of children in HBV endemic regions receiving HBV immunoprophylaxis at birth, and also observed in liver transplanted HBV carriers who received hepatitis B immunoglobulin to prevent re-infection of the graft[13-17]. Similar mutations could also arise in the natural course of HBV infection. The prevalence and clinical significance of naturally occurring mutations in full-length surface and overlapping polymerase genes of hepatitis B virus were analyzed in 42 patients with chronic hepatitis, mutations were observed in 10 patients (24 %) in the "a" determinant region[18,19].

The surface gene of HBV contains a dominant neutralizing epitope termed "a" determinant located between aa 121-149 of HBsAg, The production of antibodies to the "a" determinant after vaccination usually protects against HBV infection. The surface protein variants noted in most studies were clustered within the "a" determinant, especially the substitution of glycine for arginine at aa 145, which makes this epitope unlikely to bind to antibodies generated to wild-type HBsAg. However, other kinds of mutation outside of the "a" determinant have been described in recent years, including deleting and inserting mutations in the surface gene of HBV[20-22].

In contrast to the mutations mentioned above, an uncommon point mutation at nucleotide 336 (C to A) of HBsAg-gene occurred in our isolates, which resulted in a novel stop codon at aa 61. This finding could not be a laboratory error, because all sequences of four clones were the same. Because of this new stop codon introduction, only truncated molecules of surface antigen could be expressed, which contained only 60 amino acid residues and was lack of the "a" determinant. This unique mutation could well explain the patient' s unusual serologic pattern: HBsAg-negative, but HBeAg-positive, anti-HBs-positive and HBV DNA-positive. The novel HBsAg gene stop codon caused by a point substitution mutation upstream of the "a" determinant has not been described up to now. Our finding is very similar to the deletion mutation of HBsAg gene described by Weinberger *et al*. The deletion mutation located at the nucleotide 31 of the HBsAg gene, which led to a frame-shift and introduced a stop-codon after 21amino acids of HBsAg[23].

To initiate infection, a virus must attach to a host cell receptor via one of its surface proteins. Hepatitis B virus has three related surface proteins, small S, middle S, and large S. It is not clear which of these three proteins serves as the HBV attachment protein. It has been thought that the pre-S region or S region determines viral binding[24,25]. However, due to the lack of a susceptible cell line that could be used to test specific blocking reagents, which protein is involved in the initial stage of HBV infection is difficult to determine. The HBV DNA level in our patient was as high as 10^9/ml in serum, indicating that isolates that bear such truncated molecules on their surface (the mutant HBsAg was only equal to one-fourth of HBsAg from wild type) can well finish their life cycle including viral binding and entry. Our finding presented here provides the evidence that sequences in the pre-S region determine viral binding.

However, our finding raises a theoretical question: Cells infected with hepatitis B virus produce both virions and 20nm subviral (surface antigen) particles. Although hepatitis B virus encodes three envelope proteins, all of the information required to produce 20 nm HBsAg particles resides within the S protein[26]. The nucleotide sequence of the HBsAg gene predicts the existence of three hydrophobic domains, located at residues 4 to 28 (signal I), 80 to 100 (signal II) and 164 to 221 (signal III). Studies on certain artificial deletion mutants suggested that deletion of signal II completely destabilized the chain, and deletion of the signal III resulted in a nonsecreted chain[27]. How such a drastically shortened HBsAg which is lack of signal IIand signal III, can be able to form morphologically correct viral and subviral particles? Because when co-expressed with wild type S protein, the mutant polypeptide can be incorporated into particles and secreted, therefore, it is assumed that the presence of a minor population of intact genomes helps in replication and formation of intact virions. All virus isolates consist of a mixture of viral strains. Multiple variants have been found in a single host. Advances in molecular biology technique have revealed significant diversities in sequence of of HBV isolates. Sequencing results suggest that there were HBV quasispecies groups in chronically infected patients[28-31]. Actually, electron microscopy of serum samples containing mutated DNA from the patient reported by Weiinberger *et al*. revealed typical subviral particles with an average diameter of 17-20 nm, but did not reveal a single filamentous particle[23]. Our results show that lack of detection of HBsAg in the presence of high viral levels of replication may be caused by the existence of viral genomes harboring point mutation which results in stop codon upstream of the "a" determinant of HBsAg gene.

REFERENCES

1 **Tiollais P**, Charnay P, Vyas GN. Biology of hepatitis B Virus. *Science* 1981; **213**: 406-411

2 **Michel ML,** Tiollais P. Structure and expression of the hepatitis B virus genome. *Hepatology* 1987; **7**(Suppl): 61s-63s

3 **Krugman S**, Overby LR, Mushahwar IK, Ling CM, Frosner GG, Deinhardt F. Viral hepatitis type B: Studies on natural history and prevention re-examined. *N Engl J Med* 1979; **300**: 101-106

4 **Brechot C**, Degos F, Lugassy C, Thiers V, Zafrani S, Franco D, Bismuth H, Trepo C, Benhamou JP, Wands J, Isselbacher KJ, Tiollais P, Berthelot P. Hepatitis B virus DNA in patients with chronic liver disease and negative tests for hepatitis B surface antigen. *N Engl J Med* 1985; **312**: 270-276

5 **Sanchez-Quijano A**, Jauregui JI, Leal M, Pineda JA, Castilla A, Abad MA, Civeira MP, Garcia de Pesquera F, Prieto J, Lissen E. Hepatitis B virus occult infection in subjects with persistent isolated anti-HBc reactivity. *J Hepatol* 1993; **17**: 288-293

6 **Rehermann B**, Ferrari C, Pasquinelli C, Chisari FV. The hepatitis B virus persists for decades after patients' recovery from acute viral hepatitis despite active maintenance of a cytotoxic T-lymphocyte response. *Nat Med* 1996; **2**: 1104-1108

7 **Zhang YY**, Guo LS, Li L, Zhang YD, Hao LJ, Hansson BG, Nordenfelt E. Hepatitis B virus DNA detected by PCR in sera and liver tissues of Chinese patients with chronic liver diseases. *Chin Med J Engl* 1993; **106**: 7-12

8 **Galibert F**, Mandart E, Fitoussi F, Tiollais P, Charnay P. Nucleotide sequence of the hepatitis B virus genome (subtype ayw) cloned in *E. coli*. *Nature* 1979; **281**: 646-650

9 **Ono Y**, Onda H, Sasada R, Igarashi K, Sugino Y, Nishioka K. The complete nucleotide sequences of the cloned hepatitis B virus DNA: subtype adr and adw. *Nucleic Acids Res* 1983; **11:** 1747-1757

10 **Blum HE**. Variants of hepatitis B, C and D viruses: molecular biology and clinical significance. *Digestion* 1995; **56**: 85-95

11 **Carman WF**, Thomas HC. Genetic variation in hepatitis B virus. *Gastroenterology* 1992; **102**: 711-719

12 **Hasegawa K**, Huang J, Rogers SA, Blum HE, Liang TJ. Enhanced replication of a hepatitis B virus mutant associated with an epidemic of fulminant hepatitis. *J Virol* 1994; **68**: 1651-1659

13 **Karthigesu VD**, Allison LM, Ferguson M, Howard CR. A hepatitis B virus variant found in the sera of immunised children induces a conformational change in the HBsAg "a" determinant. *J Med Virol* 1999; **58**: 346-352

14 **He JW**, Lu Q, Zhu QR, Duan SC, Wen YM. Mutations in the "a" determinant of hepatitis B surface antigen among Chinese in-

fants receiving active postexposure hepatitis B immunization. *Vaccine* 1998; **16**: 170-173

15 **Cooreman MP**, Leroux-Roels G, Paulij WP. Vaccine-and hepatitis B immune globulin-induced escape mutations of hepatitis B virus surface antigen. *J Biomed Sci* 2001; **8**: 237-247

16 **Carman WF**, Zanetti AR, Karayiannis P, Waters J, Manzillo G, Tanzi E, Zuckerman AJ, Thomas HC. Vaccine-induced escape mutant of hepatitis B virus. *Lancet* 1990; **336**: 325-329

17 **Chen WN**, Oon CJ. Hepatitis B virus surface antigen (HBsAg) mutants in Singapore adults and vaccinated children with high anti-hepatitis B virus antibody levels but negative for HBsAg. *J Clin Microbiol* 2000; **38**: 2793-2794

18 **Hou J**, Wang Z, Cheng J, Lin Y, Lau GK, Sun J, Zhou F, Waters J, Karayiannis P, Luo K. Prevalence of naturally occurring surface gene variants of hepatitis B virus in nonimmunized surface antigen-negative Chinese carriers. *Hepatology* 2001; **34**: 1027-1034

19 **Ghany MG**, Ayola B, Villamil FG, Gish RG, Rojter S, Vierling JM, Lok AS. Hepatitis B virus S mutants in liver transplant recipients who were re-infected despite hepatitis B immune globulin prophylaxis. *Hepatology* 1998; **27**: 213-222

20 **Ogura Y**, Kurosaki M, Asahinna Y, Enomoto N, Marumo F, Sato C. Prevalence and significance of naturally occurring mutations in the surface and polymerase genes of hepatitis B virus. *J Infect Dis* 1999; **180**: 1444-1451

21 **Hou J**, Karayiannis P, Waters J, Luo K, Liang C, Thomas HC. A unique insertion in the S gene of surface antigen-negative hepatitis B virus Chinese carriers. *Hepatology* 1995; **21**: 273-278

22 **Chen HB**, Fang DX, Li FQ, Jing HY, Tan WG, Li SQ. A novel hepatitis B virus matant with A-to-G at nt551 in the surface antigen gene. *World J Gastroenterol* 2003; **9**: 304-308

23 **Weinberger KM**, Zoulek G, Bauer T, Bohm S, Jilg W. A novel deletion mutant of hepatitis B virus surface antigen. *J Med Virol* 1999; **58**: 105-110

24 **Mehdi H**, Yang X, Peeples ME. An altered form of apolipoprotein H binds hepatitis B virus surface antigen most efficiently. *Virology* 1996; **217**: 58-66

25 **Neurath AR**, Seto B, Strick N. Antibodies to synthetic peptides from the preS1 region of the hepatitis B virus (HBV) envelope (env) protein are virus-neutralizing and protective. *Vaccine* 1989; **7**: 234-236

26 **Laub O**, Rall LB, Truett M, Shaul Y, Standring DN, Valenzuela P, Rutter WJ. Synthesis of hepatitis B surface antigen in mammalian cells: expression of the entire gene and the coding region. *J Virol* 1983; **48**: 271-280

27 **Bruss V,** Ganem D. Mutational analysis of hepatitis B surface antigen particle assembly and secretion. *J Virol* 1991; **65**: 3813-3820

28 **Dong J**, Cheng J, Wang QH, Wang G, Shi SS, Liu Y, Xia XB, Li LI, Zhang GQ, Si CW. Quasispecies and variations of hepatitis B virus: core promotor region as an example. *Zhonghua Shiyan He Linchuangbing Duxue Zazhi* 2002; **16**: 264-266

29 **Mathet VL**, Feld M, Espinola L, Sanchez DO, Ruiz V, Mando O, Carballal G, Quarleri JF, D'Mello F, Howard CR, Oubina JR. Hepatitis B virus S gene mutants in a patient with chronic active hepatitis with circulating Anti-HBs antibodies. *J Med Virol* 2003; **69**: 18-26

30 **Ngui SL**, Teo CG. Hepatitis B virus genomic heterogeneity: variation between quasispecies may confound molecular epidemiological analyses of transmission incidents. *J Viral Hepat* 1997; **4**: 309-315

31 **Torresi J**. The virological and clinical significance of mutations in the overlapping envelope and polymerase genes of hepatitis B virus. *J Clin Virol* 2002; **25**: 97-106

Edited by Ma JY and Wang XL

P.O.Box 2345, Beijing 100023,China
Fax: +86-10-85381893
E-mail: wjg@wjgnet.com www.wjgnet.com

World J Gastroenterol 2003;9(7):1521-1524
World Journal of Gastroenterology
 ISSN 1007-9327

Aggregate formation of hepatitis B virus X protein affects cell cycle and apoptosis

Chang-Zheng Song, Zeng-Liang Bai, Chang-Cheng Song, Qing-Wei Wang

Chang-Zheng Song, Zeng-Liang Bai, Laboratory of Immunobiology, College of Life Sciences, Shandong University, Jinan 250100, Shandong Province, China
Chang-Zheng Song, Shandong Research Center for Medical Biotechnology, Shandong Academy of Medical Sciences, Jinan 250062, Shandong Province, China
Chang-Cheng Song, Basic Research Laboratory, National Cancer Institute at Frederick, MD 21702, USA
Qing-Wei Wang, Cancer Research Center, Qilu Hospital of Shandong University, Jinan 250012, Shandong Province, China
Correspondence to: Dr. Chang-Zheng Song, Project of Viral Vaccine, Shandong Research Center for Medical Biotechnology, Shandong Academy of Medical Sciences, Jinan 250062, Shandong Province, China. songcz@life.sdu.edu.cn
Telephone: +86-531-2919611
Received: 2002-12-28 **Accepted:** 2003-02-18

Abstract

AIM: To investigate whether the formation of aggregated HBx has a potential linking with its cellular responses.

METHODS: Recombinant HBx was expressed in Escherichia *coli* and purified by Ni-NTA metal-affinity chromatography. Anti-HBx monoclonal antibody was developed for immunocytochemical detection. Bicistronic expression vector harboring full-length DNA of HBx was employed for transfection of human HepG2 cells. Immunocytochemical staining was used to examine the intracellular HBx aggregates in cells. The effects of HBx aggregation on cell cycle and apoptosis were assessed by flow cytometry.

RESULTS: Immunocytochemical staining revealed most of the HBx was formed intracellular aggregate in cytoplasm and frequently accumulated in large granules. Flow cytometry analysis showed that HepG2 cells transfected with vector harboring HBx significantly increased apoptosis and largely accumulated in the G0-G1 phase by maintenance in serum medium for 36 hours. Control cells without HBx aggregates in the presence of serum entered S phase and proliferated more rapidly at the same time. EGFP fluorescence in HBx expression cells was significantly decreased.

CONCLUSION: Our observations show that cells with HBx aggregate undergo growth arrest and apoptosis, whereas control cells without HBx remain in growth and progression into S phase. Our data may provide helpful information to understand the biological effects of HBx aggregates on cells.

Song CZ, Bai ZL, Song CC, Wang QW. Aggregate formation of hepatitis B virus X protein affects cell cycle and apoptosis. *World J Gastroenterol* 2003; 9(7): 1521-1524
http://www.wjgnet.com/1007-9327/9/1521.asp

INTRODUCTION

Hepatitis B virus (HBV) causes transient and chronic infections of the liver. Transient infections may produce serious illness, and approximately 0.5 % terminates with fatal, fulminant hepatitis. Chronic infections may also have serious consequences: nearly 25 % terminate in untreatable liver cancer. Worldwide deaths from liver cancer caused by HBV infection probably exceed one million per year. X gene is a unique fourth open reading frame of HBV. X gene codes for a 16.5-kDa protein (X protein, HBx) and is well conserved among the mammalian hepadnaviruses[1]. HBx is a multifunctional viral regulator that modulates transcription, cell responses to genotoxic stress, protein degradation, and signaling pathways[2]. The ability of HBx to modulate cell survival is potentially relevant to viral pathogenicity in acute and chronic HBV infection as well as to the late development of hepatocellular carcinoma[3]. HBx activates signal-transduction cascades such as the Ras/Raf mitogen-activated protein kinase, Src kinase, c-Jun NH2-terminal kinase and Janus family tyrosine kinases/signal transducer and activators of transcription[4,5]. HBx targets mitochondrial calcium and activates cytosolic calcium-dependent proline-rich tyrosine kinase-2[6,7]. HBx may directly interact with transcription factors[8]. HBx is also known to play an important role in alterating gene expression, sensitizing cells to apoptosis and affect cell cycle checkpoints[2]. The fate of infected cells expressing HBx is likely to be determined by the balance between apoptotic and anti-apoptotic signals of viral, cellular, and environmental origin.

HBx expression in different cells results in distinct and opposing cellular function responses of cell cycle and apoptosis[9,10]. Most of the investigations described the effects of HBx through cellular signal-transduction pathways. Some reports suggested that HBx could induce cell death when it was expressed at high levels[11-13]. The nine residues of cysteine among 154 amino acids of HBX might involve in disulfide bridge formation and be in favor of aggregate formation[14]. Protein aggregation leads to cell cycle arrest and initiates cell death[15]. We propose that intracellular deposition of aggregated HBx may have a potential linking to its cellular responses. In this study, we reported the cytoplasmic aggregates of HBx and its effect on cell cycle and apoptosis.

MATERIALS AND METHODS

Biological and chemical materials

Restriction enzymes and T4 DNA ligase were obtained from TaKaRa Biotech (Japan). QIA express Kit including pQE-60 Vector, *E. coli* strain M15 [pREP4] and Ni-NTA Superflow was purchased from QIAGEN (USA). GeneJammer transfection reagent was from Stratagene (USA). The plasmid pSPX46, a gift of Dr. Curtis C. Harris (National Institutes of Health, USA), encodes full-length HBx of the adr subtype. The bicistronic expression vector pIRES-EGFP-HBx harboring X gene (subtype ayw) was kindly provided by Drs. Jingyu Diao and Christopher D. Richardson (University of Toronto, Canada). SABC immunocytochemical detection kit was from Wuhan Boster Biological Technology Co. (China). Other chemicals of analytical grade were from Sigma.

Construction of HBx expression vector

The coding DNA fragment was amplified by polymerase chain reaction (PCR) using the pSPX46 as a template and the 5' -PCR primer (5' -TTT CCA TGG CTG CTC GGG TGT GC-3') carrying the NcoI site before and the 3' -PCR primer (5' GCGAGATCTGGCAGAGGTGAAAAAGTTG-3') carrying the Bgl II site after the X reading frame. The PCR product was digested with NcoI and *Bgl* II and ligated into pQE-60. According to the cloning strategy, recombinant construct based on the pQE-60 vector was produced by placing the 6xHis tag at the carboxy-terminus of HBx with the protein beginning with its natural ATG start codon. pQE-60X was obtained as an expression system for biosynthesis of HBx.

Expression and purification of HBx

Recombinant pQE-60X was transformed into E. coli strain M15 [pREP4]. The culture was induced with 1 mM isopropyl β-D-thiogalactopyranoside for 4.5 hours at 37 ℃. The bacteria were harvested and lysed in a buffer containing 6 mol/L guanidine hydrochloride. The purification procedure of QIAexpress Kit was optimized. Elution with 250 mmol/L imidazole could effectively separate HBx from nickel-nitrilotriacetic acid (Ni-NTA) resins. Recombinant HBx was analysed by sodium dodecyl sulfate -polyacrylamide gel electrophoresis (SDS-PAGE). Electrophoresis was performed on 15 % polyacrylamide gel. After electrophoresis, gels were fixed in 30 % ethanol, 10 % acetic acid, and stained with Coomassie brilliant blue.

Preparation of monoclonal antibody against HBx

Balb/c mice were immunized repeatedly. Spleen cells from the most responding mouse were fused with myeloma cells (Sp-2/0) according to the routine method described by Yang *et al*[16]. Positive hybrids were selected on hypoxanthine, aminopterin and thymidine containing medium.

Cell culture and transfections

Human hepatoma cell line HepG2 was grown on coverslips or 60-mm dish and maintained in Dulbecco' s modified Eagle minimal medium containing penicillin (100 IU/ml) and streptomycin (100 mg/ml) and supplemented with 10 % fetal calf serum. Bicistronic expression vector pIRES-EGFP-HBx derived from pIRES-EGFP by adding the DNA fragments of HBx[17]. Cells at 70 % confluence were respectively transfected with pIRES-EGFP-HBx and pIRES-EGFP using GeneJammer transfection reagent. DNA transfections were performed according to the protocols supplied with the reagents.

Immunocytochemical assay

After transfection for 36 hours, HepG2 cells were washed in phosphate-buffered saline (PBS) and fixed with 90 % ethanol. SABC detection kit was used for immunocytochemical analysis. Cells were incubated with HBx monoclonal antibody for 1 hour at 37 ℃. After washed three times with PBS, cells were incubated with anti-mouse biotinylated secondary antibody. Following extensive washes with PBS, color development was demonstrated with diaminobenzidine tetrahydrochloride chromagen. Finally, the slides were counterstained with hematoxylin. Stained cells were examined using light microscopy and photographed.

Flow cytometric analysis

To assess the effect of HBx aggregation on cell cycle, apoptosis and fluorescence of enhanced green fluorescent protein (EGFP), we analyzed the transfected cells by flow cytometry for GFP fluorescence and DNA content[18]. The efficiency of transfection was verified by fluorescent signal. Cells were released by trypsinization, resuspended in PBS at a density of 2×10^6 cells/ml, and analyzed on a Becton Dickinson flow cytometer using CellQuest software.

RESULTS

Vector construction for encoding HBx

In order to develop an HBx: anti-HBx antibody system for immunocytochemical purposes, an efficient E. *coli* expression system to produce HBx in large quantity was established. HBx was expressed in E. *coli* cells harboring pQE-60X as HBx carboxy-terminally fused to six histidine residues. pQE-60X was confirmed by PCR, restriction enzymes analysis and DNA sequencing.

HBx antigen and anti-HBx monoclonal antibody

Recombinant HBx was expressed in Escherichia *coli*. Because of the high stability of HBx aggregates, the purification procedure was optimized. E. *coli* cells were lysed in a buffer containing 6 mol/L guanidine hydrochloride. Six consecutive histidine residues that placed at the carboxy-terminus of HBx facilitated Ni-NTA metal-affinity chromatography. Elution with 250 mmol/L imidazole could effectively separate HBx from Ni-NTA resins. HBx was eluted as a pure protein (Figure 1). Starting with 1L of culture, only one milligram of recombinant HBx was attained under our experimental conditions. An anti-HBx monoclonal antibody was established following the conventional approach. The anti-HBx monoclonal antibody recognized the recombinant antigen as proved by high optical density measured in a simple binding enzyme-linked immunosorbent assay. Monoclonal antibody secreted by hybridoma clone was alike optimal for immunocytochemistry.

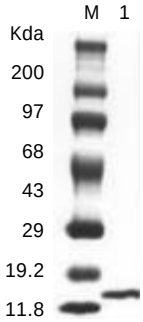

Figure 1 SDS-PAGE analyses of the purified HBx. SDS-PAGE showed a single band at the expected molecular weights (lane 1).

Immunohistochemical detection of HBx aggregates

HBx aggregate and its distribution were verified by immunocytochemistry. HBx-bearing cells exhibited positively staining by anti-HBx monoclonal antibody. Cytoplasmic HBx characteristically accumulated in large granules or strongly stained aggregates (Figure 2A, arrows). No immunoreactivity could be detected in a negative control stained by the same antibody under the same conditions (Figure 2B).

Flow cytometric analysis of HepG2 cells

A transient expression plasmid, pHBx-IRES-EGFP was used in this experiment. The vector contained HBx and EGFP reporter genes under control of a cytomegalovirus promoter and the element of internal ribosome entry site (IRES), respectively[17]. More than 80 % of human HepG2 cells could be transfected with pIRES-EGFP-HBx and pIRES-EGFP respectively as shown by fluorescence flow cytometry. A representative flow cytometric profile at the 36th is shown in Figure 3A and 3B. Results were expressed as percentage of HepG2 cells in G0-G1, G2-M and S phases of the cell cycle

(Figure 3C). Apoptosis was also monitored by flow cytometry (Figure 3C). Each value corresponded to the mean ± standard deviation of two independent experiments. Using Student's *t*-test, statistical analysis was performed. HepG2 cells transfected with vector harboring HBx were accumulated largely in the G0-G1 phase after maintenance in serum medium for 36 hours. Control cells that could not synthesize HBx protein in the presence of serum proliferated more rapidly and entered S phase at the same time.

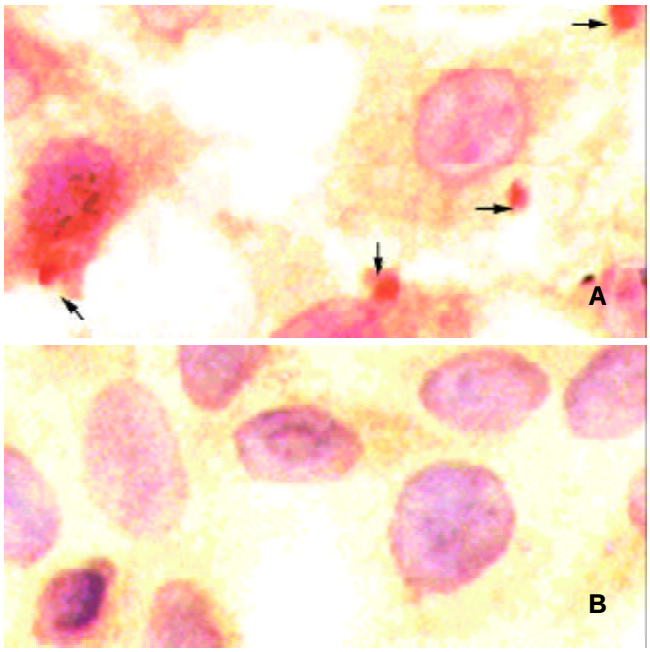

Figure 2 Immunocytochemical detection of HBx aggregates within HepG2 cells (magnification, ×400). HBx aggregates were clearly visible as granules within the cytoplasm (A). HBx could not be detected within control cells transfected with pIRES-EGFP (B).

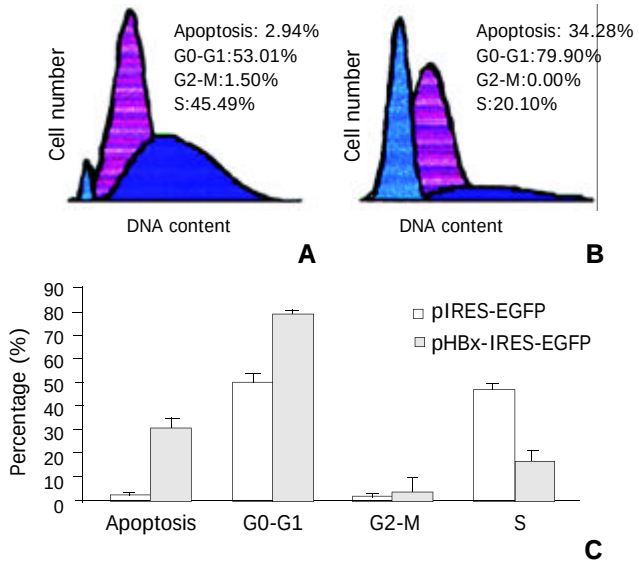

Figure 3 Flow cytometric analysis of apoptosis and cell cycle phases of HepG2 cells. (A) Control cells transfected with vector alone did not contain HBx. (B) Cells transiently transfected with the HBx expression plasmid. Apoptosis was significantly increased in HepG2 cells compared with control cells without HBx (C, $P<0.02$). Cells displayed a marked decrease in S phase ($P<0.02$) and demonstrated an evident increase in G0-G1 fraction ($P<0.01$) with control expression vector that lacked the HBx gene (C).

EGFP fluorescence was decreased in HBx transfected cells

The mean fluorescence of 10^4 EGFP positive cells was measured by fluorescence cytometer. The EGFP fluorescence value was 4.43±0.58 and 3.45±0.15 of experiments in triplicate for HepG2 cells transfected with pIRES-EGFP and pIRES-EGFP-HBx, respectively. EGFP fluorescence in HBx expression cells was significantly decreased as compared with control pIRES-EGFP ($P<0.05$).

DISCUSSION

The X open reading frame of HBV is highly conserved among all mammalian hepadnaviruses. HBx might regulate the expression of certain viral and cellular genes which are important for the creation of an environment suitable for viral propagation. HBx inhibits clonal outgrowth of cells and induces apoptosis by a p53-independent pathway. HBx expression can induce a late G1 cell cycle block prior to their counterselection by apoptosis. Furthermore, mutations in the HBx-gene evolving in hepatocellular carcinoma can abolish both HBx-induced growth arrest and apoptosis. Abrogation of the anti-proliferative and apoptotic effects of HBx by naturally occurring mutations might render the hepatocytes susceptible to uncontrolled growth and contribute to multistep hepatocarcinogenesis associated with HBV infection[18]. HBx has been shown to be able to regulate cell cycle. HBx can activate the cyclin A promoter, induce cyclin A-cyclin-dependent kinase 2 complexes, and promote cycling of growth-arrested cells into G1 through a pathway involving activation of Src tyrosine kinases[5]. HBx stimulation of Src kinases and cyclin gene expression was found to force growth-arrested cells to transit through G1 but to stall at the junction with S phase, which may be important for viral replication.

The structure feature of HBx may affect its biophysical properties including solubility, tendency toward aggregation with itself and with other proteins. Gupta *et al*.[19] purified HBx from E. *coli*, subjected the protein to air oxidation, and analyzed intramolecular disulfide bonds. They found that eight of the nine cysteines were disulphide linked in a sequential manner. The disulphide linkages were between Cys7 and Cys78, Cys17 and Cys115, Cys61 and Cys137, Cys69 and Cys143 while Cys148 was free. The disulphide arrangement in HBx followed a pattern where each cysteine was joined to the fourth cysteine. HBx is able to form intramolecular disulfide bonds even under the reducing conditions of the cytosol. With analysis of purified HBx from eukaryotic sources by using electrospray ionization mass spectrometry, Urban *et al*.[14] uncovered some components: the unmodified, monomeric, fully oxidized form with five intramolecular disulfide bridges, and its N-acetylated modification. It is not very clear whether the disulfide bridge formation is a prerequisite of HBx function, but a point mutation of Cys-69 to Ala abolishes its transactivation activity[20]. Intracellular deposition of aggregated proteins is a prominent cytopathological feature of most neurodegenerative diseases[21]. Protein aggregation is a central event in the initiation of cell death[6]. Protein aggregation directly impaires the function of the ubiquitin-proteasome system and leads to cell cycle arrest and cell death.

In view of the investigations, we proposed apoptotic effects of HBx be related to its aggregate formation. Immunohistochemical examination revealed that only a minor immunological signal of HBx was detectable in a soluble form, whereas most of the protein formed intracellular aggregates in cytoplasm. HBx frequently accumulated in large granules. Our observation could suggest that HBx transfected cells underwent growth arrest and apoptosis, whereas control cells without HBx remained in growth and progression into S phase. In addition, we used the reporter molecule EGFP to reflect the situation of

HBx expression indirectly. By counting equal number of EGFP positive cells, pIRES-EGFP-HBx transfected cells showed a weak fluorescence as compared with pIRES-EGFP transfected cells. Diao *et al.*[17] also reported that human primary hepatocytes transfected with pIRES-EGFP-HBx showed less intense fluorescent signal. HBx aggregates may affect the fluorescence intensity of EGFP in the same cell.

HBx were detected in aggregated structures and it was further showed that HBx aggregates mediated growth arrest and cell death. Our data may provide helpful information on the biological effects of HBx aggregates. The precise mechanism by which HBx aggregates could affect cell cycle and apoptosis remains to be established.

REFERENCES

1 **Seeger C**, Mason WS. Hepatitis B virus biology. *Microbiol Mol Biol Rev* 2000; **64**: 51-68

2 **Murakami S**. Hepatitis B virus X protein: a multifunctional viral regulator. *J Gastroenterol* 2001; **36**: 651-660

3 **Rui E**, de Moura PR, Kobarg J. Expression of deletion mutants of the hepatitis B virus protein HBx in E. coli and characterization of their RNA binding activities. *Virus Res* 2001; **74**: 59-73

4 **Arbuthnot P**, Capovilla A, Kew M. Putative role of hepatitis B virus X protein in hepatocarcinogenesis: effects on apoptosis, DNA repair, mitogen-activated protein kinase and JAK/STAT pathways. *J Gastroenterol Hepatol* 2000; **15**: 357-368

5 **Bouchard M**, Giannakopoulos S, Wang EH, Tanese N, Schneider RJ. Hepatitis B virus HBx protein activation of cyclin A-cyclin-dependent kinase 2 complexes and G1 transitvia a Src kinase pathway. *J Virol* 2001; **75**: 4247-4257

6 **Bouchard MJ**, Wang LH, Schneider RJ. Calcium signaling by HBx protein in hepatitis B virus DNA replication. *Science* 2001; **294**: 2376-2378

7 **Diao J**, Garces R, Richardson CD. X protein of hepatitis B virus modulates cytokine and growth factor related signal transduction pathways during the course of viralinfections and hepatocarcinogenesis. *Cytokine Growth Factor Rev* 2001; **12**: 189-205

8 **Wei W**, Dorjsuren D, Lin Y, Qin W, Nomura T, Hayashi N, Murakami S. Direct interaction between the subunit RAP30 of transcription factor IIF (TFIIF) and RNA polymerase subunit 5, which contributes to the association between TFIIF and RNA polymerase II. *J Biol Chem* 2001; **276**:12266-12273

9 **Su F**, Schneider RJ. Hepatitis B virus HBx protein sensitizes cells to apoptotic killing by tumor necrosis factor alpha. *Proc Natl Acad Sci U S A* 1997; **94**: 8744-8749

10 **Lee S**, Tarn C, Wang WH, Chen S, Hullinger RL, Andrisani OM. Hepatitis B virus X protein differentially regulates cell cycle progression in X-transforming versus nontransforming hepatocyte (AML12) cell lines. *J Biol Chem* 2002; **277**: 8730-8740

11 **Chirillo P**, Pagano S, Natoli G, Puri PL, Burgio VL, Balsano C, Levrero M. The hepatitis B virus X gene induces p53-mediated programmed cell death. *Proc Natl Acad Sci U S A* 1997; **94**: 8162-8167

12 **Terradillos O,** Pollicino T, Lecoeur H, Tripodi M, Gougeon ML, Tiollais P, Buendia MA. p53-independent apoptotic effects of the hepatitis B virus HBx protein *in vivo* and *in vitro*. *Oncogene* 1998; **17**: 2115-2123

13 **Shintani Y,** Yotsuyanagi H, Moriya K, Fujie H, Tsutsumi T, Kanegae Y, Kimura S, Saito I, Koike K. Induction of apoptosis after switch-on of the hepatitis B virus X gene mediated by the Cre/loxP recombination system. *J Gen Virol* 1999; **80**: 3257-3265

14 **Urban S**, Hildt E, Eckerskorn C, Sirma H, Kekule A, Hofschneider PH. Isolation and molecular characterization of hepatitis B virus X-protein from a baculovirus expression system. *Hepatology* 1997; **26**: 1045-1053

15 **Bence NF**, Sampat RM, Kopito RR. Impairment of the ubiquitin-proteasome system by protein aggregation. *Science* 2001; **292**: 1552-1555

16 **Yang LJ**, Sui YF, Chen ZN. Preparation and activity of conjugate of monoclonal antibody HAb18 against hepatoma F(ab')2 fragment and staphylococcal enterotoxin A. *World J Gastroenterol* 2001; **7**: 216-221

17 **Diao J**, Khine AA, Sarangi F, Hsu E, Iorio C, Tibbles LA, Woodgett JR, Penninger J, Richardson CD. X protein of hepatitis B virus inhibits Fasmediated apoptosis and is associated with up-regulation of the SAPK/JNK pathway. *J Biol Chem* 2001; **276**: 8328-8340

18 **Sirma H,** Giannini C, Poussin K, Paterlini P, Kremsdorf D, Brechot C. Hepatitis B virus X mutants, present in hepatocellular carcinoma tissue abrogate both the antiproliferative and transactivation effects of HBx. *Oncogene* 1999; **18**: 4848-4859

19 **Gupta A**, Mal TK, Jayasuryan N, Chauhan VS. Assignment of disulphide bonds in the X protein (HBx) of hepatitis B virus. *Biochem Biophys Res Commun* 1995; **212**: 919-924

20 **Arii M**, Takada S, Koike K. Identification of three essential regions of hepatitis B virus X protein for trans-activation function. *Oncogene* 1992; **7**: 397-403

21 **Schulz JB**, Dichgans J. Molecular pathogenesis of movement disorders: are protein aggregates a common link in neuronal degeneration? *Curr Opin Neurol* 1999; **12**: 433-439

Edited by Xu XQ

P.O.Box 2345, Beijing 100023,China
Fax: +86-10-85381893
E-mail: wjg@wjgnet.com www.wjgnet.com

World J Gastroenterol 2003;9(7):1525-1528
World Journal of Gastroenterology
 ISSN 1007-9327

• VIRAL HEPATITIS •

Anti-HBV effect of TAT- HBV targeted ribonuclease

Jin Ding, Jun Liu, Cai-fang Xue, Wei-dong Gong, Ying-hui Li, Ya Zhao

Jin Ding, Jun Liu, Cai-Fang Xue, Wei-Dong Gong, Ying-Hui Li, Ya Zhao, Department of Etiology, Fourth Military Medical University, Xi' an 710032, Shaanxi Province, China
Supported by National Natural Science Foundation of China, No. 30100157; Medical Research Fund of Chinese PLA, No.01MA184 and Innovation Project of FMMU, No.CX99005
Correspondence to: Professor Cai-Fang Xue or Dr. Jun Liu, Department of Etiology, Fourth Military Medical University, Xi' an 710032, Shaanxi Province, China. etiology@fmmu.edu.cn
Telephone: +86-029-3374536 **Fax:** +86-029-3374594
Received: 2003-03-05 **Accepted:** 2003-04-09

Abstract

AIM: To prepare and purify TAT-HBV targeted ribonuclease fusion protein, evaluate its transduction activity and investigate its effect on HBV replication in 2.2.15 cells.

METHODS: The prokaryotic expression vector pTAT containing TR gene was used in transforming *E.coli* BL21 (DE3) LysS and TR was expressed with the induction of IPTG. The TAT-TR fusion protein was purified using Ni-NTA-agrose and PD-10 desalting columns, and analyzed by SDS-PAGE. Transduction efficiency of TAT-TR was detected with immunofluorescence assay and the concentration of HBeAg in the supernatant of the 2.2.15 cells was determined via solid-phase radioimmunoassay (spRIA). MTT assay was used to detect the cytotoxicity of TAT-TR.

RESULTS: The SDS-PAGE showed that the TAT-TR fusion protein was purified successfully, and the purity of TAT-TR was 90 %. The visualization of TAT-TR by immunofluorescence assay indicated its high efficiency in transducing 2.2.15 cells. RIA result suggests that TAT-TR could inhibit the replication of HBV effectively, it didn't affect cell growth and had no cytotoxicity.

CONCLUSION: TAT-TR possesses a significant anti-HBV activity and the preparation of TAT-TR fusion protein has laid the foundation for the use of TR in the therapeutic trial of HBV infection.

Ding J, Liu J, Xue CF, Gong WD, Li YH, Zhao Y. Anti-HBV effect of TAT- HBV targeted ribonuclease. *World J Gastroenterol* 2003; 9(7): 1525-1528
http://www.wjgnet.com/1007-9327/9/1525.asp

INTRODUCTION

The introduction of proteins into mammalian cells has been achieved by transfection of expression vectors, microinjection, or infectious virus, *etc*. Although these approaches have been somewhat successful, the classical manipulation methods are not easily regulated and can be laborious. One approach to resolve these problems is the use of PTD-mediated protein transduction[1, 2]. Linked covalently to proteins, peptides, nucleic acids, or as in-frame fusions with full-length proteins, PTD would let them enter any cell type in a receptor and transporter independent fashion[3]. HIV-TAT is a member of protein transduction domains and appears to possess high level of protein-transduction efficiency[4,5]. TAT fusion proteins were shown to transduce into all cells and tissues present in mice[6], including those present across the blood-brain barrier[7,8]. And many, if not most, proteins may be transduced into cells by using this technology. Therefore, TAT PTD may let us address new questions in preclinical research work and even help in the treatment of human disease.

Hepatitis B is a major world-wide health problem[9-13]. Chronic infection is associated with high risk of liver cirrhosis and primary liver carcinoma[14-22]. Currently available therapies are of limited efficiency[23-35]. HBV targeted ribonuclease (TR) gene, a fusion gene of HBVc and hEDN, was constructed by Liu *et al* in our lab[36], according to the theory of capsid-targeted viral inactivation (CTVI) which is a promising strategy in anti-virus research. HBVc was used as the target molecule, which was the structure protein of HBV and was indispensable during the packaging of HBV particle. The effector molecule was hEDN, a kind of human ribonuclease that can degrade pgRNA of HBV. Transfection of 2.2.15 cells with the eukaryotic expression vector bearing TR gene suggested that TR inhibited the replication of HBV significantly[37]. Therefore, linking HIV-TAT to TR would provide us a more efficient approach to deliver TR into hepatocytes, and greatly help us to utilize TR in the treatment of HBV infection. Reported here are the purification of TAT-TR fusion protein, the identification of its transduction and the anti-HBV effect on the 2.2.15 cells. To confirm its anti-HBV mechanism, we also prepared and purified TAT-TRmut, TAT-hEDN and TAT-HBVc proteins for use as negative controls.

MATERIALS AND METHODS

Materials

Ni-NTA-agrose was purchased from Qiagen Company. PD-10 desalting columns were purchased from Amersham Pharmacia Biotech. Anti-his mAb was from Santa Cruz Company. Protein molecular mass markers, IPTG and G418, imidazole and MTT were all from Sino-American Biotech. RIA HBVeAg assay kit was purchased from Beimian Dongya Biotechnology Institute. 2.2.15 cells was a kind gift of Prof. Cheng, 302 Hospital of Chinese PLA. hEDN was purified by Li *et al*[36]. pTAT-HA/TR, TAT-HA/TRmut, pTAT-HA/hEDN and pTAT-HA/HBVc were all prepared in our Lab[38]. PET-30a/TR, PET-30a/TRmut, PET-30a/HBVc and *E.coli* BL21 (DE3) LysS were maintained in our Lab.

Methods

Expression and purification of TAT fusion proteins pTAT-HA/TR, TAT-HA/TRmut, pTAT-HA/hEDN, pTAT-HA/HBVc and pTAT-HA were employed to transform *E.coli* BL21 (DE3) LysS by using $CaCl_2$ perforation. The transformants were separately cultured in 3 mL TB amp (100 μg/L) at 37 ℃ overnight. 100 μL culture was inoculated into 10 mL fresh TB amp, and incubated for up to 4 hours at 37 ℃. Then IPTG was added to each tube to a final concentration of 100 μmol/L, and the culture was incubated for an additional 4 hours. The induced cells were harvested by centrifugation, and cell lysates were analyzed by 120 g/L SDS-PAGE. The his-tagged fusion

proteins were purified by using Ni-NTA-agrose and PD-10 desalting columns according to the manufacturer's recommendations (Qiagen and Amersham Pharmacia). The purified proteins were analyzed by 120 g/L SDS-PAGE.

Expression and purification of proteins without TAT PTD PET-30a/TR, pET-30a/TRmut, and pET-30a/HBVc transformed *E.coli* BL21 (DE3) LysS. After the analysis of expression levels, the three proteins were purified in the same way as for TAT fusion proteins.

Culture of 2.2.15 cells Cells were cultured in DMEM containing 150 mL/L fetal bovine serum at 37 ℃ in 50 mL/L CO_2 and 100 mg/L G418.

Identification of TAT fusion protein transduction 2.2.15 cells (2×10^8/L) were plated into 6-well plates with coverships, and allowed to adhere for 24 hours. TAT-TR, TAT-TRmut, TAT-hEDN, TAT-HBVc, TR, TRmut, hEDN and HBVc were added into the wells, respectively, at the final concentration of 100 nmol/L. Incubated for 30 min at 37 ℃, all cells were immediately washed with sterile PBS (pH8.0), fixed in 20 g/L paraformaldehyde and 1 g/L TritonX-100 diluted in PBS and put on ice for 30 min. Cells were washed three times with cold PBS. Non-specific epitopes were blocked by using 10 g/L BSA for 10 min at 42 ℃. Cells were washed three times with cold PBS, and then incubated with mouse anti-His mAb (1:500) for 15 min at 42 ℃. After washing three times in cold PBS, the rabbit anti-mouse IgG labeled with FITC (1:1 000) was added to each well and incubated for 10 min at 42 ℃. Rinsed with PBS for 1 hour and the coverships were mounted on slides by using 500 mL/L glycerol. The cells were observed by fluorescence microscopy.

Determination of anti-HBV effect of TAT-TR 2.2.15 cells were plated at the density of 2×10^8/L into 12-well plates. TAT-TR, TAT-TRmut, TAT-hEDN and TAT-HBVc were added into the wells, respectively, at the final concentration of 100 nmol/L. 20 μL DMEM was added into wells as mock group. Four parallels were set up for each group. 24 hours later, HBVeAg in the supernatant was determined by using spRIA kit as described by the manufacturer.

MTT assay 2.2.15 cells were plated at the density of 2×10^8/L into 96-well plates. After 24 hours, TAT-TR, TAT-TRmut, TAT-HEDN, TAT-HBVc were added into (A), (B), (C), (D) groups at the final concentration of 100 nmol/L. 20 μL DMEM was added into well (E). 72 hours later, the morphology of cells was observed through inverted microscopy and MTT was applied in each well at the final concentration of 5 g/L. After another 4 hours' culturing, 150 μL DMSO was added into all wells and the light absorbance at A_{490} was detected.

Statistical analysis

All data obtained were processed by SPSS software. $P<0.05$ was considered statistically significant.

RESULTS

Expression and purification of TAT fusion proteins

In order to obtain the fusion proteins, pTAT-HA/TR, pTAT-HA/TRmut, pTAT-HA/hEDN and pTAT-HA/HBVc were used to transform *E.coli* BL21 (DE3) LysS and expressed with the induction of IPTG. The same strain transformed by pTAT-HA was used as negative control. The expression levels were determined by 120 g/L SDS-PAGE. Four predicted new bands could be detected in the lysates of TAT fusion transformants, but not in the control. Then the proteins were purified by using Ni-NTA affinity columns and PD-10 desalting columns (Figure 1). The degrees of purity of the fusion proteins were 90 %, 88 %, 80 % and 85 % respectively.

Expression and purification of proteins without TAT PTD

In a similar fashion, pET-30a/TR, pET-30a/TRmut and pET-30a/HBVc were induced to express proteins without TAT PTD by IPTG in BL21 (DE3) LysS, and they produced proteins with predicted molecular masses (Figure 2). Then the proteins were purified by using Ni-NTA affinity columns and PD-10 desalting columns. The degrees of purity of the fusion proteins were 88 %, 76 % and 81 % respectively.

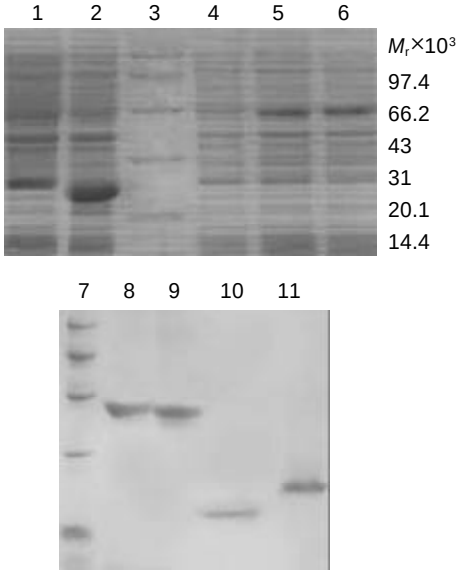

Figure 1 SDS-PAGE analysis of expression and purification for TAT fusion proteins. 1: Transformed by pTAT-HA /HBVc; 2: Transformed by pTAT-HA /hEDN; 3: Protein marker; 4: Transformed by pTAT-HA; 5: Transformed by pTAT-HA/TR; 6: Transformed by pTAT-HA/TRmut; 7: Protein marker; 8: Purified TAT-TN; 9: Purified TAT-TNmut; 10: Purified TAT-hEDN; 11. Purified TAT-HBVc.

Identification of protein transduction

To evaluate the fusion proteins' transduction ability in crossing the membrane of 2.2.15 cells. TAT-TR, TAT-TR mut, TAT-hEDN and TAT-HBVc were added in the culture media at the final concentration of 100 nmol/L. TR, TRmut, hEDN and HBVc without TAT PTD were used as negative controls. Under the fluorescence microscope, abundant fluorescence could be seen in cytoplasm of the cells transduced with TAT fusion proteins, but no fluorescence could be found in the control cells (Figure 3). This result clearly suggests that TAT fusion proteins could cross the membrane of 2.2.15 cells with high efficiency.

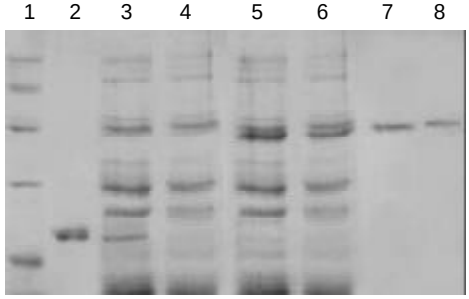

Figure 2 SDS-PAGE analysis of purified control proteins. 1: Protein marker; 2: Purified HBVc; 3: Expression product of BL21 transformed by pET30-a/HBVc; 4: Expression product of BL21 transformed by pET30-a; 5: Expression product of BL21 transformed by pET30-a /TR; 6. Expression product of BL21 transformed by pET30-a/TRmut; 7: Purified TR; 8: Purified TRmut.

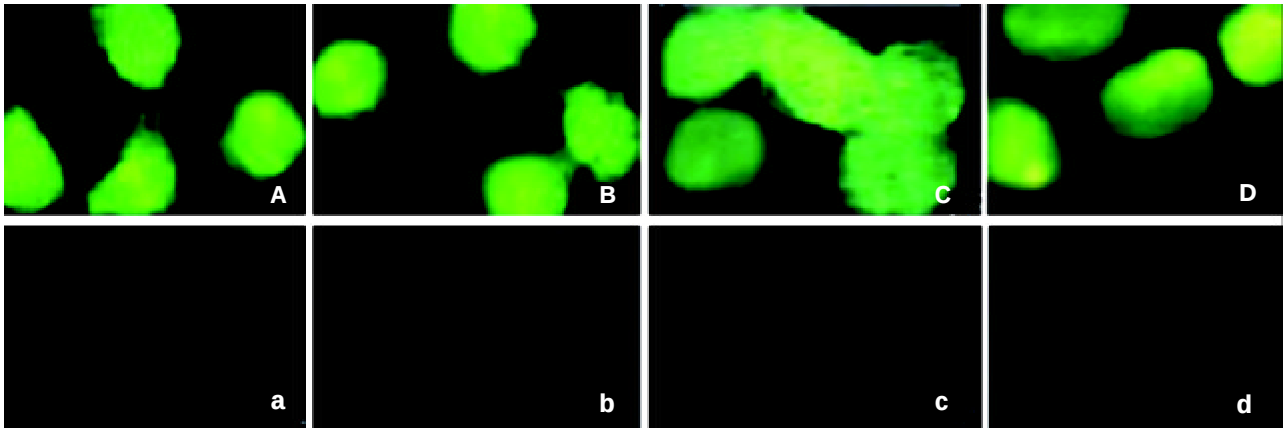

Figure 3 Detection of the transduction of the TAT fusion proteins in 2.2.15 cells. A: Added with TAT-TR; B: Added with TAT-hEDN; C: Added with TAT-HBVc; D: Added with TAT-TRmut; a: Added with TR; b: Added with hEDN; c: Added with HBVc; d: Added with TRmut.

Analysis of anti-HBV activity for TAT-TR

Statistical analysis with SPSS software showed that the mean HBeAg concentration of the TAT-TR group decreased significantly as compared with control groups (The mean difference is significant at the 0.05 level). In addition, there is no significant difference among the mean concentration of control groups (P>0.05). The HBeAg concentration of TAT-TR group decreased by 60.3 % (Figure 4).

MTT assay

After 72 hours culture, the morphology of cells was observed under inverted microscope and it was found that there was no discernable difference among the four experiment groups and the DMEM control. MTT assay showed no significant difference among the five groups. Their A_{490} absorbance values ($\bar{x}\pm s$, n=4) were 0.4875±0.018, 0.4675±0.022, 0.4690±0.028, 0.4800±0.029 and 0.4855±0.050, respectively, (P>0.05).

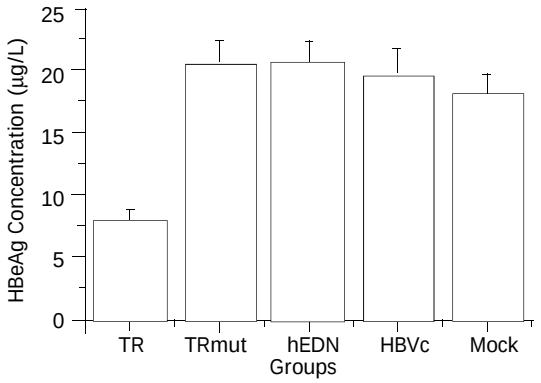

Figure 4 Comparison of HBeAg concentration between different groups.

DISCUSSION

The transduction of proteins into cells was first described in 1988 independently by Green *et al*[39] and Frankel *et al*[40]. In 1994, Faweell *et al*[5] expanded these observations by demonstrating that heterologous proteins chemically cross-linked to a 36 amino acid domain of TAT were able to transduce into cells. Subsequent to the TAT discovery, other transduction domains were identified that resided in the Antennapedia (Antp) protein from Drosophila[41] and HSV VP22 protein from HSV[42]. Although the exact mechanism of protein transduction across the cellular membrane remains unclear, PTD's widespread application has been realized. TAT-mediated transduction provides several advantages over DNA transfection, the current standard method of intracellular protein expression. Importantly, all eukaryotic cell types tested to date are susceptible to transduction, even osteoclasts, primary cells and peripheral-blood mononuclear cells, which are impervious to DNA transfection and retroviral infection, can be effectively transduced[43,44]. Additionally, as transduction occurs so rapidly (15 min rather than 12 h in serum-free media for transfection), issues of timing can be addressed. The exact intracellular concentration can also be controlled precisely just by varying the amount added to the culture medium. Furthermore, every cell in the population appears to contain a near-identical intracellular protein level[3]. Another dominant advantage of the system allows denatured fusion protein be directly applied without the laborious renature course, and thus it also provides much convenience for protein purification. Once transduced inside the cells, the denatured proteins can be correctly refolded by chaperones[45], and are capable of binding their cognate intracellular targets and performing biochemical functions.

To explore the feasibility of using PTD in the anti-HBV research work and provide an alternative strategy for treatment of hepatitis B in this study, we prepared and purified the TAT-TR fusion protein, and also other control proteins. Transduction of TAT-fusion proteins was detected by immunofluorescence assay. Strong fluorescence appeared in the cytoplasm of the cells applied with four TAT fusion proteins, but not in the control groups. These results showed the high transduction efficiency of TAT fusion proteins. We also investigated TAT-TR's anti-HBV activity by radioimmunoassay and got an exciting result. As compared with the mock group, concentration of HBeAg in TAT-TR group decreased by 60.3 %, which indicated that the purified TAT-TR possessed a potent anti-HBV activity. There was no significant difference between any other group and the mock group, suggesting HBVc or hEDN alone had no effect on HBV replication, and TRmut, a fusion molecule of HBVc with an inactivated mutant hEDN, also had no inhibitory effect. These further confirmed the anti-HBV mechanism of the HBV targeted ribonuclease. While TR was transduced into 2.2.15 cells, it could be packaged into the HBV core particles by HBVc, and then hEDN, as a ribonuclease, could degrade the pgRNA packed in the core particles, thus inhibiting the replication of HBV. We performed MTT assay to reveal whether the TAT fusion proteins were harmful to 2.2.15 cells, and the results indicate that they did not affect the growth of 2.2.15 cells and the purified TAT-TR may be applied *in vivo*. Therefore, we conclude that the TAT-HBV targeted ribonuclease fusion protein obtained in this study has laid the foundation for using TR in the therapy of HBV infection.

REFERENCES

1 **Becker-Hapak M**, McAllister SS, Dowdy SF. TAT-mediated protein transduction into mammalian cells. *Methods* 2001; **24**: 247-256
2 **Schwarze SR**, Dowdy SF. *In vivo* protein transduction: intracellular delivery of biologically active proteins, compounds and DNA. *Trends Pharmacol Sci* 2000; **21**: 45-48
3 **Schwarze SR**, Hruska KA, Dowdy SF. Protein transduction: unrestricted delivery into all cells? *Trends Cell Biol* 2000; **10**: 290-295
4 **Vives E**, Brodin P, Lebieu B. A truncated HIV-1 Tat protein basic domain rapidly translocates through the plasma membrane and accumulates in the cell nucleus. *J Biol Chem* 1997; **272**: 16010-16017
5 **Fawell S**, Seery J, Daikh Y, Moore C, Chen LL, Pepinsky B, Barsoum J. Tat-mediated delivery of heterologous proteins into cells. *Proc Natl Acad Sci USA* 1994; **91**: 664-668
6 **Schwarze SR**, Ho A, Vocero-Akbani A, Dowdy SF. *In vivo* protein transduction: delivery of a biologically active protein into the mouse. *Science* 1999; **285**: 1569-1572
7 **Nagahara H**, Vocero-Akbani AM, Snyder EL, Ho A, Latham DG, Lissy NA, Becker-Hapak M, Ezhevsky SA, Dowdy SF. Transduction of full-length TAT fusion proteins into mammalian cells: TAT-p27kip1 induces cell migration. *Natl Med* 1998; **4**: 1449-1452
8 **Chellaiah MA**, Soga N, Swanson S, McAllister S, Alvarez U, Wang D, Dowdy SF, Hruska KA. Rho-A is critical for osteoclast podosome organization, motility and bone resorption. *Biol Chem* 2000; **275**: 11993-12002
9 **Shi H**, Wang FS. Host factors in chronicity of hepatitis B virus infection and their significances in clinic. *Shijie Huaren Xiaohua Zaizhi* 2001; **9**: 66-69
10 **Befeler AS**, Di Bisceglie AM. Hepatitis B. *Infect Dis Clin North Am* 2000; **14**: 617-632
11 **Maddrey WC**. Hepatitis B: an important public health issue. *J Med Virol* 2000; **61**: 362-366
12 **Lau GK**. Hepatitis B infection in China. *Clin Liver Dis* 2001; **5**: 361-379
13 **Merican I**, Guan R, Amarapuka D, Alexander MJ, Chutaputti A, Chien RN, Hasnian SS, Leung N, Lesmana L, Phiet PH, Sjalfoellah Noer HM, Sollano J, Sun HS, Xu DZ. Chronic hepatitis B virus infection in Asian countries. *J Gastroenterol Hepatol* 2000; **15**: 1356-1361
14 **Guo SP**, Wang WL, Zhai YQ, Zhao YL. Expression of nuclear factor-kappa B in hepatocellular carcinoma and its relation with the X protein of hepatitis B virus. *World J Gastroenterol* 2001; **7**: 340-344
15 **Shi DR**, Lu L, Wang JH, Dong CL, Cong WT. HBV DNA distibution of hepatitis B virus in pancreas and liver of patients with cirrhosis. *Shijie Huaren Xiaohua Zazhi* 2000; **8**: 751-754
16 **Wu C**, Cheng ML, Ding YS, Liu RC, Li J, Wang WL, Hu L. A five -year fellow up survey of risk factor of viral hepatic cirrhosis. *Shijie Huaren Xiaohua Zazhi* 2000; **8**: 1365-1367
17 **Wang HY**, Yan RQ, Long JB, Wu QL. Cyclin D1 amplification is associated with HBV DNA intergration and pathology in human hepatocellular carcinoma. *Shijie Huaren Xiaohua Zazhi* 1999; **7**: 98-100
18 **Fan ZR**, Yang DH, Qin HR, Huang CC, Xu C, Qiu QL. Expression of IGF-I, IGF-I receptor mRNA in hepatocellular carcinomas and adjacent nontumor tissue. *Shijie Huaren Xiaohua Zazhi* 1999; **7**: 848-850
19 **Yan JC**, Ma Y, Chen WB, Shun XH. Pathological significance of expression of intrahepatic smooth muscle fiber in hepatitis B. *Shijie Huaren Xiaohua Zazhi* 2000; **8**: 1242-1246
20 **Zhai SH**, Liu JB, Liu YM, Zhang LL, Du ZH. Expression of HBsAg, HCV-Ag and AFP in liver cirrhosis and hepatocarcinoma. *Shijie Huaren Xiaohua Zazhi* 2000; **8**: 524-527
21 **Feitelson MA**. Hepatitis B virus in hepatocarcinogenesis. *J Cell Physiol* 1999; **181**: 188-202
22 **Arbuthnot P**, Kew M. Hepatitis B virus and hepatocellular carcinoma. *Int J Exp Pathol* 2001; **82**: 77-100
23 **Zhuang L**, You J, Tang BZ, Ding SY, Yan KH, Peng D, Zhang YM, Zhang L. Preliminary results of Thymosin-a1 versus interferon-á-treatment in patient with HBeAg negative and serum HBV DNA positive chronic hepatitis B. *World J Gastroenterol* 2001; **7**: 407-410
24 **Xie Q**, Guo Q, Zhou XQ, Gu RY. Effect of adenine arabinoside monophosphate coupled to lactosaminated human serum albumin on duck hepatitis B virus. *Shijie Huaren Xiaohua Zazhi* 1999; **7**: 125-126
25 **Li J**, Tang B. Effect on replication of hepatitis B virus by Chinese traditional medicine. *Shijie Huaren Xiaohua Zazhi* 2000; **8**: 945-946
26 **Zhu Y**, Wang YL, Shi L. Clinical analysis of the efficacy of interferon alpha treatment of hepatitis. *World J Gastroenterol* 1998; **4**:85-86
27 **Xu KC**, Wei BH, Yao XX, Zhang WD. Recently therapy for chronic hepatitis B virus by combined traditional Chinese and Western medicine. *Shijie Huaren Xiaohua Zaizhi* 1999; **7**: 970-974
28 **Lau GK**. Use of immunomodulatory therapy (other than interferon) for the treatment of chronic hepatitis B virus infection. *J Gastroenterol Hepatol* 2000; **15**(Suppl): E46-52
29 **Guan R**. Interferon monotherapy in chronic hepatitis B. *J Gastroenterol Hepatol* 2000; **15** (Suppl): E34-40
30 **Torresi J**, Locarnini S. Antiviral chemotherapy for the treatment of hepatitis B virus infections. *Gastroenterology* 2000; **118** (Suppl): S83-103
31 **Schiff ER**. Lamivudine for hepatitis B in clinical practice. *J Med Virol* 2000; **61**: 386-391
32 **Jarvis B**, Faulds D. Lamivudine. A review of its therapeutic potential in chronic hepatitis B. *Drugs* 1999; **58**: 101-141
33 **Malik AH**, Lee WM. Chronic hepatitis B virus infection: treatment strategies for the next millennium. *Ann Intern Med* 2000; **132**: 723-731
34 **Farrell GC**. Clinical potential of emerging new agents in hepatitis B. *Drugs* 2000; **60**: 701-710
35 **Song YH**, Lin JS, Liu NZ, Kong XJ, Xie N, Wang NX, Jin YX, Liang KH. Anti-HBV hairpin ribozyme-mediated cleavage of target RNA *in vitro*. *World J Gastroenterol* 2002; **8**: 91-94
36 **Li YH**, Liu J, Xue CF. Construction of HBV targeted ribonuclease and its expression in 2.2.15 cell line. *Xibao Yu Fenzi Mianyixue Zazhi* 2002; **18**: 217-220
37 **LiuJ**, Li YH, Xue CF, Ding J, Gong WD, Zhao Y. HBV targeted ribonuclease can inhibit HBV replication. *World J Gastroenterol* 2003; **9**: 295-299
38 **Ding J**, Liu J, Xue CF, Li YH, Gong WD. Construction and expression of prokaryotic expression vector for pTAT-HBV targeted ribonuclease fusion protein. *Xibao Yu Fenzi Mianyixue Zazhi* 2003; **19**: 49-51
39 **Green M**, Loewenstein PM. Automomous functional domains of chemically synthesized human immunodeficiency virus tat trans-activator protein. *Cell* 1988; **55**: 1179-1188
40 **Frankel AD**, Pabo Co. Cellular uptake of the tat protein from human immunodeficiency virus. *Cell* 1988; **55**: 1189-1193
41 **Derossi D**, Joliot AH, Chassaing G, Prochiantz A. The third helix of the Antennapedia homeodomain translocates through biological membranes. *J Biol Chem* 1994; **269**: 10444-10450
42 **Elloit G**, O'Hare P. Intercellular trafficking and protein delivery by a herpesvirus structural protein. *Cell* 1997; **88**: 223-233
43 **Chellaiah MA**, Soga N, Swanson S, McAllister S, Alvarez U, Wang D, Dowdy SF, Hruska KA. Rho-A is critical for osteoclast podosome organization, motility, and bone resorption. *J Biol Chem* 2000; **275**: 11993-2002
44 **Schutze-Redelmeier MP**, Gournier H, Garcia-Pons F, Moussa M, Joliot AH, Volovitch M, Prochiantz A, Lemonnier FA. Introduction of exogenous antigens into the MHC class I processing and presentation pathway by Drosophila antennapedia homeodomain primes cytotoxic T cells *in vivo*. *J Immunol* 1996; **157**: 650-655
45 **Gottesman S**, Wickner S, Maurizi MR. Protein quality control: triage by chaperones and proteases. *Genes Dev* 1997; **11**: 815-823

Edited by Lu HM

P.O.Box 2345, Beijing 100023,China
Fax: +86-10-85381893
E-mail: wjg@wjgnet.com www.wjgnet.com

World J Gastroenterol 2003;9(7):1529-1536
World Journal of Gastroenterology
 ISSN 1007-9327

Construction of hpaA gene from a clinical isolate of *Helicobacter pylori* and identification of fusion protein

Ya-Fei Mao, Jie Yan, Li-Wei Li, Shu-Ping Li

Ya-Fei Mao, Jie Yan, Li-Wei Li, Shu-Ping Li, Department of Medical Microbiology and Parasitology, College of Medical Sciences, Zhejiang University, Hangzhou 310031, Zhejiang Province, China
Supported by the Excellent Young Teacher Fund of Chinese Education Ministry and the General Research Plan of Science and Technology Department of Zhejiang Province, No. 001110438
Correspondence to: Dr. Jie Yan, Department of Medical Microbiology and Parasitology, College of Medical Sciences, Zhejiang University, 353 Yan an Road, Hangzhou 310031, Zhejiang Province, China. yanchen@mail.hz.zj.cn
Telephone: +86-571-87217385 **Fax:** +86-571-87217044
Received: 2003-03-02 **Accepted:** 2003-03-28

Abstract

AIM: To clone hpaA gene from a clinical strain of *Helicobacter pylori* and to construct the expression vector of the gene and to identify immunity of the fusion protein.

METHODS: The hpaA gene from a clinical isolate Y06 of *H. pylori* was amplified by high fidelity PCR. The nucleotide sequence of the target DNA amplification fragment was sequenced after T-A cloning. The recombinant expression vector inserted with hpaA gene was constructed. The expression of HpaA fusion protein in *E.coli* BL21DE3 induced by IPTG at different dosages was examined by SDS-PAGE. Western blot with commercial antibody against whole cell of *H.pylori* as well as immunodiffusion assay with self-prepared rabbit antiserum against HpaA fusion protein were applied to determine immunity of the fusion protein. ELISA was used to detect the antibody against HpaA in sera of 125 patients infected with *H.pylori* and to examine HpaA expression of 109 clinical isolates of *H.pylori*.

RESULTS: In comparison with the reported corresponding sequences, the homologies of nucleotide and putative amino acid sequences of the cloned hpaA gene were from 94.25-97.32 % and 95.38-98.46 %, respectively. The output of HpaA fusion protein in its expression system of pET32a-hpaA-BL21DE3 was approximately 40 % of the total bacterial proteins. HpaA fusion protein was able to combine with the commercial antibody against whole cell of *H.pylori* and to induce rabbit producing specific antiserum with 1:4 immunodiffusion titer after the animal was immunized with the fusion protein. 81.6 % of the serum samples from 125 patients infected with *H.pylori* (102/125) were positive for HpaA antibody and all of the tested isolates of *H.pylori* (109/109) were detectable for HpaA.

CONCLUSION: A prokaryotic expression system with high efficiency of *H.pylori* hpaA gene was successfully established. The HpaA expressing fusion protein showed satisfactory immunoreactivity and antigenicity. High frequencies of HpaA expression in different *H.pylori* clinical strains and specific antibody production in *H.pylori* infected patients indicate that HpaA is an excellent and ideal antigen for developing *H.pylori* vaccine.

Mao YF, Yan J, Li LW, Li SP. Construction of hpaA gene from a clinical isolate of *Helicobacter pylori* and identification of fusion protein. *World J Gastroenterol* 2003; 9(7): 1529-1536
http://www.wjgnet.com/1007-9327/9/1529.asp

INTRODUCTION

In China, chronic gastritis and peptic ulcer are the most prevalent gastric diseases and gastric cancer is one of the malignant tumors with high morbidities[1-34]. *Helicobacter pylori*, a microaerophilic, spiral and gram-negative bacillus, is recognized as a human-specific gastric pathogen that colonizes the stomaches of at least half of the world's populations[35]. Most infected individuals are asymptomatic. However, in some subjects, the infection causes acute, chronic gastritis or peptic ulceration, and plays an important role in the development of peptic ulcer and gastric adenocarcinoma, mucosa-associated lymphoid tissue (MALT) lymphoma and primary gastric non-Hodgkin's lymphoma[36-43]. This organism is categorized as a class I carcinogen pronounced by the World Health Organization[44], and direct evidence of carcinogenesis was recently demonstrated in an animal model[45,46]. Immunization against the bacterium represents a cost-effective strategy to prevent *H.pylori*-associated peptic ulcer diseases and to reduce the incidence of global gastric cancers[47]. The selection of antigenic targets is critical in the design of *H.pylori* vaccine. To date, this field is scarcely touched upon. The majority of studies focused on urease enzyme, heat shock protein, vacuolating cytotoxin, and so on[35,48-50], but rarely on *H. pylori* adhesin (HpaA) which is a flagellar sheath protein with approximately 29KDa located in the bacterial outer membrane[51]. So, in this study, a recombinant plasmid inserted with the gene (hpaA) responsible for encoding HpaA was constructed and the immunogenicity and immunoreactivity of its expression product were examined. Furthermore, the fusion protein of HpaA and its rabbit antiserum were also used to detect serum samples from *H.pylori* infected patients and *H. pylori* isolates, respectively. The results of this study will be helpful for determining whether the recombinant HpaA (rHpaA) becomes one of the good candidates as an antigen in *H.pylori* vaccine.

MATERIALS AND METHODS

Materials

A well-characterized clinical strain of *H.pylori*, provisionally named Y06, was provided by the Department of Medical Microbiology and Parasitology, College of Medical Sciences, Zhejing University. Plasmid pET32a (Promega) and *E.coli* BL21 DE3 (Promega) were used as expression vector and host cell, respectively. The primers for amplification were synthesized by BioAsia (Shanghai, China). EX Taq high fidelity PCR kit and restriction endonucleases were purchased from TaKaRa (Dalian, China). T-A cloning kit and sequencing service were offered by BBST (Shanghai, China). Rabbit antibody against the whole cell of *H.pylori* and HRP-labeling sheep antibodies against rabbit IgG and human IgG were

purchased from DACO and Jackson ImmunoResearch, respectively. The agents used in isolation and identification of *H.pylori* were purchased from Sigma and bioMérieux, etc. 126 biopsy specimens from patients with positive *H.pylori* (86 males and 40 females; age range: 6-78 years; mean age: 40.5 years) for gastroduodenoscopy in four different hospitals in Hangzhou were collected during the period of the end of 2001 to the midyear of 2002. Each of the patients consented to be enrolled in this study and all of them agreed to offer their biopsy samples. Among the 126 patients, 68 suffered from chronic gastritis (CG) in cluding 48 with chronic superficial gastritis, 10 with chronic active gastritis and 10 with chronic atrophic gastritis, and 58 patients suffered from peptic ulcer (PU) in cluding 12 with gastric ulcer, 40 with duodenal ulcer and 6 with gastric and duodenal ulcer. None of the patients had received nonsteroidal anti-inflammatory drugs or antacid drugs and antibiotics within the previous two weeks before the study. At the same time, 126 serum specimens from these patients were also collected.

Methods

Isolation and identification of clinical *H.pylori* strains Each of the biopsy specimens was homogenized with a tissue grinder and then inoculated onto Columbia agar plates supplemented with 8.0 % (V/V) sheep blood, 0.2 % (W/V) cyclodextrin, 5 mg/L trimethoprim, 10 mg/L vancomycin, 2.5 mg/L amphotericin B and 2 500 U/L polymyxin B. The plates were incubated at 37 ℃ under microaerobic conditions (5 % O_2, 10 % CO_2 and 85 % N_2) for 3 to 5 days. Isolates were identified as *H.pylori* according to typical Gram stain morphology, positive biochemical tests for urease and oxidase, and agglutination with commercial rabbit antibody against whole cell of the microbe. All of *H.pylori* isolates were stored at -70 ℃ for ELISA.

Preparation of DNA template Genomic DNA of *H.pylori* strain Y06 was extracted by routine phenol-chloroform method, DNase-free RNase digestion and phenol-chloroform extraction. The DNA template was solved in TE buffer, and its concentration and purity were determined by ultraviolet spectrophotometry[52].

Polymerase chain reaction Oligonucleotide primers were designed to amplify the whole sequence of hpaA gene from *H.pylori* strain Y06 based on the published corresponding genome sequence[51,53]. The sequence of sense primer with an endonuclease site of *BamH* I was: 5' -CCGGGATCCATGA GAGCAAATAATC-3' . The sequence of antisense primer with an endonuclease site of *EcoR* I was: 5' -CCGGAATTCTTCT TATGCGTTATTTG-3' . The total volume of PCR reaction mixture was 100 μL containing 2.5 mol· L^{-1} each dNTP, 250 nmol· L^{-1} each primer, 15 mol· L^{-1} $MgCl_2$, 3.0 U EX Taq polymerase, 200 ng DNA template and 1×PCR buffer (pH8.3). The parameters for PCR were as follows: at 94 ℃ for 5 min, one cycle; at 94 ℃ for 30 sec, at 50 ℃ for 30 sec, at 72 ℃ for 60 sec, 10 cycle; at 94 ℃ for 30 sec, at 50 ℃ for 30 sec, at 72 ℃ for 70 sec (additional 10 sec for each of the following cycles), 20 cycle, at 72 ℃ for 10 min, 1 cycle. The results of PCR were observed under UV light after electrophoresis in 15 g· L^{-1} agarose pre-stained with ethidium bromide. The expected size of target amplification fragment was 802 bp.

Cloning and sequencing The target amplification DNA fragment of hpaA gene was cloned into pUCm-T vector (pUCm-T-hpaA) by using the T-A cloning kit according to the manufacturer' s instructions. The recombinant plasmid was amplified in *E.coli* strain DH5α and then extracted by Sambrook' s method[52]. A professional company (BBST) was responsible for nucleotide sequence analysis of the inserted fragments. Two different strains of *E.coli* DH5α containing pUCm-T-hpaA and expression vector pET32a were amplified respectively and the two plasmids were extracted[52]. The plasmids were digested with *BamH* I and *EcoR* I. The target fragments of hpaA and pET32a were recovered and then ligased. The recombinant expression vector pET32a-hpaA was transformed into *E.coli* BL21DE3. pET32a-hpaA was prepared for sequencing again after the amplification in its host cell.

Expression and identification of the fusion protein The hpaA prokaryotic expression system pET32a-hpaA-BL21DE3 was rotationally cultured in LB medium at 37 ℃ under induction of isopropylthio-β-D-galactoside (IPTG) at different dosages of 1, 0.5 and 0.1 mmol· L^{-1}. The supernatant and precipitate were isolated by centrifugation after the engineering bacterium pellet was ultrasonically broken (300V, 5sec once for three times). The molecular weight, output and location of HpaA fusion protein were examined by SDS-PAGE. HpaA fusion protein was collected by Ni-NTA affinity chromatography. The immunoreactivity of HpaA fusion protein was determined by Western blot with commercial rabbit antibody against whole cell of *H.pylori* and HRP-labeling sheep antibody against rabbit IgG, respectively. Rabbits were immunized with HpaA fusion protein to obtain the antiserum. Immunodiffusion assay was applied to determine antigenicity of the fusion protein.

ELISA The antibodies against HpaA in sera of the patients infected with *H.pylori* were detected by ELISA with HpaA fusion protein at the concentration of 20 μg/mL as coated antigen, the patients' sera (1:200 dilution) as the first antibody, HRP-labeling sheep antibody against human IgG (1:4 000 dilution) as the second antibody and ortho-phenylene diamine as a substrate. The result of ELISA for a patient' s serum sample was considered as positive if its OD_{490} value was over the mean plus 3 SD of 6 cases of negative serum samples[54]. HpaA expression of clinical isolates of *H.pylori* was detected by ELISA using ultrasonic supernatant at the protein concentration of 50 μg/mL of each *H.pylori* isolate as coated antigen, the self-prepared rabbit antiserum against HpaA fusion protein (1:2 000 dilution) as the first antibody, HRP-labeling sheep antibody against rabbit IgG (1:3 000 dilution) as the second antibody and ortho-phenylene diamine as a substrate. The result of ELISA for an *H.pylori* ultrasonic supernatant was considered as positive if its OD_{490} value was over the mean plus 3 SD of 6 cases of ultrasonic supernatant at the same protein concentration of *E.coli* ATCC 25922 played as negative control[54].

Data analysis The nucleotide sequences of the cloned hpaA gene inserted in the two recombinant plasmid vectors were compared for homologies with 6 published hpaA gene sequences (X92502, NC000915, X61574, NC000921, AF479028 and U35455)[51,53,55-58] with a special molecular biological analysis soft ware.

RESULTS

PCR

Target fragment with expected size amplified from DNA template of *H.pylori* strain Y06 is shown in Figure 1.

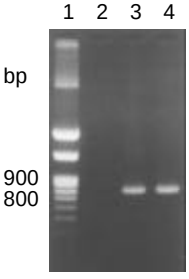

Figure 1 The target fragment of hpaA gene amplified from *H.pylori* strain Y06 (1: 100 bp DNA marker; 2: blank control; 3 and 4: the target fragment amplified from *H.pylori* strain Y06 DNA).

Nucleotide sequence analysis

The hpaA gene nucleotide sequences in the recombinant plasmid vectors of pUCm-T-hpaA and pET32a-hpaA were completely the same. The homologies of the nucleotide and putative amino acid sequences in the pUCm-T-hpaA and pET32a-hpaA compared with the published hpaA gene sequences[51,53,55-58] were from 94.25-97.32 % and 95.38-98.46 %, respectively (Figures 2, 3).

```
[1]1   ATGAGAGCAAATAATCATTTTAAAGATTTTGCATGGAAAAAATGCCTTTTAGGCGCGAGC
[2]1   ....A.....................................................T......
[3]1   ....A.A.....GG.........G.............................A.....
[4]1   ....A.A.....GG.........G.....................T.............
[5]1   ....A.A.....GG.........G.....................................T
[6]1   ....A.A.....GG.........G.....................................
[7]1   ................................................................

[1]61  GTGGTGGCTTTATTAGTGGGATGCAGCCCGCATATTATTGAAACCAATGAAGTCGCTTTG
[2]61  ...........G.....................................................
[3]61  ....................G..............................G.........
[4]61  ....................G..T..........................T......
[5]61  ................................................................
[6]61  ....G...........................................................
[7]61  ...........G..G..................................................

[1]121 AAATTGAATTACCATCCAGCTAGCGAGAAAGTTCAAGCGTTAGATGAAAAGATTTTGCTT
[2]121 ................................................................
[3]121 ............................G...................................
[4]121 ...........................................................A...
[5]121 ................................................................
[6]121 ..G.............................................................
[7]121 ...........................................................C......

[1]181 TTAAGGCCAGCTTTCCAATATAGCGATAATATCGCTAAAGAGTATGAAAACAAATTCAAG
[2]181 ..............T.....C...........T.........................
[3]181 ....A.............C........C..T.................T.........
[4]181 ....................C...........T.........................
[5]181 ....................C...........T.........................
[6]181 ..............T.....C...........T.........................
[7]181 ..............T.....C...........T.........................

[1]241 AATCAAACCGCGCTCAAGGTTGAACAGATTTTGCAAAATCAAGGCTATAAGGTTATTAGC
[2]241 ...........................................G................
[3]241 .........A....T..A......G....C...........G.....C........C.AT
[4]241 .........A....T..A......G....C...........G................AT
[5]241 ...........................................G.....C........C.AT
[6]241 ..........T..............................G................AT
[7]241 .........A....T.........G....C............................

[1]301 GTAGATAGCAGCGATAAAGACGATTTTTCTTTTGCACAAAAAAAAAGAAGGGTATTTGGCG
[2]301 ........................C........T.G......................T
[3]301 ..G..............................G.......................
[4]301 ..G..............................G......................T
[5]301 ..G.....T........................G.......................
[6]301 ..G..............................G......................T
[7]301 ........................C........T.G......................C

[1]361 GTTGCTATGAATGGCGAAATTGTTTTACGCCCCGATCCTAAAAGGACCATACAGAAAAAA
[2]361 ................................................................
[3]361 ..........T..............................A.................
[4]361 ..C.............................................................
[5]361 ................................................................
[6]361 ..C...........T..................................................
[7]361 ..C.............................................................
```

```
[1]421 TCAGAACCCGGGTTATTATTCTCCACCGGTTTGGACAAAATGGAAGGGGTTTTAATCCCG
[2]421 ..............G...........T........T.....................A
[3]421 ........................T........T.............C.........
[4]421 ........................T........T.........................
[5]421 ......................T...........T.........................
[6]421 ........T................T.................................
[7]421 ........................T.................................

[1]481 GCTGGGTTTATTAAGGTTACCATACTAGAGCCTATGAGTGGGGAATCTTTGGATTCTTTT
[2]481 ..C......G.C.....................................................
[3]481 ..C..T...G.C.....................................A.....C...
[4]481 .........G.C.....................................................
[5]481 ......................T.......................A.........
[6]481 .........G.C...........T.....................................
[7]481 .........G.C.....................................A.........

[1]541 ACGATGGATTTGAGCGAGTTGGACATTCAAGAAAAATTCTTAAAAACCACCCATTCAAGC
[2]541 .....................................................................
[3]541 ..............T.....A.....................G.....................
[4]541 .....................................................................
[5]541 ........................C.....................................
[6]541 .....................................................................
[7]541 .....................................................................

[1]601 CATAGCGGGGGGTTAGTTAGCACTATGGTTAAGGGAACGGATAATTCTAATGACGCGATC
[2]601 .....................................................................
[3]601 ........A.....................................................T......
[4]601 ........A.........................G...................A..T
[5]601 .....................................................................
[6]601 .....................................................................
[7]601 .....................................................................

[1]661 AAGAGCGCTTTGAATAAGATTTTTGCAAATATCATGCAAGAAATAGACAAAAAACTCACT
[2]661 .....................................................................
[3]661 ............................G..............G..T..G.........
[4]661 ............................G..............G..T..G.........
[5]661 ..............C.....................................................
[6]661 ........................G..G.....................................
[7]661 .....................................................G......

[1]721 CAAAAGAATTTAGAATCTTATCAAAAAGACGCCAAAGAATTAAAAGGCAAAAGAAACCGA
[2]721 ...................................G.........................
[3]721 ....G..............................G.....G...AA...G.........
[4]721 ....G..............................G.........AA...G.........
[5]721 ...................................G.....G...AA...G.........
[6]721 .....................................................................
[7]721 ...................................G.....G...AA...G.........

[1]781 TAAAAACAAATAACGCATAA
[2]781 ...
[3]781 ....G..............
[4]781 ...................
[5]781 ...
[6]781 ...................
[7]781 TAA.G..............GAA
```

Figure 2 Homology comparison of *H.pylori* hpaA gene nucleotide sequences ([1]-[6]: the reported sequence from GenBank (No. X92502, strain 11637; No. NC000915, strain 26695; No. X61574, strain 8826; No. NC_000921, strain J99; No. AF479028, strain CH-CTX1; No. U35455, strain CCUG 17874); [7]: the sequencing result of *H.pylori* strain Y06 hpaA gene. outline region: oligonucleotide primer sequences; square frame: start code and end code).

```
[1]1   MRANNHFKDFAWKKCLLGASVVALLVGCSPHIIETNEVALKLNYHPASEKVQALDEKILL
[2]1   .K..........................................................
[3]1   .KT.G............T.........................................
[4]1   .KT.G.........F.............................................
[5]1   .KT.G..........................................................
[6]1   .KT.G..............G.....................................
[7]1   ..........................................................

[1]61  LRPAFQYSDNIAKEYENKFKNQTALKVEQILQNQGYKVISVDSSDKDDFSFAQKKEGYLA
[2]61  ..............................................L..S........
[3]61  .K.....................T....E.........N...................
[4]61  ......................T....E.........N...................
[5]61  ........................................N...................
[6]61  ......................V..............N...................
[7]61  ......................T....E..................L..S........

[1]121 VAMNGEIVLRPDPKRTIQKKSEPGLLFSTGLDKMEGVLIPAGFIKVTILEPMSGESLDSF
[2]121 ........................................V................
[3]121 ...I....................................V................
[4]121 ........................................V................
[5]121 ..........................................................
[6]121 ........................................V................
[7]121 ........................................V................

[1]181 TMDLSELDIQEKFLKTTHSSHSGGLVSTMVKGTDNSNDAIKSALNKIFANIMQEIDKKLT
[2]181 ..........................................................
[3]181 ..................................................S....M.....
[4]181 ..................................................S....M.....
[5]181 ..........................................................
[6]181 ..................................................GS.........
[7]181 ..........................................................

[1]241 QKNLESYQKDAKELKGKRNR
[2]241 ....................
[3]241 ..............N....
[4]241 .R............N....
[5]241 ..............N....
[6]241 ....................
[7]241 ..............N....
```

Figure 3 Homology comparison of the putative amino acid sequences of hpaA gene ([1]-[6]: the reported sequence from GenBank (No. X92502, strain 11637; No. NC000915, strain 26695; No. X61574, strain 8826; No. NC_000921, strain J99; No. AF479028, strain CH-CTX1; No. U35455, strain CCUG 17874); [7]: the sequencing result of Hp strain Y06 hpaA gene).

Expression of target fusion protein

1, 0.5 and 0.1 mmol· L^{-1} of IPTG were able to efficiently induce the expression of HpaA fusion protein in pET32a-hpaA-BL21DE3 system. The product of HpaA fusion protein was mainly presented in ultrasonic precipitate and the output was approximately 40 % of the total bacterial proteins (Figure 4).

Immunoreactivity and antigenicity of HpaA fusion protein

The commercial rabbit antibody against the whole cell of *H.pylori* could combine with HpaA fusion protein confirmed by Western blot (Figure 5) and the titer demonstrated by immunodiffusion assay between HpaA fusion protein and rabbit antiserum against the fusion protein was 1:4.

ELISA

The mean ±SD at OD_{490} of the negative serum samples was 0.11±0.03 and the positive reference value was 0.20. The mean ±SD at OD_{490} of the negative bacterial control was 0.04±0.04 and the positive reference value was 0.16. According to the reference values, 81.6 % (102/125, another serum sample was

contaminated) of the tested patients' serum samples were positive for antibodies against HpaA fusion protein with a range of 0.54-1.84 and 100 % (109/109, other 17 isolates could not be revived from -70 ℃) of the tested *H.pylori* isolates were detectable for HpaA with a range of 0.52-1.47.

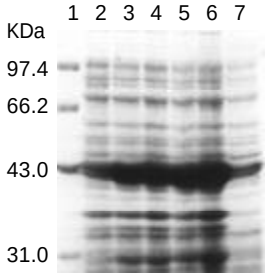

Figure 4 Expression of HpaA gene in pET32a-hpaA-BL21DE3 induced by IPTG with different dosages shown in SDS-PAGE (1: protein marker; 2: non-induced; 3-5: induced with 0.1, 0.5, 1 mmol·L^{-1} of IPTG, respectively; 6: the bacterial precipitate induced with 1 mmol·L^{-1} of IPTG; 7: the bacterial supernatant induced with 1 mmol·L^{-1} of IPTG).

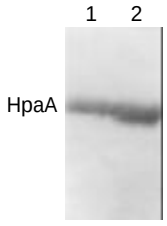

Figure 5 Western blot result of commercial rabbit antibody against whole cell of *H.pylori* and HpaA fusion protein (1 and 2: 20 μl and 40 μl of expressed HpaA product induced with 0.1 mmol·L^{-1} of IPTG, respectively).

DISCUSSION

The outer membrane is a continuous structure on the surface of gram-negative bacteria. For outer membrane proteins in the outer monolayer of bacterial membrane, they have bilateral particular significance as a potential target for protective immunity and bacterial pathogens. Outer membrane vaccines have been used with considerable success to induce protection against a number of organisms, including heat shock protein, vacuolating cytotoxin, ureases A, B of *H.pylori* and so on[59-65]. HpaA is one of the major structural outer membrane proteins of *H.pylori* and plays an important role in adhesion of the microbe[51,53]. HpaA gene is located in genome DNA of *H.pylori* and considerably conservative for its nucleotide and amino acid sequences[55,56]. Furthermore, antibody against HpaA could be found in approximately 86 % of *H.pylori* infected patients' sera and this proportion was obviously higher than that of heat shock protein (68 %) and vacuolating cytotoxin (68 %)[57] and was similar to that of urease B[64]. Therefore, HpaA is an ideal antigen candidate for *H.pylori* vaccine.

In this study, the homologies of the nucleotide and putative amino acid sequences in the cloned HpaA gene from *H.pylori* strain Y06 compared with the 6 published hpaA gene sequences[51, 53, 55-58] were as high as 94.25-97.32 % and 95.38-98.46 %, respectively, whereas the nucleotide and putative amino acid homologies among the 6 HpaA gene sequences were 93.72-98.21 % and 95.00-98.78 %. These data indicate that the mutation level of the HpaA gene of *H.pylori* strain Y06 is within the range reported by the literatures.

The results of SDS-PAGE demonstrated that the constructed expression system pET32a-hpaA-BL21DE3 was able to efficiently produce the target fusion protein presented with the form of inclusion body even if induced by IPTG at lower concentration of 0.1 mmol· L^{-1} and the output was approximately 40 % of the total bacterial proteins.

The rabbit antibody against the whole cell of *H.pylori* could recognize and combine with HpaA fusion protein confirmed by Western blot, indicating that the fusion protein has an active and satisfactory immunoreactivity. The immunodiffusion assay performed in this study demonstrated that HpaA fusion protein could efficiently induce rabbit to produce specific antibody with a higher titer against the fusion protein, which indicates that HpaA fusion protein has favorable antigenicity. The results of ELISA showed that all of the tested clinical isolates of *H.pylori* would express HpaA and the majority of *H.pylori* infected patients' sera (81.6 %) were present for the specific antibody against the microbe.

All the evidences mentioned above suggest that HpaA is an excellent and ideal antigen for developing *H.pylori* vaccine and an HpaA expression system with high efficiency was successfully constructed in this study.

REFERENCES

1 **Ye GA**, Zhang WD, Liu LM, Shi L, Xu ZM, Chen Y, Zhou DY. *Helicobacter pylori* vacA gene polymorphism and chronic gastrisis. *Shijie Huaren Xiaohua Zazhi* 2001; **9**: 593-595
2 **Lu SY**, Pan XZ, Peng XW, Shi ZL. Effect of *Hp* infection on gastric epithelial cell kinetics in stomach diseases. *Shijie Huaren Xiaohua Zazhi* 1999; **7**: 760-762
3 **Zhang Z**, Yuan Y, Gao H, Dong M, Wang L, Gong YH. Apoptosis, proliferation and p53 gene expression of *H.pylori* associated gastric epithelial lesions. *World J Gastroenterol* 2001; **7**: 779-782
4 **Lu XL**, Qian KD, Tang XQ, Zhu YL, Du Q. Detection of *H.pylori* DNA in gastric epithelial cells by in situ hybridization. *World J Gastroenterol* 2002; **8**: 305-307
5 **Yao YL**, Xu B, Song YG, Zhang WD. Overexpression of cyclin E in Mongolian gerbil with *Helicobacter pylori*-induced gastric precancerosis. *World J Gastroenterol* 2002; **8**: 60-63
6 **Guo DL**, Dong M, Wang L, Sun LP, Yuan Y. Expression of gastric cancer-associated MG7 antigen in gastric cancer, precancerous lesions and *H. pylori*-associated gastric diseases. *World J Gastroenterol* 2002; **8**: 1009-1013
7 **Peng ZS**, Liang ZC, Liu MC, Ouyang NT. Studies on gastric epithelial cell proliferation and apoptosis in *Hp* associated gastric ulcer. *Shijie Huaren Xiaohua Zazhi* 1999; **7**: 218-219
8 **Hiyama T**, Haruma K, Kitadai Y, Miyamoto M, Tanaka S, YoshiharanM, Sumii K, Shimamoto F, Kajiyama G. B-cell monoclonality in *Helicobacter pylori*-associated chronic atrophic gastritis. *Virchows Arch* 2001; **483**: 232-237
9 **Xia HHX**. Association between *Helicobacter pylori* and gastric cancer: current knowledge and future research. *World J Gastroenterol* 1998; **4**: 93-96
10 **Quan J**, Fan XG. Progress in experimental research of *Helicobacter pylori* infection and gastric carcinoma. *Shijie Huaren Xiaohua Zazhi* 1999; **7**: 1068-1069
11 **Liu HF**, Liu WW, Fang DC. Study of the relationship between apoptosis and proliferation in gastric carcinoma and its precancerous lesion. *Shijie Huaren Xiaohua Zazhi* 1999; **7**: 649-651
12 **Zhu ZH**, Xia ZS, He SG. The effects of ATRA and 5-Fu on telomerase activity and cell growth of gastric cancer cells *in vitro*. *Shijie Huaren Xiaohua Zazhi* 2000; **8**: 669-673
13 **Tu SP**, Zhong J, Tan JH, Jiang XH, Qiao MM, Wu YX, Jiang SH. Induction of apoptosis by arsenic trioxide and hydroxy camptothecin in gastric cancer cells *in vitro*. *World J Gastroenterol* 2000; **6**: 532-539
14 **Cai L**, Yu SZ, Zhang ZF. *Helicobacter pylori* infection and risk of gastric cancer in Changle County, Fujian Province, China. *World J Gastroenterol* 2000; **6**: 374-376
15 **Yao XX**, Yin L, Zhang JY, Bai WY, Li YM, Sun ZC. Htert expression and cellular immunity in gastric cancer and precancerosis. *Shijie Huaren Xiaohua Zazhi* 2001; **9**: 508-512
16 **Xu AG**, Li SG, Liu JH, Gan AH. Function of apoptosis and ex-

pression of the proteins *Bcl*-2, *p*53 and *C-myc* in the development of gastric cancer. *World J Gastroenterol* 2001; **7**: 403-406

17 **Wang X**, Lan M, Shi YQ, Lu J, Zhong YX, Wu HP, Zai HH, Ding J, Wu KC, Pan BR, Jin JP, Fan DM. Differential display of vincristine-resistance-related gene in gastric cancer SGC7901 cells. *World J Gastroenterol* 2002; **8**: 54-59

18 **Liu JR**, Li BX, Chen BQ, Han XH, Xue YB, Yang YM, Zheng YM, Liu RH. Effect of cis-9, trans-11-conjugated linoleic acid on cell cycle of gastric adenocarcinoma cell line (SGC-7901). *World J Gastroenterol* 2002; **8**: 224-229

19 **Cai L**, Yu SZ. A molecular epidemiologic study on gastric cancer in Changle, Fujian Province. *Shijie Huaren Xiaohua Zazhi* 1999; **7**: 652-655

20 **Gao GL**, Yang Y, Yang SF, Ren CW. Relationship between proliferation of vascular andothelial cells and gastric cancer. *Shijie Huaren Xiaohua Zazhi* 2000; **8**: 282-284

21 **Xue XC**, Fang GE, Hua JD. Gastric cancer and apoptosis. *Shijie Huaren Xiaohua Zazhi* 1999; **7**: 359-361

22 **Niu WX**, Qin XY, Liu H, Wang CP. Clinicopathological analysis of patients with gastric cancer in 1200 cases. *World J Gastroenterol* 2001; **7**: 281-284

23 **Li XY**, Wei PK. Diagnosis of stomach cancer by serum tumor markers. *Shijie Huaren Xiaohua Zazhi* 2001; **9**: 568-570

24 **Fang DC**, Yang SM, Zhou XD, Wang DX, Luo YH. Telomere erosion is independent of microsatellite instability but related to loss of heterozygosity in gastric cancer. *World J Gastroenterol* 2001; **7**: 522-526

25 **Morgner A**, Miehlke S, Stolte M, Neubauer A, Alpen B, Thiede C, Klann H, Hierlmeier FX, Ell C, Ehninger G, Bayerdorffer E. Development of early gastric cancer 4 and 5 years after complete remission of *Helicobacter pylori* associated gastric low grade marginal zone Bcell lymphoma of MALT type. *World J Gastroenterol* 2001; **7**: 248-253

26 **Deng DJ**. Progress of gastric cancer etiology: N-nitrosamides in the 1999s. *World J Gastroenterol* 2000; **6**: 613-618

27 **Liu ZM**, Shou NH, Jiang XH. Expression of lung resistance protein in patients with gastric carcinoma and its clinical significance. *World J Gastroenterol* 2000; **6**: 433-434

28 **Guo CQ**, Wang YP, Liu GY, Ma SW, Ding GY, Li JC. Study on *Helicobacter pylori* infection and p53, c-erbB-2 gene expression in carcinogenesis of gastric mucosa. *Shijie Huaren Xiaohua Zazhi* 1999; **7**: 313-315

29 **Cai L**, Yu SZ, Ye WM, Yi YN. Fish sauce and gastric cancer: an ecological study in Fujian Province, China. *World J Gastroenterol* 2000; **6**: 671-675

30 **Xue FB**, Xu YY, Wan Y, Pan BR, Ren J, Fan DM. Association of *H. pylori* infection with gastric carcinoma: a Meta analysis. *World J Gastroenterol* 2001; **7**: 801-804

31 **Wang RT**, Wang T, Chen K, Wang JY, Zhang JP, Lin SR, Zhu YM, Zhang WM, Cao YX, Zhu CW, Yu H, Cong YJ, Zheng S, Wu BQ. *Helicobacter pylori* infection and gastric cancer: evidence from a retrospective cohort study and nested case-control study in China. *World J Gastroenterol* 2002; **8**: 1103-1107

32 **Hua JS**. Effect of *Hp*: cell proliferation and apoptosis on stomach cancer. *Shijie Huaren Xiaohua Zazhi* 1999; **7**: 647-648

33 **Liu DH**, Zhang XY, Fan DM, Huang YX, Zhang JS, Huang WQ, Zhang YQ, Huang QS, Ma WY, Chai YB, Jin M. Expression of vascular endothelial growth factor and its role in oncogenesis of human gastric carcinoma. *World J Gastroenterol* 2001; **7**: 500-505

34 **Cao WX**, Ou JM, Fei XF, Zhu ZG, Yin HR, Yan M, Lin YZ. Methionine-dependence and combination chemotherapy on human gastric cancer cells *in vitro*. *World J Gastroenterol* 2002; **8**: 230-232

35 **Michetti P**, Kreiss C, Kotloff KL, Porta N, Blanco JL, Bachmann D, Herranz M, Saldinger PF, Corthesy-Theulaz I, Losonsky G, Nichols R, Simon J, Stolte M, Acherman S, Monath TP, Blum AL. Orla immunization with urease and *Escherichia coli* heat-labile enterotoxin is safe and immunogenic in *Helicobacter pylori*-infected adults. *Gastroenterology* 1999; **116**: 804-812

36 **Suganuma M**, Kurusu M, Okabe S, Sueoka N, Yoshida M, Wakatsuki Y, Fujiki H. *Helicobacter pylori* membrane protein 1: a new carcinogenic factor of *Helicobacter pylori*. *Cancer Res* 2001; **61**: 6356-6359

37 **Nakamura S**, Matsumoto T, Suekane H, Takeshita M, Hizawa K, Kawasaki M, Yao T, Tsuneyoshi M, Iida M, Fujishima M. Predictive value of endoscopic ultrasonography for regression of gastric low grade and grade MALT lymphomas after eradication of *Helicobactter pylori*. *Gut* 2001; **48**: 454-460

38 **Uemura N**, Okamoto S, Yamamoto S, Matsumura N, Yamaguchi S, Yamakido M, Taniyama K, Sasaki N, Schlemper RJ. *Helicobacter pylori* infection and the development of gastric cancer. *N Engl J Med* 2001; **345**: 8298-8232

39 **Morgner A**, Miehlke S, Fischbach W, Schmitt W, Muller-Hermelink H, Greiner A, Thiede C, Schetelig J, Neubauer A, Stolte M, Ehninger G, Bayerdorffer E. Complete remission of primary high-rade B-cell gastric lymphoma after cure of *Helicobacter pylori* infection. *J Clin Oncol* 2001; **19**: 2041-2048

40 **Kate V**, Ananthakrishnan N, Badrinath S. Effect of *Helicobacter pylori* eradication on the ulcer recurrence rate after simple closure of perforated duodenal ulcer: retrospective and prospective randomized controlled studies. *Br J Surg* 2001; **88**: 1054-1058

41 **Zhuang XQ**, Lin SR. Progress in research on the relationsh between Hp and stomach cancer. *Shijie Huaren Xiaohua Zazhi* 2000; **8**: 206-207

42 **Gao HJ**, Yu LZ, Bai JF, Peng YS, Sun G, Zhao HL, Miu K, Lu XZ, Zhang XY, Zhao ZQ. Multiple genetic alterations and behavior of cellular biology in gastric cancer and other gastric mucosal lesions: *H. pylori* infection, histological types and staging. *World J Gastroenterol* 2000; **6**: 848-854

43 **Yao YL**, Zhang WD. Relation between *Helicobacter pylori* and gastric cancer. *Shijie Huaren Xiaohua Zazhi* 2001; **9**: 1045-1049

44 **Goto T**, Nishizono A, Fujioka T, Ikewaki J, Mifune K, Nasu M. Local secretory immunoglobulin A and postimmunization gastritis correlated with protection against *Helicobacter pylori* infection after oral vaccination of mice. *Infect Immun* 1999; **67**: 2531-2539

45 **Watanabe T**, Tada M, Nagai H, Sasaki S, Nakao M. *Helicobacter pylori* infection induces gastric cancer in mongolian gerbils. *Gastroenterology* 1998; **115**: 642-648

46 **Honda S**, Fujioka T, Tokieda M, Satoh R, Nishizono A, Nasu M. Development of *Helicobacter pylori*-induced gastric carcinoma in mongolian gerbils. *Cancer Res* 1998; **58**: 4255-4259

47 **Hatzifoti C**, Wren BW, Morrow JW. *Helicobacter pylori* vaccine strategies-triggering a gut reaction. *Immuno Today* 2000; **21**: 615-619

48 **Kotloff KL**, Sztein MB, Wasserman SS, Losonsky GA, DiLorenzo SC, Walker RI. Safety and immunogenicity of oral inactivated whole-cell *Helicobacter pylori* vaccine with adjuvant among volunteers with or without subclinical infection. *Infect Immun* 2001; **69**: 3581-3590

49 **Dubois A**, Lee CK, Fiala N, Kleanthous H, Mehlman PT, Monath T. Immunization against natural *Helicobacter pylori* infection in nonhuman primates. *Infect Immune* 1998; **66**: 4340-4346

50 **Ikewaki J**, Nishizono A, Goto T, Fujioka T, Mifune K. Therapeutic oral vaccination induces mucosal immune response sufficient to eliminate longterm *Helicobacter pylori* infection. *Microbiol Immunol* 2000; **44**: 29-39

51 **Evans DG**, Karjalainen TK, Evans DJ, Graham DY, Lee CH. Cloning, nucleotide sequence, and expression of a gene encoding an adhesin subunit protein of *Helicobacter pylori*. *J Bacteriol* 1993; **175**: 674-683

52 **Sambrook J**, Fritsch E F, Maniatis T. Molecular Cloning, A Laboratory Manual. 2nd edition. New York: Cold Spring Harbor Laboratory Press. 1989, 1.21-1.52, 2.60-2.80, 7.3-7.35, 9.14-9.22

53 **Jones AC**, Logan RP, Foynes S, Cockayne A, Wren BW, Penn CW. A flagellar sheath protein of *Helicobacter pylori* is identical to HpaA, a putative N-acetylneuraminyllactose-binding hemagglutinin, but is not an adhesin for AGS cells. *J Bacteriol* 1997; **179**: 5643-5647

54 **Chen Y**, Wang J, Shi L. *In vitro* study of the biological activities and immunogenicity of recombinant adhesion of *Helicobacter pylori* rHpaA. *Zhonghua Yixue Zazhi* 2001; **81**: 276-279

55 **Tomb JF**, White O, Kerlavage AR, Clayton RA, Sutton GG, Fleischmann RD, Ketchum KA, Klenk HP, Gill S, Dougherty BA, Nelson K, Quackenbush J, Zhou L, Kirkness EF, Peterson S, Loftus B, Richardson D, Dodson R, Khalak HG, Glodek A, McKenney K, Fitzegerald LM, Lee N, Adams MD, Hickey EK, Berg DE, Gocayne JD, Utterback TR, Peterson JD Kelley JM, Karp PD, Smith HO, Fraser CM, Venter JC. The complete genome sequence of the gastric pathogen *Helicobacter pylori*. *Nature* 1997; **388**: 539-547

56 **Alm RA**, Ling SL, Moir DT, King BL, Brown ED, Doig PC, Smith DR, Noonan B, Guild BC, Dejonge BL, Carmel G, Tummino PJ, Caruso A, Uria-Nickelsen M, Mills DM, Lves C, Gibson R, Merberg D, Mills SD, Jiang Q, Taylor DE, Vovis GF, Trust TJ. Genomic-sequence comparison of two unrelated isolates of the human gastric pathogen *Helicobacter pylori*.. *Nature* 1999; **397**: 176-180

57 **Opazo P**, Muller I, Rollan A, Valenzuela P, Yudelevich A, Garcia-de la Guarda R, Urra S, Venegas A. Serological response to *Helicobacter pylori* recombinant antigens in Chilean infected patients with duodenal ulcer, non-ulcer dyspepsia and gastric cancer. *APMIS* 1999; **107**: 1069-1078

58 **Otoole PW**, Janzon L, Doig P, Huang J, Kostrzynska M, Trust TJ. The putative neuraminyllactose-binding hemagglutinin hpaA of *Helicobacter pylori* CCUG 17874 is a lipoprotein. *J Bacteriol* 1995; **177**: 6049-6057

59 **Hocking D**, Webb E, Radcliff F, Rothel L, Taylor S, Pinczower G, Kapouleas C, Braley H, Lee A, Doidge C. Isolation of recombinant protective *Helicobacter pylori* antigens. *Infect and Immun* 1999; **67**: 4713-4719

60 **Sheng T**, Zhang JZ. Current situation on studies of *Hp* urease. *Shijie Huaren Xiaohua Zazhi* 1999; **7**: 881-884

61 **Huang XQ**. *Helicobacter pylori* infection and gastrointestinal hormones: a review. *World J Gastroenterol* 2000; **6**: 783-788

62 **Hou P**, Tu ZX, Xu GM, Gong YF, Ji XH, Li ZS. *Helicobacter pylori* vacA genotypes and cagA status and their relationship to associated diseases. *World J Gastroenterol* 2000; **6**: 605-607

63 **Jiang Z**, Tao XH, Huang AL, Wang PL. A study of recombinant protective *H. Pylori* antigens. *World J Gastroenterol* 2002; **8**: 308-311

64 **Wu C**, Zou QM, Guo H, Yuan XP, Zhang WJ, Lu DS, Mao XH. Expression, purification and immunocharacteristics of recombination UreB protein of *H. pylori*. *World J Gastroenterol* 2001; **7**: 389-393

65 **Keenan J**, Oliaro J, Domigan N, Potter H, Aitken G, Allardyce R, Roake J. Immune response to an 18-Kilodalton outer membrane antigen identifies lipoprotein 20 as a *Helicobacter pylori* vaccine candidate. *Infect and Immun* 2000; **68**: 3337-3343

Edited by Xu XQ

P.O.Box 2345, Beijing 100023,China
Fax: +86-10-85381893
E-mail: wjg@wjgnet.com www.wjgnet.com

World J Gastroenterol 2003;9(7):1537-1540
World Journal of Gastroenterology
 ISSN 1007-9327

Density of *Helicobacter pylori* may affect the efficacy of eradication therapy and ulcer healing in patients with active duodenal ulcers

Yung-Chih Lai, Teh-Hong Wang, Shih-Hung Huang, Sien-Sing Yang, Chi-Hwa Wu, Tzen-Kwan Chen, Chia-Long Lee

Yung-Chih Lai, Sien-Sing Yang, Chi-Hwa Wu, Tzen-Kwan Chen, Chia-Long Lee, Department of Internal Medicine, Cathay General Hospital, Taipei, Taiwan, China
Teh-Hong Wang, Department of Internal Medicine, National Taiwan University Hospital, Taipei, Taiwan, China
Shih-Hung Huang, Department of Pathology, Cathay General Hospital, Taipei, Taiwan, China
Supported by the grant from Cathay General Hospital, Taipei, Taiwan
Correspondence to: Dr. Yung-Chih Lai, Department of Internal Medicine, Cathay General Hospital, 280, Jen-Ai Road, Section 4, Taipei 106, Taiwan, China. yungchihlai@hotmail.com
Telephone: +86-2-27082121 Ext. 3120 **Fax:** +86-2-27074949
Received: 2003-03-12 **Accepted:** 2003-04-11

Abstract

AIM: To evaluate the association of pre-treatment *Helicobacter pylori* (*H. pylori*) density with bacterial eradication and ulcer healing rates in patients with active duodenal ulcer.

METHODS: One hundred and four consecutive duodenal ulcer outpatients with *H. pylori* infection ascertained by gastric histopathology and ^{13}C-urea breath test (UBT) were enrolled in this study. *H. pylori* density was graded histologically according to the Sydney system (normal, mild, moderate, and marked). In each patient, lansoprazole (30 mg b.i.d.), clarithromycin (500 mg b.i.d.) and amoxicillin (1 g b.i.d.) were used for 1 week, then 30 mg lansoprazole once daily was continued for an additional 3 weeks. Follow-up endoscopy was performed at 4 weeks after completion of the therapy, and UBT was done at 4 and 8 weeks after completion of the therapy.

RESULTS: The *H. pylori* eradication rates were 88.9 %/100.0 %, 94.3 %/100.0 %, and 69.7 %/85.2 %; and the ulcer healing rates were 88.9 %/100.0 %, 94.3 %/100.0 %, and 63.6 %/77.8 % (intention-to-treat/per protocol analysis) in the mild, moderate, and marked *H. pylori* density groups, respectively. The association of pretreatment *H. pylori* density with the eradication rate and ulcer healing rate was both statistically significant (P=0.013/0.006 and 0.002/<0.001, respectively; using results of intention-to-treat/per protocol analysis).

CONCLUSION: Intragastric bacterial load may affect both the outcome of eradication treatment and ulcer healing in patients with active duodenal ulcer disease.

Lai YC, Wang TH, Huang SH, Yang SS, Wu CH, Chen TK, Lee CL. Density of *Helicobacter pylori* may affect the efficacy of eradication therapy and ulcer healing in patients with active duodenal ulcers. *World J Gastroenterol* 2003; 9(7): 1537-1540
http://www.wjgnet.com/1007-9327/9/1537.asp

INTRODUCTION

Helicobacter pylori (H. pylori) has been considered as the main cause of chronic gastritis and peptic ulcer[1]. It has been identified in 90-95 % of patients with duodenal ulcer and 60-80 % of patients with gastric ulcer[2]. Strong evidence has also shown an association between the eradication of *H. pylori* infection and the cure of peptic ulcer diseases[3-5].

Recommendations and guidelines for *H. pylori* eradication therapy have been developed rapidly during recent years. The global trend of eradication therapy has now shifted to proton pump inhibitor (PPI)-based triple therapy (a PPI and two different anti-microbials)[6], which can assure rapid symptom relief, improve ulcer healing, and reduce ulcer recurrence[7,8]. However, some cases failed to heal with this advanced PPI-based triple therapy. Patient compliance and antibiotic resistance are currently regarded as the major causes of eradication failure[9]. Several researchers have also revealed that high antral density of *H. pylori* may increase the rate of ulcer recurrence and be related with low eradication rate after triple therapy[10-12]. Intragastric bacterial load might be another factor affecting the success of eradication therapy[12]. Therefore, we conducted this study to investigate the association of *H. pylori* density in the stomach with the efficacy of eradication therapy and ulcer healing in patients with active duodenal ulcers.

MATERIALS AND METHODS

Patients

From January 2000 to June 2002, consecutive outpatients with endoscopically verified active duodenal ulcers (5 mm in diameter or larger) at Cathay General Hospital were enrolled in this study. All panendoscopic examinations were performed and interpreted by the same group of experienced endoscopists. We only enrolled patients with positive diagnosis of *H. pylori* infection proven by both histological examinations and ^{13}C-urea breath tests (UBT). To avoid interference in evaluating the status of *H. pylori*, the following patients were initially excluded before endoscopy: those who had ingested bismuth, antibiotics, anti-secretory medication, or PPI during the 4 weeks prior to the beginning of the study; those who used non-steroidal anti-inflammatory drugs; those who were pregnant or immuno-compromised, and those who had a history of gastric surgery or a previous attempt to eradicate *H. pylori*. The patients with coexisting gastric ulcers or gastric cancer were also excluded. All procedures were performed after obtaining informed consent from the patients.

The patients enrolled were treated with the same regimen of 30 mg lansoprazole b.i.d. plus 500 mg clarithromycin b.i.d. and 1 g amoxicillin b.i.d. for 7 days. After 1 week of anti-*H. pylori* therapy, 30 mg lansoprazole once daily was continued for an additional 3 weeks. From then on, either PPI or anti-secretory H_2-blocker was avoided; only oral antacids were taken for symptomatic relief when necessary. The second endoscopic examination was performed 4 weeks after completion of the therapy.

Histology

During the first endoscopic examination, three biopsies were taken from the gastric antrum (one near the incisura and the

other two on the greater and lesser curvature, 2 cm within the pyloric ring)[13]. On the follow-up endoscopic examination, two additional specimens were taken from the greater curvature of the gastric body due to the possibility of patchy distribution of *H. pylori* after eradication therapy. An "Olympus GIF-XQ 200' endoscope was used, the biopsy forceps were the "FB 25-K" type. The specimens were stained with hematoxylin-eosin and with a modified Giemsa stain. Then they were examined by experienced histopathologist who was unaware of the clinical diagnosis for the existence of *H. pylori* of the patients. The version of the visual analogue scale in the updated Sydney system was used to grade the density of *H. pylori* (4 grades: normal, no bacteria; mild, focal few bacteria; moderate, more bacteria in several areas; and marked, abundance of bacteria in most glands)[14]. If the density varied, the highest grade of density in the specimens was selected.

Urea breath test

UBTs were performed before the start of therapy and on two separate occasions, at 4 and 8 weeks after the cessation of therapy, respectively. The ^{13}C-urea used was 100 mg 99 % ^{13}C-labelled urea produced by the Institute of Nuclear Energy Research, Taiwan. Patients drank 100 ml of fresh milk as the test meal. The procedure was modified from the European standard protocol for the detection of *H. pylori*[15,16]. We chose 3 per mil for the cut-off level of the rise in the delta value of $^{13}CO_2$ at 15 min after the ingestion of ^{13}C-urea. UBT was defined as positive when the excess $\delta^{13}CO_2$ was above this value. By using this cut-off, the sensitivity and specificity of UBT were 97 % and 95 %, respectively[16].

Eradication of *H. pylori* infection was defined as negative results on UBT and histology tests at 4 weeks after the cessation of therapy or negative results on two UBTs at both 4 and 8 weeks after the cessation of therapy[17]. Healing of ulcers was defined as complete disappearance of the ulcer and non-healing as persistence of ulcers, even if the size had decreased[18].

To be included in the intention-to-treat analysis, the infection of *H. pylori* had to be confirmed using both UBT and histological examination results. When protocol violations which were likely to influence the response variable or its assessment occurred, patients were excluded from the per protocol analysis.

Statistical analysis

Chi-square or Fisher' s exact test was used to evaluate the qualitative data. ANOVA test was applied for the quantitative data. The eradication rates of *H. pylori* and healing rates of duodenal ulcers in the three groups of different *H. pylori* densities were compared using chi-square test or Fisher' s exact test and assessed on the basis of both intention-to-treat and per protocol analysis. The 95 % confidence intervals (95 % CI) were calculated. The relationship between *H. pylori* eradication and duodenal ulcer healing was evaluated by Fisher' s exact test. *P* value less than 0.05 was considered significant.

RESULTS

Patients

One hundred and ten patients were initially included in the study, but 6 patients were later excluded due to their negative results of *H. pylori*. We enrolled 104 patients who fulfilled the inclusion criteria. Table 1 shows the demographic and other baseline characteristics of the patients divided by the grade of *H. pylori* density. None of differences in variables was statistically significant. Among them, 12 patients did not complete the study because of poor compliance of taking medications (3 cases) or refusal to receive the second endoscopy (9 cases). Because we wanted to observe the results of both the eradication therapy and the ulcer healing, the patients who refused the second endoscopy were excluded. Therefore, 92 patients were included for per protocol analysis.

Table 1 Clinical characteristics of patients

	H. pylori density		
	Mild (*n*=36)	Moderate (*n*=35)	Marked (*n*=33)
Sex (male / female)	23 / 13	25 / 10	23 / 10
Age (years, Mean ±S.D.)	45.6±10.3	44.1±12.7	47.2±13.4
Smoking(yes / no)	18 / 18	20 / 15	18 / 15
Ulcer size			
< 1 cm	32	32	30
1-2 cm	4	2	3
>2 cm	0	1	0
Ulcer number			
One	34	32	30
Two	2	3	3
Drop outs	4	2	6

Eradication rate and the density of H. pylori

The overall eradication rates were 84.6 % (95 % CI: 75.9-90.7 %) in the intention-to-treat analysis set and 95.7 % (95 % CI: 88.6-98.6 %) in the per protocol set. The eradication rates of the three grades of bacterial densities had a downward trend as the bacterial load became denser (Table 2). The association was statistically significant (*P*=0.013 and 0.006, by intention-to-treat and per protocol analysis).

Table 2 Eradication rates and the density of *H. pylori*

	Eradication rates	95% CI	*P* value
Intention-to-treat			
H. pylori density			
Mild	32 / 36 (88.9%)	73.0 – 96.4 %	
Moderate	33 / 35 (94.3%)	79.5 – 99.0 %	
Marked	23 / 33 (69.7%)	51.1 – 83.8 %	
Total	88 / 104 (84.6%)	75.9 – 90.7 %	0.013[a]
Per protocol			
H. pylori density			
Mild	32 / 32 (100.0%)	86.7 – 100.0 %	
Moderate	33 / 33 (100.0%)	87.2 – 100.0 %	
Marked	23 / 27 (85.2%)	65.4 – 95.2 %	
Total	88 / 92 (95.7%)	88.6 – 98.6 %	0.006[b]

Notes: [a]Based on Chi-square test; [b]Based on Fisher' s exact test.

Healing rates of duodenal ulcer and the density of H. pylori

The healing rates of active duodenal ulcer are shown in Table 3. According to both of the intention-to-treat and per protocol analysis, the differences in the ulcer healing rates of the three grades of *H. pylori* densities were statistically significant (*P*=0.002 and <0.001, respectively). As the bacterial density increased in the stomach, the healing rate of duodenal ulcer decreased.

Relationship between H. pylori eradication and duodenal ulcer healing

Table 4 shows the positive impact of *H. pylori* eradication on duodenal ulcer healing. The association was statistically significant (*P*<0.001). Active ulcers of 97.7 % of the patients with successful *H. pylori* eradication had healed at the time of

the second endoscopic examination.

Table 3 Healing rates of duodenal ulcer and the density of *H. pylori*

	Healing rates	95% CI	*P* value
Intention-to-treat			
H. pylori density			
Mild	32 / 36 (88.9%)	73.0 – 96.4 %	
Moderate	33 / 35 (94.3%)	79.5 – 99.0 %	
Marked	21 / 33 (63.6%)	45.1 – 79.0 %	
Total	86 / 104 (82.7%)	73.8 – 89.2 %	0.002[a]
Per Protocol			
H. pylori density			
Mild	32 / 32 (100.0%)	86.7 – 100.0 %	
Moderate	33 / 33 (100.0%)	87.2 – 100.0 %	
Marked	21 / 27 (77.8%)	57.3 – 90.6 %	
Total	86 / 92 (93.5%)	85.8 – 97.3 %	<0.001[b]

Notes: [a]Based on Chi-square test; [b]Based on Fisher's exact test.

Table 4 Relationship between *H. pylori* eradication and duodenal ulcer healing

	H. pylori	
	Eradicated (*n*=88)	Not eradicated (*n*=4)
Duodenal ulcer		
Healed	86 (97.7%)[a]	0 (0.0%)
Not healed	2 (2.3%)	4 (100.0%)

[a]*P*<0.001 *vs* not eradicated group, based on Fisher's exact test.

DISCUSSION

H. pylori is an important factor in the pathogenesis of duodenal ulcer. Researchers have shown the eradication of *H. pylori* not only prevents ulcer recurrence but also aids ulcer healing[19]. Eradication of *H. pylori* has changed the natural history of duodenal ulcer and has become a standard therapy for duodenal ulcer patients[3, 4, 10].

At present, short-term (7-day) triple therapies including a PPI and two antibiotics (clarithromycin, and amoxycillin or a nitroimidazole compound) are considered as the first line in anti-*H. pylori* regimens[12]. However, despite of the high efficacy of different anti-*H. pylori* treatment schemes, a proportion of patients, varying from 10 % to 25 %, fails the first attempt to eradicate *H. pylori*[9]. Patient compliance and antibiotic resistance are currently regarded as the key factors affecting the outcome of treatment[9,12]. The evidence for other possible factors associated with lower eradication rates is somewhat sparse and equivocal. Nevertheless, several reports revealed that the patients with higher intragastric *H. pylori* load had reduced eradication rates. This association was found in both bismuth and PPI-based triple therapies[9-12]. Therefore, pre-treatment bacterial density was used by some authors to predict the success of *H. pylori* eradication in patients with chronic duodenal ulcer[10,11].

Our working hypothesis was that "the higher the intragastric *H. pylori* colonization, the less effective the short-term triple therapy". In our study, an inverse relationship between successful eradication and intragastric bacterial load was found, which is compatible with the results of other studies[9-12]. Increased bacterial density of *H. pylori* was associated with a significant reduction in the eradication rate after anti-*H. pylori* treatment. This correlation provides additional support for the importance of bacterial density as a factor in *H. pylori* eradication.

With more *H. pylori* inhabiting the antrum, the gastric mucosa will suffer greater damage by this bacteria[20, 21]. The denser infection of *H. pylori* associated with greater antral inflammation may cause lower somatostatin expression, leading to higher levels of gastrin and acid production, which may therefore predispose the duodenum to ulceration[22]. Alam *et al*[21] have shown that the prevalence of duodenal ulcer increased with increasing *H. pylori* density, and a greater likelihood of ulceration was noted among patients with high concentrations of *H. pylori*. Effective *H. pylori* eradication was found to induce good responses in peptic ulcer healing[18]. Treiber *et al* [23] reported successful *H. pyl*ori eradication therapy accelerated peptic ulcer healing even without concomitant acid suppression. In several trials, *H. pylori* eradication not only did result in greater duodenal ulcer healing, but also dramatically decreased ulcer recurrence rate 12 months following treatment[24]. The cure rates of *H. pylori* infection could be expected more than 90 % using standard triple therapy according to the Maastricht consensus guidelines, and the effective *H. pylori* eradication therapy could achieve rapid peptic ulcer healing in more than 90 % of subjects[23,25].

In our study, 86/88 cases (97.7 %) in the *H. pylori* eradication group had complete healing of ulcers, which were proven by the results of follow-up endoscopy. The association between *H. pylori* eradication and ulcer healing was statistically significant. Therefore, a positive impact of *H. pylori* eradication on peptic ulcer healing is concluded.

Intragastric bacterial load can affect the success of *H. pylori* eradication therapy, and *H. pylori* eradication can influence the healing of duodenal ulcer. Thus, the healing of duodenal ulcer might be associated with the *H. pylori* density in the stomach. According to our results, *H. pylori* density was revealed to be inversely related to ulcer healing. We asked every patient enrolled to receive follow-up endoscopic examinations so that we could observe the healing process of duodenal ulcer directly. Although some patients refused the second endoscopic examination, our results were still able to confirm the assumed association mentioned above.

Identification of pre-treatment predictors of eradication therapy is important in clinical practice. Therapeutic regimens may be tailored to individual patients according to their particular conditions. Despite the fact that high *H. pylori* density might adversely influence the efficacy of eradication therapy, patients with high intragastric bacterial loads were found to benefit from an extension of eradication regimen from 1 to 2 weeks[9]. Prolonging duration of the standard triple therapy was proposed as a way to overcome the unfavorable effects caused by high *H. pylori* density and proved to be effective[9,12].

Most patients (101/104 cases, 97.1 %) included in this study had good drug compliance. Bacterial culture and drug sensitivity test to assess the effect of antibiotic resistance were not performed. Therefore, we could not demonstrate the influence of drug resistance on eradication therapy by our results. Although some authors mentioned the resistance to antimicrobials could be considered as a statistical event and estimated as a certain proportion of the *H. pylori* population in the stomach[26], the relationship between antibiotic resistance and bacterial load of *H. pylori* has not been studied. Further investigation is warranted to elucidate this issue. The culture and susceptibility testing of *H. pylori* are time-consuming and expensive, and they are rarely performed in most developing countries[27]. In Taiwan, they are not routinely performed either. Our study may thus provide a practical option to identify the pre-treatment predictors of eradication therapy and ulcer healing when information on drug sensitivity is not available.

In conclusion, our findings reveal that pre-treatment high bacterial density of *H. pylori* in the stomach adversely affects

the success of eradication therapy and influences the healing of ulcers in patients with active duodenal ulcers, and effective *H. pylori* eradication is also shown to be significantly associated with duodenal ulcer healing. Identifying patients with high bacterial loads before treatment and making adjustments of therapeutic regimens accordingly may further improve the efficacy of eradication therapy.

ACKNOWLEDGMENTS

We would like to thank Mr. Shui-Cheng Lee (Institute of Nuclear Energy Research) for his help in the assessment of urea breath test.

REFERENCES

1 **Wewer V,** Andersen LP, Parregaard A. Treatment of *Helicobacter pylori* in children with recurrent abdominal pain. *Helicobacter* 2001; **6:** 244-248
2 **Hunt RH.** Peptic ulcer disease: defining the treatment strategies in the era of *Helicobacter pylori*. *Am J Gastroenterol* 1997; **92:** 36S-43S
3 **Moss S,** Calam J. *Helicobacter pylori* and peptic ulcers: the present position. *Gut* 1992; **33:** 289-292
4 **Hunt RH.** pH and *Hp* – gastric acid secretion and *Helicobacter pylori*: implications for ulcer healing and eradication of the organism. *Am J Gastroenterol* 1993; **88:** 481-483
5 **Graham DY,** Lew GM, Klein PD. Effect of treatment of *Helicobacter pylori* infection on the long-term recurrence of gastric or duodenal ulcer: a randomized, controlled study. *Ann Intern Med* 1992; **116:** 705-708
6 **Asaka M,** Sugiyama T, Kato M. A multicenter, double-blind study on triple therapy with lansoprazole, amoxicillin and clarithromycin for eradication of *Helicobacter pylori* in Japanese peptic ulcer patients. *Helicobacter* 2001; **6:** 254-261
7 **Penston JG.** *Helicobacter pylori* eradication: understandable caution but no excuse for inertia. *Aliment Pharmacol Ther* 1994; **8:** 369-389
8 **Logan RP,** Bardhan KD, Celestin LR. Eradication of *Helicobacter pylori* and prevention of recurrence of duodenal ulcer: a randomized double-blind, multi-centre trial of omeprazole with or without clarithromycin. *Aliment Pharmacol Ther* 1995; **9:** 417-423
9 **Maconi G,** Parente F, Russo A, Vago L, Imbesi V, Porro GB. Do some patients with *Helicobacter pylori* infection benefit from an extension to 2 weeks of a proton pump inhibitor-based triple eradication therapy? *Am J Gastroenterol* 2001; **96:** 359-366
10 **Sheu BS,** Yang HB, Su IJ, Shiesh SC, Chi CH, Lin XZ. Bacterial density of *Helicobacter pylori* predicts the success of triple therapy in bleeding duodenal ulcer. *Gastrointest Endosc* 1996; **44:** 683-688
11 **Moshkowitz M,** Konikoff FM, Peled Y. High *Helicobacter pylori* numbers are associated with low eradication rate after triple therapy. *Gut* 1995; **36:** 845-847
12 **Perri F,** Clemente R, Festa V. Relationship between the results of pre-treatment urea breath test and efficacy of eradication of *Helicobacter pylori* infection. *Ital J Gastroenterol Hepatol* 1998; **30:** 146-150
13 **Genta RM,** Graham DY. Comparison of biopsy site for the histopathologic diagnosis of *Helicobacter pylori*: a topographic study of *H. pylori* density and distribution. *Gastrointest Endosc* 1994; **40:** 342-345
14 **Dixon MF,** Genta RM, Yardley JH, Correa P. Classification and grading of gastritis. The updated Sydney system. *Am J Surg Pathol* 1996; **20:** 1161-1181
15 **Logan RP,** Polson RJ, Misiewicz JJ, Rao G, Karim NQ, Newell D, Johnson P, Wadsworth J, Waiker MM, Baron JH. Simplified single sample ^{13}Carbon urea breath test for *Helicobacter pylori*: comparison with histology, culture, and ELISA serology. *Gut* 1991; **32:** 1461-1464
16 **Wang WM,** Lee SC, Ding HJ. Quantification of *Helicobacter pylori* infection : simple and rapid ^{13}C-urea breath test in Taiwan. *J Gastroenterol* 1998; **33:** 330-335
17 **Unge P.** The OAC and OMC options. *Eur J Gastroenterol Hepatol* 1999; **11**: S9-S17
18 **Ge ZZ,** Zhang DE, Xiao SD, Chen Y, Hu YB. Does eradication of *Helicobacter pylori* alone heal duodenal ulcers? *Aliment Pharmacol Ther* 2000; **14:** 53-58
19 **Hosking SW,** Ling TK, Chung SC. Duodenal ulcer healing by eradication of *Helicobacter pylori* without anti-acid treatment: randomized controlled trial. *Lancet* 1994; **343:** 508-510
20 **McColl KE.** Pathophysiology of duodenal ulcer disease. *Eur J Gastroentrol Hepatol* 1997; **9**: S9-S12
21 **Alam K,** Schubert TT, Bologna SD, Ma CK. Increased density of *Helicobacter pylori* on antral biopsy is associated with severity of acute and chronic inflammation and likelihood of duodenal ulceration. *Am J Gastroenterol* 1992; **87:** 424-428
22 **Atherton JC**, Tham KT, Peek RM, Cover TL, Blaser MJ. Density of *Helicobacter pylori* infection *in vivo* as assessed by quantitative culture and histology. *J Infect Dis* 1996; **174:** 552-556
23 **Treiber G,** Lambert JR. The impact of *Helicobacter pylori* eradication on peptic ulcer healing. *Am J Gastroenterol* 1998; **93:** 1080-1084
24 **Williams MP,** Pounder RE. What are appropriate end-points for *Helicobacter pylori* eradication in the treatment of duodenal ulcer? *Drugs* 1998; **56:** 1-10
25 **Working Party of the European *Helicobacter pylori* Study Group**. Guidelines for clinical trials in *Helicobacter pylori* infection. *Gut* 1997; **41:** S1- S9
26 **Graham DY,** de Boer WA, Tytgat GN. Choosing the best anti-*Helicobacter pylori* therapy: effect of antimicrobial resistance. *Am J Gastroenterol* 1996; **91:** 1072-1076
27 **Lam SK,** Talley NJ. *Helicobacter pylori* consensus: report of the 1997 asia pacific consensus conference on the management of *Helicobacter pylori* infection. *J Gastroenterol Hepatol* 1998; **13:** 1-12

Edited by Xu XQ and Wang XL

P.O.Box 2345, Beijing 100023,China
Fax: +86-10-85381893
E-mail: wjg@wjgnet.com www.wjgnet.com

World J Gastroenterol 2003;9(7):1541-1544
World Journal of Gastroenterology
 ISSN 1007-9327

• BASIC RESEARCH •

Polymorphism in transmembrane region of MICA gene and cholelithiasis

Shou-Chuan Shih, Yann-Jinn Lee, Hsin-Fu Liu, Ching-Wen Dang, Shih-Chuan Chang, Shee-Chan Lin, Chin-Roa Kao

Shou-Chuan Shih, Division of Gastroenterology, Department of Medicine, Mackay Memorial Hospital; Mackay Junior School of Nursing, Taipei, Taiwan
Yann-Jinn Lee, Department of Pediatrics and Medical Research, Mackay Memorial Hospital; College of Medicine, Taipei Medical University, Taipei, Taiwan
Hsin-Fu Liu, Ching-Wen Dang, Shih-Chuan Chang, Department of Medical Research, Mackay Memorial Hospital, Taipei, Taiwan
Shee-Chan Lin, Chin-Roa Kao, Division of Gastroenterology, Department of Medicine, Mackay Memorial Hospital, Taipei, Taiwan
Supported by MMH Grant 8844 from Mackay Memorial Hospital
Correspondence to: Dr. Yann-Jinn Lee, Departments of Pediatrics and Medical Research, Mackay Memorial Hospital, 92, Section 2, Chung-Shan North Road, Taipei, Taiwan. yannlee@ms2.mmh.org.tw
Telephone: +886-2-25433535 **Fax:** +886-2-25433642
Received: 2003-04-02 **Accepted:** 2003-04-24

Abstract

AIM: To study the significance of polymorphism of MHC class I chain-related gene A (MICA) gene in patients with cholelithiasis.

METHODS: Subjects included 170 unrelated adults (83 males) with cholelithiasis and 245 randomly selected unrelated adults (130 males) as controls. DNA was extracted from peripheral leukocytes and analyzed for polymorphism of 5 alleles (A4, A5, A5.1, A6 and A9) of the MICA gene.

RESULTS: There was no significant difference in phenotype, allele, and genotype frequencies of any of the 5 alleles between cholelithiasis patients and controls.

CONCLUSION: This study demonstrates that MICA alleles studied bear no relation to cholelithiasis.

Shih SC, Lee YJ, Liu HF, Dang CW, Chang SC, Lin SC, Kao CR. Polymorphism in transmembrane region of MICA gene and cholelithiasis. *World J Gastroenterol* 2003; 9(7): 1541-1544
http://www.wjgnet.com/1007-9327/9/1541.asp

INTRODUCTION

Molecular genetics has a substantial impact on our understanding of inherited susceptibility to many diseases. There is an increased familial frequency of cholelithiasis[1], which is a prevalent disorder in Taiwan[2]. HLA gene is associated with many human diseases. It is reasonable to speculate on whether there is a correlation between cholelithiasis and HLA gene.

MICA gene is located near HLA-B on chromosome 6, and is by far the most divergent mammalian MHC class I gene known[3]. It lies 46.4 kb centromeric to HLA-B gene, and they are oriented head-to-head. It has a triplet repeat microsatellite polymorphism $(GCT)_n$ in the transmembrane region. This polymorphism consists of five alleles, with 4, 5, 6, and 9 repetitions of GCT or 5 repetitions of GCT with 1 additional nucleotide insertion (G), designated as A4, A5, A6, A9, and A5.1, respectively[4]. The alleles vary among individuals, and hence this microsatellite can be used as an informative polymorphic marker for genetic mapping and for analysis of disease susceptibility.

To date, there have been no reports investigating an association between MICA gene and cholelithiasis. We designed this study to compare MICA polymorphism among Chinese with cholelithiasis, their family members, and unaffected controls.

MATERIALS AND METHODS

Patients with cholelithiasis and controls

One hundred and seventy unrelated adult patients (83 males) with cholelithiasis were enrolled. The average age at diagnosis was 50.5±3.1 years. Cholelithiasis was documented ultrasonographically and/or after operation (75 patients underwent cholecystectomy). The ultrasonographic criterion for diagnosis of cholelithiasis was echogenic material with a postural shift and/or casting an acoustic shadow in the gallbladder. According to their number and size, ultrasonographic patterns of gallbladder stones were divided into 3 types: single, particle (multiple, larger size) and sandy (multiple, sand-like appearance). Control subjects consisted of 245 unrelated subjects (130 males) from the same area where the patients resided. They came to the hospital for physical checkups, minor operations or injuries, or evaluation of fever or abdominal pain. Those with autoimmune disorders, liver diseases, or blood diseases were excluded from the study. In addition, a total of 144 family members of 75 patients with cholelithiasis were included for further comparison. Blood was drawn from all the subjects to extract genomic DNA. All the subjects were Chinese, and they all gave written consent. The study was approved by the local ethics committee.

DNA extraction

Genomic DNA was extracted from fresh or frozen peripheral blood leukocytes by standard techniques[5, 6].

Determination of the polymorphism of $(GCT)_n$ microsatellite

Primers for analysis of microsatellite polymorphism in the transmembrane region of MICA gene, PCR primers flanking the transmembrane region (MICA5F, 5'-CCTTTTTTTCAGGGAAAGTGC-3'; MICA5R, 5'-CCTTACCATCTCCAGAAACTGC-3') were designed according to the reported sequences[3, 4]. The MICA5F primer corresponded to the intron 4 and exon 5 boundary region and MICA5R was located in intron 5[4]. MICA5R was 5' end-labelled with fluorescent dye (Applied Biosystems)[7, 8].

Polymerase chain reaction (PCR) The amplification reaction mixture (15 μl) contained 50 ng genomic DNA, 10 mM Tris-HCl (pH 9.0), 50 mM KCl, 1.5 mM $MgCl_2$, 0.01 % gelatin, 0.1 % Triton X-100, 0.2 mM of each dNTP, 0.5 mM of each primer and 0.5 unit Pro Taq DNA polymerase (Protech Technology Enterprise). PCR amplification was carried out in a GeneAmp PCR system (Applied Biosystems). The mixture

was subjected to denaturation at 95 ℃ for 5 min, followed by 10 cycles at 94 ℃ for 15 sec, at 55 ℃ for 15 sec, at 72 ℃ for 30 sec, then by an additional 20 cycles at 89 ℃ for 15 sec, at 55 ℃ for 15 sec, at 72 ℃ for 30 sec, and by a final extension at 72 ℃ for 10 min.

Analysis of triplet repeat polymorphism The amplified products were denatured at 100 ℃ for 5 min, mixed with formamide-containing stop buffer, and subjected to electrophoresis on 4 % polyacrylamide gels containing 8-M urea in an automated DNA sequencer (ABI Prism 377-18 DNA sequencer, Applied Biosystems). The number of microsatellite repeats was estimated automatically with Genescan 672 software (Applied Biosystems) by means of the local Southern method with a size standard marker of GS-350 TAMRA (Applied Biosystems)[8]. Alleles were designated according to Mizuki *et al.*[4] and Perez-Rodriguez *et al.*[9], with amplified sizes of 179 bp (A4), 182 bp (A5), 183 bp (A5.1), 185 bp (A6), 194 bp (A9), and 197 bp (A10).

Statistical analysis

Evaluation of the Hardy-Weinberg equilibrium was performed by comparing observed and expected heterozygotes and homozygotes, as well as observed and expected genotypes, using the χ^2 test[10]. Phenotype, allele, or genotype frequencies of patients and controls were compared by the χ^2 test with Yates' correction where appropriate (one expected number <5). Patients and controls positive for a factor were compared using a free statistical program on the internet[11]. *P* values were corrected using the Bonferonni inequality method for the number of comparisons[12]. Statistical significance was defined as $P<0.05$.

RESULTS

Figure 1 shows the electrophoretograms of the PCR products of 3 subjects. We did not detect A10 in any of the patients or controls. The distribution of MICA genotypes in the two groups was in Hardy-Weinberg equilibrium, i.e. observed and expected figures did not differ. No significant difference was found between patients with cholelithiasis and controls in phenotype, allele, or genotype frequencies. There were also no differences between male and female patients or between patients with different sonographic stone types. Age at diagnosis was also not correlated with allele frequency (Tables 1, 2 3). As the difference between patients and controls was not remarkable, it was not meaningful to compare the results between patients and their family members (data not shown).

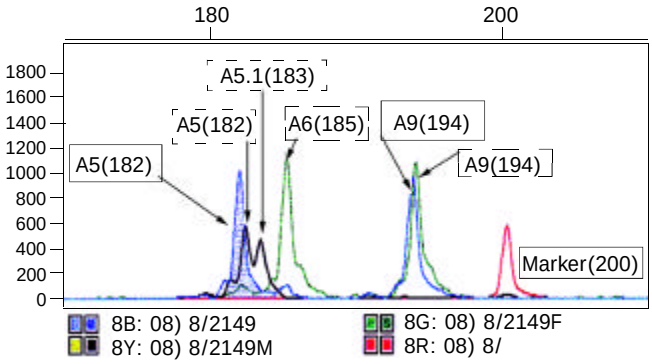

Genotypes of a subject (2149), his father (2149F), and mother (2149M)

Subject	Line	Genotype
2149	solid	A5 / A9
2149F	dash	A6 / A9
2149M	dot	A5 / A5.1

Figure 1 Electrophoretograms of the PCR products for three subjects. Amplified sizes of the alleles were 182 bp (A5), 183 bp (A5.1), 185 bp (A6), and 194 bp (A9).

Table 1 Phenotype frequencies of the polymorphism in transmembrane region of MICA gene in patients with cholelithiasis and controls

Phenotype	Patient[a]		Control[a]		Single[b]		Particle[b]		Sandy[b]		Male[c]		Female[c]	
	n	%	*n*	%	*n*	%	*n*	%	*n*	%	*n*	%	*n*	%
A4	49	28.8	69	28.2	10	35.7	24	30.0	15	24.2	30	36.1	19	21.9
A5	85	50.0	133	54.3	15	53.6	43	53.8	27	43.6	42	50.6	43	49.4
A5.1	72	42.4	113	46.1	9	32.1	32	40.0	31	50.0	33	39.8	39	44.8
A6	23	13.5	30	12.2	4	14.3	10	12.5	9	14.5	9	10.8	14	16.1
A9	64	37.7	79	32.2	11	39.3	31	38.8	22	35.5	30	36.1	34	39.1
Total	170	100	245	100	28	100	80	100	62	100	83	100	87	100

[a]$P=0.81$, [b]$P=0.441$, [c]$P=0.316$.

Table 2 Allele frequencies of the polymorphism in transmembrane region of MICA gene in patients with cholelithiasis and controls

Allele	Patient[a]		Control[a]		Single[b]		Particle[b]		Sandy[b]		Age at Dx≤50		Age at Dx≤30		Age at Dx ≤40[d]		Male[c]		Female[c]	
	n	%	*n*	%	*n*	%	*n*	%	*n*	%	*n*	%	*n*	%	*n*	%	*n*	%	*n*	%
A4	53	15.6	74	15.1	11	19.6	26	16.3	16	12.9	21	13.8	3	15.0	5	8.1	34	20.5	19	10.9
A5	105	30.9	162	33.1	18	32.1	56	35.0	31	25.0	49	32.2	6	30.0	19	30.6	51	30.7	54	31.0
A5.1	85	25.0	135	27.6	11	19.6	35	21.9	39	31.5	39	25.7	5	25.0	18	29.0	38	22.9	47	27.0
A6	24	7.1	32	6.5	4	7.1	10	6.3	10	8.1	13	8.6	2	10.0	6	9.7	10	6.0	14	8.0
A9	73	21.5	87	17.8	12	21.4	33	20.6	28	22.6	30	19.7	4	20.0	14	22.6	33	19.9	40	23.0
Total	340	100	490	100	56	100	160	100	124	100	152	100	20	100	62	100	166	100	174	100

[a]$P=0.71$, [b]$P=0.541$, [c]$P=0.415$, [d]$P=0.501$ (age ⩽ 40 *vs.* control), Dx=Diagnosis.

Table 3 Genotype frequencies of the polymorphism in transmembrane region of MICA gene in patients with cholelithiasis and controls

Genotype	Patient[a]		Control[a,b]		Single[b]		Particle[b]		Sandy[b]		Age at Dx ⩽ 50		Male[c]		Female[c]	
	n	%	*n*	%	*n*	%	*n*	%	*n*	%	*n*	%	*n*	%	*n*	%
A4 / A4	4	2.4	5	2.0	1	3.6	2	2.5	1	1.6	2	2.6	4	4.8	0	0
A4 / A5	14	8.2	22	9.0	3	10.7	8	10.0	3	4.8	6	7.9	8	9.6	6	6.9
A4 / A5.1	13	7.6	23	9.4	2	7.1	6	7.5	5	8.1	6	7.9	7	8.4	6	6.9
A4 / A6	2	1.2	8	3.3	0	0	1	1.3	1	1.6	0	0	2	2.4	0	0
A4 / A9	16	9.4	11	4.5	4	14.3	7	8.8	5	8.1	5	6.6	9	10.8	7	8.0
A5 / A5	20	11.8	29	11.8	3	10.7	13	16.3	4	6.5	8	10.5	9	10.8	11	12.6
A5 / A5.1	21	12.4	37	15.1	2	7.1	8	10.0	11	17.7	10	13.2	11	13.3	10	11.5
A5 / A6	10	5.9	11	4.5	4	14.3	3	3.8	3	4.8	7	9.2	3	3.6	7	8.0
A5 / A9	20	11.8	34	13.9	3	10.7	11	13.8	6	9.7	10	13.2	11	13.3	9	10.3
A5.1 / A5.1	13	7.6	22	9.0	2	7.1	3	3.8	8	12.9	6	7.9	5	6.0	8	9.2
A5.1 / A6	8	4.7	7	2.9	0	0	5	6.3	3	4.8	3	3.9	3	3.6	5	5.7
A5.1 / A9	17	10.0	24	9.8	3	10.7	10	12.5	4	6.5	8	10.5	7	8.4	10	11.5
A6 / A6	1	0.6	2	0.8	0	0	0	0	1	1.6	1	1.3	1	1.2	0	0
A6 / A9	2	1.2	2	0.8	0	0	1	1.3	1	1.6	1	1.3	0	0	2	2.3
A9 / A9	9	5.3	8	3.3	1	3.6	2	2.5	6	9.7	3	3.9	3	3.6	6	6.9
Total	170	100	245	100	28	100	80	100	62	100	76	100	83	100	87	100

[a]P=0.797, [b]P=0.063 (control *vs.* stone types), [c]P=0.337, Dx=Diagnosis.

DISCUSSION

Cholelithiasis is quite prevalent in Taiwan[2] and is easily detected by ultrasonography, which has become a commonly used screening tool for health maintenance exams. There is as yet no well documented method to prevent cholelithiasis formation. However, it is now well known that detecting genetic defects may lead to better surveillance or even avoidance of certain diseases. Thus it seems worthwhile to search for gene disorders in a common disease like cholelithiasis.

MHC class I genes (HLA-A, -B and -C) encode single polypeptides organized into three domains: α_1, α_2, and α_3. Their surface expression on most nucleated cells of the body depends on the noncovalent association with a fourth domain, the non-MHC-encoded polypeptide β_2-microglobulin[13]. MHC class I molecules are important in the efferent limb of immunity, which is designed to destroy cells bearing foreign antigens. Foreign peptides presented within the cell are deposited in the binding groove of MHC class I molecules and expressed on the cell surface. Cytotoxic T cells recognize them and destroy the cell[14]. Certain MHC class I molecules have been found to be associated with various diseases, including type 1 diabetes and cholelithiasis[15-18]. An even stronger association has been found with MHC class II molecules[18, 19]. The initial explanation of HLA class I associations is linkage disequilibrium between certain subtypes of MHC class I and class II molecules[19, 20]. However, other studies have suggested that there may be other loci in the MHC gene complex that also play a role[21, 22]. Further investigation of such loci nearby or within MHC class I genes, such as MICA gene, is necessary to clarify these discrepancies.

MICA gene has recently been found to be more significantly associated with disease susceptibility that had been previously reported to be associated with the HLA-B locus (HLA-B7, -B8, -B15, -B18 in Caucasians; -Bw22, and -Bw54 in Chinese; -B5, -Bw52, and -Bw54 in Japanese are reportedly associated with various diseases)[4, 7, 8, 15, 16, 23-28]. This suggests that susceptibility associated with the HLA-B locus might be due to different genotypes of MICA gene.

MICA is specifically expressed by fibroblasts, epithelial cells, keratinocytes, endothelial cells, and monocytes[3, 29]. The molecule is similar to MHC class I antigens. Thus MICA is thought to represent a second lineage of MHC antigens and possibly to play a specialized or modified role in the immune response[3]. The recruitment of γδ T cells in skin and intestinal mucosa mirrors the pattern of expression of MICA and is consistent with the hypothesis that these molecules may play a role in inflammation and in the response to stress or damage in certain tissues[29]. MICA expression is regulated by promoter heat shock elements similar to those of HSP70 genes[30]. The high levels of MICA expression in epithelial cell lines together with the upregulation of MICA after heat shock may represent a molecular mechanism for exposing stressed epithelial cells to the immune system[31]. Thus MICA may function as an indicator of cell stress and may be recognized by γδ T cells in an unusual interaction. It is possible, therefore, that MICA regulates the immune response when cells are stressed and might be involved in the development of cholelithiasis.

However, our study showed that the polymorphic MICA alleles were not significantly associated with cholelithiasis, nor were there any differences when we looked at subgroups of patients, stratified according to sex, types of gallstone, or age. The latter factor is of interest in considering the contribution of heredity *vs.* environment. These results are perhaps not surprising, since the pathogenesis of cholelithiasis in Taiwan is multifactorial[32]. Nevertheless, our demonstration of the absence of an association between MICA gene and cholelithiasis is useful in pointing future research in other directions. The fact of the increased familial frequency of cholelithiasis[1] thus remains to be explained, perhaps by studying other loci on the human chromosome.

REFERENCES

1 **Gilat T,** Feldman C, Halpern Z, Dan M, Bar-Meir S. An increased familial frequency of gallstones. *Gastroenterol* 1983; **84:** 242-246

2 **Su CH,** Lui WY, P'eng FK. Relative prevalence of gallstone diseases in Taiwan. A nationwide cooperative study. *Dig Dis Sci* 1992; **37:** 764-768

3 **Bahram S,** Bresnahan M, Geraghty DE, Spies T. A second lineage of mammalian major histocompatibility complex class I genes. *Proc Natl Acad Sci USA* 1994; **91:** 6259-6263

4 **Mizuki N,** Ota M, Kimura M, Ohno S, Ando H, Katsuyama Y, Yamazaki M, Watanabe K, Goto K, Nakamura S, Bahram S, Inoko H. Triplet repeat polymorphism in the transmembrane region of

the MICA gene: A strong association of six GCT repetitions with Behcet's disease. *Proc Natl Acad Sci USA* 1997; **94:** 1298-1303

5 **Buffone GJ,** Darlington GJ. Isolation of DNA from biological specimens without extraction with phenol. *Clin Chem* 1985; **31:** 164-165

6 **Lee HH,** Chao HT, Ng HT, Choo KB. Direct molecular diagnosis of CYP21 mutations in congenital adrenal hyperplasia. *J Med Genet* 1996; **33:** 371-375

7 **Goto K,** Ota M, Ohno S, Mizuki N, Ando H, Katsuyama Y, Maksymowych WP, Kimura M, Bahram S, Inoko H. MICA gene and ankylosing spondylitis: linkage analysis via a transmembrane-encoded triplet repeat polymorphism. *Tissue Antigens* 1997; **49:** 503-507

8 **Goto K,** Ota M, Maksymowych WP, Mizuki N, Yabuki K, Katsuyama Y, Kimura M, Inoko H, Ohno S. Association between MICA gene A4 allele and acute anterior uveitis in white patients with and without HLA-B27. *Am J Ophthalmol* 1998; **126:** 436-441

9 **Perez-Rodriguez M,** Corell A, Arguello JR, Cox ST, McWhinnie A, Marsh SG, Madrigal JA. A new MICA allele with ten alanine residues in the exon 5 microsatellite. *Tissue Antigens* 2000; **55:** 162-165

10 **Hedrick PW.** Genetics of Populations. 2nd ed. Sudbury, Massachusetts: *Jones and Bartlett Publishers* 2000: 1-553

11 **Lee YJ,** Chen MR, Chang WC, Lo FS, Huang FY. A freely available statistical program for testing association. *MD Comput* 1998; **15:** 327-330

12 **Svejgaard A,** Ryder LP. HLA and disease associations: detecting the strongest association. *Tissue Antigens* 1994; **43:** 18-27

13 **Todd JA,** Bell JI, McDevitt HO. A molecular basis for genetic susceptibility to insulin-dependent diabetes mellitus. *Trends Genet* 1988; **4:** 129-134

14 **Walker RH.** The HLA system. In: Walker RH, eds. Technical Manual. Bethesda: *American Association of Blood Banks* 1993: 287-307

15 **Singal DP,** Blajchman MA. Histocompatibility (HL-A) antigens, lymphocytotoxic antibodies and tissue antibodies in patients with diabetes mellitus. *Diabetes* 1973; **22:** 429-432

16 **Nerup J,** Platz P, Anderson OO, Christiy M, Lyngsoe J, Poulsen JE, Ryder LP, Nielsen LS, Thomsen M, Svejgaard A. HL-A antigens and diabetes mellitus. *Lancet* 1974; **2:** 864-866

17 **Papasteriades C,** Al-Mahmoud I, Papageorgakis N, Romania ST, Katsas A, Ollier W, Economidou I. HLA antigen in Greek patients with cholelithiasis. *Dis Markers* 1990; **8:** 17-21

18 **Pokorny CS,** McCaughan GW, Gallagher ND, Selby WS. Sclerosing cholangitis and biliary tract calculi-primary or secondary. *Gut* 1992; **33:** 1376-1380

19 **Solow H,** Hidalgo R, Singal DP. Juvenile-onset diabetes HLA-A, -B, -C, and-DR alloantigens. *Diabetes* 1979; **28:** 1-4

20 **Farid NR,** Sampson L, Noel P, Barnard JM, Davis AJ, Hillman DA. HLA-D-related (DRw) antigens in juvenile diabetes mellitus. *Diabetes* 1979; **28:** 552-557

21 **Raum D,** Awdeh Z, Yunis EJ, Alper CA, Gabbay KH. Extended major histocompatibility complex haplotypes in type 1 diabetes mellitus. *J Clin Invest* 1984; **74:** 449-454

22 **Robinson WP,** Barbosa J, Rich SS, Thomson G. Homozygous parent affected sib pair method for detecting disease predisposing variants: Application to insulin dependent diabetes mellitus. *Genet Epidemiol* 1993; **10:** 273-288

23 **Ota M,** Katsuyama Y, Mizuki N, Ando H, Furihata K, Ono S, Pivetti-Pezzi P, Tabbara KF, Palimeris GD, Nikbin B, Davatchi F, Chams H, Geng Z, Bahram S, Inoko H. Trinucleotide repeat polymorphism within exon 5 of the MICA gene (MHC class I chain-related gene A): allele frequency data in the nine population groups Japanese, Northern Han, Uygur, Kazakhstan, Iranian, Saudi Arabian, Greek and Italian. *Tissue Antigens* 1997; **49:** 448-454

24 **Goto K,** Ota M, Ando H, Mizuki N, Nakamura S, Inoue K, Yabuki K, Kotake S, Katsuyama Y, Kimura M, Inoko H, Ohno S. MICA gene polymorphisms and HLA-B27 subtypes in Japanese patients with HLA-B27-associated acute anterior uveitis. *Invest Ophthalmol Vis Sci* 1998; **39:** 634-637

25 **Fukuda K,** Sugawa K, Wakisaka A, Moriuchi J, Matsuura N, Sato Y. Statistical detection of HLA and disease association. *Tissue Antigens* 1985; **26:** 81-86

26 **Thomson G.** HLA disease associations: Models for the study of complex human genetic disorders. *Crit Rev Clin Lab Sci* 1995; **32:** 183-219

27 **Hawkins BR.** Human leukocyte antigens in chinese. Hong-Kong: *Hong-Kong University Press* 1987: 1-122

28 **Kobayashi T,** Tamemoto K, Nakanishi K, Kato N, Okubo M. Immunogenetic and clinical characterization of slowly progressive IDDM. *Diabetes Care* 1993; **16:** 780-788

29 **Zwirner NW,** Fernandez-Vina MA, Stastny P. MICA, a new polymorphic HLA-related antigen, is expressed mainly by keratinocytes, endothelial cells, and monocytes. *Immunogenetics* 1998; **47:** 139-148

30 **Groh V,** Bahram S, Bauer S, Herman A, Beauchamp M, Spies T. Cell stress-regulated human major histocompatibility complex class I gene expressed in gastrointestinal epithelium. *Proc Natl Acad Sci USA* 1996; **93:** 12445-12450

31 **Bahram S,** Mizuki N, Inoko H, Spies T. Nucleotide sequence of the human MHC class I MICA gene. *Immunogenetics* 1996; **44:** 80-81

32 **Ho KJ,** Lin XZ, Yu SC, Chen JS, Wu CZ. Cholelithiasis in Taiwan. Gallstones characteristics, surgical incidence, bile lipid composition and role of β-glucuronidase. *Dig Dis Sci* 1995; **40:** 1963-1973

Edited by Xu XQ and Wang XL

P.O.Box 2345, Beijing 100023,China
Fax: +86-10-85381893
E-mail: wjg@wjgnet.com www.wjgnet.com

World J Gastroenterol 2003;9(7):1545-1549
World Journal of Gastroenterology
 ISSN 1007-9327

• BASIC RESEARCH •

Improvements of postburn renal function by early enteral feeding and their possible mechanisms in rats

Li Zhu, Zong-Cheng Yang, De-Chang Chen

Li Zhu, Department of Anesthesiology, Naval General Hospital, Beijing 100037, China
Zong-Cheng Yang, Institute of Burn Research, Southwest Hospital, Third Military Medical University, Chongqing 400038, China
De-Chang Chen, Department of Critical Care Medicine, Peking Union Medical College Hospital, Chinese Academy of Medical Sciences, Beijing 100730, China
Supported by National Natural Science Foundation of China, No. 30290700
Correspondence to: Dr. Zhu Li, Department of Anesthesiology, Naval General Hospital, Beijing 100037, China. zlicu@mail.china.com
Telephone: +86-10-68589503
Received: 2003-04-02 **Accepted:** 2003-05-19

Abstract

AIM: To investigate the protective effects of early enteral feeding (EEF) on postburn impairments of renal function and their possible mechanisms.

METHODS: Wistar rats with 30 % of total body surface area (TBSA) full-thickness burn were adopted as the experimental model. The effects of EEF on the postburn changes of gastric intramucosal pH (pHi), endotoxin levels in portal vein, water contents of renal tissue, and blood concentrations of tumor necrosis factor (TNF-α), urea nitrogen (BUN), creatinine (Cr), as well as the changes of clearance of creatinine (CCr) were dynamically observed within 48 h postburn.

RESULTS: EEF could significantly improve gastric mucosal acidosis, reduce portal vein endotoxin levels and water contents of renal tissue, as well as blood concentrations of TNF-α after severe burns ($P<0.01$). The postburn elevations of BUN and BCr were not found to be recovered by EEF. However, the CCr in EEF group was greatly increased by 4.67-fold compared with that of the non-feeding burned control (16.43±2.90 *vs*. 3.52±0.79, $P<0.01$).

CONCLUSION: EEF has beneficial effects on the improvement of renal function in severely burned rats, which may be related to its increase of splanchnic blood flow, decrease of the translocation of gut-origin endotoxin and the release of inflammatory mediators.

Zhu L, Yang ZC, Chen DC. Improvements of postburn renal function by early enteral feeding and their possible mechanisms in rats. *World J Gastroenterol* 2003; 9(7): 1545-1549
http://www.wjgnet.com/1007-9327/9/1545.asp

INTRODUCTION

Acute renal failure (ARF) is one of the well-known complications after severe burns with an extremely high incidence of death[1-4]. In most circumstances, it manifests as a part of multiorgan dysfunction syndrome[5, 6] and the kidney-oriented supportive therapy so far has not achieved satisfactory results[6, 7]. In recent years, abundant researches have suggested that the translocation of gut-origin endotoxin in certain pathological conditions may lead to remote organ injury[8, 9], which may also be the major contributor to renal dysfunction[10-13]. Meanwhile, it has become increasingly apparent that early enteral feeding (EEF) in various groups of patients could produce multiple beneficial effects, including increase of blood flow to the splanchnic organs, maintenance of gut mucosal integrity, prevention of intramucosal acidosis and permeability disturbances, and alleviation of the translocation of gut-origin bacteria and endotxin[14-19]. We therefore presume that EEF might be possible to improve renal function injured by severe burns, which up to now has been seldom documented. Thus, the present study was designed to demonstrate this hypothesis, in attempt to seek ways to improve the treatment of severely injured patients, which would be no doubt of both theoretical and practical importance.

MATERIALS AND METHODS

Animals

Healthy adult Wistar rats of both sexes, weighing 220±30 g, were employed in the study. They were housed in individual metabolic cages in a temperature conditioned room (22-24 ℃) with a 12 h light-dark circle, allowed access to standard rat chow (provided by experimental animal center, Third Military Medical University) and water ad libium, and acclimatized to the surroundings for 7 days prior to the experiments.

Operative procedure

All animals were weighed and anesthetized with 1 % pentobarbitale sodium (30 mg/kg, ip). After laparotomy, a polyethylene catheter (1.5 mm in diameter) was inserted into duodenum on the anterior wall 1.5 cm from pylorus via a puncture hole made by a metal needle for enteral feeding. The catheter was appropriately fixed, tunneled under the skin and exited through the nape skin. The animals were housed and fed as described above after operation.

Burn injury and resuscitation

After a recovery period of 24 h, the animals inserted with a feeding tube were anesthetized, having their dorsal hair shaved and placed in a wooden template designed to expose 30 % of the total body surface area (TBSA), and then immersed in water at 92 ℃ for 20 seconds, which resulted in a clearly demarcated full-thickness burn. One hour after burn injury, the animals were resuscitated with 10 ml of warm 0.9 % NaCl (normal saline solution, 37 ℃) given by intraperitoneal injection. Control animals were similarly anesthetized, shaved, resuscitated but not burned.

Feeding and experimental protocol

Nutrient feeding liquid was prepared as one with a caloric of 2.1 KJ/ml before use by mixing nutritional powder (ENSURE, USA) with an appropriate amount of warm boiled water. According to different feeding regimens, the animals were randomly divided into three groups: (1) EEF group. Enteral

feeding was initiated 1 h postburn in burned animals via a feeding tube with a total caloric of 202 KJ· Kg^{-1}· 24 h^{-1}. The feeding nutrient liquid required for 24 hours was administered evenly at 6 time points. (2) Burn group. The animals were treated exactly the same as EEF group, except that the nutrient feeding liquid was substituted for the same amount of saline. (3) Control group. Only the feeding tube was inserted, whereas no tube feeding and burn were conducted. The animals in this group were allowed access to standard rat chow, nutrition liquid and water ad libium. Time points for different measurements and assays in all groups were made at 3, 6, 12, 24 and 48 h postburn, except for the determination of renal tissue water content, which was performed at 12 h after thermal injury. 24-hr urine was collected for the detection of urea nitrogen and creatinine that were used to calculate CCr. For plasma assays, rats were sacrificed by decapitation at each time point and heparinised blood was collected in a separator tube spun at 3 000 g for 10 min, decanted and frozen at -20 ℃ until analysis.

Measurements

The gastric intramucosal pH was determined with an indirect method as previously described[20] with minor modifications. Briefly, the animals were anesthetized and injected cimetidine (15 mg) intraperitoneally 1 h prior to each time point, a polyethylene catheter was inserted into gastric lumen through pylorus via a puncture hole on the anterior wall of duodenum made by a metal needle after a midline laparotomy. A 2.5-ml of normal saline was injected into gastric lumen though the catheter and removed in order to get rid of intragastric residues, then 1.5-ml of normal saline was injected and retained in the gastric lumen. After an equilibration interval of 60 min, 1 ml of saline solution was aspirated and PCO_2 was determined using the blood gas analyzer. A simultaneously obtained arterial blood sample was used to determine the [HCO_3^-]. pHi was then calculated as:

$$pHi=6.1+\log([HCO_3^-] / [PCO_2\times 0.03])$$

The multifunction-biochemical analyzer Beckman Synchron CX-7 was employed to detect urea nitrogen and creatinine in both blood and urine.

Portal plasma endotoxin levels were assayed with the limulus-amoebocyte-lysate test (LAL)[21]. Briefly, plasma samples were diluted tenfold with pyrogen-free water and heated to 75 ℃ for 5 min to overcome assay inhibition by plasma. The samples were incubated with LAL for 33 min at 37 ℃. Then the chromogenic substrate was added and the samples was incubated for another 3 min. After the reaction was stopped with acetic acid, sample optical density was read at 545 nm and the endotoxin concentration was finally expressed as Eu/ml.

Radioimmunoassay of TNF-α levels in systemic circulation was conducted according to the instructions with kits from Dong-Ya Research Institute of Immunotechnology.

Renal tissue water contents were determined with a method as reported in a previous study[22] with minor modifications. Eight renal tissue samples for each group were harvested at 12 h postburn, weighed and put in an oven at 90 ℃ for 24 h, then weighed again. The renal tissue water contents were calculated as: Renal tissue water contents=(wet weight - dry weight / wet weight)×100 %

Statistical analysis

Experimental results were analyzed by analysis of variance and *t*-tests for multiple comparisons. Data were expressed as mean ± standard error of the mean. Statistical significance was determined at $P<0.05$.

RESULTS

BUN and BCr in both EEF and Burn groups were significantly increased postburn with the peak value at 6 h. Though gradually decreased thereafter, they were still significantly higher than those of the control at 24 and 48 h time points ($P<0.01$). The beneficial effects of EEF on the renal function manifested as the improvement of CCr, in which a 4.67-fold increase was observed in EEF group as compared with burn group and the CCr value in EEF group tended to be close to that in the control (Table 1).

Gastric mucosal acidosis was significantly improved in EEF group as indicated by the elevation of gastric pHi at most of the postburn time points, however, gastric pHi in burn group was sustained in lower levels until 48 h postburn (Table 2).

Table 3 displays the changes in portal endotoxin levels after severe burns. Three hours postburn, endotoxin concentration was significantly increased in burn group and peaked at 6 h, another increase appeared at 24 h and persisted until 48 h postburn. However, the portal endotoxin levels in animals that received EEF markedly decreased at almost all time points as compared with that of the burn group.

The data for plasma TNF-α levels are shown in Table 4. In accordance with other observations, EEF could also significantly reduce TNF-α levels in systemic circulation at most postburn time points as compared with that of burnt animals.

Table 1 Effects of EEF on postburn changes of BUN, BCr and CCr ($\bar{x}\pm s$)

Group	Samples	Postbun hours (h)				
		3	6	12	24	48
EEF	40					
BUN (mmol/L)		10.30±0.67[a d]	17.67±1.52[b d]	13.73±1.43[d]	8.73±2.10[d]	7.50±1.16[d]
BCr (mmol /L)		53.77±3.20[d]	89.60±6.54[b d]	55.44±3.57[d]	46.95±2.66[d]	42.90±2.23[d]
CCr (ml/h/100g)					16.43± 2.90 [b]	
Burn	40					
BUN (mmol/L)		11.76±1.72[d]	15.42±1.74[d]	13.48±1.56[d]	9.27±1.75[d]	7.68±1.63[d]
BCr (mmol /L)		51.80±2.83[d]	71.23±2.63[d]	57.70±4.93[d]	44.75±1.69[d]	41.76±1.26[d]
CCr (ml/h/100g)					3.52 ±0.79[d]	
Control	40					
BUN (mmol/L)		4.67±0.85	4.49±0.58	4.74±0.80	4.31±0.69	4.52±0.93
BCr (mmol /L)		37.43±3.64	37.67±3.26	37.28±4.42	36.94±3.71	37.69±3. 47
CCr (ml/h/100g)					19.45±2.21	

[a]$P<0.05$, [b]$P<0.01$ *vs* Burn group; [c]$P<0.05$, [d]$P<0.01$ *vs* Control.

Table 2 Effects of EEF on postburn changes of gastric intramucosal pH ($\bar{x}\pm s$)

Group	Samples	Postbun hours (h)				
		3	6	12	24	48
EEF	50	7.119±0.078[ab]	6.943±0.089[ab]	7.074±0.037[ab]	7.285±0.098[a]	7.257±0.077[ab]
Burn	50	7.017±0.037[b]	6.826±0.049[b]	6.802±0.080[b]	6.949±0.082[b]	7.074±0.041[b]
Control	50	7.321±0.054	7.296±0.067	7.343±0.045	7.306±0.069	7.348±0.074

[a]$P<0.01$ *vs* Burn group; [b]$P<0.01$ *vs* Control.

Table 3 Effects of EEF on postburn changes of portal endotoxin level (Eu / ml, $\bar{x}\pm s$)

Group	Samples	Postbun hours (h)				
		3	6	12	24	48
EEF	40	0.683±0.072[ab]	0.797±0.085[ab]	0.542±0.078[ab]	0.725±0.061[ab]	0.461±0.049[ab]
Burn	40	1.394±0.126[b]	1.518±0.173[b]	1.124±0.133[b]	1.627±0.215[b]	1.168±0.188[b]
Control	40	0.206±0.032	0.195±0.043	0.189±0.049	0.204±0.037	0.215±0.051

[a]$P<0.01$ *vs* Burn group; [b]$P<0.01$ *vs* Control.

Table 4 Effects of EEF on postburn changes of plasma TNF-a level (ng / ml, $\bar{x}\pm s$)

Group	Samples	Postbun hours (h)				
		3	6	12	24	48
EEF	40	1.48±0.38[ab]	2.57±0.45[ab]	2.36±0.47[ab]	1.92±0.26[ab]	1.68±0.45[ab]
Burn	40	1.92±0.19[b]	4.49±0.47[b]	3.51±0.45[b]	4.07±0.71[b]	3.24±0.61[b]
Control	40	0.83±0.08	0.78±0.11	0.83±0.12	0.81±0.09	0.85±0.10

[a]$P<0.01$ *vs* Burn group; [b]$P<0.01$ *vs* Control.

For EEF, burn and control groups of animals, the renal tissue water contents reached 75.36±0.99 %, 78.94±1.56 % and 76.26±1.25 % respectively (Figure 1). It was evident that a significant decrease of renal tissue water content was seen in EEF group compared with that in burn group at 12 h postburn ($P<0.01$).

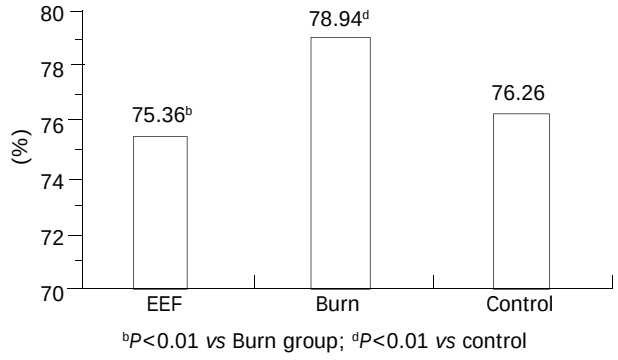

[b]$P<0.01$ *vs* Burn group; [d]$P<0.01$ *vs* control

Figure 1 Effects of EEF on water content of renal tissue 12 h postburn.

DISCUSSION

Nutritional support plays an important role in the management of critically ill patients to prevent and treat multiple organ dysfunction syndrome (MODS)[23]. Numerous clinical and animal studies have demonstrated that early enteral feeding could preserve the gut barrier function, diminish hypermetabolic response, maintain caloric intake, reduce the chance of gut origin infection and significantly shorten hospital stay following injury[14-19]. Unfortunately, the protective effects of EEF on the splanchnic function after severe traumas were relatively neglected in most of these investigations.

In a previous study, Roberts and his associates[24] observed that acute impairment of renal function inflicted by rhabdomyolysis was improved with EEF. Through 72 h dynamic observation, they found both BUN and BCr in EEF rats decreased by 65.7 % and 60 % respectively and the mortality reduced by 43 % compared with that of the animals fed with water. In contrast, in present animal model of severely thermal injury, BUN and BCr in both EEF and burn groups were significantly elevated, and no effect of EEF on the postburn changes of these variables was noted. We conjecture the phenomenon might be attributed to the more severity of the injury, difference in feeding components and blood condensation postburn. It has been reported that CCr could correlate well with the inulin clearance and exhibit renal function more accurately in the presence of acute renal failure[25]. In a animal study on renal dysfunction caused by ischemia, Mouser and his colleagues[25] demonstrated that the percentage of CCr increment in enterally fed animals was 2.5-fold higher than that in animals fed intravenously, whereas no significant changes of BUN and BCr were observed, showing that the improvement of renal function would not be always in accordance with BUN and BCr changes. In the present study, CCr in EEF animals increased by 4.67-fold compared with that in burn group, indicating that EEF could exert protective effects on the postburn renal impairment, and that aborative

attention should be paid to the selection of proper variables to perform such investigations.

The mechanisms of EEF to improve posttrauma renal function so far have not been clarified yet. It was once considered that the enhanced feeding of certain nutrients such as proteins or amino acids might increase the glomerular filtration rate (GFR). However, Mouser *et al*.[25] have shown that even with the same kind of nutrients, CCr in intravenously fed animals with renal ischemia was significantly lower than that in enterally fed animals, suggesting that the enteric factors beyond nutrients play a role in the improvement of impaired renal function. In fact, in severe traumas including burn, loss of large amount body fluids and release of stress hormones caused a sharp reduce of blood flow to many organs, especially the gastrointestinal tract and the kidney. Reduced intestinal blood flow then led to translocation of bacteria and/or their toxic products through the gut mucosa. Subsequent bacteria- and/or toxin-induced persistent and excessive release of cytokines (i.e. tumor necrosis factor, interleukins) and complement activation initiated progressive multiple organ failure and even caused death[26, 27]. In accordance with this theory, numerous studies have proposed that the renal ischemia and endotoxemia occurred in various pathological conditions be the major contributors to the renal dysfunction[10-13, 28-30].

Postprandial gut hyperemia is a locally mediated vascular response to the presence of foodstuff in the lumen, an important physiological phenomenon for food digestion and absorption. Even though in some pathological conditions, this phenomenon still exists. In burned guinea pigs, Inoue *et al*[31] using radiolabeled microspheres demonstrated that blood flow to the jejunum and cecum was higher in the diet group than in the control during initial 24 h of enteral feeding. In a dog model of splanchnic ischemia induced with endotoxin, Eleftheriadis *et al*.[32] reported that portal vein, hepatic and superior mesenteric artery blood flow, hepatic and intestinal microcirculation, hepatic tissue PO_2 and energy charge, and intestinal intramucosal pH were significantly increased after early enteral feeding, which were all reduced in the early septic condition. In the present study, we showed that postburn EEF could effectively restore reduced gastric intramucosal pH, decrease endotoxin concentrations in portal vein and TNF-α levels in systemic circulation, as well as alleviate renal tissue edema compared with burn controls. All the above indicate that in addition to provision of nutritional substrates, posttrauma EEF is most likely via a mechanism of postprandial hyperemia, to improve gut low flow and splanchnic ischemic status, to maintain gut mucosal integrity, and to block the vicious circle of mutual activation between the translocation of gut origin bacteria and their toxic products, and the release of inflammatory mediators[33], thereby reducing hypoxic and inflammatory tissue damage. However, detailed mechanisms are needed to be further studied.

The facts that EEF could improve postburn renal function are of both theoretical and practical importance. The present study revealed that EEF should not be taken merely as a method or a route for nutritional support. Its clinical value has exceeded the range of nutrition and is not limited to the locally enteric benefits as well. Although the results from the animal study can not be extrapolated directly to humans, a better understanding of the postburn EEF might lead to new ways for the further improvement in prevention and treatment of MODS posttrauma.

REFERENCES

1 **Holm C,** Horbrand F, von Donnersmarck GH, Muhlbauer W. Acute renal failure in severely burned patients. *Burns* 1999; **25**: 171-178

2 **Anlatici R,** Ozerdem OR, Dalay C, Kesiktas E, Acarturk S, Seydaoglu G. A retrospective analysis of 1083 Turkish patients with serious burns. Part 2: burn care, survival and mortality. *Burns* 2002; **28**: 239-243

3 **Kim GH,** Oh KH, Yoon JW, Koo JW, Kim HJ, Chae DW, Noh JW, Kim JH, Park YK. Impact of burn size and initial serum albumin level on acute renal failure occurring in major burn. *Am J Nephrol* 2003; **23**: 55-60

4 **Chrysopoulo MT,** Jeschke MG, Dziewulski P, Barrow RE, Herndon DN. Acute renal dysfunction in severely burned adults. *J Trauma* 1999; **46**: 141-144

5 **Davies MP,** Evans J, McGonigle RJ. The dialysis debate: acute renal failure in burns patients. *Burns* 1994; **20**: 71-73

6 **Triolo G,** Mariano F, Stella M, Salomone M, Magliacani G. Dialytic therapy in severely burnt patients with acute renal failure. *G Ital Nefrol* 2002; **19**: 155-159

7 **Tremblay R,** Ethier J, Querin S, Beroniade V, Falardeau P, Leblanc M. Veno-venous continuous renal replacement therapy for burned patients with acute renal failure. *Burns* 2000; **26**: 638-643

8 **Turnage RH,** Guice KS, Oldham KT. Endotoxemia and remote organ injury following intestinal reperfusion. *J Surg Res* 1994; **56**: 571-578

9 **LaNoue JL Jr,** Turnage RH, Kadesky KM, Guice KS, Oldham KT, Myers SI. The effect of intestinal reperfusion on renal function and perfusion. *J Surg Res* 1996; **64**: 19-25

10 **Yamaguchi H,** Kita T, Sato H, Tanaka N. Escherichia coli endotoxin enhances acute renal failure in rats after thermal injury. *Burns* 2003; **29**: 133-138

11 **Yokota M,** Kambayashi J, Tahara H, Kawasaki T, Shiba E, Sakon M, Mori T. Renal insufficiency induced by locally administered endotoxin in rabbits. *Methods Find Exp Clin Pharmacol* 1990; **12**: 487-491

12 **Heyman SN,** Rosen S, Darmon D, Goldfarb M, Bitz H, Shina A, Brezis M. Endotoxin-induced renal failure. II. A role for tubular hypoxic damage. *Exp Nephrol* 2000; **8**: 275-282

13 **Zager RA.** Escherichia coli endotoxin injections potentiate experimental ischemic renal injury. *Am J Physiol* 1986; **251**: F988-994

14 **Yamaguchi H**, Kita T, Sato H, Tanaka N. Escherichia coli endotoxin enhances acute renal failure in rats after thermal injury. *Burns* 2003; **29**: 133-138

15 **Hanna MK,** Kudsk KA. Nutritional and pharmacological enhancement of gut-associated lymphoid tissue. *Can J Gastroenterol* 2000; **14**(Suppl): 145D-151D

16 **Fukatsu K,** Zarzaur BL, Johnson CD, Lundberg AH, Wilcox HG, Kudsk KA. Enteral nutrition prevents remote organ injury and death after a gut ischemic insult. *Ann Surg* 2001; **233:** 660-668

17 **Alexander JW.** Is early enteral feeding of benefit? *Intensive Care Med* 1999; **25:** 129-130

18 **Kompan L,** Kremzar B, Gadzijev E, Prosek M. Effects of early enteral nutrition on intestinal permeability and the development of multiple organ failure after multiple injury. *Intensive Care Med* 1999; **25:** 157-161

19 **Eleftheriadis E.** Role of enteral nutrition-induced splanchnic hyperemia in ameliorating splanchnic ischemia. *Nutrition* 1999; **15:** 247-248

20 **Noc M,** Weil MH, Sun S, Gazmuri RJ, Tang W, Pakula JL. Comparison of gastric luminal and gastric wall PCO_2 during hemorrhagic shock. *Circ Shock* 1993; **40:** 194-199

21 **Buttenschoen K,** Berger D, Hiki N, Strecker W, Seidelmann M, Beger HG. Plasma concentrations of endotoxin and antiendotoxin antibodies in patients with multiple injuries: a prospective clinical study. *Eur J Surg* 1996; **162:** 853-860

22 **Jiang DJ,** Tao JY, Xu SY. Inhibitory effects of clonidine on edema formation after thermal injury in mice and rats. *Zhongguo Yaoli Xuebao* 1989; **10:** 540-542

23 **Bengmark S,** Gianotti L. Nutritional support to prevent and treat multiple organ failure. *World J Surg* 1996, **20:** 474-481

24 **Roberts PR,** Black KW, Zaloga GD. Enteral feeding improves outcome and protects against glycerol-induced acute renal failure in the rat. *Am J Respir Crit Care Med* 1997; **156:** 1265-1269

25 **Mouser JF,** Hak EB, Kuhl DA, Dickerson RN, Gaber LW, Hak LJ.

Recovery from ischemic acute renal failure is improved with enteral compared with parenteral nutrition. *Crit Care Med* 1997; **25:** 1748-1754

26 **Vincent JL.** Prevention and therapy of multiple organ failure. *World J Surg* 1996; **20:** 465-470

27 **Pastores SM,** Katz DP, Kvetan V. Splanchnic ischemia and gut mucosal injury in sepsis and the multiple organ dysfunction syndrome. *Am J Gastroenterol* 1996; **91:** 1697-1710

28 **Lugon JR,** Boim MA, Ramos OL, Ajzen H, Schor N. Renal function and glomerular hemodynamics in male endotoxemic rats. *Kidney Int* 1989; **36:** 570-575

29 **Van Lambalgen AA,** Van Kraats AA, Van den Bos GC, Stel HV, Straub J, Donker AJ, Thijs LG. Renal function and metabolism during endotoximia in rats: role of hypotention. *Circ Shock* 1991; **35:** 164-173

30 **Begany DP,** Carcillo JA, Herzer WA, Mi Z, Jackson EK. Inhibition of type IV phosphodiesterase by Ro 20-1724 attenuates endotoxin-induced acute renal failure. *J Pharmacol Exp Ther* 1996; **278:** 37-41

31 **Inoue S,** Lukes S, Alexander JW, Trocki O, Silberstein EB. Increased gut blood flow with early enteral feeding in burned guinea pigs. *J Burn Care Rehabil* 1989; **10:** 300-308

32 Eleftheriadis E, **Kazamias P,** Kotzampassi K, Koufogiannis D. Influence of enteral nutrition-induced splanchnic hyperemia on the septic origin of splanchnic ischemia. *World J Surg* 1998; **22:** 6-11

33 **Gianotti L,** Alexander JW, Nelson JL, Fukushima R, Pyles T, Chalk CL. Role of early enteral feeding and acute starvation on postburn bacterial translocation and host defense: prospective, randomized trials. *Crit Care Med* 1994; **22:** 265-272

Edited by Zhang JZ and Wang XL

P.O.Box 2345, Beijing 100023,China
Fax: +86-10-85381893
E-mail: wjg@wjgnet.com www.wjgnet.com

World J Gastroenterol 2003;9(7):1550-1553
World Journal of Gastroenterology
 ISSN 1007-9327

• BASIC RESEARCH •

Application of modified two-cuff technique and multiglycosides tripterygium wilfordii in hamster-to-rat liver xenotransplant model

Hua Guo, Yi-Jun Wu, Shu-Sen Zheng, Wei-Lin Wang, Jun Yu

Hua Guo, Yi-Jun Wu, Shu-Sen Zheng, Wei-Lin Wang, Jun Yu, Department of Hepatobiliary Surgery, First Affiliated Hospital, Medical College Zhejiang University, Hangzhou 310003, Zhejiang Province, China
Supported by Chinese Traditional Medicine Administration of Zhejiang Province Foundation, No.2000C55
Correspondence to: Dr. Hua Guo, Department of Hepatobiliary Surgery, First Affiliated Hospital, Medical College of Zhejiang University, 79 Qingchun Lu, Hangzhou 310003, Zhejiang Province, China. ggghua@mail.hz.zj.cn
Telephone: +86-571-87236857 **Fax:** +86-571-87236618
Received: 2003-01-11 **Accepted:** 2003-03-10

Abstract

AIM: To modify the hamster-to-rat liver xenotransplant technique to prevent postoperative complications, and to study the inhibiting effect of multiglycosides tripterygium wilfordii (T_{II}) on immune rejection.

METHODS: Female golden hamsters and inbred male Wistar rats were used as donors and recipients, respectively. One hundred and twelve orthotopic liver xenotransplants were performed by Kamada's cuff technique with modifications. Over 72 hour survival of the animal after operation was considered as a successful operation. When the established surgical model became stable, 30 of the latest 42 cases were divided into untreated control group (n=15) and T_{II} group (n=15) at random. Survival of recipients was observed. Liver specimens were collected at 2 and 72 h from the operated animals and postmortem, respectively, for histological study.

RESULTS: The successfully operative rate of the 30 operations was 80 %, and the survival of the control and T_{II} group was 7.1±0.35 was days and 7.2±0.52 days, respectively (t=0.087,P=0.931). The rate of conjunctival hyperemia in control group (100 %) differed significantly from that (31 %) in T_{II} group (P=0.001). Rejection did not occur in both groups within 2 h postoperatively, but became obvious in control group at 72 h after surgery and mild in T_{II} group. Although rejections were obvious in both groups at death of recipients, it was less severe in T_{II} group than in control group.

CONCLUSION: This modified Kamada's technique can be used to establish a stable hamster-to-rat liver xenotransplant model. Monotherapy with multiglycosides tripteryguiumwilfordii (30 mg· kg^{-1}· d^{-1}) suppresses the rejection mildly, but fails to prolong survival of recipients.

Guo H, Wu YJ, Zheng SS, Wang WL, Yu J. Application of modified two-cuff technique and multiglycosides tripterygium wilfordii in hamster-to-rat liver xenotransplant model. *World J Gastroenterol* 2003; 9(7): 1550-1553
http://www.wjgnet.com/1007-9327/9/1550.asp

INTRODUCTION

The hamster-to-rat liver transplant model is useful to study immunology and physiology of liver xenotransplantation (XT)[1-11], especially for the extended host response to long-surviving xenografts[12]. As it is very difficult to establish this surgical model[13], we summarized our surgical experience in producing for performing this model.

The model could serve as a tool to evaluate immunosuppressive drugs[14,15]. Tripterygium wilfordii hook F (TWHF) has been used for more than two thousand years as a traditional Chinese herb. T_{II} is extracted and refined from the root of TWHF. In recent years, T_{II} and other extracts of TWHF have been applied to allotransplantation and cardiac XT as immunosuppressive drugs with successful results[16-27]. However, the effects of T_{II} in liver XT are unknown and deserve study.

MATERIALS AND METHODS

Animals and liver xenotransplantation

Female golden hamsters (weighing 80-130 g) and inbred male Wistar rats (weighing 130-180 g) were used as donors and recipients, respectively. One hundred and twelve orthotopic liver xenotransplants were performed by Kamada's cuff technique[28] with modifications, which were outlined as follows.

Donor operation Ligaments and vessels around the liver were partially dissected while the liver was protected by wrapping film. The common bile duct was entered from anterior wall and a Teflon catheter was inserted into the lumen proximally. The proper hepatic artery was dissected but not ligated. The infrahepatic vena cava (VC) was clamped at the level of left renal vein. The liver was perfused through the abdominal aorta with 10-20 ml of cold (4 ℃) lactated Ringer's solution containing 5 U/ml of heparin. Meanwhile the thoracic cavity was opened with the thoracic aorta clamped, and the thoracic inferior VC was opened to release the perfusate. Then, the infrahepatic VC was transected at the upper part of the clamp. So the perfusate could escape from the two ends of VC. Deep ligaments around the liver were dissected while perfusing and the right suprarenal vein was ligated. At the end of perfusion, the proper hepatic artery and portal vein (PV) at the level of splenic vein were ligated and transected. The free liver was stored in lactated Ringer's solution at 0-4 ℃.

Preparation of donor liver Preparation of the donor liver was done in lactated Ringer's solution at 0-4 ℃. Two cuffs with different diameters were mounted on the PV and infrahepatic VC, respectively. The cystic duct near the common bile duct was ligated and followed by removal of the gallbladder. The suprahepatic VC was trimmed and a stitch was left on each side for suture.

Recipient operation Vessels, the common bile duct and ligaments around the recipient liver were divided, respectively. The right suprarenal vein behind the papilla lobe was ligated, the recipient liver was removed and covered with fresh film orthotopically. The suprahepatic VC was sutured, the PV was anastomosed with cuff method. The infrahepatic VC was anastomosed as the method for suprahepatic VC. Finally, the distal part of Teflon catheter in donor bile duct was inserted into the recipient bile duct and secured by a silk suture. The greater omentum was wrapped around the bile duct. The abdominal incision was closed with continuous suture.

Treatment of the animal with T_{II}

When the model became stable, 30 recipients of the latest 42 cases were divided into untreated controls (n=15) and treatment group with T_{II} 30 mg· kg^{-1}· d^{-1} (n=15) at random by gavages three days prior to operation till the end of experiment.

Liver specimens were collected at 2 and 72 h after operation or at death of the recipients, respectively, fixed in 10 % formalin, embedded in paraffin, sectioned and stained with hematoxylin and eosin for light microscopy to determine the grade of rejection.

Statistical methods

The results were analyzed by t test and Fisher' s exact test, respectively. Statistical significance was defined as a P value less than 0.05.

RESULTS

Liver xenotransplantation

One hundred and twelve operations were performed from October 2000 to March 2001. The successful rate of the latest 30 operations was 80 % (24/30). The causes of death were anesthesia accident in one case, chronic hemorrhage from the surface of donor liver in 3 cases, thrombosis in infrahepatic VC in one case and suppurate peritonitis in one case. The 6 recipients died within 72 h after operation were excluded from the experiment[14]. The average survival of 24 cases was 7.2±0.44 days.

Effects of T_{II} on survival of recipients

The average survival of the untreated controls and T_{II} group was 7.1±0.35 days and 7.2±0.52 days, respectively (t=0.087, P=0.931). Four cases in controls and 2 in T_{II} group died within 72 h after operation were eliminated from statistic study.

Effects of T_{II} on conjunctival hyperemia of recipients

The morbidity of conjunctival hyperemia was 100 % (11/11) in controls and 31 % (4/13) in T_{II} group (P=0.001). The commence time of conjunctival hyperemia in controls and T_{II} group were 4.73±0.47 days and 5.75±0.5 days, respectively (t=3.688, P=0.003).

Pus in conjunctiva was obvious in controls with conjunctival hyperemia, and three cases had ablepsia. However, no pus and ablepsia were observed in T_{II} group.

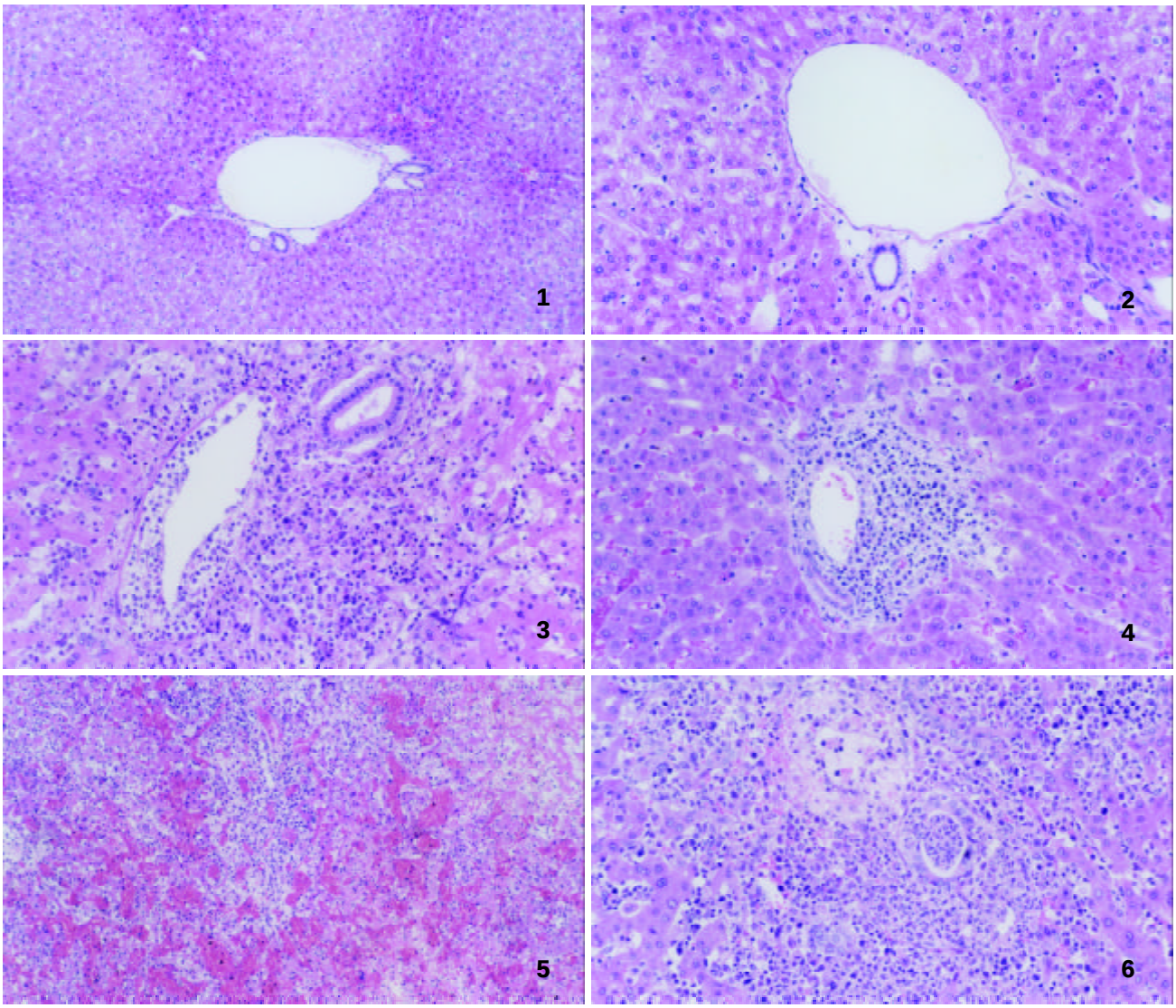

Figure 1 Histological changes of the liver in controls (HE, ×100).
Figure 2 Histological changes of the liver in T_{II} group (HE,×200).
Figure 3 Histological changes of the liver in controls (HE, ×200).
Figure 4 Histological changes of the liver in T_{II} group (HE,×200).
Figure 5 Histological changes of the liver in controls (HE,×100).
Figure 6 Histological changes of the liver in T_{II} group (HE,×200).

Histopathology

Two hours after operation The structures of hepatic lobule were normal and no inflammatory cells in portal area in both groups were observed (Figures 1 and 2).

Seventy-two hours after operation In controls, hepatic lobules were normal, numerous inflammatory cells consisting mainly of mononuclear cells and neutrophilic granulocytes infiltrated in portal area, edema could be seen in the tunica intima of interlobular veins and inflammatory cells infiltrated into subintima. However, epithelia of interlobular bile ducts were not injured (Figure 3).

In T_{II} group, the structures of hepatic lobules and interlobular veins were normal, moderate amounts of inflammatory cells were found in portal area, and epithelium of interlobular bile ducts was intact (Figure 4).

Postmortem specimens on day 7 postoperation In controls, hepatic lobules were damaged severely, inflammatory cells consisting mainly of mononuclear cells and neutrophilic granulocytes in portal area as well as massive hemorrhage were observed, interlobular vessels were disappeared and damaged epithelia of interlobular bile ducts were observed (Figure 5).

In T_{II} group, many mixed cells could also be seen in portal area, but most of the interlobular vessels and bile ducts were existed with inflammatory intima, and variable injured epithelia, hepatocytes around portal area were swollen, degenerated and partially necrotic and some liver plates were destroyed (Figure 6).

DISCUSSION

Sun *et al.*[29] firstly advocated that perfusate should enter the liver via dual vascular systems of the hepatic artery and the PV, then the liver and its structures around were divided. The authors performed 300 liver transplantations in rats, and the successful rate of operation and survival rate in one week were 92.7 % and 88.4 %, respectively. So we adopted this dual perfusion except for perfusion by PV in initial trials of 20 cases. We found that perfusion by PV could often result in incomplete perfusion in some small areas and undesirable pressure. Incomplete perfusion did not occur with dual perfusion, and due to the invariant pressure of intestinal circulation, the liver was not mechanically injured by fluctuant pressure and warm ischemia and mechancial injuries were avoided. If the donor liver was dissected at the end of complete perfusion, the vessels became pale and were difficult to be identified and were easily injured accidentally. After modification of the technique, the quality of the liver in donor was excellent in the trials and the survival time of recipient animals was similar to that in the literature[14,30,31].

We used to ligate the cystic duct, and then to remove the gallbladder and electrocauterize the bed of the gallbladder. However, it usually rendered slow hemorrhage in the bed of the gallbladder and the recipients died in hours after transplantation. So we modified the method as follows: ligating cystic duct near the common bile duct, then ligating cervix of the gallbladder and cutting gallbladder at the distal side of the ligation. No postoperative hemorrhage was observed after the modifications.

For the sake of exposing and ligating suprahepatic VC of the donor and the recipient, papilla lobe and right lobe of the liver were turned over frequently and thus were injured easily, and the recipient could die from mild hemorrhage from the surface of the graft. Sometimes, ligation of the infra-branch of suprarenal vein was mistaken for main stem with left supra-branch unligated, which rendered hemorrhage at recipient liver' s cutting and posttransplantation. Therefore, we ligated the right suprarenal vein at the end of perfusion, the structures around the donor liver were divided completely and the right suprarenal vein was exposed easily, so that liver injury and false ligation were reduced. Loop-ligation behind papilla lobe method was used to ligate the suprarenal vein of the recipient. The right suprarenal vein and part of ligaments behind the recipient liver were ligated with 5-0 silk sutures behind the papilla lobe and near the infrahepatic VC. This ligation was reliable, simple, and shortened the anhepatic phase directly.

Hamster' s liver is more fragile than that of rat. Slight press or attrition on its surface could result in contuse and chronic hemorrhage. Moreover, it has poor coagulating mechanism. Thus, fresh film has been used to protect the donor liver in operation, and the pressure on donor liver could be dispersed, the accident stab to the donor liver by instruments could be relieved to some extent and the donor liver could be kept from drying and crisping. Moreover, careful and delicate operation should not be ignored. Nevertheless, in our 30 trials, 3 of 6 failed cases died due to chronic hemorrhage on the surface of the donor liver.

We found that T_{II} at a dosage of 30 $mg\cdot kg^{-1}\cdot d^{-1}$ could not prolong the survival of the operated animal. But the rejection in T_{II} group was less severe in comparison with that of controls. We speculated that this dosage of T_{II} had certain limited immunosuppressive effect. Li *et al.*[32] found that the extracts of TWHF could inhibit human peripheral blood mononuclear cells (PBMC) in a concentration-dependent manner and the best inhibitory rate could be achieved at 72 h. Another research suggested that T_{II} at a dosage of 30 $mg\cdot kg^{-1}\cdot d^{-1}$ had no effects on the liver, kidney, heart and the total number of WBC in rat, but could inhibit the transforming of spleen lymphocytes significantly. T_{II} at this dosage could prolong the survival time of renal allotransplantation in Wistar-to-SD combination significantly. When it was combined with CsA, the survival time could be further prolonged[19]. Nevertheless, in other organ transplantations such as small intestine transplantation, whose rejection was relatively strong, and the monotherapy with T_{II} was demonstrated to have limited effects[21]. Wang *et al.*[16] applied PG27 (extract of TWHF) combined with a low dosage of CsA to hamster-to-rat cardiac xenotransplantation and all xenografts survived more than 100 days. However, they found that either PG27 or CsA had no such effects. Therefore, although a high dosage of T_{II} was given to the recipient 3 days before operation in our trials as monotherapy, the survival time of the recipient was not prolonged due to the strong rejection in this model.

In this study, conjunctival hyperemia occurred in all untreated control recipients on day 4-5 after operation, and deteriorated rapidly, even resulted in ablepsia. However, in the recipients treated with T_{II}, the sign occurred only in 31 % rats (on day 5-6 after transplantation) and ablepsia did not occur. The differences between the two groups were highly significant and the similar report has not been found in literature. We speculated that conjunctival hyperemia could be a local representation of rejection in this model. Relieving the sign with T_{II} treatment supported the hypothesis, but the exact mechanism of the sign needs to be further studied.

REFERENCES

1 **Tandin A,** Goller AL, Miki T, Lee YH, Kovscek AM, Fung JJ, Starzl TE, Valdivia LA. Concordant hamster-to-rat liver xenotransplantation leads to hyperlipidemia. *Transplant Proc* 2000; **32:** 1109

2 **Celli S,** Marto JA, Falchetto R, Shabanowitz J, Valdivia LA, Fung JJ, Hunt DF, Kelly RH. Serum protein immunogenicity: implications for liver xenografting. *Electrophoresis* 2000; **21:** 965-975

3 **Mollevi DG,** Jaurrieta E, Ribas Y, Hurtado I, Serrano T, Gomez N, de-Oca J, Fiol C, Figueras J. Liver xenotransplantation: changes in lipid and lipoprotein concentration after long-term graft survival. *J Hepatol* 2000; **32:** 655-660

4 **Tan JW,** Zhang SG, Jiang Y, Yang JM, Qian GX, Wu MC. Apoptosis in acute rejection of hamster-to-rat liver transplantation. *HBPD Int* 2002; **1:** 340-344

5 **Tan JW,** Yao HX, Yang JM, Qian GX, Wu MC. The role of spleen in rejection of concordant liver xenograft. *Zhonghua Qiguan Yizhi Zazhi* 2000; **21:** 83-85

6 **Valdivia LA,** Fung JJ, Demetris AJ, Celli S, Pan F, Tsugita M, Starzl TE. Donor species complement after liver xenotransplantation. *Transplantation* 1994; **57:** 918-922

7 **Schraa EO,** Stockmann HB, Broekhuizen AJ, Scheringa M, Schnurman HJ, Marquet RL, Ijzermans JN. IgG, but IgM, mediates hyperacute rejection in hepatic xenografting. *Xenotransplantation* 1999; **6:** 110-116

8 **Diao TJ,** Yuan TY, Li YL. Immunologic role of nitric oxide in acute rejection of golden hamster to rat liver xenotransplantation. *World J Gastroenterol* 2002; **8:** 746-751

9 **Zhang SG,** Wu MC, Tan JW, Chen H, Yang JM, Qian QJ. Expression of perforin and granzyme B mRNA in judgement of immunosuppressive effect in rat liver transplantation. *World J Gastroenterol* 1999; **5:** 217-220

10 **Valdivia LA,** Demetris AJ, Fung JJ, Celli S, Murase N, Starzl TE. Successful hamster-to-rat liver xenotransplantation under FK506 immunosuppression induces unresponsiveness to hamster heart and skin. *Transplantation* 1993; **55:** 659-661

11 **Celli S,** Valdivia LA, Fung JJ, Kelly RH. Early recipient-donor switch of the complement type after liver xenotransplantation. *Immunol Invest* 1997; **26:** 589-600

12 **Mollevi DG,** Ribas Y, Ginesta MM, Serrano T, Mestre M, Vidal A, Figueras J, Jaurrieta E. Heart and liver xenotransplantation under low-dose tacrolimus: graft survival after withdrawal of immunosuppression. *Transplantation* 2001; **71:** 217-223

13 **Tan JW,** Zhang SG, Qian GX, Wu MC. The modified for orthotopic liver transplantation model in hamster-to-rat. *Zhongguo Puwai Jichu Yu Linchuang Zazhi* 1999; **6:** 201-203

14 **Murase N,** Starzl TE, Demetris AJ, Valdivia L, Tanabe M, Cramer D, Makowka L. Hamster-to-rat heart and liver xenotransplantation with FK506 plus antiproliferative drugs. *Transplantation* 1993; **55:** 701-708

15 **Murase N,** Demetris AJ, Tanabe M, Miyazawa H, Valdivia LA, Nakamura K, Starzl TE. Effect of FK506 and antiproliferative agents for heart and liver xenotransplantation from hamster to rat. *Transplant Proc* 1993; **25:** 425-426

16 **Wang J,** Xu R, Jin R, Chen Z, Fidler JM. Immunosuppressive activity of the Chinese medicinal plant Tripterygium wilfordii. II. Prolongation of hamster-to-rat cardiac xenograft survival by combination therapy with the PG27 extract and cyclosporine. *Transplantation* 2000; **70:** 456-464

17 **He X,** Verran D, Hu C, Wang C, Li L, Wang L, Huang J, Sun J, Sheil AG. Synergistic effect of Triptergium Wilfordii Hook F [TWHF] and cyclosporine A in rat liver transplantation. *Transplant Proc* 2000; **32:** 2054

18 **Qian YY,** Shi BY, Liang CQ, Li N, Shi YC, Xia JM. Effects of total gulcosides of triptergium wilfordii (T_{II}) on the reproductive organs of transplant recipients. *Zhonghua Miniao Waike Zazhi* 2002; **23:** 209-211

19 **Zhang LL,** Sun JH. Synergistic effect of triptergium wilfordii hook f and cyclosporine A on hetertopic rat cardiac allograft survival. *Zhonghua Shiyan Waike Zazhi* 2001; **18:** 407-408

20 **Qian YY,** Shi BY, Liang CQ, Kang XJ, Shi YC, Li N, Xia JM. Total glucosides of triptergium wilfordii in the management of rats with renal allograft. *Zhonghua Miniao Waike Zazhi* 1996; **17:** 338-340

21 **Li YX,** Li N, Wu B, Li JS. The effect of Triptergium wilfordii on acute rejection in small bowel transplantation in rats. *Zhonghua Xiaoer Waike Zazhi* 2000; **21:** 49-51

22 **Wang DH,** Wang JP, Wang L. Role of triptergium wilfordii hook f($T_{\epsilon\delta}$) on pancreaticoduodenal allograft in rats. *Zhonghua Qiguan Yizhi Zazhi* 2000; **21:** 220-222

23 **Shao QX,** Yin L, Xu HX, Li LJ, Liu GZ, Cao YQ, Chen M. Using DcsMcAb and tripterygll multi-glycosidorum to prevent the rejection of heart-lung allogeneic transplantation in rats. *Zhongguo Mianyixue Zazhi* 1998; **14:** 356-359

24 **Li N,** Li JS, Li YS, Jiang ZW, Yin L, Zhao YZ. Experimental and clinical studies of small bowel allotransplantation. *Zhonghua Waike Zazhi* 1995; **33:** 11-14

25 **Qian YY,** Shi By, Liang CQ. Total glucosides of triptergium wilfordii (T_{II}) as an immuno-suppressant in kidney transplantation. *Zhonghua Miniao Waike Zazhi* 1995; **16:** 268-269

26 **Chen BJ.** Triptolide, a novel immunosuppressive and anti-inflammatory agent purified from a Chinese herb Tripterygium wilfordii Hook F. *Leuk Lymphoma* 2001; **42:** 253-265

27 **Ramgolam V,** Ang SG, Lai YH, Loh CS, Yap HK. Traditional Chinese medicines as immunosuppressive agents. *Ann Acad Med Singapore* 2000; **29:** 11-16

28 **Kamada N,** Calne RY. A surgical experience with five hundred thirty liver transplants in the rat. *Surgery* 1983; **93:** 64-69

29 **Sun JH,** Zeng QH, Wu MC. Experience with orthotopic rat liver transplantation. *Chin Med J Engl* 1990; **103:** 142-145

30 **Valdivia LA,** Monden M, Gotoh M, Hasuike Y, Kubota N, Endoh W, Okamura J, Mori T. Hepatic xenografts from hamster to rat. *Transplant Proc* 1987; **XIX:** 1158-1159

31 **Sankary HN,** Yin DP, Chong ASF, Ma LL, Blinder L, Shen JK, Foster P, Williams JW. FK506 treatment in combination with leflunomide in hamster-to-rat heart and liver xenograft transplantation. *Transplantation* 1998; **66:** 832-837

32 **Li XW,** Weir MR. Radix *Tripterygium Wilfordii*-a Chinese herbal medicine with potent immunosuppressive properties. *Transplantation* 1990; **50:** 82-86

Edited by Ren SY and Wang XL

P.O.Box 2345, Beijing 100023,China
Fax: +86-10-85381893
E-mail: wjg@wjgnet.com www.wjgnet.com

World J Gastroenterol 2003;9(7):1554-1558
World Journal of Gastroenterology
 ISSN 1007-9327

• BASIC RESEARCH •

Expression of metallothionein gene at different time in testicular interstitial cells and liver of rats treated with cadmium

Xu-Yi Ren, Yong Zhou, Jian-Peng Zhang, Wei-Hua Feng, Bing-Hua Jiao

Xu-Yi Ren, Yong Zhou, Jian-Peng Zhang, Wei-Hua Feng, Bing-Hua Jiao, Department of Biochemistry and Molecular Biology, Second Military Medical University, Shanghai 200433, China
Supported by the National Natural Science Foundation of China, No. 39970631
Correspondence to: Dr. Xu-Yi Ren, Department of Biochemistry and Molecular Biology, Second Military Medical University, Shanghai 200433, China. renxuyi2003@163.com
Telephone: +86-21-25070306-8008 **Fax:** +86-21-65334344
Received: 2002-12-30 **Accepted:** 2003-03-04

Abstract

AIM: Rodent testes are generally more susceptible to cadmium (Cd)-induced toxicity than liver. To clarify the molecular mechanism of Cd-induced toxicity in testes, we compared metallothionein (MT) gene expression, MT protein accumulation, and Cd retention at different time in freshly isolated testicular interstitial cells and liver of rats treated with Cd.

METHODS: Adult male Sprague-Dawley rats weighing 250-280 g received a s.c injection of 4.0 μmol Cd/kg and were euthanized by CO_2 asphyxiation 1 h, 3 h, 6 h, or 24 h later. Tissue was sampled and testicular interstitial cells were isolated. There were three replicates per treatment and 3 animals per replicate for RNA analyses, others, three replicates per treatment and one animal per replicate. MT1 and MT2 mRNA levels were determined by semi-quantitative RT-PCR analysis followed by densitometry scanning, and MT was estimated by the enzyme-linked immunosorbent assay (ELISA) method. Cadmium content was determined by atomic absorption spectrophotometry. The same parametersd were also analyzed in the liver, since this tissue unquestionably accumulate MT.

RESULTS: The rat testis expressed MT1 and MT2, the major isoforms. We also found that untreated animals contained relatively high basal levels of both isoform mRNA, which were increased after Cd treatment in liver and peaked at 3 h, followed by a decline. In contrast, the mRNA levels in interstitial cells peaked at 6 h. Interestingly, the induction of MT1 mRNA was lower than MT2 mRNA in liver of rat treated with Cd, but it was opposite to interstitial cells. Cd exposure substantially increased hepatic MT (3.9-fold increase), but did not increase MT translation in interstitial cells.

CONCLUSION: Cd-induced expression of MT isoforms is not only tissue dependent but also time-dependent. The inability to induce the metal-detoxicating MT-protein in response to Cd, may account for a higher susceptibility of testes to Cd toxicity and carcinogenesis compared to liver.

Ren XY, Zhou Y, Zhang JP, Feng WH, Jiao BH. Expression of metallothionein gene at different time in testicular interstitial cells and liver of rats treated with cadmium. *World J Gastroenterol* 2003; 9(7): 1554-1558
http://www.wjgnet.com/1007-9327/9/1554.asp

INTRODUCTION

Metallothionein (MT) gene expression appears to be not only tissue specific but also cell specific[1,2]. In rodents, the testes and ventral prostate have been shown to have a higher sensitivity to cadmium (Cd)-induced carcinogenesis than many other tissues[3]. These tissues have also been shown to have either no induction or a reduced expression of MT gene when animals were exposed to Cd or some other MT inducer agents[4,5]. It has been reported that testicular Cd is bound to a protein different from MT. The testicular Cd-binding protein contains less cysteine and more glutamate than MT[6]. However, some other studies have shown that MT is constitutively expressed in the whole testes or specific testicular cells at levels higher than that in some other organs, e.g. the liver, and that *in vivo* or *in vitro* Cd exposure increases MT gene expression in the testes[7-9].

Therefore, the published data are inconclusive as to whether MT exists in the testes under physiological conditions and whether this protein plays an important role in the detoxification of testicular Cd. Some of the controversies may derive from analyzing the whole testicular tissue instead of individual cell types, since MT gene expression appears to be not only tissue specific but also cell specific[1,2]. On the other hand, MT might affect testicular Cd accumulation toxicokinetically by sequestering the metal in the liver, thus diverting it from target tissues, such as the testes. It has been well established that Cd significantly enhances hepatic MT gene expression and MT synthesis. Such enhancement of liver MT might lead to lower testicular Cd uptake and toxicity.

In rodents testicular Cd appears to be localized in the interstitial tissue and a high incidence of interstitial cell (Leydig cell) tumors can occur following Cd exposure. However, testicular lesions as a result of Cd exposure have not been reported in men[10]. A single s.c. dose $\geqslant$5 μmol Cd/kg could result in a high incidence of testicular interstitial cell tumors. An elevated incidence of testicular tumors in rats was also found after chronic oral exposure to Cd. Within the interstitial tissue, Leydig cells appeared to be highly sensitive to Cd cytotoxicity[11]. However, most of the studies on MT gene expression and synthesis have been focused on the whole testes, which might mask the results on MT activity in these specific cells, since they only contributed to 11 % of parenchymal volume. Some authors investigated Cd-induction of MT expression in cultured Leydig cell lines established from Leydig cell tumors[12], but their findings gave little insight into MT synthesis in normal testicular interstitial cells or purified Leydig cells isolated from animals exposured to Cd.

Furthermore, MT gene expression is time-dependent. It was reported that both MT isoform mRNA levels in rat livers were substantially increased 4-6 h after Cd treatment, followed by a reduction and chromatography demonstrated a significant time-related increase in MT protein level. *In vitro* studies showed that MT induction was dose- and time-dependent in both Leydig and Sertoli cells[13]. Therefore some of the controversies may derive from the different study time.

In general, the studies on Cd-induced MT gene expression and MT synthesis in the testis, have been carried out under acute exposure to toxic Cd levels. It is also conceivable that

the biochemical changes occurring in the testes under such conditions of Cd toxicity might mask the molecular processes of MT gene expression at a lower Cd exposure dose.

Although there is a wealth of published information regarding MT gene expression and MT synthesis following induction by Cd[14-16], little systematic information is available on MT gene expression at different time in testes, particularly in testicular interstitial cells. The aim of this study therefore was to clone MT gene and to investigate MT gene expression, MT accumulation, and Cd retention at different time in testicular interstitial cells isolated by collagenase dispersion and density gradient centrifugation from rats treated with a non-toxic Cd dose. The same parameters in the liver were also analyzed, since this tissue unquestionably accumulated MT.

MATERIALS AND METHODS

Animals and treatments

Adult male Sprague-Dawley rats weighing 250-280 g were obtained from the Animal Center of Second Military Medical University. Rats received a single s.c. injection of 4 μmol Cd/kg and were euthanized by CO_2 asphyxiation 1 h, 3 h, 6 h, or 24 h later for RNA, total Cd, and MT analyses in interstitial cells and liver. Untreated rats (0 h) were also treated as described above. There were three replicates per treatment and 3 animals per replicate for RNA analyses, others, three replicates per treatment and one animal per replicate. Testes and liver were weighed and processed as described below.

Preparation and purification of testicular interstitial cells

Immediately after the testes were removed, these cells were decapsulated, deveined and incubated in a solution of 2 mg/ml collagenase (334 μ/mg, Type IA, Worthington Biochemical Co.) with minimum essential medium (MEM) (6 ml/2 testes) at 37 ℃ in a shaking water bath at 90 oscillations/min for 15 min. DNase (Sigma Chemical Co.) was added as needed (5-10 drops of 0.1 %) to reduce the clumping of cells to the DNA released from damaged cells. After collagenase dispersion, the digestion media were diluted with 12 ml prewarmed MEM and the tubules were allowed to settle. The resultant supernatant was centrifuged at 80×g for 10 min at 4 ℃. Crude interstitial cells from 2 testes were resuspended in ≤3 ml cold MEM and layered on the top of a linear (0-50 %) Percoll density gradient. The gradient was prepared in a LKB gradient mixer with 4 ml of a solution containing 50 % Percoll, 0.15 M NaCl, and 0.07 % bovine serum albumin (BSA) in the diluting chamber and 4 ml of an aqueous solution with 0.15 M NaCl, and 0.07 % BSA in the mixing chamber. Crude interstitial cells were then separated from other cell types by centrifugation at 800×g for 20 min in tubes (8×1.5 cm, 3 tubes for one type of cells from one sample) at 4 ℃. Purified interstitial cells formed a distinct band at 41-42 mm from the gradient bottom. Cell band was aspirated, diluted three times its volume with cold MEM to remove Percoll and centrifuged at 80×g for 10 min. Testicular interstitial cells were then suspended in a minimal volume of MEM and processed for RNA, total Cd, or MT protein analysis after aliquots was taken for cell count. Morphological observations by light microscopy showed that the purity ranged from 80 % to 85 %.

Cadmium content

Interstitial cells and liver tissue were wet-ashed in HNO_3 (u. p.)-H_2O_2 and Cd was determined by atomic absorption spectrophotometry (detection limit: 0.001ppm). Precautions were taken to avoid Cd contamination by acid-washing all glasswares and blanks were run along with the samples.

RNA extraction

Total ribonucleic acids were extracted from freshly isolated interstitial cells and liver tissue using RNAzol (GibcoBRL). Total RNA was determined by UV absorbance at 260 nm and its purity was estimated by the absorbance ratio A_{260}/A_{280} nm. In addition, RNA integrity was confirmed by ethidium bromide staining of ribosomal RNA following gel electrophoresis.

Polymerase chain reaction(PCR) primers

Oligonucleotide primers were synthesized using a DNA synthesizer (Worthington Biochemical Co.). The sequences of sense and antisense primers for rat MT-1 were 5'-ACTGCCTTCTTGTCGCTTA-3' and 5'-TGGAGGTGTA-CGGCAAGACT-3' respectively. They spanned a 310bp fragment. The sequences of sense and antisense primers for rat MT-2 were 5'-CCAACTGCCGCCTCCATTCG-3' and 5'-GAAAAAAGTGTGGAGAACCG-3' respectively, spanning a 300bp fragment. The sequences of sense and antisense primers for β-actin were 5'-CCCATTGAACACGG-CATTG-3' and 5'-GGTACGACCAGAGGCATACA-3' respectively, spanning a 236bp fragment.

Reverse transcription-PCR (RT-PCR) and products analysis

First-strand cDNA was synthesized with 1 μg total RNA, 50 pmol oligo (dT)18, 10U avian myloblastosis virus (AMV) reverse transciptase and 20U RNase inhibitor in a final 20 μl reaction mixture containing 1× reverse transcriptase buffer, 8 mM $MgCl_2$, 0.5 mM of each dNTP. The reaction mixture was incubated at 42 ℃ for 60 min. The cDNA products were stored at -20 ℃ until use.

PCR was carried out in a 25 μl reaction mixture containing 0.2 mM of each dNTP, 1 pmol of each sense and antisense primer and 0.625 unit of Taq DNA polymerase (TaKaRa), including 4 μl of cDNA products. After an initial denaturation at 95 ℃ for 5 min, amplification was carried out for approximately 27 cycles comprising 1 min at 95 ℃ for denaturation, 1 min at 55 ℃ for annealing, 1 min at 72 ℃ for extension with a final entension step at 72 ℃ for 5 min. The PCR products were applied to electrophoresis using a 2.0 % (w/v) agarose gel, which was stained with ethidium bromide and visualized under UV light. In order to confirm that there was no significant contamination in the total RNA preparation, we synthesized the first-strand DNA and performed control reactions in the absence of reverse transcriptase, and did not find any band on further PCR. In order to guarantee amplification in phase of exponential increase, we minimize the cycles of PCR in condition that the strap of gel electrophoresis could be detected. MT1 and MT2 mRNA levels were determined by RT-PCR analysis followed by densitometry scanning. All MT1 and MT2 RT-PCR products were normalized to the corresponding β-actin RT-PCR results that served as an internal control to ensure an approximate ratio of MTs mRNA.

Cloning of PCR products

PCR products were cloned using pUCm-T vector, The constructed plasmids were transfected into JM109, positive colonies were selected and the DNA sequence was analysed using a DNA sequencer (Worthington Biochemical Co.).

MT content analysis

Testicular interstitial cells were suspended in 500 μl of 10 mM Tris-HCL, pH 7.4, and lysed by sonication (3×10 s) on ice. Cytosol was then obtained by centrifugation at 18 000×g for 20 min at 4 ℃. Liver tissue was homogenated in 10 mM Tris-HCL, pH 7.4, with a glass homogenizer and a Teflon pestle. MT content analysis was performed by the enzyme-linked

immunosorbent assay (ELISA) method. The test procedure was similar to that described by Ruitenberg *et al*[17] and affinity-purified sheep anti-(rat MT) IgG was provided by Environmental Health Sciences Division, National Institute for Environmental Studies, Japan.

Statistical analysis

Data were represented as means ±S.E. of three replicates per Cd treatment or untreatment. Differences between Cd-treated (1 h, 3 h, 6 h, 24 h) and untreated rats were evaluated by Student' s *t*-test with $P<0.05$ as the limit of significance.

RESULTS

DNA sequences of RT-PCR products

After cloning the RT-PCR products described above into a pUCm-T vector, we examined their DNA sequences (Figure 1) and compared with rat liver MT1 and MT2 cDNAs. These data clearly indicate that the MT1 and MT2 genes are constitutively expressed in the rat testis.

MT1

ACTGCCTTCTTGTCGCTTACACCGTTGCTCCAGATTCACCAGATCTCGGAAT
GGACCCCAACTGCTCCTGCTCCACCGGCGGCTCCTGCACCTGCTCCAGCTC
CTGCGGCTGCAAGAACTGCAAATGCACCTCCTGCAAGAAGAGCTGCTGCT
CCTGCTGCCCCGTGGGCTGCTCCAAATGTGCCCAGGGCTGTGTCTGCAAAG
GTGCCTCGGACAAGTGCACGTGCTGTGCCTGAAGTGACGAACAGTGCTGC
TGCCCTCAGGTGTAAATAATTTCCGGACCAACTCAGAGTCTTGCCGTACAC
CTCCA

MT2

CCAACTGCCGCCTCCATTCGCCATGGACCCCAACTGCTCCTGTGCCACAGA
TGGATCCTGCTCCTGCGCTGGCTCCTGCAAATGCAAACAATGCAAATGCAC
CTCCTGCAAGAAAAGCTGCTGTTCCTGCTGCCCCGTGGGCTGTGCGAAGT
GCTCCCAGGGCTGCATCTGCAAAGAGGCTTCGGACAAGTGCAGCTGCTGC
GCCTGAAGTGGGGGCGTCCTCACAATGGTGTAAATAAAACAACGTAAGGA
ACCTAGCCTTTTTTTGTACAACCCTGACCGGTTCTCCACACTTTTTTC

Figure 1 DNA sequences of RT-PCR products from rat testis.

Cadmium content

Cadmium accumulated in the liver rapidly after its administration, but then leveled off. 24 h after Cd content in the liver increased about 10 000-fold whereas interstitial cell Cd was not detected (Figure 2). This indicated that the Cd content in interstitial cells might be below atomic absorption spectrophotometry detection limit (<1 ng/10^7 cells).

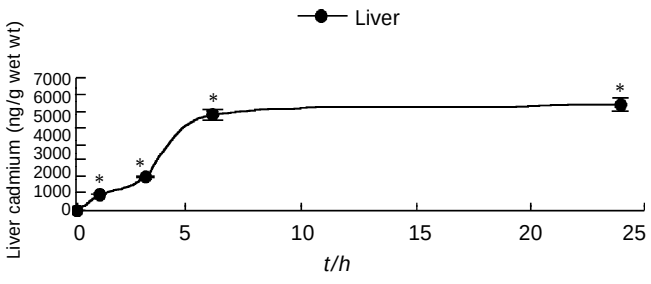

Figure 2 Time course of Cd accumulation in liver after a single subcutaneous injection of 4 μmol Cd / kg. The values were the mean ± S.E. (n=3). An asterisk indicated a significant difference (*P<0.05 *vs* control) from the untreated.

Effects of cadmium on transcription of MTs in interstitial and cells liver

To assess gene expression of both MT1 and MT2 genes, semi-quantitative RT-PCR was used. Results from the semi-quantitative RT-PCR (Figure 3) showed that untreated animals contained relatively high basal levels of both isoform mRNA, which were substantially increased after Cd treatment in the liver and peaked at 3 h, followed by a decline. In contrast, the mRNA levels in interstitial cells peaked at 6 h (Figure 3). Interestingly, the induction of MT1 mRNA was lower than MT2 mRNA in the liver of rats treated with Cd, but it was opposite to interstitial cells.

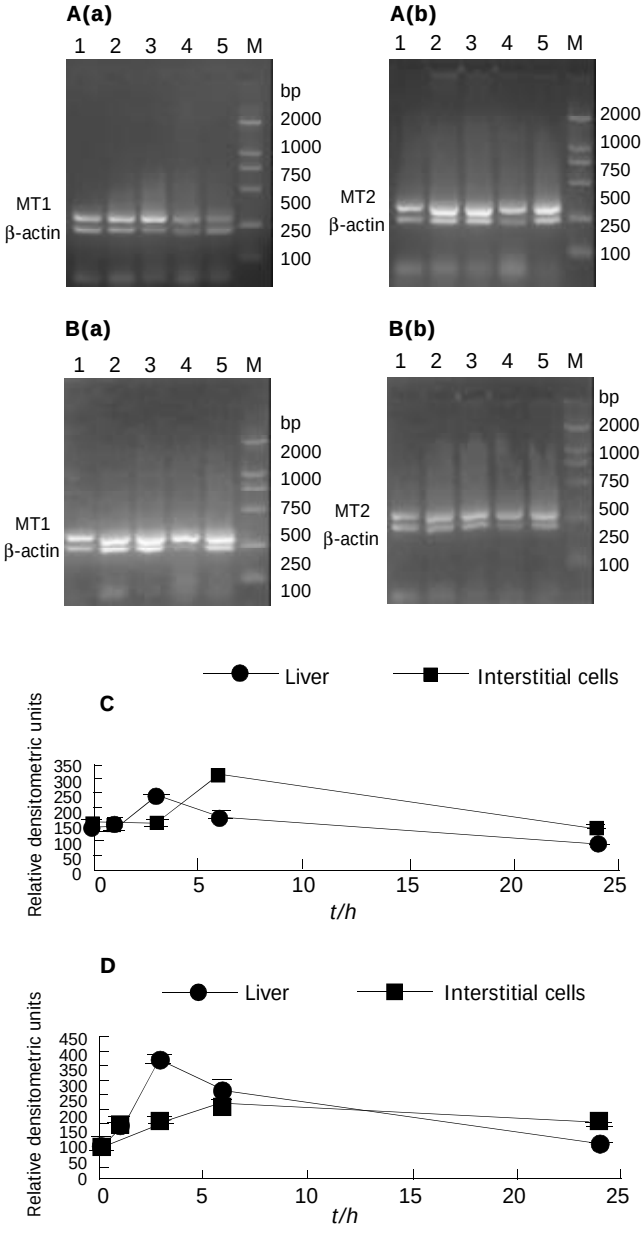

Figure 3 Effect of cadmium treatment on MT1(a) and MT2(b) mRNA levels in testicular interstitial cells (B) and the liver (A) of untreated rats (0h) and Cd-treated rats after 1 h, 3 h, 6 h, or 24 h (lanes 1-5). Values were obtained by RT-PCR analysis followed by densitometry scanning and expressed as MT1(C) or MT2(D) mRNA RT-PCR products to β-actin mRNA RT-PCR products ratio. Data represented the mean ± SE (n=9, three treatment replicates with three analyses per replicate).

Effects of cadmium on translation of MT in testicular interstitial cells and liver

In parallel to the elevation of liver Cd, the level of hepatic MT

increased significantly (3.9 hold increase) 24 h after Cd injection (Figure 4). In sharp contrast to the 3.9-fold elevation of hepatic MT, the MT in testicular interstitial cells of rats treated with Cd slightly declined as compared to untreated animals.

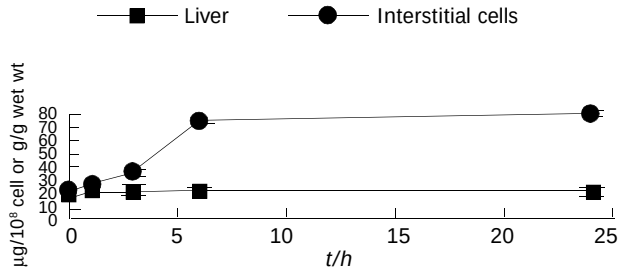

Figure 4 Metallothionein protein in testicular interstitial cells and liver of untreated and Cd-treated rats. Experimental conditions are shown in Figure 3. The values were the mean ± S.E. (n= 3).

DISCUSSION

MTs exist not only in tissues from various animal species, but also in bacteria and plants, and are thought to play essential, but as yet unknown roles in cellular processes[18-22]. MTs are known to detoxify heavy metals. However, male genital organs, particularly testis, are extremely susceptible to Cd. Thus, it has been a long-standing issue as to whether MTs are present in male genital organs or not. We have previously summarized the major points of dispute arising from earlier studies that advocated either the presence or the absence of MTs in the testis, since these earlier studies utilized indirect experimental methods to characterize testicular Cd-binding proteins. Therefore,we considered it essential to analyse directly the cDNA sequence. It has been demonstrated by RT-PCR analysis and DNA sequence analysis of the cloned PCR products that MT1 and MT2 genes are transcripted as their respective mRNA in the rat testis. The present results have clearly shown that the rat testis contains MT1 and MT2, the major isoforms of MT, thus supporting the results of earlier studies, not only in turns of the amounts of MT(-like) proteins estimated by the Cd-binding method in the rat testis, but also in regard to the localization of MT in male genital tissues.

Our observations demonstrated that MT1 and MT2 mRNAs were expressed in interstitial cells under normal physiological conditions, which confirmed the results of others in the whole testes of rats and mice. Furthermore, our results showed that both MT1 and MT2 mRNA increased, but did not translate into any higher protein in interstitial cells in response to Cd treatment. Cd-inducibility of MT1 and MT2 mRNA that we observed in freshly isolated intertitial cells, corroborated the findings of others using cultured mouse interstitial tumor cell lines exposed to Cd *in vitro*. In contrast, other reports indicated decrease, no changes, or little increases of MTs mRNA levels in the whole testes of Cd-treated rats and mice[16,23]. The discrepancy in the results among the various studies might be due to analysis of whole testicular tissue rather than isolated interstitial cells, or species and strain differences in Cd-induced MT. MT expression in male reproductive tissue might also depend on doses, time course between Cd administration and tissue sampling, age and reproductive states of the animals[24]. The present data showed that untreated animals contained relatively high basal levels of both isoforms of mRNA, which were substantially increased after Cd treatment in the liver and peaked at 3 h, followed by a decline. In contrast, the mRNA levels in interstitial cells peaked at 6 h (Figure 3). Interestingly, the induction of MT1 mRNA was lower than MT2 mRNA in the liver of rats treated with Cd, but it was opposite to interstitial cells. This indicates that Cd-induced transcription of MT gene is not only tissue-dependent, but also time-dependent. Therefore, the time selected to analyse mRNA levels might be another source of discrepancy. Furthermore, both isoforms were different from Cd-induction in different tissues or cells. The cause is unclear, and might be related to methylation status of the MT gene, since DNA methylation controls MT gene expression in murine lymphoid cells.

We also found that interstitial cells isolated from unteated animals contained relatively high basal levels of MT protein, thus supporting the results of earlier studies that MT were constitutively present in the testes at levels higher than that in many other tissues, such as the liver and kidney[25].

MT might not have any significant role in the detoxification of Cd in the testes, since 20 μmol Cd/kg destroyed the testicular endothelium of both normal mice and mice with inactivated MT1 and MT2 genes. Furthermore, mouse strain differences in Cd-induced testicular toxicity have not been reported to be correlated with testicular MT levels. In fact, resistance to Cd-induced testicular necrosis is linked to the cdm gene, which is located in a different chromosome from the genes for MT1 and MT2.

One hypothesis, which may explain why Cd-induced MT mRNA in interstitial cells was not accompanied by an increase of MT synthesis, is that MT mRNA increases were not translated into the corresponding protein. The existence of nonfunctional MT translations in interstitial cells could explain the higher susceptibility of testes than the liver to Cd toxicity. On the other hand, the absence of an increase in the MT gene translation product in interstitial cells accompanied by a significant increase in the liver of Cd-treated animals, could also be due to kinetic differences between interstitial cells and liver on the rate at which MT mRNA molecules were translated into MT or the rate of MT degradation[1]. The discrepancy between MT mRNA and MT protein in interstitial cells suggested that MT synthesis was regulated at the level of post-transcription[26], since an increase of mRNA should not result in decreased protein if regulation was only through transcription. While it is well known that MT gene expression is specifically induced by metals through metal response elements and the heavy metal induction of MT is mediated through the transcription factor MTF-1[27-29]. We not determine whether the effect of these metals on MT mRNA translation and/or protein degradation was specific to MT. Therefore it is possible that the metals have a more widespread effect on translation of genes[30-32]. However, it is clear that metals do not have a widespread effect on gene transcription through stress or nonspecific events. For example, housekeeping genes, such as β-actin or dihydrofolate reductase, in the liver and kidney of CD-1 mice were unaffected when treated with 0.6 mg cadmium/kg.

In summary, our observations clearly demonstrate that both MT mRNA and MT are constitutively expressed in isolated interstitial cells and Cd-induced expression of MT isoforms are not only tissue dependent but also time-dependent. Our findings of Cd-induced MT mRNA without increases in MT protein in interstitial cells deserve further investigation. The inability to induce metal-detoxicating MT-protein, in response to Cd, might account for the higher susceptibility of testes to Cd toxicity and carcinogenesis compared to the liver.

ACKNOWLEGEMENTS

We thank for Prof. Chiharu Tohyama for kindly providing affinity-purified sheep anti-(rat MT) IgG and Dr. Xu Qin-Hua for invaluable assistance with analysis of cadmium content.

REFERENCES

1 **Vasconcelos MH**, Tam SC, Hesketh JE, Reid M, Beattie JH. Metal- and tissue-dependent relationship between metallothionein mRNA and protein. *Toxicol Appl Pharmacol* 2002; **182**: 91-97
2 **Ren XY**, Zhou Y, Zhang JP, Feng WH, Jiao BH. Metallothionein gene expression under different time in testicular Sertoli and spermatogenic cells of rats treated with cadmium. *Reprod Toxicol* 2003; **17**: 219-227
3 **Abe T**, Yamamoto O, Gotoh S, Yan Y, Todaka N, Higashi K. Cadmium-induced mRNA expression of Hsp32 is augmented in metallothionein-I and -II knock-out mice. *Arch Biochem Biophys* 2000; **382**: 81-88
4 **Xu G**, Zhou G, Jin T, Zhou T, Hammarstrom S, Bergh A, Nordberg G. Apoptosis and p53 gene expression in male reproductive tissues of cadmium exposed rats. *Biometals* 1999; **12**: 131-139
5 **Coogan TP**, Shiraishi N, Waalkes MP. Minimal basal activity and lack of metal-induced activation of the metallothionein gene correlates with lobe-specific sensitivity to the carcinogenic effects of cadmium in the rat prostate. *Toxicol Appl Pharmacol* 1995; **132**: 164-173
6 **Mullins JE**, Fredrickson RA, Fuentealba IC, Markham RJ. Purification and partial characterization of a cadmium-binding protein from the liver of rainbow trout (Onchorynchus mykiss). *Can J Vet Res* 1999; **63**: 225-229
7 **Suzuki JS**, Kodama N, Molotkov A, Aoki E, Tohyama C. Isolation and identification of metallothionein isoforms (MT-1 and MT-2) in the rat testis. *Biochem J* 1998; **334**: 695-701
8 **Lee KF**, Lau KM, Ho SM. Effects of cadmium on metallothionein-I and metallothionein-II mRNA expression in rat ventral, lateral, and dorsal prostatic lobes: quantification by competitive RT-PCR. *Toxicol Appl Pharmacol* 1999; **154**: 20-27
9 **Katakura M**, Sugawara N. Preventive effect of selenium against the testicular injury by cadmium. *Nippon Eiseigaku Zasshi* 1999; **54**: 481-489
10 **Cook JC**, Klinefelter GR, Hardisty JF, Sharpe RM, Foster PM. Rodent Leydig cell tumorigenesis: a review of the physiology, pathology, mechanisms, and relevance to humans. *Crit Rev Toxicol* 1999; **29**: 169-261
11 **McKenna IM**, Bare RM, Waalkes MP. Metallothionein gene expression in testicular interstitial cells and liver of rats treated with cadmium. *Toxicology* 1996; **107**: 121-130
12 **Shiraishi N**, Hochadel JF, Coogan TP, Koropatnick J, Waalkes MP. Sensitivity tocadmium-induced genotoxicity in rat testicular cells is associated with minimal expression of the metallothionein gene. *Toxicol Appl Pharmacol* 1995; **130**: 229-236
13 **Wang SH**, Chen JH, Lin LY. Functional integrity of metallothionein genes in testicular cell lines. *J Cell Biochem* 1994; **55**: 486-495
14 **Liu J**, Corton C, Dix DJ, Liu Y, Waalkes MP, Klaassen CD. Genetic background but not metallothionein phenotype dictates sensitivity to cadmium-induced testicular injury in mice. *Toxicol Appl Pharmacol* 2001; **176**: 1-9
15 **Valverde M**, Fortoul TI, Diaz-Barriga F, Mejia J, Castillo ER. Induction of genotoxicity by cadmium chloride inhalation in several organs of CD-1 mice. *Mutagenesis* 2000; **15**: 109-114
16 **Zhou T**, Zhou G., Song W, Eguchi N, Lu W, Lundin E, Jin T Nordberg G. Cadmium-induced apotosis and changes in expression of p53, c-jun and MT-I genes in testes and ventral prostate of rats. *Toxicology* 1999; **142**: 1-13
17 **Ruitenberg EJ**, Steerenberg PA, Brosi BJM, Buys J. Reliability of the enzyme-linked immunosorbent assay (ELISA) for the serodiagnosis of Trichinella spiralis infections in conventionally raised pigs. *Tijdschr Diergeneeskd* 1976; **101**: 57-70
18 **Cai L**, Deng DX, Jiang J, Chen S, Zhong R, Cherian MG, Chakrabarti S. Induction of metallothionein synthesis with preservation of testicular function in rats following long term renal transplantation. *Urol Res* 2000; **28**: 97-103
19 **Waalkes MP**, Rehm S, Cherian MG. Repeated cadmium exposures enhance the malignant progression of ensuing tumors in rats. *Toxicol Sci* 2000; **54**: 110-120
20 Klaassen CD, Liu J. Metallothionein transgenic and knock-out mouse models in the study of cadmium toxicity. *J Toxicol Sci* 1998; **23**: 97-102
21 **Eid H**, Geczi L, Magori A, Bodrogi I, Institoris E, Bak M. Drug resistance and sensitivity of germ cell testicular tumors: evaluation of clinical relevance of MDR1 / Pgp, p53, and metallothionein (MT) proteins. *Anticancer Res* 1998; **18**: 3059-3064
22 **Satoh M**, Kaji T, Tohyama C. Low dose exposure to cadmium and its health effects. (3) Toxicity in laboratory animals and cultured cells. *Nippon Eiseigaku Zasshi* 2003; **57**: 615-623
23 **Shiraishi N**, Waalkes MP. Enhancement of metallothionein gene expression in male Wistar(WF / NCr) rats by treatment with calmodulin inhibitors: potential role of calcium regulatory pathways in metallothionein induction. *Toxicol Appl Pharmacol* 1994; **125**: 97-103
24 **Betka M**, Callard GV. Stage-dependent accumulation of cadmium and induction of metallothionein-like binding activity in the testis of the Dogfish shark, Squalus acanthias. *Biol Reprod* 1999; **60**: 14-22
25 **Cyr DG**, Dufresne J, Pillet S, Alfieri TJ, Hermo L. Expression and regulation of metallothioneins in the rat epididymis. *J Androl* 2001; **22**: 124-135
26 **Vasconcelos MH**, Tam SC, Beattie JH, Hesketh JE. Evidence for differences in the post-transcriptional regulation of rat metallothionein isoforms. *Biochem J* 1996; **315**: 665-671
27 **Dufresne J**, Cyr DG. Effects of short-term methylmercury exposure on metallothionein mRNA levels in the testis and epididymis of the rat. *J Androl* 1999; **20**: 769-778
28 **Radtke F**, Heuchel R, Georgiev O, Hergersberg M, Gariglio M, Dembic Z, Schaffner W. Cloned transcription factor MTF-1 activates the mouse metallothionein I promoter. *EMBO J* 1993; **12**: 1355-1362
29 **Saydam N**, Georgiev O, Nakano MY, Greber UF, Schaffner W. Nucleo-cytoplasmic trafficking of metal-regulatory transcription factorl is regulated by diverse stress signals. *J Biol Chem* 2001; **276**: 25487-25495
30 **Min KS**, Kim H, Fujii M, Tetsuchikawahara N, Onosaka S. Glucocorticoids suppress the inflammation-mediated tolerance to acute toxicity of cadmium in mice.*Toxicol Appl Pharmacol* 2002; **178**: 1-7
31 **Ozawa N**, Goda N, Makino N, Yamaguchi T, Yoshimura Y, Suematsu M. Leydig cell-derived heme oxygenase-1 regulates apoptosis of premeiotic germ cells in response to stress. *J Clin Invest* 2002; **109**: 457-467
32 **Matsuura T**, Kawasaki Y, Miwa K, Sutou S, Ohinata Y, Yoshida F, Mitsui Y. Germ cell-specific nucleocytoplasmic shuttling protein, tesmin, responsive to heavy metal stress in mouse testes. *J Inorg Biochem* 2002; **88**: 183-191

Edited by Zhang JZ and Wang XL

P.O.Box 2345, Beijing 100023,China
Fax: +86-10-85381893
E-mail: wjg@wjgnet.com www.wjgnet.com

World J Gastroenterol 2003;9(7):1559-1562
World Journal of Gastroenterology
 ISSN 1007-9327

• BASIC RESEARCH •

Effect of compound rhodiola sachalinensis A Bor on CCl_4-induced liver fibrosis in rats and its probable molecular mechanisms

Xiao-Ling Wu, Wei-Zheng Zeng, Pi-Long Wang, Chun-Tao Lei, Ming-De Jiang, Xiao-Bin Chen, Yong Zhang, Hui Xu, Zhao Wang

Xiao-Ling Wu, Pi-Long Wang, Chun-Tao Lei, Department of Gastroenterology, First Affiliated Hospital, Chongqing University of Medical Sciences, Chongqing 400016, China
Wei-Zheng Zeng, Ming-De Jiang, Xiao-Bin Chen, Yong Zhang, Hui Xu, Zhao Wang, Department of Digestion, General Hospital of Chengdu Military Command, Chengdu 610083, Sichuan Province, China
Supported by the Tenth-Five Year Plan of Medical Science Foundation of Chengdu Military Command, No. 01A009
Correspondence to: Professor Wei-Zheng Zeng, Department of Digestion, General Hospital of Chengdu Military Command, Chengdu 610083, Sichuan Province, China. zengweizheng@163.com
Telephone: +86-28-86570347
Received: 2002-11-06 **Accepted:** 2002-12-30

Abstract

AIM: To explore the anti-fibrotic effect of a traditional Chinese medicine, compound rhodiola sachalinensis A Bor on CCl_4-induced liver fibrosis in rats and its probable molecular mechanisms.

METHODS: Ninety healthy male SD rats were randomly divided into three groups: normal group (n=10), treatment group of compound rhodiola sachalinensis A Bor (n=40) and CCl_4-induced model group (n=40). The liver fibrosis was induced by CCl_4 subcutaneous injection. Treatment group was administered with compound rhodiola sachalinensis A Bor (0. 5 g/kg) once a day at the same time. Then the activities of several serum fibrosis-associated enzymes: alanine aminotransferase (ALT), aspartate aminotransferase (AST), N-acetyl-beta-D-glucosaminidase (β-NAG) and the levels of serum procollagen III (PCIII), collagen IV (CIV), hyaluronic acid (HA) were assayed. The histopathological changes were observed with HE, VG and Masson stain. The expression of TGF-β1 mRNA,α1 (I) mRNA and Na^+/Ca^{2+} exchanger (NCX) mRNA was detected by reverse transcription polymerase chain reaction (RT-PCR) *in situ*.

RESULTS: Compound rhodiola sachalinensis A Bor significantly reduced serum activities of ALT, AST, β-NAG and decreased the levels of PCIII, CIV, HA, improved the liver histopathological changes, inhibited the expression of TGF-β1 mRNA, α(I) mRNA and Na^+/Ca^{2+} exchanger mRNA in rats.

CONCLUSION: Compound rhodiola sachalinensis A Bor can intervene in CCl_4-induced liver fibrosis in rats, in which potential mechanisms may be decreasing the production of TGF-β1, reducing the production of collagen, preventing the activation of hepatic stellate cell (HSC) and inhibiting the expression of TGF-β1 mRNA, α1(I) mRNA and Na^+/Ca^{2+} exchanger mRNA.

Wu XL, Zeng WZ, Wang PL, Lei CT, Jiang MD, Chen XB, Zhang Y, Xu H, Wang Z. Effect of compound rhodiola sachalinensis A Bor on CCl_4-induced liver fibrosis in rats and its probable molecular mechanisms. *World J Gastroenterol* 2003; 9(7): 1559-1562
http://www.wjgnet.com/1007-9327/9/1559.asp

INTRODUCTION

Transforming growth factor beta 1 (TGF-β 1) is the most potent profibrogenic mediator in liver fibrosis and cirrhosis as shown in animal models and human chronic hepatic injury[1-4]. It plays critical roles in the activation of hepatic stellate cell (HSC) and the regulation of the production, degradation, and accumulation of extracellular matrix (ECM) proteins[5-7]. Recent studies have identified that TGF-beta 1 mRNA transcription is significantly increased during chronic liver injury. Thus the TGF-beta signal transduction pathway has become a new effective target for the prevention or treatment of liver fibrosis[8-11]. Several traditional Chinese herbs have been shown to have the ability of intervention in liver fibrosis[12-20], however, most of them were limited in morphological and serum studies, lacking of deep research in their molecular biological mechanisms. Our previous study has shown another Chinese medicine, compound rhodiola sachalinensis A Bor, can effectively prevent CCl_4-induced liver fibrosis in rats[21-23]. In this study, the probable biological mechanism of it, especially in the expression of TGF-beta 1 mRNA, α1(I) mRNA and Na^+/Ca^{2+} exchanger mRNA was explored.

MATERIALS AND METHODS

Animals

Male SD rats (weighing 140-160 g) were obtained from the Experimental Animal Center of Sichuan University (Chengdu, Sichuan Province, China). The rats were housed in a room with controlled temperature (15-20 ℃) and lighting (10 h light, 14 h dark). Free access to water and food was allowed during the experimental period. All the rats were randomly divided into three groups: normal group (n=10), treatment group (n=40) and model group (n=40). For model group, 300 mL/L CCl_4 in liquid paraffin was injected subcutaneously at a dose of 3 mL/kg twice weekly. The treatment group, apart from the administration of CCl_4, was fed with compound rhodiola sachalinensis A Bor 0.5 g/kg once per day. The model group was given normal food and water, received injection of liquid paraffin with the same dosage and duration as CCl_4.

At the end of the 15-week experimental period, all the rats were anesthetized with intramuscular injection of sodium pentobarbital (30 mg/kg) before sacrificed. Blood was collected from the heart and the serum obtained through centrifugation. The liver was removed rapidly, part of it was conserved in 100 mL/L neutral formalin, and the rest was frozen in a refrigerator at -20 ℃.

Serum parameters of hepatic fibrosis

Parameters of hepatic fibrosis were determined by levels of type III procollagen (PCIII), type IV collagen (CIV) and hyaluronic acid (HA),using radioimmunoassay (commercial kit obtained from Shanghai Navy Medical Institute, China). Serum activities of alanine aminotransferase (ALT) and aspartate aminotransferase (AST) were assayed by a automatic analyzer. Another serum enzyme N-acetyl-beta-D-glucosaminidase (β-NAG) was assayed with spectrophotometric method.

Table 1 Primer sequences of α1(I), TGF-β1 and Na^+/Ca^{2+} exchanger mRNA

mRNA	Upstream (5'→3')	Downstream (5'→3')
α1(I)	CAC CCT CAA GAG CCT GAG TC	GTT CGG GCT GAT GTA CCA GT
TGF-β1	CTT TGT ACA ACA GCA CCC GC	GTC AAA AGA CAG CCA CTC AGG
NCX	TAT TGC CGA ACC GGT TTA TGT	CTC GTC TCT CCA TCT GGG AC

Table 2 Liver fibrosis-associated enzymes and fibrosis markers in serum ($\bar{x}\pm s$)

Group	ALT (IU/L)	AST (IU/L)	β-NAG (μmol/L)	PCIII (μg/L)	CIV (μg/L)	HA (μg/L)
Normal	87.93±18.61[a]	104.3±32.40[a]	189.00±26.70[a]	89.99±10.85[a]	35.69±9.68[a]	112.41±45.62[a]
Model	198.64±71.02	514.59±180.22	415.77±133.37	265.54±98.21	159.67±29.64	455.79±113.55
Treatment	114.17±47.89[a]	291.62±141.75[a]	244.67±46.8[a]	164.25±45.68[a]	96.73±16.48[a]	289.35±75.68[a]

[a]$P<0.01$ *vs* model group.

Histopathological grading

Liver samples from each rat were embedded in paraffin, stained with hematoxylin-eosin (HE), Van Gieson (VG) and Masson trichrome collagen stain, and then examined under an optical microscope. Fibrosis-degree of liver sections was graded numerically based on the criteria described below: 0, no fibrosis; +, slight fibrosis, fibrosis located in the central liver lobule; +2, moderate fibrosis, widen central fibrosis; +3, severe fibrosis, fibrosis extended to the edge of liver lobule; +4, liver cirrhosis.

Molecular biological detection: RT-PCR in situ

Each liver sample embedded in paraffin was sectioned and fixed onto a poly-L-lysine covered glass. The expression of α1(I) mRNA, TGF-β1 mRNA and Na^+/Ca^{2+} exchanger (NCX) mRNA was detected with RT-PCR *in situ*. (primers obtained from Shanghai Sangon Biotechnology Co. Ltd.) (Table 1).

Statistical analysis

Data were analyzed using *t*-test and Microsoft Excel 2000.

RESULTS

Changes of serum fibrosis-associated markers

In model group, the serum activities of ALT, AST and β-NAG were significantly increased ($P<0.01$), the serum levels of PCIII, CIV and HA were also elevated ($P<0.01$). With administration of compound Rhodiola Sachalinensis A Bor (RSC), serum activities of ALT, AST, β-NAG and levels of PCIII, CIV, HA were decreased obviously ($P<0.01$), although they were still higher than those in normal group ($P<0.05$) (Table 2).

Histopathological changes of the liver

The control livers showed a normal lobular architecture with central veins and radiating hepatic cords. The staging score was 0. Subcutaneous injection of CCl_4 caused severe liver pathological damages such as: inflammation, necrosis and excessive collagen deposition. The semiquantitative staging score of hepatic fibrosis was raised to 3.53±0.68 in model group. The livers in treatment group showed less inflammation, necrosis, collagen deposition and a significantly decreased staging score of 2.43±0.47 ($P<0.05$) (Table 3, Figures 1, 2).

Molecular biological changes

Scoring method: according to the number of positive cells within one visual field on average. (-), no positive cells, scoring 0; (+), positive cells <1/3, scoring 1; (++), positive cells <2/3, scoring 2; (+++), positive cells >2/3, scoring 3. There were less positive signals of α1(I) mRNA, TGF-β1 mRNA and Na^+/Ca^{2+} exchanger mRNA detected with RT-PCR *in situ* in normal group, in which scores were 1.11, 0.75, 0.10 and the ratio of positive samples was 77.8 %, 62.5 %, 10.0 % respectively (Tables 4-6). In model group, the positive signals of RT-PCR *in situ* for α1(I) mRNA, TGF-β1 mRNA and Na^+/Ca^{2+} exchanger mRNA were significantly enhanced. The semiquantitative scores of them were increased to 2.80, 2.40, 2.30 and the ratio of positive samples rised to 100.0 %, 90.0 %, 100.0 % respectively ($P<0.01$). Treatment with RSC made the scores reduced to 1.63, 1.20, 1.50, and positive ratio lowered to 87.5 %, 80.0 %, 80.0 % respectively in comparison with model group ($P<0.05$) (Tables 4-6, Figures 3-6).

Table 3 Histopathological semiquantitative scores in the liver

Group	*n*	0	+1	+2	+3	+4	Staging scores
Normal	10	10	0	0	0	0	0[a]
Model	30	0	0	3	8	19	3.53±0.68
Treatment	35	0	2	18	13	2	2.43±0.47[b]

[a]$P<0.01$, [b]$P<0.05$ *vs* model group.

Table 4 Expression of α1 (I) mRNA (semiquantitative scores and positive ratio)

Group	*n*	-	+	++	+++	Scores	Positive ratio (%)
Normal	9	2	4	3	0	1.11[a]	77.8[b]
Model	10	0	0	2	8	2.80	100.0
Treatment	8	1	2	4	1	1.63[b]	87.5[b]

[a]$P<0.01$, [b]$P<0.05$ *vs* model group.

Table 5 Expression of TGF-β1mRNA (semiquantitative scores and positive ratio)

Group	*n*	-	+	++	+++	Scores	Positive ratio (%)
Normal	8	3	4	1	0	0.75[a]	62.5[a]
Model	10	1	1	1	7	2.40	90.0
Treatment	10	2	5	2	1	1.20[b]	80.0[b]

[a]$P<0.01$, [b]$P<0.05$ *vs* model group.

Table 6 Expression of Na^+/Ca^{2+} exchanger mRNA (semiquantitative scores and positive ratio)

Group	*n*	-	+	++	+++	Scores	Positive ratio (%)
Normal	10	9	1	0	0	0.10[a]	10.0[a]
Model	10	0	2	3	5	2.30	100.0
Treatment	10	2	3	3	2	1.50[b]	80.0[b]

[a]$P<0.01$, [b]$P<0.05$ *vs* model group.

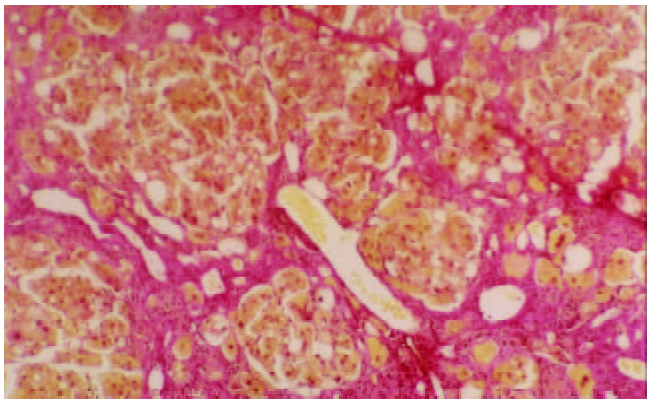

Figure 1 Liver VG staining in model rats (10×40).

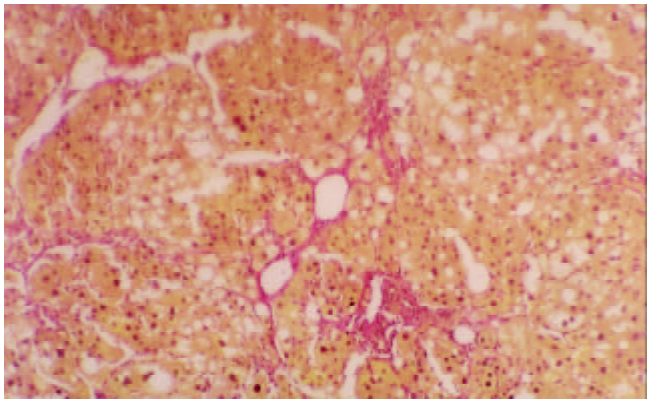

Figure 2 Liver VG staining in treatment rats (10×40).

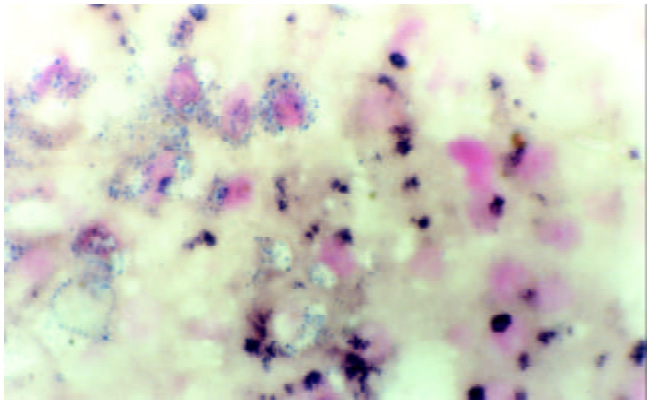

Figure 3 Expression of TGF-β1mRNA in liver of model rats (10×40).

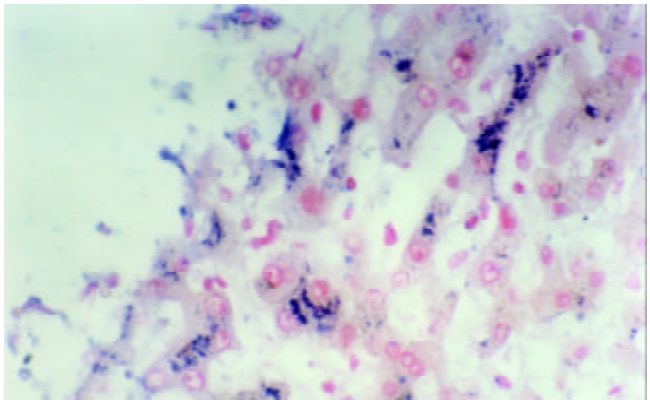

Figure 4 Expression of TGF-β1mRNA in liver of treatment rats (10×40).

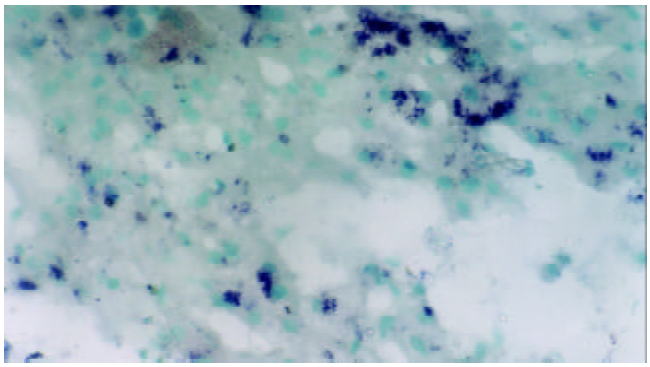

Figure 5 Expression of NCX mRNA in liver of model rats (10×40).

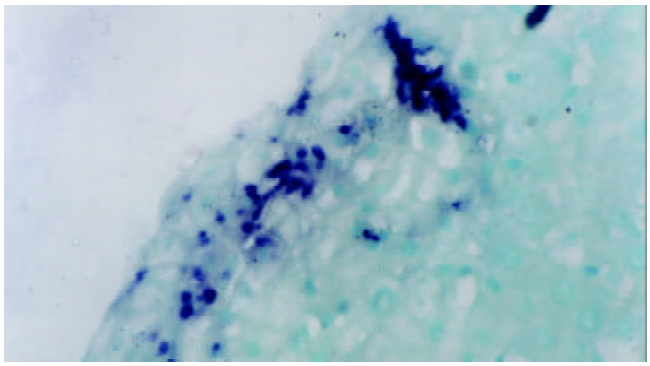

Figure 6 Expression of NCX mRNA in liver of treatment rats (10×40).

DISCUSSION

Liver fibrosis is generally preceded by chronic liver injury despite of its primary causes, including alcohol, hepatic virus, oxidant stress and other persistent damages. The activation of hepatic stellate cells (HSC) is considered to be of great importance during the long period of liver fibrosis, which is induced by some critical cytokines and then becomes the main source of most collagen proteins[24]. Among the cytokine mediating factors, transforming growth factor beta 1 (TGF-β1) has been considered as the essential profibrogenesis factor and the main target of treatment[25-31]. Additionally, Na^+/Ca^{2+} exchanger was a newly noticed factor whose expression increased along with the activation of HSC, and its real role in liver fibrosis has not been interpreted[32]. Thus, detection of the expression of TGF-β1 and Na^+/Ca^{2+} exchanger mRNA is useful in exploring the probable mechanisms of anti-fibrotic drugs.

Several drugs, including cytokines, antioxidant, chemical drugs, soluble type II receptor of TGF-β1[9, 33], antibody of TGF-β1 have been used to block liver fibrosis. But their effects are not as prosperous as we expected[1]. Besides, some traditional Chinese drugs have been found to be effective on preventing fibrogenesis and other chronic liver injury, which develop a more hopeful future in controlling liver fibrosis and cirrhosis. The present study aimed at exploring the effects of a traditional Chinese herb, compound rhodiola sachalinensis A Bor, which consists of rhodiola sachalinensis A Bor, sophora flavescens Ait and other herbs, on the prevention of CCl_4-induced liver fibrosis in rats. The potential mechanisms of RSC was explained at the same time.

In this study, chronic administration of CCl_4 caused liver fibrosis and cirrhosis as indicated by the changes of serum markers, histopathological changes, and molecular biological changes. The activities of serum fibrosis-associated enzymes, namely ALT, AST, β-NAG and contents of extracellular matrix (ECM) components (PCIII, CIV, HA) were significantly

increased along with increased expression of α1(I) mRNA, TGF-β1 mRNA and Na^+/Ca^{2+} exchanger mRNA. Under the light microscope, the liver fibrosis/cirrhosis was verified by the typical liver structure: inflammation, necrosis and excessive collagen deposition, some of the samples even had pseudolobules. With the therapy of compound rhodiola sachalinensis A Bor, serum parameters of liver fibrosis (ALT, AST, β-NAG, PCIII, CIV, HA) were significantly decreased ($P<0.01$). HE, VG and Masson stained histopathological sections showed mild inflammation, necrosis and fewer collagen deposition. The semiquantitative fibrosis staging scores were also decreased obviously ($P<0.01$). The expression of α1(I) mRNA, TGF-β1 mRNA and Na^+/Ca^{2+} exchanger mRNA was significantly inhibited using RT-PCR *in situ* ($P<0.01$). These results suggest that compound rhodiola sachalinensis A Bor may prevent experimental liver fibrosis by modulating the synthesis and releasing of critical cytokines, such as TGF-β1, thus inhibiting the activation of HSC and its production of collagen proteins. The inhibition of Na^+/Ca^{2+} exchanger mRNA may partly relate to its anti-fibrotic effects. In conclusion, traditional Chinese medicine compound rhodiola sachalinensis A Bor has significant anti-fibrogenesis effects on CCl_4-induced liver fibrosis in rats. The probable molecular mechanisms may include blocking the synthesis of TGF-β1, interfering with the activation of HSC, preventing production and deposition of collagen, and inhibiting the expression of Na^+/Ca^{2+} exchanger mRNA. The exact molecular mechanisms remain to be explored.

REFERENCES

1 **Bissell DM**, Roulot D, George J. Transforming growth factor β and the liver. *Hepatology* 2001; **34**: 859-867
2 **Liu F**, Liu JX. The role of transforming growth factor b1 in liver fobrosis. *Shijie Huaren Xiaohua Zazhi* 2000; **8**: 86-88
3 **Schuppan D,** Porov Y. Hepatic fibrosis: From bench to bedside. *J Gastroenterol Hepatol* 2002; **7**(Suppl 3): S300-S305
4 **Cui DL**, Yao XX. The serum detection of liver fibrosis. *Shijie Huaren Xiaohua Zazhi* 2000; **8**: 683-684
5 **Qin JP**, Jiang MD. The phenotype and regulation of hepatic stellate cell and liver fibrosis. *Shijie Huaren Xiaohua Zazhi* 2001; **9**: 801-804
6 **Wu JX**, Meng XJ, Chen YW, Li DG, Lu HM. Message molecular of Smads and the activation of hepatic stellate cells. *Weichangbingxue He Ganbingxue Zazhi* 2002; **11**: 197-199
7 **Shi YJ**, Tian ZB, Zhao QX. The current research of Smads protein family. *Zhonghua Fubu Jibing Zazhi* 2002; **2**: 497-500
8 **Li D,** Friedman SL. Liver fibrogenesis and the role of hepatic stellate cells: New insights and prospects for therapy. *J Gastroenterol Hepatol* 1999; **14**: 618-633
9 **George J**, Roulot D, Kotelinnsky VE, Bissell DM. *In vivo* inhibition of rat stellate cell activation by soluble transforming growth factor β type II receptor: A potential new therapy for hepatic fibrosis. *Proc Natl Acad Sci USA* 1999; **96**: 12719-12724
10 **Yoshiji H**, Kuriyama S, Yoshii J, Ikenaka Y, Noguchi R, Nakatani T, Tsujinoue H, Fukui H. Angiotensin-II type 1 receptor interaction is a major regulator for liver fibrosis development in rats. *Hepatology* 2001; **34**(4Pt 1): 745-750
11 **Jiang SL**, Yao XX, Sun YF. The treatment of liver fibrosis. *Shijie Huaren Xiaohua Zazhi* 2000; **8**: 684-686
12 **Sun YF**, Yao XX, Jiang SL. The traditional Chinese medicine treatment of liver fibrosis. *Shijie Huaren Xiaohua Zazhi* 2000; **8**: 686-687
13 **Du WD**, Zhang YE, Zhai WR, Zhou XM. Dynamic changes of type I, III and IV collagen synthesis and distribution of collagen-producing cells in carbon tetrachloride-induced rat liver fibrosis. *World J Gastroenterol* 1999; **5**: 397-403
14 **Liu P**, Liu C, Xu LM, Xue HM, Liu CH,Zhang ZQ. Effects of Fuzheng Huayu 319 recipe on liver fibrosis in chronic hepatitis B. *World J Gastroenterol* 1998; **4**: 348-353
15 **Liu CH**, Hu YY, Wang XL, Liu P, Xu LM. Effects of salvianolic acid-A on NIH / 3T3 fibroblast proliferation, collagen synthesis and gene expression. *World J Gastroenterol* 2000; **6**: 361-364
16 **Cai DY**, Zhao G, Chen JC, Ye GM, Bing FH, Fan BW. Therapeutic effect of Zijin capsule in liver fibrosis in rats. *World J Gastroenterol* 1998; **4**: 260-263
17 **Shimizu I**. Sho-saiko-to: Japanese herbal medicine for protection against hepatic fibrosis and carcinoma. *J Gastroenterol Hepatol* 2000; **15**(Suppl): d84-90
18 **Yang W**, Zeng M, Fan Z, Mao Y, Song Y, Jia Y, Lu L, Chen CW, Peng YS, Zhu HY. Prophylactic and therapeutic effect of oxymatrine on D-galactosamine-induced rat liver fibrosis. *Zhonghua Ganzangbing Zazhi* 2002; **10**: 193-196
19 **Li CX**, Li L, Lou J, Yang XW, Lei TW, Li YH, Liu J, Cheng ML, Huang LH. The protective effects of traditional Chinese medicine prescription, Han-Dan-Gan-Le, on CCl_4-induced liver fibrosis in rats. *Am J Chin Med* 1998; **16**: 325-332
20 **Liu P**, Hu YY, Liu C, Zhu DY, Xue HM, Xu ZQ, Xu LM, Liu CH, Gu HT, Zhang ZQ. Clinical observation of salvianolic acid B in treatment of liver fibrosis in chronic hepatitis B. *World J Gastroenterol* 2002; **8**: 679-685
21 **Zeng WZ**, Wu XL, Jiang MD, Chen XB, Xu H, Wang Z, Xiong BJ. The effect of rhodiola sachalinensis compound on the expression of TGF-β1 mRNA in rats of CCl_4-induced liver fibrosis. *Zhongguo Zhongxiyi Jiehe Xiaohua Zazhi* 2002; **10**: 138-141
22 **Jiang MD**, Gan XY, Xie FW, Zeng WZ, Wu XL. Effect of salidroside on the proliferation and collagen mRNA transcription in rat hepatic stellate cells stimulated by acetaldehyde. *Yaoxue Xuebao* 2002; **37**: 841-844
23 **Wu XL,** Zene WZ, Chen XB, Jiang MD, Xiong BJ, Zhang Y, Xu H. The effects of rhodiola sachalinensis A Bor on the activities of fibrosis-associated enzymes in serum and tissue in rats of CCl_4-induced liver fibrosis. *Huaxi Yaoxue Zazhi* 2002; **17**: 416-418
24 **Schuppan D**, Koda M, Bauer M, Hahn EG. Fibrosis of liver, pancreas and intestine: common mechanisms and clear targets? *Acta Gastroenterol Belg* 2000; **63**: 366-370
25 **Gressner AM,** Weiskirchen R, Breitkopf K, Dooley S. Roles of TGF-beta in hepatic fibrosis. *Front Biosci* 2002; **7**: d793-807
26 **Neuman MG,** Benhamou JP, Bourliere M, Ibrahim A, Malkiewicz I, Asselah T, Martinot-Peignoux M, Shear NH, Katz GG, Akremi R, Benali S, Boyer N, Lecomte L, Le Breton V, Le Guludec G, Marcellin P. Serum tumour necrosis factor-alpha and transforming growth factor-beta levels in chronic hepatitis C patients are immunomodulated by therapy. *Cytokine* 2002; **17**: 108-117
27 **Bissell DM.** Chronic liver injury, TGF-beta, and cancer. *Exp Mol Med* 2001; **33**: 179-190
28 **Kanzler S,** Baumann M, Schirmacher P, Dries V, Bayer E, Gerken G, Dienes HP, Lohse AW. Prediction of progressive liver fibrosis in hepatitis C infection by serum and tissue levels of transforming growth factor-beta. *J Viral Hepat* 2001; **8**: 430-437
29 **Paizis G,** Gilbert RE, Cooper ME, Murthi P, Schembri JM, Wu LL, Rumble JR, Kelly DJ, Tikellis C, Cox A, Smallwood RA, Angus PW. Effect of angiotensin II type 1 receptor blockade on experimental hepatic fibrogenesis. *J Hepatol* 2001; **35**: 376-385
30 **Deng L,** Zhou Y, Peng X, Deng H, Deng Y, Yao J. Serum markers and pathological evaluation in hepatitis fibrosis of chronic hepatitis B treated with interferon alpha. *Zhonghua Ganzangbing Zazhi* 2001; **9**: 66-67
31 **Jiang W,** Wang J, Yang C, Wang Y, Liu W, He B. Effects of antisense transforming growth factor beta receptor-I expressing plasmid on pig serum-induced rat liver fibrosis. *Zhonghua Yixue Zazhi* 2002; **82**: 1160-1164
32 **Toshio N**, Shigeki A, Kazunobu M, Masaharu F, Yoshihisa T, Masayuki I, Makoto T, Yasunobu O. Expression of the Na^+/Ca^{2+} exchanger emerges in hepatic stellate cells after activation in association with liver fibrosis. *Physiology* 1998; **95**: 5389-5394
33 **Ueno H,** Sakamoto T, Nakamura T, Qi Z, Astuchi N, Takeshita A, Shimizu K, Ohashi H. A soluble transforming growth factor beta receptor expressed in muscle prevents liver fibrogenesis and dysfunction in rats. *Hum Gene Ther* 2000; **11**: 33-42

Edited by Zhang JZ

P.O.Box 2345, Beijing 100023,China
Fax: +86-10-85381893
E-mail: wjg@wjgnet.com www.wjgnet.com

World J Gastroenterol 2003;9(7):1563-1566
World Journal of Gastroenterology
 ISSN 1007-9327

• BASIC RESEARCH •

Effect of tetramethylpyrazine on P-selectin and hepatic/renal ischemia and reperfusion injury in rats

Jin-Lian Chen, Tong Zhou, Wei-Xiong Chen, Jin-Shui Zhu, Ni-Wei Chen, Ming-Jun Zhang, Yun-Lin Wu

Jin-Lian Chen, Wei-Xiong Chen, Jin-Shui Zhu, Ni-Wei Chen, Department of Gastroenterology, Shanghai Sixth People' s Hospital, Shanghai Jiao-Tong University, Shanghai 200233, China
Tong Zhou, Department of Nephrology, Ruijin Hospital, Shanghai Second Medical University, Shanghai 200025, China
Ming-Jun Zhang, Animal Laboratory, Ruijin Hospital, Shanghai Second Medical University, Shanghai 200025, China
Yun-Lin Wu, Department of Gastroenterology, Ruijin Hospital, Shanghai Second Medical University, Shanghai 200025, China
Supported by the National Natural Science Foundation of China (No. 39970340) and the Scientific Foundation of Ministry of Public Health
Correspondence to: Jin-Lian Chen, Department of Gastroenterology, Shanghai Sixth People' s Hospital, Shanghai Jiao-Tong University, Shanghai 200233, China. cqinqin@fm365.com
Telephone: +86-21-64369181
Received: 2002-12-30 **Accepted:** 2003-02-19

Abstract

AIM: To investigate the effect of tetramethylpyrazine on hepatic/renal ischemia and reperfusion injury in rats.

METHODS: Hepatic/renal function, histopathological changes, and hepatic/renal P-selectin expression were studied with biochemical measurement and immunohistochemistry in hepatic/renal ischemia and reperfusion injury in rat models.

RESULTS: Hepatic/renal insufficiency and histopathological damage were much less in the tetramethylpyrazine-treated group than those in the saline-treated groups. Hepatic/renal P-selectin expression was down regulated in the tetramethylpyrazine-treated group.

CONCLUSION: P-selectin might mediate neutrophil infiltration and contribute to hepatic/renal ischemia and reperfusion injury. Tetramethylpyrazine might prevent hepatic/renal damage induced by ischemia and reperfusion injury through inhibition of P-selectin.

Chen JL, Zhou T, Chen WX, Zhu JS, Chen NW, Zhang MJ, Wu YL. Effect of tetramethylpyrazine on P-selectin and hepatic/renal ischemia and reperfusion injury in rats. *World J Gastroenterol* 2003; 9(7): 1563-1566
http://www.wjgnet.com/1007-9327/9/1563.htm

INTRODUCTION

Hepatic/renal ischemia-reperfusion injury is common clinically. Up to now, there has been no effective treatment for this pathological injury. Cell adhesion molecules have been found to play an important role in hepatic/renal ischemia-reperfusion injury by mediating interactions of polymorphonuclear neutrophils with endothelium. P-seletin monoclonal antibody has been demonstrated to prevent effectively reperfusion-induced hepatic/renal tissue damage[1-23]. Tetramethylpyrazine (TMP), a traditional Chinese herb, has been widely used especially in the treatment of patients with cerebral and cardiac ischemic diseases in China. Experimental study has found that TMP could protect vascular endothelial cells, and inhibit respiratory explosion and free radicals of polymorphonuclear neutrophils[24-28]. In the present study, we investigated the effect of TMP and P-selectin on hepatic ischemia and reperfusion injury in rats.

MATERIALS AND METHODS

Animal model

Ninety male Wistar rats (Shanghai Experimental Animal Center of Chinese Academy of Sciences), weighing 200±10 g, were given free access to food and water for three days before the experiments. The rats were anesthetized with 2.5 % sodium pentobarbital intraperitoneally, and randomly divided into 2 groups. In one group of rats, the ligament linking liver, diaphragm and abdominal wall were separated, the portal vein and liver artery that drain blood to left hepatic lobe were freed by blunt dissection and then blocked with a microvascular clamp for 60 minutes, then the clamp was removed, and reperfusion was performed. While in the other group, the left renal artery was freed, and blocked with a microvascular clamp for 60 minutes, then the clamp was removed and reperfusion was performed, simultaneously, the right kidney was cut off. The two groups of rats were randomly divided into TMP-treated group (n=20) and non-treated group (n=20). They were divided into subgroups according to the indicated time 1,3,6,24 hours after reperfusion. TMP or saline was intravenously injected five minutes before the reperfusion. A sham-operated group (n=5, anesthesia and opening celiac cavity, no blocking of hepatic or renal blood flow) served as control.

Collection and measurement methods of specimens

Blood and hepatic and renal tissues were harvested at the indicated time. Serum levels of aspartate aminotransferase (AST) and alanine aminotransferase (ALT), and blood urea nitrogen (BUN) and creatinine (Cr) were measured with a 747 automatic analyzor (Hitachi Boehringer Mannhein, Mannhein, Germany). Hepatic and renal tissue samples were fixed in 10 % formalin and embedded in paraffin. 5 μm thick sections were cut into and stained with hematoxylin and eosin for light microscope examination. Expression of P-selectin in hepatic/renal tissue was detected by immunohistochemistry method with a labeled streptavidin biotin (LSAB) kit (Fujian Maixin Biotechnology Co., products of Biotechnology Co. CA, USA).

Statistical analysis

Data were presented as $\bar{x}\pm s$, and Student' s t test was used to determine changes between different groups. $P<0.05$ was considered significant.

RESULTS

Histopathologic evaluation

One hour after reperfusion, visual observation revealed that the left hepatic lobe was more swollen than the right lobe, and was dark in color. Under the light microscope, interstitial congestion and infiltration of inflammatory cells were

observed. One hour after reperfusion, the renal cortex was macroscopically pale, the renal medulla displayed blood stagnation and was dark in color. Under the light microscope, edema, denaturation with different extent and necrosis of renal tubular epithelial cells were observed. Simultaneously, interstitial congestion, edema and infiltration of inflammatory cells were also observed. However, in the TMP-treated group, the outward appearance of the liver and kidney was similar to that of normal. Hepatic cells and tubular cells showed less swelling and no denaturation or necrosis, and interstitial changes were not obvious.

Hepatic and renal function evaluation

Twenty four hours after hepatic reperfusion, the serum levels of ALT (628±91 u/L) and AST (1 608±199 u/L) in the saline-treated group were much higher than those in the sham-operated group (52±11 u/L and 80±17 u/L respectively, $P<0.01$). The TMP-treated group revealed significantly lower levels of ALT (190±21 u/L) and AST (386±62 u/L) than those in the saline-treated group ($P<0.01$).

Twenty four hours after renal reperfusion, the serum levels of BUN (14.54±0.67 mmol/L) and Cr (102.2±4.67 μmol/L) were much higher in the TMP-treated group than those in the sham-operated group (7.88±0.57 mmol/L and 39.00±4.47 μmol/L, respectively, $P<0.01$). The TMP-treated group presented with significantly lower levels of BUN (11.21±0. 56 mmol/L) and Cr (70.61±4.95 μmol/L) than those in the saline-treated group ($P<0.01$).

P-selectin expression in hepatic and renal tissues

P-selectin was expressed widely within hepatic and renal tissues 1 hour after reperfusion, which was mainly distributed on small vessels of left hepatic lobe and kidney. In addition, it was also expressed on part of hepatic cellular membrane, glomerulomesangium, capillary loops, and interstitium. After treatment with TMP, there were no obvious yellow-brown positive granules in the hepatic and renal tissues, suggesting that P-selectin expression was not displayed.

DISCUSSION

Recently, the role of cell adhesion molecules and neutrophils in ischemia and reperfusion injury has aroused attention[29-50]. Ischemia reperfusion liver injury is characterized by microvascular leukocyte accumulation and massive infiltration of postischemic tissues. Primary leukocyte endothelial cell interaction(rolling) is mediated by selectins, whereas firm adherence and transendothelial migration involve immunoglobulin superfamily(intercellular adhesion molecule-1, ICAM-1) with leukocyte β_2-integrins (CD11/CD18)[51]. As a potential member of the selectin family, P-selectin has been found in both Weibel-Palade body of epithelial cells of middle and small blood vessels and α-granule of platelets. It is expressed rapidly on the surface of these cells in seconds after their activation. Furthermore, P-selectin can be up-regulated by *de novo* synthesis in the ischemia-reperfusion injury in hours. P-selectin plays an important role in inflammation by initiating neutrophil rolling, adhesion and recruitment to injured tissue[15]. Blockade of P-selectin expression or interaction with its ligands can attenuate leukocyte adherence and infiltration during ischemia and reperfusion injury. And P-selectin monoclonal antibody has been found to have protective effects on the injury[21].

Tetramethylpyrazine (TMP) is an active ingredient of Ligustium Wallich Franch. It has been shown in animal models and clinical investigations that TMP is effective on ischemic diseases such as heart, brain and lung. TMP could block the calcium channel, reduce the bioactivity of platelets and platelet aggregation, and inhibit free radicals, and has inhibitory roles in platelets and arterial thrombus formation in dogs[52]. However, the roles and mechanisms of TMP in treatment of digestive diseases have not been extensively studied.

The effect of TMP on ischemia and reperfusion injury was observed in this study based on the established rat model of hepatic/renal ischemia-reperfusion.

Hepatic and renal tissues displayed significantly histopathologic damages after hepatic/renal ischemia-reperfusion while the serum levels of ALT and AST as well as BUN and Cr were increased. It was showed that hepatic/renal injury induced by ischemia-reperfusion was remarkably attenuated when TMP was given 5 minutes before reperfusion as shown by improved hepatic/renal function and less pathologic damage. The results suggest that TMP has a protective effect on hepatic/renal reperfusion injury by inhibiting the interaction of neutrophils and endothelium.

After ischemia and reperfusion, P-selectin expression was up-regulated in hepatic and renal tissues, suggesting that P-selectin is related to hepatic/renal reperfusion injury. It was found that leukocyte rolling and recruitment were delayed when deficient mice are infected, suggesting that P-selectin is involved in the early events of inflammation mediated by leukocytes[53]. Results from this study showed that P-selectin expression in hepatic and renal tissues was inhibited in TMP-treated group. This is consistent with down-regulated expression of sialyl Lewis X, a ligand for P-selectin located mainly in neutrophils, as with anti-P-selectin therapy (unpublished data). These suggest that P-selectin might mediate neutrophil infiltration within the liver and kidney in the early stage of hepatic/renal reperfusion injury. Furthermore, blockade of P-selectin can attenuate inflammatory cell infiltration and pathological damage. Wu found that TMP could reduce significantly the number of α-granule membrane protein (GMP140) of platelets and had inhibitory effects on platelets and arterial thrombus formation in dogs. TMP can play a protective role in hepatic and renal injury caused by ischemia-reperfusion by inhibiting the adhesion and activation of neutrophils mediated by P-selectin.

In an animal model of thioacetamide (TAA) induced acute hepatotoxicity, increase of serum SGOT and SGPT produced by TAA was decreased by TMP, and increase of malondialdehyde (MDA) produced by TAA was also prevented by *in vitro* addition of TMP to liver homogenates. A rise of serum interleukin-2 was similarly prevented. The results suggest that part of hepatocellular injury induced by TAA is mediated by oxidative stress caused by the action of cytokines through lipid peroxidation, TMP may act by preventing lipid peroxidation[54]. Another study showed that the hepatoprotective effect of TMP might be in part due to its inhibitory ability on membrane lipid peroxidation and free radical formation and its free radical scavenging ability[55]. Therefore, TMP might be effective on the treatment of on reperfusion injury.

REFERENCES

1 **Funaki H**, Shimizu K, Harada S, Tsuyama H, Fushida S, Tani T, Miwa K. Essential role for nuclear factor kappaB in ischemic preconditioning for ischemia-reperfusion injury of the mouse liver. *Transplantation* 2002; **74**: 551-556

2 **Khandoga A**, Biberthaler P, Enders G, Axmann S, Hutter J, Messmer K, Krombach F. Platelet adhesion mediated by fibrinogen-intercelllular adhesion molecule-1 binding induces tissue injury in the postischemic liver *in vivo.Transplantation* 2002; **74**: 681-688

3 **Satoh S**, Suzuki A, Asari Y, Sato M, Kojima N, Sato T, Tsuchiya N, Sato K, Senoo H, Kato T. Glomerular endothelium exhibits enhanced expression of costimulatory adhesion molecules, CD80 and CD86, by warm ischemia / reperfusion injury in rats. *Lab In-*

vest 2002; **82**: 1209-1217
4 **de Rossi LW**, Horn NA, Buhre W, Gass F, Hutschenreuter G, Rossaint R. The effect of isoflurane on neutrophil selectin and beta(2)-integrin activation *in vitro*. *Anesth Analg* 2002; **95**: 583-587
5 **Burne MJ**, Rabb H. Pathophysiological contributions of fucosyltransferases in renal ischemia reperfusion injury. *J Immunol* 2002; **169**: 2648-2652
6 **Faure JP**, Hauet T, Han Z, Goujon JM, Petit I, Mauco G, Eugene M, Carretier M, Papadopoulos V. Polyethylene glycol reduces early and long-term cold ischemia-reperfusion and renal medulla injury. *J Pharmacol Exp Ther* 2002; **302**: 861-870
7 **Khandoga A**, Enders G, Biberthaler P, Krombach F. Poly(ADP-ribose) polymerase triggers the microvascular mechanisms of hepatic ischemia-reperfusion injury. *Am J Physiol Gastrointest Liver Physiol* 2002; **283**: G553-560
8 **Horie Y**, Yamagishi Y, Kato S, Kajihara M, Tamai H, Granger DN, Ishii H. Role of ICAM-1 in chronic ethanol consumption-enhanced liver injury after gut ischemia-reperfusion in rats. *Am J Physiol Gastrointest Liver Physiol* 2002; **283**: G537-543
9 **Olanders K**, Sun Z, Borjesson A, Dib M, Andersson E, Lasson A, Ohlsson T, Andersson R. The effect of intestinal ischemia and reperfusion injury on ICAM-1 expression, endothelial barrier function, neutrophil tissue influx, and protease inhibitor levels in rats. *Shock* 2002; **18**: 86-92
10 **Kubes P**, Payne D, Woodman RC. Molecular mechanisms of leukocyte recruitment in postischemic liver microcirculation. *Am J Physiol Gastrointest Liver Physiol* 2002; **283**: G139-147
11 **Leonard MO**, Hannan K, Burne MJ, Lappin DW, Doran P, Coleman P, Stenson C, Taylor CT, Daniels F, Godson C, Petasis NA, Rabb H, Brady HR. 15-Epi-16-(para-fluorophenoxy)-lipoxin A(4)-methyl ester, a synthetic analogue of 15-epi-lipoxin A(4), is protective in experimental ischemic acute renal failure. *J Am Soc Nephrol* 2002; **13**: 1657-1662
12 **Farmer DG**, Amersi F, Shen XD, Gao F, Anselmo D, Ma J, Dry S, McDiarmid SV, Shaw G, Busuttil RW, Kupiec-Weglinski J. Improved survival through the reduction of ischemia-reperfusion injury after rat intestinal transplantation using selective P-selectin blockade with P-selectin glycoprotein ligand-Ig. *Transplant Proc* 2002; **34**: 985
13 **Oktar BK**, Gulpinar MA, Bozkurt A, Ghandour S, Cetinel S, Moini H, Yegen BC, Bilsel S, Granger DN, Kurtel H. Endothelin receptor blockers reduce I/R-induced intestinal mucosal injury: role of blood flow. *Am J Physiol Gastrointest Liver Physiol* 2002; **282**: G647-655
14 **Kuzu MA**, Koksoy C, Kuzu I, Gurhan I, Ergun H, Demirpence E. Role of integrins and intracellular adhesion molecule-1 in lung injury after intestinal ischemia-reperfusion. *Am J Surg* 2002; **183**: 70-74
15 **Zhou T**, Li X, Wu P, Zhang D, Zhang M, Chen N, Dong D. Effect of anti-P-selectin monoclonal antibody on renal ischemia/reperfusion injury in rats. *Chin Med J* 2000; **113**: 790-793
16 **Stepkowski SM**, Chen W, Bennett CF, Condon TP, Stecker K, Tian L, Kahan BD. Phosphorothioate/methoxyethyl-modified ICAM-1 antisense oligonucleotides improves prevention of ischemic/reperfusion injury. *Transplant Proc* 2001; **33**: 3705-3706
17 **Deng J**, Kohda Y, Chiao H, Wang Y, Hu X, Hewitt SM, Miyaji T, McLeroy P, Nibhanupudy B, Li S, Star RA. Interleukin-10 inhibits ischemic and cisplatin-induced acute renal injury. *Kidney Int* 2001; **60**: 2118-2128
18 **Redlin M**, Werner J, Habazettl H, Griethe W, Kuppe H, Pries AR. Cariporide (HOE 642) attenuates leukocyte activation in ischemia and reperfusion. *Anesth Analg* 2001; **93**: 1472-1479
19 **Salter JW**, Krieglstein CF, Issekutz AC, Granger DN. Platelets modulate ischemia/reperfusion-induced leukocyte recruitment in the mesenteric circulation. *Am J Physiol Gastrointest Liver Physiol* 2001; **281**: G1432-1439
20 **Lindner JR**, Song J, Christiansen J, Klibanov AL, Xu F, Ley K. Ultrasound assessment of inflammation and renal tissue injury with microbubbles targeted to P-selectin. *Circulation* 2001; **104**: 2107-2112
21 **Wu P**, Li X, Zhou T, Zhang MJ, Chen JL, Wang WM, Chen N, Dong DC. Role of P-selectin and anti-P-selectin monoclonal antibody in apoptosis during hepatic/renal ischemia reperfusion injury. *World J Gastoenterol* 2000; **6**: 244-247
22 **Kojima N**, Sato M, Suzuki A, Sato T, Satoh S, Kato T, Senoo H. Enhanced expression of B7-1, B7-2, and intercellular adhesion molecule 1 in sinusoidal endothelial cells by warm ischemia/reperfusion injury in rat liver. *Hepatology* 2001; **34**: 751-757
23 **Weigand MA**, Plachky J, Thies JC, Spies-Martin D, Otto G, Martin E, Bardenheuer HJ. N-acetylcysteine attenuates the increase in alpha-glutathione S-transferase and circulating ICAM-1 and VCAM-1 after reperfusion in humans undergoing liver transplantation. *Transplantation* 2001; **72**: 694-698
24 **Huang X**, Ren P, Wen AD, Wang LL, Zhang L, Gao F. Pharmacokinetics of traditional Chinese syndrome and recipe: a hypothesis and its verification (I). *World J Gastroenterol* 2000; **6**: 384-391
25 **Zhou S**, Shao W, Zhang W. Clinical study of Astragalus injection plus ligustrazine in protecting myocardial ischemia reperfusion injury.*Zhongguo Zhongxiyi Jiehe Zazhi* 2000; **20**: 504-507
26 **Liu CF**, Lin CC, Ng LT, Lin SC. Protection by tetramethylpyrazine in acute absolute ethanol-induced gastric lesions. *J Biomed Sci* 2002; **9**: 395-400
27 **Liu CF**, Lin MH, Lin CC, Chang HW, Lin SC. Protective effect of tetramethylpyrazine on absolute ethanol-induced renal toxicity in mice. *J Biomed Sci* 2002; **9**: 299-302
28 **Li M**, Handa S, Ikeda Y, Goto S. Specific inhibiting characteristics of tetramethylpyrazine, one of the active ingredients of the Chinese herbal medicine 'Chuanxiong,' on platelet thrombus formation under high shear rates. *Thromb Res* 2001; **104**: 15-28
29 **Dragun D**, Hoff U, Park JK, Qun Y, Schneider W, Luft FC, Haller H. Prolonged cold preservation augments vascular injury independent of renal transplant immunogenicity and function. *Kidney Int* 2001; **60**: 1173-1181
30 **Young CS**, Palma JM, Mosher BD, Harkema J, Naylor DF, Dean RE, Crockett E. Hepatic ischemia/reperfusion injury in P-selectin and intercellular adhesion molecule-1 double-mutant mice. *Am Surg* 2001; **67**: 737-744
31 **Yabe Y**, Kobayashi N, Nishihashi T, Takahashi R, Nishikawa M, Takakura Y, Hashida M. Prevention of neutrophil-mediated hepatic ischemia/reperfusion injury by superoxide dismutase and catalase derivatives. *J Pharmacol Exp Ther* 2001; **298**: 894-899
32 **Maroszynska I**, Fiedor P. Leukocytes and endothelium interaction as rate limiting step in the inflammatory response and a key factor in the ischemia-reperfusion injury. *Ann Transplant* 2000; **5**: 5-11
33 **Laskowski I**, Pratschke J, Wilhelm MJ, Gasser M, Tilney NL. Molecular and cellular events associated with ischemia/reperfusion injury. *Ann Transplant* 2000; **5**: 29-35
34 **Burne MJ**, Elghandour A, Haq M, Saba SR, Norman J, Condon T, Bennett F, Rabb H. IL-1 and TNF independent pathways mediate ICAM-1/VCAM-1 up-regulation in ischemia reperfusion injury. *J Leukoc Biol* 2001; **70**: 192-198
35 **Fuller TF**, Sattler B, Binder L, Vetterlein F, Ringe B, Lorf T. Reduction of severe ischemia reperfusion injury in rat kidney grafts by a soluble P-selectin glycoprotein ligand. *Transplantation* 2001; **72**: 216-222
36 **Oe S**, Hiros T, Fujii H, Yasuchika K, Nishio T, Limuro Y, Morimoto T, Nagao M, Yamaoka Y. Continuous intravenous infusion of deleted form of hepatocyte growth factor attenuates hepatic ischemia-reperfusion injury in rats. *J Hepatol* 2001; **34**: 832-839
37 **Kobayashi A**, Imamura H, Isobe M, Matsuyama Y, Soeda J, Matsunaga K, Kawasaki S. Mac-1 (CD11b/CD18) and intercellular adhesion molecule-1 in ischemia-reperfusion injury of rat liver. *Am J Physiol Gastrointest Liver Physiol* 2001; **281**: G577-585
38 **Cabrera PV**, Blanco G, Argibay P, Hajos SE. Isoforms modulation of CD44 adhesion molecule in a murine model of ischemia and intestinal reperfusion. *Medicina* 2000; **60**: 940-946
39 **Serracino-Inglott F**, Habib NA, Mathie RT. Hepatic ischemia-reperfusion injury. *Am J Surg* 2001; **181**: 160-166
40 **Taut FJ**, Schmidt H, Zapletal CM, Thies JC, Grube C, Motsch J, Klar E, Martin E. N-acetylcysteine induces shedding of selectins from liver and intestine during orthotopic liver transplantation. *Clin Exp Immunol* 2001; **124**: 337-341
41 **Bojakowski K**, Abramczyk P, Bojakowska M, Zwolinska A, Przybylski J, Gaciong Z. Fucoidan improves the renal blood flow in the early stage of renal ischemia/reperfusion injury in the rat. *J Physiol Pharmacol* 2001; **52**: 137-143

42 **Opal SM**, Sypek JP, Keith JC Jr, Schaub RG, Palardy JE, Parejo NA. Evaluation of the safety of recombinant P-selectin glycoprotein ligand-immunoglobulin G fusion protein in experimental models of localized and systemic infection. *Shock* 2001; **15**: 285-290

43 **Zingarelli B**, Yang Z, Hake PW, Denenberg A, Wong HR. Absence of endogenous interleukin 10 enhances early stress response during post-ischaemic injury in mice intestine. *Gut* 2001; **48**: 610-622

44 **Rivera-Chavez FA**, Toledo-Pereyra LH, Martinez-Mier G, Nora DT, Harkema J, Bachulis BL, Dean RE. L-selectin blockade and liver function in rats after uncontrolled hemorrhagic shock. *J Invest Surg* 2001; **14**: 7-12

45 **Chen W**, Bennett CF, Condon TP, Stecker K, Tian L, Kahan BD, Stepkowski SM. Methoxyethyl modification of phosphorothioate ICAM-1 antisense oligonucleotides improves prevention of ischemic / reperfusion injury. *Transplant Proc* 2001; **33**: 854

46 **Ghobrial R**, Amersi F, Stecker K, Kato H, Melinek J, Singer J, Mhoyan A, Busuttil RW, Kupiec-Weglinski JW, Stepkowski SM. Amelioration of hepatic ischemia / reperfusion injury with intercellular adhesion molecule-1 antisense oligodeoxynucleotides. *Transplant Proc* 2001; **33**: 538

47 **Koksoy C**, Kuzu MA, Kuzu I, Ergun H, Gurhan I. Role of tumour necrosis factor in lung injury caused by intestinal ischaemia-reperfusion. *Br J Surg* 2001; **88**: 464-468

48 **Sun Z**, Wang X, Lasson A, Bojesson A, Annborn M, Andersson R. Effects of inhibition of PAF, ICAM-1 and PECAM-1 on gut barrier failure caused by intestinal ischemia and reperfusion. *Scand J Gastroenterol* 2001; **36**: 55-65

49 **Amersi F**, Dulkanchainun T, Nelson SK, Farmer DG, Kato H, Zaky J, Melinek J, Shaw GD, Kupiec-Weglinski JW, Horwitz LD, Horwitz MA, Busuttil RW. A novel iron chelator in combination with a P-selectin antagonist prevents ischemia / reperfusion injury in a rat liver model. *Transplantation* 2001; **71**: 112-118

50 **Wada K**, Montalto MC, Stahl GL. Inhibition of complement C5 reduces local and remote organ injury after intestinal ischemia / reperfusion in the rat. *Gastroenterology* 2001; **120**: 126-133

51 **Chen JL**, Zhou T, Chu YD, Xu HM, Li X, Zhang MJ, Zhang DH, Wu YL. Study on intercellular adhesion-1 and P-selectin in liver ischemia and reperfusion injury. *J SSMU* 1998; **10**: 63-65

52 **Zou LY**, Hao XM, Zhang GQ, Zhang M, Guo JH, Liu TF. Effect of tetramethyl pyrazine on L-type calcium channel in rat ventricular myocytes. *Can J Physiol Pharmacol* 2001; **79**: 621-626

53 **Frenette PS**, Mayadas TN, Rayburn H, Hynes RO, Wagner DD. Susceptibility to infection and altered hematopoiesis in mice deficient in both P-and E-selectins. *Cell* 1996; **84**: 563-574

54 **So EC**, Wong KL, Huang TC, Tasi SC, Liu CF. Tetramethylpyrazine protects mice against thioacetamide-induced acute hepatotoxicity. *J Biomed Sci* 2002; **9**: 410-414

55 **Liu CF**, Lin CC, Ng LT, Lin SC. Hepatoprotective and therapeutic effects of tetramethylpyrazine on acute econazole-induced liver injury. *Planta Med* 2002; **68**: 510-514

Edited by Xu XQ and Wang XL

P.O.Box 2345, Beijing 100023,China
Fax: +86-10-85381893
E-mail: wjg@wjgnet.com www.wjgnet.com

World J Gastroenterol 2003;9(7):1567-1570
World Journal of Gastroenterology
 ISSN 1007-9327

• BASIC RESEARCH •

Role of NF-κB and cytokine in experimental cancer cachexia

Wei Zhou, Zhi-Wei Jiang, Jie Tian, Jun Jiang, Ning Li, Jie-Shou Li

Wei Zhou, Zhi-Wei Jiang, Jun Jiang, Ning Li, Jie-Shou Li, Department of Surgery, School of Medicine, Nanjing University, Nanjing 210002, Jiangsu Province, China
Jie Tian, Department of Anaesthesiology, School of Life Sciences, Nanjing University, Nanjing 210002, Jiangsu Province, China
Correspondence to: Dr. Wei Zhou, Department of Surgery, Jinling Hospital, 305 East Zhongshan Road, Nanjing 210002, Jiangsu Province, China. nuzw@sohu.com
Telephone: +86-25-3685194 **Fax:** +86-25-4803956
Received: 2003-03-02 **Accepted:** 2003-03-29

Abstract

AIM: To assess the putative involvement of NF-κB and pro-inflammatory cytokines in the pathogenesis of cancer cachexia and the therapeutic efficacy of indomethacin (IND) on cachexia.

METHODS: Thirty young male BABL/c mice were divided randomly into five groups: (a) control, (b) tumor-bearing plus saline, (c) tumor-bearing plus IND (0.25 mg·kg^{-1}), (d) tumor-bearing plus IND (0.5 mg·kg^{-1}), and (e) tumor-bearing plus IND (2 mg·kg^{-1}). Colon 26 adenocarcinoma cells of murine were inoculated subcutaneously to induce cachexia. Saline and IND were given intraperitoneally daily for 7 days from the onset of cachexia to sacrifice. Food intake and body composition were documented, serum levels of TNF-α and IL-6 and activity of NF-κB in the spleen were investigated in all animals.

RESULTS: Weight loss was observed in all tumor-bearing mice. By day 16, body weights of non-tumor mice were about 72 % of healthy controls (P<0.01), and the weight of gastrocnemius was decreased by 28.7 % (P<0.01). No difference was found between groups in food intake (P>0.05). Gastrocnemius weight was increased markedly (P<0.01) after treatment of IND (0.5 mg·kg^{-1}), while the non-tumor body weights were not significantly elevated. Tumor-bearing caused a 2-3 fold increase in serum levels of both TNF-α and IL-6 (P<0.01). The concentration of TNF-α (P<0.05) and IL-6 (P<0.01) in tumor-bearing mice was reduced after administration of 0.5 mg·kg^{-1} IND for 7 days. But the level of IL-6 was slightly elevated following treatment of IND 2.0 mg·kg^{-1}. NF-κB activation in the spleen was increased in tumor-bearing mice in comparison with controls in electrophoretic mobility shift assay (EMSA). NF-κB activity was reduced in mice treated with 0.5 mg·kg^{-1} of IND, whereas a higher NF-κB activity was observed in mice treated with 2.0 mg·kg^{-1} of IND.

CONCLUSION: Colon 26 adenocarcinoma cells can induce severe cancer cachexia experimentally, and the mechanism may be partially due to the enhanced TNF-α and IL-6 in tumor-bearing animals, which is controlled by NF-κB. Low dose of indomethacin alleviates the cachexia, decreases the activation of NF-κB and the serum levels of TNF-α and IL-6, and prevents body weight loss and muscle atrophy, while no further effect is gained by a higher dosage.

Zhou W, Jiang ZW, Tian J, Jiang J, Li N, Li JS. Role of NF-κB and cytokine in experimental cancer cachexia. *World J Gastroenterol* 2003; 9(7): 1567-1570
http://www.wjgnet.com/1007-9327/9/1567.asp

INTRODUCTION

Cancer cachexia is characterized by significant weight loss even at an early course of malignancy, and reduces the quality of life of patients as well as responsiveness to chemotherapy. It is the most debilitating and life-threatening aspect of cancer and is associated with psychological distress and a lower quality of life. Thus, it is necessary to clarify the cellular and molecular biological mechanisms of cancer cachexia for the improvement of cancer treatment.

It has been well established that pro-inflammatory cytokines are important in inducing and promoting the development of experimental cancer cachexia. Most research efforts have focused on the role of cytokines of tumor necrosis factor α (TNF-α), interleukin 6 (IL-6) and interleukin 1 (IL-1)[1-4]. Many of these cytokines are responsible for weight loss, an acute phase of protein response, fat and skeletal muscle protein breakdown and elevated energy expenditure in animals and patients[5]. The nuclear factor-kappaB proteins are ubiquitous transcription factors that mediate cellular responses to a diverse array of stimuli, including lipopolysaccharide, reactive oxygen species (ROS) and several cytokines. Over the past decade, significant advances have been made in elucidation of the molecular signals leading to NF-κB activation, as well as in identification of gene regulation by NF-κB. The role of NF-κB proteins in regulating genes associated with immune system and inflammation has been extensively studied. Activation of NF-κB in immune cells upregulates the expression of cytokines, and growth factors that are essential to immune response contribute to inflammation. An autoregulatory feedback loop has been generated with production of cytokines TNF-α and IL-1. NF-κB represents an upstream element of a common pathway that produces catabolic cytokines[6-8]. Such a pathway has an obvious clinical importance in providing potential targets for therapeutic intervention to inhibit or reverse cancer cachexia.

In the present study, a cachectic model was established in mouse bearing colon 26 adenocarcinoma cells for studying the mechanism and therapies of cancer cachexia. As with human cachexia, there was a significant loss of body weight in this model, and the animals had substantial hypoglycemia and an increase of circulating pro-inflammatory cytokines that were thought to be correlative to the onset of cancer cachexia[9-12]. Early researches showed that indomethacin (IND) could prolong the mean survival time of patients with advanced solid cancer[13]. In this study, we chose IND as an anti-inflammatory agent to study its effect on peripheral blood cytokine levels and NF-κB activation in spleen. The purpose of this study was to assess the relationship of NF-κB and cancer cachexia and the role of IND in the treatment of cachexia.

MATERIALS AND METHODS

Animals and tumor implantation

BABL/c male mice aged 6-8 weeks (weighing 19-22 g) were

purchased from the Animal Center of Chinese Academy of Sciences, Shanghai, China. They had free access to standard laboratory chow and tap water, and were maintained in a temperature-controlled room (22±1 ℃) on a 12-h light-dark cycle. Thirty animals were evenly divided into five groups randomly: (a) control, (b) tumor-bearing plus saline, (c) tumor-bearing plus IND (0.25 mg· kg^{-1}, ICN, Biomedicals Inc. Ohio, USA), (d) tumor-bearing plus IND (0.5 mg· kg^{-1}), and (e) tumor-bearing plus IND (2 mg· kg^{-1}). The mice were allowed to adjust to new environment and diet for at least 1 week before experiment.

Colon 26 adenocarcinoma is appropriate for investigating cancer cachexia. This murine tumor is responsible for inducing weakness, abnormal carbohydrate metabolism, hypercorticism, and elevated levels of pro-inflammatory cytokines. Colon 26 adenocarcinoma cells were kindly supplied by Institute Materia Medica, Chinese Academy of Medical Sciences. Stock cells were passed on the BABL/c mice. Mice of passages three or four were used in the study. On day 0, a homogenate of murine colon 26 adenocarcinoma (50 mg of solid tumor tissue in 0.1 ml of sterile 0.9 % NaCl) was injected s.c. into armpits of the tumor-bearing groups. All procedures in the study were approved by the Institutional Animal Care Committee.

Experimental procedures

After inoculation of tumor cells, physical activity, fur condition, and other signs of general well being of the animals were registered. The tumor inoculation site and the tumor size were inspected. The tumor volume was estimated by using the equation $ab^2/2$, where a and b are length and width (cm) of the tumor. Body weight was monitored and food intake was measured at 10 a.m. everyday.

Significant loss of body weight was observed in tumor-bearing groups beginning on day 9 to day 16, 0.1 ml saline and variable dosages of indomethacin were given intraperitoneally to groups *b*, *c*, *d* and *e* daily for 7 days, respectively. On day 16, carcass weight was measured after removing the entire tumor. Blood samples were collected from orbital veins by removal of one side eyeballs of the animals and stored at -20 ℃ for determination of TNF-α and IL-6 by ELISA kit (Bender Medsystems, Vienna, Austria). Weight of the gastrocnemius of left hind leg was measured. The spleens were frozen in liquid nitrogen, and stored at -70 ℃ for nuclear protein extraction and electrophoretic mobility shift assay.

Nuclear protein extraction and electrophoretic mobility shift assay (EMSA)

Nuclear extracts of spleen tissues were prepared by hypotonic lyses followed by high salt extraction as references[14,15]. EMSA was performed using a commercial kit (Gel Shift Assay System; Promega, Madison, WI) as previously described. The NF-κB oligonucleotide probe, (5' -AGTTGAGGGGACTTTCCCAGGC-3'), was end-labeled with [γ-^{32}P] ATP (Free Biotech, Beijing, China) with T4-polynucleotide kinase. Nuclear protein (20 μl) was preincubated in 9 μl of a binding buffer, consisting of 10 mM Tris -Cl, pH 7.5, 1 mM $MgCl_2$, 50 mM NaCl, 0.5 mM EDTA, 0.5 mM DTT, 4 % glycerol, and 0.05 g· L^{-1} of poly-(deoxyinosinic deoxycytidylic acid) for 15 min at room temperature. After addition of 1 μl ^{32}P-labeled oligonuleotide probe, the incubation was continued for 30 min at room temperature. Reaction was stopped by adding 1 μl of gel loading buffer, and the mixture was subjected to non-denaturing 4 % polyacrylamide gel electrophoresis in 0.5×TBE buffer. The gel was vacuum-dried and exposed to X-ray film (Fuji Hyperfilm) at -70 ℃ with an intensifying screen. NF-κB was quantitated with densitometry.

Statistical analysis

Data were expressed as means ±SE. Statistical significance was determined by one-way ANOVA using SPSS 10.0. $P<0.05$ was considered statistically significant.

RESULTS

Tumors were palpable in mice initially on day 5 after inoculation of tumor cells, symptoms of cachexia began 3-4 days later. Weight loss began once a tumor grew to 1 cm^3 and a rapid loss of body weight occurred. Initial body weights of mice before experiment had no difference. By day 16, non-tumor body weights of tumor-bearing mice were about 72 % of healthy controls ($P<0.01$), and the weights of gastrocnemius were lowered by 28.7 % ($P<0.01$), though the final whole body weights were elevated because of tumor growth. Food intake between groups was not different ($P>0.05$, Table 1).

After administration of indomethacin for 1 week, the non-tumor body weights of tumor-bearing mice were increased, but had no significant difference from that in group b. The gastrocnemius weights in animals treated with 0.5 mg· kg^{-1} of IND increased significantly ($P<0.01$). But no weight gain of gastrocnemius in animals treated with IND 2.0 mg· kg^{-1} was observed. On the contrary, the tumor weight of this group was increased compared with that in saline group ($P<0.01$, data not shown). There was no evidence that IND had additional effects on appetite because quantity of food intake of mice treated with IND did not increase.

Table 1 Clinical features of tumor-bearing and non-tumor-bearing mice

Group	Initial body wt (g)	Final body wt (g)	Nontumor body wt (g)	Gastrocnemius muscle wt (mg)	Dry food intake (g· day^{-1})
Control	20.93±1.40	25.50±1.71	25.50±1.71	136.8±6.11	6.65±0.24
Tumor + saline	20.91±1.29	25.95±1.61	20.92±1.52[a]	97.5±8.32[a]	6.53±0.31
Tumor +IND(0.25 mg· kg^{-1})	20.98±1.42	27.75±2.20	21.75±1.64	95.65±13.5	6.56±0.27
Tumor +IND(0.5 mg· kg^{-1})	20.92±1.14	27.83±1.88	22.48±1.57	115.82±9.63[b]	6.70±0.32
Tumor +IND(2.0 mg· kg^{-1})	21.38±1.00	28.00±1.24	21.90±1.38	93.15±10.83	6.53±0.19

[a]$P<0.01$, *vs* control; [b]$P<0.01$, *vs* tumor + saline.

Table 2 Serum levels of TNF-α and IL-6 in mice

Parameter	Control	Tumor + saline	Tumor+IND (0.25mg· kg^{-1})	Tumor + IND (0.5mg· kg^{-1})	Tumor +IND (2.0mg· kg^{-1})
TNF-α(pg / ml)	43.24±13.37	113.83±16.91[a]	89.9±4.5	71.68±16.70[b]	110.96±20.93
IL-6 (pg / ml)	1445.82±244.20	2646.05±93.39[a]	2527.78±266.43	1983.07±219.19[c]	2733.33±201.84

[a]$P<0.01$, *vs* control; [b]$P<0.05$, *vs* tumor + saline; [c]$P<0.01$, *vs* tumor + saline.

Tumor-bearing caused a 2-3 fold increase in serum levels of both TNF-α and IL-6 (P<0.01). Administration of IND 0.5 mg· kg^{-1} for 7 days reduced the concentrations of TNF-α (P<0.05) and IL-6 (P<0.01) in tumor-bearing mice (Table 2). But level of IL-6 slightly increased after administration of 2.0 mg· kg^{-1} of IND.

EMSA experiments were performed to examine the effect of indomethacin on the activation of NF-κB induced by tumor bearing. As shown in Figure 1, NF-κB activation in spleen was increased in tumor-bearing mice, compared to controls. The tumor-bearing mice treated with 0.5 mg· kg^{-1} of indomethacin had a lower level of NF-κB than the cachectic mice without treatment. No dose-dependent response of NF-κB activity to different dose of IND treatment was observed. Instead, a higher NF-κB activity was found in the mice treated with IND 2.0 mg· kg^{-1}.

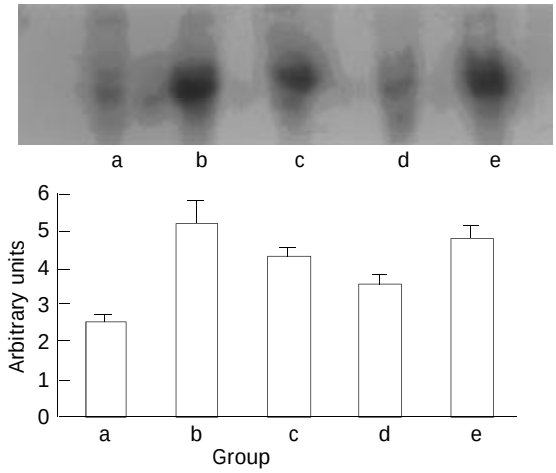

Figure 1 Activation of NF-κB in spleen. Lane a represents the control group, Lane b, c, d, e represents the group of tumor-bearing plus saline, indomethacin 0.25 mg·kg^{-1}, 0.5 mg·kg^{-1}, 2 mg·kg^{-1}, respectively.

DISCUSSION

The syndrome of cancer cachexia including progressive weight loss, particularly in skeletal muscle and adipose tissue, weakness, anemia, and often accompanied by anorexia is an important problem in the management of cancer patients. Nearly all cancer patients have significant weight loss by the time of death. Progressive wasting is an acknowledged clinical problem, it contributes to cancer mortality and may reduce the ability of patients to tolerate aggressive chemotherapy and radiotherapy. Although cachexia is frequently accompanied by anorexia, the decrease of food intake alone may be insufficient to account for cachexia because the body composition change in cachexia differs from that of starvation. Loss of skeletal muscle is more prominent in cachectic patients, leading to weakness and immobility of cancer patients eventually to death due to dysfunction of respiratory muscle. The fact that calories provided by total parenteral nutrition cannot maintain body weight of cancer patients suggests that weight loss is resulted from complex metabolic events rather than simple nutrition insufficiency[16].

Some possible mechanisms can be considered for the wasting in cachexia. It has been reported that weight loss is associated with anorexia in some tumor cachexia model[17]. But it is unlikely that the cachexia in our model was due to anorexia, because food intake was not significantly reduced while the mice were losing weight. Several cytokines are suggested to be involved in the development of cancer cachexia. The last decade has witnessed the discovery of multiple actions of cytokines on the regulation of metabolism in normal and pathophysiological conditions. Some of them are clearly involved in the wasting process that is often accompanied by chronic infection or cancer. We found that TNF-α and IL-6 levels in peripheral blood of animals were elevated while body and muscle weight decreased, which suggested the two cytokines were involved in our cachectic model. TNF-α levels were detectable in serum of pancreatic cancer patients, particularly in those with advanced disease, and these levels correlated with poor nutritional status[18]. Muscle wasting during tumor growth may be associated with the activation of non-lysosomal ubiquitin-dependent proteases associated with enhanced skeletal muscle proteolysis. This activation seems to be mediated by these cytokines, especially TNF-α, IL-6 and some other catabolic factors produced by tumors and hosts[19-22]. It was previously reported that TNF-α was partially mediated DNA fragmentation in skeletal muscle, suggesting an apoptotic phenomenon during experimental cancer-associated cachexia[23]. Production of pro-inflammatory cytokines also induces production of corresponding anti-inflammatory cytokines such as IL-15, IL-1 and IL-6 receptor antagonist, which may significantly reduce the severity of key parameters of cachexia[24-26]. Clearly the balance between pro-inflammatory and anti-inflammatory mediators may be crucial in determining the net clinical effects.

Several experiments suggested that cytokines (IL-1, IL-6, and TNF-α) induced anorexia in tumor-bearing and infected animals, and the appetite was improved in indomethacin-treated animals[17]. However, tumor-bearing mice in our experiments had no significant appetite change, and indomethacin had no obvious effect on diet consumption. So, the wasting condition in this model may have no relation with food consumption, but may be attributed to metabolic disorders. The present study confirmed previous reports demonstrating that a low dose of NASID, particularly indomethacin could inhibit cancer cachexia, whereas a high dose might be toxic[17, 27,28]. We found a low dose of indomethacin treatment could decrease TNF-α and IL-6 productions which were very important in the process of immune regulation and inflammation in this experimental model. Indomethacin also protected the host from deterioration in body composition, particularly lean body mass. It is likely that the inhibition was confined to host cell, since indomethacin caused no growth inhibition of tumors. However, contrary evidence also exists. Other reports suggested that IND appeared to suppress the growth of colon 26 as long as the tumor burden was small, whereas it facilitated the tumor growth when the tumor burden was large[29].

NF-κB is normally sequestered in the cytoplasm of nonstimulated cells and must translocate into nuclei to regulate effector gene expression. A family of inhibitory proteins, IκBs, binds to NF-κB and masks its nuclear localization signal domain and therefore controls the translocation of NF-κB. Exposure of cells to extracellular stimuli that perturb redox balance results in rapid phosphorylation, ubiquitination, and proteolytic degradation of IκBs. This process frees NF-κB from the NF-κB/IκBs complexes and enables NF-κB to translocate to the nuclei where they regulate gene transcription. Many effector genes such as those encoding cytokines and adhesion molecules are in turn regulated by NF-κB[6]. Some anti-inflammatory agents (e.g. salicylates, dexamethasone) can inhibit NF-κB, which also indicates that NF-κB is an important molecular target for modulation of inflammatory disease[30-33]. However, the identity of NF-κB, and its role in cancer cachexia still remain to be investigated. In the present study, a low baseline activity of spleen NF-κB was observed in controls, while tumor bearing increased NF-κB activities markedly. A low dose of indomethacin decreased NF-κB activities variably.

In summary, colon 26 adenocarcinoma cells could produce severe cancer cachexia, including loss of non-tumor whole

body and gastrocnemius muscle weight. The wasting condition may be partially due to the enhanced TNF-α and IL-6 production in the tumor-bearing animals, which is controlled by NF-κB. A low dose of indomethacin alleviates the wasting, decreases the activation of NF-κB, and serum level of TNF-α and IL-6, delays body weight loss and muscle atrophy. These results suggest that activation of NF-κB may play a critical role in inflammatory response of cancer cachexia. However, other possible mechanisms cannot be excluded. Indomethacin can suppress activation of NF-κB, and can be used as a reagent to improve the catabolic status in cancer cachexia. Although the present study could not clarify the definite mode of the anticachectic action of IND, the ability of IND to reverse cachexia should be considered as one of the various actions of this drug. Further studies are required to evaluate its clinical effects and mechanism in patients with cancer cachexia.

ACKNOWLEDGEMENT

We thank Dr. Genbao Feng for his technical assistance.

REFERENCES

1 **Kurzrock R.** The role of cytokines in cancer-related fatigue. *Cancer* 2001; **92**(Suppl)**:** 1684-1688
2 **Tisdale MJ.** Wasting in cancer. *J Nutr* 1999; **129**(Suppl): 243S-246S
3 **Barton BE,** Murphy TF. Cancer cachexia is mediated in part by the induction of IL-6-like cytokines from the spleen. *Cytokine* 2001; **16:** 251-257
4 **Barton BE.** IL-6-like cytokines and cancer cachexia: consequences of chronic inflammation. *Immunol Res* 2001; **23:** 41-58
5 **O'Riordain MG,** Falconer JS, Maingay J, Fearon KC, Ross JA. Peripheral blood cells from weight-losing cancer patients control the hepatic acute phase response by a primarily interleukin-6 dependent mechanism. *Int J Oncol* 1999; **15:** 823-827
6 **Baeuerle PA,** Baltimore D. NF-kappa B: ten years after. *Cell* 1996; **87:** 13-20
7 **Schwartz SA,** Hernandez A, Mark Evers B. The role of NF-kappaB / IkappaB proteins in cancer: implications for novel treatment strategies. *Surg Oncol* 1999; **8:** 143-153
8 **Wang T,** Zhang X, Li JJ. The role of NF-kappaB in the regulation of cell stress responses. *Int Immunopharmacol* 2002; **2:** 1509-1520
9 **Strassmann G,** Jacob CO, Fong M, Bertolini DR. Mechanisms of paraneoplastic syndromes of colon-26: involvement of interleukin 6 in hypercalcemia. *Cytokine* 1993; **5:** 463-468
10 **Tanaka M,** Miyazaki H, Takeda Y, Takeo S. Detection of serum cytokine levels in experimental cancer cachexia of colon 26 adenocarcinoma-bearing mice. *Cancer Lett* 1993; **72:** 65-70
11 **Strassmann G,** Fong M, Kenney JS, Jacob CO. Evidence for the involvement of interleukin 6 in experimental cancer cachexia. *J Clin Invest* 1992; **89:** 1681-1684
12 **Tanaka Y,** Eda H, Tanaka T, Udagawa T, Ishikawa T, Horii I, Ishitsuka H, Kataoka T, Taguchi T. Experimental cancer cachexia induced by transplantable colon 26 adenocarcinoma in mice. *Cancer Res* 1990; **50:** 2290-2295
13 **Lundholm K,** Gelin J, Hyltander A, Lonnroth C, Sandstrom R, Svaninger G, Korner U, Gulich M, Karrefors I, Norli B. Anti-inflammatory treatment may prolong survival in undernourished patients with metastatic solid tumors. *Cancer Res* 1994; **54:** 5602-5606
14 **Gong JP,** Liu CA, Wu CX, Li SW, Shi YJ, Li XH. Nuclear factor kB activity in patients with acute severe cholangitis. *World J Gastroenterol* 2002; **8:** 346-349
15 **Liu Z,** Yu Y, Jiang Y, Li J. Growth hormone increases lung NF-kappaB activation and lung microvascular injury induced by lipopolysaccharide in rats. *Ann Clin Lab Sci* 2002; **32:** 164-170
16 **Tisdale MJ.** Cancer anorexia and cachexia. *Nutrition* 2001; **17**: 438-442
17 **Cahlin C,** Korner A, Axelsson H, Wang W, Lundholm K, Svanberg E. Experimental cancer cachexia: The role of host-derived cytokines interleukin (IL)-6, IL-12, interferon-gamma, and tumor necrosis factor alpha evaluated in gene knockout, tumor-bearing mice on C57 Bl background and eicosanoid-dependent cachexia. *Cancer Res* 2000; **60:** 5488-5493
18 **Karayiannakis AJ,** Syrigos KN, Polychronidis A, Pitiakoudis M, Bounovas A, Simopoulos K. Serum levels of tumor necrosis factor-alpha and nutritional status in pancreatic cancer patients. *Anticancer Res* 2001; **21:** 1355-1358
19 **Llovera M,** Carbo N, Lopez-Soriano J, Garcia-Martinez C, Busquets S, Alvarez B, Agell N, Costelli P, Lopez-Soriano FJ, Celada A, Argiles JM. Different cytokines modulate ubiquitin gene expression in rat skeletal muscle. *Cancer Lett* 1998; **133:** 83-87
20 **Costelli P,** Bossola M, Muscaritoli M, Grieco G, Bonelli G, Bellantone R, Doglietto GB, Baccino FM, Fanelli FR. Anticytokine treatment prevents the increase in the activity of ATP-ubiquitin- and Ca(2+)-dependent proteolytic systems in the muscle of tumour-bearing rats. *Cytokine* 2002; **19:** 1-5
21 **Tisdale MJ**. The 'cancer cachectic factor'. *Support Care Cancer* 2003; **11**: 73-78
22 **Llovera M,** Garcia-Martinez C, Agell N, Lopez-Soriano FJ, Argiles JM. TNF can directly induce the expression of ubiquitin-dependent proteolytic system in rat soleus muscles. *Biochem Biophys Res Commun* 1997; **230:** 238-241
23 **Carbo N,** Busquets S, van Royen M, Alvarez B, Lopez-Soriano FJ, Argiles JM. TNF-alpha is involved in activating DNA fragmentation in skeletal muscle. Br J *Cancer* 2002; **86:** 1012-1016
24 **Strassmann G,** Kambayashi T. Inhibition of experimental cancer cachexia by anti-cytokine and anti-cytokine-receptor therapy. *Cytokines Mol Ther* 1995; **1:** 107-113
25 **Carbo N,** Lopez-Soriano J, Costelli P, Busquets S, Alvarez B, Baccino FM, Quinn LS, Lopez-Soriano FJ, Argiles JM. Interleukin-15 antagonizes muscle protein waste in tumour-bearing rats. *Br J Cancer* 2000; **83:** 526-531
26 **Strassmann G,** Masui Y, Chizzonite R, Fong M. Mechanisms of experimental cancer cachexia. Local involvement of IL-1 in colon-26 tumor. *J Immunol* 1993; **150:** 2341-2345
27 **Gelin J,** Andersson C, Lundholm K. Effects of indomethacin, cytokines, and cyclosporin A on tumor growth and the subsequent development of cancer cachexia. *Cancer Res* 1991; **51:** 880-885
28 **Niu Q,** Li T, Liu A. Cytokines in experimental cancer cachexia. *Zhonghua Zhongliu Zazhi* 2001; **23:** 382-384
29 **Tanaka Y,** Tanaka T, Ishitsuka H. Antitumor activity of indomethacin in mice bearing advanced colon 26 carcinoma compared with those with early transplants. *Cancer Res* 1989; **49:** 5935-5939
30 **Cai E,** Chen Z, Wu W. The effects of lipopolysaccharide and anti-inflammatory drugs on nuclear factor-kappa B in pulmonary intravascular macrophage. *Zhonghua Jiehe He Huxi Zazhi* 1999; **22:** 283-286
31 **Crinelli R,** Antonelli A, Bianchi M, Gentilini L, Scaramucci S, Magnani M. Selective inhibition of NF-κB activation and TNF-alpha production in macrophages by red blood cell-mediated delivery of dexamethasone. *Blood Cells Mol Dis* 2000; **26:** 211-222
32 **Chang CK,** Llanes S, Schumer W. Effect of dexamethasone on NF-κB activation, tumor necrosis factor formation, and glucose dyshomeostasis in septic rats. *J Surg Res* 1997; **72:** 141-145
33 **Amann R,** Peskar BA. Anti-inflammatory effects of aspirin and sodium salicylate. *Eur J Pharmacol* 2002; **447:** 1-9

Edited by Ren SY and Wang XL

P.O.Box 2345, Beijing 100023,China
Fax: +86-10-85381893
E-mail: wjg@wjgnet.com www.wjgnet.com

World J Gastroenterol 2003;9(7):1571-1575
World Journal of Gastroenterology
 ISSN 1007-9327

• BASIC RESEARCH •

Maxizyme-mediated specific inhibition on mutant-type p53 *in vitro*

Xin-Juan Kong, Yu-Hu Song, Ju-Sheng Lin, Huan-Jun Huang, Nan-Xia Wang, Nan-Zhi Liu, Bin Li, You-Xin Jin

Xin-Juan Kong, Yu-Hu Song, Ju-Sheng Lin, Huan-Jun Huang, Nan-Xia Wang, Nan-Zhi Liu, Institute of Liver Disease, Tongji Hospital, Tongji Medical College, Huazhong University of Science and Technology, Wuhan 430030, Hubei Province, China
Xin-Juan Kong, Bin Li, You-Xin Jin, State Key Laboratory of Molecular Biology, Shanghai Institute of Biochemistry, Chinese Academy of Sciences, Shanghai 200031, China
Supported by the National Natural Science Foundation of China, No.30171061
Correspondence to: Professor You-Xin Jin, State Key Laboratory of Molecular Biology, Shanghai Institute of Biochemistry, Chinese Academy of Sciences, 320 Yueyang Road, Shanghai 200031, China. yxjin@sunm.shcnc.ac.cn
Telephone: +86-21-64315030-5221 **Fax:** +86-21-64338357
Received: 2002-11-26 **Accepted:** 2003-02-19

Abstract

AIM: To evaluate the specific inhibition of maxizyme directing against mutant-type p53 gene (mtp53) at codon 249 in exon 7 (AGG→AGT) *in vitro.*

METHODS: Two different monomers of anti-mtp53 maxizyme (maxizyme right MzR, maxizyme left MzL) and control mutant maxizyme ($G^5 \rightarrow A^5$) were designed by computer and cloned into vector pBSKU6 (pBSKU6MzR, pBSKU6MzL). After being sequenced, the restrictive endonuclease site in pBSKU6MzR was changed by PCR and then U6MzR was inserted into pBSKU6MzL, the recombinant vector was named pU6Mz and pU6asMz (mutant maxizyme). Mtp53 and wild-type p53 (wtp53) gene fragments were cloned into pGEM-T vector under the T7 promoter control. The ^{32}p-labeled mtp53 transcript was the target mRNA. Cold maxizyme transcripts were incubated with ^{32}p-labeled target RNA *in vitro* and radioautographed after denaturing polyacrylamide gel electrophoresis.

RESULTS: In cell-free systems, pU6Mz showed a specific cleavage activity against target mRNA at 37 ℃ and 25 mM $MgCL_2$. The cleavage efficiency of pU6Mz was 42 %, while pU6asMz had no inhibitory effect. Wtp53 was not cleaved by pU6Mz either.

CONCLUSION: pU6Mz had a specific catalytic activity against mtp53 in cell-free system. These lay a good fundation for studying the effects of anti-mtp53 maxizyme in HCC cell lines. The results suggest that maxizyme may be a promising alternative approach for treating hepatocellular carcinoma containing mtp53.

Kong XJ, Song YH, Lin JS, Huang HJ, Wang NX, Liu NZ, Li B, Jin YX. Maxizyme-mediated specific inhibition on mutant-type p53 *in vitro. World J Gastroenterol* 2003; 9(7): 1571-1575
http://www.wjgnet.com/1007-9327/9/1571.asp

INTRODUCTION

Hepatocellular carcinoma (HCC) is one of the major causes of mortality worldwide[1,2]. Several risk factors are associated with the development of HCC including chronic infection with hepatitis B virus (HBV) and hepatitis C virus (HCV), exposure to genotoxic environmental agents such as aflatoxins. The high incidence of HCC has been observed in areas such as sub-saharan Africa, Thailand and the Southern region of China (Qidong) where concomitant infection occurs with HBV and high intake of aflatoxins[3-5]. Mutational inactivation of tumor suppressor gene p53 is very common in hepatocellular carcinoma. Indeed, p53 gene mutations, deletions or loss is a very important step during carcinogenesis and might participate in all stages of HCC development[6-9]. AGG to AGT transversion in codon 249 (the third base of codon 249) of exon 7 of p53 gene occurs in over 50 % of HCC from endemic regions, where both chronic infection with HBV and exposure to carcinogens such as aflatoxin B1(AFB1) prevail[10-13]. The p53 tumor suppressor gene product plays a crucial physiological role as a "cellular gatekeeper" by exerting a variety of effects following DNA damage[14,15]. Study of p53 as a tumor suppressor gene has attracted a large number of top scientists worldwide. But mutant p53 has drawn much less attention. Mutant p53 may not be an inactivated tumor suppressor gene, it appears to be one of the most prominent members of a new family of oncogenes[16,17]. Inactivation of p53 contributes not only to tumor progression but also to resistance of cancer cells to chemotherapy. Mutant p53 protein may possess transforming ability and can cooperate with other oncogenes in the transformation of normal cells. Mutant p53 protein has a prolonged halflife of 2 to 12 hours, resulting in higher intracellular concentrations than the wild-type protein[18,19]. Loss of ability to suppress transformation and gain of transforming potential and tumorigenicity are the properties of mutant p53 gene product.

Ribozyme is a kind of catalytic RNA which can catalyze the cleavage of sequence-specific RNA[20]. Among different types of ribozymes discovered, hammerhead ribozyme has been studied extensively for the treatment of disorders ranging from cancer to infectious disease[21-29]. However, because the limited number of cleavable sequences on target RNA, in some cases conventional ribozyme does not have precise cleavage specificity. This shortcoming may greatly limit the utility of hammerhead ribozyme[30,31]. A minizyme (minimised ribozyme) is a hammerhead ribozyme with short oligonucleotide linker instead of stem II. It has lower cleavage activity compared with that of wild-type parental hammerhead ribozyme[32,33]. Two minizymes could form an active dimeric structure. The dimmers can be homodimeric (with two identical binding sequences) or heterodimer (with two different binding sequences). In order to distinguish monomeric forms of conventional minizymes that have extremely low activity from novel heterodimer with high-level activity, the latter was designated as "maxizyme"[34-36]. Maxizyme stands for minimized, active, heterodimeric, and intelligent ribozyme. Some study showed that maxizyme could cleave chimeric genes, such as BCR-ABL mRNA, which cauases chonric myelogenous leukemia (CML)[37]. In this study, we designed maxizyme targeting mtp53 mRNA by computer and examined its cleavage activity *in vitro*.

MATERIALS AND METHODS

Materials

In vitro transcription kit and pGEM-T vector were purchased from Promega Company. Restriction endonucleases, T4 DNA ligase, RNase inhibition and DNA marker were purchased from TaKaRa Company. [α-^{32}p] dUTP was purchased from Beijing Yahui Company. *E.coli* DH5α was maintained in our laboratory. pBSKU6 vector was a generous gift from Dr.You-Xin Jin. pCMV-mtp53 (or wtp53) plasmid was kindly provided by Pro.Bert Vogelstein (Howard Hughs Medical Institute). Materials used were of analytical purity.

Maxizyme design

Maxizyme targeting mutant-type p53 (249 codon) was designed. Only after binding mutant-type p53 in codon 249 (the third base of 249 codon, AGG→AGT) can the maxizyme cleave mtp53 in 201bp site. The oligonucleotide sequences included Xba I and BamH I linker sites and were as follows: *MzL*: 5' CTA GAG AGG ATG GCT GAT GAG CGA AAG GTC TGG 3' ; 5' GAT CCC AGA CCT TTC GCT CAT CAG CCA TCC TCT3' . *MzR*: 5' CTA GAA GTT TCC ACT GAT GAG CGA AAC TCC GGG 3' ; 5' GAT CCC CGG AGT TTC GCT CAT CAG TGG AAA CTT 3' . A mutant maxizyme was designed with a sequence almost identical to that of the maxizyme except for G^5 to A^5 mutation within the catalytic core. This mutant maxizyme was expected to have no cleavage activity. They were chemically synthesized in Beckman Oligo 1000-DNA synthesizer. The structure of maxizyme against mtp53 is shown in Figure 1.

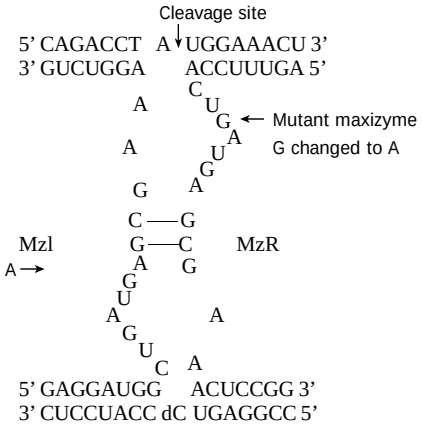

Figure 1 Structure of maxizyme against mtp53.

Methods

Construction of cell-free transcription plasmid for target RNA Mtp53 and wtp53 gene containing a cDNA fragment with 986 bases was amplified by PCR from pCMV-p53mt249 and pCMV-wtp53 vector. The PCR products were analyzed and purified by 2 % agarose gel and cloned into the transcription vector pGEM-T downstream of the T7 bacteriophage RNA promoter. The reconstructed plasmids were named as pmtp53 and pwtp53. The primers used were: upstream primer 5' GAT TCT CTT CCT CTG TGC 3' and downstream primer 5' CTT TCC ACG ACG GTG ACA 3' .

Construction of cell-free transcription plasmid for maxizyme Maxizyme targeting mtp53 was designed according to the computer software from professor Chen Nong-An (Shanghai Institute of Biochemistry of Chinese Academy of Sciences). The homologous possibility with the gene of humanbeing was excluded by consulting with RNA sequences of human cell from NCBI Genebank. The *in vitro* transcription vector pBSKU6 was digested with *Xba* I and *BamH* I restriction enzymes. The linearlized vector pBSKU6 was purified by 1 % agarose gel electrophoresis. After annealed, oligonucleotides of MzL and MzR were cloned into pBSKU6. The reconstructed plasmids were named as pBSKU6MzL and pBSKU6MzR. After being sequenced, the restrictive endonuclease site in pBSKU6MzR was changed by PCR and then U6MzR was inserted into pBSKU6MzL, the recombinant was named as pU6Mz. pBSKU6 vector contained the T7 RNA polymerase promoter for driving transcription of Mz *in vitro*. The steps of pU6Mz construction was shown in Figure 2.

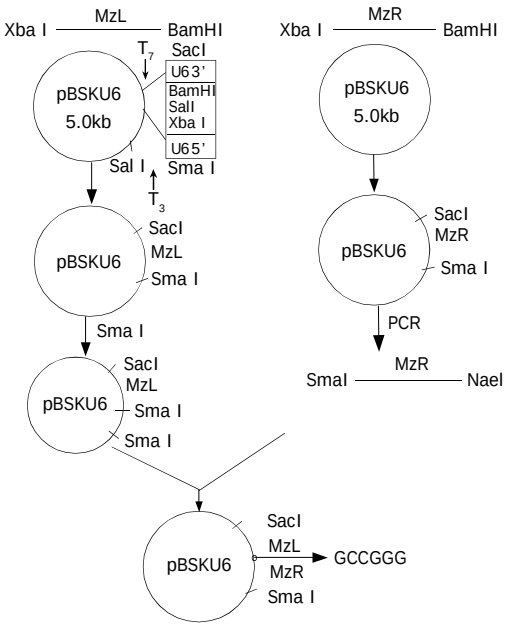

Figure 2 Steps of pU6Mz construction.

***In vitro* transcription of target RNA and maxizyme** Templates pmtp53 and pwtp53 were linearlized with Sal, while pU6Mz was linearlized with Sma I. The linearlized templates were transcribed in the presence of [α-^{32}p]dUTP (10 μl) using T7 RNA polymerase according to the manufacturer's protocol. Transcription was performed for three hours at 37 ℃ in a 50 μl final volume. The samples were purified by cutting off the autoradiograph bands after running on 8 % polyacrylamide (8 mol/l urea) gel and soaking in NES (0.5 M NH_4Ac, 0.1M EDTA, 0.1 % SDS pH 5.4) at 42 ℃ overnight. The products were precipitated by ethanol, washed once by 70 % ethanol, dissolved in DEPC-treated water and kept at -20 ℃.

***In vitro* cleavage reaction** The products of maxizyme and target RNA were quantified by measuring their radioactive cpm in 1 ul solution. The cleavage reaction was performed for 90 minutes at 37 ℃ in 25 mmol/l Tris-Cl (pH7.5) and 25 mmol/l $MgCl_2$ with cold maxizyme to [α-^{32}p] dUTP-labeled substrate ratio of 4:1 and stopped by adding 1 ul RNA loading buffer (0.25 % bromophenol blue, 0.25 % xylene cyanol FF, 20 mmol/l EDTA and saturated urea) and heated for 3 minutes at 95 ℃. The cleaved products were separated by 8 % polyacrylamide gel electrophoresis(PAGE) with 8M urea. The cleavage efficiency was calculated from cpm values of the bands of substrates (S) and products (P): cleavage efficiency=[P/(S+P)]×100 %.

RESULTS

Construction of cloning vector pU6Mz

Mz gene was successfully cloned into the vector pBSKU6. The gene complex was treated with restriction endonuclease *Sma* I and *Sac* I and analyzed by 2 % agarose gel (Figure 3). The DNA sequence analysis showed that chimeric U6 maxizyme was correct.

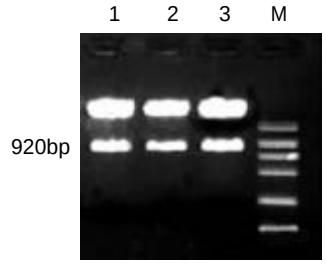

Figure 3 Restrictive enzyme analysis of recombinant plasmid pU6Mz by Sma I and Sac I. M was DNA Marker (DL2000). 1, 2, 3 were selected clones.

Identification of transcripts of pU6Mz and target RNA

The lengths of RNA transcribed from Sal I-linearlized templates of pmtp53 and pwtp53 shoud be 1002nt (Figure 4A). The transcription of pU6Mz from Sma I-linearlized templates including U6 and Mz bases shoud be 910nt (Figure 4B). The results showed that our design was correct.

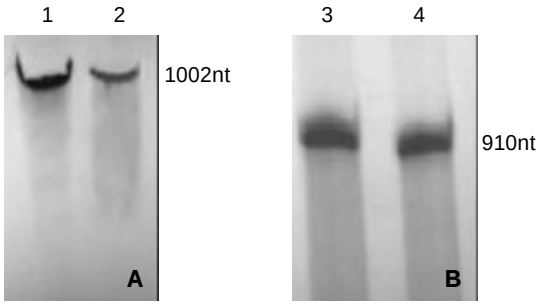

Figure 4 *In vitro* transcripts. (A) *In vitro* transcripts of wtp53 and mtp53 (1002nt). (B) *In vitro* transcripts of maxizyme and control maxizyme (910nt). lane 1: mtp53; lane 2: wtp53; lane 3: maxizyme; lane 4: control maxizyme.

In vitro cleavage reaction of Mz

Target RNA was ^{32}p-labeled. The cleavage results showed that the designed maxizyme had correct structure, it cleaved mtp53 mRNA efficiently, giving cleavage products with the expected size of 874nt and 128nt under conditions at 37 ℃ and high Mg concentration (25 mM), the cleavage efficiency was 42 %. More encouraging was that no cleavage was found with mutant maxizyme under the same conditions, and wtp53 was not cleaved by maxizyme (Figure 5).

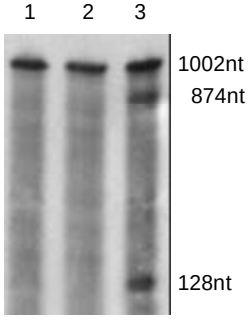

Figure 5 *In vitro* cleavage reaction. lane 1: cleavage of wtp53 by cold maxizyme; lane 2: cleavage of mtp53 by inactive cold maxizyme; lane 3: cleavage of mtp53 by cold maxizyme.

DISCUSSION

Ribozyme is a class of small catalytic RNA molecules that recognize specific substrate RNA by their complementary nucleotide sequence, and cleave the substrate RNA as an endoribonuclease at enzymatic rate. It has been demonstrated that potential utility in attenuating eukaryotic gene expression was studied in preclinical gene therapy models. Among different types of ribozymes discovered, the hammerhead ribozyme has received a great deal of attention in recent years because of its application in treatment of malignant and infectious diseases[38,39]. Many different hammerhead ribozymes targeting oncogene and HIV, HBV have been developed. The hammerhead ribozyme could cleave almost any RNA molecules containing the 3 base target recognition sequence NUX (N=any base, X is any nucleotide except G). The basic structure of a hammerhead ribozyme is composed of a catalytic core of 24 conserved bases containing helix II and two self-associating helices, I and III which are antisense to the substrate and position of ribozyme to catalyze cleavage. However, because the limited number of cleavable sequences on target RNA, in some cases conventional hammerhead ribozyme does not have precise cleavage specificity. Some scientists found that the stem II (loop II) region of hammerhead ribozyme did not appear to be directly involved in catalysis. For development of chemically systhesized ribozyme as potential therapeutic agent, it would certainly be advantageous to remove surplus nucleotides. This consideration led to the production of minizymes, which are conventional hammerhead ribozyme with a deleted stem II region. But the activities of minizyme are two or three orders of magnitude lower than those of the parental hammerhead ribozyme, suggesting that minizymes might not be suitable as gene inactivating reagents. But Kinetic and NMR analysis indicated that the minizyme was essentially inactive as a monomer but exhibited strong catalytic activity as a dimer. This dimeric structure is called maxizyme[40-42]. The maxizyme is also a metalloenzyme, its activity depends on the presence or absence of the correct formation of Mg ion-binding pocket. The maxizyme could bind to two different substrate-binding sites, one substrate-binding site functions as the "eye" that identifies the specific mRNA, wheareas the other serves as the "scissors" and cleaves the target mRNA. Some studies showed that only after binding to the target gene can the maxizyme form a cavity that captures the Mg ions.

As a novel class of ribozyme, maxizyme that targets different chimeric genes has been studied[43,45]. The chimeric gene is generated as a result of reciprocal chromosomal translocation. A well known chimeric gene is BCR-ABL gene which causes chronic myelogenous leukemia(CML). In the design of ribozyme that might cleave chimeric mRNA, it is necessary to avoid the cleavage of normal mRNA. There have been many attempts to specifically cleave chimeric BCR-ABL gene using ribozymes, but it is very difficult to cleave only chimeric gene without affecting the normal genes, such as BCR or ABL gene. Kuwabara *et al*[44] designed a maxizyme directly against BCR-ABL mRNA. The results showed that the maxizyme had extremely high specificity and high level activity not only *in vitro* but also in cultured cells. p53 mutation in 249 codon was observed in 50 % of hepatocellular carcinoma. Some studies have suggested that p53 has a gain of transforming function after mutation in addition to loss of tumor suppressor activity. Several groups have attempted to develop gene therapy methods to treat HCC via introduction of wild-type p53 cDNA into cancer cells. Unfortunately, these approaches did not result in regulated expression of p53 gene and did not reduce the expression of mutant p53 that was overexpressed in HCC cells. These shortcomings may greatly limit the utility of this gene replacement approach.

We designed a maxizyme directing against mutant-type p53 (249 codon). The cleavage results showed that the maxizyme cleaved mtp53 target mRNA efficiently. More encouraging

was that no cleavage was found in wild-type p53 under the same conditions. The activity of maxizyme must have originated from the formation of active heterodimers. So control of inactive maxizyme was also made by the mutation of a functionally indispensable ($G^5 \rightarrow A^5$) in the catalytic core. The *in vitro* cleavage reaction showed that the inactive maxizyme had no effects on target mRNA. This suggests that the cleavage effects of active maxizyme are clearly originated from the chemical cleavage. For the application of maxizyme to gene therapy, they must be expressed *in vivo* under the control of a strong promoter. Development of an efficient system for the expression of a small piece of RNA in the cell, such as antisense RNA and ribozyme, is a major challenge in nonviral gene therapy. Recently, U6 RNA has been explored to drive the expression of antisense RNA and oligonucleotide. It is much efficient than the CMV promoter which is used often[46,47]. In our study, the U6 expression system was explored for the construction of maxizyme plasmid. These lay a good fundation for the study in HCC cell lines.

In conclusion, the results of the present study showed that chimeric U6 maxizyme could cleave mtp53 mRNA *in vitro* with high efficiency. Anti-mtp53 maxizyme may be a promising tool for the treatment of hepatocellular carcinoma with an oncogenic mutation in codon 249 of p53 gene.

ACKNOWLEDGEMENTS

We would like to thank Dr Bert Vogelstein for his generous gift of plasmid p53.We also thank Mr.F Xu, Mr.XL Chen and Miss W Li for their kind help.

REFERENCES

1 **Tang ZY**. Hepatocellular carcinoma-cause,treatment and metastasis. *World J Gastroenterol* 2001; **7**: 445-454
2 **Tang ZY**. Advances in clinical research of hepatocellular carcinoma in China. *Huaren Xiaohua Zazhi* 1998; **6**: 1013-1016
3 **Lin NF**, Tang J, Ismael HS. Study on environmental etiology of high incidence areas of liver cancer in China. *World J Gastroenterol* 2000; **6**: 572-576
4 **Zhai SH**, Liu JB, Liu YM, Zhang LL, Du ZH. Expression of HBsAg, HCV-Ag and AFP in liver cirrhosis and hepatocarcinoma. *Shijie Huaren Xiaohua Zazhi* 2000; **8**: 524-527
5 **Li Y**, Tang ZY, Ye SL, Lin YK, Chen J, Xue Q, Chen J, Gao DM, Bao WH. Establishment of cell clones with different metastatic potential from the metastatic hepatocellular carcinoma cell line MHCC97. *World J Gastroenterol* 2001; **7**: 630-636
6 **Qin LL**, Su JJ, Li Y, Yang C, Ban KC, Yian RQ. Expression of IGF-II, p53, p21 and HBxAg in precancerous events of hepatocarcinogenesis induced by AFB1 and/or HBV in tree shrews. *World J Gastroenterol* 2000; **6**: 138-139
7 **Blandino G**, Levine AJ, Oren M. Mutant p53 gain of function: differential effects of different p53 mutants on resistance of cultured cells to chemotherapy. *Oncogene* 1999; **18**: 477-485
8 **Sohn S**, Jaitovitch-Groisman I, Benlimame N, Galipeau J, Batist G, Alaoui-Jamali MA. Retroviral expression of the hepatitis B virus x gene promotes liver cell susceptibility to carcinogen-induced site specific mutagenesis. *Mutation Res* 2000; **460**: 17-28
9 **Ghebranious N**, Sell S. Hepatitis B injury,male gender,aflatoxin, and p53 expression each contribute to hepatocarcinogenesis in transgenic mice. *Hepatology* 1998; **27**: 383-391
10 **Bressac B**, Kew M, Wands J, Ozturk M. Selective G to T mutations of p53 gene in hepatocellular carcinoma from southern Africa. *Nature* 1991; **350**: 429-431
11 **Prost S**, Ford JM, Taylor C, Doig J, Harrison DJ. Hepatitis B x protein inhibits p53-dependent DNA repair in primary mouse hepatocytes. *J Bio Chem* 1998; **273**: 33327-33332
12 **Liu H**, Wang Y, Zhou Q, Gui SY, Li X. The point mutation of p53 gene exon 7 in hepatocellular carcinoma from Anhui Province, a non HCC prevalent area in China. *World J Gastroenterol* 2002; **8**: 480-482
13 **Niu ZS**, Li BK, Wang M. Expression of p53 and C-myc genes and its clinical relevance in the hepatocellular carcinomatous and pericarcinomatous tissues. *World J Gastroenterol* 2002; **8**: 822-826
14 **Levine AJ**. P53 ,the cellular gatekeeper for growth and division. *Cell* 1997; **88**: 323-331
15 **Qin LX**, Tang ZY, Ma ZC, Wu ZQ, Zhou XD, Ye QH, Ji Y, Huang LW, Jia H L, Sun HC, Wang L. p53 immunohistochemical scoring: an independent prognostic marker for patients after hepatocellular carcinoma resection. *World J Gastroenterol* 2002; **8**: 459-463
16 **Doppert W**, Gohler T, Koga H, Kom E. Mutant p53: "gain of function" through perturbation of nuclear structure and function? *J Cell Biochem Suppl* 2000; **35**(Suppl): 115-122
17 **Lee YI**, Lee S, Das GC, Park US, Park SM, Lee YI. Activation of the insulin-like growth factor II transcription by aflatoxin B1 induced p53 mutant 249 is caused by activaton of transcription complexes; implications for a gain-of-function during the formation of hepatocellular carcinoma. *Oncogene* 2000; **19**: 3717-3726
18 **Koga H**, Deppert W. Identification of genomic DNA sequences bound by mutant p53 protein(Gly245->Ser) *in vivo*. *Oncogene* 2000; **19**: 4178-4183
19 **Zheng SX**, Liu LJ, Shao YS, Zheng QP, Ruan YB, Wu ZB. Relationship between ras p53 gene RNA and protein expression and HCC metastasis. *Huaren Xiaohua Zazhi* 1998; **6**: 104-105
20 **Phylactou LA**. Ribozyme and peptide-nucleic acid-based gene therapy. *Adv Drug Deliv Rev* 2000; **44**: 97-108
21 **Song YH**, Lin JS, Liu NZ, Kong XJ, Xie N, Wang NX, Jin YX, Liang KH. Anti-HBV hairpin ribozyme-mediated cleavage of target RNA *in vitro*. *World J Gastroenterol* 2002; **8**: 91-94
22 **Tanaka M**, Kijima H, Itoh J, Matsuda T, Tanaka T. Impaired expression of a human septin family gene Bradeion inhibits the growth and tumorigenesis of colorectal cancer *in vitro* and *in vivo*. *Cancer Gene Ther* 2002; **9**: 483-488
23 **Tokunaga T**, Abe Y, Tsuchide T, Hatanaka H, Oshika Y, Tomisawa M, Yoshimura M, Ohnishi Y, Kijima H, Yamazaki H, Ueyama Y, Nakamura M. Ribozyme mediated cleavage of cell-associated isoform of vascular endothelial growth factor inhibits liver metastasis of a pancreatic cancer cell line. *Int J Oncol* 2002; **21**: 1027-1032
24 **Qu Y**, Liu S, Liu B. Attenuation of telomerase activity by hammerhead ribozyme targeting the 5'-end of hTERT mRNA. *Zhonghua Yixue Yichuanxue Zazhi* 2002; **19**: 389-392
25 **Blount KF**, Grover NL, Mokler V, Beigelman L, Uhlenbeck OC. Steric interference modification of the hammerhead ribozyme. *Chem Biol* 2002; **9**: 1009-1016
26 **Huesker M**, Folmer Y, Schneider M, Fulda C, Blum HE, Hafkemeyer P. Reversal of drug resistance of hepatocellular carcinoma cells by adenoviral delivery of anti-MDR1 ribozymes. *Hepatology* 2002; **36**: 874-884
27 **Sullenger BA**, Gilboa E. Emerging clinical applications of RNA. *Nature* 2002; **418**: 252-258
28 **Xu R**, Lin J, Zhou X, Xie Q, Jin Y, Yu H, Liao D. Activity identification of anti-caspase-3 mRNA hammerhead ribozyme in both cell-free condition and BRL-3A cells. *Chinese Medical Journal(Engl)* 2001; **114**: 606-611
29 **Yu YC**, Mao Q, Gu CH, Li QF, Wang YM. Activity of HDV ribozymes to trans-cleave HCV RNA. *World J Gastroenterol* 2002; **8**: 694-698
30 **Zhang YA**, Nemunaitis J, Tong AW. Generation of a ribozyme-adenoviral vector against k-ras mutant human lung cancer cells. *Mol Biotechnol* 2000; **15**: 39-49
31 **Hammann C**, Lilley DM. Folding and activity of the hammerhead ribozyme. *Chembiochem* 2002; **3**: 690-700
32 **Sioud M**, Opstad A, Hendry P, Lockett TJ, Jennings PA, McCall MJ. A minimised hammerhead ribozyme with activity against interleukin-2 in human cells. *Biochem Biophys Res Commun* 1997; **231**: 397-402
33 **Amontov S**, Nishikawa S, Taira K. Dependence on Mg2+ ions of the activities of dimeric hammerhead minizymes. *FEBS Lett* 1996; **386**: 99-102
34 **Iyo M**, Kawasaki H, Taira K. Allosterically controllable maxizymes for molecular gene therapy. *Curr Opin Mol Ther* 2002; **4**: 154-165
35 **Tani K**. Target therapy for CML-applying maxizyme. *Nippon Rinsho* 2001; **59**: 2439-2444

36 **Kuwabara T**, Hamada M, Warashina M, Taia K. Allosterically controlled single-chained maxizymes with extremely high and specific activity.*Biomacromolecules* 2001; **2**: 788-799
37 **Kuwabara T**, Tanabe T, Warashina M, Xiong KX, Tani K, Taira K, Asano S. Allosterically controllable maxizyme-mediated suppression of progression of leukemia in mice. *Biomacromolecules* 2001; **2**: 1220-1228
38 **Morino F**, Tokunaga T, Tsuchida T, Handa A, Nagata J, Tomii Y, Kijima H, Yamazaki H, Watanabe N, Matsuzaki S, Ueyama Y, Nakamura M. Hammerhead ribozyme specifically inhibits vascular endothelial growth factor gene expression in a human hepatocellular carcinoma cell line. *Int J Oncol* 2000; **17**: 495-499
39 **Ozaki I**, Zern MA, Liu S, Wei DL, Pomerantz RJ, Duan L. Ribozyme-mediated specific gene replacement of the alphal-antitrypsin gene in human hepatoma cells. *J Hepatol* 1999; **31**: 53-60
40 **Kuwabara T**, Warashina M, Taira K. Cleavage of an inaccessible site by the maxizyme with two independent binding arms:an alternative approach to the recruitment of RNA helicases. *J Biochem (Tokyo)* 2002; **132**: 149-155
41 **Kuwabara T**, Warashina M, Taira K. Allosterically controllable maxizymes cleave mRNA with high efficiency and specificity. *Trends Biotechnol* 2000; **18**: 462-468
42 **Nakayama A**, Warashina M, Kuwabara T, Taira K. Effects of cetyltrimethylammonium bromide on reactions catalyzed by maxizymes, a novel class of metalloenzymes. *J Inorg Biochem* 2000; **78**: 69-77
43 **Hamada M**, Kuwabara T, Warashina M, Nakayama A, Taira K. Specificity of novel allosterically trans- and cis-activated connected maxizymes that are designed to suppress BCR-ABL expression. *FEBS Lett* 1999; **461**: 77-85
44 **Kuwabara T**, Warashina M, Tanabe T, Tani K, Asano S, Taira K. A novel allosterically trans-activated ribozyme, the maxizyme, with exceptional specificity in vitro and in vivo. *Mol Cell* 1998; **2**: 617-627
45 **Suwanai H**, Matsushita H, Kobayashi H, Ikeda Y, Kizaki M. A novel therapeutic technology of specific RNA inhibition for acute promyelocytic leukemia: improved design of maxizymes against PML/RARalpha mRNA. *Int J Oncol* 2002; **20**: 127-130
46 **Kuwabara T**, Warashina M, Orita M, Koseki S, Ohkawa J, Taira K. Formation of a catalytically active dimer by tRNA(Val)-driven short ribozymes. *Nat Biotechnol* 1998; **16**: 961-965
47 **Lui VW**, He Y, Huang L. Specific down-regulation of HER-2/neu mediated by a chimeric U6 hammerhead ribozyme results in growth inhibition of human ovarian carcinoma. *Mol Ther* 2001; **3**: 169-177

Edited by Yuan HT and Wang XL

P.O.Box 2345, Beijing 100023,China
Fax: +86-10-85381893
E-mail: wjg@wjgnet.com www.wjgnet.com

World J Gastroenterol 2003;9(7):1576-1579
World Journal of Gastroenterology
 ISSN 1007-9327

• CLINICAL RESEARCH •

High level of deoxycholic acid in human bile does not promote cholesterol gallstone formation

Ulf Gustafsson, Staffan Sahlin, Curt Einarsson

Ulf Gustafsson, Staffan Sahlin, Department of Surgery, Danderyd Hospital, Stockholm, Sweden
Curt Einarsson, Division of Gastroenterology and Hepatology, Department of Medicine, Huddinge University Hospital, Karolinska Institutet, Stockholm, Sweden
Supported by the grants from the Swedish Science Council
Correspondence to: Dr. Curt Einarsson, Division of Gastroenterology and Hepatology, Department of Medicine, K63, Huddinge University Hospital, SE-141 86 Stockholm, Sweden. curt.einarsson@medhs.ki.se
Telephone: +46-8-58582328 **Fax:** +46-8-58582335
Received: 2002-12-07 **Accepted:** 2002-12-22

Abstract

AIM: To study whether patients with excess deoxycholic acid (DCA) differ from those with normal percentage of DCA with respect to biliary lipid composition and cholesterol saturation of gallbladder bile.

METHODS: Bile was collected during operation through puncturing into the gallbladder from 122 cholesterol gallstone patients and 46 gallstone-free subjects undergoing cholecystectomy. Clinical data, biliary lipids, bile acid composition, presence of crystals and nucleation time were analyzed.

RESULTS: A subgroup of gallstone patients displayed a higher proportion of DCA in bile than gallstone free subjects. By choosing a cut-off level of the 90th percentile, a group of 13 gallstone patients with high DCA levels (mean 50 percent of total bile acids) and a large group of 109 patients with normal DCA levels (mean 21 percent of total bile acids) were obtained. The mean age of the patients with high DCA levels was higher than that of the group with normal levels (mean age: 62 years *vs* 45 years) and so was the mean BMI (28.3 *vs.* 24.7). Plasma levels of cholesterol and triglycerides were slightly higher in the DCA excess groups compared with those in the normal DCA group. There was no difference in biliary lipid composition, cholesterol saturation, nucleation time or occurrence of cholesterol crystals in bile between patients with high and normal levels of DCA.

CONCLUSION: Gallstone patients with excess DCA were of older age and had higher BMI than patients with normal DCA. The two groups of patients did not differ with respect to biliary lipid composition, cholesterol saturation, nucleation time or occurrence of cholesterol crystals. It is concluded that DCA in bile does not seem to contribute to gallstone formation in cholesterol gallstone patients.

Gustafsson U, Sahlin S, Einarsson C. High level of deoxycholic acid in human bile does not promote cholesterol gallstone formation. *World J Gastroenterol* 2003; 9(7): 1576-1579
http://www.wjgnet.com/1007-9327/9/1576.asp

INTRODUCTION

The two major primary bile acids formed in human liver are cholic acid (CA) and chenodeoxycholic acid (CDCA). During the enterohepatic circulation, CA and CDCA are partly 7a-dehydroxylated by microbial enzymes, yielding deoxycholic acid (DCA) and lithocholic acid, respectively[1]. Only a small amount of lithocholic acid is absorbed from the intestine, whereas DCA is efficiently reabsorbed mainly via active transport in the distal part of ileum but also by passive diffusion along the small intestine and probably also from the proximal part of colon. DCA constitutes usually 10-35 % of bile acids in the bile. However, individuals may vary widely in the proportion of DCA in bile from 0 to more than 50 % of biliary bile acids. These wide inter-individual variations in DCA probably reflect the difference in colonic flora.

According to some previous studies, the proportion of DCA in bile of patients with cholesterol gallstone is higher than that of stone-free subjects and it has been suggested that DCA may play a role in cholesterol gallstone formation[2-8]. Other authors have found a normal percentage of DCA in patients with cholesterol gallstones[9-13]. An increased proportion of DCA in the bile acid pool of gallstone patients has been associated with higher levels of 7a-dehydroxylating faecal bacteria[6,14]. In a recent study, Thomas *et al*[8] found an increased 7a-hydroxylating activity in the caecal aspirates of patients with cholesterol gallstones, which was associated with slower colonic transit time and increased percentage of DCA in fasting serum. Berr *et al*[6] have reported about a subgroup of cholesterol gallstone patients with DCA excess and increased 7a-dehydroxylating activity and levels of faecal 7a-dehydroxylating bacteria which may trigger cholesterol gallstone disease.

In a recent study including large series of gallstone patients and gallstone free subjects, we could not find a significantly higher proportion of biliary DCA in cholesterol gall-stone patients compared to pigment stone patients or gallstone-free subjects[13]. No correlation was found between the percentage of DCA and cholesterol saturation in gallbladder bile. However, a subgroup of the patients with cholesterol gallstones had a high percentage of DCA.

The purpose of this study was to study whether patients with excess DCA differed from patients with a normal percentage of DCA with respect to biliary lipid composition, cholesterol saturation, nucleation time and occurrence of cholesterol crystals in gallbladder bile.

MATERIALS AND METHODS

Patients

The patients in the present study were included in a recent report from our group dealing with lipid composition of gallbladder bile in large series of patients with cholesterol gallstones and pigment stones and gallstone free subjects undergoing elective cholecystectomy[13]. In this study, only cholesterol gallstone patients (n=122) and gallstone-free subjects (n=46) in which data on biliary bile acid composition were available were included. Data on the patients are shown in Table 1. None of the patients had clinical or laboratory evidence of diabetes mellitus, alcohol abuse or other diseases that affect the function of the kidney or the liver. The patients

Table 1 Clinical data of patients with cholesterol gallstones and gallstone free subjects

Group	*n*	Female / male ratio(% Female)	Median age years (range)	Body mass index kg / m^2(*n*)	Plasma cholesterol mmol / l (*n*)	Plasma triglycerides mmol / l (*n*)
Total gallstone	122	96 / 26 (79)	49 (18-83)	25.0±0.3 (111)	5.7±0.1 (81)	1.5±0.1 (82)
High DCA	13	10 / 3 (77)	62^b (37-74)	28.3±1.3^b (10)	6.4±0.3^a (11)	2.2±0.4^a (10)
Low DCA	109	86 / 23 (79)	45 (18-83)	24.7±0.4 (101)	5.6±0.1 (70)	1.5±0.1 (72)
Gallstone free	46	38 / 18 (83)	45 (20-71)	23.2±0.5^c (45)	5.8±0.2 (36)	1.4±0.1 (36)

Notes: Mean values ± Standard Error of the Mean. *n*=number. $^aP<0.05$ *vs* Low DCA, $^bP<0.005$ *vs* Low DCA, $^cP<0.01$ *vs* Total gallstone.

were not on any medications known to affect lipid metabolism. None of the patients received or had been treated with antibiotics prior to or during cholecystectomy. The gallstone-free patients were cholecystectomized either because of polyps, cholesterolosis or adenomyomatosis or because of frequent, recurrent right upper biliary colic and other symptoms suggestive of gallbladder dysfunction.

Informed consent was obtained from each patient before operation. The ethical aspects of the study were approved by the Ethical Committée at Karolinska Institutet, Stockholm.

Experimental procedure

All patients were hospitalized in the surgical ward. The operations were done after an overnight fasting. After opening the abdomen or in the case of a laparoscopic procedure following application of pneumoperitoneum and establishing four laparoscopic ports, the gall bladder was completely emptied of bile with a sterile needle and syringe to avoid possible stratification of bile[15]. Indicative of a functioning gallbladder was the presence of dark concentrated bile in the gallbladder and no evidence of impacted stones in the neck of the cystic duct at operation. The gall bladder was then removed. The gallstones were classified as cholesterol stones by visual inspection and when necessary by analysis in the laboratory[16,17]. All gall bladders were routinely examined by a pathologist.

Analysis of biliary lipids and calculation of cholesterol saturation

Gallbladder bile was extracted with chloroform-methanol (2/1, w/w) for measurement of cholesterol and phospholipids. Cholesterol was measured by an enzymatic method[18] and phospholipids by the method of Rouser *et al*[19]. The total bile acid concentration in one aliquot of the bile sample was measured using a 3-alpha-hydroxysteroid dehydrogenase assay[20]. Cholesterol saturation was calculated as a percentage of the predicted cholesterol solubility at the respective biliary lipid concentration and composition as described by Carey[21].

Measurement of bile acid composition

Aliquots of bile were hydrolyzed in 1 mol/L potassium hydroxide at 110 ℃ for 12 h. The conjugated bile acids were extracted with diethyl ether after acidification to pH 1 with hydrochloric acid. After preparation of trimethylsilyl ethers, the bile acids were analyzed by gas-liquid chromatography using 1 % Hi-Eff BP 8 as the stationary phase. A Pye Unicam gas chromatograph (Pye Unicam Ltd, Cambridge, UK) equipped with a 1.5 m×4 mm column was used[22].

Analysis of cholesterol crystals and nucleation time

Bile samples were examined for typical rhomboid monohydrate cholesterol crystals by polarising light microscopy on pre-warmed slides. Nucleation time (NT) was determined by the method of Holan *et al*[23] with minor modifications[24].

Statistical analysis

Data were presented as mean ± SEM. The statistical significance of differences was evaluated with Student' s *t*-test. Nucleation time was evaluated by Wilcoxon' s sum of rank test.

RESULTS

Age, body mass index and plasma lipids

As can be seen in Figure 1, a subgroup of gallstone patients displayed a higher proportion of DCA in bile than gallstone-free subjects. Choosing a cut-off level of the 90th percentile, a group of 13 gallstone patients with high DCA-levels was obtained. The proportion of DCA in the high DCA-group averaged 50 % compared with 21 % in the normal DCA-group.

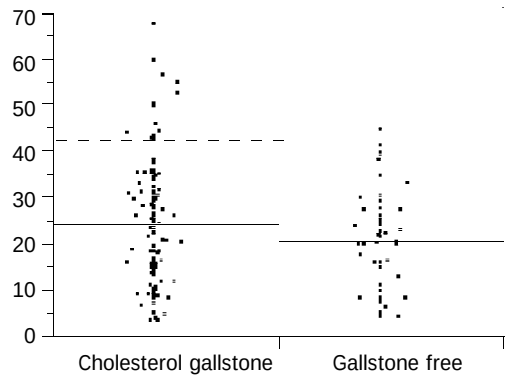

Figure 1 Deoxycholic acid levels in 122 gallstone patients and 46 gallstone free patients (Dotted line represented the 90th percentile in the gallstone patients).

The mean age of the patients with high DCA-levels was significantly higher than that of the patients with normal DCA-levels (mean ages: 62 years *vs* 45 years, Table 1). The mean body mass index (BMI) was also higher in the high DCA-group, 28.3, compared to 24.7 in the normal DCA-group ($P<0.005$). Plasma levels of cholesterol and triglycerides were slightly higher in the high DCA-group.

Lipid composition, cholesterol saturation, nucleation time and occurrence of crystals in gallbladder bile

The results are summarized in Table 2. There was no difference in biliary lipid composition, total lipid concentration or cholesterol saturation of bile between patients with high and normal levels of DCA.The molar percentage of cholesterol in cholesterol gallstone patients was significantly higher (7.8 mol %), compared to gallstone-free subjects (5.8 mol %). The total biliary lipid concentration was significantly lower in cholesterol gallstone patients compared to gallstone-free patients. Also the mean cholesterol saturation was significantly higher in gallstone patients (112 %) compared to gallstone-free subjects (79 %), ($P<0.0001$).

Table 2 Occurrence of crystals and lipid composition in gallbladder bile of patients with cholesterol gallstones and gallstone free subjects

Group (*n*)	Single stone % (*n*)	Crystals positive % (*n*)	Median nucleation time days, (range) (*n*)	Cholesterol mol %	Bile acid mol %	Phospholipids mol %	Total lipid concentration g/dl	Cholesterol saturation %
Total gallstone (122)	29 (116)	79 (112)	6 (1-56) (46)	7.8±0.3	68.6±0.6	23.6±0.4	9.4±0.4	112±4
High DCA (13)	42 (12)	73 (11)	14 (2-28) (4)	8.1±0.6	68.1±1.6	23.8±1.2	8.2±1.0	116±10
Low DCA (109)	28 (104)	79 (101)	3 (1-56) (42)	7.8±0.3	68.7±0.6	23.6±0.5	9.6±0.5	112±5
Gallstone free (46)	-	11[a] (45)	17[a] (1-35) (24)	5.8±0.3[a]	71.3±0.8	22.9±0.7	13.1±0.6[a]	79±3[a]

Notes: Mean values ± Standard Error of the Mean. *n*=Number of observations. [a]*P*<0.0001 *vs* Total gallstone.

Table 3 Bile acid composition in patients with cholesterol gallstones and gallstone free subjects

Group	*n*	Cholic acid %	Deoxycholic acid %	Chenodeoxy-cholic acid %	Lithocholic acid %	Ursodeoxy-cholic acid %
Total gallstone	122	38.9±1.0	24.2±1.2	34.5±0.9	1.0±0.1	1.3±0.2
High DCA	13	22.7±1.7	50.0±2.1	24.5±1.7	1.4±0.4	1.3±0.9
Low DCA	109	40.8±1.0	21.1±0.9	35.7±0.9	0.9±0.1	1.3±0.2
Gallstone free	46	46.1±1.6[b]	20.7±1.6	30.6±1.0[a]	0.6±1.6	1.7±0.4

Notes: Mean values ± Standard Error of the Mean. *n*=Number of observations, [a]*P*<0.05 *vs* Total gallstone, [b]*P*<0.001 *vs* Total gallstone.

There was a tendency to shorter nucleation time in patients with normal DCA-levels compared to those with high DCA-levels, but the difference did not reach statistical significance. The proportion of patients with crystals in their bile was the same between patients with high and normal levels of DCA. Nucleation time was significantly shorter in cholesterol gallstone patients compared to that in gallstone-free patients, 6 days *vs.* 17 days (*P*<0.0001). The proportion of patients with bile positive for cholesterol crystals was significantly higher among gallstone patients (79 %) compared to gallstone-free subjects (11 %), (*P*<0.0001).

Bile acid composition

The bile acid composition is summarized in Table 3. The proportion of cholic acid was significantly lower and that of chenodeoxycholic acid was higher in the gallstone patients compared to the gallstone-free patients. There was no significant difference in the proportion of deoxycholic acid, lithocholic acid or ursodeoxycholic acid between gallstone patients and gallstone-free subjects.

DISCUSSION

In the present study, a subgroup of cholesterol gallstone patients with a high proportion of DCA in the gallbladder bile, mean 50 %, was compared to gallstone patients with a normal proportion of DCA, mean 21 %. The high DCA-level was not associated with either higher cholesterol content or cholesterol saturation of bile. The proportion of patients with cholesterol crystals in the bile did not differ between patients with high and normal levels of DCA. Nor was the nucleation time shortened in patients with high DCA content. If anything, there was a tendency to longer nucleation time in patients with high DCA-levels although the difference was not significant. These results were in agreement with some previous studies, showing that a high proportion of DCA in human gallbladder bile was not associated with a higher risk for formation of cholesterol gallstones[9-13].

The gallstone patients with a high level of DCA were of older age than those with a normal level of DCA. The reason why old age is associated with a high percentage of DCA in bile is not quite apparent. Slow colonic transit has been reported to lead to high biliary proportions of DCA, probably by increasing the intestinal residence time of bile salts[2]. Recently, Thomas *et al*[8] reported that slow colonic transit in combination with increased number of colonic gram-positive anaerobes and greater 7a-dehydroxylating activity favours enhanced DCA-formation in gallstone patients. Berr *et al*[6] also found that a group of gallstone patients with DCA-excess had higher 7a-dehydroxylating activity and increased counts of 7a-dehydroxylating bacteria in feces compared with a group of patients with normal DCA, but this difference was not due to a slow intestinal transit time. In agreement with that, van der Werf *et al*[25] have previously shown that elderly persons (55-75 years old) have a higher fractional turnover of cholic acid and a higher deoxycholic acid input rate from the large bowel than young adults (20-30 years old) and this is not due to any difference in gut transit time.

Another finding of this study was that high level of DCA was also associated with high BMI. This could indicate a potential role of BMI as a confounder when analysing biliary DCA levels in studies on cholesterol gallstone patients.

To conclude, gallstone patients with excess DCA are of older age and have higher BMI than patients with normal DCA. The two groups of patients do not differ with respect to biliary lipid composition, cholesterol saturation, nucleation time or occurrence of cholesterol crystals. These findings further underline that DCA in bile does not significantly contribute to cholesterol gallstone formation.

ACKNOWLEDGMENTS

We greatly appreciate the skilful technical assistance by Ms Ingela Arvidsson and Ms Lisbet Benthin.

REFERENCES

1 **Carey MC**, Duane WC. Enterohepatic circulation. In: Arias IM, Boyer JL, Fausto N, Jakoby WB, Schachter D, Shafritz DA, eds. The liver: biology and pathobiology. *New York: Raven Press* 1994: 719-767

2 **Marcus NS,** Heaton KW. Intestinal transit, deoxycholic acid and the cholesterol saturation of bile – three inter-related factors. *Gut* 1986; **27:** 550-558

3 **Berr F,** Schreiber E, Frick U. Interrelationships of bile acid and phospholipid fatty acid species with cholesterol saturation of duodenal bile in health and gallstone disease. *Hepatology* 1992; **16:** 71-81

4 **Hussaini SH,** Pereira SP, Murphy GM, Dowling RH. Deoxycholic acid influences cholesterol solubilization and microcrystal nucle-

ation time in gallbladder bile. *Hepatology* 1995; **22:** 1735-1744
5 **Shoda J,** He BF, Tanaka N, Matsuzaki Y, Osuga T, Yamamori S, Miyazaki H, Sjövall J. Increase of deoxycholate in supersaturated bile of patients with cholesterol gallstone disease and its correlation with de novo syntheses of cholesterol and bile acids in liver, gallbladder emptying and small intestinal transit. *Hepatology* 1995; **21:** 1291-1302
6 **Berr F,** Kullak-Ublick GA, Paumgartner G, Munzing W, Hylemon PB. 7 alpha-dehydroxylating bacteria enhance deoxycholic acid input and cholesterol saturation of bile in patients with gallstones. *Gastroenterology* 1996; **111:** 1611-1620
7 **Azzaroli FG,** Mazzella G, Mazzeo C, Simoni P, Festi D, Colecchia A, Montagnani M, Martino C, Villanova N, Roda A, Roda E. Sluggish small bowel motility is involved in determining increased biliary deoxycholic acid in cholesterol gallstone patients. *Am J Gastroenterol* 1999; **94:** 2453-2459
8 **Thomas LA,** Veysey MJ, Bathgate T, King A, French G, Smeeton NC, Murphy GM, Dowling RH. Mechanism for the transit-induced increase in colonic deoxycholic acid formation in cholesterol cholelithiasis. *Gastroenterology* 2000; **119:** 806-815
9 **Van Erpecum KJ,** Portincasa P, Stolk MFJ, Van de Heijning BJM, Van der Zaag ES, Van den Broek AMWC, Van Berge Henegouwen GP, Renooij W. Effects of bile salt and phospholipid hydrophobicity on lithogenicity of human gallbladder bile. *Eur J Clin Invest* 1994; **24:** 744-750
10 **Noshiro H,** Chijiiwa K, Makino I, Nakano K, Hirota I. Deoxycholic acid in gall bladder bile does not account for the shortened nucleation time in patients with cholesterol gall stones. *Gut* 1995; **36:** 121-125
11 **Miguel JF,** Nunez L, Amigo L, Gonzalez S, Raddatz A, Rigotti A, Nervi F. Cholesterol saturation, not proteins or cholecystitis, is critical for crystal formation in human gallbladder bile. *Gastroenterology* 1998; **114:** 1016-1023
12 **Jungst D,** Muller I, Kullak-Ublick GA, Meyer G, Frimberger E, Fischer S. Deoxycholic acid is not related to lithogenic factors in gallbladder bile. *J Lab Clin Med* 1999; **133:** 370-377
13 **Gustafsson U,** Sahlin S, Einarsson C. Biliary lipid composition in patients with cholesterol and pigment gallstones and gallstone-free subjects: deoxycholic acid does not contribute to formation of cholesterol gallstones. *Eur J Clin Invest* 2000; **30:** 1099-1106
14 **Wells JE,** Berr F, Thomas LA, Dowling RH, Hylemon PB. Isolation and characterization of cholic acid 7α -dehydroxylating fecal bacteria from cholesterol gallstone patients. *J Hepatol* 2000; **32:** 4-10
15 **Tera H.** Stratification of human gallbladder bile *in vivo*. *Acta Chir Scand Supplement* 1960; **256:** 4-65
16 **Trotman BW,** Ostrow JD, Soloway RD. Pigment *vs* cholesterol cholelithiasis: comparison of stone and bile composition. *Am J Dig Dis* 1974; **19:** 585-590
17 **Whiting MJ,** Down RH, Watts JMCK. Biliary crystals and granules, the cholesterol saturation index, and the prediction of gallstone type. *Surg Gastroenterol* 1982; **1:** 17-21
18 **Roda A,** Festi D, Sama C, Mazzella G, Aldini T, Roda E, Barbara L. Enzymatic determination of cholesterol in bile. *Clin Chim Acta* 1975; **64:** 337-341
19 **Rouser G,** Fleischer S, Yamamoto A. Two dimensional thin layer chromatography separation of polar lipids and determination of phospholipids by phosphorous analysis of spots. *Lipids* 1970; **5:** 494-496
20 **Fausa O,** Skalhegg BA. Quantitative determination of bile acids and their conjugates using thin-layer chromatography and a purified 3alpha-hydroxysteroid dehydrogenase. *Scand J Gastroenterol* 1974; **9:** 249-254
21 **Carey MC.** Critical tables for calculating the cholesterol saturation of native bile. *J Lipid Res* 1978; **19:** 945-955
22 **Angelin B,** Einarsson K, Leijd B. Biliary lipid composition during treatment with different hypolipidaemic drugs. *Eur J Clin Invest* 1979; **9:** 185-190
23 **Holan KR,** Holzbach RT, Hermann RE, Cooperman AM, Claffey WJ. Nucleation time; a key factor in the pathogenesis of cholesterol gallstone disease. *Gastroenterology* 1979; **77:** 611-617
24 **Sahlin S,** Ahlberg J, Angelin B, Reihnér E, Einarsson K. Nucleation time of gall bladder bile in gallstone patients: influence of bile acid treatment. *Gut* 1991; **32:** 1554-1557
25 **Van der Werf SDJ,** Huijbregts AWM, Lamers HLM, van Berge Henegouwen GP, van Tongeren JHM. Age dependent differences in human bile acid metabolism and 7α-dehydroxylation. *Eur J Clin Invest* 1981; **11:** 425-431

Edited by Xu XQ

P.O.Box 2345, Beijing 100023,China
Fax: +86-10-85381893
E-mail: wjg@wjgnet.com www.wjgnet.com

World J Gastroenterol 2003;9(7):1580-1583
World Journal of Gastroenterology
 ISSN 1007-9327

• CLINICAL RESEARCH •

Association of *CagA* and *VacA* presence with ulcer and non-ulcer dyspepsia in a Turkish population

Kantarceken Bulent, Aladag Murat, Atik Esin, Koksal Fatih, Harputluoglu MMMurat, Harputluoglu Hakan, Karincaoglu Melih, Ates Mehmet, Yildirim Bulent, Hilmioglu Fatih

Kantarceken Bulent, Aladag Murat, Karincaoglu Melih, Hilmioglu Fatih, Division of Gastroenterology, Medical Faculty, Inonu University, Malatya, Turkey
Atik Esin, Mustafa Kemal University, Department of Pathology, Medical Faculty, Hatay, Turkey
Koksal Fatih, Department of Microbiology, Medical Faculty, Cukurova University, Adana, Turkey
Harputluoglu MMMurat, Ates Mehmet, Division of Gastroenterology, Medical Faculty, Inonu University, Malatya, Turkey
Harputluoglu Hakan, Department of Internal Medicine, Medical Faculty, Inonu University, Malatya, Turkey
Yildirim Bulent, Division of Gastroenterology, Medical Faculty, Inonu University, Malatya, Turkey
Correspondence to: Bulent Kantarceken, Zafer Mah. Mehmet Buyruk Cad. 2.Ordu karsýsý Haþimbey Apt. Dai. No: 19, 44300/ Malatya, Turkey. bkantarceken@inonu.edu.tr, bulentkc@lycos.com
Telephone: +90-422-3411199 **Fax:** +90-422-3410729(28)
Received: 2003-01-14 **Accepted:** 2003-02-25

Abstract

AIM: The mostly known genotypic virulence features, of *H. pylori* are cytotoxin associated gene A (*cagA*) and Vacuolating cytotoxin gene A (*VacA*). We investigated the association of these major virulence factors with ulcer and non-ulcer dyspepsia in our region.

METHODS: One hundred and forty two dyspeptic patients were studied (average age 44.8±15.9 years, range 15-87 years, 64 males and 78 females). Antral and corpus biopsies were taken for detecting and genotyping of *H. pylori*. 107 patients who were *H. pylori* positive by histological assessment were divided into three groups according to endoscopic findings: Duodenal ulcer (DU), gastric ulcer (GU) and non-ulcer dyspepsia (NUD). The polymerase chain reaction (PCR) was used to detect *CagA* and *VacA* genes of *H. pylori* using specific primers.

RESULTS: *H. pylori* was isolated from 75.4 % (107/142) of the patients. Of the 107 patients, 66 (61.7 %) were *cagA*-positive and 82 (76.6 %) were *VacA*-positive. *CagA* gene was positively associated with DU and GU ($P<0.01$, $P<0.02$), but not with NUD ($P>0.05$). Although *VacA* positivity in ulcer patients was higher than that in NUD group, the difference was not statistically significant ($P>0.05$).

CONCLUSION: There is a significantly positive association between *CagA* genes and DU and GU. The presence of *VacA* is not a predictive marker for DU, GU, and NUD in our patients.

Bulent K, Murat A, Esin A, Fatih K, MMMurat H, Hakan H, Melih K, Mehmet A, Bulent Y, Fatih H. Association of *CagA* and *VacA* presence with ulcer and non-ulcer dyspepsia in a Turkish population. *World J Gastroenterol* 2003; 9(7): 1580-1583
http://www.wjgnet.com/1007-9327/9/1580.asp

INTRODUCTION

Helicobacter pylori (*H. pylori*) is a gram-negative, spiral shaped microaerophilic bacterium that colonizes in the gastric mucosa in humans[1]. In the majority of individuals, infection causes asymptomatic histological chronic gastritis. A significant minority subsequently develop peptic ulcer disease (PUD), and infection with *H. pylori* is a significant risk factor for gastric carcinoma and mucosa-associated lymphoid tissue (MALT) lymphoma[2-4]. The process by which different disease patterns develop has not been fully elucidated. But two putative virulence determinants of *H. pylori* have been identified as markers of ulcerogenic strains, the cytotoxin associated gene A (*CagA*) and the vacuolating cytotoxin gene A (*VacA*) (Phenotype 1, ulcerogenic; *CagA* & *VacA*-positive, phenotype 2, non-ulcerogenic; *CagA* & *VacA*-negative). The *CagA* gene encodes a 120-140 kDa protein of unknown function in about 60-70 % of *H. pylori* strains. This gene is part of the cag pathogenicity island (PAI), a 40-kbp segment with several genes involved in cytokine production[5, 6]. Strains that do not produce the *CagA* protein generally lack the entire cag PAI. *H. pylori* strains produced by *CagA* have been detected in patients with PUD more frequently than in patients with chronic gastritis alone[7- 9]. Another virulence factor that injures epithelial cells is encoded by *VacA*. *VacA* is present nearly in all *H. pylori* strains and contains at least two variable parts[10,12]. The s-region (encoding the signal peptide) exists as s1 or s2 allelic types. Among type s1 strains, subtypes s1a, s1b, and s1c have been identified. The m-region (middle) occurs as m1 or m2 allelic types. Among type m2, two subtypes have been identified, and designated as m2a and m2b[11]. Production of the vacuolating cytotoxin is related to the mosaic structure of *VacA*. The *VacA* signal sequence type s1, but not type s2 is closely associated with *in vitro* cytotoxin activitiy, PUD, and the presence of *CagA* gene[9, 10, 12]. The m1 allele is associated with higher levels of toxin activitiy and more severe gastric epithelial damage than the m2 allele[10, 12].

MATERIALS AND METHODS

Materials

Patients and classification of endoscopic findings One hundred forty two dyspeptic patients (excluding those taking proton pump inhibitors [PPIs] and/or NSAIDs in the past month, and/or had previous *H. pylori* eradication) were studied (average age 44.8±15.9 years, range 15-87 years, 64 males and 78 females) and referred for routine endoscopy at the Department of Gastroenterology in the Turgut Özal Medical Center, Malatya, Turkey. Endoscopic findings were recorded and according to endoscopic findings, *H. pylori* positive patients were divided into three groups: Group 1: Patients with duodenal ulcer (DU); Group 2: Patients with gastric ulcer (GU); Group 3: Patients with non-ulcer dyspepsia (NUD). All the patients gave informed consent to participate in the study.

Methods

Endoscopy and detection of *H. pylori* by histological assessment During each endoscopic procedure (by Olympus

GIF XQ 240 videoendoscope), two antral and two corpus mucosal biopsy specimens were obtained by using biopsy forceps (FB-25 k; Olympus, Japan) which were cleaned with a detergent and disinfected after each examination. Two biopsy samples were transported to pathology laboratory and fixed in 10 % formalin overnight. Tissue processing was undertaken with graded ethanol solutions and clearing was made with xylene. Paraffin tissue blocks were cut into 4-5 μm sections with a rotary microtome. The sections were stained with hematoxylin-eosin and tissue Giemsa and assessed for the presence of *H.pylori* microorganisms. 107 (75.4 %) patients (average age 45.8±15.7 years, range 17-87 years, 50 males and 57 females) were found to be *H. pylori* positive and the other two biopsy specimens of those patients were transported to the microbiology laboratory for PCR examination to determine *CagA* and *VacA* status.

PCR examination Biopsy samples obtained from 107 patients with positive *H. pylori* were put into 20 % dextrose solution and stored at -20 ℃ until a sufficient number was reached for PCR assay. The transport media contained the tissue samples were discarded and the tissue samples were resuspended with 100-200 μg/ml of lysis buffer (10 mM Tris-HCL, 0.1 M EDTA, 5 % SDS, 100-200 μg/ml proteinase K). The mixture was incubated at 52 ℃ for 2 hours in a thermal cycler. 100 μl phenol-chloroform-isoamyl alcohol (25:24:1) was added into the mixture. The mixture was then vortexed and centrifuged at 5 000×g for 5 minutes. The supernatant was discarded and isoamyl alcohol (24:1) was added as much as the taken volume. The mixture was vortexed and centrifuged as described above. The supernatant was discarded and 2.5 volume of cold ethanol (70 %) was added and stored at -20 ℃ overnight. On the following day, the mixture was centrifuged at 13 000×g for 13 minutes. The supernatant was discarded and the pellet was resuspended with TE buffer and used for PCR assay. The reaction mixture (50 μl) was prepared for *CagA* as described below. 2 μl dNTP mix (200 μM/ μl of each deoxynucleotide), 1 μl primer 1(0.5 μM/1 μl of each oligonucleotide), 1 μl primer II, 1 μl taq polymerase (2.5U/ μl), 4.5 μl 10×PCR buffer, 0.5 μl $MgCl_2$ (5 μM/ μl), 35 μl distilled water, 5 μl sample DNA. PCR reaction was performed in the thermal cycler (M.J. research) with the following incubation steps: at 94 ℃ **for** 4 min (Pre-heating), 35 cycles at 94 ℃ **for** 1 min (denaturation), at 57 ℃ 1.30 min (annealing) and at 74 ℃ **for** 2 min (elongation), 1 cycle at 74 ℃ **for** 5 min post elongation. *Cag A* primers: 5' -GAT AAC AGG CAA GCT TTT GAG G-3', 5' - CTG CAA AAG ATT ATT TGG CAA GA-3' targeting 349 bp fragment. The reaction mixture was prepared for *VacA* as described below. 2 μl dNTP mix, 1 μl primer 1, 1 μl primer II, 1 μl taq polymerase, 4.5 μl 10×PCR buffer, 0.5 μl $MgCl_2$, 35 μl distilled water, 5 μl sample DNA. Then at 94 ℃ **for** 1 min (denaturation), at 63 ℃ **for** 1.30 min (annealing), at 72 ℃ **for** 1 min (elongation), 30 cycles, and at 74 ℃ **for** 5 min 1 cycle for post elongation. *VacA* primers: 5' - CCG AAG AAG CCA ATA AAA CCC CAG-3', 5' - CAA AGT CAA AAC CGT AGA GCT GGC- 3' targeting 467 bp fragment. The PCR products were analysed by 2 % agarose gel with 0.5 % ethidium bromide via electrophoresis.

Statistical analysis

Normal χ^2 analysis and Fisher' s exact χ^2 method were used for statistical evaluation of data derived from the results of the procedures mentioned above.

RESULTS

Prevalence of H. pylori infection

H. pylori infection was found in 107 of 142 patients (75.4 %).

Endoscopic findings

35 of the 107 patients had DU (32.7 %), 24 (22.4 %) GU and 48 NUD (44.9 %).

Prevalence of CagA and VacA among H. pylori positive patients

While 66 of 107 *H. pylori* strains were *CagA* positive (61.7 %), 82 of the patients were *VacA* positive (76.6 %), and 62 of the patients were both *CagA* and *VacA* positive (57.9 %).

Relation between CagA-VacA status and DU, GU, and NUD

28 of 35 patients with DU (80 %), 20 of 24 patients with gastric ulcers (83.3 %) and 18 of 48 patients with NUD (37.5 %) were *CagA* positive. The presence of *CagA* in the patients with DU and GU was significantly higher than that in the patients with NUD, respectively (P=0.007, P=0.013). *CagA* positivity was statistically lower in patients with NUD (P<0.001). 29 of 35 patients with DU (82.9 %), 21 of 24 patients with gastric ulcer (87.5 %), and 32 of 48 patients with NUD (66.7 %) were *VacA* positive. *VacA* positivity was both higher in the patients with DU and GU than that in the patients with NUD, but this difference between the groups was not statistically significant (P>0.05). We detected phenotype 1 *H. pylori*, characterized by the expression of both *CagA* and *VacA*, in 57.9 % (62 of 107) of the patients (71.4 % DU, 79.2 % GU, 37.5 % NUD patients). The prevalence of phenotype 1 was significantly higher in patients with duodenal or gastric ulcer, than that in the patients with NUD (P<0.0004, P<0.0002). Phenotype 2 *H. pylori* characterized by a lack of expression of either *CagA* or *VacA*, was found in 19.6 % of the patients (21 of 107) in our study (8.6 % DU, 8.3 % GU, 33.3 % NUD). The prevalence of phenotype 2 in the patients with NUD was significantly higher than that in patients with duodenal or gastric ulcer (P<0.01, P<0.04). The remaining 22.4 % of the total number of patients studied (24 of 107) had an intermediate phenotype, which expressed either *CagA* independent of the presence of *VacA* (CagA-positive and *VacA*-negative, 3.7 %) or vice versa (CagA-negative and *VacA* positive, 18.7 %). There was not any significant difference between the groups according to intermediate phenotypes (P>0.05) (Table 1).

DISCUSSION

The most common interaction between *H. pylori* and human is asymptomatic bacterial colonisation in the gastric mucosa, which can be continued lifelong. However, the presence of this bacterium in an individual increases the risk of serious

Table 1 Distribution of endoscopic findings according to *CagA* and *VacA* status

	CagA+	*VacA*+	*CagA*+*VacA*+ (Phenotype 1)	*CagA*+ *VacA*-	*CagA*-*VacA*+	*CagA*-*VacA*- (Phenotype 2)
DU(35)	28(80%)	29(82.8%)	25(71.4%)	3(8.6%)	4(11.4%)	3(8.6%)
GU(24)	20(83.3%)	21(87.5%)	19(79.2%)	1(4.2%)	2(8.3%)	2(8.3%)
NUD(48)	18(37.5%)	32(66.6%)	18(37.5%)	0(0.0%)	14(29.2%)	16(33.3%)
Total(107)	66(61.6%)	82(76.6%)	62(57.9%)	4(3.7%)	20(18.6%)	21(19.6%)

gastroduodenal diseases such as gastritis, GU, DU, gastric cancer and MALT lymphoma[3, 4, 13, 14]. It has been suggested that *H. pylori* may induce more or less severe gastroduodenal diseases according to the strain virulence. Two major markers of virulence, *CagA* and *VacA*, have been described in *H. pylori*. The association between putative virulence markers with ulcer and NUD was investigated in a Turkish population.

In our study, the presence of *CagA*, and both *CagA* and *VacA* was significantly more prevelent in patients with DU and GU, than those in patients with NUD ($P<0.05$). The positivity of *VacA* was higher in the patients with DU and GU than that in the patients with NUD, but difference was not statistically significant ($P>0.05$). Previous studies from different countries showed that CagA-positive strains were more common in patients with ulcer disease. CagA-positive strains were found in 79 % to 100 % of DU patients[7,8,15,18-31], 71 % to 100 % of GU patients [7-9,19,20,27,28], as compared with 37 % to 89.7 % of NUD patients[8,18-24,26-31]. In the present study, we found a significantly higher prevalence of CagA-positive strains in DU and GU than that in NUD patients (80 %, 83.3 %, and 37.5 %, respectively). It was reported from different centers that in patients with duodenal ulcer, the positivity rates of cagA, *VacA*, and both *Cag A* and *VacA* were 79-100 %, 47.5-92 %, 37-75 %, respectively[7,8,15,18-31]. The positivity rates of *Cag A*, *VacA*, and both *CagA* and *VacA* in the patients with gastric ulcer, have been reported to be 71-100 %, 40.8-75 %, and 38.8-56.6 %, respectively[7-9,19-30]. In all of these studies, the positivity of *CagA* and *VacA* was higher in the patients with DU or GU, however some was statistically significant[7-10,12,15-18,24-26,28-31] and some not[19-21,23,32,33,35- 37,39,42,43] when it was compared to patients without ulcer.

In patients with NUD, the positivity rates of *CagA* and *VacA* were reported to be 37-89.7 %[8,18,19,21-24,26,28,29] and 33.3-73 %[8,19,21-23,28-30], respectively. Nearly in all of these studies, *CagA* and *VacA* positivity rate in the patients with NUD was found to be low compared to that in the patients with ulcer, however, this difference was statistically significant in some studies[7-9, 15-18, 24-26, 28-30], but not in some others[19-21,23,27,33,35-38,41,42]. In our study, the *CagA* positivity in the patients with NUD was significantly lower than that in the ulcer patients ($P<0.01$). This supported the results of DU and GU mentioned above. Although *VacA* positivity was higher in the patients with ulcer than that in the patients with NUD, this was not statistically significant and did not seem to be an important risk factor for the development of ulcer in our patients. However, determination the *VacA* genotypes and the presence of *CagA* gene together may contribute to potential clinic determination of patients who have different levels of risk. It has been shown that *VacA* type s1/m1 strains produce more cytotoxins than type s1/m2, and that type s2/m2 strains do not produce active cytotoxins[10]. Many studies have confirmed these findings[9,12,24,25,31,38]. In this study, we couldn' t detect the *VacA* subtypes for not having their primers. Also, we had no information on the *in vitro* cytotoxin production of our strains, so we could not compare our results directly with those from other studies. If we could have determined these factors, perhaps we would find an association between *VacA* and ulcer disease. It was reported that the presence of *CagA* and *VacA* genes in *H. pylori* isolates increased the risk of gastric cancer[22,40] but some studies refused this[37,41,42]. In two studies, no statisticallly significant difference between the presence of *CagA* or *VacA* in patients with MALT lymphoma and NUD was found[8]. In another study which interrogated the importance of the presence of *CagA* for developing resistance to metronidazole, which was used in eradication therapies of *H. pylori*, an association between resistance and the presence of *CagA* was not shown. It was investigated that if the patients could be selected for gastroscopy adequately only by looking for anti *H. pylori* and anti-*CagA* serologically, and it was observed that the method was not adequate for screening, since many serious pathology and malignancy could not have been noticed by just a selection of this method[43].

Gastroduodenal lesions developed in the patients infected with *H. pylori* isolates that had *CagA* and *VacA* gene and showed differences according to regions, countries and ethnic groups. In the literature, it has been controversial that *CagA* and *VacA* positive isolates cause more serious gastroduodenal lesions[7-42]. In our study, it was seen that gastric and duodenal ulcer incidence increased in the patiens with *CagA*, and both *CagA* and *VacA* positive. Recently, it was reported similar results for *CagA* in ulcer patients from Turkey abtained by using an ELISA method[46]. Many risk factors have been determined for *H. pylori* infection (CagA, *VacA*, *IceA* etc.), but none of them is specific for disease. It has been put forward that *CagA* plays a partial role in increased mucosal inflammation, increased density of *H. pylori* in antrum, and causes more profound inhibition of mucin synthesis, DU, GU and gastric cancer[7-9,39,44], and has a protective role in Barret' s esophagitis[16,17]. However direct association was found only with IL-8 induction[32,34,45]. The *IceA* gene, considered as a virulence factor for *H. pylori* infection recently, has no disease specific features, and there is no biologic and epidemiologic evidences that *IceA* gene is a virulence factor associated with *H. pylori*[33,34]. The opinion that *VacA* genotyping may be useful clinically (for example, predicting the presence of DU) is controversial from now on[19,32, 34].

As a result, the association between, the virulence factors in *H.pylori* positive patients, clinical course and gastroduodenal lesions that develop subsequently has not been understood yet. For determining these interactions, it needs great scale and multicenter studies which examine the structural features of *H. pylori* (virulence factors), host features and environmental features together. To have definite results, study must be large enough and include different diseases and ethnic groups. Also, in our country, multicenter and large scale studies would reveal the virulence differences between different regions.

REFERENCES

1 **Warren JR**, Marshall BJ. Unidentified curved bacilli on gastric epithelium in active chronic gastritis. *Lancet* 1983; **1**: 1273-1275

2 **Parsonnet J**, Friedman GD, Vandersteen DP, Chang Y, Vogelman JH, Orentreich N, Sibley RK. *Helicobacter pylori* infection and the risk of gastric carcinoma. *N Engl J Med* 1991; **325**: 1127-1131

3 **Wotherspoon AC**, Doglioni C, Diss TC, Pan L, Moschini A, de Boni M, Isaacson PG. Regression of primary low-grade B-cell gastric lymphoma of mucosa-associated lymphoid tissue type after eradication of *Helicobacter pylori*. *Lancet* 1993; **342**: 575-577

4 An international association between *Helicobacter pylori* infection and gastric cancer. The EUROGAST Study Group. *Lancet* 1993; **341**: 1359-1362

5 **Censini S**, Lange C, Xiang Z, Crabtree JE, Ghiara P, Borodovsky M, Rappuoli R, Covacci A. cag, a pathogenicity island of *Helicobacter pylori*, encodes type I-specific and disease-associated virulence factors. *Proc Natl Acad Sci U S A* 1996; **93**: 14648-14653

6 **Covacci A**, Falkow S, Berg DE, Rappuoli R. Did the inheritance of a pathogenicity island modify the virulence of *Helicobacter pylori*? *Trends Microbiol* 1997; **5**: 205-208

7 **Martin Guerrero JM**, Hergueta Delgado P, Esteban Carretero J, Romero Castro R, Pellicer Bautista FJ, Herrerias Gutierrez JM**.** Clinical relevance of *Helicobacter pylori* CagA-positive strains: gastroduodenal peptic lesions marker. *Rev Esp Enferm Dig* 2000;**92**: 160-173

8 **Lamarque D**, Gilbert T, Roudot-Thoraval F, Deforges L, Chaumette MT, Delchier JC. Seroprevalence of eight *Helicobacter pylori* antigens among 182 patients with peptic ulcer, MALT gastric lymphoma or non-ulcer dyspepsia. Higher rate of seroreactivity against CagA and 35-kDa antigens in patients with peptic ulcer originating from Europe and Africa. *Eur J Gastroenterol Hepatol* 1999; **11**: 721-726

9 **Rudi J**, Rudy A, Maiwald M, Kuck D, Sieg A, Stremmel W. Di-

rect determination of *Helicobacter pylori* vacA genotypes and cagA gene in gastric biopsies and relationship to gastrointestinal diseases. *Am J Gastroenterol* 1999; **94**: 1525-1531

10 **Atherton JC**, Cao P, Peek RM Jr, Tummuru MK, Blaser MJ, Cover TL. Mosaicism in vacuolating cytotoxin alleles of Helicobacter pylori. Association of specific vacA types with cytotoxin production and peptic ulceration. *J Biol Chem* 1995; **270**: 17771-17777

11 **van Doorn LJ**, Figueiredo C, Sanna R, Pena S, Midolo P, Ng EK, Atherton JC, Blaser MJ, Quint WG. Expanding allelic diversity of Helicobacter pylori vacA. *J Clin Microbiol* 1998; **36**: 2597-2603

12 **Atherton JC**, Peek RM Jr, Tham KT, Cover TL, Blaser MJ. Clinical and pathological importance of heterogeneity in vacA, the vacuolating cytotoxin gene of Helicobacter pylori. *Gastroenterology* 1997; **112**: 92-99

13 **Sipponen P**, Hyvarinen H. Role of *Helicobacter pylori* in the pathogenesis of gastritis, peptic ulcer and gastric cancer. *Scand J Gastroenterol Suppl* 1993; **196**: 3-6

14 **Cullen DJE**, Collins BJ, Christiansen KJ. Long term risk of peptic ülcer disease in people with *Helicobacter pylori* infection. A community based study. *Gut* 1993; **34**: F284

15 **Lin CW**, Wu SC, Lee SC, Cheng KS. Genetic analysis and clinical evaluation of vacuolating cytotoxin gene A and cytotoxin-associated gene A in Taiwanese *Helicobacter pylori* isolates from peptic ulcer patients. *Scand J Infect Dis* 2000; **32**: 51-57

16 **Vaezi MF**, Falk GW, Peek RM, Vicari JJ, Goldblum JR, Perez-Perez GI, Rice TW, Blaser MJ, Richter JE. CagA-positive strains of *Helicobacter pylori* may protect against Barrett's esophagus. *Am J Gastroenterol* 2000; **95**: 2206-2211

17 **Loffeld RJ**, Werdmuller BF, Kuster JG, Perez-Perez GI, Blaser MJ, Kuipers EJ. Colonization with cagA-positive *Helicobacter pylori* strains inversely associated with reflux esophagitis and Barrett's esophagus. *Digestion* 2000; **62**: 95-99

18 **Hennig EE**, Trzeciak L, Regula J, Butruk E, Ostrowski J. VacA genotyping directly from gastric biopsy specimens and estimation of mixed *Helicobacter pylori* infections in patients with duodenal ulcer and gastritis. *Scand J Gastroenterol* 1999; **34**: 743-749

19 **Mahachai V**, Tangkijvanich P, Wannachai N, Sumpathanukul P, Kullavanijaya P. CagA and VacA: virulence factors of *Helicobacter pylori* in Thai patients with gastroduodenal diseases. *Helicobacter* 1999; **4**: 143-147

20 **Tokumaru K**, Kimura K, Saifuku K, Kojima T, Satoh K, Kihira K, Ido K. CagA and cytotoxicity of *Helicobacter pylori* are not markers of peptic ulcer in Japanese patients. *Helicobacter* 1999; **4**: 1-6

21 **Marshall DG**, Hynes SO, Coleman DC, O'Morain CA, Smyth CJ, Moran AP. Lack of a relationship between Lewis antigen expression and cagA, CagA, vacA and VacA status of Irish *Helicobacter pylori* isolates. *FEMS Immunol Med Microbiol* 1999; **24**: 79-90

22 **Basso D**, Navaglia F, Brigato L, Piva MG, Toma A, Greco E, Di Mario F, Galeotti F, Roveroni G, Corsini A, Plebani M. Analysis of *Helicobacter pylori* vacA and cagA genotypes and serum antibody profile in benign and malignant gastroduodenal diseases. *Gut* 1998; **43**: 182-186

23 **Holtmann G**, Talley NJ, Mitchell H, Hazell S. Antibody response to specific *H. pylori* antigens in functional dyspepsia, duodenal ulcer disease, and health. *Am J Gastroenterol* 1998; **93**: 1222-1227

24 **Evans DG**, Queiroz DM, Mendes EN, Evans DJ Jr. *Helicobacter pylori* cagA status and s and m alleles of vacA in isolates from individuals with a variety of *H. pylori*-associated gastric diseases. *J Clin Microbiol* 1998; **36**: 3435-3437

25 **Stephens JC**, Stewart JA, Folwell AM, Rathbone BJ. *Helicobacter pylori* cagA status, vacA genotypes and ulcer disease. *Eur J Gastroenterol Hepatol* 1998; **10**: 381-384

26 **Warburton VJ**, Everett S, Mapstone NP, Axon AT, Hawkey P, Dixon MF. Clinical and histological associations of cagA and vacA genotypes in *Helicobacter pylori* gastritis.*J Clin Pathol* 1998; **51**: 55-61

27 **Takata T**, Fujimoto S, Anzai K, Shirotani T, Okada M, Sawae Y, Ono J. Analysis of the expression of CagA and VacA and the vacuolating activity in 167 isolates from patients with either peptic ulcers or non-ulcer dyspepsia. *Am J Gastroenterol* 1998; **93**: 30-34

28 **Ito A**, Fujioka T, Kodama K, Nishizono A, Nasu M. Ito Virulence-associated genes as markers of strain diversity in *Helicobacter pylori* infection. *J Gastroenterol Hepatol* 1997; **12**: 666-669

29 **Donati M**, Moreno S, Storni E, Tucci A, Poli L, Mazzoni C, Varoli O, Sambri V, Farencena A, Cevenini R. Detection of serum antibodies to CagA and VacA and of serum neutralizing activity for vacuolating cytotoxin in patients with *Helicobacter pylori*-induced gastritis. *Clin Diagn Lab Immunol* 1997; **4**: 478-482

30 **Weel JF**, van der Hulst RW, Gerrits Y, Roorda P, Feller M, Dankert J, Tytgat GN, van der Ende A. The interrelationship between cytotoxin-associated gene A, vacuolating cytotoxin, and *Helicobacter pylori*-related diseases. *J Infect Dis* 1996; **173**: 1171-1175

31 **Kidd M**, Lastovica AJ, Atherton JC, Louw JA. Heterogeneity in the *Helicobacter pylori* vacA and cagA genes: association with gastroduodenal disease in South Africa? *Gut* 1999; **45**: 499-502

32 **Audibert C**, Janvier B, Grignon B, Salaun L, Burucoa C, Lecron JC, Fauchere JL. Correlation between IL-8 induction, cagA status and vacA genotypes in 153 French *Helicobacter pylori* isolates. *Res Microbiol* 2000; **151**: 191-200

33 **Zheng PY**, Hua J, Yeoh KG, Ho B. Association of peptic ulcer with increased expression of Lewis antigens but not cagA, iceA, and vacA in *Helicobacter pylori* isolates in an Asian population. *Gut* 2000; **47**: 18-22

34 **Graham DY**, Yamaoka Y. Disease-specific *Helicobacter pylori* virulence factors: the unfulfilled promise. *Helicobacter* 2000; **5**: S27-31

35 **Mukhopadhyay AK**, Kersulyte D, Jeong JY, Datta S, Ito Y, Chowdhury A, Chowdhury S, Santra A, Bhattacharya SK, Azuma T, Nair GB, Berg DE. Distinctiveness of genotypes of *Helicobacter pylori* in Calcutta. *India J Bacteriol* 2000; **182**: 3219-3227

36 **Opazo P**, Muller I, Rollan A, Valenzuela P, Yudelevich A, Garciade la Guarda R, Urra S, Venegas A. Serological response to *Helicobacter pylori* recombinant antigens in Chilean infected patients with duodenal ulcer, non-ulcer dyspepsia and gastric cancer. *APMIS* 1999; **107**: 1069-1078

37 **Kodama K**, Ito A, Nishizono A, Fujioka T, Nasu M, Yahiro K, Hirayama T, Uemura N. Divergence of virulence factors of Helicobacter pylori among clinical isolates does not correlate with disease specificity. *J Gastroenterol* 1999;**34**(Suppl 11): 6-9

38 **Pan ZJ**, van der Hulst RW, Tytgat GN, Dankert J, van der Ende A. Relation between vacA subtypes, cytotoxin activity, and disease in *Helicobacter pylori*-infected patients from The Netherlands. *Am J Gastroenterol* 1999; **94**: 1517-1521

39 **Beil W**, Enss ML, Muller S, Obst B, Sewing KF, Wagner S. Role of vacA and cagA in *Helicobacter pylori* inhibition of mucin synthesis in gastric mucous cells. *J Clin Microbiol* 2000; **38**: 2215-2218

40 **Rudi J**, Kolb C, Maiwald M, Zuna I, von Herbay A, Galle PR, Stremmel W. Serum antibodies against *Helicobacter pylori* proteins VacA and CagA are associated with increased risk for gastric adenocarcinoma. *Dig Dis Sci* 1997; **42**: 1652-1659

41 **Matsukura N**, Onda M, Kato S, Hasegawa H, Okawa K, Shirakawa T, Tokunaga A, Yamashita K, Hayashi A. Cytotoxin genes of *Helicobacter pylori* in chronic gastritis, gastroduodenal ulcer and gastric cancer: an age and gender matched case-control study. *Jpn J Cancer Res* 1997; **88**: 532-536

42 **Mitchell HM**, Hazell SL, Li YY, Hu PJ. Serological response to specific *Helicobacter pylori* antigens: antibody against CagA antigen is not predictive of gastric cancer in a developing country. *Am J Gastroenterol* 1996; **91**: 1785-1788

43 **Heikkinen M**, Janatuinen E, Mayo K, Megraud F, Julkunen R, Pikkarainen P. Usefulness of anti-*Helicobacter pylori* and anti-CagA antibodies in the selection of patients for gastroscopy. *Am J Gastroenterol* 1997; **92**: 2225-2229

44 **McGee DJ**, Mobley HL. Mechanisms of *Helicobacter pylori* infection: bacterial factors. *Curr Top Microbiol Immunol* 1999; **241**: 155-180

45 **Yamaoka Y**, Kodama T, Graham DY, Kashima K. Search for putative virulence factors of Helicobacter pylori: the low-molecular-weight (33-35 K) antigen. *Dig Dis Sci* 1998; **43**: 1482-1487

46 **Demirturk L**, Ozel AM, Yazgan Y, Solmazgul E, Yildirim S, Gultepe M, Gurbuz AK. CagA status in dyspeptic patients with and without peptic ulcer disease in Turkey: association with histopathologic findings. *Helicobacter* 2001; **6**: 163-168

Edited by Xu XQ, Wang XL and Zhu LH

P.O.Box 2345, Beijing 100023,China
Fax: +86-10-85381893
E-mail: wjg@wjgnet.com www.wjgnet.com

World J Gastroenterol 2003;9(7):1584-1588
World Journal of Gastroenterology
 ISSN 1007-9327

• CLINICAL RESEARCH •

Expression of local renin and angiotensinogen mRNA in cirrhotic portal hypertensive patient

Li Zhang, Zhen Yang, Bao-Min Shi, Da-Peng Li, Chong-Yun Fang, Fa-Zu Qiu

Li Zhang, Bao-Min Shi, Department of General Surgery, Shandong Provincial Hospital, Jinan 250021, Shandong Province, China
Zhen Yang, Fa-Zu Qiu, Department of General Surgery, Tongji Hospital, Tongji Medical College, Huazhong Science and Technology University, Wuhan 430030, Hubei Province, China
Da-Peng Li, Department of General Surgery, Shanghai First People' s Hospital, Shanghai, 200080, China
Chong-Yun Fang, Immunology Institute of Tongji Medical College, Huazhong Science and Technology University, Wuhan 430030, Hubei Province, China
Supported by the National Natural Science Foundation of China, No 30170920
Correspondence to: Li Zhang, Department of General Surgery, Shandong Provincial Hospital, Jinan 250021, Shandong Province, China. pzzl@sina.com
Telephone: 0531-5266692
Received: 2002-11-29 **Accepted:** 2003-01-13

Abstract

AIM: To investigate the expression of local renin and angiotensinogen mRNA in cirrhotic portal hypertensive patients.

METHODS: The expression of local renin and angiotensinogen mRNA in the liver, splenic artery and vein of PH patients was detected by RT-PCR analysis.

RESULTS: Expression of local renin mRNA in the liver of control group was (0.19±0.11), significantly lower than that in splenic artery(0.45±0.17)or splenic vein(0.39±0.12) respectively, (P<0.05). Expression of local angiotensinogen mRNA in the liver was (0.64±0.21), significantly higher than that in splenic artery(0.41±0.15) or in splenic vein (0.35±0.18) respectively, (P<0.05). Expression of local renin mRNA in the liver, splenic artery and vein of PH group was (0.78±0.28), (0.86±0.35) and (0.81±0.22) respectively, significantly higher than that in the control group, (P<0.05). Expression of local angiotensinogen mRNA in the liver, splenic artery and vein of PH group was (0.96±0.25), (0.83±0.18) and (0.79±0.23) respectively, significantly higher than that in the control group, (P<0.05). There was no significant difference between the liver, splenic artery and vein in the expression of local renin or local angiotensinogen mRNA in PH group, (P<0.05).

CONCLUSION: In normal subjects the expression of local renin and angiotensinogen mRNA was organ specific, but with increase of the expression of LRAS, the organ-specificity became lost in cirrhotic patients. LRAS may contribute to increased resistance of portal vein with liver and formation of splanchnic vasculopathy.

Zhang L, Yang Z, Shi BM, Li DP, Fang CY, Qiu FZ. Expression of local renin and angiotensinogen mRNA in cirrhotic portal hypertensive patient. *World J Gastroenterol* 2003; 9(7): 1584-1588
http://www.wjgnet.com/1007-9327/9/1584.asp

INTRODUCTION

The initial clues to the presence of an extrarenal or tissue RAS were suggested in the studies of hypertension. Biochemical and histologic evidences have been established for the existence of a tissue-based RAS within a variety of tissues such as blood vessels, liver, kidney, spleen. Many researchers documented that this RAS system was functionally independent of the endocrine system[1-3] and called tissue or local RAS (LRAS). Its activition includes both short and long-term regulatory roles in cardiovascular homeostasis and secondary structural changes, instead of short-term regulatory profile for endocrine RAS. Locally generated AngII plays a significant role not only in controlling the growth of vascular smooth muscle cells (VSMC), hepatocytes and hepatic satellite cells (HSC was one of the most important cells in liver fibrosis[4-6]), but also in regulating local vascular tone including hepatic microcirculation. Hyperdynamic circulation and splanchnic vasculopathy were the common pathological process and changes in cirrhotic portal hypertension[7-9], vascular and hepatic RAS may have great contribution to it. Through detection of expression of the two components of LRAS, the relationship between local renin and angiotensinogen and cirrhotic portal hypertensions was investigated.

MATERIALS AND METHODS

Materials

The liver tissues and a section of splenic artery and vein were obtained during the operation of esophagogastric devascularization and splenectomy in 20 cirrhotic portal hypertensive patients. The same samples were obtained during splenectomy and partial hepatectomy in 24 controls.

13 male and 7 female patients were included in this study with mean age of 49±21, mild or severe gastroesophageal varices and splenomagely were found in all patients.

16 male and 8 female subjects with mean age of 39±17 served as control, 12 of them underwent partial hepatectomy for hepatic trauma and 12 underwent splenectomy for splenic injury. Those with hepatitis or hypertension were excluded.

A portion of the resected tissues was routinely fixed with 10 % formalin and embedded in paraffin and cut into sections, another portion of tissues was stored in liquid nitrogens at -80 ℃ for use.

Methods

Immunohistochemical analysis To investigate splanchnic vascular changes in these patients, we took the splenic veins by using monoclonal anti-vascular smooth muscle cell α-cm-actin antibody, PCNA, and the splenic veins were stained with HE. Immunohistochemical analysis was performed according to routine methods as suggested by the manufacturer.

Preparation of specimens for electron microscopic observation Fresh vascular tissues were made into cubes of 1 mm^3 and prefixed for 2 h in 2.5 % glutaraldehyde, and then postfixed at 4 ℃ for 2 h in 1 % osmic acid. Alcohol of increasing concentrations and acetone were used for dehydration. The specimens were then embedded in epoxy resin EPON 812 and cut into ultrathin sections. Plumbum-double-staining was used to prepare the samples for ultrastructural observation under transmission electron

microscope (Opton EM 10C Model).

Reverse-transcription polymerse chain reaction (RT-PCR) Messenger RNA (mRNA) levels of local renin and angiotensinogen were assessed by RT-PCR analysis using β-actin as the house keeping gene. Total RNA was prepared from frozen tissues of the liver, splenic artery and vein. Diluted complementary DNA was cloned in a total volume of 50 μl containing DEPC 31.5 μl, buffer solution 5 μl, dNTP 4 μl, 2.5 mmol/l $mgcl_2$ 3 μl, primers 20 μmol*4 μl, cDNA 2.5 μl, and TAG 0.25 μl. The PCR conditions were at 94 ℃ for 4 min followed by 35 cycles at 90 ℃ for 30 sec, at 54 ℃ for 30 sec, and at 72 ℃ for 1 min. Total RNA was also analyzed for β-actin transcript expression and PCR for 28 cycles for β-actin.

Table 1 Primer sequences

MRNA		Sequence	Size of products
Renin	sense	5'-TCT CAG CCA GGA CAT CAT CA-3'	288bp
	antisense	5'-AGT GGA AAT TCC CTT CGT AA-3'	
Angiotensinogen			256bp
	sense	5'- TGT TGC TGC TGA GAA GAT TG-3'	
	antisense	5'-CCG AGA AGT TGT CCT GGA TG –3'	

RT-PCR products were visualized under ultraviolet and analyzed by computer which provided the data for analysis. Study values were normalized as a ratio to the β-actin signal in each sample, and each value was analyzed as a transcriptional index (transcript of the interest mRNA expression in samples of interest/β-actin mRNA expression in samples of interest).

Statistical analysis

P value <0.05 was considered statistically significant, and all variable data were summarized in terms of mean ±SD and analyzed by Student *t* test using SAS software.

RESULTS

Immunohistochemical staining

In these patients, such typical cirrhotic changes as hepatocyte degeneration, necrosis, pseudolobule formation and fibrosis were seen, and splenic vein wall was thickened and VSMC in media tunica was disorderly arranged (Figures 1,2). With α-cm-actin antibody staining method, VSMC could be seen in the intima of splenic vein, suggesting migration of VSMC from media to intima. Hyperplasia of VSMC could be seen in both splenic artery and vein by PCNA staining (Figures 3,4), there wes no obviously positive staining in the control group.

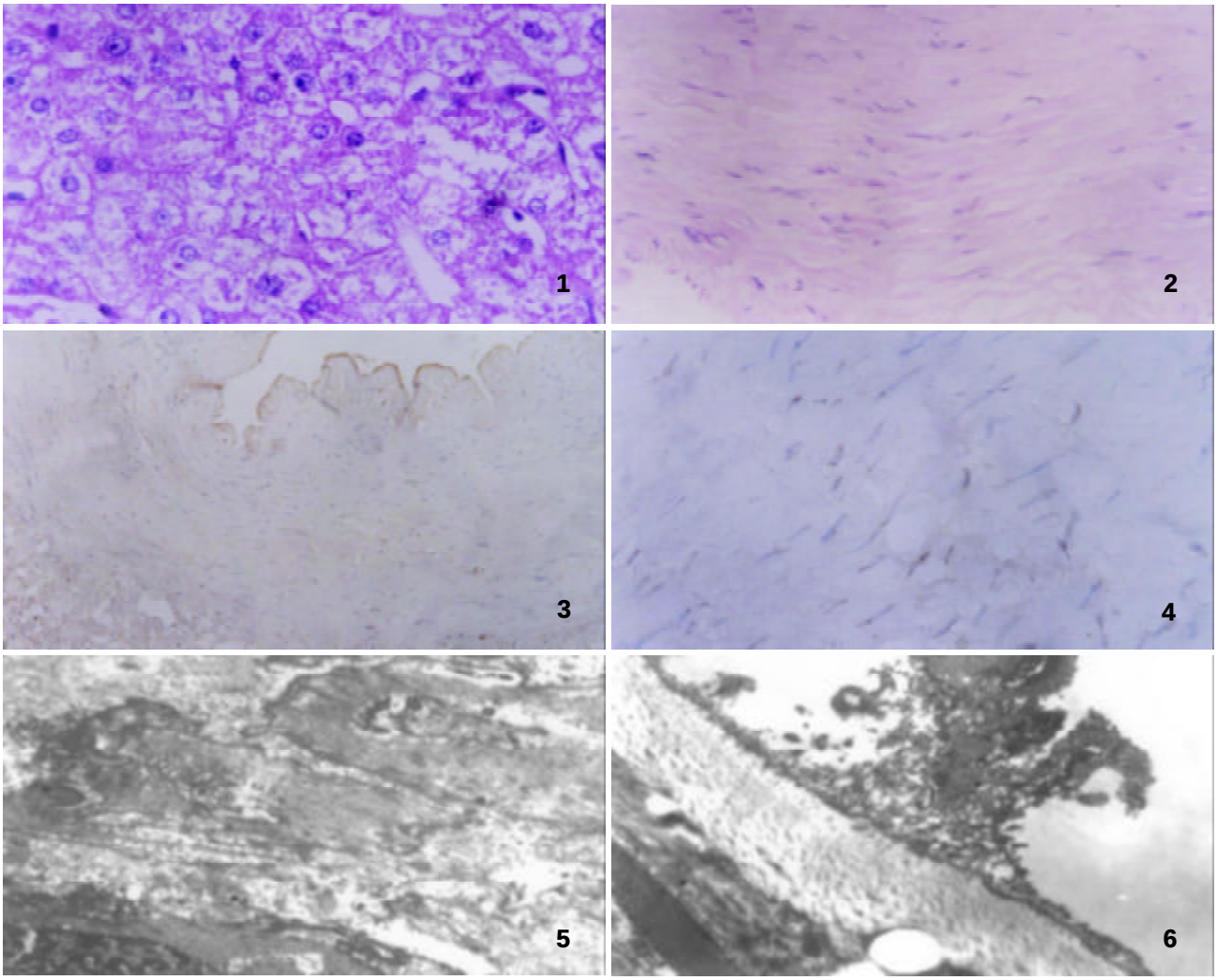

Figure 1 The liver tissue in portal hypertensive patients with HE staining × (400).
Figure 2 Splenic vein in portal hypertensive patients with HE staining method (×400).
Figure 3 Splenic vein in portal hypertensive patients by immunohistochemical staining with α-cm-actin antibody (×400).
Figure 4 Splenic vein in portal hypertensive patients by immunohistochemical staining with PCNA (×400).
Figure 5 Splenic vein of portal hypertensive patients under transmission electron microscope (×4000).
Figure 6 Splenic vein of portal hypertensive patients under transmission electron microscope (×6000).

Electron microscopic observation

In the splenic vein of these patients, endothelium was damaged with adhered thrombus, VSMC of media migrated into the subintima under transmission electron microscopy (Figures 5,6).

RT-PCR analysis

In the control group, the expression of local renin mRNA in the liver was significantly lower than that in the splenic artery or vein, $P<0.05$. Expression of local angiotensinogen mRNA in the liver was significantly higher than that in the splenic artery and vein, $P<0.05$. There was no significant difference in the expression of local renin or angiotensinogen mRNA between splenic artery and vein. ($P>0.05$, Figures 7,8,9).

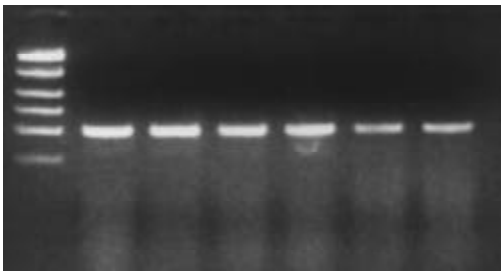

Figure 7 Expression of human β-actin mRNA (Note: from left to right there was PCR marker and lanes 1-6, figures 8,9 were the same).

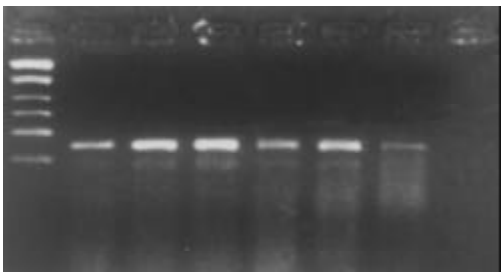

Figure 8 Expression of local renin mRNA in the liver, splenic artery and vein from the controls and cirrhotic portal hypertensive patients. Lanes 1,3,5 were splenic vein, artery and liver from controls, Lanes 2,4,6 were from patients.

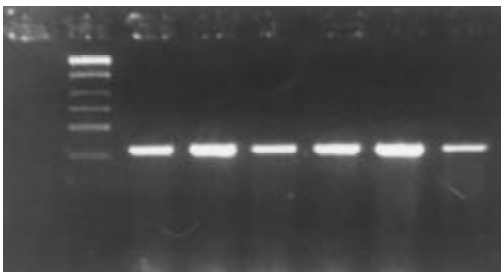

Figure 9 Expression of local angiotensinogen mRNA in the liver, splenic artery and vein from controls and portal hypertensive patients. Lanes 1,2,3 were splenic vein, artery and liver from controls, Lanes 4,5,6 were from portal hypertensive patients.

In cirrhotic portal hypertensive patient group, expression of local renin and angiotensinogen in liver, splenic artery and vein were all significantly higher than those in the controls respectively, $P<0.05$. Expression of local renin and angiotensinogen mRNA in the liver was not significantly different from those in the splenic artery or vein in PH group, $P>0.05$. The concrete data are listed in Table 2.

Table 2 Expression of local renin (Lr) and angiotensinogen (Lan) mRNA in the patient and control groups

	Control group (n=12)			Patient group (n=20)		
	Liver	Splenic artery	Splenic vein	Liver	Splenic artery	Splenic vein
Lr	0.19±0.11[a]	0.45±0.17	0.39±0.12	0.78±0.28[b]	0.86±0.35[b]	0.81±0.22[b]
Lan	0.64±0.21[a]	0.41±0.15	0.35±0.18	0.96±0.25[b]	0.83±0.18[b]	0.79±0.23[b]

The data were expressed as mean ±SD. Lr and Lan mRNA in the patient group versus those in the control group, [b]$P<0.05$. Within the same group, Lr and Lan mRNA in the liver versus those in splenic artery or vein respectively, [a]$P<0.05$.

DISCUSSION

The results demonstrated that expression of hepatic renin and angiotensinogen mRNA in cirrhotic portal hypertensive patients was significantly higher than that of the controls. Therefore the end product of LRAS, the synthesized local AngII increased and exerted a strong effect on hepatic microcirculation via its paracrine pathway.

Firstly, local AngII constricted blood vessels as well as sinusoids leading to increase of intrahepatic portal venous pressure through an increase in intracellular calcium in VSMC. Although VSMC was absent in the hepatic sinusoid, hepatic stellate cells (HSCs) expressed receptors for AngII, could also contract and increase the intrahepatic resistance[10-12].

Secondly, AngII has been shown to induce cell proliferation in various cell types, including hepatocytes and HSCs and was considered as a mediator of hepatic fibrogenesis[3,13]. Local angiotensinogen also induced increase of TGF-β mRNA expression which was an important growth promoting factor for HSC[14,15]. It was demonstrated that AngII could be a mitogenic factor for activated human HSCs through MAPK-dependent pathway[3,16]. Significant relationship was seen between high TGF-β and AngII production and the development of progressive hepatic fibrosis caused by hepatitis C virus[17,18]. AngII was also involved in the development of fibrosis in the heart and kidney through enhancement of TGF-β production[19]. *In vitro* study found that AngII could increase mRNA levels for collagen types I and III, procollagen α (I) and fibronectin in cardiac fibrosis[20]. Therefore it is possible that hepatic RAS plays an important role in the collagen synthesis, hepatic fibrosis and cirrhosis. In this study, the cirrhotic portal hypertension induced hepatic RAS activity which increased and accelerated the cirrhotic process and portal hypertension. By interrupting the vicious cycle, it was possible for medical treatment to prevent further progression of the disease. It has already been confirmed that catoprill could reduce the expression of procollagenI significantly and prevent liver fibrogenesis in a rat model of hepatic fibrosis[21-23].

The experimental data illustrated that expression of local renin and angiotensinogen mRNA in the splenic artery and vein of cirrhotic portal hypertensive patients was significantly higher than that of the controls and suggested that portal hypertension led to activation of LRAS of splenic vessels. The mechanism probably might be as follows: (1) Endothelial injury was caused by splanchnic hyperdynamic circulation and high blood flow shear, and the endothelial cells were the key site of LRAS metabolism[2]. (2) The splenic vessel wall was stretched by the increment of splanchnic blood flow. (3) Influence of other vasoactive substance.

When the expression of LRAS increased in splenic vessel, it could participate in many pathologic processes. Firstly, vascular RAS induced VSMC proliferation and enhanced progression of vascular remodeling. AngII induced hypertrophy, proliferation and migration of VSMC[24-26] with

modulation of expression of C-fos[22], C-jun, C-myc and synthesis of cytokines such as PDGF, b-FGf [23] etc. In this study, changes of VSMC in splenic vein of PH patients could be seen by HE stain, immunohistochemistry and electron microscopy. These suggested that vascular RAS was closely related with the structural alterations of the splenic vein. Response of VSMC to hypertension and injury of blood flow shear included: hypertrophy, proliferation and remodeling. As a result, the vascular RAS played an even more important role than endocrine RAS[27-30]. In addition, the matrix modulation was another key event in remodeling and vasculopathy[7,8]. Other studies reported that vascular RAS modulated the synthesis of vessel matrix via its effect on expression of PDGF and TGF-β etc[31,32]. Therefore, LRAS plays an important role in vascular remodeling and vasculopathy in portal hypertension.

Secondly, LRAS has vasoconstrictive functions. The response of splanchnic blood vessel to AngII decreased in advanced portal hypertension[33], it was due to decrease of AngII receptor on the blood vessel wall or due to the existence of post receptor dysfunction[34,35]. Furthermore, glucagon and other vasoactive substances could influence the effect of AngII on splanchnic vessel[36,37].

Thirdly, the imbalance of vasoconstrictors and vasodilators was existed in portal hypertension. Studies on vasculature showed that vascular RAS could change the response of blood vessel to other vasoactive substances[29] and *vice versa*[38]. For example, in the rabbit model of portal hypertension, the response degree of splanchnic vessel to AngII was improved by CO[33], the presence of ET could induce the local renin activity and increase sythesis of AngIIin rat mesentery artery[39], and LRAS could decrease the degradation of endogenous bradykin[30]. All the changes mentioned above could result in imbalance of vasodilators and vasoconstrictors. In this study, local renin and angiotensinogen mRNA expression in the liver was not significantly different from that in the splenic artery and vein in portal hypertensive patients, suggesting that the loss of expression of organ- specificity of LRAS components might be due to disordered metabolism of vasoactive substances.

In conclusion, increased LRAS activity in the hepatic and splenic vessels is due to cirrhotic portal hypertension, and the synthesis of local AngII increases, which contract the hepatic sinusoid, stimulate hyperplasia of HSC and proliferation of VSMC, and also interfere with the metabolism of other vasoactive substances. All these enhance the degree of cirrhosis and portal hypertension. By interruption of this vicious cycle, medical treatment may be able to improve the hemodynamic disturbance and ameliorate the splanchnic vasculopathy and to offer a new way for preventing the complications of portal hypertension[40].

REFERENCES

1 **Gricndling KK**, Murphy TJ, Alexander RW. Molecular biology of the renin-angiotensin system. *Circulation* 1993; **87**: 1816-1828
2 **Kelly MP**, Kahr O, Aalkjaer C, Cumin F, Samani NJ. Tissue expression of components of the renin-angiotensin system in experimental post-infarction heart failure in rats: effects of heart failure and angiotensin-converting enzyme inhibitor treatment. *Clin Sci* 1997; **92**: 455-465
3 **Bataller R**, Gines P, Nicolas JM, Gorbig MN, Garcia-Ramallo E, Gasull X, Bosch J, Arroyo V, Rodes J. AngiotensinII induces contraction and proliferation of human hepatic stellate cells. *Gastroenterology* 2000; **118**: 1149-1156
4 **Yao XX,** Tang YW, Yao DM, Xiu HM. Effects of Yigan Decoction on proliferation and apoptosis of hepatic stellate cells. *World J Gastroenterol* 2002; **8**: 511-514
5 **Liu XJ**, Yang L, Mao YQ, Wang Q, Huang MH, Wang YP, Wu HB. Effects of the tyrosine protein kinase inhibitor genistein on the proliferation, activation of cultured rat hepatic stellate cells. *World J Gastroenterol* 2002; **8**: 739-745
6 **Du WD,** Zhang YE, Zhai WR, Zhou XM. Dynamic changes of type I, III and IV collagen synthesis and distribution of collagen-producing cells in carbon tetracholoride-induced rat liver fibrosis. *World J Gastroenterol* 1999; **5**: 397-403
7 **Yang Z**, Zhang L, Li D, Qiu F. Pathological morphology alteration of the splanchnic vascular wall in portal hypertensive patients. *Chin Med J* 2002; **115**: 559-562
8 **Yang Z,** Liu RZ, Yang RG, Qui FZ. Pathology of endothelium, extracellular matrix and smooth muscle in gastric coronary vein of cirrhotic patients. *Zhonghua Waike Zazhi* 1996; **34**: 138-140
9 **Shi BM**, Yang Z. Vascular lesion and its mechanisms in spleen under statement of portal hypertension. *Zhonghua Yixue Zazhi* 2000; **80**: 196-198
10 **Bataller R**, Nicolas JM, Gines P, Esteve A, Nieves GM, Garcia RE, Pinzani M, Ros J,Jimenez W,Thomas AP,Arroyo V, Rodes J. Arginine vasopressin induces contraction and stimulates growth of cultured human hepatic stellate cells. *Gastroenterology* 1997; **113**: 615-624
11 **Pinzani M**, Failli P, Ruocco C, Casini A, Milani S, Baldi E, Giotti A, Gentilini P. Fat-storing cells as liver-specific pericytes. Spatial dynamics of agonist-stimulated intracellular calcium transients. *J Clin Invest* 1992; **90**: 642-646
12 **Don R**. The celluar pathogenesis of portal hypertension: stellate cell contractility, endothelin, and nitric oxide. *Hepatology* 1997; **25**: 2-5
13 **Wei HS**, Lu HM, Li DG, Zhan YT, Wang ZR, Huang X, Cheng JL, Xu QF. The regulatory role of AT1 receptor on activated HSCs in hepatic fibrogenesis: effects of RAS inhibitors on hepatic fibrosis induced by CCL(4). *World J Gastroenterol* 2000; **6**: 824-828
14 **Powell EE**, Edwards CJ, Hay JL, Andrew DC, Darrell HC, Claudia S, David MP, Julie RJ. Host genetic factors influence disease progression in chronic hepatitis C. *Hepatology* 2000; **31**: 828-833
15 **Dai WJ**, Jiang HC. Advances in gene therapy of liver cirrhosis: a review. *World J Gastroenterol* 2001; **7**: 1-8
16 **Marra F**, Grandaliano G, Valente AJ, Abboud HE. Thrombin stimulates proliferation of liver fat-storing cells and expression of monocyte chemotactic protein-1:potential role in liver injury. *Hepatology* 1995; **22**: 780-787
17 **Arved WS**, Johann F K, Christian P K. Effect of Losartan, an angiotensin II receptor antagonist, on portal pressure in cirrhosis. *Hepatology* 1999; **29**: 334-339
18 **Powell EE**, Edwards-Smith CJ, Hay JL, Clouston AD, Crawford DH, Shorthouse C, Purdie DM, Jonsson JR. Host genetic factors influence disease progression in chronic hepatitis C. *Hepatology* 2000; **31**: 828-833
19 **Lee LK**, Meyer TW, Pollock AS, Lovett DH. Endothelial cell injury intiates glomerular sclerosis in the rat remnant kidney. *J Clin Invest* 1995; **96**: 953-964
20 **Lijnen P**, Petrov V. Renin-angiotensin system, hypertrophy and gene expression in cardiac myocytes. *J Mol Cell Cardiol* 1999; **31**: 949-970
21 **Julie RJ**, Andrew DC, Yuichi A, Livia IK, Murray JH, Michael DA, David MP, Elizabeth EP. Angiotensin-converting enzyme inhibition attenuates the progression of rat hepatic fibrosis. *Gastroenterology* 2001; **121**: 148-155
22 **Wei HS**, Li DG, Lu HM, Zhan YT, Wang ZR, Huang X, Zhang J, Cheng JL, Xu QF. Effects of AT1 receptor antagonist, losartan, on rat hepatic fibrosis induced by CCL(4). *World J Gastroenterol* 2000; **6**: 540-545
23 **Yang YY**, Lin HC, Huang YT, Lee TY, Hou MC, Lee FY, Liu RS, Chang FY, Lee SD. Effect of 1-week losartan administration on bile duct-ligated cirrhotic rats with portal hypertension. *J Hepatol* 2002; **36**: 600-606
24 **Dzau VJ**. Local expression and pathophysiological role of renin-angiotensin in the blood vessels and heart. *Basic Res Cardiol* 1993; **88** (Suppl 1): 1-14
25 **Naftilan AJ**, Pratt RE, Dzau VJ. Induction of platelet-derived growth factor A-chain and c-myc gene expressions by angiotensin II in cultured rat vascular smooth muscle cells. *J Clin Invest* 1989; **83**: 1419-1423
26 **Ferns GA**, Raines EW, Sprugel KH, Motani AS, Reidy MA, Ross

R. Inhibition of neointimal smooth muscle accumulation after angioplasty by an antibody to PDGF. *Science* 1991; **253**: 1129-1132

27 **Taubman MB**, Berk BC, Izumo S, Tsuda T, Alexander RW, Nadal GB. Angiotensin II induces c-fos mRNA in aortic smooth muscle. Role of Ca^{2+} mobilization and protein kinase C activation. *J Biol Chem* 1989; **264**: 526-530

28 **Hiroshi I,** Masashi M, Richard EP, Gary HG, Victor JD. Multiple autocrine growth factors modulate vascular smooth muscle cell growth response to angiotensin II. *J Clin Invest* 1993; **91**: 2268-2274

29 **Holtz J**, Goetz RM. Vascular renin-angiotensin-system, endothelial function and atherosclerosis. *Basic Res cardiol* 1994; **89** (Suppl 1): 71-86

30 **Falkenhahn M**, Gohlke P, Paul M, Stoll M, Unger T. The renin-angiotensin system in the heart and vascular wall: new therapeutic aspects. *J Cardiovasc Pharmacol* 1994; **24** (Suppl 2):S6-13

31 **Hahn AW**, Resink TJ, Kern F, Buhler FR. Peptide vasoconstrictors, vessel structure,and vascular smooth-muscle proliferation. *J Cardiovasc Pharmacol* 1993; **22**(Suppl): S37-43

32 **Kato H**, Suzuki H, Tajima S, Ogata Y, Tominaga T, Sato A, Saruta T. Angiotensin IIstimulates collagen synthesis in cultured vascular smooth muscle cells. *J Hypertens* 1991; **9**: 17-22

33 **Sitzmann JV,** Li SS, Wu YP, Groszmann R, Bulkley GB. Decreased mesenteric vascular response to angiotensin II in portal hypertension. *J Surg Res* 1990; **48**: 341-344

34 **James VS**, Yuping Wu, Greti A, Paul AC, R Cartland B. Loss of angiotensin-II receptors in portal hypertensive rabbits. *Hepatology* 1995; **22**: 559-564

35 **Castro A**, Jimenez W, Claria J, Ros J, Martinez JM, Bosch M, Arroyo V, Piulats J, Rivera F, Rodes J. Impaired responsiveness to angiotensin II in experimental cirrhosis: role of nitric oxide. *Hepatology* 1993; **18**: 367-372

36 **Sitzmann JV**, Bulkley GB, Mitchell MC, Campbell K. Role of prostacyclin in the splanchnic hyperemia contributing to portal hypertension. *Ann Syrg* 1989; **209**: 322-327

37 **Benoit JN**, Barrowman JA, Harper SL, Kvietys PR, Granger DN. Role of humoral factors in the intestinal hyperemia associated with chronic portal hypertension. *Am J Physiol* 1984; **247**: G486-493

38 **Moller S**, Bendtsen F, Henriksen JH. Splanchnic and systemic hemodynamic derangement in decompensated cirrhosis. *Can J Gastroenterol* 2001; **15**: 94-106

39 **Rakugi H**, Tabuchi Y, Nakamaru M, Nagano M, Higashimori K, Mikami H, Ogihara T. Endothelin activates the vascular renin-angiotensin system in rat mesenteric arteries. *Biochem Int* 1990; **21**: 867-872

40 **Hulagu S**, Senturk O, Erdem A, Ozgur O, Celebi A, Karakaya AT, Seyhogullari M, Demirci A. Effects of losartan, somatostatin and losartan plus somatostatin on portal hemodynamics and renal functions in cirrhosis. *Hepatogastroenterology* 2002; **49**: 783-787

Edited by Wu XN and Zhu LH

P.O.Box 2345, Beijing 100023,China
Fax: +86-10-85381893
E-mail: wjg@wjgnet.com www.wjgnet.com

World J Gastroenterol 2003;9(7):1589-1593
World Journal of Gastroenterology
 ISSN 1007-9327

• BRIEF REPORTS •

Biliary carcinoembryonic antigen levels in diagnosis of occult hepatic metastases from colorectal carcinoma

Jaques Waisberg, Rogério T. Palma, Luís Contim Neto, Lourdes C. Martins, Maurício S. L. Oliveira, Carlos A. Nagashima, Antonio C. Godoy, Fabio S. Goffi

Jaques Waisberg, Rogério T. Palma, Luí s Contim Neto, Lourdes C. Martins, Maurí cio S. L. Oliveira, Antonio C. Godoy, Fabio S. Goffi, Surgical Gastroenterology Department, Hospital do Servidor Público Estadual, São Paulo, Brazil
Carlos A. Nagashima, Clinical Laboratory Department, Hospital do Servidor Público Estadual, São Paulo, Brazil
Correspondence to: Jaques Waisberg, M.D., Rua das Figueiras, 550 apto. 134 Bairro Jardim, 09080-300 Santo André - São Paulo - Brazil.
jaqueswaisberg@uol.com.br
Telephone: +55-11-44362461 **Fax:** +55-11-44362160
Received: 2003-02-26 **Accepted:** 2003-03-16

Abstract

AIM: To prospectively explore the role of carcinoembryonic antigen (CEA) in gallbladder bile in patients with colorectal carcinoma and the morphological and clinical features of neoplasia and the occurrence of hepatic metastases.

METHODS: CEA levels in the gallbladder and peripheral blood were studied in 44 patients with colorectal carcinoma and 10 patients with uncomplicated cholelithiasis. CEA samples were collected from the gallbladder bile and peripheral blood during the operation, immediately before extirpating the colorectal neoplasia or cholecystectomy. Values of up to 5 ng/ml were considered normal for bile and serum CEA.

RESULTS: In the 44 patients with colorectal carcinoma who underwent operation with curative intent, the average level of serum CEA was 8.5 ng/ml (range: 0.1 to 111.0 ng/ml) and for bile CEA it was 74.5 ng/ml (range: 0.2 to 571.0 ng/ml). In the patients with uncomplicated cholelithiasis who underwent cholecystectomy, the average level of serum CEA was 1.9 ng/ml (range: 1.0 to 3.5 ng/ml) and for bile CEA it was 1.2 ng/ml (range: 0.3 to 2.9 ng/ml). The average duration of follow-up time was 16.5 months (range: 6 to 48 months). Four patients who underwent extirpation of the colorectal carcinoma without evidence of hepatic metastasis and with an average bile CEA value of 213.2 ng/ml presented hepatic metastases between three and seventeen months after removal of the primary colorectal neoplasia. Three of them successfully underwent extirpation of the hepatic lesions.

CONCLUSION: High CEA levels in gallbladders of patients undergoing curative operation for colorectal carcinoma may indicate the presence of hepatic metastases. Such patients must be followed up with special attention to the diagnosis of such lesions.

Waisberg J, Palma RT, Neto LC, Martins LC, Oliveira MSL, Nagashima CA, Godoy AC, Goffi FS. Biliary carcinoembryonic antigen levels in diagnosis of occult hepatic metastases from colorectal carcinoma. *World J Gastroenterol* 2003; 9(7): 1589-1593
http://www.wjgnet.com/1007-9327/9/1589.asp

INTRODUCTION

Colorectal carcinoma is the second most common cancer type in the Western world and the liver is the organ most affected by its distant metastases[1,2]. At the time when primary tumor is extirpated, hepatic metastases are encountered in 20 to 25 % of the patients. Approximately half of the patients who have had colorectal lesions extirpated in an apparently curative manner will develop hepatic metastases postoperatively[1,3,4].

The majority of relapse monitoring programs for operated colorectal carcinoma include determinations at regular intervals of the serum concentration of carcinoembryonic antigen (CEA) and hepatic imaging via abdominal ultrasonography, tomography and/or magnetic resonance[3,5]. Nonetheless, even with such investigations, around 10 to 30 % of hepatic metastases will remain undiagnosed[4]. When lesions are present in the liver, extirpation is the treatment of choice. However, this is only possible in 20 % of such patients and only 25 % of these will achieve survival of more than 5 years[1,3,4].

In 1965, Gold and Freedman[6] described the presence of CEA in extracts from malignant tumors and fetal intestinal tissue. Today, assaying of blood CEA is utilized preoperatively and postoperatively among colorectal carcinoma patients for the detection of disease relapse[7-10].

In 1989, Yeatman *et al*[11] suggested that CEA concentration in bile could constitute a marker for detecting hepatic metastases at an earlier stage. Their hypothesis was based on the observation that CEA derived from hepatic metastases could be excreted both in bile and in blood. Since the bile volume is less than the plasma volume, rises in the detectable CEA concentration occur earlier in the gallbladder than in peripheral blood[11-13]. Yeatman and Paul *et al*[11-14] found elevated CEA concentrations in bile among patients with colorectal carcinoma and proven hepatic metastases and among patients who underwent curative extirpation without any hepatic involvement could be detected via imaging methods.

The role of CEA level in gallbladder bile remains controversial with regard to its contribution towards early detection of hepatic metastases in patients undergoing curative operation for colorectal carcinoma[15-23].

The aim of this study was to prospectively analyze the results of CEA determinations in peripheral blood and gallbladder bile among a series of patients treated by curative operation for colorectal carcinoma, relating them to morphological features of the neoplasia and hepatic relapse.

MATERIALS AND METHODS

Patients

Between 1998 and 2001, 44 patients experienced extirpation of colorectal carcinoma with curative intent. The term curative was utilized to designate an absence of macroscopic disease at the termination of the surgical procedure, verified in the report on the anatomopathological examination of the extirpated neoplastic lesions and associated structures. Samples of gallbladder bile and peripheral blood were collected during the operation, immediately before the start of excision of the neoplasia, for all patients.

This investigation was made in accordance with the ethical standards accepted by the Helsinki Declaration of the World Medical Association, adopted in 1964 and amended in 1996. The patients were aware of the study protocol and signed a statement of free and informed consent upon entering the present study.

The following were considered to be inclusion criteria: achievement of curative operation, absence of distant metastases and presence of adenocarcinoma of the large intestine confirmed by means of histopathological study of the extirpated lesion. Patients submitted to operations that were evaluated as non-curative were not included in this sample.

The clinical and morphological data were obtained by consulting the hospital records of the patients included in the study, or by interviewing the patients or their relatives at return outpatient visits.

Thirty-nine patients (88.6 %) were white, three were oriental (6.8 %) and two were black (4.5 %). Twenty-one patients (47.7 %) were male and 23 (52.3 %) were female. The average age was 63±14.7 years (range: 29 to 90 years). All patients had their preoperative diagnosis of colorectal carcinoma confirmed by biopsy specimens obtained via colonoscopy. For this, the thin sections were stained using the hematoxylin-eosin (HE) method and analyzed by a pathologist.

Neoplasia was considered to be Dukes A when it did not reach the external muscle tunica of the intestinal wall, Dukes B when it extended throughout the wall and also reached the adventitious adipose tissue, and Dukes C when lymph nodes were compromised, independent of the depth of parietal invasion.

Preoperative investigation of the presence of an extra-intestinal lesion was made via abdominal ultrasonography, abdominal tomography and chest radiography, and did not reveal metastases in any of these patients.

In ten patients with uncomplicated cholecystolithiasis who underwent elective cholecystectomy via laparotomy, blood and gallbladder bile samples were collected under the same conditions as for the patients with colorectal carcinoma. These served to furnish CEA levels in gallbladder bile for comparison purposes. All these patients were white, of whom seven (70 %) were female and three (30 %) were male. The average age was 50.8±20.1 years (range: 23 to 74 years old).

Sample collection

Blood and bile sample collection was performed during the operation. After making an inventory of the abdominal cavity, 5 ml samples of gallbladder bile were obtained via puncture of the fundic region of the gallbladder using a caliber 23 needle coupled to a plastic syringe of capacity 10 ml. Then, using another syringe of capacity 20 ml, the remainder gallbladder bile was evacuated, followed by occlusion of the location of the puncture by a pouch suture using thin atraumatic absorbable thread made of polyglycolic acid. At the start of the operation, prior to removing the colorectal neoplasia, 5 ml blood samples was collected via peripheral venous puncture in the non-dominant upper limb, divested of intravenous infusion of any solution, using a caliber 37 needle coupled to a plastic syringe of capacity 10 ml.

CEA assay

The serum and bile samples were stored in a freezer at -70 ℃ until the CEA analyses were done. A solid-phase fluoroimmunometric assay system was utilized (Delfia CEA Kit, Pharmacia, Turkü, Finland) for assaying the serum and bile CEA. The precision of the method was estimated via the coefficient of variation (c.v.), with intra-assay c.v. of 3.4 % and 2.4 % for low and high values, respectively, and inter-assay c.v. of 4.6 % and 2.8 % for the same parameters. The sensitivity of this CEA assay was 0.2 ng/ml and the upper limit on the recognition curve was 500 ng/ml. Whenever this value was exceeded, dilutions were needed for adjustment of the reactions.

The limit of normality adopted for bile CEA was 5 ng/ml which was based on the analysis of the values obtained in the group of patients who underwent cholecystectomy.

Statistical analysis

Considering the nature of the samples, non-parametric statistical tests were utilized in the evaluation of the results. Quantitative variables were represented by absolute frequency (*n*) and relative frequency (%). The statistical models utilized were arithmetic mean, standard deviation, Mann-Whitney test, Wilcoxon test and Kruskal-Wallis test. The normality of the data were tested using the Kolmogorov-Smirnov test and the homogeneity of the variance was verified using the Levene test.

In all tests, the level for the rejection of the null hypothesis was set at 0.05 % (significance level of 95 %), in accordance with the current standards in biological studies.

RESULTS

In the group of patients with colorectal carcinoma, there was a single lesion in 43 patients (97.7 %) and multiple lesions in one of them (2.3 %). The neoplasia was located in the rectum in 24 patients (54.5 %), in the cecum-ascending colon in 6 (13.7 %), in the transverse colon in 6 (13.6 %), in the sigmoid in 4 (9.1 %), in the descending colon in 2 (4.5 %), in the left flexure in 1 (2.3 %), and the lesion involved the cecum and rectum simultaneously in 1 patient (2.3 %). With regard to the degree of histopathological differentiation of the neoplasia, all the lesions were considered to be moderately differentiated. All the patients operated for colorectal carcinoma evolved without notable intercurrences and were discharged from hospital. The average duration of follow-up for the patients was 16.5 months (range: 6 to 48 months).

Concerning the Dukes classification, 2 patients (4.6 %) were classified as class A, 21 (47.7 %) as class B, and 21 (47.7 %) as class C.

Thirteen patients (29.5 %) classified as Dukes C were submitted to adjuvant chemotherapy using intravenous 5-fluorouracil over seven sessions.

In the patients with colorectal carcinoma, the average value was 8.5±18.7 ng/ml (range: 0.1 to 111.0 ng/ml) for serum CEA, and was 74.5±130.3 ng/ml for bile CEA (0.2 to 571 ng/ml) (Table 1).

In the group of patients with uncomplicated cholelithiasis, the average value was 1.94±0.8 ng/ml (range: 1.0 to 3.5 ng/ml) for serum CEA, and was 1.24±0.9 ng/ml for bile CEA (range: 0.3 to 2.9 ng/ml) (Table 2). The patients in this group were discharged from hospital with uneventful recovery.

Seventeen patients (38.6 %) presented a serum CEA value of more than 5.0 ng/ml, while 27 patients (61.4 %) exhibited a blood CEA level less than or equal to 5.0 ng/ml. With regard to bile CEA, 29 patients (65.9 %) exhibited values of more than 5.0 ng/ml, whereas 15 patients (34.1 %) had determinations of less than or equal to 5.0 ng/ml. In 35 patients (79.5 %), the bile CEA level was greater than the serum CEA level, and in nine patients (20.5 %), the serum CEA level was higher than the bile CEA level. Thirteen patients (29.5 %) simultaneously presented serum CEA and bile CEA values of more than 5 ng/ml. In 11 patients (25.0 %), the determinations obtained for serum CEA and bile CEA were less than or equal to 5.0 ng/ml.

The bile CEA values in the patients operated for colorectal carcinoma were significantly greater than those determined in the blood ($P<0.0001$) (Table 1). On the other hand, in the group of patients who underwent cholecystectomy, the bile CEA

values were significantly less than those of serum CEA (P=0.46) (Table 2). The bile CEA levels in patients with colorectal carcinoma were significantly greater (P<0.0001) than those that underwent cholecystectomy. Comparison of the bile CEA/serum CEA ratios for the colorectal carcinoma and cholecystectomy patients showed significantly greater values in the group with neoplasia of the large intestine than in those with cholecystectomy (P<0.0001) (Table 3).

Table 1 Average values for serum and bile CEA obtained from patients operated for colorectal carcinoma

Variables	Average (ng/ml)	S.D.	Minimum (ng/ml)	Maximum (ng/ml)	*n*
Serum CEA	8.5	18.7	0.1	111.0	44
Bile CEA	74.5	130.26	0.2	571.0	44

Wilcoxon (Z)=-4.614, P<0.0001 (Serum CEA *vs* Bile CEA), Notes: S.D.=standard deviation.

Table 2 Average values for serum and bile CEA obtained from patients operated for uncomplicated cholelithiasis

Variables	Average (ng/ml)	S.D.	Minimum (ng/ml)	Maximum (ng/ml)	*n*
Serum CEA	1.9	0.8	1.0 ng/ml	3.5 ng/ml	10
Bile CEA	1.2	0.9	0.3 ng/ml	2.9 ng/ml	10

Wilcoxon (Z)=-1.992, P<0.46 (Serum CEA *vs* Bile CEA), Notes: S.D.=standard deviation.

Table 3 Average values of the bile CEA/serum CEA ratio obtained from patients operated for colorectal carcinoma and cholelithiasis

Group	Variables	Average	S.D.	Minimum	Maximum	*n*
Colorectal carcinoma	Bile CEA/serum CEA	22.1	48.5	0.02	287.0	44
Cholelithiasis	Bile CEA/serum CEA	0.6	0.3	0.3	1.9	10

Mann-Whitney (U)=63.5, P<0.0001 (colorectal carcinoma group *vs* cholelithiasis group), Notes: S.D.=standard deviation.

In this study, there was no significant relationship between Dukes classification and serum CEA values (P=0.60) or bile CEA values (P=0.78). Besides, the bile and serum CEA values showed a non-significant relationship with the localization of the neoplastic lesions in the right colon, left colon or rectum (P=0.93 and P=0.53, respectively).

Four patients (9.1 %) with colorectal carcinoma showing elevated bile CEA levels who were operated on with curative intent presented evolution to hepatic metastases. They were initially diagnosed due to a rise in postoperative serum CEA levels, with an average of 8.6 ng/ml (range: 0.3 to 22.8 ng/ml). Only two of them presented increased serum CEA levels at the time of operation, although all four presented elevated bile CEA levels, with an average of 228.4 ng/ml (range: 6.6 to 571 ng/ml). They corresponded to 13.8 % of the 29 patients with elevated bile CEA. In these four patients, hepatic metastases developed on average around 9.7 months (range: 3 to 17 months) after removal of the primary colorectal lesion. Three of them were staged as Dukes C and one as Dukes B (Table 4). With the exception of the single Dukes B patient, who presented disease relapse with hepatic metastases disseminated in both lobes, the other three patients were submitted to hepatectomy for the removal of their metastases. Two of them died after removal of the hepatic lesions: one around nine months afterwards and the other 21 months afterwards. Although no necropsy was performed on these patients, there was no evidence of neoplasia recurrence up to the time of death. The third of these patients is still alive, without active disease, around eight months after extirpation of the hepatic metastases. The remaining 40 patients are alive, without signs of disease relapse, six to 48 months after removal of the primary colorectal lesion.

Table 4 Location of the lesion, Dukes staging and serum and bile CEA values, obtained from the patients operated for colorectal carcinoma with hepatic metastases during the follow-up

Case	Location	Dukes	Serum CEA (ng/ml)	Bile CEA (ng/ml)
1	Transverse colon	B	22.8	510.0
2	Rectum	C	2.1	292.0
3	Rectum	C	9.4	44.1
4	Sigmoid	C	6.6	6.6
Average			10.2	213.2

DISCUSSION

An ability to predict the appearance of hepatic metastases in patients operated on for colorectal carcinoma with curative intent could influence the use of adjuvant chemotherapy and intensify the follow-up of patients with indications for surgical treatment for lesions that could be extirpated[18,20,24-26].

Determination of bile CEA levels may be a potentially sensitive method for diagnosing hepatic metastases of colorectal carcinoma, since hepatic lesions smaller than 1 cm^3 are able to produce elevations of CEA concentrations in bile[11,16,22,26].

Huang and Tang[17] studied serum and bile CEA obtained by drainage using a preoperative duodenal tube in patients with benign affections and colorectal carcinoma, with and without hepatic metastases. These authors verified that the difference between bile CEA values in patients operated upon for colorectal carcinoma with and without hepatic metastases was significant, thus showing that the bile CEA level assisted in confirming the existence of hepatic lesions. Novell and Moura *et al*[19, 22] studied the levels of serum and bile CEA in patients with colorectal carcinoma and suggested that a determination of the bile CEA level might be useful in diagnosing concealed hepatic metastases. In the four patients of the present study who evolved with hepatic metastases, and in 29 other patients (65.9 %) who did not present metastases, the bile CEA values were also significantly greater than those for serum CEA. The average follow-up duration of 16.5 months was not yet sufficient for a conclusive evaluation of bile CEA determination as a predictive parameter for the appearance of hepatic metastases in these patients. An average follow-up for at least 60 months would increase the possibility of finding hepatic relapse of the disease and would furnish more consistent support for an assessment of the usefulness of bile CEA.

In patients with hepatic metastases of colorectal carcinoma, the concentrating capacity of the gallbladder has been singled out as the mechanism responsible for the elevated bile CEA levels in comparison with serum CEA levels[18,27-29]. The finding of elevated bile CEA values in the absence of hepatic metastases may also be credited to the fact that bile CEA is derived not only from the hepatic metastases but also from the primary tumor[29]. This situation is thought to contribute to the existence of a direct relationship between serum and bile CEA levels[13]. That is, when serum CEA levels are significantly elevated, bile CEA levels will also be, and consequently the serum CEA levels produced by the primary tumor may elevate the bile levels, even in the absence of hepatic metastases. These events could justify the findings in the present sample, in which 25 patients (86.2 %) with elevated bile CEA levels had not

presented hepatic metastases at the time of last follow-up consultation. Nonetheless, other studies[13,14,17,30] have suggested that increased CEA levels in bile in the presence of hepatic metastases are exclusively produced by neoformation in the liver, without originating in the portal circulation, indicating that patients with elevated bile CEA have silent hepatic metastatic disease. Paul *et al*[14] suggested that the bile CEA predicted hepatic disease only when collected after the removal of the primary tumor, which would avoid any significant contribution of serum CEA to bile CEA levels. It remains to be proven whether the finding of elevated serum and bile CEA levels during the extirpation of colorectal carcinoma, as occurred in 27 patients (61.4 %) of this study would constitute a selecting criterion for monitoring bile CEA levels after operation.

Yeatman *et al*[11] found elevated bile CEA levels in 70 % of their patients with colorectal carcinoma extirpated in a curative manner that had normal intraoperative hepatic ultrasonography. Over the average follow-up of 30 months for this group of patients, 13 % of them presented hepatic metastases. The result was close to that found in the present study, which observed that 9.1 % of patients had hepatic metastases over an average follow-up of 16.5 months. Li Destri *et al*[23] found a diagnostic accuracy for bile CEA of 91 % among patients operated for colorectal carcinoma with or without hepatic metastases, and 89.5 % among patients who evolved with hepatic metastases. Ishida *et al*[21] analyzed the relationship of CEA values in gallbladder bile collected during operation and in peripheral blood, with the appearance of metachronic hepatic metastases of colorectal carcinoma. In 49 patients without evidence of hepatic metastases at the time of operation, the elevated levels of bile CEA were predictive of the appearance of metachronic hepatic metastases with a 75 % sensitivity rate, 85 % specificity and 84 % accuracy. In another study, Ishida *et al*[15] showed that patients with elevated bile CEA or elevated bile CEA / serum CEA ratio could be candidates for hepatic relapse.

In the present study, four patients (9.1 %) operated for colorectal carcinoma with curative intent developed hepatic metastases after removal of the neoplastic lesion. Since the average follow-up duration for the patients was 16.5 months, it was possible that the number of patients affected by hepatic metastases and elevated bile CEA increased with the prolongation of the follow-up. This could make the determination of bile CEA levels a predictive parameter for the development of hepatic lesions.

However, other studies did not share the idea that bile CEA had a predictive value in relation to the development of hepatic metastases. Dorrance *et al*[20] determined serum and bile CEA levels in 26 patients submitted to curative surgery and followed up for an average of 63.5 months. Twelve patients (46.1 %) survived without relapse and 14 (53.8 %) died because of recurrence of neoplasia. The average value of serum CEA in the group free of disease was significantly greater than that in the group with relapse. The accuracy of serum CEA as a predictive indicator for concealed hepatic metastases was 77 %, in comparison with 72 % for bile CEA, without significant difference. The authors concluded that determination of intraoperative bile CEA levels was not more accurate than serum CEA as a predictive indicator for the occurrence of metastases among patients undergoing potentially curative surgery for colorectal carcinoma. Panaguzzi *et al*[16] studied the follow-up of patients operated for colorectal carcinoma without hepatic metastases although with elevated bile CEA levels. They concluded that, although the bile CEA levels were elevated in patients with hepatic metastases, these levels did not represent a predictive parameter for their presence in colorectal carcinoma. Garcia *et al*[18] determined the concentration of bile CEA in 24 patients with colorectal carcinoma, all of them exhibited elevated bile CEA, of whom 21 did not present evidence of hepatic metastases, while three had such lesions in the liver. These authors followed up their patients for an average of 32.3 months. Three of them developed hepatic metastases. The authors stressed that there was no clear relationship between the bile CEA values and the appearance of hepatic metastases, although they recognized that their sample was not large enough for definitive conclusions.

In our sample, nine patients (20.5 %) presented bile CEA values less than the respective values for serum CEA. One possible explanation for this fact is that the liver purification mechanisms for CEA produced by primary colorectal neoplasia might not be saturated and consequently the levels excreted into the bile would be less than into blood.

Bile CEA has apparently emerged as a promising tool for identifying patients with undiagnosed hepatic metastases. In patients with verified recurrence of neoplasia, the sensitivity of CEA determination in bile is greater than that for values found in the blood. Consequently, there could be a broadening of the indication for hepatectomy or radiofrequence ablation[31] due to hepatic metastases. Local or systemic chemotherapy procedures[32] could be introduced earlier, as could radioimmunoguided surgery or also treatments using anti-CEA monoclonal antibodies. To prove the real value of bile CEA for detecting hepatic relapses at an earlier stage, prospective studies with an adequate length of follow-up time, and standardized intervals between extirpation of colorectal neoplastic lesion and withdrawal of the bile samples, are needed.

REFERENCES

1 **Adson MA**. Resection of liver metastases: when is it worthwhile? *World J Surg* 1987; **11**: 511-520
2 **Kievit J**, Bruinvels JD. Detection of recurrence after surgery for colorectal cancer. *Eur J Cancer* 1995; **31A**: 1222-1225
3 **Fantini GA**, DeCosse JJ. Surveillance strategies after resection of carcinoma of the colon and rectum. *Surg Gynecol Obstet* 1990; **171**: 267-273
4 **Finlay IG**, McArdle CS. Occult hepatic metastases in colorectal carcinoma. *Br J Surg* 1986; **73**: 732-735
5 **Stone MD**, Kane R, Bothe A Jr, Jessup JM, Cady B, Steele GD Jr. Intraoperative ultrasound imaging of the liver at the time of colorectal cancer resection. *Arch Surg* 1994; **129**: 431-436
6 **Gold P**, Freedman SO. Demonstration of tumor-specific antigens in human colonic carcinomata by immunological tolerance and absortion techniques. *J Exp Med* 1965; **121**: 439-462
7 **Fletcher RH**. Carcinoembryonic antigen. *Ann Intern Med* 1986; **104**: 66-73
8 **Hohenberger P**, Schlag PM, Gerneth T, Herfarth C. Pre- and post-operative carcinoembryonic antigen determinations in hepatic resection for colorectal metastases. Predictive value and implication for adjuvant treatment based on multivariate analysis. *Ann Surg* 1994; **219**: 135-143
9 **King J**, Caplehorn JR, Ross WB, Morris DL. High serum carcinoembryonic antigen concentration in patients with colorectal liver metastases is associated with poor cell-mediated immunity, which is predictive of survival. *Br J Surg* 1997; **84**: 1382-1385
10 **Bakalakos EA**, Burak WE Jr, Young DC, Martin EW Jr. Is carcinoembryonic antigen useful in the follow-up management of patients with colorectal liver metastases? *Am J Surg* 1999; **177**: 2-6
11 **Yeatman TJ**, Bland KI, Copeland EM 3rd, Hollenbeck JI, Souba WW, Vogel SB, Kimura AK. Relationship between colorectal liver metastases and CEA levels in gallbladder bile. *Ann Surg* 1989; **210**: 505-512
12 **Yeatman TJ**, Kimura AK, Copeland EM 3rd, Bland KI. Rapid analysis of carcinoembryonic antigen levels in gallbladder bile. Identification of patients at high risk of colorectal liver metastasis. *Ann Surg* 1991; **213**: 113-117
13 **Paul MA**, Visser JJ, Mulder C, Blomjous JG, van Kamp GJ, Cuesta MA, Meijer S. Detection of occult liver metastases by measurement of biliary carcinoembryonic antigen concentrations. *Eur J Surg* 1996; **162**: 483-488

14 **Paul MA**, Visser JJ, Mulder C, van Kamp GJ, Cuesta MA, Meijer S. The use of biliary CEA measurements in the diagnosis of recurrent colorectal cancer. *Eur J Surg Oncol* 1997; **23**: 419-423

15 **Ishida H**, Hojo I, Gonda T, Nakajima H, Hirukawa H, Itoh M, Satoh K, Higuchi T, Toyooka M, Yoshinaga K. Measurement of bile CEA levels in patients with colorectal cancer: is it of value for diagnosis of occult liver metastases aiming at prophylactic regional hepatic chemotherapy? *Gan To Kagaku Ryoho* 1993; **20**: 1551-1554

16 **Paganuzzi M**, Onetto M, de Paoli M, Castagnola M, de Salvo L, Civalleri D, Grossi CE. Carcinoembryonic antigen (CEA) in serum and bile of colorectal cancer patients with or without detectable liver metastases. *Anticancer Res* 1994; **14**: 1409-1412

17 **Huang M**, Tang D, Li B. Evaluation of biliary CEA in the diagnosis of colorectal cancer with liver metastases. *Zhonghua Zhongliu Zazhi* 1999; **21**: 45-47

18 **Garcia** BA, Madrona AP, Ayalla MP, Paricio PP. The usefulness of determining carcinoembryonic antigen in the bile for the prognosis of the development of hepatic metastases following the resection of colorectal cancer. *Med Clin (Barc)* 1997; **108**: 396

19 **Novell F**, Trias M, Molina R, Filella X. Detection of occult liver metastases in colorectal cancer by measurement of biliary carcinoembryonic antigen. *Anticancer Res* 1997; **17**: 2743-2746

20 **Dorrance HR**, McGregor JR, McAllister EJ, O'Dwyer PJ. Bile carcinoembryonic antigen levels and occult hepatic metastases from colorectal cancer. *Dis Colon Rectum* 2000; **43**: 1292-1296

21 **Ishida H**, Yoshinaga K, Gonda T, Ando M, Hojo I, Fukunari H, Iwama T, Mishima Y. Biliary carcinoembryonic antigen levels can predict metachronous liver metastasis of colorectal cancer. *Anticancer Res* 2000; **20**: 523-526

22 **Moura RM**, Matos D, Galvão Filho MM, D'Ippolito G, Sjzenfeld J, Giuliano LM. Value of CEA level determination in gallbladder bile in the diagnosis of liver metastases secondary to colorectal adenocarcinoma. *Sao Paulo Med J* 2001; **119**: 110-113

23 **Li Destri G**, Curreri R, Lanteri R, Gagliano G, Rodolico M, Di Cataldo A, Puleo S. Biliary carcinoembryonic antigen in the diagnosis of occult hepatic metastases from colorectal cancer. *J Surg Oncol* 2002; **81**: 8-11

24 **Wang JY**, Chiang JM, Jeng LB, Changchien CR, Chen JS, Hsu KC. Resection of liver metastases from colorectal cancer: are there any truly significant clinical prognosticators? *Dis Colon Rectum* 1996; **39**: 847-851

25 **Gervaz P**, Blanchard A, Pampallona S, Mach JP, Fontolliet C, Gillet M. Prognostic value of postoperative carcinoembryonic antigen concentration and extent of invasion of resection margins after hepatic resection for colorectal metastases. *Eur J Surg* 2000; **166**: 557-561

26 **Uchino R**, Kanemitsu K, Obayashi H, Hiraoka T, Miyauchi Y. Carcinoembryonic antigen (CEA) and CEA - related substances in the bile of patients with biliary diseases. *Am J Surg* 1994; **167**: 306-308

27 **Frikart L,** Fournier K, Mach JP, Givel JC. Potential value of biliary CEA assay in early detection of colorectal adenocarcinoma liver metastases. *Eur J Surg Oncol* 1995; **21**: 276-279

28 **Svenberg T**, Hammarstrom S, Hedin A. Purification and properties of biliary glycoprotein I (BGP I). Immunochemical relationship to carcinoembryonic antigen. *Mol Immunol* 1979; **16**: 245-252

29 **Thomas P**. Studies on the mechanisms of biliary excretion of circulating glycoproteins. The carcinoembryonic antigen. *Biochem J* 1980; **192**: 837-843

30 **Tabuchi Y**, Deguchi H, Imanishi K, Saitoh Y. Comparison of carcinoembryonic antigen levels between portal and peripheral blood in patients with colorectal cancer. Correlation with histopathologic variables. *Cancer* 1987; **59**: 1283-1288

31 **Liu LX,** Jiang HC, Piao DX. Radiofrequence ablation of liver cancers. *World J Gastroenterol* 2002; **8**: 393-399

32 **Liu LX**, Zhang WH, Jiang HC. Current treatment for liver metastases from colorectal cancer. *World J Gastroenterol* 2003; **9**: 193-200

Edited by Xu XQ and Wang XL

P.O.Box 2345, Beijing 100023,China
Fax: +86-10-85381893
E-mail: wjg@wjgnet.com www.wjgnet.com

World J Gastroenterol 2003;9(7):1594-1597
World Journal of Gastroenterology
 ISSN 1007-9327

• BRIEF REPORTS •

Effects of carbon dioxide and nitrogen on adhesive growth and expressions of E-cadherin and VEGF of human colon cancer cell CCL-228

Kai-Lin Cai, Guo-Bing Wang, Li-Juan Xiong

Kai-Lin Cai, Guo-Bing Wang, General Surgery Department, Union Hospital, Tongji Medical College, Huazhong University of Science and Technology, Wuhan 430022, Hubei Province, China
Li-Juan Xiong, Infectious Disease Department, Union Hospital, Tongji Medical College, Huazhong University of Science and Technology, Wuhan 430022, Hubei Province, China
Supported by the Natural Science Foundation of Hubei Province, No. 2000J062
Correspondence to: Dr. Kai-Lin Cai, General Surgery Department, Union Hospital, Tongji Medical College, Huazhong University of Science and Technology, Wuhan 430022,Hubei Province, China. caikailin@yahoo.com.cn
Telephone: +86-27-85726405 **Fax**: +86-27-85776343
Received: 2003-03-03 **Accepted:** 2003-04-05

Abstract

AIM: To study the effects of carbon dioxide on the metastatic capability of cancer cells, and to compare them with that of nitrogen.

METHODS: The colon cancer cell CCL-228 was treated with 100 % carbon dioxide or nitrogen at different time points and then cultured under normal condition. Twelve hours after the treatment, the survival rates of suspension cells and the expressions of e-cadherin and VEGF were examined.

RESULTS: After 60 min of carbon dioxide and longer time of nitrogen treatment, the suspended cells increased and the expression of e-cadherin decreased while the expression of VEGF was enhanced significantly. And the effects of nitrogen were similar to, but weaker than, those of carbon dioxide.

CONCLUSION: Carbon dioxide may improve the metastatic capability of cancer cells and its effects are significantly stronger than that of nitrogen. A sequential use of carbon dioxide and nitrogen in pneumoperitoneum may take the advantage of both gases.

Cai KL, Wang GB, Xiong LJ. Effects of carbon dioxide and nitrogen on adhesive growth and expressions of E-cadherin and VEGF of human colon cancer cell CCL-228. *World J Gastroenterol* 2003; 9(7): 1594-1597
http://www.wjgnet.com/1007-9327/9/1594.asp

INTRODUCTION

The indications for laparoscopic surgery have expanded significantly thanks to the improved expertise and equipment. The main method to expose the operative field is carbon dioxide pneumoperitoneum. A large number of laparoscopic surgeries for gastroenteric malignant diseases, especially rectum or colon resections, have been performed. But there is a dispute on whether laparoscopic surgery is suitable for malignant diseases[1-6]. To investigate if carbon dioxide influences the metastatic capability of gastroenteric cancer cells, we studied the effects of carbon dioxide on the adhesive growth and the expression of cadherin and VEGF of a colon cancer cell line CCL-228 propagated *in vitro*. And the effects of carbon dioxide were compared with those of nitrogen. We found that, the metastatic ability of CCL-228 cells might elevate after carbon dioxide treatment and the influence of nitrogen was significantly milder than that of carbon dioxide. Based on these results, we proposed a sequential pneumoperitoneum method to reduce the side-effect but remain the safe-guard ness of carbon dioxide, *i.e.*, to establish the pneumoperitoneum with carbon dioxide and to maintain it with nitrogen, and before the end of the surgery, insufflating carbon dioxide to remove the unabsorbable nitrogen. In the present study, we evaluated the influence of the sequential gas treatment on the expression of E-cadherin and VEGF in CCL-228 cells.

MATERIALS AND METHODS

Cell culture

Human colon cancer cell line CCL-228, supplied by the Type Culture Collection Center, Wuhan University, was maintained in RPMI 1640 medium supplemented with 10 % fetal bovine serum. The cell cultures were maintained as monolayer in a plastic flask and incubated in 5 % CO_2, 95 % air at 37 ℃. The cultures were free of mycoplasma.

Carbon dioxide or nitrogen treatment

The CCL-228 cells were seeded onto 6-well plates (1×10^6 cells per well). When the button was 80 % covered, the cells were divided into two groups. Three parallel wells of cells in each group were incubated either in 100 % CO_2 (CO_2 group) or in 95 % N_2+5 % CO_2 (N_2 group) for 30, 60, 120, 180 min, respectively. To evaluate the effect of sequential pneumoperitoneum on the metastatic ability of colon cancer cells, 3 wells of CCL-228 cells were treated with CO_2 for 15 min, with nitrogen for 90 min or 150 min, and then with CO_2 again for 15 min. After the gas treatment, all cells were incubated again in 5 % CO_2, 95 % air for 12 h.

Histology

The supernate was collected and stained with typan blue, and the survival rate of the supernatant cells was estimated.

Immunohistochemistry

The adhesive growth cells were collected and stained for immunohistochemical studies on the expressions of VEGF and E-cadherin. The cell smear was fixed with cold acetone for 10 min at room temperature and rinsed with phosphate-buffered saline (PBS). The endogenous peroxidase was blocked using 3 % hydrogen peroxide for 10 min and the unspecific combined site was blocked with normal goat serum. Excessive blocking serum was drained and the samples were incubated at 40 ℃ for 18 h with the appropriate dilution of monoclonal mouse anti-human

VEGF or E-cadherin (Santa Cluz). Each sample was then rinsed with PBS and incubated for 10 min at room temperature with 50 μl of biotin-labeled goat anti-mouse IgG. The samples were then rinsed with PBS and incubated for 10 min at room temperature with 50 μl peroxidase conjugated avidin. The smears were rinsed with PBS and incubated for 5 min with diaminobenzidine. They were then washed with water and counterstained with Mayer' s hematoxylin and fixed with neutral resin. The smears were examined under microscope and positive reaction was indicated by brownish precipitate in cytoplasm.

Analysis of results

The smears were analyzed with MPZAS-500 multimedia color pathological graph analyzing system. The average integral light density (ILD) of positive staining in each sample was obtained and presented as $\bar{x}\pm s$. Results were then analyzed with Student' s *t* test.

RESULTS

Effects of CO_2 and N_2 on adhesive growth of CCL-228

Sixty min of CO_2 treatment or 120 min of N_2 treatment was sufficient to increase the rate of suspending growth cells very significantly (Table 1). The difference of rates of alive suspending cells between CO_2 and N_2 treatments was very significant after 60 min of treatment ($P<0.01$).

Table 1 Counts and survival rate of suspension CCl-228 cells after CO_2 or N_2 treatment

Duration	Counts of suspension cells (×1000 / ml)		Survival rate of suspension cells	
	CO_2 group	N_2 group	CO_2 group	N_2 group
0 min	4.2±0.1		0.884±0.011	
30 min	7.5±2.9	4.9±2.5	0.912±0.018	0.852±0.022
60 min	16.7±5.4[ab]	5.2±0.7	0.914±0.041	0.897±0.021
120 min	23.2±10.7[ac]	8.5±1.4[d]	0.904±0.034	0.912±0.023
180 min	32.1±5.5[ac]	9.7±3.3[d]	0.845±0.028	0.912±0.032

[a]$P<0.01$, *vs* the 0 min in same group; [b]$P<0.05$, *vs* N_2 group at same time; [c]$P<0.01$, *vs* N_2 group at same time; [d]$P<0.05$, *vs* 0 min in same group.

Effects of CO_2 and N_2 on expression of E-cadherin in CCL-228 cell

Both CO_2 and N_2 treatment depressed the expression of E-cadherin in CCL-228 cell (Figure 1). The expression of E-cadherin after 60 min or longer time of CO_2 treatment was significantly different from that after the same time periods of N_2 treatment. Comparing with the expression of E-cadherin before any gas treatment, 120 min or longer time of CO_2 treatment produced a very significant depression ($P<0.01$) and the same periods of N_2 treatment caused a significant depression ($P<0.05$).

Effects of CO_2 and N_2 on expression of VEGF in CCL-228 cell

Both CO_2 and N_2 treatment improved the expression of VEGF in CCL-228 cell (Figure 2). Thirty min to 120 min of CO_2 treatment caused significantly higher expression of VEGF comparing with the normal control and the same periods of N_2 treatment ($P<0.05$). CO_2 treatment for 180 min resulted in a VEGF expression significantly lower than CO_2 treatment for 120 min, but still significantly higher than normal control. As for N_2, 30 min to 180 min of treatment resulted in a continuous increase of VEGF expression.

Effects of sequential treatment with CO_2 and N_2 on expression of E-cadherin and VEGF in CCL-228 cell

The effects of sequential gas treatment for 120 min or 180 min on expression of E-cadherin and VEGF in CCL-228 cell were not significantly different from those of continuous nitrogen treatment but significantly milder than those of continuous carbon dioxide treatment (Figures 1 and 2).

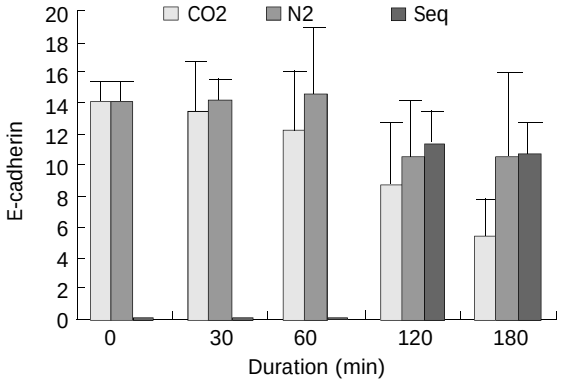

Figure 1 The expression of E-Cadherin in CCL-228 cells after gas treatment.

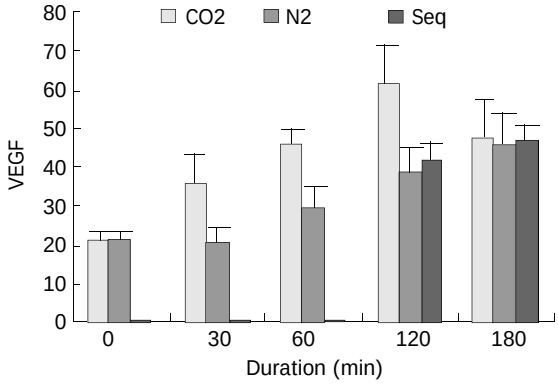

Figure 2 The expression of VEGF in CCL-228 cells after gas treatment.

DISCUSSION

It has been verified that laparoscopic surgery has many virtues such as minimal injury, less pain, sooner rehabilitation and less intervention in the immune function[7-11]. Now many gastroenteric surgeries including cancer resection could be fulfilled under laparoscope. Clinical trials have proved that laparoscopic surgery is feasible for gastroenteric malignant diseases. However, cancer metastasis in trocar site has been reported and has aroused a debate about whether laparoscopic surgery is suitable for malignant diseases. There is no consensus on if the incidence of metastasis in trocar site was accurately higher than that in the wound after open surgery[6], because the cases were few in each paper and there has been a decline in incidence of trocar site metastasis in recent reports, due to more attention paid to the wound protection during extraction of the specimen. Moreover, open surgery has been reported to increase cancer metastasis[12-15], and had more intervention in immunity. Therefore, whether laparoscopic surgery is suitable to early malignant diseases needs to be clarified by more clinical trials and further laboratory studies. In the present experiment, we studied the effect of carbon dioxide on the adhesive ness of colon cancer cells to the culture plate and the expressions of E-cadherin and VEGF. It should be noted that, the duration of carbon dioxide treatment was much longer than others because a laparoscopic surgery for gastroenteric cancer resection often lasts 2-3 hours.

We found that both carbon dioxide and nitrogen influenced the adhesive growth of CCL-228 cells. The cells in supernate increased after CO_2 or N_2 treatment. The rate of living cells in

supernate had no significant change confirmed by typan blue staining. Therefore, increase of cells in the supernate was a result of detachment of cells from the culture plate, but not the result of apoptosis or necrosis after gas treatment. It is suggested that CO_2 or N_2 could influence the adhesive ness of CCL-228 to matrix, resulting in easier metastasis by improving the detachment of cancer cells from the original lesion. We found that 30 min of CO_2 treatment caused an obvious increase of suspensive growth but the increase was not statistically significant, while 60 min and longer time produced very significant results. There were several laboratory reports on the effect of CO_2 on liver metastasis of intestinal cancer but the conclusions were controversial. We suppose that the controversy might result from a relatively short duration of pneumoperitoneum. Considering that laparoscopic surgery for malignant diseases usually needs several hours, the pneumoperitoneum time in experiments should be long enough to produce a practical result.

E-cadherin is one of the key adhesive molecules to mediate intercellular adhesion. It has been proved that, E-cadherin expression is depressed in metastatic tissues, which is helpful for the detachment of cancer cells from original lesions[16-20]. We examined the expression of E-cadherin in CCL-228 to explore if it plays a role in the influence of carbon dioxide on the adhesive growth of CCL-228. The results showed that, carbon dioxide treatment depressed E-cadherin expression and the effect was positively related to the duration of carbon dioxide treatment. Because cancer metastasis course includes the detachment of cells from the original lesion and also the settlement in the new environment, depression of adhesion has a two-edged effect on the metastasis of cancer. It is helpful for cancer cell dissemination but unfavorable to the settlement of circulating cancer cells.

The expression of VEGF is essential for cancer metastasis because it is a vital factor in tumor angiogenesis. A great deal of researches have indicated that cancer cells with higher VEGF expression results in much more persistently growing metastatic lesions, and inhibition of VEGF expression or function could interrupt the metastasis[21-25]. Therefore, we studied further the effect of carbon dioxide on VEGF expression in CCL-228 and found that it promoted VEGF expression. The promotion of VEGF expression suggests that decrease of E-cadherin expression in CCL-228 cells was not due to a general inhibition of protein synthesis by carbon dioxide, and the results implicate that carbon dioxide pneumoperitoneum was favorable for not only the detachment of cancer cells from the primary lesion but also for the growth of micrometastatic cells and their aggregation into a mass.

Many factors are supposed to be associated with the favorable effect on cancer growth and metastasis by carbon dioxide. The topical acidosis might be the main reason, and the less absorbable gases such as nitrogen and helium have less influence on metastasis[1,26,27]. In this experiment, we found that, comparing with carbon dioxide, nitrogen had a similar but much more mild effects on cancer cells. Since carbon dioxide had a significant duration-effect relationship with the expression of E-cadherin and VEGF, reduced carbon dioxide insufflation duration might be less harmful to patients with malignant diseases. Here we propose a sequential pneumoperitoneum, namely, establishing the pneumoperitoneum with carbon dioxide and maintaining it with nitrogen, and then, before the end of surgery, insufflating carbon dioxide to remove the unabsorbable nitrogen. We found that, during the 120 min or 180 min of gas treatment, when carbon dioxide was applied in the first and last 15 min but replaced with nitrogen in the time between E-cadherin and VEGF expressions were significantly different from that by persistent carbon dioxide treatment. Therefore, we think that in laparoscopic surgery for malignant diseases, the sequential pneumoperitoneum method may take the advantages of both nitrogen and carbon dioxide, as the effect of carbon dioxide on metastasis is reduced by nitrogen replacement during the operation, and the safe guard ness of carbon dioxide to prevent from gas embolism, usually happening during the establishment of pneumoperitoneum, is remained. And the remaining gas in abdomen after surgery is also carbon dioxide, which is ready to be absorbed.

REFERENCES

1 **Neuhaus SJ,** Watson DI, Ellis T, Rowland R, Rofe AM, Pike GK, Mathew G, Jamieson GG. Wound metastasis after laparoscopy with different insufflation gases. *Surgery* 1998; **123**: 579-583

2 **Schaeff B**, Paolucci V, Thomopouluis J. Port site recurrences after laparoscopic surgery. *Dig Surg* 1998; **15**: 124-134

3 **Wexner S**, Cohen SM. Port site metastases after laparoscopic colorectal surgery for cure of malignancy. *Br J Surg* 1995; **82**: 295-298

4 **Lacy AM**, Delgado S, Garcia-Valdecasas JC, Castells A, Pique JM, Grande L, Fuster J, Targarona EM, Pera M, Visa J. Port site metastases and recurrence after laparoscopic colectomy. *Surg Endosc* 1998; **12**: 1039-1042

5 **Mathew G,** Watson DI, Rofe AM, Baigrie CF, Ellis T, Jamieson GG. Wound metastases following laparoscopic and open surgery for abdominal cancer in a rat model. *Br J Surg* 1996; **83**: 1087-1090

6 **Gibson M**, Byrd C, Pierce C, Wright F, Norwood W, Gibson T, Zibari GB. Laparoscopic colon resections: a five-year retrospective review. *Am Surg* 2000; **66**: 245-248

7 **Trokel MJ**, Bessler M, Treat MR, Whelan RL, Nowygrod R. Preservation of immune response after laparoscopy. *Surg Endosc* 1994; **8**: 1385-1387

8 **Allendorf JD**, Bessler M, Whelan RL, Trokel M, Laird DA, Terry MB, Treat MR. Postoperative immune function varies inversely with the degree of surgical trauma in a murine model. *Surg Endosc* 1997; **11**: 427-430

9 **Cho JM**, LaPorta AJ, Clark JR, Schofield MJ, Hammond SL, Mallory PL 2nd. Response of serum cytokines in patients undergoing laparoscopic cholecystectomy. *Surg Endosc* 1994; **8**: 1380-1383

10 **Wexner SD**, Cohen SM, Johansen OB, Nogueras JJ, Jagelman DG. Laparoscopic colorectal surgery: a prospective assessment and current perspective. *Br J Surg* 1993; **80**: 1602-1605

11 **Evrard S**, Falkenrodt A, Park A, Tassetti V, Mutter D, Marescaux J. Influence of CO_2 pneumoperitoneum on systemic and peritoneal cell-mediated immunity. *World J Surg* 1997; **21**: 353-356

12 **Murthy SM**, Goldschmidt RA, Rao LN, Ammirati M, Buchmann T, Scanlon EF. The influence of surgical trauma on experimental metastasis. *Cancer* 1989; **64**: 2035-2044

13 **Da Costa ML**, Redmond P, Bouchier-Hayes DJ. The effect of laparotomy and laparoscopy on the establishment of spontaneous tumor metastases. *Surgery* 1998; **124**: 516-525

14 **Paik PS,** Misawa T, Chiang M, Towson J, Im S, Ortega A, Beart RW Jr. Abdominal incision tumor implantation following pneumoperitoneum laparoscopic procedure vs. standard open incision in a syngeneic rat model. *Dis Colon Rectum* 1998; **41**: 419-422

15 **Ishida H**, Murata N, Yamada H, Nakada H, Takeuchi I, Shimomura K, Fujioka M, Idezuki Y. Pneumoperitoneum with carbon dioxide enhances liver metastases of cancer cells implanted into the portal vein in rabbits. *Surg Endosc* 2000; **14**: 239-242

16 **Dorudi S**, Hanby AM, Poulsom R, Northover J, Hart IR. Level of expression of E-cadherin mRNA in colorectal cancer correlates with clinical outcome. *Br J Cancer* 1995; **71**: 614-616

17 **Jiang WG**. E-cadherin and its associated protein catenins, cancer invasion and metastasis. *Br J Surg* 1996; **83**: 437-446

18 **Kinsella AR**, Green B, Lepts GC, Hill CL, Bowie G, Taylor BA. The role of the cell–cell adhesion molecule E-cadherin in large bowel tumour cell invasion and metastasis. *Br J Cancer* 1993; **67**: 904-909

19 **Jiang WG.** Cell adhesion molecules in the formation of liver metastasis. *J Hepatobiliary Pancreat Surg* 1998; **5**: 375-382
20 **Zhou YN,** Xu CP, Han B, Li M, Qiao L, Fang DC, Yang JM. Expression of E-cadherin and beta-catenin in gastric carcinoma and its correlation with the clinicopathological features and patient survival. *World J Gastroenterol* 2002; **8**: 987-993
21 **Bruns CJ,** Liu W, Davis DW, Shaheen RM, McConkey DJ, Wilson MR, Bucana CD, Hicklin DJ, Ellis LM. Vascular endothelial growth factor is an in vivo survival factor for tumor endothelium in a murine model of colorectal carcinoma liver metastases. *Cancer* 2000; **89**: 488-499
22 **Ellis LM**, Takahashi Y, Liu W, Shaheen RM. Vascular endothelial growth factor in human colon cancer: biology and therapeutic implications. *Oncologist* 2000; **5**(Suppl 1): 11-15
23 **Kondo Y,** Arii S, Mori A, Furutani M, Chiba T, Imamura M. Enhancement of angiogenesis, tumor growth, and metastasis by transfection of vascular endothelial growth factor into LoVo human colon cancer cell line. *Clin Cancer Res* 2000; **6**: 622-630
24 **Liu DH,** Zhang XY, Fan DM, Huang YX, Zhang JS, Huang WQ, Zhang YQ, Huang QS, Ma WY, Chai YB, Jin M. Expression of vascular endothelial growth factor and its role in oncogenesis of human gastric carcinoma. *World J Gastroenterol* 2001; **7**: 500-505
25 **Tao HQ**, Lin YZ, Wang RN. Significance of vascular endothelial growth factor messenger RNA expression in gastric cancer. *World J Gastroenterol* 1998; **4**: 10-13
26 **Jacobi CA**, Sabat R, Bohm B, Zieren HU, Volk HD, Müller JM. Pneumoperitoneum with carbon dioxide stimulates growth of malignant colonic cells. *Surgery* 1997; **121**: 72-78
27 **Jacobi CA,** Wenger F, Sabat R, Volk T, Ordemann J, Muller JM. The impact of laparoscopy with carbon dioxide versus helium on immunologic function and tumor growth in a rat model. *Dig Surg* 1998; **15**: 110-116

Edited by Ma JY

P.O.Box 2345, Beijing 100023,China
Fax: +86-10-85381893
E-mail: wjg@wjgnet.com www.wjgnet.com

World J Gastroenterol 2003;9(7):1598-1600
World Journal of Gastroenterology
 ISSN 1007-9327

• BRIEF REPORTS •

Meta analysis of risk factors for colorectal cancer

Kun Chen, Jiong-Liang Qiu, Yang Zhang, Yu-Wan Zhao

Kun Chen, Jiong-Liang Qiu, Yang Zhang, Yu-Wan Zhao, Department of Epidemiology, School of Medicine, Zhejiang University, Hangzhou 310031, Zhejiang Province, China
Supported by the National Natural Science Foundation of China, No.30170828
Correspondence to: Kun Chen, Department of Epidemiology, School of Medicine, Zhejiang University, Hangzhou 310031, Zhejiang Province, China. ck@zjuem.zju.edu.cn
Telephone: +86-571-87217190
Received: 2003-03-02 **Accepted:** 2003-04-01

Abstract

AIM: To study the risk factors for colorectal cancer in China.

METHODS: A meta-analysis of the risk factors of colorectal cancer was conducted for 14 case-control studies, and reviewed 14 reports within 13 years which included 5034 cases and 5205 controls. Dersimonian and Laird random effective models were used to process the results.

RESULTS: Meta analysis of the 14 studies demonstrated that proper physical activites and dietary fibers were protective factors (pooled OR<0.8), while fecal mucohemorrhage, chronic diarrhea and polyposis were highly associated with colorectal cancer (all pooled OR>4). The stratified results showed that different OR values of some factors were due to geographic factors or different resourses.

CONCLUSION: Risks of colorectal cancer are significantly associated with the histories of intestinal diseases or relative symptoms, high lipid diet, emotional trauma and family history of cancers. The suitable physical activities and dietary fibers are protective factors.

Chen K, Qiu JL, Zhang Y, Zhao YW. Meta analysis of risk factors for colorectal cancer. *World J Gastroenterol* 2003; 9 (7): 1598-1600

http://www.wjgnet.com/1007-9327/9/1598.asp

INTRODUCTION

Meta-analysis named by Glass, is generally defined as a quantitative summary of studies in a particular area, which has addressed the same research question, and an overall summary obtained by statistically aggregating the results of the reviewed studies. It is used to improve the statistical efficiency, to evaluate the disadvantages of formulated researches, and hypothesis and to reach reliable conclusions from the mixed assortment of the potentially relevant studies to determine the most promising directions for future researches. It has been gradually applied in medicine since it was adopted in 1970s.

Colorectal cancer is one of the most malignant cancers in China and has been steadily increasing in frequency in large or middle cities[1]. Thus, in order to provide the overall information on colorectal cancer risk factors, we performed a meta analysis of the results of 14 case-control studies in China.

MATERIALS AND METHODS

Materials

The published Chinese literatures of case-control studies related to colorectal cancer risk factors from 1988 to 2000 were collected by bibliographic searches through Index of Chinese Science and Technology Data. The selection criteria of literature were as follows: The independent case-control studies were published in Chinese magazines from 1988 to 2000, each study should have the synthetic statistical index: odds ratio (*OR*), the similar research goal with the identical study method. The overall results of literature should be presented with the corresponding statistical index, the latest articles were chosen among several ones with the same sample size. Duplicated, poor quality reports or those with little information on colon cancer were discarded. Thus, 14 papers were chosen by screening, and 5 034 cases and 5 205 controls were accumulated.

Methods

Different stratified studies were performed, including studies on prevalence/death cases (CD) versus incidence cases (ND) according to different cases, studies on general population (PB) and on patients in hospital (HB). The studies were classified in rural or urban areas in the north (NOR) and those in the south (SOU) separated by the Yangtze River as the boundary. Studies were divided into colon cancer (Jca) and rectal cancer (Zca) according to the sites of cancer.

Statistical treatment

Test of equal variance was conducted before statistical analysis, and the index odds ratio (OR) was performed using the model established by Dersimonian and Laird. The fundamental principle was as follows: $y_i=lnOR_i$, with its variance: $S_i=[P_{1\,i}(1-P_{1\,i})/y_in_{1i}]+[P_{2i}(1-P_{2i})/n_{2i}]$, ($P_{1i}$ and n_{1i} are the exposing rate of the case group and the sample size, respectively; P_{2i} and n_{2i} are the corresponding parameters in control group). OR could be calculated with the confidence limit, standard error or Chi-squared value in some way if the basic data could not be acquired. If the total comprehensive effect was $\bar{y}^*$, then $\bar{y}^*=\sum(W_i^*\cdot y_i)/\sum W_i^*$, with 95 % confidence interval $\bar{y}^*\pm1.96\cdot SE(\bar{y}^*)$.

$$SE(\bar{y}^*)=1/\sum W_i^*$$
$$W_i^*=(W_i^{-1}+\Delta^2)^{-1}$$
$$W_i=S_i^{-1}$$
$$\Delta^2=max\{0,Q-(k-1)/\sum W_i-(\sum W_i^2/\sum W_i)\}$$
$$Q=\sum[W_i(y_i-\bar{y})^2]$$
$$\bar{y}=\sum(W_i\cdot y_i)/\sum W_i$$

RESULTS

The papers used in the studies are shown in Table 1. The number of literature in Zhejiang accounted for a half of the total in this country since Zhejiang had a high incidence of colorectal cancer.

Meta analysis showed that all the risk factors of colorectal cancer except alcohol drinking were significant (P<0.05), (Table 2), while proper physical activities and dietary fibers were protective factors (pooled OR was 0.6-0.8). Histories of fecal mucohemorrhage and bowel polyps were more

significantly associated with colorectal cancer (pooled OR>4) than other ones (pooled OR was 1-4).

Results of the stratified meta analysis including index cases, study area, location of cancer and origins of the controls are shown in Table 3. The pooled OR of family history of cancers differed significantly between prevalence/death cases (CD) and incidence cases (ND), which in the latter (pooled OR=3.73 [95 % confidence interval (CI) 3.14-4.44]) was one-fold more than that in the former (1.76 [1.71-1.81]). History of chronic diarrhea was more frequently significant among rectum cancers (pooled OR=4.02, $P<0.05$). However, no significant association was observed with colon cancer ($P>0.05$).

Table 1 Case-control studies on risk factors of colorectal cancer

No	Author	Area	Number of cases	Number of factors	Sources of references
1	JIAO Den-Ao	Jiashan	160	9	Zhonghua Liuxingbingxue Zazhi, 1988, 9(6): 354-357
2	WU Den-Ren	Jiashan	114	5	Shiyong Zhongliu Zazhi, 1990, 5(2): 95-99
3	YANG Gong	Shanghai	850	2	Zhonghua Liuxingbingxue Zazhi, 1992, 13(1): 30-33
4	ZHANG Cao	Beijing	250	5	Zhonghua Liuxingbingxue Zazhi, 1992, 13(6): 321-323
5	ZOU Run	Jiashan	41	10	Zhongguo Manxingbing Yufang Yu Kongzhi, 1993, 1(5): 213-215
6	MEN Fan-He	Guangdong	100	3	Diyi Junyi Daxue Xuebao, 1994,14(4): 281-283
9	LIU Xi-Yong	Jiashan	286	6	Zhongguo Manxingbing Yufang Yu Kongzhi, 1994, 2(3): 122-124
7	YANG Gong	Shanghai	1328	4	Zhonghua Liuxingbingxue Zazhi, 1994, 15(5): 299-303
8	YANG Gong			3	Zhongguo Zhongliu Linchuang, 1995, 22(6): 403-408
10	LAI Kuang-De	Dalian	129	3	Zhongguo Manxingbing Yufang Yu Kongzhi, 1995, 3(3): 106-109
11	HE Xi-Zhen	Shenyang	390	2	Shiyong Zhongliuxue Zazhi, 1996, 10(2): 64-65
12	YANG Gong	Shanghai	3166	3	Zhongliu, 1996, 16(2): 74-78
13	ZOU Run	Hangzhou	245	5	Zhejiang Yike Daxue Xuebao, 1996, 25(5): 204-206
4	LIU Ai-Zong	Hunan	153	7	Zhongguo Gonggong Weisheng, 1997, 13(4): 206-207

Table 2 Results from meta-analysis of risk factors of colorectal cancer

Factors	Number of references	Pooled *OR and* 95 % C.I.	Factors	Number of references	Pooled *OR and* 95% C.I.
(1) History of chronic diarrhea	7	4.80 (4.30~5.37)	(8) Pickled vegetables	3	1.86 (1.67~2.07)
(2) History of fecal mucohemorrhage	5	7.18 (5.06~10.21)	(9) High lipid food	3	3.16 (2.22~4.51)
(3) History of bowel polyps	5	12.69 (7.49~21.48)	(10) Proper physical activities	4	0.74 (0.72~0.77)
(4) History of constipation	4	2.23 (1.95~2.54)	(11) Alcohol drinking	5	1.06 (0.91~1.24)
(5) History of appendicitis	3	1.98 (1.71~2.28)	(12) Cigarette smoking	5	1.40 (1.10~1.77)
(6) Dietary fibers	5	0.79 (0.59~0.99)	(13) Emotional trauma	4	2.95 (2.81~3.09)
(7) Fish fry-cooked with soybean sauce	4	2.99 (2.69~3.35)	(14) Family history of cancers	7	2.27 (2.12~2.44)

(1) references: 1,2,5,7,9,13, 14 (2) references: 1,5,7,9,13 (3) references: 1,2,5,7,12
(4) references: 1,5,7,9 (5) references: 1,2,5 (6) references: 4,6,10,11,14
(7) references: 1,5,6, 7 (8) references: 2,6,14 (9) references: 4,5,14
(10) references: 4,10,13,14 (11) references: 2,5,8,13,14 (12) references: 2,5,6,8,14
(13) references: 1,4,5,7 (14) references: 1,3,4,5,6,7,14

Table 3 Results from stratified meta-analysis of risk factors of colorectal cancer

Factors	Strata	Pooled *OR and* 95% C.I.	Factors	Strata	Pooled *OR and* 95% C.I.
History of chronic diarrhea	CD[a]	6.04 (5.45~6.70)	Pickled vegetables	CD	1.58 (1.20~2.07)
	ND[a]	3.99 (2.81~5.66)		ND	2.30 (1.30~4.20)
	Jca[b]	7.01 (0.48~10.12)		Jca	1.70 (1.10~2.50)
	Zca[b]	4.02 (1.13~14.21)		Zca	1.50 (1.01~2.30)
	HB	6.60 (2.46~11.21)		HB	2.30 (1.30~4.20)
	PB	4.50 (3.90~5.17)		PB	1.58 (1.20~2.07)
Fecal muco-hemorrhage	CD[b]	9.81 (4.55~21.17)	Alcohol drinking	CD[b]	0.91 (0.71~1.17)
	ND[b]	3.60 (2.80~4.80)		ND[b]	1.65 (1.03~2.63)
	Jca[b]	2.80 (0.75-10.46)		HB[b]	1.65 (1.03~2.63)
	Zca[b]	4.56 (2.12~9.81)		PB[b]	0.91 (0.71~1.17)
History of bowel polyps	CD[a]	7.40 (4.13~13.28)	Cigarette smoking	CD[b]	0.74 (0.43~1.27)
	ND[a]	22.30 (12.40~40.01)		ND[b]	1.92 (1.49~2.47)
	Jca	17.42 (14.54~20.85)		HB[b]	1.92 (1.49~2.47)
	Zca	12.14 (3.07~28.00)		PB[b]	0.74 (0.43~1.27)
History of constipation	CD	2.53 (1.55~4.11)	Emotional trauma	Jca[b]	2.80 (1.51~3.28)
	ND	1.90 (1.50~2.40)		Zca[b]	1.63 (0.39~6.85)
	Jca[b]	3.4 (1.02~11.39)		NOR	3.36 (2.21~5.12)
	Zca[b]	0.89 (0.09~8.53)		SOU	2.53 (2.28~2.81)
Dietary fibers	CD[b]	0.43 (0.18~0.97)	Proper physical activities	CD	0.79 (0.77~0.81)
	ND[b]	1.02 (0.40~2.57)		ND	0.57 (0.35~0.90)
	NOR[b]	0.43 (0.18~0.97)		NOR[a]	0.69 (0.67~0.71)
	SOU[b]	1.02 (0.40~2.57)		SOU[a]	0.77 (0.70~0.85)
	HB[b]	0.86 (0.58~0.96)		HB	0.57 (035~0.90)
	PB[b]	0.37 (0.06~2.13)		PB	0.79 (0.77~0.81)
Fish fry-cooked with soybean	CD	2.84 (2.31~3.48)	Family history of cancers	CD[a]	1.76 (1.71~1.81)
	ND	3.20 (1.60~6.30)		ND[a]	3.73 (3.14~4.44)
	Jca[b]	7.01 (1.10~12.01)		Jca[a]	2.84 (2.58~3.13)
	Zca[b]	1.18 (0.30~8.01)		Zca[a]	1.52 (1.34~1.72)
	HB	3.20 (1.60~6.30)		HB[a]	3.73 (3.14~4.44)
	PB	2.84 (2.31~3.48)		PB[a]	1.76 (1.71~1.81)

[a]: No mutual involvement of OR by correspondent two ranges of 95 % CI was found. [b]: At least one 95 % CI of pooled OR was found including 1.00.

DISCUSSION

Environmental factors are the predominant contributors to colorectal cancer, and genetic factors show significant effects[1,3-5]. Meta analysis indicated that a variety of factors could contribute to colorectal cancer as follows.

1. **Intestinal disorders and colorectal cancer** Precancerous syndromes or diseases based on the review of Chinese literature included chronic diarrhea, fecal mucohemorrhage, polyposis, constipation, etc. Therefore, colorectal cancer should be suspected if chronic diarrhea, fecal mucohemorrhage or constipation of unknown cause occur in patients with a history of bowel polyps[2]. In addition, whether appendicitis is a risk factor of colorectal cancer remains plausible. However, it is considered as one of the risk factors since its pooled OR was 1.98 ($P<0.05$) demonstrated in this study. Because appendicitis weakens the immunological function of appendix and thus causes colorectal cancer.

2. **Diet** High fat diet was the highest risk factor of colon cancer ($OR=3.16$), followed by fish fry-cooked with soybean sauce ($OR=2.99$) and pickled vegetables ($OR=1.86$). In contrast, dietary fibers played a protective role in colorectal cancer (pooled $OR=0.79$, $P<0.05$). Fried fish with soybean sauce may generate mutagenic heterocyclic amines as red meats[6,7]. The dietary fiber may shorten the transporting time of excrement in intestines, decrease the time of carcinogens affecting intestinal mucus and reduce the growth of bacterial strains that produce carcinogens in the colonic lumen. However, no evidence was reported to suggest that high dietary fiber could reduce the incidence or recurrence of adenomatous polyps during a two to four year period[8]. In addition, many experimental findings indicated an association between diet with high calcium and vitamin D and low risk for colorectal cancer, which deserve further study[9].

3. **Physical activity, cigarette smoking and alcohol** The relationship between physical activities and colorectal cancer has been noticed recently. Studies showed that people with proper physical activities had low incidence of colorectal cancer since appropriate physical activities could decrease the random segmentation without propulsion of the intestine, and increase effective vermiculation, thus shortening the transit time of excrement in the intestine and reducing the contact between intestinal mucosa and carcinogen. No significant association was found between alcohol and colorectal cancer in meta analysis, though other studies reported that significantly lower levels of serum cholesterol and triglycerides were found in daily alcohol drinkers with colorectal adenomas[10], while cigarette smoking was regarded as a risk factor since its OR exceeded 1($P<0.05$) although it is plausible whether smoking causes colorectal cancer.

Moreover, it was suggested that long-term emotional trauma and family history of cancers were related to the increased risk of colorectal cancer. However, further work is needed to clarify the mechanism.

Bias and confounding factors can also be found in meta analysis, and so we conducted the stratified analysis as follows: (1) Since studies on the prevalence or death cases could lead to bias due to selection and exposure misclassification, stratified analysis for the index cases was performed, which showed that there was a difference between studies on the prevalence or death cases and those on the incidence cases (Table 3). (2) The results of different strata suggested that studies on incidence cases based on the population should be conducted strictly in the future. (3) Risk factors of colorectal cancer in south and in the north may be different. (4) The cause of colon cancer may not be completely the same as that of cancer in the rectum. In this study, chronic diarrhea and fecal mucohemorrhage were more frequent in cancers of rectum, while complaint of constipation, fish fry-cooked with soybean sauce and emotional trauma were more frequently seen in colon cancer.

Meta means "more comprehensive, transcending"[11]. Meta analysis has extended quickly from social sciences to medical sciences. Incidence of colorectal cancer has increased over the last decade in China, and it is necessary to study its causes. Thus, synthetic analysis was performed on the etiology of colorectal cancer in China in 12 years with meta analysis. However, the potential confounding factors may not be well controlled due to the limited literature and therefore the result may be affected. Thus, further study is required.

REFERENCES

1 **Zhang ZS**, Zhang YL. Development of research on colorectal cancer in China. *Shijie Huaren Xiaohua Zazhi* 2001; **9**: 489-494
2 **Li SR**. Strategy for the early diagnosis of colorectal cancer. *Shijie Huaren Xiaohua Zazhi* 2001; **9**: 780-782
3 **Lai MD**. Related genes of generation and development of colorectal cancer in China. *Shijie Huaren Xiaohua Zazhi* 2001; **9**: 1227-1232
4 **Sheng JQ**, Chen ZM. Screening of colorectal cancer with the related genes. *Shijie Huaren Xiaohua Zazhi* 2001; **9**: 783-785
5 **Johns LE**, Houlston RS. A systematic review and meta-analysis of familial colorectal cancer risks. *Am J Gastroenterol* 2001; **96**: 2992-3003
6 **Sweeney C**, Coles BE, Nowell S, Lang NP, Kadlubar FF. Novel marker of susceptibility to carcinogens in diet: Associations with colorectal cancer. *Toxicology* 2002; **181-182**: 83-87
7 **Norat T**, Lukanova A, Ferrari P, Riboli E. Meat consumption and colorectal cancer risk: dose-response meta-analysis of epidemiological studies. *Int J Cancer* 2002; **98**: 241-256
8 **Asano T**, Mcleod RS. Dietary fiber for the prevention of colorectal adenomas and carcinomas. *Cochrane Database Syst Rev* 2002; **2**: CD003430
9 **Lipkin M**. Update of preclinical and human studies of calcium and colon cancer prevention. *World J Gastroenterol* 1999; **5**: 461-464
10 **Fujimori S**, Kishida T, Mitsui K, Yonezawa M, Nagata K, Shibata Y, Tanaka S, Tatsuguchi A, Sato J, Yokoi K, Tanaka N, Ohaki Y, Sakamoto C, Kobayashi M. Influence of alcohol consumption on the association between serum lipids and colorectal adenomas. *Scand J Gastroenterol* 2002; **37**: 1309-1312
11 **Bailar JC**, Mosteller F. Medical uses of statistics. 2nd edition. *Waltham Mass: Nejm Books* 1992: 422-427

Edited by Ren SY and Wang XL

P.O.Box 2345, Beijing 100023,China
Fax: +86-10-85381893
E-mail: wjg@wjgnet.com www.wjgnet.com

World J Gastroenterol 2003;9(7):1601-1603
World Journal of Gastroenterology
 ISSN 1007-9327

• BRIEF REPORTS •

Expressions of PCNA, p53, p21^{WAF-1} and cell proliferation in fetal esophageal epithelia: Comparative study with adult esophageal lesions from subjects at high-incidence area for esophageal cancer in Henan, North China

Ying Xing, Yu Ning, Li-Qiang Ru, Li-Dong Wang

Ying Xing, Li-Qiang Ru, Department of Neurobiology, Tongji Medical College, Huazhong University of Science and Technology, Wuhan, 430030, Hubei Province, China
Yu Ning, Department of Physiology, College of Medicine, Zhengzhou University, Zhengzhou, 450052, Henan Province, China
Li-Dong Wang, Laboratory for Cancer Research, College of Medicine, Zhengzhou University, Zhengzhou, 450052, Henan Province, China
Supported by National Distinguished Young Scientist Foundation of China, No.30025016
Correspondence to: Dr. Li-Dong Wang, Professor of Pathology and Oncology and Ying Xing, Professor of Physiology, Laboratory for Cancer Research, College of Medicine, Zhengzhou University, Zhengzhou 450052, Henan Province, China. lidong0823@sina.com
Telephone: +86-371-6970165 **Fax:** +86-371-6970165
Received: 2003-03-02 **Accepted:** 2003-03-25

Abstract

AIM: To characterize the expression of p53, p21^{WAF-1} and proliferation-cell-nuclear-antigen (PCNA) in fetal esophageal epithelia and to determine the role of these genes in proliferation of fetal and adult esophageal epithelial cells.

METHODS: Immunohistochemical avdin-biotin peroxidase complex (ABC) method was applied to 31 cases of fetal esophageal specimens and 194 cases of adult esophageal specimens to detect the expression of p53, p21^{WAF-1} and PCNA in fetal and adult esophageal epithelia.

RESULTS: Both the PCNA positive immunostaining cell number and PCNA positive immunostaining rate in fetal esophageal epithelia (506±239) were significantly higher than those in adults, including normal epithelia (200±113) and epithelia with basal cell hyperplasia (BCH) (286±150) (P<0.05, t test). However, the number of PCNA positive immunostaining cells in adult esophageal dysplasia (719±389) and squamous cell carcinoma (SCC) (1261±545) was apparently higher than that in fetal esophageal epithelia (506±239) (P<0.05, t test). The positive immunostaining rate of P53 was 10 % (3/31) in fetal esophageal epithelia, which was significantly lower than that in adult normal esophageal epithelia (50 %), adult epithelia with basal cell hyperplasia (62 %), dysplasia (73 %) and squamous cell carcinoma (86 %) (P<0.05, Fisher's exact test). No p21^{WAF-1} positive immunostaining cells were observed in fetal esophageal epithelia. However, p21^{WAF-1} positive immunostaining cells were observed in adult esophagus with 39 % (11/28) in normal, 38 % (14/37) in BCH, 27 % (3/11) in DYS and 14 % (1/7) in SCC.

CONCLUSION: PCNA could act as an indicator accurately reflecting the high proliferation status of fetal esophageal epithelium. p53 may play an important role in growth and differentiation of fetal esophageal epithelium. p21^{WAF-1} may have no physiological function in development of fetal esophageal epithelium.

Xing Y, Ning Y, Ru LQ, Wang LD. Expressions of PCNA, p53, p21^{WAF-1} and cell proliferation in fetal esophageal epithelia: Comparative study with adult esophageal lesions from subjects at high-incidence area for esophageal cancer in Henan, North China. *World J Gastroenterol* 2003; 9(7): 1601-1603
http://www.wjgnet.com/1007-9327/9/1601.asp

INTRODUCTION

Fetal esophageal epithelium is characterized by cellular hyperproliferation. Tumor suppressor genes have been known to suppress malignant cell proliferation through encoding corresponding proteins that inhibit cell cycle. But it is still not clear whether this inhibition effect of tumor suppressor genes is also involved in the proliferative activity of fetal epithelium.

Tumor suppressor proteins p53 and p21^{WAF-1} play important roles in regulating G1 phase progression, which is the key modulation point in the cell cycle[1-8]. Proliferating cell nuclear antigen (PCNA) acts as a good marker for cell proliferation and can reflect the status of epithelium growth[9,10]. To detect the expression of these proteins would help to explore fetal esophageal epithelium proliferation status and characteristics, and to further understand the role of tumor suppressor genes in fetal esophageal epithelium growth control.

Most previous studies about fetal esophagus development focused on the influences of certain chemical factors, such as nitrosamine[11,12], and biological factors, such as alternariol[13]. There are, however, few reports about the proliferation characteristics and control of cell cycle in growth of fetal esophageal epithelium.

In this study, immunohistochemical avdin-biotin peroxidase complex (ABC) method was applied to investigate the expression of PCNA, p53 and p21^{WAF-1} in fetal esophageal epithelium and adult esophageal epithelium with different histopathological subtypes. Comparison between the expression of the above proteins in fetal and adult esophageal epithelium would provide important evidences for characteristics of fetal esophageal epithelium proliferation and the mechanisms of its cell cycle control.

MATERIALS AND METHODS

Tissue collection and processing

Thirty-one cases of fetal esophageal specimens were collected from Runan County, Taikang County, Lankao County and Zhengzhou City. The ages of the fetuses ranged from 4 months to 10 months (Table 1). No history of drug using and family history of tumor were found among all the parents of these fetuses. 194 cases of adult esophageal specimens were collected in the same areas for control of PCNA expression, among which 83 adult esophageal specimens were used for the control of p53 and p21^{WAF-1} expression. All specimens were fixed in 85 % ethanol, embedded with paraffin and serially sectioned at

5 μm. The sections were mounted onto the histostick-coated slides. Four or five adjacent ribbons were collected for histopathological diagnosis (hematoxylin and eosin stain) and immunohistochemical staining.

Table 1 Distribution of fetus sex and age

Sex	Age (months)						Mean age (months)
	4	5	6	7	8	>9	
Male	0	2	4	3	0	0	6.11±0.78
Female	2	5	4	7	3	1	6.36±1.47[a]
Total	2	7	8	10	3	1	6.29±1.30

[a]P>0.05, t-test, no significant difference was detected in the distribution of age between male and female fetuses.

Histopathologic diagnosis

Histopathological diagnosis and categorization for esophageal epithelium were based on the changes in cellular morphology and tissue architecture in reference to previous reports[14-17], and the adult esophageal epithelium was correspondingly classified as normal, basal cell hyperplasia (BCH), dysplasia (DYS) and squamous cell carcinoma (SCC).

Immunohistochemical staining (IHC)

Anti-p53 antibody is a monoclonal mouse anti-serum against p53 of human origin, and recognizes both wild and mutant type p53 (Ab-6, Oncogene Science, Manhasset, NY). Anti-PCNA antibody is a monoclonal mouse anti-serum against PCNA of human origin (Mab, DAKO, Carpinteria, CA). Anti-$p21^{WAF-1}$ antibody is a monoclonal mouse anti-serum against $p21^{WAF-1}$ of human origin, and recognizes both wild and mutant type p21 (Ab-6, Oncogene Science, Manhasset, NY). The avidin-biotin-peroxidase complex method was used for the immunostaining of p53, PCNA and $p21^{WAF-1}$ as previously reported. In brief, after dewaxing, inactivating endogenous peroxidase activity and blocking cross-reactivity with normal serum (Vectastain Elite Kit; Vector, Burlingame, CA), the sections were incubated overnight at 4 ℃ with a diluted solution of the primary antibodies (1:500 for p53, 1:200 for PCNA and 1:20 for $p21^{WAF-1}$). Location of the primary antibodies was achieved by subsequent application of a biotinylated anti-primary antibody, an avidin-biotin complex conjugated to horseradish peroxidase, and diaminobenzidine (Vectastain Elite Kit, Vector, Burlingame, CA). The slides were counter-stained by hematoxylin. Negative controls were established by replacing the primary antibody with PBS and normal mouse serum. Known immunostaining-positive slides were used as positive controls.

The criteria of positive staining for p53 and $p21^{WAF-1}$ were as previously reported[6-8, 14-16]. Quatitative analysis of PCNA immunostaining results was recorded as the number of positive staining cells per mm^2 of the tissue section[17,18]. All the immunostaining slides were observed by two pathologists independently and the final concordant results were adopted.

Statistic analysis

Fisher' s exact χ^2 test and t-test were applied for the statistical analysis and two-sided P value of less than 0.05 was considered statistically significant.

RESULTS

Histopathological results

Among the cases of fetal esophageal epithelium, the number of basal cell layers ranged from 2 to 6. Five cases contained more than 10 basal cell layers and showed a high proliferation activity. As for the cases of adult esophageal epithelium, the results of histopathological diagnosis were 31 normal cases, 106 cases with BCH, 31 cases with DYS and 26 cases with SCC.

Comparison of PCNA protein expression between fetal and subtypes of adult esophageal epithelium

PCNA positive immunostaining cells were located mainly in the basal cell layer. And the positive immunoreaction occurred mainly in the nucleolus in dark brown. The mean number of PCNA positive immunostaining cells was 506±239 per mm^2 in fetal esophageal epithelia, which was significantly higher than that in adult esophageal epithelia of normal and BCH (P<0.05, t-test), but significantly lower than that in adult esophageal epithelia with DYS and SCC (P<0.05, t-test) (Table 2).

Table 2 Quantitative comparison of PCNA expression between fetal and subtypes of adult esophageal epithelia

Histopathological subtypes	Case (n)	Number of immunostaining positive cells / mm^2
Adult normal	31	200±113
Adult BCH	106	286±150
Fetal	31	506±239[a]
Adult DYS	31	719±389
Adult SCC	26	1261±545

[a]P<0.05 *vs* t-test.

Comparison of P53 protein expression between fetal and subtypes of adult esophageal epithelia

p53 positive immunostaining cells were located mainly in the basal cell layer and the positive immunoreaction occurred mainly in the nucleoli in brown.

The positive immunostaining rate of p53 was 10 % (3/31) in fetal esophageal epithelia, which was significantly lower than that of adult normal esophageal epithelia (50 %, 14/28), adult epithelia with BCH (62 %, 23/37), DYS (73 %, 8/11) and SCC (86 %, 6/7) (P<0.05, Fisher' s exact test) (Table 3).

Table 3 Comparison of p53 expression between fetal and subtypes of adult esophageal epithelia

Histopathological subtypes	Case (n)	Positive immunostaining	
		Number	Percentage (%)
Fetal	31	3	10[a]
Adult normal	28	14	50
Adult BCH	37	23	62
Adult DYS	11	8	73
Adult SCC	7	6	86

[a]P<0.05 *vs* Fisher' s exact test.

Expression of $p21^{WAF-1}$ protein in fetal esophageal epithelia

No positive immunoreaction of $p21^{WAF-1}$ was detected in all the fetal esophageal epithelia. However, $p21^{WAF-1}$ positive immunostaining cells were observed in adult esophagus with 39 % (11/28) in normal, 38 % (14/37) in BCH, 27 % (3/11) in DYS and 14 % (1/7) in SCC.

DISCUSSION

To our knowledge, this is the first report about the role of PCNA as an indicator of proliferation status of fetal esophageal epithelium. In our study, we observed that most PCNA immunostaining positive cells were located in the basal layer

of fetal esophageal epithelium. PCNA is an important index of cell proliferation kinetics. Qian *et al*[18] found that according to the proliferation status, most cell nuclei were in the G1 phase to S phase of cell cycle in the cell clones with high proliferative activity. And the positive rate of PCNA expression increased gradually in cell nuclei with the progress of G1 phase and reached a peak when entering S phase. Our research found that all fetal esophageal epithelia showed a positive immunoreaction of PCNA and possessed high level of positive immunostaining cells per mm^2, which was much higher than that in normal adult esophageal epithelium and BCH. This result is concordant with previous theory and suggests that PCNA may act as a good marker for fetal esophageal epithelium proliferation status.

In our study, we also observed that malignant adult esophageal epithelia possessed much more PCNA positive immunostaining cells than fetal esophageal epithelia. This phenomenon is plausible. It was reported that PCNA played a role in DNA damage repair (DDR). With the presence of nucleotide excision, PCNA binds replication protein A (RPA) and constitutes a subunit of DNA polymerase δ[19,20]. Kieczkowaske *et al*[21] also supposed that PCNA could combine with hMSH6 and hMSH3, the subunits of hMutSalpha and hMutSbeta that acted as cofactors in DNA mismatch repair system. Malignant tissue was characterized by high frequencies of DNA mismatch, breakages and mutations, which would in turn induce more expression of PCNA for its repair function. As for fetal esophageal epithelia, there were few opportunities of contacting external environmental carcinogens and incurring much DNA damages and mutations. As a result, adult malignant esophageal epithelia had much more PCNA positive immunostaining cells, which implied that PCNA could potentially act as an indicator of malignant proliferation.

For the expression of p53, the positive immunostaining rate was 10 % in fetal esophageal epithelia, which was much lower than that in adult esophageal epithelia of each histopathological subtype. These differences were due to lack of induced p53 expression by external environmental factors in fetal esophageal epithelia. But in our study, there were some cases that were observed with expression of p53. Guo *et al*[11] reported that no expression of p53 was detected in fetal esophageal epithelia that had been cultured by NMBzA for up to 3 weeks. p53 supervised cell cycle through G1 phase checkpoint[21]. Then we supposed that stable expression of p53 might be required for normal cell cycle in the highly proliferative fetal esophageal epithelia. Lowe *et al*[21] found that disfigurement was not detected during development of rat fetus, which showed strong p53 expression. It was suggested that p53 possessed a protective function in fetal tissue development. Although this mechanism should be studied further, our study confirmed its existence in fetal esophageal epithelium development and maybe this function of p53 worked in a special stage of fetal esophageal epithelium proliferation and differentiation.

No positive expression of p21^{WAF-1} was observed in fetal esophageal epithelia. This protein has been reported to be trans-activated by p53 and could repair genomic DNA damages[7, 8]. Fetal esophageal epithelium encountered few outer carcinogens and few DNA damages occurred in this tissue. We hypothesize that there may not be a large number of p21^{WAF-1} required for DNA damage repair in development of fetal esophageal epithelium.

In conclusion, PCNA can reflect the proliferation status of fetal esophageal epithelium, and p53 may contribute to its development. But p21^{WAF-1} may not play a role in the process of its development. Further studies to explore the molecular mechanisms of these proteins in esophageal development should be performed to provide more pronounced evidences.

REFERENCES

1 **Wang LD**, Chen H. Alterations of tumor suppressor gene p53-Rb system and human esophageal carcinogenesis. *Shijie Huaren Xiaohua Zazhi* 2002; **9**: 367-371

2 **Shi ST**, Yang GY, Wang LD, Xue Z, Feng B, Ding W, Xing EP, Yang CS. Role of P53 gene mutations in human esophageal carcinogenesis: results from immunohistochemical and mutation analysis of carcinomas and nearby non-cancerous lesions. *Carcinogenesis* 1999; **20**: 591-597

3 **Sidransky D,** Hollstein M. Clinical implications of the p53 gene. *Annu Rev Med* 1996; **47**: 285-301

4 **Gao H**, Wang LD, Zhou Q, Hong JY, Huang TY, Yang CS. p53 tumor suppressor gene mutation in early esophageal precancerous lesions and carcinoma among high-risk populations in Henan, China. *Cancer Res* 1994; **54**: 4342-4346

5 **Bennett WP**, Hollstein MC, He A, Zhu SM, Resau JH, Trump BF, Metcalf RA, Welsh JA, Midgley C, Lane DP. Archival analysis of p53 genetic and protein alterations in Chinese esophageal Cancer. *Oncogene* 1991; **6**: 1779-1784

6 **Ohbu M**, Kobayashi N, Okayasu I. Expression of cell cycle regulatory proteins in the multistep process of oesophageal carcinogenesis: stepwise over-expression of cyclin E and p53, reduction of p21(WAF1/CIP1) and dysregulation of cyclin D1 and p27(KIP1). *Histopathology* 2001; **39**: 589-596

7 **Shirakawa Y**, Naomoto Y, Kimura M, Kawashima R, Yamatsuji T, Tamaki T, Hamada M, Haisa M, Tanaka N. Topological analysis of p21WAF1/CIP1 expression in esophageal squamous dysplasia. *Clin Cancer Res* 2000; **6**: 541-550

8 **Wang LD**, Yang WC, Zhou Q, Xing Y, Jia YY, Zhao X. Changes of p53 and Waf1p21 and cell proliferation in esophageal carcinogenesis. *China Natl J New Gastroenterol* 1997; **3**: 87-89

9 **Lohr F**, Wenz F, Haas S, Flentje M. Comparison of proliferating cell nuclear antigen (PCNA) staining and BrdUrd-labelling index under different proliferative conditions in vitro by flow cytometry. *Cell Prolif* 1995; **28**: 93-104

10 **Gillen P,** McDermott M, Grehan D, Hourihane DO, Hennessy TP. Proliferating cell nuclear antigen in the assessment of Barrett's mucosa. *Br J Surg* 1994; **81**: 1766-1768

11 **Guo YJ**, Lu SX, Liang YY. Alterations of oncogenes in human fetal esophageal epithelium induced by N-methylbenzylnitrosamine (NMBzA). *Zhonghua Zhongliu Zazhi* 1994; **16**: 407-410

12 **Lu SX**. Esophageal carcinoma in human fetus induced by N-methyl-N-benzylnitrosamine (NMBzA). *Zhonghua Zhongliu Zazhi* 1989; **11**: 401-403

13 **Zhang P.** Studies on the activation of oncogenes by alternariol monomethyl ether in human fetal esophageal epithelium. *Zhonghua Binglixue Zazhi* 1991; **20**: 14-17

14 **Chen H,** Wang LD, Guo M, Gao SG. Alterations of p53 and PCNA in cancer and adjacent tissues from concurrent carcinomas of the esophagus and gastric cardia in the same patient in Linzhou, a high incidence area for esophageal cancer in northern China. *World J Gastroenterol* 2003; **9**: 16-21

15 **Wang LD**, Shi ST, Zhou Q, Goldstein S, Hong JY, Shao P, Qiu SL, Yang CS. Changes in P53 and cyclin D1 protein level and cell proliferation in different stages of Henan esophageal and gastric-cardia carcinogenesis. *Int J Cancer* 1994; **59**: 514-519

16 **Wang LD**, Hong JY, Qiu SL, Gao HG, Yang CS. Accumulation of p53 protein in human esophageal precancerous lesions: a possible early biomarker for carcinogenesis. *Cancer Res* 1993; **53**: 1783-1787

17 **Koide N**, Yamanda T, Iida F, Usuda N, Nagata T. Immunohistochemical studies of vascular volume and proliferative activity in squamous cell carcinoma of the esophagus. *Surg Today* 1997; **27**: 99-106

18 **Qian LF,** Zhang DX, Cheng AM. Cytophotometric determination of DNA content of esophageal mucosa cells of human fetus with different monthly age and analysis of proliferation of cells in tissues. *Xi'an Yike Daxue Zazhi* 1991; **12**: 49-53

19 **Mitkova AV**, Biswas EE, Biswas SB. Cell cycle specific plasmid DNA replication in the nuclear extract of Saccharomyces cerevisiae: modulation by replication protein A and proliferating cell nuclear antigen. *Biochemistry* 2002; **41**: 5255-5265

Edited by Zhu LH and Wang XL

P.O.Box 2345, Beijing 100023,China
Fax: +86-10-85381893
E-mail: wjg@wjgnet.com www.wjgnet.com

World J Gastroenterol 2003;9(7):1604-1606
World Journal of Gastroenterology
 ISSN 1007-9327

• BRIEF REPORTS •

Vascular endothelial growth factor and microvascular density in esophageal and gastric carcinomas

Jin-Rong Du, Ying Jiang, Yan-Mei Zhang, Hong Fu

Jin-Rong Du, Ying Jiang, Yan-Mei Zhang, Hong Fu, Department of Pathology, the Second Affiliated Hospital, Harbin Medical University, Harbin 150086, Heilongjiang Province, China
Correspondence to: Dr. Jin-Rong Du, Department of Pathology, the Second Affiliated Hospital, Harbin Medical University, Harbin 150086, Heilongjiang Province, China. jying1972@yahoo.com
Telephone: +86-451-6605803
Received: 2002-11-19 **Accepted:** 2003-01-16

Abstract

AIM: To observe the relationship between the expression of vascular endothelial growth factor (VEGF), microvascular density (MVD) and the pathological characteristics of esophageal and gastric carcinomas.

METHODS: S-P immunohistochemical staining was used to investigate the expression of VEGF in all the specimens. The antibody against factor VIII-related antigen was used to display vascular endothelial cells, and MVD was examined by counting the factor VIII-positive vascular endothelial cells.

RESULTS: The positive rates of VEGF expression in esophageal carcinoma and gastric carcinoma were 81.36 % and 67.5 % respectively, and the MVD averaged 41.81±8. 44 and 34.36±9.67 respectively, which were higher than those in benign diseases. The expression of VEGF and MVD were closely correlated with the degree of differentiation, lymphatic metastasis, but not related to depth of cancer invasion. In early stage gastric carcinoma, the rate of expression of VEGF and MVD was lower than that in progressive gastric carcinomas.

CONCLUSION: The expression of VEGF is correlated with tumor angiogenesis, and VEGF plays an important role in new blood vessels formation, the expression of VEGF and MVD play an important role in tumor growth and metastasis. MVD and the expression of VEGF may be two important indexes for patients' prognosis.

Du JR, Jiang Y, Zhang YM, Fu H. Vascular endothelial growth factor and microvascular density in esophageal and gastric carcinomas. *World J Gastroenterol* 2003; 9(7): 1604-1606
http://www.wjgnet.com/1007-9327/9/1604.asp

INTRODUCTION

The growth and metastasis of solid tumor, a complex biological event, are affected by many factors. Recent research found that the growth and metastasis of tumors needed constant angiogenesis, which could provide a way for tumor metastasis through vessels, and could affect the prognosis of patients[1]. Angiogenesis is not an active process by itself, and it is controlled by some angiogenic factors and some angiogenic inhibitors[2]. Of all the angiogenic factors, vascular endothelial growth factor (VEGF) is a potent, multifunctional cytokine that exerts several important and possibly independent actions on vascular endothelium. That is its property and capacity to induce angiogenesis, which has excited the greatest interest in VEGF[3].

In this study, we used immunohistochemical method to detect VEGF expression and MVD in 59 cases of esophageal carcinoma and 80 cases of gastric carcinoma. We studied the relationship between VEGF expression and MVD and pathological features, which will help to understand the role of VEGF and angiogenesis in the growth of esophageal and gastric cancers.

MATERIALS AND METHODS

Materials

The resected specimens from 59 cases of esophageal cancer and 80 cases of gastric cancer were obtained from our hospital from January 2000 to June 2002. Of 59 cases of esophageal carcinoma, 57 were male and 2 were female, with a mean age of 57 (38 to 79). Of 80 cases of gastric carcinoma, 55 were male, 25 were female, with a mean age of 59 (35 to 69). All these specimens were clearly classified by experienced pathologists based on the depth of invasion, metastasis of lymph nodes and degree of differentiation. We collected specimens of 20 normal esophageal tissues and 20 gastric tissues as control. All of them had not received any radiotherapy or chemotherapy.

Reagents and methods

Rabbit anti-human VEGF polyclonal antibodies (RAB-0243), rabbit anti-human VIII polyclonal antibodies (RAB-0070) and ready-to-use SP immunohistochemical reagent box were purchased from FuJian Maxin Co. Ltd. Formalin-fixed, paraffin-embedded specimens were available and sectioned sequentially with a thickness of 4 μm. The sections carrying the detected antigen were stained with SP immunohistochemical method.

In this study we used lung cancer specimen that was known as positive of VEGF expression to be positive control, and with the first antibody substituted by PBS as negative control.

Results

Criteria of positive staining VEGF According to the criteria proposed by Volms *et al*[4], brown granules in the cytoplasm of tumor cells or vascular endothelial cells were identified to be positive VEGF. The sections were graded respectively according to the density (1) and the percentage (2) of positively stained tumor cells into score 0, 1, 2 and 3. If the sum of two scores (1) and (2) were 0-2, the section was considered as negative, whereas 3-6 was considered as positive VEGF.

MVD According to the criteria proposed by Weidners *et al*[5], when the cytoplasm of vascular endothelial cells was stained brown or brownish yellow, it was positive. The microvessels were counted according to the number of single endothelial cell or endothelial cell cluster showing brownish yellow granules in the cytoplasm. The sections were observed first under the low power (×40), then the most dense area of microvessel sections was selected under the high power (×200, the surface area of every vision field being 0.785 mm^2). The number of microvessel in three vision fields were counted and averaged as MVD of this specimen.

Statistical methods

Statistic analysis was performed by using the χ^2 test to dispose the expression of VEGF and the pathological features. *t* test was used to detect the relationships between the expression of VEGF and MVD, and between MVD and pathological characteristics.

RESULTS

The relationship between the expression of VEGF and pathological features of esophageal carcinoma

Of 59 cases of esophageal carcinoma, 11 cases were negative and 48 cases were positive, and the positive rate was 81.36 % (48/59). Of 20 normal esophageal tissues, 4 cases were positive, and the positive rate was 20 %. The rate of expression of VEGF in esophageal carcinoma was higher than that in normal esophageal tissue (χ^2=24.99, P<0.001). The expression of VEGF was closely related to pathological grade, that is, the poorer differentiation of the tumor, the higher expression of VEGF (χ^2=7.08, P<0.05). The cases having lymph node metastasis had significantly higher VEGF expression than those having no lymph node metastasis (χ^2=5.59, P<0.05). The VEGF expression was not related to invasion depth of tumor (Table 1).

Table 1 Relationship between expression of VEGF and MVD and pathological features of esophageal carcinoma

Pathological characteristics	*n*	VEGF				MVD	
		-	+-++	x^2	*P*	$\bar{x}\pm s$	*P*(*t*)
Degree of differentiation							
Well differentiated	27	9	18	7.08	<0.05	38.52±9.22	<0.05
Poorly differentiated	32	2	30			43.43±7.61	(*t*=2.07)
Depth of invasion							
Invading musclaris	37	7	30	0.01	>0.05	40.38±8.31	>0.05
Invading serosa	22	4	18			42.53±9.24	(*t*=0.88)
LN metastasis							
-	35	10	25	5.59	<0.05	38.22±8.54	<0.05
+	24	1	24			45.5±7.04	(*t*=3.23)

The relationship between the expression of VEGF and pathological features of gastric carcinoma

Of 80 cases of gastric carcinomas, 26 cases were negative and 54 cases were positive, and the positive rate was 67.5 % (54/80). There was no positive stain in 20 cases of gastric tissues. The expression of VEGF was closely related to degree of differentiation (χ^2=11.31, P<0.01) and lymph node metastasis (χ^2=9.32, P<0.01). As in esophageal carcinoma, the expression of VEGF had no significant difference between the different depths of invasion (χ^2=0.40, P<0.05). The expression of VEGF in early stage carcinoma was significantly lower than that in progressive stage cancer (χ^2=19.67, P<0.001) (Table 2).

The relationship between MVD and pathological features in esophageal carcinoma and gastric carcinoma

In the two carcinomas, MVD was higher than that in normal tissue, and MVD was closely related to differentiation degree of tumor and metastasis of lymph nodes, but not related to depth of invasion. In gastric carcinoma, MVD was significantly different between the different stages of carcinoma. (Table 1 and Table 2).

The relationship between VEGF expression and MVD in the two cancers

In this study, MVD was closely related to the expression of VEGF in gastric carcinoma and esophageal carcinoma, that is, the stronger the expression of VEGF, the higher the MVD. This suggested that VEGF be related to MVD and angiogenesis. VEGF and MVD were closely related to tumor growth (Table 3).

Table 2 Relationship between expression of VEGF and MVD and pathological features of gastric carcinoma

Pathological characteristics	*n*	VEGF				MVD	
		-	+-++	x^2	*P*	$\bar{x}\pm s$	*P* (*t*)
Degree of differentiation							
Well differentiated	43	21	22	11.31	<0.001	32.85±6.14	<0.01
Poorly differentiated	37	5	32			38.63±5.10	(*t*=4.53)
Depth of invasion							
Not invading serosa	39	14	25	0.40	>0.05	34.94±9.26	>0.05
Invading serosa	41	12	29			33.68±9.12	(*t*=0.30)
Tumor stage							
Early stage	21	15	6	19.67	<0.001	32.14±5.89	<0.05
Progressive stage	59	11	48			35.46±6.58	(*t*=2.04)
LN metastasis							
-	52	23	29	9.32	<0.01	33.06±5.33	<0.05
+	28	3	25			35.74±7.58	(*t*=2.07)

Table 3 Relationship between VEGF expression and MVD in the two cancers

	n	MVD	
		$\bar{x}\pm s$	*P*(*t*)
VEGF expression in esophageal carcinoma			
-	11	43.45±6.98	<0.05
+-++	48	31.30±8.74	(*t*=4.33)
VEGF expression in esophageal carcinoma			
-	26	31.08±9.54	<0.05
+-++	54	36.83±8.87	(*t*=2.65)

DISCUSSION

The importance of tumor angiogenesis in the growth and infiltration of tumor has been well known since J Folkman first proposed the hypothesis "Growth of solid tumor and the formation of metastasis are dependent on the formation of new blood vessels" in 1971. Growth of solid tumors is dependent on the induction of new blood vessels[6]. In order to maintain the unlimited growth of tumor, tumor tissue must depend on the constant and wide formation of new blood vessels, which is essential for tumors to grow beyond minimal size, providing oxygenation and nutrient perfusion as well as removal of waste products[7]. In normal organism, angiogenesis is strictly controlled, but in tumors, angiogenesis is uncontrolled and immature[8]. Controlled by angiogenic factors and angiogenic inhibitors, tumor cells, endothelial cells and other cells can produce and release VEGF protein if the local microenvironment is changed by hypoxia, *etc*[9]. Some researches proved that in tumors with foci of relative hypoxia, VEGF mRNA may be expressed not only by malignant cells but also by stromal cells[10,11]. Different tumor needs different angiogenesis factors, such as bFGF, which is a very important angiogenesis factor in fibrosarcoma. In gastroenteric tumors VEGF proved to play a key role.

VEGF, also known as VPF (vascular permeability factor), is secreted by some tumor cells. It combines with its receptors on endothelial cells. It can render venules and small veins hyperpermeable to circulatory macromolecules, and induce angiogenesis, which can induce tumor growth[12].

The human VEGF gene has been assigned to chromosome 6p21.3. Its coding region spans approximately 14kb. Native VEGF is a basic, heparin-binding homodimeric glycoprotein[13,14]. VEGF target cell is endothelial cell. On the one hand it renders microvascular hyperpermeable, so that plasma proteins and fibrinogen leak, can stimulate angiogenesis and new stroma formation. On the other hand, VEGF stimulates the endothelial cell of microvessels to proliferate, migrate and alters their pattern of gene expression[15].

More and more researches proved the important role of VEGF in tumor growth. Recently, Meada *et al*[16] found that VEGF expression was consistent with MVD, that is, MVD of gastric carcinoma with positive expression of VEGF was higher than that with negative expression of VEGF, and MVD was higher in the area where VEGF expression was positive. Toi *et al*[17] found that the positive expression of VEGF and factor VIII were detected in the samples of breast carcinoma which were poorly differentiated, with inrasive growth and lymph node metastasis. So strong expression of VEGF and factor VIII may indicate a poor prognosis.

In our study, a strong correlation was found between VEGF expression and increased tumor microvasculature, malignancy and metastasis in esophageal carcinoma and gastric carcinoma. These results indicate that VEGF and angiogenesis promoted by VEGF play important roles in cancer growth, infiltration and metastasis in esophageal and gastric carcinoma. It also implied that VEGF expression and MVD have prognostic significance. We also found that there was an obvious heterogeneity in VEGF expression and new vessel formation in cancer tissue. New tumor vessels were deficienct in constant basement membrane. This proved that the new vessels were hyperpermeable. This may facilitate the tumor cells to penetrate through the blood vessels and metastasis. VEGF expression manifested that positive cells located at the center of tumor or at the edge of the necrosis area, this may be explained by the hypoxia, which can stimulate VEGF expression and its biological activity.

In the study of the correlation of VEGF expression and MVD, we proved that VEGF was closely related with MVD in the cancer tissues of both esophageal and gastric carcinoma, this result proved VEGF could induce formation of new blood vessels. Thus VEGF expression and MVD may play important roles in tumor biological behaviors, progression and prognosis.

In conclusion, VEGF overexpression and active angiogenesis exist in esophageal carcinoma and gastric carcinoma. VEGF and MVD are closely relevant to lymph node metastasis, tumor differentiation and clinical stage. VEGF and MVD may act as two valuable indexes of tumor prognosis. These conclusions may provide an important theoretical evidence for cancer therapy through antiangiogenesis.

REFERENCES

1 **Folkman J**, Shing Y. Angiogenesis. *J Biol Chem* 1992; **267**: 10931-10934
2 **Klagsbrun M**, D' Amore PA. Regulators of angiogenesis. *Annu Rev Physiol* 1991; **53**: 217-239
3 **Dvorak HF**, Brown LF, Detmer M, Dvorak AM. Vascular permeability factor / vascular endothe lial growth factor, microvascular hyperpermeability and angiogenesis. *Am J Pathol* 1995; **146**: 1029-1039
4 **Volm M**, Koomagi R, Mattern J. Prognostic value of vascular endothelial growth factor and its receptor Flt-1 in squamous cell lung cancer. *Int J Cancer* 1997; **74**: 64-68
5 **Weidner N**, Folkman J, Pozza F, Bevilacqua P, Allred EN, Moore DH, Meli S, Gasparini G. Tumor angiogenesis: a new significant and independent prognostic indicator in early-stage breast carcinoma. *J Natl cancer Inst* 1992; **84**: 1875-1887
6 **Folkman J**. Angiogenesis and Angiogenesis inhibition:an overview. *EXS* 1997; **79**: 1-8
7 **Hanahan D**, Folkman J. Patterns and emerging mechanisms of the angiogenic switch during tumorigenesis. *Cell* 1996; **86**: 353-364
8 **Saaristo A**, Karpanen T, Alitalo K. Mechanism of angiogenesis and their use in the inhibition of tumor growth and metastasis. *Oncogene* 2000; **19**: 6122-6129
9 **Goldberg MA**, Schneider TJ. Similarities between the oxygen sensing mechanisms regulating the expression of vascular endothelial growth factor and erythropoietin. *J Biol Chem* 1994; **269**: 4355-4359
10 **Brown LF**, Berse B, Jackman RW, Tognazzi K, Manseau EJ, Senger DR, Dvorak HF. Expression of vascular permeability factor (vascular endothelial growth factor)and its receptors in adenocarcinomas of the gastrointestinal tract. *Cancer Res* 1993; **53**: 4727-4735
11 **Brown LF**, Berse B, Jackman RW, Tognazzi K, Manseau EJ, Dvorak HF, Senger DR. Increased expression of vascular permeability factor(vascular endothelial growth factor)and its receptors in kidney and bladder carcinoma. *Am J Pathol* 1993; **143**: 1255-1262
12 **Ferrara N**, Davis-Smyth T. The biology of vascular endothelial growth factor. *Endocr Rev* 1997; **18**: 4-25
13 **Tischer E**, Mitchell R, Hartman T, Silva M, Gospodarowicz D, Fiddes JC, Abraham JA. The human gene for vascular endothelial growth factor.Multiple protein forms are encoded through alternative exon splicing. *J Biol Chem* 1991; **266**: 11947-11954
14 **Vincenti V**, Cassano C, Rocchi M, Persico G. Assignment of the vascular endothelial growth factor gene to human chromosome 6p21.3. *Circulation* 1996; **93**: 1493-1495
15 **Detmar M**, Velasco P, Richard L, Claffey KP, Streit M, Riccardi L, Skobe M, Brown LF. Expression of vascular endothelial growth factor induces an invasive phenotype in human squamous cell carcinomas. *Am J Pathol* 2000; **156**: 159-167
16 **Maeda K**, Chung YS, Ogawa Y, Takatsuka S, Kang SM, Ogawa M, Sawada T, Sowa M. Prognostic value of vascular endothelial growth factor expression in gastric carcinoma. *Cancer* 1996; **77**: 858-863
17 **Toi M**, Inada K, Hoshina S, Suzuki H, Kondo S, Tominaga T. Vascular endothelial growth factor and platelet-derived endothelial cell growth factor are frequently coexpressed in highly vascularized human breast cancer. *Clin Cancer Res* 1995; **1**: 961-964

Edited by Zhang JZ and Zhu LH

P.O.Box 2345, Beijing 100023,China
Fax: +86-10-85381893
E-mail: wjg@wjgnet.com www.wjgnet.com

World J Gastroenterol 2003;9(7):1607-1610
World Journal of Gastroenterology
 ISSN 1007-9327

• BRIEF REPORTS •

Effect of P-selectin monoclonal antibody on metastasis of gastric cancer and immune function

Jin-Lian Chen, Wei-Xiong Chen, Jin-Shui Zhu, Ni-Wei Chen, Tong Zhou, Ming Yao, Dong-Qing Zhang, Yun-Lin Wu

Jin-Lian Chen, Wei-Xiong Chen, Jin-Shui Zhu, Ni-Wei Chen, Department of Gastroenterology, Shanghai Jiao-Tong University affiliated Sixth People' s Hospital, Shanghai 200233, China
Tong Zhou, **Yun-Lin Wu**, Ruijin Hospital, Shanghai Second Medical University, Shanghai 200025, China
Ming Yao, Shanghai Cancer Institute, Shanghai 200233, China
Dong-Qing Zhang, Shanghai Institute of Immunology, Shanghai 200025, China
Supported by the Youth Science Foundation of Shanghai Public Administration No.131984Y15
Correspondence to: Jin-Lian Chen, Department of Gastroenterology, Shanghai Sixth People' s Hospital, Shanghai Jiao-Tong University affiliated Sixth People' s Hospital, Shanghai 200233, China. wqq_021002@163.com
Telephone: +86-21-64369181
Received: 2003-03-02 **Accepted:** 2003-03-29

Abstract

AIM: To investigate the effect of cell adhesion molecule P-selectin monoclonal antibody (Mab) on metastasis and immune function of mice orthototopically implanted with human gastric cancer tissue.

METHODS: SCID mice were implanted orthotopically with SGC-7901 human gastric carcinoma tissue. Starting from day 3 after operation, animals were given intravenously PBS or P-selectin Mab (100 μg/injection) (for both normal mice and tumor-implanted mice with tumors), twice weekly for 3 weeks. Two animals in each group were sacrificed randomly at the 1st, 2nd, 4th week and 6th week. While T cell and B cell transformation indices were determined with the ^{3}H TdR infiltration method, the NK cell activity was detected by the LDH release method.

RESULTS: The metastatic rate in the P-selectin Mab treated group was lower than that in the PBS treated group (with tumors). The NK activity of normal mice increased over time. The immune functions (T, B cell function, NK activity) of the tumor group in the 6th week were significantly lower than those in the 4th week, but the change was attenuated by P-selectin Mab.

CONCLUSION: P-selectin Mab could suppress the metastasis of gastric cancer with no adverse effect on host immune function.

Chen JL, Chen WX, Zhu JS, Chen NW, Zhou T, Yao M, Zhang DQ, Wu YL. Effect of P-selectin monoclonal antibody on metastasis of gastric cancer and immune function. *World J Gastroenterol* 2003; 9(7): 1607-1610
http://www.wjgnet.com/1007-9327/9/1607.asp

INTRODUCTION

Gastric carcinoma is one of the most frequent tumors in China. Tumor metastasis is very common clinically. Cell adhesion molecules have been implicated to be crucial elements in the process of metastasis[1-28]. P-selectin is an adhesion molecules that mediates the cell to cell interaction of platelets and endothelial cells with neutrophils and monocytes as well as tumor cells[29]. Our previous study indicates that P-selectin expression is related to aggressive behavior, dissemination and poor prognosis of human gastric carcinomas, and P-selectin monoclonal artibody can inhibit gastric carcinoma metastasis[30-32]. The present study was performed to investigate effects of P-selectin monoclonal antibody on metastasis and immune function in SCID mouse metastaic models of human gastric cancer constructed by orthotopic implantation of histologically intact tumor tissue.

MATERIALS AND METHODS

Animal model

Forty-eight male SCID mice obtained from Shanghai Cancer Institute were 7-8 weeks old with weight of 20-25 g. Human gastric cancer SGC-7901, a poorly-differentiated adenocarcinoma line, was originally derived from a primary tumor and maintained by passage in nude mice subcutaneously.

SCID mice were randomly divided into experimental group (n=24) and normal group (n=24). Animal models in experimental group were made using orthotopic implantation of histologically intact tissue of human gastric carcinoma[33]. Tumors were resected aseptically. Necrotic tumor tissues were removed and the remaining non-necrotic tumor tissues were minced into pieces about 5-7 mm in diameter in Hank's balanced salt solution. Each of the tumor pieces was weighed and adjusted to be 150 mg with scissors. Mice were anesthetized with 4.3 % trichloraldehyde hydrate and an incision was made through the left upper abdominal pararectal line and peritoneal cavity was carefully exposed and a part of the serosal membrane in the middle of the greater curvature of the glandular stomach was mechanically injured by using scissors. A tumor piece of 150 mg was fixed on each injured site of the serosal surface. The stomach was then returned to the peritoneal cavity, and the abdominal wall and skin were closed. 3 d later, all animals implanted with intact tumor tissues received i.v. injection of PBS (group3, n=12) or P-selectin antibody (Suzhou Medical College; 100 μg/injectiom; group4, n=12) twice weekly for 3 weeks. Animals in normal group received i.v. injections of PBS (group1, n=12) or P-selectin antibody (100 μg/injection; group2, n=12).

Sample collection and pathological examination

Two mice in each group were sacrificed randomly on weeks 1, 2,and 4. The remaining animals were sacrificed at 6th week and the tumors growing on the stomach wall were removed and examined histologically. Tissues from all organs were examined for metastasis after careful macroscopic examination. The spleen of mice was harvested for detection of immune function.

Lymphocyte transformation test

Using ^{3}H TdR infiltration method, T cell transformation function was detected with Con A (5 μg/ml, Sigma), B cell function with LPS (50 μg/ml, Sigma). The spleen was made

into suspension and mononuclear cells were acquired with lymphocyte-separating fluid. The cell suspension was adjusted to 2×10^6/ml with RPMI 1640 liquid containing 10 % calf serum (GIBCO). Then 200 μl of the cell suspension was put into each well in 96-well plates. One plate was for Con A group, and another plate for LPS group. There were negative control group and experimental group for Con A or LPS group respectively, and each test had 5 repetitive wells and was cultivated under 5 % CO_2 at 37 ℃. The cell suspension in Con A group was cultivated for 3 d, while it was done for 5 d in Con A group. All wells were added up ^{3}H TdR 16 h before the end of cultivation. They were collected in filtration paper, and given 0.5 ml of scintillating liquid to detect cpm value with β-scintillator, which was presented with SI. SI amounts to cpm of experimental group/cpm of empty group.

NK activity

NK activity was detected by the 4 h LDH release method. NK cell activity (%)=

$$\frac{\text{Experimental group' s OD-Natural release group' s OD}}{\text{Max release group' s OD-Natural release group' s OD}}$$

Statistical methods

Comparisons among groups were performed by the student' s test and χ^2 test. A value of $P<0.05$ was considered significant.

RESULTS

Effects of P-selectin antibody on metastasis

All animals in each group were sacrificed randomly at the 1st, 2nd, 4th week and 6th week. Tumors grew in the implanted site. Under microscopy, the tumors demonstrated lower differentiated adenocarcinoma invadeing mucosal layer, submucosal layer and muscle layer. Tumor metastasis was observed most frequently in the regional lymph nodes and liver. It could be seen in lung, spleen and other organs.

In tumor group (Group 3), no metastasis was found at the 1st and 2nd week, but metastasis was found in 1 of 2 cases at the 4th week, in 5 of 6 cases at 6th week. However, in P-selectin antibody treated tumor group (Group 4), tumor metastasis was remarkably inhibited. No metastasis was found at 1st, 2nd, and 4th week, while it was found only in 1 of 6 mice at 6th week.

Table 1 Immune functions of mice in various groups ($\bar{x}\pm s$)

Group	Week 1	Week 2	Week 4	Week 6
T cell transformation indices (SI)				
Group 1	1.95±0.16	2.19±0.18	2.28±0.19	2.35±0.20
Group 2	2.10±0.19	2.13±0.21	2.42±0.23	2.27±0.22
Group 3	1.83±0.17	1.77±0.18	1.58±0.15	1.01±0.10[d]
Group 4	1.92±0.19	1.82±0.16	1.63±0.17	1.43±0.13[a]
B cell transformation indices (SI)				
Group 1	2.57±0.22	2.35±0.23	2.76±0.24	2.87±0.26
Group 2	2.49±0.24	2.33±0.26	2.82±0.28	2.59±0.29
Group 3	2.54±0.23	2.48±0.24	2.20±0.22	1.49±0.12[d]
Group 4	2.60±0.22	2.51±0.21	2.43±0.26	2.11±0.20[a]
NK activity (90)				
Group 1	8.66±0.78	11.21±0.99	14.22±1.22[b]	18.62±1.14[c]
Group 2	8.96±0.91	11.39±1.12	13.75±1.03	17.99±1.36
Group 3	8.12±0.81	7.63±0.74	6.75±0.62	4.17±0.52[d]
Group 4	8.00±0.73	7.61±0.83	6.97±0.62	6.24±0.63[a]

[a]$P<0.05$ *vs* group3; [b]$P<0.05$, [c]$P<0.01$ *vs* week1; [d]$P<0.05$ *vs* week4.

Effect of P-selectin antibody on immune function

The NK activity of normal mice increased over time, but no significant difference of the immune functions of T cell and B cell was found in all the groups. Over time, the immune functions (T, B cell function, NK activity) of SCID mice orthotopically implanted with tumor tissue were significantly lower in the 6th week than those in the 4th week, but the change was attenuated by P-selectin antibody ($P<0.05$) (Table 1).

DISCUSSION

Research on cell adhesion molecules and metastasis has aroused a lot of attention recently[34-50]. P-selectin (GMP140, CD62, or PADGEM) is located in alpha granules of platelets and Weibel-Palade bodies of endothelial cells. Once platelet or endothelial cell is activated by mediators such as thrombin, alpha granule and weibel-palade body membranes fuse rapidly with the plasma membrane, leading to the expression of P-selectin on the cell surface[29]. P-selectin contributes to interaction of tumor cell to cell adhesion by mediating endothelial cells and platelets with tumor cells.

We have immunohistochemically studied P-selectin expression in 60 cases of human gastric carcinomas. The study showed that P-selectin was expressed in human gastric cancer, which was detected not only on intratumoral endothelium but also on cancer cells. P-selectin expression was found higher in patients with lymph node metastasis than those without metastasis. The survival time and five-year survival rate were lower in P-selectin positive cases than those in negative cases[30-32]. Recently, our study indicated that P-selectin mRNA expression is related to tumor metastasis, and the metastasis may be inhibited by the monoclonal antibody. This finding is in accordance with Stone' s results[22]. These results suggest that selectins play an important role in metastasis by mediating the interaction of endothelial cells and platelets with cancer cells, and the metastasis can be inhibited by the monoclonal antibody.

Recently, study on anti-adhesion therapy with adhesion molecule monoclonal antibodies exhibits good clinical prospective[51-53]. However, there existed some problems. Antibody against intercellular adhesion molecule-1 (ICAM-1) might block inflammation while it inhibits the immune function of the body so that it increases the risk for infection[54,55]. The present study investigated the effects of P-selectin monoclonal antibody on tumor metastasis and immune function of SCID mice orthotopically implanted with gastric cancer tissue to lay foundation for clinical application of anti-adhesion therapy. The result indicated that P-selectin antibody could inhibit the metastasis. This is consistent with our previous study.

Results obtained in this study showed that NK activity of normal mice got higher with the passage of time. It was higher at 6th week than between 1st week and 4th week. But there had no significant change in both T cell and B cell function. The experiment suggested that mice used for metastasis models should not be too old, otherwise the metastasis rate of the mice implanted with tumor would be low. Our experiment discovered that the immune functions (T, B cell function, NK activity) of the tumor group were significantly lower in the 6th week than in the 4th week, but the change was remarkably attenuated by P-selectin antibody. No difference of the immune functions between the two groups at 1st, 2nd, 4th week was found. This result suggested that the immune functions of mice was suppressed with the development of tumor metastasis. On the other hand, the metastatic rates of tumor group were 50 % (1/2) at 4th week and 83.3 % (5/6) at 6th week, whereas it was 16.7 % (1/6) at 6th week in P-selectin antibody treated tumor group. Therefore, the improved immune function in the

antibody treated tumor group might result from the inhibition of metastasis by the P-selectin monoclonal antibody. Sharar discovered that P-selectin could not inhibit functions of neutrophils. The results suggest that P-selectin monoclonal antibody could inhibit the metastatic tendency with no harmful effect on host immune function.

REFERENCES

1 **Xin Y**, Li XL, Wang YP, Zhang SM, Zheng HC, Wu DY, Zhang YC. Relationship between phenotypes of cell-function differentiation and pathobiological behavior of gastric carcinomas. *World J Gastroenterol* 2001; **7**: 53-59

2 **Ikonen T**, Matikainen M, Mononen N, Hyytinen ER, Helin HJ, Tommola S, Tammela TL, Pukkala E, Schleutker J, Kallioniemi OP, Koivisto PA. Association of E-cadherin germ-line alterations with prostate cancer.*Clin Cancer Res* 2001; **7**: 3465-3471

3 **Tsujitani S**, Kaibara N. Clinical significance of molecular biological detection of micrometastases in gastric carcinoma. *Nippon Geka Gakkai Zasshi* 2001; **102**: 741-744

4 **Murahashi K**, Yashiro M, Takenaka C, Matsuoka T, Ohira M, Chung KH. Establishment of a new scirrhous gastric cancer cell line with loss of heterozygosity at E-cadherin locus. *Int J Oncol* 2001; **19**: 1029-1033

5 **Okada Y**, Fujiwara Y, Yamamoto H, Sugita Y, Yasuda T, Doki Y, Tamura S, Yano M, Shiozaki H, Matsuura N, Monden M. Genetic detection of lymph node micrometastases in patients with gastric carcinoma by multiple-marker reverse transcriptase-polymerase chain reaction assay. *Cancer* 2001; **92**: 2056-2064

6 **Yanagimoto K**, Sato Y, Shimoyama Y, Tsuchiya B, Kuwao S, Kameya T. Co-expression of N-cadherin and alpha-fetoprotein in stomach cancer. *Pathol Int* 2001; **51**: 612-618

7 **Chun YS**, Lindor NM, Smyrk TC, Petersen BT, Burgart LJ, Guilford PJ, Donohue JH. Germline E-cadherin gene mutations: is prophylactic total gastrectomy indicated? *Cancer* 2001; **92**: 181-187

8 **Shun CT**, Wu MS, Lin MT, Chang MC, Lin JT, Chuang SM. Immunohistochemical evaluation of cadherin and catenin expression in early gastric carcinomas: correlation with clinicopathologic characteristics and Helicobacter pylori infection. *Oncology* 2001; **60**: 339-345

9 **Xin Y**, Grace A, Gallagher MM, Curran BT, Leader MB, Kay EW. CD44V6 in gastric carcinoma: a marker of tumor progression. *Appl Immunohistochem Mol Morphol* 2001; **9**: 138-142

10 **Chan AO**, Lam SK, Chu KM, Lam CM, Kwok E, Leung SY, Yuen ST, Law SY, Hui WM, Lai KC, Wong CY, Hu HC, Lai CL, Wong J. Soluble E-cadherin is a valid prognostic marker in gastric carcinoma. *Gut* 2001; **48**: 808-811

11 **Chan JK**, Wong CS. Loss of E-cadherin is the fundamental defect in diffuse-type gastric carcinoma and infiltrating lobular carcinoma of the breast. *Adv Anat Pathol* 2001; **8**: 165-172

12 **Werner M**, Becker KF, Keller G, Hofler H. Gastric adenocarcinoma: pathomorphology and molecular pathology. *J Cancer Res Clin Oncol* 2001; **127**: 207-216

13 **Machado JC**, Oliveira C, Carvalho R, Soares P, Berx G, Caldas C, Seruca R, Carneiro F, Sobrinho-Simoes M. E-cadherin gene (CDH1) promoter methylation as the second hit in sporadic diffuse gastric carcinoma. *Oncogene* 2001; **20**: 1525-1528

14 **Tamura G**, Sato K, Akiyama S, Tsuchiya T, Endoh Y, Usuba O, Kimura W, Nishizuka S, Motoyama T. Molecular characterization of undifferentiated-type gastric carcinoma. *Lab Invest* 2001; **81**: 593-598

15 **Futamura N**, Nakamura S, Tatematsu M, Yamamura Y, Kannagi R, Hirose H. Clinicopathologic significance of sialyl Le(x) expression in advanced gastric carcinoma. *Br J Cancer* 2000; **83**: 1681-1687

16 **Lynch HT**, Grady W, Lynch JF, Tsuchiya KD, Wiesner G, Markowitz SD. E-cadherin mutation-based genetic counseling and hereditary diffuse gastric carcinoma. *Cancer Genet Cytogenet* 2000; **122**: 1-6

17 **Fukudome Y**, Yanagihara K, Takeichi M, Ito F, Shibamoto S. Characterization of a mutant E-cadherin protein encoded by a mutant gene frequently seen in diffuse-type human gastric carcinoma. *Int J Cancer* 2000; **88**: 579-583

18 **Maehara Y**, Kabashima A, Koga T, Tokunaga E, Takeuchi H, Kakeji Y, Sugimachi K. Vascular invasion and potential for tumor angiogenesis and metastasis in gastric carcinoma. *Surgery* 2000; **128**: 408-416

19 **Koseki K**, Takizawa T, Koike M, Ito M, Nihei Z, Sugihara K. Distinction of differentiated type early gastric carcinoma with gastric type mucin expression. *Cancer* 2000; **89**: 724-732

20 **Uchiyama K**, Yamamoto Y, Taniuchi K, Matsui C, Fushida Y, Shirao Y. Remission of antiepiligrin (laminin-5) cicatricial pemphigoid after excision of gastric carcinoma. *Cornea* 2000; **19**: 564-566

21 **Machado J**, Carneiro F, Sobrinho-Simoes M. E-cadherin mutations in gastric carcinoma. *J Pathol* 2000; **191**: 466-468

22 **Chen J**, Zhang Y, Chu Y. Inhibition of human stomach cancer metastasis in vivo by anti-P-selectin monoclonal antibody. *Zhonghua Yixue Zazhi* 1998; **78**: 437-439

23 **Luber B**, Candidus S, Handschuh G, Mentele E, Hutzler P, Feller S, Voss J, Hofler H, Becker KF. Tumor-derived mutated E-cadherin influences beta-catenin localization and increases susceptibility to actin cytoskeletal changes induced by pervanadate. *Cell Adhes Commun* 2000; **7**: 391-408

24 **Tamura G**, Yin J, Wang S, Fleisher AS, Zou T, Abraham JM, Kong D, Smolinski KN, Wilson KT, James SP, Silverberg SG, Nishizuka S, Terashima M, Motoyama T, Meltzer SJ. E-Cadherin gene promoter hypermethylation in primary human gastric carcinomas. *J Natl Cancer Inst* 2000; **92**: 569-573

25 **Hofler H**. Diffuse stomach carcinoma: from H&E diagnosis and molecular pathology to specific therapy. *Verh Dtsch Ges Pathol* 1999; **83**: 148-154

26 **Debruyne P**, Vermeulen S, Mareel M. The role of the E-cadherin / catenin complex in gastrointestinal cancer. *Acta Gastroenterol Belg* 1999; **62**: 393-402

27 **Park CK**, Shin YK, Kim TJ, Park SH, Ahn GH. High CD99 expression in memory T and B cells in reactive lymph nodes. *J Korean Med Sci* 1999; **14**: 600-606

28 **Stachura J**, Krzeszowiak A, Popiela T, Urbanczyk K, Pituch-Noworolska A, Wieckiewicz J, Zembala M. Preferential overexpression of CD44v5 in advanced gastric carcinoma Gosekigrades I and III. *Pol J Pathol* 1999; **50**: 155-161

29 **Chen JL**, Wu YL. Selectins and tumor metastasis. *Tumor* 1996; **16**: 43-44

30 **Chen JL**, Wu YL, Zhou T, Wang RN. Expression of P-selectin in human gastric cancer.*Shanghai Dier Yike Daxue Xuebao* 1996; **16**: 328-332

31 **Chen JL**, Wu YL, Zhou T, Wang RN, Chu YD, Xu HM. Prognostic siginificance of P-selectin expression in Chinese patients with gastric carcinoma. *J SMMU* 1999; **11**: 66-70

32 **Chen JL**, Zhang YX, Chu YD, Zhon T, Xu HM, Li ML. Inhibition of human stomach carcinoma metastasis in vivo by anti-P-selectin monoclonal antibody.*Shanghai Dier Yike Daxue Xuebao* 1998; **18**: 30-32

33 **Chen JL**, Chu YD, Zhang YX, Xu HM, Li ML. Metastatic models of human gastric carcinoma established by orthotopic implantation of histologically intact specimens in SCID mice. *Shanghai Shiyan Dongwu Kexue* 1997; **17**: 207-209

34 **Koshikawa N**, Moriyama K, Takamura H, Mizushima H, Nagashima Y, Yanoma S, Miyazaki K. Overexpression of laminin gamma2 chain monomer in invading gastric carcinoma cells. *Cancer Res* 1999; **59**: 5596-5601

35 **Becker KF**, Kremmer E, Eulitz M, Becker I, Handschuh G, Schuhmacher C, Muller W, Gabbert HE, Ochiai A, Hirohashi S, Hofler H. Analysis of E-cadherin in diffuse-type gastric cancer using a mutation-specific monoclonal antibody. *Am J Pathol* 1999; **155**: 1803-1809

36 **Jawhari AU**, Noda M, Pignatelli M, Farthing M. Up-regulated cytoplasmic expression, with reduced membranous distribution of the src substrate p120(ctn) in gastric carcinoma. *J Pathol* 1999; **189**: 180-185

37 **Nollet F**, Berx G, van Roy F. The role of the E-cadherin / catenin adhesion complex in the development and progression of cancer. *Mol Cell Biol Res Commun* 1999; **2**: 77-85

38 **Schuhmacher C**, Becker KF, Reich U, Schenk U, Mueller J, Siewert JR, Hofler H. Rapid detection of mutated E-cadherin in perito-

neal lavage specimens from patients with diffuse-type gastric carcinoma. *Diagn Mol Pathol* 1999; **8**: 66-70

39 **Hsieh HF**, Yu JC, Ho LI, Chiu SC, Harn HJ. Molecular studies into the role of CD44 variants in metastasis in gastric cancer. *Mol Pathol* 1999; **52**: 25-28

40 **Jawhari AU**, Noda M, Farthing MJ, Pignatelli M. Abnormal expression and function of the E-cadherin-catenin complex in gastric carcinoma cell lines. *Br J Cancer* 1999; **80**: 322-330

41 **Sato S**, Yokozaki H, Yasui W, Nikai H, Tahara E. Silencing of the CD44 gene by CpG methylation in a human gastric carcinoma cell line. *Jpn J Cancer Res* 1999; **90**: 485-489

42 **Yoo CH**, Noh SH, Kim H, Lee HY, Min JS. Prognostic significance of CD44 and nm23 expression in patients with stage II and stage IIIA gastric carcinoma. *J Surg Oncol* 1999; **71**: 22-28

43 **Nakanishi H**, Kodera Y, Yamamura Y, Kuzuya K, Nakanishi T, Ezaki T, Tatematsu M. Molecular diagnostic detection of free cancer cells in the peritoneal cavity of patients with gastrointestinal and gynecologic malignancies. *Cancer Chemother Pharmacol* 1999; **43**(Suppl): S32-36

44 **Taniuchi K**, Takata M, Matsui C, Fushida Y, Uchiyama K, Mori T, Kawara S, Yancey KB, Takehara K. Antiepiligrin (laminin 5) cicatricial pemphigoid associated with an underlying gastric carcinoma producing laminin 5. *Br J Dermatol* 1999; **140**: 696-700

45 **Koyama S**, Maruyama T, Adachi S. Expression of epidermal growth factor receptor and CD44 splicing variants sharing exons 6 and 9 on gastric and esophageal carcinomas: a two-color flow-cytometric analysis. *J Cancer Res Clin Oncol* 1999; **125**: 47-54

46 **Isozaki H**, Ohyama T, Mabuchi H. Expression of cell adhesion molecule CD44 and sialyl Lewis A in gastric carcinoma and colorectal carcinoma in association with hepatic metastasis. *Int J Oncol* 1998; **13**: 935-942

47 **Saito H**, Tsujitani S, Katano K, Ikeguchi M, Maeta M, Kaibara N. Serum concentration of CD44 variant 6 and its relation to prognosis in patients with gastric carcinoma. *Cancer* 1998; **83**: 1094-1010

48 **Harn HJ**, Shen KL, Liu CA, Ho LI, Yang LS, Yueh KC. Hyaluronate binding assay study of transfected CD44 V4-V7 isoforms into the human gastric carcinoma cell line SC-M1. *J Pathol* 1998; **184**: 291-296

49 **Yasui W**, Kudo Y, Naka K, Fujimoto J, Ue T, Yokozaki H, Tahara E. Expression of CD44 containing variant exon 9 (CD44v9) in gastric adenomas and adenocarcinomas: relation to the proliferation and progression. *Int J Oncol* 1998; **12**: 1253-1258

50 **Castella EM**, Ariza A, Pellicer I, Fernandez-Vasalo A, Ojanguren I. Differential expression of CD44v6 in metastases of intestinal and diffuse types of gastric carcinoma. *J Clin Pathol* 1998; **51**: 134-137

51 **Chen JL**, Zhou T, Chu YD, Xu HM, Li X, Zhang MJ, Zhang DH, Wu YL. The significance of intercellular adhesion molecule-1 and P-selectin in hepatic ischemia-reperfusion injury.*Zhongguo Weizhongbing Jijiuyixue* 1998; **10**: 670-672

52 **Chen JL**, Chu YD, Zhou T, Xu HM, Li X, Zhang MJ. Effects of P-selectin and anti-P-selectin antibody on apoptosis during liver ischemia-reperfusion injury.*Shanghai Dier Yike Daxue Xuebao* 2000; **20**: 239-241

53 **Wu P**, Li X, Zhou T, Zhang MJ, Chen JL, Wang WM, Chen N, Dong DC. Role of P-selectin and anti-P-selectin monoclonal antibody in apoptosis during hepatic/renal ischemia reperfusion injury. *World J Gastroentero* 2000; **6**: 244-247

54 **Sandborn WJ**, Targan SR. Biologic therapy of inflammatory bowel disease. *Gastroenterology* 2002; **123**: 1592-1608

55 **Burns RC**, Rivera-Nieves J, Moskaluk CA, Matsumoto S, Cominelli F, Ley K. Antibody blockade of ICAM-1 and VCAM-1 ameliorates inflammation in the SAMP-1/Yit adoptive transfer model of Crohn's disease in mice. *Gastroenterology* 2001; **121**: 1428-1436

Edited by Ren SY

P.O.Box 2345, Beijing 100023,China
Fax: +86-10-85381893
E-mail: wjg@wjgnet.com www.wjgnet.com

World J Gastroenterol 2003;9(7):1611-1614
World Journal of Gastroenterology
 ISSN 1007-9327

• BRIEF REPORTS •

Effects of heparin on liver fibrosis in patients with chronic hepatitis B

Jun Shi, Jing-Hua Hao, Wan-Hua Ren, Ju-Ren Zhu

Jun Shi, Jing-Hua Hao, Wan-Hua Ren, Ju-Ren Zhu, Center for Liver Diseases, Shandong Provincial Hospital, Jinan 250021, Shandong Province, China
Supported by Research Grant of Shandong Provincial Health Committee. No. 2001CA2CKA2
Correspondence to: Dr. Jun Shi, Center for Liver Diseases, Shandong Provincial Hospital, 342 Jing Wu Wei Qi Road, Jinan 250021, Shandong Province, China. sdshij@yahoo.com.cn
Telephone: +86-531-7938911-2450
Received: 2002-11-29 **Accepted:** 2003-03-02

Abstract

AIM: To evaluate the effects of heparin on liver fibrosis in patients with chronic hepatitis B.

METHODS: Fifty-two cases under study were divided into two groups, group A and group B. The two groups were given regular treatment and heparin/low molecular weight heparin (LMWH) treatment respectively. Hepatic functions, serum hyaluronic acid (HA) and type IV collagen levels were measured before and after the treatment, and six cases were taken liver biopsy twice.

RESULTS: After treatment, hepatic functions became significantly better in both groups. Serum HA and type IV collagen levels in group B compared with group A, decreased significantly after treatment. Collagen proliferation also decreased in group B after treatment.

CONCLUSION: Heparin/LMWH can inhibit collagen proliferation in liver tissues with hepatitis B.

Shi J, Hao JH, Ren WH, Zhu JR. Effects of heparin on liver fibrosis in patients with chronic hepatitis B. *World J Gastroenterol* 2003; 9(7): 1611-1614

http://www.wjgnet.com/1007-9327/9/1611.asp

INTRODUCTION

The treatment of liver cirrhosis is always a problem in the clinical practice. To control and stop liver fibrosis towards liver cirrhosis is of utmost importance. A recent trial indicated that heparin could inhibit the growth of Ito cells effectively *in vitro*[1], which suggested that heparin might act as an antifibrosis drug. In this study, we aimed to seek a safe and effective antifibrosis drug in 52 patients with chronic hepatitis B.

MATERIALS AND METHODS

Materials

Fifty-two patients were treated in Shandong Provincial Hospital from 1999 to 2002. There were 39 males and 13 females, age ranged from 14 to 70 years, diagnosis was made by clinical manifestations and serum hepatitis B viral markers.

Experimental design

These 52 cases were divided into two groups randomly. The treatment regime of each group is listed in Table 1.

Table 1 Treatment regimes in group A and B

Group	*n*	Treatment regime
A	18	regular treatment(GIK,diamnonium glycyrrhizinate injection,potassium magnesium aspartate,et al)
B	34	regular treatment and heparin(25mg,iv,bid) or low molecular weight heparin(6400IU,iH,qd)

Note: In group B, 18 cases were treated with heparin and 16 with low molecular weight heparin (LMWH). The LMWH was FLUX manufactured by ALFA WASSERMANN S.P.A (Italy).

All cases were treated for a course of 3 weeks. Serum alanine transaminase (ALT), prothrombin time (PT), total bilirubin (TBIL), hyaluronic acid (HA) and type IV collagen (IV-C) were measured before and after treatment. The liver tissue specimens were obtained by percutaneous needle biopsy. Ten cases in group A and sixteen in group B had liver biopsies before treatment. Six cases in group B had a second biopsy at 30-60 days after treatment.

Determination of serum HA and IV-C level

Serum HA and IV-C level was determined with radioimmunoassay. The procedures were strictly in accordance with the instructions.

Light microscopic examination

Part of the liver tissues were fixed in 10 % formalin, embedded in paraffin, and then cut into slices. The sections were stained with hematoxylin and eosin for histological study and Masson trichrome for collagen stained green.

Electron microscopic examination

Small liver blocks were fixed in 2.5 % glutaraldehyde, postfixed in 1 % OsO_4, dehydrated with ethanol, and embedded in epoxy resin. Ultrathin sections were stained with uranyl acetate and lead citrate and examined with H-800 transmitted electron microscope (Tokyo, Japan).

RESULTS

Changes of serum/plasma indexes before and after treatment

As shown in Table 2, the levels of ALT and TBIL decreased significantly after treatment, while the level of PT changed slightly only. The level of HA and IV-C in group B decreased markedly, while those in group A were elevated.

Table 2 Changes of the serum / plasma indexes before and after treatment in group A and B ($\bar{x}\pm s$)

	A		B	
	Before	After	Before	After
ALT	136.45±103.46	69.88±43.58[a]	185.58±138.54	84.93±57.14[a]
PT	17.84±3.22	15.98±2.67	18.45±4.25	18.62±3.67
TBIL	64.65±21.35	38.42±14.38[a]	69.54±26.53	31.25±17.84[a]
HA	254.43±116.37	309.48±214.03	579.59±191.45	286.45±136.54[a]
IV-C	237.5±104.44	259.3±137.65	349.56±112.43	189.8±79.63[a]

[a]$P<0.05$, *vs* before treatment.

Histologic changes before and after treatment with heparin/ LMWH

Hematoxylin and eosin staining Hepatocytes swelled and appeared balloon-like before treatment. Inflammatory cells penetrated into the interstitium. Red blood cells congregated in the sinusoids. After treatment with heparin/LMWH, the swollen hepatocytes alleviated , and the sinusoids became clearly seen (Figure 1,2).

Masson trichrome staining Collagens could be seen evidently before treatment. Some sinusoids had been compressed by collagens. After treatment with heparin/LMWH, the collagen fibers decreased significantly (Figure 3,4).

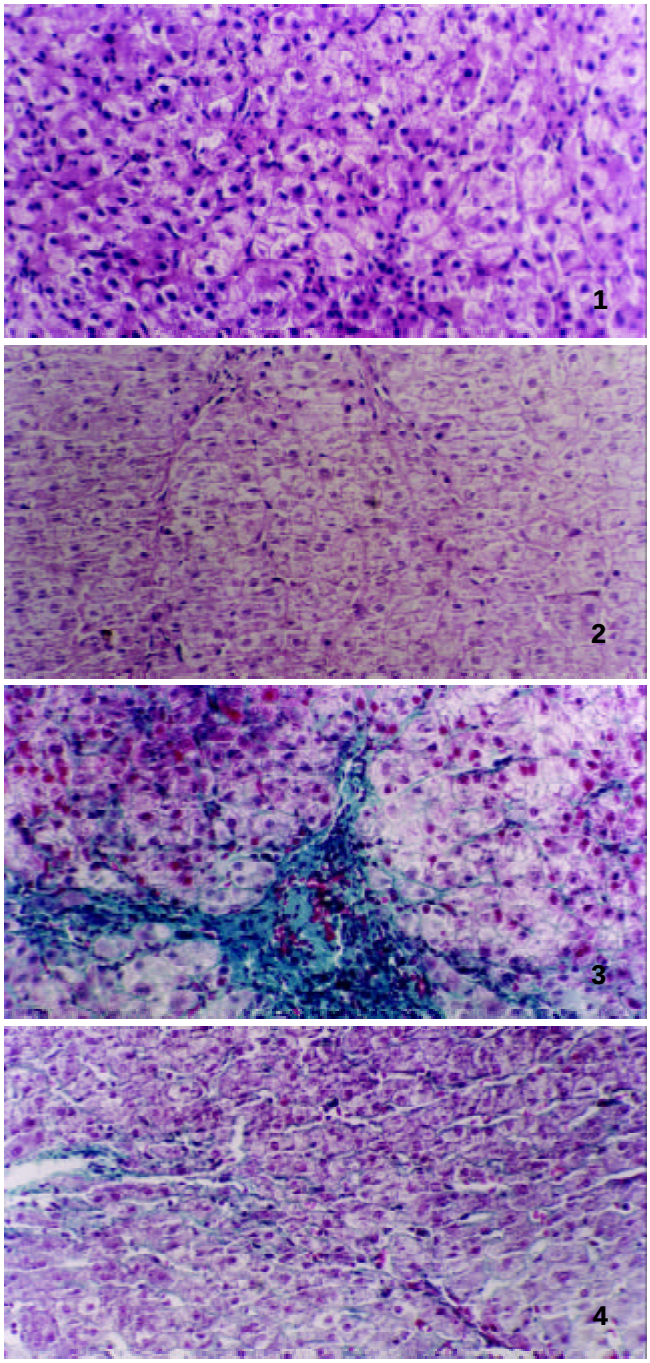

Figure 1 The liver tissue before treatment with heparin. H&E staining. ×200.
Figure 2 The liver tissue after treatment with heparin. H&E staining. ×200.
Figure 3 The liver tissue before treatment with heparin. Masson staining. ×200.
Figure 4 The liver tissue after treatment with heparin. Masson staining. ×200.

Electron microscopic observation Before treatment, hepatocytes were enlarged and cytoplasm appeared dissolved with swollen mitochondria. Base membrane was seen under the hepatic sinusoidal endothelial cells with collagen deposited in the Disse' s space. The Ito cells simulated fibroblasts. The edge of membrane looked uneven, saw-like in severe cases. The number of fat drops decreased markedly. There was microfilament-like structure in the cytoplasm, fibrils were seen around the Ito cells. After treatment, the swollen hepatocytes decreased , so did the base membrane and the depositioning collagen in the Disse' s space. The edge of Ito cells turned smooth. Several fat drops could be seen in the cytoplasm of Ito cells (Figure 5-8).

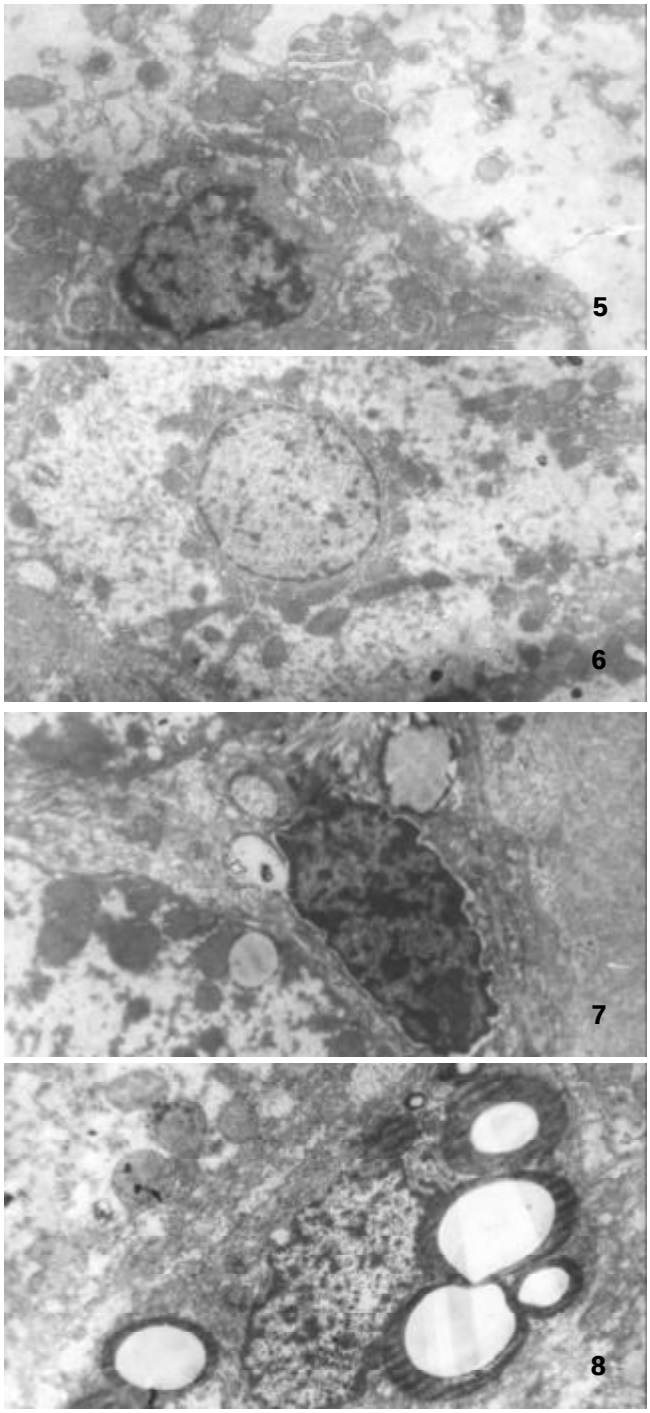

Figure 5 The hepatocyte before treatment heparin. ×6000.
Figure 6 The hepatocyte after treatment with with heparin. ×3500.
Figure 7 The Ito cell before treatment with heparin. ×5000.
Figure 8 The Ito cell after treatment with with heparin. ×5000.

DISCUSSION

Liver fibrosis is caused by the deposition of extracellular matrix (ECM)[2-3]. All cells in the liver can synthesize and secrete ECM, which regulates the proliferation, differentiation and metabolism of liver cells. The abnormal metabolism and deposition of ECM lead to liver fibrosis. It has been recognized that Ito cells have intimate relationships with liver fibrosis[4], which have been postulated to play critical roles in the development of fibrosis of the liver from viral infection, alcohol and many drugs[5,6].Ito cells are relatively inactive fibroblasts in the liver lobules. During liver fibrogenesis, cytokines such as TGF-β_1, PDGF can activate Ito cells[7-9] to acquire a myofibroblast-like phenotype characterized by increased proliferation and synthesis of ECM component[10-27].

It has been proved in animal studies that heparin can inhibit the growth of Ito cells and the expression of α-actin, types I and IV procollagen *in vitro*[1]. Our studies showed that heparin/LMWH could decrease serum HA and IV-C levels in patients with chronic hepatitis B. After treatment, the collagen fibrils in the liver tissues decreased significantly and Ito cells turned oval and fatty drops reappeared in the cytoplasm. The above results indicate that heparin/LMWH act on Ito cells.

The liver functions were improved in both group A and B after treatment. HA and IV-C levels decreased significantly in group B, in contrast, they were elevated in group A. These results suggest that the routine liver function tests could not reflect the fibrosis completely. Kopke-Aguiar *et al*[28] also proved that serum hyaluronic acid was a good marker for hepatic fibrosis at the initial phase.

Wanless *et al*[29] have studied hepatic veins of medium size (0.2 to 3 mm in diameter) in 61 cirrhotic livers. Intimal fibrosis with at least 10 % luminal narrowing was found in 70 % of cirrhotic livers. They considered that multiple layers of intimal fibrosis in some livers suggested the presence of recurrent thrombosis. In other words, thrombosis was related to intimal fibrosis and even caused obstruction of the veins. Our previous studies[30] also showed that as an anticoagulant agent, heparin could improve hepatic microcirculation significantly and lessen sinusoidal capillarization. IV-C is considered an important marker of the development of hepatic sinusoidal capillarization and may appear basal-like membrane[31,32]. Therefore, decrease of the IV-C concentration can not only reflect the improvement of hepatic microcirculation, but also inhibit the fibrosis. It can be used as antifibrosis drug together with antiviral drugs.

Heparin is cheap and safe. LMWH has a weaker effect on thrombin than heparin, but has stronger effect on Xa. 90 % of LMWH can be absorbed hypodermically and its anti-Xa effect can last for 24 hours and therefore, LMWH can be used once a day. One needs not measure the activated coagulation time (ACT) during the procedure[33]. As to the mechanisms of its antifibrosis effect ,further studies are necessary.

REFERENCES

1 **Yuan TX**, Zhang JS, Zhang YE, Chen Q. Culture of rat liver Ito cells and the observation of inhibitory effect of heparin on Ito cells. *Shanghai Yike Daxue Xuebao* 1996; **23**: 90-93

2 **Bissell DM**, Friedman SL, Maher JJ, Roll FJ. Connective tissue biology and hepatic fibrosis: report of a conferrence. *Hepatology* 1990; **11**: 488-498

3 **Schuppan D**. Structure of the extracellular matrix in normal and fibrotic liver:collagens and glycoproteins.*Semin Liver Dis* 1990; **10**: 1-10

4 **Friedman SL**. Cellular source of collagen and regulation of collagen production in liver. *Semin Liver Dis* 1990; **10**: 20-29

5 **Bataller R**, Brenner DA. Hepatic stellate cells as a target for the treatment of liver fibrosis. *Semin Liver Dis* 2001; **21**: 437-451

6 **Dai WJ**, Jiang HC. Advances in gene therapy of liver cirrhosis,a review. *World J Gastroenterol* 2001; **7**: 1-8

7 **Kinnman N,** Goria O, Wendum D, Gendron MC, Rey C, Poupon R, Housset C. Hepatic stellate cell proliferation is an early platelet-derived growth factor-mediated cellular event in rat cholestatic liver injury. *Lab Invest* 2001; **81**: 1709-1716

8 **Gandhi CR**, Kuddus RH, Uemura T, Rao AS. Endothelin stimulates transforming growth facter-β1 and collagen synthesis in stellate cells from control but not cirrhotic rat liver. *Eur J Pharmacol* 2000; **406**: 311-318

9 **Gabriel A**, Kuddus RH, Rao AS, Gandhi CR. Down-regulation of endothelin receptor by transforming growth factorβ1 in hepatic stellate cells. *Hepatol* 1999; **30**: 440-450

10 **Huang GC**, Zhang JS, Zhang YE. Effects of retinoic acid on proliferation, phenotype and expression of cyclin-dependent kinase inhibitors in TGF-β1 stimulated rat hepatic stellate cells. *World J Gastroenterol* 2000; **6**: 819-823

11 **Chen PS**, Zhai WR, Zhou XM, Zhang JS, Zhang YE, Ling YQ, Gu YH. Effects of hypoxia, hyperoxia on the regulation of expression and activity of matrix metalloproteinase-2 in hepatic stellate cells. *World J Gastroenterol* 2001; **7**: 647-651

12 **Wang JY**, Zhang QS, Guo JS, Hu MY. Effects of glycyrrhetinic acid on collagen metabolism of hepatic stellate cells at different stages of liver fibrosis in rats. *World J Gastroenterol* 2001; **7**: 115-119

13 **Eng FJ**, Friedman SL, Fibrogenesis I. New insight into hepatic stellate cell activation: the simple becomes complex. *Am J Phsiol* 2000; **279**: G7-G11

14 **Friedman SL.** Molecular regulation of hepatic fibrosis, an integrated cellular response to tissue injury. *J Biol Chem* 2000; **275**: 2247-2250

15 **Albanis E**, Friedman SL. Hepatic fibrosis. Pathogenesis and principles of therapy. *Clin Liver Dis* 2001; **5**: 315-334

16 **Paradis V**, Perlemuter G, Bonvoust F, Dargere D, Parfait B, Vidaud M, Conti M, Huet S, Ba N, Buffet C, Bedossa P. High glucose and hyperinsulinemia stimulate connective tissue growth factor expression: a potential mechanism involved in progression to fibrosis in nonalcoholic steatohepatitis. *Hepatology* 2001; **34**: 738-744

17 **Schneiderhan W**, Schmid-Kotsas A, Zhao J, Grunert A, Nussler A, Weidenbach H, Menke A, Schmid RM, Adler G, Bachem MG. Oxidized low-density lipoproteins bind to the scavenger receptor, CD36, of hepatic stellate cells and stimulate extracellular matrix synthesis. *Hepatology* 2001; **34**: 729-737

18 **Benyon RC**, Arthur MJ. Extracellular matrix degradation and the role of hepatic stellate cells. *Semin Liver Dis* 2001; **21**: 373-384

19 **Vaillant B**, Chiaramonte MG, Cheever AW, Soloway PD, Wynn TA. Regulation of hepatic fibrosis and extracellular matrix genes by the Th response: new insight into the role of tissue inhibitors of matrix metalloproteinases. *J Immunol* 2001; **167**: 7017-7026

20 **Breitkopf K**, Lahme B, Tag CG, Gressner AM. Expression and matrix deposition of latent transforming growth factor beta binding proteins in normal and fibrotic rat liver and transdifferentiating hepatic stellate cells in culture. *Hepatology* 2001; **33**: 387-396

21 **Bruck R**, Genina O, Aeed H, Alexiev R, Nagler A, Avni Y, Pines M. Halofuginone to prevent and treat thioacetamide-induced liver fibrosis in rats. *Hepatology* 2001; **33**: 379-386

22 **Watanabe T**, Niioka M, Hozawa S, Kameyama K, Hayashi T, Arai M, Ishikawa A, Maruyama K, Okazaki I. Gene expression of interstitial collagenase in both progressive and recovery phase of rat liver fibrosis induced by carbon tetrachloride. *J Hepatol* 2000; **33**: 224-235

23 **Nakamura T**, Sakata R, Ueno T, Sata M, Ueno H. Inhibition of transforming growth factor beta prevents progression of liver fibrosis and enhances hepatocyte regeneration in dimethylnitrosamine-treated rats. *Hepatology* 2000; **32**: 247-255

24 **Castera L**, Hartmann DJ, Chapel F, Guettier C, Mall F, Lons T, Richardet JP, Grimbert S, Morassi O, Beaugrand M, Trinchet JC. Serum laminin and type IV collagen are accurate markers of histologically severe alcoholic hepatitis in patients with cirrhosis. *J Hepatol* 2000; **32**: 412-418

25 **Brenner DA**, Waterboer T, Choi SK, Lindquist JN, Stefanovic B, Burchardt E, Yamauchi M, Gillan A, Rippe RA. New aspects of hepatic fibrosis. *J Hepatol* 2000; **32**(Suppl 1): 32-38

26 **Benyon RC**, Iredale JP. Is liver fibrosis reversible? *Gut* 2000; **46**: 443-446

27 **Friedman SL**. Molecular regulation of hepatic fibrosis, an integrated cellular response to tissue injury. *J Biol Chem* 2000; **275**: 2247-2250

28 **Kopke-Aguiar LA**, Martins JR, Passerotti CC, Toledo CF, Nader HB, Borges DR. Serum hyaluronic acid as a comprehensive marker to assess severity of liver disease in schistosomiasis. *Acta Trop* 2002; **84**: 117-126

29 **Wanless IR**, Wong F, Blendis LM, Greig P, Heathcote EJ, Levy G. Hepatic and portal vein thombosis in cirrhosis: possible role in development of parenchymal extinction and portal hypertention. *Hepatology* 1995; **21**: 1238-1247

30 **Hao JH**, Shi J, Ren WH, Han GQ, Wang WZ, Zhu JR, Wang SY, Xie YB. Usage of heparin in the patients with chronic hepatitis B. *Wei Xunhuan Xue Zazhi* 2001; **11**: 9-11

31 **Matsumoto S**, Yamamoto K, Nagano T, Okamoto R, Ibuki N, Tagashira M, Tsuji T. Immunohistochemical study on phenotypical changes of hepatocytes in liver disease with reference to extracelluar matrix composition. *Liver* 1999; **19**: 32-38

32 **Marcato PS**, Bettini G, Della Salda L, Galeotti M. Pretelangiectasis and telangiectasis of the bovine liver:a morphological immunohistochemical and ultrastructural study. *J comp Pathol* 1998; **119**: 95-110

33 **Khosla S**, Kunjummen B, Guerrero M, Manda R, Razminia M, Trivedi A, Vidyarthi V, Elbazour M, Ahmed A, Lubell D. Safety and efficacy of combined use of low molecular weight heparin (enoxaparin, lovenox) and glycoprotein IIb/IIIa receptor antagonist (eptifibatide,integrelin)during nonemergent coronary and peripheral vascular intervention. *Am J Ther* 2002; **9**: 488-491

Edited by Wu XN

P.O.Box 2345, Beijing 100023,China
Fax: +86-10-85381893
E-mail: wjg@wjgnet.com www.wjgnet.com

World J Gastroenterol 2003;9(7):1615-1617
World Journal of Gastroenterology
 ISSN 1007-9327

• BRIEF REPORTS •

Effect of Sea buckthorn on liver fibrosis: A clinical study

Ze-Li Gao, Xiao-Hong Gu, Feng-Tao Cheng, Fo-Hu Jiang

Ze-Li Gao, Fo-Hu Jiang, Department of Gastroenterology, Baogang Hospital, Shanghai Second Medical University, Shanghai 201900, China
Xiao-Hong Gu, Feng-Tao Cheng, Department of Gastroenterology, Yangpu District Hospital, Shanghai 200090, China
Correspondence to: Dr. Ze-Li Gao, Department of Gastroenterology, Baogang Hospital, Shanghai Second Medical University, Shanghai 201900, China. gzeli@sina.com
Telephone: +86-21-56691101-6260
Received: 2002-12-28 **Accepted:** 2003-02-18

Abstract

AIM: To appraise the effect of sea buckthorn (Hippophae rhamnoides) on cirrhotic patients.

METHODS: Fifty cirrhotic patients of Child-Pugh grade A and B were randomly divided into two groups: Group A as the treated group (n=30), taking orally the sea buckthorn extract, 15 g 3 times a day for 6 months. Group B as the control group (n=18), taking vitamin B complex one tablet, 3 times a day for 6 months. The following tests were performed before and after the treatment in both groups to determine LN, HA, collagens types III and IV, cytokines IL-6 and TNFα, liver serum albumin, total bile acid, ALT, AST and prothrombin time.

RESULTS: The serum levels of TNFα, IL-6, laminin and type IV collagen in group A were significantly higher than those in the control group. After a course of sea buckthorn treatment, the serum levels of LN, HA, collagen types III and IV, total bile acid (TBA) decreased significantly as compared with those before and after treatment in the control group. The sea buckthorn notably shortened the duration for normalization of aminotransferases.

CONCLUSION: Sea buckthorn may be a hopeful drug for prevention and treatment of liver fibrosis.

Gao ZL, Gu XH, Cheng FT, Jiang FH. Effect of Sea buckthorn on liver fibrosis: A clinical study. *World J Gastroenterol* 2003; 9 (7): 1615-1617
http://www.wjgnet.com/1007-9327/9/1615.asp

INTRODUCTION

Liver cirrhosis is a common chronic hepatic injury caused by chronic hepatitis B, ethanol consumption and metabolic disorders, etc. The patients often die of hepatic failure due to portal hypertension, bleeding of esophageal and gastric varices. Recent studies have shown that fat storing cells now called hepatic stellate cells (HSCs) are the main collagen producing cells in fibrotic liver. Under the influence of inflammatory cytokines, vitamin A- rich cells are activated, proliferating and transforming into myofibroblasts, producing extracellular matrix(ECM)[1,2]. Retinoic acid droplets and retinoic acid receptors (RAR) diminish. Recent studies have also shown that when retinyl esters and RAR contents are restored in HSC, HSCs would remain in the inactivated state. Hence HSCs are regarded as the therapeutic targets for prevention and treatment of hepatic fibrosis[3]. In this study, sea buckthorn (Hippophae rhamnoides,) was used in cirrhotic patients to determine its effect on the changes of fibrotic parameters, improvement of liver function and whether it could be used as a therapeutic antifibrotic agent.

MATERIALS AND METHODS

Subjects

Fifty patients aged 20-70 years were enrolled in this study with at least an elevation of two items of the following parameters, e,g, serum collagen types III and IV, laminin (LN), hyaluronic acid (HA). These patients were divided into treated group (group A, n=30, 25 hepatitis B cirrhosis and 5 alcoholic) and control group (group B n=20, 17 hepatitis B cirrhosis and 3 alcoholic). These two groups had similar demographic characteristics. All these patients had not taken any antifibrotic drug or immunomodulator or antiviral herbs in the past 6 months. Group A received sea buckthorn extract in fine granules (manufactured by Sichuan Pharmaceutical Co.LTD, China), 15 g, three times a day for 6 months. Group B received vitamin-B complex, 2 tablets once, 3 times a day for 6 months.

Measurement of cytokines, parameters of liver fibrosis and liver function tests

Cytokine: IL6 and TNFα were measured by enzyme-linked immunosorbent assay (ELISA). LN, HA, collagen types III and IV were measured by radioimmunoassay (RIA). Serum albumin (Alb), total bilirubin, aspartate aminotransferase (AST), alanine aminotransferase (ALT), alkaline phosphatase (ALP), conjugates, total bile acid (TBA), prothrombin time (PT) were measured by a biochemical autoanalyzer.

Statistical analysis

All data were analyzed with SAS software. The results were expressed as mean ± standard deviation, the rate of normalization of AST, ALT was analyzed by Chi-square test. LN, HA, Alb, TBA, PT, collagen types III and IV were analyzed by signed rank test (both pre-and posttreatment in the same group) and Wilcoxon rank test (between the two groups, pre-and post treatment for comparison). P value <0.05 was considered statistically significant.

RESULTS

Determination of TNFα, IL-6, LN, HA

The levels of TNFα, IL-6, LN, collagen type IV in the 50 cirrhotic patients were significantly higher than those in the controls (P<0.05). There were positive correlations between TNFα, IL-6 and LN, collagen type IV (Table 1).

Table 1 Measurements of TNFα, IL-6, LN, type IV collagen ($\bar{x}\pm s$)

Group	n	TNFα (ng/L)	IL-6 (ng/L)	LN (μg/L)	Type IV (ng/L)
A	30	19.6±3.2	15.1±2.8	374.1±31.2	250.9±22.6
B	20	6.7±1.2	3.8±1.1	99.4±6.8	51.8±4.6
t value		2.419	2.961	2.618	2.997
P value		<0.05	<0.05	<0.05	<0.05

Table 2 Normalization rates of AST,ALT ($\bar{x}$±s)

Group	AST (IU/L)		Normalization rate (%)	ALT (IU/L)		Normalization rate (%)
	Before treatment	After treatment		Before treatment	After treatment	
A	59.87±26.70	49.03±18.99	24/30(80)[a]	50.57±32.47	44.12±26.05	24/30(80)[a]
B	l54.75±20.21	47.85±23.53	10/18(56)	41.65±23.54	39.15±16.68	10/18(56)

[a]P<0.05 *vs* controls.

Table 3 Parameters of liver fibrosis ($\bar{x}$±s)

Parameters	Group	Before treatment	After treatment	Comparison of two groups	
				Stat Z	*P* value
III (ng/l)	A	428.43±196.02	149.43±75.91		
	B	423.56±251.41	169.80±138.94	0.0403	0.0394
IV (ng/l)	A	123.98±81.22	70.00±34.45		
	B	178.32±89.45	139.85±98.15	0.0393	0.0384
LN (μg/l)	A	210.91±165.12	136.51±105.56		
	B	211.56±188.91	156.00±100.00	0.0073	0.0070
HA (μg/l)	A	516.74±338.75	240.56±169.78		
	B	494.74±272.26	387.16±196.28	0.0148	0.0144

Wilcoxon rank test.

Table 4 Changes of TBA, PT, Alb ($\bar{x}$±s)

Parameters	Group	Before treatment	After treatment	Before treatment		Before/after treatment		Comparison of two groups before/after treatment	
				Stat(Z)	*P* value	Stat(t)	*P* value	Stat (S)	*P* value
TBA (ng/l)	A	38.70±27.50	22.83±12.28			189.32	0.0001		
	B	40.50±34.02	38.55±22.60	0.751	0.743	35.55	0.1922	545.0	0.0003
PT (sec)	A	14.57±0.97	13.50±0.73			7.443	0.0001		
	B	15.15±0.93	14.40±0.74	4.35	0.048	5.252	0.0001	2.21	0.1415
Alb (g/l)	A	34.07±9.35	35.13±7.13			1.205	0.238		
	B	27.45±7.41	27.40±6.25	7.02	0.010	0.053	0.958	0.48	0.4887

Signed rank test and Wilcoxon rank test.

ECM parameters and liver function tests

Remarkable changes were found in AST and ALT after sea buckthorn treatment. The rate of normalization was 80 % in the treated group and 56 % in the control group (P<0.05). No difference was found in serum albumin and prothrombin time. In group A, serum LN, HA, total bile acid (TBA), collagen types III and IV were decreased after treatment as compared with group B. There was a significant difference between the two groups (P<0.05). (Tables 2-4).

DISCUSSION

Sea buckthorn is a plant growing in severely cold region of South-west China, its fruit juice has been taken as a tonic by the local Mongolians and Tibetans. It contains a great deal of vitamins, amino acids and trace elements, which are beneficial to human health[4]. Recent studies have shown that sea buckthorn contains lots of vitamin A precursors including β carotene and unsaturated fatty acids. Zhao *et al*[5] reported that sea buckthorn could protect the liver from damage by CCl_4. A combination of an antiviral drug and sea buckthorn in treating patients with chronic hepatitis B could shorten the duration for the normalization of serum ALT. The rate of turning negative of HBeAg and HBsAg was 52.16 % and 16.67 %, respectively[6].

In the normal liver, HSCs are mainly involved in the storage of vitamin A. In addition, they synthesize extracellular matrix components, matrix degrading metalloproteinases, cytokines, and growth factors[7,8]. Following acute or chronic liver injury, HSCs are activated and undergo a process of transdifferentiation, leading to a myofibroblastic phenotype. The activated HSCs are characterized by a loss of vitamin A droplets, increase of proliferation, release of proinflammatory, profibrogenic, and promitogenic cytokines and migration to the sites of injury with increased production of extracellular matrix components and alterations in matrix protease activity and provision for the fundamental needs of tissue repair[9]. In acute or self-limited liver damage, these changes are transient, whereas in case of persistent injury, they lead to chronic inflammation with an accumulation of extracellular matrix, resulting in liver fibrosis and ultimately cirrhosis. Several growth factors and cytokines are involved in HSCs activation and proliferation, of which transforming growth factor β (TGFβ), platelet derived growth factor (PDGF), TNFα and IL-6 are probably the most important ones[10].

TNFα is not only an anticancer factor, but also participates in the process of immunologic reaction and inflammation. The synthesis of collagen and some extracellular matrices were elevated 3 fold and 2.6 fold, respectively when rat HSCs were incubated with TNFα (5.0 nmol/l) for 24 hours[11]. IL-6 is a cytokine which has many biologic functions, such as promoting cell proliferation and differentiation, regulating immune

function. Wang *et al*[12,13] reported IL-6 increased in the peripheral blood of an early animal model of liver fibrosis, and the peripheral blood level of IL-6 in cirrhotic patients was remarkably higher than that in those without[14].

HSCs represent 5-8 % of all human liver cells. They have long cytoplasmic processes which run parallel to the sinusoidal endothelial wall. The second order branches sprout out from the processes, and embrace the sinusoids. Some HSCs are in close contact with nerve endings, some of which contain neuropeptides such as substance P, neuropeptide Y, somatostatin, and calcitonin gene-related peptide[15,16].

Our previous study showed[17] that retinoic acid receptor (RAR) and cAMP of primarily cultured HSCs were reduced, as compared with those in freshly isolated HSCs. The contents of RAR and cAMP of cultured HSCs were increased after treated with all-transretinoic acid (10^{-5} Mol/L).

Based on the recent articles and our results, we may deduce that the resting HSCs are activated by TNFα and IL-6 released by Kupffer cells during the process of acute or chronic inflammation, then TNFα and IL-6 in turn stimulate Kupffer cells to release TGFβ and PDGF. Eventually, HSCs proliferation and synthesis of ECM, along with the loss of vitamin A droplets, will transform themselves into myofibroblast producing liver fibrosis[18,19].

The present study showed that sea buckthorn could reduce the serum levels of laminin, hyaluronic acid, TBA, collagen types III and IV in patients with liver cirrhosis, indicating that it may restrain the synthesis of collagen and other components of ECM. We are attempting to restore vitamin A and RAR contents of HSCs, so as to keep HSCs in a quiescent status and to prevent progression of liver fibrosis. Sea buckthorn may be a hopeful drug for prevention and treatment of liver fibrosis, but further well controlled clinical trials are required.

REFERENCES

1 **Norifumi K**, Shuichi S, Masayasu I, Tetsuo K. Effect of antioxidants, resveratrol, quercetin, and N-Acetylcysteine on the function of cultured rat hepatic stellate cells and kupffer cells. *Hepatology* 1998; **27**: 1265-1274

2 **Giuliano R,** Thomas A. Cytokines in the liver. *Eur J Gastroenterol Hepatol* 2001; **13**: 777-784

3 **Reynaert H,** Thompson MG, Thomas T, Geerts A. Hepatic stellate cells: role in microcirculation and pathophysiology of portal hypertension. *Gut* 2002; **50**: 571-581

4 **Oomah BD,** Sery C, Godfrey DV, Beveridge TH. Rheology of sea buckthorn (*Hippophae rhamnoides* L) juice. *J Agric Chem* 1999; **47**: 3546-3550

5 **Zao TD,** Cheng ZX, Liu XY, Shao JY, Ren LJ, Zhang L, Chen WC. Protective effect of the sea buckthorn oil for liver injury induced by CCl_4. *Zhongcaoyao* 1987; **18**: 22-24

6 **Huang DL,** Chang XZ, Gui HN, Tian YD, Chen LX, Li ZP, Xing L. Analysis of 156 cases of chronic hepatitis treated with sea buckthorn. *Zhongxiyi Jiehe Zazhi* 1991; **11**: 697-6980

7 **Greerts A.** History, heterogeneity, developmental biology and functions of quiescent hepatic stellate cells. *Semin Liver Dis* 2001; **21**: 311-315

8 **Schumann J,** Tiegs G. Pathophysiological mechanisms of TNF during intoxication with natural or man-made toxins. *Toxicology* 1999; **138:** 103-126

9 **Lissoos TW,** Davis BH. Pathogenesis of hepatic fibrosis and the role of cytokines. *J Clin Gastroenterol* 1992; **15**: 63-67

10 **Friedman SL**. Molecular regulation of hepatic fibrosis, an integrated cellular response to tissue injury. *J Biol Chem* 2000; **275**: 2247-2250

11 **Knittel T,** Muller L, Saile B, Ramadori G. Effect of tumor necrosis factor -alpha on proliferation, activation and protein synthesis of rat hepatic stellate cells. *J Hepatol* 1997; **27**:1067-1080

12 **Weiner FR,** Giambrone MA, Czaja MJ, Shah A, Annoni G, Takahashi S, Eghbali M, Zern MA. Ito-cell gene expression and collagen regulation. *Hepatology* 1990; **11**: 111-117

13 **Wang Q**, Xia HS, Jiang HY, Ma XX, Zhu F, Zuo LQ. The Immunologic regulation of liver in the process of rat liver fibrosis. *Zhonghua Yixue Zazhi* 1995; **75**:594-598

14 **Tili H,** Lissoos TW. Pathogenesis of hepatic fibrosis and the role of the cytokine. *Gastroenterology* 1992; **103**: 264-271

15 **Burt AD**, Le Bail B, Balabaud C, Bioulac-Sage P. Morphologic investigation of sinusoidal cells. *Semin Liver Dis* 1993; **13**: 21-38

16 **Stoyanova II,** Gulubova MV. Immunocytochemical study on the liver innervation in patients with cirrhosis. *Acta Histochem* 2000; **102**: 391-402

17 **Gao ZL**, Li DG, Lu HM.The effect of retinoic acid receptor and cAMP of HSC cell. *Weichangbingxue He Ganbingxue Zazhi* 1995; **4**: 20-22

18 **Rebecca G,** Wells. Fibrogenesis V. TGF-β signaling pathways. *Am J Physiol Gastrointest Liver Physiol* 2000; **279**: G845-G850

19 **Gangopadhyay A**, Bajenova O, Kelly TM, Thomas P. Carcinoembryonic antigen induces cytokine expression in Kuppfer cells:implications for hepatic metastasis from colorectal cancer. *Cancer Res* 1996; **56**: 4805-4810

Edited by Wu XN and Wang XL

P.O.Box 2345, Beijing 100023,China
Fax: +86-10-85381893
E-mail: wjg@wjgnet.com www.wjgnet.com

World J Gastroenterol 2003;9(7):1618-1620
World Journal of Gastroenterology
 ISSN 1007-9327

• BRIEF REPORTS •

Fatty metamorphosis of the liver in patients with breast cancer: Possible associated factors

Cheng-Hsin Chu, Shee-Chan Lin, Shou-Chuan Shih, Chin-Roa Kao, Sun-Yen Chou

Cheng-Hsin Chu, Shee-Chan Lin, Shou-Chuan Shih, Chin-Roa Kao, Sun-Yen Chou, Division of Gastroenterology, Department of Internal Medicine, Mackay Memorial Hospital, Taipei, Taiwan, China
Correspondence to: Dr. Cheng-Hsin Chu, Department of Hepatology and Gastroenterology, Mackay Memorial Hospital, Address: No. 92, Sec. 2, Chung-Shan N. Road, Taipei, Taiwan, China. suyu5288@ms14.hinet.net
Telephone: +86-2-88661107 **Fax:** +86-2-25433642
Received: 2003-02-25 **Accepted:** 2003-03-16

Abstract

AIM: To investigate the relationship between breast cancer and fatty liver in Chinese patients.

METHODS: The study group consisted of 217 patients with newly diagnosed breast cancers and the control group of 182 subjects undergoing routine health examination in the same hospital. All subjects were female and the groups were matched for date of study. Ultrasound scanning was performed by the same operator using a 3.5 mHz transducer. Steatosis of the liver was diagnosed based on the criteria of Saverymuttu *et al*. Clinical variables were statistically analyzed.

RESULTS: Fatty liver was diagnosed in 98 patients of the study group and 37 patients of the control group, a significant difference was found in incidence (98/217, 45.2 % and 37/182, 20.3 %; $P<0.0001$). On univariate analysis, fatty liver in breast cancer patients was associated with overweight, hyperlipidemia, and hepatitis. On multivariate analysis in the same patients, obesity and hyperlipidemia were significantly associated with fatty liver.

CONCLUSION: The cause of fatty liver in women with breast cancer may be multifactorial. The present study confirms its link with overweight and hyperlipidemia.

Chu CH, Lin SC, Shih SC, Kao CR, Chou SY. Fatty metamorphosis of the liver in patients with breast cancer: Possible associated factors. *World J Gastroenterol* 2003; 9(7): 1618-1620
http://www.wjgnet.com/1007-9327/9/1618.htm

INTRODUCTION

Breast cancer is a common cancer in the developed countries such as Western Europe and North America where women tend to be well-nourished. In 1973, the reported crude annual incidence rate of new breast cancer was 71.5 per 100 000 in Canada[1]. This contrasts with the incidence in Taiwanese women of 6.11 per 100 000 published in 1971[2]. However, more recent epidemiological studies revealed an increasing incidence of breast cancer with 12.46 per 100 000 in Taiwan[3]. The development of breast cancer is multifactorial. Genetic, dietary, environmental, menstrual, endocrine and ethnic factors all influence it[4]. In the course of using ultrasonography to assess liver metastases from breast cancer, we have noted a fair number of women with breast cancer who also have fatty liver. The aim of this study was to investigate the incidence and clinicopathological factors associated with fatty liver in patients with breast carcinoma.

MATERIALS AND METHODS

A hospital-based prospective study was conducted to investigate the relationship between fatty liver and breast cancer. From May 1994 to August 1997, 217 consecutive, newly diagnosed women with breast cancer were enrolled as the study group. 182 subjects presenting to the same hospital for routine health examination was served as the control group of the same period. All subjects underwent abdominal ultrasonography performed by the same operator using a 3.5 mHz transducer (Toshiba SSA-340A). Fatty liver was diagnosed in the presence of at least two of the following sonographic features: (1) increase in liver echoes, (2) loss of echoes from the wall of the portal veins, (3) exaggeration of liver and kidney echo discrepancy, and (4) ultrasonic attenuation of the liver parenchyma. Overweight was defined as a BMI >25 [body mass index = weight (kg)/height (m^2)]. Subjects were excluded if they were pregnant, on a weight reduction diet in the 6 months preceding the study, or taking cholesterol-lowering therapy or steroids. Data collected included age, the presence of hepatitis C virus antibodies with elevation of alanine aminotransferase (GPT) and aspartate aminotransferase (GOT), BMI, a history of diabetes or hyperlipidemia, drug use (contraceptives, steroids, tamoxifen, alcohol), and chemotherapy.

Statistical analysis

The chi-square test was used for univariate analysis of these factors. Statistically significant variables on univariate analysis were subsequently subjected to multivariate analysis with logistic regression. A P value less than 0.05 was considered to be statistically significant.

RESULTS

The mean age of the breast cancer patients was slightly higher than that of the controls (48.6±10.5 *vs* 46.8±12.0; $P=0.029$). None of the subjects in either group drank alcohol. Fatty liver was found in 98/217 (45.2 %) of the study group and in 37/182 (20.3 %) of the control group, with a statistically significant difference ($P<0.0001$). The breast cancer subjects were also significantly more likely to be obese than controls (124/217, 57.1 % *vs*. 45/182, 24.7 %, $P<0.0001$). There were no significant differences in the presence of hyperlipidemia or hepatitis C (Table 1).

On univariate analysis, fatty liver in subjects with breast cancer was significantly associated with overweight, hyperlipidemia, and hepatitis C but not with diabetes mellitus, tamoxifen, contraceptives, or chemotherapy (Table 2). Using logistic regression, the odds of fatty liver were increased in the breast cancer subjects in the presence of overweight (OR 1.406, $P<0.0001$) and hyperlipidemia (OR 1.206, $P=0.0473$) (Table 3).

Table 1 Clinical variables in patients with breast cancer and controls

Variables	Cases (*n*=217) Number (%)	Controls (***n***=182) Number (%)	*P*
Fatty liver			
No	119 (54.8)	145 (79.7)	
Yes	98 (45.2)	37 (20.3)	<0.0001
Overweight			
No	93 (42.9)	137 (75.3)	
Yes	124 (57.1)	45 (24.7)	<0.0001
Hyperlipidemia			
No	177 (81.6)	154 (84.6)	
Yes	40 (18.4)	28 (15.4)	0.432
Hepatitis C			
No	204 (94.0)	165 (90.6)	
Yes	13 (6.0)	17 (9.4)	0.144
Age			
Mean ± SD	48.6±10.5	46.8±12.0	0.029

Table 2 Clinical factors associated with fatty liver in patients with breast cancer (*n*=217)

Variables	Number of cases		*P*
	Fatty Liver (-)	Fatty Liver (+)	
Contraceptives			
No	117	94	
Yes	2	4	0.28
Tamoxifen			
No	25	13	
Yes	94	85	0.14
Chemotherapy			
No	52	49	
Yes	58	47	0.59
Hepatitis C			
No	116	88	
Yes	10	3	0.031
Diabetes			
No	113	92	
Yes	6	6	0.73
Overweight			
No	71	21	
Yes	48	77	<0.0001
Hyperlipidemia			
No	106	71	
Yes	13	27	0.017

Table 3 Significant variables on multivariate analysis for patients with breast cancer

Variables	Coefficient estimates and significant test			
	Coefficient	SD	*P*	Odds ratio
Overweight	0.3410	0.0474	0.0000	1.4064
Hyperlipidemia	0.0263	0.0132	0.0473	1.2066

DISCUSSION

Fatty liver is associated with alcohol abuse, obesity, malnutrition, diabetes mellitus, toxic agents, corticosteroids and endocrine imbalance. However, there had been little investigation of this disorder in relation to malignancy until Lanza reported in 1968 that a fair number of patients with known cancer had steatosis on percutaneous liver biopsy[5]. The diagnostic criteria and high accuracy of ultrasound in the detection of fatty liver were documented by Foster and Saverymuttu *et al*[6,7]. In a similar manner, an unusually high proportion of fatty liver in patients with carcinoma of breast was observed in the present study (Table 1). In this study, fatty liver was observed in 37 out of 182 (20.3 %) asymptomatic control subjects, significantly less than the 45.2 % of breast cancer subjects. Fatty liver was related to BMI, dietary fat intake, and ethnic differences. The actual incidence in the general population was varied.

The results of numerous epidemiological studies have demonstrated that the risk for breast cancer is related to a variety of factors, including age at menarche and at first childbirth, parity, level of education, previous benign breast tumor, family history of breast cancer, young age at menopause, environmental factors, ethnicity, BMI, dietary fat intake, and high central adiposity[2,8-10]. A significantly higher proportion of the breast cancer subjects were obese compared with controls (57.1 % *vs.* 15.4 %). With increasing weight, long chain fatty acid synthesis also increases, which in turn leads to lipid accumulation in the liver. It is likely that the higher incidence of fatty liver in our breast cancer subjects is related at least in part to their higher BMI.

The excess estrogen and insulin-like growth factor (IGF-1) produced by obese women have been suggested to be the key factor in promoting proliferation of mammary epithelial cells[11-14]. Furthermore, obesity may lead to delay in diagnosis, and it appears to be a poor prognostic factor[15,16].

Tamoxifen is an anti-estrogenic drug utilized in adjuvant therapy for breast cancer. Ogawa and colleagues suggested in 1998 that tamoxifen induced fatty liver in patients with breast cancer[17]. Nguyen published a study in 2001 demonstrating an increase in fatty liver and accumulation of visceral adipose tissue in breast cancer patients receiving tamoxifen[18]. Fatty liver can occur because of increased delivery of free fatty acids to the liver, increased synthesis of fatty acids in the liver, decreased β-oxidation of free fatty acids, and decreased synthesis or secretion of very low density lipoprotein[19]. Tamoxifen must therefore disarrange some of the steps in lipid metabolism[20].

There are a few reports of tamoxifen-associated steatohepatitis and multi-focal fatty infiltration of the liver[21,22]. Generally speaking, patients with fatty liver are usually symptom-free, but severe steatohepatitis may lead to liver cirrhosis in some cases. Therefore, careful attention should be paid to functional and morphological changes of the liver during tamoxifen treatment[21]. We have not yet found a significant relationship between tamoxifen and fatty liver in our subjects. This may be resulted from the insufficient length of tamoxifen treatment. Our subjects who took tamoxifen did for a mean of 12 months (range: 2-38 months), compared with a mean of 30 months (range: 4-84 months) in Nguyen' s series[18].

The clinical appearance of hepatic fatty changes may be diffuse, focal, multi-focal, the latter findings possibly mimic or harbor either primary or metastatic cancer[17,22]. Because of the possibility of liver metastases as well as the possibility of fatty liver (including the chance of progression to steatohepatitis or cirrhosis) with or without tamoxifen, it would be wise to monitor liver function and imaging in patients with breast cancer.

REFERENCES

1 **Canada S**. New primary sites of malignant neoplasms in Canada. *Publication No* 82-107, 1976

2 **Lin TM**, Chen KP, MacMahon B. Epidemiologic characteristics of cancer of the breast in Taiwan. *Cancer* 1971; **27**: 1497-1504

3 **Cheng CJ**, You SL, Lin LH, Hsu WL, Yang YW. Cancer epidemiology and control in Taiwan: a brief review. *Jpn J Clin Oncol* 2002; **32**: S66-81
4 **Boring CC**, Squires BA, Tong T. Cancer statistics, 1991. *CA Cancer J Clin* 1991; **41**: 19-36
5 **Lanza FL**, Nelson RS. Fatty metamorphosis of the liver in malignant neoplasia. Special reference to carcinoma of the breast. *Cancer* 1968; **21**: 699-705
6 **Foster KJ**, Dewbury KC, Griffith AH, Wright R. The accuracy of ultrasound in the detection of fatty infiltration of the liver. *Br J Radiol* 1980; **53**: 440-442
7 **Saverymuttu SH**, Joseph AEA, Maxell JD. Ultrasound scanning in the detection of hepatic fibrosis and steatosis. *Br Med J* 1986: **292**: 13-15
8 **Gary GE**, Pike MC, Henderson BE. Breast cancer incidence and mortality rate in different countries in relation to known risk factors and dietary practices.*Br J Cancer* 1979; **39**: 1-7
9 **Choi NW**, Howe GR, Miller AB. An epidemiologic study of breast cancer. *Am J Epidemiol* 1978; **107**: 510-521
10 **Hirayama T**. Epidemiology of breast cancer with special reference to the role of diet. *Prev Med* 1978; **7**: 173-195
11 **Kirschner MA**, Ertel N, Schneider G. Obesity, hormones, and cancer. *Cancer Res* 1981; **41**: 3711-3717
12 **Schapira DV**, Kumar NB, Lyman GH, Cox CE. Abdominal obesity and breast cancer risk. *Ann Intern Med* 1990; **112**: 182-186
13 **Peyrat JP**, Bonneterre R, Dijane J, Demaille A. IGF1 receptors in human breast cancer and their relation to estradiol and progesterone receptors. *Cancer Res* 1988; **48**: 6429-6433
14 **Kern WH**, Hegar AH, Payne JH, DeWind LT. Fatty metamorphosis of the liver in morbid obesity. *Arch Pathol* 1973; **96**: 342-346
15 **Boyd NF**, Campbell JE, Germanson T. Body weight and prognosis in breast cancer. *J Natl Cancer Inst* 1981; **67**: 785-789
16 **Senie RT**, Rosen PP, Rhodes P. Obesity at diagnosis of breast carcinoma influences duration of disease-free survival. *Ann Intern Med* 1992; **51**: 25-32
17 **Ogawa Y**, Murata Y, Nishioka A, Inomata T, Yoshida S. Tamoxifen-induced fatty liver in patients with breast cancer. *Lancet* 1998; **351**: 725
18 **Nguyen MC**, Steward RB, Banerji MA. Relationships between tamoxifen use, liver fat and body fat distribution in women with breast cancer. *Int J Obesity* 2001; **25**: 296-298
19 **Lombardi B**. Consideration on the pathogenesis of fatty liver. *Lab Invest* 1966; **15**: 1-20
20 **Louis DB**, Claude G, Cöme R. Severe lipemia induced by tamoxifen. *Cancer* 1986; **57**: 2123-2126
21 **Pino HC**, Baptista A, Camilo ME, de Costa EB, Valente A, de Moura MC. Tamoxifen-associated steatohepatitis-Report of three cases. *J Hepatol* 1995; **23**: 95-97
22 **Cai Q**, Bensen M, Greene R, Kirchner J. Tamoxifen-induced transient multifocal hepatic fatty infiltration. *Am J Gastroenterol* 2000; **95**: 277-279

Edited by Xu XQ and Zhu LH

P.O.Box 2345, Beijing 100023,China
Fax: +86-10-85381893
E-mail: wjg@wjgnet.com www.wjgnet.com

World J Gastroenterol 2003;9(7):1621-1624
World Journal of Gastroenterology
 ISSN 1007-9327

• BRIEF REPORTS •

Diarrhea and acaroid mites: A clinical study

Chao-Pin Li, Yu-Bao Cui, Jian Wang, Qing-Gui Yang, Ye Tian

Chao-Pin Li, Yu-Bao Cui, Jian Wang, Qing-Gui Yang, Ye Tian, Department of Etiology and Immunology, School of Medicine, Anhui University of Science & Technology, Huainan 232001, Anhui Province, China
Correspondence to: Dr. Chao-Pin Li, Department of Etiology and Immunology, School of Medicine, Anhui University of Science & Technology, Huainan 232001, Anhui Province, China. cpli@aust.edu.cn
Telephone: +86-554-6658770 **Fax:** +86-554-6662469
Received: 2002-12-28 **Accepted:** 2003-02-05

Abstract

AIM: To explore the characteristics of diarrhea caused by acaroid mites.

METHODS: Acaroid mites in fresh stools of 241 patients with diarrhea were separated by flotation in saturated saline. Meanwhile, skin prick test, total IgE and mite-specific IgE were detected in all patients.

RESULTS: The total positive rate of mites in stool samples of the patients was 17.01 % (41/241), the positive rates of mites in male and female patients were 15.86 % (23/145) and 18.75 % (18/96), respectively, without significant difference ($P>0.05$). The percentage of skin prick test as "+++", "++", "+", "±" and "-" was 9.13 % (22/241), 7.47 % (18/241), 5.81 % (14/241), 4.98 % (12/241) and 72.61 % (175/241), respectively. The serum levels of total IgE, mite-specific IgE in patients with and without mites in stool samples were (165.72±78.55) IU/ml, (132.44±26.80) IU/ml and (145.22±82.47) IU/ml, (67.35±45.28) IU/ml, respectively, with significant difference ($P<0.01$). The positive rate of mites in stool samples in staffs working in traditional Chinese medicine storehouses or rice storehouses (experimental group) was 26.74 % (23/86), which was significantly higher than that (11.61 %, 18/155) in people engaged in other professions ($\chi^2=8.97$, $P<0.01$).

CONCLUSION: Acaroid mites cause diarrhea and increase serum levels of total IgE and mite-specific IgE of patients, and the prevalence of diarrhea caused by acaroid mites is associated with occupations rather than the gender of patients.

Li CP, Cui YB, Wang J, Yang QG, Tian Y. Diarrhea and acaroid mites: A clinical study. *World J Gastroenterol* 2003; 9(7): 1621-1624

http://www.wjgnet.com/1007-9327/9/1621.asp

INTRODUCTION

Grain or flour mite is a serious and widespread pest of stored foodstuffs, particularly grain and grain products[1-10]. Further studies have shown that some mites with strong vitality not only live freely, feeding on a wide variety of food, but also exist in animals or human intestines. After ingesting contaminated food by mites, like grain and grain products, individuals might have diarrhea, abdominal pain, burning sensation around anus and other symptoms of gastrointestinal tract[11]. The characteristics of diarrhea caused by acaroid mites were investigated in 241 patients with diarrhea in this study.

MATERIALS AND METHODS

Patients

Two hundred and forty-one patients with diarrhea (male 145 and female 96, aged from 6 to 58 years) were divided into experimental group (n=86) including staffs working in traditional Chinese medicine storehouses (n=47) and staffs working in rice storehouses or mills (n=39), and control group (n=155) including miners (n=36), staffs of railway system (n=34), pupils (n=62) and others (n=23).

Reagents

Horse anti-human IgE and standard working solution for IgE (17 000 IU/ml) were provided by Beijing Institute of Biological Products, and horse anti-human horseradish peroxidase-IgE was provided by Third Affiliated Hospital, Shanghai Second Medical University.

Methods

History-taking, separation of mites from stool samples, skin prick test and detection of total IgE and mite-specific IgE were carried out in all 241 subjects.

History-taking Detailed information of each subject was collected via telephone and personal interview, including age, gender, present history, anamnesis, symptoms (i.e. abdominal pain, cramps, diarrhea, urodynia, cloudy urine, and urination frequency), onset and duration of symptoms, personal hygienic habits, living conditions and the date of stool samples collected.

Stool examination The stool samples were collected, the mites were separated by flotation in saturated saline and identified under microscope. Stool examination was performed three times for each person, positive specimens were labeled once either adult or larval mite, egg, or hypopus was found.

Skin prick test Skin prick test was performed with the concentration of 1:100 (W/V). After skin was disinfected, a little of extract (about 0.01 ml) was dripped on skin of the right forearm flexor, then a sterile needle was pricked into the skin through the drop of the extract for about 0.5-1 mm in depth without bloodshed. About 5 cm distal and proximal of the prick site, normal saline and histamine were used as negative and positive control, respectively. The mean diameter of the wheals or areolae was measured 15~20 min after the test. The reactions of skin prick test with the mean diameter ≧1.5 mm, ≧2 mm, ≧3 mm, ≧5 mm and ≧10 mm were regarded as ±, +, ++, +++ and ++++, respectively. Otherwise, the reaction was judged as negative[12,13].

The test extract was prepared according to WHO approved document NIBSC 82/518 in 1984. The purified fraction was prepared as follows: the mites cultured in initial medium for several months were frozen and thawed several times. A 48-h maceration in borate buffer at pH 8.5 was centrifuged. The supernatant was neutralized and submitted to acetone precipitation at gradually increasing concentrations. The fraction precipitated in 80 % acetone was isolated, washed and dried. The purified extract was lyophilized or stocked in

50 % glycerol and 5 % phenol[14-16].

Detection of total IgE and mite-specific IgE To investigate humoral immune function in individuals with diarrhea caused by acaroid mites, the levels of total IgE and mite-specific IgE in peripheral blood of mite-positive individuals were tested with ELISA. Peripheral venous blood of the subjects was withdrawn and saved in eppendorf tubes, then the optical density (OD) value was tested on enzyme labeling meters. Positive and negative control tubes were included each time. When the OD value in the tested sample was 2.1 times that or more in negative control, it was regarded as positive.

Mites separated from environment Directicopy, waterenacopy and tullgren were used to separate mites from mill floor dust, stores of traditional Chinese medicine, and traditional Chinese herbs of wolfberry fruit, ophiopogon root liquorice, boat-fruited sterculia seed and safflower, etc.

Statistical analysis

The positive rates were expressed as percentage, and t and χ^2 tests were used in statistical analysis. A probability value of less than 0.05 was considered statistically significant.

RESULTS

Stool examination

The positive rate of mites in stool samples in all the individuals was 17.01 % (41/241), and was 15.86 % (23/145) and 18.75 % (18/96), respectively in samples from male and female subjects, without significant difference (χ^2=0.34, P>0.05). The mites separated from stool samples were confirmed to be *Acarus siro*, *TyroPhagus putrescentiae*, *Dermatophagoides farinae*, *D. pteronyssinus*, *Glycyphagus domesticus*, *G.ornatus*, *Carpoglyphus lactis* and *Tarsonemus granaries*. Among 41 cases with mites in stools, adult mites, larval mites, both adult and larval mites, adult mites and eggs, adult and larval mites and eggs, larval mites and eggs, and both hypopus and eggs were found in 15, 6, 11, 3, 2, 2 and 2 cases, and the constituent ratios of them were 36.59 %, 14.63 %, 26.83 %, 7.32 %, 4.88 %, 4.88 % and 4.88 %, respectively. In addition, the statistics of this investigation showed that the case number with concentration of mites of 1-2/cm^3, 2-4/cm^3 and >5/cm^3 was 6, 12 and 23, respectively. Among the 41 mite-positive cases, 3 cases had other intestinal parasites, 6 cases had pathogenic bacteria. The remaining 32 cases had mites in stool samples only.

Skin prick test

The percentages of cases with "+++", "++", "+", "±" and "-" were 9.13 % (22/241), 7.47 % (18/241), 5.81 % (14/241), 4.98 % (12/241) and 72.61 % (175/241), respectively. The positive number of skin prick test was 54, of which, 41 subjects with mites in stools were all included. In other words, all the 22 subjects with "+++" reaction were confirmed to be mite-positive, and 14 subjects with mites in stools were found in the 18 subjects with "++" reactions, 5 subjects with mites in stools were found in the 14 subjects with "+" reaction. However, all the 41 subjects with mites in stools were positive in skin prick test.

Detection of total IgE and specific IgE

The levels of total IgE and mite-specific IgE in 41 cases with mites were higher than those in individuals without mites (P<0.01) (Table 1).

Relationship between diarrhea caused by acaroid mites and occupation

Among the 241 patients with diarrhea, the positive rate of mites in experimental group was 26.74 % (23/86), which was higher than that in control group (χ^2=8.97, P<0.01) (Table 2).

Table 1 Serum total IgE and mite-specific IgE in patients with diarrhea (IU / ml, $\bar{x}\pm s$)

Group	n	Total IgE (IU / ml)	Specific IgE (IU / ml)
Mite-positive cases	41	165.72±78.55[a]	145.22±82.47[b]
Mite-negative cases	200	132.44±26.80	67.35±45.28
Total	241	138.10±35.37	80.59±53.62

[a]P<0.01, t=4.81; [b]P<0.01, t=8.52 *vs* mite-negative cases.

Table 2 Mites in stool samples in patients with different occupations (n, %)

Groups	Cases	Positive number	Positive rate
Experimental group	86	23[c]	26.74
Staffs working in traditional Chinese medicine storehouses	47	14	29.79
Staffs working in rice storehouses or mills	39	9	23.08
Control group	155	18	11.61
Miners	36	4	11.11
Staffs of railway system	34	3	8.82
Pupils	62	8	12.90
Others	23	3	13.04
Total	241	41	17.01

[c]P<0.01, χ^2=8.97 *vs* control group.

Mites separated from work environment

Samples of mill floor dust (30 shares), stores of traditional Chinese medicine, and traditional Chinese herbs (146 species) of wolfberry fruit, ophiopogon root liquorice, boat-fruited sterculia seed, safflower and other work environment and foodstuffs were collected and separated for mites. The results showed that the number of breeding mites per gram was 91-1862, 21-186, 0-483, 10-348, 51-712, and 311-1193, in mill floor dust, traditional Chinese medicine stores, traditional Chinese herbs such as candied fruit, dry fruit, brown sugar, and expired cake. Twenty-two species of mites were separated and identified belonging to nine families, i.e. *Acaridae*, *Lardoglyphidae*, *Glycyphagidae*, *Chortoglyphidae*, *Carpoglyphidae*, *Histiostomidae*, *Pyroglyphidae*, *Tarsonemus*, *Cheyletus*. The results of this study showed that the mites separated from work environment were identical to those from stored food.

DISCUSSION

In this study, *Acarus siro*, *TyroPhagus putrescentiae*, *Dermatophagoides farinae*, *D. pteronyssinus*, *Glycyphagus domesticus*, *G.ornatus*, *Carpoglyphus lactis* and *Tarsonemus granaries* were separated from stool of patients with diarrhea. This confirmed that acaroid mites were able to parasitize in human intestines, which might play an important role in diarrhea. Like other intestinal parasites, the mites living in intestinal tract may stimulate mechanically and damage intestinal tissues with its gnathosoma, chelicera and feet[17-25]. Certainly they may also intrude into mucous and deep tissues, and cause inflammation and necrosis.

The results of this study support the idea that the patients with mites in stool samples are allergic to acaroid mites. Skin

prick test is one of the specific methods for clinical diagnosis of allergic disease. After superficial layer of skin is pierced by a special needle, interaction occurrs between the test extract and mastocytes in the brain, which causes mastocytes degranulation and inflammation-media release like histamine that is able to increase capillary telangiectasia and permeability. Thereby wheal and flush appear on the surface of skin tested[26,27]. Among the 241 patients tested with skin prick test, 54 subjects had positive reactions. This demonstrated that some of the patients with diarrhea were allergic to acaroid mites. Moreover, the results of skin prick test on 41 patients with mites in their stools were all positive. It provided the evidence that acaroid mites in intestine might lead to the allergy of patients to acaroid mites. The reason why there were no mites found in stools taken from 13 patients with positive reaction of skin prick test is that mites live in other locus besides intestines, and that mites may be missed in detection with saturated saline flotation methods.

Although the serum level of total IgE is a marker of human sensitization to extrinsic allergen, the level of specific IgE is a sensitive index for allergic reaction to acaroid mites[28-34]. In this study, the levels of specific IgE in 41 patients with mites were higher than those without mites. This provides another evidence that acaroid mites can cause allergy. The dejecta, products of metabolism, and cleaved pieces of dead mites in intestine may stimulate lymphocytes and reticuloendothelial system, and produce specific antibodies, such as IgE.

This study confirms that the prevalence of diarrhea caused by acaroid mites was associated with the patients' occupation. The positive rates of mites in stools of staffs working in traditional Chinese medicine storehouses and rice storehouses or mills were 29.79 % (14/47) and 23.08 % (9/39), respectively, which were higher than those of patients with other occupations. However, no significant association was observed between diarrheas caused by the organism with the gender of patients. The positive rates of mites in male and female patients were 15.86 % (23/145) and 18.75 % (18/96), respectively.

Eight species of acaroid mites separated from stool samples could be found in the house dust collected from traditional Chinese medicine storehouses, rice storehouses and flourmills, suggesting that the source of diarrhea caused by acaroid mites is mites in our living environment and stored food. Generally speaking, the path of the mites invading human is related to ingestion of stored food. However, some mites in dust or in air might invade intestine through mouth, or nasal cavity, gorge[35-37]. We have set up eight sampling sites in traditional Chinese medicine storehouses by dust sampler, and separated thirteen mites from dust samples collected from 640 L of air in work environment of the storehouses.

In conclusion, acaroid mites in our living and working environments may invade human intestines and cause diarrhea. The levels of total IgE, mite-specific IgE of the patients with diarrhea caused by acaroid mites increased, the prevalence was associated with the patient' s occupation rather than gender. It is suggested that separation of mites from stool samples, skin prick test and detection of total IgE and mite-specific IgE should be used in the diagnosis of diarrhea caused by acaroid mites.

REFERENCES

1 **Sun HL,** Lue KH. Household distribution of house dust mite in central Taiwan. *J Microbiol Immunol Infect* 2000; **33:** 233-236
2 **Cadman A,** Prescott R, Potter PC. Year-round house dust mite levels on the Highveld. *S Afr Med J* 1998; **88:** 1580-1582
3 **Croce M,** Costa-Manso E, Baggio D, Croce J. House dust mites in the city of Lima, Peru. *Investig Allergol Clin Immunol* 2000; **10:** 286-288
4 **Arlian LG,** Neal JS, Vyszenski-Moher DL. Reducing relative humidity to control the house dust mite *Dermatophagoides farinae. J Allergy Clin Immunol* 1999; **104:** 852-856
5 **Mumcuoglu KY,** Gat Z, Horowitz T, Miller J, Bar-Tana R, Ben-Zvi A, Naparstek Y. Abundance of house dust mites in relation to climate in contrasting agricultural settlements in Israel. *Med Vet Entomol* 1999; **13:** 252-258
6 **Arlian LG,** Neal JS, Vyszenski-Moher DL. Fluctuating hydrating and dehydrating relative humidities effects on the life cycle of Dermatophagoides farinae (Acari: Pyroglyphidae). *J Med Entomol* 1999; **36:** 457-461
7 **Racewicz M.** House dust mites (Acari: Pyroglyphidae) in the cities of Gdansk and Gdynia (northern Poland). *Ann Agric Environ Med* 2001; **8:** 33-38
8 **Solarz K.** Risk of exposure to house dust pyroglyphid mites in Poland. *Ann Agric Environ Med* 2001; **8:** 11-24
9 **Sadaka HA,** Allam SR, Rezk HA, Abo-el-Nazar SY, Shola AY. Isolation of dust mites from houses of Egyptian allergic patients and induction of experimental sensitivity by Dermatophagoides pteronyssinus. *J Egypt Soc Parasitol* 2000; **30:** 263-276
10 **Boquete M,** Carballada F, Armisen M, Nieto A, Martin S, Polo F, Carreira J. Factors influencing the clinical picture and the differential sensitization to house dust mites and storage mites. *J Investig Allergol Clin Immunol* 2000; **10:** 229-234
11 **Li CP,** Wang J. Intestinal acariasis in Anhui Province. *World J Gastroenterol* 2000; **6**: 597-600
12 **Baratawidjaja IR,** Baratawidjaja PP, Darwis A, Soo-Hwee L, Fook-Tim C, Bee-Wah L, Baratawidjaja KG. Prevalence of allergic sensitization to regional inhalants among allergic patients in Jakarta, Indonesia. *Asian Pac J Allergy Immunol* 1999; **17:** 9-12
13 **Yun YY,** KO SH, Park JW, Lee IY, Ree HI, Hong CS. Comparison of allergenic components between German cockroach whole body and fecal extracts. *Ann Allergy Asthma Immunol* 2001; **86:** 551-556
14 **Nuttall TJ,** Lamb JR, Hill PB. Characterization of major and minor Dermatophagoides allergens in canine atopic dermatitis. *Res Vet Sci* 2001; **71:** 51-57
15 **Basomba A,** Tabar AI, de Rojas DH, Garcia BE, Alamar R, Olaguibel JM, del Prado JM, Martin S, Rico P. Allergen vaccination with a liposome-encapsulated extract of Dermatophagoides pteronyssinus: a randomized, double-blind, placebo -controlled trial in asthmatic patients. *J Allergy Clin Immunol* 2002; **109:** 943-948
16 **Akcakaya N,** Hassanzadeh A, Camcioglu Y, Cokugras H. Local and systemic reactions during immunotherapy with adsorbed extracts of house dust mite in children. *Ann Allergy Asthma Immunol* 2000; **85:** 317-321
17 **Van der Geest LP,** Elliot SL, Breeuwer JA, Beerling EA. Diseases of mites. *Exp Appl Acarol* 2000; **24:** 497-560
18 **Zhou X,** Li N, Li JS. Growth hormone stimulates remnant small bowel epithelial cell proliferation. *World J Gastroentero* 2000; **6:** 909-913
19 **Fryauff DJ,** Prodjodipuro P, Basri H, Jones TR, Mouzin E, Widjaja H, Subianto B. Intestinal parasite infections after extended use of chloroquine or primaquine for malaria prevention. *J Parasitol* 1998; **84:** 626-629
20 **Zhou JL,** Xu CH. The method of treatment on protozoon diarrhea. *Shijie Huaren Xiaohua Zazhi* 2000; **8:** 93-95
21 **Herwaldt BL,** de Arroyave KR, Wahlquist SP, de Merida AM, Lopez AS, Juranek DD**.** Multiyear prospective study of intestinal parasitism in a cohort of Peace Corps volunteers in Guatemala. *J Clin Microbiol* 2001; **39:** 34-42
22 **Fan WG,** Long YH. Diarrhea in travelers. *Shijie Huaren Xiaohua Zazhi* 2000; **8:** 937-938
23 **Feng ZH.** Application of gene vaccine and vegetable gene in infective diarrhea. *Shijie Huaren Xiaohua Zazhi* 2000; **8:** 934-936
24 **Xiao YH.** Treatment of infective Diarrhea with antibiotic. *Shijie Huaren Xiaohua Zazhi* 2000; **8**: 930-932
25 **Komatsu S,** Nimura Y, Granger DN. Intestinal stasis associated bowel inflammation. *World J Gastroenterol* 1999; **5:** 518-521
26 **Davis MD,** Richardson DM, Ahmed DD. Rate of patch test reactions to a dermatophagoides mix currently on the market: a mite too sensitive? *Am J Contact Dermat* 2002; **13:** 71-73
27 **Obase Y,** Shimoda T, Tomari SY, Mitsuta K, Kawano T, Matsuse H, Kohno S. Effects of pranlukast on chemical mediators in induced sputum on provocation tests in atopic and aspirin-intolerant asthmatic patients. *Chest* 2002; **121:** 143-150

28 **Silva DA,** Gervasio AM, Sopelete MC, Arruda-Chaves E, Arruda LK, Chapman MD, Sung SS, Taketomi EA. A sensitive reverse ELISA for the measurement of specific IgE to Der p 2, a major Dermatophagoides pteronyssinus allergen. *Ann Allergy Asthma Immunol* 2001; **86:** 545-550

29 **Pumhirun P,** Jane-Trakoonroj S, Wasuwat P. Comparison of *in vitro* assay for specific IgE and skin prick test with intradermal test in patients with allergic rhinitis. *Asian Pac J Allergy Immunol* 2000; **18:** 157-160

30 **Nahm DH,** Kim HY, Park HS. House dust mite-specific IgE antibodies in induced sputum are associated with sputum eosinophilia in mite-sensitive asthmatics. *Ann Allergy Asthma Immunol* 2000; **85:** 129-133

31 **Walusiak J,** Palczynski C, Wyszynska-Puzanska C, Mierzwa L, Pawlukiewicz M, Ruta U, Krakowiak A, Gorski P. Problems in diagnosing occupational allergy to flour: results of allergologic screening in apprentice bakers. *Int J Occup Med Environ Health* 2000; **13:** 15-22

32 **Kanceljak-Macan B,** Macan J, Buneta L, Milkovic-Kraus S. Sensitization to non-pyroglyphid mites in urban population of Croatia. *Croat Med J* 2000; **41:** 54-57

33 **Morsy TA,** Saleh WA, Farrag AM, Rifaat MM. Chironomid potent allergens causing respiratory allergy in children. *J Egypt Soc Parasitol* 2000; **30:** 83-92

34 **Chew FT,** Lim SH, Goh DY, Lee BW. Sensitization to local dust-mite fauna in Singapore. *Allergy* 1999; **54:** 1150-1159

35 **Paufler P,** Gebel T, Dunkelberg H. Quantification of house dust mite allergens in ambient air. *Rev Environ Health* 2001; **16:** 65-80

36 **Roux E,** Hyvelin JM, Savineau JP, Marthan R. Human isolated airway contraction: interaction between air pollutants and passive sensitization. *Am J Respir Crit Care Med* 1999; **160:** 439-445

37 **Ponsonby AL,** Kemp A, Dwyer T, Carmichael A, Couper D, Cochrane J. Feather bedding and house dust mite sensitization and airway disease in childhood. *J Clin Epidemiol* 2002; **55:** 556-562

Edited by Ren SY and Wang XL

P.O.Box 2345, Beijing 100023,China
Fax: +86-10-85381893
E-mail: wjg@wjgnet.com www.wjgnet.com

World J Gastroenterol 2003;9(7):1625-1628
World Journal of Gastroenterology
 ISSN 1007-9327

• BRIEF REPORTS •

Modified technique for combined liver-small bowel transplantation in pigs

Zhen-Yu Yin, Xiao-Dong Ni, Feng Jiang, Ning Li, You-Sheng Li, Jie-Shou Li

Zhen-Yu Yin, Xiao-Dong Li, Feng Jiang, Research Institute of General Surgery, School of Medicine, Nanjing University, Nanjing, 210093, Jiangsu Province, China
Zhen-Yu Yin, Ning Li, You-Sheng Li, Jie-Shou Li, Research Institute of General Surgery, Nanjing PLA General Hospital, Nanjing, 210002, Jiangsu Province, China
Correspondence to: Zhen-Yu Yin, Research Institute of General Surgery, Nanjing PLA General Hospital, 305 East Zhongshan Road, Nanjing 210002, Jiangsu Province, China. davidmd@sohu.com
Telephone: +86–25-3685194 **Fax:** +86-25-4803956
Received: 2002-12-30 **Accepted:** 2003-02-08

Abstract

AIM: As the conventional combined liver-small bowel transplantation is complicated with many postoperative complications, the aim of this study was to describe a modified technique for the combined liver-small bowel transplantation with preservation of the duodenum, partial head of pancreas and hepatic biliary system in pigs.

METHODS: Composite liver/small bowel allotransplantations were undertaken in 30 long-white pigs. The graft included liver, about 3 to 4 m proximal jejunum, duodenum and partial pancreatic head. Vessels reconstructions included subhepatic vena cava-vena cava anastomosis, aorta-aorta anastomosis and portal-splenic vein anastomosis.

RESULTS: Without immunosuppressive treatment, the median survival time of the animals was 6 days (2 to 12 days), and about 76.9 % (20/26) of the animals survived for more than 4 days after operation.

CONCLUSION: The modified technique is feasible and safe for the composite liver/small bowel transplantation with duodenum and pancreas preserved in pigs. And also this technique can simplify the operation and decrease possible postoperative complications.

Yin ZY, Ni XD, Jiang F, Li N, Li YS, Li JS. Modified technique for combined liver-small bowel transplantation in pigs. *World J Gastroenterol* 2003; 9(7): 1625-1628
http://www.wjgnet.com/1007-9327/9/1625.asp

INTRODUCTION

As a result of total parenteral nutrition (TPN) induced end-stage liver disease, 60 % to 70 % of recipients of intestinal transplant procedures require simultaneous liver allografts[1,2]. Although many clinical liver/small bowel transplantations (LSBT) were reported from different medical centers[3-5], it remains an experimental procedure[6]. Compared to the widely used rat LSBT model[7,8], large animal models such as LSBT in pigs were rarely reported.

As a conventional composite liver-small bowel graft requires a loop of defunctionalized (Roux) allograft small bowel for biliary drainage[9], its posttransplant biliary complications include anastomotic leaks and obstruction in 12 % of the cases, with significantly associated morbidity and mortality in clinical reports[1]. In the present study, we modified the technique for LSBT by preserving the duodenum, partial head of pancreas and hepatic biliary system, and also we modified the conventional vena cava and the portal drainage anastomotic methods. Experience with this technique for the LSBT in pigs has not been described previously.

MATERIALS AND METHODS

Donor preparation 60 long-white pigs weighing 20-40 Kg with random sex were undertaken 30 LSBTs. The weight of the donor was generally lower than that of the corresponding recipient. No immunosuppressive treatment was given in the group.

Preoperative treatment The animals were not allowed to eat for 24 hours and drink for 4 hours before operation respectively. The gut decontamination was attempted in all donors with an oral antibiotic preparation 3 days before surgery.

After anesthesia with 25 mg/kg of intravenous pentobarbital sodium, the animal was intubated and mechanically ventilated with a mixture of oxygen, nitrous oxide and isoflurane. In addition, the standard intravenous antibiotic prophylaxis was instituted with cefotaxime at the time of surgery.

Donor surgical technique

Initial exposure and isolation of the abdominal organs The procurement varied in details but followed the standard techniques for human multiorgan retrieval[10-12]. Briefly, the donor operation was performed through a midline laparotomy. Cares should be taken not to damage the urethra of male pigs when opening the abdomen. The liver was mobilized by dividing its suspensory attachments. The right gastric and right gastroepiploic vessels were divided, and the pylorus was transected, which allowed the stomach to be reflected craniad. The proximal 3 to 4 m of jejunum (the total porcine small bowel is about 15 m) together with the liver was procured as the graft. After the redundant small bowel was dissected, its supply vessels were ligated. Then the intestinal tract was transected at the beginning of the descending colon, and then the redundant small bowel and the colon were removed from the operative field. Thus the duodenum, proximal jejunum and the aorta could be well exposed. The left gastric artery was ligated at the celiac axis.

Dissection of the vessels The suprahepatic vena cava was firstly dissected and encircled. An extensive Kocher maneuver allowed visualization of the inferior vena cava and its branch. The subhepatic vena cava was dissected and encircled. The left and right renal veins were ligated respectively.

With division of the left retroperitoneal artery, the superior mesenteric and celiac arteries were identified by extending dissection of the aorta. The right and left renal arteries were then isolated and ligated. The subrenal aorta was isolated and encircled distally for the eventual insertion of an infusion cannula. The abdominal aorta was also encircled above the celiac axis for later crossclamping when cold fluid was infused through the distal aortic cannula[13]. It should be mentioned

that dissection of the celiac trunk would always open the diaphragm and result in pneumothorax.

The splenic vein was then freed and prepared for portal perfusion cannulation after division of the splenic artery. The splenic vein should be well protected when dividing the splenic artery[14].

***In situ* cooling and removal of the organs** Unlike the clinical transplantation, it was imperative to collect the donor' s blood for the recipient operation. Before the infusion with cold solution, the donor' s blood was collected from the iliac artery. After completion of the preliminary dissections and collection of the donor' s blood, the liver and small bowel connected by the portal vein and the aortic segment were lavaged *in situ* with UW solution. Briefly, the donor was fully heparinized and the previously encircled proximal aorta was crossclamped, and the distal donor aorta was cannulated with infusion of cold UW solution. For the simultaneous portal venous infusion, a venous cannula was placed into the splenic vein and infused with the UW solution. The intrapericardial inferior vena cava and the subhepatic vena cava were transected to decompress the infused solution as in other reports[15,16]. The amount of infusion was variable (between 50 mL/Kg and 100 mL/Kg), guided by blanching the organs and estimated by palpation of the degree of cooling. If the intestine did not feel cold after limited perfusion, there was no reason for concern, providing it was blanched, further surface cooling after immersion in cold fluid was rapid as the intestine is a hollow organ[11]. It is important to avoid both venous hypertension and overperfusion of the intestine and pancreas, as overperfusion might result in duodenopancreatic and small bowel edema[13,17]. Some solution was injected into the gallbladder to lavage the bile tract.

After infusion, the graft containing liver, hepatic hilus, pancreatic-duodeno complex, spleen together with the splenic vein, and small bowel was achieved with preservation of a segment of aorta containing the superior mesenteric artery and celiac trunk in continuity. The intestine was entrapped by stapling its two ends and carried with the specimen throughout the preservation. Thus the graft was *en bloc* removed and stored in UW solution at 0 to 4 ℃.

Back table procedure Back table procedure was performed in the cold UW solution. It included suturing the orifice of suprahepatic vena cava and the proximal end of the aorta. The spleen was removed and the splenic vein was well preserved. The body and tail of the pancreas along the portal vein were isolated and transected, leaving partial pancreatic head attached to the allograft duodenum. This preserved the superior and inferior pancreatic duodenal arcades. The stump of the pancreas was stapled and then oversewn with a running suture using 4-0 polypropylene. The gallbladder was removed and a catheter was placed into the cystic duct stump for the early decompression and study of the donor biliary system during the early postoperative period.

Recipient operation

After anesthesia, a monitor was placed on the recipient. Two venous catheters were inserted for transfusion and central venous pressure monitoring. The arterial blood pressure was monitored through a thigh artery catheter.

Intestinal resection When the abdomen was opened, the small bowel and its mesentery were dissected. Most of the intestine was removed for an artificial short bowel with only about 30 cm left at each end.

Vascular preparation The subrenal aorta was exposed and encircled 2 cm under the renal artery. Small arterial and lymphatic vessels along the aorta were ligated to avoid later bleeding or lymphorrhea. Subhepatic vena cava was also dissected and encircled. The place just above the left renal vein was routinely used for the donor out-flow anastomosis. The hilar of the recipient liver was dissected. The common bile duct and the liver artery were transected while the portal vein was crossclamped with a bulldog after transection.

Hepatectomy The resection of the recipient liver was another major step. The total vascular exclusive technique for hepatectomy in human being was not suitable to the pig, so the liver was removed lobe by lobe. Since the retrohepatic vena cava in the pig was passing through the liver with numerous small hepatic veins draining to this segment besides the major hepatic veins, it was hard to be skeletonized. In order to avoid massive bleeding when dissecting the retrohepatic vena cava, a small part of the liver around the retrohepatic vena cava was always saved and oversewn.

Graft implantation and revascularization The transplantation methods varied in details but followed the principles as described previously[11]. The typical reconstruction is shown in Figure 1.

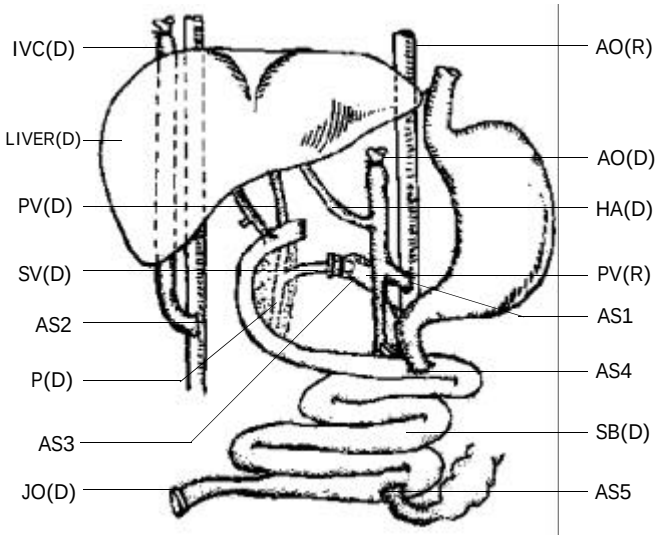

Figure 1 Composite liver/small bowel transplantation (D=donor, R=recipient, AO=aorta, HA=hepatic artery, PV=portal vein, SB=small bowel, IVC=inferior vena cava, SV=splenic vein, P=pancreas, JO=jejunum ostomy, AS1=aorta-aorta anastomosis, AS2=subhepatic vena cava- vena cava anastomosis, AS3=portal-splenic vein anastomosis, AS4=proximal jejuno-jejunal anastomosis, AS5=distal jejuno-ileal anastomosis).

The graft was placed in an orthotopic position. The arterial inflow was created via an end-to-side anastomosis of the graft aorta to the subrenal native aorta with a running polypropylene suture. Donor and recipient vena cava were anastomosed end to side. The venous outflow was a modification of the piggyback fashion with the end of the graft subhepatic vena cava anastomosed to the side of the native subhepatic vena cava.

Before reperfusion, unclamping and perfusion of the allograft liver were achieved after a lavage of 300 to 500 ml donor blood or Ringer' s solution through the splenic vein.

Anastomosis of the donor splenic vein to the recipient portal vein By using the graft splenic venous stump, a branch point left could be clamped separately and anastomosed to the recipient portal vein to allow outflow of the retained recipient viscera (stomach, pancreas, and spleen as well as the remaining native intestine). Since the splenic vein was smaller than the recipient portal vein, the cuff technique was always used for this anastomosis.

Gastrointestinal reconstruction The proximal duodenum was closed. The intestinal continuity was established proximally by end-to-side recipient-to-donor jejuno-jejunal anastomosis. The end of the recipient' s distal ileum was anastomosed to the side of the donor distal jejunum including a donor distal

intestinal vent for the early decompression and surveillance endoscopies as described in some clinical reports[18,19]. The bile was drained with a catheter in the donor' s cystic tract.

Postoperative management After operation, the animal was returned to the monitor room, where hemodynamic monitoring and mechanical ventilation were performed as needed 24 hours after operation. Due to the high rate of inflammatory complications, broad-spectrum antibacterial prophylaxis was administered once for 5 days. Lactated Ringer' s solution and parenteral nutrition were given daily until the animal was able to eat and drink.

The appearance of the allograft ostomy and the amount of ostomy output were useful clinical signs of graft dysfunction. Ostomy losses up to 100 cc/kg per day were acceptable and could be compensated by supplementary intravenous fluids.

RESULTS

After reperfusion, the liver was soft and pink with prompt bile production, evidenced through the cystic duct catheter. If the liver was harder than normal, the outflow of the liver might be obstructed and the vena cava anastomosis was required to be checked. The small bowel would be perfused well, with good mesenteric arterial inflow and venous outflow. The peristalsis and intraluminal mucous production were evident within 15 minutes after reperfusion.

Animals died suddenly after reperfusion were ruled out from the statistic series. 4 recipients died because of post reperfusion syndrome and operative techniques. The other 26 LSBT pigs had a median survival time of 6 days (from 2 to 12 days). The surgical records are shown in Table 1, and the values were expressed as median (range).

Table 1 Surgical records

Parameters	Values
Weight of the donor (KG)	22.5 (19-25)
Weight of the recipient (KG)	25 (22-38)
Length of the graft small bowel (m)	3.4 (2.8-4.2)
Weight of the graft liver (g)	760 (620-960)
Collection of the donor blood (ml)	800 (400-1200)
Cooling solution (ml)	1400 (1200-2000)
Donor operative time (hr)	3.3 (2.8-3.6)
Back table time (hr)	0.8 (0.5-1.1)
Preservation time (hr)	3.8 (3.0-4.5)
Total cold ischemia time (hr)	5.6 (3.8-6.6)
Total operative time (hr)	8.2 (7.0-11.4)
Postoperative survival time (day)	6 (2-12)
Survival rate (more than 4 days)	76.9%(20/26)

During the first three days, the intestinal graft stoma appeared healthy, and the mucosa was pink, moist, and well vascularized. No intestinal edema was found in most cases with stomal output averaging 500 ml/day and characterized by bile-stained stool. The high stomal output would decrease with time.

All liver grafts functioned immediately after serum bilirubin and transaminase levels peaked on the first postoperative day and fell rapidly thereafter.

Neither the duodenal allografts experienced signs of ischemia or stump leakage, nor experienced any biliary complication. Abdominal drains were monitored serially for amylase and lipase. Chemical pancreatitis was observed during the early postoperative period with lipase-rich fluid drainage. The biopsies of the dead animals indicated mild pancreatitis in the remained pancreas.

Histopathologic studies of the grafts showed no significant preservation injury. None of the biopsies obtained in the first postoperative week had histological evidence of submucosal bacterial invasion. The frequent cause of death was postoperative rejection convinced by the graft biopsies when the animal was dead.

DISCUSSION

Specialties of porcine anatomy and LSBT model Firstly, the porcine liver is divided into 4 relatively independent lobes. There are obvious borderlines between lobes. This is the reason why we can remove the liver lobe by lobe when total vascular exclusive technique can not be used in hepatectomy. Secondly, the porcine retrohepatic vena cava is passing through the liver parenchyma with numerous small hepatic veins outflow to this segment besides the major hepatic veins. It is dangerous to remove the liver parenchyma when dissecting the retrohepatic vena cava. This is the reason why the classic piggyback liver transplantation is not suitable to the pig. The vena cava anastomosis was modified by replacing the major hepatic vein (or suprahepatic vena cava) anastomosis in classical piggyback transplantation with the subhepatic vena cava anastomosis (Figure 1). This modification has at least three advantages in porcine LSBT: (1). It is safe to remove the liver, for the whole recipient liver is not moved to expose the retrohepatic vena cava. (2). The subhepatic vena cava anastomosis can be easily performed. (3). The subhepatic vena cava anastomosis can adjust a flexible anastomotic interval to make the aorta-aorta and the portal-splenic vein anastomosis easier.

The third difference of porcine anatomy is that the interval between the celiac axis and superior mesenteric artery is longer than that of human being. It is about 2 to 2.5 cm in general, so the Carrel patch with celiac axis and superior mesenteric artery in human LSBT is not suitable to the pig. The long segment of aorta with celiac axis and superior mesenteric artery was used in porcine LSBT. (Figure 1).

Feasibility and safety of the porcine LSBT with pancreatic head and duodenum In clinical practice, Abu-Elmagd suggested that LSBT with pancreatic head and duodenum had some advantages including avoidance of biliary complications and simplification of the operative procedure[20]. These possible advantages might exist in the animal LSBT.

The LSBT transplant procedure is a much more arduous surgical endeavor. The technique retaining the duodenum and the head of pancreas would simplify the back table preparation and avoid risks associated with dissection of the donor hepatic hilus.

Retrieval for composite grafts using the standard technique involves an obligatory reconstruction of the biliary system with a defunctionalized loop of proximal allograft jejunum[3]. In this porcine LSBT model, no biliary reconstruction is required to eliminate the source of complications such as bile leakage, bile tract stricture or even the death of recipient. Liver transplantation related biliary complication rate is about 12 %, which would result in about 19 % of death of them[21,22]. The LSBT with partial pancreas and duodenum would remarkably decrease such complications.

Without donor or recipient bowel for Roux-en-Y biliary reconstruction would enhance the potential benefits of any intestinal segment in freeing the pig for TPN, as it is directly kept in continuity with the alimentary tract.

The advantage of the composite technique is to maintain the hepatic hilus. The use of liver artery and superior mesenteric artery with a large arterial conduit would minimize the risk of hepatic artery thrombosis compared to isolated graft[18,23].

In the experiments, we found that the graft with duodenum and partial pancreas was also convenient to be implanted as compared to the standard LSBT. Only three vascular anastomoses were required, including aorta-aorta anastomosis,

vena cava-vena cava anastomosis and portal-splenic vein anastomosis. The liver artery anastomosis and biliary reconstruction are not necessary when this method is used. Since the aorta and vena cava are end-to-side anastomosed with the recipient' s aorta and vena cava partially excluded during the anastomosis. This method would avoid not only hemodynamic damages, but also possible kidney injuries, postoperative thrombus and lower limb ischemia.

Inclusion of the duodenum and pancreatic head to maintain continuity of the biliary system was associated with early postoperative allograft pancreatitis, and no significant morbidity was reported[17]. This complication was also found in our study. It could be detected by measuring pancreatic enzymes in peritoneal fluid from abdominal drains and serum pancreatic enzymes[20]. Early diagnosis and aggressive surgical management of the native pancreatitis have eliminated the need for repeated transplantation[18]. At present, the following possible ways are considered to protect the allografted pancreas from postoperative pancreatitis. (1). To limit the cold solution and the pressure of perfusion[13]. (2). To procure the pancreas entirely with the graft and avoid over-dissection of the tissue and vessels around the duodenum and pancreas[24]. (3). To ligate the pancreatic tract and suture the pancreatic interface definitely. (4). To use somatostatin after operation.

Some reports suggested that LSBT with duodenum and pancreas head preserved would neither increase the possibility of rejection nor require more immunosuppressive treatment than that of the standard LSBT without pancreas and duodenum[18,23]. The presence of allograft pancreas in the multivisceral allograft was not an important risk factor for mortality, and the incidence of rejection of the pancreas was only 12 % in some report[18]. So the technique with preservation of the pancreas is safe in composite LSBT.

In summary, the modified technique is feasible and safe for composite liver/small bowel transplantation with duodenum and pancreas preserved. This technique can simplify the operation procedure and decrease possible postoperative complications. The immunosuppressive treatment in this large animal LSBT model needs to be further studied.

REFERENCES

1 **Reyes J**, Bueno J, Kocoshis S, Green M, Abu-Elmagd K, Furukawa H, Barksdale EM, Strom S, Fung JJ, Todo S, Irish W, Starzl TE. Current status of intestinal transplantation in children. *J Pediatr Surg* 1998; **33**: 243-254

2 **Grant D**. Intestinal transplantation: 1997 report of the international registry intestal transplant. *Transplantation* 1999; **67**: 1061-1067

3 **Grant D**, Wall W, Mimeault R, Zhong R, Ghent C, Garcia B, Stilier C, Duff J. Successful small bowel/liver transplantation. *Lancet* 1990; **335**: 181-184

4 **Todo S**, Reyes J, Furukawa H, Abu-Elmagd K, Lee RG, Tzakis A, Rao AS, Starzl TE. Outcome analysis of 71 clinical intestinal transplantations. *Ann Surg* 1995; **222**: 270-280

5 **Goulet O**, Jan D, Sarnacki S, Brousse N, Colomb V, Salomon R, Cuenod B, Piloquet H, Ricour C, Revillon Y. Isolated and combined liver-small bowel transplantation in Paris: 1987-1995. *Transplant-Proc*1996; **28**: 2750

6 **Muiesan P**, Dhawan A, Novelli M, Mieli-Vergani G, Rela M, Haton ND. Isolated liver transplant and sequential small bowel transplantation for intestinal failure and related liver disease in children. *Transplantation* 2000; **69**: 2323-2326

7 **Zhong R**, He G, Sakai Y, Zhang Z, Garcia B, Li XC, Jevnikar A, Grant D. The effect of donor-recipient strain combination on rejection and graft-versus-host disease after small bowel/liver transplantation in the rat. *Transplantation* 1993; **56**: 381-385

8 **Li XC**, Zhong R, He G, Sakai Y, Garcia B, Jevnikar A, Grant D. Host immune suppression after small bowel/liver transplantation in rats. *Transplant Int* 1994; **7**: 131-135

9 **Furukawa H**, Kaubu-Elmagd K, Reyes JL. Technical aspects of intestinal transplantation In: Braverman MH, Tawas RL, eds. Surgical Technology International II, San Francisco CA. *TF Laszlo* 1994: 165-170

10 **Starzl TE**, Todo S, Tzakis A, Alessiani M, Casavilla A, Abu-Elmagd K, Fung JJ. The many faces of multivisceral transplantation. *Surg Gynecol Obstet* 1991; **172**: 335-344

11 **Casavilla A**, Selby R, Abu-Elmagd K, Tzakis A, Todo S, Retes J, Fung J, Starzl TE. Logistics and technique for combined hepatic-intestinal retrieval. *Ann Surg* 1992; **216**: 605-609

12 **Williams JW**, Sankary HN, Foster PF. Technique for splanchnic transplantation. *J Pediatr Surg* 1991; **26**: 79-81

13 **Abu-Elmagd K**, Fung J, Bueno J, Martin D, Madariaga JR, Mazariegos G, Bond G, Molmenti E, Corry RJ, Starzl TE, Reyes J. Logistics and technique for procurement of intestinal, pancreatic, and hepatic grafts from the same donor. *Ann Surg* 2000; **232**: 680-687

14 **Goyet JdVd**, Mitchell A, Mayer AD, Beath SV, McKiernan PJ, Kelly DA, Mirza D, Buckles JA. En bloc combined reduced-liver and small bowel transplants: from large donors to small children. *Transplantation* 2000; **69**: 555-559

15 **Starzl TE**, Hakala TR, Shaw BW Jr, Hardesty RL, Rosenthal TJ, Griffith BP, Iwatsuki S, Bahnson HT. A flexible procedure for multiple cadaveric organ procurement. *Surg Gybecol Obstet* 1984; **158**: 223-230

16 **Starzl TE**, Miller C, Bronznick B, Makowka L. An improved technique for multiple organ harvesting. *Surg Gybecol Obstet* 1987; **165**: 343-348

17 **Casavilla A**, Selby R, Abu-Elmagd K, Tzakis A, Todo S, Starzl TE. Donor selection and surgical technique for en bloc liver-small bowel graft procurement. *Trans Spant Proc* 1993; **25**: 2622-2623

18 **Reyes J**, Fishbein J, Bueno J, Mazariegos G, Abu-Elmagd K. Reduced-size orthotopic composite liver-intestinal allograft. *Transplantation* 1998; **66**: 489-492

19 **Todo S**, Tzakis AG, Abu-Elmagd K, Reyes J, Fung JJ, Casavilla A, Nakamura K, Yagihashi A, Jain A, Murase N. Cadaveric small bowel and small bowel-liver transplantation in humans. *Transplantation* 1992; **53**: 369-376

20 **Abu-Elmagd K**, Reyes J, Todo S, Rao A, Lee R, Irish W, Furukawa H, Bueno J, McMichael J, Fawzy AT, Murase N, Demetris J, Rakela J, Fung JJ, Starzl TE. Clinical intestinal transplantation: New perspectives and immunologic considerations. *J Am Coll Surg* 1998; **186**: 512-527

21 **Lopez RR**, Benner KG, Ivancev K, Keeffe EB, Deveney CW, Pinson CW. Management of biliary complication after liver transplantation. *Am J Surg* 1992; **163**: 519-524

22 **Greif F**, Bronsther OL, Van Thiel DH, Casavilla A, Iwatsuki S, Tzakis A, Todo S, Fung JJ, Starzl TE. The incidence, timing and management of biliary tract complications after orthotopic liver transplantation. *Ann Surg* 1994; **219**: 40-45

23 **Bueno J**, Abu-Elmagd K, Mazariegos G, Madariaga J, Fung J, Reyes J. Composite liver-small bowel allografts with preservation of donor duodenum and hepatic biliary system in children. *J Pediatr Surg* 2000; **35**: 291-296

24 **Kato T**, Romero R, Verzaro R, Misiakos E, Khan FA, Pinna AD, Nery JR, Ruiz P, Tzakis AG. Inclusion of entire pancreas in the composite liver and intestinal graft in pediatric intestinal transplantation. *Pediatr Transplant* 1999; **3**: 210-214

Edited by Yuan HT, Zhu LH and Wang XL

P.O.Box 2345, Beijing 100023,China
Fax: +86-10-85381893
E-mail: wjg@wjgnet.com www.wjgnet.com

World J Gastroenterol 2003;9(7): 1629-1632
World Journal of Gastroenterology
 ISSN 1007-9327

• BRIEF REPORTS •

In vitro assay for HCV serine proteinase expressed in insect cells

Li-Hua Hou, Gui-Xin Du, Rong-Bin Guan, Yi-Gang Tong, Hai-Tao Wang

Li-Hua Hou, Gui-Xin Du, Rong-Bin Guan, Yi-Gang Tong, Hai-Tao Wang, Department of Applied Molecular Biology, Institute of Microbiology and Epidemiology, Beijing 100071, China
Supported by the National Natural Science Foundation of China, No. 39630020
Correspondence to: Dr. Li-Hua Hou, Department of Applied Molecular Biology, Institute of Microbiology and Epidemiology, Beijing 100071, China. houlihua@sina.com
Telephone: +86-10-66948580 **Fax:** +86-10-63869835
Received: 2003-03-20 **Accepted:** 2003-04-11

Abstract

AIM: To produce the recombinant NS3 protease of hepatitis C virus with enzymatic activity in insect cells.

METHODS: The gene of HCV serine proteinase domain which encodes 181 amino acids was inserted into pFastBacHTc and the recombinant plasmid pFBCNS3N was transformed into DH10Bac competent cells for transposition. After the recombinant bacmids had been determined to be correct by both blue-white colonies and PCR analysis, the isolated bacmid DNAs were transfected into Sf9 insect cells. The bacmids DNA was verified to replicate in insect cells and packaged into baculovirus particles via PCR and electronic microscopic analysis. The insect cells infected with recombinant baculovirus were determined by SDS-PAGE and Western-blot assays. The recombinant protein was soluted in N-lauryl sarcosine sodium (NLS) and purifed by metal-chelated-affinity chromatography, then the antigenicity of recombinant protease was determined by enzyme-linked immunoabsorbant assay and its enzymatic activity was detected.

RESULTS: The HCV NS3 protease domain was expressed in insect cells at high level and it was partially solved in NLS. Totally 0.2 mg recombinant serine proteinase domain with high purity was obtained by metal-chelated-affinity chromatography from 5×10^7 cells, and both antigenicity and specificity of the protein were evaluated to be high when used as antigen to detect hepatitis C patients' sera in indirect ELISA format. *In vitro* cleavage assay corroborated its enzymatic activity.

CONCLUSION: The recombinant HCV NS3 proteinase expressed by insect cells is a membrane-binding protein with good antigenicity and enzymatic activity.

Hou LH, Du GX, Guan RB, Tong YG, Wang HT. *In vitro* assay for HCV serine proteinase expressed in insect cells. *World J Gastroenterol* 2003; 9(7): 1629-1632
http://www.wjgnet.com/1007-9327/9/1629.asp

INTRODUCTION

Hepatitis C virus, the major etiological agent of post-transfusion non-A, non-B hepatitis, is an enveloped virus obtaining a single-stranded RNA genome of approximately 9.5kb[1-3]. A single polyprotein of 3 010-3 030 amino acids is translated from this genome in the order of NH2-C-E1-E2-p7-NS2-NS3-NS4A-NS4B-NS5A-NS5B-COOH. Proteolytic procession of the viral precursor protein is required for replication and is mediated by either viral or host cell proteinases[4-7]. HCV uses a serine proteinase located at the N- terminus of NS3, to process the cleavage of four sites (3/4A, 4A/4B, 4B/5A and 5A/5B). Since the NS3 protein is very important for releasing functional proteins from the polyprotein, it has been currently targeted in the development of drugs and diagnostics[8-11].

In the absence of satisfactory cell culture, protein expression is the primary technological methods for HCV[12-14]. In this report, we described the construction of the recombinant baculovirus, designed to express the NS3 proteinase in insects. The activity of the expressed enzyme has been demonstrated by *in vitro* assay.

MATERIALS AND METHODS

Cells, vectors and strains

Spodoptera frugiperda Sf9 cells were a gift from Professor Gu Shu-Yan, Institute of Virology, CDC, China. The vector pGEX-3X-NS3N containing the gene serine proteinase located at N-terminus of HCV NS3, was constructed in our lab before[15]. The expression vector pFastBacHTc and *E.coli* DH10Bac were purchased from Invitrogen Inc.

Primers

The primers flanking the vector transfer pFastBacHTc MCS were WB538P (5' -TATTC CGGAT TATTC ATACC-3') and WHT62P (5' -TGGTA TGGCT GATTA TGAT-3'). The primers for bacmid were pUC/M13-R (5' -CAGGA AACAG CTATG AC) and pUC/M13-F (5' -GTTTT CCCAG TCACG AC-3').

Construction of recombinant transfer vector

The gene HCV NS3N serine proteinase was excised from pGEX-3X-NS3N with restriction enzyme *BamHI* and *EcoRI*, and ligated with vector pFastBacHTc. The recombinant plasmids were transformed into *E.coli* DH5α. The positive recombinants were identified with PCR and restriction enzyme digestion, then termed as pFBCNS3N.

Transposition

The recombinant transfer vector pFBCNS3N was transformed into the competent DH10Bac cells. After growth in the shaking incubator at 37 ℃ for 6 h, the cells were placed on the plates (containing 50 mg/L kanamycin, 7 mg/L gentamicin, 10 mg/L tetracycline, 40 mg/L IPTG and 100 mg/L X-gal) with serial dilution, then incubated at 37 ℃ for 48 h. The white colonies containing the recombinant bacmid, therefore, were selected for the isolation of recombinant bacmid DNA. The bacmid, termed as bacmid-NS3N, was analyzed by 0.5 % agarose gel electrophoresis to confirm the presence of high molecular weight DNA.

Production and analysis of recombinant baculovirus

9×10^5 of Sf9 cells were seeded to each well of a 6-well plate in TNM-FH medium and incubated at 27 ℃. Bacmic-NS3N was transfected into Sf9 cells using Lipofectamine reagent (Gibco

BRL) after cells attached to the wells. The supernatant was collected as virus stock when cytopathic effect appeared. At the same time, virus particles in the supernatant were precipitated using PEG8000 to extract viral genome for PCR amplification with the primers WB538P, WHT62P and pUC/M13-R, F to confirm the recombinant virus containing the interested gene. The morpha of recombinant baculovirus was observed under transmission electron microscope.

Expression and purification of serine proteinase in insect cells

Monolayer insect cells were transfected by the recombinant baculovirus at a multiplicity of infection (MOI) of 10. The cells were harvested after incubation for 72 h at 27 ℃, resuspended in lysis buffer (0.5 % NP-40, 20 mmol/L Tris-HCl pH 7.4, 150 mmol/L NaCl, 100 mg/L PMSF), and disrupted by ultrasonic. The supernatant and precipitation of the mixture were collected for SDS-PAGE and Western blotting. 5×10^7 of Sf9 cells were collected by centrifugation after transfection for 72 h to purify the recombinant serine proteinase. The cell pellet was resuspended in TNG buffer (50 mmol/L Tris-HCl pH 7.4, 0.2 % NLS (N-Lauryl Sarcosine Sodium), 10 % glycerol, 150 mmol/L NaCl, 100 mg/L PMSF), and disrupted by ultrasonic. The interested protein was purified from the supernatant by means of affinity chromatography on Ni-NTA columns (Qiagen).

In vitro assay of HCV NS3 proteinase activity

Fifteen μg recombinant serine proteinase was mixed with 15 μg substrate HCV NS5ab in 100 μl of 25 mmol/L Tris-HCl pH 7.4, 10 % glycerol, 0.5 mol/L NaCl, 10 mmol/L DTT, 0.5 % NP-40. The incubation was carried out at room temperature for different time periods and the result was read through SDS-PAGE.

Antigenicity of recombinant HCV serine proteinase

The identity of recombinant proteins was confirmed by 50 HCV-positive and 10 HCV-negative sera. Microtitre cells were coated by overnight incubation at 4 ℃ with 100 μl recombinant protein solution (10 mg/L proteins in 0.1 mol/L sodium carbonate buffer, pH 9.6). Serum samples diluted at 1:20 in PBSTM (PBS+0.3 % Tween-20+3 % fat-free milk) were added, and incubated at 37 ℃ for 1 hour after blocking. The specific binding was revealed using HRP anti-human IgG detection system(Sigma, USA).

RESULTS

Construction of recombinant transfer vector

A 540 bp fragment was excised from the plasmid pFBCNS3N with restriction endonuclease enzymes *HindIII* and *EcoRI* (Figure 1). The result showed that the construction of recombinant transfer vector was successful.

Generation of recombinant baculovirus

The recombinant baculoviruses were generated after the site-specific transposition of transfer plasmids in *E.coli*, transfection and packaging in insect cells. Large amounts of baculoviruses were observed in the nuclei of cells under transmission electron microscope (Figure 2). In PCR detection, genome DNA of the recombinant baculoviruses as template, 800 bp and 3 000 bp fragments appeared respectively with primers WB538P, WHT62P and pUC/M13-R, F. The result conformed to our previous expectation and revealed HCV serine proteinase gene existed in the genome of recombinant baculoviruses.

Efficient expression of HCV serine proteinase by recombinant baculovirus

Sf9 cells were transfected with the recombinant baculovirus at a MOI of 10, and serious CPE appeared after 72 h. The total cell extracts were separated by 15 % SDS-PAGE and stained with Coomassie blue. A predominant band at 23 kDa (approximately 20 % of total proteins) was detected in the cell extracts from bacmic-NS3N infected cells but not in the uninfected cell extracts (Figure 3A). Immunoblot analysis with the HCV-positive sera (Figure 3B) revealed that the 23 kDa protein was clearly detected in cells infected with the recombinant baculovirus.

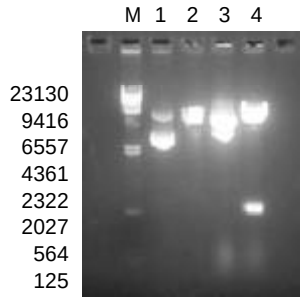

Figure 1 Restriction endonuclease enzyme analysis for recombinant bacmid. Lane M. λ / *HindIII* standard DNA molecular weight marker, Lane 1. pFastBacHTc plasmid, Lane 2. pFastBacHTc plasmid digested with *HindIII* and *EcoRI*, Lane 3. pFBCNS3N plasmid, Lane 4. pFBCNS3N plasmid digested with *HindIII* and *EcoRI*.

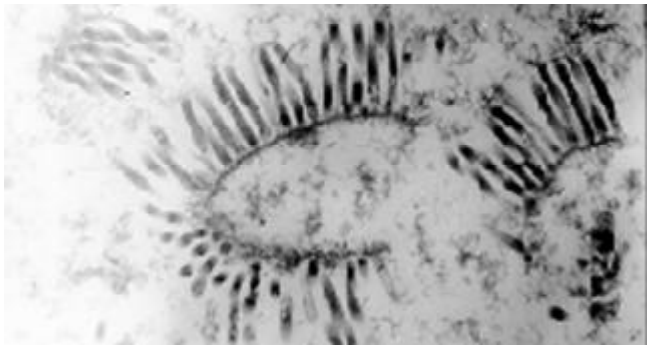

Figure 2 Recombinant bacoluvirus in insect cells under transmission electron microscope (×36 000).

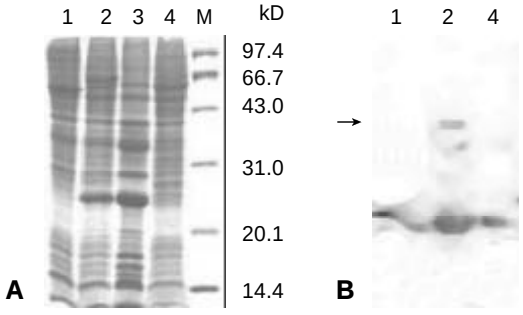

Figure 3 SDS-PAGE analysis (3A) and Western blotting analysis (3B) for the recombinant HCV serine proteinase expressed in insect cells. 3A. lane 1. untransfected Sf9 cells, lane 2. Sf9 cells transfected with rvBacNS3N, lane 3. the pellet of the cell lysate transfected with rvBacNS3N, lane 4. the supernatant of the cell lysate transfected with rvBacNS3N, Lane M. low molecular weight markers. 3B lanes 1,2,4 corresponded to Figure 3A.

Analysis of solubility of recombinant HCV serine proteinase

Though HCV serine proteinase was expressed efficiently in insect cells, a little was laid in the supernatant of the cell lysate.

Only by immunoblot analysis was the protein in the supernatant detected. Did the protein's misfolding or binding with endomembrane system in cells lead to unsoluble protein? This question was analyzed by changing the composition of the lysis buffer. When the cell lysates were dissolved in TNG buffer containing N-lauryl sarcosine sodium, more interested protein was soluble because TNG as a detergent could dissolve proteins binding with membrane. Therefore, it was presumed that the recombinant HCV serine proteinase binding with membrane resulted in its unsolubility. The HCV serine proteinase was extensively purified from 5×10^7 Sf9 cells and demonstrated a single protein band of 23kDa (more than 90 % of the total proteins by densitometric analysis) by using Ni-NTA columns. The total yield of the purified protein was about 0.2 mg.

Activity of baculovirus-expressing HCV serine proteinase in trans

In order to determine whether the baculovirus-expressing cleavage N-terminus of HCV NS3 has a proteinase activity, an *in vitro* proteolytic assay with HCV NS5ab protein (235aa) as a substrate containing the cleavage site of HCV NS5a and NS5b was designed. Figure 4 shows that the baculovirus-expressing HCV serine proteinase could cleave the substrate HCV NS5ab (about 35kDa) into bands of 24kDa and 11kDa (Figure 4). This means that the baculovirus-expressing HCV serine proteinase has a high proteolytic activity.

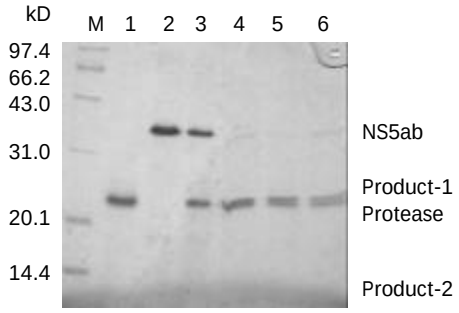

Figure 4 *In vitro* trans-cleavage at the NS5A/5B site of the recombinant HCV serine proteinase. Lane M. low molecular weight markers, lane 1. the purified HCV serine proteinase, lane 2. the substrate HCV NS5ab protetin, lanes 3-6. cleavage reaction after 0, 10, 20 and 30 min.

Antigenicity of recombinant HCV serine proteinase

Fifty HCV positive sera and 10 HCV negative sera were evaluated for their reactivities against the purified HCV serine proteinase. A high degree of immunoreactivity was observed in 30 HCV positive sera, showing good antigenicity of HCV serine proteinase.

DISCUSSION

It has been proved that HCV NS3 protein with 631 amino acids possesses both serine proteinase in its N-terminus and NTP/RNA helicase activity in its C-terminus[16]. Both *in vitro* translation and transient mammalian cells have shown that NS3 is a serine proteinase and is responsible for proteolytic processing of the non-structural region (NS3, NS4A, NS4B, NS5A and NS5B) of HCV polyprotein. Since the maturation of these non-structural proteins is the prerequisites for replication, and packaging of HCV, NS3 serine proteinase plays an important role in the life cycle of HCV and is an attractive target for antiviral therapy. We expressed only 181 amino acids in HCV NS3 N-terminus because previous experiments had corroborated it with good enzyme activity[17].

Baculovirus-insect cell expression system has two advantages over others: first, in most cases the recombinant protein in insect cells is processed, modified, and targeted to its appropriate cellular location, where it is functionally similar to its authentic counterparts. Second, high levels of heterogenous gene expression, up to 20 % of total cellular proteins, are often achieved compared with other eukaryotic expression systems[18-20]. Here we chose the Bac-to-Bac expression system which is based on site-specific transposition of an expression cassette into a baculovirus shuttle vecor (bacmid) propagated in *E.coli*[21,22]. Colonies containing the recombinant bacmid are white in a background of blue colonies that harbor the unaltered bacmid. Recombinant bacmid DNA can be rapidly isolated from small scale cultures and then is used to transfect insect cells, eliminating the need for multiple rounds of plaque purification.

In our experiment, the interested gene was efficiently expressed in insect cells through the recombinant virus BacNS3N containing HCV NS3 serine proteinase gene, and the identity of the protein was validated by use of immunoblot. But the recombinant protein predominantly lay in the insoluble part, and the solubility could not be improved even by adding 1 % NP-40 into the lysate. Overton *et al* illuminated that HCV NS3 serine proteinase expressed in insect cells was a membrane-associated protein through discontinuous sucrose density gradients and only by adding some detergents did part of the protein gain the enzyme activity[23]. Suzuki *et al* discovered that HCV serine proteinase from insect cells was soluble and active with 0.5 % NLS[24]. Therefore, the TNG buffer including NLS and glycerol was used to dissolve the pellet. The results showed that part of the recombinant protein became soluble and more proteins were soluble when enhancing the percentage of NLS and adding EDTA both. The recombinant protein fused with 6 His tag at its N- terminus could be purified through metal-chelating chromatography. Finally, 0.2 mg purified recombinant protein was obtained from 5×10^7 insect cells. An *in vitro* detection system with SDS-PAGE and staining was developed with the recombinant HCV NS5ab as a substrate. The system eliminates the need of expensive instrument and reagent, heavy work, as compared with other cleavage systems[25-27] and provides a simple and clear strategy for the screening of inhibitors against the HCV proteinase.

REFERENCES

1 **Choo QL**, Kuo G, Weiner AJ, Overby LR, Bradley DW, Houghton M. Isolation of a cDNA clone derived from a blood-borne non-A, non-B viral hepatitis genome. *Science* 1989; **244:** 359-362
2 **Kuo G**, Choo QL, Alter HJ, Gitnick GL, Redeker AG, Purcell RH, Miyamura T, Dienstag JL, Alter MJ, Stevens CE. An assay for circulating antibodies to a major etiologic virus of human non-A, non-B hepatitis. *Science* 1989; **244:** 362-364
3 **Alter MJ**, Margolis HS, Krawczynski K, Judson FN, Mares A, Alexander WJ, Hu PY, Miller JK, Gerber MA, Sampliner RE. The natural history of community-acquired hepatitis C in the United States. The Sentinel Counties Chronic non-A, non-B Hepatitis Study Team. *N Engl J Med* 1992; **327:** 1899-1905
4 **Okamoto H**, Okada S, Sugiyama Y, Kurai K, Iizuka H, Machida A, Miyakawa Y, Mayumi M. Nucleiotide sequence of the genomic RNA of hepatitis C virus isolated from a human carrier: comparison with reported isolates for conserved and divergent regions. *J Gen Virol* 1991; **72:** 2697-2704
5 **Takamizawa A**, Mori C, Fuke I, Manabe S, Murakami S, Fujita J, Onishi E, Andoh T, Yoshida I, Okayama H. Structure and organization of the hepatitis C virus genome isolated from human carriers. *J Virol* 1991; **65:** 1105-1113
6 **Grakoui A**, Wychowski C, Lin C, Feinstone SM, Rice CM. Expression and identification of hepatitis C virus polyprotein cleavage products. *J Virol* 1993; **67:** 1385-1395
7 **Shimotohno K**, Tanji Y, Hirowatari Y, Komoda Y, Kato N, Hijikata M. Processing of the hepatitis C virus precursor protein. *J Hepatol* 1995; **22**(Suppl): 87-92

8 **Yan Y**, Li Y, Munshi S, Sardana V, Cole JL, Sardana M, Steinkuehler C, Tomei L, De Francesco R, Kuo LC, Chen Z. Complex of NS3 protease and NS4A peptide of BK strain hepatitis C virus: a 2.2 A resolution structure in a hexagonal crystal form. *Protein Sci* 1998; **7**: 837-847

9 **Dymock BW**, Jones PS, Wilson FX. Novel approaches to the treatment of hepatitis C virus infection. *Antivir Chem Chemother* 2000; **11:** 79-96

10 **Llinas-Brunet M**, Bailey M, Fazal G, Ghiro E, Gorys V, Goulet S, Halmos T, Maurice R, Poirier M, Poupart MA, Rancourt J, Thibeault D, Wernic D, Lamarre D. Highly potent and selective peptide-based inhibitors of the hepatitis C virus serine protease: towards smaller inhibitors. *Bioorg Med Chem Lett* 2000; **10:** 2267-2270

11 **Bartenschlager R**. The NS3/4A proteinase of the hepatitis C virus: unravelling structure and function of an unusual enzyme and a prime target for antiviral therapy. *J Viral Hepat* 1999; **6:** 165-181

12 **Takehara T**, Hayashi N, Miyamoto Y, Yamamoto M, Mita E, Fusamoto H, Kamada T. Expression of the hepatitis C virus genome in rat liver after cationic liposome-mediated *in vivo* gene transfer. *Hepatology* 1995; **21:** 746-751

13 **Bartenschlager R**, Lohmann V. Replication of hepatitis C virus. *J Gen Virol* 2000; **81:** 1631-1648

14 **Gale M Jr**, Beard MR. Molecular clones of hepatitis C virus: applications to animal models. *ILAR J* 2001; **42:** 139-151

15 **Du GX**, Hou LH, Guan RB, Tong YG, Wang HT. Establishment of a simple assay *in vitro* for hepatitis C virus NS3 serine protease based on recombinant substrate and single-chain protease. *World J Gastroenterol* 2002; **8:** 1088-1093

16 **Grakoui A,** McCourt DW, Wychowski C, Feinstone SM, Rice CM. Characterization of the hepatitis C virus-encoded serine proteinase: determination of proteinase-dependent polyprotein cleavage sites. *J Virol* 1993; **67:** 2832-2843

17 **Tanji Y,** Hijikata M, Hirowatari Y, Shimotohno K. Identification of the domain required for trans-cleavage activity of hepatitis C virul serine proteinase. *Gene* 1994; **145:** 215-219

18 **Luckow VA.** Baculovirus systems for the expression of human gene products. *Curr Opin Biotechnol* 1993; **4**: 564-572

19 **Patterson RM**, Selkirk JK, Merrick BA. Baculovirus and insect cell gene expression: review of baculovirus biotechnology. *Environ Health Perspect* 1995; **103:** 756-759

20 **Marchal I,** Jarvis DL, Cacan R, Verbert A. Glycoproteins from insect cells: sialylated or not? *Biol Chem* 2001; **382**: 151-159

21 **Luckow VA**, Lee SC, Barry GF, Olins PO. Efficient generation of infectious recombinant baculoviruses by site-specific transposon-mediated insertion of foreign genes into a baculovirus genome propagated in *Escherichia coli*. *J Virol* 1993; **67:** 4566-4579

22 **Joubert AM**, Louw AI, Joubert F, Neitz AW. Cloning nucleotide sequence and expression of the gene encoding factor Xa inhibitor from the salivary glands of the tick, Ornithodoros savignyi. *Exp Appl Acarol* 1998; **22:** 603-619

23 **Overton H**, McMillan D, Gillespie F, Mills J. Recombinant baculovirus-expressed NS3 proteinase of hepatitis C virus shows activity in cell-based and in vitro assays. *J Gen Virol* 1995; **76:** 3009-3019

24 **Suzuki T**, Sato M, Chieda S, Shoji I, Harada T, Yamakawa Y, Watabe S, Matsuura Y, Miyamura T. *In vivo* and *In vitro* trans-cleavage activity of hepatitis C virus serine proteinase expressed by recombinant baculoviruses. *J Gen Virol* 1995; **76:** 3021-3029

25 **Shoji I,** Suzuki T, Sato M, Aizaki H, Chiba T, Matsuura Y, Miyamura T. Internal processing of hepatitis C virus NS3 protein. *Virology* 1999; **254**: 315-323

26 **Sali DL**, Ingram R, Wendel M, Gupta D, McNemar C, Tsarbopoulos A, Chen JW, Hong Z, Chase R, Risano C, Zhang R, Yao N, Kwong AD, Ramanathan L, Le HV, Weber PC. Serine protease of hepatitis C virus expressed in insect cells as the NS3/4A complex. *Biochemistry* 1998; **37:** 3392-3401

27 **Berdichevsky Y**, Zemel R, Bachmatov L, Abramovich A, Koren R, Sathiyamoorthy P, Golan-Goldhirsh A, Tur-Kaspa R, Benhar I. A novel high throughput screening assay for HCV NS3 serine protease inhibitors. *J Virol Methods* 2003; **107**: 245-255

Edited by Ma JY and Wang XL

P.O.Box 2345, Beijing 100023,China
Fax: +86-10-85381893
E-mail: wjg@wjgnet.com www.wjgnet.com

World J Gastroenterol 2003;9(8):1635-1645
World Journal of Gastroenterology
 ISSN 1007-9327

• REVIEW •

Current status of severe acute respiratory syndrome in China

Qing-He Nie, Xin-Dong Luo, Jian-Zhong Zhang, Qin Su

Qing-He Nie, Xin-Dong Luo, The Chinese PLA Center of Diagnosis and Treatment for Infectious Diseases, Tangdu Hospital, Fourth Military Medical University, Xi' an 710038, Shaanxi Province, China
Jian-Zhong Zhang, Department of Pathology, Bei jing 306 Hospital, Beijing 100101, China
Qin Su, Department of Pathology, Tangdu Hospital, Fourth Military Medical University, Xi' an, 710038, Shaanxi Province, China
Correspondence to: Dr. Qing-He Nie, The Chinese PLA Center of Diagnosis and Treatment for Infectious Diseases, Tangdu Hospital, Fourth Military Medical University, Xi' an 710038, Shaanxi Province, China. nieqinghe@hotmail.com
Telephone: +86-29-3377452 **Fax:** +86-29-3537377
Received: 2003-06-30 **Accepted:** 2003-07-06

Abstract

Severe acute respiratory syndrome (SARS), also called infectious atypical pneumonia, is an emerging infectious disease caused by a novel variant of coronavirus (SARS-associated coronavirus, SARS-CoV). It is mainly characterized by pulmonary infection with a high infectivity and fatality. SARS is swept across almost all the continents of the globe, and has currently involved 33 countries and regions, including the mainland China, Hong Kong, Taiwan, North America and Europe. On June 30, 2003, an acumulative total reached 8450 cases with 810 deaths. SARS epidemic was very rampant in March, April and May 2003 in the mainland of China and Hong Kong. Chinese scientists and healthcare workers cooperated closely with other scientists from all over the world to fight the disease. On April 16, 2003, World Health Organization (WHO) formally declared that SARS-CoV was an etiological agent of SARS. Currently, there is no specific and effective therapy and prevention method for SARS. The main treatments include corticosteroid therapy, anti-viral agents, anti-infection, mechanical ventilation and isolation. This disease can be prevented and controlled, and it is also curable. Under the endeavor of the Chinese Government, medical staffs and other related professionals, SARS has been under control in China, and Chinese scientists have also made a great contribution to SARS research. Other studies in developing new detection assays and therapies, and discovering new drugs and vaccines are in progress. In this paper, we briefly review the current status of SARS in China.

Nie QH, Luo XD, Zhang JZ, Su Q. Current status of severe acute respiratory syndrome in China. *World J Gastroenterol* 2003; 9 (8): 1635-1645

http://www.wjgnet.com/1007-9327/9/1635.asp

INTRODUCTION

On November 16, 2002, the first case of SARS patient was found in Foshan city, Guangdong Province, China[1]. Severe acute respiratory syndrome (SARS) is different from ordinary pneumonias caused by bacteria, other viruses, chlamydia and mycoplasma. The disease starts with an abrupt onset of fever, progresses swiftly, and is subjected to acute respiratory failure. Furthermore, it results in multiple organ dysfunctions with a higher infectivity and fatality. The main clinical manifestations of the patient are high fever, non-productive cough, myalgia and dyspnea. The patient has no response to any antibacterial therapy. At the beginning, the experts in Guangdong Province believed that it might be caused by a novel virus infection, and designated it as "atypical pneumonia" based on its clinical manifestations. On April 8, 2003, the State Council of the People' s Republic of China classified this illness as a legal infectious disease, and named it as infectious atypical pneumonia according to its higher infectivity, quick transmission and high mortality. The same kind of patients was found in Hong Kong and Vietnam at the end of February[2,3]. Dr. Carlo Urbani, an Italian epidemiologist working at the Hanoi Office of the World Health Organization (WHO), first reported to WHO and named this disease as severe acute respiratory syndrome. Later, Dr. Urbani caught the disease himself and died on March 29, 2003. In memory of Dr. Urbani' s great contributions in fighting against this disease, WHO formally designated this disease with unknown causes as SARS on April 16, 2003[4]. Ksiazek and his colleagues proposed that their first isolate be named the Urbani strain of SARS-associated coronavirus (SARS-CoV)[4,5].

On March 12, 2003, WHO issued a global alert of SARS outbreak, and called upon 11 laboratories (including the Institute of Virology, Center of Disease Control and Prevention, China, and Guangdong Center of Disease Control and Prevention, China) in 9 countries to join a collaborative multi-center research project on SARS. Chinese medical and health care workers have been keeping abreast of the advances in SARS research, and have achieved a number of success while fighting against SARS. In this paper, we briefly reviewed the current status of SARS research in China.

EPIDEMIOLOGY

General situation

During the period from November 16, 2002 to April 16, 2003, 13 cities had reports of SARS cases in Guangdong Province, China. Among the 13 reported cases of SARS, 3 were cooks, 3 officers, 2 farmers, 2 retired persons, 2 workers, and 1 businessman. Their age ranged from 18 to 84 years, the majority (77 %) was between 30-50 years. No evidence of mutual transmission was found between the reported cases[6]. The first case of SARS in Guangzhou was found on January 2, 2003. The epidemic broke out and reached the peak early in February, and then the incidence started to decline. As to age distribution of the patients, most patients were between 20-50 years. The patients were present in all the 13 counties and cities, but concentrated in 7-city areas, accounting for 95 % of the total cases, in which 28.7 % of the patients were healthcare workers. Of the 36 deaths, their age ranged from 5 to 89 years, and half of them were older than 60 years. Some of the deaths (38.9 %) were complicated with underlying diseases, including hypertension, diabetes, heart disease, and pulmonary emphysema. There was also a clustering trend: more than 2 patients were found in 42 families, 277 cases of healthcare workers were from 28 hospitals and institutes[7]. The incidence in Beijing had a similar feature to Guangdong (Table 1)[8]. Till June 30, 2003, an acumulative total reached 8 450 cases with 810 deaths. In the mainland of China, there were 5 327 cases

Table 1 History of SARS contact and incubation period in 80 cases

	Male (*n*, %)	Female (*n*, %)	Age (year)	Contact history	Incubation period (d)
Total	28 (35 %)	52 (65 %)	31.6±10.1	72 / 80(90 %)	7.6±4.3
Healthcare worker	13 (24.5 %)	40 (7.5 %)	30.8±8.4	49 / 53(92.5 %)	7.8±4.5
Non-healthcare worker	15 (55.6%)	12(44.4%)	36.4±12.1	23 / 27(85.2 %)	7.7±3.1

of SARS in which 348 patients died, and 1 755 cases with 298 deaths and 681 cases with 84 deaths occurred in Hong Kong and Taiwan, respectively. The national case reports showed that SARS patients were distributed in almost all professions, and healthcare workers with the infection accounted for 20-30 % at the early stage of SARS epidemic. There was no difference between both sexes in the incidence. SARS patients were found in every age group, and predominant in 20-49 years group (about 80 % of cases). The mortality in senile patients was significantly higher than that in young patients[9,10].

A professor from Zhongshan University in Guangzhou suffering from SARS stayed at Jinghua Grand Hotel, and a 28-year-old resident in Hong Kong got infected there, leading to SARS outbreak in the Prince Wales Hospital. However, a study made by Medical College of Zhongshan University indicated that at least 3 sources contributed to the outbreak early in March, that is to say, the source of SARS outbreak in Hong Kong was more than one. The mainland of China reported for the first time that no new case was found on June 2, 2003. No confirmed, suspected cases and deaths occurred for the first time on June 19, 2003 in China. Xiaotangshan Hospital, a speciality SARS hospital in Beijing, was then closed, demonstrating that a decisive victory has been won in fighting against SARS in China.

Infectious source

Currently, the known patient with SARS is the only infectious source. In the primary stage, symptoms are more obvious and it has high infectivity, while in the recovery stage, its infectivity is lost. Not all the cases have the same infectivity. Highly contagious cases are those who deliver a large amount of viruses for a long time, especially with severe cough, or those who undergo an endotracheal intubation with a splashing of droplets. Few cases with very strong infectiousness are called "super-spreader", who usually are the first cases or the first cluster of SARS patients during the outbreak. Usually, the early cases of SARS have a high infectivity and a strong pathogenicity, which would decrease later with progression of the epidemic. It is still unclear that why some individuals exposed to the patient did not contract SARS. Does occult infection of SARS exist? If yes, what role it plays in transmission and what is its epidemiologic significance? All these need to be further studied.

The initial results of epidemiologic surveys showed that the first reported cases or the first cluster of SARS were cook and market purchasers in some cities of Guangdong Province. A certain number of the sporadic cases did not have a contact history of SARS patients, from which we could deduce that there might be some other route of transmission and animal-mediated route of transmission may play a role in pathogenesis. Sources of infection may include some species of animals and the detail is unclear.

From May 23, 2003, scientists in Hong Kong and Shenzhen have collaborated in search for the origins of SARS. On the basis of population epidemic investigations, researchers have been on the track of animals infected with SARS viruses and have targeted at the wild mammal animals in their study. They have confirmed the kinship relations between these animals and human SARS viruses based on an evolutionary analysis of the SARS virus genes of different genera. It seems that they have observed the origin of the human SARS viruses based on these findings. By nearly a month of painstaking efforts, researchers have isolated 3 SARS specimens from 6 Paguma larvata. The fully genetic sequencing of one specimen showed that the SARS viruses in Paguma larvata bore 99 % homology with the SARS viruses in the human body. A further genetic analysis confirmed that SARS viruses in animals were the precursors of the SARS viruses in humans. The testing and analysis of the SARS antibody were performed in 10 people who were engaged in wild animal businesses, among them, 5 people had a positive response, indicating that the SARS viruses in wild animals may infect those who have close contacts with them. These findings have provided important evidences for further investigation of the origins of SARS viruses in humans, and their associated chains, and will lay a foundation for the future development of SARS vaccines and treatment serum. Currently, there is no strong evidence that demonstrates SARS is transmitted through animals or insects.

Route of transmission

Airborne droplets from the patient are the main route of transmission. It is not clear whether there are other transmission routes, personal touch by hands, playthings contaminated by the secretions from the patient' s respiratory tract. Close contact refers to the direct touch of the patient' s secretions and body fluid during treatment and nursing of the patients. The transmission scope is closely correlated with the environment of the ward, course of treatment, patient' s condition, time of exposure and personal protection of healthcare workers and visitors. Improper protection increases the risk of infection. Rubbing nose and eyes with the contaminated hands may also be a route of the transmission. Sexual transmission of SARS has not been confirmed, but close contact during sexual intercourse may increase the chance to get infected.

Lin *et al*[11] from the Institute of Preventive Medicine, University of Taiwan, also believed that only when respiratory symptoms appeared did the patient have infectivity. As for the route of transmission they have made the following two conclusions. The first is that the special shell antigen of SARS-CoV might come from chromosome 6q in human tissues (MCH/HLA). Once the virus enters human body, the invader is wrapped by the special tissue antigens in some individual hosts, so that the virus loses its capacity to infect other persons. Clinically, this strong tissue antigen might relate to severe leukopenia or lymphopenia in SARS patients. Once the disease progresses to respiratory distress, the lungs would try to dissolve the mucus produced by acute inflammation, by activating the body defense system to secrete proteolytic enzymes for the mucus dissolution. Meanwhile, the enzymes would also dissolve the tissue antigens of the shell, and make the virus resume its infectivity to other individuals. This clear-cut route of transmission is characterized by SARS-CoV. It has been proposed that SARS be liable to transmit among the family members because of the same type of HLA. The second is that different strains of bacteria in the sewage are able to produce proteolytic enzymes and dissolve the shell protein of SARS-CoV, and promote its infectivity to others. This mechanism might explain why SARS outbreak occurred in Amoy Garden, as well as in sporadic individuals who had been

to the epidemic regions, without direct contact with the patients. This virus can enter the human body via any part of mucosa, including respiratory tract, oral cavity, and genital tract. Owing to the higher concentration of proteolytic enzymes in the lung, SARS patients have a strong infectivity even at the early stage of the disease. Although the above hypotheses could explain some phenomena in SARS epidemiology, they need to be further confirmed.

Susceptible population

The ordinary population is very susceptible to SARS, the healthcare workers who have close contacts to the patients during the treatment and nursing, are the high-risk group. Anyone who has a history of close contact to the patients is a high-risk individual, and may exist the occult infection. In view of professions, healthcare workers are the most easily infected persons. Compared with other infectious diseases, the rate of SARS infection was very high in medical professionals, accounting for 20-30 % in some areas. It might be due to the insufficient protective measures in the early epidemic stage of SARS. But in Beijing, the rate of infection was relatively low in healthcare workers both at hospitals and at CDC. It is suggested that personal protection plays an important role in prevention of SARS among the healthcare workers. In order to protect the doctors and nurses, the Chinese Government has taken almost all the necessary preventive measures to strengthen sterilization and ventilation in the wards and to forestall medical staffs to be overworked. This is why the incidence of SARS has been kept at a lower level in the healthcare workers.

Distribution characteristics in epidemic areas

There are four kinds of SARS epidemic situation in China: (1) Epidemic area of SARS (in Zhujiang Delta of Guangdong Province, China, there was no direct relationship among the primary cases in different cities). (2) Imported SARS cases, which caused local spreading (as in Shanxi Province and Beijing, etc.). (3) Imported SARS cases, which did not cause local spreading (as in Hunan Province and Sichuan Province, etc.), and (4) no SARS cases reported.

Epidemiological statistical analysis and prediction

How will the SARS epidemic situation develop? How to control SARS effectively? Are there any scientific ways to predict the SARS epidemic situation? According to the current actual SARS epidemic situation in the world, the Center of Geosystem Science and the Key Laboratory of Geodynamics of the Chinese Academy of Sciences have studied the relationship between SARS epidemic situation and its development based on their accumulated experience for years, established the systemic dynamics model of SARS contagion, and calculated the relationship between the control of SARS epidemic situation and its development in detail. The results were identical with the current actual SARS situation in the world, and the model could predict the SARS epidemic situation. The successful establishment of this model is important to evaluate and predict SARS epidemic situations. The task group of "SARS Epidemic Trend and Control System" in Xi' an Jiaotong University made use of computers to make computing simulation with the data and theories by using the statistical methods and parameters confirmed in the epidemic transmission, and then composed the software by modifications and got the predicting cuve to meet the actual demand. They finally put forward the epidemic patterns and trend of SARS. The predicted number of increasing cases of SARS was basically identical with that publicized by the Ministry of Public Health every day.

According to the data of the diagnosed, suspected and dead cases of SARS in the world, the task group of mathematical epidemiology in the University of Science and Technology of China has established the epidemic spatial statistical model of SARS, and predicted on June 10, 2003, that the number of SARS inpatients in Beijing would be decreased below 60[12].

There are so many problems which need to be further studied. For example, our understanding of the source of SARS infection remains on the conditions of SARS patients, and little is known about its effect on sub-clinical SARS patients and animals, as well as the blood transmission and fecal-mouth transmission ,except for the short distance transmission of droplets from respiratory tract and transmission by close contacts. The reason why the incidence rate is high in young people and low in children and elderly people is not clear. What are the influence factors of the superior infectors?

ETIOLOGY

At the beginning of the study conducted by the Chinese scientists, chlamydia-like and coronavirus-like granules were found by electron microscopy in the dead bodies of SARS patients in Guangdong Province, China. Though chlamydia was thought to be the possible pathogen of SARS, it could not be confirmed in foreign laboratories due to the limited specimens for assay. Furthermore, there was not much possibility that chlamydia was the pathogen of SARS according to the clinical manifestations and therapeutic efficacy of SARS patients. Thus it might be due to the secondary infection. After the outbreak of SARS in Hong Kong, researchers isolated the avian influenza virus from a symptomatic child in Hong Kong, which was soon excluded to be the pathogen of SARS. Not long after, paramyxovirus was found in many SARS patients, but not in all the SARS patients in the further studies. However, all these findings could not be further confirmed.

The Pei Weishi Research Group of Hong Kong incubated the blood and tissue samples from SARS patients in cell lines which are not usually used to culture and isolate viruses. The genes of infected tissues were randomly screened in order to find the DNA fragments which could provide useful clues. On March 17, 2003, the cultured tissues isolated from two SARS patients could kill the cell line which is usually used to culture hepatitis A virus. In order to find the relationship between it and SARS, we observed the different reactions occurred when serum in the early and recovery stages was used to culture the tissues. Antibody reaction occurred in the former, while it did not occur in the latter. It was obvious that there was something in the culture, which was related to SARS. Nicols is the first who has found and isolated coronavirus in the tissue samples by electron microscopy. In the following days, three foreign laboratories including that in Hong Kong have confirmed almost at the same time that the pathogen of SARS is a novel kind of coronavirus.

On March 23, 2003, the Institute of Microbiology and Epidemiology, Academy of Military Medical Sciences of China, successfully isolated coronavirus from the pulmonary tissues of SARS patients and established its animal model. Based on the model, the pathogen was isolated by cell culture of samples from pulmonary tissues of the dead bodies and nasopharyngeal swabs. Coronavirus granules were found by electron microscopy in the pathological cells and their culture supernatant. The results of SARS patient serum detected by immunofluorescence staining showed that the isolated virus was closely related to SARS virus, which could induce infection of SARS in mice. The coronavirus-like granules were also found in the pulmonary tissues of mice. The cDNA fragments were amplified with RT-PCR, respectively from the pulmonary tissues of SARS dead bodies, the infected mice, and the infected

cell culture isolations. The whole genome of coronavirus was sequenced at 11pm, on April 15,2003. The sequence had 60 % homogeneity with the known coronavirus, and was about 30 000 bp long, which was identical with the results reported in Canada and USA, suggesting that it is a novel kind of coronavirus closely related with the epidemic of SARS, and may be the major pathogen of SARS.

Hong Kong University has found that some gene fragments have different sequences by comparing "6 SARS samples" from different regions (2 from Hong Kong, 2 from Guangzhou, China, 1 from Canada and 1 from USA), indicating that the "6 viruses" are different members of one family. However, it is not quite sure which one is their "mother". The inclination of the researchers is that one of the two samples from Hong Kong was similar with the two samples from Canada and USA respectively, the other one from Hong Kong was similar with the two from Guangdong, China. Further study is needed to clarify whether the members of such a family exist or they are deprived of a variety of SARS viruses.

Shanghai Institute of Life Science, Chinese Academy of Sciences, has successfully cloned the 6 main protein genes of S, M, N, E, RNA polymerase and proteinase (3CL), and found the expression samples of proteins E, N, and 3CL in the experiment of expression, isolation and purification of the important protein genes. The expression samples passed the drug virtual screening. This achievement is of great importance in the study of biological functions of SARS virus and in seeking after the vaccines and drugs against SARS virus.

The survival time of SARS virus in different conditions varies greatly. It can survive for a long time in 3 human discharges (sputum, feces, and urine) and in blood at 24 ℃, for 5 days in sputum and feces, for 10 days in urine, and for 15 days in blood, respectively. In the indoor condition, it can survive for 3 days on the surface of filter paper, cotton, wood block, soil, metal, plastic, glass, etc. SARS virus is sensitive to temperature. Its survival rate decreases with increasing temperature. It can survive for 4 days in the culture condition without serum at 37 ℃, and can be inactivated at 56 ℃ for 90 minutes, at 75 ℃ for 30 minutes, respectively.

PATHOLOGY

Macroscopically, the pulmonary tissue is swollen and extensively consolidated. The surface blood vessels are dilated and hyperemic, dot or sheet necrosis and hemorrhagic infarct can be found. Thrombi are formed in the pulmonary artery, and wine liquid flows out from the cut section.

Light microscopy

Chronic inflammatory cell infiltration can be found in trachea and bronchioles, and some necrosis tissues and a few inflammatory cells in the duct and some shed mucous epithelia. The pathology in the lung shows severe acute interstitial exudation, pulmonary interstitial and alveolar septum capillaries are severely dilated and congested, and there is a medium amount of lymphocytes, macrophages and polymorphonuclear white cells infiltrated. Some red blood cells are exudated into the alveolar septum and cavity. Pale and red fluids are exudated in most alveolar cavities, and hyaline membrane is formed in about 20-30 % alveolar cavities, but no inflammatory cells infiltrate into alveolar cavities, and focal compensatory emphysema can be seen. Diffuse alveolar epithelial cell injuries are manifested as pyknosis of chromatin to mass in alveolar epithelial cells which are distributed along the karyotheca, apoptosis of alveolar epithelial cells, vacuolar changes of nuclei in some alveolar epithelial cells. The necrosis in pulmonary tissue is not obvious and the phenomenon of lymphocytes attacking alveolar epithelial cells is not found. Regional proliferation is very active in the H type alveolar epithelial cells. Under light microscopy, some virus inclusion bodies-like structures can be observed in alveolar intraepithelial cells. The surface of pleura is smooth, subpleura stroma is edematous and loose, capillaries are dilated and congested with lymphocytes infiltrated.

Many superficial and deep lymph nodes show extensive or large regional hemorrhage and necrosis which are significant in the subcapsular region. Cell proliferation is obvious around the necrosis tissues and the phenomenon of red blood cells phagocytosed by macrophages . Hemosiderin is deposited in the cytoplasm. The lymphocyte infiltration is decreased , the lymphoid follicle structure can hardly be seen. The vascular and splenic sinusoids are greatly dilated and congested, the white pulp is decreased . Extensive and fused hemorrhage and necrosis as well as cell reactive hyperplasia are easily found.

Vacuolation can be found in a few cardiac myocytes, there are interstitial infiltration of a few lymphocytes and mild vascular dilation. The structure of hepatic lobule remains integrated. Mildly mixed hepatocellular fatty degeneration and mildly hydropic degeneration can be seen in the lobules, focal hemorrhagic inflammation and apoptotic body can be occasionally found. Liver sinusoid is dilated and congested, mild reactive hyperplasia occurs in Kupffer cells, and infiltration of lymphocytes is observed. Bilateral adrenal gland also shows focal hemorrhagic inflammation and lymphocyte infiltration which are obvious in the medulla. The structure of glomerulus is almost normal, the capillaries are dilated and congested, but no hyaline thrombus and fibrinoid necrosis can be found. Renal tubular epithelial cells are swollen, with few protein casts and tubular necrosis, there are focal hemorrhage and interstitial lymphocyte infiltration[8]. The structure of the walls of stomach and intestinal tract remains its integrity with a few lymphocytes infiltrated in the lamina propria mucosae and submucosa. Vasodilatation and congestion can also be seen. The intestinal tract shows segmental hemorrhage, and the rest changes are the same as in the stomach.

Transmission electron microscopy

The structure of pulmonary tissue remains very well, intracellular mitochondria and endoplasmic reticulum in alveolar epithelial cells and some endothelial cells of capillaries are swollen, the matrix is very loose, degranules can be found in some rough endoplasmic reticula. Chromatin in the nucleus is changed into mass shape and is not well distributed and is accumulated under the nuclear membrane. Type I alveolar epithelial cells show proliferation which is characterized by increased number, abundant chromatin, intracytoplasmic lamellar bodies, widened interspace of capillaries in the alveolar septum and increased pinocytosis vesicles in the endothelial cells. It is observed that there are many virus-like particles in most of the type II alveolar epithelial cells, bronchioles epithelial cells and intracytoplasma of some endothelial cells of capillaries in the alveolar septum which has an envelope with halation or in the shape of garland and is about 100-150 μm in size with low density in the centre, and these kinds of virus-like particles can also be seen in the dilated endoplasmic reticulum. In addition, chlamydia-like inclusion bodies at different stages which have reticular bodies, midbodies and elementary bodies can be seen in very few alveolar epithelial cells and endothelial cells. In the edema fluid of alveolar cavity, virus-like particles can be found. Proliferation of macrophages in which virus-like particles can also be found is mainly seen in the alveolar septum and alveolar cavity[19].

Many virus-like particles can be found in a few cardiac myocytes which are the same as in the lung tissues. Mild swelling of mitochondrion and endoplasmic reticulum is found in the hepatocytes, and lipid droplet with moderate electron

density is also found, and chlamydia-like inclusion bodies at different stages are seen in the cytoplasm. Some renal tubular epithelial cells show swelling and no villi, virus-like and chlamydia-like particles are also found in them. The injured immune organs mainly include the spleen, lymph nodes and bone marrow. Deposited plasma protein can be seen in the central arteries of splenic corpuscle, massive necrosis can be found in the white medulla and marginal sinus lymph tissues. Some remaining lymphocytes are at the apoptotic state. Blood vessels in the lymph nodes are severely dilated and congested, and lymphoid nodules are atrophied and disappeared, a lot of monocytes are found in the lymphatic sinus, the lymph tissue shows focal necrosis and lymphocytes show apoptosis. Hematopoietic area of myeloid tissue is decreased, granulocyte and macrophage systems are relatively inhibited, polychromatophil erythroblasts show little focal proliferation[20,21].

Tissues around the venules and the vascular walls of lung, heart, liver, kidneys, adrenal gland and striated muscles show swelling, and there are monocytes, lymphocytes, plasmocytes and neutrophilic granulocytes infiltrated.

After the nude mouse is inoculated with SARS virus, and onset of SARS occurs. The main lesions are found in the lung and liver, the alveolar cavity is microscopically very narrow even atelectatic, the alveolar septum is widened, bronchioles epithelial cells are shed. Swollen hepatocytes show hydropic degeneration and vacuolation and some hepatocyes show pyknosis and necrosis. And other anomalies include myocardial hyperemia and increased multinuclear giant cells in the spleen.

In the culture medium of Vero E6 cells infected with SARS virus, virus particles can be found under electron microscope with negative staining which is in the shape of ball with coronally arrayed processes, the end of the process is also a round shape and there is a wide interspace between processes. The diameter of the virus is about 80-120 μm. The viruses detected from the culture medium of cells infected with viruses from Beijing and Guangdong are similar.

PATHOGENESIS

The mechanism of the injury caused by SARS virus is unknown. It is suspected that there are auto-antibodies developed after the infection of SARS virus which induces the autoimmunity reaction, and the current studies cannot explain it.

The reasons why T cells of SARS patients are quickly declined in a short time after the onset of SARS are probable as following: (1) SARS virus directly attacks T cells and causes them splitting and to be destructed quickly which results in the sharp decrease of the count of T cells. (2) After the infection of SARS, SARS virus has no effect on the immune system and results in the abnormal distribution and leads to the decrease of T cells in the peripheral blood. (3) SARS virus, or its productions or its components act as a super-antigen and polyclonally activate T cells and lead the activated T cells to death and decrease of T cells in the peripheral blood.

CLINICAL MANIFESTATIONS

The analysis of the blood samples of SARS patients has shown that the latent period of SARS is at least 4 days and the longest is 17 days. This is related to the load of virus and individuality. The one who has been infected but without symptoms has no infectivity, no such cases have been reported so far.

After the patient is infected with SARS, he will have a high fever and dry cough without the symptoms of influenza such as nasal mucus, pharyngalgia, spitting white or yellow sputum. But sometimes there is some blood in the sputum, and the patient will feel short of breath, and even develop ARDS. Generally, the count of white blood cells will increase when a patient has a fever, but it is normal or below it when the SARS patient has a fever. The most prominent phenomenon is that the X-ray characteristics are not disassociated with its clinical situations. The patient with common pneumonia usually has very severe clinical manifestations and then the changes in the X-ray films can be found. But the X-ray films of SARS patients have very significant changes when the patient of SARS is not very severe, which show floccule shadows and have the trend of quick development[29-31].

The symptoms of SARS include high fever (more than 38 ℃), dry cough, shortness of breath, headache, anorexia, malaise, skin eruption and diarrhea without the common symptoms of influenza such as nasal mucus, pharyngalgia, spitting white or yellow sputum. But sometimes there is some blood in the sputum and the patient will feel short of breath, and even develop ARDS. About 7 % patients of SARS need artificial breathing. The clinical manifestations in different areas in China are shown in Table 2.

The manifestations of chest radiograph of SARS include patchy consolidation or reticular consolidation. Some patients' conditions develop very fast, large patchy consolidation is shown in the chest film and multiple lobes or bilateral lung are involved. The absorbance of the patchy consolidation is very slow. The sites and scope of pulmonary lesions in SARS patients are shown in Table 3.

Table 2 Clinical manifestations in different areas of China

	Fever (%)	Dry cough (%)	Shortness of breath (%)	Chest pain (%)	Bloody sputum (%)	Diarrhea (%)	Headache (%)	Muscle pain (%)	Inertia (%)
Guangzhou[22]	100	72.2	31.2	1.9	11.5	24.2	25.8		24.6
Guangzhou[23]	97.7	81.2	20	22.3		22.3	63.5	41.2	74.1
Guangzhou[24]	100	92		22	13	24	61	60	92
Beijing[25]	97.8	68.9	53.3		9.8	26.7		26.7	60
Beijing[26]	100	87.8	12.2						
Henan[27]	100	67	29	17		17		50	83
Hongkong[28]	100	62	20			10	20	54	

Table 3 Sites and scope of pulmonary lesions in SARS patients

	Superior lung field	Medial lung field	Inferior lung field	Hilum of lung	Multiple lobes	Total
Pachy-lung markings, small shadow	3(2.5)	5(4.2)	10(8.5)	2(1.7)	0(0)	20(16.9)
Unilateral inflammation	8(6.8)	11(9.3)	16(13.6)	0(0)	0(0)	35(29.7)
Bilateral inflammation	3(2.5)	7(5.9)	15(12.7)	0(0)	37(31.4)	62(52.5)
Total	14(11.9)	23(19.5)	41(34.7)	2(1.7)	37(31.4)	117(99.2)

The count of white blood cells of SARS patients is normal or below it, and CD4+ and CD8+ T lymphocytes are also decreased, but all these will be in the normal range after patients are fully recovered.

LABORATORY EXAMINATION

Theoretically, there are three ways to diagnose SARS: cell culture, RT-PCR and detection of antibody. All these ways are mature, so progress in the detecting techniques can be achieved in the work of prevention and cure of SARS easier than that in the study of vaccines and drugs. But cell culture and detection of antibody have no effect at the early stage of clinical diagnosis. Cell culture needs very high requirements of laboratory conditions and experienced operators, it takes a long time to isolate viruses or bacteria, and its positive rate is low. The time of the generation of antibody against SARS virus in the body is at least 10 days, and the time of the generation of IgG is at least 15-20 days. The antibody has interactions with the *in vivo* immune system, the mechanism of the generation of antibody is not clear. Whether all SARS patients have antibody after 3 weeks of infection needs to be further studied. RT-PCR is the simple and easy diagnostic method of SARS at the early stage[33-35]. Although there are many kinds of RT-PCR kits in China, it needs further improvement for its clinical use. It is needed to explore how to get the best virus nucleic acid and the best sampling time. Till today, the diagnosis still depends on the epidemiology and clinical symptoms, no methods have been found to be effective in the prevention and cure of SARS. The natural immunity adhesive function of red blood cells in two SARS cases in China was detected, and it was found that its adhesive function was lowered with aggravation of SARS. It is thought that it may be a good index indicating the degrees of the conditions of SARS patients.

Laboratory examinations, points for attention and evaluation of data

The Ministry of Public Health of PRC proposed the precautions on June 7, 2003 for guidance in practice and applications of tests supposed to be of diagnostic value for SARS.

Virus isolation by cell culture The method is used to isolate SARS virus from human respiratory secretion, blood, urine, stool and autopsy tissue samples. The positive result is considered as a reliable evidence for the presence of replicating SARS virus, and for the diagnosis of the disease or a virus-carrier status in combination with the clinical symptoms. The test must be performed by specialists in a BSL-3 laboratory. Thus, it is difficult at present to be widely used. Another weak point is that this assay is laborious and time-consuming, thereby not suitable for the quick diagnosis. Usually, the positive rate of this assay is not high, and the negative result cannot be regarded as a reliable evidence to exclude SARS. For these reasons, it is not a routine examination in clinical laboratories of most medical centers.

Detection of viral nucleic acid by polymerase-chain reaction following reverse transcription (RT-PCR) The procedure can be used for detection of SARS virus from human respiratory secretion, blood, serum, urine, stool and autopsy tissue samples. It is a quick and convenient method.

Up to date, it is not clear what time is best for sampling and what samples are optimal for the assay. Its sensitivity remains to be improved. The possibility of false negativity is considerably high. In addition, inappropriately handling of the samples often leads to laboratory pollution by the viral nucleic acids and false negative results. When the virus is detected in different samples from the same individual, or the amplification product is demonstrated repeatedly in the same sample, the positivity is established, meaning that the sample contains nucleic acids of SARS virus. For the clinically suspected patients, the positive reaction is a diagnostic parameter for SARS. For apparently healthy individuals, the positive result is a reliable evidence for the establishment of their virus-carrier status. Apparently, a negative reaction cannot be regarded as an evidence to exclude SARS or the suspected either.

Immunofluorescence test and enzyme-linked immunosorbent assay (ELISA) for antibodies to SARS virus The procedures are used to demonstrate specific SARS virus antibody from the serum. The antibody is detectable in a majority of samples from asymptomatically infected individuals and SARS patients for about 10 days, or even later for some cases, after being infected or onset of the disease.

The assays are used mainly for verification of the clinical diagnosis and for epidemiological surveys. A positive reaction obtained using sera from the convalescent suspected patients, or a four-time increase in its titer during recovery compared to that in the acute stage can be regarded as a diagnostic parameter for SARS. Occurrence of the antibody is also found in healthy individuals, reflecting the past infection of SARS virus. As for the replicating virus and its nucleic acids as described above, the antibody is not always detectable in SARS patients. A negative result, therefore, cannot be regarded as a reliable evidence to exclude the possibility of SARS.

Laboratory approaches for assays of SARS in China

A chip covering genomic sequences of all the reported coronaviruses, including SARS virus, was prepared and the detection has been established based on the microarray, as declared by Benyuan-Zhengyang Gene Technology Company Limited, China and its partner organizations in May 2003. The genotyping, conducted based on this system and similar assays, may be useful for determination of pathogenic factors and monitoring of mutations in the genomes of these viruses from different geographic areas, possibly providing some clues to the origin of SARS virus. Moreover, this system and database were designed to be an open platform, allowing the online processing and analysis of data by customers through Internet. In addition, the online exchange and management of detection data from all registered customers can provide an opportunity for the related administrations to obtain statistic information about the disease epidemics on time[37].

The virus-collecting facility, prepared by a group in Wu Jianxiong Laboratory, Dongnan University allows collection and concentration of viral particles from air, claiming to be able to process 30 liters of air per minute. According to the manufacturer, its collection efficiency can be as high as 90 %, as tested using protein particles and the inactivated viral particles. It can be used for sampling from air and viral particle concentration. In combination with PCR, the device may be applied for the detection of SARS virus contamination of the air, providing timely and dynamic data of the viral load.

A preliminary observation was made on dynamic changes of circulating T cells and serum immunoglobulin contents in 124 SARS patients by the Beijing Group of the National Emergent and Technological Action on SARS Prevention and Treatment. A marked decrease was found for all subsets of T lymphocytes examined, including those expressing CD3, CD4 and CD8, with their cell counts reduced to about one third of those of healthy individuals. This shows that the immune functions of SARS patients are severely impaired. The counts of CD4- and CD8-positive T cells were found to decrease quickly at the same time, the change was more pronounced during the period between the 10^{th} day and the 14^{th} day. This is in accordance with the disease course for most cases, its levels going up gradually two weeks after the onset with the recovery

of the patients. It appears reasonable to consider T cells to be involved in the pathogenesis of SARS.

Another apparatus, invented by Gene Company Limited and the Molecular Medical Diagnosis Center in Hong Kong based on the fast DNA hybridization, was claimed to allow the detection of SARS-associated coronavirus in patients' samples and identification of the mutated viruses within 15 minutes. Rong-An Tan, the technical spokesman of the diagnosis center, declared that the system could be used to detect SARS-associated virus from blood, saliva and secretion samples. According to him, the times requested for the detection range from 1 to 15 minutes, with 5 or 6 mutated viruses demonstrated as conducted in Guangzhou, Taiwan and Hong Kong for separate cases.

A seroassay for circulating antibody to SARS virus, namely immuno-chromatography test (ICT), is now being established in Taiwan University Hospital. As claimed by the laboratory, it is possible to determine the diagnosis of SARS at the 7th or 8th day by this assay, much earlier than RT-PCR that cannot show the positive result till the 21st day after the disease onset. The project, currently, is reported to arrive at the ultimate stage of sensitivity assessment. ICT is hoped to be an assay faster than RT-PCR by 13 days[27].

Dalian Institute of Chemistry and Physics, the Chinese Academy of Sciences, recently claimed to have established an early detection system for the virus-induced respiratory diseases with fever based on a controlled micro-current chip. They have finished the preparation of the chip and established the system. Currently, the system is under the evaluation using 9 primer pairs for the amplification following RT, with the SARS virus and parainfluenza virus RNA samples as the templates and a negative control, respectively. The system is characterized by its early detection of viral RNA even if the target sequence contained in samples is minimal in quantity. The controlled micro-current chip is also known as a chip laboratory, which is greatly different from the ordinary gene chips regarding their principles, preparation and applications. It is characterized by high-throughout and large-scale integration. Several fundamental units, involving sample preparation, biological and chemical reactions, isolation and detection, are integrated onto a single chip as small as several cm, being able to finish different reactions and to characterize their minimal-amount products[39].

Recently, artificial virus-like particles were prepared, with the SARS coronavirus nucleic acid enveloped within liposome, by a group in the Laboratory of Clinical Chemistry, Beijing Hospital under the Ministry of Public Health. The reagent may prompt technical improvement, standardization and quality control of the RT-PCR for SARS, as the kits currently available are not stable enough and require further clinical verification. The virus-like particles have been characterized by two properties: safety (non-infectious) and stability. This is of application value for the quality control of RT-PCR for SARS virus in clinical laboratories of medical centers, as well as for evaluation of new diagnostic reagents for the disease[40].

DIAGNOSIS AND DIFFERENTIAL DIAGNOSIS

Criteria for clinical diagnosis of SARS proposed by Ministry of Public Health of PRC

Epidemiological history The history evidences indicative for SARS include close contact with the patient, individuals from an infected group, having infectivity to others, and a tourist back, or a resident moving away from the epidemic regions two weeks before onset of the disease where there are SARS patients reported and the secondary infection has taken place.

Symptoms and signs The onset of the disease is acute. Fever is the first symptom, with the body temperature above 38 ℃ for most cases and chilling as one of the complaints occasionally. Headache, joint pain, fatigue and diarrhea may also be the complaints. Usually respiratory catarrh symptom is not evident. Coughing may be the manifestation, mostly a dry cough with very little sputum. Occasionally, little blood is present in the sputum. Chest distress is common, with the quick respiration, short ness of breath and even breathing difficulty in unfavorable cases. Signs of the lung disorder are usually not obvious, with some moist rales heard or pulmonary consolidation found in some cases. In a small number of the patients, fever is not the first symptom. This is particularly true for those cases operated recently or having some accompanying diseases.

Laboratory tests Usually, the count of peripheral blood leukocytes is not increased, or even decreased. The count of lymphocytes decreases in most cases examined.

Chest roentgenological examination There are various degrees of pulmonary infiltration, with many small pieces of lungs involved or in a meshwork pattern. In the fast progressing cases, massive shadows are present frequently, with multiple or bilateral lobes involved. Their resolution is usually slow. Occurrence and resolution of the roentgenological changes are not necessarily in accordance with the related symptoms and signs. For the cases not showing the changes, reexamination should be performed one or two days later.

Response to antibiotics Treatment with various antibiotics is not effective.

Diagnotic criteria For suspected cases: With positive findings in the epidemiological history + symptoms and signs + laboratory tests, or the epidemiological history + symptoms and signs + laboratory tests, or the symptoms and signs + laboratory tests + X-ray examination.

For cases with a clinical diagnosis of SARS: With positive findings in the epidemiological history + symptoms and signs + X-ray examination , or more, or the symptoms and signs + X-ray examination + no response to antibiotics , or the history + symptoms and signs + laboratory tests + X-ray examination.

For cases under medical observation: With findings in the symptoms and signs + laboratory tests.

For severe cases of SARS: SARS cases with one of the following findings: (1) a breathing difficulty, with respiratory rate exceeding 30 times per minute; (2) hypoxemia even during O_2 inhalation at 3-5 L/min, with PaO_2 below 70 mmHg and SpO_2 below 93 %, or having acute lung injury (ALI) or acute respiratory distress syndrome (ARDS); (3) multiple-lobe lesions involving more than one third of the lungs in area, or enlargement of the pulmonary lesion by more than 50 % within 48 hours as shown by chest roentgenograms; (4) shock or multiple organ dysfunction syndrome (MODS); (5) with a severe accompanying disease or a complicating infection, or with the age exceeding 50 years.

Differential diagnosis

Attention should be paid to the exclusion of other diseases or clinical syndromes such as infection of the upper respiratory tract, influenza, bacterial or fungous pneumonia, pulmonary infection complicating AIDS, legionnaires disease, pulmonary tuberculosis, epidemic hemorrhagic fever, pulmonary neoplasms, non-infectious interstitial pulmonary diseases, pulmonary edema, atelectasis, pulmonary embolism, pulmonary eosinophilic pneumonia and pulmonary vasculitis.

TREATMENT

Patients under the medical observation should receive treatment and observation in the appointed isolation ward or hospital, or under isolation observation in their homes. For the later case, the patients should live in a well-ventilated room and avoid

any close contact with other family members. They should be still under the observation of the disease-control department with their body temperature measured every day during the period. The patients, whose conditions are found to progress and to meet the criteria for SARS or the suspected during the observation, should be sent immediately to the appointed hospital by the special vehicles for isolation and treatment.

The key procedures of prevention and treatment of SARS are early detection, report, isolation and early treatment.

Treatment protocol for SARS and its suspected cases recommended by Chinese Center for Disease Control and Prevention (China CDC)

General therapy The general treatment includes adequate rest and supplement of nutrients such as fluid and vitamins, avoidance of intense and vigorous coughing. The patient' s condition should be observed intensively, since the onset of SARS within 14 days probably belongs to the progressive period in the majority of patients. Regular reexamination of chest x-rays and the functions of heart, liver and kidney are also necessary. The interval for the reinspection of chest x-rays in early phase of SARS should not be more than 3 days. SpO_2 should be checked daily.

Expectant treatment (1) Antipyretic analgesics should be used for patients with fever more than 38.5 ℃ and systemic prominent soreness. For the patients with hyperpyrexia, cooling measures should be applied such as ice compress and sponge bath with alcohol. (2) Antibechic and expectorant should be given when the patients suffer from cough and expectoration. (3) Corresponding measures should be taken when dysfunctions of multiple organs such as heart, liver and kidney take place. (4) Persistent oxygen inhalation by nasal tube should be applied early to the patients with obvious tachypnea and mild hypoxemia. (5) Aspirin medication should be avoided in children for fear of resulting in Reye syndrome.

Antibacterial treatment It is recommended to use antibiotics such as macrolides, fluoroquinolones, β-lactams and tetracyclines early in the course of SARS. Vancomycin or norvancomycin should be chosen as the preferable therapy when the infection caused by antimicrobial-resistant cocci is evidenced either clinically or experimentally.

Glucocorticoid therapy The following indications for the use of corticosteroids are proposed: Patients with severe toxic reaction and persistent high fever, and those with rapid deterioration of the chest film by increased infiltration progressing to a critical condition. The drug should be given regularly with the doses matching the actual condition of the disease and should be used with caution in children.

Selective therapy Selective therapy includes the use of antiviral agents, immunopotentiators and Chinese herbs.

Treatment of critical cases (1) Intensive care and monitoring should be applied to the patients with severe dyspnea or those who meet the criteria of a critical case. (2) Noninvasive and positive pressure ventilation is recommended for those with SaO_2 less than 93% while the oxygen inspiration is at 3-5 L/min and breath rate $\geqslant$ 30/min, in which CPAP with nasal mask is preferable. Routine level of inspiratory positive airway pressure should be set at 4-10 cmH_2O. Selection of adequate breathing masks, and persistent use of noninvasive ventilation that is interrupted no more than 30 min including hora decubitus till the disease remission are required. (3) For patients with severe dyspnea and hypoxemia, SaO_2 < 90 % or oxygenation index < 200 mmHg at 5 $L \cdot min^{-1}$ of oxygen inhalation, failure to tolerate or respond to noninvasive ventilation should be promptly followed by invasive ventilation after intubation. (4) Timely therapeutic measures should be taken once shock or MODS takes place in SARS patients and consultations of relevant experts are indicated when the treatment is limited by professional skill or poor medical equipments.

Standard treatment protocol for SARS (suspected and probable) in adult patients in Hong Kong[41]

Antibacterial treatment Levofloxacin 500 mg is given once daily intravenously or orally, or clarithromycin 500 mg is given twice daily orally plus co-amoxiclav (amoxicillin and clavulanic acid) 375 mg three times daily orally if patient is younger than 18 years, or pregnant, or suspected to have tuberculosis.

Ribavirin and methylprednisolone Combination treatment with ribavirin and methylprednisolone is given when the patient has extensive or bilateral chest radiographic involvement, or persistent chest radiographic involvement and persistent high fever for 2 days, or clinical and chest radiographic or laboratory findings suggestive of worsening, or oxygen saturation < 95 % in room air.

Standard corticosteroid regimen for 21 days Methylprednisolone 1 mg/kg is given every 8 h (3 mg/kg daily) intravenously for 5 days, then methylprednisolone 1 mg/kg is given every 12 h (2 mg/kg daily) intravenously for 5 days, followed by prednisolone 0.5 mg/kg twice daily (1 mg/kg daily) orally for 5 days, prednisolone 0.5 mg/kg daily orally for 3 days, prednisolone 0.25 mg/kg daily orally for 3 days, withdrawal of drugs.

Ribavirin regimen for 10-14 days Ribavirin 400 mg is given every 8 h (1 200 mg daily) intravenously for at least 3 days (or until condition becomes stable), followed by ribavirin 1 200 mg twice daily (2 400 mg daily) orally.

Pulsed methylprednisolone Pulsed methylprednisolone is given if clinical condition, chest radiograph, or oxygen saturation worsen (at least two of these), and lymphopenia persists, followed by methylprednisolone 500 mg twice daily intravenously for 2 days, and then standard corticosteroid regimen.

Ventilation

Non-invasive ventilation or mechanical ventilation should be considered if oxygen saturation < 96 % while O_2 > 6 L per min or if the patient complains of increasing shortness of breath.

Indications for intubation: (1) Failure to respond to non-invasive ventilation, SaO_2 less than 93 % while oxygen inspiration with facial/nasal mask at 5 L/min and progressive deterioration on chest radiography. (2) Failure to tolerate noninvasive ventilation while with severe dyspnea and hypoxemia. (3) With serious toxic reaction and rapid deteriorating conditions[42-46].

One of the important principles that should be noted in mechanical ventilation is the permission of hypercapnia that is usually performed when there are extensive pulmonary consolidation, poor compliance, and possible pneumothorax. In this way, the tidal volume and oxygen supply per minute could be reduced at the moment. SaO_2<90 % and positive end expiratory pressure (PEEP) at 10-15 cmH_2O may prevent atrophy of pulmonary alveoli and improve oxygen supply.

Academician Zhong Nanshan has recently emphasized 4 important therapies for SARS, including paying attention to fever and myalgia at the acute onset with a combination of traditional Chinese and Western medicine, prompt medication with large-dose of corticosteroids to prevent development of pulmonary fibrosis, timely application of nasal (facial) mask ventilation to improve the supply of oxygen, preventing alveolar collapse thus reducing the need for intubation and timely treatment of complications (especially super infections).

Therapeutic approaches in research

The SARS therapy with convalescent sera was firstly proposed

and used for himself by Dr. Su-Chun Jiang. Later, It was also used for the critically ill patients by Hong Kong scholars and achieved some beneficial effects[48]. However, detailed information about it has not been available.

Theoretically, the therapy is specific, but ineffective when used before severe and irreversible pathological changes take place. On the other hand, it should be screened for the pathogens that are probably transmitted via blood such as HBV, HCV and HIV in patients before the sera are used. Meanwhile, more attention should be paid to the possibility of serum sickness reaction[49, 50]. Other drugs such as protease inhibitors[51] and pulmoalveolar surfactant[52] have been under research and development.

Immunomodulators or immunopotentiators such as thymosin or thymopeptide and glutamine dipeptides have been proposed to be used in the treatment of SARS, though the current evaluation of these approaches remains absent. The therapy is based on the finding that the number of peripheral blood T lymphocytes, especially subgroups of CD4+ and CD8+, is significantly decreased in acute phase of SARS patients, suggesting that impairment of cellular immunity does occur in the early stage of SARS.

The therapies described above are the components of the whole treatment protocol for SARS. Their effectiveness and safety have not been systemically evaluated by prospective, randomized and controlled clinical trials. Therefore, it is hard to conclude which is better. SARS, a disease coming all of a sudden, is highly contagious. The researchers working in the first line of anti-SARS battle are engaged in clinical therapeutic activities. Meanwhile, they are also facing the risk to be infected. Under the circumstances, it is more difficult to perform a well and strictly designed clinical trial, and further more, plenty of concrete problems such as ethnics, research time, and lack of investigators and experimental control may also exist. Therefore it is difficult to make sure the effectiveness and safety of different therapies used in the coming months and years, if well designed trials are not performed. Notwithstanding these difficulties and problems, a reasonably designed clinical trial for SARS therapy remains to be very necessary[53].

Development of new anti-SARS drugs in China

Sivelestat sodium is the first newly developed anti-SARS drug in China that has been approved to enter clinical trials on May, 19, 2003, by State Food and Drug Administration of China. It is also the first one that has been approved to be tested in clinical trial since the rapid ratification program for anti-SARS drugs came into operation. It is an injection of chemical medicine used mainly to prevent and alleviate acute lung injury induced by PMN elastase via a mechanism of inhibiting systemic inflammatory response, with an attempt to improve pulmonary function, shorten the period of ventilation, decrease ventilator-related lung injury and other complications.

On May 21, 2003, the researchers in the Fourth Military Medical University discovered 3 polypeptides that exhibit prominent inhibitory effects on SARS virus *in vitro*, which may lay a solid foundation for the development of new polypeptide-type anti-SARS drugs. They found that a corona-like ring existed in the periphery of SARS virus and there were 4 constitutive proteins within this structure, in which the protein S plays a central role in the virus replication and invasion to human cells. These polypeptides were observed to be able to prevent coronavirus from invading the cells. Currently, these polypeptides have acquired the identification from Institute for Viral Disease Control and Prevention of China CDC. On May 15, State Intellectual Property Office of China has accepted the patent application for these findings.

A research group in the Second Military Medical University currently developed a kind of suspension containing porcine pulmoalveolar surfactant for SARS therapy, which has been approved to enter clinical trial by State Food and Drug Administration of China. It has been demonstrated by the animal study that its primary actions are to reduce pulmoalveolar surface tension, improve pulmonary ventilation and gas exchange, as well as prevent the formation of atelectasis and pulmonary edema. Furthermore, the safety, simplicity, sufferingless of this therapy make it possible to be applied in county or even in rural hospitals[54].

National Center for Drug Screening and Shanghai Institute of Materia Medica have received a considerable variety of pharmaceutical compounds, totally more than 4 000 samples, from more than 50 institutes of drug research in more than 20 domestic provinces and municipalities, as well as from that in USA and South Korea for screening new anti-SARS drugs. Co-operations among National Center for Drug Screening, Shanghai Institute of Materia Medica, Shanghai Municipal Center for Disease Control and Prevention and Academy of Military Medical Sciences have made more than 400 samples screened, in which 3 compounds, namely ZZ-I natural unity compound, an empirical prescription of Chinese medicine "Jieduwan" (detoxicating pill) and 5-hydroxytryptamine receptor antagonist DDDC-AS-001, were found to be the most powerful agents in anti-SARS efficiency among those currently screened all over the world.

TRADITIONAL CHINESE MEDICINE

The clinical characteristics of SARS are mainly manifested as prominent symptoms due to noxious heat and pathogenic dampness in most cases, which may lead to the rapid exhaustion of yin-qi and body fluids, and severe complications. Accordingly, the preventive strategy against SARS is to clear away the lung heat and toxic substances, to remove the pathogenic dampnes' s by aromatics and to supplement qi and promote the production of body fluids.

Prevention and treatment protocol for SARS and suspected cases by State Administration of Traditional Chinese Medicine of China

In order to improve the curative effects on the basis of recommended treatment protocol for SARS or suspected cases and discharge criteria by Ministry of Public Health, the following therapeutic approaches of the traditional Chinese medicine are proposed to be used in the anti-SARS treatment. It is recommended that the therapeutic principles of traditional Chinese medicine, namely diagnosis and treatment based on an overall analysis of the illness and the patient' s condition, should be performed in the treatment of SARS and suspected cases. Meanwhile, the treatment protocols should be adjusted as the patient' s condition changes.

In the early phase, the SARS patients are characterized by the impairment of pulmonary function due to noxious heat and stagnation of damp-heat, which are symptomatically categorized into 3 types of pulmonary impairment due to noxious heat, stagnation of damp heat and exterior cold and interior heat with dampness. For the cases manifested as pulmonary impairment due to noxious heat, it is suitable to promote pulmonary function by eliminating toxic heat via activating superficial channels and choosing a modified prescription of Yinqiao Powder plus Maxing Shigan Decoction. For the patients displaying stagnation of damp-heat, it is recommended to disperse the pathogenic factor out of the body by a revised recipe of Sanren Decoction plus Shengjiang Powder. When the condition is dominated by more dampness and less heat in these cases, Huopu Xialing Decoction should be adopted. For those with a manifestation of exterior cold

and interior heat, the therapeutic strategy is to clear the interior heat and ventilate the lung to get rid of toxic heat, which can be achieved by a modified prescription of Maxing Shigan Decoction plus Shengjiang Powder.

In the metaphase of SARS, the manifestations of the patients are displayed as the invasion of lung by epidemic pathogenic factors, abundant heat both in exterior and interior, accumulation of noxious heat, obstruction of Shaoyang by pathogenic factors and excessive epidemic pathogenic factors both in exterior and interior. For these patients, it is suitable to clear away heat and toxic materials, expell the lung heat and suppress the pathogenic factors with Qingfei Jiedu Decoction. A modified prescription of Ganlu Xiaodu Pill can exert the function of clearing away heat and toxic materials, eliminating dampness and keeping away filthiness, which is favorable for those with accumulated toxic heat. For patients with obstruction of Shaoyang by toxic heat, the therapeutic principles are to clear away the toxic heat at Shaoyang channel and to remove the damp-heat and a modified recipe of Haoqin Qidan Decoction should be adopted. For the patients with predominating toxic heat, pathogenic heat should be removed from blood and excessive heat should be purged. For this purpose, a modified recipe of Qiwen Baidu Decoction should be used.

In the critical phase, SARS cases are manifested as excessive accumulation of toxic heat with impaired body resistance, consumption of both qi and yin, and loss of consciousness and collapse. Accordingly, they are divided into accumulation of phlegm damp-heat blocking pulmonary vessels, stagnation of excessive pathogenic heat with deficiency of both qi and yin, excessive damp-heat weakening body resistance and blockage of breath. For the accumulation of phlegm toxic damp-heat blocking pulmonary vessels, it is helpful to invigorate qi for detoxication, eliminate phlegm for dispersing toxic damp-heat and remove blood heat for activating the channels. To achieve this purpose, Huoxie Xiefei Decoction should be used. For the patients with pulmonary stagnation of damp-heat with deficiency of both qi and yin, it is beneficial to clear away heat and promote diuresis, and to invigorate qi and nourish yin. Under the circumstances, Yifei Huazhuo Decoction is indicated. For the patients with hyperpyrexia weakening body resistance and blockage of breath, the preferable choice is to invigorate qi for restoring the vitality, dredge channels for promoting resuscitation, and choose Shenfu Decoction for getting the therapeutical purpose.

In the recovery phase, the symptoms of deficiency of both qi and yin, and deficiency of the lung and spleen, and the stagnant damp-heat are noted as the primary characteristics of SARS cases. For the former, it is recommended to nourish qi and yin, dispel pathogenic dampness to activate the channels, and to choose a modified prescription of Lishi Qinshu Yiqi Decoction. For the latter, it is reasonable to nourish qi and invigorate the spleen, which can be achieved by a modified prescription of Shenglin Baishu Powder plus Gegen Qinlian Decoction.

PROBLEMS AND COGITATION[55-57]

(1) The SARS cases reported in domestic medical literatures are all diagnosed on the basis of clinical experience without pathogenic evidences. (2) It is not worthwhile to advocate that the same contents are repeatedly reported by several papers or the same paper are repeatedly published by different journals. (3) Researches are lack of creative and constructive results or even simply repeat what have been performed overseas. (4) Most of the papers published are empty in contents with no substantive conclusions. Besides, some clinical reports are published by different journals. (5) The reasons why such inferior papers have been published are the insufficient collection of data and a lack of experience. (6) The achievements of SARS related research are exaggerated sometimes in certain domestic media, which mislead the public and should be prohibited. (7) Co-operations and communications in SARS research are seldom carried out among domestic research institutes, which deeply impressed the author when he was working in Beijing Xiaotangshan Hospital.

REFERENCES

1 **WHO**. Cumulative number of reported cases of severe acute respiratory syndrome (SARS). March 31, 2003 (http://www.who.int/csr/sarsarchive/2003-03-31/en)
2 **WHO**. Weekly epidemiological record. 14 March 2003, 78th year / 14 March 2003. http://www.who.int/wer/pdf/2003/wer7811.pdf
3 **Berned Sebastian Kamps,** Kamps-Hoffmann. 1. Timeline. SARS Reference (First Edition). May 8,2003.http://sarsreference.com/index.htm
4 **Reilley B**, Van Herp M, Sermand D, Dentico N. SARS and Carlo Urbani. *N Engl J Med* 2003; **348**: 1951-1952
5 **WHO**. Coronavirus never before seen in humans is the cause of SARS. 16 April 2003. http://www.who.int/csr/sarsarchive/2003-04-16/en/
6 **Luo HM**, Yu HJ, Ni DX, Yin WW, Gao LD, Mo JJ, Yang WZ, Yan JY, Liang Gd, Zeng G, Li LM. Etiology of infectious SARS and live survey. *Zhonghua Liuxing Bingxue Zazhi* 2003; **24**: 336-339
7 **He JF**, Peng GW, Zheng HZ, Luo HM, Liang WJ, Li LH, Guo RL, Deng ZH. An epidemiological study on the index cases of sever acute respiratory syndrome occurred in different cities among Guangdong province. *Zhonghua Liuxing Bingxue Zazhi* 2003; **24**: 347-349
8 **Lu HY**, Huo N, Xu XY, Wang GF, Li JP, Wang GQ, Li HC, Wang J, Nie LG. The epidemiologic characteristics of 80 patients with sever acute respiratory syndrome (SARS). *Beijing Daxue Xuebao (Yixueban)* 2003; **35S**: 8-11
9 **Wang M**, Du L, Zhou RH, Di B, Liu YF, Qing PZ, Wu XW, Chen XS, Qiu JC, Li ZR. Study on the epidemiology and measeures for control on severe acute respiratory syndrome in Guangzhou city. *Zhonghua Liuxing Bingxue Zazhi* 2003; **24**: 353-355
10 **Liu ZJ**, Sheng Z, He X, Huang RG, Teng RM, Ning F, Li XM, Ding LX, Lin CY. An epidemiological analysis on a input SARS case. *Zhonghua Liuxing Bingxue Zazhi* 2003; **4**: 358-359
11 **Zhonghua yixuehui**, Zhonghua yufang yixuehui, Zhonghua yiyuan guanli xuehui. Summary of academic seminar between two shores on control SARS. *Zhonghua Yixue Zazhi* 2003; **83**: 708-712
12 **Liu B**. Establishment of model of SARS space statistics in University of Science and Technology of China. http://www.gmd.com.cn/gmw/defaulta.htm, 2003.06.16
13 **Hong T**, Wang JW, Sun YL, Duan SM, Chen LB, Qu JG, Ni AP, Liang GD, Ren LL, Yang RQ, Guo F, Zhou WM, Chen J, Li DX, Xu WB, Xu H, Guo YJ, Dai SL, Bi SL, Dong XP, Ruan L. Chlamydia- like and coronavirus-like agents found in dead cases of atypical pneumonia by electron microscopy. *Zhonghua Yixue Zazhi* 2003; **83**: 632-636
14 **Zhu QY**, Qin ED, Wang CE. The isolation and identification of a novel coronavirus from patient of severe acute respiratory syndrome. *Zhongguo Gongcheng Shengwu Zazhi* 2003; **23**: 106-112
15 **Fan BC**, Jiang T, Yu M, Deng YQ, Peng WM, Chang GH, Shi BY, Liu BH, Yang BA, Zhu QY, Qing ED. Determination and analysis of 3' untranslated regions of 4 strains of SARS coronavirus isolated in China. *Zhongguo Shengwu Huaxue Yu Fenzi Shengwu Xuebao* 2003; **19**: 273-277
16 http://www.washprofile.org/chinese/sars-pathogen-042503.cfm 2003.04.25
17 **Ding YQ**. Preliminary discussion of etiology and pathogenesis of acute respiratory syndrome. *Jiefangjun Yixue Zazhi* 2003; **28**: 475-476
18 **Zhao JM**, Zhou GD, Sun YL, Wang SS, Yang JF, Mao YL, Pan D, Mao PY, Cheng Y, Wang YD, Xin SJ, Zhou XZ, Lu JY, Li L, Chen JM. Pathological and etiological findings in a dead case of sever acute respiratory syndrome of China. *Jiefangjun Yixue Zazhi* 2003; **28**: 379-382

19 **Wang CE**, Qin ED, Gan YH, Li YC, Wu XH, Cao JT, Yu M, Shi BY, Yan G, Li JF, Zhu QY. Pathological observation on suckling mice and vero E6 cells inoculated with SARS samples. *Jiefangjun Yixue Zazhi* 2003; **28**: 383-384

20 **Lai HW**, Lai RQ, Yang CH, Feng XD, Wang ZC. Pathology and ultrastructure in one infectious SARS case. *Jiefangjun Yixue Zazhi* 2003; **28S**: S34-S35

21 **Ji XL**, Tong Y, Shen MS. Mechanisms of lung injury in severe acute respiratory syndrome (SARS):histopathological analysis. *Zhonghua Weishengwuxue He Mianyixue Zazhi* 2003; **23**: 321-324

22 **Zhang FC**, Yin ZB, Tang XP, Min X. Liu JX, Chen YQ, Wang J, Chen WL, Chen WS, Jia WD, Lei CL. Clinical analysis of 260 cases with severe acute respiratory syndrome in Guangzhou areas. *Zhonghua Chuanranbing Zazhi* 2003; **21**: 84-86

23 **Peng J**, Hou JL, Guo YB, Feng XR, Chen JJ, Liu DL, Zhu YF, Jiang RL, Chen YP. Clinical characteristics of the severe acute respiratory syndrome in Guangzhou. *Zhonghua Chuanranbing Zazhi* 2003; **21**: 89-92

24 **Zhao ZW**, Zhang FC, Xu M, Huang K, Zhong WN, Cai WP, Yin ZB, Huang SD, Deng ZT, Wei M. Clinical analysis of 190 cases outbreak with atypical pneumonia in Guangzhou in spring. *Zhonghua Yixue Zazhi* 2003; **83**: 713-718

25 **Huo N**, Lu HY, Xu XY, Wang GF, Li HC,Wang GQ, Li JP, Wang J, Nie LG, Gao XM, Zhao ZD, Li J, Li YH, Zhuang H. Clinical characteristics and outcome of 45 early stage patients with SARS. *Beijing Daxue Xuebao (Yixueban)* 2003; **35S**: 19-22

26 **Gao ZC**, Zhu JH, Sun Y, Ding XL, Ma JS, Cui YX, Du XK, Gao T, He QY. Clinical investigation of nosocomial severe acute respiratory syndrome. *Zhongguo Weizhongbing Jijiu Yixue* 2003; **15**: 332-335

27 **Hu DS**, Zhang WD, Xi YL, Wen HW, Song LP, Wang WM, Dai LP, Yang WJ, Zhang MX, Kang QZ, Qiao HL, Xue LX, Duan GC, Dong ZM, Zheng YL. Epidemiological study on the outbreak of severe acute respiratory syndrome in Henan, China. *Zhengzhou Daxue Xuabao* 2003; **38**: 342-3344

28 **Chan-Yeung M**, Yu WC. Outbreak of severe acute respiratory syndrome in Hongkong special administrative region: case report. *BMJ* 2003; **326**: 850-852

29 **Ma W**, Chen GF, Li TS, Gao L, Han TZ, Liu DC. Analysis of chest x-ray manifestations in 118 patient with severe acute respiratory syndrome. *Zhongguo Weizhongbing Jijiu Yixue* 2003; **15**: 338-342

30 **Wang RG**, Sun HY, Song LY, Song W, Cui H, Li BS, Wang GF, Xu XY, Li N, Nie LG, Na J. Plain radiograph and CT features of 112 patients with SARS in acute stage. *Beijing Daxue Xuebao (Yixue ban)* 2003; **35**: 29-33

31 **Ma J**, Li N, Que CL,Li HC, Nie LG, Wang GF. Dynamic observation of the features of chest radiograph in SARS. *Beijing Daxue Xuebao(yixue ban)* 2003; **35**: 38-40

32 **Li TS**, Qiu ZF, Han Y, Zhang HW, Wamg Z, Liu ZY, Fan HW, Lv W, Yu Y, Wang HL, Zhang HY, Xie J, Zhou BD, Ma XJ, Ni AP, Wang AX, Deng GH. The alterations of T cell subjects in acute respiratory syndrome during acute phase. *Zhonghua Jianyan Yixue Zazhi* 2003; **26**: 297-299

33 **Wang Y**, Ma WL, Song YB, Xiao WW, Zhang B, Huang H, Wang HM, Ma XD, Zheng WL. Gene sequence analysis of SARS-associated coronavirus by nested RT-PCR. *Diyi Junyi Daxue Xuabao* 2003; **23**: 421-423

34 **Yang J**, Wang HZ, Chen JJ, Hou JL. Clinical detection of polymerase gene of SARS-associated coronavirus. *Diyi Junyi Daxue Xuabao* 2003; **23**: 424-427

35 **Wu XW**, Chen G, Di B, Yin AH, He YS, Wang M, Zhou XY, He LJ, Luo K, Du L. Establishment of fluorescent PCR method for detection of SARS coronavirus and the clinical trial. *Zhonghua Jianyan Yixue Zazhi* 2003; **26**: 300-301

36 **Wang HB**, Mao YL, Jiu LC, Jia L, Ma HB, Cui EB. The changes of red cell nature-immune-adhesion function in two patients with atypical pneumonia at different stages. *Zhongguo Yixue Jianyan Zazhi* 2003; **4**: 85-86

37 **Li B**. Researchers in China have developed the chip of the whole genome of SARS virus. http://www.xinhua.org/ 2003.05.08 19: 10:36

38 Taiwan University invented the way of ICT which can quickly confirm whether someone is infected with SARS. http://www.sars.ac.cn/show.php?id=5222

39 **Liu B**. Micorflow control chip can detect SARS virus. *Science and technology daily* 2003.06.16

40 **China has cloned SARS-like virus particle**. Jian kang bao,http://www.jkb.com.cn 2003.06.17

41 **Fisher DA**, Lim TK, Lim YT, Singh KS, Tambyah PA. Atypical presentations of SARS. *Lancet* 2003; **361**: 1740

42 **So LK**, Lau AC, Yam LY, Cheung TM, Poon E, Yung RW, Yuen KY. Development of a standard treatment protocol for severe acute respiratory syndrome. *Lancet* 2003; **361**: 1615-1617

43 **Lapinsky SE**, Hawryluck L. ICU management of severe acute respiratory syndrome. *Intensive Care Med* 2003; **29:** 870-875

44 **Allegra L**, Blasi F. Problems and perspectives in the treatment of respiratory infections caused by atypical pathogens. *Pulm Pharmacol Ther* 2001; **14**: 21-27

45 **Atabai K**, Matthay MA. The pulmonary physician in critical care. 5: Acute lung injury and the acute respiratory distress syndrome: definitions and epidemiology. *Thorax* 2002; **57**: 452-458

46 **The Acute Respiratory Distress Syndrome Network**. Ventilation with lower tidal volumes as compared with traditional tidal volumes for acute lung injury and the acute respiratory distress syndrome. *N Engl J Med* 2000; **342**: 1301-1308

47 **Zhong NS**. Status of diagnosis and treatment of SARS. *Zhongguo Yixue Luntanbao* 2003.4.29

48 **Jiang SC**, Wei H, Wang Y. Prevention and cure of hospital infection due to severe respiratory syndrome. *Zhonghua Yixue Zazhi* 2003; **13**: 401-404

49 **Wong VWS**, Dai D, Wu AKL, Sung JJY.Treatment of severe acute respiratory syndrome with convalescent plasma. H K MJ. http://www.hkmj.org.hk/hkmj/update/SARS/cr1606.htm

50 **WHO Recommendations on SARS and Blood Safety**. http://www.who.int/csr/sars/guidelines/ bloodsafety/en/

51 **Anand K**, Ziebuhr J, Wadhwani P, Mesters JR, Hilgenfeld R. Coronavirus main proteinase (3CLpro) Structure: Basis for Design of Anti-SARS Drugs. *Science* 2003; **300**: 1763-1767

52 **Moller JC**, Schaible T, Roll C, Schiffmann JH, Bindl L, Schrod L, Reiss I, Kohl M, Demirakca S, Hentschel R, Paul T, Vierzig A, Groneck P, Von Seefeld H, Schumacher H, Gortner L. Treatment with bovine surfactant in severe acute respiratory distress syndrome in children: a randomized multicenter study. *Intensive Care Med* 2003; **29**: 437-446

53 **Zhao RTG**. General situation of the treatment of SARS and problems needed to solve.Jian kang bao,http://www.jkb.com.cn. 2003-05-23

54 **Xiao X**, Yuan MD. http://www.xinhua.org, 2003-06-20 15:49:01

55 **Zhang JZ**. Severe acute respiratory syndrome and its lesions in digestive system. *World J Gastroenterol* 2003; **9**: 1135-1138

56 **Nie QH**, Luo XD, Hui WL. Advances in clinical diagnosis and treatment of severe acute respiratory syndrome. *World J Gastroenterol* 2003; **9**: 1139-1143

57 **Nie QH**, Luo XD, Hui WL. An emerging infectious disease: severe acute respiratory syndrome. *Shijie Huaren Xiaohua ZaZhi* 2003; **11**: 881-887

Edited by Wang XL

P.O.Box 2345, Beijing 100023,China
Fax: +86-10-85381893
E-mail: wjg@wjgnet.com www.wjgnet.com

World J Gastroenterol 2003;9(8):1646-1656
World Journal of Gastroenterology
 ISSN 1007-9327

• REVIEW •

Progress in searching for susceptibility gene for inflammatory bowel disease by positional cloning

Chang-Qing Zheng, Gang-Zheng Hu, Zhao-Shu Zeng, Lian-Jie Lin, Gin-Ge Gu

Chang-Qing Zheng, Gang-Zheng Hu, Lian-Jie Lin, Gin-Ge Gu, Department of Gastroenterology, the Second Affiliated Clinical College of China Medical University, Shenyang 110001, Liaoning Province, China
Zhao-Shu Zeng, Department of Serology, College of Forensic Medicine, China Medical University, Shenyang 110001, Liaoning Province, China
Correspondence to: Professor Chang-Qing Zheng, Department of Internal Medicine, the Second Affiliated Clinical College of China Medical University, Shenyang 110001, Liaoning Province, China. zhengchangqing88@163.com
Telephone: +86-24-83956682 **Fax:** +86-24-83956682
Received: 2003-03-03 **Accepted:** 2003-04-11

Abstract

Inflammatory bowel disease (IBD) includes two clinical subtypes: Crohn disease (CD) and ulcerative colitis (UC). The general prevalence is about 1.0-2.0 % in Western countries. It is predominantly regarded as a multifactorial disorder involving environmental factors and polygenic defects. The view was confirmed by a lot of evidences from clinical attributions and animal models, especially from epidemiological investigations. So the etiological study of IBD has been focused on searching for susceptibility genes by positional cloning, which consists of two steps: linkage analysis and association analysis. Linkage analysis has been an important method of searching for susceptibility genes to polygenic diseases as well as single-gene disorders. IBD, as a polygenic disease, has been widely investigated by linkage analysis for susceptibility gene since 1996. The paper reviewed 38 articles, which covered almost all original researches in relation to IBD and linkage analysis. So far, several loci, such as 16q, 12q, 6p and 3p, have been identified by the studies. The most striking is 16q12 (IBD1), which linked only with CD not UC in the majority of studies. Association analysis, as one essential step for positional cloning, is usually carried out by genotyping candidate genes selected by means of linkage analysis or other methods, for figuring out the frequencies of alleles and comparing the frequencies between IBD group and healthy control group to identify the specific allele. It has been established that IBD is implicated in immune disorder. So the studies were centered on the genes of NOD2/CARD15, HLA-II, cytokine, cytokine receptor and adhesion molecule. This paper reviewed 14 original articles on association between NOD2 and IBD that have been published since 2001. All results, with the exception of one report from a Japanese group, provide evidences that the three kinds of variants of NOD2 are susceptibility factors for IBD. This article also comprehensively analyzed 18 original researches of HLA gene polymorphism in IBD. We found extensive discrepancy among the conclusions and a novel hypothesis was put forward to explain the discordance. Most studies published recently on association between IBD and cytokine gene polymorphism were reviewed.

Zheng CQ, Hu GZ, Zeng ZS, Lin LJ, Gu GG. Progress in searching for susceptibility gene for inflammatory bowel disease by positional cloning. *World J Gastroenterol* 2003; 9(8): 1646-1656
http://www.wjgnet.com/1007-9327/9/1646.asp

INTRODUCTION

Inflammatory bowel disease (IBD) is composed of two clinical subtypes: Crohn disease (CD) and ulcerative colitis (UC). Its general prevalence is 0.1-0.2 % in Western countries[1]. There has been no epidemiological investigation of large scale for the prevalence or incidence of IBD in China so far, despite the facts that UC is common in China and CD has been more frequently diagnosed by clinical physicians in recent years[2]. The pathogenesis of IBD has not been clearly identified. Today, the most generally accepted pathogenesis of IBD is that IBD is resulted from abnormal immune response to enteric bacteria in individuals with susceptibility due to genetically polygenic defects. Therefore, investigators have searched human genome for the loci of susceptibility genes by linkage analysis and have achieved great success. On the other hand, association analysis, as one of the essential steps for positional cloning, was carried out by many investigators to identify the specific allele. It has established that IBD is implicated in immune disorder. Biochemical substances involved in immunoregulation are very rich and the corresponding genes are widely distributed in genome. Genome-wide linkage analysis has suggested multiple candidate regions in several chromosomes for IBD, therefore, considerable numbers of candidate genes should be selected for association analysis. In recent years, these studies were centered on the genes of NOD2/CARD15, HLA-II, cytokine, cytokine receptor and adhesion molecule. These studies were summarized in this review.

IBD IS A MULTIFACTORIAL DISEASE

There have been a number of hypotheses about the pathogenesis of IBD, but neither environmental factors, such as habit of diet and behavior, infection of microorganisms and contact of chemical or physical pathogenic agents, nor single-gene genetic disorder alone can fully explain its complex phenotypes. Thereby, it is thought to be a multifactorial disease. The view was supported by a larger amount of evidences from clinical attributions and animal models, especially epidemiologic investigations and linkage analyses.

Persuasive evidences of genetic contribution to IBD[3-12]

A. The first-degree relatives of affected individuals show about 20-50-fold increased risk of developing the disease compared with the general population for CD, and 10-20-fold increased risks for UC. Moreover, the affected siblings frequently present at similar ages and concordance rates reach up to 80 % for disease site, behavior and presence of extraintestinal manifestation. B. Twin studies have shown that the concordance rate of CD is about 20-44 % for monozygotic twins, and 3.8-6.5 % for dizygotic twins; the concordance rate of UC is about 6-16 % and 3 % respectively[6,7]. C. There are significant ethnic differences in disease frequency. For instance, the prevalence in Ashkenazi Jews is much higher than that in other races, even though they share similar living environment in the same community[8,9]. D. All genome-scanning linkage analyses detected some linkage loci, certain of which were subsequently confirmed by replication studies only involving certain

chromosomes; NOD2 was consistently identified as the susceptibility gene for CD in recent years. E. Simulation studies on animal models have showed that transgenic mice or gene-knockout mice are subject to colitis similar to human IBD, and that spontaneous colitis or hapten-induced colitis manifests fairly different in different strains of mice[10-12].

Evidence of environmental contribution

A. The concordance rate of IBD for monozygotic twins is much less than 100 %. The identical genotype with different phenotypes means that environmental factors take part in the pathogenesis of the disease[6,7]. B. Intestinal bacteria are suggested as the main environmental contributions demonstrated by many evidences: antibiotic therapy can usually induce temporary remission for most IBD cases[13], diversion of faeces stream can make distal improvement in patients with CD[14], some studies suggested that certain strains of intestinal bacteria were associated with IBD[15,16], colonization with normal enteric bacterial flora was required for the occurrence of disease in animals with CD irrespective of the underlying defect[10-12]. C. smoking is likely to be associated with the progress of IBD[17,18]. D. Migrant epidemiological studies demonstrated that population of identical ethnic background, when lived in different communities, showed discordant incidence[8,9,19,20].

IBD is not a disorder of simple mendelian inheritance[3,21-25]

Genetic disease of classic Mendelian model, which consists of Mendelian dominant and recessive genetic disorders, is a phenotype of single-gene defect and called single-gene disorder. IBD has previously been interpreted as genetic disease of Mendelian recessive model. But segregation analyses offered counter-evidence that IBD followed the principle of Mendelian inheritance. Parents of most IBD probands were healthy, frequency of siblings or children of the patients was much less than 50 %, the decline in frequency of affected second-degree relatives compared with first-degree relatives was greater than that predicted by autosomal dominant inheritance, in which the frequency was expected to decrease by 1/2 with each step. Incidence of IBD in children of affected spouses was sharply less than 100 % and a similar proportion of affected siblings and children of affected probands was inconsistent with autosomal recessive inheritance. Linkage analysis has detected several linkage loci that are distributed on a number of chromosomes.

LINKAGE ANALYSIS

It is very difficult to find the biochemical substances, which express qualitative difference between patients and healthy population by means of classical functional cloning. So linkage analysis, as the first step of positional cloning, may serve as a unique and practicable substitution for the time being. Figuring out genetic distance between marked loci and susceptibility gene by means of pedigree investigation and genotyping, then defining the approximate position of susceptibility gene in genomic map are the essential courses of linkage analysis. The dramatic progress of human genome project, which has located nearly 10 000 marker loci in genomic map, has greatly boosted positional cloning for complex genetic diseases. Epidemiological studies have identified striking genetic contributions to the etiology of IBD, but so far, studies with traditional biochemical methods have not yet identified the products with quantitative defects. Many investigators have turned to linkage analysis and have achieved great success. The important data from 38 original researches, which covered almost all articles in relation to IBD and linkage analysis that have been published since 1996, are listed in Table 1[26-63], and some aspects were reviewed as follows.

The common course of linkage analysis for IBD is: collecting families with affected sibling pairs (ASP) or affected relative pairs (ARP) $\geqslant$2 by strict ascertainment, genotyping of genome-wide or certain chromosomes according to microsatellite polymorphisms, figuring out multi-point maximal non-parametric LOD score (MLOD) and two-point LOD score by means of statistical software, inferring genetic distances of susceptibility genes to marker loci and locations in physical genome map, offering candidate genes for association analysis. The majority of investigations found certain suggestive linkage loci with various LOD score, but when defined according to different LOD thresholds, the locations or number of linkage loci were variable. In view of the traits of statistical software and quantity of subjects in most studies, we only displayed the results with MLOD $\geqslant$2.0 or 3.0, represented by ± and +. The chromosomes, on which the linkage loci strongly supported (MLOD$\geqslant$3.0) by at least one of 8 linkage analyses of genome-wide scanning located, include chromosomes 1, 3, 5, 6, 7, 12, 14, 16, 18 and 19, as well as chromosomes 4, 10, 17 and x with suggestive evidence (2.0$\leqslant$MLOD<3.0). Although there was striking discrepancy among the genome-wide scans in respect of linkage loci, almost all studies detected more than 3 linkage loci. This shows that the pathogenesis of IBD is involved in multiple genes and manifests obvious genetic heterogeneity. Several loci were supported by relative more studies, such as 16q, 12q, 6p, and 3p. Because Hugot *et al*[26] and Satsangi *et al*[27] detected strong linkage evidences for chromosomes 16, 12, 6, 3 and 7 in 1996, subsequent studies mainly focused on these chromosomes. It can be seen from Table 1 that more evidences were offered for these loci, with the exception of 16q, simply because these loci were investigated by more studies. Some loci supported by certain genome-wide scans, such as 14q, 5q, 19p, likely to harbor susceptibility genes, were less investigated.

Stratification studies demonstrated significant variances as to the degree and loci of linkage between families with severe IBD and those with only slight IBD, male patients and female patients, Jewish people and non-Jewish people, as well as between UC and CD. Some investigators examined families with CD patients only; others examined families with UC patients only, but most studies detected both families and those with mixed patients and compared the differences of linkage loci between the two groups. As shown in Table 1, there were some differences between UC and CD. The most striking is 16q12 (IBD1), which linked only with CD not UC in the majority of studies. This shows that CD and UC have some common susceptibility genes, as well as certain individual susceptibility genes. Three studies[32,47,48] found that certain loci linked only with the families with early onset of CD. All subjects examined by the studies listed in Table 1 included Caucasian or Jewish patients from Europe, Australia and northern America, but no Mongolian patients. Three studies[28,29,42] demonstrated significant differences between Jewish patients and non-Jewish patients. In respect of nationality of patients, it seems there are no remarkable differences among American, English, German, Australian, Canadian, Italian, Dutch and Belgian. But Paavola *et al*[40] examined chromosomes 1, 3, 7, 12, 14 and 16 in Finnish patients and did not find linkage loci. Fisher *et al*[33] found that some loci on chromosomes 6p, 1, 14 and 18 linked only with IBD of male sufferer. These results confirm the extensive genetic heterogeneity of IBD.

Linkage analysis is intended as an essential tactic to offer candidate genes for association analysis. We should focus our attention on the linkage loci containing some candidate genes, products of which have been suggested as pathogenic factors by other methods, as well as confirmed by subsequent replication studies. The loci meeting these conditions were briefly reviewed here.

Table 1 Data of linkage analysis

Ref	Author	Year	Subject	Scope	Linkage loci for IBD	Linkage loci for CD	Linkage loci for UC
R26	Hugot JP	1996	Caucasian CD	Autosome		16q(IBD1)+	
R27	Satsangi J	1996	Northern european IBD	Autosome	7+, 12+, 3±	7±, 12±, 3±	7+
R28	Cho JH	1998	American IBD[a]	Genome	(3q+,1p±)(non-Jewish), (3q±,4q±)[e]	16±	––
R29	Ma Y	1999	American CD[a]	Genome		14q±, 17q±[e], 5q±[e]	
R30	Hampe J	1999	European IBD[b]	Genome	1±, 6±, X±	10±, 12±, 16±	4±, X±
R31	Duerr RH	2000	American CD[a]	Genome		14q+	
R32	Rioux JD	2000	Canadian IBD	Genome	19p+, 5q+, 3p±, 6p±	5q+[f], 19p+	19p±
R33	Fisher SA	2002	European IBD	Genome	(6p+,1+,14+,18+)(male)	6p+(male)	6p+(male)
R34	Brant SR	1998	American CD[a]	3,7,12,16		16q(IBD1)±	
R35	Rioux JD	1998	Toronto IBD	3,7,12,16	– –	––	––
R36	Curran ME	1998	European IBD[b]	12,16	– –	12q±	––
R37	Annese V	1999	Italian IBD	3,6,7,12,16	16q±	16q±	16q±
R38	Vermeire S	2000	Belgian CD	3,7,12,16		––	
R39	Dechairo B	2001	European IBD	3,6,7,	6p+	––	––
R40	Paavola P	2001	Finnish IBD	1,3,7,12,14,16	– –	––	––
R41	Gavanaugh J	2001	IBD[c]	12,16	16q+	16q+	––
R42	Ohmen JD	1996	American IBD[a]	16	– –	16q±[e]	––
R43	Parkes M	1996	English IBD	16	– –	16q±	––
R44	CavanaughJA	1998	Australian CD	16		16q+(IBD1)	
R45	Mirza MM	1998	Northern european UC	16			16q±(IBD1)
R46	Porabosco P	2000	Italian IBD	16	16q+	16q+	16q+
R47	Brant SR	2000	American CD	16		16q+[f], 16q±	
R48	Akollar PN	2001	Jewish CD	16		16q+[f]	
R49	Van Heel DA	2002	European CD	16		––	
R50	Zouali H	2001	European CD	16		16q+	
R51	Hampe J	2002	European IBD	16	16p±	16q+, 16p±	––
R52	Satsangi J	1996	European IBD	6(MHC-II)	– –	––	6p(MHC-II)+
R53	Silverber MS	1999	Canadian CD	6		6p(MHC-II)±	
R54	Hampe J	1999	Northern european IBD[b]	6	6p+	6p+	6p+
R55	Yang H	1999	American CD	6		6p(MHC)+	
R56	Duerr RH	1998	Northern american IBD	12	12q±	––	––
R57	Yang H	1999	American IBD	12	– –	12q±	––
R58	Lesage S	2000	Northern european CD[d]	12		––	
R59	Parkes M	2000	American IBD	12	12q+	––	12q+
R60	Hampe J	2001	Northern european IBD[b]	3	– –	––	––
R61	Duerr RH	2002	American IBD	3	3p+	––	––
R62	Rioux JD	2001	American CD	5q		5q+	
R63	Vermeire S	2001	Belgian CD	X		Xq±	

Note: CD, CD-only family; UC, UC-only family; IBD=UC+CD+mixed family; +, convincing linkage (LOD≥3.0); ±, suggestive linkage (3.0>LOD≥2.0); —, no suggestive linkage (LOD<2.0); [a], including Jewish; [b], family from English, German and Dutch; [c], family from Northern American, European and Australian; [d], family from French and Belgian; [e], linkage only for Jewish; [f], linkage only for IBD with early onset.

Chromosome 16 As shown in Table 1, 14 out of 25 related studies found linkage loci for CD with MLOD more than 2.0 on the chromosome, additionally, some loci with suggestive score (MLOD between 1.0 and 2.0) were detected. Only 3 studies found linkage loci with UC, furthermore, 2 of them also detected linkage with CD, and the other one merely examined UC families. It can be inferred from these studies that chromosome 16 contains susceptibility gene for CD rather than UC. Chromosome 16 is comparatively short, with 98 Mb of physical length, 130.8 cm of genetic distance, and has been spaced by about 200 microsatellite markers[64]. The linkage loci suggested by the studies in Table 1 were distributed in most part of chromosome 16 (for instance, D16S409-419[26], D16S748-764[28], D16S411[42,43], D16S3136[50]), but only pericentromeric region on 16q was the most consistent linkage region. The important candidate genes in the region are NOD2, CD11integrins, CD19, Sialophorin, IL-4 receptor gene etc. NOD2 gene has been established as susceptibility gene to CD. It remains unanswered if there are other susceptibility genes in the chromosome. Hampe *et al*[51] examined additional regions with high-density experiment using 39 microsatellite markers and found three-peak logarithm of odds (LOD) scores of 2.7, 3.2, and 3.1 on proximal 16p, proximal 16q, and central 16q, respectively. Taking account of the differences of suggestive markers, it is probable that there are other susceptibility genes for CD in the chromosome.

Chromosome 12 Six out of 19 studies found suggestive linkage loci in the chromosome, 4 of them for CD, and one for UC. Though the studies with suggestive MLOD are rare, several studies found linkage loci with slightly suggestive significance (MLOD between 1.0 and 2.0) with IBD, especially with UC. This may result from the fact that the sample sizes in most studies were not large enough; furthermore, they were predominantly consisted of CD families. Parkes *et al*[59] examined 581 affected relative pairs, of which 252 were from CD-only families, 138 from UC-only families, and 191 from mixed families (the sample size was much larger than that in most of other studies, especially for UC), and found that MLOD at certain marker on chromosome 12 was 5.26 for all IBD, 3.91 for UC and 1.66 for CD. In summary, it is probable that

Table 2 Data of association analysis for NOD2

Ref year author	Subject	Main conclusion
R65, 2001	Europe CD, UC	A. Find P241S, R432R, R675W, G881R, IVS8-133delAinSCT, 980fs etc.31 variants
Hugot, JP		B. R675W, G881R, 980fs with CD, not with UC
		C. CD-GRR 3.0 at SHEM, 38.0 at HOM, 44.0 at CHEM
R66, 2001	American CD	A. 3020insC with CD
Ogura Y		B. CD-GRR 1.5 at SHEM, 17.6 at HOM
R67, 2001	German, English CD	A. 3020insC with CD, not with UC
Hampe J	UC	B. CD-GRR 2.6 at SHEM, 42.1 at HOM
R68, 2002	Europe CD, UC	A. Find 67 sequence variants, 9 of which gene frequency >5 %
Lesage S		B. R702W, G908R, 3020insC with CD, not with UC
		C. Support gene-dosage effect
R69, 2002	Europe CD, UC	A. R702W, G908R, 3020insC with CD, especially ileum CD, not with UC
Cuthbert AP		B. P628S linkage disequilibrium with the other three mutations
		C. CD-GRR 3.0 at SHEM, >22.0 at HOM or at CHEM
		D. Mutation frequency: familial CD > sporadic CD
R70, 2002	Dutch CD	A. 3020insC with CD, G2722C not with CD
Murillo L		B. No association with clinical phenotype
R71, 2002	German, Norwegian	A. R675W, G881R, 980fs with CD
Hampe J	CD	B. Especially with ileum CD
R72, 2002	Canadian CD	A. R702W, G908R, 1007fs with CD, especially ileum CD
Vermeire S		B. No difference between familial CD and sporadic CD
R73, 2002	German UC, CD	A. 3020insC with CD, not with UC
Radlmayr M		B. Association with fistula, fibrostenosis, ileocecum resection
R74, 2002	Japanese CD, UC	A. R675W, G881R, 3020insC not with CD or UC
Inoue N		
R75, 2002	Europe CD	A. R675W, G881R, 3020insC with CD
Vermeire S		B. Not with effect of Infliximb
R76, 2002	American CD	A. R702W, G908R, 1007fs with CD
Abreu MT		B. With fibrostenosis
R77, 2002	English CD	A. R702W, G908R, 1007fs with CD, especially ileum CD
Ahmad T		B. 3020insC with early onset of CD
		C. CD-GRR 2.4 at SHEM, 9.8 at HOM, 29.3 at CHEM
R49, 2002	Europe CD	A. R702W, 1007fs with CD, linkage disequilibrium with P628S
Van heel DA		B. Support gene-dosage effect

Note: CD=Crohn disease; UC=ulcerative colitis; CD-GRR=CD-genotype relative risk; SHEM=simple heterogeneous mutation; HOM= Homozygous mutation; CHEM=complex heterogeneous mutation; *P* value is uniformly set at $\leqslant$0.05; Nomenclatures were not uniform among the studies, R675W=R702W, G881R=G908R, 1007fs=980fs=3020insC.

chromosome 12 contains susceptibility genes both for CD and UC, but with only weak contributions. The most consistent microsatellite markers lay in 12q13, which is also called IBD2. The main candidate genes in the region are IFN-γ, natural resistance associated macrophage protein (MRAMP2), vitamin D receptor genes etc.

Chromosome 6 Eight out of 14 studies found linkage loci in the chromosome. There was no remarkable difference between CD and UC in terms of the number of suggestive studies or LOD score in most studies. This shows that common susceptibility genes for both CD and UC are probably located in chromosome 6. Linkage markers of most studies were distributed in 6p13, which was called IBD3 in some studies. The important candidate susceptibility genes in the region include HLA-A, HLA-B, HLA-C, HLA-E, HLA-F, HLA-G, MIC-A, MIC-B, HLA-DR, HLA-DP, HLA-DQ, HLA-DM, LMP-2, LMP-7, transporterin antigen processing (TAP)-1, TAP-2, TNF-α, TNF-β, (LT-α), heat shock proteins (HSP), complement C4, C2 genes etc.

Chromosome 3 Four out of 16 related studies found linkage loci with LOD score more than 2.0. It should be noticed that the LOD scores in 4 studies for all IBD were always higher than that for CD or UC alone and no LOD score for CD or UC alone reached 2.0 in all related studies. It may be partly due to the fact that the sample sizes were much smaller after stratifications and could not reach the threshold of statistical significance. It is very likely that there are some common susceptibility genes for CD and UC, but they probably confer slight genetic contribution to IBD, since some studies found linkage loci in the chromosome only with weakly suggestive LOD score[30,39,60]. The considerable linkage region was proximal 3p. The principal candidate genes in the region include CCR2, CCR5, IL-4RA, IL-5RA, lactotransferrin, IFN-α A2, cathelicidin antimicrobial peptide genes etc.

Chromosome 5q It was confirmed by only 3 studies involved in the chromosome. The linkage loci were located in 5q32-35, which happened to be in the region of cytokine-rich cluster and was called IBD5 in some studies. The main candidate genes are IL-3, IL-4, IL-5, IL-13, CSF-2 genes etc. The cytokines have been accepted as playing important roles in initiating IBD. So further investigations are needed.

14q11(IBD4) and 19p13 They were suggested as linkage loci in some studies. 14q11 contains the immunoloregulation members TCR-α/δ gene and 19p13 contains ICAM1, C3, TBXA2 and LTB4H genes.

ASSOCIATION ANALYSIS

Association analysis, as an essential step for positional cloning, was usually carried out by genotyping candidate genes selected by means of linkage analysis or other methods, for figuring out the frequencies of alleles and comparing the frequencies

Table 3 Data of association analysis for HLA

Ref	Year	Author	Subject	Region	Association with CD	Association with UC
R83	1995	Duerr RH	American UC	HLA-DR2		DRB1*1601-
R84	1995	Nakajima A	Japanese CD	DR, DQ, DP	(DRB1*0405,0410,DQA1*03,DQB1 *0401,0402)+, (DQA1*0102,DRB1* 1501,1302,DQB1*0602) -	
R85	1996	Reishagen M	German CD	DRB1, DQA1, DQB1	DRB1*07+, DRB1*03-	
R86	1996	Hesresbach D	French CD	HLA-I, HLA-II, TAP	DRB1*1302+, DRB1*04+[c]	
R52	1996	Satsangi J	Europe IBD	DRB, DQB		DRB1*103+, DRB1*12+
R87	1996	Danze PM	French CD	DRB1, DQB1	(DQB1*0501, DRB1*07, 01)+ (DQB1*0602 / 0603, DRB1*03)-	
R88	1996	Heresbach D	French UC	HLA-II, TAP		DRB1*03-
R89	1997	Bouma G	Dutch IBD	HLA-DR		DRB1*15+, DRB1*13-
R90	1998	Fernandez AM	Spanish UC	DRB1		DRB1*1501+, DRB1*
R91	1998	Cariappa A	American CD	DRB, DQB, DPB	Haplotype DRB3*0301 / DRB1*1302+	1502(severe)+
R92	1999	Bouma G	Dutch UC	DR, TNF-α, LT-α		DRB1*0103+, DRB1*15(female)+
R93	1999	Yoshitake S	Japanese IBD	DQ, DR, DP	DQB1*0402+, DRB1*1502-	(DRB1*1502,DRB5*0102, DQA1*0103,DQB1*06011, DPA1*0201,DPB1*0901)+, (DRB4*0101,DQA1*0302) -
R94	1999	Stokkers PC	Meta-analysis	DR, DQ, TNF-α	(DR7,DRB3*0301,DQ4)+, (DR2,DR3)-	(DR2, DR9, DRB1*0103)+, DR4 -
R95	1999	Hirv K	Estonians UC	DR, DQ, TNF-α		DRB1*1501+
R96	2001	Seki SS	Japanese UC	HLA-I, HLA-II		(MICA-TM-STR6, B52, DR2)+
R97	2002	Lantermann A	IBD[a]	DPA1	DPA1*02021(German)+	
R98	2002	Orchard TR	Europe IBD	HLA-B, DR, TNF-α	Uveitis with (B*27,B*58,DRB1*0103)	
R77	2002	Ahmad T	CD[b]	HLA-I, HLA-II TNF-α, LT-α, HSP70	(DRB1*0701,CW*0802)+, DRB1*0103(fistula)+, DRB1*1501-	

Note: UC= Ulcerative colitis; CD= Crohn disease; IBD= UC+CD; [a], German, South Africa and South Korea IBD; [b], white people CD; [c], DRB1*04 is only associated with CD with no effect to cortexin; *P* value is uniformly set at $\leqslant$0.05; +, Positive association; -, Negative association.

between IBD group and healthy control group to identify the specific allele. It has established that IBD is implicated in immune disorders. So studies have been centered on genes of NOD2/CARD15, HLA-II, cytokine, cytokine receptor and adhesion molecule.

NOD2/CARD15 mutations

Identification of NOD2 as susceptibility gene for IBD is supported by linkage analysis, association analysis and immunological function analysis. In this review, crucial information from 14 original studies on the relationship between IBD and NOD2 mutations are listed in Table 2[49, 65-77] and were comprehensively analyzed as follows. NOD1 is an intracellular protein composed of a N-terminal caspase recruitment domain (CARD), a centrally located nucleotide binding domain (NBD), and a leucine rich repeat (LRR) domain at its C-terminus which could activate nuclear factor κB (NFκB) and also promote apoptosis[78]. NOD2 was identified by searching the public database for genes encoding similar proteins to NOD1. The gene happens to be located on chromosome 16q12, a domain called IBD1 supported by most linkage analysis. NOD2 has one more CARD at its N-terminal than NOD1. It is expressed primarily in monocytes and following stimulation by bacterial lipopolysaccharide (LPS), which occurs at LRR domain, activates NF-κB.

So far, approximately one hundred sequence variants have been detected in NOD2 gene, most of which were rare mutations, and located in LRR domain. Lesage *et al* discovered 67 sequence variants in the gene, 9 out of them with gene frequencies more than 5 %. This demonstrates that NOD2 gene has high polymorphism. Of these alleles, P268S, R702W, G908R and 1007fs are consistently confirmed to be the genetic susceptibility factors to IBD. Gene frequency of P268S in general population was about 20-28 %, a little higher than other three variants. While it was remarkably higher in CD patients, transmission disequilibrium test (TDT) suggested that this was very likely to be the result of transmission disequilibrium with other three variants, but not the independent susceptibility factor to CD. R702W, G908R and 1007fs are widely considered as independent susceptibility factors. 1007fs allele frequency was different among all reports: about 1.6-3.3 % in control population and 6.6-23.7 % in CD patients. All the studies, with the exception of a report from Japanese group, strongly support the association of 1007fs with CD. Allele frequency of R702W was slightly higher than that of 1007fs, and was significantly higher in CD patients than in control population. Allele frequency of G908R was about 1.5 % and has been suggested as an independent susceptibility factor to CD, but the statistical values in some reports did not reach significant level. This may be due to its lower gene frequency. The CD-genotype relative risk of the three mutations was about 3.0 for simple heterozygote mutation, and more than 20.0 for homozygote mutation or compound heterozygote mutation. This supports the fact that mutations in NOD2 gene show a gene-dosage effect and somewhat recessive trait. Five studies, in which subjects included UC patients, did not find any persuasive evidences that the three mutations were associated with UC. It' s worthy to point out that association of the three mutations with CD was not confirmed in study by the Japanese group. The discordance is usually explained by the view that CD is a genetic disease with high locus heterogeneity or allele heterogeneity among patients from different races or different geographic territories. With respect to the association of three mutations with clinical phenotypes, most reports suggested 3 mutations were only associated with ileum CD and certain reports found they were associated with fibrostenosis, fistula or effect of medicine.

How can the mutations of NOD2 initiate CD[65,66,79-82]? Some

studies have provided evidences that NOD2 is an intracellular receptor for bacterial pathogenic agents, and expresses only in monocytes. LRR of NOD2, after being activated by lipopolysaccharide (LPS), can trigger NF-κB signal pathway, which promotes the expression of certain proinflammatory cytokines. LRR can also promote apoptosis. So it is the most likely mechanism that the mutations in NOD2 either raise sensitivity of monocyte to bacterial pathogenic agents, with the result of overexpression of certain proinflammatory cytokines, or cause deficiency of apoptosis, leading to monocyte accumulation in intestinal mucosa and chronicity of the course. There are some questions about the relation between mutations in LRR and activity of NF-κB. Though high activity of NF-κB is always found in monocytes in lamina propria of intestinal mucosa from CD patients, it descends in cells with frame-shift mutation in LRR *in vitro* when stimulated by LPS. Functional study by Hugot *et al* demonstrated that expression of a NOD2 mutant form lacking the entire LRR region results in enhanced NF-κB activity, whereas the frame-shift mutation causing a truncated protein missing the final 33 amino results in low NF-κB activity. The potential explanation may be that the truncated protein leads to elevated NF-κB when stimulated by an untested bacterial LPS and that the frame-shift mutation may have a differential effect on caspase 9 induced apoptosis. To understand the mechanism how mutations in NOD2 confer susceptibility to CD, more functional analyses should be ingeniously performed. Identification of NOD2 was a great achievement in the history of exploring genetic susceptible factor for IBD. Detecting of the mutations may well have some clinical benefits for the prediction of onset risk, classification of disease, individualization of therapy and future gene therapy, but it should not be used as a tool for diagnosis since there is about 6-9 % overall allele frequency of the three single nucleotide polymorphisms (SNPs) in general population.

HLA gene polymorphisms

HLA gene is composed of three regions: HLA-I, HLA-II and HLA-III. HLA-I mainly includes HLA-A, HLA-B and HLA-C, and HLA-II mainly contains HLA-DR, HLA-DQ, HLA-DP. The primary immunity relative genes in HLA-III region are TNF-α, TNF-β, (LT-α), complement 2 (C2), complement 4(C4). Genes in the regions are highly polymorphic. HLA-II is expressed primarily in macrophages, dendritic cells and thymic epithelial cells, playing important parts in presenting exogenous antigen. Immunologic studies have shown strong evidences that IBD is closely associated with disturbance of Th lymphocyte subclass, and that the major environmental factor inducing immune disorder is intestinal bacterial flora. T lymphocytes accept enteric antigens presented by microphages, so it is naturally viewed that sequence variants of HLA-II are likely to cause disorder of antigen presenting and result in imbalance of Th lymphocyte subclass. HLA genes located in IBD3 (6p13) were identified by linkage analysis, it is sensible to select HLA gene as candidate gene for association analysis. This review collected 18 studies published since 1995 and listed the main results in Table 3[52,77,87-98]. Most studies published before 1995 usually typed HLA by examining serum HLA antigen through immunologic assay. The studies shown in Table 3 tried to identify HLA alleles by using reliable and precise molecular biological techniques, such as specific sequence primer polymerase chain reaction (PCR-SSP), specific sequence oligonucleotide probe assay (PCR-SSO) and gene sequencing.

It could be summarized from Table 3 that polymorphisms positively or negatively associated with UC or CD are mainly located in DRB1 or DQB1, which are the key regions to determine the polymorphism of peptide-binding cleft. The sequence variants in the regions could change the affinity for distinct antigen peptides. According to serum typing, results from more than two studies suggest that UC is positively associated with DR2, DR9 and negatively associated with DR4, and that CD is positively associated with DR7, DQ4, negatively with DR2, DR3. Further genotypings by molecular biological technique found that only DRB1*0103, DRB1*1501 and DRB1*1502 were associated with UC in more than two studies. Other variants in the regions have not been confirmed to be positively or negatively associated with UC or CD. Many investigators studied the association between polymorphism and clinical phenotype (p-ANCA, sex, extent, age of onset, site of disease, effect of certain medicine, complication, certain extraintestinal symptoms), but their conclusions were not consistent. The heterogeneity was obvious between UC and CD in respect of association with polymorphisms of HLA-II genes. The alleles associated with UC or CD were not associated with the others. On the contrary, DR2, positively associated with UC in some reports, was negatively associated with CD in other reports.

Stokkers *et al*[94] carried out a meta-analysis involving 29 pieces of related reports published from 1980 to 1999 (there were some overlaps between those and reports listed in Table 2). Taking a wider view of all these studies, we discovered a remarkable characteristic: the vast majority of studies discovered certain positively or negatively associated alleles, but all the suggested alleles showed significant discrepancy (there were always both evidences and counterevidences of the association as to any of the alleles among the studies). The contradiction cannot be explained by race heterogeneity because there are discrepancies both in white people and yellow people. It cannot be convinced that sequence variants in HLA-II gene are not associated with IBD and positive results are due to confusions either from linkage disequilibrium or from coincidences resulted from high polymorphisms. In view of the functional property of HLA-II and the widespread contradictions in association analysis, we consider that polymorphism in the regions, to some extent, plays a role in initiating IBD, but the involved alleles differ between different communities (in view of geographic situation, climatic condition and dietary culture) and even between individuals in the same community. The constituent characteristics (sort, ratio, total amount and time order of all antigens) of antigen compound (all kinds of antigens) derived from intestine in one community are distinct from that in an other community. The antigen presenting cells (APC) containing certain HLA-II allele, only when disposing and presenting the antigen compound with matching constituent characteristic, can cause pathologic response. There are different predominant antigen compound in different communities, so the predominantly matching alleles implicated in IBD might be different among communities, and therefore no particular or unchanged antigen and HLA-II allele can take part in pathologic lesions in all IBD. Nevertheless, some of them may play a more dominant role in one community than in another community.

Cytokine, cytokine receptor and adhesion molecule polymorphisms

IL-1β, excreted mainly by microphages, up-regulates the expression of HLA-II, adhesion molecule and IFN-γ in an autocrine manner. It can also, through paracrine, promote activity of Th lymphocyte and play an important part in triggering immune response. IBD is regarded as the result of imbalance of Th lymphocyte subclass, thereby, IL-1β, IL-1β receptor (IL-1R), IL-1 receptor antagonist (IL-1RA), balance of IL-1β/IL-1RA may be associated with IBD. Up to date, many investigators have tried to explore association between IBD and gene polymorphism, but studies in recent years did not

find any positive results[99-101]. Nemetz *et al* found that IL-1β-511*2 allele was associated with the overexpression of IL-1β and descent of bone mineral density[102], and that IL-1β(+3953,-511) allele is associated with pathological course and patient' s condition[103]. Mwantembe *et al*[104] examined the polymorphism of IL-1β, IL-1R and IL-1RA genes by *TaqI, Pst I* and VNTR and discovered IL-1R (*TaqI-*) allele frequency was significantly higher in white patients than that in white healthy controls and Negro patients, whereas IL-1R (*Pst I-)* allele frequency was higher in Negro patients than those in white patients. IL-1β and IL-1RA genes were not located in the region which was strongly supported by linkage analysis.

TNF-α is suggested as a pathogenic factor for IBD because its concentration is usually increased in intestinal mucosa of IBD patients, and therapy of anti-TNF-α antibody Infliximb has shown satisfactory effects on refractory IBD. The gene is located in IBD3 (6p13) which is supported by linkage analysis. Most studies in recent years discovered certain alleles were associated with IBD. Van Heel *et al*[105] found (-857C) TNF-α allele was associated with IBD. Sashio *et al*[106] found TNF-α (-308G/A, -238 G/A) allele was associated with UC. Mitchell *et al*[107] found that TNF-α (-308G/A) was associated with sclerosis cholangitis. Koss *et al*[108] found that different haplotypes of TNF-α gene were associated with the expression of TNF-α. Louis *et al*[109] discovered (-308) TNF-α was associated with certain clinical phenotypes of CD. Negoro *et al*[110] discovered (-1031C, -803A, -857T) TNF-α was associated with CD. These results show that sequence variants of TNF-α gene, especially (-308G/A) may take part in the pathogenesis of IBD by enhancing the expression of TNF-α and promoting activity and proliferation of Th lymphocytes.

IL-4, expressed mainly in Th2 lymphocytes, plays an important role in regulating the balance of Th lymphocyte subclasses and induces differentiation and proliferation of B lymphocytes or microphages, thereby it is regarded as a principal factor in initiating UC. IL-4 and IL-4 receptor (IL-4R) gene are separately located in 5q31-33 (IBD5) and 16q12 (IBD1) which are supported by linkage analyses. Klein *et al* [111] and Aithal *et al*[112] found that certain alleles of the genes were associated with CD. Peng *et al* examined IL-4 polymorphisms in Chinese people and found IL-4-RP2 allele frequency was obviously higher in UC patients than in healthy control, whereas RP1 allele frequency was higher in healthy control than in UC patients[99].

IL-10, mainly excreted by Th3 or Th2 lymphocytes, can suppress the expression of IL-12 and TNF-α in natural killer cells or microphages, restrain activity or proliferation of Th1 lymphocytes. The functional deficiency of IL-10 may be an important maintenance factor for chronicity of IBD. The fact that IL-10 gene knockout mice are subject to colitis similar to human IBD is a persuasive evidence. But studies in recent years did not discover any allele was associated with IBD (allele IL-10 (-627, -1117, -1082, -592, -819) etc.)[101,107,113,114]. Koss *et al*[108] found IL-10 (-1082G/A) allele was associated with the down-regulation of IL-10 expression.

ICAM-1 plays an important role in regulating the homing of lymphocytes. Overexpression of ICAM-1 and significant lymphocyte infiltration have been found in intestinal mucosa of IBD patients. ICAM-1 gene is located in 19p13, which is supported by some linkage analysis. Yang *et al*[115,116] found that R241 allele was associated only with ANCA-positive UC. Contrarily, Braun *et al*[117] reported that ICAM-1 R241 allele and R/G241 heterogeneous mutation were much more frequent in UC patients than in healthy control irrespective of ANCA-positive or ANCA-negative.

Other investigators examined E-selection, L-selection, CCR2, CCR5, IL-6, NRAMP1 and IFN-r genes and found they had no association with IBD[95,118-121].

PROBLEMS AND PERSPECTIVES

Taking a wide view of these studies, we could find extensive discrepancies, which are usually interpreted by the view that IBD is a genetic disease with widespread heterogeneity[122]. It means that the complicated clinical phenotypes of IBD are determined by interaction of multiple genes with environmental factors. Single gene contributes little to IBD, and only polygenic defects with corresponding conformation underlie the complicated phenotypes of IBD. One phenotype may be determined by more than one conformation models of polygenic defects. Nevertheless, we should take into account of other aspects to resolve the discordant results in linkage analyses. A. Entrance criteria and clinical classifications of subjects must be controled more strictly and uniformly, since a minor mistake may influence the outcomes[123,124]. B. The microsatellite markers used by different investigators were not uniform, some investigators selected high-density markers, and others used somehow lower density markers. This could result in discrepancy conclusion. C. The sizes of sample were different among the studies, ranging from about 100 patients to more than 600 patients. Stratification studies performed using small sample sizes may cause false-negative error. Cavanaugh *et al*[41] carried out an international multicenter study, which involved 613 families from 12 study centers. By pooling of data sets, which were acquired from 12 independent centers using the same statistical method, despite the lack of convincing evidence for linkage based on data from individual center, they discovered unequivocal linkage for IBD on chromosome 16 (MLOD 5.79). D. The principle of linkage analysis is based on the view that crossing over in meiosis I is random and physical distance on chromosomes is necessarily in accord with genetic distance. The findings that significant association was found, but no linkage was suggested for the same subject group and the same loci demonstrated somehow theoretical disability of linkage analysis[49,125,126]. E. Other molecular biological mechanisms such as epigenetics may also play a role in initiating IBD[127]. In addition, if IBD is thought as a genetic disorder like familial adenomatous polyposis (certain mutations were inherited from parents, then somatic mutations were accumulated in certain cells such as macrophages or epithelial cells in intestinal mucosa or lymphoid tissue), all phenomena observed so far would not produce counterevidence. Today, linkage analysis has shed lights on genetic diseases such as diabetes mellitus, hypertension, asthma, Alzheimer' s disease and arteriosclerosis, as well as single-gene disorders. As for IBD, we have identified several linkage loci, which harbor a number of important candidate genes pending further confirmation by association analysis and functional analysis.

At present, about 30 candidate genes have been investigated by means of association analysis, and the majority of them either have no association with IBD or have not been confirmed by replication studies. With respect to HLA gene, though the majority of investigations discovered certain positively or negatively associated alleles, all the suggested alleles showed significant discrepancy. The three mutations in NOD2 gene have been consistently confirmed to be the independent susceptibility factors for CD in all-14 original studies except for one from a Japanese group, but how the variants can cause CD remains to be answered. Taking a wide view of all reports, which reached statistic significance, we discovered that frequencies of any alleles ever suggested by association analysis did not manifest a great absolute difference between patients and healthy controls. For instance, only about 20 % CD patients carried at least one of the three alleles of NOD2, whereas about 4-7 % healthy population also carried one of them. This shows that no allele ever studied demonstrates high specifity and sensitivity of the association with IBD and other

alleles need to be explored. It should be noted that the results of most studies, irrespective of positive or negative, did not absolutely ascertain the involvement of genes as susceptibility genes to IBD, since these could be confounded by a number of factors such as type I error or type II error caused by linkage disequilibrium or coincidence. In addition, there are many sequence variants in most genes, some of them are rare mutations and can only be properly analyzed in study of very large samples. Most investigators only detected variants in certain regions of the genes, instead of sequencing of whole gene of these alleles, therefore these results cannot represent the whole genes. The associations of some alleles with clinical phenotype of IBD have been detected by stratification study in many studies, but studies on the associations with the expression of cytokines involving the regulation of Th lymphocytes, were far less and more studies need to be carried out. The biochemical substances, which were ever suggested to be pathogenic factors for IBD, are of great variety, so it' s important to select proper candidate genes for association analysis. Since 1996, nearly 40 linkage analyses have identified several linkage loci in different chromosomes, such as IBD1, IBD2, IBD3, IBD4, and IBD5. Therefore, the genes located in such loci, and their products widely established as pathogenic factors for IBD, should be preferentially selected as candidate genes. Association analysis is an important method for unraveling the pathogenesis of IBD at gene level and will contribute tremendously to the understanding of IBD in the near future.

REFERENCES

1 **Probert CS**, Jayanthi V, Rampton DS, Mayberry JF. Epidemiology of inflammatory bowel disease in different ethnic and religious groups: limitations and aetiological clues. *Int J Colorectal Dis* 1996; **11**: 25-28

2 Z**heng JJ**. Incidence of inflammatory bowel disease in: Zheng JJ, Chu XQ, eds. Inflammatory bowel disease: basis and clinic. Beijing: *Science Press* 2001: 36-36

3 **Binder V**. Genetic epidemiology in inflammatory bowel disease. *Dig Dis* 1998; **16**: 351-355

4 **Heresbach D**, Gulwani-Akolkar B, Lesser M, Akolkar PN, Lin XY, Heresbach-Le Berre N, Bretagne JF, Katz S, Silver J. Anticipation in Crohn's disease may be influenced by gender and ethnicity of the transmitting parent. *Am J Gastroenterol* 1998; **93**: 2368-2372

5 **Satsangi J**, Grootscholten C, Holt H, Jewell DP. Clinical patterns of familial inflammatory bowel disease. *Gut* 1996; **38**: 738-741

6 **Tysk C,** Lindberg E, Jarnerot G, Floderus-Myrhed B. Ulcerative colitis and Crohn's disease in an unselected population of monozygotic and dizygotic Twins. A study of heritability and the inflence of smoking. *Gut* 1988; **29**: 990-996

7 **Thompson NP**, Driscoll R, Pounder RE, Wakefield AJ. Genetics versus environment in inflammatory bowel disease: result of a British twin Study. *BMJ* 1996; **312**: 95-96

8 **Roth MP,** Petersen GM, McElree C, Vadheim CM, Panish JF, Rotter JI. Familial empiric risk estimates of inflammatory bowel disease in Ashkenazi Jews. *Gastroenterology* 1989; **96**: 1016-1020

9 **Jayanthi V**, Probert CS, Pinder D, Wicks AC, Mayberry JF. Epidemiology of Crohn's disease in Indian migrants and the indigenous population in Leicestershire. *Q J Med* 1992; **82**: 125-138

10 **Blumberg RS**, Saubermann LJ, Strober W. Animal models of mucosal inflammation and their relation to human inflammatory bowel disease. *Curr Opin Immunol* 1999; **11**: 648-656

11 **Kosiewicz MM**, Nast CC, Krishnan A, Rivera-Nieves J, Moskaluk CA, Matsumoto S, Kozaiwa K, Cominelli F. Th1-type responses mediate spontaneous ileitis in a novel murine model of Crohn's disease. *J Clin Invest* 2001; **107**: 695-702

12 **Wirtz S**, Neurath MF. Animal models of intestinsl inflammation: new insight into the molecular pathogenesis and immunotherapy of inflammatory bowel disease. *Int J Colorectal Dis* 2000; **15**: 144-160

13 **Mckay DM**. Intestinal inflammation and the gut microflora. *Can J Gastroenterol* 1999; **13**: 509-516

14 **Shanahan F**. Probiotics and inflammatory bowel disease: is there a scientific rationale? *Inflamm Bowel Dis* 2000; **6**: 107-115

15 **Masseret E**, Boudeau J, Colombel JF, Neut C, Desreumaux P, Joly B, Cortot A, Darfeuille-Michaud A. Genetically related Escherichia coli strains associated with Crohn's disease. *Gut* 2001; **48**: 320-325

16 **Sutton CL,** Kim J, Yamane A, Dalwadi H, Wei B, Landers C, Targan SR, Braun J. Identification of a novel bacterial sequence associated with Crohn's disease. *Gastroenterology* 2000; **119**: 23-31

17 **Cosnes J,** Beaugerie L, Carbonnel F, Gendre JP. Smoking cessation and the course of Crohn's disease: an intervention study. *Gastroenterology* 2001; **120**: 1093-1099

18 **Tysk C,** Jarnerot G. Has smoking changed the epidemiology of ulcerative colitis? *Scand J Gastroenterol* 1992; **27**: 508-512

19 **Feehally J,** Burden AC, Mayberry JF, Probert CS, Roshan M, Samanta AK, Woods KL. Disease variations in Asians in Leicester. *Q J Med* 1993; **86**: 263-269

20 **Jayanthi V**, Probert CS, Pollock DJ, Baithun SI, Rampton DS, Mayberry JF. Low incidence of ulcerative colitis and proctitis in Bangladeshi migrants in Britain. *Digestion* 1992; **52**: 34-42

21 **Lander ES**, Schork NJ. Genetic dissection of complex traits. *Science* 1994; **265**: 2037-2048

22 **Karban A,** Eliakim R, Brant SR. Genetics of inflammatory bowel disease. *Isr Med Assoc J* 2002; **4**: 798-802

23 **Laharie D,** Debeugny S, Peeters M, Van Gossum A, Gower-Rousseau C, Belaiche J, Fiasse R, Dupas JL, Lerebours E, Piotte S, Cortot A, Vermeire S, Grandbastien B, Colombel JF. Inflammatory bowel disease in spouses and their offspring. *Gastroenterology* 2001; **120**: 816-819

24 **Orholm M**, Iselius L, Sorensen TI, Munkholm P, Langholz E, Binder V. Investigation of inheritance of chronic inflammatory bowel disease by complex segregation analysis. *BMJ* 1993; **306**: 20-24

25 **Kuster w**, Pascoe L, Purrmann J, Funk S, Majewski F, Pascoe L, Purrmann J. The genetics of Crohn disease: complex segregation analysis of a family study with 265 patients with Crohn disease and 5,387 relatives. *Am J Med Genet* 1989; **32**: 105-108

26 **Hugot JP**, Laurent-Puig P, Gower-Rousseau C, Olson JM, Lee JC, Beaugerie L, Naom I, Dupas JL, Van Gossum A, Orholm M, Bonaiti-Pellie C, Weissenbach J, Mathew CG, Lennard-Jones JE, Cortot A, Colombel JF, Thomas G. Mapping of a susceptibility locus for Crohn's disease on chromosome 16. *Nature* 1996; **379**: 821-823

27 **Satsangi J**, Parkes M, Louis E, Hashimoto L, Kato N, Welsh K, Terwilliger JD, Lathrop GM, Bell JI, Jewell DP. Two-stage genome-wide search in inflammatory bowel disease provides evidence for susceptibility loci on chromosomes 3, 7 and 12. *Nat Genet* 1996; **14**: 199-202

28 **Cho JH**, Nicolae DL, Gold LH, Fields CT, LaBuda MC, Rohal PM, Pickles MR, Qin L, Fu Y, Mann JS, Kirschner BS, Jabs EW, Weber J, Hanauer SB, Bayless TM, Brant SR. Identification of novel susceptibility loci for inflammatory bowel disease on chromosomes 1p, 3q, and 4q: evidence for epistasis between 1p and inflammatory bowel disease1. *Proc Natl Acad Sci U S A* 1998; **95**: 7502-7507

29 **Ma Y,** Ohmen JD, Li Z, Bentley LG, McElree C, Pressman S, Targan SR, Fischel-Ghodsian N, Rotter JI, Yang H. A genome-wide search identifies potential new susceptibility loci for Crohn's disease. *Inflamm Bowel Dis* 1999; **5**: 271-278

30 **Hampe J**, Schreiber S, Shaw SH, Lau KF, Bridger S, Macpherson AJ, Cardon LR, Sakul H, Harris TJ, Buckler A, Hall J, Stokkers P, van Deventer SJ, Nurnberg P, Mirza MM, Lee JC, Lennard-Jones JE, Mathew CG, Curran ME. A genomewide analysis provides evidence for novel linkages in inflammatory bowel disease in a large European cohort. *Am J Hum Genet* 1999; **64**: 808-816

31 **Duerr RH**, Barmada MM, Zhang L, Pfutzer R, Weeks DE. High-density genome scan in Crohn disease shows confirmed linkage to chromosome 14q11-12. *Am J Hum Genet* 2000; **66**: 1857-1862

32 **Rioux JD**, Silverberg MS, Daly MJ, Steinhart AH, McLeod RS, Griffiths AM, Green T, Brettin TS, Stone V, Bull SB, Bitton A, Williams CN, Greenberg GR, Cohen Z, Lander ES, Hudson TJ, Siminovitch KA. Genomewide search in Canadian families with inflammatory bowel disease reveals two novel susceptibility loci. *Am J Hum Genet* 2000; **66**: 1863-1870

33 **Fisher SA**, Hampe J, Macpherson AJ, Forbes A, Lennard-Jones JE, Schreiber S, Curran ME, Mathew CG, Lewis CM. Sex stratification of an inflammatory bowel disease genome search shows Male-specific linkage to the HLA region of chromosome 6. *Eur J Hum Genet* 2002; **10**: 259-265

34 **Brant SR,** Fu Y, Fields CT, Baltazar R, Ravenhill G, Pickles MR, Rohal PM, Mann J, Kirschner BS, Jabs EW, Bayless TM, Hanauer SB, Cho JH. American families with Crohn's disease have strong evidence for linkage to chromosome 16 but not chromosome 12. *Gastroenterology* 1998; **115**: 1056-1061

35 **Rioux JD**, Daly MJ, Green T, Stone V, Lander ES, Hudson TJ, Steinhart AH, Bull S, Cohen Z, Greenberg G, Griffiths A, McLeod R, Silverberg M, Williams CN, Siminovitch KA. Absence of linkage between inflammatory bowel disease and selected loci on chromosomes 3, 7, 12, and 16. *Gastroenterology* 1998; **115**: 1062-1065

36 **Curran ME**, Lau KF, Hampe J, Schreiber S, Bridger S, Macpherson AJ, Cardon LR, Sakul H, Harris TJ, Stokkers P, Van Deventer SJ, Mirza M, Raedler A, Kruis W, Meckler U, Theuer D, Herrmann T, Gionchetti P, Lee J, Mathew C, Lennard-Jones J. Genetic analysis of inflammatory bowel disease in a large European cohort supports linkage to chromosomes 12 and 16. *Gastroenterology* 1998; **115**: 1066-1071

37 **Annese V**, Latiano A, Bovio P, Forabosco P, Piepoli A, Lombardi G, Andreoli A, Astegiano M, Gionchetti P, Riegler G, Sturniolo GC, Clementi M, Rappaport E, Fortina P, Devoto M, Gasparini P, Andriulli A. Genetic analysis in Italian families with inflammatory bowel disease supports linkage to the IBD1 locus-a GISC study. *Eur J Hum Genet* 1999; **7**: 567-573

38 **Vermeire S**, Peeters M, Vlietinck R, Parkes M, Satsangi J, Jewell D, Rutgeerts P. Exclusion of linkage of Crohn's disease to previously reported regions on chromosomes 12, 7, and 3 in the Belgian population indicates genetic heterogeneity. *In Flamm Bowel Dis* 2000; **6**: 165-170

39 **Dechairo B**, Dimon C, van Heel D, Mackay I, Edwards M, Scambler P, Jewell D, Cardon L, Lench N, Carey A. Replication and extension studies of inflammatory bowel disease susceptibility regions confirm linkage to chromosome 6p (inflammatory bowel disease3). *Eur J Hum Genet* 2001; **9**: 627-633

40 **Paavola P,** Helio T, Kiuru M, Halme L, Turunen U, Terwilliger J, Karvonen AL, Julkunen R, Niemela S, Nurmi H, Farkkila M, Kontula K. Genetic analysis in Finnish families with inflammatory bowel disease supports linkage to chromosome 3p21.*Eur J Hum Genet* 2001; **9**: 328-334

41 **Cavanaugh J**. The IBD International Genetics Consortium. International collaboration provides convincing linkage replication in complex disease through analysis of a large pooled data set: Crohn disease and chromosome 16. *Am J Hum Genet* 2001; **68**: 1165-1171

42 **Ohmen JD**, Yang HY, Yamamoto KK, Zhao HY, Ma Y, Bentley LG, Huang Z, Gerwehr S, Pressman S, McElree C, Targan S, Rotter JI, Fischel-Ghodsian N. Susceptibility locus for inflammatory bowel disease on chromosome 16 has a role in Crohn's disease, but not in ulcerative colitis. *Hum Mol Genet* 1996; **5**: 1679-1683

43 **Parkes M,** Satsangi J, Lathrop GM, Bell JI, Jewell DP. Susceptibility loci in inflammatory bowel disease. *Lancet* 1996; **348**: 1588

44 **Cavanaugh JA**, Callen DF, Wilson SR, Stanford PM, Sraml ME, Gorska M, Crawford J, Whitmore SA, Shlegel C, Foote S, Kohonen-Corish M, Pavli P. Analysis of Australian Crohn's disease pedigrees refines the localization for susceptibility to inflammatory bowel disease on chromosome 16. *Ann Hum Genet* 1998; **62**: 291-298

45 **Mirza MM**, Lee J, Teare D, Hugot JP, Laurent-Puig P, Colombel JF, Hodgson SV, Thomas G, Easton DF, Lennard-Jones JE, Mathew CG. Evidence of linkage of the inflammatory bowel disease susceptibility locus on chromosome 16 (IBD1) to ulcerative colitis. *J Med Genet* 1998; **35**: 218-221

46 **Forabosco P**, Collins A, Latiano A, Annese V, Clementi M, Andriulli A, Fortina P, Devoto M, Morton NE. Combined segregation and linkage analysis of inflammatory bowel disease in the IBD1 region using severity to characterise Crohn's disease and ulcerative colitis. On behalf of the GISC. *Eur J Hum Genet* 2000; **8**: 846-852

47 **Brant SR**, Panhuysen CI, Bailey-Wilson JE, Rohal PM, Lee S, Mann J, Ravenhill G, Kirschner BS, Hanauer SB, Cho JH, Bayless TM. Linkage heterogeneity for the IBD1 locus in Crohn's disease pedigrees by disease onset and severity. *Gastroenterology* 2000; **119**: 1483-1490

48 **Akolkar PN,** Gulwani-Akolkar B, Lin XY, Zhou Z, Daly M, Katz S, Levine J, Present D, Gelb B, Desnick R, Mayer L, Silver J. The IBD1 locus for susceptibility to Crohn's disease has a greater impact in Ashkenazi Jews with early onset disease. *Am J Gastroenterol* 2001; **96**: 1127-1132

49 **Van Heel DA,** McGovern DP, Cardon LR, Dechairo BM, Lench NJ, Carey AH, Jewell DP. Fine mapping of the IBD1 locus did not identify Crohn disease-associated NOD2 variants: Implications for complex disease genetics. *Am J Med Genet* 2002; **111**: 253-259

50 **Zouali H**, Chamaillard M, Lesage S, Cezard JP, Colombel JF, Belaiche J, Almer S, Tysk C, Montague S, Gassull M, Christensen S, Finkel Y, Gower-Rousseau C, Modigliani R, Macry J, Selinger-Leneman H, Thomas G, Hugot JP. Genetic refinement and physical mapping of a chromosome 16q candidate region for inflammatory bowel disease. *Eur J Hum Genet* 2001; **9**: 731-742

51 **Hampe J**, Frenzel H, Mirza MM, Croucher PJ, Cuthbert A, Mascheretti S, Huse K, Platzer M, Bridger S, Meyer B, Nurnberg P, Stokkers P, Krawczak M, Mathew CG, Curran M, Schreiber S. Evidence for a NOD2-independent susceptibility locus for inflammatory bowel disease on chromosome 16p. *Proc Natl Acad Sci U S A* 2002; **99**: 321-326

52 **Satsangi J,** Welsh KI, Bunce M, Julier C, Farrant JM, Bell JI, Jewell DP. Contribution of genes of the major histocompatibility complex to susceptibility and disease phenotype in inflammatory bowel disease. *Lancet* 1996; **347**: 1212-1217

53 **Silverberg MS**. Evidence for linkage between Crohn disease and a locus near the major histocompatibility complex on chromosome 6 in a Canadian inflammatory bowel disease population. *Gastroenterology* 1999; **116**: A.820

54 **Hampe J,** Shaw SH, Saiz R, Leysens N, Lantermann A, Mascheretti S, Lynch NJ, MacPherson AJ, Bridger S, van Deventer S, Stokkers P, Morin P, Mirza MM, Forbes A, Lennard-Jones JE, Mathew CG, Curran ME, Schreiber S. Linkage of inflammatory bowel disease to human chromosome 6p. *Am J Hum Genet* 1999; **65**: 1647-1655

55 **Yang H,** Plevy SE, Taylor K, Tyan D, Fischel-Ghodsian N, McElree C, Targan SR, Rotter JI. Linkage of Crohn's disease to the major histocompatibility complex region is detected by multiple non-parametric analyses. *Gut* 1999; **44**: 519-526

56 **Duerr RH**, Barmada MM, Zhang L, Davis S, Preston RA, Chensny LJ, Brown JL, Ehrlich GD, Weeks DE, Aston CE. Linkage and association between inflammatory bowel disease and a locus on chromosome 12. *Am J Hum Genet* 1998; **63**: 95-100

57 **Yang H**, Ohmen JD, Ma Y, Bentley LG, Targan SR, Fischel-Ghodsian N, Rotter JI. Additional evidence of linkage between Crohn's disease and a putative locus on chromosome 12. *Genet Med* 1999; **1**: 194-198

58 **Lesage S**, Zouali H, Colombel JF, Belaiche J, Cezard JP, Tysk C, Almer S, Gassull M, Binder V, Chamaillard M, Le Gall I, Thomas G, Hugot JP. Genetic analyses of chromosome 12 loci in Crohn's disease. *Gut* 2000; **47**: 787-791

59 **Parkes M**, Barmada MM, Satsangi J, Weeks DE, Jewell DP, Duerr RH. The IBD2 locus shows linkage heterogeneity between ulcerative colitis and Crohn disease. *Am J Hum Genet* 2000; **67**: 1605-1610

60 **Hampe J,** Lynch NJ, Daniels S, Bridger S, Macpherson AJ, Stokkers P, Forbes A, Lennard-Jones JE, Mathew CG, Curran ME, Schreiber S. Fine mapping of the chromosome 3p susceptibility locus in inflammatory bowel disease. *Gut* 2001; **48**: 191-197

61 **Duerr RH,** Barmada MM, Zhang L. Evidence for an inflammatory bowel disease locus on chromosome 3p26: linkage, transmission / disequilibrium and partitioning of linkage. *Hum Mol Genet* 2002; **11**: 2599-2606

62 **Rioux JD**, Daly MJ, Silverberg MS, Lindblad K, Steinhart H, Cohen Z, Delmonte T, Kocher K, Miller K, Guschwan S, Kulbokas EJ, O'Leary S, Winchester E, Dewar K, Green T, Stone V, Chow C, Cohen A, Langelier D, Lapointe G, Gaudet D, Faith J, Branco N, Bull SB, McLeod RS, Griffiths AM, Bitton A, Greenberg GR, Lander ES, Siminovitch KA, Hudson TJ. Genetic variation in the 5q31 cytokine gene cluster confers susceptibility to Crohn disease. *Nat Genet* 2001; **29**: 223-228

63 **Vermeire S**, Satsangi J, Peeters M, Parkes M, Jewell DP, Vlietinck R, Rutgeerts P. Evidence for inflammatory bowel disease of a susceptibility locus on the X chromosome. *Gastroenterology* 2001; **120**: 834-840

64 **Dib C,** Faure S, Fizames C, Samson D, Drouot N, Vignal A, Millasseau P, Marc S, Hazan J, Seboun E, Lathrop M, Gyapay G, Morissette J, Weissenbach J. A comprehensive genetic map of the human genome based on 5,264 microsatellites. *Nature* 1996; **380**: 152-154

65 **Hugot JP**, Chamaillard M, Zouali H, Lesage S, Cezard JP, Belaiche J, Almer S, Tysk C, O'Morain CA, Gassull M, Binder V, Finkel Y, Cortot A, Modigliani R, Laurent-Puig P, Gower-Rousseau C, Macry J, Colombel JF, Sahbatou M, Thomas G. Association of NOD2 leucine-rich repeat variants with susceptibility to Crohn's disease. *Nature* 2001; **411**: 599-603

66 **Ogura Y**, Bonen DK, Inohara N, Nicolae DL, Chen FF, Ramos R, Britton H, Moran T, Karaliuskas R, Duerr RH, Achkar JP, Brant SR, Bayless TM, Kirschner BS, Hanauer SB, Nunez G, Cho JH. A frameshift mutation in NOD2 associated with susceptibility to Crohn's disease. *Nature* 2001; **411**: 603-606

67 **Hampe J**, Cuthbert A, Croucher PJ, Mirza MM, Mascheretti S, Fisher S,Frenzel H, King K, Hasselmeyer A, MacPherson AJ, Bridger S, van Deventer S, Forbes A, Nikolaus S, Lennard-Jones JE, Foelsch UR, Krawczak M, Lewis C, Schreiber S, Mathew CG. Association between insertion mutation in NOD2 gene and Crohn's disease in German and British populations. *Lancet* 2001; **357**: 1902-1904

68 **Lesage S**, Zouali H, Cezard JP, Colombel JF, Belaiche J, Almer S, Tysk C, O'Morain C, Gassull M, Binder V, Finkel Y, Modigliani R, Gower-Rousseau C, Macry J, Merlin F, Chamaillard M, Jannot AS, Thomas G, Hugot JP. EPWG-IBD Group; EPIMAD Group; GETAID Group. CARD15/NOD2 mutational analysis and genotype-phenotype correlation in 612 patients with inflammatory bowel disease. *Am J Hum Genet* 2002; **70**: 845-857

69 **Cuthbert AP,** Fisher SA, Mirza MM, King K, Hampe J, Croucher PJ, Mascheretti S, Sanderson J, Forbes A, Mansfield J, Schreiber S, Lewis CM, Mathew CG. The contribution of NOD2 gene mutations to the risk and site of disease in inflammatory bowel disease. *Gastroenterology* 2002; **122**: 867-874

70 **Murillo L,** Crusius JB, van Bodegraven AA, Alizadeh BZ, Pena AS. CARD15 gene and the classification of Crohn's disease. *Immunogenetics* 2002; **54**: 59-61

71 **Hampe J,** Grebe J, Nikolaus S, Solberg C, Croucher PJ, Mascheretti S, Jahnsen J, Moum B, Klump B, Krawczak M, Mirza MM, Foelsch UR, Vatn M, Schreiber S. Association of NOD2 (CARD 15) genotype with clinical course of Crohn's disease: a cohort study. *Lancet* 2002; **359**: 1661-1665

72 **Vermeire S,** Wild G, Kocher K, Cousineau J, Dufresne L, Bitton A, Langelier D, Pare P, Lapointe G, Cohen A, Daly MJ, Rioux JD. CARD15 genetic variation in a Quebec population: prevalence, genotype-phenotype relationship, and haplotype structure. *Am J Hum Genet* 2002; **71**: 74-83

73 **Radlmayr M,** Torok HP, Martin K, Folwaczny C. The c-insertion mutation of the NOD2 gene is associated with fistulizing and fibrostenotic phenotypes in Crohn's disease. *Gastroenterology* 2002; **122**: 2091-2092

74 **Inoue N**, Tamura K, Kinouchi Y, Fukuda Y, Takahashi S, Ogura Y, Inohara N, Nunez G, Kishi Y, Koike Y, Shimosegawa T, Shimoyama T, Hibi T. Lack of common NOD2 variants in Japanese patients with Crohn's disease. *Gastroenterology* 2002; **123**: 86-91

75 **Vermeire S**, Louis E, Rutgeerts P, De Vos M, Van Gossum A, Belaiche J, Pescatore P, Fiasse R, Pelckmans P, Vlietinck R, Merlin F, Zouali H, Thomas G, Colombel JF, Hugot JP. Belgian Group of Infliximab Expanded Access Program and Fondation Jean Dausset CEPH, Paris, France. NOD2/CARD15 does not influence response to infliximab in Crohn's disease. *Gastroenterology* 2002; **123**: 106-111

76 **Abreu MT,** Taylor KD, Lin YC, Hang T, Gaiennie J, Landers CJ, Vasiliauskas EA, Kam LY, Rojany M, Papadakis KA, Rotter JI, Targan SR, Yang H. Mutations in NOD2 are associated with fibrostenosing disease in patients with Crohn's disease. *Gastroenterology* 2002; **123**: 679-688

77 **Ahmad T,** Armuzzi A, Bunce M, Mulcahy-Hawes K, Marshall SE, Orchard TR,Crawshaw J, Large O, de Silva A, Cook JT, Barnardo M, Cullen S, Welsh KI, Jewell DP. The molecular classification of the clinical manifestations of Crohn's disease. *Gastroenterology* 2002; **122**: 854-866

78 **Inohara N**, Koseki T, del Peso L, Hu Y, Yee C, Chen S, Carrio R, Merino J, Liu D, Ni J, Nunez G. Nod1, an Apaf-1-like activator of caspase-9 and nuclear factor-kappaB. *J Biol Chem* 1999; **274**: 14560-14567

79 **Ogura Y,** Inohara N, Benito A, Chen FF, Yamaoka S, Nunez G. Nod2, a Nod1/Apaf-1 family member that is restricted to monocytes and activates NF-Kb. *J Bio Chem* 2001; **276**: 4812-4818

80 **Inohara N**, Ogura Y, Chen FF, Muto A, Nunez G. Hunan Nod1 confers responsiveness to bacterial lipopolysaccharides. *J Bio Chem* 2001; **276**: 2551-2554

81 **Schreiber S**, Nikolaus S, Hampe J. Activation of nuclear factor kappa B in inflammatory bowel disease. *Gut* 1998; **42**: 477-484

82 **Zareie M,** Singh PK, Irvine EJ, Sherman PM, McKay DM, Perdue MH. Monocyte/macrophage activation by normal bacteria and bacterial products: implications for altered epithelial function in Crohn's disease. *Am J Pathol* 2001; **158**: 1101-1109

83 **Duerr RH**, Neigut DA. Molecularly defined HLA-DR2 alleles in ulcerative colitis and an antineutrophil cytoplasmic antibody-positive subgroup. *Gastroenterology* 1995; **108**: 423-427

84 **Nakajima A,** Matsuhashi N, Kodama T, Yazaki Y, Takazoe M, Kimura A. HLA-linked susceptibility and resistance genes in Crohn's disease. *Gastroenterology* 1995; **109**: 1462-1467

85 **Reinshagen M,** Loeliger C, Kuehnl P, Weiss U, Manfras BJ, Adler G, Boehm BO. HLA class II gene frequencies in Crohn's disease: a population based analysis in Germany. *Gut* 1996; **38**: 538-542

86 **Hesresbach D**, Alizadeh M, Bretagne JF, Gautier A, Quillivic F, Lemarchand B, Gosselin M, Genetet B, Semana G. Investigation of the association of major histocompatibility complex genes, including HLA class I, class II and TAP genes, with clinical forms of Crohn's disease. *Eur J Immunogenet* 1996; **23**: 141-151

87 **Danze PM,** Colombel JF, Jacquot S, Loste MN, Heresbach D, Ategbo S, Khamassi S, Perichon B, Semana G, Charron D, Cezard JP. Association of HLA class II genes with susceptibility to Crohn's disease. *Gut* 1996; **39**: 69-72

88 **Heresbach D,** Alizadeh M, Reumaux D, Colombel JF, Delamaire M, Danze PM, Gosselin M, Genetet B, Bretagne JF, Semana G. Are HLA-DR or TAP genes genetic markers of severity in ulcerative colitis? *J Autoimmun* 1996; **9**: 777-784

89 **Bouma G,** Oudkerk Pool M, Crusius JB, Schreuder GM, Hellemans HP, Meijer BU, Kostense PJ, Giphart MJ, Meuwissen SG, Pena AS. Evidence for genetic heterogeneity in inflammatory bowel disease (IBD); HLA genes in the predisposition to suffer from ulcerative colitis (UC) and Crohn's disease (CD). *Clin Exp Immunol* 1997; **109**: 175-179

90 **Fernandez Arquero M**, Lopez Nava G, De la Concha EG, Figueredo MA, Santa Cruz S, Dumitru CG, Diaz Rubio M, Garcia Paredes J. HLA-DR2 gene and Spanish patients with ulcerative colitis. *Rev Esp Enferm Dig* 1998; **90**: 243-249

91 **Cariappa A,** Sands B, Forcione D, Finkelstein D, Podolsky DK, Pillai S. Analysis of MHC class II DP, DQ and DR alleles in Crohn's disease. *Gut* 1998; **43**: 210-215

92 **Bouma G**, Crusius JB, Garcia-Gonzalez MA, Meijer BU, Hellemans HP, Hakvoort RJ, Schreuder GM, Kostense PJ, Meuwissen SG, Pena AS. Genetic markers in clinically well defined patients with ulcerative colitis (UC). *Clin Exp Immunol* 1999; **115**: 294-300

93 **Yoshitake S,** Kimura A, Okada M, Yao T, Sasazuki T. HLA class II alleles in Japanese patients with inflammatory bowel disease. *Tissue Antigens* 1999; **53**: 350-358

94 **Stokkers PC,** Reitsma PH, Tytgat GN, van Deventer SJ. HLA-DR and -DQ phenotypes in inflammatory bowel disease: a meta-analysis. *Gut* 1999; **45**: 395-401

95 **Hirv K,** Seyfarth M, Uibo R, Kull K, Salupere R, Latza U, Rink L. Polymorphisms in tumor necrosis factor and adhesion molecule genes in patients with inflammatory bowel disease: associations with HLA-DR and -DQ alleles and subclinical markers. *Scand J Gastroenterol* 1999; **34**: 1025-1032

96 **Seki SS,** Sugimura K, Ota M, Matsuzawa J, Katsuyama Y, Ishizuka K, Mochizuki T, Suzuki K, Yoneyama O, Mizuki N, Honma T, Inoko H, Asakura H. Stratification analysis of MICA

triplet repeat polymorphisms and HLA antigens associated with ulcerative colitis in Japanese. *Tissue Antigens* 2001; **58**: 71-76

97 **Lantermann A**, Hampe J, Kim WH, Winter TA, Kidd M, Nagy M, Folsch UR, Schreiber S. Investigation of HLA-DPA1 genotypes as predictors of inflammatory bowel disease in the German, South African, and South Korean populations. *Int J Colorectal Dis* 2002; **17**: 238-244

98 **Orchard TR**, Chua CN, Ahmad T, Cheng H, Welsh KI, Jewell DP. Uveitis and erythema nodosum in inflammatory bowel disease: clinical features and the role of HLA genes. *Gastroenterology* 2002; **123**: 714-718

99 **Peng Z,** Hu P, Cui Y, Li C. Interleukin (IL)-1beta, IL-1 receptor antagonist and IL-4 gene polymorphisms in ulcerative colitis in the Chinese. *Zhonghua Neike Zazhi* 2002; **41**: 248-251

100 **Craggs A**, West S, Curtis A, Welfare M, Hudson M, Donaldson P, Mansfield J. Absence of a genetic association between IL-1RN and IL-1B gene polymorphisms in ulcerative colitis and Crohn disease in multiple populations from northeast England. *Scand J Gastroenterol* 2001; **36**: 1173-1178

101 **Donaldson PT**, Norris S, Constantini PK, Bernal W, Harrison P, Williams R. The interleukin-1 and interleukin-10 gene polymorphisms in primary sclerosing cholangitis: no associations with disease susceptibility / resistance. *J Hepatol* 2000; **32**: 882-886

102 **Nemetz A**, Toth M, Garcia-Gonzalez MA, Zagoni T, Feher J, Pena AS, Tulassay Z. Allelic variation at the interleukin 1beta gene is associated with decreased bone mass in patients with inflammatory bowel diseases. *Gut* 2001; **49**: 644-649

103 **Nemetz A**, Nosti-Escanilla MP, Molnar T, Kope A, Kovacs A, Feher J, Tulassay Z, Nagy F, Garcia-Gonzalez MA, Pena AS. IL1B gene polymorphisms influence the course and severity of inflammatory bowel disease. *Immunogenetics* 1999; **49**: 527-531

104 **Mwantembe O,** Gaillard MC, Barkhuizen M, Pillay V, Berry SD, Dewar JB, Song E. Ethnic differences in allelic associations of the interleukin-1 gene cluster in South African patients with inflammatory bowel disease (IBD) and in control individuals. *Immunogenetics* 2001; **52**: 249-254

105 **van Heel DA**, Udalova IA, De Silva AP, McGovern DP, Kinouchi Y, Hull J, Lench NJ, Cardon LR, Carey AH, Jewell DP, Kwiatkowski D. Inflammatory bowel disease is associated with a TNF polymorphism that affects an interaction between the OCT1 and NF-kappa B transcription factors. *Hum Mol Genet* 2002; **11**: 1281-1289

106 **Sashio H,** Tamura K, Ito R, Yamamoto Y, Bamba H, Kosaka T, Fukui S, Sawada K, Fukuda Y, Tamura K, Satomi M, Shimoyama T, Furuyama J. Polymorphisms of the TNF gene and the TNF receptor superfamily member 1B gene are associated with susceptibility to ulcerative colitis and Crohn's disease, respectively. *Immunogenetics* 2002; **53**: 1020-1027

107 **Mitchell SA,** Grove J, Spurkland A, Boberg KM, Fleming KA, Day CP, Schrumpf E, Chapman RW. European Study Group of Primary Sclerosing Cholangitis. Association of the tumor necrosis factor alpha -308 but not the interleukin 10 -627 promoter polymorphism with genetic susceptibility to primary sclerosing cholangitis. *Gut* 2001; **49**: 288-294

108 **Koss K,** Satsangi J, Welsh KI, Jewell DP. Cytokine (TNF alpha, LT alpha and IL-10) polymorphisms in inflammatory bowel diseases and normal controls: differential effects on production and allele frequencies. *Genes Immun* 2000; **1**: 185-190

109 **Louis E,** Peeters M, Franchimont D, Seidel L, Fontaine F, Demolin G, Croes F, Dupont P, Davin L, Omri S, Rutgeerts P, Belaiche J. Tumour necrosis factor (TNF) gene polymorphism in Crohn's disease (CD): influence on disease behaviour? *Clin Exp Immunol* 2000; **119**: 64-68

110 **Negoro K,** Kinouchi Y, Hiwatashi N, Takahashi S, Takagi S, Satoh J, Shimosegawa T, Toyota T. Crohn'disease is associated with novel polymorphisms in the 5'-flanking region of the tumor necrosis factor gene. *Gastroenterology* 1999; **117**: 1062-1068

111 **Klein W,** Tromm A, Griga T, Fricke H, Folwaczny C, Hocke M, Eitner K, Marx M, Duerig N, Epplen JT. Interleukin-4 and interleukin-4 receptor gene polymorphisms in inflammatory bowel diseases. *Genes Immun* 2001; **2**: 287-289

112 **Aithal GP,** Day CP, Leathart J, Daly AK, Hudson M. Association of single nucleotide polymorphisms in the interleukin-4 gene and interleukin-4 receptor gene with Crohn's disease in a British population. *Genes Immun* 2001; **2**: 44-47

113 **Aithal GP**, Craggs A, Day CP, Welfare M, Daly AK, Mansfield JC, Hudson M. Role of polymorphisms in the interleukin-10 gene in determining disease susceptibility and phenotype in inflammatory bowel disease. *Dig Dis Sci* 2001; **46**: 1520-1525

114 **Klein W,** Tromm A, Griga T, Fricke H, Folwaczny C, Hocke M, Eitner K, Marx M, Runte M, Epplen JT. The IL-10 gene is not involved in the predisposition to inflammatory bowel disease. *Electrophoresis* 2000; **21**: 3578-3582

115 **Yang H**. Analysis of ICAM-1 gene polymorphism in immunologic subsets of inflammatory bowel disease. *Exp Clin Immunogenet* 1997; **14**: 214-225

116 **Yang H,** Vora DK, Targan SR, Toyoda H, Beaudet AL, Rotter JI. Intercellular adhesion molecule 1 gene associations with immunologic subsets of inflammatory bowel disease. *Gastroenterology* 1995; **109**: 440-448

117 **Braun C,** Zahn R, Martin K, Albert E, Folwaczny C. Polymorphisms of the ICAM-1 gene are associated with inflammatory bowel disease, regardless of the p-ANCA status. *Clin Immunol* 2001; **101**: 357-360

118 **Klein W,** Tromm A, Griga T, Fricke H, Folwaczny C, Hocke M, Eitner K, Marx M, Epplen JT. The polymorphism at position -174 of the IL-6 gene is not associated with inflammatory bowel disease. *Eur J Gastroenterol Hepatol* 2001; **13**: 45-47

119 **Koss K**, Satsangi J, Welsh KI, Jewell DP. Is interleukin-6 important in inflammatory bowel disease? *Genes Immun* 2000; **1**: 207-212

120 **Stokkers PC,** de Heer K, Leegwater AC, Reitsma PH, Tytgat GN, van Deventer SJ. Inflammatory bowel disease and the genes for the natural resistance-associated macrophage protein-1 and the interferon-gamma receptor 1. *Int J Colorectal Dis* 1999; **14**: 13-17

121 **Hampe J,** Hermann B, Bridger S, MacPherson AJ, Mathew CG, Schreiber S. The interferon-gamma gene as a positional and functional candidate gene for inflammatory bowel disease. *Int J Colorectal Dis* 1998; **13**: 260-263

122 **Xia B,** Crusius JBA, Meuwissen SGM, Pea AS. Inflammatory bowel disease: definition, epidemiology, etiologic aspects, and immunogenetic studies. *World J Gastroenterol* 1998; **4**: 446-458

123 **Silverberg MS,** Daly MJ, Moskovitz DN, Rioux JD, McLeod RS, Cohen Z, Greenberg GR, Hudson TJ, Siminovitch KA, Steinhart AH. Diagnostic misclassification reduces the ability to detect linkage in inflammatory bowel disease genetic studies. *Gut* 2001; **49**: 773-776

124 **Ghosh S**. Linking genotype with phenotype in inflammatory bowel disease-Will we ever have reagent standard patients? *Dis Markers* 2000; **16**: 167-171

125 **Hampe J**, Wienker T, Nurnberg P, Schreiber S. Mapping genes for polygenic disorders: consideration for study design in the complex trait of inflammatory bowel disease. *Hum Hered* 2000; **50**: 91-101

126 **Schreiber S**. Genetics of inflammayory bowel disease: a puzzle with contradictions? *Gut* 2000; **47**: 746–747

127 **Petronis A**, Petroniene R. Epigenetics of inflammatory bowel disease. *Gut* 2000; **47**: 302-306

Edited by Yuan HJ and Wang XL

P.O.Box 2345, Beijing 100023,China
Fax: +86-10-85381893
E-mail: wjg@wjgnet.com www.wjgnet.com

World J Gastroenterol 2003;9(8):1657-1661
World Journal of Gastroenterology
 ISSN 1007-9327

• REVIEW •

RNA interference: Antiviral weapon and beyond

Quan-Chu Wang, Qing-He Nie, Zhi-Hua Feng

Quan-Chu Wang, Qing-He Nie, Zhi-Hua Feng, The Center of Diagnosis and Treatment for Infectious Diseases of Chinese PLA, Tangdu Hospital, Fourth Military Medical University, Xi' an 710038, Shaanxi Province, China
Correspondence to: Qing-He Nie, The Center of Diagnosis and Treatment for Infectious Diseases of Chinese PLA, Tangdu Hospital, Fourth Military Medical University, Xi' an 710038, Shaanxi Province, China. nieqinghe@hotmail.com
Telephone: +86-29-3377452 **Fax:** +86-29-3377452
Received: 2003-04-04 **Accepted:** 2003-05-11

Abstract

RNA interference (RNAi) is a remarkable type of gene regulation based on sequence-specific targeting and degradation of RNA. The term encompasses related pathways found in a broad range of eukaryotic organisms, including fungi, plants, and animals. RNA interference is part of a sophisticated network of interconnected pathways for cellular defense, RNA surveillance, and development and it may become a powerful tool to manipulate gene expression experimentally. RNAi technology is currently being evaluated not only as an extremely powerful instrument for functional genomic analyses, but also as a potentially useful method to develop specific dsRNA based gene-silencing therapeutics. Several laboratories have been interested in using RNAi to control viral infection and many reports in *Nature* and in *Cell* show that short interfering (si) RNAs can inhibit infection by HIV-1, polio and hepatitis C viruses in a sequence-specific manner. RNA-based strategies for gene inhibition in mammalian cells have recently been described, which offer the promise of antiviral therapy.

Wang QC, Nie QH, Feng ZH. RNA interference: Antiviral weapon and beyond. *World J Gastroenterol* 2003; 9(8): 1657-1661
http://www.wjgnet.com/1007-9327/9/1657.asp

INTRODUCTION

RNA, long upstaged by its more glamorous sibling, DNA, is turning out to have star qualities of its own. *Science* hails the electrifying discoveries of RNA interference as 2002's breakthrough of the year. RNA interference, also named RNA silencing or post transcriptional gene silencing (PTGS), is a phenomenon in which small double-stranded RNA molecules induce sequence-specific degradation of homologous single-stranded RNA[1]. RNAi activity plays a role in host-cell protection from viruses and transposons in plants and insects. From a practical perspective, RNAi can therefore be used to target gene expression and has been proved to be a very powerful technique to knock down specific genes to evaluate their physiological roles in *Caenorhabditis elegans*, *Drosophila melanogaster*, and humans[2-5].

Previous reports have show that RNAi has following important characteristics[7-11]. (1) RNAi can be induced through transfection or microinjection of long double-stranded RNA. In plants and invertebrates, the double-stranded RNA is cleaved into 19- to 23-nt RNA fragments known as small interfering RNAs (siRNA). siRNAs are double-stranded RNA (dsRNA) molecules with characteristic 2-nucleotide over hanging 3' ends. They act as intermediates in the RNA interference (RNAi) pathway, which is thought to protect cells from harmful transposons and highly repetitive sequences by targeting their RNA transcripts for endonucleolytic cleavage and subsequent exonucleolytic degradation. siRNA-directed RNA degradation is central to the antiviral response in plants, where it represents a potent form of sequence-based immunity. Only RNA molecules <30 bases in length can be used to exclusively induce RNAi in mammalian cells because longer molecules also activate the nonspecific double-stranded RNA-dependent response. (2) RNAi has amplification activity and different durations. In plants and nematodes, RNAi activity is long-term and disseminates throughout the organism via an uncharacterized amplification mechanism. In mammalian cells, amplification activity seems absent, and interference activity is transient, lasting for only 3-5 days. More recently, DNA expression vectors have been developed to express hairpin or duplex siRNA, which employ the type III class of RNA polymerase promoters to drive the expression of siRNA molecules. In addition, stable cell lines containing siRNA expression plasmids have been produced to induce RNAi over longer durations. (3) RNAi can be induced locally and then spread throughout the organism in plants, and this aspect of the process likely reflects its role in viral defense.

The power of siRNAs springs from the cellular biochemistry of the RNAi pathway. Like antisense oligonucleotides, siRNAs use sequence complementarity to target an mRNA for destruction. Unlike the antisense pathway, the RNAi pathway couples the specificity of an RNA guide to the stability and efficiency of a multiple-turnover protein enzyme. The ability to manipulate RNA interference thus sets the stage for realizing a wide variety of practical applications of biotechnology ranging from molecular farming to possibly even gene therapy in animals. Gitlin *et al*[12] showed that RNAi drastically reduced polio infection in HeLa cells. While analysing the antiviral effects of siRNA over a course of viral infection, they found that siRNA-resistant viruses turned out to carry silent base-pair mismatches in the siRNA complementary sequences. The authors argued, therefore, that if RNAi was to be used for therapeutic reasons, siRNA needed to be designed against highly conserved parts of the viral genome. Adelman et *al*[13] demonstrated that dsRNA-mediated interference also could act as a viral defense mechanism in mosquito cells. These observations are consistent with RNA interference as the mechanism of resistance to DEN-2 in transformed mosquito cells. Kay *et al*[14] went beyond the *in vitro* systems and genetically engineered mice that expressed siRNA against hepatitis C RNA to show that this technique also worked well *in vivo* to prevent viral replication. After this bumper crop of promising results, it remains to be seen how close we are to RNAi-mediated antiviral therapy. Because siRNA taps into natural gene-silencing pathways, a new form of intracellular immunization against viral infection might be just around the corner.

INTERFERING HCV

HCV genome is a single-stranded RNA that functions as both a messenger RNA and a replication template, making it an

attractive target for the study of RNA interference[15-21]. Previous results from Izumi RE' s laboratory[22] identified a small (60 nt) RNA from the yeast S. cerevisiae that specifically inhibited internal ribosome entry site (IRES)-mediated translation programmed by poliovirus (PV) and hepatitis C virus (HCV) 5' -untranslated region (5' UTR). The yeast inhibitor RNA (called RNAi) was found to efficiently compete with viral 5' UTR for binding to several cellular polypeptides that presumably play important roles in IRES-mediated translation. RNA interference offers further hope that a novel approach to silencing troublesome genes will become a valuable disease-fighting tool. But the therapy must leap many hurdles before it can be safely applied to humans. The power of small RNAs to shut down specific gene activities has now been brought to bear on an animal model of hepatitis. Mice infused with a siRNA against a cell death receptor recovered their liver function after experimentally induced injury. The work of Song *et al*[23] suggests that one type of entirely natural nucleic acid, small interfering RNAs (siRNAs), may hold promise as a therapeutic agent even without further engineering. These investigators provided the first *in vivo* evidence that infusion of siRNAs into an animal could alleviate disease, in this case hepatitis. Assembly of a siRNA strand into an RISC seemed to protect it from rapid degradation, the normal fate of small single-stranded RNA in cells. With this durability in mind, Song *et al*. set out to test whether direct infusion of siRNAs into mice might protect them from fulminant hepatitis. Both mice and humans with this disease suffered severe hepatic failure complicated with consequent encephalopathy, cerebral edema, metabolic imbalance and organ collapse. Infusing a solution of siRNA into a mouse' s tail, in massive amount, equivalent to half the animal' s blood volume protected it against hepatitis. And in animals that were already ailing, RNAi shut down the inflammation enough to allow the liver to recover. Despite the traumatic delivery method, the mice didn' t appear to suffer side effects. They gave mice injections of siRNA designed to shut down a gene called Fas, when over-activated during inflammatory response, it induced liver cells to self-destruct. The next day, the animals were given an antibody that sent Fas into hyperdrive. Control mice died of acute liver failure within a few days, but 82 % of the siRNA-treated mice remained free from serious disease and survived. About 80 % and 90 % of their liver cells incorporated the siRNA. Furthermore, the RNA molecules functioned for 10 days before fading completely after 3 weeks, lasting roughly three times longer than in previous studies. Another set of animals faced a different challenge: injections of cells with ConA, which compelled the immune system to attack the liver and produced the scarring seen in viral hepatitis. Animals infused with siRNA developed no liver damage. Silencing Fas expression with RNAi holds some therapeutic promise to prevent liver injury by protecting hepatocytes from cytotoxicity. In addition, biologists have agreeed that the best strategy would be to aim siRNA directly at hepatitis B or C viruses, but that would require a different siRNA than the one used by Song' s team. Evidences from several laboratories suggest that, in petri dishes, siRNA can stop hepatitis C from replicating. McCaffrey *et al*[24] showed that transgene expression could be suppressed in adult mice by synthetic small interfering RNAs and small-hairpin RNAs transcribed *in vivo* from DNA templates. They also showed the therapeutic potential of this technique by demonstrating effective targeting of a sequence from hepatitis C virus by RNA interference *in vivo*. Wilson *et al*[25] found RNA interference blocked gene expression and RNA synthesis from hepatitis C replicons propagated in human liver cells. Double-stranded small interfering RNA (siRNA) molecules designed to target the HCV genome were introduced through electroporation into a human hepatoma cell line (Huh-7) that contained an HCV subgenomic replicon. Two siRNA dramatically reduced virus-specific protein expression and RNA synthesis to levels that were 90 % less than those seen in cells treated with negative control siRNA. These same siRNA protected naive Huh-7 cells from challenge with HCV replicon RNA. Treatment of cells with synthetic siRNA was effective for more than 72 h, but the duration of RNA interference could be extended beyond 3 weeks through stable expression of complementary strands of the interfering RNA by using a bicistronic expression vector. These results suggest that a gene-therapeutic approach with siRNA can ultimately be used to treat HCV.

The utility of siRNA as a therapy against HCV infection will depend on the development of efficient delivery systems that induce long-lasting RNAi activity[26]. HCV is an attractive target for its localization in the liver, an organ that can be readily targeted by nucleic acid molecules and viral vectors. In future, chemically modified synthetic siRNA, with improved resistance to nucleases coupled with enhanced duration of RNAi, may become a possibility for therapeutic applications. On the other hand, gene therapy offers another possibility to express siRNA that targets HCV in a patient' s liver. Based on the above experiments, the use of siRNA as a treatment for HCV infections has great potential for use alone or in combination with conventional IFN/ribavirin therapy as means to decrease virus loads and eventually clear the persistent viruses from its host[27]. As therapeutic agents, siRNAs have enticing properties. Their actions appear to be short-lived in mammals, they are sequence specific and natural, cellular products and may therefore not produce toxic metabolites. Nonetheless, caveats for clinical use remain. Delivering siRNAs to the appropriate cells is a major challenge. siRNAs have thus far only been administered intravenously to mice by ' hydrodynamic transfection' , the rapid infusion of siRNA in a volume one-tenth the mass of the animal. Furthermore, the liver seems to be particularly receptive to exogenous RNA. Better delivery methods-such as formulation of siRNAs with compounds that promote transit across cell membranes-are clearly required before siRNAs can be used in therapy, especially to suppress gene expression in tissues other than in the liver. Nonetheless, the results of Song *et al*[23] have revealed the power of siRNAs in a disease model.

FACILITATING FUNCTIONAL GENOMICS

Until recently, RNA interference has been viewed primarily as a thorn in the side of plant molecular geneticists, limiting expression of transgenes and interfering with a number of applications that require consistent, high-level transgene expression. With our present understanding of the process, however, it is clear that RNA interference has enormous potential for engineering control of gene expression, as well as for a tool in functional genomics. It can be experimentally induced with high efficiency and targeted to a single specific gene or to a family of related genes. Likewise, dsRNA-induced TGS (transcriptional gene silencing) may have similar potential to control gene expression. Unwanted RNA interference, on the other hand, can be alleviated using viral suppressor technology or mutants impaired in silencing[28-30].

Genome-sequencing projects have provided tremendous amount of information about the genetic make-up of an organism. One way for finding out what genes do is to inactivate them, and to study the effects, in ' model' organisms. Kamath *et al*[4] used double-stranded RNAs to rapidly and transiently inactivate 16 757 of the worm' s predicted protein-coding genes. Meanwhile, Ashrafi and co-workers[31] have analysed these genes specifically to see if they had a role in regulating body fat. Together, their work has set a new standard

for systematic, genome-wide genetic studies. RNAi-based loss-of-function screens like these are tremendously powerful. Yet they have some disadvantages compared with classical genetic screening. For instance, some genes are more difficult to target by RNAi than others. And there are many non-coding RNAs, which are not translated into proteins. It remains to be seen if they are susceptible to RNAi. But there are still a vast number of protein-coding genes, from many different organisms, to study in detailed RNAi-based functional analyses, and this will keep the army of cell and molecular biologists busy for some time. Soon it will be possible to carry out RNAi-based screens in animal and human cells, using short synthetic double-stranded RNAs or plasmid- or virus-based DNA molecules that encode hairpin RNAs[32-34]. With the development of phenotypic read-outs based on cell biology, the hunt will begin.

SILENCING HIV-1

RNA interference represents an exciting new technology that may have therapeutic applications in the treatment of viral infections such as HCV and HIV. RNA interference is also found in HIV. Previous reports have shown that siRNA directed against the HIV genome can effectively inhibit virus production in cell-culture systems[35-38]. In addition, RNAi activity directed toward the major HIV receptor protein, CD4, led to decreased entry of HIV into cells[39-41]. However, replication of HIV occurred through an integrated DNA genome. Does it mean that RNAi is ineffective in clearing the virus? By targeting several regions of the HIV-1 genome, Jacque *et al*[42] showed that siRNA mediated viral genome degradation and caused downregulation of viral gene expression and they proved that RNAi worked even when the viral genome was contained within the nucleoprotein complex. They also showed that intracellularly made siRNA (transcribed from a plasmid) worked well, providing possible ways for delivering gene-therapy agents against HIV. To assess the effects of RNAi on HIV-1 infection, Novina *et al*[43] targeted both cellular and viral RNAs. The HeLa-derived cell line Magi-CCR5 (which expresses human CD4, and the chemokine receptors CCR5 and CXCR4) was transfected with short interfering RNA specific for the gene of interest and then infected with HIV-1. Cells transfected with siRNA specific for CD4 expressed CD4 mRNA at a level eight times lower than control cells, which led to a four-fold reduction in HIV-1 entry. Therefore, siRNA-directed silencing of CD4 specifically inhibited HIV entry and hence replication. Next, the viral structural protein Gag was targeted by transfecting cells with siRNA specific for the p24 component of this polyprotein. p24-siRNA-transfected cells showed a four-fold decrease in viral protein compared with controls, implying that viral amplification was inhibited by this approach. The authors also carried out transfection assays on human T cells, to assess the effect of RNAi on viral infectivity in a more physiological context. H9 cells were transfected with siRNA against green fluorescent protein (GFP) and were infected with an HIV-1 strain in which the *nef* gene was replaced with GFP. Again, silencing of viral gene expression occurred, resulting in reduced GFP and HIV-1 protein expression. These and other recent studies[44-46] show that siRNA can inhibit viral replication at several stages of infection, including very early stages, when viruses are most vulnerable. Infection can also be blocked by targeting either viral genes or host genes that are involved in the viral life cycle. It has been shown that siRNA directed against HIV-1 has the potential to be useful treatments. This study extended work by Lee *et al*[47,48] who used a vector-based RNAi strategy to silence an HIV-1 gene, and established that siRNA technology could be used to suppress multiple steps of the HIV-1 life cycle. They described a mammalian Pol III promoter system capable of expressing functional double-stranded siRNA following transfection into human cells. In the case of the 293 cells cotransfected with the HIV-1 pNL4-3 proviral DNA and the siRNA-producing constructs, they were able to achieve up to 4 logs of inhibition of expression from the HIV-1 DNA. Martinez *et al*[49] found that suppression of chemokine receptor expression by RNA interference could inhibit HIV-1 replication. Their results demonstrate that RNAi may be used to block HIV entry and replication through the blockade of cellular gene expression. Park *et al*[50] showed that HIV-1 replication was totally suppressed in a sequence-specific manner by six long dsRNAs containing the HIV-1 gag and env genes in HIV-1-infected cells. Especially, E2 dsRNA containing the major CD4-binding domain sequence of gp120, dramatically inhibited the expression of the HIV-1 p24 antigen in PBMCs for a relatively long time. Coburn *et al*[51] demonstrated that siRNA duplexes targeted against the essential Tat and Rev regulatory proteins encoded by HIV-1 could specifically block Tat and Rev expression and function. More importantly, they showed that these same siRNAs could effectively inhibit HIV-1 gene expression and replication in cell cultures, including those of human T-cell lines and primary lymphocytes. These results demonstrate the utility of RNAi for modulating the HIV replication cycle and provide the evidence that genomic HIV-1 RNA, existing within a nucleoprotein reverse-transcription complex, is amenable to siRNA-mediated degradation.

But does it actually work as an antiviral weapon? More recent studies have suggested that it does, at least in cells in culture dishes. Gitlin *et al*[12] reported that specific siRNA administered to human cells from the outside, like a drug, could enter them and protect them against infection by the rapidly multiplying poliovirus. Jacque *et al*[42], meanwhile, reported similar results in their studies with the AIDS virus HIV-1. These authors further demonstrated that if the siRNA were expressed from inside cells, rather than simply administered from the outside, the cells became largely immune to subsequent HIV-1 is infection. These results are exciting, and suggest that RNAi perfectly suitable to many antiviral applications. But one important factor is that not all viral RNA sequences are equally accessible to siRNA. Some sequences might be buried within secondary structures or within highly folded regions in target RNAs, whereas others might come form tight complexes with proteins that obscure their recognition. Optimal targets must be chosen by trial and error. Another issue is that viruses often produce mutated progeny molecules. Some of these naturally help the viruses escape immune surveillance or inhibition by drugs, but they might also prevent recognition by siRNA. To overcome this obstacle, one might need to target viral RNA sequences that are conserved and normally invariant between different strains, or to simultaneously target several viral sequences. Finally, the problem of how to deliver siRNA to cells needs to be addressed. They can certainly be delivered efficiently to cells in culture, but methods must be improved before RNAi can be used in animals, let alone patients.

FUTURE DIRECTIONS

The field of RNAi is moving at an impressive pace and generating exciting results that are clearly associated with RNA interference, transgene silencing and transposon mobilization[52-55]. Possible links to X-chromosome inactivation, imprinting and interferon response have also been suggested, but not yet firmly established. RNAi also has a considerable economic potential, especially in agriculture. A better understanding of PTGS should allow a more efficient response to viral infection and the development of transgene/host associations that can override silencing to allow the expression of interested proteins. Now that early mouse embryos are known to be susceptible to

RNAi, it will be critical to determine whether this technique can also be applied to tissue culture[56-60]. The possible repercussions of RNAi in mammals are potentially far-reaching in the fight against certain diseases such as cancer or virus/ parasite infection, as well as for the analysis of more fundamental problems in neurobiology and cell and developmental biology. In the next ten years, RNAi will probably be regarded as one of the major breakthroughs of the 2000s. A new report has shown that incubating a target mRNA with *Drosophila* embryonic extracts and the cognate dsRNA *in vitro* leads to its degradation in a process that recapitulates many of the features of RNA interference *in vivo* (including sequence specificity, length dependence and amplification). This important study has paved the way for a biochemical analysis of RNA interference. In relation to RNA interference in mammals, it is important to note that in contrast to the sequence-specific RNAi effect observed in mouse embryos, this new study has shown that incubation of an mRNA with rabbit reticulocyte lysates and dsRNA induces nonspecific mRNA degradation, one possible reason for this difference could be that the interferon response present in rabbit reticulocyte lysate is not functional in early mouse embryos[61-65].

Although antiviral RNAi technology has not yet been optimized, the phenomenon does appear to be both general and effective. In 1988, the concept of "intracellular immunization" was proposed, whereby one could express within cells inhibitory molecules (usually proteins) that could protect these cells from specific viral infections in the future[66-75]. The promise of intracellular immunization now appears to be closer to reality - although amazingly, through the use of small RNAs rather than peptides or proteins. The potential of using RNAi activity for the treatment of viral diseases and cancer has aroused a great deal of interests in the scientific community. Many laboratories have reported the use of RNAi activity in cultured cells infected with HIV, human papillomavirus, and polio or containing a variety of cancer genes. The clinical applications of RNA is just around the corner.

REFERENCES

1 **Zamore PD**. Ancient pathways programmed by small RNAs. *Science* 2002; **296**: 1265-1269
2 **Williams RW**, Rubin GM. ARGONAUTE1 is required for efficient RNA interference in Drosophila embryos. *Proc Natl Acad Sci U S A* 2002; **99**: 6889-6894
3 **Ge Q**, McManus MT, Nguyen T, Shen CH, Sharp PA, Eisen HN, Chen J. RNA interference of influenza virus production by directly targeting mRNA for degradation and indirectly inhibiting all viral RNA transcription. *Proc Natl Acad Sci U S A* 2003; **100**: 2718-2723
4 **Kamath RS**, Fraser AG, Dong Y, Poulin G, Durbin R, Gotta M, Kanapin A, Le Bot N, Moreno S, Sohrmann M, Welchman DP, Zipperlen P, Ahringer J. Systematic functional analysis of the Caenorhabditis elegans genome using RNAi. *Nature* 2003; **421**: 231-237
5 **Schwarz DS**, Hutvagner G, Haley B, Zamore PD. Evidence that siRNAs function as guides, not primers, in the Drosophila and human RNAi pathways. *Mol Cell* 2002; **10**: 537-548
6 **Pantaleo V,** Rubino L, Russo M. Replication of Carnation Italian ringspot virus defective interfering RNA in Saccharomyces cerevisiae. *J Virol* 2003; **77**: 2116-2123
7 **Dennis C**. Small RNAs: the genome's guiding hand? *Nature* 2002; **420**: 732
8 **Jia Q,** Sun R. Inhibition of gammaherpesvirus replication by RNA interference. *J Virol* 2003; **77**: 3301-3306
9 **Van Wezel R**, Liu H, Wu Z, Stanley J, Hong Y. Contribution of the zinc finger to zinc and DNA binding by a suppressor of post-transcriptional gene silencing. *J Virol* 2003; **77**: 696-700
10 **Qu F**, Ren T, Morris TJ. The coat protein of turnip crinkle virus suppresses posttranscriptional gene silencing at an early initiation step. *J Virol* 2003; **77**: 511-522
11 **Ray D**, White KA. An internally located RNA hairpin enhances replication of Tomato bushy stunt virus RNAs. *J Virol* 2003; **77**: 245-257
12 **Gitlin L**, Karelsky S, Andino R. Short interfering RNA confers intracellular antiviral immunity in human cells. *Nature* 2002; **418**: 430-434
13 **Adelman ZN**, Sanchez-Vargas I, Travanty EA, Carlson JO, Beaty BJ, Blair CD, Olson KE. RNA sicencing of dengue virus type 2 replication in transformed C6/36 mosquito cells transcribing an inverted-repeat RNA derived from the virus genome. *J Virol* 2002; **76**: 12925-12933
14 **McCaffrey AP**, Kay MA. A story of mice and men. *Gene Ther* 2002; **9**: 1563
15 **Gong GZ**, Lai LY, Jiang YF, He Y, Su XS. HCV replication in PBMC and its influence on interferon therapy. *World J Gastroenterol* 2003; **9**: 291-294
16 **Yan FM**, Chen AS, Hao F, Zhao XP, Gu CH, Zhao LB, Yang DL, Hao LJ. Hepatitis C virus may infect extrahepatic tissues in patients with hepatitis C. *World J Gastroenterol* 2000; **6**: 805-811
17 **Yu YC**, Mao Q, Gu CH, Li QF, Wang YM. Activity of HDV ribozymes to trans-cleave HCV RNA. *World J Gastroenterol* 2002; **8**: 694-698
18 **Song ZQ**, Hao F, Min F, Ma QY, Liu GD. Hepatitis C virus infection of human hepatoma cell line 7721 *in vitro*. *World J Gastroenterol* 2001; **7**: 685-689
19 **Dai YM,** Shou ZP, Ni CR, Wang NJ, Zhang SP. Localization of HCV RNA and capsid protein in human hepatocellular carcinoma. *World J Gastroenterol* 2000; **6**: 136-137
20 **Cheng JL**, Liu BL, Zhang Y, Tong WB, Yan Z, Feng BF. Hepatitis C virus in human B lymphocytes transformed by Epstein-Barr virus in vitro by in situ reverse transcriptase-polymerase chain reaction. *World J Gastroenterol* 2001; **7**: 370-375
21 **Meier V**, Mihm S, Wietzke Braun P, Ramadori G. HCV-RNA positivity in peripheral blood mononuclear cells of patients with chronic HCV infection: does it really mean viral replication? *World J Gastroenterol* 2001; **7**: 228-234
22 **Izumi RE**, Valdez B, Banerjee R, Srivastava M, Dasgupta A. Nucleolin stimulates viral internal ribosome entry site-mediated translation. *Virus Res* 2001; **76**: 17-29
23 **Song E,** Lee SK, Wang J, Ince N, Ouyang N, Min J, Chen J, Shankar P, Lieberman J. RNA interference targeting Fas protects mice from fulminant hepatitis. *Nat Med* 2003; **9**: 347-351
24 **McCaffrey AP,** Meuse L, Pham TT, Conklin DS, Hannon GJ, Kay MA. RNA interference in adult mice. *Nature* 2002; **418**: 38-39
25 **Wilson JA**, Jayasena S, Khvorova A, Sabatinos S, Rodrigue-Gervais IG, Arya S, Sarangi F, Harris-Brandts M, Beaulieu S, Richardson CD. RNA interference blocks gene expression and RNA synthesis from hepatitis C replicons propagated in human liver cells. *Proc Natl Acad Sci U S A* 2003; **100**: 2783-2788
26 **Randall G**, Grakoui A, Rice CM. Clearance of replicating hepatitis C virus replicon RNAs in cell culture by small interfering RNAs. *Proc Natl Acad Sci U S A* 2003; **100**: 235-240
27 **Zamore PD**, Aronin N. siRNAs knock down hepatitis. *Nat Med* 2003; **9**: 266-267
28 **Pomerantz RJ.** RNA interference meets HIV-1: will silence be golden? *Nat Med* 2002; **8**: 659-660
29 **Mallory AC**, Parks G, Endres MW, Baulcombe D, Bowman LH, Pruss GJ, Vance VB. The amplicon-plus system for high-level expression of transgenes in plants. *Nat Biotechnol* 2002; **20**: 622-625
30 **Caplen NJ,** Zheng Z, Falgout B, Morgan RA. Inhibition of viral gene expression and replication in mosquito cells by dsRNA-triggered RNA interference. *Mol Ther* 2002; **6**: 243-251
31 **Ashrafi K,** Chang FY, Watts JL, Fraser AG, Kamath RS, Ahringer J, Ruvkun G. Genome-wide RNAi analysis of Caenorhabditis elegans fat regulatory genes. *Nature* 2003; **421**: 268-272
32 **Miyagishi M**, Taira K. U6 promoter-driven siRNA with four uridine 3' overhangs efficiently suppress targeted gene expression in mammalian cells. *Nat Biotechnol* 2002; **20**: 497-500
33 **Nicholson RH**, Nicholson AW. Molecular characterization of a mouse cDNA encoding Dicer, a ribonuclease III ortholog involved in RNA interference. *Mamm Genome* 2002; **13**: 67-73
34 **Adelman ZN**, Blair CD, Carlson JO, Beaty BJ, Olson KE. Sindbis virus-induced silencing of dengue viruses in mosquitoes. *Insect Mol Biol* 2001; **10**: 265-273

35 **Hu WY,** Myers CP, Kilzer JM, Pfaff SL, Bushman FD. Inhibition of retroviral pathogenesis by RNA interference. *Curr Biol* 2002; **12**: 1301-1311

36 **Dector MA**, Romero P, Lopez S, Arias CF. Rotavirus gene silencing by small interfering RNAs. *EMBO Rep* 2002; **3**: 1175-1180

37 **Surabhi RM**, Gaynor RB. RNA interference directed against viral and cellular targets inhibits human immunodeficiency Virus Type 1 replication. *J Virol* 2002; **76**: 12963-12973

38 **Martinez de Alba AE**, Flores R, Hernandez C. Two chloroplastic viroids induce the accumulation of small RNAs associated with posttranscriptional gene silencing. *J Virol* 2002; 76: 13094-13096

39 **Park WS**, Miyano-Kurosaki N, Hayafune M, Nakajima E, Matsuzaki T, Shimada F, Takaku H. Prevention of HIV-1 infection in human peripheral blood mononuclear cells by specific RNA interference. *Nucleic Acids Res* 2002; **30**: 4830-4835

40 **Kitabwalla M**, Ruprecht RM. RNA interference-a new weapon against HIV and beyond. *N Engl J Med* 2002; **347**: 1364-1367

41 **Capodici J**, Kariko K, Weissman D. Inhibition of HIV-1 infection by small interfering RNA-mediated RNAinterference. *J Immunol* 2002; **169**: 5196-5201

42 **Jacque JM,** Triques K, Stevenson M. Modulation of HIV-1 replication by RNA interference. *Nature* 2002; **418**: 435-438

43 **Novina CD**, Murray MF, Dykxhoorn DM, Beresford PJ, Riess J, Lee SK, Collman RG, Lieberman J, Shankar P, Sharp PA. siRNA-directed inhibition of HIV-1 infection.*Nat Med* 2002; **8**: 681-686

44 **Wojtkowiak A**, Siek A, Alejska M, Jarmolowski A, Szweykowska-Kulinska Z, Figlerowicz M. RNAi and viral vectors as useful tools in the functional genomics of plants. Construction of BMV-based vectors for RNA delivery into plant cells. *Cell Mol Biol Lett* 2002; **7**: 511-522

45 **Xia H,** Mao Q, Paulson HL, Davidson BL. siRNA-mediated gene silencing *in vitro* and *in vivo*. *Nat Biotechnol* 2002; **20**: 1006-1010

46 **Rhodes A**, James W. Inhibition of heterologous strains of HIV by antisense RNA. *AIDS* 1991; **5**: 145-151

47 **Lee NS**, Dohjima T, Bauer G, Li H, Li MJ, Ehsani A, Salvaterra P, Rossi J. Expression of small interfering RNAs targeted against HIV-1 rev transcripts in human cells. *Nat Biotecrnol* 2002; **20**: 500-505

48 **Song E**, Lee SK, Wang J, Ince N, Ouyang N, Min J, Chen J, Shankar P, Lieberman J. RNA interference targeting Fas protects mice from fulminant hepatitis. *Nat Med* 2003; **9**: 347-351

49 **Martinez MA**, Clotet B, Este JA. RNA interference of HIV replication. *Trends Immunol* 2002; **23**: 559-561

50 **Park WS**, Miyano-Kurosaki N, Hayafune M, Nakajima E, Matsuzaki T, Shimada F, Takaku H. Prevention of HIV-1 infection in human peripheral blood mononuclear cells by specific RNA interference. *Nucleic Acids Res* 2002; **30**: 4830-4835

51 **Coburn GA**, Cullen BR. Potent and specific inhibition of human immunodeficiency virus type 1 replication by RNA interference. *J Virol* 2002; **76**: 9225-9231

52 **Couzin J**. RNA interference. Mini RNA molecules shield mouse liver from hepatitis. *Science* 2003; **299**: 995

53 **Jia Q,** Sun R. Inhibition of gammaherpesvirus replication by RNA interference. *J Virol* 2003; **77**: 3301-3306

54 **Agami R**. RNAi and related mechanisms and their potential use for therapy. *Curr Opin Chem Biol* 2002; **6**: 829-834

55 **Lin SL**, Ying SY. D-RNAi (messenger RNA-antisense DNA interference) as a novel defense system against cancer and viral infections. *Curr Cancer Drug Targets* 2001; **1**: 241-247

56 **Di Serio F**, Schob H, Iglesias A, Tarina C, Bouldoires E, Meins F Jr. Sense- and antisense-mediated gene silencing in tobacco is inhibited by the same viral suppressors and is associated with accumulation of small RNAs. *Proc Natl Acad Sci U S A* 2001; **98**: 6506-6510

57 **Vaucheret H**, Fagard M. Transcriptional gene silencing in plants: targets, inducers and regulators. *Trends Genet* 2001; **17**: 29-35

58 **Blair CD**, Adelman ZN, Olson KE. Molecular strategies for interrupting arthropod-borne virus transmission by mosquitoes. *Clin Microbiol Rev* 2000; **13**: 651-661

59 **Morel JB,** Vaucheret H. Post-transcriptional gene silencing mutants. *Plant Mol Biol* 2000; **43**: 275-284

60 **Hammond SM**, Bernstein E, Beach D, Hannon GJ. An RNA-directed nuclease mediates post-transcriptional gene silencing in Drosophila cells. *Nature* 2000; **404**: 293-296

61 **Yamamoto T**, Omoto S, Mizuguchi M, Mizukami H, Okuyama H, Okada N, Saksena NK, Brisibe EA, Otake K, Fuji YR. Double-stranded nef RNA interferes with human immunodeficiency virus type 1 replication. *Microbiol Immunol* 2002; **46**: 809-817

62 **Couzin J**. Breakthrough of the year. Small RNAs make big splash. *Science* 2002; **298**: 2296-2297

63 **Brummelkamp TR**, Bernards R, Agami R. Stable suppression of tumorigenicity by virus-mediated RNA interference. *Cancer Cell* 2002; **2**: 243-247

64 **Olson KE,** Adelman ZN, Travanty EA, Sanchez-Vargas I, Beaty BJ, Blair CD. Developing arbovirus resistance in mosquitoes. *Insect Biochem Mol Biol* 2002; **32**: 1333-1343

65 **Jiang M**, Milner J. Selective silencing of viral gene expression in HPV-positive human cervical carcinoma cells treated with siRNA, a primer of RNA interference. *Oncogene* 2002; **21**: 6041-6048

66 **Hao CQ**, Feng ZH, Zhou YX, Nie QH, Li JG, Jia ZS, Liang XS, Xie YM, Cao YZ, Kang WZ. Construction,package and identification of replication-deficient recombinant adenovirus expression vector of HCV C. *Shijie Huaren Xiaohua Zazhi* 2003; **11**: 144-147

67 **Jia ZS**, Chen L, Hao CQ, Feng ZH, Li JG, Wang JP, Cao YZ, Zhou YX. Intracellular immunization by hammerhead ribozyme against HCV. *Shijie Huaren Xiaohua Zazhi* 2003; **11**: 148-150

68 **Cheng YQ**, Nie QH, Zhou YX, Huang XF, Luo H, Yang HG. Ultrastructure characteristics of HCV infected human trophoblast cells in culture. *Shijie Huaren Xiaohua Zazhi* 2003; **11**: 151-156

69 **Liang XS**, Lian JQ, Zhou YX, Nie QH, Hao CQ. Inhibitory effect of IRES specific inhibitor RNA on HCV IRES mediated protein translation. *Shijie Huaren Xiaohua Zazhi* 2003; **11**: 157-160

70 **Sun L**, Zhou YX, Hao CQ, Feng ZH, Zhao J, Hu PZ, Fu Y, Ma FC, Chang JQ, Wang JP, Nie QH. Effect of DNA vaccine on anti-HCV infection in mice with subcutaneous inoculating tumor. *Shijie Huaren Xiaohua Zazhi* 2003; **11**: 165-168

71 **Sun Y**, Cheng RX, Feng DY, Ouyang XM, Zheng H. Effect of HCV NS3 on proliferation and phosphorylation of MAPK in human hepatocytes. *Shijie Huaren Xiaohua Zazhi* 2003; **11**: 173-177

72 **Zhang L**, Zhao GZ, Li Y, Shi LL. Dynamic changes of HVR1 quasispecies in chronic hepatitis C after IFN therapy. *Shijie Huaren Xiaohua Zazhi* 2003; **11**: 182-184

73 **Li L**, Cheng J, Li F, Wang JJ, Zhang J, Wu Q, Han P, Chen GF, Ji D, Li K. Clinical and pathological characteristics of steatohepatitis in patients with chronic hepatitis C virus infection. *Shijie Huaren Xiaohua Zazhi* 2002; **10**: 1009-1013

74 **Zhang J**, Cheng J, Li L, Liu AB, Wu Q, Li K, Dong J, Wang L, Lu YY. Apolipoprotein A I and A II in the patients infected with hepatitis C virus. *Shijie Huaren Xiaohua Zazhi* 2002; **10**: 1014-1017

75 **Cheng J**, Ren JY, Li L, Lu ZM, Li K, Hong Y, Lu YY, Wang G, Liu Y, Zhang LX, Chen JM. Liver steatosis of transgenic mice expressing hepatitis C virus structural proteins. *Shijie Huaren Xiaohua Zazhi* 2002; **10**: 1022-1026

Edited by Yuan HT and Wang XL

P.O.Box 2345, Beijing 100023,China
Fax: +86-10-85381893
E-mail: wjg@wjgnet.com www.wjgnet.com

World J Gastroenterol 2003;9(8):1662-1666
World Journal of Gastroenterology
 ISSN 1007-9327

• GASTRIC CANCER •

Growth, invasion, metastasis, differentiation, angiogenesis and apoptosis of gastric cancer regulated by expression of PTEN encoding products

Hua-Chuan Zheng, Yi-Ling Li, Jin-Min Sun, Xue-Fei Yang, Xiao-Han Li, Wei-Guo Jiang, Yin-Chang Zhang, Yan Xin

Hua-Chuan Zheng, Jin-Min Sun, Xue-Fei Yang, Yin-Chang Zhang, Yan Xin, Lab. 4, Cancer Institute, The First Affiliated Hospital of China Medical University, Shenyang 110001, Liaoning Province, China
Yi-Ling Li, Department of Digestive Diseases, The First Affiliated Hospital of China Medical University, Shenyang 110001, Liaoning Province, China
Xiao-Han Li, Wei-Guo Jiang, Department of Pathology, The Second Affiliated Hospital of China Medical University, Shenyang 110004, Liaoning Province, China
Correspondence to: Hua-Chuan Zheng, Lab. 4, Cancer Institute, The First Affiliated Hospital of China Medical University, Shenyang 110001, Liaoning Province, China. zheng_huachuan@hotmail.com
Telephone: +86-24-23256666 Ext 6351 **Fax:** +86-24-23253443
Received: 2003-03-05 **Accepted:** 2003-03-29

Abstract

AIM: To investigate expression of PTEN in gastric cancer and to explore its roles in tumorigenesis and progression of gastric cancer.

METHODS: Formalin-fixed and paraffin-embedded tissues of adjacent non-tumor mucosa and primary foci from 113 cases of gastric cancers were studied for the expression of PTEN and Caspase-3 and microvessel density (MVD) by streptavidin-peroxidase (S-P) immunohistochemistry with antibodies against PTEN, Caspase-3, and CD34. The relationship between PTEN and Caspase 3 expression and clinicopathological parameters of tumors was compared.

RESULTS: Primary gastric cancer cells expressed PTEN less frequently than adjacent epithelial cells of primary foci (54.9 % *vs* 89.4 %; P=0.000, χ^2=33.474). PTEN expression was significantly associated with invasive depth (P=0.003, rs=0.274), metastasis (P=0.036, rs=0.197), growth pattern (P=0.008, rs=0.282), Lauren's classification (P=0.000, rs=0.345), and histological classification (P=0.005, rs=0.262) of tumors, but not with tumor size (P=0.639, rs=0.045), Borrmann's classification (P=0.544, rs=0.070) or TNM staging (P=0.172, rs=0.129). PTEN expression was negatively correlated with MDV in primary gastric cancer (P=0.020, F=5.558). Primary gastric cancer cells showed less frequent immunoreactivity to Caspase-3 than adjacent epithelial cells of primary foci (32.7 % *vs* 50.4 %; P=0.007,χ^2=7.286). Caspase-3 expression was dependent of PTEN expression in primary gastric cancer cells (P=0.000, χ^2=15.266).

CONCLUSION: Down-regulated expression of PTEN plays an important role in tumorigenesis, progression, growth, differentiation and angiogenesis of gastric cancer. Low expression of PTEN can decrease expression of Caspase-3 to disorder apoptosis of tumor cells, which might explain the molecular mechanisms of PTEN contributions to tumorigenesis and progression of gastric cancer.

Zheng HC, Li YL, Sun JM, Yang XF, Li XH, Jiang WG, Zhang YC, Xin Y. Growth, invasion, metastasis, differentiation, angiogenesis and apoptosis of gastric cancer regulated by expression of PTEN encoding products. *World J Gastroenterol* 2003; 9(8): 1662-1666
http://www.wjgnet.com/1007-9327/9/1662.asp

INTRODUCTION

Human suppressor gene, PTEN/MMAC1/TEP1 (phosphatase and tensin homology deleted from chromosome ten/mutated in multiple advanced cancer 1/TGF-β-regulated and epithelial cell enriched phosphatase 1), located on chromosome 10q23. 3 encodes a dual specific protein- phospholipid phosphatase that is involved in regulation of a variety of signal transduction pathways[1]. PTEN inhibits shc' s (src-homology collagen) phosphorylation following epidermal growth factor (EGF) stimulation and therefore blocks the activation of the Ras/MAP-kinase (MAPK) pathway[2]. Another mechanism that involves the protein phosphatase activity of PTEN is dephosphorylation and inactivation of focal adhesion kinase (FAK), thus playing a crucial role of PTEN in the interaction between extracellular matrix and cytoskeleton[3,4]. Besides its function as the protein phosphase, PTEN acts as a phospholipid phosphatase with phosphatidylinosiol 3,4,5-triphosphate (PIP_3) as a substrate[5-7]. Recently, many studies have shown that there are several putative mechanisms relating to tumor suppression as follows: inhibiting cell invasion and metastasis by dephosphorylating FAK, inhibiting cell apoptosis and increasing cell growth by dephosphorylating PIP_3, restraining cell differentiation by inhibiting MAPK signal pathway[5,8,9]. Mutation or abnormal expression of PTEN protein occurs commonly in multiple tumors and significantly correlates with tumorigenesis and progression of different malignancies[10-20]. It was reportedly suggested that deletion or mutation of PTEN could enhance the expression of vascular epithelial growth factor (VEGF) and matrix metalloproteinases (MMPs), which in turn closely correlated with tumor angiogenesis and metastasis[10-14]. Jones *et al*.[15] found that activation of PTEN signal pathway could reduce expression of Caspase-3, resulting in inhibition of cellular apoptosis.

Gastric cancer is one of the commonest malignancies in China, and even in the world. In patients with gastric cancer, the natural disease process consists of carcinogenesis, metastasis and eventual death. However, the molecular aspects of carcinogenesis and progression of gastric cancer remain elusive[16-18]. In the current study, we evaluated the expression of PTEN in adjacent epithelial cells, primary gastric cancer cells and intented to find if there was any correlation between its expression and clinicopathological features and microvessel density (MVD) of gastric cancer, as well as between PTEN and Caspase-3 expression in primary foci in order to clarify its role in tumorigenesis and progression of gastric cancer.

MATERIALS AND METHODS

Patients

One hundred and thirteen cases of surgically resected specimens of gastric cancer were collected from the Second Affiliated Hospital of China Medical University from Sept, 1997 to Feb, 2001, including 83 men and 30 women. Their age ranged from 26 to 83 years, with the mean age of 57.1 years. Among them, 38 tumors were accompanied by lymph node or organ metastasis. None of the patients had received radiotherapy or chemotherapy before operation.

Preparation of tissue samples

Adjacent mucosa and primary lesions of each case were fixed in 4 % formaldehyde solution, embedded in paraffin, incised into 4 μm sections and mounted on poly-lysine-coated slides. These sections were stained by hematoxylin-and-eosin method to confirm their histological diagnosis and other microscopic characteristics.

Evaluation of clinicopathological parameters

Clinical staging for each gastric carcinoma was evaluated according to the TNM system. Gross appearance of the tumors was described according to the Borrmann' s classification. Histomorphological architecture of the tumor samples was expressed on the basis of Lauren' s and Nakamura' s classifications. Growth patterns of gastric cancer were classified in the light of Zhang' s classification. Tumor diameter, invasive depth and metastasis were determined as well.

Immunohistochemistry

Representative and consecutive sections were studied with streptavidin-peroxidase immunohistochemistry (S-P kit from Zhongshan Biotech., China). Anti-PTEN, anti-CD34 and anti-Caspase-3 antibodies were purchased from Antibody Dignostica (USA), Zhongshan (China), and DAKO (Japan), respectively. All procedures were implemented according to the product recommendation. For negative controls, sections were processed as above but treated with PBS (0.01 mol/L, pH7.4) instead of primary antibodies.

Evaluation of PTEN and Caspase-3 immunostaining

The immunoreactivity to PTEN and Caspase-3 was localized in the cytoplasm. From 5 randomly selected representative fields of each section, two independent observers counted one hundred cells. According to the proportion of positive ones in counted cells, the degree of immunostaining was graded as follows: negative(-), ≤5 %; weakly positive (+), 5-25 %; moderately positive (++), 25-50 %; and strongly positive (+++), ≥50 %.

Microvessel density counting

Modified Weidner' s method was used to calculate MVD by anti-CD34 immunohistochemistry, which was described as follows. Microvessels in sclerotic areas within tumor, where microvessels were sparse and immediately adjacent areas of unaffected gastric tissue were considered as hot points in vessel counts. Observers selected five such areas and counted individual microvessels in a 400×field (i.e. 40×objective lens and 10×ocular lens, 0.1885 mm^2 per field). Any brown staining endothelial cell or endothelial cell cluster that was clearly separated from adjacent microvessel, tumor cells, and other connective tissue elements was considered as a single, countable microvessel. They must agree on what constituted a single microvessel.

Statistical analysis

Statistical evaluation was performed using chi-square test to compare the rates between different groups, using Spearman test to analyze the rank data, and using the one-way ANOVA to differentiate the means of different groups. $P<0.05$ was considered as statistically significant. SPSS 10.0 software was employed to analyze all data.

RESULTS

PTEN expression in adjacent epithelial cells and cancer cells of primary gastric cancer

Figures 1-3 show that PTEN was positively expressed in the nuclei of adjacent epithelial cells, lymphocytes and cancer cells of primary foci of gastric cancer. In this study, epithelial cells and cancer cells were immunostained for PTEN protein in 89.4 % and 54.9 % of the tumors, respectively. There was a significant difference between them ($P<0.05$) (Table 1).

Table 1 PTEN expression in adjacent epithelial cells and cancer cells of primary gastric cancer

Groups	*n*	PTEN expression				
		-	+	++	+++	PR(%)
Adjacent epithelial cells	113	12	10	23	68	89.4
Primary cancer cells	113	51	13	11	38	54.9[a]

Notes: PR: positive rate, [a]$P=0.000$ ($\chi^2=33.474$, Pearson' R=0.385).

Table 2 Relationship between expression of PTEN in primary foci and clinicopathological features of gastric cancer

Clinicopathological features	*n*	PTEN expression					*rs*	*P* value
		-	+	++	+++	PR(%)		
Tumor size							0.045	0.639
<4 cm	47	20	6	4	17	57.4		
≥4 cm	66	31	7	7	21	53.0		
Borrmann's Classification							0.070	0.544
I/II	28	12	3	3	10	57.1		
III/IV	59	30	5	6	18	49.2		
Invasive depth							0.274	0.003
Above submucosa	26	7	4	2	13	73.1		
Muscularis propria	34	14	2	4	14	58.8		
Below subserosa	53	30	7	5	11	56.6		
Metastasis							0.197	0.036
Negative	76	28	10	8	29	62.7		
Positive	38	23	3	3	9	39.5		
TNM staging							0.129	0.172
O	18	7	4	1	6	61.1		
I	28	11	2	2	13	60.7		
II	40	19	3	5	13	52.5		
III	17	7	3	3	4	58.8		
IV	10	7	1	0	2	30.0		
Growth pattern							0.282	0.008
Mass	23	8	2	2	11	65.2		
Nest	30	12	3	4	11	60.0		
Diffuse	34	22	3	3	6	35.3		
Lauren's Classification							0.345	0.000
Intestinal type	36	8	2	6	20	77.8		
Diffuse type	57	32	10	3	12	43.9		
Mixed type	20	11	1	2	6	45.0		
Histological classification							0.262	0.005
Differentiated	53	18	3	8	24	66.0		
Undifferentiated	60	33	10	3	14	45.0		

Notes: PR: positive rate.

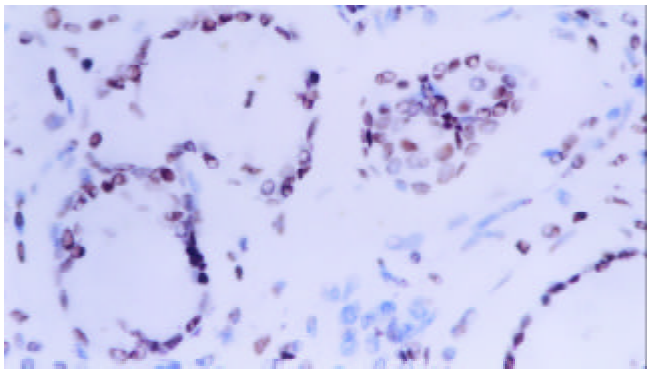

Figure 1 PTEN was immunostained in cell nuclear. It was strongly expressed in gastric epithelial cells (+++) (S-P, ×400).

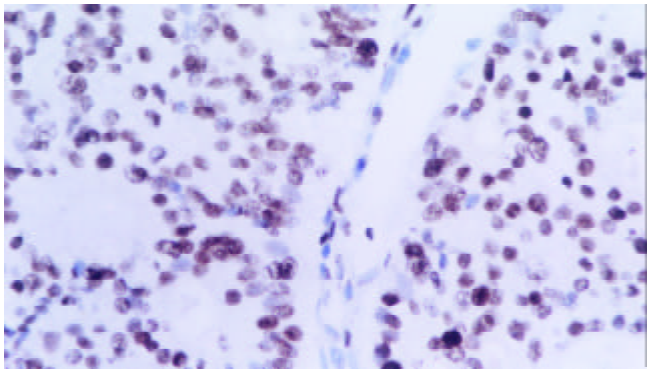

Figure 2 PTEN was strongly expressed in gastric well-differentiated adenocarcinoma (+++) (S-P, ×400).

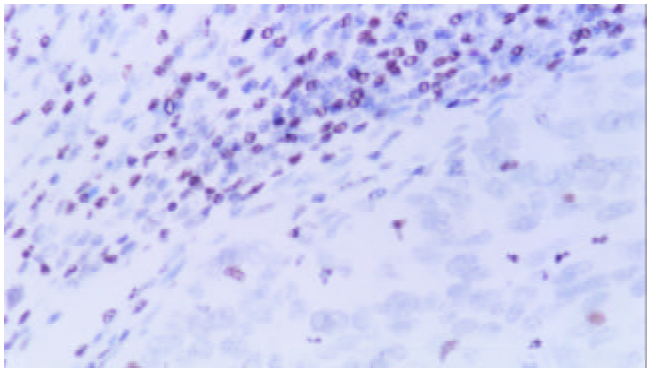

Figure 3 PTEN was negatively expressed in poorly-differentiated adenocarcinoma cells (-) and tumor infiltrated lymphocytes showed strong expression of PTEN (+++) (S-P, ×400).

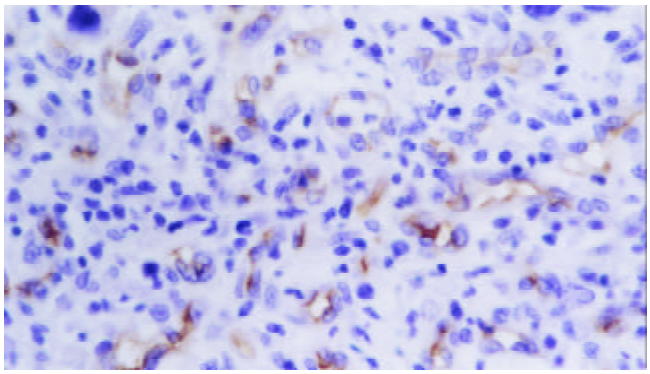

Figure 4 CD34 was located in cytoplasm and cellular membrane of vascular endothelial cells (S-P, ×400).

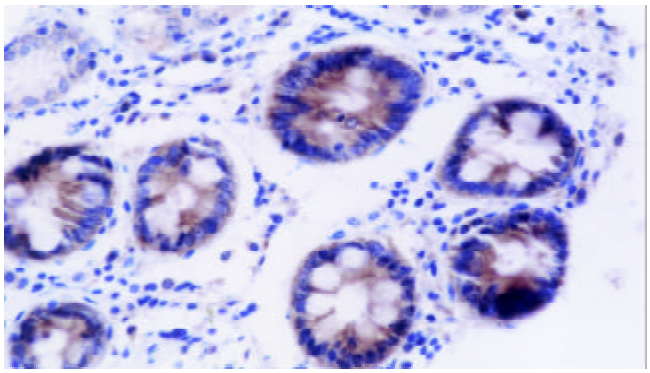

Figure 5 Caspase-3 was distributed in cytoplasm. Caspase-3 was strongly expressed in gastric epithelial cells (+++) (S-P,×400).

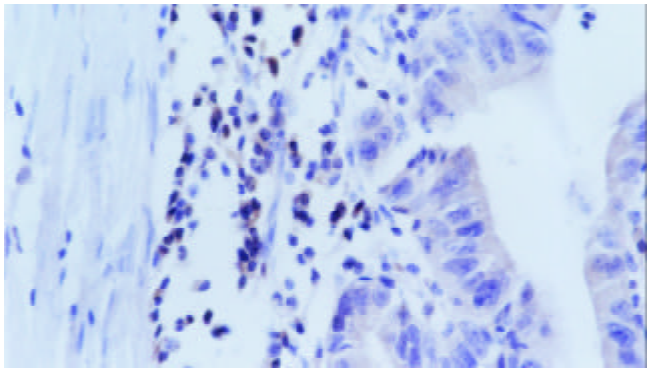

Figure 6 Caspase-3 was positively expressed in well-differentiated adenocarcinoma of stomach (++), and strongly in tumor infiltrated lymphocytes (+++) (S-P, ×400).

Correlation between PTEN expression in primary cancer cells and clinicopathological features of gastric cancer

PTEN expression in primary cancer cells was significantly associated with invasive depth, metastasis, growth pattern, Lauren's Classification, and histological classification of gastric cancer ($P<0.05$). There was no close correlation between PTEN expression and tumor size, Borrmann's Classification or TNM staging ($P>0.05$). One ANOVA analysis showed PTEN expression was negatively correlated with MDV in primary gastric cancer ($P<0.05$) (Tables 2-3, Figure 4).

Table 3 Relationship between expression of PTEN expression and MVD in primary gastric cancer

PTEN expression	*n*	MVD (mean± standard error)	*F* value	*P* value
-	51	52.53±25.47	5.558	0.020
+~+++	62	41.84±22.69		
Total	113	46.67±24.47		

Table 4 Relationship between expression of PTEN and Caspase-3 in primary gastric cancer cells

PTEN expression	*n*	Caspase-3 expression		
		-	+~+++	PR(%)
-	51	44	7	13.7[a]
+~+++	62	32	30	48.4
Total	113	76	37	32.7

Notes: PR: positive rate. [a]$P=0.000$ ($\chi^2=15.266$, Pearson's R=0.368).

Relationship between PTEN and Caspase-3 expression in primary gastric cancer cells

Figures 5-6 showed positive immunostaining of Caspase-3 in

the cytoplasm of adjacent epithelial cells, infiltrating lymphocytes, and cancer cells of primary gastric cancer. Cancer cells showed less frequent immunoreactivity to Caspase-3 than adjacent epithelial cells (32.7 % *vs* 50.4 %; $P<0.05$). Moreover, Caspase-3 expression was dependent of PTEN expression in primary gastric cancer cells ($P<0.05$) (Table 4).

DISCUSSION

Deletion or down-regulation of tumor suppressing genes plays an important role in the multiple steps of tumorigenesis and progression of gastric cancer. PTEN, a tumor-suppressing gene, makes a great contribution to cellular differentiation, reproduction and apoptosis, as well as cellular adhesion and mobility[8,9]. Some studies showed down-regulation of PTEN protein expression was due to genetic changes such as mutation, loss of heterozygosity, hypermethylation in gastric cancer, prostate cancer and breast cancer[19-21]. Our results showed that expression of PTEN decreased in primary gastric cancer cells, compared with that in adjacent epithelial cells. This revealed that genetic changes of PTEN gene could play an important role in malignant transition of gastric epithelial cells.

Low expression of PTEN gene product was involved in clinicopathological stage and metastasis of various malignancies. We found that the positive rate of PTEN was lower in gastric cancer with metastasis than that without metastasis. Additionally, the positive rate of PTEN expression tended to decrease with increase of invasive depth. These results were similar to other kinds of tumors[22-29]. Mass-type gastric cancer showed more expression of PTEN than nest-type one, the latter more than diffuse-type one, demonstrating that PTEN expression was implicated in the growth pattern of gastric cancer. These results suggest that deletion or reduced expression of PTEN protein probably facilitates the invasive and metastatic ability of gastric cancer cells. Several studies revealed that PTEN could enhance mobility and metastasis of tumor cells by regulating MMPs and VEGF[10-14]. There was another report that PTEN dephosphorylated FAK so as to be involved in cellular adhesion[30]. Deletion or reduced expression of PTEN could result in decreased cellular adhesion, increased synthesis of MMPs and VEGF, which subsequently contributed to invasion and angiogenesis of tumor tissues. These biological effects possibly underlay the prelude of invasion and metastasis of tumor. Our results revealed that reduced expression of PTEN was implicated in progression of gastric cancer probably by decreased cellular adhesion, increased cellular mobility and angiogenesis, and could act as an objective and effective marker to reflect the pathobiological behaviors of gastric cancer.

In addition, undifferentiated carcinomas showed the lower expression of PTEN than differentiated ones, suggesting that down-regulated expression of PTEN was closely associated with differentiation of gastric cancer. Diffuse-type gastric cancer showed fewer expression of PTEN than intestinal-type one. It supported that there were different tumorigenetic pathways between diffuse- and intestinal-type gastric cancer. Diffuse-type gastric cancer, the main part of which was undifferentiated, showed diffusely invasive growth pattern. It was possible that down-regulation of PTEN expression could influence the function of cellular skeleton, mobility and adhesion of cancer cells.

Angiogenesis was necessary for tumor growth, invasion and metastasis, and tumor-host interaction induced several sorts of tumor angiogenetic factors such as VEGF and MMPs to stimulate the intratumoral and peritumoral neovascularization[31,32]. In this study, we found that mean MVD was negatively related to PTEN expression in primary gastric cancer. Huang *et al.*[12] found that inhibition of endogenous endothelial PTEN by adenovirus-mediated over-expression of a dominant negative PTEN mutant in cultured endothelial cells potently enhanced a variety of VEGF-mediated cellular responses by PIP_3-kinase signaling, including cell survival, mitogenesis, and migration. In contrast, these effects of VEGF were significantly inhibited by over-expression of wild-type PTEN. Moreover, overexpression of wild-type PTEN modulated endothelial tube formation *in vitro* and vascular sprouting in an *ex vivo* model of angiogenesis. On the other hand, decreased and loss of expression of wild-type PTEN would facilitate MMPs expression which played an important role in angiogenic processes, including proliferation of endothelial cells, breakdown of the extracellular matrix and endothelial cell migration[33]. These *in vivo and in vitro* observations suggested that down-regulated expression of PTEN in gastric cancer increased angiogenesis by up-regulating VEGF and MMPs.

Some investigators found that PTEN could promote cell apoptosis, which in turn inhibited tumor growth[34]. Additionally Caspase-3 played an important role in apoptosis as an effector. Krajewska *et al.*[35] delineated for the first time some of the *in vivo* patterns of Caspase-3 expression in human tissues. Their observation that Caspase-3 was detectable in almost all types of cell implied its role in the regulation of cell life and death in a variety of types of cells as a proteinase. Our finding showed that Caspase-3 was less frequently expressed in gastric cancer cells than in adjacent epithelial cells. In addition, our study showed that expression of PTEN was positively correlated with expression of Caspase-3 in primary gastric cancer cells. Schwartzbauer *et al.*[36] found increased PTEN expression by recombinant adenovirus in cultured neonatal rat primary cardiomyocytes caused cardiomyocyte apoptosis as evidenced by increased caspase-3 activity and cleaved poly (A) DP-ribose polymerase. Furthermore, several studies suggested PTEN could enhance Fas/FasL-mediated or cytochrome-c-mediated apoptosis, whose apoptotic pathway evoked Caspase-3[34,37]. Consequently, we could infer that low expression of PTEN could decrease expression of Caspase-3 to make tumor cells apoptosis dysfunction, which underlay the theoretic basis of contribution of PTEN to tumorigenesis and progression of gastric cancer.

In conclusion, expression of PTEN and Caspase-3 is down-regulated in tumorigenesis of gastric cancer. Decreased expression of PTEN is implicated in progression of gastric cancer by decreased cell adhesion and increased angiogenesis and cell mobility. Moreover, low expression of PTEN can reduce expression of Caspase-3 to make tumor cells apoptosis disorder, which forms molecular mechanisms of PTEN contribution to tumorigenesis and progression of gastric cancer. However, a further study is necessary to directly clarify regulatory roles of PTEN and MMP-7 expression in angiogenesis of gastric cancer.

REFERENCES

1 **Steck PA,** Pershouse MA, Jasser SA, Yung WK, Lin H, Ligon AH, Langford LA, Baumgard ML, Hattier T, Davis T, Frye C, Hu R, Swedlund B, Teng DH, Tavtigian SV. Identification of a candidate tumour suppressor gene, MMAC1, at chromosome 10q23.3 that is mutated in multiple advanced cancers. *Nat Genet* 1997; **15**: 356-362

2 **Gu J**, Tamura M, Yamada KM. Tumor suppressor PTEN inhibits integrin- and growth factor-mediated mitogen-activated protein (MAP) kinase signaling pathways. *J Cell Biol* 1998; **143**: 1375-1383

3 **Tamura M**, Gu J, Takino T, Yamada KM. Tumor suppressor PTEN inhibition of cell invasion, migration, and growth: differential involvement of focal adhesion kinase and p130Cas. *Cancer Res* 1999; **59**: 442-449

4 **Tamura M**, Gu J, Tran H, Yamada KM. PTEN gene and integrin signaling in cancer. *J Natl Cancer Inst* 1999; **91**: 1820-1828

5 **Maehama T**, Dixon JE. The tumor suppressor, PTEN / MMAC1,

dephosphorylates the lipid second messenger, phosphatidylinositol 3, 4, 5-trisphosphate. *J Biol Chen* 1998; **273**: 13375-13378

6 **Hopkin K**. A surprising function for the PTEN tumor suppressor. *Science* 1998; **282**: 1027-1030

7 **Cantley LC**, Neel BG. New insight into tumor suppression: PTEN suppresses tumor formation by restraining the phosphoinositide 3-kinase / AKT pathway. *Proc Natl Acad Sci USA* 1999; **96**: 4240-4245

8 **Besson A**, Robbins SM, Yong VW. PTEN / MMAC1 / TEP1 in signal transduction and tumorigenesis. *Eur J Biochem* 1999; **263**: 605-611

9 **Waite KA**, Eng C. Protean PTEN: form and function. *Am J Hum Genet* 2002; **70**: 829-844

10 **Koul D**, Parthasarathy R, Shen R, Davies MA, Jasser SA, Chintala SK, Rao JS, Sun Y, Benvenisite EN, Liu TJ, Yung WK. Suppression of matrix metalloproteinase-2 gene expression and invasion in human glioma cells by MMAC / PTEN. *Oncogene* 2001; **20**: 6669-6678

11 **Tsugawa K**, Jones MK, Sugimachi K, Sarfeh IJ, Tarnawski AS. Biological role of phosphatase pten in cancer and tissue injury healing. *Front Biosci* 2002; **7**: E245-251

12 **Huang J**, Kontos CD. PTEN modulates vascular endothelial growth factor-mediated signaling and angiogenic effects. *J Biol Chem* 2002; **277**: 10760-10766

13 **Byzova TV**, Goldman CK, Pampori N, Thomas KA, Bett A, Shattil SJ, Plow EF. A mechanism for modulation of cellular responses to VEGF: activation of the integrins. *Mol Cell* 2000; **6**: 851-860

14 **Jiang BH**, Zheng JZ, Aoki M, Vogt PK. Phosphatidylinositol 3-kinase signaling mediates angiogenesis and expression of vascular endothelial growth factor in endothelial cells. *Proc Natl Acad Sci USA* 2000; **97**: 1749-1753

15 **Jones RG**, Elford AR, Parsons MJ, Wu L, Krawczyk CM, Yeh WC, Hakem R, Rottapel R, Woodgett JR, Ohashi PS. CD28-dependent activation of protein kinase B / Akt blocks Fas-mediated apoptosis by preventing death-inducing signaling complex assembly. *J Exp Med* 2002; **196**: 335-348

16 **Parkin DM**. Global cancer statistics in the year 2000. *Lancet Oncol* 2001; **2**: 533-543

17 **Chen XY**, van Der Hulst RW, Shi Y, Xiao SD, Tytgat GN, Ten Kate FJ. Comparison of precancerous conditions: atrophy and intestinal metaplasia in *Helicobacter pylori* gastritis among Chinese and dutch patients. *J Clin Pathol* 2001; **54**: 367-370

18 **Xin Y**, Li XL, Wang YP, Zhang SM, Zheng HC, Wu DY, Zhang YC. Relationship between phenotypes of cell-function differentiation and pathobiological behavior of gastric carcinomas. *World J Gastroenterol* 2001; **7**: 53-59

19 **Kondo K,** Yao M, Kobayashi K, Ota S, Yoshida M, Kaneko S, Baba M, Sakai N, Kishida T, Kawakami S, Uemura H, Nagashima Y, Nakatani Y, Hosaka M. PTEN / MMAC1 / TEP1 mutations in human primary renal-cell carcinomas and renal carcinoma cell lines. *Int J Cancer* 2001; **91**: 219-224

20 **Wang DS**, Rieger-Christ K, Latini JM, Moinzadeh A, Stoffel J, Pezza JA, Saini K, Libertino JA, Summerhayes IC. Molecular analysis of PTEN and MXI1 in primary bladder carcinoma. *Int J Cancer* 2000; **88**: 620-625

21 **Salvesen HB**, MacDonald N, Ryan A, Jacobs IJ, Lynch ED, Akslen LA, Das S. PTEN methylation is associated with advanced stage and microsatellite instability in endometrial carcinoma. *Int J Cancer* 2001; **91**: 22-26

22 **Lee JI**, Soria JC, Hassan KA, El-Naggar AK, Tang X, Liu DD, Hong WK, Mao L. Loss of PTEN expression as a prognostic marker for tongue cancer. *Arch Otolaryngol Head Neck Surg* 2001; **127**: 1441-1445

23 **Verma RS**, Manikal M, Conte RA, Godec CJ. Chromosomal basis of adenocarcinoma of the prostate. *Cancer Invest* 1999; **17**: 441-447

24 **McMenamin ME**, Soung P, Perera S, Kaplan I, Loda M, Sellers WR. Loss of PTEN expression in paraffin-embedded primary prostate cancer correlates with high gleason score and advanced stage. *Cancer Res* 1999; **59**: 4291-4296

25 **Rustia** A, Wierzbicki V, Marrocco L, Tossini A, Zamponi C, Lista F. Is exon 5 of the PTEN / MMAC1 gene a prognostic marker in anaplastic glioma? *Neurosurg Rev* 2001; **24**: 97-102

26 **Nozaki M**, Tada M, Kobayashi H, Zhang CL, Sawamura Y, Abe H, Ishii N, Van Meir EG. Roles of the functional loss of p53 and other genes in astrocytoma tumorigenesis and progression. *Neurooncol* 1999; **1**: 124-137

27 **Minaguchi T**, Yoshikawa H, Oda K, Ishino T, Yasugi T, Onda T, Nakagawa S, Matsumoto K, Kawana K, Taketani Y. PTEN mutation located only outside exons 5, 6, and 7 is an independent predictor of favorable survival in endometrial carcinomas. *Clin Cancer Res* 2001; **7**: 2636-2642

28 **Tada K**, Shiraishi S, Kamiryo T, Nakamura H, Hirano H, Kuratsu J, Kochi M, Saya H, Ushio Y. Analysis of loss of heterozygosity on chromosome 10 in patients with malignant astrocytic tumors: correlation with patient age and survival. *J Neurosurg* 2001; **95**: 651-659

29 **Mills GB**, Lu Y, Kohn EC. Linking molecular therapeutics to molecular diagnostics: inhibition of the FRAP / RAFT / TOR component of the PI3K pathway preferentially blocks PTEN mutant cells *in vitro* and *in vivo*. *Proc Natl Acad Sci USA* 2001; **98**: 10031-10033

30 **Maehama T**, Taylor GS, Dixon JE. PTEN and myotubularin: novel phosphoinositide phosphatases. *Annu Rev Biochem* 2001; **70**: 247-279

31 **Kim TS**, Kim YB. Correlation between expression of matrix metalloproteinas-2 (MMP-2), and matrix metalloproteinase-9 (MMP-9) and angiogenesis in colorectal adenocarcinoma. *J Korean Med Sci* 1999; **14**: 263-270

32 **Giatromanolaki A**, Koukourakis MI, Stathopoulos GP, Kapsoritakis A, Paspatis G, Kakolyris S, Sivridis E, Georgoulias V, Harris AL, Gatter KC. Angiogenic interactions of vascular endothelial growth factor of thymidine phosphorylase, and of p53 protein expression in locally advanced gastric cancer. *Oncol Res* 2000; **12**: 33-41

33 **Cox G**, O'Byrne KJ. Matrix metalloproteinases and cancer. *Anticancer Res* 2001; **21**: 4207-4219

34 **Carson JP**, Kulik G, Weber MJ. Antiapoptotic signaling in LNCaP prostate cancer cells: a survival signaling pathway independent of phosphatidylinositol 3'-kinase and Akt / protein kinase B. *Cancer Res* 1999; **59**: 1449-1453

35 **Krajewska M**, Wang HG, Krajewski S, Zapata JM, Shabaik A, Gascoyne R, Reed JC. Immunohistochemical analysis of *in vivo* patterns of expression of CPP32 (Caspase-3), a cell death protease. *Cancer Res* 1997; **57**: 1605-1613

36 **Schwartzbauer G**, Robbins J. The tumor suppressor gene PTEN can regulate cardiac hypertrophy and survival. *J Biol Chem* 2001; **276**: 35786-357893

37 **Wick W**, Furnari FB, Naumann U, Cavenee WK, Weller M. PTEN gene transfer in human malignant glioma: sensitization to irradiation and CD95L-induced apoptosis. *Oncogene* 1999; **18**: 3936-3943

Edited by Xu XQ

P.O.Box 2345, Beijing 100023,China
Fax: +86-10-85381893
E-mail: wjg@wjgnet.com www.wjgnet.com

World J Gastroenterol 2003;9(8):1667-1674
World Journal of Gastroenterology
 ISSN 1007-9327

• LIVER CANCER •

Characterization of focal hepatic lesions with contrast-enhanced C-cube gray scale ultrasonography

Wen-Ping Wang, Hong Ding, Qing Qi, Feng Mao, Zhi-Zhang Xu, Masatoshi Kudo

Wen-Ping Wang, Hong Ding, Qing Qi, Feng Mao, Zhi-Zhang Xu, Department of Ultrasound, Zhongshan Hospital of Fudan University, 180 Fenglin Road, Shanghai, 200032, China
Masatoshi Kudo, Department of Gastroenterology and Hepatology, School of Medicine, Kinki University, 377-2, Ohno-Higashi, Osaka-Sayama, 589-8511, Japan
Correspondence to: Dr. Hong Ding, Department of Ultrasound, Zhongshan Hospital of Fudan University, 180 Fenglin Road, Shanghai, 200032, China. hongding3@hotmail.com
Telephone: +86-21-64041990 Ext 2474 **Fax:** +86-21-64220319
Received: 2003-04-02 **Accepted:** 2003-05-19

Abstract

AIM: To characterize enhancement patterns of focal hepatic lesions using C-cube gray scale sonography with a microbubble contrast agent and to evaluate its usefulness in differential diagnosis of hepatic lesions.

METHODS: Fifty-four patients with 58 focal hepatic lesions were examined with Levovist-enhanced C-cube gray scale sonography. The final diagnosis of hepatic lesions was 29 primary liver cancers, 4 metastases, 8 hemangiomas, 12 focal nodular hyperplasias, 2 inflammatory pseudotumors of the liver and 3 angiomyolipomas. The initiation time of enhancement in various lesions and enhancement duration after administration of contrast agent were compared. Vascular findings in lesions were classified as peripheral enhancement, homogenous enhancement, mosaic enhancement and no enhancement depending on microbubble signals in the lesion relative to the liver parenchyma.

RESULTS: The initiation time of enhancement in hemangioma (48±12 s) was significantly later compared to other lesions ($P<0.05$). The enhancement duration of malignancies (69±33 s in primary liver cancer, 61±23 s in metastasis) was significantly shorter compared to benign lesions ($P<0.05$). Intranodular enhancement appearing at arterial phase and decreasing at portal venous phase was considered characteristic for malignancy. Intranodular enhancement did not appear earlier than the liver parenchyma, and peripheral enhancement pattern was regarded as positive findings for hemangioma. Intranodular enhancement appeared in the arterial phase, and homogenous enhancement pattern sustained in the whole portal venous phase were regarded as positive findings for focal nodular hyperplasia. No microbubble signals appeared in two inflammatory pseudotumors of the liver.

CONCLUSION: C-cube gray scale sonography can demonstrate dynamic intranodular enhancement in various focal hepatic lesions. The information provided by this methodology may be useful in the differential diagnosis of hepatic lesions.

Wang WP, Ding H, Qi Q, Mao F, Xu ZZ, Kudo M. Characterization of focal hepatic lesions with contrast-enhanced C-cube gray scale ultrasonography. *World J Gastroenterol* 2003; 9(8): 1667-1674
http://www.wjgnet.com/1007-9327/9/1667.asp

INTRODUCTION

Color Doppler ultrasonography (US) is the most widely used imaging modality in screening detection of hepatic tumors and differential diagnosis of malignancies based on tumor vascularity. Unfortunately, conventional Doppler US does not provide satisfactory results in the evaluation of tumor vascularity because of limitations such as a lack of sensitivity to slow flow and deeply located flow, inevitable motion artifacts from either respiratory or cardiac activity, and poor showing of tumor stain.

Over the past decade, great efforts have been made to improve both ultrasound instruments and echo-enhancing agents to demonstrate tumor flow more sensitively with non-invasive modalities. Harmonic imaging is a newly developed technique used with microbubble contrast agents that interact with the imaging process. The microbubbles reflect ultrasonic echoes with a low acoustic power, additionally, they resonant and emit multiple frequencies when acoustic power is sufficiently elevated[1]. Second harmonic imaging, which transmits sonographic pulses at one frequency and then selectively receives echoes at twice that frequency, has been shown to be excellent in eliminating clutter noises and displaying the slower blood flow in smaller vessels when compared to conventional Doppler US[2-5].

However, the intensity of second harmonic frequency of some microbubble contrast agents (e.g., Levovist) is lower than that of fundamental ones[1, 6]. In addition to second harmonics, the microbubbles emit multiple frequencies such as subharmonic, ultraharmonic, etc. Recently, a commercially available C-cube gray scale US (C^3-Mode™, Esaote Biomedica, Genoa, Italy) technique uses comparative digital decorrelation and a digital adaptive band pass filtering process, providing a combination of gray scale, Doppler and contrast signals. It utilizes the signal coming from the microbubbles with not only the second harmonics, but also the fundamental, sub- and ultra-harmonics from the contrast agent. Therefore, this new technique might be able to provide increased sensitivity in demonstrating slow blood flow in focal liver lesions with good spatial resolution in comparison to contrast-enhanced conventional US or second harmonic imaging.

The purpose of this study was to characterize enhancement patterns in focal hepatic lesions with contrast-enhanced C-cube gray scale US.

MATERIALS AND METHODS

Subjects

Between October 2001 and March 2002, 54 patients with clinically and histopathologically diagnosed hepatic tumors who were referred for hepatic color Doppler US were examined with C-cube gray scale US in combination with a microbubble contrast agent. All the patients gave fully informed consent for the study that had received approval from our institutional review board.

The patients consisted of 31 men and 23 women aged between 20-68 years (mean, 47 years). Contrast-enhanced C-cube gray scale US was performed 2-3 days before treatment. In patients with multiple lesions, the largest one was selected for contrast

study except 4 patients with different types of hepatic lesions. Therefore, a total of 58 hepatic lesions were studied with contrast agents. They were 29 cases of primary liver cancer (PLC) (hepatocellular carcinoma, HCC, 27; cholangiocarcinoma, 2), 8 of hemangiomas, 12 of focal nodular hyperplasias (FNH), 2 of inflammatory pseudotumors of the liver (IPT), 3 of angiomyolipomas, and 4 of metastases (gastric cancer, 1; breast cancer, 2; nasopharyngeal carcinoma, 1). Histopathological diagnosis was obtained by surgical resection or US-guided percutaneous biopsy in all the 33 malignancies, 3 hemangiomas, 7 FNHs, 2 IPTs and 3 angiomyolipomas. Other 5 hemangiomas and 5 FNHs were diagnosed according to the typical imaging findings on contrast-enhanced computed tomography (CT), magnetic resonance imaging, as well as clinical follow-up which showed no change of lesion size for more than one year.

The maximal diameters of the 58 hepatic lesions measured on conventional US were as follows: PLC, 1.1-8.2 cm (mean, 3.3 cm); metastasis, 2.2-3.5 cm (mean, 2.8 cm); hemangioma, 1.0-8.0 cm (mean, 5.5 cm); FNH, 1.1-7.3 cm (mean, 4.5 cm); angiomyolipoma, 2.4-7.3 cm (mean, 6.3 cm) and IPT, 1.7-4.1 cm (mean, 2.9 cm).

Contrast agent

The contrast agent was Levovist (Schering AG, Berlin, Germany), which is a suspension of monosaccharide microparticles (galactose) in sterile water. Microbubbles were stabilized in the microparticle suspension with an average diameter of 1.3 μm, which could traverse the pulmonary capillary bed and enhance the signal of blood. Before US examination, the agent was prepared with 5 mL of water by shaking vigorously for 5-10 s. After standing for 2 min for equilibration, a total of 2.5 g Levovist (6 mL 400 mg/mL concentration) was injected manually through a 20-gauge canula placed in an antecubital vein at a speed of 1 mL/s and flushed by an additional 5 mL of normal saline.

Imaging

Contrast-enhanced C-cube gray scale US was performed with a commercially available US system, Technos DU6 US system (Esaote Biomedica, Genoa, Italy), equipped with C^3-Mode™ technology. A convex-arrayed wide band transducer CA 421 was used at a frequency of 2-5 MHz. There were two states in contrast examination: LOW state and C^3-Mode state. At the LOW state, the system transmitted pulses at a low acoustic power with a mechanical index of 0.2-0.4 that theoretically would not destroy microbubbles. At C^3-Mode state, the system transmitted pulses at a high acoustic power with a mechanical index of 1.0-1.4 to destroy microbubbles in the scanning plane. We could transfer from the LOW state to the C^3-Mode state by simply pressing a keyboard button to obtain signals of microbubble collapse, and the system automatically returned to the LOW state then.

Conventional US was performed on all lesions before contrast-enhanced study started. An ideal plane was selected for clearly showing the lesion and the surrounding liver parenchyma. Following administration of Levovist, we monitored the same scanning plane using LOW state and obtained a series of C^3-Mode images by pressing the key button manually for 7-8 minutes. During 15-120 s after injection of Levovist, we obtained C^3-Mode images of high mechanical index every 5-10 s. After that (121-480 s after injection of Levovist), we obtained C^3-Mode images every 20-30 s. During the entire scanning procedure, we held the transducer and unfroze it during the same stage of the patient's respiration to maintain the same scanning plane. The time delay between the initiation of contrast injection and the time at which the C^3-Mode image obtained was automatically recorded on the US system.

Analysis

All US images were recorded on digital videotapes and still images were stored digitally on a hard disk in the US system. Videotapes and still images were reviewed by two authors who were unaware of the findings on other imaging modalities and the final diagnosis of the lesions.

The time of occurrence of microbubble signals in the lesion and in surrounding liver parenchyma after administration of Levovist (injection-enhancement delay time), and subsequent time of microbubble signals decreased in the lesion on C^3-Mode images (injection-decrease delay time) were carefully recorded. Enhancement decrease in a lesion was defined as the echogenicity lower in the lesion than that in the same-depth of surrounding liver parenchyma. In this way, we calculated enhancement duration of various lesions.

The entire procedure of contrast-enhanced C-cube gray scale US was classified into three phases. As vascular transit time of blood through the liver was associated with liver diseases, such as hepatic cirrhosis[7-9], we modified the scheme that Kim *et al*[10] used on dynamic CT. Arterial phase prior to the enhancement appeared in the liver parenchyma, approximately 15-50 s after administration of Levovist, and portal venous phase appeared 51-120 s after administration of Levovist, and delayed phase appeared 121 s after administration of Levovist.

Based on the enhancement of microbubble signals in the lesion relative to the surrounding liver parenchyma, vascular findings in lesions on C^3-Mode images in the arterial phase were classified as peripheral enhancement (continuous or discontinuous ring enhancement occurred in the periphery of the lesion), homogenous enhancement (enhancement occurred in the whole lesion), mosaic enhancement (enhancement occurred in some area of the lesion), and no enhancement (no microbubble signal occurred in the lesion while enhancement in the liver parenchyma occurred). All the enhancement patterns including peripheral, homogenous and mosaic enhancements were defined as positive enhancement, namely positive detection of intranodular vascularity.

All the data were normal distribution and homogeneity of variance after tested. The data were analyzed using SAS (SAS 6.04 for windows). Continuous variables were compared by means of independent *t*-test. Categorical data were analyzed with chi square test. A P value <0.05 was considered to be significant.

RESULTS

The detection rate of intranodular vascularity was 96.6 % (56/58) on C-cube gray scale US with administration of Levovist. All PLCs, metastases, hemangiomas, FNHs, and angiomyolipomas presented positive enhancement. No microbubble signals appeared in the lesions of IPT, resulting in a vascular defect when liver parenchymal perfusion was observed on C-cube gray scale US.

The initiation time of microbubble enhancement in various lesions and in the surrounding liver parenchyma after administration of Levovist, as well as enhancement duration of various lesions are listed in Table 1. Except hemangioma, all other lesions enhanced earlier than the liver parenchyma. The initiation time of enhancement in hemangioma (48±12 s after administration of Levovist) was significantly later when compared to other lesions ($P<0.05$). The enhancement in HCC (Figure 1), cholangiocarcinoma (Figure 2), and metastasis (Figure 3) decreased more rapidly when compared to benign liver lesions. The enhancement duration of malignancies (69±33 s in PLC, 59±22 s in metastasis, respectively) was significantly shorter when compared to benign liver lesions ($P<0.05$).

If the intranodular enhancement appeared at arterial phase

and enhancement decreased at portal venous phase in a lesion was considered characteristic for malignancy, the sensitivity, specificity and positive predictive values for contrast-enhanced C-cube gray scale US to differentiate malignancies from benign liver lesions were 90.9 % (30/33), 92.0 % (23/25), and 93.8 % (30/32), respectively.

Vascular findings in all lesions at the arterial phase on contrast-enhanced C-cube gray scale US are shown in Table 2. Peripheral enhancement was detected in 50.0 % (2/4) of metastases and 87.5 % (7/8) of hemangiomas, homogenous enhancement in 55.2 % (16/29) of PLCs, 100 % (12/12) of FNHs, and mosaic enhancement in 41.4 % (12/29) of PLCs, and 66.7 % (2/3) of angiomyolipomas.

With respect to the enhancement patterns on contrast-enhanced C-cube gray scale US, no specific enhancement pattern was found among malignancies. For benign liver lesions, however, the enhancement patterns were specific. After administration of Levovist, hemangioma enhanced later than the liver parenchyma, and peripheral enhancement was obtained in most hemangiomas (Figure 4). All FNHs enhanced earlier than the liver parenchyma and presented homogenous enhancement (Figure 5). Most angiomyolipomas enhanced early and showed mosaic enhancement pattern (Figure 6).

If the intranodular enhancement did not appear earlier than the surrounding liver parenchyma after administration of Levovist, and the peripheral enhancement patterns were regarded as positive findings for hemangioma, the sensitivity, specificity and positive predictive values were 87.5 % (7/8), 94.0 % (47/50) and 70.0 % (7/10), respectively.

If the intranodular enhancement appeared in the arterial phase, and the homogenous enhancement pattern sustained in the whole portal venous phase were regarded as positive findings for FNH, the sensitivity, specificity and positive predictive values were 100 % (12/12), 95.7 % (44/46) and 85.7 % (12/14), respectively.

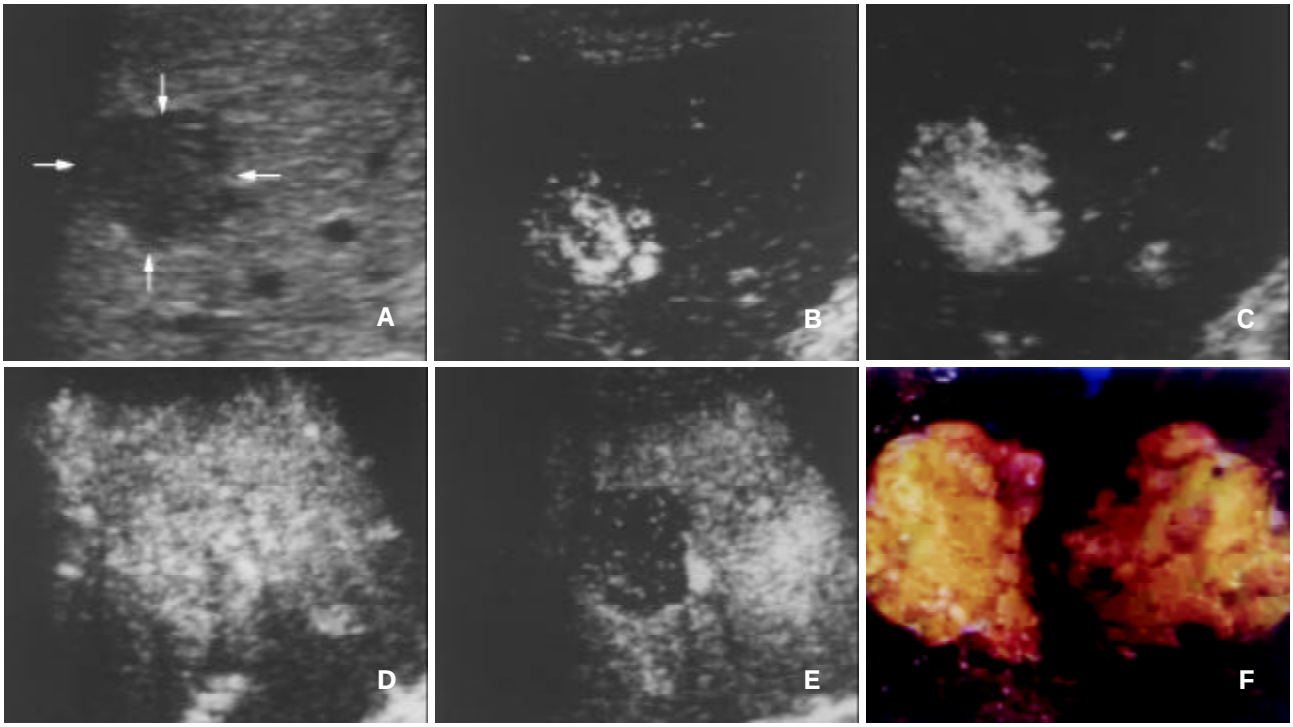

Figure 1 A 47-year-old man with hepatocellular carcinoma. A. Intercostal precontrast conventional sonography exhibits a hypoechogenic lesion (arrows) of 2.7 cm in diameter. B-E. Contrast-enhanced C-cube gray scale sonography at 23 s (B), 28 s (C) and 43 s (D) after injection of Levovist shows that intranodular signals enhance gradually and earlier than the liver parenchyma, and enhancement decreases rapidly in the portal venous phase (110 s, E). This suggests hypervascularity of hepatocellular carcinoma with an early enhancement and early wash-out of contrast. F. Gross specimen of the resected tumor exhibits a gray fish-like profile and suggests the typical appearance of hepatocellular carcinoma.

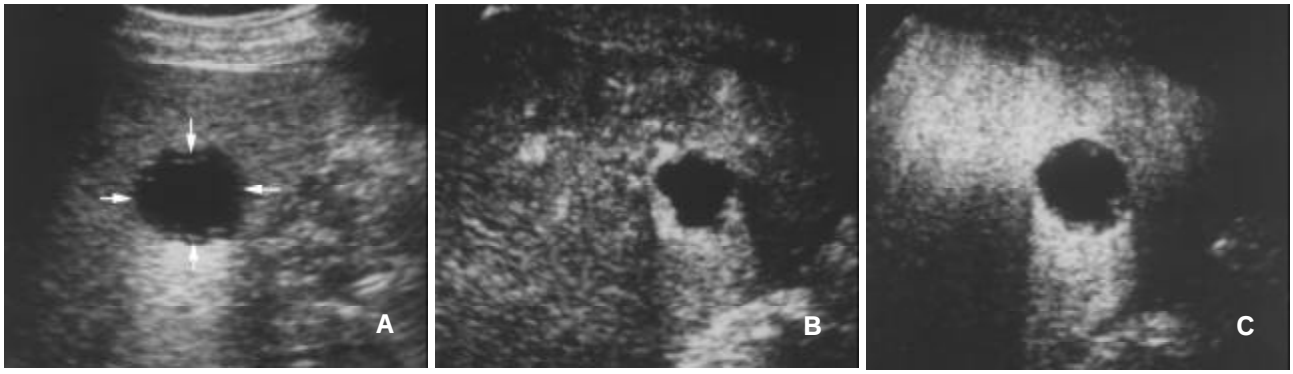

Figure 2 A 48-year-old man with metastasis of nasopharyngeal carcinoma. A. Intercostal section of precontrast conventional sonography exhibits a hypoechogenic lesion (arrows) with a diameter of 3.5 cm. B. Contrast-enhanced C-cube gray scale sonography at 24 s after injection of Levovist shows that peripheral enhancement appears at the same time with the liver parenchyma. C. Intranodular enhancement decreases at 107 s in the portal venous phase, earlier than that in the liver parenchyma.

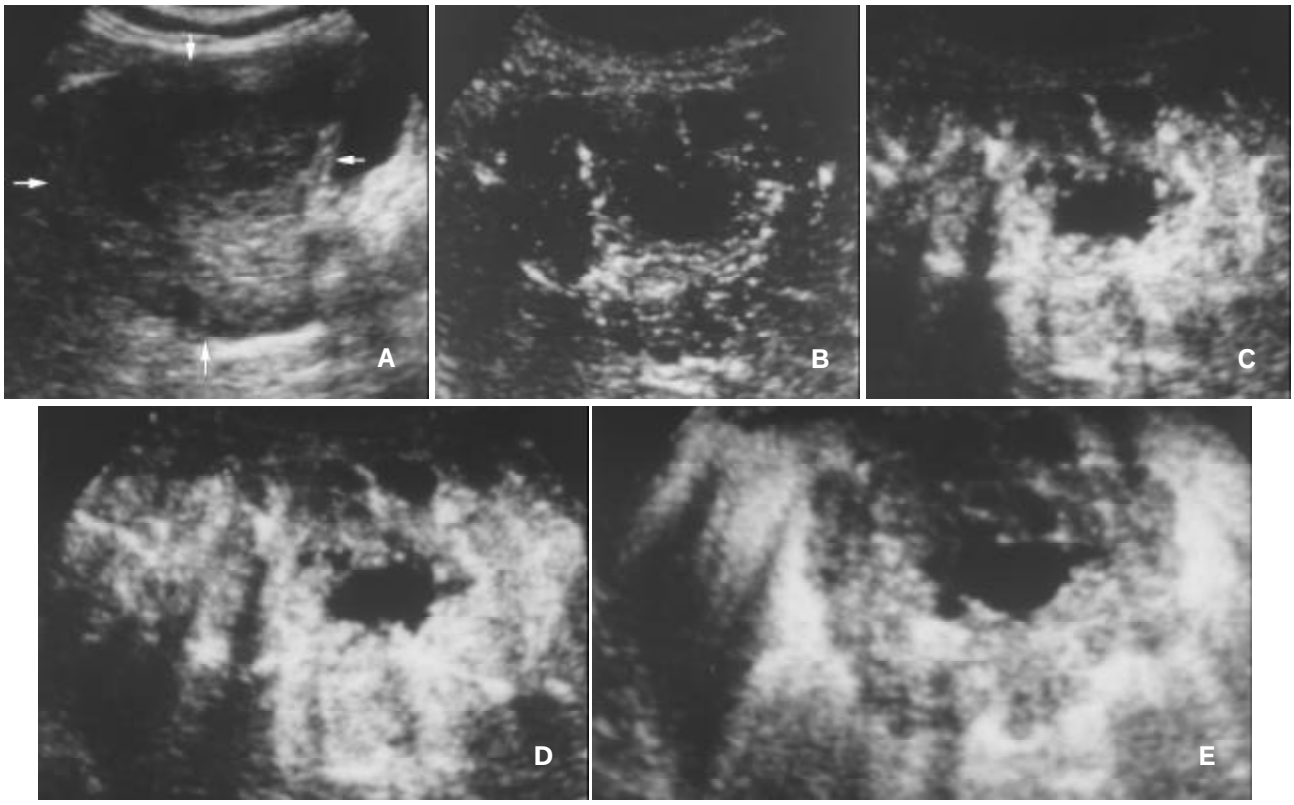

Figure 3 A 62-year-old woman with cholangiocarcinoma. A. Subcostal section of precontrast conventional sonography shows a hypoechogenic lesion (arrows) in segment V of the liver with a diameter of 8.0 cm. B-E. Contrast-enhanced C-cube gray scale sonography at 16 s (B), 20 s (C) and 25 s (D) after injection of Levovist shows that intranodular signals enhance gradually and earlier than the liver parenchyma, and enhancement decreases rapidly in the portal venous phase (78 s, E). Histopathology of US-guided percutaneous biopsy reveals cholangiocarcinoma of the liver.

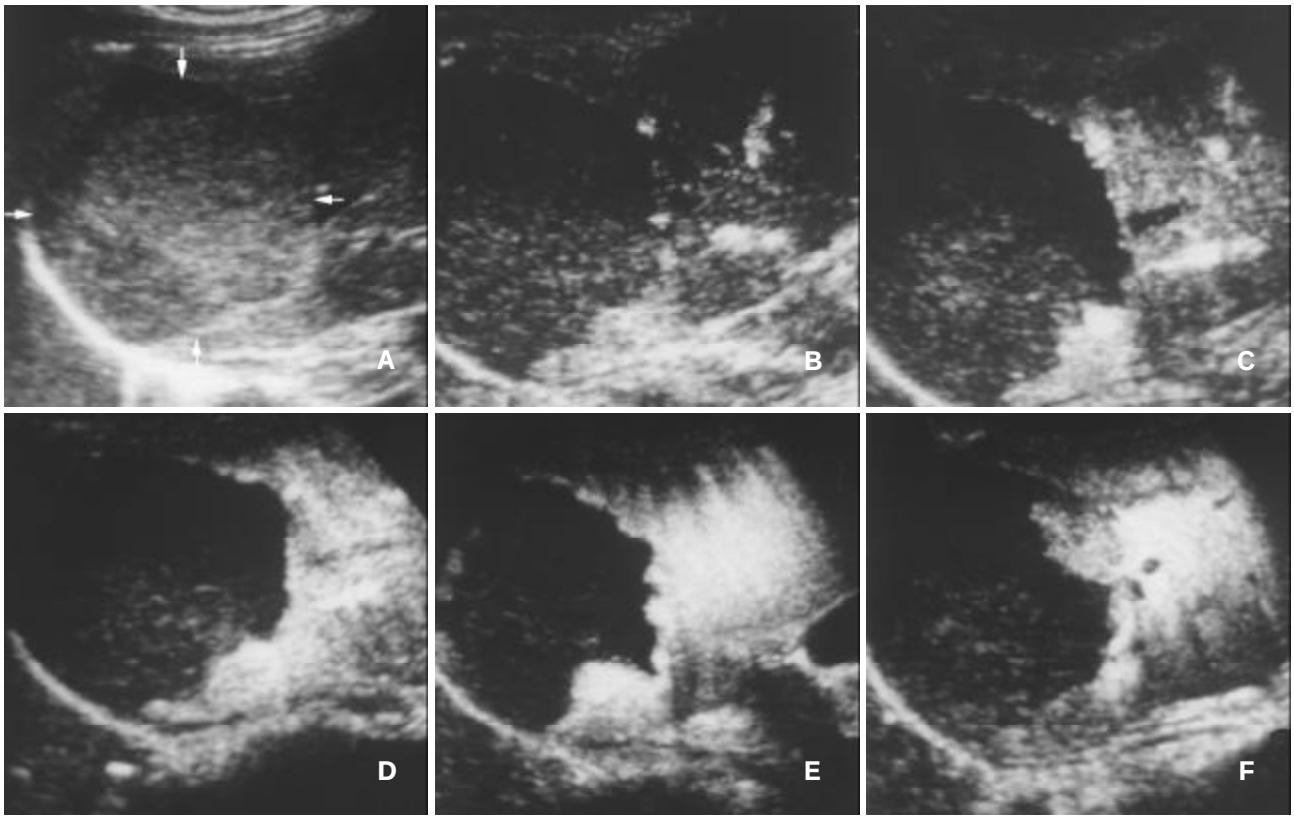

Figure 4 A 45-year-old female with hemangioma. A. Intercostal section of precontrast conventional sonography exhibits a hypoechogenic lesion (arrows) of 6.5 cm in diameter. B. Contrast-enhanced C-cube gray scale sonography at 23 s (B) after injection of Levovist shows that no microbubble signal appears in the lesion while enhancement in the liver parenchyma begins. C-F. C-cube gray scale sonography demonstrates gradual peripheral enhancement at 32 s (C), 47 s (D), 113 s (E) and 370 s (F) with a long enhancement duration.

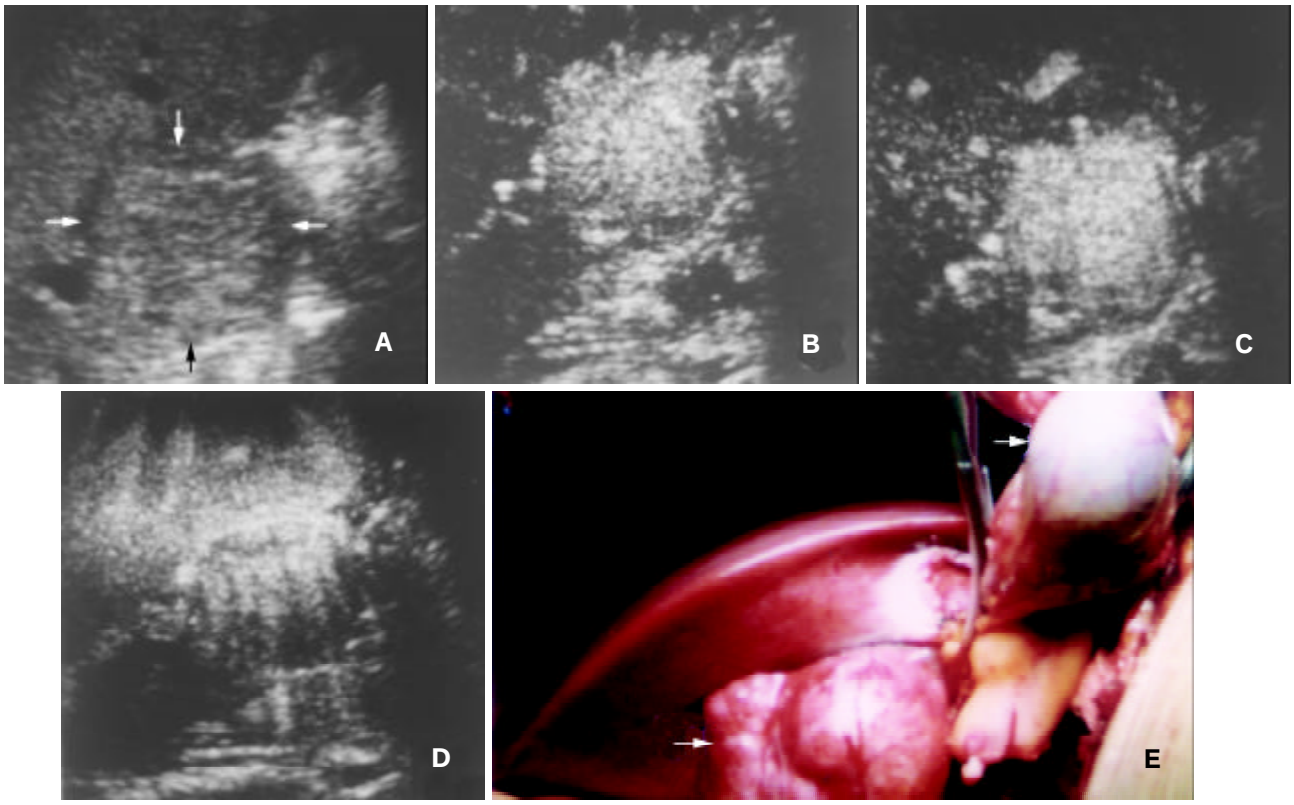

Figure 5 A 29-year-old man with focal nodular hyperplasia. A. Intercostal section of precontrast conventional sonography exhibits an isoechoic lesion (arrows) in segment V of the liver with a diameter of 4.8 cm. B-D. Contrast-enhanced C-cube gray scale sonography at 49 s (B) and 60 s (C) after injection of Levovist shows that intranodular signals enhance earlier than the liver parenchyma, and enhancement sustains in the portal venous phase until the delayed phase (140 s, D), suggestive of slow wash-out of contrast in the lesion. E. Appearance of the lesion and its surrounding organs in laparotomy. The lesion (arrow) protrudes from the liver with a smooth capsule while the gallbladder (arrowhead) is lifted with hemostatic forceps. Histopathology of the tumor revealed focal nodular hyperplasia.

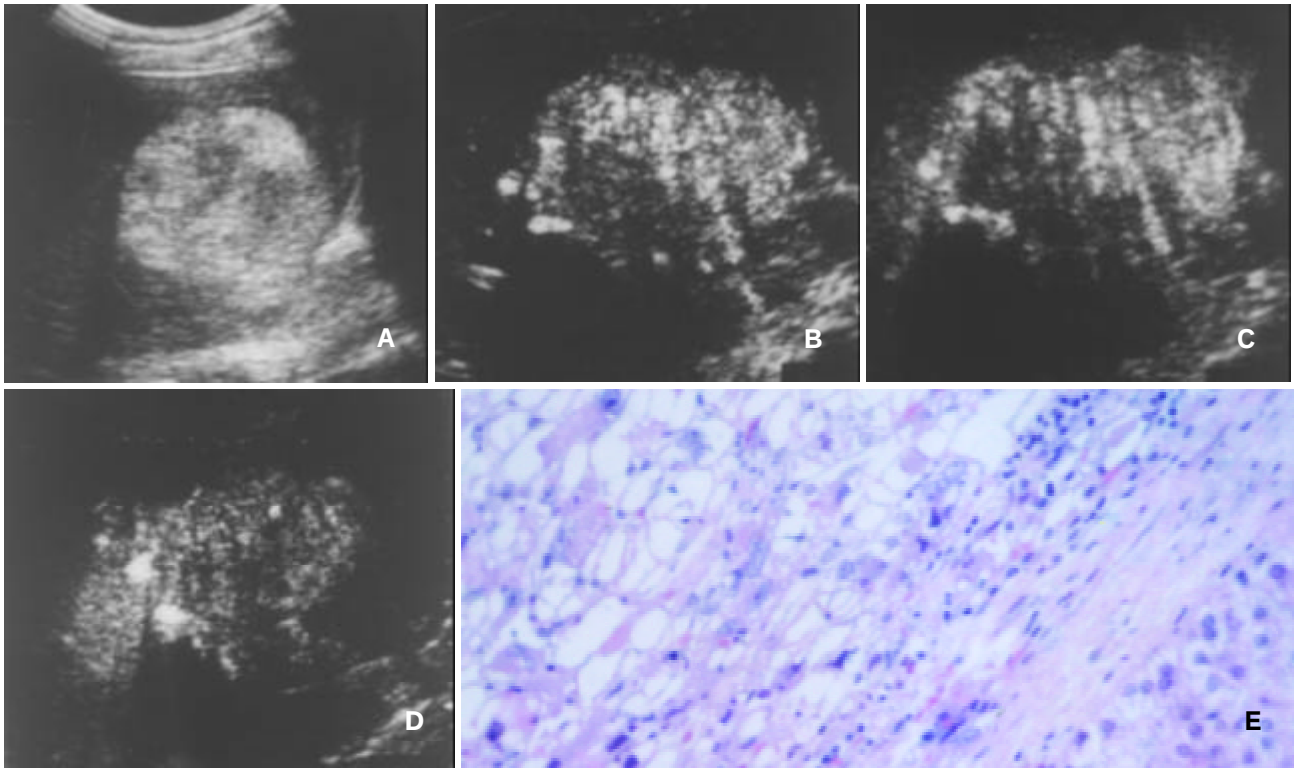

Figure 6 A 51-year-old female with angiomyolipoma. A. Subcostal section of precontrast conventional sonography exhibits a hyperechogenic lesion of 7.3 cm in diameter. B-D. Contrast-enhanced C-cube gray scale sonography at 54 s (B) and 110 s (C) after injection of Levovist shows that intranodular signals enhance earlier than the liver parenchyma with an inhomogenous enhancement pattern, and enhancement decreases in the delayed phase (206 s, D). E. Photomicrography shows defuse sheets of adipocytes and muscle cells adjacent to the noncirrhotic liver tissue, presenting a typical appearance of angiomyolipoma (HE 400).

Table 1 Hemodynamics of focal hepatic lesions on contrast-enhanced C-cube gray scale ultrasonography

Types of lesion	No. of lesions	Injection-enhancement delay time (mean±SD) (s)			Enhancement duration (mean±SD) (s)	
		Liver	Lesion	*P* Value	Lesion	*P* Value
Primary liver cancer	29	33±10	23±6	<0.05	69±33[b]	–
Metastasis	4	26±7	26±11	<0.05	59±22[c]	–
Hemangioma	8	36±8	48±12[a]	–	221±47	<0.05
Focal nodular hyperplasia	12	29±9	20±6	<0.05	196±96	<0.05
Angiomyolipoma	3	37±12	26±6	<0.05	177±90	<0.05

[a]The injection-enhancement delay time after administration of Levovist in hemangioma was significantly longer than that in other types of lesions ($P<0.05$). [b]The enhancement duration in primary liver cancer was significantly shorter than that in benign lesions ($P<0.05$). [c]The enhancement duration in metastasis was significantly shorter than that in benign lesions ($P<0.05$).

Table 2 Enhancement patterns of focal liver lesions in the arterial phase on contrast-enhanced C-cube gray scale ultrasonography

Enhancement patterns	Peripheral	Homogenous	Mosaic	Negative	Total
Primary liver cancer	1	16	12	0	29
Metastasis	2	0	2	0	4
Hemangioma	7	0	1	0	8
Focal nodular hyperplasia	0	12	0	0	12
Angiomyolipoma	0	1	2	0	3
Inflammatory pseudotumor	0	0	0	2	2
Total	10	29	17	2	58

Note: Values are number of lesions.

DISCUSSION

The characterization of focal liver lesions depends closely on their specific intranodular hemodynamics[11-14]. Various imaging modalities have been studied for demonstrating the typical vasculature of focal liver lesions. Contrast-enhanced US may be especially promising for depicting intranodular vascularity not only because of its easy performance, but also because of its particular advantages of providing dynamic flow information on a tomographic plane basis[4, 15, 16].

Levovist is the most widely used microbubble contrast agent for intravenous administration in the clinical setting. The backscatter signals caused by vibration or disruption of the microbubbles are received and used for image formation. Interval delay imaging or intermittent harmonic imaging[4, 16-19], which transmits an ultrasound beam with a flexible interval, destroys most of the microbubbles in a region of interest with high acoustic power, and permits refreshment of microbubbles in the scanning plane during the low acoustic power period due to fresh blood inflow. C-cube gray scale US is a newly available technique using interval delay scanning to destroy microbubbles in the scanning plane. With the help of the low acoustic power image on LOW state, we could obtain intranodular capillary flow signals on the same sonographic scanning plane. Moreover, a series of C^3-Mode images with microbubbles collapse provide dynamic information of enhancement patterns of focal liver lesions. Therefore, we could continuously observe the lesion of interest from the arterial phase to the delayed phase. The detailed enhancement process of each lesion could be obtained just as a single-level dynamic CT study[20]. In the present study, positive enhancement was detected in all focal liver lesions except for two IPT with complete necrosis. No false negative nodule was found on contrast-enhanced C-cube gray scale US.

The blood of normal liver is supplied both by the portal vein and by the hepatic artery, whereas the blood of most neoplastic tumors of the liver are supplied by the hepatic artery. The typical vascular patterns of PLC are high velocity signals on color Doppler US[21, 22], and high attenuation at the early phase and low attenuation at the portal venous phase relative to the liver parenchyma on dynamic CT[23]. In this study, the injection-enhancement delay time of PLC was shorter than that of the liver parenchyma after administration of Levovist, presenting an early enhancement at the arterial phase. As the portal venous phase arrived, the concentration of microbubbles in the hepatic artery decreased. We recorded the injection-decrease delay time of various focal liver lesions and found that the injection-decrease delay time of PLC was relatively shorter compared to benign liver lesions. The difference of enhancement duration between PLC and benign liver lesions was statistically significant ($P<0.05$). The hemodynamics of PLC was that, namely, it enhanced early in the arterial phase and washed out rapidly in the portal venous phase. These findings were highly corresponding to the appearance of PLC on contrast-enhanced dynamic CT[23-25].

As to intranodular enhancement patterns of PLC in the arterial phase, homogenous or mosaic enhancements were found in most lesions of PLC (96.7 %, 28/29), which were also found in other focal liver lesions.

Similarly, 4 liver matestases enhanced early in the arterial phase and the enhancement decreased rapidly in the portal venous phase, resulting in a shorter enhancement duration compared to benign liver lesions ($P<0.05$). This was probably due to their hemodynamics of mainly arterial blood supply. The enhancement patterns of metastases were peripheral or mosaic enhancements, which were also nonspecific and found in other liver lesions. Further study may be needed to clarify this results.

Hemangioma is usually rich in vessels with a sluggish blood circulation. After administration of a contrast agent, the enhancement of most hemangiomas on helical CT was a peripheral puddle pattern in the arterial phase and cotton wool sign in post vascular phase[25, 26]. On contrast-enhanced C-cube gray scale US, similarly, the injection-enhancement delay time of hemangioma was significantly longer compared to other types of focal liver lesions (Table 1). As the arterial phase ended, the

enhancement in hemangioma sustained and lasted over a long period. With respect to the enhancement patterns, peripheral enhancement was shown in most hemangiomas (87.5 %, 7/8). Since microbubbles were destroyed when they were imaged by ultrasound beam, intratumoral enhancement could not be obtained with C-cube gray scale US using 5-10 s interval transmission in relatively large hemangioma. Based upon our preliminary experience, we supposed that at least one minute of interval transmission would be needed to image the microbubbles in the center of hemangioma. The specific characteristics of hemangioma after administration of Levovist was that, in short, it enhanced slowly and mainly at the periphery of the lesion with a long period of enhancement.

Except hemangioma, other benign liver lesions including 12 FNHs and 3 angiomyolipomas demonstrated positive enhancement on contrast-enhanced C-cube gray scale US, presenting their hypervascular characteristics. These lesions enhanced early in the arterial phase and positive enhancement lasted over a long period until the delayed phase. Their enhancement duration was relatively longer compared to hepatic malignancies (P<0.05).

FNH is not a neoplasm but a hyperplastic response of liver parenchyma to the presence of a preexisting vascular malformation. FNH is a hypervascular lesion bypassing the portal venous system and exhibiting a varying degree of arteriovenous shunting[27]. On contrast-enhanced C-cube gray scale US, all FNH lesions showed early enhancement and appeared homogenously. In the portal venous and delayed phase, the intranodular enhancement was somewhat greater than that in the same-depth of surrounding liver parenchyma (Figure 5). The enhancement pattern of FNH seemed to be exclusively caused by arterial vascularization in the lesion, an absent capillary bed, and a vascular volume in excess of that of the normal liver[27-29].

Hepatic angiomyolipoma is a rare benign mesenchymal tumor, composed of a varying heterogenous mixture of three tissue components: blood vessels, smooth muscle and adipose cells. Most angiomyolipoma markedly enhanced with curved vessels in the arterial phase, and remained enhancement in the portal venous phase on spiral CT[30]. Its appearance on contrast-enhanced C-cube gray scale US was corresponding to that on helical CT. It enhanced inhomogenously because of the presence of the multiple ingredients within the lesion.

Contrast-enhanced C-cube gray scale US images microbubbles intermittently with a high mechanical index. This technique allows the detection of blood in the capillary bed, where the flow velocity is too low to be detected with Doppler US flow techniques. On the other hand, however, tumor vessel cannot be shown real-timely. It is because the microbubbles in small vessels (i.e. tumor vessels) cannot be detected with a low mechanical index on the LOW state, and real time C^3-Mode state with a high mechanical index breaks microbubbles when they are imaged. This is one limitation of C-cube gray scale US.

In conclusion, C-cube gray scale US with administration of Levovist can demonstrate dynamic intranodular enhancement in various focal hepatic lesions. The information provided by this methodology may be useful in the differential diagnosis of hepatic lesions on the basis of demonstrating characteristic appearances of various hepatic lesions. Additional study with a greater number of cases is in progress to gather additional data to support and replenish these results.

REFERENCES

1 **Calliada F**, Campani R, Bottinelli O, Bozzini A, Sommaruga MG. Ultrasound contrast agents basic principles. *Eur J Radiol* 1998; **27**(Suppl): S157-S160

2 **Kono Y**, Moriyasu F, Mine Y, Nada T, Kamiyama N, Suginoshita Y, Matsumura T, Kobayashi K, Chiba T. Gray-scale second harmonic imaging of the liver with galactose-based microbubbles. *Invest Radiol* 1997; **32**: 120-125

3 **Choi BI**, Kim TK, Han JK, Kim AY, Seong CK, Park SJ. Vascularity of hepatocellular carcinoma: assessment with contrast-enhanced second-harmonic versus conventional power Doppler US. *Radiology* 2000; **214**: 381-386

4 **Wilson SR**, Burns PN, Muradali D, Wilson JA, Lai X. Harmonic hepatic US with microbubble contrast agent: initial experience showing improved characterization of hemangioma, hepatocellular carcinoma, and metastasis. *Radiology* 2000; **215**: 153-161

5 **Maresca G**, Summaria V, Colagrande C, Manfredi R, Calliada F. New prospects for ultrasound contrast agents. *Eur J Radiol* 1998; **27**(Suppl): S171-S178

6 **Hosoki T**, Mitomo M, Chor S, Miyahara N, Ohtani M, Morimoto K. Visualization of tumor vessels in hepatocellular carcinoma. Power Doppler compared with color Doppler and angiography. *Acta Radiol* 1997; **38**: 422-427

7 **Blomley MJ**, Albrecht T, Cosgrove DO, Jayaram V, Eckersley RJ, Patel N, Taylor-Robinson S, Bauer A, Schlief R. Liver vascular transit time analyzed with dynamic hepatic venography with bolus injections of an US contrast agent: early experience in seven patients with metastases. *Radiology* 1998; **209**: 862-866

8 **Albrecht T**, Blomley MJ, Cosgrove DO, Taylor-Robinson SD, Jayaram V, Eckersley R, Urbank A, Butler-Barnes J, Patel N. Non-invasive diagnosis of hepatic cirrhosis by transit-time analysis of an ultrasound contrast agent. *Lancet* 1999; **353**: 1579-1583

9 **Bang N**, Nielsen MB, Rasmussen AN, Osterhammel PA, Pedersen JF. Hepatic vein transit time of an ultrasound contrast agent: simplified procedure using pulse inversion imaging. *Br J Radiol* 2001; **74**: 752-755

10 **Kim T**, Murakami T, Takahashi S, Tsuda K, Tomoda K, Narumi Y, Oi H, Sakon M, Nakamura H. Optimal phases of dynamic CT for detecting hepatocellular carcinoma: evaluation of unenhanced and triple-phase images. *Abdom Imaging* 1999; **24**: 473-480

11 **Kudo M**. Morphological diagnosis of hepatocellular carcinoma: special emphasis on intranodular hemodynamic imaging. *Hepatogastroenterology* 1998; **45**(Suppl 3): 1226-1231

12 **Koito K**, Namieno T, Morita K. Differential diagnosis of small hepatocellular carcinoma and adenomatous hyperplasia with power Doppler sonography. *AJR Am J Roentgenol* 1998; **170**: 157-161

13 **Brancatelli G**, Federle MP, Grazioli L, Blachar A, Peterson MS, Thaete L. Focal nodular hyperplasia: CT findings with emphasis on multiphasic helical CT in 78 patients. *Radiology* 2001; **219**: 61-68

14 **Kudo M**. Imaging diagnosis of hepatocellular carcinoma and premalignant / borderline lesions. *Semin Liver Dis* 1999; **19**: 297-309

15 **Kim TK**, Choi BI, Han JK, Hong HS, Park SH, Moon SG. Hepatic tumors: contrast agent-enhancement patterns with pulse-inversion harmonic US. *Radiology* 2000; **216**: 411-417

16 **Ding H**, Kudo M, Onda H, Suetomi Y, Minami Y, Maekawa K. Hepatocellular carcinoma: depiction of tumor parenchymal flow with intermittent harmonic power Doppler US during the early arterial phase in dual-display mode. *Radiology* 2001; **220**: 349-356

17 **Heckemann RA**, Cosgrove DO, Blomley MJ, Eckersley RJ, Harvey CJ, Mine Y. Liver lesions: intermittent second-harmonic gray-scale US can increase conspicuity with microbubble contrast material - early experience. *Radiology* 2000; **216**: 592-596

18 **Ding H**, Kudo M, Onda H, Suetomi Y, Minami Y, Maekawa K. Contrast-enhanced subtraction harmonic sonography for evaluating treatment response in patients with hepatocellular carcinoma. *AJR Am J Roentgenol* 2001; **176**: 661-666

19 **Hancock J**, Dittrich H, Jewitt DE, Monaghan MJ. Evaluation of myocardial, hepatic, and renal perfusion in a variety of clinical conditions using an intravenous ultrasound contrast agent (Optison) and second harmonic imaging. *Heart* 1999; **81**: 636-641

20 **Ueda K**, Matsui O, Kawamori Y, Nakanuma Y, Kadoya M, Yoshikawa J, Gabata T, Nonomura A, Takashima T. Hypervascular hepatocellular carcinoma: evaluation of hemodynamics with dynamic CT during hepatic arteriography. *Radiology* 1998; **206**: 161-166

21 **Gaiani S**, Casali A, Serra C, Piscaglia F, Gramantieri L, Volpe L, Siringo S, Bolondi L. Assessment of vascular patterns of small liver mass lesions: value and limitation of the different Doppler ultrasound modalities. *Am J Gastroenterol* 2000; **95**: 3537-3546

22 **Taylor KJ**, Ramos I, Carter D, Morse SS, Snower D, Fortune K. Correlation of Doppler US tumor signals with neovascular morphologic features. *Radiology* 1988; **166**(Pt 1): 57-62

23 **Lee HM**, Lu DS, Krasny RM, Busuttil R, Kadell B, Lucas J. Hepatic lesion characterization in cirrhosis: significance of arterial hypervascularity on dual-phase helical CT. *AJR Am J Roentgenol* 1997; **169**: 125-130

24 **Van Hoe LV**, Baert AL, Gryspeerdt S, Vandenbosh G, Nevens F, Van Steenbergen W, Marchal G. Dual-phase helical CT of the liver: value of an early-phase acquisition in the differential diagnosis of noncystic focal lesions. *AJR Am J Roentgenol* 1997; **168**: 1185-1192

25 **Nino-Murcia M**, Olcott EW, Jeffrey RB Jr, Lamm RL, Beaulieu CF, Jain KA. Focal liver lesions: pattern-based classification scheme for enhancement at arterial phase CT. *Radiology* 2000; **215**: 746-751

26 **Gryspeerdt S**, Van Hoe L, Marchal G, Baert AL. Evaluation of hepatic perfusion disorders with double-phase spiral CT. *Radio Graphics* 1997; **17**: 337-348

27 **Uggowitzer M**, Kugler C, Groll R, Mischinger HJ, Stacher R, Fickert P, Weiglein A. Sonographic evaluation of focal nodular hyperplasias (FNH) of the liver with a transpulmonary galactose-based contrast agent (Levovist). *Br J Radiol* 1998; **71**: 1026-1032

28 **Ruppert-Kohlmayr AJ**, Uggowitzer MM, Kugler C, Zebedin D, Schaffler G, Ruppert GS. Focal nodular hyperplasia and hepatocellular adenoma of the liver: differentiation with multiphasic helical CT. *AJR Am J Roentgenol* 2001; **176**: 1493-1498

29 **Miyayama S**, Matsui O, Ueda K, Kifune K, Yamashiro M, Yamamoto T, Komatsu T, Kumano T. Hemodynamics of small hepatic focal nodular hyperplasia: evaluation with single-level dynamic CT during hepatic arteriography. *AJR Am J Roentgenol* 2000; **174**: 1567-1569

30 **Yan F**, Zeng M, Zhou K, Shi W, Zheng W, Da R, Fan J, Ji Y. Hepatic angiomyolipoma: various appearances on two-phase contrast scanning of spiral CT. *Eur J Radiol* 2002; **41**: 12-18

Edited by Zhang JZ

P.O.Box 2345, Beijing 100023,China
Fax: +86-10-85381893
E-mail: wjg@wjgnet.com www.wjgnet.com

World J Gastroenterol 2003;9(8):1675-1678
World Journal of Gastroenterology
 ISSN 1007-9327

• LIVER CANCER •

Study on the possibility of insulin as a carrier of IUdR for hepatocellular carcinoma-targeted therapy

Xiao-Hong Ou, An-Ren Kuang, Xian Peng, Yu-Guo Zhong

Xiao-Hong Ou, An-Ren Kuang, Department of Nuclear Medicine, West China Hospital of Sichuan University, Sichuan Province, China
Xian Peng, Yu-Guo Zhong, Department of Pharmaceutical, Sichuan University, Sichuan Province, China
Supported by The National Natural Science Foundation of China, Grant No 30270415
Correspondence to: An-Ren Kuang, Department of Nuclear Medicine, West China Hospital of Sichuan University, Chengdu, China. ouxiaohong2002@xinhuanet.com
Telephone: +86-28-85422696 **Fax:** +86-28-85422696
Received: 2003-01-04 **Accepted:** 2003-02-17

Abstract

AIM: To evaluate the possibility of using insulin as a carrier for carcinoma-targeted therapy mediated by receptor, and to investigate the expression of insulin receptor in human hepatocellular carcinoma and the receptor binding characteristics of insulin-IUdR (iododeoxyuridine).

METHODS: IUdR was covalently conjugated to insulin. Receptor binding assays of ^{125}I-insulin to human hepatocellular carcinoma and its adjacent tissue were performed. Competitive displacements of ^{125}I-insulin by insulin and insulin-IUdR to bind to insulin receptor were respectively carried out. Statistical comparisons between the means were made with paired t-test at a confidence level of 95 %.

RESULTS: The data indicated that there were high- and low- affinity binding sites for ^{125}I-insulin on both hepatocellular carcinoma and its adjacent tissue. Hepatocellular carcinoma had a significantly higher Bmax for high affinity binding site than its adjacent liver tissue (P<0.05, t=2.275). Insulin-IUdR competed as effectively as insulin with ^{125}I-insulin for binding to insulin receptor. Values of $IC_{50}1$, $C_{50}2$, KI1 and KI2 for insulin-IUdR were 11.50±2.83 nmol·L^{-1}, 19.35±5.11 nmol·L^{-1}, 11.26±2.65 nmol·L^{-1} and 19.30±5.02 nmol·L^{-1} respectively, and for insulin were 5.01±1.24 nmol·L^{-1},17.75±4.86 nmol·L^{-1}, 4.85±1.12 nmol·L^{-1} and 17.69±4.81 nmol·L^{-1}, respectively. Values of $IC_{50}1$ and KI1 for insulin-IUdR were significantly higher than that for insulin (P<0.01, t=4.537 and 4.813).

CONCLUSION: It is possible to use insulin as a carrier for carcinoma-targeted therapy mediated by receptor.

Ou XH, Kuang AR, Peng X,Zhong YG. Study on the possibility of insulin as a carrier of IUdR for hepatocellular carcinoma-targeted therapy. *World J Gastroenterol* 2003; 9(8): 1675-1678
http://www.wjgnet.com/1007-9327/9/1675.asp

INTRODUCTION

Hepatocellular carcinoma is one of the most common cancers with highly uneven geographic distribution and its treatment by conventional methods is still difficult. In recent years receptor-based radiopharmaceuticals have been used for localization diagnosis and therapy of certain tumors[1-5]. Insulin may be a convenient carrier for anticancer drugs or radionuclides in targeted therapy of carcinoma, because several studies have shown there is an increased expression of insulin receptor on a variety of malignant tumor cells[6-11]. Moreover, insulin is internalized by cells possessing insulin receptor and reported in the cell nuclei subsequent to endocytosis[12-14].

S-iodo-z-deoxyuridine (IUdR), a thymidine analog, can be incorporated into the DNA of cells in the S phase. ^{125}I-IUdR has been successfully applied for the treatment of bladder cancer and hepatic metastases[15-18]. Short-range Auger electrons emitted by ^{125}I-IUdR can cause DNA double-strand broken and deliver a lethal radiation dose to the cell when it is incorporated into DNA. But when killing malignant cells, ^{125}I-IUdR also brings damage to normal tissues, such as the bone marrow, the small intestine and the large intestine. To reduce the damage, we presented a strategy for IUdR targeting delivery to hepatocellular carcinoma which exploited the efficiency and specificity of internalization afforded by the process of receptor-mediated endocytosis. IUdR was primarily used in this investigation, because it had the identical chemical and biological properties with ^{125}I-IUdR. The expression of insulin receptor in human hepatocellular carcinoma and the receptor binding characteristics of insulin-IUdR conjugate were investigated.

MATERIALS AND METHODS

Preparation of cell membrane

Hepatocellular carcinoma and its adjacent liver tissue specimens were obtained from six patients at surgery whose diagnosis was confirmed by histopathology and immediately frozen at -70 ℃ for further use. Cell membrane fractions were prepared according to established techniques[19]. Tissues were cut into pieces, put into Tris-HCL buffer (pH 7.5) and homogenized. The cell membrane fractions purified by centrifugation in a discontinuity sucrose density gradient were stored at -70 ℃. The protein concentration was determined according to Lowrry method[20].

Radioiodination of insulin

Porcine insulin was radioiodinated with the Ch-T method and purified by polyacrylamide gel electrophoresis. The radiochemical purity of ^{125}I-insulin was measured by TLC (thin layer chromatogray).

Preparation of insulin-IUdR

Insulin-IUdR was kindly synthesized by Department of Pharmaceutical, Sichuan University. Briefly, both IUdR (1.2 g) and succinic anhydride (1.5 g) were dissolved in 25 ml of pyridrine and the mixture was stirred at 70-80 ℃ for 24 hours. The solvents were evaporated under vacuum and the residue was crystallized from isopropanol.

Conjugation of IUdR-succinin to insulin was done as follows: IUdR-succinin (50 mg), EDC (100 mg) and HOBt (50 mg) were dissolved in 3 ml phosphate-buffered saline (pH=8.9) and mixed with 1 ml phosphate-buffered saline (pH=8.9) containing 25 mg insulin. The mixture was stirred at

4 ℃ for 48 hours. The precipitation was removed by filtration and pH of the solvent was adjusted to 5.5 with 0.5 mol· L^{-1} HCl. The reaction mixture was kept at 4 ℃ overnight. Thereafter, white solid precipitation was collected with filter and purified by polyacrylamine agarose gel electrophoresis. The solvents were evaporated under vacuum.

Isolated insulin-IUdR was analyzed by analytical HPLC (Beckman) with 4×200 mm ODS column. The mobile phase was 27 % (v/v) acetonitrile and 73 % 0.1 mol· L^{-1} NaH_2PO_4 (pH=0.3) at a flow rate of 0.5 ml· min^{-1}.

SDS-polyacrylamine gel electrophoresis (SDS-PAGE) was performed in 15 % polyacrylamine gel to calculate the molecular weight of insulin-IUdR.

Saturation binding assay

Cell membrane fractions (80 μg protein) of hepatocellular carcinoma or its adjacent liver tissue were incubated for 20 hours at 4 ℃ with binding buffer (NaCl 118 mmol· L^{-1} $CaCl_2$ 1.3 mmol· L^{-1} KCl 5 mmol· L^{-1} $MgSO_4$ 1.2 mmol· L^{-1} KH_2PO_4 1.2 mmol· L^{-1} pH 7.5) containing increasing concentration (5×10^3-5×10^5 cpm) of ^{125}I-insulin. The free ligands were removed by centrifugation at 2 000×g for 10 minutes after addition of 0.1 ml 0.3 % bovine γ-globulin and 0.8 mL 15.8 % PEG. Radioactivity of the membrane pellets was determined in a gamma counter for one minute as the total binding. The nonspecific binding was estimated by incubating membrane with ^{125}I-insulin in the presence of 4.3 nmol unlabeled insulin. Specific binding was obtained by subtracting nonspecific binding from total binding.

Competition binding assay

Cell membrane fractions (80 μg protein) were incubated with 5 nmol ^{125}I-insulin in the presence of increasing concentrations (10^{-12}-10^{-7} mol/L) of the unlabeled insulin or insulin-IUdR. After incubated for 20 hours at 4 ℃, the unbound ligands were removed as saturation binding assay. Radioactivity of the membrane pellets was determined in a gamma counter for one lmin as the total binding. The nonspecific binding was estimated by incubating membrane with ^{125}I-insulin in the presence of 4.3 nmol unlabeled insulin.

Statistical analysis

Binding data were calculated on a computer with receptor binding analysis software. Values are presented as means ±SD. Statistical comparisons between the means were made with paired *t*-test at a confidence level of 95 %.

RESULTS

Radioiodination of insulin

The radiochemical purity of ^{125}I-insulin was 98 % and remained over 95 % after 14 days stored at -20 ℃.

Analysis of insulin-IUdR

The recovery of insulin-IUdR was about 76.3 %. HPLC showed that isolated insulin-IUdR (retention time 13.91 min) yield was about 98 % (shown in Figure 1). The other 2 % was the insulin (8.81 min) and IUdR (3.87 min).

The calculated molecular weight of insulin-IUdR was 7179Da according to its relative position to the molecular weight marker in the SDS-PAGE pattern.

Saturation binding assay

For cell membrane of hepatocellular carcinoma and its adjacent tissue, as concentration of the radioligand increased, binding amount went up and then plateaued rapidly (Figure 2). The Scatchard plot corresponding to the saturation binding curve had a slightly curvilinear shape (Figure 3). Curvilinear Scatchard plots were characteristic of insulin binding in many other systems and had been attributed to interaction of ligand with two or more classes of sites that exhibited different affinities. Using the RBA software, the Scatchard plot of hepatocellular carcinoma could be resolved in a component with Kd=2.20 nmol· L^{-1} (Bmax=0.36 nmol/L) and another component with Kd=18.8 nmol· L^{-1} (Bmax=1.58 nmol· L^{-1}) by the computer. And that of adjacent tissue could be resolved in a component with Kd=2.21 nmol· L^{-1} (Bmax=0.33 nmol· L^{-1}) and another component with Kd=17.89 nmol· L^{-1} (Bmax=1.09 nmol· L^{-1}). Remarkably higher Bmax of high affinity insulin binding sites was identified in hepatocellular carcinoma (P<0.05).

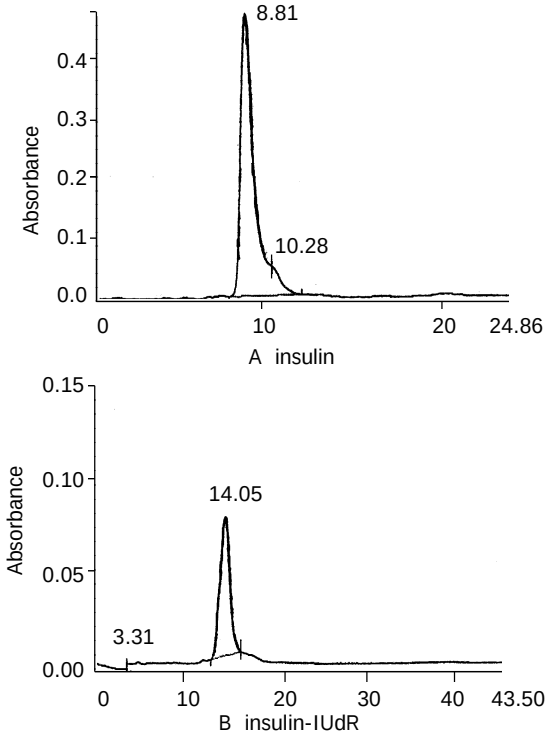

Figure 1 Insulin and insulin-IUdR analysis by HPLC. Retention time of insulin was 8.81 minutes (A); Retention time of insulin-IUdR was 13.91 minutes (B).

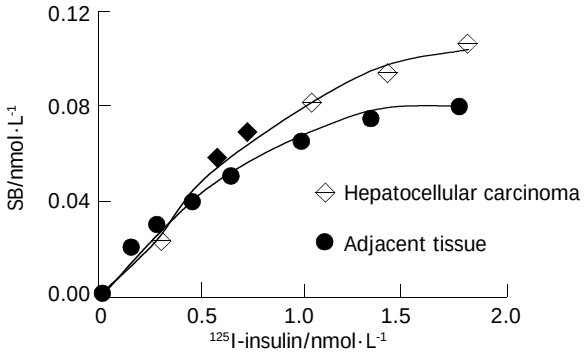

Figure 2 Saturation binding curves of ^{125}I-insulin in hepatocellular carcinoma and its adjacent tissue.

Competition binding assay

Competition displacement assays compared the ability of insulin-IUdR and unlabeled insulin to compete with ^{125}I-insulin for binding to insulin receptor in hepatocellulor carcinoma (Figure 4). The conjugate competed as effectively as insulin for binding to the insulin receptor in a dose-dependent manner. IUdR had no effect on ^{125}I-insulin binding (data not shown). Values of IC_{50} and KI for insulin-IUdR and insulin are shown

in Table 2. Although there were increased $IC_{50}1$ and KI1, the data showed that most of the receptor-binding activity of insulin-IUdR remained.

Table 1 Values of Bmax and Kd of ^{125}I-insulin binding to insulin receptor in hepatocellular carcinoma and its adjacent liver tissue (mean ±SD for six identical experiments)

	High affinity sites		Low affinity sites	
	Bmax (nmol·L^{-1})	Kd (nmol·L^{-1})	Bmax (nmol·L^{-1})	Kd (nmol·L^{-1})
Hepatocellular carcinoma	1.58±0.16[a]	2.20±0.66	0.36±0.11	18.80±7.85
Adjacent liver tissue	1.09±0.51	2.21±0.72	0.33±0.74	17.89±7.87

[a]P<0.05 *vs* adjacent liver tissue. Bmax was the maximal amount of ligand bound; Kd was the dissociation constant of the binding site for the ligand.

Table 2 Values of IC_{50} and KI for insulin-IUdR and insulin competing with ^{125}I-insulin for binding to insulin receptor on hepatocellular carcinoma (mean ±SD for four identical experiments)

	High affinity sites		Low affinity sites	
	IC_{50} (nmol·L^{-1})	KI (nmol·L^{-1})	IC_{50} (nmol·L^{-1})	KI (nmol·L^{-1})
Insulin-IUdR	11.50±2.83[b]	11.26±2.65[b]	19.35±5.11	19.30±5.02
Insulin	5.01±1.24	4.85±1.12	17.75±4.86	17.69±4.81

[b]P<0.01 *vs* insulin. IC_{50} was the concentration of competing ligand to displace radioligand binding by 50 %; KI was the dissociation constant of competing ligand.

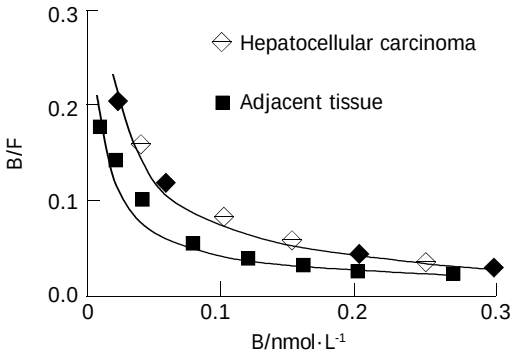

Figure 3 The Scatchard plot corresponding to the saturation binding.

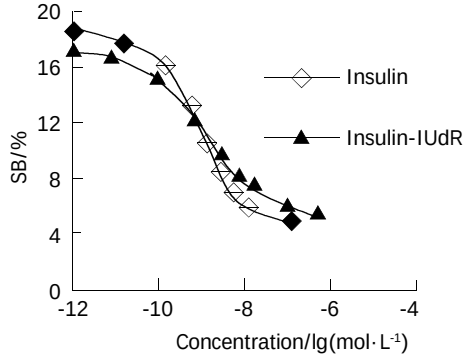

Figure 4 Competitive binding curves of ^{125}I-insulin against insulin-IUdR or insulin.

DISCUSSION

In recent years, there have been several studies on target delivery of specific gene to living cells mediated by insulin receptor. For example, Ivanova *et al* introduced a foreign DNA into early mouse and rabbit embryos by using insulin as a carrier[21], and Alexder carried out transfection of H-11 murine epithelial mammary cells as well as murine and sheep mammary glands using insulin-containing constructs that deliver DNA by receptor-mediated endocytosis[22]. Sosenkranz *et al* synthesized a soluble construct consisting of a plasmid carrying the gene of SV40 large T-antigen and an insulin-poly-L-lysine conjugate which is able to selectively transfect PLC/PRF/S human hepatoma cells possessing insulin receptors[23]. Moreover, Zhang *et al* measured the levels of luciferase gene expression in human or rat glioma cells after targeting the PIL-encapsulated plasmid DNA via human insulin receptor, the human epidermal growth factor receptor, or rat transferrin receptor. The highest levels of gene expression were obtained after targeting the insulin receptor, and this may derive from the nuclear targeting properties of this receptor system[24].

In the present study, we presented a procedure for tumor treatment which combined the targeted transportation function afforded by insulin receptor mediating endocytosis with radiotoxicity of ^{125}I-IUdR to cells at the S phase. IUdR is usually administrated by local infusion or intratumor injection. Systemic therapy is not indicated because of potential severity of undesirable side effects. Insulin used as a carrier might offer an advantage in this aspect. Firstly, most of ^{125}I-IUdR is directly delivered into the liver by insulin. Thereby, other actively dividing normal tissue can efficiently avoid being damaged. Secondly, because of overexpression of insulin receptor in tumor cells, there will be very little conjugate entering normal liver cells. At last, Auger electron' s range is about 10 nm, it is hardly harmful to cells until it is incorporated in the DNA of cells. Since IUdR can only be incorporated in the DNA of cells at the S phase[25], non-dividing tissues possessing insulin receptor will not be injured.

We found that hepatocellular carcinoma bound more ^{125}I-insulin than its adjacent liver tissue. Amir kurtaran has successfully applied ^{123}I-insulin for *in vivo* scintigraphy in the diagnosis of hepatocellular carcinoma[26]. Kuang Anren reported that ^{131}I-insulin was localized within H22 hepatoma in mice, and cleared rapidly from the rest of the body[27]. Schars reported that insulin receptor might play a role in the regulation of hepatocellular carcinoma[28]. Our finding was consistent with theirs. The results demonstrated that escalated binding site for ^{125}I-insulin was expressed in hepatocellular carcinoma. The Bmax values indicated that the increased binding of ^{125}I-insulin in hepatocellular carcinoma was due to an apparent increase in high affinity insulin receptor rather than an increase in low affinity insulin receptor. Our studies also showed that high affinity insulin receptor, constituting 87.72 % of insulin receptor on cell surface of hepatocellular carcinoma, predominated over low affinity insulin receptor. These observations indicated that more IUdR covalently linked to insulin could be transferred to the carcinoma through mediation of the overexpressed high affinity insulin receptor.

It has also been verified in *in vitro* studies that insulin-IUdR is capable of binding specifically to insulin receptor in human hepatocellular carcinoma with high affinity. Chakrabarti *et al* conjugated ^{125}I-IUdR with T101 antibody via polylysine, but the conjugate remained only 68 % immunoactivity[29]. The conjugate used was prepared by covalently linking IUdR to insulin via succine. This complex has an advantage over the conjugate linked via poly-L-lysine[30] or albumin[31] or other large molecules. Both succine and IUdR are small molecules. The small size of the complex may result in less interference in insulin binding to its receptor or other cellular proteins and may permit this complex to be processed intracellularly in a manner more identical to that of unlabelled insulin.

Why insulin-IUdR has an increased IC_{50} and KI for high affinity insulin receptor but not for low affinity receptor is unclear. It is possible that the functional sites of structural microheterogeneity in the two receptors have different sensitivity to the structural change of ligand. Competition binding assays showed that insulin-IUdR still maintained the greater part of affinity for insulin receptor. Therefore, it is not necessary to administer insulin-IUdR in a micromolar range, which may result in glucopenia.

SDS-polyacrylamine agarose gel electrophoresis showed the molecular weight of insulin-IUdR was 7 179 Da, which was equal to the total weight of one molecule of insulin (M_r=5 800 Da) and three molecules of IUdR (M_r=454 Da). It might be concluded that the ratio of insulin molarity to the IUdR is 1:3. On the basis of this molar ratio, it is calculated that for administration 100-300 MBq ^{125}I-IUdR, about 10^{-9}mol insulin was required. Administration of such a low dose of insulin in therapy would not result in glucopenia.

In summary, hepatocellular carcinoma overexpressing insulin receptor and insulin-IUdR conjugate can specifically bind to insulin receptor. This new conjugate holds promise for therapy of hepatocellular carcinoma, but further investigation into transportation of IUdR and its interactions with tumor cells during subsequent intracellular processing would be a desirable prerequisite.

REFERENCES

1 **Menda Y**, Kahn D. Somatostatin receptor imaging of non-small cell lung cancer with 99mTc depreotide. *Semin Nucl Med* 2002;**32**: 92-96

2 **Virgolini** I, Traub T, Novotny C, Leimer M, Fuger B, Li SR, Patri P, Pangerl T,Angelberger P, Raderer M, Andreae F, Kurtaran A, Dudczak R. New trends in peptide receptor radioligands. *Q J Nucl Med* 2001; **45:** 153-159

3 **Rao PS**, Thakur ML, Pallela V, Patti R, Reddy K, Li H, Sharma S, Pham HL, Diggles L, Minami C, Marcus CS. 99mTc labeled VIP analog: evaluation for imaging colorectal cancer. *Nucl Med Biol* 2001; **28**: 445-450

4 **Thakur ML**, Marcus CS, Saeed S, Pallela V, Minami C, Diggles L, Le Pham H, Ahdoot R, Kalinowski EA. 99mTc-labeled vasoactive intestinal peptide analog for rapid localization of tumors in humans. *J Nucl Med* 2000; **41**: 107-110

5 **Heppeler A**, Froidevaux S, Eberle AN, Maecke HR. Receptor targeting for tumor localisation and therapy with radiopeptides. *Curr Med Chem* 2000; **7**: 971-994

6 **Kalli KR**, Falowo OI, Bale LK, Zschunke MA, Roche PC, Conover CA. Functional insulin receptors on human epithelial ovarian carcinoma cells:implications for IGF-II mitogenic signaling. *Endocrinology* 2002; **143**: 3259-3267

7 **Vella V**, Sciacca L, Pandini G, Mineo R, Squatrito S, Vigneri R, Belfiore A. The IGF system in thyroid cancer: new concepts. *Mol Pathol* 2001; **54**: 121-124

8 **Maune S**, Gorogh T. Detection of overexpression of insulin receptor gene in laryngeal carcinoma cells by using differential display method. *Laryngorhinootologie* 2000; **79**: 438-441

9 **Spector SA**, Olson ET, Gumbs AA, Friess H, Buchler MW, Seymour NE. Human insulin receptor and insulin signaling proteins in hepatic disease. *J Surg Res* 1999; **83**: 32-35

10 **Frittitta L**, Vigneri R, Stampfer MR, Goldfine ID. Insulin receptor overexpression in 184B5 human mamary epithelial cells induces a ligand-dependent transformed phenotype. *J Cell Biochem* 1995; **57**: 666-669

11 **Freund GG**, Kulas DT, Way BA, Mooney RA. Functional insuln and insulin-like growth factor-1 receptors are preferentially expressed in multiple myeloma cell lines as compared to B-lymphoblastoid cell lines. *Cancer Res* 1994; **54**: 3179-3185

12 **Shah N**, Zhang S, Harada S, Smith RM, Jarett L. Electron microscopic visualization of insulin translocation into the cytoplasm and nuclei of intact H35 hepatoma cells using covalently linked nanogold-insulin. *Endocrinology* 1995; **136**: 2825-2835

13 **Harada S**, Smith RM, Smith JA, Jarett L. Inhibition of insulin-degrading enzyme increases translocation of insulin to the nucleus in H35 rat hepatoma cells: evidence of a cytosolic pathway. *Endocrinology* 1993; **132**: 2293-2298

14 **Harada S**, Loten EG, Smith RM, Jarett L. Nonreceptor mediated nuclear accumulation of insulin in H35 rat hepatoma cells. *J Cell Physiol* 1992; **153**: 607-613

15 **Chiou RK**, Dalrymple GV, Baranowska-Kortylewicz J, Holdeman KP, Schneiderman MH, Harrison KA, Taylor RJ. Tumor localization and systemic absorption of intravesical instillation of radio-iodinated iododeoxyuridine in patients with bladder cancer. *J Urol* 1999; **162**: 58-62

16 **Morgan RJ Jr**, Newman EM, Doroshow JH, McGonigle K, Margolin K, Raschko J, Chow W, Somlo G, Leong L, Tetef M, Shibata S, Hamasaki V, Carroll M, Vasilev S, Akman S, Coluzzi P, Wagman L, Longmate J, Paz B, Yen Y, Klevecz R. Phase I trial of intraperitoneal iododeoxyuridine with and without intravenous high-dose folinic acid in the treatment of advanced malignancies primarily confined to the peritoneal cavity: flow cytometric and pharmacokinetic analysis. *Cancer Res* 1998; **58**: 2793-2800

17 **Sondak VK**, Robertson JM, Sussman JJ, Saran PA, Chang AE, Lawrence TS. Preoperative idoxuridine and radiation for large soft tissue sarcomas: clinical results with five-year follow-up. *Ann Surg Oncol* 1998; **5**: 106-112

18 **Daghighian F**, Humm JL, Macapinlac HA, Zhang J, Izzo J, Finn R, Kemeny N, Larson SM. Pharmacokinetics and dosimetry of iodine-125-IUdR in the treatment of colorectal cancer metastatic to liver. *J Nucl Med* 1996; **37**(Suppl 4): 29s-32s

19 **Yan XQ**, Cheng ML, Liu BW, Lan TH. Study on binding assay of insulin receptor in liver cell membrane. *Zhonghua Heyixue Zazhi* 1986; **6**: 91-93

20 **Cheng YQ**. Shengwu huaxue shiyan fangfa he jishu.1. Beijing: *Science Press* 2002: 164-166

21 **Ivanova MM**, Rosenkranz AA, Smirnova OA, Nikitin VA, Sobolev AS, Landa V, Naroditsky BS, Ernst LK. Receptor-mediated transport of foreign DNA into preimplantation mammalian embryos. *Mol Reprod Dev* 1999; **54**: 112-120

22 **Sobolev AS**, Rosenkranz AA, Smirnova OA, Nikitin VA, Neugodova GL, Naroditsky BS, Shilov IN, Shatski IN, Ernst LK. Receptor mediated transfection of murine and ovine mammary glands *in vivo*. *J Biol Chem* 1998; **273**: 7928-7933

23 **Rosenkranz AA**, Yachmenev SV, Jans DA, Serebryakova NV, Murav'ev VI, Peters R, Sobolev AS. Receptor-mediated endocytosis and nuclear transport of a transfecting DNA construct. *Exp Cell Res* 1992; **199**: 323-329

24 **Zhang Y**, Boado RJ, Pardridge WM. Marked enhancement in gene expression by targeting the human insulin receptor. *J Gene Med* 2003; **5**: 157-163

25 **Toyohara J**, Hayashi A, Sato M, Tanaka H, Haraguchi K, Yoshimura Y, Yonekura Y, Fujibayashi Y. Rationale of 5-^{125}I-iodo-4'-thio-2'-deoxyuridine as a potential iodinated proliferation marker. *J Nucl Med* 2002; **43**: 1218-1226

26 **Kurtaran A**, Li SR, Raderer M, Leimer M, Muller C, Pidlich J, Neuhold N, Hubsch P, Angelberger P, Scheithauer W, Virgolini I. Technetium-99m-galactosyl- neoglycoal bumin combined with iodine-123Tyr (A14) insulin visualized human hepatocellular carcinomas. *J Nucl Med* 1995; **36**: 1875-1881

27 **Kuang AR**, Zhou LY, Liang ZL, Tan TZ, Wang CJ. Evaluation of hepatoma targeting ability with radioiodiated insulin in H22 bearing mice. *Zhonghua Heyixue Zazhi* 1999; **19**: 179-180

28 **Scharf JG**, Dombrowski F, Ramadori G. The IGF axis and hepatocarcinogenesis. *Mol Pathol* 2001; **54**: 138-144

29 **Chakrabarti MC**, Paik CH, Carrasquillo JA. Preparation and *in vitro* studies of [125I]IUDR-T101 antibody conjugate. *Cancer Biother Radiopharm* 1999; **14**: 91-98

30 **Wagner E**, Ogris M, Zauner W. Polylysine-based transfection systems utilizing receptor-mediated delivery. *Adv Drug Deliv Rev* 1998; **30**: 97-113

31 **Huckett B**, Ariatti M, Hawtrey AO. Evidence for targeted gene transfer by receptor-mediated endocytosis. Stable expression following insulin-directed entry of NEO into HepG2 cells. *Biochem Pharmacol* 1990; **40**: 253-263

Edited by Xu XQ and Zhu LH

P.O.Box 2345, Beijing 100023,China
Fax: +86-10-85381893
E-mail: wjg@wjgnet.com www.wjgnet.com

World J Gastroenterol 2003;9(8):1679-1682
World Journal of Gastroenterology
 ISSN 1007-9327

• LIVER CANCER •

Assessment of hepatic VX2 tumors of rabbits with second harmonic imaging under high and low acoustic pressures

Wen-Hua Du, Wei-Xiao Yang, Xiang Wang, Xiu-Qin Xiong, Yi Zhou, Tao Li

Wen-Hua Du, Wei-Xiao Yang, Xiang Wang, Xiu-Qin Xiong, Yi Zhou, Tao Li, Department of Ultrasonography, Daping Hospital and Research Institute of Surgery, the Third Military Medical University, Chongqing 400042, China
Supported by the National Natural Science Foundation of China, No. 30070227
Correspondence to: Wen-Hua Du, Department of Ultrasonography, Daping Hospital and Research Institute of Surgery, the Third Military Medical University, Chongqing 400042, China. duwenhua001@163.com
Telephone: +86-23-68757441
Received: 2002-10-08 **Accepted:** 2003-02-11

Abstract

AIM: To investigate the possible clinical application value of second harmonic imaging under low acoustic pressure.

METHODS: Six New Zealand rabbits, averaging 2.7±0.4 kg, were selected and operated upon to construct hepatic VX2 tumor carrier model. Hepatic VX2 tumors were imaged with B mode Ultrasonography (US), and second harmonic imaging (SHI) under high mechanic index (1.6) and low mechanic index (0.1). Echo agent was intravenously injected through ear vein at a dose of 0.01 mL/kg under B mode US and high MI SHI, and 0.05 mL/kg under low MI SHI, and then the venous channel was cleaned with sterilized saline. All the images were recorded by magnetic optics (MO), and they were analyzed further by at least two independent experienced sonographers.

RESULTS: Totally 6 hypoechoic and 3 hyperechoic lesions were found in the six carrier rabbits with a mean size about 2.1±0.4 under B mode ultrasound, they were oval or round in shape with a clear outline or a hypoechoic halo at the margin of the lesions. Contrast agent could not change the echogenicity of the lesions under B mode US and SHI under high acoustic pressure. However, it could greatly increase the real time visualization sensitivity of the lesions with SHI under low acoustic pressure.

CONCLUSION: Our results suggest that contrast enhanced SHI with low MI and a bubble non-destructive method would be much more helpful than conventional SHI in our future clinical applications.

Du WH, Yang WX, Wang X, Xiong XQ, Zhou Y, Li T. Assessment of hepatic VX2 tumors of rabbits with second harmonic imaging under high and low acoustic pressures. *World J Gastroenterol* 2003; 9(8): 1679-1682
http://www.wjgnet.com/1007-9327/9/1679.asp

INTRODUCTION

Second harmonic imaging (SHI) technique has been shown more valuable than conventional B mode ultrasonography (US). SHI involves transmitting at frequency *f* and receiving at frequency *2f*, and the contrast enhanced echoes can therefore be obtained at second harmonic frequency because of the non-linear motion of the gas bubbles when destroyed by high acoustic pressures[1,2]. However, the use of second harmonic technique under high acoustic pressure (mechanical indexes 0.6-1.2) does not usually provide ideal images because of the short duration of enhancement and no quantitative evaluation and other technical difficulties. To avoid this, new dedicated software operating at low acoustic pressure (mechanical index <0.4) has been demonstrated to produce significant harmonic answer together with a real time imaging based on the maintenance of microbubbles. Only very small amount of microbubbles would allow the evaluation of blood flow volume and blood flow in normal and pathologic tissues. Liver image has been recently proven to be the first area where microbubbles manifest similarly to that of computed tomography or magnetic resonance imaging contrast media. In particular, this technique, applied to the evaluation of perfusional pattern of hepatic mass lesions, provides a significant contribution to their detection and characteristics. In this study, we aimed to find out the features of these two ultrasonographic methods in the depiction of hepatic metastasis.

MATERIALS AND METHODS

Preparation of animal models

Six New Zealand rabbits weighing 2.6-3.2 kg, average 2.7±0.4 kg, were anaesthetized by Sumianxin (a product of the Changchun Argo-Pastoral University) at 0.2 mL/kg through intramuscular injection. Hairs over the abdominal region were moulted by 8 % sodium sulfide, then the region was cleaned by saline water. Median incision right beneath the metasternum was made to expose the right lobe of liver. A tunnel about 3 cm deep at the lobe was constructed with an ophthalmic nipper. Viable VX2 tumor masses about 2-3 mm^3 were implanted into the tunnel, locally stanched and then each layer of the abdominal wall was sutured accordingly. 2 or 3 weeks later, these rabbits were ready for use. VX2 tumor is a kind of skin squamous cancer induced by Shope virus, viable VX2 tumor could be transplanted and underwent passages in the New Zealand rabbits, and therefore was used as mimicking metastatic hepatic tumor models.

Preparation of echo contrast agent

Self made echo contrast agent was made from 5 % (g/L) human albumin and 40 % (g/L) Dextran at a ratio of 1:3 (v/v), the mixture was then undergone electromechanical sonication (Sonication machine JY92-2D was manufactured by Ninbo Xinzhi Research Institute) for 90 seconds under mechanical energy of 280 W. During the sonication process, perfluropropane gas was mixed into the mixture. Microbubbles manufactured in this way were counted by a Coulter counter, at a concentration of 1.6×10^9 bubbles/L averaging 4.3±2.1 μm.

Equipment

A transducer S8 connected to HP-5500 ultrasound system was used, second harmonic imaging was transmitted at frequency 3MHz receiving at frequency 6 MHz, conventional mechanic index was tuned to 1.6, while low mechanic index was tuned

to 0.1. During the whole process of experiment, the image depth, compensation and TGC should be kept constant.

Methods

Hepatic VX2 tumors were imaged with conventional B mode US, and second harmonic imaging (SHI) under conventional mechanic index (1.6) and low mechanic index (0.1). An intravenous bolus echo agent was injected through ear vein at a dose of 0.01 mL/kg under conventional B mode US and high acoustic pressure SHI, and 0.05 mL/kg under low acoustic pressure SHI, and then the venous channel was cleaned with sterilized saline. All the images were recorded real-timely by magnetic optics (MO), and they were analyzed further by at least two independent but experienced sonographers.

RESULTS

Features of VX2 tumor under conventional and harmonic B mode US

A total of 6 hypoechoic and 3 hyperechoic lesions were found in the six carrier rabbits with a mean size of 2.1±0.4 cm under conventional B mode ultrasound, no hyperechoic or iso echoic lesions were found. They were oval or round in shape with a clear outline or a hypoechoic halo at the margin of the lesions. Contrast images under conventional B mode US also showed no improvement at all (Figure 1).

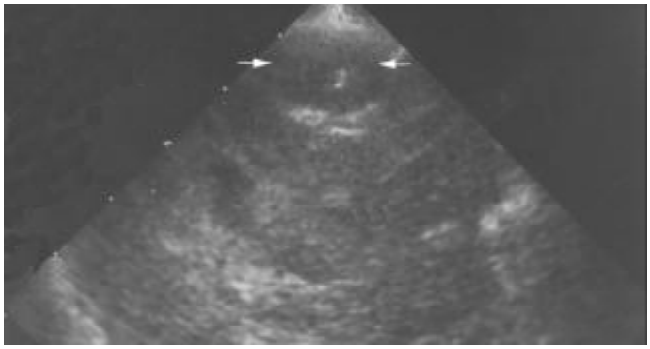

Figure 1 Image of VX2 tumor lesion under conventional B mode US. Arrow indicated the VX2 tumor lesion at the anterior part of the right lobe. It was oval and hypoechoic with a small hyperechoic scar at the center of the lesion.

VX2 tumor lesions assessed by SHI under high and low acoustic pressures

SHI under high acoustic pressure (Mechanic index 1.6) could reveal a short duration enhancement of the hepatic arteries and tumor lesions at the early phase, and an enhancement of the liver parenchyma and a decreased echo at the later phase. A pronounced arterial enhancement was also found at one side of the lesion, which might be considered as the nutrient artery of the tumor. In addition, branches of the afferent artery were seen at the same time. Interestingly, a branch vessel was also found coming from the same artery going to the other side of the lesion as shown in Figure 2a. The whole process of contrast enhanced SHI under high acoustic pressure lasted only for a few seconds.

Visualization by second harmonic imaging under low acoustic pressure was quite different from that by SHI under low acoustic pressure. The echogenicity of liver parenchyma and hepatic VX2 tumor lesions was extremely low, and no structures were observable at first. About five seconds after injection of contrast agent, image of the inferior vena cava could be observed. Again about fifteen seconds later, the contrast agent could be observed within the tumor lesion, as time went by, the afferent artery and its branches of the lesion could gradually and clearly be visualized. A suspicious branch artery was also observed going to the other side of the lesion near the afferent vessels, as what we observed by second harmonic imaging under high acoustic pressure (Figure 2b). As the contrast agent accumulated in the lesion, VX2 tumor appeared as a hyperechoic contour and even satellite lesions could also be observable just beside the original lesion (Figure 3). About 40 seconds later, arteries in the liver parenchyma gradually appeared markedly, and about 20 to 30 seconds afterwards the portal venous system could be visualized. At this stage, the tumor lesion was revealed as hypoechoic. During the last stage period, about 2 minutes after injection of contrast agent, the echogenicity of the liver parenchyma became hyperechoic, while the tumor lesion and its satellite lesion became typically hypoechoic. The whole process of visualization by second harmonic imaging under low acoustic pressure lasted for almost four minutes.

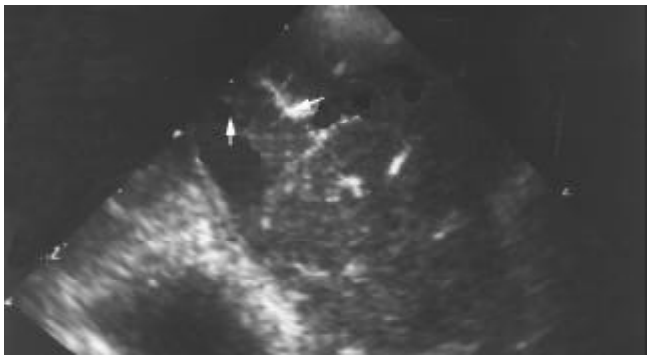

Figure 2a Image of VX2 tumor lesion under high MI second harmonic imaging. Arrow indicated the nutrient artery of same VX2 tumor lesion, and the suspicious artery of a satellite lesion.

Figure 2b Contrast enhanced second harmonic image under low MI revealed the enhancement of nutrient arteries of VX2 tumor lesion and the nutritive artery of satellite lesion.

Figure 3 Image of second harmonic under low MI. It showed the clear tumor and its satellite lesion.

DISCUSSION

The accurate recognition or exclusion of focal liver lesions was a primary objective of diagnostic imaging in patients who were suspected to have a tumor, and the detection of tumor lesions should include their number, location and size. Detection of small liver lesions may be difficult when the acoustic properties of the lesions were similar to those of the surrounding liver parenchyma[3]. The overall accuracy of US imaging in the detection of liver lesions has been shown to range from 53-77 %, but the sensitivity of milimeter nodules has been found to be as low as 20 %[4-6]. US contrast agents were originally developed and used to overcome some of the shortage of US in the assessment of lesional and parenchymal microcirculation by increasing the linear backscattering from the microvascular blood pool. The latest generation of US contrast agents prepared from perflurocarbon gases has been shown to be highly effective in enhancing Doppler signals within the macrovasculature and the microvasculature for several minutes following an intravenous bolus injection[7-9]. However, US contrast agents do not enhance the tumor lesion or parenchyma microvasculature on the fundamental gray-scale image, since the echoes from the tissues are too strong compared to the small volume of microbubbles in the microcirculation[10]. Thus these agents do not significantly improve the detectability of liver lesions when used in association with fundamental imaging, as what we have found in this study. It is necessary to take advantage of their nonlinear characteristics and selectively detect their emission of harmonics in order to increase the US sensitivity to contrast.

A dramatic improvement of contrast enhanced US was the discovery that the bursting of air-based microbubbles caused by high mechanic acoustic pressure US generated large quantities of harmonic frequencies (non-linear response). By decreasing the fundamental frequency, the contrast between highly vascularized lesions containing microbubbles and poorly vascularized tissues were increased[11-14]. Therefore, both macrovasculature and microvasculature of the liver tumor lesions could be well visualized. Some significant limitations about this technique have also been found. Due to the need of breaking air based microbubbles in order to achieve harmonics, the scans have to be started only 2-3 minutes following contrast agent bolus injection, and thus would miss completely the arterial and early portal phases. Furthermore, since all malignancies appear as hypoechoic and all benign tumors isoechoic in late phase[15], discrimination between hepatocellular carcinoma and metastasis, hemangiomas and focal nodular hyperplasia cannot be achieved. In our experiment, although contrast enhanced second harmonic imaging under high acoustic pressure could reveal an increased visualization of the tumor lesions and its surrounding liver parenchymal arteries, the major defect of this method was the short duration of visualization. A suitable method for the detection of hypervascular and hypovascular focal liver lesions should be a bubble non-destruction method with very low MI and high sensitivity for harmonics, allowing continuous real-time imaging of the whole liver and the visualization at the arterial, portal, and late phase during the same examination period with a single contrast agent administration only[16-21]. Furthermore, it should allow us to carry out perfusion and reperfusion studies following the planned bubble destruction and characterization of either hyper- or hypovascular lesions simultaneously[21-25]. We herewith reported our experimental results using this new technique, using a low MI SHI, a nearly complete cancellation of signals from stationary tissues was achieved. Prior to the injection of self-made albumin contrast agent, only high amplitude signals were visualized, such as large vessel walls and the diaphragm. After albumin contrast agent injection, a true subtraction effect was obtained due to the high level harmonic signals coming from the bubbles and the dynamic threshold suppressing low amplitude signals moving toward the transducer. In all rabbits, the whole vasculatures could be observed and studied, including an arterial phase about 15-40 seconds, an early portal phase about 40 to 50 seconds, and a complete portal phase about one and a half minutes. This result is in agreement with what has been described by Solbiati, and this "portal phase" is suggested to be "hepatic sinusoidal phases"[26-31]. The scans could be performed to study the changes of enhancement in these areas by moving the transducer throughout the liver visualizing not only the vascular phases in real time, but also any peculiar region of interest. Using this technique of second harmonic imaging under low acoustic pressure, we could therefore achieve the best visualization of macrocirculation and microcirculation simultaneously. Most interestingly, some satellite lesions, which were not found by high MI SHI, were now clearly revealed by low MI SHI as shown in Figures 2b and 3. It can be concluded that contrast enhanced ultrasonography with second harmonic imaging under low acoustic pressure is currently more sensitive than that with second harmonic imaging under high acoustic pressure in the detection of metastatic lesions as VX2 tumors. This study suggests that this new technique of low MI and microbubble non-destructive method would be much more helpful in our future clinical applications.

REFERENCES

1 **Choi BI,** Kim TK, Han JK, Kim AY, Seong CK, Park SJ. Vascularity of hepatocellular carcinoma: assessment with contrast-enhanced second-harmonic versus conventional power Doppler US. *Radiology* 2000; **214**: 381-386

2 **Kono Y,** Moriyasu F, Nada T, Suginoshita Y, Matsumura T, Toda Y, Nakamura T, Chiba T. Ultrasonographic arterial portography with second harmonic imaging: evaluation of hepatic parenchymal enhancement with portal venous flow. *J Ultrasound Med* 1999; **18**: 395-402

3 **Sirlin CB,** Girard MS, Baker KG, Steinbach GC, Deiranieh LH, Mattrey RF. Effect of acquisition rate on liver and portal vein enhancement with microbubble contrast. *Ultrasound Med Biol* 1999; **25**: 331-338

4 **Tanaka S,** Kitamura T, Ohshima A, Umeda K, Okuda S, Ohtani T, Tatsuta M, Yamamoto K. Diagnostic accuracy of ultrasonography for hepatocellular carcinoma. *Cancer* 1986; **58**: 344-347

5 **Tanaka S,** Kitamura T, Nakanishi K, Okuda S, Kojima J, Fujimoto I. Recent advances in ultrasonographic diagnosis of hepatocellular carcinoma. *Cancer* 1989; **63**: 1313-1317

6 **Tanaka S,** Kitamura T, Imaoka S, Sasaki Y, Taniguchi H, Ishiguro S. Hepatocellular carcinoma: sonographic and histologic correlation. *Am J Roentgenol* 1983; **140**: 701-707

7 **Harvey CJ,** Blomley MJ, Eckersley RJ, Cosgrove DO, Patel N, Heckemann RA, Butler-Barnes J. Hepatic malignancies: Improved detection with pulse-inversion US in late phase of enhancement with SHU508A-early experience. *Radiology* 2000; **216**: 903-908

8 **Carter R,** Hemingway D, Cooke TG, Pickard R, Poon FW, MacKillop JA, McArdle CS. A prospective study of six methods for detection of hepatic colorectal metastases. *Ann Royal Coll Surg Eng* 1996; **78**: 27-30

9 **Forsberg F,** Liu JB, Merton DA, Rawool NM, Goldberg BB. Parenchymal enhancement and tumor visualization using a new sonographic contrast agent. *J Ultrasound Med* 1995; **14**: 949-957

10 **Girard MS,** Sirlin CB, Baker KG, Hall LA, Mattrey RF. Liver tumor detection with ultrasound contrast: a blinded prospective study in rabbits. *Acad Radiol* 1998; **5**(Suppl 1): S189-191

11 **Mattrey RF,** Wrigley R, Steinbach GC, Schutt EG, Evitts DP. Gas emulsions as ultrasound contrast agents: preliminary results in rabbits and dogs. *Invest Radiol* 1994; **29**(Suppl 2): S139-S141

12 **Girard MS,** Kono Y, Sirlin CB, Baker KG, Deiranieh LH, Mattrey RF. B-mode enhancement of the liver with microbubble contrast agent: a blinded study in rabbits with VX2 tumors. *Acad Radiol* 2001; **8**: 734-740

13 **Porter TR,** Xie F. Visually discernible myocardial echocardiographic contrast after intravenous injection of solicated dextrose albumin microbubbles containing high molecular weight, less soluble gases. *J Am Coll Cardiol* 1995; **25**: 509-515
14 **Kim TK,** Han JK, Kim AY, Choi BI. Limitations of characterization of hepatic hemangiomas using a sonographic contrast agent (Levovist) and power Doppler ultrasonography. *J Ultrasound Med* 1999; **18**: 737-743
15 **Koito K,** Namieno T, Morita K. Differential diagnosis of small hepatocellular carcinoma and adenomatous hyperplasia with power Doppler sonography. *Am J Roentgenol* 1998; **170**: 157-161
16 **Gaiani S,** Casali A, Serra C, Piscaglia F, Gramantieri L, Volpe L, Siringo S, Bolondi L. Assessment of vascular patterns of small liver mass lesions: value and limitation of the different Doppler ultrasound modalities. *Am J Gastroenterol* 2000; **95**: 3537-3546
17 **Kim TK,** Choi BI, Han JK, Hong HS, Park SH, Moon SG. Hepatic tumors: contrast agent-enhancement patterns with pulse-inversion harmonic US. *Radiology* 2000; **216**: 411-417
18 **Choi BI,** Kim TK, Han JK, Chung JW, Park JH, Han MC. Power versus conventional color Doppler sonography: comparison in the depiction of vasculature in liver tumors. *Radiology* 1996, **200**: 55-58
19 **Bartolozzi C,** Lencioni R, Ricci P, Paolicchi A, Rossi P, Passariello R. Hepatocellular carcinoma treatment with percutaneous ethanol injection: evaluation with contrast-enhanced color Doppler US. *Radiology* 1998; **209**: 387-393
20 **Seidel G,** Vidal-Langwasser M, Algermissen C, Gerriets T, Kaps M. The influence of doppler system settings on the clearance kinetics of different ultrasound contrast agents. *Eur J Ultrasound* 1999; **9**: 167-175
21 **Cosgrove D.** Ultrasound contrast enhancement of tumors. *Clin Radiol* 1996; **51**(Suppl 1): 44-49
22 **Gaiani S,** Volpe L, Piscaglia F, Bolondi L. Vascularity of liver tumours and recent advances in Doppler ultrasound. *J Hepatol* 2001; **34**: 474-482
23 **Leen E,** McArdle CS. Ultrasound contrast agents in liver imaging. *Clin Radiol* 1996; **51**(Suppl 1): 35-39
24 **Cosgrove D**. Microbubble enhancement of tumour neovascularity. *Eur Radiol* 1999; **9**(Suppl 3): S413-414
25 **Strobel D,** Krodel U, Martus P, Hahn EG, Becker D. Clinical evaluation of contrast enhanced color Doppler sonography in the differential diagnosis of liver tumors. *J Clin Ultrasound* 2000; **28**:1-13
26 **Hosten N,** Puls R, Bechstein WO, Felix R. Focal liver lesions: Doppler ultrasound. *Eur Radiol* 1999; **9**: 428-435
27 **Leen E.** The role of contrast-enhanced ultrasound in the characterisation of focal liver lesions. *Eur Radiol* 2001; **11**(Suppl 3): E27-34
28 **Ramnarine KV,** Kyriakopoulou K, Gordon P, McDicken NW, McArdle CS, Leen E. Improved characterization of focal liver tumors: dynamic power Doppler imaging using NC100100 echo-enhancer. *Eur J Ultrasound* 2000; **11**: 95-104
29 **Solbiati L,** Tonolini M, Cova L, Goldberg SN. The role of contrast-enhanced ultrasound in the detection of focal liver lesions. *Eur Radiol* 2001; **11**(Suppl 3): E15-26
30 **Catalano O,** Esposito M, Lobianco R, Cusati B, Altei F, Siani A. Hepatocellular carcinoma treated with chemoembolization: assessment with contrast-enhanced doppler ultrasonography. *Cardiovasc Intervent Radiol* 1999; **22**: 486-492
31 **Blomley M,** Albrecht T, Cosgrove D, Jayaram V, Butler-Barnes J, Echersley R. Stimulated acoustic emission in liver parenchyma with Levovist. *Lancet* 1998; **351**: 568

Edited by Wu XN and Wang XL

P.O.Box 2345, Beijing 100023,China
Fax: +86-10-85381893
E-mail: wjg@wjgnet.com www.wjgnet.com

World J Gastroenterol 2003;9(8):1683-1688
World Journal of Gastroenterology
 ISSN 1007-9327

• LIVER CANCER •

Peroxisome proliferator-activated receptor gamma ligands inhibit cell growth and induce apoptosis in human liver cancer BEL-7402 cells

Ming-Yi Li, Hua Deng, Jia-Ming Zhao, Dong Dai, Xiao-Yu Tan

Ming-Yi Li, Dong Dai, Xiao-Yu Tan, Department of General Surgery, Affiliated Hospital of Guangdong Medical College, Zhangjiang 524001, Guangdong Province, China
Hua Deng, Department of Biochemistry and Molecular Biology, Beijing Institute for Cancer Research, Da Hong-Luo Chang Street, Beijing 100034, China
Jia-Ming Zhao, Central Experiment, Affiliated Hospital of Guangdong Medical College, Zhangjiang 524001, Guangdong Province, China
Correspondence to: Ming-Yi Li, Department of General Surgery, Affiliated Hospital of Guangdong Medical College, Zhangjiang 524001, Guangdong Province, China. zjmyli@sohu.com
Telephone: +86-759-2387613
Received: 2002-11-06 **Accepted:** 2003-01-28

Abstract

AIM: To investigate the characteristics of PPAR gamma ligands induced apoptosis in liver cancer cells.

METHODS: The effects of ligands for each of the PPAR gamma ligands on DNA synthesis and cell viability were examined in BEL-7402 liver cancer cells. Apoptosis was characterized by Hochest33258 staining, DNA fragmentation, TUNEL and ELISA, and cell cycle kinetics by FACS. Modulation of apoptosis related caspases expression by PPAR gamma ligands was examined by Western blot.

RESULTS: PPARgamma ligands, 15-deoxy-^{12,14}-prostaglandin J2 (15d-PGJ2) and troglitazone (TGZ), suppressed DNA synthesis of BEL-7402 cells. Both 15d-PGJ2 and TGZ induced BEL-7402 cell death in a dose dependent manner, which was associated with an increase in fragmented DNA and TUNEL-positive cells. At concentrations of 10 and 30 μM, 15d-PGJ_2 or troglitazone increased the proportion of cells with G_0/G_1 phase DNA content and decreased those with S phase DNA content. There was no significant change in the proportion of cells with G_2/M DNA content. The activities of Caspases-3, -6, -7 and -9 were increased by 15d-PGJ2 and TGZ treatment, while the activity of Caspase 8 had not significantly changed.

CONCLUSION: The present results suggest the potential usefulness of PPAR gamma ligands for chemoprevention and treatment of liver cancers.

Li MY, Deng H, Zhao JM, Dai D, Tan XY. Peroxisome proliferator-activated receptor gamma ligands inhibit cell growth and induce apoptosis in human liver cancer BEL-7402 cells. *World J Gastroenterol* 2003; 9(8): 1683-1688
http://www.wjgnet.com/1007-9327/9/1683.asp

INTRODUCTION

Peroxisome proliferator-activated receptors (PPARs) are members of the nuclear hormone receptor family. Three distinct PPARs, termed PPAR-α, PPAR-β and PPAR-γ, have been identified. PPAR-α is abundant in primary hepatocytes, where it regulates the expression of proteins involved in fatty acid metabolism. PPAR-β is the most widely distributed subtype and is often expressed at high levels. PPAR-γ is predominantly seen in adipose tissue, where it plays a critical role in regulating adipocyte differentiation. The ability of PPAR-γ to regulate cell differentiation and proliferation has inspired a number of researchers to explore the use of PPAR-γ agonists as chemotherapeutic agents[1-7]. PPAR-γ is highly expressed in human lipocarcinomas and various other human tumors including breast, lung, colon, prostate, bladder and gastric cancer[8-13]. Furthermore, prostaglandin 15d-PGJ_2 and/or troglitazone induce apoptosis and growth inhibition of human breast, lung, colon, prostate, bladder, gastric and thyroid carcinoma cells *in vitro*.

In support of the *in vitro* data, there are now many reported examples of tumor growth suppression/arrest in tumor-bearing rodent models treated with PPAR-γ agonist therapies. For example, troglitazone treatment of nude mice implanted with papillary thyroid tumors reduced tumor growth and prevented distant metastasis. Both estrogen receptor positive (MCF-7) and negative (MDA-MB-231) breast cancer cell lines undergo cell cycle arrest when treated with15d-PGJ_2 or troglitazone and similar effects are observed in rodent breast cancer *in vivo* models[14-18]. PPAR-γ ligands have been shown to inhibit growth and induce terminal differentiation of liposarcoma cells, and to inhibit growth and induce apoptosis of breast cancer cells, prostatic carcinoma, and lung cancer cells.

In the field of gastroenterology, many investigators have focused on the role of PPAR-γ in colon cancer, since PPAR-γ is highly expressed in human colon and colon tumors. The effects of PPAR-γ on colon cancer are still unclear and controversial[19-25], since PPAR-γ ligands have been reported both to promote the development and to reduce the growth rate of colon tumors. PPAR-γ ligands also inhibit the growth of human gastric carcinoma cells through induction of apoptosis[25]. However, the effects of PPAR-γ ligands on growth of human liver cancer cells have not been examined. In this study, we investigated the effects of PPAR-γ ligands 15d-PGJ_2 and troglitazone on growth of human liver cancer BEL-7402 cells and whether 15d-PGJ_2 and troglitazone affected the cell cycle, apoptosis, and Caspases activity of BEL-7402 cells.

MATERIALS AND METHODS

Cell line and reagents

Human liver cancer cell line BEL-7402 was provided by the American Type Culture Collection. Cells were grown in RPMI-1640 medium supplemented with 15 % new born bovine serum, penicillin G (100 kU/L) and kanamycin (0.1 g/L) at 37 ℃ in a 5 % CO_2-95 % air atmosphere. Anti-Caspases-3, -6, -7, -8 and -9 antibodies were obtained from Sigma Chemical Co. 15-deoxy-$\Delta^{12,14}$-prostaglandin J_2 (15d-PGJ_2) and troglitazone were

obtained from Cayman Chemical Co. All other chemicals were purchased from Sigma Chemical Co (St Louis, MO, USA).

Determination of cell proliferation rate

BEL-7402 cells (1×10^5) were seeded in 24 well plates and cultured for 24 h. The cultures were divided into three groups: the first group (control) was cultured in the RPMI1640 medium, the second group was cultured in the continuous presence of 20 μM 15-deoxy-$\triangle^{12,14}$-prostaglandin J_2 (15d-PGJ_2), the third was cultured in the continuous presence of 20 μM troglitazone. Cells were then harvested every 24 h by trypsinization and cell numbers were counted with a hemocytometer, three cultures were used for experiments at each time point.

[^{3}H] thymidine incorporation

Subconfluent cells were cultured in 24-well plates and incubated for 24 h with 5uCi of [^{3}H] thymidine. The cells were then washed 3 times with HBSS, lysed with 1M NaOH, and lysate was counted by liquid scintillation.

Hoechst 33258 staining

Cells were fixed with 4 % formaldehyde in phosphate buffered saline (PBS) for 10 min, stained by Hoechst33258 (10 mg/L) for one hour, and subjected to fluorescence microscopy. After treated with 15d-PGJ_2 or troglitazone, the morphologic changes including reduction in volume, nuclear chromatin condensation were observed.

Electron microscopy (EM)

Control BEL-7402 cells or those treated with 15-deoxy-$\triangle^{12,14}$-prostaglandin J_2 (15d-PGJ_2) or troglitazone for 48 h and that remained attached to the surface of the culture dishes were gently washed with serum-free medium, and then fixed with 2.5 % glutaraldehyde in 0.1 M sodium cacodylate buffer. These cells were scraped from the surface of the dishes and pelleted by spinning for 5 min at 10 000×g. The cells were osmicated with 1 % osmium tetroxide, then block was stained, dehydrated in graded ethanol, infiltrated with propylene oxide, and embedded with EMBED overnight and cured in a 60 ℃ oven for 48 h. Silver sections were cut with an Ultracut E microtome, collected on a formvar and carbon-coated grid, stained with uranyl acetate and Reynold's lead citrate, and viewed under a JEOL100 CX electron microscope.

Ladder detection assay

After induction of apoptosis, cells (7×10^6/sample, both attached and detached cells) were lyzed with 150 μl hypotonic lysis buffer (edetic acid 10 mM, 0.5 % Triton X-100, Tris-HCl, ph7.4) for 15 min on ice and were precipitated with 2.5 % polyethylene glycol and NaCl 1 M for 15 min at 4 ℃. After centrifugation at 16 000×g for 10 min at room temperature, the supernatant was incubated in the presence of proteinase K (0.3 g/L) at 37 ℃ for one hour and precipitated with isopropanol at -20 ℃. After centrifugation, each pellet was dissolved in 10 μl of Tris-EDTA (pH 7.6) and electrophoresed on a 1.5 % agarose gel containing ethidium bromide. Ladder formation of oligonucleosomal DNA was detected under ultraviolet light.

Detection of apoptotic DNA fragmentation

BEL-7402 cells were grown in 96-well culture plates. The cells were incubated with various doses of 15d-PGJ_2 and troglitazone for 6 h. Apoptotic DNA fragmentation was determined using a commercially available enzyme-linked immunosorbent assay (ELISA) kit from Roche Co. This assay was based on a quantitative sandwich enzyme-immunoassay directed against cytoplasmic histone-associated DNA fragments. Briefly, the cells were incubated in 200 μl of lysis buffer provided in the kit, the lysates were centrifuged, and 20 μl of the supernatant containing cytoplasmic histone-associated DNA fragments was reacted overnight at 4 ℃ in streptavidin-coated microtitrator wells with 80 μl of the immunoreagent mixture containing biotinylated anti-histone antibody and peroxidase-conjugated anti-DNA antibody. After washed, the immunocomplex-bound peroxidase was probed with 2,2' -azino-di[3-ethylbenzthiazoline sulfonate] for spectrophotometric detection at 405 nm.

TUENL assay

TUNEL assay was performed using the apoptosis detection system. Cells were fixed by 4 % paraformaldehyde in PBS overnight at 4 ℃. The samples were washed three times with PBS and permeabilized by 0.2 % Triton X-100 in PBS for 15 min on ice. After washed twice, cells were equilibrated at room temperature for 15 to 30 min in equilibration buffer(potassium cacodylate 200 mM, dithiothreitol 0.2 mM, bovine serum albumin 0.25 g/L, and cobalt chloride 2.5 mM in Tris-HCl 25 mM, pH 6.6) and then incubated in the presence of fluorescein-12-dUTP 5 μM, dATP 10 μM, edetic acid 100 μM, and terminal deoxynucleotidyl transferase at 37 ℃ for 1.5 h in the dark. The tailing reaction was terminated by 2×standard saline citrate (SSC). The samples were washed three times with PBS and analyzed by fluorescence microscopy. At least 1000 cells were counted, and the percentage of TUNEL-positive cells was determined.

Flow cytometry

For DNA content analysis, cells were treated with different concentrations of 15-deoxy-$\triangle^{12,14}$-prostaglandin J_2 (15d-PGJ_2) and troglitazone for 24 h. 1×10^6 cells were harvested, pelleted and washed with phosphate-buffered saline (PBS), and resuspended in PBS containing 20 mg/L PI and 1 g/L ribonuclease A. 10^6 fixed cells were examined under each experimental condition by flow cytometry, and percentage of degraded DNA was determined by the number of cells displaying subdiploid (sub-G_1). DNA divided by the total number of cells was examined. Cell cycle analysis was performed under the same experimental conditions and distributions were determined using the CellFit program. All measurements were carried out under the same instrumental settings.

Western blot analysis

The cells were lysed in lysis buffer [hepes 25 mM, 1.5 % Triton X-100, 1 % sodium deoxycholate, 0.1 %SDS, NaCl 0.5 M, edetic acid 5 mM, NaF 50 mM, sodium vanadate 0.1 mM, phenylmethylsulfonyl fluoride (PMSF) 1 mM, and leupeptin 0.1 g/L, pH7.8] at 4 ℃ with sonication. The lysates were centrifuged at 15 000 g for 15 min and the concentration of the protein in each lysate was determined with Coomassie brilliant blue G-250. Loading buffer (Tris-HCl 42 mM, 10 % glycerol, 2.3 % SDS, 5 % 2-mercaptoethanol and 0.002 % bromophenol blue) was then added to each lysate, which was subsequently boiled for 3 min and then electrophoresed on a SDS-polyacrylamide gel. Proteins were transferred to nitrocellulose and incubated sequentially with anti-Caspases-3, -6, -7, -8 and -9 antibodies and then with peroxidase-conjugated secondary antibodies in the second reaction. Detection was performed with enhanced chemiluminescence reagent. The results on Western blot analysis represented the average of three individual experiments.

Statistical analysis

Data were presented as the mean ± standard error of the mean, unless otherwise indicated. Multiple comparisons were examined for significant differences using analysis of variance, followed by individual comparisons with the Bonferroni post-test. Comparisons between two groups were made with the Student's *t* test. A $P<0.05$ was considered significant.

RESULTS

Effects of 15d-PGJ$_2$ and troglitazone on proliferation and cell cycle

Cells were cultured in the presence or absence of 15d-PGJ$_2$ or troglitazone and cell numbers were determined over three days. In the absence of 15d-PGJ$_2$ or troglitazone, the number of control cells doubled approximately every 24 h in RPMI 1640 medium supplemented with 10 % fetal calf serum. By contrast, in the continuous presence of 20 μM 15d-PGJ$_2$ or troglitazone' the growth of BEL-7402 cells was significantly inhibited (Figure 1A). We next examined by [^{3}H]-thymidine incorporation whether 15d-PGJ$_2$ or troglitazone affected DNA synthesis of BEL-7402 cells. Cells were treated with various doses of 15d-PGJ$_2$ or troglitazone (10, 20, 30 μM). The results showed that 15d-PGJ$_2$ or troglitazone significantly and dose-dependently inhibited [^{3}H]-thymidine incorporation into BEL-7402 cells (Figures 1B, 1C). Table 1 indicates the effects of 15d-PGJ$_2$ or troglitazone on the cell cycle distribution of BEL-7402 cells. 15d-PGJ$_2$ or troglitazone at 10 μM induced limited or no change in the cell cycle distribution of cells. At concentrations of 20 and 30 μM, 15d-PGJ$_2$ or troglitazone increased the proportion of cells with G_0/G_1 phase DNA content and decreased those with S phase DNA content. There was no significant change in the proportion of cells with G_2/M DNA content.

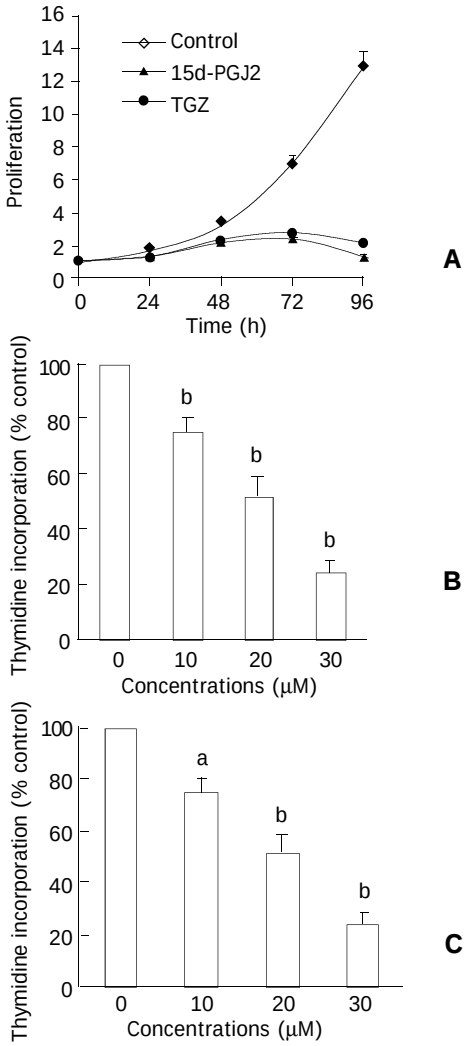

Figure 1 Concentration and time effect of 15d-PGJ2 or TGZ on growth of BEL-7402 cells. (A) BEL-7402 cells were incubated with 20 μM 15d-PGJ2 or TGZ for 12, 24, 48, 72, 96 h. (B) BEL-7402 cells were incubated with various concentrations of 15d-PGJ2 for 48 h; (C) BEL-7402 cells were incubated with various concentrations of TGZ for 48 h. The value was represented as mean ±SEM (n=3). [a]P<0.05 and [b]P<0.01 versus corresponding control group.

Effect of 15d-PGJ$_2$ or troglitazone on induction of apoptosis in BEL-7402 cells

Morphological changes 15d-PGJ$_2$ or troglitazone treatment of BEL-7402 cells altered their morphology and induced DNA strand breaks in a manner consistent with apoptosis. That the changes were indeed induced by apoptosis and not necrosis was confirmed by EM and Hoechst 33258 staining. 15d-PGJ$_2$ or troglitazone-treated cells showed compacted nuclear chromatin with fine granular masses marginated against the nuclear enveloped and condensed cytoplasm, the nuclear outline was convoluted and the organelles were preserved.

TUNEL assay To determine whether 15d-PGJ$_2$ or troglitazone has a capacity to induce apoptosis in BEL-7402 cells, exponentially growing cells were exposed to various concentrations of 15d-PGJ$_2$ or troglitazone. TUNEL assay was performed. 15d-PGJ$_2$ or troglitazone dramatically increased the number of TUNEL-positive cells in a dose-dependent manner.

DNA fragments Agarose gel electrophoresis exhibited DNA ladder formation in BEL-7402 cells after exposed to different concentrations of 15d-PGJ$_2$ or troglitazone for 48 h. Compared with control, the DNA laddering was more clearly observed by the treatment with 15d-PGJ$_2$ or troglitazone. ELISA assay also showed that 15d-PGJ$_2$ or troglitazone induced DNA fragment in a dose-dependent manner (Figure 2).

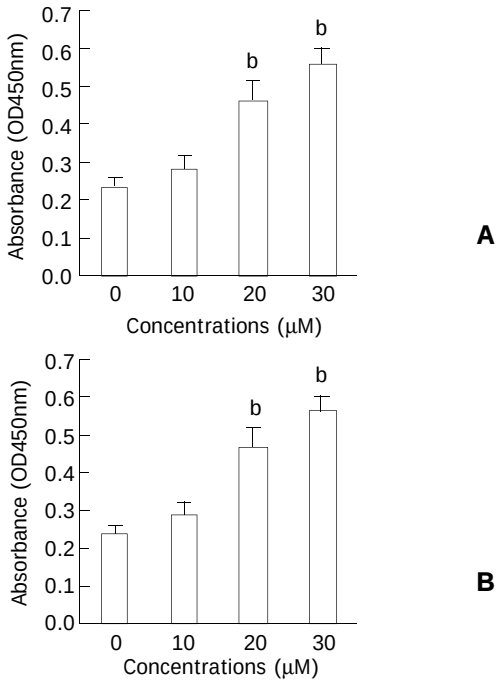

Figure 2 DNA fragmentation by ELISA assay, as measured by absorbance (OD 450 values). Culture of BEL-7402 cells for 48 h in the presence of 15d-PGJ2 / TGZ resulted in dose dependent DNA fragmentation. A) 15d-PGJ2; B) TGZ. [b]P<0.01 compared to respective control. The value was represented as mean ± SEM (n=3).

Flow cytometry In order to determine the effect of 15d-PGJ$_2$ or troglitazone on apoptosis in BEL-7402 cells, cells were exposed to 15d-PGJ$_2$ or troglitazone for 48 h, apoptotic damage of DNA was detected according to the sub-G_1 peak on a flow cytometer. Cells in sub-G_1 phase were increased from 2.1±0.3 % to 55.8±4.7 % or 50.0±4.1 % after 15d-PGJ$_2$ or troglitazone treatment (Table1).

Effect of 15d-PGJ$_2$ or troglitazone on the activities of Caspase-3, -6, -7, -8 and -9

In order to elucidate the pathway leading to apoptosis, we

examined the activation of Caspases-3, -6, -7, -8 and -9, which were reported to initiate apoptosis upon various stimuli. BEL-7402 cells treated with15d-PGJ_2 or troglitazone for 24 h were analyzed for the enzymatic activity by Western blot. The results showed that Caspases-3, -6, -7, -8 and -9 were activited after 15d-PGJ_2 or troglitazone treatment in BEL-7402 cells, while the activity of Caspase 8 had not significantly changed (Figure 3).

Table 1 Effect of 15d-PGJ2 and TGZ on cell cycle distribution and apoptosis in BEL-7402 cells

Treatment (μm)	%Cell cycle distribution			%apoptosis
	G_0/G_1	S	G_2/M	
Control	49.7±1.5	34.8±2.1	15.5±1.1	2.1±0.3
15d-PGJ2				
10	50.5±2.6	34.2±1.7	15.3±0.5	13.9±1.1[b]
20	64.8±2.9[b]	19.5±1.5[b]	15.7±0.2	33.5±2.3[b]
30	71.6±4.2[b]	14.1±0.6[b]	14.4±1.3	55.8±4.7[b]
TGZ				
10	54.2±2.1	29.4±1.3	16.6±0.9	10.3±1.1[b]
20	61.5±3.1[b]	28.2±1.7[b]	14.9±1.7	25.5±1.8[b]
30	68.9±4.8[b]	14.2±0.8[b]	16.9±1.4	50.0±4.1[b]

Cell cycle distribution was determined after 24 h of treatment in one group and apoptosis was determined after 48 h of treatment in the other group. The tabulated percentages were an average calculated on the results of three separate experiments. The value was represented as mean±SEM (n=3). [b]P<0.01 versus corresponding control group.

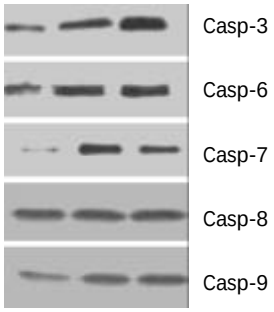

Figure 3 Western blot analysis of the activities of Caspases-3, -6, -7, -8 and –9 in human liver cancer cell line BEL-7402 cells: lane 1: control, lane 2: 30 μM TGZ treated BEL-7402 cells; lane 3: 30 μM 15d-PGJ2 treated BEL-7402 cells.

DISCUSSION

Several members of the family of nuclear hormone receptors (NHR) play crucial roles in the control of cellular homeostasis, and administration of their cognate ligands has successfully been used in cancer treatment[26-33]. The nuclear receptor superfamily includes members such as the estrogen, thyroid and glucocorticoid receptors as well as the subfamily of peroxisome proliferator-activated receptors. The PPAR family comprises PPAR-α, PPAR-β and PPAR-γ. The PPARs bind as heterodimers with retinoic-x acid receptor (RXR) to a subset of DR-1 elements, peroxisome proliferator response elements and have been shown to regulate expression of genes involved in the transport, metabolism and storage of fatty acids. Transcriptional activation of the PPAR-RXR heterodimers is enhanced upon binding of a large variety of ligands including saturated and unsaturated fatty acids, arachidonic acid derivatives and a wide range of synthetic drugs with different subtype specificities.

For the last 10 years, administration of peroxisome proliferators, PPAR-α agonists, has been known to induce hepatocarcinogenesis in rodents. However, cancer development is probably induced by mechanisms secondary to PPAR-α transcriptional activation. A role in growth regulation for the two remaining PPAR subtypes has also been suggested. Whichever, upregulaties PPAR-β expression has been associated with colon cancer and activation of PPAR-β stimulates post-confluent proliferation of pre-adipocytes. Opposite effects on cell proliferation are mediated by activation of PPAR-γ. PPAR-γ agonists could be promising therapeutic or chemopreventive agents in oncology, since they can induce apoptosis or differentiation in several tumors, by acting as inhibitors of malignancy progression. PPAR-γ activation inhibits the growth of several tumors as shown by *in intro* and *in vivo* studies performed on liposarcoma, breast cancer and leukemia. However, conflicting evidence exists on the role of PPAR-γ activation in colon cancer, where different studies have shown that PPAR-γ activation promotes tumor development or, in contrast, protects against colon cancer, depending on the cell model[34-42]. In the present study, in order to examine the effects of PPAR-γ ligands 15d-PGJ_2 or troglitazone on the BEL-7402 cell growth, we employed cell counting and [^{3}H]-thymidine incorporation assay. The results showed 15d-PGJ_2 or troglitazone significantly and concentration-dependently inhibited the growth of BEL-7402 cells. To examine whether growth inhibition of BEL-7402 cells by 15d-PGJ_2 or troglitazonem was a result of cell cycle arrest, BEL-7402 cells treated with either vehicle or 15d-PGJ_2/troglitazone were analyzed by FACScan. BEL-7402 cells treated with 15d-PGJ_2 and troglitazone exhibited decreased fractions of S phase cells from 34.8±2.1 % in controls to14.4±1.3 % and 16.9±1.4 %, respectively, resulting in a remarkable increase in accumulation if cells at G_1 phase, increased from a control level of 49.7±1.5 % to 71.6±1.5 % and 68.9±4.8 %. Therefore, the inhibitory effect of 15d-PGJ_2 or troglitazone on growth of BEL-7402 cells may thus be due in part to PPAR-γ-mediated G_1 cell cycle arrest. Similar findings of G_1 cell cycle arrest by PPAR-γ ligands have been reported for colon cancer cells and prostate cancer cells. Several reports suggested that PPAR-γ ligands affected cell cycle-related genes and proteins. Others demonstrated that PPAR-γ activation caused G_1 cell cycle arrest of fibroblasts and SV40-transformed adipogenic HIB1B cells, and that this arrest was strongly associated with loss of E2F/DP DNA binding through modulation of phosphorylation by phosphatase 2A[43-47].

Previous studies have shown that PPAR-γ activation generally promotes apoptosis and/or differentiation in several normal and tumor cells such as human breast cancer cells, human gastric cancer cells, human non-small cell lung carcinoma, human glioblastoma cells, macrophages, endothelial cells and liposarcoma. In the present study, to determine the underlying mechanisms of the growth inhibitory effect of PPAR-γ ligands, we investigated whether 15d-PGJ_2 or troglitazone acted by inducing apoptosis of liver cancer BEL-7402 cells. We performed DNA fragments and morphological changes assay EM or Hoechst 33258. The results showed that 15d-PGJ_2 or troglitazone induced apoptosis in a dose-dependent manner, indicating that growth inhibition of BEL-7402 by PPAR-γ ligands was, in part, associated with apoptosis.

Recent evidence indicates that increased expression and activation of some Caspase zymogens in tumor cells can lead to efficient inhibition of tumor cell growth, invasion and metastasis and tumor regression[48-56]. Such a Caspase-dependent cessation of tumor cell proliferation and dissemination is accomplished via an active process of tumor cells death collectively named as apoptosis. It has been demonstrated that a high level of activity of effector Caspases-3, -6, -7 and -8, in tumor cells plays a decisive role in their commitment to apoptosis[57-66]. To-date studies on zymogens of the effector

Caspases in primary human tumors showed an increased expression of procasp-3 and -6 in breast carcinoma, pancreatic carcinoma and non-small cell lung carcinoma compared to normal tissue and benign or premalignant lesions. This suggests that tumor cells of some epithelial neoplasms may acquire an increased apoptotic potential during progression at the levels of primary tumor. The zymogens of casp-3 and -7 in tumor cells can be activated by the initiator Caspases, such as casp-8 and casp-9, and by the aspartyl-specific serine proteinase granzyme B upon its perforin-assisted entry into the cytoplasm of tumor cells. Procasp-6 can be activated by casp-3 while the generated casp-6 can activate in turn the zymogen of casp-3. In the present study, in order to elucidate the pathway leading to apoptosis, we examined activation of Caspases-3, -6, -7, -8 and -9, which have been reported to initiate apoptosis upon various stimuli. BEL-7402 cells treated with15d-PGJ_2 or troglitazone for 24 h were analyzed for the enzymatic activity by Western blot. The results showed that Caspases-3, -6, -7, -8 and -9 were activited after 15d-PGJ_2 or troglitazone treatment in BEL-7402 cells, while the activity of Caspase 8 had not significantly changed, indicating that activation of Caspases plays an important role in the apoptosis induced by 15d-PGJ_2 or troglitazone.

In conclusion, the present results, together with reports by other investigators, suggest a potential usefulness of PPAR gamma ligands for chemoprevention and treatment of liver cancers. Further basic as well as clinical studies are required to develop new strategies to fight liver cancers using PPAR gamma ligands.

REFERENCES

1 **Mangelsdorf DJ**, Thummel C, Beato M, Herrlich P, Schutz G, Umesono K, Blumberg B, Kastner P, Mark M, Chambon P. The nuclear receptor superfamily: the second decade. *Cell* 1995; **83**: 835-839

2 **Spiegelman BM,** Flier JS. Adipogenesis and obesity: rounding out the big picture. *Cell* 1996; **87**: 377-389

3 **Sarraf P**, Mueller E, Jones D, King FJ, DeAngelo DJ, Partridge JB, Holden SA, Chen LB, Singer S, Fletcher C, Spiegelman BM. Differentiation and reversal of malignant changes in colon cancer through PPARgamma. *Nat Med* 1998; **4**: 1046–1052

4 **Mueller E,** Sarraf P, Tontonoz P, Evans RM, Martin KJ, Zhang M, Fletcher C, Singer S, Spiegelman BM. Terminal differentiation of human breast cancer through PPAR gamma. *Mol Cell* 1998; **1**: 465-470

5 **Kubota T,** Koshizuka K, Williamson EA, Asou H, Said JW, Holden S, Miyoshi I, Koeffler HP. Ligand for peroxisome proliferator-activated receptor gamma (troglitazone) has potent antitumor effect against human prostate cancer both *in vitro* and *in vivo*. *Cancer Res* 1998; **58**: 3344–3352

6 **Takahashi N,** Okumura T, Motomura W, Fujimoto Y, Kawabata I, Kohgo Y. Activation of PPARgamma inhibits cell growth and induces apoptosis in human gastric cancer cells. *FEBS Lett* 1999; **455**: 135-139

7 **Chinetti G,** Griglio S, Antonucci M. Activation of proliferator-activated receptors alpha and gamma induces apoptosis of human monocyte-derived macrophages. *J Biol Chem* 1998; **273**: 25573–25580

8 **Vamecq J**, Latruffe N. Medical significance of peroxisome proliferator-activated receptors. *Lancet* 1999; **354**: 141-148

9 **Tontonoz P**, Hu E, Spiegelman BM. Stimulation of adipogenesis in fibroblasts by PPAR gamma 2, a lipid-activated transcription factor. *Cell* 1994; **79**: 1147–1156

10 **Forman BM**, Tontonoz P, Chen J, Brun RP, Spiegelman BM, Evans RM. 15-Deoxy-delta 12, 14-prostaglandin J2 is a ligand for the adipocyte determination factor PPAR gamma. *Cell* 1995; **83**: 803–812

11 **Kliewer SA**, Lenhard JM, Willson TM, Patel I, Morris DC. A prostaglandin J2 metabolite binds peroxisome proliferator-activated receptor gamma and promotes adipocyte differentiation. *Cell* 1995; **83**: 813–819

12 **Mansen A**, Guardiola-Diaz H, Rafter J. Expression of the peroxisome proliferator-activated receptor (PPAR) in the mouse colonic mucosa. *Biochem Biophys Res Commun* 1996; **222**: 844–851

13 **Fajas L**, Auboeuf D, Raspe E, Schoonjans K, Lefebvre AM, Saladin R, Najib J, Laville M, Fruchart JC, Deeb S, Vidal-Puig A, Flier J, Briggs MR, Staels B, Vidal H, Auwerx J. The organization, promoter analysis, and expression of the human PPARgamma gene. *J Biol Chem* 1997; **272**: 18779–18789

14 **Okumura M**, Yamamoto M, Sakuma H, Kojima T, Maruyama T, Jamali M, Cooper D, Yasuda K. Leptin and high glucose stimulate cell proliferation in MCF-7 human breast cancer cells: reciprocal involvement of PKC-alpha and PPAR expression. *Biochim Biophys Acta* 2002; **1592**: 107

15 **Wang X**, Kilgore M. Signal cross-talk between estrogen receptor alpha and beta and the peroxisome proliferator-activated receptor gamma1 in MDA-MB-231 and MCF-7 breast cancer cells. *Mol Cell Endocrinol* 2002; **194**: 123

16 **Suchanek KM**, May FJ, Robinson JA, Lee WJ, Holman NA, Monteith GR, Roberts-Thomson SJ. Peroxisome proliferator-activated receptor alpha in the human breast cancer cell lines MCF-7 and MDA-MB-231. *Mol Carcinog* 2002; **34**: 165-171

17 **Stoll BA**. Linkage between retinoid and fatty acid receptors: implications for breast cancer prevention. *Eur J Cancer Prev* 2002; **11**: 319-325

18 **Stoll BA**. N-3 fatty acids and lipid peroxidation in breast cancer inhibition. *Br J Nutr* 2002; **87**: 193-198

19 **Inadera H,** Nagai S, Dong HY, Matsushima K. Molecular analysis of lipid-depleting factor in a colon-26-inoculated cancer cachexia model. *Int J Cancer* 2002; **101**: 37-45

20 **Dobbie Z**, Muller PY, Heinimann K, Albrecht C, D'Orazio D, Bendik I, Muller H, Bauerfeind P. Expression of COX-2 and Wnt pathway genes in adenomas of familial adenomatous polyposis patients treated with meloxicam. *Anticancer Res* 2002; **22**: 2215-2220

21 **Sunami E**, Tsuno NH, Kitayama J, Saito S, Osada T, Yamaguchi H, Tomozawa S, Tsuruo T, Shibata Y, Nagawa H. Decreased synthesis of matrix metalloproteinase-7 and adhesion to the extracellular matrix proteins of human colon cancer cells treated with troglitazone. *Surg Today* 2002; **32**: 343-350

22 **Theocharis S**, Kanelli H, Politi E, Margeli A, Karkandaris C, Philippides T, Koutselinis A. Expression of peroxisome proliferator activated receptor-gamma in non-small cell lung carcinoma: correlation with histological type and grade. *Lung Cancer* 2002; **36**: 249-255

23 **Bogazzi F**, Ultimieri F, Raggi F, Costa A, Gasperi M, Cecconi E, Mosca F, Bartalena L, Martino E. Peroxisome proliferator activated receptor gamma expression is reduced in the colonic mucosa of acromegalic patients. *J Clin Endocrinol Metab* 2002; **87**: 2403-2406

24 **Takashima T**, Fujiwara Y, Higuchi K, Arakawa T, Yano Y, Hasuma T, Otani S. PPAR-gamma ligands inhibit growth of human esophageal adenocarcinoma cells through induction of apoptosis, cell cycle arrest and reduction of ornithine decarboxylase activity. *Int J Oncol* 2001; **19:** 465-471

25 **Sato H**, Ishihara S, Kawashima K, Moriyama N, Suetsugu H, Kazumori H, Okuyama T, Rumi MA, Fukuda R, Nagasue N, Kinoshita Y. Expression of peroxisome proliferator-activated receptor (PPAR) gamma in gastric cancer and inhibitory effects of PPARgamma agonists. *Br J Cancer* 2000; **83**: 1394-1400

26 **Terashita Y**, Sasaki H, Haruki N, Nishiwaki T, Ishiguro H, Shibata Y, Kudo J, Konishi S, Kato J, Koyama H, Kimura M, Sato A, Shinoda N, Kuwabara Y, Fujii Y. Decreased peroxisome proliferator-activated receptor gamma gene expression is correlated with poor prognosis in patients with esophageal cancer. *Jpn J Clin Oncol* 2002; **32**: 238-243

27 **Chen GG**, Lee JF, Wang SH, Chan UP, Ip PC, Lau WY. Apoptosis induced by activation of peroxisome-proliferator activated receptor-gamma is associated with Bcl-2 and NF-kappaB in human colon cancer. *Life Sci* 2002; **70**: 2631-2646

28 **Evangelou A**, Letarte M, Marks A, Brown TJ. Androgen modulation of adhesion and antiadhesion molecules in PC-3 prostate cancer cells expressing androgen receptor. *Endocrinology* 2002; **143**: 3897-3904

29 **Eisen SF**, Brown HA. Selective estrogen receptor (ER) modula-

tors differentially regulate phospholipase D catalytic activity in ER-negative breast cancer cells. *Mol Pharmacol* 2002; **62**: 911-920

30 **Aoyama Y**. Experimental studies on the effects of the combined use of N-(4-hydroxyphenyl)retinamide (4-HPR) and tamoxifen (TAM) for estrogen receptor (ER)-negative breast cancer. *Kurume Med J* 2002; **49**: 27-33

31 **Galbiati E**, Caruso PL, Amari G, Armani E, Ghirardi S, Delcanale M, Civelli M. Pharmacological actions of a novel, potent, tissue-selective benzopyran estrogen. *J Pharmacol Exp Ther* 2002; **303:** 196-203

32 **Lovat PE**, Oliverio S, Ranalli M, Corazzari M, Rodolfo C, Bernassola F, Aughton K, Maccarrone M, Hewson QD, Pearson AD, Melino G, Piacentini M, Redfern CP. GADD153 and 12-lipoxygenase mediate fenretinide-induced apoptosis of neuroblastoma. *Cancer Res* 2002; **62:** 5158-5167

33 **Belev B**, Aleric I, Vrbanec D, Petrovecki M, Unusic J, Jakic-Razumovic J. Nm23 gene product expression in invasive breast cancer-immunohistochemical analysis and clinicopathological correlation. *Acta Oncol* 2002; **41:** 355-361

34 **Kintscher U**, Goetze S, Wakino S, Kim S, Nagpal S, Chandraratna RA, Graf K, Fleck E, Hsueh WA, Law RE. Peroxisome proliferator-activated receptor and retinoid X receptor ligands inhibit monocyte chemotactic protein-1-directed migration of monocytes. *Eur J Pharmacol* 2000; **401**: 259-270

35 **Hirase N**, Yanase T, Mu Y, Muta K, Umemura T, Takayanagi R, Nawata H. Thiazolidinedione suppresses the expression of erythroid phenotype in erythroleukemia cell line K562. *Leuk Res* 2000; **24**: 393-400

36 **Gurnell M**, Wentworth JM, Agostini M, Adams M, Collingwood TN, Provenzano C, Browne PO, Rajanayagam O, Burris TP, Schwabe JW, Lazar MA, Chatterjee VK. A dominant-negative peroxisome proliferator-activated receptor gamma (PPARgamma) mutant is a constitutive repressor and inhibits PPARgamma-mediated adipogenesis. *J Biol Chem* 2000; **275**: 5754-5759

37 **Asou H**, Verbeek W, Williamson E, Elstner E, Kubota T, Kamada N, Koeffler HP. Growth inhibition of myeloid leukemia cells by troglitazone, a ligand for peroxisome proliferator activated receptor gamma, and retinoids. *Int J Oncol* 1999; **15**: 1027-1032

38 **Esteller M**, Fraga MF, Paz MF, Campo E, Colomer D, Novo FJ, Calasanz MJ, Galm O, Guo M, Benitez J, Herman JG. Cancer epigenetics and methylation. *Science* 2002; **297**: 1807-1808

39 **Yamakawa-Karakida N**, Sugita K, Inukai T, Goi K, Nakamura M, Uno K, Sato H, Kagami K, Barker N, Nakazawa S. Ligand activation of peroxisome proliferator-activated receptor gamma induces apoptosis of leukemia cells by down-regulating the c-myc gene expression via blockade of the Tcf-4 activity. *Cell Death Differ* 2002; **9**: 513-526

40 **Oyama Y**, Akuzawa N, Nagai R, Kurabayashi M. PPARgamma ligand inhibits osteopontin gene expression through interference with binding of nuclear factors to A/T-rich sequence in THP-1 cells. *Circ Res* 2002; **90**: 348-355

41 **Abe A**, Kiriyama Y, Hirano M, Miura T, Kamiya H, Harashima H, Tokumitsu Y. Troglitazone suppresses cell growth of KU812 cells independently of PPARgamma. *Eur J Pharmacol* 2002; **436**: 7-13

42 **Harris SG**, Smith RS, Phipps RP. 15-deoxy-Delta 12,14-PGJ2 induces IL-8 production in human T cells by a mitogen-activated protein kinase pathway. *J Immunol* 2002; **168**: 1372-1379

43 **Anderson SP**, Yoon L, Richard EB, Dunn CS, Cattley RC, Corton JC. Delayed liver regeneration in peroxisome proliferator-activated receptor-alpha-null mice. *Hepatology* 2002; **36**: 544-554

44 **Rumi MA**, Sato H, Ishihara S, Ortega C, Kadowaki Y, Kinoshita Y. Growth inhibition of esophageal squamous carcinoma cells by peroxisome proliferator-activated receptor-gamma ligands. *J Lab Clin Med* 2002; **140**: 17-26

45 **Ohta T,** Elnemr A, Yamamoto M, Ninomiya I, Fushida S, Nishimura GI, Fujimura T, Kitagawa H, Kayahara M, Shimizu K, Yi S, Miwa K. Thiazolidinedione, a peroxisome proliferator-activated receptor-gamma ligand, modulates the E-cadherin/beta-catenin system in a human pancreatic cancer cell line, BxPC-3. *Int J Oncol* 2002; **21**: 37-42

46 **Kawakami S**, Arai G, Hayashi T, Fujii Y, Xia G, Kageyama Y, Kihara K. PPARgamma ligands suppress proliferation of human urothelial basal cells *in vitro*. *J Cell Physiol* 2002; **191**: 310-319

47 **Toyota M,** Miyazaki Y, Kitamura S, Nagasawa Y, Kiyohara T, Shinomura Y, Matsuzawa Y. Peroxisome proliferator-activated receptor gamma reduces the growth rate of pancreatic cancer cells through the reduction of cyclin D1. *Life Sci* 2002; **70**: 1565-1575

48 **Li HL**, Zhang HW, Chen DD, Zhong L, Ren XD, Si-Tu R. JTE-522, a selective COX-2 inhibitor, inhibits cell proliferation and induces apoptosis in RL95-2 cells. *Acta Pharmacol Sin* 2002; **23**:631-637

49 **Li HL**, Chen DD, Li XH, Zhang HW, Lu YQ, Ye CL, Ren XD. Changes of NF-kB, p53, Bcl-2 and caspase in apoptosis induced by JTE-522 in human gastric adenocarcinoma cell line AGS cells: role of reactive oxygen species. *World J Gastroenterol* 2002; **8**: 431-435

50 **Li HL**, Chen DD, Li XH, Zhang HW, Lu JH, Ren XD, Wang CC. JTE-522-induced apoptosis in human gastric adenocarcinoma cell line AGS cells by caspase activation accompanying cytochrome C release, membrane translocation of Bax and loss of mitochondrial membrane potential. *World J Gastroenterol* 2002; **8**: 217-223

51 **Li HL**, Ren XD, Zhang HW, Ye CL, Lv JH, Zheng PE. Synergism between heparin and adriamycin on cell proliferation and apoptosis in human nasopharyngeal carcinoma CNE2 cells. *Acta Pharmacol Sin* 2002; **23**: 167-172

52 **Li HL,** Ye KH, Zhang HW, Luo YR, Ren XD, Xiong AH, Situ R. Effect of heparin on apoptosis in human nasopharyngeal carcinoma CNE2 cells. *Cell Res* 2001; **11**: 311-315

53 **Tian G**, Yu JP, Luo HS, Yu BP, Yue H, Li JY, Mei Q. Effect of nimesulide on proliferation and apoptosis of human hepatoma SMMC-7721 cells. *World J Gastroenterol* 2002; **8**: 483-487

54 **Wu YL**, Sun B, Zhang XJ, Wang SN, He HY, Qiao MM, Zhong J, Xu JY. Growth inhibition and apoptosis induction of Sulindac on Human gastric cancer cells. *World J Gastroenterol* 2001; **7**: 796-800

55 **Wang X**, Lan M, Wu HP, Shi YQ, Lu J, Ding J, Wu KC, Jin JP, Fan DM. Direct effect of croton oil on intestinal epithelial cells and colonic smooth muscle cells. *World J Gastroenterol* 2002; **8**: 103-107

56 **Niu ZS**, Li BK, Wang M. Expression of p53 and C-myc genes and its clinical relevance in the hepatocellular carcinomatous and pericarcinomatous tissues. *World J Gastoenterol* 2002; **8**: 822-826

57 **Liu S**, Wu Q, Ye XF, Cai JH, Huang ZW, Su WJ. Induction of apoptosis by TPA and VP-16 is through translocation of TR3. *World J Gastroenterol* 2002; **8:** 446-450

58 **Xu CT**, Huang LT, Pan BR. Current gene therapy for stomach carcinoma. *World J Gastroenterol* 2001; **7**: 752-759

59 **Wu YL**, Sun B, Zhang XJ, Wang SN, He HY, Qiao MM, Zhong J, Xu JY. Growth inhibition and apoptosis induction of Sulindac on Human gastric cancer cells. *World J Gastroenterol* 2001; **7**: 796-800

60 **Hou L**, Li Y, Jia YH, Wang B, Xin Y, Ling MY, Lü S. Molecular mechanism about lymphogenous metastasis of hepatocarcinoma cells in mice. *World J Gastroenterol* 2001; **7**: 532-536

61 **Xu AG**, Li SG, Liu JH, Gan AH. Function of apoptosis and expression of the proteins Bcl-2, p53 and C-myc in the development of gastric cancer. *World J Gastroenterol* 2001; **7**: 403-406

62 **Liu XJ,** Yang L, Wu HB, Qiang O, Huang MH, Wang YP. Apoptosis of rat hepatic stellate cells induced by anti-focal adhesion kinase antibody. *World J Gastroenterol* 2002; **8**: 734-738

63 **Zhang XL**, Liu L, Jiang HQ. Salvia miltiorrhiza monomer IH764-3 induces hepatic stellate cell apoptosis via caspase-3 activation. *World J Gastroenterol* 2002; **8**: 515-519

64 **Sun BH**, Zhang J, Wang BJ, Zhao XP, Wang YK, Yu ZQ, Yang DL, Hao LJ. Analysis of in vivo patterns of caspase 3 gene expression in primary hepatocellular carcinoma and its relationship to p21(WAF1) expression and hepatic apoptosis. *World J Gastroenterol* 2000; **6**: 356-360

65 **Farilla L**, Hui H, Bertolotto C, Kang E, Bulotta A, Di Mario U, Perfetti R. Glucagon-Like Peptide-1 Promotes Islet Cell Growth and Inhibits Apoptosis in Zucker Diabetic Rats. *Endocrinology* 2002; **143:** 4397-4408

66 **Higashitsuji H**, Higashitsuji H, Nagao T, Nonoguchi K, Fujii S, Itoh K, Fujita J. A novel protein overexpressed in hepatoma accelerates export of NF-kappaB from the nucleus and inhibits p53-dependent apoptosis. *Cancer Cell* 2002; **2**: 335-346

Edited by Pang LH and Wang XL

P.O.Box 2345, Beijing 100023,China
Fax: +86-10-85381893
E-mail: wjg@wjgnet.com www.wjgnet.com

World J Gastroenterol 2003;9(8):1689-1696
World Journal of Gastroenterology
 ISSN 1007-9327

• LIVER CANCER •

S-phase delay in human hepatocellular carcinoma cells induced by overexpression of integrin b1

Yu-Long Liang, Ting-Wen Lei, Heng Wu, Jian-Min Su, Li-Ying Wang, Qun-Ying Lei, Xi-Liang Zha

Yu-Long Liang, Heng Wu, Li-Ying Wang, Qun-Ying Lei, Xi-Liang Zha, Department of Biochemistry and Molecular Biology, Shanghai Medical College, Fudan University, Shanghai 200032, China
Ting-Wen Lei, Department of Biochemistry, Guiyang Medical College, Guiyang 550004, Guizhou Province, China
Jian-Min Su, Department of Chemistry, Shanghai Medical College, Fudan University, Shanghai 200032, China
Supported by Grants from the National Natural Science Foundation of China, No.30000083 and Shanghai Municipal Government Science and Technology Committee, No.00JC14042
Correspondence to: Dr. Xi-Liang Zha, Department of Biochemistry and Molecular Biology, Shanghai Medical College, Fudan University, 138 Yi Xue Yuan Road, Shanghai 200032, China. xlzha@shmu.edu.cn
Telephone: +86-21-54237696 **Fax**: +86-21-64179832
Received: 2003-03-05 **Accepted:** 2003-04-01

Abstract

AIM: To clarify the mechanisms of integrin overexpression in negatively regulating the cell cycle control of hepatocellular carcinoma cells SMMC-7721.

METHODS: The cell cycle pattern was determined by flow cytometry. The mRNA and protein expression levels were assayed by RT-PCR and Western blot, respectively. Stable transfection was performed by Lipofectamine 2000 reagent, and cells were screened by G418.

RESULTS: Overexpression of α5β1 or β1 integrin induced S-phase delay in SMMC-7721 cells, and this delay was possibly due to the accumulation of cyclin-dependent kinase inhibitors (CKIs) $p21^{cip1}$ and $p27^{kip1}$. The decrease of protein kinase B (PKB) phosphorylation was present in this signaling pathway, but focal adhesion kinase (FAK) was not involved. When phosphorylation of PKB was solely blocked by wortmannin, $p27^{kip1}$ protein level was increased. Moreover, S-phase delay was recurred when attachment of the parental SMMC-7721 cells was inhibited by the preparation of poly-HEME, and this cell cycle pattern was similar to that of β1-7721 or α5β1-7721 cells.

CONCLUSION: S-phase delay induced by overexpression of integrin β1 subunit is attributed to the decrease of PKB phosphorylation and subsequent increases of $p21^{cip1}$ and $p27^{kip1}$ proteins, and may be involved in the unoccupied α5β1 because of lack of its ligands.

Liang YL, Lei TW, Wu H, Su JM, Wang LY, Lei QY, Zha XL. S-phase delay in human hepatocellular carcinoma cells induced by overexpression of integrin β1. *World J Gastroenterol* 2003; 9(8): 1689-1696
http://www.wjgnet.com/1007-9327/9/1689.asp

INTRODUCTION

Extracellular matrix (ECM) is consisted of many components, such as collagen, glycoproteins, elastin, and proteoglycans that in addition to providing a scaffold for tissue, regulate many fundamental cellular processes such as proliferation, survival, migration and differentiation[1,2]. Many cell types require anchorage to ECM to proliferate[3]. If lacking attachment to ECM, they will undergo anoikis[2, 4]. Integrins activate growth-promoting signaling pathways that are responsible for the anchorage, and two such pathways appear to be involved. One is that integrins facilitate growth factor-mediated activation of extracellular signal-regulated protein kinase (ERK); the other is that integrins activate the c-Jun NH_2-terminal kinase (JNK)[2, 5]. In addition, serine/threonine protein kinase, PKB, has emerged as a crucial regulator in the integrin pathway, which can be controlled through phosphatidylinositol-3' kinase (PI3K)[6]. Integrins, often together with growth factor receptors, up-regulate cyclins D and E and down-regulate CKIs $p21^{cip1}$, $p27^{kip1}$, and $p57^{kip2}$[2, 7]. This action allows cells to pass through the G1/S transition and complete the cell cycle.

Many studies, however, have demonstrated that integrins give rise to growth inhibition rather than growth stimulation[8-13]. Integrin α5β1 has been often observed to be lost in cancerous areas other than in its normal counterpart tissues[14]. It is apparent from these studies that integrin signaling may play a major role in negative control of cell growth, which may be lost in some cancer cells, and the mechanisms of this effect are not completely known yet.

In this study we have further investigated the inhibition role of integrin α5β1 in human hepatocellular carcinoma cell line, SMMC-7721. We analyzed the effect of these cells with or without adhesion to ECM. These studies identified overexpression of β1 subunit or α5β1 inhibited cell cycle progression at S-phase, and this inhibition maybe resulted from the up-regulation of cdk2 inhibitors $p21^{cip1}$ and $p27^{kip1}$ and involved in the unoccupied β1 because of relative lack of its ligands.

MATERIALS AND METHODS

Materials and antibodies

Poly-HEME, wortmannin, FN and LN were all obtained from Sigma, and geneticin (G418) was purchased from Calbiochem (San Diego, CA). Monoclonal antibodies used were directly against cyclin D1 (Santa Cruz), cdk2 (Santa Cruz), integrin β1 (BD Transduction Laboratories, Lexington, KY), phosphorylated FAK (anti-phosphotyrosine clone PT-66, Sigma) and β-actin (Santa Cruz). Goat anti-human integrin α5 polyclonal antibody was also purchased from Santa Cruz. Other antibodies used were those against FAK (Santa Cruz), $p21^{cip1}$ (Santa Cruz), $p27^{kip1}$ (Oncogene Research Products, Cambridge, MA), Ser473-phosphorylated form of PKB and PKB (Cell Signaling). Horseradish peroxidase conjugated anti-mouse, rabbit or goat IgG were purchased from Calbiochem (San Diego, CA).

Cell culture

Human hepatocellular carcinoma cell line SMMC-7721 was obtained from the Liver Cancer Institute, Zhongshan Hospital (Shanghai, China). SMMC-7721 cells were grown in RPMI 1640 medium (Gibco BRL) supplemented with 100 $mL \cdot L^{-1}$ calf bovine serum (CBS), 100×10^3 $U \cdot L^{-1}$ penicillin and 100×10^3 $U \cdot L^{-1}$ streptomycin sulfate. Integrin-overexpressing transfectant

cell lines were maintained in the same medium as above plus 500 μg/ml geneticin (Gibco BRL).

Plasmid construction and stable transfections

pECE vector containing human full-length cDNA of integrin β1 was presented generously by Dr. Mara Brancaccio (Department of Genetics, University of Torino, Torino, Italy). Complementary DNA of β1 integrin cleaved from the pECE plasmid by *EcoR* I was subcloned into pcDNA3 vector to generate pcDNA3-β1. pcDNA3-α5 expression vector was presented kindly by Dr. Sue E. Craig (School of Biological Sciences, University of Manchester, Manchester, UK). Stable transfections were performed using LIPOFECTAMINE™ 2000 (LF2000) reagent (Life Technologies, Grand Island, NY) according to the manufacturer's instructions. Briefly, logarithmically growing cells were transfected with 1 μg of plasmids and 2 μl of LF2000 reagent. At 48 h after transfection, the selective medium containing 1 mg/ml geneticin (G418) antibiotic (Calbiochem) was replaced, and then the cell clones were selected and identified.

Plating experiments

Mock and integrin transfected cells were seeded on the tissue culture plates coated with either FN (15 μg/ml) or LN (15 μg/ml), grown for 60 minutes, and followed by phase-contrast microscopy or protein extraction.

Flow cytometry

Cells were starved by exposure to SFM for 48 h, the harvested cells were then grown in normal growth medium containing 10 % CBS for 12-16 h, the time span covered the duration of normal S phase. At the end of incubation, the cells were digested with 2 mM EDTA in PBS and rinsed twice with ice-cold PBS solution, then fixed by adding them dropwise into 75 % ice-cold ethanol while vortexing, followed by incubation on ice for 60 min. The fixed cells were washed with ice-cold PBS and incubated at 37 ℃ for 30 min in 0.5 ml PBS solution containing 20 μg/ml RNase A, 0.2 % Triton X-100, 0.2 mM EDTA and 20 μg/ml of propidium iodide. DNA content was determined by FACS analysis (Becton Dickinson). The percentage of cells in G0/G1, S, and G2/M phases was determined using the Modfit program.

RNA isolation and RT-PCR

RT-PCR was performed to quantify the level of mRNA, which was isolated using Trizol system (Watson Biotechnologies, Shanghai, China) according to the manufacturer's guidelines. Complementary DNA synthesis was performed essentially as described previously[15], except that 2 μg of total RNA was used for cDNA synthesis, and the primer used was oligo $(dT)_{15}$. For amplification, 2-μl cDNA product was used in a final volume of 50 μl with 5 units of Taq polymerase (SABC, Luoyang, China). The primer pairs for $p27^{kip1}$ and $p21^{cip1}$ were described previously[16,17]. Primers for β-actin[16] were used as the internal control. The expected product sizes were p27, 471 bp; p21, 159 bp and β-actin, 412 bp.

Cell lysis and immunoblotting

Cells cultured under the same conditions as cell cycle analysis were collected, and then washed twice with ice-cold PBS and lysed in 1×SDS lysis buffer (50 mM Tris (pH 6.8), 2 % SDS, 10 % glycerol, 100 μg/ml PMSF, 10 μg/ml leupeptin and 5 mM Na_3VO_4) for 10 min on ice. Cell lysates were boiled and clarified by centrifugation at 12 000 g at 4 ℃ for 10 min. Protein concentration was determined with Hartree assay. Immunoblotting analyses using the enhanced chemiluminescence (ECL) detection system (Perfect, Shanghai, China) were carried out as described previously[18].

RESULTS

Overexpression of integrin α5β1 in SMMC-7721 cells

We transfected the full-length cDNA of genes ITGA5 (α5) or ITGB1 (β1) alone, or α5 and β1 together into a human hepatocellular carcinoma cell line, SMMC-7721, respectively. The pcDNA3 empty vector was the control plasmids, and cells transfected with pcDNA3 were regarded as the mocked cells. The overexpressed transfectant cell lines were mainly screened for increased expression of α5 or β1 in protein levels by Western analysis, and designated as α5-7721, β1-7721 and α5β1-7721, respectively. As shown in Figure 1A, integrin α5 expression was increased to 2-fold in α5-7721 or α5β1-7721 cells compared with the mocked cells. Meanwhile, β1-7721 and α5β1-7721 transfectants had more than 2.5-fold amount in integrin β1 protein level (Figure 1B). The β1 subunits appeared as two bands in Western blot because of variable post-translational modification (mainly N-glycosylation). The hypoglycosylated lower band (Figure 1B) was tentatively identified as biosynthetic precursor of β1 subunit. The band with lower migration rate (upper band in Figure 1B) of integrin β1 subunit was in hyperglycosylated forms, and mainly located in plasma membrane[19-21].

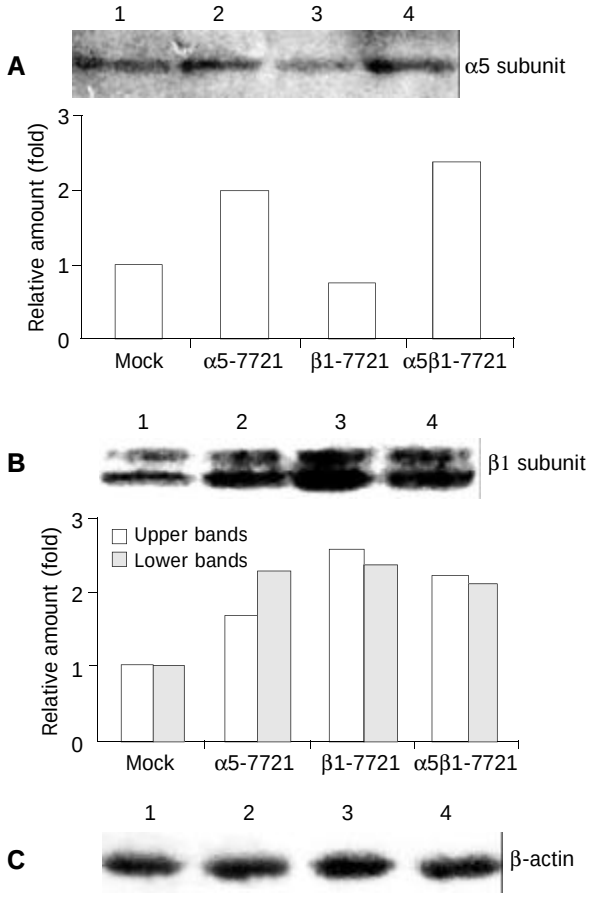

Figure 1 Integrin α5 and β1 protein levels in α5-, β1- and α5β1 transfected SMMC-7721 cells. (A) The expression level of α5 chain was increased in α5-7721 and α5β1-7721 cells. (B) Two forms of β1 integrin were due to different levels of β1-chain glycosylation. The hypoglycosylated lower band was tentatively identified as biosynthetic precursor of β1 subunit, the hyperglycosylated upper band was mature subunits, exposed in part on the cell surface (the 130-kDa product). Immunoblot assay showed that protein levels of the mature form were elevated in the transfectants, especially in β1-7721 and α5β1-7721 cells. (C) The protein level of β-actin showed an equal loading amount in each well. Lane 1, mock cells; lane 2, α5-7721; lane 3, β1-7721; lane 4, α5β1-7721. Each point in the graphs was the mean value from three separate experiments.

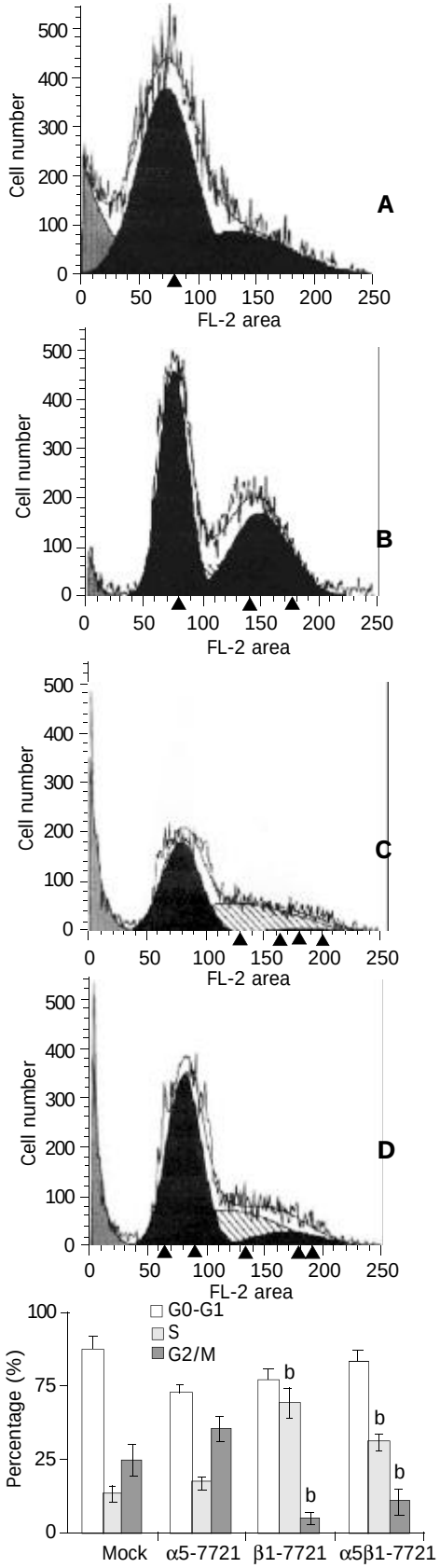

Figure 2 S-phase delay was induced in β1- and α5β1-transfectant cells. For cell cycle analysis, transfected and mocked cells were synchronized by exposure to SFM for 48 h, then grown in RPMI1640 medium containing 10 % CBS and penicillin / streptomycin solution. Twelve or 16 h later, the cells were collected and analysed for flow cytometry as described under "Materials and Methods". A, mocked cells; B, α5-7721 cells; C, β1-7721 cells; D, α5β1-7721 cells. Each bar in graph represented the mean ± SD obtained from three independent experiments. The S-phase delay was significantly different in β1-7721 and α5β1-7721 cells (n=3, ^bP<0.01 *vs* mocked cells).

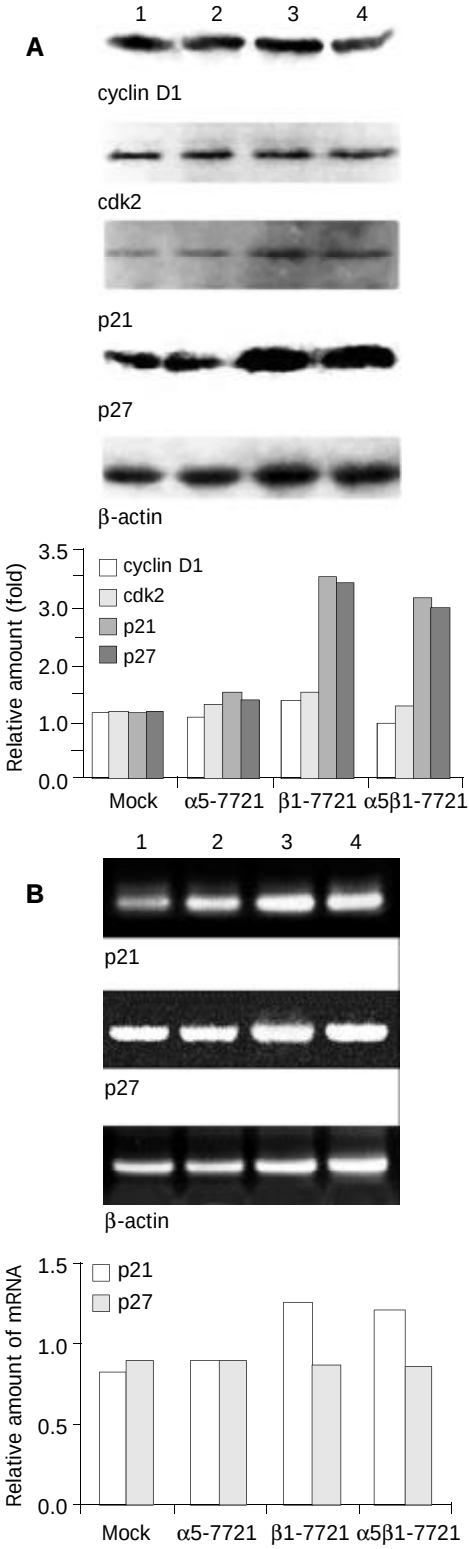

Figure 3 Message RNA and / or protein levels of cell cycle regulatory genes $p21^{cip1}$ and $p27^{kip1}$ in β1-7721 and α5β1-7721 transfectants, but not that of cyclin D1 and cdk2. (A) Immunoblot assay showed the protein level of cyclin D1 and cdk2 were not apparently affected, but $p21^{cip1}$ and $p27^{kip1}$ protein levels were increased in β1-7721 and α5β1-7721 cells. The protein level of β-actin was detected to assess the loading amount in each well in SDS-PAGE gel. (B) Message RNA levels of $p21^{cip1}$ and $p27^{kip1}$ were assessed by RT-PCR, and normalized by that of β-actin. It was apparent that mRNA level of $p21^{cip1}$ was increased in β1- and α5β1- transfected cells. However, the $p27^{kip1}$ mRNA amount was the same as control. Each result represented three separate experiments. Lane 1, mocked cell; lane 2, α5-7721; lane 3, β1-7721; lane 4, α5β1-7721.

Induction of S-phase delay by transfection of integrin β1 subunit

In the previous study, we showed that overexpression of integrin α5β1 or β1 subunit had negative effects on cell growth[11]. To elucidate the mechanisms of cell cycle perturbation induced by overexpressing integrins, flow cytometry analyses were applied. Cell cycle parameters were compared between transfected cells and mocked cells. Similar patterns of the cell cycle were found in α5-7721 and mocked cells (Figure 2). But in β1-7721 and α5β1-7721 transfectants, we observed a significant increase in fraction of cells in S phase of the cell cycle, as shown in Figure 2. This was accompanied by a decrease in proportion of cells in G2/M phases of the cell cycle. These changes were specific for the transfection events containing β1-plasmids, that is, at this point, the pattern of α5β1-7721 was similar to that of β1-7721 cells. These results were obtained from the cells synchronized partly in G0/G1 phase by exposure to serum-free medium. Therefore, these data showed that S-phase delay was probably due to enhanced production of exogenous β1 integrin.

$p21^{cip1}$ and $p27^{kip1}$ were up-regulated in β1 or α5β1 transfectant cell lines

To clarify the mechanism by which S-phase delay was induced in β1-7721 and α5β1-7721 cells, we investigated whether cyclins and cdks were involved in this situation. Expression level of cyclin D1 was examined because this protein was always referred to as a sensor molecule to the extracellular cues[22]. It was shown that cyclin D1 expression was not changed, neither was the cdk2 protein (Figure 3A). As evidenced recently, enhanced $p21^{cip1}$ and/or $p27^{kip1}$ expression was considered to be associated with G1 cell cycle arrest[23, 24], and under some circumstances, with S-phase delay in some cell types[25, 26]. So, we further examined whether β1-chain overexpression could induce $p21^{cip1}$ and $p27^{kip1}$ in β1-7721 and α5β1-7721 cells. As shown in Figure 3A, a significant increase (2-fold amount) of $p21^{cip1}$ protein levels was noted in β1-7721 and α5β1-7721 cells compared with the mocked cells or α5-7721 cells. Meanwhile, $p27^{kip1}$ protein level was also increased to 2.5-fold. We also found that the mRNA level of $p21^{cip1}$ increased, although that of $p27^{kip1}$ maintained the same as control (Figure 3B). Interestingly, we found that overexpression of β1 gene in SMMC-7721 cells induced S-phase delay in this study. The above findings showed that this S-phase delay might be attributed to the increased expression of $p21^{cip1}$ and $p27^{kip1}$.

Phosphorylated form of PKB was inhibited in β1 and α5β1 transfectants and this might result in accumulation of $p21^{cip1}$ and $p27^{kip1}$

To determine how overexpressing α5β1 integrins transferred signals from membrane to cytosol or nucleus to modulate the expression of CKIs $p21^{cip1}$ and $p27^{kip1}$, we examined the two important signaling molecules mediated by integrins, FAK and PKB. The results showed that neither FAK nor its tyrosine phosphorylated form was affected (Figure 4A). However, levels of Ser473-phosphorylated form of PKB were decreased in β1-7721 and α5β1-7721 cells in comparison with the control cells, but total amount of PKB protein was not apparently affected (Figure 4B).

In recent years, evidences have shown that activated PKB protein may phosphorylate $p21^{cip1}$, and induce its degradation through the ubiquitin-26S proteasome pathway[6,27]. But evidences indicating $p27^{kip1}$ phosphorylation by PKB are few. In this study, decrease of phosphorylated PKB (Figure 4B) and accumulation of $p27^{kip1}$ (Figure 3A) occurred concomitantly in β1-7721 or α5β1-7721 cells. To obtain support, we further performed an experiment to block the phosphorylated form of PKB. It is well known that Ser-473 phosphorylation of PKB, on behalf of its active forms, appears to be catalyzed by phosphoinositide-dependent kinase 1 (PDK1) and integrin-linked kinase (ILK)[28, 29], and that PI3K is located upstream of both ILK and PKB[6]. So the PI3K inhibitor wortmannin was explored in this study. Following serum starvation, cells were cultured in the medium with 100 nM wortmannin for 24 h or 48 h. We investigated the level of phosphorylation of PKB and $p27^{kip1}$ by immunostaining. The data showed that phosphorylation of PKB was blocked, and expression of $p27^{kip1}$ was increased at the same time compared with control cells (Figure 5). Therefore, the decrease of phosphorylated form of PKB was at least in part, responsible for $p27^{kip1}$ protein accumulation.

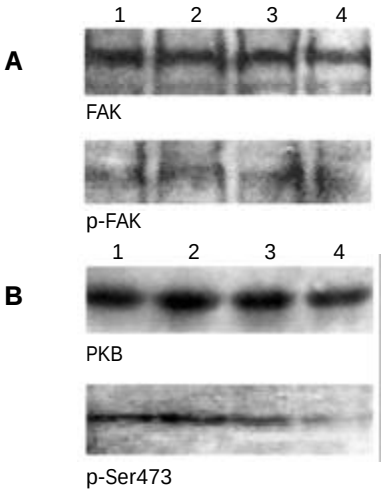

Figure 4 Activation of PKB, but not FAK, was downregulated in β1- and α5β1- transfected cells. (A) FAK activation was assessed by phosphotyrosine- specific antibody, followed by stripping and reprobing with anti-FAK antibody. (B) PKB and its Ser473-phosphorylated forms were determined by 10 % SDS-PAGE with the equal loading amount. The loading amount control is shown in Figures 1C and 3A. Lane 1, mock cells; lane 2, α5-7721; lane 3, β1-7721; lane 4, α5β1-7721. Results were representative of 4 repeated experiments.

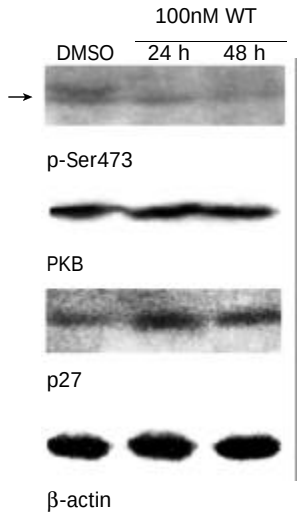

Figure 5 Ser473-phosphorylated form of PKB was decreased, but $p27^{kip1}$ protein level was increased concomitantly in SMMC-7721 parental cells treated with the PI3K inhibitor wortmannin. The parental SMMC-7721 cells were starved with serum-free medium for 48 h, then grown in normal medium / 10 % CBS containing DMSO (as control, 24 h) or 100 nM wortmannin for

the indicated times. The amount of DMSO did not exceed 0.1 %, which was determined not to damage the cells. Equal amount of wortmannin was added again after grown for 24 h. The level of Ser473-phosphorylated form of PKB (*arrow*) was declined, but $p27^{kip1}$ protein level was elevated with the treatment of wortmannin in SMMC-7721 cells. Results were representative of at least 3 repeated experiments. Abbreviation: DMSO, dimethylsulfoxide; WT, wortmannin.

Inhibition of cell cycle was possibly due to the relative lack of ECM

Integrins, in general, promote the focal adhesion protein activities such as FAK and cell cycle progression[2]. So we ponder why overexpression of integrin β1 subunit can repress the level of phosphorylated PKB and the cell cycle. Here, we performed plating experiments to elucidate its mechanism. First, we observed the morphological change of cells that were plated on LN- or FN- coated dishes and grown for 60 minutes (Figure 6). It was found that β1-7721 and α5β1-7721 cells were prone to attachment and spreading, perhaps to the cell cycle progression. Next, we determined the changes of phosphorylated FAK and phosphorylation of PKB in cells attaching on LN and FN. As mentioned above (Figure 4A), total amount of FAK and its phosphorylated forms were not affected in cells cultured in the flasks without coating of LN or FN. But the level of tyrosine phosphorylated FAK was increased in cells, which were plated on LN- or FN- coated dishes and grown for the indicated times (Figure 7A, and data not shown for FN-coated dishes). Moreover, the level of Ser473 phosphorylated form of PKB was similar to that of phosphorylated FAK under the same condition (Figure 7B, and data not shown for FN-coated dishes). Finally, protein level of $p27^{kip1}$ was declined in β1-7721 and α5β1-7721 cells (Figure 7C). These findings demonstrated that an important role of LN or FN in the molecular changes of β1-7721 or α5β1-7721 cells, especially, in PKB phosphorylation and $p27^{kip1}$ protein levels. On the contrary, when attachment of the parental cells to ECM was blocked by plating them onto poly-HEME-coated petri dishes, the percentage of cells in S-phase was increased from 13.08 % to 37.33 % (Figure 8). That is, when the parental SMMC-7721 cells were prevented from interaction with ECM through the preparation of poly-HEME, the same effects of S-phase accumulation took place as that in β1-7721 or α5β1-7721 cells. These results suggested that S-phase delay induced by overexpressing β1 in SMMC-7721 cells might be the result of the relative lack of ECM.

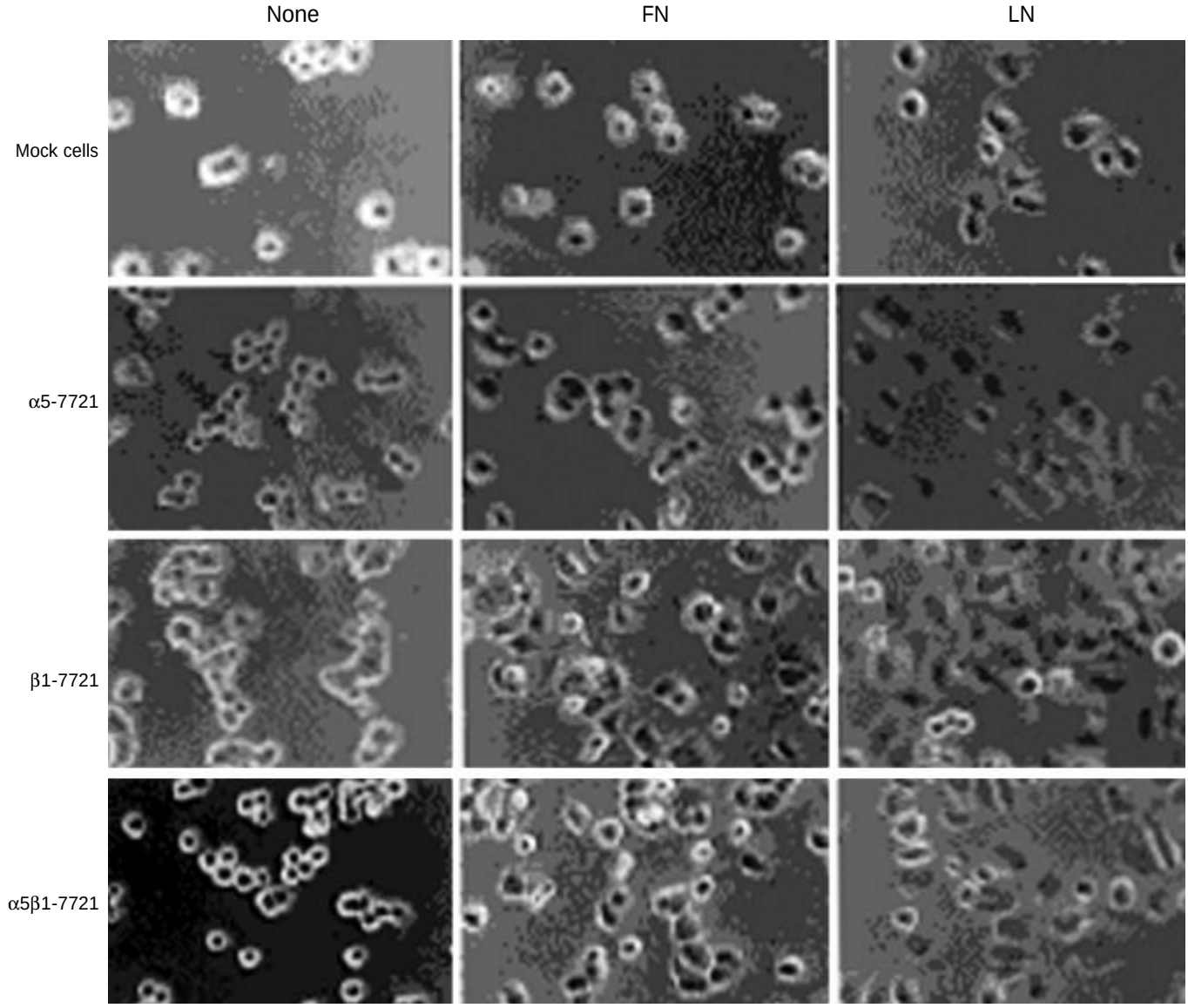

Figure 6 β1-7721 and α5β1-7721 cells subjected to spreading on fibronectin- or laminin- coated culture dishes. The mocked and transfected cells were plated on FN- or LN- coated tissue culture plates in normal medium for 60 min, then cells on the plates were photographed by phase-contrast microscopy with a digital camera. Abbreviations: FN, fibronectin; LN, laminin.

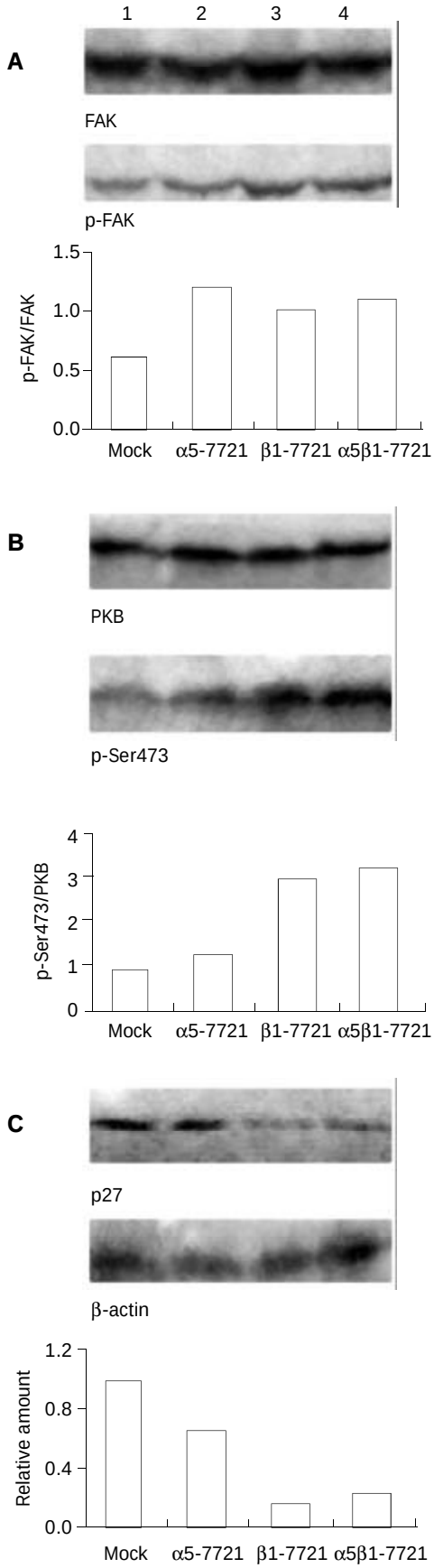

Figure 7 Effects of laminin on transfected cells. Protein levels of phosphorylated FAK (A) and Ser473-phosphorylated form of PKB (B) were increased in the transfected cells, especially in β1-7721 and α5β1-7721 cells grown in the LN-coated culture dishes for 60 minutes. (C) Under the same condition, $p27^{kip1}$ protein level was decreased in β1-7721 and α5β1-7721 cells. Lane 1, mock cells; lane 2, α5-7721; lane 3, β1-7721; lane 4, α5β1-7721. Each result represented at least 3 independent experiments.

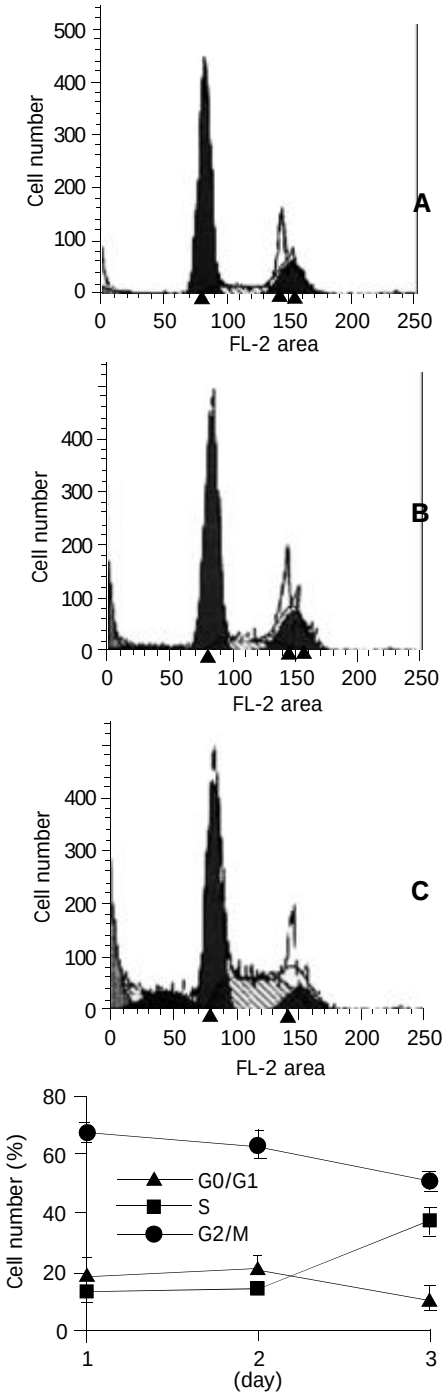

Figure 8 The percentage of cells in S phase was increased in SMMC-7721 cells plated on poly-HEME-coated petri dishes. The parental SMMC-7721 cells were plated on poly-HEME-coated petri dishes, and cultured in normal medium for 24 h (A), 48 h (B) or 72 h (C), respectively, then collected and analysed by flow cytometry. The cell cycle pattern (C) was similar to that of β1-7721 or α5β1-7721 cells.

DISCUSSION

We examined the effects of overexpressed α5β1 or β1 on tumor cell proliferation, which provide the evidence that overexpression of α5β1 or β1 inhibits the proliferation of human hepatocellular carcinoma cell line SMMC-7721 and this inhibition may be related to the insufficient ligands for overexpressed β1 integrins. This finding also demonstrated that the inhibition of cell cycle was due to a specific growth arrest at S-phase that involved an increase in the protein level of $p21^{cip1}$ and $p27^{kip1}$.

This study showed that cyclin D1 expression was not affected by transfection events. So the early G1 phase

progression may not be influenced under this condition. However, the protein levels of $p21^{cip1}$ and $p27^{kip1}$ were increased in β1 or α5β1 transfectant cells, which might be the major reason why S-phase delay occurred. It was previously reported that $p21^{cip1}$ and $p27^{kip1}$ were assembly factors rather than inhibitors of cdk4/6 kinases[30], but were inhibitors of cdk2 kinase, which is the key kinase contributing to G1/S transition and S phase progression. One CKI protein, $p21^{cip1}$, the first cyclin-dependent kinase inhibitor to be identified[31], has also a separate cdk2 binding site in its N-terminal region (amino acid 53-58) and optimal cyclin/cdk inhibition requires binding to this site as well as one of the cyclin binding domains. Furthermore, $p21^{cip1}$ interacts with proteins such as PCNA, c-Myc and E2Fs that control DNA replication and other S phase events[32]. Meanwhile, evidences have shown that $p27^{kip1}$ plays a key role in the regulation of the proliferation of tumor cells in response to signals from ECM[13]. Therefore, increased $p21^{cip1}$ and $p27^{kip1}$ proteins can induce S-phase delay in β1- and α5β1-transfected cells.

In many cell types, the intracellular concentration of $p27^{kip1}$ is mainly controlled at the posttranscriptional level, and its degradation is initiated by phosphorylation with a target enzyme, cdk2[33] or other enzymes, such as PKB[6], and completed by the ubiquitin-proteasome pathway. $p21^{cip1}$ protein can also be phosphorylated by PKB[6]. In this study, we found that PKB level of phosphorylated form was decreased in β1- or α5β1- transfected cells, accompanied by the increase of $p21^{cip1}$ and $p27^{kip1}$ to a certain extent. These findings indicate that the decrease of active form of PKB may interpret the accumulation of $p21^{cip1}$ and $p27^{kip1}$ *bona fide*, which in turn, interferes with the cell cycle at S phase.

This study suggested that overexpression of β1 or α5β1 integrin in SMMC-7721 cells could induce S-phase delay. The mechanism underlying this phenomenon may be due to two kinds of possibilities. One is "integrin-mediated death" (IMD) described by Stupack and his colleagues[34, 35], that is, an unligated integrin promotes apoptosis of cells. It is well known that α5β1 integrin, in general, acts as the effector protein of cell proliferation, such as endothelial cells in the vascular system[36]. In this study, however, we showed that overexpression of β1 or α5β1 induced S-phase delay. When cells were plated on FN/LN-coated culture dishes, they were subjected to attachment and spreading compared with the mocked and α5-7721 cells. Moreover, for the parental cells, they underwent S-phase delay and apoptosis when they were deprived of attachment by plating them on poly-HEME-coated petri dishes. Therefore, we postulated that the relative lack of ECM might be involved in S-phase delay triggered by overexpression of β1 or α5β1 integrin gene in SMMC-7721 cells. Another possibility is the trans-dominant integrin inhibition, which is defined as the occupancy of one integrin by its ligand, can inhibit the functions of other integrins[37-40]. For example, integrin α5β1 is essential for angiogenesis[36], but $\alpha_v\beta3$ may suppress the functions of integrin α5β1, if β3 integrins prevail in the endothelial cells[41]. It was reported that the basal integrin repertoire in hepatocellular carcinoma cells was characterized by the expression of several potential laminin receptors of the integrin family, such as α1β1, α2β1 and α6β1[42-47]. So the overexpression of β1 may preferentially dimerize with α1, α2 and α6, the subunits of the receptors of laminin or collagen (they were lost in this *in vitro* model). Therefore, if these α subunits are occupied, the functions of integrin α5β1 may be suppressed, including its capacity to block cell cycle arrest.

ACKNOWLEDGEMENTS

We are grateful to Dr. Mara Brancaccio from the University of Torino (Torino, Italy), and Dr. Sue E. Craig from the University of Manchester (Manchester, UK) for their gifts of the plasmids. We also acknowledge the Chinese Medicine Board (CMB) in New York, U.S.A. for its kind support to our research.

REFERENCES

1 **Lukashev ME**, Werb Z. ECM signalling: orchestrating cell behaviour and misbehaviour. *Trends Cell Biol* 1998; **8:** 437-441
2 **Giancotti FG**, Ruoslahti E. Integrin signaling. *Science* 1999; **285:** 1028-1032
3 **Assoian RK**. Anchorage-dependent cell cycle progression. *J Cell Biol* 1997; **136:** 1-4
4 **Frisch SM**, Francis H. Disruption of epithelial cell-matrix interactions induces apoptosis. *J Cell Biol* 1994; **124:** 619-626
5 **Schwartz MA**. Integrin signaling revisited. *Trends Cell Biol* 2001; **11:** 466-470
6 **Nicholson KM**, Anderson NG. The protein kinase B / Akt signalling pathway in human malignancy. *Cell Signal* 2002; **14**: 381-395
7 **Sherr CJ**, Roberts JM. CDK inhibitors: positive and negative regulators of G1-phase progression. *Genes Dev* 1999; **13:** 1501-1512
8 **Giancotti FG**, Mainiero F. Integrin-mediated adhesion and signaling in tumorigenesis. *Biochim Biophys Acta* 1994; **1198:** 47-64
9 **Giancotti FG**, Ruoslahti E. Elevated levels of the α5β1 fibronectin receptor suppress the transformed phenotype of Chinese hamster ovary cells. *Cell* 1990; **60:** 849-859
10 **Varner JA**, Emerson DA, Juliano RL. Integrin α5β1 expression negatively regulates cell growth: reversal by attachment to fibronectin. *Mol Biol Cell* 1995; **6:** 725-740
11 **Zhou GF**, Ye F, Cao LH, Zha XL. Overexpression of integrin α5β1 in human hepatocellular carcinoma cell line suppresses cell proliferation in vitro and tumorigenicity in nude mice. *Mol Cell Biochem* 2000; **207:** 49-55
12 **Wang D**, Sun L, Zborowska E, Willson JK, Gong J, Verraraghavan J, Brattain MG. Control of type II transforming growth factor-β receptor expression by integrin ligation. *J Biol Chem* 1999; **274:** 12840-12847
13 **Henriet P**, Zhong ZD, Brooks PC, Weinberg KI, DeClerck YA. Contact with fibrillar collagen inhibits melanoma cell proliferation by up-regulating $p27^{KIP1}$. *Proc Natl Acad Sci USA* 2000; **97**: 10026-10031
14 **Su JM**, Gui L, Zhou YP, Zha XL. Expression of focal adhesion kinase and α5 and β1 integrins in carcinomas and its clinical siginificance. *World J Gastroenterol* 2002; **8**: 613-618
15 **Munsterberg AE**, Lassar AB. Combinatorial signals from the neural tube, floor plate and notochord induce myogenic bHLH gene expression in the somite. *Development* 1995; **121:** 651-660
16 **Takano Y**, Kato Y, van Diest PJ, Masuda M, Mitomi H, Okayasu I. Cyclin D2 overexpression and lack of p27 correlate positively and cyclin E inversely with a poor prognosis in gastric cancer cases. *Am J Pathol* 2000; **156**: 585-594
17 **Chen B**, He L, Savell VH, Jenkins JJ, Parham DM. Inhibition of the interferon-gamma / signal transducers and activators of transcription (STAT) pathway by hypermethylation at a STAT-binding site in the $p21^{WAF1}$ promoter region. *Cancer Res* 2000; **60:** 3290-3298
18 **Kim J**, Han I, Kim Y, Kim S, Oh ES. C-terminal heparin-binding domain of fibronectin regulates integrin-mediated cell spreading but not the activation of mitogen-activated protein kinase. *Biochem J* 2001; **360:** 239-245
19 **Heino J**, Ignotz RA, Hemler ME, Crouse C, Massague J. Regulation of cell adhesion receptors by transforming growth factor-β. Concomitant regulation of integrins that share a common β1 subunit. *J Biol Chem* 1989; **264:** 380-388
20 **Bellis SL**, Newman E, Friedman EA. Steps in integrin β1-chain glycosylation mediated by TGFβ1 signaling through Ras. *J Cell Physiol* 1999; **181:** 33-44
21 **Yan Z**, Chen M, Perucho M, Friedman E. Oncogenic Ki-ras but not oncogenic Ha-ras blocks integrin β1-chain maturation in colon epithelial cells. *J Biol Chem* 1997; **272:** 30928-30936
22 **Howe A**, Aplin AE, Alahari SK, Juliano RL. Integrin signaling and cell growth control. *Curr Opin Cell Biol* 1998; **10:** 220-231
23 **Sherr CJ**, Roberts JM. Inhibitors of mammalian G1 cyclin-dependent kinases. *Genes Dev* 1995; **9:** 1149-1163
24 **Harper JW**, Adami GR, Wei N, Keyomarsi K, Elledge SJ. The p21

Cdk-interacting protein Cip1 is a potent inhibitor of G1 cyclin-dependent kinases. *Cell* 1993; **75:** 805-816

25 **Zhang Y**, Rishi AK, Dawson MI, Tschang R, Farhana L, Boyanapalli M, Reichert U, Shroot B, Van Buren EC, Fontana JA. S-phase arrest and apoptosis induced in normal mammary epithelial cells by a novel retinoid. *Cancer Res* 2000; **60:** 2025-2032

26 **Shenberger JS**, Dixon PS. Oxygen induces S-phase growth arrest and increases p53 and $p21^{WAF1/CIP1}$ expression in human bronchial smooth-muscle cells. *Am J Respir Cell Mol Biol* 1999; **21:** 395-402

27 **Brazil DP**, Hemmings BA. Ten years of protein kinase B signalling: a hard Akt to follow. *Trends Biochem Sci* 2001; **26:** 657-664

28 **Delcommenne M**, Tan C, Gray V, Rue L, Woodgett J, Dedhar S. Phosphoinositide-3-OH kinase-dependent regulation of glycogen synthase kinase 3 and protein kinase B/AKT by the integrin-linked kinase. *Proc Natl Acad Sci USA* 1998; **95:** 11211-11216

29 **Persad S**, Attwell S, Gray V, Mawji N, Deng JT, Leung D, Yan J, Sanghera J, Walsh MP, Dedhar S. Regulation of protein kinase B/Akt-serine 473 phosphorylation by integrin-linked kinase: critical roles for kinase activity and amino acids arginine 211 and serine 343. *J Biol Chem* 2001; **276:** 27462-27469

30 **Sherr CJ**. The Pezcoller lecture: cancer cell cycles revisited. *Cancer Res* 2000; **60:** 3689-3695

31 **el-Deiry WS**, Tokino T, Velculescu VE, Levy DB, Parsons R, Trent JM, Lin D, Mercer WE, Kinzler KW, Vogelstein B. WAF1, a potential mediator of p53 tumor suppression. *Cell* 1993; **75:** 817-825

32 **Dotto GP**. $p21^{WAF1/Cip1}$: more than a break to the cell cycle? *Biochim Biophys Acta* 2000; **1471:** M43-M56

33 **Elledge SJ**, Harper JW. The role of protein stability in the cell cycle and cancer. *Biochim Biophys Acta* 1998; **1377:** M61-M70

34 **Stupack DG**, Puente XS, Boutsaboualoy S, Storgard CM, Cheresh DA. Apoptosis of adherent cells by recruitment of caspase-8 to unligated integrins. *J Cell Biol* 2001; **155:** 459-470

35 **Cheresh DA**, Stupack DG. Integrin-mediated death: an explanation of the integrin-knockout phenotype? *Nat Med* 2002; **8:** 193-194

36 **Yang JT**, Rayburn H, Hynes RO. Embryonic mesodermal defects in α5 integrin-deficient mice. *Development* 1993; **119:** 1093-1105

37 **Schwartz MA**, Ginsberg MH. Networks and crosstalk: integrin signalling spreads. *Nat Cell Biol* 2002; **4:** E65-E68

38 **Blystone SD**, Graham IL, Lindberg FP, Brown EJ. Integrin αvβ3 differentially regulates adhesive and phagocytic functions of the fibronectin receptor α5β1. *J Cell Biol* 1994; **127:** 1129-1137

39 **Diaz-Gonzalez F**, Forsyth J, Steiner B, Ginsberg MH. Trans-dominant inhibition of integrin function. *Mol Biol Cell* 1996; **7:** 1939-1951

40 **Blystone SD**, Slater SE, Williams MP, Crow MT, Brown EJ. A molecular mechanism of integrin crosstalk: αvβ3 suppression of calcium/calmodulin- dependent protein kinase II regulates α5β1 function. *J Cell Biol* 1999; **145**: 889- 897

41 **Simon KO**, Nutt EM, Abraham DG, Rodan GA, Duong LT. The αvβ3 integrin regulates α5β1-mediated cell migration toward fibronectin. *J Biol Chem* 1997; **272:** 29380-29389

42 **Volpes R**, van den Oord JJ, Desmet VJ. Integrins as differential cell lineage markers of primary liver tumors. *Am J Pathol* 1993; **142:** 1483-1492

43 **Scoazec JY**, Fléjou JF, D'Errico A, Fiorentino M, Zamparelli A, Bringuier AF, Feldmann G, Grigioni WF. Fibrolamellar carcinoma of the liver: composition of the extracellular matrix and expression of cell-matrix a cell-cell adhesion molecules. *Hepatology* 1996; **24:** 1128-1136

44 **Torimura T**, Uneo T, Kin M, Inuzuka S, Sugawara H, Tamaki S, Tsuji R, Sujaku K, Sata M, Tanikawa K. Coordinated expression of integrin α6β1 and laminin in hepatocellular carcinoma. *Hum Pathol* 1997; **28:** 1131-1138

45 **Ozaki I**, Yamamoto K, Mizuta T, Kajihara S, Fukushima N, Setoguchi Y, Morito F, Sakai T. Differential expression of laminin receptors in human hepatocellular carcinoma. *Gut* 1998; **43**: 837-842

46 **Masumoto A**, Arao S, Otsuki M. Role of β1 integrins in adhesion and invasion of hepatocellular carcinoma cells. *Hepatology* 1999; **29:** 68-74

47 **Nejjari M**, Hafdi Z, Dumortier J, Bringuier AF, Feldmann G, Scoazec JY. α6β1 integrin expression in hepatocarcinoma cells: regulation and role in cell adhesion and migration. *Int J Cancer* 1999; **83:** 518-525

Edited by Zhang JZ and Wang XL

P.O.Box 2345, Beijing 100023,China
Fax: +86-10-85381893
E-mail: wjg@wjgnet.com www.wjgnet.com

World J Gastroenterol 2003;9(8):1697-1701
World Journal of Gastroenterology
 ISSN 1007-9327

• LIVER CANCER •

Comparison between chemoembolization combined with radiotherapy and chemoembolization alone for large hepatocellular carcinoma

Wei-Jian Guo, Er-Xin Yu, Lu-Ming Liu, Jie Li, Zhen Chen, Jun-Hua Lin, Zhi-Qiang Meng, Yi Feng

Wei-Jian Guo, Jie Li, Yi Feng, Department of Oncology, Xinhua Hospital of Shanghai Second Medical University, 1665 Kongjiang Road, Shanghai 200092, China
Er-Xin Yu, Lu-Ming Liu, Zhen Chen, Jun-Hua Lin, Zhi-Qiang Meng, Cancer Hospital of Fudan University, Shanghai 200032, China
Correspondence to: Wei-Jian Guo, MD, Department of Oncology, Xinhua Hospital of Shanghai Second Medical University, 1665 Kongjiang Road, Shanghai 200092, China. guoweijian1@sohu.com
Received: 2003-04-02 **Accepted:** 2003-05-19

Abstract

AIM: To investigate the efficacy of transcatheter arterial chemoembolization (TACE) combined with radiotherapy for unresectable large hepatocellular carcinoma (HCC).

METHODS: From June 1994 to June 1999, a total of 76 patients with large unresectable HCC were treated with TACE followed by external-beam irradiation. 89 patients with large HCC, who underwent TACE alone during the same period, served as the control group. Clinical features, therapeutic modalities, acute effects and survival rates were analyzed and compared between TACE plus irradiation group and TACE alone group. A multivariate analysis of nine clinical variables and one treatment variable (irradiation) was performed by the Cox proportional hazards model.

RESULTS: The clinical features and therapeutic modalities except irradiation between the two groups were comparable ($P>0.05$). The objective response rate (RR) in TACE plus irradiation group was higher than that in TACE alone group (47.4 % *vs* 28.1 %, $P<0.05$). The overall survival rates in TACE plus irradiation group (64.0 %, 28.6 %, and 19.3 % at 1, 3, 5 years, respectively) were significantly higher than those in TACE alone group (39.9 %, 9.5 %, and 7.2 %, respectively, $P=0.0001$). Cox proportional hazards model analysis showed that tumor extension and Child grade were significant and were independent negative predictors of survival, while irradiation was an independent positive predictor of survival.

CONCLUSION: TACE combined with radiotherapy is more effective than TACE alone, and is a promising treatment for unresectable large HCC.

Guo WJ, Yu EX, Liu LM, Li J, Chen Z, Lin JH, Meng ZQ, Feng Y. Comparison between chemoembolization combined with radiotherapy and chemoembolization alone for large hepatocellular carcinoma. *World J Gastroenterol* 2003; 9(8): 1697-1701
http://www.wjgnet.com/1007-9327/9/1697.asp

INTRODUCTION

Hepatocellular carcinoma (HCC) is a common cancer in Asia. In China, there has been an increasing trend in the incidence and mortality of HCC during the past two decades. The age-adjusted rate of death per 100 000/year was 20.37 in 1990's. Patients with HCC usually have a poor prognosis. Surgery is the only potential cure, and there has been a great progress in surgery over the past decades[1]. However, the overall 5-year survival rates are still not above 5 % as the number of resected cases is limited due to advanced lesions or associated liver disease[2-4]. Most of the patients with HCC are subjected to various forms of non-surgical therapy. Transcatheter arterial chemoembolization (TACE) has become one of the most popular forms of nonsurgical treatment in Asia. TACE application to HCC has demonstrated good results in reducing the size of tumor and improving survival[5-10]. However, within or around the capsule, which is supplied by both arterial and portal blood, tumor cells remain viable, which are often responsible for later recurrence[11]. Even in several prospective randomized trials, TAE failed to improve significantly the survival of patients with HCC[12,13]. Further treatment was needed to eradicate the residual tumor cells. We have found in a clinical trial that TACE combined with irradiation may be a good method for large unresectable HCC[14]. In the present study, we compared the effects of TACE plus irradiation with that of TACE alone for the treatment of large unrectable HCC.

MATERIALS AND METHODS

Patients

During the past decade, patients with unresectable HCC underwent TACE therapy as the first line treatment at the Cancer Hospital of Fudan University, but parts of patients underwent TACE combined with radiotherapy or were given percutaneous ethanol injection (PEI) in clinical trials by some doctors. Included in the present study were 76 patients with unresectable large HCC who underwent TACE combined with radiotherapy between June 1994 and June 1999. The criteria for entry into this study were as follows: (1) The tumor / liver volume ratio was not above 0.7:1. (2) The lesion was detectable by ultrasound (US) and computed tomography (CT). (3) The level of serum transaminase was under 80 IU/L. (4) There was no evidence of extrahepatic metastasis, or ascites, or severe cirrhosis (class C according to Child's classification). (5) Karnofsky performance score $\geqslant$70. During the same period, a total of 127 patients underwent TACE alone as a routine therapy. 89 patients who complied with the above criteria served as the control group. In 61 (80.0 %) patients in TACE plus irradiation group and 73 patients (82.0 %) in control group, the diagnosis of HCC was confirmed by cytological examination. Diagnosis in the remaining patients was made on the basis of characteristic findings by ultrasound, CT and angiography, and high serum α-fetoprotein (AFP) levels. None of the patients underwent surgical resection owing to advanced tumor stage and/or location of the lesion, or because of refusal of surgery. Informed consent was obtained from all patients and their relatives.

Treatments

TACE procedure was performed as follows. The tip of a catheter

was introduced into the appropriate hepatic artery, and 5-fluorouracil (1.0 g, 5-Fu, Xudong Haipu Pharmaceutical Inc., Shanghai, China) and cisplatin (40-60 mg, CDDP, Qilu Pharmaceutical Factory, Jinan, China) or doxorubicin hydrochloride (30-50 mg, Adriamycin, Main Luck Pharmaceutical Inc., Shenzhen, China) were injected, followed by a mixture of iodized oil (5-20 ml, Lipiodol, Huaihai Pharmaceutical Factory, Shanghai, China) and mitomycin C (10-20 mg, MMC, Kyowa Hakko Kogyo Co., LTD, Tokyo, Japan) was injected slowly under fluoroscopic control. In some patients embolization with a gelatin sponge (1×1×10 mm, Gelfoam. the 3rd Pharmaceutical Factory of Nanjing, Nanjing, China) was performed at the same time. TACE procedures were performed at 4 to 10 week intervals, and patients received 1 to 4 times of TACE.

In the TACE plus irradiation group, radiotherapy was started 4 to 8 weeks after TACE. Twenty-six patients with a solitary tumor within a 9 cm diameter received limited-field radiotherapy. Radiation was delivered through a pair of opposed anterior-posterior fields using a 6 MV or 18 MV linear accelerator. Field sizes ranged from 64 cm^2 to 144 cm^2. The fractions were 1.8 to 2.0 Gy daily, given five times a week. The total dose ranged from 30 Gy to 50 Gy, depending on the proportion of normal liver excluded from the high-dose volume and the Child' s grade. For 50 patients with a solitary tumor of more than 9 cm diameter or with multinodular or diffuse lesions, whole or partial liver irradiation with a moving strip technique[14] was performed. The total midline dose ranged from 19.5 to 30 Gy. Ten patients whose tumor reduced to 9 cm or smaller after whole or partial liver irradiation had a boost to residual disease to a total dose of 36 to 42Gy.

Effects evaluation

The effects on the tumor were assessed by US and CT, together with AFP levels in cases with increased baseline values. Changes in tumor size were assessed in terms of percent regressing on CT and US, using World Health Organization criteria. Cumulative survival was determined by the Kaplan-Meier method from the first day of treatment.

Statistical analysis

The difference of clinical features, therapeutic modalities, response rate (RR) and AFP decreasing rate between the 2 groups were analyzed by chi-square test. The difference of survival was assessed by log-rank test. *P* value <0.05 was considered significant.

To assess the relatively prognostic importance of factors in predicting survival, a multivariate analysis of nine clinical variables, including sex, age, AFP level, number of lesions, tumor size, tumor extension, portal thrombosis, Child grade, and Okuda stage, and one treatment variable (irradiation), was performed by Cox proportional hazards model.

RESULTS

Clinical features and therapeutic modalities

The nine clinical features before treatment in the two groups are shown in Table 1. Only the rate of two lobes invasion in TACE plus irradiation group was slightly, but not significantly higher than that in control group. The other features in two groups were similar (*P*>0.05). There was no significant difference of TACE times and spongostan use between two groups (Table 1). Thus, the clinical features and therapeutic modalities, except irradiation, were comparable between these two groups.

Effects on tumor

In the TACE plus irradiation group, 5 patients (6.6 %) showed a complete response (CR), and 31 patients (40.8 %) showed a partial response (PR). Tumor size was unchanged in 30 cases (39.5 %), and increased in 10 cases (13.2 %). The objective response rate (RR) was 47.4 %. 48 patients had increased AFP values (>20 ng/ml) before treatment. In 23 of these cases (47.9 %), AFP level reduced by more than 50 %. In the control group, CR was observed in 2 patients (2.3 %) and PR was observed in 23 patients (25.8 %). Tumor size was unchanged in 44 cases (49.4 %) and increased in 20 cases (22.5 %). The RR was 28.1 %. The rate of AFP level, reducing by more than 50 %, was 29.0 % (20/69). The RR and AFP reduction rate in the TACE plus irradiation group increased significantly compared with that in the control group (*P*<0.05).

Table 1 Clinical features and therapeutic modalities in two groups

		TACE group cases (%)	TACE plus irradiation group cases (%)	*P* value
Sex	Male	75 (84.3)	68 (89.5)	
	Female	14 (15.7)	8 (10.5)	0.327
Age	<60 years	66 (74.2)	57 (75.0)	
	⩾60 years	23 (25.8)	19 (25.0)	0.901
AFP	<400 ng/ml	45 (50.6)	42 (55.3)	
	⩾400 ng/ml	44 (49.4)	34 (44.7)	0.547
No. of lesions	Solitary	59 (66.3)	51 (67.1)	
	Multiple	30 (33.7)	25 (32.9)	0.912
Tumor	1 lobe	72 (81.9)	52 (68.4)	
extension[a]	2 lobe	17 (19.1)	24 (31.6)	0.064
Tumor size	5-10 cm	51 (57.3)	47 (61.8)	
	>10 cm	38 (42.7)	29 (38.2)	0.554
Portal	Absent	67 (75.3)	62 (81.6)	
thrombosis	Present	22 (24.7)	14 (18.4)	0.329
Child grade	A	74 (83.2)	63 (82.9)	
	B	15 (16.8)	13 (17.1)	0.996
Okuda stage	I	24 (27.0)	29 (38.2)	
	II	65 (73.0)	46 (60.5)	
	III		1 (1.3)	0.155
TACE times	1	27 (30.3)	27 (35.5)	
	2	42 (47.2)	28 (36.8)	
	3	15 (16.9)	11 (14.5)	
	4	5 (5.6)	10 (13.2)	0.253
Spongostan use	No	48 (53.9)	44 (57.9)	
	Yes	41 (46.1)	32 (42.1)	0.610

[a]Hepatic lobes were classified as two lobes: right lobe and left lobe.

Survival and Cox model analysis

In the TACE plus irradiation group, the median follow-up time was 26 months (ranged from 10 to 84 months). Fifty-two patients died, 21 patients were still alive, and the remaining 3 patients were lost to follow-up. In the control group, the median follow-up time was 24 months (ranged from 10 to 70 months). Seventy-five patients died, 9 patients were still alive, and 5 patients were lost to follow-up. The data were obtained and analyzed in January 2001.

The survival curve for patients from the two groups is shown in Figure 1. The overall survival rates at 1, 3, and 5 years from the TACE plus irradiation group were 64.0 %, 28.6 %, and 19.3 %, respectively (median survival, 19 months), and 39.9 %, 9.5 %, and 7.2 %, respectively from the control group (median survival, 10 months). The survival rates in TACE plus irradiation group were significantly higher than those in control group (*P*=0.0001).

Multivariate analysis using the Cox proportional hazards model showed that both tumor extension and Child grade were significant and independent negative predictors of survival, while irradiation was an independent positive predictor of survival (Table 2).

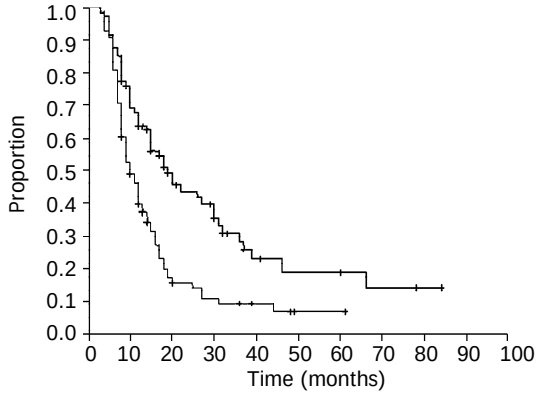

Figure 1 Cumulative survival curves for patients in two groups. The patients in TACE plus irradiation group survived significantly longer than did those in TACE alone group (P=0.0001).

Table 2 Multivariate analysis of major prognostic factors by the Cox proportional hazards model

Variabes	Regression coefficient	Hazard ratio	*P* value
Tumor extension	0.8708	2.3888	0.0016
Child grade	0.5685	1.7655	0.0200
Irradiation or not	-0.7256	0.4840	0.0002

DISCUSSION

TACE is a combination of target chemotherapy and arterial embolization that has both selective ischemic and chemotherapeutic effects on HCC. TACE is an excellent debulking procedure. Surgically resected specimens showed that TACE effectively destroyed malignant cells, not only in the main tumors, but also in daughter tumors, extracapsular invasion, and intraportal neoplastic thrombi. TACE was proved to be effective in treating HCC, and has been widely used for patients with unresectable HCC in Asia[5-10]. It was even found that the effects of TACE was comparable to that of resection in some subpopulations of patients with operable HCC[15]. However, TACE is not a curative method. Tumor cells remain viable, especially in and around the capsule, and tumors may recur by the blood supply from the collateral circulation or portal vein[11]. The long-term efficacy of TACE was disappointing. 1, 3, and 5 year survival rates were around 50 %, 20 %, and 6 %, respectively[5-10]. In the present study, the RR and 5 year survival rate in the TACE control group were 28.1 % and 7.2 %, respectively, which were approximate to the results in the literature. Nevertheless, in some prospective randomized trials, TACE therapy failed to improve the survival of patients significantly[12,13]. Segmental TACE has been shown to yield 5 year survival rate (30 %) for patients with lesions less than 5 cm, but it is suitable only for small tumors. Thus, multimodality treatments are necessary, especially for large HCC.

Radiotherapy has not played a significant role in treating HCC because of the poor tolerance of the liver. The benefit of radiotherapy is still uncertain. Whole liver irradiation at or above 35Gy in a 3-4 week period is known to cause a high incidence of radiation hepatitis, yet this dose level is not enough to control the tumor. In contrast to whole liver irradiation, small portions of the liver can be irradiated up to 50-60 Gy in 5-6 weeks without significant long-term morbidity. Limited-field high dose irradiation (40-60Gy) and three-dimension conformal radiotherapy have been found to be effective for relatively small unresectable HCC, even with portal vein thrombosis[16-20].

The combination of TACE with radiotherapy may remedy the limitation of each alone and have synergistic effects. Tumor shrinkage after TACE allows the use of smaller irradiation fields, which permits higher tumor doses and improves the normal liver tolerance. Combination therapy also serves the purpose of eliminating residual cancer cells after TACE. Furthermore, the anticancer drug retained in the tumor may have a radiosensitizing effect[21]. The anticancer drug, when it is mixed with lipiodol, has been reported to maintain relatively high concentrations in tumors as long as 27 days and decrease to a trace level after 47 days[22]. In 1990, Yoshikawa *et al*.[23] reported that the combination therapy was more effective than TACE or radiotherapy alone in a preliminary study encompassing a small number of cases. From then on, this combination regimen was carried out to treat HCC by more investigators, and was found to be an effective method for HCC[24-29]. Seong *et al*.[26] reported that 30 patients with HCC who were treated by TACE combined with radiotherapy had 3 year survival rate of 22.2 %, and a median survival of 17 months. The results of our study also suggested that TACE followed by irradiation was a promising approach for large HCC. The RR and 5 year survival rate were 47.4 % and 19.3 %, respectively, in 76 patients with very large tumors ($\geqslant$5 cm in all cases, >10 cm in 38.2 % of the cases, while two hepatic lobes were involved in 31.6 % of the cases). In addition, the results of the Cox proportional hazards model analysis showed that irradiation was an independent positive predictor of survival, and further confirmed that TACE combined with radiotherapy was more effective than TACE alone.

The results of combination therapy in the present study appeared to be comparable to those in other reports of multimodality therapy. Second-look resection after TACE yielded the highest 5 year survival rate (56 %)[30, 31], but only a few patients had the opportunity of resection following TACE. PEI after TACE yielded higher survival rates at 1, 2, and 3 years than TACE alone did[32-37], but the survival rates after 4 years dropped, and it was suitable only for tumors <8 cm. Tanaka *et al*.[37] reported that 83 patients with HCC who were treated by TACE-PEI had 5 and 7 year survival rates of 35 % and 14 %, respectively, but most of the patients (71.1 %) in their study had tumors of less than 5 cm in diameter. The results of our study showed that TACE combined with radiotherapy was effective even for very large tumors.

The optimal radiation dose in the combined therapy is unclear. It is well known that the inhibiting effect of radiotherapy on most tumors depends on the irradiation dose. It has been found that the radiation dose is a significant factor for predicting the objective response and the survival in treating HCC[14, 19], but liver tolerance should be considered at the same time. Recently, conformal radiotherapy has been introduced for the treatment of intrahepatic malignancies and dose-volume histogram analysis was used to quantify the tolerance of the liver by some investigators[20,38-40]. They suggested the irradiation dose level by normal liver volume to be radiated depended on the percentage of normal liver receiving more than 50 % of the prescribed isocenter dose, 66Gy for less than 33 %, 48Gy for 33-66 %, and 24Gy (whole liver) for more than 66 % in 1.5Gy twice a day fractionation with concurrent bromodeoxyuridine[38,39]. Introduction of conformal radiotherapy and dose-volume histogram analysis into the study of the combined therapy will help to give an optimal and tangible dose.

The Cox proportional hazards model showed that tumor extension was a significant and independent negative predictor

of survival. The prognosis of patients with invasion in two hepatic lobes was worse than that of patients with one hepatic lobe invasion. This may be because the tumor was barely controlled by combined therapy or TACE alone treatment plus the chance of metastases rose when there was invasion in two lobes. The degree of cirrhosis (classified by Child grade) is also an independent negative predictor of survival. This is in agreement with previous studies[35, 36].

In summary, our results demonstrate that TACE combined with radiotherapy is a promising treatment for large HCC. Prospectively randomized, controlled multi -center clinical trials are needed to confirm the advantageous effects of combined therapy over TACE or radiotherapy alone. In addition, further clarification about an optimal radiation dose and the optimal interval between TACE and radiotherapy are also needed.

ACKNOWLEDGEMENTS

We would like to thank Mrs. Margaret-Hiatt Rosen, Director of Admission, the Mead School, Stanford, US, for her correction of the English translation of the paper.

REFERENCES

1 **Zhou XD**, Tang ZY, Yang BH, Lin ZY, Ma ZC, Ye SL, Wu ZQ, Fan J, Qin LX, Zheng BH. Experience of 1000 patients who underwent hepatectomy for small hepatocellular carcinoma. *Cancer* 2001; **91**: 1479-1486

2 **Faivre J**, Forman D, Esteve J, Obradovic M, Sant M. Survival of patients with primary liver cancer, pancreatic cancer and biliary tract cancer in Europe. *Eur J Cancer* 1998; **34**: 2184-2190

3 **El-Serag HB**, Mason AC, Key C. Trends in survival of patients with hepatocellular carcinoma between 1977 and 1996 in the United States. *Hepatology* 2001; **33**: 62-65

4 **El-Serag HB**. Hepatocellular carcinoma: an epidemiologic view. *J Clin Gastroenterol* 2002; **35**(5 Suppl 2): S72-78

5 **Poon RT**, Ngan H, Lo CM, Liu CL, Fan ST, Wong J. Transarterial chemoembolization for inoperable hepatocellular carcinoma and postresection intrahepatic recurrence. *J Surg Oncol* 2000; **73**: 109-114

6 **Lo CM**, Ngan H, Tso WK, Liu CL, Lam CM, Poon RT, Fan ST, Wong J. Randomized controlled trial of transarterial lipiodol chemoembolization for unresectable hepatocellular carcinoma. *Hepatology* 2002; **35**: 1164-1171

7 **Savastano S**, Miotto D, Casarrubea G, Teso S, Chiesura-Corona M, Feltrin GP. Transcatheter arterial chemoembolization for hepatocellular carcinoma in patients with Child's grade A or B cirrhosis: a multivariate analysis of prognostic factors. *J Clin Gastroenterol* 1999; **28**: 334-340

8 **Sithinamsuwan P**, Piratvisuth T, Tanomkiat W, Apakupakul N, Tongyoo S. Review of 336 patients with hepatocellular carcinoma at Songklanagarind Hospital. *World J Gastroenterol* 2000; **6**: 339-343

9 **Levy I**, Verstandig A, Sasson T, Wolf D, Krichon I, Libson E, Levensart P, Papo O, Yurim O, Id A, Shouval D. Transarterial oil chemoembolization for hepatocellular carcinoma, in 100 cases. *Harefuah* 2000; **138**: 89-93

10 **Ueno K** , Miyazono N, Inoue H , Nishida H , Kanetsuki I , Nakajo M. Transcatheter arterial chemoembolization therapy using iodized oil for patients with unresectable hepatocellular carcinoma: evaluation of three kinds of regimens and analysis of prognostic factors. *Cancer* 2000; **88**: 1574-1581

11 **Tang ZY**, Yu YQ, Zhou XD, Yang BH, Lin ZY, Lu JZ, Ma ZC, Ye SL, Liu KD. Three decades' experience in surgery of hepatocellular carcinoma. *Gan To Kagaku Ryoho* 1997; **24**(Suppl): 126-133

12 **Pelletier G**, Ducreux M, Gay F, Luboinski M, Hagege H, Dao T, Van Steenbergen W, Buffet C, Rougier P, Adler M, Pignon JP, Roche A. Treatment of unresectable hepatocellular carcinoma with lipiodol chemoembolization: a multicenter randomized trial. Groupe CHC. *J Hepatol* 1998; **29**: 129-134

13 **Bruix J**, Llovet JM, Castells A, Montana X, Bru C, Ayuso MC, Vilana R, Rodes J. Transarterial embolization versus symptomatic treatment in patients with advanced hepatocellular carcinoma: results of a randomized, controlled trial in a single institution. *Hepatology* 1998; **27**: 1578-1583

14 **Guo WJ**, Yu EX. Evaluation of combined therapy with chemoembolization and irradiation for large hepatocellular carcinoma. *Br J Radiol* 2000; **73**: 1901-1907

15 **Lee HS**, Kim KM, Yoon JH, Lee TR, Suh KS, Lee KU, Chung JW, Park JH, Kim CY. Therapeutic efficacy of transcatheter arterial chemoembolization as compared with hepatic resection in hepatocellular carcinoma patients with compensated liver function in a hepatitis B virus-endemic area: a prospective cohort study. *J Clin Oncol* 2002; **20**: 4459-4465

16 **Seong J**, Park HC, Han KH, Chon CY. Clinical results and prognostic factors in radiotherapy for unresectable hepatocellular carcinoma: a retrospective study of 158 patients. *Int J Radiat Oncol Biol Phys* 2003; **55**: 329-336

17 **Tokuuye K**, Sumi M, Kagami Y, Murayama S, Kawashima M, Ikeda H, Ueno H, Okusaka T, Okada S. Radiotherapy for hepatocellular carcinoma. *Strahlenther Onkol* 2000; **176**: 406-410

18 **Seong J**, Park HC, Han KH, Lee DY, Lee JT, Chon CY, Moon YM, Suh CO. Local radiotherapy for unresectable hepatocellular carcinoma patients who failed with transcatheter arterial chemoembolization. *Int J Radiat Oncol Biol Phys* 2000; **47**: 1331-1335

19 **Park HC**, Seong J, Han KH, Chon CY, Moon YM, Suh CO. Dose-response relationship in local radiotherapy for hepatocellular carcinoma. *Int J Radiat Oncol Biol Phys* 2002; **54**: 150-155

20 **Cheng SH**, Lin YM, Chuang VP, Yang PS, Cheng JC, Huang AT, Sung JL. A pilot study of three-dimensional conformal radiotherapy in unresectable hepatocellular carcinoma. *J Gastroenterol Hepatol* 1999; **14**: 1025-1033

21 **Seong J**, Kim SH, Suh CO. Enhancement of tumor radioresponse by combined chemotherapy in murine hepatocarcinoma. *J Gastroenterol Hepatol* 2001; **16**: 883-889

22 **Raoul JL**, Heresbach D, Bretagne JF, Ferrer DB, Duvauferrier R, Bourguet P, Messner M, Gosselin M. Chemoembolization of hepatocellular carcinoma. A study of the biodistribution and pharmacokinetics of doxorubicin. *Cancer* 1992; **70**: 585-590

23 **Yoshikawa M**, Ebara M, Ohto M, Miyoshi T. A combination treatment of transcatheter arterial embolization (TAE) and irradiation for hepatocellular carcinoma (HCC): evaluation for therapeutic efficacy in comparison with TAE or irradiation alone. *Nippon Shokakibyo Gakkai Zasshi* 1990; **87**: 225-234

24 **Yamada K**, Soejima T, Sugimoto K, Mayahara H, Izaki K, Sasaki R, Maruta T, Matsumoto S, Hirota S, Sugimura K. Pilot study of local radiotherapy for portal vein tumor thrombus in patients with unresectable hepatocellular carcinoma. *Jpn J Clin Oncol* 2001; **31**: 147-152

25 **Guo WJ**, Song MZ, Yu EX. Transcatheter arterial chemoembolization combined with external radiation for primary liver cancer. *Zhonghua Zhongliu Zazhi* 1999; **21**: 25-28

26 **Seong J**, Keum KC, Han KH, Lee DY, Lee JT, Chon CY, Moon YM, Suh CO, Kim GE. Combined transcatheter arterial chemoembolization and local radiotherapy of unresectable hepatocellular carcinoma. *Int J Radiat Oncol Biol Phys* 1999; **43**: 393-397

27 **Chia-Hsien Cheng J**, Chuang VP, Cheng SH, Lin YM, Cheng TI, Yang PS, Jian JJ, You DL, Horng CF, Huang AT. Unresectable hepatocellular carcinoma treated with radiotherapy and/or chemoembolization. *Int J Cancer* 2001; **96**: 243-252

28 **Guo WJ**, Yu EX, Yi C, Wu WY, Lin JH. Prognostic factors influencing survival in patients with large hepatocellular carcinoma receiving combined transcatheter arterial chemoembolization and radiotherapy. *Zhonghua Ganzangbing Zazhi* 2002; **10**: 167-169

29 **Zeng ZC**, Tang ZY, Wu ZQ, Ma ZC, Fan J, Qin LX, Zhou J, Wang JH, Wang BL, Zhong CS. Phase I clinical trial of oral furtulon and combined hepatic arterial chemoembolization and radiotherapy in unresectable primary liver cancers, including clinicopathologic study. *Am J Clin Oncol* 2000; **23**: 449-454

30 **Fan J**, Tang ZY, Yu YQ, Wu ZQ, Ma ZC, Zhou XD, Zhou J, Qiu SJ, Lu JZ. Improved survival with resection after transcatheter arterial chemoembolization (TACE) for unresectable hepatocellular carcinoma. *Dig Surg* 1998; **15**: 674-678

31 **Tang ZY**. Hepatocellular carcinoma. *J Gastroenterol Hepatol*

2000; **15**(Suppl): G1-7

32 **Kamada K**, Kitamoto M, Aikata H, Kawakami Y, Kono H, Imamura M, Nakanishi T, Chayama K. Combination of transcatheter arterial chemoembolization using cisplatin-lipiodol suspension and percutaneous ethanol injection for treatment of advanced small hepatocellular carcinoma. *Am J Surg* 2002; **184**: 284-290

33 **Li C**, Shi Z, Hao Y. Combined percutaneous ethanol injection through liver puncture and transcatheter hepatic arterial chemoembolization for hepatocellular carcinoma. *Zhonghua Zhongliu Zazhi* 2001; **23**: 490-492

34 **Koda M**, Murawaki Y, Mitsuda A, Oyama K, Okamoto K, Idobe Y, Suou T, Kawasaki H. Combination therapy with transcatheter arterial chemoembolization and percutaneous ethanol injection compared with percutaneous ethanol injection alone for patients with small hepatocellular carcinoma: a randomized control study. *Cancer* 2001; **92**: 1516-1124

35 **Allgaier HP**, Deibert P, Olschewski M, Spamer C, Blum U, Gerok W, Blum HE. Survival benefit of patients with inoperable hepatocellular carcinoma treated by a combination of transarterial chemoembolization and percutaneous ethanol injection-a single-center analysis including 132 patients. *Int J Cancer* 1998; **79**: 601-605

36 **Lencioni R**, Paolicchi A, Moretti M, Pinto F, Armillotta N, Di Giulio M, Cicorelli A, Donati F, Cioni D, Bartolozzi C. Combined transcatheter arterial chemoembolization and percutaneous ethanol injection for the treatment of large hepatocellular carcinoma: local therapeutic effect and long-term survival rate. *Eur Radiol* 1998; **8**: 439-444

37 **Tanaka K**, Nakamura S, Numata K, Kondo M, Morita K, Kitamura T, Saito S, Kiba T, Okazaki H, Sekihara H. The long term efficacy of combined transcatheter arterial embolization and percutaneous ethanol injection in the treatment of patients with large hepatocellular carcinoma and cirrhosis. *Cancer* 1998; **82**: 78-85

38 **Dawson LA**, Normolle D, Balter JM, McGinn CJ, Lawrence TS, Ten Haken RK. Analysis of radiation-induced liver disease using the Lyman NTCP model. *Int J Radiat Oncol Biol Phys* 2002; **53**: 810-821

39 **Robertson JM**, McGinn CJ, Walker S, Marx MV, Kessler ML, Ensminger WD, Lawrence TS. A phase I trial of hepatic arterial bromodeoxyuridine and conformal radiation therapy for patients with primary hepatobiliary cancers or colorectal liver metastases. *Int J Radiat Oncol Biol Phys* 1997; **39**: 1087-1092

40 **Cheng JC**, Wu JK, Huang CM, Liu HS, Huang DY, Cheng SH, Tsai SY, Jian JJ, Lin YM, Cheng TI, Horng CF, Huang AT. Radiation-induced liver disease after three-dimensional conformal radiotherapy for patients with hepatocellular carcinoma: dosimetric analysis and implication. *Int J Radiat Oncol Biol Phys* 2002; **54**: 156-162

Edited by Zhang JZ

P.O.Box 2345, Beijing 100023,China
Fax: +86-10-85381893
E-mail: wjg@wjgnet.com www.wjgnet.com

World J Gastroenterol 2003;9(8):1702-1706
World Journal of Gastroenterology
 ISSN 1007-9327

• LIVER CANCER •

Role of preoperative selective portal vein embolization in two-step curative hepatectomy for hepatocellular carcinoma

Wu Ji, Jie-Shou Li, Ling-Tang Li, Wu-Hong Liu, Kuan-Sheng Ma, Xiang-Tian Wang, Zhen-Ping He, Jia-Hong Dong

Wu Ji, Jie-Shou Li, Ling-Tang Li, Research Institute of General Surgery, Nanjing General Hospital of Nanjing PLA Command Area, Nanjing 210002, Jiangsu Province, China
Wu Ji, Wu-Hong Liu, Xiang-Tian Wang, Department of General Surgery, Kunming General Hospital of Chengdu PLA Command Area, Kunming 650032, Yunnan Province, China
Kuan-Sheng Ma, Zhen-Ping He, Jia-Hong Dong, Hepatobiliary Surgery Center, Southwest Hospital, Third Military Medical University, Chongqing 400038, China
Correspondence to: Wu Ji, MD, Institute of General Surgery, Nanjing General Hospital of Nanjing PLA Command Area, 305 Eastern Zhongshan Road, Nanjing, 210002, Jiangsu Province, China. jiwusky@sohu.com
Telephone: +86-25-4826808 Ext 58007 **Fax:** +86-25-4820160
Received: 2002-11-06 **Accepted:** 2002-12-07

Abstract

AIM: To determine the feasibility and role of ultrasound-guided preoperative selective portal vein embolization (POSPVE) in the two-step hepatectomy of patients with advanced primary hepatocellular carcinoma (HCC).

METHODS: Fifty patients with advanced HCC who were not suitable for curative hepatectomy were treated by ultrasound-guided percutaneous transhepatic POSPVE with fine needles. The successful rate, side effects and complications of POSPVE, changes of hepatic lobe volume and two-step curative hepatectomy rate after POSPVE were observed.

RESULTS: POSPVE was successfully performed in 47 (94.0 %) patients. In patients whose right portal vein branches were embolized, their right hepatic volume decreased and left hepatic volume increased gradually. The ratio of right hepatic volume to total hepatic volume decreased from 62.4 % before POSPVE to 60.5 %, 57.2 % and 52.8 % after 1, 2 and 3 weeks respectively. The side effects included different degree of pain in liver area (38 cases), slight fever (27 cases), nausea and vomiting (9 cases). The level of aspartate alanine transaminase (AST), alanine transaminase (ALT) and total bilirubin (TBIL) increased after POSPVE, but returned to preoperative level in 1 week. After 2-4 weeks, two-step curative hepatectomy for HCC was successfully performed on 23 (52.3 %) patients. There were no such severe complications as ectopic embolization, local hemorrhage and bile leakage.

CONCLUSION: Ultrasound-guided percutaneous transhepatic POSPVE with fine needles is feasible and safe. It can extend the indications of curative hepatectomy of HCC, and increase the safety of hepatectomy.

Ji W, Li JS, Li LT, Liu WH, Ma KS, Wang XT, He ZP, Dong JH. Role of preoperative selective portal vein embolization in two-step curative hepatectomy for hepatocellular carcinoma. *World J Gastroenterol* 2003; 9(8): 1702-1706
http://www.wjgnet.com/1007-9327/9/1702.asp

INTRODUCTION

Hepatocellular carcinoma (HCC) is one of the most common malignant tumors of mankind. It threatens our life severely[1-5]. In China, HCC is responsible for about 130 000 deaths every year. It has ranked second of cancer mortality since 1990[6,7]. Surgical resection of the tumors is considered the only potentially curative therapy, and it is regarded as the first choice for the treatment of HCC. Many factors can affect hepatectomy, such as tumor size, location, multifocality and patients' status, hepatic function. Besides, 80 % of them are complicated with cirrhosis in China. So the extension of hepatectomy of HCC is greatly limited. Hepatectomy with less hepatic volume resected may be helpful to the safety of the operation, but this may not be a radical cure, and even lead to tumor residual. Hepatectomy with more hepatic volume resected will lead to postoperative hepatic failure, infection, hemorrhage and even death. So only 15 % to 30 % patients have a chance of receiving curative hepatectomy[8-10]. Most HCC patients are in late stages at the time of diagnosis. They are considered not suitable for operation. Researchers have proposed the concept of "two-step hepatectomy", and some progresses have been made in the past decades[11-15]. In 1986, Kinoshita *et al*[16] reported the experience of two-step hepatectomy after POSPVE. This is a completely new method. The purpose is to induce atrophy of the embolized (tumor) lobe and compensatory hypertrophy of the remnant lobe. The result is an increase of the remnant liver volume and a decreased ratio of resected volume to total liver volume. In recent years, reports of two-step hepatectomy after preoperative selective portal vein embolization (POSPVE) gradually increased[17-22]. But there are no such clinical reports in China.

In this study, based on an analysis of the feasibility and safety of ultrasound-guided percutaneous transhepatic POSPVE with fine needles in 50 HCC patients, we discussed the role of POSPVE in the two-step curative hepatectomy for moderate and advanced HCC.

MATERIALS AND METHODS

Eligibility of patients

This study involved 50 HCC patients. There were 36 males and 14 females. Forty three (86.0 %) patients were hepatitis surface antigen (HBsAg) positive, and 34 (68 %) were complicated with cirrhosis. Child-Pugh' s classification showed that 14 (28 %) patients were grade A, 33 (66 %) grade B, 3 (6 %) grade C. The diameter of space occupying lesions ranged from 8.1 to 16.3 cm, averaging 13.6 cm. The criteria of these patients included: HCC located in one side of the liver, with no confirmed portal vein thrombosis and distant metastasis. The ratio of hepatic volume to be resected to total hepatic volume was more than 50 % for those patients with cirrhosis and 60 % for those without cirrhosis. Those patients with coexisted morbidity-related diseases, poor life expectancy, multinodular or diffuse intrahepatic tumor, prothrombin activity less than 50 %, or platelet count lower than 50×10^9/L were excluded from the study.

Methods

One hundred microgram dolantin and 25 mg phenergan were

injected into the muscle before POSPVE. The liver, tumor and the portal vein branch to be embolized were carefully examined, located and confirmed by ultrasound. Local anesthesia was adopted with 2 % lidocaine transcutaneously down to liver surface. Under ultrasound guidance, we punctured percutaneously and transhepatically with a 21-gague PTC needle from the side of ultrasound head. When the needle was inserted into the portal vein branch to be embolized, the internal part of the needle was taken away, and dark red portal vein blood could be seen (Figure 1). Then embolic material was slowly injected into the portal vein. It consisted of a mixture of ethanol and iodized oil with a rate of 1:2. And 0.4 ml/kg was regarded as the standard dosage. Real-time ultrasonic scan showed that tiny spot echoes in the embolized portal vein branch appeared and diffused into the carcinoma. Intensified echoes appeared in some areas. After that, the fine needle was slowly pulled out. Flexible fabric bandage was used to cover the puncture spot. The patients inhaled oxygen after returning back to the ward. Changes of vital signs were monitored for 12 to 24 hours. They were given fluid infusion and anti-inflammation, hemorrhage prevention, liver function protection and analgesics treatments.

The successful rate of POSPVE, side effects and complications after POSPVE, changes of blood routine, liver function, and renal function were observed to evaluate the feasibility and safety of ultrasound-guided percutaneous transhepatic POSPVE with fine needles. Serial changes of hepatic lobe volume calculated with volume CT, ratio of right hepatic lobe volume to total hepatic volume, two-step curative hepatectomy rate after POSPVE were observed to evaluate the role of POSPVE in the two-step hepatectomy of HCC.

Statistical method

Quantitative variables were expressed as mean ± standard error of the mean. The statistical software SPSS10.0 was used. *P* value <0.05 was considered significant.

RESULTS

Feasibility and safety of POSPVE

Ultrasound-guided percutaneous transhepatic POSPVE with fine needles was successfully performed in 47 of 50 patients. The successful rate was 94.0 % (Figure 1). Three patients failed to finish the operation. The right portal vein branches were difficult to locate under ultrasound guidance because of the tumor compression in 2 of them, and one patient could not tolerate the irritation of embolic material. There were 44 right portal vein embolizations and 3 left portal vein embolizations. The side effects included different degree of pain in liver area (38 cases), slight fever (27 cases), nausea and vomiting (9 cases). The level of aspartate alanine transaminase (AST), alanine transaminase (ALT) and total bilirubin (TBIL) increased in 31 cases after POSPVE, but returned to preoperative level in 1 week. There were no such severe complications as ectopic embolization, local hemorrhage and bile leakage.

Role of POSPVE in two-step curative hepatectomy of HCC

In 44 patients whose right portal vein branches were embolized, the right hepatic volume decreased, the left hepatic volume increased and the ratio of right liver volume to total liver volume decreased gradually (Figures 2-3) (Table 1). Two to four weeks later, curative hepatectomies were successfully performed in 23 (52.3 %) patients (Figures 4-5). There were 6 irregular right hepatectomies, 15 regular right hepatectomies, and 2 right trisegmentectomies. All these 23 patients recovered smoothly, without any severe complications like hepatic failure, hemorrhage and infection. They were discharged 11 to 20 days after operations. The other 27 patients who could not receive curative hepatectomy after POSPVE were treated by transcatheter artery embolization (TAE) or chemotherapy, immune therapy and so on.

Table 1 Serial changes of liver volume and ratio of right hepatic lobe volume to total hepatic volume after right portal vein embolization

	Right liver volume (cm^3)	Left liver volume (cm^3)	Right liver volume / total liver volume (%)
Before POSPVE	592.4±98.5	352.2±65.2	62.4±7.6
1 week after POSPVE	571.7±104.0	378.6±127.9	60.5±9.3
2 weeks after POSPVE	547.7±118.3[a,c]	405.9±130.2[a,c]	57.2±11.2[a,c]
3 weeks after POSPVE	509.1±123.8[b,c,e]	446.1±143.5[b,d,e]	52.8±12.3[b,c,e]

[a]$P<0.05$, [b]$P<0.01$, *vs* before POSPVE; [c]$P<0.05$, [d]$P<0.01$, *vs* 1 week after POSPVE, [e]$P<0.05$, [f]$P<0.01$, *vs* 2 weeks after POSPVE.

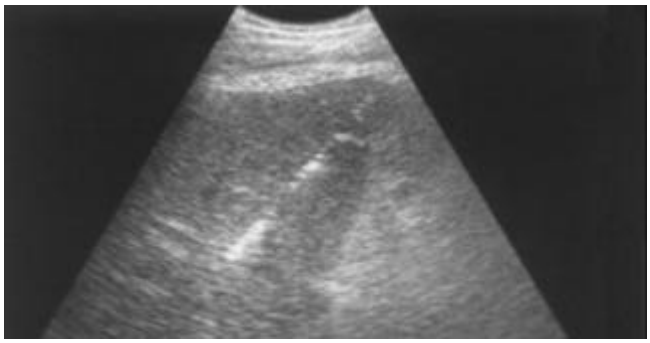

Figure 1 The fine needle was inserted into the right portal vein branch under ultrasound guidance. After embolization material was injected, tiny spot echoes appeared in the portal vein branch and diffused to the carcinoma area.

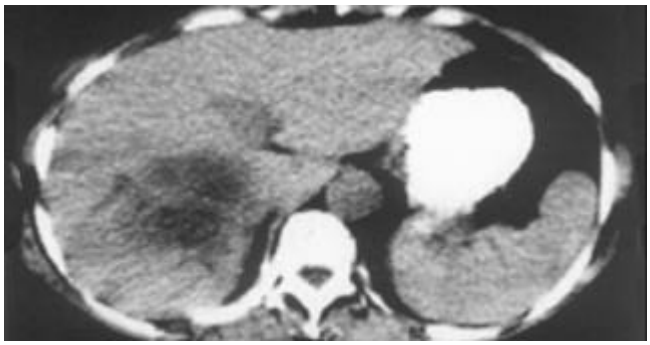

Figure 2 Before POSPVE, CT scan showed a 13.2 cm×10.8 cm HCC in the right lobe of liver. A right semihepatectomy was scheduled to perform.

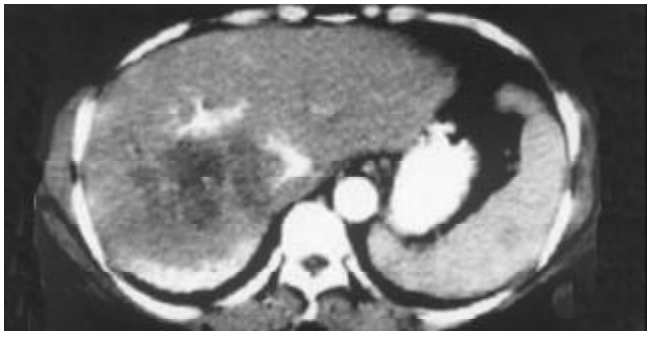

Figure 3 Three weeks after right POSPVE, CT scan showed increased volume of left lobe and decreased volume of right lobe. Iodized oil deposit still could be seen in the right portal vein branch.

Figure 4 Three weeks after right POSPVE, a right semihepatectomy was performed. In the operation, significant hypertrophy of left lobe was confirmed.

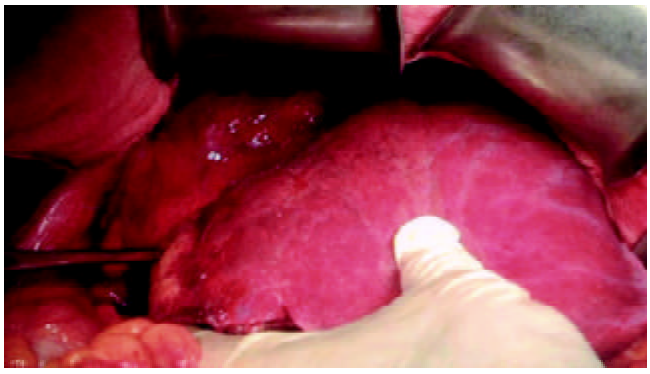

Figure 5 In the same operation, significant atrophy of right lobe and HCC could be seen. There was iodized oil deposit in the carcinoma area.

DISCUSSION

Rous and Larimore observed in 1920 that portal vein ligation in rabbit led to atrophy of the ipsilateral hepatic lobe and hypertrophy of the contralateral lobe. In 1956, Schalm confirmed it by occluding the portal vein branch. These observations provided the foundation for the study of liver regeneration after portal vein branch embolization. In 1975, Honjo found that portal vein ligation could significantly prolong the survival span of advanced HCC patients whose tumors could not be resected during operations. In 1986, Kinoshita published the first report demonstrating the efficacy of POSPVE before curative resection on primary and metastatic HCC. After that, POSPVE was gradually accepted in preparing large hepatectomy for HCC. It has been confirmed that POSPVE can extend the indication of curative hepatectomy for HCC, increase the safety of hepatectomy, and improve the long-term survival rate after the operation[23-32].

Portal vein blood supply is very important for both liver and HCC. Portal vein branch ligation or embolization results in redistribution of portal vein blood that is essential to liver regeneration. Most portal blood rich in hepatatrophic substances, such as insulin, glucagon and hepatocyte growth factor, flows toward the future remaining lobe. This leads to atrophy of the ipsilateral hepatic lobe and hypertrophy of the contralateral lobe. Harada *et al*[33] observed that POSPVE induced hepatocyte apoptosis and atrophy of the embolized lobe. Increased sinusoidal volume in this lobe may be attributable to hepatocyte deletion. Cells in the nonembolized lobe entered a highly active phase of proliferation within 2 weeks after POSPVE. Further evidences of cellular proliferation were provided by the increased nonembolized lobar volume and numerical density of hepatocyte nuclei (Nv). They concluded that the favorable role of POSPVE was attributed to a net gain of functional hepatocyte mass and early induction of hepatocyte proliferation. Shimizu *et al*[34] demonstrated that expression of proliferating cell nuclear antigen (PCNA) and mitotic index (MI) of hepatocytes in nonembolized lobe increased greatly. The amount of mitochondrial DNA-binding proteins increased 200-300 % of the preoperative level at 12 hours after ligation of left branch of the portal vein, before an increase of 390 % in mitochondrial DNA content at 24 hours, and was parallel to an increase of 240 % in mitochondrial mRNA at 12 hours. These results suggest that the energy supply for liver regeneration is achieved through enhancement of mitochondrial DNA replication as well as transcription, in which mitochondrial DNA-binding proteins probably play regulatory roles. Chijiiwa *et al*[35-37] found that the volume of nonembolized left lobe significantly increased after right POSPVE, with a significant increase in percentage of the left lobe to total liver volume. Concentrations of AMP, ADP, and ATP, and hepatic energy charge levels in the nonembolized left lobe were similar to those of the control liver. These results suggest that right POSPVE increased the volume of nonembolized left lobe, while keeping the hepatic engery charge and ATP levels similar to the control liver, thereby increasing the total amount of ATP and hepatic energy reserve of the nonembolized lobe in proportion to its volume increase at the time of surgery.

Two major techniques have been reported to access the portal vein: direct catheterization of the ileocolic vein and the percutaneous approach[38,39]. The former involves an open technique in which the ileocolic vein is cannulated at laparotomy. It is usually used when the carcinoma can not be resected during operation. This method can also be used when interventional facilities are not available for the percutaneous approach. The later can be finished under ultrasound guidance with local anesthesia. There are two major kinds of methods. One is to insert a catheter percutaneously into the portal vein branch, the other is to puncture the portal vein branch by a fine needle under ultrasound guidance. Most reports used the catheterization method. But it is technically complicated and expensive. Percutaneous approach with a fine needle is easy to perform, and patients suffer less and resume faster. But it has not been widely accepted. Its feasibility, safety and efficiency have not been discussed based on a large sample[40,41]. In this study, POSPVE with a fine needle was feasible in 47 of 50 HCC patients. The successful rate was 94.0 %. The complication rate was low, and there was no severe complication. The side effects were moderate. In 44 patients whose right portal veins were embolized, their right hepatic volume decreased and left hepatic volume increased, the ratio of hepatectomy decreased gradually. By inducing hypertrophy of the remaining liver, hepatectomies were successfully performed in 23 patients. The two-step curative hepatectomy after POSPVE was 52.3 %. All the patients recovered smoothly. It is concluded from this study that ultrasound-guided percutaneous transhepatic POSPVE with a fine needle is feasible, safe and effective. It extends the indication of curative hepatectomy for moderate and advanced HCC. This is the first report on the role of POSPVE in the treatment of HCC in China. Estimating the volume of the lobe that will remain after hepatectomy is thought to be mandatory for all patients undergoing extensive hepatic resection. If this volume is not large enough in terms of the risk of postoperative liver failure, then POSPVE is indicated. According to a criterion based on liver volumetry, POSPVE is usually indicated for patients who will undergo right trisegmentectomy, left trisegmentectomy, or right hepatectomy for cirrhosis patients. Many methods have been used to estimate the lobar volume. In this series, we used volume CT to calculate the exact volume of every lobe, and regard the ratio of hepatic volume to be resected to total hepatic

volume is more than 50 % for those patients with cirrhosis and 60 % for those without cirrhosis. The degree of hypertrophy induced in nonembolized lobe showed a large interindividual difference. It has been reported that male, diabetes mellitus and cirrhosis are negative factors, and cholestasis is a positive factor. Other factors that may influence the role of POSPVE include embolization materials and their dosage and extent[42-46]. Cyanoacrylate, lipiodol, gelatin sponge, thrombin, fibrin glue, gelfoam, and alcohol have been used as embolization materials. Their effects are controversial. We used lipidol and alcohol routinely as embolization materials throughout the study period. The functional burden placed on the liver by POSPVE using these materials was minimal and transient, as reflected in the slight elevation of AST, ALT and total bilirubin level. It was reported that the average future remaining hepatic volume increased by 28 % within 2 weeks after POSPVE. The rate of average hepatectomy decreased from 70.0 % before POSPVE to 62.2 %, and the two-step hepatectomy rate was 63.3 % to 77.4 %. But in this series, the two-step curative hepatectomy rate after POSPVE was 52.3 %. We think the main reason is that most patients in our study were male and coexisted with cirrhosis. They have been reported to be the negative regulatory factors of POSPVE. Besides, we used the method of ultrasound-guided percutaneous transhepatic POSPVE with a fine needle. It is safe, feasible and effective. The disadvantage of this method lies in that the embolization materials usually used are ethanol and iodized oil. So, it is mainly the distant branches of portal vein that are embolized. Besides, the role of ethanol is dosage dependent, while a large dosage is unbearable for most patients.

Although the concept of POSPVE appears to be well accepted and the procedure is performed ever more widely, there are a number of issues on which a general consensus has not yet been reached, such as the optimum duration between POSPVE and hepatectomy, the most suitable embolizing material and method of portal vein cannulation, the rate of technical failure and complications, and factors that accelerate or suppress the effect of POSPVE[32]. The fact that POSPVE is well tolerated might enlarge its indications in the future. POSPVE will be used not only for patients with possibly insufficient remaining liver volume after hepatectomy, but also for those whose curative operation may not be very safe.

REFERENCES

1 **Tang ZY**. Hepatocellular carcinoma-cause, treatment and metastasis. *World J Gastroenterol* 2001; **7**: 445-454
2 **Makuuchi M**, Imamura H, Sugawara Y, Takayama T. Progress in surgical treatment of hepatocellular carcinoma. *Oncology* 2002; **62**(Suppl): 74-81
3 **Fan J**, Wu ZQ, Tang ZY, Zhou J, Qiu SJ, Ma ZC, Zhou XD, Ye SL. Multimodality treatment in hepatocellular carcinoma patients with tumor thrombi in portal vein. *World J Gastroenterol* 2001; **7**: 28-32
4 **Makuuchi M**. Remodeling the surgical approach to hepatocellular carcinoma. *Hepatogastroenterology* 2002; **49**: 36-40
5 **Curley SA**, Cusack JC Jr, Tanabe KK, Stoelzing O, Ellis LM. Advances in the treatment of liver tumors. *Curr Probl Surg* 2002; **39**: 449-571
6 **Zhao WH**, Ma ZM, Zhou XR, Feng YZ, Fang BS. Prediction of recurrence and prognosis in patients with hepatocellular carcinoma after resection by use of CLIP score. *World J Gastroenterol* 2002; **8**: 237-242
7 **Qin LX**, Tang ZY. The prognostic significance of clinical and pathological features in hepatocellular carcinoma. *World J Gastroenterol* 2002; **8**: 193-199
8 **Rabe C**, Pilz T, Klostermann C, Berna M, Schild HH, Sauerbruch T, Caselmann WH. Clinical characteristics and outcome of a cohort of 101 patients with hepatocellular carcinoma. *World J Gastroenterol* 2001; **7**: 208-215
9 **Yip D**, Findlay M, Boyer M, Tattersall MH. Hepatocellular carcinoma in central sydney: a 10-year review of patients seen in a medical oncology department. *World J Gastroenterol* 1999; **5**: 483-487
10 **Fan J**, Ten GJ, He SC, Guo JH, Yang DP, Wang GY. Arterial chemoembolization for hepatocellular carcinoma. *World J Gastroenterol* 1998; **4**: 33-37
11 **Li L**, Wu PH, Li JQ, Zhang WZ, Lin HG, Zhang YQ. Segmental transcatheter arterial embolization for primary hepatocellular carcinoma. *World J Gastroenterol* 1998; **4**: 511-512
12 **Chen MS**, Li JQ, Zhang YQ, Lu LX, Zhang WZ, Yuan YF, Guo YP, Lin XJ, Li GH. High-dose iodized oil transcatheter arterial chemoembolization for patients with large hepatocellular carcinoma. *World J Gastroenterol* 2002; **8**: 74-78
13 **Wang JH**, Lin G, Yan ZP, Wang XL, Cheng JM, Li MQ. Stage II surgical resection of hepatocellular carcinoma after TAE: A report of 38 cases. *World J Gastroenterol* 1998; **4**: 133-136
14 **Sithinamsuwan P**, Piratvisuth T, Tanomkiat W, Apakupakul N, Tongyoo S. Review of 336 patients with hepatocellular carcinoma at songklanagarind hospital. *World J Gastroenterol* 2000; **6**: 339-343
15 **Schmid R**. Prospect of gastroenterology and hepatology in the next century. *World J Gastroenterol* 1999; **5**: 185-190
16 **Kinoshita H**, Sakai K, Hirohashi K, Igawa S, Yamasaki O, Kubo S. Preoperative portal vein embolization for hepatocellular carcinoma. *World J Surg* 1986; **10**: 803-808
17 **Elias D**, Ouellet JF, De Baere T, Lasser P, Roche A. Preoperative selective portal vein embolization before hepatectomy for liver metastases: long-term results and impact on survival. *Surgery* 2002; **131**: 294-299
18 **Azoulay D**, Castaing D, Smail A, Adam R, Cailliez V, Laurent A, Lemoine A, Bismuth H. Resection of nonresectable liver metastases from colorectal cancer after percutaneous portal vein embolization. *Ann Surg* 2000; **231**: 480-486
19 **Wakabayashi H**, Okada S, Maeba T, Maeta H. Effect of preoperative portal vein embolization on major hepatectomy for advanced-stage hepatocellular carcinomas in injured livers: a preliminary report. *Surg Today* 1997; **27**: 403-410
20 **Wakabayashi H**, Yachida S, Maeba T, Maeta H. Evaluation of liver function for the application of preoperative portal vein embolization on major hepatic resection. *Hepatogastroenterology* 2002; **49**: 1048-1052
21 **Tominaga M**, Ku Y, Iwasaki T, Fukumoto T, Muramatsu S, Kusunoki N, Suzuki Y, Fujino Y, Kuroda Y. Effect of portal vein embolization on function of the nonembolized lobes of the liver: Evaluation by first-pass hepatic lidocaine extraction in dogs. *Surgery* 2002; **132**: 424-430
22 **Nagino M**, Kamiya J, Kanai M, Uesaka K, Sano T, Yamamoto H, hayakawa N, Nimura Y. Right trisegment portal vein embolization for biliary tract carcinoma: Technique and clinical utility. *Surgery* 2000; **127**: 155-160
23 **Imamura H**, Shimada R, Kubota M, Matsuyama Y, Nakayama A, Miyagawa S, Makuuchi M, Kawasaki S. Preoperative portal vein embolization: an audit of 84 patients. *Hepatology* 1999; **29**: 1099-1105
24 **Gerunda GE**, Bolognesi M, Neri D, Merenda R, Miotto D, Barbazza F, Zangrandi F, Bisello M, Valmasoni M, Gangemi A, Gagliesi A, Faccioli AM. Preoperative selective portal vein embolization (PSPVE) before major hepatic resection. Effectiveness of doppler estimation of hepatic blood flow to predict the hypertrophy rate of non-embolized liver segments. *Hepatogastroenterology* 2002; **49**: 1405-1411
25 **Kubo S**, Shiomi S, Tanaka H, ShutoT, Takemura S, Mikami S, Uenishi T, Nishino Y, Hirohashi K, Kawamura E, Kinoshita H. Evaluation of the effect of portal vein embolization on liver function by (99m)tc-galactosyl human serum albumin scintigraphy. *J Surg Res* 2002; **107**: 113-118
26 **De Baere T**, Roche A, Elias D, Lasser P, Lagrange C, Bousson V. Preoperative portal vein embolization for extension of hepatectomy indications. *Hepatology* 1996; **24**: 1386-1391
27 **Abdalla EK**, Barnett CC, Doherty D, Curley SA, Vauthey JN. Extended hepatectomy in patients with hepatobiliary malignancies with and without preoperative portal vein embolization. *Arch Surg* 2002; **137**: 675-680
28 **Gerunda GE**, Neri D, Merenda R, Barbazza F, Zangrandi F,

Meduri F, Bisello M, Valmasoni M, Gangemi A, Faccioli AM. Effectiveness of preoperative selective portal vein embolization before extensive hepatic resection. *Liver Transpl* 2002; **8**: 405-407

29 **Sugawara Y**, Yamamoto J, Higashi H, Yamasaki S, Shimada K, Kosuge T, Takayama T, Makuuchi M. Preoperative portal embolization in patients with hepatocellular carcinoma. *World J Surg* 2002; **26**: 105-110

30 **Lee KC**, Kinoshita H, Hirohashi K, Kubo S, Iwasa R. Extension of surgical indications for hepatocellular carcinoma by portal vein embolization. *World J Surg* 1993; **17**: 109-115

31 **Wakabayashi H**, Ishimura K, Okano K, Karasawa Y, Goda F, Maeba T, Maeta H. Application of preoperative portal vein embolization before major hepatic resection in patients with normal or abnormal liver parenchyma. *Surgery* 2002; **131**: 26-33

32 **Tanaka H**, Hirohashi K, Kubo S, Shuto T, Higaki I, Kinoshita K. Preoperative portal vein embolization improves prognosis after right hepatectomy for hepatocellular carcinoma in patients with impaired hepatic function. *Br J Surg* 2000; **87**: 879-882

33 **Harada H**, Imamura H, Miyagawa S, Kawasaki S. Fate of the human liver after hemihepatic portal vein embolization: Cell kinetic and morphometric study. *Hepatology* 1997; **26**: 1162-1170

34 **Shimizu Y**, Suzuki H, Nimura Y, Onoue S, Nagino M, Tanaka M, Ozawa T. Elevated mitochondrial gene expression during rat liver regeneration after portal vein ligation. *Hepatology* 1995; **22**: 1222-1229

35 **Chijiiwa K**, Saiki S, Noshiro N, Kameoka N, Nakano K, Tanaka M. Effect of preoperative portal vein embolization on liver volume and hepatic energy status of the nonembolized liver lobe in humans. *Eur Surg Res* 2000; **32**: 94-99

36 **Kawai M**, Naruse K, Komatsu S, Kobayashi S, Nagino M, Nimura Y, Sokabe M. Mechanical stress-dependent secretion of interleukin 6 by endothelial cells after portal vein embolization: Clinical and experimental studies. *J Hepatol* 2002; **37**: 240-246

37 **Uemura T**, Miyazaki M, Hirai R, Matsumoto H, Ota T, Ohashi R, Shimizu N, Tsuji T, Inoue Y, Namba M. Different expression of positive and negative regulators of hepatocyte growth in growing and shrinking hepatic lobes after portal vein branch ligation in rats. *In J Mol Med* 2000; **5**: 173-179

38 **Tsuge H**, Mimura H, Kawata N, Orita K. Right portal vein embolization before extended right hepatectomy using laparoscopic catheterization of the ileocolic vein: a prospective study. *Surg Laparosc Endosc* 1994; **4**: 258-263

39 **Lu MD**, Chen JW, Xie XY, Liang LJ, Huang JF. Portal vein embolization by fine needle ethanol injection: experimental and clinical studies. *World J Gastroenterol* 1999; **5**: 506-510

40 **Seymour K**, Manas D, Charnley RM. During liver regeneration following right portal vein embolization the growth rate of liver metastases is more rapid than that of the liver parenchyma. *Br J Surg* 1999; **86**: 1482-1483

41 **Madoff DC**, Hicks ME, Vauthey JN, Charnsangavej C, Morello FA Jr, Ahrar K, Wallace MJ, Gupta S. Transhepatic portal vein embolization: anatomy, indications, and technical considerations. *Radiographics* 2002; **22**: 1063-1076

42 **Tanaka H**, Hirohashi K, Kubo S, Ikebe T, Tsukamoto T, Hamba H, Shuto T, Wakasa K, Kinoshita H. Influence of histological inflammatory activity on regenerative capacity of liver after percutaneous transhepatic portal vein embolization. *J Gastroenterol* 1999; **34**: 100-104

43 **Kaneko T**, Nakao A, Takagi H. Clinical studies of new material for portal vein embolization: Comparison of embolic effect with different agents. *Hepatogastroenterology* 2002; **49**: 472-477

44 **Yamakado K**, Takeda K, Nishide Y, Jin J, Matsumura K, Nakatsuka A, Hirano T, Kato N, Nakagawa T. Portal vein embolization with steel coil and absolute ethanol: a comparative experimental study with canine liver. *Hepatology* 1995; **22**: 1812-1818

45 **Lu MD**, YY Y, Ren W. A study of portal vein embolization with absolute ethanol injection in cirrhotic rats. *World J Gastroenterol* 1998; **4**: 415-417

46 **Lu MD**, Liang LJ, Huang JF, Ye WJ, Yang QS, Peng BG, Xie XY. Portal vein embolization with ethanol injection via a fine needle in dogs. *Surg Today* 1995; **25**: 416-420

Edited by Zhang JZ and Wang XL

P.O.Box 2345, Beijing 100023,China
Fax: +86-10-85381893
E-mail: wjg@wjgnet.com www.wjgnet.com

World J Gastroenterol 2003;9(8):1707-1712
World Journal of Gastroenterology
 ISSN 1007-9327

• COLORECTAL CANCER •

Contribution of eIF-4E inhibition to the expression and activity of heparanase in human colon adenocarcinoma cell line: LS-174T

Yu-Jie Yang, Ya-Li Zhang, Xu Li, Han-Lei Dan, Zhuo-Sheng Lai, Ji-De Wang, Qun-Ying Wang, Hai-Hong Cui, Yong Sun, Ya-Dong Wang

Yu-Jie Yang, Ya-Li Zhang, Xu Li, Han-Lei Dan, Zhuo-Sheng Lai, Ji-De Wang, Qun-Ying Wang, Hai-Hong Cui, Yong Sun, Ya-Dong Wang, Chinese PLA Institute of Digestive Disease, Nanfang Hospital, First Military Medical University, Guangzhou 510515, Guangdong Province, China
Supported by the National Natural Science Foundation of China, No. 30171053
Correspondence to: Dr. Yu-Jie Yang, Chinese PLA Institute of Digestive Disease, Nanfang Hospital, First Military Medical University, Guangzhou 510515, Guangdong Province, China. yujiey@fimmu.edu.cn
Telephone: +86-20-61641530
Received: 2003-03-04 **Accepted:** 2003-04-03

Abstract

AIM: Heparanase degrades heparan sulfate proteoglycans (HSPGs) and is a critical mediator of tumor metastasis and angiogenesis. Recently, it has been cloned as a single gene family and found to be a potential target for antimetastasis drugs. However, the molecular basis for the regulation of heparanase expression is still not quite clear. The aim of this study was to determine whether the expression of eukaryotic initiation factor 4E (eIF-4E) correlated with the heparanase level in tumor cells and to explore the correlation between heparanase expression and metastatic potential of LS-174T cells.

METHODS: A 20-mer antisense s-oligodeoxynucleotide (asODN) targeted against the translation start site of eIF-4E mRNA was introduced into LS-174T cells by lipid-mediated DNA-transfection. eIF-4E protein and mRNA levels were detected by Western blot analysis and RT-PCR, respectively. Heparanase activity was defined as the ability to degrade high molecular weight (40-100 kDa) radiolabeled HS (heparan sulfate) substrate into low molecular weight (5-15 kDa) HS fragments that could be differentiated by gel filtration chromatography. The invasive potential of tumor cell *in vitro* was observed by using a Matrigel invasion assay system.

RESULTS: The 20-mer asODN against eIF-4E specifically and significantly inhibited eIF-4E expression at both transcriptional and translational levels. As a result, the expression and activity of heparanase were effectively retarded and the decreased activity of heparanase resulted in the decreased invasive potential of LS-174T.

CONCLUSION: eIF-4E is involved in the regulation of heparanase production in colon adenocarcinoma cell line LS-174T, and its critical function makes it a particularly interesting target for heparanase regulation. This targeting strategy in antisense chemistry may have practical applications in experimental or clinical anti-metastatic gene therapy of human colorectal carcinoma.

Yang YJ, Zhang YL, Li X, Dan HL, Lai ZS, Wang JD, Wang QY, Cui HH, Sun Y, Wang YD. Contribution of eIF-4E inhibition to the expression and activity of heparanase in human colon adenocarcinoma cell line: LS-174T. *World J Gastroenterol* 2003; 9(8): 1707-1712
http://www.wjgnet.com/1007-9327/9/1707.asp

INTRODUCTION

For a malignant tumor cell to metastasize, it must break away from its neighbors, force its way through the surrounding stroma, and penetrate basement membranes to enter the stroma and the circulation. When it arrives at its destination, these steps must be repeated in reverse order[1]. A critical event in the process of cancer invasion and metastasis is therefore degradation of various constituents of the extracellular matrix (ECM) including collagen, laminin, fibronectin, and heparan sulfate proteoglycans (HSPGs). The malignant cell is able to accomplish this task through the concerted sequential action of enzymes such as metalloproteinases, serine proteases, and endoglycosidases[2,3]. Among these enzymes, an endo-β-glucuronidase (heparanase) selectively degrades the heparan sulfate chains of HSPGs which are essential and ubiquitous macromolecules associated with the cell surface and ECM of a wide range of cells and tissues[4,5]. Heparanase cleaves heparan sulfate (HS) and has been implicated in many important pathological processes, including tumor metastasis and angiogenesis[6, 7]. Therefore, heparanase plays an essential role in these pathological processes which makes it a potentially important target for cancer therapy and be helpful to investigate the mechanism, by which the expression of heparanase is regulated.

Eukaryotic initiation factor 4E (eIF-4E) is a 25 kDa mRNA cap-binding phosphoprotein that is rate-limiting for the initiation of cap-dependent mRNA translation by the eIF-4F translation initiation complex[8,9]. Overexpression of eIF-4E has been found in human carcinoma tissues and tumor cell lines. The factor (eIF-4E)[10] dramatically impacts upon the quantitative expression of key malignancy-related genes and can be considered as a critical determinant of malignancy. It seems that involvement of eIF-4E in tumor progression is more closely associated with the impact of enhanced eIF-4E activity on specific, malignancy-related molecules such as ODC, c-myc, cyclin D1, VEGF or MMP-9. Cooperative overexpression of these potent molecules leads to occurrence of tumorigenic phenotype that conspires to drive metastatic progression. The aim of this study was to determine whether eIF-4E was involved in the regulation of heparanase expression and to postulate the probable mechanism.

MATERIALS AND METHODS

Materials

Cell lines Human colon adenocarcinoma cell line LS-174T was an ATCC cell line and was maintained in RPMI 1640 supplemented with 2 mM L-glutamine and 10 % FCS at 37 ℃ in a humidified atmosphere containing 5 % CO_2.

Antisense oligonucleotides Oligonucleotides containing

phosphorothioate were customarily-made and purified with high-performance liquid chromatography. The eIF-4E antisense oligonucleotide comprised the following sequence[11]: 5' -AGTCGCCATCTTAGATCGAT-3' (20 mer), complementary to nucleotides (nt) -11 to +9 of human eIF-4E mRNA. The complementary sense sequence used was 5' -ATCGATCTA AGATGGCGACT-3' . Sense oligonucleotide was used as controls in each of the antisense oligonucleotide experiments.

Methods

Antisense oligonucleotide treatments The day before transfection, the cells were trysinized, counted and plated in a 5×10^6 cells/60-mm dish so that 90-95 % confluency was reached on the day of transfection. As it was a unique cationic lipid formulation, LIPOFECTAMlNE 2000 was more convenient in that it could be used in the presence of serum containing media, by adding it directly to the culture without washing the cells. For transfecting oligonucleotides to cells, the LIPOFECTAMlNE 2000 reagent (Invitrogen) was used according to the manufacturer' s instructions. Briefly, LIPOFECTAMlNE 2000 reagent and oligonucleotides (ODNs) were diluted separately into RPMI 1640 medium and ODNs were mixed with liposome in a charge ratio of 1:2. The mixtures were incubated at room temperature for 20 min to form complexes and then ODN-LIPOFECTAMlNE 2000 reagent complexes was added directly to each well and mixed gently by rocking the plate back and forth. The ODNs were delivered to tumor cells at the final concentration of 2 μmol/L. Tumor cells were incubated in the presence of oligonucleotides/ LIPOFECTAMlNE 2000 reagent mixture for 24 h and 48 h for RT-PCR assays or Western blot.

Semi-quantitative RT-PCR analysis of eIF-4E mRNA Total RNA was extracted by the guanidine salts and phenol-chloroform method. cDNA was prepared from 2 μg of total RNA, using poly-T as primer and MuLV reverse transcriptases (Promega). For PCR amplification, one-fourth of the reverse transcription product and 0.3 μmol/L of each oligonucleotide as primers were used. After one denaturation step at 96 ℃ for 3 minutes, 30 cycles of amplification were performed: denaturation at 94 ℃ for 45 s, annealing at 55 ℃ for 45 s, synthesis at 72 ℃ for 1 minute, and extension at 72 ℃ for 5 minutes. Oligonucleotides for eIF-4E expression analysis were sense primer 5' AGATGGCGACTGTCGAACC3' , antisense primer 5' CAGCGCCACATACATCAT3' [12]. To check cDNA quality, GAPDH was amplified using sense primer 5' CTGGCGCTGAGTACGTCGTG3' and antisense primer 5' CAGTCTTCTGGGTGGCAGTG3' . One-tenth of the amplified products was run on 2 % agarose gels in 1×Tris borate buffer and visualized with ethidium bromide.

Western blot analysis Total proteins were extracted at 48 h after transfection. Cells were lysed in RIPA buffer [10 mM Tris-HCl (pH 7.4), 1 % deoxycholate, 1 % NP40, 150 mM NaCl, 0.1 % SDS, 0.2 mM phenylmethylsulfonyl fluoride, 1 μg/ml aprotinin and 1 μg/ml leupeptin. The lysates were then centrifuged at 10 000×g for 15 min to remove debris. Protein content of the lysate was determined by using Bradford assay (Bio-Rad). For each sample, equal amounts (50 μg) of protein lysates were analyzed on a sodium dodecyl sulfate-10 % or 12 % polyacrylamide gel. Proteins were electroblotted onto Immobilon PVDF membranes (Millipore, Bedford, MA), blocked for 1 h in 5 % dry skim milk, and then incubated with the indicated antibodies. The antibodies used and their dilutions were as follows: 1:500 mouse monoclonal anti-eIF-4E (BD Biosciences), 1:700 rabbit polyclonal anti-heparanase (a kind gift from Mark D. Hulett). The secondary antibodies used were those in an enhanced chemiluminescence detection kit (Amersham) and were chosen according to the species used for the primary antibodies. Exposure times varied with the antibodies used and ranged from 5 to 60 s.

Assays for heparanase activity Heparanase activity was defined as the ability to degrade high molecular weight (40-100 kDa) radio-labeled HS substrate into low molecular weight (5-15 kDa) HS fragments[13-15], which could be differentiated by gel filtration chromatography[16,17]. Radiolabeled HS substrate was prepared by metabolically labeling the extracellular matrix with [^{35}S] as described[16,17]. Soluble substrate was made by releasing ^{35}S-labeled HS proteoglycans from the culture plate with trypsin, and incubated with cell homogenates which were prepared by suspending 10^6 cells in 0.2 ml of aq. 0.1 % (v/v) Triton X-100 and disrupted by freezing and thawing three times in a solid CO_2/ethanol mixture. Samples were taken from the above supernate fractions. Protein concentrations were estimated by a Bio-Rad Coomassie protein assay kit (Bio-Rad Laboratories) using BSA as a standard. Cell lysates containing 50 μg of protein were incubated at 37 ℃ for 24 h in 10 mM sodium phosphate-citrate buffer, pH 6.0, with 20-25 000 cpm of ^{35}S-labeled HS substrate. The incubation medium was centrifuged and the supernatant was analyzed by gel filtration on a Sepharose CL-6B column (0.7×25 cm). Fractions (0.2 ml) were eluted with PBS and their radioactivity was measured. Degradation fragments of HS side chains were eluted from Sepharose CL-6B at 0.5<Kav<0.8 (peak II). A nearly intact HSPG was eluted just after the Vo (Kav<0.2, peak I). Each experiment was repeated at least three times and the variation of elution positions (Kav values) did not exceed ±15 %. Blue dextran and phenol red were added to the sample to mark the excluded (V_0) and included (Vt) volumes, respectively.

***In vitro* invasion assays** *In vitro* invasion assays were performed using modified Boyden chambers, 24-well plates. Polycarbonate filters (8 μm porosity), used to separate the upper compartment, were coated with 50 μg Matrigel. After the lower wells were filled with 600 μl of culture media, supplemented with 0.1 % BSA and 50 μg solubilized Matrigel as a chemo-attractant. The cells in media containing 2 μM oligonucleotides, 1 % FBS at a density of 10^6 cells/ml were resuspended. Gelled Matrigel was gently washed with warmed serum free-culture media. 100 μl of the cell suspension was put onto the Matrigel. Chambers were placed in a 37 ℃ incubator with 5 % CO_2/95 % air for 48 h. Then, the cells remaining on the upper surface of the membrane were removed with a cotton swab and the filters were fixed and stained with a solution of methanol/Coomassie blue 0.1 % in acetic acid (1:3). Cells that had invaded the lower surface of the filter were counted under an inverted microscope. 10 fields per well were counted. The invasion score of untreated control cells was taken as 100 % and that of treated cells was expressed as a percentage of control. All experiments were performed in duplicate and the results from 3 separate sets of experiments were averaged.

RESULTS

Down-regulation effects of antisense oligonucleotides on eIF-4E expression

LS-174T cells were treated with either antisense oligonucleotides, sense control oligonucleotides or saline for 24 h or 48 h in the presence of liposome. By using quantitative RT-PCR analysis, a high level of eIF-4E mRNA was shown in LS-174T cell lines, and treatment with antisense oligonucleotides at concentrations up to 2 μM, induced a significant decrease in the eIF-4E mRNA expression levels compared to control groups. There was no down-regulation of eIF-4E expression in the sense oligonucleotide-treated cells (Figure 1). In order to verify that the decrease in mRNA expression levels corresponded also to

decreases in protein levels, Western blot analysis was performed (Figure 2). We used eIF-4E standard antigen (BD Transduction Laboratories) as a positive control. A significant reduction of eIF-4E protein level was observed in LS-174T cell line, treated with antisense oligonucleotides. In contrast, there was no apparent down-regulation of eIF-4E protein levels in the cells exposed to sense oligonucleotides in comparison with untreated ones.

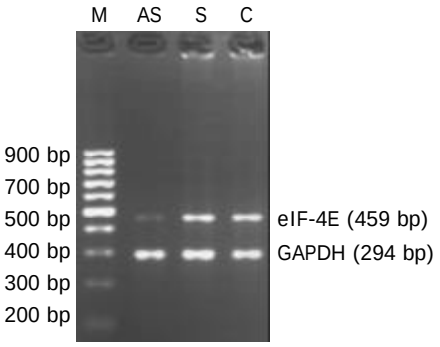

Figure 1 eIF-4E and GAPDH mRNA expression in oligonucleotide-treated human colon adenocarcinoma cells. AS. anti-sense oligonucleotide-transfected cells; S. sense oligonucleotide-transfected cells; C. cells treated with liposome only as control. LS-174T cells were treated with 2 μM oligonucleotides, according to the optimal condition of this cell line in the preliminary experimental results. The numbers under each band showed the relative amount of eIF-4E fragments normalized to that of GAPDH by densitometry. The results suggest that antisense oligonucleotides against eIF-4E inhibit eIF-4E mRNA expression in LS-174T cells, and sense oligonucleotides have no inhibitory effect on eIF-4E mRNA expression.

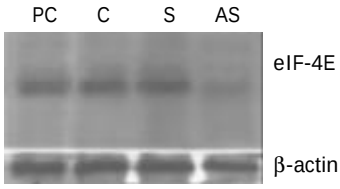

Figure 2 eIF-4E protein expression in oligonucleotide-treated colon adenocarcinoma cells. Protein extracts were prepared from oligonucleotide-treated cells at 48 h after transfection. Cell lysates were size-fractionated by 12 % SDS-PAGE, and immunodetection on the blotted membrane was performed using the eIF-4E MAb. AS, antisense oligonucleotide-treated cells; S. sense oligonucleotide-treated cells; C, cells treated with liposome only; PC, eIF-4E standard antigen (derived from a human neuroblastoma cell line) as a positive control marker.

eIF-4E down-regulation is correlated with alterations in expression of heparanase protein

It has shown that eIF-4E may be involved in regulating a variety of tumor invasion-associated molecules[10]. We investigated the relationship between eIF-4E overexpression and the effects of this expression on heparanase levels in metastatic colon adenocarcinoma cell line. Substantial alterations in the levels of both 50 kDa and 65 kDa heparanase protein expression were observed in the transfectants. In LS-174 cell lines treated with asODN, eIF-4E down-regulation appeared to be associated with the decrease in heparanase protein expression. A 50 kDa protein, corresponding to the expected active mature heparanase according to published data[18], was detected at lower levels in LS-174T cells transfected with antisense oligonucleotides. And so did a 65 kDa protein, which corresponded to the expected size for unprocessed heparanase. In the meantime, heparanase protein levels did not change apparently in the cells treated with sense oligonucleotides or liposome only. Our data demonstrated that eIF-4E did affect the expression of heparanase protein of LS-174T cells under these experimental conditions (Figure 3).

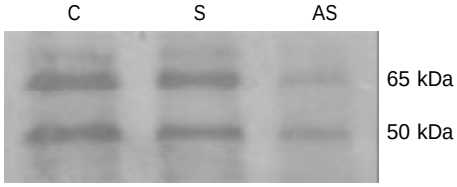

Figure 3 Western blot analysis of heparanase expression in LS-174T cells. The colon adenocarcinoma cells were lysed, and Western blot analysis was performed with an anti-human heparanase polyclonal antibody. AS, antisense oligonucleotide-treated cells; S. sense oligonucleotide-treated cells; C, cells treated with liposome only. Cells treated with antisense oligonucleotides showed markedly reduced levels of heparanase protein compared to cells treated with sense oligonucleotides or saline in the presence of liposome. The approximately 65-kDa protein represents a heparanase precursor, whereas the 50-kDa protein is a processed form, and data showed that both of them were less expressed while eIF-4E was inhibited.

Alteration in heparanase activity

Heparanase activity was determined by degradation of purified ECM [^{35}S] HS using gel filtration chromatography analysis. Degradation fragments eluted in peak II were shown to be degradation products of HS. In this experiment, incubation of an equal amount of protein with sulfate-labeled ECM resulted in release of high level HS degradation fragments (Peak II) in the samples derived from the cells treated with sense oligonucleotides or liposome alone, whereas degradation was less pronounced during incubation of ECM with extracts derived from the cells treated with antisense oligonucleotides (Figure 4). Heparanase activity was also expressed as the total amount of radioactivity eluted in peak II multiplied by the Kav of peak II, thereby representing both the total amount and the size of HS-degradation fragments. The result was consistent with heparanase expression at the protein level. Thus, the alteration of heparanase protein seen by immunostaining was also reflected by a decreased heparanase activity found in the extracts derived from the tumor cells treated with antisense oligonucleotides. These results suggested that the high levels of heparanase were parallel to over-expressed eIF-4E in LS-174T cells and the expression of heparanase might be regulated by eIF-4E in these tumor cells.

Inhibition of heparanase suppresses in vitro invasiveness of LS-174T cells

We first examined whether the variation of eIF-4E expression was associated with heparanase activity in LS-174T cells and its consequent influence on the invasive potential of these tumor cells (Figure 5). The effect of this antisense sequence on invasive capacity was studied *in vitro* by measuring the ability of tumor cells to cross a barrier composed of Matrigel. In these conditions, the invasiveness of LS-174T cells was reduced to 23 % by this antisense sequence. In a control experiment, cells treated at the same concentration of sense oligonucleotides did not show any significantly inhibitory effect on tumor cells invasion as compared to the untreated ones. These results argued that eIF-4E was involved in the regulation of heparanase expression and might further influence the invasive potential of tumor cells.

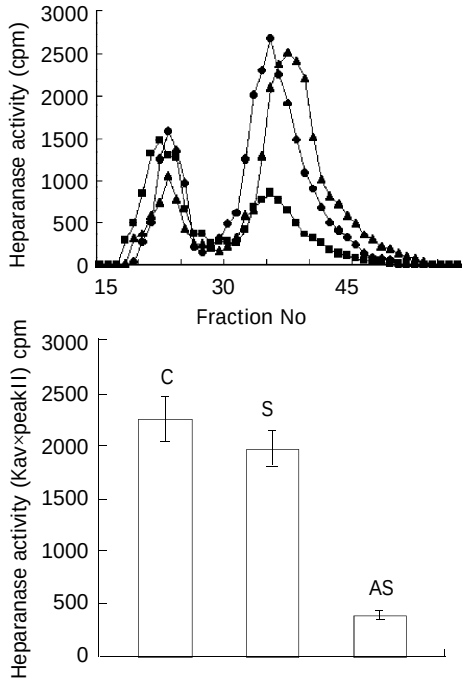

Figure 4 Effects of eIF-4E down-regulation upon enzyme activity of heparanase. Cells were treated for 48 h with antisense oligonucleotide (■), sense oligonucleotide (▲) or liposome only(◆). The soluble fraction from transfected, freezed and thawed LS-174T cells was incubated with ^{35}S-labeled HS. The incubation medium was then subjected to gel filtration over Sepharose CL-6B. Low-molecular-weight HS degradation fragments (peak II) were mainly produced during incubation with medium conditioned by sense oligonucleotide infected cells. The cells treated with antisense oligonucleotide exhibited low levels of heparanase activity as compared to untreated ones. Heparanase activity was also expressed as Kav×total cpm eluted in peak II.

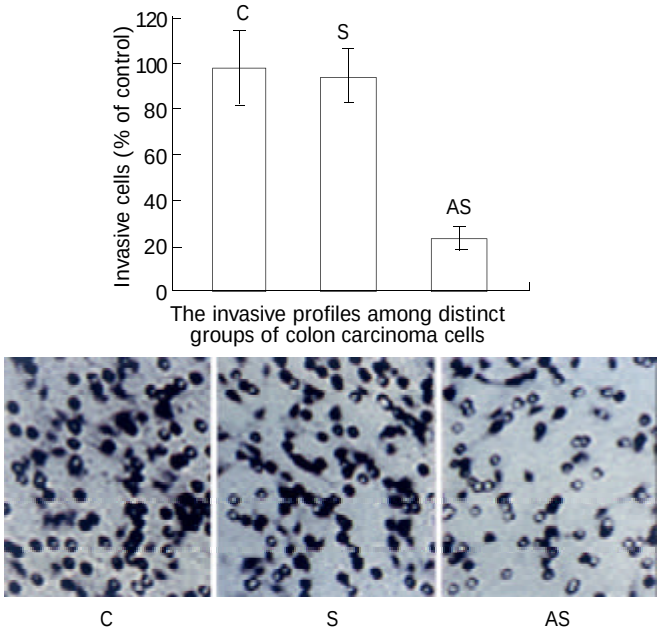

Figure 5 Invasive profiles of LS-174T cells measured *in vitro* using Matrigel as ECM barrier in modified Boyden chambers. The invasiveness of the cells on Matrigel was normalized to 100 % (control, untreated cells). Compared with the control, antisense oligonucleotide reduced invasion to 23 %. Sense sequence didn't have a significant influence on invasive potential of LS-174T cells. These results suggest that alteration of heparanase activity via inhibition of the expression of eIF-4E results in decreased invasiveness in LS-174T cells. The small rings are membrane pores.

DISCUSSION

Inhibition of tumor invasion is an attractive approach for the treatment of highly malignant tumors. Tumor cell invasion is characterized by secretion of enzymes that facilitate tumor cell spread by degrading ECM surrounding the tumors and solubilizing the vascular basement[19]. Thus, heparanase, which degrades HSPG in ECM, is an attractive target for the development of new antimetastatic drugs because of evidences implicating the enzyme in tumor cell invasion. Heparanase facilitates tumor cell invasion and metastasis by at least two different mechanisms. First, it breaks down physical barriers to invasion through degradation of HS chains of HSPGs which are the chief components in BM and ECM, not cleaved by MMPs. Second, it may regulate angiogenesis, tissue repair, inflammation and lipid metabolism by releasing HS-bound growth factor (bFGF) and lipoprotein lipase, which may be a pertinent molecular mechanism for tumor metastasis. Prior reports have mentioned that heparanase is involved in the metastatic potential of various tumor cells, however heparanase as a key regulator of tumor metastasis has not been established with regard to the lack of purified enzymes and cDNA of the gene[20-24]. Two studies concerned with cloning and sequencing of mammalian heparanase and new findings not only confirmed previous studies but revealed that heparanase played an important role in invasion and metastasis of tumor cells[25,26].

As judged by semi-quantitative RT-PCR, heparanase mRNA was increased in human malignancies and xenografts of human breast, colon, lung, prostate, ovary, and pancreas tumors, compared with the corresponding normal tissues[27]. Further support for the role of heparanase in tumour metastasis came from transfection studies where the metastatic ability of lymphoma and melanoma cell lines was substantially enhanced when they were stably transfected with the heparanase gene[25,28]. Additional evidences for heparanase involvement in tumour metastasis came from the *in vivo* administration of heparanase inhibitors, with a dramatic reduction (90 %) in the incidence of tumour metastases reported in a number of tumour models when animals were treated with heparanase inhibitors[29,30]. As to human colon carcinoma[31], heparanase mRNA and protein accumulated even at early stages in the progression of neoplastic disorders, and their levels increased gradually as cells progressed from severe dysplasia through well-differentiated to poorly differentiated colon carcinoma. Adjacent, morphologically normal colonic tissue showed no expression of the enzyme. Deeply invading colon carcinoma cells and the adjacent desmoplastic stromal fibroblasts showed high levels of heparanase mRNA and protein. These results suggest that increased expression of heparanase as in tumor cells indicates less differentiation and more invasive ness. Considering the key role of heparanase in the metastasis of tumor cells, it seems very important to investigate the mechanism by which the expression of heparanase in tumor cells is regulated. Virtually nothing is known about the factors that upregulate heparanase expression and activity in malignant cells, and the molecular basis of this upregulation at the gene level has not been delineated yet. Our research dealed with the translational regulation of heparanase via modulation of the mRNA cap-binding phosphoprotein, eIF-4E and probed the subsequent alterations of invasive potential in LS-174T cells.

To date, Overexpression of eIF-4E has been found in human carcinoma tissues and tumor cell lines. A recent publication[32] also suggested that increased expression of eIF-4E might be an early event in the development human colon cancer. Investigators have found that eIF-4E is increased in both colon adenomas and carcinomas. A compelling body of evidences now indicates that eIF-4E is centrally involved not only in

cellular transformation, but also in tumor formation, invasion and metastasis. The major intracellular signaling pathways involved in tumor growth and malignancy induce eIF-4E activity. MAP kinase activation stimulates MNK-mediated phosphorylation and activation of eIF-4E directly, while activation of the pI3 kinase/PTEN/AKT pathway ultimately yields phosphorylation and inactivation of 4E-BP1, and subsequent release of eIF-4E. Zimmer *et al*[10] indicated that increased eIF-4E activity might provide a central regulatory step facilitating tumor invasion and metastasis via upregulation of selected, potent gene products (such as bFGF, VEGF, MMP-9 and CD44v6). In this report, the colon adenocarcinoma cell line also showed expression of eIF-4E. By transfecting LS-174T cells with a 20-mer antisense s-oligodeoxynucleotide targeted against eIF-4E at well tolerated doses, eIF-4E expression was specifically and significantly inhibited at transcriptional and translational levels. Furthermore, as eIF-4E protein expression decreased, the expression and activity of heparanase were effectively retarded as well and the tumor cells also displayed a reduced invasive potential. It seems that heparanase down-regulation is closely correlated with alterations in the expression of eIF-4E. This study firstly demonstrated that eIF-4E might be involved in the regulatory processes of heparanase in colon adenocarcinoma cell line LS-174T. However, the mechanisms underlying these regulatory events remain unclear, since eIF-4E has the potential to alter gene expression at levels including translational initiation, mRNA splicing, mRNA 3' -end processing, mRNA nucleocytoplasmic transport, and protection against 5' -exonucleolytic degradation[33]. Possible roles of eIF-4E in regulatory processes of heparanase expression remain unidentified and the mechanism deserves further investigation.

Our results, together with the previous reports, indicate that constitutively high-level expression of eIF-4E in tumor cells is involved in the regulation of heparanase expression, although the exact mechanism is not quite certain. Since matrix metalloprotease 9 (MMP-9) and CD44 expression are directly related to metastatic capacity, they are certainly to be governed by enhanced eIF-4E activity. Therefore, eIF-4E antisense strategy should be an effective treatment against tumour invasion and metastasis. This targeting strategy in antisense chemistry may have practical applications in experimental or clinical anti-metastatic gene therapy of human colorectal carcinoma.

ACKNOWLEDGMENTS

This work was supported by a grant from National Natural Science Foundation of China. We thank Mr. Liu Rong, Wang Yadong for their technical assistance.

REFERENCES

1 **Poste G**, Fidler IJ. The pathogenesis of cancer metastasis. *Nature* 1980; **283**: 139-146
2 **Stetler Stevenson WG**, Aznavoorian S, Liotta LA. Tumor cell interactions with the extracellular matrix during invasion and metastasis. *Annu Rev Cell Biol* 1993; **9**: 541-573
3 **Duffy MJ**. The role of proteolytic enzymes in cancer invasion and metastasis. *Clin Exp Metastasis* 1992; **10**: 145-155
4 **Toyoshima M**, Nakajima M. Human heparanase. Purification, characterization, cloning, and expression. *J Biol Chem* 1999; **274**: 24153-24160
5 **Iozzo RV**, Murdoch AD. Proteoglycans of the extracellular environment: clues from the gene and protein side offer novel perspectives in molecular diversity and function. *FASEB J* 1996; **10**: 598-614
6 **Parish CR**, Freeman C, Hulett MD. Heparanase: a key enzyme involved in cell invasion. *Biochim Biophys Acta* 2001; **1471**: M99-108
7 **Vlodavsky I**, Friedmann Y. Molecular properties and involvement of heparanase in cancer metastasis and angiogenesis. *J Clin Invest* 2001; **108**: 341-347
8 **Rhoads RE**, Joshi-Barve S, Rinker-Schaeffer C. Mechanism of action and regulation of protein synthesis initiation factor 4E: effects on mRNA discrimination, cellular growth rate, and oncogenesis. *Prog Nucleic Acid Res Mol Biol* 1993; **46**: 183-219
9 **Sonenberg N**, Gingras AC. The mRNA 5' cap-binding protein eIF4E and control of cell growth. *Curr Opin Cell Biol* 1998; **10**: 268-275
10 **Zimmer SG**, DeBenedetti A, Graff JR. Translational control of malignancy: the mRNA cap-binding protein, eIF-4E, as a central regulator of tumor formation, growth, invasion and metastasis. *Anticancer Res* 2000; **20**: 1343-1351
11 **De Benedetti A**, Joshi-Barve S, Rinker-Schaeffer C, Rhoads RE. Expression of antisense RNA against initiation factor eIF-4E mRNA in HeLa cells results in lengthened cell division times, diminished translation rates, and reduced levels of both eIF-4E and the p220 component of eIF-4F. *Mol Cell Biol* 1991; **11**: 5435-5445
12 **Anthony B**, Carter P, De Benedetti A. Overexpression of the proto-oncogene / translation factor 4E in breast-carcinoma cell lines. *Int J Cancer* 1996; **65**: 858-863
13 **Bame KJ**, Hassall A, Sanderson C, Venkatesan I, Sun C. Partial purification of heparanase activities in Chinese hamster ovary cells: evidence for multiple intracellular heparanases. *Biochem J* 1998; **336**(Pt 1): 191-200
14 **Pikas DS**, Li JP, Vlodavsky I, Lindahl U. Substrate specificity of heparanases from human hepatoma and platelets. *J Biol Chem* 1998; **273**: 18770-18777
15 **Freeman C**, Parish CR. A rapid quantitative assay for the detection of mammalian heparanase activity. *Biochem J* 1997; **325**(Pt 1): 229-237
16 **Gilat D**, Hershkoviz R, Goldkorn I, Cahalon L, Korner G, Vlodavsky I, Lider O. Molecular behavior adapts to context: heparanase functions as an extracellular matrix-degrading enzyme or as a T cell adhesion molecule, depending on the local pH. *J Exp Med* 1995; **181**: 1929-1934
17 **Matzner Y**, Bar-Ner M, Yahalom J, Ishai-Michaeli R, Fuks Z, Vlodavsky I. Degradation of heparan sulfate in the subendothelial extracellular matrix by a readily released heparanase from human neutrophils. Possible role in invasion through basement membranes. *J Clin Invest* 1985; **76**: 1306-1313
18 **Hulett MD**, Hornby JR, Ohms SJ, Zuegg J, Freeman C, Gready JE, Parish CR. Identification of active-site residues of the pro-metastatic endoglycosidase heparanase. *Biochemistry* 2000; **39**: 15659-15667
19 **Nakajima M**, Irimura T, Di Ferrante D, Di Ferrante N, Nicolson GL. Heparan sulfate degradation: relation to tumor invasive and metastatic properties of mouse B16 melanoma sublines. *Science* 1983; **220**: 611-613
20 **Ishai-Michaeli R**, Eldor A, Vlodavsky I. Heparanase activity expressed by platelets, neutrophils, and lymphoma cells releases active fibroblast growth factor from extracellular matrix. *Cell Regul* 1990; **1**: 833-842
21 **Vlodavsky I**, Bar-Shavit R, Ishai-Michaeli R, Bashkin P, Fuks Z. Extracellular sequestration and release of fibroblast growth factor: a regulatory mechanism? *Trends Biochem Sci* 1991; **16**: 268-271
22 **Eisenberg S**, Sehayek E, Olivecrona T, Vlodavsky I. Lipoprotein lipase enhances binding of lipoproteins to heparan sulfate on cell surfaces and extracellular matrix. *J Clin Invest* 1992; **90**: 2013-2021
23 **Vlodavsky I**, Eldor A, Haimovitz-Friedman A, Matzner Y, Ishai-Michaeli R, Lider O, Naparstek Y, Cohen IR, Fuks Z. Expression of heparanase by platelets and circulating cells of the immune system: possible involvement in diapedesis and extravasation. *Invasion Metastasis* 1992; **12**: 112-127
24 **Eccles SA**. Heparanase: breaking down barriers in tumors. *Nat Med* 1999; **5**: 735-736
25 **Vlodavsky I**, Friedmann Y, Elkin M, Aingorn H, Atzmon R, Ishai-Michaeli R, Bitan M, Pappo O, Peretz T, Michal I, Spector L, Pecker I. Mammalian heparanase: gene cloning, expression and function in tumor progression and metastasis. *Nat Med* 1999;

5: 793-802

26 **Hulett MD**, Freeman C, Hamdorf BJ, Baker RT, Harris MJ, Parish CR. Cloning of mammalian heparanase, an important enzyme in tumor invasion and metastasis. *Nat Med* 1999; **5**: 803-809

27 **McKenzie E**, Tyson K, Stamps A, Smith P, Turner P, Barry R, Hircock M, Patel S, Barry E, Stubberfield C, Terrett J, Page M. Cloning and expression profiling of Hpa2, a novel mammalian heparanase family member. *Biochem Biophys Res Commun* 2000; **276**: 1170-1177

28 **Vlodavsky I**, Elkin M, Pappo O, Aingorn H, Atzmon R, Ishai-Michaeli R, Aviv A, Pecker I, Friedmann Y. Mammalian heparanase as mediator of tumor metastasis and angiogenesis. *Isr Med Assoc J* 2000; **2**(Suppl): 37-45

29 **Miao HQ**, Elkin M, Aingorn E, Ishai-Michaeli R, Stein CA, Vlodavsky I. Inhibition of heparanase activity and tumor metastasis by laminarin sulfate and synthetic phosphorothioate oligodeoxynucleotides. *Int J Cancer* 1999; **83**: 424-431

30 **Parish CR**, Freeman C, Brown KJ, Francis DJ, Cowden WB. Identification of sulfated oligosaccharide-based inhibitors of tumor growth and metastasis using novel *in vitro* assays for angiogenesis and heparanase activity. *Cancer Res* 1999; **59**: 3433-3441

31 **Friedmann Y**, Vlodavsky I, Aingorn H, Aviv A, Peretz T, Pecker I, Pappo O. Expression of heparanase in normal, dysplastic, and neoplastic human colonic mucosa and stroma. Evidence for its role in colonic tumorigenesis. *Am J Pathol* 2000; **157**: 1167-1175

32 **Rosenwald IB**, Chen JJ, Wang S, Savas L, London IM, Pullman J. Upregulation of protein synthesis initiation factor eIF-4E is an early event during colon carcinogenesis. *Oncogene* 1999; **18**: 2507-2517

33 **Rhoads RE**. Cap recognition and the entry of mRNA into the protein synthesis initiation cycle. *Trends Biochem Sci* 1988; 13: 52-56

Edited by Zhang JZ and Wang XL

P.O.Box 2345, Beijing 100023,China
Fax: +86-10-85381893
E-mail: wjg@wjgnet.com www.wjgnet.com

World J Gastroenterol 2003;9(8):1713-1718
World Journal of Gastroenterology
 ISSN 1007-9327

• COLORECTAL CANCER •

Refinement of heterozygosity loss on chromosome 5p15 in sporadic colorectal cancer

Shi-Feng Xu, Zhi-Hai Peng, Da-Peng Li, Guo-Qiang Qiu, Fang Zhang

Shi-Feng Xu, Zhi-Hai Peng, Da-Peng Li, Guo-Qiang Qiu, Fang Zhang, Department of General Surgery, Shanghai First People' s Hospital, Shanghai 200080, China
Supported by the National Natural Science Foundation of China, No. 30080016
Correspondence to: Dr. Zhi-Hai Peng, Department of General Surgery, Shanghai First People' s Hospital, 85 Wujin Road, Shanghai 200080, China. pengpzhb@online.sh.cn
Telephone: +86-21-63240090 Ext 3102
Received: 2003-03-20 **Accepted:** 2003-04-17

Abstract

AIM: To refine the loss of heterozygosity on chromosome 5p15 and to identify the new tumor suppressor gene (s) in colorectal tumorigenesis.

METHODS: Sixteen polymorphic microsatellite markers were analyzed on chromosome 5 and another 6 markers were applied on chromosome 5p15 in 83 cases of colorectal and normal DNA by PCR. PCR products were electrophoresed on an ABI 377 DNA sequencer. Genescan 3.1 and Genotype 2.1 software were used for LOH scanning and analysis.

RESULTS: We observed 2 distinct regions of frequent allelic deletions on Chromosome 5, at D5S416 on 5p15 and D5S428-D5S410 on 5q. Another 6 polymorphric microsatellite markers were applied to 5p15 and the minimal region of frequent loss of heterozygosity was established on 5p15 spanning the D5S416 locus.

CONCLUSION: Through our detailed deletion mapping studies, we have found a critical and precise location of 5p deletions, 5p15.2-5p15.3, which must contain one or more unknown tumor suppressor gene (s) of colorectal cancer.

Xu SF, Peng ZH, Li DP, Qiu GQ, Zhang F. Refinement of heterozygosity loss on chromosome 5p15 in sporadic colorectal cancer. *World J Gastroenterol* 2003; 9(8): 1713-1718
http://www.wjgnet.com/1007-9327/9/1713.asp

INTRODUCTION

Colorectal cancer is one of the most common malignant tumors threatening people' s health[1,2]. Its occurrence has been rising over the past 3 decades[3]. Now, colorectal cancer is the second cause of death in Western countries, and the fourth in China[4]. It is clear that improvement in its prognosis will not be achieved without a better understanding of its etiology and tumor biology. In recent years, the genetic basis of human tumors has been increasingly elucidated. A growing number of studies have shown that the molecular events controlling tumorigenesis involve abnormal cell growth promoted by activation of proto-oncogenes and/or inactivation of tumor suppressor genes[5,6]. Identification of novel tumor suppressor genes has been facilitated by loss of heterozygosity (LOH) studies that have guided the localization of minimally deleted regions on chromosomes[6,7]. In colorectal cancers, frequent allelic loss has been identified on chromosomes 5q (30 %), 8p (40 %), 17p (75-80 %), 18q (80 %), and 22q (20-30 %)[8,9].

Previous allelotype analyses of chromosome 5 in colorectal cancer mainly focused on the long arm (5q), where a high frequency of allelic deletions of 5q21-22 was reported, implicating the *APC/MCC* genes[10-13]. However, alterations of the short arm of chromosome 5 have not been studied extensively in colorectal cancers. In this study, 16 polymorphic microsatellite markers were applied to chromosome 5. As a result of the high frequence of LOH on the loci of D5S416, another 6 microsatellite markers from chromosomal region 5p15, spanning the D5S416 were precisely localized.

MATERIALS AND METHODS

Materials

This study was based on 83 patients with colorectal cancer including 40 men and 43 women, who were treated at the Surgical Department in Shanghai First People' s Hospital, China, between 1998 and 1999. The patients' age ranged from 31 to 84 years with a median of 66. All the patients were confirmed by pathology, and staged by Duke' s criteria. Eight, 21, 40, 14 cases were of Duke' s stages A, B, C and D, respectively. 23 cases were well differentiated, 39 moderately differentiated, 6 poorly differentiated adenocarcinoma, and 15 cases were mucinous adenocarcinoma. HNPCC patients were ruled out by Amsterdam criteria[14,15]. Each patient gave his were or her informed consent for the use of his or her tissues in this study.

Methods

DNA extraction The cancerous and adjacent normal tissues were freshly frozen within 30 min after being removed. These tissues were then cut into cubes of approximately 2 mm^3 and immediately frozen in liquid nitrogen. DNA was extracted using standard methods with proteinase K digested and phenol/chloroform purified.

Microsatellite markers and PCR Initially, 83 cases of colorectal cancer were analyzed by PCR using 16 microsatellite markers which were mapped to chromosome 5. DNA samples were analyzed as normal/tumor pairs using primers for the following microsatellite loci(location/heterozygosity): D5S1981-(5P15.3/0.73), D5S406-(5P15.3/0.78), D5S630-(5P15.3/0.89), D5S416(5P15.2/0.77), D5S419-(5P13.3/0.80), D5S418-(5P13.1/0.80), D5S407-(5q11.2/0.86), D5S647-(5q12.2/0.82), D5S424-(5q13.2/0.76), D5S428-(5q14.1/0.76), D5S2027-(5q21.1/0.78), D5S471-(5q23.1/0.75), D5S2115-(5q31.1/0.76), D5S410-(5q33.2/0.79), D5S400-(5q35.1/0.81), D5S408-(5q35.3/0.73). As a result of the high frequency of LOH in D5S416, 6 additional microsatellite markers from chromosomal region 5p15 were employed to span the D5S416 locus. DNA samples were also analyzed as normal/tumor pairs for the following microsatellite loci (location/heteozygosity): D5S1987-(5p15.3/0.87), D5S1991-(5p15.3/0.68), D5S1954-

(5p15.3/0.69), D5S1963-(5p15.2/0.69), D5S2114-(5P15.2/0.87), D5S486-(5p15.1/0.74). Polymorphic microsatellite markers were analyzed by PCR (GeneAmp PCR System 9700, PE Applied Biosystems Fostercity CA, USA). PCR conditions were as follows: 5 μl total volume with approximately 1.4 ng of DNA as a template with 10× standard buffer, 0.3 μl Mg^{2+}, 0.8 μl deoxynucleotide triphosphates, 0.3 unit of Hot-start taq polymerase and 0.06 ml of each oligonucleotide primer, with the forward primer fluorescence labeled with HEX, FAM or NED. The "touch-down" was applied. Cycling conditions consisted of 3 stages: an initial denaturation at 96 ℃ for 12 min in stage I; 14 cycles each at 94 ℃ for 20 s, at 63-56 ℃ for 1 min (decrease 0.5 ℃ per cycle) and at 72 ℃ for 1 min in stage II, 35 cycles each at 94 ℃ for 20 s, at 56 ℃ for 1 min and at 72 ℃ for 1 min in stage III.

LOH analysis A portion of each PCR product (0.5 μl) was combined with 0.1 μl of Genescan 500 size standard (PE Applied Biosystems Fostercity CA, USA) and 0.9 ul of formamide loading buffer. After denaturation at 96 ℃ for 5 min, the products were electrophoresed on a 5 % polyacrylamide gel on an ABI 377 DNA sequencer (PE Applied Biosystems Fostercity CA, USA) for 3 hours. Genotype 2.1 software displayed individual gel lanes as electrophoretograms with a given size, height, and area for each detected fluorescent peak. Stringent criteria were used to score the samples. Alleles were defined as the two highest peaks within the expected size range. A ratio of T1:T2/N1:N2 of less than 0.67 or greater than 1.50 was scored as a loss of heterozygosity (Figure 1). Most amplifications of normal DNA produced two PCR products indicating heterozygosity. A single fragment amplified from normal DNA (homozygote) and those PCR reactions in which fragments were not clearly amplified, were scored as not informative. The LOH frequency of a locus was equal to the ratio between allelic loss and informative cases.

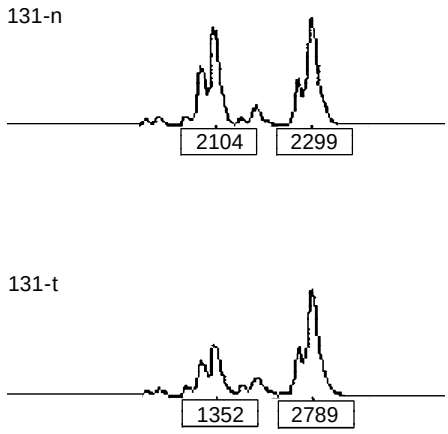

Figure 1 Representative LOH in tumor. "*n*" is normal DNA, "*t*" is tumor DNA. The peak heights are indicated below the corresponding alleles. Allele ratio=(t1:t2)/(n1:n2)=(1 352:2 789)/(2 104:2 299)=0.53. Allele ratio of less than 0.67 or greater than 1.50 was scored as LOH.

RESULTS

LOH analysis of colorectal cancers

Eighty-three colorectal cancers were analyzed for LOH at the 16 marker loci spanning chromosome 5 with the following most likely order: pter-D5S1981-D5S406-D5S630-D5S416-D5S419-D5S418-D5S407-D5S647-D5S424-D5S641-D5S428-D5S2027-D5S471-D5S2115-D5S410-D5S400-D5S408-qter[16] (Table 1 and Figure 2). We observed 2 distinct regions of frequent allelic deletions on chromosomes at D5S416 on 5p15 and D5S428-D5S410 on 5q.

LOH mapping of 5p15 region

The chromosomal region spanning D5S416 locus on chromosome 5p was further investigated using a saturation mapping strategy with another 6 microstellite markers that are localized and closely spaced within this region (Figure 3). Eighty-three paired normal and tumor DNA samples were analyzed for LOH at these loci which further refined the resolution of the deletion map to a genomic segment of approximately 1 centimorgan (cM) and established the minimal region of frequent chromosomal loss at D5S416 locus. Based on the databases described previously, the most likely order of these markers was pter-D5S630-D5S1987-D5S1991-D5S1954-D5S1963-D5S416-D5S2114-D5S486[16] (Table 2). Overall, preferential deletions of D5S416 were observed in 26/54 colorectal cancers and deletions of the 2 markers, D5S1954 and D5S1963 (approximately 1 cM centromeric to D5S416), were seen in 33.3 % (16/48) and 21.1 % (12/57), respectively. Thus, the majority of observed interstitial deletions were localized within a 1 cM genomic segment encompassing the D5S416 locus.

Table 1 The ratios of LOH of all loci on chromosome 5

Loci	Map location	Number of informative cases (%)	LOH No (%)
D5S1981	p15.3	24 (28.92)	3 (12.50)
D5S406	p15.3	26 (31.33)	5 (19.23)
D5S630	p15.3	65 (78.31)	8 (12.31)
D5S416	**p15.2**	**54 (65.06)**	**26 (48.15)**
D5S419	p13.3	63 (75.90)	7 (11.11)
D5S418	p13.1	66 (79.52)	15 (22.73)
D5S407	q11.2	51 (61.45)	10 (19.61)
D5S647	q12.2	74 (89.16)	16 (21.62)
D5S424	q13.2	36 (43.37)	8 (22.22)
D5S428	**q14.1**	**61 (73.49)**	**23 (37.70)**
D5S2027	**q21.1**	**46 (55.42)**	**15 (32.61)**
D5S471	**q23.1**	**62 (74.70)**	**24 (38.71)**
D5S2115	**q31.1**	**59 (71.08)**	**19 (32.20)**
D5S410	**q33.2**	**18 (21.69)**	**8 (44.44)**
D5S400	q35.1	28 (33.73)	4 (14.39)
D5S408	q35.3	61 (73.49)	6 (9.84)

Table 2 The ratios of LOH of the loci on 5p15 region

Loci	Map location	Space of two loci (cM)	Number of informative cases (%)	LOH No (%)
D5S630	p15.3	2.2	65 (78.31)	8 (12.31)
D5S1987	p15.3	4.7	67 (80.31)	11 (16.42)
D5S1991	p15.3	0.6	50 (60.24)	6 (12.00)
D5S1954	**p15.3**	**0.1**	**48 (57.83)**	**16 (33.33)**
D5S1963	**p15.2**	**0.8**	**57 (68.67)**	**12 (21.05)**
D5S416	**p15.2**	1.0	**54 (65.06)**	**26 (48.15)**
D5S2114	p15.2	2.2	53 (63.86)	7 (13.21)
D5S486	p15.1		60 (72.29)	10 (16.67)

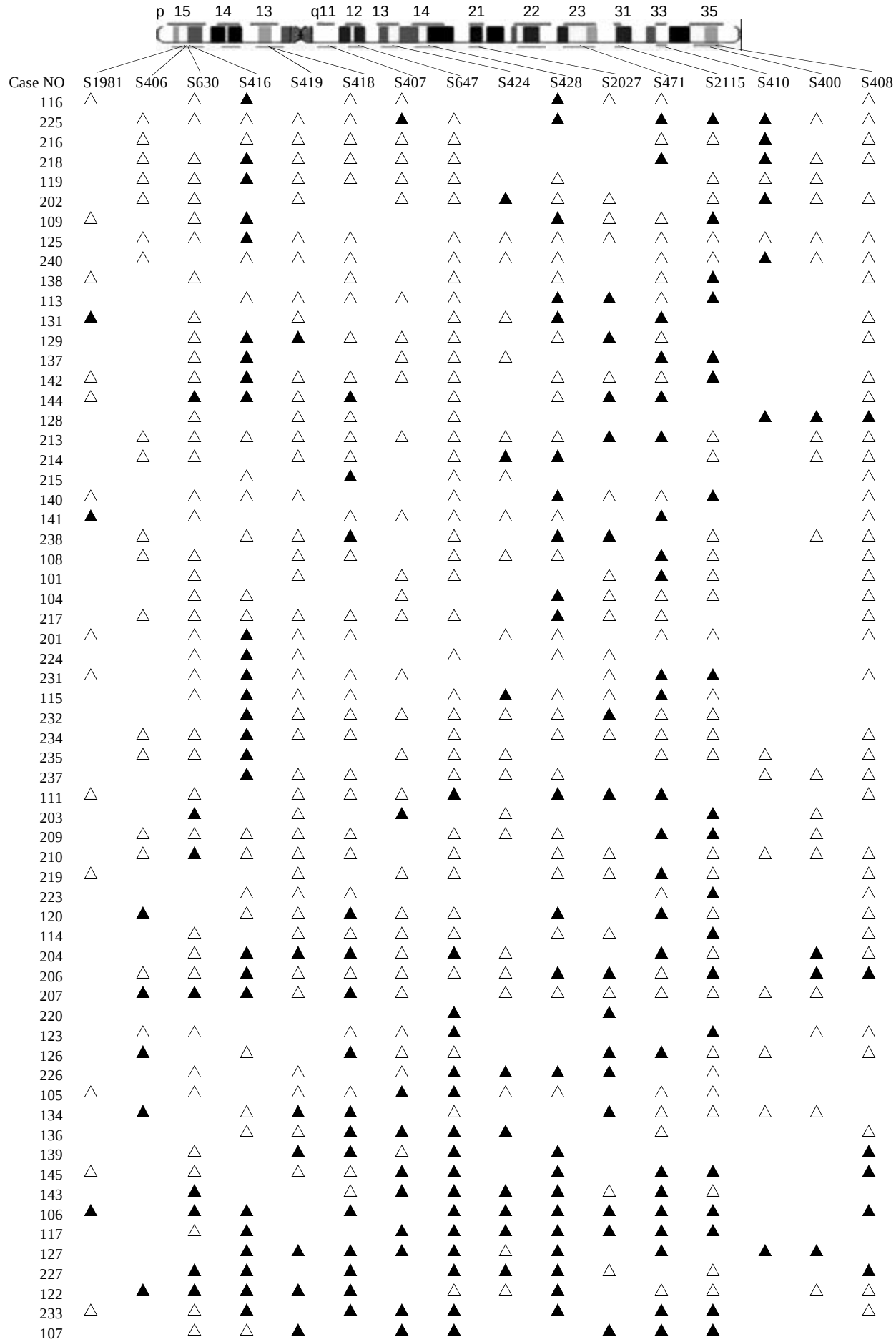

Figure 2 LOH map of chromosome 5 in colorectal cancer. ▲ LOH; △ retaining heterozygosity; neither ▲ or △ is non-informative. We can clearly figure out the two regions of the high rates of LOH on chromosome 5, one is D5S416 on 5p15, the other is D5S428-D5S410 on 5 q.

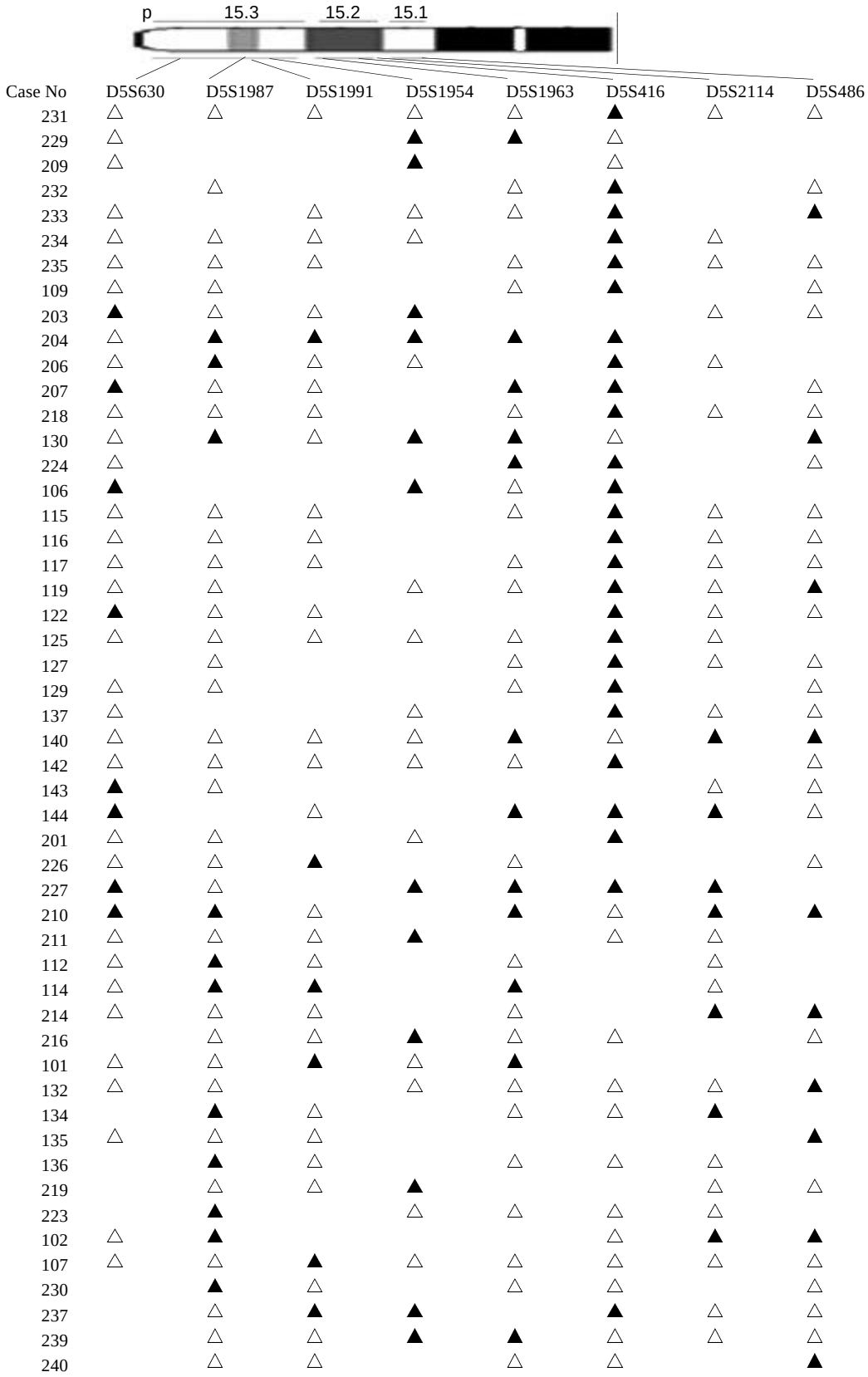

Figure 3 LOH map of 5p15 in colorectal cancer. ▲ LOH; △ retaining heterozygosity; neither ▲ or △ is non-informative.

DISCUSSION

Inactivation of tumor suppressor genes appears to be one of the genetic mechanisms involved in the development of colorectal cancer[17-19]. This process includes mutation of one allele, followed by a deletion of the remaining one (LOH) or homozygous deletion of both alleles[20]. Allelic deletions detected as LOH have been proved useful for mapping regions of DNA that contain tumor suppressor genes. LOH at specific chromosomal regions strongly suggests the existence of tumor suppressor genes at the relevant segment[21,22]. We performed deletion mapping analyses of chromosome 5 markers in 83 sporadic colorectal cancers, using 16 microsatellite markers. Analysis of the deletion map (Figure 2), together with the frequency of LOH obtained for each locus (Table 1) allowed us to identify two regions on chromosome 5 displaying high rates of LOH.

The 5q14-q22 region (D5S428-D5S410) has been frequently deleted in colorectal cancer. Ashton-Rickardt is the first author to describe the *APC/MCC* region as being frequently deleted in sporadic colorectal cancer[10]. Since then, several reports have indicated a high frequency of LOH at this region[11-13]. Our study also identified it, which proved our ways right.

The other region is 5p15 (D5S416). Further mapping of 5p15 region defined a minimal region of frequent deletion spanning the D5S416 locus (Figure 3). Based on this map, the majority of allelic deletions were localized within 1 cM chromosomal segment encompassing the 3 loci (D5S1954, D5S1963 and D5S416). Of these, D5S416 was the most frequently deleted locus (48.15 %), while the other 2 markers, D5S1954 and D5S1963, demonstrated allelic losses of 33.33 % and 21.05 %, respectively. Thus, the high LOH frequency and the patterns of allelic losses of chromosome 5p15.2-5p15.3 suggest that this region may be preferentially deleted in colorectal cancer and could potentially harbor important tumor suppressor genes in colorectal development and progression. A database search has identified four candidate genes, *PDCD6*[23-27], *TERT*[28-29], *T RIP13*[30,31] and *POLS*[32-34] with suggestive tumor suppressor gene functions. The programmed cell death gene, *PDCD6*, is a member of the family of intracellular Ca^{2+}-binding proteins and a part of the apoptotic machinery controlled by T-cell receptor (TCR) Fas, and glucocorticoid signals[23-27]. *TERT* encodes a reverse transcriptase required for the replication of chromosome termini and plays a role in telomere elongation. Although telomerase expression is a hallmark of cancer[35], the mice lacking the RNA component of telomerase (mTERC) exhibit progressive telomere shortening and chromosomal instability associated with epithelial tumors[28]. *TRIP13*, thyroid receptor interacting protein 13, is a transcription factor that regulates expression of a variety of specific target genes such as the human papilloma virus type16 E1(HPV16E1) which is important in cervical carcinoma[30,31]. *POLS* gene, a topoisomerase-related functional protein-4-1, encodes polymerase (DNA directed) signal within the deleted region. The yeast homolog TRF4 plays a critical role in chromosome segregation by coordinating between DNA replication and sister chromatid cohesion[32, 33]. The data strongly support the importance of the *POLS* gene, which is critical for TRF4' s essential and repair functions. Cell cycle analysis has revealed that *TRF4/POLS* is associated with chromosomes in G1, S and G2 phases[34]. The presence of these genes at the 5p15.2-5p15.3 interval suggests that they may target tumor suppressor genes of these deletions in colorectal cancer. It will be helpful for us to find the tumor suppressor genes through studying their functions.

In summary, through our detailed deletion mapping studies, we have found a critical and precise location of 5p deletions, 5p15.2-5p15.3, which must contain one or more unknown tumor suppressor gene(s) of colorectal cancer.

REFERENCES

1 **Zhang ZS**, Zhang YL. Progress in research of colorectal cancer in China. *Shijie Huaren Xiaohua Zazhi* 2001; **9**: 489-494

2 **Zhang YL**, Zhang ZS, Wu BP, Zhou DY. Early diagnosis for colorectal cancer in China. *World J Gastroenterol* 2002; **8**: 21-25

3 **Becker N.** Epidemiology of colorectal cancer. *Radiologe* 2003; **43**: 98-104

4 **Yu JP**, Dong WG. Current situation about early diagnosis of cancer of large intestine. *Shijie Huaren Xiaohua Zazhi* 1999; **7**: 553-554

5 **Lasko D**, Cavenee W, Nordenskjold M. Loss of constitutional heterozygosity in human cancer. *Annu Rev Genet* 1991; **25:** 281-314

6 **Cliby W**, Ritland S, Hartmann L, Dodson M, Halling KC, Keeney G, Podratz KC, Jenkins RB. Human epithelial ovarian cancer allelotype. *Cancer Res* 1993; **53**: 2393-2398

7 **Peng Z,** Ling Y, Bai S. Loss of heterozygosity on chromosome 3 in sporadic colorectal carcinoma. *Zhonghua Yixue Zazhi* 2001; **81**: 336-339

8 **Vogelstein B**, Fearon ER, Kern SE, Hamilton SR, Preisinger AC, Nakamura Y, White R. Allelotype of colorectal carcinomas. *Science* 1989; **244**: 207-211

9 **Weber TK**, Conroy J, Keitz B, Rodriguez-Bigas M, Petrelli NJ, Stoler DL, Anderson GR, Shows TB, Nowak NJ. Genome-wide allelotyping indicates increased loss of heterozygosity on 9p and 14q in early age of onset colorectal cancer. *Cytogenet Cell Genet* 1999; **86**: 142-147

10 **Ashton-Rickardt PG,** Dunlop MG, Nakamura Y, Morris RG, Purdie CA, Steel CM, Evans HJ, Bird CC, Wyllie AH. High frequency of APC loss in sporadic colorectal carcinoma due to breaks clustered in 5q21-22. *Oncogene* 1989; **4**: 1169-1174

11 **Okamoto M**, Sato C, Kohno Y, Mori T, Iwama T, Tonomura A, Miki Y, Utsunomiya J, Nakamura Y, White R. Molecular nature of chromosome 5q loss in colorectal tumors and desmoids from patients with familial adenomatous polyposis. *Hum Genet* **85**: 595-599

12 **Iacopetta B**, DiGrandi S, Dix B, Haig C, Soong R, House A. Loss of heterozygosity of tumour suppressor gene loci in human colorectal carcinoma. *Eur J Cancer* 1994; **30A**: 664-670

13 **Zhang F**, Zhou C, Ling Y, Qiu G, Bai S, Liu W, He L, Peng Z. Allelic analysis on chromosome 5 in sporadic colorectal cancer patients. *Zhonghua Zhongliu Zazhi* 2002; **24**: 458-460

14 **Vasen HF**, Mecklin JP, Khan PM, Lynch HT. The international collaborative group on hereditary non-polyposis colorectal cancer (ICG-HNPCC). *Dis Colon Rectum* 1991; **34**: 424-425

15 **Vasen HFA**, Watson P, Mecklin JP, Lynch HT. New clinical criteria for hereditary nonpolyposis colorectal cancer(HNPCC, Lynch syndrome) proposed by the International Collaborative group on HNPCC. *Gastroenterology* 1999; **116**: 1453-1456

16 http://www.ncbi.nlm.nih.gov/mapview/maps.cgi?org=hum&chr=5

17 **Kataoka M**, Okabayashi T, Johira H, Nakatani S, Nakashima A, Takeda A, Nishizaki M, Orita K, Tanaka N. Aberration of p53 and DCC in gastric and colorectal cancer. *Onco/Rep* 2000; **7**: 99-103

18 **Zhou CZ**, Peng ZH, Zhang F, Qiu GQ, He L. Loss of heterozygosity on long arm of chromosome 22 in sporadic colorectal carcinoma. *World J Gastroenterol* 2002; 8: 668-673

19 **Komarova NL,** Lengauer C, Vogelstein B, Nowak MA. Dynamics of genetic instability in sporadic and familial colorectal cancer. *Cancer Biol Ther* 2002; **1**: 685-692

20 **Dong JT.** Chromosomal deletions and tumor suppressor genes in prostate cancer. *Cancer Metastasis Rev* 2001; **20**: 173-193

21 **Baker SJ**, Fearon ER, Nigro JM, Hamilton SR, Preisinger AC, Jessup JM, Van Tuinen P, Ledbetter DH, Barker DF, Nakamura Y, White R, Vogelstein B. Chromosome 17 deletions and p53 gene mutations in colorectal carcinomas. *Science* 1989; **244**: 217-221

22 **Kinzler KW**, Nibert MC, Vogelstein B, Bryan TM, Levy DB, Smith KJ, Preisinger AC, Hamiton SR, Hedge P, Markham A, Carlson M, Joslyn G, Groden J. Identification of gene located at chromosome 5q21 that is mutated in colorectal cancers. *Science* 1991; **251**: 1366-1370

23 **Vito P**, Lacana E, D'Adamio L. Interfering with apoptosis: Ca (2+)-binding protein ALG-2 and Alzheimer's disease gene ALG-3. *Science* 1996; **271:** 521-524

24 **Krebs J,** Klemenz R. The ALG-2/AIP-complex, a modulator at the interface between cell proliferation and cell death? A hypothesis. *Biochim Biophys Acta* 2000; **1498**: 153-161

25 **Jung YS**, Kim KS, Kim KD, Lim JS, Kim JW, Kim E. Apoptosis-linked gene 2 binds to the death domain of Fas and dissociates from Fas during Fas-mediated apoptosis in Jurkat cells. *Biochem Biophys Res Commun* 2001; **288:** 420-426

26 **Krebs J,** Saremaslani P, Caduff R. ALG-2: a Ca2+ -binding modulator protein involved in cell proliferation and in cell death. *Biochim Biophys Acta* 2002; **1600**: 68-73

27 **Kitaura Y,** Satoh H, Takahashi H, Shibata H, Maki M. Both ALG-2 and peflin, penta-EF-hand (PEF) proteins, are stabilized by dimerization through their fifth EF-hand regions. *Arch Biochem Biophys* 2002; **399**: 12-18

28 **Artandi SE,** Chang S, Lee SL, Alson S, Gottlieb GJ, Chin L,

DePinho RA. Telomere dysfunction promotes non-reciprocal translocations and epithelial cancers in mice. *Nature* 2000; **406:** 641-645

29 **Poole JC,** Andrews LG, Tollefsbol TO. Activity, function, and gene regulation of the catalytic subunit of telomerase (hTERT). *Gene* 2001; **269**: 1-12

30 **Lee JW,** Choi HS, Gyuris J, Brent R, Moore DD. Two classes of proteins dependent on either the presence or absence of thyroid hormone for interaction with the thyroid hormone receptor. *Mol Endocrinol* 1995; **9**: 243-254

31 **Yasugi T,** Vidal M, Sakai H, Howley PM, Benson JD. Two classes of human papillomavirus type 16 E1 mutants suggest pleiotropic conformational constraints affecting E1 multimerization, E2 interaction, and interaction with cellular proteins. *J Virol* 1997; **71:** 5942-5951

32 **Wang Z**, Castano IB, De Las Penas A, Adams C, Christman MF. Pol kappa: A DNA polymerase required for sister chromatid cohesion. *Science* 2000; **289:** 774-779

33 **Carson DR,** Christman MF. Evidence that replication fork components catalyze establishment of cohesion between sister chromatids. *Proc Natl Acad Sci U S A* 2001; **98**: 8270-8275

34 **Wang Z,** Casatano IB, Adams C, Vu C, Fitzhugh D, Christman MF. Structure / function analysis of the *Saccharomyces* cerevisiae Trf4 / Pol Sigma DNA polymerase. *Genetics* 2002; **160**: 381-391

35 **Granger MP,** Wright WE, Shay JW. Telomerase in cancer and aging. *Crit Rev Oncol Hematol* 2002; **41**: 29-40

Edited by Ma JY and Wang XL

P.O.Box 2345, Beijing 100023,China
Fax: +86-10-85381893
E-mail: wjg@wjgnet.com www.wjgnet.com

World J Gastroenterol 2003;9(8):1719-1724
World Journal of Gastroenterology
 ISSN 1007-9327

• COLORECTAL CANCER •

Isolation of a novel member of small G protein superfamily and its expression in colon cancer

Wei Yan, Wen-Liang Wang, Feng Zhu, Sheng-Quan Chen, Qing-Long Li, Li Wang

Wei Yan, Wen-Liang Wang, Feng Zhu, Sheng-Quan Chen, Qing-Long Li, Li Wang, Department of Pathology, Xijing Hospital, Fourth Military Medical University, Xi' an 710032, Shaanxi Province, China
Supported by National Natural Science Foundation of China, No. 30270667
Correspondence to: Professor Wen-Liang Wang, Department of Pathology, Xijing Hospital, Fourth Military Medical University, Xi' an 710032, Shaanxi Province, China. wlwang@fmmu.edu.cn
Telephone: +86-29-3224893 **Fax:** +86-29-3284284
Received: 2003-03-02 **Accepted:** 2003-03-26

Abstract

AIM: APMCF1 is a novel human gene whose transcripts are up-regulated in apoptotic MCF-7 cells. In order to learn more about this gene's function in other tumors, we cloned its full length cDNA and prepared its polyclonal antibody to investigate its expression in colon cancers with immunohistochemistry.

METHODS: With the method of 5' rapid amplification of cDNA end (RACE) and EST assembled in GenBank, we extended the length of APMCF1 at 5' end. Then the sequence encoding the APMCF1 protein was amplified by RT-PCR from the total RNA of apoptotic MCF-7 cells and cloned into the prokaryotic expression vector pGEX-KG to construct recombinant expression vector pGEX-APMCF1. The GST-APMCF1 fusion protein was expressed in *E. coli* and used to immunize rabbits to get the rabbit anti-APMCF1 serum. The specificity of polyclonal anti-APMCF1 antibody was determined by Western blot. Then we investigated the expression of Apmcf1 in colon cancers and normal colonic mucosa with immunohistochemistry.

RESULTS: A cDNA fragment with a length of 1 745 bp was obtained. APMCF1 was mapped to chromosome 3q22.2 and spanned at least 14.8 kb of genomic DNA with seven exons and six introns contained. Bioinformatic analysis showed the protein encoded by APMCF1 contained a small GTP-binding protein (G proteins) domain and was homologous to mouse signal recognition particle receptor β(SRβ). A coding region covering 816 bp was cloned and polyclonal anti-APMCF1 antibody was prepared successfully. The immunohistochemistry study showed that APMCF1 had a strong expression in colon cancer.

CONCLUSION: APMCF1 may be the gene coding human signal recognition particle receptor β and belongs to the small-G protein superfamily. Its strong expression pattern in colon cancer suggests it may play a role in colon cancer development.

Yan W, Wang WL, Zhu F, Chen SQ, Li QL, Wang L. Isolation of a novel member of small G protein superfamily and its expression in colon cancer. *World J Gastroenterol* 2003; 9(8): 1719-1724
http://www.wjgnet.com/1007-9327/9/1719.asp

INTRODUCTION

Apoptosis or programmed cell death (PCD) is a form of cell death in human and other multicellular organisms[1-15]. It is a genetically controlled program of cellular selfdestruction, which is of central importance to the development and homeostasis of almost all animals, and also a highly regulated process involving a large number of genes that are conserved in all metazoans. A variety of genes have been found to take part in the process of apoptosis, such as the TNF/FasL family, the Bcl-2 family, the ICE/CED-3 family, oncogenes, tumor suppressor genes and the genes encoding heat shock proteins[16-24]. APMCF1 is a novel human gene fragment we cloned in 1999. Its transcript was found to be up-regulated in apoptotic MCF-7 cells, which might play a role in apoptosis of tumor cells[25]. As its 5' end is not complete, the functional study of this gene has not been performed. In order to learn more about this gene' s biological functions, we extended its 5' cDNA end and found it was a gene homologous to mouse SRβ. Then polyclonal antibody against this gene' s product was prepared and protein expression of APMCF1 in human colon cancer and normal colonic mucosa was examined with immunohistochemistry method.

MATERIALS AND METHODS

Main reagents

Reverse transcription kit was from TaKaRa. Pfu and Tf1 Taq DNA polymerase were from Promega. TRIzol Reagent was from Gibco. Retinoid acid (RA) was from Sigma.

Cell lines and specimens

MCF-7 cell line was kept by our lab oratory and maintained in DMEM medium supplemented with 100 mL/L fetal bovine serum. The cells were induced to apoptosis by RA with the method described before[25]. Fifty five tissue specimens of colon cancer and 5 tissue specimens of normal colonic mucosa were obtained from surgically resected tissues of patients with hepatocellular carcinoma in Xijing Hospital of Fourth Military Medical University. The tumor tissues consisted of 25 well-differentiated, 23 moderately differentiated, and 7 poorly differentiated colon cancer specimens, All the tissues were fixed in 100mL/L buffered formalin phosphate and embedded in paraffin wax.

5' RACE

A human EST named AGENCOURT_8343738 was initially identified with APMCF1 cDNA sequence(AF141882) by running a BLASTN search against the public database of ESTs (dbEST). It shared 98 % identification with APMCF1 but had more than 325 nucleotide acids at the 5' end. Then we designed a reverse transcription primer against this sequence. The total RNA extracted from the apoptotic MCF-7 cells with TRIzol reagent according to the manufacturer' s instructions was used as reverse transcription template. While transcription, 5' cap sequence was added according to the protocol of SMART™ PCR cDNA synthesis kit (Clontech). RT-PCR was

performed using the cap sequence as a sense primer, reverse transcription primer as a antisense primer. The sequences of the primers were as follows: sense primer (cap sequence), 5' TACGGCTGCGAGAAGACGACAGAA 3', and antisense primer, 5' CAGGCAATTTTAGCCAGCCATTT 3' (reverse transcription primer). A total of 30 cycles of PCR reactions were performed: at 95 ℃ for 15 s, at 68 ℃ for 5 min. Then 5 μL PCR products was extracted as a template for the next 30 cycles with the same PCR parameters. The resulting PCR fragment (810 bp) was subcloned into the pEGM-T easy vector (Promega) for sequencing.

Bioinformatics

The fragment of 810 bp was used as a bait to search the Genbank database and a homologous sequence FLJ14619 was found. Then all these ESTs were retrieved and a coontig was assembled from overlapping ESTs. A full length cDNA sequence of APMCF1 was obtained and identified in human genomic database. The putative cleavage site of the signal peptide was predicted by using Signal P server (http://www.cbs.dtu.dk/services/Signal P). The gene localization of APMCF1 on the chromosome was analyzed with the HTGS database (http://www.ncbi.nlm.nih.gov).

Construction of recombinant pGEX-APMCF1

The entire APMCF1 coding region was amplified by PCR by using upstream and downstream primers, which introduce a *Bam*HI and *Sal* I site respectively according to the conjunct sequence. The sequences of the primers were as follows: sense primer, 5' AGGATCCTCATCCATGGCTTCCG 3', and antisense primer, 5' ACGCGTCGACCTGCCTCTCAGGCAAT 3'. The PCR product was cloned into the pGEM-T easy vector for sequencing. Then the fragment containing the ORF of APMCF1 was released from the recombinant plasmid by cutting with *Bam*HI and *Sal* I, and subcloned into the prokaryotic expression vector pGEX-KG. The recombinant plasmid was termed pGEX-APMCF1.

Preparation of polyclonal antibody to APMCF1

The GST-APMCF1 fusion protein was expressed in *E. coli* DH5α and purified on glutathione-Sepharose 4B according to the manufacturer's instructions. After the purified protein was separated by 100 g/L sodium dodecylsulfate-poluacrylamide gel electrophoresis (SDS-PAGE), it was then transferred from the gel to nitrocellulose. The specific strip corresponding to the antigenic protein was excised and cut into very small pieces for immunizing rabbits. The specificity of the anti-APMCF1 antibodies was identified by Western blot.

Immunohistochemical staining

All the colon cancer specimens were fixed in 100 mL/L buffered formalin and embedded in paraffin. ABC technique was adopted for immunohistochemical staining. Briefly, deparaffinized sections were treated with 30 mL/L H_2O_2 in methanol for 30 minutes to abolish the endogenous peroxidase activity. Sections were further blocked with 10 mL/L normal goat serum for 0.5 hour, followed by incubation with polyclonal rabbit anti-APMCF1 serum (1:100) at 4 ℃ overnight. The sections were then washed in phosphate buffer solution (PBS) (0.01 mol/L, pH 7.2) and sequentially incubated with biotinylated goat anti-rabbit IgG followed by avidin-biotin horseradish peroxidase complex following the manufacturer's instructions (ABC kit, Sigma. USA). Staining was developed by immersing slides in 0.5 g/L diaminobenzidine tetrahydrochloride (DAB) with 3.3 g/L hydrogen peroxide. All slides were counterstained with haematoxylin, dehydrated and mounted. PBS substituting for the primary antibody was used as the negative control.

The intensity of staining for APMCF1 in colon cancer tissues and normal colonic mucosa tissues was scored for each specimen on a scale of 0 to 3, in which 0=negative staining, 1=weakly positive staining, 2=moderately positive staining, and 3=strongly positive staining. The percentage of positive cells in each specimen was estimated and scored on a scale of 0 to 4, in which 0=negative, 1=positive staining in 1 % to 25 % of cells counted, 2 in 26 % to 50 %, 3 in 51 % to 75 %, and 4 in 76 % to 100 %. Each section was evaluated for the sum of these two parameters. Group means of expression scores of APMCF1 antigens were compared by using ANOVA followed by Fisher's protected *t* test. $P<0.05$ was considered statistically significant.

RESULTS

Identification of human APMCF1

With 5' RACE and assembled homologous ESTs, the 5' end of original APMCF1 cDNA sequence was extended successfully. The length of new sequence was 1 745 bp. It was mapped to chromosome 3q22.2 and spanned at least 14.8 kb of genomic DNA with seven exons and six introns contained. Sequence analysis revealed that APMCF1 encoded a protein of 271 aa, with an ATG initiation codon at nt 17-19. The deduced APMCF1 protein contained no putative N-glycosylation site, and no typical signal cleavage site was revealed by searching on the signal P server. There was a transmembrane helice from 37 aa to 54 aa predicted by the method of TMpred. It contained a small GTP-binding protein (G proteins) domain and it was homologous to mouse signal recognition particle receptor β(SRβ) both in nucleic acid and amino acid sequence by 86 % and 89 % respectively. Further analysis showed that APMCF1 protein was homologous to gene products of SRβ from species ranging from mice to yeast. This indicated that APMCF1 protein was a human SRβ gene and also was a well conserved protein (Figure 1).

Identification of polyclonal antibody to APMCF1

To detect APMCF1 protein, we generated anti-human APMCF1 antibody by immunizing rabbit with the purified GST-APMCF1 fusion protein. On immunoblots, this anti-APMCF1 antibody specifically recognized GST-APMCF1 fusion protein, the dominant band was the expected 56-ku molecular size. No band was evident in the blot of the same samples using a preimmune rabbit serum. When the antibody was preabsorbed with GST-APMCF1 fusion protein, the corresponding band was no longer observed, confirming the antibody specificity (Figure 2).

Expression of APMCF1 in colon cancer

Fifty five cases of colon cancer tissues and 5 cases of normal colonic mucosa were examined for expression of APMCF1 by using immunohistochemistry. Specific cytoplasmic staining for APMCF1 was observed in 44 out of 55 cases of carcinomas (80 %) and 4 out of 5 normal mucosa. All of the positive samples had cytoplasmic staining, suggesting that APMCF1 might be a cytoplasmic protein. The positive ratios of APMCF1 in well-differentiated, moderately differentiated, and poorly differentiated carcinomas were 80 %, 74 % and 86 % respectively. A significantly high expression level of APMCF1 was found in poorly and moderately differentiated colon cancer, compared with that of normal tissue (Figures 3). There were also differences between different histological grades of colon cancer, but these differences did not reach statistical significance (Table 1).

A

```
                                                    a cca cgc gtc tca tcc
17   atg gct tcc gcg gac tcg cgc cgg gtg gca gat ggc ggc ggt gcc
      M   A   S   A   D   S   R   R   V   A   D   G   G   G   A
62   ggg ggc acc ttc cag ccc tac cta gac acc ttg cgg cag gag ctg
      G   G   T   F   Q   P   Y   L   D   T   L   R   Q   E   L
107  cag cag acg gac cca acg ctg ttg tca gta gtg gtg gcg gtt ctt
      Q   Q   T   D   P   T   L   L   S   V   V   V   A   V   L
152  gcg gtg ctg ctg acg cta gtc ttc tgg aag tta atc cgg agc aga
      A   V   L   L   T   L   V   F   W   K   L   I   R   S   R
197  agg agc agt cag aga gct gtt ctt ctt gtt ggc ctt tgt gat tcc
      R   S   S   Q   R   A   V   L   L   V   G   L   C   D   S
242  ggg aaa acg ttg ctc ttt gtc agg ttg tta aca ggc ctt tat aga
      G   K   T   L   L   F   V   R   L   L   T   G   L   Y   R
287  gac act cag acg tcc att act gac agc tgt gct gta tac aga gtc
      D   T   Q   T   S   I   T   D   S   C   A   V   Y   R   V
332  aac aat aac agg ggc aat agt ctg acc ttg att gac ctt ccc ggc
      N   N   N   R   G   N   S   L   T   L   I   D   L   P   G
377  cat gag agt ttg agg ctt cag ttc tta gag cgg ttt aag tct tca
      H   E   S   L   R   L   Q   F   L   E   R   F   K   S   S
422  gcc agg gct att gtg ttt gtt gtg gat agt gca gca ttc cag cga
      A   R   A   I   V   F   V   V   D   S   A   A   F   Q   R
467  gag gtg aaa gat gtg gct gag ttt ctg tat caa gtc ctc att gac
      E   V   K   D   V   A   E   F   L   Y   Q   V   L   I   D
512  agt atg ggt ctg aag aat aca cca tca ttc tta ata gcc tgc aat
      S   M   G   L   K   N   T   P   S   F   L   I   A   C   N
557  aag caa gat att gca atg gca aaa tca gca aag tta att caa cag
      K   Q   D   I   A   M   A   K   S   A   K   L   I   Q   Q
602  cag ctg gag aaa gaa ctc aac acc tta cga gtt acc cgt tct gct
      Q   L   E   K   E   L   N   T   L   R   V   T   R   S   A
647  gcc ccc agc aca ctg gac agt tcc agc act gcc cct gct cag ctg
      A   P   S   T   L   D   S   S   S   T   A   P   A   Q   L
692  ggg aag aaa ggc aaa gag ttt gaa ttc tca cag ttg ccc ctc aaa
      G   K   K   G   K   E   F   E   F   S   Q   L   P   L   K
737  gtg gag ttc ctg gag tgc agt gcc aag ggt gga aga ggg gac gtg
      V   E   F   L   E   C   S   A   K   G   G   R   G   D   V
782  ggc tct gct gac atc cag gac ttg gag aaa tgg ctg gct aaa att
      G   S   A   D   I   Q   D   L   E   K   W   L   A   K   I
827  gcc tga gag gca gct cta aag cac aag acc tgg atg tgt gac aca
      A   *
872  cag ttt tgg aaa aag gtc tgt ggt agt ctg gag ttg atg agg aag
917  ggg tac aag atg tgg tta gaa aca ttt ctt tgt tct gga aac aaa
962  gta ctg ttg aaa cca gct tgg aat ttt ttt ttt ttt ttt ttt taa
1007 gtt cag ttc tcc ctt atg gct gcc ttt caa aca agt acc ttt tat
1052 ctg atg cct gta tct tcc ctt tgt taa ggt gta act tga tgt agg
1097 gtc aag gtt ttt gtg aca aca ggc aga ctc cac aca gag agg ata
1142 tga tga gaa tat ggc cat cac ctg aaa agt ttt ctt atc ttc tgt
1187 gct ttt ggt ccc tgg aaa caa atc cgc cta tgt atg aag cta gtt
1232 gat ttc cag ttg cac tat ttc cag ttg cct ctg aag ttc aca ggc
1277 aat aca ttg tct agt cct ttg cga att tct ctg att tgt ggg cac
1322 agt tat gaa gtt tcc cca cat gtg aag aca ggt aca aaa tag cag
1367 agc caa gca gac agt ggg tct att ctt cat tag ctc agt gac ttg
1412 tcc aca ctc gtc tta gca ctt acg ttt caa aag ctt gtc aca aac
1457 cct tgg agt cat tcc cag ata ata gaa ctg gaa atg ata aat ccc
1502 cta atg cca agg gtc tag tgt gtt ctt agt ggt tat act ggg aag
1547 tgt gtg gag att tag gtg ctg ctc tgc tgc tct gga tgg ctg aag
1592 gct cct ggg cca tct tca tgt gct gct tga aga gct cct att ttg
1637 tac tcc tgg cta gaa tgc tgt gga aca aat aca aag tga aaa aag
1682 ttc tct gta gat ttc tga agt gca tat tca ttg atg cca aga aaa
1727 aaa aaa agt tgc ctt ttt g
```

B

```
APMCF1       (1) MASADSRRVADGGGAGGTFQPYLDTLRQELQQTDPTLLSVVVAVLAVLLT
Mouse        (1) MASANTRRVGDG--AGGAFQPYLDSLRQELQQRDPTLLSVAVALLAVLLT
C. elegan    (1) -------------------------MDKIDFNDPTTLAVLATAVIGLLT
Drosophila   (1) -----MDKLNEN-----ARQ------RKQIKLGEIDTGPIIVALLLGFIA
Saccharomyces(1) -------------------------MLSNTLIIACLLVIGTTIALIAVQ

APMCF1      (51) LVFWKLIRSRRSSQRAVLLVGLCDSGKTLLFVRLLT--GLYRDTQTSITD
Mouse       (49) LVFWKFIWSRKSSQRAVLFVGLCDSGKTLLFVRLLT--GQYRDTQTSITD
C. elegan   (25) VLLLVLKSFASSNKNRVLFVGLMDCGKTTIFTQLSQKEAEYPTTTKTYTS
Drosophila  (35) VAIFVILRRRSAGRKDFLLTGLSESGKSAIFMQLIH--GKFPATFTSIKE
Saccharomyces(25) KASSKTGIKQKSYQPSIIIAGPQNSGKTSLLTLLTT--DSVRPTVVSQEP

APMCF1      (99) SCAVYRVNNNRGNSLTLIDLPGHESLRLQFLERFKSS---AGAIVFVVDS
Mouse       (97) SSAIYKVNNNRGNSLTLIDLPGHESLRFQLLDRFKSS---ARAVVFVVDS
C. elegan   (75) MVENKITLRIKDKEKEIIDYPGNDRLRQKLIENHLHSR-SLLRIVFVVDS
Drosophila  (83) NVGDYRTG-S--ASARLVDIPGHYRVRDKCLELYKHR---AKGIVFVVDS
Saccharomyces(73) LSAADYDG----SGVTLVDFPGHVKLRYKLSDYLKTRAKFVKGLIFMVDS

APMCF1     (146) AAFQREVKDVAEFLYQVLIDSMG-LKNTPSFLIACNKQDIAMAKSAKLIQ
Mouse      (144) AAFQREVKDVAEFLYQVLIDSMA-LKNSPSLLIACNKQDIAMAKSAKLIQ
C. elegan  (124) AAFSKNARDVAELFYTVALEN----VDKVPILIACHKQDLSLAKTEKVIR
Drosophila (127) VTAHKDIRDVADFLYTILSDS---ATQPCSVLVLCNKQDQTTAKSAQVIK
Saccharomyces(119) TVDPKKLTTTAEFLVDILSITESSCENGIDILIACNKSELFTARPPSKIK

APMCF1     (195) QQLEKELNTLRVTRS-----AAPSTLYSSSTAPAQLGKKGKE-FEFSQLP
Mouse      (193) QQLEKELNTLRVTRS-----AAPSTLDSSSTAPAQLGKKGKE-FEFSQLP
C. elegan  (170) NSLEKEIGLINKSRA-----AALIGTDGSEEKRSTLTDTGID-FKWEDLK
Drosophila (174) SLLESELHTVRDTRSR----KLQSVGDEDGSKSITLGKPGRD-FEFSHIA
Saccharomyces(169) DALESEIQKVIERRKKSLNEVERKINEEDYAENTLDVLQSTDGFKFANLE

APMCF1     (239) -LKVEFLECSAKGGRGDVGSADIQDLEKWLAKIA
Mouse      (237) -LKVEFLECSAKGGRGDTGSADIQDLEKWLAKIA
C. elegan  (214) KQEVSFVSTSSNSE--DFG---VHEIASFVRA--
Drosophila (219) -QNIQFAEASAK----DT---ELDPLTDWLARLL
Saccharomyces(219) ASVVAFEGSINK----RK----ISQWREWIDEKL
```

Figure 1 Nucleotide and Predicted Amino Acid Sequence of the APMCF1 cDNA and sequence alignment of APMCF1 wth the protein from other species. A: The full-length gene sequence and amino acids sequence of APMCF1; B: Alignment was done by using the Align software in Vector NTI. Dark gray background shows identity with at lease five aligned residues in different species. The gray region represents the sequence conserved among different species.

Table 1 Expression of APMCF1 in colon cancer and normal colon

Histological type	*n*	Expression of APMCF1	Positive rate (%)
A) Well differentiated	25	4.20±1.02	80
B) Moderately differentiated	23	4.78±1.10	74
C) Poorly differentiated	7	5.18±1.89	86
D) Normal	5	3.84±1.73	80

Expression score (mean ± SE) in different histological grades of colon cancer and normal colon tissue. Statistically significant differences: B *versus* D, $P<0.05$; C *versus* D, $P<0.01$.

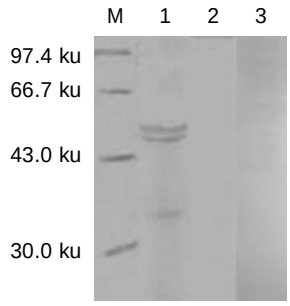

Figure 2 Immunoblotting of APMCF1 in GST-APMCF1 (56 ku) using antiserum, normal rabbit serum before immunization and antiserum preabsorbed with GST-APMCF1. M: Protein marker; 1: antiserum; 2: rabbit serum before immune from GST-APMCF1; 3: antiserum absorbed in the peptides used for immunization (control antibody).

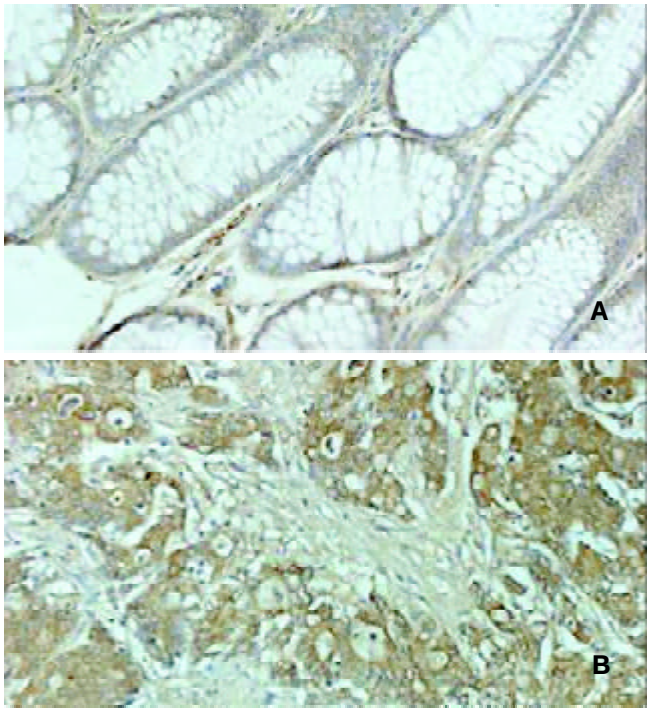

Figure 3 Expression of AMPCF1 in normal colon tissue and colon cancer (×200). A. Normal colon tissue; B. Colon cancer.

DISCUSSION

We have successfully extended the 5' end of APMCF1. The new sequence contains an open-reading frame of 816 bp that encodes a protein with a predicted molecular mass of 30ku. By searching the GenBank, it was found that the amino acid sequence of APMCF1 was homologous to mouse signal recognition particle receptor β(SRβ) and conserved in several other species, including *Caenorhabditis elegans*, *Saccharomyces cerevisia* and *Drosophila melanogaster*. This indicates that APMCF1 is likely a human SRβ gene and also a well conserved protein. The conservation of APMCF1 implies that it may have a very important function, since it remains stable during the evolution of species[26,27].

The mammalian SRP receptor, also known as docking protein, is composed of two subunits, SRα and SRβ. Based on the study results in mouse and canine, both of them are required to target nascent secretory and membrane proteins to the membrane of endoplasmic reticulum (ER). SRβ anchors alpha subunit to the ER membrane during this course[26,28-30]. The result of conserved domain searching showed that APMCF1 containd a GTPase domain closely related to ADP-ribosylation factor family (ARF) and Sar1p-like members of the Ras-family of small GTPases, suggesting it belongs to the small GTP-binding protein (G proteins) superfamily[31-36].

Over 100 members of the Ras superfamily of GTPases have been found so far. Based on both their sequence homology and function, they have been subdivided into at least six families: Ras, Rho, Rab, Arf, Ran, and Rad/Gem[37-42]. Each family, in turn, is comprised of several members with distinct expression, cellular localization and biological activities. Among these members, both Ras and Rho GTPases can mediate key cellular processes in response to diverse stimuli, such as cell growth, apoptosis, lipid metabolism, cytoarchitecture, membrane trafficking, and transcriptional regulation. The Rab and Sar1/Arf families regulate vesicle trafficking, and the Ran family regulates nucleocytoplasmic transport and microtubule organization. However, the negative aspect of these multifunctional proteins arises in the context of scenarios that cause their constitutive activation (i.e. point mutations or overexpression) and render them insensitive to regulatory signals. In this case, these GTPases trigger specific signals that lead to uncontrolled cell growth, enhanced angiogenesis, inhibition of apoptosis, and genetic instability, all of which result in tumor development[43-48].

From the analysis of bioinfomatics we can see that APMCF1 might be a new member of small-G protein superfamily. It may have the potential function to regulate the survival, proliferation, differentiation and apoptosis of cells as well as other small-G protein members such as Ras and Rho. Preliminary studies also showed that transcripts of APMCF1 were up-regulated in apoptotic MCF-7 cells, indicating it might play a role in apoptosis of tumor cells. So it is necessary to know expression pattern of APMCF1 in various tissues, especially in tumors. In the present study, APMCF1 was expressed highly in poorly and moderately differentiated colon cancers compared with that in normal colon mucosa, perhaps indicating its possible biological function in tumor development. It is early to say there are some relationship between the expression of APMCF1 and tumorigenesis before further study has been done. But it will be very interesting and worthy to further study these aspects in the future.

REFERENCES

1 **Lan J**, Xiong YY, Lin YX, Wang BC, Gong LL, Xu HS, Guo GS. *Helicobacter pylori* infection generated gastric cancer through p53-Rb tumor-suppressor system mutation and telomerase reactivation. *World J Gastroenterol* 2003; **9**: 54-58

2 **Guo XZ**, Shao XD, Liu MP, Xu JH, Ren LN, Zhao JJ, Li HY, Wang D. Effect of bax, bcl-2 and bcl-xL on regulating apoptosis in tissues of normal liver and hepatocellular carcinoma. *World J Gastroenterol* 2002; **8**: 1059-1062

3 **Hengartner MO**. The biochemistry of apoptosis. *Nature* 2000; **407**: 770-776

4 **Li HL**, Chen DD, Li XH, Zhang HW, Lu YQ, Ye CL, Ren XD.

Changes of NF-kB, p53, Bcl-2 and caspase in apoptosis induced by JTE-522 in human gastric adenocarcinoma cell line AGS cells: role of reactive oxygen species. *World J Gastroenterol* 2002; **8**: 431-435

5 **Qin LX**, Tang ZY. The prognostic molecular markers in hepatocellular carcinoma. *World J Gastroenterol* 2002; **8**: 385-392

6 **Javelaud D**, Besancon F. Inactivation of p21WAF1 sensitizes cells to apoptosis via an increase of both p14ARF and p53 levels and an alteration of the Bax/Bcl-2 ratio. *J Biol Chem* 2002; **277**: 37949-37954

7 **Huang ZH**, Fan YF, Xia H, Feng HM, Tang FX. Effects of TNP-470 on proliferation and apoptosis in human colon cancer xenografts in nude mice. *World J Gastroenterol* 2003; **9**: 281-283

8 **Chen G**, Goeddel DV. TNF-R1 signaling: a beautiful pathway. *Science* 2002; **296**: 1634-1635

9 **Shi M**, Wang FS, Wu ZZ. Synergetic anticancer effect of combined quercetin and recombinant adenoviral vector expressing human wild-type p53, GM-CSF and B7-1 genes on hepatocellular carcinoma cells *in vitro*. *World J Gastroenterol* 2003; **9**: 73-78

10 **Hatoum A**, El-Sabban ME, Khoury J, Yuspa SH, Darwiche N. Overexpression of retinoic acid receptors alpha and gamma into neoplastic epidermal cells causes retinoic acid-induced growth arrest and apoptosis. *Carcinogenesis* 2001; **22**: 1955-1963

11 **Daigle JL**, Hong JH, Chiang CS, McBride WH. The role of tumor necrosis factor signaling pathways in the response of murine brain to irradiation. *Cancer Res* 2001; **61**: 8859-8865

12 **Yu JL**, Rak JW, Coomber BL, Hicklin DJ, Kerbel RS. Effect of p53 status on tumor response to antiangiogenic therapy. *Science* 2002; **295**: 1526-1528

13 **Holtzman MJ**, Green JM, Jayaraman S, Arch RH. Regulation of T cell apoptosis. *Apoptosis* 2000; **5**: 459-471

14 **Afford S**, Randhawa S. Apoptosis. *Mol Pathol* 2000; **53**: 55-63

15 **Liu JW**, Tang Y, Shen Y, Zhong XY. Synergistic effect of cell differential agent-II and arsenic trioxide on induction of cell cycle arrest and apoptosis in hepatoma cells. *World J Gastroenterol* 2003; **9:** 65-68

16 **Urquhart JL**, Meech SJ, Marr DG, Shellman YG, Duke RC, Norris DA. Regulation of Fas-mediated apoptosis by N-ras in melanoma. *J Invest Dermatol* 2002; **119**: 556-561

17 **Nikitin AY**, Liu CY, Flesken-Nikitin A, Chen CF, Chen PL, Lee WH. Cell lineage-specific effects associated with multiple deficiencies of tumor susceptibility genes in Msh2(-/-)Rb(+/-) mice. *Cancer Res* 2002; **62**: 5134-5138

18 **Suzuki Y**, Honma T, Hayashi S, Ajioka Y, Asakura H. Bcl-2 expression and frequency of apoptosis correlate with morphogenesis of colorectal neoplasia. *J Clin Pathol* 2002; **55**: 212-216

19 **Schmitz I**, Kirchhoff S, Krammer PH. Regulation of death receptor-mediated apoptosis pathways. *Int J Biochem Cell Biol* 2000; **32**: 1123-1136

20 **Chen Y**, Wu Q, Song SY, Su WJ. Activation of JNK by TPA promotes apoptosis via PKC pathway in gastric cancer cells. *World J Gastroenterol* 2002; **8**: 1014-1018

21 **Cohen O**, Kimchi A. DAP-kinase: from functional gene cloning to establishment of its role in apoptosis and cancer. *Cell Death Differ* 2001; **8**: 6-15

22 **Baliga BC**, Kumar S. Role of Bcl-2 family of proteins in malignancy. *Hematol Oncol* 2002; **20**: 63-74

23 **Broceno C**, Wilkie S, Mittnacht S. RB activation defect in tumor cell lines. *Proc Natl Acad Sci U S A* 2002; **99**: 14200-14205

24 **Neurath MF**, Finotto S, Fuss I, Boirivant M, Galle PR, Strober W. Regulation of T-cell apoptosis in inflammatory bowel disease: to die or not to die, that is the mucosal question. *Trends Immunol* 2001; **22**: 21-26

25 **Yan W**, Li Q, Zhu F. Apoptosis-related genes cloned by improved subtractive hybridization. *Zhonghua Zhongliu Zazhi* 2001; **23**: 193-195

26 **Miller JD**, Tajima S, Lauffer L, Walter P. The beta subunit of the signal recognition particle receptor is a transmembrane GTPase that anchors the alpha subunit, a peripheral membrane GTPase, to the endoplasmic reticulum membrane. *J Cell Biol* 1995; **128**: 273-282

27 **Boettner B**, Van Aelst L. The role of Rho GTPases in disease development. *Gene* 2002; **286**: 155-174

28 **Hortsch M**, Labeit S, Meyer DI. Complete cDNA sequence coding for human docking protein. *Nucleic Acids Res* 1988; **16**: 361-362

29 **Exton JH**. Regulation of phospholipase D. *FEBS Lett* 2002; **531**: 58-61

30 **Ehrhardt A**, Ehrhardt GR, Guo X, Schrader JW. Ras and relatives-job sharing and networking keep an old family together. *Exp Hematol* 2002; **30**: 1089-1106

31 **Vaidehi N**, Floriano WB, Trabanino R, Hall SE, Freddolino P, Choi EJ, Zamanakos G, Goddard WA 3rd. Prediction of structure and function of G protein-coupled receptors. *Proc Natl Acad Sci U S A* 2002; **99**: 12622-12627

32 **Bacher G**, Pool M, Dobberstein B. The ribosome regulates the GTPase of the beta-subunit of the signal recognition particle receptor. *J Cell Biol* 1999; **146**: 723-730

33 **Larsen N,** Samuelsson T, Zwieb C. The Signal Recognition Particle Database (SRPDB). *Nucleic Acids Res* 1998; **26**: 177-178

34 **Bacher G**, Lutcke H, Jungnickel B, Rapoport TA, Dobberstein B. Regulation by the ribosome of the GTPase of the signal-recognition particle during protein targeting. *Nature* 1996; **381**: 248–251

35 **Alto NM**, Soderling J, Scott JD. Rab32 is an A-kinase anchoring protein and participates in mitochondrial dynamics. *J Cell Biol* 2002; **158**: 659-668

36 **Raugei G**, Ramponi G, Chiarugi P. Low molecular weight protein tyrosine phosphatases: small, but smart. *Cell Mol Life Sci* 2002; **59**: 941-949

37 **Shimada J**, Shakhnovich EI. The ensemble folding kinetics of protein G from an all-atom Monte Carlo simulation. *Proc Natl Acad Sci U S A* 2002; **99**: 11175-11180

38 **Lambert JM**, Lambert QT, Reuther GW, Malliri A, Siderovski DP, Sondek J, Collard JG, Der CJ. Tiam1 mediates Ras activation of Rac by a PI (3) K-independent mechanism. *Nat Cell Biol* 2002; **4**: 621-625

39 **Malumbres M**, Pellicer A. RAS pathways to cell cycle control and cell transformation. *Front Biosci* 1998; **3**: d887-912

40 **Bar-Sagi D**, Hall A. Ras and Rho GTPases: a family reunion. *Cell* 2000; **103**: 227-238

41 **Henriksson ML**, Sundin C, Jansson AL, Forsberg A, Palmer RH, Hallberg B. Exoenzyme S shows selective ADP-ribosylation and GTPase-activating protein (GAP) activities towards small GTPases *in vivo*. *Biochem J* 2002; **367**(Pt 3): 617-628

42 **Thompson PW**, Randi AM, Ridley AJ. Intercellular adhesion molecule (ICAM)-1, but not ICAM-2, activates RhoA and stimulates c-fos and rhoA transcription in endothelial cells. *J Immunol* 2002; **169**: 1007-1013

43 **Aresta S**, De Tand-Heim MF, Beranger F, De Gunzburg J. A novel Rho GTPase-activating-protein interacts with Gem, a member of the Ras superfamily of GTPases. *Biochem J* 2002; **367**(Pt 1): 57-65

44 **Neves SR**, Ram PT, Iyengar R. G protein pathways. *Science* 2002; **296**: 1636-1639

45 **Aznar S**, Lacal JC. Rho signals to cell growth and apoptosis. *Cancer Lett* 2001; **165**: 1-10

46 **Price LS**, Collard JG. Regulation of the cytoskeleton by Rho-family GTPases:implications for tumour cell invasion. *Semin Cancer Biol* 2001; **11**: 167-173

47 **Hall A**. Rho GTPases and the actin cytoskeleton. *Science* 1998; **279**: 509-514

48 **Takai Y**, Sasaki T, Matozaki T. Small GTP-binding proteins. *Physiol Rev* 2001; **81**: 153-208

Edited by Zhu LH

P.O.Box 2345, Beijing 100023,China
Fax: +86-10-85381893
E-mail: wjg@wjgnet.com www.wjgnet.com

World J Gastroenterol 2003;9(8):1725-1728
World Journal of Gastroenterology
 ISSN 1007-9327

• COLORECTAL CANCER •

Effect of retinoic acid on cell proliferation kinetics and retinoic acid receptor expression of colorectal mucosa

Hong-Bo Wei, Xiao-Yan Han, Wei Fan, Gui-Hua Chen, Ji-Fu Wang

Hong-Bo Wei, Xiao-Yan Han, Department of Gastrointestinal Surgery, The Third Affiliated Hospital, Sun Yat-Sen University, Guangzhou 510630, China
Wei Fan, Department of Nuclear Medicine, Cancer Center, Sun Yat-Sen University, Guangzhou 510060, China
Gui-Hua Chen, Ji-Fu Wang, Department of Gastrointestinal Surgery, The First Affiliated Hospital, Sun Yat-Sen University, Guangzhou 510080, China
Supported by Natural Science Foundation of Guangdong Province, No.010742
Correspondence to: Dr. Hong-Bo Wei, Department of Gastrointestinal Surgery, The Third Affiliated Hospital, Sun Yat-Sen University, Guangzhou 510630, China. drwhb@21cn.com
Telephone: +86-20-85516867 Ext 2228
Received: 2002-08-24 **Accepted:** 2003-02-11

Abstract

AIM: To investigate the effect of retinoic acid (RA) on cell proliferation kinetics and retinoic acid receptor (RAR) expression of colorectal mucosa.

METHODS: One hundred sixty healthy male Wistar rats were randomly divided into 4 groups. Rats in groups I and II were subcutaneously injected with dimethylhydrazine (DMH) (20 mg/kg, once a week,) for 7 to 13 weeks, while groups III and IV were injected with normal saline. Rats in groups II and III were also treated with RA (50 mg/kg, every day, orally) from 7th to 15th week, thus group IV was used as a control. The rats were killed in different batches. The expressions of proliferating cell nuclear antigen (PCNA), nucleolar organizer region-associated protein (AgNOR) and RAR were detected.

RESULTS: The incidence of colorectal carcinoma was different between groups I (100 %) and II (15 %) (P<0.01). The PCNA indices and mean AgNOR count in group II were significantly lower than those in group I (F=5.418 and 4.243, P<0.01). The PCNA indices and mean AgNOR count in groups I and II were significantly higher than those in the groups III and IV (in which carcinogen was not used) (F=5.927 and 4.348, P<0.01). There was a tendency in group I that the longer the induction with DMH the higher PCNA index and AgNOR count expressed (F=7.634 and 6.826, P<0.05). However, there was no such tendency in groups II, III and IV (F=1.662 and 1.984, P>0.05). The levels of RAR in normal and cancerous tissues in groups treated with RA were significantly higher than those in groups not treated with RA (F=6.343 and 6.024, P<0.05).

CONCLUSION: RA decreases the incidence of colorectal carcinoma induced by DMH. Colorectal cancer tissue is associated with abnormal expression of PCNA, AgNOR and RAR. RA inhibits the expression of PCNA and AgNOR, and increases RAR concentration in colorectal tissues.

Wei HB, Han XY, Fan W, Chen GH, Wang JF. Effect of retinoic acid on cell proliferation kinetics and retinoic acid receptor expression of colorectal mucosa. *World J Gastroenterol* 2003; 9(8): 1725-1728
http://www.wjgnet.com/1007-9327/9/1725.asp

INTRODUCTION

The occurrence and development of colorectal carcinoma usually need a long and multistep process. Intervention treatment to block the canceration course from precancerous lesion of colorectal carcinoma is an important step to decrease the incidence of colorectal carcinoma. Some results obtained from *in vitro* experiments have shown that retinoic acid (RA) plays a role in blocking canceration induced by carcinogen and promotes normal differentiation of leucocythemia cells[1-3]. However, the effect of RA on colorectal carcinoma, especially on cell proliferation kinetics and the expression of retinoic acid receptor (RAR) of colorectal mucosa, has not be reported. To provide theoretic data on prevention and treatment of colorectal carcinoma, we investigated the effect of RA on cell proliferation kinetics and expression of RAR of colorectal mucosa.

MATERIALS AND METHODS

Animals and groups

One hundred sixty healthy male Wistar rats (body weight 134±12 g) were randomly divided into 4 groups. There were 40 rats in each group. Rats in group I and II were subcutaneously injected with dimethylhydrazine (DMH) (20 mg/kg, once a week,) for 7 to 13 weeks, while groups III and IV were injected with normal saline. Rats in groups II and III were treated with RA (50 mg/kg, every day, orally) from 7th to 15th week, group IV was used as a control. Eight rats in each group were killed randomly at 7th, 14th and 21st week in each group. The other rats were killed at 28th week. The number of colorectal carcinoma lesions was examined, and the normal colorectal tissues were also collected. The colorectal samples were fixed with 10 % formalin and embedded in paraffin. The expression of proliferating cell nuclear antigen (PCNA) and nucleolar organizer region-associated protein (AgNOR) was studied.

Detection of PCNA and AgNOR

Normal colorectal tissues (n=8) and the colorectal tissues (n=8) free of cancer induced by DMH after 7, 14, 21 and 28 weeks, were included. The samples including well-differentiated adenocarcinoma (n=8) and poorly differentiated adenocarcinoma (n=8) were also collected.

The immunohistochemical staining method was used to detect PCNA indices[4-7]. Representative regions with a double blind method were selected, and at least 1 000 cells were counted. The rates of positive cells over total cells counted were defined as the PCNA indices. Ploton one-step method was used for the detection of AgNOR count[8-11].

Detection of retinoic acid receptor (RAR)

Specimen disposal The mesentery tissues were removed and

part of the colorectal tissues was cut to pieces and placed in DMEM buffer. A tissue was homogenated by a high speed disperser, 4 000 r.min^{-1} for 10 min and a homogenizer 4 000 r.min^{-1} for 30 min and then by centrifugation 1 000 r. min^{-1} for 30 min. The buffer was added to the deposit, and the suspension was centrifugated, 750 r. min^{-1}for 15 min. Finally, the deposit was made to nucleus fluid. DNA concentration was determined by the dimethylamine method. The rest part of tissues was treated with liguid nitrogen and preserved in an ultra cold storage freezer.

Receptor radio-ligand binding test[16-20] All the procedures of the test were carried out at 4 ℃. 0.1 ml of nucleus fluid and 0.05 ml of 3H-atRA (2×10^{-6} mol/L) and 0.05 ml of buffer were mixed at different concentrations (the end concentration was 0.1-10 nM, with 6 concentration points). At the same time, the control test tube of non-specific binding was 200-time of unlabelled 9-cis-atRA. After 20 h, the reaction mixture was filtered with a multi-head collecting device and the free RA was removed, and examined by the filter membrane method. Saturation binding curve, Scatchard diagram and receptor maximum dissociation constant KD were analyzed by a receptor radio-ligand binding analyzing software.

Statistical analysis

Experimental results were analyzed by variance analysis and chi-square test with SPSS software. Statistical significance was determined at $P<0.05$.

RESULTS

Incidence of colorectal carcinoma

At the 14th week after induction, 12.5 % of rats in group I developed colorectal carcinoma, but colorectal carcinoma was not found in group II. At the 21st and 28th weeks, the incidence of colorectal carcinoma reached 60 % and 100 % respectively in group I, compared with 12 % and 20 % respectively in group II. There were significant differences between the two groups ($P<0.05$ and $P<0.01$). All the carcinomas were adenocarcinomas. In group I, 12 cases of adenocarcinoma were well-differentiated and 9 cases were poorly-differentiated. All the 4 cases in group II were well-differentiated (Table 1).

Table 1 Incidence (%) of colorectal carcinoma in the groups

Weeks	*n*	Number of cancer			
		I	II	III	IV
7	8	0	0	0	0
14	8	1(12.5)	0	0	0
21	8	5(60.5)	1(12.5)	0	0
28	15	15(100.0)	3(20.0)	0	0

Expression of PCNA indices

At the 7th week, PCNA indices reached 96.75±6.88 and 95.50±14.01, respectively, in group I and group II, which were significantly higher than those in group III and group IV (34.38±6.30 and 33.63±4.75, respectively, $P<0.01$). In metaphase and late-phase, PCNA indices in group I and group II were continuously increased, especially in group I. PCNA indices in group I reached 168.13±14.34 at the 28th week and approached the level of well-differentiated adenocarcinoma (169.13±11.68), but were still significantly lower than that of poorly-differentiated adenocarcinoma (181.63±23.38, $P<0.05$). Analysis of variance showed that there was a tendency in group I that the longer the induction with DMH the higher the PCNA index ($F=7.634$, $P<0.05$). However, there was no such tendency in groups II, III and IV ($F=1.662$, $P>0.05$).

In comparison between the groups, the results showed that PCNA indices in group I and group II were significantly higher than those in groups III and IV at all stages of carcinoma induction ($F=5.927$, $P<0.01$). Moreover, PCNA index in group I was significantly higher than that in groups II at all stages ($F=5.418$, $P<0.01$), except at the 7th week (Table 2).

Table 2 Expression of PCNA indices in groups

Weeks	*n*	I	II	III	IV
7	8	96.75±6.88	95.50±14.01	34.38±6.30	33.63±4.75
14	8	110.88±15.51	97.88±8.90	35.13±3.91	35.88±2.17
21	8	149.50±15.15	98.25±25.09	36.00±3.46	34.13±4.39
28	8	168.13±14.34	98.88±25.30	35.88±4.29	33.13±4.32
Well-differentiated adenocarcinoma	8	169.13±11.68	-	-	-
Poorly differentiated adenocarcinoma	8	181.63±23.38	-	-	-

Expression of AgNOR count

At the 7th week, AgNOR count reached 3.78±0.88 and 3.71±9.95, respectively, in group I and group II, which was significantly higher than that in group III and group IV ($P<0.05$). As the time of induction with DMH prolonged, the AgNOR count in group I was continuously increased. Analysis of variance showed that there was a tendency in group I that the longer the induction with DMH the higher the AgNOR count ($F=6.826$, $P<0.05$). However, there was no such tendency in groups II, III and IV ($F=1.984$, $P>0.05$). At the 28th week, the AgNOR count already approached the level of well-differentiated adenocarcinoma, but was still significantly lower than that of poorly-differentiated adenocarcinoma ($P<0.05$).

In comparison between the groups, the results showed that the AgNOR counts in group I and group II were significantly higher than those in groups III and IV at all stages of carcinoma induction ($F=4.348$, $P<0.05$). The AgNOR count was significantly higher in group I than that in group II at all stages ($F=4.243$, $P<0.05$), except at the 7th week (Table 3).

Table 3 Expression of AgNOR count in groups

w	*n*	AgNOR count ($\bar{x}\pm s$)			
		I	II	III	IV
7	8	3.78±0.88	3.71±0.95	2.17±0.53	2.45±1.06
14	8	5.15±1.87	4.30±0.84	2.20±0.86	2.16±0.80
21	8	7.54±0.73	4.39±0.62	2.20±0.77	2.49±0.90
28	8	9.37±0.71	4.75±0.98	2.35±1.01	2.38±1.04
Well-differentiated adenocarcinoma	8	9.93±1.47	-	-	-
Poorly-differentiated adenocarcinoma	8	11.14±1.86	-	-	-

Table 4 RAR count (fmol/μg DNA) and KD (nmol) in cells. ($\bar{x}\pm s$)

Group	*n*	Bmax	KD
I	6	1.16±0.34	1.99±0.25
II	6	1.78±0.36	2.16±0.18
III	6	2.61±0.55	2.39±0.43
IV	6	2.64±0.22	2.45±0.23
Cancer tissue	6	1.02±0.21	1.74±0.16

Expression of RAR

Six samples of colorectal and cancer tissues were collected randomly from groups I, II, III and IV respectively. Expressions

of RAR were detected, Bmax and KD were calculated. The Bmax and KD in group I approached the level of cancer tissues (1.02±0.21 and 1.74±0.16, $P>0.05$). The Bmax and KD in group II were significantly higher than those in group I, but significantly lower than those in groups III and IV, ($F=6.343$ and 6.024, $P<0.05$).

DISCUSSION

Recently, the mechanism of preventing carcinoma by RA has been studied by scholars all over the world. Some researchers reported that leukaemia cells could respond to the effect of differentiation induced by RA to put up the potential of diphasic differentiation[21-23]. Some reported that RA could result in reversion of liver cancer cells[24,25]. In our research, we found that the incidence of carcinoma developed in RA treatment group (group II) was significantly lower than that in group I during inducetion. The results showed that retinoic acid (RA) had an effect on blocking canceration induced by carcinogen and decreased the incidence of colorectal cancer.

PCNA is the 36 KD polypeptide which is synthesized and expressed just in proliferating cells. It has been proved that PCNA expression is related to cell generation cycle[11,12]. Expression of PCNA increases in G_1 phase gradually, reaches pinnacle in S phase, and decreases in G_2/M phase. It plays an important role in understanding cell generation state to detect PCNA indices. The higher the PCNA expression, the higher the cell malignancy trend[12-15]. Our experimental results showed that there was a tendency in group I that the longer the interval induced by DMH, the higher the PCNA index would be ($P<0.05$). At the 28th week, the PCNA indices already approached the level of well-differentiated adenocarcinoma, but were still significantly lower than that of poorly-differentiated adenocarcinoma ($P<0.05$). The PCNA indices in group II were higher than those in groups III and IV, but still lower than those in group I. RA may have an effect on blocking canceration induced by carcinogen and decreasing the incidence of colorectal carcinoma. The mechanism is not clear, maybe it is related to blocking the transition of cancer cells from G_0/G_1 phase to S_1,G_2+M phase. Our results also showed that RA could not block canceration entirely.

AgNOR is the biochemical symbol of rDNA and transcription. AgNOR count can reflect the cell active state and cell malignant trend of carcinoma[8-10]. We found that AgNOR count of colorectal mucosa cells in group II was significantly lower than that in group I, but significantly higher than that in groups III and IV during the period of inducement. The reasonable explanation was that RA could inhibit the process of canceration induced by carcinogen but could not block canceration entirely.

Our results showed that there were plenty of RARs in colorectal tissues. The normal RAR contents in colorectal cells were 2.64 f mol/μg DNA, and KD was 2.45 nmol. However, RAR contents in colorectal cancer cells decreased significantly (1.02 f mol/μg DNA, and 1.74 nmol). It is possible that the development of colorectal carcinoma is related to abnormal expression of RAR, and especially decrease of RAR content. After interference treatment with RA, the expression of RAR increased. The carcinogenic course induced by DMH was slowed down distinctly. The results revealed that RA had an effect on inhibiting cellular proliferation and RA could regulate the expression of RAR[24-30].

There are plenty of similarities between human colorectal cancer and experimental colorectal cancer. However, it is possible that colorectal cancer occurs in total colorectal mucosa under the action of carcinogenic factor. It is possible that clinical application of RA can inhibit the precancerous lesion of colorectal carcinoma, block the canceration course, and decrease the incidence of colorectal cancer[31-35]. It is expected that clinical application of RA after colorectal operation would prevent and decrease the recurrence of carcinoma.

REFERENCES

1 **Adachi Y**, Itoh F, Yamamoto H, Iku S, Matsuno K, Arimura Y, Imai K. Retinoic acids reduce matrilysin (matrix metalloproteinase 7) and inhibit tumor cell invasion in human colon cancer. *Tumour Biol* 2001; **22**: 247-253

2 **Szeto W**, Jiang W, Tice DA, Rubinfeld B, Hollingshead PG, Fong SE, Dugger DL, Pham T, Yansura DG, Wong TA, Grimaldi JC, Corpuz RT, Singh JS, Frantz GD, Devaux B, Crowley CW, Schwall RH, Eberhard DA, Rastelli L, Polakis P, Pennica D. Overexpression of the retinoic acid-responsive gene Stra6 in human cancers and its synergistic induction by Wnt-1 and retinoic acid. *Cancer Res* 2001; **61**: 4197-4205

3 **Paulsen JE**, Lutzow-Holm C. *In vivo* growth inhibition of human colon carcinoma cells (HT-29) by all-trans-retinoic acid, difluoromethylornithine, and colon mitosis inhibitor, individually and in combination. *Anticancer Res* 2000; **20**: 3485-3489

4 **Wu W**, Zhang X, Yan X, Wang J, Zhang J, Li Y. Expressions of beta-catenin, p53 and proliferating cell nuclear antigen in the carcinogenesis of colorectal adenoma. *Zhonghua Zhongliu Zazhi* 2002; **24**: 264-267

5 **Boonsong A**, Curran S, McKay JA, Cassidy J, Murray GI, McLeod HL.Topoisomerase I protein expression in primary colorectal cancer and lymph node metastases. *Hum Pathol* 2002; 33: 1114-1119

6 **Izawa H**, Yamamoto H, Ikeda M, Ikeda K, Fukunaga H, Yasui M, Ikenaga M, Sekimoto M, Monden T, Matsuura N, Monden M. Analysis of cyclin D1 and CDK expression in colonic polyps containing neoplastic foci: a study of proteins extracted from paraffin sections. *Oncol Rep* 2002; **9**: 1313-1318

7 **Kohno H**, Tanaka T, Kawabata K, Hirose Y, Sugie S, Tsuda H, Mori H. Silymarin, a naturally occurring polyphenolic antioxidant flavonoid, inhibits azoxymethane-induced colon carcinogenesis in male F344 rats. *Int J Cancer* 2002; **101**: 461-468

8 **Barnett KT**, Fokum FD, Malafa MP. Vitamin E succinate inhibits colon cancer liver metastases. *J Surg Res* 2002; **106**: 292-298

9 **Lavezzi AM**, Ottaviani G, De Ruberto F, Fichera G, Matturri L. Prognostic significance of different biomarkers (DNA content, PCNA, karyotype) in colorectal adenomas. *Anticancer Res* 2002; **22**: 2077-2081

10 **McKay JA**, Douglas JJ, Ross VG, Curran S, Loane JF, Ahmed FY, Cassidy J, McLeod HL, Murray GI. Analysis of key cell-cycle checkpoint proteins in colorectal tumours. *J Pathol* 2002; **196**: 386-393

11 **Ohishi T**, Kishimoto Y, Miura N, Shiota G, Kohri T, Hara Y, Hasegawa J, Isemura M. Synergistic effects of (-)-epigallocatechin gallate with sulindac against colon carcinogenesis of rats treated with azoxymethane. *Cancer Lett* 2002; **177**: 49-56

12 **Yamada Y**, Yoshimi N, Hirose Y, Matsunaga K, Katayama M, Sakata K, Shimizu M, Kuno T, Mori H. Sequential analysis of morphological and biological properties of beta-catenin-accumulated crypts, provable premalignant lesions independent of aberrant crypt foci in rat colon carcinogenesis. *Cancer Res* 2001; **61**: 1874-1876

13 **Hung LC**, Pong VF, Cheng CR, Wong FI, Chu RM. An improved system for quantifying AgNOR and PCNA in canine tumors. *Anticancer Res* 2000; **20**: 3273-3280

14 **Derenzini M**, Trere D, Pession A, Govoni M, Sirri V, Chieco P. Nucleolar size indicates the rapidity of cell proliferation in cancer tissues. *J Pathol* 2000; **191**: 181-186

15 **Eminovic-Behrem S**, Trobonjaca Z, Petrovecki M, Dobi-Babic R, Dujmovic M, Jonjic N. Prognostic significance of DNA ploidy pattern and nucleolar organizer regions (AgNOR) in colorectal carcinoma. *Croat Med J* 2000; **41**: 154-158

16 **Ofner D**. *In situ* standardised AgNOR analysis: a simplified method for routine use to determine prognosis and chemotherapy efficiency in colorectal adenocarcinoma. *Micron* 2000; **31**: 161-164

17 **Sugai T**, Nakamura SI, Habano W, Uesugi N, Sato H, Yoshida T, Orii S. Usefulness of proliferative activity, DNA ploidy pattern and p53 products as diagnostic adjuncts in colorectal adenomas and intramucosal carcinomas. *Pathol Int* 1999; **49**: 617-625

18 **Nanashima A**, Yamaguchi H, Shibasaki S, Sawai T, Yasutake T, Tsuji T, Nakagoe T, Ayabe H. Proliferation of hepatic metastases of colorectal carcinoma: relationship to primary tumours and prognosis after hepatic resection. *J Gastroenterol Hepatol* 1999; **14**: 61-66
19 **Guan RJ**, Ford HL, Fu Y, Li Y, Shaw LM, Pardee AB. Drg-1 as a differentiation-related, putative metastatic suppressor gene in human colon cancer. *Cancer Res* 2000; **60**: 749-755
20 **Lee MO**, Han SY, Jiang S, Park JH, Kim SJ. Differential effects of retinoic acid on growth and apoptosis in human colon cancer cell lines associated with the induction of retinoic acid receptor beta. *Biochem Pharmacol* 2000; **59**: 485-496
21 **Sarraf P**, Mueller E, Smith WM, Wright HM, Kum JB, Aaltonen LA, de la Chapelle A, Spiegelman BM, Eng C.Loss-of-function mutations in PPAR gamma associated with human colon cancer. *Mol Cell* 1999; **3**: 799-804
22 **Nicke B**, Riecken EO, Rosewicz S. Induction of retinoic acid receptor beta mediates growth inhibition in retinoid resistant human colon carcinoma cells. *Gut* 1999; **45**: 51-57
23 **Zheng Y**, Kramer PM, Lubet RA, Steele VE, Kelloff GJ, Pereira MA. Effect of retinoids on AOM-induced colon cancer in rats: modulation of cell proliferation, apoptosis and aberrant crypt foci. *Carcinogenesis* 1999; **20**: 255-260
24 **Teraishi F**, Kadowaki Y, Tango Y, Kawashima T, Umeoka T, Kagawa S, Tanaka N, Fujiwara T. Ectopic p21sdi1 gene transfer induces retinoic acid receptor beta expression and sensitizes human cancer cells to retinoid treatment. *Int J Cancer* 2003; **103**: 833-839
25 **Narayanan BA**, Narayanan NK, Simi B, Reddy BS. Modulation of inducible nitric oxide synthase and related proinflammatory genes by the omega-3 fatty acid docosahexaenoic acid in human colon cancer cells. *Cancer Res* 2003; **63**: 972-979
26 **Wei HB**, Wang JF, Chen GH. Effect of retinoic acid (RA) on the T-lymphocyte subsets and T-cell colony of patients with colorectal cancer. *Ai Zheng* 2003; **22**: 202-205
27 **Lee MO**, Kang HJ. Role of coactivators and corepressors in the induction of the RARbeta gene in human colon cancer cells. *Biol Pharm Bull* 2002; **25**: 1298-1302
28 **Tao L**, Kramer PM, Wang W, Yang S, Lubet RA, Steele VE, Pereira MA.Altered expression of c-myc, p16 and p27 in rat colon tumors and its reversal by short-term treatment with chemopreventive agents. *Carcinogenesis* 2002; **23**: 1447-1454
29 **Ahmed KM**, Shitara Y, Takenoshita S, Kuwano H, Saruhashi S, Shinozawa T. Association of an intronic polymorphism in the midkine (MK) gene with human sporadic colorectal cancer. *Cancer Lett* 2002; **180**: 159-163
30 **Li Y**, Zhang H, Xie M, Hu M, Ge S, Yang D, Wan Y, Yan B. Abundant expression of Dec1/stra13/sharp2 in colon carcinoma: its antagonizing role in serum deprivation-induced apoptosis and selective inhibition of procaspase activation. *Biochem J* 2002; **367** (Pt2): 413-422
31 **Ye J**, Lu H, Zhou J, Wu H, Wang C. Inhibitory effect of all-trans-retinoid and polyphenon-100 on microsatellite instability in a colon cancer line. *Zhonghua Yixue Yichuanxue Zazhi* 2002; **19**: 190-193
32 **Wong NA**, Pignatelli M. Beta-catenin-a linchpin in colorectal carcinogenesis? *Am J Pathol* 2002; **160**: 389-401
33 **Lamprecht SA**, Lipkin M. Cellular mechanisms of calcium and vitamin D in the inhibition of colorectal carcinogenesis. *Ann N Y Acad Sci* 2001; **952**: 73-87
34 **Paulsen JE**, Elgjo K. Effect of tumour size on the *in vivo* growth inhibition of human colon carcinoma cells (HT-29) by colon mitosis inhibitor. *In Vivo* 2001; **15**: 397-401
35 **Parlesak A**, Menzl I, Feuchter A, Bode JC, Bode C. Inhibition of retinol oxidation by ethanol in the rat liver and colon. *Gut* 2000; **47**: 825-831

Edited by Xia HHX and Wang XL

P.O.Box 2345, Beijing 100023,China
Fax: +86-10-85381893
E-mail: wjg@wjgnet.com www.wjgnet.com

World J Gastroenterol 2003;9(8):1729-1733
World Journal of Gastroenterology
 ISSN 1007-9327

• COLORECTAL CANCER •

Expression of tumor related genes NGX6, NAG-7, BRD7 in gastric and colorectal cancer

Xiao-Mei Zhang, Shou-Rong Sheng, Xiao-Yan Wang, Jie-Ru Wang, Jiang Li

Xiao-Mei Zhang, Xiao-Yan Wang, Department of Digestion Medicine, Xiangya Hospital, Central South University, Changsha 410008, Hunan Province, China
Shou-Rong Sheng, Department of Digestion Medicine, The Third Xiangya Hospital, Central South University, Changsha 410013, Hunan Province, China
Jie-Ru Wang, Jiang Li, Carcinoma Research Institute, Xiangya Medical School, Central South University, Changsha 410078, Hunan Province, China
Supported by the Natural Science Foundation of Hunan Province No.01JJY2102 and the National "863 Program" of China, No.102-10-01-05
Correspondence to: Dr. Shou-Rong Sheng, Department of Digestion Medicine, The Third Xiangya Hospital, Central South University, Changsha 410013, Hunan Province, China. tangyy@public.cs.hn.cn
Telephone: +86-731-4316667 **Fax:** +86-731-4316667
Received: 2003-04-02 **Accepted:** 2003-05-19

Abstract

AIM: NGX6, NAG-7 and BRD7 genes are tumor related genes, which have been newly cloned by positional candidate cloning strategy. This study was designed to investigate the expression levels of NGX6, NAG-7 and BRD7 genes in human gastric and colorectal cancer tissues, and their corresponding normal tissues, and to investigate whether these genes play a role in the pathogenesis of gastric and colorectal cancers.

METHODS: Reverse transcription-polymerase chain reaction (RT-PCR), dot hybridization and Northern blot analysis were used to compare the expression levels of NGX6, NAG-7 and BRD7 genes in 34 gastric cancer tissues and 34 colorectal cancer tissues with their corresponding normal tissues of the same patients, respectively.

RESULTS: Among the 34 colorectal cancer specimens and the 34 gastric cancer specimens, the expression of NGX6 in 25 colorectal cancer tissues was absent or very weak (73.5 %) by RT-PCR analysis. The down-regulation rate of NGX6 in colorectal cancer tissues was significantly higher than that in corresponding normal tissues (26.5 %,9/34) ($P<0.005$). Moreover, the down-regulation of NGX6 was significantly correlated with lymph node and/or distance metastases. Patients with lymph node and/or distance metastasis had much higher down-regulation rate of NGX6 than patients without metastases (93.8 % *vs* 55.6 %, $P<0.05$). However no correlation was found between the expression of NGX6 and pathologic type of colorectal cancer in this study, and also the expression of NGX6 did not display any difference between gastric cancer and corresponding normal tissues (58.8 % *vs* 70.6 %, $P>0.25$). Dot hybridization and Northern blot analysis confirmed the results of RT-PCR. Furthermore, NAG-7 and BRD7 mRNA was not up- or down-regulated in gastric and colorectal cancers compared with their corresponding normal tissues in our study.

CONCLUSION: The down-regulation of NGX6 may be closely associated with tumorigenesis and metastasis of colorectal carcinoma. However, it may not contribute to the development and progression of gastric carcinoma. In addition, the expression levels of NAG-7, and BRD7 did not alter in gastric and colorectal cancers. This seems to suggest that NAG-7 and BRD7 genes may not play a role in gastric and colorectal carcinogenesis.

Zhang XM, Sheng SR, Wang XY, Wang JR, Li J. Expression of tumor related genes NGX6, NAG-7, BRD7 in gastric and colorectal cancer. *World J Gastroenterol* 2003; 9(8): 1729-1733
http://www.wjgnet.com/1007-9327/9/1729.asp

INTRODUCTION

Gastric cancer (GC) is a leading cause of carcinoma morbidity and mortality in China[1]. Meanwhile, the occurrence of colorectal cancer (CRC) has been rising in the past 3 decades. At present, CRC is the fourth cause of death in China[2,3]. It is well known that a multistep process associated with multiple gene abnormalities including inactivation of tumor suppressor genes and activation of oncogenes may be related to the occurrence of these diseases, but the molecular basis of these diseases is still not well understood[4-11]. Recently modern molecular genetic analyses have clarified that multiple chromosome alterations are frequently found in GC and CRC[12-16]. Nonrandom and significant losses of heterozygosity (LOH) at 9p, 3p and 6q have been detected to be more significant by cytogenetic studies, indicating that there may be more than one tumor suppressor gene (TSG) associated with GC and CRC located in these regions[17-24]. Unfortunately, homozygous deletions and point mutations of the known tumor suppressor genes such as p16/MTS1 gene (9p21),VHL gene (3p25-26), PPARγ gene (3p24.2-25) and FHIT gene (3p14.2) have seldom been observed in GC and CRC. These results suggest that these genes might not play important roles in gastric and colorectal tumorigenesis, and several other tumor suppressor genes in these region may contribute to the occurrence and development of GC and CRC[25-33]. NGX6, NAG-7 and BRD7 genes located at 9p21-22, 3p25 and 6q22.1-6q22.33, respectively, are novel tumor related genes cloned by positional candidate cloning strategy. In previous studies, all of them were found to be potential tumor suppressor genes associated with nasopharyngeal carcinoma (NPC)[34-39]. To investigate whether NGX6, NAG-7 and BRD7 genes also play a role in the pathogenesis of gastric and colorectal carcinoma, we analyzed the expression levels of NGX6, NAG-7 and BRD7 genes in 34 human gastric carcinoma tissues, 34 human colorectal carcinoma tissues and their corresponding normal tissues by RT-PCR, dot hybridization and Northern blot analysis.

MATERIALS AND METHODS

Tumor specimens

Fresh surgical specimens of thirty-four gastric carcinomas (GC), thirty-four colorectal carcinomas (CRC) and their corresponding normal tissues were obtained from the Xiang

ya Hospital Affiliated to Central South University from January 2000 to July 2000. All tumor specimens were confirmed by pathological diagnosis. Each freshly resected specimen was immediately stored in liquid nitrogen until analysis. Histologically, in the 34 cases of gastric carcinoma, 4 were well-differentiated adenocarcinomas, 22 poorly-differentiated adenocarcinomas, 6 signet ring cell carcinomas and 2 mucoid carcinomas. There were 18 males and 16 females, their age ranged from 30 to 68 years (mean age, 51.7 years). Six cases had lymph node and/or distance metastases. In the 34 cases of colorectal carcinoma, 6 were poorly-differentiated adenocarcinomas, 27 well-differentiated adenocarcinomas and 1 signet ring cell carcinoma. There were 20 males and 14 females, their age ranged from 17 to 72 years (mean age, 47.4 years). Sixteen cases had lymph node and/or distance metastases. No patient had received chemotherapy or radiation therapy before surgery.

RT-PCR

Total RNA was isolated using Trizol reagent (Gibco-BRL, Gaithersburg, MD, USA) according to the protocol provided by the manufacturer. After being treated with DNase-I (Promega), 1-2 μg of total RNA was reversely transcribed into complementary DNA (cDNA) with oligo (dT) using cDNA synthesis kit (Promega). Then 1 μl cDNA product was used as the template to amplify specific fragments in a 25 μl reaction mixture. The PCRs were performed using Taq polymerase and the buffer (Promega) supplied with 0.2 mM dNTPs and 0.2 μM primers. RT-PCR reaction was carried out with an initial denaturation at 95 ℃ for 5 min, followed by 35 cycles at 94 ℃ for 50 s, annealing temperature (56 ℃) for 50 s, at 72 ℃ for 60 s, and final extension at 72 ℃ for 10 min. At the same time, a housekeeping gene, $GAPDH_1$ or $GAPDH_2$ was amplified as an internal control to normalize the relative levels of cDNA, in which primers generated a PCR product of 475 bp or 760 bp. An aliquot (10 μl) of each reaction products was analyzed by 1.0 % agarose gel electrophoresis.

Primers corresponding to NGX6, NAG-7 and BRD7 sequences were designed with WWW Primer Picking (Primer 3) and synthesized by TaKaRa. Gene-specific forward and reverse primers for NGX6, NAG-7 and BRD7 genes were designed to produce PCR products of 780 bp, 466 bp and 270 bp, respectively. Primer sequences were as follows: NGX6F1, 5'-GAA CGT GGT GGA AAT ACA GA-3'; NGX6R1, 5'-TTC TAC ATC TTC TTT GGC CC-3'; NAG-7F1, 5'-ACATCAGCTTGGAGTTATTGA-3'; NAG-7R1,5'-GAAATGTACCACCCTACA-3'; BRD7F1, 5'-TGGAAGCCTCTCACAAGCT-3'; BRD7R1, 5'-TGTGTACTAATGCCATGAT-3'; $GAPDH_1$F1, 5'-GTCATCCATGACAACTTTGGTATC-3'; $GAPDH_1$R1, 5'-CTGTAGCCAAATTCGTTGTCATAC-3'; $GAPDH_2$F1, 5'-CGAGATCCCTCCAAAATCAA-3'; $GAPDH_2$R1, 5'-TGCTGTAGCCAAATTCGTTG-3'.

Northern blot analysis

Total RNA was isolated from human gastric and colorectal carcinomas and their corresponding normal tissues by Trizol reagent (Gibco-BRL), and transferred to nylon membrane according to the standard procedure. Hybridization was performed as previously described. 30 μg RNA was separated by electrophoresis through denaturing agarose gels, and blotted onto the nylon membranes (Clontech). RNA was permanently attached to the membrane by UV illumination for 150 s (GS Gene Linker, Bio-Rad, USA), and the membranes were dried in a vacuum at 80 ℃ for 2 h and sealed in a plastic bag for use. The hybridization probes were obtained by RT-PCR amplification. NGX6, NAG-7 and BRD7 cDNA probes were random-prime labeled with [α-^{32}P]dCTP using primer-a-gene random labeling kit (Promega, USA) following the protocol. Hybridization with RNA blots was carried out at 68 ℃ overnight in Express Hyb TM hybridization solution (Clontech) in rolling bottles. The membranes were washed twice at room temperature in 2×saline sodium citrate (SSC), 0.05 % SDS for 10 min, once at 42 ℃ in 1×SSC, 0.1 % SDS for 15 min and once at 50 ℃ in 0.1×SSC, 0.1 % (w/v) SDS for 30 min, exposure to film (Eastman Kodak, Rochester, NY, USA) for 4 d at -70 ℃. After exposure, the blot was again hybridized with a GAPDH probe.

Dot blot analysis

GAPDH and NGX6, NAG-7 and BRD7 cDNA fragments containing open reading frame from cDNA of gastric or colorectal carcinoma samples were obtained by RT-PCR. These cDNAs were reclaimed and purified by using a Kit according to the instruction of its manufacturer (Shanghai Huashun Co.). After alkali dissolution, GAPDH and NGX6, NAG-7 and BRD7 cDNA were blotted onto nylon membranes. cDNA permanently was attached to the membrane by UV illumination for 150 s, and the membranes were dried in a vacuum at 80 ℃ for 2 h to fix the cDNA. 10 μg total RNA was isolated from 10 cases of human gastric carcinomas, 10 cases of colorectal carcinomas and 10 cases of each corresponding normal tissues respectively, and was reversely-transcribed into cDNA probes with oligo (dT) and [α-^{32}P] dCTP using cDNA synthesis kit after treated with DNase I and RNasin at 37 ℃ for 1 h to remove contaminated DNA (1 μg total RNA of each case was used). Then the four cDNA probes were hybridized with GAPDH and NGX6, NAG-7 and BRD7 cDNA blots respectively as Northern hybridization described above.

Statistical analysis

Chi-square test was used for the comparison between two groups. A P value less than 0.05 was considered statistically significant.

RESULTS

Expression of NGX6, NAG-7 and BRD7 genes in gastric and colorectal cancer tissues by RT-PCR

In 34 pairs of CRC and corresponding normal tissues, 25 (73.5 %) showed decreased or absent expression of NGX6 in cancer samples compared with their corresponding normal tissues. The expression of NGX6 in colorectal carcinoma was significantly lower than that in normal tissues (χ^2=15.06, P<0.005). Representative cases of NGX6 expression detected by RT-PCR are shown in Figure 1. The down-regulation rate of NGX6 in the patients with lymph-node and/or distance metastases was 93.8 % (15/16), significantly higher than that in those without lymph-node or distance metastases (55.6 %, 10/18) (P<0.05). The down-regulation rates of NGX6 in well differentiated and poorly differentiated adenocarcinomas were 46.2 % and 85.7 %, respectively. There was no apparent relevance between NGX6 down-expression and pathologic type of colorectal carcinomas (P>0.05).

In 34 pairs of GC and their corresponding normal tissue specimens, NGX6 expression was detected in 20 GC tissues (58.8 %) and 24 corresponding normal tissues (70.6 %) as an expected PCR product of 780 bp in length. The expression level of NGX6 did not display any difference between gastric carcinoma and its corresponding normal tissues (χ^2=1.03, P>0.05).

NAG-7 expression was detected in 88.2 % (30/34) GC tissues and 82.3 % (28/34) corresponding normal tissues as well as in 76.2 % (26/34) CRC tissues and 76.2 % (26/34) corresponding normal tissues as an expected PCR product of 466 bp in length. BRD7 expression was detected in all samples

as an expected PCR product of 270 bp in length. The expression level of NAG-7 and BRD7 did not display any significant difference between cancer samples and normal tissues (P>0.05).

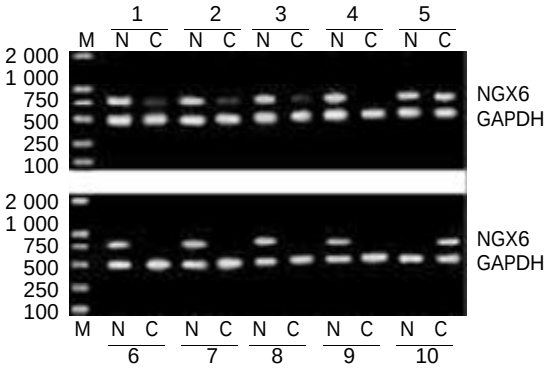

Figure 1 Expression of NGX6 in colorectal carcinoma and its corresponding normal tissues was examined by RT-PCR. The RT-PCR products with NGX6 primers produced 780 bp fragments and GAPDH primers produced 466 bp fragments. Lane M, DL-2000 marker; Lane N, normal tissues; Lane C, colorectal carcinoma tissues. This figure showed the representative results from several individual patients.

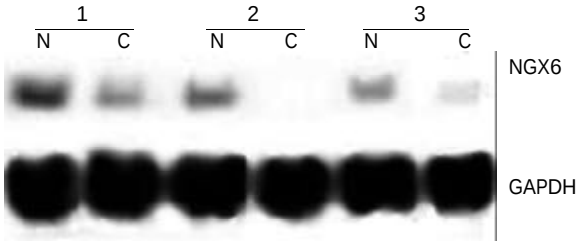

Figure 2 Northern blot was used to detect the expression abundance of NGX6 gene in human colorectal carcinoma and its adjacent normal tissues. The expression level of NGX6 was down-regulated in colorectal carcinoma tissues. C, human colorectal carcinoma tissue; N, adjacent normal colorectal tissue.

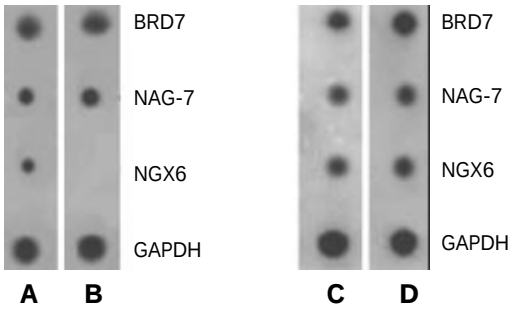

Figure 3 Dot hybridization analysis of NGX6, NAG-7 and BRD7 gene expression profiles in human colorectal and gastric carcinomas and their corresponding normal tissues. NGX6, NAG-7 and BRD7 cDNAs obtained by RT-PCR were blotted onto nylon membranes (Clontech) respectively. The membranes were respectively hybridized with each type of cDNA probes. (A: corresponding normal colorectal epithelial tissues, B: colorectal carcinoma, C: corresponding normal gastric epithelial tissues, D: gastric carcinoma.) NGX6 was down-regulated in colorectal carcinoma tissues, however it was expressed at the same level in the gastric cancer samples and normal tissues.

Expression of NGX6, NAG-7 and BRD7 genes in gastric and colorectal carcinoma tissues by Northern blot analysis and dot hybridization

Northern blot analysis and dot hybridization were performed to further investigate the expression of NGX6, NAG-7 and BRD7. Northern blot analysis showed that NGX6 was expressed as one single transcript of 2.4 kb, corresponding well with the size of the cloned cDNA. NGX6 was strongly expressed in its corresponding normal colorectal epithelial tissues, whereas faint signals or no signals were found in colorectal carcinoma tissues. Representative cases of NGX6 expression detected by Northern hybridization are shown in Figure 2. However, no signals were discerned in gastric carcinoma and its corresponding normal epithelial tissues. NAG-7 and BRD7 mRNA was expressed at the same level in the cancer samples and normal tissues. The results of dot hybridization were consistent with those of Northern analysis. Both dot hybridization and Northern analysis confirmed the results of RT-PCR. The expression of NGX6 was significantly down-regulated in colorectal carcinoma tissues.

DISCUSSION

NGX6, NAG-7 and BRD7 genes located at 9p21-22, 3p25 and 6q22.1-6q22.33 respectively are novel tumor related genes that were cloned by positional candidate cloning strategy. The cDNA sequence of NGX6, NAG-7 and BRD7 genes compared with Genbank and EMBO database using the BLAST program has verified that all of them are unique genes with no homology to any previously reported human genes, and their GenBank accession numbers are AF188239, AF086709 and AF179285, respectively. The NGX6 gene encodes a transmembrane protein of 338 amino acids containing four transmembrane regions, an EGF-like domain signature and a number of potential phosphorylation sites for protein kinase C (PKC), casein kinase II, tyrosine kinase and several N-myristylation sites. The NAG-7 gene encodes a transmembrane protein of 94 amino acids including one PKC phosphorylation site and one myristylation site. The BRD7 gene encodes a protein of 508 amino acids including a bromodomain and several important phosphorylation sites. In our previous study, their mRNA expression levels in nasopharyngeal carcinoma (NPC) cells were all significantly lower than those in normal nasopharyngeal epithelium. The proliferation rate of NPC cells was slower after transfection with these genes. The growth of xenografts was also inhibited after the transfected cells were injected into nude mice *in vivo*. These results suggest that the downregulation of these genes might play important roles in the occurrence and development of NPC[34-39].

Allelic imbalance or loss of heterozygosity (LOH) studies have been used to identify regions on chromosomes that may contain putative tumor suppressor genes. Deletions of chromosome 9p, 3p, and 6q regions have been observed at a high frequency in many types of sporadic tumors, including gastric and colorectal cancers[17-24]. NGX6, NAG-7 and BRD7 genes located at 9p21-22, 3p25 and 6q22.1-6q22.33 respectively, are the frequent sites of LOH in GC and CRC. We were interested in investigating if expression of NGX6, NAG-7 and BRD7 genes was altered in GC and CRC. In this study, RT-PCR, Northern blot and dot hybridization were used to detect the expression abundance of the three genes in gastric and colorectal carcinoma tissues, as well as their corresponding normal tissues. The results of RT-PCR showed that the down-regulation rate of NGX6 in colorectal carcinoma tissues with lymph-node or distant metastases was significantly higher than that both in its corresponding normal tissues (P<0.005) and in carcinomas without lymph-node or distant metastases (P<0.05). Dot hybridization and Northern analysis confirmed the results of RT-PCR. However, no significant correlation was found between the expression of NGX6 and pathologic type of colorectal carcinomas. The results suggest that down-regulation of NGX6 might be closely associated with the

development, progression and metastasis of CRC. It is reasonable to predict that the NGX6 gene plays an important role in suppressing CRC tumorigenesis; losses of its function may contribute to the development of CRC. Deletion of this gene may occur as a later event associated with tumor progress, and may contribute to the metastatic potential of CRC. So, it is speculated that NGX6 gene located on chromosomes 9p21-22 may be a candidate tumor suppressor gene and a putative metastasis suppressor gene associated with CRC. The possible mechanism of this gene suppressing CRC tumorigenesis remains unclear. We speculated that the possible mechanism might be as follows. Firstly, NGX6 gene may be involved in cell cycle regulation and play an important role in tumor growth suppression. Our previous studies showed that significant accumulation of cells in the G0-G1 fraction was observed in HNE_1 cell transfected with NGX6 gene by using flow cytometric analysis, and several genes related to cell cycle and transcription regulation were differentially expressed in NGX6 overexpressed nasopharyngeal carcinoma cells by cDNA array assay[34,35,40]. Combined with our data presented here, it is reasonable to speculate that deletion or down-regulation of NGX6 gene in colorectal cancer may contribute to tumor cell proliferation and tumor metastasis. Secondly, NGX6 gene encodes a putative transmembrance protein including an important structural feature-EGF-like domain signature. In our study, NGX6 gene was significantly down-regulated in CRC, indicating that NGX6 protein might function as an inhibited membrane receptor or a negative growth factor in the initiation and progression of CRC. However, many previous studies showed that the proteins with EGF-like domains such as EGF, TGF-a were overexpressed in tumor tissues and might play a role in promoting tumor growth and metastasis[41-43]. Recently, Williams *et al*[44] identified two novel mucin genes, which encoded two putative transmembrane mucins with EGF-like domains and were commonly downregulated in colorectal carcinoma. This detection further confirmed that the transmembrance protein with EGF-like domain could act as a suppressive membrane receptor or a negative growth factor. Finally, NGX6 gene may exert functions by up-regulating and down-regulating some proteins. Recently, Li *et al*[45] found that seven proteins were up-regulated and seven proteins were down-regulated in NGX6 transfected cells using high-resolution two-dimensional electrophoresis. These proteins included Fas, zinc-finger protein (ZNF), RAB, and Ah receptor-interacting protein (AIP), which may affect the signaling pathway, alter the cell metabolism, and inhibit cell proliferation, induce cell apoptosis and prevent tumor invasion. Therefore, all these protein roles on cells indicate that NGX6 gene has the capacity to suppress both NPC and CRC tumorigenesis.

In this study, we did not find the existence of up- or down-regulated NGX6 in 34 gastric carcinoma specimens and their corresponding normal tissues by RT-PCR. The expression of NAG-7 and BRD7 genes did not display any significant difference between gastric and colorectal carcinomas and their corresponding normal tissues. The results of RT-PCR were also confirmed by Northern blot analysis and dot hybridization. This seems to suggest that NAG-7 and BRD7 genes play no roles in the pathogenesis of gastric and colorectal carcinomas, and NGX6 gene may not contribute to the occurrence and development of gastric carcinoma.

In summary, the results of this study have shown that NGX6 is down-regulated in colorectal carcinoma, and the down-regulation of this gene has a close correlation with lymph node or distant metastasis of CRC, suggesting that NGX6 plays an important role in tumor suppression. However the mechanism of this gene is still unclear. Further studies are needed to better understand the function of this novel gene and its role in CRC tumorigenesis *in vivo*.

REFERENCES

1 **Deng DJ**. Progress of gastric cancer etiology: N-nitrosamides 1999s. *World J Gastroenterol* 2000; **6**: 613-618
2 **Zhang YL**, Zhang ZS, Wu BP, Zhou DY. Early diagnosis for colorectal cancer in China. *World J Gastroenterol* 2002; **8**: 21-25
3 **Yu J P,** Dong WG. Current situation about early diagnosis of cancer of large intestine. *Shijie Huaren Xiaohua Zazhi* 1999; **7**: 553-554
4 **Fiocca R,** Luinetti O, Villani L, Mastracci L, Quilici P, Grillo F, Ranzani GN. Molecular mechanisms involved in the pathogenesis of gastric carcinoma: interactions between genetic alterations, cellular phenotype and cancer histotype. *Hepatogastroenterology* 2001; **48**: 1523-1530
5 **Yustein AS**, Harper JC, Petroni GR, Cummings OW, Moskaluk CA, Powell SM. Allelotype of gastric adenocarcinoma. *Cancer Res* 1999; **59**: 1437-1441
6 **Song ZJ**, Gong P, Wu YE. Relationship between the expression of iNOS,VEGF,tumor angiogenesis and gastric cancer. *World J Gastroenterol* 2002; **8**: 591-595
7 **Liu LX**, Liu ZH, Jiang HC, Qu X, Zhang WH, Wu LF, Zhu AL, Wang XQ, Wu M. Profiling of differentially expressed genes in human gastric carcinoma by cDNA expression array. *World J gastroenterol* 2002; **8**: 580-585
8 **He XS**, Su Q, Chen ZC, He XT, Long ZF, Ling H, Zhang LR. Expression, deletion [was deleton] and mutation of p16 gene in human gastric cancer. *World J Gastroenterol* 2001; **7**: 515-521
9 **Li XG**, Song JD, Wang YQ. Differential expression of a novel colorectal cancer differentiation-related gene in colorectal cancer. *World J Gastroenterol* 2001; **7**: 551-554
10 **Lou MJ**, Lai MD. Identification of differentially expressed genes in normal mucosa, adenoma and adenocarcinomas of cilon by SSH. *World J Gastroenterol* 2001; **7**: 726-731
11 **Hu JY**, Li GC, Wang WM, Zhu JG, Li YF, Zhou GH, Sun QB. Transfection of colorectal cancer cells with chemokine MCP-3 (monocyte chemotactic protein-3) gene retards tumor growth and inhibits tumor metastasis. *World J Gastroenterol* 2002; **8**: 1067-1072
12 **Wang Y**, Zheng E, Ke Y. Studies of loss of heterozygosity (LOH) in Chinese human gastric cancer tissues. *Zhonghua Zhongliu Zazhi* 1998; **20**: 116-118
13 **Gayet J**, Zhou XP, Duval A, Rolland S, Hoang JM, Cottu P, Hamelin R. Extensive characterization of genetic alterations in a series of human colorectal cancer cell lines. *Oncogene* 2001; **20**: 5025-5032
14 **Lai MD**. Gene changes of Chinese colorectal cancer. *Shijie Huaren Xiaohua Zazhi* 2001; **9**: 1227-1232
15 **Qin LX**. Chromosomal aberrations related to metastasis of human solid tumors. *World J Gastroenterol* 2002; **8**: 769-776
16 **Zhou CZ**, Peng ZH, Zhang F, Qiu GQ, He L. Loss of heterozygosity on long arm of chromosome 22 in sporadic colorectal carcinoma. *World J Gastroenrerol* 2002; **8**: 668-673
17 **Chetty R**, Naidoo R, Tarin M, Sitti C. Chromosome 2p, 3p, 5q and 18q status in sporadic gastric cancer. *Pathology* 2002; **34**: 275-281
18 **Weber TK**, Conroy J, Keitz B, Rodriguez-Bigas M, Petrelli NJ, Stoler DL, Anderson GR, Shows TB, Nowak NJ. Genome-wide allelotyping indicates increased loss of heterozygosity on 9p and 14q in early age of onset colorectal cancer. *Cytogenet Cell Genet* 1999; **86**: 142-147
19 **Martignetti JA**, Gelb BD, Pierce H, Picci P, Desnick RJ. Malignant fibrous histiocytoma: inherited and sporadic forms have loss of heterozygosity at chromosome bands 9p21-22-evidence for a common genetic defect. *Genes Chromosomes Cancer* 2000; **27**: 191-195
20 **Zhang Y**, Lai M. Microsatellite alterations on chromosome 9p21-22 in sporadic colorectal cancer. *Zhonghua Binglixue Zazhi* 1999; **28**: 418-421
21 **Kim NG**, Kim JJ, Ahn JY, Seong CM, Noh SH, Kim CB, Min JS, Kim H. Putative chromosomal deletions on 9P, 9Q and 22Q occur preferentially in malignant gastrointestinal stromal tumors. *Int J Cancer* 2000; **85**: 633-638
22 **Carvalho B**, Seruca R, Buys CH, Kok K. Novel expressed sequences obtained by means of a suppression subtractive hybridisation analysis from the 6q21 region that is frequently deleted in gastric cancer. *Eur J Cancer* 2002; **38**: 1126-1132
23 **Carvalho B**, van der Veen A, Gartner F, Carneiro F, Seruca R, Buys CH, Kok K. Allelic gains and losses in distinct regions of chromosome 6 in gastric carcinoma. *Cancer Genet Cytogenet* 2001; **131**: 54-59

24 **Carvalho B**, Seruca R, Carneiro F, Buys CH, Kok K. Substantial reduction of the gastric carcinoma critical region at 6q16.3-q23.1. *Genes Chromosomes Cancer* 1999; **26**: 29-34

25 **Gunther T**, Schneider-Stock R, Pross M, Manger T, Malfertheiner P, Lippert H, Roessner A. Alterations of the p16/MTS1-tumor suppressor gene in gastric cancer. *Pathol Res Pract* 1998; **194**: 809-813

26 **Shim YH**, Kang GH, Ro JY. Correlation of p16 hypermethylation with p16 protein loss in sporadic gastric carcinomas. *Lab Invest* 2000; **80**: 689-695

27 **Tsujie M**, Yamamoto H, Tomita N, Sugita Y, Ohue M, Sakita I, Tamaki Y, Sekimoto M, Doki Y, Inoue M, Matsuura N, Monden T, Shiozaki H, Monden M. Expression of tumor suppressor gene p16(INK4) products in primary gastric cancer. *Oncology* 2000; **58**: 126-136

28 **Dai CY**, Furth EE, Mick R, Koh J, Takayama T, Niitsu Y, Enders GH. p16 (INK4a) expression begins early in human colon neoplasia and correlates inversely with markers of cell proliferation. *Gastroenterology* 2000; **119**: 929-942

29 **Trzeciak L**, Hennig E, Kolodziejski J, Nowacki M, Ostrowski J. Mutations, methylation and expression of CDKN2a/p16 gene in colorectal cancer and normal colonic mucosa. *Cancer Lett* 2001; **163**: 17-23

30 **Noguchi T**, Muller W, Wirtz HC, Willers R, Gabbert HE. FHIT gene in gastric cancer: association with tumour progression and prognosis. *J Pathol* 1999; **188**: 378-381

31 **Thiagalingam S**, Lisitsyn NA, Hamaguchi M, Wigler MH, Willson JK, Markowitz SD, Leach FS, Kinzler KW, Vogelstein B. Evaluation of the FHIT gene in colorectal cancers. *Cancer Res* 1996; **56**: 2936-2939

32 **Wijnhoven BP**, Lindstedt EW, Abbou M, Ijzendoorn Y, de Krijger RR, Tilanus HW, Dinjens WN. Molecular genetic analysis of the von Hippel-Lindau and human peroxisome proliferator-activated receptor gamma tumor-suppressor genes in adenocarcinomas of the gastroesophageal junction. *Int J Cancer* 2001; **94**: 891-895

33 **Miyakis S**, Sourvinos G, Liloglou TL, Stathopoulos GP, Field JK, Spandidos DA. The Von Hippel-Lindau (VHL) tumor-suppressor gene is not mutated in sporadic human colon adenocarcinomas. *Int J Cancer* 2000; **88**: 503-505

34 **Yang JB**, Bin LH, Li ZH, Zhang XF, Qian J, Zhang BC, Zhou M, Xie Y, Deng LW, Li GY. Refined localization and cloning of a novel putative tumor suppressor gene associated with nasopharyngeal carcinoma on chromosome 9p21-22. *Aizheng* 2000; **19**: 6-9

35 **Yang J,** Tang X, Deng L. Detailed deletion mapping of chromosome 9p21-22 in nasopharyngeal carcinoma. *Zhonghua Zhongliu Zazhi* 1999; **21**: 419-421

36 **Xie Y**, Deng L, Jiang N, Zhan F, Cao L, Qiu Y, Tang X, Li G. Molecular cloning of a novel gene located on chromosome 3p25.3 and an analysis of its expression in nasopharyngeal carcinoma. *Zhonghua Yixue Yichuan Xue Zazhi* 2000; **17**: 225-228

37 **Xie Y**, Bin L, Yang J, Li Z, Yu Y, Zhang X, Cao L, Li G. Molecular cloning and characterization of NAG-7: a novel gene downregulated in human nasopharyngeal carcinoma. *Chin Med J (Engl)* 2001; **114**: 530-534

38 **Yu Y**, Zhang BC, Xie Y, Cao L, Zhou M, Zhan FH, Li GY. Analysis and molecular cloning of differentially expressing genes in nasopharyngeal carcinoma. *Shengwu Huaxue Yu Shengwu Wuli Xuebao* 2000; **32**: 327-332

39 **Yu Y**, Xie Y, Cao L, Zhang BC, Zhou M, Zhan FH, Li GY. Molecular Cloning and functional primary study of a novel candidate tumor suppressor gene related with nasopharyngeal carcinoma. *Shengwu Huaxue Yu Shengwu Wuli Jinzhan* 2000; **27:** 319-324

40 **Ma J**, Li J, Zhou J, Li XL, Tang K, Zhou M, Yang JB, Yan Q, Shen SR, Hu GX, Li GY. Profiling genes differentially expressed in NGX6 overexpressed nasopharyngeal carcinoma cells by cDNA array. *J Cancer Res Clin Oncol* 2002; **128**: 683-690

41 **Choi JH**, Kim HC, Lim HY, Nam DK, Kim HS, Yi SY, Shim KS, Han WS. Detection of transforming growth factor-alpha in the serum of gastric carcinoma patients. *Oncology* 1999; **57**: 236-241

42 **Xia L**, Yuan YZ, Xu CD, Zhang YP, Qiao MM, Xu JX. Effects of epidermal growth factor on the growth of human gastric cancer cell and the implanted tumor of nude mice. *World J Gastroenterol* 2002; **8**: 455-458

43 **Ghanem MA**, Van Der Kwast TH, Den Hollander JC, Sudaryo MK, Mathoera RB, Van den Heuvel MM, Noordzij MA, Nijman RJ, van Steenbrugge GJ. Expression and prognostic value of epidermal growth factor receptor, transforming growth factor-alpha, and c-erb B-2 in nephroblastoma. *Cancer* 2001; **92**: 3120-3129

44 **Williams SJ**, McGuckin MA, Gotley DC, Eyre HJ, Sutherland GR, Antalis TM. Two novel mucin genes down-regulated in colorectal cancer identified by differential display. *Cancer Res* 1999; **59**: 4083-4089

45 **Li J**, Tan C, Xiang Q, Zhang X, Ma J, Wang JR, Yang J, Li W, Shen SR, Liang S, Li G. Proteomic detection of changes in protein synthesis induced by NGX6 transfected in human nasopharyngeal carcinoma cells. *J Protein Chem* 2001; **20**: 265-271

Edited by Zhang JZ and Wang XL

P.O.Box 2345, Beijing 100023,China
Fax: +86-10-85381893
E-mail: wjg@wjgnet.com www.wjgnet.com

World J Gastroenterol 2003;9(8):1734-1738
World Journal of Gastroenterology
 ISSN 1007-9327

• COLORECTAL CANCER •

Transcriptional gene expression profiles of HGF/SF-met signaling pathway in colorectal carcinoma

Xue-Nong Li, Yan-Qing Ding, Guo-Bing Liu

Xue-Nong Li, Yan-Qing Ding, Department of Pathology, First Military Medical University, Guangzhou 510515, Guangdong Province, China
Guo-Bing Liu, Department of Obstetrics & Gynecology, Nanfang Hospital, Guangzhou 510515, Guangdong Province, China
Supported by National Natural Science Foundation of China, No. 30170486 and No.30170423
Correspondence to: Dr. Xue-Nong Li, Department of Pathology, First Military Medical University, Guangzhou 510515, Guangdong Province, China. leexue0@163.com
Telephone: +86-20-61648223
Received: 2002-12-28 **Accepted:** 2003-04-01

Abstract

AIM: To explore the transcriptional gene expression profiles of HGF/SF-met signaling pathway in colorectal carcinoma to understand mechanisms of the signaling pathway at so gene level.

METHODS: Total RNA was isolated from human colorectal carcinoma cell line LoVo treated with HGF/SF (80 ng/L) for 48 h. Fluorescent probes were prepared from RNA labeled with cy3-dUTP for the control groups and with cy5-dUTP for the HGF/SF-treated groups through reverse-transcription. The probes were mixed and hybridized on the microarray at 60 ℃ for 15-20 h, then the microarray was scanned by laser scanner (GenePix 4000B). The intensity of each spot and ratios of Cy5/Cy3 were analyzed and finally the differentially expressed genes were selected by GenePix Pro 3.0 software. 6 differential expression genes (3 up-regulated genes and 3 down-regulated genes) were selected randomly and analyzed by β-actin semi-quantitative RT-PCR.

RESULTS: The fluorescent intensities of built-in negative control spots were less than 200, and the fluorescent intensities of positive control spots were more than 5000. Of the 4004 human genes analyzed by microarray, 129 genes (holding 3.22 % of the investigated genes) revealed differential expression in HGF/SF-treated groups compared with the control groups, of which 61 genes were up-regulated (holding 1.52 % of the investigated genes) and 68 genes were down-regulated (holding 1.70 % of the investigated genes), which supplied abundant information about target genes of HGF/SF-met signaling.

CONCLUSION: HGF/SF-met signaling may up-regulate oncogenes, signal transduction genes, apoptosis-related genes, metastasis related genes, and down-regulate a number of genes. The complexity of HGF/SF-met signaling to control the gene expression is revealed as a whole by the gene chip technology.

Li XN, Ding YQ, Liu GB. Transcriptional gene expression profiles of HGF/SF-met signaling pathway in colorectal carcinoma. *World J Gastroenterol* 2003; 9(8): 1734-1738
http://www.wjgnet.com/1007-9327/9/1734.asp

INTRODUCTION

HGF/SF-met signaling is a pathway by stimulation of c-met via its ligand hepatocyte growth factor /scatter factor (HGF/SF), leading to a considerable variety of biological and biochemical effects on the cells[1-3]. HGF/SF, a multifunctional cell growth factor, is yielded by interstitial cells such as fibroblast, neuroglial cell, glial cell, fat-storing cell and macrophage[3,4]. It binds to the c-met receptor specifically, inducing a series of conformational changes of signaling proteins by activating JAK[5], phosphatidylinositol 3-kinase (PI-3 K)[6], phospholipase C-γ[7], Raf-1 kinase[8] etc, by which it transmits the signal to the nuclear transcription machines to control certain gene transcription and expressions. Finally it affects the cell proliferation, differentiation, locomotion and other cell functions[9-12]. HGF/SF has been proved to have mitogen, motogen, morphogen activity for almost all epithelial cells, and to promote adhesiveness, invasiveness, motion and metastasis and stimulation for blood vessel growth of cancer cells[8-13]. It was revealed to have anti-cytotoxin and anti-apoptosis for cancer cells in the recent investigation[11,12]. It is evidenced that abnormal activation of HGF/SF-met signaling plays an important or critical causal role in tumor progression and invasion and metastasis. However, little is known about the target genes and gene expression profiles by which HGF/SF exerts biological functions through start-up of transcriptional gene expression.

In the present study, we aimed to explore the transcriptional gene expression profiles by activating HGF/SF-met signaling in colorectal carcinoma cells using the microarray technology by which thousands of genes could be detected at the same time.

MATERIALS AND METHODS

Reagents

Hepatocyte growth factor/scatter factor (HGF/SF), ethidium bromide(EB), and SDS were purchased from Sigma. AMV reverse transcriptase, oligo(dT), dNTP, Taq, and agarose were Promega products. Trypsin, Cy3-dUTP, and Cy5-dUTP were purchased from Amersham Phamacia, and Oligotex mRNA midi kit from Qiagen, and other reagents from Shanghai Biostar Co.

Cells and cell culture

Human colorectal carcinoma cell line LoVo was routinely cultured in RPMI-1640 medium with 10 % FCS, incubated at 37 ℃ with 5 % CO_2. The well-grown cells at the logarithmic growth phase were treated with HGF/SF (80 ng/L) for 24-48 h in the same medium containing 2.5 % FCS. The blank control groups were treated with D-Hanks solution in the same culture condition as HGF/SF-treated groups. Triduplication of the experiments was for the microarray assay.

Construction of microarrays

The genes for HGEC-40S microarray containing 4096 cDNA spots (including 92 negative and positive control spots) were provided by Shanghai Biostar Co. These genes were amplified by PCR with universal primers and then purified by the routine method[13-15]. The purity of PCR products was supervised by agarose electrophoresis and then the PCR products were

dissolved in 3 X SSC solution. The target genes were spotted on siliconlated slides (TeleChem Inc) by using Cartesian 7500 spotting robotics (Cartesian Inc), then hydrated for 2 h, dried for 0.5 h, UV cross-linked by UVP CL-1000 at 65 mJ/cm, and then treated with 0.2 % SDS(10min), H_2O (10 min) and 0.2 % $NaBH_4$ (10 min). Finally the slides were dried again and ready for use.

Probe preparation

Total RNA was isolated from human colorectal carcinoma cell line LoVo by the routine method[13-15]. And then they were tested by hot-stabilization experiments and RNA electrophoresis. cDNA probes were prepared through reverse transcription in 50 μl reaction system in reference to Schena *et al*[15]. The fluorescent probes derived from cDNA reverse-transcripted from RNA were labeled with cy3-dUTP for the control groups and with cy5-dUTP for the HGF/SF-treated groups. The two kinds of probes were mixed equally after ethanol precipitation, then inspissated by vacuum to 50 μl, purified by using S-200 columns, and finally dissolved in hybridizing solution (20 μl 5×SSC+0.2 % SDS).

Microarray hybridization[16-19]

After denatured at 95 ℃ water bath, the microarray was prehybridized with 6 μl hybridization solutions 1 and 2 (Biostar) at 42 ℃ for 6 h. The probe mixtures were added on the prehybridized microarray, denatured at 95 ℃ for 5 min, then inoculated in hybridization cabin at 60 ℃ for 15-20 h. After the glass cover was removed, the microarray was washed in solutions 1 (2×SSC+0.2 % SDS), and 2 (0.1×SSC+0.2 % SDS) and 3 (0.1×SSC) for 10 min each, then dried at room temperature.

Detection and analysis

GenePix 4000B laser scanner (Axon) was used to scan microarray, with laser power 3.72 and photomultiplier tube volts 750. GenePix Pro 3.0 software was used for analysis of intensity of each spot and ratio of Cy5/Cy3 from the acquired images. The intensities of Cy3 and Cy5 were normalized by a coefficient according to the ratio of the located 40 housekeeping genes. The standards for differentially expressed genes were as follows: the ratio of Cy5/Cy3 was more than 4 or less than 0.25, and the intensity value of Cy3 and Cy5 was more than 200.

Verification by RT-PCR[20,21]

RT-PCR primers were designed by Omiga 2.0 software with basic reaction parameters as follows: primer length 18-22 bp, primer % GC 40-60 %, primer Tm 55 ℃; PCR products length 100-600 bp, PCR products % GC 40-60 %, and PCR products Tm 82.5 ℃. The primer sequences were as follows:

CAMK4 (321 bp): 5' GAGACCCTTCTCCAATCC3'
5' GAACTTCAAAACCCACAGC 3'
SHPG (555 bp): 5' ACATCTCCCCTTTGCTAACG 3'
5' GCCACAGTACCCTCATAACTCC 3'
Heregulin (424 bp): 5' TGCTCAACAGCAACATCC 3'
5' TCATACATCTGCCCCTCC 3'
p130 (523 bp): 5' GCACTTCAGTGTTCTAATCG 3'
5' GGCTATTCTCCTTAATGTACC 3'
DAP-1 (322 bp): 5' ACATGAGACACCACATTCC 3'
5' ACGACACAGTTGCTGACC 3'
TRAMP (381 bp): 5' ATTCGCAAGAAAAGCACC 3'
5' GTAGAACGCACTAAGCTGACC 3'
β-actin (206 bp): 5' GGCGGCACCACCATGTACCCT 3'
5' AGGGGCCGGACTCGTCATCATACT 3'

Components of the reverse transcription reaction system were as follows: oligo (dT) 0.5 μl, AMV5x buffer 4 μl, dNTP (10 mM) 1 μl RNasin (20u/ μl) 1 μl, AMV (10u/ μl) 0.5 μl, and DEPC-treated water 12 μl. Components of PCR reaction system were as follows: 10X PCR buffer 2 μl, cDNA 5 μl, dNTP (10 mM) 1 μl, forward primer 1 μl (1 μM), reverse primer 1 μl (1 μM), β-actin forward primer 0.5 μl (0.2 μM), β-actin reverse primer 0.5 μl (0.2 μM), Taq DNA polymerase (2U/ μl) 1 μl, and DEPC-treated water 8 μl, PCR amplification consisted of 35 cycles of denaturation for 60-90 s at 94 ℃, annealing for 60-90 s at 56 ℃, and extension for 90-120 s at 72 ℃. After 35 turns of the cycle, it ended after extension at 72 ℃ for 7 min. DEPC-treated water was replaced with DNA template for the negative control. 1.5 % agarose gel electrophoresis with ethidium bromide was used for the analysis of PCR products. Bandleader 3.0 software was applied to detect the density of bands of PCR products. The value of gene expression was calculated from percent of the ratio of band density of PCR product and the band density of β-actin.

Statistical methods

Data for gene expression were analyzed by two sided Student' s *t* test using SPSS 10.0 software and the significant value was $P<0.05$.

RESULTS

Total RNA electrophoresis and hot-stabilization test

The values of D_{260}/D_{280} for control and HGF/SF-treated groups were 2.022, 2.103 respectively. After hot stabilization test the 18S and 28S bands of total RNA extracts were as clear as before the test (Figure 1).

Microarray quality control

The fluorescent intensities of built-in negative control including rice U2 RNA gene, HCV coat protein gene, spotting solution (without DNA) as blank spots were lower than 200, while the intensities of built-in 40 house-keeping genes as positive control spots were larger than 5000. Normalization coefficient was 1.028. The odds of spot average intensities with background for HGF/SF-treated groups and the control groups were 10.254, 12.856 respectively. The ratio of Cy5/Cy3 by self-check test was 0-1.7, with the average 1.0112.

Scanning results of microarray

The scanning images for HGF/SF-treated groups labeled with Cy5 and images for control groups labeled with Cy3 showed lower noise background and appropriate spot intensity of signal with clear circle appearance. The overlaying image for bicolor fluorescence label is shown in Figure 2.

Filter of the differential expression genes

Of the 4 004 human genes analyzed by microarray, 129 differential expression genes were identified by the filter standard mentioned above. Among the 129 differential expression genes, 61 genes were up-regulated and 68 genes were down-regulated. The up-regulated genes by HGF/SF-met signaling consisted of cell growth factor genes, cell surface receptor genes, angiogenesis genes, cell cycle positive-regulation genes, calcium-, MAPK signaling-related genes and nuclei-receptor genes, etc. The down-regulated genes by HGF/SF-c-met signaling were cell death correlation receptor genes, transmembrane-4 superfamily, cell cycle negative- regulation genes, calcium-, MAPK signaling-related negative genes, cytoskeleton rearrangement inhibitor, anti-oncogene and protease inhibitor, etc.

Results of RT-PCR

To validate the reliability of microarray results, 6 differential expression genes (3 up-regulated genes and 3 down-regulated genes) were selected randomly and analyzed by β-actin semi-quantitative RT-PCR. Expressions of the 6 differential genes by RT-PCR were confirmed to be consistent with the results of microarray (shown in Figure 3 and Figure 4). The average

relative densities of bands detected by Bandlead 3.0 computer program showed significant differences (P<0.05) between HGF/SF-treated groups and control groups except SHPG, heregulin, and DAP-1 groups.

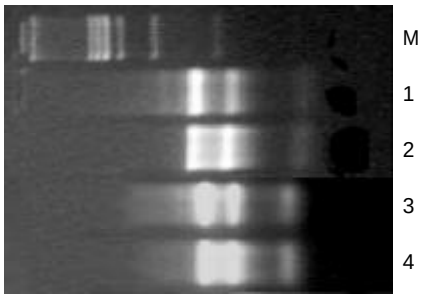

Figure 1 Result of total RNA electrophoresis and hot-stabilization test. M: PCR marker; 1: RNA of HGF/SF-treated group; 2: RNA of control group; 3: RNA of HGF/SF-treated group after hot-treatment; 4: RNA of control group after hot-treatment.

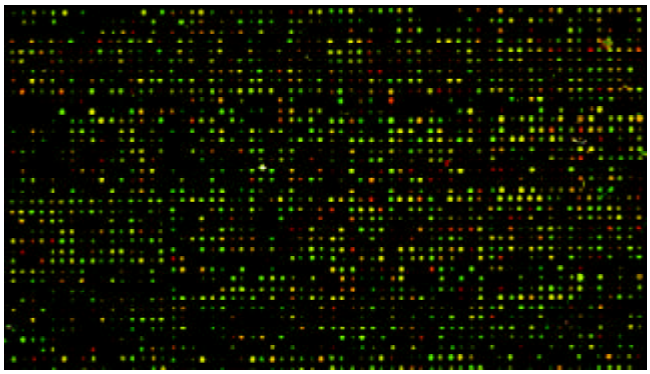

Figure 2 The overlaying image for bicolor fluorescence label on gene chip. red: high expression; green: low expression; yellow: no change in expression.

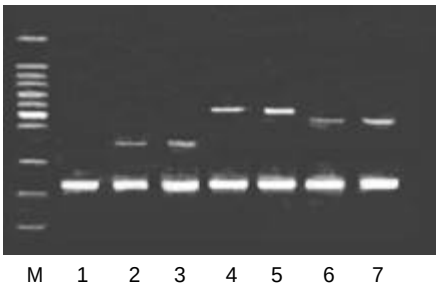

Figure 3 Result of RT-PCR for up-regulated genes. M: 100 bp DNA ladder marker; 1: negative control; 2: CAMK4 blank control; 3: CAMK4 HGF 80 ng/ml; 4: SHPG blank control; 5: SHPG HGF 80 ng/ml; 6: Heregulin blank control; 7: Heregulin HGF 80 ng/ml.

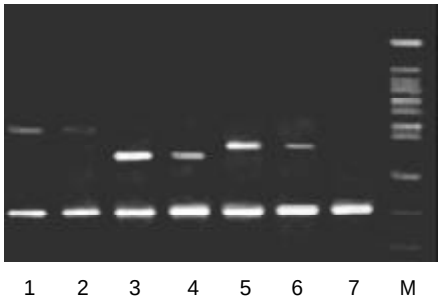

Figure 4 Result of RT-PCR for down-regulated genes. 1: p130 blank control; 2: p130 HGF 80 ng/ml; 3: DAP-1 blank control; 4: DAP-1 HGF 80 ng/ml; 5: TRAMP blank control; 6: TRAMP HGF 80 ng/ml; 7: negative control; M: 100 bp DNA ladder marker.

DISCUSSION

Reliability of the microarray assay

Gene chip, or DNA chip, including oligonucleotide chip synthesized *in situ* and cDNA microarray by direct-spot or cDNA array[22-24], is a key technique platform[25-27] in post-genome times for its striking superiority of high-throughput, high-parallelity, high-sensitivity, micromation and automatization. cDNA microarray is a mature and widespread technique. Its stability, reliability and reproducibility have been confirmed by many investigators[28-31]. The microarray experiment in this research was successful and under strict quality control, with mRNA in good quality and no degradation tested by the test of hot-stabilization. In our experiment the built-in positive and negative control showed the qualified results, the scanning images showed lower noise background, and the positive spots indicated high intensity of signal with clear circle appearance. All the parameters such as odds of spot average intensity with background for the HGF/SF-treated group and for the control, normalization coefficient, and ratio of Cy5/Cy3 by self-check test were in accord with theoretic values of successful experiment. The expressions of the 6 differential expression genes randomly selected by RT-PCR were confirmed to be consistent with the results of microarray. These results indicate satisfactory reliability of the microarray experiment.

Superiority of microarray for study of target genes related to the HGF/SF-met signaling

It has been evidenced that HGF/SF-met signaling plays an important, even a critical role in tumor progression, invasion and metastasis. Hamasuna *et al*[32] showed that HGF/SF activated membrane type metalloproteinases (MT1-MMP) in dosage-related manner and decreased wild-type metalloproteinases inhibitor TIMP-2 mRNA. They indicated that glioblastoma cells U251 excreted more MMP-2 protein and MMP-2 mRNA expression increased by 2.5 fold by HGF/SF stimulation. Abouader *et al*[33] argued that HGF/SF-met signaling was a key molecule path for control of glioblastoma cells growth, progression, invasion and metastasis. Recently Webb *et al*[34] have confirmed that HGF/SF-met-uPA -plasmin pathway exists in some tumor cell lines and is related to invasion, metastasis and other malignant behaviors. Only a few genes can be investigated by the traditional technology of molecular biology and the whole transcriptional gene expression profiles of HGF/SF-met signaling pathway can hardly be explored. In this paper the transcriptional gene expression profiles of HGF/SF-met signaling pathway in colorectal carcinoma cells were discussed for the first time so as to explore the target genes related to the signaling pathway. The results indicated that HGF/SF-met signaling might activate oncogenes, signal transduction genes, apoptosis-related genes, metastasis related genes and many other genes with up-regulation effects, and meanwhile it might down-regulate a number of genes. It is suggested that a complex signaling-adjusting-gene-expression network may be in existence, and contribute to extensive gene transcription effects and comprehensive biological roles. The complexity of HGF/SF-met signaling to control the gene expression was revealed as a whole by the gene chip technology, by which it manifested incomparable superiority.

Transcriptional gene expression profiles of HGF/SF-met signaling

Of the 4 004 human genes analyzed by microarray (totally 4 096 spots, subtracted 92 built-in positive and negative control

spots), 129 genes (holding 3.22 % of the investigated genes) revealed differential expression in the HGF/SF-treated groups compared with the control groups, which supplied abundant information about target genes of HGF/SF-met signaling. Among the 129 differential expression genes, 61 genes were up-regulated (holding 1.52 % of the investigated genes), and 68 genes were down-regulated (holding 1.70 % of the investigated genes). The expressions of some differential genes analyzed by microarray, for instance, collagenase IV[35], catenin[36], were consistent with the results reported in literatures that they were uncovered by traditional technology. Still a number of genes with differential expression not reported previously were found in our investigation. Some of them are genes with unknown function. Some genes with elevated expression by HGF/SF stimulation not reported previously are listed as following: Syndeans-2, calmodulin-dependent protein kinase IV(CaMK4), cadherein 8, protocadherin, calcium-dependent serine protein kinase (CASK), human keractnocyte growth factor(KGF), Heregulin, angiogenin, *etc*. In a word, the up-regulated genes by HGF/SF stimulation usually belong to cell growth factor genes, cell surface receptor genes, angiogenesis genes, cell cycle positive-regulation genes, calcium-, MAPK signaling-related genes, transcription factor, cytoskeleton regulation genes, and nuclei-receptor genes. These up-regulation genes stimulating cell growth, promoting cell transformation, resisting apoptosis, facilitating cell locomotion, accelerating signal conduction, and promoting vascularization and extracellular matrix lysis[37-44], may provide a foundation for mitogen, motogen, and morphogen activity in HGF/SF-met signaling pathway further.

Versatile effects on down-regulated gene expression by HGF/SF-met signaling have been found in this microarray assay. The genes of reduced expression by HGF/SF stimulation not reported previously include dual-specificity phosphatase 6 (DUSP6), SPINT2 (serine protease inhibitor, Kunitz-type 2, hepatocyte growth factor activator inhibitor type 2), TIMP1(tissue inhibitor of metalloproteinases 1), elastase inhibitive factor, TAPA1(Target of antiproliferative antibody 1, CD81), MRP-1 (motility-related protein 1, CD9), PRB2/p130, pRB2/p107, TRAMP (TNF receptor-related apoptosis mediating protein, DR3), WD40, DAP-1, etc. On the whole, the adjustability of multi-aspects and multi-targets in down-regulation of gene expression in colorectal carcinoma cells by HGF/SF-met signaling was revealed by microarray assay. The down-regulated genes by HGF/SF stimulation usually belong to cell death correlated receptor genes, transmembrane-4 superfamily, cell cycle negative-regulation genes, calcium and MAPK signaling-related negative genes, cytoskeleton rearrangement inhibitors, anti-oncogene and protease inhibitors. These genes are responsible for the negative control of cell function, which makes reinforcement and maintenance in stimulation of cell growth, promotion of cell transformation, resistance to apoptosis, facilitation for cell locomotion, acceleration of signal transduction, promotion of vascularization and lysis of extracellular matrix[45-56]. These are another annotation for mitogen, motogen, and morphogen activity of HGF/SF-met signaling pathway in tumor progression, also the first confirmation of pluripotency and versatility in regulation of gene expression by HGF/SF-met signaling.

The transcriptional gene expression profiles induced by HGF/SF-met signaling pathway in the colorectal carcinoma cells were described by cDNA microarray technology, and meanwhile the complexity and pluripotency of regulation in gene expression were also revealed for the first time. A majority of the genes with differential expression can be explained by the existing scientific theories, although some of them have unknown-function and a few of them cannot be explained reasonably for the time being, which deserve further investigation.

REFERENCES

1 **Stuart KA,** Riordan SM, Lidder S, Crostella L, Williams R, Skouteris GG. Hepatocyte growth factor / scatter factor-induced intracellular signalling. *Int J Exp Pathol* 2000; **81:** 17-30

2 **Ueoka Y**, Kato K, Kuriaki Y, Horiuchi S, Terao Y, Nishida J, Ueno H, Wake N. Hepatocyte growth factor modulates motility and invasiveness of ovarian carcinomas via Ras-mediated pathway. *Br J Cancer* 2000; **82:** 891-899

3 **Delehedde M,** Sergeant N, Lyon M, Rudland PS, Fernig DG. Hepatocyte growth factor / scatter factor stimulates migration of rat mammary fibroblasts through both mitogen-activated protein kinase and phosphatidylinositol 3-kinase / Akt pathways. *Eur J Biochem* 2001; **268:** 4423-4429

4 **Liu ZX**, Nickel CH, Cantley LG. HGF promotes adhesion of ATP-depleted renal tubular epithelial cells in MAPK-dependent manner. *Am J Physiol Renal Physiol* 2001; **281**: 62-70

5 **Rodrigues GA**, Park M, Schlessinger J. Activation of the JNK pathway is essential for transformation by the Met oncogene. *EMBO J* 1997; **16**: 2634-2645

6 **Awasthi V,** King RJ. PKC, p42 / p44 MAPK, and p38 MAPK are required for HGF-induced proliferation of H441 cells. *Am J Physiol Lung Cell Mol Physiol* 2000; **279**: 942-949

7 **Day RM**, Cioce V, Breckenridge D, Castagnino P, Bottaro DP. Differential signaling by alternative HGF isoforms through c-Met: activation of both MAP kinase and PI 3-kinase pathways is insufficient for mitogenesis. *Oncogene* 1999; **18:** 3399-3406

8 **Abounader R**, Ranganathan S, Kim BY, Nichols C, Laterra J. Signaling pathways in the induction of c-met receptor expression by its ligand scatter factor / hepatocyte growth factor in human glioblastoma. *J Neurochem* 2001; **76:** 1497-1508

9 **Sipeki S**, Bander E, Buday L, Farkas G, Bacsy E, Ways DK, Farago A. Phosphatidylinositol 3-kinase contributes to Erk1 / Erk2 MAP kinase activation associated with hepatocyte growth factor-induced cell scattering. *Cell Signal* 1999; **11**: 885-890

10 **Wong AS**, Leung PC, Auersperg N. Hepatocyte growth factor promotes in vitro scattering and morphogenesis human cervical carcinoma cells. *Gynecol Oncol* 2000; **78**: 158-165

11 **Hiscox S,** Jiang WG. Association of the HGF / SF receptor, c-met, with the cell-surface adhesion molecule, E-cadherin, and catenins in human tumor cells. *Biochem Biophys Res Commun* 1999; **261:** 406-411

12 **Kitamura S,** Kondo S, Shinomura Y, Kanayama S, Miyazaki Y, Kiyohara T, Hiraoka S, Matsuzawa Y. Met / HGF receptor modulates bcl-w expression and inhibits apoptosis in human colorectal cancers. *Br J Cancer* 2000; **83:** 668-673

13 **Luo YQ,** Wu MC, Cong WM. Gene expression of hepatocyte growth factor and its receptor in HCC and nontumorous liver tissues. *World J Gastroenterol* 1999; **5:** 119-121

14 **Liu LX**, Jiang HC, Liu ZH, Zhou J, Zhang WH, Zhu AL, Wang XQ, Wu M. Integrin gene expression profiles of human hepatocellular carcinoma. *World J Gastroenterol* 2002; **8:** 631-637

15 **Schena M,** Shalon D, Heller R, Chai A, Brown PO, Davis RW. Parallel human genome analysis: microarray-based expression monitoring of 1000 genes. *Proc Natl Acad Sci U S A* 1996; **93:** 10614-10619

16 **Heller RA**, Schena M, Chai A, Shalon D, Bedilion T, Gilmore J, Woolley DE, Davis RW. Discovery and analysis of inflammatory disease-related genes using cDNA microarrays. *Proc Natl Acad Sci U S A* 1997; **94**: 2150-2155

17 **Schena M,** Shalon D, Davis RW, Brown PO. Quantitative monitoring of gene expression patterns with a complementary DNA microarray. *Science* 1995; **270:** 467-470

18 **Shirota Y,** Kaneko S, Honda M, Kawai HF, Kobayashi K. Identification of differentially expressed genes in hepatocellular carcinoma with cDNA microarrays. *Hepatology* 2001; **33:** 832-840

19 **Raouf A**, Seth A. Discovery of osteoblast-associated genes using cDNA microarrays. *Bone* 2002; **30:** 463-471

20 **Verhofstede C,** Fransen K, Marissens D, Verhelst R, van der Groen G, Lauwers S, Zissis G, Plum J. Isolation of HIV-1 RNA from plasma: evaluation of eight different extraction methods. *J Virol Methods* 1996; **60**: 155-159

21 **Mannhalter C,** Koizar D, Mitterbauer G. Evaluation of RNA isolation methods and reference genes for RT-PCR analyses of rare target RNA. *Clin Chem Lab Med* 2000; **38:** 171-177

22 **Orr MS,** Scherf U. Large-scale gene expression analysis in molecular target discovery. *Leukemia* 2002; **16:** 473-477
23 **Bashyam MD**. Understanding cancer metastasis: an urgent need for using differential gene expression analysis. *Cancer* 2002; **94**: 1821-1829
24 **Ramaswamy S**, Golub TR. DNA microarrays in clinical oncology. *J Clin Oncol* 2002; **20:** 1932-1941
25 **Lakhani SR**, Ashworth A. Microarray and histopathological analysis of tumours: the future and the past? *Nat Rev Cancer* 2001; **1:** 151-157
26 **Bertucci F,** Houlgatte R, Nguyen C, Viens P, Jordan B R, Birnbaum D. Gene expression profiling of cancer by use of DNA arrays: how far from the clinic? *Lancet Oncol* 2001; **2:** 674-682
27 **Balmain A.** Cancer genetics: from Boveri and Mendel to microarrays. *Nat Rev Cancer* 2001; **1:** 77-82
28 **Xu S,** Mou H, Lu G, Zhu C, Yang Z, Gao Y, Lou H, Liu X, Cheng Y, Yang W. Gene expression profile differences in high and low metastatic human ovarian cancer cell lines by gene chip. *Chin Med J* 2002; **115:** 36-41
29 **Lu T,** Liu J, Le Cluyse EL, Zhou YS, Cheng ML, Waalkes MP. Application of cDNA microarray to the study of arsenic-induced liver diseases in the population of Guizhou, China. *Toxicol Sci* 2001; **59:** 185-192
30 **Shen XZ,** Chow JF, Koo MW, Cho CH. Gene expression profiles in gastric mucosa of sleep deprivation rats. *World J Gastroenterol* 2000; **6:** 754-758
31 **Cheung ST,** Chen X, Guan XY, Wong SY, Tai LS, Ng IO, So S, Fan ST. Identify metastasis-associated genes in hepatocellular carcinoma through clonality delineation for multinodular tumor. *Cancer Res* 2002; **62**: 4711-4721
32 **Hamasuna R,** Kataoka H, Moriyama T, Itoh H, Seiki M, Koono M. Regulation of matrix metalloproteinase-2 (MMP-2) by hepatocyte growth factor / scatter factor (HGF / SF) in human glioma cells: HGF / SF enhances MMP-2 expression and activation accompanying up-regulation of membrane type-1 MMP. *Int J Cancer*, 1999; **82:** 274-281
33 **Abounader R,** Ranganathan S, Lal B, Fielding K, Book A, Dietz H, Burger P, Laterra J. Reversion of human glioblastoma malignancy by U1 small nuclear RNA / ribozyme targeting of scatter factor / hepatocyte growth factor and c-met expression. *J Natl Cancer Inst* 1999; **91:** 1548-1556
34 **Webb CP,** Hose CD, Koochekpour S, Jeffers M, Oskarsson M, Sausville E, Monks A, Vande Woude GF. The geldanamycines are potent inhibitor of the hepatocyte growth factor / scatter factor-Met-urokinase plasminogen activator-plasmin proteolytic netwok. *Cancer Res*, 2000; **60:** 342-349
35 **Nabeshima K,** Inoue T, Shimao Y, Okada Y, Itoh Y, Seiki M, Koono M. Front-cell-specific expression of membrane-type 1 matrix metalloproteinase and gelatinase A during cohort migration of colon carcinoma cells induced by hepatocyte growth factor / scatter factor. *Cancer Res* 2000; **60:** 3364-3369
36 **Hiscox S,** Jiang WG. Hepatocyte growth factor / scatter factor disrupts epithelial tumour cell-cell adhesion: involvement of beta-catenin. *Anticancer Res* 1999; **19:** 509-517
37 **Contreras HR,** Fabre M, Granes F, Casaroli-Marano R, Rocamora N, Herreros AG, Reina M, Vilaro S. Syndecan-2 expression in colorectal cancer-derived HT-29 M6 epithelial cells induces a migratory phenotype. *Biochem Biophys Res Commun* 2001; **286:** 742-751
38 **Munesue S,** Kusano Y, Oguri K, Itano N, Yoshitomi Y, Nakanishi H, Yamashina I, Okayama M. The role of syndecan-2 in regulation of actin-cytoskeletal organization of Lewis lung carcinoma-derived metastatic clones. *Biochem J* 2002; **363:** 201-209
39 **Tamura N,** Tai Y, Sugimoto K, Kobayashi R, Konishi R, Nishioka M, Masaki T, Nagahata S, Tokuda M. Enhanced expression and activation of Ca(2+) / calmodulin-dependent protein kinase IV in hepatocellular carcinoma. *Cancer* 2000; **89:** 1910-1916
40 **Williams CL,** Phelps SH, Porter RA. Expression of Ca2+ / calmodulin-dependent protein kinase types II and IV, and reduced DNA synthesis due to the Ca2+ / calmodulin-dependent protein kinase inhibitor KN-62 (1-[N,O-bis(5-isoquinolinesulfonyl)-N-methyl-L- tyrosyl]-4-phenyl piperazine) in small cell lung carcinoma. *Biochem Pharmacol* 1996; **51:** 707-715
41 **Wilson SE,** Weng J, Chwang EL, Gollahon L, Leitch AM, Shay JW. Hepatocyte growth factor (HGF), keratinocyte growth factor (KGF), and their receptors in human breast cells and tissues: alternative receptors. *Cell Mol Biol Res* 1994; **40:** 337-350
42 **Hijazi MM,** Thompson EW, Tang C, Coopman P, Torri JA, Yang D, Mueller SC, Lupu R. Heregulin regulates the actin cytoskeleton and promotes invasive properties in breast cancer cell lines. *Int J Oncol* 2000; **17:** 629-641
43 **Etoh T,** Shibuta K, Barnard GF, Kitano S, Mori M. Angiogenin expression in human colorectal cancer: the role of focal macrophage infiltration. *Clin Cancer Res* 2000; **6:** 3545-3551
44 **Lixin R,** Efthymiadis A, Henderson B, Jans DA. Novel properties of the nucleolar targeting signal of human angiogenin. *Biochem Biophys Res Commun* 2001; **284**: 185-193
45 **Rao CN,** Lakka SS, Kin Y, Konduri SD, Fuller GN, Mohanam S, Rao JS. Expression of tissue factor pathway inhibitor 2 inversely correlates during the progression of human gliomas. *Clin Cancer Res* 2001; **7:** 570-576
46 **Kataoka H,** Uchino H, Denda K, Kitamura N, Itoh H, Tsubouchi H, Nabeshima K, Koono M. Evaluation of hepatocyte growth factor activator inhibitor expression in normal and malignant colonic mucosa. *Cancer Lett* 1998; **128:** 219-227
47 **Longo N,** Yanez-Mo M, Mittelbrunn M, de la Rosa G, Munoz ML, Sanchez-Madrid F, Sanchez-Mateos P. Regulatory role of tetraspanin CD9 in tumor-endothelial cell interaction during transendothelial invasion of melanoma cells. *Blood* 2001; **98:** 3717-3726
48 **Hashida H,** Takabayashi A, Tokuhara T, Taki T, Kondo K, Kohno N, Yamaoka Y, Miyake M. Integrin alpha3 expression as a prognostic factor in colon cancer: Association with MRP-1 / CD9 and KAI1 / CD82. *Int J Cancer* 2002; **97:** 518-525
49 **Luo D,** Liu QF, Gove C, Naomov NV, Su JJ, Williams R. Analysis of N-ras gene mutation and p53 gene expression in human hepatocellular carcinomas. *World J Gastroenterol* 1998; **4:** 97-99
50 **Wang L,** Lu W, Chen YG, Zhou XM, Gu JR. Comparison of gene expression between normal colon mucosa and colon carcinoma by means of messenger RNA differential display. *World J Gastroenterol* 1999; **5:** 533-534
51 **Sun BH,** Zhang J, Wang BJ, Zhao XP, Wang YK, Yu ZQ, Yang DL, Hao LJ. Analysis of in vivo patterns of caspase 3 gene expression in primary hepatocellular carcinoma and its relationship to p21(WAF1) expression and hepatic apoptosis. *World J Gastroenterol* 2000; **6:** 356-360
52 **Wu BP,** Zhang YL, Zhou DY, Gao CF, Lai ZS. Microsatellite instability, MMR gene expression and proliferation kinetics in colorectal cancer with famillial predisposition. *World J Gastroenterol* 2000; **6:** 902-905
53 **Berditchevski F,** Odintsova E. Characterization of integrin-tetraspanin adhesion complexes: role of tetraspanins in integrin signaling. *J Cell Biol* 1999; **146:** 477-492
54 **Tanaka N,** Ogi K, Odajima T, Dehari H, Yamada S, Sonoda T, Kohama G. pRb2 / p130 protein expression is correlated with clinicopathologic findings in patients with oral squamous cell carcinoma. *Cancer* 2001; **92:** 2117-2125
55 **Paggi MG,** Giordano A. Who is the boss in the retinoblastoma family? The point of view of Rb2 / p130, the little brother. *Cancer Res* 2001; **61:** 4651-4654
56 **Classon M,** Dyson N. p107 and p130: versatile proteins with interesting pockets. *Exp Cell Res* 2001; **264:** 135-147

Edited by Zhao P and Wang XL

P.O.Box 2345, Beijing 100023,China
Fax: +86-10-85381893
E-mail: wjg@wjgnet.com www.wjgnet.com

World J Gastroenterol 2003;9(8):1739-1742
World Journal of Gastroenterology
 ISSN 1007-9327

• VIRAL HEPATITIS •

Pathogenicity of GB virus C on virus hepatitis and hemodialysis patients

Wan-Fu Zhu, Li-Min Yin, Peng Li, Jian Huang, Hui Zhuang

Wan-Fu Zhu, Li-Min Yin, Peng Li, Jian Huang, Hui Zhuang, Department of Microbiology, School of Basic Medical Sciences, Peking University, Beijing 100083, China
Supported by the National Natural Science Foundation of China, No.39870695
Correspondence to: Professor Wan-Fu Zhu, Department of Microbiology, School of Basic Medical Sciences, Peking University, Beijing 100083, China. zhuwanfu@sun.bjmu.edu.cn
Telephone: +86-10-82801599 **Fax:** +86-10-82801599
Received: 2003-01-04 **Accepted:** 2003-02-13

Abstract

AIM: To determine the pathogenicity of GB virus C (GBV-C) on liver and the effects of its co-infection on the clinical features and prognosis of patients with hepatitis B and C.

METHODS: Cross-sectional study was carried out in 413 patients with acute, chronic hepatitis B or liver cirrhosis, and in 67 hemodialysis patients. A 20-month prospective cohort study was carried out in 95 hepatitis B and 80 hepatitis C patients. A reverse transcriptase nested polymerase chain reaction (RT-nPCR) of the 5'-noncoding region was used to detect circulating GBV-C RNA. Liver function was determined by an automated analyzer for all patients.

RESULTS: The prevalence of GBV-C in the high-risk populations with the virus transmitted via blood was high, ranging from 16.2 to 28.8 %. Co-infection with GBV-C in hepatitis B patients did not affect the clinical features of the disease or liver function. The dialysis patients infected with GBV-C alone did not develop functional changes to the liver. Prospective cohort study showed that GBV-C co-infection did not affect the clinical features, prognosis or negative serum conversion rate of chronic hepatitis B and C.

CONCLUSION: The results suggest that GBV-C has no marked pathogenicity on liver, so it may not be a hepatitis virus.

Zhu WF, Yin LM, Li P, Huang J, Zhuang H. Pathogenicity of GB virus C on virus hepatitis and hemodialysis patients. *World J Gastroenterol* 2003; 9(8): 1739-1742
http://www.wjgnet.com/1007-9327/9/1739.asp

INTRODUCTION

Hepatitis B and C viruses (HBV, HCV) jointly contribute to 90 % of cases of post-transfusion non-A, non-B hepatitis (HNANB). The remaining 10 % of cases could not be attributed to any of the other known hepatitis viruses or other factors such as alcohol, drug, or any disease related causes[1,2]. These cases are named non-A-E hepatitis (HNA-E) and may be caused by an unknown viral agent. In 1995 and 1996, GB virus-C (GBV-C) and hepatitis G virus (HGV) were cloned by Simons *et al.* and Linnen *et al.*, respectively, in the United States[3,4]. Sequence analysis revealed that these two viruses had 85 % and 95 % identical nucleotide and amino acid sequences, respectively. And now these two viruses are named as GBV-C. Initially, GBV-C was isolated from the serum of patients with HNA-E[3,4]. However, there are still a lot of arguments up to now on the pathogenicity of GBV-C on liver and on whether GBV-C is an aetiological agent of HNA-E[5,6]. The prevalence of GBV-C in patients with chronic hepatitis B or chronic hepatitis C is very common, because of the similar transmission routes[7-12]. In the present study, we investigated the prevalence of GBV-C and evaluated its pathogenicity on liver with a cross-sectional study in 413 patients with acute, chronic hepatitis B, or liver cirrhosis, and in 67 hemodialysis patients. We also carried out a 20-month prospective cohort study in 95 patients with chronic hepatitis B and 80 patients with chronic hepatitis C. The results suggest that GBV-C has no marked pathogenicity on liver, so it may not be a new hepatitis virus.

MATERIALS AND METHODS

Patients

A total of 413 inpatients with confirmed diagnoses of acute, chronic hepatitis B or liver cirrhosis in two hospitals for infectious diseases in Beijing from January to December 2000 were enrolled in this study. Anti-HAV IgM, anti-HCV, anti-HDV and anti-HEV antibodies were all negative in these patients. Serum samples of the inpatients were collected and tested to assess liver biochemical characteristics on the day of admission. The rest serum was tested and stored at -80 ℃ for pathogen analysis.

Serum samples of hemodialysis patients with renal failure were collected from 67 patients in 3 general hospitals from December 2001 to March 2002 in Beijing. All samples were stored at -30 ℃ before analysis.

A cohort of 95 patients with chronic hepatitis B and 80 patients with chronic hepatitis C was enrolled from villages of a county in Zhoukou area, Henan Province. All patients were infected with HBV or HCV from 1991 to 1992 as a consequence of blood donation. All the patients had persistently elevated serum alanine aminotransferase (ALT) (at least 1.5 times the upper limit of the normal level) and were positive for serum HBV DNA or HCV RNA as detected by PCR or RT-PCR, respectively. All the patients were negative for serum anti-HAV IgM and anti-HEV. The average disease course of these patients was 3 years when investigation and confirming diagnosis were carried out in April 1994. All the patients of the cohort showed no evidence of liver cirrhosis or hepatocellular carcinoma in regular ultrasonic graphic examinations. All the patients were followed up twice, i.e., 6 and 20 months after the first investigation.

Laboratory examination

For GBV-C RNA detection, RNA was first extracted from 50 μl of serum using a commercial RNA extraction kit (Promega, Z5110). Reverse transcriptase and nested polymerase chain reactions (RT-nPCR), 35 cycles for two round, were performed using a PCR machine (SABC Thinker Series II, Sino-American Biotechnology Company, China). The primers used were from

the 5' -noncoding region of the GBV-C genome, outer primers (sense, 5' -TCTTGGTAGCCACTATAGGTG-3' , and antisense, 5' -GGCAAAGCCTATTGGTCAAG-3'), and inner primers (sense, 5' -AGAAAGAGCACGGTCCACAG-3' , and antisense, 5' -CCACTGGTCCTTGTCAACTC-3'). The amplified product (158 base pairs) was visualized under ultraviolet light after gel electrophoresis and stained with ethidium bromide. GBV-C RNA was assessed in duplicate sera and scored as positive only when consistent results were obtained. Liver biochemistry tests including alanine aminotransferase (ALT), aspartate aminotransferase (AST), total bilirubin (TBil), direct bilirubin (DBil), total protein (Tp), and serum albumin/globulin ratio (A/G) were measured with an automated analyzer.

Statistical analysis

Data in the text and tables were expressed as $\bar{x}\pm s$. Student' s *t*-test and one-way analysis of variance were used for statistical analysis according to the data obtained. For all tests, *P* values less than 0.05 were considered to be statistically significant, and *P* values less than 0.01 were considered to be greatly statistically significant.

RESULTS

Of the serum samples from 413 patients infected with HBV, 67 were co-infected with GBV-C (16.22 %). 169 cases had integrated clinical data. The patients suffering from acute, chronic hepatitis B or liver cirrhosis were grouped on the basis of the presence or absence of GBV-C co-infection, and the levels of ALT, AST, TBil, DBil, Tp of the different groups were compared (Table 1).

Results shown in Table 1 indicated that there was no significant difference in the serum biochemistry characteristics of 3 types of patients (acute, chronic hepatitis B and liver cirrhosis) between GBV-C RNA infected group and non-infected group ($P>0.05$).

11 of the 67 dialysis patients were GBV-C RNA positive (16.42 %) and the positive rate of GBV-C RNA increased with the number of times of dialysis. The comparison of serum ALT and AST levels in 67 patients infected with different viruses is shown in Table 2.

Table 2 Comparison of serum ALT and AST in dialysis patients with different virus infection

Group	*n*	Average dialysis times	ALT/IU·L^{-1}	AST/IU·L^{-1}
(1) HBV DNA(+) HCV RNA(-) GBV-C RNA(-)	11	243.75±224.53	31.63±22.32	35.12±18.06
(2) HBV DNA(-) HCV RNA(+) GBV-C RNA(-)	6	306.67±296.41	30.67±9.45	25.00±12.28
(3) HBV DNA(-) HCV RNA(-) GBV-C RNA(+)	8	353.40±309.45	20.67±11.72	17.00±1.00
(4) HBV DNA(-) HCV RNA(-) GBV-C RNA(-)	37	116.45±103.02	15.37±6.83	20.00±7.04

Table 1 Comparison of biochemistry characteristics in all types of patients with or without GBV-C infection

Group	*n*	ALT/IU·L^{-1}	AST/IU·L^{-1}	TBil/μmol·L^{-1}	DBil/μmol·L^{-1}	Tp/g·L^{-1}
Acute hepatitis B						
GBV-C RNA(+)	13	1173.92±961.98	565.69±405.32	5.18±3.47	3.54±2.66	68.44±12.14
GBV-C RNA(-)	33	1380.27±906.14	620.06±405.32	6.52±6.61	4.57±4.51	67.84±12.42
Chronic hepatitis B						
GBV-C RNA(+)	24	366.33±237.36	289.42±201.32	6.48±7.34	3.98±4.50	71.30±8.57
GBV-C RNA(-)	35	312.91±432.82	227.29±292.17	3.29±5.58	2.21±4.24	71.06±7.66
Liver cirrhosis						
GBV-C RNA(+)	30	71.67±74.13	96.73±87.21	5.54±7.44	3.62±5.33	66.46±8.75
GBV-C RNA(-)	34	92.68±80.33	106.15±94.81	7.67±10.30	5.20±5.80	62.58±10.99
Total						
GBV-C RNA(+)	67	400.51±585.36	255.22±301.71	5.73±6.81	3.69±4.46	68.80±9.61
GBV-C RNA(-)	102	578.63±807.04	314.98±345.05	5.85±7.85	3.87±4.80	67.21±10.92

No significant difference ($P>0.05$) was found in all the biochemistry characteristics between hepatitis B patients with or without GBV-C infection.

Table 3 Comparison of biochemistry characteristics between chronic hepatitis B patients with or without GBV-C infection

GBV-C RNA	*n*	A/G	ALT/IU·L^{-1}	AST/IU·L^{-1}	TBil/μmol·L^{-1}
(1) Positive group	24	1.65±0.26	90.84±48.43	43.21±31.56	5.91±1.86
(2) Negative group	71	1.63±0.21	95.36±51.96	44.45±38.07	7.66±1.95

No significant difference ($P>0.05$) was found in all the biochemistry characteristics between the two groups.

Table 4 Comparison of biochemistry characteristics between chronic hepatitis C patients with or without GBV-C infection

GBV-C RNA	*n*	A/G	ALT/IU·L^{-1}	AST/IU·L^{-1}	TBil/μmol·L^{-1}
(1) Positive group	23	1.82±0.30	110.23±59.61	45.96±40.11	4.53±1.55
(2) Negative group	57	1.65±0.25	97.65±56.74	52.94±48.00	5.77±1.73

No significant difference ($P>0.05$) was found in all the biochemistry characteristics between the two groups.

On statistic analysis, ALT levels were significantly different between groups 1 and 4 ($P<0.01$) and groups 2 and 4 ($P<0.05$). AST levels were also significantly different between groups 1 and 4 ($P<0.01$). The results showed a significant elevation in the levels of ALT and AST in hemodialysis patients infected with HBV or HCV compared with that in those not infected with the two viruses. Significant difference ($P<0.05$) was found in dialysis times between groups 2 and 4, and groups 3 and 4. Three patients had abnormal liver function (ALT>40 IU/L, AST>40 IU/L), among them one was infected with HCV, the other two were infected with HBV. Serum ALT and AST levels were normal in patients with GBV-C infection alone.

A cohort study was carried out in 95 patients with chronic hepatitis B and 80 patients with chronic hepatitis C enrolled from villages in Henan Province. Serum GBV-C was positive in 24 (25.26 %) chronic hepatitis B patients and 23 (28.75 %) chronic hepatitis C patients (Tables 3 and 4).

When following up the patients 6 months later, we found that 23 of the 95 chronic hepatitis B patients (24.21 %) became HBV DNA negative and 21 of the 80 (26.25 %) chronic hepatitis C patients became HCV RNA negative. GBV-C RNA could not be detected in 12.50 % (3/95) chronic hepatitis B patients and in 17.39 % (4/80) chronic hepatitis C patients. Table 5 and Table 6 show the biochemistry characteristics of chronic hepatitis B and C patients.

Table 5 Comparison of biochemistry characteristics between chronic hepatitis B patients with or without GBV-C infection at the 6-month follow-up

Group	*n*	A/G	ALT/IU·L^{-1}	AST/IU·L^{-1}	TBil/μmol·L^{-1}
(1) HBV DNA(+) GBV-C RNA(+)	14	1.74±0.19	93.29±60.67	29.14±13.87	7.64±5.47
(2) HBV DNA (+) GBV-C RNA (-)	58	1.73±0.18	62.33±41.67	27.68±11.99	6.10±2.09
(3) HBV DNA (-) GBV-C RNA (+)	7	1.61±0.11	30.00±7.80	21.57±8.18	7.57±3.41
(4) HBV DNA (-) GBV-C RNA (-)	16	1.64±0.14	32.65±17.01	26.65±11.96	7.71±2.76

Significant difference ($P<0.05$) was found only in ALT between group 1 and group 3, group 2 and group 4. No significant difference ($P>0.05$) was found in other biochemistry characteristics among the 4 groups.

Table 6 Comparison of biochemistry characteristics between chronic hepatitis C patients with or without GBV-C infection at the 6-month follow-up

Group	*n*	A/G	ALT/IU·L^{-1}	AST/IU·L^{-1}	TBil/μmol·L^{-1}
(1) HCV RNA(+) GBV-C RNA(+)	11	1.76±0.17	127.11±82.12	41.13±19.07	7.49±5.82
(2) HCV RNA(+) GBV-C RNA (-)	48	1.82±0.20	71.62±47.74	26.05±12.49	7.97±3.91
(3) HCV RNA (-) GBV-C RNA(+)	8	1.60±0.13	33.11±8.08	22.97±9.78	7.26±4.25
(4) HCV RNA (-) GBV-C RNA (-)	13	1.60±0.14	30.74±20.01	24.65±11.84	7.65±3.23

Significant difference ($P<0.05$) was found both in ALT between group 1 and group 3, group 2 and group 4, and in AST between group 1 and group 4. No significant difference ($P>0.05$) was found in other biochemistry characteristics among the 4 groups.

At the 20-month follow up, the biochemistry characteristics of chronic hepatitis B and C patients were compared between two groups: one with and the other without GBV-C co-infection (Tables 7 and 8). At this time point, 26.0 % (25/95) chronic hepatitis B patients and 20.0 % (16/80) chronic hepatitis C patients were lost in the follow up.

Table 7 Comparison of biochemistry characteristics between chronic hepatitis B patients with or without GBV-C infection after 20 months

Group	*n*	ALT/IU·L^{-1}	AST/IU·L^{-1}
(1) HBV DNA(+) GBV-C RNA(+)	8	52.13±44.90	44.25±28.42
(2) HBV DNA (+) GBV-C RNA (-)	30	44.40±37.26	34.67±24.23
(3) HBV DNA (-) GBV-C RNA (+)	8	28.14±15.36	25.29±17.21
(4) HBV DNA (-) GBV-C RNA (-)	24	25.15±11.59	25.73±13.16

Significant difference ($P<0.05$) was found only in ALT and AST between group 1 and group 3, and group 2 and group 4.

Table 8 Comparison of biochemistry characteristics between chronic hepatitis C patients with or without GBV-C infection after 20 months

Group	*n*	ALT/IU·L^{-1}	AST/IU·L^{-1}
(1) HCV RNA(+) GBV-C RNA(+)	6	72.24±73.87	49.29±48.49
(2) HCV RNA(+) GBV-C RNA (-)	22	42.43±39.10	32.91±30.57
(3) HCV RNA (-) GBV-C RNA(+)	7	26.98±24.47	25.11±19.07
(4) HCV RNA (-) GBV-C RNA (-)	29	25.39±13.16	26.74±16.99

Significant difference ($P<0.05$) was found only in ALT and AST between group 1 and group 3, and group 2 and group 4.

After 20-month follow up, correlation was seen between the abnormal levels of the liver biochemistry characteristics and HBV DNA in chronic hepatitis B patients. However, no correlation was found between the abnormal levels of the liver function and co-infection with GBV-C. The same result was found in chronic hepatitis C patients. During the period of follow up for 20 months, 50.00 % (8/16) hepatitis B patients with GBV-C infection and 44.44 % (24/54) hepatitis B patients without GBV-C infection became HBV DNA undetectable. 53.85 % (7/13) hepatitis C patients with GBV-C infection and 56.86 % (29/51) hepatitis C patients without GBV-C infection became HCV RNA undetectable. The rates of negative serum conversion of HBV DNA and HCV RNA were not significantly different between the two groups.

DISCUSSION

Since GBV-C was cloned, there have been a lot of arguments on the pathogenicity of GBV-C. Although a number of reports have indicated that GBV-C can induce acute, chronic, and even fulminant hepatitis[13-16], most of the clinical observations have demonstrated that GBV-C infection alone has little significance in causing liver damage in human[17-20]. There were 363 research publications on GBV-C/HGV in MEDLINE database from 1999 to February 2001, among which only 8 supported GBV-C pathogenicity on the liver. Most researches implicated that no correlation existed between GBV-C and liver diseases. Patients with HBV or HCV co-infected with GBV-C did not have different clinical manifestations and outcomes when compared with patients with HBV or HCV infection alone[21-23].

GBV-C, HBV and HCV have a similar route of transmission. Many of the reports limited their research on the prevalence of GBV-C in hepatitis B and hepatitis C patients and had relatively small numbers of cases. Therefore, it was difficult for them to draw a definite conclusion on GBV-C pathogenicity on the liver. The subjects of this study were a large sample in the high-risk population with GBV-C infection (hepatitis B, hepatitis C and hemodialysis patients). This work combined the cross-sectional and prospective cohort studies and applied the methods of cross-experimental design and analysis. Therefore, it could analyze more reasonably the pure effects of GBV- C infection on liver.

All data in this study were pooled from experiments carried out by many graduate students and repeated many times. Hepatitis B, hepatitis C and hemodialysis patients belonged to the high-risk population transmitted via blood. Previous investigations have shown that there was no significant difference between the prevalence rates of GBV-C in patients with HNA-E and of the aforementioned high-risk population (P>0.05)[23-25]. So these findings do not support the argument that GBV-C was the etiological factor of HNA-E. No significant difference was seen in the abnormal level of liver biochemistry characteristics between positive and negative serum GBV-C RNA in acute, chronic hepatitis B or liver cirrhosis patients (P>0.05). But the abnormal level of liver biochemistry characteristics correlated well with HBV DNA. Therefore, these results demonstrated that co-infection with GBV-C did not affect the liver biochemistry characteristics and illness. Infection with HBV or HCV could elevate the level of liver enzymes (ALT and AST) in hemodialysis patients, but infection with GBV-C did not demonstrate such effects. So these results showed that the hemodialysis patients had no abnormal liver biochemistry characteristics when infected with GBV-C alone without the known hepatitis virus co-infection. The dynamic observation in 3 follow-ups of the cohort of chronic hepatitis B and C patients during a period of 20 months indicated that co-infection with GBV-C did not significantly affect the illness, outcome or rate of negative serum conversion. In summary, this work demonstrates that, though GBV-C is highly prevalent in high-risk populations with virus infection via blood, it seems to have no pathogenicity on the liver and therefore may not be a hepatitis virus.

ACKNOWLEDGMENTS

We are very grateful to Prof. Liu Shu-Lin for his revision of the manuscript.

REFERENCES

1 **Alter HJ,** Seeff LB. Transfusion associated hepatitis. In: Zuckerman AJ, Thomas HC, eds. Viral Hepatitis. *London: Churchill Livingstone* 1998: 489-513
2 **Karayiannis P,** Pickering J, Zampino R, Thomas HC. Natural history and molecular biology of hepatitis G virus / GB virus C. *Clin Diagn Virol* 1998; **10**: 103-111
3 **Simons JN,** Leary TP, Dawson GJ, Pilot-Matias TJ, Muerhoff AS, Schlauder GG, Desai SM, Mushahwar IK. Isolation of novel virus-like sequences associated with human hepatitis. *Nat Med* 1995; **1**: 564-569
4 **Linnen J,** Wages J Jr, Zhang-Keck ZY, Fry KE, Krawczynski KZ, Alter H, Koonin E, Gallagher M, Alter M, Hadziyannis S, Karayiannis P, Fung K, Nakatsuji Y, Shih JW, Young L, Piatak M Jr, Hoover C, Fernandez J, Chen S, Zou JC, Morris T, Hyams KC, Ismay S, Lifson JD, Kim JP. Molecular cloning and disease association of hepatitis G virus: a transfusion-transmissible agent. *Science* 1996; **271**: 505-508
5 **Grassi M,** Mammarella A, Sagliaschi G, Granati L, Musca A, Traditi F, Pezzella M. Persistent hepatitis G virus (HGV) infection in chronic hemodialysis patients and non-B, non-C chronic hepatitis. *Clin Chem Lab Med* 2001; **39**: 956-960
6 **De Filippi F,** Lampertico P, Soffredini R, Rumi MG, Lunghi G, Aroldi A, Tarantino A, Ponticelli C, Colombo M. High prevalence, low pathogenicity of hepatitis G virus in kidney transplant recipients. *Dig Liver Dis* 2001; **33**: 477-479
7 **Halasz R,** Weiland O, Sallberg M. GB virus C / hepatitis G virus. *Scand J Infect Dis* 2001; **33**: 572-580
8 **Kleinman S.** Hepatitis G virus biology, epidemiology, and clinical manifestations: Implications for blood safety. *Transfus Med Rev* 2001; **15**: 201-212
9 **Li G,** Ma HH, Lau GK, Leung YK, Yao CL, Chong YT, Tang WH, Yao JL. Prevalence of hepatitis G virus infection and homology of different viral strains in southern China. *World J Gastroenterol* 2002; **8**: 1081-1087
10 **Yan J,** Chen LL, Luo YH, Mao YF, He M. High frequencies of HGV and TTV infections in blood donors in hangzhou. *World J Gastroenterol* 2001; **7**: 637-641
11 **Yan J,** Dennin RH. A high frequency of GBV-C / HGV coinfection in hepatitis C patients in Germany. *World J Gastroenterol* 2000; **6**: 833-841
12 **Yan J**, Chen LL, Lou YL, Zhong XZ. Investigation of HGV and TTV infection in sera and saliva from non-hepatitis patients with oral diseases. *World J Gastroenterol* 2002; **8**: 857-862
13 **Kocabas E,** Antmen B, Yarkin F, Serin M, Aksungur P, Tanyeli A, Kilinc Y, Aksaray N. Prevalence of GB virus C / hepatitis G virus infection in pediatric patients receiving multiple transfusions in southern Turkey. *Turk J Pediatr* 1999; **41**: 81-90
14 **Tanaka T,** Hess G, Tanaka S, Kohara M. The significance of hepatitis G virus infection in patients with non-A to C hepatic diseases. *Hepatogastroenterology* 1999; **46**: 1870-1873
15 **Yoshiba M,** Okamoto H, Mishiro S. Detection of the GBV-C hepatitis virus genome in serum from patients with fulminant hepatitis of unknown aetiology. *Lancet* 1995; **346**: 1131-1132
16 **Xu JZ,** Yang ZG, Le MZ, Wang MR, He CL, Sui YH. A study on pathogenicity of hepatitis G virus. *World J Gastroenterol* 2001; **7**: 547-550
17 **Sathar M,** Soni P, York D. GB virus C / hepatitis G virus (GBV-C / HGV): still looking for a disease. *Int J Exp Pathol* 2000; **81**: 305-322
18 **Pessoa MG,** Terrault NA, Detmer J, Kolberg J, Collins M, Hassoba HM, Wright TL. Quantitation of hepatitis G and C viruses in the liver: evidence that hepatitis G virus is not hepatotropic. *Hepatology* 1998; **27**: 877-880
19 **Sarrazin C,** Ruster B, Lee JH, Kronenberger B, Roth WK, Zeuzem S. Prospective follow-up of patients with GBV-C / HGV infection: specific mutational patterns, clinical outcome, and genetic diversity. *J Med Virol* 2000; **62**: 191-198
20 **Shindo M,** Arai K, Okuno T. Long-term follow-up of hepatitis G virus / GB virus C replication in liver during and after interferon therapy in patients coinfected with hepatitis C and G viruses. *J Gastroenterol* 1999; **34**: 680-687
21 **Fattovich G,** Ribero ML, Favarato S, Azzario F, Donato F, Giustina G, Fasola M, Pantalena M, Portera G, Tagger A. Influence of GB virus-C / hepatitis G virus infection on the long-term course of chronic hepatitis B. *Liver* 1998; **18**: 360-365
22 **Kao JH,** Chen PJ, Lai MY, Chen W, Chen DS. Effects of GB virus-C / hepatitis G virus on hepatitis B and C viremia in multiple hepatitis virus infections. *Arch Virol* 1998; **143**: 797-802
23 **Yu ML,** Chuang WL, Dai CY, Lu SN, Wang JH, Huang JF, Chen SC, Lin ZY, Hsieh MY, Tsai JF, Wang LY, Chang WY. The serological and molecular epidemiology of GB virus C / hepatitis G virus infection in a hepatitis C and B endemic area. *J Infect* 2001; **42**: 61-66
24 **Li P,** Zhu WF, An WF, Li ZJ, Wang SP, Zhuang H. Cohort study on pathogenicity of hepatitis G virus mixed infection with hepatitis B and C virus. *Zhongguo Gonggong Weisheng* 2002; **18**: 911-913
25 **Huang J,** Zhu WF, Li Z, Sun JY, Hao W, Wang XM, Li P, Zhuang H. Pathogenicity study of hepatitis G virus mixed infection in chronic hepatitis B and C patients. *Ziran Kexue Jinzhan* 2002; **12**: 307-310

Edited by Pang LH

P.O.Box 2345, Beijing 100023,China
Fax: +86-10-85381893
E-mail: wjg@wjgnet.com www.wjgnet.com

World J Gastroenterol 2003;9(8):1743-1746
World Journal of Gastroenterology
 ISSN 1007-9327

• VIRAL HEPATITIS •

Novel assay of competitively differentiated polymerase chain reaction for screening point mutation of hepatitis B virus

Xiao-Mou Peng, Xue-Juan Chen, Jian-Guo Li, Lin Gu, Yang-Su Huang, Zhi-Liang Gao

Xiao-Mou Peng, Xue-Juan Chen, Jian-Guo Li, Lin Gu, Yang-Su Huang, Zhi-Liang Gao, Department of Infectious Diseases, the Third Affiliated Hospital, Zhongshan University, Guangzhou 510630, Guangdong Province, China
Supported by the Science Foundation of Guangdong Province, No. 99M04801G
Correspondence to: Xiao-Mou Peng, Department of Infectious Diseases, the Third Affiliated Hospital, Zhongshan University, Guangzhou 510630, China. xiaomoupeng@hotmail.com
Telephone: +86-20-85516867 Ext 2019 **Fax:** +86-20-85515940
Received: 2003-04-12 **Accepted:** 2003-05-17

Abstract

AIM: Point mutation, one of the commonest gene mutations, is the most important molecular pathogenesis of cancer and chronic infection. The commonest methods for detection of point mutation are based on polymerase chain reaction (PCR). These techniques, however, cannot be used in large scale screening since they are neither accurate nor simple. For this reason, this study established a novel method of competitively differentiated PCR (CD-PCR) for screening point mutation in clinical practice.

METHODS: Two competitively differentiated primers for mutant-type and wild-type templates respectively with an identically complemented region in 3' end except for last 2 base pairs and a different non-complemented region in 5' end were designed. Thus, competitive amplification might be carried out at a lower annealing temperature at first, and then differentiated amplification at a higher annealing temperature when primers could not combine with initial templates. The amplification was performed in one-tube. The products of CD-PCR were detected using microplate hybridization assay. CD-PCR was evaluated by detecting G1896A variant of hepatitis B virus (HBV) in form of recombinant plasmids and in sera from patients with hepatitis B, and compared with allele-specific PCR (AS-PCR) and competitive AS-PCR.

RESULTS: CD-PCR was successfully established. It could clearly distinguish wild-type and mutant-type plasmid DNA of G1896A variant when the amount of plasmid DNA was between 10^2-10^8copies/reaction, while for AS-PCR and competitive AS-PCR, the DNA amount was between 10^2-10^4copies/reaction. CD-PCR could detect one copy of G1896A variant among 10-100 copies of wild-type plasmid DNA. The specificity of CD-PCR was higher than those of AS-PCR and competitive AS-PCR in the detection of HBV G1896A variant in sera from patients with hepatitis B. CD-PCR was independent of the amount of HBV DNA in serum. HBV G1896A variant was more often found in HBeAg (-) patients with a lower level of detectable viremia than that with a higher level of detectable viremia (P=0.0192).

CONCLUSION: CD-PCR is more specific since it is less influenced by the amount of initial templates and the cross amplification between mutant- and wild-type amplified products. It is also simple and time-saving. Thus, CD-PCR might be useful in routine gene typing and point mutation screening. HBV G1896A or other more important mutations have to be routinely detected in patients with a detectable level of viremia after HBeAg/antibody conversion in clinical practice.

Peng XM, Chen XJ, Li JG, Gu L, Huang YS, Gao ZL. Novel assay of competitively differentiated polymerase chain reaction for screening point mutation of hepatitis B virus. *World J Gastroenterol* 2003; 9(8): 1743-1746
http://www.wjgnet.com/1007-9327/9/1743.asp

INTRODUCTION

Point mutation is one of the commonest gene mutations not only in human genome but also in genome of pathogens. It is the most important molecular pathogenesis of cancer and chronic infection[1-3]. The commonest method for detecting point mutation is based on polymerase chain reaction (PCR), which can be divided into two types. One type is to analyze the PCR products using direct sequencing, restriction fragment length polymorphism and single strand conformation polymorphism[4-7]. This type of technique is usually accurate, but cannot be used in routine clinical examination since it needs additional manipulation. The other type is allele specific-PCR (AS-PCR), sequence specific-PCR or amplification refractory mutation system[8-13]. This type of techniques is usually simple, but its specificity is influenced by the amount of initial templates of PCR. This deficiency was not so obvious when this type of methods was used to detect point mutation or gene typing of human gene in the past since the initial templates in these samples could be controlled[8,12,13]. Some investigators, however, have made efforts to improve AS-PCR by introducing competitive mechanism, and established the so-called bidirectional AS-PCR and competitive PCR in order to decrease the influence of the amount of initial templates on its specificity[14-19]. AS-PCR has been used to detect point mutation of pathogens recently[10, 20-22]. However, the specificity of AS-PCR in detection of pathogen mutations was challenged by uncontrollable amount of initial templates and the requisition of high sensitivity. For these reasons, a novel method of competitively differentiated polymerase chain reaction (CD-PCR) was established in this study and compared with AS-PCR and competitive AS-PCR in the detection of G1896A variant of HBV.

MATERIALS AND METHODS

Materials

One hundred serum samples with (hepatitis B surface antigen) HBsAg(+), anti-(hepatitis B e antigen) HBe(+) and anti-(hepatitis B core antigen) HBc(+), 60 serum samples with HBsAg(+), HBeAg(+) and anti-HBc(+) and 40 serum samples without HBV serum markers were collected. The serum markers were demonstrated by enzyme-linked immunoabsorbent assay. Recombinant plasmid pG1896A was constructed as described

before[23]. TZ19U-HBV that contained double copies of HBV DNA (adw) was a gift from Professor Huang Zhimin (Zhongshan University, Guangzhou, China) and was used as wild-type DNA control. T4 DNA ligase and pfu DNA polymerase were purchased from Promega (USA). DNA gel extraction kits and plasmid isolation kits were purchased from Qiagen (Germang). Anti-digoxigenin and anti-fluorescein labeled with horseradish peroxidase were purchased from Roche (USA). Primers shown in Table 1 were designed with the Omega 2 software and synthesized in Bioasia Biological Engineering Company (Shanghai, China).

Table 1 Primers and probes for detecting of HBV G1896A variant

Denomination	Sequence(5'→3')
BIO-PCP	BIO-GAGAC TCTAA GGCTT CTCGA TACAG AGCTG AGG
PCA	GCAGT ATGGT GAGGT GAGCA ATGCT CAG
DIG-PCMd	DIG-CTCAC GCTAC ATTGT GTGCC TTGGG TGGCT TCA
DIG-PCMc	DIG-TGTGC CTTGG GTGGC TTCA
FLU-PCWd	FLU-GTCCG TAGTC TCGTT GTGCC TTGGG TGGCT TGG
FLU-PCWc	FLU-TGTGC CTTGG GTGGC TTGG
PCS	CCACC GTGAA CGCCC ATCAG
PCSc	CCCGA ATTCC ACCGT GAACG CCCAT CAG
PCAc	CCCAA GCTTG CAGTA TGGTG AGGTG AGCAA TG

BIO: the abbreviation of biotin; DIG: the abbreviation of digoxigenin; FLU: the abbreviation of fluorescein.

Methods

Principles of CD-PCR Two competitively differentiated primers (CDP) with different labels in 5' end were designed. CDP had a complemented region of 17-20 bp long with penultimate mismatch and a 3' terminus matching the mutant or the normal bases of the templates. The annealing temperature of this part was about 52-54 ℃. There was also a non-complemented region of 14 bp long, which was different from each other in 5' end. The total annealing temperature of CDP was about 75-80 ℃. PCR was performed in one tube. Competitive amplification was performed first when CDP competed for templates under lower annealing temperature. After certain amounts of products of each primer were obtained, differentiated amplification was then performed under higher annealing temperature when CDP could only use its own products as templates. This amplification model would keep the products ratio of mutant and wild templates and allow the templates to be fully amplified.

G1896A variant detected by CD-PCR Wild-type and G1896A mutant-type plasmids were used for the optimization of CD-PCR. A total volume of 30 μl was used in the final conditions of PCR reaction. The reaction mixture consisted of 10 mmol/L Tris-HCl, pH 8.5,50 mmol/L KCl, 1.5 mmol/L $MgCl_2$, 0.2 mmol/L dNTPs, 2U pfu DNA polymerase, 20 pmol FLU-PCWd, 20 pmol DIG-PCMd, 20 pmol PCA and 5 μl plasmid or extracted DNA. The cycling conditions were as follows: 3 cycles (first set) at 94 ℃ for 40 s, at 52 ℃ for 40 s and at 72 ℃ for 90 s followed by 35 cycles (second set) at 94 ℃ for 40 s, and at 72 ℃ for 90 s. The PCR products were then hybridized with solidified biotin-labeled probe PCP in two wells of microplate. The color reaction was obtained after captured PCR products reacted with anti-DIG or anti-FLU respectively, which were conjugated with horseradish peroxidase.

G1896A variant detected by competitive AS-PCR Except for the replacement of primer FLU-PCWd and DIG-PCMd with primer FLU-PCWc and DIG-PCMc, the components of competitive AS-PCR were similar to CD-PCR. The cycling conditions were as follows: 25 cycles (first set) at 94 ℃ for 40 s, at 60 ℃ for 40 s, and at 72 ℃ for 90 s followed by 10 cycles (second set) at 94 ℃ for 40 s, at 52 ℃ for 40 s, and at 72 ℃ for 90 s. The PCR products were then detected similar to CD-PCR.

G1896A variant detected by AS-PCR Except for the absence of FLU-PCWc, the components and the cycling conditions were similar to competitive CD-PCR. The PCR products were visualized under an ultraviolet transilluminator.

Quantification of serum HBV DNA by fluorescent quantitive PCR The HBV DNA level of 200 sera was detected using fluorescent quantitive PCR following the instruction (Taqmen, Roche).

DNA sequencing A fragment of HBV precore in positive or negative sera by all three methods and in sera that were positive for AS-PCR and competitive AS-PCR, and negative for CD-PCR was analyzed using DNA sequencing after it was amplified using primers PCSc and PCAc and cloned into plasmid pUC19.

RESULTS

Detection of HBV G1896A variant in recombinant plasmid DNA

The typical results of HBV G1896A variant detected by means of AS-PCR, competitive AS-PCR and CD-PCR are shown in Figure 1. To detect G1896A variant, the sensitivity of AS-PCR was 10^3 copies/reaction, and there was non-specific amplification when the amount of wild-type initial templates was higher than 10^4 copies/reaction. For competitive AS-PCR, the wild-type and mutant-type plasmid DNA could be clearly distinguished when the initial templates were 10^2-10^4 copies/reaction. CD-PCR could clearly distinguish them in the range of 10^2-10^8 copies/reaction. There was some degree of non-specific reaction when the amount of initial templates was higher than 10^4 copies/reaction, but the difference of color intensities between wild-type and mutant-type product wells was obvious. CD-PCR could detect one variant G1896A copy among 100 wild-type copies of DNA when the initial templates were 10^2-10^5 copies/reaction, but one out of 10 copies when the initial templates were 10^5-10^8 copies/reaction.

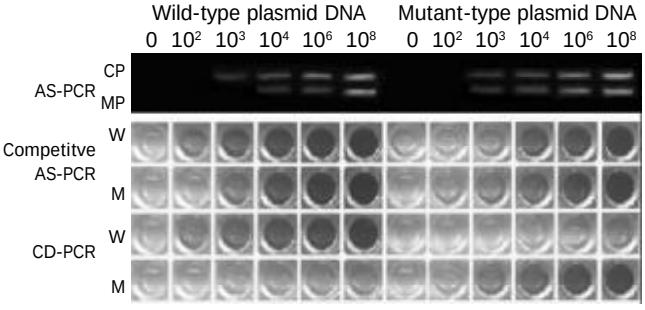

Figure 1 HBV G1896A variant detected by AS-PCR, competitive AS-PCR and CD-PCR using its wild-type or mutant-type recombinant plasmid DNA as objects. CP: common product band; MP: mutant product band; W: wild-type products; M: mutant-type products.

Detection of HBV G1896A variant in sera

Among 200 sera, HBV DNA was positive in 104 cases using AS-PCR, in 119 cases using competitive AS-PCR and in 122 cases using CD-PCR. The sensitivity for HBV DNA detection by CD-PCR was similar to that of competitive AS-PCR, but higher than that of AS-PCR (χ^2=5.47, P=0.0193). The results of G1896A variant in sera are shown in Table 2. Among the 104 cases with positive HBV DNA detected by all the three methods, there were 33 positive cases, and 31 negative cases

of G1896A variant detected by both CD-PCR and AS-PCR, and 40 cases that were positive by AS-PCR but not by CD-PCR.

Table 2 HBV G1896A variant and its relationship with HBV serum markers

	Cases	CD-PCR(%)		CAS-PCR(%)		AS-PCR(%)	
		HBV DNA(+)	G1896A variant	HBV DNA(+)	G1896A variant	HBV DNA(+)	G1896A variant
HBsAg(+)/ HBeAg(+)	60	100.0	6.7	100.0	63.3[b]	93.3	55.0[b]
HBsAg(+)/ HBeAg(-)	100	62.0[c]	38.0	59.0	46.0	48.0	40.0
HBsAg(-)/ HBeAg(-)	40	0	0	0	0	0	0

[b]$P<0.01$, compared with group of CD-PCR, χ^2 test, [c]$P<0.05$, compared with group of AS-PCR, χ^2 test.

The results of DNA sequencing

HBV G1896A mutation was confirmed by DNA sequencing in 3 positive sera by all the three methods, and excluded in 3 negative sera by all the three methods and in 4 sera that were positive by AS-PCR and competitive AS-PCR, but negative by CD-PCR.

The relationship between G1896A variant and HBV DNA level

The relationship between G1896A variant detected by AS-PCR, competitive AS-PCR and CD-PCR and HBV DNA level in the sera is shown in Table 3. More G1896A variants were found in patients with positive HBeAg by AS-PCR and competitive AS-CR. These could be false positives. These false-positive findings occurred more often in patients with a higher level of HBV DNA in serum. CD-PCR seemed more specific since only 4 patients were found to be infected with both wild-type HBV and G1896A variants in HBeAg positive cases. By CD-PCR, HBV G1896A variant was more often found in HBeAg (-) patients with a lower level of viremia (P=0.0192).

Table 3 Relationship between G1896A variant and HBV DNA level in serum

	HBeAg(+)(n=56)		HBeAg(-) (n=48)	
	$\leqslant 10^6$copies / ml (n=14)	$>10^6$ copies / ml(n=42)	$\leqslant 10^6$ copies / ml(n=28)	$>10^6$ copies / ml(n=20)
AS-PCR	2	31	21	19
Competitive AS-PCR	2	35	23	20
CD-PCR	2	2	21[a]	8

[a]Compared with HBeAg(-) group with a level higher than 10^6 copies / ml of HBV DNA in serum, Fisher's exact possibility test, P=0.0192.

DISCUSSION

AS-PCR has been considered as a simplest and quickest method for the detection of known point mutations[5,10-19]. False positive results, however, seem inevitable since the amplification of wild-type templates by allele-specific or sequence-specific primers for mutant-type templates can not be completely prevented. Once non-specific products occur, they will be amplified subsequently. Thus the ratio of specific and non-specific products will decrease, and become even smaller as the plateau of PCR reaches at the late stage. It is understandable that false band will occur when a large amount of initial templates or too many cycles are used in AS-PCR. To improve the specificity of AS-PCR, the specificity of primers was designed by introducing penultimate mismatch[24], and the cycles of specific amplification were reduced by introducing basic amplification[6,25]. The application of competitive mechanism is another important step to improve AS-PCR.

Competitive AS-PCR and bidirectional or tetra-primer AS-PCR are common assays that have a competitive mechanism[6,14-19,25]. Bidirectional or tetra-primer AS-PCR is in fact a competition for PCR system, while competitive AS-PCR is the competition for both templates and PCR system. However, these PCRs can not exclude the non-specific amplification from initial templates in each cycle. For competitive AS-PCR, it is possible to reduce the influence of initial templates, but a new problem will occur, which is that the initial products will become the templates for non-specific amplification in subsequent cycles. This might be the underlying mechanism that the competitive AS-PCR seemed worse than AS-PCR in this study. Therefore, to reduce the influence of the initial templates and products would be a very important measure to improve AS-PCR assay on specificity of amplification

For CD-PCR, competitive amplification was performed first, and followed by differentiated amplification, which was different from competitive AS-PCR. This protocol would allow allele- or sequence-specific amplification to begin at a low level of templates. Thus, the influence of initial templates could be controlled to a minimal level. After a few cycles, differentiated amplification was carried out under higher annealing temperature at which primers could not combine with initiated templates and the initial products could not be used as templates for non-specific amplification in subsequent cycles under higher annealing temperature either. These might be the mechanisms that CD-PCR had much better performance than that of AS-PCR and competitive AS-PCR in this study. The molecular weights of wild-type and mutant-type products were the same, therefore, products of CD-PCR could not be distinguished by electrophoresis. It was convenient and time-saving when microplate hybridization assay was used to demonstrate the products in this study. Automatic detection was possible too when CD-PCR was adapted to real-time fluorescent PCR assay as used in AS-PCR or competitive AS-CR[26,27]. CD-PCR could also be used by combining with other high resolution techniques[28,29]. It could be used in gene typing for organ transplantation or gene polymorphism in addition to the detection of gene point mutations as AS-PCR[30,31].

Detectable viremia was found in sera of some patients with hepatitis B after HBeAg/antibody conversion[32-34]. This type of viremia resulted in G1896A mutation in 60.4 % out of such patients, especially in patients with a much lower level of HBV DNA. This result is conformable to the fact that the replication ability of G1896A variant has decreased[35], and suggests that G1896A or other more important mutations have to be detected in patients with a detectable level of viremia after HBeAg/ antibody conversion in clinical practice.

REFERENCES

1 **Bressac B**, Kew M, Wands J, Ozturk M. Selective G to T mutations of p53 gene in hepatocellular carcinoma from southern Africa. *Nature* 1991; **350**: 429-431

2 **Steinberg JL**, Yeo W, Zhong S, Chan JY, Tam JS, Chan PK, Leung NW, Johnson PJ. Hepatitis B virus reactivation in patients undergoing cytotoxic chemotherapy for solid tumours: precore / core mutations may play an important role. *J Med Virol* 2000; **60**: 249-255

3 **Yoo BC**, Park JW, Kim HJ, Lee DH, Cha YJ, Park SM. Precore and core promoter mutations of hepatitis B virus and hepatitis B e antigen-negative chronic hepatitis B in Korea. *J Hepatol* 2003; **38**: 98-103

4 **Chen RY**, Edwards R, Shaw T, Colledge D, Delaney WE 4th, Isom

H, Bowden S, Desmond P, Locarnini SA. Effect of the G1896A precore mutation on drug sensitivity and replication yield of lamivudine-resistant HBV *in vitro*. *Hepatology* 2003; **37**: 27-35

5 **Peng XM**, Peng WW, Yao JL. Codon 249 mutations of p53 gene in development of hepatocellular carcinoma. *World J Gastroenterol* 1998; **4**: 125-127

6 **Peng XM**, Yao CL, Chen XJ, Peng WW, Gao ZL. Codon 249 mutations of p53 gene in non-neoplastic liver tissues. *World J Gastroenterol* 1999; **5**: 324-326

7 **Ding Y**, Le XP, Zhang QX, Du P. Methylation and mutation analysis of p16 gene in gastric cancer. *World J Gastroenterol* 2003; **9**: 423-426

8 **Suzuki F**, Suzuki Y, Tsubota A, Akuta N, Someya T, Kobayashi M, Saitoh S, Arase Y, Ikeda K, Kumada H. Mutations of polymerase, precore and core promoter gene in hepatitis B virus during 5-year lamivudine therapy. *J Hepatol* 2002; **37**: 824-830

9 **Moses JH**, Greville WD, Downes J, McClenahan W, Kennedy A, Dunckley H. A new HLA-A*02 allele, A*0234, detected by polymerase chain reaction using sequence-specific primers (PCR-SSP). *Tissue Antigens* 2000; **55**: 175-177

10 **Ma CL**, Fang DX, Chen HB, Li FQ, Jin HY, Li SQ, Tan WG. A mutation specific polymerase chain reaction for detecting hepatitis B virus genome mutations at nt551. *World J Gastroenterol* 2003; **9**: 509-512

11 **Hodgson DR**, Foy CA, Partridge M, Pateromichelakis S, Gibson NJ. Development of a facile fluorescent assay for the detection of 80 mutations within the p53 gene. *Mol Med* 2002; **8**: 227-237

12 **Stoehr R**, Knuechel R, Boecker J, Blaszyk H, Schmitt R, Filbeck T, Hofstaedter F, Hartmann A. Histologic-genetic mapping by allele-specific PCR reveals intraurothelial spread of p53 mutant tumor clones. *Lab Invest* 2002; **82**: 1553-1561

13 **Kirby GM**, Batist G, Fotouhi-Ardakani N, Nakazawa H, Yamasaki H, Kew M, Cameron RG, Alaoui-Jamali MA. Allele-specific PCR analysis of p53 codon 249 AGT transversion in liver tissues from patients with viral hepatitis. *Int J Cancer* 1996; **68**: 21-25

14 **Waterfall CM**, Eisenthal R, Cobb BD. Kinetic characterisation of primer mismatches in allele-specific PCR: a quantitative assessment. *Biochem Biophys Res Commun* 2002; **299**: 715-722

15 **Horvath AD**, Kirov SA, Karaulanov EE, Ganev VS. Detection of apoB-100 R3500Q mutation by competitive allele-specific polymerase chain reaction. *J Clin Lab Anal* 2001; **15**: 256-259

16 **Sasvari-Szekely M**, Gerstner A, Ronai Z, Staub M, Guttman A. Rapid genotyping of factor V Leiden mutation using single-tube bidirectional allele-specific amplification and automated ultrathin-layer agarose gel electrophoresis. *Electrophoresis* 2000; **21**: 816-821

17 **Hamajima N**, Saito T, Matsuo K, Kozaki K, Takahashi T, Tajima K. Polymerase chain reaction with confronting two-pair primers for polymorphism genotyping. *Jpn J Cancer Res* 2000; **91**: 865-868

18 **Hamajima N**, Saito T, Matsuo K, Tajima K. Competitive amplification and unspecific amplification in polymerase chain reaction with confronting two-pair primers. *J Mol Diagn* 2002; **4**: 103-107

19 **McKinzie PB**, Parsons BL. Detection of rare K-ras codon 12 mutations using allele-specific competitive blocker PCR. *Mutat Res* 2002; **517**: 209-220

20 **Gramegna M**, Lampertico P, Lobbiani A, Colucci G. Detection of the hepatitis B virus major pre-core mutation by the amplification refractory mutation system technique. *Res Virol* 1993; **144**: 307-309

21 **Nainan OV**, Khristova ML, Byun K, Xia G, Taylor PE, Stevens CE, Margolis HS. Genetic variation of hepatitis B surface antigen coding region among infants with chronic hepatitis B virus infection. *J Med Virol* 2002; **68**: 319-327

22 **Kinoshita M**, Seno T, Fukui T, Shin S, Tsubota A, Kumada H. A detection method for point mutation in the precore region of human hepatitis B virus (HBV)-DNA using mutation-site-specific assay. *Clin Chim Acta* 1994; **228**: 83-90

23 **Peng XM**, Gu L, Chen XJ, Huang YS, Gao ZL. The Defect and Improvement of Allele-specific PCR during Detection of G1896A Variant of Hepatitis B Virus. *J Practical Med* 2003; **19**: 467-469

24 **Fishbein WN**, Davis JI, Foellmer JW, Nieves S, Merezhinskaya N. A Competitive Allele-specific Oligomers Polymerase Chain Reaction Assay for the cis Double Mutation in AMPD1 that is the Major Cause of Myo-adenylate Deaminase Deficiency. *Mol Diagn* 1997; **2**: 121-128

25 **Hersberger M**, Marti-Jaun J, Hanseler E, Speck RF. Rapid detection of the CCR2-V64I, CCR5-A59029G and SDF1-G801A polymorphisms by tetra-primer PCR. *Clin Biochem* 2002; **35**: 399-403

26 **Glaab WE**, Skopek TR. A novel assay for allelic discrimination that combines the fluorogenic 5' nuclease polymerase chain reaction (TaqMan) and mismatch amplification mutation assay. *Mutat Res* 1999; **430**: 1-12

27 **Suemizu H**, Ohnishi Y, Maruyama C, Tamaoki N. Two-color allele-specific polymerase chain reaction (PCR-SSP) assay of the leptin receptor gene (Leprdb) for genotyping mouse diabetes mutation. *Exp Anim* 2001; **50**: 435-439

28 **Tian H**, Brody LC, Fan S, Huang Z, Landers JP. Capillary and microchip electrophoresis for rapid detection of known mutations by combining allele-specific DNA amplification with heteroduplex analysis. *Clin Chem* 2001; **47**: 173-185

29 **McClay JL**, Sugden K, Koch HG, Higuchi S, Craig IW. High-throughput single-nucleotide polymorphism genotyping by fluorescent competitive allele-specific polymerase chain reaction (SNiPTag). *Anal Biochem* 2002; **301**: 200-206

30 **Donohoe GG**, Laaksonen M, Pulkki K, Ronnemaa T, Kairisto V. Rapid single-tube screening of the C282Y hemochromatosis mutation by real-time multiplex allele-specific PCR without fluorescent probes. *Clin Chem* 2000; **46**: 1540-1547

31 **See D**, Kanazin V, Talbert H, Blake T. Electrophoretic detection of single-nucleotide polymorphisms. *Biotechniques* 2000; **28**: 710-714

32 **Seo Y**, Yoon S, Nakaji M, Yano Y, Nagano H, Ninomiya T, Hayashi Y, Kasuga M. Hepatitis B virus DNA in anti-HBe-positive asymptomatic Carriers. *Intervirology* 2003; **46**: 43-49

33 **Yotsuyanagi H**, Hino K, Tomita E, Toyoda J, Yasuda K, Iino S. Precore and core promoter mutations, hepatitis B virus DNA levels and progressive liver injury in chronic hepatitis B. *J Hepatol* 2002; **37**: 355-363

34 **Yuen MF**, Sablon E, Yuan HJ, Hui CK, Wong DK, Doutreloigne J, Wong BC, Chan AO, Lai CL. Relationship between the development of precore and core promoter mutations and hepatitis B e antigen seroconversion in patients with chronic hepatitis B virus. *J Infect Dis* 2002; **186**: 1335-1338

35 **Karino Y**, Toyota J, Sato T, Ohmura T, Yamazaki K, Suga T, Nakamura K, Sugawara M, Matsushima T, Hino K. Early mutation of precore (A1896) region prior to core promoter region mutation leads to decrease of HBV replication and remission of hepatic inflammation. *Dig Dis Sci* 2000; **45**: 2207-2213

Edited by Yuan HT and Wang XL

P.O.Box 2345, Beijing 100023,China
Fax: +86-10-85381893
E-mail: wjg@wjgnet.com www.wjgnet.com

World J Gastroenterol 2003;9(8):1747-1751
World Journal of Gastroenterology
 ISSN 1007-9327

Identification of *H. pylori* strain specific DNA sequences between two clinical isolates from NUD and gastric ulcer by SSH

Feng-Chan Han, Min Gong, Han-Chong Ng, Bow Ho

Feng-Chan Han, Min Gong, Han-Chong Ng, Bow Ho, Department of Microbiology, Faculty of Medicine, National University of Singapore, 5 Science Drive 2, Singapore 117595, Republic of Singapore
Supported by the NMRC-Sponsored Project, Grant number: R-182-000-037-213
Correspondence to: Feng-Chan Han, Institute of Genetic Diagnosis, Fourth Military Medical University, 169 Changle West Road, Xi' an 710033, Shaanxi Province, China. biohanfc@hotmail.com
Telephone: +86-29-3374772 **Fax:** +86-29-3285729
Received: 2003-04-08 **Accepted:** 2003-05-17

Abstract

AIM: The genomes of *Helicobacter pylori* (*H. pylori*) from different individuals are different. This project was to identify the strain specific DNA sequences between two clinical *H. pyl*ori isolates by suppression subtractive hybridization (SSH).

METHODS: Two clinical *H. pylori* isolates, one from gastric ulcer (GU, tester) and the other from non-ulcer dyspepsia (NUD, driver), were cultured and the genomic DNA was prepared and submitted to *Alu* I digestion. Then two different adaptors were ligated respectively to the 5'-end of two aliquots of the tester DNA fragments and SSH was made between the tester and driver DNA. The un-hybridized tester DNA sequences were amplified by two sequential PCR and cloned into pGEM-T-Easy Vector. The tester strain specific inserts were screened and disease related DNA sequences were identified by dot blotting.

RESULTS: Among the 240 colonies randomly chosen, 50 contained the tester strain specific DNA sequences. Twenty three inserts were sequenced and the sizes ranged from 261 bp to 1 036 bp. Fifteen inserts belonged to the *H.pylori* plasmid pHPO100 that is about 3.5 kb and codes a replication protein A. Other inserts had patches of homologous to the genes of *H.pylori* in GenBank. Various patterns of dot blots were given and no GU strain unique DNA sequences were found when 4 inserts were used as probes to screen the genomic DNA from 27 clinical isolates, 8 from GU, 12 from duodenum ulcer (DU), 4 from GU-DU, 2 from NUD and 1 from gastric cancer (GC). But a 670 bp DNA fragment (GU198) that was a bit homologous to the 3'-end of the gene of thymidylate kinase was positive in 7 GU strains (7/8), 3 GU-DU strains (3/4) and 3 DU strains (3/12). A 384 bp fragment (GU79) of the replication gene A (repA) was positive only in 4 *H.pylori* isolates, 2 from GU and 2 from GU-DU.

CONCLUSION: Differences exist in the genes of different *H.pylori* isolates. SSH is very effective to screen *H.pylori* strain specific DNA sequences between two clinical isolates, and some of these sequences may have clinical significance.

Han FC, Gong M, Ng HC, Ho B. Identification of *H. pylori* strain specific DNA sequences between two clinical isolates from NUD and gastric ulcer by SSH. *World J Gastroenterol* 2003; 9(8): 1747-1751
http://www.wjgnet.com/1007-9327/9/1747.asp

INTRODUCTION

Helicobacter pylori (*H. pylori*) is a microaerophilic Gram-negative bacterium that colonizes the stomach in more than half of the world population. It is the causative agent of chronic gastritis and contributes to peptic ulcer[1, 2] and also plays an important role in the pathogenesis of gastric cancer[3-16]. When one is infected by this bacterium, the clinical outcome depends on the interaction of virulent effects of the bacterium, the host response, and the environment[18]. The genomes of *H.pylori* from different individuals are quite different and each one contains about 1 600 genes, among which almost 320 genes are dispensable and 100 genes are strain unique[17-19]. Genes that are present in one strain and absent or substantially different in the others can be of great biological interest[20].

H. pylori strains with the cag pathogenicity island (PAI) can induce more severe inflammation, proliferation and apoptosis in the gerbil mucosa than do the strains partial or complete lack of the cag PAI[21]. In contrast to the $CagA^-$ *H. pylori* infection, $CagA^+$ *H. pylori* infection is associated with a higher prevalence of p53 mutation in gastric adenocarcinoma[22]. In addition to the *cag* island, other polymorphic loci that appear clinically relevant have to be identified.

We screened the strain specific DNA sequences between two clinical isolates and tried further to identify the disease related sequences. Different methods, such as microarray[19,21], and subtractive hybridization[18, 23,24] could be used for bacterial strain specific DNA screening. Suppression subtractive hybridization (SSH), in which the genomic DNA sample containing the sequences of interest is called "tester", and the reference sample is called "driver", is a powerful approach for assessing the DNA sequence differences among the closely related bacterial strains.

MATERIALS AND METHODS

H.pylori growth and genomic DNA extraction

H. pylori clinical isolates preserved in the brain heart infusion broth (BHI, Gibco) supplemented with 100 mL/L horse serum (Gibco) and 200 mL/L glycerol (BDH) were inoculated on the *H.pylori* selective chocolate blood agar containing 40 g/L blood agar base No.2 (Oxoid) and 50 mL/L horse blood (Gibco). Antibiotics were also used at the following concentrations: vancomycin (Sigma) 3 mg/L, trimethoprim (Sigma) 5 mg/L, nalidixic acid (Sigma) 10 mg/L and amphotericin B (Sigma) 2 mg/L. The plates were incubated in microaerobic atmosphere (50 mL/L CO_2) in a CO_2 incubator (Forma Scientific) at 37 ℃ for up to 5 days. *H.pylori* genomic DNA was extracted following Bow's method[25].

Driver and tester DNA preparations

The subtractive DNA library was made by using the PCR-select bacterial genome subtraction kit (Clontech) with Akopyants NS's method (*Proc Natl Acad Sci U S A.* 1998;95: 13108) as reference, but with some change at certain procedures. Genomic DNA of an *H.pylori* strain from gastric ulcer (GU) was used as the tester, and DNA of a strain from non-ulcer dyspepsia (NUD) was used as the driver. The

sequences of the adaptors and primers were listed as followings: adaptor 1, 5'-CTAATACGACTCACTATAGGGCTCGAGCGGCCGCCCGGGCAGGT-3',5'-ACCTGCCCGG-3',adaptor 2R, 5'-CTAATACGACTCACTATAGGGCAGCGTGGTCGCGGCCGAGGT-3',5'-ACCTCGGCCG-3',P1,5'-CTAATACGACTCACTATAGGGC-3', NP1, 5'-TCGAGCGGCCGCCCGGGCAGGT-3', NP2, 5'-AGCGTGGTCGCGGCCGAGGT-3'. In brief, 4 μg of the tester or driver genomic DNA was digested with 40 units of *Alu*I (New England Biolabs) in 400 μL reaction volume at 37 ℃ for 16 hours. The DNA fragments were then extracted with phenol and precipitated with ethanol, and resuspended in sterile distilled water at a final concentration of 300 mg/L. Two aliquots of tester DNA (120 ng each) were ligated separately to the two adaptors (2 μmol/L final concentration) at 16 ℃ for 16 hours, each in a total volume of 10 μL, with 1 μL (New Engl and Biolabs, 400 units) of T4 DNA ligase in the buffer supplied by the manufacturer. After ligation, 1 μL of 0.2 mol/L EDTA was added, and the sample was heated at 70 ℃ for 5 minutes to inactivate the ligase and then stored at -20 ℃.

Suppression subtractive hybridization

Two microliters of the driver DNA fragments (600 ng) were added to 1 μL (12 ng) of each adaptor-ligated tester DNA (50:1 ratio). One microliter of 4×hybridization buffer (2 mol/L NaCl, 200 mmol/L Hepes, pH 8.0, 0.8 mmol/L EDTA) was added to each tube, and the solution was overlaid with a drop of mineral oil. The DNA fragments were then denatured at 98 ℃ for 2 minutes, and allowed to anneal at 65 ℃ for 1.5 hours. After the first hybridization, the two samples (one with adaptor 1, the other with adaptor 2R) were combined and 300 ng more heat-denatured driver DNA dissolved in 2 μL of 1× hybridization buffer was added. The 10 μL mixture was allowed to hybridize at 65 ℃ for an additional 14 hours. After being diluted to 200 μL with dilution buffer (50 mmol/L, NaCl, 20 mmol/L Hepes, pH8.3, 0.2 mmol/L EDTA), the sample was heated at 65 ℃ for 10 minutes, and stored at -20 ℃.

The first and second PCRs

The first PCR mixture (25 μL) containing 1 μL of the above diluted DNA, 1 μL of 10 μmol/L PCR primer P1, 2 μL of 2.5 mmol/L dNTPs, 2.5 μL of 10×PCR reaction buffer, and 5 μL of the Advantage 2 Polymerase Mix (Clontech) was incubated in a thermal cycler (Perkin-Elmer 2400) at 72 ℃ for 2 minutes and subjected to 25 cycles at 94 ℃ for 30 s, at 66 ℃ for 30 s, and at 72 ℃ for 1.5 minutes. Seven microliters of the PCR products were analyzed by 15 g/L agarose gel electrophoresis. The products were then diluted 40-fold in 10 mmol/L Tris· HCl (pH 7.5). The second PCR mixture (25 μL) contained 1 μL of the diluted first PCR products, 1 μL of the nest PCR primers (NP1 and NP2, 10 μmol/L each), 2 μL of 2.5 mmol/L dNTPs, 2.5 μL of 10×PCR reaction buffer, and 5 μL of the Advantage 2 Polymerase Mix. The cycling program was 12 cycles at 94 ℃ for 30 s, at 68 ℃ for 30 s, and at 72 ℃ for 1.5 minutes, followed by further extension at 72 ℃ for 5 minutes. The PCR products were analyzed by 15 g/L agarose gel electrophoresis, purified by using the Quaquick Spin PCR Purification Kit (Qiagen) and cloned into the pGEM- T Easy Vector (Promega) following the protocols. The recombinant plasmids were transformed into *E. coli Top*[10], which was then cultured overnight on the selective agar plates containing 20 μL of 50 g/L ampicillin, 35 μL of 100 mmol/L IPTG and 40 μL of 20 g/L X-gal. White colonies were randomly picked and suspended in 100 μL of Luria-Bertani medium containing ampicillin in an eppendorf tube and cultured at 37 ℃ for 2 hours. One microliter of the cell suspension, after being frozen and thawed three times, was used as templates and the inserts were amplified under condition as in the second PCR except for 25 cycles. The sizes of the inserts were identified by agarose gel electrophoresis.

Strain specific insert screening and disease related DNA sequence identification

One microliter of each PCR product (10 ng) was dotted on the Hybond N+ membrane (Amersham) in duplicating forms and DNA fixation was carried out by irradiation under a UV transilluminator (Vilber Lourmat) for 5 minutes. The *Alu*I-digested DNA fragments of the tester and driver *H.pylori* were used as probes and dot blotting was preformed using the ECL direct nucleic acid labeling and detection system (Amersham Phamacia Biotech). The pre-hybridization and hybridization were carried out in the hybridization oven (Amersham) at 42 ℃ for 1 hour and 12 hours respectively. After stringently washing the Hybond N+ membrane (twice for 20 minutes in 6 mol/L Urea, 4 g/L SDS and 0.1×SSC, and twice for 5 minutes in 2× SSC), the chemiluminenscence signals were detected by exposure of the Hyperfilm to the membrane for 5 to 30 minutes. The inserts that gave positive results to the tester probes and negative to the driver probes were sequenced using a Big Dye Terminator DNA sequencing kit (Perkin-Elmer) and ABI automated sequencer. The sequences were then submitted to gene and protein homologous analysis. In the same way, by dotting 100 ng of each genomic DNA from different *H.pylori* isolates on the membrane and using the inserts interested as probes, the disease related DNA sequences were identified. In the above cases, 1 ng of each probe DNA was dotted on the membrane to be used as positive control.

RESULTS

Tester strain specific DNA sequencing and homologous analysis

After SSH between the tester and driver DNA fragments, about 900 colonies grew on the ampicillin plates and two thirds of them were white in color. Two hundred and forty white colonies

Table 1 Homologous analysis of some strain specific DNA sequences

Inserts	GenBank accesion No.	Homolog/genes or proteins	DNA matches
GU79	AF056496	*H.pylori* plasmid pHPO100/ RepA, $2e^{-53}$	1882-2265
GU150	AE000629	Carbamoyl-phosphate synthetase, $3e^{-29}$	1029-1229
GU185	AE000595	Putative outer membrane p1, $7e^{-24}$	2993-3177
GU198	AE001560	Thymidylate kinase, $2e^{-10}$	640-717
GU210	AE000590	Hypothetical protein , $3e^{-33}$	789-396
GU212	AE000531	Type II restriction enzyme R protein, $4e^{-26}$	1-597
GU223	AE000647	Hypothetical protein, $4e^{-16}$	7724-8193
GU234	AE000650	Site specific DNA-methyltransferase, $3e^{-54}$	9070-8752
GU235	AE000547	Toxin-like outer membrane protein, $2e^{-64}$	13943-14494

were randomly chosen and the inserts were amplified using the primers as in the nest PCR. By dotting and fixing the equal amount of each PCR product in replica form on the membrane, dot blotting was carried out using the *Alu*I digested DNA fragments as probes (Figure 1). Fifty tester strain specific DNA sequences were screened and 23 of them were sequenced. The sizes of the inserts ranged from 261 to 1 036 bp. Blast analysis showed that, of the 23 inserts sequenced, 15 belonged to parts of the *H.pylori* plasmid pHPO100 (Table1 only shows GU79) and 2 of them contained the same fragment. The size of this plasmid is 3 520 bp, which codes a replication protein A (RepA, 1 842-2 765) and an unknown protein (2 762-3 520). The other 8 inserts were homologous to genes of *H.pylori* in GenBank to different extent (Table1).

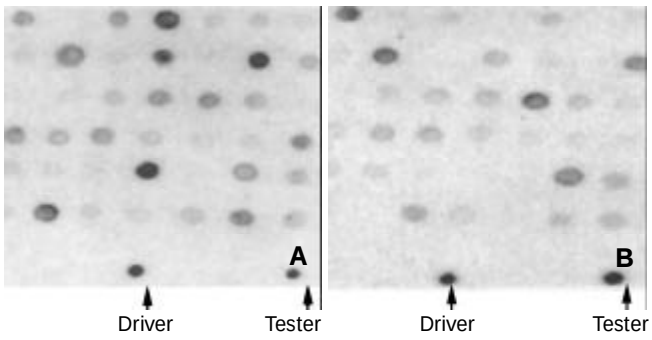

Figure 1 Dot blotting to screen the tester strain specific inserts by using the *Alu* I digested tester DNA (A) and driver DNA (B) as probes. The arrowheads indicate the spots of positive controls.

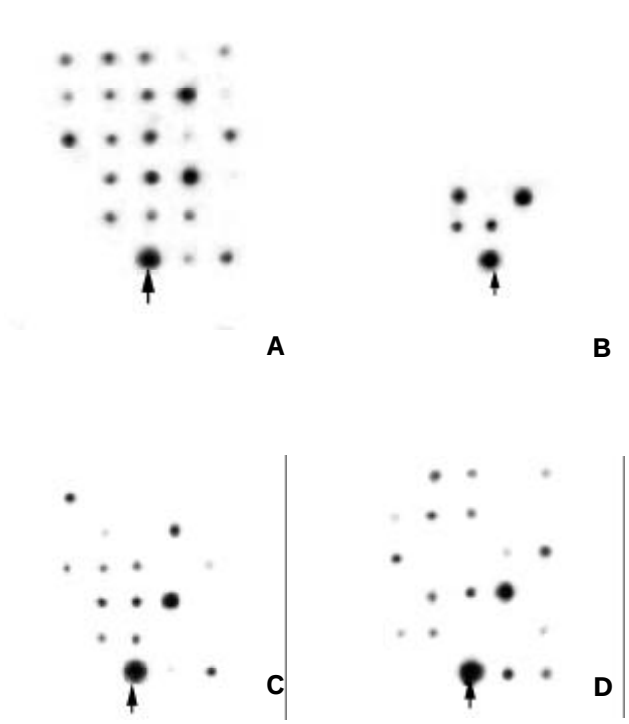

Figure 2 Dot blotting for identification the disease related DNA sequences in 27 different clinical isolates by using GU210 (A), GU79 (B), GU198 (C) and GU235 (D) as probes. The arrowheads indicate the spots of positive controls.

Disease related DNA sequence screening

We next chose 4 tester strain specific DNA sequences as probes to screen the genomic DNA of *H.pylori* with different clinical background, 8 from GU, 12 from duodenum ulcer (DU), 4 from GU-DU, 2 from NUD and 1 from gastric cancer (GC), to know if some of them were specific for the GU isolates. We found that the 4 different inserts gave 4 different dot blotting profiles (Figure 2) and there were no GU strain unique sequences. But a DNA fragment GU198 (670 bp) that was a bit (78 bp) homologous to the 3' -end of the gene of hymidylate kinase was positive in 7 of the 8 GU strains, 3 of the 4 GU-DU strains, and 3 of the 12 DU strains. It was also positive in one of the 2 NUD strains and the GC strain. The replication gene A fragment GU79 (384 bp) was positive in 4 *H.pylori* isolates, 2 from GU and 2 from GU-DU.

DISCUSSION

A remarkable feature of *H.pylori* is the high diversity of its genomic DNA[26-29]. Clinical isolates of *H.pylor*i from different individuals show enormous variations in their genomes or genes[30-33]. The genetic diversity is represented in many forms, including point mutations and inserted sequences[34]. Such variation has given rise to the notion that *H. pylori* has a very plastic genome, and that such plasticity confers a selective advantage on a bacterium that must co-evolve with its host over the course of decades[17]. Based on this, it is conceivable that there are different DNA sequences between two genomes of *H.pylori* with different clinical background.

SSH is a powerful technique that has been applied to research in many different fields. In studies of eukaryotic systems, application of subtraction techniques typically focuses on differential gene expression between two cDNA populations rather than differences between genomes (Diatchenko L. *Proc Natl Acad Sci U S A* 1996; 93: 6025). This is because eukaryotic genomes are too complex for existing subtraction technologies. In contrast, bacterial genomes are considerably smaller, and are even less complex than many eukaryotic cDNA populations. Thus, subtraction methods can be used to identify sequences that are present in one bacterial genome, but absent in another. It requires only about several micrograms of genomic DNA, takes only several days, and does not involve the physical separation of single strain and double strain molecules. Furthermore, the suppression PCR prevents undesirable amplification while enrichment of target molecules proceeds. Even so, the conditions of the SSH were carefully optimized in this experiment. By comparing the genomic DNA digestion efficiency of *Hae* III, *Rsa* I and *Alu* I, *Alu* I was finally selected. The time of the adaptor ligation should be within 16 hours to avoid ligation between the DNA fragments. The ratio of tester and driver DNA was 1:50 in the first hybridization. In this way, we established a GU strain specific DNA sequence library.

When we used the tester and driver DNA fragments as probes to hybridize separately with different PCR products of the subtracted inserts, the tester specific DNA sequences were screened. Of the 23 sequenced DNA fragments, 15 were homologous to the *H.pylori* plasmid pHPO100. The size of this plasmid is about 3.5 kb and codes a replication protein A, which appears to be the predominant plasmid replication protein of *H. pylori* and has the highly conserved (76-96 %) amino acid sequence and may play an important role in the DNA sequence exchange between plasmid and the chromosome[35]. Thus the protein may increase the gene diversity and have the pathogenic significance. Other inserts had patches of homologous to the genes of different *H.pylori* proteins in GenBank. The results indicate that SSH can be used to screen the strain specific DNA sequences between clinical isolates even though the dominant subtracted fragments come from the plasmid of the tester strain.

When we tried to find out if some of the tester strain specific DNA sequences were unique to GU strains, no such DNA sequences were identified. Whereas a DNA fragment GU198

that is partly homologous to the gene of thymidylate kinase was positive in 7 of the 8 GU strains, 3 of the 4 GU-DU strains, and only 3 of the 12 DU strains. This is also of clinical significance. Study on identification of this DNA fragment is still going on.

Several aspects regarding the identification of disease related DNA sequences need to be discussed. First, the tester strain specific DNA sequences mean that, comparing with the driver strain, these sequences are unique to the tester strain, other strains from GU patients may share or may not share these sequences. Second, since the strain specific genes account for about 6 % of the whole genes of a given *H.pylori* strain[19], more colonies should be screened and more DNA fragments be used to identify the disease specific DNA sequences. Third, dot blotting can be used as a primary screening method, and, if possible, Southern blotting be employed for further identification. Fourth, it is better to choose the plasmid free *H. pylori* for the strain specific DNA sequence screening. Since the copies of a plasmid in the bacterium are often more than that of a gene in its genome, amplification of the subtracted gene sequences coming from the genome would be suppressed in the PCR and, as a result, the dominant strain specific DNA sequences would belong to the plasmid. Although about 50 % of *H. pylori* strains carry cryptic plasmids ranging in size from 2 to about 100 kb[35,36], the role of these plasmids is not well understood. In this investigation, the repA gene was positive in 4 *H.pylori* strains, 2 from GU (2/8), and 2 from GU-DU (2/4). This may be due to the homologous of the genomic DNA to the repA or the insertion of the repA fragment into the genome (De Ungria MC. *Plasmid* 1999; 41: 97) or the plasmid DNA being not eliminated during genomic DNA preparation. Study on the relationship between repA gene and the disease state of the patients is also necessary.

Anyway, we have successfully screened some tester strain specific DNA sequences by SSH, and this study is one of the few attempts trying to identify the disease specific genes using *H.pylori* clinical isolates[23]. Though we failed to get the disease specific DNA sequences, we believe that, at least, some tester strain specific sequences may have significantly high positive rates in strains with similar background to the tester strain. This may aid in the effective diagnosis and treatment of *H. pylori* infection and have the potential value for pathogenic investigation of this bacterium.

ACKNOWLEDGEMENT

Mr. Mun-Fai Loke, from Department of Microbiology, National University of Singapore, prepared some of the *H. pylori* clinical isolates.

REFERENCES

1 **Israel DA**, Peek RM. Pathogenesis of *Helicobacter pylori*-induced gastric inflammation. *Aliment Pharmacol Ther* 2001; **15**: 1271-1290
2 **Sanders MK,** Peura DA. *Helicobacter pylori*-Associated Diseases. *Curr Gastroenterol Rep* 2002; **4**: 448-454
3 **Dawsey SM**, Mark SD, Taylor PR, Limburg PJ. Gastric cancer and *H pylori*. *Gut* 2002; **51**: 457-458
4 **Blaser MJ**. Linking *Helicobacter pylori* to gastric cancer. *Nat Med* 2000; **6**: 376-377
5 **Unger Z**, Molnar B, Pronai L, Szaleczky E, Zagoni T, Tulassay Z. Mutant p53 expression and apoptotic activity of *Helicobacter pylori* positive and negative gastritis in correlation with the presence of intestinal metaplasia. *Eur J Gastroenterol Hepatol* 2003; **15**: 389-393
6 **Yang Y,** Deng CS, Peng JZ, Wong BC, Lam SK, Xia HH. Effect of *Helicobacter pylori* on apoptosis and apoptosis related genes in gastric cancer cells. *Mol Pathol* 2003; **56**: 19-24
7 **Wang RT**, Wang T, Chen K, Wang JY, Zhang JP, Lin SR, Zhu YM, Zhang WM, Cao YX, Zhu CW, Yu H, Cong YJ, Zheng S, Wu BQ. *Helicobacter pylori* infection and gastric cancer: evidence from a retrospective cohort study and nested case-control study in China. *World J Gastroenterol* 2002; **8**: 1103-1107
8 **Meining A**, Riedl B, Stolte M. Features of gastritis predisposing to gastric adenoma and early gastric cancer. *J Clin Pathol* 2002; **55**: 770-773
9 **Lan J,** Xiong YY, Lin YX, Wang BC, Gong LL, Xu HS, Guo GS. *Helicobacter pylori* infection generated gastric cancer through p53-Rb tumor-suppressor system mutation and telomerase reactivation. *World J Gastroenterol* 2003; **9**: 54-58
10 **Cai L**, Yu SZ, Zhang ZF. *Helicobacter pylori* infection and risk of gastric cancer in Changle County, Fujian Province, China. *World J Gastroenterol* 2000; **6**: 374-376
11 **Liu HF**, Liu WW, Fang DC, Wang GA, Teng XC. Relationship between *Helicobacter pylori* infection and gastric precancerous lesions: a follow-up study. *Shijie Huaren XiaohuaZazhi* 2002; **10**: 912-915
12 **Miehlke S**, Kirsch C, Dragosics B, Gschwantler M, Oberhuber G, Antos D, Dite P, Lauter J, Labenz J, Leodolter A, Malfertheiner P, Neubauer A, Ehninger G, Stolte M, Bayerdorffer E. *Helicobacter pylori* and gastric cancer: current status of the Austrian in Czech German gastric cancer prevention trial (PRISMA Study). *World J Gastroenterol* 2001; **7**: 243-247
13 **Yao YL**, Xu B, Song YG, Zhang WD. Overexpression of cyclin E in Mongolian gerbil with *Helicobacter pylori*-induced gastric precancerosis. *World J Gastroenterol* 2002; **8**: 60-63
14 **Zhang Z,** Yuan Y, Gao H, Dong M, Wang L, Gong YH. Apoptosis, proliferation and p53 gene expression of *H. pylori* associated gastric epithelial lesions. *World J Gastroenterol* 2001; **7**: 779-782
15 **Xue FB,** Xu YY, Wan Y, Pan BR, Ren J, Fan DM. Association of *H.pylori* infection with gastric carcinoma: a Meta analysis. *World J Gastroenterol* 2001; **7**: 801-804
16 **Liu HF**, Liu WW, Fang DC, Wang GA, Teng XC. Effect of *Helicobacter pylori* infection on bax protein expression in patients with gastric precancerous lesions. *Shijie Huaren Xiaohua Zazhi* 2003; **11**: 22-24
17 **Bjorkholm BM**, Oh JD, Falk PG, Engstrand LG, Gordon JI. Genomics and proteomics converge on *Helicobacter pylori*. *Curr Opin in Microbiol* 2001; **4**: 237-245
18 **Agron PG**, Macht M, Radnedge L, Skowronski EW, Miller W, Andersen GL. Use of subtractive hybridization for comprehensive surveys of prokaryotic genome differences. *FEMS Microbiology Letters* 2002; **10468**: 1-8
19 S**alama N,** Guillemin K, McDaniel TK, Sherlock G, Tompkins L, Falkow S. A whole genome microarray reveals genetic diversity among *Helicobacter pylori* strains. *Proc Natl Acad Sci U S A* 2000;**97**: 14668-14673
20 **Blaser MJ,** Berg DE. *Helicobacter pylori* genetic diversity and risk of human disease. *J Clin Invest* 2001; **107**: 767-773
21 I**srael DA**, Salama N, Arnold CN, Moss SF, Ando T, Wirth HP, Tham KT, Camorlinga M, Blaser MJ, Falkow S, Peek RM Jr. *Helicobacter pylori* strain-specific differences in genetic content, identified by microarray, influence host inflammatory responses. *J Clin Invest* 2001; **107**: 611-620
22 **Shibata A**, Parsonnet J, Longacre TA, Garcia MI, Puligandla B, Davis RE, Vogelman JH, Orentreich N, Habel LA. CagA status of *Helicobacter pylori* infection and p53 gene mutations in gastric adenocarcinoma.*Carcinogenesis* 2002; **23**: 419-424
23 **Kersulyte D,** Velapatino B, Dailide G, Mukhopadhyay AK, Ito Y, Cahuayme L, Parkinson AJ, Gilman RH, Berg DE. Transposable element ISHp608 of *Helicobacter pylori*: nonrandom geographic distribution, functional organization, and insertion specificity. *J Bacteriol* 2002; **184**: 992-1002
24 **Kersulyte D**, Mukhopadhyay AK, Shirai M, Nakazawa T, Berg DE. Functional organization and insertion specificity of IS607, a chimeric element of *Helicobacter pylori*. *J Bacteriol* 2000; **182**: 5300-5308
25 **Hua JS**, Zheng PY, Fong TK, Mar KM, Bow H. *Helicobacter pylori* acquistion of metronidazole resistance by natural transformation *in vitro*. *World J Gastroenterol* 1998; **4**: 385-387

26 **Suerbaum S**. Genetic variability within *Helicobacter pylori*. *Int J Med Microbiol* 2000; **290**: 175-181

27 **Yakoob J,** Hu GL, Fan XG, Yang HX, Liu SH, Tan DM, Li TG, Zhang Z. Diversity of *Helicobacter pylori* among Chinese persons with *H. pylori* infection. *APMIS* 2000; **108**: 482-486

28 **Israel DA**, Salama N, Krishna U, Rieger UM, Atherton JC, Falkow S, Peek RM Jr. *Helicobacter pylori* genetic diversity within the gastric niche of a single human host. *Proc Natl Acad Sci U S A* 2001; **98**: 14625-14630

29 **Nobusato A**, Uchiyama I, Kobayashi I. Diversity of restriction-modification gene homologues in *Helicobacter pylori*. *Gene* 2000; **259**: 89-98

30 **Tomasini ML**, Zanussi S, Sozzi M, Tedeschi R, Basaglia G, De Paoli P. Heterogeneity of cag Genotypes in *Helicobacter pylori* Isolates from Human Biopsy Specimens. *J Clin Microbiol* 2003; **41**: 976-980

31 **Ji WS**, Hu JL, Qiu JW, Peng DR, Shi BL, Zhou SJ, Wu KC, Fan DM. Polymorphism of flagellin A gene in *Helicobacter pylori*. *World J Gastroenterol* 2001; **7**: 783-787

32 **Pride DT**, Meinersmann RJ, Blaser MJ. Allelic Variation within *Helicobacter pylori* babA and babB. *Infect Immun* 2001; **69**: 1160-1171

33 **Azuma T,** Yamakawa A, Yamazaki S, Fukuta K, Ohtani M, Ito Y, Dojo M, Yamazaki Y, Kuriyama M. Correlation between variation of the 3' region of the cagA gene in *Helicobacter pylori* and disease outcome in Japan. *J Infect Dis* 2002; **186**: 1621-1630

34 **Nobusato A**, Uchiyama I, Ohashi S, Kobayashi I. Insertion with long target duplication: a mechanism for gene mobility suggested from comparison of two related bacterial genomes. *Gene* 2000; **259**: 99-108

35 **Hofreuter D**, Haas R. Characterization of two cryptic *Helicobacter pylori* plasmids: a putative source for horizontal gene transfer and gene shuffling. *J Bacteriol* 2002; **184**: 2755-2766

36 **Hosaka Y**, Okamoto R, Irinoda K, Kaieda S, Koizumi W, Saigenji K, Inoue M. Characterization of pKU701, a 2.5-kb plasmid, in a Japanese *Helicobacter pylori* isolate. *Plasmid* 2002; **47**: 193-200

Edited by Zhang JZ

P.O.Box 2345, Beijing 100023,China
Fax: +86-10-85381893
E-mail: wjg@wjgnet.com www.wjgnet.com

World J Gastroenterol 2003;9(8):1752-1755
World Journal of Gastroenterology
 ISSN 1007-9327

Seroprevalence of *Helicobacter pylori* in school-aged Chinese in Taipei City and relationship between ABO blood groups

Tzee-Chung Wu, Liang-Kung Chen, Shinn-Jang Hwang

Tzee-Chung Wu, Division of Gastroenterology and Nutrition, Children' s Medical Center, Taipei Veterans General Hospital; School of Medicine, National Yang-Ming University, Taipei, Taiwan
Liang-Kung Chen, Shinn-Jang Hwang, Department of Family Medicine, Taipei Veterans General Hospital; School of Medicine, National Yang-Ming University, Taipei, Taiwan
Correspondence to: Dr. Tzee-Chung Wu, Division of Gastroenterology and Nutrition, Children' s Medical Center, Taipei Veterans General Hospital, No. 201, Shih-Pai Road Sec 2, Taipei, 11217 Taiwan. tcwu@vghtpe.gov.tw
Telephone: +886-2-2875-7190 **Fax**: +886-2-2876-7109
Received: 2003-04-02 **Accepted:** 2003-04-24

Abstract

AIM: To explore the seropositive rate of antibodies against *H. pylori* (anti-HP) in Taipei City and to compare the relationship of ABO blood groups and *H. pylori* infection.

METHODS: In 1993, high school students in Shih-Lin District were randomly selected for blood samplings by their registration number at school. In addition, similar procedures were performed on the well-children clinics of Taipei Veterans General Hospital. Besides, randomly selected sera from the adults who took the physical examination were recruited for evaluation. Informed consents were obtained from all the subjects before blood samplings and parents were simultaneously informed for those who were younger than 18-year-old. Blood tests for anti-HP and ABO blood groupings were performed by enzyme-linked immunosorbent assay. Chi square tests were used for the comparisons between seroprevalence of *H. pylori* and ABO blood groups.

RESULTS: Totally, 685 subjects were recruited (260 children aged 1-14 years, 425 high school students aged 15-18 years) were evaluated, and another 88 adult healthy volunteers were studied as well for comparison. The age-specific seropositive rate of anti-HP was 1.3 % at age 1-5 years, 7.7 % at age 6-10 years, and 11.5 % at age 11-14 years. The seroprevalence of *H. pylori* infection was abruptly increased in young adolescence: 18.6 % at age 15 years, 28.1 % at age 16 years, 32.4 % at age 17 years and 41.0 % at age 18 years, respectively. In the 425 high school students, ABO blood groupings were performed, which disclosed 48.5 % (206/425) of blood group O, 24 % (102/425) of blood group A, 21.8 % (93/425) of blood group B and 5.6 % (24/425) of blood group AB. In comparison of the subjects with blood group O and the other blood groups, no statistical significance could be identified in the seroprevalence of *H. pylori* (P=0.99).

CONCLUSION: The seroprevalence of *H. pylori* infection in Taipei City in adults is similar to the developed countries, and the abrupt increase of *H. pylori* during high school may be resulted from marked increase of interpersonal social activities. Although blood group O was reported to be related to *H. pylori* infection in previous literature, we found no association between *H. pylori* infection and ABO blood groups.

Wu TC, Chen LK, Hwang SJ. Seroprevalence of *Helicobacter pylori* in school-aged Chinese in Taipei City and relationship between ABO blood groups. *World J Gastroenterol* 2003; 9 (8): 1752-1755
http://www.wjgnet.com/1007-9327/9/1752.asp

INTRODUCTION

Helicobacter pylori (*H. pylori*) infection is the most common chronic bacterial infection in the world. Previous seroepidemiologic studies indicated that about 50 % of adults in the developed countries and nearly 90 % of adults in the developing countries were positive of serum antibodies against *H. pylori*[1]. Chronic *H. pylori* infection may be related to several conditions, including chronic gastritis[2,3], peptic ulcer disease[4,5], primary gastric lymphoma (mostly mucosa-associated lymphoid tissue, MALToma)[6,7], and gastric adenocarcinoma[8,9].

The seroprevalence of *H. pylori* infection of adults in Taiwan varied from 54.4 % to 59 % in previous reports, which was similar to developed countries[10-12]. However, the seroprevalence of *H. pylori* infection was low in the preschool children in Taiwan. The seropositive rate of antibodies against *H. pylori* was 8.1 % in 2 551 healthy preschool children aged 3-6 years[13], and it was significantly increased to 21.1 % in young adolescence[14]. Therefore, marked increase of interpersonal social activities during the school age was proposed to be the most likely source of *H. pylori* infection.

People with blood group O have been noted to be more susceptible to peptic ulcer disease for decades without appropriate explanations[15,16]. In 1993, Boren *et al*[17] reported that people with blood group O had more *H. pylori* receptors, and Lewis^b antigens mediated the attachment of *H. pylori* to the gastric mucosa. Furthermore, higher density of colonization of *H. pylori* was noted in the gastric mucosa of people with blood group O[18]. However, absence of correlation between *H. pylori* infection and ABO blood groups was reported in some following studies[19,20].

In Taiwan, blood group O was reported to correlate with the prevalence of *H. pylori* infection in patients with gastroduodenal diseases[21], but it remained unknown for those asymptomatic individuals who were infected by *H. pylori*. Therefore, we conducted a study to evaluate the relationship between *H. pylori* and ABO blood groups in those healthy volunteers in Taipei City to clarify the possible association.

MATERIALS AND METHODS

We conducted a cross-sectional survey among senior high schools in the Shih-Lin District, Taipei City in 1993. All the recruited subjects were randomly selected in each age group (from 15 to 18) according to the registration number in schools. Blood samplings were performed after the informed consents were signed by themselves or their parents (if the subjects were younger than 18-year-old). In addition, children at age 1 to 14 years from the well-children clinics of Taipei Veterans General Hospital were recruited if their parents agreed with the study

and signed the informed consents. Moreover, we randomly collected the sera of adults who underwent physical examinations from the Department of Physical Examination to evaluate the seroprevalence of *H. pylori*. This study was evaluated and approved by the Ethical Committee of Taipei Veterans General Hospital.

The blood samples were centrifuged and the sera were stored in aliquot at -80 ℃ until analysis. The serum antibodies against *H. pylori* were tested by the commercial enzyme-linked immunosorbent assay (ELISA) kit (HEL-P test, AMRAD, Sydney, Australia). In addition, ABO blood groupings were also done by the ELISA test (Gamma Biologicals, Houston, TX, USA). ABO blood groupings were not performed in children from the well-children clinics because we reserved the sera from the blood samplings in the beginning, which were not possible for ABO blood groupings by the commercial kit.

Data of the recruited individuals were expressed in categories. The comparisons of seroprevalence of *H. pylori* between each ABO blood group were evaluated by chi-square test or Fisher' s exact test if appropriate. A *P* value of less than 0.05 would be considered statistically significant. All the available data were analyzed by a computer program (SPSS, Chicago, IL, USA).

RESULTS

Totally, 685 subjects were recruited, including 260 children aged 1-14 years from the Well-children Clinic, and 425 young adolescents aged 15-18 years from high school students in Shih-Lin District, Taipei City. In addition, sera of 88 randomly selected subjects from the Department of Physical Examination were evaluated for the referential seroprevalence of *H. pylori* in adults (Table 1).

Table 1 Age and sex distribution of seroprevalence of antibodies against *Helicobacter pylori* (anti-HP), and comparisons between sex and age groups

Age	Male		Female		*P*
	Anti-HP (+)/*n*	(%)	Anti-HP (+)/*n*	(%)	
1-5	0/26	0	1/42	2.4	0.32
6-10	4/39	10.3	2/39	5.1	0.40
11-14	9/53	17.0	3/51	5.9	0.08
Subtotal	13/118	11.0	6/132	4.5	0.06
15	7/34	20.6	11/63	17.5	0.72
16	9/38	23.7	27/90	30	0.46
17	21/65	32.3	24/74	32.4	0.99
18	14/41	34.1	11/20	55.0	0.14
Subtotal	51/179	28.5	73/246	29.7	0.79
Adults	27/49	55.1	19/39	48.7	0.56
Total	91/346	26.3	98/417	23.5	0.37

The age-specific seropositive rate of antibodies against *H. pylori* was 1.3 % at age 1-5 years, 7.7 % at age 6-10 years, and 11.5 % at age 11-14 years. The seroprevalence of *H. pylori* infection abruptly increased in young adolescence: 18.6 % at age 15 years, 28.1 % at age 16 years, 32.4 % at age 17 years and 41.0 % at age 18 years, respectively. In randomly selected adults, the seropositive rate of anti-HP reached 52.3% (Figure 1).

In the 425 randomly selected high school students, ABO blood groupings were performed, which disclosed 48.5 % (206/425) blood group O, 24 % (102/425) blood group A, 21.8 % (93/425) blood group B and 5.6 % (24/425) blood group AB. Further analysis on the ABO blood groupings and seroprevalence of *H. pylori* demonstrated that seropositive rate of anti-HP was 27.7 % (57/206) in blood group O, 31.4 % (32/102) in blood group A, 30.1 % (28/93) in blood group B, and 29.2 % (7/24) in blood group AB (Table 2). In comparison of the subjects with blood group O with the other blood groups, no statistical difference could be identified in the seroprevalence of *H. pylori* (*P*=0.98). Neither was the difference significant among the groups as for being vulnerable to *H. pylori* infection.

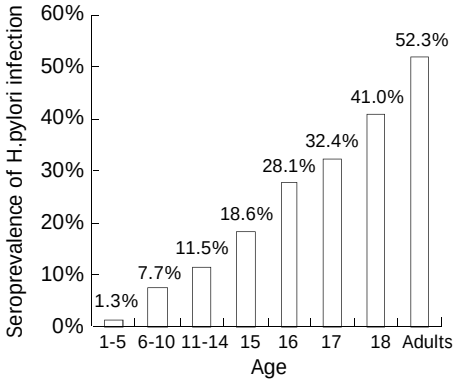

Figure 1 Age-specific seroprevalence of *H. pylori* infection in 773 healthy subjects in Taipei.

Table 2 Relationship of ABO blood groups and seropositivity of antibodies against *Helicobacter pylori* (anti-HP) infection

Blood group	Serum anti-HP (+)	Serum anti-HP (-)	*P*
O	57 (27.7%)	149 (72.3%)	-
A	32 (31.4%)	70 (68.6%)	0.99
B	28 (30.1%)	65 (69.9%)	0.99
AB	7 (29.2%)	17 (60.8%)	0.99
Total	124 (100%)	301 (100%)	

DISCUSSION

H. pylori infection is the most prevalent chronic bacterial infection in the world. Despite of the worldwide infection, the transmission pattern remains uncertain. *H. pylori* infection is rare before first two decades of life in developed countries, ranging from 6 % to 16 %[22-24]. However, children in Gambia and Nigeria are almost all infected by *H. pylori* at age of 5 years[25,26]. According to the previous reports, the seroprevalence of *H. pylori* infection in Taiwanese preschool children (3-6 years old) was 8.1 %, with the age-dependent progression (4.5 % in 3-year-old children, 4.4 % in 4-year-old children, 9.4 % in 5-year-old children, and 11.7 % in 6-year-old children)[13]. Furthermore, the seropositivity of antibodies against *H. pylori* was reported to be 21.1 % in adolescents[14], and 54.4 % in adults over 30-year-old in Taiwan[10]. Moreover, age-specific prevalence of *H. pylori* infection in patients with gastroduodenal diseases was 11.1 % in those aged 1 to 20, 73.1 % at age 21-30, and 79.8 % at age 51-60 in Central Taiwan[27]. In this seroepidemiological study, we also found a similar pattern of age-dependent progression. However, the seroprevalence of *H. pylori* in this study (1.3 % at age 1-5 years, 7.7 % at age 6-10 years, and 11.5 % at age 11-14 years) was significantly lower than that in the Taiwan islandwide survey. The better socioeconomic status in Taipei City may account for the differences of seroprevalence of *H. pylori* infection. However, the seroprevalence of *H. pylori* infection among adults in Taipei City was about the average of the Taiwan islandwide survey.

The transmission pattern of *H. pylori* currently remains uncertain, but the role of fecal-oral route seems to be minor[28,29]. The genotypic study did not support oral-oral transmission

pattern of *H. pylori* infection, either[30]. Intrafamilial and person-to-person transmission has been shown being more important in *H. pylori* infection[31,32]. Risk factors analysis of *H. pylori* infection has been extensively performed including gender, race, family income, type of housing, location of housing, water supply, health status, and keeping pets, but only the socioeconomic status was better confirmed[33-36]. Broutet *et al* [37] proposed that male gender deserve more attention in epidemiological studies of *H. pylori* infection. In this study, the male predominance of *H. pylori* infection was observed. However, similar findings were not supported in previous epidemiological reports despite of different areas, ethnicity, and age[38-41]. The sex difference of *H. pylori* infection at age 11-14 years was unclear, which deserves further investigations.

The seropositive rate of anti-HP increased abruptly in subjects at age 15 years to 18 years (18.6 % to 41.0 %) in this study. The estimated annual incidence was 7.5 % in this cross-sectional survey, which might be resulted from the extensive social activities at this stage. On the other hand, smoking is an important factor in *H. pylori* infection, particularly in young adults[42,43]. Most smokers start smoking at their young adolescence. Therefore, smoking may be another explanation of such an abrupt increase of *H. pylori* infection among people aged 15 to 18.

People with blood group O were found more susceptible to peptic ulcer disease for decades without known cause until the relationship between Lewis^b antigens and the attachment of *H. pylori* to gastric mucosa was observed[15-18]. However, the correlation between *H. pylori* infection and ABO blood types was not supported in some reports[19,20]. Nevertheless, Lin *et al*[21] demonstrated the close relationship between *H. pylori* infection and blood group O patients with gastroduodenal diseases in Central Taiwan. In our study, healthy individuals rather than symptomatic patients with blood group O were not particularly vulnerable to *H. pylori* infection.

In conclusion, the abrupt increase of *H. pylori* infection in high school students was noted with the estimated yearly incidence to be 7.5 %. Subjects with blood group O do not increase clinical susceptibility to *H. pylori* infection than those with other blood groups.

REFERENCES

1 **Megraud F.** Epidemiology of *Helicobacter pylori* infection. *Gastroenterol Clin North Am* 1993; **22:** 73-88
2 **Czinn SJ,** Dahms BB, Jacobs GH, Kaplan B, Rothstein FC. Campylobacter-like organisms in association with symptomatic gastritis in children. *J Pediatr* 1986; **109**: 80-83
3 **Ashorn M.** What are the specific features of *Helicobacter pylori* gastritis in children? *Ann Med* 1995; **27:** 617-620
4 **Rauws EA,** Tytgat GN. Cure of duodenal ulcer associated with eradication of *Helicobacter pylori*. *Lancet* 1990; **1:** 1233-1235
5 **Macarthur C,** Saunders N, Feldman W. *Helicobacter pylori*, gastroduodenal disease, and recurrent abdominal pain in children. *JAMA* 1995; **273:** 729-734
6 **Wotherspoon AC.** Gastric lymphoma of mucosa-associated lymphoid tissue and *Helicobacter pylori*. *Annu Rev Med* 1998; **49:** 289-299
7 **Wu TC,** Chen LK, Lai CR. Primary gastric lymphoma associated with *Helicobacter pylori* in a child. *J Ped Gastroenterol Nutr* 2001; **32:** 608-610
8 **Parsonnet J,** Friedman GD, Vandersteen DP, Chang Y, Vogelman JH, Orentreich N, Sibley RK. *Helicobacter pylori* infection and the risk of gastric carcinoma. *N Engl J Med* 1991; **325:** 1127-1131
9 **Nomura A,** Stemmermann GN. *Helicobacter pylori* and gastric cancer. *J Gastroenterol Hepatol* 1993; **8:** 294-303
10 **Lin JT,** Wang JT, Wang TH, Wu MS, Lee TK, Chen CJ. *Helicobacter pylori* infection in a randomly selected population, healthy volunteers, and patients with gastric ulcer and gastric adenocarcinoma. A seroprevalence study in Taiwan. *Scand J Gastroenterol* 1993; **28:** 1067-1072
11 **Lin JT,** Wang JT, Wu MS, Wang TH, Lee TK, Chen CJ. Seroprecalence study of *Helicobacter pylori* infection in patients with gastroduodenal diseases. *J Formos Med Assoc* 1994; **93:** 122-127
12 **Lin JT,** Wang LY, Wang JT, Wang TH, Tang CS, Chen CJ. A nested case-control study on the association between *Helicobacter pylori* infection and gastric cancer risk in a cohort of 9775 men in Taiwan. *Anticancer Res* 1995; **15:** 603-606
13 **Lin DB,** Nieh WT, Wang HM, Hsiao MW, Ling UP, Changlai SP. Seroepidemiology of *Helicobacter pylori* infection among preschool children in Taiwan. *Am J Trop Med Hyg* 1999; **61:** 554-558
14 **Wang LY,** Lin JT, Cheng YW, Chou SSJ, Chen SJ. Seroepidemiology of *Helicobacter pylori* among adolescents in Taiwan. *Chin J Microbiol Immunol* 1996; **29:** 10-17
15 **Clark CA,** Wyn EJ, Haddock DRW, Howel-Evans AW, McConnell RB, Sheppard PM. ABO blood groups and secretor character in duodenal ulcer. *Br Med J* 1956; **2:** 725-731
16 **Mentis A,** Blackwell CC, Weir DM, Spiliadis C, Dailianas A, Skandalis N. ABO blood group, secretor status, and detection of *Helicobacter pylori* among patients with gastric or duodenal ulcers. *Epidemiol Infect* 1991; **106:** 221-229
17 **Boren T,** Falk P, Roth KA, Larson G, Normark S. Attachment of *H. pylori* to human gastric epithelium mediated by blood type group antigens. *Science* 1993; **262:** 1892-1895
18 **Atherton JC,** Tham KT, Peek RM Jr, Cover TL, Blaser MJ. Density of *Helicobacter pylori* infection *in vivo* as assessed by quantitative culture and histology. *J Infect Dis* 1996; **174:** 552-556
19 **Loffeld RJ,** Stobberingh E. *Helicobacter pylori* and ABO blood groups. *J Clin Pathol* 1991; **44:** 516-517
20 **Niv Y,** Fraser G, Delpre G, Neeman A, Leiser A, Samra Z. *Helicobacter pylori* infection and blood groups. *Am J Gastroenterol* 1996; **91:** 101-104
21 **Lin CW,** Chang YS, Wu SC, Cheng KS. *Helicobacter pylori* in gastric biopsies of Taiwanese patients with gastroduodenal diseases. *Jpn J Med Sci Biol* 1998; **51:** 13-23
22 **De Giacomo C,** Lisato L, Negrini R, Licardi G, Maggiore G. Serum immune response to Helicobacter pylori in children: epidemiologic and clinical applications. *J Pediatr* 1991; **199:** 205-210
23 **Thomas JE,** Whatmore AM, Barer MR, Eastham EJ, Kehoe MA. Serodiagnosis of *Helicobacter pylori* infection in children. *J Clin Microbiol* 1990; **28:** 2641-2646
24 **Oderda G,** Vaira D, Holton J. Age-related increase of *Helicobacter pylori* prevalence in symptom-free and in dyspeptic children. *Lancet* 1992; **340:** 671-672
25 **Holcombe C,** Tsimiri S, Elridge J, Jones DM. Prevalence of antibody to *Helicobacter pylori* in children in northern Nigeria. *Trans R Soc Trop Med Hyg* 1993; **87:** 19-21
26 **Sullivan PB,** Thomas JE, Wight DG, Neale G, Eastham EJ, Corrah T. *Helicobacter pylori* in Gambian children with chronic diarrhea and malnutrition. *Arch Dis Child* 1990; **65:** 189-191
27 **Lin CW,** Chang YS, Lai PY, Cheng KS. Prevalence and heterogeneity of *Helicobacter pylori* in gastric biopsies of patients with gastroduodenal diseases. *J Microbiol Immunol Infect* 1997; **30:** 61-71
28 **Webb PM,** Knight T, Newell DG, Elder JB, Forman D. *Helicobacter pylori* transmission: evidence from a comparison with hepatitis A virus. *Eur J Gastroenterol Hepatol* 1996; **8:** 439-441
29 **Lin DB,** Tsai TP, Yang CC. Association between seropositivity of antibodies against hepatitis A virus and *Helicobacter pylori*. *Am J Trop Med Hyg* 2000; **63:** 189-191
30 **Luman W,** Zhao Y, Ng HS, Ling KL. *Helicobacter pylori* infection is unlikely to be transmitted between partners: evidence from genotypic study in partners of infected patients. *Eur J Gastroenterol Hepatol* 2002; **14:** 521-528
31 **Tindberg Y,** Bengtsson C, Granath F, Blennow M, Nyren O, Granstrom M. *Helicobacter pylori* infection in Swedish school children: lack of evidence of child-to-child transmission outside the family. *Gastroenterology* 2001; **121:** 310-316
32 **Wizla-Derambure N,** Michaud L, Ategbo S, Vincent P, Ganga-Zandzou S, Turck D, Gottrand F. Familial and community environmental risk factors for *Helicobacter pylori* infection in children and adolescents. *J Ped Gastroenterol Nutr* 2001; **33:** 58-63
33 **Graham DY,** Malaty HM, Evans DG, Evans DJ Jr, Klein PD, Adam E. Epidemiology of *Helicobacter pylori* in an asymptomatic popu-

lation in the United States. Effect of age, race, and socioeconomic status. *Gastroenterology* 1991; **100:** 1495-1501

34 **Fiedorek SC,** Malaty HM, Evans DL, Pumphrey CL, Casteel HB, Evans DJ Jr, Granham DY. Factors influencing the epidemiology of *Helicobacter pylori* infection in children. *Pediatrics* 1991; **88:** 578-582

35 **Stone MA,** Taub N, Barnett DB, Mayberry JF. Increased risk of infection with *Helicobacter pylori* in spouses of infected subjects: observations in a general population sample from the UK. *Hepato-Gastroenterology* 2000; **47:** 433-436

36 **Brown LM.** *Helicobacter pylori*: epidemiology and routes of transmission. *Epidemiologic Reviews* 2000; **22:** 283-297

37 **Broutet N,** Sarasqueta AM, Sakarovitch C, Cantet F, Lethuaire D, Megraud F. *Helicobacter pylori* infection in patients consulting gastroenterologists in France: prevalence is linked to gender and region of residence. *Eur J Gastroenterol Hepatol* 2001; **13:** 677-684

38 **Elitsur Y,** Short JP, Neace C. Prevalence of *Helicobacter pylori* infection in children from urban and rural West Virginia. *Dig Dis Sci* 1998; **43:** 773-778

39 **Sinha SK,** Martin B, Sargent M, McConnell JP, Bernstein CN. Age at acquisition of *Helicobacter pylori* in a pediatric Canadian First Nations population. *Helicobacter* 2002; **7:** 76-85

40 **Leal-Herrera Y,** Torres J, Perez-Perez G, Gomez A, Monath T, Tapia-Conyer R, Munoz O. Serologic IgG response to urease in *Helicobacter pylori*-infected persons from Mexico. *Am J Trop Med Hyg* 1999; **60:** 587-592

41 **Lin JT,** Wang LY, Wang JT, Wang TH, Chen CJ. Ecological study of association between *Helicobacter pylori* infection and gastric cancer in Taiwan. *Dig Dis Sci* 1995; **40:** 385-388

42 **Brenner H,** Rothenbacher D, Bode G, Adler G. Relation of smoking and alcohol and coffee consumption to active *Helicobacter pylori* infection: cross sectional study. *Br Med J* 1997; **315:** 1489-1492

43 **Kopanski Z,** Schlegel-Zawadzka M, Golec E, Witkowska B, Micherdzinski J, Cienciala A, Kustra Z. The significance of selected epidemiologico-clinical factors in the prevalence of the *Helicobacter pylori* infection in young males. *Eur J Med Res* 1997; **2:** 358-360

Edited by Xu XQ

P.O.Box 2345, Beijing 100023,China
Fax: +86-10-85381893
E-mail: wjg@wjgnet.com www.wjgnet.com

World J Gastroenterol 2003;9(8):1756-1761
World Journal of Gastroenterology
 ISSN 1007-9327

Construction and characterization of bivalent vaccine candidate expressing HspA and M_r18 000 OMP from *Helicobacter pylori*

Zheng Jiang, Ai-Long Huang, Xiao-Hong Tao, Pi-Long Wang

Zheng Jiang, Xiao-Hong Tao, Pi-Long Wang, Department of Gastroenterology, the First Affiliated Hospital, Chongqing University of Medical Sciences, Chongqing 400016, China
Ai-Long Huang, Institute of Viral Hepatitis, Chongqing University of Medical Sciences, Chongqing 400010, China
Correspondence to: Dr. Zheng Jiang, Department of Gastroenterology, the First Affiliated Hospital, Chongqing University of Medical Sciences, Chongqing 400016, China. jianggooddoctor@mail.china.com
Telephone: +86-23-68891218
Received: 2003-01-11 **Accepted:** 2003-03-10

Abstract

AIM: To construct a recombinant vector which can express outer membrane protein (OMP) with M_r18 000 and heat shock protein A (HspA) from *Helicobacter pylori* (*H. pylori*) in *E. coli* BL21, and to exploit the possibility for obtaining the vaccine conferring protection from *H. pylori* infection.

METHODS: The target gene of HspA was amplified from *H. pylori* chromosome by PCR, and then inserted into the prokaryotic expression vector pET32a (+) by restrictive endonuclease enzyme *kpn* I, *Bam*H I simultaneously. The recombinant vector was used to sequence, and then together with pET32a (+)/Omp_{18}, digested by restrictive endonuclease enzyme *Hind* III and *Bam*H I simultaneously. pET32a(+)/HspA and Omp_{18} were recovered from 1 % agarose gel by gel kit, and ligated with T_4 ligase by *Bam*H I digested viscidity end. The recombinant plasmid of pET32a(+)/HspA/Omp_{18} was transformed and expressed in *E. coli* BL21 (DE3) under induction of IPTG. After purification, its antigenicity of the fusion protein was detected by Western blot.

RESULTS: Enzyme digestion analysis and sequencing showed that the target genes were inserted into the recombinant vector, composed of 891 base pairs, encoded objective polypeptides of 297 amino acid residues. Compared with GenBank reported by Tomb *et al,* there were 1.3 % and 1.4 % differences in obtained *H. pylori* nucleotide sequence and amino acid residues, respectively. SDS-PAGE analysis showed that relative molecule mass (M_r) of the expressed product was M_r 51 000, M_r of protein expressed by pET32a (+) was about M_r 20 000, and soluble expression product accounted for 18.96 % of total bacterial protein. After purification with Ni^{+2}-NTA agarose resins, the purification of recombinant fusion protein was about 95 %. Western blot showed that recombinant fusion protein could be recognized by the patients' serum infected with *H. pylori* and anti-Omp_{18} monoclone, suggesting that this protein had good antigenicity.

CONCLUSION: The gene coding for *H. pylori* M_r18 000 OMP and HspA was cloned and expressed successfully. The results obtained lay the foundation for development of *H. pylori* protein vaccine and a quick diagnostic kit.

Jiang Z, Huang AL, Tao XH, Wang PL. Construction and characterization of bivalent vaccine candidate expressing HspA and M_r18 000 OMP from *Helicobacter pylori*. *World J Gastroenterol* 2003; 9(8): 1756-1761
http://www.wjgnet.com/1007-9327/9/1756.asp

INTRODUCTION

Helicobacter pylori (*H.pylori*) is a microaerophilic, spiral and gram-negative bacillus first isolated from human gastric antral epithelium in 1982. It has been recognized as a human-specific gastric pathogen that colonizes the stomaches of at least half the world's population[1], and there are approximately thousands of newly infected people annually. Most infected individuals are asymptomatic. However, in some individuals, their infections are associated with the development of peptic ulcer, gastric adenocarcinoma, mucosa-associated lymphoid tissue (MALT) lymphoma and primary gastric non-Hodgkin's lymphoma[2-20], moreover with extradigestive diseases[21-37]. This organism was recently categorized as a class I carcinogenetic factor by the World Health Organization, and direct evidence of carcinogenesis was recently demonstrated in an animal model[38,39]. Although there are many methods for eradication of *H. pylori* infection, such as bi-, tri- drug therapy, the definitive curative effects were acquired by using a serial of antibiotics, which has led to resistant *H. pylori*. Meantime medical side effects, patients' endurance and compliance were challenged. This has drawn increasing interests of scientists in developing *H. pylori* vaccine so as to reduce and prevent *H. pylori* infection, extinct diseases associated with *H. pylori* infection. Immunization against this bacterium represents a cost-effective strategy to reduce global *H. pylori*-gastric cancer and peptic ulcer rates[40]. To date, *H. pylori* vaccine candidate antigens identified include urease enzyme, VacA, and so on[41-50]. M_r18 000 and HspA are outer membrane proteins of *H. pylori*, and the vaccines prepared with M_r18 000 OMP and HspA respectively were used to inoculate Balb/c mice, 70-80 % of experimental mice were protected. In order to acquire a better immunocompetent effect, some investigators suggested that bi-valent antigen vaccine was possibly superior to single antigen. So in this study, the recombinant plasmid encoding *H. pylori* M_r18 000 OMP and HspA genes was constructed and expressed in BL21 to explore the possibility for obtaining a vaccine conferring protection from *H. pylori* infection.

MATERIALS AND METHODS

Material

A well-characterized strain of *H. pylori* was afforded by the Department of Microbiology, Chongqing University of Medical Sciences. Top10, BL21 *E.coli* strains and pET32a (+), pET32a(+)/Omp_{18} plasmid, anti-Omp_{18} antibody were provided by the Institute of Viral Hepatitis of Chongqing University of Medical Sciences. Restriction endonuclease enzymes (*Kpn* I, *Hind* III, *Bam*HI) and T_4DNA ligase were purchased from Promega, *Tag*DNA polymerase was produced by the Immunology Department of Beijing University of Medical Sciences. Isopropyl-β-D-thiogalactopyranoside (IPTG), dNTP and oligonucleotide primers were obtained from Sigma.

Cloning of H.pylori HspA gene

Oligonucleotide primers were designed to amplify *H. pylori* open reading frame (ORFs) of HspA based on GenBank. The primers had a *KpnI* site incorporated into the 5' end and a *Bam*HI site at the 3' end and their sequences were as follows (5'-3'): CCGGTACCATGAAGTTTCAACCATTAGG (forward) and CCGGATCCGTGTTTTTTGTGATCATGAC (reverse). The reverse 5' end stop codon TAA was banned. Genomic DNA prepared from Chinese *H. pylori* strains was used as the template in PCR. The PCR consisted of 30 cycles of denaturation at 94 ℃ for 60 s, annealing at 52 ℃ for 50 s, and an extension step at 72 ℃ for 50 s. The products were visualized on 10 g· L^{-1} agarose gel and purified using a PCR purification kit. After digestion with the restriction endonuclease enzymes *Bam*HI and *KpnI* simultaneously, the purified products were cloned into the compatible sites of the expression vector pET32a (+) by using T_4 DNA ligase at a molar ratio of 4:1 at 4 ℃ overnight.

Construction of recombinant plamids

After the above connected products were transfected into Top10, pET32a(+)/HspA was selected and identified by the methods reported by Jiang *et al*[51]. After pET32a(+)/HspA and pET32a(+)/Omp_{18} were digested by restrictive endonuclease enzymes *Bam*HI and *Hind* III simultaneously, the segments of Omp_{18} and pET32a(+)/HspA were recycled by gel extract kit, and ligated by using T_4 DNA ligase at a molar ratio of 4:1 at 4 ℃ overnight. pET32a(+)/HspA /Omp_{18} was selected, appraised by PCR or enzyme digestion (Figure 1).

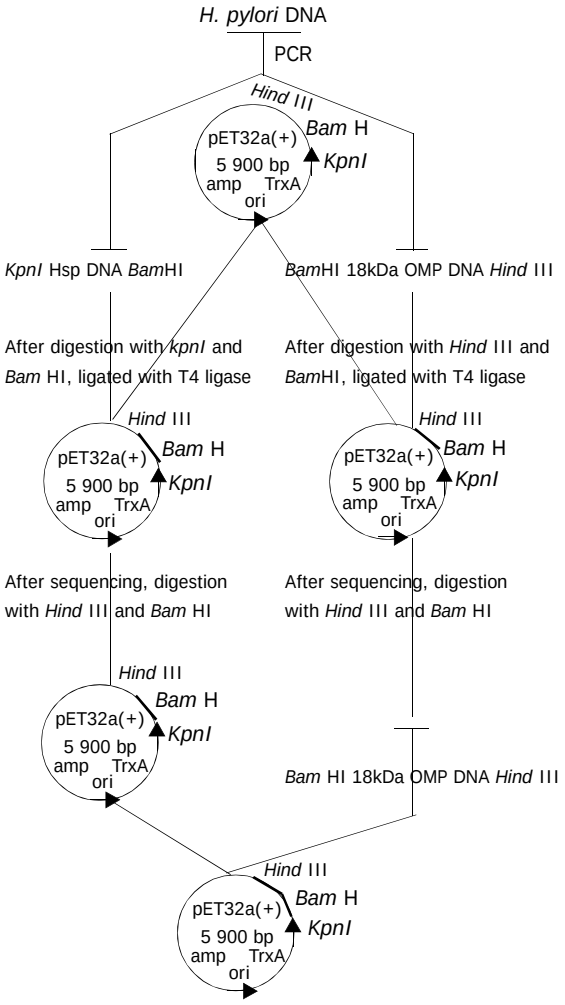

Figure 1 Schematic construction of plasmid pET32a(+)/HspA-Omp_{18}.

Extraction and expression of recombinant plasmid

The single bacterial colony (Top10/pET32a (+)/HspA/Omp_{18}) was picked, and cultivated in 2 ml LB broth containing 100 mg· L^{-1} of ampicillin, at 300 r· min^{-1} at 37 ℃ overnight, then recombinant plasmids were extracted according to the manufacturer's instructions, in the meantime, identified by PCR and restriction endonuclease enzyme digestion. The recombinant plasmid was transfected into competent BL21 (DE3) *E.coli* strains by using standard procedures reported by Jiang *et al*. BL21 *E.coli* strains containing recombinant plasmid were grown until mid-log phase (optical density at 600 nm=0.5 to 1.0), and then induced to express recombinant fusion protein by adding 1 mmol· L^{-1} IPTG for 4 h. Following induction, bacteria were harvested by centrifugation at 12 000 r· min^{-1} for 2 min, resuspended in protein-buffer and seethed for 5 min. Total proteins were electrophoresed on 150 g· L^{-1} SDS-PAGE gel and stained with Coomassie. The rate of recombinant fusion protein to total protein was deduced by Image Master Totallab v1.11 software.

Immunoblotting analysis of the recombinant fusion protein

Due to C end of recombinant fusion antigen with six histidines, the recombinant fusion antigen was purified by using Ni^{2+}-NTA agarose resin. Briefly, 500 ml of bacteria cultivated suspension was prepared, centrifugated, resuspended with the buffer liquid (50 mmol· L^{-1} phosphate, 300 mmol· L^{-1} NaCl, pH 7.0), and sonicated by ultrasonic wave with the energy of 600W×35 % for 40 min, and ultracentrifugated for 15 min at 10 000 r· min^{-1} at 4 ℃. The sonicated recombinant fusion antigen was purified by using Ni^{2+}-NTA agarose resin with abluent (50 mmol· L^{-1} phosphate, 300 mmol· L^{-1} NaCl, 20 mmol· L^{-1} imidazole, pH 7.80) and lavation (50 mmol· L^{-1} phosphate, 300 mmol· L^{-1} NaCl, 250 mmol· L^{-1} imidazole, pH 7.80) respectively, and quantified. The antigenicity of expressed recombinant fusion protein was determined by immunoblotting. Following electrophoretic transfer of SDS-PAGE-separated (150 g· L^{-1} acrylamide) recombinant fusion protein to 0.45 μm pore size PVDF membrane, and after a 30-min wash in tris-saline blotting buffer, antigen-impregated PVDF strips were incubated with the sera of patients infected with *H. pylori* and anti-Omp_{18} antibody for 2 h at RT. After a washing, the protein was detected by incubating the strips in alkaline phosphatase-conjugated goat anti-man IgG antibody for 1 h at RT.

RESULTS

PCR amplification of H.pylori HspA gene

According to literature[55], *H. pylori* HspA ORF was amplified by PCR with Chinese *H. pylori* strain's chromosomal DNA as the templates. The cloning products were electrophoresed and visualized by10 g· L^{-1} agarose gel (Figure 2). It revealed that the size of HspA DNA fragment amplified by PCR was between 250-500 base pairs, and contained a gene of approximately 357 nucleotides, and was compatible with the previous reports[55].

Identification of recombinant vector by PCR or restriction enzyme digestion

pET32a(+)/HspA identification by PCR After the single colony of Top10 *E. coli* /recombinant pET32a(+)/HspA was picked and incubated in 2 ml LB broth containing 100 mg· L^{-1} of ampicillin at 300 r· min^{-1} at 37 ℃ overnight, then 50 μl was incubated and seethed for 10 min, with the genomes of supernate and recombinant vector as templates respectively, products were amplified by PCR under the condition as mentioned above. The PCR products were visualized by 10

g· L^{-1} agarose gel electrophoresis (Figure 3). It indicated that recombinant plasmid contained the objective gene. At the same time, it was successful in transfecting recombinant plasmid into Top10 *E. coli*.

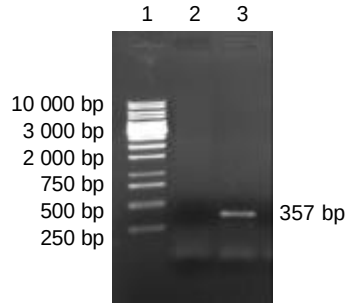

Figure 2 10 g·L^{-1} agarose gel electrophoresis of HspA DNA fragment amplified by PCR from Helicobacter pylori. Lane 1. PCR marker, Lane 2. Negative control, Lane 3. PCR products.

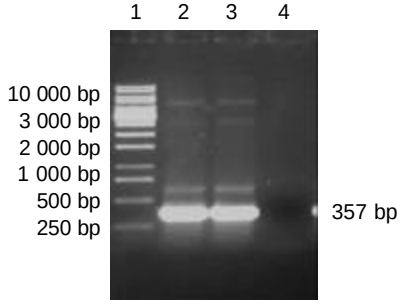

Figure 3 The identification of recombinant vector by PCR. Lane 1. DNA Marker, Lane 2, 3. PCR products with the template of Top10/recombinant vector, and recombinant vector respectively, Lane 4. Negative control.

pET32a(+)/HspA-Omp$_{18}$ identification by restriction enzyme digestion Recombinant plasmids pET32a(+)/HspA-Omp$_{18}$ were digested by single, bi-, tri-enzyme digestion with *Hind*III, *KpnI* and *Bam*HI, respectively, then digestive products were visualized on 10 g· L^{-1} agarose gel (Figure 4). It demonstrated that recombinant plasmids were digested to 357 bp, 528 bp DNA fragment, and contained the objective gene.

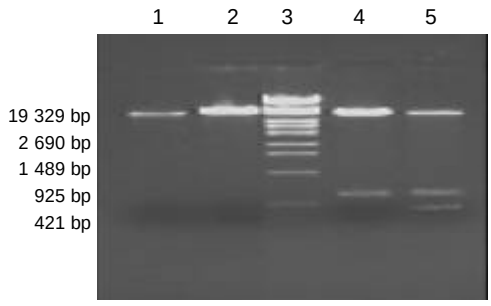

Figure 4 Identification of recombinant plasmid by restriction enzyme digestion. Lane 1. pET32a(+)/HspA digested by *Bam*HI, Lane 2. pET32a(+)/HspA-Omp$_{18}$ digested by *Bam*HI, Lane 3. DNA marker, Lane 4. pET32a(+)/HspA-Omp$_{18}$ digested by *Bam*HI and *Hind* III simultaneously, Lane 5. pET32a(+)/HspA-Omp$_{18}$ digested by kpnI, *Bam*HI and *Hind* III simultaneously.

Sequence analysis of cloned HspA, M_r18 000 OMP nucleotide

The nucleotide sequence of the cloned genes M_r18 000 OMP and HspA inserted into pET32a (+) was analyzed by automated sequencing across the cloning junction, using the universal primer T_7. The results showed that the cloned genes M_r18 000 OMP and HspA were connected by *Bam*H I enzyme digestion adhesion end. The cloned HspA genes contained 357 nucleotides with a promoter codon coding a putative protein of 119 amino acid residues with a calculated molecular mass of M_r13 000, and provided a putative signal peptide. Compared with previous reports, 5 base pairs of the cloned gene and 2 amino acid residues (G→D, A→S) encoded were changed. The cloned gene M_r18 000 OMP and its encoding protein sequences were published in GenBank (AF374387).

Analysis of the recombinant fusion protein

After pET32a(+)/HspA-Omp$_{18}$ was transfected into BL21 *E. coli* strains, the strains with high expressions of fusion proteins were selected. BL21 (DE3) *E.coli* strains containing recombinant plasmid were grown until mid-log phase (optical density at 600 nm=0.4 to 0.6), and then induced to express recombinant fusion protein by adding of 1 mmol· L^{-1} IPTG for 4 h. Following induction, bacteria were harvested by centrifugation at 12 000 r· min^{-1} for 5 min, resuspended in protein-buffer and seethed for 5 min. Total protein was electrophoresed on 150 g· L^{-1} SDS-PAGE gel and stained with Coomassie. Its molecular mass was M_r 51 000 by 150 g· L^{-1} SDS-PAGE gel analysis. After the recombinant bacteria were sonicated by ultrasonic wave and ultracentrifuged (10 000 r· min^{-1}, 15 min, 4 ℃), the level of soluble fusion protein in the supernate was about 18.96 % of total cellular protein. After purification by Ni^{2+}-NTA agarose resin columniation, the purity of recombinant fusion protein was about 95 % (Figure 5).

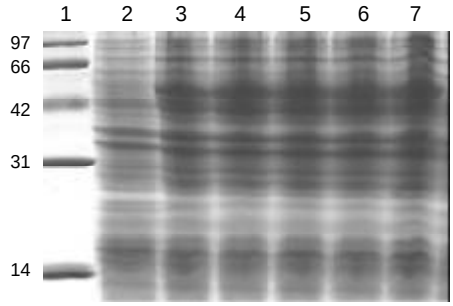

Figure 5 150 g·L^{-1} SDS-PAGE of total protein in recombinant vector expressed in BL21 *E.coli*. Lane 1. Standard protein marker (M_r 14; 31; 42; 66; 97×10^3), Lane 2. Bacterial protein expressed in BL21 after induction for 4 hours with IPTG, Lane 3-7. Expression of recombinant vector in BL21 after induction for 4 h with IPTG.

Antigenicity of recombinant fusion protein

After bacteria BL21/pET32a(+)/HspA-Omp$_{18}$, BL21/pET32a (+), BL21/pET32a(+)/HspA were induced to cultivate by adding of 1 mmol· L^{-1} IPTG for 4 h respectively, 1 ml of cultivated medium was respectively ultracentrifuged, resuspended in protein-buffer and seethed for 5 min. Total protein was electrophoresed on 150 g· L^{-1} SDS-PAGE gel, and then the proteins of SDS-PAGE-separated (150 g· L^{-1} acrylamide) were transferred to 0.45 μm pore size PVDF membrane at 14V, at 4 ℃ overnight. Following a 30-min wash in tris-saline blotting buffer, antigen-impregated PVDF strips were incubated with the sera of patients infected with *H. pylori* and anti-Omp$_{18}$ antibody for 2 h at RT. After a washing, the proteins were detected by incubating the strips in alkaline phosphatase-conjugated goat anti-man IgG antibody for 1 h at RT. In this study, antigen-impregated PVDF strips of BL21/pET32a(+)/HspA-Omp$_{18}$ were recognized by anti-Omp$_{18}$ antibody, showing brown strip corresponding to the site of the

recombinant fusion protein. Antigen-impregated PVDF strips of BL21/pET32a(+)/HspA were recognized by patient' s sera infected with *H. pylori*, also showing brown strip corresponding to the site of the fusion protein, while antigen-impregated PVDF strips of BL21/pET32a(+) were not recognized by patient' s sera infected with *H. pylori* (Figure 6).

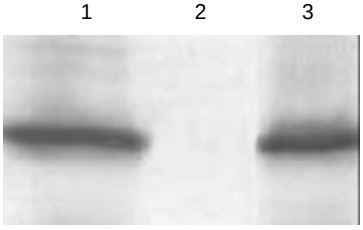

Figure 6 Antigenic analysis of the expression of recombinant vector by Western blot. Lane 1. BL21 / pET32a(+) / HspA-Omp$_{18}$, Lane 2. BL21 / pET32a(+), Lane 3. BL21 / pET32a(+) / HspA.

DISCUSSION

Heat shock phenomena were found by a geneticist Ritossa in studying on change of drosophila cell chromosome stimulated by heat in 1962. Heat shock protein, found by Tissiers *et al* in 1974, indwells in man, microbe, foliage, and animal. It belongs to secretory protein, and accounts for 5 % of total cellular proteins. When cells are stimulated by environment, Hsps are induced to synthesize. A series of heat shock proteins, such as HspA, HspB, Hsp60, and Hsp70, synthesized by *H. pylori*, play a significant role in *H. pylori* pathogenesis, for example, taking part in regulation of cell immunization, initiating auto-immunoreaction of gastric epithelial cell, serving as a promotor in development of chronic gastric pathological changes, and mediating recognition and adhesion of pathogens with host. HspA and HspB genes encode 118, 545 amino acid residues respectively, corresponding to calculated molecular mass of M_r 13 000, 58 200. HspA is consisted of two domains: N domain is conservative sequence, associated with immune appearance; C domain is composed of 27 amino acid residues, including 8 histidines, and 4 cysteines. So the frame is a nickel combinative region, and plays a role in nickel ion translation and presentation. The experiments suggested that HspA, B were important factors in *H. pylori* conglutination and *H. pylori* active proteins stabilization under the extremely unfavorable conditions, meantime they increase urease activity. Others suggested that Hsp60 and HopZ (*H. pylori* outer membrane protein Z) of *H. pylori* were associated with *H. pylori* adhesion. HspA and HspB were homologous with *E. coli* GroEs and GroEI, associated with auto-immunoreaction, which might lead to the production of damaging auto-antibody. Animal experiments demonstrated that mice fed with HspA, B resulted in coronary artery sclerosis[52].

The outer membrane is a continuous structure on the surface of gram-negative bacteria and an asymmetric bilayer with phospholipids in the inner monolayer and the bulky glycolipid lipopolysaccharide (LPS). In the outer monolayer, *H. pylori* as bacterial pathogens, has particular significance as a potential target for inducing host protective immunity and escaping from the host' s immune system. Outer membrane vaccines have been used with considerable success to induce protection against a number of organisms, including the heat shock protein in *H. pylori*, urease A, and B. M_r18 000 OMP is a lipoprotein (Lpp20) belonging to other outer membrane protein[53]. In an earlier study, immunoreactive species-specific M_r19 500 *H. pylori* OMP actually was Lpp20-M_r18 000 OMP. The Lpp20 antigen appears to be commonly expressed in all *H. pylori* strains examined so far. Furthermore, no cross-reaction was shown when antibodies (polyclonal and monoclonal) to *H. pylori* Lpp20 were used to immunoscreen closely related species of helicobacter, campylobacter, or a diverse range of other bacteria. It shows that the Lpp20 gene to be unique to *H. pylori*[54]. Keenan *et al* demonstrated the protein was expressed on the surface of the bacteria by immunolabeling of *H. pylori* with gold-labeled anti-Lpp20 antibodies. Bacterial lipoproteins have been well described, not only as vaccine target candidates, but also as immunostimulatory molecules.

In order to overcome the weak antigenicity of a single antigen, *H. pylori* M_r18 000 OMP and HspA gene were amplified by PCR, and inserted into pET32a(+) vector simultaneously in our study. The pET32a(+) vector was designed for cloning and high-level expression of peptide sequences with the 109aa Trx.· Tag™ thioredoxin protein. Cloning sites were available to produce objective proteins also containing cleavable His· Tag and s· Tag™ sequences for detection and purification. The expressed protein of pET32a(+) vector had a putative molecular mass of M_r 20 000, so the expression of recombinant vector was a fusion protein with a calculated molecular mass of M_r 51 000, consistent with our results. Compared with the reports, 1.8 % of the cloned genes was mutated, and 1.7 % of amino acid residues was changed. The reasons for the discrepancy might be as follows: (1) *H. pylori* chromosomal DNA as templates was different, (2) there were heterogeneity among *H. pylori* strains, and (3) *H. pylori* was provided with the ability of transformation, which could lead to *H. pylori* variation and genome reset[54]. But there was much homogeneity between them.

Todoroki *et al*[55] investigated the effect of DNA vaccines encoding *H. pylori*-heat shock proteins A and B (pcDNA3.1-hspA and -hspB) on inducing immune responses against *H. pylori* in mice. C57BL/six mice aged 5 weeks were immunized by a single injection of 10microg of pcDNA3.1-hspA and pcDNA3.1-hspB into intracutaneous tissue. Plasmid DNA lacking the inserted Hsp was injected as a control. The results demonstrated that DNA vaccines encoding *H. pylori*-Hsp induced significant immune response against *H. pylori*, decreased gastric mucosal inflammation, indicating that a pcDNA3.1-hspA or -hspB DNA vaccine can be a new approach against *H. pylori* in human. Jiang *et al*[51] reported that recombinant fusion OMP$_{18}$ protein also had good antigenicity. While being an immunogenic marker, the patient sera infected with *H. pylori* M_r 18 000 Omp antigen showed high sensitivity and specificity[56]. Moreover, a significant association was found between the serologic response to M_r 18 000 Omp antigen and malignant outcome of *H. pylori* infection[57]. So the serum test for detecting antibody with lower-molecular-weight proteins of *H. pylori* could be used to identify *H. pylori*-infected patients at risk of peptic ulcer or malignancy. A recently published study also identified M_r 18 000 Omp as a candidate following the successful immunization of mice with purified recombinant antigen. In our study, the purified M_r 51 000 recombinant fusion HspA-Omp$_{18}$ protein could be recognized by patients' sera infected with *H. pylori* and anti-Omp$_{18}$ monoclonal antibody, and the purified M_r 33 000 recombinant fusion HspA protein could also be recognized by patients' sera. The results demonstrated that recombinant fusion protein had good antigenicity. These showed that M_r 51 000 recombinant fusion HspA-Omp$_{18}$ protein would not only provide HspA characteristics, but possess M_r 18 000 Omp specialty. Meantime, M_r 51 000 recombinant fusion HspA-Omp$_{18}$ protein was suggested to be a true vaccine candidate and not merely an immunogenic marker for *H. pylori* infection.

In addition to construction of the recombinant vector, looking for living carriers would be a key step. Immunization via the mucosal or intracutaneous-inoculated route offers the advantage that has the potential to stimulate both mucosal and systemic immunity. It is simple, safe and can be used for the

immunization of a large population. Bacillus Calmette-Guerin (BCG), the attenuated strain of mycobacterium bovid and the current vaccine against tuberculosis, has been widely used as a living, innately immunogenic vehicle for multiple protective recombinant antigens for vaccines against pathogenic microorganisms. With the aim of developing a recombinant vaccine, vaccines against human immunodeficiency virus, diphtheria, pertussis, tetanus (DPT), and parasite[58-68] have been investigated. We are developing a living carrier-BCG to provide a mucosal or intracutaneous-inoculated vaccine vector to deliver M_r 51 000 recombinant fusion HspA-Omp_{18} protein to antigen-presenting cells on mucosal surface. We believe that before long, *H. pylori* vaccine could be constructed successfully for eradicating *H. pylori* infection and *H. pylori* associated diseases.

REFERENCES

1 **Michetti P**, Kreiss C, Kotloff KL, Porta N, Blanco JC, Bachmann D, Herranz M, Saldinger PF, Corthesy-Theulaz I, Losonsky G, Nichols R, Simon J, Stolte M, Ackerman S, Monath TP, Blum AL. Oral immunization with urease and Escherichia coli heat-labile Enterotoxin is safe and immunogenic in *Helicobacter pylori*-infected adults. *Gastroenterology* 1999; **116**: 804-812

2 **Hiyama T**, Haruma K, Kitadai Y, Masuda H, Miyamoto M, Ito M, Kamada T, Tanaka S, Uemura N, Yoshihara M, Sumii K, Shimamoto F, Chayama K. Clinicopathological features of gastric mucosa-associated lymphoid tissue lymphoma: a comparison with diffuse large B-cell lymphoma without a mucosa-associated lymphoid tissue lymphoma component. *J Gastroenterol Hepatol* 2001; **16**: 734-739

3 **Nakamura S**, Matsumoto T, Suekane H, Takeshita M, Hizawa K, Kawasaki M, Yao T, Tsuneyoshi M, Iida M, Fujishima M. Predictive value of endoscopic ultrasonography for regression of gastric low grade and high grade MALT lymphomas after eradication of *Helicobacter pylori*. *Gut* 2001; **48**: 454-460

4 **Uemura N**, Okamoto S, Yamamoto S, Matsumura N, Yamaguchi S, Yamakido M, Taniyama K, Sasaki N, Schlemper RJ. *Helicobacter pylori* infection and the development of gastric cancer. *N Engl J Med* 2001; **345**: 784-789

5 **Kate V**, Ananthakrishnan N, Badrinath S. Effect of *Helicobacter pylori* eradication on the ulcer recurrence rate after simple closure of perforated duodenal ulcer: retrospective and prospective randomized controlled studies. *Br J Surg* 2001; **88**: 1054-1058

6 **Xue FB**, Xu YY, Wan Y, Pan BR, Ren J, Fan DM. Association of H. pylori infection with gastric carcinoma: a Meta analysis. *World J Gastroenterol* 2001; **7**: 801-804

7 **Xia HHX**, Fan XG, Talley NJ. Clarithromycin resistance in *Helicobacter pylori* and its clinical relevance. *World J Gastroenterol* 1999; **5**: 263-265

8 **Peng ZS**, Liang ZC, Liu MC, Ouang NT. Studies on gastric epithelial cell proliferation and apoptosis in *Hp* associated gastric ulcer. *Shijie Huaren Xiaohua Zazhi* 1999; **7**: 218-219

9 **Xiao SD**, Liu WZ. Current statue in treatment of *Hp* infection. *Shijie Huaren Xiaohua Zazhi* 1999; **7**: 3-4

10 **Meyer JM**, Silliman NP, Dixon CA, Siepman NY, Sugg JE, Hopkins RJ. *Helicobacter pylori* and early duodenal ulcer status post-treatment: a review. *Helicobacter* 2001; **6**: 84-92

11 **Casella G**, Buda CA, Maisano R, Schiavo M, Perego D, Baldini V. Complete regression of primary gastric MALT-lymphoma after double eradication *Helicobacter pylori* therapy: role and importance of endoscopic ultrasonography. *Anticancer Res* 2001; **21**(2B): 1499-1502

12 **Hurenkamp GJ**, Grundmeijer HG, Van Der Ende A, Tytgat GN, Assendelft WJ, Van Der Hulst RW. Arrest of chronic acid suppressant drug use after successful *Helicobacter pylori* eradication in patients with peptic ulcer disease: a six-month follow-up study. *Aliment Pharmacol Ther* 2001; **15:** 1047-1054

13 **Guo CQ**, Wang YP, Liu GY, Ma SW, Ding GY, Li JC. Study on *Helicobacter pylori* infection and-p^{53}, c-erbB-2 gene expression in carcinogenesis of gastric mucosa. *Shijie Huaren Xiaohua Zazhi* 1999; **7**: 313-315

14 **Hiyama T**, Haruma K, Kitadai Y, Masuda H, Miyamoto M, Ito M, Kamada T, Tanaka S, Uemura N, Yoshihara M, Sumii K, Shimamoto F, Chayama K. Clinicopathological features of gastric mucosa-associated lymphoid tissue lymphoma: a comparison with diffuse large B-cell lymphoma without a mucosa-associated lymphoid tissue lymphoma component. *J Gastroenterol Hepatol* 2001; **16**: 734-739

15 **Hu PJ**. *Hp* and gastric cancer: challenge in the research. *Shijie Huaren Xiaohua Zazhi* 1999; **7**: 1-2

16 **Quan J**, Fan XG. Progress in experimental research of *Helicobacter pylori* infection and gastric cancinoma. *Shijie Huaren Xiaohua Zazhi* 1999; **7**: 1068-1069

17 **Delchier JC**, Lamarque D, Levy M, Tkoub EM, Copie-Bergman C, Deforges L, Chaumette MT, Haioun C. *Helicobacter pylori* and gastric lymphoma: high seroprevalence of CagA in diffuselarge B-cell lym phoma but not in low-grade lymphoma of mucosa-associatedlymphoid tissue type. *Am J Gastroenterol* 2001; **96**: 2324-2328

18 **Morgner A**, Miehlke S, Fischbach W, Schmitt W, Muller-Hermelink H, Greiner A, Thiede C, Schetelig J, Neubauer A, Stolte M, Ehninger G, Bayerdorffer E. Complete remission of primary high-grade B-cell gastric lymphoma after cure of *Helicobacter pylori* infection. *J Clin Oncol* 2001; **19**: 2041-2048

19 **Zhang XQ**, Lin SR. Progress in research on the relationship between *Hp* and stomach cancer. *Shijie Huaren Xiaohua Zazhi* 2000; **8**: 206-207

20 **Hua JS**. Effect of *Hp*: cell proliferation and apoptosis on stomach cancer. *Shijie Huaren Xiaohua Zazhi* 1999; **7**: 647-648

21 **Armitage GC**. Periodontal infections and cardiovascular disease-how strong is the association? *Oral Dis* 2000; **6**: 335-350

22 **Tsai CJ**, Huang TY. Relation of *Helicobacter pylori* infection and angiographically demonstrated coronary artery disease. *Dig Dis Sci* 2000; **45**: 1227-1232

23 **Gocyk W**, Niklinski T, Olechnowicz H, Duda A, Bielanski W, Konturek PC, Konturek SJ. *Helicobacter pylori*, gastrin and cyclooxygenase-2 in lung cancer. *Med Sci Monit* 2000; **6**:1085-1092

24 **Tsang KW**, Lam WK, Kwok E, Chan KN, Hu WH, Ooi GC, Zheng L, Wong BC, Lam SK. *Helicobacter pylori* and upper gastrointestinal symptoms in bronchiectasis. *Eur Respir J* 1999; **14**: 1345-1350

25 **Caselli M**, Zaffoni E, Ruina M, Sartori S, Trevisani L, Ciaccia A, Alvisi V, Fabbri L, Papi A. *Helicobacter pylori* and chronic bronchitis. *Scand J Gastroenterol* 1999; **34**: 828-830

26 **Dauden E**, Jimenez-Alonso I, Garcia-Diez A. *Helicobacter pylori* and idiopathic chronic urticaria. *Int J Dermatol* 2000; **39**: 446-452

27 **Ojetti V**, Armuzzi A, De-Luca A, Nucera E, Franceschi F, Candelli M, Zannoni GF, Danese S, Di-Caro S, Vastola M, Schiavino D, Gasbarrini G, Patriarca G, Pola P, Gasbarrini A. *Helicobacter pylori* infection affects eosinophilic cationic protein in the gastric juice of patients with idiopathic chronic urticaria. *Int Arch Allergy Immunol* 2001; **125**: 66-72

28 **Vainio E**, Huovinen S, Liutu M, Uksila J, Leino R. Peptic ulcer and *Helicobacter pylori* in patients with lichen planus. *Acta Derm Venereol* 2000; **80**: 427-429

29 **Szlachcic A**, Sliwowski Z, Karczewska E, Bielanski W, Pytko-Polonczyk J, Konturek SJ. *Helicobacter pylori* and its eradication in rosacea. *J Physiol Pharmacol* 1999; **50**: 777-786

30 **Avci O**, Ellidokuz E, Simsek I, Buyukgebiz B, Gunes AT. *Helicobacter pylori* and Behcet's disease. *Dermatology* 1999; **199**: 140-143

31 **Yazawa N**, Fujimoto M, Kikuchi K, Kubo M, Ihn H, Sato S, Tamaki T, Tamaki K. High seroprevalence of *Helicobacter pylori* infection in patients with systemic sclerosis: association with esophageal involvement. *J Rheumatol* 1998; **25**: 650-653

32 **Emilia G**, Longo G, Luppi M, Gandini G, Morselli M, Ferrara L, Amarri S, Cagossi K, Torelli G. *Helicobacter pylori* eradication can induce platelet recovery in idiopathic thrombocytopenic purpura. *Blood* 2001; **97**: 812-814

33 **Parkinson AJ**, Gold BD, Bulkow L, Wainwright RB, Swaminathan B, Khanna B, Petersen KM, Fitzgerald MA. High prevalence of *Helicobacter pylori* in the Alaska native population and association with low serum ferritin levels in young adults. *Clin Diagn Lab Immunol* 2000; **7**: 885-888

34 **Konno M**, Muraoka S, Takahashi M, Imai T. Iron-deficiency anemia associated with *Helicobacter pylori* gastritis. *J Pediatr Gastroenterol Nutr* 2000; **31**: 52-56

35 **Annibale B**, Lahner E, Bordi C, Martino G, Caruana P, Grossi C, Negrini R, Delle-Fave G. Role of *Helicobacter pylori* infection in

pernicious anaemia. *Dig Liver Dis* 2000; **32**: 756-762
36 **Choe YH**, Kwon YS, Jung MK, Kang SK, Hwang TS, Hong YC. *Helicobacter pylori*-associated iron-deficiency anemia in adolescent female athletes. *J Pediatr* 2001; **139**: 100-104
37 **Kaptan K**, Beyan C, Ural AU, Cetin T, Avcu F, Gulsen M, Finci R, Yalcin A. *Helicobacter pylori*-is it a novel causative agent in Vitamin B12 deficiency? *Arch Intern Med* 2000; **160**: 1349-1353
38 **Watanabe T**, Tada M, Nagai H, Sasaki S, Nakao M. *Helicobacter pylori* infection induces gastric cancer in Mongolian Gerbils. *Gastroenterol* 1998; **115**: 642-648
39 **Honda S**, Fujioka T, Tokieda M, Satoh R, Nishizono A, Nasu M. Development of *Helicobacter pylori*-induced gastric carcinoma in Mongolian Gerbils. *Cancer Res* 1998; **58**: 4255-4259
40 **Hatzifoti C**, Wren BW, Morrow JW. *Helicobacter pylori* vaccine strategies-triggering a gut reaction. *Immuno Today* 2000; **21**: 615-619
41 **Dieterich C**, Bouzourene H, Blum AL, Corthesy-Theulaz IE. Urease-based mucosal immunization against Helicobacter heilmannii infection induces corpus atrophy in mice. *Infect Immun* 1999; **67**: 6206-6209
42 **Liu X**, Hu J, Zhang X, Fan D. Oral immunization of mice with attenuated Salmonella typhimurium expressing *Helicobacter pylori* urease B subunit. *Chin Med J* 2002; **115**: 1513-1516
43 **Lee CK**, Soike K, Hill J, Georgakopoulos K, Tibbitts T, Ingrassia J, Gray H, Boden J, Kleanthous H, Giannasca P, Ermak T, Weltzin R, Blanchard J, Monath TP. Immunization with recombinant Helicobacter pylori urease decreases colonization levels following experimental infection of rhesus monkeys. *Vaccine* 1999; **17:** 1493-1505
44 **Solnick JV**, Canfield DR, Hansen LM, Torabian SZ. Immunization with recombinant *Helicobacter pylori* urease in specific-pathogen-free rhesus monkeys (Macaca mulatta). *Infect Immun* 2000; **68**: 2560-2565
45 **Satin B**, Del Giudice G, Della Bianca V, Dusi S, Laudanna C, Tonello F, Kelleher D, Rappuoli R, Montecucco C, Rossi F. The neutrophil-activating protein (HP-NAP) of *Helicobacter pylori* is a protective antigen and a major virulence factor. *J Exp Med* 2000; **191**: 1467-1476
46 **Chen Y**, Zhang ZS, Wang JD, Zhou DY. Cloning and expression of adhesion gene hpaA of *Helicobacter pylori*. *J First Mil Med Univ* 2000; **20**: 210-213
47 **Chen Y**, Wang J, Shi L. *In vitro* study of the biological activities and immunogenicity of recombinant adhesin of *Heliobacter pylori* rHpaA. *Zhonghua Yixue Zazhi* 2001; **81**: 276-279
48 **Kim BO**, Shin SS, Yoo YH, Pyo S. Peroral immunization with *Helicobacter pylori* adhesin protein genetically linked to cholera toxin A2B subunits. *Clin Sci* 2001; **100**: 291-298
49 **Kotloff KL**, Sztein MB, Wasserman SS, Losonsky GA, DiLorenzo SC, Walker RI. Safety and immunogenicity of oral inactivated whole-cell Helicobacter pylori vaccine with adjuvant among volunteers with or without subclinical infection. *Infect Immun* 2001; **69**: 3581-3590
50 **Goto T**, Nishizono A, Fujioka T, Ikewaki J, Mifune K, Nasu M. Local secretory immunoglobulin A and postimmunization gastritis correlate with protection against *Helicobacter pylori* infection after oral vaccination of mice. *Infect Immun* 1999; **67**: 2531-2539
51 **Jiang Z**, Tao XH, Huang AL, Wang PL. A study of recombinant protective *H. pylori* antigens. *World J Gastroenterol* 2002; **8**: 308-311
52 **Metzler B**, Mayr M, Oietrich H, Singh M, Wiebe E, Xu Q, Wick G. Inhibition of arteriosclerosis by T-cell depletion in normocholesterolemic rabbits immunized with heat shock protein 65. *Arterioscler thromb vasc boil* 1999; **19**: 1905-1911
53 **Keenan J**, Oliaro J, Domigan N, Potter H, Aitken G, Allardyce R, Roake J. Immune response to an 18-kilodalton outer membrane antigen identifies Lipoprotien 20 as a *Helicobacter pylori* vaccine candidate. *Infect Immun* 2000; **68**: 3337-3343
54 **Alm RA**, Bina J, Andrews BM, Dolg P, Hancock REW, Trust TJ. Comparative genomics of *Helicobacter pylori*: analysis of the outer membrane protein families. *Infect immun* 2000; **68**: 4155-4168
55 **Todoroki I**, Joh T, Watanabe K, Miyashita M, Seno K, Nomura T, Ohara H, Yokoyama Y, Tochikubo K, Itoh M. Suppressive effects of DNA vaccines encoding heat shock protein on *Helicobacter pylori*-induced gastritis in mice. *Biochem Biophys Res Commun* 2000; **277**: 159-163
56 **Shiesh SC**, Sheu BS, Yang HB, Tsao HJ, Lin XZ. Serologic response to lower-molecular-weight proteins of *Helicobacter pylori* is related to clinical outcome of *Helicobacter pylori* infection in Taiwmn. *Dig Dis Sci* 2000; **45**: 781-788
57 **Raymond J**, Sauvestre C, Kalach N, Bergeret M, Dupont C. Immunoblotting and serology for diagnosis of *Helicobacter pylori* infection in children. *Pediatr Infect Dis J* 2000; **19**: 118-121
58 **Kawahara M**, Hashimoto A, Toida I, Honda M. Oral recombinant mycobacterium bovis bacillus calmette-guerin expressing HIV-1 antigens as a freeze-dried vaccine induces long-term, HIV-specific mucosal and systemic immunity. *Clin Immunol* 2002; **105**: 326-331
59 **Kawahara M**, Matsuo K, Nakasone T, Hiroi T, Kiyono H, Matsumoto S, Yamada T,Yamamoto N, Honda M. Combined intrarectal / intradermal inoculation of recombinant mycobacterium bovis bacillus calmette-guerin (BCG) induces enhanced immune responses against the inserted HIV-1 V3 antigen. *Vaccine* 2002; **21**: 158-166
60 **Young SL**, O'Donnell MA, Buchan GS. IL-2-secreting recombinant bacillus Calmette Guerin can overcome a Type 2 immune response and corticosteroid-induced immunosuppression to elicit a Type 1 immune response. *Int Immunol* 2002; **14**: 793-800
61 **Young S**, O'Donnell M, Lockhart E, Buddle B, Slobbe L, Luo Y, De Lisle G, Buchan G. Manipulation of immune responses to Mycobacterium bovis by vaccination with IL-2- and IL-18-secreting recombinant bacillus Calmette Guerin. *Immunol Cell Biol* 2002; **80**: 209-215
62 **Zheng C**, Xie P, Chen Y. Recombinant Mycobacterium bovis BCG producing the circumsporozoite protein of Plasmodium falciparum FCC-1 / HN strain induces strong immune responses in BALB / c mice. *Parasitol Int* 2002; **51**: 1-7
63 **Mederle I**, Bourguin I, Ensergueix D, Badell E, Moniz-Peireira J, Gicquel B, Winter N. Plasmidic versus insertional cloning of heterologous genes in Mycobacterium bovis BCG: impact on *in vivo* antigen persistence and immune responses. *Infect Immun* 2002; **70**: 303-314
64 **Zheng C**, Xie P, Chen Y. Immune response induced by recombinant BCG expressing merozoite surface antigen 2 from Plasmodium falciparum. *Vaccine* 2001; **20**: 914-919
65 **Chujoh Y**, Matsuo K, Yoshizaki H, Nakasatomi T, Someya K, Okamoto Y, Naganawa S, Haga S, Yoshikura H, Yamazaki A, Yamazaki S, Honda M. Cross-clade neutralizing antibody production against human immunodeficiency virus type 1 clade E and B' strains by recombinant Mycobacterium bovis BCG-based candidate vaccine. *Vaccine* 2001; **20**: 797-804
66 **Hiroi T**, Goto H, Someya K, Yanagita M, Honda M, Yamanaka N, Kiyono H. HIV mucosal vaccine: nasal immunization with rBCG-V3J1 induces a long term V3J1 peptide-specific neutralizing immunity in Th1- and Th2-deficient conditions. *J Immunol* 2001; **167**: 5862-5867
67 **Ohara N**, Matsuoka M, Nomaguchi H, Naito M, Yamada T. Protective responses against experimental Mycobacterium leprae infection in mice induced by recombinant Bacillus Calmette-Guerin over-producing three putative protective antigen candidates. *Vaccine* 2001; **19**: 1906-1910
68 **Luo Y**, Chen X, Szilvasi A, O'Donnell MA. Co-expression of interleukin-2 and green fluorescent protein reporter in mycobacteria: *in vivo* application for monitoring antimycobacterial immunity. *Mol Immunol* 2000; **37**: 527-536

Edited by Zhang JZ, Zhu LH and Wang XL

P.O.Box 2345, Beijing 100023,China
Fax: +86-10-85381893
E-mail: wjg@wjgnet.com www.wjgnet.com

World J Gastroenterol 2003;9(8):1762-1766
World Journal of Gastroenterology
 ISSN 1007-9327

cagA and vacA genotype of *Helicobacter pylori* associated with gastric diseases in Xi'an area

Wen Qiao, Jia-Lu Hu, Bing Xiao, Kai-Chun Wu, Dao-Rong Peng, John C Atherton, Hui Xue

Wen Qiao, Hui Xue, Department of Gastroenterology, First Hospital, Xi' an Jiaotong University, Xi' an 710061, Shaanxi Province, China
Jia-Lu Hu, Kai-Chun Wu, Dao-Rong Peng, Department of Gastroenterology, Xijing Hospital, Fourth Military Medical University, Xi' an 710032, Shaanxi Province, China
Bing Xiao, Department of Gastroenterology, Nanfang Hospital, First Military Medical University, Guangzhou 510515, Guangdong Province, China
John C Atherton, Division of Gastroenterology and Institute of Infections and Immunity, University Hospital, Nottingham NG7 2UH, England
Correspondence to: Dr. Wen Qiao, Department of Gastroenterology, First Hospital, Xi' an Jiaotong University, Xi' an 710061, Shaanxi Province, China. xhy1202@ sohu.com
Telephone: +86-29-5324101 **Fax:** +86-29-5263190
Received: 2003-01-11 **Accepted:** 2003-03-05

Abstract

AIM: To establish stock of clinical *Helicobacter pylori* (*H. pylori*) isolates, to perform cagA and vacA typing of these isolates, to evaluate the relationship between genotypes of cagA and vacA and upper gastrointestinal diseases and to assess the association of vacA genotypes with presence of the pathogenicity marker-cagA.

METHODS: Clinical *H.pylori* strains were isolated from the antrum of 259 patients in Clumbia agar. The isolated *H. pylori* strains were identified by histology, and16SrRNA PCR. CagA genotypes were detected by colony hybridization, the probe was derived from the cloned plasmid PcagA, and digested by *Eco*RI-*Hin*dIII and the isolated PcagA DNA fragment was radioactively labelled by the random priming method. vacA genes types (s,m)and subtypes (s1a, s1b, s2) were typed by PCR. Vacuolating toxin was detected with neutral red absorb test. The results were treated statistically by χ^2 test, *t* test, and rank sum test.

RESULTS: A total of 192 clinical *H.pylori* strains were isolated and the stock of *Helicobacter pylori* was established. The total positive rate of cagA was 87 % in all gastric diseases, and 95 % in gastric cancer group. There was a difference between gastric cancer group and the other groups ($P<0.05$) except duodenal ulcer group. The expression of type s1 of vacA was more than type s2 ($P<0.05$), and, the expression of type m1 was equal to type m2. In gastric cancer group, there was a difference between s1a and s1b ($P<0.05$), and s1a was more than s1b. Vacuolating toxins were more in Xi'an area isolates.

CONCLUSION: The cagA$^+$ vacA type s1 clinical isolates are more in Xi'an area, but this can not serve as an index to predict gastric cancer.

Qiao W, Hu JL, Xiao B, Wu KC, Peng DR, Atherton JC, Xue H. cagA and vacA genotype of *Helicobacter pylori* associated with gastric diseases in Xi'an area. *World J Gastroenterol* 2003; 9 (8): 1762-1766
http://www.wjgnet.com/1007-9327/9/1762.asp

INTRODUCTION

Helicobacter pylori (*H. pylori*) is an important human pathogen that causes chronic gastritis and is associated with development of peptic ulcer diseases, and gastric malignancies[1]. Epidemiological studies have shown that *H. pylori* is a class 1 carcinogen for gastric adenocarcinoma, which is one of the most common cancers worldwide, and the odds ratio for developing gastric cancer is 3.8 to 8.7 in *H.pylori* infected subjects[2-6]. The pathophysiological mechanism by which *H.pylori* leads to gastric cancer has not yet been defined, although many hypotheses have been put forward.

The genetic variability among *H.pylori* strains is relatively high[7]. Approximately 50-60 % of *H. pylori* strains contain cytotoxin-associated (cagA) gene and consequently produce 128 ku CagA protein[8,9]. The presence of cagA is associated with gastric cancer, gastric mucosal atrophy, and duodenal ulcer. CagA is a part of a large genomic entity, designating the pathogenicity (cag) island[10,11], which contains multiple genes that are related to the virulence and pathogenicity of *H. pylori* strains. Therefore, the presence of cagA can be considered as a marker for this genomic pathogenicity island and is associated with more virulent *H.pylori* strains.

Another important virulence factor, produced by approximately 50 % of *H. pylori* strains, is a cytotoxin that induces formation of vacuolates in mammalian cells *in vitro* and leads to cell death[12]. The toxin is encoded by vacA gene, which is virtually present in all *H.pylori* strains[13]. The existence of different allelic variants in two parts of this gene has been described[14-17]. The N-terminal signal (s) region occurs as either a s1a, s1b or s2 allele. The middle (m) region is present as a m1 or m2 allele. The mosaic structure of vacA gene accounts for differences in cytotoxin production between strains[18-20].

The aim of this study was to detect and type the virulence-associated cagA and vacA genes of clinical *H.pylori* isolates in Xi'an area of China. Finally, the clinical relevance of vacA and cagA genotyping was investigated with gastric cancer and precancerous conditions.

MATERIALS AND METHODS

Bacterial isolation and culture

A total of 192 *H.pylori* isolates were obtained from patients undergoing upper gastrointestinal examination. The diagnosis obtained by endoscopy and histology was recorded for all the patients from whom the strains were isolated. Following primary isolation, *H.pylori* strains were grown on Columbia agar with 50 mL/L frozen-melting sheep blood, 100 mL/L fetal bovine serum, and Skirrow's antibiotic supplement in a microaerophilic atmosphere for 5 days at 37 ℃, then frozen at -70 ℃. Most of the strains were frozen four to six passages after primary isolation. Subsequent analyses were performed on strains derived from the frozen stocks. The isolated *H.pylori* strains were identified by histology, and16SrRNA PCR.

Plasmid DNA preparation

A signal bacteria clone was incubated at 37 ℃ overnight, harvested, and suspended in 0.5 mol/L EDTA-1M Tris-HCl

(pH 8.0), 10 mol/L NaOH and 100 g/L SDS was added, mixed, then 5 mol/L KAc and ice HAc were added. The mixture was centrifuged at 12 000 r/min for 10 min. The supernatant was extracted with phenol-chloroform followed by with chloroform. After extraction, the DNA solution was mixed with absolute ethanol and 3 mol/L NaAc at -20 ℃ for 20 min, washed with 700 mL/L ethanol, and dried. The DNA pellet was suspended in TE (10 mmol/L Tris-HCl, 1 mmol/L pH8.0 EDTA), and stored at -20 ℃.

DNA probes

The probe was derived from the cloned plasmid PcagA, and digested by *Eco*RI-*Hin*dIII. The enzyme digestion segment of PcagA was retrieved by DNA purification reagent kit (Baotaike Biotechnology Company). The isolated PcagA DNA fragment was radioactively labelled by the random priming method.

Colony hybridization

SDS of 100 g/L was added in fresh *H.pylori* liquid for 10 min, 2×SSC (1×SSC is 0.15 mol/L NaCl plus 0.015 mol/L sodium citrate) for 5 min, then *H.pylori* degeneration liquids were dotted on NC membranes which had been treated by 2×SSC, heated at 80 ℃ for 2 h. The membranes were put into pre-hybridization liquid (1×Denhardt, 1 g/L SDS, 5×SSC, 500 g/L deionised fomamide) at 42 ℃ for 3 h, then α-^{32}P labeled probes were added at 43.5 ℃ overnight. The membrane filters were subsequently washed once in 2×SSC-5 g/L SDS and three times in 0.1×SSC-1 g/L SDS, then exposed to X-ray film and their radioactivity was self-developing at -20 ℃ for 48 h. The film was developed and then fixed.

H.pylori chromosomal DNA extracts

Fresh *H. pylori* strains were harvested, suspended in 0.1 mol/L NaCl-10 mmol/L Tris-HCl-1 mmol/L EDTA (pH 8.0), and incubated at 37 ℃ for 15 min. NH_4Ac was added and the mixture was placed on ice for 5 min and extracted once with chloroform, mixed with isopropanol and placed on ice for 10 min. After extraction, the DNA solution was mixed with absolute ethanol at -20 ℃ for 1 h, washed with 700 mL/L ethanol, and dried. The DNA pellet was suspended in distilled water and stored at -20 ℃.

VacA genotyping

The vacA was typed by PCR. Table 1 shows the primer sequence of vacA. And Table 2 shows the system of PCR. The reaction condition was at 94 ℃ for 1 min, at 52 ℃ for 1 min, and at 72 ℃ for 1 min for 35 cycles and extension at 72 ℃ for 6 min. The PCR product was analyzed by 20 g/L agarose gel. The reference *H.pylori* strains were 60 190 (s1a/m1), 84 183 (s1b/m1) and 86 313 (s2/m2).

Cytotoxicity test on hela cells

Hela cells were cultured in plastic flasks in Dulbecco' s modified Eagle' s medium (DMEM) containing 25 mmol/L HEPES buffer (N-2-hydroxyethylpiperazine-N' -2-ethanesulfonic acid, pH7.2) and 100 g/L fetal bovine serum. Cells were maintained at 37 ℃ in a 50 mL/L CO_2 atmosphere. After cultured for 24 h, the cells were suspended with trypsin-EDTA and seeded in 96-well titration plates to make the density of cells of 10^4 per well. The supernatant prepared by water extracts from different strains was diluted two-fold from 1:2 to 1:32 and incubated with Hela cells for 12 h, then added 0.5 g/L neutral red- normal saline for 5 min, washed 3 times with 2 g/L BAS-normal saline and added HCl-ethanol. The absorbance was detected at 540 nm. When the detected value was more than 3 times of the negative control, it was defined as a positive result.

Table 2 The system of PCR

Constituents	Volume / per tube (μL)	Final concentration
Water	36	
10×PCR buffer	5	1×
4dNTP, 2.5mmol/L /each	4	0.2mmol/L each
primer 1.25 μmol/L	1	0.5 μmol/L
primer 2.25 μmol/L	1	0.5 μmol/L
$MgCl_2$, 50 mmol/L	1.5	1.5 mmol/L
Taq DNA polymerase, 5MU/L	0.5	0.1 MU/L
Template DNA	1	

Statistical analysis

χ^2 test, *t* test, and rank sum test were used for statistical analysis.

RESULTS

Presence of cagA gene

The presence of cagA gene was investigated in all clinical isolates by colony hybridization. *Eco*RI-*Hin*dIII-digested chromosomal DNA (Figure 1) was probed with an α ^{32}P-labelled DNA fragement internal to cagA. Typical examples of the results obtained with colony hybridization are reported in Figure 2. Of the 192 clinical isolates, 165 strains (86 %) had a positive hybridization dot, while 27 strains (14 %) did not show hybridization dot. In the 192 strains, the positive rate of gastric cancer group was 95 %, chronic superficial gastritis (CSG) 77 %, chronic atrophic gastritis (CAG) 86 %, gastric ulcer (GC) 69 %, and duodenal ulcer (DU) 95 %. There were differences between CAG and GU (P<0.05), and between GU and DU (P<0.05), but there were no statistical differences between CSG and CAG (P>0.05), and between CSG and GU (P>0.05).

Presence of signal sequence typing of vacuolating toxin gene

The signal sequence gene was typed by PCR in all *H. pylori* clinical isolates. The products of s1 and s2 were 259 bp and 286 bp, respectively. In the 192 strains, 174 strains (90.6 %) were s1 type, and 18 strains (9.4 %) were s2. The subtypes of s1 were typed by two pairs of primers (SS1-F/VA1-R and SS3-

Table 1 Oligonucleotide primers used for vacA typing

Gene and region amplified	Genotype identified	Primer designation	Primer sequence	Size of PCR product(bp)
Mid-region	m1/m2	VAG-F	5'CAATCTGTCCAATCAAGCGAG3'	567/642
		VAG-R	5'GCGTCAAAATAATTCCAAGG3'	
Signal sequence	s1/s2*	VA1-F	5'ATGGAAATACAACAAACACAC3'	259/286*
		VA1-R	5'CTGCTTGAATGCGCCAAAC3'	
	s1a	SS1-F#	5'GTCAGCATCACACCGCAAC3'	190
	s1b	SS3-F#	5'AGCGCCATACCGCAAGAC3'	187

vacA types s1 and s2 were differentiated on the size of the PCR product. # Used with reverse primer VA1-R.

F/VA1-R) (Table 3 and Figure 3). The product of s1a and s1b was 190 bp and 187 bp, respectively. In the 174 s1 type strains, 111 strains (63.8 %) were s1a, and 63 strains (36.2 %) were s1b (Figures 4, 5).

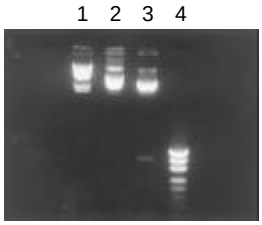

Figure 1 Restriction endonuclease *Eco*RI, *Hin*dIII digests of PcagA. 1. λDNA *Hin*dIIImarker, 2. PcagA, 3. Fragement digested by *Eco*RI-*Hin*dIII, 4. PUC18/MSPI marker.

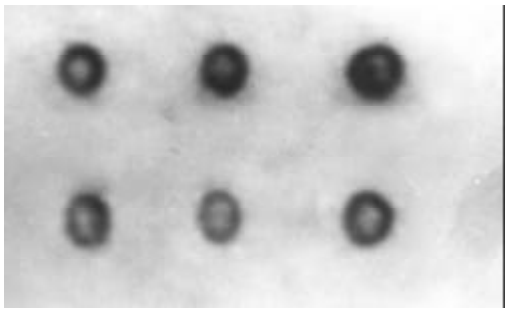

Figure 2 Colony hybridization detection of cagA. The positive hybridization dot.

Figure 3 PCR typing of vacA signal sequence. 1.PCR marker, 2. Type s2, 3. Type s1, 4. Standard strain 86313, 5. Standard strain 60 190.

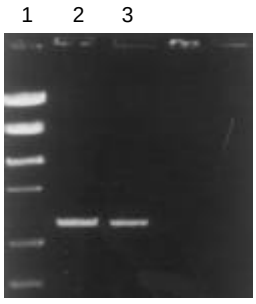

Figure 4 PCR typing of vacA s1a. 1. PCR marker, 2. Clinical isolates, 3. Standard strain 84 183.

Presence of middle region typing of vacuolating toxin gene

The middle region gene was also typed by PCR in all *H. pylori* clinical isolates. The products of m1 and m2 were 567 bp and 642 bp, respectively. In the 192 strains, 99 strains (51.6 %) were m1 type, and 93 strains(48.4%) were m2, (Table 4 and Figure 6).

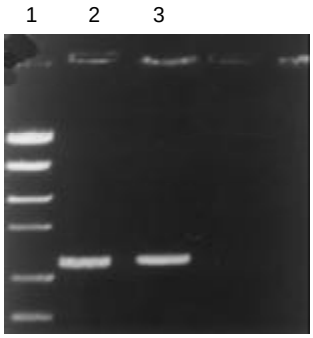

Figure 5 PCR typing of vacA mid-region. 1. PCR marker, 2. Clinical isolates, 3. Standard strain 84 183.

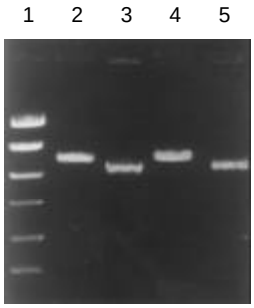

Figure 6 PCR typing of vacA s1a. 1. PCR marker, 2.Type m2, 3. Type m1, 4. Standard strain 86 313, 5. Standard strain 60 190.

Table 3 *H.pylori* signal sequence typing and gastric diseases

s type	GC	CSG	CAG	GU	DU	Total(%)
s1a	43a	14	37	5	12	111(57.8)
s1b	10	13	25	8	7	63(32.8)
s2	3	4	7	3	1	18(9.4)
Total	56	31	69	16	20	192(100.0)

[a]$P<0.05$ *vs* GU, CSG, CAG.

Table 4 *H.pylori* signal sequence typing and gastric diseases

m type	GC	CSG	CAG	GU	DU	Total(%)
m1	31	13	36	7	12	99(51.6)
m2	25	18	33	9	8	93(48.4)
Total	56	31	69	16	20	192(100.0)

No difference at all.

Presence of middle region typing and signal sequence of vacuolating toxin gene

In the 192 strains, 65 strains (33.9 %) were sla/m1, 34 strains (17.7 %) s1b/m1, 46 strains (24.0 %) s1a/m2, 29 strains (15.1 %) s1b/m2, and 18 strains (9.4 %) s2/m2.

Relationship between vacA typing and detecting of vacuolating cytotoxin activity in vitro

The maximum diluting times of positive result were the value of vacuolating toxin. Based on the maxium diluting unit, the strains were divided into three types: high toxin ($\geqslant$8), low toxin (1-8) and none toxin (less than 1). In the 192 strains, high toxin was 90 strains (46.9 %), low toxin 62 (32.3 %) and none toxin 40 (20.8 %, Table 5).

Relationship between cagA and vacA subtype

In the 165 cagA gene positive strains, 165 strains (100 %)

were vacA s1 type; 97 strains (58.8 %) vacA m1 type, and 78 strains (46.2 %, Table 6) vacA m2 type.

Table 5 Relationship between vacA typing and grade of vacuolating cytotoxin activity

vacA type	Grade of vacuolating cytotoxin activity		
	None	Low	High
s1a	5	38	68
s1b	17	24	22
s2	18	0	0
m1	10	30	59
m2	30	32	31

$P<0.05$, each group *vs* s1a, s1b, s2.

Table 6 Relationship between vacA typing, cagA gene and gastric diseases for 192 *H. pylori* isolates

vacA type	cagA+					Total(%)
	GC	CSG	CAG	GU	DU	
s1a	43	14	37	4	12	110(66.7)
s1b	10	10	22	6	7	55(33.3)
s2	0	0	0	0	0	0(0.0)
m1	31	12	36	6	12	97(58.8)
m2	22	12	23	4	7	78(46.2)

DISCUSSION

H. pylori is the major causative agent of chronic superficial gastritis and plays a central role in the etiology of peptic ulcer disease. Evidence suggests that *H. pylori* infection pre-exists in gastric carcinoma and precancerous lesions, and is a risk for development of gastric carcinoma. Cittelly showed that lower frequencies of cytotoxic genotypes such as cagA and vacA s1m1 were observed in patients with NAG (non atrophic gastritis), when compared to patients with GC (gastric cancer) or PU (peptic ulcer). He suggested that vacA and cagA could be used as markers for increased virulence. In 1994, *H. pylori* was designated as a class I carcinogen by the World Health Organization[21,22]. *H. pylori* infection is high among Chinese people (the infected rate is 40-70 %), and also high in gastric cancer. The mortality of gastric cancer ranks the first among malignancies. The results of epidemiologic surveys on the relationship between *H. pylori* and gastric cancer show that infection of *H.pylori* in Lanzhou, an area with a high occurrence of gastric cancer, is higher than that in Guangzhou, an area with a low occurrence of gastric cancer[23, 24].

Recent researches suggested that the positive cytotoxin-associated gene A of *H.pylori* was about 60 %. This toxin can induce severe inflammation of gastric mucosa and is related with peptic ulcer and gastric cancer[25]. We detected the cagA gene in 192 clinical strains by colony hybridization, with a total positive rate of 86 %. In gastric cancer and duodenal ulcer, *H.pylori* infection rate (91 %) was the highest in all gastric diseases. In gastric ulcer group it was the lowest, only 69 %. Our results suggest that positive cagA of *H.pylori* isolated strains is related with gastric diseases in Xi' an area, Because the expression of cagA positive strains in gastric cancer group was higher than that in chronic gastritis group and the difference was apparent ($P<0.05$). CagA can increase the serious consequences of carcinogenesis from chronic inflammation. The detectable rate of CagA antibody in human group in high occurrence region of gastric cancer was obviously higher than that in low occurrence area. Some researches have also proved that cagA positive strains are easy to cause inflammation of gastric mucosa and can stimulate hyperplasia of gastric mucosal cells. Many studies have shown that there is a relationship between cagA positive antibody and peptic ulcer and gastric cancer. One research suggested that development of more prominent gastritis and severe atrophy in cagA (+) patients was an indicator for the importance of cagA rather than *H. pylori* load. Our research was consistent with theirs[26, 27].

All strains have the gene encoding toxin vacA, but its structure varies, especially in the mid-region which may be type m1 or m2 and the region encoding the signal sequence (type s1a, s1b or s2). The final structure is a mosaic, and all combinations of signal sequence and mid-region types are found except s2/m1. A strain' s vacA structure determines its *in vitro* cytotoxin activity, with type m1 vacA being more active than type m2, type s1a being more active than type s1b, and type s2 vacA not producing detectable activity. Our results showed that the main genotype was s1a in gastric cancer group, and there was an apparent difference between s1a and s1b ($P<0.05$), and the s2 genotype was seldom found. In the meantime, there was no apparent difference between m1 and m2 ($P>0.05$). The expression of s1a type was different among gastric cancer, gastric ulcer, and chronic gastritis. In gastritis group, there was no difference between s1a type and s1b type. Andreson' s research showed that the presence of the cagA gene was correlated with that of vacA signal sequence type s1a. However, no clear differences were found in the distribution of cagA and vacA genotypes among patients with peptic ulcer or chronic gastritis in Estonia. The reason why the different regional distribution can cause different genotype of *H.pylori* is not clear[28].

Our results showed that the infected *H.pylori* in Xi' an area was mainly toxin strains. In the meantime, the expression of s1a and s1b in the toxin strains was obviously different ($P<0.05$), and there was no significant difference between m1 and m2 ($P>0.05$). This suggests that s2 type can not produce detectable vacuolating toxin, and s1 type can produce the toxin. The middle-region is not obviously related to toxin production. The toxin produced by s2 type may not effectively pass through cellular membrane[29].

In cagA positive strains, the main vacA subtype was s1a, about 67 %, and s1b was only 33 %, and there was an apparent difference between these two subtypes ($P<0.05$). But there was no difference between m1 and m2 ($P>0.05$). We found that s1 type was related with gastric cancer[30].

Inactivation of multiple antioncogenes and *H.pylori* infection may be involved in the development and progress of gastric carcinoma, and *H.pylori* infection may be associated with the inactivation of some oncogenes[31]. The genotype expression of *H.pylori* in gastric cancer was mainly $cagA^+$/s1a strains in Xi' an area, but this can not serve as an index to predict gastric cancer. The main genotype of vacA in chronic gastritis, gastric ulcer and duodenal ulcer is s1, but there is no difference between s1a, s1b, m1 and m2.

REFERENCES

1 **YaoYL**, Zhang WD. The relationship between *Helicobacter pylori* and gastric cancer. *Shijie Huaren Xiaohua Zazhi* 2001; **9**: 1045-1049

2 **Zhuang XQ**, Lin SR. Research of *Helicobacter pylori* infection in precancerous gastric lesions. *World J Gastroenterol* 2000; **6**: 428-429

3 **Vandenplas Y**. *Helicobacter pylori* infection. *World J Gastroenterol* 2000; **6**: 20-31

4 **Zhong Z**, Yuan Y, Gao H, Dong M, Wang L, Gong YH. Apoptosis, proliferation and p53 gene expression of *H. pylori* associated gastric epithelial lesions. *World J Gastroenterol* 2001; **7**: 779-782

5 **Gao H**, Wang JY, Shen XZ, Liu JJ. Effect of *Helicobacter pylori* infection on gastric epithelial cell proliferation. *World J Gastroenterol* 2000; **6**: 442-444

6 **Zhuang XQ**, Lin SR. Study on the relationship between *Helicobactr pylori* and gastric cancer. *Shijie Huaren XiaoHuaZazhi* 2000; **8**: 206-207

7 **Figueiredo C**, Van Doorn LJ, Nogueira C, Soares JM, Pinho C, Figueira P, Quint WG, Carneiro F. *Helicobacter pylori* genotypes are associated with clinical outcome in Portuguese patients and show a high prevalence of infections with multiple strains. *Scand J Gastroenterol* 2001; **36**: 128-135

8 **Li XJ**, Yan XJ, Liu ZG, Su CZ. Expression, purification and clinical research of *Helicobacter pylori* cytotoxin-associated gene A. *Shijie Huaren Xiaohua Zazhi* 2002; **10**: 271-274

9 **Abasiyanik MF**, Sander E, Salih BA. *Helicobacter pylori* anti-CagA antibodies: Prevalence in symptomatic and asymptomatic subjects in Turkey. *Can J Gastroenterol* 2002; **16**: 527-532

10 **Kidd M,** Lastovica AJ, Atherton JC, Louw JA. Conservation of the cag pathogenicity island is associated with vacA alleles and gastroduodenal disease in south african *Helicobacter pylori* isolates. *Gut* 2001; **49**: 11-17

11 **Hu WJ**, Li NS, Wang SL, Liu J, Tu ZX, Xu GM. Difference between cagA and cagM in cag I of *Helicobacter pylori* isolated from Chinese patients. *Shijie Huaren Xiaohua Zazhi* 2001; **9**: 405-409

12 **Ye GA**, Zhang WD, Liu LM, Shi L, Xu ZM, Chen Y, Zhou DY. vacA gene of *Helicobacter pylori*. *Shijie Huaren Xiaohua Zazhi* 2001; **9**: 593-595

13 **van Doorn LJ**. Detection of *Helicobacter pylori* virulence-associated genes. *Expert Rev Mol Diagn* 2001; **1**: 290-298

14 **Lin CW**, Wu SC, Lee SC, Cheng KS. Genetic analysis and clinical evaluation of vacuolating cytotoxin gene A and cytotoxin-associated gene A in taiwanese *Helicobacter pylori* isolates from peptic ulcer patients. *Scand J Infect Dis* 2000; **32**: 51-57

15 **Fallone CA**, Barkun AN, Gottke MU, Best LM, Loo VG, Veldhuyzen van Zanten S, Nguyen T, Lowe A, Fainsilber T, Kouri K, Beech R. Association of *Helicobacter pylori* genotype with gastroesophageal reflux disease and other upper gastrointestinal diseases. *Am J Gastroenterol* 2000; **95**: 659-669

16 **Shiesh SC**, Sheu BS, Yang HB, Tsao HJ, Lin XZ. Serologic response to lower-molecular-weight proteins of H. pylori is related to clinical outcome of *H. pylori* infection in Taiwan. *Dig Dis Sci* 2000; **45**: 781-788

17 **Yao YL**, Xu B, Song YG, Zhang WD. Overexpression of cyclin E in mongolian gerbil with *Helicobacter pylori*-induced gastric precancerosis. *World J Gastroenterol* 2002; **8**: 60-63

18 **Ji KY**, Hu FL. The development of *Helicobacter pylori* and cytokines. *Shijie Huaren Xiaohua Zazhi* 2002; **10**: 503-508

19 **Hou P**, Tu ZX, Xu GM, Gong YF, Ji XH, Li ZS. *Helicobacter pylori* vacA genotypes and cagA status and their relationship to associated diseases. *World J Gastroenterol* 2000; **6**: 605-607

20 **She FF**, Su DH, Lin JY, Zhou LY. Virulence and potential pathogenicity of coccoid *Helicobacter pylori* induced by antibiotics. *World J Gastroenterol* 2001; **7**: 254-258

21 **Xue FB,** Xu YY, Wan Y, Pan BR, Ren J, Fan DM. Association of *H. pylori* infection with gastric carcinoma: a meta analysis. *World J Gastroenterol* 2001; **7**: 801-804

22 **Cittelly DM**, Huertas MG, Martinez JD, Oliveros R, Posso H, Bravo MM, Orozco O. *Helicobacter pylori* genotypes in non atrophic gastritis are different of the found in peptic ulcer, premalignant lesions and gastric cancer in colombia. *Rev Med Chil* 2002; **130**: 143-151

23 **Wang GT**.The relationship between CagA/VacA strains and chronic gastric diseases. *Shijie Huaren XiaoHuaZazhi* 2001; **9**: 1335-1338

24 **Chen JP**, Shen DM, Yang ZB. CagA+ *Hp* broth culture filtrates induced malignant transformation on human gastric epithelial cells. *Shijie Huaren Xiaohua Zazhi* 2001; **9**: 617-621

25 **Wang CD**, Li JS, Chen LY. CagA and VacA do not predict *Helicobacter pylori*-associated gastroduodenal diseases. *Shijie Huaren Xiaohua Zazhi* 2002; **10**: 533-535

26 **Cai L**, Yu SZ, Zhang ZF. *Helicobacter pylori* infection and risk of gastric cancer in Changle County, Fujian Province, China. *World J Gastroenterol* 2000; **6**: 374-376

27 **Zhou JC**, Xu CP, Zhang JZ. The research development of cagA/CagA of *Helicobacter pylori* mocular biology. *Shijie Huaren XiaoHuaZazhi* 2001; **9**: 560-562

28 **Demirturk L**, Ozel AM, Yazgan Y, Solmazgul E, Yildirim S, Gultepe M, Gurbuz AK. CagA status in dyspeptic patients with and without peptic ulcer disease in turkey: Association with histopathologic findings. *Helicobacter* 2001; **6**: 163-168

29 **Andreson H**, Loivukene K, Sillakivi T, Maaroos HI, Ustav M, Peetsalu A, Mikelsaar M. Association of cagA and vacA genotypes of *Helicobacter pylori* with gastric diseases in estonia. *J Clin Microbiol* 2002; **40**: 298-300

30 **Park SM**, Park J, Kim JG, Yoo BC. Relevance of vacA genotypes of *Helicobacter pylori* to cagA status and its clinical outcome. *Korean J Intern Med* 2001; **16**: 8-13

31 **Wang XD**, Fang DC, Li W, Du QX, Liu WW. A study on relationship between infection of *Helicobacter pylori* and inactivation of antioncogenes in cancer and pre-cancerous lesion. *Shijie Huaren Xiaohua Zazhi* 2001; **9**: 984-987

Edited by Ma JY

P.O.Box 2345, Beijing 100023,China
Fax: +86-10-85381893
E-mail: wjg@wjgnet.com www.wjgnet.com

World J Gastroenterol 2003;9(8):1767-1771
World Journal of Gastroenterology
 ISSN 1007-9327

• BASIC RESEARCH •

Expression and activities of three inducible enzymes in the healing of gastric ulcers in rats

Jin-Sheng Guo, Chi-Hin Cho, Wei-Ping Wang, Xi-Zhong Shen, Chuen-Lung Cheng, Marcel Wing Leung Koo

Jin-Sheng Guo, Chi-Hin Cho, Wei-Ping Wang, Xi-Zhong Shen, Chuen-Lung Cheng, Marcel Wing Leung Koo, Department of Pharmacology, Faculty of Medicine, University of Hong Kong, Hong Kong
Jin-Sheng Guo, Xi-Zhong Shen, Division of Gastroenterology, Zhongshan Hospital, Fu Dan University, Shanghai 200032, China
Correspondence to: Marcel Wing Leung Koo, Department of Pharmacology, Faculty of Medicine, University of Hong Kong, Pokfulam, Hong Kong. wlkoo@hkusua.hku.hk
Telephone: +852-28199256 **Fax:** +852-28170859
Received: 2003-04-04 **Accepted:** 2003-05-20

Abstract

AIM: To explore the roles of nitric oxide synthase (NOS), heme oxygenase (HO) and cyclooxygenase (COX) in gastric ulceration and to investigate the relationships of the expression and activities of these enzymes at different stages of gastric ulceration.

METHODS: Gastric ulcers (kissing ulcers) were induced by luminal application of acetic acid. Gastric tissue samples were obtained from the ulcer base, ulcer margin, and non-ulcerated area around the ulcer margin at different time intervals after ulcer induction. The mRNA expression and protein levels of inducible and constitutive isoforms of NOS, HO and COX were analyzed with RT-PCR and Western blotting methods. The activities of the total NOS, inducible NOS (iNOS), HO, and COX were also determined.

RESULTS: Differential expression of inducible iNOS, HO-1 and COX-2 and enzyme activities of NOS, HO and COX were found in the gastric ulcer base. High iNOS expression and activity were observed on day 1 to day 3 in severely inflamed ulcer tissues. Maximum expressions of HO-1 and COX-2 and enzyme activities of HO and COX lagged behind that of iNOS, and remained at high levels during the healing phase.

CONCLUSION: The expression and activities of inducible NOS, HO-1 and COX-2 are found to be correlated to different stages of gastric ulceration. Inducible NOS may contribute to ulcer formation while HO-1 and COX-2 may promote ulcer healing.

Guo JS, Cho CH, Wang WP, Shen XZ, Cheng CL, Koo MWL. Expression and activities of three inducible enzymes in the healing of gastric ulcers in rats. *World J Gastroenterol* 2003; 9 (8): 1767-1771

http://www.wjgnet.com/1007-9327/9/1767.asp

INTRODUCTION

Nitric oxide synthase (NOS), heme oxygenase (HO) and cyclooxygenase (COX) are three important enzymes with constitutive and inducible isoforms. NOS catabolizes L-arginine to L-citrulline and nitric oxide (NO)[1,2], COX converts arachidonic acid to bioactive prostanoids[3,4], while HO metabolizes heme to biliverdin, carbon monoxide, and iron[5,6]. All these products play important roles in physiological and pathological conditions. The constitutive forms, namely eNOS, HO-2 and COX-1, are normally expressed in cells and tissues. Their expressions and activities are unaffected or only marginally modified during the process of inflammation. On the contrary, the inducible isoforms, namely iNOS, HO-1 and COX-2, are highly inducible in acute and chronic inflammation[7-9]. These induced enzymes may directly mediate the inflammatory reaction or contribute to the resolution of inflammation. Although the inducible property of these enzymes in inflammation has been proven and widely studied, their expression and activities at different stages of gastric ulceration have not been well defined. In this study, the temporal changes in the expressions and activities of these enzymes in rat stomaches during inflammation and ulcer healing were examined.

MATERIALS AND METHODS

Animals

The protocol of the study was approved by the Committee on the Use of Live Animals for Teaching and Research of University of Hong Kong. Male SD rats (weighing between 150-170 g) were fed on a standard laboratory diet (Ralston Purina Co., Chicago, IL) and kept inside a room with well-regulated temperature (22±1 ℃), humidity (65-70 %), and day/night cycle (12 h/12 h). The rats were starved for 24 h and water withdrawn 1 hour before the operation of the induction of gastric ulcer.

Preparation of gastric kissing ulcers

Gastric kissing ulcers were induced by luminal application of an acetic acid solution as previously described[10,11]. Briefly, the abdomen was opened under ether anesthesia, and the stomach was exposed. The anterior and posterior walls of the stomach were clamped together by a clip with metal rings of 11 mm internal diameter attached to both ends. Acetic acid solution (60 %, v/v) of 0.12 mL was injected with a syringe through the forestomach into the gastric lumen between the two rings. The acid solution was withdrawn 45 s later into the same syringe, and the operating site was disinfected with 70 % ethanol. Thereafter the animals were allowed to feed on standard diet and tap water *ad libitum* until collection of gastric tissue samples.

Sample collection

The rats were killed by ether anesthetization at 2 h, 6 h, 12 h, 1 d, 2 d, 3 d, 5 d, 8 d, and 15 d after ulcer induction and their stomachs were excised. The stomach was opened along the greater curvature and rinsed with cold normal saline, then blotted dry. The ulcer area (mm^2) was traced onto a transparency and then copied to a grid paper with 1 mm^2 square. The ulcer area was determined by counting the numbers of square it covered. Gastric tissues from the ulcer base, ulcer margin (1-2 mm adjacent to the ulcer base) and intact tissues around the ulcer margin were obtained and immediately frozen

in liquid nitrogen before storage at -70 ℃ until used for reverse transcription polymerase chain reaction (RT-PCR), Western blot and enzyme activities analysis. Gastric samples obtained from each time point were also fixed in 10 % buffered formalin for histological examinations. Gastric tissues from the rats without kissing ulcers were used as the control.

Histology

Paraffin embedded sections were prepared and hematoxylin and erosin staining (H&E) was used for morphological examinations of histological changes during tissue inflammation and ulcer healing.

RT-PCR analysis of mRNA expression

Total RNA was isolated from gastric tissues using Trizol reagent (Gibico BRL, Gathersburg, MD, USA). First strand complementary DNA (cDNA) was synthesized from 5 μg RNA by using oligo $(dT)_{20}$ primer with the thermoscript RT-PCR system (Gibico BRL). PCR cycles were performed for amplification of iNOS, eNOS, COX-1, COX-2, HO-1, HO-2 and β-actin cDNA using a PCR thermal cycler (Gene Amp PCR System 9700; Perkin-Elmer Corp., Norwalk, CT, USA) and oligonucleotides (Gibico BRL) of sequences are listed in Table 1. The number of PCR cycles was adjusted carefully to avoid saturation of the amplification system. PCR products were visualized by UV illumination (Bio-Rad, Hercules, CA, USA) after electrophoresis through 1 % agarose gel containing 0.5 μg/mL ethidium bromide. The gel photographs were scanned with a computerized densitometer (Multi-Analyst, Bio-Rad, Hercules, CA).

Table 1 Primer sequences of iNOS, eNOS, COX-1, COX-2, HO-1, HO-2 and β-actin

Primer	Primer sequences	Amplicon-length (bp)
HO-1	Sense: 5'-CAGTCGCCTCCAGAGTTTCC-3'	
	Antisense: 5'-TACAAGGAGGCCATCACCAGC-3'	284
HO-2	Sense: 5'-AGAAGTATGTGGATCGGA-3'	
	Antisense: 5'-TACTCAGGTCCAAGGCA-3'	242
COX-1	Sense: 5'-TGCTGCTGAGAAGGGAGTTCATTC-3'	
	Antisense: 5'-CAAGTCACACACACGGTTATGCTC-3'	403
COX-2	Sense: 5'-ACACTCTATCACTGGCATCC-3'	
	Antisense: 5'-GAAGGGACACCCTTTCACAT-3'	584
iNOS	Sense: 5' -TGGCTTGCCCTTGGAAGTTTCTC-3'	
	Antisense: 5'-TCCAGGCCATCTTGGTGGCAAGA-3'	574
eNOS	Sense: 5'-TACGGAGCAGCAAATCCAC-3'	
	Antisense: 5'-CAGGCTGCAGTCCTTTGATC-3'	812
β-actin	Sense:5'-GTGGGGCGCCCCAGGCACCA-3'	
	Antisense: 5'-CTCCTTAATGTCACGCACGATTTC-3'	540

Western blot analysis of NOS, HO and COX proteins

Gastric tissues for the analysis of protein expressions of iNOS, eNOS, HO-1, HO-2, COX-1 and COX-2 were homogenized in a proteinase inhibitor buffer (50 mmol/L Tris HCl, pH 7.5, 150 mmol/L NaCl, 0.5 % α-cholate sodium, 0.1 % SDS, 2 mmol/L EDTA, 1 % Triton X-100, 10 % glycerol, 1 mmol/L PMSF and aprotinin) and then centrifuged at 10 000 rpm for 15 min at 4 ℃. The supernatant was collected and the protein content was determined with dye-binding (Bio-Rad) method. 30 μg of total protein was loaded onto SDS-polyacrylamide gel and blotted onto hybrid C membranes (Amersham Life Science, Little Chalfont, Buckinghamshire, England) by electrophoresis. Pre-stained rainbrow recombinant protein molecular weight markers (Amersham International plc, Little Chalfont, Buckinghamshire, England) were used for molecular weight determinations. Membranes were blocked with blocking buffer containing 5 % fat free milk powder, 10 mmol/L Tris-HCl (pH 7.5), 100 mmol/L NaCl and 0.1 % Tween 20 for 1 h at room temperature. The blots were incubated overnight at 4 ℃ with 1:500 dilution of polycolonal antibodies against HO-1 and HO-2 (Stress-Gen, Victoria, Canada), monoclonal antibodies against iNOS and eNOS (Transduction Lab, Lexington, Kentucky, USA), polyclonal antibodies against COX-1 and COX-2 (Santa Cruz Biotechnology INC, Santa Cruz, California, USA). After washed in washing buffer for 30 min, the membranes were treated with HRP conjugated secondary antibody (1:5 000) (Bio-Rad) for 1 h at room temperature followed by another 30 min of washing. The ECL Western blotting system (Amersham Life Sciences) was used in accordance to the manufacturer's instructions for chemiluminescence of proteins, and the blots were then exposed to photographic films (Fuji Photo Film Co., Tokyo, Japan).

Determination of NOS activity

NOS activity in the gastric tissue was measured as the ability of tissue homogenates to convert L-[^{3}H]-arginine to L-[^{3}H]-citrulline[12]. Gastric samples were homogenized at 4 ℃ in a buffer containing 10 mmol/L HEPES (pH 7.2), 320 mmol/L surcose, 0.1 mmol/L EDTA, 1 mmol/L dithiothreitol, 10 μg/mL leupeptin, 2 μg/mL aprotinin (Sigma, St. Louis, MO, USA) and 1 mmol/L PMSF (Sigma), then centrifuged at 12 000 rpm for 30 min at 4 ℃. The supernatant was collected and the protein contents were measured. 100 μL of supernatant was then mixed with a buffered solution consisting of 0.7 mmol/L NADPH, 150 μmol/L $CaCl_2$, 7 mmol/L L-valine, 10 mmol/L HEPES (pH 7.2) and 1μ Ci [^{3}H]-L-arginine (Gibico BRL) and incubated at 37 ℃ for 30 min to determine the total NOS activity. For determination of the iNOS activity, 1 mmol/L EGTA was used to inhibit the activity of calcium-dependent constitutive eNOS. The reaction was stopped by adding 50 μL 20 % perchloric acid, 160 mL 1 mmol/L NaOH and 540 mL dilution solution containing 1 mmol/L each of L-arginine and DL-citrulline. The newly formed L-[^{3}H]-citrulline was separated from L-[^{3}H]-arginine by passing the reaction mixture over 1 mL AG50W-X8 resin columns (Bio-Rad), and the eluted labelled material was measured using a Beckman scintillation counter (LS-6500, Beckman Instrument, USA). The final result was expressed as pmol of L-[^{3}H]-citrulline formed per milligram of protein per 30 min.

Determination of HO activity

Heme oxygenase activity was measured as the ability of tissue homogenates to metabolize heme to bilirubin[13]. In brief, gastric tissues were homogenized in 0.1 mol/L potassium phosphate-buffered saline (pH 7.4) and centrifuged at 12 000 rpm for 30 min. Then 500 μL supernatant (about 4 mg total protein) was added to an equal volume of reaction mixture (2 mmol/L $MgCl_2$, 30 μmol/L hemin, 30 mg rat liver cytosol, 0.2 U glucose-6-phosphate dehydrogenase, 2 mmol/L glucose-6-phosphate, and 0.8 mmol/L NADPH), and incubated at 37 ℃ in the dark for 1 h. The formed bilirubin was extracted with benzene and the absorbance of bilirubin at 462 nm was measured against a baseline absorbance at 530 nm. Heme oxygenase activity was expressed as μg of bilirubin formed/mg protein per hour. The protein content in the supernatant was determined by dye-binding method with BSA as a standard.

Assessment of COX activity

Cyclooxygenase activity was measured as the ability of tissue homogenates to metabolize arachidonic acid to PGE_2 according to the method described by Tomlinson and Vane[7, 8]. Gastric tissues were homogenized at 4 ℃ in proteinase inhibitory

buffer containing 50 mmol/L Tris-Cl (pH 7.4), 3.15 % trisodium citrate, 1 mmol/L PMSF, 0.2 mmol/L leupeptin. The protein concentration in the homogenates was measured. Homogenates were incubated at 37 ℃ for 30 min in the presence of excess arachidonic acid (30 mmol/L). The samples were then boiled and centrifuged at 12 000 rpm for 30 min. The concentration of PGE_2 in the supernatant was measured by immunoassay, using R&D PGE_2 kits (R&D Systems, Inc. Minneapolis, MN, USA). Results were expressed as ng PGE_2 produced per mg protein in 30 min.

Statistical analysis

All the data were expressed as mean ± S.E.M. Statistical analysis was performed using Student' s *t*-test. Values of $P<0.05$ were considered statistically significant.

RESULTS

Morphology and histology

Two symmetrical ulcers were induced in the anterior and posterior walls of the stomach by acetic acid injection. The ulcer base was denuded of mucosal layers because of the necrotic changes and it reepithelized gradually during ulcer healing. Histological accumulation of neutrophils was found at 6 h and prominent inflammatory infiltration was observed at the ulcer base on day 1 to day 3 after ulcer induction. This period was defined as the inflammatory stage of gastric ulceration. After 3 days, the ulcer healed rapidly and was characterized by a reduction in ulcer area (Figure 1). There was intensive proliferation of epithelial cells at the ulcer margin, accompanied by the development of granulation tissues with angiogenesis. The period from day 3 onwards was considered to be the healing phase of gastric ulceration. Complete reepithelization of the ulcer craters was found in some stomaches on day 15 after ulcer induction.

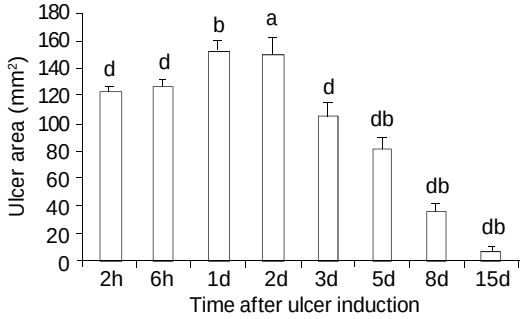

Figure 1 Sequential change of ulcer areas at different time points after ulcer induction. Significant decrease of ulcer area was found on day 3 after ulcer induction. The data were represented as mean ± S. E. M of 20 rats in each group, $^aP<0.05$ *vs* the 2 h group; $^bP<0.001$ *vs* the 2 h group; $^dP<0.001$ *vs* the day 1 group.

Expression of HO, NOS and COX mRNA

Basal levels of COX-2 and HO-1 mRNA expression were detected in normal and non-ulcerated gastric tissues around the ulcers, while expression of iNOS mRNA could only be detected in the ulcer tissue 6 h after ulcer induction. Dramatic increase in mRNA expression of HO-1, iNOS and COX-2 was found from 6 h onwards. High level of iNOS expression persisted for only 3 days then declined rapidly over the healing phase. The expression of HO-1 and COX-2 mRNA remained at high levels during the healing stage from day 3 to day 8. Unlike their inducible isoforms, mRNA expression of HO-2, eNOS and COX-1 was relatively stable. The HO-2 mRNA appeared to be slightly increased in the ulcer base at 12 h after ulcer induction (Figure 2).

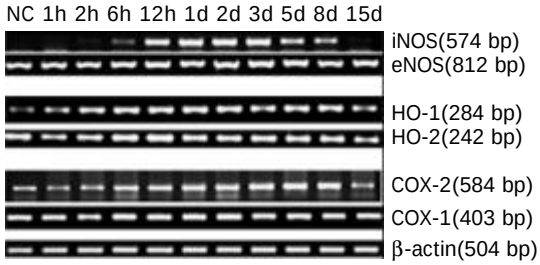

Figure 2 Time course of mRNA expression of inducible and constitutive isoforms of NOS, HO and COX in the ulcer bases. NC=normal control group.

Western blot analysis of HO, NOS and COX

A basal level of HO-1 protein was found in normal gastric tissues, while the iNOS and COX-2 proteins were undetectable. Acetic acid-induced ulceration resulted in a transient loss of HO-1 protein at 2 h, but re-appeared at 6 h and then increased persistently until its peak expression on day 3 to day 5. Its level decreased but still remained higher than normal during day 5 to day 15, at which the ulcer decreased in size and reepithelized.

Expression of COX-2 protein was found to be induced 6 h after ulcer induction and peaked on day 5. Afterwards it remained at a high level during the healing stage. Unlike HO-1 and COX-2, high level of iNOS protein was only detected at the inflammatory stage from day 1 to day 3. The protein expressions of HO-2, eNOS and COX-1 were relatively stable. Transient losses of eNOS and COX-1 proteins were observed at 2 h after acetic acid injection, and then gradually returned to normal levels during the healing process. The level of HO-2 protein was slightly increased after ulcer induction and peaked on day 1, then returned to normal level during ulcer healing (Figure 3).

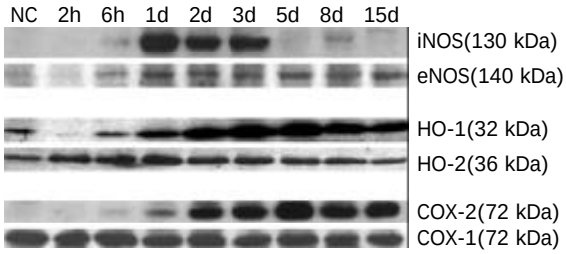

Figure 3 Western blot analysis of the protein levels of inducible and constitutive isoforms of NOS, HO and COX in the ulcer bases at different time after ulcer induction. NC= normal control group.

Expressions of iNOS and COX-2 in the ulcer margin were lower than those in ulcer base during the inflammatory phase. HO-1 expression in the ulcer margin was higher than that in non-ulcerated tissue but lower than that in the ulcer base both in the inflammatory and healing stages.

Enzyme activities of HO, NOS and COX

Marked increase of HO, NOS and COX activities at the ulcer base was found 6 h after ulcer induction. High level of iNOS activity was detected in ulcer base on day 1 to day 3, which was in consistent with the Western blot findings of iNOS protein expression. Similar trend was found in the margins but to a lesser extent (Figure 4). The activity of HO increased in 6 h and peaked on day 2, then remained at an elevated level on day 3 to day 8 (Figure 5). COX activity was persistently increased during the healing stage and was markedly elevated on day 15. Similar trend was found in the margin tissues but to a lesser extent (Figure 6). The trends for HO, NOS and COX activities in the ulcer margin were similar to those found in the ulcer base but with a lower value.

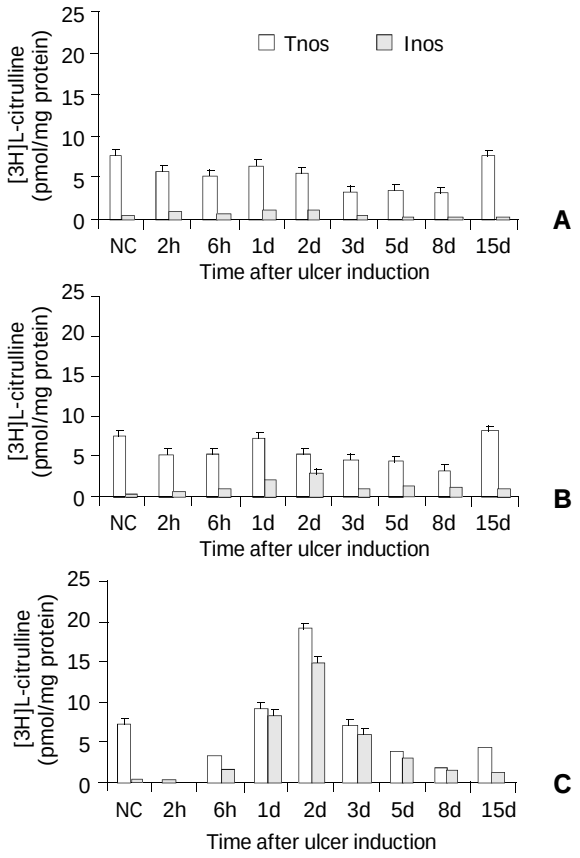

Figure 4 Total NOS (tnos) and iNOS (inos) activities at the non-ulcerated tissues (A), margins (B), and ulcer base (C) of acetic acid induced gastric ulcer. Each bar represents the mean ± S.E.M of 8 rats in each group. NC=normal control group.

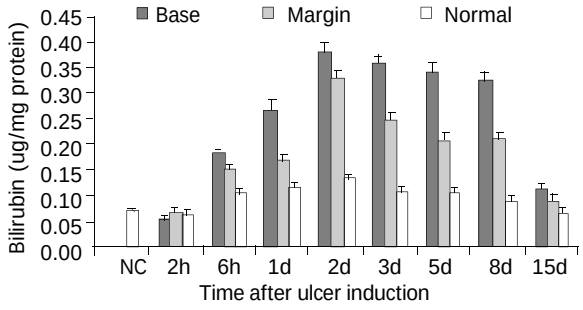

Figure 5 HO activities in the gastric tissues of normal control rats (NC) and the non-ulcerated tissues, ulcer margins and ulcer bases of acetic acid induced gastric ulcer. Each bar represents the mean ± S. E. M of 8 rats in each group.

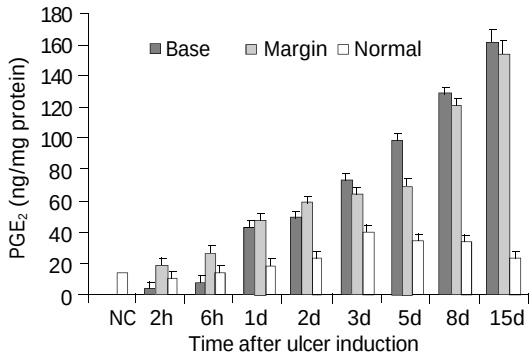

Figure 6 COX activities in the gastric tissues of normal control rats (NC) and the non-ulcerated tissues, ulcer margins and ulcer bases of acetic acid induced gastric ulcer. Each bar represents the mean ± S.E.M of 8 rats in each group.

DISCUSSION

In this study, the expression and activity patterns of NOS, HO and COX were investigated in rats with acetic acid-induced kissing ulcers. The results showed that the inducible isoforms of HO-1, iNOS and COX-2 were all up-regulated during the inflammatory phase. High expression and activity of iNOS were found to coincide with severe inflammation in the ulcer tissue, suggesting that it could be contributed by inflammatory cells that were involved in the inflammatory process. Maximum expressions and activities of HO-1 and COX-2 were found during the ulcer healing phase and thus they might play a role in ulcer healing.

It has been found that NO released from endothelial cells and neuronal cells by the constitutive isoform of NO synthase has regulatory roles in blood flow, motility and secretion. It also protects the gastrointestinal tract against injurious substances. NO produced from inflammatory cells by the inducible isoform of NOS has antimicrobial, antitumor and cytotoxic effects, but excessive amount may lead to peroxynitrite formation, protein tyrosine nitration, hydroxyl radical production and tissue damage[14, 15]. The present study also demonstrated that overexpression of iNOS on day 1 and day 2 after ulcer induction was accompanied by enlargement of ulcer crater. The expression of iNOS protein and activity were observed to be declined when the ulcer began to heal. NO generated from iNOS may also play a beneficial role during ulcer healing by inducing apoptosis in inflammatory cells[16].

The roles of HO-1 and COX-2 in gastric ulcer healing have not been clearly defined. HO-1 has been shown to possess cyto-protective and anti-inflammatory actions. Its expression is associated with the resolution of non-immune as well as immune-driven inflammation[9]. The role of HO-1 as an inflammatory defensive factor may be due to its conversion of oxidant heme to antioxidants biliverdin and bilirubin. It also elevates intracellular free iron levels to facilitate ferritin up-regulation, and regulation of vascular tension through CO generation. Moreover, a recent study has found that CO is able to inhibit the expression of lipopolysaccharide-induced pro-inflammatory cytokines and increase the anti-inflammatory cytokine through a pathway involving the mitogen-activated protein kinases (MAPK)[17]. Besides a role in resolution of inflammation, evidence has also been found that HO-1 may participate in the regulation of endothelial cells activation, proliferation and angiogenesis[18,19], which is essential for wound healing. In this study, the expression and activity of HO-1 were significantly elevated during early ulcer healing and this could be due to the contributory actions of HO-1 in inflammatory resolution and angiogenesis in tissue regeneration.

High expression of COX-2 protein and enzymatic activity of COX at the late ulcer healing stage were observed in this study. The expression of COX-1 protein was relatively stable, thus the change of COX activity might mainly be due to the change of protein level and activity of COX-2. Since tissue remodeling which includes reepithelization of gastric mucosa, maturation of granulation tissue, and reconstruction of extracellular matrix (ECM) mainly occurs at the late ulcer healing stage, the results of this study suggest that COX-2 may play an essential role in these remodeling processes. This is supported by the fact that non-selective as well as selective COX-2 inhibitors delay ulcer healing and prevent regeneration of the mucosa, maturation and angiogenesis in the ulcer base[20-26].

There may be interactions among NOS, HO and COX. HO may modulate NOS and COX systems since they are all heme-containing enzymes. NO and NO donors have been found to stimulate HO-1 expression in different cell lines[27-31] and NO was found to be able to stabilize HO-1 mRNA[32]. On the other hand, HO-1 may have a negative feedback regulation on NO production. Induction of HO-1 by cadmium, bismuth salts,

heme, and nitric oxide (NO) donors have been shown to inhibit the expression of iNOS[33, 34], while inhibition of HO-1 by its inhibitor enhanced iNOS expression. In the present study, a dramatic decrease of iNOS expression and activity was accompanied by an increase in expression and activity of HO-1 on day 5 after ulcer induction. This inverse relationship between iNOS and HO-1 expression and activities supports the existence of close interaction among these enzymes.

In summary, differential expression and activity patterns of inducible enzymes of iNOS, HO-1 and COX-2 during gastric ulceration and healing were found in the present study. The results indicate that iNOS may contribute to tissue inflammation during ulcer formation, while HO-1 and COX-2 may promote ulcer healing, since their expression and activities correlate with the resolving of inflammation and remodeling of ulcer tissues. Close interaction between iNOS and HO-1 may exist because the decrease of iNOS expression and activity coincide with the increase in expression and activity of HO-1. However, further experiments that enroll the use of selective blockers of these inducible enzymes should be conducted to substantiate these conclusions.

ACKNOWLEDGMENT

The authors wish to thank Hon Chueng Leung and Hau Leung So for their excellent technical assistance. This research was supported by RGC grant of the Hong Kong Research Council.

REFERENCES

1 **Griffith OW,** Stuehr DJ. Nitric oxide synthases: properties and catalytic mechanism. *Annu Rev Physiol* 1995; **57:** 707-736
2 **Marletta MA.** Nitric oxide synthase structure and mechanism. *J Biol Chem* 1993; **268:** 12231-12234
3 **DeWitt DL.** Prostaglandin endoperoxide synthase: regulation of enzyme expression. *Biochim Biophys Acta* 1991; **1083**: 121-134
4 **Marnett LJ,** Rowlinson SW, Goodwin DC, Kalgutkar AS, Lanzo CA. Arachidonic acid oxygenation by COX-1 and COX-2. Mechanisms of catalysis and inhibition. *J Biol Chem* 1999; **274:** 22903-22906
5 **Abraham NG,** Drummond GS, Lutton JD, Kappas A. The biological significance and physiological role of heme oxygenase. *Cell Physiol Biochem* 1996; **6:** 129-168
6 **Maines MD,** Trakshel GM, Kutty RK. Characterization of two constitutive forms of liver microsomal heme oxygenase. Only one molecular species of the enzyme is inducible. *J Biol Chem* 1986; **261:** 411-419
7 **Tomlinson A,** Appleton I, Moore AR, Gilroy DW, Willis D, Mitchell JA, Willoughby DA. Cyclo-oxygenase and nitric oxide synthase isoforms in rat carrageenin-induced pleurisy. *Br J Pharmacol* 1994; **113:** 693-698
8 **Vane JR,** Mitchell JA, Appleton I, Tomlinson A, Bishop-Bailey D, Croxtall J, Willoughby DA. Inducible isoforms of cyclooxygenase and nitric-oxide synthase in inflammation. *Proc Natl Acad Sci USA* 1994; **91:** 2046-2050
9 **Willis D,** Moore AR, Willoughby DA. Heme oxygenase isoform expression in cellular and antibody-mediated models of acute inflammation in the rat. *J Pathol* 2000; **190:** 627-634
10 **Chow JY,** Ma L, Zhu M, Cho CH. The potentiating actions of cigarette smoking on ethanol-induced gastric mucosal damage in rats. *Gastroenterology* 1997; **113:** 1188-1197
11 **Tsukimi Y,** Okabe S. Validity of kissing gastric ulcers induced in rats for screening of antiulcer drugs. *J Gastroenterol Hepatol* 1994; **9:** S60-S65
12 **Tepperman BL,** Brown JF, Whittle BJ. Nitric oxide synthase induction and intestinal epithelial cell viability in rats. *Am J Physiol* 1993; **265:** G214-G218
13 **Ishikawa K,** Sato M, Yoshida T. Expression of rat heme oxygenase in Escherichia coli as a catalytically active. Full-length form that binds to bacterial membrances. *Eur J Biochem* 1991; **202:** 161-165
14 **Beckman JS,** Koppenol WH. Nitric oxide, superoxide and peroxynitrite: the good, the bad, and ugly. *Am J Physiol* 1996; **271:** C1424-C1437
15 **Cho CH.** Current roles of nitric oxide in gastrointestinal disorders. *J Physiol Paris* 2001; **95:** 253-256
16 **Akiba Y,** Nakamura M, Mori M, Suzuki H, Oda M, Kimura H, Miura S, Tsuchiya M, Ishii H. Inhibition of inducible nitric oxide synthase delays gastric ulcer healing in the rat. *J Clin Gastroenterol* 1998; **27:** S64-S73
17 **Otterbein LE,** Bach FH, Alam J, Soares M, Tao Lu H, Wysk M, Davis RJ, Flavell R A, Choi AM. Carbon monoxide has anti-inflammatory effects involving the mitogen-activated protein kinase pathway. *Nat Med* 2000; **6:** 422-428
18 **Brouard S,** Otterbein LE, Anrather J, Tobiasch E, Bach FH, Choi AM, Soares MP. Carbon monoxide generated by heme oxygenase 1 suppresses endothelial cell apoptosis. *J Exp Med* 2000; **192:** 1015-1026
19 **Deramaudt BM,** Braunstein S, Remy P, Abraham NG. Gene transfer of human heme oxygenase into coronary endothelial cells potentially promotes angiogenesis. *J Cell Biochem* 1998; **68:** 121-127
20 **Mizuno H,** Sakamoto C, Matsuda K, Wada K, Uchida T, Noguchi H, Akamatsu T, Kasuda M. Induction of cyclooxygenase 2 in gastric mucosal lesions and its inhibition by the specific antagonist delays healing in mice. *Gastroenterology* 1997; **112:** 387-397
21 **Hudson N,** Balsitis M, Everitt S, Hawkey CJ. Angiogenesis in gastric ulcers: impaired in patients taking non-steroidal anti-inflammatory drugs. *Gut* 1995; **37:** 191-194
22 **Jones MK,** Wang H, Peskar BM, Levin E, Itani RM, Sarfeh, IJ, Tarnawski AS. Inhibition of angiogenesis by nonsteroidal anti-inflammatory drugs: insight into mechanisms and implications for cancer growth and ulcer healing. *Nat Med* 1999; **5:** 1418-1423
23 **Shigeta JJ,** Takahashi S, Okabe S. Role of cyclooxygenase-2 in the healing of gastric ulcers in rats. *J Pharmacol Exp Ther* 1998; **287:** 1383-1390
24 **Sun WH,** Tsuji S, Tsujii M, Gunawan ES, Sawaoka H, Kawai N, Iijima H, Kimura A, Kakiuchi Y, Yasumaru M, Sasaki Y, Kawano S, Hori M. Cyclo-oxygenase-2 inhibitors suppress epithelial cell kinetics and delay gastric wound healing in rats. *J Gastroenterol Hepatol* 2000; **15:** 752-761
25 **Brzozowski T,** Konturek PC, Konturek SJ, Sliwowski Z, Pajdo R, Drozdowicz D, Ptak A, Hahn EG. Classic NSAID and selective cyclooxygenase (COX)-1 and COX-2 inhibitors in healing of chronic gastric ulcers. *Microsc Res Tech* 2001; **53:** 343-353
26 **Brzozowski T,** Konturek PC, Konturek SJ, Schuppan D, Drozdowicz D, Kwiecien S, Majka J, Nakamura T, Hahn E. Effect of local application of growth factors on gastric ulcer healing and mucosal expression of cyclooxygenase-1 and –2. *Digestion* 2001; **64:** 15-29
27 **Alcaraz MJ,** Habib A, Lebret M, Creminon C, Levy-Toledano S, Maclouf J. Enhanced expression of heam oxygenase-1 by nitric oxide and antiinflammatory drugs in NIH 3T3 fibroblasts. *Br J Pharmacol* 2000; **130:** 57-64
28 **Hara E,** Takahashi K, Takeda K, Nakayama M, Yoshizawa M, Fujita H, Shirato K, Shibahara S. Induction of heme oxygenase-1 as a response in sensing the signals evoked by distinct nitric oxide donors. *Biochem Pharmacol* 1999; **58:** 227-236
29 **Durante W,** Kroll MH, Christodoulides N, Peyton KJ, Schafer AI. Nitric oxide induces heme oxygenase-1 gene expression and carbon monoxide production in vascular smooth muscle cells. *Circ Res* 1997; **80:** 557-564
30 **Hartsfield CL,** Alam J, Cook JL, Choi AMK. Regulation of heme oxygenase-1 gene expression in vascular smooth muscle cells by nitric oxide. *Am J Physiol* 1997; **273:** L980-L988
31 **Saudau K,** Pfeilschifter J, Brüne B. Nitrosative and oxidative stress induced heme oxygenase-1 accumulation in rat mesangial cells. *Eur J Pharmacol* 1998; **342:** 77-84
32 **Bouton C**, Demple B. Nitric oxide-inducible expression of heme oxygenase-1 in human cells. Translation-independent stabilization of the mRNA and evidence for direct action of nitric oxide. *J Boil Chem* 2000; **275**: 32688-32693
33 **Cavicchi M,** Gibbs L, Whittle BJ. Inhibition of inducible nitric oxide synthase in the human intestinal epithelial cell line, DLD-1, by the inducers of heme oxygenase-1, bismuth salts, and nitric oxide donors. *Gut* 2000; **47:** 771-778

Edited by Xu XQ and Wang XL

P.O.Box 2345, Beijing 100023,China
Fax: +86-10-85381893
E-mail: wjg@wjgnet.com www.wjgnet.com

World J Gastroenterol 2003;9(8):1772-1776
World Journal of Gastroenterology
 ISSN 1007-9327

• BASIC RESEARCH •

Role of TFF in healing of stress-induced gastric lesions

Shi-Nan Nie, Xiao-Ming Qian, Xue-Hao Wu, Shi-Yu Yang,Wen-Jie Tang, Bao-Hua Xu, Fang Huang, Xin Lin, Dong-Yan Sun, Hai-Chen Sun, Zhao-Shen Li

Shi-Nan Nie, Xiao-Ming Qian, Xue-Hao Wu, Shi-Yu Yang, Wen-Jie Tang, Bao-Hua Xu, Fang Huang, Xin Lin, Dong-Yan Sun, Hai-Chen Sun, Emergency Department, Nanjing General Hospital of Nanjing Command/Clinical School of Medical College of Nanjing University, Nanjing 210002, Jiangsu Province, China
Zhao-Shen Li, Department of Gastroenterology, Changhai Hospital, Second Military Medical University, Shanghai, 200433, China
Supported by the Key Project of the Tenth-Five-Year Plan Foundation of PLA, No.01Z059
Correspondence to: Shi-Nan Nie, Emergency Department, Nanjing General Hospital of Nanjing Command/Clinical School of Medical College of Nanjing University, Nanjing 210002, Jiangsu Province, China. shnnie630504@.sohu.com
Telephone: +86-25-4826808-58143
Received: 2003-03-05 **Accepted:** 2003-04-01

Abstract

AIM: To determine the changes of pS2 and ITF of TFF expression in gastric mucosa and the effect on ulcer healing of pS2, ITF to Water-immersion and restraint stress (WRS) in rats.

METHODS: Wistar rats were exposed to single or repeated WRS for 4 h every other day for up to 6 days.Gastric mucosal blood flow (GMBF) was measured by LDF-3 flowmeter and the extent of gastric mucosal lesions were evaluated grossly and histologically. Expression of pS2 and ITF mRNA was determined by RT-PCR. Immunohistochemistry was used to further detect the expression of pS2 and ITF.

RESULTS: WRS applied once produced numerous gastric mucosal erosions, but the number of these lesions gradually declined and GMBF restored at 2, 4, 8 h after stress. The area of gastric mucosal lesion was reduced by 64.9 % and GMBF was increased by 89.8 % at 8 h. The healing of stress-induced ulcerations was accompanied by increased expression of pS2 (0.51±0.14 *vs* 0.77±0.11, $P<0.01$) and ITF (0.022±0.001*vs* 0.177±0.010, $P<0.01$). The results were demonstrated further by immunohistochemistry of pS2 (0.95±0.11 *vs* 1.41±0.04, $P<0.01$) and ITF (0.134±0.001*vs* 0.253±0.01,$P<0.01$). With repeated WRS, adaptation to this WRS developed, the area of gastric mucosal lesions was reduced by 22.0 % after four consecutive WRS. This adaptation to WRS was accompanied by increased GMBF (being increased by 94.2 %), active cell proliferation in the neck region of gastric glands, and increased expression of pS2 (0.37±0.02 *vs* 0.77±0.01, $P<0.01$) and ITF (0.040± 0.001*vs* 0.372±0.010, $P<0.01$). The result was demonstrated further by immunohistochemistry of pS2 (0.55±0.04 *vs* 2.46±0.08, $P<0.01$) and ITF (0.134±0.001*vs* 0.354±0.070, $P<0.01$).

CONCLUSION: TFF may not only participate in the early phase of epithelial repair known as restitution(maked by increased cell migration),but also play an important role in the subsequent,protracted phase of glandular renewal(made by cell proliferation).

Nie SN, Qian XM, Wu XH, Yang SY, Tang WJ, Xu BH, Huang F, Lin X, Sun DY, Sun HC, Li ZS. Role of TFF in healing of stress-induced gastric lesions. *World J Gastroenterol* 2003; 9(8): 1772-1776
http://www.wjgnet.com/1007-9327/9/1772.asp

INTRODUCTION

Stress ulcer is a highly prevalent clinical complication. Fully understanding the mechanism of healing of stress-induced gastric lesions not only deepens our insights into stress ulcer, but also provides new ways for its prevention and treatment in clinical practice. The mechanism of the recovery of gastric mucosa after stress exposure has not been fully explained, the healing of stress ulcerations is a complex process which is affected by different factors. Current research has found that a variety of peptides are considered to play a crucial role in the control of mucosal integrity and repair. Among them, an important role was attributed to epidermal growth factor and transforming growth factor alpha[1-3].

Recently, a group of new peptides has been discovered, called TFF (trefoil factor family or trefoil peptides) because of their uniquely distinctive cysteine-rich "three-leaf" secondary structure, which probably protects these peptides from degradation by luminal acid and proteases within gastrointestinal tract. pS2 and intestinal trefoil factor (ITF) belong to the growing family of trefoil peptides[4,5].

The physiological role of TFF is poorly understood so far. The aim of the present study was to investigate the expression of pS2 and ITF in gastric mucosa of rats undergone WRS, and to probe the role of TFF in the early phase of epithelial repair of stress-induced gastric lesion.

MATERIALS AND METHODS

Induction of gastric adaptation to WRS: Thirty male Wistar rats, weighing 210-250 g (purchased from Xipuer-Bikai Experimental Animal Co. LTD, Shanghai) which had been fasted for 24 h with free access to water, were used. The animals were deprived of water 1 h before the experiment and divided into normal control group (n=6) and experimental control group (n=24). After being fasted for 24 h, the rats of normal control group were lightly anesthetized with ether and tied up on the rat board, the abdomen was opened, the stomach was exposed and GMBF was measured in the oxyntic gland area, gastric mucosa was sampled. The rats of experimental control group were divided into four subgroups (6 in each group) and exposed to WRS[6] for 4 h. They were killed either immediately (0 time: namely 0 h) or after 2 h, 4 h, 8 h. GMBF was measured and gastric mucosa was sampled as described below.

The rats of experimental control group were divided into four subgroups (6 each group) and exposed to repeated WRS[7]: The rats of group I were lightly anesthetized with ether, tied up on the rat board and exposed to WRS for 4 h by placing in water at 20-23 ℃ to the rat's xyphoid level at 10:00 AM on day 1. Then the rats were anesthetized with pentobarbital (30 mg· kg^{-1} i.p.), GMBF was measured and gastric mucosa was sampled. the rats of group II were treated similarly except that after WRS, they were removed from water and placed at

room temprature, and refed with food and water until 10:00 AM the next day, and starved again for 24 h, WRS was repeated. the rats of group III and IV were exposed to the 3rd or 4th WRS as described above.

Measurement of GMBF: GMBF was measured by using laser Doppler flowmetry (LDF-3 flowmeter, Nankai University, Tianjin, China). In brief, the rats were anesthetized with pentobarbital (30 mg· kg^{-1} i.p.), the abdomen was opened, the stomach was exposed and transected, the gastric contents were gently evacuated to the exterior through the cut made in the forestomach.Then, an optical probe was placed gently 0.5 mm above perpendicular to the mucosal surface in the oxyntic gland area to monitor GMBF displayed in mV (value of Doppler signal voltage) on the digital panel of the flowmeter. When GMBF became stable, four points were selected for measurement (one point for 1 minute) and the average value was calculated and expressed as *U/mV*.

Appreciation of UI: Mucosal lesions were evaluated by the score systems reported by Nie S[7]. Briefly, after the measurement of GMBF, the stomach was dissected out and opened along the greater curvature. The stomach was then examined with a 10×magnifier for the presence of erosions and scored as follows: 1 point for small round hemorrhagic erosion, 2 points when the length of hemorrhagic erosion was less than 1 mm, 3 points when the length was 1-2 mm, 4 points when the length was 2-3 mm, 5 points when the length was longer than 4 mm. The score value multiplied 2 when the width of erosion was larger than 1 mm.

Reverse-transcriptase-polymerase chain reaction (RT-PCR) for detection of messenger RNA (mRNA) for pS2 and ITF: The stomachs were removed from rats with intact gastric mucosa and from those exposed to single or repeated stress. Mucosal specimens (about 100 mg) were scraped off using a slide glass and immediately snap frozen in liquid nitrogen and stored at -80 ℃ until analysis. Total RNA was isolated from mucosal samples using a guanidium isothiocyanate/phenol chloroform single step extraction kit from Stratagene (Gibco BRL,USA). Following precipitation, the RNA was resuspended in RNAse-free TE buffer and the concentration was estimated by absorbance at 260 nm wavelength. Furthermore, the quality of each RNA sample was determined by running the agarosefomaldehyde electrophoresis. RNA samples were stored at -80 ℃ until analysis.

Single-strand cDNA was generated from 5 μg of total cellular RNA using StrataScript™ reverse transcriptase (Gibco BRL,USA) and oligo (dT) primers (Gibco BRL,USA). Briefly, 5 μg of total RNA was used as the template to synthesize complementary DNA with 2.5 U of Maloney murine leukemia virus reverse transcriptase in 5 μl of buffer containing 10 mM Tris-HCl, pH 8.3; 50 mM KCl, 5 mM $MgCl_2$; 1 mM of each deoxyribonucleoside triphosphate; 2.5 mM of oligo (dt) primers and 1.4 U μl^{-1} RNAse blocker. Reverse-transcription was performed at room temperature for 20 min, then at 37 ℃ for 15 min, at 90 ℃ for 5 min and at 5 ℃ for 10 min. The resulting complementary DNA was used as a template for subsequent polymerase chain reaction (PCR).

A 124-base pair (bp) fragment of pS_2 was amplified from single-stranded DNA by polymerase chain reaction (PCR) using two oligonucleotide primers for pS_2 sequence: Sense primer, 5' -CCATGGAGCACAAGGTGACCTG-3' and antisense primer, 5' -GGGAAGCCACAATTTATTCT-3' . A 221-base pair (bp) fragment of ITF was amplified from single-stranded DNA by polymerase chain reaction (PCR) using two oligonucleotide primers to ITF sequence: Sense primer, 5' -ATGGAGACCAGAGCCTTCTGGAC-3' and antisense primer, 5' -AGAGGTTTGAAGCACCAGGGC-3' . Concomitantly, amplification of the 521 bp fragment of rat β-actin was performed on the same RNA samples to assess RNA integrity, two oligonucleotide primers to β-actin sequence: Sense primer, 5' -TGGGACGATATGGAGAAGAT-3' and antisense primer, 5' -ATTGCCGATAGTGATGACCT-3' . The nucleotide sequences of the primers for pS_2 were based on the pulished cDNA sequences encoding pS2[8] and the nucleotide sequences of the primers for ITF were based on the published cDNA sequences encoding ITF[9]. The primers were synthesized by Bo-Ya Biotechnical Co. LTD, Shanghai, China.

Reaction mixture for PCR contained cDNA template (2 μl), 50 pmol of each primer, and 2.5 U of Termus aquaticus DNA (Promega) in 10 mM Tris-HCl (pH 8.8), 50 mM KCl, 1.5 mM $MgCl_2$, 0.5 mM dNTPs in a volume of 50 μl. RT blanks (no RNA included) were incubated in each analysis. The mixture was overlaid with 25 μl of mineral oil to prevent evaporation. Amplification was performed using a DNA thermal cycler for 35 cycles, each of which consisted of 2 min at 94 ℃ for denaturation, 45 s at 52 ℃ (pS_2) and at 50 ℃ (ITF) for annealing, and 1 min at 72 ℃ for extension. The final cycle included extension for 5 min at 72 ℃ to ensure full extension of the product. The number of amplification cycles was previously determined to keep amplification in linear to avoid the "plateau effect" associated with increased numbers of PCR cycles. 8 μl of each PCR -product was electrophoresed on 1.6 % agarose gel stained with ethidium bromide, and then visualized under UV light. Location of predicted PCR-product was confirmed by using DNA digest phix 174/Hae III as a stained size marker. The gel was then photographed under UV transillumination. In addition to size analysis by agarose gel electrophoresis,specificity of the primer pair for pS_2 and ITF was assessed by sequencing PCR products. For quantification,we determined the intensity of polymerase chain reaction products on the negative film of gel photographs according to Konturek PC *et al*[10]. Expression of the products was quantified using video image analysis system (TanonGIS-1000, Tanon Technical Co, LTD, Shanghai, China). An index of messenger RNA expression was determined in each sample using the following equation according to Konturek PC *et al*[11].

Immunocytochemistry: For histological assessment, the other half of the stomach was fixed in 10 % formalin, embedded in paraffin, and stained with hematoxylin and eosin. For immunohistochemistry, serial sections obtained from these paraffin blocks were dewaxed and rehydrated. Endogenous peroxidase was blocked with 3 % hydrogen peroxide for 15 min. Sections were then incubated for 35 min with a specific monoclonal antibody against pS_2 and ITF (Asgiraud, Italy), washed and incubated with biotinylated rabbit anti-mouse antibody. After 35 min incubation in avidin-biotin complex, the sections were incubated for 2 min in peroxidase substrate (diaminobenzidine, PBS, in addition to 0.3 percent of hydrogen peroxide) and counterstained with haematoxylin.

The intensity of pS_2 and ITF staining (Mean score) for each cell was graded according to the criteria described by Nie *et al*[6]. as follows: 0=no staining, I=weakly positive, II=moderately positive (cytoplasm positive but other cytoplasmic details also visible), or III=densely stained. The staining intensity was calculated in 300 consecutive cells in three regions of the gastric mucosa: Surface epithelium (top), neck region (neck) and basal portions of the gastric glands (base). The mean intensity per section and region was calculated. Negative control sections were processed immunohistochemically after replacing the primary antibody with an irrelevant monoclonal antibody or phosphate-buffered-saline (PBS).

Statistical analysis: Results were presented as *means±SD*. Statistical comparisons were made by Student' s *t* test.The linearly relevant analysis was applied to analyse the relationship between two variants, *P* values less than 0.05 were considered statistically significant.

RESULTS

Gastric lesion induced by single or repeated WRS: WRS applied once produced numerous gastric mucosal erosions in oxyntic mucosa with the mean lesion number of 45.32±1.41 per rat. No microscopic evidence of damage occurred in the forestomach. Microscopical examination of the mucosa after 4 h stress revealed widespread damage of the surface epithelium with many cells sloughed off into the gastric lumen and focal area of deep haemorrhagic necrosis (Figure 1). The number of stress lesions was gradually declined at 2, 4, 8 h after the end of stress. UI was reduced to about 20.8 % of the initial number at 8 h after the end of stress (Table 1). With repeated WRS, adaptative cytoprotection against stress was developed, UI in II, III, IV groups markedly reduced as compared with group I (P<0.01). UI after four consecutive WRS was 22 % of UI after one WRS. Cell proliferation in the neck regions of gastric glands was activated (Figure 2, Table 2).

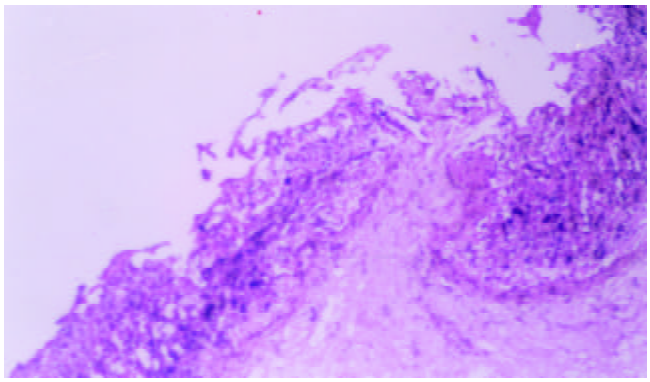

Figure 1 Necrosis appeared as craters in rats after exposed to single WRS for 4 h (HE×200).

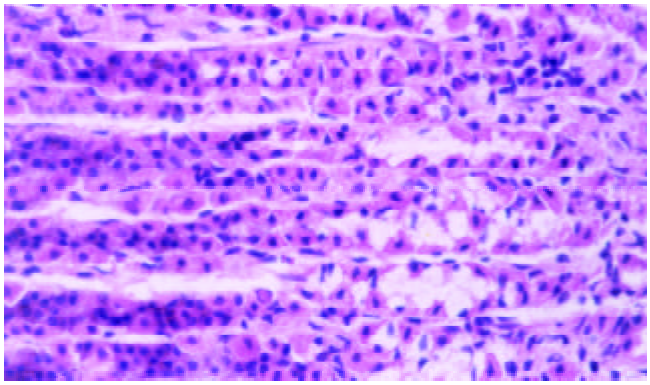

Figure 2 Foveolae and neck region elongated and the mucosa appeared thicker after rats exposed to 4th WRS for 4 h(HE×400).

Change of GMBF after single or repeated WRS: GMBF of normal rats was 424.70±7.72*U/mV*. GMBF significantly decreased after single exposure to WRS and restored at 2, 4, 8 h after the end of stress. It increased up to 94.5 % of normal value at 8 h after the end of stress (Table 1). GMBF of normal rats was 484.01±10.97*U/mV*. GMBF significantly decreased after single exposure to WRS.With repetitive challenge with WRS, there was an adaptive increase of it in experimental group, and GMBF of groups II, III, IV markedly increased as compared with that of group I (P<0.01). After the 4th time of WRS, the value of GMBF was almost restored to normal level (94.2 % of normal value). There was a significantly negative relevance between GMBF and UI (r=-0.953, P<0.01) (Table 2).

Expressions of pS_2 and ITF mRNA and immunohistochemical staining for expression of pS_2 and ITF proteins during recovery from stress damage: The expressions of pS_2 and ITF could be detected in normal gastric mucosa. They were expressed mainly in the regenerative zone of cytoplasm and weaker expressions were found at the basal portions of the gastric glands. The expressions of pS_2 and ITF in single WRS significantly decreased and was absent in the necrotic region, whereas repeated WRS significantly increased expression of pS_2 and ITF. In addition to the regenerative zone,other areas including the lumen of gastric glands also expressed pS_2 and ITF.

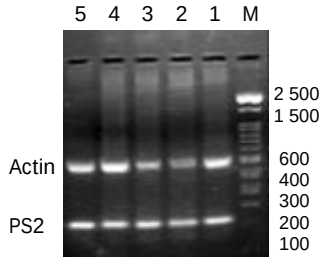

Figure 3 Messenger RNA expression of pS_2 mRNA and β-actin in gastric mucosa of rats after single exposure to WRS and in control intact rats (M=PCR size marker, 1=control group, 2=group 1, 3=group 2, 4=group 3, 5=group 4).

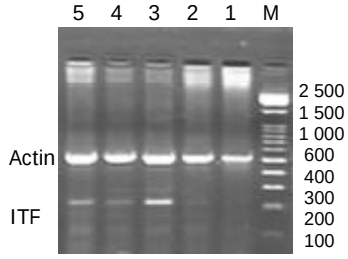

Figure 4 Messenger RNA expression of ITF mRNA and β-actin in gastric mucosa of rats after single exposure to WRS and in control intact rats (M=PCR size marker, 1=control group, 2=group 1, 3=group 2, 4=group 3, 5=group 4).

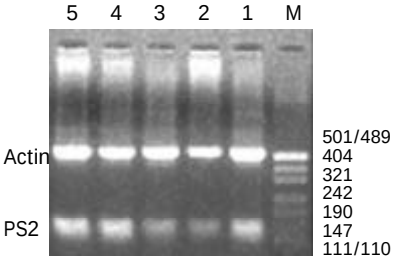

Figure 5 Messenger RNA expression of pS_2 mRNA and β-actin in gastric mucosa of rats after repeated exposure to WRS and in control intact rats (M=PCR size marker, 1=control group, 2=group I, 3=group II, 4=group III, 5=group IV).

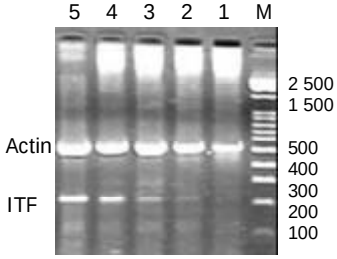

Figure 6 Messenger RNA expression of ITF mRNA and β-actin in gastric mucosa of rats after repeated exposure to WRS and in control intact rats (M=PCR size marker, 1=control group, 2=group I, 3=group II, 4=group III, 5=group IV).

Table 1 Changes of expression of pS_2, ITF, GMBF and UI in gastric mucosa after exposed to WRS

Group	GMBF (*U* / mV)	UI	Mean score (pS_2)	pS_2 / β-actin	Mean score (ITF)	ITF / β-actin
Control	424.70±7.72	0.00	1.65±0.03	0.78±0.11	0.003±0.001	0.004±0.0002
experimental						
1	274.56±13.0[b]	45.32±1.41	0.95±0.11[b]	0.51±0.14[b]	0.134±0.001[b]	0.022±0.01[b]
2	371.35±15.27[bd]	18.31±1.47[d]	1.63±0.14[d]	0.78±0.13[d]	0.259±0.01[bd]	0.287±0.008[bd]
3	417.451±12.31[d]	11.38±1.31[d]	1.53±0.13[bd]	0.71±0.12[d]	0.136±0.04[ad]	0.112±0.009[d]
4	401.32±8.95[d]	9.54±1.27[d]	1.41±0.04[bd]	0.77±0.11[ad]	0.235±0.01[bd]	0.177±0.01[ad]

[a]*P*<0.05 *vs* control group; [b]*P*<0.01 *vs* control group; [c]*P*<0.05 *vs* group 1; [d]*P*<0.01 *vs*r group 1.

Table 2 Changes of expression of pS_2, ITF, GMBF and UI in gastric mucosa after exposed to repeated WRS

Group	GMBF(*U* / mV)	UI	Mean score (pS_2)	pS_2 / β-actin	Mean score (ITF)	ITF / β-actin
Control	484.01±10.97	0.00	2.01±0.14	0.63±0.01	0.0003±0.001	0.004±0.0004
experimental						
I	321.87±8.85[b]	47.23±1.20	0.55±0.04[b]	0.37±0.02[b]	0.134±0.001[b]	0.040±0.001[b]
II	418.35±7.94[bd]	30.54±1.12[d]	1.51±0.03[bd]	0.42±0.01[bd]	0.194±0.05[bd]	0.108±0.009[bd]
III	446.09±10.98[bd]	20.75±1.54[d]	2.55±0.11[bd]	0.72±0.02[bd]	0.281±0.015[bd]	0.265±0.009[bd]
IV	455.95±11.81[bd]	10.39±1.18[d]	2.46±0.08[bd]	0.77±0.01[bd]	0.354±0.07[bd]	0.372±0.01[bd]

[a]*P*<0.05 *vs* control group; [b]*P*<0.01 *vs* control group; [c]*P*<0.05 *vs* group I; [d]*P*<0.01 *vs* group I.

The expressions of pS2 and ITF mRNA were increased during the healing after single WRS (pS2: 0.51±0.14 *vs* 0.77±0.11, *P*<0.01; ITF: 0.022±0.001*vs* 0.177±0.010, *P*<0.01) (Figure 3, 4). The same results were observed by immunohistochemistry (pS2: 0.95±0.11 *vs* 1.41±0.04, *P*<0.01; ITF: 0.134±0.001*vs* 0.253±0.01, *P*<0.01). With repeated WRS, adaptative cytoprotection against stress was developed.The expression of pS2 and ITF mRNA was increased by using RT-PCR (pS2: 0.37±0.02 *vs* 0.77±0.01, *P*<0.01; ITF: 0.040±0.001*vs*0.372±0.010, *P*<0.01) (Figure 5,6) and immunohistochemistry (pS2: 0.55±0.04 *vs* 2.46±0.08, *P*<0.01; ITF: 0.134±0.001*vs* 0.354±0.070, *P*<0.01). There was a significantly negative relevance between expressions of pS_2 or ITF and UI (*r*=-0.921, *P*<0.01; *r*=-0.965, *P*<0.01), and positive relevance was found between expressions of pS_2 or ITF and GMBF (*r*=0.826, *P* <0.05; *r*=0.854, *P*<0.05) (Table 2).

DISCUSSION

The cytoprotective functions in protecting gastrointestinal tract against ongoing damage may be accomplished in several ways, and evidences for participation in both the early phase of epithelial repair known as restitution (marked by increased cell migration but no proliferation), and in the subsequent, protracted phase of glandular renewal (marked by proliferation, differentiation and migration) have been published[12-14].

This study assessed for the first time immunohistochemical and RT-PCR analyses of pS2, ITF expression in rat gastric mucosa after exposure to water immersion and restrained stress. Our observation showed that expression of pS2 and ITF in gastric mucosa was enhanced shortly after the stress, leading us to hypothesize that this process might be mediated by pS2 and ITF.

The importance of trefoil peptides in the process of response to the damage action of strong irritants has not yet been evaluated.The members of the trefoil peptide family, including pS2 and ITF, share a common structural feature, which is a motif of six cysteine residues termed a trefoil or a P domain. There are increasing evidences that pS2 and ITF are important in maintaining the integrity of gastric mucosa and involved in the repair of ulcerated areas in gastrointestinal tract[15-19]. This is supported by an observation that increased expressions of pS2 and ITF were found in the ulcer-associated cell lineage (UACL), which is a glandular structure that develops in the area of gastrointestinal tract adjacent to ulcerated mucosa[20]. This is supported by the findings obtained from *in vitro* study which showed that pS2 and ITF exhibited a mitogenic effect on different cell lines[21,22]. Moreover, exogenously recombinant TFF has been shown to significantly attenuate the extent of acute mucosal injury induced by a variety of ulcerogens such as 96 % ethanol, indomethacin or stress[23], indicating that this peptide does exhibit gastroprotective activity.

The present study showed that, WRS applied once produced numerous gastric mucosal erosions. UI gradually declined at 2, 4, 8 h after the end of stress, the expression of pS2 and ITF was increased during the healing of stress-induced ulceration, there was not a correlation between the expression of pS2 or ITF and UI.

The facts that pS2 or ITF is over-expressed in gastric mucosa immediately after stress injury and that this peptide stimulates cell migration, strongly suggest that it might mediate the early phase healing of acute gastric lesion called restitution[24-28].

It has also been proposed that trefoil peptide family contribute to gastric mucosal defence and repair by affecting cell proliferation[29,30].

In the present study, we found this adaptation was accompanied by an increased mucosal cell proliferation and enhanced expressions of mRNA for pS2 and ITF, suggesting the involvement of pS2 and ITF in the adaptation process.

The major finding of this report was the demonstration for the first time that gastric adaptation to WRS involved overexpressions of mRNA for pS2 and ITF and an increased rate of cell proliferation in gastric mucosa, and enhanced cell proliferation was preceded by overexpressions of pS_2 and ITF mRNA, although the expressions of mRNA for pS_2 and ITF decreased in initial phase after exposure of gastric mucosa to WRS, suggesting that this trefoil peptide contributes to cell proliferation.

The present study also showed that with repeated WRS, adaptative cytoprotection against stress was developed, the mucosal lesions reduced markedly after 2nd, 3rd and 4th WRS. The expression of pS2 and ITF was increased. There was a significantly negative relevance between expressions of pS2 or ITF and UI.

After the 4th WRS, GMBF was almost restored to normal level. Therefore, during the process of tolerant cytoprotection, GMBF, UI and expression of pS2 and ITF showed regular

changes and there was a good relationship beween them.

Indeed, we have confirmed that WRS-adapted mucosa exhibits an augment GMBF, but it is not clear whether this factor could directly or indirectly account for the mucosal adaptation, or what could be the mechanism of this mucosal hyperemia in the stomach. TGFα has been shown to increase GMBF[2,31], while TFF can promote synthesis of TGFα. So hyperemia observed during the development of adaptation can be mediated, at least in part by the release of this peptide.

REFERENCES

1 **Brzozowski T,** Konturek SJ, Majka J, Dembinski A, Drozdowicz D. Epidermal growth factor, polyamines, and prostaglandins in healing of stress-induced gastric lesions in rats. *Dig Dis Sci* 1993; **38**: 276-283

2 **Konturek SJ,** Brzozowski T, Majka J, Dembinski A, Slomiany A, Slomiany BL. Transforming growth factor alpha and epidermal growth factor in protection and healing of gastric mucosal injury. *Scand J Gastroenterol* 1992; **27**: 649-655

3 **Konturek PC,** Ernst H, Brzozowski T, Ihlm A, Hahn EG, Konturek SJ. Expression of epidermal growth factor and transforming growth factor-alpha after exposure of rat gastric mucosa to stress. *Scand J Gastroenterol* 1996; **31**: 209-216

4 **Podolsky DK.** Mechanisms of regulatory peptide action in the gastrointestinal tract: trefoil peptides. *J Gastroenterol* 2000; **35** (Suppl 12): 69-74

5 **Tran CP,** Cook GA, Yeomans ND, Thim L, Giraud AS. Trefoil peptide TFF2 (spasmolytic polypeptide) potently accelerates healing and reduces inflammation in a rat model of colitis. *Gut* 1999; **44**: 636-642

6 **Nie SN,** Li ZS, Zhan XB, Gong YF, Tu ZX, Gong YF. Role of the pS2 in healing of stress-induced gastric lesions. *Wei Chang Bing Xue* 2002; **7**: 20-23

7 **Nie S,** Li Z, Zhan X, Tu Z, Xu G, Gong Y, Man X. Role of the pS (2) in gastric mucosa adaptative cytoprotection from stress. *Zhonghua Yixue Zazhi* 2002; **82**: 172-175

8 **Itoh H,** Tomita M, Uchino H, Kobayashi T, Kataoka H, Sekiya R, Nawa Y. cDNA cloning of rat pS2 peptide and expression of trefoil peptides in acetic acid-induced colitis. *Biochem J* 1996; **318**: 939-944

9 **Nie SN,** Li ZS, Zhan XB, Xu GM, Tu ZX, Gong YF. Role of the pS2,ITF in the early phase of epithelial repaire of stress-induced gastric lesion. *Jiefangjun Yixue Zazhi* 2002; **27**: 182-185

10 **Brzozowski T,** Konturek PC, Konturek SJ, Stachura J. Gastric adaptation to aspirin and stress enhances gastric mucosal resistance against the damage by strong irritants. *Scand J Gastroenterol* 1996; **31**: 118-125

11 **Konturek PC,** Brzozowski T, Pierzchalski P, Kwiecien S, Pajdo R, Hahn EG, Konturek SJ. Activation of genes for spasmolytic peptide, transforming growth factor alpha and for cyclooxygenase (COX)-1 and COX-2 during gastric adaptation to aspirin damage in rats. *Aliment Pharmacol Ther* 1998; **12**: 767-777

12 **Podolsky DK.** Mucosal immunity and inflammation. V. Innate mechanisms of mucosal defense and repair: The best offense is a good defense. *Am J Physiol* 1999; **277**: G495-499

13 **Wright NA.** Aspects of the biology of regeneration and repair in the human gastrointestinal tract. *Philos Trans R Soc Lond B Biol Sci* 1998; **353**: 925-933

14 **Podolsky DK.** Healing the epithelium: Solving the problem from two sides. *J Gastroenterol* 1997; **32**: 122-126

15 **Farrell JJ,** Taupin D, Koh TJ, Chen D, Zhao CM, Podolsky DK, Wang TC. TFF2/SP-deficient mice show decreased gastric proliferation, increased acid secretion, and increased susceptibility to NSAID injury. *J Clin Invest* 2002; **109**: 193-204

16 **Ulaganathan M,** Familari M, Yeomans ND, Giraud AS, Cook GA. Spatio-temporal expression of trefoil peptide following severe gastric ulceration in the rat implicates it in late-stage repair processes. *J Gastroenterol Hepatol* 2001; **16**: 506-512

17 **Longman RJ,** Douthwaite J, Sylvester PA, Poulsom R, Corfield AP, Thomas MG, Wright NA. Coordinated localisation of mucins and trefoil peptides in the ulcer associated cell lineage and the gastrointestinal mucosa. *Gut* 2000; **47**: 792-800

18 **McKenzie C,** Thim L, Parsons ME. Topical and intravenous administration of trefoil factors protect the gastric mucosa from ethanol-induced injury in the rat. *Aliment Pharmacol Ther* 2000; **14**: 1033-1040

19 **Cook GA,** Thim L, Yeomans ND, Giraud AS. Oral human spasmolytic polypeptide protects against aspirin-induced gastric injury in rats. *J Gastroenterol Hepatol* 1998; **13**: 363-370

20 **Alison MR,** Chinery R, Poulsom R, Ashwood P, Longcroft JM, Wright NA. Experimental ulceration leads to sequential expression of spasmolytic polypeptide, intestinal trefoil factor, epidermal growth factor and transforming growth factor alpha mRNAs in rat stomach. *J Pathol* 1995; **175**: 405-414

21 **Chinery R,** Coffey RJ. Trefoil peptides: Less clandestine in the intestine. *Science* 1996; **274**: 204

22 **Mashimo H,** Wu DC, Podolsky DK, Fishman MC. Impaired defense of intestinal mucosa in mice lacking intestinal trefoil factor. *Science* 1996; **274**: 262-265

23 **Babyatsky MW,** deBeaumont M, Thim L, Podolsky DK. Oral trefoil peptides protect against ethanol- and indomethacin-induced gastric injury in rats. *Gastroenterology* 1996; **110**: 489-497

24 **Saitoh T,** Mochizuki T, Suda T, Aoyagi Y, Tsukada Y, Narisawa R, Asakura H. Elevation of TFF1 gene expression during healing of gastric ulcer at non-ulcerated sites in the stomach: Semiquantification using the single tube method of polymerase chain reaction. *J Gastroenterol Hepatol* 2000; **15**: 604-609

25 **Poulsen SS,** Thulesen J, Christensen L, Nexo E, Thim L. Metabolism of oral trefoil factor 2 (TFF2) and the effect of oral and parenteral TFF2 on gastric and duodenal ulcer healing in the rat. *Gut* 1999; **45**: 516-522

26 **Dossinger V,** Kayademir T, Blin N, Gott P. Down-regulation of TFF expression in gastrointestinal cell lines by cytokines and nuclear factors. *Cell Physiol Biochem* 2002; **12**: 197-206

27 **Ito S,** Lacy ER, Rutten MJ, Critchlow J, Silen W. Rapid repair of injured gastric mucosa. *Scand J Gastroenterol Suppl* 1984; **101**: 87-95

28 **Konturek PC,** Brzozowski T, Konturek SJ, Elia G, Wright N, Sliwowski Z, Thim L, Hahn EG. Role of spasmolytic polypeptide in healing of stress-induced gastric lesions in rats. *Regul Pept* 1997; **68**: 71-79

29 **Konturek PC.** Physiological, immunohistochemical and molecular aspects of gastric adaptation to stress, aspirin and to *H. pylori*-derived gastrotoxins. *J Physiol Pharmacol* 1997; **48**: 3-42

30 **Modlin IM,** Poulsom R. Trefoil peptides: Mitogens, motogens, or mirages? *J Clin Gastroenterol* 1997; **25**(Suppl 1): S94-100

31 **Tepperman BL,** Soper BD. Effect of epidermal growth factor, transforming growth factor alpha and nerve growth factor on gastric mucosal integrity and microcirculation in the rat. *Regul Pept* 1994; **50**: 13-21

Edited by Zhao P and Wang XL

P.O.Box 2345, Beijing 100023,China
Fax: +86-10-85381893
E-mail: wjg@wjgnet.com www.wjgnet.com

World J Gastroenterol 2003;9(8):1777-1780
World Journal of Gastroenterology
 ISSN 1007-9327

• BASIC RESEARCH •

Cloning of human 15ku selenoprotein gene from H9 T cells

Ke-Jun Nan, Chun-Li Li, Yong-Chang Wei, Chen-Guang Sui, Zhao Jing, Hai-Xia Qin, Li-Jun Zhao, Bo-Rong Pan

Ke-Jun Nan, Chun-Li Li, Yong-Chang Wei, Chen-Guang Sui, Zhao Jing, Hai-Xia Qin, Department of Medical Oncology, First Hospital of Xi' an Jiaotong University, Xi' an 710061, Shaanxi Province, China
Li-Jun Zhao, The University of Georgia, Athens, Ga 30602, USA
Bo-Rong Pan, Department of Oncology, Xijing Hospital, Fourth Military Medical University, Xi' an 710032, Shaanxi Province, China
Supported by Science and Technology Research and Development Project of Shaanxi Province, No. 2002K10-G1
Correspondence to: Dr. Chun-Li Li, Department of Medical Oncology, First Hospital of Xi' an Jiaotong University, 1 Jiangkang Road, Xi' an 710061, Shaanxi Province, China. chun128@sohu.com
Telephone: +86-29-5324036 **Fax:** +86-29-5324086
Received: 2003-03-03 **Accepted:** 2003-03-29

Abstract

AIM: To clone human 15ku selenoprotein gene.

METHODS: H9 human T cells were cultured in RPMI1640 medium supplemented with 100 mL /L fetal calf serum. mRNA was isolated from the cells. cDNA library was constructed by RT-PCR. The human 15ku selenoprotein gene was obtained by PCR and cloned into T vector and sequenced.

RESULTS: A unique cDNA fragment about 1 244 bp was obtained. Sequence analysis identified an open reading frame within the cDNA. The gene had an in-frame TGA, which encoded selenocysteine (Sec), and a 3'-UTR SECIS element, which was required for synthesis of selenoprotein. The predicted protein molecular mass was about 15ku (162 residues). The result was identical with human liver 15ku selenoprotein gene published in Genbank.

CONCLUSION: Human 15ku selenoprotein gene can be successfully obtained from T cell line.

Nan KJ, Li CL, Wei YC, Sui CG, Jing Z, Qin HX, Zhao LJ, Pan BR. Cloning of human 15ku selenoprotein gene from H9 T cells. *World J Gastroenterol* 2003; 9(8): 1777-1780
http://www.wjgnet.com/1007-9327/9/1777.asp

INTRODUCTION

The trace element selenium (Se) is an essential human nutrient[1]. It has been shown to prevent cancers, especially liver and stomach cancers[2] in both epidemiological studies and clinical supplementation trials[3]. However, the mechanism by which Se suppresses tumor development remains unknown. Se is present in known human selenoproteins as amino acid selenocysteine (Sec)[4]. Sec is the active form of Se in selenoproteins and has important biological functions. Recently, a human 15ku selenoprotein (Sep15) containing Se in the form of Sec was identified. It was an acid protein with a PI value of 4.5. It was recently identified in human T cells[5, 6] and was present in various human tissues, such as liver, kidney, testis and brain, but it was highly expressed in epithelial cells of the prostate gland[6] and thyroid[5]. The level of this selenoprotein was reduced substantially in hepatocellular carcinoma[7] and in a malignant prostate cell line[8]. Furthermore, epidemiological data have indicated a statistically significant inverse correlation between Se in the diet and occurrence of liver cancer. These facts have provoked our interest to study Sep15. The recent finding that the gene of Sep15 was located on human chromosome 1p31, often affected in human cancer[9], also supports the hypothesis that this protein might play a role in the development of cancers[5]. To get a better understanding of the relationship between Sep15 and tumor, and the mechanism by which it suppresses the tumor, we firstly cloned the gene of this selenoprotein.

MATERIALS AND METHODS

Materials

H9 T cell line was purchased from ATCC. RPMI1640 was purchased from Gibco. Fetal bovine serum was from Hangzhou Sijiqing Company. Main biochemical reagents of T vector, T4 DNA ligase, *Taq* DNA polymerase and Trizol reagent were from Promega. Small amount plasmid extraction kit and PCR products purification kit were from Huashun Shengwu Engineering Company. Bacteria species JM109 was from the Department of Biochemistry of the Fourth Military Medical University. Agarose was from Huamei Shengwu Engineering Company. The restriction endonuclease *Not* I was from Takara. RNA extraction kit was from Promega. RT-PCR kit was from American Bior' s Company. The primers were synthesized by Georgia University of America. The forward primer was 5'-AGCGATGGCGGCTGGGCCGAG-3'. The backward primer was 5'-GATTTTTGAAACTTTTTATTTATA-3'.

Methods

mRNA extraction of H9 T cells H9 T cells were cultured in the RPMI1640 containing new born bovine serum under the condition of 50 mL/L CO_2 at 37 ℃ in a CO_2 incubator. About 10^7 H9 T cells were absolutely split with trizol reagent. Total RNA was extracted with chloroform, deposited with isopropanol, then dried at 37 ℃. mRNA was isolated with a mRNA purification kit from Promega[10]. The procedure in details was performed according to the instructions of the kit.
RT-PCR[11] By using the reverse transcription system from Promega[12], cDNA synthesis was performed according to the following instructions. mRNA previously extracted and random hexamers were used to synthesize first strand of cDNA[13], which was used to synthesize the double-strand DNA in the latter PCR[14]. PCR was performed as follows[15, 16]. The total volume of the PCR amplification system was 100 μL. First, 10 μL reverse transcription reaction liquid, 4 μL 20 pmol/L primers (each 2 μL), 8 μL 10 mmol/L dNTP, 10 μL 10×PCR reaction liquid, and 10U *Taq*DNA were added consecutively, then water was added to a total volume of 100 μL. The PCR was performed by incubating at 94 ℃ for 2 min, at 94 ℃ for 1 min, at 55 ℃ for 1 min, at 72 ℃ for 1 min, totally 35 cycles. The reaction mixture was incubated at 72 ℃ for 7 min. Finally all the PCR products were used for 10 g/L agarose gel electrophoresis to purify the products. Purification was performed according to the instructions of the gel extraction kit from Huashun Company.
Linkage and conversion 5 μL T vector, 1 μL T_4DNA ligase,

1 μL 10×buffer were added into previously purified PCR products, incubated at 16 ℃ overnight. 5 μL linkage products was picked up to infect competence bacteria of JM109. The conversion products were spread on a LB agarose plate containing ampicillin at 37 ℃ overnight.

Restriction endonuclease digestion and evaluation First, 3 monoclonal colonies were randomly chosen, and put into 10 g/L LB containing ampicillin, the culture was shaken at 37 ℃ overnight in air bath, then the plasmid of $P^{GEM\text{-}T\text{-}15ku\text{-}selenoprotein}$ was extracted. The procedure was performed according to the instructions of the low-dose plasmid extraction kit from Huashun Company. 5 μL previously extracted plasmid was digested with *Not* I. The reaction system containing 5 μL plasmid, 1 μL *Not* I, 2 μL 10×BSA buffer, 2 μL 10×H buffer, 2 μL 10×TritonX-100, and 8 μL sterilized water was performed at 37 ℃ for 3 hours. Finally 5 μL reaction mixture was used for 10 g/L agarose gel electrophoresis for 45 minutes. At the same time, the plasmid DNA was sent to the laboratory of Georgia University in America to sequence the DNA.

RESULTS

Sep15 gene amplification

After 35 cycles of RT-PCR, 5 μL PCR products were used for 10 g/L agarose gel electrophoresis. When compared with the DNA marker, cDNA fragment was between 1 000 bp and 2 000 bp. It was coincident with the length of purposed gene (Figure 1).

Figure 1 Agarose gel electrophoresis of RT-PCR amplified Sep15 gene fragment.

Sep15 gene cloning and its digestion and evaluation

After 3 monoclonal colonies were randomly chosen, the plasmid was extracted and digested with *Not* I. Then, 5 μL was used for 10 g/L agarose gel electrophoresis, the straps were found to be coincident with the length of purposed gene (Figure 2).

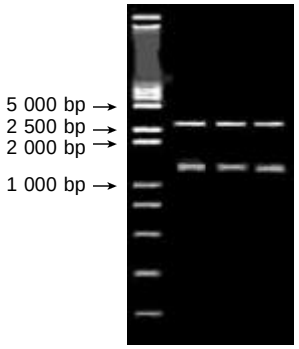

Figure 2 *Not* I cut plasmid of $P^{GEM\text{-}T\text{-}15ku\text{-}selenoprotein}$.

DNA sequencing

The sequencing of $P^{GEM\text{-}T\text{-}15ku\text{-}selenoprotein}$ showed that the Sep15 gene we cloned was completely coincident with the sequence in GenBank. It was 100 % homology with the human Sep15 gene. The sequences were as follows.

```
   1 agcgatggcg gctgggccga gtgggtgtct ggtgccggcg tttgggctac ggttgttgtt ggcgactgtg
  71 cttcaagcgg tgtctgcttt tggggcagag ttttcatcgg aggcatgcag agagttaggc ttttctagca
 141 acttgctttg cagctcttgt gatcttctcg gacagttcaa cctgcttcag ctggatcctg attgcagagg
 211 atgctgtcag gaggaagcac aatttgaaac caaaaagctg tatgcaggag ctattcttga agtttgtgga
 281 tgaaaattgg gaaggttccc tcaagtccaa gcttttgtta ggagtgataa acccaaactg ttcagaggac
 351 tgcaaatcaa gtatgtccgt ggttcagacc ctgtattaaa gcttttggac gacaatggga acattgctga
 421 agaactgagc attctcaaat ggaacacaga cagtgtagaa gaattcctga gtgaaaagtt ggaacgcata
 491 taaatcttgc ttaaattttg tcctatcctt ttgttacctt atcaaatgaa atattacagc acctagaaaa
 561 taatttagtt ttgcttgctt ccattgatca gtcttttact tgaggcatta aatatctaat taaatcgtga
 631 aatggcagta tagtccatga tatctaagga gttggcaagc ttaacaaaac ccatttttta taaatgtcca
 701 tcctcctgca tttgttgata ccactaacaa aatgctttgt aacagacttg cggttaatta tgcaaatgat
 771 agtttgtgat aattggtcca gttttacgaa caacagattt ctaaattaga gaggttaaca agacagatga
 841 ttactatgcc tcatgtgctg tgtgctcttt gaaaggaatg acagcagact acaaagcaaa taagatatac
 911 tgagcctcaa cagattgcct gctcctcaga gtctctccta tttttgtatt acccagcttt ctttttaata
 981 caaatgttat ttatagttta caatgaatgc actgcataaa aactttgtag cttcattatt gtaaaacata
1050 ttcaagatcc tacagtaaga gtgaaacatt cacaaagatt tgcgttaatg aagactacac agaaaacctt
1121 tctagggatt tgtgtggatc agatacatac ttggcaaatt tttgagtttt acattcttac agaaaagtcc
1191 atttaaaagt gatcatttgt aagaccaaaa tataaataaa aagtttcaaa aatc
```

DISCUSSION

Se was recognized as an essential trace element in human and animal' s life by WHO in 1978. The relationship between Se and many kinds of disease including cancer is a hot point of medical research[17, 18]. Usually, Se is incorporated into proteins in the forms of selenocysteine (Sec) and selenomethionine (SeMet). The term "selenoprotein" is restricted to the proteins which contain Se in the form of selenocysteine[19]. Selenoproteins are distinguished from proteins which nonspecifically incorporate selenomethionine not contributing to the biological function of the Se. About 21 specific selenoproteins have been identified in mammals and bacteria, and 18 of them could have biological functions attributed to them. Mammalian Se-containing proteins can be divided into three groups: proteins containing nonspecifically incorporated Se, specific Se-binding proteins, and specific selenocysteine-containing selenoproteins[5]. Selenoproteins with a known function identified so far include five glutathione peroxidases, two deiodinases, several thioredoxin reductases, and selenophosphate synthetase 2. Sep15, selenoprotein P, selenoprotein W, an 18-ku selenoprotein and several selenoproteins identified in silico from nucleotide sequence databases have been found to contain selenocysteine, but their functions are not known. Gel electrophoretic separation of tissue samples from rats labeled with ^{75}Se showed the existence of further Se-containing proteins[5].

It has been shown that Se could prevent cancer in a variety of animal model systems[20, 21]. Both epidemiological studies and supplementation trial supported its efficacy in humans[22]. However, the mechanism by which Se suppresses tumor development remains unknown[23]. Se is present in known human selenoproteins as selenocysteine. Selenocysteine represents the 21st amino acid and is encoded by UGA triplet in selenoprotein mRNA[24, 25]. Although UGA most often functions as a stop codon, UGA-encoded incorporation of selenocysteine into the growing polypeptide is determined by the presence of a specific stem-loop secondary structure within the 3' -untranslated region of the selenoprotein mRNA[26]. Sep15 was firstly found in human T cells, and it contains a selenocysteine residue encoded by TGA. Its coding sequence has no homology to known protein-encoding genes. Computer analysis of transcript map databases indicated that this gene included five exons and four introns[27]. Recent findings indicate that the chromosome, in which the gene of Sep15 is located, is a genetic locus commonly mutated or deleted in human

cancers. One in-frame TGA codon and two stem loop structures resembling selenocysteine insertion sequence (SECIS) elements were identified in the 3' -untranslated region of the gene, and only one of them was functional[9]. Examination of the available cDNA sequence of this protein revealed that two polymorphisms were located at position 811(C/T) and 1 125 (G/A)[28] within the 3' -untranslated region. They were organized into two alleles, C^{811}/G^{1125} and T^{811}/A^{1125} in the 68 %/32 % frequency distribution. These 3' -untranslated region polymorphisms resulted in changes in selenocysteine incorporation into protein and different response. To Se supplementation[9]. Human epidemiological studies have revealed that Se has a negative correlation with the occurrence of prostate cancer[29, 30] and lung cancer[31]. Moreover, recent investigations have shown that Se supplementation may be effective on the reduction of common human cancers, including prostate cancer[9], colon[32] cancer and lung cancer. Northern blot analysis of the human Sep15 mRNA demonstrated that the expression of Sep15 was significantly decreased in malignant prostate cancer cell line and in hepatocellular carcinoma cell line. The Sep15 protein levels in liver tumors, adjacent tissues, and normal hepatic tissue were significantly different. The Sep15 level was significantly decreased in tumors compared with that in the normal control. It was consistent with the observation that Sep15 protein was not detectable in mouse prostate adenocarcinoma cells, while normal mouse prostate showed a strong signal with Sep15 protein-specific antibodies.

Different expression patterns of the Sep15 protein in normal and malignant tissues, the occurrence of polymorphism associated with protein expression, the role of Se in differential regulation of polymorphisms, and loss of heterozygosity at the Sep15 locus in certain human tumor types make us suggest that Sep15 may be involved in cancer development[28]. We have cloned the gene of Sep15 in our country for the first time in order to study the expression of Sep15 protein in different tissue, its structure, function and the relationship with cancer due to the worldwide cancer[33-37] , and digestive in china[38-40].

REFERENCES

1 **Yu MW,** Horng IS, Hsu KH, Chiang YC, Liaw YF, Chen CJ. Plasma selenium levels and risk of hepatocellular carcinoma among men with chronic hepatitis virus infection. *Am J Epidemiol* 1999; **150**: 367-374

2 **Trobs M,** Renner T, Scherer G, Heller WD, Geiss HC, Wolfram G, Haas GM, Schwandt P. Nutrition, antioxidants, and risk factor profile of nonsmokers, passive smokers and smokers of the Prevention Education Program (PEP) in Nuremberg, Germany. *Prev Med* 2002; **34**: 600-607

3 **Popova NV**. Perinatal selenium exposure decreases spontaneous liver tumorogenesis in CBA mice. *Cancer Lett* 2002; **179**: 39-42

4 **Leblondel G,** Mauras Y, Cailleux A, Allain P. Transport measurements across Caco-2 monolayers of different organic and inorganic selenium: influence of sulfur compounds. *Biol Trace Elem Res* 2001; **83**: 191-206

5 **Behne D,** Kyriakopoulos A. Mammalian selenium-containing proteins. *Annu Rev Nutr* 2001; **21**: 453-473

6 **Korotkov KV,** Kumaraswamy E, Zhou Y, Hatfield DL, Gladyshev VN. Association between the 15-kDa selenoprotein and UDP-glucose:glycoprotein glucosyltransferase in the endoplasmic reticulum of mammalian cells. *J Biol Chem* 2001; **276**: 15330-15336

7 **Chin-Thin W,** Wei-Tun C, Tzu-Ming P, Ren-Tse W. Blood concentrations of selenium, zinc, iron, copper and calcium in patients with hepatocellular carcinoma. *Clin Chem Lab Med* 2002; **40**: 1118-1122

8 **Klein EA,** Thompson IM, Lippman SM, Goodman PJ, Albanes D, Taylor PR, Coltman C. SELECT: the selenium and vitamin E cancer prevention trial: rationale and design. *Prostate Cancer Prostatic Dis* 2000; **3**: 145-151

9 **Kumaraswamy E,** Malykh A, Korotkov KV, Kozyavkin S, Hu Y, Kwon SY, Moustafa ME, Carlson BA, Berry MJ, Lee BJ, Hatfield DL, Diamond AM, Gladyshev VN. Structure-expression relationships of the 15-kDa selenoprotein gene. Possible role of the protein in cancer etiology. *J Biol Chem* 2000; **275**: 35540-35547

10 **Li SW,** Gong JP, Wu CX, Shi YJ, Liu CA. Lipopolysaccharide induced synthesis of CD14 proteins and its gene expression in hepatocytes during endotoxemia. *World J Gastroenterol* 2002; **8**: 124-127

11 **Liu LX,** Jiang HC, Liu ZH, Zhou J, Zhang WH, Zhu AL, Wang XQ, Wu M. Integrin gene expression profiles of human hepatocellular carcinoma. *World J Gastroenterol* 2002; **8**: 631-637

12 **Jiang RL,** Lu QS, Luo KX. Cloning and expression of core gene cDNA of Chinese hepatitis C virus in cosmid pTM3. *World J Gastroenterol* 2000; **6**: 220-222

13 **Li Y,** Yang L, Cui JT, Li WM, Guo RF, Lu YY. Construction of cDNA representational difference analysis based on two cDNA libraries and identification of garlic inducible expression genes in human gastric cancer cells. *World J Gastroenterol* 2002; **8**: 208-212

14 **Li Y,** Lu YY. Applying a highly specific and reproducible cDNA RDA method to clone garlic up-regulated genes in human gastric cancer cells. *World J Gastroenterol* 2002; **8**: 213-216

15 **Zhao Y,** Wu K, Xia W, Shan YJ, Wu LJ, Yu WP. The effects of vitamin E succinate on the expression of c-jun gene and protein in human gastric cancer SGC-7901 cells. *World J Gastroenterol* 2002; **8**: 782-786

16 **Xue YW,** Zhang QF, Zhu ZB, Wang Q, Fu SB. Expression of cyclooxygenase-2 and clinicopathologic features in human gastric adenocarcinoma. *World J Gastroenterol* 2003; **9**: 250-253

17 **Ujiie S,** Kikuchi H. The relation between serum selenium value and cancer in Miyagi, Japan: 5-year follow up study. *Tohoku J Exp Med* 2002; **196**: 99-109

18 **Hara S,** Shoji Y, Sakurai A, Yuasa K, Himeno S, Imura N. Effects of selenium deficiency on expression of selenoproteins in bovine arterial endothelial cells. *Biol Pharm Bull* 2001; **24**: 754-759

19 **Mostert V.** Selenoprotein P: properties, functions, and regulation. *Arch Biochem Biophys* 2000; **376**: 433-438

20 **Riondel J,** Wong HK, Glise D, Ducros V, Favier A. The effect of a water-dispersible beta-carotene formulation on the prevention of age-related lymphoid neoplasms in mice. *Anticancer Res* 2002; **22**: 883-888

21 **Popova NV.** Perinatal selenium exposure decreases spontaneous liver tumorogenesis in CBA mice. *Cancer Lett* 2002; **179**: 39-42

22 **Nakaji S,** Fukuda S, Sakamoto J, Sugawara K, Shimoyama T, Umeda T, Baxter D. Relationship between mineral and trace element concentrations in drinking water and gastric cancer mortality in Japan. *Nutr Cancer* 2001; **40**: 99-102

23 **Calvo A,** Xiao N, Kang J, Best CJ, Leiva I, Emmert-Buck MR, Jorcyk C, Green JE. Alterations in gene expression profiles during prostate cancer progression: functional correlations to tumorigenicity and down-regulation of selenoprotein-P in mouse and human tumors. *Cancer Res* 2002; **62**: 5325-5335

24 **Korotkov KV,** Novoselov SV, Hatfield DL, Gladyshev VN. Mammalian selenoprotein in which selenocysteine (Sec) incorporation is supported by a new form of Sec insertion sequence element. *Mol Cell Biol* 2002; **22**: 1402-1411

25 **Zhang W,** Cox AG, Taylor EW. Hepatitis C virus encodes a selenium-dependent glutathione peroxidase gene. Implications for oxidative stress as a risk factor in progression to hepatocellular carcinoma. *Med Klin* 1999; **94** (Suppl 3): 2-6

26 **Mansur DB,** Hao H, Gladyshev VN, Korotkov KV, Hu Y, Moustafa ME, El-Saadani MA, Carlson BA, Hatfield DL, Diamond AM. Multiple levels of regulation of selenoprotein biosynthesis revealed from the analysis of human glioma cell lines. *Biochem Pharmacol* 2000; **60**: 489-497

27 **Hatfield DL,** Gladyshev VN. How selenium has altered our understanding of the genetic code. *Mol Cell Biol* 2002; **22**: 3565-3576

28 **Hu YJ,** Korotkov KV, Mehta R, Hatfield DL, Rotimi CN, Luke A, Prewitt TE, Cooper RS, Stock W, Vokes EE, Dolan ME, Gladyshev VN, Diamond AM. Distribution and functional consequences of nucleotide polymorphisms in the 3'-untranslated region of the human Sep15 gene. *Cancer Res* 2001; **61**: 2307-2310

29 **Brooks JD,** Metter EJ, Chan DW, Sokoll LJ, Landis P, Nelson WG, Muller D, Andres R, Carter HB. Plasma selenium level before diagnosis and the risk of prostate cancer development. *J Urol* 2001;

166: 2034-2038

30 **Gasparian AV,** Yao YJ, Lu J, Yemelyanov AY, Lyakh LA, Slaga TJ, Budunova IV. Selenium compounds inhibit I kappa B kinase (IKK) and nuclear factor-kappa B (NF-kappa B) in prostate cancer cells. *Mol Cancer Ther* 2002; **1**: 1079-1087

31 **Trobs M,** Renner T, Scherer G, Heller WD, Geiss HC, Wolfram G, Haas GM, Schwandt P. Nutrition, antioxidants, and risk factor profile of nonsmokers, passive smokers and smokers of the Prevention Education Program (PEP) in Nuremberg, Germany. *Prev Med* 2002; **34**: 600-607

32 **Casimiro C.** Etiopathogenic factors in colorectal cancer. Nutritional and life-style aspects. 2. *Nutr Hosp* 2002; **17**: 128-138

33 **Sun XW,** Shen BZ, Shi MS, Dai XD. Relationship between CD44v6 expression and risk factors in gastric carcinoma patients. *Shijie Huaren Xiaohua Zazhi* 2002; **10**: 1129-1132

34 **Zhou HB,** Zhang JM, Yan Y. Inactivation of DPC4 gene in colorectal carcinoma. *Shijie Huaren Xiaohua Zazhi* 2002; **10**: 1140-1142

35 **Zhou XD,** Yu JP, Ran ZX, Luo HS, Yu BP. Expression of cFLIP and p53 mutation in adenocarcinoma of colon. *Shijie Huaren Xiaohua Zazhi* 2002; **10**: 536-539

36 **Dong K,** Li B, Qin Y, Li CZ, Lui JY, Sun ZL, Sun ZF. Methylation pattern analysis in CpG islands of p15 and p16 tumor suppressor genes in pancreatic carcinoma tissue. *Shijie Huaren Xiaohua Zazhi* 2002; **10**: 1264-1267

37 **Cui M,** Zhang HJ, An LG. Tumor growth Inhibition by polysaccharide from Coprinus comatus. *Shijie Huaren Xiaohua Zazhi* 2002; **10**: 287-290

38 **Gong JQ,** Fang CH. Relationship between the oval cells and development of hepatocellular carcinoma in rats. *Shijie Huaren Xiaohua Zazhi* 2002; **10**: 1133-1139

39 **Yang L**, Wang YP, Wu DY, Zhang SM, Li JY, Zhang YC, Xin Y. Pathological behaviors and molecular mechanisms of signet-ring cell carcinoma and mucinous adenocarcinoma of stomach: a comparative study. *Shijie Huaren Xiaohua Zazhi* 2002; **10**: 516-524

40 **Zhu JS,** Zhu L, Wang L, Zhuang QX, Hu B, Da W, Chen WX, Chen GQ, Ma JQ. Autologous peripheral blood stem cell combined with high-dose arterial chemotherapy for advanced gastric cancer. *Shijie Huaren Xiaohua Zazhi* 2002; **10**: 1408-1411

Edited by Xu XQ and Wang XL

P.O.Box 2345, Beijing 100023,China
Fax: +86-10-85381893
E-mail: wjg@wjgnet.com www.wjgnet.com

World J Gastroenterol 2003;9(8):1781-1785
World Journal of Gastroenterology
 ISSN 1007-9327

• BASIC RESEARCH •

X-ray induced L02 cells damage rescued by new anti-oxidant NADH

Fa-Quan Liu, Ji-Ren Zhang

Fa-Quan Liu, Ji-Ren Zhang, Department of Oncology, Zhujiang Hospital, First Military Medical University, Guangzhou 510282, Guangdong Province, China
Supported by Healthcare Research Fundation of the Tenth Five-Year Plan of PLA, No, 01MA138
Correspondence to: Fa-Quan Liu, Department of Oncology, Zhujiang Hospital,First Military Medical University, Guangzhou, 510282, China. liufaquan@163.net
Telephone: +86-20-85143202 **Fax:** +86-20-85143200
Received: 2002-08-06 **Accepted:** 2002-10-18

Abstract

AIM: To explore molecular mechanism of nicotinamide adenine dinucleotide (NADH) antagonization against X-ray induced L02 cells damage.

METHODS: L02 liver cells were cultured in RPMI 1640, exposed to X-ray irradiation and continued to culture in the presence or absence of NADH. Cellular viability was analyzed by routine MTT methods. The percent age of apoptotic cells and positive expressions of p53, bax and bcl-2, fas, fasL proteins were determined by FCM. Level of intracellular ROS was determined by confocal microscope scanning. Morphological change was detected by scanning electron micrograph.

RESULTS: The viability of L02 cells was decreased with increasing dose of X-ray irradiation. NADH could not only eliminate the apoptosis induced by X-ray irradiation, but also up-regulate expression of bcl-2 protein and down-regulate expression of p53, bax, fas and fasL proteins ($P<0.05$). At the same time, NADH could reduce level of intracellular ROS in radiated L02 cells.

CONCLUSION: NADH has marked anti-radiation effect, its mechanism may be associated with up-regulation of bcl-2 expression and down-regulation of p53, bax fas and fasL expression, as well as decline of intracellular ROS. However, further investigation of its mechanism is worthwhile.

Liu FQ, Zhang JR. X-ray induced L02 cells damage rescued by new anti-oxidant NADH. *World J Gastroenterol* 2003; 9(8): 1781-1785
http://www.wjgnet.com/1007-9327/9/1781.asp

INTRODUCTION

Recent radiobiological studies have demonstrated that ionizing radiation can induce cell death. Exposure of cell to ionizing radiation over a wide dose range results in activation of cellular response pathways, including p53-dependent and p53-independent ways[1,2]. At the same time, apoptosis resulted from a coordinate sequence of biochemical events eventually leads to cell death. Among these,the generation of ROS with perturbation of prooxidant/antioxidant ratio, alterations in mitochondria structure and $\triangle \Psi m$, and diminutions of plasma membrane potential have been investigated[3,4]. The stabilized electrochemical gradient relies on a functional ion exchange via the electrogenic transporter Na+/K+-ATPase. Na+/K+-ATPase is an energy hungry process which consumes a major of cellular ATP production. Therefore, there may be a decrease of ATP level when apoptosis starts within a few minutes after ionizing irradiation. NADH, an important coenzyme, participates in three carboxyl cycles and ultimately produces ATP molecules. We added NADH to L02 cells undergoing X-ray irradiation *in vitro*, and observed change of survivals and apoptosis as well as radiation associated proteins which take part in signal transduction of apoptosis.

MATERIALS AND METHODS

Reagents

NADH (purity: 97 %) was gifted by Professor Birkmay from Chemical Department of Graz University. Monoclonal mouse anti-p53, bcl-2, bax antibodies and rat anti-Fas, FasL antibodies were from Beijing Zhongshan Biotechnology Company. PI/Annexin V kits were purchased from Immunotech (France). High FITC-labeled goat anti-mouse antibodies were from Zhongshan Company. H_2DCF probe was purchased from America Molecular Probe Company.

Cell lines and culture

Normal human liver cell line L02 was purchased from Shanghai Institute of Cell Biology, Chinese Academy of Sciences. The cells were cultured in RPMI 1640 supplemented with streptomycin (50 U/ml), glutamate (2 mM) and 10 % fetal bovine serum.

Induction of apoptosis

The L02 cells were seeded in 6-well tissue cultured plates, the supernatant was discarded and 0.01 M PBS (pH 7.4) was added. The L02 cells were X-ray-irradiated with 2.5, 5.0 and 7.5 Gy. The cells were then cultured in a complete medium in the presence or absence of NADH at a concentration of 400 ug/ml, respectively. Non-irradiated culture served as control.

MTT cell viability assay

The cells were seeded into 96-well dishes (5×10^3 cells/well), incubated for 24 h to allow attachment, treated with X-ray at 5.0 Gy, and continued to culture for 12, 24, 36, 48 h in the presence or absence of NADH. Absorbance was read at 570 nm by using DG3022 ELISA according to the routine MTT methods. The cellular viability was calculated as the amount of MTT uptake[5].

Assessment of apoptotic cells

The L02 cells were seeded at 5×10^4-5×10^5/ml in 6 well tissue cultured plates and cultured for 48 hours in RPMI-1640 medium containing 10 % FBS. Apoptosis was induced by X-ray irradiation, the LO2 cells were continued to culture for 24 h. A total of 5×10^5-5×10^6/ml cells were collected by centrifugation at 200 g (×5 min) and washed twice with ice-cold PBS (pH 7.4). Percent age of apoptosis was detected by flow cytometry according to PI/Annexin V kits.

Scanning electron microscope

24 hours following exposure to 2.5 Gy X-ray radiation, the L02 cells were fixed for 1 hour at room temperature using 4 % glutaraldehyde in PBS and proceeded for scanning electron microscopy as routine methods.

Protein expression of bcl-2, bax, fas, FasL and p53

The L02 cells were collected and then washed twice with ice-cold PBS, followed by fixation in 0.5 % paraformaldehyde at 4 ℃ for 30 min. The fixated cells were treated with PBS containing 0.1 % Triton-100 and washed twice. The treated cells of every tube were divided into five tubes and washed. The supernatant was aspirated. The antibodies against bcl-2, bax, p53, fas, FasL were added into each tube, mixed and incubated for 1 h at 37 ℃. The cells were washed twice and the FITC-labeled second antibodies were added for 30 min at 37 ℃. Then, the cells were washed twice with ice-cold PBS and resuspended with 500 μl PBS. 10 000 events were analyzed and the positive rate of protein expression was detected by FCM.

Determination of intracellular ROS concentration

The cell suspension was dispensed into special culture plates at a density of 2×10^4 cells per ml and incubated at 37 ℃, 5 % CO_2 for 48 h. The supernatant was removed and replaced with Hank' s solution , then exposed to 2.5 Gy X-ray radiation. The supernatant was discarded at once, and replaced with RPMI-1640 medium with or without NADH at a concentration of 400 ug/ml for 4 h, respectively. Non-irradiated culture served as control, followed by washing three times with Hank' s solution. Measurement of intracellular ROS concentration was described in literature. Briefly, the cells were loaded with 0.5 ml H_2DCF in DMSO solution at 5 μg/ml and incubated at 37 ℃ for 30 min. After washed three times with PBS, 0.5 ml PBS was loaded and the change of intracellular ROS was detected by scanning fluorescence intensity under confocal microscope.

RESULTS

X-ray treatment inhibited growth of L02 cells

The L02 cells were treated with different doses of X-ray irradiation. Cell survival was determined after 12, 24, 36, 46 h. Inhibition of growth in X-ray treated cells occurred in a dose-dependent manner (Figure 1). Survival of L02 cells decreased as the dose of X-ray increased. It was most obvious at 24 h post-irradiation.

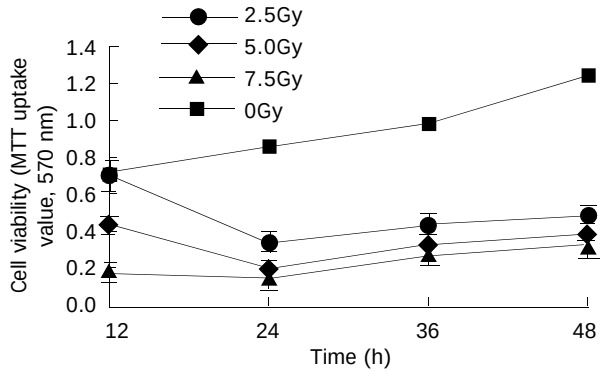

Figure 1 X-ray induced inhibition of growth of L02 cells.

NADH antagonized apoptosis of X-ray treated L02 cells

The L02 cells were treated with 2.5, 5.0, 7.5 Gy X-ray irradiation, then post-incubated in fresh complete RPMI 1640 medium containing NADH or NADH free drug for 24 h. Percent age of apoptosis was determined by FCM using PI/ Annexin V stain method. The results showed that NADH diminished apoptosis of L02 cells exposed to X rays. The percent age of apoptosis was (7.08±2.34) %, (28.16±2.46) %, (47.30±3.43) % in the absence of NADH. However, it was (6.04±0.86) %, (8. 25±1.64) %, (15.30±1.98) % in the presence of NADH. The difference was significant between L02 cells treated with 5.0 Gy,7.5 Gy X rays and cultured for 24 h in the presence of NADH and L02 cells cultured in the absence of NADH ($P<0.05$). These findings suggested that NADH was involved in cytoprotection by blocking the induction of apoptosis.

NADH rescued L02 cells damage from X-ray radiation

X-ray radiation could induce L02 cells damage. As shown in Figure 2, Part(b) and part(c) represented different morphologic changes of 2.5 Gy X-ray radiated L02 cells in the absence or presence of NADH. Part(a) represented the shamly irradiated L02 cells, which had normal liver cell surface structure with normal protuberance and volume. But, Part(b) had decreased protuberance and atrophy. However, degree of damage in L02 cells of part(c) group was becoming less than that of part(b). These suggested that NADH could rescue L02 cells damage from X-ray irradiation.

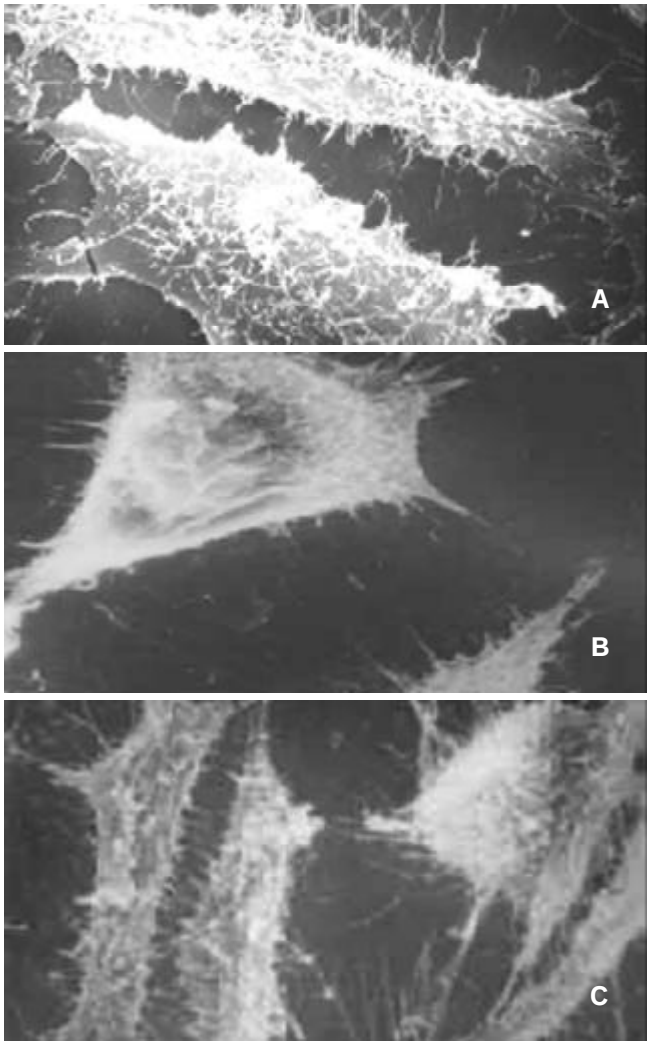

Figure 2 The result of scan electron microscopy. (a) Normal liver cell surface structure. (b) Irradiated hepatocytes with atrophy and decreased protuberance. (c) Morphological changes of hepatocytes irradiated and incubated in the presence of NADH.

Expression of p53, bax, bcl-2, Fas and Fas-L in L02 cells

The results of FCM analysis for p53, bax, bcl-2, Fas and FasL protein expression in X-ray irradiated and mockly irradiated

L02 cells are summarized in Table 1. Significantly high levels of p53, bax, Fas and Fas-L protein expression were detected in cells irradiated and cultured in the absence of NADH than in those cells cultured in the presence of NADH and mockly irradiated, but expression of bcl-2 protein tended to be low in L02 cells. Our results showed that NADH up-regulated expression of bcl-2 protein and down-regulated expression of p53, bax, bcl-2, Fas and FasL protein in L02 cells undergoing X ray irradiation. It might be one of the mechanisms that NADH rescues L02 cells injury from ionizing irradiation.

Table 1 Effect of NADH on regulation of apoptosis associated proteins in L02 cells treated with X-ray (n=3, $\bar{x}\pm s$)

Group	p53	Fas	FasL	bcl-2	bax
Mock IR	22.40±0.91	7.01±0.21	66.66±1.60	5.27±0.12	74.71±1.81
IR	37.4±1.11[a]	13.40±0.78[a]	74.40±1.09[a]	2.22±0.18[a]	86.76±2.14[a]
IR+NADH	26.93±6.73	11.29±1.40	68.93±1.88	3.62±1.34	71.60±2.92

Based on *t* test, "Mock IR" represented L02 cells of non-irradiated group. "IR+NADH" represented L02 cells irradiated and continued to culture in the presence of NADH. [a]P<0.05 *vs* Mock IR group and IR+NADH group.

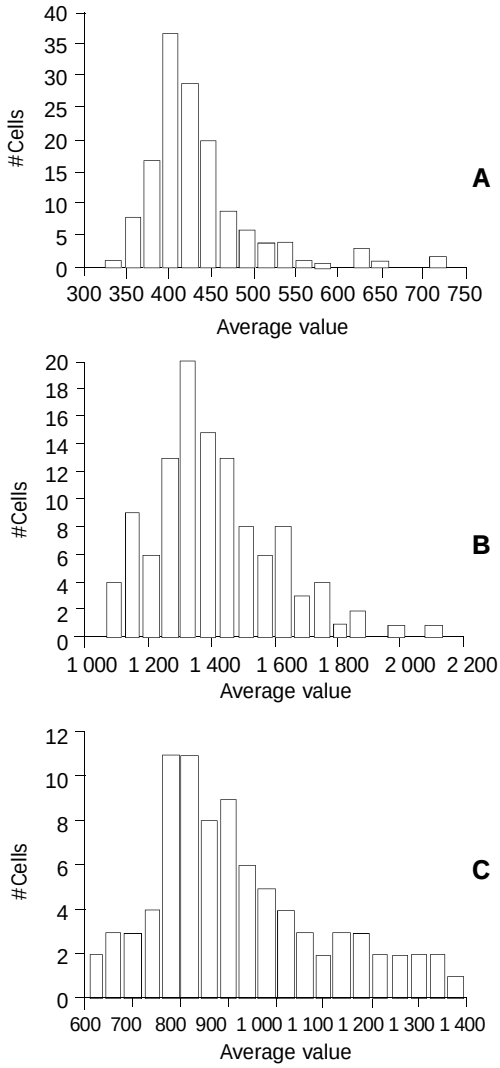

Figure 3A The change of intracellular H_2O_2 production in L02 cells cultured with or without NADH for 4 h after X-ray irradiation. (a) Sham irradiation group. (b and c) X-ray treated (2.5 Gy) L02 cells were respectively cultured in the absence or presence of NADH. Mean value of fluorescence was calculated according to the number of L02 cells. [a]P<0.05 compared with sham irradiation (a) and test group (c).

Determination of intracellular ROS

Figure 3A and Figure 3B show that 2.5 Gy X-ray irradiation increased the level of intracellular ROS after 4 h irradiation in L02 cells compared with that in L02 cells of sham irradiation group. However, NADH could reverse the effect of X-ray irradiation.

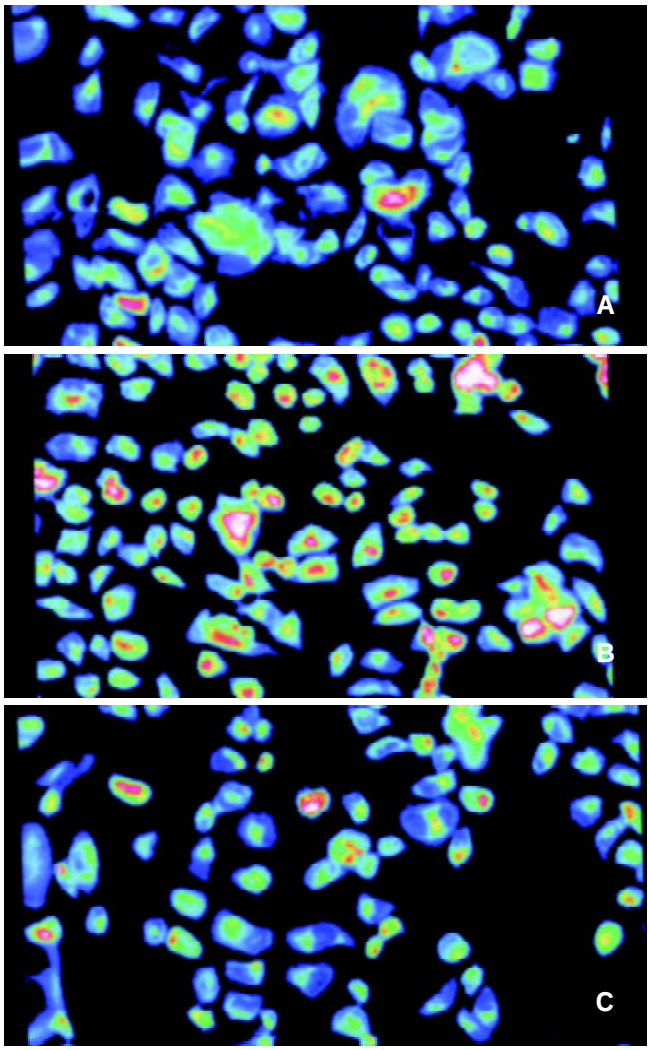

Figure 3B The graph showed the cell fluorescence change of intracellular ROS by confocal microscope scanning in L02 cells of different treatment.

DISCUSSION

When a cell exposed to ionizing irradiation, at least two signal-generating targets are activated, one at the membrane and the other at the DNA. Signal may also originate in cytoplasm[6,7]. These signal targets ultimately result in cell death or non-death stress response. Apoptosis, also called programmed cell death (PCD),is a peculiar form of cell death characterized by several morphological and biochemical aspects which are different from necrosis, an other form of death. X-ray irradiation is one of the ionizing radiations, which can cause both membrane and DNA damage to cells and result in cell apoptosis. How ionizing radiation triggers apoptosis is not known. It was reported that apoptosis mediated by DNA damage occurred via p53-dependent and p53-independent pathways[1,2]. However, several pathways of apoptosis have been reported. One of these is the Fas/FasL pathway, which involves binding of a death receptor to a death domain, initiating a cascade of proteases that leads to cell apoptosis[8]. In the present study, we tested whether apoptosis induced by X-ray irradiation

occurred via DNA damage or Fas/FasL pathway. Our results demonstrated that X-ray irradiation led to cell apoptosis by increasing positive rate of L02 cells expressing p53 and bax proteins, and decreasing positive rate of bcl-2 protein. At the same time, Fas and FasL expression in L02 cells exposed to irradiation was up-regulated as compared with that in mockly irradiated-cells.

Cellular sensitivity to radiation reflects a culmination of distinct molecular pathway including DNA repair, cell cycle checkpoint fidelity, and particularly apoptosis. Several oncogenes and tumor suppressor genes play a pivotal role in modulating the response of cells to radiation. An important molecule, p53, initiates responses to DNA damage, and affects the sensitivity of cells to apoptosis. Functional inactivation of p53 is associated with resistance to radiotherapy. Overexpression of wtp53 gene was found to be associated with increased cellular sensitivity to apoptosis induced by ionizing irradiation[9,10]. Bcl-2, an important regulator of apoptosis, was found to be associated with anti-apoptosis response. Over expression of bcl-2 by transferring bcl-2 gene into deficient cells has been associated with increased cellular resistance to induction of apoptosis by a variety of DNA-damaging agents including ionizing irradiation, drugs. However, bax, another member of bcl-2 family, as an inhibitor of apoptosis, can bind bcl-2 to form homo- and heterodimers. Rate of bcl-2 to bax may determine the extent to which apoptosis is induced or suppressed[11,12]. At the same time, high expression of wild - type p53 protein induced by ionizing irradiation appears to regulate expression of bcl-2, bax, p21 and p16 genes[13]. Our results showed that X-ray radiation induced DNA damage resulted in an increase of positivity of p53 and bax protein expression, and decrease of bcl-2 protein expression in L02 cells. But it is necessary to further confirm whether p53 may regulate expression of bcl-2 and bax genes.

Recently, it has been suggested that Fas/FasL system plays a key role in the regulation of apoptosis. Fas is located on the plasma membrane of hepatocytes abundantly, and FasL, a glycoprotein of 40 kd is located on the plasma membrane of the lymphocytes. The interaction of the Fas ligand and Fas receptor initiates a chemical process in the cells that leads to apoptosis. Fas, named CD95, expresses in alcoholic liver disease, viral hepatitis, hepatocarcinomas, and hepatocirrhosis[14-16]. Fas-FasL interaction may contribute to hepatocyte apoptosis in these patients. It was rarely reported that apoptosis induced by ionizing irradiation occurred via Fas-FasL interaction pathway, particularly apoptosis induced by Fas-FasL interaction itself in hepatocytes. It was recently reported that the Fas/Fas ligand system was involved in modulating keratocyte apoptosis induced by UV irradiation[17]. Newton reported that apoptosis induced by ionizing radiation required p53 and was regulated by the Bcl-2 protein family but did not require signals transduced by Fas and FADD/MORT1[18]. Our experiment indicated that X-ray irradiation enhanced the positive rate of L02 cells expressing Fas and FasL protein as compared with shamly irradiated cells. It is suggested that FasL-Fas interaction play an important role in liver cell apoptosis induced by X-ray irradiation. It is different from the model in which ionizing irradiation triggers apoptosis via p53-dependent activation of caspase-9.

Several biochemical alterations, including excessive generation of reactive oxygen species (ROS), calcium flux, Caspase activation, have been shown to be essential in cell apoptosis[19-21]. ROS plays a pivotal role in ionizing irradiation -induced cell apoptosis[22-24]. ROS, as a signal molecule, could regulate gene expression and mitochondria membrane potential[25,26]. Free radicals are an integral part of metabolism and formed continuously in the body. Many sources of stress heat, irradiation, hyperoxia, inflammation and any increases in metabolism including exercise, injury, and even repair processes lead to increased production of free radicals and associated reactive oxygen or nitrogen species (ROS/RNS)[27-29]. Evidences have shown that free radicals have important functions in the signal network of cells, including induction of growth and apoptosis and as killing tools of immunocompetent cells[30,31]. Massive intervention into the redox state by pharmaceutical doses of exogenous antioxidants should be considered with caution due to the ambiguous role of free radicals in regulation of growth, apoptosis, and cytotoxicity of immunocompetent cells. Our results showed that X-ray irradiation could give rise to increases of ROS generation after 4 h irradiation, but NADH could reverse the effect of X-ray irradiation, lower the level of intracellular ROS. These results indicated that NADH rescued L02 cells damage from X-ray irradiation by regulation of ROS generation.

NADH, a kind of important coenzyme, takes part in triggering biological anti-oxidation and regulating the expression of membrane glycoprotein receptors[32]. But it was seldom reported that NADH played a role in antagonizing ionizing irradiation induced apoptosis and regulating expression of membrane receptors. Recently, it was reported that the content of intracellular NADH changed after UV or ionizing irradiation[33,34]. Most of the results indicated that the content of intracellular NADH declined after ionizing irradiation or PDT treatment by confocal microscope scanning analysis. Pogue reported that the endogenous fluorescence signal attributable to reduced nicotinamide adenine dinucleotide (NADH) was measured in response to photodynamic therapy (PDT)-induced damage. Measurements on cells *in vitro* have showed that NADH fluorescence decreased relatively to that of controls after treatment with a toxic dose of PDT, as measured within 30 min after treatment. Similarly, assays of cell viability indicated that mitochondria function was reduced immediately after treatment in proportion to the dose delivered[35]. It was seldom reported that signal transduction molecules changed after ionizing irradiation by extraneously added NADH. Recent studies of repairing ionizing irradiation injury focused on antioxidant drugs. Bush reported that NAC could protect immune function and regulate expression of oncogenes in bone marrow cells exposed to ionizing irradiation[36]. Zhou found that bilobalide might block PC12 cells from reactive oxygen species-induced apoptosis in the early stage and then attenuate the elevation of c-Myc, p53, and Bax and activation of Caspase-3[37]. Our results indicated that expression of p53, bax, Fas and FasL proteins was up-regulated and expression of bcl-2 protein was down-regulated in L02 cells undergoing X-ray irradiation. However, when L02 cells undergoing X-ray irradiation continued to culture in the presence of NADH, expression of p53, bax, Fas and FasL proteins were down-regulated and expression of bcl-2 protein was up-regulated. At the same time, level of intracellular ROS declined, survival of cell increased. Our observations provide evidence that NADH is a new kind of radiation protector.

REFERENCES

1 **Caelles C**, Helmberg A, Karin M. p53-dependent apoptosis in the absence of transcriptional activation of p53-target genes. *Nature* 1994; **370**: 220-223

2 **Strasser A**, Harris AW, Jacks T, Cory S. DNA damage can induce apoptosis in proliferating lymphoid cells via p53-independent mechanisms inhibitable by Bcl-2. *Cell* 1994; **79**: 329-339

3 **Zamzami N**, Marchetti P, Castedo M, Zanin C, Vayssiere JL, Petit PX, Kroemer G. Reduction in mitochondrial potential constitutes an early irreversible step of programmed lymphocyte death *in vivo*. *J Exp Med* 1995; **181**: 1661-1672

4 **Zamzami N**, Marchetti P, Castedo M, Decaudin D, Macho A, Hirsch T, Susin SA, Petit PX, Mignotte B, Kroemer G. Sequence

reduction of mitochondrial transmembrane potential and generation of reactive oxygen species in early programmed cell death. *J Exp Med* 1995; **182**: 367-377

5 **Weller M**, Schmidt C, Roth W, Dichgans J. Chemotherapy of human malignant glioma: prevention of efficacy by dexamethasone? *Neurology* 1997; **48**: 1704-1709

6 **Godar DE,** Thomas DP, Miller SA, Lee W. Long-wavelength UVA radiation induces oxidative stress, cytoskeletal damage and hemolysis. *Photochem Photobiol* 1993; **57**: 1018-1026

7 **Liu ZG**, Baskaran R, Lea-Chou ET, Wood LD, Chen Y, Karin M, Wang JY. Three distinct signalling responses by murine fibroblasts to genotoxic stress. *Nature* 1996; **384**: 273-276

8 **Friesen C**, Herr I, Krammer PH, Debatin KM. Involvement of the CD95(APO-1/FAS) receptor/ligand system in drug-induced apoptosis in leukemia cells. *Nat Med* 1996; **2**: 574-577

9 **Burger H,** Nooter K, Boersma AW, Kortland CJ, Van den Berg AP, Stoter G. Expression of p53, p21/WAF/CIP, Bcl-2, Bax, Bcl-x, and Bak in radiation-induced apoptosis in testicular germ cell tumor lines. *Int J Radiat Oncol Biol Phys* 1998; **41**: 415-424

10 **Bandoh N**, Hayashi T, Kishibe K, Takahara M, Imada M, Nonaka S, Harabuchi Y. Prognostic value of p53 mutations, bax, and spontaneous apoptosis in maxillary sinus squamous cell carcinoma. *Cancer* 2002; **94**: 1968-1980

11 **Findley HW**, Gu L, Yeager AM, Zhou M. Expression and regulation of Bcl-2, Bcl-xl, and Bax correlate with p53 status and sensitivity to apoptosis in childhood acute lymphoblastic leukemia. *Blood* 1997; **89**: 2986-2993

12 **Latonen L**, Taya Y, Laiho M. UV-radiation induces dose-dependent regulation of p53 response and modulates p53-HDM2 interaction in human fibroblasts. *Oncogene* 2001; **20**: 6784-6793

13 **Miyashita T**, Krajewski S, Krajewska M, Wang HG, Lin HK, Liebermann DA, Hoffman B, Reed JC. Tumor suppressor p53 is a regulator of bcl-2 and bax gene expression *in vitro* and *in vivo*. *Oncogene* 1994; **9**: 1799-1805

14 **Hayashi N**, Mita E. Involvement of Fas system-mediated apoptosis in pathogenesis of viral hepatitis. *J Viral Hepat* 1999; **6**: 357-365

15 **Abdulkarim B**, Sabri S, Deutsch E, Vaganay S, Marangoni E, Vainchenker W, Bongrand P, Busson P, Bourhis J. Radiation-induced expression of functional Fas ligand in EBV-positive human nasopharyngeal carcinoma cells. *Int J Cancer* 2000; **86**: 229-237

16 **Li ZY**, Zou SQ. Fas counterattack in cholangiocarcinoma: a mechanism for immune evasion in human hilar cholangiocarcinomas. *World J Gastroenterol* 2001; **7**: 860-863

17 **Podskochy A**, Fagerholm P. The expression of Fas ligand protein in ultraviolet-exposed rabbit corneas. *Cornea* 2002; **21**: 91-94

18 **Newton K**, Strasser A. Ionizing radiation and chemotherapeutic drugs induce apoptosis in lymphocytes in the absence of Fas or FADD/MORT1 signaling. Implications for cancer therapy. *J Exp Med* 2000; **191**: 195-200

19 **Chan WH**, Yu JS. Inhibition of UV irradiation-induced oxidative stress and apoptotic biochemical changes in human epidermal carcinoma A431 cells by genistein. *J Cell Biochem* 2000; **78**: 73-84

20 **Pu Y**, Chang DC. Cytosolic Ca^{2+} signal is involved in regulating UV-induced apoptosis in hela cells. *Biochem Biophys Res Commun* 2001; **282**: 84-89

21 **Zhao QL**, Kondo T, Noda A, Fujiwara Y. Mitochondrial and intracellular free-calcium regulation of radiation-induced apoptosis in human leukemic cells. *Int J Radiat Biol* 1999; **75**: 493-504

22 **Li HL**, Chen DD, Li XH, Zhang HW, Lu YQ, Ye CL, Ren XD. Changes of NF-kB, p53, Bcl-2 and caspase in apoptosis induced by JTE-522 in human gastric adenocarcinoma cell line AGS cells: role of reactive oxygen species. *World J Gastroenterol* 2002; **8**: 431-435

23 **Lam M**, Oleinick NL, Nieminen AL. Photodynamic therapy-induced apoptosis in epidermoid carcinoma cells. Reactive oxygen species and mitochondrial inner membrane permeabilization. *J Biol Chem* 2001; **276**: 47379-47386

24 **Lin CP**, Lynch MC, Kochevar IE. Reactive oxidizing species produced near the plasma membrane induce apoptosis in bovine aorta endothelial cells. *Exp Cell Res* 2000; **259**: 351-359

25 **Ferlini C**, De Angelis C, Biselli R, Distefano M, Scambia G, Fattorossi A. Sequence of metabolic changes during X-ray-induced apoptosis. *Exp Cell Res* 1999; **247**: 160-167

26 **Kang CD**, Jang JH, Kim KW, Lee HJ, Jeong CS, Kim CM, Kim SH, Chung BS. Activation of c-jun N-terminal kinase/stress-activated protein kinase and the decreased ratio of Bcl-2 to Bax are associated with the auto-oxidized dopamine-induced apoptosis in PC12 cells. *Neurosci Lett* 1998; **256**: 37-40

27 **Chen YC**, Tsai SH, Lin-Shiau SY, Lin JK. Elevation of apoptotic potential by anoxia hyperoxia shift in NIH3T3 cells. *Mol Cell Biochem* 1999; **197**: 147-159

28 **Fehrenbach E**, Northoff H. Free radicals, exercise, apoptosis, and heat shock proteins. *Exerc Immunol Rev* 2001; **7**: 66-89

29 **Gorman AM**, Heavey B, Creagh E, Cotter TG, Samali A. Anti-oxidant-mediated inhibition of the heat shock response leads to apoptosis. *FEBS Lett* 1999; **445**: 98-102

30 **Elbim C**, Pillet S, Prevost MH, Preira A, Girard PM, Rogine N, Matusani H, Hakim J, Israel N, Gougerot-Pocidalo MA. Redox and activation status of monocytes from human immunodeficiency virus-infected patients: relationship with viral load. *J Virol* 1999; **73**: 4561-4566

31 **Goldshmit Y**, Erlich S, Pinkas-Kramarski R. Neuregulin rescues PC12-ErbB4 cells from cell death induced by H(2)O(2). Regulation of reactive oxygen species levels by phosphatidylinositol 3-kinase. *J Biol Chem* 2001; **276**: 46379-46385

32 **Birkmayer GJ**, Birkmayer W. Stimulation of endogenous L-dopa biosynthesis-a new principle for the therapy of Parkinson's disease: the clinical effect of nicotinamide adenine dinucleotide (NADH) and nicotinamide adenine dinucleotidephosphate (NADPH). *Acata Neurol Scand Suppl* 1989; **126**: 183-187

33 **Obi-Tabot ET**, Hanrahan LM, Cachecho R, Beer ER, Hopkins SR, Chan JC, Shapiro JM, LaMorte WW. Change in hepatocyte NADH fluorescence during prolonged hypoxia. *J Surg Res* 1993; **55**: 575-580

34 **Cristovao L**, Lechner MC, Fidalgo P, Leitao CN, Mira FC, Rueff J. Absence of stimulation of poly(ADP-ribose) polymerase activity in patients predisposed to colon cancer. *Br J Cancer* 1998; **77**: 1628-1632

35 **Pogue BW**, Pitts JD, Mycek MA, Sloboda RD, Wilmot CM, Brandsema JF, O'Hara JA. *In vivo* NADH fluorescence monitoring as an assay for cellular damage in photodynamic therapy. *Photochem Photobiol* 2001; **74**: 817-824

36 **Bush JA**, Ho VC, Mitchell DL, Tron VA, Li G. Effect of N-acetylcysteine on UVB-induced apoptosis and DNA repair in human and mouse keratinocytes. *Photochem Photobiol* 1999; **70**: 329-333

37 **Zhou LJ**, Zhu XZ. Reactive oxygen species-induced apoptosis in PC12 cells and protective effect of bilobalide. *J Pharmacol Exp Ther* 2000; **293**: 982-988

Edited by Wen CY and Wang XL

P.O.Box 2345, Beijing 100023,China
Fax: +86-10-85381893
E-mail: wjg@wjgnet.com www.wjgnet.com

World J Gastroenterol 2003;9(8):1786-1790
World Journal of Gastroenterology
 ISSN 1007-9327

• BASIC RESEARCH •

Effect of gastrin on differentiation of rat intestinal epithelial cells *in vitro*

Zhou Wang, Wei-Wen Chen, Ru-Liu Li, Bin Wen, Jing-Bo Sun

Zhou Wang, Wei-Wen Chen, Ru-Liu Li, Bin Wen, Piwei Institute, Guangzhou University of TCM, Guangzhou, 510405, Guangdong Province, China
Jing-Bo Sun, The Second Affiliated Hospital of Guangzhou University of TCM, Guangzhou, 510120, Guangdong Province, China
Supported by the Major State Basic Research Development Program of China (973 Program) No.G19990544 and the National Natural Science Foundation of China, No.39970906
Correspondence to: Dr. Wei-Wen Chen, Piwei Institute, Guangzhou University of TCM, Guangzhou, 510405, Guangdong Province, China. chenww@gzhtcm.edu.cn
Telephone: +86-20-36585080 **Fax:** +86-20-36586563
Received: 2003-03-04 **Accepted:** 2003-04-03

Abstract

AIM: To investigate the effect of gastrin on differentiation of IEC-6 cell line *in vitro*.

METHODS: IEC-6 cells were incubated with gastrin. On day 7 after treatment, cell morphology was examined by light microscope, and on day 20, the cellular ultrastructures were examined by electron microscope. After exposure to gastrin for 6 hours, villin mRNA was analyzed by reverse transcription-polymerase chain reaction, and on day 7, the expression of villin was examined by immunocytochemical analysis with laser confocal microscope.

RESULTS: After exposure to gastrin, IEC-6 cells showed differentiated phenotypes as villas enterocytes and contained an abundance of plasma, small nuclei with nucleoli, and were arranged regularly. There were numerous microvilli around edge of the cells, and several cells showed columnar structures. Villin mRNA expression in cytoplasm was increased in comparison with control.

CONCLUSION: Differentiated characteristics of villus enterocytes and phenotypic changes of rat intestinal epithelial cells (IEC-6) are induced by gastrin, and the effects of gastrin are correlated to increased villin expression.

Wang Z, Chen WW, Li RL, Wen B, Sun JB. Effect of gastrin on differentiation of rat intestinal epithelial cells *in vitro*. *World J Gastroenterol* 2003; 9(8): 1786-1790
http://www.wjgnet.com/1007-9327/9/1786.asp

INTRODUCTION

Gastrin stimulates cell proliferation in gastric mucosa under physiological conditions[1]. Studies have demonstrated that gastrin many increase ornithine decarboxylase activity of IEC-6 cells, cause intracellular polyamine synthesis, and therefore promote cell proliferation[2,3] and migration[4]. Polyamine has been demonstrated to be closely correlated to cytoskeleton reconstitution, an important process of cellular differentiation[5-9], but it is not clear yet whether gastrin plays roles in differentiation of IEC-6 cells. This study was to investigate gastrin-induced morphological changes of intestinal epithelial cell (IEC-6) and the intracellular expression of villin.

MATERIALS AND METHODS

Cell culture

IEC-6 cells (ATCC, Rockville, MD) were grown at 37 ℃ in a 900 mL· L^{-1} air-100 mL· L^{-1} CO_2 atmosphere in Dulbecco' s modified Eagle' s medium (pH7.2) containing 50 g· L^{-1} dFBS, 10 mg· L^{-1} insulin, 50 mg· L^{-1} gentamycin sulfate, and subcultured once a week. When cultured cells became confluence, they were dissociated with 0.5 g· L^{-1} trypsin and 0.2 g· L^{-1} EDTA, and seeded into 6-well cell culture plates. Pentagastrin (Sigma. Louis, MO) was dissolved in two or three drops of 300 g· L^{-1} ammonium hydroxide (sterile), the solution was adjusted to pH 7.5, and then diluted with medium to 62.5 mg· L^{-1} before use.

Morphology

Light microscopy Monolayer of IEC-6 cells was prepared on glass coverslips, which were placed in 6-well cell culture plates (Corning Glass Works). The cells were seeded at a concentration of 1.0×10^5 per well, and incubated at 37 ℃ in a 900 mL· L^{-1} air-100 mL· L^{-1} CO_2 atmosphere for 24 h. The media containing cDMEM 2 000 μL, PBS 490 μL and 10 μL pentagastrin solution were replaced to make a final concentration of pentagastrin 250 μg· L^{-1} in culture. The medium in control group was the same as that in the treatment group except gastrin. Cells were harvested on day 7 from the initial treatment. The coverslips were removed and fixed for 15 min at room temperature in 3.5 % paraformaldehyde in PBS, washed with distilled water, followed by HE staining and examined under light microscope.

Electron microscopy The cells were seeded in 6-well cell culture plates with a concentration of 1.0×10^5 per well under the same culture condition as above. Cultured cells were harvested on day 20 from the initial treatment of gastrin, washed with PBS, fixed in 2 % glutaraldehyde, postfixed in 1 % osmium tetroxide, dehydrated, and embedded in Epon, and examined under electron microscope.

Villin expression

mRNA level analysis After incubated with gastrin for 6 hours, cultured cells were harvested for extraction of total RNA with RNA TRIzol reagent (Gibco, Gaithersburg, MD). Isolation was performed according to the manufacturer' s protocols. The concentration of extracted RNA was determined. RT-PCR kit (Gibco, Gaithersburg, MD) was used for RT-PCR reaction following the attached protocol of the product. The primers (Seagon, Shanghai, China) were synthesized according to sequences of rat villin gene (GenBank™ accession number M98454) as follows: coding strand primer: 5' -ATG CCC AAG TCA AAG GCT CTC TCA ACA TCA C-3' , noncoding strand primer: 5' -TGC AAC AGT CGC TGG ACA TCA CAG G-3' [10]. The reference primers (Seagon, Shanghai, China) were according to sequences of rat β-actin gene (GenBank™ accession number AB028846) as follows: coding strand primer: 5' -TTC CAG CCT TCC TTC CTG G-3' , noncoding strand primer: 5' -TTG CGC TCA GGA GGA GCA AT-3' . 2 μL of

RT products was added to the PCR master mix. After incubation at 94 ℃ for 2 min, reaction was done for 35 cycles at 94 ℃ for 60 s, at 55 ℃ for 60 s, and at 72 ℃ for 30 s. The expected cDNA amplification products were 408 bp for villin and 238 bp for β-actin. After electrophoresis on agarose gel and staining with ethidium bromide, DNA bands were visualized with an ultraviolet transilluminator.

Protein level analysis On day 7 from the initial treatment, cultured cells were fixed for 15 min at room temperature in 3.5 % paraformaldehyde in PBS, and washed three times. For study of villin expression, the cells were permeabilized by incubation with 0.2 % Triton X-100 in PBS for 4 min, washed three times with PBS, and then treated with goat serum for 10 min. The permeabilized cells were incubated with goat anti-rat antibody with dilution of 1:100 in PBS (Santa Cruz) for 2 hours at room temperature, washed, and then incubated with FITC-conjugated rabbit anti-goat IgG with dilution of 1:50 in PBS (Sigma. Louis, MO). The treated cells were visualized under TCS SP confocal laser scanning microscope (Leica, Heidelberg, Germany).

RESULTS

Effect of gastrin on morphology of IEC-6 cells

Light microscopy Seven-days after treatment with gastrin, cells were arranged regularly with an abundance of plasma, and small nuclei with nucleoli. Typically differentiated cells showed a tendency to form microvilli on the edge, and remarkable cytoskeleton-like structure, which was similar to cytoskeleton distribution in well-differentiated enterocytes. Cells in control group contained sparse plasma, large nuclei without nucleoli, and were arranged irregularly (Figure1).

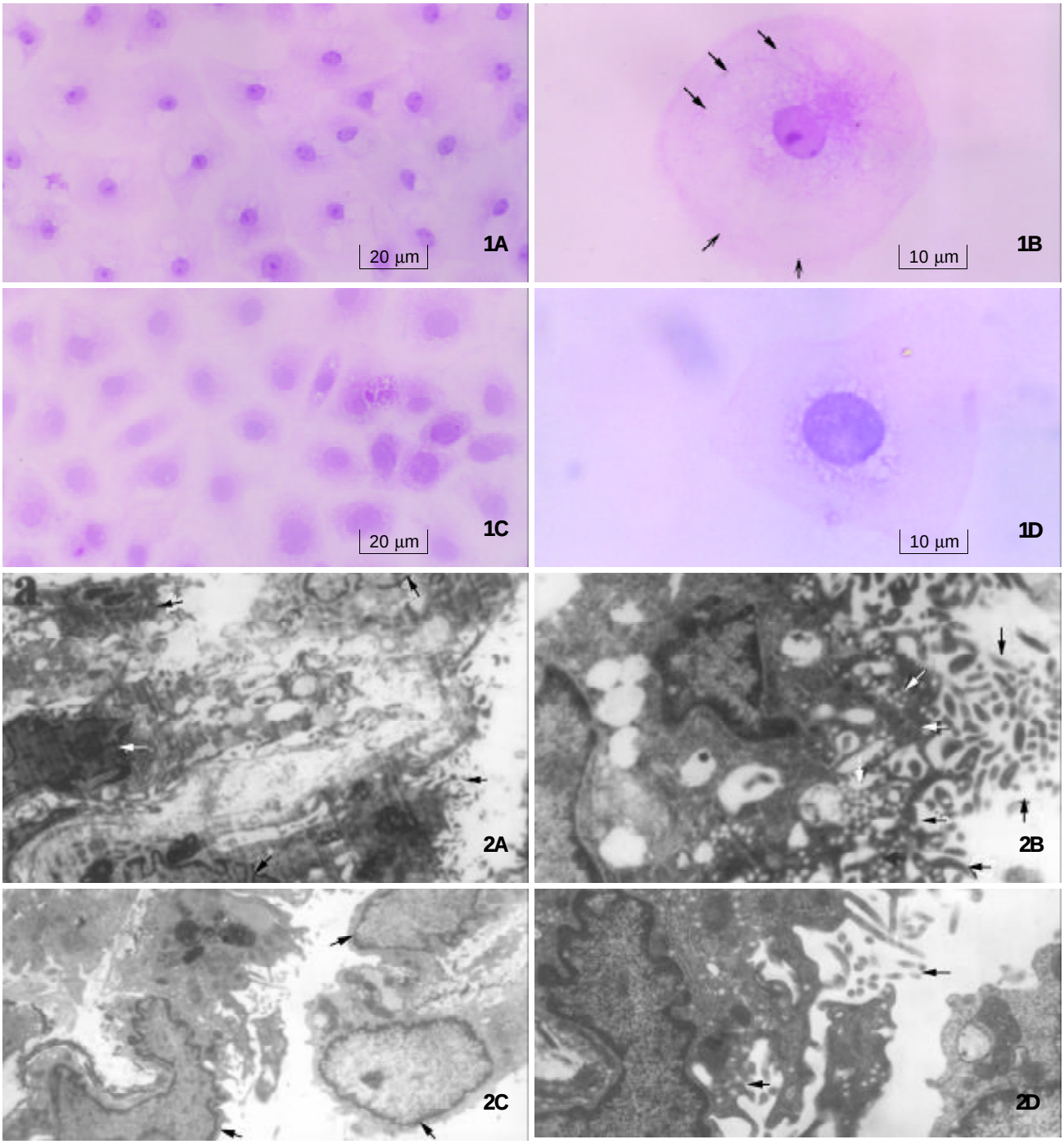

Figure 1 Morphology of IEC-6 cells. a: Gastrin-treated cells(250×) contained an abundance of plasma, small nuclei with nucleoli, and were arranged regularly. b: One of gastrin-treated cells (400×) showed the tendency to form microvilli on the edge(open

arrows), and cytoskeleton-like staining in plasma (solid arrows). c: Control cells (250×) contained sparse plasma, large nuclei without nucleoli, and were in irregular arrangement and immature shape. d: One of control cells (400×) showed no tendency to form microvilli on the edge, and nucleus was relatively larger and had no nucleolus.

Figure 2 Ultrastructural changes of IEC-6 cells. a: Gastrin-treated cells (5 000×, bar=1 μm) showed columnar structures(the nuclei were shown by open arrows) with numerous microvilli on the edge (solid arrows). b: Gastrin-treated cells (12 000×, bar=500 nm)developed numerous microvilli (open arrows) and lots of endocytic vesicles appeared under the apical membrane (solid arrows). c: Control cells (5 000×, bar=1 μm) were thin and flat. Relatively large nuclei (open arrows) and scanty plasma were observed. d: Only sparse microvilli (open arrow) and endocytic vesicles (solid arrow) were seen in control cells (12 000×, bar=500 nm).

Electron microscopy Twenty days after 20-day treatment with gastrin, numerous microvilli appeared on the edge of IEC-6 cells, many endocytic vesicles occurred under the apical membrane, and columnar structures were seen in some cells. Control cells were thin and flat, the nuclei were relatively large with scanty of cytoplasm. Only sparse microvilli were observed on the edge of control cells, and few endocytic vesicles were noticed (Figure 2).

Effect of gastrin on villin expression in IEC-6 cells

mRNA level After exposure to gastrin for 6 hours, villin mRNA expression in gastrin-treated cells was stronger than that in control cells (Figure 3).

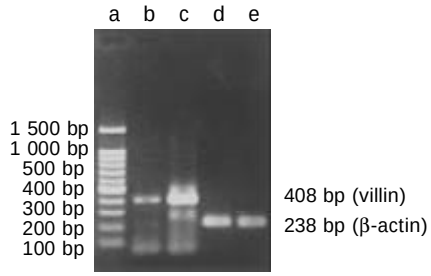

Figure 3 RT-PCR products from IEC-6 cells on agarose electrophoresis. a: Marker (brighter band: 500 bp), b: Control, c: Gastrin treated cells, d: β-actin(Control), e: β-actin (Gastrin).

Protein level On day 7 after treatment, plenty of cytoplasmic villins were observed obviously in gastrin-treated cells and few in control cells (Figure 4).

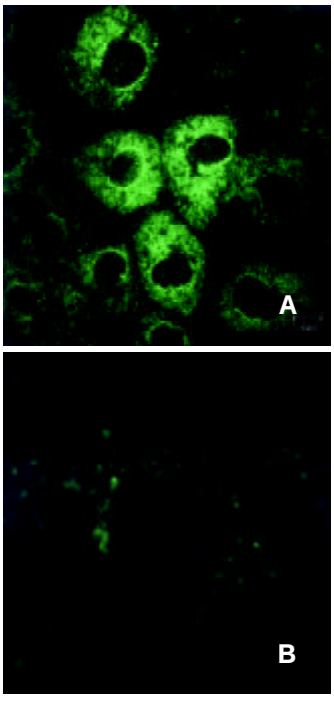

Figure 4 Villin expression in IEC-6 cells. a: Gastrin-treated cells (800×), b: Control cells (800×).

DISCUSSION

The barrier function of intestine is based on the physiological renewal or pathological repair of intestinal epithelia. The process includes proliferation, migration and terminal differentiation of the crypt cells. Development and differentiation of intestinal epithelia proceed in at least two distinct steps: the conversion of a nonepithelial cell to a protoepithelium, followed by a process of terminal differentiation. Terminal differentiation continues to occur in adult animals in the intestine[11], and is the last process. It not only indicates the completion of renewal or repair and the degree of differentiation, but also determines whether the new epithelia have physiological functions. There are two morphological characteristics in differentiated intestinal epithelia. One is the columnar shape cells with microvilli at the apical membrane, the other is organization of intestinal epithelial cells on a basement membrane into multicellular structures.

Intestinal epithelial cells (IEC-6) have features of undifferentiated small intestinal crypt cells[12], and are often used as a model of intestinal mucosal repair and cell differentiation[13,14]. The differentiation of intestinal crypt cell is a complex process, which is controlled by multiple factors. It has been known that several genes, such as p38 mitogen-activated protein kinases (p38MAPK)[15], Cdx gene family[16-20], pancreatic-duodenal homeobox (Pdxs) gene[21-23], sucrase-isomaltase (SI) gene[18,24,25], villin[26], activin[27], provoke cells towards the phenotype of differentiated villus enterocytes. Some cytokines such as epidermal growth factor (EGF)[6,7], insulin, insulin-like growth factor (IGF)-I and II[28,29], transforming growth factor (TGF)-β1[29], glucagon-like peptide-2 (GLP-2)[30] also have effects on the process. Astragalus injection could promote IEC-6 cell differentiation by inducing ODC activity and polyamine biosynthesis[31].

Moreover, the interaction between cells or between cells and extracellular matrix (ECM) also plays an important role in differentiation of IEC-6 cells[32]. Both humoral and matrix factors from intestinal mesenchyme are involved in intestinal epithelial differentiation and these factors appear to be organ specific[33,34]. And in conjunction with cell-cell contact and/or ECM, many regulatory cytokines such as enteroglucagon, interleukin-2 (IL-2), fibroblast growth factor (FGF), and EGF family members lead to specific differentiation signals[35]. Cdx2 gene provokes pleiotropic effects triggering cells towards the phenotype of differentiated villus enterocytes, but its expression is also modulated by basement membrane components[18].

Previous studies on differentiation of IEC-6 cells have found that laminin can lead the organization of IEC-6 cells on a basement membrane into multicellular structures[36], and the down-regulation of c-jun expression mediated by laminin might result in the event[37]. IEC-6 cell culture on Englebreth-Holm-Swarm (EHS) extracellular matrix proteins also displays morphological changes, correlated with loss of nuclear localization of c-myc protein and development of cell surface alkaline phosphatase (ALP) enzymatic activity[14]. And it has been documented that striking morphological and functional alterations can be induced by glucocorticoid in IEC-6 cells. These effects are consistent with the activation or modulation of multiple genes important in physiological functions of

absorptive villous cells[38]. Other data showed differentiation of IEC-6 cells was associated with upregulation of 11β-hydroxysteroid dehydrogenase (11β-HSD2) activity[39]. Members of the Cdx gene family play a fundamental role in both the establishment of the intestinal phenotype during development and maintenance of this phenotype via transcriptional activation of differentiated intestinal genes[40-43].

Our results showed that significantly morphological changes were observed in IEC-6 cells treated with gastrin in comparison with control group. The cells were in regular arrangement. Typically differentiated cell had an abundance of cytoplasm and a small nucleus containing nucleolus. There was a tendency to form microvilli and cytoskeleton-like structures were observed in the cytoplasm. Twenty-days after treatment of gastrin, a great number of microvilli appeared on the edges of the cells, and several cells displayed a simple columnar structure, and were fundamentally different from adenocarcinoma-like differentiation induced by Cdx1 transfection, which exhibited stratified columnar structure[16]. The absence of a multilayer structure indicated that these cells did not lose their contact inhibition characteristics, and they were not tumor cells. The existence of lots of endocytic vesicles as found under the apical membrane was also a typical feature of terminally differentiated enterocytes[11,44]. These results indicated that the cells might have the function of endocytosis as well as enterocytes. In control cells, only few microvilli were observed on the edge of cells with few endocytic vesicles.

Villin is one of the actin-binding proteins which have been reported to play a major role in the formation of the microvillus core bundle[45]. These proteins are known to modulate the dynamics of the actin cytoskeleton by mediating the state of actin polymerization and the spatial arrangement of actin protofilaments[46-49]. Villin may also respond to the apical calcium gradient, fragmenting actin microfilaments (MFs), and thus locally facilitate actin remodeling[50], and has a very important role in the alteration of cell morphology. The villin mRNA was expressed at high levels in the small intestine, to a lesser degree in the colon, and was not detected in the brain or liver[51]. The results indicate that villin is a kind of intestine-specific structure protein. In HT-29 cells, increase of villin mRNA levels was consistent with the process of enterocyte differentiation. Similarly, villin gene expression was induced in Caco-2 cells during postconfluence differentiation[51]. Immunolocalization studies on the distribution of the brush border-specific microvillar protein, villin, in human colonic mucosa indicated that localization of this protein was disrupted in certain dysplastic and neoplastic states. Thus, the expression and/or distribution of brush border-specific proteins such as villin may be useful markers for defects in the differentiation state of enterocytes[52].

Changes of cellular morphology and expression of mRNA and protein of villin in IEC-6 were investigated in order to observe the effects of gastrin on the differentiation of IEC-6 cells. The results showed that gastrin could obviously up-regulate villin expression at both mRNA and protein levels. These results were in consistent with the morphological alterations of these cells, and indicated that there was causality between the two events, i.e., gastrin induced characteristic features of differentiated enterocytes may account for its up-regulation to villin expression in IEC-6 cells. All these results indicate that gastrin can promote differentiation of IEC-6 cells, which is correlated to the up-regulation of villin expression.

ACKNOWLEDGEMENTS

We are grateful to Professor Peixun Wang, Associate Professors Weiwei Lei and Qin Xu, and Dr. Haibin Wang for their technical advice and excellent assistance.

REFERENCES

1 **Jonson L**, Bundgaard JR, Johnsen AH, Rourke IJ. Identification and expression of gastrin and cholecystokinin mRNAs from the turtle, Pseudemys scripta: evidence of tissue-specific tyrosyl sulfation(1). *Biochim Biophys Acta* 1999; **1435**: 84-93

2 **Wang JY**, McCormack SA, Viar MJ, Johnson LR. Secretin inhibits induction of ornithine decarboxylase activity by gastrin in duodenal mucosa and IEC-6 cells. *Am J Physiol* 1994; **267**(2Pt 1): G276-G284

3 **Zhang ZL**, Chen WW. Proliferation of intestinal crypt cells by gastrin-induced ornithine decarboxylase. *World J Gastroenterol* 2002; **8**: 183-187

4 **McCormack SA**, Wang JY, Viar MJ, Tague L, Davies PJ, Johnson LR. Polyamines influence transglutaminase activity and cell migration in two cell lines. *Am J Physiol* 1994; **267**(3Pt 1): C706-C714

5 **McCormack SA**, Wang JY, Johnson LR. Polyamine deficiency causes reorganization of F-actin and tropomyosin in IEC-6 cells. *Am J Physiol* 1994; **267**(3Pt 1): C715-C722

6 **McCormack SA**, Blanner PM, Zimmerman BJ, Ray R, Poppleton HM, Patel TB, Johnson LR. Polyamine deficiency alters EGF receptor distribution and signaling effectiveness in IEC-6 cells. *Am J Physiol* 1998; **274**(1Pt 1): C192-C205

7 **McCormack SA**, Ray RM, Blanner PM, Johnson LR. Polyamine depletion alters the relationship of F-actin, G-actin, and thymosin beta4 in migrating IEC-6 cells. *Am J Physiol* 1999; **276**(2Pt 1): C459-C468

8 **Teti D,** Visalli M, McNair H. Analysis of polyamines as markers of (patho)physiological conditions. *J Chromatogr B Analyt Technol Biomed Life Sci* 2002; **781**: 107-149

9 **Weiss TS,** Bernhardt G, Buschauer A, Thasler WE, Dolgner D, Zirngibl H, Jauch KW. Polyamine levels of human colorectal adenocarcinomas are correlated with tumor stage and grade. *Int J Colorectal Dis* 2002; **17**: 381-387

10 **Pinto D,** Robine S, Jaisser F, El Marjou FE, Louvard D. Regulatory sequences of the mouse villin gene that efficiently drive transgenic expression in immature and differentiated epithelial cells of small and large intestines. *J Biol Chem* 1999; **274**: 6476-6482

11 **Hikita C,** Vijayakumar S, Takito J, Erdjument-Bromage H, Tempst P, Al-Awqati Q. Induction of terminal differentiation in epithelial cells requires polymerization of hensin by galectin 3. *J Cell Biol* 2000; **151**: 1235-1246

12 **Quaroni A**, Wands J, Trelstad RL, Isselbacher KJ. Epithelioid cell cultures from rat small intestine. Characterization by morphologic and immunologic criteria. *J Cell Biol* 1979; **80**: 248-265

13 **Wroblewski R,** Jalnas M, Van Decker G, Bjork J, Wroblewski J, Roomans GM. Effects of irradiation on intestinal cells *in vivo* and *in vitro*. *Histol Histopathol* 2002; **17**: 165-177

14 **Wood SR,** Zhao Q, Smith LH, Daniels CK. Altered morphology in cultured rat intestinal epithelial IEC-6 cells is associated with alkaline phosphatase expression. *Tissue Cell* 2003; **35**: 47-58

15 **Houde M**, Laprise P, Jean D, Blais M, Asselin C, Rivard N. Intestinal epithelial cell differentiation involves activation of p38 mitogen-activated protein kinase that regulates the homeobox transcription factor Cdx2. *J Biol Chem* 2001; **276**: 21885-21894

16 **Soubeyran P**, Andre F, Lissitzky JC, Mallo GV, Moucadel V, Roccabianca M, Rechreche H, Marvaldi J, Dikic I, Dagorn JC, Iovanna JL. Cdx1 promotes differentiation in a rat intestinal epithelial cell line. *Gastroenterology* 1999; **117**: 1326-1338

17 **Freund JN**, Domon-Dell C, Kedinger M, Duluc I. The Cdx-1 and Cdx-2 homeobox genes in the intestine. *Biochem Cell Biol* 1998; **76**: 957-969

18 **Lorentz O**, Duluc I, Arcangelis AD, Simon-Assmann P, Kedinger M, Freund JN. Key role of the Cdx2 homeobox gene in extracellular matrix-mediated intestinal cell differentiation. *J Cell Biol* 1997; **139**: 1553-1565

19 **Taylor JK**, Levy T, Suh ER, Traber PG. Activation of enhancer elements by the homeobox gene Cdx2 is cell line specific. *Nucleic Acids Res* 1997; **25**: 2293-2300

20 **Moucadel V,** Soubeyran P, Vasseur S, Dusetti NJ, Dagorn JC, Iovanna JL. Cdx1 promotes cellular growth of epithelial intestinal cells through induction of the secretory protein PAP I. *Eur J Cell Biol* 2001; **80**: 156-163

21 **Yamada S**, Kojima H, Fujimiya M, Nakamura T, Kashiwagi A, Kikkawa R. Differentiation of immature enterocytes into

enteroendocrine cells by Pdx1 overexpression. *Am J Physiol Gastrointest Liver Physiol* 2001; **281**: G229-G236

22 **Yoshida S,** Kajimoto Y, Yasuda T, Watada H, Fujitani Y, Kosaka H, Gotow T, Miyatsuka T, Umayahara Y, Yamasaki Y, Hori M. PDX-1 induces differentiation of intestinal epithelioid IEC-6 into insulin-producing cells. *Diabetes* 2002; **51**: 2505-2513

23 **Kojima H,** Nakamura T, Fujita Y, Kishi A, Fujimiya M, Yamada S, Kudo M, Nishio Y, Maegawa H, Haneda M, Yasuda H, Kojima I, Seno M, Wong NC, Kikkawa R, Kashiwagi A. Combined expression of pancreatic duodenal homeobox 1 and islet factor 1 induces immature enterocytes to produce insulin. *Diabetes* 2002; **51**: 1398-1408

24 **Suh E**, Traber PG. An intestine-specific homeobox gene regulates proliferation and differentiation. *Mol Cell Biol* 1996; **16**: 619-625

25 **Taylor JK**, Boll W, Levy T, Suh E, Siang S, Mantei N, Traber PG. Comparison of intestinal phospholipase A / lysophospholipase and sucrase-isomaltase genes suggest a common structure for enterocyte-specific promoters. *DNA Cell Biol* 1997; **16**: 1419-1428

26 **Braunstein EM**, Qiao XT, Madison B, Pinson K, Dunbar L, Gumucio DL. Villin: A marker for development of the epithelial pyloric border. *Dev Dyn* 2002; **224**: 90-102

27 **Sonoyama K**, Rutatip S, Kasai T. Gene expression of activin, activin receptors, and follistatin in intestinal epithelial cells. *Am J Physiol Gastrointest Liver Physiol* 2000; **278**: G89-G97

28 **Jehle PM**, Fussgaenger RD, Blum WF, Angelus NK, Hoeflich A, Wolf E, Jungwirth RJ. Differential autocrine regulation of intestine epithelial cell proliferation and differentiation by insulin-like growth factor (IGF) system components. *Horm Metab Res* 1999; **31**: 97-102

29 **Kojima H**, Hidaka H, Matsumura K, Fujita Y, Nishio Y, Maegawa H, Haneda M, Yasuda H, Fujimiya M, Kikkawa R, Kashiwagi A. Concerted regulation of early enterocyte differentiation by insulin-like growth factor I, insulin, and transforming growth factor-beta1. *Proc Assoc Am Physicians* 1998; **110**: 197-206

30 **Kitchen PA**, Fitzgerald AJ, Goodlad RA, Barley NF, Ghatei MA, Legon S, Bloom SR, Price A, Walters JR, Forbes A. Glucagon-like peptide-2 increases sucrase-isomaltase but not caudal-related homeobox protein-2 gene expression. *Am J Physiol Gastrointest Liver Physiol* 2000; **278**: G425-G428

31 **Zhang ZL,** Chen WW. Effect of astragalus injection in promoting IEC-6 cell differentiation through activating ornithine decarboxylase. *Zhongguo Zhongxiyi Jiehe Zazhi* 2002; **22**: 439-443

32 **Wolpert S**, Wong ML, Bass BL. Matrix alters the proliferative response of enterocytes to growth factors. *Am J Surg* 1996; **171**: 109-112

33 **Ferretti E**, Li S, Wang J, Post M, Moore A. Mesenchymal regulation of differentiation of intestinal epithelial cells. *J Pediatr Gastroenterol Nutr* 1996; **23**: 65-73

34 **Karlsson L**, Lindahl P, Heath JK, Betsholtz C. Abnormal gastrointestinal development in PDGF-A and PDGFR-α deficient mice implicates a novel mesenchymal structure with putative instructive properties in villus morphogenesis. *Development* 2000; **127**: 3457-3466

35 **Burgess AW**. Growth control mechanisms in normal and transformed intestinal cells. *Philos Trans R Soc Lond B Biol Sci* 1998; **353**: 903-909

36 **Olson AD**, Pysher T, Bienkowski RS. Organization of intestinal epithelial cells into multicellular structures requires laminin and functional actin microfilaments. *Exp Cell Res* 1991; **192**: 543-549

37 **Wolpert SI**, Lally KM, Li J, Wang JY, Bass BL. Extracellular matrix modulates enterocyte growth via downregulation of c-jun but is independent of p21 and p27 expression. *J Gastrointest Surg* 1999; **3**: 319-324

38 **Quaroni A**, Tian JQ, Goke M, Podolsky DK. Glucocorticoids have pleiotropic effects on small intestinal crypt cells. *Am J Physiol* 1999; **277**(5Pt 1): G1027-G1040

39 **Pacha J,** Lisa V, Miksik I. Effect of cellular differentiation on 11beta-hydroxysteroid dehydrogenase activity in the intestine. *Steroids* 2002; **67**: 119-126

40 **Suh E**, Chen L, Taylor J, Traber PG. A homeodomain protein related to caudal regulates intestine-specific gene transcription. *Mol Cell Biol* 1994; **14**: 7340-7351

41 **Moucadel V,** Totaro MS, Dell CD, Soubeyran P, Dagorn JC, Freund JN, Iovanna JL. The homeobox gene Cdx1 belongs to the p53-p21(WAF)-Bcl-2 network in intestinal epithelial cells. *Biochem Biophys Res Commun* 2002; **297**: 607-615

42 **Soubeyran P**, Haglund K, Garcia S, Barth BU, Iovanna J, Dikic I. Homeobox gene Cdx1 regulates Ras, Rho and PI3 kinase pathways leading to transformation and tumorigenesis of intestinal epithelial cells. *Oncogene* 2001; **20**: 4180-4187

43 **Patterson AP,** Chen Z, Rubin DC, Moucadel V, Iovanna JL, Brewer HB Jr, Eggerman TL. Developmental regulation of apolipoprotein B mRNA editing is an autonomous function of small intestine involving homeobox gene Cdx1. *J Biol Chem* 2003; **278**: 7600-7606

44 **Vijayakumar S,** Takito J, Hikita C, Al-Awqati Q. Hensin remodels the apical cytoskeleton and induces columnarization of intercalated epithelial cells: processes that resemble terminal differentiation. *J Cell Biol* 1999; **144**: 1057-1067

45 **Athman R,** Louvard D, Robine S. The epithelial cell cytoskeleton and intracellular trafficking. III. How is villin involved in the actin cytoskeleton dynamics in intestinal cells? *Am J Physiol Gastrointest Liver Physiol* 2002; **283**: G496-G502

46 **Glenney JR Jr**, Bretscher A, Weber K. Calcium control of the intestinal microvillus cytoskeleton: its implications for the regulation of microfilaments organizations. *Proc Natl Acad Sci U S A* 1980; **77**: 6458-6462

47 **Mooseker MS**, Graves TA, Wharton KA, Falco N, Howe CL. Regulation of microvillus structure: calcium-dependent solation and cross-linking of actin filaments in the microvilli of intestinal epithelial cells. *J Cell Biol* 1980; **87**(3Pt 1): 809-822

48 **Ferrary E,** Cohen-Tannoudji M, Pehau-Arnaudet G, Lapillonne A, Athman R, Ruiz T, Boulouha L, El Marjou F, Doye A, Fontaine JJ, Antony C, Babinet C, Louvard D, Jaisser F, Robine S. *In vivo*, villin is required for Ca(2+)-dependent F-actin disruption in intestinal brush borders. *J Cell Biol* 1999; **146**: 819-830

49 **Coluccio LM**, Bretscher A. Reassociation of microvillar core proteins: making a microvillar core *in vitro*. *J Cell Biol* 1989; **108**: 495-502

50 **Vidali L,** Hepler PK. Actin and pollen tube growth. *Protoplasma* 2001; **215**: 64-76

51 **Hodin RA**, Shei A, Meng S. Transcriptional activation of the human villin gene during enterocyte differentiation. *J Gastrointest Surg* 1997; **1**: 433-438

52 **Carboni JM,** Howe CL, West AB, Barwick KW, Mooseker MS, Morrow JS. Characterization of intestinal brush border cytoskeletal proteins of normal and neoplastic human epithelial cells. A comparison with the avian brush border. *Am J Pathol* 1987; **129**: 589-600

Edited by Ren SY and Wang XL

P.O.Box 2345, Beijing 100023,China
Fax: +86-10-85381893
E-mail: wjg@wjgnet.com www.wjgnet.com

World J Gastroenterol 2003;9(8):1791-1794
World Journal of Gastroenterology
 ISSN 1007-9327

• BASIC RESEARCH •

Role of nucleation of bile liquid crystal in gallstone formation

Hai-Ming Yang, Jie Wu, Jin-Yi Li, Lin Gu, Min-Fei Zhou

Hai-Ming Yang, Jie Wu, Lin Gu, Department of Physics and Mathematics, Kunming Medical College, Kunming 650031, Yunnan Province, China
Jin-Yi Li, Department of Physics, Yunnan Normal University, Kunming 650092, Yunnan Province, China
Min-Fei Zhou, Department of Hepato-biliary Surgery, The Second Affiliated Hospital of Kunming Medical College, Kunming 650101, Yunnan Province, China
Supported by the National Natural Sciencce Foundation of China, No. 39960024, and Applied Basic Research Fund of Yunnan Provincial Science and Technology Committee, No. 1999C 0064M and Science Foundation of Yunnan Education Committee, No. 9912073
Correspondence to: Hai-Ming Yang, Physics and Mathematics Department of Kunming Medical College, 191 West Renming Road, Kunming 650031, Yunnan Province, China. yanghaiming88@hotmail.com
Telephone: +86-871-5338812
Received: 2003-01-04 **Accepted:** 2003-02-16

Abstract

AIM: To explore the role of bile liquid crystal in the process of gallbladder stone formation and to provide bases for preventing and treating cholelithiasis.

METHODS: 46 guinea pigs, half males and half females, were randomly divided into control group and stone-causing group. Normal feed and stoneleading feed were used respectively to raise guinea pigs in the control group and stone-causing group. The guinea pigs were killed in three batches during the raising period. Under polarizing microscope, the pattern changes of bile liquid crystal in the gallbladder biles of the guinea pigs in the control group and stone-causing group were dynamicly observed respectively in single-blind trial.

RESULTS: It was found that there were few crystals in the guinea pigs' biles of the control group, and their Malta cross was small and scattered, and existed in single form. With the increase of the feeding days, bile liquid crystals grew and Malta cross became bigger with their distribution densified, denser somewhere, but always existed in single form. While those of the stone-causing group had more bile liquid crystals, Malta cross was big and merged in strings. With the increase of the feeding days, bile liquid crystals grew in amount and strings of Malta cross increased and became bigger. The crosses in strings were arranged more and more regularly and they gradually changed into stone crystals.

CONCLUSION: Formation of gallbladder stone is a process of nucleation from different substances, and the causing-stone gallbladder bile is a constantly supersaturated solution, and bile liquid crystal is a nucleation factor in the formation of gallbladder stones. The process of nucleation includes gathering, merging and phase-changing of bile liquid crystals. The process of gathering, merging of bile liquid crystal is the key to nucleation.

Yang HM, Wu J, Li JY, Gu L, Zhou MF. Role of nucleation of bile liquid crystal in gallstone formation. *World J Gastroenterol* 2003; 9(8): 1791-1794
http://www.wjgnet.com/1007-9327/9/1791.asp

INTRODUCTION

Bile liquid crystal is a type of liquid crystal in the living beings' bile. Since American scholar Olszewski *et al*[1] found the substance of liquid crystal in the bile liquid of human body in 1973, some scholars at home and abroad have explored the matter of liquid crystal in the living beings' bile[2-4], but the relation between bile liquid crystal and formation of gallbladder stone has not been clarified so far. In order to explore the role of bile crystal in the process of gallbladder-stone formation and to provide certain bases for the prevention and treatment of gallbladder stone, we made dynamic observations and studied on the nucleation of bile liquid crystal in gallbladder stone through animal tests in guinea pigs.

MATERIALS AND METHODS

Materials

46 guinea pigs (provided by the animal branch of the Scientific Research Department in Kunming Medical College, with qualified animal testing certificate issued by Yunnan Province), each weighing about 300 grams, half males and half females, were randomly divided into control group (n=23) and stone-causing group (n=23).

Methods

Animal raising The control group was given normal feed which was provided by the animal branch of the Scientific Research Department in Kunming Medical College, while the stone-causing group was given stoneleading feed. The two groups were separately raised in flocks, with free access to water containing 1 % vitamin C.

Stone-causing feed The components of the stone-causing feed were as follows: starch 25 %, bran 25 %, glucose 12 %, lard 1.5 %, cholesterol 1.5 %, normal feed 35 %[5]. They were mixed evenly and made granule with feed machine.

Sample preparation Guinea pigs were killed in three batches. The first batch was killed after raised for 10 days, with 5 pigs in each group, totally 10 pigs in the 2 groups. The 2nd batch was killed after raised for 25 days, with 5 pigs in each group, totally 10 pigs in the 2 groups. The 3rd batch was killed after raised for 60 days, with 13 pigs in each group, totally 26 pigs in the 2 groups. The pigs were whacked at head to stupor with a blood vessel forceps, immediately cut open belly and their cystic duct was blocked with a blood vessel forceps to take out gallbladder and all bile. The bile was centrifugalized for 30 minutes with a China-made TGL-16B bench centrifuge, 4 000 r/min, and observed under polarizing microscope.

Polarizing microscope observation A China-made W-104 micro-sample advancer (precision of 0.2 μL) was used to stratify the centrifuged bile and drip 6.0 μL of it on a carrier flake, then it was covered with the cover-glass and the bile naturally spread out to form slices. Under an advanced polarizing microscope (BHSP model of Olympus, Japan), the pattern changes of the bile liquid crystal in the process of gallbladder stone formation were observed.

RESULTS

Patterns change of bile liquid crystals in control group

Under the perpendicular polarized microscope, the

morphological changes of bile liquid crystal in the gallbladder bile of guinea pigs in the control group were observed, and it was found that there were few matters of liquid crystal in gallbladder bile, and that the interference pattern, named Malta cross, was small and scattered, in single form. With the increase of the feeding days, bile liquid crystals grew larger and Malta cross became bigger with their distribution densified unevenly, but always existed in single form, as shown in Figure 1 (a), (b), (c) and (d). No regularly shaped stone crystal was found in the biles.

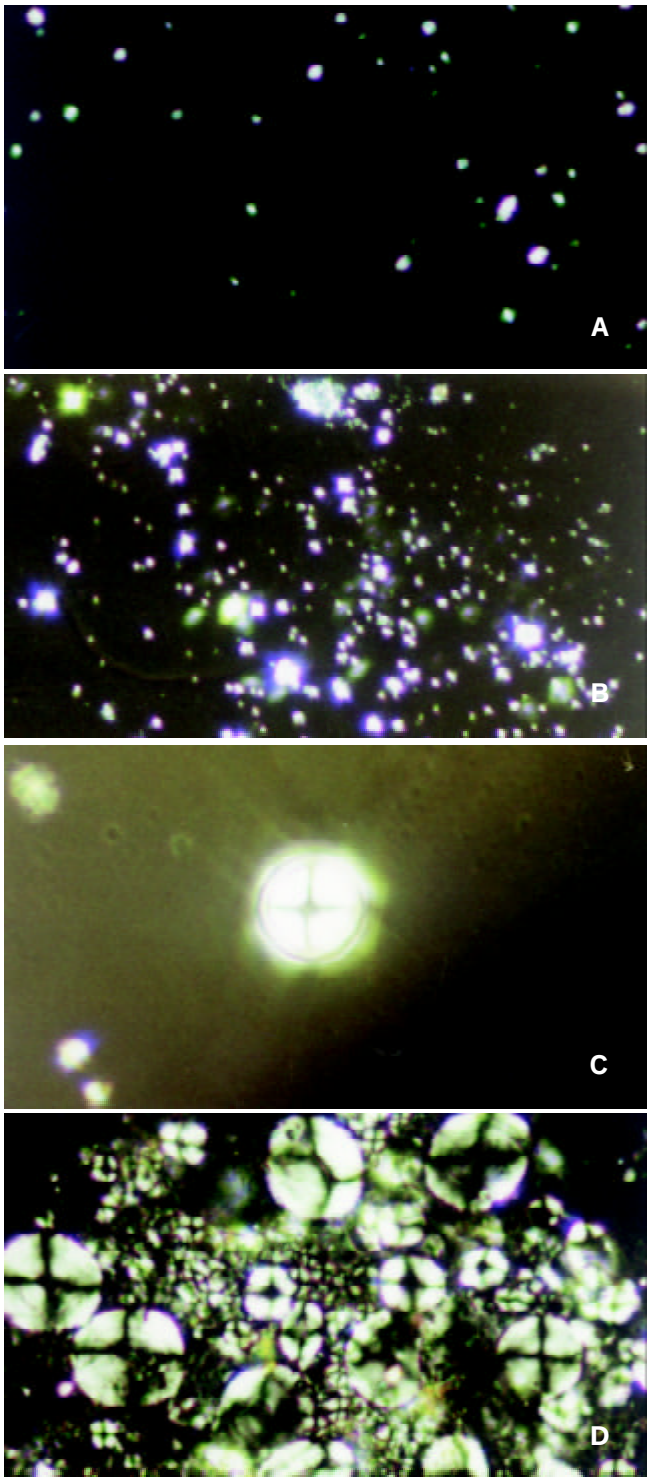

Figure 1 Malta cross showed in bile liquid crystals in gallbladders of guinea pigs in the control group: (a) Small and scattered crosses (10 days, ×400). (b) The crosses gradually grew in size and number (25 days, ×400). (c) Single big crosses (25 days, ×400). (d) Densely distributed crosses (60 days, ×400).

The pattern changes of bile liquid crystals in the stone-causing group

Under the polarizing microscope, the morphological changes of bile liquid crystal in guinea pigs' gallbladders in stone-causing group were observed, and it was found that there were more matters of liquid crystal in gallbladder biles, and that the interference pattern, Malta cross was big and merged into strings. With the increase of the feeding days, bile liquid crystals grew in number and strings of Malta crosses increased and became bigger. The crosses in strings were arranged more regularly so that they gradually phase-changed into stone crystals, as shown in Figure 2 (a), (b), (c) and (d). It exhibited variously shaped stone crystals in the biles, as shown in Figure 3 (a), (b), (c) and (d).

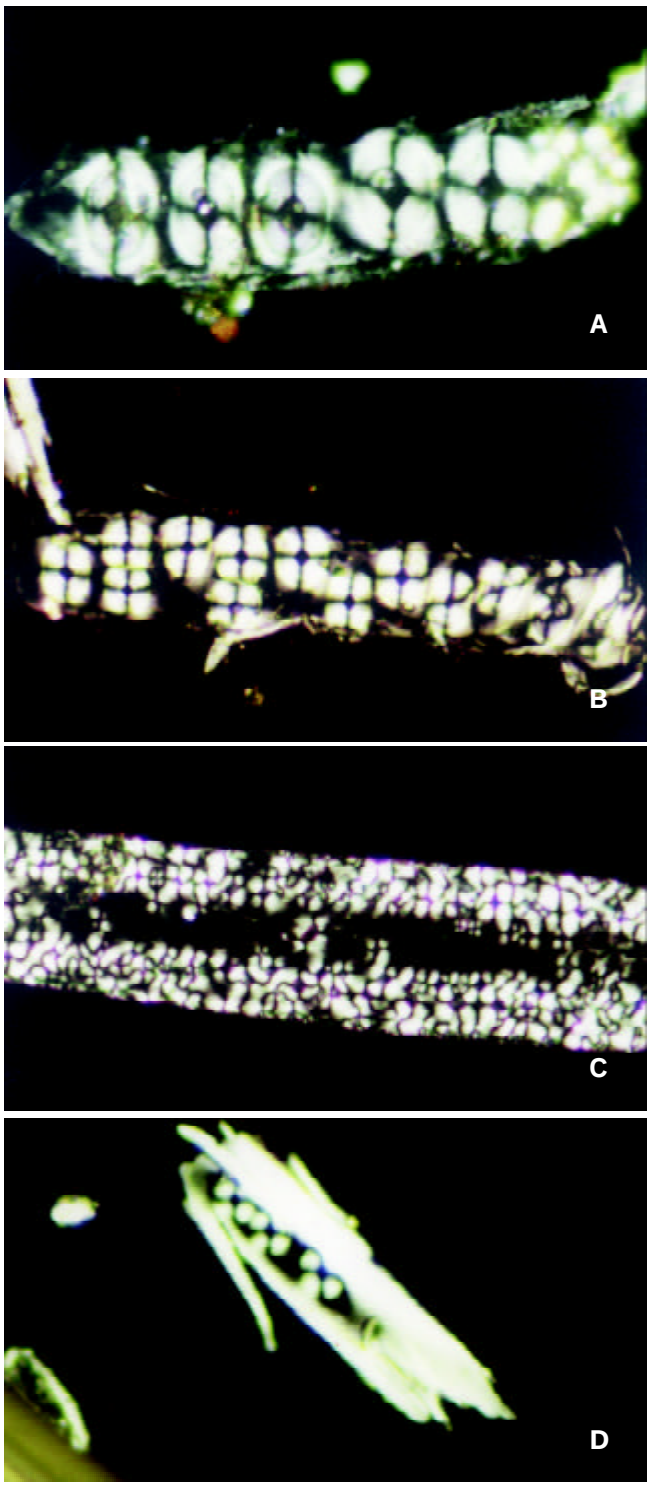

Figure 2 Malta cross shown in bile liquid crystals in gallblad-

ders of guinea pigs in the stone-causing group: (a) The cross merged into strings (10 days, ×400). (b) Gradually growing strings of the cross (25 days, ×200). (c) Strings of the cross in phase-changing (60 days, ×400). (d) Stone crystals nucleated by strings of the cross (60 days, ×200).

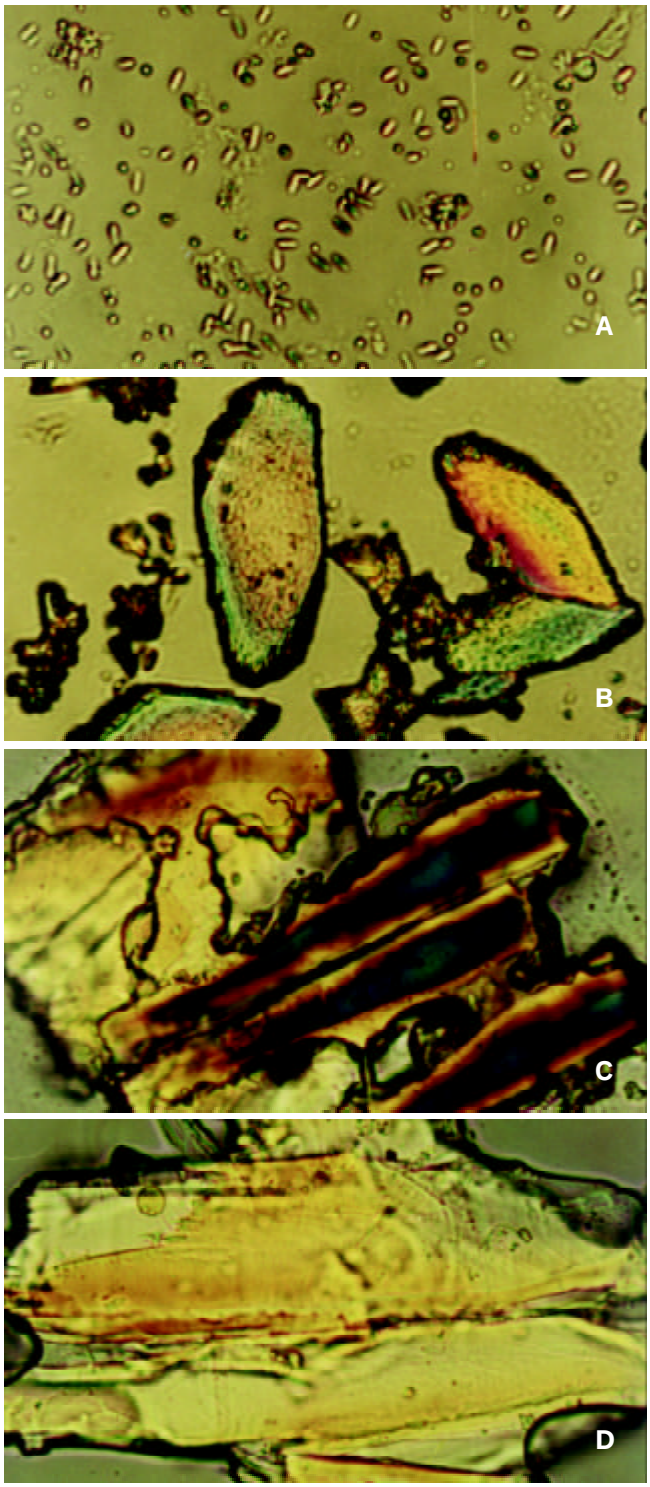

Figure 3 Gallbladder stone crystals in bile of the stone-causing group.

DISCUSSION

The cause of gallbladder stone is very complicated, various factors are involved[5-9]. The basic factor is now considered to be the change of compositions and physical-chemistry characteristics of biles, which results in cholesterol in the state of super-saturation in the bile. And it is very likely to form crystals, which is then deposited to form gallbladder stones. It also causes imbalance between nucleation-leading factors and antinucleation factors and abnormal function of the gallbladder and so on[10-19]. From the viewpoint of crystallogeny, in a system of solution, the precondition for solute to be separated out and to form crystal is that the solute in the system must be in the state of super-saturation, which is an unstable state in thermodynamics. Only in this state, can the solute be crystallized and separated out. The formation of crystals has two steps of nucleation and crystallization, it firstly forms a crystalline nucleus containing hundreds of molecules, then crystals grow. In a system of solution, spontaneous nucleation of solute often requires a very high degree of saturation, the supersaturated solution in this state is called unstably supersaturated solution. When a certain type of special nucleating factors is added, supersaturated solution of a relatively low degree also can produce nucleation, which is called heterogeneous nucleation, and the supersaturated solution in this state is called substably supersaturated solution[20,21]. Homogeneous nucleation of bile cholesterol requires a very high degree of saturation (estimated at about 300 %), which is not possible to occur in human body, and even less possible in guinea pigs' body. So the formation of gallbladder-stone should be a process of heterogeneous nucleation, stone-causing gallbladder bile should be a substably supersaturated solution, and bile liquid crystal should be a type of nucleating factors for gallbladder stones.

As we observed under the polarizing microscope, there were many substances of liquid crystal in the gallbladder bile of the guinea pigs in the stone-causing group, which were big and string of Malta crosses. With the increase of the feeding days, bile liquid crystals grew in number, more and more strings of Malta cross appeared and steadily became bigger and bigger, and their arrangement became more and more regular, and gradually phase-changed into stone crystals. These have proved that the formation of gallbladder stone is indeed a process of heterogeneous nucleation, and stone-causing gallbladder bile is a type of substably supersaturated solution, and that bile liquid crystal is a type of nucleating factors in gallbladder-stone. Its process of nucleation is such that bile liquid crystals get together, merge and phase change. In another word, single Malta crosses assemble into strings, then merge as slices, and finally phase-change into crystals. The assemblage and merger of bile liquid crystals are the key for nucleation. Although there were also substances of liquid crystal existing in gallbladder biles in the control group and bile crystals also increased with feeding time, they neither assembled nor merged, and Malta crosses always existed in single forms which were unable to nucleate to form stone. If some way can be found to prevent or retard the assemblage and merger of bile liquid crystals, i. e., formation of the nucleus, it will be of a great significance in theory and practice for prevention and treatment of cholelithiasis.

Cholesterol can not dissolve in water, but it can dissolve in bile. The concentration of cholesterol in bile is about 10-20 mmol/L, this concentration is about 10^6 times[22] denser than that of the solubility of cholesterol in water. Studies concerned pointed out that cholesterol in bile maintained its state of dissolution in forms of micelle and vesicle. Micelle is the polymer of cholesterol, phosphatide and cholate, while vesicle is the compound of cholesterol and phosphatide[23-31]. These two form a system of thermodynamic balance in bile so that they are interlinked and interconverted, and play the role of modulation for dissolution and separation of cholesterol. Under the effect of nucleation-leading factors and antinucleation factors in bile, vesicles in bile assemble, merge and separate out crystalline nuclei of cholesterol which then gradually grow up to form stones[32]. As we observed under the polarizing microscope, single Malta cross in bile liquid crystal of guinea pigs in stone-causing group, gradually assembled into strings,

then merged into slices, and finally phase-changed into stone crystals. The present study supports the above viewpoints from the studies of morphology. Whether bile crystal is such a kind of vesicles or vesicles aggregate and what factors cause or stop bile liquid crystal assembling and merging, still need to be further studied.

REFERENCES

1 **Olszewski MF**, Holzbach RT, Saupe A, Brown GH. Liquid crystals in human bile. *Nature* 1973; **242**: 336-337
2 **Yang HM,** Wu J, Li JY, Zhou JL, He LJ, Xu XF. Optic properties of bile liquid crystals in human body. *World J Gastroenterol* 2000; **6**: 248-251
3 **Yang H**, Wu J, Cu L, Zhou J, He L, Cao S. The optical properties of bile liguid crystals in organisms. *Chin J Biomedi Engin* 1999; **8**: 67-68
4 **Savina LV**, Kokueva OV, Golovanva ES, Kadygrob GV. Crystallooptic structures of bile in chronic acalculous cholecystitis. *Eksp Klin Gastroenterol* 2002; **128**: 59-62
5 **Han TQ,** Jiang ZY, Zhang SD. Research progress in formation of gallstone. *Zhongguo Shiyong Waike Zazhi* 2001; **21**: 123-125
6 **Zhang SD,** Han TQ. Prospects for studies of gallstone. *Waike Lilun Yu Shijian* 1999; **4**: 5-6
7 **Nishioka T,** Tazuma S, Yamashita G, Kajiyama G. Partial replacement of bile salts causes marked changes of cholesterol crystallization in supersaturated model bile systems. *Biochem J* 1999; **340**: 445-451
8 **Wang DQ,** Cohen DE, Lammert F, Carey MC. No pathophysiologic relationship of soluble biliary proteins to cholesterol crystallization in human bile. *J Lipid Res* 1999; **40**: 415-425
9 **Rubin M**, Pakula R, Konikoff FM. Microstructural analysis of bile: relevance to cholesterol gallstone pathogenesis. *Histol Histopathol* 2000; **15**: 761-770
10 **Wu ZD**. Surgery. 5th ed. Beijing: *People's Health Publishing House* 2002: 617-619
11 **Yu JP,** Sheng ZX, Luo HS. Practical Digestive Diseases. 1st ed. Beijing: *Science Press* 1999: 1228-1232
12 **Yang GH**. Pathology. 5th ed. Beijing: *People's Health Publishing House* 2001: 217-218
13 **Zhao JC,** Shu Y, Cheng NS, Xiao LJ, Zhu H. Changes of cholesterol metabolism in cholesterol gallstone formation in the rabbit. *Zhongguo Putong Waike Zazhi* 2000; **9**: 124-128
14 **Li QR,** Gong YH, Zhou JP, Gao Q, Pang BZ. Formation of gallstones by feeding on high cholesterol diet. *Zhonghua Linchuang Ganzangbingxue Zazhi* 2002; **18**: 320-321
15 **Zhang JH,** Yang KZ, Han BL. The kinetic mechanism of gallstone formation. *Zhongguo Putong Waike Zazhi* 2001; **16:** 424-426
16 **Ye SA,** Tang WH. Research progress in gallbladder's effect in the process of gallstone formation. *Guowai Yixue Waike Fence* 2001; **28**: 221-223
17 **Liu CL,** Higuchi WI. Cholesterol crystallite nucleation in supersaturated model biles from a thermodynamic standpoint. *Biochim Biophys* 2002; **1588**: 15-25
18 **Jirsa M,** Groen AK. Role of biliary proteins and non-protein factors in kinetics of cholesterol crystallisation and gallstone growth. *Front Biosci* 2001; **6**: E154-167
19 **Qin YL,** Tang WH. Research progress in glycoprotein in gallstone. *Guowai Yixue Waike Fence* 1999; **26**: 344-347
20 **Zhang KC,** Zhang LH. Crystal Growth Science and Technology. 2nd Edition. Beijing: *Science Press* 1997: 178-182
21 **Cheng JZ**. Modern Crystal Chemistry-Theories and Technique. 1st Edition. Beijing: *Higher Education Press* 2001: 126-131
22 **Zhang QY**. Diseases of the Biliary System. 1st Edition. Nanjing: *Jiangsu Science and Technology Press* 1997: 167
23 **Luk A**S, Kaler EW, Lee SP. Structural mechanisms of bile salt-induced growth of small unilamellar cholesterol-lecithin vescicles. *Biochemistry* 1997; **36**: 5633-5644
24 **Prigun NP,** Korolevich AN. Changes in human biliary vesicle sizes in pathological states. *Biofizika* 2002; **47**: 1095-1100
25 **Portincasa P,** Venneman NG, Moschetta A, van den Berg A, Palasciano G, vanBerge-Henegouwen GP, van Erpecum KJ. Quantitation of cholesterol crystallization from supersaturated model bile. *J Lipid Res* 2002; **43**: 604-610
26 **Venneman NG,** Huisman SJ, Moschetta A, vanBerge-Henegouwen GP, van Erpecum KJ. Efects of hydrophobic and hydrophilic bile salt mixtures on cholesterol crystallization in model biles. *Biochim Biophys Acta* 2002; **1583**: 221-228
27 **Moschetta A,** vanBerge-Henegouwen GP, Portincasa P, Palasciano G, van Erpecum KJ. Cholesterol crystallization in model biles: effects of bile salt and phospholipid species composition. *J Lipid Res* 2001; **42**: 1273-1281
28 **Moschetta A**, Frederik PM, Portincasa P, vanBerge-Henegouwen GP, van Erpecum KJ. Incorporation of cholesterol in sphingomyelin-phosphatidylcholine vesicles has profound effects on detergent-induced phase transitions. *J Lipid Res* 2002; **43**: 1046-1053
29 **Moschetta A**, vanBerge-Henegouwen GP, Portincasa P, Renooij WL, Groen AK, van Erpecum KJ. Hydrophilic bile salts enhance differential distribution of sphingomyelin and phosphatidylcholine between micellar and vesicular phases: potential implications for their effects *in vivo*. *J Hepatol* 2001; **34**: 492-499
30 **Eckhardt ER**, Moschetta A, Renooi j W, Goerdayal SS, van Berge-Henegouwen GP, van Erpecum KJ. Asymmetric distribution of phosphatidylcholine and sphingomyelin between micellar and vesicular phases. Potential implications for canalicular bile formation. *J Lipid Res* 1999; **40**: 2022-2033
31 **Sakomoto M**, Tazuma S, Chayama K. Less hydrophobic phosphatidylcholine species simplify biliary vesicle morphology, but induce bile metastability with a broad spectrum of crystal forms. *Biochem J* 2002; **362**: 105-112
32 **Gantz DL,** Wang DQ, Garey MC, Small DM. Cryoelectron microscopy of a nucleating model bile in vitreous ice: formation of primordial vesicles. *Biophys J* 1999; **76**: 1436-1451

Edited by Xu XQ and Zhu LH

P.O.Box 2345, Beijing 100023,China
Fax: +86-10-85381893
E-mail: wjg@wjgnet.com www.wjgnet.com

World J Gastroenterol 2003;9(8):1795-1798
World Journal of Gastroenterology
 ISSN 1007-9327

• BASIC RESEARCH •

Toxicities and therapeutic effect of 5-fluorouracil controlled release implant on tumor-bearing rats

Yin-Cheng He, Ji-Wei Chen, Jun Cao, Ding-Yu Pan, Jian-Guo Qiao

Yin-Cheng He, Ji-Wei Chen, Jun Cao, Ding-Yu Pan, Jian-Guo Qiao, Department of General Surgery, Zhongnan Hospital, Wuhan University, Wuhan 430071, Hubei Province, China
Correspondence to: Dr. Yin-Cheng He, Department of General Surgery, Zhongnan Hospital, Wuhan University, Wuhan 430071, Hubei Province, China. w030508h@public.wh.hb.cn
Telephone: +86-27-67812963
Received: 2002-12-10 **Accepted:** 2003-01-16

Abstract

AIM: To investigate the toxicities, biodistribution and anticancer effect of 5-fluorouracil controlled release implant (5-FUCI) on Walker 256 carcinosarcoma cells in Wistar rats.

METHODS: Experiment 1: Wistar rats were randomly divided into three groups (27 rats per group). Blank implant was implanted in left lobe of the liver, and rats were treated with saline solution (in group A) or 5-fluorouracil (subcutaneous injection, group B). 5-FUCI was inserted in left lobe of the liver (group C). The gastrointestinal and hematological toxicities were observed and contents of element F in group C were assayed. Experiment 2: on day 6 after Walker-256 carcinosarcoma transplantation in left lobe of the liver, 5-FUCI was implanted in right lobe of the liver (group E) or left lobe (group F), and rats in control group (group D) were inserted blank implant. Tumor inhibition rate and survival time were investigated.

RESULTS: 5-FUCI showed no obvious toxic effect, extraction of Evan's blue from gastrointestinal tissue was normal, the peripheral white blood cells and bone marrow nucleated cells were not reduced, compared with control group ($P>0.05$). Histological examination revealed that there were no visible changes in small intestinal mucosa, The concentration of 5-fluorouracil in left lobe of the liver was 9.84, 28, 34 times as much as those of right lobe of the liver, heart and kidney respectively after the implantation in group C. They kept a high level of fluorouracil in left lobe of the liver, ranging from (4.414±0.482) % to (7.800±0.804) %, for eight weeks. Survival days were 28.0±2.2, 30.0±3.2 and 38.7±6.7 d in group D, E and F, respectively.

CONCLUSION: 5-FUCI shows no obvious toxicities to gastrointestinal tract and myelotoxicity. After implantation, it kept a high level of 5- fluorouracil in surrounding tissues of the implant for eight weeks. Its antitumor effect on Walker-256 carcinosarcoma is demonstrated.

He YC, Chen JW, Cao J, Pan DY, Qiao JG. Toxicities and therapeutic effect of 5-fluorouracil controlled release implant on tumor-bearing rats. *World J Gastroenterol* 2003; 9(8): 1795-1798
http://www.wjgnet.com/1007-9327/9/1795.asp

INTRODUCTION

5-Fluorouracil (5-FU) is one of the most widely used chemotherapeutic drugs in the treatment of malignant gastrointestinal cancers[1-7], but its use has been limited by is systemic toxicities, i.e. severe gastrointestinal toxicities, hematological side effects, and severe disturbance in bone marrow[8,9]. Moreover, 5-FU has a serum half-life of only 10 minutes[10-13], further limiting its usefulness. To maximize the therapeutic effect of 5-FU and minimize any adverse effect, we developed silicone as a polymer matrix, and 5-FU as a model drug to prepare a controlled-release implant of 5-fluorouracil (5-FUCI, Figure 1) for delivering agents directly to the site of the tumor. Tube-type pellets made of silastic elastomer were of 2 mm in outer diameter, 0.5 mm in wall thickness and 25 mm in length. Per pellet contained 13.2 mg of 5-FU. The daily delivery dose of 5-FU was approximately 30 $\mu g \cdot d^{-1}$, zero-order release profiles lasted for 24 weeks *in vitro* (unpublished data). This study investigated its toxicities as compared with standard systemic therapy, the biodistribution of 5-FU after 5-FUCI was implanted in the liver of rats, and therapeutic effect on the Walker-256 carcinosarcoma in the liver of Wistar rats. Two experiments were performed.

MATERIALS AND METHODS

Experiment 1: Toxicity evaluation and biodistribution of 5-FUCI

5-FUCI and blank implant 5-FUCI and blank implants were prepared and kindly provided by Prof. Huaiying Wu (from Shanghai Medical University, China). 5-Fu was purchased from Shanghai Haipu Pharmaceutical Company.

Animals Adult male Wistar rats, weighing 300-320 g, were obtained from the Experimental Animal Center of Wuhan University, China. They were housed in stock cages (3 rats per cage) and given free access to water and the commercial laboratory rodent diet. Twelve hours prior to experiment, the rats were fasted, but allowed free access to water.

Implantation and treatment The rats were anesthetized with i.p. of sodium pentobarbital (40 $mg \cdot kg^{-1}$). All procedures were carried out aseptically. Then, they were randomly divided into three groups (27 rats per group) and received implantations.

Group A: A blank implant was implanted in left lobe of the liver. Subcutaneous injection of 1 ml saline solution was administered (daily×7, weekly×7).

Group B: A blank implant was implanted in left lobe of the liver. 5-FU (10 $mg \cdot kg^{-1}$) was subcutaneously injected (daily×7, weekly ×7).

Group C: 5-FUCI was implanted in left lobe of the liver. 1 ml saline solution was subcutaneously injected (daily×7, weekly ×7).

Counts of WBC and bone marrow nucleated cells Three rats per group were respectively anesthetized weekly, counts of the peripheral white blood cells and bone marrow nucleated cells were assessed. The jugular vein was isolated and received injection of 1 % Evan' s blue solution (1.0 $mg \cdot kg^{-1}$). The rats were killed by cervical dislocation at 45 min postinjection.

Toxicity evaluation of small intestine Two cm sections of the proximal jejunum were cut and weighed, and treated with 40 % trichloroacetic acid solution (1:8, w/v), then left at 25 ℃ overnight and centrifuged at 1 500 g for 10 min. The upper aqueous phase was collected and extraction of Evan' s blue

was measured by spectrophotometer.

Morphological changes of small intestinal mucosa The small intestine segments were collected, and haematoxylin and eosin stained slides were used. The area of small intestinal mucosal cells and integrated optical density (IOD) of inner mucosal surface of the small intestine were measured by using image analysis system (IBAS, Kontron Co. Ltd., Germany).

Assay of element F in group C To evaluate the biodistribution of 5-FU postimplantation, major organs (left/right lobe of the liver, heart, kidney) in group C were resected, adherent blood was removed and weighed. The contents of F were measured by an electron probe analyzer (JCXA-733, JEDL Co. Ltd., Japan).

Experiment 2: Antitumor activities of 5-FUCI

Preparation of TB rats Walker-256 carcinosarcoma cells were obtained from Chinese Center of Culture Preservation. On day 0 following laparotomy, 10^7 tumor cells of approximately 0.1 ml of cell suspension were transplanted in left lobe of the liver under slight ketamine anesthesia.

5-FUCI transplantation and treatment On day 6 after tumor transplantation, the tumor-bearing (TB) rats were randomly assigned to three groups (12 rats per group) for treatment and reoperated for insertion of 5-FUCI or blank implant.

Group D: The TB rats were treated by intratumoral implantation of a blank implant in left lobe of the liver.

Group E: 5-FUCI was implanted in right lobe of the liver.

Group F: The TB rats were treated by intratumoral implantation of 5-FUCI in left lobe of the liver.

Tumor volume and survival days On day 21, six rats per group were sacrificed, solid tumors were excised, weighed and the rate of tumor inhibition was calculated by the formula: (the tumor volume of control group- tumor volume of experimental group)/(the tumor volume of control group)×100 %. The life span of rest rats was investigated.

Pathological examination The tumor tissues taken from control group and experimental group were embedded in paraffin, and 5 μm sections were taken, stained with hematoxylin-eosin, and observed under light microscope to examine the therapeutic effect of 5-FUCI.

Statistical analysis

The differences between the mean values were analyzed for significance using the Student' s *t* test for independent samples. Survival time was examined with time sequence examination. $P \leqslant 0.05$ was considered to be statistically significant.

RESULTS

Changes of counts of WBC and bone marrow nucleated cells before and after treatment

Counts of the peripheral white blood cells in group B decreased from 11.5 g· L^{-1} before chemotherapy to 2.0 g· L^{-1} 3 weeks after treatment, but the data were not significantly different in group C compared with control group (group A, $P>0.05$). Counts of the bone marrow nucleated cells after subcutaneous injection of 5-FU decreased from 41.4×10^9· L^{-1} to 24.0×10^9· L^{-1}, and the data were normal in groups A and C ($P>0.05$).

Small intestinal mucosal image analysis

Morphological changes of small intestinal mucosa are listed in Tables 1 and 2.

Gastrointestinal toxicity

Gastrointestinal toxicity was positive by correlated with extraction of Evan' s blue from gastrointestinal tract. The results of extraction of Evan' s blue from small intestine are shown in Table 3.

Table 1 Changes of area of small intestinal mucosal cells (μm^2)

Time (weeks)	Group A	Group B	Group C
2	38.98±8.16	47.16±3.29	31.32±7.76[b]
4	35.07±5.70	42.25±4.42	28.81±1.98[b]
6	38.11±1.89	36.97±3.44	30.17±5.00
8	29.91±1.34	-	29.72±0.97
Mean	35.68±5.78	42.13±5.48[a]	30.00±4.15[ab]

[a]$P<0.05$ *vs* group A; [b]$P<0.05$ *vs* group B.

Table 2 Changes of IOD of inner mucosal surface of small intestine

Time (weeks)	Group A	Group B	Group C
2	0.406±0.020	0.248±0.069	0.453±0.051
4	0.417±0.110	0.290±0.017	0.409±0.024[b]
6	0.379±0.042	0.335±0.055	0.453±0.081
8	0.508±0.083	-	0.352±0.041[a]
Mean	0.427±0.080	0.295±0.051[a]	0.417±0.063[b]

[a]$P<0.05$ *vs* group A; [b]$P<0.05$ *vs* group B.

Table 3 Changes of extraction of Evan's blue from small intestine (μg· g^{-1})

Time (weeks)	Group A	Group B	Group C
0	0.860±0.051	0.840±0.045	0.870±0.035
1	0.903±0.045	0.980±0.145	0.847±0.083
2	0.797±0.086	1.123±0.172	1.243±0.169[a]
3	0.880±0.240	1.273±0.231	0.813±0.081[b]
4	0.917±0.349	1.275±0.230	0.823±0.067[b]
5	0.793±0.100	1.320±0.110[a]	0.863±0.115[b]
6	0.993±0.276	1.427±0.227	0.813±0.099[b]
7	0.890±0.226	1.010±0.014	0.923±0.250
8	0.873±0.116	-	0.853±0.131
Mean	0.881±0.183	1.253±0.323[a]	0.898±0.179[b]

[a]$P<0.05$ *vs* group A; [b]$P<0.05$ *vs* group B.

Biodistribution of 5-FU after implantation

After 5-FUCI implantation, the local high accumulation of 5-FU was demonstrated in the adjacent tissue surrounding 5-FUCI implant (in left lobe of the liver). On the other hand, the concentration of 5-FU was lower in right lobe of the liver, heart and kidney (Table 4).

Table 4 Contents of element F in group C in major organs (%)

Time (weeks)	Left lobe of liver	Right lobe of liver	Heart	Kidney
2	7.800±0.804	0.782±0.084[a]	0.143±0.050[ab]	0.174±0.144[ab]
4	6.560±0.694	0.645±0.233[a]	0.300±0.131[a]	0.272±0.136[a]
6	6.269±1.383	0.784±0.362[a]	0.288±0.232[a]	0.141±0.061[ab]
8	4.414±0.482	0.334±0.143[a]	0.162±0.067[a]	0.184±0.120[a]

[a]$P<0.05$ *vs* left lobe of the liver; [b]$P<0.05$ *vs* right lobe of the liver.

Observations of the anticancer effect

Changes of tumor volume and survival time in cancer-bearing rats are listed in Table 5. One animal in group F survived to the end of the experiment (50 days) and no viable tumor was found.

Table 5 Changes of tumor volume and survival days in tumor-bearing rats

Group	Tumor volume (cm^3)		Tumor inhibition rates (%)	Survival days (d)
	6 days of transplantation	21 days of transplantation		
Group D	0.021±0.010	2.762±1.384	-	28.0±2.2
Group E	0.030±0.014	1.844±0.904	33.2	30.0±3.2
Group F	0.027±0.012	0.102±0.117[ab]	96.3[b]	38.7±6.7[ab]

[a]$P<0.05$ *vs* group D, [b]$P<0.05$ *vs* group E.

Results of pathologic examination

5-FUCI implantation had no apparent pathological changes in the heart, liver, kidney and small intestine in group C. Some local effects of 5-FUCI were observed. The tumor cell proliferation in group D was very active (Figure 2). A number of focal necrosis were observed in group E (Figure 3) Most necrotic tissues were found at a distance of up to 1 cm from the implant in group F(Figure 4).

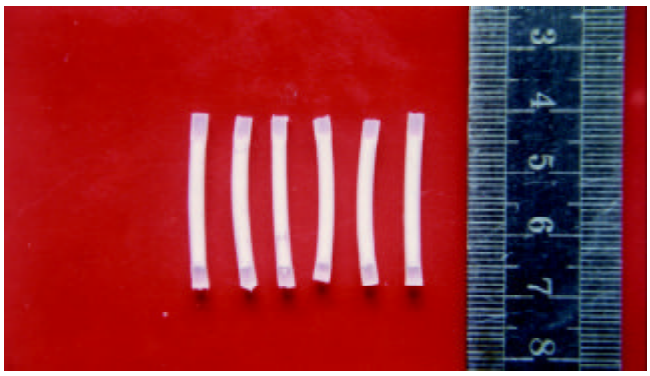

Figure 1 5-FUCI.

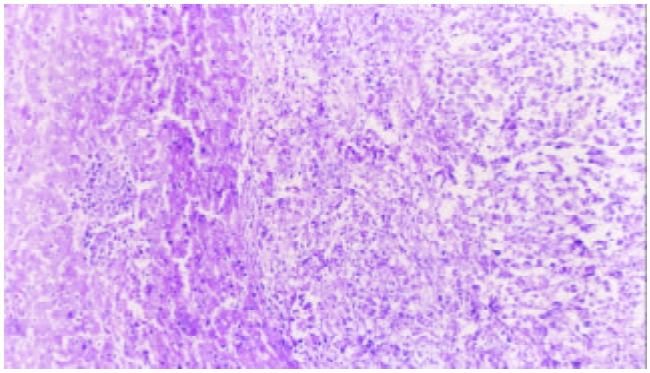

Figure 2 Tumor section (HE×100): tumor cell proliferation was active in group D.

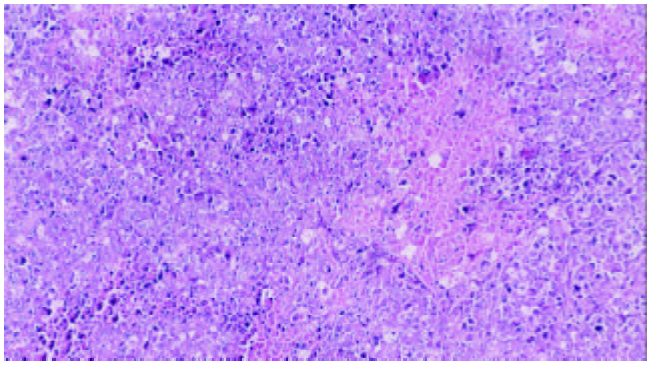

Figure 3 Tumor section (HE×100): a number of focal necrosis observed in group E.

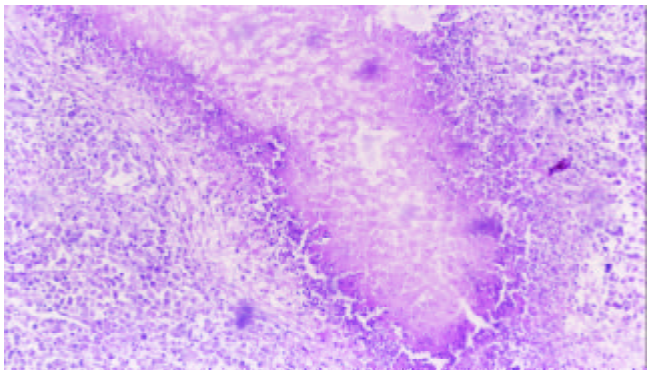

Figure 4 Tumor section (HE×100): the island of necrosis and lymphocytes infiltrated around the necrotic tissue found in group F.

DISCUSSION

Controlled release implant is a newly developed agent[14-17]. Different from other kinds of common or slow-released agents, it is capable of being administered through implantation to target organ, and can result in a therapeutically suitable plasma concentration of agents for an extended period of time[18-22], and exert a full antitumor action, despite the short half-life of drugs[23,24].

This study illustrated that the concentration of 5-FU in left lobe of the liver was 9.84, 28 and 34 times as much as that in right lobe of the liver, heart and kidney respectively after the implantation. It kept a high level of 5-FU in surrounding tissues of the implant, ranging from (4.414±0.482) % to (7.800±0.804) %, for eight weeks. 5-FUCI not only provided higher drug and /or drug metabolite concentrations in the tumor than the drug administered as an aqueous solution s.c. or systemically, but also resulted in a prolonged exposure of the tumor tissue to the drug and /or its metabolites. Consequently, 5-FUCI would be expected to improve effectiveness and to minimize the systemic toxicity associated with current systemic therapy of 5-FU[25-28].

New insights indicate that the toxicity of 5-FU is dose dependent, frequent low-dose infusions are less toxic to host than less frequent higher doses. No sign of systemic toxicities of 5-FUCI was detected because the daily delivery dose of 5-FUCI was only approximately 30 $\mu g \cdot d^{-1}$.

In previous studies, Smith *et al* demonstrated the sensitivity of tumor cells to 5-FU and dependence on drug concentration and exposure time[25,29]. If the exposure time was increased, the required drug concentration could be reduced. For example, the concentration of 5-FU that inhibited growth of 50-90 % (IC_{50}, IC_{90}) of BxPC-3 pancreatic cancer cells was eight to ten times less with a 72-h drug exposure than with a 24-h exposure[29]. We have shown that delivery of drugs administrated in 5-FUCI resulted in growth inhibition of Walker-256 carcinosarcoma cells that could hardly be accomplished with s.c. 5-FU solution.

Controlled release implant may enhance the pharmacological alternatives for the treatment of malignant tumors. Some researches have proved that tumor cell growth could be inhibited at a distance of 0.5-5 cm from the implant[30-32]. Therefore an implant needs to be inserted in many sites for multicenter or >5 cm neoplasms in outer diameter.

The data indicated that silicone pellets were transparent, and without fracture or apparent degradation after 8 weeks of implantation. In addition, a fibrous capsule was not detected around the pellets. Release of 5-FU from these pellets allows the drug to remain in the plasma for 1 to 8 weeks, in spite of its short plasma half-life (10 min)[10-13]. This was an

improvement compared with the injection of drugs. Administration of 5-FU by implantation of silastic elastomer seems to be a good candidate for 5-FU therapy. It suggests that 5-FUCI is a novel clinical approach and can offer an effective local chemotherapy.

REFERENCES

1 **Aboagye EO**, Saleem A, Cunningham VJ, Osman S, Price PM. Extraction of 5-fluorouracil by tumor and liver: a noninvasive positron emission tomography study of patients with gastrointestinal cancer. *Cancer Res* 2001; **61**: 4937-4941

2 **Xiao HB**, Cao WX, Yin HR, Lin YZ, Ye SH. Influence of L-methionine-deprived total parenteral nutrition with 5-fluorouracil on gastric cancer and host metabolism. *World J Gastroenterol* 2001; **7**: 698-701

3 **Liu LX**, Zhang WH, Jiang HC, Zhu AL, Wu LF, Qi SY, Piao DX. Arterial chemotherapy of 5-fluorouracil and mitomycin C in the treatment of liver metastases of colorectal cancer. *World J Gastroenterol* 2002; **8**: 663-667

4 **Chen XX**, Lai MD, Zhang YL, Huang Q. Less cytotoxicity to combination therapy of 5-fluorouracil and cisplatin than 5-fluorouracil alone in human colon cancer cell lines. *World J Gastroenterol* 2002; **8**: 841-846

5 **Cao S**, Rustum YM. Synergistic antitumor activity of irinotecan in combination with 5-fluorouracil in rats bearing advanced colorectal cancer: role of drug sequence and dose. *Cancer Res* 2000; **60**: 3717-3721

6 **Yoshikawa R**, Kusunoki M, Yanagi H, Noda M, Furuyama JI, Yamamura T, Hoshimoto-Tamaoki T. Dual antitumor effects of 5-fluorouracil on the cell cycle in colorectal carcinoma cells: a novel target mechanism concept for pharmacokinetic modulating chemotherapy. *Cancer Res* 2001; **61**: 1029-1037

7 **Van Kuilenburg AB**, Haasjes J, Richel D, Zoetekouw L, Van Lenthe H, De Abreu RA, Maring JG, Vreken P, Van Gennip AH. Clinical implications of dihydropyrimidine dehydrogenase (DPD) deficiency in patients with severe 5-fluorouracil-associated toxicity: identification of new mutations in the *DPD* gene. *Clin Cancer Res* 2000; **6**: 4705-4712

8 **Di Paolo A**, Danesi R, Falcone A, Cionini L, Vannozzi F, Masi G, Allegrini G, Mini E, Bocci G, Conte PF, Del Tacca M. Relationship between 5-fluorouracil disposition, toxicity and dihydropyrimidine dehydrogenase activity in cancer patients. *Ann Oncol* 2001; **12**: 1301-1306

9 **Van Kuilenburg AB**, Haasjes J, Richel DJ, Zoetekouw L, Van Lenthe H, De Abreu RA, Maring JG, Vreken P, Van Gennip AH. Clinical implications of dihydropyrimidine dehydrogenase (DPD) deficiency in patients with severe 5-fluorouracil-associated toxicity: identification of new mutations in the *DPD* gene. *Clin Cancer Res* 2000; **6**: 4705-4712

10 **Fraile RJ**, Baker LH, Buroker TR, Horwitz J, Vaitkevicius VK. Pharmacokinetics of 5-fluorouracil administered orally, by rapid intravenous and by slow infusion. *Cancer Res* 1980; **40**: 2223-2228

11 **Yi YM**, Yang TY, Pan WM. Preparation and distribution of 5-fluorouracil (125)I sodium alginate-bovine serum albumin nanoparticles. *World J Gastroenterol* 1999; **5**: 57-60

12 **Kuan HY**, Smith DE, Ensminger WD, Knol JA, De Remer SJ, Yang Z, Stetson PL. Regional pharmacokinetics of 5-fluorouracil in dogs: role of the liver, gastrointestinal tract, and lungs. *Cancer Res* 1998; **58**: 1688-1694

13 **Schlemmer HP**, Becker M, Bachert P, Dietz A, Rudat V, Vanselow B, Wollensack P, Zuna I, Knopp MV, Weidauer H, Wannenmacher M, Van Kaick G. Alterations of intratumoral pharmacokinetics of 5-fluorouracil in head and neck carcinoma during simultaneous radiochemotherapy. *Cancer Res* 1999; **59**: 2363-2369

14 **Saltzman WM**, Fung LK. Polymeric implants for cancer chemotherapy. *Adv Drug Deliv Rev* 1997; **26**: 209-230

15 **Dash AK**, Cudworth GC 2nd. Therapeutic applications of implantable drug delivery systems. *J Pharmacol Toxicol Methods* 1998; **40**: 1-12

16 **Takahashi T**. Development and clinical application of drug delivery systems for cancer treatment. *Int J Clin Oncol* 2002; **7**: 206–218

17 **Einmahl S**, Zignani M, Varesio E, Heller J, Veuthey JL, Tabatabay C, Gurny R. Concomitant and controlled release of dexamethasone and 5-fluorouracil from poly(ortho ester). *Int J Pharm* 1999; **185**: 189-198

18 **Itokazu M**, Kumazawa S, Wada E, Wenyi Y. Sustained release of adriamycin from implanted hydroxyapatite blocks for the treatment of experimental osteogenic sarcoma in mice. *Cancer Lett* 1996; **107**: 11-18

19 **Ramchandani M**, Robinson D. *In vitro* and *in vivo* release of ciprofloxacin from PLGA 50:50 implants. *J Control Release* 1998; **54**: 167-175

20 **Wang G**, Tucker IG, Roberts MS, Hirst LW. *In vitro* and *in vivo* evaluation in rabbits of a controlled release 5-fluorouracil subconjunctival implant based on poly (d, L-lactide-co-glycolide). *J Control Release* 1998; **54**: 167-175

21 **Kong Q**, Kleinschmidt-Demasters BK, Lillehei KO. Intralesionally implanted cisplatin cures primary brain tumor in rats. *J Surg Oncol* 1997; **64**: 268-273

22 **Kitchell BK**, Orenberg EK, Brown DM, Hutson C, Ray K, Woods L, Luck E. Intralesoinal sustained-release chemotherapy with therapeutic implants for treatment of canine sun-induced squamous cell carcinoma. *Eur J Cancer* 1995; **31**: 2093-2098

23 **Ning S**, Yu N, Brown DM, Kanekal S, Knox SJ. Radiosensitization by intratumoral administration of cisplatin in a sustained-release drug delivery system. *Radiother Oncol* 1999; **50**: 215-223

24 **Maeda M**, Moriuchi S, Sano A, Yoshimine T. New drug delivery system for water-soluble drugs using silicone and its usefulness for local treatment: application of GCV-silicone to GCV / HSV-tk gene therapy for brain tumor. *J Control Release* 2002; **84**: 15-25

25 **Smith JP**, Kanekal S, Patawaran MB, Chen JY, Jones RE, Orenberg EK, Yu NY. Drug retention and distribution after intratumoral chemotherapy with fluorouracil / epinephrine injectable gel in human pancreatic cancer xenografts. *Cancer Chemother Pharmacol* 1999; **44**: 267-274

26 **Tang WX**, Cheng PY, Luo YP, Wang RX. Interaction between cisplatin, 5-fluorouracil and vincristine on human hepatoma cell line (7721). *World J Gastroenterol* 1998; **4**: 418-420

27 **Deng LY**, Zhang YH, Xu P, Yang SM, Yuan XB. Expression of IL 1beta converting enzyme in 5-FU induced apoptosis in esophageal carcinoma cells. *World J Gastroenterol* 1999; **5**: 50-52

28 **Jin J**, Huang M, Wei HL, Liu GT. Mechanism of 5-fluorouracil required resistance in human hepatocellular carcinoma cell line Bel(7402). *World J Gastroenterol* 2002; **8**: 1029-1034

29 **Smith JP**, Stock E, Orenberg EK, Yu NY, Kanekal S, Brown DM. Intratumoral chemotherapy with a sustained-release drug delivery system inhibits growth of human pancreatic cancer xenografts. *Anticancer Drugs* 1995; **6**: 717-726

30 **Harper E**, Dang W, Lapidus RG, Garver RI Jr. Enhanced efficacy of a novel controlled release paclitaxel formulation (PACLIMER Delivery System) for local-regional therapy of lung cancer tumor nodules in mice. *Clin Cancer Res* 1999; **5**: 4242-4248

31 **Williams JA**, Dillehay LE, Tabassi K, Sipos E, Fahlman C, Brem H. Implantable biodegradable polymers for IUdR radiosensitization of experimental human malignant glioma. *J Neurooncol* 1997; **32**: 181-192

32 Yuan X, Fahlman C, Tabassi K, Williams JA. Synthetic, implantable, biodegradable polymers for controlled release of radiosensitizers. *Cancer Biother Radiopharm* 1999; **14**: 177-186

Edited by Zhang JZ and Wang XL

P.O.Box 2345, Beijing 100023,China
Fax: +86-10-85381893
E-mail: wjg@wjgnet.com www.wjgnet.com

World J Gastroenterol 2003;9(8):1799-1803
World Journal of Gastroenterology
 ISSN 1007-9327

• BASIC RESEARCH •

TLR4 mediates LPS-induced HO-1 expression in mouse liver: Role of TNF-α and IL-1β

Yong Song, Yi Shi, Li-Hua Ao, Alden H. Harken, Xian-Zhong Meng

Yong Song, Yi Shi, Department of Respiratory Diseases, Nanjing Jinling Hospital, School of Medicine, Nanjing University, Nanjing 210002, Jiangsu Province, China
Li-Hua Ao, Alden H. Harken, Xian-Zhong Meng, Department of Surgery, Box C-320, Health Sciences Center, University of Colorado, 4200 E. 9th Avenue, Denver, CO 80262, USA
Correspondence to: Yong Song, M.D., Ph D., Department of Respiratory Diseases, Nanjing Jinling Hospital, School of Medicine, Nanjing University, Nanjing 210002, Jiangsu Province, China. yong_song6310@yahoo.com
Telephone: +86-25-4810453 **Fax:** +86-25-4809843
Received: 2003-01-18 **Accepted:** 2003-03-03

Abstract

AIM: Heme oxygenase (HO)-1 catalyzes the conversion of heme to biliverdin, iron and carbon monoxide. HO-1 is induced by many stimuli including heme, Hb, heat stress, lipopolysaccharide (LPS) and cytokines. Previous studies demonstrated that LPS induced HO-1 gene activation and HO-1 expression in liver. However, the mechanisms of LPS-induced HO-1 expression in liver remain unknown. The effect of toll-like receptor-4 (TLR4) on LPS-induced liver HO-1 expression and the role of TNF-α and IL-1β in this condition were determined.

METHODS: HO-1 expression was determined by immunofluorescent staining and immunoblotting. Double immunofluorescent staining was performed to determine the cell type of HO-1 expression in liver.

RESULTS: A low dose of LPS significantly increased HO-1 expression in the liver which was localized in Kupffer cells only. Furthermore, HO-1 expression was enhanced by three doses of LPS. HO-1 expression was significantly inhibited in the liver of TLR4 mutant mice. While the liver HO-1 expression in TNF KO mice was much lower than that in C57 mice following the same LPS treatment, IL-1β KO had a slight influence on liver HO-1 expression following LPS treatment.

CONCLUSION: The present results confirm that macrophages are the major source of HO-1 in the liver induced by LPS. This study demonstrates that TLR4 plays a dominant role in mediating HO-1 expression following LPS. LPS-induced HO-1 expression is mainly mediated by endogenous TNF-α, but only partially by endogenous IL-1β.

Song Y, Shi Y, Ao LH, Harken AH, Meng XZ. TLR4 mediates LPS-induced HO-1 expression in mouse liver: Role of TNF-α and IL-1β. *World J Gastroenterol* 2003; 9(8): 1799-1803
http://www.wjgnet.com/1007-9327/9/1799.asp

INTRODUCTION

Heme oxygenase (HO) catalyzes the degradation of heme into biliverdin, iron and carbon monoxide[1-3]. Heme oxygenase has three known isoforms that consist of the inducible isoform heme oxygenase-1 (HO-1), the constitutive isoform heme oxygenase-2 and heme oxygenase-3. HO-1 is induced not only by its substrate, hemin, but also by oxidative stress, heat stress, UV irradiation, heavy metals, lipopolysaccharide (LPS) and cytokines[4-8]. This diversity of HO-1 inducers has provided further support for the speculation that HO-1 may play a vital function in maintaining cellular homeostasis, and some studies suggest that HO-1 can serve as a key biological molecule in the adaptation and/or defense against oxidative stress.

LPS is generally regarded as a key initiating factor in the pathogenesis of septic shock, and it stimulates inflammatory cells to produce cytokines, and other inflammatory mediators. HO-1 is induced by LPS in some cultured cell models *in vitro*[4,9], and also in lungs[10], kidneys and spleen[11,12] *in vivo*. It has been reported that HO-1 is induced in the liver after administration of LPS[11,13,14], but little is known about the mechanism of LPS-induced HO-1 expression in liver.

Studies have demonstrated that LPS induces cellular response by the signaling molecules belonging to the Toll-like receptor (TLR) family[15]. So far, six members (TLR1-6) have been reported and two of these, TLR2 and TLR4, have been shown to be essential for the recognition of distinct bacterial cell wall components[15,16]. TLR4 recognizes LPS, lipoteichoic acid and Taxol[17-19]. Recently, it was demonstrated that TLR4 mediated heat shock protein 60 signaling[20]. Although TLR4 is clearly critical to LPS signaling, the role of TLR4 in LPS-induced HO-1 expression has remained unclear. TLR4 mutation attenuates LPS-induced NF-κB activation and the production of cytokines[21,22]. Previous studies showed that cytokines, TNF-α, IL-α, or IL-1β induced HO-1 expression *in vitro*[8,23,24]. Do endogenous cytokines, TNF-α and IL-1β play a role in LPS-induced HO-1 expression?

The purposes of this study were to examine: the time course and localization of HO-1 expression in the liver by LPS stimulation, the role of TLR4 in LPS-induced liver HO-1 expression, whether LPS-induced HO-1 expression is dependent on TNF-α, and whether IL-1β plays a role in LPS-induced HO-1 expression.

MATERIALS AND METHODS

Animals

Male mice of the C57 BL/6, BALB/cJ and C.C3H-Tlr4Lps-d (TLR4 mutant) aged 8-10 weeks were obtained from Jackson Laboratory (Bar Harbor, ME). TNF-α knockout (TNF KO) mice of the same age range were generous gifts from Dr. David Riches of National Jewish Medical and Research Center (Denver, CO). IL-1β knockout (IL-1KO) mice were obtained from National Jewish Medical and Research Center (Denver, CO). The mice were kept on a 12-h light/dark cycle with free access to food and water. All animal experiments were approved by the University of Colorado Health Science Center Animal Care and Research Committee. During experiments, all the animals received humane care in compliance with the "Guide for the Care and Use of Laboratory Animals" [DHEW Publication No. (NIH) 85-23, revised in 1985, Office of Science and Health Reports, DRR/NIH, Bethesda, MD 20205].

Chemicals and reagents

Rabbit polyclonal antibody to HO-1 and the recombinant rat HO-1 were purchased from StressGen Biotechnologies Corp (Victoria, BC, Canada). Rat monoclonal antibody to mouse CD 68 was purchased from Serotec (Oxford, UK). Rat IgG and Cy3-conjugated goat anti-rabbit IgG were purchased from Jackson ImmunoResearch Laboratories (West Grove, PA). Fluorescein-conjugated wheat germ agglutinin was obtained from Molecular Probes (Eugene, OR). LPS (Escherichia coli, O55:B5) and all other chemicals were obtained from Sigma (St Louis, MO).

Experimental protocols

To determine HO-1 expression in the liver, the mice received either LPS (0.5 mg/kg) or normal saline by tail vein injection. To determine a time course of HO-1 expression, a single dose, two or three doses of LPS were used in each every 24 hours. After anesthesia and heparinization (40 mg/kg of pentobarbital sodium, ip), the liver tissue samples were prepared for the assessment of HO-1 expression. A portion of the liver tissue was embedded in a tissue-freezing medium and frozen in dry-ice-chilled isopentane. The remaining liver tissue was frozen in liquid nitrogen. All the samples were stored at -70 ℃ prior to use.

Immunofluorescent detection of HO-1 expression

Liver HO-1 expression was determined by immunofluorescent staining as previously described[25]. Tissue cryosections (5 μm thick) were prepared with a cryostat (IEC Minotome plus, Needham Heights, MA) and collected on poly-l-lysine-coated slides. All incubations were performed at room temperature. Sections were treated with a mixture of 70 % acetone and 30 % methanol for 5 min, and then fixed with 3 % paraformaldehyde for 20 min. Sections were washed with PBS, blocked with 10 % normal goat serum for 30 min, and incubated for 1 h with a polyclonal rabbit anti-HO-1 antibody (1:300 in PBS containing 1 % bovine serum albumin). Control sections were incubated with nonimmune rat IgG (5 mg/ml). After washed with PBS, sections were incubated with Cy3-conjugated goat anti-rabbit IgG (1:300 dilution with PBS containing 1 % bovine serum albumin). The cell surface was counterstained with fluorescein-conjugated wheat germ agglutinin, and the nucleus with *bis*-benzimide. The sections were mounted with aqueous media. Microscopic analysis was performed with a Leica DMRXA digital microscope (Germany) equipped with Slidebook software (I. I. I. Inc., Denver, CO).

Double immunofluorescent staining of HO-1 and macrophage

Double immunofluorescent staining was performed to determine the cell type stained positively of HO-1. CD68 (macrophages)-positive cells were studied. Tissue cryosections (5-μm thick) were prepared, fixed as described for staining of HO-1. Sections were blocked with 5 % normal goat serum + 5 % normal donkey serum for 30 min. Then slides were incubated for 1 h with a rat monoclonal antibody to mouse macrophages (CD68, 1:200) and rabbit polyclonal antibody to HO-1 (1:300). Control sections were incubated with non-immune rat IgG and rabbit IgG. After washed with PBS, the sections were incubated with Cy3-conjugated donkey anti-rat IgG (CD68) and FITC-conjugated goat anti-rabbit IgG (HO-1). The nucleus was counterstained with *bis*-benzimiade. The sections were washed with PBS, and then mounted on aqueous mounting media. Microscopic observation and photography were performed as described above.

Immunoblotting of HO-1

Liver tissue was homogenized with 4 volumes of homogenate buffer (PBS containing the protease inhibitor cocktail and 1 % Triton X100, pH 7.4), and centrifuged at 10 000×g for 20 min at 4 ℃. The resulting supernatant was collected and stored at -70 ℃ for immunoblotting of HO-1. Aliquots of protein (60 μg/lane) in the liver tissue homogenate were separated on a 4-20 % SDS-polyacrylamide gel (Bio-Rad, Hercules, CA). Separated proteins were blotted onto a nitrocellulose membrane (Bio-Rad, Hercules, CA), and equal loading was confirmed by densitometric assessment of protein band staining with Ponceau S solution. The membrane was rinsed in PBS and blocked for 1 h at room temperature with 5 % dry milk in PBS. The membrane was then incubated with a polyclonal rabbit anti-HO-1 antibody (1:1 000 dilution with 5 % dry milk in PBST) at room temperature for 1 h. Following an incubation with HRP-conjugated goat anti-rabbit IgG (1:10 000 dilution with 5 % dry milk in PBST), HO-1 bands were developed using ECL and visualized by exposure to Kodak X-Omat film (Eastman Kodak, Rochester, NY).

Statistical analysis

Data were expressed as mean ± standard error of the mean (SE). An analysis of variance (ANOVA) was performed with Statview 4.0 statistical analysis software (SAS Institute, Cary, NC), and a difference was accepted as significant if the P value was smaller than 0.05 as verified by the Bonferroni/ Dunn post hoc test.

RESULTS

Time course of liver HO-1 expression following LPS administration

Liver HO-1 expression in C57 mice after LPS administration was assessed by immunofluorescent staining and immunoblotting. HO-1 had low basal level expression in control liver by immunofluorescent staining (Figure 1A), but was barely detectable by immunoblotting (Figure 1B). A low dose (0.5 mg/kg) of LPS significantly increased HO-1 expression in the liver at 24 h after LPS administration. Furthermore, HO-1 expression was enhanced by three doses of LPS (Figure 1A and Figure 1B). The integrated intensity of HO-1 expression was significantly increased in liver of LPS-treated mice as compared with sham treatment mice (Figure 1C, $P<0.05$). However, cellular HO-1 level went down if animals were allowed to recover for 48 h following the last LPS injection, then gradually declined to control level at 72 h (data not shown).

Cell type involved in liver HO-1 expression

HO-1 protein was barely detectable in parenchymal liver cells following LPS stimulation, whereas high amounts of HO-1 were detectable in interstitial cells. To further characterize the cell types expressing HO-1, we attempted to localize the cell type(s) responsible for LPS-induced HO-1 expression in liver by double immunofluorescent staining. Rat anti-mouse CD68 monoclonal antibody and rabbit anti-HO-1 polyclonal antibody were used. We found that lower percentages of Kupffer cells exhibited positive staining for HO-1 in sham treatment. After three doses of LPS treatment, the majority of CD68 positive cells (>90 %) were HO-1 positive (Figure 2).

Effect of TLR4 on liver HO-1 expression

To examine the mechanism of regulation of liver HO-1 expression in response to LPS, we used C.C3H-Tlr4Lps-d mice, mice of TLR4 mutation. In BALB/cJ (wild type) mice, LPS-induced HO-1 expression in liver was comparable to C57 mice. In contrast, liver HO-1 expression in TLR4 mutant mice was significantly inhibited following the same treatment with LPS (Figure 3). These results suggested that mutation of

TLR4 exerted a dominant effect on liver HO-1 expression after LPS treatment.

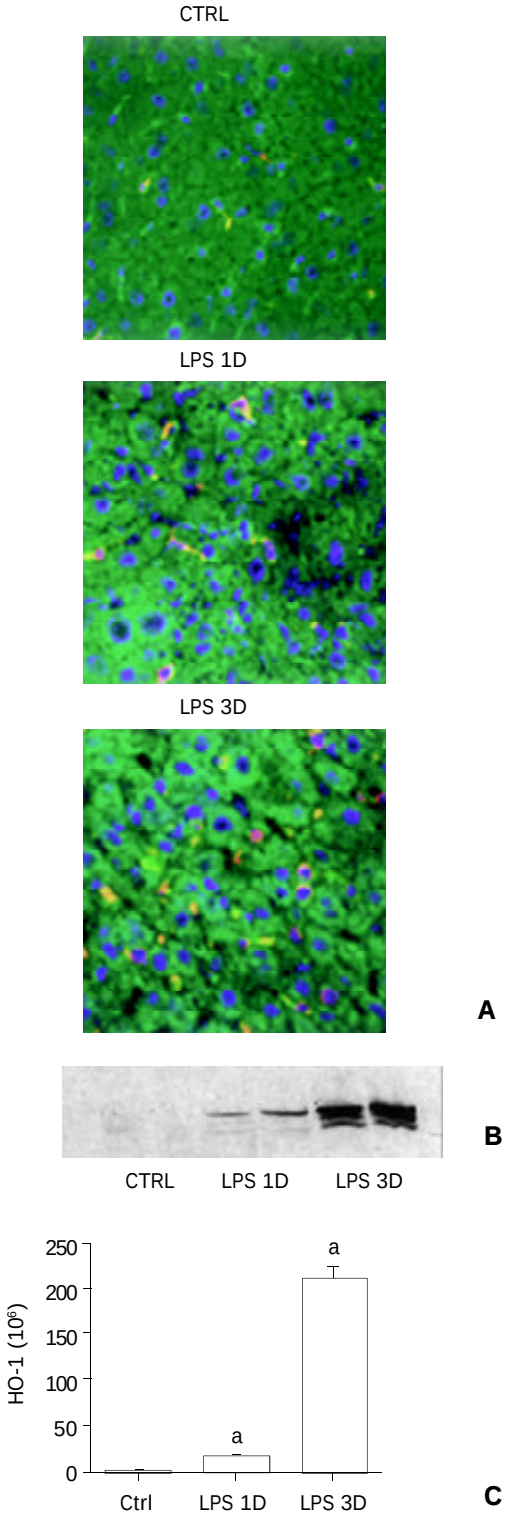

Figure 1 Liver HO-1 expression in wild type mice. A: Immunofluorescent detection of HO-1 in liver. After different doses of LPS or sham treatment, liver HO-1 expression of wild type (C57) mice were visualized by immunofluorescent staining with a specific rabbit polyclonal antibody against HO-1 followed by indocarbocyanine (Cy3)-conjugated anti-rabbit IgG (red). The cell surface was counterstained with fluorescein-conjugated wheat germ agglutinin (green), and the nucleus was counterstained with *bis*-benzimide (blue). HO-1 was present in liver of sham-treated animals (Ctrl). A single dose of LPS treatment increased liver HO-1 expression (LPS 1D). Furthermore, HO-1 expression was enhanced by three doses of LPS treatment (LPS 3D, magnification ×400). B: Immunoblotting detection of HO-1 in liver. C57 mice were treated with vehicle (Ctrl), single dose of LPS (LPS 1D) and three doses of LPS (LPS 3D). Liver tissue was homogenized, and immunoblotting analysis was performed. HO-1 protein was detected by immunoblotting with polyclonal rabbit antibody against HO-1. Data were representative of at least 2 experiments. C: Immunofluorescent staining to quantitate HO-1 expression. Liver HO-1 expression was determined by immunofluorescent staining. Integrated intensity of HO-1 positive signal was masked and quantified by using Slidebook software (I. I. I. Inc., Denver, CO). $^aP<0.05$ *vs.* sham.

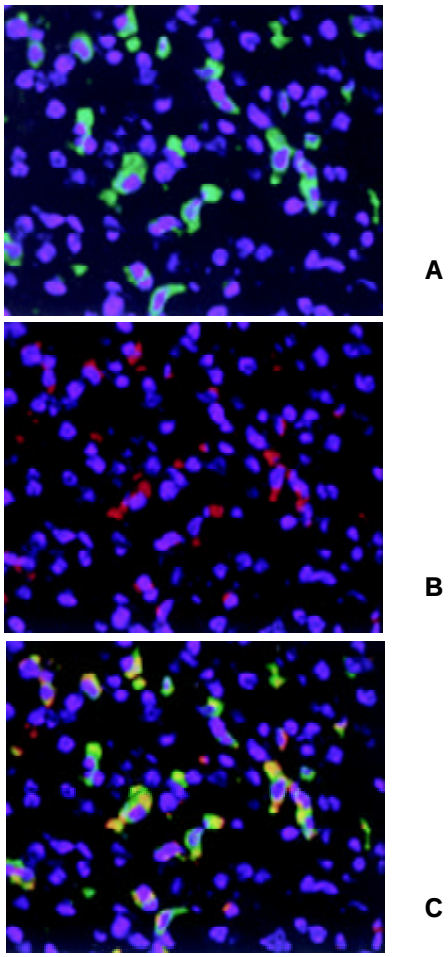

Figure 2 Double immunofluorescent staining of HO-1 localization in liver. After three doses of LPS treatment, HO-1 and CD68 in liver tissue were detected by double immunofluorescent staining with polyclonal rabbit antibody against HO-1 followed by FITC-conjugated anti-rabbit IgG (green) and monoclonal rat antibody against mouse CD68 followed by Cy3-conjugated anti-rat IgG (red). Cell nuclei were counterstained with *bis*-benzimide (blue). A: HO-1; B: Macrophages (Kupffer cells); C: HO-1 + Macrophages. magnification ×400.

Effect of TNF knockout on HO-1 expression

LPS is a potent inducer of TNF-α. Recent evidence suggests that LPS-induced TNF-α production is mediated through TLR4. Previous study demonstrated that TNF-α induced HO-1 expression in endothelial cells. Does TNF-α play an important role in LPS-induced HO-1 expression in liver? To examine the mechanism of regulation of liver HO-1 expression in response to LPS, we used C.C3H-Tlr4Lps-d mice, mice of TLR4 mutation. In BALB/cJ (wild type) mice, LPS-induced HO-1 expression in liver was comparable to C57 mice. In contrast, liver HO-1 expression in TLR4 mutant mice was significantly inhibited following same treatment as wild type mice (Figure 3). These results suggested that TLR4 exerted a dominant effect on liver HO-1 expression following LPS treatment.

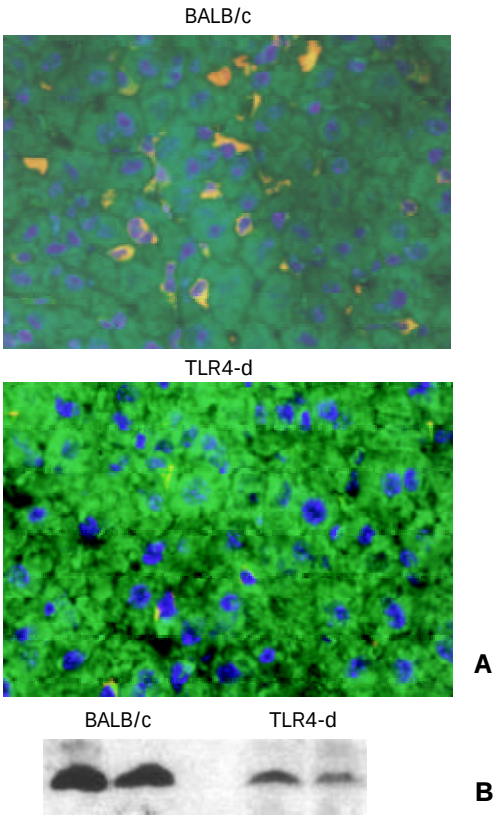

Figure 3 Effect of TLR4 mutation on liver HO-1 expression. A: Immunofluorescent detection of HO-1 in liver. After three doses of LPS treatment, liver HO-1 expression was visualized by immunofluorescent staining with a specific rabbit polyclonal antibody against HO-1, followed by indocarbocyanine (Cy3)-conjugated anti-rabbit IgG (red). The cell surface was counterstained with fluorescein-conjugated wheat germ agglutinin (green), and the nucleus was counterstained with *bis*-benzimide (blue). Liver HO-1 expression was abrogated in TLR4 mutated mice following LPS, but neither was influenced in BALB/c (control) mice (magnification ×400). B: Immunoblotting detection of HO-1 in liver. BALB/c and TLR4 mutated mice were treated with three doses of LPS. Liver tissue was homogenized, and immunoblotting analysis was performed. HO-1 protein was detected by immunoblotting with polyclonal rabbit antibody against HO-1. Data were representative of at least 2 experiments.

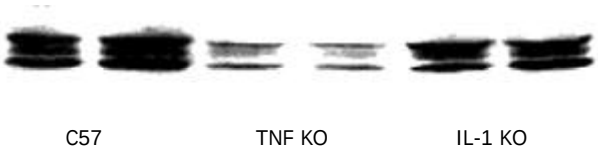

Figure 4 Effect of TNF KO and IL-1 KO on liver HO-1 expression. Immunoblotting detection of HO-1 in liver. C57, TNF KO and IL-1 KO mice were treated with three doses of LPS. Liver tissue was homogenized, and immunoblotting analysis was performed. HO-1 protein was detected by immunoblotting with polyclonal rabbit antibody against HO-1. Data were representative of at least 2 experiments.

Effect of IL-1b knockout on HO-1 expression

IL-1β is characteristically present in many inflammatory disorders. Although previous studies showed that IL-1β induced HO-1 expression *in vitro*, little is known about the role of endogenous IL-1β in LPS-induced HO-1 expression. We determined liver HO-1 expression in IL-1β KO mice. Mice were treated with LPS same as C57 mice. Compared with C57 mice, mice of IL-1β KO showed only a slight difference in liver HO-1 expression following LPS treatment (Figure 4), indicating that the expression of HO-1 following LPS was partially mediated by endogenous IL-1β.

DISCUSSION

In this study, we found that a low dose of LPS significantly increased HO-1 expression only in macrophages of wild type mice. This effect was further enhanced by the same dose of LPS for 3 consecutive days. However, HO-1 expression was significantly inhibited in TLR4 mutant mice. While liver HO-1 expression in TNF KO mice was much lower than that in C57 mice following the same LPS treatment, IL-1 KO had a slight influence on liver HO-1 expression following LPS treatment. The present results confirmed that macrophages were the major source of HO-1 in the lungs and liver as induced by LPS. This study demonstrated that TLR4 played a dominant role in mediating HO-1 expression following LPS. LPS-induced HO-1 expression was mainly mediated by endogenous TNF, but only partially by endogenous IL-1.

HO-1 is the rate-limiting enzyme in heme catabolism, and is also known as heat shock protein 32. Previous studies demonstrated that HO-1, besides its role in heme degradation, may also play a vital function in maintaining cellular homeostasis[26]. HO-1 is induced not only by its substrate, hemin, but also by oxidative stress, heat stress, UV irradiation, heavy metals, LPS and cytokines[4-8]. It has also been reported that HO-1 is induced in liver after LPS administration[11,13,14]. But most of studies just determined the changes of HO-1 mRNA in liver. Little is known about the time course and localization of HO-1 protein expression in liver. We examined liver HO-1 expression following LPS. We found that HO-1 had a low basal level expression in normal mouse liver by immunofluorescent staining. A low dose of LPS significantly increased HO-1 expression in the liver at 24 h after LPS administration. HO-1 expression was enhanced by three doses of LPS. Induction of HO-1, however, went down when animals were allowed to recover 48 h following the last LPS injection, then gradually declined to the control level by 72 h (data not shown). These results indicate that LPS-induced HO-1 expression in liver is in a dose-dependent fashion. Furthermore, we detected and localized HO-1 using immunofluorescent double staining. Hepatocytes were involved in the removal of plasma hemoglobin and some studies suggested that LPS mediated HO-1 mRNA accumulation in hepatocytes[7,13]. Interestingly, in the present study, most of HO-1 positive signals were co-localized in Kupffer cells. This finding formed a contrast to those from other animal models by hemin and LPS treatment. It is possible that the differences of experimental design, i.e, different stimuli, doses, and animals may lead to different results. In addition, the method of HO-1 staining by others was different from ours, it could be a reason for different expression of HO-1 in liver. Kupffer cells are the first line defense and effector cells in liver inflammatory response. The present results confirm that Kupffer cells are the major source of HO-1 in liver induced by LPS. HO-1 expression in Kupffer cells may play a protective role by inducing an adaptive hepatocellular stress response after LPS stimulation.

Studies demonstrated that LPS induced a cellular response by the signaling molecules belonging to the Toll-like receptor family[15]. TLR4 has been shown to be essential for the recognition of LPS, lipoteichoic acid (LTA) and Taxol[17-19]. Recently, it was demonstrated that TLR4 mediated heat shock protein 60 signaling[20]. Although TLR4 is clearly critical to LPS signaling, the role of TLR4 in LPS-induced HO-1 expression has remained unclear. To examine the mechanism of regulation of liver HO-1 expression in response to LPS, we determined liver HO-1 expression in TLR4 mutant mice. Liver

HO-1 expression in TLR4 mutant mice was significantly inhibited following the same treatment as wild type mice. This result suggests that TLR4 exerts a dominant effect on liver HO-1 expression after LPS treatment.

TNF-α is a pleiotropic early response cytokine and is rapidly produced by LPS stimulation. To determine the role of TNF-α in HO-1 expression following LPS *in vivo*, we subjected TNF KO mice to the same treatment as C57 mice. This treatment could also result in liver HO-1 expression comparable to that in the liver of C57 mice. We found that liver HO-1 expression in TNF KO mice was much lower than that in C57 mice following the same LPS treatment. This result suggests that LPS induces HO-1 expression mainly through endogenous TNF.

As an important inflammatory cytokine, IL-1 (IL-1α and IL-1β) induces HO-1 expression in endothelial cells and pancreatic islets[23-28]. Toll-like receptors belong to the IL-1 receptor family containing repeated leucine-rich motifs in their extracellular portion and are linked to a signaling pathway that involves the IL-1-receptor-associated kinase and NF-κB. It is likely that IL-1-induced HO-1 expression is mediated by TLR4. But it is unclear about the role of endogenous IL-1 in LPS-induced liver HO-1 expression. So, in the present study, IL-1 KO mice were used to determine liver HO-1 expression following LPS induction. Mice were treated with LPS the same as C57 mice. Compared with C57 mice, IL-1β KO has a slight influence on liver HO-1 expression following LPS treatment of IL-1β KO mice, indicating that the expression of HO-1 following LPS is partially mediated by endogenous IL-1β.

Taken together, the current study *in vivo* showed that TLR4 mutation attenuated LPS-induced HO-1 production in tissues. This provides a strong support to the hypothesis that TLR4 plays an important role in HO-1 signals. However, some aspects of its action remain unknown. What are the down stream signals of TLR4? In this context, future investigations are necessary to determine the signal transduction pathway of HO-1 expression induced by LPS.

REFERENCES

1 **Maines, MD.** The heme oxygenase system: a regulator of second messenger gases. *Annu Rev Pharmacol Toxicol* 1997; **37**: 517-554

2 **Maines, MD.** Heme oxygenase: function, multiplicity, regulatory mechanisms, and clinical applications. *FASEB J* 1988; **2**: 2557-2568

3 **Otterbein LE,** Choi AM. Heme oxygenase: colors of defense against cellular stress. *Am J Physiol Lung Cell Mol Physiol* 2000; **279**: L1029-L1037

4 **Camhi SL,** Alam J, Otterbein L, Sylvester SL, Choi AM. Induction of heme oxygenase-1 gene expression by lipopolysaccharide is mediated by AP-1 activaion. *Am J Respir Cell Mol Biol* 1995; **13**: 387-398

5 **Choi AM,** Alam J. Heme oxygenase-1: Function, regulation, and implication of a novel stress-inducible protein in oxidant-induced lung injury. *Am J Respir Cell Mol Biol* 1996; **5**: 9-19

6 **Keyse SM,** Tyrrell RM. Heme oxygenase is the major 32-kDa stress protein induced in human skin fibroblasts by UVA radiation, hydrogen peroxide, and sodium arsenite. *Proc Natl Acad Sci USA* 1989; **86**: 99-103

7 **Otterbein L,** Sylvester SL, Choi AM. Hemoglobin provides protection against lethal endotoxemia in rats: the role of heme oxygenase-1. *Am J Respir Cell Mol Biol* 1995; **13**: 595-601

8 **Terry CM,** Clikeman JA, Hoidal JR, Callahan KS. Effect of tumor necrosis factor-α and interleukin-1α on heme oxygenase-1 expression in human endothelial cells. *Am J Physiol* 1998; **274**(3Pt 2): H883-H891

9 **Camhi SL,** Alam J, Wiegand GW, Chin BY, Choi AM. Transcriptional activation of the HO-1 gene by lipopolysacchsride is mediated by 5' distal enhancers: role of reactive oxygen intermediates and AP-1. *Am J Respir Cell Mol Biol* 1998; **18**: 226-234

10 **Carraway MS,** Ghio AJ, Taylor JL, Piantadosi CA. Induction of ferritin and heme oxygenase-1 by endotoxin in the lung. *Am J Physiol* 1998; **275** (3Pt 1): L583-L592

11 **Oshiro S,** Takeuchi H, Matsumoto M, Kurata S. Transcriptional activation of heme oxygenase-1 gene in mouse spleen,liver and kidney cells after treatment with lipopolysacchride or hemoglobin. *Cell Biol Int* 1999; **23**: 465-474

12 **Suzuki T,** Takahashi T, Yamasaki A, Fujiwara T, Hirakawa M, Akagi R. Tissue-specific gene expression of heme oxygenase-1 (HO-1) and non-specific delta-aminolevulinate synthase (ALAS-N) in a rat model of septic multiple organ dysfunction syndrome. *Biochem Pharmacol* 2000; **60:** 275-283

13 **Bauer I,** Wanner GA, Rensing H, Alte C, Miescher EA, Wolf B, Pannen BH, Clemens MG, Bauer M. Expression pattern of heme oxygenase isoenzymes 1 and 2 in normal and stress-exposed rat liver. *Hepatology* 1998; **27**: 829-838

14 **Rizzardini M,** Zappone M, Villa P, Gnocchi P, Sironi M, Diomede L, Meazza C, Monshouwer M, Cantoni L. Kupffer cell depletion partially prevents hepatic heme oxygenase 1 messenger RNA accumulation in systemic inflammation in mice: role of interleukin 1beta. *Hepatology* 1998; **27**: 703-710

15 **Means TK,** Golenbock DT, Fenton MJ. The biology of toll-like receptors. *Cytokine Growth Factor Rev* 2000; **11**: 219-232

16 **Medvedev AE,** Kopydlowski KM, Vogel SN. Inhibition of lipopolysaccharide-induced signal transduction in endotoxin-tolerized mouse macrophages: dysregulation of cytokine, chemokine, and toll-like receptor 2 and 4 gene expression. *J Immnuol* 2000; **164**: 5564-5574

17 **Kawasaki K,** Akashi S, Shimazu R, Yoshida T, Miyake K, Nishijima M. Mouse toll-like receptor 4 MD-2 complex mediates lipopolysaccharide-mimetic signal transduction by Taxol. *J Biol Chem* 2000; **275**: 2251-2254

18 **Means TK,** Lien E, Yoshimura A, Wang S, Golenbock DT, Fenton MJ. The CD14 ligands lipoarabinomannan and lipopolysaccharide differ in their requirement for toll-like receptors. *J Immunol* 1999; **163**: 6748-6755

19 **Takeuchi O,** Hoshino K, Kawai T, Sanjo H, Takada H, Ogawa T, Takeda K, Akira S. Differential roles of TLR2 and TLR4 in recognition of gram-negative and gram-positive bacterial cell wall components. *Immunity* 1999; **11**: 443-451

20 **Ohashi K,** Burkart V, Flohe S, Kolb H. Cutting edge: heat shock protein 60 is a putative endogenous ligand of the toll-like receptor-4 complex. *J Immunol* 2000; **164**: 558-561

21 **Means TK,** Jones BW, Schromm AB, Shurtleff BA, Smith JA, Keane J, Golenbock DT, Vogel SN, Fenton MJ. Differnetial effects of a toll-like receptor antagonist on mycobacterium tuberculosis-induced macrophage response. *J Immunol* 2001; **166**: 4074-4082

22 **Nill MR,** Oberyszyn TM, Ross MS, Oberyszyn AS, Robertson FM. Temporal sequence of pulmonary cytokine gene expression in response to endotoxin in C3H / HeN endotoxin-sensitive and C3H / HeJ endotoxin-resistant mice. *J Leukoc Biol* 1995; **58**: 563-574

23 **Terry CM,** Clikeman JA, Hoidal JR, Callahan KS. TNF-α and IL-1α induce heme oxygenase-1 via protein kinase C, Ca^{2+}, and phospholipase A2 in endothelial cells. *Am J Physiol* 1999; **276**(5Pt 2): H1493-H1501

24 **Ye J,** Laychock SG. A protective role for heme oxygenase expression in pancreatic islets exposed to interleukin-1b. *Endocrinology* 1998; **139**: 4155-4163

25 **Song Y,** Ao L, Calkins CM, Raeburn CD, Harken AH, Meng X. Differential cardiopulmonary recruitment of neutrophils during hemorrhagic shock: a role for ICAM-1? *Shock* 2001; **16**: 444-448

26 **Horvath I,** MacNee W, Kelly FJ, Dekhuijzen PNR, Phillips M, Doring G, Choi AMK, Yamaya M, Bach FH, Willis D, Donnelly LE, Chung KF, Barnes PJ. "Haemoxygenase-1 induction and exhaled markers of oxidative stress in lung diseases", summary of the ERS research seminar in Budapest, Hungary, September,1999. *Eur Respir J* 2001; **18**: 420-430

27 **Kyokane T,** Norimizu S, Taniai H, Yamaguchi T, Takeoka S, Tsuchida E, Naito M, Nimura Y, Ishimura Y, Suematsu M. Carbon monoxide from heme catabolism protects against hepatobiliary dysfunction in endotoxin-treated rat liver. *Gastroenterology* 2001; **120**: 1227-1240

28 **West MA,** Bennet T, Seatter SC, Clair L, Bellingham J. LPS pretreatment reprograms macrophage LPS-stimulated TNF and IL-1 release without protein tyrosine kinase activation. *J Leukoc Biol* 1997; **61**: 88-95

Edited by Lu HM and Wang XL

P.O.Box 2345, Beijing 100023,China
Fax: +86-10-85381893
E-mail: wjg@wjgnet.com www.wjgnet.com

World J Gastroenterol 2003;9(8):1804-1807
World Journal of Gastroenterology
 ISSN 1007-9327

• BASIC RESEARCH •

Contractile effects and intracellular Ca^{2+} signalling induced by emodin in circular smooth muscle cells of rat colon

Tao Ma, Qing-Hui Qi, Wen-Xiu Yang, Jian Xu, Zuo-Liang Dong

Tao Ma, Qing-Hui Qi, Jian Xu, Zuo-Liang Dong, Department of Surgery, General Hospital of Tianjin Medical University, Tianjin 300052, China
Wen-Xiu Yang, Division of Biophysics, Department of Physics, Nankai University, Tianjin 300071, China
Supported by the National Natural Science Foundation of China, No.30171198
Correspondence to: Qing-Hui Qi, Department of Surgery, General Hospital of Tianjin Medical University, Tianjin 300052, China. mataoemail@yahoo.com.cn
Telephone: +86-22-84283767
Received: 2003-01-11 **Accepted:** 2003-03-10

Abstract

AIM: To investigate whether emodin has any effects on circular smooth muscle cells of rat colon and to examine the mechanism underlying its effect.

METHODS: Smooth muscle cells were isolated from the circular muscle layer of Wistar rat colon and the cell length was measured by computerized image micrometry. Intracellular Ca^{2+} ($[Ca^{2+}]i$) signalling was studied in smooth muscle cells using Ca^{2+} indicator Fluo-3 AM on a laser-scanning confocal microscope.

RESULTS: Emodin dose-dependently induced smooth muscle cells contraction. The contractile responses induced by emodin were inhibited by preincubation of the cells with ML-7 (an inhibitor of MLCK). Emodin caused a large, transient increase in $[Ca^{2+}]i$ followed by a sustained elevation in $[Ca^{2+}]i$. The emodin –induced increase in $[Ca^{2+}]i$ was unaffected by nifedipine, a voltage-gated Ca^{2+}-channel antagonist, and the sustained phase of the rising of $[Ca^{2+}]i$ was attenuated by extracellular Ca^{2+} removal with EGTA solution. Inhibiting Ca^{2+} release from ryanodine-sensitive intracellular stores by ryanodine reduced the peak increase in $[Ca^{2+}]i$. Using heparin, an antagonist of IP_3R, almost abolished the peak increase in $[Ca^{2+}]i$.

CONCLUSION: Emodin has a direct excitatory effect on circular smooth muscle cells in rat colon mediated via Ca^{2+}/CaM dependent pathways. Furthermore, emodin-induced peak $[Ca^{2+}]i$ increase may be attributable to the Ca^{2+} release from IP_3 sensitive stores, which further promote Ca^{2+} release from ryanodine-sensitive stores through CICR mechanism. Additionally, Ca^{2+} influx from extracellular medium contributes to the sustained increase in $[Ca^{2+}]i$.

Ma T, Qi QH, Yang WX, Xu J, Dong ZL. Contractile effects and intracellular Ca^{2+} signalling induced by emodin in circular smooth muscle cells of rat colon. *World J Gastroenterol* 2003; 9(8): 1804-1807

http://www.wjgnet.com/1007-9327/9/1804.asp

INTRODUCTION

Emodin (1, 3, 8-trihydroxy-6-methylanthraquinone) is an anthraquinone derivative isolated from *Rheum palmatum*[1]. Pharmaceutical preparations based on *Rheum palmatum* have been widely used in China for hundreds of years to treat gastrointestinal disorders[2-4]. The reported biological effects of emodin include antitumor, antibacterial and anti-inflammatory actions[5-7]. Emodin also possesses prokinetic effect on gastrointestinal smooth muscle. Stimulatory actions of emodin on gastrointestinal smooth muscle have been described in several studies, and emodin-induced contractions have been related to calcium ions[8-10]. However, the effects of emodin on the contractility of smooth muscle cells have not yet been explored. Thus, the present study was designed to determine whether emodin had any effects on circular smooth muscle cells of rat colon and to examine the mechanism underlying its effects.

MATERIALS AND METHODS

Materials

Fluo-3 AM (Molecular Probes,USA) was dissolved in DMSO (Sigma) and stored at -20 ℃. Pluronic F-127, collagenase type II, emodin, nifedipine, ryanodine, heparine, Egtazic acid (EGTA), trypsin inhibitor and HEPES were all purchased from Sigma Co. Ltd, USA. DMEM was purchased from GIBCO Co, USA, other chemicals were from LianXing BIO Co. Ltd (Beijing). Nifedipine, ryanodine and heparin were all dissolved in standard buffer and kept at 4 ℃.

Methods

Preparation of dispersed smooth muscle cells Smooth muscle cells were isolated from the circular muscle layer of Wistar rat colon as previously described with slight modifications[11]. Briefly, muscle strips were digested for 30 min at 31 ℃ in HEPES medium containing 0.1 % type II collagenase and 0.01 % trypsin inhibitor. The partly digested strips were washed with PBS, and muscle cells were allowed to disperse spontaneously for 30 min. The cells were harvested by filtration through 500 μm Nitex filter and centrifuged at 350 g for 10 min, and the filtrate (cell suspension) was equilibrated for 20 min before the experiment. For some experiments, cells were permeabilized with a brief exposure to saponin (75 μg/ml for 4 min) and equilibrated in a cytosolic buffer.

Measurement of muscle cell contraction Contraction was measured in smooth muscle cells by computerized image micrometry as described previously[12]. An aliquot consisting of 1×10^4 cells in 0.25 ml of medium was added to 0.1 ml of a solution containing the test agents. The reaction was interrupted at 1 min by adding 0.1 ml of acrolein at a final concentration of 0.1 %. Individual cell length was measured by computerized image micrometry. The average length of cells in the control state or after adding test agents was obtained from 50 cells randomly. The contractile response was defined as the decrease in the average length of the 50 cells and expressed in percentage as compared with control length.

Measurements of $[Ca^{2+}]i$ in smooth muscle cells Changes in $[Ca^{2+}]i$ were estimated by fluorescence measurement using

Ca^{2+} indicator Fluo-3 AM as described elsewhere[13], using a laser scanning confocal microscope(Radiance 2000; Bio-rad, Hertfordshire, UK).

Freshly dissociated smooth muscle cells were seeded onto glass coverslips and incubated with Fluo-3 working solution (Fluo-3 AM 5 μmol and Pluronic F-127 0.03 % dissolved in standard buffer) at 37 ℃ under an atmosphere of 5 % CO_2. After a loading period of 30 min, the cells were washed with PBS to remove extracellular Fluo-3 AM and incubated for an additional 20 min to allow complete desterilization of the cytosolic Fluo-3 AM.

Coverslips mounted on the chamber slide (Molecular Probe) were placed on the stage of the microscope. The fluorescence in the cell was excited at 488 nm by an argon-ion laser, emission at wavelength between 515-545 nm was detected by a photomultiplier. Changes in the Fluo-3 fluorescence intensity indicating fluctuations in cytosolic Ca^{2+} were recorded using T-series acquisition. After stable baseline fluorescence intensity was measured, 10 μl of an agent was added to extracellular medium to yield a 1/100 concentration, and the fluorescence intensity was recorded. The ratio representing the intracellular calcium variations related to the basal level was calculated. Baseline and sustained phases of agonist induced [Ca^{2+}]i were determined from the average of 5 data points. Peak [Ca^{2+}]i was determined from the average of 3 data points including the absolute maximum of the response.

Statistical analysis

Data represented means ± standard error of the mean. Values of *n* were the numbers of cells. Student' s *t*-test was performed and a *P*-value of less than 0.05 was considered statistically significant.

RESULTS

Effect of emodin on smooth muscle cell length

In resting state, the average length of isolated smooth muscle cells was 81.27±6.29 μm. The application of emodin to freshly isolated smooth muscle cells induced a reduction in cell length. This reduction in cell length reflected contraction of the smooth muscle cells. Emodin at concentrations of 5 to 100 μmol/L induced a concentration-dependent contraction (Figure 1). Maximal contraction of 17.26±3.51 % was observed with 50 μmol/L of emodin. In order to determine the signal mechanism underlying emodin-induced contraction, the effect of ML-7, an inhibitor of MLCK, on the cell contraction induced by emodin was examined. 36.61±4.69 % of the contractile response induced by 50 μmol/L emodin was inhibited by preincubation of the cells with ML-7(Figure 2).

Role of calcium in emodin-induced responses

The exposure of freshly isolated smooth muscle cells to emodin (50 μmol/L) induced an increase in [Ca^{2+}]i. The emodin-induced increase in [Ca^{2+}]i was a biphasic rise, consisting of a transient peak followed by a decline to steady-state level that remained significantly above baseline during scanning (Figures 3 and 4).

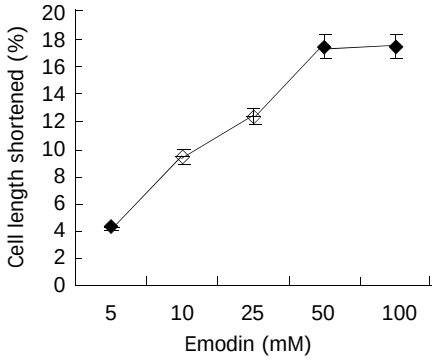

Figure 1 Contractile effect of emodin on isolated smooth muscle cell. Values were calculated as means ± SE from 3 experiments.

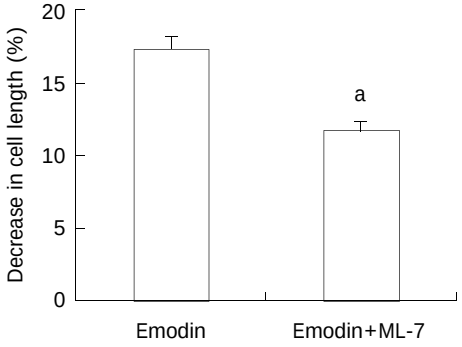

Figure 2 Effect of ML-7 on emodin-induced contraction of smooth muscle cells. Values were means ±SE of 3 experiments. [a]*P*<0.05 by Student's *t*-test.

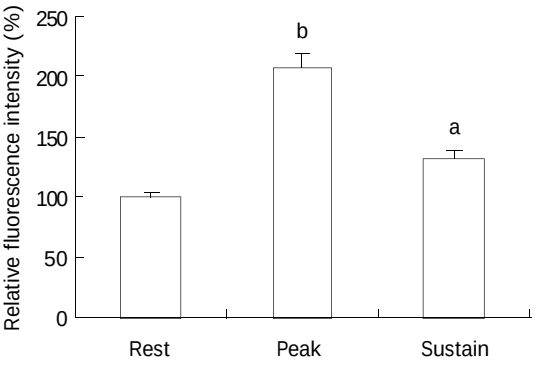

Figure 4 Average peak and sustained changes in [Ca^{2+}]i in response to emodin (50 μmol / L). [a]*P*<0.05, [b]*P*<0.001.

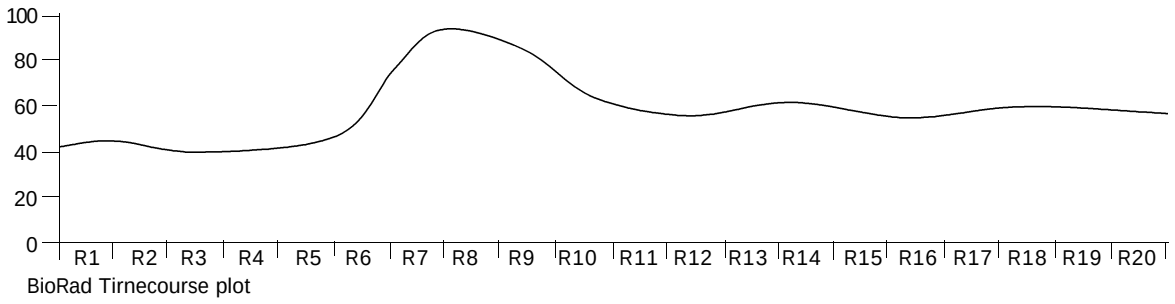

Figure 3 Timecourse changes of [Ca^{2+}]i induced by emodin in a circular colonic smooth muscle cells (analysed by BioRad Laserpix software).

To determine whether the emodin-induced increase in $[Ca^{2+}]i$ required calcium influx from extracellular medium, the effect of nifedipine, an antagonist of voltage-gated Ca^{2+} channel in response to emodin was investigated. Emodin was applied after 15 min-exposure to nifedipine. Exposing smooth muscle cells to nifedipine had no effect on the increase in $[Ca^{2+}]i$ induced by emodin ($P>0.05$). To further evaluate the role of extracellular Ca^{2+} influx to the emodin-induced rise in $[Ca^{2+}]i$, emodin was applied to cells incubation with Ca^{2+}-free extracellular solution. Removal of extracellular Ca^{2+} by EGTA solution significantly reduced the sustained changes in $[Ca^{2+}]i$ (Figure 4, $P<0.05$) compared with the sustained increase in $[Ca^{2+}]i$ induced by emodin, and had no effect on peak changes in $[Ca^{2+}]i$ (Figure 4, $P>0.05$).

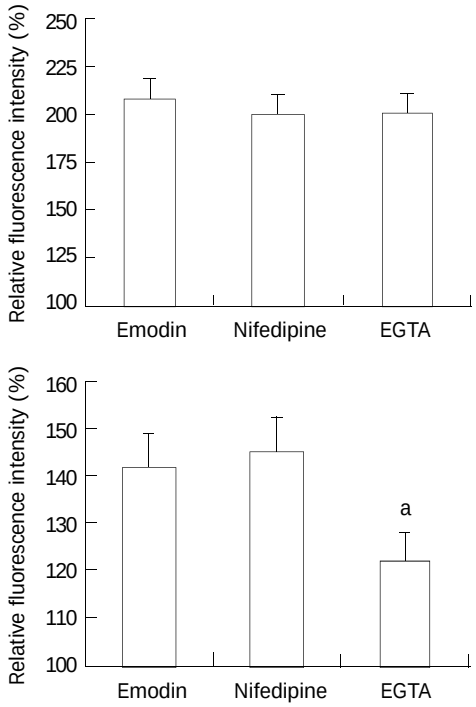

Figure 5 Average peak (top) and sustained (bottom) changes in $[Ca^{2+}]i$ in response to emodin under control conditions, in the presence of nifedipine, and EGTA solution. $n=15$. $^aP<0.05$ *vs* emodin group.

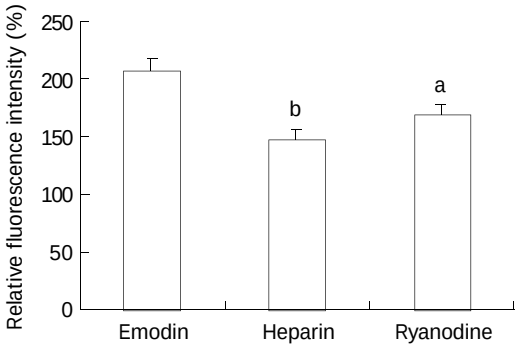

Figure 6 Effect of ryanodine and heparin on the change in $[Ca^{2+}]i$ induced by emodin. $n=15$ $^aP<0.05$ *vs* emodin group $^bP<0.01$ *vs* emodin group.

Because emodin-induced peak increase in $[Ca^{2+}]i$ was not affected by pretreatment with EGTA and nifedipine, the contribution of calcium release from the intracellular stores to the changes in $[Ca^{2+}]i$ in response to emodin was examined. Smooth muscle cells were pretreated for 10 min with ryanodine (10^{-5}M) to inhibit Ca^{2+} release from ryanodine-sensitive intracellular stores. Ryanodine markedly attenuated the peak increase in $[Ca^{2+}]i$ in response to emodin (Figure 5, $P<0.05$). In order to examine the role of IP_3 in emodin-induced increases in $[Ca^{2+}]i$, the effect of low molecular weight heparin, a specific IP_3 receptor antagonist was tested. Heparin did not diffuse across the plasma membrane, therefore, it was used in permeablized smooth muscle cells. In permeablized smooth muscle cells, the peak rise in $[Ca^{2+}]i$ induced by emodin was almost abolished by incubation with 10 μg/ml heparin (Figure 5).

DISCUSSION

The contractile effects of emodin on gastrointestinal smooth muscle have been described in several reports[8-10]. In this study, we have attempted to investigate the effects of emodin on circular smooth muscle cells of rat colon and to examine the mechanisms underlying its effects.

The result of this study showed that emodin had a direct contractile effect on smooth muscle cells freshly isolated from rat colon, as application of emodin resulted in a decrease in cell length. It was also found that exposure of smooth muscle cells to emodin induced an increase in $[Ca^{2+}]i$, and the rising in $[Ca^{2+}]i$ induced by emodin was a biphasic rise in $[Ca^{2+}]i$ consisting of a rapid, transient peak followed by a decline to sustained level that remained elevated than baseline. The involvement of calcium in emodin-induced contraction was in agreement with previous studies[9,10], reporting that emodin-induced contractions were related to calcium ion.

Calcium is believed to be the crucial signal for tension generation or shortening of smooth muscle cells[11-16]. The increase in $[Ca^{2+}]i$ induced by contractile agonists in smooth muscle cells is accompanied by Ca^{2+}/CaM-dependent activation of myosin light chain (MLC) kinase, leading to activation of myosin ATPase and cell contraction[14,17-19]. In these experiments, suppression of Ca^{2+}/CaM-dependent MLCK activity with ML-7 while maintaining Ca^{2+} mobilization partly inhibited emodin-induced cell contraction. This implies that Ca^{2+}/CaM-dependent MLCK signal pathway is involved in emodin-induced cell contraction.

Regulation of intracellular Ca^{2+} concentration ($[Ca^{2+}]i$) in smooth muscle cells involves multiple mechanisms[14,15,20]. Increases in $[Ca^{2+}]i$ can be resulted from either the transplasma membrane flux through plasma membrane Ca^{2+} channels or release of Ca^{2+} from intracellular stores, with a relative contribution from these two Ca^{2+} pools varying in different smooth muscle cells and in response to different stimuli[21-23]. The present study demonstrated that both Ca^{2+} influx and release of Ca^{2+} from intracellular sources contributed to the emodin-induced increase in $[Ca^{2+}]i$ in smooth muscle cells.

Removal of extracellular Ca^{2+} by EGTA solution caused a reduction of sustain phase of $[Ca^{2+}]i$ in response to emodin indicated extracellular Ca^{2+} contributed to the sustained elevation in $[Ca^{2+}]i$. Furthermore, compared with EGTA, blockade of L-type Ca^{2+} channel with nifedipine had no effect on the increase in $[Ca^{2+}]i$ induced by emodin. These results suggest that extracellular Ca^{2+} is essential for the sustain phase of $[Ca^{2+}]i$ and extracellular Ca^{2+} influx did not occur through L-type Ca^{2+} channel. These results also indicate that Ca^{2+} release from intracellular sources may be the main resources for the peak increases in $[Ca^{2+}]i$ induced by emodin.

Because pretreatment with EGTA and nifedipine had no effect on emodin-induced peak increase in $[Ca^{2+}]i$, it seemed likely that the portion of peak emodin-induced Ca^{2+} transient mainly depended on the calcium release from intracellular stores. The sarcoplasmic reticulum (SR) is the physiological intracellular source and sink of activator Ca^{2+} in smooth muscle cells[15,24]. The SR of smooth muscle is endowed with two different types of Ca^{2+} release channels, i.e. inositol 1, 4, 5-triphosphate receptors (IP_3Rs) and ryanodine receptors

(RyRs)[14,15,24-26]. Pretreating cells with ryanodine, a RyRs antagonist, attenuated but did not abolish the peak in $[Ca^{2+}]i$. In contrast, heparin, which inhibits the IP_3 binding to its receptor, almost abolished the peak component of the Ca^{2+} transient. These observations suggest that the residual Ca^{2+} peak observed in the presence of ryanodine is due to release of Ca^{2+} from IP_3-sensitive stores, and Ca^{2+} release through RyR receptors is possibly linked with the Ca^{2+}-induced Ca^{2+}-release (CICR). CICR means a process that a rise in $[Ca^{2+}]i$ resulted from extracellular Ca^{2+} influx or Ca^{2+} release from IP_3-sensitive store triggers further calcium release from RYR in the SR[14, 26-29]. Ryanodine receptors contain Ca^{2+} binding sites, allowing increased $[Ca^{2+}]i$ to initiate release from intracellular calcium stores[30,31]. CICR has been demonstrated to occur in a number of studies. On the basis of our findings, it appears to be operative in emodin-induced increase of $[Ca^{2+}]i$ in rat colonic smooth muscle cells.

Taken together, the results of this study indicate that emodin has a direct excitatory effect on circular smooth muscle cells from rat colon and its effect is mediated via Ca^{2+}/CaM-dependent MLCK signal pathway. The data suggest that the emodin-induced peak increases in $[Ca^{2+}]i$ primarily depend on Ca^{2+} release from IP_3 sensitive stores, which trigger Ca^{2+} release from ryanodine-sensitive stores through CICR mechanism. Additionally, Ca^{2+} influx from extracellular medium contributes to the sustained increase in $[Ca^{2+}]i$ observed in response to emodin.

ACKNOWLEDGE

We thank Professor Chang Chen for revising this article.

REFERENCES

1 **Liang JW**, Hsiu SL, Wu PP, Chao PD. Emodin pharmacokinetics in rabbits. *Planta Med* 1995; **61**: 406-408

2 **Xia Q**, Jiang JM, Gong X, Chen GY, Li L, Huang ZW. Experimental study of Tong Xia purgative method in ameliorating lung injury in acute necrotizing pancreatitis. *World J Gastroenterol* 2000; **6**: 115-118

3 **Chen H**, Wu X, Guan F. Protective effects of tongli gongxia herbs on gut barrier in rat with multiple organ dysfunction syndrome. *Zhongguo Zhongxiyi Jiehe Zazhi* 2000; **20**: 120-122

4 **You SY**, Wu XZ, Liu ML. Effects of dachengqi decoction on gut hormones and intestinal movement after cholecystectomy. *Zhongguo Zhongxiyi Jiehe Zazhi* 1994; **14**: 522-524

5 **Lee HZ**. Effects and mechanisms of emodin on cell death in human lung squamous cell carcinoma. *Br J Pharmacol* 2001; **134**: 11-20

6 **Lee HZ**. Protein kinase C involvement in aloe-emodin- and emodin-induced apoptosis in lung carcinoma cell. *Br J Pharmacol* 2001; **134**: 1093-1103

7 **Kuo YC**, Meng HC, Tsai WJ. Regulation of cell proliferation, inflammatory cytokine production and calcium mobilization in primary human T lymphocytes by emodin from Polygonum hypoleucum Ohwi. *Inflamm Res* 2001; **50**: 73-82

8 **Jin ZH**, Ma DL, Lin XZ. Study on effect of emodin on the isolated intestinal smooth muscle of guinea-pigs. *Zhongguo Zhongxiyi Jiehe Zazhi* 1994; **14**: 429-431

9 **Li JY**, Yang WX, Hu WW, Wang J, Jin ZG, Wang XY, Xu WS. Effects of emodin on the activity of K channel in guinea pig taenia coli smooth muscle cells. *Yaoxue Xuebao* 1998; **33**: 321-325

10 **Yang WX**, Wang J, Li JY, Yu Y, Xu WS. Characteristics of emodin evoked $[Ca^{2+}]i$ and inhibition of GDP in guinea pig taenia coli cells. *Shengwu Wuli Xuebao* 2001; **17**: 165-169

11 **Wang P**, Bitar KN. RhoA regulates sustained smooth muscle contraction through cytoskeletal reorganization of HSP27. *Am J Physiol* 1998; **275**(6Pt 1): 1454-1462

12 **Yamada H**, Strahler J, Welsh MJ, Bitar KN. Activation of MAP kinase and translocation with HSP27 in bombesin-induced contraction of rectosigmoid smooth muscle. *Am J Physiol* 1995; **269** (5Pt 1): 683-691

13 **Jacques D**, Sader S, El-Bizri N, Chouffani S, Hassan G, Shbaklo H. Neuropeptide Y induced increase of cytosolic and nuclear Ca^{2+} in heart and vascular smooth muscle cells. *Can J Physiol Pharmacol* 2000; **78**: 162-172

14 **Sanders KM**. Invited review: mechanisms of calcium handling in smooth muscles. *J Appl Physiol* 2001; **91**: 1438-1449

15 **Bolton TB**, Prestwich SA, Zholos AV, Gordienko DV. Excitation-contraction coupling in gastrointestinal and other smooth muscles. *Annu Rev Physiol* 1999; **61**: 85-115

16 **Makhlouf GM**, Murthy KS. Signal transduction in gastrointestinal smooth muscle. *Cell Signal* 1997; **9**: 269-276

17 **Sayeski PP**, Ali MS, Bernstein KE. The role of Ca^{2+} mobilization and heterotrimeric G protein activation in mediating tyrosine phosphorylation signaling patterns in vascular smooth muscle cells. *Mol Cell Biochem* 2000; **212**: 91-98

18 **Fan J**, Byron KL. Ca^{2+} signalling in rat vascular smooth muscle cells: a role for protein kinase C at physiological vasoconstrictor concentrations of vasopressin. *J Physiol* 2000; **524**(Pt 3): 821-831

19 **White C**, Mc Geown JG. Regulation of basal intracellular calcium concentration by the sarcoplasmic reticulum in myocytes from the rat gastric antrum. *J Physiol* 2000; **529**(Pt 2): 395-404

20 **Carl A**, Lee HK, Sanders KM. Regulation of ion channels in smooth muscles by calcium. *Am J Physiol* 1996; **271**(1Pt 1): 9-34

21 **McCarron JG**, Flynn ER, Bradley KN, Muir TC. Two Ca^{2+} entry pathways mediate $InsP_3$-sensitive store refilling in guinea-pig colonic smooth muscle. *J Physiol* 2000; **525**(Pt 1): 113-124

22 **Takeuchi M**, Watanabe J, Horiguchi S, Karibe A, Katoh H, Baba S, Shinozaki T, Miura M, Fukuchi M, Kagaya Y, Shirato K. Interaction between L-type Ca^{2+} channels and sarcoplasmic reticulum in the regulation of vascular tone in isolated rat small arteries. *J Cardiovasc Pharmacol* 2000; **36**: 548-554

23 **van Helden DF**, Imtiaz MS, Nurgaliyeva K, Von der Weid P, Dosen PJ. Role of calcium stores and membrane voltage in the generation of slow wave action potentials in guinea-pig gastric pylorus. *J Physiol* 2000; **524**(Pt 1): 245-265

24 **Flynn ER**, Bradley KN, Muir TC, McCarron JG. Functionally separate intracellular Ca^{2+} stores in smooth muscle. *J Biol Chem* 2001; **276**: 36411-36418

25 **Kotlikoff ML**, Wang YX, Xin HB, Ji G. Calcium release by ryanodine receptors in smooth muscle. *Novartis Found Symp* 2002; **246**: 108-119

26 **Ji G**, Barsotti RJ, Feldman ME, Kotlikoff MI. Stretch-induced calcium release in smooth muscle. *J Gen Physiol* 2002; **119**: 533-544

27 **Collier ML**, Ji G, Wang Y, Kotlikoff MI. Calcium-induced calcium release in smooth muscle: loose coupling between the action potential and calcium release. *J Gen Physiol* 2000; **115**: 653-662

28 **Morgan JM**, Gillespie JI. The modulation and characterisation of the Ca^{2+}-induced Ca^{2+} release mechanism in cultured human myometrial smooth muscle cells. *FEBS Lett* 1995; **369**: 295-300

29 **Henkel CC**, Asbun J, Ceballos G, del Carmen Castillo M, Castillo EF. Relationship between extra and intracellular sources of calcium and the contractile effect of thiopental in rat aorta. *Can J Physiol Pharmacol* 2001; **79**: 407-414

30 **Somlyo AP,** Somlyo AV. The sarcoplasmic reticulum: then and now. *Novartis Found Symp* 2002; **246**: 258-268

31 **Chambers P**, Neal DE, Gillespie JI. Ryanodine receptors in human bladder smooth muscle. *Exp Physiol* 1999; **84**: 41-46

Edited by Zhang JZ and Zhu LH

P.O.Box 2345, Beijing 100023,China
Fax: +86-10-85381893
E-mail: wjg@wjgnet.com www.wjgnet.com

World J Gastroenterol 2003;9(8):1808-1814
World Journal of Gastroenterology
 ISSN 1007-9327

• CLINICAL RESEARCH •

Relationship between telomerase activity and its subunit expression and inhibitory effect of antisense hTR on pancreatic carcinoma

Jia-Hua Zhou, Hong-Mei Zhang, Quan Chen, Dong-Dong Han, Fei Pei, Li-Shan Zhang, De-Tong Yang

Jia-Hua Zhou, Quan Chen, Dong-Dong Han, De-Tong Yang, Department of Biliary-pancreatic Surgery, Zhongda Hospital of Southeast University, Nanjing, Jiangsu Province, 210009, China
Hong-Mei Zhang, Li-Shan Zhang, Genetic Center, Southeast University, Nanjing, Jiangsu Province, 210009, China
Fei Pei, Department of General Surgery of Huangshi Central Hospital, Huangshi, Hubei Province, 435000, China
Supported by the Applied Basic Research Programs of Science and Technology Commission Foundation of Jiangsu Province, No BJ98080 (1998-2001)
Correspondence to: Jia-Hua Zhou, Department of Biliary-pancreatic Surgery, Zhongda Hospital Affiliated to Southeast University, 87 Dingjiaqiao, Nanjing 210009, Jiangsu Province, China. zhoujiahua@hotmail.com
Telephone: +86-25-3249268 **Fax:** +86-25-3272356
Received: 2002-10-08 **Accepted:** 2003-02-09

Abstract

AIM: To directly investigate the relationship between telomerase activity and its subunit expression and the inhibitory effect of antisense hTR on pancreatic carcinogenesis.

METHODS: We examined the telomerase activity and its subunit expression by cell culture, polymerase chain reaction (PCR), PCR-silver staining, PCR-ELISA, DNA sequencing, MTT and flow cytometry methods.

RESULTS: PCR-silver staining and PCR-ELISA methods had the same specificity and sensitivity as the TRAP method. Telomerase activity was detected in the extract of the 10^{th}, $20^{th}$and 30^{th} passages of P3 cells,while it was absent in fibroblasts. Furthermore, after the 30th generation, the proliferation period of fibroblast cells was significantly prolonged. Telomerase activity and hTERTmRNA were detected in two pancreatic carcinoma cell lines, but were found to be negative in human fibroblast cells. Telomerase activity and hTERTmRNA were tested in pancreatic carcinoma specimens of 24 cases. The telomerase activity was positive in 21 of the 24 cases (87.5 %), and the hTERTmRNA in 20 cases (83.3 %). In adjacent normal tissues positive rates were both 12.5 %. There was a significant difference between the two groups. This indicated a significant correlation between the expression level of telomerase activity and histologic differentiation, metastasis and advanced clinical stage of pancreatic carcinoma. Our findings showed that the expressions of hTR and TP1mRNA were not correlated with the activity of telomerase but the expression of hTERTmRNA was. After treatment with PS-ODNs, telomerase activity in P_3 cells weakened and the inhibiting effect became stronger with an increase in PS-ODNs concentration. There was a significant difference between different PS-ODN groups ($P<0.05$). Inhibition of telomerase activity occurred most significant with PS-ODN1.The results of the FCM test of pancreatic cancer P_3 cells showed an increase in the apoptotic rate with increasing PS-ODN1 and PS-ODN2 concentrations.

CONCLUSION: The expression of telomerase activity has a significant relationship to carcinogenesis. A strong correlation exists between telomerase activity and hTERTmRNA expression. The up-regulation of hTERTmRNA expression may play a critical role in human carcinogenesis. The expression of telomerase activity and its subunit level in pancreatic carcinoma significantly correlate with the clinical stage of pancreatic carcinoma and hence, may be helpful in its diagnosis and prognosis. The anti-hTR complementary to the template region of hTR is sufficient to inhibit P3 cell telomerase activity and cell proliferation *in vitro*, and can lead to a profound induction of programmed cell death.

Zhou JH, Zhang HM, Chen Q, Han DD, Pei F, Zhang LS, Yang DT. Relationship between telomerase activity and its subunit expression and inhibitory effect of antisense hTR on pancreatic carcinoma. *World J Gastroenterol* 2003; 9(8): 1808-1814
http://www.wjgnet.com/1007-9327/9/1808.asp

INTRODUCTION

Telomerase is a DNA-dependent RNA polymerase[1] carrying template features. It is different from reverse transcriptase, DNA polymerase of commonly pure proteins. The activated telomerase takes the 3' distal end of telomeres as the primer and its RNA component acts as the template. The protein component of telomerase regulates the catalytic activity in the synthesis of telomere repetitive sequence to maintain the telomere length. Human telomerase mainly consists of three subunits-human telomerase RNA (hTR), human telomerase-associated protein 1(TP_1) and human telomerase reverse transcriptase (hTERT). Telomerase activity has been found in most human tumor cells[2], while there is no evident expression in normal human tissues other than in germ cells, hemopoietic stem cells and cuticle basal cells[3,4]. This suggests that telomerase is a broad spectrum tumor marker[5-9]. It is recognized that activation of telomerase and stability of telomere length are necessary for tumor immortalization. However, it has been found that expression of hTERTmRNA is obviously related to telomerase activity. It is suggested that up-regulation of the expression level of hTERTmRNA is a key factor in the formation of tumor cells.

Human pancreatic cancer is one of the most frequent tumors. The present clinical treatment however has a low curative effect. The mortality rate of human pancreatic cancer is very high. Post-operative metastases are common and less than 3 % of patients have a survival rate of 5-years. In recent years, a close relationship has been found between telomerase and pancreatic cancer. By cell culture, PCR-silver staining, PCR-ELISA, RT-PCR, DNA sequencing technology, MTT and Flow cytometry methods, we have investigated the expression of telomerase activity and its subunits in pancreatic cancer cell line, fibroblasts, and in pancreatic cancer samples of 24 cases and their adjacent normal tissues. The purpose of this research was to explore the relationship between the biological behavior and clinico-pathological characteristics of human pancreatic cancer, as well as the inhibitory effects of hTR antisense oligonucleotide on pancreatic cancer cells.

MATERIALS AND METHODS

Cell lines and tissuse samples

In this study, the pancreatic cancer P_3 cells were provided by Peking Union Medical College Hospital, PaTu-8801 cells were provided by Shanghai Changhai Hospital, and the human skin fibroblasts were developed in the Zhongda Hospital. Cancer tissues and adjacent normal tissues from 24 patients with pancreatic cancer were provided and assayed by the Surgical Department of Zhongda Hospital Affiliated to Southeast University and Jiangsu Provincial People·s Hospital. These samples were frozen at -80 ℃ within 15 min after surgical removal and stored until use. Of the 24 patients, 13 were male and 12 female.Their age ranged between 55-74 years with an average of 63 years.

Cell culture

Culture of the pancreatic cancer P_3 cells and PaTu-8801 cells: P_3 cells and human skin fibroblasts were cultured in 1640 culture medium and PaTu-8801 cells in DMEM culture medium (high glucose content) with 10 % inactivated calf serum and all were put in 5 % CO_2 at 37 ℃ for generational culture at 100 % RH.

Telomerase assay

Telomerase extracts and assays of activity were done as TRAP method. Briefly frozen pancreatic tissue samples of approximately 200 mg were homogenized in 200 μl of lysis reagent containing 5 % CHPAS (3-(3-cholamidopropyl dimethyammonio)-1-propanesulfonate lysis buffer, Roche Co.). The cells obtained by cell culture were also treated with lysis reagent containing 5 % CHPAS (Roche Co.). After 30 min of incubation on ice,the lysates were centrifuged at 16 000×g (tissue) or 34 000×g (cell) for 20 min at 4 ℃, and the supernatants were rapidly frozen in liquid nitrogen and stored at -80 ℃ until use. In the extracts from frozen tissues, the concentration of protein was measured using the Coomassie brilliant blue method. BCA. Extracts of 293 cell line with telomerase activity were used as the standard, while extracts obtained by inactivation for 10 min at 94 ℃ or treated with RNase for 10 min at 37 ℃ were used as the negative control. For cell samples, aliquots corresponding to extracts derived from approximately 10^2, 10^3, 10^4, 10^5 cells were used for TRAP assay. Extracts of tissues containing 0.06, 0.6 and 6 μg of protein were used for TRAP assay. Each extract specimen was assayed in 25 μl reaction mixture (Roche Co assay kit containing dNTP, Taq enzyme, biotin tagged TS primer and CX primer) which was diluted to 50 μl with DEPC water solution. After 30 min incubation at 25 ℃ for telomerase-mediated extension of the TS primer, the reaction mixture was heated at 94 ℃ for 5 min and then subjected to 30 PCR cycles at 94 ℃ for 30 s, at 50 ℃ for 30 s and at 72 ℃ for 50 s and then extended for 10 min at 72 ℃. Firstly, the PCR product went through enzyme-linked immunosorbent assay (PCR-ELISA) containing DIG-labeled probes (Roche Co assay kit). After spectrophotometric determination, the absorbance value A(=A_{450}-A_{690}) was calculated. The result was positive if A >0.2. Secondly, the PCR product was electrophoresed on a 10 % polyacrylamide gel. The telomerase activity was positive if the specific band appeared. For each sample of pancreatic carcinoma tissue, the intensity of telomerase was graded according to the different contents of protein in the extract specimen. A sample intensity of telomerase was represented as (-) if the specimen containing 6 μg extracted protein was tested to be negative, or (+) if the specimen containing 6 μg extracted protein was tested positive. If both sample specimens containing 6 μg and 0.6 μg extracted protein were tested positive, while the specimen containing 0.06 μg extracted protein was tested to be negative, it was represented by (++), and (+++) if all three specimens containing 6 μg, 0.6 μg, and 0.06 μg extracted protein were tested positive[10].

Expression of the subunit of telomerase

Analysis of the expression of each telomerase subunit was performed by RT-PCR amplification[11-13]. hTERT mRAN was amplified by using the primer pair (145 bp): LT5 5' -CGGA AGAGTATCTGGAGCAA-3' , LT6 5' -GGATGAAGCGGA GTCTGGA-3' . TP1 mRAN was amplified by using the primer pair (340 bp), TP1.1 5' -TCAAGCCAAACCTGAATCTGAG-3' , TP1.2 5' -CCCCGAGTGAATCTTTCTACGC-3' . hTR was amplified by using the primer pair (134 bp): F3b 5' -TCTAACCCTAACTGAGAAGGGCGTAG-3' , R3c 5' -GTTTGCTCTAGAATGAACGGTGGAAG-3' . The efficiency of cDNA synthesis from each sample was estimated by PCR with glyceraldehyde-3-phosphate-dehydrogenase (GAPDH)-specific primers of (450 bp): K136 5' -CTCAGACACCATG GGGAAGGTGA-3' ,K137 5' -ATGATCTTGAGGCTG TTGTCATA-3' . cDNA was synthesized in 20 μl of reaction mixture containing 5×RT Buffer 4 μl, RNasin 0.5 μl, total RNA 1 μl, and MLV 0.8 μl with 1 μl random primers. The reaction mixture was incubated at 94 ℃ for 5 min before it was heated at 95 ℃ for 5 min to inactivate MLV. To amplify the cDNA 2 μl aliquots of the reversely-transcribed cDNA was subjected to 35 cycles of PCR in 50 μl containing 10×buffer (10 mM Tris-HCl (pH8.3), 25 mM $MgCl_2$, 500 mM KCl) 10 mM dNTP 1 μl, 25 mM $MgCl_2$ 2-3 μl, Taq enzyme 4 unit and 10 pM of specific primers 22 μ1. After heated at 94 ℃ for 5 min, each cycle consisted of de-naturation at 94 ℃ for 45 s, annealing at 56 ℃ for 45 s (hTERT) or at 61 ℃ for 45 s (hTR) or at 60 ℃ for 45 s (TP_1) and extension at 72 ℃ for 90 s and then extended at 72 ℃ for 10 min. PCR products were electrophoresed on 3 % agarose gel with ladder marker to determine the concentrations and purity of PCR amplified products. hTERTmRNA PCR products were sequenced (sent to Shanghai Biolottering Co, Ltd.).

Inhibitory effects of antisense hTR

Four nucleotides were synthesized as hTR template sequence (5' -CUAACCCUAAC-3') and modified by thiophosphoric acid. They were PS-ODN1: 5' -GTTAGG-3' (antisense), PS-ODN2: 5' -GTTAGGGTTAG-3' (antisense), PS-ODN3: 5' -CCTAAC-3' (pro-sense), and a PS-ODN4 with random sequence: 5' -AACTCGTAGTC-3' . After 5×10 P_3 cells and human fibroblasts were inoculated into culture bottles and replaced the old culture medium with a fresh one after 24-h-lasting cultivation, the cells stuck to the wall of bottle. The test group was arranged PS-ODN1, PS-ODN2, PS-ODN3, PS-ODN4 so that each had four concentrations, 3.16 μmol/L, 10 μmol/L, 31.6 μmol/L, and 100 μmo1/L. They were added into the culture bottles, respectively. Additional sets were the control groups which had no PS-ODN. The following tests were conducted when obvious change in cytomorphology was observed under the optical microscope. Firstly, P_3 and human fiber forming monolayer anchorage-dependent cells were digested. The suspended cells were cultured in RPMI 1640. After the suspended cell liquor was inoculated into a 96-cave culture board (100 μ1 per cave), 20 μ1 of freshly prepared 5 mg/ml MTT solution was added into each cave. This was incubated for 4 h at 37 ℃, the culture medium in the caves was discarded, and then dimethyl sulfoxide (DMSO) 150 μ1 was added into each cave to be shaken for 10 min to solve the crystal. The activity of succinic dehydrogenase (SDH) was determined according to the optical absorbance of the content in each cave at 540 μm in an enzyme-linked immunoassay analyzer. Secondly, after 2×10^6 P_3 cells were treated with each

of the different PS-ODNs, the activity of telomerase extracts was assayed according to the TRAP, PCR-ELISA and polyacrylamidedel gel (10 %) electrophoresis (PAGE). The telomerase extract of 293 cell line was taken as the positive control. The extract that was subjected to inactivation for 10 min at 94 ℃ or RNase treatment for 10 min at 37 ℃ was taken as the negative control. Finally, the single cell suspension was prepared by digesting anchorage-dependent cells after treatment with PS-ODN1 and PS-ODN2, respectively. It was cool-washed three times, and then centrifuged for 10 min at 2 000 rpm. After the supernatant was discarded and dried, precooled 95 % alcohol was added and the sample was placed into a refrigerator at 4 ℃ for 1 h, and then incubated with 10 μg/ml RNase at 4 ℃ for 3 h. The apoptotic rate and the cell cycle distribution of pancreatic cancer cells were analyzed by a flow cytometer (DB Corp. United States) after 1 ml propidium iodide comprehensive staining solution was added in an ice-bath for 15 min. Data were collected by Cellquest software and analyzed by Mmodift Lt software.

Statistic analysis

The data were processed by *t*-test and variance analysis. The *P* value was determined according to the *t* value, *F* value and FI value.

RESULTS

Cell culture

There were morphological changes in the fibroblasts (HE stain) of the 32nd generation, such as karyopyknosis, cytoplasmic concentration, and cell body shrinkage. No changes were found in P_3 cells. P_3 cells, and fibroblasts of the 10th, 20th, and 30th generations were used to detect the activity of telomerase in this test. All results were positive for P_3 cells, and negative for fibroblasts (Figure 1).

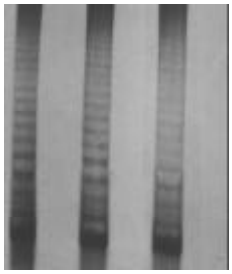

Figure 1 Telomerase activity of fibroblasts and P_3 cells of different generations (1, 3 and 5 were P_3 cells of the 10th, 20th, and 30th generations; 2, 4, and 6 were fibroblasts of the 10th, 20th, and 30th generations).

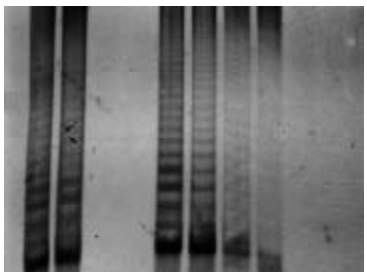

Figure 2 Specificity and sensitivity of telomerase activities in P3 cells (1, 293 cells as the positive control; 2,104 P_3 cells; 3, treated with RNase; 4, heat treated; 5, 6, 7, and 8 were 103, 102, 101, and 100 P_3 cells, respectively; 9, the lytic liquid).

Telomerase assay

The protein content was calculated from the sample extract, and standard curves were prepared by using the data. The protein contents in the sample extracts were determined by Coomassie brilliant blue method. PCR-silver staining method was used to detect the activities of telomerase in 10 cells or 1 μg protein extracted from a sample. PCR-ELISA method had a same sensitivity as PCR-silver staining (Figure 2).

The results were positive for the activity of telomerase in pancreatic cancer cells, and negative for fibroblasts. There were 21 cases whose telomerase activity was detected in the 24 pancreatic cancer tissues by PCR-ELISA or PCR silver staining. Four cases of them were (+++), 11 cases (++), and 6 cases (+). The rate of positive findings was 87.5 %. However, there were only 3 cases with telomerase activity (+) was found in adjacent normal tissues, with a positive rate of 12.5 % (Figure 3).

Figure 3a Telomerase activity of tumor and normal pancreas (T: tumor; N: normal).

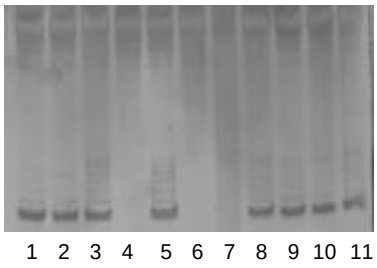

Figure 3b Semiquantitative telomerase activity of tumor and normal pancreas (1 2 3; 5 4 6; 9 10 11: T_{10}, T_{15} T_{18} 6 μg 0.6 μg 0.06 μg; 7: negative control, 8: positive control; T: tumor).

Detection of telomerase subunit

Pancreatic cancer cell P_3, and PaTu-8801 were taken as the positive control, while the fibroblast was taken as the negative control. There were 20 cases which expressed hTERTmRNA in cancer tissues of 24 cases, and 3 cases expressed hTERTmRNA in the adjacent normal tissues. 4 of 24 cases of cancer tissue did not express hTR and 3 cases of the adjacent normal tissues did not express hTR. Two cases tested were negative for TP_1 (Figure 4).

The cDNA sequencing of hTERTmRNA PCR products showed that there were 143 base groups that were significant sequences between the 51st and the 193rd base groups.The homology with hTERTcDNA reached 98.6 %, proving that the amplification products were the hTERTcDNA sequence amplified from hTERT.

Relationship between the expression of telomerase activities and its subunit with human pancreatic cancer, its biological behavior and clinico-pathological characteristics

Table 1 shows the relationship between telomerase activity

and tumor and adjacent normal tissue of pancreas.

Table 1 Telomerase activity of tumor and normal pancreas

	Cases	Telomerase activity	hTERTmRNA
Tumor	24	21[a]	20[b]
Normal	24	3	3

[a]P<0.01 (FI=28.82); [b]P<0.01 (FI=25.42).

There were significant differences in the expressions of telomerase activity and hTERTmRNA between pancreatic cancer tissues and adjacent normal tissues

Table 2 shows the relationship between telomerase activity and biological behavior of human pancreatic carcinoma.

Table 2 The relationship between telomerase activity and biological behavior of human pancreatic carcinoma

Biological behavior	Telomerase activity		
	–	+	AverageA (+)
Age	63.15±0.45	62.50±0.31	1.21±0.11
Sex			
Male	1	12	1.22±0.13
Female	2	9	1.15±0.44
Pathologic type			
Cystadenocarcinoma	1	1	1.19
Duct cell adenocystoma	2	19	1.13±0.39
Mucinous adenocystoma		1	1.22
Histologic differentiation			
Well-diff.	3	3	0.66±0.33[a]
Mod-diff.		10	1.10±0.16
Poorly-diff.		8	1.46±0.12
Invasion stage			
Non-invasive	1	3	0.86±0.31
Invasive	2	18	1.20±0.35
Lymphnode metastasis			
Absent	1	6	0.88±0.31[b]
Present	2	15	1.31±0.24
TNM stage			
I	1	1	1.19
II		5	0.81±0.35[c]
III	2	10	1.28±0.24
IV		5	1.34±0.12

[a]P<0.01 (F=26.06); [b]P<0.01 (t=3.22); [c]P<0.01 (F=9.31).

A correlation existed between the expression level of telomerase activity in pancreatic cancer tissues with histologic differentiation, presence of lymph node metastasis, and clinical TNM stage of the tumor (no significant difference between stages III and IV). However, in pancreatic cancer patients no correlation was found between the expression level of telomerase activities and age or sex of patients, pathologic category or tumor infiltration.

Table 3 shows the relationship between telomerase activity and telomerase subunit.

There was also an obvious correlation between expression of hTERT and telomerase activities in pancreatic cancer tissues, but no correlation was found between expressions of hTR and TPlmRNA and telomerase activities.

In 24 pancreatic cancer tissues and adjacent normal tissues, their hTR/GAPDH ratios were 0.592±0.056 and 0.510±0.059, respectively. No difference was found in the expression level of hTR.

Table 3 The relationship between telomerase activity and telomerase subunit

Telomerase activity	hTERT[a]		HTR[b]		TP1[c]	
	+	-	+	-	+	-
Tumor						
+	18	3	19	2	20	2
-	2	1	1	2	2	0
Normal						
+	1	2	3	0	3	0
-	1	20	18	3	19	2

[a]P>0.05 (χ^2=0.5); [b]P<0.01 (χ^2=13.76); [c]P<0.01(χ^2=15.70).

Inhibitory effects of antisense hTR

In the control groups, pancreatic cancer cells extended in polygon, showed large differences in their size and shape. The cells were more transparent, strong refractive, overlapped to grow after fully covering the bottom of the bottle and mitotic figures increased. After treatment with PS-ODN1 and PS-ODN2, morphologic changes of cells were obvious-refractiv, intercellular space became larger and the cells gradually became round, crenated, and fell off[14]. Occasionally, ballooning could be seen. When P_3 cells and human fibroblasts were treated with four PS-ODNs for reflecting the survival rate of cells, the results of SDH activity are shown in Table 4 and Table 5. There was a significant difference in the effects between the different PS-ODN groups (P<0.05). Along with an increase in concentrations of PS-ODN1 and PS-ODN2, the survival rate of cells significantly decreased. There was a significant difference between different concentrations in the same groups (P<0.05). No significant difference was found between PS-ODN1 and PS-ODN2. It was found that PS-ODN3 also might cause a decrease in SDH activity,but the decrease was less obvious than that of the former two. Inhibition of SDH activity occurred earliest with PS-ODN1. Comparison between different PS-ODNs and different concentrations of any PS-ODN (P<0.05) showed that the four PS-ODNs of any concentration had no significant effect on the survival rate of normal human fibroblasts.

Table 4 The viability of PS-ODNs treated P3 cells (%, $\bar{x}\pm s$)

PS-ODN	C1(3.16) V(%, $\bar{x}\pm s$)	C2(10) V(%, $\bar{x}\pm s$)	C3(31.6) V(%, $\bar{x}\pm s$)	C4(100) V(%, $\bar{x}\pm s$)
PS-ODN1	92.16±4.2	80.39±5.9	58.11±3.4	33.34±4.6
PS-ODN2	93.40±2.6	84.22±3.6	74.10±3.8	27.35±2.4
PS-ODN3	91.74±4.1	88.75±7.1	86.38±6.7	81.37±5.3
PS-ODN4	94.23±3.3	92.36±5.2	93.72±4.9	91.54±4.4

a.C is the concentration (unit). A is absorbance at 540 μm. V (%) is survival rate. V=$A_{CONTRAL\ GROUP}$*100 %.

Table 5 The viability of normal fibroblasts treated with PS-ODNs (%, $\bar{x}\pm s$)

PS-ODN	C1(3.16) V(%, $\bar{x}\pm s$)	C2(10) V(%, $\bar{x}\pm s$)	C3(31.6) V(%, $\bar{x}\pm s$)	C4(100) V(%, $\bar{x}\pm s$)
PS-ODN1	104.16±6.4	100.48±3.9	107.20±8.4	103.04±5.7
PS-ODN2	100.80±5.4	97.12±6.7	99.52±7.0	106.72±6.4
PS-ODN3	94.72±4.7	90.56±6.1	92.80±6.8	95.36±3.5
PS-ODN4	100.16±5.6	104.48±5.3	99.04±7.6	106.40±9.2

a.C is the concentration (unit). A is absorbance at 540 μm. V (%) is survival rate. V=$A_{CONTRAL\ GROUP}$*100 %.

After P_3 cells were treated by four PS-ODNs, their telomerase activity was detected using the PCR-ELISA method. The results showed that there was a significant difference between different PS-ODN groups ($P<0.05$). PS-ODN1 and PS-ODN2 showed similar results when different concentration groups were compared ($P<0.05$), suggesting that telomerase activity in P_3 cells weakened and the inhibiting effect became stronger with increasing concentration. There was no significant difference of telomerase activity between the different concentration groups of PS-ODN3 and PS-ODN4 ($P>0.05$) (Table 6). The results of quantitative tests of telomerase activity in PS-ODNs-treated P_3 cells by TRAP-PAGE silver staining method are shown in Figure 5. After treatment by PS-ODN1 and PS-ODN2, the telomerase activity in P_3 cells was positive. The brightness of the bands darkened with increasing PS-ODN1 and PS-ODN2 concentrations, and expression of the telomerase activity had a tendency to be depressed.

Table 6 Telomerase assay of PS-ODN treated P3 cells ($\bar{x}\pm s$)

PS-ODN	C0(0) B($\bar{x}\pm s$)	C1(3.16) B($\bar{x}\pm s$)	C2(10) B($\bar{x}\pm s$)	C3(31.6) B($\bar{x}\pm s$)	C4(100) B($\bar{x}\pm s$)
PS-ODN1	2.25±0.56	1.53±0.23	1.20±0.15	0.97±0.12	0.65±0.47
PS-ODN2	2.25±0.56	1.66±0.46	1.40±0.44	0.69±0.29	0.49±0.32
PS-ODN3	2.25±0.56	2.28±0.32	2.32±0.37	2.26±0.31	2.19±0.26
PS-ODN4	2.25±0.56	2.16±0.35	2.24±0.50	2.27±0.43	2.13±0.38

a.C0 (0 μmol/L) is the control group. B is telomerase activity.

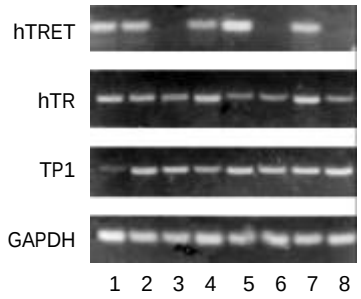

Figure 4 Telomerase subunit expression of pancreatic carcinoma (1: P3; 2: PaTu-8801; 3: fibroblast cell line; 4, 5, 7: tumor; 6, 8: normal).

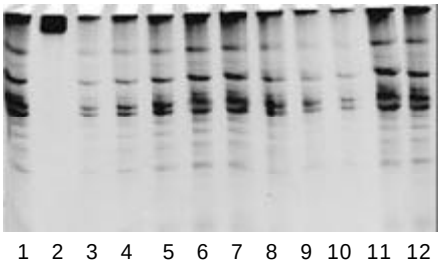

Figure 5 Telomerase activity after treated with PS-ODN in P3 cell line (1: positive control; 2: negative control; 3-6: 100 μmol/L, 31.60 μmol/L, 10 μmol/L, 3.16 μmol/L PS-ODN1 groups; 7-10: 3.16 μmol/L,10 μmol/L, 31.60 μmol/L, 100 μmol/L PS-ODN2 group; 11: 100 μmol/L PS-ODN3 group; 12: 100 μmol/L PS-ODN4 groups).

The FCM results of pancreatic cancer P_3 cells showed the apoptotic rate of cells increased along with increasing PS-ODN1 and PS-ODN2 concentrations. Fifty days or so after continuous treatment of the cells at 100 μM concentration of PS-ODN1 and PS-ODN2, the apoptotic rate of cells was 81.03 % and 70.75 %, respectively. The cycle distribution increased from 86.51 % and 83.89 % to 94.53 % and 95.39 % for cells in stage G_o/G_1, and reduced from 13.49 % and 16.11 % to 5.47 % and 2.11 % for cells in stage S, respectively (Figure 6).

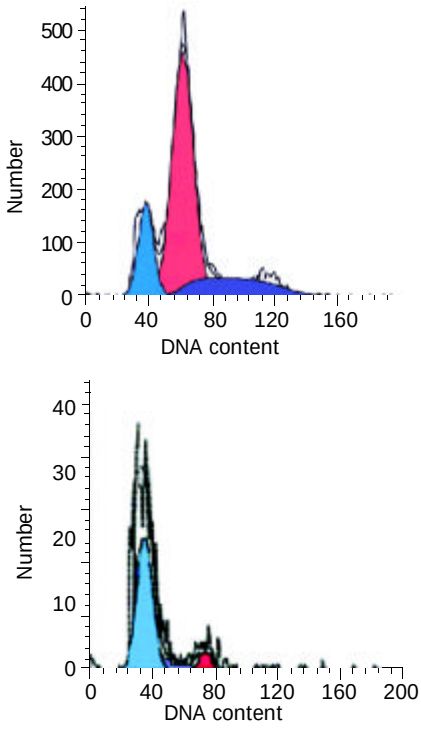

Figure 6 The apoptotic rate of P3 cells by the FCM test after treatment in P_3 cells with PS-ODN. A: PS-ODN1 10 μmol/L group; B: PS-ODN1 100 μmol/L group.

DISCUSSION

The activation of telomerase and maintenance of telomere length are essential for tumor cell immortalization. The positive rate of telomerase activity was 85-95 % in patients with pancreatic cancer, much higher than that in patients with benign pancreatic diseases[15-18]. Therefore, it can be deduced that there is a close link between telomerase activity and metastatic potential of pancreatic cancer cells[19].

The 10th, 20th, and 30th generations of cultured tumor cells and fibroblasts showed a significant difference in their telomerase activities. The results showed a positive telomerase activity for tumor cells, whereas it was absent in all generations of fibroblasts. After the 30th generation, the fibroblast cell proliferation period was obviously elongated, and part of the cells were found to have morphologic changes such as karyopyknosis, cytoplasmic concentration and cell-body shrinkage on HE stain. These findings indicate that telomerase is involved in immortalization of pancreatic cancer cells.

Hiyama *et al*[15]. reported positive telomerase activity was found in 43 cases. Among them, five cases were found to have a low level of telomerase activity expression in the adjacent normal tissues. In 24 pancreatic cancer samples, the positive rate of telomerase activity was 87.5 %, while there were 3 cases whose telomerase activity appeared in the adjacent normal tissue, a positive rate of 12.5 %. Of the three cases, one was proven to be infiltrated by tumor cells. The positive rate of hTERTmRNA in pancreatic cancer samples was 83.3 %, and 12.5 % in the adjacent normal tissue.

The results of this study support the theory that telomerase is involved in the formation of pancreatic cancer. It is a consensus that the prognosis is poor in patients with low differentiation and wide infiltration of human pancreatic cancer, i.e., those falling into the TNM stages III-IV of the

pancreatic cancer[20-22]. By statistic analysis, our data showed that there was a definite correlation between the expression level of telomerase activity in pancreatic cancer and histologic differentiation, presence of lymph node metastasis and TNM staging of the tumor. However, no significant correlation was found between it and age, sex of the subjects, pathologic category and degree of infiltration. Along with increasing expression level of telomerase, the tumor showed a higher lymph node metastasis. Therefore, the prognosis became much worse. We did not perform any post-operative follow-up studies.Tang *et al*[22] reported that patients with pancreatic endocrine neoplasm who were positive in telomerase expression usually had a shorter life expectancy than those who were negative in telomearse expression.

In the tumor cell line with positive telomerase expression, hTERTmRNA was found to have a higher expression level, whereas it was absent in normal tissues. In 21 cases of pancreatic cancer tissues with positive telomerase activity, hTERTmRNA was detected in 18 cases and only one case was found to be positive in the adjacent normal tissue which showed no telomerase activity.

Statistic analysis showed a significant correlation between hTERTmRNA and telomerase activity. Therefore, it may be thought that expression of hTERT is an important factor in governing telomerase activity[23, 24] and that up-regulation of hTERTmRNA expression may play an important role in the formation of pancreatic cancer. However hTERTmRNA was detected in two of the pancreatic cancer samples in which no telomerase activity was found. This may be explained by the following factors: (1) The expression level of each subunit or an equilibrium state between their expression levels determines the activity of telomerase; (2) Modification of the telomerase subunit after its transcription may have a regulating effect on the enzyme activity; (3) telomerase inhibitor existing in the cell extract reduces the activity of telomerase. Furthermore, there were 3 cases whose telomerase activity was detected, while the expression of hTERTmRNA showed negative results. There may be other factors to determine the activity of telomerase in this latter situation.

This study found that though the expression level of hTR in pancreatic cancer tissue was higher than that in adjacent normal tissue, it had no statistical significance. hTR itself cannot reflect the activity of telomerase. However, its function is essential for the activity of telomerase. This point is consistent with other studies[25-28].

It was found in our study that inhibition of the growth of P_3 cells by PS-ODN1 occurred the earliest. This was probably not only due to the smaller PS-ODN1 molecules entering cells, but also due to two important basic UC groups at the junction of the closed hTR templates. No significant effect was found on the survival rate of the P_3 cells in the random sequence group, while slight inhibition of P_3 cells growth was found in the pro-sense group. This could be explained as the pro-sense oligonucleotide competed against telomerase RNA in quantity and space, thus impeding the attachment of telomere with RNA template zone to a certain degree[29]. The results showed that inhibition of PS-ODN1 and PS-ODN2 on the growth of P_3 cells was dosage-dependent. This implies that after hTR template is closed, telomerase can no longer bring its activity into full play. Therefore it can be concluded that hTR is involved in the regulation of telomerase activity[30].

FCM results showed that the apoptotic rate of P_3 cells would increase along with increase of the concentrations of antisense oligonucleotide, at the same time, cells in G_0/G_1 stage increased in quantity while those in S stage decreased. This suggests that treatment with PS-ODN1 and PS-ODN2 may block the cells at G_0/G_1 stage and induce apoptosis.

In regard to the relationship between telomerase activity and cell cycle, it was thought[31] that the tolemerase activity was regulated in the cell cycle-leading mode. It was also thought that tolemerase should be activated at the DNA replication stage as tolemerase activity was essential to maintain tolemere. This activity is not required at the non- replication stage of the cell cycle. Telomerase has different activity at different stages of the cell cycle, its highest rate is at S stage, lowest at G_2/M stage, and almost no activity at G_0/G_1 stage. Our results support this point of view.

We simultaneously observed the influence of PS-ODNs on SDH activity and proliferation of normal human fibroblasts. The results showed that it had a significantly inhibitory effect on the metabolism and proliferation of cells. Therefore, it can be assumed that the effect of antisense hTR is cell-specific, and has no harmful action on normal cells.

Our study suggested that there was no correlation between the expression of TPlmRNA and telomerase activity in pancreatic cancer. However, the function of TP1 is still not clearly known, and it may be related to interaction with protein. TP1 may play a role in the interface between telomerase and telomere conjugated proteins. Modification after transcription of TPlmRNA may regulate the telomerase activity.

In conclusion, telomerase may be taken as a subsidiary parameter for the diagnosis and outcome of pancreatic cancer. For preoperative patients, detection of the telomerase activity may be conducted on blood, or pancreatic juice and duct cells taken from ERCP on fine needle aspiration specimens for early diagnosis[32-35]. Antisense oligonucleotide can reduce the activity of telomerase in pancreatic cancer P_3 cells, inhibit the growth of P_3 cells, promote changes in cell cycle and induce their apoptosis[36, 37].

REFERENCES

1 **Greider CW,** Blackburn EH. A telomeric sequence in the RNA of tetrahymena telomerase required for telomere repeat synthesis. *Nature* 1989; **337**: 331-337

2 **Kim NW,** Piatyszek MA, Prowse KR, Harley CB, West MD, Ho PL, Coviello GM, Wright WE, Weinrich SL, Shay JW. Specific association of human telomerase activity with immortal cells and cancer. *Science* 1994; **266**: 2011-2015

3 **Wan M,** Li WZ, Duggan BD, Felix JC, Zhao Y, Dubeau L. Telomerase activity in benign and malignant epithelial ovarian tumors. *J Natl Cancer Inst* 1997; **89**: 437-441

4 **Harle-Bachor C,** Boukamp P. Telomerase activity in the regenerative basal layer of the epidermis inhuman skin and in immortal and carcinoma-derived skin keratinocytes. *Proc Natl Acad Sci U S A* 1996; **93**: 6476-6481

5 **Wang J,** Liu X, Fang J. Expression and clinical significance of telomerase catalytic subunit gene in lung cancer and its correlations with genes related to drug resistance and apoptosis. *Zhonghua Zhongliu Zazhi* 1999; **21**: 350-353

6 **Zhang YL,** Zhang ZS, Wu BP, Zhou DY. Early diagnosis for colorectal cancer in China. *World J Gastroenterol* 2002; **8**: 21-25

7 **Shen ZY**, Xu LY, Li EM, Cai WJ, Chen MH, Shen J, Zeng Y. Telomere and telomerase in the initial stage of immortalization of esophageal epithelial cell. *World J Gastroenterol* 2002; **8**: 357-362

8 **Qin LX,** Tang ZY. The prognostic molecular markers in hepatocellular carcinoma. *World J Gastroenterol* 2002; **8**: 385-392

9 **Yao XX,** Yin L, Sun ZC. The expression of hTERT mRNA and cellular immunity in gastric cancer and precancerosis. *World J Gastroenterol* 2002; **8**: 586-590

10 **Kojima H,** Yokosuka O, Imazeki F, Saisho H, Omata M. Telomerase activity and telomere length in hepatocellular carcinoma and chronic liver disease. *Gastroenterology* 1997; **112**: 493-500

11 **Suzuki T,** Suzuki Y, Fujioka T. Expression of the catalytic subunit associated with telomerase gene in human urinary bladder cancer. *J Urol* 1999; **162**: 2217-2220

12 **Takakura M,** Kyo S, Kanaya T, Tanaka M, Inoue M. Expression of human telomerase subunits and correlation with telomerase

activity in cervical cancer. *Cancer Res* 1998; **58**: 1558-1561

13 **Lanham S,** Herbert A, Watt P. HPV detection and measurement of HPV-16,telomerase, and survivin transcripts in colposcopy clinic patients. *J Clin Pathol* 2001; **54**: 304-308

14 **Zhang FX,** Zhang XY, Fan DM, Deng ZY, Yan Y, Wu HP, Fan JJ. Antisense telomerase RNA induced human gastric cancer cell apoptosis. *World J Gastroenterol* 2000; **6**: 430-432

15 **Hiyama E,** Kodama T, Shinbara K, Iwao T, Itoh M, Hiyama K, Shay JW, Matsuura Y, Yokoyama T. Telomerase activity is detected in pancreatic cancer but not in benign tumors. *Cancer Res* 1997; **57**: 326-331

16 **Tsutsumi M,** Tsujiuchi T, Ishikawa O, Majima T, Yoshimoto M, Sasaki Y, Fukuda T, Oohigashi H, Konishi Y. Increased telomerase activities in human pancreatic duct adenocarcinomas. *Jpn J Cancer Res* 1997; **88**: 971-976

17 **Buchler P,** Conejo-Garcia JR, Lehmann G, Muller M, Emrich T, Reber HA, Buchler MW, Friess H. Real-time quantitative PCR of telomerase mRNA is useful for the differentiation of benign and malignant pancreatic disorders. *Pancreas* 2001; **22**: 331-340

18 **Iwao T**, Hiyama E, Yokoyama T, Tsuchida A, Hiyama K, Murakami Y, Shimamoto F, Shay JW, Kajiyama G. Telomerase activity for the preoperative diagnosis of pancreatic cancer. *J Natl Cancer Inst* 1997; **89**: 1621-1623

19 **Sato N,** Maehara N, Mizumoto K, Nagai E, Yasoshima T, Hirata K, Tanaka M. Telomerase activity of cultured human pancreatic carcinoma cell lines correlates with their potential for migration and invasion. *Cancer* 2001; **91**: 496-504

20 **Ohta K**, Kanamaru T, Morita Y, Hayashi Y, Ito H, Yamamoto M. Telomerase activity in hepatocellular carcinoma as a predictor of postoperative recurrence. *J Gastroenterol* 1997; **32**: 791-796

21 **Suda T,** Isokawa O, Aoyagi Y, Nomoto M, Tsukada K, Shimizu T, Suzuki Y, Naito A, Igarashi H, Yanagi M, Takahashi T, Asakura H. Quantitation of telomerase activity in hepatocellular carcinoma: a possible aid for a prediction of recurrent diseases in the remnant liver. *Hepatology* 1998; **27**: 402-406

22 **Tang SJ,** Dumot JA, Wang L, Memmesheimer C, Conwell DL, Zuccaro G, Goormastic M, Ormsby AH, Cowell J. Telomerase activity in pancreatic endocrine tumors. *Am J Gastroenterol* 2002; **97**: 1022-1030

23 **Meyerson M,** Counter CM, Eaton EN, Ellisen LW, Steiner P, Caddle SD, Ziaugra L, Beijersbergen RL, Davidoff MJ, Liu Q, Bacchetti S, Haber DA, Weinberg RA. HEST2, the putative human telomerase catalytic subunit gene, is up-regulated in tumor cells and during immortalization. *Cell* 1997; **90**: 785-795

24 **Nakamura TM,** Morin GB, Chapman KB, Weinrich SL, Andrews WH, Lingner J, Harley CB, Cech TR. Telomerase catalytic subunit homologs from fission yeast and human. *Science* 1997; **277**: 955-959

25 **Muller M**, Krause H, Heicappell R, Tischendorf J, Shay JW, Miller K. Comparison of human telomerase RNA and telomerase activity in urine for diagnosis of bladder cancer. *Clin Cancer Res* 1998; **4**: 1949-1954

26 **Kanaya T**, Kyo S, Takakura M, Ito H, Namiki M, Inoue M. hTERT is a critical determinant of telomerase activity in renal-cell carcinoma. *Int J Cancer* 1998; **78**: 539-543

27 **Kyo S**, Kanaya T, Takakura M, Tanaka M, Yamashita A, Inoue H, Inoue M. Expression of human telomerase subunits in ovarian malignant, borderline and benign tumors. *Int J Cancer* 1999; **80**: 804-809

28 **Harrington L**, McPhail T, Mar V, Zhou W, Oulton R, Bass MB, Arruda I, Robinson MO. A mammalian telomerase-associated protein. *Science* 1997; **275**: 973-977

29 **Yuan X**, Zhang B, Ying J, Wang H, Zhang H, Hou L, Wu B. Expression of antisense telomerase genes suppressing human cancer malignant phenotypes *Zhonghua Binglixue Zazhi* 1999; **28**: 356-360

30 **Teng L,** Chen S, Thomas JF. Stable expression of antisense hTR inhibits *in vitro* pancreatic cancer cell growth. *Chin Med J (Engl)* 2002; **115**: 1196-1200

31 **Zhu X**, Kumar R, Mandal M, Sharma N, Sharma HW, Dhingra U, Sokoloski JA, Hsiao R, Narayanan R. Cell cycle-dependent modulation of telomerase activity in tumor cells. *Proc Natl Acad Sci U S A* 1996; **93**: 6091-6095

32 **Inoue H,** Tsuchida A, Kawasaki Y, Fujimoto Y, Yamasaki S, Kajiyama G. Preoperative diagnosis of intraductal papillary-mucinous tumors of the pancreas with attention to telomerase activity. *Cancer* 2001; **91**: 35-41

33 **Myung SJ,** Kim MH, Kim YS, Kim HJ, Park ET, Yoo KS, Lim BC, Wan Seo D, Lee SK, Min YI, Kim JY. Telomerase activity in pure pancreatic juice for the diagnosis of pancreatic cancer may be complementary to K-ras mutation. *Gastrointest Endosc* 2000; **51**: 708-713

34 **Seki K**, Suda T, Aoyagi Y, Sugawara S, Natsui M, Motoyama H, Shirai Y, Sekine T, Kawai H, Mita Y, Waguri N, Kuroiwa T, Igarashi M, Asakura H. Diagnosis of pancreatic adenocarcinoma by detection of human telomerase reverse transcriptase messenger RNA in pancreatic juice with sample qualification. *Clin Cancer Res* 2001; **7**: 1976-1981

35 **Pearson AS**, Chiao P, Zhang L, Zhang W, Larry L, Katz RL, Evans DB, Abbruzzese JL. The detection of telomerase activity in patients with adenocarcinoma of the pancreas by fine needle aspiration. *Int J Oncol* 2000; **17**: 381-385

36 **Sato N,** Mizumoto K, Nagai E, Tanaka M. Telomerase as a new target for pancreatic cancer treatment. *J Hepatobiliary Pancreat Surg* 2002; **9**: 322-327

37 **Pirocanac EC**, Nassirpour R, Yang M, Wang J, Nardin SR, Gu J, Fang B, Moossa AR, Hoffman RM, Bouvet M. Bax-induction gene therapy of pancreatic cancer. *J Surg Res* 2002; **106**: 346-351

Edited by Lu HM and Wang XL

P.O.Box 2345, Beijing 100023,China
Fax: +86-10-85381893
E-mail: wjg@wjgnet.com www.wjgnet.com

World J Gastroenterol 2003;9(8):1815-1818
World Journal of Gastroenterology
 ISSN 1007-9327

• CLINICAL RESEARCH •

p53 protein expression and CA19.9 values in differential cytological diagnosis of pancreatic cancer complicated with chronic pancreatitis and chronic pancreatitis

De-Qing Mu, Guo-Feng Wang, Shu-You Peng

De-Qing Mu, Shu-You Peng, Department of Surgery, the Second Affiliated Hospital, Medical College of Zhe Jiang University, Hang Zhou 310009, Zhe Jiang Province, China
Guo-Feng Wang, Department of Pathology, the Second Affiliated Hospital, Medical College of Zhe Jiang University, Hang Zhou 310009, Zhe Jiang Province, China
Correspondence to: Dr. De-Qing Mu, Department of Surgery, the Second Affiliated Hospital, Medical College of Zhe Jiang University, Hangzhou 310009 Zhe jiang Province, China. samier-1969@163.com
Telephone: +86-0571-87783762
Received: 2003-01-11 **Accepted:** 2003-03-05

Abstract

AIM: To evaluate p53 protein overexpression and to measure serum CA19.9 concentrations in cytological diagnosis of patients with suspected pancreatic cancer.

METHODS: 24 patients with suspected pancreatic cancer due to chronic pancreatitis, had a pancreatic mass determined by imaging methods. The serum CA19.9 concentration was measured by solid phase radioimmunoassay. On laparotomy, puncture biopsy was performed, and specimens were divided into two parts for cytological diagnosis and detection of p53 protein.

RESULTS: Cytology offered a sensitivity of 0.63, a specificity of 1.00, and an accuracy of 0.63. p53 protein analysis offered a sensitivity of 0.44, a specificity of 1.00, and an accuracy of 0.73. CA19.9 offered a sensitivity of 0.44, a specificity of 0.80, and an accuracy of 0.67. The combined cytology and p53 protein analysis showed a sensitivity of 0.78, a specificity of 1.00, and an accuracy of 0.92. Cytology and CA19.9 showed a sensitivity of 0.67, a specificity of 0.80, an accuracy of 0.67. combined cytology and p53 protein analysis and CA19.9 showed a sensitivity of 0.78, a specificity of 0.80, and an accuracy of 0.79.

CONCLUSION: Superior to any single test, the combined approach is helpful for the differential diagnosis of pancreatic cancer complicated with chronic pancreatitis.The combined cytology and p53 protein analysis offers the best diagnostic efficacy.

Mu DQ, Wang GF, Peng SY. p53 protein expression and CA19.9 values in differential cytological diagnosis of pancreatic cancer complicated with chronic pancreatitis and chronic pancreatitis. *World J Gastroenterol* 2003; 9(8): 1815-1818
http://www.wjgnet.com/1007-9327/9/1815.asp

INTRODUCTION

The differential diagnosis of pancreatic cancer (PC) complicated with and chronic pancreatitis (CP) is difficult because of their common clinical symptoms and overlapping findings. Increased pancreatic adenocarcinoma risk in chronic pancreatitis patients has renewed the interest in early tumour diagnosis and in the differentiation of neoplastic and chronic inflammatory ductal changes[1, 2]. If a pancreatic mass is discovered by the imaging method, cytological examination is required to make a conclusive diagnosis. Owing to a large number of cases without a conclusive diagnosis[3], it would be worthy to diagnose it with other methods. Genomic alterations in p53 tumour-suppressor gene and overexpression of p53 protein are frequently found in pancreatic cancer, but rarely in chronic pancreatitis. An elevated serum CA19.9 concentrations is found in a high proportion of patients with pancreatic cancer and this is considered to be the standard serum marker for adenocarcinoma of the pancreas. In the current study, we retrospectively evaluated overexpression of p53 protein, serum CA19.9, and cytology in the diagnosis of pancreatic cancer.

MATERIALS AND METHODS

Materials

24 patients,19 men and 5 women, with a mean age 58.6 years, (range 41-69 years,) with jaundice, weight loss, and abdominal pain, underwent pancreatectomy in our hospital between January 1995 and December 2001 because of high suspicion of pancreatic cancer arising from chronic pancreatitis. Preoperatively, they were found to have a mass in the pancreas by CT and ERCP. 19 masses were located in pancreatic head, two in the body, and two in the tail, 1 with three foci.

Methods

CA19.9 determination The serum samples were stored at -20 ℃ for CA19.9 by solid phase radioimmunoassay. A value of 37 U/ml was the upper limit of normal.

Cytological examination Puncture biopsy of the pancreas was performed during laparotomy, and the specimen was divided into two parts: one part was used for making fresh smears, after papanicolaou staining. The presence of malignant cells and suspicious cells were examined under microscope (Figures 1-2). The other part was employed for immunohistochemical analysis.

Immunohistochemical analysis The sample was fixed in buffered formaldehyde and paraffin-embeded. Histological sections (5 μm) were prepared, mounted on poly-L-lysine-coated slides and dried for 12 to 24 h at 37 ℃. Immunohistochemistry was performed with the avidin-biotin complex (ABC) kit[4] using the monoclonal antibody which recognizes both mutant and wild-type p53.

The result was graded as either negative or positive. The specimen was considered to positive when >5 % of the tissure component was unequivocally immunoreactive in the appropriate cellular compartment (Figure 3).

Histological examination The resected specimens were fixed in 10 % formaldehyde and sliced into 5 mm sections and stained with hematoxylin-eosin. The presence or absence of cancer was microscopically determined.

Statistical analysis

Statistical analysis was performed with STATISTICA for Windows. Differences between the results of two groups were tested with one-sided *t* test. A *P* value <0.05 was considered statistically significant.

RESULTS

Histological diagnosis

9 patients were diagnosed as pancreatic cancer complicated with chronic pancreatitis, including carcinoma of the pancreas head in 6 cases; carcinoma of the body and/or tail of pancreas in 2 cases, multifocal cancer with three foci in 1 case. The other 15 patients were confirmed to be chronic pancreatitis, including 13 cases with inflammatory mass in the head of pancreas, and two cases with adenoma in the body and/or tail of pancreas.

To compare with histological diagnosis, cytology offered a conclusive diagnosis in 5 of 24 cases. The cytological report was not conclusive in 19 cases (9 cases with suspicious cells and 8 cases with insufficient material, and two cases without non-malignant cell) (Figures 1,2).

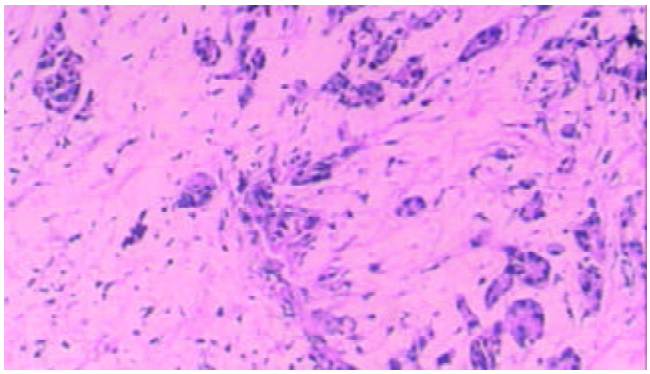

Figure 1 A little glandublar tissue and a large amount of fibrotic tissue.

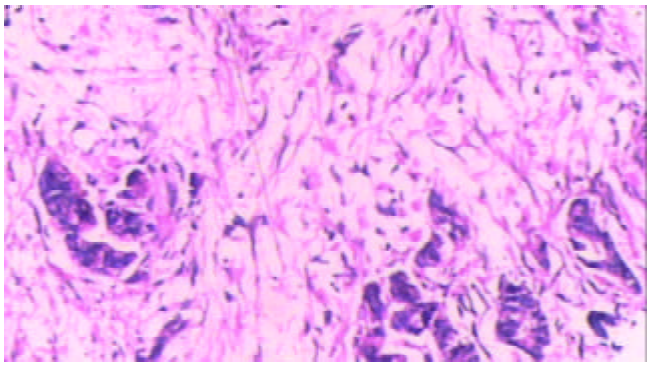

Figure 2 A few cancerous cells scattered in fibrotic gland tissue. (Papanicolaou staining, original magnification ×200).

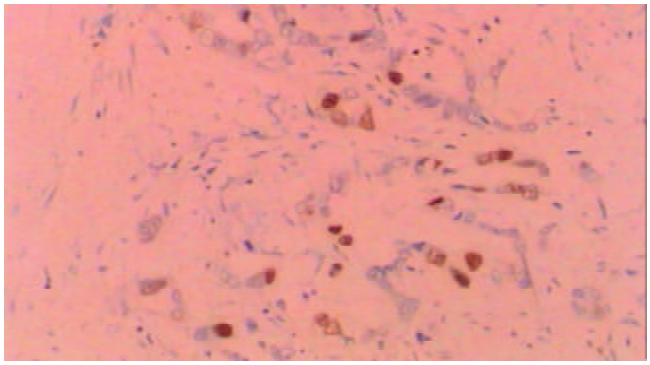

Figure 3 Yellow-brownly stained nuclei of p53 positive cells (ABC, original magnification ×400).

The presence of malignant cells in puncture samples was detected in 5 of 9 pancreatic cancer patients confirmed by histological examination. According to cytological diagnosis. The incidence of p53 protein overexpression and CA19.9 values ovre shown in Table 1.

Table 1 Patients with p53 protein overexpression and high serum CA19.9 with cytologically diagnosed pancreatic disease (*n*=24)

Histological diagnosis	Cytology				
	Patient *n*(%)	Malignant cells	Suspicious cells	Insufficient material	Non-malignant cells
Malignant diseases					
PC	9(37.5) p53(+)	2/5	1/1	1/1	0/2
	CA19.9≥37 U/ml	3/5	1/1	0/1	0/2
Benign disease					
IMH	13(54.2) p53(+)	0	0/5	0/4	0/4
	CA19.9≥37 U/ml	0	2/5	1/4	0/4
Adenoma	2(8.3)p53(+)	0	0/2	0	0
	CA19.9≥37 U/ml	0	0/2	0	0

PC: pancreatic cancer; IMH: inflammatory mass of the head of pancreas.

Table 2 Assay effectiveness in patients with pancreatic diseases (*n*=24)

Assay	Sensitivity TP/(TP+FN)	Specificity TN/(FP+TN)	Predictive value of positive test TP/(TP+FP)	Efficiency (TP+TN)/Total
Cytology alone	5/(5+3)=0.63	10/(0+10)=1.00	5/(5+0)=1.00	(5+10)/24=0.63
CA19.9>37 U/ml	4/(4+5)=0.44	12/(3+12)=0.80	4/(4+3)=0.57	(4+12)/24=0.67
P53(+)	4/(4+5)=0.44	15/(0+15)=1.00	4/(4+0)=1.00	(4+15)/24=0.79
Cytology+CA19.9	6/(6+3)=0.67	12/(12+3)=0.80	6/(6+3)=0.67	(6+12)/24=0.67
Cytology+P53	7/(7+2)=0.78	15/(15+0)=1.00	7/(7+0)=1.00	(7+15)/24=0.92
Cytology+P53+CA19.9	7/(7+2)=0.78	12(3+12)=0.80	7(7+3)=0.70	(7+12)/24=0.79

TP: true-positive; FN: false-negative; FP: false-positive; TN: true-negative.

p53 protein overexpression (shown by immunohistochemical staining) was positive in 4 of 9 patients with pancreatic cancer (Figure 3), and negative in the remaining 20 specimens. The combination of p53 protein overexpression and cytology offered a78 % sensitivity and a 100 % specificity.

Using the cut-off value of 37 U/ml as the normal upper limit, CA19.9 measurement identified 4 of 9 pancreatic carcinomas (range=41-480 U/ml). Additionally, high concentrations were also detected in 3 cases of chronic pancreatitis with a mass (range=210-1 200 U/ml). CA19.9 positivity in the chronic pancreatitis patient was related to common bile duct obstruction. The combined CA 19.9 and cytological assay showed a sensitivity of 67 % and a specificity of 80 %.

Combination of cytological analysis, P53 protein overexpression and CA19.9

Since all positive cytologies carried a final diagnosis of carcinoma, the main diagnostic contribution of p53 and CA19. 9 in the pancreatic cancer group was at the time when the cytology was suspicious or not contributory. Either test contributed to the final diagnosis of pancreatic adenocarcinoma in 4 out of 9 cases: in one case both were positive, in another case p53 protein showed overexpression but CA19.9 value was lower than 37 U/ml. None of the patients with chronic pancreatitis was positive for both markers. The sensitivity of the combined approach was 78 % with a specificity of 80 %. Both the sensitivity and efficiency of the combined approach (cytology, CA19.9, and p53 protein overexpression) were significantly higher than that of either test alone (P<0.01). Both the sensitivity and efficiency of combination of cytology and p53 were higher than that of combination of cytology, p53 and CA19.9 (P<0.05). Finally both the sensitivity and efficiency of the combined approach of cytology, p53 and CA19.9 were better than that of combination of cytology and CA19.9 (P<0.05) (Table 2).

DISCUSSION

Much effort has been devoted to achieve an optimum standard for conventional imaging procedures to increase the sensitivity and specificity of these diagnostic tools. Among which CT, ERCP are the mainstay for pancreatic cancer detection[5,6]. However, these morphologically oriented procedures, have an unsolved drawback ie, the inability to differentiate tumour tissue from pancreatic masses caused by chronic pancreatitis. Therefore, this has limited their application in patients with a suspected resectable mass for the decision of surgical exploration. FNA biopsy of the primary tumor has a significantly false negative rate due to the inflammatory response around the tumor, which accounts for the lower sensitivity[3]. According to a 1986 review, the average sensitivity was approximately 80 %[7]. A more recent, large, single-institution series reported a sensitivity of 72.5 %[8]. FNA-cytological distinction between chronic pancreatitis and pancreatic cancer is occasionally difficult because chronic pancreatitis can induce morphological changes similar to those seen in well differentiated adenocarcinoma[9]. This explains the equivocal results found in two kinds of pancreatic diseases, which can not be discriminated by clinical and imaging tests. In addition, the accuracy of cytology examination also depends on the quality and number of cells. The reported sensitivities of ERCP aspiration cytology, brush cytology, FNA biopsies, and forceps biopsies were in the range of 22 % to 71 %, and the use of multimethod samplings increased the sensitivity to 50-78 %[10]. Even with endoscopic ultrasonography-guided FNA biopsy, there were also false negative results[11]. Sometimes the accuracy of cytology might be damaged by poor staining or inadequate fixation[12]. The distinction between chronic pancreatitis and well-differentiated adenocarcinoma is difficult and it remains to find whether artificial intelligence algorithms can prove themselves useful in the cytologically differential diagnosis of carcinoma and chronic pancreatitis[9].

The greatest usefulness of carbohydrate antigen CA19.9 is its performance in detecting pancreatic cancer using a cutoff upper limit of 37 U/ml[13-16]. However, it can be confusing to interpret elevated concentrations of CA19.9, because the elevated concentration of CA19.9 used for the diagnosis of pancreatic cancer can also be seen in benign conditions such as pancreatitis[17-19], and conversely CA19.9 may be low in malignant conditions[20]. As shown in Table 1 and Table 2, the application of CA19-9 for differentiating cancer from chronic pancreatitis was disappointing in our study because of its low sensitivity and specificity, which were only 44 % and 80 %, similar to those reported by Okaga *et al*[21]. This may be explained by the elevation of CA19.9 in benign inflammatory conditions as well as in malignant diseases. According to Ker *et al*[22] CA19.9 is synthesized by normal biliary ductal cells. In benign biliary obstruction, epithelial cells will proliferate, and as a result, more CA19.9 may be secreted and leaks out into the bloodstream. The other mechanism concerning the false serum elevation of tumour markers in chronic pancreatitis has been shown to be a disturbed antigen polarity[23].

p53 gene abnormalities are considered to play an important role in the carcinogenesis of pancreatic cancer present in almost half of pancreatic cancer, but uncommon in chronic pancreatitis[24-26].

Studies on p53 abnormalities generally look for overexpression or persistence of the p53 protein, or for mutations in the genic sequence. Mutations of p53 gene lead to an accumulation of p53 protein reaching detectable concentrations by immunohistochemistry. In contrast, production of the wild type p53 gene is undetectable because of its short half-life. Thus there seems to be a good correlation between the overexpression of p53 protein and p53 gene mutations[27]. The p53 protein concentrations are correlated with percentage of p53 gene alterations[28,29]. In 40-60 % of pancreatic carcinomas, mutations of p53 gene and the increased accumulation of p53 protein have been shown by both direct sequencing and immunohistochemistry[30,31]. Both methods require tissue specimens. In comparison with cytology the, biggest advantage of gene analysis is no need to search for integrity or large number of cells. This method is sensitive enough to detect 3-30 mutant copies in the presence of 300 000 normal copies of the gene (which would be the equivalent to 0.01 ng of mutant DNA in 1 mcg of total DNA)[32]. In our series we found p53 protein overexpression in suspicious cells and insufficient materials.

In the current study, we analyzed the relative and combined contributions of the detection of p53 protein and CA19.9 concentration to the cytological diagnosis of pancreatic cancer when there was a clinical suspicion of pancreatic cancer corroborated by imaging diagnostic technique. In FNA samples, overexpressions were detected in 44 % of carcinoma. Fortunately no false-positives were detected even in the subset of chronic pancreatitis patients with a mass. Using a cut-off upper limit of 37 U/ml, the high CA19.9 concentrations were not strongly suggestive of pancreatic cancer. Although CA19. 9 is superior to any single markers elevated, it is not suitable for determining the nature of a pancreatic mass in patients with chronic pancreatitis. Similar results were also reported by other authors[33].

The combination of cytology and p53 offered the best diagnostic procedure. In four out of 9 patients with PC, the p53 protein overexpression contributed much to supporting the cytological diagnosis. Therefore, p53 protein overexpressions in FNAs are specific for pancreatic cancer, but CA19.9 values are not. Interestingly, none of the patients with chronic pancreatitis was positive for both markers,

suggesting that the combination of cytology and p53 might be useful in distinguishing PC and CP.

In conlusion, p53 protein analysis enhanced the diagnostic sensitivity of cytological evaluation in chronic pancreatitis patients with clinical suspicion of pancreatic cancer, especially in those with inconclusive cytological results such as the presence of suspicious cells or insufficient cellular material. In this case, p53 protein overexpression analysis offered a highly specific test although it was rarely employed as a clinical decision-making process.The previous clinical evidence also indicated the diagnostic benefit provided by p53 and other molecular marker analysis[34, 35], with an accumulation of more patients in such a study, there will be growing facilities for differentiating PC from CP.

REFERENCES

1 **Lowenfels AB**, Maisonneuve P, Cavallini G, Ammann RW, Lankisch PG, Andersen JR, Dimagno EP, Andren-Sandberg A, Domellof L. International pancreatitis study group. *N Engl J Med* 1993; **328**: 1433-1437

2 **Apple SK**, Hecht JR, Lewin DN, Jahromi SA, Grody WW, Nieberg RK. Immunohistochemical evaluation of k-ras,p53, and HER-2/neu expression in hyperplastic, dysplastic, and carcinomatous lesions of the pancreas: evidence for multistep carcinogenesis. *Hum Pathol* 1999; **30**: 123-129

3 **Robins DB**, Katz RL, Evans DB, Atkinson EN, Green L. Fine needle aspiration of the pancreas.In quest of accuracy. *Acta Cytol* 1995; **39**: 1-10

4 **Kawesha A**, Ghaneh P, Andren-Sandberg A, Ograed D, Skar R, Dawiskiba S, Evans JD, Campbell F, Lemoine N, Neoptolemos JP. K-ras oncogene subtype mutations are associated with survival but not expression of p53, p16(INK4A), p21(WAF-1), cyclin D1, erbB-2 and erbB-3 in resected pancreatic ductal adenocarcinoma. *Int J Cancer* 2000; **89**: 469-474

5 **Rosewicz S**, Wiedenmann B. Pancreatic carcinoma. *Lancet* 1997; **349**: 485-489

6 **Sheridan MB**, Ward J, Guthrie JA, Spencer JA, Craven CM, Wilson D, Guillou PJ, Robinson PJ. Dynamic contrast-enhanced MR imaging and dual-phase helical CT in the preoperative assessment of suspected pancreatic cancer: a comparative study with receiver operating characteristic analysis. *Am J Roentgenol* 1999; **173**: 583-590

7 **Bret PM**, Nicolet V, Labadie M. percutaneous fine-needle aspiration biopsy of the pancreas. *Diagn Cytopathol* 1986; **2**: 221-227

8 **Lerma E**, Musulen E, Cuatrecasas M, Martinez A, Montserrat E, Prat J. Fine needle aspiration cytology in pancreatic pathology. *Acta Cytol* 1996; **40**: 683-686

9 **Yeaton P**, Sears RJ, Ledent T, Salmon I, Kiss R, Decaestecker C. Discrimination between chronic pancreatitis and pancreatic adenocarcinoma using artificial intelligence-related algorithms based on image cytometry-generated variables. *Cytometry* 1998; **32**: 309-316

10 **Lee JG**, Leung J. Tissue sampling at ERCP in suspected pancreatic cancer. *Gastrointest Endosc Clin N Am* 1998; **8**: 221-235

11 **Gress F**, Gottlieb K, Sherman S, Lehman G. Endoscopic ultrasonography-guided fine-needle aspiration biopsy of suspected pancreatic cancer. *Ann Intern Med* 2001; **134**: 459-464

12 **Nakaizumi A**, Tatsuta M, Uehara H, Yamamoto R, Takenaka A, Kishigami Y, Takemura K, Kitamura T, Okuda S. Cytologic examination of pure pancreatic juice in the diagnosis of pancreatic carcinoma. The endoscopic retrograde intraductal catheter aspiration cytologic technique. *Cancer* 1992; **70**: 2610-2614

13 **Farini R**, Fabris C, Bonvicini P, Piccoli A, del Favero G, Venturini R, Panucci A, Naccarato R. CA 19-9 in the differential diagnosis between pancreatic cancer and chronic pancreatitis. *Eur J Cancer Clin Oncol* 1985; **21**: 429-432

14 **Steinberg WM**, Gelfand R, Anderson KK, Glenn J, Kurtzman SH, Sindelar WF, Toskes PP. Related Articles, Links Comparison of the sensitivity and specificity of the CA19-9 and carcinoembryonic antigen assays in detecting cancer of the pancreas. *Gastroenterology* 1986; **90**: 343-349

15 **Safi F**, Beger HG, Bittner R, Bucher M, Krautzberger W. CA19-9 and pancreatic adenocarcinoma. *Cancer* 1986; **57**: 779-783

16 **Kim HJ**, Kim MH, Myung SJ, Lim BC, Park ET, Yoo KS, Seo ISK, Min YI. A new strategy for the application of CA19-9 in the differentiation of pancreaticobiliary cancer: analysis using a receiver operating characteristic curve. *Am J Gastroenterol* 1999; **94**: 1941-1946

17 **Wakasugi H**, Funakoshi A, Iguchi H, Takase M, Inoue M, Ohshima A, Seo Y. Pancreatic carcinoma associated with chronic pancreatitis. *Intern Med* 1999; **38**: 951-956

18 **Uno K**, Azuma T, Nakajima M, Yasuda K, Hayakumo T, Mukai H, Sakai T, Kawai K. Clinical significance of cathepsin E in pancreatic juice in the diagnosis of pancreatic ductal adenocarcinoma. *J Gastroenterol Hepatol* 2000; **15**: 1333-1338

19 **Ridwelski K**, Meyer F, Fahlke J, Kasper U, Roessner A, Lippert H. Value of cytokeratin and CA19-9 antigen in immunohistological detection of disseminated tumor cells in lymph noodes in pancreas carcinoma. *Chirurg* 2001; **72**: 920-926

20 **Shimura T**, Tsutsumi S, Hosouchi Y, Kojima T, Kon Y, Yonezu M, Kuwano H. Clinical significance of soluble form of HLA class I molecule in Japanese patients with pancreatic cancer. *Hum Immunol* 2001; **62**: 615-619

21 **Okaga M**, Karasawa H, Kobayashi T, Satsukime N, Miki R. Effect of biliary tract obstruction and cholangitis on serum CA 19-9 levels. *Nippon Shokakibyo Gakkai Zasshi* 1985; **82**: 1418

22 **Ker CG**, Chen JS, Lee KT, Sheen PC, Wu CC. Assessment of serum and bile levels of CA19-9 and CA125 in cholangitis and bile duct carcinoma. *J Gastroenterol Hepatol* 1991; **6**: 505-508

23 **Satomura Y**, Sawabu N, Takemori Y, Ohta H, Watanabe H, Okai T, Watanbe K, Matsuno H, Konishi F. Expression of various sialyated carbohydrate antigens in malignant and nonmalignant pancreatic tissues. *Pancreas* 1991; **6**: 448-458

24 **Casey G**, Yamanaka Y, Friess H, Kobrin MS, Lopez ME, Buchler M, Beger HG, Korc M. p53 mutations are common in pancreatic cancer and are absent in chronic pancreatitis. *Cancer Lett* 1993; **69**: 151-160

25 **Tomaszewska R**, Karcz D, Stachura J. An immunohistochemical study of the expression of bcl-2 and p53 oncoproteins in pancreatic intraepithelial neoplasia and pancreatic cancer. *Int J Pancreatol* 1999; **26**: 163-171

26 **Yamaguchi K**, Chijiiwa K, Noshiro H, Torata N, Kinoshita M, Tanaka M. K-ras codon 12 point mutation and p53 mutation in pancreatic diseases. *Hepatogastroenterology* 1999; **46**: 2575-2581

27 **Boschman CR**, Stryker S, Reddy JK, Rao MS. Expression of p53 protein in precursor lesions and adenocarcinoma of human pancreas. *Am J Pathol* 1994; **145**: 1291-1295

28 **Luo JC,** Neugut AI, Garbowski G, Forde KA, Treat M, Smith S, Carney WP, Brandt-Rauf PW. Levels of p53 antigen in the plasma of patients with adenomas and carcinomas of the colon. *Cancer Lett* 1995; **91**: 235-240

29 **Fontanini G**, Vignati S, Bigini D, Merlo GR, Ribecchini A, Angeletti CA, Basolo F, Pingitore R, Bevilacqua G. Human non-small cell lung cancer: p53 protein accumulation is an early event and persists during metastatic progression. *J Pathol* 1994; **174**: 23-31

30 **Barton CM**, Staddon SL, Hughes CM, Hall PA, O'Sullivan C, Kloppel G, Theis B, Russel RC, Neoptolemos J, Williamson RC. Abnormalities of the p53 tumour suppressor gene in human pancreatic cancer. *Br J Cancer* 1992; **64**: 1076-1082

31 **Scarpa A**, Capelli P, Mukai K, Zamboni G, Oda T, Iacono C, Hirohashi S. Pancreatic adenocarcinomas frequently show p53 gene mutations. *Am J Pathol* 1993; **142**: 1534-1543

32 **Tada M**, Omata M, Kawai S, Saisho H, Ohto M, Saiki RK, Sninsky JJ. Detection of ras gene mutations in pancreatic juice and peripheral blood of patients with pancreatic adenocarcinoma. *Cancer Res* 1993; **53**: 2472-2474

33 **Wakasugi H**, Funakoshi A, Iguchi H, Takase M, Inoue M, Oshima A, Seo Y. Pancreatic carcinoma associated with chronic pancreatitis. *Intern Med* 1999; **38**: 951-956

34 **Pellegata NS**, Sessa F, Renault B, Bonato M, Leone BE, Solcia E, Ranzani GN. K-ras and p53 gene mutations in pancreatic cancer: ductal and nonductal tumors progress through different genetic lesions. *Cancer Res* 1994; **54**: 1556-1560

35 **Yamaguchi Y**, Watanabe H, Yrdiran S, Ohtsubo K, Motoo Y, Okai T, Sawabu N. Detection of mutations of p53 tumor suppressor gene in pancreatic juice and its application to diagnosis of patients with pancreatic cancer: comparson with k-ras mutations. *Clin Cancer Res* 1999; **5**: 1147-1153

Edited by Lu HM and Wang XL

P.O.Box 2345, Beijing 100023,China
Fax: +86-10-85381893
E-mail: wjg@wjgnet.com www.wjgnet.com

World J Gastroenterol 2003;9(8):1819-1823
World Journal of Gastroenterology
 ISSN 1007-9327

• CLINICAL RESEARCH •

Pancreatic cancer mortality in China (1991-2000)

Li Wang, Gong-Huan Yang, Xing-Hua Lu, Zheng-Jing Huang, Hui Li

Li Wang, Hui Li, Department of Epidemiology, School of Basic Medical Sciences, PUMC, Institute of Basic Medical Sciences, CAMS, Beijing, 100005, China
Gong-Huan Yang, Zheng-Jing Huang, Institute of Epidemiology and Microbiology, Center for Disease Control and Prevention of China, Beijing, 100050, China
Xing-Hua Lu, Department of Internal Medicine, Peking Union Hospital, Beijing, 100730, China
Supported by the Ministry of Public Health, No. 20010102
Correspondence to: Li Wang, Graduate School of Peking Union Medical College, 9 Dongdan 3 Tiao, Beijing, 100730, China. wangli0528@vip.sina.com
Telephone: +86-10- 65237943 **Fax**: +86-10-65284767
Received: 2003-03-02 **Accepted:** 2003-03-29

Abstract

AIM: To describe the mortality rate of pancreatic cancer and its distribution in China during the period of 1991-2000.

METHODS: Based on the data of demography and death collected through China's Disease Surveillance Point System (DSPS) over the period of 1991-2000, the distribution of death rate of pancreatic cancer was described in terms of age group, gender, calendar year, rural/urban residence and administrative district.

RESULTS: A total of 1 619 death cases attributed to pancreatic cancer (975 men and 644 women) were reported by DSPS during 1991-2000. The reported, adjusted and age-standardized mortality rates increased from 1.46, 1.75, and 2.18 per 100 000 populations in 1991 to 2.38, 3.06, and 3.26 per 100 000 populations in 2000. The majority (69.62 %) of the deaths of pancreatic cancer were seen in the age group of 60 years and older. The mortality rate was higher in men than in women, but the male to female death rate ratios decreased during the 10 years. Our data also showed that the death rate of pancreatic cancer in urban areas was about 2-4 fold higher than that in rural areas, and in Northeast and East China, the death rates were higher than those in the other 5 administrative districts.

CONCLUSION: The death rate due to pancreatic cancer was rising during the period of 1991-2000 and the peak mortality of pancreatic cancer might arrive in China.

Wang L, Yang GH, Lu XH, Huang ZJ, Li H. Pancreatic cancer mortality in China (1991-2000). *World J Gastroenterol* 2003; 9 (8): 1819-1823

http://www.wjgnet.com/1007-9327/9/1819.asp

INTRODUCTION

Pancreatic cancer is one of the most formidable malignant tumors worldwide. It is difficult to diagnose at early stage, unresectable at the time of diagnosis with extremely poor survival rate due to its inaccessible location, proximity to other vital organs, and inherently aggressive pattern of growth[1,2]. The death to incidence ratio of pancreatic cancer is approximately 0.98-0.99:1[3,10]. With more than 27 000 people died from pancreatic cancer each year, it is the fourth leading cause of cancer death in the United States[4]. Some sporadic reports have shown that the mortality rates of pancreatic cancer in China have increased constantly over the last decades[5-7]. But there is little descriptive documentation countrywide on its epidemiology. By analyzing the death data from China's Disease Surveillance Point System (DSPS), we presented the first report on the mortality from pancreatic cancer and its distribution among the surveillance population during the period of 1991-2000 in China.

MATERIALS AND METHODS

Materials

All mortality data were collected from the population who resided in 145 DSPs (Disease Surveillance Points) of China. The DSPS was originated in the beginning of 1980s for the surveillance of morbidity and mortality, and the present system was established in 1989. DSPs were selected from an official list of all neighborhoods in urban areas and villages in rural areas using stratified multistage sampling. The strata was involved in geographic areas (urban or rural status: within the rural areas, stratification into 4 levels based on indicators of mortality and socioeconomic status). In 1989, 145 surveillance points with a total population of around 10 million under surveillance (Table 1) were chosen, and scattered in 31 provinces, autonomous regions, or municipalities in China. Comparisons among the DSP population and the whole population over the country showed no significant differences in terms of socioeconomic conditions, population constitution, and health status. Such comparisons were made annually[8].

The obtained information related to death in China was based on the causes of death reported by qualified physicians on medical death certificates. The underlying causes of death were ascertained following the procedures specified by the World Health Organization in the (Manual of the International Statistical Classification of Diseases, Injuries, and Causes of Death), ninth revision (ICD-9). If the death causes of the deceased were either uncertain, or out of accord with the classification standards or could not be coded with ICD-9, the registry staff would clarify and/or justify the causes of death through interviewing the relatives of the patient or consulting his or her physicians.

Evaluation on data quality

Since the beginning of the disease surveillance, the National Center of DSPs had developed a series of quality control and evaluation system to examine data quality from DSPs every year, to assure that the surveillance data over the period of 1991-2000 were reliable and valuable for estimating the mortality of surveillance population. The quality of the data was evaluated as follows: (1) The demographic data and distribution of population by age and gender were credible and suitable for a denominator for calculating the rates since the United Nations Integrated Index of Population[9] fluctuates between 15 and 20. (2) The cases with uncertain death causes accounted for around 5 % of all death cases. (3) Three types of medical evidences from medical records or files were used for

Table 1 Population distribution by age group in DSPs during 1991-2000 in China (10 000)[a]

Age group	1991	1992	1993	1994	1995	1996	1997	1998	1999	2000
0-	18.52	15.74	13.84	13.56	11.47	11.60	12.00	10.40	9.92	10.17
1-	72.69	66.59	64.06	64.94	57.60	60.96	61.20	52.76	49.51	50.16
5-	88.94	83.27	79.72	83.66	76.27	80.52	82.40	70.60	66.62	69.51
10-	91.70	87.86	81.64	83.12	75.32	79.54	87.59	73.59	73.60	79.71
15-	106.24	96.25	90.63	94.48	82.97	90.43	94.27	81.45	78.51	83.92
20-	105.41	101.42	97.64	101.40	88.72	95.43	98.82	83.81	81.04	83.31
25-	99.66	98.06	93.77	95.82	86.55	92.23	97.02	83.60	81.07	83.60
30-	82.29	80.92	77.13	81.59	75.30	82.17	84.81	73.89	73.50	76.26
35-	77.87	77.00	75.00	76.67	68.58	73.37	76.82	68.56	67.84	70.99
40-	60.53	61.85	60.06	63.28	60.86	65.06	67.89	61.70	59.62	60.93
45-	48.19	48.48	47.51	50.14	47.67	51.95	54.45	50.14	49.87	52.72
50-	44.32	43.93	42.62	44.74	41.93	44.51	46.30	41.76	41.83	44.05
55-	40.80	40.08	39.46	40.59	37.76	40.99	41.62	37.14	37.10	38.55
60-	33.19	32.92	32.91	33.93	31.45	34.80	35.64	32.22	31.98	33.01
65-	25.73	25.45	25.94	26.65	24.50	27.56	28.54	26.10	25.93	27.17
70-	17.85	18.32	18.31	19.16	17.60	19.66	19.82	18.13	18.18	18.95
75-	11.18	11.64	11.73	12.33	11.24	12.21	12.39	11.25	11.28	11.86
80-	5.92	6.33	6.14	6.64	5.86	6.77	6.66	6.09	6.35	6.55
85+	2.81	2.59	2.90	3.08	3.17	3.67	3.38	3.13	3.30	3.51
Total	1033.84	998.70	961.01	995.78	904.82	973.43	1011.62	886.32	867.05	904.93

[a]Population of the surveillance points with poor quality deleted.

the diagnosis and classification of the causes of death, including autopsy or biopsy, laboratory or radiology tests (clinical diagnosis), and inference after death (without certain documentation from biopsy or radiology test, but making highly suspicious diagnosis in terms of clinical symptoms, signs and some laboratory tests). Cases of pancreatic cancer, diagnosed using pathological test and clinical test, accounted for 31.56 % and 64.13 % respectively, the remaining (4.31 %) was determined by inference diagnosis. The percentage of cases diagnosed at different levels of hospitals was as follows: 92 % by hospitals of county grade and above (36.4 % by provincial grade and 29.1 % by municipal grade). This showed that the diagnosed death causes were credible and could be used for data analysis. (4) Validation was undertaken through periodic under-reporting surveys. A stratified three-stage cluster sampling design was adopted by each DSP to obtain the under-reporting rate. The overall under-reporting rate for mortality fluctuated between 12.25 % and 22.46 %.

Analysis methods

Based on the surveillance data from the DSPs during the period of 1991-2000, the distribution of death rate of pancreatic cancer was described by age group, gender, calendar year, rural/urban residence and administrative district. The reported death rate was expressed as the reported number of deaths of pancreatic cancer per 100 000 populations per year. The adjusted death rate was calculated with the formula, reported death rate/(1-under-reporting rate) and the age-standardized rate was calculated with the indirect method in terms of World Standard Population (*http://www3.who.int/whosis/discussion_papers/htm/paper31.htm)*. All analyses were conducted using software EPI 2000.

RESULTS

During 1991-2000, 504 604 death cases were reported in DSPs population. The reported death rate fluctuated between 507.67 and 546.60 per 100 000 populations in 1991-2000. The adjusted death rate remained relatively stable in 1991-1997 and increased gradually after 1997. But the age-standardized death rate decreased slightly during the 10 years.

Table 2 Mortality rate of pancreatic cancer during 1991-2000 in China (1/100 000)

Year	Death number	Reported death rate	Adjusted death rate	Age-standardized death rate	Deaths due to tumor (%)[a]
1991	151	1.46	1.75	2.18	1.83
1992	139	1.39	1.60	1.92	1.66
1993	129	1.34	1.54	1.80	1.51
1994	142	1.43	1.63	1.90	1.69
1995	145	1.60	1.85	2.12	1.79
1996	161	1.65	1.91	2.14	1.75
1997	168	1.66	1.92	2.18	1.86
1998	183	2.06	2.66	2.92	2.10
1999	186	2.16	2.78	2.96	2.23
2000	215	2.38	3.06	3.26	2.26

[a]Calculated by reported death rate.

Eighty six thousand five hundred and fifty six patients died from tumor in the 10 years, accounting for 17.15 % of total death cases reported in DSPs population. The reported, adjusted and age-standardized death rate for tumor increased from 79.86, 95.57 and 118.74 per 100 000 in 1991 to 104.91, 135.30 and 145.63 in 2000 respectively, with a steady increase on average of 3.08 %, 3.94 % and 2.29 % per year. Tumor contributed 15.65 % of all deaths in 1991, and 19.23 % in 2000. Tumor ranked the third of death cause in all death cases during 1991-1998, and went up to the second rank in 1999-2000.

One thousand six hundred and nineteen deaths were attributed to pancreatic cancer during the 10 years, accounting for 1.87 % of all deaths due to tumors. The reported, adjusted and age-standardized mortality rate increased by 5.53 %, 6.41 % and 4.57 % annually, from 1.46, 1.75, 2.18 per 100 000 populations in 1991 to 2.38, 3.06, and 3.26 per 100 000 populations in 2000. Pancreatic cancer accounted for 1.83 %

of all deaths due to tumor in 1991 and 2.26 % in 2000, with the 6-8th rank for men and the 9-10th for women. The details and the time trend are shown in Table 2.

The death rate of pancreatic cancer was closely related to age. The majority (69.62 %) of the deaths of pancreatic cancer were seen in the age group of 60 years and more, while fewer cases (3.95 %) were found among people aged less than 40 years. Table 3 also shows the changing trend of annual mortality in all age groups during the 10 years. The annual mortality rates in the 10 years fluctuated around 2 per 100 000 populations in the age group of 45 to 54 years, but the rates were higher than 10 per 100 000 populations in the group aged 65 to 84 years, approximately 5-fold difference between these groups. Around 2-fold increase was found in the mortality in the last few years compared with that at the beginning of 1990' s in people aged over 65 years.

Table 3 Reported death rate of pancreatic cancer by age during 1991-2000 in China (1 / 100 000)

Age group	1991	1992	1993	1994	1995	1996	1997	1998	1999	2000
0-	0.00	0.00	0.00	0.00	0.00	0.00	0.00	0.00	0.00	0.00
15-	0.19	0.00	0.05	0.00	0.06	0.00	0.05	0.00	0.00	0.00
25-	0.22	0.11	0.00	0.11	0.12	0.06	0.16	0.19	0.26	0.06
35-	0.51	0.14	0.89	0.64	0.46	0.36	0.41	1.15	0.63	0.53
45-	2.70	2.06	2.44	0.95	1.45	1.76	2.38	2.50	2.84	1.65
55-	6.49	6.71	4.01	6.58	6.94	6.73	6.99	6.78	6.37	7.27
65-	9.18	10.74	9.49	9.17	9.98	11.86	11.17	13.11	16.55	18.87
75-	10.53	10.01	11.76	14.23	18.13	13.17	11.03	18.45	16.45	23.36
85+	17.82	7.74	6.89	13.01	6.32	16.36	14.79	15.98	9.08	17.10
Total	1.46	1.39	1.34	1.43	1.60	1.65	1.66	2.06	2.15	2.37

Of all the reported death cases of pancreatic cancer between 1991 and 2000, 975 were diagnosed in men and 644 in women. The mortality rates of pancreatic cancer by gender are presented in Table 4. The data showed that all the reported, adjusted and age-standardized rates in males increased during the 10 years, from 1.86, 2.23, and 2.94 per 100 000 populations in 1991 to 2.70, 3.48, and 3.87 per 100 000 populations in 2000, with an increase on average of 4.23 %, 5.07 % and 3.10 % per year respectively. All these rates in female increased from 1.05, 1.25, and 1.49 to 2.04, 2.63 and 2.68 per 100 000 populations, with an annual average increase of 7.66 %, 8.61 % and 6.74 %. The male to female standardized death rate ratios decreased from 1.97 in 1991 to 1.44 in 2000.

The distribution of pancreatic cancer differed among the administrative districts (Table 5). The reported death rates in Northeast and East China were higher than those in the other 5 districts. After adjusted by the under-reporting rates for different districts, the rates of Northeast and East China were still higher than the latter (Figure 1).

Table 5 Reported death rate of pancreatic cancer by the administrative district of DSPs, China, 1991-2000 (1 / 100 000)

Year	North China	Northeast China	East China	Central China	South China	Northwest China	Southwest China
1991	2.22	1.23	2.52	0.85	1.26	1.28	1.14
1992	1.43	2.43	2.10	0.86	0.90	1.93	1.15
1993	2.01	0.70	2.75	0.95	0.74	0.76	0.71
1994	1.27	3.18	2.62	1.13	0.60	0.88	0.92
1995	1.67	3.30	3.33	1.01	0.73	0.91	1.08
1996	1.68	3.37	3.34	1.27	1.07	0.67	0.78
1997	2.08	3.39	3.01	0.96	0.89	1.17	1.37
1998	1.80	4.26	4.04	1.31	0.51	1.61	1.85
1999	1.83	4.72	5.51	1.28	0.89	1.29	1.15
2000	1.55	6.96	4.31	1.26	1.48	0.73	1.79

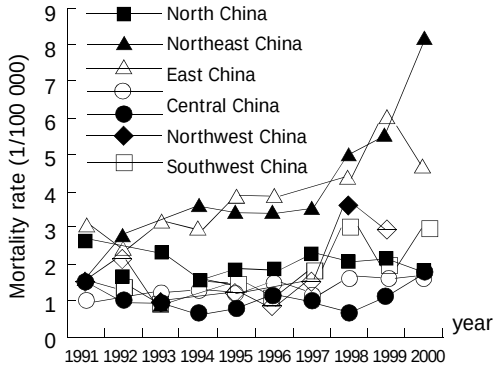

Figure 1 The adjusted mortality rate of pancreatic cancer by different districts, China, 1991-2000.

The distribution of pancreatic cancer was variable among rural and urban areas as well. The reported mortality rates in the urban areas were much higher than those in the rural areas. After adjusted by the differential under-reporting rates, the adjusted rates in the urban areas were still higher than those in the rural areas. And the death rates of pancreatic cancer displayed an increasing trend for both rural and urban areas during the period of 1991-2000 (Table 6). In 1991 the reported death rate of pancreatic cancer was 3.37 per 100 000 populations in the urban areas and 0.91 in the rural areas, and the adjusted death rates were 3.97 and 1.09, respectively. In 2000, the correspondent rates were 5.53 and 1.54, 7.32 and

Table 4 Mortality rate of pancreatic cancer by gender during 1991-2000 in China (1 / 100 000)

Year	Male				Female			
	Death number	Reported death rate	Adjusted death rate	Age-standardized rate	Death number	Reported death rate	Adjusted death rate	Age-standardized rate
1991	98	1.86	2.23	2.94	53	1.05	1.25	1.49
1992	97	1.90	2.19	2.77	42	0.86	0.99	1.13
1993	81	1.66	1.90	2.36	48	1.02	1.17	1.29
1994	79	1.56	1.78	2.24	63	1.29	1.47	1.62
1995	94	2.04	2.36	2.87	51	1.15	1.33	1.44
1996	90	1.82	2.10	2.47	71	1.48	1.72	1.85
1997	98	1.89	2.20	2.61	70	1.41	1.63	1.76
1998	106	2.34	3.02	3.45	77	1.77	2.28	2.40
1999	108	2.44	3.15	3.57	78	1.83	2.36	2.40
2000	124	2.70	3.48	3.87	91	2.04	2.63	2.68

1.97, respectively. Between 1991 and 2000, the reported and adjusted death rates increased by 5.02 % and 7.03 % per year in the urban areas and 6.02 % and 6.80 % in the rural areas, respectively.

Table 6 Mortality rate of pancreatic cancer by areas during 1991-2000 in China (1/100 000)

Year	Reported death rate			Adjusted death rate		
	Urban	Rural	Ratio of urban to rural	Urban	Rural	Ratio of urban to rural
1991	3.37	0.91	3.70	3.97	1.09	3.64
1992	3.00	0.92	3.26	3.37	1.06	3.18
1993	3.25	0.81	4.01	3.65	0.93	3.93
1994	3.50	0.84	4.17	3.84	0.96	4.00
1995	3.63	0.99	3.67	4.28	1.14	3.75
1996	4.12	0.88	4.68	4.86	1.01	4.81
1997	3.80	1.02	3.73	4.47	1.18	3.79
1998	3.77	1.56	2.42	4.99	2.00	2.50
1999	3.89	1.61	2.42	5.15	2.07	2.49
2000	5.53	1.54	3.59	7.32	1.97	3.72

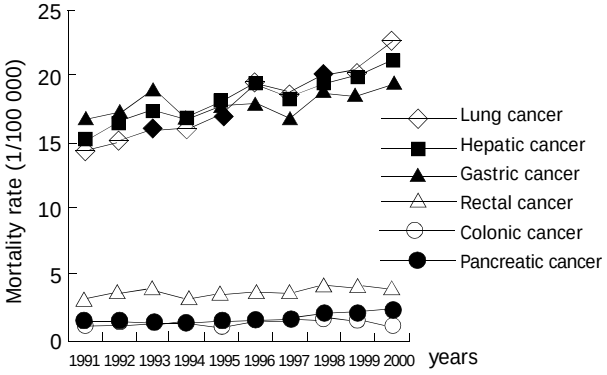

Figure 2 The trend of reported mortality of pancreatic cancer and some major cancers in DSP, China, 1991-2000.

Figure 2 shows the dynamic trend of mortality rate of pancreatic cancer and other common tumors. The increasing trend of pancreatic cancer paralleled the slight variation seen in rectal and colonic cancer, while the death rates of hepatic, stomach and lung cancers changed more remarkablely.

DISCUSSION

Our data analysis was performed based on the data of demography and death, collected through DSPs over the period from 1991 to 2000. The DSPS data were of good representative ness due to their selection by probability sampling and their rigorous management[8] and therefore the results derived from surveillance population can be inferred to health status of national population. The assessment of indicators used for data quality evaluation, including the United Nations Integrated Index on Population, the proportion of cases with uncertain death cause, the diagnosis evidence of pancreatic cancer and the under-reporting rate, demonstrates that these data are reliable and the mortality rate of pancreatic cancer derived from the DSPs data might be used to estimate the death level over the whole community. However, the mortality rates reported in this study might be lower in view of the impact of technology development in the diagnosis of pancreatic cancer and its nonspecific clinical symptoms.

Pancreatic cancer may be one of the diseases that are correlated with industrialization. Reports from the studies on the mortality of pancreatic cancer worldwide in 1990 suggested that majority deaths (66 %) occurred in developed countries[10]. WHO reported[11] the age-standardized mortality rates of pancreatic cancer in Western developed countries such as the United States, the United Kingdom, Australia, and Japan, ranged from 6 to 8 per 100 000 in males, and 4 to 6 in females, which were about 2-4 times higher than that in China (about 2 to 3 per 100 000 in males and 1 to 3 in females) in the same period. But in these countries, the mortality rate of pancreatic cancer, both in males and females, have leveled off and even dropped by the end of last century. And in some Asian countries, such as South Korea and Singapore, the age-standardized rates of pancreatic cancer are also higher than those in China, even though not reaching the peak yet[11]. In addition, we have seen a rapid increasing of death rates of pancreatic cancer in China, particularly among those aged over 65 years in the recent decade. The reported, adjusted and age-standardized death rates of pancreatic cancer have increased by 62.33 %, 74.86 % and 49.54 % respectively. This is, to some extent, explained by the improved diagnosis and cancer death registration since pancreatic cancer is difficult to be diagnosed and classified[31], but it is also probably attributed to the increased risk factors associated with industrialization, such as diet- and smoking-related factors as well as life-style changes[21,22]. At present, little is known about the etiology of pancreatic cancer. Cigarette smoking is the only firmly established factor[17, 25-28], with a 1. 2- to 3.1-fold increase in risk. Smoking, however, cannot by itself totally explain the increasing trends. There is less certainty concerning the risks associated with a range of dietary factors. Some studies have reported an increased risk with higher consumption of meat, protein and cholesterol and lower consumption of fruits and vegetables[27-30].

The role of life-style and dietary factors[27-30] in the etiology of pancreatic cancer is also supported by the higher mortality rates observed in the urban areas. Of course, the higher rates in the urban areas could be partly attributed to the improved diagnosis. Also our data showed that the death rates of pancreatic cancer were not identical in different administrative districts. The mortality rate was considerably higher in Northeast and East China than that in the other 5 districts, and the reasons led to this difference need to be discussed further, but a partial reason might be associated with higher level of industrialization and urbanization in these areas.

The mortality rate of pancreatic cancer was strongly related to age in our study. Our study indicated that the majority of death cases of pancreatic cancer occurred in the age group of 60 years or older, and the patients aged less than 45 years only accounted for 3.95 %, almost the same as the results in other studies[12-17]. Similar to the other studies[11,14,18-20], our data have also found the gender difference between male and female. And the mortality from pancreatic cancer in males was higher than that in females, but the male to female mortality rate ratio showed a decreased trend in the period of 1991-2000.

Our study indicated that the increasing trend of mortality rate of pancreatic cancer paralleled that of rectal cancer. And other studies have also shown that there are remarkable similarities between the increased incidence of pancreas cancer and breast cancer in women and prostate cancer in men, and bowel cancer in both sexes over approximately the same period[23,24]. Dietary- and smoking- factors as the common risk factors may be relevant to the similarly increased trends of breast[33], prostate[32], bowel[34] and pancreatic cancers.

It is suggested that with the entry into an aging society and urbanization in China, the peak mortality of pancreatic cancer arrive soon in the next few decades. Therefore, it is crucial to carry out further studies on the etiology of pancreatic cancer and set up screening indicators earlier to reduce the number of deaths from pancreatic cancer.

REFERENCES

1 **Warshaw AL,** Fernandez-del Castillo C. Pancreatic carcinoma. *N Engl J Med* 1992; **326:** 455-465
2 **Williamson RC.** Pancreatic cancer: the greatest oncological challenge. *Br Med J* 1988; **296**: 445-446
3 **Devesa SS,** Blot WJ, Stone BJ, Miller BA, Tarone RE, Fraumeni JF Jr. Recent cancer trends in the United States. *J Natl Cancer Inst* 1995; **87**: 175-182
4 **Greenlee RT**, Murray T, Bolden S, Wingo PA. Cancer statistics, 2000. *CA Cancer J Clin* 2000; **50**: 7-33
5 **Qian MF**, Wang XH, Ma XY, Lei TH, Yao KY. Aresearch on the epidemiologic trend and mortality with cancer in Jiashan County. *Zhongguo zhongliu* 2001; **10:** 381-383
6 **Tan YD**, Jin YS, Lu XJ, Zhu YH. The change of death spectrum for major malignancies in Xiaoshan from 1970s to 1990s. *Zhejiang Zhongliu* 2000; **6:** 128-129
7 **Men BY**, Li SY, Wang Y, Gao HY, Zhang WL, Wang F, Liu L. A comparison between the results of cancer mortalities in 1972-1975 and in 1992-1994 in a rural areas of Shanxi proivince. *Zhonghua Liuxing Bingxue Zazhi* 1997; **33**: 5-8
8 **Yang GH**, Zhen XW, Zen G, Wang LS, Chen YL, Chen AP, Huang ZJ, Ge WM. Selection of DSP points in the second stage and their presentation. *Zhonghua Liuxing Bingxue Zazhi* 1992; **13**: 197-201
9 Department of Control Disease of MOPH, Chinese Academy of Preventive Medicine. A series of reports on Chinese disease surveillance: 1995 annual report on Chinese disease surveillance. *Beijing, China: People's Medical Publishing House* 1997: 9
10 **Pisani P,** Parkin DM, Bray F, Ferlay J. Estimates of the worldwide mortality from 25 cancers in 1990. *Int J Cancer* 1999; **83**: 18-29
11 **Worldwide cancer mortality statistics**. [cited 2002-06]. Available form: URL: http / / www-depdb.iarc.fr / who / menu.htm.
12 **Lillemoe KD,** Yeo CJ, Cameron JL. Pancreatic cancer: state-of-the-art care. *CA Cancer J Clin* 2000; **50**: 241-268
13 **Tan HP,** Smith J, Garberoglio CA. Pancreatic adenocarcinoma: an update. *J Am Coll Surg* 1996; **183**: 164-184
14 **Oomi K,** Amano M. The epidemiology of pancreatic disease in Japan. *Pancreas* 1998; **16**: 233-237
15 **Lillemoe KD**. Pancreatic disease in the elderly patient. *Surg Clin North Am* 1994; **74:** 317-344
16 **Hedberg M,** Anderson H, Borgstrom A, Janzon L, Larsson SA. Rising incidence of pancreatic carcinoma in middle-aged and older women-time trends 1961-90 in the city of Malmo, Sweden. *Br J Cancer* 1996; **73:** 843-846
17 **Nilsen TI,** Vatten LJ. A prospective study of lifestyle factors and the risk of pancreatic cancer in nord-trondelag, Norway. *Cancer Causes and Control* 2000; **11:** 645-652
18 **Niederhuber JE,** Brennan MF, Menck HR. The national cancer data base report on pancreatic cancer. *Cancer* 1995; **76**: 1671-1677
19 **Zheng T,** Holford TR, Ward BA, McKay L, Flannery J, Boyle P. Time trend in pancreatic cancer incidence in Connecticut, 1935-1990. *Int J Cancer* 1995; **61**: 622-627
20 **Karlson BM,** Ekbom A, Josefsson S, McLaughlin JK, Fraumeni JF Jr, Nyren O. The risk of pancreatic cancer following pancreatitis: an association due to confounding? *Gastroenterology* 1997; **113:** 587-592
21 Chinese Academy of Preventive Medicine, Dept. of Disease Control of Ministry of Health, P. R. China, Chinese Association of Smoking or Health, Office of Committee of the National Patriotic Health Campaign. Smoking and health in China, 1996 national prevalence survey of smoking pattern. *Beijing, China: China Science and Technology Press* 1997: 2-4
22 **Yang GH**. The transition of health mode and the control strategy on chronic disease in China. *Zhongguo Manxingbing Yufang yu Kongzhi* 2001; **9**: 145-148
23 **Stephens FO.** The increased incidence of cancer of the pancreas: is there a missing dietary factor? Can it be reversed? *Aust N Z J Surg* 1999; **69:** 331-335
24 **Jin F,** Devesa SS, Zheng W, Blot WJ, Fraumeni JF Jr, Gao YT. Cancer incidence trends in urban Shanghai, 1972-1989. *Int J Cancer* 1993; **53**: 764-770
25 **Coughlin SS,** Calle EE, Patel AV, Thun MJ. Predictors of pancreatic cancer mortality among a large cohort of united states adults. *Cancer Causes Control* 2000; **11:** 915-923
26 **Chiu BC,** Lynch CF, Cerhan JR, Cantor KP. Cigarette smoking and risk of bladder, pancreas, kidney and colorectal cancers in Iowa. *Ann Epidemiol* 2001; **11:** 28-37
27 **Stolzenberg-Solomon RZ,** Pietinen P, Barrett MJ, Taylor PR, Virtamo J, Albanes D. Dietary and other methyl-group availability factors and pancreatic cancer risks in a cohort of male smokers. *Am J Epidemiol* 2001; **153**: 680-687
28 **Baghurst PA,** McMichael AJ, Slavotinek AH, Baghurst KI, Boyle P, Walker AM. A case-control study of diet and cancer of the pancreas. *Am J Epidemiol* 1991; **134**: 167-179
29 **Farrow DC, Davis S.** Diet and the risk of pancreatic cancer in men. *Am J Epidemiol* 1990; **132**: 423-431
30 **Norell SE,** Ahlbom A, Erwald R, Jacobson G, Lindberg-Navier I, Olin R, Tornberg B, Wiechel KL. Diet and pancreatic cancer: a case-control study. *Am J Epidemiol* 1986; **124**: 894-902
31 **La Vecchia C,** Lucchini F, Negri E, Boyle P, Maisonneuve P, Levi F. Trends in cancer mortality in Europe, 1955-1989: I, Digestive sites. *Eur J Cancer* 1992; **28:** 132-235
32 **Shirai T,** Asamoto M, Takahashi S, Imaida K. Diet and prostate cancer. *Toxicology* 2002; **181-182**: 89-94
33 **Wolff MS,** Britton JA, Wilson VP. Environmental risk factors for breast cancer among African-American women. *Cancer* 2003; **97** (Suppl): 289-310
34 **Tiemersma EW,** Kampman E, Bueno de Mesquita HB, Bunschoten A, van Schothorst EM, Kok FJ, Kromhout D. Meat consumption, cigarette smoking, and genetic susceptibility in the etiology of colorectal cancer: results from a Dutch prospective study. *Cancer Causes Control* 2002; **13**: 383-393

Edited by Yuan HT and Wang XL

P.O.Box 2345, Beijing 100023,China
Fax: +86-10-85381893
E-mail: wjg@wjgnet.com www.wjgnet.com

World J Gastroenterol 2003;9(8):1824-1827
World Journal of Gastroenterology
 ISSN 1007-9327

• CLINICAL RESEARCH •

Influence of acute hyperglycemia in human sepsis on inflammatory cytokine and counterregulatory hormone concentrations

Wen-Kui Yu, Wei-Qin Li, Ning Li, Jie-Shou Li

Wen-Kui Yu, Wei-Qin Li, Ning Li, Jie-Shou Li, Medical College of Nanjing University, Research Institute of General Surgery, Jinling Hospital, Nanjing 210002, Jiangsu Province, China
Supported by the Key Project of the Tenth-Five-year plan Foundation of PLA, No. 01Z011
Correspondence to: Wen-Kui Yu, Research Institute of General Surgery, Jinling Hospital, 305 Zhongshan East Road, Nanjing 210002, Jiangsu Province, China. yudrnj@163.com
Telephone: +86-25-4826808 Ext 58067
Received: 2002-12-28 **Accepted:** 2003-02-16

Abstract

AIM: In human sepsis, a prominent component of the hypermetabolite is impaired glucose tolerance (IGT) and hyperglycemia. Elevations in plasma glucose concentration impair immune function by altering cytokine production from macrophages. We assessed the role of glucose in the regulation of circulating levels of insulin, glucagon, cortisol, IL-6 and TNF-α in human sepsis with normal or impaired glucose tolerance.

METHODS: According to the results of intravenous glucose tolerance test, forty patients were classified into two groups: control group (n=20) and IGT group (n=20). Plasma glucose levels were acutely raised in two groups and maintained at 15 mmol/L for 3 hours. Plasma insulin, glucagon and cortisol levels were measured by radioimmunoassay, the levels of TNF-α and IL-6 were detected by ELISA.

RESULTS: In IGT group, the fasting concentrations of plasma glucose, insulin, glucagon, cortisol, IL-6 and TNF-α levels were significantly higher than those in control group (P<0.05). During clamp, the control group had a higher average amount of dextrose infusion than the IGT group (P<0.01). In control group, plasma insulin levels rose from a basal value to a peak at an hour (P<0.05) and maintained at high levels. Plasma glucagon levels descended from a basal value to the lowest level within an hour (P<0.01) and low levels were maintained throughout the clamp. In IGT group, plasma insulin was more significantly elevated (P<0.01), and plasma glucagon levels were not significantly declined. Plasma cortisol levels were not significantly changed in two groups. In control group, plasma IL-6 and TNF-α levels rose (P<0.01) within 2 hours of the clamp and returned to basal values at 3 hours. In IGT group, increased levels of plasma cytokine lasted longer than in control group (3 hours *vs*. 2 hours, P<0.05), and the cytokine peaks of IGT group were higher (P<0.05) than those of control group.

CONCLUSION: Acute hyperglycemia pricks up hyperinsulinemia and increases circulating cytokine concentrations and these effects are more pronounced in sepsis with IGT. This suggests a potential modulation of immunoinflammatory responses in human sepsis by hyperglycemia.

Yu WK, Li WQ, Li N, Li JS. Influence of acute hyperglycemia in human sepsis on inflammatory cytokine and counterregulatory hormone concentrations. *World J Gastroenterol* 2003; 9(8): 1824-1827
http://www.wjgnet.com/1007-9327/9/1824.asp

INTRODUCTION

Severe human sepsis is associated with hypermetabolic stress response, and affects protein, carbohydrate and lipid metabolism throughout the body[1-7]. A prominent component of hypermetabolic stress response is hyperglycemia and impaired glucose tolerance (IGT). The mechanisms of stress hyperglycemia are well known[8]. Counterreglulatory hormone and excess cytokine result in insulin resistance, and many hospitalized patients are insulin deficient for a variety of reasons (e.g. old age, pancreatitis, hypothermia, hypoxemia). Excess dextrose infusion is an often-overlooked contributor to hyperglycemia[9].

The harm of acute hyperglycemia in stress response patients has been demonstrated in several clinical and experimental conditions[10-12]. An increased susceptibility to infections in the presence of hyperglycemia has long been known in patients with diabetes[10,11,13]. And recent investigations have demonstrated that elevations in plasma glucose concentration impair immune function by altering cytokine production from macrophages, diminishing lymphocyte proliferation, and depressing intracellular bactericidal activity of leukocytes[14-17]. Furthermore, in the issue of circulation, Esposito K. argued hyperglycemia acutely increased circulating cytokine concentrations, and this effect was more pronounced in group with IGT[18]. But former researches focused on normal human being, diabetes or critically ill patients, etc. and rarely concentrated on severe human sepsis.

The present study was to test whether circulating levels of hormones and cytokines are regulated by glucose levels in sepsis, and to measure serum insulin, glucagon, cortisol, TNF-α, and IL-6 concentrations during acute hyperglycemia in septic patients with normal or impaired glucose tolerance (IGT).

MATERIALS AND METHODS

Subjects

The subjects of this study were the patients admitted from January 5 to November 1, 2002 to the medical SICU of Jinling Hospital in Nanjing. Forty patients (23 men, 17 women) with a mean (s.d.) age of 52.2 (15.6) years with abdominal or pelvic sepsis were studied. Patients with diabetes mellitus, trauma, human immunodeficiency virus disease, end-stage renal disease, end-stage hepatic disease, the patients receiving immunosuppressive agents were excluded. Forty patients were divided into two groups according to normal (control group, n=20) or impaired (IGT group, n=20) glucose tolerance (Table 1). The patients' glucose tolerance was assessed by intravenous glucose tolerance test (IVGTT). After an overnight fast each patient underwent IVGTT: a 50 % glucose solution (glucose 0.5 gm/kg of body weight) was injected into the femoral vein

for 2 minutes. Patients in IGT group had a 2-hour plasma glucose value between 7.7 mmol/L and 11 mmol/L, and the control group had normal glucose tolerance (2-hour plasma glucose value below 7.7 mmol/L). Informed consent was obtained from all participating patients or their surrogates.

Severity of sepsis and underlying diagnosis

Sepsis was defined by the American College of Chest Physicians-Society of Critical Care Medicine consensus statement by an identifiable site of infection and evidence of a systemic inflammatory response manifested by at least three of the following criteria: (1) temperature, >38 ℃ or <36 ℃; (2) heart rate, >90 beats per minute; (3) respiratory rate, >20 breaths per minute; (4) white blood cell count, >12 000/mm^3 or <4 000/mm^3[19]. Patients meeting enrollment criteria were entered within 24 h. The cause of sepsis was severe acute pancreatitis (n=11), colorectal anastomotic dehiscence (n=9), perforated diverticular disease (n=9), gastroduodenal perforation (n=7), gallbladder perforation (n=3) and spontaneous splenic abscess (n=1). Sepsis severity was scored using the method of Elebute and Stoner[20]. This scoring procedure takes into account the site of infection, bacteriology, body temperature, secondary effects (e.g. jaundice) and various haematological and biochemical variables, such as white cell count and plasma albumin concentration.

Study protocol

After 12-hour fast overnight, the patients were placed in a supine comfortable position with the sickroom temperature between 20 ℃ and 24 ℃. Intravenous lines were inserted into a large antecubital vein of one arm for infusions and into a dorsal vein of the contralateral arm for blood sampling. Patency was preserved in a slow saline infusion (0.9 % NaCl). After withdrawal of baseline blood samples, plasma glucose concentrations were acutely raised with a bolus injection of 0.25 g/kg glucose followed by a varying 30 % glucose infusion to achieve steady-state plasma glucose concentrations of about 15 mmol/L for 180 minutes.

Analysis

Samples for analysis of plasma glucose were collected in tubes containing a trace of sodium fluoride. Plasma glucose was determined according to the glucose oxidase method with an autoanalyzer (Beckman Instruments). Serum samples for measuring hormone and cytokine level were stored at -80 ℃ until assay. Commercially available kits were used for radioimmunoassay of plasma insulin, glucagon and cortisol concentrations. Serum concentrations of TNF-α, IL-6 were determined in duplicate with commercially available kits (R&D Systems). Dilution curves of serum samples were parallel to those of standard. Intra-assay and interassay coefficients of variation were 3.8 % and 5.8 % for TNF-α, 2.8 % and 3.3 % for IL-6.

Statistical analysis

Results were given as mean ±SD. One-way ANOVA was used to compare baseline data, followed by Scheffé's test for pairwise comparisons. Multiple comparison tests were made with ANOVA, followed by post hoc analysis (Student-Newman-Keuls test) to locate the significant difference indicated by ANOVA. A value of P<0.05 was considered statistically significant. Data were analysed using Statistical Package for the Social Sciences computer software (SPSS 11.0).

RESULTS

During the 7-month study period 46 patients were collected, however analysis was limited to 40 patients with complete and available data. IGT group had higher admission severity scores than control group (APACHE Ⅱ, 10 (7-15) *vs*. 7 (4-10), sepsis score, 13 (8-19) *vs*. 8 (6-13); P<0.05). In IGT group, the levels of fasting plasma glucose, insulin, glucagon, cortisol, IL-6 and TNF-α levels were significantly higher than those in control group (Table 1). During the clamp, plasma glucose became stabilized at 15 mmol/L with oscillations not exceeding 5 % of the prefixed value. The control group had a higher average amount of dextrose infusion than IGT group (0.68±0.31 g/kg *vs*. 0.42±0.16 g/kg; P<0.01).

Table 1 Details of control and IGT groups

Variable	Control group (n=20)	IGT subject (n=20)
Age, y	41±4	42±6
Sex, M/F, n	13/7	12/8
Body mass index, kg/m2	21.11±1.22	20.12±1.43
Plasma glucose, mmol/L	5.22±0.89	7.23±0.73[a]
Plasma insulin, pmol/L	72.00±14.83	82.95±10.23[a]
Plasma glucagon, pmol/L	80.75±12.98	90.90±15.54[a]
Plasma cortisol, mmol/L	0.68±0.11	0.79±0.12[b]
IL-6, pg/ml	3.18±0.64	3.63±0.43[a]
TNF-α, pg/ml	4.66±0.70	5.99±0.76[b]
APACHE Ⅱ score	7(4-10)	10(7-15)[a]
Sepsis score	10(8-16)	15(10-25)[a]

All data were the mean (s.d.), except APACHE Ⅱ score and sepsis score which were the median (range). APACHE, acute physiology and chronic health evaluation. [a]P<0.05 *vs*. control group. [b]P<0.01 *vs* control group.

Counterregulatory hormone

During the clamp, plasma insulin levels increased from a basal level of 72.00±14.83 pmol/L to a peak of 83.40±14.29pmol/L within one hour (P<0.05) and maintained at high levels in control group. Whereas, plasma insulin levels increased more significantly in IGT group (P<0.01) (Figure 1). In control group, plasma glucagon levels decreased from a basal value of 80.75±12.98 pmol/L to the lowest level of 74.70±11.40 pmol/L within an hour (P<0.01) and low levels maintained, and was not significantly declined in IGT group during the entire observation period (Figure 2). Plasma cortisol was not significantly changed in two groups (Figure 3).

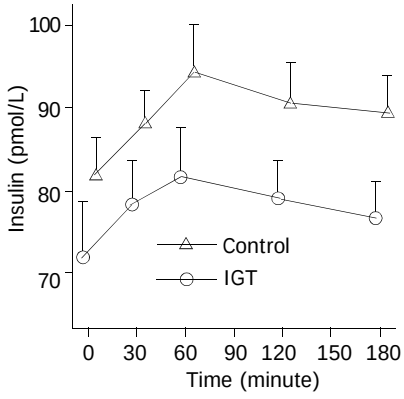

Figure 1 Circulation insulin levels during hyperglycemia clamps in 20 patients of control group (○-○) and in 20 patients of IGT group (△-△). Mean ± S.E.M. in human sepsis. Plasma insulin levels rose from a basal value to a peak within an hour (P<0.01) and high levels maintained in two groups.

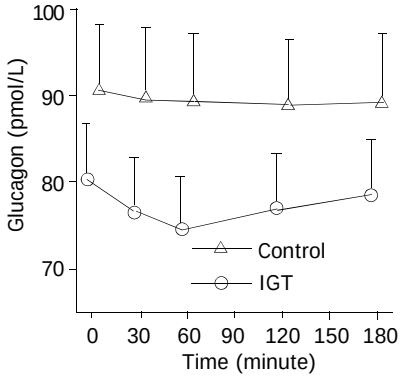

Figure 2 Circulation glucagon levels during hyperglycemia clamps in 20 patients of control group (○-○) and in 20 patients of IGT group (△-△). Mean ± S.E.M. in human sepsis. In control group, plasma glucagon levels decreased from a basal value to the lowest level within half an hour (P<0.01) and a low level maintained, and was not significantly declined in IGT group in the entire observation period.

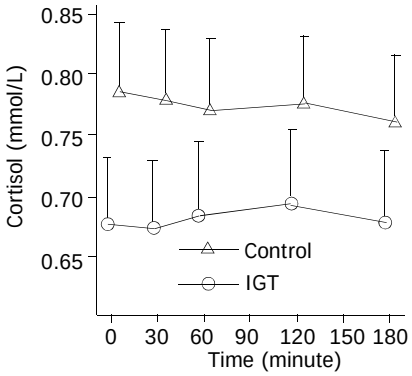

Figure 3 Circulation cortisol levels during hyperglycemia clamps in 20 patients of control group (○-○) and in 20 patients of IGT group (△-△). Mean ± S.E.M. in human sepsis. There were no significant changes in two groups.

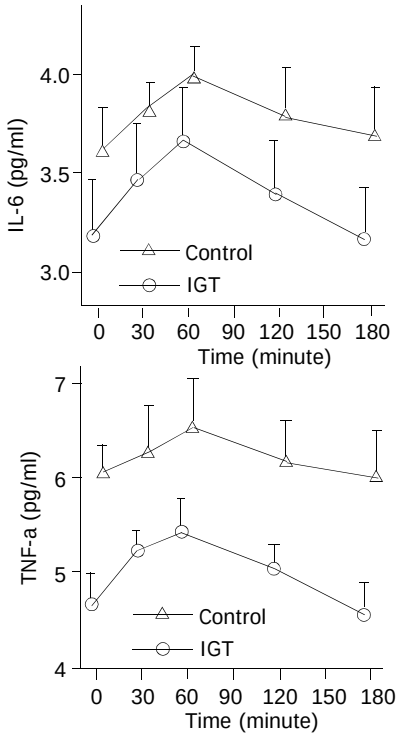

Figure 4 Circulation IL-6, TNF-α levels during hyperglycemia clamps in 20 patients of control group (○-○) and in 20 patients of IGT group (△-△). Mean ± S.E.M. in human sepsis. In two groups, plasma IL-6, TNF-α levels rose from a basal value to a peak within 1 hour (P<0.01). In IGT group, increased level of plasma TNF-α, IL-6 during the clamping lasted longer than in control group (3 hours *vs*. 2 hours; P<0.05).

Inflammatory cytokine

In control group, plasma IL-6 levels increased from a basal value of 3.18±0.64 pg/mL to a peak of 3.67±0.57 pg/mL within 1 hour (P<0.01) and returned to basal level at 3 hours. Fasting plasma TNF-α levels were 4.66±0.70 pg/mL, they peaked at 1 hour (5.4±0.64 pg/mL, P<0.01), and returned to baseline at 3 hours. In IGT group, increased levels of plasma cytokine during the clamp lasted longer than in control group (3 hours *vs*. 2 hours; P<0.05) (Figure 4, 5).

DISCUSSION

In this study, we found that IGT group had higher admission severity scores than control group, and had high plasma concentrations of counterregulatory hormones and inflammatory cytokines. During the clamp, IGT group had a less average amount of dextrose infusion than control group. In IGT patients, a short term of hyperglycemia after glucose infusion failed to adjust the plasma concentration of counterregulatory hormones to maintain glucose homeostasis. Acute hyperglycemia in control and in IGT patients induced an increase in plasma IL-6, TNF-α concentrations and insulin levels, and the effect was amplified by IGT group. These results indicate that hyperglycemia in human sepsis with IGT is more easy to be revoked, and plays a potential modulation role in immunoinflammatory responses.

The mechanisms for "stress IGT" are well known. Human sepsis is accompanied by a marked increase in plasma concentration of counterregulatory hormones, i.e. glucagons, epinephrine, cortisol and growth hormone that affect glucose homeostasis. These hormones can lead to significant reductions in insulin sensitivity through poorly understood mechanisms likely related to alterations in insulin signal pathway[21]. Counterregulatory hormones also enhance lipolysis and level of free fatty acids (FFA) which may contribute additional defects to the defective insulin action. Cytokine, TNF-α and IL-6 may exert their influence indirectly by stimulating counterregulatory hormone secretion and by direct action themselves[22-24]. TNF-α and IL-6 individually and synergistically increase net glucose flux through resistance to insulin actions in muscle and liver via poorly understood post-receptor mechanisms[25]. Hepatic insulin resistance leads to ongoing glucose production even in hyperglycemia[26]. Peripheral insulin resistance decreases sketetal muscle glucose uptake and reduces glucose clearance, which leads to the development of IGT and even hyperglycemia.

After glucose infusion, in normal group, glucagon and glucose concentrations reduced by host insulin were sufficient and inhibited hepatic gluconeogenesis and glycogenolysis and prevented glucose production[27]. In contrast, in IGT group, glucose infusion failed to suppress endogenous glucose production despite accompanying hyperinsulinemia. Using stable isotopes, it was demonstrated that hepatic glucose production was -150 % of the normal resting post-absorptive values of healthy subjects in spite of provision of total parenteral nutrition with dextrose at rates exceeding the basal energy expenditure[28].

Glucose-based nutrition in septic patients may cause marked hyperinsulinemia due to peripheral insulin resistance[29]. Hyperinsulinemia associated with glucose-based nutrition in sepsis might augment proinflammatory cytokine production and stress response in septic patients[30]. The present findings

also demonstrated that acute hyperglycemia affected concentration of plasma cytokines in human sepsis, and this effect was more pronounced in IGT patients. *In vitro* studies using supraphysiological glucose concentration (>22 mmol/l) showed an increase in TNF-α and IL-6 secretion from healthy human mononuclear cells[31]. Furthermore, increased synthesis of TNF-α has been reported both in rat uterine cells cultured *in vitro* with increasing concentrations of glucose[32] and in placental tissue explants from women with gestational diabetes incubated with high glucose (25 mmol/l)[33]. Human monocytes produced by IL-6 in healthy volunteers increased during 24-hour incubation in high-glucose medium[34]. These findings are in accordance with our observations *in vivo*, suggesting a potential modulation of immunoinflammatory response by carbohydrates.

In summary, IGT in sepsis is associated with marked changes in plasma concentrations of counterregulatory hormones and inflammatory cytokines, and these changes partially account for the fact that IGT easily develops acute hyperglycemia during glucose infusion. Acute hyperglycemia pricks up hyperinsulinemia and increases circulating cytokine concentrations. This suggests a potential role of hyperglycemia in inflammatory responses in human sepsis.

REFERENCES

1 **Wu XN**. Current concept of pathogenesis of severe acute pancreatitis. *World J Gastroenterol* 2000; **6**: 32-36
2 **Netea MG**, Van der Meer JW, Kullberg BJ. Sepsis-theory and therapies. *N Engl J Med* 2003; **348**: 1600-1602
3 **Han DW**. Intestinal endotoxemia as a pathogenetic mechanism in liver failure. *World J Gastroenterol* 2002; **8**: 961-965
4 **Douglas RG**, Shaw JH. Metabolic response to sepsis and trauma. *Br J Surg* 1989; **76**: 115
5 **Wray CJ**, Mammen JM, Hasselgren PO. Catabolic response to stress and potential benefits of nutrition support. *Nutrition* 2002; **18**: 971-977
6 **Wu XN**. Treatment revisited and factors affecting prognosis of severe acute pancreatitis. *World J Gastroenterol* 2000; **6**: 663-665
7 **Chen QP**. Enteral nutrition and acute pancreatitis. *World J Gastroenterol* 2001; **7**: 185-192
8 **Mesotten D**, Van Den Berghe G. Clinical potential of insulin therapy in critically ill patients. *Drugs* 2003; **63**: 625-636
9 **Hirsch IB**. In-patient hyperglycemia-are we ready to treat it yet? *J Clin Endocrinol Metab* 2002; **87**: 975-977
10 **Beckman JA**, Goldfine AB, Gordon MB, Creager MA. Ascorbate restores endothelium-dependent vasodilation impaired by acute hyperglycemia in humans. *Circulation* 2001; **103**: 1618-1623
11 **Mizock BA**. Alterations in fuel metabolism in critical illness: hyperglycaemia. *Best Pract Res Clin Endocrinol Metab* 2001; **15**: 553-551
12 **Vasa FR**, Molitch ME. Endocrine problems in the chronically critically ill patient. *Clin Chest Med* 2001; **22**: 193-208
13 **Alexiewicz JM**, Kumar D, Smogorzewski M, Massry SG. Elevated cytosolic calcium and impaired proliferation of B lymphocytes in type II diabetes mellitus. *Am J Kidney Dis* 1997; **30**: 98-104
14 **Losser MR**, Bernard C, Beaudeux JL, Pison C, Payen D. Glucose modulates hemodynamic, metabolic, and inflammatory responses to lipopolysaccharide in rabbits. *J Appl Physiol* 1997; **83**: 1566-1574
15 **Reinhold D**, Anosorge S, Scheeicher ED. Elevated glucose levels stimulate transforming growth factor-beta 1 (TGF-beta 1), suppress interleukin IL-2, IL-6 and IL-10 Production and DNA synthesis in peripheral blood mononuclear cells. *Horm Metab Res* 1996; **28**: 267-270
16 **Gregory R**, McElveen J, Tattersall RB, Todd I. The effects of 3-hydroxybutyrate and glucose on human T cell responses to Candida albicans. *FEMS Immunol Med Microbiol* 1993; **7**: 315-320
17 **Moises RS**, Heidenreich KA. Glucose regulates expression of Gi-proteins in cultured BC3H-1 myocytes. *Biochem Biophys Res Commun* 1992; **182**: 1193-1200
18 **Esposito K**, Nappo F, Marfella R, Giugliano G, Giugliano F, Ciotola M, Quagliaro L, Ceriello A, Giugliano D. Inflammatory cytokine concentrations are acutely increased by hyperglycemia in humans: role of oxidative stress. *Circulation* 2002; **106**: 2067-2072
19 American College of Chest Physicians / Society of Critical Care Medicine Consensus Conference: definitions for sepsis and organ failure and guidelines for the use of innovative therapies in sepsis. *Crit Care Med* 1992; **20**: 864-874
20 **Elebute EA**, Stoner HB. The grading of sepsis. *BR J Surg* 1983; **70**: 29-31
21 **Shamoon H**, Hendler R, Sherwin RS. Altered responsiveness to cortisol, eipinephrine and glucagon in insulin-infused juvenile-onset diabetes A mechanism for diabetic instability. *Diabetes* 1980; **29**: 284-291
22 **Zhang GL**, Wang YH, Teng HL, Lin ZB. Effects of aminoguanidine on nitric oxide production induced by inflammatory cytokines and endotoxin in cultured rat hepatocytes. *World J Gastroenterol* 2001; **7**: 331-334
23 **Webber J.** Abnormalities in glucose metabolism and their relevance to nutrition support in the critically ill. *Curr Opin Clin Nutr Metb Care* 1998; **1**: 191-194
24 **Wang P**, Li N, Li JS, Li WQ. The role of endotoxin, TNF-α, and IL-6 in inducing the state of growth hormone insensitivity. *World J Gastroenterol* 2002; **8**: 531-536
25 **Chang HR**, Bistrian B. The role of cytokines in the catabolic consequences of infection and injury. *J Parenter Enteral Nutr* 1998; **22**: 156-166
26 **Wolfe RR**. Substrate utilization / insulin resistance in sepsis / trauma. *Balliere's Clin Endocrinol Metab* 1997; **11**: 645-657
27 **Rizza RA**, Mandarino LJ, Gerich JE. Dose-response characteristics for effects of insulin on production and utilization of glucose in man. *Am J Physiol* 1981; **240**: E630-E639
28 **Tappy L**, Schwarz JM, Schneiter P, Cayeux C, Revelly JP, Fagerquist CK, Jequier E, Chiolero R. Effects of isoenergetic glucose-based or lipid-based parenteral nutrition on glucose metabolism, de novo lipogenesis, and respiratory gas exchanges in critically ill patients. *Crit Care Med* 1998; **26**: 860-867
29 **Saeed M**, Carlson GL, Little RA, Irving MH. Selective impairment of glucose storage in human sepsis. *Br J Surg* 1999; **86**: 813-821
30 **Soop M**, Duxbury H, Agwunobi AO, Gibson SM, Hopkins SJ, Childs C, Cooper RG, Maycock P, LittLe RA, Carlson GL. Euglycemic hyperinsulinemia augments the cytokine and endocrine responses to endotoxin in humans. *Am J Physiol Endocrinol Metab* 2002; **282**: E1276-E1285
31 **Morohoshi M**, Fujisawa K, Uchimura I, Numano F. Glucose-dependent interleukin 6 and necrosis factor production by human peripheral blood monocytes in vitro. *Diabetes* 1996; **45**: 954-959
32 **Pampfer S**, Vanderheyden I, De Hertogh R. Increased synthesis of tumor necrosis factor-alpha in uterine explants from pregnant diabetic rats and in primary cultures of uterine cells in high glucose. *Diabetes* 1997; **46**: 1214-1224
33 **Coughlan MT**, oliva K, Georgiou HM, Permezel JM, Rice GE. Glucose-induced release of tumor necrosis factor-alpha from human placental and adipose tissues in gestational diabetes mellitus. *Diabet Med* 2001; **18**: 921-927
34 **Morohoshi M**, Fujisawa K, Uchimura I, Numano F. The effect of glucose and advanced glycosylation end products on IL-6 production by human monocytes. *Ann N Y Acad Sci* 1995; **748**: 562-570

Edited by Ren SY and Wang XL

P.O.Box 2345, Beijing 100023,China
Fax: +86-10-85381893
E-mail: wjg@wjgnet.com www.wjgnet.com

World J Gastroenterol 2003;9(8):1828-1831
World Journal of Gastroenterology
 ISSN 1007-9327

• CLINICAL RESEARCH •

Percentage of peak-to-peak pulsatility of portal blood flow can predict right-sided congestive heart failure

Jui-Ting Hu, Sien-Sing Yang, Yun-Chih Lai, Cheng-Yen Shih, Cheng-Wen Chang

Jui-Ting Hu, Yun-Chih Lai, Cheng-Yen Shih, Liver Unit, Cathay General Hospital, Taipei, Taiwan
Sien-Sing Yang, Liver Unit, Cathay General Hospital, Taipei and Medical Faculty, China Medical College, Taichung, Taiwan
Cheng-Wen Chang, Department of Cardiology, Cathay General Hospital, Taipei, Taiwan
Correspondence to: Sien-Sing Yang, MD., Liver Unit, Cathay General Hospital, 280, Jen-Ai Road, Sec. 4, Taipei 106, Taiwan yangss@cgh.org.tw
Telephone: +886-2-2708-2121 Ext 3123 **Fax:** +886-2-2707-4949
Received: 2003-03-28 **Accepted:** 2003-04-24

Abstract

AIM: To study the change of portal blood flow for the prediction of the status of right-sided heart failure by using non-invasive way.

METHODS: We studied 20 patients with rheumatic and atherosclerotic heart diseases. All the patients had constant systemic blood pressure and body weight 1 week prior to the study. Cardiac index (CI), left ventricular end-diastolic pressure (LVEDP), mean aortic pressure (AOP), pulmonary wedge pressure (PWP), mean pulmonary arterial pressure (PAP), mean right atrial pressure (RAP), right ventricular end-diastolic pressure (RVEDP) were recorded during cardiac catheterization. Ten patients with RAP <10 mmHg were classified as Group 1. The remaining 10 patients with RAP ⩾10 mmHg were classified as Group 2. Portal blood velocity profiles were studied using an ultrasonic Doppler within 12 h after cardiac catheterization.

RESULTS: CI, AOP, and LVEDP had no difference between two groups. Patients in Group 1 had normal PWP (14.6±7.3 mmHg), PAP (25.0±8.2 mmHg), RAP (4.7±2.4 mmHg), and RVEDP (6.4±2.7 mmHg). Patients in Group 2 had increased PWP (29.9±9.3 mmHg), PAP (46.3±13.2 mmHg), RAP (17.5±5.7 mmHg), and RVEDP (18.3±5.6 mmHg) (P<0.001). Mean values of maximum portal blood velocity (Vmax), mean portal blood velocity (Vmean), cross-sectional area (Area) and portal blood flow volume (PBF) had no difference between 2 groups. All the patients in Group 1 had a continuous antegrade portal flow with a mean percentage of peak-to-peak pulsatility (PP) 27.0±8.9 % (range: 17-40 %). All the patients in Group 2 had pulsatile portal flow with a mean PP 86.6±45.6 (range: 43-194 %). One patient had a transient stagnant and three patients had a transient hepatofugal portal flow, which occurred mainly during the ventricular systole. Vmax, Vmean and PBF had a positive correlation with CO (P<0.001) but not with AOP, LVEDP, PWP, PAP, RAP, and RVEDP. PP showed a good correlation (P<0.001) with PWP, PAP, RAP, and RVEDP but not with CI, AOP, and LVEDP. All the patients with PP >40 % had a right-sided heart failure with a RAP=10 mmHg.

CONCLUSION: The measurement of PP change is a simple and non-invasive way to identify patients with right heart failure.

Hu JT, Yang SS, Lai YC, Shih CY, Chang CW. Percentage of peak-to-peak pulsatility of portal blood flow can predict right-sided congestive heart failure. *World J Gastroenterol* 2003; 9 (8): 1828-1831
http://www.wjgnet.com/1007-9327/9/1828.asp

INTRODUCTION

Hepatic artery and portal vein contribute to the hepatic blood inflow. In cirrhotic patients, oral nitroglycerin can reduce portal blood flow due to systemic hypotension[1-4]. Congestive heart failure, systemic hypotension and the use of hypotensive agents can decrease cardiac output. The reduced cardiac out put and systemic hypotension can decrease the portal inflow volume. Marked reduction of hepatic inflow may cause ischemic hepatitis. Patients with cardiopulmonary diseases may develop ischemic hepatitis with abnormal serum ALT levels[5,6].

On the other hand, right-sided congestive heart failure can result in the increase of pressure in inferior vena cava and hepatic veins[6,7]. The liver in passive "backward" congestion status can develop hepatomegaly and synchronous pulsation, and the liver histology shows engorged and dilated terminal hepatic veins, atrophy of hepatocytes and eventually cardiac cirrhosis. The high pressure of the hepatic veins can transmit through the liver to result in post-sinusoidal portal hypertension and cardiac ascites. The diameter of portal vein has been proved to correlate with right atrial pressure[8]. Thus, right-sided heart failure can affect portal vein flow patterns.

The role of heart function in portal blood flow remains uncertain. Therefore, we studied the changes of portal blood flow in patients with different degree of right-sided heart failure using non-invasive ultrasonic Dopper[5,8-11].

MATERIALS AND METHODS

We studied the portal blood velocity profiles in 20 patients (9 males, 11 females, mean age: 49±16 years) who underwent cardiac and/or Swan-Ganz catheterizations for cardiovascular disorders (16 rheumatic heart disease cases, 4 atherosclerotic heart disease cases) to compare the portal profiles of 20 healthy volunteers. Although all the patients took medications affecting the hemodynamics such as isosorbide dinitrate and furosemide, their systemic blood pressure and body weight were constant for at least 1 week prior to the study. Patients with fever, infection, and shock were excluded. All the patients had no past history of liver disease, alcoholism or other metabolic disorders such as chronic renal failure or diabetes mellitus. None underwent transfusion or under cardiac inotropic agents. All the patients had an abdominal sonographic examination excluding chronic liver disease or splenomegaly. Patients with severe dyspnea were excluded if they were not able to remain on supine position for the study of ultrasonic Doppler.

Cardiac profiles including cardiac index (CI), left ventricular end-diastolic pressure (LVEDP), mean aortic pressure (AOP), pulmonary wedge pressure (PW), mean pulmonary arterial

pressure (PAP), mean right atrial pressure (RAP), right ventricular end-diastolic pressure (RVEDP) were recorded during the cardiac and Swan-Ganz catheterizations. Ten patients with PAP <10 mmHg (range: 1-7 mmHg) without right heart failure were classified as Group 1. The other 10 patients with right heart failure and RAP=10 mmHg (range: 10-28 mmHg) were classified as Group 2.

We studied the portal profiles using an ultrasonic Doppler composed of a real-time mechanical sector scanner and a 3.5 mHz pulsed Doppler flowmeter (Aloka Echo Camera Model SSD-650, Tokyo) within 12 h after cardiac catheterization. After more than 8 h fasting, portal profiles were measured in supine position for more than 30 min. Portal blood flow was measured from the main portal vein with the patient in expiratory apnea. We located the cursor in the main portal vein at a site just entering or immediately after entering the liver and opened the gate of cursor as wide as possible to include the inner diameter of the main portal vein. We corrected the flow angle formed by the directions of ultrasonic beam and the portal blood flow below 55 degree to minimize the variation caused by the angle of insonation. The Doppler signal could be viewed on the screen and heard through a build-in speaker. Portal blood flow was measured by the same physician to avoid inter-observer variations[12].

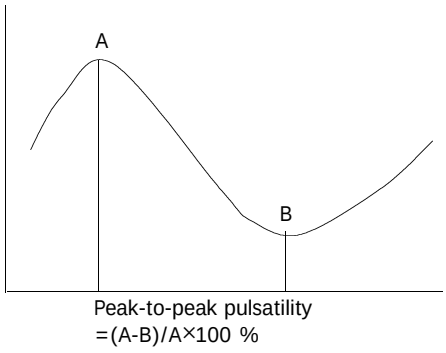

Figure 1 Mean portal blood velocity (Vmean) was calculated (cm/s) by the equation of "Vmean=0.57×maximum portal blood velocity (Vmax)".

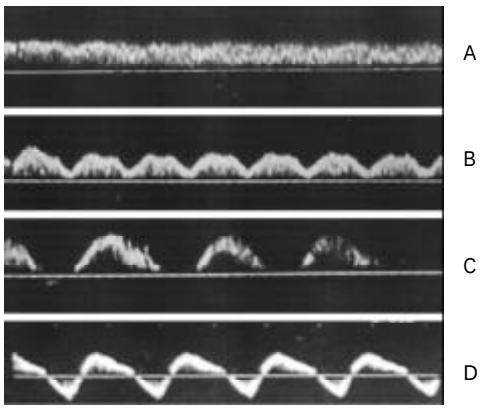

Figure 2 Representative waveform of portal blood flow from patients with normal (A; PP: 17 %), transiently reduced (B; PP: 60 %), stagnant (C; PP: 100 %) or retrograde (D; PP: 194 %) portal blood flow.

For each measurement, at least 3 reproducible patterns were made to calculate the mean maximum portal blood velocity (Vmax) over a period of 4 seconds to ensure the measurement accuracy. Mean portal blood velocity (Vmean) was calculated (cm/s) by the equation of "Vmean=0.57×Vmax" as described by Moriyasu *et al* (Figure 1)[13]. Cross-sectional area (Area) was also recorded (cm^2) at the site of main portal vein where portal blood velocity was measured. The direction of portal blood velocity, antegrade or retrograde, was also measured. Positive signal above the zero velocity indicated the flow toward the transducer and vice versa. Portal blood flow volume (PBF) was obtained (ml/min) by the equation "PBF=Area×Vmean ×60"[12,13]. The percentage of peak-to-peak pulsatility (PP) was calculated by the equation of PP=(maximum-minimum)/maximum frequency shift (Figure 1)[5,10,12]. The waveforms were classified as continuous (PP=40 %; Figure 2A), decreased (PP 41-99 %; Figure 2B), stagnant (PP=100 %; Figure 2C), and retrograde (PP >100 %; Figure 2D).

The study protocol was reviewed and approved by the Institutional Review Committee under the guidelines of the 1975 Declaration of Helsinki. Statistical analysis was performed using Student's *t*-test and linear regression as appropriate.

RESULTS

The clinical and biochemical data are shown in Table 1. All the controls had normal blood chemistries. All the patients had normal serum bilirubin, and prothrombin time. The mean serum albumin levels were lower in Group 1 (3.9±0.7 g/dL, $P<0.02$) and Group 2 (3.7±0.5 g/dL, $P<0.01$) than Controls. The serum ALT levels were all less than two times of the upper normal limit. Group 2 patients (35±20 IU/L) had a higher mean serum ALT activity than that of the controls (24±6 IU/L, $P<0.05$) but not statistically different from that of Group 1 (23±8 IU/L). Group 2 (59±29 IU/L) had a higher mean AST level than those of Group 1 (31±11 IU/L, $P=0.004$) and controls (21±6 IU/L, $P<0.001$). The higher serum AST activities, were supposed to be related to ischemic hepatitis. The other clinical and biochemical data between Group 1 and 2 showed no statistical difference.

Table 1 Clinical and biochemical data of patients with congestive heart failure ($\bar{x}\pm s$)

	Control	Group 1	Group 2
Gender (M/F)	10/10	4/6	5/5
Age (y)	46±12	50±13	47±19
Total protein (g/dL)	7.5±0.6	7.1±0.8	6.9±1.1
Albumin (g/dL)	4.3±0.2	3.9±0.7	3.7±0.5
Total serum bilirubin (mg/dL)	0.9±0.4	1.3±0.8	1.4±0.8
AST (IU/L)	21±6	31±11	59±29
ALT (IU/L)	24±6	23±8	35±20
Prolonged prothrombin time (s)	-	1.1±0.9	1.4±0.8

The CI [3.0±1.4 L/(min· m^2); range: 2.3-8.6 L/(min· m^2) *vs* 2.4±0.5 L/(min· m^2); range: 2.8-4.2 L/(min· m^2)], AOP (87.8±11.7 mmHg; range: 65-100 mmHg *vs* 87.6±16.5 mmHg; range: 65-115 mmHg), and LVEDP (12.2±9.3 mmHg; range: 4-40 mmHg *vs* 22.8±13.0 mmHg; range: 10-40 mmHg) were not statistically different between Group 1 and 2 (Table 2). All the Group 1 patients had normal PWP (mean: 14.6±7.3 mmHg; range: 5-40 mmHg), PAP (mean: 25.0±8.2 mmHg; range: 16-48 mmHg), RAP (mean: 4.7±2.4 mmHg; range: 1-10 mmHg), and RVEDP (mean: 6.4±2.7 mmHg; range: 4-14 mmHg). All the group 2 patients had abnormally higher PWP (mean: 29.9±9.3 mmHg; range: 13-38 mmHg), PAP (mean: 46.3±13.2 mmHg; range: 25-65 mmHg), RAP (mean: 17.5±5.7 mmHg; range: 12-28 mmHg), and RVEDP (mean: 18.3±5.6 mmHg; range: 9-26 mmHg) than those of Group 1 patients ($P<0.001$).

Table 2 Cardiac profiles in patients with congestive heart failure [$\bar{x}\pm s$, (n)]

	Group 1	Group2
CI [L/(min· m²)]	3.0±1.4 (6)	2.4±0.5 (7)
AOP (mmHg)	87.8±11.7 (9)	87.6±16.5 (8)
LVEDP (mmHg)	12.2±9.3(10)	22.8±13.0(9)
PWP (mmHg)	14.6±7.3(9)	29.9±9.3[a] (9)
PAP (mmHg)	25.0±8.2(10)	46.3±13.2[a] (9)
RAP (mmHg)	4.7±2.4(10)	17.5±5.7[a] (10)
RVEDP (mmHg)	6.4±2.7(10)	18.3±5.6[a] (10)

[a]P<0.001 *vs* group 1.

The mean values of Vmax (24.5±4.9 cm/s; range: 17-33 cm/s *vs* 21.5±6.1 cm/s; range: 16-33 cm/s), Vmean (14.0±2.9 cm/s; range: 9.7-18.8 cm/s *vs*12.3±3.5 cm/s; range: 8.6-13.7 mmHg), area (0.80±0.17 cm²; range: 0.64-1.13 cm² *vs* 0.94±0.18 cm²; range: 0.79-1.33 cm²) and PBF (678±239 ml/min; range: 373-1120 ml/min *vs* 684±191 ml/min; range: 432-922 ml/min) between Group 1 and 2 did not show any statistical difference (Table 3). All the 10 patients in Group 1 had a continuous antegrade portal flow with a mean PP 27.0±8.9 % (range: 17-40 %). The mean PP of the remaining 10 patients in Group 2 was 86.6±45.6 % (range: 43-194 %); all the patients had a pulsatile portal blood flow with PP >40 %. 6, 1 and 3 patients had transiently reduced, stagnant, and hepatofugal portal blood flow, respectively. The transiently reduced, stagnant and retrograde flow occurred mainly immediately after the corresponding ventricular systole. Different from earlier reports, we have observed that the decreased or reversed portal blood flow did not occur during ventricular systole in 3 patients with ventricular premature depolarizations or atrial fibrillation (Figure 3).

Table 3 Portal profiles in patients with congestive heart failure ($\bar{x}\pm s$)

	Control (n=20)	Group1 (n=10)	Group2 (n=10)
Vmax (cm/s)	20.1±3.1	24.5±4.9	21.5±6.1
Vmean (cm/s)	11.2±1.9	14.0±2.9	12.3±3.5
Area (cm²)	1.01±0.20	0.80±0.17	0.94±0.18
PBF (ml/min)	685±136	678±239	684±191
PP (%)	23.3±6.3	27.0±8.9	86.6±45.6[a]

[a]P<0.001 *vs* control and group 1.

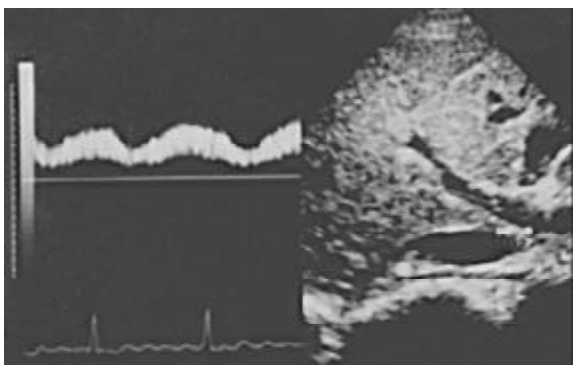

Figure 3 Occurrence of reduced portal blood flow immediately after ventricular systole.

By using linear correlation, Vmax, Vmean and PBF had a positive correlation with CI (P<0.001) but not with AOP, LVEDP, PWP, PAP, RAP, and RVEDP. PP showed a good correlation with PWP, PAP, RAP, and RVEDP (P<0.001) but did not show any correlation with CI, AOP, and LVEDP. PP had no correlation with Vmax, Vmean and PBF.

DISCUSSION

In the present study, all the 10 patients with RA=10 mmHg had a PP>40 %. On the contrary, all the patients with RAP <10 mmHg had a PP 40 % or less. It suggested these patients developed transiently reduced, stagnant or hepatofugal portal blood flow. 4 (36 %) of the patients with RAP=10 mmHg had a retrograde portal blood flow with a PP >100 %. Therefore, the portal blood flow can be retrograde during severe right heart failure[13]. Furthermore, RAP, PWP and RVEDP have a good correlation with PP. Thus, the waveforms of portal blood flow correlate well with right heart function[14]. Therefore, the measurement of PP change is a simple and non-invasive way to identify patients with right heart failure[9,15].

In the present study, AOP did not correlate with PP and "estimated" PBF[12,13,16]. Actually, all the patients had preserved AOP and only 1 patient whose AOP was 2.3 L/(min· m²) with RAP< 10 mmHg had AOP less than 2.6 L/(min· m²). Thus, right heart failure rather than reduced CI is responsible for PP changes[5,17-19]. Furthermore, "estimated" portal inflow showed no difference between patients with high and low RAP. Since the portal inflow can be transiently reduced, stagnant or hepatofugal during severe right heart failure, the "actual" portal inflow volume should be lower than the "estimated" volume[20]. As a consequence, the "estimated" volume does not represent the "actual" portal inflow volume. Hence, the correlation among "actual" PBF, AOP and RAP warrants further study.

Portal blood flow contributes to 90 % of blood flow and 50 % of oxygen supply of the liver. Therefore, portal inflow plays an important role in the delivery of oxygen to the liver[16]. It has been well known that cirrhosis with portal hypertension can result in reduced PP[16,21,22]. However, the volume of portal inflow varies due to the occurrence of collaterals or the presence of portal hypertension. In alcoholic cirrhosis, oral nitroglycerin can cause systemic hypotension to reduce portal inflow[1-4,22,23]. In the present study, all the patients did not experience systemic hypotension. Therefore, their transiently reduced, stagnant or hepatofugal portal blood flow was not likely to be related to systemic hypotension[15,24].

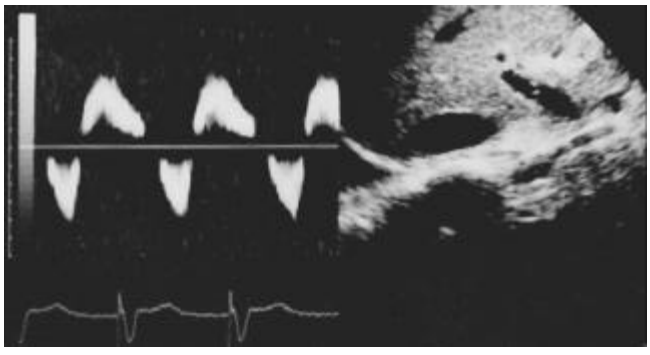

Figure 4 The occurrence of transient hepatofugal portal blood flow immediately after ventricular systole.

In the present study, the occurrence of transiently reduced (Figure 3), stagnant or hepatofugal (Figure 4) portal blood flow was immediately after ventricular systole[14,24,25]. The increased PP in those patients with RAP=10 mmHg suggests that the portal inflow is transiently reduced immediately after ventricular systole. The occurrence of transiently stagnant or hepatofugal portal blood flow may impair the delivery of

oxygen to the liver. It is well known that left heart failure and systemic hypotension can decrease hepatic inflow to cause ischemic hepatitis with a higher AST level[15,26]. However, it is not uncommon that some patients with heart failure have both abnormally higher serum ALT and LDH levels even without systemic hypotension clinically[5,6,24]. Thus, the occurrence of transiently reduced, stagnant or hepatofugal portal blood flow may in part explain the relatively higher AST levels in those patients with RAP=10 mmHg than those <10 mmHg.

ACKNOWLEDGMENT

A part of the present data was presented at the VIII World Congress of Ultrasound in Medicine and Biology, Buenos Aires, 1997, Ultrasound in Medicine and Biology 1997;23:22.

REFERENCES

1 **Yang SS**, Ralls PW, Korula J. The effect of oral nitroglycerin on portal vein flow. *J Chin Gastroenterol* 1991; **13**: 173-177
2 **Nagy I,** Szilvassy Z. Tolerance to nitroglycerin in rats with experimental liver cirrhosis: an *in vitro* study on aortic rings. *Hepatology* 1998; **1:** 71
3 **Garcia-Taso G,** Groszmann RJ. Portal hemodynamic during nitroglycerin administration in cirrhotic patients. *J hepatol* 1987; **7:** 805-809
4 **Gibson PR,** Mclean AJ, Dudley FJ. The hypotensive effect of oral nitroglycerin on portal venous pressure in patients with cirrhotic portal hypertension. *J Gastroenterol Hepatol* 1986; **1:** 201-206
5 **Yang SS,** Wu CH, Chen TK, Lee CL, Lai YC, Chen DS. Portal blood flow in acute hepatitis with and without ascites: A noninvasive measurement using ultrasonic Doppler. *J Gastroenterol Hepatol* 1995; **10:** 36-41
6 **Pannen BH.** New insights into the regulation of hepatic blood flow after ischemia and reperfusion. *Anesth Analg* 2002; **94:** 1448-1457
7 **Shen B,** Younossi ZM, Dolmatch B, Newman JS, Henderson JM, Ong JP, Gramlich T, Yamani M. Patent ductus venosus in an adult presenting as pulmonary hypertension, right-sided heart failure, and portosystemic encephalopathy. *Am J Med* 2001; **110:** 657-660
8 **Catalano D,** Caruso G, DiFazzio S, Carpinteri G, Scalisin N, Trovato GM. Portal vein pulsatility ratio and heart failure J. *Clin Ultrasound* 1998; **26:** 27-31
9 **Tang SS,** Shimizu T, Kishimoto R, Kodama Y, Miyasaka K. Analysis of portal venous waveform after living related liver transplantation with pulsed Doppler ultrasound. *Clin Transplant* 2001; **15:** 380-387
10 **Koslin DB,** Mulligan SA, Berland LL. Duplex assessment of the portal venous system. *Semin Ultrasound CT MR* 1992; **13:** 22-33
11 **Bolondi L,** Gaiani S, Barbara L. Accuracy and reproducibility of portal flow measurement by Doppler US. *J hepatol* 1991; **13:** 269-273
12 **Sabba C,** Weltin GG, Cicchetti DV, Ferraioli G, Taylor KJ, Nakamura T, Moriyasu F, Groszmann RJ. Observer variability in echo-Doppler measurements of portal flow in cirrhotic patients and normal volunteers. *Gastroenterology* 1990; **98:** 1603-1611
13 **Moriyasu F,** Nishida O, Ban N, Nakamura T, Miura K, Sakai M, Miyake T, Uchino H. Measurement of portal vascular resistance in patients with portal hypertension. *Gastroenterology* 1986; **90:** 710-717
14 **Rengo C,** Brevetti G, Sorrentino G, D'Amato T, Imparato M, Vitale DF, Acanfora D, Rengo F. Portal vein pulsatility ratio provides a measure of right heart function in chronic heart failure. *Ultrasound Med Biol* 1998; **24:** 327-332
15 **Hosoki T,** Arisawa J, Marukawa T, Tokunaga K, Kuroda C, Kozuka T, Nakano S. Portal blood flow in congestive heart failure: pulsed duplex sonographic findings. *Radiology* 1990; **174:** 733
16 **Valla D,** Flejou JF, Lebrec D, Bernuau J, Rueff B, Salzmann JL, Benhamou JP. Portal hypertension and ascites in acute hepatitis: clinical, hemodynamic and histological correlations. *Hepatology* 1989; **10:** 482-487
17 **Moriyasu F,** Nishida O, Ban N, Nakamura T, Miura K, Sakai M, Uchino H, Miyake T. "Congestion index" of the portal vein. *AJR Am J Roentgenol* 1986; **146:** 735-739
18 **Bihari DJ,** Gimson AE, Williams R. Cardiovascular, pulmonary and renal complications of fulminant hepatic failure. *Semin Liver Dis* 1986; **6:** 119-128
19 **Sherlock S.** Vasodilatation associated with hepatocellular disease: Relation to functional organ failure. *Gut* 1990; **31:** 365-367
20 **Lebrec D**. Pharmacological treatment of portal hypertension: presnt and future. *J Hepatology* 1998; **28:** 896-907
21 **Chiu KW,** Changchien CS, Liaw YF, Yang SS. Albumin gradient and portal vein velocity in severe viral hepatitis patients complicated with ascites. *Hepatogastroenterology* 2000; **47:** 1700-1702
22 **Ozaki CF,** Anderson JC, Liebeman RP, Rikker LF. Duplex ultrasonography as a noninvasive technique for assessing portal hemodynamics. *Am J Surg* 1988; **155:** 70-75
23 **Bosch J,** Garcia-Pagan JC. Complication of cirrhosis. I. Portal Hypertension. *J Hepatol* 2000; **32:** 141-156
24 **Wachsberg RH,** Needleman L, Wilson DJ. Portal vein pulsatility in normal and cirrhotic adults without cardiac disease. *J Clin Ultrasound* 1995; **23:** 33
25 **Abu-Yousef MM,** Milam SG, Faner RM. Pulsatile portal vein flow: a sign of tricuspid regurgitation on duplex Doppler sonography. *AJR Am J Roentgenol* 1990; **155:** 785
26 **Taourel P,** Blanc P, Dauzat M, Chabre M, Pradel J, Gallix B, Larrey D, Bruel JM. Doppler study of mesenteric, hepatic, and portal circulation in alcoholic cirrhosis: relationship between quantitative Doppler measurements and the severity of portal hypertensive and hepatic failure. *Hepatology* 1998; **28:** 932-936

Edited by Xu XQ and Wang XL

P.O.Box 2345, Beijing 100023,China
Fax: +86-10-85381893
E-mail: wjg@wjgnet.com www.wjgnet.com

World J Gastroenterol 2003;9(8):1832-1833
World Journal of Gastroenterology
 ISSN 1007-9327

• BRIEF REPORTS •

Efficacy of saccharomyces boulardii with antibiotics in acute amoebiasis

Fariborz Mansour-Ghanaei, Najaf Dehbashi, Kamyar Yazdanparast, Afshin Shafaghi

Fariborz Mansour-Ghanaei, Afshin Shafaghi, Gastrointestinal and Liver Diseases Research Center, Guilan University of Medical Sciences, Rasht, Iran
Najaf Dehbashi, Department of Gastroenterology, Shiraz University of Medical Sciences, Shiraz, Iran
Kamyar Yazdanparast, Department of Microbiology, Shiraz University of Medical Sciences, Shiraz, Iran
Correspondence to: Professor Fariborz Mansour-Ghanaei, Gastrointestinal and Liver Diseases Research Center, Guilan University of Medical Sciences, Sardar-e-jangle Ave, Razi Hospital, Rasht 41448-95655, Iran. ghanaei@gums.ac.ir
Telephone: +98-131-5535116 **Fax:** +98-131-2232514
Received: 2003-04-12 **Accepted:** 2003-05-24

Abstract

AIM: To compare the efficacy of antibiotics therapy alone with antibiotics and saccharomyces boulardii in treatment of acute amebiasis.

METHODS: In a double blind, random clinical trial on patients with acute intestinal amoebiasis, 57 adult patients with acute amoebiasis, diagnosed with clinical manifestations (acute mucous bloody diarrhea) and amebic trophozoites engulfing RBCs found in stool were enrolled in the study. Regimen 1 included metronidazole (750 mg Tid) and iodoquinol (630 mg Tid) for 10 days. Regimen 2 contained capsules of lyophilized saccharomyces boulardii (250 mg Tid) orally in addition to regimen 1. Patients were re-examined at two and four weeks after the treatment, and stool examination was performed at the end of week 4. Student's *t*-test, χ^2 and McNemar's tests were used for statistical analysis.

RESULTS: Three patients refused to participate. The other 54 patients were randomized to receive either regimen 1 or regimen 2 (Groups 1 and 2 respectively, each with 27 patients). The two groups were similar regarding their age, sex and clinical manifestations. In Group 1, diarrhea lasted 48.0±18.5 hours and in Group 2, 12.0±3.7 hours ($P<0.0001$). In Group 1, the durations of fever and abdominal pain were 24.0±8.8 and 24.0±7.3 hours and in Group 2 they were 12.0±5.3 and 12.0±3.2 hours, respectively ($P<0.001$). Duration of headache was similar in both groups. At week 4, amebic cysts were detected in 5 cases (18.5 %) of Group 1 but in none of the Group 2 ($P<0.02$).

CONCLUSION: Adding saccharomyces boulardii to antibiotics in the treatment of acute amebiasis seems to decrease the duration of clinical symptoms and cyst passage.

Mansour-Ghanaei F, Dehbashi N, Yazdanparast K, Shafaghi A. Efficacy of saccharomyces boulardii with antibiotics in acute amoebiasis. *World J Gastroenterol* 2003; 9(8): 1832-1833
http://www.wjgnet.com/1007-9327/9/1832.asp

INTRODUCTION

Intestinal amoebiasis is caused by the protozoan entamoeba histolytica. This organism feeds on the intestinal contents without any invasion to human tissue. It occasionally invades the intestinal wall and causes dysentery. It may also spread from the bowel to the liver and other organs and cause abscess in these organs. In addition, it may persist as cysts in the intestine and the patients become long-term cyst carriers, most of whom remain asymptomatic[1,2].

In most cases, the organism is avirulent but it may become virulent under different circumstances like immune suppression, malnutrition and alterations in intestinal flora[3,4].

Entamoeba histolytica is common all over the world but is more virulent in areas with low hygienic standards and in tropical and subtropical regions[1].

A luminal amebicide achieving high concentrations in the intestine like iodoquinol, paromomycin or diloxanide furoate is usually used to treat cysts. Tissue amebicides with high concentrations in the blood like the nitroimidazoles (especially metronidazole) are the cornerstone of treatment of invasive amoebiasis[5].

Saccharomyces boulardii is saprophytic, thermophylic yeast, which is found growing applications in the prevention and treatment of human septic enteritis[6,7]. The optimal temperature for this yeast to grow is 37 ℃. The gastric juice has no effect on it and it grows all along the gastrointestinal tract. It is used clinically as an oral lyophilized preparation[8]. No significant side effects have been reported with its consumption[9-11].

We assessed the effects of adding saccharomyces boulardii to the standard treatment for invasive amoebiasis.

To compare the routine treatment by means of metronidazole and iodoquinol with metronidazole, iodoquinol and saccharomyces boulardii in the treatment of acute amoebiasis, we performed this study on 57 patients at Shahid Beheshti Educational and Therapeutic Center in Shiraz during one-year period from March 21, 1995 to March 21, 1996.

MATERIALS AND METHODS

Patients with acute amebic dysentery who consented to participate were enrolled. The diagnosis was made according to compatible clinical presentations (acute mucous bloody diarrhea, fever and abdominal pain) and presence of amoeba trophozoite engulfing RBCs in diarrheal stool. Pregnant females, those on maintenance of hemodialysis, steroids or chemotherapy were excluded. The patients were then randomized to receive either metronidazole 750 mg and iodoquinol 650 mg thrice a day for 10 days (Group 1) or the same medication plus lyophilized saccharomyces boulardii (Ultra-levure®, Bio codex, Montrougo, France) 250 mg orally thrice a day (Group 2).

The patients were followed up at two and four weeks. At each visit in addition to recording patients' symptoms and possible adverse effects, pill count was performed. At the end of week 4, another stool examination (fresh spread and floatation) was done. Student's *t*-test, Chi-square and McNemar's tests were used for statistical analysis.

RESULTS

57 consenting patients were randomized (29 in Group 1 and 28 in Group 2). Two patients from Group 1 and one from Group

2 were excluded because of non-compliance. There were 12 (44.4 %) females in Group 1 and 10 (37 %) females in Group 2. Mean age was 29.3 years in Group 1 and 30.8 years in Group 2. Table 1 shows frequency of clinical findings in both groups. The two groups were comparable regarding their clinical presentations, too.

Table 1 Clinical manifestations in two therapeutic groups

	Regimen 1	Regimen 2	*P*
Diarrhea	27 (100 %)	27 (100%)	-
Fever	6 (22.2 %)	7 (26%)	N.S
Abdominal pain	19 (70.4 %)	22 (81.5%)	N.S
Headache	20 (74.1 %)	18 (66.7%)	N.S

N.S=Not significant.

As shown in Table 2, adding saccharomyces boulardii to the usual treatment of acute amebic dysentery decreased the mean duration of diarrhea to almost 25 % ($P<0.0001$) and the duration of abdominal pain and fever to almost half ($P<0.001$). Headache lasted almost equally in the two groups.

Table 2 Time of recovery from main clinical findings

	Regimen 1 (h)	Regimen 2 (h)	*P*
Diarrhea	48.0±18.5	12.0±3.7	<0.0001
Fever	24.0±8.8	12.0±5.3	<0.001
Abdominal pain	24.0±7.3	12.0±3.2	<0.001
Headache	24.0±8.6	24.0±7.9	N.S

N.S=not significant.

Amebic cysts were found in stool specimens of 5 patients (18.5 %) in group 1 and none in group 2 at week 4 ($P<0.02$, Table 3).

Table 3 Amebic cyst carriers in the fourth week after the treatment

	Regimen 1	Regimen 2
Cyst absent	22 (81.5 %)	27 (100 %)
Cyst present	5 (18.5 %)	0 (0 %)

DISCUSSION

Saccharomyces boulardii is a saprophytic yeast which is recommended for the prevention and treatment of septic enteritis[6,7] especially diarrhea caused by clostridium difficile[8,12,13]. It can also reduce the incidence of traveler' s diarrhea[12] and prevent the occurrence of diarrhea in acutely ill patients fed by nasogastric tube[14, 15]. Other diseases in which saccharomyces boulardii has been achieved some success include antibiotic associated colitis[11, 16] and Crohn' s disease[9]. Considering its inhibitory activity on enteropathogens and its anti-diarrheal characteristics, it has also been used in children with diarrhea[17]. Saccharomyces boulardii has been shown to have trophical effects on the small intestine in healthy human volunteers[18].

The exact mechanism by which this yeast prevents or improves diarrhea is still unclear. Saccharomyces boulardii may cause its trophic effect on the small intestine by releasing spermine and spermidine[6]. This yeast can hinder the cholera toxin excretion in the jejunum of mice.

Our data showed that co-administration of lyophilized saccharomyces boulardii with conventional treatment for acute amebic colitis significantly decreased the duration of symptoms and chances of cyst carriers after 4 weeks. This may be due to its potential to restore the beneficial normal flora of the gut, although the precise mechanism of the action remains to be elucidated. Considering the lack of any reported adverse reactions to this product, if our results are reproduced by other investigators, then lyophilized saccharomyces boulardii would be a very useful addition to the treatment of acute amebic dysentery.

ACKNOWLEDGMENT

We would like to thank Dr. Amirhossein Bagherzadeh, the member of Gastrointestinal & Liver Diseases Research Center, Guilan University of Medical Sciences, for his help in preparing and reviewing this manuscript.

REFERENCES

1 **Nanda R,** Baveja U, Anand BS. Entamoeba Histolytica cyst passers: clinical features and outcome in untreated subjects. *Lancet* 1984; **2:**301-303
2 **Lai SW,** Lin HC, Lin CC. Clinical analysis of a dysentery outbreak in Taichung, Taiwan .*Chung Hua Min Kuo Hsiao Erh Ko I Hsueh Hui Tsa Chih* 2000; **41:** 18-21
3 **Lewis EA,** Antia AU. Amoebic colitis. *Trop Med Hyg* 1969; **112:**633-638
4 **Neal RA.** Pathogenesis of amoebiasis. *Gut* 1971; **12:** 482-486
5 **Reed SL.** Amebiasis and infection with free- living amebas. In: Braunwald E, eds. Harrison's principles of internal medicine. *New york: McGraw-Hill* 2001: 1199-1203
6 **Buts JP,** De-Keyser N, De-Raedemaeker L. Saccharomyces boulardii enhances rat intestinal enzyme expression by endoluminal release of polyamines. *Pediatr Res* 1994; **36:** 522-527
7 **Muller J,** Remus N, Harms KH. Mycoserological study of the treatment of paediatric cystic fibrosis patients with saccharomyces boulardii. *Mycoses* 1995; **38:**119-123
8 **Corthier G,** Dubos F, Ducluzeau R. Prevention of C difficile induced mortality in gnotobiotic mice by Saccharomyces boulardii. *Can J Microbiol* 1986; **32:** 894-896
9 **Plein K,** Hotz J. Therapeutic effects of saccharomyces boulardii on mild residual symptoms in a stable phase of Crohn's disease with special respect to chronic diarrhea- a pilot study. *Z Gastroenterol* 1993; **31:** 129-134
10 **Kollaritsch H,** Holst H, Grobara P, Wiedermann G. Prevention of traveler's diarrhea with saccharomyces boulardii. Results of a placebo controlled double - blind study. *Fortschr Med* 1993; **111:** 152-156
11 **McFarland LV,** Surawicz CM, Greenberg RN. A randomized placebo - controlled trial of saccharomyces boulardii in combination with standard antibiotics for clostridium difficile disease. *JAMA* 1994; **271:** 1913-1918
12 **Pothoulakis C,** Kelly CP, Joshi MA. Saccharomyces boulardii in inhibits clostridium difficile toxin A binding and enterotoxicity in rat ileum. *Gastroenterology* 1993; **104:** 1108-1115
13 **Castagliuolo I,** LaMont JT, Nikulasson ST, Pothoulakis C**.** Saccharomyces boulardii protease inhibits clostridium difficile toxin A effects in rat ileum. *Infect Immun* 1996; **64:** 5225-5232
14 **Bleichner G,** Blehaut H, Mentec H, Moyse D. Saccharomyces boulardii prevents diarrhea in critically ill tube-fed patients. A multicenter randomized double- blind placebo - controlled trial. *Intensive Care Med* 1997; **23:** 517-523
15 **Surawicz CM,** Elmer GW, Speelman P. Prevention of antibiotic-associated diarrhea by saccharomyces boulardii: A prospective study. *Gastroenterology* 1989; **96:** 981-988
16 **McFarland LV,** Surawicz CM, Greenberg RN, Elmer GW. Prevention of β- Lactam - associated diarrhea by saccharomyces boulardii compared with placebo. *Am J Gastroenterol* 1995; **90:** 439-448
17 **Saavedra J.** Probiotics and infectious diarrhea. *Am J Gastroenterol* 2000; **95:** S16-S18
18 **Jahn HU,** Ullrich R, Schneider T, Liehr RM, Schieferdecker HL, Holst H, Zeitz M. Immunological and trophical effects of saccharomyces boulardii on the small intestine in healthy human volunteers. *Digestion* 1996; **57:** 95-104

Edited by Xu XQ

P.O.Box 2345, Beijing 100023,China
Fax: +86-10-85381893
E-mail: wjg@wjgnet.com www.wjgnet.com

World J Gastroenterol 2003;9(8):1834-1835
World Journal of Gastroenterology
 ISSN 1007-9327

• BRIEF REPORTS •

Prevalence of amebiasis in inflammatory bowel disease in Turkey

Sebnem Ustun, Hande Dagci, Umit Aksoy, Yuksel Guruz, Galip Ersoz

Sebnem Ustun, Department of Gastroenterology, School of Medicine, University of Ege, 35100, Bornova, Izmir, Turkey
Hande Dagci, Department of Parasitology, School of Medicine, University of Ege, 35100, Bornova, Izmir, Turkey
Umit Aksoy, Department of Parasitology, School of Medicine, University of Dokuz Eylul, Izmir, Turkey
Yuksel Guruz, Department of Parasitology, School of Medicine, University of Ege, 35100, Bornova, Izmir, Turkey
Galip Ersoz, Department of Gastroenterology, School of Medicine, University of Ege, 35100, Bornova, Izmir, Turkey
Correspondence to: Sebnem Ustun, Department of Gastroenterology, School of Medicine, University of Ege, 35100, Bornova, Izmir, Turkey. sustun@med.ege.edu.tr
Telephone: +90-232-3881969
Received: 2003-03-28 **Accepted:** 2003-04-20

Abstract

AIM: To explore the prevalence of amebiasis in inflammatory bowel disease (IBD) in Turkey.

METHODS: In this study, amoeba prevalence in 160 cases of IBD, 130 of ulcerative colitis and 30 of Crohn's disease were investigated in fresh faeces by means of wet mount+Lugol's iodine staining, modified formol ethyl acetate and trichrome staining methods and to compare the diagnostic accuracy of wet mount+Lugol's iodine staining, modified formol ethyl acetate and trichrome staining methods in the diagnosis of *Entamoeba histolytica (E. histolytica)*/ *Entamoeba dispar (E. dispar).*

RESULTS: *E. histolytica/E. dispar* cysts and trophozoites were found in 14 (8.75 %) of a total of 160 cases, 13 (10.0 %) of the 130 patients with ulcerative colitis and 1 (3.3 %) of the 30 patients with Crohn's disease. As for the 105 patients in the control group who had not any gastrointestinal complaints, 2 (1.90 %) patients were found to have *E. histolytica* /*E. dispar* cysts in their faeces. Parasite prevalence in the patient group was determined to be significantly higher than that in the control group (Fischer's Exact Test, $P<0.05$). When the three methods of determining parasites were compared with one another, the most effective one was found to be trichrome staining method (Kruskal-Wallis Test, $P<0.01$).

CONCLUSION: Consequently, amoeba infections in IBD cases have a greater prevalence compared to the normal population. The trichrome staining method is more effective for the detection of *E. histolytica* /*E. dispar* than the wet mount+Lugol's iodine staining, modified formol ethyl acetate methods.

Ustun S, Dagci H, Aksoy U, Guruz Y, Ersoz G. Prevalence of amebiasis in inflammatory bowel disease in Turkey. *World J Gastroenterol* 2003; 9(8): 1834-1835
http://www.wjgnet.com/1007-9327/9/1834.asp

INTRODUCTION

Amebiasis, which affects nearly 500 million people in the world, is more prevalent in developing countries in particular[1]. It is difficult to distinguish IBD from colitis associated with amoeba according to both symptomatic and endoscopic appearance of the colon. It is not even possible to establish a differential diagnosis by means of microscopic examination. Sometimes IBD can co-exist with amebiasis. This, of course, leads to confusion in the diagnosis and treatment of the disease[2].

This study was planned to consider amoeba in the cases diagnosed as IBD in the gastroenterology clinic and to compare the accuracy of wet mount + Lugol's iodine staining, modified formol ethyl acetate and trichrome staining methods in the diagnosis of *E. histolytica/E. dispar*.

MATERIALS AND METHODS

160 people who were diagnosed as IBD by endoscopic, histopathologic, radiologic and laboratory examinations at our clinic were included in this study which was carried out between January 2000 and June 2001. Of all the cases, 130 were diagnosed as ulcerative colitis and 30 as Crohn's disease. 105 people of even age and sex distribution who had not any gastrointestinal complaints and reported to the district health centre with other complaints were assessed as the control group. Fresh faeces samples taken from these people were examined immediately using the wet mount+Lugol's iodine staining, modified formol ethyl acetate and trichrome staining methods.

Fisher's exact test was applied to the groups (ulcerative colitis, Crohn's disease and control) for a comparison of amoeba frequency among them. The assessment of wet mount+Lugol's iodine staining, modified formol ethyl acetate methods used in the diagnosis of *E. histolytica/E. dispar*, was conducted by calculation of sensitivity, specificity, negative predictive value, positive predictive value and rate of accuracy.

RESULTS

In our study in which the prevalence of *E. histolytica/E. dispar* in IBD was investigated, we found *E. histolytica/E. dispar* cysts and trophozoits in 14 (8.75 %) of the 160 IBD cases. *E. histolytica/E. dispar* cysts and/or trophozoits were also determined in 13 (10.0 %) of the 130 patients with ulcerative colitis and 1 (3.3 %) of the 30 Crohn's disease patients (Table 1). Frequency of *E. histolytica/E. dispar* in patients with IBD was significantly higher than that in the control group (Fisher's exact test, $P<0.05$). When the groups of patients with IBD were compared with the control group separately, the frequency of *E. histolytica/E. dispar* in patients with ulcerative colitis was significantly higher than that in the control group. For Crohn's disease, on the other hand, it was not significantly different from the control group. A comparison between the patients with ulcerative colitis and those with Crohn's disease revealed that *E. histolytica/E. dispar* were more significantly frequent in the patients with ulcerative colitis (Fisher's exact test, $P<0.05$). When the three methods of determining parasites were compared with one another, the most effective one was found to be trichrome staining method as can be seen in Table 1 (Kruskal-Wallis test, $P<0.01$). The sensitivity of wet

mount+Lugol' s iodine staining, modified formol ethyl acetate methods was found to be quite low as compared to the trichrome staining method (36 %, 64 %, respectively) (Table 2).

Table 1 Number and methods for determination of *E. histolytica* determined in cases with IBD diagnosis and control group

	Wet mount ± Lugol's iodine staining	Modified formol ethyl acetate	Trichrome staining method	Total (none of parasite / patient)
Ulcerative colitis	5*(%3.84)	8*(%6.15)	13*(%10.0)	13 / 130
Crohn's disease	-	1*(%3.33)	1*(%3.33)	1 / 30
Control group	1*(%0.95)	2*(%1.90)	2*(%1.90)	2 / 105

*The parasite was determined by more than one method (+).

Table 2 Comparison of wet mount+Lugol's iodine, modified formol ethyl acetate methods with trichrome staining method

	Modified formol ethyl acetate (%)	Wet mount+Lugol's iodine staining (%)
Sensitivity	64	36
Specificity	99	98
False negatives	36	64
False positives	0.1	0.1
Positive predictive value	90	63
Negative predictive value	97	95
Rate of accuracy	97	93

DISCUSSION

Few studies have been performed in Turkey on this particular subject. In a study they carried out in the Province of Istanbul between April 1994 and July 1995. Bayramicli *et al*[3] explored the presence of amebiasis in 19 patients being investigated with a preliminary diagnosis of ulcerative colitis and found *E. histolytica* in 69 % of the cases. In a study they carried out in the Province of Antalya to determine the rate of amebiasis in 43 patients with ulcerative colitis. Suleymanlar *et al*[4] found *E. histolytica* cysts and trophozoites in 22 (54 %) of the patients. These values are higher than those we have found. The reason for this is the fact that the incidence of *E. histolytica/E. dispar* has been diminishing in Turkey in recent years.

Prokopowicz *et al*[5] determined 5 cases of amebiasis (4.85 %) among 103 patients with ulcerative colitis and claimed that this rate was significant in the treatment of chronic ulcerative colitis patients. We have obtained a higher rate than that of Prokopowicz in our study in which we found *E. histolytica/E. dispar* cysts and trophozoites in 13 (10.0 %) of 130 patients with ulcerative colitis**.** This was due to the environmental factors as high temperature and humidity, which are effective in and around Izmir, as well as lower immune resistance against the infection in addition to poorer hygiene. Chan *et al*[6] presented three cases with ulcerative colitis and *E. histolytica* infection and mentioned the problems to be faced during treatment.

In conclusion, amoeba infection in IBD cases, especially in patients with ulcerative colitis is more prevalent compared to the normal population. A differential diagnosis is extremely important for IBD and amebiasis cases. Therefore, we believe that *E. histolytica/E. dispar* must be explored in the faeces before planning a diagnostic scheme for cases diagnosed as IBD. In addition, the sensitivity of wet mount+Lugol' s iodine staining and modified formol ethyl acetate methods was found to be low in this study. Therefore, we think it would be necessary to use the trichrome staining method in the investigation of *E. histolytica/E. dispar* in patients with IBD diagnosis.

REFERENCES

1 **Andersen PL**. Amebiasis. *Ugeskr Laeger* 2000; **162:** 1537-1541
2 **Hansen LH,** Lund C. Amebiasis-a differential diagnosis from inflammatory bowel disease. *Ugeskr Laeger* 1998; **160:** 5514-5515
3 **Bayramicli OU,** Dalay R, Konuksal F, Kilic G, Akbayir N, Ovunc O. Ulseratif kolitle amebiasisin birlikteligi. *Turk J Gastroenterol* 1997; **8:** 94-96
4 **Süleymanlar I,** Atilgan S, Ertugrul C, Isitan F. Ulseratif kolit ve intestinal amebiasis birlikteligi ve tedavide karsilasilan sorunlar. *Gastroenteroloji* 1996; **7:** 22
5 **Prokopowicz D,** Zagorski K, Kramarz P. Amoebiasis-a problem in patients with ulcerative colitis. *Wiad Lek* 1994; **47:** 248-251
6 **Chan KL,** Sung JY, Hsu R, Liew CT. The association of the amoebic colitis and chronic ulcerative colitis. *Singapore Med J* 1995; **36:** 303-305

Edited by Xu XQ and Wang XL

P.O.Box 2345, Beijing 100023,China
Fax: +86-10-85381893
E-mail: wjg@wjgnet.com www.wjgnet.com

World J Gastroenterol 2003;9(8):1836-1839
World Journal of Gastroenterology
 ISSN 1007-9327

• BRIEF REPORTS •

Meta analysis of propranolol effects on gastrointestinal hemorrhage in cirrhotic patients

Jin-Wei Cheng, Liang Zhu, Ming-Jun Gu, Zhe-Ming Song

Jin-Wei Cheng, Liang Zhu, Zhe-Ming Song, Department of Gastroenterology, Changzheng Hospital, Second Military Medical University, Shanghai 200003, China
Ming-Jun Gu, Department of Endocrinology, Changzheng Hospital, Second Military Medical University, Shanghai 200003, China
Supported by the National Natural Science Foundation of China, No. 19872074
Correspondence to: Dr. Liang Zhu, Department of General Medicine, Changzheng Hospital, Second Military Medical University, Shanghai 200003, China. jinnwave@sohu.com
Telephone: +86-21-63610109 Ext 73181 **Fax:** +86-21-63520020
Received: 2002-12-24 **Accepted:** 2003-02-24

Abstract

AIM: To assess the effects of propranolol as compared with placebo on gastrointestinal hemorrhage and total mortality in cirrhotic patients by using meta analysis of 20 published randomized clinical trials.

METHODS: A meta analysis of published randomized clinical trials was designed. Published articles were selected for study based on a computerized MEDLINE and a manual search of the bibliographies of relevant articles. Data from 20 relevant studies fulfilling the inclusion criteria were retrieved by means of computerized and manual search. The reported data were extracted on the basis of the intention-to-treat principle, and treatment effects were measured as risk differences between propranolol and placebo. Pooled estimates were computed according to a random-effects model. We evaluated the pooled efficacy of propranolol on the risk of gastrointestinal hemorrhage and the total mortality.

RESULTS: A total of 1 859 patients were included in 20 trials, 931 in the propranolol groups and 928 as controls. Among the 652 patients with upper gastrointestinal tract hemorrhage, 261 patients were treated with propranolol, and 396 patients were treated with placebo or non-treated. Pooled risk differences of gastrointestinal hemorrhage were -18 % [95 % CI, -25 %, -10 %] in all trials, -11 % [95 % CI, -21 %, -1 %] in primary prevention trials, and -25 % [95 % CI, -39 %, -10 %] in secondary prevention trials. A total of 440 patients died, 188 in propranolol groups and 252 in control groups. Pooled risk differences of total death were -7 % [95 % CI, -12 %, -3 %] in all trials, -9 % [95 % CI, -18 %, -1 %] in primary prevention trials, and -5 % [95 % CI, -9 %, -1 %] in secondary prevention trials.

CONCLUSION: Propranolol can markedly reduce the risks of both primary and recurrent gastrointestinal hemorrhage, and also the total mortality.

Cheng JW, Zhu L, Gu MJ, Song ZM. Meta analysis of propranolol effects on gastrointestinal hemorrhage in cirrhotic patients. *World J Gastroenterol* 2003; 9(8): 1836-1839
http://www.wjgnet.com/1007-9327/9/1836.asp

INTRODUCTION

Gastrointestinal hemorrhage due to portal hypertension is a leading cause of death in patients with cirrhosis. The first episode of bleeding is fatal in 40 % to 50 % of such patients and two-thirds die within 1 year. It has been shown that treatment with propranolol can reduce portal venous pressure[1], portal blood flow[2] and superior portosystemic collateral blood flow[3] and its efficacy on preventing gastrointestinal hemorrhage has been assessed in many randomized clinical trials. Some trials have been primary, in which the drug was used to prevent hemorrhage in patients who have not bled, some have been secondary with the drug used to prevent rebleeding. Numerous primary and secondary prevention studies concluded that propranolol treatment decreased the incidence of gastrointestinal hemorrhage. Thus far, however, randomized clinical trials usually included small sample sizes and showed conflicting results, which hindered researchers drawing conclusions from the trials.

In meta analysis each treated group is compared with controls from the same study, and the treatment effect is combined across all studies, to provide information both about the presence of any significant effect and about its size. We have made extensive efforts to find all relevant studies by means of computerized and manual search. Then we combined all the studies including primary and secondary, to assess the effectiveness of propranolol as compared with placebo on the prevention of gastrointestinal hemorrhage.

MATERIALS AND METHODS

This meta analysis was performed according to a protocol determined before the study, and the widely accepted methodological recommendations[4-6]. Measurement of treatment effectiveness was determined on the basis of primary or recurrent gastrointestinal hemorrhage, and mortality.

Selection of trials

Studies that fulfilled the following criteria were included in the present meta analysis: (a) propranolol was compared with placebo; (b) patients were randomly assigned to the treatment regimen, and studies were prospective; (c) patients with cirrhosis of liver were included; (d) outcomes of primary or recurrent bleeding, and death were assessed; (e) results were published as abstracts or full reports.

Study identification

Pertinent studies were retrieved from MEDLINE database by using the search terms "propranolol", "cirrhosis" and "gastrointestinal hemorrhage" and by limiting the search to reports of clinical trials and studies with human patients. In addition, a manual search was performed by checking the reference lists from articles or reviews to identify studies not yet included in MEDLINE database. When the results of a single study were reported in more than one publication, only the most recent and complete data were included in the meta-analysis. Finally, twenty randomized clinical trials that fulfilled the criteria were identified, fifteen were published in full form[7-21], and five in abstract form[22-26].

Data extraction

Data from each randomized clinical trial were extracted by two independent reviewers (Jin-Wei Cheng, Liang Zhu). For each study and each type of treatment, the following data were extracted: number of patients, and number of each outcome. Numeric discrepancies between the two independent data extractions were resolved after discussion.

Statistical methods

All comparisons were performed according to the randomly assigned treatment (intended-treatment analysis). Because of different clinical characteristics among study groups, and varying sample sizes, we assumed that heterogeneity was present even not statistically significant, and we decided to combine data by using a random-effects model to achieve more conservative estimates[27].

For all the outcomes, the pooled estimates were computed with the method of DerSimonian and Laird[27]. Summary point estimates and 95 % confidence interval (CI) were reported. Risk differences less than zero denoted an advantage for propranolol. Those more than zero denoted an advantage for placebo. 95 % CIs of risk differences not including 0 denoted a statistically significant advantage.

RESULTS

All trials

A total of 1 859 patients were included in the twenty trials, 931 in the propranolol groups and 928 as controls.

Table 1 Point estimates and 95 % CIs of the risk difference of gastrointestinal hemorrhage

	Prapranolol group		Control group		Risk difference and its 95 % CI (%)
	Total	Bled	Total	Bled	
Primary prevention					
Pascal (1984)	34	1	35	9	-23 [-38, -7]
Mills (1987)	38	19	43	33	-27 [-47, -6]
Pascal (1987)	118	20	112	30	-10 [-20, 1]
Italian (1988)	85	16	89	27	-12 [-24, 1]
Strauss (1988)	20	4	16	4	-5 [-33, 23]
Colman (1990)	23	8	25	2	27 [5, 49]
Andreani (1990)	43	2	41	13	-27 [-43,-11]
Conn (1991)	51	4	51	14	-20 [-34, -5]
Prova (1991)	68	23	72	19	7 [-8, 23]
Subtotal	480	97	484	151	-11 [-21, -1]
Overall effect			*Z*=-2.15	*P*=0.03	
Secondary prevention					
Burroughs (1983)	26	14	22	13	-5 [-33, 23]
Lebrec (1984)	38	6	36	23	-48 [-68,-29]
Cerbelaud (1986)	42	17	42	33	-38 [-57,-19]
Villeneuve (1986)	42	32	37	30	-5 [-23, 13]
Queuniet (1987)	51	29	48	31	-8 [-27, 11]
Marbet (1988)	10	2	10	9	-70 [-101,-39]
Colombo (1989)	32	8	30	14	-22 [-45, 2]
Sheen (1989)	18	8	18	15	-39 [-68,-10]
Garden (1990)	38	20	43	36	-31 [-50,-12]
Colman (1990)	26	9	26	13	-15 [-42, 11]
Perez-Ayuso (1991)	26	16	28	24	-24 [-47, -1]
Calès (1999)	102	3	104	4	-1 [-6, 4]
Subtotal	451	164	444	245	-25 [-39,-10]
Overall effect			*Z*=-3.34	*P*=0.0008	
All trials					
Total	931	261	928	396	-18 [-25, -10]
Overall effect			*Z*=-4.38	*P*=0.00001	

In the 20 trials, among the 652 patients with upper gastrointestinal tract hemorrhage, 261 were treated with propranolol, and 396 were treated with placebo or not treated. The overall weighted bleeding rate was 31 % for propranolol and 48 % for controls. The pooled risk difference was -18 % [95 % CI, -25 %, -10 %], and the reduction had statistical significance (Z=-4.38, P<0.001, Table 1).

A total of 440 patients died, 188 in propranolol groups and 252 in control groups. The overall weighted bleeding rate was 17 % after propranolol treatment and 24 % after placebo treatment. The pooled risk difference was -7 % [95 % CI, -12 %, -3 %], and the reduction due to propranolol also was statistically significant (Z=-3.44, P<0.001, Table 2).

In ten trials, the overall weighted rate of death due to bleeding was 6 % in propranolol groups and 12 % in controls. The pooled risk difference was -5 % [95 % CI, -9 %, -2 %] (Z=-3.12, P=0.002).

Table 2 Point estimates and 95 % CIs of the risk difference of death

	Prapranolol group		Control group		Risk difference and its 95 % CI (%)
	Total	Death	Total	Death	
Primary prevention					
Pascal (1984)	34	1	35	13	-34 [-51, -17]
Mills (1987)	38	15	43	19	-5 [-26, 17]
Pascal (1987)	118	25	112	40	-15 [-26, -3]
Italian (1988)	85	30	89	22	11 [-3, 24]
Strauss (1988)	20	7	16	7	-9 [-41, 23]
Colman (1990)	23	6	25	7	-2 [-27, 23]
Andreani (1990)	43	13	41	18	-14 [-34, 7]
Conn (1991)	51	8	51	11	-6 [-21, 9]
Prova (1991)	68	7	72	14	-9 [-21, 3]
Subtotal	480	112	484	151	-9 [-18, -1]
Overall effect			*Z*=-2.11	*P*=0.03	
Secondary prevention					
Burroughs (1983)	26	4	22	5	-7 [-30, 15]
Lebrec (1984)	38	3	36	8	-14 [-30, 2]
Cerbelaud (1986)	42	5	42	12	-17 [-33, 0]
Villeneuve (1986)	42	19	37	14	7 [-14, 29]
Queuniet (1987)	51	12	48	13	-4 [-21, 14]
Marbet (1988)	10	1	10	3	-20 [-54, 14]
Colombo (1989)	32	4	30	7	-11 [-30, 8]
Sheen (1989)	18	0	18	2	-11 [-28, 6]
Garden (1990)	38	14	43	19	-7 [-29, 14]
Colman (1990)	26	1	26	1	0 [-10, 10]
Perez-Ayuso (1991)	26	4	28	7	-10 [-31, 12]
Calès (1999)	102	9	104	10	-1 [-9, 7]
Subtotal	451	76	444	101	-5 [-9, -1]
Overall effect			*Z*=-2.26	*P*=0.02	
All trials					
Total	931	188	928	252	-7 [-12, -3]
Overall effect			*Z*=-3.44	*P*=0.0006	

Primary prevention

There were 964 patients in the nine primary prevention trials. Of the total 480 patients treated with propranolol, 97 patients bled from upper gastrointestinal tract, the overall weighted rate was 20 %. And 112 patients died, the overall weighted rate was 22 %. In the control groups (484 patients), the overall weighted rate of bleeding was 31 % (151 patients), and that of death was 31 % (151 patients).

The pooled risk difference of bleeding was -11 % [95 %CI, -21 %, -1 %], and that of death was -9 % [95 % CI, -18 %, -1 %]. Both of the reduction due to propranolol had statistical

significance (Table 1, Table 2).

Death due to bleeding was reported in 5 primary prevention trials, the overall weighted rate was 6 % in propranolol groups and 10 % in controls. The pooled risk difference was -4 % [95 % CI, -8 %, 0 %] (Z=-2.06, P=0.04).

Secondary prevention

Among the 895 patients in the twelve secondary prevention trials, 451 were treated with propranolol and 444 were treated with placebo.

The number of patients with bleeding was 164 in propranolol groups and 245 in control groups, the overall weighted rate was 39 % and 63 % respectively. The pooled risk difference of hemorrhage was -25 % [95 % CI, -39 %, -10 %], which had statistical significance (Z=-3.34, P<0.001, Table 1).

In all secondary prevention trials, the total number of patients died after propranolol treatment was 76, and 101 in controls. The overall weighted rate of death was 13 % and 20 % respectively. The pooled risk difference of death was -5 % [95% CI, -9 %, -1 %], and the reduction was statistically significant (Z=-2.26, P=0.02, Table 2).

In 5 recurrent prevention trials, the overall weighted rate of death due to bleeding was 6 % after propranolol treatment and 15 % in controls. The pooled risk difference was -8 % [95% CI, -15 %, -2 %] (Z=-2.53, P=0.01).

DISCUSSION

Propranolol reduces portal pressure, portal blood flow, and superior portosystemic collateral blood flow, so it can reduce the variceal pressure to prevent upper gastrointestinal hemorrhage[1-3]. However, reduction of the risk of gastrointestinal bleeding could not be replicated in some trials[7, 19, 21]. In the present meta analysis, we reviewed 20 randomized clinical trials to assess the efficacy of propranolol on gastrointestinal hemorrhage. The overall results showed that propranolol significantly reduced the risk of upper gastrointestinal tract bleeding, with a same effect on survival.

The beneficial effect of propranolol on both first and recurrent gastrointestinal hemorrhage was observed in all but six of the trials. The average rate of gastrointestinal hemorrhage was 28 % in patients treated with propranolol, but 43 % in controls, suggesting that this interventional therapy is highly effective on prevention of upper gastrointestinal tract bleeding. The results also demonstrated the efficacy of propranolol on preventing the first episode or recurrence of upper gastrointestinal tract bleeding in patients with cirrhosis. In the six trials, propranolol used to prevent variceal bleeding was proved to be ineffective, four were published in full form[7,10,19,21], and two in abstract form[25, 26].

The results of this meta analysis showed that propranolol significantly affected survival in all trials, primary prevention trials, or secondary trials. The average mortality was 20 % in patients treated with propranolol, but 27 % in controls. The reduction in total mortality was consistent with a limited effect on death due to bleeding. Other causes of death, including liver failure, sepsis, and the development of hepatocellular carcinoma, were not affected by propranolol.

Although the beta-blockade effect of propranolol can decrease hepatic blood flow, which may in turn induce deterioration of liver function in cirrhotic patients, but hepatic decompensation has been rarely encountered in patients treated with propranolol. In addition, other adverse effects of propranolol such as hypotension (3.6 %), heart failure (2.2 %), arrhythmia (1.4 %), bronchial spasm (2.7 %), dizziness (2.0 %), asthenia (3.4 %) etc were rarely encountered.

Endoscopic sclerotherapy is a conventional treatment for reducing the risk of recurrent bleeding, and long-term survival may also improve[28-33]. Another meta analysis which we conducted showed that the average recurrent bleeding rate was 42 % after endoscopic sclerotherapy, but was only 36 % in propranolol groups, and 55 % in control group in our present meta analysis. A randomized clinical trial suggested that the efficacy of combined sclerotherapy and propranolol on the primary prevention of hemorrhage in cirrhotic patients with varices was the same as propranolol alone[34]. In other words, endoscopic sclerotherapy did not consistently improve survival. Sclerotherapy, like propranolol, is associated with a low incidence of side-effects, but side effects such as esophageal perforation, may be life-threatening. The technique also is more time demanding on both physicians and patients.

In conclusion, the results of this meta analysis of the existing controlled trials show that propranolol is an effective means of reducing both the incidence of bleeding from upper gastrointestinal tract and the total mortality, and has the advantage of being safe and cost-effective. The combined data indicate that propranolol reduces the risk of bleeding or rebleeding by about 20 %, in both primary and secondary prevention and it also reduces mortality. The primary prevention trials, which included patients with obvious varices at high risk of bleeding, clearly show a beneficial effect. Based upon the analysis we would recommend a long-term treatment of gastrointestinal hemorrhage with propranolol. However, for many patients with portal hypertension without obvious varices, large prospective multicenter trials are indicated to determine the preventive benefit of propranolol. Further comparative trials of propranolol versus sclerotherapy are required to identify which is superior for secondary prevention of gastrointestinal hemorrhage.

REFERENCES

1 **Luca A**, Garcia-Pagan JC, Feu F, Lopez-Talavera JC, Fernandez M, Bru C, Bosch J, Rodes J. Noninvasive measurement of femoral blood flow and portal pressure response to propranolol in patients with cirrhosis. *Hepatology* 1995; **21**: 83-88

2 **Albillos A**, Perez-Paramo M, Cacho G, Iborra J, Calleja JL, Millan I, Munoz J, Rossi I, Escartin P. Accuracy of portal and forearm blood flow measurements in the assessment of the portal pressure response to propranolol. *J Hepatol* 1997; **27**: 496-504

3 **Escorsell A**, Bordas JM, Feu F, Garcia-Pagan JC, Gines A, Bosch J, Rodes J. Endoscopic assessment of variceal volume and wall tension in cirrhotic patients: effects of pharmacological therapy. *Gastroenterology* 1997; **113**: 1640-1646

4 **Egger M**, Smith GD, Phillips AN. Meta-analysis: principles and procedures. *BMJ* 1997; **315**: 1533-1537

5 **Egger M**, Smith GD. Meta-Analysis. Potentials and promise. *BMJ* 1997; **315**: 1371-1374

6 **Pogue J**, Yusuf S. Overcoming the limitations of current meta-analysis of randomised controlled trials. *Lancet* 1998; **351**: 47-52

7 **Burroughs AK**, Jenkins WJ, Sherlock S, Dunk A, Walt RP, Osuafor TO, Mackie S, Dick R. Controlled trial of propranolol for the prevention of recurrent variceal hemorrhage in patients with cirrhosis. *N Engl J Med* 1983; **309**: 1539-1542

8 **Lebrec D**, Poynard T, Bernuau J, Bercoff E, Nouel O, Capron JP, Poupon R, Bouvry M, Rueff B, Benhamou JP. A randomized controlled study of propranolol for prevention of recurrent gastrointestinal bleeding in patients with cirrhosis: a final report. *Hepatology* 1984; **4**: 355-358

9 **Villeneuve JP**, Pomier-Layrargues G, Infante-Rivard C, Willems B, Huet PM, Marleau D, Viallet A. Propranolol for the prevention of recurrent variceal hemorrhage: a controlled trial. *Hepatology* 1986; **6**: 1239-1243

10 **Queuniet AM**, Czernichow P, Lerebours E, Ducrotte P, Tranvouez JL, Colin R. Controlled study of propranolol in the prevention of recurrent hemorrhage in cirrhotic patients. *Gastroenterol Clin Biol* 1987; **11**: 41-47

11 **Pascal JP**, Cales P. Propranolol in the prevention of first upper gastrointestinal tract hemorrhage in patients with cirrhosis of the liver and esophageal varices. *N Engl J Med* 1987; **317**: 856-861

12 **The Italian Multicenter Project for Propranolol in Prevention of Bleeding**. Propranolol for prophylaxis of bleeding in cirrhotic patients with large varices: a multicenter, randomized clinical trial. *Hepatology* 1988; **8**: 1-5

13 **Marbet UA**, Straumann A, Gyr KE, Beglinger C, Schaub N, Bogtlin J, Loosli J, Kiowski W, Ritz R, Stalder GA. Reduction in early recurrence of variceal bleeding by propranolol. *Scand J Gastroenterol* 1988; **23**: 369-374

14 **Colombo M**, de Franchis R, Tommasini M, Sangiovanni A, Dioguardi N. Beta-blockade prevents recurrent gastrointestinal bleeding in well-compensated patients with alcoholic cirrhosis: a multicenter randomized controlled trial. *Hepatology* 1989; **9**: 433-438

15 **Sheen IS**, Chen TY, Liaw YF. Randomized controlled study of propranolol for prevention of recurrent esophageal varices bleeding in patients with cirrhosis. *Liver* 1989; **9**: 1-5

16 **Garden OJ**, Mills PR, Birnie GG, Murray GD, Carter DC. Propranolol in the prevention of recurrent variceal hemorrhage in cirrhotic patients. A controlled trial. *Gastroenterology* 1990; **98**: 185-190

17 **Andreani T**, Poupon RE, Balkau BJ, Trinchet JC, Grange JD, Peigney N, Beaugrand M, Poupon R. Preventive therapy of first gastrointestinal bleeding in patients with cirrhosis: results of a controlled trial comparing propranolol, endoscopic sclerotherapy and placebo. *Hepatology* 1990; **12**: 1413-1419

18 **Conn HO**, Grace ND, Bosch J, Groszmann RJ, Rodes J, Wright SC, Matloff DS, Garcia-Tsao G, Fisher RL, Navasa M, Drewniak SJ, Atterbury CE, Bordas JM, Lerner E, Bramante C. Propranolol in the prevention of the first hemorrhage from esophagogastric varices: A multicenter, randomized clinical trial. The Boston-New Haven-Barcelona Portal Hypertension Study Group. *Hepatology* 1991; **13**: 902-912

19 **The PROVA Study Group**. Prophylaxis of first hemorrhage from esophageal varices by sclerotherapy, propranolol or both in cirrhotic patients: a randomized multicenter trial. *Hepatology* 1991; **14**: 1016-1024

20 **Perez-Ayuso RM**, Pique JM, Bosch J, Panes J, Gonzalez A, Perez R, Rigau J, Quintero E, Valderrama R, Viver J, Esteban R, Rodrigo L, Bordas JM, Rodes J. Propranolol in prevention of recurrent bleeding from severe portal hypertensive gastropathy in cirrhosis. *Lancet* 1991; **337**: 1431-1434

21 **Cales P**, Oberti F, Payen JL, Naveau S, Guyader D, Blanc P, Abergel A, Bichard P, Raymond JM, Canva-Delcambre V, Vetter D, Valla D, Beauchant M, Hadengue A, Champigneulle B, Pascal JP, Poynard T, Lebrec D. Lack of effect of propranolol in the prevention of large oesophageal varices in patients with cirrhosis: a randomized trial. French-Speaking Club for the Study of Portal Hypertension. *Eur J Gastroenterol Hepatol* 1999; **11**: 741-745

22 **Pascal JP**. Prophylactic treatment of variceal bleeding in cirrhotic patients with propranolol: a multicentric randomized study. *Hepatology* 1984; **4**: 1092

23 **Cerbelaud P**, Lavignolle A, Perrin D, Jutel P, Beaujard E, Colomb P, Le Bodic L. Propranolol et prevention des recidives de rupture de varice oesophagienne du cirrhotique. *Gastroenterol Clin Biologique* 1986; **10**: 18

24 **Mills PR**, Garden OJ, Birnie GG, Carter DC. Propranolol in the prevention of further variceal hemorrhage in cirrhosis. *Gastroenterology* 1987; **92**: 1755

25 **Strauss E**, de Sa MFG, Albano A, Lacet CMC, Leite MO, Maffei RA. A randomized controlled trial for the prevention of the first upper gastrointestinal bleeding due to portal hypertension in cirrhosis: sclerotherapy or propranolol versus control groups. *Hepatology* 1988; **8**: 1395

26 **Colman J**, Jones P, Finch C, Dudley F. Propranolol in the prevention of variceal haemorrhage in alcoholic cirrhotic patients. *Hepatology* 1990; **12**: 851

27 **Der Simonian R**, Laird N. Meta-analysis in clinical trials. *Control Clin Trials* 1986; **7**: 177-188

28 **de la Pena J**, Rivero M, Sanchez E, Fabrega E, Crespo J, Pons-Romero F. Variceal ligation compared with endoscopic sclerotherapy for variceal hemorrhage: prospective randomized trial. *Gastrointest Endosc* 1999; **49**: 417-423

29 **Umehara M**, Onda M, Tajiri T, Toba M, Yoshida H, Yamashita K. Sclerotherapy plus ligation versus ligation for the treatment of esophageal varices: a prospective randomized study. *Gastrointest Endosc* 1999; **50**: 7-12

30 **Masci E**, Stigliano R, Mariani A, Bertoni G, Baroncini D, Cennamo V, Micheletti G, Casetti T, Tansini P, Buscarini E, Ranzato R, Norberto L. Prospective multicenter randomized trial comparing banding ligation with sclerotherapy of esophageal varices. *Hepatogastroenterology* 1999; **46**: 1769-1773

31 **Hou MC**, Lin HC, Kuo BI, Lee FY, Chang FY, Lee SD. The rebleeding course and long-term outcome of esophageal variceal hemorrhage after ligation: comparison with sclerotherapy. *Scand J Gastroenterol* 1999; **34**: 1071-1076

32 **Hata Y**, Hamada E, Takahashi M, Ota S, Ogura K, Shiina S, Okamoto M, Okudaira T, Teratani T, Maeda S, Koike Y, Sato S, Obi S, Tanaka T, Kawabe T, Shiratori Y, Kawase T, Nomura M, Omata M. Endoscopic variceal ligation is a sufficient procedure for the treatment of oesophageal varices in patients with hepatitis C liver cirrhosis: comparison with injection sclerotherapy. *J Gastroenterol Hepatol* 1999; **14**: 236-240

33 **Gotoh Y**, Iwakiri R, Sakata Y, Koyama T, Noda T, Matsunaga C, Ogata SI, Ishibashi S, Sakata H, Tsunada S, Fujimoto K. Evaluation of endoscopic variceal ligation in prophylactic therapy for bleeding of oesophageal varices: a prospective, controlled trial compared with endoscopic injection sclerotherapy. *J Gastroenterol Hepatol* 1999; **14**: 241-244

34 **Avgerinos A**, Armonis A, Manolakopoulos S, Rekoumis G, Argirakis G, Viazis N, Vlachogiannakos J, Adamopoulos A, Kanaghinis T, Raptis SA. Endoscopic sclerotherapy plus propranolol versus propranolol alone in the primary prevention of bleeding in high risk cirrhotic patients with esophageal varices: a prospective multicenter randomized trial. *Gastrointest Endosc* 2000; **51**: 652-658

Edited by Xu JY and Wang XL

P.O.Box 2345, Beijing 100023,China
Fax: +86-10-85381893
E-mail: wjg@wjgnet.com www.wjgnet.com

World J Gastroenterol 2003;9(8):1840-1843
World Journal of Gastroenterology
 ISSN 1007-9327

• BRIEF REPORTS •

Inhibition of hepatitis B virus by a novel L-nucleoside, b-L-D4A and related analogues

Jin-Ming Wu, Ju-Sheng Lin, Na Xie, Kuo-Huan Liang

Jin-Ming Wu, Ju-Sheng Lin, Na Xie, Kuo-Huan Liang, Institute of liver diseases, Tongji Medical College, Huazhong University of Science and Technology, Wuhan 430030, China
Jin-Ming Wu, Department of Digestive Medicine, the First Affiliated Hospital, Wenzhou Medical College, Wenzhou 325000, Zhejiang Province, China
Supported by National Natural Science Foundation of China, No. 39970858
Correspondence to: Dr. Ju-Sheng Lin, Institute of Liver Diseases, Tongji Medical College, Huazhong University of Science and Technology, Wuhan430030, Hubei Province, China. linjusheng2001@163.net
Telephone: +86-27-83662578
Received: 2003-01-04 **Accepted:** 2003-02-17

Abstract

AIM: To explore the inhibition of β-L-D4A on hepatitis B virus (HBV) in 2.2.15 cells derived from HepG2 cells transfected with HBV genome.

METHODS: 2.2.15 cells were plated at a density of 5×10^4 per well in 12-well tissue culture plates, and treated with various concentrations of β-L-D4A for 6 days. In the end, 5 μl of medium was used for the estimation of HBsAg and HBeAg, the other medium was processed to obtain virions by a polyethlene glycol precipitation method. At the same time, intracellular DNA was also extracted and digested with HindIII. Both DNAs were subjected to Southern blot, hybridized with a ^{32}P-labeled HBV probe and autoradiographed. Intensity of the autoradiographic bands was quantitated by densitometric scans of computer and ED_{50} was calculated. Then Hybond-N membrane was washed and rehybridized with a ^{32}P-labeled mtDNA-specific probe, and effect of β-L-D4A on mitochondrial DNA was studied. 2.2.15 cells were also seeded in 24-well tissue culture plates, and cytotoxicity with different concentrations was examined by MTT method. ID_{50} was calculated. Structure-activity relationships between D2A and D4A were also studied as above.

RESULTS: Autoradiographic bands were similar between supernatant and intracellular HBV DNA. Episomal HBV DNA was inhibited in a dose-dependent manner. ED_{50} was 0.2 μM. HBsAg or HBeAg was not apparently decreased, and inhibition of mitochondrial DNA was not obvious. The experiment of cytotoxicity gained ID_{50} at 200 μM.

CONCLUSION: β-L-D4A possesses potent inhibitory effects on the replication of HBV *in vitro* with little cytotoxicity and mitochondrial toxicity, TI value is 1000. It is expected to be developed as a new clinically anti-HBV drug.

Wu JM, Lin JS, Xie N, Liang KH. Inhibition of hepatitis B virus by a novel L-nucleoside, β-L-D4A and related analogues. *World J Gastroenterol* 2003; 9(8): 1840-1843
http://www.wjgnet.com/1007-9327/9/1840.asp

INTRODUCTION

Like interferon, nucleoside analogues have become the focus of investigations of anti-HBV drugs[1]. However, most anti-HBV nucleoside analogues tested to date have at best only transient and limited effects in a small percentage of the general population of HBV-infected individuals and exist moderately to seriously side effects[2,3]. Vidarabine, ribavirin, acyclovir, ganciclovir, famciclovir, fialuridine, etc. have not been used widely. In recent years, considerable interest has been focused on the use of 2', 3'-dideoxynucleosides (DDNs) for the treatment of chronic HBV infection[4]. DDNs are phosphorylated to triphosphate in cells, which in turn specifically inhibits the viral polymerase, terminates the elongation of HBV DNA, showing potent anti-HBV activities with relatively low cellular toxicities[5].

Lamivudine as one of DDNs has been used widely in clinic, and has a rapidly potent anti- HBV effect, but there is a rebound of HBV DNA after treatment, and drug resistance and viral mutants may appear after a long-term treatment with lamivudine[6]. Thus it is important to search for more effective agents against HBV, even with an improved therapeutic index. In this report, 2', 3'-didehydro-2', 3'-dideoxyadenine (β-L-D4A), a novel L-Nucleoside was demonstrated to effectively block the production of HBV in 2.2.15 cells *in vitro*. Mitochondrial effects and cytotoxicity were also investigated to evaluate the potential use of these compounds in treatment of HBV infection.

MATERIALS AND METHODS

Compounds and agents

β-L-D4A was synthesized by ourselves with the help of Pharmaceutic College of Wuhan University and identified by infrared, mass spectra, nuclear-magnetic resonance. Lamivudine, ddC' D-D4A, L-D2A, D-D2A were provided by Professor Cheng YC (School of Medicine, Yale University, New Haven, CT). All compounds were dissolved in phosphate-buffered saline (pH 7.4).

Determination of anti-HBV activity in 2.2.15 cells

2.2.15 cells (clonal cells derived from hepG2 cells that were transfected with a plasmid containing HBV DNA) that could secrete heptitis B virions, kindly provided by Prof. Cheng, were incubated in DMEM medium with 10 % (vol/vol) fetal bovine serum, 100 IU/mL penicillin and 100 μg/mL streptomycin at 37 ℃ in a moist atomosphere containing 5 % CO_2/95 % air. The cells were inoculated at a density of 5×10^4/ml per well in 12-well tissue culture plates. The compounds studied were added to the medium 3 days after the inoculation. The cells were grown in the presence of drugs for 9 days with changes of medium every 3 days. On the 12th day, the culture medium was havested. An aliquot of the culture medium (5 μl) was used for estimation of HBV surface antigen (HBsAg) and HBV e antigen (HBeAg). The remaining medium was processed to obtain virions by a polyethylene glycol precipitation method[7]. The viral DNA recovered from the secreted particles was subjected to Southern blot analysis. Cellular DNA was isolated according to the standard protocols. Inhibition of viral DNA replication was determined by comparison of the viral DNA from drug-treated

and nontreated cultures. The level of inhibition was determined by hybridization of the blots to an HBV-specific probe followed by autoradiography. Quantitation of the autoradiographs was performed by density scanning with a computer software.

Effect of b-L-D4A on mitochondrial DNA

Since some of the nucleosides used in the treatment of HBV, such as FIAU[8], could affect liver function, especially mitochondrial function, a detailed analysis of the effect of β-L-D4A on mitochondrial DNA synthesis was carried out. 2.2.15 cells were cultured as above and after 24 h in culture, treatment with the compounds was initiated. β-L-D4A was added at concentrations of 0.4 μM and 10 μM in DMEM. Cultures treated with 0.4 μM 2' 3' -dideoxycytidine (ddC) were maintained in parallel as positive controls for damage of mitochondrial DNA. Blank control was also set. Cellular DNA was isolated according to the standard protocols and digested with restriction enzyme BamH I. Hybridizations and detection of the mitochodrial DNA were done according to the laboratory manual of molecular cloning. The probe was cytochrome oxidase III DNA labeled by ^{32}pdCTP.

Cytotoxicity

Cells were inoculated at a density of 5×10^3/ml per well in 24-well tissue culture plates. After 24 h in culture, the cells were treated with various concentrations of β-L-D4A in DMEM for 3 days. Then 3-(4, 5-dimethylthiazol-2-yl)-2, 5-diphenyltetrazolium bromide (MTT) assays were performed using the cell titer kit™ (Promega) following the standard procedure with the following exceptions. At the time points described as illustrations, 15 μl MTT reagent was added per well, allowed to incubate for 30 minutes, after which 130 μl stop/lysis buffer was added. Plates were sealed with Parafilm™ and left overnight at room temperature to allow solubilization of the formazan salt product. Absorbance was measured at 750 nm and 570 nm using a Thermomax (Molecular Devices, San Jose, CA), or a cytoFluor microplate reader (PE Biosystems, Foster City, CA). The data were normalized (A570-A750 nm) and the mean absorbance (5 wells/concentration) was plotted against drug concentration. The ID_{50} values were calculated as described above.

Determination of effects of b-L-D4A on HBsAg and HBeAg

HBsAg and HBeAg in the culture medium were determined according to the protocols supplied by the manufacturer. Essentially, the culture medium was appropriately diluted with phosphate-buffered saline and absorbed on the surface of plates coated by antibody to HBsAg or HBeAg. After an incubation period, the plates were washed and incubated in orthophenylene diamine. After a 30-min incubation, the reaction was terminated by adding 1N sufuric acid. The A_{490} of the final reaction was read. Appropriate positivity and negativity were assayed along with the samples.

RESULTS

Structure-activity relationships

The 2.2.15 cell line was used to evaluate the antiviral activities of ddA analogues: D-D4A, L-D2A, D-D2A (Structures are shown in Figure 1). The antiviral effects were measured by an analysis of extracellular HBV DNA. The experiment revealed that the inhibition of HBV DNA was more strong by L-isomer than by D-isomer and much more notable by L-D4A than by L-D2A (Figure 2).

Dosage-activity relationships

Inhibition of HBV DNA replication by β-L-D4A was evident as demonstrated by the amount of DNA obtained from the secreted viral particles as well as from the intracellular episomal particles. Concentrations of β-L-D4A ranging from 0.08 μM to 10 μM produced a dose-dependent inhibition (Figure 3). The intensity of autoradiographic bands for extracellular HBV DNA was quantitated by densitometric scans of computer and ED_{50} was calculated at 0.2 μM(Figure 4). Analysis of the intracellular episomal HBV DNA reflected similar trends in inhibition (Figure 5).

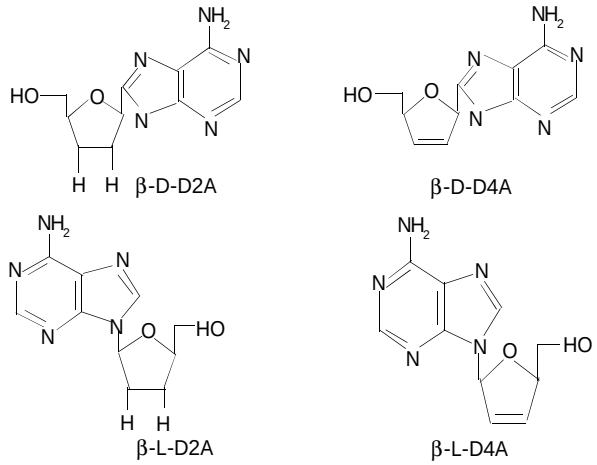

Figure 1 Structures of β-L-D4A and analogues.

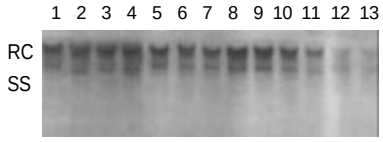

Figure 2 Inhibition of isomers of D4A and D2A on HBV DNA replication in supernatant. Lane 1 as negative control; lanes 2, 3, 4 as D-D2A at 2 μM, 4 μM and 8 μM, respectively; lanes 5, 6, 7 as L-D2A at 2 μM, 4 μM and 8 μM, respectively; lanes 8, 9, 10 as D-D4A at 2 μM, 4 μM and 8 μM, respectively; lanes 11, 12, 13 as L-D4A at 2 μM, 4 μM and 8 μM, respectively. RC: relaxed circular HBV DNA; SS: single-stranded HBV DNA.

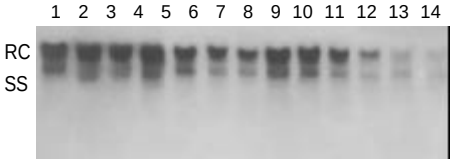

Figure 3 Inhibition on replication of extracellular HBV DNA by β-L-D4A. lanes 1, 2 as negative control; lanes 3, 4 as lamivudine at 1 μM; lanes 5, 6 as β-L-D4A at 10 μM; lanes 7, 8 as β-L-D4A at 2 μM; lanes 9, 10 as β-L-D4A at 0.4 μM; lanes 11, 12 as β-L-D4A at 0.08 μM; lanes 13, 14 as blank control ($HepaG_2$). RC: relaxed circular HBV DNA; SS: single-stranded HBV DNA.

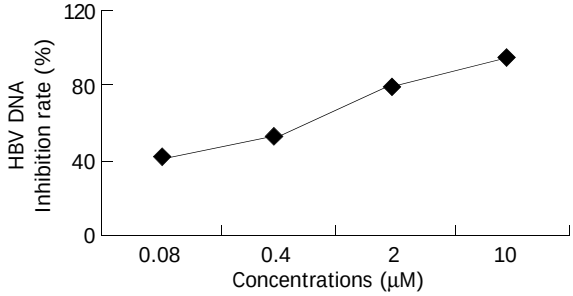

Figure 4 Inhibition on replication of extracellular HBV DNA by β-L-D4A.

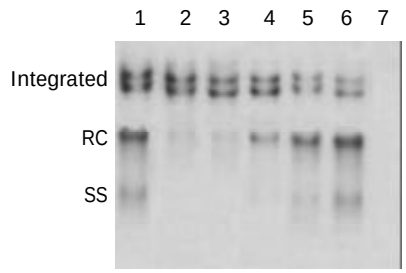

Figure 5 Inhibition on replication of intracellular HBV DNA by β-L-D4A. lane 1 as negative control; lane 2 as lamivudine at 1 μM; lane 3 as β-L-D4A at 10 μM; lane 4 as β-L-D4A at 2 μM; lane 5 as β-L-D4A at 0.4 μM; lane 6 as β-L-D4A at 0.08; lane 7 as blank control (HepaG2). RC: relaxed circular HBV DNA; SS: single-stranded HBV DNA.

Effect of b-L-D4A on mitochondrial DNA

Hybridization of intracellular DNA to a cytochrome oxidase III was done to evaluate the effect of β-L-D4A on mitochondrial DNA. Mitochondrial DNA levels treated with 0.4 μM and 10 μM β-L-D4A were nearly similar to the blank control, but were obviously lower for ddC at 0.4 μM (Figure 6).

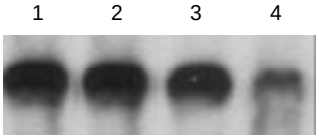

Figure 6 Toxicity of mitochondrial DNA. lane 1 as blank control; lane 2 as β-L-D4A at 0.4 μM; lane 3 as β-L-D4A at 10 μM; lane 4 as ddC at 0.4 μM.

Cytotoxicity of b-L-D4A

β-L-D4A did not show evident toxicity to 2.2.15 cells even at a concentration of 10 μM, but at high concentrations it had cytotoxicity, with 50 % inhibitory concentration (ID_{50}) of 200 μM, The data are shown in Table 1 and Figure 7.

Table 1 Effect-dosage relationship of inhibition of cell growth by β-L-D4A

Dosage (μM)	*n*	A value ($\bar{x}$±*s*)	Inhibition rate (%)
50	3	0.84±0.22	22.3
100	3	0.75±0.16	36.0
150	3	0.73±0.12	37.2
200	3	0.67±0.21	50.4
250	3	0.53±0.15	73.5
300	3	0.43±0.25	89.2
0	3	2.01±0.23	0

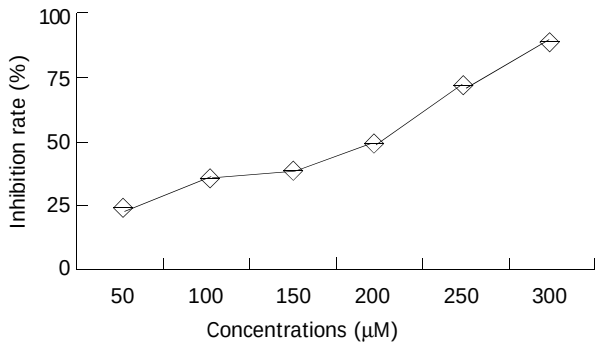

Figure 7 Effect of β-L-D4A on cell growth curve.

Effects of b-L-D4A on HBsAg and HBeAg

Measurements of the levels of viral surface antigen and e antigen from the media of cultures treated with β-L-D4A revealed that β-L-D4A had no significant inhibitory effect on HBsAg and HBeAg at low concentrations, but had marked effect of reducing HBsAg and HBeAg at 2 μM and 10 μM, significantly different from the blank group ($P<0.05$ or $P<0.01$, respectively) (Shown in Table 2).

Table 2 Effect-dosage relationship of inhibition of HBsAg and HBeAg by β-L-D4A

Dosage(μM)	*n*	HBsAg		HBeAg	
		P / N value ($\bar{x}$±*s*)	Inhibition rate(%)	P / N value ($\bar{x}$±*s*)	Inhibition rate (%)
0.08	3	2.96±0.18	13.7	4.98±0.23	5.5
0.4	3	2.84±0.22	22.3	4.97±0.15	5.7
2	3	2.75±0.16[a]	36.0	4.88±0.25	9.4
10	3	2.73±0.12[a]	37.2	4.02±0.33[b]	37.5
Blank	3	3.09±0.21	0	5.27±0.27	0

[a]$P<0.05$; [b]$P<0.01$ *vs* blank control.

DISCUSSION

One rational approach to the development of drugs for the treatment of HBV infection in patients is to identify those compounds that specifically inhibit HBV DNA replication[9,10]. Since deoxynucleoside analogues were found to be effective on a variety of viruses, several compounds have been tested *in vitro* and *in vivo* against hepadnaviruses[9-12]. The selectivity of these compounds against HBV in general is assessed by their relative potency against HBV versus cellular toxicity[13-16]. Cytotoxicity studies are usually conducted by growth retardation assays that measure cell growth in the presence of compounds tested for three or four generations[17]. This growth retardation assay could not, however, detect delayed cytotoxicity of deoxynucleoside analogues such as ddC that have an effect on cellular mtDNA synthesis. Since mitochondria play an important role in organ function, it was hypothesized that the delayed toxicity as shown by peripheral neuropathy (e.g., observed in patients treated with ddC analogs) could be due to decreases in mtDNA[18]. In this study, in addition to assessing their anti-HBV activities, compounds were examined for their effects on 4-day cell growth and on mtDNA.

Deoxynucleosides such as D2A and D4A can exist as (+)- or (-)- enatiomers. From the results we got, we could see that (-)-isomers were superior to (+)-isomers, and β-L-D4A was the most potent inhibitor of HBV replication in 2.2.15 cells, which could almost completely block HBV DNA replication at a concentration of 4 μM. However, (+) -isomers were almost inactive against HBV replication when tested up to 8 μM, mechanism of which might be in that the compounds could be deaminated intracellularly to the inactive analogues as reported before[19].

β-L-D4A was the most potent inhibitor of HBV replication in 2.2.15 cells from our results. No effects on mtDNA were observed. Cell growth retardation with the administration of β-L-D4A at low concentrations was not evident, but at high concentrations, β-L-D4A began to show cytotoxicity in a dose-dependent manner with 50 % inhibitory concentration (ID_{50}) of 200 μM. Since β-L-D4A does not inhibit mtDNA synthesis at concentrations that inhibit virus production, the delayed toxicity, such as peripheral neuropathy, associated with the treatment of ddC[20] may not occur. In addition, β-L-D4A is not toxic to proliferting cells at concentrations that completely block the synthesis of HBV virion, suggesting that acute bone

marrow toxicity may not be a concern. The study on dosage-activity relationships showed that β-L-D4A could inhibit HBV DNA replication in a markedly dose-dependent manner with 50 % inhibitory concentration (ED_{50}) of 0.2 μM. As the therapeutic index (TI value) was equal to ID_{50}/ ED_{50}, we got the TI value of β-L-D4A at 1 000. TI of lamivudine was 750 as reported in another article[21]. Therefore β-L-D4A like lamivudine possesses potent anti-HBV replication effect and has a higher TI value. In addition to that, β-L-D4A shows inhibition of expression of HBV antigens at high concentrations, indicating that β-L-D4A may be able to decrease the levels of HBsAg and HBeAg with a long term use.

About the mechanism of action of β-L-D4A, we think it is likely the inhibition of viral DNA polymerase, chain-termination resulted from incorporation into elongated DNA strand, or both. The mechanism needs to be further explored.

On the basis of the study of nucleoside analogs against HIV, human immunodeficiency virus resistant to ddC is not cross resistant to the thymidine analog zidovudine[22]. This permits the possibility of HBV treatment with β-L-D4A in the event of resistance to cytosine analogs as lamivudine. Furthermore, possibilities of a combined therapy of β-L-D4A and lamivudine for HBV can be explored.

REFERENCES

1 **Bridges EG,** Cheng YC. Use of novel beta-L(-)-nucleoside analogues for treatment and prevention of chronic hepatitis B virus infection and hepatocellular carcinoma. *Prog Liver Dis* 1995; **13**: 231-245

2 **Freiman JS**, Mc Caughan GW. Current limitations to nucleoside analogue therapy for chronic hepatitis B virus infection in the liver transplant and non-transplant settings. *J Gastroenterol Hepatol* 2000; **15**: 227-229

3 **Pan-Zhou XR**, Cui L, Zhou XJ, Sommadossi JP, Darley-Usmar VM. Differential effects of antiretroviral nucleoside analogs on mitochondrial function in HepG2 cells. *Antimicrob Agents Chemother* 2000; **44**: 496-503

4 **Van Draanen NA,** Tisdale M, Parry NR, Jansen R, Dornsife RE, Tuttle JV, Averett DR, Koszalka GW. Influence of stereochemistry on antiviral activities and resistance profiles of dideoxycytidine nucleosides. *Antimicrob Agents Chemother* 1994; **38**: 868-871

5 **Zoulim F.** Therapy of chronic hepatitis B virus infection: inhibition of the viral polymerase and other antiviral strategies. *Antiviral Res* 1999; **44**: 1-30

6 **Lai CL,** Yuen MF. Profound suppression of hepatitis B virus replication with lamivudine. *J Med Virol* 2000; **61**: 367-373

7 **Hawkins AE,** Zuckerman MA, Briggs M, Gilson RJ, Goldstone AH, Brink NS, Tedder RS. Hepatitis B nucleotide sequence analysis: linking an outbreak of acute hepatitis B to contamination of a cryopreservation tank. *J Virol Methods* 1996; **60**: 81-88

8 **Tennant BC,** Baldwin BH, Graham LA, Ascenzi MA, Hornbuckle WE, Rowland PH, Tochkov IA, Yeager AE, Erb HN, Colacino JM, Lopez C, Engelhardt JA, Bowsher RR, Richardson FC, Lewis W, Cote PJ, Korba BE, Gerin JL. Antiviral activity and toxicity of fialuridine in the woodchuck model of hepatitis B virus infection. *Hepatology* 1998; **28**: 179-191

9 **Chu CK,** Boudinot FD, Peek SF, Hong JH, Choi Y, Korba BE, Gerin JL, Cote PJ, Tennant BC, Cheng YC. Preclinical investigation of L-FMAU as an anti-hepatitis B virus agent. *Antivir Ther* 1998;**3** (Suppl 3): 113-121

10 **Colacino JM.** Mechanisms for the anti-hepatitis B virus activity and mitochondrial toxicity of fialuridine (FIAU). *Antiviral Res* 1996; **29**: 125-139

11 **Lin JS,** Kira T, Gullen E, Choi Y, Qu F, Chu CK, Cheng YC. Structure-activity relationships of L-dioxolane uracil nucleosides as anti-Epstein Barr virus agents. *J Med Chem* 1999; **42**: 2212-2217

12 **Ma T,** Pai SB, Zhu YL, Lin JS, Shanmuganathan K, Du J, Wang C, Kim H, Newton MG, Cheng YC, Chu CK. Structure-activity relationships of 1-(2-Deoxy-2-fluoro-beta-L-arabinofuranosyl) pyrimidine nucleosides as anti-hepatitis B virus agents. *J Med Chem* 1996; **39**: 2835-2843

13 **Kotra LP,** Xiang Y, Newton MG, Schinazi RF, Cheng YC, Chu CK. Structure-activity relationships of 2'-deoxy-2', 2'-difluoro-L-erythro-pentofuranosyl nucleosides. *J Med Chem* 1997; **40**: 3635-3644

14 **Qiu YL,** Ptak RG, Breitenbach JM, Lin JS, Cheng YC, Kern ER, Drach JC, Zemlicka J**.** (Z)- and (E)-2-(hydroxymethylcyclopropylidene)-methylpurines and pyrimidines as antiviral agents. *Antivir Chem Chemother* 1998; **9**: 341-352

15 **Qiu YL,** Ksebati MB, Ptak RG, Fan BY, Breitenbach JM, Lin JS, Cheng YC, Kern ER, Drach JC, Zemlicka J**.** (Z)- and (E)-2-((hydroxymethyl) cyclopropylidene) methyladenine and -guanine. New nucleoside analogues with a broad-spectrum antiviral activity. *J Med Chem* 1998; **41**: 10-23

16 **Du J,** Surzhykov S, Lin JS, Newton MG, Cheng YC, Schinazi RF, Chu CK**.** Synthesis, anti-human immunodeficiency virus and anti-hepatitis B virus activities of novel oxaselenolane nucleosides. *J Med Chem* 1997; **40**: 2991-2993

17 **Lu X,** Gong S, Monks A, Zaharevitz D, Moscow JA. Correlation of nucleoside and nucleobase transporter gene expression with anti-metabolite drug cytotoxicity. *J Exp Ther Oncol* 2002; **2**: 200-212

18 **Hostetler KY,** Korba BE, Sridhar CN, Gardner MF. Antiviral activity of phosphatidyl-dideoxycytidine in hepatitis B-infected cells and enhanced hepatic uptake in mice. *Antiviral Res* 1994; **24**: 59-67

19 **Gudmundsson KS,** Tidwell J, Lippa N, Koszalka GW, van Draanen N, Ptak RG, Drach JC, Townsend LB. Synthesis and antiviral evaluation of halogenated beta-D- and -L-erythrofuranosylbenzimidazoles. *J Med Chem* 2000; **43**: 2464-2472

20 **Dalakas MC,** Semino-Mora C, Leon-Monzon M**.** Mitochondrial alterations with mitochondrial DNA depletion in the nerves of AIDS patients with peripheral neuropathy induced by 2'3'-dideoxycytidine (ddC). *Lab Invest* 2001; **81**: 1537-1544

21 **Leung N.** Liver disease-significant improvement with lamivudine. *J Med Virol* 2000; **61**: 380-385

22 **Descamps D,** Flandre P, Joly V, Meiffredy V, Peytavin G, Izopet J, Tamalet C, Zeng AF, Harel M, Lastere S, Aboulker JP, Yeni P, Brun-Vezinet F. Effect of zidovudine resistance mutations on virologic response to treatment with zidovudine or stavudine, each in combination with lamivudine and indinavir. *J Acquir Immune Defic Syndr* 2002; **31**: 464-471

Edited by Xu XQ and Wang XL

P.O.Box 2345, Beijing 100023,China
Fax: +86-10-85381893
E-mail: wjg@wjgnet.com www.wjgnet.com

World J Gastroenterol 2003;9(8):1844-1847
World Journal of Gastroenterology
 ISSN 1007-9327

• BRIEF REPORTS •

Generation and characterization of transgenic mice expressing tamoxifen-inducible cre-fusion protein specifically in mouse liver

Huan-Zhang Zhu, Jian-Quan Chen, Guo-Xiang Cheng, Jing-Lun Xue

Huan-Zhang Zhu, Istitute of Pathology, Southwest Hospital, Third Military Medical University, Chongqing 400038, China
Jian-Quan Chen, Guo-Xiang Cheng, Shanghai Transgenic Research Center, Shanghai 201203, China
Huan-Zhang Zhu, Jing-Lun Xue, State Key Laboratory of Genetic Engineering, Institute of Genetics, School of Life Sciences, Fudan University, Shanghai 200433, Chian
Supported by the National Natural Science Foundation of China No.30070380
Correspondence to: Jing-Lun Xue, State Key Laboratory of Genetic Engineering, Institute of Genetics, School of Life Sciences, Fudan University, Shanghai 200433,Chian. jlxue@fudan.ac.cn or Guo-Xiang Cheng, Shanghai Transgenic Research Center, Shanghai 201203, China. chenggx@cngenon.com
Telephone: +86-21-65642424
Received: 2003-01-04 **Accepted:** 2003-02-24

Abstract

AIM: To establish transgenic mice expressing tamoxifen-inducible Cre-ERt recombinase specifically in the liver and to provide an efficient animal model for studying gene function in the liver and creating various mouse models mimicking human diseases.

METHODS: Alb-Cre-ERt transgenic mice were produced by microinjecting the construct with Cre-ERt fusion gene of DNA fragments into fertilized eggs derived from inbred C57BL/6 strain. Transgenic mice were identified by using PCR and Southern blotting. Expression of Cre-ERt fusion gene was analyzed in the liver, kidney, brain and lung from F1 generation transgenic mice at 8 weeks of age by reverse transcription (RT)-PCR.

RESULTS: Four hundred and fourteen fertilized eggs of C57 BL/6 mice were microinjected with recombinant Alb-Cre-ERt DNA fragments, and 312 survival eggs injected were transferred to the oviducts of 12 pseudopregnant recipient mice, 6 of 12 recipient mice became pregnant and gave birth to 44 offsprings. Of the 44 offsprings, two males and one female carried the hybrid Cre-ERt fusion gene. Three mice were determined as founders, and were back crossed to set up F1 generations with other inbred C57BL/6 mice. Transmission of Cre-ERt fusion gene in F1 offspring followed Mendelian rules. The expression of Cre-ERt mRNA was detected only in the liver of F1 offspring from two of three founder mice.

CONCLUSION: Transgenic mice expressing tamoxifen-inducible Cre-ERt recombinase under control of the liver-specific promoter are preliminary established.

Zhu HZ, Chen JQ, Cheng GX, Xue JL. Generation and characterization of transgenic mice expressing tamoxifen-inducible cre-fusion protein specifically in mouse liver. *World J Gastroenterol* 2003; 9(8): 1844-1847
http://www.wjgnet.com/1007-9327/9/1844.asp

INTRODUCTION

The liver plays a central role in regulation of carbohydrate, lipid, and urea metabolism as well as in production of most plasma proteins and detoxification of exogenous chemicals. The ability to create defined genetic modifications *in vitro* and *in vivo* provides a promising way to understand relevant functions of numerous hepatic genes in health and disease. Ligand-dependent chimeric Cre recombinases are powerful tools to induce specific DNA rearragements in cultured cells and mice[1-3]. To introduce defined genetic modifications in a temporally controlled manner in the liver, an alternative approach is to establish transgenic mice expressing tamoxifen-inducible Cre recombinase under control of the liver specific promoter. To this end, we constructed the fusion gene of Cre and the ligand binding domain (LBD) of a mutated human estrogen receptor (ER) that recognizes anti-estrogen 4-hydroxytamoxifen (4-OHT), Cre-ERt , under control of a liver-specific regulatory sequence from the mouse albumin gene. By using microinjection technology, two transgenic mice lines expressing Cre-ERt only in the liver were finally obtained.

MATERIALS AND METHODS

Materials

Restriction enzymes and other reagents Enzymes *Eco*RI, *Sma*I, *Sac*II *Hin*dIII, *Bam*HI, *Bgl* I, T4 DNA ligase, dNTP, Taq DNA polymerase, MMLV reverse transcriptase, etc, were purchased from NEB, Sangon and Sigma companies, respectively.
Mice C57BL/6, ICR mice (clean animal) were purchased from Laboratory Animal Center, Shanghai, China.

Methods

Construction of recombinant plasmid Construction of the Alb-Cre-ERt (Figure 1) was performed according to Sambrook *et al*[4]. In brief, a 0.6 Kb *Sma*I-*Sac*II fragment containing CMV promoter from plasmid pCMV-Cre-ERt (kindly provided by Prof. Chambon P) was replaced with a 2.3 Kb *Sac*II-*Eco*RV fragment containing albumin enhancer and promoter (alb e/p) from p2335A (kindly provided by Prof. Palmiter). Identity of the constructs was confirmed by restriction enzyme mapping and DNA sequence analysis.

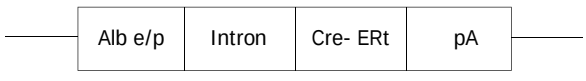

Figure 1 Structure of alb-Cre-ERt expression vector. The DNA fragments contained albumin gene promoter/enhancer (alb e/p), rabbit β-globin intron, fusion gene of Cre-ERt, and polyadenylation site (pA).

Production of transgenic mice Transgenic mice were generated by standard methods[5]. In brief, the transgene construct was linearized using *Bgl* l. The fragment was gel-purified with QIAGEN Kit. After diluted to 1 μg/ml final concentration in microinjection buffer, DNA was microinjected into the male pronucleus of fertilized C57BL/

6 mice oocytes. Then injected eggs were transplanted into the oviduct of pseudopregnant mice. Operated mice got pregnant and gave birth. Selected mice were bred with wild-type animals to establish transgenic lines that were maintained at heterozygosity.

Detection of transgenic integration Genomic DNA was extraction from transgenic mice tails (about 1-1.5 cm) at 4 weeks of age. Total DNA was extracted with the method described by Sambrook[4].

PCR assay The primers were designed on Cre gene sequence and synthesized by Cybersyn Biotechnology Company. The sequence of primers for PCR was as follows: the 5' primer for Cre was 5' -ATC CGA AAA GAA AAC GTT GA-3' and the 3' primer was 5' -ATC CAG GTT ACG GAT ATA G T-3' . The PCR reaction condition contained 2 μl of 10×PCR Buffer, 0.4 μl of 25 mM Mg^{2+}, 1 μl of 15 mM dNTP, 1 μl of 10 pmol each of primer, 2u of Taq DNA polymerase, 1 μg sample DNA. A 20 μl total reaction volume was obtained by adding sterile water, the reaction procedure of PCR was: beginning at 95 ℃ for 5 min, then 30 cycles at 94 ℃ denature for 30 s, annealing at 58 ℃ for 40 s and extension at 72 ℃ for 40 s, final extension at 72 ℃ for 10 min. 1.8 % agarose gel was prepared and 10 μl PCR products was loaded in the gel, then electrophoresed at 80 voltage for 40 min, the result of electrophoresis was observed.

Southern blot analysis Southern-blotting analysis was performed with the following standard procedures[4]: 10 μg tail DNA was digested with *Eco*RI and separated by electrophoresis on a 0.6 % agarose gel, and transferred onto a nylon membrane (Boehringer Mannheim). The nylon membrane was prehybridized for 5 h at 42 ℃ and hybridized overnight with a probe from a 0.7 kb *Bam*HI-*Xho*I Cre fragment that was a random primer labeled using α-32P dCTP (Amersham Pharmacia Biotech Inc). Bands were detected by X-ray film after 6 days of exposure.

Detection of Cre-ERt mRNA synthesis in mice The level of Cre-ERt mRNA was estimated by RT-PCR. Total RNA was isolated from F1 generation of 4 weeks old mouse tissues (liver, kidney, brain and lung) by Sambrooks method[4]. The upstream primer was 5' -CAGAACCTGAAGATGTTCG-3' and downstream was 5' -GGATCATCAGCTACACCAG-3' , resulting in a 505 bp fragment of the Cre-ERt cDNA. First stranded cDNA was synthesized as follows: The reverse transcriptase reactions contained 1 μg RNA, 5 μl of 10×PCR Buffer, 3 μl of 15 mM dNTP, 1 μl of RNasin (80 u/μl), 2 μl 10 pmol upstream primer, 1 μl MMLV(200 u). A 50 μl total reaction volume was obtained by adding sterile DEPC treated water. Reaction conditions were at 48 ℃ for 45 min for reverse transcription. The products of reverse transcriptase reactions were used directly in PCR reactions, adding 2 u Taq DNA polymerase, 3 μl of 10 pmol upstream/downstream primers, respectively. PCR denaturation was at 96 ℃ for 2 min, then for 35 cycles of reaction (denaturation at 94 ℃ for 30 s, annealing at 62 ℃ for 40 s, extension at 72 ℃ for 40 s, and a final extension at 72 ℃ for 7 min).

RESULTS

Identity of constructs

The *Sma*I-*Sac*II (blunted) fragment containing Cre-ERt of plasmid pCMV-Cre-ERt was isolated; the *Sac*II (blunted)-*Eco*RV fragment containing albumin enhancer and promoter (alb e/p) of p2335A were isolated, respectively. The two individual fragments were ligated to generate palb-Cre-ERt. The identity of palb-Cre-ERt was confirmed by restriction enzyme mapping (Figure 2) and DNA sequence analysis (data not shown), indicating that the albumin enhancer and promoter were correctly inserted and linked.

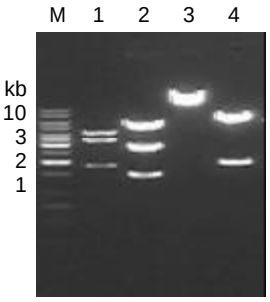

Figure 2 Identification of palb-Cre-ERt recombinant. M: GeneRuler 1 kb DNA Laddar, 1: recombinant-*Hin*dIII, 2: recombinant-*Sca*I, 3: recombinant-*Eco*RV, 4:Vector-*Hin*dIII.

Establishment of Cre-ERt transgenic mice

Recombinant Cre-ERt DNA fragment was microinjected into the male pronucleus of the 414 fertilized eggs of C57 BL/6 mice, and 312 survival eggs injected were transferred to the oviducts of 12 pseudopregnant recipient mice, 6 of 12 recipient mice became pregnant and gave birth to 44 offspring mice. The survial rate and birth rate of zygotes were 75 % (312/414) and 14 % (44/312), respectively. DNA extracted from tails of 44 offspring mice was screened by PCR assay and Southern blot analysis (Figure 3). The results showed that three mice carried the Cre-ERt gene. Three mice(two male, one female) were determined as founders. Total integration rate and efficiency of transgene were 6 % (3/44) and 0.7 % (3/414), respectively.

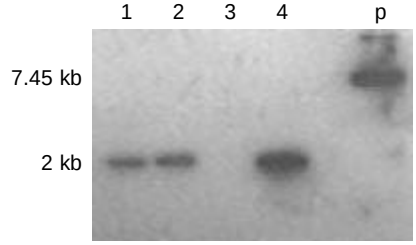

Figure 3 A part of mice was screened by Southern blot analysis. P: positive plasmid, 1,2,4: positive mice(2kb), 3: negative mice.

Stable transgenic mice of Cre-ERt

The founders were back crossed to set up F1 offsprings with other inbred C57BL/6 mice or transgenic littermates, respectively. All offsprings were screened by PCR (Figure 4), indicating that the integrated Cre-ERt gene was stably transmitted to subsequent generations (Table 1).

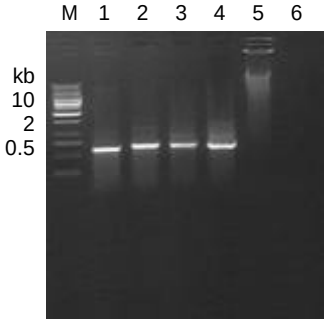

Figure 4 Electrophoresis analysis of PCR products amplified from DNA obtained from F1 mice tail tissues. Lanes 1-4 (transgenic mice) : positive bands (600 bp), lane 5: normal mouse (negative control), lane 6: blank control, M: Generuler of 1Kb DNA landar.

Table 1 Transmission rate of Alb Cre-ERt transgene to offspring

Founder line	Sex	No. of littermates	No. of offsprings	No. of transgenic mice	Ratio (%)
1	M	3	12	5	41.6
2	M	4	18	8	44.4
3	F	2	9	5	55.5

Expression of Cre-ERt gene in F1 mice

We performed RT-PCR to examine whether Cre-ERt transgene expressed only in liver tissues of F1 mice of transgenic mice lineages. The RT-PCR product (505 bp) was detected only in the liver of two of three transgenic mouse lineage (Figure 5).

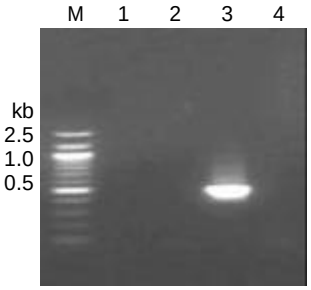

Figure 5 Electrophoresis analysis of RT-PCR products from transgenic mice. Lane 1: kidney tissue, lane 2: brain tissue, lane 3: liver (505 bp), lane 4: lung, M: Generuler of 100 bp DNA laddar.

DISCUSSION

By using transgenic mice carrying Cre recombinase under the control of a liver-specific promoter, the spatial window of gene modification can be strictly fixed to the liver. More recently, the generation and characterization of transgenic mice carrying Cre recombinase under the control of constitutive liver-specific promoters have been described[5-8]. These investigators used the constructs in which either mouse albumin regulation elements and α-fetoprotein enhancers or promoters and upstream enhancers of rat albumin gene were used to drive the Cre recombinase expression. These lines, AlfpCre, AlbCre, and Albumin-cre, allowed precise targeting of gene modifications in the liver. Nevertheless, the time of recombination remained strictly dependent on the promoter activity in these transgenic mice. In AlfpCre mice, Cre was shown to be constitutively active shortly after the appearance of the liver bud. Using the AlfpCre mice, mutagenesis of hepatic genes that serves essential functions during development could result in embryonic lethality, thus precluding analysis of their putative functions at subsequent stages. As for the temporal control of Cre expression in the liver, it was possible by using adenoviruses carrying the Cre transgene[9-11]. However, the immune response led to elimination of infected cells and could have deleterious effects on the general health status of mice[12]. An alternative approach for the temporal regulation of Cre activity is to create chimeric Cre fused to mutated ligand-binding domains of steroid hormone receptors which are insensitive to the endogenous ligands but still responsive to synthetic drugs. At present, tamoxifen-inducible Cre recombination can be achieved in many tissues of Cre-ERt transgenic adult mice and in developing mouse embryo as well as in cultured cells[13-18]. By combining the use of liver-specific promoters driving the expression of Cre and a ligand-activated Cre, gene modifications could be achieved in the liver at selected time points. Tannour-Louet *et al.*[19] established transgenic mice expressing tamoxifen-inducible Cre-mer recombinase under the control of the transthyretin promoter (TTR-Cre ind), the result showed a high recombination efficiency in the fetal and adult liver after treatment with 4-OHT. Imai *et al.*[20] established transgenic mice expressing tamoxifen-inducible Cre-ERt recombinase under control of the human 1-antitrypsin promoter, the result showed a low recombination efficiency, making it useful only to produce genetic chimeras which are not suitable for hepatic gene inactivation. In this study, the promoter and upstream enhancer of the mouse albumin gene were used to drive tamoxifen-inducible Cre-ERt recombinase expression for producing transgenic mice. After injecting the construct into oocytes, two lines expressing Cre-ERt in the liver, but not in other tested organs, were finally obtained. The results demonstrated that the promoter and upstream enhancer of the mouse albumin gene were liver-specific expression.

When the transgene results from random integration of a DNA fragment injected into a fertilized egg' s pronucleus, its level of expression in the resulting transgenic animal varied and depended upon certain factors, such as integration site, transgene cope number, genetic background of mouse, promoter/enhancer of fusion gene, etc. In this study, we only got two transgenic mice lines expressing Cre-ERt in the liver from three founder mice. The result was consistent with that of Imai *et al.*[20] in which three of 20 transgenic founder animals expressed Cre-ERt in the liver. These results indicate that not every transgenic founder mouse expresses Cre recombinase effectively, the chromosomal integration site may affect the expression pattern of transgenes.

Taken together, we have produced transgenic mice expressing Cre-ERt gene specific in the liver. This work will certainly permit a better understanding of hepatic gene functions and establish various mouse models mimicking human diseases.

ACKNOWLEDGEMENT

We thank Prof. Chambon P of Universite Louis Pasteur for providing plasmid pCMV Cre-ERt, Prof. Palmiter of University of Washington for plasmid p2335A, Prof. Orkin SH of Howard Hughes Medical Institute for Rosa26 reporter mice. This work was also supported by the Postdoctoral Foundation of China.

REFERENCES

1 **Rossant J**, McMahon A. "Cre"-ating mouse mutants- a meeting review on conditional mouse genetics. *Genes Dev* 1999; **13**: 142-145
2 **Le Y**, Sauer B. Conditional gene knockout using Cre recombinase. *Mol Biotechnol* 2001; **17**: 269-275
3 **Metzger D**, Chambon P. Site- and time-specific gene targeting in the mouse. *Mehods* 2001; **24**: 71-80
4 **Sambrook J**, Fritsch EF, Maniatis T. "Molecular Cloning: A Laboratory Manual," 2nd ed. *Cold Spring Harbor Laboratory Press, Cold Spring Harbor, New York* 1989: 9.31-9.61
5 **Hogan B**, Costantini f, Lacy E. Manipulating the mouse embryo: A laboratory manual. *Cold Spring Harbour, Cold Spring Harbor Laboratory, New York* 1980: 116-188
6 **Kellendonk C**, Opherk C, Anlag K, Schutz G, Tronche F. Hepatocyte- specific expression of Cre recombinase. *Genesis* 2000; **26**: 151-153
7 **Postic C,** Magnuson MA. DNA excision in liver by an albumin-Cre transgene occurs progressively with age. *Genesis* 2000; **26**: 149-150
8 **Yakar S**, Liu JL, Stannard B, Butler A, Accili D, Sauer B, LeRoith D. Normal growth and development in the absence of hepatic insulin- like growth factor I. *Proc Natl Acad Sci U S A* 1999; **96**: 7324-7329
9 **Wang Y**, Krushel LA, Edelman GM. Targeted DNA recombination *in vivo* using an adenovirus carrying the cre recombinase gene. *Proc Natl Acad Sci U S A* 1996; **93**: 3932-3936
10 **Rohlmann A**, Gotthardt M, Willnow TE, Hammer RE, Herz J. Sustained somatic gene inactivation by viral transfer of Cre recombinase. *Nat Biotechnol* 1996; **14**: 1562-1565

11 **Okuyama T**, Fujino M, Li XK, Funeshima N, Kosuga M, Saito I, Suzuki S, Yamada M. Efficient Fas-ligand gene expression in rodent liver after intravenous injection of a recombinant adenovirus by the use of a Cre-mediated switching system. *Gene Ther* 1998; **5**: 1047-1053
12 **Akagi K**, Sandig V, Vooijs M, Van Der Valk M, Giovannini M, Strauss M, Berns A. Cre-mediated somatic site-specific recombination in mice. *Nucleic Acids Res* 1997; **25**: 1766-1773
13 **Hayashi S**, McMahon AP. Efficient recombination in diverse tissues by a tamoxifen-inducible form of Cre: a tool for temporally regulated gene activation/inactivation in the mouse. *Dev Biol* 2002; **15**: 305-318
14 **Zheng B**, Zhang Z, Black CM, de Crombrugghe B, Denton CP. Ligand-dependent genetic recombination in fibroblasts: a potentially powerful technique for investigating gene function in fibrosis. *Am J Pathol* 2002; **160**: 1609-1611
15 **Vallier L**, Mancip J, Markossian S, Lukaszewicz A, Dehay C, Metzger D, Chambon p, Samarut J, Savatie P. An efficient system for conditional gene expression in embryonic stem cells and in their *in vitro* and *in vivo* differentiated derivatives. *Proc Natl Acad Sci U S A* 2001; **98**: 2467-2472
16 **Brocard J,** Warot X, Wendling O, Messaddeq N, Vonesch JL, Chambon P, Metzger D. Spatio-temporally controlled site-specific somatic mutagenesis in the mouse. *Proc Natl Acad Sci U S A* 1997; **94**: 14559-14563
17 **Li M**, Indra AK, Warot X, Brocard J, Messddeq N, Kato S, Metzger D, Chambon P. Skin abnormalities generated by temporally controlled RXRα mutations in mouse epidermis. *Nature* 2000; **407**: 633-636
18 **Utomo AR**, Nikitin AY, Lee WH. Temporal, spatial, and cell type-specific control of Cre-mediated DNA recombination in transgenic mice. *Nat Biotechnol* 1999; **17**: 1091-1096
19 **Tannour-Louet M**, Porteu A, Vaulont S, Kahn A, Vasseur-Cognet M. A tamoxifen-inducible chimeric Cre recombinase specifically effective in the fetal and adult mouse liver. *Hepatology* 2002; **35**: 1072-1081
20 **Imai T**, Chambon P, Metzger D. Inducible site-specific somatic mutagenesis in mouse hepatocytes. *Genesis* 2000; **26**: 147-148

Edited by Xu XQ and Wang XL

P.O.Box 2345, Beijing 100023,China
Fax: +86-10-85381893
E-mail: wjg@wjgnet.com www.wjgnet.com

World J Gastroenterol 2003;9(8):1848-1852
World Journal of Gastroenterology
 ISSN 1007-9327

• BRIEF REPORTS •

Concurrent hyperglycemia does not influence the long-term prognosis of unresectable hepatocellular carcinomas

Xiao-Ping Li, Zhen Chen, Zhi-Qiang Meng, Wen-Xia Huang, Lu-Ming Liu

Xiao-Ping Li, Zhen Chen, Zhi-Qiang Meng, Wen-Xia Huang, Lu-Ming Liu, Department of Liver Neoplasms, Cancer Hospital, Fudan University, Shanghai 200032, China
Correspondence to: Xiao-Ping Li, Department of Liver Neoplasms, Cancer Hospital, Fudan University, Shanghai 200032, China. lxpmy@sohu.com
Telephone: +86-021-64175590-1308
Received: 2003-03-04 **Accepted:** 2003-04-01

Abstract

AIM: The association has been established between the disorder of carbohydrate metabolism and liver cancer. However, little is known regarding the impact of concurrent hyperglycemia on prognosis of hepatocellular carcinoma (HCC). The present study aimed at solving this problem.

METHODS: A total of 225 patients included in this study, were admitted from January 1998 to December 2001 for an unresectable HCC proven by histological and imaging examinations. Most of the patients received interventional treatment, radiation and biotherapy. Response was evaluated by computerized tomography (CT) scan conducted 4-6 weeks following completion of the treatment, and then every 3 months. Survival was calculated from the beginning of treatment using the Kaplan-Meier method. Pretreatment, treatment and follow-up variables with possible prognostic significance were analyzed. A stepwise multivariate analysis was performed using the Cox regression model, and a prognostic index was obtained.

RESULTS: No differences were observed in survival parameters between the patients with and without hyperglycemia, median survival times of the patients were being 26±3.46 months and 29.5±2.04 months, respectively, and the 3-year survival rate was 8.36 % and 9.62 %, respectively. The univariate analysis indicated that there were several survival-associated variables including serum AFP level, clinical stage, Child-Pugh grade, method of treatment, size and number of tumor nodule (s). However, only the clinical stage, Child-Pugh grade and the treatment procedure were proved to be independent prognostic factors in the multivariate analysis.

CONCLUSION: This study indicates that hyperglycemia does not influence the long-term prognosis of HCC, and concurrent hyperglycemia should not be considered as an unfavorable prognostic factor during the treatment of patients with HCC.

Li XP, Chen Z, Meng ZQ, Huang WX, Liu LM. Concurrent hyperglycemia does not influence the long-term prognosis of unresectable hepatocellular carcinomas. *World J Gastroenterol* 2003; 9(8): 1848-1852
http://www.wjgnet.com/1007-9327/9/1848.asp

INTRODUCTION

Hepatocellular carcinoma (HCC) is the most common cancer of human liver in the world[1]. Its increasing incidence and mortality have been observed in China and some other countries. Both case-control and cohort studies have associated chronic viral hepatitis with its development[2,3]. The majority (60-80 %) of HCCs are found in livers with cirrhosis, frequently in a macronodular type in Southeast Asia and causally linked with chronic infection of hepatitis B virus (HBV) or hepatitis C virus (HCV)[3].

A large body of evidences have demonstrated that chronic liver diseases are associated with an increased incidence of glucose intolerance and diabetes[4-7]. The glucose intolerance is one of the most frequent complications in patients with HCC. Hypoglycemia is often considered as a paraneoplastic syndrome of HCC. The incidence of hyperglycemia or diabetes, however, is also increasing[8-10], accounting for 5-15 % of cases with HCC. Hyperglycemia and HCC may be found simultaneously. In some patients, HCC occurs following hyperglycemia[11]. In fact, diabetes mellitus (DM) has been considered as a risk factor for HCC development in addition to other well known factors[11-13]. In clinical views, hyperglycemia may need specific pharmacological treatment, dietary restrictions, or both procedures. It appears logical to regard hyperglycemia as an unfavorable factor during the prognosis evaluation of HCC, but this remains unsettled. A Japanese group has described the long-term impact of diabetes mellitus on the prognosis of HCC after resection[14]. Much more HCCs, however, are found at advanced stages in this country, and hence cannot be resected. For this reason, we conducted the study to evaluate the possible impact of concurrent hyperglycemia on the peri-treatment outcome and long-term survival in a large series of consecutive patients with unresectable HCCs.

MATERIALS AND METHODS

The survey involved 230 HCC patients consecutively admitted from January 1998 to December 2001. In 2002, all the clinical records of these patients were retrospectively examined, and the following clinical and laboratory indices were collected, including the values of AST, ALT, alkaline phosphatase (AP), γ-glutamyl-transpeptidase (γ-GT), prothrombin time (PT), serum bilirubin, serum proteins, albumin, γ-globulins, platelet number and glucose control. Of these, 225 cases with a complete clinical record were included. They were comprised of 180 males and 45 females, and their ages ranged from 32 to 76 years (mean ±SD, 53.19±12 years). A diagnosis of HCC was made by the ultrasound-guided transcutaneously fine-needle aspiration and subsequently by cytological examinations in 184 cases, and for the other cases the diagnosis was made by a combined consideration of the history, physical examinations, α-fetoprotein (AFP) levels and noninvasive imaging procedures. Indications for HBV and HCV infection were found in 125 and 15 patients, respectively.

Of the 225 patients examined, 28 had hyperglycemia, as determined with the concentration of plasma glucose exceeding 6.8 mmol/L in at least 2 fasting samples for each case or with the active treatment with insulin or oral hypoglycemic drugs necessary to control blood glucose levels. No consideration was given to those who had slight alternations in glucose

metabolism, such as impaired glucose tolerance demonstrated through an oral glucose tolerance test according to the criteria of World Health Organization[15,16], and those who had no evidence of glycosuria, because the test was performed in about 20 % of cases. Of the 28 hyperglycemic patients, 8 had overt diabetes mellitus when admitted to our department, and 20 had hyperglycemia identified after the diagnosis of HCC. The clinical and laboratory data are listed in Table 1.

As treatment for HCC, 146 patients received transcatheter arterial chemoembolization (TACE), 20 received radiotherapy only, 30 were treated by TACE and local radiotherapy, 14 by percutaneous ethanol injection therapy (PEIT), 162 received biotherapy.

TACE was performed with infusion of Fluorouracil or 5-FUDR (1.0 g), cisplatin (40-60 mg), followed by chemoembolization with a mixture of iodized oil and doxorubicin (40-60 mg) or mitomycin (10-20 mg), or with gelatin-sponge particles for the embolization. Radiotherapy was performed using a Co^{60} or 18-MV linear accelerator[17]. CT scan was performed to determine the radiation fields, and then whole or partial liver irradiation was conducted using the moving-strip technique or local radiotherapy covering tumors with generous margins (2-3 cm). The irradiation dose was 40-50 Gy daily in 1.8 fractions. During the treatment, the patients were monitored weekly with a complete blood count and liver function tests. For the concurrent hyperglycemia, one patient used dietary therapy, 13 received insulin therapy, and 6 took hypoglycemic drugs.

Effects of the treatments were evaluated based on serial CT scans 4-6 weeks following completion of the therapies and then every one to three months. The complete disappearance of the tumor was regarded as complete remission (CR), a decrease of over 50 % in tumor size as partial remission (PR), a decrease of less than 50 % or no change as stable disease (SD), and progression as progressive disease (PD). The response rate was calculated for CR or PR, and the SD cases were considered as non-responsive. Survival was estimated from the starting date of treatment according to the Kaplan-Meier method.

After the procedures as described above, the outcome of patients was investigated by visiting their families. Follow-up was carried out for all the subjects regularly for more than 6 months, with a median follow-up period of 25 months. The follow-up program included measurement of serum AFP and ultrasonography or CT scan every 3 months. The patients with recurrence were managed with various therapeutic methods including TACE, PEIT and/or biotherapy.

Statistical analysis

The data collected were presented as mean ± standard deviation. Continuous laboratory values were clustered to obtain two samples of approximately equal size. Statistical comparison between groups was performed using the χ^2 test with the Yates' correction for nominal data, and the Student's *t* test for numerical data.Kaplan -Meier survival plots were built to evaluate the prognostic values of individual indices, and compared using the log rank test. The same method was used for univariate analysis of survival. The univariate analysis was also carried out with age, sex, etiology and liver function parameters measured at the beginning of observation to establish their predictive value for survival. Baseline variables included in the univariate analysis were also analyzed by multivariate analysis using the step-wise forward Cox regression model to assess their predictive value with respect to survival. To check proportionality of risk factors with time, we plotted the log of cumulative hazards against time, demonstrating parallel behaviors in the two groups of patients separately with low- and high-risk values of selected prognostic covariates. All statistical analyses were computerized using the softpackage SPSS 10.0 (SPSS Inc., Chicago, Illinois). $P<0.05$ was considered statistically significant.

RESULTS

Hyperglycemia was found in 28 of the 225 patients when they were admitted. No difference in other clinical or laboratory indices was present between the groups with and without detectable hyperglycemia at the time (Table 1). Hyperglycemia was treated by insulin alone in 13, by oral hypoglycemic agents in 9, by diet therapy in 2, and by a combination of insulin and oral hypoglycemic agents in 4 patients. Table 1 shows a comparison of the clinicopathological data between hyperglycemic and non-hyperglycemic patients under the treatment for HCC.

The mean age of hyperglycemic patients was higher than that of non-hyperglycemic patients, but the difference was not significant. The two groups were comparable regarding their pathological factors such as size of the largest tumor nodules, number of tumor nodules, clinical stage and Child-Pugh grade. No significant difference was found between these two groups in other laboratory data such as total bilirubin, platelet count, prothrombin time and initial treatment.

Table 1 Clinicopathological data of hyperglycemic and non-hyperglycemic patients with HCC

Variables	With hyperglycemia (*n*=28)	Wthout hyperglycemia (*n*=197)
Age (year)	55±1.99	51.91±1.08
HBsAg(+/-)	15/13	110/87
Cirrhosis (+/-)	20/8	133/64
Gender (male/female)	23/5	157/40
Laboratory data		
ALT (U/L)	48.91±10.41	39.82±11.21
PT (s)	12.24±0.20	12.67±0.23
Albumin (g/L)	39.63±6.35	35.81±7.86
Total bilirubin (μmmol/L)	12.32±7.15	13.54±8.97
Platelet count ($\times10^9$/L)	158.41±18.14	155.75±7.37
TNM stage (I/II/III/IVa/IVb)[a]	0/3/12/5/8	0/32/76/48/41
Child-Pugh grades (A/B/C)	22/5/1	165/30/2
Sizes of the largest tumor (cm)	3.80±6.30	3.50±6.75
Initial treatment (TACE/radiotherapy/TACE+radiotherapy/PEI/biotherapy)	18/3/5/3/15	128/17/15/11/147

[a]The criteria for TNM classification were based on the criteria of UICC(1987).

During the follow up, 73 patients, 10 with and 63 without hyperglycemia, died of the hyperglycemic complications or from liver-related causes. Intrahepatic spreading was observed in 10 of them, and extrahepatic metastases occurred in 12 of the patients. Among them, 4 were complicated with lung metastases, 2 with bone metastases, 5 with para-aortic lymph node metastases, 1 with lung and bone metastases, 1 with lung and brain metastases and 1 with bone and para-aortic lymph node metastases. All of these patients received treatments according to their liver function status.

Response rates were calculated for the groups with and without hyperglycemia, which were 21.4 % and 20 %, respectively. The difference was not significant ($P>0.05$; Table 2).

Table 2 Comparison of treatment responses between the groups with (HG) and without hyperglycemia (Non-HG)

Groups	Response rate	CR (%)	PR(%)	NC(%)	PD(%)
HG	21.4(6/28)	7.1(2/28)	14.3(4/28)	53.6(15/28)	25.0(7/28)
Non-HG	23.4(46/197)	8.1(16/197)	15.2(30/197)	48.2(95/197)	28.4(56/197)
P values	0.821	0.858	0.896	0.596	0.706

The one-, two- and three-year survival rate was 51 %, 31 % and 8 % respectively for the hyperglycemia group, and was 60 %, 30 % and 10 %, respectively for the group without detectable hyperglycemia. Median survival times of these two groups were 26.0±3.5 months and 29.5±2.0 months, respectively. Figure 1 shows the overall cumulative survival after treatment.

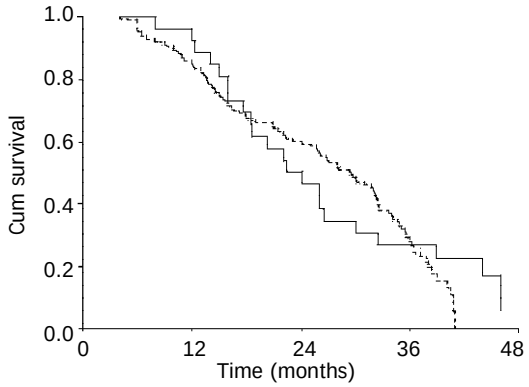

Figure 1 Kaplan-Meier survival curves for HCC patients with (green) and without hyperglycemia (red).

The incidence of complications included in this survey is shown in Table 3. The post-embolization syndrome consisted of abdominal pain, fever apparently unrelated to the tumor, and, slight or severe nausea, was seen in almost all the patients. Narcotics, anti-emetics and acetaminophen were given to relieve the symptoms. The main complications of TACE and radiotherapy included hepatic insufficiency or infarction, tumor rupture, upper gastrointestinal tract (GI) bleeding. Slight increase in serum bilirubin (n=20), elevation of serum transaminase (n=45), ascites (n=14), leukopenia (n=46) and thrombocytopaenia (n=15) were also seen during the therapies. These side effects were transient or easily controlled with medications in most cases. Two patients died of acute hepatic failure immediately after TACE, five died of hepatic encephalopathy and 2 died of severe GI bleeding. Thirty patients without hyperglycemia showed TACE- or radiotherapy-related complications, while ten with hyperglycemia showed complications after treatment and the symptoms were more severe. There was a significant difference between these two groups in the occurrence of complications.

Table 3 Incidence of complications during follow-up

Complication	With hyperglycemia		Without hyperglycemia		*P* value
	I-II	III-IV	I-II	III-IV	
Leucopoenia	6	8	22	10	0.000
Erythrocytopenia	5	1	16	2	0.049
Thrombocytopenia	2	1	10	2	0.359
Reaction of GI system	3	0	12	0	0.359
Impairment of liver function	5	1	13	0	0.008
Impairment of renal function	1	0	2	0	0.270

The univariate analysis showed that AFP level, clinical stage, Child-Pugh grade, treatment procedure, size of tumor and number of tumor nodules were independent factors predicting survival for all patients, but hyperglycemia was not. The effects of possible prognostic factors are shown in Table 4.

The Cox proportional hazards model showed that clinical stage, Child-Pugh grade and treatment procedure employed were independent factors predicting survival (Table 5). The 3-year survival rate was 1 % for Stage T4 cases and 15 % for others. The patients with T4 disease had a significantly shorter survival (P=0.0049). When the survival rates were compared according to Child-Pugh grade, patients of grade A survived significantly longer than those of grade B or C. The 3-year survival rate was 11.1 % and 0 %, respectively. The treatment procedure employed also had similar impacts on the survival. The 3-year survival rate for patients treated with TACE alone, radiotherapy alone and radiotherapy combined with TACE was 8 %, 4 % and 25 %, respectively (P=0.0042).

Table 4 Association between various clinical parameters after treatment and the survival

Clinical status		*n*	Cumulative survival rate (%)			Median survival (± SE, months)	*P* value
			1-year	2-year	3-year		
Overall		225	58.5	30.6	9.4	28.0±1.40	
Age (year)	<60	130	59.4	27.4	9.1	28.1±2.37	
	⩾60	95	57.3	35.4	9.7	26.8±2.60	0.815
HBV	Negative	100	61.8	31.2	9.69	29.3±2.01	
	Positive	125	54.4	29.9	8.97	26.1±3.63	0.876
AFP	<400	129	66.1	34.4	10.9	30.0±2.38	
(ng/ml)	⩾400	96	47.8	25.4	6.9	22.2±4.05	0.001
Hyperglycemia	Negative	28	51.1	30.7	8.36	26.0±3.46	
	Positive	197	59.7	30.5	9.62	29.5±2.04	0.231
Tumor	<6 cm	124	67.4	38.1	12.1	31.7±1.99	
size (cm)	⩾6 cm	101	47.0	19.9	5.42	21.0±3.55	0.028
Number of	Solitary	152	67.6	34.7	10.4	29.3±1.40	
tumors	Multiple	73	52.0	21.3	7.1	25.8±4.73	0.041
Child pugh	A	187	65.1	34.7	11.1	31.0±1.65	
	B or C	38	28.4	9.5	0	12.1±2.49	0.002
Clinical	Non-T4 disease	121	69.5	39.3	15.3	32.1±1.13	
stage	T4 disease	104	44.6	18.6	1.43	20.9±2.17	0.018
Method of	TACE	181	56.4	27.1	8.48	26.8±1.43	
treatment	Radiotherapy	23	58.3	29.2	4.17	32.6±9.85	
	TACE+ radiotherapy	21	77.8	63.0	25.2	37.8±6.62	0.0001

Table 5 Significant factors predicting survival tested by the Cox proportional hazards model

Variable	Coefficient	SE	Coefficient/ SE	*P* value
Clinical stage	0.8014	0.2695	2.9737	0.0019
Child-Pugh grade	0.3275	0.0657	4.9574	0.0001
Method of treatment	1.2144	0.3672	3.3072	0.0005

DISCUSSION

It is not surprising that many interactions exist between the liver and endocrine system demonstrated by some clinical and laboratory parameters. Liver diseases can result in endocrine disorders, and some endocrine disorders may affect the liver[18]. The role of the liver in glucose homeostasis is important. The regulation of hepatic glucose uptake involves a complex interaction of neural and hormonal mechanisms. HCC is often complicated with cirrhosis, and carbohydrate intolerance is seen in approximately 50 % of patients with

cirrhosis. The carbohydrate intolerance is most likely due to profound biochemical and physiologic derangements concurrent with advanced liver diseases, including portal-systemic shunting of glucose, elevated glucagon or growth hormone level, peripheral and/or hepatic resistance to insulin, malnutrition, elevated level of free fatty acids and hypokinemia[19,20]. Therefore, hyperglycemia or diabetes mellitus is often seen in HCC patients. Relatively mild hypoglycemia occurs in rapidly growing HCC among Chinese patients as a part of an end-stage illness[18], but their definite association remains lack of unequivocal evidences.

Accumulated data have associated diabetes with an increased risk for primary liver cancer[21-25]. One possible mechanism might be the proposed growth-stimulating and/or apoptosis-suppressing effects of insulin. This is particularly true for the tissues harboring preneoplastic or neoplastic lesions[26]. We observed that 68 % (153/225) of HCCs occurred in the liver with cirrhosis, and 8 of the patients had known diabetes mellitus before the diagnosis of HCC. Based on our observations, however, it is not clear whether cirrhosis and HCC were the causes or consequence of hyperglycemia and diabetes mellitus, or these two groups of disorders were merely clinically concurrent rather than causally linked.

To date, the knowledge is limited about the treatment of HCC complicated with hyperglycemia. Diabetes mellitus is regarded as an unfavorable factor in determining surgical resection for HCC patients[27-29]. Hepatic operation and anesthesia may have profound metabolic effects, potentially exacerbating the preexisting diabetes by insulin deficiency, its reduced secretion or insensitivity. This may diminish phagocyte functions, and thus impairs the resistance to infection and delays wound healing. Diabetes may also result in some cardiovascular diseases, neuropathy and nephropathy. All these factors will increase the morbidity and mortality of surgical procedures. Diabetes mellitus has been reported to be the only independent risk factor for liver failure after major hepatic resection of HCC patients with a low remnant liver volume. Ikeda *et al*[14] reported 342 hepatectomies for HCCs, the 10-year survival rate was 12.6 % and 24.6 % for diabetic and non-diabetic patients, respectively. Thus, diabetes mellitus complicated with hepatocellular carcinoma was proposed to be a high-risk condition for the higher morbidity and a shorter survival after operation. However, this notion was not approved by several recent observations carried out in Hong Kong[29], Japan[30,31] and Taiwan[27].

The impact of diabetes mellitus on the function of the liver with end-stage diseases remains obscure. Toyoda *et al*. pointed out that the presence of diabetes mellitus didn' t necessarily correlate with the severity of cirrhosis. In the present study, most of the cases of hyperglycemia did not show any symptom of diabetes, and might be simply regarded as carbohydrate intolerance, a subclinical stage to overt diabetes mellitus. Therefore, the influence of hyperglycemia on liver functions is not obvious, as indicated by the data we presented here. On the other hand, non-surgical treatments, as employed in this study, may help to reserve hepatic intracellular energy during the treatment and achieve a better peri-operational outcome, compared to those more stressful surgical procedures. Our data also showed that concurrent hyperglycemia did not significantly influence the overall survival of HCC patients after non-surgical treatment. Certainly, patients with hyperglycemia and HCC are a heterogeneous group, which is partly linked to a genetic alteration, and patients with the so-called hepatogenous hyperglycemia, are mainly associated with the acquired insulin resistance. These two conditions may have different metabolic abnormalities and possible different outcomes.

Our study was partly retrospective, and only a small number of patients underwent an oral glucose tolerance test during hospitalization, so we could not say some patients with hyperglycemia were diabetes. The prevalence of hyperglycemia in this series was higher than that reported in several previous studies. On the other hand, fasting glucose and detailed data about the treatments were available for most cases. In this survey, it was difficult to clearly identify these subgroups. Approximately 50 % of the patients had hyperglycemia before the diagnosis of HCC, whereas patients with hyperglycemia superimposed on cirrhosis were more likely to have hepatogenous hyperglycemia. Gentilini *et al*.[32] held that distinction as to either cirhhosis or diabetes occurring first did not substantially help classify patients. Carefully prospective studies are needed to answer this question.

Tumor stage was confirmed as an independent prognostic factor in our series. Patients who had non-T4 diseases survived significantly longer than those with T4 diseases. This is in agreement with a previous study[33], so we need to detect and treat liver cancer earlier[34,35]. Recently, many articles reported that combined TACE and radiotherapy might significantly increase survival rate[17,33,36].Cheng *et al*.[33]reported that the 2-year survival rate was 13 % and 55 % for patients treated with radiotherapy alone and with combined TACE and radiotherapy (P=0.0003), respectively. Our studies also confirmed this. We are currently using three dimensional conformal radiotherapy (3-DCRT) and applying the dose-volume model for every patient. With the advances in treatment planning, local radiotherapy can be more safely delivered and further studies are required to elucidate the efficacy of these regiments.

In summary, our data suggest that hyperglycemia does not significantly influence the long-term prognosis of patients who receive the proper non-surgical treatment. The T4 disease is associated with an unfavorable pognosis. Patients with Child-Pugh grade B or C have a higher risk. Further studies are needed to evaluate the impact of hyperglycemia on patients with HCC.

REFERENCES

1 **Chan AO**, Yuen MF, Hui CK, Tso WK, Lai CL. A prospective study regarding the complications of transcatheter intraarterial lipiodol chemoembolization in patients with hepatocellular carcinoma. *Cancer* 2002; **94**: 1747-1752

2 **Takano S**, Yokosuka O, Imazaki F, Tagawa M, Omata M. Incidence of hepatocellular carcinoma in chronic hepatitis B and C: A prospective study of 251 patients. *Hepatology* 1995; **21**: 650-655

3 **Hadziyannis S**, Tabor E, Kaklamani E, Tzonou A, Stuver S, Tassopoulos N, Mueller N, Trichopoulos D. A case-control study of hepatitis B and C virus infections in the etiology of hepatocellular carcinoma. *Int J Cancer* 1995; **60**: 627-631

4 **Kingston ME**, Ali MA, Atiyeh M, Donnelly RJ. Diabetes mellitus in chronic active hepatitis and cirrhosis. *Gastroenterology* 1984; **87**: 688-694

5 **Hadziyannis S**, Karamanos B. Diabetes mellitus and chronic hepatitis C virus infection. *Hepatology* 1999; **29**: 604-605

6 **Caronia S**, Taylor K, Pagliaro L, Carr C, Palazzo U, Petrik J, O'Rahilly S, Shore S, Tom BD, Alexander GJ. Further evidence for an association between non-insulin-dependent diabetes mellitus and chronic hepatitis C virus infection. *Hepatology* 1999; **30**: 1059-1063

7 **Petit JM**, Bour JB, Galland-Jos C, Minello A, Verges B, Guiguet M, Brun JM, Hillon P. Risk factors for diabetes mellitus and early insulin resistance in chronic hepatitis C. *J Hepatology* 2001; **35**: 279-283

8 **Nelson R**, Persky V, Davis F, Becker E. Excess risk of primary liver cancer in patients with diabetes mellitus. *J Natl Cancer Inst* 1997; **89**: 327-328

9 **Czyzyk A**, Szczepanik Z. Diabetes mellitus and cancer. *Eur J Intern Med* 2000; **11**: 245-252

10 **Petrides AS**, Vogt C, Schulze-Berge D, Matthews D, Strohmeyer G. Pathogenesis of glucose intolerance and diabetes mellitus in cirrhosis. *Hepatology* 1994; **19**: 616-627

11 **Fujino Y**, Mizoue T, Tokui N, Yoshimura T. Prospective study of

diabetes mellitus and liver cancer in Japan. *Diabetes Metab Res Rev* 2001; **17**: 374-379

12 **La Vecchia C**, Negri E, Franceschi S, D'Avanzo B, Boyle P. A case-control study of diabetes mellitus and cancer risk. *Br J Cancer* 1994; **70**: 950-953

13 **El-Serag HB**, Richardson PA, Everhart JE. The role of diabetes in hepatocellular carcinoma: a case-control study among United States Veterans. *Am J Gastroenterol* 2001; **96**: 2462-2467

14 **Ikeda Y**, Shimada M, Hasegawa H, Gion T, Kajiyama K, Shirabe K, Yanaga K, Takenaka K, Sugimachi K. Prognosis of hepatocellular carcinoma with diabetes mellitus after hepatic resection. *Hepatology* 1998; **27**: 1567-1571

15 **American Diabetes Association**. Report of the expert committee on the diagnosis and classification of diabetes mellitus. *Diabetes Care* 2003; **26**: S5-20

16 **Fajans SS**. Classification and diagnosis of diabetes. In: *Ellenberg and Rifkin's diabetes mellitus*. 5th .New York: *McGraw-Hill* 2000:369

17 **Guo WJ**, Yu EX. Evaluation of combined therapy with chemoembolization and irradiation for large hepatocellular carcinoma. *Br J Radiol* 2000; **73**: 1091-1097

18 **Marks JB**, Skyler JS. The liver and the endocrine system. In: *Schiff's diseaseas of the liver*. Vol 1. 8th. Philadelphia: *Lippincott-Raven* 1998: 479-481

19 **Holstein A**, Hinze S, Thiessen E, Plaschke A, Egberts EH. Clinical implications of hepatogenous diabetes in liver cirrhosis. *J Gastroenterol Hepatol* 2002; **17**: 677-681

20 **Yeh CN**, Chen MF, Lee WC, Jeng LB. Prognostic factors of hepatic resection for hepatocellular carcinoma with cirrhosis: univariate and multivariate analysis. *J Surg Oncol* 2001; **81**: 195-202

21 **Deans C**, Leslie P. Hepatocellular carcinoma. *Lancet* 1999; **354**: 253-254

22 **LaVecchia C**, Negri E, Decarli A, Franceschi S. Diabetes mellitus and the risk of primary liver cancer. *Int J Cancer* 1997; **73**: 204-207

23 **Braga C**, LaVecchia C, Negri E, Franceschi S. Attributable risks for hepatocellular carcinoma in northern Italy. *Eur J Cancer* 1997; **33**: 629-634

24 **Adami HO**, Chow WH, Nyren O, Berne C, Linet MS, Ekbom A, Wolk A, McLaughlin JK, Fraumeni JF Jr. Excess risk of primary liver cancer in patients with diabetes mellitus. *J Natl Cancer Inst* 1996; **88**: 1472-1477

25 **Wideroff L**, Gridley G, Mellemkjaer L, Chow WH, Linet M, Keehn S, Borch-Johnsen K, Olsen JH. Cancer incidence in a population-based cohort of patients hospitalized with diabetes mellitus in Denmark. *J Natl Cancer Inst* 1997; **89**: 1360-1365

26 **Yu MC**, Tong MJ, Govindarajan S, Henderson BE. Nonviral risk factors for hepatocellular carcinoma in a low-risk population, the non-Asians of Los Angeles County, California. *J Natl Cancer Inst* 1991; **83**: 1820-1826

27 **Chen MF**, Jeng LB, Lee WC. Surgical results in patients with hepatitis virus-related hepatocellular carcinoma in Taiwan. *World J Surg* 2002; **26**: 742-747

28 **Shimada M**, Takenaka K, Fujiwara Y, Gion T, Shirabe K, Yanaga K, Sugimachi K. Risk factors linked to postoperative morbidity in patients with hepatocellular carcinoma. *Br J Surg* 1998; **85**:195-198

29 **Poon RT**, Fan ST, Wong J. Does diabetes mellitus influence the perioperative outcome or long term prognosis after resection of hepatocellular carcinoma? *Am J Gastroenterol* 2002; **97**: 1480-1488

30 **Toyoda H**, Kumada T, Nakano S, Takeda I, Sugiyama K, Kiriyama S, Tanikawa M, Sone Y, Hisanaga Y. Impact of diabetes mellitus on the prognosis of patients with hepatocellular carcinoma. *Cancer* 2001; **91**: 957-963

31 **Nagasue N**, Yamanoi A, El-Assal ON, Ohmori H, Tachibana M, Kimoto T, Kohno H. Major compared with limited hepatic resection for hepatocellular carcinoma without underlying cirrhosis: A retrospective analysis. *Eur J Surg* 1999; **165**: 638-646

32 **Gentilini P**, Laffi G, La Villa G, Romanelli RG, Buzzelli G, Casini-Raggi V, Melani L, Mazzanti R, Riccardi D, Pinzani M, Zignego AL. Long course and prognostic factors of virus-induced cirrhosis of the liver. *Am J Gastroenterol* 1997; **92**: 66-72

33 **Cheng JC**, Chuang VP, Cheng SH, Huang AT, Lin YM, Cheng TI, Yang PS, You DL, Jian JJ, Tsai SY, Sung JL, Horng CF. Local radiotherapy with or without transcatheter arterial chemoembolization for patients with unresectable hepatocellular carcinoma. *Int J Radiat Oncol Biol Phys* 2000; **47**: 435-442

34 **Li L**, Wu PH, Mo YX, Lin HG, Zheng L, Li JQ, Lu LX, Ruan CM, Chen L. CT arterial portography and CT hepatic artetiography in detection of micro liver cancer. *World J Gastroenterol* 1999; **5**: 225-227

35 **Sithnamsuwan P**, Piratvisuth T, Tanomkiat W, Apakupakui N, Tongyoo S. Review of 336 patients with hepatocellular carcinoma at Songkianagarind hospital. *World J Gastroenterol* 2000; **6**: 339-343

36 **Chia-Hsien Cheng J**, Chuang VP, Cheng SH, Lin YM, Cheng TI, Yang PS, Jian JJ, You DL, Horng CF, Huang AT. Unresectable hepatocellular carcinoma treated with radiotherapy and/or chemoembolization. *Int J Cancer* 2001; **96**: 243-252

Edited by Su Q and Wang XL

P.O.Box 2345, Beijing 100023,China
Fax: +86-10-85381893
E-mail: wjg@wjgnet.com www.wjgnet.com

World J Gastroenterol 2003;9(8):1853-1855
World Journal of Gastroenterology
 ISSN 1007-9327

• BRIEF REPORTS •

Expression of class I MHC molecule, HSP70 and TAP in human hepatocellular carcinoma

Xiao-Ling Deng, Wei Chen, Mei-Ying Cai, Da-Peng Wei

Xiao-Ling Deng, Wei Chen, Mei-Ying Cai, Da-Peng Wei, Immunology Department, West China Medical Center of Sichuan University, Chengdu 610044, Sichuan Province, China
Supported by the National Natural Science Foundation of China, No. 30070855
Correspondence to: Da-Peng Wei, Immunology Department, West China Medical Center of Sichuan University, Chengdu 610044, Sichuan Province, China. dengxiaoling@163.com
Telephone: +86-28-85501259
Received: 2002-12-22 **Accepted:** 2003-01-18

Abstract

AIM: To demonstrate whether class I MHC molecule, transporter associated with antigen processing (TAP), and heat-shock proteion70 (HSP70) expressed in liver cancer cells before the design and construction of CTL vaccine against hepatocellular carcinoma (HCC).

METHODS: We studied 30 HCC specimens by labeled streptavidin biotin (LSAB) method of immunohistochemistry.

RESULTS: The results showed that the majority of HCC cells investigated naturally expressed class I MHC and TAP, which were different from other tumor cells. Furthermore, we found that HSP70 expressed not only in cellular cytoplasm, but also on the cell surface in HCC.

CONCLUSION: Our findings indicate that our understanding about immune escape mechanisms employed by HCC cells may be further improved. It is important to design and construct CTL vaccine against HCC.

Deng XL, Chen W, Cai MY, Wei DP. Expression of class I MHC molecule, HSP70 and TAP in human hepatocellular carcinoma. *World J Gastroenterol* 2003; 9(8): 1853-1855
http://www.wjgnet.com/1007-9327/9/1853.asp

INTRODUCTION

It is commonly accepted that tumor rejection is mediated by lymphocytes, and most notably, by cytotoxic T lymphocytes (CTL). The recognization of a tumor cell by CTL is regulated by interactions between T-cell receptor and antigenic peptide -MHC complex. TAP, HSP70 and class I MHC molecule are important components in endogenous processing of peptides through the MHC class I pathway. Among many proteins that contribute to MHC class I assembly, TAP complex is one of the most important components. It translocates endogenously processed peptides from cytosol into ER for binding to class I MHC, resulting in surface presentation of these complexes to CTL. Most of the studies described the defect of endogenous processing function in tumors such as melanomas, cervical carcinomas, and renal cell carcinomas[1-3]. These findings suggest that TAP down-regulation might represent an important mechanism for immune escape of malignant cells in tumors. Another importantly associated presentation protein is heat-shock proteion70 (HSP70). HSP70 has long been known to be located in the cytoplasm, where it performs chaperoning function. Recent studies have also indicated that conditional over-expression of HSP70 in target cells enhances the susceptibility to CTL[4]. Moreover, HSP70 may enhance TAP function[5]. Therefore, there is an increasing realization that expression of these molecules on tumor cell surface may potentially affect CTL-mediated recognition.

HCC is one of the most malignant cancers. However, to date most of the studies that described expressions of class I MHC, TAP, and HSP70 were carried out with cell lines[6]. Limited information is available about these molecules in HCC tumor tissues. Nevertheless, it is important to demonstrate whether these molecules can also be expressed in HCC *in vivo* before the design and construction of CTL vaccine against HCC.

MATERIALS AND METHODS

Human tissues

Thirty pathological samples were obtained from surgically resected tissues of HCC patients in West China Medical Center of Sichuan University. The specimens were frozen immediately in liquid nitrogen. Cryostat sections (4 μm) were prepared and stored at -70 ℃. Pathological diagnoses were made based on routinely processed HE sections.

Main reagents

Mouse anti-human HLA-ABC (DAKO Corp., working dilutions 1:100), rabbit anti-human TAP (Chemicon International, Inc., working dilutions 1:1 000), mouse anti-human HSP70 (DAKO Corp., working dilutions 1:50), biotin labeled goat anti-mouse IgG and goat anti-rabbit IgG, HRP-labeled streptavidin and avidin biotin blocking system were all purchased from Beijing Zhongshan Corp.

Immunohistochemistry

The frozen sections were fixed in cold acetone for 10 min. 3 % H_2O_2 containing methanol was added to block endogenous peroxidase. Fixed sections were incubated with normal goat serum for blocking and subsequently with mAb (HLA-ABC, TAP and HSP70 respectively) or PBS as control at 37 ℃ for 2 h, then washed with PBS. After incubation with biotin labeled goat anti-mouse IgG or goat anti-rabbit IgG for 30 min at 37 ℃, and washed as before, HRP-labeled streptavidin was added. The following incubation and washing were exactly the same as above. Finally, freshly prepared substrate DAB was added for color development. The reaction was stopped with tap water rinse and then counterstained with hematoxylin and mounted for examination.

RESULTS

Expression of class I MHC molecule

Strongly positive staining of class I MHC molecule was presented in all cases of HCC. The staining was mainly located

on the membrane of the liver cancer cells, in the cytoplasm, and the perinuclear area. The staining showed granular pattern (Figure 1).

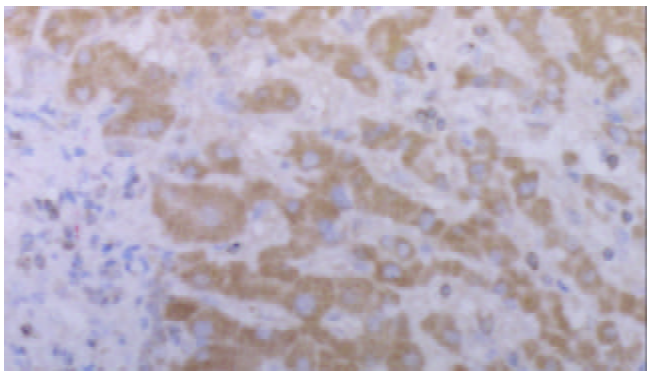

Figure 1 Displayed class I MHC molecule in hepatocellular carcinoma (×180).

The positive staining was mainly located on the membrane of the liver cancer cells. Some of the cells showed positive staining in the cytoplasm and the perinuclear area.

HSP70 expression

Tumor cells as well as adjacent non-neoplastic hepatocytes displayed intense and extensive positive staining. The staining was uniform throughout the specimen. The cytoplasmic staining showed granular pattern. The membranous staining displayed linear pattern, which made the interface between cells very clear (Figure 2).

Staining was typically uniform throughout the specimen. The cytoplasmic staining showed granular pattern. The membranous staining displayed linear pattern, which made the border between cells very clear.

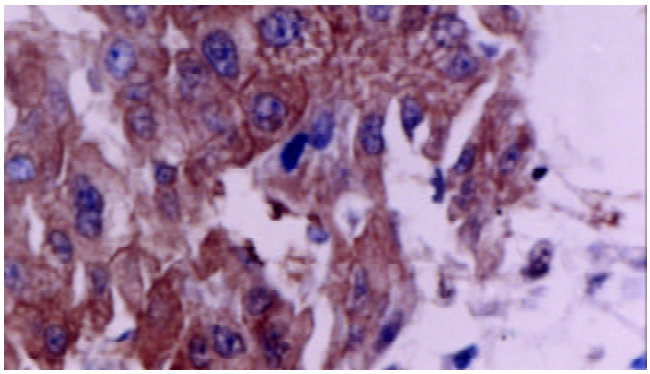

Figure 2 Hepatocellular carcinoma stained for HSP70 (×350).

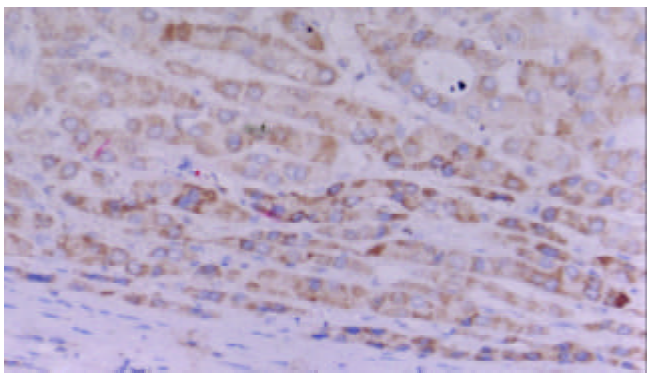

Figure 3 Hepatocellular carcinoma stained for TAP (×100).

TAP expression

Positive staining for TAP was present in 29 of 30 cases. The staining was located in the cytoplasm and the perinuclear area. It showed granular intracytoplasmic pattern accompanied by variable staining intensity. Faint or negative staining was observed within sinusoids (Figure 3).

It showed granular intracytoplasmic pattern accompanied by variable staining intensity. Hepatocytes beside the sinusoid were more intensely stained than cells in the central tissues.

DISCUSSION

In this study we examined the expressions of class I MHC, TAP, and HSP70 in 30 HCC samples by immunohistochemical methods. The results showed that the majority of HCC investigated naturally expressed TAP, which was different from other tumors. This is consistent with the results of several other groups. Kurokohchi *et al*[6] examined TAP mRNA and HLA antigen in seven HCC cell lines. They found that only one HCC cell line (HuH-7) had low expression of HLA-B and C and TAP mRNA. All the other lines expressed high levels of both TAP mRNA and HLA. They speculated posttranscriptional events or failure to transport and load peptides for MHC might allow HCC cells to escape from CTL. Whereas our results suggested HCC cells with the expression of TAP might be more susceptible to host immunity. Recently, Alimonti *et al*[7] reported that TAP expression provided a general method for improving the recognition of malignant cells. They transfected TAP gene into the TAP^- cell line and introduced it into tumor-burdened individuals. The result showed that TAP could improve tumor cell immunogenicity and host survival. This would be of a potential significance for the tumors with deficiency in components of antigen-processing molecules. However, Seliger *et al*[8,9] identified the structural alterations of TAP in the MHC class I antigen-processing pathway in melanoma after analyzing the sequence of TAP. The possibility of structural transformation of TAP in HCC cells could not be excluded and needs to be further studied.

As our understanding of the molecular aspects of the class I processing pathway has been improved, there is an increasing realization that expression of class I MHC antigen on cell surface is crucial for recognition by CTL. It is well established that many tumors escape T cell recognition by loss or down regulation of class I molecule expression on the surface of tumor cells. Previous reports described a correlation between HLA loss and TAP gene defects in some tumors[10]. So we also analyzed the expression of class I MHC on the surface of hepatocytes in HCC. Our investigation showed that most liver cancer cells in HCC tissues had strong class I MHC antigen expression. This is consistent with the results of several other groups[6,11]. The possible mechanism for the appearance of class I MHC antigen on hepatocytes remains controversial. One of the possibilities is that the expression of class I MHC antigen on HCC cells is related with viral infection. Sung *et al*[12] found that HCC patients were infected by HBV. Zhou *et al*[13] suggested cytokines such as γ-interferon released by T lymphocytes infiltrated in HCC tissues might be contributed to the expression of class I MHC molecules. The other possibility is that malignant transformation in HCC is characterized by expression of class I MHC molecules[11]. Although the underlying molecular mechanism is not well understood, the expression of class I MHC antigen on HCC cells may influence the behavior of tumor cells and has a significant effect on the reactivity of host immune system against HCC cells.

Earlier work suggested that HSP70 was shown to accumulate in the cytoplasm and the perinuclear area by cellular stress, such as non-lethal heat shock. In this study, we demonstrated

that HSP70 expressed not only in cytoplasm, but also on the surface of cells in HCC. Most members of the HSP families do not possess signal peptides. So it is still unclear how these proteins are transported to the cell membrane. Morimoto *et al*[14] postulated that some HSP might be transported to the cell surface via autoregulatory mechanism like in normal cells. Our results indicate that HSP70 may be transported to the cell surface after binding to MHC molecules. The main reason of this speculation is that class I MHC is found on the membrane of HCC cells. HSP70 is known to have strong protein-binding capacities. Therefore, it is reasonable to suggest that MHC class I may be the best candidate. It is interesting that cell-surface localization of HSP70 may make it possible to increase the immunogenicity of HCC cells. Many evidences have shown that HSPs expressing on affected cell types is recognized by the immune system[15]. Binder *et al*[16] recently identified HSP-chaperoned peptides introduced into cytosol were quite efficient as compared with free peptides. They even suggested that HSP70 was involved not only in the afferent end of this process by chaperoning partially or fully unfolded polypeptide chains, but also in chaperoning the resulting antigenic peptides to the TAP complex. These evidences indicate that HSP70 expressing on the surface of cells may be potentially promising target molecules for the immunotherapy of HCC.

On the whole, our data suggest that HCC cells express TAP, HSP70, and class I MHC. The results indicate that the mechanism of HCC cellular escape should be re-evaluated. Especially when designing immunotherapeutic strategies for HCC, it is very important to consider the potential problems associated with the ability of tumor cells to present target epitopes for immune recognition. Moreover, it needs to stress that tumor progression is dependent on multiple factors. Several scenarios have been proposed to be responsible for tumor immune-escape mechanisms, including production of suppressive cytokines by tumor cells, and expression of Fas ligand on tumor cells[17]. A recent study from Chai *et al*[18] suggested that T cell-expressed CD80 had a regulatory function and played a key role in the induction of T cell unresponsiveness by co-stimulation-deficient antigen presentation. So elucidation of the immune deficiency against cancer progression has been a difficult task because no single mechanism can explain the complicated cancer-host immune interactions. It is important to determine a more appropriate approach of combining different strategies to control the outgrowth of HCC cells.

REFERENCES

1 **Seliger B**, Ritz U, Abele R, Bock M, Tampe R, Sutter G, Drexler I, Huber C, Ferrone S. Immune escape of melanoma: first evidence of structural alterations in two distinct components of the MHC class I antigen processing pathway. *Cancer Res* 2001; **61:** 8647-8650

2 **Ritz U**, Momburg F, Pilch H, Huber C, Maeurer MJ, Seliger B. Deficient expression of components of the MHC class I antigen processing machinery in human cervical carcinoma. *Int J Oncol* 2001; **19**: 1211-1220

3 **Dovhey SE**, Ghosh NS, Wright KL. Loss of interferon-gamma inducibility of TAP1 and LMP2 in a renal cell carcinoma cell line. *Cancer Res* 2000; **60**: 5789-5796

4 **Dressel R**, Lubbers M, Walter L, Herr W, Gunther E. Enhanced susceptibility to cytotoxic T lymphocytes without increase of MHC class. I antigen expression after conditional overexpression of heat shock protein 70 in target cells. *Eur J Immunol* 1999; **29:** 3925-3935

5 **Chen D**, Androlewicz MJ. Heat shock protein 70 moderately enhances peptide binding and transport by the transporter associated with antigen processing. *Immunol Lett* 2001; **75:** 143-148

6 **Kurokohchi K**, Carrington M, Mann DL, Simonis TB, Alexander-Miller MA, Feinstone SM, Akatsuka T, Berzofsky JA. Expression of HLA class I molecules and the transporter associated with antigen processing in hepatocellular carcinoma. *Hepatology* 1996; **23:** 1181-1188

7 **Alimonti J**, Zhang QJ, Gabathuler R, Reid G, Chen SS, Jefferies WA. TAP expression provides a general method for improving the recognition of malignant cells *in vivo*. *Nat Biotechnol* 2000; **18:** 515-520

8 **Seliger B**, Ritz U, Abele R, Bock M, Tampe R, Sutter G, Drexler I, Huber C, Ferrone S.Immune escape of melanoma: first evidence of structural alterations in two distinct components of the MHC class I antigen processing pathway. *Cancer Res* 2001; **61:** 8647-8650

9 **Seliger B**, Bock M, Ritz U, Huber C. High frequency of a non-functional TAP1/LMP2 promoter polymorphism in human tumors. *Int J Oncol* 2002; **20:** 349-353

10 **Cromme FV**, Airey J, Heemels MT, Ploegh HL, Keating PJ, Stern PL, Meijer CJ, Walboomers JM. Loss of transporter protein, encoded by the TAP-1 gene, is highly correlated with loss of HLA expression in cervical carcinomas. *J Exp Med* 1994; **179:** 335-340

11 **Paterson AC**, Sciot R, Kew MC, Callea F, Dusheiko GM, Desmet VJ. HLA expression in human hepatocellular carcinoma. *Br J Cancer* 1988; **57:** 369-373

12 **Sung CH**, Hu CP, Hsu HC, Ng AK, Chou CK, Ting LP, Su TS, Han SH, Chang CM. Expression of class I and class II major histocompatibility antigens on human hepatocellular carcinoma. *J Clin Invest* 1989; **83:** 421-429

13 **Zhou DX**, Taraboulos A, Ou JH, Yen TS. Activation of class I major histocompatibility complex gene expression by hepatitis B virus. *J Virol* 1990; **64:** 4025-4028

14 **Morimoto RI**. Cells in stress: transcriptional activation of heat shock genes. *Science* 1993; **259:** 1409-1410

15 **Schueller G**, Paolini P, Friedl J, Stift A, Dubsky P, Bachleitner-Hofmann T, Jakesz R, Gnant M. Heat treatment of hepatocellular carcinoma cells: increased levels of heat shock proteins 70 and 90 correlate with cellular necrosis. *Anticancer Res* 2001; **21:** 295-300

16 **Binder RJ**, Blachere NE, Srivastava PK. Heat shock protein-chaperoned peptides but not free peptides introduced into the cytosol are presented efficiently by major histocompatibility complex I molecules. *J Biol Chem* 2001; **276:** 17163-17171

17 **Restifo NP**. Not so Fas: Re-evaluating the mechanisms of immune privilege and tumor escape. *Nat Med* 2000; **6:** 493-495

18 **Chai JG**, Vendetti S, Amofah E, Dyson J, Lechler R. CD152 ligation by CD80 on T cells is required for the induction of unresponsiveness by costimulation- deficient antigen presentation. *J Immunol* 2000; **65:** 3037-3042

Edited by Xu JY and Wang XL

P.O.Box 2345, Beijing 100023,China
Fax: +86-10-85381893
E-mail: wjg@wjgnet.com www.wjgnet.com

World J Gastroenterol 2003;9(8):1856-1858
World Journal of Gastroenterology
 ISSN 1007-9327

• BRIEF REPORTS •

Diagnosis and treatment of hepatic angiomyolipoma in 26 cases

Ning Ren, Lun-Xiu Qin, Zhao-You Tang, Zhi-Quan Wu, Jia Fan

Ning Ren, Lun-Xiu Qin, Zhao-You Tang, Zhi-Quan Wu, Jia Fan, Liver Cancer Institute and Zhongshan Hospital, Fudan University, Shanghai 200032, China
Correspondence to: Ning Ren, Liver Cancer Institute and Zhongshan Hospital, Fudan University, Shanghai 200032, China. ningren@zshospital.com
Telephone: +86-21-64041990-3078 **Fax:** +86-21-64037181
Received: 2003-03-12 **Accepted:** 2003-04-11

Abstract

AIM: To summarize the experience of the diagnosis and treatment of hepatic angiomyolipoma (HAML).

METHODS: The clinical, imaging and pathological features, and treatment strategies of 26 patients with HAML treated at the authors' institute between October 1998 and January 2003 were retrospectively analyzed. All the patients received liver resection and were followed up till the study. Immunohistochemical assays were performed with a panel of antibodies.

RESULTS: There was an obvious female predominance (21:5), and most of the patients (18/26) had no symptoms. Heterogeneous high echo was found in ultrasonography and punctiform or filiform vascular distribution pattern was found in color Doppler-sonography in most of the lesions (21/26). All of the 5 lesions further enhanced with Levovist showed early and prolonged enhancement. At contrast-enhanced spiral CT, the soft-tissue components of 24 lesions were markedly enhanced in the arterial phase and 18 lesions remained enhanced in the portal venous phase. MRI was performed in 9 patients, and showed hypointensity or hyperintensity on T1-weighted images and heterogeneous hyperintensity on T2-weighted images. Histopathologically, all lesions were composed of adipose tissues, smooth muscle and blood vessels with different proportions. Most lesions showed positive immunohistochemical staining for HMB45 (26/26), A103 (24/26) and SMA (24/26). All of the 26 patients showed a benign course with no sign of recurrence.

CONCLUSION: Preoperative radiological diagnosis of HAML is possible. The demonstration of intratumoral fat and central vessels is helpful in the diagnosis. HMB45, A103 and SMA are promising markers for pathologic diagnosis of HAML, and surgical resection is effective for the treatment of HAML.

Ren N, Qin LX, Tang ZY, Wu ZQ, Fan J. Diagnosis and treatment of hepatic angiomyolipoma in 26 cases. *World J Gastroenterol* 2003; 9(8): 1856-1858
http://www.wjgnet.com/1007-9327/9/1856.asp

INTRODUCTION

Hepatic angiomyolipoma (HAML) is a rare benign mesenchymal neoplasm of the liver. Since its first description by Ishak in 1976[1], not more than 200 cases have been reported in the English literatures[2-7]. However, with recent progress in imaging diagnostic techniques, the reported cases of HAML are increasing in number, and the significance of accurate diagnosis is becoming more important clinically. The purpose of this study was to investigate the clinical, imaging and pathological features of HAML and to summarize our experience in the diagnosis and treatment of this disease.

MATERIALS AND METHODS

Patients and clinical data

Twenty-six patients with HAML were surgically treated in Liver Cancer Institute of Fudan University from October 1998 to January 2003. There was a marked female predominance (21/26) and the mean age was 44.3 with a range of 31 to 64 years. Most of the patients (18/26) had no symptoms and were detected incidentally by medical check-up. Seven of 26 patients had symptoms caused by tumor oppression and one patient had slight fever as a chief complaint. The average tumor size at detection was 6.1 cm ranging from 1.5 to 15 cm. None of them was found complicated with a diagnosis of tuberous sclerosis and renal AML. Concomitant hepatic hemangioma was found in one patient. None of them had the history of hepatitis virus infection. Serum alpha-fetoprotein (AFP) levels were all within normal limits.

Imaging examinations

All of the patients underwent ultrasonography, color Doppler-sonography and computer tomography (CT) examinations. Nine patients also received magnetic resonance imaging (MRI) examination.

Treatment and follow-up

Limited partial liver resections were performed in 19 patients, left lateral lobectomy in 4, left hemihepatectomy in 2, and right hemihepatectomy in 1. All the patients have been followed up till the study.

Pathological and immunochemical assays

Routine histopathological examination with hematoxylin and eosin staining was performed. Immunohistochemical studies were performed by the EnVision™ method using a panel of antibodies (HMB45, A103, smoothmuscle actin, S100, Vimentin and CK8) in all of the tumor tissues.

RESULTS

Imaging features

Most lesions (21/26) showed heterogeneous high echo in ultrasonography, and punctiform or filiform vascular distribution pattern in color Doppler-sonography. Five lesions were further enhanced with Levovist, and all of them were found to have early and prolonged enhancement.

In contrast-enhanced spiral CT examination, the soft-tissue components of 24 lesions were markedly enhanced in the arterial phase, and 18 lesions remained enhanced in the portal venous phase.

MRI was performed in 9 patients, hypointensity or hyperintensity was found on T1-weighted images and heterogeneous hyperintensity on T2-weighted images.

Histopathological and immunochemical characteristics

The tumors were well circumscribed but no obvious capsule could be found. The non-tumorous liver parenchyma was normal, and no cirrhosis was found. All tumors were composed of adipose tissues, smooth muscle and blood vessels in different proportions. In immunohistochemical studies, most tumors were positive for HMB45 (26/26), A103 (24/26), SMA (24/26), S100 (20/26) and Vimentin (16/26), but negative for CK8 (22/26).

Treatment and prognosis

All of the 26 patients received hepatectomy. Six patients were followed-up for more than one year and finally decided to receive operation because of the enlargement of the lesions. All the patients have been followed up since their surgical resection. No recurrence was found in any patient during the follow-up period.

DISCUSSION

Angiomyolipoma, which occurs relatively frequent in kidney, is a rare benign mesenchymal neoplasm of the liver. The tumor size of HAML at the first diagnosis is variable, ranging from 0.1 cm to ⩾36 cm. Clinically, most of the patients have no symptoms and are detected incidentally by medical check-ups. Patients with large tumors usually have some symptoms caused by tumor compression. The diagnosis of HAML before operation mainly depends on imaging examination.

According to our experience, typical performance of HAML is a smoothly contoured heterogeneous high echo lesion, with a well-defined border separating it from adjacent normal hepatic tissues by ultrasonography and punctiform or filiform vascular distribution pattern by color Doppler-sonography. In further enhanced imaging with Levovist, the tumor showed early and prolonged enhancement. The lesions appeared as hypodense, and adipose dense could be found in pre-contrast CT scans. In the arterial phase, the soft-tissue components of the lesions were markedly enhanced and central vessels could be found. In the portal venous phase, the lesions remained in enhancement[8]. As reported, the adipose fraction of HAML varied from 5 % to 90 %, so adipose signals could be found on MRI in most lesions. Sakamoto *et al*.[9] described MRI studies showing extensive enhancement on gadolinium-enhanced images. In addition, fat could be seen with great sensitivity on T1-weighted images as high-signal intensity. However, HAML showed various patterns of imaging features, because the relative proportions of vessels, muscle and fat varied widely from tumor to tumor. So, although diagnosis may be suggested by imaging methods, histological confirmation remains mandatory.

Histopathologically, in our study, most tumors were well-circumscribed, but not encapsulated. The lesions were composed of adipose tissue, smooth muscle and blood vessels in different proportions. The tissue components in the tumor were highly variable from case to case, and even between different areas of the same mass. According to the line of differentiation and predominance of tissue components, Tsui *et al*.[6] subcategorized the tumors into mixed, lipomatous (⩾ 70 % fat), myomatous (⩽ 10 % fat), and angiomatous types. We found that the mixed type was the most common category which comprised sheets of epithelioid muscle cells admixed with islands of adipocytes, abnormal vessels, and frequently, hematopoietic cells. Some authors advocated to diagnose HAML by fine-needle aspiration (FNA)[10], for the presence of adipocytes was a clue to the diagnosis. However, adipose tissue might be a minute fraction of HAML, in which FNA diagnosis may be difficult. So we think that immunohistochemical examination may be the only authoritative method to diagnose HAML. According to our results, all the 26 tumors were positive for HMB45, the staining was intense, granular, and concentrated in tumor cell perinuclear cytoplasm. For A103, 24 tumors showed strongly and diffusely granular cytoplasmic staining in the majority of myoid cells, the staining in the other two was only focal. Smooth muscle actin (SMA) staining was weak to moderate in epithelioid cells and strong in spindle cells in 24 tumors. So HMB45, A103 and SMA are promising markers in pathologic diagnosis of HAML.

Exclusion of hepatocellular carcinoma (HCC) is the most important issue in the diagnosis of HAML, because both kinds of the lesions show similar imaging characteristics, including rich blood flow detected in Doppler-sonography, early enhancement in CT contrast scan, etc. Most of the patients with HAML had no histories of hepatitis virus infection or negative for hepatitis marker, and had no liver cirrhosis, and AFP level was normal, which might be helpful in the differential diagnosis. In CT contrast scan, there are also differences in the peak time and duration of enhancement between HAML and HCC. Ahmadi *et al*.[11] reported that HAML showed early and prolonged enhancement (>4 min) with delayed peak enhancement at 40-80 seconds, as opposed to HCC which had peak enhancement at 10 seconds and absent or minimally delayed enhancement. Further more, differentiation from HCC with fatty metamorphosis can also be made based on the angiomyolipomas prolonged tumor enhancement (>6 min) relative to HCC. Fat suppression MRI was also reported to be successful in distinguishing HAML from HCC[12].

HAML is a benign lesion and often grows slowly without any clinical symptom, so conservative treatment with close follow-up is recommended after diagnosis. For the rarity of the cases most of which are diagnosed by pathology after operation, there has been no report about culture doubling time or growth velocity of HAML yet. In this series, one patient was followed up for five years before operation, the tumor increased from 4 cm to 10 cm in size. Another one was followed up for thirteen years before operation, the size of tumor increased from 1.5 cm to 5 cm.

Spontaneous rupture, later recurrence and vascular invasion of HAML have been reported[13-15]. So surgery may be recommended for patients with symptoms, for patients in whom diagnostic imaging can not exclude malignancy, and for patients in whom the tumor enlarges obviously in short time or shows extrahepatic growth and has a risk of spontaneous rupture. All our cases received hepatectomy and have been followed up till the study for a period between 1 month and 52 months, no mortality and serious morbidity were found in these patients. Follow-up information of the 26 cases showed a benign course with no signs of recurrences. So surgical resection is safe and effective for the treatment of HAML.

REFERENCES

1 **Bakhotmah MA**, Yamasaki S. Hepatic angiomyolipoma. *HPB Surg* 1994; **8**: 133-137
2 **Ji Y**, Zhu X, Xu J, Zhou J, Tan Y, Wang J, Fan J, Zhou Y. Hepatic angiomyolipoma: a clinicopathologic study of 10 cases. *Chin Med J* 2001; **114**: 280-285
3 **Yeh CN**, Chen MF, Hung CF, Chen TC, Chao TC. Angiomyolipoma of the liver. *J Surg Oncol* 2001; **77**: 195-200
4 **Barnard M**, Lajoie G. Angiomyolipoma: immunohistochemical and ultrastructural study of 14 cases. *Ultrastruct Pathol* 2001; **25**: 21-29
5 **Sajima** S, Kinoshita H, Okuda K, Saito N, Hashino K, Sugimoto R, Eriguchi N, Aoyagi S. Angiomyolipoma of the liver-a case report and review of 48 cases reported in Japan. *Kurume Med J* 1999; **46**: 127-131
6 **Tsui WM**, Colombari R, Portmann BC, Bonetti F, Thung SN,

Ferrell LD, Nakanuma Y, Snover DC, Bioulac-Sage P, Dhillon AP. Hepatic angiomyolipoma: a clinicopathologic study of 30 cases and delineation of unusual morphologic variants. *Am J Surg Pathol* 1999; **23**: 34-48

7 **Nonomura A**, Mizukami Y, Kadoya M. Angiomyolipoma of the liver: a collective review. *J Gastroenterol* 1994; **29**: 95-105

8 **Yan F**, Zeng M, Zhou K, Shi W, Zheng W, Da R, Fan J, Ji Y. Hepatic angiomyolipoma: various appearances on two-phase contrast scanning of spiral CT. *Eur J Radiol* 2002; **41**: 12-18

9 **Sakamoto Y**, Inoue K, Ohtomo K, Mori M, Makuuchi M. Magnetic resonance imaging of an angiomyolipoma of the liver. *Abdom Imaging* 1998; **23**: 158-160

10 **Messiaen T,** Lefebvre C, Van Beers B, Sempoux C, Cosyns JP, Geubel A. Hepatic angiomyo(myelo)lipoma: difficulties in radiological diagnosis and interest of fine needle aspiration biopsy. *Liver* 1996; **16**: 338-341

11 **Ahmadi T**, Itai Y, Takahashi M, Onaya H, Kobayashi T, Tanaka YO, Matsuzaki Y, Tanaka N, Okada Y. Angiomyolipoma of the liver: significance of CT and MR dynamic study. *Abdom Imaging* 1998; **23**: 520-526

12 **Hooper LD**, Mergo PJ, Ros PR. Multiple hepatorenal angiomyolipomas: diagnosis with fat suppression, gadolinium-enhanced MRI. *Abdom Imaging* 1994; **19**: 549-551

13 **Guidi G**, Catalano O, Rotondo A. Spontaneous rupture of a hepatic angiomyolipoma: CT findings and literature review. *Eur Radiol* 1997; **7**: 335-337

14 **Croquet V**, Pilette C, Aube C, Bouju B, Oberti F, Cervi C, Arnaud JP, Rousselet MC, Boyer J, Cales P. Late recurrence of a hepatic angiomyolipoma. *Eur J Gastroenterol Hepatol* 2000; **12**: 579-582

15 **Dalle I**, Sciot R, de Vos R, Aerts R, van Damme B, Desmet V, Roskams T. Malignant angiomyolipoma of the liver: a hitherto unreported variant. *Histopathology* 2000; **36**: 443-450

Edited by Ma JY

P.O.Box 2345, Beijing 100023,China
Fax: +86-10-85381893
E-mail: wjg@wjgnet.com www.wjgnet.com

World J Gastroenterol 2003;9(8):1859-1862
World Journal of Gastroenterology
 ISSN 1007-9327

• BRIEF REPORTS •

Expression of telomerase activity and oxidative stress in human hepatocellular carcinoma with cirrhosis

Dao-Yong Liu, Zhi-Hai Peng, Guo-Qiang Qiu, Chong-Zhi Zhou

Dao-Yong Liu, Department of General Surgery, Shanghai No.5 People' s Hospital, Shanghai 200240, China
Zhi-Hai Peng, Guo-Qiang Qiu, Chong-Zhi Zhou, Department of General Surgery, Shanghai First People' s Hospital, Shanghai 200080, China
Supported by Science and Technology Foundation of Shanghai, No. 984119001
Correspondence to: Dr. Zhi-Hai Peng, Department of General Surgery, Shanghai First People' s Hospital, 85 Wujin Road, Shanghai 200080, China. pengpzhb@online.sh.cn
Received: 2003-03-04 **Accepted:** 2003-05-11

Abstract

AIM: To study the expression and significance of telomerase activity and oxidative stress in hepatocellular carcinoma (HCC) with cirrhosis.

METHODS: In this study, TRAP-ELISA assay was used to determine telomerase activity in 21 cases of HCC as well as in 23 cases of hepatic cirrhosis. Malondialdehyde (MDA), glutathione S-transferase (GST) and total anti-oxidative capacity (T-AOC) were also examined in the same samples with human MDA, GST and T-AOC kits.

RESULTS: Eighteen of 21 cases of HCC were found to have increased telomerase activity, whereas only three of the 23 non-cancerous cirrhotic samples were found to have weak telomerase activity, and the difference was significant ($P<0.001$). No significant difference in telomerase activity was detected according to different tumor size, tumor stage, histological grade, HBsAg, contents of albumin, bilirubin, ALT, AFP, r-GT and platelet. There were significant differences between HCC and cirrhosis in the expression of MDA, GST and T-AOC respectively. Telomerase activity correlated positively with the content of MDA ($P<0.05$).

CONCLUSION: Telomerase activation is the early event of carcinogenesis, which is not correlated with clinicopathological factors of HCC. The dysfunction of the anti-oxidative system is closely correlated with the progression from cirrhosis to hepatocellular carcinoma. Oxidative stress may contribute partly to telomerase activation.

Liu DY, Peng ZH, Qiu GQ, Zhou CZ. Expression of telomerase activity and oxidative stress in human hepatocellular carcinoma with cirrhosis. *World J Gastroenterol* 2003; 9(8): 1859-1862
http://www.wjgnet.com/1007-9327/9/1859.asp

INTRODUCTION

Telomeres correspond to the ends of eukaryotic chromosomes and are specialized structures containing unique (TTAGGG)n repeats[1]. Telomeres protect the chromosomes from DNA degradation, end to end fusions, rearrangements, and chromosome loss[2]. Because cellular DNA polymerases cannot replicate the 5' end of the linear DNA molecule, the number of telomere repeats decreases (by 50-200 nucleotides/cell division) during aging of normal somatic cells. Shortening of telomeres may control the proliferative capacity of normal cells[3]. Telomerase, a ribonucleicacid-protein complex, adds hexameric repeats of 5'-TTAGGG-3' to the end of telomeres to compensate for the progressive loss[4]. Although normal somatic cells do not express telomerase, immortalized cells such as tumor cells express this enzyme[5]. More recently, HeLa cells transfected with an antisense human telomerase were found to lose telomeric DNA and to die after 23 to 26 doublings[6]. Pertersen *et al*. found that the rate of shortening of telomere restriction fragments in human fibroblasts could be accelerated significantly by oxidative stress[7]. Importantly, after treatment of cells with short single stranded telomeric G-rich DNA fragments, glioblastoma cells recovered from the arrest and showed enhanced telomerase activity and elongated telomeres[8].

However, the mechanisms of activation and regulation of telomerase have not been establishednd. Cell line data indicate that a telomere length-dependent mechanism is the major pathway. On the other hand, normal lymphocytes up-regulate telomerase activity upon antigen and mitogen stimulation *in vitro* and *in vivo*. This indicates that telomere length-dependent mechanisms may be important or specific to different cell types for regulation of telomerase activation[9]. Only a few studies have specifically examined the relationship between telomerase activity in tumors and the status of oxidative stress. Our data implied that genetic defects in HCC facilitated the reactivation of telomerase activity, a process that might be associated with the increased expression of oxidative stress.

MATERIALS AND METHODS

Sample collection and processing

All 21 HCC specimens were sampled from patients who had undergone curative hepatectomy. Patients who had received radiotherapy or chemotherapy before operation were excluded. Liver cirrhosis tissues were obtained from those who had received hepatic biopsy in the operation for hypersplenia. Informed consent was obtained from all patients for subsequent use of their resected tissues. These specimens were immediately dissected into small pieces under aseptic condition within half an hour after removed, snap frozen in liquid nitrogen and stored at -80 ℃ until extracts for telomerase activity analysis and determination of oxidative stress.

Telomerase assay

Frozen tissue samples (100 μg) were homogenized in 500 μL of freshly made ice-cold lysis buffer. After 30 min incubation on ice, the lysate was centrifuged for 20 min at 16 000 g, and the supernatant was transferred to fresh tubes and used as tissue extracts for the telomerase assay. The protein concentrations were determined. Telomerase activity was assayed by the TRAP-ELISA kit, a polymerase chain reaction (PCR)-based on an improved version of the original method described by Kim *et al*[10]. In brief, aliquots of tissue extract containing 40 μg protein were added to 50 μL reaction mixtures containing

0.1 μg substrate oligonucleotide (TS) primer, TSK (internal control) template. The reaction mixtures were incubated at 25 ℃ for 20 min and then amplified for 33 cycles of PCR at 94 ℃ for 30 s, at 50 ℃ for 30 s, and at 72 ℃ for 90 s, then preserved at 4 ℃ for ELISA reaction process. 5 μg PCR product was taken for ELISA reaction. The value at A450 was read within 30 min. Telomerase activity equaled A450 for experimental well minus A450 for control well. The strength of telomerase activity was defined as follows: ++, >0.4; +, >0.2; -, <0.2.

MDA, GST and T-AOC determination

Frozen tissue samples (100 mg) were homogenized in 1.0 mL, the homogenized samples were centrifuged for 15 min at 3 000 r/min, and the supernatant was transferred to fresh tubes. After the protein concentrations were determined, MDA, GST and T-AOC were assayed with human MDA, GST and T-AOC kit (Jiancheng Biological Technical Institute, Nanjing, China).

Statistics analysis

Contingency table methods were used to analyze the univariate association between telomerase activity and clinicopathological data (age, sex, tumor grade, tumor size, and liver status). Significance was confirmed by Fisher's exact test. The association between telomerase activity and oxidative stress was investigated by Pearson correlation analysis test. All calculations were performed using the SPSS version 10.0 statistical software package, and the results were considered statistically significant at $P<0.05$.

RESULTS

Telomerase activity in HCC and hepatic cirrhosis

Telomerase positive cells were used as a positive control for assessing telomerase activity in clinical specimens. We measured telomerase activity in surgically resected specimens from 21 cases of HCC and 23 cases of liver cirrhotic tissue. Telomerase activity was detected in 18 of the 21 HCC specimens (85.7 %), but it was detected only in 3 of 23 samples of liver cirrhosis (13.4 %). There was a significant difference in telomerase activity between HCC and hepatic cirrhosis ($P<0.001$). There was no significant difference in telomerase activity in regard to different tumor size, tumor stage, histological grade, HBsAg, contents of albumin, bilirubin, ALT, AFP, r-GT and platelet (Table 1).

Table 1 Relationship between telomerase activity and clinicopathologic factors in HCC

	Telomerase activity		
	High	Low or loss	*P* value
Tumor size (cm)	7.7±3.5	7.1±3.6	0.664
Tumor grade (high / low)	9 / 4	4 / 4	0.245
Tumor stage (early / advanced)	6 / 7	3 / 5	0.327
ALT (normal / abnormal)	9 / 2	6 / 4	0.212
Bilirubin (normal / elevated)	9 / 2	9 / 1	0.414
Platelet (normal / decreased)	9 / 2	7 / 3	0.324
HbsAg (positive / negetive)	6 / 5	7 / 3	0.272
AFP (>400U / <400U)	7 / 5	5 / 5	0.309
Albumin (g / L)	39.2±5.6	39.3±4.2	0.946
Globulin (g / L)	28.6±5.3	26.8±6.5	0.423
γ-GT(U)	115.2±98.7	108.9±69.5	0.814

Expression of MDA, GST and T-AOC in HCC and hepatic cirrhosis

The content of MDA was 84.76±26.98 nM/ml in HCC, while it was 49.49±23.03 nM/ml in hepatic cirrhosis, and the difference was significant between them ($P<0.001$). Nevertheless, the contents of GST and T-AOC were lower in HCC than those in hepatic cirrhosis ($P<0.001$).

Table 2 Expression of MDA, GST and T-AOC ($\bar{x}\pm s$)

	HCC	Cirrhosis	*P* value
MDA (nM / ml)	84.76±26.98	49.49±23.03	<0.001
GST (U / mg)	8.18±5.59	18.70±5.20	<0.001
T-AOC (U / mg)	0.257±0.241	0.689±0.302	<0.001

Telomerase activity and content of MDA

The relationship between telomerase activity and oxidative stress was investigated by Pearson correlation analysis. Tumor specimes with a higher level of MDA expressed increased telomerase activity ($r=0.496$, $P<0.05$).

DISCUSSION

HCC is the most common solid tumor worldwide, being responsible for more than 1 million deaths annually, especially in Eastern Asia and South Africa[11], which ranks eighth in frequency among cancers in the world[12]. It is one of the few human cancers in which an underlying etiology can be identified in most cases, and has a background of chronic inflammatory liver disease caused by viral infection that induces cirrhosis[13]. However, it is not clear how these disorder results in HCC. The reactivation of telomerase activity may play a significant role in hepatocarcinogenesis.

Telomerase is a ribonucleoprotein complex[14] that is thought to add telomeric repeats onto the ends of chromosomes during the replicative phase of the cell cycle. Telomeres have classically been regarded as a simple linear structure, possibly capped by specific proteins. However, this simple structural view was challenged. Recent data have shown that the structure of human telomeres might be more complicated than originally thought[15]. Three different mechanisms were currently thought to contribute to telomere shortening: the so-called end replication problem, the C-strand degradation model and single-strand damage[16]. Both the end replication problem and the C-strand degradation model of telomere shortening do not take into account the possibility that the shortening rate of telomeres depends on external influences, especially oxidative stress-dependent DNA damage. von Zglonicki *et al* demonstrated that the telomere shortening rate could be either accelerated or decelerated by a modification of the amount of oxidative stress[17].

Recently, a highly sensitive PCR based TRAP assay for measuring telomerase activity that also includes an improved method of detergent lysis has been developed[10]. This assay allows more uniform extraction of telomerase from a small number of cells than conventional techniques, in which telomerase first synthesizes extension products that then serve as templates for PCR amplification. The simplicity and increased sensitivity of this assay have resulted in a dramatic increase in the investigation of telomerase expression. In this study, telomerase activity was positive in 18 of 21 HCC specimens (85.7 %), which suggested that telomerase activation was a universal event in human hepatocellular carcinoma. However, undetectable telomerase activity has been reported by others in about 10 % of tumors samples[18,19]. Some immortal cell lines without detectable telomerase activity have been described that were characterized by long and heterogenous telomeres[20,21]. These observations might indicate the presence of a telomerase-independent mechanism for telomere length maintenance in these tumors.

It is well documented that telomerase activity is detectable in the majority of cancers but rarely in normal somatic tissue. Some studies have demonstrated that some types of somatic cells express low levels of telomerase activity[22-24]. In particular physiologically regenerating somatic cells, such as hematopoietic cells, epithelial cells of skin or intestine, and endometrial cells, have been shown low levels of telomerase activity. In this study, low telomerase activity was detected in 3 of 23 cirrhotic specimens. One possible explanation for this finding was that these cirrhotic tissue samples may also contained probable cancer cell, infiltration of lymphoid cells, or dysplasia cells. Finally, demographic and clinical information of patients, such as tumor size, tumor stage, histological grade, HBsAg, albumin, bilirubin, ALT, AFP, r-GT and platelet were not correlated with the telomerase activity.

Many lines of evidence indicate that telomerase is reversibly regulated[25]. Resting lymphocytes express little telomerase activity, but stimulation of specific antigen receptors on the cell plasma membrane markedly increases telomerase activity[26-29]. High-level sun light exposure of normal human skins results in an increased incidence of telomerase activation[30]. Human hematopoietic cells with γ-rays[31], or human carcinoma cell lines with X-rays[32] induce the activation of telomerase. Activated telomerase in cancer cells is repressed when the cells leaves the cell cycle and become quiescent[33-37]. Nevertheless, the mechanisms of telomerase regulation, such as its suppression in normal human somatic cells and activation in neoplastic cells, are far from established.

Telomeres are believed to protect the ends of chromosomes against exonuclease and ligases, to prevent the activation of DNA-damage checkpoints, and to counteract loss of terminal DNA-segments that occurs when linear DNA is replicated[2,38,39]. Oikawa *et al* demonstrated that oxidative stress induced DNA damage at the 5' site of 5' -GGG-3' in the telomere sequence, and the telomeric G triplet was especially sensitive to cleavage by oxidative damage[40,41]. Moreover, it was shown that oxidative stress increased the frequency of S1 nuclease-sensitive sites, especially in telomeres[42,43]. However, it was unknown whether oxidative stress was associated with the telomerase activity in human tissue specimens. In this study, the expression of malondialdehyde, glutathione S-transferase and total anti-oxidative capacity were examined in the same samples. There were higher levels of the expression of glutathione S-transferase and total anti-oxidative capacity in hepatic cirrhosis specimens, while enhanced expression of malondialdehyde was found in HCC specimens. The difference between HCC and hepatic cirrhosis was significant (P<0.05). These findings suggested that the dysfunction of the anti-oxidative system was closely correlated with the progression from hepatic cirrhosis to hepatocellular carcinoma. Other studies also showed that HCC patients with higher anti-oxidative capacity levels survived longer after hepatectomy[44].

Henle *et al*. found that the telomeric G triplet was especially sensitive to cleavage by oxidative damage. In MRC-5 fibroblasts and U87 glioblastoma cells, oxidative stress-mediated production of single-strand damage in telomeres was concomitant to cell cycle arrest. This response can be modeled by treatment of cells with short single stranded telomeric G-rich DNA fragments. Recovery from it is accompanied by up-regulation of telomerase activity and elongation of telomeres[45]. The gene transcription of TERT is an essential rate-limiting step in telomerase activation and may be subjected to multiple levels of control and regulated by different factors in different cellular contexts[46]. In the present study we found that telomerase activity correlated positively with the content of MDA (P<0.05). One possible explanation for this observation was that telomere shortening might be accelerated by oxidative stress when telomere reached critical length, which caused the gene transcription of TERT, and telomerase was activated. Buchkovich *et al*[47] first demonstrated that in primary human leukocytes stimulated with phytohemagglutinin, telomerase activity was increased by more than 10-fold as naturally quiescent cells entered the cell cycle. In an animal model, treatment with an antagonist of growth hormone-releasing hormone dramatically decreased telomerase activity in xenografted U-87-MG human glioblastoma cells[46]. Their research was the first demonstration of a signaling pathway in normal cells that regulated telomerase, and paved the way for experimental analysis of "upstream" regulators. The possibility of a relationship between upstream regulators and oxidative stress is an important issue for future experimental studies on control of telomerase activity.

Although tumor cells have a much shorter telomere length, telomeres shorten with rates between 15 and 76 bp/PD in different culture. Too much time[48] is needed to reach the critical length of telomeres in tumor cells. However, oxidative stress may increase the rate of telomere shortening by the site-specific DNA damage in the telomere sequence. Thus, combination treatment[7] of oxidative stress and telomerase inhibitor in cancer cells will accelerate greatly the telomere shortening. Telomeres might shorten quickly to the point which is no longer able to divide.

REFERENCES

1 **Blackburn EH.** Structure and function of telomeres. *Nature* 1991; **350**: 569-573
2 **de Lange T.** Activation of telomerase in a human tumor. *Proc Natl Acad Sci U S A* 1994; **91**: 2882-2885
3 **Harley CB**, Futcher AB, Greider CW. Telomeres shorten during ageing of human fibroblasts. *Nature* 1990; **345**: 458-460
4 **Greider CW**, Blackburn EH. Identification of a specific telomere terminal transferase activity in Tetrahymena extracts. *Cell* 1985; **43**: 405-413
5 **Chiu CP**, Dragowska W, Kim NW, Vaziri H, Yui J, Thomas TE, Harley CB, Lansdorp PM. Differential expression of telomerase activity in hematopoietic progenitors from adult human bone marrow. *Stem Cells* 1996; **14**: 239-248
6 **Feng J**, Funk WD, Wang SS, Weinrich SL, Avilion AA, Chiu CP, Adams RR, Chang E, Allsopp RC, Yu J. The RNA component of human telomerase. *Science* 1995; **269**: 1236-1241
7 **Petersen S**, Saretzki G, von Zglinicki T. Preferential accumulation of single-stranded regions in telomeres of human fibroblasts. *Exp Cell Res* 1998; **239**: 152-160
8 **Saretzki G**, Sitte N, Merkel U, Wurm RE, von Zglinicki T. T e - lomere shortening triggers a p53-dependent cell cycle arrest via accumulation of G-rich single stranded DNA fragments. *Oncogene* 1999; **18**: 5148-5158
9 **Norrback KF**, Dahlenborg K, Carlsson R, Roos G. Telomerase activation in normal B lymphocytes and non-Hodgkin's lymphomas. *Blood* 1996; **88**: 222-229
10 **Kim NW,** Piatyszek MA, Prowse KR, Harley CB, West MD, Ho PL, Coviello GM, Wright WE, Weinrich SL, Shay JW. Specific association of human telomerase activity with immortal cells and cancer. *Science* 1994; **266**: 2011-2015
11 **Qin LX,** Tang ZY. The prognostic significance of clinical and pathological features in hepatocellular carcinoma. *World J Gastroenterol* 2002; **8**: 193-199
12 **Tang ZY.** Hepatocellular carcinoma-cause, treatment and metastasis. *World J Gastroenterol* 2001; **7**: 445-454
13 **Schafer DF**, Sorrell MF. Hepatocellular carcinoma. *Lancet* 1999; **353**: 1253-1257
14 **Meyne J**, Ratliff RL, Moyzis RK. Conservation of the human telomere sequence (TTAGGG)n among vertebrates. *Proc Natl Acad Sci U S A* 1989; **86**: 7049-7053
15 **Griffith JD**, Comeau L, Rosenfield S, Stansel RM, Bianchi A, Moss H, de Lange T. Mammalian telomeres end in a large duplex loop. *Cell* 1999; **97**: 503-514
16 **von Zglinicki T**. Role of oxidative stress in telomere length regulation and replicative senescence. *Ann N Y Acad Sci* 2000; **908**:

99-110
17 **von Zglinicki T**, Pilger R, Sitte N. Accumulation of single-strand breaks is the major cause of telomere shortening in human fibroblasts. *Free Radic Biol Med* 2000; **28**: 64-74
18 **Hsieh HF**, Harn HJ, Chiu SC, Liu YC, Lui WY, Ho LI. Telomerase activity correlates with cell cycle regulators in human hepatocellular carcinoma. *Liver* 2000; **20**: 143-151
19 **Shoji Y**, Yoshinaga K, Inoue A, Iwasaki A, Sugihara K. Quantification of telomerase activity in sporadic colorectal carcinoma: association with tumor growth and venous invasion. *Cancer* 2000; **88**: 1304-1309
20 **Rogan EM**, Bryan TM, Hukku B, Maclean K, Chang AC, Moy EL, Englezou A, Warneford SG, Dalla-Pozza L, Reddel RR. Alterations in p53 and p16INK4 expression and telomere length during spontaneous immortalization of Li-Fraumeni syndrome fibroblasts. *Mol Cell Biol* 1995; **15**: 4745-4753
21 **Strahl C**, Blackburn EH. Effects of reverse transcriptase inhibitors on telomere length and telomerase activity in two immortalized human cell lines. *Mol Cell Biol* 1996; **16**: 53-65
22 **Hiyama K**, Hirai Y, Kyoizumi S, Akiyama M, Hiyama E, Piatyszek MA, Shay JW, Ishioka S, Yamakido M. Activation of telomerase in human lymphocytes and hematopoietic progenitor cells. *J Immunol* 1995; **155**: 3711-3715
23 **Yasumoto S**, Kunimura C, Kikuchi K, Tahara H, Ohji H, Yamamoto H, Ide T, Utakoji T. Telomerase activity in normal human epithelial cells. *Oncogene* 1996; **13**: 433-439
24 **Kyo S**, Takakura M, Kohama T, Inoue M. Telomerase activity in human endometrium. *Cancer Res* 1997; **57**: 610-614
25 **Liu JP**. Studies of the molecular mechanisms in the regulation of telomerase activity. *FASEB J* 1999; **13**: 2091-2104
26 **Igarashi H**, Sakaguchi N. Telomerase activity is induced in human peripheral B lymphocytes by the stimulation to antigen receptor. *Blood* 1997; **89**: 1299-1307
27 **Hu BT**, Lee SC, Marin E, Ryan DH, Insel RA. Telomerase is upregulated in human germinal center B cells *in vivo* and can be re-expressed in memory B cells activated *in vitro*. *J Immunol* 1997; **159**: 1068-1071
28 **Hathcock KS**, Weng NP, Merica R, Jenkins MK, Hodes R. Cutting edge: antigen-dependent regulation of telomerase activity in murine T cells. *J Immunol* 1998; **160**: 5702-5706
29 **Weng NP**, Hathcock KS, Hodes RJ. Regulation of telomere length and telomerase in T and B cells: a mechanism for maintaining replicative potential. *Immunity* 1998; **9**: 151-157
30 **Ueda M**, Ouhtit A, Bito T, Nakazawa K, Lubbe J, Ichihashi M, Yamasaki H, Nakazawa H. Evidence for UV-associated activation of telomerase in human skin. *Cancer Res* 1997; **57**: 370-374
31 **Leteurtre F**, Li X, Gluckman E, Carosella ED. Telomerase activity during the cell cycle and in gamma-irradiated hematopoietic cells. *Leukemia* 1997; **11**: 1681-1689
32 **Hyeon Joo O**, Hande MP, Lansdorp PM, Natarajan AT. Induction of telomerase activity and chromosome aberrations in human tumour cell lines following X-irradiation. *Mutat Res* 1998; **401**: 121-131
33 **Sharma HW**, Sokoloski JA, Perez JR, Maltese JY, Sartorelli AC, Stein CA, Nichols G, Khaled Z, Telang NT, Narayanan R. Differentiation of immortal cells inhibits telomerase activity. *Proc Natl Acad Sci U S A* 1995; **92**: 12343-12346
34 **Holt SE**, Wright WE, Shay JW. Regulation of telomerase activity in immortal cell lines. *Mol Cell Biol* 1996; **16**: 2932-2939
35 **Bestilny LJ**, Brown CB, Miura Y, Robertson LD, Riabowol KT. Selective inhibition of telomerase activity during terminal differentiation of immortal cell lines. *Cancer Res* 1996; **56**: 3796-37802
36 **Xu D**, Gruber A, Peterson C, Pisa P. Supression of telomerase activity in HL60 cells after treatment with differentiating agents. *Leukemia* 1996; **10**: 1354-1357
37 **Savoysky E**, Yoshida K, Ohtomo T, Yamaguchi Y, Akamatsu K, Yamazaki T, Yoshida S, Tsuchiya M. Down-regulation of telomerase activity is an early event in the differentiation of HL60 cells. *Biochem Biophys Res Commun* 1996; **226**: 329-334
38 **Morin GB**. Is telomerase a universal cancer target? *J Natl Cancer Inst* 1995; **87**: 859-861
39 **Sharma HW**, Maltese JY, Zhu X, Kaiser HE, Narayanan R. Telomeres, telomerase and cancer: is the magic bullet real? *Anticancer Res* 1996; **16**: 511-515
40 **Oikawa S**, Kawanishi S. Site-specific DNA damage at GGG sequence by oxidative stress may accelerate telomere shortening. *FEBS Lett* 1999; **453**: 365-368
41 **Henle ES**, Han Z, Tang N, Rai P, Luo Y, Linn S. Sequence-specific DNA cleavage by Fe2+-mediated fenton reactions has possible biological implications. *J Biol Chem* 1999; **274**: 962-971
42 **von Zglinicki T**, Saretzki G, Docke W, Lotze C. Mild hyperoxia shortens telomeres and inhibits proliferation of fibroblasts: a model for senescence? *Exp Cell Res* 1995; **220**: 186-193
43 **Sitte N**, Saretzki G, von Zglinicki T. Accelerated telomere shortening in fibroblasts after extended periods of confluency. *Free Radic Biol Med* 1998; **24**: 885-893
44 **Lin MT**, Wang MY, Liaw KY, Lee PH, Chien SF, Tsai JS, Lin-Shiau SY. Superoxide dismutase in hepatocellular carcinoma affects patient prognosis. *Hepatogastroenterology* 2001; **48**: 1102-1105
45 **Wick M**, Zubov D, Hagen G. Genomic organization and promoter characterization of the gene encoding the human telomerase reverse transcriptase (hTERT). *Gene* 1999; **232**: 97-106
46 **Kiaris H**, Schally AV. Decrease in telomerase activity in U-87MG human glioblastomas after treatment with an antagonist of growth hormone-releasing hormone. *Proc Natl Acad Sci U S A* 1999; **96**: 226-231
47 **Buchkovich KJ**, Greider CW. Telomerase regulation during entry into the cell cycle in normal human T cells. *Mol Biol Cell* 1996; **7**: 1443-1454
48 **Kondo S**, Tanaka Y, Kondo Y, Hitomi M, Barnett GH, Ishizaka Y, Liu J, Haqqi T, Nishiyama A, Villeponteau B, Cowell JK, Barna BP. Antisense telomerase treatment: induction of two distinct pathways, apoptosis and differentiation. *FASEB J* 1998; **12**: 801-811

Edited by Zhang JZ

P.O.Box 2345, Beijing 100023,China
Fax: +86-10-85381893
E-mail: wjg@wjgnet.com www.wjgnet.com

World J Gastroenterol 2003;9(8):1863-1865
World Journal of Gastroenterology
 ISSN 1007-9327

• BRIEF REPORTS •

Relationship between nuclear morphometry, DNA content and resectability of pancreatic cancer

Yin-Cheng He, Wei Peng, Jian-Guo Qiao, Jun Cao, Ji-Wei Chen

Yin-Cheng He, Jian-Guo Qiao, Jun Cao, Ji-Wei Chen, Department of General Surgery, Zhongnan Hospital, Wuhan University, Wuhan 430071, Hubei Province, China
Wei Peng, Medical College, Jingmen Technical College, Jingmen 448000, Hubei Province, China
Correspondence to: Dr. Yin-Cheng He, Department of General Surgery, Zhongnan Hospital, Wuhan University, Wuhan 430071, Hubei Province, China. w030508h@public.wh.hb.cn
Telephone: +86-27-67812963
Received: 2003-05-11 **Accepted:** 2003-06-04

Abstract

AIM: To investigate the association of nuclear morphometry and DNA content with resectability of pancreatic cancer.

METHODS: A total of 36 patients with pancreatic adenocarcinoma were divided into resectable group and unresectable group. The nuclear morphometry and DNA contents of tumor cells were analyzed by IBAS autoimagine analyzer from paraffin-embedded materials. Localization size, histological type and grade, and clinical stage of the tumor were evaluated. Factors influencing resectability of pancreatic cancer were investigated using stepwise regression analysis.

RESULTS: Statistical significance was found in nuclear DNA content (integrated optical density, IOD) of tumor cells (1.64±0.41 *vs* 2.96±0.55), DNA ploidy, ages (46.5±5.3 years *vs* 58.6±0.7 years) and tumor volumes (298.1±101.5 cm^3 *vs* 634.7±512.5 cm^3) in both groups ($P<0.05$), and no difference was found in the nuclear morphometry ($P>0.05$). The rates of diploid/tetraploid and aneuploid were 66.7 % and 33.3 % in resectable group respectively, and 38.9 % and 62.1 % in unresectable group, respectively ($P<0.05$). IOD (X_{12}), ploidy status (X_{13}) and clinical stage (X_3) were radical resectable indicators with statistical significance. The regression equation for resectability was $Y=-9.2053+3.5428X_{12}+2.5390X_{13}-2.3001X_3$ ($RR=0.8780$, $P<0.01$).

CONCLUSION: There is a high correlation between resectability of pancreatic cancers and their DNA contents, DNA ploidy status and clinical stage.

He YC, Peng W, Qiao JG, Cao J, Chen JW. Relationship between nuclear morphometry, DNA content and resectability of pancreatic cancer. *World J Gastroenterol* 2003; 9(8): 1863-1865
http://www.wjgnet.com/1007-9327/9/1863.asp

INTRODUCTION

Pancreatic cancer is a highly malignant tumor, and has the most dismal prognosis among abdominal malignancies[1-6]. The overall five-year survival for all the patients is only 0.4 %. Patients who undergo radical resection have five-year survival rates between 10-24 %[1,3,4]. The traditional approach to patients has been surgical procedure, but approximately 10 % to 20 % of cancers of the pancreatic head, body and tail can be resected for potential cure[7-9]. The reason is the topographical peculiarities of the pancreas and the biological aggressiveness are involved. Recent results indicated that there was a relation between DNA ploidy, DNA content of tumor cell nuclei and the biological behaviour of tumors[10-15]. The present study was to investigate the effect of the clinical characteristics, nuclear morphometry and DNA contents of pancreatic cancer on its resectability.

MATERIALS AND METHODS

Patients and group

A total of 36 patients with pancreatic carcinoma were enrolled in this study. There were 20 men and 16 women with a mean age of 52.7±8.4 years (range 32-72 years). They were followed up from 1999 to December 2002. No patient had received preoperative chemotherapy and radiotherapy. The patients were divided into: resectable group and unresectable group (18 patients per group). In resectable group, 15 patients underwent radical resection with Whipple' s procedure, 2 splenopancreatectomy and 1 total pancreatectomy. In unresectable group, palliative bypass of the biliary tree and/or the duodenum was performed in 14 patients and biopsy in 4 patients. Criteria for unresectability included definite liver metastases, tumor spread to the whole pancreas proved by needle biopsy on operation, obstruction or invasion of the portal or mesenteric veins, and/or tumor encasement of the celiac or superior mesenteric arteries. Localization size, histological type, histological grade, and clinical stage of the tumor were evaluated for each patient.

Preparation of sections

From paraffin blocks, areas with high contents of neoplastic parenchymal cells were selected. Sections about 50 to 100 μm thick were cut from these parts and deparaffinized. The two 5 μm slides were preparated, one was stained with hematoxylin and eosin for confirmation of the presence of pancreatic cancer cells in the 50 μm sections, the other was stained with Feulgen method for DNA measurement.

Feulgen reaction

The cell nuclei were stained by the classic Feulgen reaction. The sections were deparaffinized and washed with distilled water. Cells were hydrolyzed (1 N HCl at 25 ℃ for 2-3 minutes, 1N HCl at 60 ℃ for 10-12 minutes, 1 N HCl at 25 ℃ for 2-3 minutes) and washed with distilled water again, then stained with Schiff ' s reagents for 80 minutes at room temperature, treated with freshly prepared sulfurous acid rinse 3 times (3-6 minutes), and washed in running tap water for 10 minutes. After dehydration, sections were coverslipped for DNA analysis.

Image analysis

Morphological characteristics and nuclear DNA content of tumor cells were measured by IBAS image analyzer (Kontron Company, Germany). The light was a halogen lamp (12V, 100W). Measurements were made using an interferential filter centered at 546 nm. Lymphocytes admixed with the tumor cells on the sections were used as internal control cells in the

procedure. At least 100 structurally identified neoplastic cell nuclei, selected at random on three different areas, were analyzed in each specimen. The structural identification was based on conventional cytodiagnostic criteria such as nuclear shape and chromatin texture. Morphological characteristics [nuclear areas, perimeter (μm), length of minor axis (μm), length of major axis (μm), form factor (FF)] and nuclear DNA content of tumor cells (integrated optical density, IOD) were analyzed. FF was calculated using the following equation: $FF= 4\pi A/P^2$. Where A is nuclear areas (μm^2), and *P* is nuclear perimeter (μm).

DNA ploidy

The same investigator made all measurements with no previous knowledge of coded clinical data. The DNA histograms were divided into three groups[16]. Type A with one stemline within the diploid region (1.5-2.5 C) and a G_2 fraction in the tetraploid region, type B with one stemline in the tetraploid region (3.5-4.5 C) and a G_2 fraction in the octoploid region, independent of the presence of a diploid stemlione, and type C with a stemline outside the diploid/ tetraploid region or a mosaic pattern.

Statistical analysis

All the data were input into a microcomputer, and statistical evaluation was carried out using the SPSS 10.0 statistical package. Differences between the mean values were analyzed for significance using the Student' s *t* test. Fisher' s exact probability test (two tailed) was used to assess the constituent ratio between two groups because of N of valid cases <40. To establish a relation between independent variables (X_1-X_{13}, Table 1) and dependent variables (Y, resectabiliry), stepwise regression analysis was used. The difference was considered significant when *P* value was less than 0.05.

RESULTS

Histological examination

The 36 cases consisted of 33 ductal adenocarcinoma, 1 acinus cell carcinoma, 1 mucinous carcinoma, and 1 adenosquamous carcinoma.

Nuclear morphometry and DNA contents

Nuclear morphometry and DNA contents are shown in Table 1. Statistical significance was found in IOD, ages and tumor volumes between resectable group and unsectable group ($P<0.05$). No difference was found in the nuclear morphometry of tumor cells when resectable group with unsectable group were compared ($P>0.05$, Table 1).

Nuclear DNA content of tumor cells (IOD) versus *clinical pathologic parametesr*

Relationships between IOD and clinical pathologic characteristics are presented in Table 1. Except for clinical stage (correlation coefficient $r=0.683$, $P<0.05$), no statistically significant relationship was found between IOD and age ($r=0.201$, $P>0.05$), tumor cell sources ($r=0.209$), histological grade ($r=0.167$), site ($r=0.235$), size ($r=0.312$), nuclear areas ($r=0.184$), perimeter ($r=0.085$), minor axis ($r=0.202$), major axis ($r=0.206$) and form factor ($r=0.149$).

Correlation analysis of resectability

Relationships between resectability and clinical pathologic characteristics were analyzed using Pearson correlation analysis. Correlation coefficients "*r*" are listed in Table 1. Age, clinical stage, site, size, IOD and ploidy status were covariates independently associated with resectability of pancreatic cancer.

Table 1 Relationship between DNA contents, clinical characteristics and resectability

Variable Factor		Resectable group	Unresectable group	Correlation coefficient (*r*)
X_1	Age (years)	46.5±5.3	58.6±0.7[a]	0.536[b]
X_2	Tumor cells (*n*)			0.387
	Ductal	17(94%)	16(89%)	
	Other	1(6%)	2(11%)	
X_3	Clinical stage (*n*)[c]			0.605[b]
	Stage I	9(50%)	0(0%)[a]	
	Stage II	8(44%)	3(17%)	
	Stage III	1(6%)	11(61%)[a]	
	Stage IV	0(0%)	4(22%)	
X_4	Histological grade (*n*)			0.394
	Kloppel I	5(28%)	3(17%)	
	Kloppel II	6(33%)	9(50%)	
	Kloppel III	7(39%)	6(33%)	
X_5	Site (n)[c]			-0.545[b]
	Head of pancreas	16(89%)	10(56%)[a]	
	Other	2(11%)	8(44%)[a]	
X_6	Size (cm^3)	298.1±101.5	634.7±512.5[a]	0.575[b]
X_7	Nuclear areas (μm^2)	33.37±8.42	34.74±6.93	0.478
X_8	Perimeter (μm)	24.90±4.02	25.60±3.02	0.367
X_9	Minor axis (μm)	5.56±0.68	5.67±0.57	0.482
X_{10}	Major axis (μm)	8.31±1.10	8.56±0.93	0.434
X_{11}	Form factor	0.75±0.05	0.70±0.06	0.376
X_{12}	IOD	1.64±0.41	2.96±0.55[a]	0.787[b]
X_{13}	DNA ploidy (*n*)			0.735[b]
	Diploid / tetraploid	12(67%)	7(39%)[a]	
	Aneuploid	6(33%)	11(61%)[a]	

[a]$P<0.05$, *vs* resectable group, [b]$P<0.05$, *T* test, [c]$P<0.05$, resectable group *vs* unresectable group

Stepwise regression analysis of resectability

Resectability predictors were evaluated in a stepwise regression model. In this model, stepwise regression analysis demonstrated that IOD (X_{12}), ploidy status (X_{13}) and clinical stage (X_3) were statistically significant resectable indicators after backward elimination ($F=2.80$). The regression equation for resectability was $Y=-9.2053+3.5428X_{12}+2.5390X_{13}-2.3001X_3$ ($RR=0.8780$, $P<0.01$). IOD remained to be the most important predictor, ploidy status was th second important one, followed by clinical stage according to variable *F* values.

DISCUSSION

The prognosis of pancreatic cancer though remarkable diagnosis and therapeutic advances, have led many surgeons to question whether patients with pancreatic cancer should be submitted to radical surgery[17-20]. Nevertheless, the only chance for longterm survival and cure is undoubtedly related to the feasibility of radical surgery. Therefore, many surgeons have investigated the resectability of pancreatic cancer. Although the biologic behavior and location of the tumor are the most common predictors reliable factors that may predict resectability before laparotomy are waiting to be found[21-26].

DNA aneuploidy is one of the markers of malignant tumour cells. Aneuploidy DNA pattern may be related to the development of distant organ metastases, invasion and prognosis[27-29]. Weger *et al*[16] investigated the relationship between DNA ploidy status and resectability of pancreatic cancer, in which 77 cases were studied by automatic DNA image cytometry, and the authors found that the radical resectable rates of diploid, tetraploid and aneuploid tumors were 87.5 %, 48.6 % and 25.9 % respectively. Joensuu *et al* found that only 3 of 15 resected pancreatic cancers had

aneuploid DNA content, whereas 35 of 47 nonresected pancreatic cancers had aneuploid, and the patients with diploid tumors lived longer than patients with aneupoid cancers. These findings suggested that the biological behavior of tumor could influence life span and resectability[30], which was in agreement with our study. Nuclear morphometry (nuclear area, perimeter, length of minor axis, length of major axis and form factor) was not significant between resectable group and unresectable group (P>0.05), but the tumor cellular DNA contents and ploidies in resectable group were different from those in unresectable group (P<0.05). It is suggested that there may be some difference between both groups at molecular levels, despite no difference was found in nuclear morphometry. Table 1 shows that the rates of diploid/tetraploid and aneuploid were 66.7 % and 33.3 % in resectable group, and 38.9 % and 62.1 % in unresectable group, respectively (P<0.05). The resectable rate of aneuploid tumor was lower than that of diploid/tetraploid. Compared with diploid cells, metabolism of the aneuploid cells was significantly accelerated, and the tumor cells underwent more rapid differentiation and proliferation, and had higher levels of DNA synthesis, accompanied by high DNA contents and DNA ploidy levels. According to our findings, there was a high correction between resectability of tumors and their quantitative DNA contents, DNA ploidy status. That is to say, radical or palliative resection of tumors is principally determined by DNA contents and ploidy status of tumor nuclei. Tumor tissue could be easily obtained in most cases by ultrasound guided percutaneous fine needle aspiration biopsy before operation[31]. Therefore, DNA image analysis for aspirated cellular materials may provide important preoperative information, and may help surgeons plan for radical or palliative procedure. We are convinced that the clinical application of preoperative imaging techniques and DNA measurements as a guide to select patients for surgical resection will become mature in the near future.

REFERENCES

1 **Li YJ**, Ji XR. Relationship between expression of E-cadherin-catenin complex and clinicopathologic characteristics of pancreatic cancer. *World J Gastroenterol* 2003; **9**: 368-372
2 **Postier RG**, Lerner MR, Lightfoot SA, Vannarath R, Lane MM, Hanas JS, Brackett DJ. DNA ploidy and markovian analysis of neoplastic progression in experimental pancreatic cancer. *J Histochem Cytochem* 2003; **51**: 303-309
3 Zheng M, Liu LX, Zhu AL, Qi SY, Jiang HC, Xiao ZY. K-ras gene mutation in the diagnosis of ultrasound guided fine-needle biopsy of pancreatic masses. *World J Gastroenterol* 2003; **9**: 188-191
4 **Shankar A**, Russell RC. Recent advances in the surgical treatment of pancreatic cancer. *World J Gastroenterol* 2001; **7**: 622-626
5 Yoshida T, Matsumoto T, Sasaki A, Morii Y, Aramaki M, Kitano S. Prognostic factors after pancreatoduodenectomy with extended lymphadenectomy for distal bile duct cancer. *Arch Surg* 2002; **137**: 69-73
6 **Wagman R**, Grann A. Adjuvant therapy for pancreatic cancer: current treatment approaches and future challenges. *Surg Clin North Am* 2001; **81**: 667-681
7 **Gebhardt C**, Meyer W, Reichel M, Wunsch PH. Prognostic factors in the operative treatment of ductal pancreatic carcinoma. *Langenbecks Arch Surg* 2000; **385**: 14-20
8 **Warshaw AL**, Gu ZY, Wittenberg J, Waltman AC. Preoperative staging and assessment of resectability of pancreatic cancer. *Arch Surg* 1990; **125**: 230-233
9 **Durup Scheel-Hincke J**, Mortensen MB, Qvist N, Hovendal CP. TNM staging and assessment of resectability of pancreatic cancer by laparoscopic ultrasonography. *Surg Endosc* 1999; **13**: 967-971
10 **Bazan V**, Migliavacca M, Zanna I, Tubiolo C, Corsale S, Calo V, Amato A, Cammareri P, Latteri F, Grassi N, Fulfaro F, Porcasi R, Morello V, Nuara RB, Dardanoni G, Salerno S, Valerio MR, Dusonchet L, Gerbino A, Gebbia N, Tomasino RM, Russo A. DNA ploidy and S-phase fraction, but not p53 or NM23-H1 expression, predict outcome in colorectal cancer patients. Result of a 5-year prospective study. *J Cancer Res Clin Oncol* 2002; **128**: 650-658
11 **Berczi C**, Bocsi J, Bartha I, Math J, Balazs G. Prognostic value of DNA ploidy status in patients with rectal cancer. *Anticancer Res* 2002; **22**: 3737-3741
12 **El-Rayes BF**, Maciorowski Z, Pietraszkiewicz H, Ensley JF. Comparison of DNA content parameters in paired, fresh tissue pretreatment biopsies and surgical resections from squamous cell carcinoma of the head and neck. *Otolaryngol Head Neck Surg* 2003; **128**: 169-177
13 **Sugai T**, Uesugi N, Nakamura S, Habano W, Jiao YF, Noro A, Takahashi H, Akasaka I, Higuchi T. Evolution of DNA ploidy state and DNA index in colorectal adenomas and carcinomas using the crypt isolation technique: New hypothesis in colorectal tumorigenesis. *Pathol Int* 2003; **53**: 154-162
14 **Tsutsui S**, Ohno S, Murakami S, Kataoka A, Kinoshita J, Hachitanda Y. Prognostic significance of the combination of biological parameters in breast cancer. *Surg Today* 2003; **33**: 151-154
15 **Huang JJ**, Yeo CJ, Sohn T, Lillemoe KD, Sauter PK, Coleman J, Hruban RH, Cameron JL. Quality of life and outcomes after pancreaticoduodenectomy. *Ann Surg* 2000; **6**: 890-898
16 **Weger AR**, Glaser KS, Schwab G, Oefner D, Bodner E, Auer GU, Mikuz G. Quantitative nuclear DNA content in fine needle aspirates of pancreatic cancer. *Gut* 1991; **32**: 325-328
17 **Sohn TA**, Yeo CJ, Cameron JL, Koniaris L, Kaushal S, Abrams RA, Sauter PK, Coleman J, Hruban RH, Lillemoe KD. Resected adenocarcinoma of the pancreas-616 patients: results, outcomes and prognostic indicators. *J Gastrointest Surg* 2000; **4**: 567-579
18 **Liu B**, Staren E, Iwamura T, Appert H, Howard J. Effects of Taxotere on invasive potential and multidrug resistance phenotype in pancreatic carcinoma cell line SUIT-2. *World J Gastroenterol* 2001; **7**: 143-148
19 **Zhang LJ**, Chen KN, Xu GW, Xing HP, Shi XT. Congenital expression of mdr-1 gene in tissues of carcinoma and its relation with pathomorphology and prognosis. *World J Gastroenterol* 1999; **5**: 53-56
20 **Guo XZ**, Friess H, Shao XD, Liu MP, Xia YT, Xu JH, Buchler MW. KAI1 gene is differently expressed in papillary and pancreatic cancer: influence on metastasis. *World J Gastroenterol* 2000; **6**: 866-871
21 **G House M**, Campbell K, D Schulick R, Leach S, J Yeo C, Horton K, Fishman E, L Cameron J, D Lillemoe K. PANCREAS Surgery 123. Predicting Resectability of Periampullary Tumors With 3-Dimensional Computed Tomography. *J Gastrointest Surg* 2003; **7**: 296
22 **Catalano C**, Laghi A, Fraioli F, Pediconi F, Napoli A, Danti M, Reitano I, Passariello R. Pancreatic carcinoma: the role of high-resolution multislice spiral CT in the diagnosis and assessment of resectability. *Eur Radiol* 2003; **13**: 149-156
23 Saftoiu A, Ciurea T. The role of imaging for the evaluation of pancreatic cancer resectability. *Rom J Gastroenterol* 2002; **11**: 78-79
24 **John TG**, Wright A, Allan PL, Redhead DN, Paterson-Brown S, Carter DC, Garden OJ. Laparoscopy with laparoscopic ultrasonography in the TNM staging of pancreatic carcinoma. *World J Surg* 1999; **23**: 870-881
25 **Lim JE**, Chien MW, Earle CC. Prognostic factors following curative resection for pancreatic adenocarcinoma: a population-based, linked database analysis of 396 patients. *Ann Surg* 2003; **237**: 74-85
26 **Merchant NB**, Conlon KC, Saigo P, Dougherty E, Brennan MF. Positive peritoneal cytology predicts unresectability of pancreatic adenocarcinoma. *J Am Coll Surg* 1999; **188**: 421-426
27 **Xu L**, Zhang SM, Wang YP, Zhao FK, Wu DY, Xin Y. Relationship between DNA ploidy,expression of ki-67 antigen and gastric cancer metastasis. *World J Gastroenterol* 1999; **5**: 10-11
28 **Alanen KA**, Joensuu H, Klemi PJ, Marin S, Alavaikko M, Nevalainen TJ. DNA ploidy in pancreatic neuroendocrine tumors. *Am J Clin Pathol* 1990; **93**: 784-788
29 **Alanen KA**, Joensuu H, Klemi PJ, Marin S, Alavaikko M, Nevalainen TJ. DNA ploidy in pancreatic neuroendocrine tumors. *Am J Clin Pathol* 1990; **93**: 784-788
30 **Joensuu H**, Alanen KA, Klemi PJ. Doubts on "curative" resecti on of pancreatic cancer. *Lancet* 1989; **1**: 953-954
31 **Williams DB**, Sahai AV, Aabakken L, Penman ID, van Velse A, Webb J, Wilson M, Hoffman BJ, Hawes RH. Endoscopic ultrasound guided fine needle aspiration biopsy: a large single centre experience. *Gut* 1999; **44**: 720-726

Edited by Zhang JZ and Wang XL

P.O.Box 2345, Beijing 100023,China
Fax: +86-10-85381893
E-mail: wjg@wjgnet.com www.wjgnet.com

World J Gastroenterol 2003;9(8):1866-1870
World Journal of Gastroenterology
 ISSN 1007-9327

• BRIEF REPORTS •

Early protective effect of ischemic preconditioning on small intestinal graft in rats

Shu-Feng Wang, Guo-Wei Li

Shu-Feng Wang, Department of General Surgery, First Hospital, Xi' an Jiaotong University, Xi' an 710061, Shannxi Province, China
Guo-Wei Li, Department of General Surgery, Second Hospital, Xi' an Jiaotong University, Xi' an 710004, Shannxi Province, China
Supported by The National Natural Science Foundation of China, No.30271275
Correspondence to: Dr. Shu-Feng Wang, Department of General Surgery, First Hospital, Xi' an Jiaotong University, Xi' an 710061, Shannxi Province, China. dawnwsf@sina.com
Telephone: +86-29-5271909
Received: 2003-01-18 **Accepted:** 2003-03-10

Abstract

AIM: To investigate the early protective effect of ischemic preconditioning on small intestinal graft in rats.

METHODS: SD rats were randomly divided into the following groups: sham operation group (S group, *n*=6), small bowel transplantation group (SBT group, *n*=12), ischemic preconditioning plus small bowel transplantation group (ISBT group, *n*=12). Heterotopic SBT was performed with a technique modified from that described by Monchik *et al*.When the graft was revascularized successfully and reperfused for 1 h, samples were obtained from the different groups. Laminin was analyzed with immunohistochemical staining. Quantitative analysis of laminin positive signals was performed using image acquiring analysis system. Apoptotic epithelia of small intestinal graft were detected by the TdT-mediated dUTP nick end labeling method. The morphological change of epithelial basement membrane was observed by transmission electron microscopy.

RESULTS: The mean optical density value of laminin positive signals was 39.52±2.60, 13.53±0.44, 25.40±1.79, respectively, in S, SBT and ISBT groups. The average optical density value of laminin positive products in SBT group was sharply lower than that in S group ($P<0.05$). However, the mean optical density value of laminin positive products in ISBT group was significantly higher than that in SBT group ($P<0.05$). The apoptotic index (AI) in S, SBT and ISBT group was 2.2±0.83,30.8±3.2, 13.2±2.86, respectively. The AI in SBT group was significantly higher than that in S group ($P<0.05$), and AI in ISBT group was sharply lower than that in SBT group ($P<0.05$). On transmission electron microscopy, the epithelial basement membrane in S group stayed normal, but in SBT group it became disrupted and collapsed, even disappeared. The lesion of epithelial basement membrane in ISBT group was slighter compared with that in SBT group.

CONCLUSION: Ischemic preconditioning has an early protective effect on epithelial cells and extracellur matrix of small intestinal graft. Inhibition of epithelial cell apoptosis may be one of the mechanisms of ischemic preconditioning.

Wang SF, Li GW. Early protective effect of ischemic preconditioning on small intestinal graft in rats. *World J Gastroenterol* 2003; 9(8): 1866-1870
http://www.wjgnet.com/1007-9327/9/1866.asp

INTRODUCTION

Small bowel transplantation (SBT) has been advocated as the preferred therapy for patients with irreversible intestinal failures such as short bowel syndrome[1-6]. In recent years, although potent immunosuppressive agents have been used, rejection rate of small intestinal grafts still amounts to 50 %[7]. Primary graft rejection and reperfusion damage involved in loss of small intestine function after transplantation are still the major obstacle to SBT[8-10]. Postischemic reperfusion damage, a nonspecific injury, may enhance graft immunogenicity and is likely to play an important role in the development of early specific and late rejection-related events, and threatens graft function and graft survival[11]. Therefore, it has important clinical significance for SBT if reperfusion injury of the graft could be ameliorated or prevented.

Studies have indicated that ischemic preconditioning can alleviate reperfusion injury of tissues or organs. Ischemic preconditioning (IPC) refers to a phenomenon in which a tissue is rendered resistant to the deleterious effects of prolonged ischemia and reperfusion by prior exposure to brief periods of vascular occlusion[12]. With regard to organ transplantation, the beneficial effect of IPC has been previously described in transplantation procedures involving in ameliorating heart preservation injury and liver reperfusion damage[13,14], but its protective capacity against reperfusion injury in small bowel transplantation has not completely defined. Lately, Sola *et al*[15]. have shown that the release of lactate dehydrogenase (marker of cell injury) decreases markedly during small intestinal graft preservation and reperfusion, and morphological change of graft improves greatly, after IPC was carried out. Extracelluar matrix is the early target of reperfusion injury[16]. Epithelial cell apoptosis of small intestinal graft is the major mode of cell death[17]. But no study has covered the effect of IPC on them. So this study was to investigate the protective effect of ischemic preconditioning on epithelial cells and extracelluar matrix of intestinal graft in rats.

MATERIALS AND METHODS

Animal preparation

Healthy male Sprague-Dawley (SD) rats, weighing 280±20 g, provided by Medical Experiment Animal Center, Xi' an Jiaotong University, were housed in standard animal facilities and fed with commercially available rat chow and tap water *ad libitum* for 1 week before test to acclimatize the laboratory. They were maintained on a 12 h light/dark cycle.

Experimental design

SD rats were used as donors and recipients. They were randomly divided into the following groups: (1) sham operation group (S group, *n*=6), in which animals were only subjected

to anesthesia and laparotomy; (2) heterotopic segmental small bowel transplantation group (SBT group, *n*=12), in which the donor and recipient were paired according to the similar body weight; (3) IPC plus SBT group (ISBT group, *n*=12). IPC was carried out before the graft was harvested. Namely, the superior mesenteric artery was occluded for 10 min with a microsurgical atraumatic vascular clamp, then it was released, and the graft was reperfused for 10 min. The following surgical procedures were the same as SBT group.

Heterotopic small bowel transplantation

Heterotopic SBT was performed with a technique modified from that described by Monchik and others scholars[18-21]. All animals were fasted for 12 h, but had free access to water before operation. They were anesthetized with pentobarbital sodium solution (2 %, 35 mg/kg) intraperitoneally. After perfused *in situ* with cold lactated Ring' s solution, the small intestine 5 cm distal to the Treitz ligament was harvested from donor rat with a vascular pedicle including portal vein (PV) and aorta segment with superior mesenteric artery, and stored at 4 ℃ in lactated Ringer' s solution for 1 h. After left nephrectomy, left renal vein and abdominal aorta of the recipient were isolated. The graft was revascularized by end-to-side anastomosis between donor aorta and recipient aorta using continuous 9-0 non-traumatic nylon suture and end-to-end anastomosis between donor PV and the left renal vein of the recipient using a cuff technique. The recipient' s own intestine was left intact. During transplantation, mean warm ischemia time of graft was 25-30 min, and the longest did not exceed 40 min[22].

Immuohistochemical staining and evaluation

When the graft was revascularized successfully and reperfused for 1 h, samples were obtained from the different groups. Specimens were fixed in 4 % paraformaldehyde, embeded in paraffin, sliced 4 μm thick, and stained by the SP methods. A polyclonal antirat laminin antibody (Boster Biotech, Wuhan, China) was used at concentration of 1:100. DAB was used for visualization. For negative control, the slides were treated with PBS instead of primary antibody.

Laminin is one of the major components of epithelial basement membrane. It was regarded as positive signals when epithelial basement membrane became brownish yellow. Quantitative analysis of positive products was performed using image acquiring analysis system (Leica QWin500CW, Germany). The image system randomly selected five visual fields per slice to measure the optical density value, using the average value as the mean optical density.

Detection of cell apoptosis

Apoptosis was detected on sections from paraformaldehyde-fixed and paraffin-embedded blocks by the terminal deoxynucleotidyl-transferase (TdTase) mediated d-UTP-biotin nick end labeling (TUNEL) method[23]. Apoptosis assay with a detection kit from Bochinger Mannheim Germany, conformed to the manufacturer' s protocol strictly. The nuclei of apoptotic cells were stained brown as detected under light microscope, and apoptotic cells were quantified by calculating the apoptotic index (apoptotic cells/10 high-power fields)[24]. Negative control was designed by PBS instead of TdTase.

Transmission electron microscopy

For transmission electron microscopy, intestinal fragments of approximately 2 mm^3 obtained from different groups, were fixed in 2.5 % glutaraldehyde for 3 h, rinsed in PBS, then postfixed in 1 % osmium tetroxide for 2 h. Samples were dehydrated in graded alcohols, and embedded in Epon 812, cut on an ultramicrotome and stained with uranyl acetate and lead citrate. Ultrathin sections were viewed using transmission electron microscopy (Hitachi H-600).

Statistical analysis

Data were expressed as mean ± standard error of the mean. One-way analysis of variance (ANOVA) was used for multiple comparisons with Student Newman Keylls (SNK) test. Significant difference was assumed when $P<0.05$.

RESULTS

Quantitative analysis of laminin expression in different groups

As seen from Table 1, the mean optical density value of laminin positive products in SBT group was sharply lower than that in S group ($P<0.05$). However, after IPC was carried out, the mean optical density value of positive products in ISBT group was higher, compared with that in SBT group ($P<0.05$). It indicated that IPC had a protective effect on the basement membrane, one of the components of extracelluar matrix.

Table 1 Expression of laminin in different groups

Group	*n*	Mean optical density value
S	6	39.52±2.60
SBT	6	13.53±0.44[a]
ISBT	6	25.40±1.79[b]

[a]$P<0.05$ *vs* S group q=29.87, [b]$P<0.05$ *vs* SBT group q=13.64.

Cell apoptosis in different groups

As shown in Figure 1 and Table 2 in S group, apoptotic epithelial cells at villus tip were found only occasionally. However, after the graft underwent 60 min of cold ischemia and 60 min of warm reperfusion, many apoptotic cells appeared at villus tip of the graft in SBT group, The AI in SBT groups was significantly higher than that in S group ($P<0.05$), but the number of apoptotic cells at villus tip of the graft decreased sharply after transient IPC was carried out. The AI in ISBT group was sharply lower than that in SBT group ($P<0.05$). It showed that the mechanism of IPC was also involved in inhibition of epithelial cell apoptosis induced by ischemia and reperfusion in small intestinal graft.

Table 2 AI of epithelial cells of small intestinal graft in different groups

Group	*n*	AI
S	6	2.2±0.83
SBT	6	30.8±3.2[a]
ISBT	6	13.2±2.86[b]

[a]$P<0.05$ *vs* S group q=25.33 [b]$P<0.05$ *vs* SBT group q=15.59.

Morphological analysis of epithelial basement membrane

Under light microscope, epithelial basement membrane was stained brownish yellow in S, SBT and ISBT groups, but there was an obvious difference in the structure of epithelial basement membrane. Basement membrane in S group showed line-shaped continuous normal structure, however, it became disrupted and collapsed, even disappeared in SBT group. The lesion of basement membrane in ISBT group was slighter compared with that in SBT group. Under transmission electron microscope, the morphological change of epithelial basement membrane was the same as that under light microscopy (Figure 2).

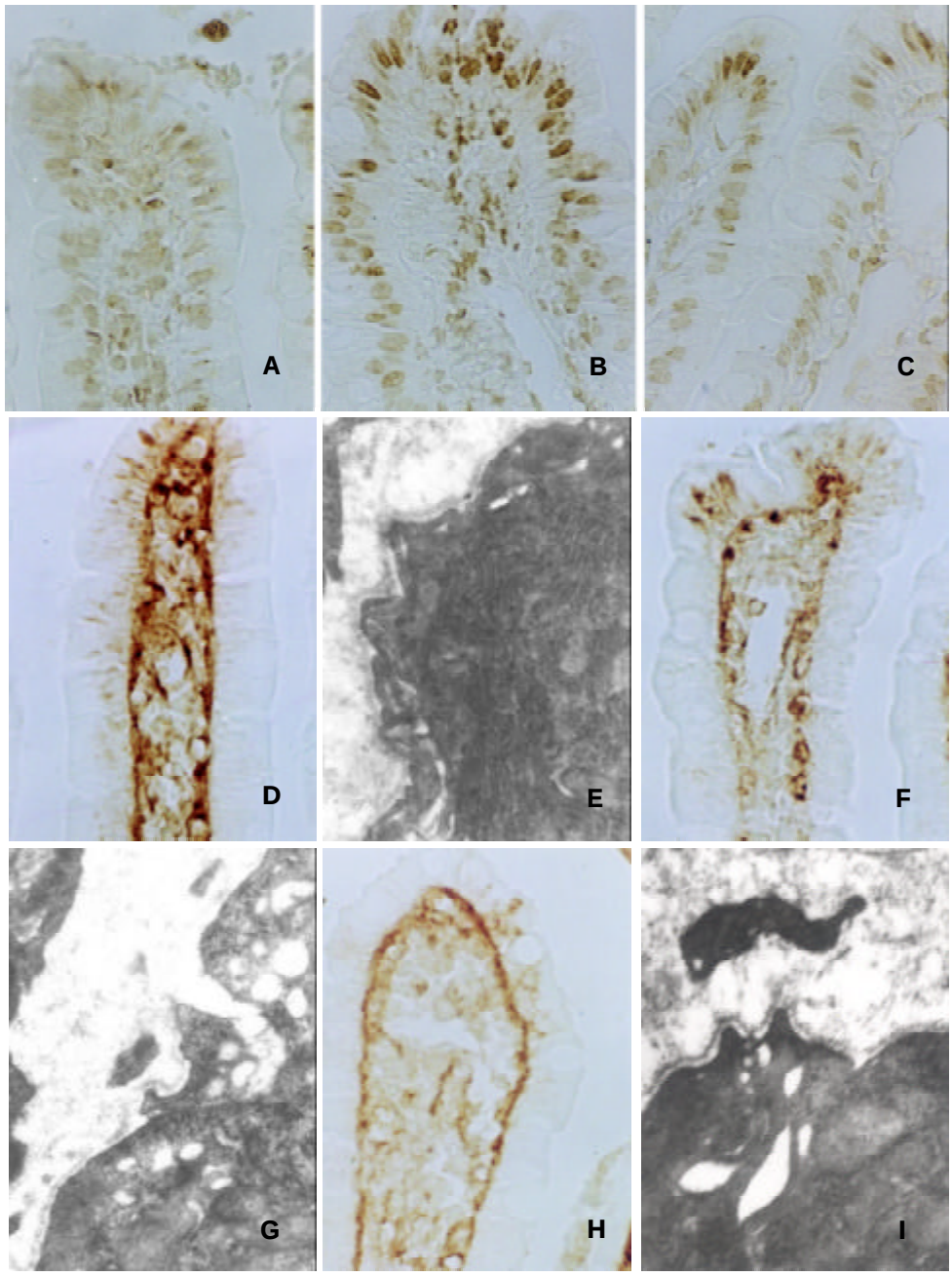

Figure 1 Light micrographs of apoptotic cells detected by TUNEL method (original magnification ×400). A: In S group, TUNEL signals were only observed accidentally at villi tip. B: In SBT group, many TUNEL signals appeared at villi tip of the graft. C: In ISBT group, after IPC was carried out, TUNEL signals decreased significantly at villi tip of the graft.

Figure 2 Light and electron micrographs (LM and EM) of morphological change of epithelial basement membrane (BM) (LM, original magnification ×400, EM, original magnification ×20 000). D and E: In S group, BM showed line-shaped, continuous normal structure. F and G: In SBT group, BM became disrupted and collapsed, even disappeared. H and I: In ISBT group, after IPC was function carried out, the lesion of BM was slighter, compared with that in SBT group.

DISCUSSION

Available evidences indicate that the small intestinal mucosa is susceptible to postischemic reperfusion, 15 minutes of ischemia alone could induce detectable mucosal injury, and reperfusion exacerbates the mucosal injury[25]. Under physiological conditions, the gut shows a remarkable rate of turnover, and a rapid regeneration of the epithelial layer has also been reported after intestinal hypoxia/reperfusion. Taguchi *et al*. have found that 15 minutes of ischemia and 1 h reperfusion could result in increase of the expression of proliferation cell nuclear antigen (PCNA) in small intestine[26]. PCNA, a kind of nuclear protein that produces or expresses in proliferative cells, is a significant cell-regulated nuclear protein for DNA-polymerase δ. So PCNA is a marker for proliferative cells[27-29]. The increase of small intestinal PCNA expression after 1 h reperfusion indicates that the repair process of epithelia is initiated by ischemia and reperfusion. In order to discover the deleterious effect of reperfusion and protective effect of IPC, respectively, on epithelia and extracelluar matrix of the small intestinal graft, and to prevent influence on graft due to the recovery of epithelia during reperfusion, the present study was designed to obtain specimens from different groups 1 h after reperfusion when the vascular anastomosis had finished.

The protective effect of IPC was first described in heart[30], and many comprehensive studies on IPC indicated that it could be divided into two major classes. One is the early phase of protection that appears 1-3 h after IPC, and the other is the late phase of protection that appears 24 h after IPC (the second

window of protection). Lately, this protective effect has been also demonstrated in the small intestine[31]. Although the effects of IPC on small intestine are not completely understood, several studies suggested that they were involved in transient increase of nitric oxide synthesis, activation of K_{ATP} channel, release of calcitonin gene-related peptide and endogenous opioid peptides, and inhibition of P-selectin expression in small intestine[32-36]. Apoptosis regulates many physiological and pathological processes. The influence of IPC on cell apoptosis in small bowel graft is not well known. Apoptosis is a major mode of epithelial death and peaks at 60 min during reperfusion period, in comparison, necrosis was relatively minor[37,38]. Therefore, loss of intestinal epithelia is a consequence of apoptosis during reperfusion. In the present experiment, apoptotic epithelial cells at villus tip were found accidentally in S group. Under physiological circumstances, apoptosis was reported to be an important mechanism of epithelial cell renewal. However, in SBT group after the graft underwent 60 min of cold ischemia and 60 min of warm reperfusion, many apoptotic cells appeared at villus tip of the graft. Compared with S group, the number of apoptotic cells was significantly higher. It indicated that apoptosis was initiated by ischemia and reperfusion in the graft. But in ISBT group, after transient IPC was carried out, the number of apoptotic cells at villus tip of the graft decreased sharply, in comparison with that in SBT group. It suggests that the mechanism of IPC may also involve the inhibition of epithelial cell apoptosis induced by ischemia and reperfusion in small intestinal graft.

Extracelluar matrix proteins provide structural support and maintenance, and also modulate a number of cell functions such as repair and immunity[39]. Laminin, an active glycoprotein with many biological functions, is one of the most abundant components of epithelial basement membrane[40]. It may play an important role in regulating cell-cell interactions, cell migration and differentiation. Laminin can be produced by epithelial and endothelial cells. In the present study, after laminin expression was evaluated by immunohistochemical staining and analyzed by quantitative analysis system, it was found that intestinal epithelial basement membrane in S group appeared line-shaped continuous structure, but it became decomposed and disrupted, even disappeared in SBT group. Compared with the average optical density value of laminin positive expression signals in S group, it was significantly lower in SBT group. Hence, it proved again that epithelial basement membrane was an early target of reperfusion injury. The small bowel contains a large reservoir of mediators, such as reactive oxygen radicals, various protease and cytokines, as well as adhesion molecules[41]. During reperfusion, laminin regulates polymorphonuclear cells to adhere and migrate to epithelial villus, and it is reactive oxygen radicals and various proteases released from polymorphonuclear cells that decompose epithelial basement membrane, meanwhile reperfusion injury damages the ability of epithelial cells to produce laminin. So, more damage and less production result in the collapse of epithelial basement membrane. In accordance with immunohistochemical results, under transmission electron microscopy, intestinal epithelial basement membrane in S group kept normal, but it showed disruption, even disappeared in SBT group. After IPC, the morphological change of epithelial basement membrane in ISBT group improved greatly, and the mean optical density value of laminin positive expression signals became higher, compared with that in SBT group. Under transmission electron microscope, the reperfusion injury degree of basement membrane in ISBT group was slighter than that in SBT group. It indicates strongly that IPC has protective effects on extracelluar matrix of small intestinal graft, and the beneficial effect may appear at early phase after IPC.

In summary, the present study demonstrates that ischemic preconditioning has an early protective effect on epithelial cells and extracelluar matrix of small intestinal graft. Inhibition of epithelial cell apoptosis initiated by reperfusion may be one of the mechanisms of IPC. With regard to organ transplantation, IPC may have a substantial impact on clinical practice. Alleviation of reperfusion injury of graft by IPC can enhance the function grafts and prolong their survival.

REFERENCES

1 **Platell CF**, Coster J, McCauley RD, Hall JC. The management of patients with the short bowel syndrome. *World J Gastroenterol* 2002; **8**: 13-20
2 **Kato T**, Ruiz P, Thompson JF, Eskind LB, Weppler D, Khan FA, Pinna AD, Nery JR, Tzakis AG. Intestinal and multivisceral transplantation. *World J Surg* 2002; **26**: 226-237
3 **Park BK**. Intestinal transplantation in pediatric patients. *Prog Transplant* 2002; **12**: 97-113
4 **Kaufman SS**. Small bowel transplantation: selection criteria, operative techniques, advances in specific immunosuppression, prognosis. *Curr Opin Pediatr* 2001; **13**: 425-428
5 **Dionigi P**, Alessiani M, Ferrazi A. Irreversible intestinal failure, nutrition support, and small bowel transplantation. *Nutrition* 2001; **17**: 747-750
6 **Reyes J**. Intestinal transplantation for children with short bowel syndrome. *Semin Pediatr Surg* 2001; **10**: 99-104
7 **Ghanekar A,** Grant D. Small bowel transplantation. *Curr Opin Crit Care* 2001; **7**: 133-137
8 **Farmer DG**, Amersi F, Shen XD, Gao F, Anselmo D, Ma J, Dry S, McDiarmid SV, Shaw G, Busuttil RW, Kupiec-Weglinski J. Improved survival through the reduction of ischemia-reperfusion injury after rat intestinal transplantation using selective P-selectin blockade with P-selectin glycoprotein ligand-Ig. *Transplant Proc* 2002; **34**: 985
9 **Guo WH**, Chan KL, Fung PP, Chan KW, Tam PK. Nitric oxide protects segmental intestinal grafts from ischemia and reperfasion injury. *Transplant Proc* 2000; **32**: 1297-1298
10 **Carey HV**, Mangino MJ, Southard JH. Changes in gut function during hibernation: implications for bowel transplantation and surgery. *Gut* 2001; **49**: 459-461
11 **Massberg S**, Messmer K. The nature of ischemia / reperfusion injury. *Transplant Proc* 1998; **30**: 4217-4223
12 **Sola A**, Rosello-Catafau J, Alfaro V, Pesquero J, Palacios L, Gelpi E, Hotter G. Modification of glyceraldehyde-3-phosphate dehydrogenase in response to nitric oxide in intestinal preconditioning. *Transplantation* 1999; **67**: 1446-1452
13 **Karck M**, Rahmanian P, Haverich A. Ischemic preconditioning enhances donor heart preservation. *Transplantation* 1996; **62**: 17-22
14 **Yin DP**, Sankary HN, Chong AS, Ma LL, Shen J, Foster P, Williams JW. Protective effect of ischemic preconditioning on liver preservation-reperfusion injury in rats. *Transplantation* 1998; **66**: 152-157
15 **Sola A**, De Oca J, Gonzalez R, Prats N, Rosello-Catafau J, Gelpi E, Jaurrieta E, Hotter G. Protective effect of ischemic preconditioning on cold preservation and reperfusion injury associated with rat intestinal transplantation. *Ann Surg* 2001; **234**: 98-106
16 **Mueller AR**, Platz KP, Heckert C, Hausler M, Guckelberger O, Schuppan D, Lobeck H, Neuhaus P. Extracellular matrix: an early target of preservation / reperfusion injury and acute rejection after small bowel transplantation. *Transplant Proc* 1998; **30**: 2569-2571
17 **Shah KA**, Shurey S, Green CJ. Characterization of apoptosis in intestinal ischaemia-reperfusion injury - a light and electron microscopic study. *Int J Exp Pathol* 1997; **78**: 355-363
18 **Monchik GJ**, Russell PS. Transplantation of small bowel in the rat: technical and immunological considerations. *Surgery* 1971; **70**: 693-702
19 **Wu XT**, Li JS, Zhao XF, Zhuang W, Feng XL. Modified techniques of heterotopic total small intestinal transplantation in rats. *World J Gastroenterol* 2002; **8**: 758-762
20 **Li YX**, Li JS, Li N. Improved technique of vascular anastomosis for small intestinal transplantation in rats. *World J Gastroenterol* 2000; **6**: 259-262

21 **Li YX**, Li JS, Li N. Surgical technique for intestinal transplantation in rats. *Huaren Xiaohua Zazhi* 1998; **6**: 667-669

22 **Giele HP**, Heel KA, Storrie A, McCauley RD, Hall JC. Warm ischaemia time in a model for small bowel transplantation. *Microsurgery* 1996; **17**: 438-443

23 **Wu MY**, Liang YR, Wu XY, Zhuang CX. Relationship between Egr-1 gene expression and apoptosis in esophageal carcinoma and precancerous lesions. *World J Gastroenterol* 2002; **8**: 971-975

24 **Farber A**, Connors JP, Friedlander RM, Wagner RJ, Powell RJ, Cronenwett JL. A specific inhibitor of apoptosis decreases tissue injury after intestinal ischemia-reperfusion in mice. *J Vasc Surg* 1999; **30**: 752-760

25 **Noda T**, Iwakiri R, Fujimoto K, Matsuo S, Aw TY. Programmed cell death induced by ischemia-reperfusion in rat intestinal mucosa. *Am J Physiol* 1998; **274**: G270-276

26 **Taguchi T**, Shima Y, Nakao M, Fujii Y, Tajiri T, Ogita K, Suita S. Activation of immediate early genes in relation to proliferation and apoptosis of enterocytes after ischemia-reperfusion injury of small intestine. *Transplant Proc* 2002; **34**: 983

27 **Zhao ZQ**, Liu FL, Zhang L. Expressions of C-fos PCNA and Bax in intestine after ischemia and in dogs. *Shijie Huaren Xiahua Zazhi* 2001; **9**: 1021-1026

28 **Luo YQ**, Ma LS, Zhao YL, Wu KC, Pan BR, Zhang XY. Expression of proliferating cell nuclear antigen in polyps from large intestine. *World J Gastroenterol* 1999; **5**: 160-164

29 **Prelich G**, Tan CK, Kostura M, Mathews MB, So AG, Downey KM, Stillman B. Functional identity of proliferating cell nuclear antigen and a DNA polymerase-delta auxiliary protein. *Nature* 1987; **326**: 517-520

30 **Murry CE**, Jennings RB, Reimer KA. Preconditioning with ischemia: a delay of lethal cell injury in ischemic myocardium. *Circulation* 1986; **74**: 1124-1136

31 **Aksoyek S**, Cinel I, Avlan D, Cinel L, Ozturk C, Gurbuz P, Nayci A, Oral U. Intestinal ischemic preconditioning protects the intestine and reduces bacterial translocation. *Shock* 2002; **18**: 476-480

32 **Vlasov TD**, Smirnov DA, Nutfullina GM. Preconditioning of the small intestine to ischemia in rats. *Neurosci Behav Physiol* 2002; **32**: 449-453

33 **Yang SP**, Hao YB, Wu YX, Dun W, Shen LH, Zhang Y. Ischemic preconditioning mediated by activation of KATP channels in rat small intestine. *Zhongguo Yaoli Xuebao* 1999; **20**: 341-344

34 **Dun Y**, Hao YB, Wu YX, Zhang Y, Zhao RR. Protective effects of nitroglycerin-induced preconditioning mediated by calcitonin gene-related peptide in rat small intestine. *Eur J Pharmacol* 2001; **430**: 317-324

35 **Zhang Y**, Wu YX, Hao YB, Dun Y, Yang SP. Role of endogenous opioid peptides in protection of ischemic preconditioning in rat small intestine. *Life Sci* 2001; **68**: 1013-1019

36 **Davis JM**, Gute DC, Jones S, Krsmanovic A, Korthuis RJ. Ischemic preconditioning prevents postischemic P-selectin expression in the rat small intestine. *Am J Physiol* 1999; **277**: H2476-2481

37 **Ikeda H**, Suzuki Y, Suzuki M, Koike M, Tamura J, Tong J, Nomura M, Itoh G. Apoptosis is a major mode of cell death caused by ischaemia and ischaemia / reperfusion injury to the rat intestinal epithelium. *Gut* 1998; **42**: 530-537

38 **Fukuyama K**, Iwakiri R, Noda T, Kojima M, Utsumi H, Tsunada S, Sakata H, Ootani A, Fujimoto K. Apoptosis induced by ischemia-reperfusion and fasting in gastric mucosa compared to small intestinal mucosa in rats. *Dig Dis Sci* 2001; **46**: 545-549

39 **Fujisaki** S, Kimizuka K, Park E, Tomita R, Fukuzawa M, Matsumoto K. Immunohistochemical analysis in the extracellular matrix during acute rejection of small bowel grafts in rats. *Transplant Proc* 2000; **32**: 1316-1317

40 **Liu CQ**, Ye JX, Jin B. Components of the extracelluarr matrix. *Shijie Huaren Xiaohua Zazhi* 2002; **10**: 53-54

41 **Mueller AR**, Platz KP, Heckert C, Hausler M, Schuppan D, Lobeck H, Neuhaus P. Differentiation between preservation reperfusion injury and acute rejection after small bowel transplantation. *Transplant Proc* 1998; **30**: 2657-2659

Edited by Zhang JZ and Wang XL

P.O.Box 2345, Beijing 100023,China
Fax: +86-10-85381893
E-mail: wjg@wjgnet.com www.wjgnet.com

World J Gastroenterol 2003;9(8):1871-1873
World Journal of Gastroenterology
 ISSN 1007-9327

• BRIEF REPORTS •

Outcome of gallbladder preservation in surgical management of primary bile duct stones

Ming-Guo Tian, Wei-Jin Shi, Xin-Yuan Wen, Hai-Wen Yu, Jing-Shan Huo, Dong-Feng Zhou

Ming-Guo Tian, Xin-Yuan Wen, Hai-Wen Yu, Jing-Shan Huo, Dong-Feng Zhou, Department of Hepatobiliary Surgery, Affiliated Hospital of Jining Medical College, Jining 272129, Shandong Province, China
Wei-Jin Shi, Department of General Surgery, Ren Ji Hospital of Shanghai Second Medical University, Shanghai 200001, China
Correspondence to: Dr. Ming-Guo Tian, Department of Hepatobiliary Surgery, Affiliated Hospital of Jining Medical College, Jining City 272129, Shandong Province, China. tian88@hotmail.com
Telephone: +86-537-2903270 **Fax:** +86-537-2213030
Received: 2003-02-25 **Accepted:** 2003-03-29

Abstract

AIM: To evaluate the methods and outcome of gallbladder preservation in surgical treatment of primary bile duct stones.

METHODS: Thirty-five patients with primary bile duct stones and intact gallbladders received stone extraction by two operative approaches, 23 done through the intrahepatic duct stump (RBD-IDS, the RBD-IDS group) after partial hepatectomy and 12 through the hepatic parenchyma by retrograde puncture (RBD-RP, the RBD-RP group). The gallbladders were preserved and the common bile duct (CBD) incisions were primarily closed. The patients were examined postoperatively by direct cholangiography and followed up by ultrasonography once every six months.

RESULTS: In the RBD-IDS group, residual bile duct stones were found in three patients, which were cleared by a combination of fibrocholedochoscopic extraction and lithotripsy through the drainage tracts. The tubes were removed on postoperative day 22 (range: 16-42 days). In the RBD-RP group, one patient developed hemobilia and was cured by conservative therapy. The tubes were removed on postoperative day 8 (range: 7-11 days). Postoperative cholangiography showed that all the gallbladders were well opacified, contractile and smooth. During 54 (range: 6-120 months) months of follow-up, six patients had mildly thickened cholecystic walls without related symptoms and further changes, two underwent laparotomies because of adhesive intestinal obstruction and gastric cancer respectively, three died of cardiopulmonary diseases. No stones were found in all the preserved gallbladders.

CONCLUSION: The intact gallbladders preserved after surgical extraction of primary bile duct stones will not develop gallstones. Retrograde biliary drainage is an optimal approach for gallbladder preservation.

Tian MG, Shi WJ, Wen XY, Yu HW, Huo JS, Zhou DF. Outcome of gallbladder preservation in surgical management of primary bile duct stones. *World J Gastroenterol* 2003; 9(8): 1871-1873
http://www.wjgnet.com/1007-9327/9/1871.asp

INTRODUCTION

The gallbladder is important for digestion. Cholecystectomy can give rise to postoperative symptoms such as flatulent dyspepsia, abdominal pain, distention, heart burn, obstipation and diarrhea[1-5], and may lead to increase of incidence of carcinoma of the proximal colon[6]. Many patients with primary bile duct stones do not have stones in the gallbladders. However, as T-tube drainage after common bile duct (CBD) exploration may cause adhesion and subsequent cholecystitis and stone formation, these intact gallbladders are often concomitantly resected. Since 1991, we have adopted retrograde biliary drainage instead of T-tube drainage for primary bile duct stones. Thirty-five intact gallbladders have been thus preserved.

MATERIALS AND METHODS

Patients

Thirty-five patients with primary bile duct stones and intact gallbladders received retrograde biliary drainage (RBD) between December 1991 and December 2001. The age of the patients ranged from 29 to 70 (mean 44) years. Preoperative diagnosis was made by ultrasonography and in some cases by a combination with percutaneous transhepatic cholangiography (PTC). During the operation, the gallbladders were normal in appearance and no stones and lesions were found by intraoperative ultrasonography (IOUS). Stones extracted from the bile ducts had the typical features of pigment stones with brown color and soft quality. Stone distribution and the operation methods are shown in Table 1. Postoperatively, all the patients were routinely examined by direct cholangiography and followed up once every six months by ultrasonography. The follow-up duration ranged from 6 to 120 (mean 54 months) months.

Table 1 Stone distribution and operation methods

Stone distribution	Cases	Operation methods	Cases
Left hepatic	11	RBD-IDS&II, III segmentectomy	15
Extrahepatic	8	RBD-RP	12
Intra-and extrahepatic	8	RBD-IDS & left hepatectomy	6
Bilateral hepatic	7	RBD-IDS & III segmentectomy	1
Segment VII	1	RBD-IDS & VII segmentectomy	1
Total	35	Total	35

Notes: RBD-RP: retrograde biliary drainage by retrograde puncture, RBD-IDS: retrograde biliary drainage through intrahepatic duct stump.

Methods

RBD through intrahepatic duct stump (RBD-IDS) After partial hepatectomy for intrahepatic bile duct stones, biliary tract exploration was done by fibrocholedochoscopy through the intrahepatic bile duct stump. The CBD was incised in the patient with big concurrent extrahepatic bile duct stones which could not be extracted retrogradely. The RBD tube was placed through the hepatic duct stump and the CBD incision was closed primarily. In case of suspected residual stones, the RBD

tube was sheathed by a tube of larger bore from the abdominal wall to the lumen of the stump.

RBD by retrograde puncture (RBD-RP) After CBD exploration and stone clearance, a guide sheath was inserted into the right hepatic duct, with the tip as deep in the duct as possible. The direction was regulated with IOUS to avoid injury of large blood vessels. An 8Fr cannula fitting over a matching stylet was inserted through the guide sheath and pushed forward until the tip came out of the liver. From the other end, an 8Fr Silastic drainage tube was inserted over the guide wire which was introduced through the cannula. When the tip of the drainage tube emerged in the CBD incision, the guide wire, retrograde cannula and guide sheath were retracted together. The end of the drainage tube was brought out of the abdominal wall subcostally. The CBD incision was primarily closed. Intraoperative cholangiography was done to rule out residual stones in some suspected cases.

RESULTS

In the RBD-IDS group, postoperative drainage of bile was 340-780 ml/d (mean 440±140 ml/d). The drainage tubes were removed on postoperative day 16-42 (mean 22 days). Residual stones were found in three cases. After four weeks, stone extraction started through the tracts with the help of fibrocholedochoscope and ultrasonic lithotriptor. All patients had the stones cleared after 2-5 sessions of extraction. In the RBD-RP group, postoperative drainage of bile was 150-800 ml/d (mean 520±210 ml/d). Bile drainage was interrupted intermittently in two patients owing to blockage of the tubes and it resumed to draining after flushing with normal saline. The drainage tubes were removed on postoperative day 7-11 (mean 8 days). Hemobilia occurred in one earlier treated patient. She recovered soon after conservative therapy. No tube dislocation or residual stones occurred in this series.

Postoperative cholangiography of both methods showed that the extrahepatic bile ducts had no stricture at the sites of CBD incisions. The preserved gallbladders were well opacified, contractile and smooth (Figure 1). During the follow-up, six patients were found to have rough and mildly thickened cholecystic walls at 12-36 months after operation. However, these patients had no related symptoms and no further changes afterwards. Two patients underwent laparotomies because of adhesive intestinal obstruction and gastric cancer, respectively. Three died of cardiopulmonary diseases. No stones occurred in the preserved gallbladders.

Figure 1 Direct cholangiogram showed that the preserved gallbladder was well opacified and contractile.

DISCUSSION

A high recurrent rate of gallbladder stone after successful extracorporeal shock wave lithotripsy and dissolution has been documented by many reports[7-11]. However, the gallbladders after endoscopic sphincterotomy for common bile duct calculi rarely formed stones[12-14]. One explanation for the difference of the results is that sphincterotomy decreases fasting volume of the gallbladder and increases its contraction ability[15, 16]. Another is that the primary bile duct pigment stone is different from the cholecystic cholesterol one in both epidemiology[17-21] and pathogenesis[22-26]. It is therefore generally considered that both kinds of stones are different diseases[26]. The results of this study also showed that the gallbladders preserved during operation of the patients with primary bile duct stones had no tendency to form stones. As most gallbladders of the patients with primary intrahepatic bile duct stones are not affected, concomitant cholecystectomy during surgical extraction of stones or liver resection in these patients seems unjustified.

T-tube drainage after choledochostomy or after liver resection is a conventional method for primary bile duct stones. However, many reports in recent decades have demonstrated the problems it brought about[27,28]. The long tube-bearing not only results in inconvenience, but also causes pathological changes of the CBD[29]. T-tube tract can also adhere to the gallbladder and impair its function. Therefore, intact gallbladder is often concomitantly resected during these operations. In recent years, several alternatives to T-tube drainage have been reported[30-33]. However, preservation of the gallbladder during surgical management of primary bile duct stones and its long-term outcome have not been reported yet. After retrograde biliary drainage, the function of the gallbladder will not be impaired by tube stimulation or tube induced local adhesion because the gallbladder does not contact the drainage tube. This study also demonstrated that both methods had respective advantages over T-tube placement in residual stone management and the duration of tube-bearing.

Therefore, we conclude that retrograde biliary drainage is an optimal method for preservation of gallbladder during surgical management of primary bile duct stones.

REFERENCES

1 **Ure BM**, Troidl H, Spangenberger W, Lefering R, Dietrich A, Eypasch EP, Neugebauer E. Long-term results after laparoscopic cholecystectomy. *Br J Surg* 1995; **82**: 267-270

2 **Sand J**, Pakkala S, Nordback I. Twenty to thirty year follow-up after cholecystectomy. *Hepatogastroenterology* 1996; **43**: 534-537

3 **Ros E**, Zambon D. Postcholecystectomy symptoms. A prospective study of gall stone patients before and two years after surgery. *Gut* 1987; **28**: 1500-1504

4 **McNamara DA**, O'Donohoe MK, Horgan PG, Tanner WA, Keane FB. Symptoms of esophageal reflux are more common following laparoscopic cholecystectomy than in a control population. *Ir J Med Sci* 1998; **167**: 11-13

5 **Carrilho-Ribeiro L**, Serra D, Pinto-Correia A, Velosa J, De Moura MC. Quality of life after cholecystectomy and after successful lithotripsy for gallbladder stones: a matched-pairs comparison. *Eur J Gastroenterol Hepatol* 2002; **14**: 741-744

6 **Alley PG**, Lee SP. The increased risk of proximal colonic cancer after cholecystectomy. *Dis Colon Rectum* 1983; **26**: 522-524

7 **Pelletier G**, Raymond JM, Capdeville R, Mosnier H, Caroli-Bosc FX. Gallstone recurrence after successful lithotripsy. *J Hepatol* 1995; **23**: 420-423

8 **Plauletzki J**, Holl J, Sackmann M, Neubrand M, Klueppelberg U, Sauerbruch J, Paumgartner G. Gallstone recurrence after direct contact dissolution with methyl tert-butyl ether. *Dig Dis Sci* 1995; **40**: 1775-1781

9 **Benes J**, Chmel J, Blazek O, Marecek Z. Extracorporeal shock wave lithotripsy of gallstones with oral dissolution: results in course of ten years in czech republic in correlation to indication criteria. *Sb Lek* 2001; **102**: 17-22

10 **Chen P**, Wang BS, He LQ. Multifactorial analysis of recurrence of cholecy stolithiasis in Shanghai area. *World J Gastroenterol* 1999; **5**: 31-33

11 **Janssen J**, Johanns W, Weickert U, Rahmatian M, Greiner L. Long-term results after successful extracorporeal gallstone lithotripsy: outcome of the first 120 stone-free patients. *Scand J Gastroenterol* 2001; **36**: 314-317

12 **Kwon SK**, Lee BS, Kim NJ, Lee HY, Chae HB, Youn SJ, Park SM. Is cholecystectomy necessary after ERCP for bile duct stones in patients with gallbladder in situ? *Korean J Intern Med* 2001; **16**: 254-259

13 **Benattar JM**, Caroli-Bosc FX, Harris AG, Dumas R, Delmont J. Endoscopic sphincterotomy for common bile duct calculi in patients without stones in the gallbladder. *Dig Dis Sci* 1993; **38**: 2225-2227

14 **Tanaka M**, Ikeda S, Yoshimoto H, Matsumoto S. The long term fate of the gallbladder after endoscopic sphincterotomy. *Am J Surg* 1987; **154**: 505-509

15 **Sugiyama M**, Atomi Y. Long term effects of endoscopic sphincterotomy on gall bladder motility. *Gut* 1996; **39**: 856-859

16 **Sharma BC**, Agarwal DK, Baijal SS, Negi TS, Choudhuri G, Saraswat VA. Effect of endoscopic sphincterotomy on gall bladder bile lithogenicity and motility. *Gut* 1998; **42**: 288-292

17 **Kawai M**, Iwahashi M, Uchiyama K, Ochiai M, Tanimura H, Yamaue H. Gram-positive cocci are associated with the formation of completely pure cholesterol stones. *Am J Gastroenterol* 2002; **97**: 83-88

18 **Lee DK**, Tarr PI, Haigh WG, Lee SP. Bacterial DNA in mixed cholesterol gallstones. *Am J Gastroenterol* 1999; **94**: 3502-3506

19 **Ko CW**, Lee SP. Gallstone formation: local factors. *Gastroenteral Clin North Am* 1999; **28**: 99-115

20 **Sandstad O**, Osnes T, Skar V, Urdal P, Osnes M. Structure and composition of common bile duct stones in relation to duodenal diverticula, gastric resection, cholecystectomy and infection. *Digestion* 2000; **61**: 181-188

21 **Makino I**, Chijiiwa K, Higashijima H, Nakahara S, Kishinaka M, Kuroki S, Mibu R. Rapid cholesterol nucleation time and cholesterol gall stone formation after subtotal or total colectomy in humans. *Gut* 1994; **35**: 1760-1764

22 **Donovan JM**. Physical and metabolic factors in gallstone pathogenesis. *Gastroenterol Clin North Am* 1999; **28**: 75-97

23 **Higashijima H**, Ichimiya H, Nakano T, Yamashita H, Kuroki S, Satoh H, Chijiiwa K, Tanaka M. Deconjugation of bilirubin accelerates coprecipitation of cholesterol, fattyacids, and mucin in human bile - *in vitro* study. *J Gastroenterol* 1996; **31**: 828-835

24 **Diehl AK**, Schwesinger WH, Holleman DR Jr, Chapman JB, Kurtin WE. Clinical correlates of gallstone composition: distinguishing pigment from cholesterol stones. *Am J Gastroenterol* 1995; **90**: 967-972

25 **Ho KJ**, Lin XZ, Yu SC, Chen JS, Wu CZ. Cholelithiasis in Taiwan: Gallstone characteristics, surgical incidence, bile lipid composition, and role of beta-glucuronidase. *Dig Dis Sci* 1995; **40**: 1963-1973

26 **Sarli L**, Gafa M, Bonilauti E, Longinotti E, Carreras F, Pietra N, Peracchia A. Pigment vs. cholesterol microlithiasis: comparison of clinical features, bacteriology, stone and gallbladder composition. *Hepatogastroenterology* 1989; **36**: 156-159

27 **Wills VL**, Gibson K, Karihaloot C, Jorgensen JO. Complications of biliary T-tube after choledochotomy. *ANZ J Surg* 2002; **72**: 177-180

28 **Corbett CR**, Fyfe NC, Nicholls RJ, Jackson BT. Bile peritonitis after removal of T-tubes from the common bile duct. *Br J Surg* 1986; **73**: 641-643

29 **Lee SH,** Burhenne HJ. Extrahepatic bile duct angulation by T-tube: the elbow sign. *Gastrointest Radiol* 1991; **16**: 157-158

30 **Zhi QH**. New development of biliary surgery in China. *World J Gastroenterol* 2000; **6**: 187-192

31 **Tsunoda T**, Kusano T, Furukawa M, Eto T, Tsuchiya R. Common bile duct exploration--primary closure of the duct with retrograde transhepatic biliary drainage. *Jpn J Surg* 1991; **21**: 162-166

32 **Tian MG**, Wen XY, Liu ZY, Cao HX, Li H. Operative percutaneous transhepatic biliary catheterization by retrograde puncture. *Zhongguo Putong Waike Zazhi* 1995; **4**: 91-93

33 **Goseki N**, Methaste A, Gen T, Ito K, Endo M. Extraperitoneal retrograde transhepatic biliary drainage for common bile duct exploration for prevention of tube dislodgement and its earlier removal. *Dig Surg* 1998; **15**: 12-14

Edited by Xu XQ

P.O.Box 2345, Beijing 100023,China
Fax: +86-10-85381893
E-mail: wjg@wjgnet.com www.wjgnet.com

World J Gastroenterol 2003;9(8):1874-1877
World Journal of Gastroenterology
 ISSN 1007-9327

• BRIEF REPORTS •

Effects of neurotrophins on gastrointestinal myoelectric activities of rats

Ning-Li Chai, Lei Dong, Zong-Fang Li, Ke-Xin Du, Jian-Hua Wang, Li-Kun Yan, Xi-Lin Dong

Ning-Li Chai, Lei Dong, Xi-Lin Dong, Department of Digestion, Second Affiliated Hospital, Xi' an Jiaotong University, Xi' an 710004, Shaanxi Province, China
Zong-Fang Li, Department of General Surgery, Second Affiliated Hospital, Xi' an Jiaotong University, Xi' an 710004, Shaanxi Province, China
Ke-Xin Du, Functional Center of Medical School, Xi' an Jiaotong University, Xi' an 710061, Shaanxi Province, China
Jian-Hua Wang, Li-Kun Yan, Department of General Surgery, Shaanxi Provincial People' s Hospital, Xi' an 710068, Shaanxi Province, China
Supported by the National Natural Science Foundation of China, No. 30170414
Correspondence to: Lei Dong, Department of Digestion, Second Affiliated Hospital, Xi' an Jiaotong University, Xi' an 710004, Shaanxi Province, China. csxlily@ hotmail.com
Telephone: +86-29-8024005 **Fax:** +86-29-7231758
Received: 2003-01-18 **Accepted:** 2003-03-10

Abstract

AIM: To observe the effects of mouse nerve growth factor (NGF), rat recombinant brain derived neurotrophic factor (rm-BDNF) and recombinant human neurotrophin-3 (rh-NT-3) on the gastrointestinal motility and the migrating myoelectric complex (MMC) in rat.

METHODS: A randomized, double-blinded, placebo-controlled experiment was performed. 5-7 days after we chronically implanted four or five bipolar silver electrodes on the stomach, duodenum, jejunum and colon, 21 experimental rats were coded and divided into 3 groups and injected NGF, rm-BDNF, rh-NT-3 or placebo respectively via tail vein at a dose of 20 $\mu g \cdot kg^{-1}$. The gastrointestinal myoelectrical activity was recorded 2 hours before and after the test substance infusions in these consciously fasting rats.

RESULTS: The neurotrophins-induced pattern of activity was characterized by enhanced spiking activity of different amplitudes at all recording sites, especially in the colon. In the gastric antrum and intestine, only rh-NT-3 had increased effects on the demographic characteristics of electrical activities ($P<0.05$), but did not affect the intervals of MMCs. In the colon, all the three kinds of neurotrophins could significantly increase the frequency, amplitude and duration levels of spike bursts, and also rh-NT-3 could prolong the intervals of MMC in the transverse colon (25±11 min *vs* 19±6 min, $P<0.05$). In the distal colon rh-NT-3 could evoke phase III-like activity and disrupt the MMC pattern, which was replaced by a continuously long spike bursts (LSB) and irregular spike activity (ISA) for 48±6 min.

CONCLUSION: Exogenous neurotrophic factors can stimulate gut myoelectric activities in rats.

Chai NL, Dong L, Li ZF, Du KX, Wang JH, Yan LK, Dong XL. Effects of neurotrophins on gastrointestinal myoelectric activities of rats. *World J Gastroenterol* 2003; 9(8): 1874-1877
http://www.wjgnet.com/1007-9327/9/1874.asp

INTRODUCTION

Many basic studies have shown that neurotrophins play fundamental roles in the differentiation, survival and maintenance of peripheral and central neurons[1-5] and have suggested the possible use of neurotrophins as therapeutic tools for degenerative neuronal disorders[6]. Neurotrophic factors comprise nerve growth factor (NGF), brain-derived neurotrophic factor (BDNF), neurotrophin-3 (NT-3), NT-4/5, and NT-6[7-9]. These factors signal their effects through specific tyrosine-kinase (trk) receptors[10,11]. In addition to the high sequence homology of neurotrophins, neurotrophic factors including NT-3, BDNF and NGF are also highly conserved across species (mouse, rat and human)[13].

In a clinical study of patients with a variety of neurologic disorders treated with rh-NT-3 or recombinant human BDNF (rh-BDNF), they were found to have alterations of bowel function, and a dose-related tendency to increasing frequency of stools or having "diarrhea"[14]. Studies also have proved that exogenous neurotrophic factors stimulate gut motility and accelerate colonic transit in health and constipation[14]. This suggests that the action of rh-NT-3 and rh-BDNF on the gastrointestinal tract parallels their effect on the central nervous system. Review of the clinical reports suggested an increased frequency of bowel movements with less impressive effects on stool consistency[15], but the mechanism is unclear so far.

All the conclusions of previous studies lead to the hypothesis that neurotrophins alter bowel motor function, leading to increased frequency of bowel movements. In order to assess the action of neurotrophins on gut motility, in the present study we injected respectively NGF, rm-BDNF and rh-NT-3 via tail vein and registered the electrical activities with chronically implanted electrodes in fasting rats.

MATERIALS AND METHODS

Animal preparation

21 healthy Sprague-Dawley (SD) rats, weighing 250-300 (mean 276±17) g, 15 male and 6 female, individually housed, fed on chow pellets and water *ad libitum*, were used for these experiments. After fasted for 24 h, the rats were intraperitoneally anesthetized with sodium pentobarbital 30 $mg \cdot kg^{-1}$ (ip) A segment of the small intestine was exposed through a midline incision. Four or five bipolar insulated silver electrodes made by teflon-coated wire (0.5 mm in outer diameter, 20 cm in length) were implanted into the muscular layer of the bowel with a needle as a trocar. 1 mm of the wire was exposed near the implanted end, and the interval between pairs of electrodes should be 2.0-3.0 mm. The electrodes were placed on the gastric antrum at 5 mm proximal to the pylorus, on the duodenum and jejunum respectively at 5 cm and 20 cm distal to the pylorus, and on the transverse colon 5 cm distal to the ileocaecal junction. Among the 21 experimental animals, 9 were implanted electrodes on the distal colon 10 cm distal to the ileocaecal junction at the same time. The bundled electrode wires were grasped by the clamp through a silastic tube (2.4 mm in diameter), which then passed

through the subcutaneous tunnel from the abdominal incision to the back of the shoulder exit. Following surgery, the rats were individually housed, and allowed 5 to 7 days to recover from the surgery.

Motility recordings

The animals were fasted for 8 h with free access to water. The experiments were performed in conscious rats. The electromyographic (EMG) recordings were monitored by using a polygraph (Biolap98, Chengdu, China), with time constant set at 0.01 s, gain set at 1 000, the filtering at lower and higher frequencies set at 0.3 Hz and 100 Hz, respectively. The amplitudes of contractions were recorded in microvolts and the paper speed was 5 cm· h^{-1}.

Experimental procedure

A randomized, double-blinded, placebo-controlled experiment was performed. The rats were coded and divided into 3 groups, 7 animals in each group. On each experimental day, at the beginning of the experiments, the gastrointestinal myoelectrical activity was recorded for 2 h for each rat, and during this period at least 3 MMCs appeared. Then, the test substances were infused through the tail vein. The substances were dissolved immediately before use in normal saline. In each group, 2 rats were placed as control that received placebo (vehicle), 0.2 mL saline containing 250 μg bovine serum albumin (BSA, Sigma), the other 5 received 0.2 ml saline containing neurotrophins at a dose of 20 μg· kg^{-1}. Of them, 3 were placed electrodes on the distal colon as well. The three groups were injected them NGF (Sigma), rm-BDNF (Sigma) and rh-NT-3 (Sigma), respectively. After tail vein injection, the gastrointestinal myoelectrical activity of the rats was continuously recorded at least for 2 h. The codes of rats were not released (sealed) for analysis until all the EMG recordings and the entire data set for statistical studies were completed.

Statistical analysis

The results were expressed as $\bar{x}\pm s$ unless otherwise stated. Student' s *t* test was used to compare the different paired values before and after the test substance administration in the 3 groups. It was considered to be statistically significant when $P<0.05$.

RESULTS

Gastrointestinal myoelectrical activity during fasting

About 1 week later, among the 93 pairs of electrodes, 2 pairs implanted on the gastric antrum failed possibly due to the their slipping off, the other 91 pairs continued to function until the study was completed. A typical pattern of myoelectrical activity in the fasting state was observed in all rats (Figure 1, Table 1). Of the totally 238 activity fronts recorded in fasting rats under control, we observed that 199 (80 %) started in the duodenum.

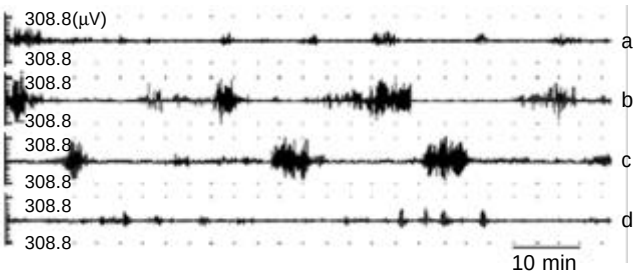

Figure 1 Electrical activity recorded directly from four electrode sites on the gastric antrum (a) at 5 mm proximal to the pylorus, on the duodenum (b) and jejunum (c) respectively at 5 cm and 20 cm distal to the pylorus, and on the transverse colon (d) at 5 cm distal to the ileocaecal junction in one fasting rat.

The antral myoelectrical activity was characterized by the presence of spike bursts, superimposed at 34.5 % of the

Table 1 Effects of neurotrophins (20 μg· kg^{-1}) on gut myoelectric activity profiles 2 h before and 1 h after administration. ($\bar{x}\pm s$)

Parameter	Site	*n*	NGF treatment		rm-BDNF treatment		rh-NT-3 treatment		Placebo treatment	
			Before	After	Before	After	Before	After	Before	After
	Antrum	5	1.6±0.5	1.6±0.5	1.6±0.5	1.6±0.5	1.6±0.5	1.8±0.6[a]	1.6±0.5	1.6±0.5
Frequency of	Duodenum	5	16.2±5.4	17.5±5.8	15.9±5.2	17.2±5.9	16.3±5.6	20.1±9.3[a]	16.3±5.4	16.5±5.6
spike bursts	Jejunum	5	12.1±2.8	13.5±3.4	11.9±2.6	13.2±3.7	12.2±2.7	16.5±7.1[a]	12.5±2.9	12.4±2.8
(min^{-1})	Transverse colon	5	0.6±0.1	0.8±0.1[a]	0.6±0.1	0.8±0.1[a]	0.6±0.1	0.9±0.2[b]	0.6±0.1	0.6±0.1
	Distal colon*	3	0.5±0.1	0.7±0.1[a]	0.5±0.1	0.7±0.1[a]	0.5±0.1	0.9±0.2[b]		
	Antrum	5	180.2±18.6	182.3±19.1	181.3±17.9	182.5±20.4	180.6±17.9	185.2±22.1[a]	180.9±18.8	180.4±18.9
Amplitude of	Duodenum	5	306.5±73.6	308.8±72.7	306.7±72.9	308.4±72.4	306.5±72.7	314.6±81.8[a]	305.6±74.2	306.2±74.5
spike bursts	Jejunum	5	295.8±87.2	297.4±88.5	296.5±88.1	298.6±89.3	295.6±86.7	313.8±98.3[b]	296.8±87.3	295.8±88.5
(μV)	Transverse colon	5	138.7±32.1	142.5±35.9[a]	139.4±33.4	145.5±38.8[a]	139.5±33.3	160.3±47.5[b]	137.9±31.8	139.1±32.5
	Distal colon*	3	142.9±29.9	163.5±40.1[a]	141.2±27.3	160.5±37.4[a]	142.6±29.1	173.4±35.4[b]		
	Antrum	5	4.8±1.1	4.8±1.2	4.7±1.2	4.9±1.3	4.8±1.2	4.9±1.5	4.8±1.2	4.8±1.2
Duration of	Duodenum	5	6.5±2.7	6.6±3.1	6.5±2.8	6.6±3.2	6.5±2.8	11.5±6.8[a]	6.5±2.8	6.5±2.7
spike bursts	Jejunum	5	6.7±3.1	6.8±3.2	6.7±3.1	6.9±3.4	6.8±3.2	12.9±8.3[a]	6.8±3.2	6.8±3.2
(s)	Transverse colon	5	9.3±2.2	14.3±6.2[a]	9.3±2.2	13.5±7.2[a]	9.3±2.3	15.3±7.5[a]	9.3±2.2	9.3±2.3
	Distal colon*	3	12.7±2.7	17.8±3.8[a]	12.7±2.7	19.7±4.7[a]	12.7±2.8	46.2±7.3[b]		
	Antrum	5	10.1±3.1	11.3±4.0	10.2±3.4	11.3±4.3	10.1±3.1	12.3±6.2	10.3±3.3	10.2±3.1
Intervals	Duodenum	5	15.3±5.4	16.9±6.1	16.1±5.5	17.2±6.2	15.5±5.5	17.3±7.5	15.6±5.5	15.6±5.2
of MMC	Jejunum	5	16.8±5.8	18.2±7.4	17.1±5.9	18.9±7.6	16.8±5.8	19.1±9.1	16.4±5.6	16.4±5.6
(min)	Transverse colon	5	18.4±6.0	19.7±6.1	19.3±6.1	21.0±7.5	18.9±6.0	25.1±11.1[a]	19.2±6.2	19.7±6.3
	Distal colon*	3	19.7±4.1	22.2±8.0	20.8±5.3	23.5±8.4	19.9±4.2	-		

[a]$P<0.05$, [b]$P<0.01$ *vs* before, * There were 3 among 5 experimental rats in the three groups placed bipolar electrodes at distal colon.

rhythmic oscillatory potentials corresponding to the slow wave rhythm. In fasting rats, the pattern of spike bursts of the small intestine was organized into cyclic MMCs that occurred at regular 15.6±5.4 min intervals and were propagated from the duodenum to the jejunum at 2 to 3 cm· min^{-1}. Each MMC was a cycle consisting of four phases: a period of silence (slow wave), namely phase I lasting 7.3±0.8 min, which was followed sequentially by a period of ISA (irregular spike activity), namely phase II lasting 4.1±0.9 min, and phase III of intense RSA (regular spike activity) lasting 3.6±1.1 min. Phase IV was the last period from the end of phase III to the start of phase I lasting 0.9±0.3 min. The intervals between the MMCs were measured from the end of one activity before to the end of the next one.

The pattern of colonic myoelectrical activity was characterized by randomly occurring spike bursts at a frequency of 0.6±0.07 per minute in the transverse colon and 0.5±0.09 per minute in the distal colon.

Effects of neurotrophins on the gastrointestinal and colon myoelectric activity

The effect of neurotrophins on the gastrointestinal motility was established within 2 to 4 min after commencement of the infusion. The neurotrophin-induced pattern of activity was characterized by enhanced spiking activity of different amplitudes at all recording sites, especially at the colon, which continued about 50±8 min and gradually returned to normal complexes. There was no significant difference in demographic characteristics before and after placebo treatment. Table 1 summarizes the effect of neurotrophins on the different electromyographic parameters before and after treatment.

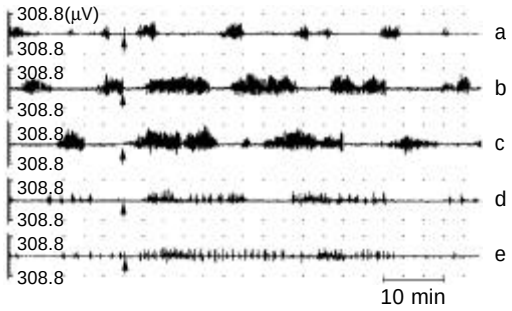

Figure 2 The effects of rh-NT-3 on the myoelectric activities respectively recorded from gastric antrum (a), duodenum (b), jejunum (c), transverse colon (d), and distal colon (e) in one case. The arrows indicated the time point of rh-NT-3 injection via tail vein at a dose of 20 μg·kg^{-1}.

In the gastric antrum and intestine of fasting rats, administration of 20 μg· kg^{-1} mouse NGF and rm-BDNF didn' t significantly increase electrical activities (P>0.05), whereas intravenous infusion of 20 μg· kg^{-1} rh-NT-3 could increase the frequency, amplitude and duration of spike bursts (P<0.05, Table 1), but did not affect the intervals of MMCs (Figure 2).

In the colon, treatment with mouse NGF and rm-BDNF prolonged the duration as well as increased the frequency and amplitude of spike bursts (P<0.05, Table 1) without alterations of MMC intervals. In the transverse colon, rh-NT-3 not only significantly increased the electrical activities, but also prolonged the intervals of MMC (25±11 min *vs* 19±6 min, P<0.05) (Figure 2). The distal colon electromyogram recordings in 3 cases implanted bipolar electrodes on the distal colon, showed that rh-NT-3 could evoke phase III-like activity and disrupt the MMC pattern that were replaced by a continuous long spike bursts (LSB) and irregular spike activity (ISA) for 48±6 min (Figure 2).

DISCUSSION

Previous studies showed that rm-BDNF and rh-NT-3 caused diarrhea in a dose-related manner[15] and that exogenous neurotrophic factors accelerated colonic transit and increased stool frequency in humans[14]. The present studies were carried out to evaluate comparatively the effects of NGF, rm-BDNF and rh-NT-3 on the gastrointestinal myoelectric activity in fasting rats. The study firstly showed that neurotrophin-induced pattern of activity was characterized by enhanced spiking activity of different amplitudes at all recording sites, especially in the colon. The MMCs were firstly described in the small intestine of fasting dogs and its presence was observed in several species, including rats. In the present studies, MMC was also observed in fasting rats and found that in gastric antrum and intestine, only rh-NT-3 had enhanced effects on demographic characteristics of electrical activities (P<0.05), but did not affect the intervals of MMCs. In the colon, not only all the three kinds of neurotrophins infusion could significantly increase the frequency, amplitude and duration of spike bursts, but also rh-NT-3 could prolong the intervals of MMC in the transverse colon (25±11 min *vs* 19±6 min, P<0.05), and in the distal colon, rh-NT-3 could evoke phase III-like activity and disrupt the MMC pattern, which was replaced by continuous LSB and ISA for 48±6 min. Thus the present results indicate that exogenous neurotrophic factors can stimulate gut myoelectric activity in rats. The recording of myoelectrical activity by means of chronically implanted electrodes in rats is a suitable experimental animal model to investigate the mechanism of action of neurotrophins on intestinal motility.

Our conclusion is consistent with the previous ones. Probably it can contribute to the explanation of the mechanisms of the rapid onset of diarrhea in clinical trials with these neurotrophins, that neurotrophins lead to increases of bowel motor, as a result the gastrointestinal contents are transmitted too quickly, leading to diarrhea for the water having not been fully absorbed.

Two mechanisms mediating the actions of neurotrophins on neuromuscular function are considered: trophic effects or a direct effect on neurotransmission[22]. The neurotrophins have long-term trophic actions, including prolongation of survival and speeding up phenotypic maturation of many types of neurons[16-19]. These functions are mediated by the Trk family of tyrosine kinase receptors[20-23]. Modulation of neurotransmission has been shown by acute or short-lived effects of neurotrophins[24,25]. For example, BDNF modulates neurotransmitter synthesis, increases neuronal excitability, and provides long-term synaptic potentiation of neurons[26], and it has been reported that NT-3 stimulates the expression of SP and neurotrophins, enhances not only synthesis but also storage of acetylcholine (Ach) in cultured septal neurons[27]. The time of the onset of effects on bowel movements with exogenous r-metHuBDNF and r-merHuNT-3 suggested direct actions on the neuromuscular apparatus or a very rapid trophic or regenerative effect on gut neuromuscular function. The other study suggested that the mechanism of rh-NT-3 excitation of colonic muscle involved increased noncholinergic contractility and decreased NANC neurotransmission with reduction in number of nitric oxide synthase (NOS) neurons. The abundance of BDNF protein in certain internal organs suggests that this neurotrophin may regulate the function of adult visceral sensory and motor neurons.

We are not quite clear why different enhancements of neurotrophins accelerating gut transition in the stomach, duodeno-jejunum and colon are possibly associated with the receptors of different neurotrophin distribution in gastrointestinal tract. Decreased trk C expression may reflect developmental abnormalities in Hirschsprung' s disease and idiopathic slow-transit constipation (STC)[28]. Further studies are needed to elucidate the precise mechanism by which neurotrophins

influence smooth muscle contractility and/or enteric nerve functions in the human gastrointestinal tract.

Gut motility disorder is common in clinical practice[29-33], and its suitable treatment should be studied[34-38]. In this respect, our data indicate that neurotrophins are the promising agents capable of modifying transit in the entire gastrointestinal tract and may provide novel treatments for patients with disturbed gut motility, such as Hirschspnmg' s disease[28, 39].

REFERENCES

1 **Shao Y,** Akmentin W, Toledo-Aral JJ, Rosenbaum J, Valdez G, Cabot JB, Hilbush BS, Halegoua S. Pincher, a pinocytic chaperone for nerve growth factor/TrkA signaling endosomes. *J Cell Biol* 2002; **157:** 679-691

2 **Chiabrando GA,** Sanchez MC, Skornicka EL, Koo PH. Low-density lipoprotein receptor-related protein mediates in PC12 cell cultures the inhibition of nerve growth factor-promoted neurite outgrowth by pregnancy zone protein and alpha2-macroglobulin. *J Neurosci Res* 2002; **70:** 57-64

3 **Groth R,** Aanonsen L. Spinal brain-derived neurotrophic factor (BDNF) produces hyperalgesia in normal mice while antisense directed against either BDNF or trkB, prevent inflammation-induced hyperalgesia. *Pain* 2002; **100:** 171-181

4 **Mizoguchi Y,** Monji A, Nabekura J. Brain-derived neurotrophic factor induces long-lasting Ca^{2+}-activated K^+ currents in rat visual cortex neurons. *Eur J Neurosci* 2002; **16:** 1417-1424

5 **Bartlett SE,** Reynolds AJ, Weible M, Hendry IA. Phosphatidylinositol kinase enzymes regulate the retrograde axonal transport of NT-3 and NT-4 in sympathetic and sensory neurons. *J Neurosci Res* 2002; **68:** 169-175

6 **Alberch J,** Perez-Navarro E, Canals JM. Neuroprotection by neurotrophins and GDNF family members in the excitotoxic model of Huntington's disease. *Brain Res Bull* 2002; **57:** 817-822

7 **Stucky C,** Shin JB, Lewin GR. Neurotrophin-4: a survival factor for adult sensory neurons. *Curr Biol* 2002; **12:** 1401-1404

8 **Caleo M,** Menna E, Chierzi S, Cenni MC, Maffei L. Brain-derived neurotrophic factor is an anterograde survival factor in the rat visual system. *Curr Biol* 2000; **10:** 1155-1161

9 **von Bartheld CS,** Wang X, Butowt R. Anterograde axonal transport, transcytosis, and recycling of neurotrophic factors: the concept of trophic currencies in neural networks. *Mol Neurobiol* 2001; **24:** 1-28

10 **Schneider MB,** Standop J, Ulrich A, Wittel U, Friess H, Andren-Sandberg A, Pour PM. Expression of nerve growth factors in pancreatic neural tissue and pancreatic cancer. *J Histochem Cytochem* 2001; **49:** 1205-1210

11 **Shinoda M,** Hidaka M, Lindqvist E, Soderstrom S, Matsumae M, Oi S, Sato O, Tsugane R, Ebendal T, Olson L. NGF, NT-3 and Trk C mRNAs, but not TrkA mRNA, are upregulated in the paraventricular structures in experimental hydrocephalus. *Childs Nerv Syst* 2001; **17:** 704-712

12 **Ricci A,** Greco S, Mariotta S, Felici L, Bronzetti E, Cavazzana A, Cardillo G, Amenta F, Bisetti A, Barbolini G. Neurotrophins and neurotrophin receptors in human lung cancer. *Am J Respir Cell Mol Biol* 2001; **25:** 439-446

13 **Mukai J,** Hachiya T, Shoji-Hoshino S, Kimura MT, Nadano D, Suvanto P, Hanaoka T, Li Y, Irie S, Greene LA, Sato TA. NADE, a p75NTR-associated cell death executor, is involved in signal transduction mediated by the common neurotrophin receptor p75NTR. *J Biol Chem* 2000; **275:** 17566-17570

14 **Coulie B,** Szarka LA, Camilleri M, Burton DD, McKinzie S, Stambler N, Cedarbaum JM. Recombinant human neurotrophic factors accelerate colonic transit and relieve constipation in humans. *Gastroenterology* 2000; **119:** 41-50

15 **The BDNF Study Group.** A controlled trial of recombinant methionyl human BDNF in ALS: The BDNF study Group (phase III). *Neurology* 1999; **52:** 1427-1433

16 **Ciccolini F,** Svendsen CN. Neurotrophin responsiveness is differentially regulated in neurons and precursors isolated from the developing striatum. *J Mol Neurosci* 2001; **17:** 25-33

17 **Guarino N,** Yoneda A, Shima H, Puri P. Selective neurotrophin deficiency in infantile hypertrophic pyloric stenosis. *J Pediatr Surg* 2001; **36:** 1280-1284

18 **Ip FC,** Cheung J, Ip NY. The expression profiles of neurotrophins and their receptors in rat and chicken tissues during development. *Neurosci Lett* 2001; **301:** 107-110

19 **Carr MJ,** Hunter DD, Undem BJ. Neurotrophins and asthma. *Curr Opin Pulm Med* 2001; **7:** 1-7

20 **Roux PP,** Barker PA. Neurotrophin signaling through the p75 neurotrophin receptor. *Prog Neurobiol* 2002; **67:** 203-233

21 **Wiesmann C,** de Vos AM. Nerve growth factor: structure and function. *Cell Mol Life Sci* 2001; **58:** 748-759

22 **Galter D,** Unsicker K. Brain-derived neurotrophic factor and trkB are essential for cAMP-mediated induction of the serotonergic neuronal phenotype. *J Neurosci Res* 2000; **61:** 295-301

23 **Ichinose T,** Snider WD. Differential effects of TrkC isoforms on sensory axon outgrowth. *J Neurosci Res* 2000; **59:** 365-371

24 **Skup M,** Dwornik A, Macias M, Sulejczak D, Wiater M, Czarkowska-Bauch J. Long-term locomotor training up-regulates TrkB(FL) receptor-like proteins, brain-derived neurotrophic factor, and neurotrophin 4 with different topographies of expression in oligodendroglia and neurons in the spinal cord. *Exp Neurol* 2002; **176:** 289-307

25 **Heppenstall PA,** Lewin GR. BDNF but not NT-4 is required for normal flexion reflex plasticity and function. *Proc Natl Acad Sci U S A* 2001; **98:** 8107-8112

26 **Baldelli P,** Novara M, Carabelli V, Hernandez-Guijo JM, Carbone E. BDNF up-regulates evoked GABAergic transmission in developing hippocampus by potentiating presynaptic N- and P/Q-type Ca2+ channels signalling. *Eur J Neurosci* 2002; **16:** 2297-2310

27 **Malcangio M,** Ramer MS, Boucher TJ, McMahon SB. Intrathecally injected neurotrophins and the release of substance P from the rat isolated spinal cord. *Eur J Neurosci* 2000; **12:** 139-144

28 **Facer P,** Knowles CH, Thomas PK, Tam PK, Williams NS, Anand P. Decreased tyrosine kinase C expression may reflect developmental abnormalities in Hirschsprung's disease and idiopathic slow-transit constipation. *Br J Surg* 2001; **88:** 545-552

29 **Yang M,** Fang DC, Long QL, Sui JF, Li QW, Sun NX. Effects of gastric pacing on the gastric myoelectrical activity of a canine model of gastric motor disorders. *Shijie Huaren Xiaohua Zazhi* 2002; **10:** 1152-1156

30 **Platell CFE,** Coster J, McCauley RD, Hall JC. The management of patients with the short bowel syndrome. *World J Gastroenterol* 2002; **8:** 13-20

31 **Zhou X,** Li YX, Li N, Li JS. Effect of bowel rehabilitative therapy on structural adaptation of remnant small intestine: animal experiment. *World J Gastroenterol* 2001; **7:** 66-73

32 **Xie DP,** Chen LB, Liu CY, Liu JZ, Liu KJ. Effect of oxytocin on contraction of rabbit proximal colon *in vitro*. *World J Gastroenterol* 2003; **9:** 165-168

33 **Xie DP,** Li W, Qu SY, Zheng TZ, Yang YL, Ding YH, Wei YL, Chen LB. Effect of areca on contraction of colonic muscle strips in rats. *World J Gastroenterol* 2002; **8:** 350-352

34 **Liu CY,** Chen LB, Liu PY, Xie DP, Wang PS. Effects of progesterone on gastric emptying and intestinal transit in male rats. *World J Gastroenterol* 2002; **8:** 338-341

35 **Wang X,** Zhong YX, Zhang ZY, Lu J, Lan M, Miao JY, Guo XG, Shi YQ, Zhao YQ, Ding J, Wu KC, Pan BR, Fan DM. Effect of L-NAME on nitric oxide and gastrointestinal motility alterations in cirrhotic rats. *World J Gastroenterol* 2002; **8:** 328-332

36 **Peng X,** Feng JB, Yan H, Zhao Y, Wang SL. Distribution of nitric oxide synthase in stomach myenteric plexus of rats. *World J Gastroenterol* 2001; **7:** 852-854

37 **Wang X,** Zhong YX, Lan M, Zhang ZY, Shi YQ, Lu J, Ding J, Wu KC, Jin JP, Pan BR, Fan DM. Screening and identification of proteins mediating senna induced gastrointestinal motility enhancement in mouse colon. *World J Gastroenterol* 2002; **8:** 162-167

38 **Wang X,** Lan M, Wu HP, Shi YQ, Lu J, Ding J, Wu KC, Jin JP, Fan DM. Direct effect of croton oil on intestinal epithelial cells and colonic smooth muscle cells. *World J Gastroenterol* 2002; **8:** 103-107

39 **Camilleri M,** Lee JS, Viramontes B, Bharucha AE, Tangalos EG. Insights into the pathophysiology and mechanisms of constipation, irritable bowel syndrome, and diverticulosis in older people. *J Am Geriatr Soc* 2000; **48:** 1142-1150

Edited by Xu XQ, Wang XL and Zhu LH

P.O.Box 2345, Beijing 100023,China
Fax: +86-10-85381893
E-mail: wjg@wjgnet.com www.wjgnet.com

World J Gastroenterol 2003;9(8):1878-1880
World Journal of Gastroenterology
 ISSN 1007-9327

• BRIEF REPORTS •

Intestinal permeability in patients after surgical trauma and effect of enteral nutrition versus parenteral nutrition

Xiao-Hua Jiang, Ning Li, Jie-Shou Li

Xiao-Hua Jiang, Ning Li, Jie-Shou Li, Research Institute of General Surgery, Medical School of Nanjing University, Nanjing 210002, Jiangsu Province, China
Correspondence to: Xiao-Hua Jiang, Research Institute of General Surgery, Medical School of Nanjing University, Nanjing 210002, Jiangsu Province, China. dr_jxh@163.com
Telephone: +86-25-3593192 **Fax:** +86-25-4803956
Received: 2003-03-04 **Accepted:** 2003-04-03

Abstract

AIM: To study the intestinal permeability (IP) following stress of abdominal operation and the different effects on IP of enteral nutrition (EN) and parenteral nutrition (PN).

METHODS: Forty patients undergoing abdominal surgery were randomized into EN group and PN group. Each group received nutritional support of the same nitrogen and calorie from postoperative day (POD) 3 to POD 11. On the day before operation (POD-1), POD 7 and POD 12, 10 g of lactulose and 5 g of mannitol were given orally, and urine was collected for 6 hours. Urine excretion ratios of lactulose and mannitol (L/M) were measured.

RESULTS: L/M ratios of EN group on POD-1, POD 7 and POD 12 were 0.026±0.017, 0.059±0.026, 0.027±0.017, respectively, and those of PN group were 0.025±0.013, 0.080±0.032, 0.047±0.021, respectively. Patients of both groups had elevated L/M ratios on POD 7 *vs*. POD-1. However the ratio returned toward control level in EN group by POD 12. In contrast, PN group still had elevated L/M ratios on POD 12.

CONCLUSION: L/M ratio increases for a period of time after surgical trauma and the loss of gut mucosal integrity can be reversed by substitution of enteral nutrition.

Jiang XH, Li N, Li JS. Intestinal permeability in patients after surgical trauma and effect of enteral nutrition versus parenteral nutrition. *World J Gastroenterol* 2003; 9(8): 1878-1880
http://www.wjgnet.com/1007-9327/9/1878.asp

INTRODUCTION

Apart from the major function for digestion and absorption of nutrients, intestine also acts as "a central organ of stress". In many pathological conditions such as severe trauma, operation, chemotherapy and acute severe pancreatitis, intestine is a barrier to prevent microorganisms and toxins in the lumen from spreading to distant tissues and organs.

Nutritional support has been used in clinical care for more than forty years. Total parenteral nutrition (TPN) is the form of nutritional support most suitable to patients with gut failure, in which it is lifesaving[1]. However, studies have found that TNP has many disadvantages, such as gut barrier dysfunction and bacterial translocation. Enteral nutrition may not have these disadvantages[2-4].

Many studies have demonstrated that intestinal permeability (IP) can reflect gut barrier function[5,6]. When the integrity of gut mucosal barrier is damaged, increased intestinal permeability may occur. The excretion ratio of L/M of urine has been used to measure intestinal permeability[7]. However, few studies have directly compared the effect of EN versus PN on intestinal permeability after surgical trauma. Therefore, the present study was to observe intestinal permeability following operation and to investigate the different effects of enteral nutrition and parenteral nutrition on IP.

MATERIALS AND METHODS

Patients

A prospective and randomized study was designed. Forty patients with digestive tract tumor were enrolled. All the patients had normal liver and kidney functions but no metabolic diseases. Informed consent was obtained from all the patients preoperatively.

All the patients were randomized intraoperatively after complete resection of tumor. The groups were defined as follows. EN group: Patients received enteral nutrition via jejunostomy tube or nasojejunal tube starting from POD 3. All the tubes were placed approximately 20 cm distal to the ligament of Treitz. PN group: Patients received total parenteral nutrition via central venous catheter starting from POD 3. Control group: It consisted of twenty healthy volunteers. All controls underwent an overnight fast and took the test solution orally.

Nutrition

All the patients of the two groups received isonitrogenous (0.1728 g/Kg/d) and isocaloric (30 Kcal/Kg/d) nutritional support starting from POD 3. The aim of enteral or parenteral nutrition was to meet 50 % of nutritional requirements according to the protocol and GI tolerance of the patient on POD3, 75 % on the next day and 100 % on POD5.

EN group: Patients received Isosource (Novartis Corp, Switzerland) fluid polymeric formulation containing 14 % protein, 29 % fat, 57 % carbohydrate calories. Nutrient solution was given at a steady speed.

PN group: Patients received total parenteral nutrition. Amino acids, fat, glucose and minerals were mixed and infused steadily.

Lactulose/mannitol test

Intestinal permeability was performed on POD-1, POD7 and POD12. All the patients fasted for at least 6 hours and their bladders were emptied before the test. The test solution consisted of 10 g of lactulose and 5 g of mannitol in a total volume of 50 mL with osmotic pressure 1 200 mOsm/L. The solution was given via the jejunostomy tubes or by nasojejunal or oral routes. The urine volume was collected for the subsequent 6 hours. One hour after the test started, the patients were encouraged to drink. After 2 h, liberal intake of food was allowed. The urine volume was recorded, and 10-mL portion was frozen and stored at -80 ℃.

Analysis

Urinary lactulose and mannitol were assayed using high-

pressure liquid chromatography (HPLC) as described by Willems D and colleagues[8]. Calibration was performed on a daily basis with authentic standards at multiple concentrations, and the experimental standards were diluted so that the areas of all peaks fell within the calibration range. Fractional excretions (lactulose and mannitol) and L/M ratios were calculated. Fractional excretion was defined as the fraction of the gavaged dose recovered in the urine sample, and L/M ratio was a ratio of fractional excretions (lactulose-mannitol).

Statistical analysis

Statistical analysis was performed using analysis of variance (ANOVA) when comparing mean L/M ratios within groups and by an independent *t* test for differences between groups and *vs* control. Enumeration data were analyzed by χ^2 square test. Differences were considered significant when $P<0.05$, and obviously significant when $P<0.01$. All values were expressed as means ±SD.

RESULTS

Patients ' general data

From April 2000 to July 2001, forty patients with digestive tract tumors were randomized to receive enteral nutrition or total parenteral nutrition. Preoperative and procedure related data for the two groups are listed in Table 1.

Table 1 Comparison of preoperative and procedure related data between experimental groups

	EN group	PN group
Age (y)	50.8±14.9	53.1±15.6
Sex (M / F)	13 / 7	11 / 9
Weight (Kg)	60.0±6.8	61.3±12.3
Cancer of stomach	15	11
Cancer of colon	5	9
Complete gastrectomy	7	5
Partial gastrectomy	8	6
Left hemicolectomy	4	5
Right hemicolectomy	1	4

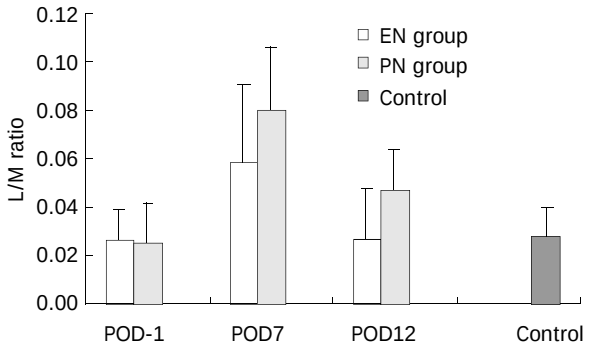

Figure 1 Mean ratio of recovered lactulose to mannitol (L / M) in the urine. A significant elevated ratio was seen on POD7 *vs* that on POD-1 in both groups ($P<0.01$). Significant decreases in the ratio were seen in both groups on POD12 *vs* POD7 ($P<0.01$). The L / M ratio of EN group was significantly lower than PN group on POD7 ($P<0.05$) and on POD12 ($P<0.01$).

Intestinal permeability

Figure 1 depicts the mean L/M ratios for all groups. On POD-1, there were no significant differences in EN group (0.026±0.017) and PN group (0.025±0.013) *vs* control (0.028±0.012) ($P>0.05$). Also there was no significant difference in EN group *vs* PN group ($P>0.05$). On POD7, there was one-fold to two-fold increase in the L/M ratios in both EN group (0.059±0.026) and PN group (0.080±0.032) *vs* that on POD-1 ($P<0.01$). However, there was a significant difference between PN group and EN group ($P<0.05$). On POD12, there was a significant difference in L/M ratios in both EN group and PN group *vs.* that on POD7 ($P<0.01$). However, there was a decreasing trend in L/M ratio in EN group (0.027±0.017) *vs.* that on POD-1 ($P>0.05$), while there was a significant difference in PN group (0.047±0.021) *vs.* that on POD-1 ($P<0.01$). There was a significant difference between PN group and EN group on POD12 ($P<0.01$).

DISCUSSION

Small intestinal permeability has been used to quantify the damage of gut mucosal barrier[9,10]. Intestinal permeability changes have been detected by oral administration of probes such as ^{51}Cr-EDTA, sucrose, lactulose, cellobiose, and polyethylene glycol[11-14]. The measurement of urinary excretion of nonmetabolized sugars has been widely used as a noninvasive method to assess mucosal integrity of the small bowel[15-17]. Monosaccharides such as mannitol and L-rhamnose pass through the transcellular routes of aqueous pores, reflecting the degree of absorption of small molecules (0.65 nm). Disaccharides, including lactulose and cellobiose, pass through the intercellular junctional complexes and extrusion zones at the villous tips, reflecting the permeability of large molecules (0.93 nm). The permeabilities of mono- and disaccharides are usually compared and expressed as an excretion ratio such as lactulose/mannitol or lactulose/L-rhamnose in urine samples. Lactulose and mannitol represent ideal compounds for measuring differential sugar absorption because they have a negligible affinity for the monosaccharide transport system and are passively absorbed and not metabolized before urine excretion. Intraindividual differences in gastric emptying, small intestinal transit, and urinary excretion are therefore eliminated[5-7,16].

Several enzymatic, colorimetric, and thin-layer chromatographic methods have been developed for the determination of lactulose and mannitol[5,6]. However, most of them are time-consuming and do not allow a simultaneous assay of both sugars. More recently, gas chromatographic and HPLC procedures have been proposed to overcome these problems[8,18]. Data from our study suggested that HPLC was a good method of measuring lactulose and mannitol. Our data also showed that L/M ratios could reflect intestinal permeability.

Sepsis, systemic inflammatory response and trauma in both animal and human are associated with gut mucosal damage and dysfunction[19-21]. Gut dysfunction is a common problem, resulting in loss of gut mucosal barrier selectivity, increased permeability to various hydrophilic solutes and translocation of bacterial products into the circulation, which may then further increase the inflammatory response in distant organs, leading to multiple organ dysfunction and death[22]. As a result, many authors considered the gut as an "engine" that drived sepsis. One possible contributory mechanism to endotoxin-induced gut mucosal damage was the increased apoptosis[11]. Inflammatory mediators enhanced apoptosis in a large number of cell lines. In intact animals, increased cardiac and hepatic apoptosis during sepsis might contribute to sepsis-related dysfunction of those organs. Thus paracellular tight junction may be injured and intestinal permeability increases. Our study showed an increased permeability after the stress of surgical trauma.

Nowadays nutritional support has become a routine therapy method. In the stress condition, proper nutritional support may provide necessary nutrients, reduce clinical complications and

promote patients' recovery from illness[3]. Total parenteral nutrition (TPN) provides significant benefits to surgical patients. However, there are still many complications. The effects of total parenteral nutrition on the gastrointestinal tract include decreasing brush-border hydrolase and nutrient-transporter activity, increasing mucosal permeability, and decreasing microvillus height[23-25]. Thus TPN is complicated by bacterial translocation (BT). Enteral nutrition after stress can maintain immunocompetence, and promote wound healing. Furthermore, it is considered that enteral nutrition can maintain gut barrier integrity, reduce septic complications[26] and the risk of death of critical care patients[3, 27]. In our study, we used L/M ratio as a marker to reflect gut mucosal barrier. On POD7, L/M ratios in both EN group and PN group were elevated, but L/M ratio of EN group was significantly lower than that of PN group. And on POD12, L/M ratio of EN group returned to the level of POD-1, while L/M ratio of PN group was still higher than that of POD-1 and EN group.

It is concluded that L/M ratio increases in a period of time after surgical trauma and institution of enteral nutrition can reverse the loss of gut mucosal integrity.

REFERENCES

1 **Jeejeebhoy KN**. Total parenteral nutrition: potion or poison? *Am J Clin Nutr* 2001; **74**: 160-163
2 **Windsor AC**, Kanwar S, Li AG, Barnes E, Guthrie JA, Spark JI, Welsh F, Guillou PJ, Reynolds JV. Compared with parenteral nutrition, enteral feeding attenuates the acute phase response and improves disease severity in acute pancreatitis. *Gut* 1998; **42**: 431-435
3 **Minard G**, Kudsk KA. Nutritional support and infection: does the route matter? *World J Surg* 1998; **22**: 213-219
4 **Zhu L**, Yang ZC, Li A, Cheng DC. Protective effect of early enteral feeding on postburn impairment of liver function and its mechanism in rats. *World J Gastroenterol* 2000; **6**: 79-83
5 **Travis S**, Menzies I. Intestinal permeability: functional assessment and significance. *Clin Sci* 1992; **82**: 471-488
6 **Bjarnason I**, MacPherson A, Hollander D. Intestinal permeability: an overview. *Gastroenterology* 1995; **108**: 1566-1581
7 **Barboza Junior MS**, Silva TM, Guerrant RL, Lima AA. Measurement of intestinal permeability using mannitol and lactulose in children with diarrheal diseases. *Braz J Med Biol Res.* 1999; **32**: 1499-1504
8 **Willems D**, Cadranel S, Jacobs W. Measurement of urinary sugars by HPLC in the estimation of intestinal permeability: evaluation in pediatric clinical practice. *Clin Chem* 1993; **39**: 888-890
9 **Meddings JB**, Gibbons I. Discrimination of site-specific alterations in gastrointestinal permeability in the rat. *Gastroentology* 1998; **114**: 83-92
10 **Wu CT**, Huang XC, Li ZL. Intestinal mucosal permeability increase and intestinal bacterial translocation. *Shijie Huaren Xiaohua Zazhi* 1999; **7**: 605-606
11 **Uil JJ**, van Elburg RM, van Overbeek FM, Mulder CJ, VanBerge-Henegouwen GP, Heymans HS. Clinical implications of the sugar absorption test: intestinal permeability test to assess mucosal barrier function. *Scand J Gastroenterol Suppl* 1997; **223**: 70-78
12 **Fink MP**. Gastrointestinal mucosal injury in experimental models of shock, trauma, and sepsis. *Crit Care Med* 1991; **19**: 627-641
13 **Smecuol E**, Bai JC, Sugai E, Vazquez H, Niveloni S, Pedreira S, Maurino E, Meddings J. Acute gastrointestinal permeability responses to different non-steroidal anti-inflammatory drugs. *Gut* 2001; **49**: 650-655
14 **Blomquist L**, Bark T, Hedenborg G, Norman A. Evaluation of the lactulose / mannitol and 51Cr-ethylenediaminetetraacetic acid / 14C-mannitol methods for intestinal permeability. *Scand J Gastroenterol* 1997; **32**: 805-812
15 **Smecuol E**, Bai JC, Vazquez H, Kogan Z, Cabanne A, Niveloni S, Pedreira S, Boerr L, Maurino E, Meddings JB. Gastrointestinal permeability in celiac disease. *Gastroenterology* 1997; **112**: 1129-1136
16 **Dong HL**. Intestinal permeability test and its clinical significance. *Shijie Huaren Xiaohua Zazhi* 2000; **8**: 562-563
17 **Tibble JA**, Bjarnason I. Non-invasive investigation of inflammatory bowel disease. *World J Gastroenterol* 2001; **7**: 460-465
18 **Smecuol E**, Bai JC, Sugai E, Vazquez H, Niveloni S, Pedreira S, Maurino E, Meddings J. Acute gastrointestinal permeability responses to different non-steroidal anti-inflammatory drugs. *Gut* 2001; **49**: 650-655
19 **Deitch EA**. Intestinal permeability is increased in burn patients shortly after injury. *Surgery* 1990; **107**: 411-416
20 **Wang W**, Smail N, Wang P, Chaudry IH. Increased gut permeability after hemorrhage is associated with upregulation of local and systemic IL-6. *J Surg Res* 1998; **79**: 39-46
21 **Sun XQ**, Fu XB, Zhang R, Lu Y, Deng Q, Jiang XG, Sheng ZY. Relationship between plasma D(-)-lactate and intestinal damage after severe injuries in rats. *World J Gastroenterol* 2001; **7**: 555-558
22 **Peng YZ**, Yuan ZQ, Xiao GX. Effects of early enteral feeding on the prevention of enterogenic infection in severely burned patients. *Burns* 2001; **27**: 145-149
23 **Li J**, Langkamp-Henken B, Suzuki K, Stahlgren LH. Glutamine prevents parenteral nutrition-induced increases in intestinal permeability. *J Parenter Enteral Nutr* 1994; **18**: 303-307
24 **Helton WS**. The pathophysiologic significance of alterations in intestinal permeability induced by total parenteral nutrition and glutamine. *J Parenter Enteral Nutr* 1994; **18**: 289-290
25 **Illig KA**, Ryan CK, Hardy DJ, Rhodes J, Locke W, Sax HC. Total parenteral nutrition-induced changes in gut mucosal function: atrophy alone is not the issue. *Surgery* 1992; **112**: 631-637
26 **Braunschweig CL**, Levy P, Sheean PM, Wang X. Enteral compared with parenteral nutrition: a meta-analysis. *Am J Clin Nutr* 2001; **74**: 534-542
27 **Omura K**, Hirano K, Kanehira E, Kaito K, Tamura M, Nishida S, Kawakami K, Watanabe Y. Small amount of low-residue diet with parenteral nutrition can prevent decreases in intestinal mucosal integrity. *Ann Surg* 2000; **231**: 112-118

Edited by Zhao P and Wang XL

P.O.Box 2345, Beijing 100023,China
Fax: +86-10-85381893
E-mail: wjg@wjgnet.com www.wjgnet.com

World J Gastroenterol 2003;9(8):1881-1883
World Journal of Gastroenterology
 ISSN 1007-9327

• BRIEF REPORTS •

Single-dose daclizumab induction therapy in patients with liver transplantation

Lu-Nan Yan, Wei Wang, Bo Li, Shi-Chun Lu, Tian-Fu Wen, Qi-Yuan Lin, Yong Zeng, Nan-Sheng Cheng, Ji-Chun Zhao, Yue-Meng Dai

Lu-Nan Yan, Wei Wang, Bo Li, Shi-Chun Lu, Tian-Fu Wen, Qi-Yuan Lin, Yong Zeng, Nan-Sheng Cheng, Ji-Chun Zhao, Yue-Meng Dai, Liver Transplantation Center, West China Hospital, Sichuan University, Chengdu 610041, Sichuan Province, China
Correspondence to: Dr. Lu-Nan Yan, Department of Surgery, West China Hospital, Sichuan University, Chengdu 610041, Sichuan Province, China. yanlunan@hotmail.com
Telephone: +86-28-85422072 **Fax:** +86-28-85423724
Received: 2002-06-20 **Accepted:** 2002-10-17

Abstract

AIM: To investigate the efficacy and safety of a single-dose daclizumab induction therapy in orthotopic liver transplantation (OLTx).

METHODS: A retrospective study was made for 54 cases of OLTx in recent three years. The daclizumab group consisted of 23 cases of OLTx who received single-dose of 2 mg/kg intravenously after postoperative 24 hours. The control group consisted of the remaining 31 patients. Additional immunosuppressors included steroids, mycomphenolate mofetil, facrolimus or microemulsion cyclosporine used in all patients. Meta-statistical analysis was made for general data, incidence of acute rejection and infection, postoperative clinical course, complications and prognosis between two groups.

RESULTS: Pretransplant demographies were not significantly different between two groups. In the induction group there were significantly less acute rejection episodes (5 of 23, 21.74 %) than those in the control group (12 of 31, 38.71 %), which were proved by pathologic diagnosis ($P<0.05$). The incidence of infection at the early stage was not significantly different between two groups.

CONCLUSION: Induction therapy with single-dose of daclizumab is safe and effective and appears to be able to reduce the incidence of acute rejection.

Yan LN, Wang W, Li B, Lu SC, Wen TF, Lin QY, Zeng Y, Cheng NS, Zhao JC, Dai YM. Single-dose daclizumab induction therapy in patients with liver transplantation. *World J Gastroenterol* 2003; 9(8): 1881-1883
http://www.wjgnet.com/1007-9327/9/1881.asp

INTRODUCTION

One of the key elements for successful liver transplantation is to effectively prevent acute rejection in patients with liver transplantation. Even the routine immunosuppressants such as azathioprin (AZA), cyclosporin (CSA), mycomphenolate mofetil (MMF) and tacrolinous (FK506)were used, the acute rejection rate in liver transplantation was still as high as 30-40 %[1-3]. Daclizumab, a humanized form of murine monoclonal antibody, has been recently shown to be able to decrease the acute rejection in liver transplanted recipients[4-7].

In this retrospective study, whether daclizumab induction therapy was effective and safe in orthotopic liver transplantation (OLTx) was evaluated.

MATERIALS AND METHODS

General data

We retrospectively reviewed the results of 54 consecutive OLTx performed from February, 1999 to January, 2002 at the West China Hospital in Sichuan University. There were 44 males and 10 females,their age ranged from 11 to 68 years old (average 38.98 years old). 42 patients had benign hepatic diseases, 29 had cirrhosis due to hepatitis B, 2 had diffusive intrahepatic stones with liver cirrhosis, 1 had alcoholic cirrhosis, 1 had polycystic liver with cirrhosis, 2 had Budd-Chari' s syndrome, 3 had unibobar carolis syndrome, 1 had alcoholic cirrhosis and 3 had alveolar echinococcosis. 12 patients had hepatocellular carcinoma. According to the Child' s classification, 39 of the 54 patients were grade A, 2 were grade B and 13 were grade C. According to the classification of the united network of organ share (UNOS), 14 were grade I, 40 were grade II.

Among them, 14 cases were performed emergency liver transplantation because of acute hepatic failure with severe jundice (total bilirubin 129-676 nmol/L), large volume of ascites (2 500-11 000 ml) or severe coagulopathy, and 4 cases had hepatic enphacelopathy. 23 patients received induction therapy with daclizumab and 31 patients were managed with conventional immunosuppression (non induction). In the control group (non-induction), oral cyclosporin was administered at a dosage of 6-10 mg/kg/day, starting within 24 hours before the operation. Dosage adjustments were based on achieving servm level of CSA between 200 ng and 300 ng/dL. Patients received methylprednisolone during surgery 200 mg intravenously, which was decreased by 40 mg daily over a period of 5 days. On postoperative day 5, patients started to administer prednisone at 20 mg/day. MMF was administered at a dosage of 0.75 g, twice daily.

In the induction group, daclizumab was given 2 mg/kg intravenously within the postoperative 24 hours, cyclosporin, steroid and MMF were identical to the control group.

Tacrolimas was used in patients with CSA toxicity and occasionally as the primary therapy.

Diagnosis of rejection

Rejection was suspected by biochemical evidence of deteriorating liver function and/or clinical signs. Pathological examimation was done in all patients suspected of rejection. The patients in both groups received methyprednisolone every day for the treatment of acute rejection at 500 mg intravenously for 3 days.

Concomitant therapy

The patients in both groups received losec for prophylaxis of stress ulcer (40 mg, intravenously, daily). Cephaloxin was used for postoperative infection prophylaxis. HBV-DNA positive patients were given lamivudine (100 mg, orally, daily). The

patients accompanied by suspected virus infection were treated with acyclovir (800 mg, orally twice daily) or ganciclovir (5 mg/kg , intravenously twice daily).

Liver transplantation

Operative procedures were performed according to standard surgical techniques, and all grafts were perfused with the University of Wisconsin solution[8]. Veno-venous bypass was used in all cases. Buct-to-duct over a T-tube biliary anastomosis or choledochojejunostomy was performed.

Statistical analysis

All the patients received a minimum follow-up for 60 days. Values of the descriptive variables between groups were compared with a nonparainetric wilcoxon rank sum test. Chi-square test or Fisher exact test was used to evaluate the data of the independent groups.

RESULTS

Survival rate

The general data of patients in this study are shown in Table 1, which were similar in two groups.

Table 1 General data in two groups

	Induction group (n=23)	Non-induction group (n=31)
Average age(yr)	39.17(19-68)	38.76(11-57)
Male / female	21 / 2	23 / 8
Indication with		
Liver cirrhosis	15	18
Liver cancer	6	6
Other	2	7
UNOS classification		
Grade I	5	10
Grade II	18	21
Child classification		
Grade A	4	9
Grade B	2	0
Grade C	17	22
Blood type		
ABO-identical	14	23
ABO-compatible	9	8

The 1-, 3-, and 6-month survival rate in patients receiving the induction therapy with daclizumab was 91.3 %, 86.9 % and 86.9 %, respectively *vs* 90.0 %, 83.9 % and 83.9 %, respectively for patients not receiving induction therapy (P>0.05). There was a significant difference between two groups. Six months after the transplantation, 20 of the 23 patients with daclizumab induction were still alive. Deaths occurred in this group were due to the following rensons: complications of intercereberal bleeding (1case), heart failure (1case) and pulmonary infection (1case). In the non induction group, 26 of 31 patients surrived for 6 months. Deaths occurred in this group were due to the following rensons: complications of intracerebral bleeding (1case), pulmonary fungus infection (2case), MOF(1case) and recurrent of cancer (1case).

No patients in either group developed primary dysfunction or died of blood vessel complications.

Complications

Complications especially infection were less in the induction group than those in the non induction group, without significant difference (Table 2).

Table 2 Postoperative complications in two groups

	Induction (n=23)	Non-induction (n=31)
Intraperitoneal bleeding	1	3
Ascite infection	0	1
Stress ulcer bleeding	1	3
Stress ulcer perforation	0	1
Pulmonary infection	5	11
Heart failure	1	3
Biliary leakage	1	3
Chronic oral ulcer	2	3
Bowel fungal infection	1	2
Intracerebral bleeding	1	3
Total	13	32

Rejection

Overall, in the first month, acute rejection occurred less in patients of the daclizumab induction group than that in the non-induction group(21.74 % *vs* 38.71 %, P<0.05). None in either group had acute rejection after the first month and occurred chronic rejection during the first 6 months. None in the induction group and one patient in the noninduction group had OKT_3 added to their immunosuppression for intractable rejection.

Tolerance of daclizumab

None in the daclizumab group required reduction of their dose or cessation of daclizumab for side effects. Daclizumab was well tolerated without apparently clinical or biochemical toxicity.

DISCUSSION

In the recent 30-40 years, with the development of organ transplantation biology, many immunosuppressive agents have been introduced to reduce the incidence of acute rejection[9-12]. The introduction of azathioprine (AZA) was in 1960s by Starzl. Cyclosporin A has (CSA) achieved long-term survival rade since early 1980s[13-17], and occurrenc of tacrolimus (FK506)[18-22] and mycomphenolate mofetil (MMF)[23-27] has prolonged the long-term survival. In spite of these major advances in liver transplantation, there are a number of problems associated with its use. For example, the incidence of acute rejection is still as high as 30-40 %[1].

Thus, the next advance that is required in immunosuppression in recipients with liver transplantation is an agent that can either decrease the rejection without increase of toxicity or decrease toxicity with maintenance of effective immunosuppression.

Daclizumab, a humanized anti-IL-2R a-chain (CD25) antibody, is a new immunosuppressant, its proposed actions include blockade of signaling *via* the high-affinity IL-2R, down-modulation of CD25, depletion of CD25+ cells, and interaction with its FC fragments and FCRs on activated T cells[28, 29]. Induction therapy with daclizumab has been shown effective in preventing acute rejection in kidney transplantation patients[30-32]. Routine use of antibody induction therapy in liver transplantation has not gained widespread acceptance[1].

This study explored the results of adding daclizumab to conventional immunosuppressive therapy in 23 liver recipients with liver transplantation compared to the results in 31 control recipients. It was found that adding daclizumab appeared to be able to decrease the incidence of acute rejection from 38.71 % to 21.74 % without any apparent toxicity or opportunistic infections.

In this study, a different dosing schedule for daclizumab was used. Ciancio *et al* reported their dosing schedule was that daclizumab (1 mg/kg) was given on the day of surgery and every other week for a total of 5 doses[31]. Devin' s schedule

was that the first dose (2 mg/kg) was given before organ engraftment and the second dose (1 mg/kg) was given on postoperative day 5[1]. Both results suggest the efficacy of their dosing schedule. Our dosage of daclizumab was smaller than that in other transplant centers, but we still found that daclizumab appeared to be able to reduce the incidence of acute rejection singnificantly without apparent toxicity and was well tolerated. In conclusion, the induction therapy with single-dose of daclizumab is safe and effective.

REFERENCES

1 **Eckhoff DE**, Mcguire B, Sellers M, Contreras J, Frenette L, Young C, Hudson S, Bynon JS. The safety and efficacy of a two-dose daclizumab (zenapax) induction therapy in liver transplant recipients. *Transplantation* 2000; **69**: 1867-1872

2 **Kwekkeboom J**, Zondervan PE, Kuijpers MA, Tilanus HW, Metselaar HJ. Fine-needle aspiration cytology in the diagnosis of acute rejection after liver transplantation. *Br J Surg* 2003; **90**:246-247

3 **Ramji A**, Yoshida EM, Bain VG, Kneteman NM, Scudamore CH, Ma MM, Steinbrecher UP, Gutfreund KS, Erb SR, Partovi N, Chung SW, Shapiro J, Wong WW. Late acute rejection after liver transplantation: the Western Canada experience. *Liver Transpl* 2002; **8**: 945-951

4 **Levy GA.** Neoral is superior to FK506 in liver transplantation. *Transplant Proc* 1998; **30**: 1812-1815

5 **Niemeyer G**, Koch M, Light S, Kuse ER, Nashan B. Long-term safety, tolerability and efficacy of daclizumab (zenapax) in a two-dose regimen in liver transplant recipients. *Am J Transplant* 2002; **2**: 454-460

6 **Carswell CI,** Plosker GL, Wagstaff AJ. Daclizumab: a review of its use in the management of organ transplantation. *Biodrugs* 2001; **15**: 745-773

7 **Koch M,** Niemeyer G, Patel I, Light S, Nashan B. Pharmacokinetics, pharmacodynamics, and immunodynamics of daclizumab in a two-dose regimen in liver transplantation. *Transplantation* 2002; **73**: 1640-1646

8 **Yan LN,** Li B, Lu SC, Jin LR, Wen TF, Wu XD, Jia QB, Zhou Y, Wu YT. Orthotopic liver transplantation: a report of 15 cases. *Zhonghua Qiguan Yizhi Zazhi* 2000; **21**: 275-277

9 **Ankersmit HJ**, Roth G, Zuckermann A, Moser B, Obermaier R, Taghavi S, Brunner M, Wieselthaler G, Lanzenberger M, Ullrich R, Laufer G, Grimm M, Wolner E. Rapamycin as rescue therapy in a patient supported by biventricular assist device to heart transplantation with consecutive ongoing rejection. *Am J Transplant* 2003; **3**: 231-234

10 **Rose ML**, Smith J, Dureau G, Keogh A, Kobashigowa J. Mycophenolate mofetil decreases antibody production after cardiac transplantation. *J Heart Lung Transplant* 2002; **21**: 282-285

11 **Calmus Y,** Scheele JR, Gonzalez-Pinto I, Jaurrieta EJ, Klar E, Pageaux GP, Scudamore CH, Cuervas-Mons V, Metselaar HJ, Prestele H, Girault D. Immunoprophylaxis with basiliximab, a chimeric anti-interleukin-2 receptor monoclonal antibody, in combination with azathioprine-containing triple therapy in liver transplant recipients. *Liver Transpl* 2002; **8**: 123-131

12 **Agha IA**, Rueda J, Alvarez A, Singer GG, Miller BW, Flavin K, Lowell JA, Shenoy S, Howard TK, Ramachandran V, Irish W, Schnitzle MA, Brennan DC. Short course induction immunosuppression with thymoglobulin for renal transplant recipients. *Transplantation* 2002; **73**: 473-475

13 **Calne RY,** Rolles K, White DJ, Thiru S, Evans DB, Mcmaster P, Dunn DC, Graddock GN, Henderson RG, Aziz S, Lewis P. Cyclosporin A initially as the only immunosuppressant in 34 recipients of cadaveric organs: 32 kidneys, 2 pancreases, and 2 livers. *Lancet*, 1979; **2**: 1033-1036

14 **Lerut JP**, Ciccarelli O, Mauel E, Gheerardhyn R, Talpe S, Sempoux C, Laterre PF, Roggen FM, Van Leeuw V, Otte JB, Gianello P. Adult liver transplantation and steroid-azathioprine withdrawal in Cyclosporine (Sandimmun)-based immunosuppression - 5 year results of a prospective study. *Transpl Int* 2001; **14**: 420-428

15 **Venkiteswaran K**, Sgoutas DS, Santanam N, Neylan JF. Tacrolimus, Cyclosporine and plasma lipoproteins in renal transplant recipients. *Transpl Int* 2001; **14**: 405-410

16 **Gonwa TA**, Hricik DE, Brinker K, Grinyo JM, Schena FP. Sirolimus Renal Function Study Group Improved renal function in sirolimus-treated renal transplant patients after early Cyclosporine elimination. *Transplantation* 2002; **74**: 1560-1567

17 **Meier-Kriesche HU**, Kaplan B. Cyclosporine microemulsion and tacrolimus are associated with decreased chronic allograft failure and improved long-term graft survival as compared with sandimmune. *Am J Transplant* 2002; **2**: 100-104

18 **Fung JJ,** Todo S, Tzakis A, Demetris A, Jain A, Abu-Elmaged K, Alessiani M, Starzl TE. Conversion of liver allograft recipients from Cyclosporine to FK506-based immunosuppression: benefits and pitfalls. *Transplant Proc* 1991; **23**(1Pt 1): 14-21

19 **Kato T,** Sato Y, Kurasaki I, Yamamoto S, Hirano K, Nakatsuka H, Kobayashi T, Kameyama H, Watanabe T, Hatakeyama K. FK506 may suppress liver injury during the early period following living-related liver transplantation. *Transplant Proc* 2003; **35**: 79

20 **Chen JW**, Pehlivan M, Gunson BK, Buckels JA, McMaster P, Mayer D. Ten-year results of a randomised prospective study of FK506 versus Cyclosporine in management of primary orthotopic liver transplantation. *Transplant Proc* 2002; **34**: 1507-1510

21 **Ahmad SM**, Stegman Z, Fructhman S, Asbell PA. Successful treatment of acute ocular graft-versus-host disease with tacrolimus (FK506). *Cornea* 2002; **21**: 432-433

22 **Vincenti F**, Jensik SC, Filo RS, Miller J, Pirsch J. A long-term comparison of tacrolimus (FK506) and Cyclosporine in kidney transplantation: evidence for improved allograft survival at five years. *Transplantation* 2002; **73**: 775-782

23 **Lebranchu Y**, Bridoux F, Buchler M, Le Meur Y, Etienne I, Toupance O, Hurault de Ligny B, Touchard G, Moulin B, Le Pogamp P, Reigneau O, Guignard M, Rifle G. Immunoprophylaxis with basiliximab compared with antithymocyte globulin in renal transplant patients receiving MMF-containing triple therapy. *Am J Transplant* 2002; **2**: 48-56

24 **Boggi U**, Vistoli F, Coppelli A, Marchetti P, Rizzo G, Mosca F. Use of basiliximab in conjunction with either Neora / MMF / steroids or Prograf / MMF / steroids in simultaneous pancreas-kidney transplantation. *Transplant Proc* 2001; **33**: 3201-3202

25 **Ciancio G**, Burke GW, Miller J. Current treatment practice in immunosuppression. *Expert Opin Pharmacother* 2000; **1**: 1307-1330

26 **Mouly-Bandini A**. A new immunosuppressor: CellCept. *Presse Med* 2001; **30**: 66-67

27 **Wu MJ**, Shu KH, Cheng CH, Chen CH, Lian JD. MMF-based regimen in maintenance therapy after kidney transplantation. *Transplant Proc* 2000; **32**: 1748-1750

28 **Van Assche G**, Dalle I, Noman M, Aerden I, Swijsen C, Asnong K, Maes B, Ceuppens J, Geboes K, Rutgeerts P. A pilot study on the use of the humanized anti-interleukin-2 receptor antibody daclizumab in active ulcerative colitis. *Am J Gastroenterol* 2003; **98**: 369-376

29 **Krueger JG**, Walters IB, Miyazawa M, Gilleaudeau P, Hakimi J, Light S, Sherr A, Gottlieb AB. Successful *in vivo* blockade of CD25 (high-affinity interleukin 2 receptor) on T cells by administration of humanized anti-Tac antibody to patients with psoriasis. *J Am Acad Dermatol* 2000; **43**: 448-458

30 **Light JA**, Sasaki TM, Ghasemian R, Barhyte DY, Fowlkes DL. Daclizumab induction / tacrolimus sparing: a randomized prospective trial in renal transplantation. *Clin Transplant* 2002; **16** (Suppl 7): 30-33

31 **Ciancio G,** Burke GW, Suzart K, Mattiazzi A, Rosen A, Zilleruello G, Abitbol C, Montane B, Miller J. Effect of daclizumab, tacrolimus, and mycophenolate mofetil in pediatric first renal transplant recipients. *Transplant Proc* 2002; **34**: 1944-1945

32 **Vincenti F**, Kirkman R, Light S, Bumgardner G, Pescovitz M, Halloran P, Neylan J, Wilkinson A, Ekberg H, Gaston R, Backman L, Burdick J. Interleukin-2-receptor blockade with daclizumab to prevent acute rejection in renal transplantation. *N Engl J Med* 1998; **338**: 161-165

Edited by Xu XQ and Wang XL

P.O.Box 2345, Beijing 100023,China
Fax: +86-10-85381893
E-mail: wjg@wjgnet.com www.wjgnet.com

World J Gastroenterol 2003;9(9):1885-1891
World Journal of Gastroenterology
 ISSN 1007-9327

• REVIEW •

Combined interventional therapies of hepatocellular carcinoma

Jun Qian, Gan-Sheng Feng, Thomas Vogl

Jun Qian, Gan-Sheng Feng, Department of Radiology, Xiehe Hospital, Tongji Medical College, Huazhong University of Science and Technology, Wuhan 430022, Hubei Province, China
Thomas Vogl, Department of Diagnostic and Interventional Radiology, J. W. Goethe University of Frankfurt, Theodor-Stern-Kai 7, 60590 Frankfurt, Germany
Correspondence to: Dr. Jun Qian, M.D. Department of Radiology, Xiehe Hospital, Tongji Medical College, Huazhong University of Science and Technology, Wuhan 430022, Hubei Province, China. junqian_tjmc@yahoo.com.cn
Telephone: +86-27-85726432 **Fax:** +86-27-85727002
Received: 2003-03-04 **Accepted:** 2003-04-11

Abstract

Hepatocellular carcinoma (HCC) is one of the most common malignancies in the world, responsible for an estimated one million deaths annually. It has a poor prognosis due to its rapid infiltrating growth and complicating liver cirrhosis. Surgical resection, liver transplantation and cryosurgery are considered the best curative options, achieving a high rate of complete response, especially in patients with small HCC and good residual liver function. In nonsurgery, regional interventional therapies have led to a major breakthrough in the management of unresectable HCC, which include transarterial chemoembolization (TACE), percutaneous ethanol injection (PEI), radiofrequency ablation (RFA), microwave coagulation therapy (MCT), laser-induced thermotherapy (LITT), etc. As a result of the technical development of locoregional approaches for HCC during the recent decades, the range of combined interventional therapies has been continuously extended. Most combined multimodal interventional therapies reveal their enormous advantages as compared with any single therapeutic regimen alone, and play more important roles in treating unresectable HCC.

Qian J, Feng GS, Vogl T. Combined interventional therapies of hepatocellular carcinoma. *World J Gastroenterol* 2003; 9(9): 1885-1891
http://www.wjgnet.com/1007-9327/9/1885.asp

INTRODUCTION

Hepatocellular carcinoma (HCC) is a highly malignant tumour with a very high morbidity and mortality, carrying a poor prognosis and presenting considerable management[1]. The treatment of patients with HCC has been evolving in the past years.

Liver resection remains a good treatment for HCC in patients with cirrhosis[2]. The best results are obtained in patients with small, non-invasive tumours[3]. However, only a small number of patients are suitable for curative resection due to many factors such as multicentric tumours, extrahepatic metastases, early vascular invasion, coexisting advanced liver cirrhosis and comorbidities[4,5]. Liver transplantation seems to be the choice for monofocal HCC less than 5 cm in diameter and in selected cases of plurifocal HCC[6], but may be limited by availability of donor organs and a long waiting time[7-9]. Cryosurgery destroys neoplastic tissue by application of cold and affords a better chance of cure because of predictable necrosis even for HCC larger than 3 cm, but its use is limited by a high complication rate[10].

Local methods for tumour ablation, which include transarterial chemoembolization (TACE), percutaneous ethanol injection (PEI), radiofrequency ablation (RFA), microwave coagulation therapy (MCT), laser-induced thermotherapy (LITT), are promising extensions of tumour therapy, especially in patients with limited liver function, unresectable tumours, or multifocal tumours[11]. Since TACE was introduced as a palliative treatment in patients with unresectable HCC, it has become one of the most common forms of interventional therapy[12-15]. TACE has been shown to reduce systemic toxicity and increase local effects and thus improve the therapeutic results[14, 16]. However, its perceived benefit for survival has not been substantiated in randomized trials, presumably because its anticancer effect is offset by its adverse effect on liver function. Its therapeutic effect is also limited by the lack of appropriate and reliable embolic agents and when the tumour is infiltrative in nature or is hypovascular, too large or too small[17-19]. PEI is widely used with excellent results for small, encapsulated tumours in livers with less than three HCCs, but it is not suitable for patients having coagulopathy or ascites[19]. While RFA results in a higher rate of complete necrosis and requires fewer treatment sessions than PEI, the complication rate is higher with RFA than with PEI[20]. MCT under local anaesthesia is a minimally invasive and effective therapy when carried out on a single occasion to treat HCC located near the liver surface[21]. MCT may be superior to PEI for the local control of moderately or poorly differentiated small HCC[22, 23]. MR-guided LITT is another local effective therapy with low morbidity in malignant liver tumours with a maximum quantity of 5 and a size of < or = 5 cm[24,25], but local recurrence can occur even in small HCC, while this drawback is infrequent[26]. Biotherapy will play a certain role in the treatment of HCC, however, the results are still controversial[27].

It is well known that improving the overall therapeutic effects of liver cancer depends on the combined therapies. The purpose of combined interventional therapies for HCC is to give full play to the merits of various therapeutic schemes, to overcome their shortcomings and to get combined effects that are impossible to obtain from any single therapeutic regimen. The general principles of combined interventional therapies for HCC are to destroy the tumour as completely as possible, to increase their therapeutic efficiencies but not the side effects and complications, to keep the liver function and immunity of patients in a better condition, and to choose the suitable combined therapeutic plan individually. In this paper, the current status of combined interventional therapies for unresectable HCC are reviewed.

COMBINATION OF TACE AND SURGERY

The role of pre- and postoperative transarterial chemoembolization (TACE)

Zhang *et al* suggested that TACE could be performed 2-4 times preoperatively within 6 months according to tumour size, range, location, hepatic function, and TACE effect. It was reported

the 5-year disease-free survival rate was 56.8 % with a mean time of 90.1 months and the 1-, 3- and 5- year survival rates were 79.7 %, 65 % and 56 %, respectively[28,29]. Gerunda *et al* suggested that TACE was able to improve HCC and significantly reduce the incidence of early and overall HCC recurrence and related death after resection[30]. It has been confirmed that pre-operative TACE can necrotize the main lesion and temporarily arrest portal diffusion of neoplastic cells by acting on microvascular infiltration[31]. Nakano *et al* recommended that preoperative TACE should be performed in HCC patients only when LHL15 (the ratio of liver to heart-plus-liver radioactivity of Tc-GSA 15 minutes after injection) was less than 0.91[32]. However, Huang *et al* and Wu *et al* suggested that preoperative TACE for resectable large HCC should be avoided because it could not provide complete necrosis in large tumours and could result in delayed surgery and difficulty in the treatment of recurrent lesions, without any benefit[33,34]. It is concluded that TACE of HCC prior to liver transplantation has no influence on the recurrent rate[35]. However, a more detailed study of this treatment for HCC has not yet been reported. Clavien *et al* demonstrated that cryosurgery after TACE was feasible for cirrhotic livers with HCC and could increase the cure rate of large tumours. TACE might reduce the risk of hemorrhage after cryosurgery, but could also increase the risk of hepatic failure in patients with poor hepatic function. The 5-year survival rate could be raised to 79 %[36].

The results of Lin *et al* indicate that postoperative TACE is useful for prevention and treatment of HCC. It helps improve survival of surgically treated HCC patients[37]. Randomized trials to accurately define the position of this combined technique are needed.

COMBINATION OF TACE AND PEI

Percutaneous ethanol injection (PEI) is widely used with excellent results for small, encapsulated tumours in livers with less than three HCCs[19,38-40]. Ethanol in PEI acts by diffusing within the cells, which causes immediate dehydration of cytoplasmic proteins with consequent coagulation necrosis followed by fibrosis, and by entering the circulation, which induces necrosis of endothelial cells and platelet aggregation with consequent thrombosis of small vessels followed by ischemia of the neoplastic tissues. Advantages for using PEI include[41-43]: no remarkable damage to the remaining parenchyma, relative safety, easy repetition when new lesions appear as in the majority of patients followed for 5 years, application anywhere due to its low cost and easy operation, and fairly good long-term results.

PEI can be carried out either in patients with HCC who have poor hepatic function or in elderly patients (age > or = 70 years)[40,44]. Long-term survival rates of PEI-treated patients are similar to those obtained in matched patients submitted to partial hepatectomy[38, 40, 42]. Livraghi *et al* reported in 746 HCCs with cirrhosis treated by PEI, the 5-year survival rates for single HCC < 5 cm were 47 % for Child A, 29 % for Child B and 0 % for Child C, respectively[45].

PEI has been performed in many hospitals and is now categorized as a potentially curative procedure for patients with HCC. However, the long-term prognosis remains disappointed because of the high recurrent rate among patients with HCC after PEI, especially in those with high levels of alphafetoprotein (AFP) and those without peritumoral capsule or with large lesions and cirrhosis[39,44]. In fact, histological examination of HCC lesions after PEI reveals that viable tissue remains in portions isolated by septa or in extracapsular or intracapsular invasion. It has been demonstrated that the high vascularity of HCC promotes an early wash-out of injected ethanol, so that PEI for patients with hypervascular tumours may be less effective than for patients with hypovascular tumours[46,47].

Combined TACE and PEI is a therapeutic option that has been recently proposed to overcome the weakness of each of the two procedures in the treatment of large HCC[48-50]. The rationale for combination of the two treatments relies on the fact that after TACE tumour consistency is markedly decreased and intratumoral septa are usually disrupted, as a result of the necrotic phenomena induced by the procedure. These histopathologic changes make subsequent treatment with PEI easier, as they provide enhanced ethanol diffusion within the tumour. Consequently, higher doses of ethanol than those used in conventional PEI can be injected, enabling complete and homogeneous perfusion even of large lesions. Moreover, treatment with PEI is facilitated by the TACE-derived fibrous wall around the lesion, which favours a better retention of the injected ethanol within the tumour[46,50,51]. The 5-year survival rate was 50 % in the TACE/PEI group and was 22 % in the TACE group[52]. A favourable outcome of this combined therapy can be expected in patients with solitary and encapsulated HCC (low Okuda stage, AFP level <100 ng/ml), compensatory cirrhosis, and absence of portal vein thrombosis[42,49,51,53].

COMBINATION OF TACE AND RFA

Radiofrequency thermal ablation (RFA) is a minimally invasive and safe technique for the nonsurgical treatment of HCC. Similar to other ablation techniques, the treatment strategy depends on several factors, such as the patient' s clinical status, the stage of liver cirrhosis and of HCC. RFA can be performed percutaneously, laparoscopically or after laparotomy[54]. RFA achieves complete tumour necrosis for small HCC (< or = 3.5 cm in diameter) with fewer treatment sessions compared with PEI, and can also create large volumes of tumour necrosis in a shorter period of time than either laser or microwave therapy. Curley and Izzo suggested that RFA could be performed for unresectable hepatic malignancies less than 6.0 cm in diameter[55]. In addition, equipments used for RFA were less expensive than either laser or microwave equipments[56]. RFA provides local control of advanced liver tumours with low recurrence and acceptable morbidity[57-62]. However, the complication rate is higher with RFA than with PEI[20].

The combination of TACE and RFA induces larger coagulation necrosis areas than RFA without any possibility of revascularization[63-66]. RFA performed after TACE effectively treats HCC larger than those suitable for segmental TACE or RFA application alone[63]. Bloomston *et al* reported that one-year survival was greater in patients undergoing TACE and RFA than TACE alone (100 % *vs* 67 %, P=0.04). Mean survival was longer after TACE with RFA compared with TACE alone (25.3 months +/- 15.9 *vs*. 11.4 months +/- 7.3, P<0.05). No patients suffered significant complications in that study[66]. For multifocal recurrence, RFA can be useful as a complementary technique for lesions not completely treated by TACE[67].

COMBINATION OF TACE AND MCT

It is well known that percutaneous microwave coagulation therapy (MCT) under local anesthesia is a palliative and effective therapy when carried out on a single occasion to treat HCC located near the liver surface, and it can be safely performed under direct visual guidance[21]. MCT may be superior to PEI for the local control of moderately or poorly differentiated small HCC[22, 23]. MCT is also superior to PEI for treating patients with HCC < or = 15 mm in diameter. In such patients with well-differentiated HCC, PEI is as effective

as MCT[68].

The combined therapy of MCT applied within 1-2 days of TACE can effectively treat HCC >2.0 cm but <3.0 cm in dimension. A few microwave electrode insertions and microwave irradiations are needed[69]. Ishikawa *et al* suggested that MCT destroyed the peripheral part of the tumour that might remain viable after TAE, but combination therapy with transarterial embolization (TAE) was preferable, especially when a viable part existed within tumours[70]. However, larger scale clinical trials are required to define the role of this combined therapy in the strategy of oncology.

COMBINATION OF TACE AND LITT

Patients with larger and more than two HCC nodules have a relatively high incidence of recurrence of HCC in the remnant liver, even when coagulation by PEI, MCT or RFA is complete[71-73].

Laser-induced thermotherapy (LITT) is another minimally invasive and attractive method for destroying relatively larger tumours within solid organs by causing carbonization and vaporization in tissue[24,72-75]. MR-guided LITT is a local effective therapy with low morbidity for malignant liver tumours with a maximum quantity of 5 and a size of < or = 5 cm[24,25]. LITT may be also equivalent to limited hepatic resection and may influence long-term survival, achieving results comparable to those of segmentectomies, but local recurrence can occur even in small HCC, while this drawback is infrequent[26].

The rationale for combination of TACE and LITT is based on the fact that LITT can reduce the volume of viable tissue and improve the lesion within the range of TACE effectiveness. Moreover, in the case of multiple lesions in the same patient, it is possible to treat the small lesions with LITT alone and to reduce the number of hepatic segments requiring TACE[74]. Pacella *et al* achieved complete response with a single segmental TACE session in 21 (70 %) of the 30 patients and reported that the 1-, 2-, and 3-year local recurrent rate was 7 % in large HCC, respectively. Complete tumour necrosis was achieved in all 15 (100 %) small HCCs. The 1-, 2-, and 3-year cumulative survival rates were 92 %, 68 %, and 40 %, respectively. The mean number of sessions needed to control large HCC was 4.2[74]. LITT seems to be more beneficial and advisable in combination with TACE for treating patients with relatively larger and multiple HCCs.

COMBINATION OF TACE AND RADIATION

A number of studies have shown the experimental and clinical therapeutic effectiveness of combination of external/interstitial radiation and TACE[76-82]. Delivering the highest irradiation dose within the tolerance of the liver is the key to improve the long-term effect.

Intra-arterial injection of radioactive lipiodol has shown promising results in patients with HCC and portal obstruction. Raoul *et al*. reported that overall survival rates at 6 months, 1, 2, 3, and 4 years were 69 %, 38 %, 22 %, 14 % and 10 %, in the ^{131}I-labeled lipiodol group and 66 %, 42 %, 22 %, 3 %, and 0 % in the chemoembolization group, respectively. In terms of patient survival and tumor response, radioactive ^{131}I-labeled lipiodol and chemoembolization were equally effective in the treatment of HCC, but tolerance to ^{131}I-labeled lipiodol was significantly better[83].

Guo *et al* and Tazawa *et al* regarded the combination of TACE and radiotherapy as an alternative and permissible treatment for large unresectable HCC, and it might be useful to reverse portal vein tumor thrombi in patients with good hepatic function reserve[79, 80]. It was reported the cumulative survival rates of 1, 3 and 5 years were 59.4 %, 28.4 % and 15. 8 %, respectively[80]. Cheng *et al* demonstrated that this combined therapy was associated with better control of HCC than radiation given alone, probably due to the selection of patients with favorable prognosis for the combined treatment[82]. However, it has been reported that the survival of patients with combined TACE and radiotherapy was similar to that with TACE as the only treatment, while a significant portion of the patients treated with radiotherapy developed extrahepatic metastasis[81]. In another study, Yasuda *et al* also confirmed that radiotherapy combined with TAE and PEI did not clearly show improvement of the survival. However, it could effectively control large HCC with minimal toxicity[84].

Whether this therapeutic method can really increase the survival rate of patients suffering from liver cancer, should be determined by further prospective and comparative studies.

COMBINATION OF TACE AND IMMUNOTHERAPY

In the past few years, combined targeting locoregional immunochemotherapy has been reported with encouraging results[85, 86].

OK-432, a biological response modifier (BRM) derived from the weakly virulent Su strain of *Streptococcus pyogenes*, has been applied in combination with locoregional chemotherapy or transarterial embolization for treating HCC in clinic. OK-432 can augment the anti-tumour effect of anticancer agents (cisplatin/mitomycin), because OK-432 itself has a direct cytotoxic and cytostatic activity against tumour cells and inhibits DNA and RNA synthesis in tumour cells. Chemotherapy can also increase the susceptibility of tumour cells to cytotoxic effector cells including lymphocytes, macrophages and neutrophils activated by OK-432 through direct damage or modulation of surface antigens by chemotherapy[87]. In addition, anticancer agents can eliminate the suppressor cells or suppressor factors in the blood or effusion, resulting in augmented anticancer activity of OK-432-activated immunopotentiating cells, especially T-cells[88, 89].

Based on the results of histologic examination in Japan, transarterial immunoembolization (TIE) seems to be more effective than conventional TAE against extracapsular invasion and intrahepatic metastasis in clinic. Data on disease-free survival and recurrence site suggest TIE may be a useful preoperative treatment[90,91]. Such combined transarterial immuno-chemoembolization merits further clinical investigation in patients with unresectable HCC and immunoincompetence.

Other BRMs such as tumor necrosis factor (TNF), cytotoxic T lymphocyte (CTL), tumor infiltrating lymphocyte (TIL) have not been used in TACE in clinic up to now.

COMBINATION OF TACE AND GENE THERAPY

Gene therapy is one of the more promising approaches for patients with advanced liver tumour. Experimental and clinical studies have been reported using cytokine genes (tumor necrosis factor, interleukin-2, interferon), suicide and p53 genes, retrovirus, adenovirus and Epstein-barr virus as vector, AFP enhancer, intraarterial administration, etc.[92-99].

Adenovirus-mediated gene therapy of experimental HCC is hindered by its low transduction efficacy *in vivo*[92]. Gene therapy for cancer requires efficient, selective gene transfer to cancer cells. The delivery of anticancer agents and iodized oil esters as embolic agents through hepatic artery is known as TACE[93]. Shiba *et al* speculated that genes might be efficiently and selectively transferred for HCC using iodized oil esters because these esters might remain together with a genetic vector within HCC selectively[93]. Clinical trials have begun to evaluate the efficacy of gene transfer of cytotoxic genes to metastatic

colorectal tumors through hepatic artery infusion[92]. The efficiency of trans-arterial gene delivery has also been compared to that of intra-tumoral injection. The results of Seol *et al* indicate that gene expression in patients with liver tumour can be enhanced by trans-arterial delivery of the liposome-DNA complex[94].

Combination of TACE and gene therapy leads to a higher transfer rate and higher concentration of drugs without major side-effects and remains an attractive field for clinical application[92,95,96].

COMBINATION OF TACE AND ANTIANGIOGENESIS THERAPY

Development of tumor angiogenesis-targeting agents is often referred to as a new concept in anticancer therapy, and antiangiogenic agents have the following clinical implications. They may overcome drug resistance in solid tumours. Identification of the angiogenic factors in serum or microvessels in tumors can allow the efficacy of the new agents to be quantified. Antiangiogenic agents have low toxicity due to their selective effect on tumour vasculature. Their combination with anticancer agents may potentiate their anticancer effects[100-104]. For the best clinical results, anti-angiogenic therapy should be used in combination with other adjuvant therapies[105-109].

TNP-470 is the first angio-inhibitor which has entered into phase III clinical trial. TNP-470 (AGM-1470) is a fumagillin analogue which inhibits proliferation and migration of endothelial cells and capillary vessel formation at cytostatic but not cytotoxic concentrations. It is believed that ischaemic hypoxia and necrosis induced by TACE stimulate angiogenesis in the residual viable HCC[110]. TNP-470 inhibits the proliferation of new microvascular channels and consequently the development of multiple arterial collaterals[111]. TNP-470 may be particularly effective in inhibiting extrahepatic collaterals and may make it possible to perform TAE repeatedly[112].

Combination treatment of animals showed that TNP-470 potentiated the anticancer effects of some cytotoxic and biological agents[113], but the terminal plasma half-life of TNP-470 was short and the drug was rapidly cleared from the circulation after a single 1-hour infusion[114]. The use of embolic substances (micropheres and medium-chain triglyceride solution), in which TNP-470 is very stable, prolonged retention of the anticancer drug at the tumour site, and augmented the efficacy of anticancer therapy[115]. TAE combined with TNP-470 may enhance the anticancer effect of TAE alone in the treatment of HCC without severe side effects on the liver or body weight gain[116]. This anticancer effect can be enhanced by coadministration of doxorubicin hydrochloride aqueous solution[117].

By combining antiangiogenic agents with TACE used in the treatment of HCC, the limitations of each therapeutic approach will be overcome, leading to enhanced efficacy with diminished toxicity. However, the optimal strategy for the use, monitoring, and validation of antiangiogenic agents in clinic remains unclear.

COMBINATION OF TACE AND TRADITIONAL CHINESE MEDICINAL THERAPY

Traditional Chinese medicinal therapy has gained wide acceptance as a safe, palliative and effective treatment even in patients with large HCC and cirrhosis in China.

Bletilla striata (BS) is a common Chinese medicinal herb and is usually used as an embolic material in TACE for HCC. Its compositions are mucilage, starch, and a little volatile oil[118]. The mechanisms of embolization by BS are attributable to the following factors such as non-absorbent property, mechanical obstruction, effect on coagulative and anticoagulative systems and secondary obstruction due to the injury to wall of blood vessels[119, 120]. Zheng *et al* have confirmed that BS powder has an adherent function and can diffuse slowly in blood flow, leading to mechanical blockade of vessels. The rough surface of BS powder can disintegrate local blood platelets and its mucilage component can make locked erythrocytes agglutinate, thus shortening the clotting time and prothrombin time and causing formation of secondary thrombi[118]. It has also been hypothesized that BS can slowly diffuse into the liver parenchyma around the tumour in colloidal forms, leading to prolonged anticancer effect and inhibition of collateralisation and metastasis of tumour[121]. Compared with gelfoam embolus, BS has the following characteristics. It can produce extensive and permanent vascular embolization, while it cannot be absorbed by body tissue. After embolization, tumour necrosis and shrinkage are significant with less collateral circulation that forms later. The mucilage component of BS is a wide-spectrum anticancer element that may inhibit tumor occurrence and development[118,121]. The 1-, 2- and 3-year survival rates were 44.9 %, 33.6 % and 33.6 % in BS group, and were 48.9 %, 31.1 % and 16.0 % in gelfoam group, suggesting that BS is superior to gelfoam as an embolizing agent, and the transarterial administration of BS may provide a beneficial therapeutic modality for HCC[122].

CONCLUSION

In summary, despite the number of treatment options, HCC usually has a poor prognosis and is one of the malignancies to be cured. The range of treatment options is fairly wide, and the choice is not always easy, given the number of variables to be assessed.

Combined interventional therapies are superior to any single therapy for improving the prognosis and survival of patients with HCC. More multi-center randomized experimental and clinical studies are required to define the indications and role of these combined modalities for treating unresectable HCC.

REFERENCES

1 **Qin LX**, Tang ZY. The prognostic significance of clinical and pathological features in hepatocellular carcinoma. *World J Gastroenterol* 2002; **8**: 193-199

2 **Parks RW**, Garden OJ. Liver resection for cancer. *World J Gastroenterol* 2001; **7**: 766-771

3 **Franco D**, Usatoff V. Resection of hepatocellular carcinoma. *Hepatogastroenterology* 2001; **48**: 33-36

4 **Alsowmely AM**, Hodgson HJ. Non-surgical treatment of hepatocellular carcinoma. *Aliment Pharmacol Ther* 2002; **16**: 1-15

5 **Yan FH**, Zhou KR, Cheng JM, Wang JH, Yan ZP, Da RR, Fan J, Ji Y. Role and limitation of FMPSPGR dynamic contrast scanning in the follow-up of patients with hepatocellular carcinoma treated by TACE. *World J Gastroenterol* 2002; **8**: 658-662

6 **Colella G**, Bottelli R, De Carlis L, Sansalone CV, Rondinara GF, Alberti A, Belli LS, Gelosa F, Iamoni GM, Rampoldi A, De Gasperi A, Corti A, Mazza E, Aseni P, Meroni A, Slim AO, Finzi M, Di Benedetto F, Manochehri F, Follini ML, Ideo G, Forti D. Hepatocellular carcinoma: comparison between liver transplantation, resective surgery, ethanol injection, and chemoembolization. *Transpl Int* 1998; **11**: 193-196

7 **Durand F**, Belghiti J. Liver transplantation for hepatocellular carcinoma. *Hepatogastroenterology* 2002; **49**: 47-52

8 **Wong LL**. Current status of liver transplantation for hepatocellular cancer. *Am J Surg* 2002; **183**: 309-316

9 **Wu MC**, Shen F. Progress in research of liver surgery in China. *World J Gastroenterol* 2000; **6**: 773-776

10 **Poon RT**, Fan ST, Tsang FH, Wong J. Locoregional therapies for hepatocellular carcinoma: a critical review from the surgeon's perspective. *Ann Surg* 2002; **235**: 466-486

11 **Sturm JW**, Keese MA, Bonninghoff RG, Wustner M, Post S. Lo-

cally ablative therapies of hepatocellular carcinoma. *Onkologie* 2001; **24** (Suppl 5): 35-45
12 **Achenbach T**, Seifert JK, Pitton MB, Schunk K, Junginger T. Chemoembolization for primary liver cancer. *Eur J Surg Oncol* 2002; **28**: 37-41
13 **Mizoe A**, Yamaguchi J, Azuma T, Fujioka H, Furui J, Kanematsu T. Transcatheter arterial embolization for advanced hepatocellular carcinoma resulting in a curative resection: report of two cases. *Hepatogastroenterology* 2000; **47**: 1706-1710
14 **Llovet JM**, Real MI, Montana X, Planas R, Coll S, Aponte J, Ayuso C, Sala M, Muchart J, Sola R, Rodes J, Bruix J. Barcelona Liver Cancer Group. Arterial embolisation or chemoembolisation versus symptomatic treatment in patients with unresectable hepatocellular carcinoma: a randomised controlled trial. *Lancet* 2002; **359**: 1734-1739
15 **Li L**, Wu PH, Li JQ, Zhang WZ, Lin HG, Zhang YQ. Segmental transcatheter arterial embolization for primary hepatocellular carcinoma. *World J Gastroenterol* 1998; **4**: 511-512
16 **Chen MS**, Li JQ, Zhang YQ, Lu LX, Zhang WZ, Yuan YF, Guo YP, Lin XJ, Li GH. High-dose iodized oil transcatheter arterial chemoembolization for patients with large hepatocellular carcinoma. *World J Gastroenterol* 2002; **8**: 74-78
17 **Qian J,** Truebenbach J, Graepler F, Pereira P, Huppert P, Eul T, Wiemann G, Claussen C. Application of poly-lactide-co-glycolide-microspheres in the transarterial chemoembolization in an animal model of hepatocellular carcinoma. *World J Gastroenterol* 2003; **9**: 949-948
18 **Fan J**, Ten GJ, He SC, Guo JH, Yang DP, Wang GY. Arterial chemoembolization for hepatocellular carcinoma. *World J Gastroenterol* 1998; **4**: 33-37
19 **Lin DY**, Lin SM, Liaw YF. Non-surgical treatment of hepatocellular carcinoma. *J Gastroenterol Hepatol* 1997; **12**: 319-328
20 **Livraghi T**, Goldberg SN, Lazzaroni S, Meloni F, Solbiati L, Gazelle GS. Small hepatocellular carcinoma: treatment with radiofrequency ablation versus ethanol injection. *Radiology* 1999; **210**: 655-661
21 **Seki S**, Sakaguchi H, Kadoya H, Morikawa H, Habu D, Nishiguchi S, Shiomi S, Kitada T, Kuroki T. Laparoscopic microwave coagulation therapy for hepatocellular carcinoma. *Endoscopy* 2000; **32**: 591-597
22 **Seki T**, Wakabayashi M, Nakagawa T, Imamura M, Tamai T, Nishimura A, Yamashiki N, Okamura A, Inoue K. Percutaneous microwave coagulation therapy for patients with small hepatocellular carcinoma: comparison with percutaneous ethanol injection therapy. *Cancer* 1999; **85**: 1694-1702
23 **Itamoto T**, Katayama K, Fukuda S, Fukuda T, Yano M, Nakahara H, Okamoto Y, Sugino K, Marubayashi S, Asahara T. Percutaneous microwave coagulation therapy for primary or recurrent hepatocellular carcinoma: long-term results. *Hepatogastroenterology* 2001; **48**: 1401-1405
24 **Vogl TJ**, Straub R, Eichler K, Woitaschek D, Mack MG. Malignant liver tumors treated with MR imaging-guided laser-induced thermotherapy: experience with complications in 899 patients (2,520 lesions). *Radiology* 2002; **225**: 367-377
25 **Vogl TJ**, Mack MG, Straub R, Zangos S, Engelmann K, Eichler K. Percutaneous laser ablation of malignant liver tumors. *Zentralbl Chir* 2001; **126**: 571-575
26 **Pacella CM**, Bizzarri G, Magnolfi F, Cecconi P, Caspani B, Anelli V, Bianchini A, Valle D, Pacella S, Manenti G, Rossi Z. Laser thermal ablation in the treatment of small hepatocellular carcinoma: results in 74 patients. *Radiology* 2001; **221**: 712-720
27 **Tang ZY**. Hepatocellular carcinoma-cause, treatment and metastasis. *World J Gastroenterol* 2001; **7**: 445-454
28 **Zhang Z**, Liu Q, He J, Yang J, Yang G, Wu M. The effect of preoperative transcatheter hepatic arterial chemoembolization on disease-free survival after hepatectomy for hepatocellular carcinoma. *Cancer* 2000; **89**: 2606-2612
29 **Fan J**, Yu Y, Wu Z. Liver resection after transcatheter hepatic arterial chemoembolization for hepatocellular carcinoma and curative effect analysis. *Zhonghua Waike Zazhi* 1997; **35**: 710-712
30 **Gerunda GE**, Neri D, Merenda R, Barbazza F, Zangrandi F, Meduri F, Bisello M, Valmasoni M, Gangemi A, Faccioli AM. Role of transarterial chemoembolization before liver resection for hepatocarcinoma. *Liver Transpl* 2000; **6**: 619-626
31 **Di Carlo V**, Ferrari G, Castoldi R, De Nardi P, Bergamo C, Taccagni G, Salvioni M, Angeli E, Venturini M, Del Maschio A. Pre-operative chemoembolization of hepatocellular carcinoma in cirrhotic patients. *Hepatogastroenterology* 1998; **45**: 1950-1954
32 **Nakano H**, Yoshida K, Takeuchi S, Kumada K, Yamaguchi M, Jaeck D. Liver scintigraphy is useful for selecting candidates for preoperative transarterial chemoembolization among patients with hepatocellular carcinoma and chronic liver disease. *Am J Surg* 1999; **178**: 385-389
33 **Huang J**, He X, Lin X, Zhang C, Li J. Effect of preoperative transcatheter arterial chemoembolization on tumor cell activity in hepatocellular carcinoma. *Chin Med J* 2000; **113**: 446-448
34 **Wu CC**, Ho YZ, Ho WL, Wu TC, Liu TJ, P'eng FK. Preoperative transcatheter arterial chemoembolization for resectable large hepatocellular carcinoma: a reappraisal. *Br J Surg* 1995; **82**: 122-126
35 **Veltri A**, Grosso M, Martina MC, Ciancio A, David E, Salizzoni M, Soldano U, Galli J, Fava C. Effect of preoperative radiological treatment of hepatocellular carcinoma before liver transplantation: a retrospective study. *Cardiovasc Intervent Radiol* 1998; **21**: 393-398
36 **Clavien PA**, Kang KJ, Selzner N, Morse MA, Suhocki PV. Cryosurgery after chemoembolization for hepatocellular carcinoma in patients with cirrhosis. *J Gastrointest Surg* 2002; **6**: 95-101
37 **Lin Z**, Ren Z, Xia J. Appraisal of postoperative transcatheter arterial chemoembolization (TACE) for prevention and treatment of hepatocellular carcinoma recurrence. *Zhonghua Zhongliu Zazhi* 2000; **22**: 315-317
38 **Huo TI**, Huang YH, Wu JC, Lee PC, Chang FY, Lee SD. Survival benefit of cirrhotic patients with hepatocellular carcinoma treated by percutaneous ethanol injection as a salvage therapy. *Scand J Gastroenterol* 2002; **37**: 350-355
39 **Ishii H**, Okada S, Nose H, Okusaka T, Yoshimori M, Takayama T, Kosuge T, Yamasaki S, Sakamoto M, Hirohashi S. Local recurrence of hepatocellular carcinoma after percutaneous ethanol injection. *Cancer* 1996; **77**: 1792-1796
40 **Koda M**, Murawaki Y, Mitsuda A, Ohyama K, Horie Y, Suou T, Kawasaki H, Ikawa S. Predictive factors for intrahepatic recurrence after percutaneous ethanol injection therapy for small hepatocellular carcinoma. *Cancer* 2000; **88**: 529-537
41 **Livraghi T**. Role of percutaneous ethanol injection in the treatment of hepatocellular carcinoma. *Dig Dis* 2001; **19**: 292-300
42 **Livraghi T**. Percutaneous ethanol injection in the treatment of hepatocellular carcinoma in cirrhosis. *Hepatogastroenterology* 2001; **48**: 20-24
43 **Allgaier HP**, Deibert P, Olschewski M, Spamer C, Blum U, Gerok W, Blum HE. Survival benefit of patients with inoperable hepatocellular carcinoma treated by a combination of transarterial chemoembolization and percutaneous ethanol injection - a single-center analysis including 132 patients. *Int J Cancer* 1998; **79**: 601-605
44 **Teratani T**, Ishikawa T, Shiratori Y, Shiina S, Yoshida H, Imamura M, Obi S, Sato S, Hamamura K, Omata M. Hepatocellular carcinoma in elderly patients: beneficial therapeutic efficacy using percutaneous ethanol injection therapy. *Cancer* 2002; **95**: 816-823
45 **Livraghi T**, Giorgio A, Marin G, Salmi A, de Sio I, Bolondi L, Pompili M, Brunello F, Lazzaroni S, Torzilli G. Hepatocellular carcinoma and cirrhosis in 746 patients: long-term results of percutaneous ethanol injection. *Radiology* 1995; **197**: 101-108
46 **Dimitrakopoulou-Strauss A**, Strauss LG, Gutzler F, Irngartinger G, Kontaxakis G, Kim DK, Oberdorfer F, van Kaick G. Pharmacokinetic imaging of 11C ethanol with PET in eight patients with hepatocellular carcinomas who were scheduled for treatment with percutaneous ethanol injection. *Radiology* 1999; **211**: 681-686
47 **Tanaka K**, Nakamura S, Numata K, Kondo M, Morita K, Kitamura T, Saito S, Kiba T, Okazaki H, Sekihara H. The long term efficacy of combined transcatheter arterial embolization and percutaneous ethanol injection in the treatment of patients with large hepatocellular carcinoma and cirrhosis. *Cancer* 1998; **82**: 78-85
48 **Koda M**, Murawaki Y, Mitsuda A, Oyama K, Okamoto K, Idobe Y, Suou T, Kawasaki H. Combination therapy with transcatheter arterial chemoembolization and percutaneous ethanol injection compared with percutaneous ethanol injection alone for patients with small hepatocellular carcinoma: a randomized control study. *Cancer* 2001; **92**: 1516-1524
49 **Lencioni R**, Paolicchi A, Moretti M, Pinto F, Armillotta N, Di Giulio M, Cicorelli A, Donati F, Cioni D, Bartolozzi C. Combined transcatheter arterial chemoembolization and percutaneous etha-

nol injection for the treatment of large hepatocellular carcinoma: local therapeutic effect and long-term survival rate. *Eur Radiol* 1998; **8**: 439-444

50 **Kirchhoff T**, Chavan A, Galanski M. Transarterial chemoembolization and percutaneous ethanol injection therapy in patients with hepatocellular carcinoma. *Eur J Gastroenterol Hepatol* 1998; **10**: 907-909

51 **Lencioni R**, Cioni D, Donati F, Bartolozzi C. Combination of interventional therapies in hepatocellular carcinoma. *Hepatogastroenterology* 2001; **48**: 8-14

52 **Kamada K**, Kitamoto M, Aikata H, Kawakami Y, Kono H, Imamura M, Nakanishi T, Chayama K. Combination of transcatheter arterial chemoembolization using cisplatin-lipiodol suspension and percutaneous ethanol injection for treatment of advanced small hepatocellular carcinoma. *Am J Surg* 2002; **184**: 284-290

53 **Acunas B**, Rozanes I. Hepatocellular carcinoma: treatment with transcatheter arterial chemoembolization. *Eur J Radiol* 1999; **32**: 86-89

54 **Allgaier HP**, Galandi D, Zuber I, Blum HE. Radiofrequency thermal ablation of hepatocellular carcinoma. *Dig Dis* 2001; **19**: 301-310

55 **Curley SA**, Izzo F. Radiofrequency ablation of hepatocellular carcinoma. *Minerva Chir* 2002; **57**: 165-176

56 **Livraghi T**, Goldberg SN, Lazzaroni S, Meloni F, Ierace T, Solbiati L, Gazelle GS. Hepatocellular carcinoma: radio-frequency ablation of medium and large lesions. *Radiology* 2000; **214**: 761-768

57 **Shibata T**, Iimuro Y, Yamamoto Y, Maetani Y, Ametani F, Itoh K, Konishi J. Small hepatocellular carcinoma: comparison of radio-frequency ablation and percutaneous microwave coagulation therapy. *Radiology* 2002; **223**: 331-337

58 **Buscarini L**, Buscarini E, Di Stasi M, Vallisa D, Quaretti P, Rocca A. Percutaneous radiofrequency ablation of small hepatocellular carcinoma: long-term results. *Eur Radiol* 2001; **11**: 914-921

59 **Bowles BJ**, Machi J, Limm WM, Severino R, Oishi AJ, Furumoto NL, Wong LL, Oishi RH. Safety and efficacy of radiofrequency thermal ablation in advanced liver tumors. *Arch Surg* 2001; **136**: 864-869

60 **Ikeda M**, Okada S, Ueno H, Okusaka T, Kuriyama H. Radiofrequency ablation and percutaneous ethanol injection in patients with small hepatocellular carcinoma: a comparative study. *Jpn J Clin Oncol* 2001; **31**: 322-326

61 **Jiang HC**, Liu LX, Piao DX, Xu J, Zheng M, Zhu AL, Qi SY, Zhang WH, Wu LF. Clinical short-term results of radiofrequency ablation in liver cancers. *World J Gastroenterol* 2002; **8**: 624-630

62 **Yamasaki T**, Kurokawa F, Shirahashi H, Kusano N, Hironaka K, Okita K. Percutaneous radiofrequency ablation therapy with combined angiography and computed tomography assistance for patients with hepatocellular carcinoma. *Cancer* 2001; **91**: 1342-1348

63 **Buscarini L**, Buscarini E, Di Stasi M, Quaretti P, Zangrandi A. Percutaneous radiofrequency thermal ablation combined with transcatheter arterial embolization in the treatment of large hepatocellular carcinoma. *Ultraschall Med* 1999; **20**: 47-53

64 **Bloomston M**, Binitie O, Fraiji E, Murr M, Zervos E, Goldin S, Kudryk B, Zwiebel B, Black T, Fargher S, Rosemurgy AS. Transcatheter arterial chemoembolization with or without radiofrequency ablation in the management of patients with advanced hepatic malignancy. *Am Surg* 2002; **68**: 827-831

65 **Kurokohchi K**, Watanabe S, Masaki T, Hosomi N, Funaki T, Arima K, Yoshida S, Nakai S, Murota M, Miyauchi Y, Kuriyama S. Combination therapy of percutaneous ethanol injection and radiofrequency ablation against hepatocellular carcinomas difficult to treat. *Int J Oncol* 2002; **21**: 611-615

66 **Kurokohchi K**, Watanabe S, Masaki T, Hosomi N, Funaki T, Arima K, Yoshida S, Miyauchi Y, Kuriyama S. Combined use of percutaneous ethanol injection and radiofrequency ablation for the effective treatment of hepatocellular carcinoma. *Int J Oncol* 2002; **21**: 841-846

67 **Nicoli N**, Casaril A, Marchiori L, Mangiante G, Hasheminia AR. Treatment of recurrent hepatocellular carcinoma by radiofrequency thermal ablation. *J Hepatobiliary Pancreat Surg* 2001; **8**: 417-421

68 **Horigome H**, Nomura T, Saso K, Itoh M. Standards for selecting percutaneous ethanol injection therapy or percutaneous microwave coagulation therapy for solitary small hepatocellular carcinoma: consideration of local recurrence. *Am J Gastroenterol* 1999; **94**: 1914-1917

69 **Seki T**, Tamai T, Nakagawa T, Imamura M, Nishimura A, Yamashiki N, Ikeda K, Inoue K. Combination therapy with transcatheter arterial chemoembolization and percutaneous microwave coagulation therapy for hepatocellular carcinoma. *Cancer* 2000; **89**: 1245-1251

70 **Ishikawa M**, Ikeyama S, Sasaki K, Sasaki K, Miyauchi T, Fukuda Y, Miyake H, Harada M, Terashima Y, Yogita S, Tashiro S. Intraoperative microwave coagulation therapy for large hepatic tumors. *J Hepatobiliary Pancreat Surg* 2000; **7**: 587-591

71 **Izumi N**, Asahina Y, Noguchi O, Uchihara M, Kanazawa N, Itakura J, Himeno Y, Miyake S, Sakai T, Enomoto N. Risk factors for distant recurrence of hepatocellular carcinoma in the liver after complete coagulation by microwave or radiofrequency ablation. *Cancer* 2001; **91**: 949-956

72 **Vogl TJ**, Mack MG, Roggan A, Straub R, Eichler KC, Muller PK, Knappe V, Felix R. Internally cooled power laser for MR-guided interstitial laser-induced thermotherapy of liver lesions: initial clinical results. *Radiology* 1998; **209**: 381-385

73 **Vogl TJ**, Muller PK, Hammerstingl R, Weinhold N, Mack MG, Philipp C, Deimling M, Beuthan J, Pegios W, Riess H. Malignant liver tumors treated with MR imaging-guided laser-induced thermotherapy: technique and prospective results. *Radiology* 1995; **196**: 257-265

74 **Pacella CM**, Bizzarri G, Cecconi P, Caspani B, Magnolfi F, Bianchini A, Anelli V, Pacella S, Rossi Z. Hepatocellular carcinoma: long-term results of combined treatment with laser thermal ablation and transcatheter arterial chemoembolization. *Radiology* 2001; **219**: 669-678

75 **Vogl TJ**, Muller PK, Mack MG, Straub R, Engelmann K, Neuhaus P. Liver metastases: interventional therapeutic techniques and results, state of the art. *Eur Radiol* 1999; **9**: 675-684

76 **Leung SW**, Huang EY, Cheng YF, Lu SN. Conformal radiation therapy for hepatoma with portal vein thrombosis. *Br J Radiol* 2000; **73**: 550-552

77 **Seong J**, Keum KC, Han KH, Lee DY, Lee JT, Chon CY, Moon YM, Suh CO, Kim GE. Combined transcatheter arterial chemoembolization and local radiotherapy of unresectable hepatocellular carcinoma. *Int J Radiat Oncol Biol Phys* 1999; **43**: 393-397

78 **Seong J**, Park HC, Han KH, Lee DY, Lee JT, Chon CY, Moon YM, Suh CO. Local radiotherapy for unresectable hepatocellular carcinoma patients who failed with transcatheter arterial chemoembolization. *Int J Radiat Oncol Biol Phys* 2000; **47**: 1331-1335

79 **Guo WJ**, Yu EX. Evaluation of combined therapy with chemoembolization and irradiation for large hepatocellular carcinoma. *Br J Radiol* 2000; **73**: 1091-1097

80 **Tazawa J**, Maeda M, Sakai Y, Yamane M, Ohbayashi H, Kakinuma S, Miyasaka Y, Nagayama K, Enomoto N, Sato C. Radiation therapy in combination with transcatheter arterial chemoembolization for hepatocellular carcinoma with extensive portal vein involvement. *J Gastroenterol Hepatol* 2001; **16**: 660-665

81 **Chia-Hsien Cheng J**, Chuang VP, Cheng SH, Lin YM, Cheng TI, Yang PS, Jian JJ, You DL, Horng CF, Huang AT. Unresectable hepatocellular carcinoma treated with radiotherapy and/or chemoembolization. *Int J Cancer* 2001; **96**: 243-252

82 **Cheng JC**, Chuang VP, Cheng SH, Huang AT, Lin YM, Cheng TI, Yang PS, You DL, Jian JJ, Tsai SY, Sung JL, Horng CF. Local radiotherapy with or without transcatheter arterial chemoembolization for patients with unresectable hepatocellular carcinoma. *Int J Radiat Oncol Biol Phys* 2000; **47**: 435-442

83 **Raoul JL**, Guyader D, Bretagne JF, Heautot JF, Duvauferrier R, Bourguet P, Bekhechi D, Deugnier YM, Gosselin M. Prospective randomized trial of chemoembolization versus intra-arterial injection of 131I-labeled-iodized oil in the treatment of hepatocellular carcinoma. *Hepatology* 1997; **26**: 1156-1161

84 **Yasuda S**, Ito H, Yoshikawa M, Shinozaki M, Goto N, Fujimoto H, Nasu K, Uno T, Itami J, Isobe K, Shigematsu N, Ebara M, Saisho H. Radiotherapy for large hepatocellular carcinoma combined with transcatheter arterial embolization and percutaneous ethanol injection therapy. *Int J Oncol* 1999; **15**: 467-473

85 **Kountouras J**, Boura P, Kouklakis G. Locoregional immunochemotherapy in hepatocellular carcinoma. *Hepatogastroenterology* 2002; **49**: 1109-1112

86 **Sato T**. Locoregional immuno(bio)therapy for liver metastases. *Semin Oncol* 2002; **29**: 160-167

87 **Uehara K**, Ichida T, Sugahara S, Ishikawa T, Yamagiwa S, Yoshida Y, Nomoto M, Katoh M, Satoh H, Watanabe H, Abo T, Asakura

H. Systemic administration of liposome-encapsulated OK-432 prolongs the survival of rats with hepatocellular carcinoma through the induction of IFN-gamma-producing hepatic lymphocytes. *J Gastroenterol Hepatol* 2002; **17**: 81-90

88 **Nio Y**, Nagami H, Tamura K, Tsubono M, Nio M, Sato M, Kawabata K, Hayashi H, Shiraishi T, Imai S, Tsuchitani T, Mizuta J, Nakagawa M, Fukumoto M. Multi-institutional randomized clinical study on the comparative effects of intracavital chemotherapy alone versus immunotherapy alone versus immunochemotherapy for malignant effusion. *Br J Cancer* 1999; **80**: 775-785

89 **Oka M**, Hazama S, Yoshino S, Shimoda K, Suzuki M, Shimizu R, Yano K, Nishida M, Suzuki T. Intraarterial combined immunochemotherapy for unresectable hepatocellular carcinoma: preliminary results. *Cancer Immunol Immunother* 1994; **38**: 194-200

90 **Yoshida T**, Sakon M, Umeshita K, Kanai T, Miyamoto A, Takeda T, Gotoh M, Nakamura H, Wakasa K, Monden M. Appraisal of transarterial immunoembolization for hepatocellular carcinoma: a clinicopathologic study. *J Clin Gastroenterol* 2001; **32**: 59-65

91 **Kanai T**, Monden M, Sakon M, Gotoh M, Umeshita K, Hasuike Y, Nakano H, Monden T, Murakami T, Nakamura H. New development of transarterial immunoembolization (TIE) for therapy of hepatocellular carcinoma with intrahepatic metastases. *Cancer Chemother Pharmacol* 1994; **33**: 48-54

92 **Gerolami R**, Cardoso J, Bralet MP, Cuenod CA, Clement O, Tran PL, Brechot C. Enhanced in vivo adenovirus-mediated gene transfer to rat hepatocarcinomas by selective administration into the hepatic artery. *Gene Ther* 1998; **5**: 896-904

93 **Shiba H**, Okamoto T, Futagawa Y, Ohashi T, Eto Y. Efficient and cancer-selective gene transfer to hepatocellular carcinoma in a rat using adenovirus vector with iodized oil esters. *Cancer Gene Ther* 2001; **8**: 713-718

94 **Seol JG**, Heo DS, Kim HK, Yoon JH, Choi BI, Lee HS, Kim NK, Kim CY. Selective gene _expression in hepatic tumor with transarterial delivery of DNA / liposome / transferrin complex. *In Vivo* 2000; **14**: 513-517

95 **Iwazawa T**, Chau GY, Mori T, Dookeran KA, Rubin JT, Watkins S, Robbins PD, Lotze MT, Tahara H. Potent antitumor effects of intra-arterial injection of fibroblasts genetically engineered to express IL-12 in liver metastasis model of rat: no additional benefit of using retroviral producer cell. *Cancer Gene Ther* 2001; **8**: 17-22

96 **Alfke H**, Kalinowski M, Nocken F, Klose KJ. A review of molecular radiology. I: Gene therapy. *Rofo Fortschr Geb Rontgenstr Neuen Bildgeb Verfahr* 2000; **172**: 949-956

97 **Kwon HC**, Kim JH, Kim KC, Lee KH, Lee JH, Lee BH, Lee KH, Jang JJ, Lee CT, Lee H, Kim CM. *In vivo* antitumor effect of herpes simplex virus thymidine kinase gene therapy in rat hepatocellular carcinoma: feasibility of adenovirus-mediated intra-arterial gene delivery. *Mol Cells* 2001; **11**: 170-178

98 **Gerolami R**, Cardoso J, Lewin M, Bralet MP, Sa Cunha A, Clement O, Brechot C, Tran PL. Evaluation of HSV-tk gene therapy in a rat model of chemically induced hepatocellular carcinoma by intratumoral and intrahepatic artery routes. *Cancer Res* 2000; **60**: 993-1001

99 **Humphreys MJ**, Ghaneh P, Greenhalf W, Campbell F, Clayton TM, Everett P, Huber BE, Richards CA, Ford MJ, Neoptolemos JP. Hepatic intra-arterial delivery of a retroviral vector expressing the cytosine deaminase gene, controlled by the CEA promoter and intraperitoneal treatment with 5-fluorocytosine suppresses growth of colorectal liver metastases. *Gene Ther* 2001; **8**: 1241-1247

100 **Westphal JR**, Ruiter DJ, De Waal RM. Anti-angiogenic treatment of human cancer: pitfalls and promises. *Int J Cancer* 2000; **86**: 870-873

101 **Rosen L**. Antiangiogenic strategies and agents in clinical trials. *Oncologist* 2000; **5**(Suppl 1): 20-27

102 **Keshet E**, Ben-Sasson SA. Anticancer drug targets: approaching angiogenesis. *J Clin Invest* 1999; **104**: 1497-1501

103 **Tomanek RJ**, Schatteman GC. Angiogenesis: new insights and therapeutic potential. *Anat Rec* 2000; **261**: 126-135

104 **Burrows FJ**, Thorpe PE. Vascular targeting-a new approach to the therapy of solid tumors. *Pharmacol Ther* 1994; **64**: 155-174

105 **Folkman J**. New perspectives in clinical oncology from angiogenesis research. *Eur J Cancer* 1996; **32A**: 2534-2539

106 **Kuiper RA**, Schellens JH, Blijham GH, Beijnen JH, Voest EE. Clinical research on antiangiogenic therapy. *Pharmacol Res* 1998; **37**: 1-16

107 **Drixler TA**, Voest EE, van Vroonhoven TJ, Rinkes IH. Angiogenesis and surgery: from mice to man. *Eur J Surg* 2000; **166**: 435-446

108 **Zetter BR**. Angiogenesis and tumor metastasis. *Annu Rev Med* 1998; **49**: 407-424

109 **O'Reilly MS**. The combination of antiangiogenic therapy with other modalities. *Cancer J* 2002; **8**(Suppl 1): 89-99

110 **Kim YB**, Park YN, Park C. Increased proliferation activities of vascular endothelial cells and tumour cells in residual hepatocellular carcinoma following transcatheter arterial embolization. *Histopathology* 2001; **38**: 160-166

111 **Mugitani T**, Taniguchi H, Takada A, Yamaguchi A, Masuyama M, Hoshima M, Takahashi T. TNP-470 inhibits collateralization to complement the anti-tumour effect of hepatic artery ligation. *Br J Cancer* 1998; **77**: 638-642

112 **Charnsangavej C**, Chuang VP, Wallace S, Soo CS, Bowers T. Work in progress: transcatheter management of primary carcinoma of the liver. *Radiology* 1983; **147**: 51-55

113 **Ogawa H**, Sato Y, Kondo M, Takahashi N, Oshima T, Sasaki F, Une Y, Nishihira J, Todo S. Combined treatment with TNP-470 and 5-fluorouracil effectively inhibits growth of murine colon cancer cells *in vitro* and liver metastasis *in vivo*. *Oncol Rep* 2000; **7**: 467-472

114 **Figg WD**, Pluda JM, Lush RM, Saville MW, Wyvill K, Reed E, Yarchoan R. The pharmacokinetics of TNP-470, a new angiogenesis inhibitor. *Pharmacotherapy* 1997; **17**: 91-97

115 **Yanai S**, Okada H, Saito K, Kuge Y, Misaki M, Ogawa Y, Toguchi H. Antitumor effect of arterial administration of a medium-chain triglyceride solution of an angiogenesis inhibitor, TNP-470, in rabbits bearing VX-2 carcinoma. *Pharm Res* 1995; **12**: 653-657

116 **Yanai S**, Okada H, Misaki M, Saito K, Kuge Y, Ogawa Y, Toguchi H. Antitumor activity of a medium-chain triglyceride solution of the angiogenesis inhibitor TNP-470 (AGM-1470) when administered via the hepatic artery to rats bearing Walker 256 carcinosarcoma in the liver. *J Pharmacol Exp Ther* 1994; **271**: 1267-1273

117 **Kamei S**, Okada H, Inoue Y, Yoshioka T, Ogawa Y, Toguchi H. Antitumor effects of angiogenesis inhibitor TNP-470 in rabbits bearing VX-2 carcinoma by arterial administration of microspheres and oil solution. *J Pharmacol Exp Ther* 1993; **264**: 469-474

118 **Zheng C**, Feng G, Liang H. Bletilla striata as a vascular embolizing agent in interventional treatment of primary hepatic carcinoma. *Chin Med J* 1998; **111**: 1060-1063

119 **Feng XS**, Qiu FZ, Xu Z. Experimental studies of embolization of different hepatotropic blood vessels using Bletilla striata in dogs. *J Tongji Med Univ* 1995; **15**: 45-49

120 **Qian J**, Feng G, Liang H. Action of DDPH in the interventional treatment of portal hypertension induced by liver cirrhosis in rabbits. *J Tongji Med Univ* 1998; **18**: 108-112

121 **Zheng C**, Feng G, Zhou R. New use of Bletilla striata as embolizing agent in the intervention treatment of hepatic carcinoma. *Zhonghua Zhongliu Zazhi* 1996; **18**: 305-307

122 **Feng G**, Kramann B, Zheng C, Zhou R. Comparative study on the long-term effect of permanent embolization of hepatic artery with Bletilla striata in patients with primary liver cancer. *J Tongji Med Univ* 1996; **16**: 111-116

Edited by Zhu LH and Wang XL

P.O.Box 2345, Beijing 100023,China
Fax: +86-10-85381893
E-mail: wjg@wjgnet.com www.wjgnet.com

World J Gastroenterol 2003;9(9):1892-1896
World Journal of Gastroenterology
 ISSN 1007-9327

• ESOPHAGEAL CANCER •

Using yeast two-hybrid system to identify ECRG2 associated proteins and their possible interactions with ECRG2 gene

Yong-Ping Cui, Jian-Bo Wang, Xin-Yu Zhang, Mei-Xia Bi, Li-Ping Guo, Shih-Hsin Lu

Yong- Ping Cui, Jian-Bo Wang, Xin-Yu Zhang, Mei-Xia Bi, Li-Ping Guo, Shih-Hsin Lu, Department of Etiology and Carcinogenesis, Tumor Hospital, Peking Union Medical College & Chinese Academy of Medical Sciences, Beijing 100021, China
Supported by G1998051204 the Major State Basic Research Development Program of China, No.G1998051204
Correspondence to: Shih-Hsin Lu, Ph.D, Department of Etiology and Carcinogenesis, Tumor Hospital, Peking Union Medical College & Chinese Academy of Medical Sciences, Beijing 100021, China. shlu@public.bta.net.cn
Telephone: +86-10-67712368 **Fax:** +86-10-67712368
Received: 2002-11-19 **Accepted:** 2003-01-16

Abstract

AIM: To identify esophageal cancer related gene2 (ECRG2) associated proteins and their possible interactions with ECRG2 gene.

METHODS: In the yeast forward two-hybrid system, ECRG2 was fused with the DNA-binding domain (DBD) of Gal4 and human fetal liver cDNA library was fused with the transcriptional activation domain (AD) of Gal4. We performed a high-stringency scale procedure to screen ECRG2 against human fetal liver cDNA library and characterized positives by sequence analysis.

RESULTS: We found the following 9 putatively associated proteins. They were metallothionein2A, metallothionein1H, metallothionein1G, ferritin, erythrocyte membrane protein band4.2, mitochondrial ribosomal protein S12, hypothetical protein FLJ10101, and a novel gene whose cDNA was found to have no strong homology to any other previously characterized gene whose DDBJ/EMBL/GenBank accession number is AF422192 mapped to human chromosome 14q31.

CONCLUSION: MT, a potential interaction partner for ECRG2, might be involved in the regulation of cell proliferation and apoptosis, and in various physiological processes. Determination of a reliability score for each single protein-protein interaction, especially interaction of ECRG2 and MT, permits the assignment of ECRG2 and unannotated proteins to biological pathways. A further understanding of the association between ECRG2 and MT should facilitate the functions of ECRG2 gene.

Cui YP, Wang JB, Zhang XY, Bi MX, Guo LP, Lu SH. Using yeast two-hybrid system to identify ECRG2 associated proteins and their possible interactions with ECRG2 gene. *World J Gastroenterol* 2003; 9(9): 1892-1896
http://www.wjgnet.com/1007-9327/9/1892.asp

INTRODUCTION

Esophageal cancer (EC) is one of the most common malignancies worldwide with the highest mortality and prevalencet in certain areas of China with a higher incidence[1-2]. It has been found some of tumor suppressor genes and oncogenes are involved in the EC initiation and development[3, 4]. However, so far no gene directly related to EC has been identified. By comparing the differential gene expression between normal esophageal epithelia and esophageal cancer using the technique of mRNA differential display, we have cloned a new gene ECRG2 (GenBank Accession No. AF268198) whose expression was found to be down-regulated in some malignant tissues such as esophageal carcinoma tissue, colon cancer and brain tumor tissues, and most common in esophageal cancer tissues. Although SMART online (http://www.smart.embl-heidelberg.de) has shown that ECRG2 gene contains a characteristic KAZAL-type conserved domain and belongs to the KAZAL-type related serine proteinase inhibitor family, little has been known about its function in normal cellur activities, other than suppressing neoplasia. In order to further reveal its biological roles, we therefore tried to identify ECRG2 associated proteins in the present study by the GAL4-based yeast two-hybrid system using the full-length ECRG2 cDNA as a bait to screen the human fetal liver cDNA library.

MATERIALS AND METHODS

Yeast strains

Matchmaker GAL4 two-hybrid system 3 and vector pACT2 containing the human fetal liver cDNA library were obtained from Clontech. Yeast strain AH109 (MATa, trp 1-901, leu2-3, 112, ura 3-52, his3-200, gal4△, gal80△, LYS2: $GAL1_{UAS}$-$GAL1_{TATA}$-HIS3, $GAL2_{UAS}$-$GAL2_{TATA}$-ADE2, URA3: $MEL1_{UAS}$-$MEL1_{TATA}$-LacZ) was used to screen the library and to verify protein-protein interactions, which could eliminate false positives by using three reporters-ADE2, HIS3, and MEL1 (or LacZ)-under the control of GAL4 upstream activating sequences (UASs) and TATA boxes. Among these reporters ADE2 provided strong nutrition selection, HIS3 gave a selection reducing false positive incidence, and MEL1 or LacZ encoding β-galactosidase could be assayed on X-α-gal indicator plates.

Plasmid constructs

Vector pGBkT7 expressing proteins were fused with amino acids 1-147 of the GAL4 DNA binding domain (DNA-BD), pGADT7 expressing proteins were fused with amino acids 768-881 of the GAL4 activation domain (AD). The control plasmids pGBKT7-53, pGBKT7-lam, pGADT7-T, pCL1 were from Clontech. Plasmid pGBKT7-ECRG2 encoding full-length (85 amino acids) ECRG2 gene fused in frame with the GAL4 DNA binding domain was constructed by inserting the PCR-generated fragment into the EcoRI and BamHI sites of pGBKT7. Plasmid pGADT7-ECRG2 encoding full-length ECRG2 gene fused in frame with GAL4 activation domain was constructed by inserting the PCR-generated fragment into the EcoRI and BamHI sites of pGADT7.

Library tittering and amplification

For tittering library, an aliquot of the library plasmid was thawed and mixed on ice by gentle vortexing. Then 1μl of library plasmid was transferred to 1 ml of LB broth, which was mixed and named dilution A ($1:10^3$). By the same way,

another library plasmid diluent dilution B ($1:10^6$) was obtained. The prewarmed LB/amp plates were prepared by inoculating them in 1 μl of dilution A mixed with 50 μl of LB broth, or 50 μl and 100 μl of dilution B where respectively incubated on LB/amp plates at 30 ℃ for 48 h. The library titer was calculated as follows: Dilution A: counted colonies$\times10^3\times10^3$=cfu/ml, Dilution B: (counted colonies/plating volume)$\times10^3\times10^3\times10^3$ =cfu/ml. For the library amplification, LB/amp plates were inoculated with the library plasmids at such a high density that the resulting colonies could be easily confluent (-20 000-40 000 cfu per 150-mm plate) and reach at least 2-3 times as the library original plasmid number to ensure the better screening results. After incubated at 30 ℃ for 48 h, colonies were scraped, mixed with adequate volume of LB broth and shake-cultured in a flask at 30 ℃ for 2 h. One-third of the library culture was set aside for plasmid preparation.

Verification of activation of reporter gene by pGBKT7-ECRG2

Plasmid pGBKT7-ECRG2 was independently transformed into strain AH109. The transformants were assayed for β-galactosidase activity by selecting them on SD/-Trp/-Leu/X-α-Gal. Positive control, pCL1, was performed in parallel.

Library transformation and screening

Plasmid pGBkT7-ECRG2 was used as a bait in two-hybrid screening of human fetal liver cDNA libraries by MATCHMAKER Two-Hybrid System 3 protocol (Clontech). The yeast strain AH109 was sequencely transformed with pGBKT7-ECRG2 and a human fetal liver cDNA library in the pACT2 vector (Clontech) was obtained by the lithium acetate method. Transformants expressing both the bait and interacting prey proteins were selected on SD/-Trp/-Leu/-His/-Ade and incubated at 30 ℃ for 5-7 days. β-galactosidase activity was tested using the filter lift assay to identify the positive colones.

Isolating plasmid DNA from putatively positive yeast clones, rescuing AD/library plasmids and retesting protein interaction in yeast

Approximately 3×10^6 colonies were screened and 146 positive clones were identified. cDNA inserts of the positive clones were amplified by PCR using primers complementary to the sequence of pACT2 vector (5' T ACC ACT ACA ATG GAT3' and 5' GTG AAC TTG CGG GGT TTT TCA GTA TCT ACG A3'). Subsequently, pACT2-cDNA constructs were isolated from positive yeast colonies, as recommended by the supplier, transformed into super-competent *E. coli* DH5α by electroporation, grown under selection, re-isolated and analyzed by restriction digests. The uniquely purified constructs were then re-tested against the original pGBKT7-ECRG2 bait construct. To ensure the interactions were specific, the positive clones were also tested against an irrelevant bait protein laminC and grown on SD/-Ade/-His/-Leu/-Trp/X-α-Gal to test the specificity of interactions.

Sequence Ad/library inserts and blast online (http://www.ncbi.nlm.nih.gov/blast)

The positive inserts were sequenced and analyzed by comparison to the GenBank sequence data bank.

RESULTS

Library tittering and amplification

The titer of human fetal liver cDNA library was 3.17×10^9cfu/ml counted by dilution method. The number of separate colonies was 1.05×10^7. We amplified it in 150 mm×500 plates, about 1×10^8 (3.5 μl original cDNA library) colonies and the library plasmids were successfully isolated.

Verification of activation reporter genes by pGBKT7-ECRG2

Plasmid pGBKT7-ECRG2 was independently transformed into AH109. After β-galactosidase activity assay, the AH109 transformed pGBKT7-ECRG2 did not appear blue colonies, but the positive control, pCL1, appeared as is shown in Figure 1. It was verified that pGBKT7-ECRG2 construct did not activate reporter genes and was suitable for the yeast two-hybrid system (Figure 1).

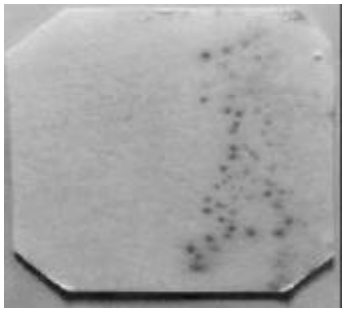

Figure 1 Colony-lift filter assay for β-galactosidase activity. Left: β-galactosidase activity of AH109 transformed with pGBKT7-ECRG2. Right: β-galactosidase activity of AH109 transformed with pCL1 (positive control). The results showed that pCL1 could activate reporter genes, but pGBKT7-ECRG2 could not.

Yeast two-hybrid screen of cellular proteins interacting with ECRG2 protein

To identify proteins associated with the ECRG2 protein, ECRG2's ORF was synthesized as a translational fusion of a DNA-binding domain (DBD) and used as the bait for screening of a human fetal liver yeast two-hybrid cDNA library. Of 3×10^6 transformants screened, 146 clones grew in the absence of tryptophan, lencine, histidine, adenine and expressed β-galactosidase activity. pACT2/cDNA plasmids were successfully isolated and duplicates were eliminated by HaeIII digestion (Figure 2). After elimination, 26 uniquely positive clones were further retested for specificity of β-galactosidase expression. After retransformation, 9 independent positive clones were identified and sequenced (Table 1).

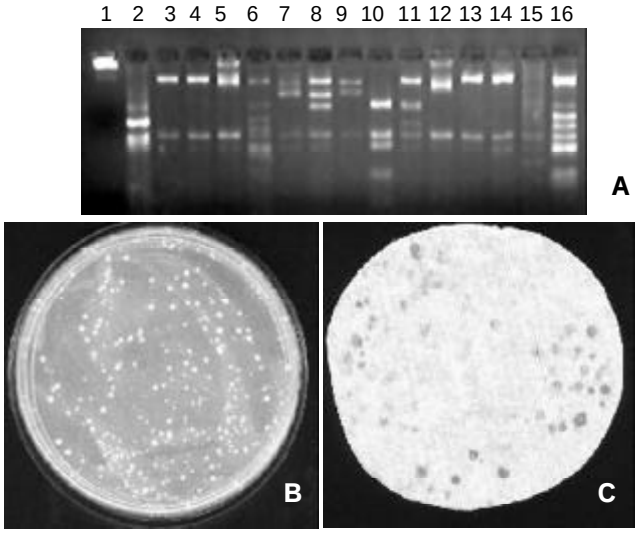

Figure 2 Positive colonies screened by yeast two-hybrid system using full-length cDNA of ECRG2 as baits. A: PCR products of positive clones digested with HaeIII restriction enzyme. Lane 1: λDNA/EcoRI+HindIII Marker, Lanes 2-16: positive colonies, B: $Trp^+/Leu^+/His^+/Ade^+$ positive clone growing on the $SD/Trp^-/Leu^-/His^-/Ade^-$ plate, C: colony-lift filter assay for β-galactosidase activity.

Table 1 Yeast two-hybrid screening using ECRG2 as baits

Yeast transformation	Transformation efficiency[a] (cfu / μg library)	Transformation yield[b]	His$^+$,Ade$^+$, Laz$^+$[c]	True positives
1	2.46×10^5	9×10^5	48	3
2	3.17×10^5	1.3×10^6	63	4
3	2.32×10^5	8×10^5	35	2
Total		3×10^6	146	9

[a]: Transformation efficiency (transformants / μg) = transformation yield ÷ amount of library DNA in μg). [b]: Transformation yield (total transformants) = [(colonies / plate) ÷ (volume / plate)] ×[(volume of total reaction) ÷ (dilution factor)]. [c]: β-galactosidase activity of the positive colonies assayed by β-galactosidase filter lift assay.

Database: All GenBank+EMBL+DDBJ+PDB sequences (but no EST, STS, GSS, or phases 0, 1 or 2 HTGS sequences)

1,431,609 sequences; 7,058,003,641 total letters

Taxonomy reports

Distribution of 259 blast hits on the query sequence

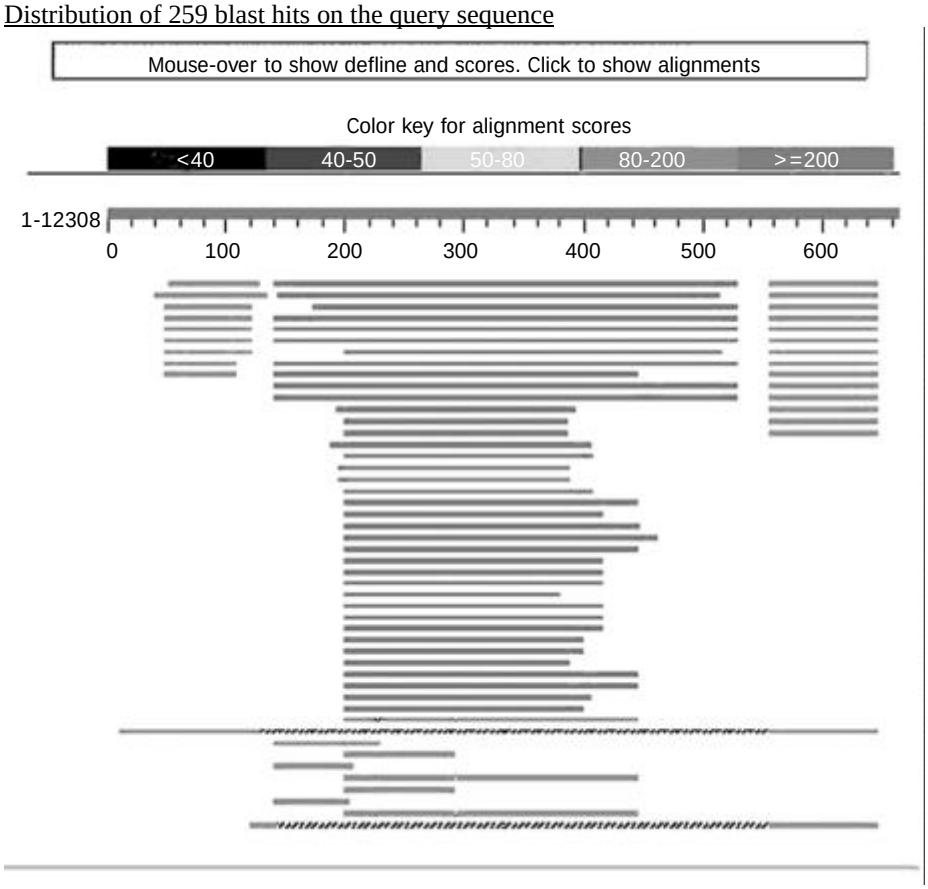

Score E

Sequences producing significant alignments: (bits) Value

gi|13937856|gb|BC007034.1|BC007034 Homo sapiens, metallothi... 755 0.0 **L U**
gi|37120|emb|V00594.1|HSTHIO Human mRNA for metallothionein... 698 0.0 **U**
gi|18043898|gb|BC019382.1| Mus musculus, metallothionein 2A... 682 0.0 **U**
gi|18370038|gb|AC074378.4| Homo sapiens chromosome 4 clone ... 613 e-172
gi|20270509|ref|NG_001158.1| Homo sapiens metallothionein 2... 605 e-170 **L**
gi|187530|gb|J00272.1|HUMMET2PS Human metallothionein-II ps... 605 e-170 **L**
gi|1495465|emb|X97260.1|HSMTISO2 H.sapiens mRNA for metallo... 597 e-168 **U**
gi|187529|gb|M13074.1|HUMMET2PG Human metallothionein II pr... 589 e-165
gi|38121|emb|V01532.1|MOTHI2 Monkey complementary DNA codin... 496 e-137
gi|20146733|gb|AC026461.9| Homo sapiens chromosome 16 clone... 450 e-123
gi|467308|gb|J00271.1|HUMMET2 Human metallothionein-II gene... 442 e-121 **L**
gi|187527|gb|M26637.1|HUMMET2AB Human metallothionein II mR... 389 e-105 **L**
gi|5174763|ref|NM_005953.1| Homo sapiens metallothionein 2A... 369 3e-99 **L U**

Figure 3 Blast results of MT2A.

GSS, or phase 0, 1 or 2 HTGS sequences)
Taxonomy reports
Distribution of 114 Blast Hits on the Query Sequence

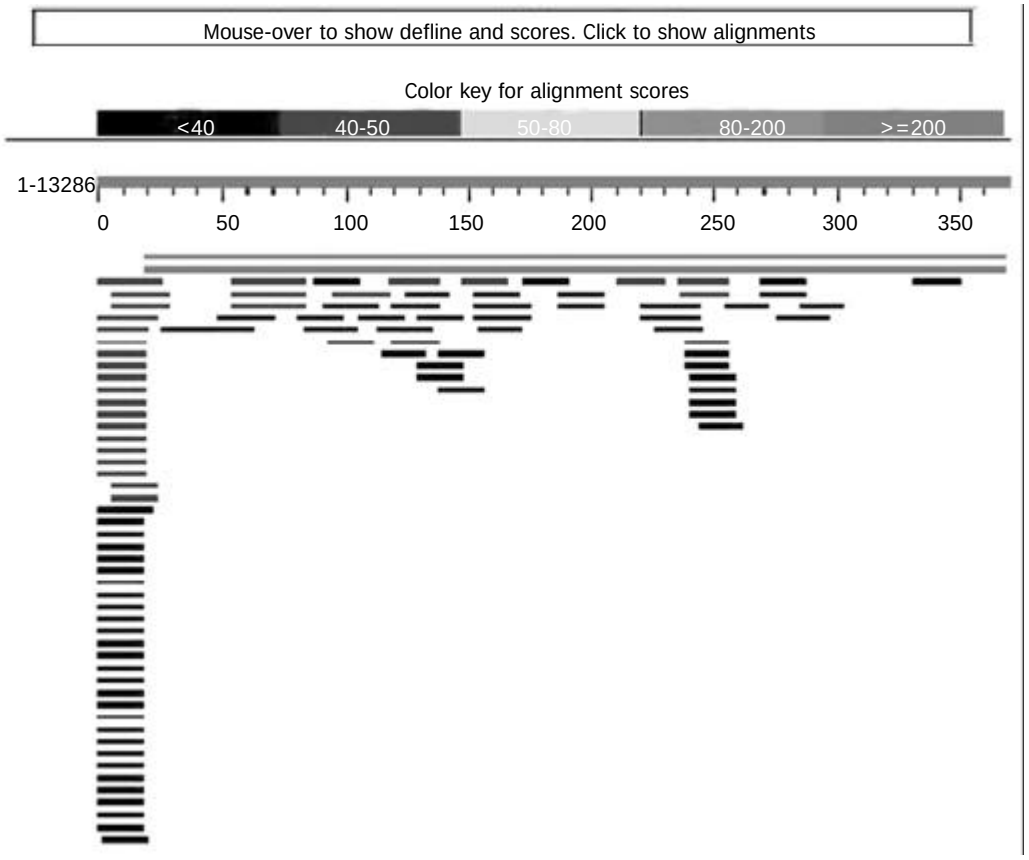

Sequences producing significant alignments:		Score (bits)	E Value
gi|23334560|gb|AF422192.1|	Homo sapiens esophagus cancer-re...	696	0.0
gi|15282087|emb|AL117190.6|CNS01DRF	Human chromosome 14 DNA...	696	0.0

Figure 4 Blast results of AF422192.

Bioinformatics

Blast online (http://www.ncbi.nlm.nih.gov/blast) showed the genes identified by the yeast two-hybrid approach were metallothionein 2A(MT2A), metallothionein 1H, metallothionein 1G, ferritin, erythrocyte membrane protein band 4.2, hemoglobin, mitochondrial ribosomal protein S12, hypothetical protein FLJ10101, and a novel gene whose cDNA was found to have no strong homology to any other previously characterized gene whose GenBank accession No.is AF422192.

DISCUSSION

Protein-protein interactions played important roles in almost all events that took place in a cell[6]. Because proteins often assembled into large complexes to perform discrete activities, the characterization of the interaction pattern of a protein could provide considerable assistance in the elucidation of the functions of that protein[7]. The availability of complete genome sequences now permits the development of tools for functional biology on a proteomic scale. Among those, the yeast two-hybrid system is the choice to detect protein-protein interactions[8,9]. The ECRG2 gene is a novel candidate of tumor suppressor gene identified from human esophageal carcinoma. Identifying the function of ECRG2 gene product may provide opportunities to elucidate the esophageal cancer mechanisms and its role in tumor development and progression. The yeast-two-hybrid approach could find novel partners for known function proteins and identify the function of a novel protein by identifying well-characterized interacting partners[10]. So, we searched for associated proteins with a yeast-two-hybrid system using the ECRG2 cDNA fragment as baits.

Our results showed that ECRG2 gene did not activate transcription by itself and was suitable for yeast two-hybrid. On screening a human fetal liver cDNA library, we identified 9 putative clones as associated proteins, which included metallothionein 2A (MT2A), metallothionein 1H, metallothionein 1G. Metallothioneins (MTs) are a family of low molecular weight, cysteine-rich, metal ion-binding proteins which are wildly distributed in various species. MTs were thought to be involved in heavy-metal detoxification, intracellular trace elements storage and scavenging free radicals. Recently, emerging data suggested that MTs had a close relationship with tumors. They might play important roles in carcinogenic and apoptotic process and differentiation of tumor cells[11-23]. In addition, MTs were attributed to affording tumor cell resistance to some important chemotherpeutic agents[24]. Using immunohistochemical-staining method, MTs have been localized intensively in various types of human tumors in organs and tissues such as skin, kidneys, prostate, tests, gallbladder, colon, breast and endometrium[25-34]. Since

human metallothioneins are closely linked with tumor, it is possible for us to understand the cellular functions of the ECRG2 protein through its linkage to MT2A. The other associated clone is a novel gene whose cDNA was found to have no strong homology to any other previously characterized gene whose GenBank Accession No.is AF422192. There are also 5 clones including ferritin, erythrocyte membrane protein band 4.2, hemoglobin, mitochondrial ribosomal protein S12 and hypothetical protein FLJ10101. Determination of a reliability score for each single protein-protein interaction, especially interaction of ECRG2 and MTs, permits the assignment of ECRG2 and unannotated proteins to biological pathways. A further understanding of the association between ECRG2 and MT should facilitate the functions of ECRG2 gene.

REFERENCES

1 **Lu SH**. Alterations of oncogenes and tumor suppressor genes in esophageal cancer in China. *Mutat Res* 2000; **467**: 343-353
2 **Zhou J,** Zhao LQ, Xiong MM, Wang XQ, Yang GR, Qiu ZL, Wu M, Liu ZH. Gene expression profiles at different stages of human esophageal squamous cell carcinoma. *World J Gastroenterol* 2003; **9**: 9-15
3 **Montesano R,** Hollstein M, Hainaut P. Genetic alterations in esophageal cancer and their relevance to etiology and pathogenesis: a review. *Int J Cancer* 1996; **69**: 225-235
4 **Xiong XD**, Xu LY, Shen ZY, Cai WJ, Luo JM, Han YL, Li EM. Identification of differentially expressed proteins between human esophageal immortalized and carcinomatous cell lines by two-dimensional electrophoresis and MALDI-TOF-mass spectrometry. *World J Gastroenterol* 2002; **8**: 777-781
5 **Su T**, Liu HL, Lu SH. Cloning and identification of cDNA fragments related to human esophageal cancer. *Zhonghua Zhongliu Zazhi* 1998; **20**: 254-257
6 **Blackstock WP**, Weir MP. Proteomics: quantitative and physical mapping of cellular proteins. *Trends Biotechnol* 1999; **17**: 121-127
7 **Emmert-Buck MR**, Gillespie JW, Pawletz CP, Ornstein DK, Basrur V, Appella E, Wang QH, Huang J, Hu N, Taylor P, Petricoin EE 3rd. An approach to proteomic analysis of human tumors. *Mol Carcinog* 2000; **27**: 158-165
8 **Fromont-Racine M**, Rain JC, Legrain P. Toward a functional analysis of the yeast genome through exhaustive two-hybrid screens. *Nature Genet* 1997; **16:** 277-282
9 **Toby GG**, Golemis EA. Using the yeast interaction trap and other two-hybrid-based approaches to study protein-protein interactions. *Methods* 2001; **24**: 201-217
10 **Chambers G**, Lawrie L, Cash P, Murray GI. Proteomics: a new approach to the study of disease. *J Pathol* 2000; **192**:280-288
11 **Zhang XH**, Takenaka I. Incidence of apoptosis and metallothionein expression in renal cell carcinoma. *Br J Urol* 1998; **81**: 9-13
12 **Tan Y**, Sinniah R, Bay BH, Singh G. Metallothionein expression and nuclear size in benign, borderline, and malignant serous ovarian tumours. *J Pathol* 1999; **189**: 60-65
13 **Takaba K**, Saeki K, Suzuki K, Wanibuchi H, Fukushima S. Significant overexpression of metallothionein and cyclin D1 and apoptosis in the early process of rat urinary bladder carcinogenesis induced by treatment with N-butyl-N-(4-hydroxybutyl) nitrosamine or sodium L-ascorbate. *Carcinogenesis* 2000; **21**: 691-700
14 **Jayasurya A**, Bay BH, Yap WM, Tan NG, Tan BK. Proliferative potential in nasopharyngeal carcinoma: correlations with metallothionein expression and tissue zinc levels. *Carcinogenesis* 2000; **21**: 1809-1812
15 **Hiura T**, Khalid H, Yamashita H, Tokunaga Y, Yasunaga A, Shibata S. Immunohistochemical analysis of metallothionein in astrocytic tumors in relation to tumor grade, proliferative potential, and survival. *Cancer* 1998; **83**: 2361-2369
16 **Hishikawa Y**, Kohno H, Ueda S, Kimoto T, Dhar DK, Kubota H, Tachibana M, Koji T, Nagasue N. Expression of metallothionein in colorectal cancers and synchronous liver metastases. *Oncology* 2001; **61**: 162-167
17 **Abdel-Mageed AB**, Agrawal KC. Activation of nuclear factor kappaB: potential role in metallothionein-mediated mitogenic response. *Cancer Res* 1998; **58**: 2335-2338
18 **Aloia TA**, Harpole DH Jr, Reed CE, Allegra C, Moore MB, Herndon JE D' Amico TA. Tumor marker expression is predictive of survival in patients with esophageal cancer. *Ann Thorac Surg* 2001; **72**: 859-866
19 **Joseph MG**, Banerjee D, Kocha W, Feld R, Stitt LW, Cherian MG. Metallothionein expression in patients with small cell carcinoma of the lung: correlation with other molecular markers and clinical outcome. *Cancer* 2001; **92**: 836-842
20 **Ebert MP**, Gunther T, Hoffmann J, Yu J, Miehlke S, Schulz HU, Roessner A, Korc M, Malfertheiner P. Expression of metallothionein II in intestinal metaplasia, dysplasia, and gastric cancer. *Cancer Res* 2000; **60**: 1995-2001
21 **Jin R**, Chow VT, Tan PH, Dheen ST, Duan W, Bay BH. Metallothionein 2A expression is associated with cell proliferation in breast cancer. *Carcinogenesis* 2002; **23**: 81-86
22 **Jayasurya A**, Bay BH, Yap WM, Tan NG. Correlation of metallothionein expression with apoptosis in nasopharyngeal carcinoma. *Br J Cancer* 2000; **82**: 1198-1203
23 **Cherian MG**, Howell SB, Imura N, Klaassen CD, Koropatnick J, Lazo JS, Waalkes MP. Role of metallothionein in carcinogenesis. *Toxicol Appl Pharmacol* 1994; **126**: 1-5
24 **Jasani B**, Schmid KW. Significance of metallothionein overexpression in human tumours. *Histopathology* 1997; **31**: 211-214
25 **Huang GW**, Yang LY. Metallothionein expression in hepatocellular carcinoma. *World J Gastroenterol* 2002; **8**: 650-653
26 **Rossen K**, Haerslev T, Hou-Jensen K, Jacobsen GK. Metallothionein expression in basaloid proliferations overlying dermatofibromas and in basal cell carcinomas. *Br J Dermatol* 1997; **136**: 30-34
27 **Zhang XH**, Jin L, Sakamoto H, Takenaka I. Immunohistochemical localization of metallothionein in human prostate cancer. *J Urol* 1996; **156**: 1679-1681
28 **Giuffre G**, Barresi G, Sturniolo GC, Sarnelli R, D'Inca R, Tuccari G. Immunohistochemical expression of metallothionein in normal human colorectal mucosa, in adenomas and in adenocarcinomas and their associated metastases. *Histopathology* 1996; **29**: 347-354
29 **Kuo T**, Lo SK. Immunohistochemical metallothionein expression in thymoma: correlation with histological types and cellular origin. *Histopathology* 1997; **30**: 243-248
30 **Shukla VK**, Aryya NC, Pitale A, Pandey M, Dixit VK, Reddy CD, Gautam A. Metallothionein expression in carcinoma of the gallbladder. *Histopathology* 1998; **33**: 154-157
31 **Zelger B**, Hittmair A, Schir M, Ofner C, Ofner D, Fritsch PO, Bocker W, Jasani B, Schmid KW. Immunohistochemically demonstrated metallothionein expression in malignant melanoma. *Histopathology* 1993; **23**: 257-264
32 **Goulding H**, Jasani B, Pereira H, Reid A, Galea M, Bell JA, Elston CW, Robertson JF, Blamey RW, Nicholson RA. Metallothionein expression in human breast cancer. *Br J Cancer* 1995; **72**: 968-972
33 **Douglas-Jones AG**, Schmid KW, Bier B, Horgan K, Lyons K, Dallimore ND, Moneypenny IJ, Jasani B. Metallothionein expression in duct carcinoma in situ of the breast. *Hum Pathol* 1995; **26**: 217-222
34 **Uozaki H**, Horiuchi H, Ishida T, Iijima T, Imamura T, Machinami R. Overexpression of resistance-related proteins (metallothioneins, glutathione-S-transferase pi, heat shock protein 27, and lung resistance-related protein) in osteosarcoma. Relationship with poor prognosis. *Cancer* 1997; **79**: 2336-2344

Edited by Zhu L and Wang XL

P.O.Box 2345, Beijing 100023,China
Fax: +86-10-85381893
E-mail: wjg@wjgnet.com www.wjgnet.com

World J Gastroenterol 2003;9(9):1897-1899
World Journal of Gastroenterology
 ISSN 1007-9327

• ESOPHAGEAL CANCER •

FT-IR spectroscopic analysis of normal and cancerous tissues of esophagus

Jian-Sheng Wang, Jing-Sen Shi, Yi-Zhuang Xu, Xiao-Yi Duan, Li Zhang, Jing Wang, Li-Ming Yang, Shi-Fu Weng, Jin-Guang Wu

Jian-Sheng Wang, Jing-Sen Shi, Xiao-Yi Duan, Department of Oncological Surgery, First Hospital of Xi' an Jiaotong University, Xi' an 710061, Shaanxi Province, China
Yi-Zhuang Xu, Li Zhang, Li-Ming Yang, Shi-Fu Weng, Jin-Guang Wu, Institute of Chemistry and Molecular Engineering, Peking University, Beijing 100871, China
Jing Wang, Department of Pathology, Oral Medical Hospital, Peking University, Beijing 100871, China
Supported by the National Natural Science Foundation of China, No. 39730160
Correspondence to: Jing-Sen Shi, Laboratory of Hepatobiliary Surgery, First Hospital of Xi' an Jiaotong University, Xi' an 710061, Shaanxi Province, China. wjsdxy@263.net
Telephone: +86-29-5323527 **Fax:** +86-29-5263190
Received: 2003-05-12 **Accepted:** 2003-06-02

Abstract

AIM: To investigate the special Fourier transform infrared spectroscopy (FT-IR) spectra in normal and cancerous tissues of esophagus.

METHODS: Twenty-seven pairs of normal and cancerous tissues of esophagus were studied by using FT-IR and the special spectra characteristics were analyzed in different tissues.

RESULTS: Different spectra were found in normal and cancerous tissues. The peak at 1 550/cm was weak and wide in cancerous tissues but strong and high in normal tissues.The ratio of *I* 1 647/*I* 1 550 was 2.0 in normal tissues and 2.36 in cancerous tissues ($P<0.05$). The ratio of *I* 1 550/*I* 1 080 was 4.5 in normal tissues and 3.4 in cancerous tissues ($P<0.01$). The peak at 1453 /cm was higher than at 1 402/cm in normal tissue and lower than at 1 402/cm in cancerous tissues.

CONCLUSION: The results indicate that FTIR may be used in clinical diagnosis.

Wang JS, Shi JS, Xu YZ, Duan XY, Zhang L, Wang J, Yang LM, Weng SF, Wu JG. FT-IR spectroscopic analysis of normal and cancerous tissues of esophagus. *World J Gastroenterol* 2003; 9(9): 1897-1899
http://www.wjgnet.com/1007-9327/9/1897.asp

INTRODUCTION

Esophageal carcinoma is still one of the malignant tumors that challenges clinical oncologists. In China, there are about 1 300 000 new patients diagnosed as esophageal carcinoma each year[1]. At present, the best way to diagnose the disease is fiber endoscopy, which can not only look steadily at the lesion to get information of the size, location, ect, but also obtain the tissues of suspected portions for pathological examinations. Although endoscopy has been widely used in diagnosis and differential diagnosis of esophageal diseases, about 20 percent of esophageal cancer in early stage can not be detected and diagnosed by this technology because it is limited by the experience of the operator and affected by the atypical clinical manifestations of the disease[2].

Thus, it is the very goal to develop an accurate, quick, convenient, and inexpensive method for detecting early cancer of esophagus at molecular level. With the development of vibrational spectroscopic technologies, their application in cancer research has been reported. Among these technologies, Fourier transform infrared spectroscopy (FT-IR) has been extensively employed in the fields of biology and chemical engineering to get information about the structural and chemical/physical properties at molecular level. Recently, some researches about the application of FT-IR in cancer have been reported[3-8]. In fact, the results of our previous research have already shown its advantages in clinical and scientific applications[9-14]. But the study on the spectra of esophageal tissues is still preliminary. In the present work, we examined the cancerous and normal tissues of esophagus with FT-IR in order to put some light on the combination of FT-IR and endoscopy.

MATERIALS AND METHODS

Tissue preparation

Twenty-seven fresh tissues of esophageal cancer were obtained from the First Hospital of Xi' an Jiaotong University. The tissues were washed with normal saline solution and sampled immediately after removed during the operation. Two pieces of the tissues about 1 cm in diameter were taken, one was cut off from the center of the lesion and the other was from the distant edge of the removed tissues. Each tissue was divided into two equal parts, one was frozen with liquid nitrogen and the other was fixed with 10 % formalin, embedded in paraffin and stained with hematoxylin and eosin for pathological examination. All the 27 patients were diagnosed before operation as squamous cell carcinoma with endoscopic biopsy. There were 15 males and 12 females, aged 41 to 71 years old, and averaged 58 years.

Spectral measurements

The spectra were recorded on a Nicolet Magna 750 FT-IR spectrometer with a mercury cadmium telluride (MCT) detector. No special sample preparation was needed in the experiment. The sample was defrosted at room temperature, and the measurements were carried out by putting the mucosal surface and cancer side (the section side of cancer tissue) of tissue on the attenuated total reflectance (ATR) probe. A total of 64 scans were recorded at a resolution of 4/cm at the region of 900 to 4 000/cm. The samples were frozen again for reexamination after FT-IR scanning.

RESULTS

Significant differences were found between normal and malignant esophageal tissues in the FT-IR spectra except one sample.

At the range of 1 800-1 500/cm, the amide band II at about 1 550/cm was weak and broad in malignant tissues, and was

strong and sharp in normal tissues (Figure 1). The relative intensity of *I* 1 647/*I* 1 550 of malignant tissues was higher than that of normal tissues (Figure 2). The ratio of *I* 1 647/*I* 1 550 was 2.0 in malignant tissues and 2.36 in normal tissues, with a statistically significant difference ($P<0.05$). The wave number of amide band I in normal tissues was about 1-6/cm higher than that in malignant tissues, without statistically significant difference ($P>0.05$).

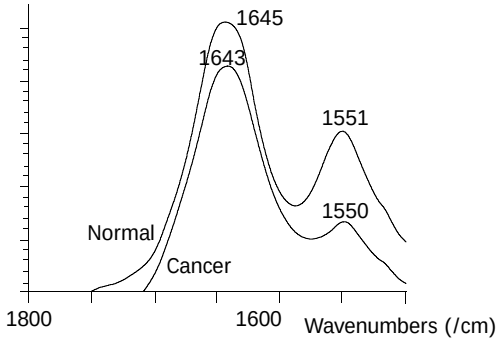

Figure 1 The spectra of the normal and cancer tissues at 1 800/cm-1 500/cm area.

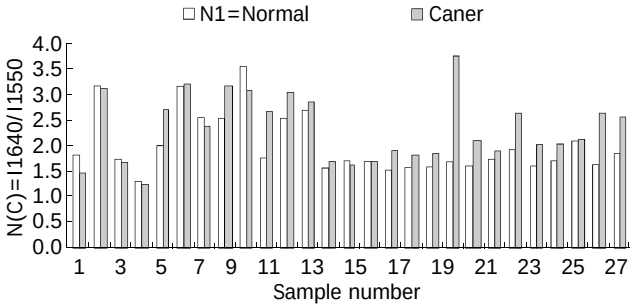

Figure 2 The ratio of *I* 1 640/*I* 1 550 of normal and cancer tissues.

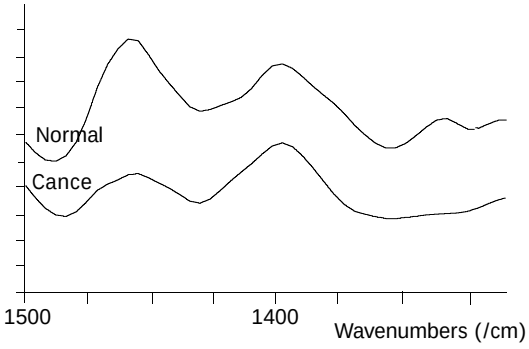

Figure 3 The spectra of the normal and cancer tissues at 1 400/cm-1 500/cm area.

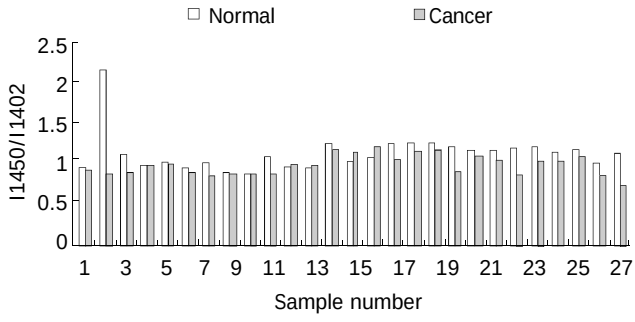

Figure 4 The ratio of *I* 1 450/*I* 1 402 of normal and cancer tissues.

At the range of 1 500-1 400/cm, two typical bands at about 1 453/cm and 1 402/cm could be seen in all the studied samples. The intensity of the band at 1 453/cm in normal tissues was higher than that in malignant tissues (Figure 3). The relative intensity of *I* 1 454/*I* 1 400 is shown in Figure 4.

The band at 1 080/cm was higher and stronger in malignant tissues than that in normal tissues. The ratio of *I* 1 080/ *I* 1540 was higher in malignant tissues. In normal tissues, a peak at 1 745/cm was seen in 6 cases, but none was seen in malignant tissues. At the range of 2 800-3 000/cm, three peaks (2 965/cm, 2 926/cm, and 2 853/cm) were seen in 25 of 27 normal tissues and only in 5 of both normal and malignant tissues. For these 5 cases, the ratio of *I* 1 226/*I* 3 380 was higher in normal tissues. For a pair of samples, in which the same spectra were found by FT-IR, the regular pathological examination showed that the two samples were normal tissues of esophagus.

DISCUSSION

The pathogenesis and development of esophageal carcinoma are a multi-step process that is controlled by many genes and affected by many factors[15-24]. The cooperation of oncogene' s activation and anti-oncogene' s inactivation causes the relative changes of contents and structures of protein, nuclear acid, sugar and fat in cells[25-31]. FT-IR could provide information about molecular structure, which makes it possible to reflect the changes of protein, nuclear acid, sugar and fat in cells and the structure changes of space array of the molecule, thus the diagnosis of cancer cells could be made at the molecular level[32-34].

Significant differences between normal and malignant esophageal tissues were seen in FT-IR spectra in this study. They might be caused by the changes of content and space array of protein, nuclear acid, sugar and fat in cells. For the bands of protein, amide bands I and II, the amide band II at about 1 550/cm was weak and broad in malignant tissues and was strong and sharp in normal tissues. The relative intensity of *I* 1 647/*I* 1 550 of malignant tissues was higher than that of normal tissues. At the range of 1 500-1 400/cm, the relative intensity of *I* 1 454/*I* 1 402 was higher in normal tissues than that in malignant tissues.

The peak at 1 745/cm was caused by the stretching vibration of carbonyl, the peaks at 2 852/cm and 2 930/cm were absorption spectra of the symmetry and asymmetry stretching vibrations of methylene, the peaks at 2 873/cm and 2 958/cm were absorption spectra of the symmetry and asymmetry stretching vibrations of methyl. Because triglyceride contains lots of methyl, methylene and carbonyl, so the differences of FT-IR spectra in normal and malignant tissues at those area were caused by the different contents of lipid substance in the tissues. The decreased lipid substance in malignant tissues might be related to the following factors. Firstly, the fast growth of cancer needs more nutrition and energy, therefore it might utilize lipid to supply nutrition and energy, which cause the lipid substance not to be accumulated in cancer cells and tissues. The second reason is that normal cell and tissues, including fat cells, are excluded mechanically by proliferating malignant tissues of the tumor.

One of the most important characteristics of cancer cells is the increased DNA content in cells caused by the endless replication of DNA, which is presented with enlarged and dark stained nuclei under light microscopy. The peak at 1 080/cm was caused by symmetry stretching vibrations of phospholipids. In this study, we found the peak at 1 080/cm was stronger and higher in malignant tissues than that in normal tissues and the ratio of *I* 1 080/*I* 1 540 was higher in malignant tissues, indicating that DNA content in malignant tissues is significantly higher than that in normal tissues.

REFERENCES

1 **Shiozaki H,** Tahara H, Kobayashi K, Yano H, Tamura S, Imamoto H, Yano T, Oku K, Miyata M, Nishiyama K, Kubo K, Mori T. Endoscopic screening of early esophageal cancer with the lugol dye method in patients with head and neck cancers. *Cancer* 1990; **66:** 2086-2071

2 **Tachimori Y,** Kato H. Diagnosis and surgery of esophageal cancer. *Crit Rev Oncol/Hematol* 1998; **28:** 57-71

3 **Yamada T,** Miyoshi N, Ogawa T, Akao K, Fukuda M, Ogasawara T, Kitagawa Y, Sano K. Observation of molecular changes of a necrotic tissue from a murine carcinoma by Fourier-transform infrared microspectroscopy. *Clin Cancer Res* 2002; **8:** 2010-2014

4 **Argov S,** Ramesh J, Salman A, Sinelnikov I, Goldstein J, Guterman H, Mordechai S. Diagnostic potential of Fourier-transform infrared microspectroscopy and advanced computational methods in colon cancer patients. *J Biomed Opt* 2002; **7:** 248-254

5 **Yano K,** Ohoshima S, Gotou Y, Kumaido K, Moriguchi T, Katayama H. Direct measurement of human lung cancerous and noncancerous tissues by fourier transform infrared microscopy: can an infrared microscope be used as a clinical tool? *Anal Biochem* 2000; **287:** 218-225

6 **Romeo MJ,** Wood BR, Quinn MA, McNaughton D. Removal of blood components from cervical smears: Implications for cancer diagnosis using FTIR spectroscopy. *Biopolymers* 2003; **72:** 69-76

7 **Wong PT,** Senterman MK, Jackli P, Wong RK, Salib S, Campbell CE, Feigel R, Faught W, Fung Kee Fung M. Detailed account of confounding factors in interpretation of FTIR spectra of exfoliated cervical cells. *Biopolymers* 2002; **67:** 376-386

8 **Ramesh J,** Kapelushnik J, Mordehai J, Moser A, Huleihel M, Erukhimovitch V, Levi C, Mordechai S. Novel methodology for the follow-up of acute lymphoblastic leukemia using FTIR microspectroscopy. *J Biochem Biophys Methods* 2002; **51:** 251-261

9 **Peng Q,** Xu YZ, Li WH, Zhou XS, Wu JG. FTIR study on the normal and tumor gastrointestinal tissues. *Spectroscopy and Spectral Analysi* 1998; **18:** 528-531

10 **Xu YZ,** Soloway RD, Lin XF, Zhi X, Weng SF, Wu QG, Shi JS, Sun WX, Zhang TX, Wu JG, Xu DF, Xu GX. Fourier transform infrared (FT-IR) mid-IR spectroscopy separates normal and malignant tissue from the colon and stomach. *Gastroenterology* 2000; **118** (Suppl 2): 6438

11 **Wu JG,** Xu YZ, Sun CW, Soloway RD, Xu DF, Sun QG, Weng SF, Xu GX. Distinguishing malignant from normal oral tissues using FTIR fiber-optic techniques. *Biopolymers* 2001; **62:** 185-192

12 **Ma J,** Wang JS, Soloway RD, Xu YZ, Wang F, Zhang L, Yang LM, Shi JS, Wu JG. Separation of normal from diseased hepatocytes using Fourier transform infrared (FT-IR) spectroscopy: A basis for histologic characterization and quantitation. *Gastroenterology* 2002(Suppl); **122:** 1467

13 **Weng SF,** Ling XF, Song YY, Xu YZ, Li WH, Zhang X, Yang L, Sun W, Zhou X, Wu J. FTIR fiber optics and FT-Raman spectroscopic studies for the diagnosis of cancer. *Am Clin Lab* 2000; **19:** 20

14 **Wang JS,** Shi JS, Xu YZ, Weng SF, Wu JG. Preliminary FT-IR study on the normal, inflammatory and malignant tissues of gallbladder. *Zhonghu Gandan Waike Zazhi* 2002; **8:** 196

15 **Zhou J,** Zhao LQ, Xiong MM, Wang XQ, Yang GR, Qiu ZL, Wu M, Liu ZH. Gene expression profiles at different stages of human esophageal squamous cell carcinoma. *World J Gastroenterol* 2003; **9:** 9-15

16 **Xu M,** Jin YL, Fu J, Huang H, Chen SZ, Qu P, Tian HM, Liu ZY, Zhang W. The abnormal expression of retinoic acid receptor-β, p53 and Ki67 protein in normal, premalignant and malignant esophageal tissues. *World J Gastroenterol* 2002; **8:** 200-202

17 **Wang AH,** Sun CS, Li LS, Huang JY, Chen QS. Relationship of tobacco smoking, CYP1A1, GSTM1 gene polymorphism and esophageal cancer in Xi'an. *World J Gastroenterol* 2002; **8:** 49-53

18 **Chen H,** Wang LD, Guo M, Gao SG, Guo HQ, Fan ZM, Li JL. Alterations of p53 and PCNA in cancer and adjacent tissues from concurrent carcinomas of the esophagus and gastric cardia in the same patient in Linzhou, a high incidence area for esophageal cancer in northern China. *World J Gastroenterol* 2003; **9:** 16-21

19 **Li J,** Feng CW, Zhao ZG, Zhou Q, Wang LD. A preliminary study on ras protein expression in human esophageal cancer and precancerous lesions. *World J Gastroenterol* 2000; **6:** 278-280

20 **Li X,** Lu JY, Zhao LQ, Wang XQ, Liu GL, Liu Z, Zhou CN, Wu M, Liu ZH. Overexpression of ETS2 in human esophageal squamous cell carcinoma. *World J Gastroenterol* 2003; **9:** 205-208

21 **Millar CB,** Guy J, Sansom OJ, Selfridge J, MacDougall E, Hendrich B, Keightley PD, Bishop SM, Clarke AR, Bird A. Enhanced CpG mutability and tumorigenesis in MBD4-deficient mice. *Science* 2002; **297:** 403-405

22 **Gao HJ,** Yu LZ, Bai JF, Peng YS, Sun G, Zhao HL, Miu K, Lü XZ, Zhang XY, Zhao ZQ. Multiple genetic alterations and behavior of cellular biology in gastric cancer and other gastric mucosal lesions: *H pylori* infection, histological types and staging. *World J Gastroenterol* 2000; **6:** 848-854

23 **Wang N,** Liu ZH, Ding F, Wang XQ, Zhou CN, Wu M. Down-regulation of gut-enriched Kruppel-like factor expression in esophageal cancer. *World J Gastroenterol* 2002; **8:** 966-970

24 **Wiseman BS,** Werb Z. Stromal effects on mammary gland development and breast cancer. *Science* 2002; **296:** 1046-1049

25 **Ginn-Pease ME,** Eng C. Increased nuclear phosphatase and tensin homologue deleted on chromosome 10 is associated with G(0)-G(1) in MCF-7 cells. *Cancer Res* 2003; **63:** 282-286

26 **Ferrando AA,** Neuberg DS, Staunton J, Loh ML, Huard C, Raimondi SC, Behm FG, Pui CH, Downing JR, Gilliland DG, Lander ES, Golub TR, Look AT. Gene expression signatures define novel oncogenic pathways in T cell acute lymphoblastic leukemia. *Cancer Cell* 2002; **1:** 75-87

27 **Kabarowski JHS,** Zhu K, Le LQ, Witte ON, Xu Y. Lysophosphatidylcholine as a ligand for the immunoregutatory receptor G2A. *Science* 2001; **293:** 702-705

28 **Rincon-Arano H,** Rosales R, Mora N, Rodriguez-Castaneda A, Rosales C. R-Ras promotes tumor growth of cervical epithelial. *Cancer* 2003; **97:** 575-585

29 **Arboleda MJ,** Lyons JF, Kabbinavar FF, Bray MR, Snow BE, Ayala R, Danino M, Karlan BY, Slamon DJ. Overexpression of AKT2/protein kinase B beta leads to up-regulation of beta 1 integrins, increased invasion, and metastasis of human breast and ovarian cancer cells. *Cancer Res* 2003; **63:** 196-206

30 **Kunkel M,** Reichert TE, Benz P, Lehr HA, Jeong JH, Wieand S, Bartenstein P, Wagner W, Whiteside TL. Overexpression of Glut-1 and increased glucose metabolism in tumors are associated with a poor prognosis in patients with oral spuamous cell carcinoma. *Cancer* 2003; **97:** 1015-1024

31 **Wu BW,** Wu Y, Wang JL, Lin JS, Yuan SY, Li A, Cui WR. Study on the mechanism of epidermal growth factor-induced proliferation of hepatoma cells. *World J Gastroenterol* 2003; **9:** 271-275

32 **Dovbeshko GI,** Chegel VI, Gridina NY, Repnytska OP, Shirshov YM, Tryndiak VP, Todor IM, Solyanik CI. Surface enhanced IR absorption of nucleic acids from tumor cells: FTIR reflectance study. *Biopolymers* 2002; **67:** 470-486

33 **Lasch P,** Pacifico A, Diem M. Spatially resolved IR microspectroscopy of single cells. *Biopolymers* 2002; **67:** 335-338

34 **Neviliappan S,** Fang Kan L, Tiang Lee Walter T, Arulkumaran S, Wong PT. Infrared spectral features of exfoliated cervical cells, cervical adenocarcinoma tissue, and an adenocarcinoma cell line (SiSo). *Gynecol Oncol* 2002; **85:** 170-174

Edited by Zhang JZ and Wang XL

P.O.Box 2345, Beijing 100023,China
Fax: +86-10-85381893
E-mail: wjg@wjgnet.com www.wjgnet.com

World J Gastroenterol 2003;9(9):1900-1903
World Journal of Gastroenterology
 ISSN 1007-9327

Down-regulation of γ-synuclein in human esophageal squamous cell carcinoma

Cui-Qi Zhou, Shuang Liu, Li-Yan Xue, Yi-Hua Wang, Hong-Xia Zhu, Ning Lu, Ning-Zhi Xu

Cui-Qi Zhou, Shuang Liu, Yi-Hua Wang, Hong-Xia Zhu, Ning-Zhi Xu, Laboratory of Cell and Molecular Biology, Cancer Institute and Cancer Hospital, Chinese Academy of Medical Sciences, Peking Union Medical College, Beijing 100021, China
Li-Yan Xue, Ning Lu, Department of Pathology, Cancer Institute and Cancer Hospital, Chinese Academy of Medical Sciences, Peking Union Medical College, Beijing 100021, China
Supported by the National Natural Science Foundation of China, No. 39925020, and from State Key Basic Research Program, No. G1998051204
Correspondence to: Dr. Ning Zhi Xu, Laboratory of Cell and Molecular Biology, Cancer Institute and Cancer Hospital, Chinese Academy of Medical Sciences, Peking Union Medical College, Beijing 100021, China. xningzhi@public.bta.net.cn
Telephone: +86-10-67738220 **Fax:** +86-10-67767548
Received: 2003-03-20 **Accepted:** 2003-04-11

Abstract

AIM: To investigate gene expression pattern of human γ-synuclein gene in human esophageal squamous cell carcinoma (ESCC) by using semi-quantitive reverse transcription polymerase chain reaction (RT-PCR), and to study the role of γ-synuclein in the development of human ESCC.

METHODS: Semi-quantitive RT-PCR of 27 pairs of specimens of human ESCC tissues and corresponding normal tissues was used to investigate the expression pattern of γ-synuclein in ESCC. 9706/γ-syn cells in which γ-synuclein was overexpressed were obtained through cloning γ-synuclein gene by PCR and transfecting it into ESCC 9706 cells, then selecting with G-418 for 14 days. The biological effects of γ-synuclein were measured and compared between 9706/γ-syn and 9706/vec cells by cell growth curve and soft agar assay.

RESULTS: RT-PCR showed that γ-synuclein gene was expressed in all the 27 cases of normal epithelial tissues, while downregulation of γ-synuclein was observed in 16 out of the 27 cases (59.3 %) of ESCC. There were also 6 cases of ESCC tissues with a high expression level of γ-synuclein mRNA. In functional analysis we found that over-expression of γ-synuclein in ESCC 9706 cells could inhibit the growth rate and transformation ability of ESCC 9706 cells.

CONCLUSION: The low expression level of γ-synuclein in human ESCC and the biological effects of γ-synuclein over-expression on ESCC 9706 cells suggest that γ-synuclein may play a role as a negative regulator in the development of human ESCC.

Zhou CQ, Liu S, Xue LY, Wang YH, Zhu HX, Lu N, Xu NZ. Down-regulation of γ-synuclein in human esophageal squamous cell carcinoma. *World J Gastroenterol* 2003; 9(9): 1900-1903
http://www.wjgnet.com/1007-9327/9/1900.asp

INTRODUCTION

Synucleins are a family of small, highly conserved soluble proteins that are predominantly expressed in neural tissues and certain tumors[1,2]. There are at least three members of this family in vertebrates: α-, β-, γ-synuclein. All synucleins contain a highly conserved amino-terminal domain that includes several repeated domains displaying variation of a KTKEGV consensus sequence and a less conserved carboxy-terminal domain that includes a preponderance of acidic residues[1,2]. The α- and β-synuclein proteins are found primarily in brain tissues and in association with pathological lesions of neurodegenerative diseases[3,4]. While γ-synuclein, initially termed breast cancer-specific gene 1 (BCSG1)[5], is found in the peripheral nervous system and retina, and it may affect the integrity of the neurofilament network[4-6]. Furthermore, over-expression of γ-synuclein has been recently shown in several types of cancer, including breast and ovarian cancer, suggesting that it may be involved in a certain number of human cancers[5,7].

γ-synuclein gene was first isolated from a human breast tumor cDNA library, and therefore named breast cancer-specific gene 1 (BCSG1)[5], soon after it was determined to be a new member of the synuclein family[8]. The human γ-synuclein maps to chromosome region 10q23, and is composed of five exons and transcribed into an mRNA of about 1 kb, coding 127 amino acids[8,9]. It was reported that γ-synuclein was over-expressed in infiltrating breast ductal carcinoma and ovarian cancer[7]. Other studies have shown that over-expression of γ-synuclein in breast and ovarian cancer cells may enhance the motility and invasiveness *in vitro* and metastasis *in vivo* of breast cancer[10,11].

Human esophageal squamous cell carcinoma (ESCC) is one of the most common malignant tumors in China, and its etiology and pathogenesis remain to be determined[12]. However, it has been reported that many oncogenes and tumor suppressor genes are closely related to ESCC, such as *c-myc*, cyclin D1, p53[13-15]. In the present study, we first examined the expression pattern of γ-synuclein in 27 cases of ESCC. It was unexpected that γ-synuclein was down regulated in 16 out of 27 cases of ESCC compared to their corresponding normal tissues, rather than over-expressed in tumor tissues. In order to further explore the role of γ-synuclein in the development of ESCC, we cloned human γ-synuclein gene and transfected it into ESCC 9706 cell line. Our data demonstrated that the ectopic expression of γ-synuclein in ESCC cell line could inhibit cell growth in dish and colony formation in soft agar. In conclusion, unlike in breast and ovarian cancers, γ-synuclein might play a role as a tumor suppressor in the development of human ESCC.

MATERIALS AND METHODS

Tissue sample

Twenty-seven carcinomatous tissues and the corresponding normal tissues were obtained from surgically resected esophageal carcinoma in Cancer Hospital. Fresh samples were dissected manually to remove connective tissues and stored immediately at -80 ℃ until analysis. Carcinoma tissues were obtained from poorly, moderately, and well differentiated squamous epithelial cell carcinomas. The corresponding

normal tissues were obtained from the distant edge of dissected esophagus. Each tissue sample contained over 80 % of normal or tumor epithelial cells.

RNA extraction and semi-quantitative RT-PCR

Total RNA was extracted from paired specimens of primary esophageal cancer and non-cancerous esophageal epithelial tissues with TRIZOL reagent (Invitrogen) according to the manufacturer' s protocol.

Five micrograms of total RNA extracted from paired esophageal carcinoma were used as a template respectively to synthesize cDNA in 25 μl reaction mixture with 2.5 mM oligo $d(T)_{16}$ primers and M-MLV Reverse Transcriptase (Promega) at 37 ℃ for 1 h followed by 85 ℃ for 10 min. PCR was performed in 20 μl reaction mixture [1×taq buffer (Dingguo Company), 100 ng template cDNA, 200 μM of each dNTPs, 0.5 μM of each primers and 2 U Taq] as follows: at 95 ℃ for 5 min followed by 20 cycles at 95 ℃ for 1 min, at 61 ℃ for 1 min, at 72 ℃ for 1 min, and the final step of extension was for 10 min at 72 ℃. Sequences of the PCR primers for γ-synuclein are as follows: Upper primer: 5' CGGGATCCACCATGGATGTCTTCAAGAAG 3' . Lower primer: 5' CCGCTCGAGCTAGTCTCCCCCACTCTG 3' .

The reaction products were visualized by electrophoresis of 5 ul reaction mixture at 70 V for 40 min in 2 % agarose gel containing 0.5 μg/ml ethidium bromide, and quantitated by densitometry using a dual-intensity transilluminator equipped with Gel -Pro Analyzer version 3.1. β-actin was used as internal control.

Cell culture and transfection

Human ESCC 9706 cell line (kindly provided by Dr. Mingrong Wang) was grown in Dulbecco' s modified Eagle' s medium containing 10 % heat-inactivated fetal bovine serum (Gibico BRL)[16]. Transfection was performed in 80 % confluent cells using LipofectAMINE (Invitrogen) according to the manufacturer' s protocol. Stable transfectants were obtained by G418 selection for about 14 days.

Cell lysis and Western blot

Total cell lysate was prepared in cell lysis buffer (1 % NP-40, 137 mM NaCl, 20 mM Tris pH=7.4, 1 mM DTT, 10 % glycerin, 10 μg/ml Aprotinin, 2 mM sodium orthavanadate, 100 uM PMSF). After incubation for 30 min on ice, cells were scraped from the culture dish, and the mixture was centrifuged at 12 000 g for 10 min at 4 ℃. The protein concentration of the clarified lysate was determined using a BCA kit with BSA as a standard (Periece).

Equal amounts of total protein from cell lysate were resolved on 15 % SDS-PAGE. For western blot analysis, proteins separated by SDS-PAGE were transferred to nitrocellulose (PROTRAN, Schleicher&Schuell). Firstly the filters were incubated in a blocking solution (5 % fat-free dry milk, 2 % BSA in TBS) for 1 h at room temperature. Then the filters were incubated with primary antibody, added with a blocking solution at 1:1 000 dilution, for 1 h at room temperature. After washed three times with TTBS (0.5 % Tween-20 in TBS), the filters were subsequently incubated for 40 min with HRP (horseradish peroxidase) conjugated secondary antibody (Zhongshan Company). The filters were washed as above and developed using a Luminol detection system (Santa Cruz). Before re-blotting, the filters were stripped by incubation for 30 min in stripping buffer (2 % SDS, 62.5 mM Tris.Cl pH=6.7, 100 mM 2-mercaptoethanol) at 50 ℃.

Cell growth assay

Growth on plastic culture dish 2×10^4 cells from 9706/γ-syn and 9706/vec cell line were seeded in triplicate of 24-well plates and cultured in DMEM plus 1 % FBS and 10 % FBS. At each time point, cells were trypsinized to single cell suspension and counted on a Coulter counter set at >10 μm in diameter.

Anchorage -independent growth in soft agar According to standard protocol, 200 ESCC 9706 cells were suspended in 1 mL of 0.3 % agarose medium containing DMEM plus 10 % FBS and layered onto a 2 mL bed of 0.6 % agarose in a 35 mm dish with grids. Plates were incubated for about 14 days, and the colonies were stained with 0.2 % p-iodonitroterazolium violet and photographed.

RESULTS

Expression pattern of γ-synuclein in human esophageal squamous cell carcinoma (ESCC)

Expression pattern of γ-synuclein in human ESCC was examined using semi-quantitative RT-PCR approach. Figure 1 shows a 384 bp γ-synuclein fragment from ESCC tissues and relatively normal tissues, and a 200 bp β-actin fragment as an internal control by electrophoresis in 2 % agarose gel. The γ-synuclein gene was expressed in all the 27 cases of normal esophageal epithelial tissues, while down-regulation of γ-synuclein gene was observed in 16 out of the 27 cases (59.3 %) of ESCC. There were also 6 cases of ESCC tissues with high expression level of γ-synuclein mRNA (Table 1). These results indicated that γ-synuclein might play a negative role in carcinogenesis of human ESCC.

Table 1 Expression pattern of human γ-synuclein in human esophageal squamous cell carcinoma

γ-synuclein RT-PCR	Cases (percentage)
Down-regulated	16 (59.3%)
Up-regulated	6 (22.2%)
No change	5 (18.5%)
Total	27 (100%)

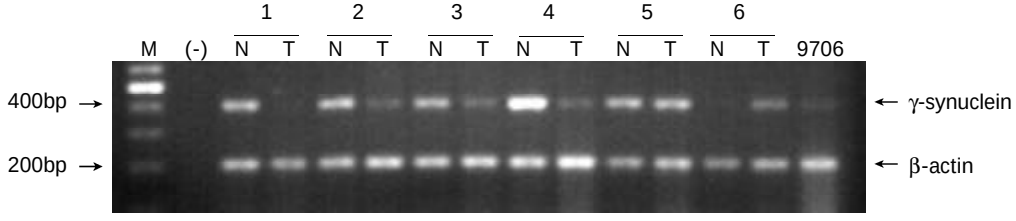

Figure 1 Simi-quantitative RT-PCR analysis of human γ-synuclein mRNA in human esophageal squamous cell carcinoma. The γ-synuclein fragment (384 bp) was amplified by 20 cycles PCR using the paired primers as indicated in Material and Methods. Five micrograms of total RNA isolated from human ESCC tissues and corresponding normal tissues were used as templates for cDNA synthesis respectively. β-actin was used as an internal control. T: esophageal squamous cell carcinoma tissue, N: corresponding normal tissue, 9706: human ESCC 9706 cell line, (-): negative control, M: 100 bp DNA marker.

Inhibition of growth rate and transformation ability of human ESCC 9706 cells by γ-synuclein

RT-PCR results led us to investigate the role of γ-synuclein in carcinogenesis of human ESCC. Firstly we amplified the γ-synuclein cDNA fragment from fetal brain cDNA and cloned it into the pcDNA3.0 vector to generate HA-tagged γ-synuclein expression plasmids. Then we transfected γ-synuclein expression plasmid and pcDNA3.0 vector into ESCC 9706 cells respectively. After 14 days selection with G418 (300 μg/ml), we obtained the stable transfectants named 9706/γ-syn and 9706/vec cells. The expression of transfected γ-synuclein was verified by Western blot analysis (Figure 2). To determine whether γ-synuclein over-expression affected the growth of ESCC 9706 cells, cells from 9706/γ-syn and 9706/vec were seeded in triplicate of 24-well plate in DMEM plus 1 % FBS and 10 % FBS. According to the growth curve we observed that 9706/γ-syn cells grew more slowly than control cells, whether in low or high serum medium in dishes (Figure 3). Furthermore, we confirmed the negative effect of γ-synuclein on ESCC 9706 cells by soft agar assay in which 9706/γ-syn cells displayed much smaller and fewer colonies than 9706/vec cells (Figure 4), indicating that γ-synuclein had the ability to inhibit the transformation activity of ESCC 9706 cells, and might act as a negative regulator in the development of human ESCC.

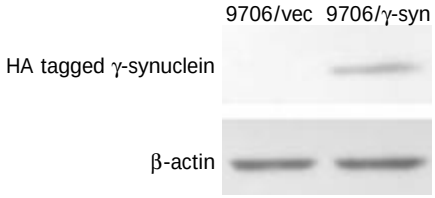

Figure 2 Identification of exogenous γ-synuclein expression in 9706/γ-syn stable cell line. Exogenous HA tagged γ-synuclein was detected by Western blot using anti-HA antibody in 9706/γ-syn cells. β-actin was used as internal control.

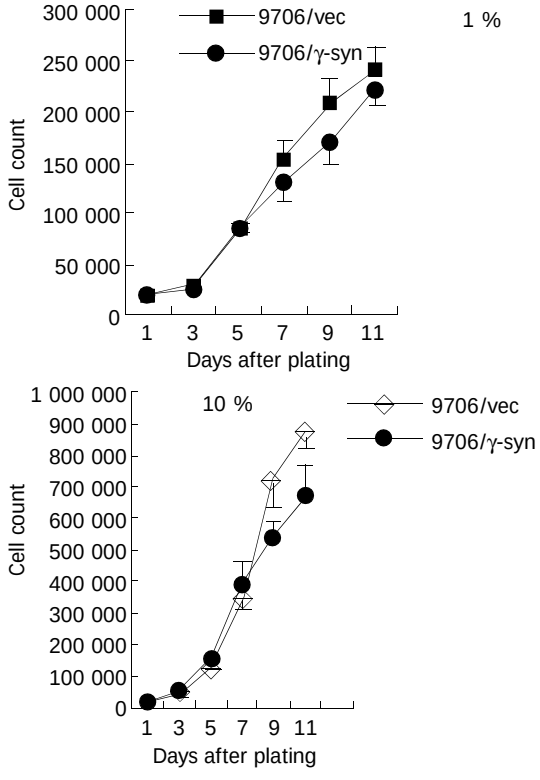

Figure 3 Effect of γ-synuclein over-expression on cell growth of 9706 cells with 1 % and 10 % FBS respectively. ESCC 9706/γ-syn and 9706/vec were seeded in triplicate of 24-well plate in DMEM plus 1 % FBS and 10 % FBS. The growth curve showed that 9706/γ-syn cells grew more slowly than that of control cells, both in low and high serum medium in dishes.

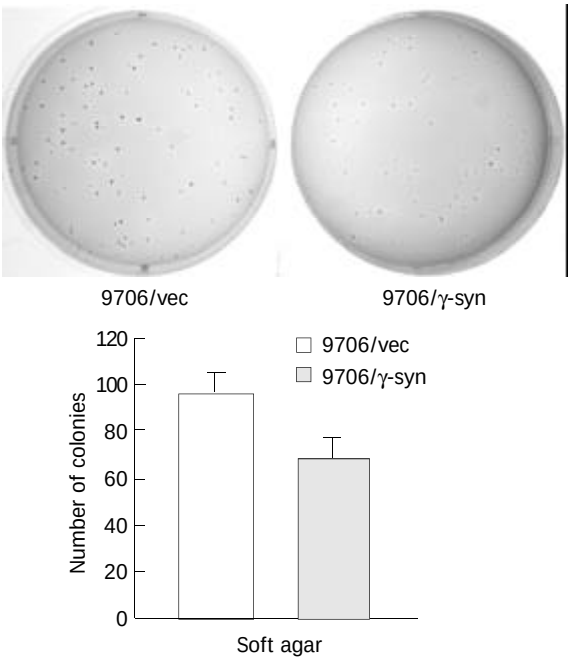

Figure 4 Colony formation of ESCC 9706 cells transfected with vector and γ-synuclein. 200 cells from each of the cell pools were plated in six-well plates. After 14 days, the colonies were stained with 0.2 % p-iodonitroterazolium violet and photographed. The number of colonies per well was quantified. Experiments were repeated three times with consistent and reproducible results.

DISCUSSION

Human esophageal squamous cell carcinoma (ESCC) is one of the most common malignant tumors in China[12]. Although the etiological agents have yet to be identified, studies have shown a series of genetic events involving the development of this cancer[13-15,17]. Identification of the genetic changes in ESCC as well as in other cancers will provide diagnostic and prognostic markers and molecular targets for treatment, intervention and prevention of human cancers.

It was reported that γ-synuclein was over-expressed in breast and ovarian cancer[5,7]. In the current study, we intended at first to detect the expression of γ-synuclein in esophageal squamous cell carcinoma (ESCC). However, γ-synuclein was unexpectedly down regulated in some 60 % tumor samples (16 out of 27 cases), compared to the corresponding normal tissues, rather than over-expressed in tumor tissues such as in breast and ovarian cancer. On the other hand, γ-synuclein was detected in all the 27 normal esophageal tissues. Furthermore, consistent with our observation that the expression of γ-synuclein was lower in tumor tissue than in surrounding non-tumor tissue in ESCC, after transfection of human ESCC cells into ESCC 9706 cells and selection with G-418, the transfectants expressing γ-synuclein (9706/γ-syn) grew remarkably slower than 9706/vec cells in low or high serum medium in dishes (Figure 3). It also displayed much smaller and fewer colonies than 9706/vec cells in soft agar (Figure 4), indicating that γ-synuclein has the ability to inhibit the transformation activity of ESCC 9706 cells. Therefore our present study suggests that γ-synuclein may be a negative regulator in tumorigenesis of human ESCC, unlike that in breast and ovarian cancer as an oncogene.

It is not unexpected to find out that the biological and

biochemical functions of the same gene are different in different cells or tissues from different tumors, since the development of tumors is a complex multigene-related phenomenon and the result of a multistep process involving a series of genetic events. As shown in our study, the manner and effect of γ-synuclein in human ESCC were different from those in breast and ovarian cancer. Moreover it was previously shown by others that in A2780 and OVCAR5 cells (ovarian cancer cell lines) with over-expressed γ-synuclein, the activated ERK1/2 was increased 2- to 3-fold. In contrast, in HEK293 cells (human embryonic kidney cells), γ-synuclein over-expression did not increase ERK activation level[18]. Likewise, the same status was also observed in many other studies, among which GKLF/KLF4 (gut-enriched Krüppel-like factor/ Krüppel-like factor 4) gene was a good example. GKLF/KLF4 encodes a zinc finger transcription factor and belongs to a big family[19]. It is the same as γ-synuclein as it is over-expressed in breast cancer[20], while down regulated in ESCC[21]. In addition, Annexin I (lipocortin I) gene is another very similar case. Annexin I is a phospholipid binding protein which is implicated in various cell activities, including proliferation, differentiation and apoptosis[22]. Studies showed that annexin I protein was actually over-expressed in human tumors including breast cancer, hepatocellular carcinoma[23,24]. However, it was also found that annexin I protein expression was decreased in human esophageal and prostate cancers[25,26]. p21 (Waf1/Cip1), one of the best broad-specificity inhibitors of CDK, acts as a suppressor in most tumors. But in some tumors, including ESCC, p21 (Waf1/Cip1) is over-expressed, acting as an oncogene to promote carcinogenesis and tumor progression[27].

Despite the fact that the mechanism by which γ-synuclein protein is involved in carcinogenesis of human tumors remains unclear, the data presented here have shown that γ-synuclein is down-regulated in ESCC, and is over-expressed in breast and ovarian cancer[5,7]. To shed new light on the role of γ-synuclein in oncogenesis, more studies are certainly needed to determine how γ-synuclein is down- regulated or up-regulated in tumors and what the physiological functions of γ-synuclein are during the development of human tumors.

ACKNOWLEDGMENT

We are grateful to Dr. Mingrong Wang for generously providing the human ESCC 9706 cell line.

REFERENCES

1 **Lavedan C**. The synuclein family. *Genome Res* 1998; **8**: 871-880
2 **George JM**. The synucleins. *Genome Biol* 2002; **3**: REVIEWS 3002
3 **Mukaetova-Ladinska EB**, Hurt J, Jakes R, Xuereb J, Honer WG, Wischik CM. Alpha-synuclein inclusions in Alzheimer and Lewy body diseases. *J Neuropathol Exp Neurol* 2000; **59**: 408-417
4 **Li JY**, Henning Jensen P, Dahlstrom A. Differential localization of alpha-, beta- and gamma-synucleins in the rat CNS. *Neuroscience* 2002; **113**: 463-478
5 **Ji H**, Liu YE, Jia T, Wang M, Liu J, Xiao G, Joseph BK, Rosen C, Shi YE. Identification of a breast cancer-specific gene, BCSG1, by direct differential cDNA sequencing. *Cancer Res* 1997; **57**: 759-764
6 **Buchman VL**, Hunter HJ, Pinon LG, Thompson J, Privalova EM, Ninkina NN, Davies AM. Persyn, a member of the synuclein family, has a distinct pattern of expression in the developing nervous system. *J Neurosci* 1998; **18**: 9335-9341
7 **Bruening W**, Giasson BI, Klein-Szanto AJ, Lee VM, Trojanowski JQ, Godwin AK. Synucleins are expressed in the majority of breast and ovarian carcinomas and in preneoplastic lesions of the ovary. *Cancer* 2000; **88**: 2154-2163
8 **Lavedan C**, Leroy E, Dehejia A, Buchholtz S, Dutra A, Nussbaum RL, Polymeropoulos MH. Identification, localization and characterization of the human gamma-synuclein gene. *Hum Genet* 1998; **103**: 106-112
9 **Ninkina NN**, Alimova-Kost MV, Paterson JW, Delaney L, Cohen BB, Imreh S, Gnuchev NV, Davies AM, Buchman VL. Organization, expression and polymorphism of the human persyn gene. *Hum Mol Genet* 1998; **7**: 1417-1424
10 **Jia T**, Liu YE, Liu J, Shi YE. Stimulation of breast cancer invasion and metastasis by synuclein gamma. *Cancer Res* 1999; **59**: 742-747
11 **Liu J**, Spence MJ, Zhang YL, Jiang Y, Liu YE, Shi YE. Transcriptional suppression of synuclein gamma (SNCG) expression in human breast cancer cells by the growth inhibitory cytokine oncostatin M. *Breast Cancer Res Treat* 2000; **62**: 99-107
12 **Wang DX**, Li W. Advances in esophageal neoplasms etiology. *Shijie Huaren Xiaohua Zazhi* 2000; **8**: 1029-1030
13 **Mandard AM**, Hainaut P, Hollstein M. Genetic steps in the development of squamous cell carcinoma of the esophagus. *Mutat Res* 2000; **462**: 335-342
14 **Raja S**, Godfrey TE, Luketich JD. The role of tumor suppressor genes in esophageal cancer. *Minerva Chir* 2002; **57**: 767-780
15 **Zou JX**, Wang LD, Shi ST, Yang GY, Xue ZH, Gao SS, Li YX, Yang CS. p53 gene mutations in multifocal esophageal precancerous and cancerous lesions in patients with esophageal cancer in high-risk northern China. *Shijie Huaren Xiaohua Zazhi* 1999; **7**: 280-284
16 **Han Y**, Wei F, Xu X, Cai Y, Chen B, Wang J, Xia S, Hu H, Huang X, Han Y, Wu M, Wang M. Establishment and comparative genomic hybridization analysis of human esophageal carcinomas cell line EC9706. *Zhonghua Yixue Yichuanxue Zazhi* 2002; **19**: 455-457
17 **Zhou J**, Zhao LQ, Xiong MM, Wang XQ, Yang GR, Qiu ZL, Wu M, Liu ZH. Gene expression profiles at different stages of human esophageal squamous cell carcinoma. *World J Gastroenterol* 2003; **9**: 9-15
18 **Pan ZZ**, Bruening W, Giasson BI, Lee VM, Godwin AK. Gamma-synuclein promotes cancer cell survival and inhibits stress- and chemotherapy drug-induced apoptosis by modulating MAPK pathways. *J Biol Chem* 2002; **277**: 35050-35060
19 **Shields JM,** Christy RJ, Yang VW. Identification and characterization of a gene encoding a gut-enriched Krüppel-like factor expressed during growth arrest. *J Biol Chem* 1996; **271**: 20009-20017
20 **Foster KW,** Frost AR, McKie-Bell P, Lin CY, Engler JA, Grizzle WE, Ruppert JM. Increase of GKLF messenger RNA and protein expression during progression of breast cancer. *Cancer Res* 2000; **60**: 6488-6495
21 **Wang N,** Liu ZH, Ding F, Wang XQ, Zhou CN, Wu M. Down-regulation of gut-enriched Krüppel-like factor expression in esophageal cancer. *World J Gastroenterol* 2002; **8**: 966-970
22 **Gerke V**, Moss SE. Annexins: from structure to function. *Physiol Rev* 2002; **82**: 331-371
23 **Ahn SH**, Sawada H, Ro JY, Nicolson GL. Differential expression of annexin I in human mammary ductal epithelial cells in normal and benign and malignant breast tissues. *Clin Exp Metastasis* 1997; **15**: 151-156
24 **Masaki T**, Tokuda M, Ohnishi M, Watanabe S, Fujimura T, Miyamoto K, Itano T, Matsui H, Arima K, Shirai M, Maeba T, Sogawa K, Konishi R, Taniguchi K, Hatanaka Y, Hatase O, Nishioka M. Enhanced expression of the protein kinase substrate annexin in human hepatocellular carcinoma. *Hepatology* 1996; **24**: 72-81
25 **Xia SH**, Hu LP, Hu H, Ying WT, Xu X, Cai Y, Han YL, Chen BS, Wei F, Qian XH, Cai YY, Shen Y, Wu M, Wang MR. Three isoforms of annexin I are preferentially expressed in normal esophageal epithelia but down-regulated in esophageal squamous cell carcinomas. *Oncogene* 2002; **21**: 6641-6648
26 **Paweletz CP**, Ornstein DK, Roth MJ, Bichsel VE, Gillespie JW, Calvert VS, Vocke CD, Hewitt SM, Duray PH, Herring J, Wang QH, Hu N, Linehan WM, Taylor PR, Liotta LA, Emmert-Buck MR, Petricoin EF 3rd. Loss of annexin 1 correlates with early onset of tumorigenesis in esophageal and prostate carcinoma. *Cancer Res* 2000; **60**: 6293-6297
27 **Roninson IB**. Oncogenic functions of tumour suppressor p21 (Waf1/Cip1/Sdi1): association with cell senescence and tumour-promoting activities of stromal fibroblasts. *Cancer Lett* 2002; **179**: 1-14

Edited by Zhu LH

P.O.Box 2345, Beijing 100023,China
Fax: +86-10-85381893
E-mail: wjg@wjgnet.com www.wjgnet.com

World J Gastroenterol 2003;9(9):1904-1908
World Journal of Gastroenterology
 ISSN 1007-9327

• GASTRIC CANCER •

Inhibitory effect of octreotide on gastric cancer growth via MAPK pathway

Chun-Hui Wang, Cheng-Wei Tang, Chun-Lun Liu, Li-Ping Tang

Chun-Hui Wang, Cheng-Wei Tang, Department of Gastroenterology, West China Hospital, Sichuan University, Chengdu 610041, Sichuan Province, China
Chun-Lun Liu, Li-Ping Tang, Department of Gastroenterology, The First Hospital, Chongqing University of Medical Sciences, Chongqing 400016, China
Supported by the National Natural Science Foundation of China for Excellent Young Scientists, No. 39725012 and the National Natural Science Foundation of China, No. 30170418
Correspondence to: Cheng-Wei Tang, Department of Gastroenterology, West China Hospital, Sichuan University, Chengdu 610041, Sichuan Province, China. cwtang@medmail.com.cn
Telephone: +86-28-85422383
Received: 2003-04-07 **Accepted:** 2003-05-19

Abstract

AIM: Somatostatin and its analogues may suppress the growth of various tumor cells. However, the effect of octreotide on growth of gastric adenocarcinoma is still largely unknown. This study was to explore if octreotide could inhibit the growth of gastric adenocarcinoma and its probable mechanisms.

METHODS: Proliferation of gastric cancer cell line affected by octreotide was determined by ^{3}H-thymidine incorporation. After xenografts of human gastric cancer were implanted orthotopically in stomach, nude mice were administrated octreotide for 8 weeks. The mRNA of somatostatin receptor in the SGC-7901 cells was detected by reverse transcription polymerase chain reaction technique. Extracellular signal-regulated protein kinase and c-Fos in gastric cancer tissues were measured by immunohistochemistry and Western blot. Activator protein-1 binding activity was examined by electrophoretic mobility sift assay.

RESULTS: ^{3}H-thymidine incorporation into SGC-7901 cells was significantly decreased by octreotide in a concentration dependent manner. Either size or weight of tumors treated with octreotide was significantly reduced *in vivo*. The inhibition rate for tumor was 62.3 % in octreotide group. The genes of somatostatin receptors 2 and 3 were expressed in SGC-7901 gastric cancer cell lines. Extracellular signal-regulated protein kinase and c-Fos protein level were decreased in gastric adenocarcinoma treated with octreotide. Moreover, fetal calf serum stimulated activator protein-1 binding activity could be suppressed by octreotide potentially.

CONCLUSION: Inhibition of sequential molecular events in MAPK pathway may interpret the mechanisms underlying the effect of octreotide on the growth of gastric adenocarcinoma.

Wang CH, Tang CW, Liu CL, Tang LP. Inhibitory effect of octreotide on gastric cancer growth via MAPK pathway. *World J Gastroenterol* 2003; 9(9): 1904-1908
http://www.wjgnet.com/1007-9327/9/1904.asp

INTRODUCTION

Somatostatin (SST) is a widely distributed neuropeptide that negatively regulates a number of cellular processes, including exocrine and endocrine, neurotransmission and cell proliferation[1-6]. Many studies have shown that SST and its analogues suppress the growth of normal and tumor cells in various types[7-11]. The biological effects of SST are mediated through five subtypes of SST receptors (SSTR) that belong to a family of G-protein-coupled receptors. The mechanisms responsible for the inhibitory effects of SST are related to many signal transduction pathways including control of cytosolic free calcium, adenylate cyclase, protein kinase C and SHP-1 activation[12-14]. The activator protein-1 (AP-1) family transcription factors have been implicated in the control of proliferation, apoptosis and malignant transformation. SST may inhibit the expression of c-Fos and binding of AP-1[15-18]. Advanced gastric adenocarcinoma still appears to be poor in its prognosis. Chemotherapy or radiation therapy has generally shown some clinical response but little survival advantage and is intolerable in many patients. Therefore, other therapeutic regimens for gastric adenocarcinoma need to be evaluated. The purpose of this study was to investigate the inhibitory effect of SST analog, octreotide on the growth of gastric cancer and the role of mitogen-activated protein kinases (MAPK) in cell proliferation after SSTR binding.

MATERIALS AND METHODS

Assay of [methyi-^{3}H]-thymidine incorporation

Gastric cancer cell line SGC-7901 was obtained from Cell Research Institute (Shanghai, China). The cells were cultured in RPMI1640 (Hyclon Inc, USA) containing 10 % FCS, 100 U/ml penicillin and streptomycin at 37 ℃ in 5 % CO_2 atmosphere. After incubated for 24 hours in FCS free culture, cells were treated with octreotide (Novatis Pharma AG, Switzerland) for 22 h and then exposed to [methyi-^{3}H]-thymidine (1 μCi suspended in 1 ml of RPMI1640) in the same medium for 2 h. The radioactivity was measured by a liquid scintillation counter (Becman LS1801, USA).

Animal experimental procedure

Xenografts were initiated by subcutaneous injection of 2×10^6 cells into the right flanks of nude mice (Balb/c *nu/nu*). Tumors after 4 weeks were aseptically dissected and mechanically minced. Pieces of tumor tissue in 3 mm^3 were transplanted under serosa of stomach[19]. Two groups of mice (6 each group) were given octreotide at 100 μg/kg, s.c. or saline as control each day. After 8 weeks, tumors were excised and weighed. Tumor tissue was fixed in buffer neutral formalin for histological examination. The inhibition rate (%) was expressed as (weight of tumor in control group - weight of tumor in octreotide group)/weight of tumor in control group×100 %.

Detection of mRNA for SSTR subtypes on SGC-7901 gastric carcinoma cell line with RT-PCR

Total RNA was isolated using the Tripure RNA isolation kit (Roche limited, Hong Kong). First-strand cDNA was

produced by Moloney murine leukemia virus reverse transcriptase (MBI, USA), primers for SSTR-2 (sense, 5' -ATGGACATGGCGGATGA-GCCACTC-3' ; antisense, 5' -TACTGGTTTGGAGGTCTCCATTGAG-3'), SSTR-3 (sense, 5' -TGGGCACCCTCGTGCCAGCGG-3' ; antisense, 5' -GGG-CGGCCGCTCCTGCCCG-C-3'), β-actin (sense, 5' -GACTACCTCATGAAGATCCT-3' ; antisense, 5' -GCGGAT-GTCCACGTCACACT- 3'). For SSTR-2, amplification runs consisted of an initial denaturation a 94 ℃ for 5 min, following by 35 cycles of denaturation (at 94 ℃ for 1 min), annealing (at 55 ℃ for 70 s) and extension (at 72 ℃ for 2 min), which were then linked to a final polishing step at 72 ℃ for 10 min. Cycling parameters were approximately the same as for SSTR-3 except that the annealing temperature was at 65 ℃[20].

Detection of ERK and c-Fos with immunohistochemical staining and Western bloting

Tissue sections of gastric xenografts from control or octreotide group were incubated with 0.3 % hydrogen peroxide for 30 min and then in normal goat serum for 30 min to block endogenous peroxidase activity and unspecific binding sites, respectively. Immunohistochemical staining was performed with rabbit polyclonal IgG specific for human ERK and c-Fos (Santa Cruz Biotechnology, Inc., USA) in a dilution of 1:100 overnight at 4 ℃. The tissue sections were thereafter treated with biotinylated secondary antibodies in a dilution of 1:200 (Boster, Wuhan, China) and antibody-binding sites were finally visualized by avidin-biotin peroxidase complex solution (Boster, Wuhan, China) and 3' , 3' -diaminobenzidine. Protein extracted from SGC-7901 cells was incubated in loading buffer and heated at 100 ℃ for 10 min. The samples were loaded in lane and resolved on a 8 % SDS-PAGE gel, transferred to nitrocellulose, and incubated with rabbit polyclonal antibody for either the c-Fos or ERK at 4 ℃ overnight. Filters were then washed three times in blocking solution and incubated with horseradish peroxidase-linked immunoglobulin followed by exposure to enhanced chemiluminescence Western bloting luminal reagent (Promega, USA).

Measurement of AP-1 binding activity with electrophoretic mobility shift assay (EMSA)

Nuclear protein was isolated as follows: 5×10^6 SGC-7901 cells were lysed with buffer A (0.6 % NP-40, 150 mM NaCl, 10 mM HEPES [pH 7.9, 1 mM EDTA, 0.5 mM PMSF]) on ice for 5 min, and nuclei were pelleted by centrifugation at 5 000 g for 10 min. Nuclear lyses of the pellet were performed using buffer B [25 % glycerol, 20 mM HEPES (pH 7.5), 420 mM NaCl, 1.2 mM $MgCl_2$, 0.2 mM EDTA, 0.5 mM DTT, 0.5 mM PMSF, 2 mM benzamidine, 5 μg/ml aprotin, 5 μg/ml leupeptin] for 30 min on ice. Samples were then centrifuged at 12 000 g for 10 min and the supernatant was retained. Protein determination was performed using Coomassie blue assay (Sigma).

SGC-7901 cells were grown to confluence in a 6-well plate. After serum starvation for 24 h, the cells were incubated with either 20 % FCS alone or octreotide (1×10^{-5}M) for 2 h. At the end of incubation, nuclear protein was extracted as described above. The ^{32}P-labled DNA probe was added and incubated for 30 min at room temperature. DNA binding activity was measured from free probe on a 7 % non-denaturing polyacrylamide gel (PAGE) in TBE buffer. The gel was then dried for 1 h and autoradiographed at -80 ℃. AP-1 oligonucleotide probe consensus was 5' -CGCTTGATGAGTCAGCCGGAA-3' . Bands were quantified with Image Master™ VDS analysis software.

Statistical analysis

Statistical significance was determined by the Studen' s *t*-test. Differences with P values <0.05 were considered statistically significant. All data were shown as the mean ± standard division.

RESULTS

Anti-proliferative effect of octreotide on SGC-7901 cell lines in vitro

Octreotide in 1×10^{-5}M-1×10^{-9}M potentially decreased ^{3}H-thymidine incorporation into DNA of SGC-7901 cells in a dose-dependent manner (r=-0.9, P<0.01). The inhibitory rate was 32.2 % at concentration of 1×10^{-5}M octreotide (Figure 1).

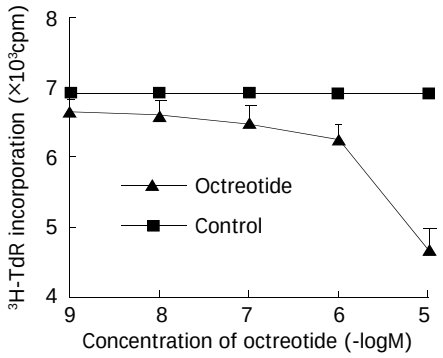

Figure 1 Effects of octreotide on ^{3}H-thymidine incorporation of SGC-7901 cell. Each value was the mean ± SD of three separate experiments in which duplicate determinations were made.

Inhibition of the growth of orthotopic tumors in nude mice in vivo

At necropsy, xenografts were found in all stomaches of nude mice. The weight of tumor in animals receiving octreotide was 0.77±0.14 g with 62.3 % reduction (P<0.01) as compared with control tumors that weighed 2.04±0.29 g. The transplanted gastric adenocarcinomas were confirmed by histological examination. Compared with control group, tissue differentiation of transplanted gastric cancer did not show notable change between two groups. No side effect was observed in all animals.

Expression of SSTR-2 and SSTR-3 in human gastric cancer

The mRNA of SSTR-2 and SSTR-3 was detected in SGC-7901 cells with RT-PCR (Figure 2). The band located between 994 bp-1 543 bp was the cDNA of SSTR-2 in 1 104 bp. The band located between 377 bp-515 bp was the cDNA of SSTR-3 in 447 bp.

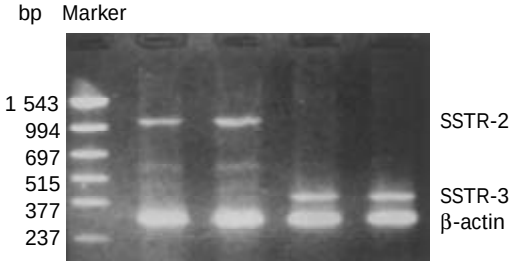

Figure 2 Expression of mRNA for SSTR-2 and SSTR-3 in SGC-7901 cells.

Inhibition of octreotide on expression of ERK

Immunohistochemical staining revealed that ERK was strongly positive in gastric adenocarcinomas. Expression of ERK in tumor tissues could be suppressed by octreotide (Figure 3). Quantitatively, ERK in SGC-7901 cells determined by Western blot was also significantly inhibited by octreotide (Figure 4).

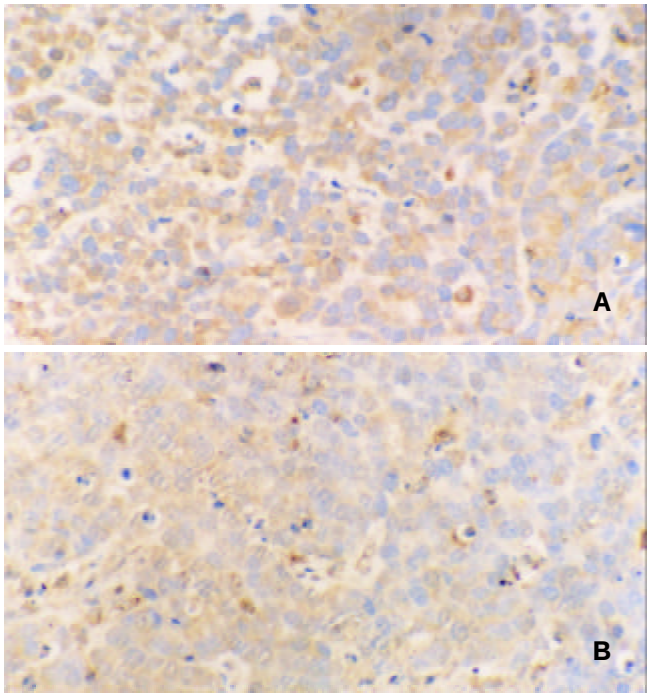

Figure 3 Immunohistochemical staining for ERK in tissues of transplanted gastric cancer in nude mice. A. control, B. octreotide group (200×).

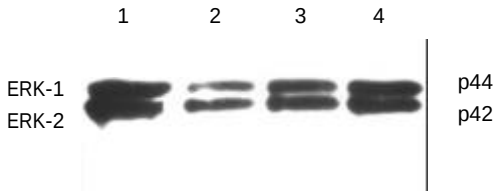

Figure 4 Western blot analysis of ERK in SGC-7901 cells. 1. control, 2. octreotide 1×10^{-5} M, 3. octreotide 1×10^{-6} M, 4. octreotide 1×10^{-7} M.

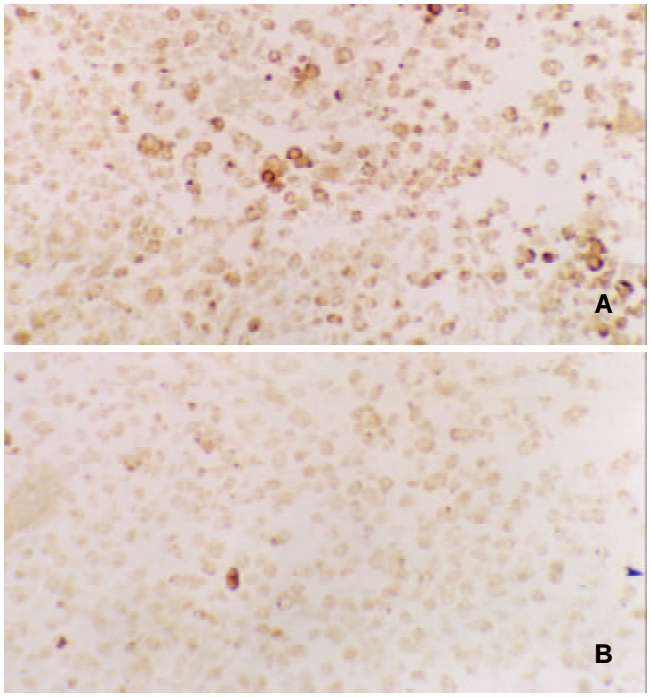

Figure 5 Immunohistochemical staining for c-Fos in tissues of transplanted gastric cancer in nude mice. A. control, B. ctreotide group (200×).

Inhibition of octreotide on expression of c-Fos

Expression of c-Fos in tumor tissues could be suppressed by octreotide (Figure 5). Quantitatively, c-Fos in SGC-7901 cells determined by Western blot was also significantly inhibited by octreotide (Figure 6).

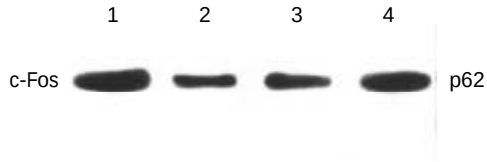

Figure 6 Western blot analysis of c-Fos in SGC-7901 cells. 1. control, 2. Octreotide 1×10^{-5} M, 3. Octreotide 1×10^{-6} M, 4. Octreotide 1×10^{-7} M.

Down-regulation of AP-1 binding activity by octreotide

As depicted in Figure 7, AP-1 binding activity could be stimulated by fetal calf serum. After addition of octreotide, the binding activity of AP-1 was reduced about 53 %.

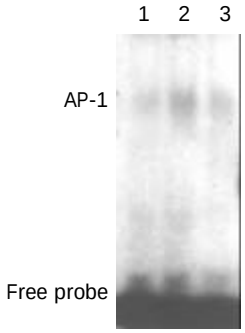

Figure 7 Effects of octreotide on AP-1 binding activity of SGC-7901 cells. 1. control, 2. FCS stimulated, 3. FCS stimulated and octreotide.

DISCUSSION

This study showed that octreotide potentially decreased ^{3}H-thymidine incorporation into gastric adenocarcinoma cell line in a dose-dependent manner. It reflected the suppression of DNA synthesis in SGC-7901 cells and reduction of tumor cells in S phase of cell cycle. Furthermore, the direct inhibitory effect of octreotory on gastric cancer *in vitro* might be attributed to the interaction of SST with its specific cellular receptors on the cell lines.

We successively established the model of *in situ* transplanted tumor in nude mice with human gastric cancer cell lines, the xenografts *in situ* were found in all stomaches of nude mice in this study. The inhibition rate for tumor was 60 % in octreotide group. This result *in vivo* was consistent with the observation *in vitro* described above. Early evidence that somatostatin analogs could inhibit the proliferation of somatostatin receptor-negative neoplasm suggested that octreotide probably acted indirectly on tumors through the inhibition of releasing some peptides or growth factors such as insulin, EGF, gastrin and IGF-1, which promote tumor growth[21-25]. Therefore, the arrested growth of transplanted gastric tumor in nude mice treated with octreotide may be either mediated directly by SST receptors or achieved indirectly via inhibition of various growth factors.

Five subtypes of SSTR, SSTR-1 to SSTR-5, have been cloned and functionally characterized during the last decade[26,27]. Natural SST is a non-selective ligand for all SSTR subtypes. Short synthetic SST analogs, however, such as octreotide and lanreotide demonstrate specific binding only to the subgroup

consisting of SSTR-2, SSTR-3 and SSTR-5[28,29]. Since no specific agonist, antagonist or antibody against individual SSTR subtype was available, detection of SSTR subtype was usually performed through analysis of corresponding mRNA. Using RT-PCR technique, to our knowledge, we demonstrated the gene expression of human SSTR-2 and SSTR-3 in SGC-7901 cell line. It afforded the further evidence for the deduction that the anti-proliferative effects of octreotide on gastric cancer might be mediated directly by SSTR-2 or SSTR-3.

The binding of SST to its receptors in native membranes triggered the intracellular signaling pathways through the activation of G proteins[30-32]. Particular interest has been devoted recently to the regulation of MAPK pathway by SSTR, which might represent an important facet of signaling. The basic assembly of the MAPK pathway was a three-component module and included three kinases that establish a sequential activation pathway[33-36]. More than a dozen of mammalian MAPK family members have been discovered, which include the ERK1/ERK2, p38 MAPK, and JNK/SAPK pathways. The activation of MAPK might be translocated to the nucleus, where these kinases phosphorylate target transcription factors such as AP-1[35,37-39]. In the present study, expression of both ERKs and c-Fos could be inhibited by octreotide. Since the expression of c-Fos is regulated by ERKs, down-regulated expression of c-Fos in gastric cancer cell lines may reflect either suppression of ERKs protein or direct effect of octreotide on c-Fos.

Accumulated data have suggested the important role of AP-1 activation in pre neoplastic-to-neoplastic transformation in cell culture and animal models. AP-1 was a critical mediator of tumor promotion in a diversity of processes[40-43]. AP-1 was best characterized as a heterodimers of c-Fos and c-Jun[44]. For this reason, the expression level and activity of c-Fos were crucial to AP-1 activation[45]. Numerous reports have confirmed that inhibition of c-Fos or c-Jun leads to inhibition of cellular proliferation. In this study, the decreased availability of c-Fos protein by octreotide led to less binding to the AP-1 site. As a result, AP-1 activity stimulated by 20 % FCS could be inhibited. The ability of AP-1 complex binding to its specific DNA elements was suppressed. Therefore, the proliferation signals of gastric cancer cell could not be transcribed.

In conclusion, the results obtained in the present study show that octreotide is able to inhibit the growth of gastric cancer *in vitro* and *in vivo*. The mechanisms may involve the down-regulation of ERKs or c-Fos expressions and binding activity of AP-1.

REFERENCES

1 **Zaki M**, Koduru S, McCuen R, Vuyyuru L, Schubert ML. Amylin, released from the gastric fundus, stimulates somatostatin and thus inhibits histamine and acid secretion in mice. *Gastroenterology* 2002; **123**: 247-255

2 **Yao YL**, Xu B, Zhang WD, Song YG. Gastrin, somatostatin, and experimental disturbance of the gastrointestinal tract in rats. *World J Gastroenterol* 2001; **7**: 399-402

3 **Tirone TA**, Norman MA, Moldovan S, DeMayo FJ, Wang XP, Brunicardi FC. Pancreatic somatostatin inhibits insulin secretion via SSTR-5 in the isolated perfused mouse pancreas model. *Pancreas* 2003; **26**: E67-E73

4 **Li YY**. Mechanisms for regulation of gastrin and somatostatin release from isolated rat stomach during gastric distention. *World J Gastroenterol* 2003; **9**: 129-133

5 **Sun FP**, Song YG, Cheng W, Zhao T, Yao YL. Gastrin, somatostatin, G and D cells of gastric ulcer in rats. *World J Gastroenterol* 2002; **8**: 375-378

6 **Wang XB**, Wang X, Zhang NZ. Inhibition of somatostatin analog octreotide on human gastric cancer cell MKN45 growth *in vitro*. *Shijie Huaren Xiaohua Zazhi* 2002; **10**: 40-42

7 **Wang CH**, Tang CW. Inhibition of activator protein-1 on the growth of gastric cancer by octreotide. *Ai Zheng* 2002; **21**: 850-854

8 **Zalatnai A**, Timar F. *In vitro* antiangiogenic effect of sandostatin (octreotide) on the proliferation of the placental vessels. *Anticancer Res* 2002; **22**: 4225-4227

9 **Guillermet J**, Saint-Laurent N, Rochaix P, Cuvillier O, Levade T, Schally AV, Pradayrol L, Buscail L, Susini C, Bousquet C. Somatostatin receptor subtype 2 sensitizes human pancreatic cancer cells to death ligand-induced apoptosis. *Proc Natl Acad Sci U S A* 2003; **100**: 155-160

10 **Wang C**, Tang C, Tang L. Inhibition effects of octreotide on the growth of hepatocellular carcinoma *in vitro* and *in vivo*. *Zhonghua Yixue Zazhi* 2001; **81**: 1194-1197

11 **Zhang QX**, Dou YL, Shi XY, Ding Y. Expression of somatostatin mRNA in various differentiated types of gastric carcinoma. *World J Gastroenterol* 1998; **4**: 48-51

12 **Petrucci C**, Cervia D, Buzzi M, Biondi C, Bagnoli P. Somatostatin-induced control of cytosolic free calcium in pituitary tumor cells. *Br J Pharmacol* 2000; **129**: 471-484

13 **Hipkin RW**, Wang Y, Schonbrunn A. Protein kinase C activation stimulates the phosphorylation and internalization of the sst2A somatostatin receptor. *J Bio Chem* 2000; **275**: 5591-5599

14 **Thangaraju M**, Sharma K, Liu D, Shen SH, Srikant CB. Interdependent regulation of intracellular acidification and SHP-1 in apoptosis. *Cancer Res* 1999; **59**: 1649-1654

15 **Held-Feindt J**, Forstreuter F, Pufe T, Mentlein R. Influence of the somatostatin receptor sst2 on growth factor signal cascades in human glioma cells. *Brain Res Mol Brain Res* 2001; **87**: 12-21

16 **Yamashita M**, Dimayuga P, Kaul S, Shah PK, Regnstrom J, Nilsson J, Cercek B. Phosphatase activity in the arterial wall after balloon injury: effect of somatostatin analog octreotide. *Lab Invest* 1999; **79**: 935-944

17 **Ubeda M**, Vallejo M, Habener JF. CHOP enhancement of gene transcription by interactions with Jun/Fos AP-1 complex proteins. *Mol Cell Biol* 1999; **19**: 7589-7599

18 **Baumeister H**, Kreuzer OJ, Roosterman D, Schafer J, Meyerhof W. Cloning, expression, pharmacology and tissue distribution of the mouse somatostatin receptor subtype 5. *J Neuroendocrinol* 1998; **10**: 283-290

19 **Furukawa T**, Fu X, Kubota T, Watanabe M, Kitajima M, Hoffman RM. Nude mouse metastatic models of human stomach cancer constructed using orthotopic implantation of histologically intact tissue. *Cancer Res* 1993; **53**: 1204-1208

20 **Douziech N**, Calvo E, Coulombe Z, Muradia G, Bastien J, Aubin RA, Lajas A, Morisset J. Inhibitory and stimulatory effects of somatostatin on two human pancreatic cancer cell lines: a primary role for tyrosine phospatase SHP-1. *Endocrinology* 1999; **140**: 765-777

21 **Spoerri PE**, Caballero S, Wilson SH, Shaw LC, Grant MB. Expression of IGFBP-3 by human retinal endothelial cell cultures: IGFBP-3 involvement in growth inhibition and apoptosis. *Invest Ophthalmol Vis Sci* 2003; **44**: 365-369

22 **Pollak MN**, Schally AV. Mechanisms of antineoplastic action of somatostatin analogs. *Proc Soc Exp Biol Med* 1998; **217**: 143-152

23 **Mansky PJ**, Liewehr DJ, Steinberg SM, Chrousos GP, Avila NA, Long L, Bernstein D, Mackall CL, Hawkins DS, Helman LJ. Treatment of metastatic osteosarcoma with the somatostatin analog OncoLar: significant reduction of insulin-like growth factor-1 serum levels. *J Pediatr Hematol Oncol* 2002; **24**: 440-446

24 **Burghardt B**, Barabas K, Marcsek Z, Flautner L, Gress TM, Varga G. Inhibitory effect of a long-acting somatostatin analogue on EGF-stimulated cell proliferation in Capan-2 cells. *J Physiol Paris* 2000; **94**: 57-62

25 **He SW**, Shen KQ, He YJ, Xie B, Zhao YM. Regulatory effect and mechanism of gastrin and its antagonists on colorectal carcinoma. *World J Gastroenterol* 1999; **5**: 408-416

26 **Patel YC**. Molecular pharmacology of somatostatin receptor subtypes. *J Endocrinol Invest* 1997; **20**: 348-367

27 **Rocheville M**, Lange DC, Kumar U, Sasi R, Patel RC, Patel YC. Subtypes of the somatostatin receptor assemble as functional homo- and heterodimers. *J Biol Chem* 2000; **275**: 7862-7869

28 **Patel YC**, Srikant CB. Subtype selectivity of peptide analogs for all five cloned human somatostatin receptor ($hsstr_{1-5}$). *Endocrinology* 1994; **135**: 2814-2817

29 **Mearadji A**, Breeman W, Hofland L, van Koetsveld P, Marquet R, Jeekel J, Krenning E, van Eijck C. Somatostatin receptor gene therapy combined with targeted therapy with radiolabeled octreotide: a new treatment for liver metastases. *Ann Surg* 2002; **236**: 722-729

30 **Brown PJ**, Schonbrunn A. Affinity purification of a somatostatin receptor-G-protein complex demonstrates specificity in receptor-G-protein coupling. *J Biol Chem* 1993; **268**: 6668-6676
31 **Vasilaki A**, Georgoussi Z, Thermos K. Somatostatin receptors (sst2) are coupled to Go and modulate GTPase activity in the rabbit retina. *J Neurochem* 2003; **84**: 625-632
32 **Komatsuzaki K**, Terashita K, Kinane TB, Nishimoto I. Somatostatin type V receptor activates c-Jun N-terminal kinases via Galpha(12) family G proteins. *Biochem Biophys Res Commun* 2001; **289**:1211-1217
33 **Widmann C**, Gibson S, Jarpe MB, Johnson GL. Mitogen-activated protein kinase: conservation of a three-kinase module from yeast to human. *Physiol Rev* 1999; **79**: 143-180
34 **Cobb MH**. MAP kinase pathways. *Prog Biophys Mol Biol* 1999; **71**: 479-500
35 **Chen Y**, Wu Q, Song SY, Su WJ. Activation of JNK by TPA promotes apoptosis via PKC pathway in gastric cancer cells. *World J Gastroenterol* 2002; **8**: 1014-1018
36 **Feng DY**, Zheng H, Tan Y, Cheng RX. Effect of phosphorylation of MAPK and Stat3 and expression of c-fos and c-jun proteins on hepatocarcinogenesis and their clinical significance. *World J Gastroenterol* 2001; **7**: 33-36
37 **Eriksson M**, Leppa S. Mitogen-activated protein kinases and activator protein 1 are required for proliferation and cardiomyocyte differentiation of P19 embryonal carcinoma cells. *J Biol Chem* 2002; **277**: 15992-16001
38 **Rosenberger SF**, Finch JS, Gupta A, Bowden GT. Extracellular signal-regulated kinase 1/2-mediated phosphorylation of JunD and FosB is required for okadaic acid-induced activator protein-1 activation. *J Biol Chem* 1999; **274**: 1124-1130
39 **Liu S**, Wu Q, Chen ZM, Su WJ. The effect pathway of retinoic acid through regulation of retinoic acid receptor α in gastric cancer cells. *World J Gastroenterol* 2001; **7**: 662-666
40 **Ding M**, Dong Z, Chen F, Pack D, Ma WY, Ye J, Shi X, Castranova V, Vallyathan V. Asbestos induces activator protein-1 transactivation in transgenic mice. *Cancer Res* 1999; **59**: 1884-1889
41 **Huang C**, Huang Y, Li J, Hu W, Aziz R, Tang MS, Sun N, Cassady J, Stoner GD. Inhibition of benzo(a)pyrene diol-epoxide-induced transactivation of activated protein 1 and nuclear factor kappaB by black raspberry extracts. *Cancer Res* 2002; **62**: 6857-6863
42 **Arnott CH**, Scott KA, Moore RJ, Hewer A, Phillips DH, Parker P, Balkwill FR, Owens DM. Tumour necrosis factor-alpha mediates tumour promotion via a PKC alpha- and AP-1-dependent pathway. *Oncogene* 2002; **21**: 4728-4738
43 **Zhong S**, Quealy JA, Bode AM, Nomura M, Kaji A, Ma WY, Dong Z. Organ-specific activation of activator protein-1 in transgenic mice by 12-o-tetradecanoylphorbol-13- acetate with different administration methods. *Cancer Res* 2001; **61**: 4084-4091
44 **Karin M**, Liu Z, Zandi E. AP-1 function and regulation. *Curr Opin Cell Biol* 1997; **9**: 240-246
45 **Faubert BL**, Kaminski NE. AP-1 activity is negatively regulated by cannabinol through inhibition of its protein components, c-fos and c-jun. *J Leukoc Biol* 2000; **67**: 259-266

Edited by Zhang JZ and Wang XL

P.O.Box 2345, Beijing 100023,China
Fax: +86-10-85381893
E-mail: wjg@wjgnet.com www.wjgnet.com

World J Gastroenterol 2003;9(9):1909-1914
World Journal of Gastroenterology
 ISSN 1007-9327

• GASTRIC CANCER •

Inhibitory effects of *c*9, *t*11-conjugated linoleic acid on invasion of human gastric carcinoma cell line SGC-7901

Bing-Qing Chen, Yan-Mei Yang, Yan-Hui Gao, Jia-Ren Liu, Ying-Ben Xue, Xuan-Lin Wang, Yu-Mei Zheng, Jing-Shu Zhang, Rui-Hai Liu

Bing-Qing Chen, Yan-Mei Yang, Jia-Ren Liu, Ying-Ben Xue, Xuan-Lin Wang, Yu-Mei Zheng, Jing-Shu Zhang, Department of Nutrition and Food Hygiene, Public Health College, Harbin Medical University, Harbin 150001, Heilongjiang Province, China
Yan-Hui Gao, Chinese Center for Disease Control and Prevention, the Center for Endemic Disease Control, China
Rui-Hai Liu, Department of Food Science and Toxicology, 108 Stocking Hall, Cornell University, Ithaca, NY 14853-7201, USA
Supported by the National Natural Science Foundation of China, No. 30070658
Correspondence to: Bing-Qing Chen, Department of Nutrition and Food Hygiene, Public Health College, Harbin Medical University, 199 Dongdazhi Street, Nangang District, Harbin 150001, Heilongjiang Province, China. bingqingchen@sina.com
Telephone: +86-451-3608014 **Fax:** +86-451-3648617
Received: 2003-03-10 **Accepted:** 2003-05-11

Abstract

AIM: To investigate the effect of *c*9, *t*11-conjugated linoleic acid (*c*9, *t*11-CLA) on the invasion of human gastric carcinoma cell line and its possible mechanism of preventing metastasis.

METHODS: Using reconstituted basement membrane invasion, chemotaxis, adhesion, PAGE substrate zymography and RT-PCR assays, we analyzed the abilities of invasion, direct migration, adhesion of intracellular matrix, as well as the activity of type IV collagenase and expression of tissue inhibitor of metalloproteinase (TIMP)-1 and TIMP-2 mRNA in SGC-7901 cells which were treated with gradually increased concentrations (25, 50, 100 and 200 μmol/L) of *c*9, *t*11-CLA for 24 h.

RESULTS: At the concentrations of 200 μmol/L, 100 μmol/L and 50 μmol/L, *c*9,*t*11-CLA suppressed the invasion of SGC-7901 cells into the reconstituted basement membrane by 53.7 %, 40.9 % and 29.3 %, respectively, in comparison with the negative control. Only in the 200 μmol/L *c*9,*t*11-CLA group, the chemotaxis of SGC-7901 cells was inhibited by 16.0 % in comparision with the negative control. C9,*t*11-CLA also could inhibit the adhesion of SGC-7901 cells to laminin, fibronectin and Matrigel, increase the expression of TIMP-1 and TIMP-2 mRNA, and reduce type IV collagenase activities in the serum-free medium supernatant of SGC-7901 cells.

CONCLUSION: *c*9,*t*11-CLA can inhibit the invasion of SGC-7901 cells at multiple procedures in tumor metastasis cascade, which may be associated with the induction of TIMP-1 and TIMP-2 mRNA expression.

Chen BQ, Yang YM, Gao YH, Liu JR, Xue YB, Wang XL, Zheng YM, Zhang JS, Liu RH. Inhibitory effects of *c*9, *t*11-conjugated linoleic acid on invasion of human gastric carcinoma cell line SGC-7901. *World J Gastroenterol* 2003; 9(9): 1909-1914
http://www.wjgnet.com/1007-9327/9/1909.asp

INTRODUCTION

Conjugated linoleic acid (CLA) refers to a class of positional and geometrical isomers of linoleic acid (18:2) with conjugated double bonds. The conjugated double bonds are mainly located at sites 9 and 11 or 10 and 12, and each double bond may be in the *cis* or *trans* configuration[1-5]. CLA exists in dairy products and meat of ruminants, the former is the principal source of CLA, of which *c*9, *t*11-CLA is the major isomer and represents 85-90 % of total CLA in bovine milk[1]. CLA is mainly produced from linoleic acid by rumen bacteria during biohydrogenation[6], although CLA can also be synthesized in non-ruminants by Δ9-desaturase from *trans*-11 18:1, another intermediate in rumen biohydrogenation[7]. The level of CLA in human adipose tissue has been reported to be associated with the consumption of dairy fat[8]. Besides, CLA can be synthesized in the laboratory and commercially synthesized CLA is available as a dietary supplement and has been shown to be non-toxic[9].

CLA is a potent cancer preventive agent and has chemoprotective properties[10-20]. In animal models of chemical carcinogenesis, CLA has been shown to inhibit skin papillomas[10,11], forestomach neoplasia[12,13] and mammary tumors[14-20]. Several studies[21-28] suggest that CLA is cytostatic and cytotoxic to a variety of human cancer cells, including hepatoma, malignant melanoma, colorectal cancer, breast carcinomas, and gastric cancer cells. Moreover, CLA also plays a role in reducing the tumor size and inhibiting the metastasis of transplanted human breast cancer cells and prostate cancer cells in SCID mice[29,30].

Gastric cancer is one of the most common malignancies in China[31-34] and its metastasis is the major cause of death in cancer patients. Our previous studies have revealed that *c*9, *t*11-CLA is an effective agent to prevent gastric cancer[13,35,36], and could inhibit the invasion of mouse melanoma[37]. However, it is unclear whether *c*9,*t*11-CLA influences on the metastasis of gastric cancer. Thus, we investigated the effect of *c*9,*t*11-CLA on the metastasis of human gastric carcinoma cell line SGC-7901.

MATERIALS AND METHODS

Materials

*c*9,*t*11-CLA with 98 % purity, was obtained from Dr. Rui-Hai Liu (Food Science and Toxicology, Department of Food Science, Cornell University, Ithaca, NY, USA). It was dissolved in ethanol and then diluted to the following concentrations: 25 μmol/L, 50 μmol/L, 100 μmol/L and 200 μmol/L, respectively.

Methods

Cell culture Human gastric adenocarcinoma cells (SGC-7901) purchased from Cancer Research Institute of Beijing (China) were cultured at 37 ℃ in PRMI 1640 (Gibco Co.) medium supplemented with fetal calf serum (100 ml/L), penicillin (100×10^3U/L), streptomycin (100 mg/L) and L-glutamine (2 mmol/L). The pH was maintained at 7.2-7.4 by

equilibration with 5 % CO_2. The SGC-7901 cells were sub-cultured with EDTA.

In vitro invasion assay Invasion assay assessing the ability of cells to invade a synthetic basement membrane was performed in transwell chambers (Costar Co. USA) with a polycarbonate filter of 8.0 μm pore size, separating the upper and lower chambers. The top surface of the polycarbonate filter was coated with Matrigel, the bottom with fibronectin. SGC-7901 cells (2×10^5) treated with different concentration of *c*9, *t*11-CLA (25, 50, 100, and 200 μmol/L) for 24 h were added to the upper transwell chamber in 100 μl of serum-free RPMI 1640 medium containing 0.1 % bovine serum albumin (BSA, Gibco Co.) and 600 μl of serum-free BSA-RPMI 1640 medium was added to the lower chamber. After 4 h, the filters were fixed in methanol and stained with hematoxylin and eosin (HE). The noninvading cells on the top surface of the filter membrane were removed with a cotton swab. Cells on the bottom surface of the filter were counted and the cell means were obtained from five high-power fields under a light microscope. The inhibitory rate (IR) was calculated as follows:

$$IR(\%)=\frac{\text{Number of invasive cells in negative control group}-\text{Number of invasive cells in test groups}}{\text{Number of invasive cells in negative control group}}\times100$$

Chemotaxied-motion assay The assay also was performed in transwell chambers (Costar Co. USA) with a polycarbonate filter of 8.0 μm pore size separating the upper and lower chambers. The bottom surface of filter was coated with fibronectin. The lower chambers were filled with 600 μl of serum-free BSA-RPMI 1640 medium. SGC-7901 cells (2×10^5) treated with different concentrations of *c*9,*t*11-CLA (25, 50, 100, and 200 $\mu mol\cdot L^{-1}$) for 24 h were added to the upper chambers, the chambers then were treated the same as invasion assay. SGC-7901 cells that migrated from the upper chamber to the bottom surface of the filter were counted and the means of cell numbers from five high-power fields under a light microscope were calculated. The inhibitory rate (IR) was calculated as follows:

$$IR(\%)=\frac{\text{Number of cells in negative control group}-\text{Number of cells in test groups}}{\text{Number of cells in negative control group}}\times100$$

Cell adhesion assay 96-well plates (Nunc. Co.) were incubated at 37 ℃ with laminin or fibronectin or Matrigel for 1 h and then blocked with phosphate-buffered saline (PBS) containing 10 g/L BSA for another 1 h at the same temperature. The SGC-7901 cells exposed to different concentrations of *c*9,*t*11-CLA (25, 50, 100, and 200 μmol/L) for 24 h were suspended in serum-free medium at a density of 8×10^5 cells/ml. Then 0.1 ml of SGC-7901 cells suspension was added to each well, and incubated at 37 ℃ for 1 h. The plates were washed three times in PBS to remove the unattached cells, then the remaining SGC-7901 cells in 96-well plates were reacted with MTT for 4 h at 37 ℃, then were solubilized with DMSO, and the absorbance of each well was measured at 570 nm with an ELX800 microplate reader (Bio-TEK Co.). Results were expressed as the percentage of total cells, assuming that the adhesion of cells in control represented 100 %.

Zymography Zymography was used for the analysis of MMP activity secreted into the culture medium of cell lines as described[38]. SGC-7901 cells were seeded at a density of 8×10^4 cells/pore in 24 well plates (Nunc. Co.) and maintained in 400 μl of serum-free medium containing different concentrations of *c*9,*t*11-CLA (25, 50, 100, and 200 μmol/L) for 24 h. After centrifugation at 500 g for 10 min, the supernatant was collected and stored at -20 ℃. SDS-PAGE was performed on gradient gels that contained 1.0 g/L gelatin (Amresco Co.) and run for 3-4 h under nondenaturing conditions. After electrophoresis, the gels were incubated in 2.5 % Triton X-100 for 1 h and then incubated in substrate buffer [50 μmol/L Tris (pH 7.5), 10 mmol/L $CaCl_2$, 200 mmol/L NaCl and 1 μmol/L $ZnCl_2$] for 12-16 h at 37 ℃. After incubation, the gels were stained in a solution containing 1 g/L Coomassie blue R250 for 4 h, and destained with 45 % methanol and 10 % acetic acid untill clear bands were shown.

RT-PCR SGC-7901 cells were treated at different concentrations of *c*9,*t*11-CLA (25, 50, 100, and 200 μmol/L) for 24 h and collected by centrifugation. Total RNA was isolated using Trizol reagent according to the manufacturer' s instructions. The concentrations and purity of total RNA were determined by DUR 640 nucleic acid and protein analyzer (Beckman, USA). The first-strand cDNA was synthesized from 5 μg of total RNA using 50 pmol of oligo (dT) primers, 10 units of AMV reverse transcriptase XL) (TAKAKA Biotechnology, Dalian Co.), 20 units RNase Inhibitor, 5×buffer and 10 mmol/L each dNTP in a total volume of 20 μl. PCRs were performed using respectively primers for TIMP-1, TIMP-2 and β-actin. The primer sequences are described in Table1. PCR was carried out in 25 μl volume containing 4 μl of cDNA template, 10×PCR buffer, 20 μmol/L each primer, 2.5 mmol/L dNTP mixture, 2.5 unit of Taq Polymerase. After denaturation at 94 ℃ for 5 min, the reaction mixtures were subjected to 35 cycles of PCR amplification in PCT-100™ programmable thermal controller (MJ Research Inc., USA). Each cycle consisted of 1 min of denaturation at 94 ℃, a primer specific annealing temperature and period (at 58 ℃ for 45 s for TIMP-1, at 58 ℃ for 30 s for TIMP-2, at 55 ℃ for 30 s for β-actin) and extension at 72 ℃ (1.5 min for TIMP-1, 1 min for TIMP-2, 45 s for β-actin).

Table 1 Primer sequence and size of expected PCR products

Primer	Sequence	Lengh (bp)
β-actin sense	5'-AAGGATTCCTATGTGGGC-3'	532
antisense	5'-CATCTCTTGCTCGAAGTC-3'	
TIMP-1 sense	5'-CTGTTGGCTGTGAGGAATGCACAG-3'	106
antisense	5'-TTCAGAGCCTTGGAGGAGCTGGTC-3'	
TIMP-2 sense	5'-AGACGTAGTGATCGGGCCA-3'	490
antisense	5'-GTACCACGCGCAAGAACCT-3'	

The amplified products were separated in 20 $g\cdot L^{-1}$ agarose gel and stained with ethidium bromide. After electrophoresis, the gel was observed and photographed under ultraviolet reflector. The density and area of each band were analyzed using ChemiImager™ 4000 digital system (Alpha Innotech Corporation, USA).

Statistical analysis

Analysis of data was performed using the Student' s *t* test. A value of $P<0.05$ was considered as statistically significant.

RESULTS

Effect of c9,t11-CLA on invasion in SGC-7901 cells

As shown in Table 2, the invasive abilities of SGC-7901 cells treated with 50 μmol/L, 100 μmol/L, and 200 μmol/L of *c*9, *t*11-CLA were significantly lower than those of the negative control group ($P<0.01$), and the inhibitory rates were 53.7 %, 40.9 % and 29.3 %, respectively. At 25 μmol/L *c*9,*t*11-CLA, the invasive ability of SGC-7901 cells did not differ from that of the negative control group ($P>0.05$). The effect of *c9*,

t11-CLA on the invasive ability of SGC-7901 cells is shown in Figure1.

Table 2 Effect of c9,t11-CLA on invasive ability of SGC-7901 cells

Groups	Invasive cell number (x±s)	Inhibitory frequency(%)
200 μmol/L	23.2±2.9[a]	53.7
100 μmol/L	29.6±3.3[a]	40.9
50 μmol/L	35.4±2.8[a]	29.3
25 μmol/L	44.9±3.1	10.4
Negative control	50.1±4.6	0

[a]P<0.01, compared with the negative control group.

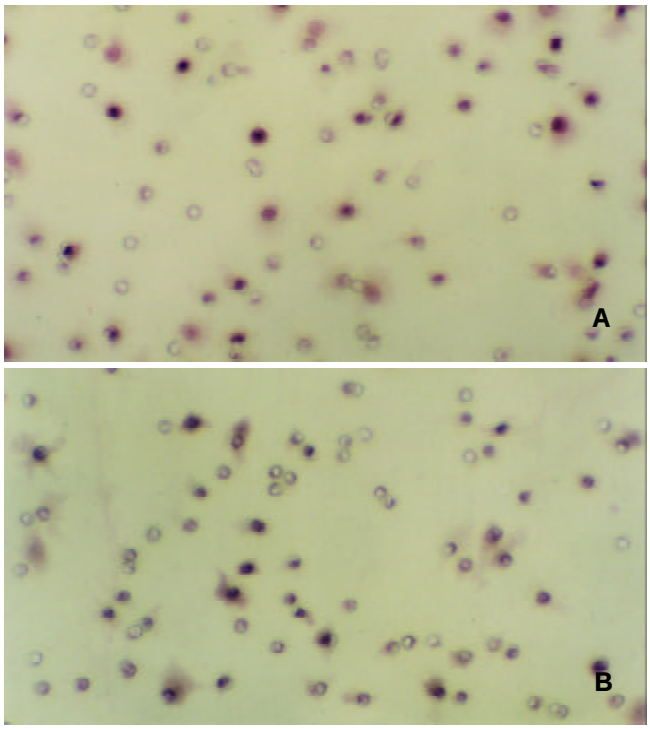

Figure 1 Effect of *c*9, *t*11-CLA on invasion of SGC-7901 cells detected by reconstituted basement membrane invasion assay (100×). A: There are more invading SGC-7901 cells in the negative control group. B: There are less invading SGC-7901 cells in the 200 μmol/L *c*9,*t*11-CLA group.

Effect of c9,t11-CLA on Chemotaxic migration ability in SGC-7901 cells

The chemotaxic ability of SGC-7901 cells at 200 μmol/L *c*9,*t*11-CLA was lower than that of the negative control group (P<0.05) and the inhibitory rate was 16.0 %. At 100 μmol/L, 50 μmol/L and 25 μmol/L of *c*9,*t*11-CLA, the chemotaxic ability of SGC-7901 cells did not differ from that of the negative control group (P>0.05). The effect of *c*9,*t*11-CLA on the chemotaxic migration ability of SGC-7901 cells is shown in Figure 2.

Table 3 Effect of *c*9,*t*11-CLA on migration ability of SGC-7901 cells

Groups	Cell number ($\bar{x}$±s)	Inhibitory frequency(%)
200 μmol/L	50.8±3.3[a]	16.0
100 μmol/L	52.5±3.1	13.2
50 μmol/L	54.4±3.9	10.1
25 μmol/L	55.0±4.4	10.1
Negative control	60.5±4.2	0

[a]P<0.05, compared with the negative control group.

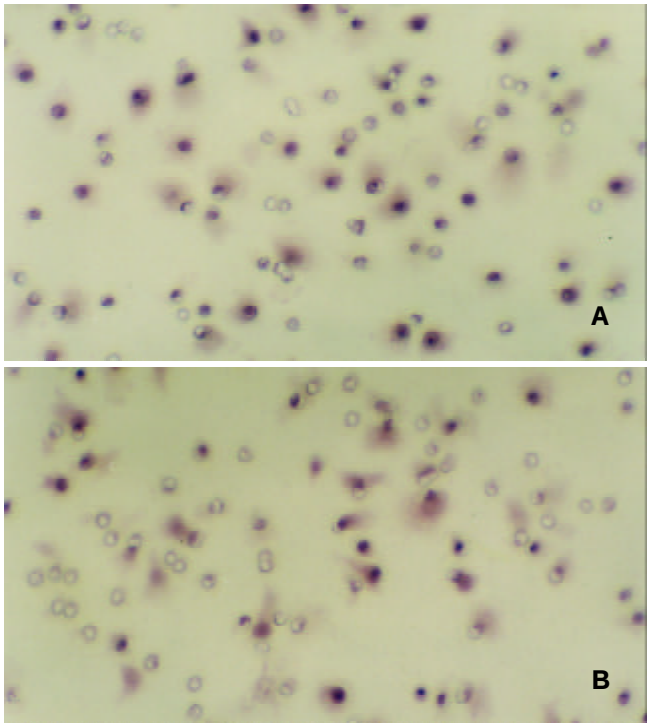

Figure 2 Effect of *c*9,*t*11-CLA on chemotaxic migration of SGC-7901 cells detected by chemotaxied-motion assay (100×). A: There are more invading SGC-7901 cells in the negative control group. B: There are less invading SGC-7901 cells in the 200 μmol/L *c*9, *t*11-CLA group.

Effect of c9,t11-CLA on attachment ability in SGC-7901 cells

As shown in Figure 3, at levels of 25 μmol/L, 50 μmol/L, 100 μmol/L and 200 μmol/L *c*9, *t*11-CLA could decrease the attachment to FN, LN or Matrigel ability of SGC-7901 cells and the inhibitory effect was positively correlated with the concentration of *c*9, *t*11-CLA.

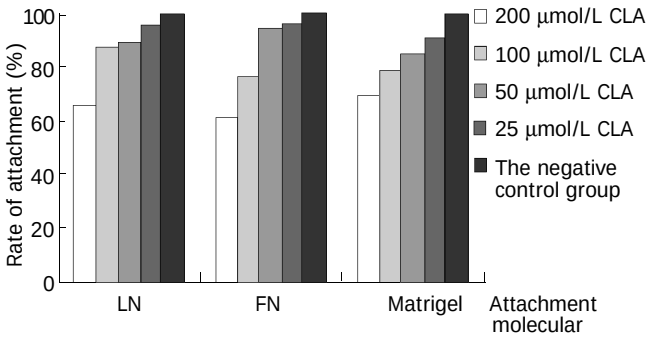

Figure 3 Effect of c9, t11-CLA on the attachment ability of SGC-7901 cells.

Effect of c9,t11-CLA on collagenase ability in SGC-7901 cells

As shown in Figure 4 and Figure 5, at levels of 200 μmol/L, 100 μmol/L and 50 μmol/L *c9, t*11-CLA significantly reduced 92 kDa type IV collagenase (MMP-9) activity in the serum-free medium supernatant of SGC-7901 cells, but at 25 μmol/L *c9, t*11-CLA, the collagenase ability did not differ from that in the negative control group. *c*9, *t*11-CLA did not influence on the 72 kDa collagenase (MMP2) activity.

Effect of c9,t11-CLA on expression of TIMP-1and TIMP-2 mRNA in SGC-7901 cells

The expression of TIMP-1 and TIMP-2 mRNA of SGC-7901 cells treated at different concentrations of *c*9,*t*11-CLA increased in comparison with that of the negative control group. As the

concentrations of *c*9,*t*11-CLA increased, the expression of TIMP-1and TIMP-2 mRNA was upregulated. Moreover, the increase of TIMP-2 mRNA expression was more obvious (Figure 6,7).

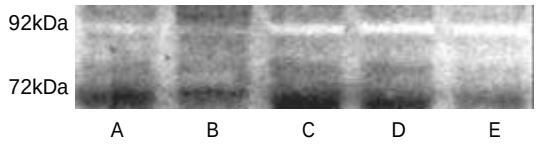

Figure 4 Effects of *c*9,*t*11-CLA on Gelatinase secretion in SGC-7901 cells detected by zymography. A, B, C, D are 200 μmol/L, 100 μmol/L, 50 μmol/L, 25 μmol/L *c*9,*t*11-CLA, respectively. E is the negative control group.

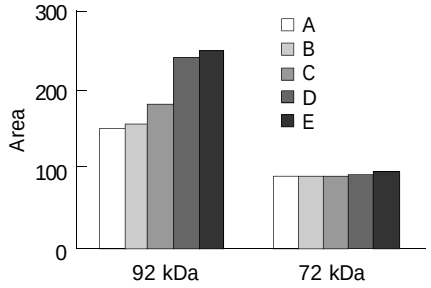

Figure 5 Quantitation of 92 and 72 kDa type IV Collagenase levels in SGC-7901 cells by ChemiImager 4000. A, B, C, D are 200 μmol/L, 100 μmol/L, 50 μmol/L, 25 μmol/L *c*9,*t*11-CLA, respectively. E is the negative control group.

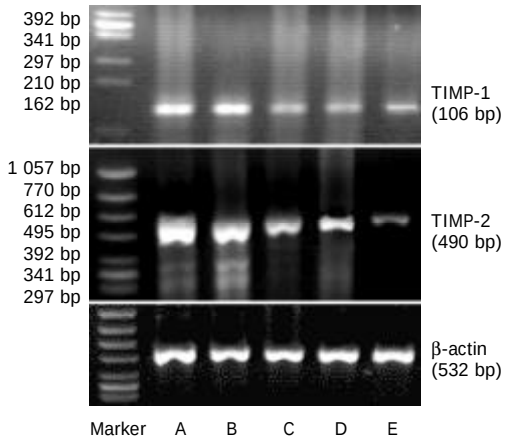

Figure 6 Effects of *c*9, *t*11-CLA on expression of TIMP-1 mRNA and TIMP-2 mRNA in SGC-7901 cells detected by RT-PCR. Top: Expression of TIMP-1 mRNA. Middle: Expression of TIMP-2 mRNA. A, B, C, D are 20 μmol/L, 100 μmol/L, 50 μmol/L, 25 μmol/L *c*9, *t*11-CLA, respectively. E is the negative control group.

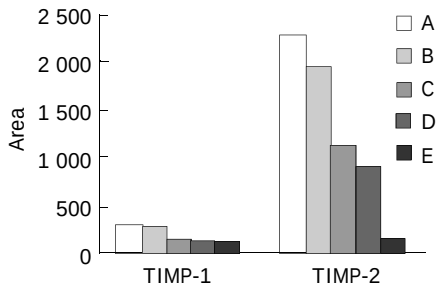

Figure 7 Quantitation of TIMP-1 and TIMP-2 mRNA levels in the SGC-7901 cells by ChemiImager 4000. A, B, C, D are 200 μmol/L, 100 μmol/L, 50 μmol/L, 25 μmol/L *c*9,*t*11-CLA, respectively. E is the negative control group.

DISCUSSION

Metastasis is a multistage process involving interactions between tumor cells and extracellular matrix (ECM). Metastasis of cancer cells required several sequent steps, including changes in cell-ECM interaction, disconnection of intercellular adhesions, separation of single cell from tumor tissue, degradation of ECM, migration of tumor cells into the ECM, invasion of lymph and blood vessels, immunologic escape in the circulatory system, adhesion to endothelial cells, extravasation from lymph and blood vessels, proliferation of cells and induction of angiogenesis[39]. The complex metastasis cascade could be described as cell attachment to the extracellular matrix, proteolytic dissolution of the matrix, and movement of cells through the digested barrier[40]. Therefore, tumor metastasis can be inhibited by blocking attachment, invasion and motility. *In vitro* invasion, attachment, proteolytic dissolution of the matrix and movement are required for tumor cell through Matrigel and polycarbonate, thus the reconstituted basement membrane invasion assay could better reflects the invasion ability of tumor. This study showed that the invasion ability of SGC-7901 cells treated with 200 μmol/L, 100 μmol/L and 50 μmol/L of *c*9, *t*11-CLA was significantly inhibited, which was consistent with the study result from mice melanoma[37]. We conclude that CLA can inhibit the invasion and metastasis of mice melanoma and human gastric adenocarcinoma.

Many studies indicated the importance of cancer cell-matrix interaction. Cell and matrix interactions promoted cell migration, proliferation, and ECM degradation[39-43]. Also, it has been shown that prevention of tumor cell adhesion and migration was related to the inhibition of tumor cell invasion into the basement membrane, and agents inhibiting cell attachment *in vitro* decreased the invasion and metastatic potential of tumor cells *in vivo*. Therefore, cellular interactions with ECM, which promote adhesion and migration, were thought to be required for tumor invasion, migration, and metastasis. We demonstrated that after incubated with 200 μmol/L, 100 μmol/L and 50 μmol/L of *c*9,*t*11-CLA for 1 h, the attachment to extracellular matrix component of SGC-7901 cells was significantly reduced, which was consistent with our previous finding[37], indicating CLA could inhibit the attachment to extracellular matrix component of tumor cells. However, in previous study we found that CLA could not affect the direct migration of B16-MB cells and in this study we observed that 200 μmol/L CLA could reduce the direct migration of SGC-7901 cells. Therefore, attachment of tumor cells to matrix inhibited by *c*9, *t*11-CLA may be a mechanism for the inhibition of invasion and needs further study.

Basement membrane is a barrier for tumor invasion and metastasis. Tumor cell invasion through the ECM was an essential process in cancer metastasis[42]. Matrix metalloproteinases (MMPs) were important enzymes for the proteolysis of extracellular matrix proteins such as collagen, laminin and fibronectin[44]. Most MMPs were synthesized and secreted from the cells as proenzymes[45]. Human MMP-2 (gelatinase A/72kD type IV collagenase) and MMP-9 (gelatinase B/92kD type IV collagenase) were thought to be the key enzymes for degrading IV collagen, which is a principal structural protein of the basement mmebrane[46]. Studies revealed that increased production of MMPs was correlated with the invasion, metastasis, and angiogenesis of tumors[47]. In this study, we found that *c*9, *t*11-CLA significantly reduced 92 kDa type (MMP9) activities in the serum-free medium supernatant of SGC-7901 cells, but had no effect on 72 kDa collagenase (MMP2), showing that CLA could inhibit the ability of tumor cells to degrade basement membrane via reduction of type IV collagenase activities. MMPs activity is regulated by tissue inhibitors of metalloproteinase (TIMPs).

There have been four members of the TIMP family determined up to date, of which TIMP-1 and TIMP-2 were best characterized as inhibitors of all known MMPs[44]. We found that TIMP-1 and TIMP-2 mRNA expression increased in SGC-7901 cells treated with *c*9,*t*11-CLA,indicating that *c*9,*t*11-CLA may inhibit the MMPs activity via inducing the expression of TIMP-1 and TIMP-2 mRNA and then inhibit the metastasis of SGC-7901 cells.

In conclusion, *c*9, *t*11-CLA inhibits several essential steps of metastasis in SGC-7901 cells. It can inhibit cell-matrix component interaction, reduce the activity of MMPs and increase the expression of TIMP1 and TIMP2 mRNA. Its mechanism in SGC-7901 cells metastasis needs to be studied further.

ACKNOWLEDGEMENTS

We are grateful to Dr. Rui-Hai Liu from Cornell University for providing 98 % purity of *c*9, *t*11-CLA.

REFERENCES

1 **Sebedio JL**, Gnaedig S, Chardigny JM. Recent advances in conjugated linoleic acid research. *Curr Opin Clin Nutr Metab Care* 1999; **2**: 499-506
2 **Pariza MW**, Park Y, Cook ME. Mechanisms of action of conjugated linoleic acid: evidence and speculation. *Proc Soc Exp Biol Med* 2000; **223**: 8-13
3 **Pariza MW**, Park Y, Cook ME. Conjugated linoleic acid and the control of cancer and obesity. *Toxicol Sci* 1999; **52**(Suppl 2): 107-110
4 **Whigham LD**, Cook ME, Atkinson RL. Conjugated linoleic acid: implications for human health. *Pharmacol Res* 2000; **42**: 503-510
5 **MacDonald HB**. Conjugated linoleic acid and disease prevention: a review of current knowledge. *J Am Coll Nutr* 2000; **19**(Suppl 2): 111S-118S
6 **Kim YJ**, Liu RH, Bond DR, Russell JB. Effect of linoleic acid concentration on conjugated linoleic acid production by Butyrivibrio fibrisolvens A38. *Appl Environ Microbiol* 2000; **66**: 5226-5230
7 **Santora JE**, Palmquist DL, Roehrig KL. Trans-vaccenic acid is desaturated to conjugated linoleic acid in mice. *J Nutr* 2000; **130**: 208-215
8 **Jiang J**, Wolk A , Vessby B. Relation between the intake of milk fat and the occurrence of conjugated linoleic acid in human adipose tissue. *Am J Clin Nutr* 1999; **70**: 21-27
9 **Scimeca JA**. Toxicological evaluation of dietary conjugated linoleic acid in male Fischer 344 rats. *Food Chem Toxicol* 1998; **36**: 391-395
10 **Belury MA**, Nickel KP, Bird CE , Wu Y. Dietary conjugated linoleic acid modulation of phorbol ester skin tumor promotion. *Nutr Cancer* 1996; **26**: 149-157
11 **Pariza MW**, Hargraves WA. A beef-derived mutagenesis modulator inhibits initiation of mouse epidermal tumors by 7,12-dimethylbenz(a)anthracene. *Carcinogenesis* 1985; **6**: 591-593
12 **Ha YL**, Storkson J, Pariza MW. Inhibition of benzo(a)pyrene-induced mouse forestomach neoplasia by conjugated dienoic derivatives of linoleic acid. *Cancer Res* 1990; **50**: 1097-1101
13 **Zhu Y**, Qiou J, Chen B, Liu RH. The inhibitory effect of conjugated linoleic acid on mice forestomach neoplasia induced by benzo(a)pyrene. *Zhonghua Yufang Yixue Zazhi* 2001; **35**: 19-22
14 **Ip C**, Jiang C, Thompson HJ, Scimeca JA. Retention of conjugated linoleic acid in the mammary gland is associated with tumor inhibition during the post-initiation phase of carcinogenesis. *Carcinogenesis* 1997; **18**: 755-759
15 **Ip C**, Singh M, Thompson HJ, Scimeca JA. Conjugated linoleic acid suppresses mammary carcinogenesis and proliferative activity of the mammary gland in the rat. *Cancer Res* 1994; **54**: 1212-1215
16 **Ip C**, Banni S, Angioni E, Carta G, McGinley J, Thompson HJ, Barbano D , Bauman D. Conjugated linoleic acid-enriched butter fat alters mammary gland morphogenesis and reduces cancer risk in rats. *J Nutr* 1999; **129**: 2135-2142
17 **Thompson H**, Zhu Z, Banni S, Darcy K, Loftus T, Ip C. Morphological and biochemical status of the mammary gland as influenced by conjugated linoleic acid: implication for a reduction in mammary cancer risk. *Cancer Res* 1997; **57**: 5067-5072
18 **Banni S**, Angioni E, Casu V, Melis MP, Carta G, Corongiu FP, Thompson H, Ip C. Decrease in linoleic acid metabolites as a potential mechanism in cancer risk reduction by conjugated linoleic acid. *Carcinogenesis* 1999; **20**: 1019-1024
19 **Kimoto N**, Hirose M, Futakuchi M, Iwata T, Kasai M, Shirai T. Site-dependent modulating effects of conjugated fatty acids from safflower oil in a rat two-stage carcinogenesis model in female Sprague-Dawley rats. *Cancer Lett* 2001; **168**: 15-21
20 **Ip C**, Ip MM, Loftus T, Shoemaker S, Shea-Eaton W. Induction of apoptosis by conjugated linoleic acid in cultured mammary tumor cells and premalignant lesions of the rat mammary gland. *Cancer Epidemiol Biomarkers Prev* 2000; **9**: 689-696
21 **Shultz TD**, Chew BP, Seaman WR , Luedecke LO. Inhibitory effect of conjugated dienoic derivatives of linoleic acid and beta-carotene on the *in vitro* growth of human cancer cells. *Cancer Lett* 1992; **63**: 125-133
22 **Igarashi M** , Miyazawa T. Newly recognized cytotoxic effect of conjugated trienoic fatty acids on cultured human tumor cells. *Cancer Lett* 2000; **148**: 173-179
23 **Igarashi M**, Miyazawa T. The growth inhibitory effect of conjugated linoleic acid on a human hepatoma cell line, HepG2, is induced by a change in fatty acid metabolism, but not the facilitation of lipid peroxidation in the cells. *Biochim Biophys Acta* 2001; **1530**: 162-171
24 **Park Y**, Allen KG , Shultz TD. Modulation of MCF-7 breast cancer cell signal transduction by linoleic acid and conjugated linoleic acid in culture. *Anticancer Res* 2000; **20**: 669-676
25 **O'Shea M**, Devery R, Lawless F, Murphy J, Stanton C. Milk fat conjugated linoleic acid (CLA) inhibits growth of human mammary MCF-7 cancer cells. *Anticancer Res* 2000; **20**: 3591-3601
26 **O'Shea M**, Stanton C, Devery R. Antioxidant enzyme defence responses of human MCF-7 and SW480 cancer cells to conjugated linoleic acid. *Anticancer Res* 1999; **19**: 1953-1959
27 **Cunningham DC**, Harrison LY, Shultz TD. Proliferative responses of normal human mammary and MCF-7 breast cancer cells to linoleic acid, conjugated linoleic acid and eicosanoid synthesis inhibitors in culture. *Anticancer Res* 1997; **17**: 197-203
28 **Schonberg S**, Krokan HE. The inhibitory effect of conjugated dienoic derivatives (CLA) of linoleic acid on the growth of human tumor cell lines is in part due to increased lipid peroxidation. *Anticancer Res* 1995; **15**: 1241-1246
29 **Visonneau S**, Cesano A, Tepper SA, Scimeca JA, Santoli D, Kritchevsky D. Conjugated linoleic acid suppresses the growth of human breast adenocarcinoma cells in SCID mice. *Anticancer Res* 1997; **17**: 969-973
30 **Cesano A**, Visonneau S, Scimeca JA, Kritchevsky D, Santoli D. Opposite effects of linoleic acid and conjugated linoleic acid on human prostatic cancer in SCID mice. *Anticancer Res* 1998; **18**: 1429-1434
31 **Liu LX**, Liu ZH, Jiang HC, Qu X, Zhang WH, Wu LF, Zhu AL, Wang XQ, Wu M. Profiling of differentially expressed genes in human Gastric carcinoma by cDNA expression array. *World J Gastroenterol* 2002; **8**: 580-585
32 **Song ZJ**, Gong P, Wu YE. Relationship between the expression of iNOS,VEGF, tumor angiogenesis and gastric cancer. *World J Gastroenterol* 2002; **8**: 591-595
33 **Shi XY**, Zhao FZ, Dai X, Ma LS, Dong XY, Fang J. Effect of jianpiyiwei capsule on gastric precancerous lesions in rats. *World J Gastroenterol* 2002; **8**: 608-612
34 **Zhao AG**, Zhao HL, Jin XJ, Yang JK, Tang LD. Effects of Chinese Jianpi herbs on cell apoptosis and related gene expression in human gastric cancer grafted onto nude mice. *World J Gastroenterol* 2002; **8**: 792-796
35 **Liu J**, Chen B, Liu R, Lu G. Inhibitory effect of conjugated linoleic acid on human gastric carcinoma cell line. *Weisheng Yanjiu* 1999; **28**: 353-357
36 **Liu JR**, Li BX, Chen BQ, Han XH, Xue YB, Yang YM, Zheng YM, Liu RH. Effect of *cis*-9,*trans*-11-conjugated linoleic acid on cell cycle of gastric adenocarcinoma cell line(SGC-7901). *World J Gastroenterol* 2002; **8**: 224-229
37 **Xue Y**, Chen B, Zheng Y, Yuan L. Effects of conjugated linoleic acid on the metastasis of mouse melanoma B16-MB. *Wei Sheng Yan Jiu* 2001; **30**: 37-39

38 **Ries C**, Loher F, Zang C, Ismair MG, Petrides PE. Matrix metalloproteinase production by bone marrow mononuclear cells from normal individuals and patients with acute and chronic myeloid leukemia or myelodysplastic syndromes. *Clin Cancer Res* 1999; **5**: 1115-1124

39 **Yoon SO,** Kim MM, Chung AS. Inhibitory effect of selenite on invasion of HT1080 tumor cells. *J Biol Chem* 2001; **276**: 20085-20092

40 **Ara T,** Deyama Y, Yoshimura Y, Higashino F, Shindoh M, Matsumoto A, Fukuda H. Membrane type 1-matrix metalloproteinase expression is regulated by E-cadherin through the suppression of mitogen-activated protein kinase cascade. *Cancer Lett* 2000; **157**: 115-121

41 **Seftor RE**, Seftor EA, Gehlsen KR, Stetler-Stevenson WG, Brown PD, Ruoslahti E, Hendrix MJ. Role of the alpha v beta 3 integrin in human melanoma cell invasion. *Proc Natl Acad Sci U S A* 1992; **89**: 1557-1561

42 **Nakahara H**, Nomizu M, Akiyama SK, Yamada Y, Yeh Y, Chen WT. A mechanism for regulation of melanoma invasion. Ligation of alpha6beta1 integrin by laminin G peptides. *J Biol Chem* 1996; **271**: 27221-27224

43 **Giancotti FG**, Ruoslahti E. Integrin signaling. *Science* 1999; **285**: 1028-1032

44 **Kim MH**, Kitson RP, Albertsson P, Nannmark U, Basse PH, Kuppen PJ, Hokland ME, Goldfarb RH. Secreted and membrane-associated matrix metalloproteinases of IL-2-activated NK cells and their inhibitors. *J Immunol* 2000; **164**: 5883-5889

45 **Nagase H**, Woessner JF Jr. Matrix metalloproteinases. *J Biol Chem* 1999; **274**: 21491-21494

46 **Andela VB**, Schwarz EM, Puzas JE, O'Keefe RJ, Rosier RN. Tumor metastasis and the reciprocal regulation of prometastatic and antimetastatic factors by nuclear factor kappaB. *Cancer Res* 2000; **60**: 6557-6562

47 **Westermarck J**, Kahari VM. Regulation of matrix metalloproteinase expression in tumor invasion. *FASEB J* 1999; **13**: 781-792

Edited by Ren SY and Wang XL

P.O.Box 2345, Beijing 100023,China
Fax: +86-10-85381893
E-mail: wjg@wjgnet.com www.wjgnet.com

World J Gastroenterol 2003;9(9):1915-1919
World Journal of Gastroenterology
 ISSN 1007-9327

• GASTRIC CANCER •

Degradation of retinoid X receptor a by TPA through proteasome pathway in gastric cancer cells

Xiao-Feng Ye, Su Liu, Qiao Wu, Xiao-Feng Lin, Bing Zhang, Jia-Fa Wu, Ming-Qing Zhang, Wen-Jin Su

Xiao-Feng Ye, Su Liu, Qiao Wu, Xiao-Feng Lin, Bing Zhang, Jia-Fa Wu, Ming-Qing Zhang, Wen-Jin Su, Key Laboratory of the Ministry of Education for Cell Biology and Tumor Cell Engineering, School of Life Sciences, Xiamen University, Xiamen 361005, Fujian Province, China
Supported by the National Natural Science Foundation of China, No. 30170477, and the National Natural Science Foundation of Fujian Province, No. 0110004
Correspondence to: Wu Qiao, Ph.D, Key Laboratory of the Ministry of Education for Cell Biology and Tumor Cell Engineering, School of Life Sciences, Xiamen University, Xiamen 361005, Fujian Province, China. xgwu@xmu.edu.cn
Telephone: +86-592-2187959 **Fax:** +86-592-2086630
Received: 2003-03-03 **Accepted:** 2003-05-16

Abstract

AIM: To investigate and determine the mechanism and signal pathway of tetradecanoylphorbol-1, 3-acetate (TPA) in degradation of RXRα.

METHODS: Gastric cancer cell line, BGC-823 was used in the experiments. The expression level of RXRα protein was detected by Western blot. Nuclear and cytoplasmic protein fractions were prepared through lysis of cell and centrifugation. Localization and translocation of RXRα were observed under laser-scanning confocal microscope through labeling specific anti-RXRα antibody and corresponding immunofluorescent antibody as secondary antibody. Different inhibitors were used as required.

RESULTS: In BGC-823 cells, RXRα was expressed in the nucleus. When cells were treated with TPA, expression of RXRα was repressed in a time-dependent and TPA-concentration-dependent manner. Meanwhile, translocation of RXRα from the nucleus to the cytoplasm occurred, also in a time-dependent manner. When cells were pre-incubated with proteasome inhibitor MG132 for 3 hrs, followed by TPA for another 12 hrs, TPA-induced RXRα degradation was inhibited. Further observation of RXRα translocation in the presence of MG132 showed that MG-132 could block TPA-induced RXRα redistribution. Conversely, when RXRα translocation was inhibited by LMB, an inhibitor for blocking protein export from the nucleus, TPA could not repress expression of RXRα.

CONCLUSION: TPA could induce the degradation of RXRα protein in BGC-823 cells, and this degradation is time- and TPA-concentration-dependent. Furthermore, the degradation of RXRα by TPA is via a proteasome pathway and associated with RXRα translocation from the nucleus to the cytoplasm.

Ye XF, Liu S, Wu Q, Lin XF, Zhang B, Wu JF, Zhang MQ, Su WJ. Degradation of retinoid X receptor α by TPA through proteasome pathway in gastric cancer cells. *World J Gastroenterol* 2003; 9 (9): 1915-1919
http://www.wjgnet.com/1007-9327/9/1915.asp

INTRODUCTION

Retinoid receptors are nuclear receptors, and belong to members of the steroid and thyroid hormone receptor superfamily[1-4]. As retinoid receptor ligands, retinoids exert their effects on proliferation and differentiation through regulating the transcriptional and post-transcriptional activities of retinoid receptors[5-8]. Besides retinoids, other agents such as tetradecanoylphorbol-1, 3-acetate (TPA), and nerve growth factor (NGF), have an effect on retinoid receptor regulation[9-11]. Although up-regulation of retinoid receptor mRNA by retinoids has been demonstrated among a number of different types of cells[12-15], it is also indicated that retinoid receptors are degraded through a distinct pathway[16]. However, little is known how and where retinoid receptors are degraded, especially when other agents, rather than their ligands, are used to stimulate carcinoma cells.

Eukaryotic cells contain multiple proteolysis systems, which are mainly responsible for degradation of proteins in the extracellular milieu[17]. The multicomplex 26S proteasome contains two 19S regulatory complexes and a 20S catalytic core complex that may be responsible for 80-90 % of protein degradation in the cells[18,19]. It has been reported that proteasomes play an important role in thymocyte apoptosis and inflammatory response[20-23]. Proteasome inhibitors can induce cell apoptosis, accompanied by activation of several Caspases, such as Caspase-3 and Caspase-7[24,25]. In contrast, proteasome inhibitors may prevent cells from apoptosis through promoting resistance of cells at higher temperature and toxicity[26-28].

Retinoid receptors can be divided into two types, retinoic acid receptor (RAR) and retinoid X receptor (RXR)[29-32]. Usually, to regulate retinoid receptor by retinoid is preferential to measure its mRNA level, little has been done on retinoid receptor protein itself. Recently, Tanaka *et al*. pointed out that although retinoic acid caused up-regulation of RARα and RARγ mRNA, it down-regulated the expression of RARα and RARγ protein in breast cancer cell line MCF-7[16]. This evidence suggests that the mechanism of retinoic acid on transcriptional or post-transcriptional activity of retinoid receptor is quite different. In the course of investigating the effect of TPA on RXR protein expression, we found that TPA could down-regulate the expression of RXRα protein effectively in gastric cancer cells. In present study, we focused on the mechanism of TPA in RXRα degradation. The results demonstrated that degradation of RXRα by TPA was proteasome-dependent in gastric cancer cells. More importantly, both degradation and proteasome-dependency of RXRα were associated with translocation of RXRα protein. These findings may provide a novel insight into the cross-talk between degradation and translocation of retinoid receptor and TPA signaling pathway.

MATERIALS AND METHODS

Cancer cell line

Human gastric cancer cell line, BGC-823, was obtained from the Institute of Cell Biology in Shanghai. The cells were maintained in RPMI-1640 medium, supplemented with 10 % FCS, 1 mM glutamine, and 100 u/ml penicillin.

Detection of western blot[9, 33]

Cells treated by different agents were harvested, and suspended in RIPA buffer (10 mmol/L Tris (pH 7.4), 150 mmol/L NaCl, 1 % Triton X-100, 1 % deoxycholic acid, 0.1 % SDS, 5 mmol/L EDTA (pH 8.0), 1 mmol/L PMSF). Protein concentration was determined using the Bio-Rad protein assay system according to the manufacturer' s instructions (Bio-Rad Hereules, CA). Total protein (50 μg) was subjected to SDS-PAGE and transferred to nitrocellulose membrane for Western blot analysis. The membrane was subsequently blocked with 5 % dry milk in TBS-T and then immunnoblotted with the corresponding antibody. Protein was detected using the ECL kit (Peirce) according to the manufacturer' s directions. Before incubation with antibody, the same membrane was stained by ponceau S (Sigma) to show the amount of protein used in each well. The intensities of bands indicated by Western blot were quantified by a densitometer. To separate the cytoplasmic and nuclear fractions, cells were suspended in 500 μl of 10 mM Tris-Cl (pH 7.8), 1 % Nonidet P-40, 10 mM mercaptoethanol, 0.5 mM phenylmethylsulfonyl fluoride, 1 mg/L leupeptin and 1 mg/L aprotinin for 2 min at 0 ℃, then 500 μl of DDW was added, and the cells were allowed to swell for 2 min. Cells were sheared by 10 passages through a 22 gauge needle. The nuclear and cytoplasmic fraction was obtained by centrifugation at 4 000×g for 5 min. The supernatant was cytoplasmic fraction and pellet was nuclear fraction.

Immunofluorescent labeling and confocal microscopy[9, 34]

Cells were cultured on a cover glass overnight, then treated with various agents. After washed with PBS, cells were fixed in 4 % paraformaldehyde. To identify RXRα protein, cells were firstly incubated with anti-RXRα IgG antibody (Santa Cruz), and then reacted with corresponding FITC-conjugated anti-IgG (Pharmingen) as secondary antibody. To visualize nuclei, cells were stained with propidium iodine (50 mg/L) containing 100 mg of DNase-free RNase A per liter. Fluorescent images were observed and analyzed under laser-scanning confocal microscope (Bio-Rad MRC-1024ES).

RESULTS

TPA induces degradation of RXRa

Western blot analysis was carried out to investigate the effect of TPA on the expression level of RXRα protein. When BGC-823 cells were treated at different concentrations of TPA (ranging from 100-1.0 g/L) for 24 hrs, the expression of RXRα protein showed a concentration-dependent decrease (Figure 1A), 87 % reduction of RXRα protein expression was observed at the concentration of 100 g/L TPA determined by a densitometer (Figure 1B). Similar repressing tendency was also seen in time-course of TPA treatment. As shown in Figure 1A-B, treatment of cells with TPA for different time periods caused a marked down-regulation of RXRα protein in BGC-823 cells. After 24 hr of TPA treatment, the expression of RXRα protein was almost inhibited. Thus, TPA could induce the degradation of RXRα protein in BGC-823 cells. Moreover, this degradation was time- and TPA concentration-dependent.

TPA induces RXRa translocation

To determine the effect of TPA on the subcellular localization of RXRα, immunofluorescent labeling of RXRα protein was performed and observed under laser-scanning confocal microscope. The result indicated that RXRα was accumulated in the nuclei in intact BGC-823 cells (Figure 2A). Treatment of TPA resulted in redistribution of RXRα protein in a time-dependent manner. When cells were treated with TPA for 6 hrs, RXRα protein started to be translocated from the nucleus to the cytoplasm, and after 12 h of treatment, RXRα protein was completely accumulated in the cytoplasm, and after 24 h of treatment, most of the RXRα protein became localized in the cytoplasm, but little in the nucleus (Figure 2A). To further confirm this translocation, nuclear and cytoplasmic fractions were prepared from BGC-823 cells, and the protein extracts were analyzed by Western blot. It clearly showed that in the intact BGC-823 cells, RXRα was expressed mainly in the nucleus (Figure 2B). TPA treatment resulted in a time-dependent shift of RXRα protein from nuclear portion to cytoplasmic portion. The maximum cytoplasmic RXRα accumulation occurred in the 12 h TPA treatment, and after 24 h TPA treatment, trace RXRα was detected in the nucleus, mostly in the cytoplasm (Figure 2B). Accordingly, this result was in agreement with that of Figure 2A, strongly suggesting that the translocation of RXRα did occur in the course of TPA treatment.

To verify that cytoplasmic RXRα protein was originated from nuclear RXRα, rather than being synthesized in the cytoplasm, cells were pre-incubated with cycloheximide

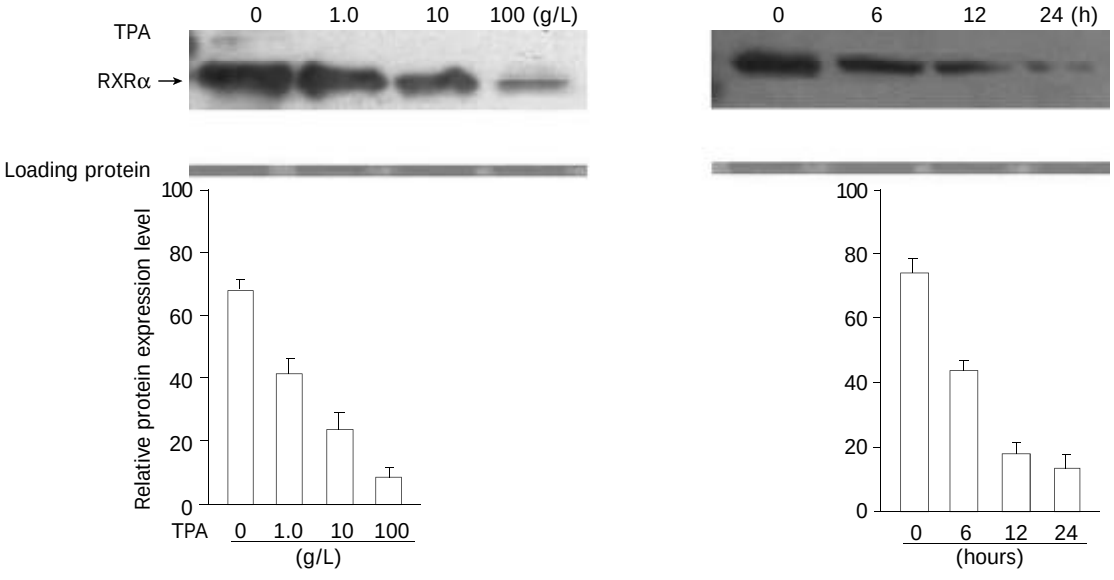

Figure 1 Effect of TPA on expression of RXRα protein. Cells were treated at different concentrations of TPA or different time periods. (A) Expression of RXRα was detected by Western blot. The amount of protein used in each lane was indicated by staining with ponceau S. (B) The intensity of each band shown in Figure 1A was quantified by a densitometer.

(CHX) for 3 hrs to specifically prevent new cytoplasmic protein synthesis[35]. Confocal microscopy observation showed that RXRα protein was seen only in the nucleus when cells were treated with CHX alone (Figure 2A), indicating that cytoplasmic protein synthesis was inhibited by CHX effectively. However, when cells were continuously incubated with TPA for another 24 hrs, RXRα protein was still translocated into the cytoplasm (Figure 2A). Therefore, it convincingly demonstrated that cytoplasmic RXRα protein was from the nucleus.

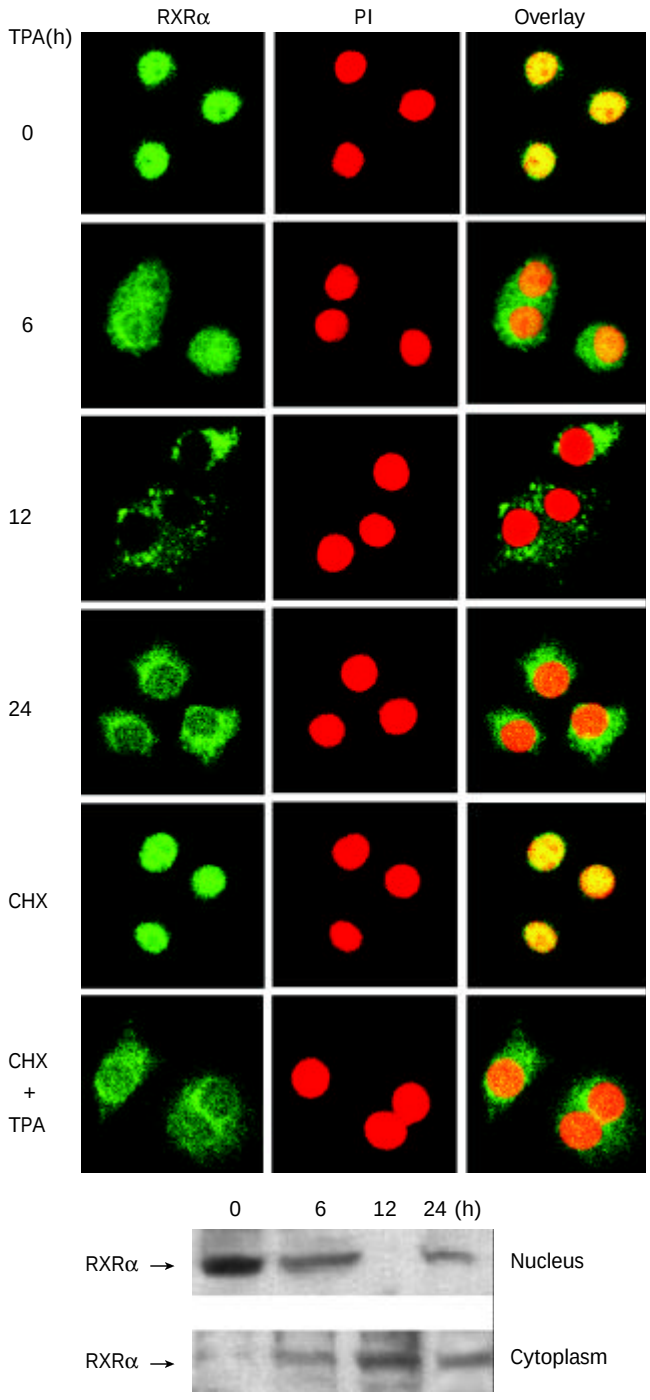

Figure 2 Translocation of RXRα from the nucleus to the cytoplasm induced by TPA. Cells were treated with TPA for different time periods or CHX (10 g/L) for 3 hrs as required. (A) Cells were immunostained with anti-RXRα antibody followed by corresponding FITC-conjugated anti-IgG secondary antibody to show RXRα protein. Simultaneously, cells were stained with PI to display the nucleus. The fluorescent image was observed under laser-scanning confocal microscope. (B) Nuclear and cytoplasmic fractions were prepared as described in the Materials and Methods. RXRα was revealed by Western blot.

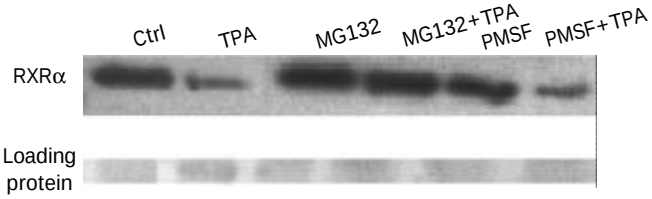

Figure 3 Effect of different agents, including TPA, MG132 (10 μmol/L) and PMSF (100 mg/L), on expression of RXRα. Cells were pre-treated with MG132 or PMSF for 3 hrs, followed by TPA for another 24 hrs. RXRα expression was analyzed by Western blot.

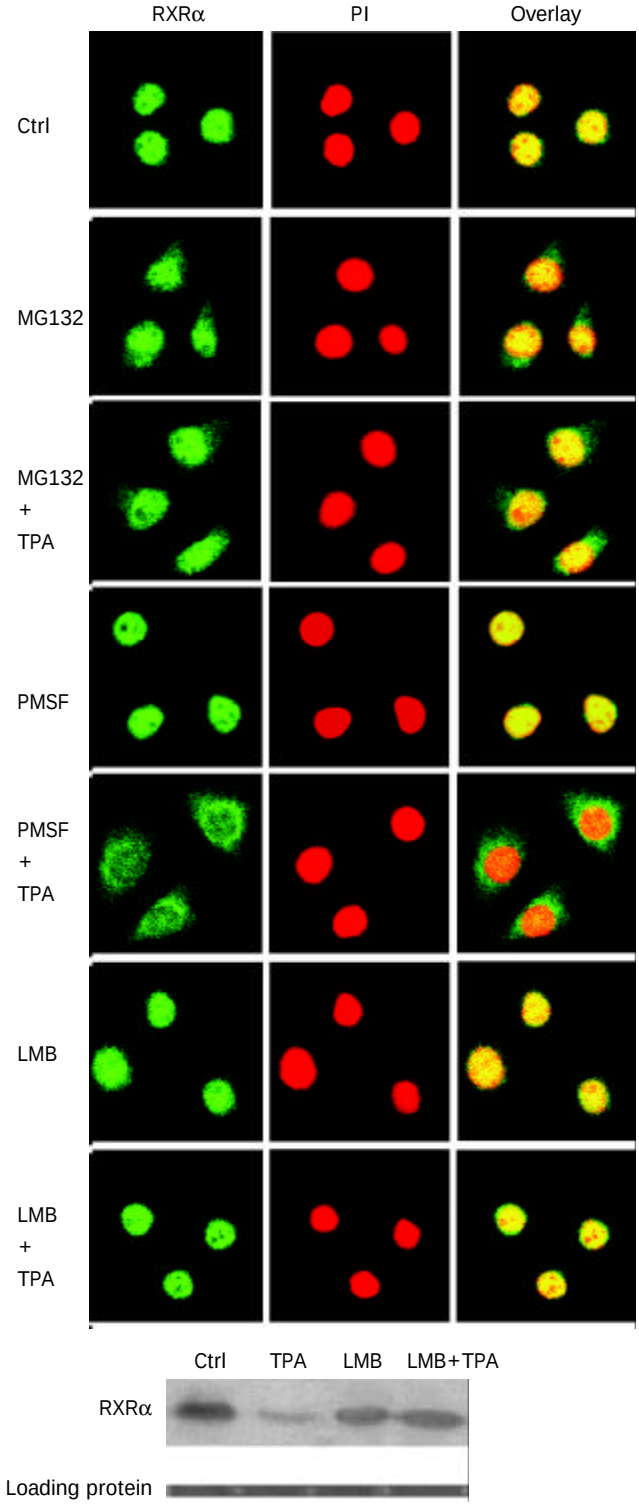

Figure 4 Effect of different agents, including TPA, MG132, PMSF and LMB (1 ng/ml), on translocation and expression of

RXRα. Cells were pre-treated with different inhibitors for 3 hrs as required, followed by TPA treatment for another 12 hrs. (A) Translocation of RXRα in response to different agents, observed under laser-confocal microscope. (B) Expression of RXRα induced by different agents, revealed by Western blot.

Effect of proteasome inhibitor on RXRa degradation

To determine whether the degradation of RXRα by TPA was 26S proteasome-dependent, BGC-823 cells were incubated with proteasome-specific inhibitor MG132[16,18] in the absence or presence of TPA. Western blot analysis showed that MG132 was able to inhibit TPA-induced RXRα degradation (Figure 3). By contrast, when PMSF, a potent inhibitor of protease but not specific-inhibitor of proteasome[36], was used as a positive control, it could not inhibit TPA-induced RXRα degradation, TPA still down-regulated expression of RXRα (Figure 3). Thus, this result suggested that TPA-induced degradation of RXRα occurred through the proteasome pathway.

RXRa translocation by TPA is proteasome-dependent

To determine the relationship between RXRα translocation and proteasome pathway, the behavior of RXRα translocation in the presence of MG132 was investigated. Confocal microscopy observation showed that cells treated with MG132 alone for 3 hrs could hardly induce RXRα protein translocation into the cytoplasm, majority of RXRα protein was localized in the nucleus, but very little in the cytoplasm. After TPA treatment for another 12 hrs, most of RXRα protein remained in the nucleus, similar to MG132 treatment alone (Figure 4A). As a positive control, when PMSF was used to treat cells alone, RXRa was not translocated, still in the nucleus. However, when cells were continuously incubated with TPA, translocation of RXRα was detected (Figure 4A). Thus, it clearly revealed that MG132 and PMSF had different effects on inducing RXRα translocation, MG132 could inhibit TPA-induced translocation of RXRa protein, and RXRα translocation induced by TPA was proteasome-dependent.

In addition, we used another inhibitor LMB, an inhibitor of protein export from the nucleus[37,38], to block RXRα protein nucleocytoplasmic translocation, and then determine whether this blockage could affect TPA-induced RXRα degradation. As shown in Figure 4A, when LMB was incubated with cells alone for 3 hrs, or followed by TPA treatment for another 12 hrs, RXRα was not translocated into the cytoplasm, indicating that LMB did block RXRα translocation no matter TPA existed or not. Under such circumstances, TPA could not repress the expression level of RXRα protein (Figure 4B). These results clearly indicated that TPA-induced RXRα degradation was not only proteasome-dependent, but also translocation-dependent.

DISCUSSION

The redistribution of proteins between nucleus and cytoplasm is an important event for the regulation of their activities and the execution of their functions[39-41]. For example, phosphorylation is needed for redistribution of some proteins. In some cases, phosphorylation of a protein promotes its entry from the cytoplasm to the nucleus[41], in other cases, it causes the protein translocation from the nucleus to the cytoplasm[41,42]. Our study showed that degradation of RXRα protein by TPA was associated with its translocation from the nucleus to the cytoplasm. In gastric cancer BGC-823 cells, TPA could down-regulate the expression of RXRα protein significantly, and this repression was time-dependent and TPA-concentration-dependent (Figure 1A). In the treatment of cells with TPA for 24 hrs, 87 % of RXRα protein expression was inhibited (Figure 1B). Moreover, we found that RXRα was translocated from the nucleus to the cytoplasm as degraded by TPA, also in a time-dependent manner (Figure 2A). However, when this translocation was blocked by LMB (Figure 4A), degradation of RXRα by TPA was not detected by Western blot (Figure 4B). Therefore, it clearly demonstrated that TPA-induced RXRα degradation was time-dependent and translocation-dependent.

Although we have detected the degradation of RXRα by TPA during the translocation of RXRα, its molecular mechanism is still largely unknown. More evidences revealed that the proteasome played not only a proteolytic role in protein degradation, but also a non-proteolytic role in transcriptional elongation, nuclear excision repair, and protein trafficking[43-48]. To determine whether degradation of RXRα was responsible for proteasome pathway, we used MG132, a specific proteasome inhibitor, to study the potential linkage among RXRα degradation, translocation and proteasome pathway. The results showed that inhibition of proteasome function by MG132 could repress TPA-induced RXRα degradation (Figure 3), and further block TPA-induced RXRα translocation (Figure 4A), which strongly supported the non-proteolytic role of the proteasome in protein translocation. Accordingly, it is likely that regulation of post-transcriptional activity of RXRα through the proteasome pathway may be involved in multiple mechanisms.

Recently, Tanaka *et al*. found that incubation of breast cancer cells MCF-7 with 10^{-6} mol/L retinoic acid induced a rapid breakdown of both RARα and RARγ in spite of the accumulation of their mRNA[16]. Eliezer *et al*. also pointed out that retinoic acid-induced degradation of RARs and RXRs could play an important role in the control of the activity of RAR/RXR heterodimer[49]. These reports, at least, provide a crucial clue: retinoid receptor (including RARs and RXRs) activity may be regulated through a distinct mechanism at transcriptional or post-transcriptional level, and formation of heterodimer/or homodimer between these receptors is essential. In our previous studies, we found that RXR could form heterodimer with RAR in the presence of retinoic acid[50]. Moreover, we have indicated that besides RAR, RXR also formed heterodimer with Nur77, an orphan receptor, bound to the RARβ (retinoic acid receptor β) promoter, and then induced RARβ expression, which is critical for inducing apoptosis and inhibiting cell growth in carcinoma cells[15,50]. Therefore, it is likely that degradation and translocation of RXRα by TPA are not a simple event. RXRα might form heterodimer with some proteins, such as Nur77 or RAR, then export from the nucleus to exert its function in the cytoplasm. But, at least, it has been confirmed that the RXRα is degraded through a proteasome pathway in the present study.

REFERENCES

1 **Kastner P**, Mark M, Chambon P. Nonsteroid nuclear receptors: what are genetic studies telling us about their role in real life? *Cell* 1995; **83**: 859-869

2 **Mangelsdorf DJ**, Evans RM. The RXR heterodimers and orphan receptors. *Cell* 1995; **83**: 841-850

3 **Zhang XK**, Pfahl M. Regulation of retinoid and thyroid hormone action through homodimeric receptors. *Trends Endocrinol Metab* 1993; **4**: 156-162

4 **Xu M**, Jin YL, Fu J, Huang H, Chen SZ, Qu P, Tian HM, Liu ZY, Zhang W. The abnormal expression of retinoic acid receptor-β, *P*53 and Ki67 protein in normal, premalignant and malignant esophageal tissues. *World J Gastroenterol* 2002; **8**: 200-202

5 **Gudas LJ**, Sporn MB, Roberts AB. Cellular biology and biochemistry of the retinoids. In: Sporn MB, Roberts AB, Goodman DS, eds. The retinoids. *New York: Raven Press* 1994: 443-520

6 **Lotan R**. Effect of the vitamin A and its analogs (retinoids) on normal and neoplastic cells. *Biochim Biophs Acta* 1981; **605**: 33-91

7 **Roberts AB**, Sporn MB. Cellular biology and biochemistry of the retinoids. In: Sporn MB, Roberts AB, Goodman DS, eds. The retinoids. *Orlando, Fla: Academic Press* 1984; **2**: 209-286

8 **Liu JR**, Li BX, Chen BQ, Han XH, Xue YB, Yang YM, Zheng YM, Liu RH. Effect of cis-9, trans-11-conjugated linoleic acid on cell cycle of gastric adenocarcinoma cell line (SGC-7901). *World J Gastroenterol* 2002; **8**: 224-229

9 **Wu Q**, Liu S, Ye XF, Huang ZW, Su WJ. Dual roles of Nur77 in selective regulation of apoptosis and cell cycle by TPA and ATRA in gastric cancer cells. *Carcinogenesis* 2002; **23**: 1583-1592

10 **Katagiri Y**, Takeda K, Yu ZX, Ferrans VJ, Ozato K, Guroff G. Modulation of retinoid signalling through NGF-induced nuclear export of NGFI-B. *Nature Cell Biol* 2000; **2**: 435-440

11 **Xia M**, Xue SB, Xu CS. Shedding of TNFR1 in regenerative liver can be induced with TNFa and PMA. *World J Gastroenterol* 2002; **8**: 1129-1133

12 **Liu S**, Wu Q, Chen ZM, Su WJ. The effect pathway of retinoic acid through regulation of retinoic acid receptor alpha in gastric cancer cells. *World J Gastroenterol* 2001; **7**: 662-666

13 **Liu Y**, Lee MO, Wang HG, Li Y, Michael K, Reed CJ, Zhang XK. Retinoic acid receptor β mediates the growth-inhibitory effect of retinoic acid by promoting apoptosis in human breast cancer cells. *Mol Cell Biol* 1996; **16**: 1138-1149

14 **Li Y**, Dawson MI, Agadir A, Lee MO, Jong L, Hobbs PD, Zhang XK. Regulation of RAR β expression by RAR- and RXR-selective retinoids in human lung cancer cell lines: effect on growth inhibition and apoptosis induction. *Int J Cancer* 1998; **75**: 88-95

15 **Wu Q**, Dawson MI, Zheng Y, Hobbs PD, Agadir A, Jong L, Li Y, Liu R, Lin B, Zhang XK. Inhibition of trans-retinoic acid-resistant human breast cancer cell growth by retinoid X receptor-selective retinoids. *Mol Cell Biol* 1997; **17**: 6598-6608

16 **Tanaka T**, Rodriguez de la Concepcion ML, De Luca LM. Involvement of all-trans-retinoicacid in the breakdown of retinoic acid receptors alpha and gamma through proteasomes in MCF-7 human breast cancer cells. *Biochem Pharmacol* 2001; **61**: 1347-1355

17 **Ciechanover A**, Schwartz AL. The ubiquitin-mediated proteolytic pathway: mechanisms of recognition of the proteolytic substrate and involvement in the degradation of native cellular proteins. *FASEB J* 1994; **8**: 182-191

18 **Lin HK**, Altuwaijri S, Lin WJ, Kan PY, Collins LL, Chang C. Proteasome activity is required for androgen receptor transcriptional activity via regulation of androgen receptor nuclear translocation and interaction with coregulators in prostate cancer cells. *J Biol Chem* 2002; **277**: 36570-36576

19 **Lee DH**, Goldberg AL. Proteasome inhibitors: valuable new tools for cell biologists. *Trends Cell Biol* 1998; **8**: 397-403

20 **Kloetzel PM**, Soza A, Stohwasser R. The role of the proteasome system and the proteasome activator PA28 complex in the cellular immune response. *Biol Chem* 1999; **380**: 293-297

21 **Hirsch T**, Dallaporta B, Zamzami N, Susin SA, Ravagnan L, Marzo I, Brenner C, Kroemer G. Proteasome activation occurs at an early, premitochondrial step of thymocyte apoptosis. *J Immunol* 1998; **161**: 35-40

22 **Grimm LM**, Goldberg AL, Poirier GG, Schwartz LM, Osborne BA. Proteasomes play an essential role in thymocyte apoptosis. *EMBO J* 1996; **15**: 3835-3844

23 **Schwartz AL**, Ciechanover A. The ubiquitin-proteasome pathway and pathogenesis of human diseases. *Annu Rev Med* 1999; **50**: 57-74

24 **Wagenknecht B**, Hermisson M, Groscurth P, Liston P, Krammer PH, Weller M. Proteasome inhibitor-induced apoptosis of glioma cells involves the processing of multiple caspases and cytochrome c release. *J Neurochem* 2000; **75**: 2288-2297

25 **Qiu JH**, Asai A, Chi S, Saito N, Hamada H, Kirino T. Proteasome inhibitors induce cytochrome c-caspase-3-like protease-mediated apoptosis in cultured cortical neurons. *J Neurosci* 2000; **20**: 259-265

26 **Lee DH**, Goldberg AL. Proteasome inhibitors cause induction of heat shock proteins and trehalose, which together confer thermotolerance in Saccharomyces cerevisiae. *Mol Cell Biol* 1998; **18**: 30-38

27 **Milligan SA**, Nopajaroonsri C. Inhibition of NF-kappa B with proteasome inhibitors enhances apoptosis in human lung adenocarcinoma cells *in vitro*. *Anticancer Res* 2001; **21**: 39-44

28 **Watanabe K**, Kubota M, Hamahata K, Lin Y, Usami I. Prevention of etoposide-induced apoptosis by proteasome inhibitors in a human leukemic cell line but not in fresh acute leukemia blasts. A differential role of NF-kappab activation. *Biochem Pharmacol* 2000; **60**: 823-830

29 **Benbrook D**, Lernhardt E, Pfahl M. A new retinoic acid receptor identified from a hepatocellular carcinoma. *Nature* 1988; **333**: 669-672

30 **Brand N**, Petkovich M, Krust A, Chambon P, de The H, Marchio A, Tiollais P, Dejean A. Identification of a second human retinoic acid receptor. *Nature* 1988; **332**: 850-853

31 **Leid M**, Kastner P, Lyons R, Nakshatri H, Saunders M, Zacharewski T, Chen JY, Staub A, Garnier JM, Mader S, Chambon P. Purification, cloning, and RXR identity of the HeLa cell factor with which RAR or TR heterodimerizes to bind target sequences efficiently. *Cell* 1992; **68**: 377-395

32 **Mangelsdorf DJ**, Ong ES, Dyck JA, Evans RM. Nuclear receptor that identifies a novel retinoic acid response pathway. *Nature* 1990; **345**: 224-229

33 **Liu S**, Wu Q, Ye XF, Cai JH, Huang ZW, Su WJ. Induction of apoptosis by TPA and VP-16 is through translocation of TR3. *World J Gastroenterol* 2002; **8**: 446-450

34 **Wu Q**, Liu S, Ding L, Ye XF, Su WJ. PKCa translocation from mitochondria to nucleus is closely related to induction of apoptosis in gastric cancer cells. *Science in China* 2002; **45**: 237-245

35 **Jilek F**, Huttelova R, Petr J, Holubova M, Rozinek J. Activation of pig oocytes using calcium ionophore: effect of protein synthesis inhibitor cycloheximide. *Anim Reprod Sci* 2000; **63**: 101-111

36 **Eitel K**, Wagenknecht B, Weller M. Inhibition of drug-induced DNA fragmentation, but not cell death of glioma cells by non-caspase protease inhibitors. *Cancer Letters* 1999; **142**: 11-16

37 **Yoshida M**, Nishikawa M, Nishi K, Abe K, Horinouchi S, Beppu T. Effects of leptomycin B on the cell cycle of fibroblasts and fission yeast cells. *Exp Cell Res* 1990; **187**: 150-156

38 **Fornerod M**, Ohno M, Yoshida M, Mattaj IW. CRM1 is an export receptor for leucine-rich nuclear export signals. *Cell* 1997; **90**: 1051-1060

39 **Nigg EA**. Nucleocytoplasmic transport: signals, mechanisms and regulation. *Nature* 1997; **386**: 779-787

40 **Kaffman A**, Rank NM, O'Neill EM, Huang LS, O'Shea EK. The receptor Msn5 exports the phosphorylated transcription factor Pho4 out of the nucleus. *Nature* 1998; **396**: 482-486

41 **Ben-Levy R**, Hooper S, Wilson R, Paterson HF, Marshall CJ. Nuclear export of the stress-activated protein kinase p38 mediated by its substrate MAPKAP kinase-2. *Curr Biol* 1998; **8**: 1049-1057

42 **Jans DA**, Hubner S. Regulation of protein transport to the nucleus: central role of phosphorylation. *Physiol Rev* 1996; **76**: 651-685

43 **Pickart CM**. Ubiquitin enters the new millennium. *Mol Cell* 2001; **8**: 499-504

44 **Shenoy SK**, McDonald PH, Kohout TA, Lefkowitz RJ. Regulation of receptor fate by ubiquitination of activated beta 2-adrenergic receptor and beta-arrestin. *Science* 2001; **294**: 1307-1313

45 **Yu A**, Malek TR. The proteasome regulates receptor-mediated endocytosis of interleukin-2. *J Biol Chem* 2001; **276**: 381-385

46 **Ferdous A**, Gonzalez F, Sun L, Kodadek T, Johnston SA. The 19S regulatory particle of the proteasome is required for efficient transcription elongation by RNA polymerase II. *Mol Cell* 2001; **7**: 981-991

47 **Gillette TG**, Huang W, Russell SJ, Reed SH, Johnston SA, Friedberg EC. The 19S complex of the proteasome regulates nucleotide excision repair in yeast. *Genes Dev* 2001; **15**: 1528-1539

48 **Lommel L**, Chen L, Madura K, Sweder K.The 26S proteasome negatively regulates the level of overall genomic nucleotide excision repair. *Nucleic Acids Res* 2000; **28**: 4839-4845

49 **Kopf E**, Plassat JL, Vivat V, de The H, Chambon P, Rochette-Egly C. Dimerization with retinoid X receptors and phosphorylation modulate the retinoic acid-induced degradation of retinoic acid receptors alpha and gamma through the ubiquitin-proteasome pathway. *J Biol Chem* 2000; **275**: 33280-33288

50 **Wu Q**, Li Y, Liu R, Agadir A, Lee MO, Liu Y, Zhang X. Modulation of retinoic acid sensitivity in lung cancer cells through dynamic balance of orphan receptors nur77 and COUP-TF and their heterodimerization. *EMBO J* 1997; **16**: 1656-1669

Edited by Ma JY

P.O.Box 2345, Beijing 100023,China
Fax: +86-10-85381893
E-mail: wjg@wjgnet.com www.wjgnet.com

World J Gastroenterol 2003;9(9):1920-1924
World Journal of Gastroenterology
 ISSN 1007-9327

• GASTRIC CANCER •

Screening and identification of mimotope of gastric cancer associated antigen MGb1-Ag

Zhe-Yi Han, Kai-Chun Wu, Feng-Tian He, Quan-Li Han, Yong-Zhan Nie, Ying Han, Xiao-Nan Liu, Jian-Yong Zheng, Mei-Hong Xu, Tao Lin, Dai-Ming Fan

Zhe-Yi Han, Kai-Chun Wu, Quan-Li Han, Yong-Zhan Nie, Ying Han, Dai-Ming Fan, Institute of Digestive Diseases, Xijing Hospital, Fourth Military Medical University, Xi'an 710033, Shaanxi Province, China
Feng-Tian He, Department of Biochemistry, Third Military Medical University, Chongqing, 400038, China
Xiao-Nan Liu, Jian-Yong Zheng, Department of Surgery, Xijing Hospital, Fourth Military Medical University, Xi'an 710033, Shaanxi Province, China
Mei-Hong Xu, Department of Gerontology, 323 Hospital of PLA, Xi' an 710054, Shaanxi Province, China
Tao Lin, Department of Gastroenterology, 451 Hospital of PLA, Xi' an 710054, Shaanxi Province, China
Supported by the National High Technology Research and Development Program (863 Program) of China, No. 2001AA215421
Correspondence to: Dr. Kai-Chun Wu, Institute of Digestive Diseases, Xijing Hospital, Fourth Military Medical University, Xi' an 710032, Shaanxi Province, China. kaicwu@fmmu.edu.cn
Telephone: +86-29-3375229 **Fax:** +86-29-2539041
Received: 2002-10-17 **Accepted:** 2002-11-16

Abstract

AIM: Using a monoclonal antibody against gastric cancer antigen named MGb1 to screen a phage-displayed random peptide library fused with coat protein pIII in order to get some information on mimotopes.

METHODS: Through affinity enrichment and ELISA screening, positive clones of phages were amplified. 10 phage clones were selected after three rounds of biopanning and the ability of specific binding of the positive phage clones to MGb1-Ab were detected by ELISA assay (DNA sequencing was performed and the amino acid sequences were deduced) By blocking test, specificity of the mimic phage epitopes was identified.

RESULTS: There were approximately 200 times of enrichment about the titer of bound phages after three rounds of biopanning procedures. DNA of 10 phage clones after the third biopanning was assayed and the result showed that the positive clones had a specific binding activity to MGb1-Ab and a weak ability of binding to control mAb or to mouse IgG. DNA sequencing of 10 phage clones was performed and the amino acid sequences were deduced. According to the homology of the amino acid sequences of the displayed peptides, most of the phage clones had motifs of H(x)Q or L(x)S. And these 10 phage clones could also partly inhibit the binding of MGb1-Ab to gastric cancer cell KATO-III. The percentage of blocking was from (21.0±1.6) % to (39.0±2.7) %.

CONCLUSION: Motifs of H(x)Q and L(x)S selected and identified show a high homology in the mimic epitopes of gastric cancer associated antigen. There may be one or more clones which can act as candidates of tumor vaccines.

Han ZY, Wu KC, He FT, Han QL, Nie YZ, Han Y, Liu XN, Zheng JY, Xu MH, Lin T, Fan DM. Screening and identification of mimotope of gastric cancer associated antigen MGb1-Ag. *World J Gastroenterol* 2003; 9(9): 1920-1924
http://www.wjgnet.com/1007-9327/9/1920.asp

INTRODUCTION

Filamentous bacteriophages have been used extensively in recent years for the display large repertoires of peptides on their surface[1-3]. These peptides can be expressed by cloning random oligonucleotides at the end of the genes encoding the phage coat proteins[4]. Phage display system has many advantages such as efficacy of biopanning, ability of amplification and linkage of the displayed peptide with its encoding DNA sequence within the phage particle, enabling quick and simple elucidation of binding sequences. Numerous papers have shown that this approach is successful with an extraordinarily wide range of protein targets, such as structural proteins, signal transduction proteins, receptors, serum proteins, oncoproteins and so on. It is also possible to select phage display peptides that mimic the original characteristics of antigen binding to specific antibodies without previous knowledge of the antigen structure[5-9]. In this respect, phage display technology has been well established as an important experimental approach in the development of novel vaccines and drugs. Antigens and epitopes play important roles in immune responses to tumors. To select the possible mimotopes of gastric cancer, a random phage display peptide library constructed on pIII was screened by biopanning with MGb1-Ab, a monoclonal antibody against gastric cancer, as a selective molecule.

MATERIALS AND METHODS

Materials

Monoclonal antibody The hybridoma cell line which secretes mouse mAb MGb1 (its immunoglobulin type is IgG) against gastric carcinoma -associated antigens was established by our laboratory. This hybridoma was prepared by taking human gastric carcinoma cell line KATOIII as antigen, and the immunized mouse spleen cells were fused with SP2/0 according to routine procedures for mAb preparation[10-15]. The mAb in ascitic fluid was prepared by intraperitoneal injection of hybridoma cells into Balb/c mouse and collected at the aseptic environment. Then the mAb was purified by saturated ammonium sulfate precipitation and DEAE-52 anion exchange chromatography[16,17].

Random peptide library and bacteria The library used was purchased from New England Biolabs Company, containing approximately 2.8×10^9 different phage clones, which composed of the genome of the filamentous phage. The phages in this library were engineered to express a recombinant form of gene III containing a degenerated DNA insert encoding random 7-mer peptide. The recombinant gene III was under the control of LacZ promoter. And all the sub-major coat proteins pIII were recombinants. The ER2537 strain of *E.coli*

was used for culture of phage. Bacteria were cultured in LB medium without any antibiotics.

Methods

Amplification of phages Infections were carried out by incubating phages for 10-15 min at room temperature with ER2537 at the number ratio of 3-5:1(bacteria: phages). And the bacteria were cultured for another 4.5 h at 37 ℃. The supernatants from the culture where phages existed were collected. The culture supernatants of infected bacteria were collected, where bacteria secreted phages. The solution of 200 g· L^{-1} PEG 2.5 mol· L^{-1} NaCl was added into the supernatant at the volume ratio to supernatant of 1:5. And the mixture was incubated for 1 h at 4 ℃. After centrifuged at 10 000 g, the precipitated phages were pelleted, and then resuspended in Tris-buffered saline (TBS). The protocols of PEG precipitation were repeated. Phages from a culture supernatant volume of 5 mL were usually resuspended in a final volume of 150 μL TBS. The titer of the phages was then assayed.

Assay of phage titer The prepared phages were 10-fold serial diluted in LB with the suggested dilution ranges: 10^8-10^{11} for amplified phage culture supernatants and10^1-10^4 for unamplified biopanning eluates. A single colony of ER2537 in 5 mL LB was cultured with shaking until mid-log phase. 200 μL of bacteria culture reached mid-log phase was dispensed into microfuge tubes and then 10 μL of diluted phages per tube was vortexed quickly and incubated at room temperature for 1-5 min. Bacteria infected with phages were transfered to a culture tube containing 3 mL 45 ℃ LB/agarose at the top and immediately poured onto a pre-warmed LB/IPTG/X-gal plate and spread evenly after vortexed. Plates were cooled for 5 min, inverted and incubated overnight at 37 ℃. Plaques on plates were counted.

Biopanning Three rounds of biopanning were carried out with mAb-MGb1. During the first round, a ELISA well was used as the solid phage. It was coated by incubating overnight with aliquots of mAb (100 mg· L^{-1}) in the coating buffer (carbonate-bicarbonate buffer, pH9.6) at 4 ℃ in a humid atmosphere, then washed with TBS for 6 times, blocked in TBS-10 g· L^{-1} BSA. One aliquot of the library containing 2×10^{11} pfu phages in 100 μL TBS-0.5 g· L^{-1} BSA was added to the mAb coated well, incubated for 1 h at 37 ℃. Unbound phages were removed and the well was washed 6 times with TBS-1 g· L^{-1} Tween-20. Eluting buffer (0.2 mol· L^{-1} glycine with its pH adjusted to 2.2 by HCl) was added for 10 min, then removed and neutralized by adding of Tris-HCl (pH 9.0). Phages eluted from each round were used to infect exponential phase ER2537. After cultured for 4.5 h, phages in the supernatant were precipitated by PEG. The second and third rounds of biopanning were followed as described above except that unbound phages were washed 20 times with TBS-0.5 % Tween-20. After neutralization in the third round of biopanning, the eluted phages were planted on the LB medium directly and cultured overnight at 37 ℃.

ELISA to identify positive phage clones ELISA was carried out as routine procedures[18-26]. ELISA wells were coated by incubating overnight with mAb-MGb1 (100 mg· L^{-1}) in the coating buffer (carbonate-bicarbonate buffer, pH9.6) at 4 ℃ in a humid atmosphere, washed 6 times with TBS, blocked with TBS-50 g· L^{-1} BSA. Single clone of phage expressing the recombinant form of gene III containing the peptide insert was incubated in LB for 4.5 h. The coated wells were incubated for 1h at 37 ℃ with supernatant from such cultures and then the horseradish peroxidase (HRP) labeled mouse-anti-M13 antibody diluted to a volume ratio of 1:5 000 in blocking buffer was added. TMB was used as a substrate for HRP and the absorbance of each well was read at 450 nm.

Extraction of single strand DNA of phages and DNA sequencing Single strand DNA was prepared from 1.5 mL overnight cultures by extraction and purification by using a single strand of M13 extraction and purification kit (Huashun Bio. Com., China). The culture supernatant of infected bacteria containing phages at the volume of 1.2 mL was transferred to sterile 1.5 mL Eppendorf tubes. 200 μL precipitate buffer was added. The mixture was cooled on ice for 15 min. After centrifugation for 5 min at 10 000 g, the supernatant was discarded and the precipitate was preserved for DNA extraction. Phages were lysed in 500 μL lysis buffer for 2 min at room temperature. The product was transfered to a column containing resin that could absorb DNA. After centrifugation for 15 s, DNA absorbed in resin was washed twice with ethanol and eluted with 20 μL Tris buffer. Single strand DNA of phages was extracted and 5 μL of product was run on a 10 g· L^{-1} agarose gel in 1×TAE. DNA bands were detected by ethidium bromide staining and visualized by UV light photography. Sequencing procedures were carried out by using a auto-sequence apparatus ABI PRISMTM310 (PE Com. U.S.A.). 100 ng of such single strand DNA was used as a template. The oligonucleotide 5' -CCC TCA TAG TTA GCG TAA CG-3' , complementary to the genomic DNA of the phage and the downstream of the insert, was used as a primer.

Blocking test ELISA wells were coated with KATOIII (1×10^5 cells per well), washed 6 times with PBS, blocked for 2 h. MAb MGb1 was mixed with 1×10^{10} pfu individual phages for 1 h at 37 ℃ and then the mixture was added into the KATOIII coated wells, incubated for another 1 h. The HRP labeled goat-anti-mouse IgG diluted to a volume ratio of 1:5 000 in the blocking buffer was added then. TMB was used as a substrate for HRP and the absorbance of each well was read at 450 nm[27].

RESULTS

Biopanning

The ratios of output/input phages in three biopanning rounds are listed in Table 1. The ratio of the last round was about 100 times higher than that of the first round. It indicated that the specific phages were enriched.

Table 1 Yields of washed phages

Round	Input phages(pfu)	Output phages(pfu)	Yields/%
1	2.0×10^{11}	5.8×10^{4}	2.9×10^{-5}
2	2.0×10^{11}	3.2×10^{5}	1.6×10^{-4}
3	2.0×10^{11}	4.0×10^{6}	2.0×10^{-3}

Selection of phage clones

MGb1 mAb with specificity to gastric carcinoma was used to screen the library of phages containing random 7-mer peptide inserts. After three rounds of biopanning, some individual phage clones were isolated and screened by ELISA to identify those of interests which bound strongly to the antibody, and 10 clones of them which gave a clear positive signal and had the highest absorbance at 450 nm were selected.

Detection of antigenic specificity of the final-eluted phage by sandwich ELISA

MGb1 mAb was immobilized on the ELISA wells in which the selected phage clones were added. HRP labeled anti-M13 mAb was then used to detect the captured phages. As negative control, anti-endotoxin mAb and mouse IgG were used to replace the coating and the binding antibodies. The results revealed that the selected phages could react to mAb MGb1 specifically, and had weak ability of binding to unrelated antibodies such as anti-endotoxin mAb and mouse IgG (Figure 1).

Extraction of single strand DNA of phages

The length of all phage clones was the same as M13 single strand DNA marker, which indicated that single strand DNA of phages was prepared well and there were no other kinds of phages contaminated (Figure 2).

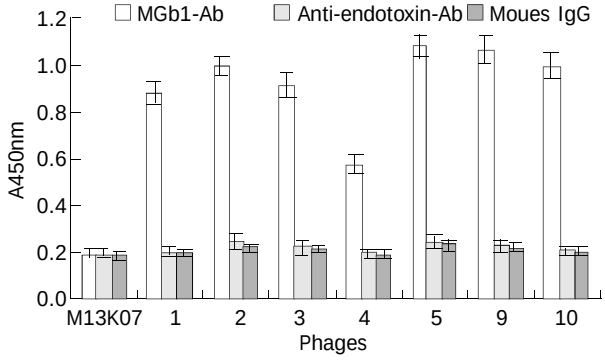

Figure 1 Binding of phages to MGb1-Ab by ELISA at the third round.

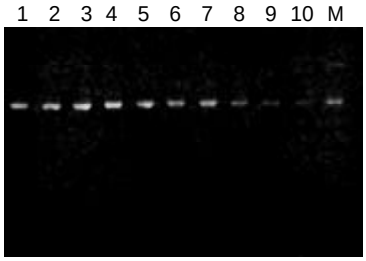

Figure 2 Electrophoresis of single strand DNA of phage clones (lanes1-10: Single strand DNA of phage clones; lane M: M13 single strand DNA marker).

Identification of motifs amongst the sequences of phage clone inserts

The selected 10 clones were sequenced and motifs could be identified amongst the deduced amino sequences of phage clone inserts for mAb MGb1. According to the homology of amino acid sequences of the displayed peptides, some preserved mimotope information was obtained. Most phage clones had motifs of H(x)Q and L(x)S (Figure 3).

K 5: VP**Q**QKFR
K 7: VP**Q**QKFR
K 2: **H**S**Q** IS **S** Y
K10: QPT**HQL**T
K1: Q**HQL**P**S**D
K3: S**L**L**S**TPQ
K6: S**L**L**S**TPQ
K8: S**L**L**S**TPQ
K9: LRPTL**S**C
K4: LPMRPIV

Figure 3 Amino acid sequences of inserts in phage clones.

Blocking test

If the selected clones contained epitopes or mimotopes of the native antigen, then they should be presented to block the binding of mAb MGb1 to gastric cancer cell-line KATOIII. To test this hypothesis, 7 of representative phage clones were used in a blocking test. Wild-type phage M13 was used as a negative control (whose absorbance at 450 nm was represented by *B*) to ensure that blocking of binding of the mAb to gastric cancer cell-line KATOIII was due to the phage insert (whose absorbance at 450 nm was represented by *A*) rather than the mere physical presence of phages. The blocking percentage of each phage was (25.6±1.3) %, (34.6±2.5) %, (32.6±1.8) %, (21.0±1.6) %, (39.0±2.7) %, (36.3±3.2) %, (29.5±1.9) %, respectively (Figure 4), compared with wells to which no phage was added (whose absorbance at 450 nm was represented by *C*), which was calculated using the formula: blocking %=[(*C*-*B*)-(*C*-*A*)]/*A*×100 %.

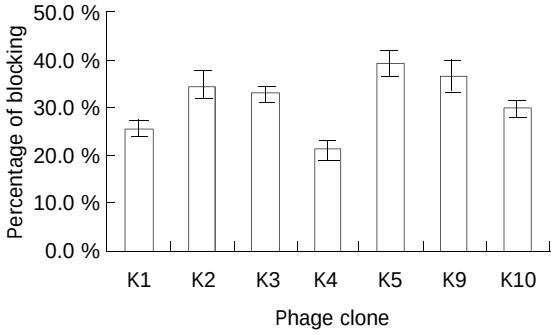

Figure 4 The blocking percentage of phage display peptides to MGb1-Ag by ELISA.

DISCUSSION

Gastric cancer is one kind of malignant tumors with complicated mechanism and is the leading cause of death in China[27-51]. Biotherapy is a new way for human to combat gastric cancer[52-63]. Tumor antigens play important roles in the induction of immune responses[64-66], which are predominantly focused on specific antigenic sites, known as epitopes. Identification of B-cell epitopes can be used to design peptide vaccines against tumor and is actively pursued in many laboratories. Since antibodies recognize B-cell epitopes that are mainly located on the surface of molecules, the native conformation of the antigen is a critical parameter for this interaction to occur. Early studies on the antigenicity of globular proteins suggested that antibodies recognized amino acids which either constituted a short linear stretch along the polypeptide chain (continuous or linear B-cell epitopes), or were brought together by the juxtaposition of the polypeptide chains when the protein was in its native conformation (discontinuous or conformational B-cell epitopes)[67].

Considerable attention has been paid to the difficulties in identifying the structural characteristics of B-cell epitopes. A number of empirical approaches have been employed to predict B-cell epitopes from the primary amino acid sequence of the protein including identification of regions of hydrophilicity, solvent accessibility, protrusion, atomic mobility and secondary structures. But many of them identify linear B-cell epitopes instead of discontinuous epitopes. B-cell epitopes are entities that can be defined only by their mutual complementarity. Phage display random peptide library offers a convenient way to select phage display peptides that mimic the original characteristics of antigen binding to specific antibodies[68,69]. One of the advantages of screening random peptide libraries to identify B-cell epitopes is that there is no need to know the amino acid sequence of the protein against which the antibody has been elicited. Since peptide libraries provide a rich source of mimic antigens, identification of B-cell epitopes has been greatly simplified.

In the present study, to select the possible mimotopes of gastric cancer, a random phage display peptide library constructed on pIII was screened by biopanning using MGb1-Ab as a selective molecule. After three biopanning procedures, there was a remarkable enrichment in the titer of bound phages.

Then, 10 phage clones were selected from the third biopanning and ELISA. Their single strand DNA was sequenced and the amino acid sequences were deduced. According to the homology of amino acid sequences of the displayed peptides, some preserved epitope information was obtained. Most phage clones had motifs of H(X)Q or L(X)S. The results of ELISA showed that the positive phage clones had a specific binding activity with MGb1-Ab and could inhibit the binding of MGb1-Ab to gastric cancer cell line KATO-III.

Since the binding site of an antibody is not unique for a single antigen, several mimotopes with different amino acid sequences can be recognized by binding to different subsites within the binding site[70-72]. To date, little is known about the structure and amino acid sequence of parental antigen MGb1, so we can not tell the exact characteristics of the peptides selected from the 7-mer random peptide library. Research should be done to further characterize the mimotopes recognized by mAb MGb1.

REFERENCES

1 **Li R**, Hoess RH, Bennett JS, DeGrado WF. Use of phage display to probe the evolution of binding specificity and affinity in integrins. *Protein Eng* 2003; **16**: 65-72
2 **Korpimaki T**, Rosenberg J, Virtanen P, Lamminmaki U, Tuomola M, Saviranta P. Further improvement of broad specificity hapten recognition with protein engineering. *Protein Eng* 2003; **16**: 37-46
3 **Hsiao KC**, Brissette RE, Wang P, Fletcher PW, Rodriguez V, Lennick M, Blume AJ, Goldstein NI. Peptides identify multiple hotspots within the ligand binding domain of the TNF receptor 2. *Proteome Sci* 2003; **1**: 1
4 **Willats WG**. Phage display: practicalities and prospects. *Plant Mol Biol* 2002; **50**: 837-854
5 **Perlman H**, Bradley K, Liu H, Cole S, Shamiyeh E, Smith RC, Walsh K, Fiore S, Koch AE, Firestein GS, Haines GK 3rd, Pope RM. IL-6 and matrix metalloproteinase-1 are regulated by the cyclin-dependent kinase inhibitor p21 in synovial fibroblasts. *J Immunol* 2003; **170**: 838-845
6 **Baker AH**. Development and use of gene transfer for treatment of cardiovascular disease. *J Card Surg* 2002; **17**: 543-548
7 **Naik RR**, Stringer SJ, Agarwal G, Jones SE, Stone MO. Biomimetic synthesis and patterning of silver nanoparticles. *Nat Mater* 2002; **1**: 169-172
8 **Pichurin PN**, Guo J, Estienne V, Carayon P, Ruf J, Rapoport B, McLachlan SM. Evidence that the complement control protein-epidermal growth factor-like domain of thyroid peroxidase lies on the fringe of the immunodominant region recognized by autoantibodies. *Thyroid* 2002; **12**: 1085-1095
9 **Taylor PC**. Anti-TNFalpha therapy for rheumatoid arthritis: an update. *Intern Med* 2003; **42**: 15-20
10 **Yang LJ**, Wang WL. Preparation of monoclonal antibody against apoptosis-associated antigens of hepatoma cells by subtractive immunization. *World J Gastroenterol* 2002; **8**: 808-814
11 **Ji Y**, Ling MY, Li Y, Xie H. Effect of cell fusion on metastatic ability of mouse hepatocarcinoma cell lines. *World J Gastroenterol* 1999; **5**: 22-24
12 **Liu JW**, Li KZ. Pancreatic cancer, oncogene and anti oncogene. *Shijie Huaren Xiaohua Zazhi* 2001; **9**: 72-73
13 **Xu HY**, Song JD. Application of TAA-LEA in the diagnosis of precancer and early stage cancer of colon. *Shijie Huaren Xiaohua Zazhi* 1999; **7**: 992
14 **Shi YQ**, Xiao B, Miao JY, Li MF, Qiao TD, Chen BJ, Chen Z, Han JL, Zhou SJ, Fan DM. A novel cDNA fragment associated with gastric cancer drug resistance screened from a library by mAb MGr1. *Huaren Xiaohua Zazhi* 1998; **6**: 656-659
15 **Chen ZN**, Bian HJ, Jiang JL. Kecent progress in anti-hepatoma monoclonal antibody and its application. *Huaren Xiaohua Zazhi* 1998; **6**: 461-462
16 **Si XH**, Yang LJ. Extraction and purification of TGFbeta and its effect on the induction of apoptosis of hepatocytes. *World J Gastroenterol* 2001; **7**: 527-531
17 **Sun K**, Jin BQ, Feng Q, Zhu Y, Yang K, Liu XS, Dong BQ. Identification of CD226 ligand on colo205 cell surface. *World J Gastroenterol* 2002; **8**: 1008-1013
18 **Zheng PY**, Hua J, Ng HC, Yeoh KG, Bow H. Expression of Lewis (b) blood group antigen in *Helicobacter pylori* does not interfere with bacterial adhesion property. *World J Gastroenterol* 2003; **9**: 122-124
19 **Du DW**, Jia ZS, Li GY, Zhou YY. HBV DNA vaccine with adjuvant cytokines induced specific immune responses against HBV infection. *World J Gastroenterol* 2003; **9**: 108-111
20 **Tang NH**, Chen YL, Wang XQ, Li XJ, Yin FZ, Wang XZ. Construction of IL-2 gene-modified human hepatocyte and its cultivation with microcarrier. *World J Gastroenterol* 2003; **9**: 79-83
21 **Shi M**, Wang FS, Wu ZZ. Synergetic anticancer effect of combined quercetin and recombinant adenoviral vector expressing human wild-type p53, GM-CSF and B7-1 genes on hepatocellular carcinoma cells *in vitro*. *World J Gastroenterol* 2003; **9**: 73-78
22 **Wang KX**, Li CP, Wang J, Tian Y. Cyclospore cayetanensis in Anhui, China. *World J Gastroenterol* 2002; **8**: 1144-1148
23 **Zhao CY**, Liu JX, Tang HH, Feng ZJ, Zhen Z, Zhang SH. Significance of IL-2 and related indexes in patients with hepatitis and hepatocellular carcinoma. *Huaren Xiaohua Zazhi* 1998; **6**: 479-481
24 **Ren JM**, Zou QM, Wang FK, He Q, Chen W, Zen WK. PELA microspheres loaded *H pylori* lysates and their mucosal immune response. *World J Gastroenterol* 2002; **8**: 1098-1102
25 **Jiao XY**, Shi JS, Ren H, Chen WK, Pan ML, Chang DM, He JJ, Hao XY, Zhou LS, Han Y. Effects of radical cholecystectomy on nutritional and immune status of patients with gallbladder carcinoma. *Shijie Huaren Xiaohua Zazhi* 1999; **7**: 394-396
26 **Wu YD**, Song XQ, Zhou DN, Hu XH, Gan YQ, Li ZG, Liao P. Expermental and clinical study on targeting treatment of liver cancer using radionuclide anti AFP antibody MMC double bomb. *Shijie Huaren Xiaohua Zazhi* 1999; **7**: 387-390
27 **Liu HJ**, Guo XL, Dong M, Wang L, Yuan Y. Association between pepsinogen C gene polymorphism and genetic predisposition to gastric cancer. *World J Gastroenterol* 2003; **9**: 50-53
28 **Yin T**, Ji XL, Shen MS. Relationship between lymph node sinuses with blood and lymphatic metastasis of gastric cancer. *World J Gastroenterol* 2003; **9**: 40-43
29 **Xin Y**, Zhao FK, Zhang SM, Wu DY, Wang YP, Xu L. Relationship between CD44v6 expression and prognosis in gastric carcinoma patients. *Shijie Huaren Xiaohua Zazhi* 1999; **7**: 210-214
30 **Liu HF**, Liu WW, Fang DC, Men RF, Wang ZH. Apoptosis and its relationship with Fas ligand expression in gastric carcinoma and its precancerous lesion. *Shijie Huaren Xiaohua Zazhi* 1999; **7**: 561-563
31 **Cui DX**, Yan XJ, Zhang L, Zhao JR, Jiang M, Guo YH, Zhang LX, Bai XP, Su CZ. Screening and its clinical significance of 6 fragments of highly expressing genes in gastric cancer and precancerous mucosa. *Shijie Huaren Xiaohua Zazhi* 1999; **7**: 770-772
32 **Yang L**, Kuang LG, Zheng HC, Li JY, Wu DY, Zhang SM, Xin Y. PTEN encoding product: a marker for tumorigenesis and progression of gastric carcinoma. *World J Gastroenterol* 2003; **9**: 35-39
33 **Wang GS**, Wang MW, Wu BY, You WD, Yang XY. A novel gene, GCRG224, is differentially expressed in human gastric mucosa. *World J Gastroenterol* 2003; **9**: 30-34
34 **Wang RT**, Wang T, Chen K, Wang JY, Zhang JP, Lin SR, Zhu YM, Zhang WM, Cao YX, Zhu CW, Yu H, Cong YJ, Zheng S, Wu BQ. *Helicobacter pylori* infection and gastric cancer: evidence from a retrospective cohort study and nested case-control study in China. *World J Gastroenterol* 2002; **8**: 1103-1107
35 **Hu JK**, Chen ZX, Zhou ZG, Zhang B, Tian J, Chen JP, Wang L, Wang CH, Chen HY, Li YP. Intravenous chemotherapy for resected gastric cancer: meta-analysis of randomized controlled trials. *World J Gastroenterol* 2002; **8**: 1023-1028
36 **Fu QG**, Meng FD, Shen XD, Guo RX. Efficacy of intraperitoneal thermochemotherapy and immunotherapy in intraperitoneal recurrence after gastrointestinal cancer resection. *World J Gastroenterol* 2002; **8**: 1019-1022
37 **Chen Y**, Wu Q, Song SY, Su WJ. Activation of JNK by TPA promotes apoptosis via PKC pathway in gastric cancer cells. *World J Gastroenterol* 2002; **8**: 1014-1018
38 **Guo DL**, Dong M, Wang L, Sun LP, Yuan Y. Expression of gastric cancer-associated MG7 antigen in gastric cancer, precancerous lesions and *H pylori*-associated gastric diseases. *World J Gastroenterol* 2002; **8**: 1009-1013

39 **Zhang FX**, Deng ZY, Zhang XY, Kang SC, Wang Y, Yu XL, Wang H, Bian XH. Telomeric length associated with prognosis in human primary and metastatic gastric cancer. *Shijie Huaren Xiaohua Zazhi* 2000; **8**: 153-155

40 **Zhou LY**, Chen CY, Liang P, Chen LY. ICAM-1 and VCAM-1 expressions on benign gastric mucosa and gastric adenocarcinoma associated with Helicobacter pylori infection. *Shijie Huaren Xiaohua Zazhi* 2000; **8**: 279-281

41 **Liu HF**, Liu WW, Fang DC, Yang SM, Wang RQ. Bax gene expression and its relationship with apoptosis in human gastric carcinoma and precancerous lesions. *Shijie Huaren Xiaohua Zazhi* 2000; **8**: 665-668

42 **Wang B**, Shi LC, Zhang WB, Xiao CM, Wu JF, Dong YM. Expression and significance of p16 gene in gastric cancer and its precancerous lesions. *Shijie Huaren Xiaohua Zazhi* 2001; **9**: 39-42

43 **Ning XX**, Wu KC, Shi YQ, Wang X, Zhao YQ, Fan DM. Construction and expression of gastric cancer MG7 mimic epitope fused to heat shock protein 70. *Shijie Huaren Xiaohua Zazhi* 2001; **9**: 892-896

44 **Jiang YA**, Zhang YY, Luo HS, Xing SF. Mast cell density and the context of clinicopathological parameters and expression of p185, estrogen receptor, and proliferating cell nuclear antigen in gastric carcinoma. *World J Gastroenterol* 2002; **8**: 1005-1008

45 **Liu JR**, Chen BQ, Yang YM, Wang XL, Xue YB, Zheng YM, Liu RH. Effect of apoptosis on gastric adenocarcinoma cell line SGC-7901 induced by cis-9, trans-11-conjugated linoleic acid. *World J Gastroenterol* 2002; **8**: 999-1004

46 **Zhang H**, Wu J, Meng L, Shou CC. Expression of vascular endothelial growth factor and its receptors KDR and Flt-1 in gastric cancer cells. *World J Gastroenterol* 2002; **8**: 994-998

47 **Zhou YN**, Xu CP, Han B, Li M, Qiao L, Fang DC, Yang JM. Expression of E-cadherin and catenin in gastric carcinoma and its correlation with the clinicopathological features and patient survival. *World J Gastroenterol* 2002; **8**: 987-993

48 **Wu K**, Li Y, Zhao Y, Shan YJ, Xia W, Yu WP, Zhao L. Roles of Fas signaling pathway in vitamin E succinate-induced apoptosis in human gastric cancer SGC-7901 cells. *World J Gastroenterol* 2002; **8**: 982-986

49 **Zhao AG**, Zhao HL, Jin XJ, Yang JK, Tang LD. Effects of Chinese Jianpi herbs on cell apoptosis and related gene expression in human gastric cancer grafted onto nude mice. *World J Gastroenterol* 2002; **8**: 792-796

50 **Fang DC**, Luo YH, Yang SM, Li XA, Ling XL, Fang L. Mutation analysis of APC gene in gastric cancer with microsatellite instability. *World J Gastroenterol* 2002; **8**: 787-791

51 **Zhao Y**, Wu K, Xia W, Shan YJ, Wu LJ, Yu WP. The effects of vitamin E succinate on the expression of c-jun gene and protein in human gastric cancer SGC-7901 cells. *World J Gastroenterol* 2002; **8**: 782-786

52 **Li N**, Xu CP, Song B, Liu WW, Wang X, Zhang CS, Xu YJ, Feng DX. Studies on the anti invasive character of TIMP2 gene transfected gastric carcinoma cells. *Huaren Xiaohua Zazhi* 1998; **6**: 663-666

53 **Xiao B**, Shi YQ, Zhao YQ, You H, Wang ZY, Liu XL, Yin F, Qiao TD, Fan DM. Transduction of fas gene or bcl-2 antisense RNA sensitizes cultured drug resistant gastric cancer cells to chemotherapeutic drugs. *Huaren Xiaohua Zazhi* 1998; **6**: 675-679

54 **Shi YQ**, Xiao B, Miao JY, Zhao YQ, You H, Fan DM. Construction of eukaryotic expression vector pBK fas and MDR reversal test of drug resistant gastric cancer cells. *Shijie Huaren Xiaohua Zazhi* 1999; **7**: 309-312

55 **Pan X**, Ke CW, Pan W, He X, Cao GW, Qi ZT. Killing effect of DT / VEGF system on gastric carcinoma cell. *Shijie Huaren Xiaohua Zazhi* 2000; **8**: 393-396

56 **Guo JC**, Li JC, Fan DM, Qiao TD, Zhang XY. Regulation of HSP70 expression in human gastric cancer cell line SGC7901 by gene transfection. *Shijie Huaren Xiaohua Zazhi* 1999; **7**: 773-776

57 **Luo ZB**, Luo YH, Lu R, Jin HY, Zhang BP, Xu CP. Immunohistochemical study on dendritic cells in gastric mucosa of patients with gastric cancer and precancerous lesions. *Shijie Huaren Xiaohua Zazhi* 2000; **8**: 400-402

58 **Guo SY**, Gu QL, Liu BY, Zhu ZG, Yin HR, Lin YZ. Experimental study on the treatment of gastric cancer by TK gene combined with mIL-2 gene. *Shijie Huaren Xiaohua Zazh*i 2000; **8**: 974-978

59 **Liu DH**, Zhang W, Su YP, Zhang XY, Huang YX. Constructions of eukaryotic expression vector of sense and antisense VEGF-165 and its expression regulation. *Shijie Huaren Xiaohua Zazhi* 2001; **9**: 886-891

60 **Xiao B**, Shi YQ, Zhao YQ, You H, Wang ZY, Liu XL, Yin F, Qiao TD, Fan DM. Transduction of Fas gene or Bcl-2 antisense RNA sensitizes cultured drug resistant gastric cancer cells to chemotherapeutic drugs. *World J Gastroenterol* 1998; **4**: 421-425

61 **Chen B**, Zhang XY, Zhang YJ, Zhou P, Gu Y, Fan DM. Antisense to cyclin D1 reverses the transformed phenotype of human gastric cancer cells. *World J Gastroenterol* 1999; **5**: 18-21

62 **Zhang FX**, Zhang XY, Fan DM, Deng ZY, Yan Y, Wu HP, Fan JJ. Antisense telomerase RNA induced human gastric cancer cell apoptosis. *World J Gastroenterol* 2000; **6**: 430-432

63 **Yin F**, Shi YQ, Zhao WP, Xiao B, Miao JY, Fan DM. Suppression of P gp induced multiple drug resistance in a drug resistant gastric cancer cell line by overexpression of Fas. *World J Gastroenterol* 2000; **6**: 664-670

64 **Xiao LF**, Luo LQ, Zou Y, Huang SL. Study of the phenotype of PBLs activated by CD28 / CD80 and CD2 / CD58 and acting with hepatoma cells and the restricted usage of TCR Vβ gene subfamily. *Shijie Huaren Xiaohua Zazhi* 1999; **7**: 1044-1046

65 **Zheng CX**, Zhan WH, Zhao JZ, Zheng D, Wang DP, He YL, Zheng ZQ. The prognostic value of preoperative serum levels of CEA, CA19-9 and CA72-4 in patients with colorectal cancer. *World J Gastroenterol* 2001; **7**: 431-434

66 **Li XW**, Ding YQ, Cai JJ, Yang SQ, An LB, Qiao DF. Studies on mechanism of Sialy Lewis-X antigen in liver metastases of human colorectal carcinoma. *World J Gastroenterol* 2001; **7**: 425-430

67 **Messmer BT**, Sullivan JJ, Chiorazzi N, Rodman TC, Thaler DS. Two human neonatal IgM antibodies encoded by different variable-region genes bind the same linear peptide: evidence for a stereotyped repertoire of epitope recognition. *J Immunol* 1999; **162**: 2184-2192

68 **Sanderson SD**, Cheruku SR, Padmanilayam MP, Vennerstrom JL, Thiele GM, Palmatier MI, Bevins, RA. Immunization to nicotine with a peptide-based vaccine composed of a conformationally biased agonist of C5a as a molecular adjuvant. *Int Immunopharmacol* 2003; **3**: 137-146

69 **Zhang WY**, Wan Y, Li DG, Tang Y, Zhou W. A mimotope of pre-S2 region of surface antigen of viral hepatitis B screened by phage display. *Cell Res* 2001; **11**: 203-208

70 **Bracci L**, Pini A, Lozzi L, Lelli B, Battestin P, Spreafico A, Bernini A, Niccolai N, Neri P. Mimicking the nicotinic receptor binding site by a single chain Fv selected by competitive panning from a synthetic phage library. *J Neurochem* 2001; **78**: 24-31

71 **Scherf T**, Kasher R, Balass M, Fridkin M, Fuchs S, Katchalski-Katzir E. A beta -hairpin structure in a 13-mer peptide that binds alpha -bungarotoxin with high affinity and neutralizes its toxicity. *Proc Natl Acad Sci U S A* 2001; **98**: 6629-6634

72 **MacDonald NJ**, Shivers WY, Narum DL, Plum SM, Wingard JN, Fuhrmann SR, Liang H, Holland-Linn J, Chen DH, Sim BK. Endostatin binds tropomyosin. A potential modulator of the antitumor activity of endostatin. *J Biol Chem* 2001; **276**: 25190-25196

Edited by Xu XQ and Wang XL

P.O.Box 2345, Beijing 100023,China
Fax: +86-10-85381893
E-mail: wjg@wjgnet.com www.wjgnet.com

World J Gastroenterol 2003;9(9):1925-1929
World Journal of Gastroenterology
 ISSN 1007-9327

• GASTRIC CANCER •

Variations of mitochondrial D-loop region plus downstream gene 1 2S rRNA-tRNA^{phe} and gastric carcinomas

Cheng-Bo Han, Fan Li, Yu-Jie Zhao, Jia-Ming Ma, Dong-Ying Wu, Yu-Kui Zhang, Yan Xin

Cheng-Bo Han, Dong-Ying Wu, Yan Xin, Tumor Institute, First Affiliated Hospital, China Medical University, Shenyang, 110001, Liaoning Province, China
Fan Li, Department for High Ranking Officials, First Affiliated Hospital, China Medical University, Shenyang 110001, Liaoning Province, China
Yu-Jie Zhao, Jia-Ming Ma, Yu-Kui Zhang, Biochip Center, China Medical University, Shenyang 110001, Liaoning Province, China
Supported by the National Natural Science Foundation of China, No.30070845 and the Natural Science Foundation of Liaoning Province, No.2001101001
Correspondence to: Dr. Yan Xin, The Fourth Laboratory of Tumor Institute, The First Affiliated Hospital, China Medical University, Shenyang 110001, Liaoning Province, China. yxin@hotmail.com
Telephone: +86-24-23256666 Ext 6351 **Fax**: +86-24-23252377
Received: 2003-03-20 **Accepted:** 2003-04-11

Abstract

AIM: To explore the instabilities, polymorphisms and other variations of mitochondrial D-loop region and downstream gene 12S rRNA-tRNA^{phe} in gastric cancers, and to study their relationship with gastric cancer.

METHODS: Three adjacent regions (D-loop, tRNA^{phe} and 12S rRNA) were detected for instabilities, polymorphisms and other variations via PCR amplification followed by direct DNA sequencing in 22 matched gastric cancerous tissues and para-cancerous normal tissues.

RESULTS: PolyC or $(CA)_n$ instabilities were detected in 13/22(59.1 %) gastric cancers and 9/22(40.9 %) in the control (P>0.05). There existed 2/12(16.7 %) and 6/10(60 %) alterations of 12S rRNA-tRNA^{phe} in well differentiated gastric cancers and poorly differentiated ones, respectively (P<0.05). Some new variations were found, among which np 318 and np 321 C-T transitions in D-loop region were two of the five bases for H-strand replication primer. np 523 AC-deletion and np 527 C-T transition occurred at mtTF1 binding site (mtTFBS), which were associated with the transcription of downstream mitochondrial genome. Seven samples showed the np 16 182 polyC instabilities, five of which simultaneously showed np 16 189 T-C transitions.

CONCLUSION: There is no statistic significance of instabilities and polymorphisms in mitochondrial D-loop region between gastric cancerous and para-cancerous normal tissues, which suggests that the instability might relate to heredity or be dependent on aging. There is a significant correlation between differentiation degree of gastric cancer and variant frequencies of 12S rRNA-tRNA^{phe}. The poorly differentiated gastric cancers are more prone to 12S rRNA-tRNA^{phe} variations, or gastric cancers with 12S rRNA-tRNA^{phe} variations are more likely to be poorly differentiated. np 16 189 T-C transition may be one of the important reasons for polyC instability in gastric cancer.

Han CB, Li F, Zhao YJ, Ma JM, Wu DY, Zhang YK, Xin Y. Variations of mitochondrial D-loop region plus downstream gene 1 2S rRNA-tRNA^{phe} and gastric carcinomas. *World J Gastroenterol* 2003; 9 (9): 1925-1929
http://www.wjgnet.com/1007-9327/9/1925.asp

INTRODUCTION

Gastric carcinoma is one of the most common cancers in the world. The pathogenesis of gastric carcinoma is complex and multifactorial, among which environmental and biological factors (excessive nitrite salt intake and *Helicobacter pylori* infection) are important risk factors for gastric cancer, but no clear mechanism has been understood as that of colon cancer[1]. Mitochondrial DNA (mtDNA) is a 16 569-bp double stranded, closed circular molecule, which encodes polypeptides participating in oxidative phosphorylation and synthesis of ATP[2]. Compared to nuclear DNA, mtDNA is more susceptible to damage by mutagens and has a high mutant rate[3], because of the lack of protective action by histones and the limited capacity of damage repairing system as in yeast and most nuclear genomes[4]. 12S rRNA and tRNA^{phe} are downstream adjacently coding regions of mitochondrial D-loop region, and could reflect the molecular damage of mtDNA[5]. Mitochondrial D-loop region, containing H-strand origin, H-strand promoter, mtTF1 binding site and conserved sequence block, etc, are involved in the replication and transcription of mtDNA. Genetic instabilities, especially at the D-loop region which is associated with the replication error (RER) phenotype caused by disruption of the DNA mismatch repair system (MMR), are potentially involved in the maintenance of structure and function or even the expression of other mitochondrial genes, and probably also involved in the progressive stage of the disease[6,7].

MATERIALS AND METHODS

Materials

Gastric cancer and para-cancerous normal tissues were taken from the resected specimens of 22 patients with gastric cancer who underwent surgery between 1999 and 2002 in the First Affiliated Hospital of China Medical University. They were all diagnosed pathologically by HE-stained section and classified according to WHO' s histological classifications of gastric carcinoma.

Methods

DNA preparation 30 mg of cancerous tissues and matched normal tissues were homogenized using homogenizer for 30 s, and then digested in 1 ml of 10 mM Tris-HCl, 0.1 M EDTA (pH 7.4) containing 0.1 mg/ml proteinase K and 0.5 % sodium dodecyl sulfate. DNA was extracted twice with an equal volume of phenol/chloroform/isoamyl alcohol (25:24:1), then with chloroform/isoamyl alcohol (24:1) once. DNA was precipitated with 1/10 volume of 3 M sodium acetate (pH7.4) and two volumes of ethanol, and then rinsed with 70 % ethanol. The precipitated DNA was recovered in 50 μl of 10 mM Tris-HCl, 0.1 mM EDTA (pH 8.0).

PCR amplification of D-loop and 12S rRNA- tRNA^{phe} PCR amplification was carried out in a final volume of 50 μl containing 200 ng total DNA, 0.5 μM of each primer, 2.5 mM $MgCl_2$, 200 μM of each dNTP, and 2.5 U Taq DNA polymerase (TaKaRa Ex Taq™). Primers were as follows: Primer pair 1: F4-5' CACAGGTCTATCACCCTATTAACCA-3' , R1604-5' CTGGTTCGTCCAAGTGCA-3' ; Primer pair 2: F15974-5' ACTCCACCATTAGCACCCAAA-3' , R16564-5' TGATGTCTTATTTAAGGGGAACGT-3' . PCR (an initial incubation at 94 ℃ for 4 min, followed by 30 cycles at 94 ℃ for 30 s, at 60 ℃ for 30 s, and at 72 ℃ for 2 min; the final step at 72 ℃ was extended to 4 min) was performed in a Biometra Personal PCR system.

DNA sequencing of PCR products PCR products were sent to United Gene Technology Company, Ltd, Shanghai, China for direct sequencing.

RESULTS

Alterations in D-loop region, 12SrRNA and tRNA^{phe} of mtDNA

Two types of instabilities were detected in D-loop region, which were PolyC and $(CA)_n$ instabilities. PolyC instability existed in two regions; one was between np305 and np317, the other between np16 182 and np16 194. Some normal and cancerous tissues contained two distinct variations of mtDNA, especially the $(C)_n$ repeat number (Figures 1A-C). Instabilities including polyC and $(CA)_n$ were found in 13/22(59.1 %) gastric cancerous tissues and in 9/22 (40.9 %) normal tissues (P>0.05) (Table 1). Some new alterations were found in D-loop region, 12SrRNA and tRNA^{phe} (Table 2), among which np 318 and np 321 C-T transitions in D-loop region were two of the five bases for H-strand replication primer (GCTTC) (Figure 1C). np 523 AC-deletion and np 527 C-T transition (Figures 1D,E) occurred at mtTF1 binding site (mtTFBS), which was associated with the transcription of downstream mitochondrial genome. But no alteration was found in the major H-strand promoter (HSP1) and the minor H-strand promoter (HSP2). Seven samples showed the np 16 182 polyC instabilities, five of which simultaneously showed np 16 189 T-C transition (Figure 1F).

Relationship between instabilities of D-loop and variations of 12SrRNA-tRNA^{phe}

np523 AC deletion and np527 C-T transition in mtTFBS did not cause replication error of downstream gene 12S rRNA and tRNA^{phe}. Downstream gene of HPR containing 318 C-T and np321 C-T transitions exhibited a previously unknown np611 G insertion in tRNA^{phe} (Figure 1G) and np 716 T-G transition in 12S rRNA (Figure 1H). In addition, its downstream variations increased. Maybe, the variations of D-loop more or less influenced downstream replication. Elements of transcription and translation for D-loop and coding region 12S rRNA-tRNA^{phe} are shown in Figure 2.

Relationship between variations of 12S rRNA-tRNA^{phe} and differentiation of gastric cancer

Two of twelve well differentiated cancerous tissues (moderately and well differentiated tubular adenocarcinoma and papillary adenocarcinoma) and two of normal tissues showed variations in mitochondrial 12SrRNA-tRNA^{phe}(P>0.05); Moreover, six of ten poorly differentiated cancerous tissues (poorly differentiated adenocarcinoma, signet-ring cell carcinoma and mucinous adenocarcinoma) and four of ten normal tissues showed variations in 12SrRNA-tRNA^{phe}(P>0.05) (Table 1). Compared the data from the two groups of different cancerous tissues (2/12 and 6/10 respectively), the discrepancy was obvious (P<0.05).

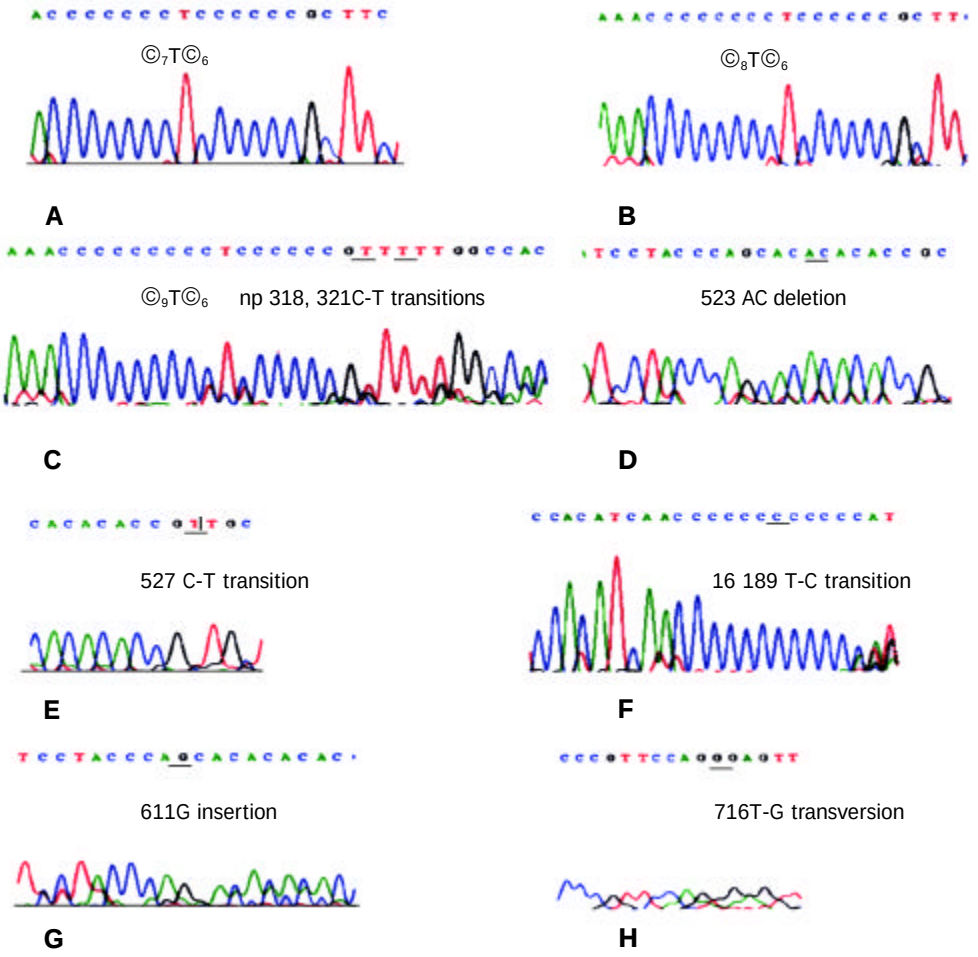

Figure 1 Sequencing results of instabilities and some variations in D-loop and 12S rRNA-tRNA^{phe}.

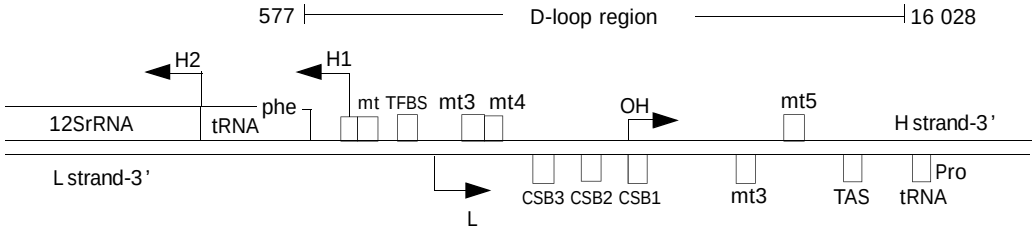

Figure 2 Elements of transcription and translation for mitochondrial coding region 12S rRNA-tRNA^{phe} and non-coding D-loop region. Non-coding D-loop region and genes encoding 12S rRNA and tRNA^{phe} are shown with boxes on the H-strand and L-strand of mtDNA. H1 and H2 are start sites for transcription of H-strand. L is start site for transcription of L-strand. O_H is the primary origin of H-strand. mt3, mt4 and mt5 are control elements. TAS: termination-associated sequence. CSB: Conserved Sequence Block.

Table 1 Variant frequencies of D-loop region, 12S rRNA and tRNA^{phe} in gastric cancers and para-cancerous tissues

Type	*n*	Variation frequency *vs* controls		
		D-loop	12S rRNA	tRNA^{phe}
Papillary adenocarcinoma	4	3/2	0/0	-[c]
Well differentiated adenocarcinoma	4	1/1	0/1[a]	-[c]
Moderately differentiated adenocarcinoma	4	2/1	2/1	-[c]
Poorly differentiated adenocarcinoma	4	3/2	3/2[b]	1/0
Signet-ring cell carcinoma	3	2/1	1/0	-[c]
Mucous adenocarcinoma	3	2/2	2/2[b]	1/0
Total	22	13/9	8/6	2/0

A: np 772 A-T transition was only found in normal tissues. B: One of variations in para-cancerous tissue was not the same as cancerous tissue. C: No variation was found.

Table 2 Instabilities and variations of mitochondrial D-loop and 12s rRNA-tRNA^{phe} in 22 patients with gastric carcinoma

Map locus	Map position	Description	Variant position	Variation
HV2	57-372	Hypervariable segment 2	73	A-G
OHR	110-441	H-strand origin	143	G-A
			146	T-C
			152	T-C
			204	T-C
CSB1	213-235	Conserved sequence block I	235	A-G
TFX	233-260	mtTF1 binding site	235	A-G
			263	A-G
TFY	276-303	mtTF1 binding site	-	-[b]
CSB2	299-315	Conserved sequence block II	310	CTCC
			312	TCCCCC
HPR	317-321	Replication primer	318(317)	C-T[a]
			321(320)	C-T[a]
CSB3	346-363	Conserved sequence block III	340	C-T
			343	C-T[a]
			345	C-T[a]
MT4H	371-379	mt4 H-strand control element	-	-[b]
MT3H	384-391	mt3 H-strand control element	-	-[b]
LSP	392-445	L-strand promoter	-	-[b]
TFL	418-445	mtTF1 binding site	481	C-T
			483	C-A
			489	T-C
			514	CACA
TFH	523-550	mtTF1 binding site	523	AC-del[a]
			527	C-T[a]
HSP1	545-567	Major H-strand promoter	-	-[b]
TF	577-647	tRNA phenylalanine	611	G ins[a]
			641	A-T
HSP2	645-645	Minor H-strand promoter		
RNR1	648-1601	12S rRNA	652	G-ins[a]
			709	G-A
			716	T-del[a]
				T-G*
			728	C-T
			745	A-G[a]
			757	A-T
			760	A-T[a]
			772	A-T[a]
			1106	T-C
			1160	A-G
			1226	C-T
HV1	16024-16383	Hypervariable segment 1	16182	AA-CC[a]
			16189	T-C
TAS	16157-16172	Termination-associated sequence	-	-[b]
MT5	16194-16208	Control element	16194	A-G

Notes: A: variations not found previously, B: relatively stable and no variation of base, del: deletion, "ins": insertion, CC or CA: insertion characteristics of instability.

DISCUSSION

The mitochondrial genome is particularly susceptible to mutations because of the high level of reactive oxygen species (ROS) generated in the organelle[8-10], coupled with a low level of mismatch repair gene (MMR)[11-13]. D-loop is the most variable part of human mitochondrial genome[14] and is hard to ascertain whether some variation is a mutation or not because of complex reasons such as different variations of mtDNA in different subjects[15,16], more polymorphism sites[17,18], age dependent variation[19,20], linkage disequilibrium and recombination[21-23], etc. In addition, mutated mtDNA often occurs together with wild-type mtDNA (heteroplasmic) no matter in normal tissues or in abnormal portions[24,25]. So far, most researches about the mutant positions in mtDNA have been limited to coding regions of mtDNA.

The variations, including point mutation, *per se* are mostly non-causative, and can not affect the mitochondrial function of tumor cells because sequence variation can be primarily found in individual normal tissues. These variations may occur during aging due to oxygen radical-induced mtDNA damage[8-10,26,27], mtDNA polymerase errors[28], or due to the activation of genes involved in error-prone DNA repair[11-13]. The mutations may become amplified because of an intracellular replicative advantage of mtDNA molecules. The cells with amplified mtDNA may then take over the whole population due to their clonal growth advantage[29].

The variations found in this study occurred in the middle of the promoter for mtDNA H-strand transcription, at a position with high affinity for the mtTF1 transcription factor, in the coding sequence of the RNA primer for H-strand synthesis, or within H-strand origin of DNA synthesis initiation. These variations occurred in DNA sequences that either unwound and bent because of mtTF1 binding at the same or an adjacent position, or formed persistent RNA-DNA hybrids giving rise to an R-loop with a tRNA-like cloverleaf structure at one or more origins of H-strand synthesis. These conformational changes would likely expose single stranded DNA stretches, which might be more susceptible to oxygen radical damage[10].

However, little is known about mtDNA mutation status in gastric tumors except a few reports[30-33]. Tamura *et al*[30] found two mutations, 10 polymorphisms in 45 Japanese individuals with gastric cancer, but did not find alterations of mononucleotide or dinucleotide repeats such as polyC and $(CA)_n$ in D-loop region. He thought that non-instability was related with ethnic difference. We have some doubt about Tamura' s viewpoint. First, how to explain the absence and the presence of mitochondrial instability coexisted in the same population? Second, our conclusion of mitochondrial PolyC instability is similar to the research results by Alonso[31] and Habano[32] among Westerners. According to human origin based on the mitochondrial genome[34-36], Chinese and Westerners came from different ancestors[37,38]. It supports our opinion that there is no ethnic difference regarding the absence or presence of D-loop instability in gastric cancer. And it was also found that D-loop instability occurred more often in poorly differentiated gastric cancers than in well differentiated ones, but no statistic significance existed. On the contrary, there existed a significant correlation between the differentiation degree of gastric cancer and the variant frequency of 12S rRNA-tRNA^{phe}, suggesting that poorly differentiated gastric cancers are more prone to variations of mitochondrial coding region 12SrRNA-tRNA^{phe}, or conversely, gastric cancers with more mitochondrial 12S rRNA-tRNA^{phe} variations have a tendency to become poorly differentiated with the presence of other carcinogenic factors. But, Habano *et al*[32] thought mtDNA mutations contributed to gastric tumorigenesis of intestinal type. Further studies are needed to eventually verify whether mutant mtDNA is related to degree of differentiation or to intestinal type of gastric cancer (according to Lauren' s classification of gastric carcinoma), which is closely related to environmental carcinogenic factors.

We thought that mitochondrial genome of gastric carcinoma was more subjected to mononucleotide or dinucleotide mutation, which may be resulted from functional loss of MMR. MMR system has been found in yeast strains, in which MSH1 and MSH2 are involved in mitochondrial and nuclear DNA repair systems respectively[39]. No MSH1 homologue has been found in mammalian cells. Therefore it remains uncertain whether an MMR system plays a role in the maintenance of mammalian mitochondrial genome. np 16 182 C-T transition may be an important reason for np 16 189 PolyC instability.

Endogenous and exogenous etiological factors could cause mitochondria oxidative stress by different ways, and make equilibrium disorder of oxidization and anti-oxidization[40,41], which damages mtDNA and mitochondrial double lipid membranes, thus disturbing electron transmission and ATP synthesis. Further damage may change the permeability of mitochondrial membrane, and influence the exchange of ions and macromolecules, even the process of apoptosis[42,43]. In fact, we are not sure whether some special variations and increased variant frequency of mtDNA are the causes of gastric tumorigenesis or just the results of gastric tumorigenesis. It is possible that mtDNA mutations are just the results of clonal expansion of spontaneous somatic mutations that occur at a very low frequency during previous replication of this precursor cell, and become apparent both by clonal expansion of the cell and by predominant selection and later become homoplasmic or at least somewhat predominant within the cell. It also indicates that frequencies and types of mtDNA mutation reflect hidden genetic and environmental actions. If it is true that increased frequencies of mitochondrial variations (especially the mutation) are related to differentiation level of gastric cancer, it must be the result of mtDNA genomic action on nuclear genome directly or indirectly.

REFERENCES

1 **Xin Y**, Li XL, Wang YP, Zhang SM, Zheng HC, Wu DY, Zhang YC. Relationship between phenotypes of cell-function differentiation and pathobiological behavior of gastric carcinomas. *Word J Gastroenterol* 2001; **7**: 53-59

2 **Taanman JW**. The mitochondrial genome: structure transcription, translation and replication. *Biochim Biophys Acta* 1999; **1410**: 103-123

3 **Li JM**, Cai Q, Zhou H, Xiao GX. Effects of hydrogen peroxide on mitochondrial gene expression of intestinal epithelial cells. *World J Gastroenterol* 2002; **8**: 1117-1122

4 **Polyak K**, Li Y, Zhu H, Lengauer C, Willson JK, Markowitz SD, Trush MA, Kinzler KW, Vogelstein B. Somatic mutations of the mitochondrial genome in human colorectal tumors. *Nat Genet* 1998; **20**: 291-293

5 **Savre-Train I**, Piatyszek MA, Shay JW. Transcription of deleted mitochondrial DNA in human colon adenocarcinoma cells. *Hum Mol Genet* 1992; **1**: 203-204

6 **Bianchi NO**, Bianchi MS, Richard SM. Mitochondrial genome instability in human cancers. *Mutat Res* 2001; **488**: 9-23

7 **Maximo V**, Soares P, Seruca R, Rocha AS, Castro P, Sobrinho-Simoes M. Microsatellite instability, mitochondrial DNA large deletions, and mitochondrial DNA mutations in gastric carcinoma. *Genes Chromosomes Cancer* 2001; **32**: 136-143

8 **Lee I**, Bender E, Kadenbach B. Control of mitochondrial membrane potential and ROS formation by reversible phosphorylation of cytochrome c oxidase. *Mol Cell Biochem* 2002; **234**: 63-70

9 **Lee I**, Bender E, Arnold S, Kadenbach B. New control of mitochondrial membrane potential and ROS formation-a hypothesis. *Biol Chem* 2001; **382**: 1629-1636

10 **Atlante A**, Calissano P, Bobba A, Azzariti A, Marra E, Passarella S. Cytochrome c is released from mitochondria in a reactive oxygen species (ROS)-dependent fashion and can operate as a ROS

scavenger and as a respiratory substrate in cerebellar neurons undergoing excitotoxic death. *J Biol Chem* 2000; **275**: 37159-37166
11 **Bianchi MS**, Bianchi NO, Bailliet G. Mitochondrial DNA mutations in normal and tumor tissues from breast cancer patients. *Cytogenet Cell Genet* 1995; **71**: 99-103
12 **Yamamoto H**, Tanaka M, Katayama M, Obayashi T, Nimura Y, Ozawa T. Significant existence of deleted mitochondrial DNA in cirrhotic liver surrounding hepatic tumor. *Biochem Biophys Res Commun* 1992; **182**: 913-920
13 **Penta JS**, Johnson FM, Wachsman JT, Copeland WC. Mitochondrial DNA in human malignancy. *Mutat Res* 2001; **488**: 119-133
14 **Wallace DC**. Mitochondrial diseases in man and mouse. *Science* 1999; **283**: 1482-1488
15 **Li Y**, Zuo L, Ke Y, Cheng A, Shu L, Ren W. Polymorphism of mitochondrial DNA region V in Bouyei people and Miao people living in Guizhou Province of China. *Zhonghua Yixue Yichuanxue Zazhi* 2002; **19**: 138-140
16 **Sun YH**, Wang W, Liu SY, He SP, Shao XL, Xie ZX, Deng FJ, Liu Y, Tong JG, Wu QJ. Genetic diversity analysis of mitochondrial D-loop region of Chinese sucker (Myxocyprinus asiaticus). *Yichuan Xuebao* 2002; **29**: 787-790
17 **Yaffe MP**. The machinery of mitochondrial inheritance and behavior. *Science* 1999; **283**: 1493-1497
18 **Hibi K**, Nakayama H, Yamazaki T, Takase T, Taguchi M, Kasai Y, Ito K, Akiyama S, Nakao A. Detection of mitochondrial DNA alterations in primary tumors and corresponding serum of colorectal cancer patients. *Int J Cancer* 2001; **94**: 429-431
19 **Michikawa Y**, Mazzucchelli F, Bresolin N, Scarlato G, Attardi G. Aging-dependent large accumulation of point mutations in the human mtDNA control region for replication. *Science* 1999; **286**: 774-779
20 **Dillin A**, Hsu AL, Arantes-Oliveira N, Lehrer-Graiwer J, Hsin H, Fraser AG, Kamath RS, Ahringer J, Kenyon C. Rates of behavior and aging specified by mitochondrial function during development. *Science* 2002; **298**: 2398-2401
21 **Awadalla P**, Eyre-Walker A, Smith JM. Linkage disequilibrium and recombination in hominid mitochondrial DNA. *Science* 1999; **286**: 2524-2525
22 **Wiuf C**. Recombination in human mitochondrial DNA? *Genetics* 2001; **159**: 749-756
23 **Thomas S**, Prabhu R, Pulimood A, Balasubramanian KA. Heat preconditioning prevents enterocyte mitochondrial damage induced by surgical manipulation. *J Surg Res* 2002; **108**: 138-147
24 **Nishikawa M**, Nishiguchi S, Shiomi S, Tamori A, Koh N, Takeda T, Kubo S, Hirohashi K, Kinoshita H, Sato E, Inoue M. Somatic mutation of mitochondrial DNA in cancerous and noncancerous liver tissue in individuals with hepatocellular carcinoma. *Cancer Res* 2001; **61**: 1843-1845
25 **Kotake K**, Nonami T, Kurokawa T, Nakao A, Murakami T, Shimomura Y. Human livers with cirrhosis and hepatocellular carcinoma have less mitochondrial DNA deletion than normal human livers. *Life Sci* 1999; **64**: 1785-1791
26 **Mandavilli BS**, Santos JH, Van Houten B. Mitochondrial DNA repair and aging. *Mutat Res* 2002; **509**: 127-151
27 **Chung YM**, Bae YS, Lee SY. Molecular ordering of ROS production, mitochondrial changes, and caspase activation during sodium salicylate-induced apoptosis. *Free Radic Biol Med* 2003; **34:** 434-442
28 **Pinz KG**, Shibutani S, Bogenhagen DF. Action of mitochondrial DNA polymerase γ at sites of base loss or oxidative damage. *J Biol Chem* 1995; **270**: 9202-9206
29 **Habano W**, Nakamura S, Sugai T. Microsatellite instability in the mitochondrial DNA of colorectal carcinomas: evidence for mismatch repair systems in mitochondrial genome. *Oncogene* 1998; **17**: 1931-1937
30 **Tamura G**, Nishizuka S, Maesawa C, Suzuki Y, Iwaya T, Sakata K, Endoh Y, Motoyama T. Mutations in mitochondrial control region DNA in gastric tumours of Japanese patients. *Eur J Cancer* 1999; **35**: 316-319
31 **Alonso A**, Martin P, Albarran C, Aquilera B, Garcia O, Guzman A, Oliva H, Sancho M. Detection of somatic mutations in the mitochondrial DNA control region of colorectal and gastric tumors by heteroduplex and single-strand conformation analysis. *Electrophoresis* 1997; **18**: 682-685
32 **Habano W**, Sugai T, Nakamura SI, Uesugi N, Yoshida T, Sasou S. Microsatellite instability and mutation of mitochondrial and nuclear DNA in gastric carcinoma. *Gastroenterology* 2000; **118**: 835-841
33 **Maximo V**, Soares P, Seruca R, Sobrinho-Simoes M. Comments on: Mutations in mitochondrial control region DNA in gastric tumours of Japanese patients. *Eur J Cancer* 1999; **35**:1407-1408
34 **Ingman M**, Kaessmann H, Paabo S, Gyllensten U. Mitochondrial genome variation and the origin of modern humans. *Nature* 2000; **408**: 708-713
35 **Gray MW**, Burger G, Lang BF. Mitochondrial evolution. *Science* 1999; **283**: 1476-1481
36 **Heddi A**, Stepien G, Benke PJ, Wallace DC. Coordinate induction of energy gene expression in tissues of mitochondrial disease patients. *J Biol Chem* 1999; **274**: 22968-22976
37 **Chen W**, Li Y, Chen Y, Feng H, Fu S, Zhang G, Li P. A study on polymorphism of mitochondrial DNA D loop in the Han nationality in China. *Zhonghua Yixue Yichuanxue Zazhi* 1999; **16**: 246-248
38 **Jin H**, Wu L, Wang W, Shi L. Mitochondrial DNA polymorphism in the Han, Miao, Buyi, and Shui ethnic groups from Guizhou province. *Yichuan Xuebao* 1995; **22**: 1-11
39 **Asumendi A**, Morales MC, Alvarez A, Arechaga J, Perez-Yarza G. Implication of mitochondria-derived ROS and cardiolipin peroxidation in N- (4-hydroxyphenyl) retinamide-induced apoptosis. *Br J Cancer* 2002; **86**: 1951-1956
40 **Herrera B**, Alvarez AM, Sanchez A, Fernandez M, Roncero C, Benito M, Fabregat I. Reactive oxygen species (ROS) mediates the mitochondrial-dependent apoptosis induced by transforming growth factor (beta) in fetal hepatocytes. *FASEB J* 2001; **15**: 741-751
41 **Zhou HP**, Wang X, Zhang NZ. Early apoptosis in intestinal and diffuse gastric carcinomas. *World J Gastroenterol* 2000; **6**: 898-901
42 **Susin SA**, Lorenzo HK, Zamzami N, Marzo I, Snow BE, Brothers GM, Mangion J, Jacotot E, Costantini P, Loeffler M, Larochette N, Goodlett DR, Aebersold R, Siderovski DP, Penninger JM, Kroemer G. Molecular characterization of mitochondrial apoptosis-inducing factor. *Nature* 1999; **397**: 441-446
43 **Shen ZY**, Shen J, Li QS, Chen CY, Chen JY, Yi Z. Morphological and functional changes of mitochondria in apoptotic esophageal carcinoma cells induced by arsenic trioxide. *World J Gastroenterol* 2002; **8**: 31-35

Edited by Zhu LH and Wang XL

P.O.Box 2345, Beijing 100023,China
Fax: +86-10-85381893
E-mail: wjg@wjgnet.com www.wjgnet.com

World J Gastroenterol 2003;9(9):1930-1934
World Journal of Gastroenterology
 ISSN 1007-9327

• GASTRIC CANCER •

Effects of allicin on both telomerase activity and apoptosis in gastric cancer SGC-7901 cells

Li Sun, Xu Wang

Li Sun, Xu Wang, Department of Oncology, Affiliated Hospital of Xuzhou Medical College, Xuzhou 221002, Jiangsu Province, China
Supported by the Natural Science Foundation of Jiangsu Province, No. BJ98110
Correspondence to: Xu Wang, Affiliated Hospital of Xuzhou Medical College, 99 Huaihai West Road, Xuzhou 221002, Jiangsu Province, China. wangxuling@eYou.com
Telephone: +86-516-5603193 **Fax:** +86-516-5601527
Received: 2002-10-30 **Accepted:** 2003-03-21

Abstract

AIM: To investigate the effects of allicin on both telomerase activity and apoptosis in gastric cancer SGC-7901 cells.

METHODS: The gastric cancer SGC-7901 adenocarcinoma cells were treated with allicin and the cell cycle, inhibitory rate, apoptosis, telomerase activity and morphologic changes were studied by MTT assay, flow cytometry (FCM), TRAP-PCR-ELISA assay, light microscope, electron microscope respectively. Results were compared with that of AZT (3'-Azido-3'-deoxythymidine).

RESULTS: SGC-7901 cells were suppressed after exposure to allicin of 0.016 mg/ml, 0.05 mg/ml, and 0.1 mg/ml for 48 h. Compared with the control, the difference was significant ($P<0.05$). Allicin could induce apoptosis of the cells in a dose-dependent and non-linear manner and increase the proportion of cells in the G_2/M phase. Compared with the control, the difference was significant in terms of the percentage of cells in the G_2/M phase ($P<0.05$). Allicin could inhibit telomerase activity in a time-dependent and dose-dependent pattern. After exposure to allicin at 0.016 mg/ml for 24 hours, SGC-7901 cells showed typical morphologic change.

CONCLUSION: Allicin can inhibit telomerase activity and induce apoptosis of gastric cancer SGC-7901 cells. Allicin may be more effective than AZT.

Sun L, Wang X. Effects of allicin on both telomerase activity and apoptosis in gastric cancer SGC-7901 cells. *World J Gastroenterol* 2003; 9(9): 1930-1934
http://www.wjgnet.com/1007-9327/9/1930.asp

INTRODUCTION

The relationship between telomere, telomerase and cancer has been the hotspot of study since Kim found telomerase activity in cancer in 1994. It was reported that telomerase activity and malignancy had a close association. Telomerase activity was detected in approximately 80-90 % of immortal cells. In contrast, telomerase activity was not detected in most mature somatic cells[1-3]. The observed differences in telomerase activity in normal *versus* tumor derived cells led to the hypothesis that the activation of telomerase might be essential to tumor progression and the proliferation of tumor cells, and that telomerase might represent a suitable target for highly specific anti-cancer therapies[4,5]

Gastric cancer is the most common alimentary tract cancer in China in terms of incidence. It is one of the malignancies that do serious harm to people's health with a high mortality and are short of effective therapeutic methods. Researchers are not only trying to enchance the therapeutic effects of the current methods but also working hard to find new ways and medicines to treat gastric cancer. We have studied the relationship between telomere, telomerase and malignancies, and tried to find new medicines to treat gastric cancer since 1997 in our laboratory. The results suggest that the presence of telomerase activity itself can be used as an excellent tool for the early diagnosis of cancer[6-8]. We carried out further studies to try to find out medicines from traditional Chinese herbs, which can inhibit telomerase activity and provide a new therapeutic approach on gastric cancer. Allicin is the bulb of Allium. Epidemiological studies and animal experiments have suggested that several garlic-derived compounds have potential anticarcinogens[8-13]. Allicin is one of them, but the mechanism of anticancer is not clearly demonstrated. In this paper, we first studied the effect of 3'-Azido-3'-deoxythymidine (AZT) on telomerase activity and apoptosis. Then the test was continued by using cheap allicin, instead of the expensive AZT. The results were compared between allicin and AZT.

MATERIALS AND METHODS

Materials

Allicin was obtained from HeFeng Pharmaceutical Company (15 mg/ml, Batch Number: 010101). AZT was purchased from Sigma Company. Human gastric adenocarcinoma SGC-7901 cell line was obtained from the Cell Biology Institute of Chinese Academy of Sciences. RPMI-1640 was the product of GBICO. Fetal bovine serum (FBS) was purchased from Tianjin Hematological Diseases Research Institute. Trypsin, tetrazolium bromide (MTT), ribonuclease A, DMSO and propidium iodide (PI) were purchased from the Sino-American Hua Mei Biotechnology Company of Beijing. The telomerase detection kits were obtained from the Sino-American Hua Mei Biotechnology Company of Shanghai.

Methods

Cell culture Cells were maintained in RPMI-1640 supplemented with 10 % fetal bovine serum (FBS), streptomycin (100 μg/ml) and penicillin (100 IU/ml) at 37 ℃ in a humidified atmosphere containing 5 % CO_2.

Effect of allicin on cell proliferation of SGC-7901 cells SGC-7901 cells were suspended at a concentration of 5×10^4/ml. Then 200 μl of the cell suspension was placed in each well of a replicate 96-well microtiter plate. The cells were allowed to adhere overnight. Then different concentrations (0.016 mg/ml, 0.05 mg/ml, 0.1 mg/ml) of allicin were added to the cells. MTT assay was performed after 48 h growth. 40 μl of 5 mg/ml of MTT was added to each well followed by incubation for 4 h at 37 ℃. The formazan crystals were dissolved in 200 μl DMSO and the absorbance measured by enzyme-linked immunosorbent assay (ELISA). Optical density value (OD)

was measured at a wavelength of 570 nm. Each assay was performed three times and the average results were calculated.

Effect of allicin on telomerase activity of SGC-7901 cell Cultured cells in logarithmic growth were digested by 0.25 % trypsin and suspended at a concentration of 2×10^4/ml, then 5 ml was placed into a cell culture flask of 25 ml and allowed to adhere overnight. Cells were harvested after 12 h, 24 h, and 36 h. Cells were washed once with PBS and scraped into a wash buffer, The cells were washed in the buffer, homogenized in 150 μl cell lysis buffer, and incubated on ice for 30 min. Cell homogenates were then centrifuged at 12 000×g for 20 min at 4 ℃. The supernatants were recovered and snap-frozen in liquid nitrogen and stored at -80 ℃. The TRAP-PCR-ELISA assay was performed using a telomerase detection kit. In brief, 2 μl of tissue extract and 48 μl TRAP reaction mixture were placed into tubes, PCR was then performed at 94 ℃ for 120 s and at 94 ℃ for 30 s, at 48 ℃ for 30 s, at 72 ℃ for 90 s for 35 cycles. The PCR products (25 μl) were hybridized to a digoxigenin (DIG)-labelled telomeric repeat specific detection probe. The PCR products were immobilized via the biotin-labelled primer to a streptavidin-coated microtiter plate. The immobilized PCR products were detected with a peroxidase-conjugated anti-DIG antibody and visualized following addition of the stop reagent. The microtitre plate was assessed on an enzyme-linked immunosorbent assay (ELISA) plate reader at a wavelength of 490 nm.

Effect of allicin on the cell cycle of SGC-7901 cells Cell culture was the same as before, and treated with allicin. Cultured cells were harvested after 24 h and fixed with 70 % cold ethanol for 4 h. The percentage of the cells in different cell cycle was determined by a flow cytometer. Analysis of the DNA content was done by using FACSalibur. Briefly, 1×10^5 cells were suspended in 0.2 % Triton-X-100/PBS solution containing 0.5 % ribonuclease A, After incubation for 20 min, DNA was stained with 50 ug/ml of propidum iodide (PI), then applied to flow cytometer analysis at the inspiring wavelength of 488 nm.

Effect of allicin on morphological changes of SGC-7901 cells Observations under light microscope The cells were treated with 0.016 mg/ml allicin for 24 h, 48 h, then morphological changes were observed under the inverted light microscope and photographed.

Observations under transmission electron microscope (TEM) For TEM, SGC-7901 cells were incubated in culture dishes with allicin for 24 h. A total of 5×10^6 cells were pelleted at 12 000×g for 5 min and washed twice with PBS. Cells were fixed in 2.5 % cold glutaraldehyde, 0.1 M of sodium cacodylate/ 1 % sucrose buffer for 24 h. The cells were washed three times with PBS, then postfixed in 1 % osmium tetroxide (60 min), encapsulated in 1 % agar, stained with uranyl acetate and phosphotungstic acid, and dehydrated in a series of graded ethanolic solutions, finished with propylene oxide before finally embedded in Epon 812-Araldite mixture. Ultrathin sections (50 nm) were cut on a LKL-208 ultramicrotome and placed under 200 mesh standard copper grids, examined with an HA-600 transmission electron microscope.

Statistical analysis

The oneway test was used to evaluate the significance of cell proliferation, cell cycle and apoptosis. The ANOVA was used to evaluate the significance of telomerase activity. $P<0.05$ was considered statistically significant.

RESULTS

Effects of allicin, AZT on cell proliferation

SGC-7901 cells were treated with different concentrations of allicin for 48 h. MTT assay was used to measure cell proliferation. The results are shown in Figure 1. Allicin could inhibit gastric cancer cell proliferation in A dose-dependent pattern. Allicin' s action was notably stronger than AZT (Figure 2). At the highest concentration, the inhibitory rate of allicin on SGC-7901 was 89 %, while that of AZT was only 52.6 %.

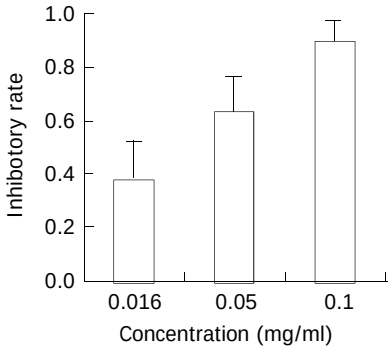

Figure 1 Effect of allicin on cell proliferation.

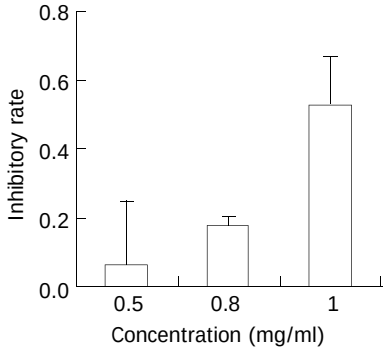

Figure 2 Effect of AZT on cell proliferation.

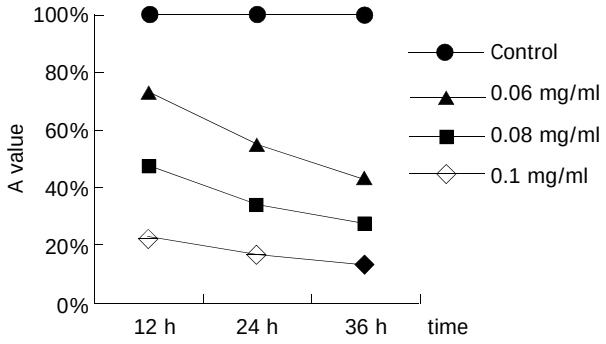

Figure 3 Effect of allicin on telomerase activity.

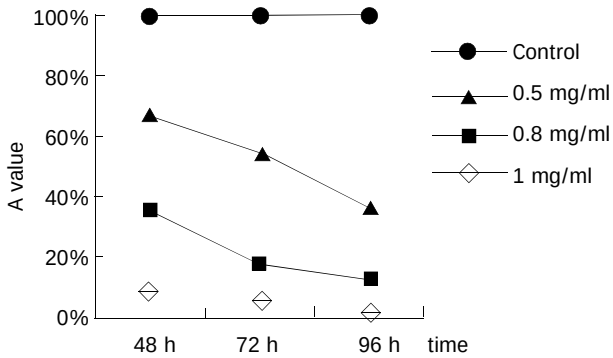

Figure 4 Effect of AZT on telomerase activity.

Effects of allicin on telomerase activity

The cells were harvested after treated at different concentrations of allicin for 12 h, 24 h, and 36 h, respectively. SGC-7901

cells were treated by AZT for 48 h, 72 h, 96 h. Then the cells were harvested. The telomerase activity was measured by TRAP-PCR-ELISA assay. The results suggested that both allicin and AZT could inhibit telomerase activity by different degrees (Figures 3 and 4).

Effects of allicin on cell cycle and apoptosis

Three different concentrations of allicin acted on SGC-7901 cells for 24 h, the flow cytometry results showed the sub-G1 wave which was the apoptosis wave. Allicin could induce apoptosis in a dose-dependent and non -linear manner (Figure 5). At the same time allicin could change the cell cycle of SGC-7901 cell. In a certain range of concentrations, when the concentration increased, the cells of G_2/M phase increased (Figure 6). As shown in Figures 7 and 8, AZT could also change the cells cycle. It could increase the cells of S phase and induce apoptosis in a dose-dependent and non-linear manner.

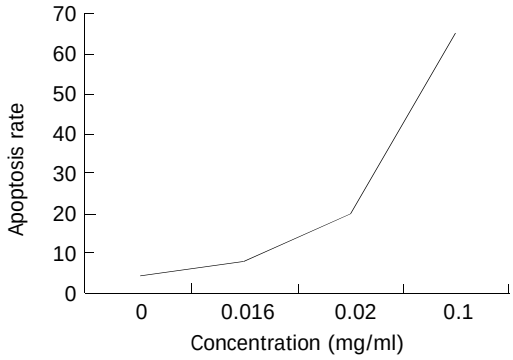

Figure 5 Effect of allicin on apoptosis.

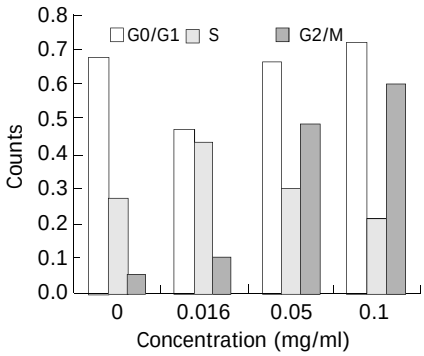

Figure 6 Effect of allicin on cells cycle.

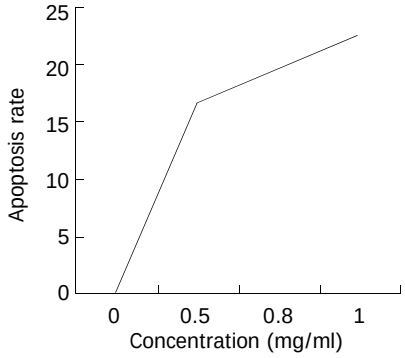

Figure 7 Effect of AZT on apoptosis.

Effect of allicin on SGC-7901 cell morphological changes

The results of light microscopy Cells became round after treated with allicin for 24 h and the intercellular gaps were loose. After 48 h, the cells were crimpled and floated. There were a lot of fragments around the cells.

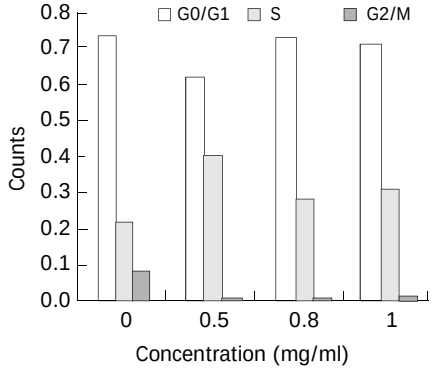

Figure 8 Effect of AZT on cell cycle.

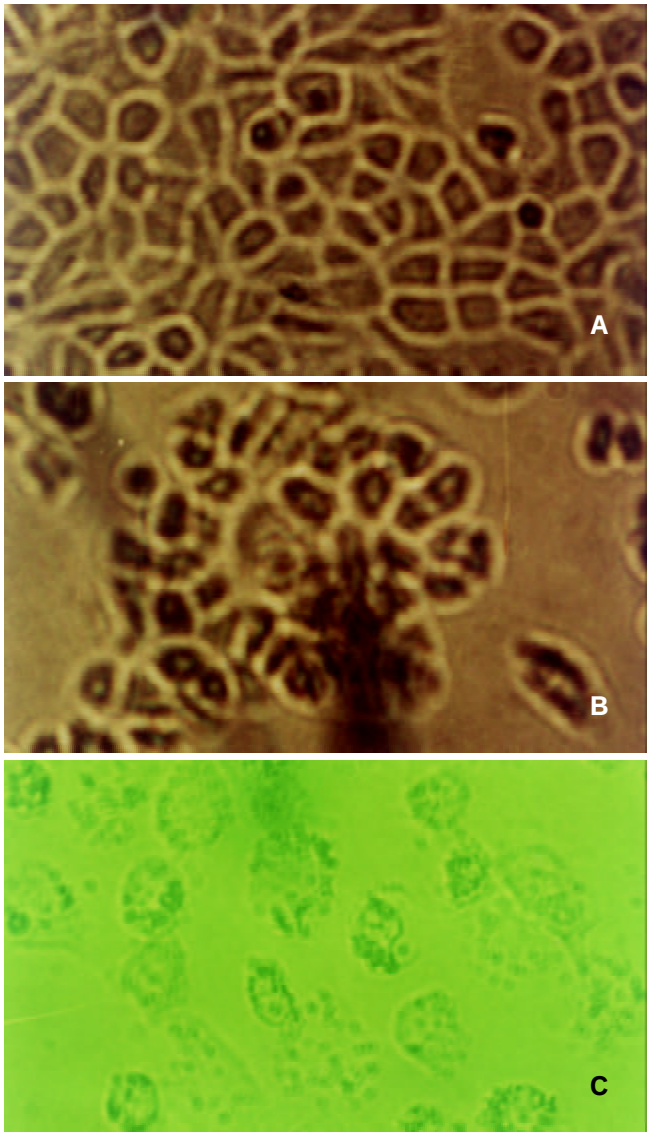

Figure 9 Allicin-induced morphological changes of SGC-7901 cells under light microscope. A: Control, ×400; B: Treated with 16 μg / ml allicin for 24 h, ×400; C: 16 μg / ml allicin for 48 h, ×400.

Results of transmission electron microscopy SGC-7901 cells had big nucleoli and aberrant nuclei. There were a lot of prominences of microvilli on the surface of cell membranes. After treated with allicin for 24 h, the prominence was disappeared and nuclei deflated, but the cell membranes were intact.

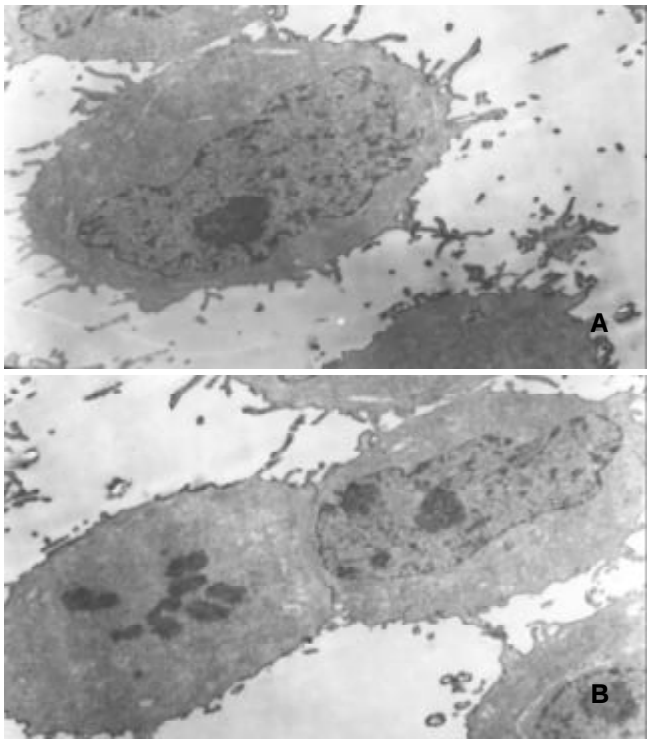

Figure 10 Allicin-induced morphological changes of SGC-7901 cells under electron microscope. A: Control, ×3 500; B: Treated with 16 ug/ml allicin for 24 h, ×3 500.

DISCUSSION

Telomeres, the ends of eukaryotic chromosomes, are composed of tandemly repeated guanine-rich sequences 5' TTAGGG3' [14]. However, due to the nature of DNA synthesis, the 5' ends of telomeres are shortened by 50-100 bp with each round of cell division. When the telomere reaches a certain critical length, the cell cannot undergo division. This has been described as the "end-replication" problem of linear chromosomes[15-17]. Telomerase is a ribonucleoprotein and its internal RNA component serves as a template for directing the appropriate telomeric sequences onto the 3' end of a telomeric primer, and then the cells can continue to divide[18]. To date, three major components of telomerase, namely, human telomerase RNA component (hTR), human telomerase-associated protein (TP) and human telomerase catalytic subunit (hTERT) have been identified[19]. Recent studies have demonstrated a close correlation between telomerase activity and hTERT expression[19,20]. In a number of laboratories, experiments have shown that down-regulation of telomerase activity can be used to treat cancer[21-28]. AZT, which has been among the most extensively studied reverse transcriptase inhibitors, is a telomerase inhibitor that works on hTERT. AZT can effectively cause telomere shortening and inhibit telomerase activity in cancer cells. The results have shown that tumor incidence is reduced and survival is prolonged, at the same time the number and size of spontaneous metastases are also decreased. But AZT has toxical effects and is so expensive that it cannot be used widely[27-29]. Allicin, which has been used to decrease blood pressure, cholesterol and as an antioxidant, antimicrobial, etc[30-33], has little toxicity and is easily available. In the current study, the SGC-7901 cells were treated at different concentrations of allicin and AZT. The results strongly suggest that allicin can effectively inhibit telomerase activity in a time- and dose-dependent manner. This study also indicates that allicin can induce cell apoptosis (arrest in G_2/M phase). The cause of apoptosis is related to decreased telomerase activity. When telomerase activity degrades, telomere shortens, mitoses of cells are arrested, which leads to cell apoptosis[34]. It was reported that apoptosis inhibitor Bcl-2 could modulate telomerase activity. Overexpression of Bcl-2 leads to a significant enchancement in the level of telomerase activity. On the other hand, with down-regulation of Bcl-2 expression, telomerase activity also decreases[35-37]. Some researches found that the mechanism of degraded Bcl-2 expression by allicin was through the secondary messengers, namely cAMP, PKC of the second signal system, which led to overexpression of Fas and Bax, and at the same time the Bcl-2 expression decreased[38]. But the telomerase activity modulation is a complex system[39]. We were unable to rigorously determine if decrease of telomerase activity after treatment by allicin was associated with the down-regulation of Bcl-2.

Furthermore, this work also provides a direct comparison between two classes of medicine, both of which can inhibit telomerase activity and induce apoptosis. Allicin is more effective than AZT. At the same time, both Allicin and AZT can arrest the cells in different cell cycle phases. Allicin arrests cells at the G_2/M phase while AZT does at the S phase, indicating that the mechanism of allicin on telomerase activity inhibition is different from that of AZT and telomerase activity is lack of cell cycle regulation[40-42]. In conclusion, our results may provide important insights into using allicin as a therapeutic approach against neoplasm.

REFERENCES

1 **Kim NW,** Piatyszek MA, Prowse KR, Harley CB, West MD, Ho PL, Coviello GM, Wright WE, Weinrich SL, Shay JW. Specific association of human telomerase activity with immortal cells and cancer. *Science* 1994; **266**: 2011-2015
2 **Harley CB.** Telomere loss: mitotic clock or genetic time bomb? *Mutat Res* 1991; **256**: 271-282
3 **Rhyu MS.** Telomeres, telomerase, and immortality. *J Natl Cancer Inst* 1995; **87**: 884-894
4 **Neidle S,** Kelland LR. Telomerase as an anti-cancer target: current status and future prospects. *Anticancer Drug Des* 1999; **14**: 341-347
5 **Zhou HP,** Wang X, Zhang NZ. Early apoptosis in intestinal and diffuse gastric carcinomas. *World J Gastroenterol* 2000; **6**: 898-901
6 **Guo T,** Wang X, Wang XY, Wang W, Liu Y, Zhang P, Shi YX, Zhang ZM, Sun QS, Xue T, Liu ZF, Zhu SY, Mao XF. The value of detecting telomerase activity on early diagnosis of lung cancer. *Zhongguo Feiai Zazhi* 2001; **4**: 37-40
7 **Peng MQ,** Wang X, Zhu SY, Luo T, Gu T, Yan YL, Liu H. The value of CT scan and detection of telomerase activity in biopsy specimens for early diagnosis of lung carcinoma. *Linchuang Fangshe Xue Zazhi* 2002; **21**: 1-4
8 **Wang XB,** Wang X, Zhang NZ. Inhibition of somatostatin analog Octreotide on human gastric cancer cell MKN-45 growth *in vitro*. *Shijie Huaren Xiaohua Zazhi* 2002; **10**: 40-42
9 **Li Y,** Lu YY. Applying a highly specific and reproducible cDNA RDA method to clone garlic up-regulated genes in human gastric cancer cells. *World J Gastroenterol* 2002; **8**: 213-216
10 **Li Y,** Yang L, Cui JT, Li WM, Guo RF, Lu YY. Construction of cDNA representational difference analysis based on two cDNA libraries and identification of garlic inducible expression genes in human gastric cancer cells. *World J Gastroenterol* 2002; **8**: 208-212
11 **Li X,** Xie J, Li W. Garlic oil induces differentiation and apoptosis of human gastric cancer cell line. *Zhonghua Zhongliu Zazhi* 1998; **20**: 325-327
12 **Arivazhagan S,** Nagini S, Santhiya ST, Ramesh A. Protection of N-methyl-N'-nitro-N-nitrosoguanidine-induced *in vivo* clastogenicity by aqueous garlic extract. *Asia Pac J Clin Nutr* 2001; **10**: 238-241
13 **Takezaki T,** Gao CM, Wu JZ, Ding JH, Liu YT, Zhang Y, Li SP, Su P, Liu TK, Tajima K. Dietary protective and risk factors for esophageal and stomach cancers in a low-epidemic area for stomach cancer in Jiangsu Province, China: comparison with those in a high-epidemic area. *Jpn J Cancer Res* 2001; **92**: 1157-1165
14 **Tang F,** Zhou J, Gu L. *In vivo* and *in vitro* effects of selenium-

enriched garlic on growth of human gastric carcinoma cells. *Zhonghua Zhongliu Zazhi* 2001; **23**: 461-464
15 **Kimsh SH,** Kaminker P, Campisi J. Telomeres, aging and cancer: in search of a happy ending. *Oncogene* 2002; **21**: 503-511
16 **Harley CB,** Futcher AB, Greider CW. Telomeres shorten during ageing of human fibroblasts. *Nature* 1990; **345**: 458-460
17 **Huffman KE,** Levene SD, Tesmer VM, Shay JW, Wright WE. Telomere shortening is proportional to the size of the G-rich telomeric 3'-overhang. *J Biol Chem* 2000; **275**: 19719-19722
18 **De Lange T.** Activation of telomerase in a human tumor. *Proc Natl Acad Sci U S A* 1994; **91**: 2882-2885
19 **Harley CB.** Telomerase is not an oncongene.*Oncogene* 2002; **21**: 494-502
20 **Collins K,** Mitchell JR. Telomerase in the human organism. *Oncogene* 2002; **21**: 564-579
21 **Jong HS,** Park YI, Kim S, Sohn JH, Kang SH, Song SH, Bang YJ, Kim NK. Up-regulation of human telomerase catalytic subunit during gastric carcinogenesis. *Cancer* 1999; **86**: 559-565
22 **Corey DR.** Telomerase inhibition, oligonucleotides, and clinical trials. *Oncogene* 2002; **21**: 631-637
23 **Elayadi AN,** Demieville A, Wancewicz EV, Monia BP, Corey DR. Inhibition of telomerase by 2'-O-(2-methoxyethyl) RNA oligomers: effect of length, phosphorothioate substitution and time inside cells. *Nucleic Acids Res* 2001; **29**: 1683-1689
24 **Tamura Y,** Tao M, Miyano-Kurosaki N, Takai K, Takaku H. Inhibition of human telomerase activity by antisense phosphorothioate oligonucleotides encapsulated with the transfection reagent, FuGENE6, in HeLa cells. *Antisense Nucleic Acid Drug Dev* 2000; **10**: 87-96
25 **Yegorov YE,** Akimov SS, Akhmalisheva AK, Semenova IV, Smirnova YB, Kraevsky AA, Zelenin AV. Blockade of telomerase function in various cells. *Anticancer Drug Des* 1999; **14**: 305-316
26 **Yokoyama Y,** Takahashi Y, Shinohara A, Wan X, Takahashi S, Niwa K, Tamaya T. The 5'-end of hTERT mRNA is a good target for hammerhead ribozyme to suppress telomerase activity. *Biochem Biophys Res Commun* 2000; **273**: 316-321
27 **Herbert BS,** Pongracz K, Shay JW, Gryaznov SM, Shea-Herbert B. Oligonucleotide N3'- - >P5' phosphoramidates as efficient telomerase inhibitors. *Oncogene* 2002; **21**: 638-642
28 **Melana SM,** Holland JF, Pogo BG. Inhibition of cell growth and telomerase activity of breast cancer cells *in vitro* by 3'-azido-3'-deoxythymidine. *Clin Cancer Res* 1998; **4**: 693-696
29 **Tejera AM,** Alonso DF, Gomez DE, Olivero OA. Chronic *in vitro* exposure to 3'-azido-2', 3'-dideoxythymidine induces senescence and apoptosis and reduces tumorigenicity of metastatic mouse mammary tumor cells. *Breast Cancer Res Treat* 2001; **65**: 93-99
30 **Komata T,** Kanzawa T, Kondo Y, Kondo S. Telomerase as a therapeutic target for malignant gliomas. *Oncogene* 2002; **21**: 656-663
31 **Mohamadi A,** Jarrell ST, Shi SJ, Andrawis NS, Myers A, Clouatre D, Preuss HG. Effects of wild versus cultivated garlic on blood pressure and other parameters in hypertensive rats. *Heart Dis* 2000; **2**: 3-9
32 **Neil HA,** Silagy CA, Lancaster T, Hodgeman J, Vos K, Moore JW, Jones L, Cahill J, Fowler GH. Garlic powder in the treatment of moderate hyperlipidaemia: a controlled trial and meta-analysis. *J R Coll Physicians Lond* 1996; **30**: 329-334
33 **Liao F,** Jiao L. Ligustrazine, allicin and shear-induced platelet aggregation. *Clin Hemorheol Microcirc* 2000; **22**: 167-168
34 **Ankri S,** Mirelman D. Antimicrobial properties of allicin from garlic. *Microbes Infect* 1999; **1**: 125-129
35 **Hackett JA,** Greider CW. Balancing instability: dual roles for telomerase and telomere dysfunction in tumorigenesis. *Oncogene* 2002; **21**: 619-626
36 **Mandal M**, Kumar R. Bcl-2 modulates telomerase activity. *J Biol Chem* 1997; **272**: 14183-14187
37 **Fan Y**, Lin GJ, Qian LP, Xu ZD, Li H. Effects of β-elemene on both telomerase activity and expression of Bcl-2 gene of gastric cancer SGC-7901 cell. *Shanghai Yixue* 2001; **24**: 490-492
38 **Johnson VL,** Cooper IR, Jenkins JR, Chow SC. Effects of differential overexpression of Bcl-2 on apoptosis, proliferation, and telomerase activity in Jurkat T cells. *Exp Cell Res* 1999; **251**: 175-184
39 **Li Y,** Liu JH, Zhao Q, Fan LF, Yu YM, Wang LL, Zhao XF, Zhang TD, Zhang TP, Ma TX, Liu PY. The study of allicin inducing BGC-823 human gastric adenocarcinoma cells apoptosis. *Zhongguo Zhongxi Yi Jiehe Waike Zazhi* 2001; **7**: 307-310
40 **Kyo S,** Inoue M. Complex regulatory mechanisms of telomerase activity in normal and cancer cells:how can we apply them for cancer therapy? *Oncogene* 2002; **21**: 688-697
41 **Holt SE,** Wright WE, Shay JW. Regulation of telomerase activity in immortal cell lines. *Mol Cell Biol* 1996; **16**: 2932-2939
42 **Holt SE,** Aisner DL, Shay JW, Wright WE. Lack of cell cycle regulation of telomerase activity in human cells. *Proc Natl Acad Sci U S A* 1997; **94**: 10687-10692

Edited by Zhu LH and Wang XL

P.O.Box 2345, Beijing 100023,China
Fax: +86-10-85381893
E-mail: wjg@wjgnet.com www.wjgnet.com

World J Gastroenterol 2003;9(9):1935-1939
World Journal of Gastroenterology
 ISSN 1007-9327

• GASTRIC CANCER •

Apoptosis-inducing effect of recombinant Caspase-3 expressed by constructed eukaryotic vector on gastric cancer cell line SGC7901

Yuan-Gen Fu, Yao-Jun Qu, Kai-Chun Wu, Hui-Hong Zhai, Zhi-Guo Liu, Dai-Ming Fan

Yuan-Gen Fu, Department of Biochemistry and Molecular Biology, Medical College, Shantou University, Shantou 515031, Guangdong Province, China
Yiao-Jun Qu, Department of Digestive Disease, Longgang Center Hospital, Shenzhen 518116, Guangdong Province, China
Yuan-Gen Fu, Kai-Chun Wu, Zhi-Guo Liu, Dai-Ming Fan, Institute of Digestive Diseases, Fourth Military Medical University, Xi' an 710032, Shaanxi Province, China
Hui-Hong Zhai, Department of Digestive Diseases, The First Hospital, Ningxia Medical College, Yinchuan 759901, Ningxia Hui Autonomous Region, China
Correspondence to: Dai-Ming Fan, Institute of Digestive Diseases, Xijing Hospital, Fourth Military Medical University, 17 Changlexi Road, Xi' an 710032, Shaanxi Province, China. steven_fu65@yahoo.com.cn
Telephone: +86-29-3375229 **Fax:** +86-29-2539041
Received: 2002-09-13 **Accepted:** 2002-10-29

Abstract

AIM: To investigate the apoptosis-inducing effect of Caspases-3 expressed by constructed eukaryotic vector on gastric cancer cell line SGC7901.

METHODS: PCR was employed to amplify the sequences of both small and large subunits of Caspases-3. Its products were separately cloned into the *Sma* I site of pBluescript KS$^+$ to generate both plasmids pBS/SS and pBS/LS. The small subunit fragment was excised from plasmid pBS/SS with *Bam*H I and then inserted into the *Bam*H I site of plasmid pBS/LS preceding that of the large subunit to yield plasmid pBS/Rev-Caspase-3. Rev-Caspase-3 cDNA was excised with *Kpn* I+*Xba* I and then subcloned into plasmid pcDNA3.1 (+) to construct Rev-Caspase-3 eukaryotic expression vector pcDNA/Rev-Caspase-3, which was used to transiently transfect SGC7901 cell line. Cell count, MTT assay and electron microscopy were used to confirm the antiproliferation and apoptosis-inducing effect of Rev-Caspase-3 expression on gastric cancer cells.

RESULTS: Plasmid pBS/Rev-Caspase-3 and eukaryotic expression vector pcDNA/Rev-Caspase-3 were successfully constructed. SGC7901 cells were transiently transfected by either pcDNA/Rev-Caspase-3 or pcDNA3.1 (+) for 24, 48, 72, and 96 h respectively. Cell growth was measured by cell count and MTT assay. In cell count assay, the cell numbers were 1.8×10^6, 1.55×10^6, 2.0×10^6, and 3.1×10^6 in the experimental group and 2.5×10^6, 3.1×10^6, 4.0×10^6, and 5.7×10^6 in the control group at 24, 48, 72 and 96 h respectively. The growth of SGC7901 cells was suppressed by Rev-Caspase-3 in a time-dependent manner ($P<0.05$). The results of MTT assay were similar to that of cell count ($P<0.05$). The characteristics of apoptosis such as chromatin condensation, crescent formation and margination were seen and more obvious with time in the given-experimental period in the experimental group, but not easily observed in the control group.

CONCLUSION: The expression of Rev-Caspase-3 by the constructed eukaryotic vector can significantly induce apoptosis of gastric cancer cell line SGC7901, which may exhibit a potential way in gastric cancer gene therapy.

Fu YG, Qu YJ, Wu KC, Zhai HH, Liu ZG, Fan DM. Apoptosis-inducing effect of recombinant Caspase-3 expressed by constructed eukaryotic vector on gastric cancer cell line SGC7901. *World J Gastroenterol* 2003; 9(9): 1935-1939
http://www.wjgnet.com/1007-9327/9/1935.asp

INTRODUCTION

Apoptosis is closely related to tumor[1-10]. Although there are many factors involved in apoptotic program[11-14], Caspases are shown to play a major role in the transduction of the apoptotic signal and the execution of apoptosis in mammalian[15-19]. Caspases belong to cysteine proteases family[20] and share several common features such as all homologous to interleukin-1-β-converting enzyme (ICE)[21] containing conserved QACR/QGC sequence[22] existing as inactive zymogens activated by cleavages specific internal ASP residues in interdomain linkers being able to cleave their substrates ASP residues, and consisting of prodomain, small subunit and large subunit.

So far 15 members of Caspases have been reported in the literature. According to their structure and function, Caspases are divided into two classes, the initiator and executor Caspases. The initiator Caspases carry long prodomain, and can process and activate their own and other inactive Caspase zymogens when triggered by a death signal[23,24]. The executor Caspases such as Caspases-3, however, lack the long prodomain and remain to be dormant until the initiator Caspases activate them by direct proteolysis[25]. Once activated, they dismantle cell regulatory components rapidly, leading to the typical changes observed in cell apoptosis[26-28].

Interestingly, by making small subunit fragment preceding that of the large subunit, Srinivasula *et al*[29] constructed a recombinant Caspases-3, which could simulate the three-dimensional structure of activated Caspases-3 and was capable of being catalyzed and inducing MCF-7 cell apoptosis without initiator Caspases' proteolysis. In this study, the eukaryotic expression vector of recombinant Caspases-3 was constructed and the apoptosis-inducing effect of its expression on SGC7901 cell line was observed.

MATERIALS AND METHODS

Subclone of both small and large subunits

Plasmid pcDNA/Caspases-3 contains all the cDNA sequences of Caspases-3 gene. It was used as template to amplify the sequences of small and large subunits of Caspases-3 by PCR. The sequences of four pairs of primers were as follows: LS-forward (P1), 5' -ATG GAG AAC ACT GAA AAC TCA G-3' ; LS-reverse (P2), 5' -GTC ATC ATC AAC ACC TCA GTC T-3' ; SS-forward (P3), 5' -GGA TCC ATG ATT GAG ACA GAC AGT GG-3' ; SS-reverse (P4), 5' -ATC AAC TTC ATC GTG ATA AAA ATA GAG TTC-3' .

PCR was performed in 50 μl reactive volume containing 2 μl cDNA, 5 μl PCR buffer, 2 μl dNTP, 1 μl primer, and 1 μl Taq DNA polymerase. The samples were subjected to 30 thermal cycles for 5 min at 95 ℃ for pre-denaturation, for 30 s at 94 ℃ for denaturing, for 30 s at 56 ℃ for annealing, for 50 s at 72 ℃ for extension, and for 7 min at 72 ℃ for final extension after the last cycle. The PCR products were separately cloned into the *Sma* I site of pBluescript KS+ to construct pBS/SS and pBS/LS, which were confirmed by *Sma* I digestion and DNA sequencing.

Construction of recombinant Caspases-3 (Rev-Caspaes-3)

The small subunit fragment was excised from plasmid pBS/SS with *Bam*H I and then inserted into the *Bam*H I site of plasmid pBS/LS to yield plasmid pBS/Rev-Caspases-3 with the small subunit fragment preceding that of the large subunit, which was verified with *Bam*H I+*Kpn* I digestion and PCR method. The primers were SS-forward and LS-reverse.

Construction of Rev-Caspases-3 eukaryotic expression vector pcDNA/Rev-Caspases-3

Eukaryotic expression vector pcDNA3.1 (+) was cleaved and linearized with *Kpn* I+*Nhe* I, meanwhile, Rev-Caspases-3 cDNA was excised from plasmid pBS/Rev-Caspases-3 with *Kpn* I+ *Xba* I. Both fragments were ligated each other with T_4 DNA ligase to produce plasmid pcDNA/Rev-Caspases-3, which was proved with *Stu* I+*Kpn* I.

Cell line and cell curltrue

Cell line SGC7901 was derived from a moderately-differentiated gastric adenocarcinoma and characterized extensively. It was maintained in RPMI 1640 medium supplemented with 10 % fetal bovine serum, 200 IU· ml^{-1} penicillin and 50 μg· ml^{-1} streptomycin at 37 ℃ in a humidified atmosphere of 5 % CO_2.

Cell transfection, cell count and electron microscopy

Cells were seeded in a 6-well plate with 2×10^5 cells per well 24 h prior to transfection when they were cultured to a confluency of about 90 %. Cell transfection was performed according to the manufacturers' instructions. Briefly, a transfection mixture was prepared by adding 6 μg of plasmid DNA and 20 μl lipofectame (GIBCO BRL) to 500 μl serum-free RPMI1640. After incubated at room temperature for 20 min, the transfection mixture was added to the cells to be cultivated for 4 h at 37 ℃ when the media containing the transfection mixture was exchanged for growth medium. Cells were harvested and counted at 24, 48, 72, and 96 h after transfection. Some cells were fixed in 40 g· L^{-1} glutaraldehyde, then post-fixed in osmium tetroxide and embedded in Epon. Ultrathin sections were prepared, stained with wranyl acetate and lead citrate, examined under a transmission electron microscope to identify the morphological changes of apoptosis.

MTT assay

Antiproliferation effects of recombinant Caspases-3 were measured by MTT assay. SGC7901 cells were seeded in 96-well microtitre plates with 1×10^4 cells per well and incubated overnight in 100 μl of culture media. Then the cells were transiently transfected with 0.3 μg DNA of plasmid pcDNA/Rev-Caspases-3 for 24, 48, 72, and 96 h respectively. The cells were added with 100 μl MTT (1g· L^{-1}) and further incubated for 4 h. After supernatant was removed, the cells were added with 100 μl DMSO per well and cultivated for 30 min. The absorbance at 490 nm was measured by a micro-ELISA reader. At the same time, the SGC7901 cells transfected with plasmid pcDNA3.1 (+) were served as control. Each assay was repeated three times.

Statistics

Comparison of the data among the groups was carried out using the Bonferroni-Dun multiple comparisons. In each case, *P* values less than 0.05 were considered statistically significant.

RESULTS

Construction of Rev-Caspaes-3 and pcDNA/Rev-Caspases-3

The construction strategies of recombinant Caspases-3 and eukaryotic expression plasmid pcDNA/Rev-Caspases-3 are shown in Figure 1.

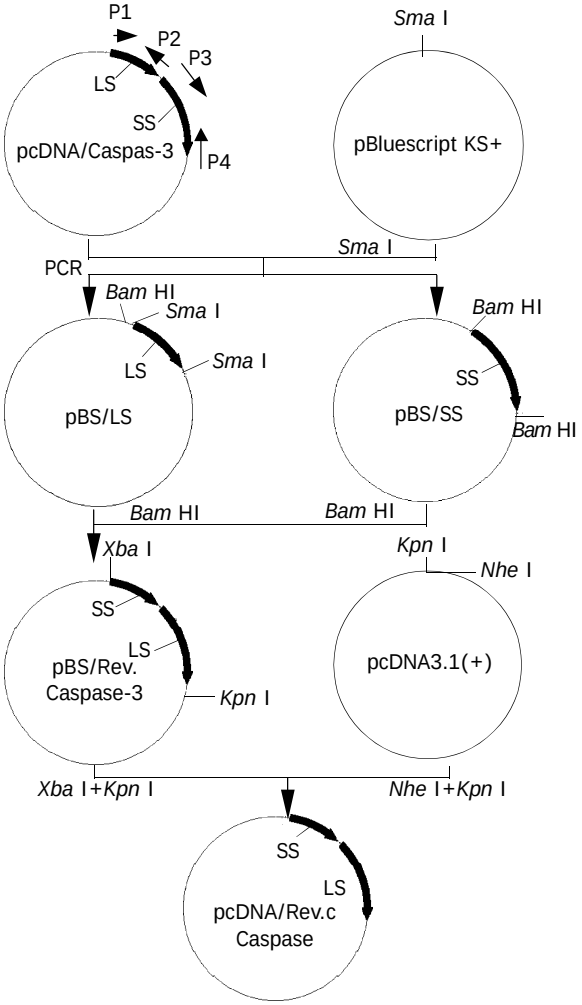

Figure 1 Schematic map of constructions of recombinant Caspases-3 and eukaryotic expression plasmid pcDNA/Rev-Caspases-3.

Both small and large subunit sequences of Caspases-3 were successfully amplified by PCR and subsequently cloned into *Sma* I site of pBluescript KS+ to yield pBS/SS and pBS/LS respectively, which were confirmed by *Sma* I digestion and DNA sequencing. The small subunit fragment was excised from plasmid pBS/SS with *Bam*H I and cloned into *Bam*H I site of plasmid pBS/LS to form recombinant plasmid pBS/Rev-Caspases-3 with the small subunit fragment located in-frame 5' to that of the large subunit, which was identified by PCR using SS-forward and LS-reverse as primers. The length of PCR product was 882 bp (Figure 2). Rev-Caspases-3 cDNA was excised from plasmid pBS/Rev-Caspases-3 with *Kpn* I+ *Xba* I and orientatively cloned into *Kpn* I and *Nhe* I site of eukaryotic expression vector pcDNA3.1(+) to construct plasmid pcDNA/Rev-Caspases-3, which was proved by the digestion of *Stu* I+*Kpn* I with a 550 bp fragment release (Figure 3).

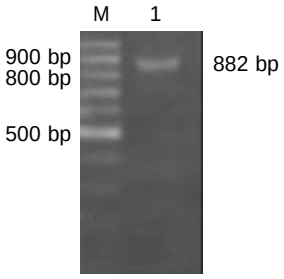

Figure 2 Identification of plasmid pBS/Rev-Caspase-3 by PCR with SS-forward and LS-reverse as primers. M: 100 bp ladder DNA marker, 1: PCR product, 882 bp.

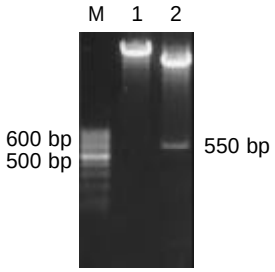

Figure 3 Enzyme digestion analysis of plasmid pcDNA/Rev-Caspase-3. M: 100 bp ladder DNA marker, 1: pcDNA/Rev-Caspase-3 cut with *Stu* I, 2: pcDNA/Rev-Caspase-3 cut with *Stu* I+*Kpn* I.

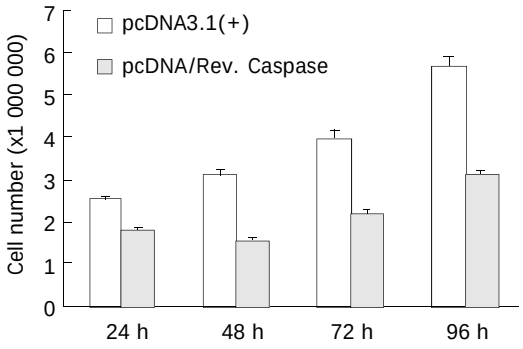

Figure 4 Comparison of cell count between SGC7901 cells transfected with pcDNA3.1(+) and pcDNA/Rev. Caspase.

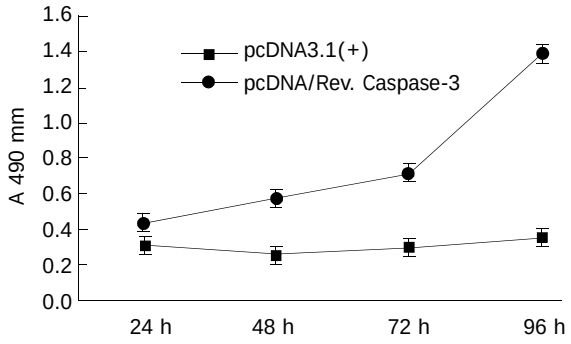

Figure 5 Comparison of MTT assays between SGC7901 cells transfected with pcDNA3.1(+) and pcDNA/Rev.Caspase-3.

Effect of Rev-Caspases-3 on SGC7901 cell growth

SGC7901 cells were transiently transfected by either pcDNA/Rev-Caspases-3 (the experimental group) or pcDNA3.1 (+) (the control group) for 24, 48, 72, and 96 h respectively. Cell growth was measured by cell count and MTT assay. In cell count assay, the cell numbers were 1.8×10^6, 1.55×10^6, 2.0×10^6, and 3.1×10^6 in the experimental group and 2.5×10^6, 3.1×10^6, 4.0×10^6, and 5.7×10^6 in the control group at 24, 48, 72, and 96 h respectively. The growth of SGC7901 cells was suppressed by Rev-Caspases-3 in a time-dependent manner (Figure 4, $P<0.05$). The results of MTT assay were similar to that of cell count (Figure 5, $P<0.05$).

Induction of apoptosis in SGC7901 by Rev-Caspases-3

The ultrastructural characteristics of apoptosis such as chromatin condensation, crescent formation, and margination were seen by electron microscopy in the experimental group, which were more obvious with time in the given-experimental period and not easily observed in the control group (Figure 6).

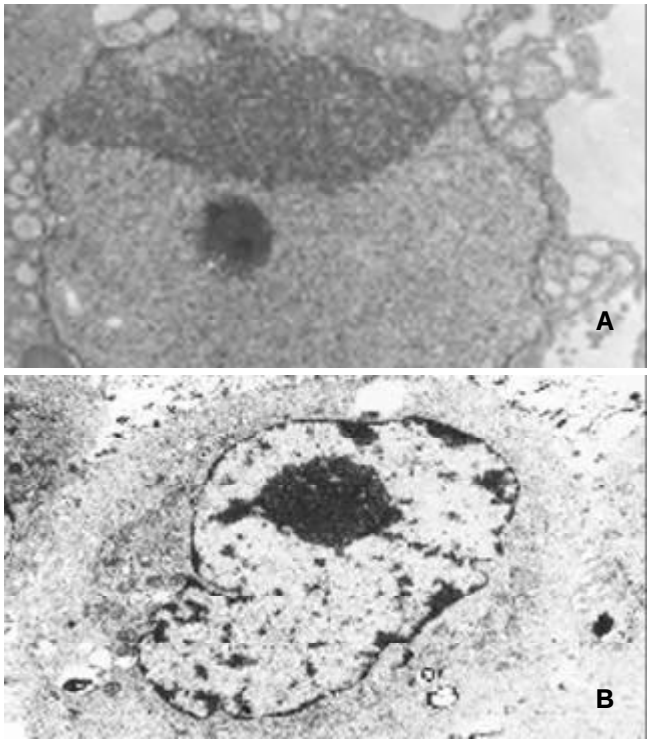

Figure 6 Electron microscopy of SGC7901 cells transfected with pcDNA3.1 (+) or pcDNA/Rev.Caspases-3. A: SGC7901 transfected with pcDNA/Rev. Caspases-3. Notice the chromatin condensation, crescent formation, original margination (×5 000); B: SGC7901 transfected with pcDNA3.1 (+), Notice no characteristics of apoptosis (×5000).

DISCUSSION

Caspases belong to cysteine protease family. So far, more than 15 members of Caspases have been reported in the literature, and most of them play a major role in apoptosis, participating in the initiation and execution of programmed cell death[30-33]. Based on their structure and function, Caspases are classified into two groups, initiator (such as Caspases-2,-8 and 10) and executor Caspases (such as Caspases-3, -6 and 7)[33-35]. Structurally, Caspase is made up of prodomain, large and small subunits, of which prodomain is located in N-terminus, small subunit in C-terminus and large subunit between. Initiator Caspases bear a long prodomain, whereas the executor Caspases do not[36-38].

Caspases are synthesized as harmless inactive zymogens and generally activated by cleavages specific internal ASP residues present in interdomain linkers, which manifests as a hierarchical process. When triggered by a death signal, the initiator Caspases are recruited through their long prodomain by specialized adaptor molecules to form the death-inducing signaling complex (DISC) or Apaf. Because of the trimeric

nature of the DISC, three Caspase molecules are brought close, which will be useful to activate initiator Caspases[39-40]. When activated, the initiator Caspase can activate itself and other inactive caspase zymogens including executor Caspases that are activated by direct proteolysis. The activated executors then rapidly dismantle important cellular components, leading to cell apoptosis.

The three-dimensional structure of activated Caspases-3 has been shown that the C-terminus of large subunit and the N-terminus of small subunit are separated far from each other, whereas the N-terminus of large subunit and C-terminus of small subunit are closed to each other[41,42]. Based on these observations, Srinivasula *et al*[29] successfully engineered recombinant Caspases-3 and -6 precursors by switching their subunits order at a gene level, in which the small subunit fragment was fused in frame N terminal to that of the large subunit. Thus the N terminus of small subunit and the C terminus of large subunit are free, while the C terminus of the small subunit and the N terminus of the large subunit are connected each other through a linker. These recombinant molecules could be activated spontaneously to induce apoptosis in MCF-7 cells independent of initiator Caspases. Jia *et al*[43] have also confirmed the apoptosis-inducing effect of recombinant Caspases-3 on HeLa cells.

Gastric carcinoma is one of the most common causes of malignancy-related death in China[44-48]. In the present study, to test the effect of recombinant Caspases-3 on gastric cancer cell, we constructed a eukaryotic expression vector of constitutively active recombinant Caspases-3 and used it to transiently transfect gastric cancer cell SGC7901. The results showed that the expressed recombinant Caspases-3 could inhibit the growth of SGC7901 in a time dependent manner. In addition, the apoptosis-inducing effect of recombinant Caspases-3 on SGC7901 was also evident. This study demonstrates the possible use of recombinant Caspases-3 in gastric cancer gene therapy. But the effects of growth inhibition and apoptosis induction conducted by recombinant Caspases-3 on other cell lines of gastric cancer or on gastric cancer cell *in vivo* need to be further investigated.

REFERENCES

1 **Sauer G**, Deissler H, Kurzeder C, Kreienberg R. New molecular targets of breast cancer therapy. *Strahlenther Onkol* 2002; **178**: 123-133

2 **Castiglioni P**, Martin-Fontecha A, Milan G, Tomajer V, Magni F, Michaelsson J, Rugarli C, Rosato A, Bellone M. Apoptosis-dependent subversion of the T-lymphocyte epitope hierarchy in lymphoma cells. *Cancer Res* 2002; **62**: 1116-1122

3 **Paczesny S**, Beranger S, Salzmann JL, Klatzmann D, Colombo BM. Protection of mice against leukemia after vaccination with bone marrow-derived dendritic cells loaded with apoptotic leukemia cells. *Cancer Res* 2001; **61**: 2386-2389

4 **Amin S**, Robins RA, Maxwell-Armstrong CA, Scholefield JH, Durrant LG. Vaccine-induced apoptosis: a novel clinical trial end point? *Cancer Res* 2000; **60**: 3132-3136

5 **Li HL,** Chen DD, Li XH, Zhang HW, Lu YQ, Ye CL, Ren XD. Changes of NF-kB, p53, Bcl-2 and caspase in apoptosis induced by JTE-522 in human gastric adenocarcinoma cell line AGS cells: role of reactive oxygen species. *World J Gastroenterol* 2002; **8**: 431-435

6 **Feng RH**, Zhu ZG, Li JF, Liu BY, Yan M, Yin HR, Lin YZ. Inhibition of human telomerase in MKN-45 cell line by antisense hTR expression vector induces cell apoptosis and growth arrest. *World J Gastroenterol* 2002; **8**: 436-440

7 **Tao HQ**, Zou SC. Effect of preoperative regional artery chemotherapy on proliferation and apoptosis of gastric carcinoma cells. *World J Gastroenterol* 2002; **8**: 451-454

8 **Wu k**, Zhao Y, Liu BH, Li Y, Liu F, Guo J, Yu WP. RRR-α-tocopheryl succinate inhibits human gastric cancer SGC-7901 cell growth by inducing apoptosis and DNA synthesis arrest. *World J Gastroenterol* 2002; **8**: 26-30

9 **Zhang Z**, Yuan Y, Gao H, Dong M, Wang L, Gong YH. Apoptosis, proliferation and *P*53 gene expression of *H pylori* associated gastric epithelial lesions. *World J Gastroenterol* 2001; **7**: 779-782

10 **Henry F**, Bretaudeau L, Hequet A, Barbieux I, Lieubeau B, Meflah K, Gregoire M. Role of antigen-presenting cells in long-term antitumor response based on tumor-derived apoptotic body vaccination. *Pathobiology* 1999; **67**: 306-310

11 **Wiley SR**, Schooley K, Smolak PJ, Din WS, Huang CP, Nicholl JK, Sutherland GR, Smith TD, Rauch C, Smith CA, Goodwin RG. Identification and characterization of a new member of the TNF family that induces apoptosis. *Immunity* 1995; **3**: 673-682

12 **Sheridan JP**, Marsters SA, Pitti RM, Gurney A, Skubatch M, Baldwin D, Ramakrishnan L, Gray CL, Baker K, Wood WI, Goddard AD, Godowski P, Ashkenazi A. Control of TRAIL-induced apoptosis by a family of signaling and decoy receptors. *Science* 1997; **277**: 818-821

13 **Wei XC**, Wang XJ, Chen K, Zhang L, Liang Y, Lin XL. Killing effect of TNF-related apoptosis inducing ligand regulated by tetracycline on gastric cancer cell line NCI-N87. *World J Gastroenterol* 2001; **7**: 559-562

14 **Golstein P**. Cell death: TRAIL and its receptors. *Curr Biol* 1997; **7**: 750-753

15 **Choi YH,** Kim MJ, Lee SY, Lee YN, Chi GY, Eom HS, Kim ND, Choi BT. Phosphorylation of p53, induction of Bax and activation of Caspases during beta-lapachone-mediated apoptosis in human prostate epithelial cells. *Int J Oncol* 2002; **21**: 1293-1299

16 **Grabarek J**, Du L, Johnson GL, Lee BW, Phelps DJ, Darzynkiewicz Z. Sequential Activation of Caspases and Serine Proteases (Serpases) During Apoptosis. *Cell Cycle* 2002; **1**: 124-131

17 **Knoblach SM**, Nikolaeva M, Huang X, Fan L, Krajewski S, Reed JC, Faden AI. Multiple Caspases are activated after traumatic brain injury: evidence for involvement in functional outcome. *J Neurotrauma* 2002; **19**: 1155-1170

18 **Shiraga S**, Adamus G. Mechanism of CAR syndrome: anti-recoverin antibodies are the inducers of retinal cell apoptotic death via the caspase 9- and caspase 3-dependent pathway. *J Neuroimmunol* 2002; **132**: 72-82

19 **Hetz CA**, Hunn M, Rojas P, Torres V, Leyton L, Quest AF. Caspase-dependent initiation of apoptosis and necrosis by the Fas receptor in lymphoid cells: onset of necrosis is associated with delayed ceramide increase. *J Cell Sci* 2002; **115**(Pt 23): 4671-4683

20 **Harvey NL**, Kumar S. The role of Caspases in apoptosis. *Adv Biochem Eng Biotechnol* 1998; **62**: 107-128

21 **Alnemri ES**, Livingston DJ, Nicholson DW, Salvesen G, Thornberry NA, Wong WW, Yuan J. Human ICE/CED-3 protease nomenclature. *Cell* 1996; **87**: 171

22 **Cohen GM**. Caspases: the executioners of apoptosis. *Biochem J* 1997; **326**(Pt 1): 1-16

23 **Fernandes-Alnemri T**, Armstrong RC, Krebs J, Srinivasula SM, Wang L, Bullrich F, Fritz LC, Trapani JA, Tomaselli KJ, Litwack G, Alnemri ES. *In vitro* activation of CPP32 and Mch3 by Mch4, a novel human apoptotic cysteine protease containing two FADD-like domains. *Proc Natl Acad Sci U S A* 1996; **93**: 7464-7469

24 **Srinivasula SM**, Ahmad M, Fernandes-Alnemri T, Litwack G, Alnemri ES. Molecular ordering of the Fas-apoptotic pathway: the Fas/APO-1 protease Mch5 is a CrmA-inhibitable protease that activates multiple Ced-3/ICE-like cysteine proteases. *Proc Natl Acad Sci U S A* 1996; **93**: 14486-14491

25 **Li P**, Nijhawan D, Budihardjo I, Srinivasula SM, Ahmad M, Alnemri ES, Wang X. Cytochrome c and dATP-dependent formation of Apaf-1/caspase-9 complex initiates an apoptotic protease cascade. *Cell* 1997; **91**: 479-489

26 **Nicholson DW**, Thornberry NA. Caspases: killer proteases. *Trends Biochem Sci* 1997; **22**: 299-306

27 **Salvesen GS**, Dixit VM. Caspases: intracellular signaling by proteolysis. *Cell* 1997; **91**: 443-446

28 **Meller R**, Skradski SL, Simon RP, Henshall DC. Expression, proteolysis and activation of Caspases 6 and 7 during rat C6 glioma cell apoptosis. *Neurosci Lett* 2002; **324**: 33-36

29 **Srinivasula SM**, Ahmad M, MacFarlane M, Lou Z, Huang Z, Fernandes-Alnemri T, Alnemri ES. Generation of constitutively active recombinant Caspases-3 and –6 by rearrangement of their subunits. *J Biol Chem* 1998; **273**: 10107-10111

30 **Huo J**, Luo RH, Metz SA, Li G. Activation of caspase-2 mediates the apoptosis induced by GTP-depletion in insulin-secreting

(HIT-T15) cells. *Endocrinology* 2002; **143**: 1695-1704
31 **Distelhorst CW**. Recent insights into the mechanism of glucocorticosteroid-induced apoptosis. *Cell Death Differ* 2002; **9**: 6-19
32 **Heinke MY**, Yao M, Chang D, Einstein R, dos Remedios CG. Apoptosis of ventricular and atrial myocytes from pacing-induced canine heart failure. *Cardiovasc Res* 2001; **49**: 127-134
33 **Riedl SJ**, Fuentes-Prior P, Renatus M, Kairies N, Krapp S, Huber R, Salvesen GS, Bode W. Structural basis for the activation of human procaspase-7. *Proc Natl Acad Sci U S A* 2001; **98**: 14790-14795
34 **Riedl SJ**, Renatus M, Schwarzenbacher R, Zhou Q, Sun C, Fesik SW, Liddington RC, Salvesen GS. Structural basis for the inhibition of Caspases-3 by XIAP. *Cell* 2001; **104**: 791-800
35 **Cuvillier O**, Edsall L, Spiegel S. Involvement of sphingosine in mitochondria-dependent Fas-induced apoptosis of type II Jurkat T cells. *J Biol Chem* 2000; **275**: 15691-15700
36 **Huang Y**, Shin NH, Sun Y, Wang KK. Molecular cloning and characterization of a novel Caspases-3 variant that attenuates apoptosis induced by proteasome inhibition. *Biochem Biophys Res Commun* 2001; **283**: 762-769
37 **Seol DW**, Billiar TR. A caspase-9 variant missing the catalytic site is an endogenous inhibitor of apoptosis. *J Biol Chem* 1999; **274**: 2072-2076
38 **Meergans T**, Hildebrandt AK, Horak D, Haenisch C, Wendel A. The short prodomain influences Caspases-3 activation in HeLa cells. *Biochem J* 2000; **349**(Pt 1): 135-140
39 **Yang X**, Chang HY, Baltimore D. Autoproteolytic activation of pro-Caspases by oligomerization. *Mol Cell* 1998; **1**: 319-325
40 **Muzio M**, Stockwell BR, Stennicke HR, Salvesen GS, Dixit VM. An induced proximity model for caspase-8 activation. *J Biol Chem* 1998; **273**: 2926-2930
41 **Mittl PR**, Di Marco S, Krebs JF, Bar X, Karanewsky DS, Priestle JP, Tomaselli KJ, Grutter MG. Structure of recombinant human CPP32 in complex with the tetrapeptide acetyl-Asp-Val-Ala-Asp fluoromethyl ketone. *J Biol Chem* 1997; **272**: 6539-6547
42 **Rotonda J**, Nicholson DW, Fazil KM, Gallant M, Gareau Y, Labelle M, Peterson EP, Rasper DM, Ruel R, Vaillancourt JP, Thornberry NA, Becker JW. The three-dimensional structure of apopain/CPP32, a key mediator of apoptosis. *Nat Struct Biol* 1996; **3**: 619-625
43 **Jia LT**, Yu CJ, Xu YM, Zhu F, Peng WD, Su CZ, Wang CJ, Yang AG. Construction and effect of Caspases-3 fusion proteins and their apoptosis induction in HeLa cells. *Disi Junyi Daxue Xuebao* 2001; **12**: 1057-1060
44 **Wang CD**, Chen YL, Wu T, Liu YR. Association between lowe expression of somatostatin receptor II gene and lymphoid metastasis in patients with gastric cancer. *Shijie Huaren Xiaohua Zazhi* 1999; **7**: 864-866
45 **Gu HP**, Ni CR, Zhan RZ. Relationship between CD15 mRNA and its protein expression and gastric carcinoma invasion. *Shijie Huaren Xiaohua Zazhi* 2000; **8**: 851-854
46 **Wang DX**, Fang DC, Liu WW. Study on alteration of multiple genes in intestinal metaplasia, atypical hyperplasia and gastric cancer. *Shijie Huaren Xiaohua Zazhi* 2000; **8**: 855-859
47 **Guo SY**, Gu QL, Liu BY, Zhu ZG, Yin HR, Lin YZ. Experimental study on the treatment of gastric cancer by TK gene combined with mIL-2 gene. *Shijie Huaren Xiaohua Zazhi* 2000; **8**: 974-978
48 **Wu YL**, Sun B, Zhang XJ, Wang SN, He HY, Qiao MM, Zhang J, Xu JY. Growth inhibition and apoptosis induction of Sulindac on Human gastric cancer cells. *World J Gastroenterol* 2001; **7**: 796-800

Edited by Zhu L, Zhang JZ and Wang XL

P.O.Box 2345, Beijing 100023,China
Fax: +86-10-85381893
E-mail: wjg@wjgnet.com www.wjgnet.com

World J Gastroenterol 2003;9(9):1940-1945
World Journal of Gastroenterology
 ISSN 1007-9327

• LIVER CANCER •

Experimental study on therapeutic effect of *in vivo* expression of Cell I-Hep II recombinant polypeptide of fibronectin on murine H22 hepatocellular carcinoma

Gui-Mei Zhang, Yan Yang, Bo Huang, Hui Xiao, Dong Li, Zuo-Hua Feng

Gui-Mei Zhang, Yan Yang, Bo Huang, Hui Xiao, Dong Li, Zuo-Hua Feng, Department of Biochemistry and Molecular Biology, Tongji Medical College, Huazhong University of Science and Technology, Wuhan 430030, Hubei Province, China
Supported by grants of National Development Program (973) for Key Basic Research (No. 2002CB513100) and the National Natural Science Foundation of China (No. 39870763)
Correspondence to: Dr. Zuohua Feng, Department of Biochemistry and Molecular Biology, Tongji Medical College, Huazhong University of Science and Technology, Wuhan 430030, Hubei Province, China. fengzhg@public.wh.hb.cn
Telephone: +86-27-83657574 **Fax:** +86-27-83657574
Received: 2003-03-20 **Accepted:** 2003-04-11

Abstract

AIM: To investigate the inhibitory effect of *in vivo* expression of expressing plasmid pCH510 of recombinant fibronectin polypeptide (CH50) on hepatocellular carcinoma and the improved therapeutic effect of pCH510 in combination with chemotherapeutic agents and Hsp70-H22 hepatocarcinoma antigen peptide on tumor.

METHODS: Mice were inoculated with H22 hepatocarcinoma cells. The chemotactic effect of the expression of plasmid pCH510 on immunocytes was observed after *in vivo* transfection, tissue slicing and HE staining. Inhibitory effect of transfection with pCH510 on murine tumor originated from different inoculative doses was observed. The inhibitory effect of immediate transfection with pCH510 after chemotherapy on tumor was compared with that of transfection 5 days after chemotherapy. The change of function and amount of mouse peritoneal macrophages and the peripheral blood immunocytes resulted from administration of chemotherapeutic agents were detected. The peptides mixture was prepared from H22 hepatocarcinoma cells. pCH510 + Hsp70-H22 antigen peptides were injected into tumor-bearing mice with or without chemotherapy, to observe the inhibitory effects on tumor.

RESULTS: At the tumor tissue site injected with pCH510, there were a great number of immunocytes which mainly were macrophages, lymphocytes and neutrophils. Transfection of plasmid pCH510 inhibited significantly the murine tumor induced by different inoculative doses. The inhibitory effect was negatively correlated with the inoculative dose. The therapeutic effect was not improved by immediate transfection with pCH510 after chemotherapy, but was significantly improved by transfection with pCH510 5 days after chemotherapy. Chemotherapeutic agent decreased the number of immunocytes and suppressed their activation *in vivo*. After injection of drug, the amount of immunocytes was the lowest from d 1 to d 3 and returned to normal level on the 10^{th} day. Transfection with plasmid pCH510 alone could inhibit tumor induced by the inoculation with 10^4 H22 cells. The tumor originated from the inoculation with 10^5 H22 cells was inhibited by pCH510+Hsp70-H22 antigen peptides and that from the inoculation with 10^6 H22 cells was inhibited by pCH510+Hsp70-H22 antigen peptides in combination with chemotherapeutic agents.

CONCLUSION: *In vivo* expression of pCH510 recruits immune cells, inhibits tumor growth, and enhances the efficacy of chemotherapy. But the proper timing of combining chemotherapy with pCH510 must be taken into great account. The synergism of pCH510 and Hsp70-H22 peptides can improve the efficacy, which could be further enhanced if they are used following chemotherapy. Chemotherapeutic agent + pCH510 + Hsp70-H22 peptides is a promising therapeutic approach of combination treatment of tumor.

Zhang GM, Yang Y, Huang B, Xiao H, Li D, Feng ZH. Experimental study on therapeutic effect of *in vivo* expression of Cell I-Hep II recombinant polypeptide of fibronectin on murine H22 hepatocellular carcinoma. *World J Gastroenterol* 2003; 9(9): 1940-1945
http://www.wjgnet.com/1007-9327/9/1940.asp

INTRODUCTION

Hepatocellular carcinoma (HCC) is a common malignant tumor with an increasing incidence, and remains a disease with a poor and dismal prognosis, and all forms of currently available conventional therapies are rarely beneficial[1]. Surgical resection is incapable of removing all HCC cells and so is chemotherapy[2]. However, in recent years, biotherapy has been reported with promising results as a new therapeutic approach of hepatocellular carcinoma[1-7]. On the other hand, the extraordinary versatility of gene therapy opens new possibilities for the treatment of hepatocellular carcinoma[8-10].

Fibronectin (FN) is an extracellular matrix glycoprotein which exists in extracellular matrix (cellular-type) and in blood (plasma-type). It is composed of multiple functional domains including cell-binding domain and heparin-binding domain, and additional regions such as EDA, EDB and V region that arise through alternative splicing. Recombinant peptides with different functional domains produce different effects on tumor cells. Hep II-V bifunctional-domain recombinant peptide can promote tumor invasion[11]. In contrast, Cell I-Hep II bifunctional-domain recombinant peptide has an inhibitory effect on adhesion, invasion, and spreading of tumor cells[12,13]. Fragments of fibronectin have chemotactic effect on immunocytes. David A.Norris[14] reported that fragments of fibronectin cleaved by enzymes were chemotactic to human peripheral blood monocytes, but intact FN was inactive. Doherty[15] also reported that FN fragments containing cell-binding domain could recruit macrophages. The chemotactic effect is mediated by the interaction between cell-binding domain and β1 integrin receptor on the cell surface[16,17]. These characteristics indicate the great potential of FN in tumor therapy. We have expressed in *E.coli* and purified recombinant

FN polypeptide containing Cell I-Hep II bifunctional-domain. The peptide has the activities of chemotaxis, macrophage activation, as well as inhibitory effect on tumor growth and metastasis[18]. On this basis, the eukaryotic expressing plasmid pCH510 of Cell I-Hep II bifunctional-domain recombinant polypeptide was constructed[19]. The main purpose of the study was to investigate the chemotactic effect on immunocytes and therapeutic effectiveness on mouse H22 hepatocellular carcinoma of *in vivo* expression of pCH510, and the role of *in vivo* expression of pCH510 in combined treatment of tumor, and to analyze the factors influencing the effect of combined treatment so as to provide experimental basis for potential use of pCH510 in tumor therapy.

MATERIALS AND METHODS

Reagents

Mouse H22 hepatocarcinoma cell line was purchased from China Center for Type Culture Collection (CCTCC, Wuhan). BALB/c mice were purchased from Medical Experimental Animal Center of Hubei Province. Eukaryotic expression plasmid pCH510 of Cell I-Hep II bifunctional-domain recombinant polypeptide CH50 of human fibronectin was constructed in our lab. Recombinant human heat shock protein 70 was expressed and purified in our laboratory. Mitomycin C (MMC) was the product of Zhejiang Hisun Pharmaceutical Corporation. IFN-γ and MTT were purchased from Sigma Co.

Inoculation of mouse with H22 cells

H22 cells were suspended in PBS at the concentrations of 1×10^8/ml, 1×10^7/ml, 1×10^6/ml, 1×10^5/ml respectively. 100 μl of the suspension was injected into the muscle of mouse at right hind limb. The inoculative doses were 1×10^7, 1×10^6, 1×10^5, 1×10^4, respectively.

Chemotaxis test for immunocytes of pCH510 transfection in hind limb muscle of tumor-bearing mice

After inoculation with 1×10^6 H22 cells, mice were randomly divided into 2 groups, 9 mice in each group, for the injection of 100 μg of plasmid pCH510, 100 μg of plasmid pcDNA3.1 respectively. The next day after inoculation, mice in each group were given an injection at the inoculation site. The tissue specimens from muscle tissue of injection site were prepared on day 1, 2, 3 after plasmid transfection, 3 mice from each group each day.

Inhibition test of tumor growth by pCH510 transfection

The mice in different groups were each inoculated with 1×10^7, 1×10^6, 1×10^5, 1×10^4 of H22 tumor cells respectively. Starting from d 2, the mice in each group were given an injection of 100 μg of plasmid pCH510 every day for 10 times at the inoculation site. The mice in control group were given an injection of control plasmid pcDNA3.1. The mice were dissected to measure the weight of tumor at different time after inoculation: on the 7th day for 1×10^7 inoculative dose, on the 10th day for 1×10^6, on the 14th day for 1×10^5, and on the 21st day for 1×10^4.

Inhibition test of pCH510 in combination with chemotherapy

The mice were inoculated with 1×10^6 H22 cells, and randomly divided into six groups designated as A, B, C, D, E, F (day 0). On day 1, the mice in group B were injected at inoculation site with 100 μg of plasmid pCH510, for 10 days. On day 2, the mice in Groups C, D, E, F were injected at inoculation site with 50 μg MMC. On day 3, the mice in group E were injected at inoculation site with 100 μg of plasmid pCH510, for 10 days. On day 6, the mice in group F were injected at inoculation site with 100 μg of plasmid pCH510, for 15 days. The mice in groups A, B, C were dissected to measure the weight of tumor on the 15th day, the mice in groups D, E, F were dissected to measure the weight of tumor on the 21st day.

Assay for function of mouse peritoneal macrophages after injection of MMC

Macrophages were collected from murine abdominal cavity 4 hours and 24 hours after ip injection of 50 μg MMC. The macrophages were cultured *in vitro* in the presence of IFN-γ and CH50. The activation and NO production of macrophages were determined after 48 hour cell culture by MTT.

Assay for amount of immunocytes in peripheral blood of mouse after injection of MMC

The mice were randomly divided into two groups for ip injection of 50 μg MMC and PBS respectively (designated as day 0). On days 1, 3, 5, 7, 9, 11, blood was collected from murine orbital vein, the cells were counted following the removal of red cells. At the same time, macrophages were collected from murine peritoneal cavity and counted.

Preparation of Hsp70-H22 antigen peptides

H22 tumor antigen peptides and Hsp70 were prepared according to the method described previously[20]. Hsp70 and peptides mixture from cells were mixed to bind each other[20]. Briefly, peptides and Hsp70, at the concentrations of 75 μg/ml and 250 μg/ml respectively, were mixed and incubated at 37 ℃ for 2 h in the presence of 1 mM of ADP and 1 mM of $MgCl_2$.

Inhibition test of pCH510 with Hsp70-H22 peptide on tumor growth

The mice were randomly divided into eight groups. Four groups were inoculated with 10^5 of H22 cells, the other four groups were inoculated with 10^6 of H22 cells (designated as day 0). On day 1, the mice in different groups were given injection of pCH510 + Hsp70-H22 antigen peptides, pCH510, Hsp70-H22 antigen peptide, and saline respectively, every other day for 9 times. The mice were dissected to measure the weight of tumor on the 21st day (for control group, on the 14th day or 10th day).

Inhibition test of chemotherapy + pCH510 +Hsp70-H22 antigen peptide on tumor growth

The mice were randomly divided into five groups and inoculated with 10^6 of H22 cells into the hind limb (designated as day 0). On day 1, the mice were injected with 50 μg of MMC at the inoculation site (the control group was given saline). On day 5, the mice injected with MMC were given injection of pCH510 + Hsp70-H22 antigen peptide, pCH510, Hsp70-H22 antigen peptide, and saline respectively, every other day for 14 times. The mice were dissected to measure the weight of tumor at different times: saline group on the 10th day, MMC group on the 15th day, MMC + pCH510 and MMC + Hsp70-H22 antigen peptide groups on the 30th day, and another MMC + pCH510 + Hsp70-H22 antigen peptide group on the 40th day. The size of tumor was observed.

Statistical analysis

The *t* test was used for statistical analysis. *P* value less than 0.05 was considered as significantly different.

RESULTS

Chemotaxis for immune cells of pCH510 expression in tumor tissue

Tumor cells in control group grew rapidly. On the 3rd day after inoculation, tumor nodes were observed. In the tissue section

of control group, there were a large amount of tumor cells which invaded muscle tissues. In the experimental group, tumor node was not observed. In the tissue section, tumor cells were distributed locally. There were a large amount of macrophages and lymphocytes in connective tissues and many neutrophils and lymphocytes on the edge of tumor and muscle tissues. Immune cells were seldom seen in normal muscle tissues which were not invaded by tumor cells (Figures 1 and 2).

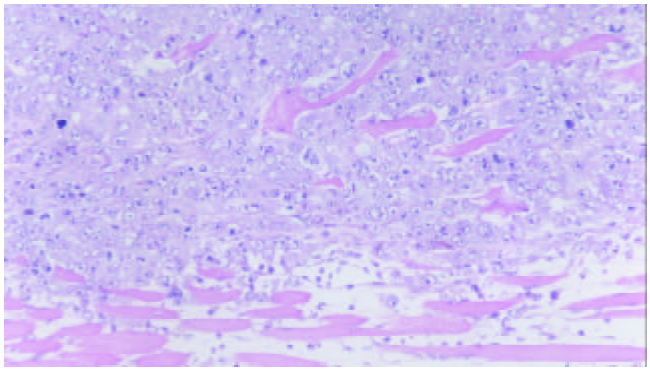

Figure 1 Control group: tumor cells grew rapidly and invaded the normal muscles (×200).

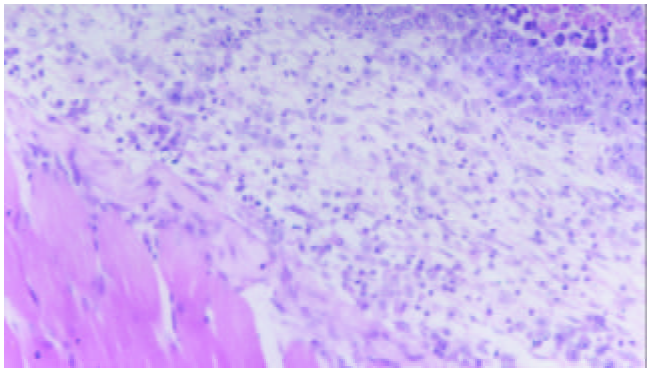

Figure 2 pCH510 group: transfection of pCH510 recruited macrophages, lymphocytes and neutrophils (×200).

Inhibitory effects of pCH510 on tumor growth

Plasmid pCH510 had inhibitory effects on murine tumor induced by different inoculative doses and the effect was negatively correlated with the inoculative dose. The lower the inoculative dose was, the more significant the effect. For 10^4 of tumor cells inoculation, pCH510 could completely inhibit the tumor growth in a period of 20 days (Table 1).

Table 1 Inhibitory effect of pCH510 on murine tumor inoculated with different doses of tumor cells

Inoculative doses	*n*	Dissecting time (d)	Tumor weight (g, $\bar{x}$±*s*)	
			Control	pCH510
10^4	8	21	2.19±0.35	0[a]
10^5	8	14	2.27±0.38	0.62±0.17[a]
10^6	8	10	2.32±0.42	1.35±0.24[a]
10^7	8	7	2.37±0.33	1.88±0.32[b]

[a]P<0.05 *vs* control; [b]P<0.01 *vs* control.

Effect of interval between injection of MMC and pCH510 on therapeutic efficacy

Chemotherapeutic agent alone or pCH510 alone could inhibit tumor growth. After chemotherapy, the effect was not improved by immediate 10-day pCH510 transfection. The tumor grew much slower if the mice were given 15-day pCH510 transfection 5 days after chemotherapy, suggesting that pCH510 in combination with chemotherapeutic agent in this way could significantly improve therapeutic effectiveness (Table 2).

Table 2 Inhibitory effect of pCH510 in combination with chemotherapy on murine tumor

Groups	*n*	Tumor weight (g, $\bar{x}$±*s*)	
		d 11	d 21
A: control	8	2.12±0.38	
B: pCH510 (d 2 to d11)	8	0.82±0.21[a]	
C: chemo I	8	0[a]	
D: chemo II	8		1.58±0.31
E: MMC+pCH510 (d 2 to d 11)	8		1.49±0.28
F: MMC+pCH510 (d 6 to d 20)	8		0.42±0.12[b]

[a]P<0.01 *vs* control; [b]P<0.01 *vs* chemo II.

Effect of MMC on the function and amount of macrophages in vivo

The metabolic activity of macrophages from murine abdominal cavity was inhibited by injection of MMC after 4 hours and 24 hours *in vivo*. The level of NO released by macrophage decreased significantly (Table 3). After injection with MMC intraperitoneally, the number of macrophage from murine peritoneal cavity and mononuclear cells from peripheral blood decreased dramatically. The number of immune cells reached the lowest from d 1 to d 3, and started recovery from d 5 and returned to normal level on the 11th day (Figure 3).

Table 3 Effects of MMC on activity of macrophages

Groups	*n*	4 h		24 h	
		Metabolism OD_{570},($\bar{x}$±*s*)	NO mol/L, ($\bar{x}$±*s*)	Metabolism OD_{570},($\bar{x}$±*s*)	NO mol/L, ($\bar{x}$±*s*)
Control	6	0.35±0.06	29.9±5.1	0.32±0.04	28.8±6.3
MMC	6	0.15±0.03[a]	16.5±4.3[a]	0.16±0.04[a]	13.9±5.4[a]

[a]P<0.01 *vs* control.

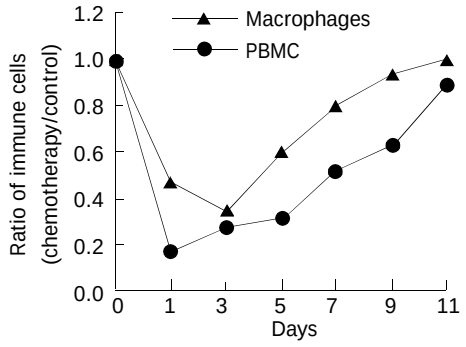

Figure 3 Numerical change of mouse celiac macrophages and peripheral blood mononuclear cells (PBMC) after injection of MMC.

Synergic effects of pCH510 with Hsp70-H22 peptides on inhibition of H22 tumor growth

pCH510 in combination with Hsp70-H22 peptides could produce a much stronger inhibitory effect on H22 tumor in mice. Although the tumor from 10^6 of H22 cells inoculation was not completely inhibited, the tumor from 10^5 of H22 cells inoculation was completely inhibited (Table 4).

Table 4 Inhibitory effect of pCH510+Hsp70-H22 antigen peptide complex on murine tumor

Group	*n*	10^5 H22 cells inoculation		10^6 H22 cells inoculation	
		Dissecting time (d)	Tumor weight (g, $\bar{x}\pm s$)	Dissecting time (d)	Tumor weight (g, $\bar{x}\pm s$)
Control	8	14	3.24±1.22	10	3.45±1.31
pCH510 plasmid	8	21	2.38±0.84	21	2.72±1.28
Hsp70-H22 peptide	8	21	1.44±0.45	21	2.58±0.93
Hsp70-H22 peptide+pCH510	8	21	0[b]	21	1.76±0.66[a]

[a]$P<0.05$ *vs* control; [b]$P<0.01$ *vs* control.

Table 5 Inhibitory effect of chemotherapy+pCH510+Hsp70-H22 peptide on murine tumor

Group	*n*	H22 cell inoculating	Dissecting time (d)	Tumor weight (g, $\bar{x}\pm s$)
Control	8	10^6	10	3.28±1.12
MMC	8	10^6	15	2.82±0.94
MMC+pCH510	8	10^6	30	1.51±0.53
MMC+Hsp70-H22 peptide	8	10^6	30	0.62±0.22[b]
MMC+pCH510+Hsp70-H22 peptide	8	10^6	40	0[a]

[a]$P<0.01$ *vs* control; [b]$P<0.05$ *vs* (MMC+pCH510).

Inhibitory effects of chemotherapy+pCH510+Hsp70-H22 peptides on tumor growth

For tumor from 10^6 of H22 cells inoculation, the anti-tumor efficacy was significantly different if chemotherapeutic agent was used in combination with other agents. Compared with the protocols of chemotherapy in combination with Hsp70-H22 peptides and chemotherapy in combination with pCH510, the anti-tumor effect of chemotherapy in combination with both pCH510 and Hsp70-H22 peptides was the most powerful, which could completely inhibit the growth of residual tumor after chemotherapy (Table 5).

DISCUSSION

Tumor immuno-therapy comprises non-specific and specific immuno-therapy. The former includes some cytokines such as IL-12, IL-18, TNF-α, as well as some immune cells such as macrophages, natural killer cells and so on. The latter is cell-mediated immunity which is produced by the activation of $CD4^+$ and $CD8^+$ T cells stimulated by tumor specific antigen. Immuno-therapy holds great promise as an effective weapon against residual tumor cells after chemotherapy. Cell I-HepII double-domain polypeptide and CH50 can recruit macrophages and lymphocytes by chemotaxis, activate macrophages to inhibit the growth of tumor by non-specific immune response. It has a great potential in tumor therapy. It has been reported that fibronectin fragments containing Cell I-domain inhibited tumor invasion and metastasis[21,22]. Our results showed that recombinant FN polypeptide recruited immune cells into the local tumor tissue, increasing the local anti-tumor immunity. A large number of immune cells gathered around the tumor tissue which had been transfected with pCH510. Moreover, comparing the result of pCH510 transfection on the first day after inoculation with those of the other groups, the distribution of tumor cells was much more limited and the invasion of tumor cells to normal tissue was delayed, suggesting that transfection with pCH510 could inhibit tumor growth and invasion at the early stage of tumor growth.

Plasmid pCH510 had inhibitory effect on murine tumor from different inoculative doses and the effects was negatively correlated with the inoculative dose. The lower the inoculative dose was, the more significant the effect was. For 10^4 of tumor cells inoculation, pCH510 could completely inhibit the tumor growth in a period of 20 days. Chemotherapeutic agent kills tumor cells rapidly and powerfully. For 10^6 of tumor cells inoculation, the tumor did not grow within 11 days after chemotherapy. At the same time, the tumor weight in pCH510 transfection group was over 0.5 g, suggesting that chemotherapy should be chosen first to kill residual tumor cells after surgery.

It had an inhibitory effect on tumor growth no matter chemotherapeutic agent or pCH510 was used alone. But neither was powerful enough. When we tried to enhance the antitumor efficacy by combining anticancer drugs with immune modulator CH50, we found that the therapeutic effectiveness was not improved as we had expected by immediate 10-day transfection with pCH510 after chemotherapy. And there was no direct evidence to testify the inhibition of the expression of the plasmid by chemotherapy. CH50 plays an anti-tumor role by regulating host immune response. So we tried to find out the response pattern of host immune system to chemotherapy and the proper timing of transferring pCH510 after chemotherapy. Our results showed that chemotherapeutic agent not only decreased the number of immunocytes but also suppressed their activation. After injection of MMC, the amount of immunocytes was the lowest from d 1 to d 3 and returned to normal level on the 10^{th} day. Similar phenomenon was observed when dendritic cell (DC) counts and function were assayed in peripheral blood of lymphoma and solid tumor patients before and after chemotherapy[23]. The DC counts declined significantly within the first week from the start of chemotherapy, recovered in the second week, and exceeded the baseline values in the third week[23]. The count of immunocytes dropping to the lowest point means that the cytotoxicity of the drug is over. At this moment the host immune system is most severely damaged. If H22 cells were inoculated to the mice on the third day after chemotherapy, the tumor grew more fast than non-chemotherapy control (data not presented), suggesting that immuno-therapy was needed after chemotherapy. But immediate pCH510 transfection after chemotherapy recruited very few inactivated immune cells, as a result, the therapeutic effectiveness was not improved. In contrast, the therapeutic effectiveness was significantly improved by 15-day transfection with pCH510 5 days after chemotherapy. The proper timing of combining chemotherapy with pCH510 was on the 3^{rd} and 5^{th} day after chemotherapy.

Besides proper timing, another influential factor on

therapeutic effectiveness was the dose of chemotherapeutic drug which has also been reported recently[24-26]. One of the disadvantages of conventional chemotherapy is the cytotoxic side effect. How to make full use of the cytotoxicity to tumor cells and lower the side effects is the basis of evaluating the drug dose. In pilot experiments, four doses of MMC were set as following: 150 μg, 100 μg, 50 μg and 25 μg. Two of eight mice died from 150 μg MMC. None of the mice died from 100 μg MMC, but they were accompanied by obtuse reactions, light weight and lackluster hair. For 50 μg and 25 μg MMC, the mice were agile and no obvious side effects were found. Therefore, 50 μg of MMC was the suitable dose for mouse in our experiment. Our results were consistent with those of related reports[27, 28], which showed that combined treatment with low-dose chemotherapy could achieve better efficacy.

The growth of tumor from 10^6 of H22 inoculation was slowed down by chemotherapy in comparison with the tumor from 10^4 of H22 inoculation without treatment. Transfection with plasmid pCH510 alone did inhibit the tumor from 10^4 of H22 inoculation, but not the tumor from 10^6 of H22 inoculation with chemotherapy, suggesting that chemotherapy had a dual effect on tumor growth: on the one hand, they killed tumor cells, on the other hand, they promoted tumor growth by damaging host immune system. Furthermore, improvement of the therapeutic effectiveness by a single immune factor combined with chemotherapy was limited. The best way is the combination of chemotherapy with several kinds of synergic immune modulators. In tumor cells, there are a great amount of over-expressed proteins which can be cleaved into small peptides. These peptides can be used as tumor antigens to induce specific antitumor immune response. At present, only limited antigen peptides are identified, including MAGE-1, MAGE-3, HER-2/neu, and MUC-1[29]. On the other hand, the immunity of multi-valence CTLs induced by mixed antigen peptides from tumor cells is stronger than that of monovalence CTL induced by a given antigen peptide[30]. Heat shock protein 70, as a molecular chaperon, can bind antigen peptide to form Hsp70-peptide complex. The complex presents the antigen peptide to antigen presenting cells (APC) mediated by high affinity receptors on the surface of APC to induce CD_8^+ CTL response[31-35]. In addition to CD_8^+ CTL response, the Hsp70-peptides can also induce CD_4^+ T cell response and NK cell reaction[36]. Our experiment demonstrated that mixed antigen peptides obtained from H22 hepatocarcinoma cells, bound to Hsp70, could induce the production of $CD8^+$ CTLs which could kill specifically H22 cells and inhibit experimental tumor growth *in vivo*[20]. It is theoretically practical that immune cells recruited by pCH510 can be activated by Hsp70-H22 peptide to produce powerful anti-tumor immunity, which was verified by our experiment. The results in this paper showed that the combination of non-specific immune response with specific immune response could be a better strategy for the treatment of tumor. The Cell I-Hep II recombinant polypeptide expressed by plasmid pCH510 could recruit macrophages and other immune cells *in vivo*, activate macrophages and produce non-specific antitumor immunity. Hsp70-H22 peptides could specifically activate $CD4^+$, $CD8^+$ T cells to produce specific anti-tumor immunity. Immune cells were recruited into the tumor tissue by the expressed product of pCH510 and activated by Hsp70-H22 peptides, producing a much stronger anti-tumor immunity.

Nowadays tumor immuno-therapy is focused on specific immune response induced by antigens such as using tumor antigen peptides, tumor idiotype antibody[37]. Tumor antigen peptides can be obtained by some methods such as phage display[38], isolation from Hsp70, hsp90, and gp96-peptide complex[39, 40]. But it is difficult to get mixed antigen peptides, and the complex obtained by the latter method is very little. In this paper we provided a new method which is simple and effective, to obtain mixed antigen peptides from tumor cells by freezing and thawing, heating and acid precipitating.

Transfection with plasmid pCH510 alone could inhibit the tumor originated from 10^4 inoculative dose of H22 cells. The tumor originated from 10^5 inoculative dose of H22 was inhibited by pCH510+Hsp70-H22 antigen peptides. Following the treatment with MMC, the two factors could inhibit the tumor from 10^6 inoculative dose of H22. These results indicate that immuno-therapy is just effective on a small amount of tumor cells. The chemotherapeutic agent is the indispensable agent once the tumor load is high. Chemotherapeutic agents can kill tumor cells rapidly and powerfully, but not completely. Combination of anticancer drugs and immune modulators is necessary. And the combination of pCH510 and Hsp70-peptides has been proved to be one of the choices for the treatment of residual tumor after chemotherapy.

In summary, recombinant polypeptide CH50 is a promising non-specific immune modulator. It can be expressed *in vivo* to inhibit experimental tumor growth. The inhibitory effect can be further improved by combining pCH510 with Hsp70-tumor antigen peptides. Furthermore, the two immune modulators can synergize with chemotherapeutic agents to treat tumor. But chemotherapeutic agents damage the host immune sysytem, so that immuno-therapy has no effect within 3 or 5 days after chemotherapy. For different immuno-therapy agents, different chemotherapeutic drugs and different patients, the combining pattern is possibly different. Individualized treatment regimen should be adopted.

REFERENCES

1 **Kountouras J**, Boura P, Kouklakis G. Locoregional immunochemotherapy in hepatocellular carcinoma. *Hepatogastroenterology* 2002; **49**: 1109-1112

2 **Tang ZY**. Hepatocellular carcinoma-cause, treatment and metastasis. *World J Gastroenterol* 2001; **7**: 445-454

3 **Fan J**, Wu ZQ, Tang ZY, Zhou J, Qiu SJ, Ma ZC, Zhou XD, Ye SL. Multimodality treatment in hepatocellular carcinoma patients with tumor thrombi in portal vein. *World J Gastroenterol* 2001; **7**: 28-32

4 **Shi BM**, Wang XY, Mu QL, Wu TH, Liu HJ, Yang Z. Angiogenesis effect on rat liver after administration of expression vector encoding vascular endothelial growth factor D. *World J Gastroenterol* 2003; **9**: 312-315

5 **Shi M**, Wang FS, Wu ZZ. Synergetic anticancer effect of combined quercetin and recombinant adenoviral vector expressing human wild-type p53, GM-CSF and B7-1 genes on hepatocellular carcinoma cells *in vitro*. *World J Gastroenterol* 2003; **9**: 73-78

6 **Liu JW**, Tang Y, Shen Y, Zhong XY. Synergistic effect of cell differential agent-II and arsenic trioxide on induction of cell cycle arrest and apoptosis in hepatoma cells. *World J Gastroenterol* 2003; **9**: 65-68

7 **Wang X**, Liu FK, Li X, Li JS, Xu GX. Retrovirus-mediated gene transfer of human endostatin inhibits growth of human liver carcinoma cells SMMC7721 in nude mice. *World J Gastroenterol* 2002; **8**: 1045-1049

8 **Mohr L**, Geissler M, Blum HE. Gene therapy for malignant liver disease. *Expert Opin Biol Ther* 2002; **2**: 163-175

9 **Ruiz J**, Mazzolini G, Sangro B, Qian C, Prieto J. Gene therapy of hepatocellular carcinoma. *Dig Dis* 2001; **19**: 324-332

10 **Sangro B**, Qian C, Schmitz V, Prieto J. Gene therapy of hepatocellular carcinoma and gastrointestinal tumors. *Ann N Y Acad Sci* 2002; **963**: 6-12

11 **Kapila YL**, Niu J, Johnson PW. The high affinity heparin-binding domain and the V region of fibronectin mediate invasion of human oral squamous cell carcinoma cells *in vitro*. *J Biol Chem* 1997; **272**: 18932-18938

12 **Saiki I**, Yoneda J, Kobayashi H, Igarashi Y, Komazawa H, Ishizaki Y, Kato I, Azuma I. Antimetastatic effect by anti-adhesion therapy with cell-adhesive peptide of fibronectin in

combination with anticancer drugs. *Jpn J Cancer Res* 1993; **84**: 326-335

13 **Yoneda J**, Saiki I, Kobayashi H, Fujii H, Ishizaki Y, Kato I, Kiso M, Hasegawa A, Azuma I. Inhibitory effect of recombinant fibronectin polypeptides on the adhesion of liver-metastatic lymphoma cells to hepatic sinusoidal endothelial cells and tumor invasion. *Jpn J Cancer Res* 1994; **85**: 723-734

14 **Norris DA**, Clark RA, Swigart LM, Huff JC, Weston WL, Howell SE. Fibronectin fragment (s) are chemotactic for human peripheral blood monocytes. *J Immunol* 1982; **129**: 1612-1618

15 **Doherty DE**, Henson PM, Clark RA. Fibronectin fragments containing the RGDS cell-binding domain mediate monocyte migration into the rabbit lung. A potential mechanism for C5 fragment-induced monocyte lung accumulation. *J Clin Invest* 1990; **86**: 1065-1075

16 **Hauzenberger D**, Klominek J, Sundqvist KG. Functional specialization of fibronectin- binding β1-integrins in T lymphocyte migration. *J Immunol* 1994; **153**: 960-971

17 **Harler MB**, Wakshull E, Filardo EJ, Albina JE, Reichner JS. Promotion of neutrophil chemotaxis through differential regulation of β1 and β2 integrins. *J Immunol* 1999; **162**: 6792-6799

18 **Zhang G**, Feng Z, Zhang H, Fan Q, Li D. Augmentation of recombinant fibronectin polypeptide CH50 on the antitumor function of macrophages. *J Tongji Med Univ* 1998; **18**: 5-9

19 **Li D**, Feng Z, Ye S, Zhang G, Zhang H, Huang B, Xiao H. Construction and expression of eukaryotic expressing vector pCH510 of polypeptide CH50 and its chemotaxis and antitumor function by *in vivo* transfection. *J Tongji Med Univ* 2001; **21**: 1-5

20 **Feng ZH**, Huang B, Zhang GM, Li D, Wang HT. Investigation on the effect of peptides mixture from tumor cells inducing anti-tumor specific immune response. *Science in China* 2002; **45**: 361-369

21 **Van Golen KL**, Bao L, Brewer GJ, Pienta KJ, Kamradt JM, Livant DL, Merajver SD. Suppression of tumor recurrence and metastasis by a combination of the PHSCN sequence and the antiangiogenic compound tetrathiomolybdate in prostate carcinoma. *Neoplasia* 2002; **4**: 373-379

22 **Saito N**, Mitsuhashi M, Hayashi T, Narumo C, Nagata H, Soyama K, Kameoka S, Harumiya S, Fujimoto D. Inhibition of hepatic metastasis in mice treated with cell-binding domain of human fibronectin and angiogenesis inhibitor TNP-470. *Int J Clin Oncol* 2001; **6**: 215-220

23 **Markowicz S**, Skurzak HM, Walewski J. A method for directly determining the number of dendritic cells and for evaluation of their function in small amounts of human peripheral blood. *Arch Immunol Ther Exp* 2001; **49**: 51-57

24 **Hanahan D**, Bergers G, Bergsland E. Less is more, regularly: metronomic dosing of cytotoxic drugs can target tumor angiogenesis in mice. *J Clin Invest* 2000; **105**: 1045-1047

25 **Klement G**, Baruchel S, Rak J, Man S, Clark K, Hicklin DJ, Bohlen P, Kerbel RS. Continuous low-dose therapy with vinblastine and VEGF receptor-2 antibody induces sustained tumor regression without overt toxicity. *J Clin Invest* 2000; **105**: R15-24

26 **Vacca A**, Iurlaro M, Ribatti D, Minischetti M, Nico B, Ria R, Pellegrino A, Dammacco F. Anti angiogenesis is produced by nontoxic doses of vinblastine. *Blood* 1999; **94**: 4143-4155

27 **Bello L**, Carrabba G, Giussani C, Lucini V, Cerutti F, Scaglione F, Landre J, Pluderi M, Tomei G, Villani R, Carroll RS, Black PM, Bikfalvi A. Low-dose chemotherapy combined with an antiangiogenic drug reduces human glioma growth *in vivo*. *Can cer Res* 2001; **61**: 7501-7506

28 **Ng CP**, Bonavida B. A new challenge for successful immunotherapy by tumors that are resistant to apoptosis: two complementary signals to overcome cross-resistance. *Adv Cancer Res* 2002; **85**: 145-174

29 **Wang RF**, Rosenberg SA. Human tumor antigens for cancer vaccine development. *Immunol Rev* 1999; **170**: 85-100

30 **Heiser A**, Maurice MA, Yancey DR, Wu NZ, Dahm P, Pruitt SK, Boczkowski D, Nair SK, Ballo MS, Gilboa E, Vieweg J. Induction of polyclonal prostate cancer-specific CTL using dendritic cells transfected with amplified tumor RNA. *J Immunol* 2001; **166**: 2953-2960

31 **Arnold-Schild D**, Hanau D, Spehner D, Schmid C, Rammensee HG, de la Salle H, Schild H. Cutting edge: receptor-mediated endocytosis of heat shock proteins by professional antigen-presenting cells. *J Immunol* 1999; **162**: 3757-3760

32 **Castellino F**, Boucher PE, Eichelberg K, Mayhew M, Rothman JE, Houghton AN, Germain RN. Receptor-mediated uptake of antigen / heat shock protein complexes results in major histocompatibility complex class I antigen presentation via two distinct processing pathways. *J Exp Med* 2000; **191**: 1957-1964

33 **Basu S**, Binder RJ, Ramalingam T, Srivastava PK. CD91 is a common receptor for heat shock proteins gp96, hsp90, hsp70,and calreticulin. *Immunity* 2001; **14**: 303-313

34 **Blachere NE**, Li Z, Chandawarkar RY, Suto R, Jaikaria NS, Basu S, Udono H, Srivastava PK. Heat shock protein-peptide complexes, reconstituted *in vitro*, elicit peptide-specific cytotoxic T lymphocyte response and tumor immunity. *J Exp Med* 1997; **186**: 1315-1322

35 **Castelli C**, Ciupitu AM, Rini F, Rivoltini L, Mazzocchi A, Kiessling R, Parmiani G. Human heat shock protein 70 peptide complexes specifically activate antimelanoma T cells. *Cancer Res* 2001; **61**: 222-227

36 **Tamura Y**, Peng P, Liu K, Daou M, Srivastava PK. Immunotherapy of tumors with autologous tumor-derived heat shock protein preparations. *Science* 1997; **278**: 117-120

37 **Timmerman JM**, Singh G, Hermanson G, Hobart P, Czerwinski DK, Taidi B, Rajapaksa R, Caspar CB, Van Beckhoven A, Levy R. Immunogenicity of a plasmid DNA vaccine encoding chimeric idiotype in patients with B-cell lymphoma. *Cancer Res* 2002; **62**: 5845-5852

38 **Wu Y**, Wan Y, Bian J, Zhao J, Jia Z, Zhou L, Zhou W, Tan Y. Phage display particles expressing tumor-specific antigens induce preventive and therapeutic anti-tumor immunity in murine p815 model. *Int J Cancer* 2002; **98**: 748-753

39 **Ishii T**, Udono H, Yamano T, Ohta H, Uenaka A, Ono T, Hizuta A, Tanaka N, Srivastava PK, Nakayama E. Isolation of MHC class I-restricted tumor antigen peptide and its precursors associated with heat shock proteins hsp70, hsp90, and gp96. *J Immunol* 1999; **162**: 1303-1309

40 **Belli F**, Testori A, Rivoltini L, Maio M, Andreola G, Sertoli MR, Gallino G, Piris A, Cattelan A, Lazzari I, Carrabba M, Scita G, Santantonio C, Pilla L, Tragni G, Lombardo C, Arienti F, Marchiano A, Queirolo P, Bertolini F, Cova A, Lamaj E, Ascani L, Camerini R, Corsi M, Cascinelli N, Lewis JJ, Srivastava P, Parmiani G. Vaccination of metastatic melanoma patients with autologous tumor-derived heat shock protein gp96-peptide complexes: clinical and immunologic findings. *J Clin Oncol* 2002; **20**: 4169-4180

Edited by Zhu LH and Wang XL

P.O.Box 2345, Beijing 100023,China
Fax: +86-10-85381893
E-mail: wjg@wjgnet.com www.wjgnet.com

World J Gastroenterol 2003;9(9):1946-1949
World Journal of Gastroenterology
 ISSN 1007-9327

• LIVER CANCER •

Pathomorphological study on location and distribution of Kupffer cells in hepatocellular carcinoma

Kai Liu, Xu He, Xue-Zhong Lei, Lian-San Zhao, Hong Tang, Li Liu, Bing-Jun Lei

Kai Liu, Xu He, Xue-Zhong Lei, Lian-San Zhao, Hong Tang, Li Liu, Bing-Jun Lei, Division of Molecular Biology of Infectious Disease Key Laboratory of Biotherapy of Human Disease, Ministry of Education, West China Hospital of Sichuan University, Chengdu 610041, Sichuan Province, China
Supported by the National Natural Science Foundation of China, No.39670812
Correspondence to: Lian-San Zhao, Division of Molecular Biology of Infectious Disease Key Laboratory of Biotherapy of Human Disease, Ministry of Education, West China Hospital of Sichuan University, Chengdu 610041, Sichuan Province, China
Telephone: +86-28-85422635 **Fax:** +86-28-85422113
Received: 2003-03-20 **Accepted:** 2003-04-14

Abstract

AIM: To clarify the location and distribution of Kupffer cells in hepatocellular carcinoma (HCC), and to investigate their role in hepatocarcinogenesis.

METHODS: Kupffer cells were immunohistochemically stained by streptavadin-peroxidase conjugated method (S-P). The numbers of Kupffer cells in cancerous, para-cancerous and adjacent normal liver tissues of 48 HCCs were comparatively examined.

RESULTS: The mean number of Kupffer cells in cancerous, para-cancerous and adjacent normal liver tissues was 12.7±6.8, 18.1±8.2 and 18.9±7.9 respectively. The number of Kuppfer cells in cancerous tissues was significantly lower than that in para-cancerous tissues (t=2.423, P<0.05) and adjacent normal liver tissues (t=2.521, P<0.05). As tumor size increased, the number of Kupffer cells in cancerous tissues significantly decreased (F=4.61, P<0.05). Moreover, there was also a significant difference in the number of Kupffer cells among well-differentiated, moderately-differentiated and poorly-differentiated cases(F=4.49, P<0.05).

CONCLUSION: This study suggests that decrease of Kupffer cells in HCCs may play an important role in the carcinogenesis of HCC, the number of Kupffer cells in HCC is closely related to the size and differentiation grade of the tumor.

Liu K, He X, Lei XZ, Zhao LS, Tang H, Liu L, Lei BJ. Pathomorphological study on location and distribution of Kupffer cells in hepatocellular carcinoma. *World J Gastroenterol* 2003; 9(9): 1946-1949
http://www.wjgnet.com/1007-9327/9/1946.asp

INTRODUCTION

Kupffer cells are important in maintaining homeostasis and in host anti-tumor defense mechanism[1-5]. It is thought that Kupffer cells are resident macrophages in the liver and are one kind of the sinusoidal endothelial cells[6]. Previously, Kupffer cells were not considered to exist in hepatocellular carcinoma (HCC) tissues. Recently, some studies revealed that Kupffer cells were also present in early-stage and well-differentiated HCC. Because small and well-differentiated HCCs could maintain an environment similar to that of normal sinusoids, Kupffer cells may also exist in these HCCs[7,8].

Unfortunately, whether Kupffer cells could exist in poorly-differentiated or large HCCs remaines unidentified. Nevertheless, the difference of Kupffer cells among variable tissue types is not clear. The relationship between the decrease of Kupffer cells and carcinogenesis of HCC also needs to be clarified.

In the present study, we pathomorphologically examined the localization and distribution of Kupffer cells in 48 cases of HCCs samples embracing cancerous tissues, corresponding para-cancerous tissues and adjacent normal liver tissues.

MATERIALS AND METHODS

Tissues and specimen

Tissues of forty-eight primary HCCs including cancerous tissues, corresponding para-cancerous tissues and adjacent normal liver tissues were obtained with the informed consent of patients who underwent hepatectomy at the West China Hospital of Sichuan University. The surgically resected tissues were fixed in 10 % formalin, embedded in paraffin, cut into 5 μm sections and stained with hematoxylin-eosin. Histopathological diagnosis and classification were made by the same pathologist.

Immunohistochemical staining

The SP method was used, and the first antibody was mouse-anti-human monoclonal CD68 antibody (DAKO, dilution 1: 50). The operation procedure was according to the instructions of SP kit which was purchased from DAKO, Glostrup, Denmark. DAB was used for coloration. The dark brown granules in cytoplasm were taken as CD68 positive reaction. Negative mouse serum and PBS were respectively used to replace 1st antibody as negative control and blank control.

Identification of Kupffer cells

Among the cells which were anti-CD68 antibody positive, those in the blood space of cancerous tissues or the sinusoids of noncancerous tissues with a stellate or spindle shape were evaluated as Kupffer cells.

Determination of Kupffer cell numbers

The number of Kupffer cells was counted in five randomly selected visual fields under a microscope (×200) for each specimen. Then the average Kupffer cell number of each specimen was determined.

Statistical analysis

The data of Kupffer cells were expressed as mean ± standard deviation (Mean ± SD), and the differences in the values of different groups were analyzed by t test and F test. The criterion of significance was set at P<0.05.

RESULTS

Kupffer cells in HCC specimens

Kupffer cells were present in the cancerous tissues of 45 out

of 48 cases of HCCs (93.8 %). The only 3 specimens in which no Kupffer cells were found were all poorly-differentiated HCCs. Kupffer cells were found in the para-cancerous tissues and adjacent normal liver tissues of all 48 HCCs.

Number of Kupffer cells and histological grades

The mean number of Kupffer cells in cancerous, para-cancerous and adjacent normal liver tissues was 12.7±6.8,18.1±8.2 and 18.9±7.9 respectively. The number of Kuppfer cells in cancerous tissues was significantly lower than that in para-cancerous tissues and adjacent normal liver tissues (P<0.05) (Table 1). The number of Kupffer cells in cancerous tissues of well, moderately and poorly differentiated HCCs was 18.4±4.2, 11.2±6.2 and 5.2±4.9, respectively (Table 2).The number of Kupffer cells in cancerous tissues significantly decreased as the histological grades decreased (P<0.05) (Figure 1).

Table 1 Kupffer cell number in different tissue types

Tissue type	*n*	Kupffer cell number ($\bar{x}$±*s*)
Cancerous tissue	48	12.7±6.8
Para-cancerous tissue	48	18.1±8.2[a]
Adjacent normal liver tissue	48	18.9±7.9[b]

[a]P<0.05 *vs*. cancerous tissues, [b]P<0.05 *vs*. cancerous tissues.

Table 2 Realationship between Kupffer cell number, tumor size, and differentiation degree

	n	Kupffer cell number ($\bar{x}$±*s*)
Tumor size (diameter)		
<3 cm	12	17.4±4.8[a]
3-5 cm	17	12.5±6.3[a]
>5 cm	19	7.9±5.8[a]
Differentiation degree		
Well- differentiated	11	18.4±4.2[b]
Moderately- differentiated	20	11.2±6.2[b]
Poorly- differentiated	17	5.2±4.9[b]

[a]P<0.05 *vs*. among three groups, [b]P<0.05 *vs*. among three groups.

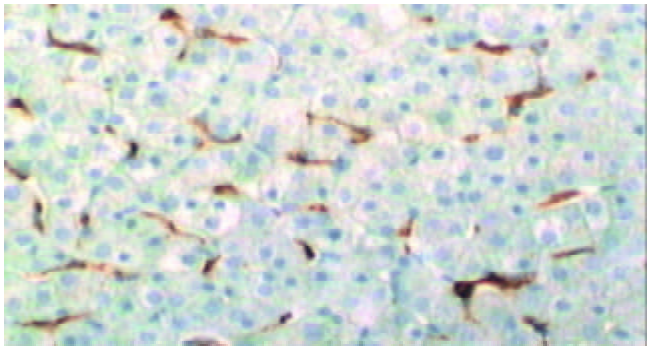

Figure 1 Kupffer cells in cancerous tissues of well-differentiated HCC ×200.

Relationship between the number of Kupffer cells and tumor size

Among the 48 HCCs, 12 cases had a tumor size <3 cm, 17 between 3-5 cm and 19 >5 cm. Mean Kupffer cell number in the cancerous tissues of the three groups was 17.4±4.8, 12.5± 6.3 and 7.9±5.8 respectively (Table 2).The three poorly-differentiated cases of HCCs in which there was no Kupffer cell in cancerous tissues all had a diameter >5 cm. Mean Kupffer cell number in cancerous tissues of HCCs which had a diameter <3 cm was significantly higher than that of the cases of HCCs which had a diameter between 3-5 cm or >5 cm (P<0.05). In addition, Kupffer cell number in cancerous tissues of tumors which had a diameter between 3-5 cm differed significantly from that of the cases of HCCs which had a diameter >5 cm (Figures 2 and 3). As the tumor size increased, the Kupffer cell number decreased significantly (P<0.05).

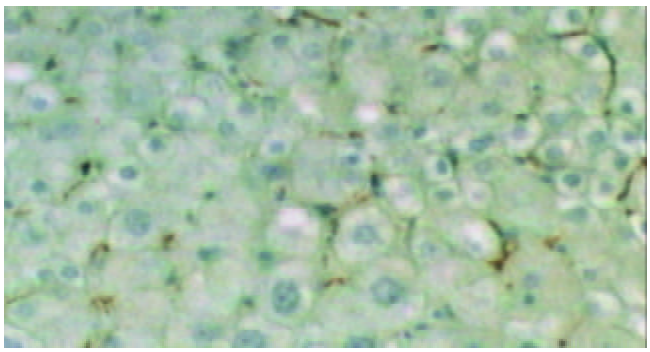

Figure 2 Kupffer cells in cancerous tissues of poorly-differentiated HCC (tumor diameter 3.5 cm) ×200.

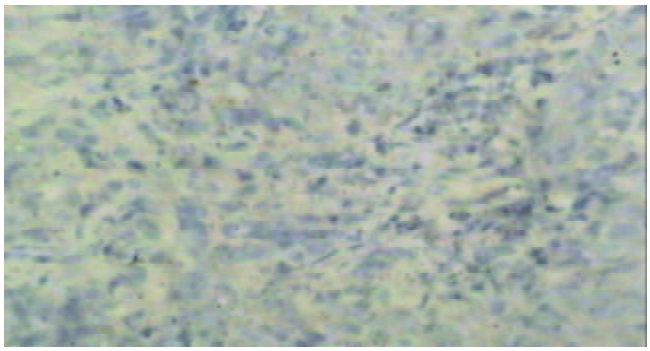

Figure 3 No Kupffer cell in cancerous tissues of poorly-differentiated HCC (tumor diameter 7.8 cm) ×200.

DISCUSSION

Kupffer cells are important in the host defense mechanism including normal metabolism, phagocytosis, cytokine generation and anti-tumor effects. They are also involved in the pathogenesis of liver diseases such as viral hepatitis, alcohoic liver injury, chemically mediated liver injury, liver fibrosis, ischemia and reperfusion injury in liver transplantation, and hepatocyte regeneration[9-23]. Functional capability of Kupffer cells is considered to decrease when the liver is impaired. Usually, light-microscope is used to identify Kupffer cells by confirming the presence of lipofuscin and hemosiderin pigments in the cytoplasm. Moreover, Kupffer cells can be identified by monitoring their unique ultra-structures. For example, they have numerous vesicles, well-developed lamillipodia in cytoplasm and lysosomes in various sizes. In this study, we used anti-CD68, an anti-human macrophage antibody, to identify macrophages. CD68 was expressed not only in the residential macrophages such as Kupffer cells, but also in the migrating macrophages. In view of this fact, Kupffer cells cannot be identified merely by being anti-CD68 positive. Morphological observations are also required to distinguish between these two cell types. For example, migrating macrophages are usually oval and contain abundant cytoplasm, while Kupffer cells usually have spindle or stellate-shaped cytoplasm and partly adhere to the sinusoidal endothelial cells[24-29].

The origin of Kupffer cells in normal liver tissues remains

unidentified. One hypothesis postulates that Kupffer cells are originated from the macrophages which have been present in the premordial liver at the embryonal stage. The other hypothesis proposes that monocytes which are originated from bone marrow arrive, settle in the sinusoids and then differentiate into Kupffer cells. There are two possible mechanisms of Kupffer cells existing in cancerous tissues of HCC. (1) Under the environmental condition similar to normal sinusoids, migrating macrophages in the blood space change into Kupffer cell-like cells. (2) Kupffer cells in normal liver tissue are maintained in the cancerous tissues. Our results showed that all the three poorly differentiated HCCs contained no Kupffer cell in cancerous tissues. Moreover, Kupffer cells in cancerous tissues of poorly differentiated HCCs were significantly less than those of well or moderately differentiated HCCs. In view of the fact that the morphology of poorly differentiated cancerous tissues is quite different from that of normal liver tissue, the former hypothesis may be more reasonable. We also found Kupffer cell number in para-cancerous and adjacent normal liver tissues had no statistical difference, probably due to the fact that para-cancerous tissues present in the blood space closer to the normal sinusoids. On the other hand, Kupffer cells were found to be activated in the pathogenesis of liver injuries such as early-stage fibrosis and fatty liver hepatitis. Under these conditions the sinusoid structures usually were not destroyed seriously and Kupffer cell number did not decrease significantly[30-32].

The mechanism responsible for the tumoricidal activities of Kupffer cells is not completely known. Kupffer cells may execute their anti-tumor effect via increasing the production of some cytotoxic molecules such as NO, TNF-α and IFN-γ, which may inhibit the growth of tumor by damaging cellular DNA and inducing apoptosis. When implanted into normal and cirrhotic rat livers, rat HCC cells grew much more progressively in cirrhotic livers than in normal livers. Meanwhile, Kupffer cells were decreased profoundly in cirrhotic livers, resulting in markedly impaired phagocytic activity. Furthermore, profound decrease production of Kupffer cell-related cytokines was found to in cirrhotic livers[1,5,33]. Previous studies also found that Kupffer cells might play an important role in controlling occurrence and progression of liver metastasis. The possible pathway of Kupffer cells against liver metastasis might be that tumor cells were apoptotic via the Fas-Fas ligand system induced by TNF-α released from Kupffer cells[34-36]. When the liver is chemically injured, Kupffer cells may release biologically active mediators that promote the pathogenic process. Though there is evidence that indicates Kupffer cells play a stimulatory role in liver regeneration, presently Kupffer cells are thought to have the potential to exert both stimulatory and inhibitory influences on hepatocyte proliferation[37-40]. Some research suggested that in viral hepatitis, Kupffer cells were activated and expressed high levels of CD80, CD40 and class-II MHC molecules, thus acquiring the phenotype of antigen presenting cells (APCs)[41].

Enhanced magnetic resonance imaging (MRI) has been used to detect hepatic tumors[42]. The method utilizes selective taken-up mechanism of superparamagnetic iron oxide (SPIO) or chondroitin sulfate iron colloid into the reticuloendothelial cells such as Kupffer cells of the liver. Our findings indicated that the number Kupffer cells in cancerous tissues decreased significantly as the tumor size increased and histological grade decreased. Therefore, the enhanced MRI which utilizes the function of Kupffer cells can be useful in estimation of histological degree of HCC. Imai *et al*[43] studied histologically proven tumors including 31 HCCs and 6 dysplastic nodules by SPIO-enhanced MRI, and proposed that SPIO-enhanced MRI reflect Kupffer cell number in HCCs and dysplastic nodules and be useful in assessing the histological grades of HCCs, especially poorly-differentiated and moderately-differentiated cases. Recently, Kitamura *et al*[44] reported 18 HCCs detected by color Doppler sonography had either a marked reduction in the number or absence of Kupffer cells. In conclusion, the present study has shown that Kupffer cells are important in preventing development of HCCs, and tumor metastases. They are also involved in the pathogenesis of chemically mediated liver injury and viral hepatitis. Further study on the biological characteristics and function of Kupffer cells will contribute to the early diagnosis of hepatic tumors and new treatment strategies.

REFERENCES

1 **Chen GG**, Lau WY, Lai PB, Chun YS, Chak EC, Leung BC, Lam IK, Lee JF, Chui AK. Activation of Kupffer cells inhibits tumor growth in a murine model system. *Int J Cancer* 2002; **99**: 713-720

2 **Ramadori G**, Armbrust T. Cytokines in the liver. *Eur J Gastroenterol Hepatol* 2001; **13**: 777-784

3 **Johnson SJ,** Burr AW, Toole K, Dack CL, Mathew J, Burt AD. Macrophage and hepatic stellate cell responses during experimental hepatocarcinogenesis. *J Gastroenterol Hepatol* 1998; **13**: 145-151

4 **Ju C,** Reilly TP, Bourdi M, Radonovich MF, Brady JN, George JW, Pohl LR. Protective role of Kupffer cells in acetaminophen-induced hepatic injury in mice. *Chem Res Toxicol* 2002; **15**: 1504-1513

5 **Zhu HZ,** Ruan YB, Wu ZB, Zhang CM. Kupffer cell and apoptosis in experimental HCC. *World J Gastroenterol* 2000; **6**: 405-407

6 **Toth CA,** Thomas P. Liver endocytosis and Kupffer cells. *Hepatology* 1992; **16**: 255-266

7 **Torimura T,** Ueno T, Inuzuka S, Kin M, Ohira H, Kimura Y, Majima Y, Sata M, Abe H, Tanikawa K. The extracellular matrix in hepatocellular carcinoma shows different localization patterns depending on the differentiation and the histological pattern of tumors: immunohistochemical analysis. *J Hepatol* 1994; **21**: 37-46

8 **Nakashima O,** Sugihara S, Kage M, Kojiro M. Pathomorphologic characteristics of small hepatocellular carcinoma: a special reference to small hepatocellular carcinoma with indistinct margins. *Hepatology* 1995; **22**: 101-105

9 **Tsujimoto T,** Kuriyama S, Yamazaki M, Nakatani Y, Okuda H, Yoshiji H, Fukui H. Augmented hepatocellular carcinoma progression and depressed Kupffer cell activity in rat cirrhotic livers. *Int J Oncol* 2001; **18**: 41-47

10 **Takeishi T,** Hirano K, Kobayashi T, Hasegawa G, Hatakeyama K, Naito M. The role of Kupffer cells in liver regeneration. *Arch Histol Cytol* 1999; **62**: 413-422

11 **Sakaida I,** Hironaka K, Terai S, Okita K. Gadolinium chloride reverses dimethylnitrosamine (DMN)-induced rat liver fibrosis with increased matrix metalloproteinases (MMPs) of Kupffer cells. *Life Sci* 2003; **72**: 943-959

12 **Luckey SW,** Petersen DR. Activation of Kupffer cells during the course of carbon tetrachloride-induced liver injury and fibrosis in rats. *Exp Mol Pathol* 2001; **71**: 226-240

13 **Melgert BN,** Olinga P, Van Der Laan JM, Weert B, Cho J, Schuppan D, Groothuis GM, Meijer DK, Poelstra K. Targeting dexamethasone to Kupffer cells: effects on liver inflammation and fibrosis in rats. *Hepatology* 2001; **34**(4 Pt 1): 719-728

14 **Bautista AP.** Impact of alcohol on the ability of Kupffer cells to produce chemokines and its role in alcoholic liver disease. *J Gastroenterol Hepatol* 2000; **15**: 349-356

15 **Enomoto N,** Ikejima K, Bradford BU, Rivera CA, Kono H, Goto M, Yamashina S, Schemmer P, Kitamura T, Oide H, Takei Y, Hirose M, Shimizu H, Miyazaki A, Brenner DA, Sato N, Thurman RG. Role of Kupffer cells and gut-derived endotoxins in alcoholic liver injury. *J Gastroenterol Hepatol* 2000; **15**(Suppl): D20-D25

16 **Vollmar B,** Siegmund S, Richter S, Menger MD. Microvascular consequences of Kupffer cell modulation in rat liver fibrogenesis. *J Pathol* 1999; **189**: 85-91

17 **Yamaguchi R,** Yano H, Nakashima Y, Ogasawara S, Higaki K, Akiba J, Hicklin DJ, Kojiro M. Expression and localization of vascular endothelial growth factor receptors in human hepatocellular carcinoma and non-HCC tissues. *Oncol Rep* 2000; **7**: 725-729

18 **Nakopoulou L,** Stefanaki K, Vourlakou C, Manolaki N, Gakiopoulou H, Michalopoulos G. Bcl-2 protein expression in

acute and chronic hepatitis, cirrhosis and hepatocellular carcinoma. *Pathol Res Pract* 1999; **195**: 19-24

19 **Wang JY,** Zhang QS, Guo JS, Hu MY. Effects of glycyrrhetinic acid on collagen metabolism of hepatic stellate cells at different stages of liver fibrosis in rats. *World J Gastroenterol* 2001; **7**: 115-119

20 **Hsu CM,** Wang JS, Liu CH, Chen LW. Kupffer cells protect liver from ischemia-reperfusion injury by an inducible nitric oxide synthase-dependent mechanism. *Shock* 2002; **17**: 280-285

21 **Zhu XH,** Qiu YD, Shen H, Shi MK, Ding YT. Effect of matrine on Kupffer cell activation in cold ischemia reperfusion injury of rat liver. *World J Gastroenterol* 2002; **8**: 1112-1116

22 **Schauer RJ,** Bilzer M, Kalmuk S, Gerbes AL, Leiderer R, Schildberg FW, Messmer K. Microcirculatory failure after rat liver transplantation is related to Kupffer cell-derived oxidant stress but not involved in early graft dysfunction. *Transplantation* 2001; **72**: 1692-1699

23 **Nie QH**, Cheng YQ, Xie YM, Zhou YX, Cao YZ. Inhibiting effect of antisense oligonucleotides phosphorthioate on gene expression of TIMP-1 in rat liver fibrosis. *World J Gastroenterol* 2001; **7**: 363-369

24 **Sharifi S,** Hayek J, Khettry U, Nasser I. Immunocytochemical staining of Kupffer and endothelial cells in fine needle aspiration cytology of hepatocellular carcinoma. *Acta Cytol* 2000; **44**: 7-12

25 **Brown KE,** Brunt EM, Heinecke JW. Immunohistochemical detection of myeloperoxidase and its oxidation products in Kupffer cells of human liver. *Am J Pathol* 2001; **159**: 2081-2088

26 **Longchampt E,** Patriarche C, Fabre M. Accuracy of cytology vs. microbiopsy for the diagnosis of well-differentiated hepatocellular carcinoma and macroregenerative nodule. Definition of standardized criteria from a study of 100 cases. *Acta Cytol* 2000; **44**: 515-523

27 **Luhrs H,** Illert B, Timmermann W, Volk H, Scheppach W, Menzel T. Ultrastructural alterations of primary human liver sinusoidal cells in patients treated for peritonitis *J Invest Surg* 2002; **15**: 209-218

28 **Klockars M,** Reitamo S. Tissue distribution of lysozyme in man. *J Histochem Cytochem* 1975; **23**: 932-940

29 **Mathew J,** Hines JE, Toole K, Johnson SJ, James OF, Burt AD. Quantitative analysis of macrophages and perisinusoidal cells in primary biliary cirrhosis. *Histopathology* 1994; **25**: 65-70

30 **Yamamoto T,** Hirohashi K, Kaneda K, Ikebe T, Mikami S, Uenishi T, Kanazawa A, Takemura S, Shuto T, Tanaka H, Kubo S, Sakurai M, Kinoshita H. Relationship of the microvascular type to the tumor size, arterialization and dedifferentiation of human hepatocellular carcinoma. *Jpn J Cancer Res* 2001; **92**: 1207-1213

31 **Baldus SE,** Zirbes TK, Weidner IC, Flucke U, Dittmar E, Thiele J, Dienes HP. Comparative quantitative analysis of macrophage populations defined by CD68 and carbohydrate antigens in normal and pathologically altered human liver tissue. *Anal Cell Pathol* 1998; **16**: 141-150

32 **Huang X,** Li DG, Wang ZR, Wei HS, Cheng JL, Zhang YT, Zhou X, Xu QF, Li X, Lu HM. Expression changes of activin A in the development of hepatic fibrosis. *World J Gastroenterol* 2001; **7**: 37-41

33 **Nakopoulou L,** Stefanaki K, Vourlakou C, Manolaki N, Gakiopoulou H, Michalopoulos G. Bcl-2 protein expression in acute and chronic hepatitis, cirrhosis and hepatocellular carcinoma. *Pathol Res Pract* 1999; **195**: 19-24

34 **Song E,** Chen J, Ouyang N, Wang M, Exton MS, Heemann U. Kupffer cells of cirrhotic rat livers sensitize colon cancer cells to Fas-mediated apoptosis. *Br J Cancer* 2001; **84**: 1265-1271

35 **Miyagawa S,** Miwa S, Soeda J, Kobayashi A, Kawasaki S. Morphometric analysis of liver macrophages in patients with colorectal liver metastasis. *Clin Exp Metastasis* 2002; **19**: 119-125

36 **Lau WY,** Chen GG, Lai PB, Chun YS, Leung BC, Chak EC, Lee JF, Chui AK. Induction of Fas and Fas ligand expression on malignant glioma cells by Kupffer cells, a potential pathway of antiliver metastases. *J Surg Res* 2001; **101**: 44-51

37 **Nanji AA.** Role of Kupffer cells in alcoholic hepatitis. *Alcohol* 2002; **27**: 13-15

38 **Hoebe KH,** Witkamp RF, Fink-Gremmels J, Van Miert AS, Monshouwer M. Direct cell-to-cell contact between Kupffer cells and hepatocytes augments endotoxin-induced hepatic injury. *Am J Physiol Gastrointest Liver Physiol* 2001; **280**: G720-728

39 **Schumann J,** Wolf D, Pahl A, Brune K, Papadopoulos T, van Rooijen N, Tiegs G. Importance of Kupffer cells for T-cell-dependent liver injury in mice. *Am J Pathol* 2000; **157**: 1671-1683

40 **Bautista AP.** Impact of alcohol on the ability of Kupffer cells to produce chemokines and its role in alcoholic liver disease. *J Gastroenterol Hepatol* 2000; **15**: 349-356

41 **Burgio VL,** Ballardini G, Artini M, Caratozzolo M, Bianchi FB, Levrero M. Expression of co-stimulatory molecules by Kupffer cells in chronic hepatitis of hepatitis C virus etiology. *Hepatology* 1998; **27**: 1600-1606

42 **Lim JH,** Choi D, Cho SK, Kim SH, Lee WJ, Lim HK, Park CK, Paik SW, Kim YI. Conspicuity of hepatocellular nodular lesions in cirrhotic livers at ferumoxides-enhanced MR imaging: importance of Kupffer cell number. *Radiology* 2001; **220**: 669-676

43 **Imai Y,** Murakami T, Yoshida S, Nishikawa M, Ohsawa M, Tokunaga K, Murata M, Shibata K, Zushi S, Kurokawa M, Yonezawa T, Kawata S, Takamura M, Nagano H, Sakon M, Monden M, Wakasa K, Nakamura H. Superparamagnetic iron oxide-enhanced magnetic resonance images of hepatocellular carcinoma: correlation with histological grading. *Hepatology* 2000; **32**: 205-212

44 **Kitamura H,** Kawasaki S, Nakajima K, Ota H. Correlation between microbubble contrast-enhanced color doppler sonography and immunostaining for Kupffer cells in assessing the histopathologic grade of hepatocellular carcinoma: preliminary results. *J Clin Ultrasound* 2002; **30**: 465-471

Edited by Zhu LH and Wang XL

P.O.Box 2345, Beijing 100023,China
Fax: +86-10-85381893
E-mail: wjg@wjgnet.com www.wjgnet.com

World J Gastroenterol 2003;9(9):1950-1953
World Journal of Gastroenterology
 ISSN 1007-9327

• LIVER CANCER •

Expression and significance of RhoC gene in hepatocellular carcinoma

Wei Wang, Lian-Yue Yang, Zhi-Li Yang, Gen-Wen Huang, Wei-Qun Lu

Wei Wang, Lian-Yue Yang, Zhi-Li Yang, Gen-Wen Huang, Wei-Qun Lu, Liver Cancer laboratory, Department of General Surgery, Xiangya Hospital, Central South University, Changsha 410008, Hunan Province, China
Supported by the grant from National Key Technologies R and D Program, No.2001BA703B05 and the grant from Hunan Province Developing Planning Committee, No.2001-907
Correspondence to: Lian-Yue Yang, Department of General Surgery, Xiangya Hospital, Changsha, 410008, Hunan Province, China. lianyueyang@hotmail.com
Telephone: +86-731-4327326 **Fax**: +86-731-4327332
Received: 2003-03-04 **Accepted:** 2003-04-05

Abstract

AIM: To investigate the expression of RhoC gene in hepatocellular carcinoma (HCC) and to evaluate the relationship between RhoC gene expression and invasion and metastasis of HCC.

METHODS: mRNA expression level of RhoC gene was examined by reverse transcription-polymerase chain reaction (RT-PCR) in 25 cases of HCC and para-cancerous normal liver tissues. In addition, mutation of RhoC gene was examined by polymerase chain reaction-single strand conformational polymorphism (PCR-SSCP).

RESULTS: The mRNA expression levels of RhoC in tumor tissues were significantly higher than those in para-cancerous normal liver tissues (1.8±1.1 *vs* 1.0±0.7, $P<0.01$). The metastatic lesions outside of liver also showed significantly higher RhoC mRNA levels than corresponding tumor tissues in liver (3.3±0.5 *vs* 2.0±0.7, $P<0.01$). There were significant associations between RhoC gene expression and certain clinical and pathological findings, including cell differentiation, vein invasion, number of tumor nodes and metastatic lesions. Mutation of RhoC gene was not found by PCR-SSCP.

CONCLUSION: The RhoC gene may be related to malignant transformation and development of HCC and may play an important role in the invasion and metastasis of HCC by overexpression but not mutation.

Wang W, Yang LY, Yang ZL, Huang GW, Lu WQ. Expression and significance of RhoC gene in hepatocellular carcinoma. *World J Gastroenterol* 2003; 9(9): 1950-1953
http://www.wjgnet.com/1007-9327/9/1950.asp

INTRODUCTION

Hepatocellular carcinoma (HCC) is one of the most common malignancies in the world, and is the second-leading cause of cancer death among males in China[1]. It is generally accepted that the high incidence of recurrence and metastasis is the most crucial prognostic factor for patients with HCC[2]. Transcellular migration of tumor cells through host structures, such as endothelium of blood vessels and methothelium of visceral cavity is crucial in cancer invasion and metastasis[3].

RhoC GTPase is a member of Ras-superfamily of small guanosine triphosphatases (GTPases), which shuttles between an inactive GDP-bound state and an active GTP-bound state and exhibits intrinsic GTPase activities[4]. Activation of Rho protein leads to assembly of the actin-myosin contractile filaments into focal adhesion complexes that lead to cell polarity and facilitate motility[5]. Recently, emerging data have suggested that RhoC gene play important roles in tumorigenesis and metastasis of tumor cell[6]. The expression level of RhoC in metastatic regions of pancreas cancer has been reported to be higher than that in primary lesion[7]. Genome-wide analysis of gene expression has revealed that RhoC gene was involved in vascular invasiveness of hepatocellular carcinoma[8]. We hypothesized that RhoC might play a critical role in tumorigenesis and invasion and metastasis of HCC. In the present study, we investigated the expression of RhoC gene in HCC and evaluated the relationship between RhoC gene expression and clinical and pathological characteristics of HCC.

MATERIALS AND METHODS

Patients and tissue preparation

Twenty-five fresh HCC specimens and corresponding para-cancerous normal liver tissues were obtained by surgical resection in Xiangya Hospital between March 2002 and August 2002. Further more, four cases of corresponding metastatic lesions or hepatic vein tumor thrombosis were obtained as well. The patients with HCC were consisted of 22 men and 3 women and were ranged from 28 to 73 (mean ±SD=53). We divided the 25 patients from six aspects: tumor <5 cm in diameter 7 cases and ⩾5 cm 18 cases, I-II in cell differentiation 9 cases and III-IV 16 cases; the number of tumor nodes ⩾2 15 cases and <2 10 cases, with capsule formation 12 cases and without it 13 cases, with microscopy portal vein tumor thrombosis 13 cases and without it 12 cases, with metastatic nodes outside of liver 5 cases and without it 20 cases. All specimens were examined under a microscope after haematoxylin and eosin (H&E) staining.

RNA extraction and RT-PCR

Total RNA was isolated using Trizol reagent (GIBCO BRL, USA) and cDNA was synthesized from the RNA by M-MLV reverse transcriptase (Promega, USA) with oligodT primers (Sangon Technology, CHINA), The primer sequences of RhoC and β_2-microglobulin which was used as an internal quantitative control for the amplification were as follows: the upstream primers of RhoC and β_2-microglobulin were 5' -TCCTCAT CGTCTTCAGCAAG-3' and 5' -ACCCCCACTGAAAAAG ATGA-3' , the downstream primers of RhoC and β_2-microglobulin were 5' -CTGCAATCCGAAAGAAGCTG-3' and 5' -ATCTTCAAACCTCCATGATG-3' . The condition of PCR was as follows: 32 cycles of denaturing at 94 ℃ for 40 s, annealing at 56 ℃ for 30 s and extending at 72 ℃ for 1 min. The bands representing amplified products were analyzed by Stratagene Eagle-eye scanner. RhoC gene expression was

presented by the relative yield of PCR product from target sequence to that from β_2-microglobulin gene.

PCR-SSCP-sliver staining analysis

Because RhoC is homologous with ras gene and mutation of ras is frequent in HCC, PCR-SSCP-sliver staining analysis was performed to determine gene mutation of RhoC. We examined exon I of RhoC. The primers were designed as follows: upstream 5'-CTGCAATCCGAAAGAAGCTG-3' and downstream 5'-CTGCAATCCGAAAGAAGCTG-3'. PCR reaction was performed by denaturing at 94 ℃ for 40 s, annealing at 55 ℃ for 30 s and extending at 72 ℃ for 1 min for 35 cycles. PCR samples were denatured at 99 ℃ for 10 min and electrophoresed with 8 % non-denaturing polyacrylamide gel at 40v for 5 hours. After electrophoresis, the gel was fixed in 10 % alcohol for 10 min, washed twice with distilled water for 2 min, silver reaction was performed (silver nitrate 1 g, topped up with distilled water to 500 ml) for 10 min, then washed with distilled water for 30 s, finally the gel was developed (sodium hydroxide 3.75 g, formaldehyde 2.7 ml, topped up with distilled water to 500 ml) for 10 min.

Statistical analysis

The results of RT-PCR were statistically analyzed using the Student's *t* test. Fisher's exact test was used to determine the relationship between RhoC expression and clinical and pathological characteristics of HCC. A value of $P<0.05$ was considered statistically significant.

RESULTS

RhoC gene was expressed in HCC tissues and para-cancerous normal liver tissues of all the 25 cases. There were significant differences in the expression level of RhoC gene between carcinoma tissues and para-cancerous normal liver tissues (mean ±SD, 1.8±1.1 *vs* 1.0±0.7 respectively) (Figure 1). Metastatic lesions or hepatic vein tumor thrombosis showed significantly higher RhoC mRNA levels than primary carcinoma tissues (mean ±SD, 3.3±0.5 *vs* 1.8±1.1 respectively). Based on the ratio of RhoC expression in tumor to corresponding para-cancerous normal liver tissues ($\overline{X}_t/\overline{X}_p=1.8$), the 25 patients were divided into two groups: overexpression group (14 cases) and high-expression group (11 cases). Fisher's exact test analysis demonstrated a significant difference in some aspects between the two groups ($P<0.05$) including cell differentiation, vein invasion, number of tumor nodes and metastatic lesions. The difference in vein invasion between the two groups was statistically significant ($P<0.01$) (Table 1). Mutation of RhoC was not found in all cases of HCC.

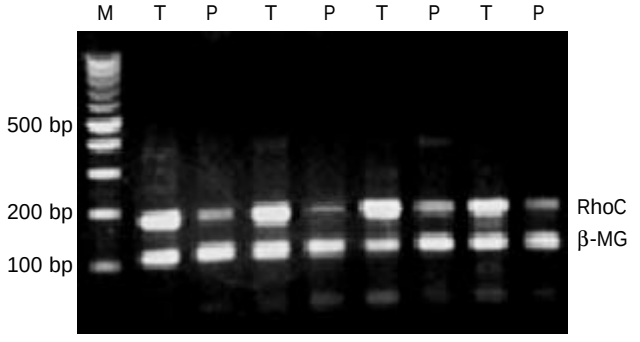

Figure 1 Expression of RhoC mRNA in hepatocellular carcinoma. M: DNA marker T: tumor P: para-cancerous normal liver tissues. PCR product of RhoC was 183 bp; PCR product of β_2-microglobulin was 120 bp. RhoC mRNA levels were significantly higher in tumor than para-cancerous normal liver tissues.

Table 1 The relationship between RhoC mRNA expression and clinical and pathological features of HCC patients

Variables	Overexpression of RhoC (*n*)	High-expression of RhoC (*n*)	Fisher's test
Sex			
Male	12	10	$P>0.05$
Female	2	1	
Tumor size (cm)			
⩾5 cm	12	6	$P>0.05$
<5 cm	2	5	
Histological grade			
I-II	2	7	$P<0.05$
III-IV	12	4	
Number of tumor nodes			
⩾2	11	4	$P<0.05$
<2	3	7	
Capsule formation			
Positive	5	7	$P>0.05$
Negative	9	4	
Portal vein thrombosis			
Positive	11	2	$P<0.01$
Negative	3	9	
Metastatic node out of liver			
Present	5	0	$P<0.05$
Absent	9	11	

DISCUSSION

RhoGTPases are members of the ras superfamily of GTP-binding protein, which act as molecular switches, cycling between an active GTP-bound and inactive GDP-bound states. Eighteen members have been identified and the most extensively characterized members are Rho, Rac and cdc42[5]. Early studies showed that Rho protein regulated cell morphology and actin cytoskeleton, however it is now clear that they also affect gene expression, cell proliferation and cell survival[9]. Emerging data have showed that RhoGTPases are more important for the evolution of cancer than initially thought, and several reports indicated that RhoGTPases directly participated in the evolution of cancer. For instance, activated Rho protein mutants were capable of transforming fibroblast and dominant inhibitory mutants of Rho protein blocked transformation by ras[10]. Furthermore, Rho protein could upregulate cyclinD_1 and downregulate CDKIs through ETS, AP-1 and NF-KB[11-19]. These indicate that Rho protein is important in tumorigenesis. RhoC is a member of Rho family and it has been shown that overexpression of RhoC induce the malignant transformation of immortalized human mammary epithelial cells. RhoC is overexpressed in pancreatic ductal adenocarcinoma and inflammatory breast cancer[7,20]. Furthermore, there is a causal link between RhoC overexpression and inflammatory breast cancer. Based on these results, we hypothesized that RhoC might be involved in tumorigenesis of HCC. We detected the expression level of RhoC mRNA in 25 patients with HCC by RT-PCR. Our results showed that RhoC gene expression was significantly higher in tumor portion than that in corresponding para-cancerous normal liver tissues. Furthermore, we also found that tumor with RhoC overexpression appeared poorer in cell differentiation than those with high-expression of RhoC gene. These suggest that overexpression of RhoC gene is related to the degree of differentiation of HCC and RhoC expression level could be a useful prognostic indicator.

Metastasis and invasion of HCC were a multistep process, and the molecular and cellular mechanisms of which were not

fully understood, although cell motility has been shown to play a pivotal role in metastasis and invasion of HCC[21]. RhoC is involved in cytoskeletal reorganization, specifically in the formation of actin stress fibers and focal adhesion contacts[22]. Numerous *in vitro* studies have indicated that RhoC protein and its effector ROCK are clearly implicated in *vivo* models of tumor-cell dissemination[23]. Overexpression of RhoC gene was found in metastatic lesions of inflammatory breast cancer and pancreatic ductal adenocarcinoma. RhoC gene was also found to be correlated with vascular invasion and tumor differentiation in human HCC by using cDNA microarray[8]. In the present study metastatic lesions or hepatic vein tumor thrombosis showed significantly higher RhoC mRNA level than primary carcinoma tissues. Expression level of RhoC gene was correlated with vein invasion, number of tumor nodes and metastatic lesions. Especially, the difference between two groups in microscopy hepatic vein tumor thrombosis indicated greater significance. These results indicate that RhoC has a close relationship with invasion and metastasis of HCC. The possible reasons may be as follows: (1) Disruption of cell polarity, which plays an important role in the epithelial-mesenchymal transformation that is observed in more aggressive tumors[24,25]. (2) Contribution to the loss of adherens junctions[26-28]. (3) Increase of motility and ability to remodel ECM, which requires tumor cells to become locally invasive[29-32]. However, the exact mechanisms need to be explored further.

Given the results that RhoC protein is important in determining the behavior of cancer cells, it is surprising that mutants of RhoC-analogous of oncogenic ras have not been found in our research. Similar results were observed in pancreatic ductal adenocarcinoma[7]. In fact, several lines of evidence indicate that not mutation but the switch of Rho protein between GTP- and GDP-bound states are important in the transformation of malignant tumor[33]. Overexpression level of RhoC may contribute to a faster GTP-GDP cycling station. Taken together, our findings indicate that RhoCGTPase is related to tumorigenesis of HCC. Overexpression but not mutation of RhoC may enhance the invasion and metastasis of HCC. The molecular basis for overexpression of RhoC remains to be elucidated. What are the most important factors regulating the expression level of RhoC and how does RhoC gene regulate effector protein will be the subject of our future studies. When upstream and downstream signaling pathways are explored, these findings will provide new potential targets for the prognostication or prevention of invasion and metastasis of HCC[34].

ACKNOWLEDGEMENT

We are grateful to Fa-Qing Tang, Jian-Qing Yang, and He-Li Liu for their technical advice and Min-Juan Lin for her statistical support.

REFERENCES

1 **Tang ZY**. Hepatocellular carcinoma-cause, treatment and metastasis. *World J Gastroenterol* 2001; **7**: 445-454
2 **Qin LX**, Tang ZY. The prognostic significance of clinical and pathological features in hepatocellular carcinoma. *World J Gastroenterol* 2002; **8**: 193-199
3 **Korn WM**. Moving toward an understanding of the metastatic process in hepatocellular carcinoma. *World J Gastroenterol* 2001; **7**: 777-778
4 **Bishop AL**, Hall A. Rho GTPases and their effector proteins. *Biochem J* 2000; **348**(Pt 2): 241-255
5 **Van Aelst L**, D'Souza-Schorey C. Rho GTPases and signaling networks. *Genes Dev* 1997; **11**: 2295-2322
6 **Sahai E,** Marshall CJ. RHO-GTPases and cancer. *Nat Rev Cancer* 2002; **2**: 133-142
7 **Suwa H**, Ohshio G, Imamura T, Watanabe G, Arii S, Imamura M, Narumiya S, Hiai H, Fukumoto M. Overexpression of the RhoC gene correlates with progression of ductal adenocarcinoma of the pancreas. *Br J Cancer* 1998; **77**: 147-152
8 **Okabe H**, Satoh S, Kato T, Kitahara O, Yanagawa R, Yamaoka Y, Tsunoda T, Furukawa Y, Nakamura Y. Genome-wide analysis of gene expression in human hepatocellular carcinomas using cDNA microarray: identification of genes involved in viral carcinogenesis and tumor progression. *Cancer Res* 2001; **61**: 2129-2137
9 **Hall A**. Rho GTPases and the actin cytoskeleton. *Science* 1998; **279**: 509-514
10 **Qiu RG,** Chen J, McCormick F, Symons M. A role for Rho in Ras transformation. *Proc Natl Acad Sci U S A* 1995; **92**: 11781-11785
11 **Vojtek AB**, Cooper JA. Rho family members: activators of MAP kinase cascades. *Cell* 1995; **82**: 527-529
12 **Marinissen MJ,** Chiariello M, Gutkind JS. Regulation of gene expression by the small GTPase Rho through the ERK6 (p38 gamma) MAP kinase pathway. *Genes Dev* 2001; **15**: 535-553
13 **Cammarano MS**, Minden A. Dbl and the Rho GTPases activate NF kappa B by I kappa B kinase (IKK)-dependent and IKK-independent pathways. *J Biol Chem* 2001; **276**: 25876-25882
14 **Olson MF**, Paterson HF, Marshall CJ. Signals from Ras and Rho-GTPases interact to regulate expression of $p21^{Waf1/cip1}$. *Nature* 1998; **394**: 295-299
15 **Adnane J**, Bizouarn FA, Qian Y, Hamilton AD, Sebti SM. p21 (WAF1/CIP1) is upregulated by the geranylgeranyltransferase I inhibitor GGTI-298 through a transforming growth factor beta- and Sp1-responsive element: involvement of the small GTPase RhoA. *Mol Cell Biol* 1998; **18:** 6962-6970
16 **Hirai A**, Nakamura S, Noguchi Y, Yasuda T, Kitagawa M, Tatsuno I, Oeda T, Tahara K, Terano T, Narumiya S, Kohn LD, Saito Y. Geranylgeranylated Rho small GTPase(s) are essential for the degradation of p27Kip1 and facilitate the progression from G1 to S phase in growth-stimulated rat FRTL-5 cells. *J Biol Chem* 1997; **272**: 13-16
17 **Weber JD**, Hu W, Jefcoat SC Jr, Raben DM, Baldassare JJ. Ras-stimulated extracellular signal-related kinase 1 and RhoA activities coordinate platelet-derived growth factor-induced G1 progression through the independent regulation of cyclin D1 and p27. *J Biol Chem* 1997; **272**: 32966-32971
18 **Shaulian E**, Karin M. AP-1 in cell proliferation and survival. *Oncogene* 2001; **20**: 2390-2400
19 **Hinz M,** Krappmann D, Eichten A, Heder A, Scheidereit C, Strauss M. NF-kappaB function in growth control: regulation of cyclin D1 expression and G0/G1-to-S-phase transition. *Mol Cell Biol* 1999; **19**: 2690-2698
20 **Van Golen KL,** Wu ZF, Qiao XT, Bao LW, Merajver SD. RhoC GTPase, a novel transforming oncogene for human mammary epithelial cells that partially recapitulates the inflammatory breast cancer phenotype. *Cancer Res* 2000; **60**: 5832-5838
21 **Donald CD**, Cooper CR, Harris-Hooker S, Emmett N, Scanlon M, Cooke DB 3rd. Cytoskeletal organization and cell motility correlates with metastatic potential and state of differentiation in prostate cancer. *Cell Mol Biol (Noisy-le-grand)* 2001; **47**: 1033-1038
22 **Ridley AJ**. Rho-GTPases and cell migration. *J Cell Sci* 2001; **114** (Pt 15): 2713-2722
23 **Clark EA,** Golub TR, Lander ES, Hynes RO. Genomic analysis of metastasis reveals an essential role for RhoC. *Nature* 2000; **406**: 532-535
24 **Zondag GC,** Evers EE, ten Klooster JP, Janssen L, van der Kammen RA, Collard JG. Oncogenic Ras downregulates Rac activity, which leads to increased Rho activity and epithelial-mesenchymal transition. *J Cell Biol* 2000; **149**: 775-782
25 **Somlyo AV,** Bradshaw D, Ramos S, Murphy C, Myers CE, Somlyo AP. Rho-kinase inhibitor retards migration and *in vivo* dissemination of human prostate cancer cells. *Biochem Biophys Res Commun* 2000; **269**: 652-659
26 **Braga VM**, Betson M, Li X, Lamarche-Vane N. Activation of the small GTPase Rac is sufficient to disrupt cadherin-dependent cell-cell adhesion in normal human keratinocytes. *Mol Biol Cell* 2000; **11**: 3703-3721
27 **Bhowmick NA,** Ghiassi M, Bakin A, Aakre M, Lundquist CA,

Engel ME, Arteaga CL, Moses HL. Transforming growth factor-beta1 mediates epithelial to mesenchymal transdifferentiation through a RhoA-dependent mechanism. *Mol Biol Cell* 2001; **12**: 27-36

28 **Sander EE**, van Delft S, ten Klooster JP, Reid T, van der Kammen RA, Michiels F, Collard JG. Matrix-dependent Tiam1/Rac signaling in epithelial cells promotes either cell-cell adhesion or cell migration and is regulated by phosphatidylinositol 3-kinase. *J Cell Biol* 1998; **143**: 1385-1398

29 **Khanna C,** Khan J, Nguyen P, Prehn J, Caylor J, Yeung C, Trepel J, Meltzer P, Helman L. Metastasis-associated differences in gene expression in a murine model of osteosarcoma. *Cancer Res* 2001; **61**: 3750-3759

30 **Matsui T**, Maeda M, Doi Y, Yonemura S, Amano M, Kaibuchi K, Tsukita S, Tsukita S. Rho-kinase phosphorylates COOH-terminal threonines of ezrin/radixin/moesin (ERM) proteins and regulates their head-to-tail association. *J Cell Biol* 1998; **140**: 647-657

31 **Engers R,** Springer E, Michiels F, Collard JG, Gabbert HE. Rac affects invasion of human renal cell carcinomas by up-regulating tissue inhibitor of metalloproteinases (TIMP)-1 and TIMP-2 expression. *J Biol Chem* 2001; **276**: 41889-41897

32 **Matsumoto Y**, Tanaka K, Harimaya K, Nakatani F, Matsuda S, Iwamoto Y. Small GTP-binding protein, Rho, both increased and decreased cellular motility, activation of matrix metalloproteinase 2 and invasion of human osteosarcoma cells. *Jpn J Cancer Res* 2001; **92**: 429-438

33 **Schnelzer A,** Prechtel D, Knaus U, Dehne K, Gerhard M, Graeff H, Harbeck N, Schmitt M, Lengyel E. Rac1 in human breast cancer: overexpression, mutation analysis, and characterization of a new isoform, Rac1b. *Oncogene* 2000; **19**: 3013-3020

34 **Kleer CG,** van Golen KL, Zhang Y, Wu ZF, Rubin MA, Merajver SD. Characterization of RhoC expression in benign and malignant breast disease: a potential new marker for small breast carcinomas with metastatic ability. *Am J Pathol* 2002; **160**: 579-584

Edited by Yuan HT and Wang XL

P.O.Box 2345, Beijing 100023,China
Fax: +86-10-85381893
E-mail: wjg@wjgnet.com www.wjgnet.com

World J Gastroenterol 2003;9(9):1954-1958
World Journal of Gastroenterology
 ISSN 1007-9327

• LIVER CANCER •

Study on relationship between expression level and molecular conformations of gene drugs targeting to hepatoma cells *in vitro*

Dong-Ye Yang, Fang-Gen Lu, Xi-Xiang Tang, Shui-Ping Zhao, Chun-Hui Ouyang, Xiao-Ping Wu, Xiao-Wei Liu, Xiao-Ying Wu

Dong-Ye Yang, Fang-Gen Lu, Xi-Xiang Tang, Chun-Hui Ouyang, Xiao-Ping Wu, Xiao-Wei Liu, Department of Gastroenterology, Xiangya Second Hospital, Central South University, Changsha 410011 & Institute of Sheng Life Gene Drugs, Changsha 410003, Hunan, China
Shui-Ping Zhao, Department of Cardiovascularology, Xiangya Second Hospital, Central South University, Changsha 410011, Hunan, China
Xiao-Ying Wu, Department of Electron Microscope, Xiangya Medical School, Central South University, Changsha 410011, Hunan, China
Supported by the National Natural Science Foundation of China, No. 39570355 & Hunan Health Bureau Foundation, No. Y02-038
Correspondence to: Dr. Fang-Gen Lu, Department of Gastroenterology, Xiangya Second Hospital, Central South University, Changsha 410011, Hunan Province, China. irisyang89@hotmail.com
Telephone: +86-731-4456022 **Fax:** +86-731-4806490
Received: 2002-07-01 **Accepted:** 2002-07-22

Abstract

AIM: To increase exogenous gene expression level by modulating molecular conformations of targeting gene drugs.

METHODS: The full length cDNAs of both P_{40} and P_{35} subunits of human interleukin 12 were amplified through polymerase chain reaction (PCR) and cloned into eukaryotic expressing vectors pcDNA3.1(±) to construct plasmids of P(+)/IL-12, P(+)/P_{40} and P(-)/P_{35}. These plasmids were combined with ASOR-PLL to form two targeting gene drugs [ASOR-PLL-P(+)/IL-12 and ASOR-PLL-P(+)/P_{40} + ASOR-PLL-P(-)/P_{35}] in optimal ratios. The conformations of these two drugs at various concentrations adjuvant were examined under electron microscope (EM) and the drugs were transfected into HepG2 (ASGr+) cells. Semi-quantitative reverse transcription polymerase chain reaction (RT-PCR) was performed with total RNA extracted from the transfected cells to determine the hIL12 mRNA transcript level. The hIL12 protein in the cultured supernatant was measured with enzyme-linked immunosorbent assay (ELISA) 48 hours after transfection.

RESULTS: Targeting gene drugs, whose structures were granular and circle-like and diameters ranged from 25 nm to 150 nm, had the highest hIL-12 expression level. The hIL-12 expression level in the group co-transfected with ASOR-PLL-P(+)/P_{40} and ASOR-PLL-P(-)/P_{35} was higher than that of ASOR-PLL-P(+)/IL-12 transfected group.

CONCLUSION: The molecular conformations of targeting gene drugs play an important role in exogenous gene expression level, the best structures are granular and circle-like and their diameters range from 25 nm to 150 nm. The sizes and linking styles of exogenous genes also have some effects on their expression level.

Yang DY, Lu FG, Tang XX, Zhao SP, Ouyang CH, Wu XP, Liu XW, Wu XY. Study on relationship between expression level and molecular conformations of gene drugs targeting to hepatoma cells *in vitro*. *World J Gastroenterol* 2003; 9(9): 1954-1958
http://www.wjgnet.com/1007-9327/9/1954.asp

INTRODUCTION

In hepatoma gene therapy, the technical difficulty is that exogenous gene expression level is too low to achieve therapeutic effecets on in target cells[1]. Studies have been focused on improving gene therapeutic vector, restraining the lysosome activity in target cells, increasing exogenous gene outputs from endosomal vesicles, and modifying their transcription elements[2-7]. Whether there are some relationships between molecular conformation of gene drugs and exogenous gene expression level is not clear. Asialoorosomucoid (ASOR), the specific ligand of asialoglycoprotein receptor on the surface of hepatocytes, can be combined covalently with poly-l-lysine (PLL) to form a soluble DNA transfection vector[8-10]. Human interleukin 12 (hIL-12), also named as cytotoxin lymphocyte maturation factor or natural killer cell stimulatory factor, plays a key regulatory role in humoral immune reactions and explicits bioactivities of antivirus, antitumor and antimetastasis[11-14]. After constructing a hIL12 (human interleukin 12) double-subunit co-expressing plasmid and single-subunit gene expression plasmids, we linked them with ASOR-PLL through electrostatic interactions to form two targeting gene drugs-ASOR-PLL-DNA complexes, then examined their molecular shapes and sizes at various concentration of adjuvant under transmission electron microscope. We compared exogenous gene expression levels to select the best molecular conformation of the complexes 48 hours after transfecting them into HepG2 (ASGr+) cells, and found the means to improve the expression efficiency in target cells on the basis of molecular conformations of gene drugs.

MATERIALS AND METHODS

Materials

Eukaryotic expressing plasmids [pcDNA3.1(+/-)] and host bacteria *E. coli* JM109 were obtained from the National Laboratory of Medical Genetics of China. Plasmids purification kit 2500 was purchased from Qiagen (Chatsworth CA). All the restriction endonuclease enzymes were purchased from New England Biolabs (Beverly MA). Minimum essential medium (MEM), Trizol and lipofectamine were purchased from GibcoBRL (Grand Island NY). RT-PCR kit was purchased from Promega (Madison WI). hIL-12 (P70) ELISA kit was purchased from Pharmingen (San Diego CA). Hepatoma cells (HepG2) were obtained from China Center of Type Culture Collection (CCTCC). Newborn bovine serum was purchased from Sijiqing (Hangzhou, China). Chloroquine was a gift from Shanghai Zhong-Xi Pharmaceutical Company. All other reagents were of analytical grade from various companies in China. ASOR-PLL was prepared by ourselves.

Methods

Construction of double-subunit co-expressing plasmid of human interleukin12 The full length cDNAs of P_{40} and P_{35} subunits were amplified from human embryonic kidney by RT-PCR based on sequences deposited in Genbank (P_{40} accession number AF180563, P_{35} accession number AF180562), and cloned into pcDNA3.1(+/-) to obtain P(+)/P_{40} and P(-)/P_{35}

plasmids. The segments-P_{35}-polyA and -cmv-P_{40}-were amplified from P(-)/P_{35} and P(+)/$_{P40}$ by using the following primers IL40F, IL40R, IL35F, IL35R. They were then ligated and cloned into pcDNA3.1(+) to obtain double-subunit co-expressing plasmid P(+)/IL-12 (Table 1).

Table 1 Primers for amplifying human interleukin 12

P_{40} subunit primary PCR primers:
up stream (6044) 5'-atg tgt cac cag cag ttg gtc atc-3'
down stream (6045) 5'-gga tca gaa cct aac tgc agg gca c-3'
P40 subunit secondary PCR primers:
up stream (3479) 5'-aag gta ccg caa gat gtg tca cca gca g-3'
Kpn I
down stream (3480) 5'-gac tcg agc tgg atc aga acc taa ctg c-3'
Xho I
P_{35} subunit PCR primers:
up stream (3477) 5'-aag cta gca atg tgg ccc cct ggg tca g –3'
Nhe I
down stream (3478) 5'-ggg gta cct ttt agg aag cat tca gat g-3'
Kpn I
-cmv-P_{40}- segment PCR primers:
up stream (IL 40F) 5'-atg cat gga ggt cgc tga gta gtc –3'
Nsi I
down stream (IL40R) 5'-c atg cat cct agg tag aag gca cag tcg agg ct-3'
Nsi I Avr II
-P_{35}-polyA- segment PCR primers:
up stream (IL35-F) 5'-a cct agg cta gag aac cca ctg ctt ac-3'
Avr II
down stream (IL35R) 5'-tac ccc cta gag ccc cag-3'

Observation under transmission electron microscope After the three plasmids were mixed and incubated with ASOR-PLL at various molecular weight ratios for 40 minutes at room temperature, the mixture was electrophoresed in a 0.8 % agarose gel retardation system to determine its optimal ratio. ASOR-PLL-P(+)/P_{40}, ASOR-PLL-P(-)/P_{35} and ASOR-PLL-P (+)/IL-12 formed in optimal ratios were the two targeting gene drugs. These two drugs (plasmid DNA 0.9 μg) were formed at various concentrations of adjuvant (0, 0.1 M, 0.2 M, 0.3 M, 0.4 M, 1.5 M), then their A_{260} values were measurated and examined under a transmission electron microscope after contrast staining by 2 % uranyl acetate (*bar*=100 nm).

Cell culture and transfection HepG2 cells were cultured to 2×10^7 in minimum essential media plus 15 % fetal bovine serum (37 ℃, 5 % CO_2), and then subcultured in 12-well plates at 1:3 ratio. After the cells were cultured to 60-70 % confluence, the 6 molecule conformations of ASOR-PLL-P(+)/IL-12 and the combined ASOR-PLL-P(+)/P_{40} and ASOR-PLL-P(-)/P_{35} were transfected into the cells using liposome transfection as positive control. There were three wells in each group and the total transfected plasmid DNA was 4.5 μg for each well. During transfection, chloroquine was used (the final concentration was 100 μM*)* to restrain lysosome activity[15,16].

Detection of hIL12 expression Total RNA of transfected HepG2 was extracted by using Trizol 48 hours after transfection. mRNA expression of P_{40} and P_{35} was determined with semi-quantitative RT-PCR using β-actin as an internal control. hIL12 protein in the supernatant was measured using ELISA.

RESULTS

Construction of P(+)P_{40}, P(-)P_{35} and P(+)IL12 plasmids

The full length cDNAs of P_{40} and P_{35} subunits were amplified from human embryonic kidney and cloned into pcDNA3.1 (+/-). P (+)/P_{40} plasmids (6.4 kb) could be cut by KpnI and Xho I to produce two bands: 5.4 kb and 1.007 kb while P (-)/P_{35} plasmids could be cut Kpn I and Nhe I to produce 5.4 kb and 823 bp bands (Figure 1). The segments of -P_{35}-polyA and -cmv-P_{40}- were ligated and cloned into pcDNA3.1 (+) to get P(+)/IL-12 (8.51 kb). P(+)/IL-12 could be cut by Nhe I and Not I (2.5 kb and 6 kb) or by BamH I (2 kb and 6.5 kb) or linearized by Avr II (8.51 kb) (Figure 2).

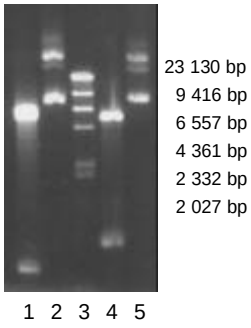

Figure 1 Electrophoresis of P(-)/P_{35}, P(+)/P_{40} and their bands after restrictive endonuclease enzyme digestion in a 0.8 % agarose gel. 1. P(-)/P_{35} plasmid digested by Kpn I and Nhe I. 2. P (-)/P_{35} plasmid. 3. Marker (λDNA/Hind III). 4. P(+)/P_{40} plasmid. 5. of P(+)/P_{40} plasmid cut by Kpn I and Xho I.

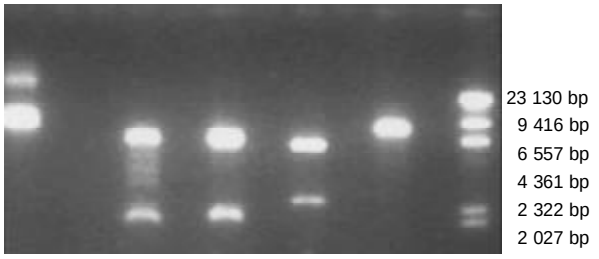

Figure 2 Electrophoresis of recombinant expression plasmid P(+)/IL-12 and the bands after restriction enzyme digestion in a 0.8 % agarose gel (Marker: λDNA/Hind III).

Molecular conformations of targeting gene drugs at various concentrations of adjuvant under transmission electron microscope

The optimal ratios of ASOR-PLL: DNA were as follow: ASOR-PLL:P(+)/IL-12=4:1, ASOR-PLL:P (+)/P_{40}[P(-)/P_{35}]=2:1. ASOR-PLL-DNA complexes which formed in 0, 0.1 M, 0.2 M, 0.3 M, 0.4 M, 1.5 M adjuvant were examined under a transmission electron microscope. The molecular conformations of gene drugs showed divarication-like (ψ-DNA) without adjuvant or in 0.3 M adjuvant, the drug molecules were condensed to granules or "doughnut"-like structures with diameters of 25 nm-300 nm in 0.1 M, 0.2 M and 0.4 M adjuvant. Their conformations varied greatly in 1.5 M adjuvant. The structure of ASOR-PLL-P(+)/IL-12 was rod-like or granule-like. The structures of ASOR-PLL-P(+)/P_{40} and ASOR-PLL-P(-)/P_{35} were both divarication-like (Figure 3).

Detection of hIL-12 expression 48 hours after drugs with different molecular conformations were transfected into HepG2 cells

Total RNA was extracted and semi-quantitative RT-PCR was performed using β-actin as an internal control. hIL12 mRNA levels were increased in both liposome-transfected and ASOR-PLL transfected groups. mRNA levels in ASOR-PLL groups varied with different concentrations of adjuvant (data not shown).

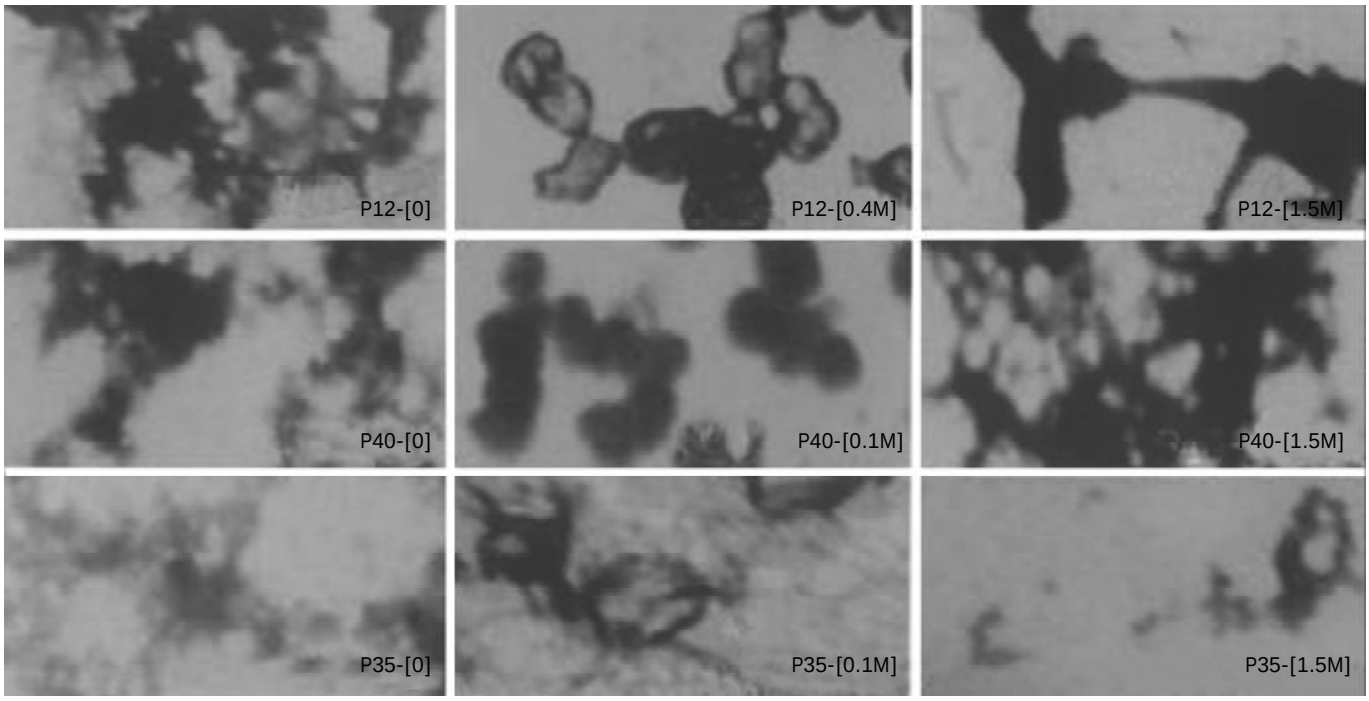

Figure 3 Differently structural features of targeting gene drugs (ASOR-PLL-DNA complexes) at various concentrations of adjuvant under transmission electron microscope. (The *bar* equals 100 nm, amplified 40 000 times).

ELISA results showed that the highest expression level of hIL12 was achieved in cells transfected with ASOR-PLL-P(+)/IL-12 in 0.4 M adjuvant, while the same level of expression was achieved when ASOR-PLL-P(+)/P_{40} and ASOR-PLL-P(-)/P_{35} were co-transfected into HepG2 cells in 0.1 M adjuvant. The expression levels in both groups went down to the lowest points in 1.5 M adjuvant. The expression levels in ASOR-PLL-P(+)/P_{40} and ASOR-PLL-P(-)/P_{35} co-transfected group were higher than those in ASOR-PLL-P(+)/IL-12 group at the same concentrations (Figure 4).

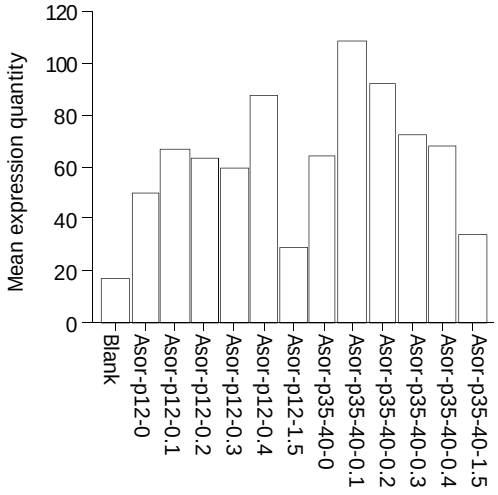

Figure 4 ELISA results of hIL-12 expressed in cell supernatant 48 hours after targeting gene drugs at various adjuvant concentrations were transfected into HepG2.

DISCUSSION

Gene transfection system mediated by receptor-ligand binding, which possesses some advantages for gene therapy, including transferring foreign genes to target cells specifically, being safer without mutation and infection caused by viral vectors, expressing functional proteins without integrating foreign genes into genomic DNA, and unlimited foreign gene size theoretically[17-19], is a potential gene therapy vector which can substitute viral vectors. ASOR is the ligand of ASG receptor (ASGr) which locates specifically on the surface of hepatocytes, and can bind to ASGr specifically[20,21]. Through the positively charged linking molecule PLL which binds to negatively charged DNA molecules through electrostatic interactions, ASOR can transfer foreign DNA molecules into hepatocytes or some hepatoma cells (ASGr+) and express the functional proteins. In 1987, Wu GY and Wu CH firstly transfected reporter gene chloramphenicol acetyltransfectase (CAT) to hepatoma cells (HepG2) by using ASOR-PLL[8]. Ever since, ASOR-PLL has been applied to various therapeutic genes targeting for hepatocytes or some hepatoma cells *in vivo* or *in vitro*[17,22,23]. However, the low expression efficiency of exogenous genes restricts its application to clinic use.

hIL-12 is a double-subunit cytokine discovered in recent years[24], which can promote Th0 cells to differentiate Th1 cells to enhance cell immunity[25]. It can also activate T cells and NK cells to proliferate and secrete IFN-γ to improve humoral immunity[26,27]. Therefore, it plays a role in antivirus, antiprimary tumors and antimetastasis[11-14]. Till now ASOR-PLL has not been used in transferring human interleukin 12 gene to HepG2. We constructed hIL12 double-subunit co-expressing plasmid P(+)/IL12 and single-subunit gene expressing plasmids P(+)/P_{40} and P(-)/P_{35}, and bound them to ASOR-PLL at various adjuvant concentrations and measured A_{260} values of the mixtures (data not shown). ASOR-PLL-P(+)/IL-12 showed the lowest A_{260} value in 0.4 M adjuvant which indicated the least dissociated DNA molecules and the highest hIL-12 expression level, while ASOR-PLL-P(+)/P_{40} and ASOR-PLL-P(-)/P_{35} showed the same result in 0.1 M adjuvant. Though ASOR-PLL-DNA complexes showed lower A_{260} values in 1.5 M adjuvant, most of the HepG2 cells could not stand such a high concentration of adjuvant and died 4 hours after they were transfected, which explained why the expression level of hIL-12 was low. These results indicate that foreign genes (hIL12) can be transferred into target cells (HepG2) through ligand (ASOR) binding to receptors (ASGr), and then endocytosed by cells as reported by Huckett *et al*[28]. The less

dissociated DNA molecules existed in the mixture, more ASOR-PLL-DNA complexes were formed, the higher efficiency of expressing hIL12 was achieved.

Pearales *et al* thought that ligand-DNA complex molecules in a receptor- mediated DNA transfection system must have a relatively high DNA concentration and certain molecule conformations to assist DNA to be transfected into target cells and express functional proteins[17]. To achieve this goal, DNA molecules need to be condensed to a smaller size, and the conformation of aggregated multiple ligand-DNA molecules (such as Ψ-DNA) inhibited gene expression. In our studies, shapes of the molecules under transmission electron microscope showed that ASOR-PLL-P(+)/IL-12 molecules were circle-like structures ("doughnut") with diameters of 50-100 nm in 0.4 M adjuvant, which produced the highest hIL-12 expression. ASOR-PLL-P(+)/P_{40} molecules were granular structures with diameters of 40-125 nm in 0.1 M adjuvant and ASOR-PLL-P(-)/P_{35} molecules were circle-like structures with diameters of 75-150 nm at the same concentration of adjuvant, both of them also achieved the highest hIL12 expression. Although ASOR-PLL-P(+)/P_{40} molecules formed granular structures with diameters of 25-75 nm in 0.2 M adjuvant, ASOR-PLL-P(-)/P_{35} molecules were concentrated to form lumps with diameters of 100-200 nm at this concentration of adjuvant. Since ASOR-PLL-P(+)/P_{40} and ASOR-PLL-P(-)/P_{35} needed to be co-transfected to express functional hIL-12, there were more factors affecting hIL-12 expression in this situation. Meanwhile, the size and the GC/AT ratio of foreign DNA molecules also affected exogenous gene expression[17]. In our studies, the smaller molecular diameters of ASOR-PLL-DNA complexes (25-150 nm), the more condensed DNA molecules and the tighter combination of DNA molecules and ASOR-PLL could lead to higher hIL-12 expression.

In general, single-subunit gene plasmids [P(+)/P_{40} and P(-)/P_{35}] co-expression mediated by ASOR-PLL could induce higher hIL12 expression than that of double-subunit genes co-expressing plasmid transfection. The possible reasons might be the following: (1) There was a certain amount of ASGr on the surface of target cells, when the same amount of DNA was used to transfect cells, ASOR-PLL-P(+)/P_{40} and ASOR-PLL-P(-)/P_{35} were co-transfected at 1:1 ratio, and ASOR could bind to ASGr more thoroughly with a relatively larger amount of ASOR, compared with ASOR-PLL-P(+)/IL-12 transfection. (2) Since the P_{40} and P_{35} subunits cDNAs were cloned in tandem into the polycloning site of pcDNA3.1(+) in which P_{40} cDNA located directly next to P_{35} cDNA, they might interfere reciprocally during transcription, and could not produce P_{40} and P_{35} subunits proportionally. However, P_{40} and P_{35} subunits must combine at 1:1 ratio to form functional hIL-12[12,25].

Another study[29], used atomic force microscope to examine DNA molecules binding to PL, ASOR-PLL and orosomucoid, and found that the optimal conformations of DNA complex molecules for foreign genes expression were solenoid-like or rod-like in diameters of 300 nm-400 nm. The condition to obtain these conformations was that ASOR was combined covalently to 10 kDa PL (Lys: nt$\geqslant$5:1), and linked to DNA molecules. In our studies, PLL was a mixture of 26 kDa, 10 kDa and 4 kDa PLL. The ratio of 10 kDa PL: nucleotide was less than 5:1 in our targeting gene drugs, so hIL-12 expression in ASOR-PLL transfection group was lower than that in liposome transfection group (data not shown).

In summary, the gene transfection system mediated by receptor-ligand binding is a prospective gene therapy strategy, and the expression level of foreign genes has a relationship with the amount of binding DNA, conformation of the complex and characteristics of the linking molecules PLL. Since hIL-12 consists of two subunits (P_{40} and P_{35}), more factors are involved in hIL-12 expression, including the way P_{40} and P_{35} genes enter into the target cells, conformations of the two ASOR-PLL-DNA complexes and interactions of the two complexes. Our studies may contribute to improving hIL-12 expression and applying hIL-12 to clinical hepatoma gene therapy research.

ACKNOWLEDEMENTS

This research work was carried out in National Laboratory of Medical Genetics of China. We sincerely thank academician Xia Jia-hui and everyone in the lab for their help.

REFERENCES

1 **Schuster MJ**, Wu GY. Gene therapy for hepatocellular carcinoma: progress but many stones yet unturned. *Gastroenterology* 1997; **112**: 656-659
2 **Ruiz J**, Qian C, Priet J. Gene therapy for liver tumor: principles and applications. *Digestion* 1998; **59** (Suppl 2): 92-96
3 **Zabner J**, Fasbender AJ, Moninger T, Poellinger KA, Welsl MJ. Cellular and molecular barriers to gene transfer by a cationic lipid. *J Biol Chem* 1995; **207**: 18997-19007
4 **Mitry RR,** Mansour MR, Havlik R, Habib NA. Gene therapy for liver tumor. *Adv Exp Med Biol* 2000; **465**: 193-205
5 **Han J**, Yeom Y. Specific gene therapy transfer mediated by galactosylated poly-L-lysine into hepatoma cells. *Int J Pharm* 2000; **202**: 151-160
6 **Curiel DT**, Wagner E, Cotton M, Birnstiel ML, Li C, Loechel S, Agarwal S, Hu P. High efficiency gene transfer mediated by adenovirus coupled to DNA polylysine complexes via an antibody bridge. *Hum Gene Ther* 1992; **3**: 147-154
7 **Cho CW**, Cho YS, Lee HK, Yeom YI, Park SN, Yoon DY. Improvement of receptor-mediated gene delivery to HepG2 cells using an amphiphilic gelling agent. Biotechnol. *Appl Biochem* 2000; **32**: 21-26
8 **Wu GY**, Wu CH. Receptor-mediated *in vitro* gene transformation by a soluble DNA carrier system. *J Biol Chem* 1987; **262**: 4429-4432
9 **Wu GY**, Wu CH. Receptor-mediated gene delivery and expression *in vivo*. *J Biol Chem* 1988; **263**: 14621-14624
10 **Wu CH**, Walton CM, Wu GY. Targeted gene transfer to liver using protein-DNA complexes. *Methods Mol Med* 2002; **69**: 15-23
11 **Lamont AG**, Adorini L. IL-12; a key cytokine in immune regulation. *Immunol Today* 1996; **17**: 214-217
12 **Trinchieri G**, Scott P. The role of interleukin 12 in the immune response, disease and therapy. *Immunol Today* 1994; **15**: 460-463
13 **Sun Y**, Qian C, Peng D, Prieto J. Gene transfer to liver cancer cells of B7-1 plus interleukin12 changes immunoeffector induced by interleukin 12 alone. *Hum Gene Ther* 2000; **11**: 127-138
14 **Hirschowitz EA**, Maama HA, Evoy D, Lieberman MD, Daly J, Crystal RG. Regional treatment of hepatic micrometastasis by adenovirus vector-mediated delivery of interleukin-2 and interleukin-12 cDNAs to the hepatic parenchyma. *Cancer Gene Ther* 1999; **6**: 491-498
15 **Uherek CH,** Wels W. DNA-carrier proteins for targeted gene delivery. *Advanced Drug Delivery Reviews* 2000; **44**: 153-166
16 **Ciftci K**, Levy RJ. Enhanced plasmid DNA transfection with lysosomotropic agents in cultured fibroblasts. *Int J Pharm* 2001; **218**: 81-92
17 **Perales JC**, Grossmann GA, Molas M, Liu G, Ferkol T, Harpst J, Oda H, Hanson RW. Biochemical and functional characterization of DNA complexes capable of targeting genes to hepatocytes via the asialoglycoprotein receptor. *J Biol Chem* 1997; **272**: 7398-7407
18 **Wu GY**, Wu CH. Receptor-mediated delivery of foreign genes to hepatocytes. *Adv Drug Deli Rev* 1998; **29**: 243-248
19 **Perales JC**, Ferkol T, Molas M, Hanson RW. An evaluation of receptor-mediated gene transfer using synthetic DNA-ligand complexes. *Eur J Biochem* 1994; **226**: 255-266
20 **Ashwell G**, Harford J. Carbohydrate-specific receptors of the liver. *Annu Rev Biochem* 1982; **51**: 531-554
21 **Fallon RJ**, Schwartz AL. Asialoglycoprotein receptor phosphorylation and receptor-mediated endocytosis in hepatoma cells.

Effect of phorbol esters. *J Biol Chem* 1988; **263**: 13159-13166
22 **Wu GY**, Wilson MJ, Shalaby F, Grossman M, Shafritz DA, Wu CH. Receptor-mediated gene delivery *in vivo*. *J Biol Chem* 1991; **266**: 14338-14342
23 **Perales JC**, Ferkol T, Beegen H, Ratnoff OD, Hanson RW. Gene transfer *in vivo*: sustained expression and regulation of genes introduced into the liver by receptor-targeted uptake. *Proc Natl Acad Sci USA* 1994; **91**: 4086-4090
24 **Wolf SF**, Temple PA, Kobayashi M, Young D, Dicig M, Lowe L, Dzialo R, Fitz L, Ferenz C, Hewick RM. Cloning of cDNA for natural killer cell stimulatory factor, a heterodimeric cytokine with multiple biologic effect of T and natural killer cells. *J Immunol* 1991; **146**: 3074-3081
25 **Trinchieri G**. Interleukin-12 and its role in the generation of Th1 cells. *Immunol Today* 1993; **14**: 335-338
26 **Yoshimoto T**, Wang CR, Yoneto T, Waki S, Sunaga S, Komagata Y, Mitsuyama M, Miyazaki J, Nariuchi H. Reduced T helper 1 responses in IL-12 p40 transgenic mice. *J Immunol* 1998; **160**: 588-594
27 **Robertson MJ**, Soiffer RJ, Wolf SF, Manley TJ, Donahue C, Young D, Herrmann SH, Ritz J. Response of human natural killer (NK) cells to NK cell stimulatory factor (NKSF): cytolytic activity and proliferation of NK cells are differentially regulated by NKSF. *J Exp Med* 1992; **175**: 779-788
28 **Huckett B**, Ariatti M, Hawtrey AO. Evidence for targeted gene transfer by receptor-mediated endocytosis. *Biochem Pharmacol* 1990; **40**: 253-263
29 **Hansma HG**, Golan R, Hsieh W, Lollo CP, Mullen-Ley P, Kwoh D. DNA condensation for gene therapy as monitored by atomic force microscope. *Nucleic Acids Research* 1998; **26**: 2481-2487

Edited by Bo XN and Wang XL

P.O.Box 2345, Beijing 100023,China
Fax: +86-10-85381893
E-mail: wjg@wjgnet.com www.wjgnet.com

World J Gastroenterol 2003;9(9):1959-1962
World Journal of Gastroenterology
 ISSN 1007-9327

• LIVER CANCER •

Potential inhibition of cytochrome P450 3A4 by propofol in human primary hepatocytes

Li-Qun Yang, Wei-Feng Yu, Yun-Fei Cao, Bin Gong, Qing Chang, Guang-Shun Yang

Li-Qun Yang, Wei-Feng Yu, Yun-Fei Cao, Department of Anesthesiology, Eastern Hepatobiliary Surgery Hospital, the Second Military Medical University, Shanghai 200438, China
Bin Gong, Qing Chang, Department of Thorax-Cardiosurgery, Changhai Hospital, the Second Military Medical University, Shanghai 200438, China
Guang-Shun Yang, Department of Clinical Surgery, Eastern Hepatobiliary Surgery Hospital, the Second Military Medical University, Shanghai 200438, China
Supported by the grant from Military Medical Science Foundation of China, No.98Q050
Correspondence to: Dr. Wei-Feng Yu, Department of Anesthesiology, Eastern Hepatobiliary Surgery Hospital, the Second Military Medical University, Shanghai 200438, China. liqunyang@yahoo.com
Telephone: +86-21-25070783 **Fax:** +86-21-25070783
Received: 2003-01-18 **Accepted:** 2003-03-10

Abstract

AIM: Hepatic cytochrome P450 isoenzymes constitute a superfamily of hemoproteins that play a major role in the metabolism of endogenous compounds and in the detoxification of xenobiotic molecules. P450 3A4 is one of the most important forms in human being, and mediates the metabolism of around 70 % of therapeutic drugs and endogenous compounds. Propofol, a widely used intravenous anesthetic drug, is known to inhibit cytochrome P450 activities in isolated rat hepatocytes. The goal of this study was to evaluate the potential efficacy of propofol on P450 3A4 in a dose-dependent manner to understand its drug-drug interaction.

METHODS: Hepatocytes were isolated from liver specimens from hepatic angioma patients undergone hepatic surgery. Primary incubated hepatocytes were treated with 0, 0.01, 0.05, 0.1, 0.5, and 1.0 mM propofol for 24 hours. P450 3A4 activity was measured with Nash's colorimetry. The protein expression was assessed by Western blot analysis.

RESULTS: A dose-dependent inhibitory effect of propofol was observed in cytochrome P450 3A4 activity. A minimal dosage of propofol (0.01 mM) induced a significant inhibition of P450 3A4 activity, although its regular dosages (0.01-0.1 mM) showed no inhibitory effect on the cellular protein expression of P450 3A4.

CONCLUSION: Propofol may be a potential CYP3A4 inhibitor as this anesthetic can inhibit isoenzyme activity significantly and reduce the metabolic rate of CYP3A4 substrates. This inhibition occurs at post-expression level, and concentration of propofol used clinically does not affect CYP3A4 protein expression. propofol may thus induce drug interaction of cytochrome P450 3A4 activity at the dosage used clinically.

Yang LQ, Yu WF, Cao YF, Gong B, Chang Q, Yang GS. Potential inhibition of cytochrome P450 3A4 by propofol in human primary hepatocytes. *World J Gastroenterol* 2003; 9(9): 1959-1962
http://www.wjgnet.com/1007-9327/9/1959.asp

INTRODUCTION

Cytochrome P450 enzymatic system is essential for the biotransformation of xenobiotics and drugs, and is a superfamily of haemoproteins[1]. One group of particular interest for those caring for the critically ill is CYP 3A4, which metabolizes many drugs used in the critical patients, including midazolam, lignocaine, alfentanil, erythromycin and cyclosporin[2,3]. Propofol (2, 6-diisopropylphenol) is widely used for anesthetic induction as well as for chronic sedation in ICU. Unlike midazolam, propofol does not undergo phase I metabolism, but is metabolized mostly through direct glucuronidation in the liver. Recent works have shown that several cytochrome P450 isoforms do participate in its metabolism, especially the CYP2B6 isoform. Both *in vitro* and *in vivo*, the inhibitory effects of propofol on cytochrome P450 activities have been already described, thus, propofol may potentially alter the metabolism of many co-administered anesthetics such as alfentanil and midazolam. However, the mechanism of propofol' s inhibitory effect still remains unclear[4-6].

Since primary cultures of human hepatocytes represent a unique *in vitro* system to study the potential of drugs to induce phase I and phase II enzymatic reaction involved in drug metabolism. Many researchers have successfully used human hepatocyte cultures to investigate the effect of various drugs on cytochrome P-450 induction and drug metabolism[7,8]. The goal of this study was to evaluate the inhibitory effect of propofol on cytochrome P450 and its 3A4 isoform activities, as well as of on protein expression of CYP3A4 isoform during 24 hours culture.

MATERIALS AND METHODS

Materials

Propofol was kindly provided by Astra-Zeneca. Rabbit anti-human CYP3A4 polyclonal antibody was purchased from Chemicon (*San Diego, CA*). HRP taged sheep anti-rabbit antibody was purchased from PharMingen (*Mannheim, Germany*). Collagenase IV glucose 6-phosphate, erythromycin, Lowry' s phenol reagent, glucose 6-phosphate transferase, acetate ammonium, acetyl-acetone, and NADP were purchased from Sigma Chemical (*St. Louis, MO*). Newborn calf serum was obtained from GIBCO (Paisley, UK). RPMI 1640 medium was purchased from Seromed (*Berlin, Germany*). dexamethasone and insulin were obtained from BioWhittaker (*Walkersville, MD*). Penicillin G/streptomycin were obtained from Gibco Laboratories (*Grand Island, NY*). All other reagents used in this study were of AR or CP grade.

Isolation and culture of human hepatocytes

Surgical liver biopsies (30-50 g) were taken from hepatic angioma patients undergone hepatic surgery after informed consent was obtained. Patients had no known liver lesions, nor had they received P450s induced medication during the weeks before surgery. None of the patients was habitual consumers of alcohol or other drugs. A total of 8 liver biopsy specimens (from ten men and two women) were used. The patients aged from 18 to 54 years. Human hepatocytes were

isolated using modified collagenase digestive technique according to the method of Liddle[9]. Liver tissues were cut into small pieces about 1 mm^3 and washed three times by 4 ℃ equilibrium liquid to remove the leftover blood, then the liver pieces were digested for 30 min by RPMI 1640 medium containing 0.05 % collagenase. The dissociated hepatocytes were placed into cold Hanks medium for 3 times and centrifugated at 600 rpm for 40 s, at 800 rpm for 50 s and at 1 000 rpm for 60 s. Percoll-gradient centrifugation (1 000-1 200 r/min,10 min) was required to get rid of remained blood thoroughly. Concentration and density of Percoll liquid were 35 % (V/V) and 1.08-1.09 g/ml respectively. Viability at plating was greater than 90 % after trypan blue elimination and hepatocytes were plated in RPMI 1640 medium supplemented with 10^{-7} M dexamethasone, 10^{-7} M insulin, 100 U/ml penicillin G, 100 μg/ml streptomycin, and 5 % bovine calf serum. The hepatocytes (3×10^6) were plated onto 60-mm culture plates previously coated with type I (rat-tail) collagen. The cells were allowed to attach for 4 h at 37 ℃ and 5 % CO2, during which the media were replaced with serum-free media with the supplements listed above and changed every 24 h thereafter.

Treatment of cultures

For CYP inhibition experiments, propofol was dissolved in dimethylsulfoxide and added to cultured human hepatocytes at a final concentration of 0.01, 0.05, 0.1, 0.5 and 1.0 mM, respectively (concentration of DMSO in culture medium was 0.1 % v/v). Treatments were started after medium renewal, and stopped after 24 hrs of co-culture in fresh RPMI 1640 medium, the control cells were run parallelily.

Cellular lysates protein and CYP3A4 activity assays

Total protein concentration of cellular lysates was determined by the method of Lowry *et al*[10]. The spectra were recorded using a Shimadzu UV-250 double-beam spectrophotometer. The final protein concentration of cellular lysates was adjusted to 0.2 mg/ml using Tris-HCl buffer (pH 7.4). CYP3A4 specific activity was determined by N-demethylation of erythromycin using the Nash method listed above[11].

Immunoquantitation of CYP3A4 isoform protein by Western blot analysis

Cellular lysates were obtained from cultured human hepatocytes, which were incubated with propofol for the indicated time points and resolved by SDS-PAGE with vertical mini-gel electrophoresis equipment. Samples of liver microsomal protein (10 μg/lane) were denatured in 10 μl loading buffer (4 ml distilled water, 1 ml 0.5M Tris-HCl, pH 6.8, 0.8 ml glycerol, 1.6 ml 10 % w/v SDS, 0.4 ml-mercaptoethanol, 0.05 ml 0.05 % w/v pyronin Y) and were separated on a 10 % w/v resolving gel. Proteins were transferred from the polyacrylamide gel to the nitrocellulose sheets by electrophoresis, and probed with rabbit anti-human CYP3A4 polyclonal antibody (not cross-reactive with other rat P450s) according to the protocol. CYP3A4 protein was detected by conjugation to the primary antibody by a HRP-linked sheep anti-rabbit second antibody using diaminobenzidine as a substrate[12].

Statistical analysis

The data were analyzed using χ^2 test. $P<0.05$ was considerd statistically significant.

RESULTS

Inhibition of CYP3A4 activity by propofol in hepatocytes primary culture

Information on the donor livers is presented in Table 1. We first determined the inhibition of propofol in primary cultures of human hepatocytes. The hepatocytes were treated with propofol at concentrations of 0.01, 0.05, 0.1, 0.5 and 1.0 mM respectively for 24 h, then we investigated the effect of propofol on Cyp3A4 activity determined by N-demethylation of erythromycin in the medium, as shown in Figure 1. A significant decrease of CYP3A4 activity was detected in hepatocytes pretreated even with 0.01 and 0.05 mM propofol which were relatively lower, and the inhibitory effect showed a dose-dependent increase when the concentration of propofol was higher. Compared with the controls, the total cellular lysate protein in the cultured medium remained unchanged in all groups.

Table 1 Informations of donors and their drug history

HH	Age (y)	Gender (F/M)	Drug history	Cell viability %
1	42	M	Fentanyl, ranitidine, dopamine	88
2	38	M	Vercuronium, fentanyl, ephedrine	86
3	18	M	Vasopressin, phenobarbital, rocuronium	90
4	26	F	Phenobarbital, fentanyl, vercuronium	92
5	39	F	Mlidozolam, fentanyl, lidocaine	80
6	54	M	Phenobarbital, rocuronium	84
7	49	M	Fentanyl, ephedrine	87
8	44	M	Fentanyl, ranitidine, dopamine	85

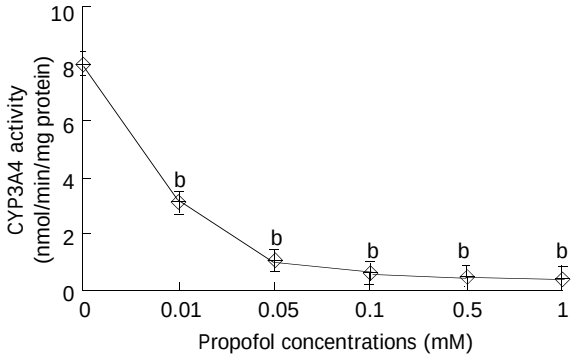

Figure 1 Effect of propofol on CYP3A4 activity in primary cultured hepatocytes. Hepatocytes prepared from donors were treated for 24 h with 0, 0.01, 0.05, 0.1, 0.5, and 1.0 mM propofol. At the end of this time, the medium was changed and erythromycin at 0.4 mM was added to the cells. After incubated for 30 min, aliquots of the medium were removed, and N-demethylation of erythromycin activity was determined as described above. Each value represented the mean of triplicate treatments with SD indicated by the vertical bars. ^{b}:$P<0.01$.

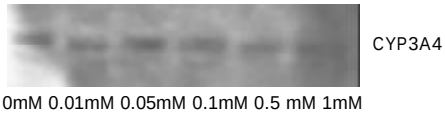

Figure 2 Effect of propofol on CYP3A protein expression. Hepatocytes prepared from donors were treated for 24 h with 0, 0.01, 0.05, 0.1, 0.5, and 1.0 mM propofol. CYP3A was analyzed in sonicates of whole cells as described in the paragraph of Materials and Methods. 20 micrograms of sonicated protein were applied per well.

Change of CYP3A4 isoform protein

Hepatocytes were treated with propofol at a concentration of 0.01, 0.05, 0.1, 0.5 and 1.0 mM, respectively for 24 hrs, and total protein synthesis was measured as described previously (Kostrubsky *et al*., 1997). The data in Figure 2 show a high expression of CYP3A4 proteins in hepatocytes, but

concentrations of propofol used clinically did not decrease total protein synthesis, even very high concentration of propofol (0.5 and 1.0 mM) could slightly reduce the hepatic CYP3A4 protein expression after 24 hours of culture. That meant the regular dosages used clinically (0.01-0.1 mM) had no significantly inhibitory effect on the cellular protein expression of P450 3A4.

DISCUSSION

In vitro studies with hepatic cells, in particular the human cultured hepatocytes, have offered a defined system for studying the direct effects of individual xenobiotic molecules on the regulation of hepatic CYP expression and activity in man[13]. This approach does not require any prior knowledge of the metabolism or disposition of the test compound, but instead uses the ability of a drug to induce or inhibit the metabolism of isoform-specific substrates, such as the conversion of testosterone to 6-hydroxytestosterone or N-demethylation of erythromycin by CYP3A[14]. This method by utilizing intact human hepatocytes for studying the metabolic activities, but not the microsomal suspensions, can provide quick and reproducible estimates of CYP3A metabolic capacity and protein levels. Primary cultures of human hepatocytes are responsive to induction of CYPs and can be used to assess the interactions resulted from the effect of CYPs during multiple drug therapy. The present study was conducted to examine the potential down-regulation by propofol on CYP expression. To this end, specific monooxygenase activities for CYP3A4 isozymes and *de novo* CYP protein synthesis were examined[15,16].

In our studies, the activity of CYP3A4 isoform in 8 Chinese patients was obviously lower than that of others reported in Caucasians. Although CYP3A4 drug metabolising activities vary widely among individuals, it has a unimodal population distribution and does not appear to be subjected to genetic polymorphism as is seen with other CYP isoforms (2D6, 2C9 and 2C19)[17-20]. The wide interrace variability is likely, in part, to be caused by ethnic or cultural differences, perhaps related to an interaction between habit and diet. Hence we could not draw any conclusion about the normal distribution character istics of CYPs in Chinese, because of the limited sample number and experimental conditions. More detailed and complete studies should be performed for analysing the distribution of CYPs among Chinese in the near future[21].

Propofol has been shown to interfere with the metabolism of alfentanil and sufentanil by inhibiting CYP2B1 and CYP1A1. Propofol inhibits CYP2E1 only to a limited extent as its molecules are too large to bind effectively to the active sites of the enzyme. Thus, propofol may potentially alter the metabolism of co-administered drugs such as alfentanil and sufentanil, but it does not effectively inhibit the metabolism of volatile agents (enflurane, sevoflurane, methoxyflurane) by CYP2E1[22-24]. This is the first report on whether different concentrations of propofol can down-regulate the protein expression of CYP3A4 in hepatocytic primary culture. According to the present result, we could see the regular dosages used clincially (0.01-0.1 mM) had no inhibitory effect on the cellular protein expression of P450 3A4, although a minimum dosage of propofol (0.01 mM) induced a significant inhibition of P450 3A4 activity. The intrinsic inhibition mechanisms of propofol on P450s have been investigated by several groups but still remain unclear[25,26]. It has been demonstrated that propofol exhibits a concentration dependent inhibitory effect on CYP2B1 and 1A1 by binding to the haemoiety of the enzymes. Some researchers have used homologic P450 models, they postulated plausible mechanisms for enzyme catalysis, inhibition, and activation, based on its 3D structure. The sites of effect that propofol binds to CYP3A4 hemeprotein maybe 214, 218 active site residues, then competitive inhibition of propofol and other CYP3A4 substrates may occur because active sites of P450s have been occupied[27] . This postulation may explain the potential inhibitory mechanism of propofol on CYP3A4.

In the present study, a dosage-dependent inhibitory effect of propofol was observed on cytochrome P450 3A4 activity, while the mean plasma concentration of propofol in clinical TCI anesthesia was 0.01-0.05 mM as described by others[28-30], indicating that a minimum clinical dosage of propofol (0.01 mM) could induce a significant inhibition of P450 3A4 activity. Since CYP3A4 is a predominant isoform of CYP3A in adult humans, change of hepatic CYP3A4 activity will change the metabolism of most therapeutic drugs. Firstly, a large number of intravenous anesthetics and sedative agents (including diazepam, midozolam, fentanyl, lidocaine, etc.) are substrates of CYP3A4 isoform, N-hydroxylation and N-dealkylation reactions of anesthetics can be reduced when propofol administration causes drug accumulation, oversedation and postoperative awake delay[31, 32]. Secondly, amiodarone, quinidine, nifedipine, berhomine and cyclosporin are also eliminated through CYP3A4, thus competitive inhibition should be noticed and avoided especially when more than one substrates are administrated by patients with impaired liver function. These findings are in accordance with pharmacokinetic studies that have shown reduced clearance of midozolam when conbined with fentanyl in cirrhotics, but overdosage of anti-arrhythmics have a greater clinical signifiance than that of other drugs[33,34]. Thirdly, as CYP3A4 also plays an important role in biotransformation and detoxification of many endogenous substrates, reduction of CYP3A4 activity may result in inactivation of endogenous substances including cholesterol, bile acid, sex hormones and glucocorticoids, thus causing more extensive physiopathologic changes in patients with hepatic diseases. These changes, in turn, will affect the drug metabolic enzymes[35,36].

REFERENCES

1 **Nebert DW**, Nelson DR, Coon MJ, Estabrook RW, Feyereisen R, Fujii-Kuriyama Y, Gonzalez FJ, Guengerich FP, Gunsalus IC, Johnson EF. The P450 superfamily: update on new sequences, gene mapping and recommended nomenclature. *DNA Cell Biol* 1991; **10**: 1-10

2 **Guengerich FP**. Cytochrome P-450 3A4: regulation and role in drug metabolism. *Annu Rev Pharmacol Toxicol* 1999; **39**: 1-17

3 **Paine MF,** Wagner DA, Hoffmaster KA, Watkins PB. Cytochrome P450 3A4 and P-glycoprotein mediate the interaction between an oral erythromycin breath test and rifampin. *Clin Pharmacol Ther* 2002; **72**: 524-535

4 **Oda Y,** Hamaoka N, Hiroi T, Imaoka S, Hase I, Tanaka K, Funae Y, Ishizaki T, Asada A. Involvement of human liver cytochrome P4502B6 in the metabolism of propofol. *Br J Clin Pharmacol* 2001; **51**: 281-285

5 **Chen TL,** Chen TG, Tai YT, Chang HC, Chen RM, Lin CJ, Ueng TH. Propofol inhibits renal cytochrome P450 activity and enflurane defluorination in vitro in hamsters. *Can J Anaesth* 2000; **47**: 680-686

6 **Guitton J,** Buronfosse T, Desage M, Flinois JP, Perdrix JP, Brazier JL, Beaune P. Possible involvement of multiple human cytochrome P450 isoforms in the liver metabolism of propofol. *Br J Anaesth* 1998; **80**: 788-795

7 **LeCluyse EL.** Human hepatocyte culture systems for the in vitro evaluation of cytochrome P450 expression and regulation. *Eur J Pharm Sci* 2001; **13**: 343-368

8 **Morel F,** Langouet S, Maheo K, Guillouzo A. The use of primary hepatocyte cultures for the evaluation of chemoprotective agents. *Cell Biol Toxicol* 1997; **13**: 323-329

9 **Liddle C,** Goodwin BJ, Tapner M. Culture and transfection of mammalian primary hepatocytes and hepatocyte-derived cell lines. *J Gastroenterol Hepatol* 1998; **13**: 855-858

10 **Lowry OH**, Passonneau JV. Some recent refinements of quantitative histochemical analysis. *Curr Probl Clin Biochem* 1971; **3**: 63-84
11 **Hover CG**, Kulkarni AP. Lipoxygenase-mediated hydrogen peroxide-dependent N-demethylation of N, N-dimethylaniline and related compounds. *Chem Biol Interact* 2000; **124**: 191-203
12 **Kostrubsky VE,** Ramachandran V, Venkataramanan R, Dorko K, Esplen JE, Zhang S, Sinclair JF, Wrighton SA, Strom SC. The use of human hepatocyte cultures to study the induction of cytochrome P-450. *Drug Metab Dispos* 1999; **27**: 887-894
13 **Li AP,** Maurel P, Gomez-Lechon MJ, Cheng LC, Jurima-Romet M. Preclinical evaluation of drug-drug interaction potential: present status of the application of primary human hepatocytes in the evaluation of cytochrome P450 induction. *Chem Biol Interact* 1997; **107**: 5-16
14 **Zhou Q,** Yao TW, Zeng S. Chiral metabolism of propafenone in rat hepatic microsomes treated with two inducers. *World J Gastroenterol* 2001; **7**: 830-835
15 **Guillouzo A,** Morel F, Fardel O, Meunier B .Use of human hepatocyte cultures for drug metabolism studies. *Toxicology* 1993; **82**: 209-219
16 **Mode A.** Sexually differentiated expression of genes encoding the P4502C cytochromes in rat liver-a model system for studying the action of growth hormone. *Reprod Fertil Suppl* 1993; **46**: 77-86
17 **Tenneze L**, Tarral E, Ducloux N, Funck-Brentano C. Pharmacokinetics and electrocardiographic effects of a new controlled-release form of flecainide acetate: Comparison with the standard form and influence of the CYP2D6 polymorphism. *Clin Pharmacol Ther* 2002; **72**: 112-122
18 **Rau T**, Heide R, Bergmann K, Wuttke H, Werner U, Feifel N, Eschenhagen T. Effect of the CYP2D6 genotype on metoprolol metabolism persists during long-term treatment. *Pharmacogenetics* 2002; **12**: 465-472
19 **Zheng YX**, Chan P, Pan ZF, Shi NN, Wang ZX, Pan J, Liang HM, Niu Y, Zhou XR, He FS. Polymorphism of metabolic genes and susceptibility to occupational chronic manganism. *Biomarkers* 2002; **7**: 337-346
20 **Dahl ML**. Cytochrome p450 phenotyping / genotyping in patients receiving antipsychotics: useful aid to prescribing? *Clin Pharmacokinet* 2002; **41**: 453-470
21 **Bertilsson L.** Geographical / interracial differences in polymorphic drug oxidation. Current state of knowledge of cytochromes P450 (CYP) 2D6 and 2C19. *Clin Pharmacokinet* 1995; **29**: 192-209
22 **Vuyk J.** Clinical interpretation of pharmacokinetic and pharmacodynamic propofol-opioid interactions. *Acta Anaesthesiol Belg* 2001; **52**: 445-451
23 **Gemayel J,** Geloen A, Mion F. Propofol-induced cytochrome P450 inhibition: an *in vitro* and *in vivo* study in rats. *Life Sci* 2001; **68**: 2957-2965
24 **Miller E,** Park GR. The effect of oxygen on propofol-induced inhibition of microsomal cytochrome P450 3A4. *Anaesthesia* 1999; **54**: 320-322
25 **McKillop D**, Wild MJ, Butters CJ, Simcock C. Effects of propofol on human hepatic microsomal cytochrome P450 activities. *Xenobiotica* 1998; **28**: 845-853
26 **Chen TL,** Wang MJ, Huang CH, Liu CC, Ueng TH. Difference between *in vivo* and *in vitro* effects of propofol on defluorination and metabolic activities of hamster hepatic cytochrome P450-dependent mono-oxygenases. *Br J Anaesth* 1995; **75**: 462-466
27 **Szklarz GD**, Halpert JR. Molecular basis of P450 inhibition and activation: implications for drug development and drug therapy. *Drug Metab Dispos* 1998; **26**: 1179-1184
28 **Lehmann A,** Boldt J, Thaler E, Piper S, Weisse U. Bispectral index in patients with target-controlled or manually-controlled infusion of propofol. *Anesth Analg* 2002; **95**: 639-644
29 **Macquaire V,** Cantraine F, Schmartz D, Coussaert E, Barvais L. Target-controlled infusion of propofol induction with or without plasma concentration constraint in high-risk adult patients undergoing cardiac surgery. *Acta Anaesthesiol Scand* 2002; **46**: 1010-1016
30 **Irwin MG,** Hui TW, Milne SE, Kenny GN. Propofol effective concentration 50 and its relationship to bispectral index. *Anaesthesia* 2002; **57**: 242-248
31 **Ahonen J,** Olkkola KT, Salmenpera M, Hynynen M, Neuvonen PJ. Effect of diltiazem on midazolam and alfentanil disposition in patients undergoing coronary artery bypass grafting. *Anesthesiology* 1996; **85**: 1246-1252
32 **Oda Y**, Mizutani K, Hase I, Nakamoto T, Hamaoka N, Asada A. Fentanyl inhibits metabolism of midazolam: competitive inhibition of CYP3A4 *in vitro*. *Br J Anaesth* 1999; **82**: 900-903
33 **Nims RW**, Prough RA, Jones CR, Stockus DL, Dragnev KH, Thomas PE, Lubet RA. *In vivo* induction and *in vitro* inhibition of hepatic cytochrome P450 activity by the benzodiazepine anticonvulsants clonazepam and diazepam. *Drug Metab Dispos* 1997; **25**: 750-756
34 **Iribarne C**, Dreano Y, Bardou LG, Menez JF, Berthou F. Interaction of methadone with substrates of human hepatic cytochrome P450 3A4. *Toxicology* 1997; **117**: 13-23
35 **Ourlin JC**, Handschin C, Kaufmann M, Meyer UAA. Link between cholesterol levels and phenobarbital induction of cytochromes P450. *Biochem Biophys Res Commun* 2002; **291**: 378-384
36 **Staudinger J**, Liu Y, Madan A, Habeebu S, Klaassen CD. Coordinate regulation of xenobiotic and bile acid homeostasis by pregnane X receptor. *Drug Metab Dispos* 2001; **29**: 1467-1472

Edited by Wu XN and Wang XL

P.O.Box 2345, Beijing 100023,China
Fax: +86-10-85381893
E-mail: wjg@wjgnet.com www.wjgnet.com

World J Gastroenterol 2003;9(9):1963-1967
World Journal of Gastroenterology
 ISSN 1007-9327

• LIVER CANCER •

Experimental study of anti-tumor effects of polysaccharides from *Angelica sinensis*

Peng Shang, Ai-Rong Qian, Tie-Hong Yang, Min Jia, Qi-Bing Mei, Chi-Hin Cho, Wen-Ming Zhao, Zhi-Nan Chen

Peng Shang, Wen-Ming Zhao, School of Life Science and Technology, Xi' an Jiaotong University, Xi' an 710054, Shaanxi Province, China
Peng Shang, Ai-Rong Qian, Zhi-Nan Chen, Department of Cell Biology, Fourth Military Medical University, Xi' an 710032, Shaanxi Province, China
Tie-Hong Yang, Min Jia, Qi-Bing Mei, Department of Pharmacology, Fourth Military Medical University, Xi' an 710032, Shaanxi Province, China
Chi-Hin Cho, Department of Pharmacology, Faculty of Medicine, University of Hong Kong, Hong Kong, China
Supported by RGC grant from the University of Hong Kong and the Hong Kong Research Grant Council (HKU7257-98M), and grants from the Hi-Tech Research & Development Program of China (2001AA215061)
Correspondence to: Dr. Zhi-Nan Chen, Department of Cell Biology, Fourth Military Medical University, Xi' an 710032, Shaanxi Province, China. chcerc2@fmmu.edu.cn. Dr. Qi-Bing Mei, Department of Pharmacology, Fourth Military Medical University, Xi' an 710032, Shaanxi Province, China. qbmei@hotmail.com
Telephone: +86-29-3374547
Received: 2003-04-07 **Accepted:** 2003-05-21

Abstract

AIM: To investigate the *in vivo* anti-tumor effects of total polysaccharide (AP-0) isolated from *Angelica* sinensis (Oliv.) Diels (Danggui) on mice and the *in vitro* inhibitory effects of AP-0 and its sub-constituents (AP-1, AP-2 and AP-3) on invasion and metastasis of human hepatocellular carcinoma.

METHODS: Three kinds of murine tumor models *in vivo*, sarcoma 180 (S180), leukemia L1210 and Ehrlich ascitic cancer (EAC) were employed to investigate the anti-tumor effects of AP-0. For each kind of tumor model, three experimental groups were respectively given AP-0 at doses of 30, 100 and 300 mg/kg by *ip* once a day for 10 days. Positive control groups were respectively given Cy at a dose of 30 mg/kg for S180 and leukemia L1210, and 5-FU at a dose of 20 mg/kg for EAC. On d 11, mice bearing S180 were sacrificed and the masses of tumors, spleens and thymus were weighed. The average living days of mice bearing EAC and of mice bearing L1210 were observed, and the rates of life prolongation of each treatment were calculated, respectively. The inhibitory effects of APs on hepatoma invasion and metastasis *in vitro* were investigated by employing human hepatocellular carcinoma cell line (HHCC) with the Matrigel invasion chamber, adhesion to extracelluler matrix and chemotatic migration tests, respectively.

RESULTS: AP-0 had no obviously inhibitory effect on the growth of S180, but it could significantly decrease the thymus weights of the mice bearing S180. AP-0 could significantly reduce the production of ascitic liquids and prolong the life of mice bearing EAC. AP-0 could also increase the survival time of mice bearing L1210. AP-0 and AP-2 had significantly inhibitory effects on the invasion of HHCC into the Matrigel reconstituted basement membrane with the inhibitory rates of 56.4 % and 68.3 %, respectively. AP-0, AP-1, AP-2 and AP-3 could influence the adhesion of HHCC to extracellular matrix proteins (Matrigel and fibronectin) at different degrees, among them only AP-3 had significant blocking effect on the adhesion of HHCC to fibronectin with an inhibitory rate of 30.3 %. AP-0, AP-1 and AP-3 could partially inhibit the chemotactic migration abilities of HHCC.

CONCLUSION: The experimental findings suggest that total polysaccharide of *Angelica* sinensis (Oliv.) Diels (Chinese Danggui) possesses anti-tumor effects on experimental tumor models *in vivo* and inhibitory effects on invasion and metastasis of hepatocellular carcinoma cells *in vitro*.

Shang P, Qian AR, Yang TH, Jia M, Mei QB, Cho CH, Zhao WM, Chen ZN. Experimental study of anti-tumor effects of polysaccharides from *Angelica sinensis. World J Gastroenterol* 2003; 9(9): 1963-1967
http://www.wjgnet.com/1007-9327/9/1963.asp

INTRODUCTION

The Chinese herbal medicine Danggui, root of *Angelica sinensis* (Oliv.) is widely used in traditional Chinese medical therapy of various diseases as well as a healthful food tonic and spice for thousands of years. Being called the "female ginseng", it is excellent as an all purpose women's herb[1]. Danggui can be used for anemia due to chronic renal failure (CRF)[2] and can enhance hematopoiesis by stimulating macrophages, fibroblasts, lymphocytes in hematopoietic inductive microenvironment and muscle tissue to secrete hematopoietic growth factors. Gastrointestinal protective effects[3,4] and the mechanism[5,6] of polysaccharides from *Angelica sinensis* in rats have been reported. Effects of *Angelica* polysaccharides on blood coagulation and platelet aggregation[7] and the protective effect of the polysaccharides-enriched fraction from *Angelica sinensis* on hepatic injury[8] were also studied. A low molecular weight polysaccharide from *Angelica sinensis* (Oliv.) Diels showed strong anti-tumor activity on Ehrlich ascitic cancer bearing mice and also exhibited immunostimulating activities, both *in vitro* and *in vivo*[9] (Choy *et al*. *Am J Chin Med*, 1994; 22:137). Polysaccharides from three kinds of edible fungi showed inhibitory activities on the proliferation of human hepatoma SMMC-7721 cells and mouse implanted S180 tumor[10]. Apoptosis of hepatoma cells SMMC-7721 could be induced by polysaccharides from *Ginkgo biloba* seeds[11]. In China, hepatocellular carcinoma with high invasiveness and recurrence has ranked second of cancer mortality since 1990s. Anti-invasion and metastasis is currently one of the major targets of hepatoma studies[12,13]. Some polysaccharides involve in the process of tumor invasion and progression, such as heparin, heparan sulfate and hyaluronan[14-16]. The anti-metastasis effects and their pharmacological mechanisms of modified citrus pectin[17] and protein-bound polysaccharide (PSK) have been studied recently[18-20]. However, the anti-tumor effects on other kinds of tumors and the anti-invasion

and metastasis effects of polysaccharides from *Angelica sinensis* (Oliv.) Diels have not been studied. In the present study, the anti-tumor effects of total polysaccharide (AP-0) on mice bearing transplanted sarcoma 180, leukemia L1210 and Ehrlich ascitic cancer (EAC) were investigated. The *in vitro* inhibitory effects of AP-0 and its sub-constituents, AP-1, AP-2 and AP-3 on the abilities of invasion and metastasis of human hepatocellular carcinoma were also tested by employing HHCC cell line.

MATERIALS AND METHODS

Animals and cell lines

Male BALB/c mice, weighing 18-22 g, were used in S180 and EAC experiments, and male DBA/2 mice, weighing 18-22 g, were used in L1210 experiment. All the mice were raised in a clear room with controlled temperature and humidity. Animals were free to drink tap water. Human hepatocellular carcinoma cell line (HHCC) was purchased from Type Culture Collection of Chinese Academy of Sciences, Shanghai, China. Human embryo dermal fibroblast cell line (Fb) was kindly presented by Dr. JT Han (Department of Plastic Surgery, Fourth Military Medical University).

Polysaccharides from Angelica sinensis

Fresh roots of *Angelica sinensis* (Oliv.) were picked in autumn from Minxian County, Gansu Province, China. Total polysaccharide (AP-0) was isolated by ethanol precipitation after boiling water extraction. The sub-constituents, AP-1, AP-2 and AP-3 from AP-0 were obtained by multi-precipitation treated with CTAB, H_3BO_3, NaOH, acetic acid and ethanol according to Yamada *et al*[21]. The physical-chemical characteristics of APs were analyzed and determined (Shang P, *et al*. *Disi Junyi Daxue Xuebao*, 2001;22:1311; *Chin Pharmaceutical J*, 2000;35:332). The contents of total carbohydrate, uronic acids and proteins in AP-0, AP-1, AP-2 and AP-3 were 97.0 %, 21.0 % and 3.0 %; 97.0 %, 17.2 % and 3.0 %; 83.0 %, 25.7 % and 17 %; 97.0 %, 8.6 % and 3 %, respectively. All of APs' solution was dispensed with sterile *N S* in the laminar flow bench.

Mice transplanted tumor models and Angelica polysaccharide (AP-0) treatments

Mice model of S180 was established by inoculating 5×10^6 S180 cells into left armpit of each mouse. From the next day following tumor cells inoculation (d 1) to the 10^{th} day (d 10), mice in 3 experimental groups were administrated *ip* AP-0 at doses of 30, 100 and 300 mg/kg, once daily, respectively. Positive and negative control groups were given Cy at a dose of 30 mg/kg and *N S* of 20 mg/kg, once daily, respectively. On d 11, the mice were sacrificed, and the weights of tumor, spleen and thymus were recorded. Mice model of EAC was made by injecting *ip* 2.5×10^6 EAC cells into each mouse. From the second day of tumor cells inoculation (d 1) to the 10^{th} day (d 10), mice in 3 experimental groups were given AP-0 *ip* at doses of 30, 100 and 300 mg/kg, once daily, respectively. Positive and negative control groups were given 5-FU at a dose of 20 mg/kg and *N.S*. of 20 mg/kg, respectively. The average survival time of less than 60 days each group was observed and the effects of AP-0 on prolongation were calculated. Mice model of L1210 was made by injecting *ip* 1×10^5 L_{1210} cells into each mouse. From the next day of tumor cells inoculation (d 1) to the 10^{th} day (d 10), mice in 3 experimental groups were given AP-0 *ip* at doses of 30, 100 and 300 mg/kg, once daily, respectively. Positive and negative control groups were given Cy at a dose of 30 mg/kg and *NS* of 20 mg/kg. The average survival time of less than 30 days of each group was observed and the rates of life prolongation were calculated.

Anti-invasion tests of angelica polysaccharides in vitro

Experimental methods employed in this part were based on previous report[22] with a slight modification.

AP-0-AP-3' s inhibitory effects on HHCC invasion into reconstituted basement membrane Each inner membrane of Millicell chamber (Millipore, USA) was paved with 40 μL Matrigel (BD Bioscience, USA) and dried in the laminar bench at room temperature. The Matrigel-Millicells of co-cultured HHCC and Fb, with each Milicell containing 150 μL (1.5×10^5) cells cultured in DMEM supplemented with 1 mL/L bovine calf serum (BCS), were put into 24-well microplates (Nunc, Sweden) containing 10 μg fibronectin (FN, GIBCO, USA) as a chemotactic agent in 200 μL DMEM (GIBCO, U S A.) supplemented with 1 mL/L BCS. AP-0, AP-1, AP-2 and AP-3 at a dose of 50 μL (7.0 mg/ml) were added into the Millicell. After the microplates and Millicells were incubated for 20 hours at 37 ℃, 50 mL/L CO_2 (Heraeus, Germany), each upper surface of membrane was scrubbed 3 times with a cotton swab. All of the membranes were fixed with 950 mL/L ethanol and then taken off for HE staining. HHCC cells infiltrated into the membrane were counted under a high power microscope. All experiments were performed in triplicate.

Inhibition of AP-0-AP-3 on HHCC adhesion to extracellular matrix proteins Each well of the 96-well microplates was coated with FN and Matrigel, 2 μg for each one, respectively. The coated wells were allowed to dry, then 20 μL 10 g/L BSA was added into each well and incubated for 1 hour. The wells were washed with PBS. Each well containing 200 μL (2×10^5) HHCC and 50 μL (7.0 g/L) APs was incubated for 2 hours at 37 ℃, 50 mL/L CO_2. After each well was washed 3 times with 200 μL PBS, 40 μg MTT was added into each one and incubated for 4 hours at 37 ℃, 50 mL/L CO_2. Then the liquid was removed, and 200 μL DMSO was added into each well. The absorbance of each well was detected by a microplate Reader (Bio-Rad 450, USA) at 490 nm. Triplicate determinations were performed at each data point.

Influences of AP-0-AP-3 on HHCC chemotactic migration The outer-surface of each Millicell was paved with 10 μg FN as a chemotactic agent. 150 μL (1.5×10^5) HHCC cells cultured in DMEM supplemented with 1 mL/L BCS, was added into each Millicell. Then the Millicells were cultured in 24-well microplates containing 200 μL DMEM supplemented with 1 mL/L BCS in each well. AP-0, AP-1, AP-2 and AP-3 at doses of 50 μL (7.0 g/L) were added into the Millicells respectively. After the microplates containing Millicells were incubated for 20 hours at 37 ℃, 50 mL/L CO_2, each upper surface of the membrane was scrubbed 3 times with a cotton swab. Then the membranes were fixed with 950 mL/L ethanol and taken off for HE staining. The HHCC cells infiltrated into the membrane were counted under a high power microscope. All experiments were performed in triplicate.

Statistical analysis

Differences of weights, cell counts and absorbance between the experimental and control groups were examined by using ANOVA (analysis of variance). Differences of life prolongation rates were examined by Cox proportional hazards regression.

RESULTS

Effects of Angelica polysaccharide (AP-0) on mice transplanted tumors

Influences of AP-0 on immunological organs of mice bearing S180 Although the differences of tumor's weights between the three AP-0 groups and N.S. control group were not significant, thymus weights of mice receiving AP-0 were significantly lighter than those of mice treated by N.S. Whereas,

thymus weights of mice receiving AP-0 were significantly heavier than those of mice treated by Cy (Table 1). Thymus weights of mice receiving doses of AP-0 at 100 mg/kg (P<0.05), 30 mg/kg and 300 mg/kg (P<0.01) were lighter than those of *NS* group. The thymus weights of mice receiving doses of dAP-0 at 30 mg/kg (P<0.05), 100 mg/kg and 300 mg/kg (P<0.01) were heavier than those of Cy group.

Table 1 Masses of body, tumor, thymus and spleen of mice bearing S180 10 days after being treated with AP-0, Cy and *N S* ($\bar{x}$±s)

Group	Mice (n) (d10/d0)	m (body) (g)	m (tumor) (g)	m (thymus) (mg)	m (spleen) (g)
N S	10/10	25±3	2.6±0.8[d]	69±17	0.25±0.08[d]
Cy	9/9	19±3[b]	1.2±0.4	16±10[b]	0.06±0.02
AP-0					
30 mg/kg	9/10	22±5	2.8±1.0[d]	35±19[bd]	0.22±0.13[d]
100 mg/kg	8/10	22±3	2.7±0.5[d]	46±16[ad]	0.20±0.08[d]
300 mg/kg	7/10	22±2	3.0±1.3[d]	44±14[bd]	0.34±0.14[d]

[a]P<0.05, [b]P<0.01 *vs N S*, [d]P<0.01 *vs* Cy.

Effects of AP-0 on mice bearing EAC The average weight of mice in each group receiving AP-0 treatment was far significantly lighter than that of *NS* group, suggesting that the amounts of ascitic fluid produced in the mice of experimental groups were less than those of *NS* groups (Table 2). The survival time of each AP-0 treated group was longer than that of *NS* group within 60 day observation. However, significant difference was found only between the AP-0 300 mg/kg treated group and *NS* group (Table 2).

Table 2 Survival and body masses of mice bearing EAC after being treated with AP-0

Group	n	Survival time (days)	Life prolongation rate (%)	m (body)/(g) ($\bar{x}$±s)	
				d 0	d 10
N S	10	14.1	0.0	19.9±0.9	42.2±1.9
5-FU	10	60.0	325.0	20.2±0.9	24.7±3.6[b]
AP-0					
30 mg/kg	10	26.5	89.7	19.8±1.6	36.5±5.2[b]
100 mg/kg	10	18.4	30.5	19.4±1.2	35.8±3.0[b]
300 mg/kg	10	36.0	155.3[a]	19.3±1.0	31.3±3.8[b]

[a]P<0.05 *vs N S*, [b]P<0.001 *vs N S*.

Effects of AP-0 on mice bearing L1210 The survival time of mice receiving AP-0 at doses of 30 mg/kg and 100 mg/kg was longer than that of *NS* group within 30 day observation. Only 30 mg/kg group had a significant difference compared with N.S. group (Table 3). The effect was not dose-dependent.

Table 3 Survival of mice with L1210 after being treated with AP-0 ($\bar{x}$±s)

Group	n	Survival time (days)	Life prolongation rate (%)
N S	0	15.0	0.0
Cy	5	30.0	200.0
AP-0			
30 mg/kg	1	25.0	66.7[a]
100 mg/kg	0	23.5	56.7
300 mg/kg	0	15.0	0.0

[a]P<0.05 *vs N S*.

Effects of Angelica polysaccharides on invasion and metastasis of hepatocellular carcinoma in vitro

Inhibition of AP-0-AP-3 on HHCC infiltrating into reconstituted basement membrane AP-0, AP-1, AP-2 and AP-3 could inhibit HHCC cells to infiltrate into the reconstituted basement membrane with inhibitory rates of 56.4 %, 38.6 %, 68.3 % and 26.7 %, respectively. Among them, AP-0 and AP-2 had significant inhibitory effects (P<0.05) compared with the control (Table 4).

Table 4 Inhibition of *Angelica* polysaccharides on infiltration and migration of HHCC

Group	Infiltration		Migration	
	Infiltrated cells ($\bar{x}$±s)	Inhibitory rate(%)	Migrated cells ($\bar{x}$±s)	Inhibitory rate (%)
Control	20.2±18.5	0.0	23.6±18.7	0.0
AP-0	8.8±9.2[a]	56.4	29.5±17.8	\
AP-1	12.4±9.5	38.6	14.4±4.8	39. 0
AP-2	6.4±2.9[a]	68.3	17.0±7.9	28.0
AP-3	14.8±14.5	26.7	16.3±9.0	30.9

[a]P<0.05 *vs* Control.

Influences of AP-0-AP-3 on HHCC adhesion to extracellular matrix proteins AP-0, AP-1, AP-2 and AP-3 could inhibit HHCC cells adhesion to Matrigel and FN by different degrees. However, only AP-3 could significantly inhibit adhesion of HHCC cells to FN (Table 5).

Table 5 Influence of *Angelica* polysaccharides on adhesion of HHCC to Matrigel and fibronectin

Group	Matrigel		Fibronectin	
	A 490 nm ($\bar{x}$±s)	Inhibitory rate (%)	*A* 490nm ($\bar{x}$±s)	Inhibitory rate (%)
Control	0.131±0.029	0.0	0.099±0.023	0.0
AP-0	0.114±0.006	12.9	0.098±0.017	1.0
AP-1	0.118±0.037	9.9	0.082±0.004	17.2
AP-2	0.105±0.018	19.8	0.073±0.014	26.0
AP-3	0.098±0.020	25.2	0.069±0.008[a]	30.3

[a]P<0.05 *vs* Control.

Influences of AP-0-AP-3 on HHCC chemotactic migration abilities AP-0 had no inhibitory effect on the migration of HHCC cells, but its sub-constituents AP-1, AP-2 and AP-3 had weak inhibitory effects on the migration of HHCC cells into membranes, with no statistical significance compared with *N.S.*group (P<0.05, Table 4).

DISCUSSION

Polysaccharides from various kinds of herbal medicines or plants have extensive pharmacological activities. Since Letinan, a polysaccharide from *Lentinus edodes* (Berk.) Sing (Chihara, *et al*. *Nature*. 1969;22:687-688) was discovered to inhibit mouse sarcoma 180, a lot of plant polysaccharides have been investigated into their anti-tumor effects and the related mechanisms (Chihara, *et al*, *Nature*. 1970;225:943-944; Maeda Y, *et al*. *Nature*.1971;229:634). In the present study, we examined systematically the anti-tumor effects of polysaccharides from Chinese Danggui (*Angelica sinensis*) in mice according to the criteria of anti-tumor drug evaluation. AP-0 might have no direct inhibition on murine solid tumor S180, but it could significantly decrease the weights of thymus

of mice bearing S180. Gu *et al* (*Bull Acad Mil Med Sci*.1986;10: 401) reported that two types of polysaccharides from *Angelica* could not only decrease the weights of thymus, but also decrease the amounts of peripheral T and B lymphocytes of normal and tumor-bearing mice. Maeda believed that the tumor-inhibiting effect of Lentinan was mediated by T lymphocytes. Our results of the S180 experiments suggested that AP-0 had significant influences on thymus of mice, but the effects were not strong enough to inhibit the growth of tumor. By using body-mass as an indicator of the amount of ascitic fluid produced in EAC-mice, we discovered that AP-0 inhibited the production of ascitic fluid and prolonged the survival of the mice. Kumazawa, *et al* (*Immunology*. 1982; 47:75) previously found that AIP, which was an immunostimulating polysaccharide separated from hot water extract of *Angelica acutiloba* Kitagawa (Yamato Tohki), prolonged the survival of mice bearing EAC. Likewise, AP-0 inhibited the production of ascitic fluid and prolonged the life of mice bearing L1210. The results of *in vivo* experiments suggested that AP-0 had obvious anti-tumor effects on murine ascitic tumors (AEC and L1210), and also affected the immune organ (thymus) of mice bearing S180. Immunostimulatory activities found in the polysaccharides from *Panax ginseng*, *Spirulina platensis*, *Aphanizomenon flos-aquae and Chlorella pyrenoidosa* also suggested that immuno-mediated effects might be the main mechanism of polysaccharides' anti-tumor actions[23,24]. Polysaccharides with potent anti-tumor effects have been used clinically for cancer immunotherapy combined with radiotherapy and chemotherapy [25-27].

Invasion and metastasis are essential characteristics of malignant tumors. Tumor invasion and metastasis are a multi-step process associated with multiple-factors, such as adhesion and migration of tumor cells, degradation of exracellular matrix (ECM), and angiogenesis[28]. Molecules existing in ECM and receptors or ligands existing on the surfaces of tumor cells played critical roles in invasion and metastasis[29,30]. Polysaccharides, such as proteoglycans and glycosaminoglycans are the main constituents of ECM. Liu *et al*[15] demonstrated that heparan sulfate glycosaminoglycan coat presenting on tumor cells contained bioactive sequences that impinged on tumor-cell growth and metastasis. Hyaluronan, an extracellular polysaccharide that has been implicated in tumor invasion, was one of the major constituents of stromal myxoid changes[16]. As to the polysaccharides from herbal medicines or plants, their anti-metastatic effects have been reported. Modified citrus pectin (MCP), a nondigestible, water-soluble polysaccharide fiber derived from citrus fruit, given orally, inhibited carbohydrate-mediated tumor growth, angiogenesis, and metastasis *in vivo*[17] . Protein-bound polysaccharide PSK inhibited tumor invasiveness by down-regulation of TGF-beta1, uPA, MMP-2 and MMP-9 expressed in two human tumor cell lines, pancreatic cancer cell line (NOR-P1) and gastric cancer cell line (MK-1P3) [18]. Enhancement of HLA class-I expression on tumor cells after PSK treatment might be one of the mechanisms responsible for the induction of anti-tumor immunity by PSK[19].

The present anti-metastasis study employed human hepatocellular carcinoma cell (HHCC) co-cultured with fibroblast, a kind of important stromal cell, to test the inhibitory effects of AP-0, AP-1, AP-2 and AP-3 on metastasis *in vitro*. The results of our experiments showed that AP-0 and its sub-constituents could inhibit the infiltration, adhesion and migration of HHCC by different degrees. By analyzing the biological-effect and chemical-composition, we found that there might be some relationship between the anti-invasion activities and the uronic acids containing APs. AP-0 and AP-3 had the strongest anti-degradation effects on basement membrane, and also possessed the highest amounts of uronic acids of 210 g/kg and 257 g/kg among the 4 polysaccharides from *Angelica*. On the other hand, AP-3 with the lowest content of uronic acids had the most effective anti-adhesion action on HHCC cells to FN among the 4 polysaccharides. The polysaccharides rich in anion groups, such as heparin and heparan sulfate, are closely related to the action between cells and ECM. Based on this, it is proposed that AP rich in uronic acides act as analogues of natural polysaccharides in ECM, and exhibit their anti-metastasis effects.

The findings in the present study suggest that polysaccharides from *Angelica* not only have anti-tumor effects on murine tumors of S180, EAC and L1210 *in vivo*, but also can inhibit invasion of HHCC *in vitro*.

REFERENCES

1 **Hardy ML**. Herbs of special interest to women. quiz 327-329. *J Am Pharm Assoc (Wash)* 2000; **40**: 234-342

2 **Bradley RR**, Cunniff PJ, Pereira BJ, Jaber BL. Hematopoietic effect of Radix *Angelica sinensis* in a hemodialysis patient. *Am J Kidney Dis* 1999; **34**: 349-354

3 **Cho CH**, Mei QB, Shang P, Lee SS, So HL, Guo X, Li Y. Study of the gastrointestinal protective effects of polysaccharides from *Angelica sinensis* in rats. *Planta Med* 2000; **66**: 348-351

4 **Ye YN**, So HL, Liu ES, Shin VY, Cho CH. Effect of polysaccharides from *Angelica sinensis* on gastric ulcer healing. *Life Sci* 2003; **72**: 925-932

5 **Ye YN**, Liu ES, Shin VY, Koo MW, Li Y, Wei EQ, Matsui H, Cho CH. A mechanistic study of proliferation induced by *Angelica sinensis* in a normal gastric epithelial cell line. *Biochem Pharmacol* 2001; **61**: 1439-1448

6 **Ye YN**, Koo MW, Li Y, Matsui H, Cho CH. *Angelica sinensis* modulates migration and proliferation of gastric epithelial cells. *Life Sci* 2001; **68**: 961-968

7 **Yang T**, Jia M, Mei Q, Shang P. Effects of *Angelica* polysaccharide on blood coagulation and platelet aggregation. *Zhong Yao Cai* 2002; **25**: 344-345

8 **Ye YN**, Liu ES, Li Y, So HL, Cho CC, Sheng HP, Lee SS, Cho CH. Protective effect of polysaccharides-enriched fraction from *Angelica sinensis* on hepatic injury. *Life Sci* 2001; **69**: 637-646

9 **Choy YM**, Leung KN, Cho CS, Wong CK, Pang PK. Immunopharmacological studies of low molecular weight polysaccharide from Angelica sinensis. *Am J Chin Med* 1994; **22**: 137-145

10 **Jiang SM**, Xiao ZM, Xu ZH. Inhibitory activity of polysaccharide extracts from three kinds of edible fungi on proliferation of human hepatoma SMMC-7721 cell and mouse implanted S180 tumor. *World J Gastroenterol* 1999; **5**: 404-407

11 **Chen Q**, Yang GW, An LG. Apoptosis of hepatoma cells SMMC-7721 induced by Ginkgo biloba seed polysaccharide. *World J Gastroenterol* 2002; **8**: 832-836

12 **Tang ZY**. Hepatocellular carcinoma-cause, treatment and metastasis. *World J Gastroenterol* 2001; **7**: 445-454

13 **Korn WM**. Moving toward an understanding of the metastatic proc ess in hepatocellular carcinoma. *World J Gastroentero* 2001; **7**: 777-778

14 **Smorenburg SM**, Van Noorden CJ. The complex effects of heparins on cancer progression and metastasis in experimental studies. *Pharmacol Rev* 2001; **53**: 93-105

15 **Liu D**, Shriver Z, Venkataraman G, El Shabrawi Y, Sasisekharan R. Tumor cell surface heparan sulfate as cryptic promoters or inhibitors of tumor growth and metastasis. *Proc Natl Acad Sci U S A* 2002; **99**: 568-573

16 **Wernicke M**, Pineiro LC, Caramutti D, Dorn VG, Raffo MM, Guixa HG, Telenta M, Morandi AA. Breast cancer stromal myxoid changes are associated with tumor invasion and metastasis: a central role for hyaluronan. *Mod Pathol* 2003; **16**: 99-107

17 **Nangia-Makker P**, Hogan V, Honjo Y, Baccarini S, Tait L, Bresalier R, Raz A. Inhibition of human cancer cell growth and metastasis in nude mice by oral intake of modified citrus pectin. *J Natl Cancer Inst* 2002; **94**: 1854-1862

18 **Zhang H**, Morisaki T, Matsunaga H, Sato N, Uchiyama A, Hashizume K, Nagumo F, Tadano J, Katano M. Protein-bound

polysaccharide PSK inhibits tumor invasiveness by down-regulation of TGF-beta1 and MMPs. *Clin Exp Metastasis* 2000; **18**: 343-352

19 **Iguchi C**, Nio Y, Takeda H, Yamasawa K, Hirahara N, Toga T, Itakura M, Tamura K. Plant polysaccharide PSK: cytostatic effects on growth and invasion; modulating effect on the expression of HLA and adhesion molecules on human gastric and colonic tumor cell surface. *Anticancer Res* 2001; **21**: 1007-1013

20 **Fisher M**, Yang LX. Anticancer effects and mechanisms of polysaccharide-K (PSK): implications of cancer immunotherapy. *Anticancer Res* 2002; **22**: 1737-1754

21 **Yamada H**, Kiyohara H, Cyong JC, Kojima Y, Kumazawa Y, Otsuka Y. Studies on polysaccharides from Angelica acutiloba. Part 1. Fractionation and biological properties of polysaccharides. *Planta Med* 1984; **50**: 163-167

22 **DeRoock IB**, Pennington ME, Sroka TC, Lam KS, Boeden GT, Bair EL, Cress AE. Synthetic peptides inhibit adhension of human tumor cells to extracellular matrix proteins. *Cancer Res* 2001; **61**: 3308-3313

23 **Shin JY**, Song JY, Yun YS, Yang HO, Rhee DK, Pyo S. Immunostimulating effects of acidic polysaccharides extract of Panax ginseng on macrophage function. *Immunopharmacol Immunotoxicol* 2002; **24**: 469-482

24 **Pugh N**, Ross SA, ElSohly HN, ElSohly MA, Pasco DS. Isolation of three high molecular weight polysaccharide preparations with potent immunostimulatory activity from Spirulina platensis, aphanizomenon flos-aquae and Chlorella pyrenoidosa. *Planta Med* 2001; **67**: 737-742

25 **Xie FY**, Zeng ZF, Huang HY. Clinical observation on nasopharyngeal carcinoma treated with combined therapy of radiotherapy and ginseng polysaccharide injection. *Zhongguo Zhongxiyi Jiehe Zazhi* 2001; **21**: 332-324

26 **Yunmbam MK**, Wellstein A. The bacterial polysaccharide tecogalan blocks growth of breast cancer cells *in vivo*. *Oncol Rep* 2001; **8**: 161-164

27 **Kidd PM**. The use of mushroom glucans and proteoglycans in cancer treatment. *Altern Med Rev* 2000; **5**: 4-27

28 **Li Y**, Tang ZY, Ye SL, Liu YK, Chen J, Xue Q, Chen J, Gao DM, Bao WH. Establishment of cell clones with different metastatic potential from the metastatic hepatoc ellular carcinoma cell line MHCC97. *World J Gastroenterol* 2001; **7**: 630-636

29 **Liu LX**, Jiang HC, Liu ZH, Zhou J, Zhang WH, Zhu AL, Wang XQ, Wu M. Integrin gene expression profiles of human hepatocellular carcinoma. *World J Gastroenterol* 2002; **8**: 631-637

30 **Su JM**, Gui L, Zhou YP, Zha XL. Expression of focal adhesion kinase and α5 and β1 integrins in carcinomas and its clinical significance. *World J Gastroenterol* 2002; **8**: 613-618

Edited by Zhu LH

P.O.Box 2345, Beijing 100023,China
Fax: +86-10-85381893
E-mail: wjg@wjgnet.com www.wjgnet.com

World J Gastroenterol 2003;9(9):1968-1971
World Journal of Gastroenterology
 ISSN 1007-9327

• LIVER CANCER •

Effects of hydroxyapatite nanoparticles on proliferation and apoptosis of human hepatoma BEL-7402 cells

Zhi-Su Liu, Sheng-Li Tang, Zhong-Li Ai

Zhi-Su Liu, Sheng-Li Tang, Zhong-Li Ai, Department of General Surgery, Zhongnan Hospital of Wuhan University, Wuhan 430071, Hubei Province, China
Correspondence to: Dr Zhi-Su Liu, Department of General Surgery, Zhongnan Hospital of Wuhan University, Wuhan 430071, Hubei Province, China. hyfr@mail.wh.cei.gov.cn
Telephone: +86-27-87331752 **Fax:** +86-27-87330795
Received: 2002-12-22 **Accepted:** 2003-04-05

Abstract

AIM: To study the effect of hydroxyapatite (HAP) nanoparticles on human hepatoma cell line BEL-7402 *in vitro*.

METHODS: The human hepatoma cell line BEL-7402 was cultured and treated with HAP nanoparticles at various concentrations. Growth suppression was detected with MTT colorimetric assay, cell apoptotic alterations were evaluated by cytochemical staining (Hoechst 33258), transmission electron microscopy (TEM), and flow cytometry (FCM).

RESULTS: HAP nanoparticles inhibited the growth of hepatoma cells in a dose-dependent manner, with IC_{50} values of 29.30 mg/L. Treated with 50-200 mg/L HAP nanoparticles for 48 h, BEL-7402 cells apoptosis with nuclear chromatin condensation and fragmentation as well as cell shrinkage and the formation of apoptotic bodies were observed under cytochemical staining and transmission electron microscopy. FCM analysis showed hypodiploid peaks on histogram, the apoptotic rates at the concentrations of 50, 75, 100, 150 and 200 mg/L of HAP nanoparticles were 20.35±2.23 %, 25.35±1.92 %, 29.34±4.61 %, 44.92±3.78 % and 53.64±3.49 %, respectively, which were all significantly higher than that of control group 2.23±0.14 %. There was a significant correlation between HAP nanoparticle concentration and apoptotic rate (r=0.994, P<0.01).

CONCLUSION: HAP nanoparticles not only inhibit proliferation but also induce apoptosis of human hepatoma cell line BEL-7402 *in vitro*.

Liu ZS, Tang SL, Ai ZL. Effects of hydroxyapatite nanoparticles on proliferation and apoptosis of human hepatoma BEL-7402 cells. *World J Gastroenterol* 2003; 9(9): 1968-1971
http://www.wjgnet.com/1007-9327/9/1968.asp

INTRODUCTION

Hepatocellular carcinoma (HCC) is the most common primary malignant tumor of the liver. Although progress in diagnosis and treatment of hepatic carcinoma has been made in recent years, its prognosis is still poor. Exploring new materials for treatment and investigating the mechanism are important. With the development of nanometer technology, hydroxyapatite nanoparticle, a novel inorganic material, was found to be able to inhibit tumor cell proliferation. However, there was yet no report about the effects of hydroxyapatite nanoparticles on the growth and apoptosis of human hepatoma cell line BEL-7402. Therefore, the present study was designed to study the inhibitory effect of hydroxyapatite nanoparticles on human hepatoma cells and its mechanism to provide a theoretical basis for its clinical use.

MATERIALS AND METHODS

Hydroxyapatite nanoparticles were obtained from Institute of Biomaterials, East China University of Science and Technology. Stock solution was made at the concentration of 400 mg/L with RPMI 1640 and diluted to working concentration before use. RPMI 1640, fetal calf serum (FCS) and MTT were purchased from GIBCO. RNase, proteinase K, propidium iodide (PI) and Hoechst 33258 were products of Sigma Chemical Co.

Cell line and culture

Human hepatoma BEL-7402 cells were provided by China Center for Type Culture Collection of Wuhan University (CCTCC). The cells were grown as monolayers in RPMI1640 medium supplemented with 10 % heat-inactived fetal calf serum and incubated in humidified incubator with 5 % CO_2 in air at 37 ℃.

Assay of cell proliferation

MTT[3-(4,5-dimethythiazoyl-2-yl) 2,5-diphenyltetrozoliumbromide] colorimetric analysis was used to measure the cytocide rate of HAP nanoparticles. Well-growing BEL-7402 cells were collected and seeded in 96-well plates at 1×10^5/ml density 100 μl cell suspension per well. When the cells anchored to the plates, the culture medium was replaced with fresh medium containing various concentrations of HAP nanoparticles (0, 12.5, 25, 50, 75, 100, 150 and 200 mg/L). Eight duplicate wells were set up in each sample. After incubated at 37 ℃, 5 % CO_2 for 48 h, 5 g/L MTT 20 μl was added to each well and cultured for another 4 h. The MTT medium was discarded and warm dimethylsulfoxide (DMSO) 200 μl was added. Absorbance was measured at 490 nm. Cellular proliferation inhibition rate (CPIR) was calculated using the following formula: CPIR=(1-average A value of experimental group / average A value of control group)×100 %.

Cytochemical staining of apoptotic cells

Cells treated with 50, 75, 100, 150 and 200 mg/L HAP nanoparticles for 48 h were harvested and fixed with 1:3 glacial acetic acid/methanol twice, first for 5 min and then for 10 min and washed with phosphate buffer solution (PBS). Cells were resuspended in Hoechst 33258 solution (Hoechst 33258 dissolved in PBS, 5 mg/L) and incubated at room temperature for 45 min in the dark. Aliquots of 100 μl/ml were placed on a glass slide and observed under an Olympus BH-2 fluorescence microscope after dried thoroughly.

Transmission electron microscopy assay

The BEL-7402 cells were seeded in culture flasks. Three culture

bottles were divided into treatment group and control group. When the cells anchored to the plates, various concentrations (0, 50 and 100 mg/L) of HAP nanoparticles were added and the cells were incubated at 37 ℃, 5 % CO_2 for 48 h. Hepatoma cells were then digested by 0.25 % trypsinase and collected. After rinsed with PBS, the cells were prefixed with 3 % glutaraldehyde for 30 min, post-fixed with 1 % osmic acid, dehydrated in graded ethanol, embedded in Epon 812 mixture, and cut into sections on an ultramicrotome. The cells were observed under Hitachi H-600 electron microscopy.

Flow cytometric analysis

The suspended single cell solutions subjected to treatment with HAP nanoparticles at different concentrations (0, 50, 75, 100, 150 and 200 mg/L) for 48 h were harvested. Each group had three culture bottles. Cells were washed with PBS, fixed with 70 % ethanol at -20 ℃ for 30 min and stored at 4 ℃ overnight, then washed with PBS again, treated with 100 mg/L RNase 100 μl at 37 ℃ for 30 min and stained with 50 mg/L PI 100 μl at 4 ℃ for 30 min in darkness. Apoptotic cells were assayed using FACSort Becton Dickinson Flow Cytometer at 488nm and data were analyzed with CELLQuest Software. For each sample, 6000 cells were measured.

Statistical analysis

All data were expressed as mean ± standard deviation. Statistical analysis was performed by *t* test using software SPSS11.0 for Windows. $P<0.05$ was considered significant.

RESULTS

Effect of HAP nanoparticles at various concentrations on the growth of BEL-7402 cells

After 48 h treatment, HAP nanoparticles produced a dose-dependent inhibition of cell growth (Table 1). Correlation analysis displayed a significantly positive correlation between the concentration of HAP and inhibition rate (IR) (r=0.931, $P<0.01$). Regression equation was as follows: $y_{concentration}=966.09 x^3_{IR}-292.20x_{IR}+54.63$, the half effective inhibitory concentration (IC_{50}) =29.30mg/L.

Table 1 Inhibitory effect of HAP nanoparticles on hepatoma cell line BEL-7402

Concentrations (mg/L)	A_{490nm} ($\bar{x}\pm s$)	Inhibition rate (%)	*t vs* control
0(control)	0.9325±0.0337		
12.5	0.5275±0.0440[bd]	43.29±6.11	16.68
25	0.4025±0.0440[b]	56.90±3.71	51.20
50	0.3950±0.0593[b]	57.74±5.37	37.43
75	0.4038±0.0245[b]	56.61±3.61	29.10
100	0.3913±0.0323[b]	58.05±3.05	46.20
150	0.3188±0.0236[bd]	65.78±2.83	42.30
200	0.2588±0.0270[bd]	72.25±7.75	53.79

[a]$P<0.05$, [b]$P<0.01$ *vs* 0 mg/L group; [c]$P<0.05$, [d]$P<0.01$ *vs* 25 mg/L group.

Fluorescence microscopic observation

Hoechst 33258 is a specific DNA-binding fluorochrome and under the fluorescence microscope it exhibits a green fluorescence. As shown in Figure 1, in the control group, the nucleus was big and round, with a smooth nuclear membrane, free of condensation and fragmentation. However, smaller nuclei, increased density of nuclear chromatin, fragmentation of nucleus and apoptotic body formation were easily identified in HAP nanoparticles treated groups. The higher the concentration of HAP nanoparticles, the more apoptotic cells there were. Apoptotic rate was counted under fluorescence microscopy, there were 18.68 %, 22.27 %, 33.49 %, 49.03 %, 57.16 % at 50, 75, 100, 150 and 200 mg/L concentration, respectively.

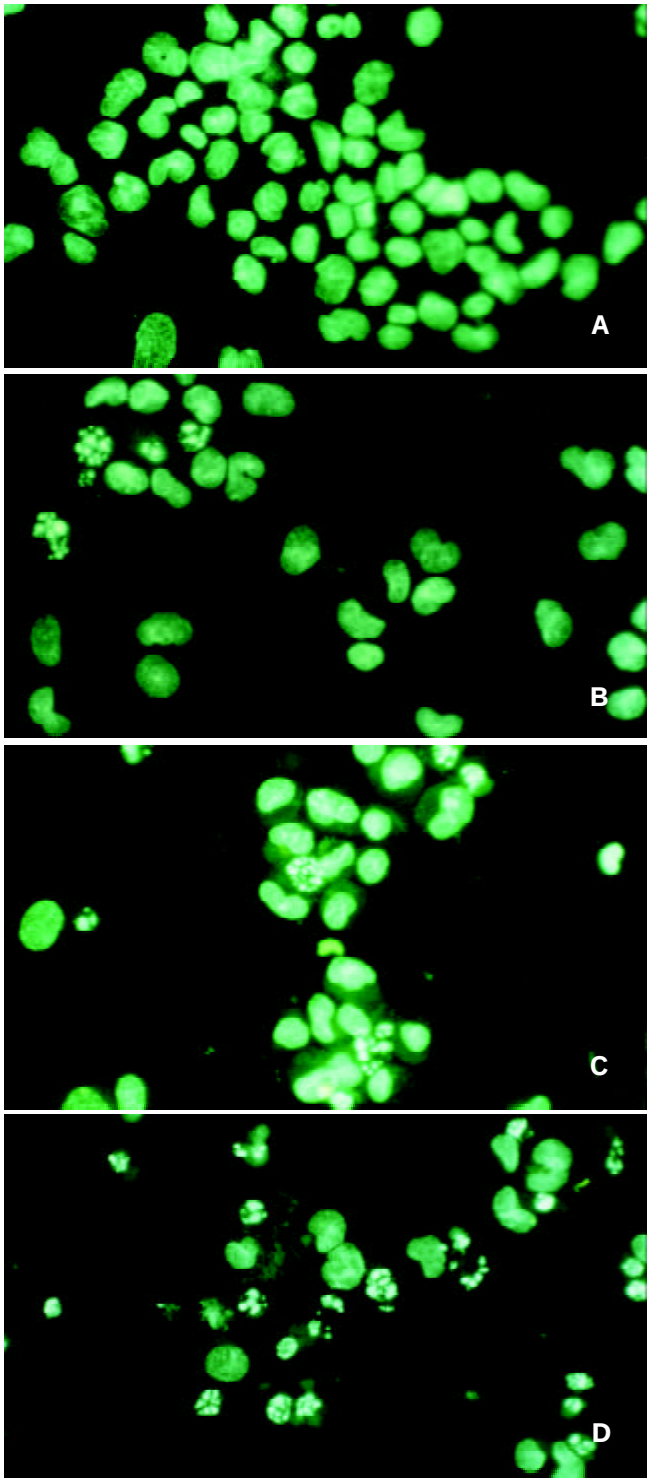

Figure 1 Fluorescence microscopy for apoptosis induced by HAP nanoparticles for 48 h (×200). A: Control; B: 50 mg/L; C: 100 mg/L; D: 200 mg/L.

Transmission electron microscopic observation

Under transmission electron microscopy, control cells were big and round, with intact nuclear membrane and low density in nuclear chromatin (Figure 2A). However, the cells treated with HAP nanoparticles exhibited characteristics of apoptosis

including cell membrane shrinkage, cytoplasm budding, condensation and fragmentation of nuclear chromatin adjacent to nuclear membrane (Figure 2B).

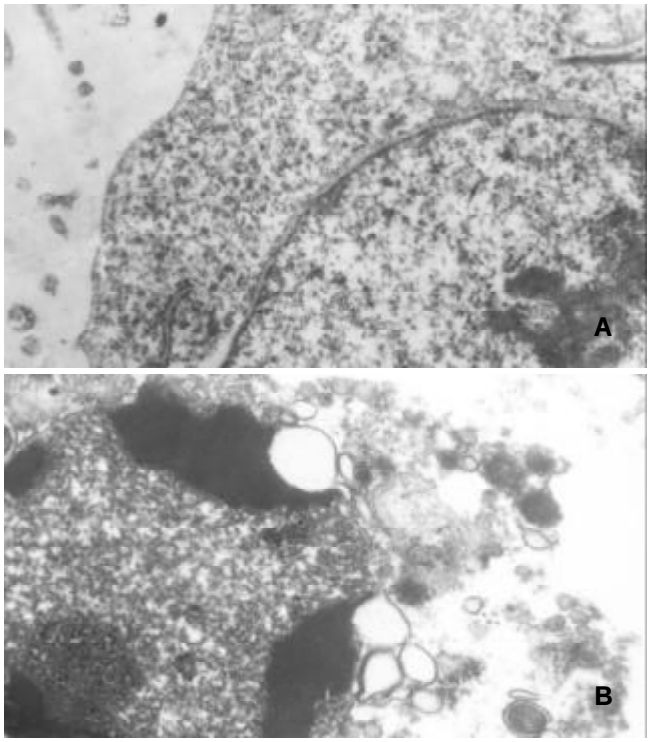

Figure 2 TEM ultrastructural changes of apoptosis induced by HAP nanoparticles for 48 h. A: Control ×15 000; B: 10 mg/L ×10 000.

Flow cytometry analysis

The hypodiploid peak appearing before the G_1 phase on histogram was called apoptotic peak, which indicated reduced DNA content in apoptotic cells in FCM analysis. Table 2 shows that apoptotic rates increased with increasing concentrations of HAP nanoparticles. Correlation analysis showed a significantly positive correlation between concentration of HAP nanoparticles and apoptotic rate (r=0.994, P<0.01).

Table 2 Apoptotic rates of HAP nanoparticles on hepatoma cell line BEL-7402

Concentrations (mg/L)	Apoptotic rate (%)	*t vs* control
0(control)	2.23±0.14	
50	20.35±2.23[b]	13.32
75	25.35±1.92[b]	22.55
100	29.34±4.61[b]	10.50
150	44.92±3.78[b c]	20.30
200	53.64±3.49[b d]	24.51

[a]P<0.05, [b]P<0.01 *vs* 0 mg/L group; [c]P<0.05, [d]P<0.01 *vs* 50 mg/L group.

DISCUSSION

Hydroxyapatite nanoparticles used in this study was synthesized by sol-gel method, with uniform particle size of 50 nm and was well dispread. After human hepatoma BEL-7402 cells treated at various concentrations of hydroxyapatite nanoparticles for 48 h, MTT colorimetric analysis showed that nanoparticles could significantly inhibit the proliferation of BEL-7402 cells, with IC_{50} values of 29.30 mg/L. Moreover, the inhibitory rates at 25, 50, 75 and 100 mg/L concentration of HAP nanoparticles were all more than 50 %, but there was no statistical difference among the four treatment groups, which indicated the tolerance of human hepatoma BEL-7402 cells subjected to HAP nanoparticles. This would provide some experimental basis for its clinical use.

With cytochemical staining and under transmission electron microscopy, typical apoptotic alterations such as cells shrinkage, nuclear chromatin condensation and fragmentation, cytoplasmic budding and formation of apoptotic bodies were observed after BEL-7402 cells were treated by HAP nanoparticles for 48 h. Quantified by FCM, the higher the concentration of HAP nanoparticles, the more apoptotic cells there were. The apoptotic rates were in accordance with the results counted under fluorescence microscopy. At the same time, no statistical difference was found among the 50, 75 and 100 mg/L groups, in which the tolerance of BEL-7402 cells subjected to HAP nanoparticles was identified. Therefore, the present study demonstrated that HAP nanoparticles could induce human hepatoma cell apoptosis *in vitro*. This might be the first report regarding the antineoploastic mechanism of HAP nanoparticles on human hepatoma cells through apoptotic induction.

Kerr *et al* first described the concept of apoptosis. It is the programmed death of cells by fragmentation of DNA, cell shrinkage, followed by cell fragmentation and formation of membrane vesicles called apoptosis bodies. A variety of studies have revealed that the uncontrolled growth of neoplasm is not only due to the over proliferation but also due to the loss of natural apoptosis[1-19]. Therefore, exploring new medicine that could induce cancer cell apoptosis would be helpful for neoplasm treatment[20-23]. To date, chemotherapeutic medicines, growth inhibitor analogs, arsenic and various Chinese herbal medicines have been testified to suppress tumor cell growth by inducing cell apoptosis[24-38].

In this study, hydroxyapatite nanoparticles inhibited human hepatoma BEL-7402 cell growth and induced apoptosis, which may add a new way to use nanopaticles for tumor treatment. Further studies are needed to clarify the mechanism of apoptosis induced by hydroxyapatite nanoparticles.

REFERENCES

1 **He SW**, Shen KQ, He YJ, Xie B, Zhao YM. Regulatory effect and mechanism of gastrin and its antagonists on colorectal carcinoma. *World J Gastroenterol* 1999; **5**: 408-416
2 **Tian G**, Yu JP, Luo HS, Yu BP, Yue H, Li JY, Mei Q. Effect of nimesulide on proliferation and apoptosis of human hepatoma SMMC-7721 cells. *World J Gastroenterol* 2002; **8**: 483-487
3 **Tao HQ**, Zou SC. Effect of preoperative regional artery chemotherapy on proliferation and apoptosis of gastric carcinoma cells. *World J Gastroenterol* 2002; **8**: 451-454
4 **Liu S,** Wu Q, Ye XF, Cai JH, Huang ZW, Su WJ. Induction of apoptosis by TPA and VP-16 is through translocation of TR3. *World J Gastroenterol* 2002; **8**: 446-450
5 **Qin LX**, Tang ZY. The prognostic molecular markers in hepatocellular carcinoma. *World J Gastroenterol* 2002; **8**: 385-392
6 **Tanaka S**, Akaike T, Fang J, Beppu T, Ogawa M, Tamura F, Miyamoto Y, Maeda H. Antiapoptotic effect of haem oxygenase-1 induced by nitric oxide in experimental solid tumour. *Br J Cancer* 2003; **88**: 902-909
7 **Shigeno M**, Nakao K, Ichikawa T, Suzuki K, Kawakami A, Abiru S, Miyazoe S, Nakagawa Y, Ishikawa H, Hamasaki K, Nakata K, Ishii N, Eguchi K. Interferon-alpha sensitizes human hepatoma cells to TRAIL-induced apoptosis through DR5 upregulation and NF-kappaB inactivation. *Oncogene* 2003; **22**:1653-1662
8 **Perez EA**, Gandara DR, Edelman MJ, O'Donnell R, Lauder IJ, DeGregorio M. Phase I trial of high-dose tamoxifen in combination with cisplatin in patients with lung cancer and other advanced malignancies. *Cancer Invest* 2003; **21**: 1-6
9 **Lin HL**, Lui WY, Liu TY, Chi CW. Reversal of Taxol resistance in hepatoma by cyclosporin A: involvement of the PI-3 kinase-AKT

1 pathway. *Br J Cancer* 2003; **88**: 973-980
10 **Yamashita H**, Iwase H, Toyama T, Fujii Y. Naturally occurring dominant-negative Stat5 suppresses transcriptional activity of estrogen receptors and induces apoptosis in T47D breast cancer cells. *Oncogene* 2003; **22**: 1638-1652
11 **Shen ZY**, Shen J, Li QS, Chen CY, Chen JY, Yi Z. Morphological and functional changes of mitochondria in apoptotic esophageal carcinoma cells induced by arsenic trioxide. *World J Gastroenterol* 2002; **8**: 31-35
12 **Shen ZY**, Shen WY, Chen MH, Shen J, Cai WJ, Yi Z. Nitric oxide and calcium ions in apoptotic esophageal carcinoma cells induced by arsenite. *World J Gastroenterol* 2002; **8**: 40-43
13 **Sun ZJ**, Pan CE, Liu HS, Wang GJ. Anti-hepatoma activity of resveratrol *in vitro*. *World J Gastroenterol* 2002; **8**: 79-81
14 **Wu YL**, Sun B, Zhang XJ, Wang SN, He HY, Qiao MM, Zhong J, Xu JY. Growth inhibition and apoptosis induction of Sulindac on Human gastric cancer cells. *World J Gastroenterol* 2001; **7**: 796-800
15 **Li J**, Yang XK, Yu XX, Ge ML, Wang WL, Zhang J, Hou YD. Overexpression of p27 (KIP1) induced cell cycle arrest in G 1 phase and subsequent apoptosis in HCC-9204 cell line. *World J Gastroenterol* 2000; **6**: 513-521
16 **Chen YN**, Chen JC, Yin SC, Wang GS, Tsauer W, Hsu SF, Hsu SL. Effector mechanisms of norcantharidin-induced mitotic arrest and apoptosis in human hepatoma cells. *Int J Cancer* 2002; **100**: 158-165
17 **Sun BH**, Zhao XP, Wang BJ, Yang DL, Hao LJ. FADD and TRADD expression and apoptosis in primary hepatocellular carcinoma. *World J Gastroenterol* 2000; **6**: 223-227
18 **Pals DR**, Thompson CB. Cell metabolism in the regulation of programmed cell death. *Trends Endocrinol Metab* 2002; **13**: 75-78
19 **Shan CM**, Li J. Study of apoptosis in human liver cancers. *World J Gastroenterol* 2002; **8**: 247-252
20 **Misawa M**, Tauchi T, Sashida G, Nakajima A, Abe K, Ohyashiki JH, Ohyashiki K. Inhibition of human telomerase enhances the effect of chemotherapeutic agents in lung cancer cells. *Int J Oncol* 2002; **21**: 1087-1092
21 **Shoieb AM**, Elgayyar M, Dudrick PS, Bell JL, Tithof PK. *In vitro* inhibition of growth and induction of apoptosis in cancer cell lines by thymoquinone. *Int J Oncol* 2003; **22**: 107-113
22 **Satomi D**, Takiguchi N, Koda K, Oda K, Suzuki H, Yasutomi J, Ishikura H, Miyazaki M. Apoptosis and apoptosis-associated gene products related to the response to neoadjuvant chemotherapy for gastric cancer. *Int J Oncol* 2002; **20**: 1167-1171
23 **Tu SP**, Zhong J, Tan JH, Jiang XH, Qiao MM, Wu YX, Jiang SH. Induction of apoptosis by arsenic trioxide and hydroxy camptothecin in gastriccancer cells *in vitro*. *World J Gastroenterol* 2000; **6**: 532-539
24 **Zhao AG**, Zhao HL, Jin XJ, Yang JK, Tang LD. Effects of Chinese Jianpi herbs on cell apoptosis and related gene expression in human gastric cancer grafted onto nude mice. *World J Gastroenterol* 2002; **8**: 792-796
25 **Li JM**, Zhou H, Cai Q, Xiao GX. Role of mitochondrial dysfunction in hydrogen peroxide-induced apoptosis of intestinal epithelial cells. *World J Gastroenterol* 2003; **9**: 562-567
26 **Ma L**, Tai H, Li C, Zhang Y, Wang ZH, Ji WZ. Photodynamic inhibitory effects of three perylenequinones on human colorectal carcinoma cell line and primate embryonic stem cell line. *World J Gastroenterol* 2003; **9**: 485-490
27 **Zhang JK**, Li J, Zhang J, Chen HB, Chen SB. Antitumor immunopreventive and immunotherapeutic effect in mice induced by hybrid vaccine of dendritic cells and hepatocarcinoma *in vivo*. *World J Gastroenterol* 2003; **9**: 479-484
28 **Li QF**, Ou-Yang GL, Peng XX, Hong SG. Effects of tachyplesin on the regulation of cell cycle in human hepatocarcinoma SMMC-7721 cells. *World J Gastroenterol* 2003; **9**: 454-458
29 **Zhou HB**, Zhu JR. Paclitaxel induces apoptosis in human gastric carcinoma cells. *World J Gastroenterol* 2003; **9**: 442-445
30 **Zhou HB**, Yan Y, Sun YN, Zhu JR. Resveratrol induces apoptosis in human esophageal carcinoma cells. *World J Gastroenterol* 2003; **9**: 408-411
31 **Liu WB**, Yang CQ, Jiang W, Wang YQ, Guo JS, He BM, Wang JY. Inhibition on the production of collagen type I, III of activated hepatic stellate cells by antisense TIMP-1 recombinant plasmid. *World J Gastroenterol* 2003; **9**: 316-319
32 **Huang ZH**, Fan YF, Xia H, Feng HM, Tang FX. Effects of TNP-470 on proliferation and apoptosis in human colon cancer xenografts in nude mice. *World J Gastroenterol* 2003; **9**: 281-283
33 **Wu BW**, Wu Y, Wang JL, Lin JS, Yuan SY, Li A, Cui WR. Study on the mechanism of epidermal growth factor-induced proliferation of hepatoma cells. *World J Gastroenterol* 2003; **9**: 271-275
34 **Chen C**, Liu FK, Qi XP, Li JS. The study of chemiluminescence in gastric and colonic carcinoma cell lines treated by anti-tumor drugs. *World J Gastroenterol* 2003; **9**: 242-245
35 **Xie DP**, Chen LB, Liu CY, Liu JZ, Liu KJ. Effect of oxytocin on contraction of rabbit proximal colon *in vitro*. *World J Gastroenterol* 2003; **9**: 165-168
36 **Shi M**, Wang FS, Wu ZZ. Synergetic anticancer effect of combined quercetin and recombinant adenoviral vector expressing human wild-type p53, GM-CSF and B7-1 genes on hepatocellular carcinoma cells *in vitro*. *World J Gastroenterol* 2003; **9**: 73-78
37 **Liu JW**, Tang Y, Shen Y, Zhong XY. Synergistic effect of cell differential agent-II and arsenic trioxide on induction of cell cycle arrest and apoptosis in hepatoma cells. *World J Gastroenterol* 2003; **9**: 65-68
38 **Rocken C**, Carl-McGrath S. Pathology and pathogenesis of hepatocellular carcinoma. *Dig Dis* 2001; **19**: 269-278

Edited by Ma JY and Wang XL

P.O.Box 2345, Beijing 100023,China
Fax: +86-10-85381893
E-mail: wjg@wjgnet.com www.wjgnet.com

World J Gastroenterol 2003;9(9):1972-1975
World Journal of Gastroenterology
 ISSN 1007-9327

• COLORECTAL CANCER •

Mad2 and p53 expression profiles in colorectal cancer and its clinical significance

Gang-Qiang Li, Hao Li, Hong-Fu Zhang

Gang-Qiang Li, Hao Li, Hong-Fu Zhang, Department of Pathology, Anhui Medical University, Hefei, 230032, Anhui Province, China
Supported by Natural Science Fund of Anhui Province, No.01043717
Correspondence to: Gang-Qiang Li, Department of Pathology, Chinese PLA 455 Hospital, Shanghai 200052, China. lgqfm@163.com
Telephone: +86-21-62800157-2163
Received: 2003-03-28 **Accepted:** 2003-05-21

Abstract

AIM: To investigate the expression of tumor suppressor gene p53 and spindle checkpoint gene Mad2, and to demonstrate their expression difference in colorectal cancer and normal mucosa and to evaluate its clinical significance.

METHODS: Western blot and immunohistochemistry methods were used to analyze the expression of Mad2 in colorectal cancer and its corresponding normal mucosa. The expression of p53 was detected by immunohistochemistry method in colorectal cancer and its corresponding normal mucosa.

RESULTS: Mad2 was significantly overexpressed in colorectal cancer compared with corresponding normal mucosa ($P<0.001$), and it was not related to the differentiation of adenocarcinoma and other clinical factors ($P>0.05$).The ratio of Mad2 protein in cancer tissue (C) to that in its normal mucosa tissue (N) was higher than 2, which was more frequently observed in patients with lymph gland metastasis ($P<0.05$). p53 protein expression was not observed in normal mucosa. The rate of p53 positive expression in adenocarcinomas was 52.6 %. There was a significant difference between adenocarcinomas and normal mucosa($P<0.001$), which was not related to the differentiation degree of adenocarcinoma and other clinical factors ($P>0.05$).

CONCLUSION: Defect of spindle checkpoint gene Mad2 and mutation of p53 gene are involved mainly in colorectal carcinogenesis and C/N>2 is associated with prognosis of colorectal cancer.

Li GQ, Li H, Zhang HF. Mad2 and p53 expression profiles in colorectal cancer and its clinical significance. *World J Gastroenterol* 2003; 9(9): 1972-1975
http://www.wjgnet.com/1007-9327/9/1972.asp

INTRODUCTION

Accurate chromosomal segregation is essential for cell survival and genomic stability. Genomic instability is a common feature of human cancer and is thought to be an important contributor to the malignant phenotype[1,2]. At least two categories of instability have been described: CIN and MIN. CIN is characterized by an alteration in chromosome number and is commonly detected as aneuploidy. The fact that the majority of human cancer cells exhibit gains or losses of chromosomes suggests that CIN may contribute to tumorigenesis[3-5]. In yeast, a loss of mitotic checkpoint frequently leads to abnormal chromosome number, resulting in aneuploidy or polyploidy[6]. The mitotic checkpoint, known as the spindle assembly checkpoint, detects errors occurred in the spindle structure or in alignment of the chromosomes on the spindle, and delays chromosome segregation and anaphase onset until the defects are corrected. Two major groups of mitotic checkpoint genes, budding uninhibited by benomyl (BUB) 1-3 and mitotic arrest defect (MAD) 1-3, have been identified in budding yeast[7]. Mammalian homologues of the yeast mitotic checkpoint protein have also been characterized[8-10].

To date, the vast majority of studies about mitotic checkpoint have focused on cancer cell lines. Little data are available on Mad2 in colorectal adenocarcinoma. In this study, the authors used Western blot and immunohistochemical technique to examine the expression of Mad2 and p53 in colorectal cancer to elucidate the relation of Mad2 and p53 to carcinogenesis and clinical pathological factors.

MATERIALS AND METHODS

Specimens

Cancer tissues and corresponding normal tissues were obtained from the First Affiliated Hospital of Anhui Medical University from October 2000 to May 2001. No patient had been treated with anti-neoplasm therapy before tumor removal. Thirty eight patients (21 males, 17 females, aged between 28 to 81 years, median age 54.8 years) were as follows: 25 cases of well differentiated adenocarcinoma, 5 cases of moderately differentiated adenocarcinoma, 8 cases of poorly differentiated adenocarcinoma. Parts of the tissues were embedded in OCT, immediately frozen in liquid nitrogen. The other parts were fixed in 10 % formalin, embedded in paraffin, cut into 4 μm serial sections.

Reagents

Mad2 polyclonal rabbit antibodes against human were provided by China Science and Technology University. HEPES, SDS and Polycrylamide were purchased from Sigma Biological Technology Ltd., USA. Immuno-blot nitrocellulose filter membrane was purchased from OSMONICS Biological Technology Ltd., USA. p53, goat anti-rabbit IgG-HRP and S-P immunohistochemical kit were purchased from Beijing Zhongshan Biological Technology Ltd.

Western blot

Both cancer and its corresponding normal frozen tissues were minced and homogenized in buffer (10 mM HEPES, 113 mM mannitol , 37 mM sucrose, 1mM EDTA) for 5 min on ice. After spun at 15 000 rpm for 20 min at 4 ℃, supernatants were collected and frozen at -20 ℃ until use. Protein concentration was measured by modified Lowry protein assay. Samples containing 40 μg total protein were electrophoretically separated and transferred to an immuno-blot nitrocellulose filter membrane. The membranes were blocked overnight at 4 ℃ with 5 % skim milk. The blots were incubated with rabbit polyclonal anti-Mad2 antibody at 1:200 dilution in 5 % skim milk for 1 h at 37 ℃ and were incubated with goat anti-rabbit IgG-HRP at 1:50 dilution in 5 % skim milk for 30 min at 37 ℃.

Following treatment with DAB, the blots were exposed to a gel image system and measured.

Immunohistochemistry

Immunohistochemical staining was performed using S-P method, anti-Mad2 antibody was diluted to 1:120. Anti-p53 was ready to use reagent. A negative control was dyed according to the above method with the primary antibody substituted by animal serum. The standard of positive Mad2 protein expression was stained with brown-yellow color mainly in cell plasma, p53 positive expression was stained in nucleus. A semi-quantitative evaluation was used to determine positively expressed cells by viewing 10 vision fields at ×400[11]. Negative (-) indicated cells were stained less than 10 %, mild positive (+) showed 11-25 % cells were stained, moderately positive (++) demonstrated 26-50 % cells was stained, strong positive (+++) revealed over 50 % cells were stained. The later three grades were all regarded as positive.

Statistical analysis

The data were analyzed by SPSS version 10.0. Fisher' s exact test or χ^2 test was used for statistical analysis. $P<0.05$ was considered statistically significant.

RESULTS

Expression of Mad2 protein

We analyzed the results measured by gel image system. Mad2 protein in cancer tissue was significantly overexpressed compared with that in corresponding normal tissues ($P<0.001$). (Figure4)The calculated ratio of Mad2 protein in cancer tissues (C) to that in corresponding normal tissues (N) was 2.07±1.87, ranging from 0.31 to 4.68, indicating that Mad2 expression was approximately 2-fold higher in cancer tissue than in normal tissue. Furthermore, we analyzed the association between the C/N ratio of Mad2 expression and clinicopathological parameters including histological differentiation and lymph node metastasis. The results are summarized in Table 1. No significant difference was found among well differentiated, moderately differentiated, and poorly differentiated adenocarcinomas. However, C/N>2 was found to be related with lymph node metastasis ($P<0.05$).

Table 1 Relationship between C / N ratio of Mad2 expression and histologic differentiation and lymph node metastasis

Groups	*n*	Mad2		Positive (%)	*P*
		C / N>2	C / N<2		
Differentiation					
WD	25	10	15	40 %	
MD	5	2	3	40 %	
PD	8	2	6	25 %	[a]P=0.737
Lymph node metastasis					
Absent	32	9	23	28%	
Present	6	5	1	83.3%	[b]P=0.01

A: comparison among groups of colorectal cancer, B: comparison between absent and present, WD: well differentiated adenocarcinoma, MD: moderately differentiated adenocarcinoma, PD: poorly differentiated adenocarcinoma.

The positive signals of Mad2 protein were brown-yellow stains mainly in cell plasma, and strength of color was directly proportional to positive percentage (Figures 1,2). Positive expression of Mad2 protein was detected in 33 out of 38(86.8 %) colorectal cancers, and 18 out of 38 (47.4 %) normal tissues. There was a significant difference between colorectal cancer and normal tissues ($P<0.001$). However, no significant difference was found among well differentiated, moderately differentiated, and poorly differentiated adenocarcinomas. The expression of Mad2 in colorectal cancer was not related with lymph node metastasis (Table 2).

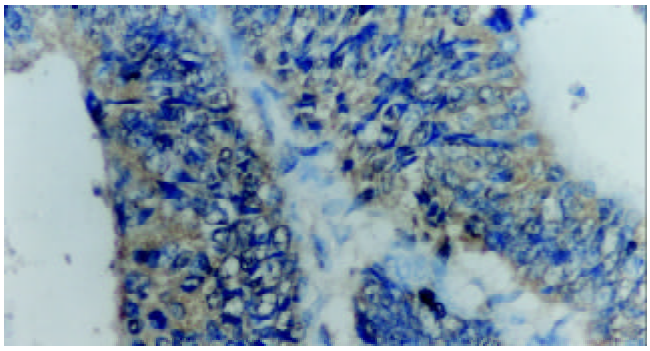

Figure 1 Strongly positive expression of Mad2 in tubular adenocarcinoma. S-P ×400.

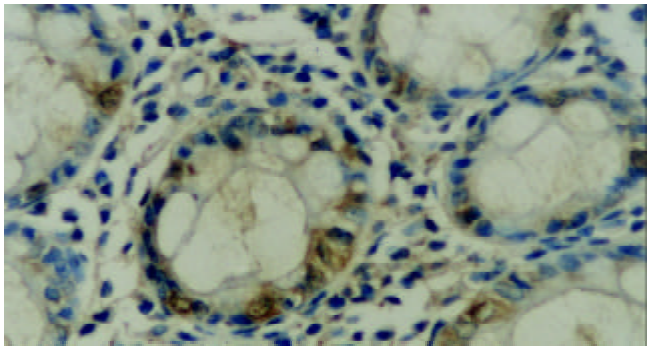

Figure 2 Weakly positive expression of Mad2 in normal mucosa S-P ×400.

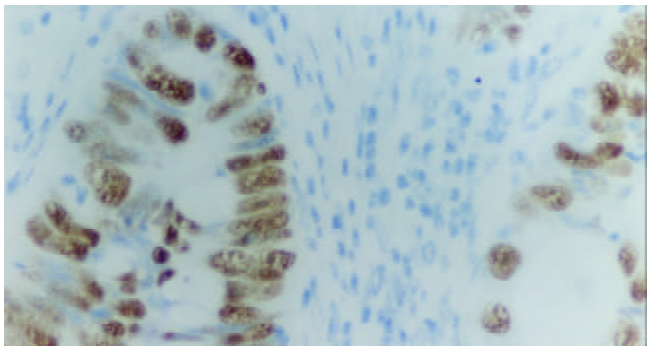

Figure 3 Strongly positive expression of p53 in tubular adenocarcinoma. S-P ×400.

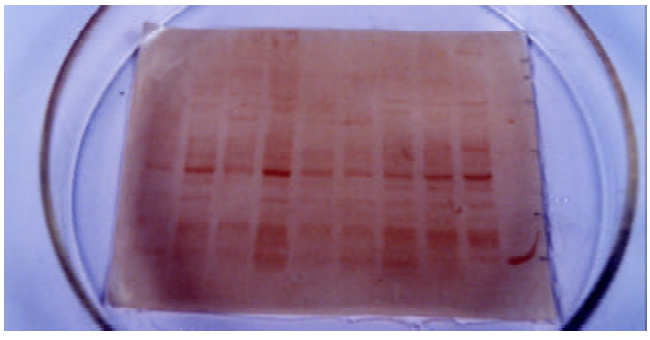

Figure 4 Mad2 protein expression in normal tissue and colorectal Cancer. 1: standard molecular weight; 2: Mad2 in

poorly differentiated adenocarcinoma; 3: Mad2 in corresponding normal tissue; 4: Mad2 in well differentiated adenocarcinoma; 5: Mad2 in corresponding normal tissue; 6: Mad2 in moderately differentiated adenocarcinoma; 7: Mad2 in corresponding normal tissue.

Table 2 Relationship between expression of Mad2 protein and histologic differentiation and lymph node metastasis

Groups	*n*	Mad2		Positive(%)	*P*
		+	-		
Normal tissue	38	18	20	47.4%	
Adenocarcinoma	38	33	5	86.8%	[a]*P*<0.001
WD	25	23	2	92%	
MD	5	5	0	100 %	
PD	8	5	3	62.5 %	[b]*P*=0.064
Lymph node metastasis					
Absent	32	29	3	90.6 %	
Present	6	4	2	66.7 %	[c]*P*=0.169

[a]: comparison between normal tissue and adeocarcinama, [b]: comparison among groups of colorectal cancer, [c]: comparison between absence and presence.

Correlation between Mad2 protein and p53

The percentage of positive p53 expression was 52.6 % (20/38) in colorectal cancer(Figure3), no such protein expression was observed in normal tissue. We analyzed the correlation between Mad2 protein and p53 expression by χ^2 test. There was a significantly positive correlation between the expressions of Mad2 and p53(P<0.05).

DISCUSSION

Kinetochores are linked to both chromosomes and microtubules, and play an important role in the generation of mitotic checkpoint signals. The function of kinetochores was to ensure that chromosomes were not segregated until each of them was aligned and attached to the spindle[12,13]. The majority of protein associated with mitotic checkpoint function have been shown to localize at kinetochores unattached to microtubules[14,15]. It has been proposed that the mitotic checkpoint proteins, especially Mad2 be crucial for generating the "wait" signal to prevent the onset of anaphase after microtubule disruption[16-18]. Previous studies indicated that mutations of mitotic checkpoint protein gene or lower expression of mitotic checkpoint protein might lead to the failure of mitotic checkpoint function, which might in turn lead to tumorigenesis, especially aneuploid cancer. Li and benezra reported that one breast cancer cell line with a mitotic checkpoint defect expressed Mad2 at a level one-third less than that of diploid normal cell lines[8]. Recently, Takahashi *et al* reported mitotic checkpoint function was impaired in 4 (44 %) out of 9 human lung cancer cell lines[19]. In the present study, the expressions of Mad2 and p53 protein were examined in colorectal cancer and its corresponding normal tissues. Mad2 expression in colorectal cancer was higher than that in its corresponding normal tissues. Our results on the expression of Mad2 were not consistent with the reduced Mad2 expression in a breast cancer cell[8]. We speculate it might be the surrounding in which cell lived that led to the expression difference. In addition, positive expression of Mad2 was found in normal tissues to some extent. In budding yeast, the amount of Mad2 protein appeared to be constant during the cell cycle, although the level of Clb2p, a mitotic cycle cyclin, changed regularly in response to cell progression[20]. Similarly, a certain amount of Mad2 protein is thought to be required to maintain the normal checkpoint system in human cell. Loren *et al* showed that subtle differences in Mad2 protein level markedly altered checkpoint function. Therefore, inactivation of Mad2 would be sufficient to create a haplo-insufficient effect and the loss of mitotic checkpoint control[21]. The most convincing evidence of the role of mitotic checkpoint defect in CIN in mammalian cells obtained in two recent studies showed that disrupting of Mad2 expression resulted in CIN. CIN cells became aneuploidy, a hallmark of cancer associated with aggressive tumor behavior and a poor prognosis[21,22]. Very recently, Poelzl *et al* reported that estrogen receptor β, which might be involved in the regulation of cellular proliferation, interacted with Mad2 directly and specifically[23]. The Mad2 protein also interacted with the cytoplasmic domain of insulin receptors, which was thought to be a regulator of cellular growth[24,25]. Mad2 protein overexpressed in cancer tissues was exclusively present in the cytoplasm of cancer cells. We speculate that cytoplasmic Mad2 protein may enhance the positive regulatory action of estrogen receptor β and insulin receptor on cellular proliferation. We also discovered that there was a significantly positive correlation between the expressions of Mad2 and p53 (P<0.05). Orr-Weaver *et al*. thought aneuploidy resulted from defect of Mad2 and other unknown factor could increase the rate at which tumor suppressors, such as p53, were lost[17]. p53 gene was the most frequently mutated gene in human cancer[26-28]. One of its roles was to ensure that when DNA damaged cells were arrested in G1, it attempted to repair their DNA before it was replicated[29,30]. In some cell types, p53 induced apoptosis when overexpressed and was required for apoptosis in response to severe DNA damage[31,32]. p53 might directly activate death genes such as BAX, or down-regulate survival genes such as BCL-2[33-35]. So when p53 gene mutates, aneupoidy from defect of Mad2 might escape from apoptosis and go on its mitosis, finally develop to malignant tumor.

The C/N ratio of Mad2 protein was found to be associated with lymph node metastasis. A C/N ratio greater than 2 was observed more frequently in patients with lymph node metastasis. Therefore, a C/N ratio >2 may be clinically an important indicator for lymph node metastasis of colorectal cancer.

In conclusion, the protein level of Mad2 is higher in colorectal cancer tissues than in normal tissues. The higher the protein level in colorectal cancer tissues is, the more frequently lymph node metastasis. Since the difference in the protein level between colorectal cancer and normal mucosa is easily detected by immunohistochemistry, Mad2 protein might be a good marker of lymph node metastasis of colorectal cancer.

REFERENCES

1 **Mitelman F**, Mertens F, Johansson B. A breakpoint map of recurrent chromosomal rearrangements in human neoplasia. *Nat Genet* 1997; **15:** 417-474

2 **Rooney PH**, Murray GI, Stevenson DA, Haites NE, Cassidy J, Mcleod HL. Comparative genomic hybridization and chromosomal instability in solid tumors. *Br J Cancer* 1999; **80:** 862-873

3 **Lengauer C**, Kinzler KW, Vogelstein B. Genetic instabilities in human cancers. *Nature* 1998; **396:** 643-649

4 **Lengauer C**, Kinzler KW, Vogelstein B. Genetic instability in colorectal cancers. *Nature* 1997; **386:** 623-627

5 **Lengauer C**, Kinzler KW, Vogelstein B. DNA methylation and genetic instability in colorectal cancer cells. *Proc Natl Acad Sci USA* 1997; **94:** 2545-2550

6 **Li R**, Murray AW. Feedback control of mitosis in budding yeast. *Cell* 1991; **66:** 519-531

7 **Hoyt MA**, Totis L, Roberts BT. S.cerevisiae genes required for cell cycle arrest in response to loss of microtubule function. *Cell* 1991; **66:** 507-517

8 **Li Y**, Benezra R. Identification of a human mitotic checkpoint gene: hsMAD2. *Science* 1996; **274:** 246-248

9 **Taylor SS**, McKeon F. Kinetochore localization of murine Bub1 is required for normal mitotic timing and checkpoint response

to spindle damage. *Cell* 1997; **89:** 727-735
10 **Jin DY**, Spencer F, Jeang KT. Human T cell leukemia virus type 1 oncoprotein Tax targets the human mitotic checkpoint protein MAD1. *Cell* 1998; **93:** 81-91
11 **Barnes DM**, Dublin EA, Fisher CJ, Levison D A, Millis RR. Immunohistochemical detection of p53 protein in mammary carcinoma: an important new independent indicator of prognosis? *Hum Pathol* 1993; **24:** 469-476
12 **Rudner AD**, Murray AW. The spindle assembly checkpoint. *Curr Opin Cell Biol* 1996; **8:** 773-780
13 **Amon A**. The spindle checkpoint. *Curr Opin Genet Dev* 1999; **9**: 69-75
14 **Waters JC**, Chen RH, Murray AW, Salmon ED. Localization of Mad2 to kinetochores depends on microtubule attachment, not tension. *J Cell Biol* 1998; **141:** 1181-1191
15 **Sharp-Baker H**, Chen RH. Spindle checkpoint protein Bub1 is required for kinetochore localization of Mad1, Mad2, Bub3, and CENP-E, independently of its kinase activity. *J Cell Biol* 2001; **153:** 1239-1250
16 **Pennisi E**. Cell division gatekeepers identified. *Science* 1998; **279:** 477-478
17 **Orr-Weaver TL,** Weinberg RA. A checkpoint on the road to cancer. *Nature* 1998; **392:** 223-224
18 **Shah JV**, Cleveland DW. Waiting for anaphase: Mad2 and the spindle assembly checkpoint. *Cell* 2000; **103:** 997-1000
19 **Takahashi T**, Haruki N, Nomoto S, Masuda A, Saji S, Osada H, Takahashi T. Identification of frequent impairment of the mitotic checkpoint and molecular analysis of the mitotic checkpoint genes, hsMAD2 and p55CDC, in human lung cancers. *Oncogene* 1999; **18**: 4295-4300
20 **Chen RH**, Brady DM, Smith D, Murray AW, Hardwick KG. The spindle checkpoint of budding yeast depends on a tight complex between the Mad1 and Mad2 proteins. *Mol Biol Cell* 1999; **10:** 2607-2618
21 **Michel LS**, Liberal V, Chatterjee A, Kirchwegger R, Pasche B, Gerald W, Dobles M, Sorger PK, Murty VV, Benezra R. MAD2 haploinsufficiency causes premature anaphase and chromosome instability in mammalian cells. *Nature* 2001; **409:** 355-359
22 **Dobles M**, Liberal V, Scott ML, Benezra R, Sorger PK. Chromosome missegregation and apoptosis in mice lacking the mitotic checkpoint protein Mad2. *Cell* 2000; **101:** 635-645
23 **Poelzl G**, Kasai Y, Mochizuki N, Shaul PW, Brown M, Mendelsohn ME. Specific association of estrogen receptor beta with the cell cycle spindle assembly checkpoint protein MAD2. *Proc Natl Acad Sci USA* 2000; **97:** 2836-2839
24 **O'Neill TJ**, Zhu Y, Gustafson TA. Interaction of MAD2 with the carboxyl terminus of the insulin receptor but not with the IGFIR. Evidence for release from the insulin receptor after activation. *J Biol Chem* 1997; **272:** 10035-10040
25 **Gliozzo B**, Sung CK, Scalia P, Papa V, Frasca F, Sciacca L, Giorgino F, Milazzo G, Goldfine ID, Vigneri R, Pezzino V. Insulin-stimulated cell growth in insulin receptor substrate-1-deficient ZR-75-1 cells is mediated by a phosphatidylinositol-3-kinase independent pathway. *J Cell Biochem* 1998; **70:** 268-280
26 **Nigro JM**, Baker SJ, Preisinger AC, Jessup JM, Hostetter R, Cleary K, Bigner SH, Davidson N, Baylin S, Devilee P. Mutations in the p53 gene occur in diverse human tumour types. *Nature* 1989; **342:** 705-708
27 **Hollstein M**, Rice K, Greenblatt MS, Soussi T, Fuchs R, Sorlie T, Hovig E, Smith-Sorensen B, Montesano R, Harris CC. Database of p53 gene somatic mutations in human tumors and cell lines. *Nucleic Acids Res* 1994; **22:** 3551-3555
28 **Greenblatt MS**, Bennett WP, Hollstein M, Harris CC. Mutations in the p53 tumor suppressor gene: clues to cancer etiology and molecular pathogenesis. *Cancer Res* 1994; **54:** 4855-4878
29 **Kuerbitz SJ**, Plunkett BS, Walsh WV, Kastan MB. Wild-type p53 is a cell cycle checkpoint determinant following irradiation. *Proc Natl Acad Sci U S A* 1992; **89:** 7491-7495
30 **Nelson WG**, Kastan MB. DNA strand breaks: the DNA template alterations that trigger p53-dependent DNA damage response pathways. *Mol Cell Biol* 1994; **14:** 1815-1823
31 **Lowe SW**, Schmitt EM, Smith SW, Osborne BA, Jacks T. p53 is required for radiation-induced apoptosis in mouse thymocytes. *Nature* 1993; **362:** 847-849
32 **Hermeking H**, Eick D. Mediation of c-Myc-induced apoptosis by p53. *Science* 1994; **265:** 2091-2093
33 **Miyashita T**, Krajewski S, Krajewska M, Wang HG, Lin HK, Liebermann DA, Hoffman B, Reed JC. Tumor suppressor p53 is a regulator of bcl-2 and bax gene expression *in vitro* and *in vivo*. *Oncogene* 1994; **9:** 1799-1805
34 **Miyashita T,** Reed JC. Tumor suppressor p53 is a direct transcriptional activator of the human bax gene. *Cell* 1995; **80:** 293-299
35 **White E**. Life, death, and the pursuit of apoptosis. *Genes Dev* 1996; **10:** 1-15

Edited by Zhu LH and Wang XL

P.O.Box 2345, Beijing 100023,China
Fax: +86-10-85381893
E-mail: wjg@wjgnet.com www.wjgnet.com

World J Gastroenterol 2003;9(9):1976-1980
World Journal of Gastroenterology
 ISSN 1007-9327

• COLORECTAL CANCER •

Effects of DNA methylation on expression of tumor suppressor genes and proto-oncogene in human colon cancer cell lines

Jing-Yuan Fang, Juan Lu, Ying-Xuan Chen, Li Yang

Jing-Yuan Fang, Juan Lu, Ying-Xuan Chen, Li Yang, Shanghai Institute of Digestive Diseases, Renji Hospital, Shanghai Second Medical University, Shanghai 200001, China
Supported by the National Natural Science Foundation of China, No.30170413, and Ph.D Funds from the Ministry of Education of China, No.199946, and the Key Subject Funds of Shanghai Education Committee to Jing-Yuan Fang
Correspondence to: Dr. Jing-Yuan Fang, Shanghai Institute of Digestive Diseases, 145 Shandong Zhong Road, Shanghai 200001, China. jingyuanfang@yahoo.com
Telephone: +86-21-63200874 **Fax:** +86-21-63266027
Received: 2002-12-22 **Accepted:** 2003-01-14

Abstract

AIM: To investigate the effects of DNA methylation on the expression of tumor suppressor genes and proto-oncogene in human colon cancer cell lines.

METHODS: Three colon cancer cell lines (HT-29, SW1116 and Colo-320) treated with different concentrations of DNA methyltransferase inhibitor, 5-aza-2'-deoxycytidine (5-aza-dC) were used to induce DNA demethylation. The expressions of $p16^{INK4A}$, $p21^{WAF1}$, *APC* and *c-myc* genes were observed by using RT-PCR. The methylation status of $p16^{INK4A}$ promoter in HT-29 cells was also determined by methylation-specific PCR (MSP).

RESULTS: Weak expressions of $p16^{INK4A}$ and *APC* in the three colon cancer cells were detected, and $p21^{WAF1}$ expression was not found in SW1116 and Colo-320 cells before treatment. After treatment of 1 μmol/L but not 10 μmol/L of 5-aza-dC, the methylation level of $p16^{INK4A}$ gene promoter decreased significantly, and the hypomethylation led to the up-regulation of $p16^{INK4A}$ gene transcription in HT-29 cells. In the cell lines of SW1116 and Colo-320, $p16^{INK4A}$ and *APC* mRNA expressions were obviously enhanced after treatment of either 10 μmol/L or 5 μmol/L 5-aza-dC for 24 h. However, no evidence was found that methylation regulated the expression of $p21^{WAF1}$ and *c-myc* genes in human colon cancer cell lines.

CONCLUSION: Expression of $p16^{INK4A}$ and *APC* genes is regulated by DNA methylation in three human colon cancer cell lines.

Fang JY, Lu J, Chen YX, Yang L. Effects of DNA methylation on expression of tumor suppressor genes and proto-oncogene in human colon cancer cell lines. *World J Gastroenterol* 2003; 9 (9): 1976-1980

http://www.wjgnet.com/1007-9327/9/1976.asp

INTRODUCTION

DNA methylation is the main epigenetic modification after replication in humans[1]. DNA (cytosine-5)-methyltransferase (DNMT) catalyzes the transfer of a methyl group from S-adenosyl-L-methionine (SAM) to C5 of cytosine within CpG dinucleotide sequences in genomic DNA of higher eukaryotes. The expression of some genes can be frequently inactivated by reversible epigenetic events rather than genetic events[2,3].

Colon cancer is one of the most common tumors worldwide. The loss of $p21^{WAF1}$, $p16^{INK4A}$ and adenomatous polyposis coli (*APC*) gene expression, or/and the over-expression of *c-myc* gene are believed to play a crucial role in colon carcinogenesis[4]. As described in our previous review[5], mutation of $p16^{INK4A}$ was not found but the frequency of hypermethylation was 10-53 % in colon cancer. Previous studies by two independent groups of investigators have demonstrated that inactivation of $p16^{INK4A}$ in human colon tissue might be due to *de novo* methylation of promoter-associated CpG island[6-8]. Colon cancer cell lines, Colo-320[9-11] and SW1116[12-14], were frequently used in molecular biological experiments.

To date, most of these studies were focused on aberrant methylation in a single gene. However, little is known about the regulation of methylation on the expression of several tumor suppressor genes and proto-oncogenes in the same human colon cancer cell line. Furthermore, several clinical trials indicated that methylation inhibitor, 5-aza-2'-deoxycytidine (5-aza-dC) was devoid of antitumour activity in adult patients with colon cancer[15-17]. We want to know whether 5-aza-dC induces over-expression of proto-oncogene while regulates the transcription of tumor suppressor gene.

In this study, we investigated the transcriptional level of $p16^{INK4A}$, $p21^{WAF1}$, *APC* tumor suppressor genes, and *c-myc* proto-oncogenes. We examined whether the expression of these genes was influenced by methylation in colon cancer cell lines. The focus of this work was to gain a better understanding of the factors involved in regulating DNA methylation.

MATERIALS AND METHODS

Cell culture

Colon cancer-derived cell lines HT-29, Colo-320 and SW1116 were maintained by serial passages in MEM containing 10 % heat-inactivated FCS, 20 mmol/L of L-glutamine, 62.5 mg/L of penicillin, and incubated at 37 ℃ using standard tissue culture incubators as described previously[18]. The cells were plated as 10^6 cells onto per 100-mm dish.

Treatment with 5-aza-dC

5-aza-dC was a DNMT inhibitor[19]. To assess the expression of $p16^{INK4A}$, $p21^{WAF1}$, *APC* and *c-myc* genes by 5-aza-dC, colon cancer cell lines were exposed to different concentrations (1 μmol/L and 10 μmol/L for HT-29 cells; 2 μmol/L, 5 μmol/L and 10 μmol/L for Colo-320 and SW1116 cells) of 5-aza-dC (Sigma, St. Louis, MO) for 24 hours and 72 hours. The control cultures were treated simultaneously with PBS. The media were changed, DNA and RNA were harvested at various time points, respectively. We did not find cytotoxics reactions from 5-aza-dC, even at 10 μmol/L concentration.

Reverse transcription polymerase chain reaction (RT-PCR)

Total RNA was isolated by using a commercial kit (Trizol)

according to the manufacturer's instructions (Gibco BRL). Reverse transcription reactions using 5 μg of total RNA in a total reaction volume of 20 μl were performed with Superscript II reverse transcriptase (Life Technologies, Inc.). The mRNA transcription levels of *p16^{INK4A}*, *p21^{WAF1}*, *APC* and *c-myc* genes were evaluated by using RT-PCR. Primer sequence and PCR reaction for each primer are shown in Table 1. For control of RT-PCR, a 612 bp (322 bp for *p16^{INK4A}* RT-PCR in HT-29) fragment of β-*actin* cDNA was also amplified. The density of bands in RT-PCR were quantitated by using a molecular dynamics phosphorImager (Nucleo Tech Inc., San Mateo, CA), which were normalized to the amount of total RNA as determined by the density of β-*actin* band from RT-PCR[16]. RT-PCR was performed three times at least.

Methylation-Specific PCR (MSP) for p16^{INK4A}

We followed Clark's method of bisulfite treatment[20] with some modifications as follows. Two μg of total genomic DNA (from at least two independent treatments corresponding to RT-PCR experiments) was isolated by using QIAamp DNA blood mini kit (QIAGEN Inc.), then denatured by NaOH and modified by sodium bisulfite solution (2.35 mol/L) containing hydroquinone (0.04 mol/L)) freshly prepared. The bisulfite-treated DNA was desalted using Wizard DNA clean up kit (Promega). To amplify the *p16^{INK4A}* promoter, we used 0.1 μg aliquot of converted DNA. Methylation of the 5' CpG island in *p16^{INK4A}* gene was also determined in samples from HT-29 cells treated by 5-aza-dC. The bisulfite treated DNA was amplified by PCR using primers specific for the methylated or unmethylated primer. The GenBank accession number, sequences of primers and program of PCR are also shown in Table 1. PCR product was directly loaded onto 3 % agarose gels and electrophoresed. The gel was stained with ethidium bromide and directly visualized under UV illumination.

RESULTS

Methylation in p16^{INK4A} promoter in HT-29 cells treated with 5-ada-dC

We examined the methylation status of *p16^{INK4A}* following 5-aza-dC treatment using MSP. Bisulfite treatment converted the cytosine residues in the genomic DNA to uracil, which were amplified as thymine during subsequent PCR. As shown in Figure 1, HT-29 cells showed a positive 150-151 bp band for methylated and unmethylated specific primer sets for *p16^{INK4A}* respectively, indicating that *p16^{INK4A}* gene was partially methylated in this cell line. The methylated bands for *p16^{INK4A}* gene in the mock treated HT-29 cells were consistently stronger than the products of 5-aza-dC treated HT-29 cells. Thus, the product level from PCR using unmethylated primer was significantly higher, and methylated product level was correspondingly lower in HT-29 cells treated with 5-aza-dC.

Three days after treatment with 1 μm of 5-aza-dC, MSP revealed a significant increase in the amount of unmethylated product (Figure 1). These results suggested that *p16^{INK4A}* gene was a target of the decreased methylation level in HT-29 cells treated with 5-aza-dC.

Restoration of p16^{INK4A} gene expression by 5-aza-dC

We initially tried to find out whether there were expressions of several tumor suppressor genes such as *p16^{INK4A}*, *p21^{WAF1}* and *APC*, and proto-oncogene *c-myc* in human colon cancer cell lines HT-29 (*p16^{INK4A}* only), Colo-320 and SW1116. mRNA levels of the above genes were investigated by using semiquantitative RT-PCR. *p16^{INK4A}* gene was expressed in these three cell lines slightly prior to the treatment with 5-aza-dC.

In the first part of the present study, we examined the possibility of methylation on expression regulation of *p16^{INK4A}* in three colon cancer cell lines. Increased levels of *p16^{INK4A}* expression were seen in HT-29 cells treated with lower (1 μmol/L, 24 hours) but not higher (10 μmol/L, 24 hours) concentrations of 5-aza-dC (Figure 2, Table 2). In contrast, 5-aza-dC induced transcription of *p16^{INK4A}* at higher concentration (10 μmol/L)) for 24 hours or 72 hours, but not at the lower concentration (2 μmol/L or 5 μmol/L) for the same duration (Figures 3A and 3B, lanes 3 and 4, Table 3).

Table 2 The expression of *p16^{INK4A}* gene in HT-29 cells (the band density)

5-aza-dC conc	Mock treated	1 μM, 24 h	10 μM, 24 h
Density	2257.7	2782.5	1975.3

The density of each band from RT-PCR in each lane of Figure 2 was normalized to the amount of total RNA as determined by the density of band in RT-PCR for β-*actin*.

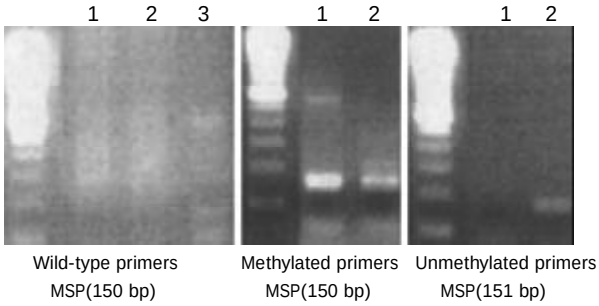

Figure 1 5-aza-dC induced hypomethylation of the promoter of *p16^{INK4A}* gene in HT-29 cells. Lane 1, untreated; lane 2, 5-aza-dC treated; lane 3, untreated with bisulfite. MSP was performed with the specific primers described in the Materials and Methods.

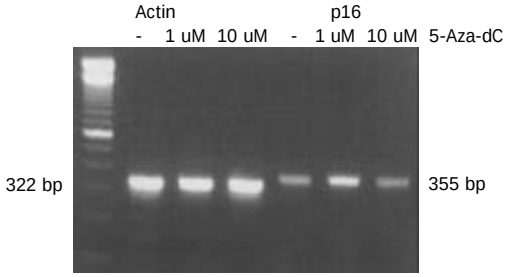

Figure 2 Up-regulated mRNA level of *p16^{INK4A}* by 5-aza-dC in HT-29 cells. RT-PCR was performed as described in Materials and Methods. β-*actin* was used as a loading / amplification control.

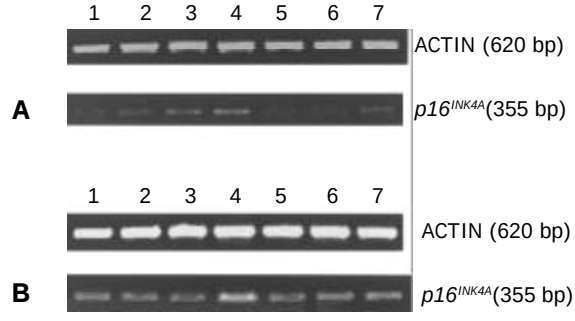

Figure 3 5-aza-dC increased the transcription of *p16^{INK4A}* gene in Colo-320 (A) and SW1116 cells. Lane 1: mock treatment. Lanes 2-7: after 5-aza-dC treatment; lane 2: 2 μmol/L, 24 h; lane 3: 5 μmol/L, 24 h; lane 4: 10 μmol/L, 24 h; lane 5: 2 μmol/L, 72 h; lane 6: 5 μmol/L, 72h; lane 7: 10 μmol/L, 72 h. The density of bands shown in Table 3.

Table 1 Sequences of primers and program of PCR

Primers	Sense(5'→3')	Antisense(5'→3')	Size of product and PCR condition	GenBank accession number
β-actin RT-PCR	GGA GTC CTG	CTA GAA GCA	322 bp	XM004814
(for *p16*^{INK4A} RT-	TGG CAT CCA CG	TTT GCG GTG GA	94 ℃ 3 m; 94 ℃ 30 s, 60 ℃	
PCR in HT-29)			1 m, 72 ℃ 1 m, 27 X; 72 ℃ 5 m	
β-*actin* RT-PCR	GGC ATC GTG	GCT GGA AGG	612 bp	BC023204
(for RT-PCR	ATG GAC TCC G	TGG ACA GCG A	94 ℃ 5 min; 92 ℃ 40 s, 58 ℃ 40 s,	
in other cells)			72 ℃ 50 s, 30 X; 72 ℃ 5 min	
p16^{INK4A}	CCC GCT TTC	TTA TTT GAG	355 bp	L27211
RT-PCR	GTA GTT TTC AT	CTT TGG TTC TG	94 ℃ 5 min; 94 ℃ 1 min,58 ℃ 1 min,	
			72 ℃, 1 min, 35 X; 72 ℃ 5 min	
APC	GAG ACA GAA	GTA AGA TGA TTG	170 bp	AF209032
RT-PCR	TGG AGG TGC TGC	GAA TTA TCT TCT A	95 ℃ 5 min; 95 ℃ 1 min, 53 ℃ 1 min,	
			72 ℃, 1 min, 35 X; 72 ℃ 5 min	
p21^{WAF1}	CAG GGG ACA	GGG CGG CCA	335 bp	NM_000389
RT-PCR	GCA GAG GAA GA	GGG TAT GTA C	94 ℃ 5 min; 94 ℃ 1 min, 58 ℃ 1 min,	
			72 ℃ 1 min, 35 X; 72 ℃ 5 min	
c-myc	CCA ACA GGA	CTC GGT CAC CAT	290 bp	V00568
RT-PCR	GCT ATG ACC TC	CTC CAG CT	94 ℃ 5 min; 94 ℃ 1 min, 52 ℃ 1 min,	
			72 ℃, 1 min, 35 X; 72 ℃ 5 min	
p16^{INK4A} MSP	CAG AGG GTG	CGG GCC GCG	140 bp	X94154
(Wild-type)	GGG CGG ACC CGC	GCC GTG G	95 ℃ 5 min; 95 ℃ 1 min, 65 ℃ 2 min, 72 ℃ 3 min,	
			5 X; 95 ℃ 30 s, 65 ℃ 30 s, 72 ℃ 1 min, 35 X; 72 5 min	
p16^{INK4A} MS	TTA TTA GAG GGT	GAC CCC GAA CCG	150 bp	X94154
P-methyl-primers	GGG GCG GAT CGC	CGA CCG TAA	95 ℃ 5 min; 95 ℃ 1 min, 65 ℃ 2 min, 72 ℃ 3 min,	
			5 X; 95 ℃ 30 s, 65 ℃ 30 s, 72 ℃ 1 min, 35 X; 72 ℃ 5 min	
p16^{INK4A}	TTA TTA GAG GGT	CAA CCC CAA ACC	151 bp	X94154
MSP-unmethyl	GGG GTG GAT TGT	ACA ACC ATA A	95 ℃ 5 min; 95 ℃ 1 min, 60 ℃ 2 min, 72 ℃ 3 m ℃,	
primers			5 X; 95 ℃ 30 s, 60 ℃ 30 s, 72 ℃ 1 min, 35 X; 70 ℃ 5 min	

Table 3 Expression of *p16*^{INK4A} gene in SW1116 and Colo-320 cells (the band density)

5-aza-dC treatment	Mock treated	2 μmol/L, 24 h	5 μmol/L, 24 h	10 μmol/L, 24 h	2 μmol/L, 72 h	5 μmol/L, 72 h	10 μmol/L, 24 h
SW1116	1494.7	2055.5	2436.9	3487.3	1592.0	2074.8	2774.0
Colo-320	809.1	860.6	829.2	1298.8	875.7	923.5	1189.6

The density of each band from RT-PCR in each lane of Figure 3 was normalized to the amount of total RNA as determined by the density of band in RT-PCR for β-*actin*.

Table 4 Expression of *APC* gene in SW1116 and Colo-320 cells (the band density)

5-aza-dC treatment	Mock treated	2 μmol/L, 24 h	5 μmol/L, 24 h	10 μmol/L, 24 h	2 μmol/L, 72 h	5 μmol/L, 72 h	10 μmol/L, 24 h
SW1116	786.2	1481.2	782.6	796.9	802.9	1173.5	1236.8
Colo320	1804.6	2388.2	4055.2	1923.9	1803.0	3197.8	3271.7

The density of each band from RT-PCR in each lane of Figure.4 was normalized to the amount of total RNA as determined by the density of band in RT-PCR for β-*actin*.

5-aza-dC increased transcription level of APC gene

To identify whether the transcription level of *APC* was regulated by DNA methylation in human colon cancer cell lines, we cultured Colo-320 and SW1116 cells with or without 5-aza-dC treatment for 24 hours and 72 hours. The data from RT-PCR implied that before incubation with 5-aza-dC, the levels of *APC* transcription in these cells were lower (Figure 4, line 1, Table 4). Incubation for 24 hours with 5-aza-dC resulted in the accumulation of *APC* mRNA, whose levels remained unchanged during the 72 hour incubation period. *APC* mRNA levels were normalized with respect to the level of β-*actin* mRNA, which did not change during culture with 5-aza-dC (Figure 4, Table 4). RT-PCR was repeated twice and the results were consistent.

The effectiveness of 5-aza-dC on the expression of *APC* was high even at lower concentration (2 μmol/L), suggesting that methylation-induced silencing of this gene was the primary event. Restoration of *APC* expression by 5-aza-dC treatment confirmed a causal relationship between DNA hypermethylation and *APC* silencing in colon cancer cell lines Colo-320 and SW1116.

5-aza-dC treatment failed to induce expression of p21^{WAF1} *and c-myc in Colo-320 and SW1116 cells*

To further define the modification status of *p21*^{WAF1} and *c-myc* expression in colon carcinogenesis, we attempted to observe whether their transcription levels would change after treatment with DNMT inhibitor. Although no expression of *p21*^{WAF1} and

significant over-expression of *c-myc* were seen in mock treatment. Our current study revealed that almost no change in activity was seen when these two cell lines Colo-320 and SW1116 cells were treated by 5-aza-dC. In other words, regulation of methylation on the expression of $p21^{WAF1}$ and *c-myc* genes was not found (data not shown).

Taken these together, it was suggested that the methylation silencing transcription be localized at specific regions of the chromatin. Other mechanisms might play a role in controlling the activity of $p21^{WAF1}$ and *c-myc* genes in colon cancer cell lines Colo-320 and SW1116.

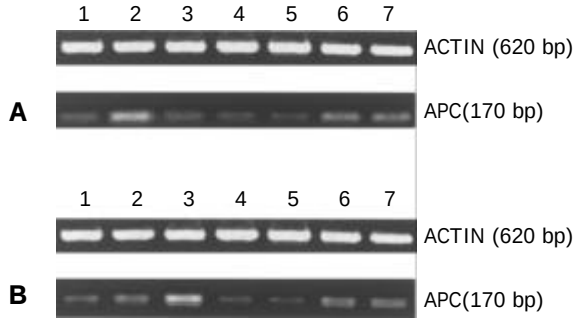

Figure 4 5-aza-dC increased the transcription of *APC* gene in Colo-320 (A) and SW1116 cells. Lane 1: mock treatment. Lanes 2-7: after 5-aza-dCtreatment; lane 2: 2 μmol/L, 24 h; lane 3: 5 μmol/L, 24 h; lane 4: 10 μmol/L, 24 h; lane 5: 2 μmol/L, 72 h; lane 6: 5 μmol/L, 72 h; lane 7: 10 μmol/L, 72 h. The density of bands shown in Table 4.

DISCUSSION

Compelling evidences for the role of epigenetic modification on the regulation of gene transcription have been published[21-26]. $p16^{INK4A}$ was a tumor suppressor gene originally identified by Serrano *et al*[27], and the methylation profile of $p16^{INK4A}$ promoter differed in each cancer type[28]. Several studies indicat that 5-aza-dC induced growth inhibition might be resulted from the release of methylation silenced cell cycle regulatory gene $p16^{INK4A}$[29]. *APC* gene hypermethylation is frequent but not universal in colon cancer cell line. Previous studies showed that $p21^{WAF1}$ transcription was regulated by histone acetylation, another modification of epigenetics in human colon cancer[30], but little is known about the effect of DNA methylation on this gene expression.

In the current study, our findings indicated firstly that $p16^{INK4A}$ was expressed in these three human colon cancer cell lines, and *APC* was expressed with $p21^{WAF1}$ inactivated in Colo-320 and SW1116 cells. 5-aza-dC induced hypomethylation of $p16^{INK4A}$ promoter and the restoration of $p16^{INK4A}$ transcription, suggesting that DNA methylation is the major regulation mechanism for $p16^{INK4A}$ in HT-29, Colo-320 and SW1116 cells. Previously it was suggested that lack of $p21^{WAF1}$ expression appeared to be the result of hypermethylation of it' s promoter region, as $p21^{WAF1}$ protein expression could be induced by growth of Rat-1 cells in the presence of 5-aza-dC[31]. However, the influence of methylation on $p21^{WAF1}$ gene expression was dependent on differentiation of cells and tissues[30]. An important finding from this study indicated that reduction of DNA methylation might not play a crucial role in the regulation of $p21^{WAF1}$ transcription in human colon cancer cell lines, Colo-320 and SW1116.

c-Myc proto-oncoprotein has been found to be deregulated in colon cancer. Over-expression of c-Myc in tissue culture caused an increase in cell proliferation with a shortened G1 phase, whereas loss of c-Myc resulted in slow growth and longer G1 phase[32]. Over-expression and abnormal intracellular location of the product of proto-oncogene *c-myc* in colon dysplasia and neoplasia might be related to the alteration in epigenetic mechanisms controlling the function of this gene [33]. Although hypomethylation of *c-myc* in human tumors has also been reported, it is not clear whether demethylation induces the over-expression of *c-myc* in human tumor cell lines. This paper reports that 5-aza-dC did not up-regulate *c-myc* transcription, while the expression of $p16^{INK4A}$ and *APC* tumor suppressor genes responded to 5-aza-dC treatment in colon cancer cell lines. The reason why 5-aza-dC failed to colon cancer treatment was not due to *c-myc* over-expression from demethylation.

In conclusion, our study results support the concept that there are significant differences in the regulatory response to DNA methylation in different genes including tumor suppressor gene and proto-oncogene, even in the same colon cancer cell lines Colo-320 or SW1116.

ACKNOWLEDGEMENTS

We are grateful to Ms.Hong-Yin Zhu and Ju-Fang Tong for performing the RT-PCR and cell culture, and Dr.Xie-Ning Wu for his assistance in preparing this manuscript.

REFERENCES

1 **Baylin SB,** Herman JG, Graff JR, Vertino PM, Issa JP. Alterations in DNA methylation:a fundamental aspect of neoplasia. *Adv Cancer Res* 1998; **72:** 141-196
2 **Herman JG,** Latif F, Weng Y, Lerman MI, Zbar B, Liu S, Samid D, Duan DS, Gnarra JR, Linehan WM, Baylin SB. Silencing of the VHL tumor-suppressor gene by DNA methylation in renal carcinoma. *Proc Natl Acad Sci USA* 1994; **91:** 9700-9704
3 **Nakayama S,** Sasaki A, Mese H, Alcalde RE, Tsuji T, Matsumura T. The E-cadherin gene is silenced by CpG methylation in human oral squamous cell carcinomas. *Int J Cancer* 2001; **93:** 667-673
4 **Nagai MA,** Habr-Gama A, Oshima CT, Brentani MM. Association of genetic alterations of c-myc, c-fos, and c-Ha-ras proto-oncogenes in colorectal tumors. Frequency and clinical significance. *Dis Colon Rectum* 1992; **35:** 444-451
5 **Fang JY,** Xiao SD. Alteration of DNA methylation in gastrointestinal carcinogenesis. *J Gastroenterol Hepatol* 2001; **16:** 960-968
6 **Vettese-Dadey M,** Grant PA, Hebbes TR, Crane-Robinson C, Allis CD, Workman JL. Acetylation of histone H4 plays a primary role in enhancing transcription factor binding to nucleosomal DNA *in vitro*. *EMBO J* 1996; **15:** 2508-2518
7 **Herman JG,** Merlo A, Mao L, Lapidus RG, Issa JP, Davidson NE, Sidransky D, Baylin SB. Inactivation of the CDKN2/p16/MTS1 gene is frequently associated with aberrant DNA methylation in all common human cancers. *Cancer Res* 1995; **55:** 4525-4530
8 **Gonzalez-Zulueta M,** Bender CM, Yang AS, Nguyen T, Beart RW, Van Tornout JM, Jones PA. Methylation of the 5'CpG island of the p16/CDKN2 tumor suppressor gene in normal and transformed human tissues correlates with gene silencing. *Cancer Res* 1995; **55:** 4531-4535
9 **Russo P,** Malacarne D, Falugi C, Trombino S, O'Connor PM. RPR-115135,a farnesyl transferase inhibitor, increases 5-FU-cytotoxicity in ten human colon cancer cell lines: Role of p53. *Int J Cancer* 2002; **100**: 266-275
10 **Mori H,** Niwa K, Zheng Q, Yamada Y, Sakata K, Yoshimi N. Cell proliferation in cancer prevention; effects of preventive agents on estrogen-related endometrial carcinogenesis model and on an in vitro model in human colorectal cells. *Mutat Res* 2001; **480-481:** 201-207
11 **Ding X,** Flatt PR, Permert J, Adrian TE. Pancreatic cancer cells selectively stimulate islet beta cells to secrete amylin. *Gastroenterology* 1998; **114:** 130-138
12 **Rylova SN,** Amalifitano A, Persaud-Sawin DA, Guo WX, Chang J, Jansen PJ, Proia AD, Boustany RM. The CLN3 gene is a novel molecular target for cancer drug discovery. *Cancer Res* 2002; **62:** 801-808
13 **Gao Z,** Gao Z, Fields JZ, Boman BM. Tumor-specific expression

of anti-mdr1 ribozyme selectively restores chemosensitivity in multidrug-resistant colon-adenocarcinoma cells. *Int J Cancer* 1999;**82:** 346-352

14 **Shiraki K,** Tsuji N, Shioda T, Isselbacher KJ, Takahashi H. Expression of Fas ligand in liver metastases of human colonic adenocarcinomas. *Proc Natl Acad Sci USA* 1997; **94:** 6420-6425

15 **Moertel CG,** Schutt AJ, Reitemeier RJ, Hahn RG. Phase II study of 5-azacytidine (NSC-102816) in the treatment of advanced gastrointestinal cancer. *Cancer Chemother Rep* 1972; **56:** 649-652

16 **Bellet RE,** Mastrangelo MJ, Engstrom PF, Strawitz JG, Weiss AJ, Yarbro JW. Clinical trial with subcutaneously administered 5-azacytidine (NSC-102816). *Cancer Chemother Rep* 1974; **58:** 217-222

17 **Abele R,** Clavel M, Dodion P, Bruntsch U, Gundersen S, Smyth J, Renard J, van Glabbeke M, Pinedo HM. The EORTC early clinical trials cooperative group experience with 5-aza-2'-deoxycytidine (NSC 127716) in patients with colo-rectal, head and neck, renal carcinomas and malignant melanomas. *Eur J Cancer Clin Oncol* 1987; **23**: 1921-1924

18 **Fang JY,** Mikovits JA, Bagni R, Petrow-Sadowski CL, Ruscetti FW. Infection of lymphoid cells by integration-defective human immunodeficiency virus type 1 increases de novo methylation. *J Virol* 2001; **75:** 9753-9761

19 **Bender CM,** Gonzalgo ML, Gonzales FA, Nguyen CT, Robertson KD, Jones PA. Roles of cell division and gene transcription in the methylation of CpG islands. *Mol Cell Biol* 1999; **19:** 6690-6698

20 **Clark SJ,** Harrison J, Paul CL, Frommer M. High sensitivity mapping of methylated cytosines. *Nucleic Acids Res* 1994; **22:** 2990-2997

21 **Usadel H,** Brabender J, Danenberg KD, Jeronimo C, Harden S, Engles J, Danenberg PV, Yang S, Sidransky D. Quantitative adenomatous polyposis coli promoter methylation analysis in tumor tissue, serum, and plasma DNA of patients with lung cancer. *Cancer Res* 2002; **62:** 371-375

22 **Jin Z,** Tamura G, Tsuchiya T, Sakata K, Kashiwaba M, Osakabe M, Motoyama T. Adenomatous polyposis coli (APC) gene promoter hypermethylation in primary breast cancers. *Br J Cancer* 2001; **85:** 69-73

23 **Shibata DM,** Sato F, Mori Y, Perry K, Yin J, Wang S, Xu Y, Olaru A, Selaru F, Spring K, Young J, Abraham JM, Meltzer SJ. Hypermethylation of HPP1 is associated with hMLH1 hypermethylation in gastric adenocarcinomas. *Cancer Res* 2002; **62:** 5637-5640

24 **To KF,** Leung WK, Lee TL, Yu J, Tong JH, Chan MW, Ng EK, Chung SC, Sung JJ. Promoter hypermethylation of tumor-related genes in gastric intestinal metaplasia of patients with and without gastric cancer. *Int J Cancer* 2002; **102:** 623-638

25 **Shen L**, Ahuja N, Shen Y, Habib NA, Toyota M, Rashid A, Issa JP. DNA methylation and environmental exposures in human hepatocellular carcinoma. *J Natl Cancer Inst* 2002; **94:** 755-761

26 **Norrie MW**, Hawkins NJ, Todd AV, Meagher AP, O'Connor TW, Ward RL. The role of hMLH1 methylation in the development of synchronous sporadic colorectal carcinomas. *Dis Colon Rectum* 2002; **45:** 674-680

27 **Serrano M,** Hannon GJ, Beach D. A new regulatory motif in cell-cycle control causing specific inhibition of cyclin D/CDK4. *Nature* 1993; **366:** 704-707

28 **Esteller M,** Corn PG, Baylin SB, Herman JG. A gene hypermethylation profile of human cancer. *Cancer Res* 2001; **61:** 3225-3229

29 **Bender CM,** Pao MM, Jones PA. Inhibition of DNA methylation by 5-aza-2'-deoxycytidine suppresses the growth of human tumor cell lines. *Cancer Res* 1998; **58:** 95-101

30 **Fang JY,** Lu YY. Effects of histone acetylation and DNA methylation on $p21^{WAF1}$ regulation. *World J Gastroenterol* 2002; **8:** 400-405

31 **Allan LA,** Duhig T, Read M, Fried M. The $p21^{WAF1/CIP1}$ promoter is methylated in Rat-1 cells: Stable restoration of p53-dependent $p21^{WAF1/CIP1}$ expression after transfection of a genomic clone containing the $p21^{WAF1/CIP1}$ gene. *Mol Cell Biol* 2000; **20:** 1291-1298

32 **Bush A,** Mateyak M, Dugan K, Obaya A, Adachi S, Sedivy J, Cole M. C-myc null cells misregulate cad and gadd45 but not other proposed c-Myc targets. *Genes Dev* 1998; **12:** 3797-3802

33 **Sharrard RM,** Royds JA, Rogers S, Shorthouse AJ. Patterns of methylation of the *c-myc* gene in human colorectal cancer progression. *Br J Cancer* 1992; **65:** 667-672

Edited by Zhu LH and Wang XL

P.O.Box 2345, Beijing 100023,China
Fax: +86-10-85381893
E-mail: wjg@wjgnet.com www.wjgnet.com

World J Gastroenterol 2003;9(9):1981-1984
World Journal of Gastroenterology
 ISSN 1007-9327

• COLORECTAL CANCER •

Telomerase activity and cell apoptosis in colon cancer cell by human telomerase reverse transcriptase gene antisense oligodeoxynucleotide

Ying-An Jiang, He-Sheng Luo, You-Yuan Zhang, Li-Fang Fan, Chong-Qing Jiang, Wei-Jin Chen

Ying-An Jiang, He-Sheng Luo, Department of Gastroenterology, Renming Hospital of Wuhan University, Wuhan 430060, Hubei Province, China
Li-Fang Fan, Department of Pathology, Medical College of Wuhan University, Wuhan 430071, Hubei Province, China
Chong-Qing Jiang, Department of General surgery, Zhongnan Hospital of Wuhan University, Wuhan 430071, Hubei Province, China
You-Yuan Zhang, Department of Pathology, Central Hospital of Huangshi City, Huangshi 435000, Hubei Province, China
Wei-Jin Chen, Department of Medical information, Central Hospital of Huangshi City, Huangshi 435000, Hubei Province, China
Supported by the Science and Technology Research Project of Hubei Province, No.2002AA301C72
Correspondence to: Ying-An Jiang, Central Hospital of Huangshi City, 43 Wuhan Road, Huangshi 435000, Hubei Province China. weijin@hs.hb.cninfo.net
Telephone: +86-714-6283783 **Fax:** +86-714-6233931
Received: 2003-03-04 **Accepted:** 2003-04-19

Abstract

AIM: To evaluate the effect of human telomerase reverse transcriptase (hTERT) gene antisense oligodeoxynucleotide (As-ODN) on telomerase activity and cell apoptosis in colon cancer cell line SW480.

METHODS: As-ODN was transfected into cells SW480 by liposomal transfection. Cultured cells were divided into three groups: ASODN (5'GGAGCGCGCGGCATCGCGGG-3'), sense oligodeoxynucleotide (5'-CCCGCGATGCCGCGCGCTCC-3', S-ODN) and control. The concentration of oligodeoxynucleotide and lipsome was 10 μmol/L and 16 mg/L, respectively. The activity of telomerase was examined by telomeric repeat amplification protocol (TRAP)-enzyme-linked immunosorbent assay (ELISA), and cell apoptosis was observed by morphology and flow cytometry in each group.

RESULTS: Telomerase activity began to be down-regulated or inhibited when cells SW480 were treated with As-ODN for 72 h, and cell apoptosis was induced.

CONCLUSION: It is suggested that hTERT As-ODN might specially inhibit the activity of telomerase in colon cancer cells and it is further proved that the hTERT gene has a significant correlation with telomerase activity. Further evidence is needed to prove whether hTERT As-ODN is a potential tool for the treatment of colon cancer.

Jiang YA, Luo HS, Zhang YY, Fan LF, Jiang CQ, Chen WJ. Telomerase activity and cell apoptosis in colon cancer cell by human telomerase reverse transcriptase gene antisense oligodeoxynucleotide. *World J Gastroenterol* 2003; 9(9): 1981-1984
http://www.wjgnet.com/1007-9327/9/1981.asp

INTRODUCTION

Telomeres, the distal ends of human chromosomes, are comprised of simple, repetitive and G-rich hexameric sequences (TTAGGG) and are vital for chromosomal stability and replication. Telomerase is a ribonucleoprotein polymerase which adds telomeric sequences onto the ends of chromosomes to compensate for DNA end replication[1,2]. Telomerase activity in humans was detected in germline and tumor tissues as well as in established cultured cell lines[3]. In normal somatic cells, the absence or low expression of telomerase was thought to result in progressive telomeric shortening with each cell division[4,5]. Therefore, it has been suggested that reactivation of telomerase is a critical step in tumorigenesis and that interference with the regulation of telomerase activity may serve as a basis for cancer therapy[6,7]. Here we report the effect of SW480, a human colon cancer line, after transfected with antisense hTERT and investigated the potential value of telomerase as a target for antisense gene therapy in colon cancer.

MATERIALS AND METHODS

Cell culture

SW480 cells, a human colon cancer cell line, generously supplied by Department of Biology, Wuhan University, Wuhan, China, were maintained in RPMI 1640-10 % fetal bovine serum, supplemented with 1 mmol/L L-glutamine, 100 U/ml penicillin plus 100 μg/ml of streptomycin at 37 ℃ under 5 % CO_2.

Cell counting

Cells were counted with 5 g/L of trypan blue staining.

Oligodeoxynucleotides synthesis

Oligodeoxynucleotides synthesis was designed as described by Feng L[8,9]. Antisense oligodeoxynucleotides (As-ODN) with sequence 5' GGAGCGCGCGGCATCGCGGG-3' , which can recognize the RNA template region of telomerase, and sense oligo- deoxynucleotides (S-ODN), with 5' CCCGCGATGCC GCGCGCTCC 3' were prepared on the 391 DNA synthesizer, synthesized by SBS Bio-technology Engineering Company of Beijing. The synthesized oligodeoxynucleotides were subjected to electrophoresis (PAGE) and purified (300 V, 1.5 h).

Transfection of oligodeoxynucleotides

The phosphorothiate oligodeoxynucleotides (ODNs) transfection was performed with liposomal transfection reagent DOSPER (Roche Diagnostic GmbH) according to the manufacturer' s protocol. Briefly, cells were plated onto 6-well plates and incubated until the cells reached 70-80 % confluency. Before the transfection, DOSPER was diluted with serum-free medium. Then, the desired amount of ODNs was incubated for 15 minutes with diluted DOSPER. The ODNs/ DOSPER mixture (100 μl) was added dropwise in 900 μl serum-free RPMI 1640. After incubation for 6 hours at 37 ℃, 1 ml RPMI 1640 containing 20 % FBS was added into each well. Cells were harvested and analysed after 48, 72, 96 and 120 hours, respectively.

Table 1 Effect of telomerase activity in SW480 cells by ODNs ($\bar{x}\pm s$)

Groups	Active duration				
	24 h	48 h	72 h	96 h	120 h
As-ODN 10 μmol/L	0.648±0.057	0.324±0.029	0.283±0.072	0.189±0.093	0.172±0.114
S-ODN 10 μmol/L	1.082±0.249	1.272±0.372	1.204±0.190	0.902±0.193	0.909±0.146
Positive control	1.336±0.231	1.376±0.238	1.354±0.186	1.298±0.172	1.246±0.169
Negative control	0.339±0.181	0.312±0.139	0.283±0.086	0.072±0.039	0.057±0.028

Telomerase assay

Polymerase chain reaction enzyme linked immunosorbent assay (PCR-ELISA) was performed following the instructions from Roche Diagnostics GmbH of Germany. Briefly, 2×10^6 cells were isolated, mixed with 200 μl protein extraction buffer, and left on ice for 30 minutes. 175 μl supernatant was collected after centrifugation (16 000×g, 20 minutes, 4 ℃). PCR was performed in 50 μl supernatant containing 25 μl transfer reaction mixture, 2 μl protein extract and 2 μl primers, and added to 23 μl nuclease-free water. The PCR condition was as follows: at 25 ℃ for 30 minutes for primer elongation, and at 94 ℃ for 5 minutes for telomerase inactivation. Amplification for 30 cycles under the condition at 94 ℃ for 30 s for denaturation, at 50 ℃ for 30 for annealing, and at 72 ℃ for 90 s for polymerization. Five μl of amplified product and 20 μl denaturated reagent were incubated at room temperature, 225 μl hybridyzation buffer was then added and mixed, and 100 μl of them was distributed in the wells of a microtitering plate. After 2 hours of incubation (37 ℃, 300 rpm), the anti-DIG-POD 100 μl working solution was added and incubated for another 30 minutes followed by adding 100 μl TMB substrate solution, and 100 μl stop reagent was added at last. The OD value in each well was read at the wave length of 450 nm and 655 nm on a microtiter plate reader (Bio-RAD Model 550 microplate reader). The results OD_{450} minus OD_{655} >1.5 unit using a protein extract from immortalized telomerase-positive human embryonic kidney cell (293 cells) were judged as a positive control. The negative control was considered as OD_{450} minus OD_{655} <0.2 unit by reading the protein extract pretreated with RNase A at 65 ℃ for 10 minutes. Telomerase activity was considered positive when the value of OD_{450} minus OD_{655} of a sample was at least 0.2 units higher than that of the negative control, otherwise it would be negative. Each sample was examined for more than twice. The final value was presented as $\bar{x}\pm s$ after a statistical treatment by using *t* test.

Cytologic morphology

Cytologic morphological changes were observed under the Olympus optical microscope and Hitach transmission electron microscope.

Detection of apoptotic cells by flow cytometry

Cells were fixed and stained with propidium iodide (PI, Sigma product). The DNA content of each cell was analyzed by a FACSORT flow cytometry (Becton Dickinson). Briefly, cells were trypsinized, washed once in ice-cold PBS, and incubated with annexin-V- fluoroescein/PI, and then analyzed immediately with FACSORT flow cytometry. All data were analyzed using Cell Quest software.

Statistical analysis

Results were expressed as the means ±SD. Statistical analyses were carried out with the software package SPSS10.0. A *P* value <0.05 was considered statistically significant.

RESULTS

Effect of telomerase activity in SW480 cells by antisense hTERT ODNs

As-ODN (10 μmol/L) and S-ODN (10 μmol/L) were transfected into SW480 cells, and the cells were collected at 24, 48, 72, 96 and 120 hours after transfection, respectively. Telomerase activities were measured by TRAP-ELISA. Results were as the followings. (1) Telomerase activity of SW480, transferred with As-ODN, was greatly inhibited when compared with that in the S-ODN. (2) Telomerase activity of SW480, transferred with As-ODN, at 72 and 96 hours after transfection was significantly lower than that at 24 hours, respectively. (3) Telomerase activity of SW480, transferred with As-ODN, was significantly lower than that in the positive control, as shown in Table 1. These findings suggested that this inhibitory action was sequence specific and in a time-dependent manner.

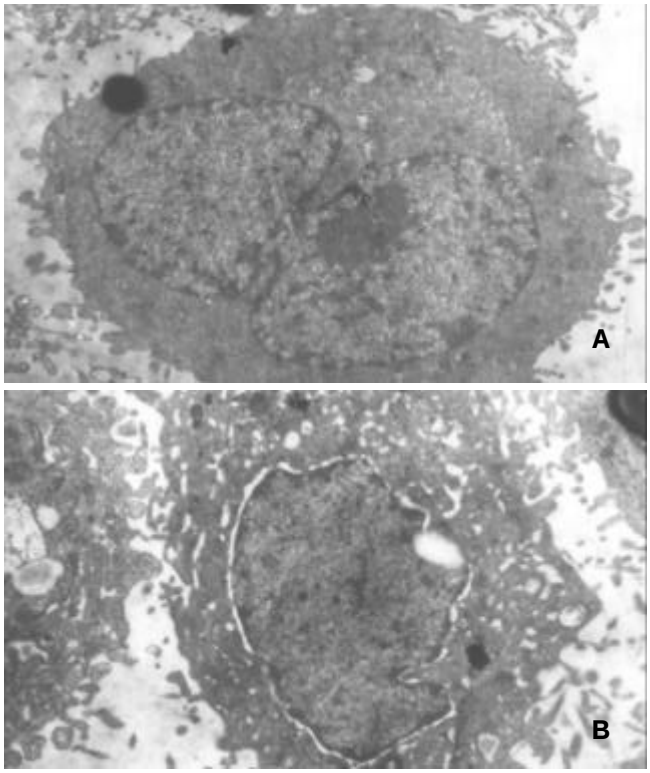

Figure 1 Morphplogic observation under transmission electron microscope. A: cell had no apoptotic features; and B: cell rounded up off the plastic, exhibiting cytoplasmic blebbing, fragmentation and chromatin condensation, features of apoptosis.

Effect of antisense hTERT ODNs on induction of SW480 cells apoptosis

Cytologic morphological changes Cytologic morphology of SW480, transferred with 10 μmol/L As-ODN for 3 days was observed under the Olympus optical microscope and Hitachi

transmission electron microscope. It was found that cells rounded up off the plaste, exhibiting cytoplasmic blebbing, fragmentation and chromatin condensation, and features of apoptosis. No apoptotic features (normal morphology) were observed in SW480 transferred with 10 μmol/L S-ODN (Figure 1).

Detection of apoptotic cells To determine the apoptotic rate, SW480 was treated with 10 μmol/L As-ODN and S-ODN for 2 days. After permeabilization, cells were stained with propidium iodide and analysed with flow cytometry. The apoptotic rate of SW480 cells transfected with As-ODN increased (at 48 hours, 4.82±0.39; 72 hours, 8.76±0.14; and 96 hours, 9.25±0.37, respectively, $P<0.001$), but no significant changes of apoptosis were observed in SW480 cells transferred with 10 μmol/L S-ODN as shown in Table 2, which indicated that this apoptotic induction was sequence specific and in a time-dependent manner.

Table 2 Effect of ODNs on induction of SW480 cells apoptosis ($\bar{x}\pm s$)

Groups	Active duration		
	48 h	72 h	96 h
As-ODN 10 μmol/L	4.82±0.39	8.76±0.14	9.25±0.37
S-ODN 10 μmol/L	2.08±0.38	2.96±0.47	2.19±0.29
hTERT blank	1.47±0.14	1.49±0.21	1.44±0.19

DISCUSSION

Three major components of telomerase, i.e. human telomerase RNA component (hTR), human telomerase-associated protein (TEP1), and human telomerase catalytic subunit (hTERT), have been identified[8,10-14]. hTR, functioning as a template for telomere elongation by telomerase, has been cloned from humans and mice[8,15] and expressed both in cancer and normal tissues, although its level was inclined to increase with tumor progression[16]. Human telomerase-associated protein (TEP1), as a human homolog of the Tetrahymena telomerase p80, was expressed ubiquitously and did not correlate with levels of telomerase activity[10,12]. hTERT, the catalytic protein subunit of human telomerase, contained the reverse transcriptase motif[12,13]. High levels of hTERT expression were observed in telomerase positive cell lines but not in telomerase negative primary fibroblasts[12]. hTERT was the limiting component necessary for the restoration of telomerase activity in normal diploid cells which was expressed transiently[17,18]. Recent studies have demonstrated telomerase activity was significantly associated with hTERT mRNA expression but not with hTR or TEP1 mRNA expression. These findings provide strong evidences that the expression of hTERT was a rate-limiting determinant of the enzymatic activity of human telomerase and that the up-regulation of hTERT expression might play a critical role in human carcinogenesis[19]. Previously, many studies[20-23] demonstrated that antisense oligonucleotides against human telomerase RNA resulted in inhibition of telomerase activity and induction of apoptosis in ovarian cancer cells and prostate cancer cells.

In our study, we found that transfection of SW480 with antisense-hTERT ODNs at a concentration of 10 μmol/L significantly inhibited the telomerase activity and induce apoptosis, when compared with positive control cells. The S-ODN with sense sequence did not affect the telomerase activity and induce apoptosis of transfected cells, indicating that this inhibitory and inducing action was sequence specific and in a time-dependent manner.

Recently, it has been shown that telomerase activity was the dominant mechanism providing telomere maintenance to human immortalized cells. The findings that the ability of cells with long telomeres to proliferate in the absence of telomerase demonstrated that telomerase activity did not require basic replicative functions of these cells, instead, telomerase activity appeared to be required to maintain a minimum telomere length[24]. However, the exact mechanisms of how telomerase activity is regulated in tumor cells remain poorly understood. Some researchers have shown that telomerase activity was correlated with the growth rate of immortal cells[25-27], whereas others found no significant association between telomerase activity and proliferative index in the tissue specimens from breast carcinoma[28], gastric carcinoma[29], and Wilm' s tumor[30]. Based on the recent findings, we did not observe any correlation between telomerase activity and proliferative index.

Some other studies, have shown that cells expressing high telomerase activity were more resistant to apoptosis than those with low telomerase expression[22,31,32], and that treatment with antisense telomerase inhibited the telomerase activity and subsequently induced either apoptosis or differentiation, and that regulation of these two distinct pathways might depend on the expression of ICE (Interleukin-1β-converting enzyme) or CDKIs (Cylin-dependent kinase inhibitors)[20]. Interestingly, inhibition of telomerase with an antisense telomerase expression vector not only decreased telomerase activity but also increased the susceptibility to cisplatin-induced apoptotic cell death in cisplatin- resistant U251-MG cells[22].

Inhibition of telomerase activity has been proposed as a potential approach to the treatment of human malignancy. It is suggested that telomerase inhibition may serve as an effective tool for eliminating tumor cells that have short telomeres. Such tumors may provide reasonable targets for the agents that inhibit telomerase. These experiments await the development of specific inhibitors for the components of the telomerase complex.

REFERENCES

1 **Blackburn EH.** Structure and function of telomeres. *Nature* 1991; **350**: 569-573

2 **Nakamura TM,** Morin GB, Chapman KB, Weinrich SL, Andrews WH, Lingner J, Harley CB, Cech TR. Telomerase catalytic subunit homologs from fission yeast and human. *Science* 1997; **277**: 955-959

3 **Holt SE,** Shay JW, Wright WE. Refining the telomere-telomerase hypothesis of aging and cancer. *Nat Biotechnol* 1996; **14**: 836-839

4 **Hoos A,** Hepp HH, Kaul S, Ahlert T, Bastert G, Wallwiener D. Telomerase activity correlates with tumor aggressiveness and reflects therapy effect in breast cancer. *Int J Cancer* 1998; **79**: 8-12

5 **Kyo S,** Takakura M, Tanaka M, Kanaya T, Inoue M. Telomerase activity in cervical cancer is quantitatively distinct from that in its precursor lesions. *Int J Cancer* 1998; **79**: 66-70

6 **Dahsc R,** Ficdler W, Ernst G. Telomeres and telomerase: biological and clinical importance. *Clin Chem* 1997; **43**: 708-714

7 **Yan P,** Coindre JM, Benhattar J, Bosman FT, Guillou L. Telomerase activity and human telomerase reverse transcriptase mRNA expression in soft tissue tumors: correlation with grade, histology, and proliferative activity. *Cancer Res* 1999; **59**: 3166-3170

8 **Feng J,** Funk WD, Wang SS, Weinrich SL, Avilion AA, Chiu CP, Adams RR, Chang E, Allsopp RC, Yu J. The RNA component of human telomerase. *Science* 1995; **269**: 1236-1241

9 **Norton JC,** Piatyszek MA, Wright WE, Shay JW, Corey DR. Inhibition of human telomerase activity by peptide nucleic acids. *Nat Biotechnol* 1996; **14**: 615-619

10 **Harrington L,** Mcphail T, Mar V, Zhou W, Oulton R, Bass MB, Arruda I, Robinson MO. A mammalian telomerase-associated protein. *Science* 1997; **275**: 973-977

11 **Nakayama J,** Saito M, Nakamura H, Matsuura A, Ishikawa F. TLP1: a gene encoding a protein component of mammali telomerase is a novel member of WD repeats family. *Cell* 1977; **88**: 875-884

12 **Nakamura TM,** Morin GB, Chapman KB, Weinrich SL, Andrews WH, Lingner J, Harley CB, Cech TR. Telomerase catalytic subunit homologs from fission yeast and human. *Science* 1997; **277**: 955-959

13 **Meyerson M,** Counter CM, Eaton EN, Ellisen LW, Steiner P, Caddle SD, Ziaugra L, Beijersbergen RL, Davidoff MJ, Liu Q, Bacchetti S, Haber DA, Weinberg RA. hEST2, the putative human telomerase catalytic subun gene, is up-regulated in tumor cells and during immortalization. *Cell* 1997; **90**: 785-795

14 **Kilian A,** Bowtell DD, Abud HE, Hime GR, Venter DJ, Keese PK Duncan EL, Reddel RR, Jefferson RA. Isolation of a candidate human telomerase catalytic subunit gene, which reveals complex splicing pattern in different cell types. *Hum Mol Genet* 1997; **6**: 2011-2019

15 **Blasco MA,** Funk W, Villeponteau B, Greider CW. Functional characterization and developmental regulation of mouse telomerase RNA. *Science* 1995; **269**: 1267-1270

16 **Avilion AA,** Piatyszek MA, Gupta J, Shay JW, Bacchetti S, Greider CW. Human telomerase RNA and telomerase activity in immortal cell lines and tumor tissues. *Cancer Res* 1996; **56**: 645-650

17 **Weinrich SL,** Pruzan R, Ma L, Ouellette M, Tesmer VM, Holt S, Bodnar AC, Lichtsteiner S, Kim NW, Trager JB, Taylor RD, Carlos R, Andrews WH, Wright WE, Shay JW, Harley CB, Morin GB. Reconstitution of human telomerase with the template RNA component hTR and the catalytic protein subunit hTRT. *Nat Genet* 1997; **17**: 498-502

18 **Counter CM,** Meyerson M, Eaton EN, Ellisen LW, Caddle SD, Haber DA, Weinberg RA. Telomerase activity is restored in human cells by ectopic expression of hTERT (hEST2), the catalytic subunit of telomerase. *Oncogene* 1998; **16**: 1217-1222

19 **Ito H,** Kyo S, Kanaya T, Takakura M, Inoue M, Namiki M. Expression of human telomerase subunits and correlation with telomerase activity in urothelial cancer. *Clin Cancer Res* 1998; **4**: 1603-1608

20 **Kondo S,** Tanaka Y, Kondo Y, Hitomi M, Barnett GH, Ishizaka Liu J, Haqqi T, Nishiyama A, Villeponteau B, Cowell JK, Bai BP. Antisense telomerase treatment: induction of two distinct pathways, apptosis and differentiation. *FASEB J* 1998; **12**: 801-811

21 **Kondo S,** Kondo Y, Li G, Silverman RH, Cowell JK. Targeted therapy of human malignant glioma in a mous model by 2-5A antisense directed against telomerase RNA. *Oncogene* 1998; **16**: 3323-3330

22 **Kondo Y,** Kondo S, Tanaka Y, Haqqi T, Barna BP, Cowell JK. Inhibition of telomerase increases the susceptibility of human malignant glioblastoma cells to cisplatin-indueed apoptosis. *Oncogene* 1998; **16**: 2243-2248

23 **Kondo Y,** Koga S, Komata T, Kondo S. Treatment of prostate cancer *in vitro* and *in vivo* with 2-5A-antitelomerase RNA component. *Oncogene* 2000; **19**: 2205-2211

24 **Zhang X,** Mar V, Zhou W, Harrington L, Robinson MO. Telomere shortening and apoptosis in telomerase-inhibited human tumor cells. *Genes Dev* 1999; **13**: 2388-2399

25 **Belair CD,** Yeager TR, Lopez PM, Reznikoff CA. Telomerase activity: a biomarker of cell proliferation, not malignant transformation. *Proc Natl Acad Sci U S A* 1997; **94**: 13677-13682

26 **Holt SE,** Glinsky VV, Ivanova AB, Glinsky GV. Resistance to apoptosis in human cells conferred by telomerase function and telomere stability. *Mol Carcinog* 1999; **25**: 241-248

27 **Greider WC.** Telomerase activity, cell proliferation, and cancer. *Proc Natl Acad Sci U S A* 1998; **95**: 90-92

28 **Bednarek AK,** Sahin A, Brenner AJ, Johnston DA, Aldaz CM. Analysis of telomerase activity levels in breast cancer: positive detection at the in situ breast carcinoma stage. *Clin Cancer Res* 1997; **3**: 11-16

29 **Okusa Y,** Shinomiya N, Ichikura T, Mochizuki H. Correlation between telomerase activity and DNA ploidy in gastric cancer. *Oncology* 1998; **55**: 258-264

30 **Dome JS,** Chung S, Bergemann T, Umbricht CB, Saji M, Carey LA, Grundy PE, Perlman EJ, Breslow NE, Sukumar S. High telomerase reverse transeriptase (hTERT) messenger RNA level correlates with tumor recurrence in patients with favorable histology Wilms' tumor. *Cancer Res* 1999; **59**: 4301-4307

31 **Fu W,** Begley JG, Killen MW, Mattson MP. Anti-apoptotic role of telomerase in phcochromecytoma cells. *J Biol Chem* 1999; **274**: 7264-7271

32 **Holt SE,** Shay JW. Role of telomerase in cellular proliferation and cancer. *J Cell Physiol* 1999; **180**: 10-18

Edited by Ma JY

P.O.Box 2345, Beijing 100023,China
Fax: +86-10-85381893
E-mail: wjg@wjgnet.com www.wjgnet.com

World J Gastroenterol 2003;9(9):1985-1989
World Journal of Gastroenterology
 ISSN 1007-9327

• COLORECTAL CANCER •

Differences in endoscopic classification of early colorectal carcinoma between China and Japan: A comparative study

Ren-Min Zhu, Fang-Yu Wang, Ichiro Hirata, Ken-Ichi Katsu, Shu-Dong Xiao, Zhong-Lin Yu, Zhi-Hong Zhang, Zhao-Min Xu

Ren-Min Zhu, Fang-Yu Wang, Department of Gastroenterology, Jinling Hospital, Nanjing 210002, Jiangsu Provincce, China
Ichiro Hirata, Ken-Ichi Katsu, The Second Department of Internal Medicine, Osaka Medical College, Takatsuki 569-8686, Osaka, Japan
Shu-Dong Xiao, Shanghai Institute of Digestive Diseases, Shanghai 200001, China
Zhong-Lin Yu, Department of Gastroenterology, Capital Medical University, Beijing 100050, China
Zhi-Hong Zhang, Zhao-Min Xu, Department of Gastroenterology, Gulou Hosiptal, Nanjing 210008, China
Supported by Japan-China Sasagawa Medical Fellowship (1999, 22th)
Correspondence to: Ren-Min Zhu, Department of Gastroenterology, Jinling Hospital, Nanjing 210002, Jiangsu Province, China. wangf65@yahoo.com
Received: 2003-05-11 **Accepted:** 2003-06-02

Abstract

AIM: To compare the differences in the endoscopic classification of early colorectal carcinoma (CRC) between Japan and China.

METHODS: Ten cases of early CRC were included in the study. After reviewing the color pictures of these cases, 5 Japanese endoscopists and 5 Chinese endoscopists made their classificatory diagnosis individually using the current Japanese classification, and indicated their findings on which the diagnosis was based.

RESULTS: Some lesions diagnosed by the Japanese endoscopists as IIa or IIa plus IIc, were classified as Is or Isp by the Chinese endoscopists. For superficial lesions consisting of elevation plus central depression, IIa plus depression, IIa plus IIc or IIc plus IIa were classified according to the ratio of elevated area/depressed area. However, international as well as interobserver difference still existed in the classification of such lesions. In addition, most Chinese endoscopists overlooked slightly depressed part on the top of a protruded lesion. Laterally spreading tumor, a special type of IIa, was identified as LST by some Japanese endoscopists.

CONCLUSION: Discrepancies on macroscopic classification for early CRC do exist between Japanese and Chinese endoscopists, which are found not only in terminology but also in recognition of some lesions. In order to develop a universal classification, it needs for international communication and cooperation.

Zhu RM, Wang FY, Hirata I, Katsu KI, Xiao SD, Yu ZL, Zhang ZH, Xu ZM. Differences in endoscopic classification of early colorectal carcinoma between China and Japan: A comparative study. *World J Gastroenterol* 2003; 9(9): 1985-1989
http://www.wjgnet.com/1007-9327/9/1985.asp

INTRODUCTION

ColorectaI carcinoma (CRC) is the most common cancer of digestive system in the Western countries[1,2]. Recently, however, with the westernization of life style and dietary habits, its morbidity and mortality have also increased considerably in both China and Japan[3,4]. A series of clinical studies in many countries have all shown that both CRC incidence and mortality can be significantly reduced by a systematic screening program including endoscopic examination of the large bowel[5-8]. As a result, endoscopic diagnosis and treatment for early lesions have become more and more important in the management of CRC all over the world[9]. Undoubtedly, a worldwide agreed endoscopic classification for early CRCs will be very useful in clinical practice as well as in research[10,11].

Early CRC, according to the Japanese definition, refers to colorectal carcinoma that has not invaded beyond the submucosal layer[12]. Japanese endoscopists have developed their endoscopic classification for early CRCs since the early 1970s, and kept on modifying it. This definition of early CRC, however, has not been formally accepted in the Western countries, where Duke' s classification has been widely used for decades[13,14]. So far there has been no such classification for early CRCs in America and Europe[15]. On the contrary, Chinese doctors hold the same opinion as Japanese on the definition of early CRC, and have established a classification slightly different from the Japanese one. Up to now there has been no comparative study on endoscopic classification of early CRCs between Japan and China. lt is unclear whether Japanese classification can be easily understood and used outside of Japan[16]. This study was conducted in an attempt to clarify these questions and, particularly to evaluate the validity and feasibility of the current Japanese classification.

MATERIALS AND METHODS

Ten typical cases of early CRC were selected in this study from the Second Department of Internal Medicine in Osaka Medical College, Japan. All the diagnoses were proved pathologically, according to the results of nine adenocarcinomas and one adenoma. Five Japanese and five Chinese expert endoscopists were asked to review the colonoscopic pictures of these cases, including those before and after indigocarmine spraying. After viewing the pictures, all the endoscopists individually made their classificatory diagnosis of these cases and indicated the findings on which they based for each classificatory diagnosis. In addition, Chinese doctors were also asked for a comment on the current Japanese classification.

Doctors included in this study all majored in gastroenterological endoscopy. Hereafter their names were alphabetically listed as follows: Ichiro Hirata, Masahiro Itoh, Hiroshi Kashida, Hideki Mitooka, Seiji Shinmizu, Shu-dong Xiao, Zhao-min Xu, Zhong- lin Yu, Zhi-hong Zhang and Ren-min Zhu. The current Japanese classification, established by Japanese Research Society for Cancer of Colon, Rectum and Anus, was used as the referring classification in this study[17].

RESULTS

The results of classification are shown in Table 1. From Table

1, the following differences were indicated in macroscopic classification between Japanese and Chinese doctors.

Table 1 Differences in classification of 10 early CRCs between Japanese and Chinese endoscopists

Case	Classificatory diagnosis	
	Japanese (5)	Chinese (5)
1	IIa+IIc(5)	Is(4), IIa+IIc(1)
2	IIa+IIc(4), Isp+llc(1)	Isp(3), Isp+IIc(1), IIa(1)
3	IIc+IIa(3), IIc(2)	IIc+IIa(4), IIc(1)
4	IIc+IIa(3),IIa+IIc(1),IIa+dep.(1)	IIa+IIc(3), IIc+IIa(2)
5	IIa+dep.(3), IIa(2)	IIa+IIc(3), IIa(2)
6	Ip+IIc(4), IIa+IIc(1)	Ip(3), Ip+IIc(1), IIa+IIc(1)
7	LST(3),IIa agg. (2)	IIa
8	IIa(3), LST(2)	IIb(3), IIa(2)
9	LST(3), IIa(1), IIc(1)	IIc(3), IIb(1), IIa+IIc(1)
10	LST(3), IIa(1), IIc+IIa(1)	IIc+IIa(4), IIa(1)

[a]The numbers in parentheses are numbers of endoscopists; [b]IIa agg. IIa aggregating type.

Distinctly elevated lesions between type I and type II

Case 1 was a distinctly elevated lesion with a diameter of 15 mm and a height of 3.6 mm. The central depression became clear after indigocarmine spraying. This one was classified as IIa plus lIc by all the five Japanese and one Chinese endoscopists, while it was regarded as Is by other four Chinese endoscopists. Case 2 was a protruded lesion with a central depression. The diameter and height were 10 mm and 5.5 mm respectively (Figure 1). It was diagnosed as type IIa plus lIc by all but one Japanese endoscopist, while classified as lsp by three of five Chinese endoscopists. One Japanese and one Chinese endoscopist diagnosed it as Isp plus IIc, while one Chinese endoscopist classified it as IIa.

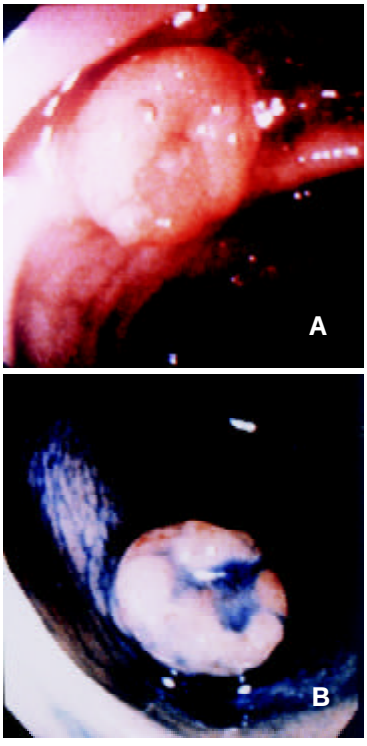

Figure 1 Submucusal adenocarcinoma with a diameter of 10 mm and a height of 5.5 mm. A: before indigocarmine staining, B: after indigocarmine staining.

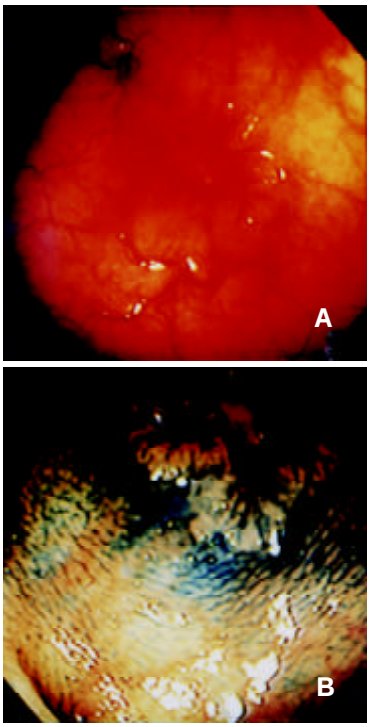

Figure 2 Mucosal adenocarcinoma with a diameter of 13 mm and a height of 1.5 mm. A: before indigocarmine staining, B: after indigocarmine staining.

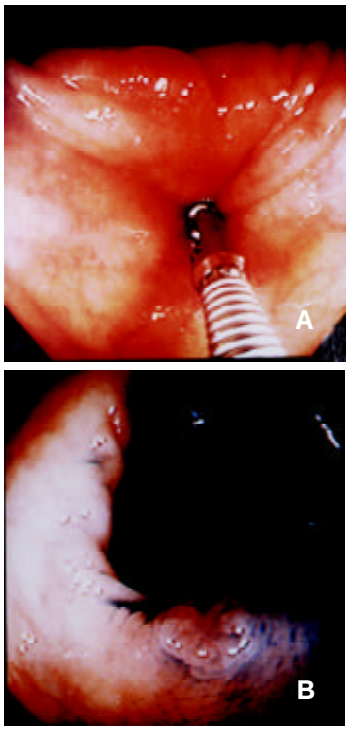

Figure 3 Adenoma with a diameter of 5 mm. A: before indigocarmine staining, B: after indigocarmine staining.

Superficial lesions consisting of elevation with depression

Case 3 was a typical superficially depressed lesion, with a slight circumferential elevation (1.5 mm), which was ambiguous before indigocarmine spraying (Figure 2). Three Japanese and four Chinese endoscopists diagnosed it as IIc plus IIa, while the rest three endoscopists classified it as IIc. Case 4 was a superficial lesion consisting of elevation plus central depression, and it was difficult to judge which part was larger even after indigocarmine spraying. Three Japanese and two

Chinese endoscopists classified it as IIc plus lIa, three Chinese and one Japanese endoscopists classified it as IIa plus IIc, and one Japanese endoscopist diagnosed it as IIa plus depression.

Superficial lesions consisting of elevation with linear depression

Case 5 was a small adenoma consisting of elevation with linear depression (Figure 3). Three Japanese endoscopists diagnosed it as IIa plus depression, while three Chinese endoscopists classified it as IIa plus IIc. The other two Japanese and two Chinese endoscopists diagnosed it as IIa.

Type I lesions with depression on the top

Case 6 was a protruded lesion with a peduncle and a depression on the center of the top (Figure 4). All but one Japanese endoscopist diagnosed it as Ip plus IIc, while three Chinese classified it as Ip. One Chinese endoscopist agreed with most Japanese, while one Japanese and one Chinese endoscopist classified it as IIa plus IIc.

Laterally spreading tumors

Case 7 was an extensively superficial elevated lesion with a diameter of 26 mm. Three Japanese doctors diagnosed it as LST granular type, and the other 2 Japanese doctors classified it as IIa aggregating type. However, five Chinese doctors all regarded it as IIa (Figure 5).

Case 8 was also a superficially elevated lesion with a diameter of 15 mm. The surface was rather smooth as compared to Case 7. Two Japanese endoscopists regarded it as LST non-granular type, three Chinese endoscopists diagnosed it as II b, while the rest five doctors classified it as IIa.

Case 9 was an extensive superficially elevated lesion with some depression, its diameter was 20 mm. Three Japanese doctors diagnosed it as LST plus "pseudo-depression", while three Chinese and one Japanese doctor regarded it as IIc. The rest doctors classified it as IIb, IIa, or IIa plus IIc, respectively.

Case 10 was also a superficial lesion extending horizontally with some depression, which was regarded as "pseudo-depression" in LST by three Japanese doctors. One Japanese and 4 Chinese doctors classified it as II c plus IIa (Figure 6).

Figure 4 Submucosal adenocarcinoma with a diameter of 8 mm. A: before indigocarmine staining, B: after indigocarmine staining.

Figure 5 Mucosal adenocarcinma with a diameter of 26 mm. A: before indigocarmine staining, B: after indigocarmine staining.

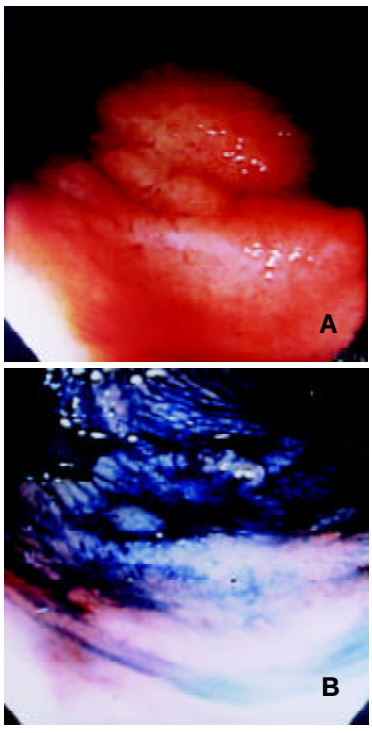

Figure 6 Submucosal adenocarcinoma with a diameter of 28 mm. A: before indigocarmine staining, B: after indigocarmine staining.

DISCUSSION

The endoscopic classification of early CRC in China was established on the basis of the Japanese classification for early gastric cancer, and has remained unchanged so far[18]. The Japanese classification, however, was developed 30 years ago and has been modified continually since then. Even so, the discrepancies are still common among Japanese colonoscopists, especially on the classification of type II lesions consisting of

elevation plus depression[19]. This was illustrated best in a recent panel discussion in Japan[20,21]. Most doctors in China regard the current Japanese classification as a comprehensive one, although some new concepts seem to be complicated and confusable. One of the differences between two classifications is that IIb, IIc and IIc plus IIa are not included in the Chinese one, for lack of such experiences in China[22]. Moreover, Chinese endoscopists are not familiar with the concept of IIa plus depression and LST. Actually, reports on superficial early CRC are few in China, which deal with depressed type. Most early CRC cases reported by Chinese endoscopists were the so-called local canceration of polyps and/or adenomas, which were diagnosed mainly after endoscopic polypectomy[23]. All these facts may explain why there are some differences in endoscopic classification of early CRC between doctors from two countries.

Some elevated lesions classified as type II in Japan might be diagnosed as Is or Isp by Chinese endoscopists. Case 1 and Case 2 were two examples. It should be emphasized that the definitions of type I and type II are exactly the same in Japan and in China. Therefore, the difference here was not in terminology but in interpretation of the same findings. In other words, the judging criteria for the height of a lesion were not the same in two countries. It is suggested that IIa should be the lesion with its height/diameter less than 1/2, therefore those with their height/diameter lager than 1/2 should be included in type I[24]. Now that the ratio for case 2 is 5.5/10, just a little bit larger than 1/2. It might be difficult to measure the accurate height of a lesion during endoscopic examination because of air-induced deformation[25]. This might be one of the reasons why international and interobserver differences occurred in the classification of such lesions.

For lesions that consist of superficial elevation plus superficial depression, many (if not all) Japanese endoscopists may classify them as IIa plus llc or IIc plus IIa, according to the ratio of elevation/depression, i.e. the large one is regarded as the main part and described first[26,27]. This is also the case in China[18]. Although international difference is not significant, interobserver differences still exist in classifying these lesions, which were indicated in case 3 and case 4.

In Japan, IIa plus depression has been used to refer to a small superficially elevated lesion with pseudo-depression or linear depression, which is always found to be adenoma pathologically[28]. This kind of lesion may appear to be IIa plus IIc or IIc plus IIa after dye spraying, although it has no well-demarcated depression. However, the current Chinese classification is not comprehensive, and does not include IIa plus depression. Furthermore, many new techniques such as chromoendoscopy or magnifying endoscopy has not been widely used in China[29,30]. Although the current Japanese classification was presented to the Chinese endoscopists, the definition of IIa plus depression might be too difficult to be understood completely in such a short time. There is no wonder that some Chinese endoscopists either overestimated the linear depression or simply neglected it, thus case 5 was diagnosed of either as IIa plus IIc or as IIa.

Similarly, to a protruded lesion with depression on the top, many Chinese endoscopists either not knew or simply neglected the depressed parts, thus diagnosed it as Is, Isp or Ip, while it should be classified as Is plus IIc, Isp plus IIc and Ip plus IIc, respectively according to most Japanese colonoscopists[31]. This tendency was indicated in case 1, case 2 and case 6.

LST, according to the definition recommended by Kudo, refers to a superficially elevated lesion that mainly grows horizontally rather than vertically, and its largest diameter is no less than 10 mm[32]. It is also suggested that LST should be classified into two subtypes, granular and non-granular, and the former may be further divided into homogeneous and mixed nodular. Our results indicated that international as well as inter-observer discrepancies were significant in the classification of such lesions. For case 7, the so-called mixed nodular LST or IIa aggregating type in Japan, Chinese endoscopists usually diagnosed it as IIa, though they also pointed out that it was a clustered nodular lesion[33]. The difference here might be just a difference in terminology.

Interestingly, three out of five Chinese endoscopists classified case 8 as IIb, which was regarded as LST non-granular type by most Japanese doctors. IIb has been defined as a lesion that is on the same level with the surrounding normal mucus in both Japanese and Chinese definition[34,35]. That is to say, Chinese endoscopists might have overlooked or simply neglected the slight elevation in case 8.

Case 9 and case 10 were rather complicated lesions, which were classified differently because the interpretations were different to the depressed parts of these lesions[36]. For those who classified them as LST, "pseudo-depression" was used to refer the depressed parts, and for those who classified them as IIc or IIc plus IIa, "authentic" rather than "pseudo" depression was interpretated, while for those who classified them as IIa, the so-called "pseudo-depression" was simply neglected.

In conclusion, differences in the endoscopic classification of early CRC do exist between Japan and China. In order to develop a universal endoscopic classification for early CRC, it needs for international communication and cooperation.

ACKNOWLEDGEMENTS

We thank Drs. Seiji Shinmizu, Masahiro Itoh, Hideki Mitooka and Hiroshi Kashida for their expert assistance in this study.

REFERENCES

1 **Bond JH**. Colorectal cancer screening. *Curr Opin Oncol* 1998; **10**: 461-466
2 **Breen N**, Wagener DK, Brown ML, Davis WW, Ballard-Barbash R. Progress in cancer screening over a decade: results of cancer screening from the 1987, 1992, and 1998 National Health Interview Surveys. *J Natl Cancer Inst* 2001; **93**: 1704-1713
3 **Wan J**, Zhang ZQ, Zhu C, Wang MW, Zhao DH, Fu YH, Zhang JP, Wang YH, Wu BY. Colonoscopic screening and follow-up for colorectal cancer in the elderly. *World J Gastroenterol* 2002; **8**: 267-269
4 **Kudo SE**, Hara E. New trends in diagnosis and treatment of depressed and flat type neoplasms in colon and rectum. *Nippon Shokakibyo Gakkai Zasshi* 2002; **99**: 463-468
5 **Schroy PC**, Heeren T, Bliss CM, Pincus J, Wilson S, Prout M. Implementation of on- site screening sigmoidoscopy positively influences utilization by primary care providers. *Gastroenterology* 1999; **117**: 304-311
6 **Smith GA**, Oien KA, O'Dwyer PJ. Frequency of early colorectal cancer in patients undergoing colonoscopy. *Br J Cancer* 1999; **86**: 1328-1331
7 **Koka VK**, Potti A, Fraiman GN, Hanekom D, Hanley JF. An epidemiological study evaluating the relationship of distance from a tertiary care cancer center to early detection of colorectal carcinoma. *Anticancer Res* 2002; **22**: 2481-2483
8 **Dove-Edwin I**, Thomas HJ. Review article: the prevention of colorectal cancer. *Aliment Pharmacol Ther* 2001; **15**: 323-336
9 **Hart AR**, Wicks AC, Mayberry JF. Colorectal cancer screening in asymptomatic populations. *Gut* 1995; **36**: 590-598
10 **Fujii T**, Rembacken BJ, Dixon MF, Yoshida S, Axon AT. Flat adenomas in the United Kingdom: are treatable cancers being missed? *Endoscopy* 1998; **30**: 437-443
11 **Read TE**, Kodner IJ. Colorectal cancer: risk factors and recommendations for early detection. *Am Fam Physician* 1999; **59**: 3083-3092
12 **Kudo S**, Kashida H, Nakajima T, Tamura S, Nakajo K. Endoscopic diagnosis and treatment of early colorectal cancer. *World J Surg* 1997; **21**: 694-701
13 **Sternberg A**, Sibirsky O, Cohen D, Blumenson LE, Petrelli NJ. Validation of a new classification system for curatively resected colorectal adenocarcinoma. *Cancer* 1999; **86**: 782-792

14 **Schlemper RJ**, Itabashi M, Kato Y, Lewin KJ, Ridell RH, Shimoda T, Sipponen P, Stolte M, Watanabe H. Differences in the diagnostic criteria used by Japanese and Western pathologists to diagnose colorectal carcinoma. *Cancer* 1998; **82**: 60-69

15 **Mainprize KS**, Mortensen NJ, Warren BF. Early colorectal cancer: recognition, classification and treatment. *Br J Cancer* 1998; **85**: 469-476

16 **Smith RA**, Cokkinides V, Von Eschenbach AC, Levin B, Cohen C, Runowicz CD, Sener S, Saslow D, Eyre HJ. American Cancer Society guidelines for the early detection of cancer. *CA Cancer J Clin* 2002; **52**: 8-22

17 **Japanese Research Society for Cancer of the Colon, Rectum and Anus**. General rules for clinical and pathological studies on cancer of colon, rectum and anus (6th ed). *Tokyo: KinbaraShuppan* 1998: 32-36

18 **Zhang YL**, Zhang ZS, Wu BP, Zhou DY. Early diagnosis for colorectal cancer in China. *World J Gastroenterol* 2002; **8**: 21-25

19 **Kudo S**, Kashida H, Tamura S, Nakajima T. The problem of "flat" colonic adenoma. *Gastrointest Endosc Clin N Am* 1997; **7**: 87-98

20 **Hirata L.** Issues in macroscopic classification of early colorectal carcinoma¨Dmy criterion in diagnosis. *Stomach and Intestine* 1999; **34**: 23

21 **Ishiguro A**, Uno Y, Ishiguro Y, Munakata A, Morita T. Correlation of lifting versus non-lifting and microscopic depth of invasion in early colorectal cancer. *Gastrointest Endosc* 1999; **50**: 329-333

22 **Schlemper RJ**, Hirata I, Dixon MF. The macroscopic classification of early neoplasia of the digestive tract. *Endoscopy* 2002; **34**: 163-168

23 **Li Z**, Zhang S, An D, Chen F, Gong J. Diagnosis and treatment of early colorectal cancer. *Zhonghua Waike Zazhi* 2000; **38**: 352-354

24 **Baba Y,** Suzuki Y, Kobayashi M, Azumaya M, Takeuchi M, Shioji K, Honma T, Narisawa R, Ajioka Y, Asakura H. Superficial depressed-type cancer monitored by colonoscopy through the early phase of invasion. *Endoscopy* 2002; **34**: 738-741

25 **Okabe S**, Arai T, Maruyama S, Murase N, Tsubaki M, Endo M. A clinicopathological investigation on superficial early invasive carcinomas of the colon and rectum. *Surg Today* 1998; **28**: 687-695

26 **Tsuda S**, Veress B, Toth E, Fork FT. Flat and depressed colorectal tumours in a southern Swedish population: a prospective chromoendoscopic and histopathological study. *Gut* 2002; **51**: 550-555

27 **Yoshida S**. Endoscopic diagnosis and treatment of early cancer in the alimentary tract. *Digestion* 1998; **59**: 502-508

28 **Kiesslich R**, von Bergh M, Hahn M, Hermann G, Jung M. Chromoendoscopy with indigocarmine improves the detection of adenomatous and nonadenomatous lesions in the colon. *Endoscopy* 2001; **33**: 1001-1006

29 **Hurlstone DP**, Fujii T, Lobo AJ. Early detection of colorectal cancer using high-magnification chromoscopic colonoscopy. *Br J Surg* 2002; **89**: 272-282

30 **Kuramoto S**, Mimura T, Yamasaki K, Kobayashi K, Hashimoto M, Sakai S, Kaminishi M, Oohara T. Flat cancers do develop in the polyp-free large intestine. *Dis Colon Rectum* 1997; **40**: 534-539

31 **Kato H**, Haga S, Endo S, Hashimoto M, Katsube T, Oi I, Aiba M, Kajiwara T. Lifting of lesions during endoscopic mucosal resection (EMR) of early colorectal cancer: implications for the assessment of resectability. *Endoscopy* 2001; **33**: 568-573

32 **Kudo S**, Kashida H, Tamura T, Kogure E, Imai Y, Yamano H, Hart AR. Colonoscopic diagnosis and management of nonpolypoid early colorectal cancer. *World J Surg* 2000; **24**: 1081-1090

33 **Kudo S**, Tamegai Y, Yamano H, Imai Y, Kogure E, Kashida H. Endoscopic mucosal resection of the colon: the Japanese technique. *Gastrointest Endosc Clin N Am* 2001; **11**: 519-535

34 **Saitoh Y**, Obara T, Watari J, Nomura M, Taruishi M, Orii Y, Taniguchi M, Ayabe T, Ashida T, Kohgo Y. Invasion depth diagnosis of depressed type early colorectal cancers by combined use of videoendoscopy and chromoendoscopy. *Gastrointest Endosc* 1998; **48**: 362-370

35 **Nagata S**, Tanaka S, Haruma K, Yoshihara M, Sumii K, Kajiyama G, Shimamoto F. Pit pattern diagnosis of early colorectal carcinoma by magnifying colonoscopy: clinical and histological implications. *Int J Oncol* 2000; **16**: 927-934

36 **Rembacken BJ**, Fujii T, Cairns A, Dixon MF, Yoshida S, Chalmers DM, Axon AT. Flat and depressed colonic neoplasms: a prospective study of 1000 colonoscopies in the UK. *Lancet* 2000; **355**: 1211-1214

Edited by Zhang JZ and Wang XL

P.O.Box 2345, Beijing 100023,China
Fax: +86-10-85381893
E-mail: wjg@wjgnet.com www.wjgnet.com

World J Gastroenterol 2003;9(9):1990-1994
World Journal of Gastroenterology
 ISSN 1007-9327

• COLORECTAL CANCER •

Role of COX-2 in carcinogenesis of colorectal cancer and its relationship with tumor biological characteristics and patients' prognosis

Ai-Wen Wu, Jin Gu, Jia-Fu Ji, Zhen-Fu Li, Guang-Wei Xu

Ai-Wen Wu, Jin Gu, Jia-Fu Ji, Guang-Wei Xu, Department of Surgery, Peking University, School of Oncology, Beijing Cancer Hospital, Beijing Institute for Cancer Research, Beijing 100036, China
Zhen-Fu Li, Department of Biochemistry, Peking University, School of Oncology, Beijing Cancer Hospital, Beijing Institute for Cancer Research, Beijing 100036, China
Correspondence to: Dr. Jin Gu, Fucheng Road, No.52, Haidian District, Beijing 100036, China. zlguj@bjmu.edu.cn
Telephone: +86-10-88141032 **Fax**: +86-10-88122437
Received: 2003-05-10 **Accepted:** 2003-06-02

Abstract

AIM: Recent clinical epidemiological studies have demonstrated the preventive effect of non-steroidal anti-inflammatory drugs (NSAIDs) against colorectal cancer. The underlying mechanism might be the inhibition of rate-limiting enzyme cyclooxygenase-2 (COX-2) in metabolism of arachidonic acid. The role of COX-2 in carcinogenesis of colorectal cancer and its relationship with tumor biological characteristics and patients' prognosis still remain unclear. This study was to investigate the role of COX-2 expression in carcinogenesis of colorectal cancer and its relationship with tumor biological characteristics and patients' prognosis.

METHODS: A total of 139 colorectal cancers and 19 adenomas surgically treated in School of Oncology, Peking University, from January 1993 to September 2001 were retrospectively studied. COX-2 expression was detected with tissue microarray (TMA) and immunohistochemistry (IHC) procedure. The association between COX-2 expression and clinicopathological features and its influence on patients' prognosis were studied.

RESULTS: COX-2 expression was strong in colorectal cancer, moderate in adenoma and weak in normal mucosa, which demonstrated statistically significant difference (χ^2=46.997, P<0.001). COX-2 expression had no association with clinicopathological features such as gross type, differentiation, invasion depth, vessel emboli and TNM staging. Cox proportional hazards modeling analysis and Log rank test revealed no prognostic role of COX-2 expression in colorectal cancer patients.

CONCLUSION: COX-2 may play an important role in the early stage of carcinogenesis, and its expression in colorectal cancer is not associated with clinicopathological features and patients' prognosis.

Wu AW, Gu J, Ji JF, Li ZF, Xu GW. Role of COX-2 in carcinogenesis of colorectal cancer and its relationship with tumor biological characteristics and patients' prognosis. *World J Gastroenterol* 2003; 9(9): 1990-1994

http://www.wjgnet.com/1007-9327/9/1990.asp

INTRODUCTION

Cyclooxygenase (COX) is one of the rate-limiting enzymes in metabolism of arachidonic acid that catalyzes the arachidonic acid into a series of products such as prostaglandins and other eicosanoids. It has two isoforms, COX-1 and COX-2. COX-2 acts as both superoxidase and peroxidase that can transform arachidonic acid into PGG_2, then PGH_2. COX-2 is inducibly expressed in many human tissues by cytokines, oncogenes and tumor promoters[1-3]. Recent clinical epidemiological studies have demonstrated the preventive effect of COX inhibitors[4-6]. Cellular and animal experimental studies indicated its relevance to tumor invasion, metastasis, cell apoptosis, cell cycle, and body immunity[7]. Carcinogenesis and development of colorectal cancer are multistep and multistage processes involving cumulative effects of many genes[8,9]. It would contribute to cancer prevention and treatment to illuminate the role of COX-2 in the carcinogenesis of colorectal cancer.

MATERIALS AND METHODS

Patients and tissues

A total of 170 patients underwent surgical treatment in School of Oncology, Peking University, from January 1993 to September 2001 were retrospectively studied. All the patients including 70 males and 69 females (M:F=1.01:1) with median age 59 years (22-89) received pathological examination. There were 4, 12, 4, 3, 4, 6, 21 and 85 cases of the cancer located in ileocecum, ascending colon, hepatic flexture, tranverse colon, splenic flexture, descending colon, sigmoid colon and rectum, respectively. As to the invasion depth, one case was in mucosa, 5 in submucosa, 29 in muscularis propria, 60 in serosa or adventitia, 40 beyond serosa or adventitia or in adjacent tissue. All the patients were followed up till October 2001.

Another 19 cases of colorectal adenomas and 29 normal colorectal tissues concurrently resected were selected for study, including 8 tubular adenomas, 7 villous adenomas and 4 tubulavillous adenomas.

Tissue array preparation

Formalin-fixed and paraffin-embedded tissues were subjected to routine sectioning of 3-5 μm thickness and HE staining. Two typical tumor spots were chosen under microscopy for each case and marked on the corresponding spot on the tissue block. Then cyclinderic tissue columns were punctured with tissue arrayer (Beecher Instruments, USA) in the marked area and transferred to corresponding receiver pore of the prepared block. The tissue array block was then completed according to the predetermined scheme. The block was heated at 40 ℃ for 15 min and the surface was flattened for subsequent section of 5 μm thickness[10].

Immunohistochemical staining

Two step immunohistochemical staining was used for COX-2 detection. Tissue sections were dewaxed in xylene for 30 min, rehydrated through graded alcohol to PBS, then inmmersed in

3 % hydrogen peroxide at room temperature for 10 min to quench endogeneous peroxidase activity. After washed with PBS, the sections were subjected to antigen retrieval in boiling sodium citrite buffer (0.01M, pH 6.0) for 10 min (microwave 450W). After cooled at room temperature, and washed with PBS and distilled water sequentially, 100 μl of diluted anti-COX-2 murine antibody from Cayman Chemical, USA (1:200) was applied for each section. Then the slides were incubated overnight in a humidified chamber. After washed with PBS, each of the sections was incubated at 37 ℃ for 45 min with 100 μl of goat anti-mouse IgG from Zhongshan Biological Corp, Beijing, China. After washed with PBS again, the sections were subjected to sequential 3, 3-diaminobenzidine (DAB Kit, Zhongshan Biological Corp, Beijing, China) for immune complex visualization and then counterstained with haemotoxylin for 30 seconds. Formalin-fixed and paraffin-embedded sections of human colon carcinoma with strong staining served as positive control whereas PBS instead of antibody as negative control. The COX-2 staining was independently reviewed by two immunohistochemistry experts. Microscopically, the slides with no staining in negative control and specific dark yellow staining of cytoplasm and neuclear membrane in positive control were eligible for further analysis. Semiquantitative scoring system was adopted according to the staining intensity: 0 for no staining, 1 for weak yellow, 2 for dark yellow and 3 for brown staining with granular distribution. The mean score was used for statistical analysis and the threshold for positivity was 2[11].

Statistical analysis

All statistical analyses were carried out with SPSS software, 10.0, USA. The relationship between COX-2 expression and categorical variables was compared with χ^2 test or Fisher two-sided exact test. Continuous variables were analyzed with *t* test and $P<0.05$ was considered significant. Cox proportional hazards model and Log rank test as well as Kaplan-Meier were used for multivariate analysis of prognostic factors and survival estimation[12].

RESULTS

Localization of COX-2 protein

Immunohistochemical assay demonstrated that COX-2 protein was located in the cytoplasm and nuclear membrane. The staining was weak yellow, dark yellow and brown at a low power field and diffuse or granular staining at a high power field under microscopy (Figures 1A-C).

Expression of COX-2 in colorectal tissues

A weak staining of COX-2 was observed in normal tissue with a positive rate of 24.1 % (7/29). COX-2 expression was relatively stronger in adenoma and the rate of positivity was 57.9 % (11/19) (Figure 1D). COX-2 expression was much stronger in the tumor cells with dark yellow or brown staining with occasional granular distributions. Some sections revealed gradual staining escalation from normal mucosa, adenoma to carcinoma. 84.9 % of the cancer tissues scored not lower than 2 were considered positive, which much higher than those in normal and adenomatous tissues ($P<0.01$).

Relationship between COX-2 expression and clinicopathological factors of colorectal cancer

The study failed to find the correlation between COX-2 expression in tumor and factors such as age and gender of the patients, tumor location, size, gross type, differentiation, invasion depth, vessel emboli, lymph node metastasis, haemotogenous metastasis and TNM staging (Table 1).

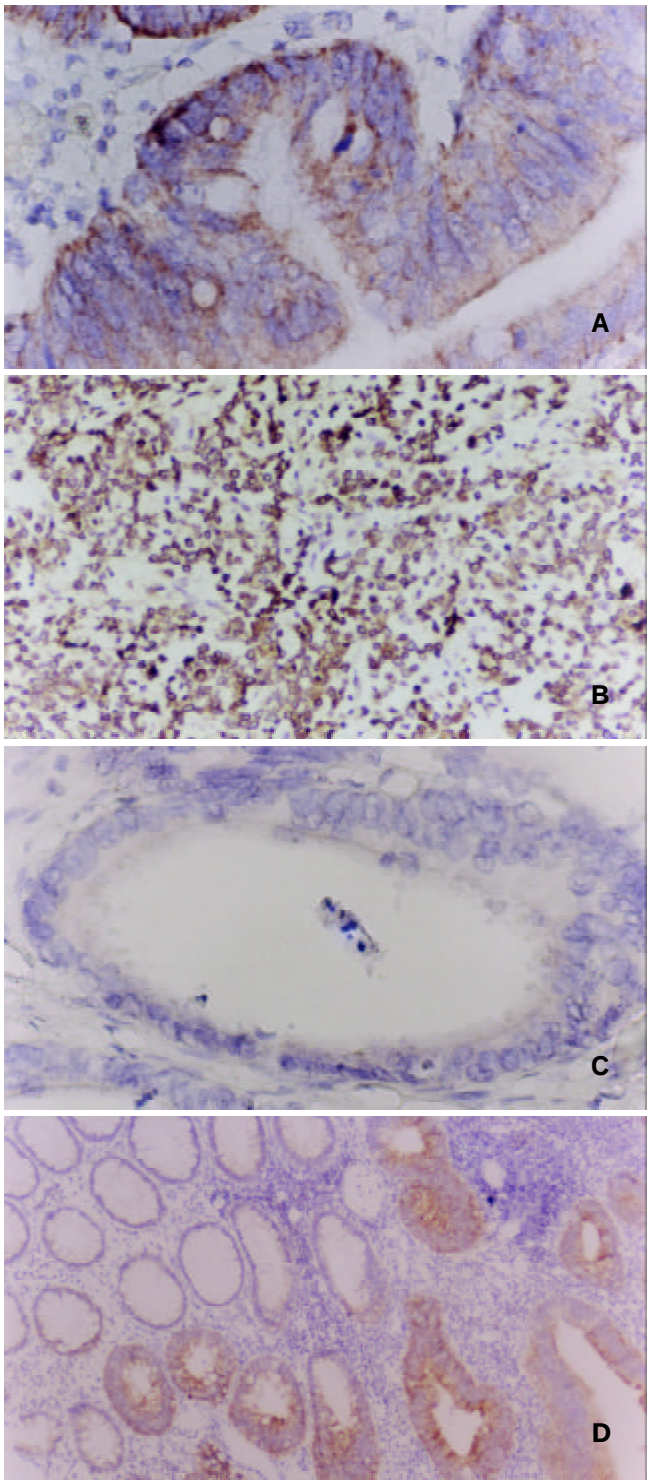

Figure 1 A: Well-differentiated adenocarcinoma of colon, COX-2 immunostaining, ×400; B: Poorly-differentiated adenocarcinoma of colon, COX-2 immunostaining, ×400; C: Negative control, COX-2 immunostaining, ×400; D: Adenoma of colon, COX-2 immunostaining, ×200.

Prognostic factor analysis of colorectal cancer patients

The median follow-up period was 55 months for the whole group (1-106 months). Two cases were missed and the follow-up rate was 98.5 %. Two and five-year survival rates of the whole group were 79.9 % and 61.6 %, respectively.

Eligible prognostic factors such as age and gender of the patients, tumor location, size, gross type, differentiation, invasion depth, vessel emboli, lymph node metastasis, COX-2 expression and TNM staging were introduced into the Cox proportional hazards model and analyzed using the backward:

wald method. The results demonstrated that TNM staging and vessel emboli were independent prognostic factors while COX-2 expression did not affect the prognosis of colorectal cancer patients (Figure 2).

Table 1 Relationship between COX-2 expression and clinicopathological factors in colorectal cancer

Item	Total	COX-2 positive	Positive rate (%)	χ^2 value	*P* value
Gender				0.557	0.455
Male	70	61	87.1		
Female	69	57	82.6		
Tumor location				0.006	0.939
Colon	54	46	85.1		
Rectum	85	72	84.7		
Gross type				0.330	0.848[a]
Protruding or fungoid	59	50	84.7		
Ulcerative	76	65	85.5		
Infiltrative	4	3	75.0		
Differentiation				3.917	0.417[a]
Papillary	3	3	100.0		
Well-differentiated	56	49	87.5		
Moderately-differentiated	52	42	80.8		
Poorly-differentiated	11	8	72.7		
Mucinous / signet cell	17	16	94.1		
Invasion depth				0.188	0.910
Mucosa to muscularis propria	35	29	82.8		
Serosa or adventitia	60	51	85.0		
Extraserosa or extraadventitia	44	38	86.4		
TNM staging				0.985	0.811[a]
Stage I	32	26	81.3		
Stage II	50	43	86.0		
Stage III	44	37	84.1		
Stage IV	13	12	92.3		
Vessel emboli				0.003	0.955
Yes	39	33	84.6		
No	100	85	85.0		
Lymph node metastasis				0.234	0.628
Yes	53	44	83.0		
No	86	74	86.0		
Haemotogenous metastasis				1.108	0.292
Yes	40	32	80.0		
No	86	75	87.2		
Age	57.2±3.1	57.3±1.2	0.962[b]		
Maximal diameter (cm)	4.3±0.3	4.6±2.9	0.599[b]		

[b]refers to with *t* test, others with χ^2 test or Fisher two side exact test; [a]refers to that more than 25 % of the theoretical values were less than 5 and no statistical significance was reached even after the combination.

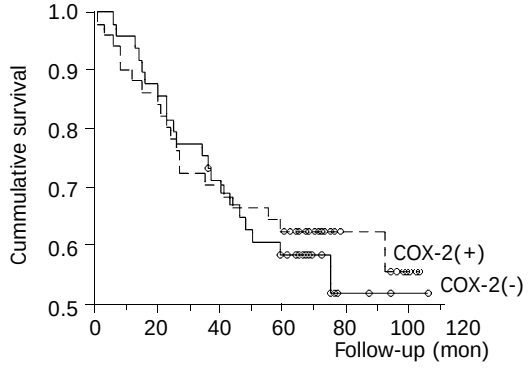

Figure 2 COX-2 expression and patients' survival (Kaplan-Meier curve).

DISCUSSION

Cumulative studies have demonstrated that COX-2 plays an important role in the carcinogenesis and development of many kinds of human cancers such as colorectal cancer[7,13], gastric cancer[14,15], lung cancer[16] and esophageal cancer[17]. Most of the colorectal cancers are derived from adenomas. Many genes are involved in the course from normal colorectal mucosa, adenoma to cancer such as APC, DCC, p53, etc[9,18-23]. The rate of COX-2 expression increases with the course of cancer development. As identified in our study, we found that most normal tissues with negative or weak positive staining had a positive rate of 24.1 % (7/29), adenomatous tissues stained stronger had a positive rate of 57.9 % (11/19), while the positive rate in cancer reached 84.9 %. A statistically significant difference existed (χ^2=46.997, P<0.001) among the three groups. In addition, some sections revealed a significant trend of gradual staining escalation from normal mucosa, adenoma to carcinoma. The present data indicated that COX-2 might be involved in early carcinogenesis, which was also supported by animal experiments. Oshima *et al*[24] found that when the COX-2 gene in a familiar adenomatous polyposis mouse model Apc Δ 716 was knocked out, the number of colon polyps decreased and the size reduced significantly. The same inhibitory effect was noted when the specific COX-2 inhibitor was used[13,25]. As stated in the prospective study on 60 000 people, the relative risk factor for colorectal cancer was reduced to 0.60 when more than 16 tablets of aspirin, a non-specific COX-2 inhibitor, was taken daily[4]. This conclusion was verified by subsequently prospective randomized trials[5,6,26,27].

The characteristics of invasion and metastasis are acquired when carcinogenesis of epithelial cells in colon mucosa occurs. Thus cancer cells might invade through the mucosa, submucosa, muscularis propria and even the adventitia to the adjacent tissues. When blood and lymphatic vessels are invaded, metastasis might occur. Invasion and metastasis are also a multistage process[28] involving many genes including COX-2. Caco-2 cell line, when transfected with COX-2, acquires increased invasiveness. It was found that COX-2 overexpressing Caco-2 cells increased about 6 times in its ability of invasion and had more lateral extension. Furthermore, metallioproteinase-2 was activated and the expression of membrane-type metallioproteinase also increased 2.8 times than the control[29], indicating the involvement of COX-2 and its metabolites in tumor invasion[30]. Tomazawa *et al*[31] injected mouse cell line colon-26 into the tail vein of VALA/C mice with simultaneous administration of JTE-52, a selective COX-2 inhibitor, into the abdominal cavity. The results showed that JTE-52 group with COX-2 overexpression had less lung metastasis than the control, but no difference was found in the group with low COX-2 expression. Therefore, COX-2 expression might be associated with metastasis of colorectal cancer, especially haematogenous metastasis.

Few clinical data are available on the relationship between COX-2 expression and clinicopathological characteristics of colorectal cancer. Thus we carried out this study in 170 colorectal cancer patients surgically treated in our institution with tissue microarray assay and tried to illustrate the relationship between COX-2 expression and clinicopathological factors of colorectal cancer. For certain reasons, only 139 cases could be analyzed and 84.9 % of the cases were positively stained according to our modified criteria of staining intensity, which combined the Masanaga' s criteria[11] with characteristics of tissue microarray technique. Among the 107 cases of advanced colorectal cancer, the expression rate of COX-2 was 86.1 %, 84.1 %, 92.3 % in stages II, III, and IV respectively. Even in stage I, COX-2 expression could reach 81.3 %. The data

indicated that COX-2 expressed high in cancer tissues. Further analysis showed that COX-2 protein expression increased with the invasion depth, its positive rate was 80 %, 82.8 %, 85 % to 86.4 % from submucosa, muscularis, serosa/adventitia to extraserosa/extraadventitia and adjacent tissues respectively, though it did not reach statistical significance (P=0.910).

Two pathways for colorectal cancer metastasis are the lymphatic and haemotogenous pathways. Masunaga *et al*[11] reported that there was a significant difference between the two groups with less or more than 3 metastatic lymph nodes based on their study in 100 patients. However, no statistical difference was found between the two groups with/without or <3 or ⩾3 lymph nodes metastasis in our study. It was inconsistent with the results of Masunaga *et al*[11]. One hundred and twenty-two colorectal cancer patients had no haemotogenous metastasis preoperatively. Forty cases of haemotogenous metastasis were found at the end of follow-up, in which 32 COX-2 positive patients had carcinoma (32/107) while 8 out of 19 COX-2 negative patients had haemotogenous metastasis. Still no correlation was found between COX-2 expression and haemotogenous metastasis. Contrary to our results, Tomozawa *et al*[32] from Japan demonstrated that COX-2 expression was correlated with haemotogenous metastasis especially in the recurrence of colorectal cancer both in clinical studies and in animal experiments. High COX-2 expression group showed a higher rate of haemotogenous metastasis. As an explanation, tumor invasion and metastasis are such a complex course that involves multiple genes. Thus, the role of one single gene should be carefully evaluated.

Few studies are available on COX-2' s role as a prognostic factor, and there are still different opinions[11,31]. Reports from Tomazawa *et al*[32] indicated that COX-2 expression was the only significant prognostic factor while the traditional TNM staging did not reach statistical significance. Our study introduced 13 eligible prognostic factors such as age and gender of the patients, tumor location, size, gross type, differentiation, invasion depth, vessel emboli, lymph node metastasis, COX-2 expression and TNM staging into the analysis, and found that TNM staging and vessel emboli could serve as independent prognostic factors instead of COX-2 expression. This was consistent to the results from Masunaga *et al* that also demonstrated that prognosis involved many factors and many genes, and expression of one single gene was not sufficient to determine the patients' prognosis.

In conclusion, our study found that COX-2 protein expression increased gradually from normal tissue, adenoma to carcinoma and no association existed between COX-2 expression and clinicopathological factors as well as prognosis of colorectal cancer patients. Therefore, it is concluded that COX-2 may play an important role in the early stage of carcinogenesis. Though involvement of COX-2 has been established, further study is needed to clarify its role in the development of colorectal cancer.

REFERENCES

1 **Williams CS**, Mann M, DuBios RN. The role of cyclooxygenases in inflammation, cancer, and development. *Oncogene* 1999; **18**: 7908-7916

2 **Egil F**. Biochemistry of cyclooxygenase (COX-2) inhibitors and molecular pathology of COX-2 in neoplasia. *Crit Rev Clin Lab Sci* 2000; **37**: 431-502

3 **Subbaramaiah K**, Dannenberg AJ. Cyclooxygenase2: a molecular target for cancer prevention and treatment. *Trends Pharmaco Sci* 2003; **24**: 96-102

4 **Thun MJ**, Hennekenn CH. Aspirin and other non-steroidal anti-inflammatory drugs and the risk of cancer development. In: DeVitt VT, Hellman S, Rosenberg SA. Cancer: principles and practice of oncology. 6th edition. Philadelphia: *Lippincott Williams & Wilkins Press, U S A* 2001: 601-607

5 **Kawamori T**, Rao CV, Seibert K, Reddy BS. Chemopreventive activity of celecoxib, a specific cyclooxygenase-2 inhibitor, against colon carcinogenesis. *Cancer Res* 1998; **58**: 409-412

6 **Reddy BS**, Rao CV, Seibert K. Evaluation of cyclooxygenase-2 inhibitor for potential chemopreventive properties in colon carcinogenesis. *Cancer Res* 1996; **56**: 4566-4569

7 **Dannenberg AJ**, Zakim D. Chemoprevention of colorectal cancer through inhibition of cyclooxygenase-2. *Semin Oncol* 1999; **26**: 499-504

8 **Fearon ER**, Vogelstein B. A genetic model for colorectal tumorigenesis. *Cell* 1990; **61**: 759-767

9 **Dicato M**, Berchem G, Duhem C, Ries F. The biology of colorectal cancer. *Semin Oncol* 2000; **27**(5 Suppl 10): 2-9

10 **Kononen J**, Bubendorf L, Kallioniemi A, Barlund M, Schraml P, Leighton S, Torhorst J, Mihatsch MJ, Sauter G, Kallioniemi OP. Tissue microarrays for high-throughput molecular profiling of tumor specimens. *Nat Med* 1998; **4**: 844-847

11 **Masunaga R**, Kohno H, Dhar DK, Ohno S, Shibakita M, Kinugasa S, Yoshimura H, Tachibana M, Kubota H, Nagasue N. Cyclooxygenase-2 expression correlates with tumor neovascularization and prognosis in human colorectal carcinoma patients. *Clin Cancer Res* 2000; **6**: 4064-4068

12 **Ni ZZ**. Medical Statistics.2nd ed. Beijing: *People's Medical Publishing House* 2000: 17-136

13 **Eberhart CE**, Coffey RJ, Radhika A, Giardiello FM, Ferrenbach S, DuBois RN. Up-regulation of cyclooxygenase 2 gene expression in human colorectal adenomas and adenocarcinomas. *Gastroenterology* 1994; **107**: 1183-1188

14 **Ohno R**, Yoshinaga K, Fujita T, Hasegawa K, Iseki H, Tsunozaki H, Ichikawa W, Nihei Z, Sugihara K. Depth of invasion parallels increased cyclooxygenase-2 levels in patients with gastric carcinoma. *Cancer* 2001; **91**: 1876-1881

15 **Saukkonen K**, Nieminen O, van Rees B, Vilkki S, Harkonen M, Juhola M, Mecklin JP, Sipponen P, Ristimaki A. Expression of cyclooxygenase-2 in dysplasia of the stomach and in intestinal-type gastric adenocarcinoma. *Clin Cancer Res* 2001; **7**: 1923-1931

16 **Wolff H**, Saukkonen K, Anttila S, Karjalainen A, Vainio H, Ristimaki A. Expression of cyclooxygenase-2 in human lung carcinoma. *Cancer Res* 1998; **58**: 4997-5001

17 **Shamma A**, Yamamoto H, Doki Y, Okami J, Kondo M, Fujiwara Y, Yano M, Inoue M, Matsuura N, Shiozaki H, Monden M. Up-regulation of cyclooxygenase-2 in squamous carcinogenesis of the esophagus. *Clin Cancer Res* 2000; **6**: 1229-1238

18 **Sedivy R**, Wolf B, Kalipciyan M, Steger GG, Karner-Hanusch J, Mader RM. Genetic analysis of multiple synchronous lesions of the colon adenoma-carcinoma sequence. *J Cancer* 2000; **82**: 1276-1282

19 **Edmonston TB**, Cuesta KH, Burkholder S, Barusevicius A, Rose D, Kovatich AJ, Boman B, Fry R, Fishel R, Palazzo JP. Colorectal carcinomas with high microsatellite instability: defining a distinct immunologic and molecular entity with respect to prognostic markers. *Hum Pathol* 2000; **31**: 1506-1514

20 **Takayama T**, Ohi M, Hayashi T, Miyanishi K, Nobuoka A, Nakajima T, Satoh T, Takimoto R, Kato J, Sakamaki S, Niitsu Y. Analysis of K-ras, APC, and beta-catenin in aberrant crypt foci in sporadic adenoma, cancer, and familial adenomatous polyposis. *Gastroenterology* 2001; **121**: 599-611

21 **Takebayashi Y**, Nakayama K, Kanzaki A, Miyashita H, Ogura O, Mori S, Mutoh M, Miyazaki K, Fukumoto M, Pommier Y. Loss of heterozygosity of nucleotide excision repair factors in sporadic ovarian, colon and lung carcinomas: implication for their roles of carcinogenesis in human solid tumors. *Cancer Lett* 2001; **174**: 115-125

22 **Jaiswal AS**, Narayan S. p53-dependent transcriptional regulation of the APC promoter in colon cancer cells treated with DNA alkylating agents. *J Biol Chem* 2001; **276**: 18193-18199

23 **Kolligs FT**, Bommer G, Goke B. Wnt / beta-catenin / tcf signaling: a critical pathway in gastrointestinal tumorigenesis. *Digestion* 2002; **66**: 131-144

24 **Oshima M**, Dinchuk JE, Kargman SL, Oshima H, Hancock B, Kwong E, Trzaskos JM, Evans JF, Taketo MM. Suppression of intestinal polyposis in Apc delta716 knockout mice by inhibi-

tion of cyclooxygenase 2 (COX-2). *Cell* 1996; **87**: 803-809

25 **Hao X**, Bishop AE, Wallace M, Wang H, Willcocks TC, Maclouf J, Polak JM, Knight S, Talbot IC. Early expression of cyclo-oxygenase-2 during sporadic colorectal carcinogenesis. *J Pathol* 1999; **187**: 295-301

26 **Reddy BS**, Rao CV. Novel approaches for colon cancer prevention by cyclooxygenase-2 inhibitors. *J Environ Pathol Toxicol Oncol* 2002; **21**: 155-164

27 **Azumaya M**, Kobayashi M, Ajioka Y, Honma T, Suzuki Y, Takeuchi M, Narisawa R, Asakura H. Size-dependent expression of cyclooxygenase-2 in sporadic colorectal adenomas relative to adenomas in patients with familial adenomatous polyposis. *Pathol Int* 2002; **52**: 272-276

28 **Lynch HT**, Fusaro RM, Lynch JF. Cancer genetics in the new era of molecular biology. *Ann N Y Acad Sci* 1997; **833**: 1-28

29 **Tsujii M**, Kawano S, DuBois RN. Cyclooxygenase-2 expression in human colon cancer cells increases metastatic potential. *Proc Natl Acad Sci U S A* 1997; **94**: 3336-3340

30 **Attiga FA**, Fernandez PM, Weeraratna AT, Manyak MJ, Patierno SR. Inhibitors of prostaglandin synthesis inhibit human prostate tumor cell invasiveness and reduce the release of matrix metalloproteinases. *Cancer Res* 2000; **60**: 4629-4637

31 **Tomazawa S**, Nagawa H, Tsuno N, Hatano K, Osada T, Kitayama J, Sunami E, Nita ME, Ishihara S, Yano H, Tsuruo T, Shibata Y, Muto T. Inhibition of haematogenous metastasis of colon cancer in mice by a selective COX-2 inhibitor, JTE-522. *Br J Cancer* 1999; **81**: 1274-1279

32 **Tomozawa S**, Tsuno NH, Sunami E, Hatano K, Kitayama J, Osada T, Saito S, Tsuruo T, Shibata Y, Nagawa H. Cyclooxygenase-2 overexpression correlates with tumour recurrence, especially haematogenous metastasis, of colorectal cancer. *Br J Cancer* 2000; **83**: 324-328

Edited by Zhang JZ and Wang XL

P.O.Box 2345, Beijing 100023,China
Fax: +86-10-85381893
E-mail: wjg@wjgnet.com www.wjgnet.com

World J Gastroenterol 2003;9(9):1995-1998
World Journal of Gastroenterology
 ISSN 1007-9327

• COLORECTAL CANCER •

Inhibitory effects of docetaxel on expression of VEGF, bFGF and MMPs of LS174T cell

Xue-Liang Guo, Geng-Jin Lin, Hong Zhao, Yong Gao, Li-Ping Qian, San-Rong Xu, Li-Na Fu, Qing Xu, Jie-Jun Wang

Xue-Liang Guo, Geng-Jin Lin, Hong Zhao, Li-Ping Qian, San-Rong Xu, Department of Gastroenterology, Huashan Hospital, Fudan University, Shanghai 200032, China
Yong Gao, Qing Xu, **Jie-Jun Wang,** Medical oncology, Changzheng Hospital, Second Military Medical University, Shanghai 200003, China
Li-Na Fu, Department of Gastroenterology, Shandong Provincial Hospital, Ji' nan 250021, China
Correspondence to: Geng-Jin Lin, Department of Gastroenterology, Huashan Hospital, Fudan University, Shanghai 200032, China. guoxueliang@ hotmail.com
Telephone: +86-21-65790000-4036
Received: 2002-11-12 **Accepted:** 2002-12-30

Abstract

AIM: To study the effects of non-cytotoxic concentrations of docetaxel on some important angiogenic factors of LS174T Cells.

METHODS: The non-cytotoxic concentration of docetaxel and the activity of gelatinase were determined with MTT and gelatin zymography respectively, the expression of VEGF (vascular endothelial growth factor), bFGF (basic fibroblast growth factor), MMP (matrix metalloproteinase) 2 and MMP 9 was investigated with RT-PCR and Western blot.

RESULTS: The maximum non-cytotoxic concentration of docetaxel on LS174T Cells was 1.0 ng/ml. Compared with the solvent control group, 0.1, 0.5, 1.0 ng/ml of docetaxel could downregulate the expression of VEGF, bFGF, MMP 2 and MMP 9 and suppress the activity of gelatinase.

CONCLUSION: Our study suggests that the non-cytotoxic concentrations of docetaxel have strong antiangiogenic activity on LS174T Cells, which suggests docetaxel may be a promising antiangiogenic agent.

Guo XL, Lin GJ, Zhao H, Gao Y, Qian LP, Xu SR, Fu LN, Xu Q, Wang JJ. Inhibitory effects of docetaxel on expression of VEGF, bFGF and MMPs of LS174T cell. *World J Gastroenterol* 2003; 9 (9): 1995-1998

http://www.wjgnet.com/1007-9327/9/1995.asp

INTRODUCTION

It has been demonstrated that angiogenesis is vital to the growth and metastasis of human cancers, thus it represents a potential therapeutic target and has become a new spotlight in tumor study fields[1-7]. Colorectal carcinoma is one of the most common malignant tumors, and the present therapeutic methods such as surgery, chemotherapy and other adjuvant methods have their own limits. Previous studies showed that the growth and metastasis of colorectal carcinoma depended intimately on angiogenesis as well[8-10], thus it is important to explore a potential way of inhibiting angiogenesis to increase its cure rate. Docetaxel, which is derived from Taxus baccata, is a cytoskeleton toxic chemotherapeutical agent. It can break the dynamic equilibrium of mitosis and cell division, hence it can induce apoptosis by preventing microtubule disassembly after binding to tubulin[11-13]. It has been proven to have positive effects on tumors such as non small cell lung cancer (NSCLC), breast cancer, ovarian cancer and some other refractory and metastatic cancerous diseases. Recently, docetaxel has been proven to hold antiangiogenic activity[14,15], but whether its antiangiogenic properties are linked to its cytotoxic role or not remains unclear, and we know little about its mechanism as yet. In this communication, our aim was to explore the effects of non-cytotoxic concentrations of docetaxel on VEGF, bFGF, MMP' s expression of LS174T Cells *in vitro*.

MATERIALS AND METHODS

Judgment of non-cytotoxic concentration of docetaxel

Docetaxel (Rhone-Poulenc Rorer, France) was disolved in solvent vehicle (13 % ethanol), then diluted to working concentrations of 0.1, 0.01 μg/ml with sterilized normal saline (NS). LS174T Cells (Shanghai Institute of Cell Biology, Chinese Academy of Sciences) were cultured in RPMI 1640 (Gibco BRL) supplemented with 10 % fetal bovine serum. The cultured cells were seeded on a 96-well plate with 5 000 cells in each well. 72 h later, at 80 % confluency, the culture medium was changed to the RPMI 1640 containing 1 % bovine serum, docetaxel solvent various concentration of docetaxel were added. The experiments were divided into docetaxel solvent control group and docetaxel 0.1, 0.2, 0.5, 1.0, 2.0, 5.0, 10.0 ng/ml groups. 24 h later, 15 μl MTT [3-(4, 5-dimethylthiazol-2-yl)-2, 5-dipheny-ltetrazolium bromide] was added into each well, and the cells were incubated for another 4 h, then the fluid was cast, 150 μl DMSO was added. After vibrated for 10 min, the 490 nm absorpance value was determined with microplate reader apparatus (Labsystem Wellscan-MK-3, Finland). The ratio value of each group and the blank control group was taken as the relative MTT A value. Finally, we determined the maximum non-cytotoxic concentration of docetaxel on LS174T Cells and the trypan blue staining results.

Gelatin zymography

The cultured LS174T Cells at 80 % confluency were treated with docetaxel solvent and various concentrations of docetaxel. The cells were classified into docetaxel solvent control group and docetaxel 0.1, 0.5, 1.0 ng/ml group. 24 h later, we collected the supernatant of the cells, and concentrated it with Amicon filters to 10 % of initial volume. Each sample was guaranteed to contain the same amount of total protein, gelatin zymography was performed in 10 % polyacrylamide in the presence of 0.1 % gelatin as described previously[16-18]. Identification of transparent bands at 92 000 and 72 000 dalton on the Coomassie blue background of the slab gel was considered positive for the presence of enzymatic activity. The collagenase activity was semi-quantified with densitometry of Image Quant software program.

Western blot

The cell culture, drug treatment and groups classified methods

were the same as the gelatin zymography experiment. All samples containing 10 μg total proteins were loaded into 7.5 % polyacrylamide-SDS gel, electrophoresed for 3 h (apparatus of Amersham Pharmacia Biotech), and transferred onto the nitrocellulose membrane. The membrane was subjected to immunoblotting with anti-mouse monoclonal antibody MMP 2 and MMP 9 or anti-rabbit polyclonal antibody VEGF and bFGF (Oncogene corp), then conjuncted with the second antibody anti-mouse IgG-HRP or anti-rabbit IgG-HRP (Santa Cruz Biotechnology, California). Immunodetections were carried out using Western blot chemiluminescence reagent (Santa Cruz Biotechnology, California). The target bands of the gel were semi-quantified by using densitometry of image Quant software program. The ratio value of each group and the blank control group was taken as the relative value.

RT-PCR

The cell culture, drug treatment and group classified methods were the same as the gelatin zymography experiment. Total RNA (extract kit of QIAgen) extracted from LS174T Cells was transcribed into cDNA (Roche), reverse transcription reaction was performed at 42 ℃ for 60 min, then denaturated at 94 ℃ for 5 min. The cDNA was then amplified with PCR by using Taq DNA polymerase. PCR (apparatus of Hybaid) was performed for 32 cycles with denaturation at 94 ℃ for 50 s, annealing at 55 ℃ for 45 s, and elongation at 72 ℃ for 50 s, and extension for 7 min after completion of all cycles. The amplified PCR products were analyzed on 1 % agarose gel electrophoresis after stained with ethidium bromide. PCR primers (Saibaisheng, China) used to detect each factor were as follows: VEGF, sense strand 5'-CACATAGGAGAGATGAGCTTC-3', antisense strand 5'-CCGCCTCGGCTTGTCACAT-3', the length of product was 210 bp; bFGF, sense strand 5'-TGGTATGTGGCACTGAAACG-3', antisense strand 5'-CTCAATGACCTGGCGAAGAC-3', the length of product was 734 bp; MMP2, sense strand 5'-CCTGGGCAACAA ATATGAGA-3', anti- sense strand 5'-ACAGTCCGCCAA ATGAACC-3', the length of product was 426 bp; MMP9, sense strand 5'-TCCCTGGAGACCTGAGAACC-3', antisense strand 5'-GTCGTCGGTGTCGTAGTTGG-3', the length of product was 659 bp; GAPDH, sense strand 5'-ATCCCATCACCATCTTCCAG-3', antisense strand 5'-ATGAGTCCTTCCACGATACCA-3', the length of product was 310 bp. The quantified method of target PCR products was the same as above. The ratio value of each group and the GAPDH group was taken as the relative value.

Statistical analysis

Data were expressed as mean ±SD. Significant differences were determined by using ANOVA in statistical software SPSS10.0. The level of significance was $P<0.05$.

RESULTS

Non-cytotoxic concentration of docetaxel

The mean relative MTT A values of blank control group, docetaxel solvent control, 0.1, 0.2, 0.5, 1.0, 2.0, 5.0, 10.0 ng/ml groups were 1.000±0.17, 0.995±0.28, 0.993±0.15, 0.990±0.18, 0.985±0.14, 0.981±0.11, 0.848±0.12, 0.657±0.08, 0.485±0.06 respectively. There were no significant differences between the first six groups ($P>0.05$), there were significant differences between other groups ($P<0.01$) (Table 1). Combined these with the trypan bule staining results, we determined 1.0 ng/ml as the maximum non-cytotoxic concentration of docetaxel to LS174T cells in the present study.

Gelatin zymography

Gelatin zymography result revealed prominent 92 000 and 72 000 dalton bands (Figure 1), there was expression of MMP2 and MMP9 in the LS174T cells culture supernatant. The semi-analysis results showed that 0.1, 0.2, 0.5, 1.0 ng/ml docetaxel could downregulate two matrix metalloproteases, the activity of MMP9 was higher than that of MMP2, there were significant differences between these groups.

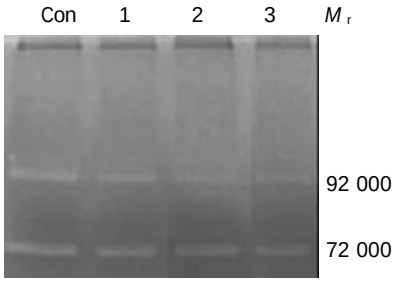

Figure 1 Inhibition of gelatinase activity of LS174T cell by docetaxel. After treated with 0.1, 0.2, 0.5, 1.0 ng / ml concentration of docetaxel,the activity of MMP2 AND 9 was inhibited. Representative results from three independent experiments: Con. docetaxel solvent control group; 1-3: 0.1, 0.5, 1.0 ng / mL concentrations of docetaxel.

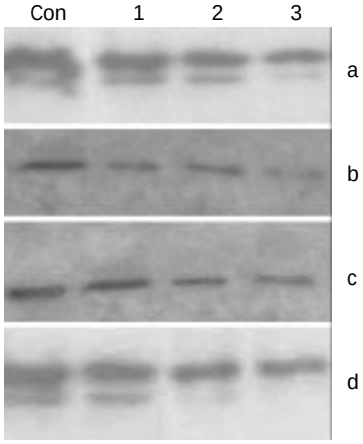

Figure 2 Inhibition of expression of proteins of LS174T cell by docetaxel. After treated with 0.1, 0.2, 0.5, 1.0 ng / ml concentration of docetaxel, the level of VEGF, bFGF, MMP2, MMP9 protein of LS174T cell was inhibited by docetaxel respectively. Representative results from three independent experiments. a. b. c. d. VEGF, bFGF, MMP2, MMP9 proteins (M_r. was 22 000, 18 000, 72 000 and 92 000) of LS174T cell; Con: docetaxel solvent control group, 1-3: 0.1, 0.5, 1.0 ng / mL concentrations of docetaxel.

Table 1 Effects of docetaxel on proliferation of LS174T ($\bar{x}\pm s$, $n=10$)

Group	Blank control	Solvent control	Docetaxel (ng / ml)						
			0.1	0.2	0.5	1.0	2.0	5.0	10.0
A Value	1.000±0.17[a]	0.995±0.28[a]	0.993±0.15[a]	0.990±0.18[a]	0.985±0.14[a]	0.981±0.11[a]	0.848±0.12[b]	0.657±0.08[b]	0485±0.06[b]

[a]$P>0.05$ *vs* between these groups, [b]$P<0.01$ *vs* other groups.

Western blot

The X-ray film was scanned (Figure 2), the semi-analysis results showed the amount of VEGF, bFGF, MMP2 and MMP9 decreased as the concentration of docetaxel increased, there were significant differences between these groups. The level of VEGF, MMP9 was higher than that of bFGF, MMP2.

RT-PCR

Agrose gel was scanned, the semi-analysis results showed the content of VEGF, MMP9 was higher than that of bFGF, MMP2, the content of bFGF was the lowest (Figure 3). The expression of VEGF, bFGF, MMP2 and MMP9 was inhibited by various concentration of docetaxel in a dose-dependent manner, and there were significant differences between these groups. However, steady state expression of GAPDH (as internal control) was observerd in all cases.

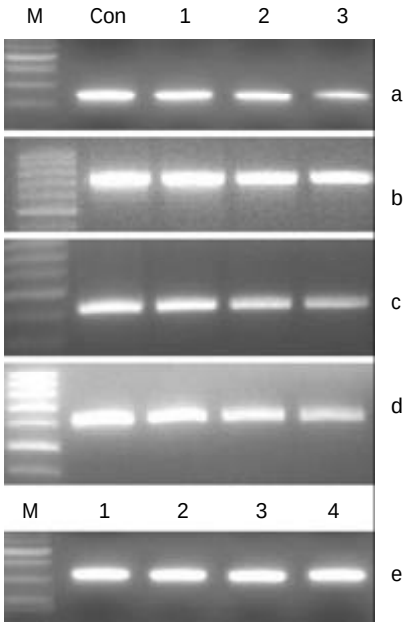

Figure 3 Inhibition of expression of mRNA of LS174T cell by docetaxel. After treated with 0.1, 0.2, 0.5, 1.0 ng/ml concentration of docetaxel, the level of VEGF, bFGF, MMP2, MMP9 protein of LS174T cell was inhibited by docetaxel respectively. Representative results from three independent experiments. a. b. c. d. e. VEGF, bFGF, MMP2, MMP9 mRNA and GAPDH (210 bp, 734 bp, 426 bp, 659 bp and 310 bp, 500 bp). Con: docetaxel solvent control group, a. b. c. d; 1-3: 0.1, 0.5, 1.0 ng/mL concentrations of docetaxel. M: marker, e; 1-4: internal control groups.

DISCUSSION

It has been demonstrated that the antitumor action of taxanes contributes to their antiangiogenic activity. Taxanes were found to inhibit angiogenesis by suppressing the proliferation, migration, and capillary formation of endothelial cells both in *in vitro* and *in vivo* models, it could inhibit the endothelial cells (HUVEC) migration with an IC50 of 0.01 nM[9,19-21]. However, little is known about the effects of docetaxel on angiogenesis related factors till now. Because of docetaxel's cytotoxic characteristic, it is important to verdict its non-cytotoxic concentration. Combined with MTT experiment and the trypan blue staining, our results indicated that 1.0 ng/ml was the maximum non-cytotoxic concentration of docetaxel in LS174T Cells.

LS174T Cells line, as a moderately differentiated adenocarcinoma with a moderately invasive ability, is one of very common colorectal carcinomas. Its characteristic is similar to that of most common carcinomas, so the present study holds definite clinical significance. And our study showed there was expression of VEGF, bFGF, MMP2 and MMP9 factors in the LS174T Cells at the gene and protein levels[22-26], which suggests angiogenesis may play a very important role in LS174T cells related tumors.

According to our current work, non-cytotoxic concentration of docetaxel could downregulate the expression of VEGF, bFGF in LS174T Cells, which are the triggers of angiogenesis. VEGF stimulates the degradation of ECM as well as the proliferation, migration and capillary formation of endothelial cells[23, 27-31], while bFGF has growth-stimulating and invasion-promoting effects on the angiogenesis process[32,33]. From the facts mentioned above, we suppose that the drug has a strong antiangiogenic action whose mechanism might be mainly related to the supressing effect on neoangiogenesis from the very beginning. Our results indicated that non-cytotoxic concentrations of docetaxel also could supress the expression of MMP2 and MMP9 and reduce their activities. MMP2 and MMP9 play a vital role in the turnover of basement membrane collagen type IV and type I which exert a crucial effect on the formation of new capillary sprouts and neoangiogenesis[15,34-36]. Baseing on the above facts, we speculate that the drug can prevent degradation of the vascular basement membrane, thus further inhibit neoangiogenesis.

We also found the inhibitory effects of docetaxel on VEGF and MMP9 are stronger than those on bFGF, MMP2. We suppose it owes to docetaxel's relative selectivity, or the higher level of VEGF and MMP9. In addition, there are complex correlating regulations among these four factors. And the direct and indirect effects of docetaxel cannot be distinguished clearly as yet, which well deserves further investigation.

Whether docetaxel's antiangiogenic property is linked to its cytotoxic role or not needs further elucidation. Schimming *et al*[37] determined whether inhibition of neoangiogenesis played a role in docetaxel's antitumor efficacy. Since no reduction in blood vessels occurred in tumors unresponsive to docetaxel, they thought the inhibition of neoangiogenesis in docetaxel responsive tumors was likely to be the result of a decrease in angiogenic stimuli due to docetaxel's cytotoxic action. Vacca *et al*[38] reported that both cytotoxic and non-cytotoxic doses of docetaxel displayed a dose-dependent antiangiogenic activity in the mouse embryo fibroblasts, human Kaposi's sarcoma, breast, endometrial carcinoma and lymphoid tumor *in vitro* and *in vivo*. Our results are in coincidence with theirs.

In conclusion, our study suggests that antiangiogenic property of docetaxel is not linked to its cytotoxicity. Docetaxel under cytotoxic concentration has strong antiangiogenic activity on LS174T Cells, with its mechanism mainly through the inhibitory effects on VEGF, bFGF and MMPs. Docetaxel in low concentration may be a promising antiangiogenic agent for tumor treatment.

REFERENCES

1 **Song ZJ,** Gong P, Wu YE. Relationship between the expression of iNOS, VEGF, tumor angiogenesis and gastric cancer. *World J Gastroenterol* 2002; **8**: 591-595
2 **Xiong B,** Gong LL, Zhang F, Hu MB, Yuan HY. TGF beta1 expression and angiogenesis in colorectal cancer tissue. *World J Gastroenterol* 2002; **8**: 496-498
3 **Qin LX,** Tang ZY. The prognostic molecular markers in hepatocellular carcinoma. *World J Gastroenterol* 2002; **8**: 385-392
4 **Gu ZP,** Wang YJ, Li JG, Zhou YA. VEGF165 antisense RNA suppresses oncogenic properties of human esophageal squamous cell carcinoma. *World J Gastroenterol* 2002; **8**: 44-48
5 **Tang ZY,** Sun FX, Tian J, Ye SL, Liu YK, Liu KD, Xue Q, Chen J, Xia JL, Qin LX, Sun HC, Wang L, Zhou J, Li Y, Ma ZC, Zhou XD,

Wu ZQ, Lin ZY, Yang BH. Metastatic human hepatocellular carcinoma models in nude mice and cell line with metastatic potential. *World J Gastroenterol* 2001; **7**: 597-601

6 **Sun HC,** Li XM, Xue Q, Chen J, Gao DM, Tang ZY. Study of angiogenesis induced by metastatic and non-metastatic liver cancer by corneal micropocket model in nude mice. *World J Gastroenterol* 1999; **5**: 116-118

7 **Tao HQ,** Lin YZ, Wang RN. Significance of vascular endothelial growth factor messenger RNA expression in gastric cancer. *World J Gastroenterol* 1998; **4**: 10-13

8 **Kondo Y,** Arii S, Furutani M, Isigami S, Mori A, Onodera H, Chiba T, Imamura M. Implication of vascular endothelial growth factor and p53 status for angiogenesis in noninvasive colorectal carcinoma. *Cancer* 2000; **88**: 1820-1827

9 **Andre T,** Kotelevets L, Vaillant JC, Coudray AM, Weber L, Prevot S, Parc R, Gespach C, Chastre E. Vegf, Vegf-B, Vegf-C and their receptors KDR, FLT-1 and FLT-4 during the neoplastic progression of human colonic mucosa. *Int J Cancer* 2000; **86**: 174-181

10 **Lee JC,** Chow NH, Wang ST, Huang SM. Prognostic value of vascular endothelial growth factor expression in colorectal cancer patients. *Eur J Cancer* 2000; **36**: 748-753

11 **Liu B,** Staren E, Iwamura T, Appert H, Howard J. Taxotere resistance in SUIT Taxotere resistance in pancreatic carcinoma cell line SUIT 2 and its sublines. *World J Gastroenterol* 2001; **7**: 855-859

12 **Liu B,** Staren E, Iwamura T, Appert H, Howard J. Effects of Taxotere on invasive potential and multidrug resistance phenotype in pancreatic carcinoma cell line SUIT-2. *World J Gastroenterol* 2001; **7**: 143-148

13 **Ciardiello F,** Caputo R, Bianco R, Damiano V, Fontanini G, Cuccato S, De Placido S, Bianco AR, Tortora G. Inhibition of growth factor production and angiogenesis in human cancer cells by ZD1839 (Iressa), a selective epidermal growth factor receptor tyrosine kinase inhibitor. *Clin Cancer Res* 2001; **7**: 1459-1465

14 **Klauber N,** Parangi S, Flynn E, Hamel E, D'Amato RJ. Inhibition of angiogenesis and breast cancer in mice by the microtubule inhibitors 2-methoxyestradiol and taxol. *Cancer Res* 1997; **57**: 81-86

15 **Sweeney CJ,** Miller KD, Sissons SE, Nozaki S, Heilman DK, Shen J, Sledge GW Jr. The antiangiogenic property of docetaxel is synergistic with a recombinant humanized monoclonal antibody against vascular endothelial growth factor or 2-methoxyestradiol but antagonized by endothelial growth factors. *Cancer Res* 2001; **61**: 3369-3372

16 **Chen PS,** Zhai WR, Zhou XM, Zhang JS, Zhang YE, Ling YQ, Gu YH. Effects of hypoxia, hyperoxia on the regulation of expression and activity of matrix metalloproteinase-2 in hepatic stellate cells. *World J Gastroenterol* 2001; **7**: 647-651

17 **Luca M,** Huang S, Gershenwald JE, Singh RK, Reich R, Bar-Eli M. Expression of interleukin-8 by human melanoma cells upregulates MMP-2 activity and increases tumor growth and metastasis. *Am J Pathol* 1997; **151**: 1105-1113

18 **Spiridonidis CH,** Laufman LR, Jones J, Rhodes VA, Wallace K, Nicol S. Phase I study of docetaxel dose escalation in combination with fixed weekly gemcitabine in patients with advanced malignancies. *J Clin Oncol* 1998; **16**: 3866-3873

19 **Belotti D,** Vergani V, Drudis T, Borsotti P, Pitelli MR, Viale G, Giavazzi R, Taraboletti G. The microtubule-affecting drug paclitaxel has antiangiogenic activity. *Clin Cancer Res* 1996; **2**: 1843-1849

20 **Lau DH,** Xue L, Young LJ, Burke PA, Cheung AT. Paclitaxel (Taxol): an inhibitor of angiogenesis in a highly vascularized transgenic breast cancer. *Cancer Biother Radiopharm* 1999; **14**: 31-36

21 **Fennelly D,** Aghajanian C, Shapiro F, O'Flaherty C, McKenzie M, O'Connor C, Tong W, Norton L, Spriggs D. Phase I and pharmacologic study of paclitaxel administered weekly in patients with relapsed ovarian cancer. *J Clin Oncol* 1997; **15**: 187-192

22 **Zhu JW,** Yu BM, Ji YB, Zheng MH, Li DH. Upregulation of vascular endothelial growth factor by hydrogen peroxide in human colon cancer. *World J Gastroenterol* 2002; **8**: 153-157

23 **Bianco C,** Tortora G, Baldassarre G, Caputo R, Fontanini G, Chine S, Bianco AR, Ciardiello F. 8-Chloro-cyclic AMP inhibits autocrine and angiogenic growth factor production in human colorectal and breast cancer. *Clin Cancer Res* 1997; **3**: 439-448

24 **Matsuoka T,** Yashiro M, Sawada T, Ishikawa T, Ohira M, Chung KH. Inhibition of invasion and lymph node metastasis of gastrointestinal cancer cells by R-94138, a matrix metalloproteinase inhibitor. *Anticancer-Res* 2000; **20**: 4331-4338

25 **Guo WJ,** Li J, Ling WL, Bai YR, Zhang WZ, Cheng YF, Gu WH, Zhuang JY. Influence of hepatic arterial blockage on blood perfusion and VEGF, MMP-1 expression of implanted liver cancer in rats. *World J Gastroenterol* 2002; **8**: 476-479

26 **Liu DH,** Zhang XY, Fan DM, Huang YX, Zhang JS, Huang WQ, Zhang YQ, Huang QS, Ma WY, Chai YB, Jin M. Expression of vascular endothelial growth factor and its role in oncogenesis of human gastric carcinoma. *World J Gastroenterol* 2001; **7**: 500-505

27 **Tang YC,** Li Y, Qian GX. Reduction of tumorigenicity of SMMC-7721 hepatoma cells by vascular endothelial growth factor antisense gene therapy. *World J Gastroenterol* 2001; **7**: 22-27

28 **Xue JT,** Wu J, Meng L, Dong ZW, Shou CC. Expression of VEGF (121) in gastric carcinoma MGC803 cell line. *World J Gastroenterol* 2000; **6**: 281-283

29 **Jiang YF,** Yang ZH, Hu JQ. Recurrence or metastasis of HCC: predictors, early detection and experimental antiangiogenic therapy. *World J Gastroenterol* 2000; **6**: 61-65

30 **Assy N,** Paizi M, Gaitini D, Baruch Y, Spira G. Clinical implication of VEGF serum levels in cirrhotic patients with or without portal hypertension. *World J Gastroenterol* 1999; **5**: 296-300

31 **Lee CG,** Heijn M, di Tomaso E, Griffon-Etienne G, Ancukiewicz M, Koike C, Park KR, Ferrara N, Jain RK, Suit HD, Boucher Y. Anti-Vascular endothelial growth factor treatment augments tumor radiation response under normoxic or hypoxic conditions. *Cancer Res* 2000; **60**: 5565-5570

32 **Fu XB,** Yang YH, Sun TZ, Gu XM, Jiang LX, Sun XQ, Sheng ZY. Effect of intestinal ischemia-reperfusion on expressions of endogenous basic fibroblast growth factor and transforming growth factor betain lung and its relation with lung repair. *World J Gastroenterol* 2000; **6**: 353-355

33 **Yang YH**, Fu XB, Sun TZ, Jiang LX, Gu XM. bFGF and TGFbeta expression in rat kidneys after ischemic/reperfusional gut injury and its relationship with tissue repair. *World J Gastroenterol* 2000; **6**: 147-149

34 **Hou L,** Li Y, Jia YH, Wang B, Xin Y, Ling MY, Lü S. Molecular mechanism about lymphogenous metastasis of hepatocarcinoma cells in mice. *World J Gastroenterol* 2001; **7**: 532-536

35 **Wang Q,** Lin ZY, Feng XL. Alterations in metastatic properties of hepatocellular carcinoma cell following H-ras oncogene transfection. *World J Gastroenterol* 2001; **7**: 335-339

36 **Stearns ME,** Wang M. Taxol blocks processes essential for prostate tumor cell (PC-3 ML) invasion and metastases. *Cancer Res* 1992; **52**: 3776-3781

37 **Schimming R,** Hunter NR, Mason KA, Milas L. Inhibition of tumor neo-angiogenesis and induction of apoptosis as properties of docetaxel (taxotere). *Mund Kiefer Gesichtschir* 1999; **3**: 210-212

38 **Vacca A,** Ribatti D, Iurlaro M, Merchionne F, Nico B, Ria R, Dammacco F. Docetaxel versus Paclitaxel for antiangiogenesis. *J Hematother Stem Cell Res* 2002; **11**: 103-118

Edited by Wu XN and Wang XL

P.O.Box 2345, Beijing 100023,China
Fax: +86-10-85381893
E-mail: wjg@wjgnet.com www.wjgnet.com

World J Gastroenterol 2003;9(9):1999-2003
World Journal of Gastroenterology
 ISSN 1007-9327

• VIRAL HEPATITIS •

Clinical and experimental study on therapeutic effect of umbilical cord blood transplantation on severe viral hepatitis

Xiao-Peng Tang, Xu Yang, Hui Tan, Yi-Ling Ding, Min Zhang, Wen-Long Wang

Xiao-Peng Tang, Xu Yang, Min Zhang, Wen-Long Wang, Research Center of Liver Diseases, the Second Xiangya Hospital, Zhongnan University, Changsha 410011, Hunan Province, China
Hui Tan, Yi-Ling Ding, Department of Gynaecology and Obstetrics, the Second Xiangya Hospital, Zhongnan University, Changsha 410011, Hunan Province, China
Supported by the National Natural Science Foundation of China, No.39870651
Correspondence to: Dr. Xiao-Peng Tang, Research Center of Liver Diseases, the Second Xiangya Hospital, Zhongnan University, Changsha 410011, Hunan Province, China. xiaopeng59@yahoo.com.cn
Telephone: +86-731-2221570
Received: 2003-03-02 **Accepted:** 2003-04-09

Abstract

AIM: To investigate the therapeutic effect of umbilical cord blood transplantation (UCBT) on patients with severe viral hepatitis and on liver lesions in rats.

METHODS: One hundred and fifty three patients with severe viral hepatitis were included in the study between April 1990 and July 2002. The patients were treated with adult plasma transfusion (control), UCBT, plasma exchange (PE) and UCBT combined with PE (UCBT+PE) respectively. The therapeutic effectiveness was evaluated by serial determinations of liver function, lipids and immune function in all patients before and after the treatment. The model of experimental hepatic failure was constructed in SD rats by injecting carbon tetrachloride. Then, the rats were given normal saline, adult plasma or neonate cord blood intraperitoneally. After detection of liver function, the rats were killed and morphological changes of the liver were microscopically observed.

RESULTS: UCBT group and UCBT+PE group had much better improvement in liver and immune functions than control group and PE group. The patients in UCBT+PE group had the best clinical efficacy. UCBT was safe and had no side effects. The animal experiment showed significant improvements in liver function and survival rate in neonate cord blood group as compared with adult plasma group. The histopathology of rat's liver indicated that neonate cord blood application could decrease the liver injury and increase hepatocellular regeneration.

CONCLUSION: UCBT demonstrated a good therapeutic effect on severe viral hepatitis and no obvious side effects. Umbilical cord blood can attenuate the liver lesions and reproduce hepatocyte. The treatment of UCBT combined with PE was much better than that of single plasma exchange, thus UCBT can enhance the therapeutic effect of plasma exchange on severe viral hepatitis.

Tang XP, Yang X, Tan H, Ding YL, Zhang M, Wang WL. Clinical and experimental study on therapeutic effect of umbilical cord blood transplantation on severe viral hepatitis. *World J Gastroenterol* 2003; 9(9): 1999-2003
http://www.wjgnet.com/1007-9327/9/1999.asp

INTRODUCTION

In 1987, a child with Fanconi' s anaemia received an allogeneic transplant using the cryopreserved umbilical cord blood (UCB). As a result, the potential of UCB as a source of haemopoietic stem cells for transplantation rapidly became a field of intense clinical and scientific interest. Because UCB is a relatively easily available starting material, it has been increasingly used as an alternative source of hematopoietic stem cells in allogeneic transplantation. Many umbilical cord blood banks have been established. The engrafting cells in UCB are found to be significantly higher than those in adult bone marrow or in mobilized peripheral blood from normal donors. It has been found that multipotent adult progenitor cells (MAPCs) can differentiate into hepatocyte-like cells *in vitro*[1]. Neurons, astrocytes and oligodendrocytes can be propagated *in vitro* from UCB cells[2,3]. The evidences indicate that stem cells can differentiate into hepatocytes[4,5]. This study evaluated the therapeutic effectiveness of UCBT on severe hepatitis, and tried to find a new therapy for severe viral hepatitis.

MATERIALS AND METHODS

Grouping and treatment

One hundred and fifty-three inpatients with severe viral hepatitis were included in the study from April 1990 to July 2002. These patients had a history of hepatitis for more than 8 weeks, with severe hepatic dysfunction, rapidly progressive jaundice, abdominal distention, asthenia, ascites, coagulopathy, encephalopathy and hepatorenal syndrome. The patients were randomly divided into control (adult plasma) group: 39 patients (36 male and 3 female) with a mean age of 39.4 years (range 17-56 years), UCBT group: 38 patients (37 male and 1 female) with a mean age of 41.2 years (range 13-62 years), PE group: 45 patients (43 male and 2 female) with a mean age of 37.5 years (range 21-58 years), and UCBT+PE group: 31 patients (all were male) with a mean age of 43.2 years (range 13-65 years). The patients were treated with 200 ml of fresh adult plasma/ blood transfusion (in control group and PE group) or 200 ml of umbilical cord blood transplantation (in UCBT group and UCBT+PE group) intravenously each time, one to three times a week for two to four weeks. Plasma exchange given was 1 500-3 000 ml each time, one to three times every week and totally two to five times. The rate of plasma separation and the flow rate of plasma exchange were controlled at the speed of 5-15 mL/min and 15-25 mL/min, respectively.

Collection and storage of umbilical cord blood

Immediately after the birth of the baby, the umbilical cord was cut off and the baby was separated from the placenta and mother. A sterile needle was inserted into the umbilical vein and the placental blood was drawn into a sterile blood collection bag containing ACD-B anticoagulant, provided by Shanghai Blood Center. Once the collection was complete, the specimen was packaged and sent to blood bank for processing and storage at low temperatures. The maternal blood sample was also collected for infectious disease analysis.

Equipment
PE was performed with COBE Spectra™ Auto PBSC version 6.0 apheresis system (COBE BCT, Inc. Colorado, USA).

Animals and experimental design
Male SD rats, weighing 150 to 180 g, were purchased from the Laboratory Animal Center, Xiangya Medical College, Zhongnan University. On the first and second day carbon tetrachloride was injected into each rat (1 ml/100 g) intraperitoneally to establish an acute liver failure model. On the third day several rats were killed as acute liver failure models and the livers were taken for histopathological examination, the other 81 survived rats were randomly assigned to control group (n=24), normal saline group (n=16), adult plasma group (n=22), and neonate cord blood group (n=19). Rats in groups 2-4 were intraperitoneally given 1 ml/100 g· d^{-1} normal saline, adult plasma or neonate cord blood respectively for five days and no treatment was given in group 1. On the eighth day, after detection of the liver function, all survived rats were killed and sections of liver tissues were taken immediately for histopathological examination. Excised liver tissues were fixed in 10 % neutralized formaldehyde, embedded in paraffin, and then routinely stained with hematoxylin and eosin.

Statistical analysis
The data were expressed as means ± standard deviation ($\bar{x}\pm s$), and the differences between the value of different groups were analysed by the t test or χ^2 test (SPSS version 9.0). The criterion of significance was set at P<0.05.

RESULTS

Changes of patient's liver function
There was no difference in liver function (Alb, ALT, serum total bilirubin and prothrombin activity) among all the groups before treatment. Alb and prothrombin activity (PTA) were much lower than normal but serum total bilirubin (TBil) was remarkably higher than normal in all groups before treatment. Alb and PTA increased in all groups after treatment. As compared with control group, the degrees of Alb and PTA increase were higher in UCBT group, PE group and much higher in UCBT+PE group (P<0.05). The change of ALT level was not significant after treatment in all groups. Serum TBil contents significantly decreased after treatment in UCBT group, PE group and UCBT+PE group (P<0.05), (Table 1).

Influence of UCBT and PE on immune functions of the patients
Immune functions of the patients were markedly improved after treatment in UCBT group and UCBT+PE group. The values of $CD4^+$, active T lymphocytes and IL2 were significantly increased after treatment in UCBT group and UCBT+PE group (P<0.05). However no significant change of the values was observed in control group and PE group. There was no significant difference of $CD8^+$ lymphocytes before and after treatment in all groups (Table 2).

Side effect and safety
No side effect or negative response was found in UCBT group. Three patients in control group, ten patients in PE group and eight patients in UCBT+PE group had rashes during the treatment. Four patients had fever in PE group. No fatal side effect was observed in all groups.

Survival of rats
On the eighth day, 89.5 % (17/19) rats survived in neonate cord blood group, 54.5 % (12/22) in adult plasma group, 31.3 % (5/16) in normal saline group and 25.0 % (6/24) in control group respectively. The survival rate of rats in neonate cord blood group was significantly higher than that in adult plasma group (P<0.05), normal saline group and control group (P<0.01).

Biochemical parameters of rats
The serum levels of ALT and TBil in neonate cord blood group were significantly lower than those in adult plasma group (P<0.05), normal saline group and control group (P<0.01). Meanwhile the serum level of AFP in neonate cord blood group was significantly higher than that in the other three groups (P<0.01), (Table 3).

Histopathology of rats
Histopathology of model rats' livers revealed lobular disarray, ballooning degeneration, fatty degeneration, inflammatory cell infiltration in the portal zone and areas of parenchyma, cholestasis and massive necrosis of hypatocytes (Figure 1). All indicated that there was an acute liver failure in model rats. After five-day treatment of neonate cord blood, hepatocellular necrosis and mononuclear cell infiltration were greatly decreased and only spotty hepatocellular necrosis occurred. Meanwhile

Table 1 Changes of biochemical parameters of patients before and after treatment ($\bar{x}\pm s$)

Group	ALT(u·L^{-1})		TBil (μmol·L^{-1})		Alb(g·L^{-1})		PTA(%)	
	Before	After	Before	After	Before	After	Before	After
Control	112.4±37.2	98.5±23.6	315.1±43.2	263.7±105.2	31.3±5.1	32.5±2.6	33.5±4.7	43.5±6.7
UCBT	95.6±31.9	84.3±35.7	376.3±55.1	203.1±85.4^{bc}	30.6±4.2	35.6±2.4^{a}	31.5±3.6	45.8±5.4^{a}
PE	116.3±44.1	81.9±42.5	356.6±48.5	195.6±103.7^{bc}	28.5±3.6	36.9±5.1^{bc}	28.8±7.2	48.3±7.5^{b}
UCBT+PE	104.5±38.6	85.3±36.2	405.7±59.4	173.2±125.6^{bc}	30.7±4.4	37.7±3.5^{bc}	29.7±6.5	52.3±10.2^{bc}

^{a}P<0.05 *vs* before treatment, ^{b}P<0.01 *vs* before treatment, ^{c}P<0.05 *vs* control group.

Table 2 Parameters of cellular and humoral immune of patients before and after treatment ($\bar{x}\pm s$)

Group	Active T lymphocyte (%)		$CD4^+$ lymphocyte (%)		$CD8^+$ lymphocyte (%)		IL2 (u· ml^{-1})	
	Before	After	Before	After	Before	After	Before	After
Control	35.6±7.5	44.1±14.3	32.7±5.3	35.6±8.2	22.5±3.6	23.7±5.2	41.3±10.5	48.6±21.5
UCBT	33.2±8.7	51.6±12.5^{ab}	30.5±6.9	44.3±11.6^{a}	23.2±4.7	25.6±9.5	44.5±9.6	62.7±28.6^{ab}
PE	36.1±6.3	42.7±16.9	29.5±8.2	34.7±7.4	20.4±6.9	26.7±8.4	48.6±11.3	51.3±31.9
UCBT+ PE	31.9±8.5	58.9±25.4^{ab}	27.1±7.3	48.5±21.3^{ab}	18.3±8.5	28.4±11.2	36.2±10.8	64.8±27.5^{ab}

^{a}P<0.05 *vs* before treatment, ^{b}P<0.05 *vs* control group.

obviously hepatocellular regeneration was observed in neonate cord blood group (Figure 2). There was no significant histopathological difference between control group and normal saline group. Multilobular necrosis and numerous lymphocytic infiltrations were noted, and no evident hepatocellular regeneration was demonstrated in control group and normal saline group (Figure 3). Local necrosis, moderate degree of lymphocytic infiltration and a few focal hepatocyte regenerations were observed in adult plasma group (Figure 4), (Table 4).

Table 3 Biochemical parameters of rats after treatment ($\bar{x}\pm s$)

Group	ALT($u \cdot L^{-1}$)	TBil ($\mu mol \cdot L^{-1}$)	AFP($\mu g \cdot L^{-1}$)
Control group	1025.3±36.9	78.6±3.4	21.5±13.8
Normal saline group	1016.8±318.2	65.6±18.3	23.7±15.9
Adult plasma group	365.6±118.4[a]	36.2±9.5[a]	28.9±18.7
Neonate cord blood group	186.7±39.5[bc]	14.3±6.0[bc]	686.4±186.5[bd]

[a]$P<0.05$ *vs* control group and normal saline group, [b]$P<0.01$ *vs* control group and normal saline group, [c]$P<0.05$ *vs* adult plasma group, [d]$P<0.01$ *vs* adult plasma group.

Table 4 Histological examinations of rats' liver after treatment ($\bar{x}\pm s$)

Groups	Ballooning degeneration	Fatty degeneration	Hepatocellular necrosis	Hepatocellular regeneration
Control group	+++	+++	+++	--
Normal saline group	+++	+++	+++	--
Adult plasma group	++	++	++	+
Neonate cord blood group	+	+	+	+++

+++: severe / extremely remarkable, ++: medium, +: mild, -: no / non-obvious.

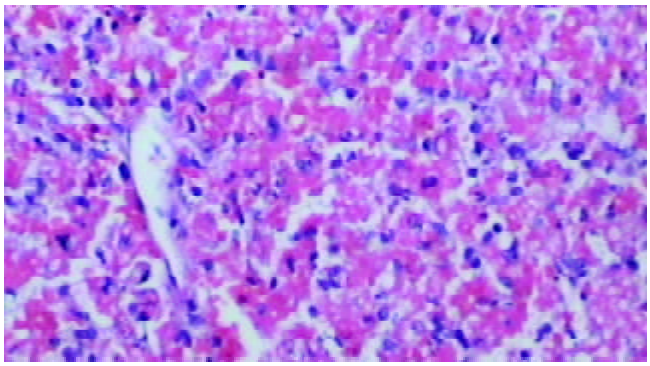

Figure 1 Liver tissue from an acute liver failure model rat (HE 200×).

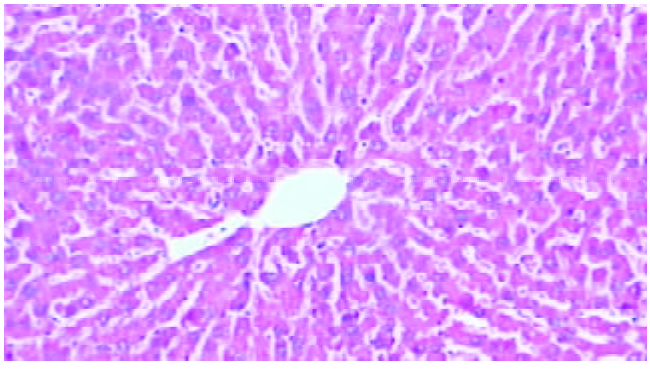

Figure 2 Liver tissue from a rat in neonate cord blood group (HE 100×).

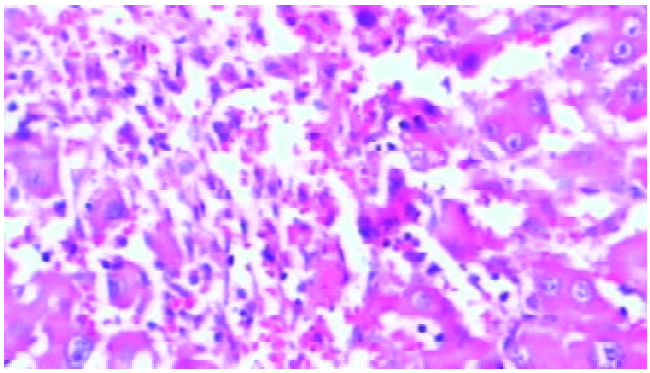

Figure 3 Liver tissue from a rat in control group and normal saline group (HE 400×).

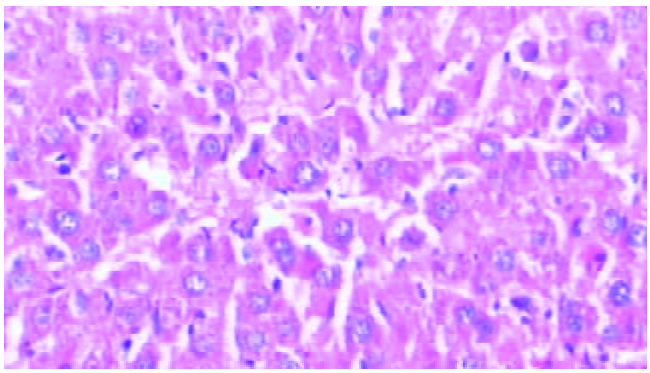

Figure 4 Liver tissue from a rat in adult plasma group (HE 200×).

DISCUSSION

Severe hepatitis is the most ominous manifestation of viral hepatitis. The overall mortality rate of patients with severe hepatitis in stage III to IV coma averages 70-80 %. The management of severe hepatitis includes conventional medical management, plasma exchange, charcoal hemoperfusion, bioartificial liver system and liver transplantation, but the therapeutic effectiveness of all these therapies is not satisfactory. Thus, it is an urgent challenge to find a new reliable therapy for severe hepatitis. Umbilical cord blood (UCB) is the blood that remains in the placenta and umbilical cord after birth. Until recently the placenta and umbilical cord blood were discarded after delivery as a medical waste. The presence of hematopoietic progenitor cells (HPC) in UCB was demonstrated in 1974. Experimental evidences have shown that UCB is a rich source of hematopoietic stem/progenitor cells (HSPC). However, it was not until 1989 that experimental and clinical studies were published, indicating that human UCB could be used in clinical settings. In same year, the first hematopoietic cell transplant in which UCB was used instead of bone marrow as the source of hematopoietic cells was reported. The hematopoietic system of a child with Fanconi's anemia was reconstituted by means of UCB from an HLA-identical sibling. Since then, there has been an expanding interest in the use of UCB as an alternate source of HSPC for transplantation[6]. Some data suggested that UCB was a better source of hematopoietic stem cells than bone marrow[7]. Recipients of cord-blood transplants from HLA-identical siblings have a lower incidence of acute and chronic GVHD than recipients of bone marrow transplants from HLA-identical siblings[8]. Frozen immature human UCB cells can be stored for more than 15 years, and efficiently retrieved, and remain effective for clinical transplantation[9]. After injected into developing neonatal mouse brains, immunodepleted mouse stem cells (MSCs) differentiated into astrocytes and neurons[10].

Intravenous administration of human UCB can reduce neurological deficiency in the rat after traumatic brain injury[11]. Transplantation of genetically marked bone marrow into immunodeficient mice revealed that marrow-derived cells migrated into areas of induced muscle degeneration, underwent myogenic differentiation, and participated in the regeneration of damaged fibers[12]. Experiments demonstrated the cardiomyogenic potential of hematopoietic stem cells[13] and the presence of circulating stem cells with osteogenic and adipogenic differentiation potential in human UCB. Hematopoiesis and the hepatic environment are known to have a close relationship at the time of liver development and systemic diseases. Transplanted cells isolated from bone marrow of rodents and humans have been shown to differentiate into oval cells, which are considered to be hepatic stem cells and hepatocytes in the liver. Purified hematopoietic stem cells have been shown to be able to replace original liver cells in mice with hereditary tyrosinemia. Intravenous injection of adult bone marrow cells in the $FAH^{-/-}$ mouse rescued the mouse and restored the biochemical function of its liver[14]. Hematopoietic stem cells can contribute to the hepatocyte lineage in humans and in rodent models of liver disease and regeneration[15] and adult human liver cells can derive from stem cells originating in the bone marrow or circulation outside the liver[16-18]. Hepatocytes can derive from bone marrow cells after irradiation in the absence of severe acute injury[19]. Adult bone marrow cells have tremendous differentiating capacity as they can also differentiate into epithelial cells of the liver, lung, GI tract, and skin[20, 21]. Human mesenchymal stem cells are thought to be multipotent cells, which are present in adult marrow, that can replicate as undifferentiated cells and have the potential to differentiate to lineages of mesenchymal tissues, including bone, cartilage, fat, tendon, muscle, and marrow stroma[22]. Transdetermination consequent to cell fusion could underlie many observations attributing to an intrinsic plasticity of tissue stem cells[23,24].

UCB can easily be collected and cryopreserved and has a number of significant advantages over bone marrow such as no risk to the donor, no donor attrition, minimal risk of viral transmission, immediate availability, high rate of engraftment, more tolerant of tissue mismatches and lower rate of rejection.

In the present study, we observed that TBil content reduced and Alb, PTA increased after treatment in all groups, especially in UCBT group, PE group and UCBT+PE group. The best therapeutic effectiveness was shown in UCBT+PE group. The effects of reducing Tbil content and increasing Alb and PTA in UCBT+PE group were more significant than those in control group ($P<0.01$) and PE group ($P<0.05$). This indicates that UCBT can enhance the therapeutic effectiveness of PE on severe hepatitis. Although the effect in UCBT+PE group was also better than that in UCBT group, the difference was not significant ($P<0.05$). The therapeutic effectiveness in UCBT group was significantly better than that in control group ($P<0.05$), indicating that UCB can more effectively improve liver function than adult plasma. The reason may be that stem cells derived from UCB can differentiate into hepatocytes and cholangiocytes in a culture system simulating liver regeneration and containing cholestatic serum, which is similar to the condition of patients with severe hepatitis[25-28].

We also found that active T lymphocytes, $CD4^+$ lymphocytes and IL2 were evidently increased after treatment in UCBT group and UCBT+PE group, but no significant improvement of immune function was found in control group and PE group. The results indicate that UCB can improve the immune function of patients with severe hepatitis. It may be because stem cells derived from UCB can differentiate into lymphocytes and reconstitute thymic function[29-32].

The animal experiment demonstrated that the survival rate of rats in neonate cord blood group was significantly higher than that in adult plasma group ($P<0.05$), control group and normal saline group ($P<0.01$), and the ALT and TBil values in neonate cord blood group were obviously lower than those in control groups, saline group ($P<0.01$) and adult plasma group ($P<0.05$). The histopathological examination of rats' livers showed that only mild hepatocyte necrosis and mononuclear cell infiltration were present in the rats of neonate cord blood group after treatment, but massive hepatocyte necrosis and numerous lymphocytic infiltrations were found in other groups. There was obvious hepatocellular regeneration in neonate cord blood group after treatment. However, there was only a few local hepatocellular regenerations in adult plasma group and no hepatocellular regeneration in normal saline group and control group after treatment. All of these indicate that neonate cord blood can protect liver, decrease hepatic injury and promote hepatocellular regeneration. It implies that there are some liver regeneration stimulating factors in neonate cord plasma and some stem cells in neonate cord blood can differentiate into hepatocytes.

Moreover, no side effect or negative response was found in the patients of UCBT group during whole treatment. It showed a high safety in UCB administration. Transient fever, rash and allergic shock were noticed in some patients in control group, PE group and UCBT+PE group. The results indicate that UCBT is much safer than adult fresh plasma transfusion.

In conclusion, this study shows that UCBT can improve liver function and immune function of patients with severe hepatitis, enhance the therapeutic effectiveness of PE, alleviate hepatic injury and promote hepatocellular regeneration. The study indicates that UCBT is a new reliable and safe therapy for severe hepatitis.

REFERENCES

1 **Schwartz RE,** Reyes M, Koodie L, Jiang Y, Blackstad M, Lund T, Lenvik T, Johnson S, Hu WS, Verfaillie CM. Multipotent adult progenitor cells from bone marrow differentiate into functional hepatocyte-like cells. *J Clin Invest* 2002; **109**: 1291-1302

2 **Buzanska L,** Machaj EK, Zablocka B, Pojda Z, Domanska-Janik K. Human cord blood-derived cells attain neuronal and glial features *in vitro*. *J Cell Sci* 2002; **115**(Pt 10): 2131-2138

3 **Brazelton TR,** Rossi FM, Keshet GI, Blau HM. From marrow to brain: expression of neuronal phenotypes in adult mice. *Science* 2000; **290**: 1775-1779

4 **Petersen BE,** Bowen WC, Patrene KD, Mars WM, Sullivan AK, Murase N, Boggs SS, Greenberger JS, Goff JP. Bone marrow as a potential source of hepatic oval cells. *Science* 1999; **284**: 1168-1170

5 **Fiegel HC,** Lioznov MV, Cortes-Dericks L, Lange C, Kluth D, Fehse B, Zander AR. Liver-specific gene expression in cultured human hematopoietic stem cells. *Stem Cells* 2003; **21**: 98-104

6 **Rocha V,** Cornish J, Sievers EL, Filipovich A, Locatelli F, Peters C, Remberger M, Michel G, Arcese W, Dallorso S, Tiedemann K, Busca A, Chan KW, Kato S, Ortega J, Vowels M, Zander A, Souillet G, Oakill A, Woolfrey A, Pay AL, Green A, Garnier F, Ionescu I, Wernet P, Sirchia G, Rubinstein P, Chevret S, Gluckman E. Comparison of outcomes of unrelated bone marrow and umbilical cord blood transplants in children with acute leukemia. *Blood* 2001; **97**: 2962-2971

7 **Kim DK,** Fujiki Y, Fukushima T, Ema H, Shibuya A, Nakauchi H. Comparison of hematopoietic activities of human bone marrow and umbilical cord blood CD34 positive and negative cells. *Stem Cells* 1999; **17**: 286-294

8 **Rocha V,** Wagner JE Jr, Sobocinski KA, Klein JP, Zhang MJ, Horowitz MM, Gluckman E. Graft-versus-host disease in children who have received a cord-blood or bone marrow transplant from an HLA-identical sibling. Eurocord and international bone marrow transplant registry working committee on alternative donor and stem cell sources. *N Engl J Med* 2000; **342**: 1846-1854

9 **Broxmeyer HE,** Srour EF, Hangoc G, Cooper S, Anderson SA, Bodine DM. High-efficiency recovery of functional hematopoi-

etic progenitor and stem cells from human cord blood cryopreserved for 15 years. *Proc Natl Acad Sci U S A* 2003; **100**: 645-650

10 **Kopen GC,** Prockop DJ, Phinney DG. Marrow stromal cells migrate throughout forebrain and cerebellum, and they differentiate into astrocytes after injection into neonatal mouse brains. *Proc Natl Acad Sci U S A* 1999; **96**: 10711-10716

11 **Lu D,** Sanberg PR, Mahmood A, Li Y, Wang L, Sanchez-Ramos J, Chopp M. Intravenous administration of human umbilical cord blood reduces neurological deficit in the rat after traumatic brain injury. *Cell Transplant* 2002; **11**: 275-281

12 **Ferrari G,** Cusella-De Angelis G, Coletta M, Paolucci E, Stornaiuolo A, Cossu G, Mavilio F. Muscle regeneration by bone marrow-derived myogenic progenitors. *Science* 1998; **279**: 1528-1530

13 **Jackson KA,** Majka SM, Wang H, Pocius J, Hartley CJ, Majesky MW, Entman ML, Michael LH, Hirschi KK, Goodell MA. Regeneration of ischemic cardiac muscle and vascular endothelium by adult stem cells. *J Clin Invest* 2001; **107**: 1395-1402

14 **Lagasse E,** Connors H, Al-Dhalimy M, Reitsma M, Dohse M, Osborne L, Wang X, Finegold M, Weissman IL, Grompe M. Purified hematopoietic stem cells can differentiate into hepatocytes *in vivo*. *Nat Med* 2000; **6**: 1229-1234

15 **Austin TW,** Lagasse E. Hepatic regeneration from hematopoietic stem cells. *Mech Dev* 2003; **120**: 131-135

16 **Alison MR,** Poulsom R, Jeffery R, Dhillon AP, Quaglia A, Jacob J, Novelli M, Prentice G, Williamson J, Wright NA. Cell differentiation: Hepatocytes from non-hepatic adult stem cells. *Nature* 2000; **406**: 257

17 **Theise ND,** Nimmakayalu M, Gardner R, Illei PB, Morgan G, Teperman L, Henegariu O, Krause DS. Liver from bone marrow in humans. *Hepatology* 2000; **32**: 11-16

18 **Strain AJ,** Crosby HA. Hepatic stem cells. *Gut* 2000; **46**: 743-745

19 **Theise ND,** Badve S, Saxena R, Henegariu O, Sell S, Crawford JM, Krause DS. Derivation of hepatocytes from bone marrow cells in mice after radiation-induced myeloablation. *Hepatology* 2000; **31**: 235-240

20 **Overturf K,** Al-Dhalimy M, Finegold M, Grompe M. The repopulation potential of hepatocyte populations differing in size and prior mitotic expansion. *Am J Pathol* 1999; **155**: 2135-2143

21 **Krause DS,** Theise ND, Collector MI, Henegariu O, Hwang S, Gardner R, Neutzel S, Sharkis SJ. Multi-organ, multi-lineage engraftment by a single bone marrow-derived stem cell. *Cell* 2001; **105**: 369-377

22 **Pittenger MF,** Mackay AM, Beck SC, Jaiswal RK, Douglas R, Mosca JD, Moorman MA, Simonetti DW, Craig S, Marshak DR. Multilineage potential of adult human mesenchymal stem cells. *Science* 1999; **284**: 143-147

23 **Terada N,** Hamazaki T, Oka M, Hoki M, Mastalerz DM, Nakano Y, Meyer EM, Morel L, Petersen BE, Scott EW. Bone marrow cells adopt the phenotype of other cells by spontaneous cell fusion. *Nature* 2002; **416**: 542-545

24 **Ying QL,** Nichols J, Evans EP, Smith AG. Changing potency by spontaneous fusion. *Nature* 2002; **416**: 545-548

25 **Avital I,** Feraresso C, Aoki T, Hui T, Rozga J, Demetriou A, Muraca M. Bone marrow-derived liver stem cell and mature hepatocyte engraftment in livers undergoing rejection. *Surgery* 2002; **132**: 384-390

26 **Avital I,** Inderbitzin D, Aoki T, Tyan DB, Cohen AH, Ferraresso C, Rozga J, Arnaout WS, Demetriou AA. Isolation, characterization, and transplantation of bone marrow-derived hepatocyte stem cells. *Biochem Biophys Res Commun* 2001; **288**: 156-164

27 **Romanov YA,** Svintsitskaya VA, Smirnov VN. Searching for alternative sources of postnatal human mesenchymal stem cells: candidate MSC-Like cells from umbilical cord. *Stem Cells* 2003; **21**: 105-110

28 **Austin TW,** Lagasse E. Hepatic regeneration from hematopoietic stem cells. *Mech Dev* 2003; **120**: 131-135

29 **Ferrandina G,** Pierelli L, Perillo A, Rutella S, Ludovisi M, Leone G, Mancuso S, Scambia G. Lymphocyte recovery in advanced ovarian cancer patients after high-dose chemotherapy and peripheral blood stem cell plus growth factor support: clinical implications. *Clin Cancer Res* 2003; **9**: 195-200

30 **Down JD,** White-Scharf ME. Reprogramming immune responses: enabling cellular therapies and regenerative medicine. *Stem Cells* 2003; **21**: 21-32

31 **Peggs KS,** Verfuerth S, D'Sa S, Yong K, Mackinnon S. Assessing diversity: immune reconstitution and T-cell receptor BV spectratype analysis following stem cell transplantation. *Br J Haematol* 2003; **120**: 154-165

32 **Hakim FT,** Gress RE. Reconstitution of thymic function after stem cell transplantation in humans. *Curr Opin Hematol* 2002; **9**: 490-496

Edited by Zhu LH and Wang XL

P.O.Box 2345, Beijing 100023,China
Fax: +86-10-85381893
E-mail: wjg@wjgnet.com www.wjgnet.com

World J Gastroenterol 2003;9(9):2004-2008
World Journal of Gastroenterology
 ISSN 1007-9327

• VIRAL HEPATITIS •

Role of hepatitis B virus infection in pathogenesis of IgA nephropathy

Nian-Song Wang, Zhao-Long Wu, Yue-E Zhang, Mu-Yi Guo, Lv-Tan Liao

Nian-Song Wang, Department of Nephrology, the Sixth Affiliated Hospital of Shanghai Jiaotong University, 600 Yushan Road, Shanghai 200233, China
Zhao-Long Wu, Lv-Tan Liao, Department of Nephrology, Zhongshan Hospital, Fudan University, 180 Fenglin Road, Shanghai 200032, China
Yue-E Zhang, Mu-Yi Guo, Department of Pathology, Fu Dan University, 136 Yixue Road, Shanghai 200032, China
Supported by the National Natural Science Foundation of China, N0. 39770292
Correspondence to: Nian-Song Wang, Department of Nephrology, The Sixth Affiliated Hospital of Shanghai Jiaotong University, 600 Yushan Road, Shanghai 200233, China. wangniansong@yahoo.com.cn
Telephone: +86-21-64369181-8393 **Fax:** +86-21-64701361
Received: 2003-03-02 **Accepted:** 2003-04-19

Abstract

AIM: To investigate the role of hepatitis B virus (HBV) in the pathogenesis of IgA nephropathy (IgAN).

METHODS: HBV antigens (HBAg, or HBsAg, HBcAg, and HBeAg) in renal tissues with IgAN were detected by immunohistochemical technique. The distribution and localization of HBV DNA were observed by using *in situ* hybridization. Southern blot analysis was performed to reveal the state of renal HBV DNA.

RESULTS: Among 100 patients with IgAN, HBs antigenemia was detected in 18 patients (18.00 %). HBAg in renal tissues was detected in 31 patients (31.00 %), the positive rate of HBAg, HBsAg and HBcAg was 64.52 % (20/31), 32.26 % (10/31), 32.26 % (10/31), respectively in glomeruli. HBcAg was also found in tubular epithelia and interstitia, which was 45.16 % (14/31) and 6.45 % (2/31), respectively. Five out of six cases with positive HBV DNA by *in situ* hybridization were proved to be HBV DNA positive by Southern blot analysis, and all were of the integrated form. Eight specimens were demonstrated to be HBV DNA positive by *in situ* hybridization, which was localized in the nuclei of tubular epithelial cells and glomerular mesangial cells as well as in infiltrated interstitial lymphocytes.

CONCLUSION: There is a relationship between HBV infection and IgAN. In addition to the humoral immune damage mediated by HBAg-HBAb immune complex, the cellular mechanism mediated by HBV originating from renal cells *in situ* may be also involved in the pathogenesis of IgAN.

Wang NS, Wu ZL, Zhang YE, Guo MY, Liao LT. Role of hepatitis B virus infection in pathogenesis of IgA nephropathy. *World J Gastroenterol* 2003; 9(9): 2004-2008
http://www.wjgnet.com/1007-9327/9/2004.asp

INTRODUCTION

The association between chronic hepatitis B virus (HBV) infection and glomerular diseases was first described in 1971[1], and various morphological patterns including membranous nephropathy, membranoproliferative glomerulonephritis (MN), mesangial proliferative glomerulonephritis (MPGN), minimal change nephropathy, and IgA nephropathy have been reported since then[1-28]. IgA nephropathy is considered the most common glomerular disease worldwide. Its prevalence varies considerably among and within countries, yet the pathogenetic mechanisms still remain largely uncertain[29,30]. Coexistence of mesangial proliferative glomerulonephritis with predominant mesangial IgA deposits and persistent hepatitis B virus surface antigenemia was first reported in five patients by Nagy *et al*[4], and later in some other reports[13,15,17,25,27], but the number of IgA nephropathy was fewer. Since China is an endemic area of hepatitis B virus (HBV) infection, and there is an incidence of 32 % IgA nephropathy in primary glomerulonephritis, according to a clinical analysis of 1001 cases by Li *et al*[31]. The relationship between IgA nephropathy and HBV infection is attracting increasing attention. In order to clarify the possible role of HBV infection in the pathogenesis of IgA nephropathy, we detected the serum HBV marker, HBV antigens (HBsAg, HBcAg, HBeAg) in renal tissues by immunohistochemistry technique, and HBV DNA in renal tissues by *in situ* hybridization and Southern bolt analysis.

MATERIALS AND METHODS

Patients

One hundred patients with IgA nephropathy who were admitted to our hospital during the period from 1982 to 1993 were included in the study. Their clinical data were complete and pathological diagnoses were confirmed by light microscopy and immunofluorescence examination (fresh renal tissue was used for immunofluorescence). The criteria for patients selection were no prior history of jaundice or liver disease, no previous history of blood transfusion, normal liver functions, no history of intravenous drug addiction, absence of cryoglobulinemia, and no clinical and laboratory evidences of secondary renal lesions such as lupus nephritis, *Henoch-Schonlein* purpura glomerulonephritis. All the patients received the following laboratory tests of urinalysis, serum creatinine and blood urea concentration, proteinuria, creatinine clearance at varying intervals during the study period. None had liver biopsies. Five patients without any HBV infection markers in serum or renal tissue were used as control. The following serial investigations were performed.

Serologic tests for HBV markers

Tests for HBV antigens and antibodies were performed before renal biopsy and regularly thereafter. Double antibody sandwich ELISA was used for detecting HBsAg and HBeAg, while double antigen ELISA was used for detecting anti-HBs and antibody competitive ELISA for detecting anti-HBe and anti-HBc. The kits of the test reagents were purchased from Shanghai Medical Laboratory.

Immunohistochemistry

The biopsy tissue was cut into three to four pieces. One piece

was fixed in 95 % ethanol and processed for 4 μm thick paraffin sections, which were stained by hematoxylin and eosin (HE) and periodic acid silver methanamine (PASM). The second piece was embedded in OCT compound (Miles Inc., Elkhart Inc., USA), and cut into 5 μm thick sections for detecting IgG, IgA, IgM and C_3 with direct immunofluorescence. The relevant antibodies were labelled with fluorescein (FITC) (Dako Corporation, Santa Barbara, CA, USA). The third piece was prefixed with 0.25 % glutaldehyde and postfixed with 1 % osmium and cut into ultrathin sections by conventional methods for electron microscopic observation. The fourth part was freshly preserved at -70 ℃ for Southern blot analysis.

Detection of HBVAg in renal tissue

The immunohistochemistry method was used mainly to detect the distribution of immunoglobulin, HBsAg, HBcAg, and HBeAg. The 4 μm thick tissue sections were digested with 0.05 % trypsin for 15 min at 37 ℃ to expose the epitopes of HBeAg, HBsAg and HbcAg. The ABC (Avidin-Biotin-Peroxidase) complex method kit for examining HBeAg and rabbit-anti-HBcAg in peroxidase-antiperoxidase (PAP) complex kit were purchased from Dako Company (Dakopatts, Denmark, U.S.A.). The PAP kit for HBcAg, and horseradish peroxidase-labelled goat anti-human IgG, IgA, IgM for immunofluorescence examination, and other antibodies were prepared by the Department of Pathology, Shanghai Medical University. The first antibodies for HBV antigens were goat anti-HBs, mouse anti-HBe and rabbit anti-HBcAg, respectively. The specificity of staining for HBV antigens was determined by blocking and absorption procedures as previously described by Lai *et al*[2]. Cross reactivities of anti-HBV antigen (s) with each other and with immunoglobulins, complements, and fibrinogen, normal and sclerosed glomerular tissues from HBsAg-negative controls were not found. Normal sheep and rabbit sera were used as negative control.

In situ hybridization

Paraffin fixed 4 μm thick sections were used for *in situ* hybridization. The digoxigenin labelled full-length HBV DNA probe prepared from an HBV plasmid clone of pBR322 and labelled with digoxigenin by random labelling and detection kit[32] were provided by Beijing Hepatitis Research Institute. The main procedures of *in situ* hybridization were as follows: (1) Paraffin fixed sections were dewaxed by conventional methods and digested with proteinase K (Sigma,0.5 mg/ml in Tris-HCL,0.01 mol/L pH 7.2) at 37 ℃ for 15 min and washed in 0.2 % glycine/0.01 % phosphate buffered saline (PBS) at pH 7.4. (2) The sections were fixed in 4 % paraformaldehyde at room temperature for 10 min. (3) The sections were then treated with 0.2 % acetic anhydride/triethanolamine (0.1 mol/L pH 8.0) at RT for 10 min. (4) The sections were treated with prehybridized medium (5×standard saline citrate (SSC)/0.1 % N-lauroylsarcosine/0.02 % sodium dodecylsulfate (SDS)/0.1 % blocking solution of BK) at room temperature for 15 min (5) Digoxigenin labelled HBV DNA probe was added (400 ng/mL), denatured at 100 ℃ for 10 min, hybridized at 60 ℃ for 16-20 h and washed in 2×SSC, 0.2×SSC, 0.1×SSC and 0.1 % Tween 20/buffer 1 (according to BK) sequentially, (6) Then it was pretreated with 5 % normal sheep serum/3 % bovine serum albumin (BSA) at room temperature for 20 min. (7) Sheep anti-digoxigenin labelled with alkaline phosphatase was added (BK) at 37 ℃ for 2 h, then washed in 0.1 % Tween 20/buffer III (according to BK). (8) it was then visualized by nitroblue tetrazolium salt(NBC)/5-bromo-4-chloro-3 indolyphosphate koluidium salt (BCIP;BK).

Examination of *in sit*u hybridization was retrospectively performed within several days by the same person. The specificity of *in situ* hybridization was confirmed by the negative controls. For example, the specific HBV DNA-digoxigenin probe was omitted, pBR328 DNA- digoxigenin probe was used (BK) instead of the HBV DNA- digoxigenin probe, DNase (Sigma, Chemical Co., St Louis, MO, USA 100 ug/mL) was digested.

Southern blot analysis

The fresh specimens preserved at -70 ℃ were processed for the detection of renal HBV DNA by Southern blot analysis. The ^{32}P(a)-dCTP labelled HBV DNA probe and the procedures used were the same as reported previously[18-27].

RESULTS

Serologic findings

Of the 100 patients in this study, 52 were males and 48 were females, (ranging 18-62 years, average 32.8 years). Eighteen patients were found to be HBsAg positive in their sera. Serum HBeAg was detected in four patients. Positive anti-HBe, HBcAb and anti-HBs were found in 7, 13, and 1 patients, respectively.

Detection of HBVAg in renal tissue

Detectable rate of HBAg (HBsAg, HBcAg and HBeAg) in glomeruli and renal tubules by immunohistochemistry was 31 % (31/100). The glomerular distribution of positive HBAg in 31 cases was as follows. Twenty cases were HBAg positive in the glomeruli, including HBsAg in 10 (32.26 %), and HBcAg in 10 (32.26 %). In addition, HBcAg was deposited in tubular epithelial cells (14 cases, 45.16 %) and renal interstitia (2 cases, 6.45 %). Three out of 20 cases were found to be HBeAg positive in glomerular cells (15 %). The distribution of HBAg in glomeruli varied either in capillary loops or in mesangial region or both. Both HBsAg and HBcAg were located in the cytoplasm of tubular epithelium. Occasionally HBcAg could be visualized in the nuclei of tubular cells.

Serologic and clinical findings

Among the 31 patients with positive HBVAg in renal tissues, eight were found to be HBsAg positive in their sera. Serum HBeAg was detected in one patient, HBeAb was positive in three patients, HBcAb was positive in seven patients. Clinical findings showed gross hematuria in 9 cases, microscopic hematuria in 5 cases, proteinuria in 6 cases, nephrotic syndrome in 5 cases, chronic renal failure in 2 cases and hypertension in 4 cases.

Detection of HBV DNA in renal tissue by in situ hybridization

HBV DNA was detected in eight out of the 31 specimens of renal tissues by *in situ* hybridization. Among the eight patients, four were found to be HBsAg positive in their sera. HBeAg was detected in one patient, HBeAb was positive in two patients, HBcAb was positive in four patients and HBsAb was positive in one patient. HBVAg was positive in the renal tissue, HBcAg was positive in glomerular cells and tubular cells in 7 and 3 cases respectively. HBsAg was positive in 1 and 4 cases, respectively. Eight cases were demonstrated to be HBV DNA positive in tubular epithelia by *in situ* hybridization, the positive rate was 100 % (Figure 1). The amount of HBV DNA positive cells varied in different cases. The positive signal of hybridization was localized within the nucleus. HBV DNA was detected in glomeruli in 6 out of the 8 specimens, the positive rate was 75 % (Figure 2).

Detection of HBV DNA in renal tissue by Southern blot

Five out of the 6 specimens with positive HBV DNA in glomeruli were found to be HBV DNA positive by Southern

blot analysis, the positive rate was 83.33 %. All of these positive specimens were identified to be the integrated form of HBV DNA , and none was identified as non-replicating free form of HBV DNA with a single band of signals at 3.2 Kb in length. The integrated HBV DNA by Southern blot analysis showed a high molecular weight single band before digestion, and revealed irregular multiple bands after ECoRI restrictive enzyme treatment.

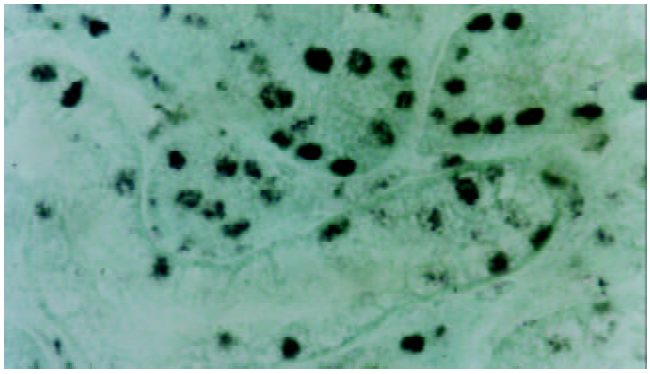

Figure 1 HBV DNA signals detected in nuclei of tubular cells by *in situ* hybridization. X200

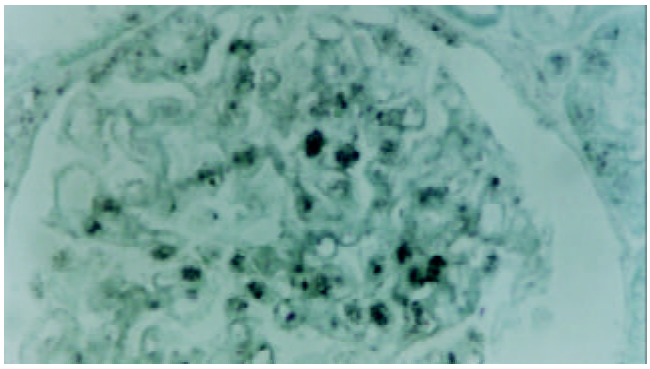

Figure 2 HBV DNA signals detected in nuclei of glomerular mesangial cells by *in situ* hybridization. X400

Relationship of positive HBV infectious markers in sera and HBAg and HBV DNA in renal tissues

The appearance of HBV infection markers in sera and HBAg and HBV DNA in renal tissues of the 8 cases of IgAN is shown in Table 1.

Neither HBAg nor HBV DNA was found in the sera or renal tissues in the five control cases of IgA nephropathy.

DISCUSSION

IgA nephropathy has been confirmed to be an immune complex-mediated glomerulonephritis defined morphologically by mesangial deposition of IgA, but the etiology is still uncertain[29,30]. The etiologic role of HBV antigenemia and HBV antigen deposition in IgA nephropathy remains speculative. It most likely involved mesangial and subendothelial trapping of circulating immune complexes (CICs), and the observations that preformed CICs primarily resulted in mesangial and subendothelial deposits supported this mechanism[29,30]. The possible role of HBV antigens was highly suspected especially in endemic areas of HBV infection such as in Southeastern Asia[13,27]. Many efforts have been contributed to this field[13,15,17,25,27], yet the data are scattered and incomplete because of the difficulty in obtaining tissue specimens, complicated clinical settings, and less specific and sensitive detection techniques. Lai *et al*[13] reported HBs antigenemia was detected in 21 out of 122 patients (17.2 %), which was significantly higher than the prevalence of HBsAg carriers in the general population ($P<0.01$). Humoral immune responses triggered by HBAg-HBAb immune complexes were traditionally regarded as the mechanism of tissue injury resulting in HBV-glomerulonephritis (GN). HBsAg, HBcAg and HBeAg with immunoglobulins and complement deposits in the glomeruli of HBV-GN have been demonstrated in many investigations[1-28]. It remains perplexing why some chronic HBsAg carriers develop IgAN whereas some develop membranous glomerulonephritis (MGN) or mesangiocapillary glomerulonephritis (MCGN). This could well be related to HBV antigens as well as the size and charge properties of HBV antigens and their antibodies. The nephrogenicity of the three different kinds of HBAg was therefore suggested. Takekosh[5], Ito[6], Hirose[8], and Zhang[15] emphasized that the molecular weight of HBeAg was the smallest (1×10^5), enabling it to pass through the glomerular basement membrane and to result in the formation of subepithelial dense deposits by microscopy. This is the well known morphologic characteristics of MGN. Local formation of antigen and antibody complexes has been well established to induce diffuse subepithelial immune deposits and proteinuria characteristic of HBV-MGN. Therefore, HBeAg is considered to be nephrogenic for MGN[5-8,15]. In contrast, the large size of HBsAg[2-4,7,9,13,15,25,27] and anionic nature of IgAN[27,29,30] favor the mesangial localization of HBsAg-anti-HBs complexes in HBV-IgAN. However, high frequencies of HBsAg (3×10^6) and HBcAg (8×10^6) were also detected in the capillary loops of glomeruli of MGN by other investigators[1,6,17,20,25,34].

Glomerular detection of HBV DNA has been reported in the kidneys of chronic HBsAg carriers with different glomerulonephritis[13,20,35], yet the consistency of these findings

Table 1 Detection results of HBV infection markers in sera and HBAg and HBV DNA in renal tissues in 8 cases of IgA nephropathy

Case	Age	Sex	Course	Serum HBVmarkers					Renal HBAg				Renal HBV DNA		
				HBAg		HBAb			T		G		ISH		Southern blot
				HBsAg	HBeAg	HBsAb	HBeAb	HBcAb	HBsAg	HBcAg	HBsAg	HBcAg	T	G	
1	30	F	4a	+	-	-	-	+	-	+	+	+	+	+	+
2	32	M	8m	+	-	-	-	-	-	+	+	-	+	+	+
3	35	M	2a	-	-	-	-	-	-	+	+	-	+	+	+
4	38	M	13a	+	-	-	+	+	-	+	-	+	+	+	+
5	35	F	5a	-	-	+	-	-	+	-	-	-	+	-	-
6	36	F	7m	+	-	-	-	+	+	-	+	+	+	+	+
7	32	M	2m	-	-	-	+	-	-	+	-	-	+	-	-
8	26	M	6a	-	-	-	-	+	-	+	+	-	+	+	+

F, female. M, male. d, day. m, month. a, year. T, tubules. G, glomeruli. ISH, *in situ* hybridization. +, positive. -, negative.

remains controversial, since some investigators have been unable to detect similar findings in chronic HBV carriers with coexisting membranous nephropathy[36]. This issue is of importance in understanding the pathogenesis of HBV-related glomerulonephritis. Therefore, with the help of *in situ* hybridization (ISH) and Southern blot analysis for HBV DNA, and highly sensitive and specific biological techniques, we found evidence for the presence of viral transcription in glomerular cells and renal tubular epithelia, which supported an etiological role of HBV in some chronic HBsAg carriers who developed coexisting glomerulonephritis[18,19,23,24,26,27]. Thereafter, the question of whether the existence of HBV DNA in renal tissue of glomerulonephritis is a general phenomenon and what role HBV DNA plays in the pathogenesis of renal tissue injury has been raised. In this serial investigation of 8 cases of IgAN, we found that HBV DNA detectable rate by *in situ* hybridization was 100 %. The positive frequencies were relevant to HBV antigenaemia and the detectable renal HBAg by immunohistochemistry. Since the presence of HBcAg in glomeruli might be not only from HBV DNA positive glomerular cells but also from circulation, the detectable rate of HBcAg in glomeruli has a close correlation with serum HBV antigenaemia and HBV DNA both in serum and renal tissue. The presence of HBcAg and HBV DNA in tubular epithelia might indicate HBV replication in epithelial cells, which were consistent with other studies in transgenic mice revealing the expression of viral genome of HBcAg or HBeAg only in epithelial cells[37-39]. In our study, 5 out of 6 patients with positive HBV DNA by *in situ* hybridization were HBV DNA positive by Southern blot analysis, all of them were integrated form. Since the number and molecular weight of the bands of HBV DNA signals of integrated form varied, it was suggested that HBV DNA integration was random. The infected cells with free form of HBV DNA, consisting of full genome of HBV, might theoretically express HBAg. However, if only some fragments of HBV DNA integrated into the chromosomes of the host cells randomly, whether the cells expressed HBAg would depend on whether the integrated part was consisted of certain intact HBAg genomes and their matched promotors as the elements of franking sequence of HBV DNA. Therefore, the kidney might carry dormant HBV DNA after HBV infection[19,23,27] (as found in the liver) or expressed HBAg to trigger immune reaction and result in tissue injury, which might be mediated by HBAg-HBAb immune complexes together with complements. Meanwhile, another possibility arises that HBV infected renal cells with the target HBcAg expression might activate T lymphocytes the relevant lymphokines to result in increased permeability of glomerular epithelial cells and glomerular basement membrane (nephrotic syndrome) or proliferation of glomerular cells (proliferative glomerulonephritis or IgAN).

Immune regulation defect was hypothesized to play a key role in the pathogenesis of IgA nephropathy[29]. Immune system disorder seemed to be related with secondary infections such as HBV infection or activation of HBV infection[40-42]. In IgA nephropathy patients, the spectrum of antibodies could be extended from both fixed and circulating endogenous antigens[30]. Studies of T lymphocytes suggested that increased T help (CD4) lymphocytes and decreased T suppresser (CD8) lymphocytes occurred with exacerbation of the disease, but overproduction of IgA was probably the consequence of the involvement of both T and B lymphocytes. This might provide some clue to the elevated serum concentration of IgA in our patients. However, whether clearance impairment of IgA immune complexes in hepatic and splenic phagocytic system or elevated levels of CICs involve in the pathogenesis of IgAN are yet to be determined.

We found that HBAg in renal biopsy specimens was mainly glomerular and renal tubular HBsAg and HBcAg. They are large molecular weight antigens forming CIC after binding to appropriate antibodies. It is believed that HBsAg preferentially deposites in mesangial region and subendothelial cells, while HBeAg as a part of viral nucleoprotein is expected to be capable of inducing membranous nephropathy by preferentially depositing along capillary walls. Since HBV DNA genome was detected in glomerular mesangium of patients with HBV associated glomerulonephritis[25], the possibility of immune complex formation *in situ* couldnot be excluded. It is noteworthy that, although many previous studies described the predominant deposition of HBV in glomeruli similar to ours, HBV DNA (ISH) was confirmed to exist extensively in glomeruli, renal tubules, interstitium and capsule[26]. This phenomenon could be attributed to the sensitive and specific techniques employed. Lai *et al* noticed that HBV DNA was found mainly in cytoplasm of proximal tubular epithelia but not in glomerular cells[24]. Zhang had the similar finding[23]. Whether HBV DNA in renal tubules represents endocytosis of HBV DNA in urinary filtrates or the direct invasion of HBV needs further study. In addition, mesangial IgA deposition was possibly resulted from the structural immunological or physicochemical abnormality in IgA nephropathy[29]. Recently Zhang *et al* examined T cell subsets infiltration in interstitia of HBV-GN by immunohistochemistry with monoclonal antibodies against CD3, CD4 and CD8, and found that there were certain relationships between the expression of HBcAg in tubular epithelial cells and the amount of phenotypes of infiltrated T cells in interstitia[23]. There is a possibility that such a relationship might be involved in the frequent occurrence of tubular atrophy with prominent interstitial inflammation and persistent clinical course in some HBV-GN patients.

Our investigation by both *in situ* hybridization and Southern blot analysis revealed that the presence of HBV DNA in renal tissues of IgAN patients with coexisting HBV antigenaemia appeared to be a general phenomenon among IgAN patients in Shanghai, China. Evidences showed that the renal tissue was infected with HBV, HBAg deposited in glomeruli was not only from circulation but also from infected glomerular cells. However, this study did not provide conclusive evidences for the hypothesis. It is suggested that cellular immune mechanism might be involved in the pathogenesis of HBV-GN in addition to humoral immune injury. These concepts might better our understanding of the pathogenesis of HBV related IgAN both theoretically and clinically.

In conclusion, our findings indicate that the host tissue tropism of HBV is not limited to hepatocytes, and active viral transcription is present in glomerular cells and tubular epithelia. Hepatitis B virus might be the etiologic agent of some chronic HBsAg carriers with coexisting IgA nephropathy. There is a relationship between HBV infection and IgAN. In addition to humoral immune injury mediated by HBAg-HBAb immune complexes, cellular mechanism mediated by HBV originating from renal cells *in situ* might also be involved in the pathogenesis of IgAN.

REFERENCES

1 **Combes B**, Shorey J, Barrera A, Stastny P, Eigenbrodt EH, Hull AR, Carter NW. Glomerulonephritis with deposition of Australia antigen-antibody complexes in glomerular basement membrane. *Lancet* 1971; **2:** 234-237

2 **Knieser MR**, Jenis EH, Lowenthal DT, Bancroft WH, Burns W, Shalhoub R. Pathogenesis of renal disease associated with viral hepatitis. *Arch Pathol* 1974; **97:** 193-200

3 **Brzosko WJ**, Krawczynski K, Nazarewicz T, Morzycka M, Nowoslawski A. Glomerulonephritis associated with hepatitis-B surface antigen immune complexes in children. *Lancet* 1974; **2:** 477-482

4 **Nagy J**, Bajtai G, Brasch H, Sule T, Ambrus M, Deak G, Hamori A. The role of hepatitis B surface antigen in the pathogenesis of glomerulopathies. *Clin Nephrol* 1979; **12:** 109-116

5 **Takekoshi Y**, Tanaka M, Miyakawa Y, Yoshizawa H, Takahashi K, Mayumi M. Free "small' and IgG-associated "large" hepatitis B e antigen in the serum and glomerular capillary walls of two patients with membranous glomerulonephritis. *N Eng J Med* 1979; **300:** 814-819

6 **Ito H**, Hattori S, Matusda I, Amamiya E, Hajikano H, Yoshizawa H, Miyakawa Y, Mayumi M. Hepatitis B e antigen-mediated membranous glomerulonephritis. Correlation of ultrastructural changes with HBeAg in the serum and glomeruli. *Lab Invest* 1981; **44:** 214-220

7 **Furuse A**, Hattori S, Terashima T, Karashima S, Matsuda I. Circulating immune complex in glomerulonephropathy associated with hepatitis B virus infection. *Nephron* 1982; **31:** 212-218

8 **Hirose H**, Udo K, Kojima M, Takahashi Y, Miyakawa Y, Miyamoto K, Yoshizawa H, Mayumi M. Deposition of hepatitis B e antigen in membranous glomerulonephritis: identification by F(ab') 2 fragments of monoclonal antibody. *Kidney Int* 1984; **26:** 338-341

9 **Zhang YE**, Guo MY, Yin JF, Wong NP, Zhang XR, Wang YX, Qiu CL. Immunopathological study of hepatitis B virus immune complex glomerulonephritis. *Zhonghua Shensangbing Zazhi* 1986; **2:** 127-130

10 **Takeda S**, Kida H, Katagiri M, Yokoyama H, Abe T, Hattori H. Characteristics of glomerular lesions in hepatitis virus infection. *Am J Kidney Dis* 1988; **11:** 57-62

11 **Lai KN**, Lai FM, Chan KW, Chow CB, Tong KL, Vallance-Owen J. The clinico-pathologic features of hepatitis B virus-associated glomerulonephritis. *Q J Med* 1987; **63:** 323-333

12 **Ishihara T**, Akamatsu A, Takahashi M, Yamashita Y, Yokota T, Nagasawa T, Gondo T, Kawano H, Kawamura S, Uchino F. Ultrastructure of kidney from three patients with HBeAg-associated nephropathy with special reference to virus-like particles in the glomerular tufts. *Acta Pathol Jpn* 1988; **38:** 339-350

13 **Lai KN**, Lai FM, Tam JS, Vallance-Owen J. Strong association between IgA nephropathy and hepatitis B surface antigenemia in endemic areas. *Clin Nephrol* 1988; **29:** 229-234

14 **Thyagarajan SP**, Thirunalasundari T, Subramanian S, Panchanadam M, Nammalwar BR, Prabha V, Vijayakumar, Jayaraman M. Serum and tissue positivity for hepatitis B virus markers in histopathologically proven glomerulonephropathies. *J Med Microbiol* 1989; **29:** 243-249

15 **Zhang YE**, Guo MY, Ying YY. Further study on the immunopathology of hepatitis B virus associated glomerulonephritis. *Zhonghua Neike Zazhi* 1990; **29:** 526-529

16 **Zhou WZ**, Zhang WL, Geng L. Glomerulonephropathy associated with hepatitis B virus (HBV) infection. *Zhonghua Neike Zazhi* 1990; **29:** 530-533

17 **Johnson RJ**, Couser WG. Hepatitis B infection and renal disease: clinical, immunopathogenetic and therapeutic considerations. *Kidney Int* 1990; **37:** 663-676

18 **Fang LJ**, GuoYQ, Zhang YE, Gu JR, Jiang HQ. The study on HBV DNA state in renal tissue of children HBV associated glomerulonephritis. *Zhonghua Shenzangbing Zazhi* 1992; **8:** 65-67

19 **Fang LJ**, Shen FY, Guo YQ, Wu ZL, Lu FM, Zhang YE, Guo MY, Zhang XR. Hepatitis B virus associated nephritis in adults and children. *Zhonghua Chuanran Bingxue Zazhi* 1996; **14:** 92-95

20 **Lin CY**. Hepatitis B virus deoxyribonucleic acid in kidney cells probably leading to viral pathogenesis among hepatitis B virus associated membranous nephropathy patients. *Nephron* 1993; **63:** 58-64

21 **Yan HP**, Lang ZW, Huang DZ. Preparation of digoxigenin labelled probe and detection of HBV DNA in liver and extrahepatic tissue with in situ hybridization. *Zhonghua Neike Zazhi* 1994; **33:** 168-171

22 **Zhang YE**, Fang LJ, Ma XL, Guo MY, Du WD, Zhai WR, Wu ZL, Lin SY, Gu JR. Hepatitis B virus infection and pathogenesis of glomerulonephritis. *Zhonghua Binglixue Zazhi* 1995; **24:** 341-344

23 **Zhang YE**, Ma XL, Fang LJ, Lin SY, Wu ZL, Gu JR. The existence and significance of hepatitis B virus DNA in glomerulonephritis. *Nephrology* 1996; **2:** 119-125

24 **Lai KN**, Ho RT, Tam JS, Lai FM. Detection of hepatitis B virus DNA and RNA in kidneys of HBV related glomerulonephritis. *Kidney Int* 1996; **50:** 1965-1977

25 **Magil A**. IgA nephropathy and membranous nephropathy associated with hepatitis B surface antigenemia. *Hum Pathol* 1988; **19:** 615

26 **Ma XL**, Zhang XR, Du WD, Zhu TF, Zhao ZH, Zhang YE. Detection of HBV DNA and HBAg in renal tissue of IgA nephropathy by using double staining technology. *Shanghai Yile Daxue Xuebao* 1997; **24:** 293-294

27 **Wang NS**, Wu ZL, Zhang YE, Liao LT, Guo MY. Is there relationship between IgA nephropathy (IgAN) and hepatitis B virus (HBV)? *Zhonghua Shenzangbing Zazhi* 1996; **12:** 276-278

28 **He XY**, Fang LJ, Zhang YE, Sheng FY, Zhang XR, Guo MY. In situ hybridization of hepatitis B DNA in hepatitis B associated glomerulonephritis. *Pediatr Nephrol* 1998; **12:** 117-120

29 **Endo Y**, Kanbayashi H. Etiology of IgA nephropathy syndrome. *Pathol Int* 1994; **44:** 1-13

30 **Galla JH**. IgA nephropathy. *Kidney Int* 1995; **47:** 377-387

31 **Li L**, Li LS, Chen HP, Zhou HZ, Ji DX, Tang Z, Yu YS, Bai XY, Zhou H, Zhang JH. Primary glomerulonephritis in China: Analysis of 1001 cases. *Chin Med J* 1989; **102:** 159-164

32 **Yan HP**, Lang ZW, Huang DZ. Preparation of digoxigenin labelled probe and detection of HBV DNA in liver and extrahepatic tissue with in situ hybridization. *Zhonghua Neike Zazhi* 1994; **33:** 168-171

33 **Gauthier VJ**, Striker GE, Mannik M. Glomerular localization of preformed immune complexes prepared with anionic antibodies or with cationic antigens. *Lab Invest* 1984; **50:** 636-644

34 **Li CY**. Treatment of hepatitis B virus-associated membranous nephropathy with recombined alpha-interferon. *Kidney Int* 1995; **47:** 225-230

35 **Dejean A**, Lugassy C, Zafrani S, Tiollais P, Brechot C. Detection of hepatitis B virus DNA in pancreas, kidney, and skin of two human carriers of the virus. *J Gen Virol* 1984; **65**(Pt 3): 651-655

36 **Yu YP**, Wang HY, Chen ML. An in situ hybridization and immunofluorescent double staining study on the pathogenesis of HBV in kidney disease. *Zhonghua Neike Zazhi* 1990; **29:** 538-540

37 **Lai KN**, Tam JS, Lin HJ, Lai FM. The therapeutic dilemma of the usage of corticosteroid in patients with membranous nephropathy and persistent hepatitis B virus surface antigenemia. *Nephron* 1990; **54:** 12-17

38 **Farza H**, Hadchouel M, Scotto J, Tiollais P, Babinet C, Pourcel C. Replication and gene expression of hepatitis B virus in a transgenic mouse that contains the complete viral genome. *J Virol* 1988; **62:** 4144-4152

39 **Araki K**, Miyazaki J, Hino O, Tomita N, Chisaka O, Matsubara K, Yamamura K. Expression and replication of hepatitis B virus genome in transgenic mice. *Proc Natl Acad Sci U S A* 1989; **86:** 207-211

40 **Nolasco FE**, Cameron JS, Hartley B, Coelho A, Hildreth GR. Intraglomerular T cells and monocytes in nephritis: study with monoclonal antibodies. *Kidney Int* 1987; **31:** 1160-1166

41 **Mondelli M**, Vergani GM, Alberti A, Vergani D, Portmann B, Eddleston AL, Williams R. Specificity of T lymphocyte cytotoxicity to autologous hepatocytes in chronic hepatitis B virus infection: evidence that Tcells are directed against HBV core antigen expressed on hepatocytes. *J Immunol* 1982; **129:** 2773-2778

42 **Yoakum GH**, Korba BE, Lechner JF, Tokiwa T, Gazdar AF, Seeley T, Siegel M, Leeman L, AutrupH, Harris CC. High-frequency transfection and cytopathology of the hepatitis B virus core antigen gene in human cells. *Science* 1983; **28:** 385-389

Edited by Zhu LH and Wang XL

P.O.Box 2345, Beijing 100023,China
Fax: +86-10-85381893
E-mail: wjg@wjgnet.com www.wjgnet.com

World J Gastroenterol 2003;9(9):2009-2011
World Journal of Gastroenterology
 ISSN 1007-9327

• VIRAL HEPATITIS •

Abnormal immunity and gene mutation in patients with severe hepatitis-B

Jing-Yan Wang, Pei Liu

Jing-Yan Wang, Pei Liu, Department of Infectious Diseases, the Second Hospital, China Medical University, Shenyang 110004, Liaoning Province, China
Supported by the National Natural Science Foundation of China, No.39370649
Correspondence to: Pei Liu M.D., Ph.D., Department of Infectious Diseases, the Second Hospital, China Medical University, Shenyang 110004, Liaoning Province, China. syliupei2003@yahoo.com.cn
Telephone: +86-24-83956962 **Fax:** +86-24-23891973
Received: 2003-03-10 **Accepted:** 2003-04-19

Abstract

AIM: To evaluate the abnormal immunity and gene mutation at precore 1896 site in patients with severe hepatitis-B.

METHODS: This study included 23 patients with severe hepatitis-B, 22 patients with acute hepatitis-B and 20 controls. Mutation at precore 1896 site of HBV gene was confirmed with restriction fragment length polymorphism (RFLP) analysis. Cytokines including TNF-α, IFN-γ, IL-6, and IL-8 were measured with ELISA, and T subgroups were detected with alkaline phosphatase anti alkaline phosphatase (APAAP) technique.

RESULTS: In patients with severe hepatitis-B, the infective rate of HBV mutant strain was 52.5 % (12/23), and only one patient with acute hepatitis-B was infected with the mutant strain. The percentage of CD8+ T lymphocyte was obviously lower (0.16±0.02 %) and the ratio of CD4+/CD8+ was obviously higher (2.35±0.89) in mutant group than in wild-type group (0.28±0.05 % and 1.31±0.18 %, respectively, $P<0.01$ or $P<0.05$). The levels of cytokines in patients with severe hepatitis-B were higher (TNF-α 359.0±17.2 ng/L, IFN-γ 234.7±16.5 ng/L, IL-6 347.5±31.3 ng/L, IL-8 181.1±19.6 ng/L) than those in acute hepatitis-B (TNF-α 220.6±8.9 ng/L, IFN-γ 174.9±12.0 ng/L, IL-6 285.8±16.5 ng/L, IL-8 118.4±5.1 ng/L, $P<0.01$ or 0.05). In patients with severe hepatitis-B, the levels of IFN-γ and IL-6 were higher in mutant group (273.4±26.6 ng/L, 387.7±32.5 ng/L) than in wild-type group (207.8±12.8 ng/L, 300.9±16.3 ng/L). The mortality of patients infected with HBV mutant strain was higher (100 %) than that with wild-type (0.9 %).

CONCLUSION: In severe hepatitis-B, the infective rate of HBV mutant strain was high. The mutant strain induces more severe immune disorders in host, resulting in the activation of lymphocyte and release of cytokines. HBV DNA mutates easily in response to the altered immunity. Ultimately liver damage is more prominent.

Wang JY, Liu P. Abnormal immunity and gene mutation in patients with severe hepatitis-B. *World J Gastroenterol* 2003; 9(9): 2009-2011
http://www.wjgnet.com/1007-9327/9/2009.asp

INTRODUCTION

HBV destroys hepatocytes by changing the host immune system after its invasion into the body. Various clinical types of hepatitis are associated with different immune status of the body. The serious damage of hepatocytes constitutes the pathological basis of severe hepatitis. At present, studies about the mechanism of hepatocytic damage in severe hepatitis B focus mainly on HBV gene mutation and immunologic abnormalities. HBV gene mutation at precore 1896 site has been already detected with restriction fragment length polymorphism (RFLP). In this study, we explored the relationships between HBV gene mutation and immune status in severe hepatitis. T subgroups in peripheral blood and levels of TNF-α, IFN-γ, IL-6, and IL-8 associated with severe hepatitis were measured.

MATERIALS AND METHODS

Patients

From 1995 to 1998, 45 patients with severe hepatitis or acute hepatitis were included in this study. There were 23 cases (17 men and 6 women) of severe hepatitis and 22 cases (15 men and 7 women) of acute hepatitis. The patients with severe hepatitis aged from 8 to 62 years and those with acute hepatitis from 11 to 65 years. The diagnosis was based on the diagnostic criteria revised at the National Infectious Disease and Parasitosis Conference in 1999 (Xian, china). All samples were obtained on the day of admission. The serological markers of HBsAg and HBV DNA were positive, and those of HAV, HCV, HDV, HEV, anti-EBV-IgM, and anti-CMV-IgM were all negative.

We also studied 20 healthy blood donors aged from 25 to 43 years, including 16 men and 4 women. They had no serological markers of HAV, HBV, HCV, HDV, HEV, and their liver functions were normal.

Analysis of restriction fragment length polymorphism (RFLP)[1]

Two pairs of primers were used in the analysis of RFLP. The primers used for the first round of PCR were 5'-GGCGAGGGAGTTCTTCTTCTAGGGG-3' (2 394 to 2 370 nucleotides) and 5'-CTGGGAGGAGTTGGGGGAGG AGATT-3' (1 730 to 1 754 nucleotides). The primers for the second round of PCR were 5'-CAAGCTGTGCCTTGGGTG GCCTT-3' (1 873 to 1 895 nucleotides), which was a mismatch primer, and 5'-GGAAAGAAGTCAGAAGGCAA-3' (1 974 to 1 955 nucleotides). All of the primers were synthesized by the Shanghai Cytobiology Institute. Huamei Company provided dNTP, PGEM-7Zf(+)Hae III, and the marker of DNA molecular weight. Bsu 36 I enzyme and relevant buffer, TaqDNA polymerase and PCR buffer were from Promega Company. HBV DNA was extracted from serum samples by using the standard method. Serum (100 μl) was treated with proteinase K, phenol and chloroform, and then precipitated with ethanol. The final products served as the amplification template of PCR. The fluorescent zone after electrophoresis was observed by ultraviolet light.

Staining of T subgroups

Monocytes were purified from the samples of anticoagulant blood using lymphocytic laminated fluid. The monoclonal

antibodies to CD4+ and CD8+ were purchased from DAKO (Denmark). The percentages of CD4+ and CD8+ were counted under microscope after staining with APAAP.

Detection of cytokines

The kits of TNF-α, IFN-γ, IL-6, and IL-8 were produced by the Genzyme Company (USA). The four cytokines were detected with ELISA. The first antibody was biological antibody and the second one was peroxidase-labelled streptavidin.

Statistical analysis

All values were expressed as means ± standard deviation. Chi-square test was performed. It was considered statistically significant when the *P* value was less than 0.05.

RESULTS

Mutation at precore 1896 site of HBV DNA from patients with severe hepatitis B

Among the 23 cases of severe hepatitis, 8 were simple infection of the mutant strain, 4 coinfection of the wild and mutant strains, and 11 simple infection of the wild strain. Only 1 case had mutation in precore region among the 22 cases of the acute hepatitis.

Effects of mutation at HBV DNA precore 1896 site on status of T subgroups in peripheral blood from patients with severe hepatitis

As shown in Table 1, the percentage of CD8+ in patients with severe hepatitis in mutant group (0.16±0.02) decreased more obviously than that in patients in the wild-type group (0.28±0.05), and the ratio of CD4+/CD8+ in mutation group (2.35±0.89) increased more significantly than that in wild-type group (1.31±0.18).

Table 1 Status of T subgroups in the peripheral blood from patients with severe hepatitis (%, $\bar{x}\pm s$)

Group	*n*	CD3+	CD4+	CD8+	CD4+/CD8+
Control	20	0.60±0.17	0.46±0.05	0.33±0.03	1.39±0.18
AH	22	0.61±0.06	0.38±0.04[a]	0.33±0.04	1.16±0.20
FH	23	0.53±0.07[a]	0.37±0.03[a]	0.25±0.06[a]	1.63±0.30[a]
Mutation	12	0.15±0.08	0.37±0.12	0.16±0.02[b]	2.35±0.89[b]
Wild	11	0.56±0.04	0.36±0.04	0.28±0.05	1.31±0.18

[a]$P<0.01$ *vs* control; [b]$P<0.05$ *vs* wild type. AH: acute hepatitis, FH: severe hepatitis.

Serum levels of TNF-α, IFN-γ, IL-6 and IL-8 from patients with mutation at HBV DNA precore 1896 site in severe hepatitis

Serum levels of TNF-α, IFN-γ, IL-6, and IL-8 in patients with mutation at HBV DNA precore 1896 site in patients with severe hepatitis are shown in Table 2.

The levels of IFN-γ and IL-6 in patients with severe hepatitis in mutant group (273.4±26.6 ng/L, 387.7±32.5 ng/L) increased more significantly than that in patients in the wild-type group (207.8±12.8 ng/L, 300.9±16.3 ng/L) ($P<0.05$).

The dynamic changes of the 4 cytokines are shown in Figure 1 and Figure 2. IFN-γ reached a peak and then decreased rapidly at the early stage of severe hepatitis with infection of mutant strain and acute hepatitis with infection of wild- type. TNF-α and IL-6 increased in acute stage and reached the highest level accompanied by the most severe jaundice, then decreased gradually. Both maintained a high level for a long time in severe hepatitis. IL-8, TNF-α, and IL-6 experienced the same change in severe hepatitis with mutation at HBV DNA precore 1896 site (173.5±10.7 ng/L, 356.6±18.1 ng/L, 387.7±32.5 ng/L) as in the course of acute hepatitis with infection of wild-type (173.1±11.3 ng/L, 328.4±14.6 ng/L, 300.9±16.3 ng/L).

All of the 12 patients in the mutant group died, and only 1 died among 11 patients in the wild-type group.

Table 2 The serum levels of TNF-α, IFN-γ, IL-6, and IL-8 in patients with mutation in HBV DNA precore 1896 site (ng/L, $\bar{x}\pm s$)

Group	*n*	TNF-α	IFN-γ	IL-6	IL-8
Control	20	146.7±9.4	65.0±7.7	231.1±16.4	110.2±2.9
AH	22	220.6±8.9	174.9±12.0	285.8±16.5	118.4±5.1
FH	23	359.0±17.2[bc]	234.7±16.5[bc]	347.5±31.3[bd]	181.1±19.6[a]
Mutation	12	356.6±18.1	273.4±26.6[e]	387.7±32.5[e]	173.5±10.7
Wild	11	328.4±14.6	207.8±12.8	300.9±16.3	173.1±11.3

[a]$P<0.05$ *vs* control; [b]$P<0.01$ *vs* control; [c]$P<0.05$ *vs* AH; [d]$P<0.01$ *vs* AH; [e]$P<0.05$ *vs* wild strain. AH: acute hepatitis, FH: severe hepatitis.

DISCUSSION

Severity of hepatitis caused by HBV varies greatly. The mechanisms determining the course and outcome of hepatitis B have not been known. Many investigations suggested that HBV was not directly cytopathic. The injury was mediated by the immune response[2]. Injury of hepatocytes in acute hepatitis was mediated by CD8+ CTLs recognizing the core protein of HBV presented in association with HLA class I proteins[3]. TNF-α and IFN-γ played indispensable roles in liver injury mediated by Th1 cells specific to HBV surface antigen[4]. Muto *et al*[5] suggested that the main immunologic abnormalities in severe hepatitis were due to TNF-α produced by monocytes in peripheral blood. Pretreatment with anti-TNF-α mAb in animal model strongly blocked Th1 cell-inducible liver injury[6]. TNF-α might be enhanced in animal models with impaired liver metabolism[7], and serum TNF-α took part in the pathogenesis of chronic hepatic failure of HBV infection[8]. The study of transgenic mice indicated that IFN-γ triggered the widespread hepatocellular necrosis. The cytopathic effect of IFN-γ was indirect, presumably due to recruitment and activation of antigen nonspecific host inflammatory cells. Immunopathological changes induced by CTL contributed to immunopathogenesis of viral hepatitis during hepatitis B virus infection in humans. IFN-γ activated the killing activity of CTL[9] and had killing activity to regenerating hepatocytes. Similarly, IL-6 was involved in the activation of NK cells and CTLs, inducing their killing activity to hepatocytes.

The serum levels of TNF-α, IFN-γ, IL-6, and IL-8 in patients with severe hepatitis were significantly higher than those in patients with acute hepatitis, and peripheral CD8+ was obviously lower, especially in mutant group. These findings suggest that cytokines and immunocytes associated with inflammation may play roles in the pathogenesis of severe hepatitis. TNF-α, IFN-γ and IL-6 may involve in hepatocytic necrosis and apoptosis. Remarkable increase of IL-8 leads to accumulation of CTL which gets direct and immediate assess to the target hepatocytes and the resident intrahepatic macrophages, and this constitutes the immunopathological basis of hepatocyte killing. CTLs that enter and reside in the liver, have the ability to bind to and kill the HBsAg-positive hepatocytes, and to activate an intrahepatic inflammatory response[4].

Omata *et al*[10] reported in 1991 that HBV DNA precore 1896 site mutation had some relationship with severe hepatitis B. Translational termination codon which was produced after

a point mutantion from G to A at nucleotide 1896 of precore region of hepatitis B virus DNA, converting tryptophan (TGG) to a stop codon (TAG) would interrupt the synthesis of HBeAg precursor protein, that may decrease or eliminate HBeAg. The presence of mutant viral strain is associated with and may be involved in the pathogenesis of severe hepatitis B and exacerbation of chronic hepatitis B. In our study the mortality was extremely high in patients with HBV DNA precore 1896 site mutation. It might be related to the immunologic abnormalities in severe hepatitis induced by HBV DNA precore 1896 site mutation[11]. It was also found that the percentages of CD8+ in the peripheral blood in patients with severe hepatitis in mutant group were much lower than those in patients in wild-type group, which was the result of the relative diminish of CD8+ infiltrating into the liver tissue in severe hepatitis. Meanwhile, the levels of IFN-γ and IL-6 increased significantly in severe hepatitis, indicating that HBeAg not only had effects on the regulation of CTL in killing hepatocytes, but also had certain effect on producing cytokines by the immunocytes. A cross-reactivition of c and e antigens at the T cell recognition sites was found by examining T cell responses to recombinant c and e antigens. When the expression of HBeAg on the surface of hepatocytes decreased or disappeared, the attacking action of specific CTL to c antigen and the target antigen through T cell-mediated cytotoxicity enhanced, resulting in massive necrosis of hepatocytes with HBV infection and deterioration of hepatitis because specific CTL bound to HBcAg which is the most possible main target for immune hepatocytolysis on hepatocytic nuclei was obviously increased[12-14]. HBV strains with mutation in the precore region that abort the translation of hepatitis B e antigen precursor, resulted in the formation of HBeAg-minus phenotype. Circulating HBeAg has been proposed as a viral strategy to induce immunotolerance[15]. Its absence, therefore, would accelerate inflammatory activity in the liver[16] which could be relevant to the pathogenesis of severe hepatitis. On the other hand, HBeAg and HBcAg were expressed simultaneously in hepatocytic membrane with HBV infection and became the target antigen of CTL[17]. Meanwhile, the activity of T suppressor cell (Ts) was weakened. As a result, the ability of Ts to regulate T cells specific to HBc/HBeAg was decreased. So the production of specific CTL to HBc/HBeAg was increased and hepatocytic necrosis exacerbated. Our investigation indicated that in severe hepatitis the abnormal immunity of patients in mutant group was due to the following aspects: (1) The levels of cytokines were abnormal compared with the wild-type, particularly IFN-γ. (2) Hepatocytic apoptosis induced by IL-6 produced by monocytes and vascular endotheliocytes might take part in the pathogenesis of fulminant hepatitis. (3) Overexpression of TNF receptors induced by IFN-γ in hepatocytes might correlate with the severe liver damage[18]. (4) Activation and aggregation of CTL in the liver enhanced the killing activity to hepatocytes and caused deterioration of liver damage. It is thus speculated that in severe hepatitis, HBV mutation might be resulted from response to immune defense reaction of the host body, or conversely, mutant HBV DNA might produce more significant immune disorders in the host body. Clinically, exploration for HBV gene mutation in patients with acute hepatitis might provide some useful hints for estimating the state of illness and predicting the prognosis.

REFERENCES

1 **Niitsuma H,** Ishii M, Miura M, Toyota T. Detection of HBV precore mutation by PCR-RFLP. *Nippon Rinsho* 1995; **53 Suppl (Pt 2)**: 316-320

2 **Chu CM.** Natural history of chronic hepatitis B virus infection in adults with emphasis on the occurrence of cirrhosis and hepatocellular carcinoma. *J Gastroenterol Hepatol* 2000; **15(Suppl)**: E25-30

3 **Bertoletti A,** Sette A, Chisari FV, Penna A, Giuberti T, Levrero M, De Carli M, Fiaccadori F, Ferrari C. Natural variants of cytotoxic epitopes are T-cell receptor antagonists for antiviral cytotoxic T cells. *Nature* 1994; **369:** 407-410

4 **Ohta A,** Sekimoto M, Sato M, Koda T, Nishimura S, Iwakura Y, Sekikawa K, Nishimura T. Indispensable role for TNF-alpha and IFN-gamma at the effector phase of liver injury mediated by Th1 cells specific to hepatitis B virus surface antigen. *J Immunol* 2000; **165**: 956-961

5 **Muto Y,** Nouri-Aria KT, Meager A, Alexander GJ, Eddleston AL, Williams R. Enhanced tumour necrosis factor and interleukin-1 in fulminant hepatic failure. *Lancet* 1988; **2:** 72-74

6 **Tanaka Y,** Takahashi A, Watanabe K, Takayama K, Yahata T, Habu T, Nishimura T. A pivotal role of IL-12 in Th1-dependent mouse liver injury. *Int Immunol* 1996; **8:** 569-576

7 **Lehmann V,** Freudenberg MA, Galanos C. Lethal toxicity of lipopolysaccharide and tumor necrosis factor in normal and D-galactosamine-treated mice. *J Exp Med* 1987; **165:** 657-663

8 **Zhang DF,** Ren H, Jia XP, Zhou YS. Serum tumor necrosis factor (TNF) in the pathogenesis of clinical hepatic failure of HCV and / or HBV infection. *Chin Med J* 1993; **106:** 335-338

9 **Ando K,** Moriyama T, Guidotti LG, Wirth S, Schreiber RD, Schlicht HJ, Huang SN, Chisari FV. Mechanisms of class I restricted immunopathology: A transgenic mouse model of fulminant hepatitis. *J Exp Med* 1993; **178:** 1541-1554

10 **Omata M,** Ehata T, Yokosuka O, Hosoda K, Ohto M. Mutations in the precore region of hepatitis B virus DNA in patients with fulminant and severe hepatitis. *N Engl J Med* 1991; **324:** 1699-1704

11 **Sato S,** Suzuki K, Akahane Y, Akamatsu K, Akiyama K, Yunomura K, Tsuda F, Tanaka T, Okamoto H, Miyakawa Y. Hepatitis B virus strains with mutations in the core promoter in patients with fulminant hepatitis. *Ann Intern Med* 1995; **122**: 241-248

12 **Yamada G,** Takaguchi K, Matsuda K, Nishimoto H, Takahashi M, Fujiki S, Mizuno M, Kinoyama S, Tsuji T. Immunoelectron microscopic observation of intrahepatic HBeAg in patients with chronic hepatitis B. *Hepatology* 1990; **12:** 133-140

13 **Hadziyannis SJ,** Vassilopoulos D. Hepatitis B e antigen-negative chronic hepatitis B. *Hepatology* 2001; **34(4Pt1):** 617-624

14 **Park YN,** Han KH, Kim KS, Chung JP, Kim S, Park C. Cytoplasmic expression of hepatitis B core antigen in chronic hepatitis B virus infection: role of precore stop mutants. *Liver* 1999; **19:** 199-205

15 **Milich DR,** Jones JE, Hughes JL, Price J, Raney AK, Mclachlan A. Is a function of the secreted hepatitis B e antigen to induce immunologic tolerance in utero? *Proc Natl Acad Sci U S A* 1990; **87:** 6599-6603

16 **Brunetto MR,** Giarin MM, Oliveri F, Chiaberge E, Baldi M, Alfarano A, Serra A, Saracco G, Verme G, Will H. Wild-type and e antigen-minus hepatitis B viruses and course of chronic hepatitis. *Proc Natl Acad Sci U S A* 1991; **88:** 4186-4190

17 **Yotsuyanagi H,** Hino K, Tomita E, Toyoda J, Yasuda K, Iino S. Precore and core promoter mutations, hepatitis B virus DNA levels and progressive liver injury in chronic hepatitis B. *J Hepatol* 2002; **37:** 355-363

18 **Ruggiero V,** Tavernier J, Fiers W, Baglioni C. Induction of the synthesis of tumor necrosis factor receptors by interferon-gamma. *J Immunol* 1986; **136:** 2445-2450

Edited by Zhu LH and Wang XL

P.O.Box 2345, Beijing 100023,China
Fax: +86-10-85381893
E-mail: wjg@wjgnet.com www.wjgnet.com

World J Gastroenterol 2003;9(9):2012-2016
World Journal of Gastroenterology
 ISSN 1007-9327

• VIRAL HEPATITIS •

Spontaneous viral clearance after 6-21 years of hepatitis B and C viruses coinfection in high HBV endemic area

Chun-Lei Fan, Lai Wei, Dong Jiang, Hong-Song Chen, Yan Gao, Ruo-Bing Li, Yu Wang

Chun-Lei Fan, Lai Wei, Dong Jiang, Hong-Song Chen, Yan Gao, Ruo-Bing Li, Yu Wang, Institute of Hepatology, People' s Hospital, Peking University, Beijing 100044, China
Supported by the National Key Technologies Research and Development Program of China during the Tenth Five-Year Plan, No. 2001BA705B06; the Major State Basic Research Development Program of China (973 Program), No.G1999054106
Correspondence to: Dr. Lai Wei, Institute of Hepatology, People' s Hospital, Peking University, 11 Xizhimen South Street, Beijing 100044, China. w1114@hotmail.com
Telephone: +86-10-68314422 Ext 5730 **Fax:** +86-10-68318386
Received: 2003-04-10 **Accepted:** 2003-05-19

Abstract

AIM: To investigate the clinical and virological course of coinfection by hepatitis B virus (HBV) and hepatitis C virus (HCV) in China.

METHODS: We enrolled 40 patients with chronic HBV and HCV coinfection (Group BC), 16 patients with chronic HBV infection (Group B) and 31 patients with chronic HCV infection (Group C). They infected HBV and/or HCV during 1982 to 1989. Sera of all the 87 patients were collected in 1994 and 2002 respectively. We detected biochemical and virologic markers and serum HBV DNA and HCV RNA levels of all the patients. B-type ultrasound detection was performed in some patients.

RESULTS: In Group BC, 67.5 % of the patients cleared HBsAg, and 92.5 % of the patients cleared HBeAg. The clearance rate of HBV DNA was 87.5 %. There was no significant difference of HBV clearance between Group BC and Group B. In Group BC, 85.7 % of males and 47.4 % of females cleared HBV, and males were easier to clear HBV (χ^2=6.686, P=0.010). Such a tendency was also found in Group B. The clearance rate of HCV RNA in Group BC was 87.5 %, significantly higher than that in Group C (χ^2=22.963, P<0.001). Less than 40 % of the patients in all groups had elevated liver enzyme values. The highest value of alanine aminotransferase (ALT) was 218 u/L (normal range for ALT is 0-40 u/L). In most patients the ultrasonogram presentations changed mildly.

CONCLUSION: The clinical manifestations of patients with HBV/HCV coinfection are mild and occult. High clearance rate of HBV and easy to clear HBV in male patients are the characteristics of HBV infection in adults in China. HBV can inhibit HCV replication, but no evidence has been found in our data that HCV suppresses HBV replication.

Fan CL, Wei L, Jiang D, Chen HS, Gao Y, Li RB, Wang Y. Spontaneous viral clearance after 6-21 years of hepatitis B and C viruses coinfection in high HBV endemic area. *World J Gastroenterol* 2003; 9(9): 2012-2016
http://www.wjgnet.com/1007-9327/9/2012.asp

INTRODUCTION

Hepatitis B virus (HBV) and hepatitis C virus (HCV) are the most common causes of chronic liver diseases worldwide. Both viruses could induce chronic hepatitis, which may progress to cirrhosis and eventually to hepatocellular carcinoma (HCC). Because HBV and HCV share similar transmission routes, coinfection seems to be frequent. Seroprevalence studies have shown that coinfection of HCV is detected in around 10 % to 15 % of patients with chronic HBV infection, although the prevalence may vary from country to country[1-3]. Earlier studies in chimpanzees showed that replication of pre-existing HBV was inhibited by superinfection of NANB hepatitis virus (HCV)[4]. Some clinical observations indicate that HCV may inhibit HBV expression and even act as the major cause of chronic hepatitis[5-8]. And it was also reported that HBV might suppress replication of HCV[9-12]. The histopathological findings and clinical outcome in some of these cases were contradictory. Some researchers found that HBV and HCV coinfection could significantly increase the risk of development of fulminant hepatitis and also cirrhosis and HCC[2,13-16]. But others showed neither exacerbation nor diminution of histopathological changes in patients with HBV/HCV coinfection[17]. Coinfection does not play an important role in the development of HCC[18,19]. Furthermore, in patients with HBV and HCV coinfection after orthotopic liver transplantation, presence of HCV may improve their clinical outcome as compared with HBV infection alone[20].

Our previous study showed that the history of patients infected with HCV in China was different from that in Western countries[21]. At the same time, we enrolled a group of patients with chronic HBV and/or HCV infection during 1982 to 1988. Sera of all the 87 patients were collected in 1994 and 2002 respectively. We analyzed the biochemical and virologic markers and serum HBV DNA and HCV RNA levels in patients with chronic coinfection and compared the results with the patients with single HBV or HCV infection. The clinical and virological course of coinfection of HBV and HCV in China was investigated.

MATERIALS AND METHODS

Patients

Eighty seven patients with chronic HBV and/or HCV infection were native individual blood donors in Hebei Province of China, who had the history of drawing plasma from the blood and transfusion back of the blood cells during 1982-1989. The serum samples of these patients were collected in 1994 and 2002, and stored without thawing at -70 ℃. We detected the serological markers of HBV and HCV in all the patients in 1994 and 2002 respectively. All the patients were divided into 3 groups: Group BC (HBV and HCV coinfected group including 40 cases), Group B (single HBV infected group including 16 cases), and Group C (single HCV infected group including 31 cases). There was no significant difference in the number of patients, age and sex distribution, and duration of infection among the groups (Table 1). No patient had received treatment of immunosuppressors or antiviral agents such as interferon. And all the patients were negative for anti-HDV and anti-HIV. None of them had a history of auto-immune disease, and alcohol abuse.

Table 1 Clinical data for patients with HBV and/or HCV infection

	Group BC	Group B	Group C	Statistical value
Number of patients	40	16	31	
Sex (male/female)	21/19	6/10	15/16	χ^2=1.030, *P*>0.05
Age (y)[a]	39±5 (29-50)	40±6 (31-53)	39±3 (32-44)	F=0.48, *P*>0.05
Time of infection (y)[a]	16±5 (14-21)	16±5 (14-21)	17±4 (14-21)	F=2.27, *P*>0.05
Serological markers (1994)				
HBsAg +	34 (85.0 %)	16 (100 %)	0	
HBeAg +	11 (27.5 %)	7 (43.8 %)	0	
HBVDNA +	37 (92.5 %)	14 (87.5 %)	0	
HCVRNA +	11 (27.5 %)	0 (0 %)	19 (61.3 %)	
Anti-HCV	39 (97.5 %)	0 (0 %)	31 (100.0 %)	

[a]Data were expressed as mean ±SD (range).

Serological examination

Serum anti-HBs, anti-HBe, anti-HBc and HBeAg were detected by commercially available enzyme-linked immunosorbent assay (ELISA) kits (RADIM, Italia). HBsAg, anti-HIV and anti-HDV were tested by ELISA kits (Organon Teknika China Ltd). Testing of anti-HCV was performed by the third-generation of ELISA kits (Ortho Diagnostic Systems Inc. NJ). Liver enzymes, such as alanine aminotransferase (ALT), aspartate aminotransferase (AST), total bilirubin (TBIL), gamma glutamyl transferase (GGT) and alkaline phosphatase (ALP) were determined using HITACHI 7170 biochemistry analyzer. Serum AFP was measured by radioimmunoassay. A value greater than 20 ng/ml was considered abnormal.

Quantitative detection of HBV DNA and HCV RNA

Serum HBV DNA and HCV RNA concentrations were determined by a programmable high-speed thermal cycler (Light Cycler II; Roche Diagnostics, Mannheim, Germany) for fluorescence quantitative polymerase chain reaction (FQ-PCR) using a commercially available kit (PG Biotech Co., Ltd., China). For HBV DNA FQ-PCR, the detection limit of the method was 500 genome copies/ml. For HCV RNA, the sensitivity limit of the method was about 1 000 genome copies/ml.

Statistical analysis

All the data were presented as the mean ±SD. χ^2 test or Fisher' s exact test was used for categorical variables. The statistical package for social sciences (SPSS, Chicago, IL), version 10.0, was used for statistical analyses. Significance was set at a *P* value of less than 0.05.

RESULTS

Spontaneous clearance of HBV (Table 2)

HCV did not influence the clearance of HBV in Group BC Persistent negative HBsAg and HBV DNA in serum and liver enzyme was considered as a criterion for HBV clearance[22, 23]. In Group BC, 27 of the 40 patients (67.5 %) cleared HBV, and in Group B, 7 of the 16 patients (43.8 %) cleared HBV. No significant difference was found between the two groups (χ^2=2.703, *P*=0.100) (Table 2). It was suggested that HCV had no effect on the elimination of HBV.

Spontaneous clearance of HBV in the course of chronic HBV infection Forty patients with coinfection of HBV and HCV had acquired the viruses for 6 to 13 years. Six of them (15 %) cleared HBsAg, 29 of them (72.5 %) cleared HBeAg, and 3 of them (7.5 %) cleared HBV DNA spontaneously in 1994 (Table 2). While in Group B, all the patients were positive for HBsAg and HBV DNA, and 10 of them (62.5 %) cleared HBeAg in 1994. In Group BC, 27 patients (67.5 %) cleared HBsAg, 37 patients (92.5 %) cleared HBeAg, and 35 patients (87.5 %) cleared HBV DNA in 2002. No significant difference was found between the two groups (Table 2). It was suggested that HBV could be cleared even after 6 years of infection in adults.

Influence of sex and serum virus load on the clearance of HBV In Group BC, 85.7 % (18/21) of the males cleared HBV, but only 47.4 % (9/19) of the malas cleared HBV. The HBV clearance rate of males was significantly higher than that of females (*P*<0.05). In Group B, the spontaneous HBV clearance rates were 66.7 % (4/6) and 30 % (3/10) in males and females respectively, but no statistical difference was found between them. It showed that males seemed easier to clear HBV (Table 2). According to the criteria of HBV clearance[22,23], 10 of the 16 patients (62.5 %) in Group BC with a high HBV DNA level had cleared HBV in 2002. Among the 24 patients who had low HBV DNA level, 17 patients (70.8 %) cleared HBV. There was no significant difference between the high and low HBV DNA level groups in Group BC (*P*>0.05). In Group B, 3 of the 9 patients (33.3 %) with a high HBV DNA level cleared HBV in 2002. While in 7 patients whose serum HBV level in 1994 was lower than 10^5 genomic copies/ml, 4 patients (57.1 %) cleared HBV (*P*>0.05) (Table 2). It was suggested that the level of virus load had no effect on the clearance of HBV infection.

Table 2 Clearance of serum HBV markers in Group BC and Group B

	Group BC (*n*=40, %)		Group B (*n*=16, %)	
HBsAg clearance				
Until 1994	6	(15%)	0	(0%)
Until 2002	27	(67.5%)	8	(50%)
HBeAg clearance/seroconversion				
HBeAg clearance				
Until 1994	29	(72.5%)	10	(62.5%)
Until 2002	37	(92.5%)	14	(87.5%)
HBeAg seroconversion	22	(55.5%)	12	(75%)
HBV DNA clearance				
Until 1994	3	(7.5%)	2	(12.5%)
Until 2002	35	(87.5%)	13	(81.2%)
HBV clearance	27	(67.5%)	7	(43.8%)
Male	18	(85.7%)[a]	4	(66.7%)
Female	9	(47.4%)[b]	3	(30%)
Low HBV DNA level group				
(<10^5 copies/ml)	17	(70.8%)	4	(57.1%)
High HBV DNA level group				
(≥10^5 copies/ml)	10	(62.5%)	3	(33.3%)

Note. [a] *vs.* [b]χ^2=6.686, *P*=0.010.

Spontaneous clearance of HCV RNA

In Group BC, 29 of the 40 patients cleared HCV RNA (72.5 %) in 1994. Thirty five patients (87.5 %) cleared HCV RNA in 2002. Two patients who were negative for HCV RNA in 1994 became positive in 2002. In Group C, 12 of the 31 patients cleared HCV RNA (38.7 %) in 1994, and 10 patients (32.3 %) cleared HCV RNA in 2002. Three patients who were formerly

negative for HCV RNA became positive in 2002. In 1994 and 2002, the clearance rate of HCV RNA in Group BC was higher than that in Group C (P<0.01) (Table 3).

Table 3 HCV RNA clearance rate in Group BC and Group C

	Group BC (n=40, %)	Group C (n=31, %)	Statistics value
HCV RNA clearance			
Until 1994	29 (72.5%)[a]	12 (38.7%)[b]	χ^2=8.173, (a *vs.* b) P<0.05
Until 2002	35 (87.5%)[c]	10 (32.3%)[d]	χ^2=22.963, (c *vs.* d) P<0.001
Male	17 (80.9%)	3 (20%)	
Female	18 (94.7%)	7 (43.8%)	

Relationship between HBV DNA and HCV RNA

Forty patients with HBV and HCV coinfection were dovided into 3 groups based on their serum HBV DNA levels in 1994. Within each of the groups, the patients were reclassified based on their serum HCV RNA viral load in 1994 (Table 4). Neither inverse nor positive correlation was found between HBV DNA and HCV RNA levels in the coinfected patients. However, detection of the sera of coinfected patients collected in 2002 showed that one who was positive for HBV DNA in 1994 was negative for HCV RNA. On the contrary, one who was positive for HCV RNA in 1994 was negative for HBV DNA. The fact that HBV DNA and HCV RNA could not be found in the same patient at the same time suggested that HBV and HCV were cleared one by one.

Table 4 Relationship of serum HBV and HCV load in 1994

HCV RNA (copies / ml)	HBV DNA(copies / ml)			Total amount
	$<10^3$	10^3-10^5	$\geqslant 10^5$	
$<10^3$	2	14	12	28
10^3-10^5	1	5	3	9
$\geqslant 10^5$	0	2	1	3
Total amount	3	21	16	40

P=0.918.

Table 5 Type B ultrasonic presentations in patients with HBV and / or HCV infection

	Normal	Mild	Medium	Severe	Fatty liver	Not detected	Total
Group BC	4	0	2	1	3	30	10
Group B	8	0	2	0	3	3	13
Group C	0	13	14	1	2	1	31

Clinical outcome of patients with HBV and HCV coinfection

All the patients had no apparent symptoms and physical signs of liver diseases. In Group BC, 10 of them (25 %) had abnormal liver enzyme values, and the highest value of ALT was 218 u/L with a mean of 95±72 (u/L) (normal range for ALT is 0-40 u/L). Five patients in Group B and 12 in Group C had elevated liver enzyme values. The rate of abnormal biochemical values was similar among the groups. The mean of elevated ALT values was 69±33 (u/L) in Group B and 53±16 (u/L) in Group C. Fifty three of the patients underwent B type ultrasound detection, and most of them had mild or moderate abnormal ultrasonic manifestations according to the criteria formulated by Chinese Medical Association[24] (Table 5). Other liver enzyme values such as TBIL, ALP, GGT and AFP were in the normal range in all the patients, and no one was found to have HCC.

DISCUSSION

All the patients were individual blood donors with chronic HBV and/or HCV infection. They have never received interferon or other antiviral agent treatment, thus our data partly reflected the natural history of HBV and HCV coinfection.

High clearance rate of both viruses, and mild clinical manifestations of coinfection were the prominent findings in this study. It may have some relationship with the special characteristics of the patients. First, different from those who got HBV and HCV coinfection sporadically, the patients in our study were all individual blood donors, and had a history of taking plasma from the blood and transfusion back of the blood cells. Second, they were adults when they acquired the infection. During 1982 to 1989, they provided the blood 5-15 times, and 200 to 400 ml each time. Third, they were the natives of certain villages in Hebei Province and their blood was collected in the same hospitals. These characteristics of the patients may have some relationships with the high clearance rate of HBV in Group BC and Group B. The mechanism needs to be further studied. After 14 to 21 years of HBV and HCV coinfection, 87.5 % of the patients have cleared HCV RNA. Researchers in Western countries reported that the spontaneous clearance rate of HCV RNA was less than 15 % in adults with HCV infection, and 34 % in patients with coinfection[25]. The history of HCV infection in China was different from that in Western countries, 29 % of the patients who got HCV infection after blood transfusion for 12 to 25 years have cleared the virus, and the clinical manifestations were occult[21]. This may be the reason of different characteristics of patients with coinfection in China from those in Western countries.

With regard to the relationship of HBV/HCV coinfection and clinical outcome, most researchers found that coinfection of HBV and HCV could cause more severe liver damage than single infection[2,13-16]. While in this study, neither patients with coinfection nor patients with single HBV or HCV infection had obvious symptoms and signs of liver diseases. Twenty five percent of patients with coinfection had elevated liver enzyme values. The mean of elevated ALT values was 95±72 u/L, while other liver enzyme values such as TBIL, ALP, and GGT were in the normal range. In most patients the ultrasonic presentations changed mildly. Good clinical outcome was one of the main characteristics of the patients with coinfection in this study. It was reported that in patients with HBV and HCV coinfection after orthotopic liver transplantation, the presence of HCV might improve the clinical outcome as compared with HBV infection alone[20]. Utili *et al*[25] followed up a group of cancer survival children who acquired HBV and HCV during treatment of neoplasia for a median period of 13 years, in which the patients went though a chronic indolent course of the liver disease, 59 % of them lost one or both viruses over time.

The clearance rate of HCV RNA in Group BC was 87.5 % in 2002, significantly higher than that in Group C (32.3 %) (P<0.05), and Group BC had a higher clearance rate of HCV RNA compared with Group C (P<0.05) (Table 3) in 1994. It was suggested that in HBV and HCV coinfection group the two viruses had mutual interference, and HBV suppressed HCV replication. While in Group BC, the patients who were positive for HCV RNA in 1994 were negative for HBV DNA in 2002, and vice versa. Previous studies also found that HBV could inhibit HCV replication and took the leading role in chronic hepatitis[9-12]. Acute HBV superinfection of patients with chronic HCV infection could suppress their pre-existing HCV, and the timing or sequence of infection was a factor influencing the outcome of viral interactions[22, 26]. The mechanism might

be that antiviral cytokines such as IFN-γ and TNF-α produced by non-T cells in the event of superinfection could inhibit the pre-existing virus[27]. *In vitro* experiments showed that when HBV DNA and HCV RNA were co-transfected into HuH7 cells, HBV DNA suppressed HCV RNA secretion, and HCV RNA also suppressed HBsAg secretion in comparison with either of HCV RNA or HBV DNA transfection alone[28].

Former studies showed that HCV could inhibit HBV replication[5-8, 29], but in this study, no statistical difference was found in the clearance rate of HBsAg, HBeAg and HBV DNA between Group BC and Group B. We did not find any relationship between serum HCV RNA and HBV DNA levels in patients with coinfection. The small number of patients in Group B might result in statistical discrepancy. Anyway, no evidence was found in this study to support that HCV could affect HBV replication.

Considering that China is a highly endemic area of HBV, and most of patients with chronic HBV infection acquired the virus in their infancy, our data may partly reflect the natural history of HBV infection in adults. Its characteristics are as follows.

High clearance rate of HBV and indolent course of the infection After 14 to 21 years of infection, the clearance rates of HBsAg, HBeAg and HBV DNA in Group BC were 67.5 %, 92.5 % and 87.5 %, while in Group B, the clearance rates of these markers were 50 %, 87.5 % and 81.5 % respectively, and no significant difference was found between the two groups. It was reported that 5-10 % of chronically infected patients cleared HBV DNA and HBeAg spontaneously each year, and this might be followed by clearance of HBsAg[30,31]. In Taiwan the annual clearance rate of HBsAg was 0.43 %[32]. European Association for the Study of the Liver (EASL) reported that in Western countries, about 1-2 % of HBV carriers became HBsAg negative each year, while in endemic areas the rate of HBsAg clearance was lower (0.05-0.08 % per year)[23]. In chronic coinfection the clearance rate of HBsAg seemed higher than that in single HBV infection, and 2.03 % of patients in Taiwan cleared HBsAg annually[32]. In this study, either in patients with HBV/HCV coinfection or in HBV single infection, the clearance rate of HBsAg was higher than that ever reported. And they had mild clinical manifestations and no evidence to progress to more severe diseases.

It seemed easier for man to eliminate HBV We found in Group BC, most of the males (85.7 %) cleared HBV, and only 47.4 % of females did so ($P<0.05$). In Group B, no statistical difference was found, which might be due to a small number of cases. It was also reported in a long-term follow-up study that 88.9 % of the patients who cleared HBsAg were males[32].

The virus load did not influence the clearance rate of HBV There is no statistically significant difference of clearance rate of HBV between different virus load groups.

In short, mild and occult clinical manifestations and high clearance rate of both viruses were the characteristics of patients with HBV/HCV coinfection. High clearance rate of HBV in male patients was a clinical feature in adults with HBV infection. HBV could inhibit HCV replication, but no evidence was found that HCV could suppress HBV replication.

REFERENCES

1 **Liaw YF**. Role of hepatitis C virus in dual and triple hepatitis virus infection. *Hepatology* 1995; **22**: 1101-1108

2 **Crespo J**, Lozano JL, de la Cruz F, Rodrigo L, Rodriguez M, San Miguel G, Artinano E, Pons-Romero F. Prevalance and significance of hepatitis C viremia in chronic active hepatitis B. *Am J Gasteoenterol* 1994; **89**: 1147-1151

3 **Rodriguez M**, Navascues A, Martinez A, Suarez S, Riestra S, Sala P, Gonzalez M, Rodrigo L. Prevalence of antibody to hepatitis C virus in chronic HBsAg carriers. *Arch Virol* 1992; **4** (Suppl): 327-328

4 **Bradley DW**, Maynard JE, McCaustland KA. Non-A, non-B hepatitis chimpanzees: interference with acute hepatitis A virus and chronic hepatitis B virus infections. *J Med Virol* 1983; **11**: 207-213

5 **Liaw YF**, Tsai SL, Chang JJ, Sheen IS, Chien RN, Lin DY, Chu CM. Displacement of hepatitis B virus by hepatitis C virus as the cause of continuing chronic hepatitis. *Gastroenterology* 1994; **106**: 1048-1053

6 **Crespo J**, Lozano JL, Carte B. Viral replication in patients with concomitant hepatitis B and C virus infections. *Eur J Clin Microbiol Infect Dis* 1997; **16**: 445-451

7 **Pontisso P**, Gerotto M, Ruvoletto MG, Fettovich G, Chemello L, Tisminetzky S, Baralle F, Alberti A. Hepatitis C genotypes in patients with dual hepatitis B and C virus infection. *J Med Virol* 1996; **48**: 157-160

8 **Pontisso P**, Ruvoletto MG, Fattovich G, Chemello L, Gallorini A, Ruol A, Alberti A. Clinical and virological profiles in patients with multiple hepatitis virus infections. *Gastroenterology* 1993; **105**: 1529-1533

9 **Ohkawa K**, Hayashi N, Yuki N, Masuzawa M, Kato M, Yamamoto K, Hosotsubo H, Deguchi M, Katayama K, Kasahara A. Long term follow-up of hepatitis B virus and hepatitis C virus replication levels in chronic hepatitis patients co-infected with both viruses. *J Med virol* 1995; **46**: 258-264

10 **Sheen IS**, Liaw YF, Lin DY, Chu CM. Role of hepatitis C virus infection in spontaneous hepatitis B surface antigen clearance during chronic hepatitis B virus infection. *J Infect Dis* 1992; **165**: 831-834

11 **Zarski JP**, Bohn B, Bastie A, Pawlotsky JM, Baud M, Bost-Bezeaux F, Nhieu JT, Seigneurin JM, Buffet C, Dhumeaux D. Characteristic of patients with dual infection by hepatitis B and C viruses. *J Hepat* 1998; **28**: 27-33

12 **Shirazi LK**, Petermann D, Muller C. Hepatitis B virus DNA in sera and liver tissue of HBeAg negative patients with chronic hepatitis C. *J Hepatol* 2000; **33**: 785-790

13 **Ishikawa T**, Ichida T, Yamagiwa S, Sugahara S, Uehara K, Okoshi S, Asakura H. High viral loads, serum alanine aminotransferase and gender are predictive factors for the development of hepatocellular carcinoma from viral compensated liver cirrhosis. *J Gastroenterol Hepatol* 2001; **16**: 1274-1278

14 **Chiaramonte M**, Stroffolini T, Vian A, Stazi MA, Floreani A, Lorenzoni U, Lobello S, Farinati F, Naccarato R. Rate of incidence of hepatocellular carcinoma in patients with compensated viral cirrhosis. *Cancer* 1999; **85**: 2132-2137

15 **Sagnelli E**, Coppola N, Scolastico C, Mogavero AR, Filippini P, Piccinino F. HCV genotype and "silent" HBV coinfection: two main risk factors for a more severe liver disease. *J Med Virol* 2001; **64**: 350-355

16 **Lee DS**, Huh K, Lee EH, Lee DH, Hong KS, Sung YC. HCV and HBV coexist in HBsAg-negative patients with HCV viraemia: Possibility of coinfection in these patients must be considered in HBV-high endemic area. *J Gastroen Hepatol* 1997; **12**: 855-861

17 **Colombari R**, Dhillon AP, Piazzola E, Tomezzoli AA, Angelini GP, Capra F, Tomba A, Scheuer PJ. Chronic hepatitis in multiple virus infection: histopathological evaluation. *Histopathology* 1993; **22**: 319-325

18 **Shiratori Y**, Shiina S, Zhang PY, Ohno E, Okudaira T, Payawal DA, Ono-Nita SK, Imamura M, Kato N, Omata M. Does dual infection by hepatitis B and C viruses play an important role in the pathogenesis of hepatocellular carcinoma in Japan? *Cancer* 1997; **80**: 2060-2067

19 **Ruiz J**, Sangro B, Cuende JI, Beloqui O, Riezu-Boj JI, Herrero JI, Prieto J. Hepatitis B and C virus infections in patients with hepatocelluar carcinoma. *Hepatology* 1992; **16**: 637-641

20 **Huang EJ**, Wright TL, Lake JR, Combs C, Ferrell LD. Hepatitis B and hepatitis C coinfections and persistent hepatitis B infections: clinical outcome and liver pathology after transplantation. *Hepatology* 1996; **23**: 296-404

21 **Wei L**, Wang QX, Xu XY, Wan H, Gao Y, Tian XL, Yu M, Sun DG, Fan CL, Jin J, Fan WM, Yi LM, Zhu WF, Chen HS, Zhuang H, Wang Y. 12-25-year follow-up of hepatitis C virus infection in a rural area of Hebei Province, *Beijing Daxue Xuebao [Yixue Ban]* 2002; **34**: 574-578

22 **Sagnelli E**, Coppola N, Messina V, Caprio D, Marrocco C, Marotta

A, Onofrio M, Scolastico C, Filippini P. HBV superinfection in hepatitis C virus chronic carriers, viral interaction, and clinical course. *Hepatology* 2002; **36**: 1285-1291

23 **EASL International consensus conference on hepatitis B**. 13-14 September, 2002: Geneva, Switzerland. Consensus statement (short version). *J Hepatol* 2003; **38**: 533-540

24 **Chinese Medical Association**. The Programme for prevention and cure of viral hepatitis. *Zhonghua Ganzangbing Zazhi* 2000; **8**: 324-329

25 **Utili BR**, Zampio R, Bellopede P, Marracino M, Ragone E, Adinolfi LE, Ruggiero G, Capasso M, Indolfi P, Casale F, Martini A, Tullio TD. Dual or single hepatitis B and C virus infection in childhood cancer survivior: long term follow-up and effect of interferon treatment. *Blood* 1999; **94**: 4046-4052

26 **Liaw YF**, Yeh CT, Tsai SL. Impact of acute hepatitis B virus superinfection on chronic hepatitis C virus infection. *Am J Gastroenterol* 2000; **95**: 2978-2980

27 **Chisari FV**. Viruses, immunity, and cancer: lessons from hepatitis B. *Am J Pathol* 2000; **156**: 1117-1132

28 **Uchida T**, Kaneita Y, Gotoh K, Kanagawa H, Kouyama H, Kawanishi T, Mima S. Hepatitis C virus is frequently coinfected with serum marker-negative hepatitis B virus: probable replication promotion of the latter as demonstrated by *in vitro* cotransfection. *J Med Virol* 1997; **52**: 399-405

29 **Jardi R**, Rodriguez F, Buti M, Costa X, Cotrina M, Galimany R, Esteban R, Guardia J. Role of hepatitis B, C,and D viruses in dual and triple infection: influence of viral genotype and hepatitis B precore and basal core promoter mutations on viral replicative interference. *Hepatology* 2001; **34**: 404-410

30 **Bonino F**, Rosina F, Rizzetto M, Rizzi R, Chiaberge E, Tardanico R, Callea F, Verme G. Chronic hepatitis in HBsAg carriers with serum HBV-DNA and anti-HBe. *Gastroenterology* 1986; **90**: 1268-1273

31 **Lohiya G**, Lohiya S, Ngo VT, Crinella R. Epidemiology of hepatitis B e antigen and antibody in mentally retarded HBsAg carriers. *Hepatology* 1986; **6**: 163-166

32 **Sheen IS**, Liaw YF, Lin DY, Chu CM. Role of hepatitis C and delta viruses in the termination of chronic hepatitis B surface antigen carrier atate: a multivariate analysis in a longitudinal follow-up study. *J Infect Dis* 1994; **170**: 358-361

Edited by Zhang JZ and Wang XL

P.O.Box 2345, Beijing 100023,China
Fax: +86-10-85381893
E-mail: wjg@wjgnet.com www.wjgnet.com

World J Gastroenterol 2003;9(9):2017-2020
World Journal of Gastroenterology
 ISSN 1007-9327

• VIRAL HEPATITIS •

Detection of T lymphocyte subsets and mIL-2R on surface of PBMC in patients with hepatitis B

Ke-Xia Wang, Jiang-Long Peng, Xue-Feng Wang, Ye Tian, Jian Wang, Chao-Pin Li

Ke-Xia Wang, Jiang-Long Peng, Xue-Feng Wang, Ye Tian, Jian Wang, Chao-Pin Li, School of Medicine, Anhui University of Science and Technology, Huainan 232001, Anhui Province, China
Correspondence to: Dr. Chao-Pin Li, Department of Etiology and Immunology, School of Medcine, Anhui University of Science and Technology, Huainan 232001, Anhui Province, China. cpli@aust.edu.cn
Telephone: +86-554-6658770 **Fax:** +86-554-6662469
Received: 2003-03-02 **Accepted:** 2003-06-02

Abstract

AIM: To study the levels of T lymphocyte subsets and membrane interleukin-2 receptor (mIL-2R) on surface of peripheral blood mononuclear cells (PBMCs) of patients with hepatitis B and its role in the pathogenesis of hepatitis B.

METHODS: The levels of T lymphocyte subsets and mIL-2R in PBMC before and after being stimulated with PHA were detected by biotin-streptavidin (BSA) technique in 196 cases of hepatitis B.

RESULTS: In patients with hepatitis B, the levels of CD_3^+, CD_4^+ cells, and the ratio of CD_4^+ cells/CD_8^+ cells were lower, but the level of CD_8^+ cells was higher than those in normal controls (42.20±6.01 *vs* 65.96±6.54, 38.17±5.93 *vs* 41.73±6.40, 0.91±0.28 *vs* 1.44±0.31, 39.86±6.36 *vs* 30.02±4.54, $P<0.01$). The total expression level of mIL-2R in PBMC before and after being stimulated with PHA was also lower than those in normal controls (3.47±1.55 *vs* 4.52±1.49, 34.03±2.94 *vs* 37.95±3.00, $P<0.01$). In all the patients with hepatitis B, the levels of T lymphocyte subsets and mIL-2R in PBMC with HBV-DNA (+) were lower than those with HBV-DNA (-), which were significantly different (39.57±7.11 *vs* 44.36±5.43, 34.36±7.16 *vs* 40.75±5.87, 37.82±6.54 *vs* 41.72±6.21, 0.88±0.33 *vs* 0.99±0.27, 2.82±1.62 *vs* 3.85±1.47, 31.56±3.00 *vs* 35.84±2.83, $P<0.01$). In addition, the levels of CD_3^+, CD_4^+, CD_8^+ cells, the ratio of CD_4^+ cells /CD_8^+ cells and mIL-2R among different courses of hepatitis B were all significantly different ($F=3\ 723.18$, $P<0.01$. $F=130.43$, $P<0.01$. $F=54.01$, $P<0.01$. $F=2.99$, $P<0.05$. $F=7.16$, $P<0.01$).

CONCLUSION: Both cellular and humoral immune functions are obviously in disorder in patients with hepatitis B, which might be closely associated with the chronicity in patients.

Wang KX, Peng JL, Wang XF, Tian Y, Wang J, Li CP. Detection of T lymphocyte subsets and mIL-2R on surface of PBMC in patients with hepatitis B. *World J Gastroenterol* 2003; 9(9): 2017-2020
http://www.wjgnet.com/1007-9327/9/2017.asp

INTRODUCTION

Hepatitis B virus (HBV) parasitizing in hepatocytes is a pathogen of viral hepatitis B, which easily develops into hepatic fibrosis and cirrhosis, even hepatocellular carcinoma. But the pathogenesis of hepatitis B is very complex and has not been clarified until now. Generally, it is not HBV itself that damages hepatocytes directly, but the results of function disorder of cell-mediated immunity[1-18]. Peripheral blood mononuclear cells (PBMCs), which are aggregation of abundant immunologically competent cells, such as T lymphocytes, natural killer cells and lymphokine activated killer, likely play an important role in anti-HBV infection. Interleukin-2 (IL-2) has a crucial role in several immunologic functions. Its effect is dependent on the conjugation with membrane interleukin-2 receptor (mIL-2R) expressed on surface of activated T lymphocytes and other immunocompetent cells and can release from them. Biotin-streptavidin (BSA) has a high specificity and sensitivity. In order to study possible changes of T lymphocyte subsets and mIL-2R on surface of peripheral blood mononuclear cells (PBMC) of patients with hepatitis B and its role in the pathogenesis of hepatitis B, 196 patients with acute and chronic hepatitis B were detected by the BSA methods in this study. The results suggest that there is a state of depression rather than of activation of T lymphocyte subsets and mIL-2R system in viral hepatitis B, and that the pathogenesis of viral hepatitis B is related to the cellular and humoral immune function of patients.

MATERIALS AND METHODS

Subjects

According to the diagnotic criteria passed by the 10th National Conference on Viral Hepatitis and Hepatopathy 2000 (Xi' an), 196 patients with hepatitis B (male 113 and female 83), aged 19-52 years (average 34.6 years), were chosen from our affiliated teaching hospitals. Among them, 24 patients were HBsAg-positive without symptoms, 22 with acute hepatitis B, 46 with slight chronic hepatitis, 37 with moderate chronic hepatitis, 26 with severe chronic hepatitis, 15 with severe hepatitis, 18 with posthepatitic cirrhosis and 8 with hepatocellular carcinoma. In addition, the controls were selected from HBsAb-positive volunteers (n=10) and normal blood donors from the local central blood bank (n=20), aged 10-45 years (average 32.6 years).

Reagents and instruments

Antibodies against T lymphocyte subsets were provided by Shanghai Jing' an Medical Institute, Ficoll-Hypaque sedimentation gradients were offered by Shanghai Second Reagent Factory, and HBV-DNA reagents were made in Shanghai Middle Asia Gene Institute. Carbon dioxide incubator (MDF-135) was made in Japan.

Samples

Five mL peripheral vein blood 5 mL from each patient with hepatitis B and the controls was collected at 8:00 a.m., and 2.5 ml was distributed in a sterile test tube and 2.5 mL into an anticoagulant test tube with heparin.

Separation of PBMC and detection of T cell subsets, mIL-2R

After the heparinized anticoagulant blood was mixed with equal volume of Hanks' liquid without Ca^{2+} and Mg^{2+}, PBMC were harvested from heparinized whole blood by centrifugation

Table 1 Detection of T lymphocyte subsets and mIL-2R in PBMC of patients with hepatitis B ($\bar{x}$±s,%)

Group	*n*	CD_3^+	CD_4^+	CD_8^+	CD_4^+/CD_8^+	mIL-2R	
						Silent	Induced
Control	30	65.96±6.54[a]	41.73±6.40[b]	30.02±4.54[c]	1.44±0.31[d]	4.52±1.49[e]	37.95±3.00[f]
Anti-HBs (+)	10	66.34±5.16	42.82±6.52	29.03±4.50	1.51±0.27	5.06±1.45	40.26±3.10
NBD	20	65.80±6.92	41.20±6.36	30.45±4.62	1.39±0.33	4.24±1.52	36.30±2.95
Hepatitis B	196	42.20±6.01[a]	38.17±5.93[b]	39.86±6.36[c]	0.91±0.28[d]	3.47±1.55[e]	34.03±2.94[f]
A HBsAg (+)	24	58.83±7.44[g]	41.34±5.16[h]	35.34±7.15[i]	1.20±0.33[j]	3.94±1.75[k]	35.05±3.05[l]
AH	22	57.38±7.73[g]	40.21±6.12[h]	39.47±6.25[i]	1.01±0.30[j]	3.67±1.68[k]	34.22±2.25[l]
SCH	46	38.54±7.56[g]	39.56±6.44[h]	41.10±7.64[i]	0.98±0.31[j]	3.44±1.40[k]	31.96±3.80[l]
MCH	37	40.14±5.85[g]	37.22±5.38[h]	41.45±6.23[i]	0.88±0.25[j]	3.25±1.50[k]	32.81±2.76[l]
SCH	20	40.01±6.23[g]	35.51±6.33[h]	42.86±5.58[i]	0.81±0.22[j]	3.06±1.56[k]	33.83±3.52[l]
SH	15	37.85±6.54[g]	34.57±6.20[h]	42.92±5.65[i]	0.80±0.21[j]	3.95±1.54[k]	33.85±2.65[l]
PC	18	38.72±6.22[g]	36.11±4.23[h]	41.89±8.98[i]	0.90±0.19[j]	3.31±1.60[k]	31.55±2.34[l]
HC	8	39.44±6.78[g]	34.15±5.50[h]	43.46±7.88[i]	0.83±0.24[j]	3.36±1.68[k]	30.38±2.15[l]

[a]t=19.9295, [a]P<0.001. [b]t=3.0300, [b]P<0.01. [c]t=8.1551, [c]P<0.001. [d]t=9.5153, [d]P<0.001. [e]t=3.4722, [e]P<0.001. [f]t=6.7832, [f]P<0.001. [g]F=3723.18, [g]P<0.01. [h]F=130.43, [h]P<0.01. [i]F=54.01, [i]P<0.01. [j]F=2.99, [j]P<0.05. [k]F=7.16, [k]P<0.01. [l]F=1.60, [l]P>0.05. NBD: normal blood donors, A HBsAg (+): asymptomatic HBsAg (+),AH: acute hepatitis, SCH: slight chronic hepatitis, MCH: moderate chronic hepatitis, SCH: severe chronic hepatitis, SH: severe hepatitis, PC: posthepatitic cirrhosis, HC: hepatocellular carcinoma.

Table 2 Detection of T lymphocyte subsets and mIL-2R in PBMC with HBV-DNA (+) before and after induced with PHA ($\bar{x}$±s,%)

Group	*n*	CD_3^+	CD_4^+	CD_8^+	CD_4^+/CD_8^+	mIL-2R	
						Silent	Induced
Control	30	65.96±6.54	41.73±6.40	30.02±4.54	1.44±0.31	4.52±1.49	37.95±3.00
Anti-HBs (+)	10	66.34±5.16	42.82±6.52	29.03±4.50	1.51±0.27	5.06±1.45	40.26±3.10
NBD	20	65.80±6.92	41.20±6.36	30.45±4.62	1.39±0.33	4.24±1.52	36.30±2.95
Hepatitis B	196	42.20±6.01	38.17±5.93	39.86±6.36	0.91±0.28	3.47±1.55	34.03±2.94
HBV-DNA(+) of PBMC	118	39.57±7.11[a]	34.36±7.16[b]	37.82±6.54[c]	0.88±0.33[d]	2.82±1.62[e]	31.56±3.00[f]
HBV-DNA(-) of PBMC	78	44.36±5.43[a]	40.75±5.87[b]	41.72±6.21[c]	0.99±0.27[d]	3.85±1.47[e]	35.84±2.83[f]

[a]t=5.3466, [a]P<0.001. [b]t=6.8525, [b]P<0.01. [c]t=4.2414, [c]P<0.001. [d]t=2.5641, [d]P<0.05. [e]t=4.6355, [e]P<0.001. [f]t=10.0352, [f]P<0.001. NBD: normal blood donors.

on Ficoll-Hypaque sedimentation gradient and diluted to (1-3)×10^6· L^{-1}cells suspension with RPMI 1640 culture liquid. Ten μL suspension of PBMC was smeared on sheet glass pores so that the cells with CD_3^+, CD_4^+, CD_8^+ and the rest phrase of mIL-2R could be detected. Of the PBMC suspension, 0.5 mL was mixed with RPMI 1640 culture liquid, which had PHA 200 μg· L^{-1}. The cells were grown in continuous culture (37 ℃, 50 mL· $L^{-1}CO_2$ in atmosphere) for 72 h and its mIL-2R induced by PHA could be measured by the antibodies against membranes of T cells.

Immunocytochemical method of biotin- streptavidin system (BSA)

The different monoclonal antibodies (mAb) against CD_3, CD_4, CD_8 and Tac with biotin and SA-HRP were smeared on different sheet glasses. These smears were left dry naturally and fixed with acetone for 15-20 min. The cells were incubated in continuous culture (37 ℃, 50 mL· $L^{-1}CO_2$ in atmosphere) for 30 min. The immune sheet glass pores were measured after being stained with the color-developing agent and several washings with Tris buffer solution (TBS). The total number of 200 PBMCs was counted and its positive cells were statistically analyzed with the help of high power lens. The positive criterion was that the color of cell membrane was brown, if not being negative.

Detection of HBV-DNA

The levels of HBV-DNA in serum and PBMC were detected with negative, positive and vacuity controls being set up each time. After routine process, the samples were placed at 94 ℃ for 300 s for denaturation at first, then at 94 ℃ for 30 s, at 55 ℃ for 30 s and at 72 ℃ for 30 s.After 35 cycles, the samples were extended at 72 ℃ for 300 s. After electrophoresis in 2 % sepharose with ethidium bromide (EB) for 20 min, products of amplification were observed with infrared-transmission meters. Samples with orange fluorescent bands as the positive controls were considered to be positive, while the others were negative.

Statistical analysis

Statistical analysis was made by *t* and *F* tests.

RESULTS

The results showed that the percentages of CD_3^+ and CD_4^+ cells, and the ratio of CD_4^+ cells /CD_8^+ cells were lower, the percentage of CD_8^+ cells was higher, and the levels of mIL-2R before and after stimulation with PHA were lower in patients with hepatitis B than those in normal controls (P<0.01). Among different courses of hepatitis B, T lymphocyte subsets and mIL-2R were all significantly different from each other. The detailed results are shown in Tables 1 and 2.

DISCUSSION

Recently, studies have shown that patients with hepatitis B are usually accompanied by disorder of immune function, and hepatocytic damage is mainly caused by immunological

injury[15-30]. Immunologically competent cells and cytokines are the key points for body to eliminate hepatitis B virus[12]. Alterations of T lymphocyte subsets are an important reason for the disorder of immune function due to HBV infection. A lots of cytokines, especially IL-2, can facilitate proliferation of immunologically competent cells[14,31-37], such as T lymphocytes, natural killer cells and lymphokine activated killer cells. While IL-2 is conjugated with mIL-2R on surface of the proper target cells, it will be efficient in immunoregulation. In order to further explore the pathogenesis of hepatitis B, we designed a series of correlation experiments to detect the levels of T lymphocyte subsets and mIL-2R on surface of PBMC in patients with hepatitis B.

CD_3^+, CD_4^+ and CD_8^+ cells are major function subgroups of T cells and play an important role in response to HBV infection, which can reflect the situations of cellular immune function and immunoregulation and are usually regarded as a valuable index to forecast the changes of patients' immunity[11,38-47]. In this study, the percentages of CD_3^+, CD_4^+ cells and the ratio of CD_4^+ cells /CD_8^+ cells decreased, and CD_8^+ cells increased, suggesting that disorders of cellular immune function and pathologic damages occurred in the 196 patients with hepatitis B detected by the method of BSA.

PBMCs are easily infected by HBV[48,49]. When entering into PBMCs, HBV can integrate with host cells and interfere with metabolism of cells, and can depress the expression of CD_3^+ and CD_4^+. As seen in this study, the expression levels of T lymphocyte subsets between positive and negative HBV-DNA and HBV-DNA in PBMC were significantly different (P<0.01).

mIL-2R plays a key role in biologic effect of IL-2 and its expression levels can reflect the course of T cell activity and the immune situation of body[50]. From this study, we can see the expression levels of mIL-2R in PBMCs in silence and induction were lower in hepatitis B patients than in normal controls (P<0.01), and the expression levels of mIL-2R in PBMCs were lower in HBV-DNA positive patients than in HBV-DNA negative patients (P<0.01). After stimulation with PHA, the levels of mIL-2R obviously increased, which showed that mIL-2R could be induced by PHA, but its expression levels were still significantly lower than those in normal controls (P<0.001). In addition, due to deterioration and chronicity of hepatitis B, the expression levels of mIL-2R had a tendency of descent in the patients. These also showed that T cell activity was interfered and humoral immune function was decreased in patients with hepatitis B.

The levels of CD_3^+, CD_4^+, CD_8^+ cells (P<0.01), the ratio of CD_4^+ cells /CD_8^+ cells (P<0.01) and mIL-2R (P<0.05) among different courses of hepatitis B were all significantly different, which suggested that there is a close correlation between levels of T lymphocyte subsets and different courses of hepatitis B. According to the above findings, it is concluded that in patients with hepatitis B, there is an obvious disorder of cellular and humoral immune functions, and a close relationship between the body's immune function and the course of illness. While infecting PBMC, HBV can interfere with the normal metabolism of these cells, and prevent lymphocytic membranes from accepting signals from antigen presenting cells (APC), and depress the expression of mIL-2R. All of these do no good to eliminating HBV and contribute to chronicity of hepatitis B.

REFERENCES

1 **Wei J**, Wang YQ, Lu ZM, Li GD, Wang Y, Zhang ZC. Detection of anti-preS1 antibodies for recovery of hepatitis B patients by immunoassay. *World J Gastroenterol* 2002; **8**: 276-281

2 **Liu DX**. A new hypothesis of pathogenetic mechanism of viral hepatitis B and C. *Med Hypotheses* 2001; **56**: 405-408

3 **Tennant BC**, Gerin JL. The woodchuck model of hepatitis B virus infection. *ILAR J* 2001; **42**: 89-102

4 **Kao JH**, Chen DS. Global control of hepatitis B virus infection. *Lancet Infect Dis* 2002; **2**: 395-403

5 **Bernardi M**, Biselli M, Gramenzi A. Chronic hepatitis B. Recent advances in diagnosis and treatment. *Recenti Prog Med* 2002; **93**: 397-402

6 **Torbenson M**, Thomas DL. Occult hepatitis B. *Lancet Infect Dis* 2002; **2**: 479-486

7 **Ohkubo K**, Kato Y, Ichikawa T, Kajiya Y, Takeda Y, Higashi S, Hamasaki K, Nakao K, Nakata K, Eguchi K. Viral load is a significant prognostic factor for hepatitis B virus-associated hepatocellular carcinoma. *Cancer* 2002; **94**: 2663-2668

8 **Tai DI**, Lo SK, Kuo CH, Du JM, Chen CJ, Hung CS, Chu CM. Replication of hepatitis B in HBsAg-positive siblings. *J Viral Hepat* 2002; **9**: 272-279

9 **Marusawa H**, Osaki Y, Kimura T, Ito K, Yamashita Y, Eguchi T, Kudo M, Yamamoto Y, Kojima H, Seno H, Moriyasu F, Chiba T. High prevalence of anti-hepatitis B virus serological markers in patients with hepatitis C virus related chronic liver disease in Japan. *Gut* 1999; **45**: 284-288

10 **Izzo F**, Cremona F, Ruffolo F, Palaia R, Parisi V, Curley SA. Outcome of 67 patients with hepatocellular cancer detected during screening of 1125 patients with chronic hepatitis. *Ann Surg* 1998; **227**: 513-518

11 **Sing G**, Butterworth L, Chen X, Bryant A, Cooksley G. Composition of peripheral blood lymphocyte populations during different stages of chronic infection with hepatitis B virus. *J Viral Hepat* 1998; **5**: 83-93

12 **Bertoletti A**, Ferrari C, Fiaccadori F. Role of the cell-mediated immune response in the pathogenesis of hepatitis B virus infection: possible immune-therapeutic strategies. *Acta Biomed Ateneo Parmense* 1996; **67**: 87-93

13 **Michalak TI,** Hodgson PD, Churchill ND. Posttranscriptional inhibition of class I major histocompatibility complex presentation on hepatocytes and lymphoid cells in chronic woodchuck hepatitis virus infection. *J Virol* 2000; **74**: 4483-4494

14 **Tulek N**, Saglam SK, Saglam M, Turkyilmaz R, Yildiz M. Soluble interleukin-2 receptor and interleukin-10 levels in patients with chronic hepatitis B infection. *Hepatogastroenterology* 2000; **47**: 828-831

15 **Helvaci M**, Ozkaya B, Ozbal E, Ozinel S, Yaprak I. Efficacy of interferon therapy on serum fibronectin levels in children with chronic hepatitis B infection. *Pediatr Int* 1999; **41**: 270-273

16 **Park YN**, Han KH, Kim KS, Chung JP, Kim S, Park C. Cytoplasmic expression of hepatitis B core antigen in chronic hepatitis B virus infection: role of precore stop mutants. *Liver* 1999; **19**: 199-205

17 **Ilan Y**, Chowdhury JR. Induction of tolerance to hepatitis B virus: can we 'eat the disease' and live with the virus? *Med Hypotheses* 1999; **52**: 505-509

18 **Khettry U**, Anand N, Gordon FD, Jenkins RL, Tahan SR, Loda M, Lewis WD. Recurrent hepatitis B, hepatitis C, and combined hepatitis B and C in liver allografts: a comparative pathological study. *Hum Pathol* 2000; **31**: 101-108

19 **Webster GJ**, Reignat S, Maini MK, Whalley SA, Ogg GS, King A, Brown D, Amlot PL, Williams R, Vergani D, Dusheiko GM, Bertoletti A. Incubation phase of acute hepatitis B in man: dynamic of cellular immune mechanisms. *Hepatology* 2000; **32**: 1117-1124

20 **Chemin I**, Ohgaki H, Chisari FV, Wild CP. Altered expression of hepatic carcinogen metabolizing enzymes with liver injury in HBV transgenic mouse lineages expressing various amounts of hepatitis B surface antigen. *Liver* 1999; **19**: 81-87

21 **Chomarat P**, Rice JM, Slagle BL, Wild CP. Hepatitis B virus-induced liver injury and altered expression of carcinogen metabolising enzymes: the role of the HBx protein. *Toxicol Lett* 1998; **102-103**: 595-601

22 **Nakamoto Y**, Guidotti LG, Kuhlen CV, Fowler P, Chisari FV. Immune pathogenesis of hepatocellular carcinoma. *J Exp Med* 1998; **188**: 341-350

23 **Hayashi N**, Mita E. Fas system and apoptosis in viral hepatitis. *J Gastroenterol Hepatol* 1997; **12**: S223-226

24 **Sarin SK**, Thakur V, Guptan RC, Saigal S, Malhotra V, Thyagarajan SP, Das BC. Profile of hepatocellular carcinoma in India: an insight into the possible etiologic associations. *J Gastroenterol Hepatol* 2001; **16**: 666-673

25 **Shoenfeld Y**, Aron-Maor A. Vaccination and autoimmunity-'vaccinosis': a dangerous liaison? *J Autoimmun* 2000; **14**: 1-10

26 **Trobonjaca Z**, Kroger A, Stober D, Leithauser F, Moller P, Hauser H, Schirmbeck R, Reimann J. Activating immunity in the liver. II. IFN-beta attenuates NK cell-dependent liver injury triggered by liver NKT cell activation. *J Immunol* 2002; **168**: 3763-3770

27 **Rapicetta M**, Ferrari C, Levrero M. Viral determinants and host immune responses in the pathogenesis of HBV infection. *J Med Virol* 2002; **67**: 454-457

28 **Tanner MS**. Mechanisms of liver injury relevant to pediatric hepatology. *Crit Rev Clin Lab Sci* 2002; **39**: 1-61

29 **Rivero M**, Crespo J, Fabrega E, Casafont F, Mayorga M, Gomez-Fleitas M, Pons-Romero F. Apoptosis mediated by the Fas system in the fulminant hepatitis by hepatitis B virus. *J Viral Hepat* 2002; **9**: 107-113

30 **Okumura A**, Ishikawa T, Yoshioka K, Yuasa R, Fukuzawa Y, Kakumu S. Mutation at codon 130 in hepatitis B virus (HBV) core region increases markedly during acute exacerbation of hepatitis in chronic HBV carriers. *J Gastroenterol* 2001; **36**: 103-110

31 **Moe SM**, Zekonis M, Harezlak J, Ambrosius WT, Gassensmith CM, Murphy CL, Russell RR, Batiuk TD. A placebo-controlled trial to evaluate immunomodulatory effects of paricalcitol. *Am J Kidney Dis* 2001; **38**: 792-802

32 **Huang YH**, Wu JC, Tao MH, Syu WJ, Hsu SC, Chi WK, Chang FY, Lee SD. DNA-Based immunization produces Th1 immune responses to hepatitis delta virus in a mouse model. *Hepatology* 2000; **32**: 104-110

33 **Akbar SM**, Abe M, Masumoto T, Horiike N, Onji M. Mechanism of action of vaccine therapy in murine hepatitis B virus carriers: vaccine-induced activation of antigen presenting dendritic cells. *J Hepatol* 1999; **30**: 755-764

34 **Livingston BD**, Alexander J, Crimi C, Oseroff C, Celis E, Daly K, Guidotti LG, Chisari FV, Fikes J, Chesnut RW, Sette A. Altered helper T lymphocyte function associated with chronic hepatitis B virus infection and its role in response to therapeutic vaccination in humans. *J Immunol* 1999; **162**: 3088-3095

35 **Lau GK**, Nanji A, Hou J, Fong DY, Au WS, Yuen ST, Lin M, Kung HF, Lam SK. Thymosin-alpha1 and famciclovir combination therapy activates T-cell response in patients with chronic hepatitis B virus infection in immune-tolerant phase. *J Viral Hepat* 2002; **9**: 280-287

36 **Priimiagi LS**, Tefanova VT, Tallo TG, Shmidt EV, Solomonova OV, Tuisk TP, Kikosh GV, Krupskaia LM, Lisitsyna SA. Th1-cytokines in chronic hepatitis B and C. *Vopr Virusol* 2002; **47**: 23-27

37 **Wang FS**, Xing LH, Liu MX, Zhu CL, Liu HG, Wang HF, Lei ZY. Dysfunction of peripheral blood dendritic cells from patients with chronic hepatitis B virus infection. *World J Gastroenterol* 2001; **7**: 537-541

38 **Chen M**, Sallberg M, Thung SN, Hughes J, Jones J, Milich DR. Nondeletional T-cell receptor transgenic mice: model for the CD4 (+) T-cell repertoire in chronic hepatitis B virus infection. *J Virol* 2000; **74**: 7587-7599

39 **Lin CM**, Wang FH. Selective modification of antigen-specific CD4 (+) T cells by retroviral-mediated gene transfer and *in vitro* sensitization with dendritic cells. *Clin Immunol* 2002; **104**: 58-66

40 **Lau GK**, Suri D, Liang R, Rigopoulou EI, Thomas MG, Mullerova I, Nanji A, Yuen ST, Williams R, Naoumov NV. Resolution of chronic hepatitis B and anti-HBs seroconversion in humans by adoptive transfer of immunity to hepatitis B core antigen. *Gastroenterology* 2002; **122**: 614-624

41 **Sing GK**, Li D, Chen X, Macnaughton T, Lichanska AM, Butterworth L, Ladhams A, Cooksley G. A molecular comparison of T lymphocyte populations infiltrating the liver and circulating in the blood of patients with chronic hepatitis B: evidence for antigen-driven selection of a public complementarity-determining region 3 (CDR3) motif. *Hepatology* 2001; **33**: 1288-1298

42 **Fei GZ**, Sylvan SP, Yao GB, Hellstrom UB. Quantitative monitoring of serum hepatitis B virus DNA and blood lymphocyte subsets during combined prednisolone and interferon-alpha therapy in patients with chronic hepatitis B. *J Viral Hepat* 1999; **6**: 219-227

43 **Polat Eyigun C**, Yasar Avci I, Sengul A, Hacibektasoglu A, Van Thiel DH. Immune status of individuals with differing clinical courses of HBV infection. *Hepatogastroenterology* 1999; **46**: 1890-1894

44 **Im EH**, Lee BS, Sung JK, Lee SO, Lee KT, Lee SM, Kim SH, Seo KS, Kim JH, Kim SG, Kim NJ, Lee HY. T cell subsets in chronic hepatitis B and the effect of prednisolone withdrawal and interferon alpha-2b. *Korean J Intern Med* 1999; **14**: 1-8

45 **Schirmbeck R**, Wild J, Reimann J. Similar as well as distinct MHC class I-binding peptides are generated by exogenous and endogenous processing of hepatitis B virus surface antigen. *Eur J Immunol* 1998; **28**: 4149-4161

46 **Bertoletti A**, D'Elios MM, Boni C, De Carli M, Zignego AL, Durazzo M, Missale G, Penna A, Fiaccadori F, Del Prete G, Ferrari C. Different cytokine profiles of intraphepatic T cells in chronic hepatitis B and hepatitis C virus infections. *Gastroenterology* 1997; **112**: 193-199

47 **Chen M**, Sallberg M, Thung SN, Hughes J, Jones J, Milich DR. Modeling the T-helper cell response in acute and chronic hepatitis B virus infection using T-cell receptor transgenic mice. *Antiviral Res* 2001; **52**: 99-111

48 **Jiang R**, Feng X, Guo Y, Lu Q, Hou J, Luo K, Fu N. T helper cells in patients with chronic hepatitis B virus infection. *Chin Med J* 2002; **115**: 422-424

49 **Sobao Y,** Tomiyama H, Sugi K, Tokunaga M, Ueno T, Saito S, Fujiyama S, Morimoto M, Tanaka K, Takiguchi M. The role of hepatitis B virus-specific memory CD8 T cells in the control of viral replication. *J Hepatol* 2002; **36**: 105-115

50 **Wang JP**, Li XH, Zhu Y, Wang AL, Lian JQ, Jia ZS, Xie YM. Detection of serum sIL-2R, IL-6, IL-8, TNF-α and lymphocytes subsets, mIL-2R in patients with chronic hepatitis B. *Shijie Huaren Xiaohua Zazhi* 2000; **8**: 763-766

Edited by Zhang JZ and Wang XL

P.O.Box 2345, Beijing 100023,China
Fax: +86-10-85381893
E-mail: wjg@wjgnet.com www.wjgnet.com

World J Gastroenterol 2003;9(9):2021-2024
World Journal of Gastroenterology
 ISSN 1007-9327

Stability of randomly amplified polymorphic DNA fingerprinting in genotyping clinical isolates of *Helicobacter pylori*

Feng-Chan Han, Han-Chong Ng, Bow Ho

Feng-Chan Han, Han-Chong Ng, Bow Ho, Department of Microbiology, Faculty of Medicine, National University of Singapore, 5 Science Drive 2, Singapore 117595, Republic of Singapore
Supported by the National Medical Research Council (NMRC) Sponsored Project, No. R-182-000-037-213
Correspondence to: Feng-Chan Han, Institute of Genetic Diagnosis, Fourth Military Medical University, 169 Changle West Road, Xi' an710033, Shaanxi Province,China. biohanfc@hotmail.com
Telephone: +86-29-3374772 **Fax:** +86-29-3285729
Received: 2003-03-02 **Accepted:** 2003-05-11

Abstract

AIM: *H pylori* genomes are highly diversified. This project was designed to genotype *H pylori* isolates by the polymerase chain reaction (PCR)-based randomly amplified polymorphic DNA (RAPD) fingerprinting technique and to verify its stability by Southern blotting and DNA sequencing.

METHODS: Clinical isolates of *H pylori* were cultured from gastric antra and cardia of 73 individuals, and genomic DNA was prepared for each isolate. RAPD was carried out under optimized conditions. 23S rDNA was regarded as an internal control, and a 361 bp rDNA fragment (RDF) was used as a probe to screen the RAPD products by Southern blotting. Ten RDFs from different clinical isolates and the flanking regions (both upstream and downstream) of four RDFs were amplified and sequenced.

RESULTS: *H pylori* isolates from different individuals had different RAPD profiles, but the profiles for isolates cultured from different gastric sites of a given individual were identical in all but one case. Isolates from 27 individuals were RDF positive by Southern blotting. Sequences of the RDFs and their flanking regions were almost the same between the RDF positive and negative isolates as determined by Southern blotting. There was no binding site for random PCR primer inside the sequences.

CONCLUSION: RAPD is very useful in genotyping *H pylori* grossly on a large scale. However, it seems unstable in amplification of low yield fragments, especially those that do not appear as visible bands on the agarose gel stained with EB, since the primer is partially matched to the template.

Han FC, Ng HC, Ho B. Stability of randomly amplified polymorphic DNA fingerprinting in genotyping clinical isolates of *Helicobacter pylori*. *World J Gastroenterol* 2003; 9(9): 2021-2024
http://www.wjgnet.com/1007-9327/9/2021.asp

INTRODUCTION

H pylori is a spiral, Gram-negative bacterium, which chronically infects more than half of population worldwide, and is implicated in gastritis, peptic ulcer and gastric cancer[1-12]. One of its features is high genome diversity[13-15]. Clinical isolates of *H pylori* from different individuals show enormous variation in their genomic fingerprints[16-18]. Studies based on the two sequenced genomes of *H pylori* strains (i.e. 26695 and J99) have revealed that among the *H pylori* genes, 22 % are dispensable and about 6 % are unique[14,15]. Sequence variation of certain genes or regions, such as the cag pathogenicity island[19, 20], *vacA*[21], *babA* and *babB*[22], drug resistant genes[23-26] and restriction-modification genes[27-29], is also remarkable. For a given individual, the genes of the colonized strain even change over the course of colonization[17, 30]. Genotyping of the bacterium is important for the epidemiological and pathogenic investigation, and genes that are present in one strain but absent or substantially different in others can be of great interest biologically.

The polymerase chain reaction (PCR)-based randomly amplified polymorphic DNA (RAPD) method has widely applied to the distinction of *H pylori* isolates due to its sensitivity, efficiency and promptness[16, 17]. However, problems with its stability or reproducibility arise. In this study, we obtained RAPD fingerprints of clinical isolates of *H pylori* under optimized conditions, and then determined the stability of RAPD products by Southern blotting and DNA sequencing techniques.

MATERIALS AND METHODS

H pylori culture

Clinical isolates of *H pylori* cultured from gastric antra and cardia of 73 patients, 12 with gastric ulcer (GU), 18 with duodenum ulcer (DU), 8 with both GU and DU, and 25 with non-ulcer dyspepsia (NUD), were selected for this study. Each isolate preserved in the brain heart infusion broth (BHI, Gibco, Edinburgh, UK) supplemented with 100 mL/L horse serum and 200 mL/L glycerol was inoculated onto *H pylori* selective chocolate blood agar containing 40 g/L blood agar base No.2 (Oxoid, Basingstoke, UK) and 50 mL/L horse blood (Gibco, Edinburgh, UK). Antibiotics (Sigma, St. Louis, MO, USA) were used at the following concentrations: 3 mg/L vancomycin, 5 mg/L trimethoprim, 10 mg/L nalidixic acid and 2 mg/L amphotericin B. The plates were incubated in a microaerobic atmosphere (50 mL/L CO_2) in a CO_2 incubator (Forma Scientific, Marietta, OH, USA) at 37 ℃ for up to 5 days.

Extraction of genomic DNA

H pylori cells on the plates were harvested by using a sterile swab, and transferred into an Eppendorf tube containing 1.5 mL TE buffer (10 mmol/L Tris-HCl, pH 8.0; 1 mmol/L EDTA, pH 8.0). The suspension was centrifuged at 8 000 g for 10 min and washed once with TE buffer. The pellet was then suspended in 800 μL TE buffer was incubated with 10 μL of 100 g/L lysozyme (Sigma, St. Louis, MO, USA) at 37 ℃ for 30 min. The suspension was then lysed with 100 μL of 100 g/L sodium dodecyl sulfate (SDS) by incubating at 37 ℃ for another 30 min. Then 5 μL of proteinase K (10 g/L) (Boehninger, Mannheim, Germany) was added into the mixture and incubated at 56 ℃ for 1 h. Afterward, *H pylori* DNA was purified by extracting twice with equal volume of phenol and once with equal volume of chloroform, followed by centrifugation at 12 000 g for 10 min each time. The supernatant

was transferred into a new Eppendorf tube, and precipitated with 2 volume of absolute ethanol and 20 μL of 3 M sodium acetate at -20 ℃ overnight. The DNA preparation was centrifuged at 12 000 g for 20 min and washed once with 700 mL/L ethanol. The pellet was then vacuum-dried and suspended in 50 μL distilled water. RNase A was added at the final concentration of 20 mg/L. After incubated at room temperature for 30 min, DNA concentration was determined spectrophotometrically.

RAPD for genomic DNA

A universal primer was chosen for the PCR-based RAPD, according to the paper of Akopyanz, *et al*[31], to fingerprint the genomic DNA. The primer was 5-AAGAGCCCGT-3. The volume of the PCR mixture was 25 μL containing 50 ng of *H pylori* genomic DNA, 20 pmol primer, 1 unit of Taq DNA polymerase, 0.25 mmol/L dNTPs, 10 mmol/L Tris-HCl, 50 mmol/L KCl, 2 mmol/L $MgCl_2$ and 0.1 g/L gelatin (Promega, Madison WI, USA). PCR was performed with a thermal cycler (Perkin-Elmer 2400, Boston, MA, USA) consisting of an initial step at 94 ℃ for 5 min. This was followed by 39 cycles of denaturation at 94 ℃ for 1 min, annealing at 36 ℃ for 1 min and extension at 72 ℃ for 1 min. Ten microlitres of the PCR products were electrophoresed in 10 g/L horizontal agarose gel in TBE buffer at 68 V for 2 h. The gels were stained with ethidium bromide (EB, 1 mg/L) and photographed.

DNA fragment cloning and sequencing

At first, two primers were designed: RDF1-CGCAAGCTTCC ACACAGAACCAC, and RDF2-CGCGGATCCGGAC CTTTACTACAAC. A 23S rDNA fragment (RDF) was amplified according to the gene sequence reported[32]. The PCR mixture was 40 μL in volume containing 4 μL of 10×polymerase buffer, 2 μL of genomic DNA (20 ng) from the reference strain NCTC11637, 1 μL (2 units) of Taq DNA polymerase, 4 μL of 2.5 mmol/L dNTPs, and 4 μL of 10 mmol/L primers. The sample was subjected to denaturation at 94 ℃ for 3 min. The PCR program was 30 cycles at 94 ℃ for 30 s, at 55 ℃ for 45 s, and at 72 ℃ for 1 min, followed by an extra extension at 72 ℃ for 5min. The PCR product (10 μL) was then electrophoresed in a 15 g/L agarose gel. DNA was recovered by using QIAEXÐagarose gel extract kits (Qiagen, Santa Clarita, CA, USA). The purified PCR product was then cloned into the *pT-Adv* vector (Clontech, Palo Alto, CA, USA) and transformed into *E. coli Top*^{10}, which was then inoculated on the selective plates containing 20 μL of 50 g/L ampicillin, 35 μL of 100 mmol/L IPTG and 40 μL of 20 g/L X-gal. White colonies were randomly picked up, suspended in 5 mL of Luria-Bertani medium containing ampicillin (50 mg/L) and cultured at 37 ℃ overnight. The recombinant plasmid was extracted by using Qiaprep spin miniprep kit (Qiagen, Santa Clarita, CA, USA). In the same way, RDFs from different *H pylori* isolates were amplified and cloned into the *pGEM-T-Easy* Vector (Promega, Madison, WI, USA). Then, A 23S rDNA fragment (1 050 bp) containing the RDF in the middle was also amplified from different *H pylori* isolates by using the primers DMSR1-TAAGTTCGCGATAAGGTGTGC and DMSR1-GGTTCCTGCTTAGATGCTTTC. The inserts in the recombinant plasmids and the RDF flanking regions were sequenced by using the Big dye terminator DNA sequencing kit (Perkin-Elmer, Boston, MA, USA) and ABI automated sequencer (GMI, Minnesota, USA).

Southern blotting

Southern blotting was carried out following the protocol provided in the Enhanced chemiluminescence (ECL) direct nucleic acid labeling and detection system (Amersham Pharmacia Biotech, Buckinghamshire, UK). In brief, after agarose gel electrophoresis of the RAPD products, the DNA was submitted to denaturation by immersing the gel (200 cm^2) in 200 ml buffer containing 0.5 mol/L NaOH and 1.5 mol/L NaCl for 30 min. Then the gel was neutralized in 200 ml of 0.5 mol/L Tris-HCl and 1.5 mol/L NaCl (pH 7.5) for 30 min. Afterward, the DNA was transferred to the Hybond N^+ membrane (Amersham Pharmacia Biotech, Buckinghamshire, UK) by using a capillary blotting apparatus. DNA fixation was carried out by exposing the membrane to an UV transilluminator (Vilber Lourmat, Marne la Vallee Cedex 1, France) for 5 min. RDF sequenced and digested by *EcoR* I from *pT-Adv* vector was used as a probe. The pre-hybridization and hybridization were performed in a buffer containing 0.5 mol/L NaCl and 50 g/L blocking agent in a hybridization oven at 42 ℃ for 1 h and 5 h respectively. After stringency washing (twice for 20 min in 6 mol/L urea, 4 g/L SDS and 0.1×standard saline citrate, SSC; twice for 5 min in 2×SSC), chemiluminenscence signals were detected by exposing the hyperfilm to the membrane for 5 to 30 min in a dark room.

RESULTS

H pylori gene profiles identified by RAPD

For all *H pylori* isolates from the 73 individuals, bacterial growth, genomic DNA extraction and RAPD were carried out under the same conditions. RAPD products were analyzed by 10 g/L agarose gel electrophoresis (Figures 1 and 2), which showed that *H pylori* from gastric antra of different individuals had different RAPD profiles whereas the isolates from antrum and cardia of the same individual had almost identical RAPD profiles with only one exception (lanes 5C and 5A in Figure 1).

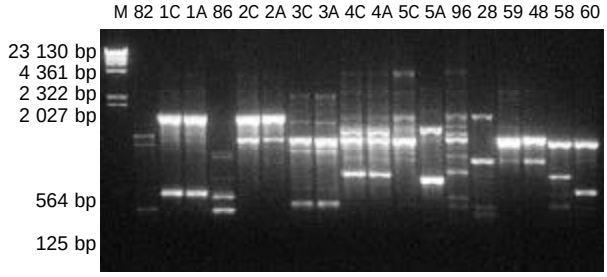

Figure 1 10 g/L agarose gel electrophoresis of RAPD products of *H pylori* isolates. M: λDNA Hind III markers; 82, 86, 96, 28, 59, 48, 59 and 60: Designations of *H pylori* isolates; A: Antrum; C: Cardia.

Probe preparation

The sequence of RDF from the reference strain NCTC11637 was 99 % identical to that reported in the GenBank. It was a 361 bp fragment of the 23S rDNA (from 2 133 to 2 493), which is just inside the loop (2 134-2 684) to form peptidyltransferase center in the ribosome. The fragment was then used as a probe in Southern blotting to investigate if the random PCR primer would pick up the same fragment with the same amount from genomes of different clinical isolates of *H pylori*.

Southern blotting

Firstly, the sensitivity of Southern blotting, in which the RDF was used as both target and probe, was determined by using the ECL system. The results showed that the sensitive limitation of this system was 4 pg. Then, the probe was used to screen the RAPD products of different *H pylori* isolates. Parts of the results are shown in Figure 2. *H pylori* isolates from 27 of the

73 individuals were RDF positive, and the darkness of the blots was quite different from one isolate to another. As the size of the RAPD fragment hybridized with the RDF was bigger (about 400 bp) than that of the RDF, at least one primer binding site would be outside the RDF region.

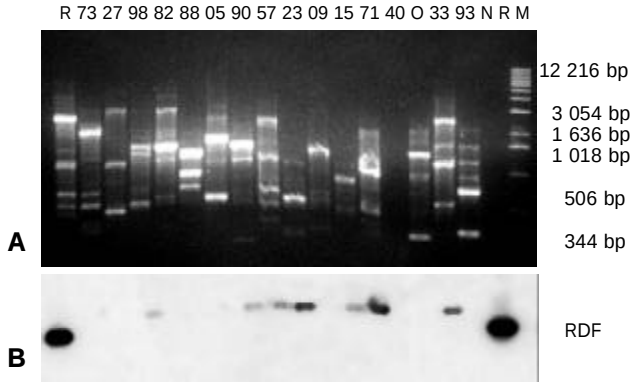

Figure 2 Results of agarose gel electrophoresis of RAPD products (A) and Southern blotting (B). A: 10 g/L agarose gel electrophoresis of RAPD products of *H pylori* isolates; M: 1 Kb DNA ladder; 73, 27, 98, 82, 88, 05, 90, 57, 23, 09, 15, 71, 40, 33 and 93: Designations of the *H pylori* isolates; N: *H pylori* reference strain NCTC11637; R: 1 ng RDF loaded in the well; O: Template blank control; B: Southern blotting results using the RDF as a probe, the dark blots on either side of Picture B corresponding to the 1 ng RDF in the agarose gel in Picture A.

Sequencing RDFs and their flanking regions

In order to know if there were sequence differences that might facilitate the binding of the random primer, the RDFs and their flanking regions from different *H pylori* isolates were sequenced. Firstly, the RDFs from 10 different *H pylori* isolates were cloned for sequencing. The isolates with designated numbers of 15, 22, 38, 58, 90 and 93 were RDF positive and the isolates 20, 41, 84 and 90 were RDF negative in Southern blotting. Blast analysis of the sequenced results exhibited that the RDFs from the 10 isolates were quite similar.

The rates of identity were 98 % to 100 %. There was no random primer binding siteinside the RDFs. Next, the RDF flanking regions were sequenced by using the PCR products directly. Four isolates were used. Sequences of the upstream regions or the downstream regions of RDFs were also quite similar (98 % to 99 % identity) between the RDF positive isolates (numbers 38 and 93) and the RDF negative isolates (numbers 84 and 90) in Southern blotting, and there was no random primer binding site inside the upstream regions or the downstream regions.

DISCUSSION

It is known that DNA fingerprints of clinical *H pyori* isolates are highly diversified[16,17] and the fingerprinting profiles are changeable even for the isolates from different parts of the stomach in a single host[33,34]. The results in this study were basically in according with those obtained in the previous studies. The gene diversity of *H pylori* is associated with certain diseases[20, 35,36], and clinical background and geographic origin of the isolates may be responsible for the changes[37].

It is always considered that the gene of rRNA is relatively conservative, and two copies of 23S rDNA exist in *H pylori* genome[32,38]. Theoretically, when the RDF probe is used to screen the RAPD products of different clinical isolates, Southern blotting profiles should be the same. However, our results showed that the Southern blotting profiles of 23S rDNA from different *H pylori* isolates were also polymorphic. Since genomes of different *H pylori* isolates contain almost identical RDF as well as the flanking regions and the same amount of genomic DNA was used as the templates in this study, instability of using RAPD to amplify this gene fragment at the pg level might be responsible for the results.

The random primer was first proposed for fingerprinting of *H pylori* by Akopyanz *et al*[31]. They recommended the primer since it had a relative high CG content and could be used to distinguish different *H pylori* isolates. In fact, when one employs this primer, there will be numerous potentially amplifiable fragments and only a few of them are visible on agarose gels after EB staining. This depends on the matching extent of the primer to the genomic DNA. For the bright or visible bands, the primer may be completely or mostly matched, but for the light or invisible bands, the primer is probably partially matched.

In conventionally used PCR, the specificity depends mainly on the properties of the primers and the annealing temperature. However, in PCR-based RAPD, the random primer is only 10 mers and the annealing temperature is 36 ℃. Therefore, specificity of amplification is relatively low. Since we could not find any primer binding site inside or outside the RDF region in this experiment, we propose that, for amplification of the RDF, the primer be partially matched to the genomic DNA, and thus, the profiles of RAPD and Southern blotting are diversified.

From our experience, RAPD depends highly on the quality and quantity of the template. If we make a comparison between two RAPD profiles of a given *H pylori* isolate, the concentration, purity and even the integrity of the DNA templates should be considered. The RAPD results will be quite different if the genomic DNA is prepared using two different methods. Sometimes different PCR machines might also give different results. So, when we employed this method, we had tried to treat every sample under the same conditions, and handled the DNA preparation carefully. Even so, RAPD seems to be unstable in amplification of low yield fragments, especially those that do not appear as visible binds in agarose gel electrophoresis.

RAPD has reasonable discriminatory power[39] and is effective for *H pylori* genotyping grossly on large scale. But stability of this method should be taken into consideration.

Although we found many strain specific RAPD profiles in this study, using the RAPD-based methods to screen *H pylori* strain specific genes are not recommended. To identify strain specific genes, the PCR sequencing techniques are more reliable and reproducible.

ACKNOWLEDGEMENT

We are grateful to Ms. Min Gong and Yan-Wing Ho, and also Mr. Mun-Fai Loke, Department of Microbiology, National University of Singapore, for their help in the preparation of *H pylori* isolates.

REFERENCES

1 **Israel DA**, Peek RM. Pathogenesis of *Helicobacter pylori*-induced gastric inflammation. *Aliment Pharmacol Ther* 2001; **15**: 1271-1290
2 **Sanders MK,** Peura DA. *Helicobacter pylori*-Associated Diseases. *Curr Gastroenterol Rep* 2002; **4**: 448-454
3 **Dawsey SM**, Mark SD, Taylor PR, Limburg PJ. Gastric cancer and *H pylori*. *Gut* 2002; **51**: 457-458
4 **Blaser MJ.** Linking *Helicobacter pylori* to gastric cancer. *Nat Med* 2000; **6**: 376-377
5 **Blaser MJ,** Berg DE. *Helicobacter pylori* genetic diversity and risk of human disease. *J Clin Invest* 2001; **107**: 767-773
6 **Wang RT**, Wang T, Chen K, Wang JY, Zhang JP, Lin SR, Zhu YM, Zhang WM, Cao YX,Zhu CW, Yu H, Cong YJ, Zheng S, Wu BQ. *Helicobacter pylori* infection and gastric cancer: evidence from

a retrospective cohort study and nested case-control study in China. *World J Gastroenterol* 2002; **8**: 1103-1107
7 **Meining A**, Riedl B, Stolte M. Features of gastritis predisposing to gastric adenoma and early gastric cancer. *J Clin Pathol* 2002; **55**: 770-773
8 **Han SR**, Zschausch HC, Meyer HG, Schneider T, Loos M, Bhakdi S, Maeurer MJ. *Helicobacter pylori:* clonal population structure and restricted transmission within families revealed by molecular typing. *J Clin Microbiol* 2000; **38**: 3646-3651
9 **Shibata A,** Parsonnet J, Longacre TA, Garcia MI, Puligandla B, Davis RE, Vogelman JH, Orentreich N, Habel LA. CagA status of *Helicobacter pylori* infection and p53 gene mutations in gastric adenocarcinoma. *Carcinogenesis* 2002; **23**: 419-424
10 **Lan J,** Xiong YY, Lin YX, Wang BC, Gong LL, Xu HS, Guo GS. *Helicobacter pylori* infection generated gastric cancer through p53-Rb tumor-suppressor system mutation and telomerase reactivation. *World J Gastroenterol* 2003; **9**: 54-58
11 **Cai L**, Yu SZ, Zhang ZF. *Helicobacter pylori* infection and risk of gastric cancer in Changle County, Fujian Province, China. *World J Gastroenterol* 2000; **6**: 374-376
12 **Liu HF**, Liu WW, Fang DC, Wang GA, Teng XC. Relationship between *Helicobacter pylori* infection and gastric precancerous lesions: a follow-up study. *Shijie Huaren Xiaohua Zazhi* 2002; **10**: 912-915
13 **Israel DA**, Salama N, Arnold CN, Moss SF, Ando T, Wirth HP, Tham KT, Camorlinga M, Blaser MJ, Falkow S, Peek RM Jr. *Helicobacter pylori* strain-specific differences in genetic content, identified by microarray, influence host inflammatory responses. *J Clin Invest* 2001; **107**: 611-620
14 **Salama N**, Guillemin K, McDaniel TK, Sherlock G, Tompkins L, Falkow S. A whole- genome microarray reveals genetic diversity among *Helicobacter pylori* strains. *Proc Natl Acad Sci U S A* 2000; **97**: 14668-14673
15 **Bjorkholm BM**, Oh JD, Falk PG, Engstrand LG, Gordon JI. Genomics and proteomics converge on *Helicobacter pylori*. *Curr Opin Microbiol* 2001; **4**: 237-245
16 **Yakoob J,** Hu GL, Fan XG, Yang HX, Liu SH, Tan DM, Li TG, Zhang Z. Diversity of *Helicobacter pylori* among Chinese persons with *H pylori* infection. *APMIS* 2000; **108**: 482-486
17 **Israel DA**, Salama N, Krishna U, Rieger UM, Atherton JC, Falkow S, Peek RM Jr. *Helicobacter pylori* genetic diversity within the gastric niche of a single human host. *Proc Natl Acad Sci U S A* 2001; **98**: 14625-14630
18 **Sillakivi T**, Aro H, Ustav M, Peetsalu M, Peetsalu A, Mikelsaar M. Diversity of *Helicobacter pylori* genotypes among Estonian and Russian patients with perforated peptic ulcer, living in Southern Estonia. *FEMS Microbiol Lett* 2001; **195**: 29-33
19 **Peters TM**, Owen RJ, Slater E, Varea R, Teare EL, Saverymuttu S. Genetic diversity in the *Helicobacter pylori* cag pathogenicity island and effect on expression of anti-CagA serum antibody in UK patients with dyspepsia. *J Clin Pathol* 2001; **54**: 219-223
20 **Dong Q,** O'Sullivan M, Hall W, Herra C, Kean C, O'Morain C, Buckley M. Identification of a new segment involved in cagA 3' region variation of *Helicobacter pylori*. *FEMS Immunol Med Microbiol* 2002; **25**: 51-55
21 C**atalano M**, Matteo M, Barbolla RE, Jimenez Vega DE, Crespo O, Leanza AG, Toppor J, Antelo P. *Helicobacter pylori* vacA genotypes, cagA status and ureA-B polymorphism in isolates recovered from an Argentine population. *Diagn Microbiol Infect Dis* 2001; **41**: 205-210
22 **Pride DT**, Meinersmann RJ, Blaser MJ. Allelic Variation within *Helicobacter pylori* babA and babB. *Infect Immun* 2001; **69**: 1160-1171
23 **Yakoob J**, Fan X, Hu G, Liu L, Zhang Z.Antibiotic susceptibility of *Helicobacter pylori* in the Chinese population. *J Gastroenterol Hepatol* 2001; **16**: 981-985
24 **Piana A,** Are BM, Maida I, Dore MP, Sotgiu G, Realdi G, Mura I. Genotypic characterization of clarithromycin-resistant *Helicobacter pylori* strains. *New Microbiol* 2002; **25**: 123-130
25 **Gerrits MM**, de Zoete MR, Arents NL, Kuipers EJ, Kusters JG.16S rRNA mutation-mediated tetracycline resistance in *Helicobacter pylori*. *Antimicrob Agents Chemother* 2002; **46:** 2996-3000
26 **Jeong JY**, Mukhopadhyay AK, Dailidiene D, Wang Y, Velapatino B, Gilman RH, Parkinson AJ, Nair GB, Wong BC, Lam SK, Mistry R, Segal I, Yuan Y, Gao H, Alarcon T, Brea ML, Ito Y, Kersulyte D, Lee HK, Gong Y, Goodwin A, Hoffman PS, Berg DE. Sequential inactivation of rdxA (HP0954) and frxA (HP0642) nitroreductase genes causes moderate and high-level metronidazole resistance in *Helicobacter pylori*. *J Bacteriol* 2000; **182**: 5082-5090
27 **Nobusato A**, Uchiyama I, Kobayashi I. Diversity of restriction-modification gene homologues in *Helicobacter pylori*. *Gene* 2000; **259**: 89-98
28 **Lin LF**, Posfai J, Roberts RJ, Kong H. Comparative genomics of the restriction-modification systems in *Helicobacter pylori*. *Proc Natl Acad Sci U S A* 2001; **98**: 2740-2745
29 **Takata T**, Aras R, Tavakoli D, Ando T, Olivares AZ, Blaser MJ. Phenotypic and genotypic variation in methylases involved in type II restriction-modification systems in *Helicobacter pylori*. *Nucleic Acids Res* 2002; **30**: 2444-2452
30 **Kuipers EJ**, Israel DA, Kusters JG, Gerrits MM, Weel J, van Der Ende A, van Der Hulst RWM, Wirth HP, Höök-Nikanne J, Thompson SA, Blaser MJ. Quasispecies development of *Helicobacter pylori* observed in paired isolates obtained years apart from the same host. *J Infect Dis* 2000; **181**: 273-282
31 **Akopyanz N,** Bukanov NO, Westblom TU, Kresovich S, Berg DE. DNA diversity among clinical isolates of *Helicobacter pylori* detected by PCR-based RAPD fingerprinting. *Nucleic Acids Res* 1992; **20**: 5137-5142
32 **Taylor DE**, Ge Z, Purych D, Lo T, Hiratsuka K. Cloning and sequence analysis of two copies of a 23S rRNA gene from *Helicobacter pylori* and association of clarithromycin resistance with 23S rRNA mutations. *Antimicrob Agents Chemother* 1997; **41**: 2621-2628
33 **Wong BC**, Wang WH, Berg DE, Fung FM, Wong KW, Wong WM, Lai KC, Cho CH, Hui WM, Lam SK. High prevalence of mixed infections by *Helicobacter pylori* in Hong Kong: metronidazole sensitivity and overall genotype. *Aliment Pharmacol Ther* 2001; **15**: 493-503
34 **Thoreson AC,** Hosseini N, Svennerholm AM, Bolin I. Different *Helicobacter pylori* strains colonize the antral and duodenal mucosa of duodenal ulcer patients. *Helicobacter* 2000; **5**: 69-78
35 **Azuma T,** Yamakawa A, Yamazaki S, Fukuta K, Ohtani M, Ito Y, Dojo M, Yamazaki Y, Kuriyama M**.** Correlation between variation of the 3' region of the cagA gene in *Helicobacter pylori* and disease outcome in Japan. *J Infect Dis* 2002; **186**: 1621-1630
36 **Arents NL,** van Zwet AA, Thijs JC, Kooistra-Smid AM, van Slochteren KR, Degener JE, Kleibeuker JH, van Doorn LJ. The importance of vacA, cagA, and iceA genotypes of *Helicobacter pylori* infection in peptic ulcer disease and gastroesophageal reflux disease. *Am J Gastroenterol* 2001; **96**: 2603-2608
37 **Göttke MU**, Fallone CA, Barkun AN, Vogt K, Loo V, Trautmann M, Tong JZ, NguyenTN, Fainsilber T, Hahn HH, Körber J, Lowe A, Beech RN. Genetic variability determinants of *Helicobacter pylori*: influence of clinical background and geographic origin of isolates. *J Infect Dis* 2000; **181**: 1674-1681
38 **Van Doorn LJ**, Glupczynski Y, Kusters JG, Megraud F, Midolo P, Maggi-Solca N, Queiroz DMM, Nouhan N, Stet E, Quint WGV. Accurate prediction of macrolide resistance in *Helicobacter pylori* by a PCR line probe assay for detection of mutations in the 23S rRNA gene: multicenter validation study. *Antimicrob Agents Chemother* 2001; **45**: 1500-1504
39 **Burucoa C**, Lhomme V, Fauchere JL. Performance criteria of DNA fingerprinting methods for typing of *Helicobacter pylori* isolates: experimental results and meta-analysis. *J Clin Microbiol* 1999; **37**: 4071-4080

Edited by Xia HHX

P.O.Box 2345, Beijing 100023,China
Fax: +86-10-85381893
E-mail: wjg@wjgnet.com www.wjgnet.com

World J Gastroenterol 2003;9(9):2025-2029
World Journal of Gastroenterology
 ISSN 1007-9327

• BASIC RESEARCH •

Ischemic preconditioning decreases C-X-C chemokine expression and neutrophil accumulation early after liver transplantation in rats

Yong Jiang, Xiao-Ping Gu, Yu-Dong Qiu, Xue-Mei Sun, Lei-Lei Chen, Li-Hua Zhang, Yi-Tao Ding

Yong Jiang, Xiao-Ping Gu, Yu-Dong Qiu, Yi-Tao Ding, Department of Hepatobiliary Surgery, Gulou Hospital, Medical Department of Nanjing University, Nanjing 210008, Jiangsu Province, China
Xue-Mei Sun, Lei-Lei Chen, Department of Biochemical Assay, Gulou Hospital, Medical Department of Nanjing University, Nanjing 210008, Jiangsu Province, China
Li-Hua Zhang, Department of Pathology, Gulou Hospital, Medical Department of Nanjing University, Nanjing 210008, Jiangsu Province, China
Yong Jiang, Department of Hepatobiliary Surgery, Changzhou First People's Hospital, Changzhou 213003, Jiangsu Province, China
Supported by the Chinese Medical Administration Bureau of Jiangsu Province, No.SZ9902
Correspondence to: Dr. Yong Jiang, Department of Hepatobiliary Surgery, Changzhou First People's Hospital, Changzhou 213003, Jiangsu Province, China. yyjiang8888@hotmail.com
Telephone: +86-519-6102280 **Fax:** +86-25-3317016
Received: 2003-04-08 **Accepted:** 2003-10-04

Abstract

AIM: Polymorphonuclear neutrophil (PMN) plays a major role in liver ischemia/reperfusion injury. Protective effect of ischemic preconditioning (IP) has been confirmed in liver ischemia/reperfusion injury. The purpose of this study was to investigate the effect of IP on C-X-C chemokine expression and PMNs recruitment early after liver transplantation.

METHODS: Male Sprague-Dawley rats were used as donors and recipients of orthotopic liver transplantation (OLT). The donor liver was stored 24 hours in University of Wisconsin (UW) solution at 4 ℃ pre-implantation. IP was done by clamp of the portal vein and hepatic artery of the donor liver for 10 minutes followed by reperfusion for 10 minutes before harvesting. The neutrophilic infiltration in liver was quantified using a myeloperoxidase (MPO) assay. Intragraft expression of macrophage inflammatory protein-2 (MIP-2) mRNA was investigated with in situ hybridization. The serum levels of MIP-2 and tumor necrosis factor (TNF)-α were also monitored.

RESULTS: After liver transplantation without IP, the hepatic MPO increased significantly compared with sham operated group. In IP group, PMN in liver indicated by MPO was reduced significantly. In situ hybridization showed no MIP-2 mRNA in sham group but dramatic expression in hepatocytes in non-IP group. In IP group, MIP-2 mRNA was significantly down-regulated. Similarly, serum MIP-2 and TNF-α levels were significantly elevated in non-IP group and both were reduced in IP group.

CONCLUSION: IP might protect graft liver from preservation-reperfusion injury after OLT through down-regulating C-X-C chemokine expression of hepatocytes, and alleviating PMNs recruitment after reperfusion.

Jiang Y, Gu XP, Qiu YD, Sun XM, Chen LL, Zhang LH, Ding YT. Ischemic preconditioning decreases C-X-C chemokine expression and neutrophil accumulation early after liver transplantation in rats. *World J Gastroenterol* 2003; 9(9): 2025-2029
http://www.wjgnet.com/1007-9327/9/2025.asp

INTRODUCTION

Liver transplantation as an effective therapy for end-stage liver diseases has been accepted. Though preservation techniques have been greatly improved, ischemia/reperfusion injury resulting in primary liver nonfunction still poses significant clinical problems and contributes to mortality[1-2]. Jaeschke *et al*.[3-6] established that there were two distinct phases of liver injury after warm ischemia and reperfusion. The initial phase of injury which is far less than that observed at later time points is characterized by Kupffer cell-induced oxidant stress. Events occurred during the initial phase including activation of Kupffer cells, initiate a complex inflammatory pathway that culminates in hepatic accumulation of neutrophils[7]. Recruited neutrophils directly damage hepatocytes by releasing oxidants and proteases and are responsible for the later phase of liver injury induced by ischemia/reperfusion. Activated PMN has also been implicated as a vital factor in the development of ischemia/reperfusion injury in both experimental and clinical liver transplantations[8-11].

C-X-C chemokines are a group of molecules that have both inflammatory and repairable properties and are best known for their neutrophil chemotactic properties[12,13]. MIP-2, belonging to C-X-C chemokines has been shown not only to regulate PMN recruitment from vascular compartment to the tissues[14] but also to cause PMN activation[15]. Kataoka *et al*. demonstrated that MIP-2 played a crucial role in PMN recruitment and activation after liver transplantation[10].

IP is a process of a short period of ischemia and reperfusion, which leads to an unexpected resistance to a long-term ischemia/reperfusion injury. It has been documented in several organs, including the liver[16-19]. In experimental liver transplantation, IP has been confirmed as an effective strategy for protecting the grafts from ischemia/reperfusion injury[20]. But few studies have been performed on whether and how IP effects PMNs accumulation and activation in protecting grafted liver from ischemia/reperfusion injury after liver transplantation. In this study, we therefore investigated the effect of IP on PMNs recruitment, as well as MIP-2 expression in grafted livers, to determine the role of C-X-C chemokine expression and PMNs recruitment in protecting grafted liver from prolonged preservation/reperfusion injury early after OLT.

MATERIALS AND METHODS

Animals

Male Spraque Dawley rats weighing 200 to 250 g were used as donors and recipients. They were housed in pathogen-free conditions with a 12-hr light-dark cycle and were allowed to drink water and fasted for 14 hours before operation. All experiments were performed in compliance with the standards for animal use and care set by Institutional Animal Care Committee.

Surgical procedures

OLT. Liver transplantation was performed according to Kamada's cuff-technique[21] with minor modifications. Before liver harvesting, 1 mL saline containing 50 units of heparin was given intravenously, and the donor liver was perfused *in situ* via the portal vein with 20 mL of cold physiological saline

solution to which 50 units of heparin was added. Following cuff preparation, the liver was stored in a beaker containing University of Wisconsin solution at 4 ℃ for 24 hours. At the end of storage, the liver was slowly flushed with 20 mL of cold (4 ℃) Ringer' s lactate and transplanted orthotopically into a recipient animal. The hepatic artery was not reconstructed.

IP. Before harvesting donor liver, the portal vein and hepatic artery were interrupted by placing a bulldog clamp for 10 min. Reflow was initiated by removing of the clamp for another 10 min.

In sham group, the left phrenic vein and the right suprarenal vein were ligated and the hepatic artery was freed by ligating and dividing.

Experimental design

All rats were randomly divided into: sham groups, non-IP group and IP group. To obtain blood and tissue samples, six animals were killed in non-IP and IP group after 1, 2, 4 and 6 hr of reperfusion and four animals at each time point in sham group. Plasma samples were collected from inferior vena cava, and separated by centrifugation, and median lobe of the liver was carefully excised and stored at -80 ℃ for analysis. Serum levels of alanine aminotransferase (ALT) and lactate dehydrogenase (LDH) were measured using standard clinical automated analysis. Serum levels of MIP-2 (IBL Immuno-Biological Laboratories, Hamburg) and TNF-α (R & D Systems, Inc) were measured using commercial enzyme-linked immunosorbent assay kits, respectively.

MPO assay

MPO was used as a marker of pulmonary and hepatic neutrophil infiltration[22]. MPO activity was measured photometrically employing 3, 3' , 5, 5' -tetramethylbenzidine as a substrate. Frozen liver tissues were macerated, homogenized, sonicated, and centrifuged at 4 000 g for 12 minutes at 4 ℃ as described previously[22]. MPO activity was measured in the supernatant, with calculations based on the absorbance change at 460 nm. All values were normalized to tissue weight.

Hybridization

Chunks (1 cm^3) from fresh rat liver were immediately fixed in 4 % paraformaldehyde at 4 ℃ for 8 h and dehydrated through graded ethanol, then embedded in paraffin and sectioned. The sections were layered onto glass slides by standard procedures. Five μm thick sections were cut for analysis. They were deparaffinized with xylene and quickly rehydrated through graded ethanol. The deparaffinized sections were quenched from endogenous peroxidase activity in 3 % H_2O_2 diluted in methanol. Then, the expression of MIP-2 mRNA was detected in rat liver tissue sections using a commercial ISH kit (TBD biotech Co.). All solutions of it were RNase free. The sections were digested using solution I (0.4 % pepsin, 0.1 M Hcl, TBD biotech Co.), then washed in 0.5 M PBS twice for 5 minutes each. The non-specific IgG binding sites were blocked with blocking solution I (1.5 % normal blocking serum, TBD biotech Co.) at RT and excess serum was blotted from the sections. Then, the sections covered with coverslips were prehybridized with a prehybridized solution (formamide, standard saline citrate, 100×denhardt' s, SDS, sperm DNA, TBD biotech Co.) at 37 ℃ for 4 h in a sealed humidity chamber. The sections were washed twice in 0.5 M PBS and hybridized with digitoxin-labeled oligonucleotide probe synthesized by TBD cooperation Lab, (5' -CCACTCGCCAGCTCCTCAATGCTGTACTGGT CCTGCTCCT-3'). Hybridization was performed at 38 ℃ overnight in a humidity chamber, and washed in 2×SSC, 0.5×SSC, 0.2×SSC for 5 minutes each. In the following step, the sections were blocked with blocking solution II (25 μg/ml avidin, TBD biotech Co.) for 15 minutes at RT, then excess solution was blotted. The sections covered by coverslips were incubated with biotinylated mouse anti-digitoxin antibody (TBD Biotech Co.) for 1 h at 37 ℃ in a sealed humidity chamber and washed three times in 0.01 M PBS for 5 minutes each. The sections were incubated with streptavidin-biotin-peroxidase complex (TBD Biotech Co.) at 37 ℃ for 1 h and washed three times in 0.01 M PBS for 5 minutes each. The complex was detected with DAB (0.1 % diaminonbenzidine, 0.02 % hydrogen peroxide, TBD Biotech Co.) in sections and counterstained with hematoxylin (Sigma). The first negative control group was performed in which the mouse anti-digitoxin antibody was substituted with normal mouse serum and the second was performed with RNase (20 μg/ml, Sigma) before hybridization. The last one was hybridized without any oligonucleotide probe.

Histology study

Liver samples were fixed in 4 % neutral buffered formalin, paraplast-embedded and cut into 4 μm thick sections, and stained with hematoxylin-eosin according to the standard procedures.

Statistical analysis

The data were expressed as mean ± SEM. Means of different groups were compared using a one-way ANOVA. The Student *t* test was performed to evaluate the significant differences between groups. Significance was determined at $P<0.05$.

RESULTS

Serum levels of ALT, LDH

Both ALT (A) and LDH (B) were significantly elevated after OLT without IP, compared with sham-operated group. When the liver grafts were pretreated with IP, the increases in ALT and LDH were relatively reduced to the non-IP group in each time point respectively (Figure 1).

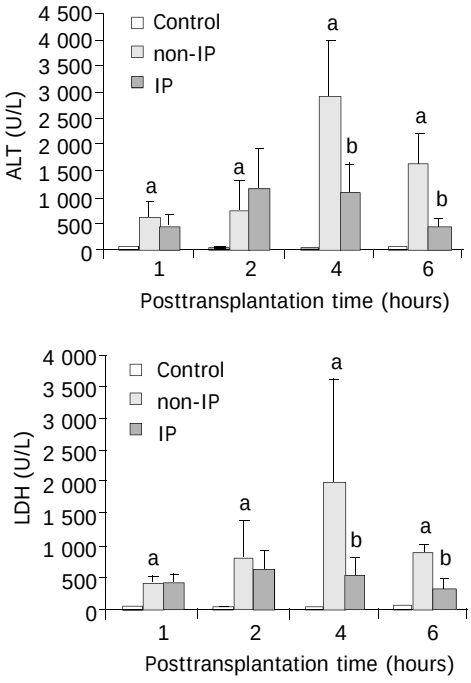

Figure 1 Changes in serum ALT (A) and LDH (B) levels. The serum ALT and LDH levels were significantly elevated in non-IP groups compared with sham-operated group ($^aP<0.01$, non-IP group *vs* sham-operated group). After IP, the increase was significantly reduced at 4 and 6 hour points after reperfusion ($^bP<0.05$, IP group *vs* non-IP group).

Hepatic PMNs accumulation

PMNs accumulation in the grafted livers was assessed by investigating the levels of MPO. Figure 2 shows changes in PMNs accumulation in three groups. The increases in non-IP groups were significantly reduced in IP group, especially at 4 and 6 hour points after reperfusion.

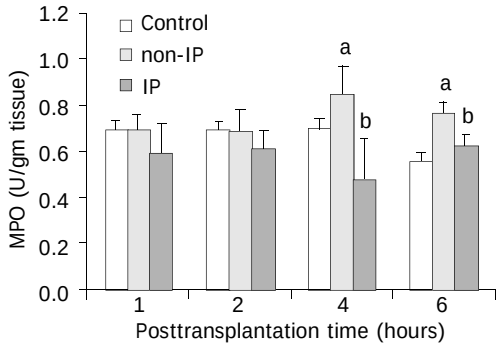

Figure 2 Changes of PMNs accumulation in grafted liver. PMNs accumulation was assessed by investigating the levels of MPO. The increase in non-IP groups was significantly reduced in IP groups, especially at 4 and 6 hour points after reperfusion ($^aP<0.05$, non-IP group *vs* sham-operated group. $^bP<0.05$, IP group *vs* non-IP group).

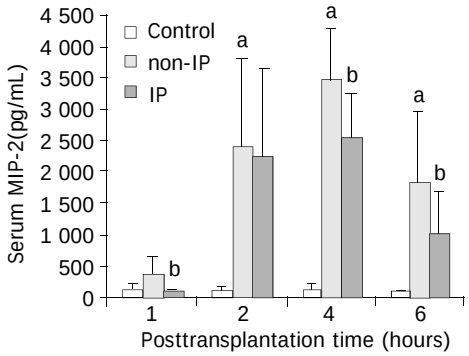

Figure 3 Changes in serum MIP-2 levels. MIP-2 was significantly increased in non-IP group compared with sham-operated group ($^aP<0.01$, non-IP group *vs* sham-operated group). After IP, the increase was significantly reduced at 1, 4 and 6 hours after reperfusion ($^bP<0.05$, IP group *vs* non-IP group).

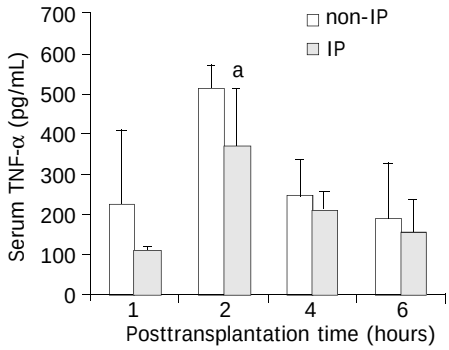

Figure 4 Changes in serum TNF-α levels. The levels of serum TNF-α were decreased to an extent in each time point respectively in IP group compared with non-IP group, especially at 2 hours after reperfusion. The decrease was significant ($^aP<0.05$, IP group *vs* non-IP group).

Serum levels of MIP-2, TNF-α

In non-IP group, MIP-2 increased significantly in each time point and peaked at 4 hours after reperfusion compared with the sham operated group. In IP group, the increases were reduced in each time point respectively (Figure 3). Similar results of TNF-α were obtained. But interestingly, the levels of TNF-α peaked at 2 hours in all three groups in this study (Figure 4).

Intragraft MIP-2 mRNA expression

In situ hybridization was performed at 4 hour point after reperfusion in all three groups (Figure 5). MIP-2 mRNA was not detectable in sham operated group (A). MIP-2 mRNA in the non-IP group (B) was remarkably up-regulated at 4 hour point and after IP(C), the expression was detectable at a lower level. It was emphasized that the MIP-2 mRNA was mostly expressed in hepatocytes in grafted livers.

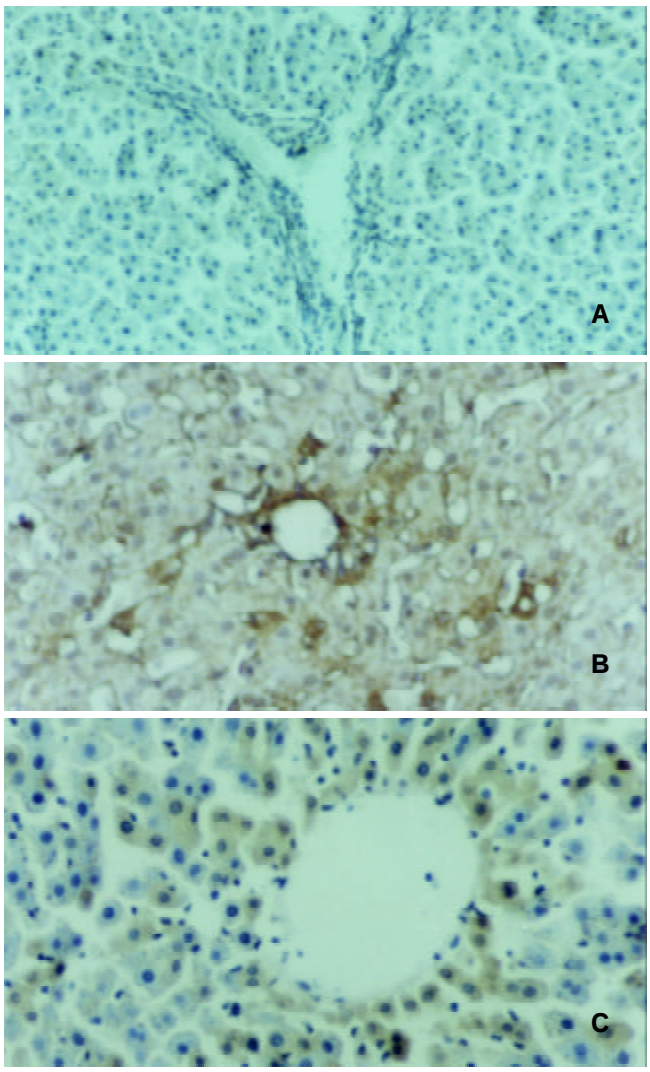

Figure 5 Intragraft MIP-2 mRNA expression. In situ hybridization was performed at 4 hours point after reperfusion in all three groups. MIP-2 mRNA was not detectable in sham operated group (A), and remarkably up-regulated in non-IP group (B), and after IP, the expression was detectable at a lower level (C). MIP-2 mRNA was mostly expressed in hepatocytes in grafted livers.

Histological changes of grafts

Similar to serum transferase indicating liver function, histological change of the graft showed that 24 hours cold storage in UW solution and reperfusion resulted in grafted liver damage. After IP and OLT, the damage was ameliated.

DISCUSSION

In this study, we demonstrated that 24 hours cold storage in

UW solution and reperfusion (OLT) resulted in grafted liver injury indicated by serum transferase and histological changes. In this process, TNF-α and C-X-C chemokines (i.e., MIP-2) were stimulated, and induced PMN-mediated tissue damage. Also we demonstrated that IP protected the grafted liver from prolonged cold preservation-reperfusion injury through down-regulation of TNF-α and MIP-2 and attenuation of PMNs accumulation. *In situ* hybridization revealed that MIP-2 mRNA was mostly expressed in hepatocytes.

IP is a phenomenon in which a short period of ischemia leads to unexpected resistance of subsequently prolonged preservation-reperfusion injury. It was found in the heart and named by Murry *et al* in 1986[16]. Recently it was reported that the phenomenon of preconditioning of the heart could be extended to the models of liver resection[19] and liver transplantation[20]. The role of IP in reducing myocardial and liver ischemic injury has been widely documented[23-26]. However, the mechanism of its protective effect remains unclear.

It is well known that accumulated PMNs in the grafted liver sinusoids might be important effector cells in the pathogenesis of liver preservation-reperfusion injury after OLT[8-11]. In this study, an increased serum level of MPO in non-IP group was synchronized with elevated serum ALT and LDH levels. The reactive oxygen and proteases released by activated PMNs might promote progressive hepatocellular damage[27]. This study demonstrated that IP decreased PMNs accumulation to protect the grafted liver from prolonged ischemia/reperfusion injury after OLT.

As the functions of cellular adhesion molecules were concerned, C-X-C chemokines (i.e., MIP-2) were intricately involved in the process of PMNs recruitment[28]. During warm hepatic ischemia/reperfusion injury, early production of proinflammatory mediators such as TNF-α has been documented[29-32]. Kataoka *et al*. revealed that TNF-α could stimulate C-X-C chemokine production in hepatocytes of prolonged ischemia-reperfusion injury after OLT[10]. Kupffer cell stimulation during extended cold preservation might result in overresponse and excessive production of TNF-α in the initial phase of reperfusion[33]. Then, TNF-α released from Kupffer cells might act locally on hepatocytes and other cells, resulting in increased C-X-C chemokine expression. This study demonstrated IP could interrupt this complex cascade of inflammatory mediators and ameliate the grafted liver damage after OLT. MIP-2 mRNA of hepatocytes performed by *in situ* hybridization was expressed in a lower level in IP group compared with non-IP group. And serum levels of TNF-α and MIP-2 in recipients also decreased significantly after IP.

In conclusion, IP can protect grafted livers from prolonged preservation-reperfusion injury in a rat liver transplantation model. One possible mechanism of its protective effect in the initial phase after reperfusion may be that IP interrupts the chain reaction of preservation-reperfusion injury in which excessive TNF-α released from activated Kupffer cells induces local expression of C-X-C chemokines of hepatocytes and accumulation of PMNs which play an important role in mediating the liver graft injury. Obviously, the preservation-reperfusion injury leading to primary nonfunction of grafted liver after OLT is multifactorial, and multi-mediators take part in it and intercross one another. Further experiments to define the protective role of IP in preservation-reperfusion injury should be performed.

ACKNOWLEDGEMENTS

We are grateful to Dr. Xin-Hua Zhu for his technical assistance in establishing rat liver transplantation models, Ms. Ru-Tian Li for her help with the statistical analysis, Dr. Qing-Xiang Xu and Dr. Xi-Tai Sun for their helpful discussions.

REFERENCES

1 **Ploeg RJ,** D'Alessandro AM, Knechtle SJ, Stegall MD, Pirsch JD, Hoffmann RM, Sasaki T, Sollinger HW, Belzer FO, Kalayoglu M. Risk factors for primary dysfunction after liver transplantation: a multivariate analysis. *Transplantation* 1993; **55**: 807-813

2 **Clavien PA,** Harvey PR, Strasberg SM. Preservation and reperfusion injuries in liver allografts. An overview and synthesis of current studies. *Transplantation* 1992; **53**: 957-978

3 **Jaeschke H,** Smith CV, Mitchell JR. Reactive oxygen species during ischemia-reflow injury in isolated perfused rat liver. *J Clin Invest* 1988; **81**: 1240-1246

4 **Jaeschke H,** Farhood A. Neutrophil and Kupffer cell-induced oxidant stress and ischemia-reperfusion injury in rat liver. *Am J Physiol* 1991; **260**(3 Pt1): G355-G362

5 **Jaeschke H,** Bautista AP, Spolarics Z, Spitzer JJ. Superoxide generation by Kupffer cells and priming of neutrophils during reperfusion after hepatic ischemia. *Free Radic Res Commun* 1991; **15**: 277-284

6 **Jaeschke H.** Reactive oxygen and ischemia / reperfusion injury of the liver. *Chem Biol Interact* 1991; **79**: 115-136

7 **Jaeschke H,** Farhood A, Smith CW. Neutrophils contribute to ischemia / reperfusion injury in rat liver *in vivo*. *FASEB J* 1990; **4**: 3355-3359

8 **Takei Y,** Marzi I, Gao WS, Gores GJ, Lemasters JJ, Thurman RG. Leukocyte adhesion and cell death following orthotopic liver transplantation in the rat. *Transplantation* 1991; **51**: 959-965

9 **Marzi I,** Knee J, Buhren V, Menger M, Trentz O. Reduction by superoxide dismutase of leukocyte-endothelial adherence after liver transplantation. *Surgery* 1992; **111**: 90-97

10 **Kataoka M,** Shimizu H, Mitsuhashi N, Ohtsuka M, Wakabayashi Y, Ito H, Kimura F, Nakagawa K, Yoshidome H, Shimizu Y, Miyazaki M. Effect of cold-ischemia time on C-X-C chemokine expression and neutrophil accumulation in the graft liver after orthotopic liver transplantation in rats. *Transplantation* 2002; **73**: 1730-1735

11 **Pesonen EJ,** Hockerstedt K, Makisalo H, Vuorte J, Jansson SE, Orpana A, Karonen SL, Repo H. Transhepatic neutrophil and monocyte activation during clinical liver transplantation. *Transplantation* 2000; **69**: 1458-1464

12 **Oppenheim JJ,** Zachariae CO, Mukaida N, Matsushima K. Properties of the novel proinflammatory supergene "intercrine" cytokine family. *Annu Rev Immunol* 1991; **9**: 617-648

13 **Miller MD,** Krangel MS. Biology and biochemistry of the chemokines: a family of chemotactic and inflammatory cytokines. *Crit Rev Immunol* 1992; **12**: 17-46

14 **Watanabe K,** Konishi K, Fujioka M, Kinoshita S, Nakagawa H. The neutrophil chemoattractant produced by the rat kidney epithelioid cell line NRK-52E is a protein related to the KC / gro protein. *J Biol Chem* 1989; **264**: 19559-19563

15 **Frevert CW,** Farone A, Danaee H, Paulauskis JD, Kobzik L. Functional characterization of rat chemokine macrophage inflammatory protein-2. *Inflammation* 1995; **19**: 133-142

16 **Murry CE,** Jennings RB, Reimer KA. Preconditioning with ischemia: a delay of lethal cell injury in ischemic myocardium. *Circulation* 1986; **74**: 1124-1136

17 **Heurteaux C,** Lauritzen I, Widmann C, Lazdunski M. Essential role of adenosine, adenosine A1 receptors, and ATP-sensitive K+ channels in cerebral ischemic preconditioning. *Proc Natl Acad Sci U S A* 1995; **92**: 4666-4670

18 **Hotter G,** Closa D, Prados M, Fernandez-Cruz L, Prats N, Gelpi E, Rosello-Catafau J. Intestinal preconditioning is mediated by a transient increase in nitric oxide. *Biochem Biophys Res Commun* 1996; **222**: 27-32

19 **Peralta C,** Hotter G, Closa D, Gelpi E, Bulbena O, Rosello-Catafau J. Protective effect of preconditioning on the injury associated to hepatic ischemia-reperfusion in the rat: role of nitric oxide and adenosine. *Hepatology* 1997; **25**: 934-937

20 **Yin DP,** Sankary HN, Chong AS, Ma LL, Shen J, Foster P, Williams JW. Protective effect of ischemic preconditioning on liver preservation-reperfusion injury in rats. *Transplantation* 1998; **66**: 152-157

21 **Kamada N,** Calne RY. Orthotopic liver transplantation in the rat. Technique using cuff for portal vein anastomosis and biliary drainage. *Transplantation* 1979; **28**: 47-50

22 **Peralta C,** Fernandez L, Panes J, Prats N, Sans M, Pique JM, Gelpi E, Rosello-Catafau J. Preconditioning protects against systemic disorders associated with hepatic ischemia-reperfusion through blockade of tumor necrosis factor-induced P-selectin up-regulation in the rat. *Hepatology* 2001; **33**: 100-113
23 **Koeppel TA,** Thies JC, Schemmer P, Trauner M, Gebhard MM, Otto G, Post S. Inhibition of nitric oxide synthesis in ischemia / reperfusion of the rat liver is followed by impairment of hepatic microvascular blood flow. *J Hepatol* 1997; **27**: 163-169
24 **Gao W,** Washington MK, Bentley RC, Clavien PA. Antiangiogenic agents protect liver sinusoidal lining cells from cold preservation injury in rat liver transplantation. *Gastroenterology* 1997; **113**: 1692-1700
25 **Saavedra JE,** Billiar TR, Williams DL, Kim YM, Watkins SC, Keefer LK. Targeting nitric oxide (NO) delivery *in vivo*: Design of a liver-selective NO donor prodrug that blocks tumor necrosis factor-α-induced apoptosis and toxicity in the liver. *J Med Chem* 1997; **40**: 1947-1954
26 **Kim YM,** de Vera ME, Watkins SC, Billiar TR. Nitric oxide protects cultured rat hepatocytes from tumor necrosis factor-α-induced apoptosis by inducing heat shock protein 70 expression. *J Biol Chem* 1997; **272**: 1402-1411
27 **Jaeschke H,** Farhood A, Bautista AP, Spolarics Z, Spitzer JJ, Smith CW. Functional inactivation of neutrophils with a Mac-1(CD11b / CD18)monoclonal antibody protects against ischemia-reperfusion injury in rat liver. *Hepatology* 1993; **17**: 915-923
28 **Luster AD.** Chemokines-chemotactic cytokines that mediate inflammation. *N Engl J Med* 1998; **338**: 436-445
29 **Colletti LM,** Kunkel SL, Walz A, Burdick MD, Kunkel RG, Wilke CA, Strieter RM. Chemokine expression during hepatic ischemia / reperfusion-induced lung injury in the rat. The role of epithelial neutrophil activating protein. *J Clin Invest* 1995; **95**: 134-141
30 **Lentsch AB,** Yoshidome H, Cheadle WG, Miller FN, Edwards MJ. Chemokine involvement in hepatic ischemia / reperfusion injury in mice: roles for macrophage inflammatory protein-2 and KC. *Hepatology* 1998; **27**: 1172-1177
31 **Yoshidome H,** Lentsch AB, Cheadle WG, Miller FN, Edwards MJ. Enhanced pulmonary expression of CXC chemokines during hepatic ischemia / reperfusion-induced lung injury in mice. *J Surg Res* 1999; **81**: 33-37
32 **Hisama N,** Yamaguchi Y, Miyanari N, Ichiguchi O, Goto M, Mori K, Ogawa M. Ischemia-reperfusion injury: the role of Kupffer cells in the production of cytokine-induced neutrophil chemoattractant, a member of the interleukin-8 family. *Transplant Proc* 1995; **27**: 1604-1606
33 **Arii S,** Monden K, Adachi Y, Zhang W, Higashitsuji H, Furutani M, Mise M, Fujita S, Nakamura T, Imamura M. Pathogenic role of Kupffer cell activation in the reperfusion injury of cold-preserved liver. *Transplantation* 1994; **58**: 1072-1077

Edited by Bo XN and Wang XL

P.O.Box 2345, Beijing 100023,China
Fax: +86-10-85381893
E-mail: wjg@wjgnet.com www.wjgnet.com

World J Gastroenterol 2003;9(9):2030-2035
World Journal of Gastroenterology
 ISSN 1007-9327

• BASIC RESEARCH •

Antitumor mechanism of antisense cantide targeting human telomerase reverse transcriptase

Qing-You Du, Xiao-Bo Wang, Xue-Jun Chen, Wei Zheng, Sheng-Qi Wang

Qing-You Du, Xiao-Bo Wang, Sheng-Qi Wang, Beijing Institute of Radiation Medicine, Beijing 100850, China
Xue-Jun Chen, Wei Zheng, College of Medicine, Zhejiang University, Hangzhou 31006, Zhejiang Province, China
Supported by the National Natural Science Foundation of China, No. 39870879, and the Special Funds for Major State Basic Research of China, No. G1998051103
Correspondence to: Sheng-Qi Wang, Beijing Institute of Radiation Medicine, 27 Tai-ping Road, Beijing 100850, China. sqwang@nic.bmi.ac.cn
Telephone: +86-10-66932211 **Fax:** +86-10-68214653
Received: 2003-03-12 **Accepted:** 2003-05-24

Abstract

AIM: To investigate the anti-tumor mechanism of antisense oligodeoxynucleotide cantide against hTERT.

METHODS: Tumor cells were cultured overnight and grown to 50-60 % confluence. HepG2 and SMMC-7721 were treated with cantide mixed with lipofectin, or lipofectin alone. After inducted for 6 h at 37 ℃, 10 % FCS in DMEM was replaced in each well. After the treatment repeated twice to three times in each concentration of cantide, hTERT mRNA and protein expression were measured by RT-PCR and Western blot analysis, respectively. Telomerase activity was determined by TRAP-ELISA assay. CPP32- and ICE-like activity was also investigated using CasPACE assay system at 48 h after cantide treatment, and apoptosis was evaluated using the DeadEnd assay at 24, 48 and 72 h after cantide treatment.

RESULTS: Compared to the control cells, the cells treated with cantide showed a dose-dependent decrease in hTERT mRNA levels at 24 h and in protein levels at 48 h respectively. The telomerase activity was decreased as the concentration of cantide increased at 48 h. At the concentration of 800 nM, the telomerase activity in the treated HepG2 and SMMC-7721 cells was only 17.1 % ($P<0.01$) and 20.3 % ($P<0.01$) of that in untreated cells. The levels of CPP32-like protease activity in HepG2 and SMMC-7721 increased by 2.8- and 3.0-fold ($P<0.05$) at 48 h, and the levels of ICE-like protease activity also increased by 2.6- and 3.2-fold ($P<0.05$) respectively. The percentage of apoptosis in HepG2 and SMMC-7721 cells treated with 800 nM cantide at 72 h was 63 % and 52 % ($P<0.01$), respectively. By contrast, 8 % and 9 % of the cells were apoptosis after 72 h treatment with lipofectin alone.

CONCLUSION: Cantide can decrease telomerase activity by inhibiting the expression of hTERT gene and has a rapid anti-tumor effect through inducing the Caspase-dependent apoptosis. The rapid inhibitory effect of cantide on tumor growth demonstrates its feasibility in cancer treatment.

Du QY, Wang XB, Chen XJ, Zheng W, Wang SQ. Antitumor mechanism of antisense cantide targeting human telomerase reverse transcriptase. *World J Gastroenterol* 2003; 9(9): 2030-2035
http://www.wjgnet.com/1007-9327/9/2030.asp

INTRODUCTION

Telomerase is a unique ribonucleoprotein enzyme responsible for adding the telomeric repeats onto the 3' ends of chromosome[1]. Telomerase plays an important role in the development of cellular immortality and oncogenesis[2,3]. Previous studies have shown that telomerase activity is found in 85-90 % of all human tumors, but not in their adjacent normal cells[4,5]. This makes telomerase a good target not only for cancer diagnosis, but also for the development of novel therapeutic agents[6,7].

The research of antisense oligodeoxynucleotides (ODN) is an area of heightened interest in the field of telomerase inhibition[8]. Antisense ODNs have been investigated on the inhibition of telomerase and suppression of tumor growth. But most of these antisense ODNs were designed to target the hTR template, and they did not reduce telomerase activity and tumor growth effectively[9-12]. It has been shown that expression of hTERT is closely associated with telomerase activity in human tumor cells while all human somatic cells constitutively contain hTR. Therefore, to significantly inhibit telomerase activity, hTERT might be more attractive as a target than hTR[13,14]. A series of antisense oligonucleotides were designed based on hTERT mRNA secondary structure. It has been demonstrated that an antisense oligonucleotide cantide has a strong inhibitory effect on tumor cell growth. The cytotoxic effect of a specific cantide antisense was also assessed by using the sense, random and mismatched ODN, only cantide had potent inhibitory effect on proliferation of tumor cells[15], and *in vivo* treatment of HepG2 tumor xenografts with cantide antisense ODN significantly retarded the growth of these tumors (data unpublished). To investigate the possible mechanism of antitumor effect of cantide, an *in vitro* study was performed in this report.

MATERIALS AND METHODS

Cell culture

Human hepatocellular carcinoma cells (HepG2, SMMC-7721) were obtained from Chinese National Cancer Institute, Chinese Academy of Medical Sciences, Beijing. Cells were cultured in Dulbecco's modified Eagle's medium supplemented with 10 % fetal bovine serum (GIBCO BRL, Grand Island, NY), 100 U/ml penicillin and 100 μg/ml streptomycin at 37 ℃ with 5 % CO_2.

Synthesis of oligonucleotides

The following specific PCR primers were synthesized by an applied biosystems 391 DNA synthesizer and purified by OPC (Perkin-Elmer, Foster city, CA). For β_2-microglobulin, sense (5'-TTCAGGTTTACTCACGTCATCC-3') and antisense (5'-CCAAATGCGGCATCTTCAAACCC-3'), amplification of 317 bp DNA fragment. For hTERT, sense (5'-TCTACCGGAAGAGTGTCTGGAGCAA-3') and antisense (5'-GCGCCCACGACGTAGTCCATGTTCA-3'), amplification of 202 bp DNA fragment. The selection of antisense ODNs against hTERT was described previously[15]. The sequence of the cantide was 5'-ACTCACTCAGGCCTC AGACT-3'. The phosphorothioate cantide was synthesized

on solid supports using Oligo Pilot II DNA (Amersham-Pharmacia, Piscataway, NJ) and purified by HPLC (Waters Delta Prep 4000) with SOURCE 15Q (Amersham-Pharmacia), and the purity of cantide was over 95 %.

Analysis of hTERT mRNA by RT-PCR

A total of 1.5×10^5 cells were seeded in a 6-well plate, and treated with 50, 100, 200, 400 or 800 nM cantide respectively mixed with 4 μl lipofectin (Invitrogen, Carlsbad, CA) according to the manufacturer' s instructions. The first day of treatment was designated as day 0. After 24 h, total RNA was isolated using TRIZOL (Invitrogen) by a single-step phenol-extraction method as templates. Subsequent RT-PCR reaction was performed using a reverse transcription system (RT-PCR kit, Promega, Madison, WI.). Briefly, first strand cDNA was synthesized using a Oligo $(dT)_{15}$ primer at 42 ℃ for 30 min. PCR reaction for hTERT and β_2-microglobulin was performed in a single reaction of 20 μl volume. The latter served as a control following 28 cycles of denaturing at 95 ℃ for 45 s, annealing at 58 ℃ for 40 s, and extending at 72 ℃ for 40 s. At this PCR condition, the amplification showed linearity as was determined experimentally (data not shown). PCR products were run on a 2.0 % agarose gel and visualized by ethidium bromide staining, and the intensities were then measured by scanning the gel with Gel Doc 1000 (Bio-Rad, Hercules, CA). Inhibition of hTERT mRNA was calculated by normalized intensity ratio hTERT: β_2-microglobulin of control sample according to the following formula:

$$\text{Inhibition percentage (\%)}=\left(1-\frac{A_{\text{sample}}\times A_{0\ \text{control}}}{A_{\ \text{control}}\times A_{0\ \text{sample}}}\right)\times 100.$$

A_{sample}: the intensity of hTERT PCR product in cells treated with cantide and lipofectin, $A_{0\ sample}$: the intensity of hTERT PCR product in cells treated with lipofectin alone, $A_{control}$: the intensity of β-actin product in cells treated with cantide and lipofectin, $A_{0\ control}$, the intensity of β-actin product in cells treated with lipofectin alone.

Analysis of hTERT protein

The levels of hTERT protein in cells treated with cantide were measured by scanning the density of bands on Western blot. The treatment of cantide was performed using the same method as for the hTERT mRNA level analysis described above. After 48 h of transfection, cells were collected by trypsinization and lysed in a lysis buffer containing 9.1 mM Na_2HPO_4, 1.7 mM NaH_2PO_4 (pH 7.4), 150 mM NaCl, 1 % NP-40, 0.5 % sodium deoxycholate, 0.1 % SDS, 100 μg/ml PMSF, 1 μg/ml aprotinin and 1 mM sodium orthovanadate for 30 min on ice. Equal amount (60 μg) of proteins was run on a 6 % SDS-PAGE gel, and transferred onto Hybond-polyvinylidene difluoride membranes (Amersham, Arlington Heights, IL). The transferred membrane was incubated first with primary antibodies against hTERT (Santa Cruz Biotechnology, Santa Cruz, CA) or primary antibodies against actin, and followed with peroxidase-linked secondary antibody, and finally the ECL Western blot system (Promega) was used for developing the bands. The intensity of the bands was scanned by Gel Doc 1 000 (Bio-Rad), and the inhibition percentage (%) was calculated according to the following formula: inhibition percent=$(1-A_{sample}/A_{control})\times100$.

Telomerase activity (TRAP-ELISA) assay

TRAP-ELISA was performed using the Telo*TAGGG* and Telomerase PCR ELISA kit (Roche, Indianapolis, IN) following the manufacturer' s instructions. Telomerase levels were determined after 48 h treatment of cantide (400 nM) transfected using the method as for the hTERT mRNA level analysis described above. These cells were grown in 24-well plates. Cells were homogenized in 200 μl lysis buffer and incubated on ice for 30 min. To determine the specificity of the assay, all protein samples were preheated for 10 min at 70 ℃ to inactivate telomerase and tested in parallel in the assay. 5 μg of each extract was assayed in 50 μl reaction mixture containing 25 μl of reaction mixture and 5 μl of the internal standard. After incubated at 25 ℃ for 30 min, the reaction mixture was then subjected to PCR amplification in a thermal cycler for 20 cycles at 94 ℃ for 30 s, at 50 ℃ for 30 s, and at 72 ℃ for 90 s. Subsequently, ELISA reaction was performed following the manufacturer' s instructions.

DeadEnd assay

Apoptosis of treated tumor cells was detected using TUNEL technique. Cells (5×10^3/well) were plated in 96-well dishes and treated with cantide at a final concentration of 400 nM. At 24, 48, and 72 h after transfection, modified TUNEL assay was performed using DeadEnd colorimetric apoptosis detection system (Promega) according to the manufacturer' s instructions. Briefly, cells were harvested, washed and fixed on silanized microscope slides. Biotinylated nucleotide was incorporated at the 3' -OH DNA ends using terminal deoxynucleotidyl transferase (TdT). Streptavidin-HRP was then bound to these biotinylated nucleotides, which were detected using hydrogen peroxide and diaminobenzidine (DAB). With this procedure, apoptotic cell nuclei were stained dark brown. Stained cells were observed under a light microscope.

Caspase activity assay

Caspase (CPP32-like and ICE-like) activity was evaluated using CaspACE assay system fluorometry (Promega) according to the protocol provided by the manufacturer. Cells were plated in flasks and treated with 400 nM cantide mixed with lipofectin. At 48 h after cantide treatment, cells were harvested and washed, lysed by subjecting to four cycles of freezing and thawing, and centrifuged at 16 000 g for 20 min at 4 ℃. The same amount of supernatant was pipetted into a 96-well plate, then the following items were added into each well, namely 32 μl buffer, 2 μl DMSO, 100 μl DTT (100 mM), 2 μl of appropriate substrate (2.5 mM). The final volume was 100 μl. Blank (without cells extracts) and negative control (with inhibitor) reaction mixtures were also prepared simultaneously. After incubated at 30 ℃ for 60 min, the fluorescence of the reactions at an excitation wavelength of 355 nm and emission wavelength of 460 nm was measured. Caspase activity was determined in duplicate cells. Relative fluorescence units (△FU) were calculated according to the formula: $\triangle FU=(FU_{assay}-FU_{blank})-(FU_{negative}-FU_{blank})$.

Statistics

The data were expressed as means ± standard deviation (SD), statistical analysis was performed by Student' s-*t*-test (two-tailed).All data represented at least two independent experiments.

RESULTS

Effect of cantide on hTERT mRNA expression

It has been suggested antisense ODNs may inhibit gene expression through diverse effects on transcription and translation, inhibition of mRNA transcription can occur through formation of triple helixes with complementary regions in DNA, and/or mRNA can be cleaved by recruitment of the endogenous nuclease RNase-H to catalyze the degradation of ODN-RNA dimmers[16]. Therefore, the mRNA level of hTERT was determined by semi-quantitative RT-PCR. A 202 bp DNA

fragment of hTERT gene and a 317 bp DNA fragment of β_2-microglobulin gene were amplified by RT-PCR with specific primers, respectively. Figure 1A shows that the mRNA expression level of hTERT was decreased as the concentration of cantide treatment increased at 24 h when compared to the untreated cells, while the mRNA level of β_2-microglobulin as a control was almost unchanged. As shown in Figure 1B, after treatment with 800 nM cantide normalized according to the levels of β_2-microglobulin, the relative inhibition rate of hTERT mRNA expression was 74.4 % (P<0.01) and 68.4 % (P<0.01) in treated tumor cells HepG2 and SMMC-7721, respectively.

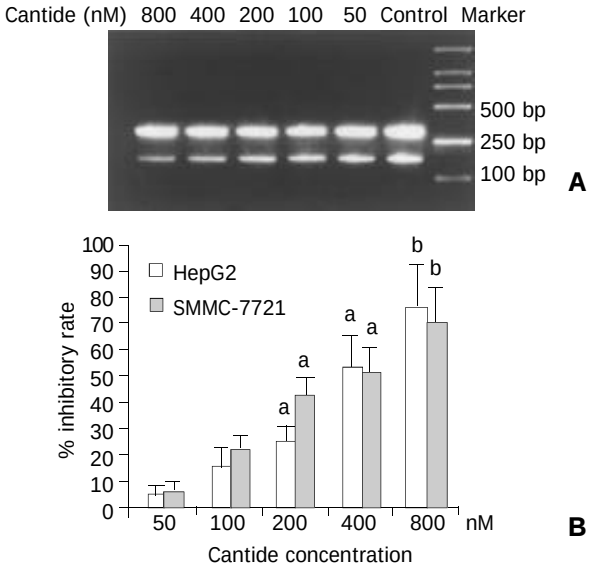

Figure 1 Inhibitory effects of cantide on mRNA level of hTERT. A: Electrophoresis of PCR products of hTERT gene and β_2-microglobulin gene in HepG2 cells treated with cantide. B: Quantitation of inhibitory percentage of hTERT mRNA in treated cells. Each level of PCR product of hTERT gene was quantitated and normalized by the level of β_2-microglobulin. Inhibitory rate was calculated by comparing to the control cells. The results were expressed as means ± SD from three independent experiments. [a]P<0.05 *vs* the cells treated with lipofectin alone, [b]P<0.01 *vs* the cells treated with lipofectin alone.

Western blot analysis was performed to determine the effect of cantide treatment on hTERT protein level in tumor cells. Figure 2A shows that the protein level of hTERT was decreased as the concentration of cantide increased at 48 h compared to the untreated cells. The relative inhibition percentage of hTERT protein was 67.8 % (P<0.01) and 66.2 % (P<0.01) in HepG2 and SMMC-7721 cells treated with 800 nM cantide, respectively (Figure 2B).

These results indicated that cantide inhibited hTERT gene expression in a dose-dependent manner after 48 h treatment.

Down-regulation of telomerase activity

It was shown that the expression of hTERT gene appeared to correlate with the level of telomerase enzymatic activity in many human tumor cells[17,18]. To investigate whether the telomerase activity was affected in tumor cells treated with cantide, a TRAP-ELISA assay was performed. Figure 3 shows that the decrease of telomerase activity was observed after 48 h of treatment at various concentrations of cantide. Moreover, the decrease of telomerase activity was approximately correlated with the concentration of cantide. At the concentration of 800 nM, the relative telomerase activity in the treated HepG2 and SMMC-7721 cells was only 17.1 % (P<0.01) and 20.3 % (P<0.01) of that in untreated cells at 48 h, respectively. These findings suggested that treatment of cantide decreased the telomerase activity in a dose-dependent manner by direct inhibition of the hTERT gene expression.

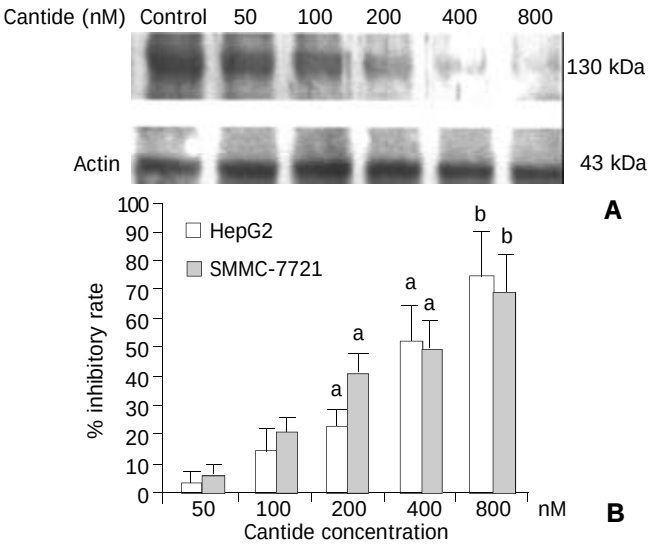

Figure 2 Inhibitory effects of cantide on protein level of hTERT. A: Western blot analysis of hTERT protein in HepG2 cells treated with cantide. B: Inhibitory percentage of hTERT protein in treated cells compared to the control cells. Each level of hTERT protein was quantitated. Inhibitory rate was calculated by comparing to the control cells. The results were expressed as means ± SD of two independent experiments. [a]P<0.05 *vs* the cells treated with lipofectin alone, [b]P<0.01 *vs* the cells treated with lipofectin alone.

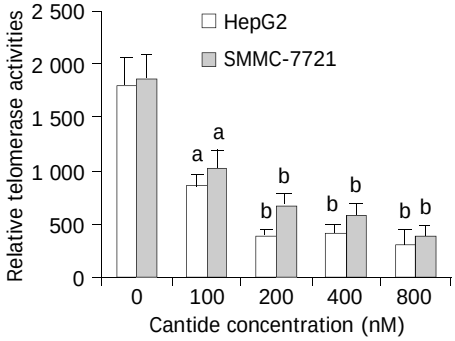

Figure 3 Comparison of telomerase activity in HepG2 and SMMC-7721 cells treated with cantide. 48 h after treatment with cantide, cells extract was tested for telomerase activity by TRAP-ELISA assay. The results were expressed as means ± SD from three independent experiments. [a]P<0.05 *vs* the cells treated with lipofectin alone, [b]P<0.01 *vs* the cells treated with lipofectin alone.

Induction of apoptosis with cantide

The DeadEnd colorimetric apoptosis detection system labeled fragmented DNA *in situ* and was used for detecting apoptosis, which was used to investigate whether cantide induced apoptosis in tumor cells. Figure 4A shows the staining of HepG2 cells 72 h after treatment. The cells treated with lipofectin alone showed very few stained cells (Figure 4 Aa). In contrast, most of the cells treated with cantide were intensively stained (Figure 4 Ab). To quantify the extent of apoptosis, the percentage of stained cells from a total of 200 cells was determined in each treatment group. As shown in Figure 4B, the percentage of apoptotic cells after cantide treatment was increased both in a time-dependent manner and in a dose-dependent manner. The percentage of stained cells in HepG2 and SMMC-7721 cells treated with 800 nM cantide at 72 h was 63 % and 52 % (P<0.01), respectively. By contrast, 8 % and 9 % cells were stained after 72 h treatment with

lipofectin alone. These results suggested that the cytotoxic effect of cantide was mainly due to induction of apoptosis.

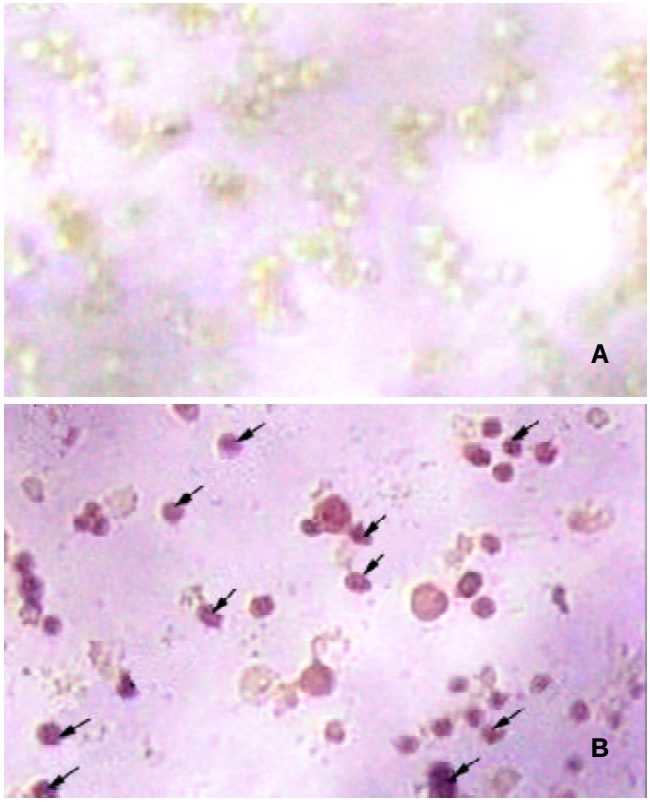

Figure 4 Apoptotic features of tumor cells. The DeadEnd kit was utilized for the assay. A: staining of the cells treated with (a) lipofectin alone and (b) cantide in combination with lipofectin. The arrows showed the representative cells with dark brown staining, 100×. B: the percentage of TUNEL-positive cells treated with cantide. c: HepG2 cells, d: SMMC-7721 cells. The results were expressed as means ± SD from three independent experiments.

Activation of Caspase

It was shown that Caspases were the main factor in the apoptotic pathway[19,20]. We investigated whether Caspase was involved in the anti-tumor effect by utilizing a Caspase activity detection assay. We observed that ICE- and CPP32-like protease activity in tumor cell treated with cantide reached the highest point at 48 h (data not shown). The levels of CPP32-like protease activity in HepG2 and SMMC-7721 were increased 2.8- and 3.0-fold respectively at 48 h ($P<0.05$) compared to the cells treated with lipofectin alone, and the levels of ICE-like protease activity were also increased 2.6- and 3.2-fold ($P<0.05$) at 48 h, respectively (Figure 5). These results clearly indicated the involvement of Caspases family (at least ICE- and CPP-like) in the induction of apoptosis by cantide treatment.

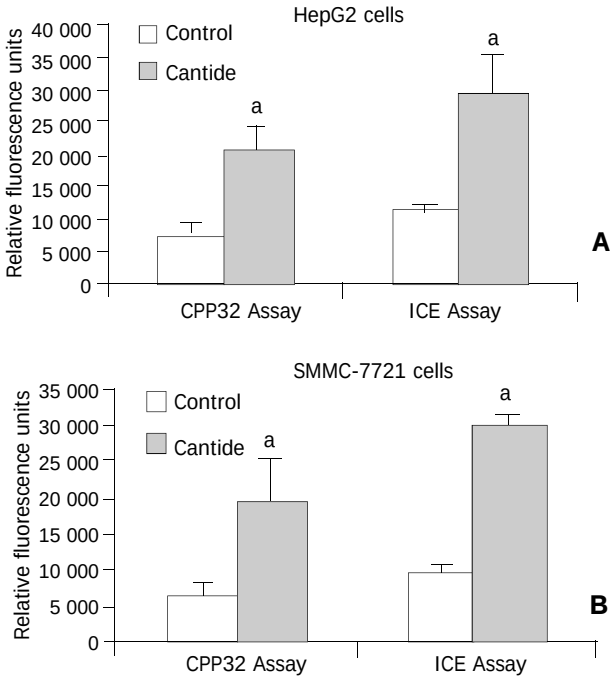

Figure 5 Measurement of CPP32- and ICE-like protease activities in tumor cells treated with cantide. Two days after treatment with cantide, cell lysates were tested for CPP32- and ICE-like protease activities.The results were expressed as means ± SD from three independent experiments. A: HepG2 cells, B: SMMC-7721 cells. $^aP<0.05$ *vs* the cells treated with lipofectin alone.

DISCUSSION

The hypothesis of telomerase mechanism is supported by the idea that progressive shortening of telomeres regulates the lifespan of cells, with each cell division, telomeres are shortened by 50-200 bp.When telomeres become critically short, the cells turn to growth arrest[21,22]. The rate of telomere DNA shortening is regulated by telomerase expression and activity[23]. Therefore, telomerase inhibitors might be useful as anticancer agents, but there will be an expected log phase between the time when telomerase is inhibited and the time when telomere of cancer cells is shortened sufficiently to produce detrimental effects on cell proliferation[24]. It takes approximately 1 month to induce cell death in tumor cells following telomerase inhibition by transfection of antisense hTR vector[25]. Our previous study has shown that cantide has a rapid inhibitory effect on tumor growth 3 days after *in vitro* treatment[15], and this striking effect is unlikely to be interpreted by the hypothesis that cantide is acting specifically through a telomere-dependent mechanism because the cells have not undergone sufficient cell divisions to significantly shorten their telomeres. It is likely that there might be other mechanisms for the antitumor effect of cantide.

In this study, we detected apoptosis in tumor cells just 3 days after cantide treatment in a dose-dependent manner. Taking previous reports on antisense hTR vector and our studies together into consideration, it is likely to raise the possibility that antitumor effect of cantide occurs through following two pathways: 1) A short-term effect on apoptosis is induced rapidly by cantide. 2) A long-term effect on

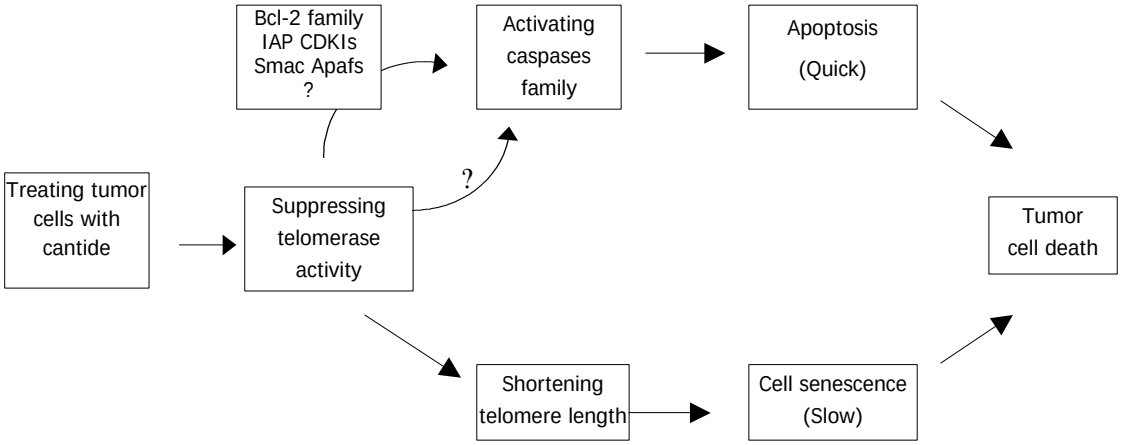

Figure 6 Two possible pathways of antitumor effect of cantide. IAP: inhibitors of apoptosis, CDKIs: cycin-dependent kinase inhibitors, Apafs: apoptotic protease activating factors.

telomerase activity is inhibited, and cell death is caused when telomere length is critically shortened by telomeric DNA.

It has been demonstrated that Caspase is a central executioner of apoptosis machinery, and over-expression and activation of Caspases in human cells lead to apoptosis[26,27]. To date, fourteen mammalian Caspases have been described. Among them, two subfamilies have been categorized based on amino acid sequence, substrate and inhibitor specificities. They are ICE-like proteases and CPP32-like proteases[28]. In this study, we found that both CPP32- and ICE-like proteases were increased 2 or 3-fold in tumor cells compared to the control cells 2 days after cantide treatment. Based on this evidence, the rapid antitumor effect of cantide may be due to active induction of Caspase-dependent apoptosis. Cantide can activate Caspase activity and lead to rapid cell death via apoptotic pathways, and might be a potential therapeutic agent for the treatment of cancer.

It has been found that 2-5A antisense ODN could cause profound cell death in prostate cancer cells and ovarian cancer cells, but not in fibroblast cells and normal ovarian epithelial cells without telomerase activity[12, 29]. Furthermore, suppression of TERT levels and function in embryonic mouse hippocampal neurons in culture could significantly increase their vulnerability to cell death induced by amyloid beta-peptide, and over-expression of TERT in pheochromocytoma cells could result in decrease of vulnerability to amyloid beta-peptide-induced apoptosis[13]. In addition, hTERT gene could be transfected into telomerase negative human embryo lung fibroblasts, the telomerase-expression cells could elongate telomeres and increase resistance to apoptosis induced by hydroxyl radicals[30]. We detected the down-regulation of hTERT mRNA gene expression, and found a significant decrease in telomerase activity after cantide treatment. The decrease was correlated with the concentration of cantide. Based on the observation above, we speculate that telomerase plays another role in addition to maintaining the telomere length, disturbance of this function will cause a rapid cell death by activating the Caspases. In accordance to that hypothesis, Cao *et al*[31] have also reported that telomerase plays roles not only in up-regulating cell proliferative life span, but also in supporting cell proliferative rate by a mechanism involving telomere lengthening-independent activity. Therefore, there should be some proteins that deliver messages between telomerase and Caspase, and further studies using techniques such as biochip or yeast two-hybrid system are necessary to find certain associated molecules.

In summary, our results have shown that cantide can effectively inhibit hTERT gene expression, decrease telomerase activity, and trigger apoptosis through activation of Caspase family. Apoptosis induction may be one of the potential mechanisms of cantide-medicated inhibition for tumor cell growth. Continuous cantide treatment might shorten the telomere to a size that leads to cell senescence (Figure 6). The treatment with cantide may be a potential strategy for cancer with telomerase activity.

REFERENCES

1 **Holt SE**, Shay JW. Role of telomerase in cellular proliferation and cancer. *J Cell Physiol* 1999; **180**: 10-18
2 **Shen ZY,** Xu LY, Li EM, Cai WJ, Chen MH, Shen J, Zeng Y. Telomere and telomerase in the initial stage of immortalization of esophageal epithelial cell. *World J Gastroenterol* 2002; **8**: 357-362
3 **Granger MP**, Wright WE, Shay JW. Telomerase in cancer and aging. *Crit Rev Oncol Hematol* 2002; **41**: 29-40
4 **Shay JW**, Bacchetti S. A survey of telomerase activity in human cancer. *Eur J Cancer* 1997; **33**: 787-791
5 **Kim NW**. Clinical implications of telomerase in cancer. *Eur J Cancer* 1997; **33:** 781-786
6 **Helder MN**, Jong S, Vries EG, Zee AG. Telomerase targeting in cancer treatment: new developments. *Drug Resist Updat* 1999; **2:** 104-115
7 **Stewart SA**, Weinberg RA. Telomerase and human tumorigenesis. *Semin Cancer Biol* 2000; **10:** 399-406
8 **Blackburn EH**. Switching and signaling at the telomere. *Cell* 2001; **106:** 661-673
9 **Wang X**, Zhang Z, Xu Y, Chen S, Xiong W. Inhibition of telomerase activity and induction of apoptosis in lung cancer cell by human telomerase reverse transcriptase gene antisense oligodeoxynucleotide. *Zhonghua Neike Zazhi* 2002; **41**: 175-178
10 **Adah SA**, Bayly SF, Cramer H, Silverman RH, Torrence PF. Chemistry and biochemistry of 2', 5'-oligoadenylate-based antisense strategy. *Curr Med Chem* 2001; **8:** 1189-1212
11 **Mukai S**, Kondo Y, Koga S, Komata T, Barna BP, Kondo S. 2-5A antisense telomerase RNA therapy for intracranial malignant gliomas. *Cancer Res* 2000; **60:** 4461-4467
12 **Koga S**, Kondo Y, Komata T, Kondo S. Treatment of bladder cancer cells *in vitro* and *in vivo* with 2-5A antisense telomerase RNA. *Gene Ther* 2001; **8:** 654-658
13 **Ulaner GA**, Hu JF, Vu TH, Giudice LC, Hoffman AR. Telomerase activity in human development is regulated by human telomerase reverse transcriptase (hTERT) transcription and by alternate splicing of hTERT transcripts. *Cancer Res* 1998; **58:** 4168-4172
14 **Zhu H**, Fu W, Mattson MP. The catalytic subunit of telomerase protects neurons against amyloid beta-peptide-induced apoptosis. *J Neurochem* 2000; **75:** 117-124
15 **Wang SQ**, Lin L, Chen ZD, Lin RX, Chen SH, Guan W, Wang XH. Effect of antisense oligonucleotides targeting telomerase catalytic subunit on tumor cell proliferation *in vitro*. *Chinese Sci Bulletin* 2002; **47:** 993-997

16 **Green DW**, Roh H, Pippin J, Drebin JA. Antisense oligonucleotides: an evolving technology for the modulation of gene expression in human disease. *J Am Coll Surg* 2000; **191**: 93-105
17 **Counter CM**, Meyerson M, Eaton EN, Ellisen LW, Caddle SD, Haber DA, Weinberg RA. Telomerase activity is restored in human cells by ectopic expression of hTERT (hEST2), the catalytic subunit of telomerase. *Oncogene* 1998; **16**: 1217-1222
18 **Chang JT**, Chen YL, Yang HT, Chen CY, Cheng AJ. Differential regulation of telomerase activity by six telomerase subunits. *Eur J Biochem* 2002; **269**: 3442-3450
19 **Takahashi A**. Caspase: executioner and undertaker of apoptosis. *Int J Hematol* 1999; **70:** 226-232
20 **Habn WC**, Meyerson M. Telomerase activation, cellular immortalization and cancer. *Ann Med* 2001; **33**: 123-129
21 **Yang Y**, Chen Y, Zhang C, Huang H, Weissman SM. Nucleolar localization of hTERT protein is associated with telomerase function. *Exp Cell Res* 2002; **277**: 201-209
22 **Klingelhutz AJ**. The roles of telomeres and telomerase in cellular immortalization and the development of cancer. *Anticancer Res* 1999; **19**: 4823-4830
23 **Feng J**, Funk WD, Wang SS, Weinrich SL, Avilion AA, Chiu CP, Adams RR, Chang E, Allsopp RC, Yu J, Le S, West MD, Harley CB, Andrew WH, Greider CW, Villeponteau B. The RNA component of human telomerase. *Science* 1995; **269**: 1236-1241
24 **White LK**, Wright WE, Shay JW. Telomerase inhibitors. *Trends Biotech* 2001; **19:** 114-120
25 **Kondo Y**, Koga S, Komata T, Kondo S. Treatment of prostate cancer *in vitro* and *in vivo* with 2-5A-anti-telomerase RNA component. *Oncogene* 2000; **19:** 2205-2211
26 **Kumar S**. Regulation of caspase activation in apoptosis: implications in pathogenesis and treatment of disease. *Clin Exp Pharmacol Physiol* 1999; **26:** 295-303
27 **Shi Y**. Mechanisms of caspase activation and inhibition during apoptosis. *Mol Cell* 2002; **9**: 459-470
28 **Van de Craen M**, Van Loo G, Pype S, Van Criekinge W, Van den Drande I, Molemans F, Fiers W, Declercq W, Vandenabeele P. Identification of a new caspase homologue: caspase-14. *Cell Death Differ* 1998; **5**: 838-846
29 **Kushner DM**, Paranjape JM, Bandyopadhyay B, Cramer H, Leaman DW, Kennedy AW, Silverman RH, Cowell JK. 2-5A antisense directed against telomerase RNA produces apoptosis in ovarian cancer cells. *Gynecol Oncol* 2000; **76:** 183-192
30 **Ren JG**, Xia HL, Tian YM, Just T, Cai GP, Dai YR. Expression of telomerase inhibits hydroxyl radical-induced apoptosis in normal telomerase negative human lung fibroblasts. *FEBS Lett* 2001; **488:** 133-138
31 **Cao Y**, Li H, Mu FT, Ebisui O, Funder JW, Liu JP. Telomerase activation causes vascular smooth muscle cell proliferation in genetic hypertension. *FASEB J* 2002; **16**: 96-98

Edited by Zhang JZ and Wang XL

P.O.Box 2345, Beijing 100023,China
Fax: +86-10-85381893
E-mail: wjg@wjgnet.com www.wjgnet.com

World J Gastroenterol 2003;9(9):2036-2039
World Journal of Gastroenterology
 ISSN 1007-9327

• BASIC RESEARCH •

Activation of phosphorylating-p38 mitogen-activated protein kinase and its relationship with localization of intestinal stem cells in rats after ischemia-reperfusion injury

Xiao-Bing Fu, Feng Xing, Yin-Hui Yang, Tong-Zhu Sun, Bao-Chen Guo

Xiao-Bing Fu, Feng Xing, Yin-Hui Yang, Tong-Zhu Sun, Bao-Chen Guo, Wound Healing and Cell Biology Laboratory, Institute of Burns, 304 Hospital, Trauma Center of Postgraduate Medical College, Beijing 100037, China
Supported by the National Basic Science and Development Program (973 Program, No. G1999054204), Grant for National Distinguished Young Scientists, No. 39525024, Grant for National Natural Science Foundation of China, No. 30170966, 30230370
Correspondence to: Xiao-Bing Fu, MD, Wound Healing and Cell Biology Laboratory, 304 Hospital, Institute of Burns, Trauma Center of Postgraduate Medical College, 51 Fu Cheng Road, Beijing 100037, China. fuxb@cgw.net.cn
Telephone: +86-10-66867396 **Fax:** +86-10-88416390
Received: 2003-05-10 **Accepted:** 2003-06-07

Abstract

AIM: To investigate the expression of phosphorylating p38 mitogen-activated protein kinase (MAPK) in rat small intestine after ischemia-reperfusion (I/R) insult and its relationship with the localization of intestinal stem cells.

METHODS: Forty-eight Wistar rats were divided randomly into three groups, namely intestinal ischemia-reperfusion group (R), intestinal ischemia group (I) and sham-operated control group (C). In group I, the animals were killed 45 minutes after superior mesenteric artery (SMA) occlusion, while in group R the rats sustained SMA occlusion for 45 minutes and reperfusion for 2, 6, 12 or 24 hours respectively. In sham-operated control group, SMA was separated, but without occlusion. The activity of plasma diamine oxidase (DAO) was determined. Intestinal tissue samples were also taken for histological analysis and immunohistochemical analysis of MAPK p38 detection and intestinal stem cell localization.

RESULTS: The changes in histological structure and plasma DAO levels indicated that the intestinal barrier was damaged after intestinal I/R injury. In group C and I, each crypt contained 5-6 p38 MAPK positive cells, which were mainly located in the lower region of the crypts. This was consistent with the distribution of intestinal stem cells. The presence of positive cells in crypts increased with the time of reperfusion and reached its peak at 12 hours after reperfusion (35.6 %).

CONCLUSION: After intestinal I/R injury, the expression of phosphorylating-p38 MAPK in small intestine increased with the duration of reperfusion, and its distribution coincided with that of intestinal stem cells and their daughter cells, indicating that phosphorylating-p38 might be a possible marker of intestinal stem cells.

Fu XB, Xing F, Yang YH, Sun TZ, Guo BC. Activation of phosphorylating-p38 mitogen-activated protein kinase and its relationship with localization of intestinal stem cells in rats after ischemia-reperfusion injury. *World J Gastroenterol* 2003; 9(9):2036-2039
http://www.wjgnet.com/1007-9327/9/2036.asp

INTRODUCTION

The four principal differentiated cell lineages of the intestinal epithelium are derived from a common multipotent stem cell located near the base of each crypt. It is observed that normally there are about 1-4 stem cells in each small intestinal crypt. These crypt stem cells are divided to produce a daughter stem cell as well as more rapidly to replicate transit cells, which in turn undergo 4-6 rapid cell divisions in the proliferative zone located in the lower half of each crypt[1,2]. The mitogen-activated protein kinase (MAPK) cascade, a cytoplasm protein kinase which requires dual phosphorylation on specific threonine and tyrosine residues for their activation, can transmit the mitogen or the differentiating signals from the cell surface into the nucleus, thus regulating the gene expression. p38MAPK is an important member of the MAPK family[3-5]. There has been hardly any report to explore the expression characteristics of phosphorylating-p38 mitogen-activated protein kinase (MAPK) in rat small intestine after ischemia-reperfusion (I/R) insult and its relationship with the localization of intestinal stem cells. In the present study, we used SMA occlusion rats as an animal model to determine the expression of phosphorylating-p38 MAPK after intestinal I/R injury, and to investigate its relationship with small intestinal stem cells.

MATERIALS AND METHODS

Animal model and experimental design

Forty-eight healthy male Wistar rats (Animal Centre, Chinese Academy of Military Medical Sciences) weighing 200-250 g were used. After 1 week adaption in our animal centre and 12 hours fasting and free drinking just before the experiment, the animals were anaesthetised with 3 % sodium pentobarbital. Ischemia/reperfusion injury was produced by clamping the superior mesenteric artery (SMA) for 45 minutes and loosing the splint to form reperfusion injury. The animals were divided randomly into ischemia-reperfusion insult group (R), ischemia only group (I) and sham-operated control group (C). According to the different periods after reperfusion, group R was further divided into 2, 6, 12 and 24 hours subgroups. In group C, SMA was separated but without occlusion, and samples were taken after exposure of SMA for 45 minutes. In group I, animals were killed after occlusion for 45 minutes. In group R, rats were killed at different time points after reperfusion. Blood samples and intestinal tissue biopsies were taken. Blood samples were centrifuged and serum was frozen to measure plasma diamine oxidase (DAO). Tissue biopsies were fixed with 4 % paraformaldehyde for immunohistochemical detection of MAPK p38 and localization of stem cells.

Detection index

Plasma DAO activity Plasma DAO activity was determined according to references 6 and 7.

Histological staining Polyformalin fixed, paraffin embedded small intestinal samples were also cut into 5 μm thick sections,

deparaffinized in xylene, and rehydrated in graded ethanol, and then stained with haematoxylin-eosine (HE) for histological observation under light microscope (Olympus, Japan).

Measurement of phosphorylated forms of p38 MAPK

Formalin-fixed, paraffin-embedded small intestinal tissues were used to measure the phosphorylated forms of p38 MAPK by immunohistochemistry. Immunohistochemistry was performed according to the instructions of the Power Vision™ kit (Santa Cruze, USA). Briefly, sections (5 μm) were dewaxed and rehydrated in graded alcohols. Endogenous peroxidase activity was quenched, antigen retrieval was performed by heating for 20 minutes at 100 ℃ in 0.01 mol/L sodium citrate. The primary monoclonal antibody for p38 MAPK (Cell Signaling Technology, Inc., USA) was diluted 1:100 with the dilute buffer and incubated for 40 minutes at 37 ℃. Then sections were incubated with HRP-conjugated secondary antibody (Santa Cruz, USA) for 20 minutes at 37 ℃. Positive expression was detected with diaminobenzidine (DAB, Sigma, St. Louis, MO, USA). Sections were lightly counterstained with hematoxylin, dehydrated in graded alcohols, and mounted. As negative control, the sections were processed in the same way as above, but PBS was used as primary antibody instead of the p38 MAPK monoclonal antibodies.

Results determination

The results of positive staining cells and their distribution were observed under 10 times eyepiece and 40 times object-lens microscope. Visions of relatively good morphology of crypts were chosen to count the positive staining cells. Among the cells in the centre of crypt basement, positive staining cells and negative cells were counted upward till reaching the boundary to villus. Fifty intestinal crypts were required for counting, and then the ratio of positive cells were calculated and analyzed.

Statistical analysis

Data were expressed as mean ± standard error. Comparisons between groups of data were analyzed by Students *t* test. *P* values <0.05 were considered as statistically significant.

RESULTS

Histological changes

It was found under light microscopy that reperfusion resulted in the damage of intestinal barrier. HE staining showed that partial loss of mucosa was observed after 2 hours of reperfusion, while at 6 hours after reperfusion, the damage of epithelial cells of intestinal mucosa, hemorrhage and necrosis were observed and accompanied by inflammatory cell infiltration in intestinal wall.

Changes of plasma DAO activity

Plasma DAO levels elevated from 2 hours after reperfusion in all groups, and reached their peak at 6 hours, which was an increase of 1.7 fold as compared with those in normal controls ($P<0.05$), and then decreased gradually, almost back to normal at 24 hours after the reperfusion (Table 1).

Table 1 Changes of plasma DAO activities in different groups

Groups	DAO activity (U / ml)	Groups	DAO activity (U / ml)
Group C	0.70±0.19	Group R6	1.20±0.24[b]
Group I	0.76±0.16	Group R12	1.00±0.28[a]
Group R2	0.90±0.23	Group R24	0.80±0.17

[a]$P<0.05$, [b]$P<0.01$ compared with control.

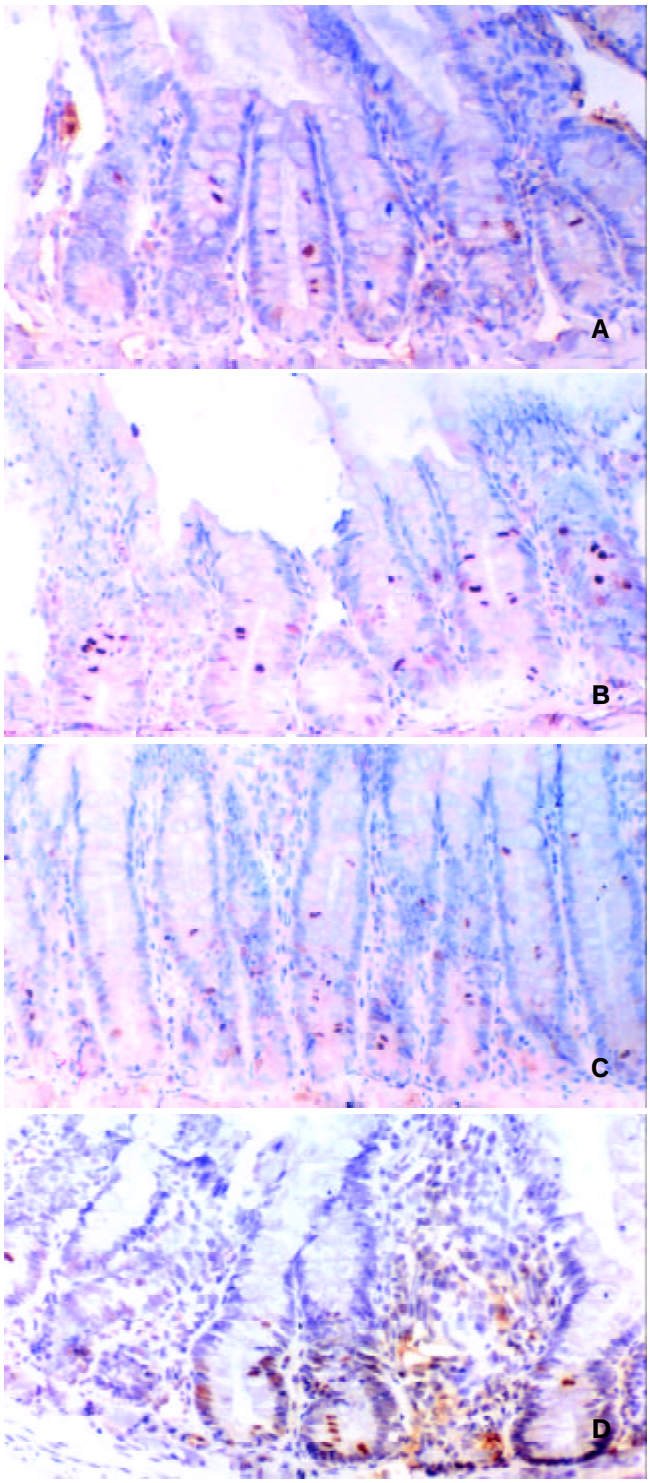

Figure 1 The expression of phosphorylated p38 MAPK in control group (A), ischemia group (B), ischemia-reperfusion 6 h (C) and 12 h (D) groups. The positive expression of p38 MAPK signals was localized mainly in the lower half of the crypts and in the cytoplasm of the crypt cells. The positively stained cells increased remarkably after 6 hours, and reached their peak at 12 hours after reperfusion, which was about 35.6 % of the total cells in crypts. At this stage, the positive staining was primarily localized in nucleus of crypt cells.

P38 MAPK expression

The immunohistochemical staining for phosphorylated forms of p38 MAPK was evaluated and summarized in Table 2. In groups C and I, there were only 5-6 p38 MAPK positive staining cells in each crypt, which were localized mainly in the lower half of the crypts and in the cytoplasm of the crypt cells. When the cell in base of crypt was regarded as layer 1,

then upward was counted till reaching the boundary to villus, there were normally about 30 cell layers. The p38 MAPK positive staining cells were mainly localized between layers 2 and 10, few positive cells were seen beyond this scale. The number was decreased slightly after 2 hours of reperfusion. The positively stained cells increased remarkably after 6 hours, and peaked at 12 hours after reperfusion, which was about 35.6 % of the total cells in crypts. At this stage, the positive staining was primarily localized in the nuclei of crypt cells. The number of positive cells was decreased and almost returned to normal after 24 hours of reperfusion. A few positive cells were found in the matrix of villus. However, no positive cells were observed in the epithelium of villus (Figure 1).

Table 2 Ratio of p38 MAPK positively stained cells to total cells in small intestinal crypts ($\bar{x}\pm s$)

Groups	Expression ratio (%)	Groups	Expression ratio (%)
Group C	15.6±1.5	Group R6	27.0±1.8[a]
Group I	14.0±1.0	Group R12	35.6±2.6[b]
Group R2	10.5±0.8	Group R24	19.3±2.1

[a]$P<0.05$, [b]$P<0.01$ compared with control.

DISCUSSION

It has become the center to study the internal organ injury and repair after severe trauma and burns in recent years and a new focus to study stem cells and intestinal organ repair[8-13]. Especially, the regulatory effects of growth factors and stem cells in internal organs are the very important field[14,15]. However, little is known about the molecular mechanisms that regulate the dynamics of stem cell replication or stem cell fate in intestinal epithelium during either normal epithelial renewal or regeneration of a functional epithelium after injury. Unfortunately, there have been no sensitive markers which can be used to identify the intestinal stem cells. In the previous studies, some positive expression of both PCNA and Ki67 in G1 phase stem cells, transit cells and other daughter cells was observed, which made them unable to act as markers for stem cells, thus becoming extremely difficult to study intestinal stem cells[16-18]. This finding raises a basic question: is there any other index which can be used as the suitable marker for stem cells?

Mitogen-activated protein kinases (MAPK) are mainly composed of the "extracellular signal regulated" p42/p44 MAPK and "stress-regulated" (SR-MAPKs) stress-activated protein kinases (SAPKs)/c-Jun N-terminal kinases (JNKs) and the p38-MAPKs. On stimulation, MAPKs translocations to the nuclei where they may phosphorylate nuclear transcription factors, thus regulating gene expression[19,20]. Philips *et al*[21] found from an *in vitro* study of mouse embryo fibroblasts, that inhibiting the activation of p38 could improve the expression of cyclin A, which is closely related to cell proliferation. p38 not only promotes the apoptosis in hematopoietic cells containing some stem cell properties, but also mediates the proliferating effect of IL-1. Various MAPK subtypes have synergetic effects[22]. p38 may have a dual function, and is tissue specific. Its effect depends on the injury degree, period and its activated condition. p38 also has a close correlation with the activation of upstream and downstream components of signaling pathways.

p38γ, a subtype of p38, is involved in myoblast differentiation[23] and its expression is enhanced with hypoxia. p38γ mediates the signaling pathway of DNA damage induced by γ ray, which protects DNA from radiative damage by stopping the cells in G2 phase. p38 may exert its effect by different subtypes.

Up to date, the studies of p38 in intestinal cells have remained on *in vitro* tissues and cultured cells. It has been concluded that p38 is related to the differentiation of intestinal crypts and villi[24]. The results of this study showed that in normal rat small intestinal cells, phosphorylated forms of p38 MAPK were mainly located in the base of crypts and cytoplasm of crypt cells, and very few in the nuclei. This localization was similar to those of intestinal stem cells demonstrated by other investigations[1,2]. These positive cells might be composed of stem cells, daughter stem cells as well as more rapidly replicating transit cells. After 45 minutes' ischemia insults, no significant difference was found in the number of p38 positive cells, indicating that ischemia can not activate p38 pathway. Positively stained p38 cells increased markedly after 6 hours of reperfusion, which might be a result of activation of p38 MAPK signaling pathway. DAO is located in the upper part of intestinal mucosa in human as well as in mammals, and is a highly active intracellular enzyme. Changes in DAO activity are an ideal index to investigate intestinal barrier function damage after trauma, especially changes in plasma DAO activity[25-28]. Our histological observations and DAO examinations showed that I/R injury induced the damage of intestinal barrier function. The activation of p38 MAPK might be mediated by LPS, TNFα and peroxides generated after small intestinal damage. However we found no positively stained p38 cells in villus epithelial cells both in normal and injured intestines, which was different from the previous *in vitro* studies. This might be related to the ischemia period, injury degree we chose in the study and the distribution of p38 MAPK and its subtypes in small intestines[29-31].

In summary, our results indicate that intestinal I/R injury can induce the activation of p38 MAPK pathway. The positively expressed cell number and their localization are more likely close to intestinal stem cells. Compared with PCNA and Ki67, the distribution and expression characteristics of p38 MAPK are similar to the intestinal stem cells. Based on these data, we suppose that p38 MAPK may not be an ideal marker for intestinal stem cells, it is more close to the goal and worthy of further investigation.

REFERENCES

1 **Gordon JI,** Hermiston ML. Differentiation and self-renewal in the mouse gastrointestinal epithelium. *Curr Opin Cell Biol* 1994; **6:** 795-803

2 **Potten CS,** Booth C, Pritchard DM. The intestinal epithelial stem cell: the mucosal governor. *Int J Exp Pathol* 1997; **78**: 219-243

3 **Marshall CJ**. Specificity of receptor tyrosine kinase signaling: transient versus sustained extracellular signal-regulated kinase activation. *Cell* 1995; **80:** 179-185

4 **Seger R,** Krebs EG. The MAPK signaling cascade. *FASEB J* 1995; **9:** 726-735

5 **Marais R,** Wynne J, Treisman R. The SRF accessory protein Elk-1 contains a growth factor-regulated transcriptional activation domain. *Cell* 1993; **73**: 381-393

6 **Li JY,** Yu Y, Hao J, Jin H, Xi HJ. Determination of deamine oxdase activity in intestinal tissue and blood using spectrophotometry. *An Ji Suan He Sheng Wu Zi Yuan* 1996; **18**: 28-30

7 **Brandt RB,** Siegel SA, Waters MG, Bloch MH. Spectrophotometric assay for D-(-)-Lactate in plasma. *Anal Biochem* 1980; **102**: 39-46

8 **Fu X**, Sheng Z, Wang Y, Ye Y, Xu M, Sun T, Zhou B. Basic fibroblast growth factor reduces the gut and liver morphologic and functional injuries after ischemia and reperfusion. *J Trauma* 1997; **42:** 1080-1085

9 **Yang YH,** Fu XB, Sun TZ, Jiang LX, Gu XM. bFGF and TGFβ expression in rat kidneys after ischemic / reperfusional gut injury and its relationship with tissue repair. *World J Gastroenterol* 2000; **6**: 147-149

10 **Fu XB,** Yang YH, Sun XQ, Sun TZ, Gu XM, Sheng ZY. Protective effects of endogenous basic fibroblast growth factor activated by 2, 3 butanedion monoxime on functional changes of ischemic

intestine, liver and kidney in rats. *Zhongguo Weizhongbing Jijiu Yixue* 2000; **12**: 69-72

11 **Yang YH,** Fu XB, Sun TZ, Jiang LX, Gu XM. The effect of exogenous basic fibroblast growth factor on hepatic endogenous basic fibroblast growth factor and fibroblast growth factor receptor expression after intestinal ischemia-reperfusion injury. *Zhongguo Weizhongbing Jijiu Yixue* 1999; **11**: 734-736

12 **Fu XB,** Yang YH, Sun TZ, Sun XQ, Gu XM, Chang GY, Sheng ZY. Effects of inhibition or anti-endogenous basic fibroblast growth factor on functional changes in intestine, liver and kidneys in rats after gut ischemia-reperfusion injury. *Zhongguo Weizhongbing Jijiu Yixue* 2000; **12**: 465-468

13 **Yang YH,** Fu XB, Sun TZ, Jiang LX, Gu XM. Renal endogenous expression of basic fibroblast growth factor and transforming growth factor βafter intestinal ischemia-reperfusion injury. *Zhongguo Weizhongbing Jijiu Yixue* 1999; **11**: 203-205

14 **Dignass AU**, Tsunekawa S, Podolsky DK. Fibroblast growth factors modulate intestinal epithelial cell growth and migration. *Gastroenterology* 1994; **106**: 1254-1262

15 **Estival A**, Monzat V, Miquel K, Gaubert F, Hollande E, Korc M, Vaysse N, Clemente F. Differential regulation of fibroblast growth factor (FGF) receptor-1 mRNA and protein by two molecular forms of basic FGF. Modulation of FGFR-1 mRNA stability. *J Biol Chem* 1996; **271**: 5663-5670

16 **Bach SP**, Renehan AG, Potten CS. Stem cells: the intestinal stem cell as a paradigm. *Carcinogenesis* 2000; **21**: 469-476

17 **Rhoads JM**, Argenzio RA, Chen W, Rippe RA, Westwick JK, Cox AD, Berschneider HM, Brenner DA. L-glutamine stimulates intestinal cell proliferation and activates mitogen-activated protein kinases. *Am J Physiol* 1997; **272**(5 Pt 1): G943-953

18 **Houchen CW**, George RJ, Sturmoski MA, Cohn SM. FGF-2 enhances intestinal stem cell survival and its expression is induced after radiation injury. *Am J Physiol* 1999; **276**(1 Pt 1): G249-258

19 **Paris F**, Fuks Z, Kang A, Capodieci P, Juan G, Ehleiter D, Haimovitz-Friedman A, Cordon-Cardo C, Kolesnick R. Endothelial apoptosis as the primary lesion initiating intestinal radiation damage in mice. *Science* 2001; **293**: 293-297

20 **Nishida E,** Gotoh Y. The MAP kinase cascade is essential for diverse signal transduction pathways. *Trends Biochem Sci* 1993; **18**: 128-131

21 **Philips A,** Roux P, Coulon V, Bellanger JM, Vie A, Vignais ML, Blanchard JM. Differential effect of Rac and Cdc42 on p38 kinase activity and cell cycle progression of nonadherent primary mouse fibroblasts. *J Biol Chem* 2000; **275:** 5911-5917

22 **Birkenkamp KU,** Dokter WH, Esselink MT, Jonk LJ, Kruijer W, Vellenga E. A dual function for p38 MAP kinase in hematopoietic cells: involvement in apoptosis and cell activation. *Leukemia* 1999; **13**: 1037-1045

23 **Lechner C,** Zahalka MA, Giot JF, Moller NP, Ullrich A. ERK6, a mitogen-activated protein kinase involved in C2C12 myoblast differentiation. *Proc Natl Acad Sci U S A* 1996; **93**: 4355-4359

24 **Houde M,** Laprise P, Jean D, Blais M, Asselin C, Rivard N. Intestinal epithelial cell differentiation involves activation of p38 mitogen-activated protein kinase that regulates the homeobox transcription factor CDX2. *J Biol Chem* 2001; **276:** 21885-21894

25 **Bragg LE**, Thompson JS, West WW. Intestinal diamine oxidase levels reflect ischemic injury. *J Surg Res* 1991; **50**: 228-233

26 **Murray MJ,** Barbose BS, Cobb CF. Serum D (-)-lactate levels as a predictor of acute intestinal ischemia in a rat model. *J Surg Res* 1993; **54:** 507-509

27 **Murray MJ,** Gonze MD, Nowak LR, Cobb CF. Serum D (-)-lactate levels as an aid to diagnosing acute intestinal ischemia. *Am J Surg* 1994; **167:** 575-578

28 **Sun XQ,** Fu XB, Zhang R, Lü Y, Deng Q, Jiang XG, Sheng ZY. Relationship between plasma D(-)-lactate and intestinal damage after severe injuries in rats. *World J Gastroenterol* 2001; **7:** 555-558

29 **Oliver BL,** Sha'afi RI, Hajjar JJ. Transforming growth factor-alpha and epidermal growth factor activate mitogen-activated protein kinase and its substrates in intestinal epithelial cells. *Proc Soc Exp Biol Med* 1995; **210**: 162-170

30 **Goke M,** Kanai M, Lynch-Deraney K, Podolsky DK. Rapid mitogen-activated protein kinase activation by transforming growth factor alpha in wounded rat intestinal epithelial cells. *Gastroenterology* 1998; **114**: 697-705

31 **Aliaga JC,** Deschenes C, Beaulieu JF, Calvo EL, Rivard N. Requirement of the MAP kinase cascade for cell cycle progression and differentiation of human intestinal cells. *Am J Physiol* 1999; **277**(3Pt 1): G631-G641

Edited by Ma JY and Wang XL

P.O.Box 2345, Beijing 100023,China
Fax: +86-10-85381893
E-mail: wjg@wjgnet.com www.wjgnet.com

World J Gastroenterol 2003;9(9):2040-2044
World Journal of Gastroenterology
 ISSN 1007-9327

• BASIC RESEARCH •

Gadolinium chloride and salvia miltiorrhiza compound ameliorate reperfusion injury in hepatocellular mitochondria

Wen-Hai Zhang, Jin-Sheng Wang, Yong Zhou, Jian-Yi Li

Wen-Hai Zhang, Jin-Sheng Wang, Yong Zhou, Jian-Yi Li, Department of General Surgery, Second Affiliated Hospital, China Medical University, Shenyang 110022, Liaoning Province, China
Supported by the National Science Foundation of Liaoning Province, No. 619025
Correspondence to: Dr. Wen-Hai Zhang, Department of General Surgery, Second Affiliated Hospital, China Medical University, 39. Huaxiang Road, Tiexi District, Shenyang 110022, Liaoning Province, China. surgeonzwh@163.net
Telephone: +86-24-25943022
Received: 2003-03-28 **Accepted:** 2003-05-11

Abstract

AIM: To investigate the effect of gadolinium chloride ($GaCl_3$) and salvia miltiorrhiza compound (SMCo) on ischemia and reperfusion (I/R) injury in hepatocellular mitochondria.

METHODS: Wistar rats were randomly to divided into control group, $GaCl_3$ group, SMCo group and $GaCl_3$ + SMCo group (n=15 each). $GaCl_3$ (7 mg· kg^{-1}) was injected into tail vein on d 1 and d 2 in contrast group. SMCo (2 ml· kg^{-1}) was injected into muscle on d 1 and d 2 in SMCo group. $GaCl_3$+SMCo group received both $GaCl_3$ (iv) and SMCo (im) injection. Control group received saline injection only. On d 3, all the rats were subjected to 2 h ischemia in the middle and left lobes of the liver, followed by reperfusion for 2 h, 6 h and 18 h respectively. The level of serum alanine aminotransferase (ALT) and malondialdehyde (MDA) in hepatocellular mitochondria was measured. Pathological changes in hepatic tissue and in hepatocellular mitochondria were determined with optical microscope and electronic microscope,respectively.

RESULTS: Remarkablly pathohistological and biochemical changes were detected after 6 h of I/R. Compared with control, the level of ALT was decreased in $GaCl_3$, SMCo and $GaCl_3$+SMCo treated groups (1 314.0±278.7 *vs* 809.4±196.1, 716.6±242.8 and 837.2±190.6 IU· L^{-1}, respectively. P<0.05). Similarly, the level of MDA was decreased in $GaCl_3$, SMCo and $GaCl_3$+SMCo treated groups (293.1±51.1 *vs* 190.8±55.5, 214.3±32.9 and 221.0±47.3 nmol· g^{-1}, respectively, P<0.05). Accordingly, in control group, swelling, degeneration, focal necrosis, infiltration of leucocyte were found in reperfused tissue under an optical microscope, and mitochondria swelling, rupture and even breakdown were seen under an electronic microscope. These pathohistological and ultrastructural damages caused by I/R were greatly attenuated in $GaCl_3$, SMCo and $GaCl_3$+SMCo treated groups. However, there was no additive effect observed when $GaCl_3$ and SMCo were used together.

CONCLUSION: Both $GaCl_3$ and SMCo can alleviate the I/R injury in hepatocellular mitochondria.

Zhang WH, Wang JS, Zhou Y, Li JY. Gadolinium chloride and salvia miltiorrhiza compound ameliorate reperfusion injury in hepatocellular mitochondria. *World J Gastroenterol* 2003; 9 (9): 2040-2044

http://www.wjgnet.com/1007-9327/9/2040.asp

INTRODUCTION

Lipid peroxide is one of the main mechanisms that cause ischemia and reperfusion (I/R) injury in the liver[1,2]. The degree of change in lipid peroxide and configuration of hepatocellular mitochondria primarily determine the severity of I/R injury[3]. Previous studies have shown that the number of Kupffer cell as well as its function are activated in response to I/R in the liver, which can be specifically inhibited by gadolinium chloride ($GdCl_3$)[4,5]. Salvia miltiorrhiza compound (SMCo) is widely used to treat many kinds of diseases in clinic, because it can scavenge oxygen free radicles, therefore reducing oxidative stress[6,7]. Reducing I/R injury constitutes a big clinical challenge and depends on the elucidation of the pathological and molecular process of I/R injury. The aim of the present study was to investigate the roles of lipid peroxide and configuration of hepatocellular mitochondria in response to I/R as well as the effect of $GaCl_3$ and SMCo on the process.

MATERIALS AND METHODS

Animals

Wistar rats (male, 8 wk old, weight 200-250 g) were randomly divided into control group, $GaCl_3$ group, SMCo group, $GaCl_3$+SMCo group (n=15 each).

Application of drugs

Gadolinium chloride hexahydrate (Wako pure medicine, Japan) was dissolved in physiological saline (2 g· L^{-1}), which was injected into tail vein at a dose of 7 mg· kg^{-1} on d 1 and d 2 in $GaCl_3$ group. Salvia miltiorrhiza compound (First Shanghai pharmacy) was injected into hind limb muscle at a dose of 2 ml· kg^{-1} on d 1 and d 2 in SMCo group. The $GaCl_3$+SMCo group received both $GaCl_3$ and SMCo injection. The control group received saline only on d 1 and d 2.

Ischemia and reperfusion

On d 3, after 12 h fasting, each rat was anesthetized with sodium thiopental at a dose of 50 mg· kg^{-1} (im). A midline incision was made to expose the liver vessels. The arteries to middle and left lobes of the liver were dissected and the blood flow was blocked with a pair of vessel clamps. The abdomen was then closed. The blood flow was restored by releasing the clamps after 2 h. The blood reperfusion in each group lasted for 2 h, 6 h and 18 h respectively (n=5 for each time point).

Assay of serum alanine aminotransferase (ALT)

The blood sample was taken from heart 2 h, 6 h and 18 h after reperfusion for ALT assay.

Preparation and observation of hepatocellular mitochondria

The liver was excised and washed with saline solution, cleaned with filter paper and then homogenized with 0.25 g· L^{-1} saccharose - EDTA solution. The homogenized solution was centrifugated for 10 min in 1 000 g of centrifugal force, and the supernatant was taken out and centrifugated again for 15 min in 7 000 g. The deposit after second centrifugation, which contained mitochondria, was reserved. All approaches were

performed at 4 ℃ and each procedure was repeated three times to make mitochondria pure.

The separated mitochondria was fixed by entering 2 ml of 25 g· L^{-1}-tris phosphoric acid glutaradehyde for 2 h and then dehydrated bleach routinely. After embedded with EPSONB for 48 h, an extreme thin slice was made and lead acetate-uranium double staining was performed. The ultrastructure of mitochondria was observed under electronic microscopy.

Determination of MDA in mitochondria

The separated mitochondria were mixed with 0.125 mol· L^{-1} kalium chloride up to 1 ml. The content of MDA in hepatocellular mitochondria was determined with biuret reaction at the 525 nm of wave.

Pathohistological observation of hepatic tissue

The hepatic tissue fixed with formaldehyde was embedded into paraffine, slices were made and stained with HE. Pathological changes were observed under optical microscopy.

Statistical analysis

Analysis of variance and Student-newman-Keuls test were used to determine the difference between groups. The results were considered statistically significant when $P<0.05$.

RESULTS

ALT assay

In control group, ALT became significantly activated 6 h after reperfusion. In $GaCl_3$, SMCo and $GaCl_3$+SMCo treated groups, ALT levels were all significantly inhibited compared with control group (Table 1).

Table 1 Change of serum ALT (IU/L, $\bar{x}\pm s$, n=5)

Group	I/R 2h	I/R 6h	I/R 18h
Control	825.8±337.5	1314.0±278.7	1071.2±201.1
$GdCl_3$	1120.8±145.5	809.4±196.1[a]	864.8±213.6
SMC	618.8±312.5	710.6±242.8[a]	899.6±227.3
$GdCl_3$ + SMC	623.8±340.9	837.2±190.6[a]	903.0±244.6

[a]$P<0.05$ *vs* contrast.

MDA assay

The dynamic changes of MDA were identical to the pattern of ALT (Table 2).

Table 2 Change of MDA in mitochondria (nmol· g^{-1}, $\bar{x}\pm s$, n=5)

Group	I/R 2h	I/R 6h	I/R 18h
Control	489.3±291.9	293.1±51.1	480.0±420.9
$GdCl_3$	440.5±581.7	190.8±55.5[a]	196.8±74.0
SMC	242.6±123.1	214.5±32.9[a]	281.4±118.8
$GdCl_3$ + SMC	191.8±44.4	221.0±47.3[a]	280.7±139.2

[a]$P<0.05$ *vs* contrast.

Pathological changes of hepatic tissue

In the control group, the major change of hepatocytes after 2 h of I/R was swelling without necrosis. The swelling became more and more severe with some scattered and focal necrosis and deposition of fibrin in central lobular vein after 6 h of I/R. In addition to obvious swelling, denaturalization and necrosis were seen after 18 h of I/R, which were associated with destroyed hepatic sinuses and infiltration of numerous white blood cells. In $GaCl_3$, SMCo and $GaCl_3$+SMCo groups, there was no necrosis 2 h and 6 h after I/R, and the hepatocyte swelling and denaturalization were much less than those in control group. In treated groups, the hepatic structure was maintained with less necrosis and infiltration of leucocyte 18 h after I/R.

Morphological changes of hepatocellular mitochondria

The I/R injury in hepatocellular mitochondria became more severe with the prolongation of I/R time in control group. It was obvious that swelling, rupture of inner membrane ridge, damage or even breakdown of mitochondrial structure with outline only (Figures 1-3). The changes in $GaCl_3$ and SMCo group were less severe than those in control group. Except for slight swelling, the structure of mitochondria was unchanged. The protective effects of $GaCl_3$ and SMCo against I/R damage on mitochondria were seen not only 2 h, 6 h, and 18 h after I/R (Figures 4-9). The effect of $GaCl_3$+SMCo combination on mitochondria was similar to that of either $GaCl_3$ or SMCo alone.

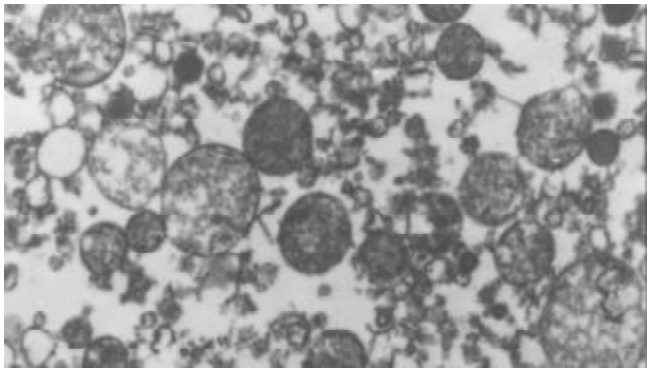

Figure 1 Hepatocellular mitochondria in I/R 2 h in control group, ×10 K.

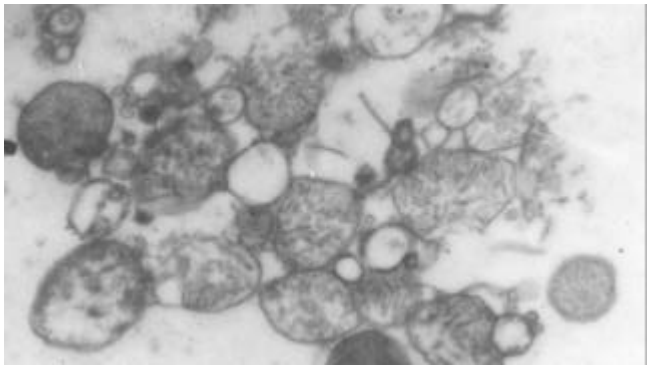

Figure 2 Hepatocellular mitochondria in I/R 6 h in control group, ×10 K.

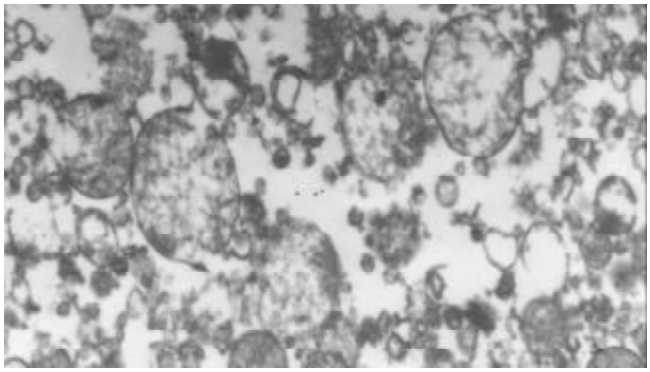

Figure 3 Hepatocellular mitochondria in I/R 18 h in control group, ×10 K.

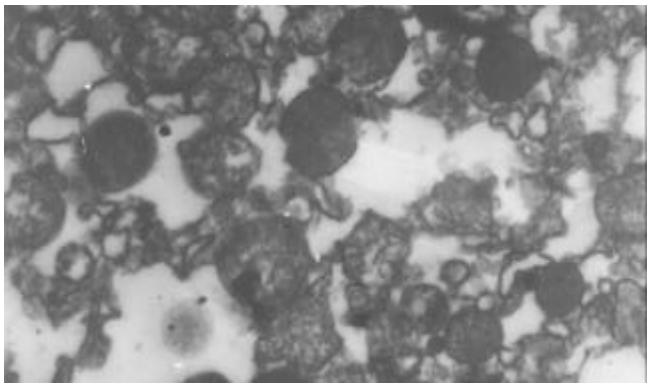

Figure 4 Hepatocellular mitochondria in I/R 2 h in $GdCl_3$ group, ×10 K.

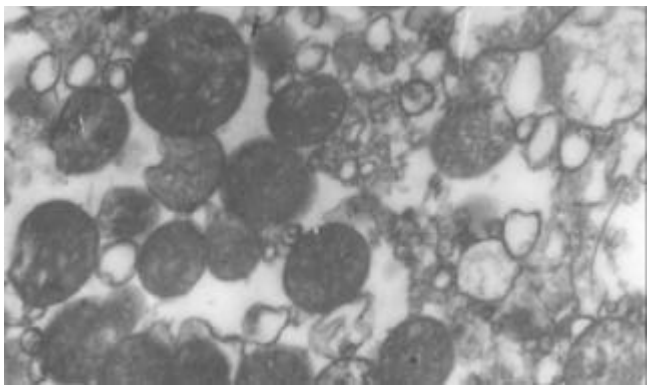

Figure 5 Hepatocellular mitochondria in I/R 6 h in $GdCl_3$ group, ×10 K.

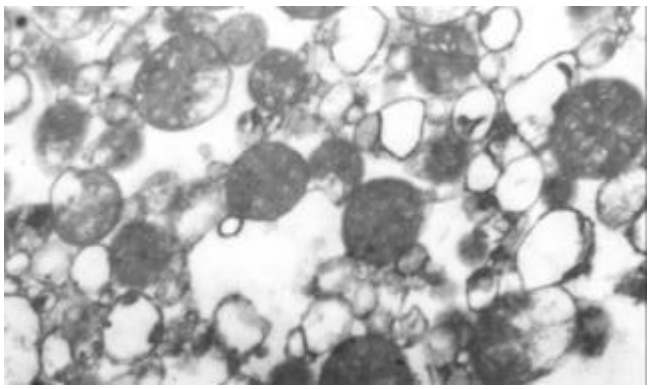

Figure 6 Hepatocellular mitochondria in I/R 18 h in $GdCl_3$ group, ×10 K.

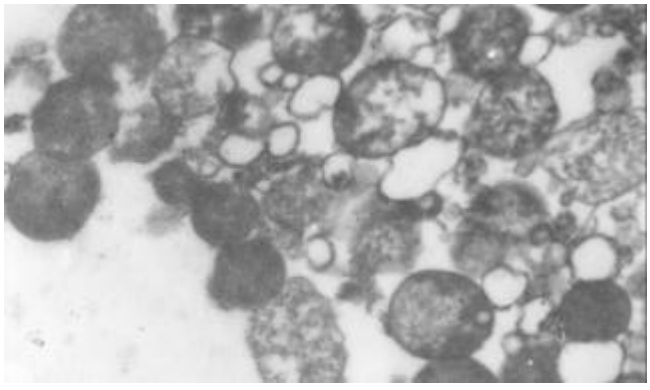

Figure 7 Hepatocellular mitochondria in I/R 2 h in SMCo group, ×10 K.

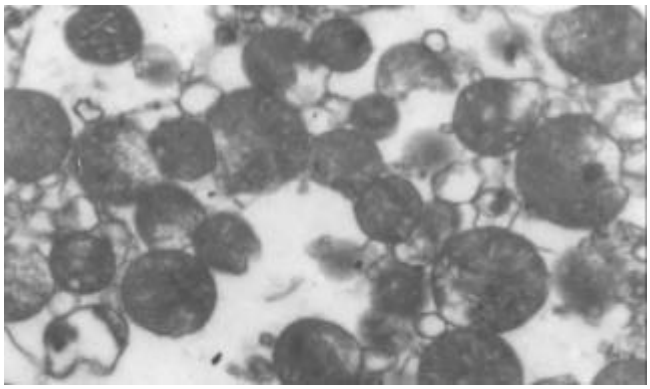

Figure 8 Hepatocellular mitochondria in I/R 6 h in SMCo group, ×10 K.

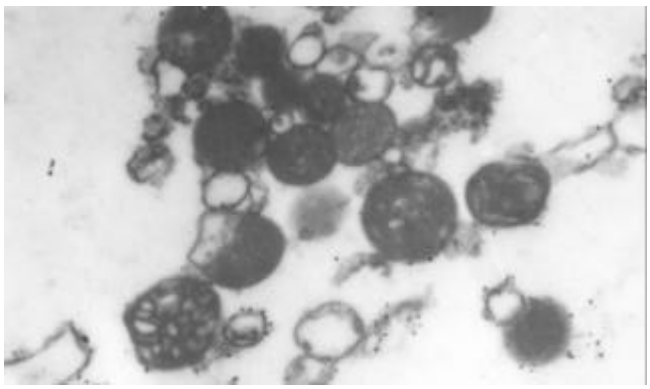

Figure 9 Hepatocellular mitochondria in I/R 18 h in SMCo group, ×10 K.

DISCUSSION

Hepatocellular mitochondria are the place of energy metabolism in hepatocytes. In response to the process of I/R, the mitochondrion produces excessive oxidative free radicle, which in turn result in lipid peroxidation of the mitochondria membrane, therefore, causing mitochondria damage. Sammut observed that the degree of I/R injury in renal mitochondria of rabbit was associated with the preserved time of the kidney. The longer the cold preserved time was, the easier the I/R injury developed[8]. Leducq found that opening of mitochondrial permeability transition pore resulted in mitochondrial and energetic dysfunction of the liver during normothermic reperfusion[9]. These studies have directly or indirectly proved that I/R injury in hepatocellular mitochondria is closely related with the structure of hepatocellular mitochondria and the extent of damage in function[10].

Effect of $GaCl_3$ on I/R injury in hepatocellular mitochondria

The experimental results from the present study showed that ALT increased after 2 h of I/R, and reached the highest value after 6 h of I/R in control group, indicating that I/R injury in hepatic tissues is maximized 6 h after I/R. Previous studies have suggested that activation of Kupffer cells is involved in the injury process at the early stage of liver I/R. $GaCl_3$ can effectively blockade the function of Kupffer cells and reduce the secretion of cytokines and reactive oxygen species from activated Kupffer cells, so that MDA in hepatocellular mitochondria is inhibited[11]. The fact that both ALT and MDA in mitochondria in $GaCl_3$ group were markedly decreased because of the use of $GaCl_3$ suggests that inhibition of Kupffer cells can protect the hepatic function[12]. This study also showed that there was no significant decrease in ALT and MDA 18 h

after I/R, which was in agreement with the hypothesis that inhibition of Kupffer cells could only decrease the injury in the liver at the early stage of I/R. These biochemistry alterations are in parallel to the pathohistological changes. In control group, slight but detectable structural change was seen after 2 h, severe changes including necrosis and denaturalization were seen after 6 h, and more severe changes were seen after 18 h following I/R. In the mean time, by inhibiting Kupffer cells, $GaCl_3$ remarkably ameliorated those detrimental changes, in particular, 6 h after I/R. It should be pointed out that the role played by Kupffer cells is only one of the factors that is involved I/R injury in the liver. In addition to $GaCl_3$, other endogenous and exogenous compounds have also shown protective effects. For example, hepatocyte growth factor could reduce the impairment of both hepatocytes and sinusoidal endothelial cells[13]. Administration of epoprostenol could decrease hepatocellular I/R injury in transplanted liver[14], and nonselective endothelin-1 receptor antagonists could improve hepatic microcirculatory impairment[15]. Special neutrophil eastase inhibitor[16], tissue factor pathway inhibitor[17], adenosine[18], precondition of low-dose TNF-α[19] or ischemic precondition[20,21], etc, could alleviate I/R injury. All of these suggest that I/R is a complicated process. Although the potential role of Kupffer cells in I/R injury is still controversial[22,23], our data provide the strongest evidence in favor of its important role because blockade of Kupffer cells greatly reduces I/R injury in hepatocellular mitochondria.

Effect of SMCo on I/R injury of hepatocellular mitochondria

Our data showed that SMCo treatment decreased the content of MDA in mitochondria in SMCo group. As a scavenger of oxygen free radicls, the SMCo can effectively inhibit lipid peroxidation in hepatocellular mitochondria[24,25], apoptosis of cells[26], and adhesion of neutrophil[27], etc, and accordingly protect hepatocellular mitochondria. Whereas simple inhibition of lipid peroxidation is not enough to prevent entirely the occurrence of I/R injury since a lot of factors are involved. Our results imply that SMCo can protect the function and structure of mitochondria, maintain energy metabolism of hepatocytes, and thereby reduce significantly I/R injury in the liver. Because a lot of factors are involved in I/R injury, it is understandable that inhibition of lipid peroxidation by SMCo can improve, but not prevent I/R injury.

Although both $GaCl_3$ and SMCo are able to alleviate I/R injury in hepatocellular mitochondria when used separately, there is no additive effect when used in combination. We speculate that the two compounds act at different level in a same mechanism. While $GaCl_3$ inhibits mainly the functions of Kupffer cells, decreases the production of oxygen free radicls, SMCo is mainly to promote microcirculation and to restrain lipid peroxidation. Therefore, the effect of SMCo will become insignificant when oxygen free radicls are reduced when $GaCl_3$ is used.

In conclusion, both $GaCl_3$ and SMCo can ameliorate I/R injury in hepatocellular mitochondria at some extent.

REFERENCES

1 **Nguyen WD**, Kim DH, Alam HB, Provido HS, Kirkpatrick JR. Polyethylene glycol-superoxide dismutase inhibits lipid peroxidation in hepatic ischemia / reperfusion injury. *Crit Care* 1999; **3**: 127-130

2 **Rhoden E**, Pereira-Lima L, Lucas M, Mauri M, Rhoden C, Pereira-Lima JC, Zettler C, Petteffi L, Bello-Klein A. The effects of allopurinol in hepatic ischemia and reperfusion: experimental study in rats. *Eur Surg Res* 2000; **32**: 215-222

3 **Jeon BR**, Lee SM. S-adenosylmethionine protects post-ischemic mitochondrial injury in rat liver. *J Hepatol* 2001; **34**: 395-401

4 **Kojima Y**, Suzuki S, Tsuchiya Y, Konno H, Baba S, Nakamura S. Regulation of pro-inflammatory and anti-inflammatory cytokine responses by Kupffer cells in endotoxin-enhanced reperfusion injury after total hepatic ischemia. *Transpl Int* 2003; **16**: 231-240

5 **Lazar G Jr**, Paszt A, Kaszaki J, Duda E, Szakacs J, Tiszlavicz L, Boros M, Balogh A, Lazar G. Kupffer cell phagocytosis blockade decreases morbidity in endotoxemic rats with obstructive jaundice. *Inflamm Res* 2002; **51**: 511-518

6 **Sugiyama A**, Zhu BM, Takahara A, Satoh Y, Hashimoto K. Cardiac effects of salvia miltiorrhiza / dalbergia odorifera mixture, an intravenously applicable Chinese medicine widely used for patients with ischemic heart disease in China. *Circ J* 2002; **66**: 182-184

7 **Peng B,** Du J, Jia Q, Qiao A, Wu Y, Liu X, Qiang Q. The effect of salvia miltiorrhiza and shengmai on inflammatory mediator and renal function of post-operative patients with obstructive jaundice. *Huaxi Yike Daxue Xuebao* 2001; **32**: 587-589

8 **Sammut IA**, Burton K, Balogun E, Sarathchandra P, Brooks KJ, Bates TE, Green CJ. Time-dependent impairment of mitochondrial function after storage and transplantation of rabbit kidneys. *Transplantation* 2000; **69**: 1265-1275

9 **Leducq N**, Delmas-Beauvieux MC, Bourdel-Marchasson I, Dufour S, Gallis JL, Canioni P, Diolez P. Mitochondrial and energetic dysfunctions of the liver during normothermic reperfusion: protective effect of cyclosporine and role of the mitochondrial permeability transition pore. *Transplant Proc* 2000; **32**: 479-480

10 **Grattagliano I**, Vendemiale G, Lauterburg BH. Reperfusion injury of the liver: role of mitochondria and protection by glutathione ester. *J Surg Res* 1999; **86**: 2-8

11 **Zhu XH**, Qiu YD, Shen H, Shi MK, Ding YT. Effect of matrine on Kupffer cell activation in cold ischemia reperfusion injury of rat liver. *World J Gastroenterol* 2002; **8**: 1112-1116

12 **Von Frankenberg M**, Golling M, Mehrabi A, Nentwich H, Thies J, Schaeffer F, Jahnke C, Bud O, Gebhard MM, Otto G, Thurman RG, Herfarth C, Klar E. Destruction of Kupffer's cells increases total liver blood flow and decreases ischemia reperfusion injury in pigs. *Transplant Proc* 1999; **31**: 3253-3254

13 **Takeda Y**, Arii S, Kaido T, Niwano M, Moriga T, Mori A, Hanaki K, Gorrin-Rivas MJ, Ishii T, Sato M, Imamura M. Morphologic alteration of hepatocytes and sinusoidal endothelial cells in rat fatty liver during cold preservation and the protective effect of hepatocyte growth factor. *Transplantation* 1999; **67**: 820-828

14 **Klein M**, Geoghegan J, Wangemann R, Bockler D, Schmidt K, Scheele J. Preconditioning of donor livers with prostaglandin I_2 before retrieval decreases hepatocellular ischemia-reperfusion injury. *Transplantation* 1999; **67**: 1128-1132

15 **Mitsuoka H**, Suzuki S, Sakaguchi T, Baba S, Miwa M, Konno H, Nakamura S. Contribution of endothelin-1 to microcirculatory impairment in total hepatic ischemia and reperfusion injury. *Transplantation* 1999; **67**: 514-520

16 **Soejima Y**, Yanaga K, Nishizaki T, Yoshizumi T, Uchiyama H, Sugimachi K. Effect of specific neutrophil elastase inhibitor on ischemia / reperfusion injury in rat liver transplantation. *J Surg Res* 1999; **86**: 150-154

17 **Yoshimura N**, kobayashi Y, Nakamura K, Yamagishi H, Oka T. The effect of tissue factor pathway inhibitor on hepatic ischemic reperfusion injury of the rat. *Transplantation* 1999; **67**: 45-53

18 **Chen XH**, Bao MS, Li ZZ. Effects of adenosine and its mechanism in ischemic preconditioning in rat liver *in vivo*. *Shijie Huaren Xiaohua Zazhi* 1999; **7**: 298-299

19 **Teoh N**, Leclercq I, Pena AD, Farrell G. Low-dose TNF-alpha protects against hepatic ischemia-reperfusion injury in mice: implications for preconditioning. *Hepatology* 2003; **37**: 118-128

20 **Koti RS**, Yang W, Dashwood MR, Davidson BR, Seifalian AM. Effect of ischemic preconditioning on hepatic microcirculation and function in a rat model of ischemia reperfusion injury. *Liver Transpl* 2002; **8**: 1182-1191

21 **Kumamoto Y**, Suematsu M, Shimazu M, Kato Y, Sano T, Makino N, Hirano KI, Naito M, Wakabayashi G, Ishimura Y Kitajima M.

Kupffer cell-independent acute hepatocellular oxidative stress and decreased bile formation in post-cold-ischemic rat liver. *Hepatology* 1999; **30**: 1454-1463

22 **Schauer RJ**, Gerbes AL, Vonier D, op den Winkel M, Fraunberger P, Bilzer M. Induction of cellular resistance against Kupffer cell-derived oxidant stress: A novel concept of hepatoprotection by ischemic preconditioning. *Hepatology* 2003; **37**: 286-295

23 **Tsukamoto S**, Ohkohchi N, Fukumori T, Orii T, Asakura T, Takayama J, Shibuya H, Kato H, Satomi S. Elimination of Kupffer cells and nafamostat mesilate rinse prevent reperfusion injury in liver grafts from agonal non-heart-beating donors. *Transplantation* 1999; **67**: 1396-1403

24 **Jiang SL**, Yao XX, Lu T. Inhibitory effect of Danshen on lipid peroxidation in mitochondria of hepatic fibrosis in rats. *Shijie Huaren Xiaohua Zazhi* 2002; **10**: 1253-1256

25 **Liu P**, Hu Y, Liu C, Zhu D. Effects of salviainolic acid A (SA-A) on liver injury: SA-A action on hepatic peroxidation. *Liver* 2001; **21**: 384-390

26 **Zhang XL,** Liu L, Jiang HQ. Salvia miltiorrhiza monomer IH 764-3 induces hepatic stellate cell apoptosis via caspase-3 activation. *World J Gastroenterol* 2002; **8**: 515-519

27 **Ren de C**, Du GH, Zhang JT. Inhibitory effect of the water-soluble extract of salvia miltiorrhiza on neutrophil-endothelial adhesion. *Jpn J Pharmacol* 2002; **90**: 276-280

Edited by Su Q and Wang XL

P.O.Box 2345, Beijing 100023,China
Fax: +86-10-85381893
E-mail: wjg@wjgnet.com www.wjgnet.com

World J Gastroenterol 2003;9(9):2045-2049
World Journal of Gastroenterology
 ISSN 1007-9327

• BASIC RESEARCH •

Effects of low-calorie diet on steatohepatitis in rats with obesity and hyperlipidemia

Jian-Gao Fan, Lan Zhong, Zheng-Jie Xu, Li-Yan Tia, Xiao-Dong Ding, Min-Sheng Li, Guo-Liang Wang

Jian-Gao Fan, Lan Zhong, Zheng-Jie Xu, Li-Yan Tia, Xiao-Dong Ding, Guo-Liang Wang, Department of Gastroenterology, Shanghai First People' s Hospital, Jiaotong University, Shanghai 200080, China
Min-Sheng Li, Department of Pathology, Medical School, Fudan University, Shanghai 200032, China
Supported by the National Natural Science Fundation of China, No: 3980051; Shanghai Youth Scientic and Technological Moring Star Plan, No: 2000QB14010
Correspondence to: Jian-Gao Fan, Department of Gastroenterology, Shanghai, First People' s Hospital, Shanghai 200080, China. fanjg@citiz.net
Telephone: +86-21-63240090 **Fax:** +86-21-63240825
Received: 2003-03-10 **Accepted:** 2003-04-19

Abstract

AIM: To evaluate the effects of low calorie diet (LCD) on nonalcoholic steatohepatitis (NASH) in rats with obesity and hyperlipidemia.

METHODS: 29 Sprague-Dawley (SD) rats were randomly divided into three groups. The animals in control (*n*=9) and NASH group (*n*=10) were fed on standard rat diet and high fat diet respectively for 12 weeks, ten rats in LCD group were fed on high fat diet for 10 weeks and then low calorie diet for 2 weeks. At the end of the experiment, body weight, abdominal adipose content, liver function, and hepatopathological changes were examined to evaluate the effect of different feeding protocols on the experimental animals.

RESULTS: There was no death of animal in the experimental period. All rats in the NASH group developed steatohepatitis according to liver histological findings. Compared with the control group, body weight (423.5±65.2 *vs* 351.1±43.0 g, *P*<0.05), abdominal adipose content (14.25±1.86 *vs* 9.54±1.43, *P*<0.05), liver index (3.784±0.533 *vs* 2.957±0.301 %, *P*<0.01), total serum cholesterol (1.60±0.41 *vs* 1.27±0.17 mmol/L,*P*<0.05) and free fatty acids (728.2±178.5 *vs* 429.2±96.7 mmol/L, *P*<0.01), serum alanine aminotransferase (1 257.51±671.34 *vs* 671.34±118.57 nkat/L, *P*<0.05) and aspartic aminotransferse (2 760.51±998.66 *vs* 1 648.29±414.16 nkat/L, *P*<0.01) were significantly increased in the NASH group. Whereas, when rats were fed on LCD protocol, their body weight (329.5±38.4 g, *P*<0.01), abdominal adipose content (310.21±1.52 g, *P*<0.05), liver index (3.199±0.552 %, *P*<0.05), and serum alanine aminotransferase (683.03±245.49 nkat/L, *P*<0.05) were significantly decreased, and the degree of hepatic steatosis (*P*<0.05) was markedly improved compared with those in the NASH group. However, no significant difference was found in serum lipid variables and hepatic inflammatory changes between the two groups.

CONCLUSION: LCD might play a role in the prevention and treatment of obesity and hepatic steatosis in SD rats, but it exerts no significant effects on both serum lipid disorders and hepatic inflammatory changes.

Fan JG, Zhong L, Xu ZJ, Tia LY, Ding XD, Li MS, Wang GL. Effects of low-calorie diet on steatohepatitis in rats with obesity and hyperlipidemia. *World J Gastroenterol* 2003; 9(9): 2045-2049 http://www.wjgnet.com/1007-9327/9/2045.asp

INTRODUCTION

Non-alcoholic steatohepatitis (NASH) is a hepatic disorder with the histopathological features of alcohol-induced liver disease that occurs in individuals who do not consume a large amount of alcohol. In recent years it has been believed to be a progressive liver disease that can lead to cirrhosis and even hepatocellular carcinoma. Unfortunately, up to the present its pathogenesis remains unknown. An empirical management of this disease in clinical practice, in which weight is reducted by a low-calorie diet (LCD), has been recommended to treat those patient with overweight and obesity. However, inappropriate caloric restrictions would lead to metabolic disorder, even promote hepatic portal inflammation, fibrosis, bile stasis and focal necrosis[1-8]. In the present study, we established a rat model of NASH with overwight/obesity and hyperlipidemia by chronically feeding high-fat diet to evaluate the protective effects of LCD on the metabolic changes of this disease to provide experimental evidence for the NASH treatment strategy.

MATERIALS AND METHODS

Animals

Male Spraque-Dawley rats weighing 140-160 g obtained from Shanghai Experimental Animal Center (Shanghai, China) were used in the present study. The rats were housed in plastic cages with a wire-mesh to isolate them from a hygienic bed and exposed to a 12-hour controlled light cycle. The rats were given free access to food and water under controlled humidity (55 %) and temperature (23+/-1 ℃). All protocols for animal experimentation and maintenance were approved by the Animal Ethics Committee in our university and conformed to the highest international standards of humane care.

Reagents

Cholesterol was from Huamei Company (Shanghai, China). Lard oil was prepared in our laboratory. Alanine aminotransferase (ALT) and aspartic aminotransferase (AST) assay kits were purchased from Sheneng Company (Shanghai). Free fatty acid (FFA), triglycerides (TG) and total cholesterol (TCH) assay kits were obtained from Zhicheng Company (Shanghai). Albumin (A) and total protein (TP) assay kits were provided by Shanghai Institution of Bio-products. Rabbit polyclonal anti-human lysozyme antibody was from Shanghai Biogenex Company. Mouse anti-human α-smooth muscle actin (α-SMA) was from Dako Company (Carpinteria, CA, USA). The second antibody for immunochemistry assay was from American Antibody Company (Greenwich, USA).

Experimental protocol

After fed on standard rat diet for one week, Spraque-Dawley rats were randomly divided into three groups. Animals in the control (*n*=9) and NASH group (*n*=10) were fed on standard

rat diet and high fat diet (a standard diet supplemented with 10 % lard oil and 2 % cholesterol) respectively for 12 weeks, while the rats in the LCD group (n=10) were fed on high fat diet for 10 weeks and then on low-calorie diet (70 kcal/kg/day accounting for 1/3 of the daily needs of a healthy rat) for 2 weeks. One rat of NASH group was harvested at week 10 for the demonstration of hepatopathological changes. The animals were weighed before experiment and one day prior to sacrifice. Blood samples were obtained by aorta abdominalis puncture at the time of sacrifice, and the resulting serum was stored at -20 ℃ until analysis. Meanwhile, liver samples were rapidly excised, weighed and frozen at -70 ℃, or fixed in 4 % buffered formaldehyde solution until use.

Blood biochemical analyses

Serum biochemical parameters such as ALT, AST, A, TP, TG, TCH and FFA were automatically analyzed with a multifunctional biochemistry analyzer Olympus AU1000.

Histopathological examination

Hepatic sections were prepared and stained with hematoxylin and eosin (H&E) for routine histopathological examination. Some sections were stained with VG carbazotic acid for detection of fibrosis. Ultromicrotomy was performed for transmission electron microscopy (JEM-1200EX, Japan). Hepatocytes involved in lobular fatty infiltration were counted in H&E stained sections. The severity of steatosis was graded on the basis of the extent of parenchyma involved. Grade 1 (+): <33 % of hepatocytes were involved. Grade 2(++): 33 % to 66 % of hepatocytes were involved. Grade 3(+++): >66 % of hepatocytes were involved. Normal(-): no hepatocytes were involved[4,9]. Knodell histological activity index (HAI) and modified HAI by Tailin Wang were used to determine hepatic necroinflammatory activity[9-11] scored by the severity of portal inflammation (P), intralobular inflammation(L), piecemeal necrosis (PN) and bridging necrosis (BN). The score from 1 to 4 was in accordance with the severity of lesions and the total score was calculated as P+L+2 (PN+BN). The number of Kupffer's cells and activated hepatic stellate cells was determined by immunohistochemistry using lysozyme and α-SMA antibody respectively. All samples were evaluated blindly by the same pathologist and confirmed by the other researcher.

Statistics

Data were expressed as mean ± SD unless otherwise specified. The Student t test was used to test individual differences. Rank samples were analyzed by Rank-sum test. Rate comparison was analyzed by u test. A value of P<0.05 was considered to be statistically significant.

RESULTS

General information

During the experimental period, the body weight of the rats fed on high-fat diet increased quickly. By the end of the 10th week, the body weight of high-fat fed rats was significantly increased compared with the controls. At the same time,we randomly harvested one of the high-fat fed rats for hepatopathological examination, which showed liver steatosis with mild intralobular inflammation. Biochemical analysis indicated that serum TCH, FFA, ALT, AST levels in this rat were higher than normal. However, rats in LCD group fed on low-calorie diet were fretful and inflammable, their bellicose and body weight stopped increasing.No animal died during the experimental period.

Body and liver weight changes

At the end of the experiment, the body weight of animals in the NASH group was 20 % higher than that in the control group (t=2.281, P<0.05). The liver index (liver weight/body weight ×100 %) and the abdominal adipose content in this group were also significantly increased compared with the controls (t=4.097 and 2.891, P<0.01and 0.05 respectively). Compared with the NASH group, the body weight,liver index and abdominal adipose content in the LCD group decreased significantly (t=3.928, 2.411, 2.632. P<0.01, 0.05, 0.05 respectively) (Table 1).

Table 1 Changes of body weight and liver index

Groups	n	Body weight/g	Liver index 100 %	Abdominal adipose/g
Control	9	351.1±43.0	2.957±0.301	9.54±1.43
NASH	10	423.5±65.2[a]	3.784±0.533[b]	14.25±1.86[a]
LCD	10	329.5±38.4[c]	3.199±0.552[d]	10.21±1.52[d]

[a]P<0.05, [b]P<0.01 *vs* control. [c]P<0.01, [d]P<0.05 *vs* NASH group.

Changes of serum lipids and glucose

At the end of the experiment, serum TCH and FFA in the NASH group were significantly higher than those in the controls (t=2.242 and 4.462; P<0.05 and 0.01 respectively), whereas serum TG level remained unchanged. Compared with the NASH group, serum TCH level in the LCD group was significantly increased (t=2.152, P<0.05) and FFA level was only slightly increased (P>0.05), whereas TG level was significantly decreased (t=4.435, P<0.001), even signicantly less than that in the control group (P<0.001), with a trend of decreased blood glucose (Table 2).

Table 2 Changes of major plasma lipid parameters

Groups	n	TG mmol/L	TCH mmol/L	FFA mmol/L
Control	9	0.63±0.22	1.27±0.17	429.2±96.7
NASH	10	0.62±0.10	1.60±0.41[a]	728.2±178.5[b]
LCD	10	0.39±0.13[c]	2.04±0.50[d]	771.3±124.4

[a]P<0.05, [b]P<0.01 *vs* control. [c]P<0.001, [d]P<0.05 *vs* NASH group.

Liver function

At the end of 12 weeks, serum ALT and AST levels were significantly increased in the NASH group compared with those in the controls (t=2.576 and 3.103, P<0.05 and 0.01 respectively). Compared with the NASH group, serum ALT level in LCD group was significantly decreased (t=2.541, P<0.05), whereas serum AST level only displayed a decreasing trend in plasma (P>0.05). There were no significant differences in plasma albumin levels and albumin-globulin ratio among these groups of rats (Table 3).

Table 3 Alternations of some biochemical variables in rat liver function

Groups	n	ALT nkat/L	AST nkat/L	A g/L	A/G
Control	9	671.34±118.57	1648.29±414.16	25.13±4.61	0.71±0.11
NASH	10	1257.51±671.34[a]	2760.51±998.66[b]	27.40±2.04	0.73±0.08
LCD	10	683.03±245.49[c]	2344.68±539.41	24.51±4.69	0.71±0.16

[a]P<0.05, [b]P<0.01 *vs* control. [c]P<0.05 *vs* NASH group.

Hepatopathological manifestations

At the end of the experiments, no specific findings were observed during the hepatohistological examination in the

controls. Under light microscope, sections stained with H&E in the NASH group showed moderate to severe macrovesicular steatosis which was diffusely distributed throughout the liver lobule, and parenchymal inflammation with both acute and chronic inflammatory cells accompanying focal necrosis. In 80 % of the samples, mild portal inflammation was noted, compared with lobular inflammation, and 20 % samples were accompanied by piecemeal necrosis. The score of HAI was significantly higher than that in the controls (3.4±2.1 *vs* 0.8±0.8, t=3.461, P<0.01) (Figures 1, 2). No obvious liver fibrosis was found in VG carbazotic acid stained sections. Immunohistochemical analysis showed that lysozyme and α-SMA positively stained cells in the NASH group were significantly increased compared with the controls.

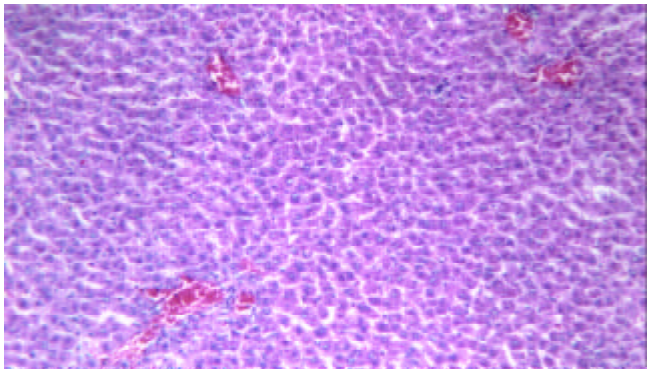

Figure 1 Light microscopy for control liver tissue, normal liver histology. H&E×100.

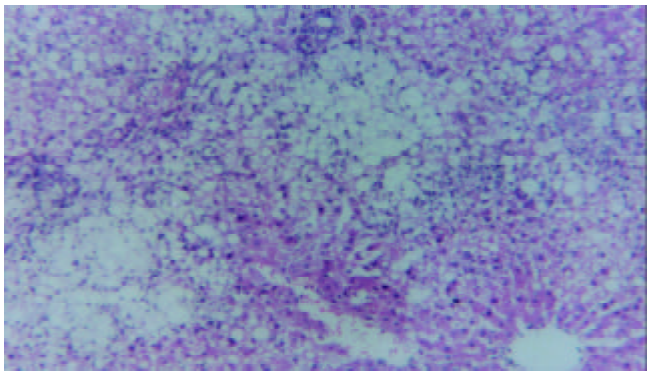

Figure 2 Light microscopy for liver tissue from a 12-week treated rat in NASH group, severe macrovesicular steatosis with mixed parenchymal inflammation and spotty focal necrosis. H&E×100.

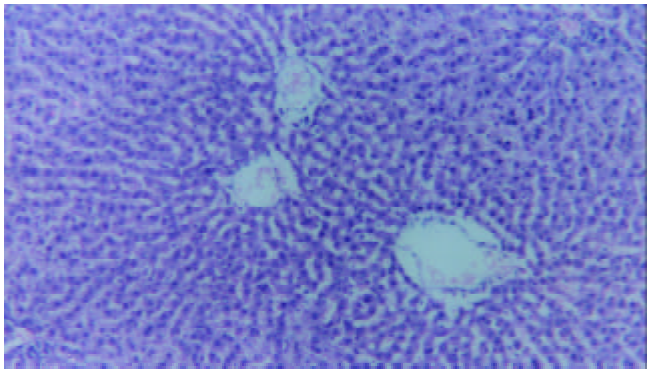

Figure 3 Light microscopy for liver tissue from a rat treated with LCD during 12-week experiment, the pathological changes of liver were obviously improved compared with the NASH group. H&E×100.

Compared with the NASH group, the liver steatosis in the LCD group was significantly reduced (P<0.05) (Figure 3, Table 4). However the score of HAI only had a trend of decrease (2.5±1.0 *vs* 3.4±2.1, P>0.05). There were no differences in the number of positive cells stained by lysozyme and α-SMA and liver fibrosis on VG stained sections between LCD and NASH groups. The liver histological findings were almost normalized in 1 sample of the LCD group.

Table 4 Severity of hepatic steatosis in rats of different groups

Groups	*n*	-	+	++	+++
Control	9	9			
NASH	10		3	6	1
LCD	10	3	5	2	

Rank sum test: P<0.05.

DISCUSSION

Non-alcoholic steatohepatitis (NASH) can be defined pathologically as severe steatohepatitis that is not resulted from alcohol,drug or any other singly identifiable causes. NASH is becoming a common liver disease and probably has a similar risk of progression to cirrhosis as chronic hepatitis C. No treatment has been yet proven to be efficient. Those who are overweight and suffer from NASH should be considered to employ a weight reduction program. Diet is an important component of weight-reduction regimen[1-8]. However, no controlled studies are available as for the value of diet in the management of NASH, further researches are needed to evaluate the effect of diet modalities on NASH either by clinical trial or by animal experiment[1,2,5,12].

In a recent study, liver tests and fatty infiltration were significantly improved in 15 obese patients with NASH treated with a restricted diet (25 kcal/kg· day) plus exercise for months. Improvement in the degree of inflammation and fibrosis was also achieved in some patients[13]. However, in another report, five obese patients stopped eating for some time and lost 14-30 kg within 1 month. Hepatic fat content decreased in three of them, but fibrosis became more prominent in four out of the five patients[14]. In addition, in another series, 41 morbidly obese patients with NASH had a median weight loss of 34 kg during the treatment with a very low calorie formula diet (388 kcal/day). The liver fat infiltration was also significantly improved. However, a fifth of the patients, particularly those had more pronounced reduction of liver fat and faster weight loss, developed mild portal inflammation or fibrosis[15]. It is well known that rapid weight reduction would lead to excessive fat catabolism, and marked elevation of FFA and lack of essential amino acids in serum and liver, which might finally induce or aggravate steatohepatitis and liver fibrosis[16-20].So, the adequate rate and degree of weight reduction remain to be established. Further studies are necessary to determine the appropriate caloric restrictions and the formula for obese patients with NASH[21-23].

No ideal animal model has yet been established for NASH research[24-31]. We have therefore established a model of this disease in rats by continuous feeding on a diet rich in fat and cholesterol for 12 weeks[17-19]. These animals were overweight and showed abnormal increase of abdominal fat (standing for trunk obesity), as well as markedly elevated levels of serum TCH, FFA and aminotransferase. Moderate to severe steatosis combined with intralobular inflammation and spotty necrosis was found in their hepatopathological examinations. Although fibrosis was absent on VG staining, we found that hepatic stellate cells and Kupffer cells were activated and proliferated,

suggesting that liver fibrosis might be inevitable[32,33]. Our subsequent research also demonstrated that feeding on a high fat diet for 24 weeks could induce steatohepatitis with liver fibrosis[34,35]. This animal model was easily established with low mortality (0 %) and high reproductive rate (100 %). Furthermore, this model was similar to that of the human disease, suggesting that this rat model is suitable for investigating the pathogenesis and prevention and treatment of NASH[30,33]. However, our model has some shortcomings. Firstly, the hepatopathological changes in this rat model were not entirely consistent with those in patients with NASH. Specifically, zone 3 involvement was not dominant. Moreover, no Mallory Hyaline bodies were found in sections stained by H&E. Secondly, NASH is often associated with hypertriglyceridemia which was not observed in this model.

The weight reduction diets recommended for NASH with obesity are slimming, low-calorie diet (LCD) and very-low calorie diet (VLCD). Slimming diets involve caloric intake of 1 200-1 800 kcal per day for adults, which is slightly less than that of normal diet, while LCD involves an intake of 600-1 200 kcal per day for adults and VLCD involves a caloric intake of 200-600 kcal per day[5,8,36]. Patients with moderate or severe obesity are usually put on LCD for weight reduction. In contrast, VLCD is seldom used clinically because of severe complications[5,8,36,37]. In our study, we took a caloric intake protocal for the animal model that belongs to LCD according to caloric calculation (70 kcal/kg· day *vs* 210 kcal/kg· day for rats).

While the rats fed on a high fat diet for 10 weeks were overweight and developed hyperlipidemia and fatty liver, a subsequent 2 weeks on LCD made both of their overweight and hyperlipidemia alleviated. In contrast,an additional two weeks on the high fat diet led to the development of more severe obesity,hyperlipidemia and steatohepatitis. These findings suggest that altering a high fat or high calorie diet to LCD may have markedly positive effects on obesity, hyperlipidemia and combined fatty liver, while continuation on the fat-rich diet may lead to the development of steatohepatitis. Since the rats in our LCD group developed hypercholesterolemia and hypoglyceridemia with a trend to increase serum FFA. Some of their liver samples were still found to have hepatocyte necrosis and inflammatory cell infiltration, indicating that LCD therapy for 2 weeks may be not quite enough to reverse steatohepatitis.

In summary, this study indicates that it might be difficult to resolve steatohepatitis by merely short-term LCD therapy, long-term appropriate diet control or concurrent administration of medications that can directly reduce the severity of liver damage may be reasonable alternatives for the treatment of NASH patients with obesity[2,3,5,23,24].

REFERENCES

1 Nonalcoholic steatohepatitis clinical research network. *Hepatology* 2003; **37:** 244

2 American Gastroenterological Association medical position statement: Nonalcoholic fatty liver disease. *Gastroenterology* 2002; **123:** 1702-1704

3 **Sanyal AJ.** AGA technical review on nonalcoholic fatty liver disease. *Gastroenterology* 2002; **123:** 1705-1725

4 **Angulo P.** Nonalcoholic fatty liver diseaes. *N Engl J Med* 2002; **346:** 1221-1231

5 **Angulo P,** Lindor KD. Treatment of nonalcoholic fatty liver: present and emerging therapies. *Semin Liver Dis* 2001; **21:** 81-88

6 **Fan JG,** Zeng MD. Classification and diagnostic strategies of non-alcoholic fatty liver diseases. *Zhonghua Ganzangbing Zazhi* 2003; **11:** 127-128

7 **Fan JG.** Steatohepatitis studies in China. *Shijie Huaren Xiaohua Zazhi* 2001; **9:** 6-10

8 **Shen L,** Fan JG, Shao Y, Zeng MD, Wang JR, Luo GH, Li JQ, Chen SY. Prevalence of nonalcoholic fatty liver among administrative officers in Shanghai:an epidemiological survey. *World J Gastroenterol* 2003; **9:** 1106-1110

9 **Brunt EM,** Janney CG, Di Bisceglie AM, Neuschwander-Tetri BA, Bacon BR. Nonalcoholic steatohepatitis:a proposal for grading and staging the histological lesions. *Am J Gastroenterol* 1999; **94:** 2467-2474

10 **Sonsuz A,** Basaranoglu M, Ozbay G. Relationship between aminotransferase levels and histopathological findings in patients with nonalcoholic steatohepatitis. *Am J Gastroenterol* 2000; **95:** 1370-1371

11 **Knodell RG,** Ishak KG, Black WC, Chen TS, Craig R, Kaplowitz N, Kiernan TW, Wollman J. Formulation and application of a numerical scoring system for assessing histological activity in asymptomatic chronic active hepatitis. *Hepatology* 1981; **1:** 431-435

12 **Eriksson S,** Eriksson KF, Bondesson L. Nonalcoholic steatohepatitis in obesity:a reversible condition.Acta Med Scand 1986; **220:** 83-88

13 **Vajro P,** Fontanella A, Perna C, Orso G, Tedesco M, De Vincenzo A. Persistent hyperaminotransferasemia resolving after weight reduction in obese children. *J Pediatr* 1994; **125:** 239-241

14 **Rozental P,** Biava C, Spencer H, Zimmerman HJ. Liver morphology and function tests in obesity and during total starvation. *Am J Dig Dis* 1967; **12:** 198-208

15 **Andersen T,** Gluud C, Franzmann MB, Christoffersen P. Hepatic effects of dietary weight loss in morbidly obese subjects. *J Hepatol* 1991; **12:** 224-229

16 **Capron JP,** Delamarre J, Dupas JL, Braillon A, Degott C, Quenum C. Fasting in obesity: another cause of liver injury with alcoholic hyaline?*Dig Dis Sci* 1982; **27:** 265-268

17 **Drenick EJ,** Simmons F, Murphy JF. Effect on hepatic morphology of treatment of obesity by fasting,reducing diets,and small bowel bypass. *N Engl J Med* 1970; **282:** 829-834

18 **Biourge V,** Groff JM, Fisher C, Bee D, Morris JG, Rogers QR. Nitrogen balance,plasma free amino acid concentrations and urinary orotic acid excretion during long-term fasting in cats. *J Nutr* 1994; **124:** 1094-1103

19 **Lu LG,** Zeng MD, Li JQ, Hua J, Fan JG, Fan ZP, Qiu DK. Effect of lipid on proliferation and activation of rat hepatic stellate cells (I). *World J Gastroenterol* 1998; **4:** 497-499

20 **Lu LG,** Zeng MD, Li JQ, Hua J, Fan JG, Qiu DK. Study on the role of free fatty acids in proliferation of rat hepatic stellate cells (II). *World J Gastroenterol* 1998; **4:** 500-502

21 **Fan JG,** Shao Y, Hong J. Effects of transfer growth factor beta, tumor necrosis factor alpha and neutral lipids on biological behaviors of L-02 cell lines. *Zhonghua Ganzangbing Zazhi* 2002; **10:** 388

22 **Fan J,** Zhong L, Wang G, Tian L, Wu W, Li M. Influence of ursodeoxycholic acid on the therapeutic effects of low-calorie diet in obesity and hyperlipidemia rats with steatohepatitis. *Zhonghua Ganzangbing Zazhi* 2002; **10:** 43-45

23 **Fang JW,** Fan JG. Current therapy strategies for nonalcoholic fatty liver disease. *Zhonghua Ganzangbing Zazhi* 2003; **11:** 120-122

24 **Fan JG.** Therapeutic strategies for nonalcoholic fatty liver disease. *Zhonghua Ganzangbing Zazhi* 2003; **11:** 111

25 **Koteish A,** Diehl AM. Animal models of steatosis. *Semin Liver Dis* 2001; **21:** 89-104

26 **Weltman MD,** Farrell GC, Liddle C. Increased hepatocyte CYP2E1 expression in a rat nutritional model of hepatic steatosis with inflammation. *Gastroenterology* 1996; **111:** 1645-1653

27 **Yang SQ,** Lin HZ, Lane MD, Clemens M, Diehl AM. Obesity increases sensitivity to endotoxin liver injury:implications for the pathogenesis of steatohepatitis. *Proc Natl Acad Sci U S A* 1997; **94:** 2557-2562

28 **Fan JG,** Chen LH, Xu ZJ, Zeng MD. Overexpression of hepatic plasminogen activator inhibitor type 1 mRNA in rabbits with fatty liver. *World J Gastroenterol* 2001; **7:** 710-712

29 **Fan J,** Chen L, Zeng M, Xu Z, Wang G, Wu X. Effects of pravastatin on hepatic plasminogen activator inhibitor 1 mRNA expression in rabbits with fatty liver. *Chung Hua Kan Tsang Ping Tsa Chih* 2000; **8:** 70-72

30 **Fan J,** Zeng M, Li J. Correlation between hepatic fat, lipid

peroxidation and hepatic fibrosis in rats chronically fed with ethanol and/or high fat diet. *Zhonghua Neike Zazhi* 1997; **36:** 808-811

31 **Wu J,** Norton PA. Animal models of liver fibrosis. *Scand J Gastroenterol* 1996; **31:** 1137-1143

32 **Fan J,** Xu M. Relationship between fatty liver and atherosclerosis, and coronary atherosclerotic heart disease. *Zhonghua Ganzangbing Zazhi* 2002; **10:** 150-151

33 **Fan J,** Zhong L, Wang G, Wu X, Li M, Jing D, Zhang P. The role of Kupffer cells in non-alcoholic steatohepatitis of rats chronically fed with high-fat diet. *Zhonghua Ganzangbing Zazhi* 2001; **9:** 16-18

34 **Xu ZJ,** Fan JG, Wang GL, Ding XD, Tian LY, Zheng XY. Rat model of nonalcoholic steatohepatitis with fibrosis by a fat-rich diet. *Shijie Huaren Xiaohua Zazhi* 2002; **10:** 392-396

35 **Fan JG,** Xu ZJ, Wang GL, Ding XD, Tian LY, Zheng XY. Change of serum endotoxin level in the progress of nonalcoholic steatohepatitis in rats. *Zhonghua Ganzangbing Zazhi* 2003; **11:** 73-76

36 **Biourge VC,** Groff JM, Munn RJ, Kirk CA, Nyland TG, Madeiros VA, Morris JG, Rogers QR. Experimental induction of hepatic lipidosis in cats. *Am J Vet Res* 1994; **55:** 1291-1302

37 **Biourge VC,** Massat B, Groff JM, Morris JG, Rogers QR. Effects of protein, lipid, or carbohydrate supplementation on hepatic lipid accumulation during rapid weight loss in obese cats. *Am J Vet Res* 1994; **55:** 1406-1415

Edited by Zhu L and Wang XL

P.O.Box 2345, Beijing 100023,China
Fax: +86-10-85381893
E-mail: wjg@wjgnet.com www.wjgnet.com

World J Gastroenterol 2003;9(9):2050-2053
World Journal of Gastroenterology
 ISSN 1007-9327

• BASIC RESEARCH •

Kangxian ruangan keli inhibits hepatic stellate cell proliferation mediated by PDGF

Ling Yang, Chi-Zhi Zhang, Qing-Jing Zhu

Ling Yang, Department of Traditional Chinese Medicine, Union Hospital, Tongji Medical college, Huazhong University of Science and Technology, Wuhan 430022, Hubei Province, China
Chi-Zhi Zhang, Qing-Jing Zhu, Institute of Liver Diseases, Affiliated Hospital of Hubei College of Traditional Chinese Medicine, Wuhan 430061, Hubei Province, China
Supported by the Natural Science Foundation of Hubei Province, No. 2000J042, and the Science Research Foundation of the Education Office of Hubei Province, No. 2000A06010
Correspondence to: Dr. Ling Yang, Department of Traditional Chinese Medicine, Union Hospital, Tongji Medical college, Huazhong University of Science and Technology, Wuhan 430022, Hubei Province, China. hepayang@163.com
Telephone: +86-27-85726395
Received: 2002-10-04 **Accepted:** 2003-03-12

Abstract

AIM: To investigate the effect of Kangxian ruangan keli (KXR) on hepatic stellate cell (HSC) proliferation mediated by platelet-derived growth factor (PDGF) and the underlying mechanism.

METHODS: In a serum-free culture system, HSCs were treated with a KXR preparation for 24 hours, followed by stimulation with PDGF-BB for 24 hours. Then the cells were incubated again in the medium containing KXR for 3 hours stimulated with PDGF-BB for 5 minutes, and collected. The proliferation of HSC was examined using an MTT assay and flow cytometry. Tyrosine phosphorylation was detected with Western blotting and visualized by the enhenced chemiluminescent (ECL) method.

RESULTS: The OD values for the HSCs growing in the media without and with addition of PDGF were 0.17±0.06 and 0.82±0.05, respectively. The PDGF-induced increase was hindered remarkably by KXR preparation in a dose-dependent manner. The reaction values for the systems with 5 mg/mL, 2.5 mg/mL and 1.25 mg/mL of KXR were 0.28±0.03, 0.37±0.02 and 0.43±0.04, respectively. Moreover, the percentages of S-phase cells in these KXR-containing culture systems were 10.95±1.35, 32.76±1.07 and 43.19±1.09, respectively, all of which were significantly lower than that in the culture free of KXR (68.24±2.72). In addition, the values for tyrosine-phosphorylated protein in HSCs treated with 5 mg/mL and 1.25 mg/mL of KXR were 0.1349±0.0072 and 0.1658±0.0025, respectively, which were smaller than that in the cells treated only with PDGF-BB (0.1813±0.0117).

CONCLUSION: Within the dose range used in the present study, KXR preparation shows an inhibitory effect on HSC proliferation induced by PDGF. The mechanism of this process may involve interference with tyrosine phosphorylation mediated by PDGF.

Yang L, Zhang CZ, Zhu QJ. Kangxian ruangan keli inhibits hepatic stellate cell proliferation mediated by PDGF. *World J Gastroenterol* 2003; 9(9): 2050-2053
http://www.wjgnet.com/1007-9327/9/2050.asp

INTRODUCTION

Hepatic fibrosis, a frequent pathologic change in a number of chronic liver diseases and an essential process during development of cirrhosis, is characterized by excessive proliferation of hepatic stellate cells (HSCs) and subsequent deposition of extracellular matrix (ECM)[1-6]. For this reason, HSC is regarded as one of the key cell types involved in progression of liver fibrosis, and is considered as a therapeutic target for treatment of hepatic fibrosis. Among several growth factors shown to be involved in the process, platelet-derived growth factor (PDGF) is the most potent mitogen for HSCs[7,8]. Hence, PDGF and its downstream target molecules or cell types may be potential targets for interventional therapies of hepatic fibrosis[9].

Kangxian ruangan keli (KXR) is an authorized granular herbal preparation, which has been used in the clinical fields for almost 30 years and is believed to be able to promote blood circulation, phlegm elimination and to soften and resolve hard mass based on traditional Chinese medicine. Our clinical and experimental data have demonstrated its effect on chronic liver diseases[10]. It may also be preventive to the fibrogensis induced by CCl_4 and inhibitory to HSC proliferation[11-14]. However, its mechanism is unknown. In this study, the effect of KXR on PDGF-mediated HSC proliferation was assessed *in vitro* using a serum-free culture system.

MATERIALS AND METHODS

Reagents

HSC-T6, a cell line from activated HSCs, was kindly provided by Prof. Liemin Xu in Institute of Liver Diseases, Shanghai University of Traditional Chinese Medicine. DMEM medium and fetal calf serum were purchased from Gibco (Life Technologies, Inc., Gaithersburg, MD, USA). PDGF-BB, propidium iodide and Fura-2/AM were purchased from Sigma (St. Louis, MO, USA). The antibody to phosphotyrosine was purchased from Santa Cruz Biotechnology Inc. (Santa Cruz, CA, USA). The SuperSignal West Pico chemiluminescent substrate was purchased from Pierce Chemicals (Rockford, IL, USA).

Cell culture

HSCs were grown in DMEM medium containing 100 mL/L fetal calf serum, 1×10^{-5} U/L penicillin, 100 mg/L streptomycin, 1 % L-glutamine and 0.1 mmol/L HEPES, and cultured at 37 ℃ in an incubator with 5 % CO_2. KXR consists of several berbs including *Radix Salviae Miltiorrhizae, Rhizoma Zedoariae, Sargassum, Carapax Trionycis*[15]. The granular preparation was made in the Affiliated Hospital of Hubei Collage of Traditional Chinese Medicine, containing 2 g of crude herbs in each gram KXR. The preparation was dissolved in DMEM medium, and sterilized by filtration through a 0.45 μm filter. Following preincubation in the serum-free medium for 24 hours, the cells were grown and incubated for 48 hours, separately in the following media: 1) Only serum-free DMEM medium as a control, 2) The serum-free medium containing 10 ng/mL PDGF-BB, 3) before the addition of PDGF-BB

(10 ng/mL), different amounts of KXR (1.25 mg/mL, 2.5 mg/mL and 5 mg/mL, separately) were extracted in the serum-free medium for 3 h.

Evaluation of cell growth

Cells were seeded in 96-well plates at a density of 1×10^8 cells/L. After treated as above, the cells were incubated with DMEM containing 1 mg/ml of 3-(4, 5-dimethylthiazol-2-yl)-2, 5-diphenyltetrazolium bromide (MTT) for 4 h at 37 ℃. The resulted precipitate was resolved by addition of dimethyl sulfoxide and incubation for 2 min. Cell growth was assessed using an enzyme-linked immunosorbent assay reader (Bio-Tek, Houston, USA) with the test wavelength at 570 nm and expressed as optical density (OD) values. The inhibition of HSC proliferation was expressed as inhibitory rate [(OD value of PDGF group - OD value of KXR group)/OD value of PDGF group]×100 %.

The cell proliferation was also described by the growth curves. HSCs were plated in 24-well dishes at a density of 1×10^5 cells/well in a complete culture medium. After 24 h (day 0), cells were washed twice with the serum-free medium and then divided and treated as described above. Cell counting was performed on triplicate wells on days 0, 2 and 4 following preparation of cell suspensions by digestion with trypsin. Fresh serum-free medium containing PDGF-BB (10 ng/ml) with or without KXR was added to the remaining wells on day 2.

The HSC proliferation kinetics was described by flow cytometry. The cells were plated in 10-cm dishes at a density of 1×10^8 cells/L in the complete culture medium. After treated as described above, cells were harvested by digestion with trypsin and washed twice with PBS. After overnight fixation with cold ethanol at 4 ℃, cells were washed twice with PBS and suspended in the buffer containing 30 μg/mL propidium iodide, 0.1 % Tritonx-100, 37 mg/mL EDTA and 0.1 % ribonuclease A. Samples were incubated in a dark chamber at room temperature for 30 minutes and stored at 4 ℃ before use. Cell fluorescence was measured by FACSCalibur flow cytometer (Becton Dickson, San Diego, CA,USA) and assessed by the Cellquest software.

Tyrosine phosphorylation assay

Subconfluent HSCs were cultured in a serum-free medium for 24 h, then in the medium with or without KXR for another 24 h. Following the culture with the presence of 10 ng/ml PDGF-BB for 24 h, cells were treated with KXR for 3 h, and incubated again in the medium containing 10 ng/ml PDGF-BB for 5 min. After washed with ice-cold PBS, the cell monolayers were harvested and suspended in a lysis buffer [1 % NP-40, 0.5 % sodium deoxycholate, 0.1 % sodium dodecyl sulfate (SDS), 150 mmol/L NaCl, 1 mmol/L ethyleneglycol-bis-(β-aminoethylether)-N, N, N', N'-tetraacetic acid, 1 mmol/L phenylmethylsulfonyl fluoride, 500 μg/mL leupepin, 1 mmol/L sodium orthovanadate, 50 mmol/L sodium fluorid, 10 mmol/L Tris-HCl, pH7.2[16]] for 30 min on ice. The lysates were clarified by centrifugation at 16 000 g for 10 min at 4 ℃, and protein concentrations were determined using Bradford' s method[16].

Proteins were electrophoresed on a 0.1 % SDS-7 % polyacrylamide gel using a Mini apparatus (Bio-Rad Laboratories, Hercules, CA, USA). The resolved proteins were transferred to a nitrocellulose filter by a transfer apparatus (Bio-Rad Laboratories, Hercules, CA,USA). After the blocking in a blocking buffer [5 % BSA,1 % hen egg albumin, 10 mmol/L Tris.Cl, pH7.4, 0.15 mol/L NaCl] for 60 min, the filter was incubated with a mouse monoclonal antibody to phosphotyrosine (1:1 000) for 120 min. Following the washing for 15 minutes respectively in a TN buffer (containing 10 mmol/L Tris pH7.4, 0.15 mol/L NaCl) and a TN buffer containing 0.05 % NP-40, the incubation was done with a peroxidase-conjugated goat antibody (1:2 000) against mouse IgG at room temperature for 60 min. The antigen-antibody complexes were visualized by an enhanced chemiluminescent (ECL) reaction[16]. The reaction intensities were assessed with an image analyzer (HPIAS-1000, Tongji Medical college Huazhong University of Science & Technology,Wuhan,China).

Statistical analysis

Results were expressed as mean ± standard deviation. Differences between groups were described by the Student *t* test. $P<0.05$ was considered significant.

RESULTS

Effect of KXR on PDGF-mediated HSC Proliferation

An inhibitory effect was observed by the MTT assay (Table 1) and cell counting (Figure 1) for KXR to PDGF-mediated HSC proliferation, which was in a dose-dependent manner. HSC growth response to PDGF stimulation with or without the presence of KXR was assessed by cell counting (Figure 1). PDGF-BB, with its concentration at 10 ng/mL, significantly increased HSC growth after 2 to 4 days of incubation, in comparison to the medium free of PDGF ($P<0.01$). This response was markedly inhibited by pretreatment with KXR ($P<0.01$), which was not associated with any detectable cytotoxic effects in the dose range used.

Table 1 Effects of KXR on PDGF-mediated HSC proliferation (mean ±s)

Groups	KXR concentration (mg/mL)	OD values	Inhibitory rate (%)
Control		0.17±0.06[b]	-
PDGF		0.82±0.05	0.00
KXR treatment before	5	0.28±0.03[b]	65.9
PDGF stimulation	2.5	0.37±0.02[b]	54.9
	1.25	0.43±0.04[b]	47.6

[b]$P<0.01$ *vs* PDGF group.

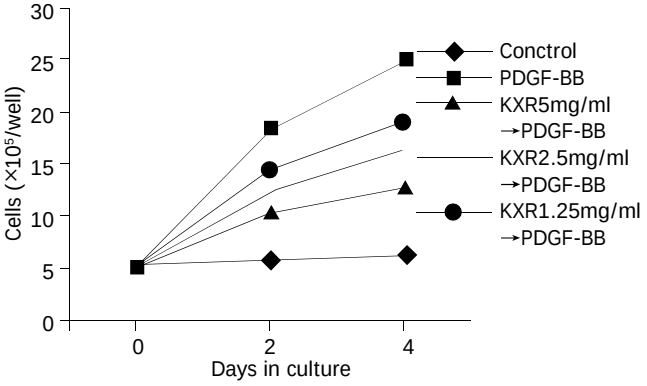

Figure 1 Effect of Kangxian Ruangan Granule on PDGF-induced cell proliferation in HSC-T6 cell line.

KXR affects cell cycle of HSC

Flow cytometry showed a reduction in G0/G1-phase cell fraction and an increase in the S-phase cell fraction for the HSCs exposed to PDGF. Pretreatment with KXR inhibited the PDGF-mediated response for the cells in S phase, the result was in agreement with the data obtained by MTT assay. However, the G0/G1-phase cell fraction was similar to that without KXR pretreatment (Table 2). It indicated that KXR treatment was inhibitory to the PDGF-induced progression of

the cell cycle beyond the G_1 phase. The effect seemed to be dose-dependent ($P<0.01$).

Table 2 Effect of KXR on cell cycle progression of HSCs mediated by PDGF (mean ±s)

Groups	*n*	HSC fractions at (%)		
		G_0-G_1 phase	S phase	G_2-M phase
Control	6	94.67±2.17	4.13±0.92	1.20±0.47
PDGF 10 ng/ml	6	20.18±1.12	68.24±2.72	11.18±1.93
KXR 5 mg/ml→PDGF	6	83.64±3.68[b]	10.95±1.35[b]	5.41±0.98[b]
KXR 2.5 mg/ml→PDGF	6	62.58±4.52[b]	32.76±1.07[b]	4.66±0.81[b]
KXR 1.25 mg/ml→PDGF	6	48.18±3.37[b]	43.19±1.09[b]	8.63±0.71[a]

[a]$P<0.05$, [b]$P<0.01$ *vs* PDGF group.

Effect of KXR on PDGF-induced tyrosine phosphorylation

As shown in Figure 2 and Table 3, treatment of KXR resulted in a reduction in the content of tyrosine-phosphorylated proteins, the result was in accordance with its effects on cell proliferation and kinetics.

Figure 2 Effect of KXR on the expression of tyrosine-phosphorylated proteins induced by PDGF (Western blot). Lanes 1 to 4 were loaded with HSC lysates from the control, PDGF groups, and the PDGF groups with pretreatment of KXR at 1.25 mg/mL and 5 mg/mL, respectively.

Table 3 Effect of KXR on the contents of tyrosine-phosphorylated proteins in HSCs stimulated by PDGF (mean ±s)

Groups	*n*	Intensities of tyrosine-phosphorylated proteins
Control	4	0.1199±0.0037
PDGF 10 mg/ml	4	0.1813±0.0117
KXR 1.25 mg/ml+PDGF	4	0.1658±0.0025[a]
KXR 5 mg/ml+PDGF	4	0.1349±0.0072[b]

[a]$P<0.05$, [b]$P<0.01$ *vs* PDGF group.

DISCUSSION

KXR is a granular herb preparation mainly composed of *Salviae Miltiorrhizae, Rhizoma Zedoariae, Sargassum* and *Carapax Trionycis*. It has been reported that *Salviae Miltiorrhizae* exhibits a series of important effects including anti-inflammation, anti-oxidation and retardation of HSC proliferation[17,18]. Its extract has been shown to induce HSC apoptosis[19,20]. The oil from *Rhizoma Zedoariae* was reported to be inhibitory to the proliferation of fibroblast cells and hepatocellular carcinoma cells[21,22]. It was pointed out that *Sargassum* could be helpful for the elimination of reactive oxygen species which were believed to be important factors in the progression of fibrosis[23]. Our previous clinical and experimental observations[10-14] have approved these effects using decoction preparation of KXR in patients with chronic hepatitis or cirrhosis and in rats with CCL_4-induced liver fibrosis.

HSCs are a key cell type during liver fibrogenesis. Its activation is characterized by the myofibroblast-like phenotypes including an elevated proliferation rate, expression of α-smooth muscle actin, synthesis and excretion of some extracellular matrix components[4,24]. Recently, the phenotypic transformation has been linked to some cytokines, including PDGF, and their intracellular signal transduction pathways[6,25-30].

Among many polypeptide growth factors potentially involved in chronic hepatitis, PDGF, a dimmer of two chains referred to as A-chain and B-chain, has been shown to be the most potent mitogen for cultured HSCs isolated from rat, mouse or human liver. Of the three possible dimeric forms, including AA, AB and BB, PDGF-BB has been shown to be most effective[1,6-8,30]. Tyrosine protein kinase plays an important role in the PDGF-mediated activation and proliferation of HSCs[32,33]. PDGF binds to the extracellular domain of its receptor, PDGF-Rβ, results in the receptor molecule autophosphorylation, which allows the docking of numerous signaling cascades, such as PI3-K, Raf-MEK-MAPK, Na^+/H^+ and Ca^{2+}, leading to cell division and chemotaxis[6,34-38]. In the current study, we showed that KXR blocked PDGF-stimulated mitogenesis and DNA synthesis, and inhibited PDGF-induced autophosphorylation of tyrosine. These results suggest KXR may have the effects as those of tyrosine phosphorylation inhibitors. Clearly, more data are needed to elucidate the effect of KXR on tyrosine phosphorylation and its underlying mechanism.

REFERENCES

1 **Friedman SL**. Cytokines and fibrogenesis. *Semin Liver Dis* 1999; **19**: 129-140
2 **Jiang HQ**, Zhang XL. Progress in the study of pathogenesis in hepatic fibrosis. *Shijie Huangren Xiaohua Zazhi* 2000; **8**: 687-689
3 **Wang JY**, Zhang QS, Guo JS, Hu MY. Effects of lycyrrhetinic acid on collagen metabolism of hepatic stellate cells at different stages of liver fibrosis in rats. *World J Gastroenterol* 2001; **7**: 115-119
4 **Reeves HL**, Friedman SL. Activation of hepatic stellate cells-a key issue in liver fibrosis. *Front Biosci* 2002; **7**: d808-d826
5 **Pinzani M**, Marra F, Carloni V. Signal transduction in hepatic stellate cells. *Liver* 1998; **18**: 2-13
6 **Marra F**, Gentilini A, Pinzani, M, Choudhury GG, Parola M, Herbst H, Dianzani MU, Laffi G, Abboud HE, Gentilini P. Phosphatidylinositol 3-kinase is required for platelet-derived growth factor's actions on hepatic stellate cells. *Gastroenterology* 1997; **112**: 1297-1306
7 **Kinnman N**, Goria O, Wendum D, Gendron MC, Rey C, Poupon R, Housset C. Hepatic stellate cell proliferation is an early platelet-derived growth factor-mediated cellular event in rat cholestatic liver injury. *Lab Invest* 2001; **81**: 1709-1716
8 **Iwamoto H**, Nakamuta M, Tada S, Sugimoto R, Enjoji M, Nawata H. Platelet-derived growth factor receptor tyrosine kinase inhibitor AG1295 attenuates rat hepatic stellate cell growth. *J Lab Clin Med* 2000; **135**: 406-412
9 **Bataller R,** Brenner DA. Hepatic stellate cells as a target for the treatment of liver fibrosis. *Semin Liver Dis* 2001; **21**: 437-451
10 **Zhang CZ**, Yan HM, Wang L. Effect of Kangxian Ruangan Chongji on 31 cases of liver cirrhosis. *Zhongxiyi Jiehe Ganbing Zazhi* 1999; **2**: 19-20
11 **Xiong YQ**, Yan HM, Zhang CZ. Experimental study of the Kangxian Ruangan granute on anti-hepatic fibrosis in rats. *Zhongguo Shiyan Fangjixue Zazhi* 2000; **6**: 28-30
12 **Yang L,** Zhu QJ, Zhang CZ. Serapharmlocogical effect of Kangxian Ruangan Chongji on expression of type I procollagen and transforming growth factor β_1 mRNA in hepatic stellate cells. *Zhongguo Zhongyi Jichu Yixue Zazhi* 2001; **8**: 38-40
13 **Yang L**, Cheng HQ, Zhu QJ, Zhang CZ. Effects of Kangxian Ruangan Granules on platelet-derived growth factor (PDGF) induced cell cycle and intercellular calium concentration of hepatic stellate cells. *Zhongxiyi Jiehe Ganbing Zazhi* 2002; **1**: 20-22
14 **Zhou Z**, Zhang CZ, Chen J, Zhou P. Serapharmlocogical effect

of Kangxian Ruangan Chongji on hepatic stellate cell proliferation. *Zhongyaocai* 2001; **24**: 809-810

15 **Feng H,** Zhang H, Tang D. Study on preparation and quality of Kangxian Ruangan Granule. *Zhongxiyi Jiehe Ganbing Zazhi* 2000; **4**: 31-32

16 **Ausubel F**. Short protocols in molecular biology. 1st ed. *Beijing: Science Publishing House* 1999: 687-693

17 **Liu CH,** Liu P, Hu YY, Xu LM, Tan YZ, Wang ZN, Liu C. Effects of salvianolic acid-A on rat hepatic stellate cell proliferation and collagen production in culture. *Acta Pharmacol Sin* 2000; **21**: 721-726

18 **Liu P**, Liu CH, Wang HN, Hu YY, Liu C. Effect of salvianolic acid B on collagen production and mitogen-activated protein kinase activity in rat hepatic stellate cells. *Acta Pharmacol Sin* 2002; **23**: 733-738

19 **Zhang XL**, Liu L, Jiang HQ. Salvia miltiorrhiza monomer IH764-3 induces hepatic stellate cell apoptosis via caspase-3 activation. *World J Gastroenterol* 2002; **8**: 515-519

20 **Yao XX,** Tang YW, Yao DM, Xiu HM. Effects of Yigan Decoction on proliferation and apoptosis of hepatic stellate cells. *World J Gastroenterol* 2002; **8**: 511-514

21 **Shi LC,** Wu WY, Zhang WB, Qu YQ, Tan M, Xiao CM. Effect of curcuma aramatica oil on proliferating cell nuclear antigen of hepatoma in mice. *Shijie Huangren Xiaohua Zazhi* 1999; **7**: 156-157

22 **Xin JJ**, Li GY, Cui KY. Effects of algae-selenium polysaccharide on immune function of mice. *Zhongguo Haiyang Yaowu* 1999; **3:** 36-38

23 **Zheng G**, Hao J, Jia GR, Zhong HM, Song YM. Effects of algin on preventing liver fibrosis in rat. *Zhongguo Haiyang Yaowu* 1997; **1**: 30-32

24 **Pinzani M**, Marra F. Cytokine receptors and signaling in hepatic stellate cells. *Semin Liver Dis* 2001; **21**: 397-416

25 **Iredale JP**. Hepatic stellate cell behavior during resolution of liver injury. *Semin Liver Dis* 2001; **21**: 427-436

26 **Shen H**, Huang GJ, Gong YW. Effect of transforming growth factor beta and bone morphogenetic proteins on rat hepatic stellate cell proliferation and trans-differentiation. *World J Gastroenterol* 2003; **9**: 784-787

27 **Huang GC**, Zhang JS. Signal transduction in activated hepatic stellate cells. *Shijie Huaren Xiaohua Zazhi* 2001; **9**: 1056-1060

28 **Britton RS**, Bacon BR. Intracellular signaling pathways in stellate cell activation. *Alcohol Clin Exp Res* 1999; **23**: 922-925

29 **Maeda N**, Kawada N, Seki S, Arakawa T, Ikeda K, Iwao H, Okuyama H, Hirabayashi J, Kasai K, Yoshizato K. Stimulation of proliferation of rat hepatic stellate cells by galectin-1 and galectin-3 through different intracellular signaling pathways. *J Biol Chem* 2003; **278**: 18938-18944

30 **Tahashi Y**, Matsuzaki K, Date M, Yoshida K, Furukawa F, Sugano Y, Matsushita M, Himeno Y, Inagaki Y, Inoue K. Differential regulation of TGF-beta signal in hepatic stellate cells between acute and chronic rat liver injury. *Hepatology* 2002; **35**: 49-61

31 **Pinzani M**. PDGF and signal transduction in hepatic stellate cells. *Front Biosci* 2002; **7**: d1720-d1726

32 **Liu XJ**, Yang L, Mao YQ, Wang Q, Huang MH, Wang YP, Wu HB. Effects of the tyrosine protein kinase inhibitor genistein on the proliferation, activation of cultured rat hepatic stellate cells. *World J Gastroenterol* 2002; **8**: 739-745

33 **Carloni V**, Pinzani M, Giusti S, Romanelli RG, Parola M, Bellomo G, Failli P, Hamilton AD, Sebti SM, Laffi G, Gentilini P. Tyrosine phosphorylation of focal adhesion kinase by PDGF is dependent on *ras* in human hepatic stellate cells. *Hepatology* 2000; **31**: 131-140

34 **Marra F**, Arrighi MC, Fazi M, Caligiuri A, Pinzani M, Romanelli RG, Efsen E, Laffi G, Gentilini P. Extracellular signal-regulated kinase activation differentially regulates platelet-derived growth factor's actions in hepatic stellate cells, and is induced by *in vivo* liver injury in the rat. *Hepatology* 1999; **30**: 951-958

35 **Carloni V,** Defranco RM, Caligiuri A, Gentilini A, Sciammetta SC, Baldi E, Lottini B, Gentilini P, Pinzani M. Cell adhesion regulates platelet-derived growth factor-induced MAP kinase and PI-3 kinase activation in stellate cells. *Hepatology* 2002; **36**: 582-591

36 **Reeves HL**,Thompson MG, Dack CL, Burt AD, Cay CP. The role of phosphatidic acid in platelet-derived growth factor–induced proliferation of rat hepatic stellate cells. *Hepatology* 2000; **31**: 95-100

37 **Di Sario A**, Bendia E, Svegliati Baroni G, Ridolfi F, Bolognini L, FeliciangeliG, Jezequel AM, Orlandi F, Benedetti A. Intracellular pathways mediating Na+/H+ exchange activation by platelet-derived growth factor in rat hepatic stellate cells. *Gastroenterology* 1999; **116**: 1155-1166

38 **Di Sario A**, Bendia E, Taffetani S, Marzioni M, Candelaresi C, Pigini P, Schindler U, Kleemann HW, Trozzi L, Macarri G, Benedetti A. Selective Na+/H+ exchange inhibition by cariporide reduces liver fibrosis in the rat. *Hepatology* 2003; **37**: 256-266

Edited by Su Q

P.O.Box 2345, Beijing 100023,China
Fax: +86-10-85381893
E-mail: wjg@wjgnet.com www.wjgnet.com

World J Gastroenterol 2003;9(9):2054-2059
World Journal of Gastroenterology
 ISSN 1007-9327

• BASIC RESEARCH •

Role of calcium-activated potassium currents in CNP-induced relaxation of gastric antral circular smooth muscle in guinea pigs

Hui-Shu Guo, Zheng-Xu Cai, Hai-Feng Zheng, Xiang-Lan Li, Yi-Feng Cui, Zuo-Yu Wang, Wen-Xie Xu, Sang-Jin Lee, Young-Chul Kim

Hui-Shu Guo, **Hai-Feng Zheng, Xiang-Lan Li, Yi-Feng Cui, Zuo-Yu Wang, Wen-Xie Xu,** Department of Physiology, College of Medicine, Yanbian University, Yanji 133000, Jilin Province, China
Wen-Xie Xu, Center of Experiment, Affiliated Hospital of College of Medicine, Yanbian University, Yanji 133000, Jilin Province, China
Zheng-Xu Cai, the First Clinical Hospital of Jilin University, Changchun 130000, Jilin Province, China
Sang-Jin Lee, Young-Chul Kim, Department of Physiology, College of Medicine, Chungbuk National University, Cheongju, Chungbuk, 361-763, Korea
Supported by the National Natural Science Foundation of China, No. 30160028
Correspondence to: Dr. Wen-Xie Xu, Department of Physiology, College of Medicine, Yanbian University, Juzi 121 Street, Yanji 133000, Jilin Province, China. wenxiexu@ybu.edu.cn
Telephone: +86-433-2660586 **Fax:** +86-433-2659795
Received: 2003-05-13 **Accepted:** 2003-06-27

Abstract

AIM: To investigate ion channel mechanism in CNP-induced relaxation of gastric circular smooth muscle in guinea pigs.

METHODS: Spontaneous contraction of gastric smooth muscle was recorded by a four -channel physiograph. The whole cell patch-clamp technique was used to record calcium-activated potassium currents and membrane potential in the gastric myocytes isolated by collagenase.

RESULTS: C-type natriuretic peptide (CNP) markedly inhibited the spontaneous contraction in a dose-dependent manner in gastric circular smooth muscle in guinea pigs. Ly83583, an inhibitor of guanylate cyclase, weakened CNP-induced inhibition on spontaneous contraction but Zaparinast, an inhibitor of cGMP sensitive phosphoesterase, potentiated CNP-induced inhibition in gastric circular smooth muscles. The inhibitory effects of CNP on spontaneous contraction were blocked by tetrathylammonium (TEA), a nonselective potassium channel blocker. CNP hyperpolarized membrane potential from -60.0 mV±2.0 mV to -68.3 mV±3.0 mV in a single gastric myocyte. CNP increased calcium-activated potassium currents ($I_{K(ca)}$) in a dose-dependent manner in gastric circular myocytes. CNP also increased the spontaneously transient outward currents (STOCs). Ly83583 partly blocked CNP-induced increase of calcium-activated potassium currents, but Zaparinast potented the effect.

CONCLUSION: CNP inhibits spontaneous contraction, and potassium channel may be involved in the process in gastric circular smooth muscle of guinea pigs. CNP-induced increase of $I_{K(ca)}$ is mediated by a cGMP dependent pathway.

Guo HS, Cai ZX, Zheng HF, Li XL, Cui YF, Wang ZY, Xu WX, Lee SJ, Kim YC. Role of calcium-activated potassium currents in CNP-induced relaxation of gastric antral circular smooth muscle in guinea pigs. *World J Gastroenterol* 2003; 9(9): 2054-2059
http://www.wjgnet.com/1007-9327/9/2054.asp

INTRODUCTION

Currently, there are six members in the natriuretic peptides (NP) family, including ANP, BNP, CNP, DNP, MNP and VNP. They are distributed in the whole body[1-4], and exhibit natriuresis-diuresis and vasorelaxation, keep electrolyte homeostasis and other qualities. In gastrointestinal tract, the studies mainly focused on absorption, secretion and intestinal motility[5-7]. Our previous study[8,9] indicated that natriuretic peptide receptor (NPR) was distributed in the gastric smooth muscle of rats, and NP inhibited gastric motility in rats, guinea pigs and humans.

There are different views about the mechanism of NP physiological function. Some scholars mentioned that NP did not exert physiological function by cGMP pathway. For example, Carvajal *et al*[10] indicated that natriuretic peptide-induced relaxation of pregnant myometrium was mediated by a novel mechanism, which was independent of GC-A or GC-B activation, cGMP generation, or clearance receptor activation. However, most scholars supported the views that NP exerted many physiological functions by cyclic guanosine monophosphate (cGMP) and that ion channel participated in the process. McCann *et al*[11] showed that ANP activated guanylyl cyclase that converted guanosine triphosphate (GTP) into cGMP. cGMP activated protein kinase G (PKG), which regulated Na+ channels to reduce heart rate and the force of contraction, thus decreasing cardiac output. Carini *et al*[12] demonstrated that ANP enhanced hepatocytic resistance to hypoxia by cGMP-PKC- Na+ channels pathway in rats. Kanwal *et al*[13] showed that NP regulated release of some neurotransmitters by activating L-type calcium channel in rats. Our previous study demonstrated that CNP significarntly inhibited spontaneous contraction of gastric smooth muscle, and the inhibitory effect was mediated by cGMP pathway in rats[9].

To investigate the ionic channel mechanism in CNP-induced relaxation of gastric circular smooth muscle in guinea pigs, the conventional whole cell patch clamp technique was used to record calcium-activated potassium currents, so that the relationship between $I_{K(ca)}$ and CNP-induced relaxationship could be cleared up.

MATERIALS AND METHODS

Preparation of muscle strips and documentation of contractive activity

EWG/B guinea pigs of either sex, weighing (300±50) g bred by Experimental Animal Center of Jilin University, were anaesthetised by a lethal dose of intravenous pentobarbital sodium (50 mg/kg). The abdomen of each rat was opened along the midline and the stomach was removed and placed in a pre-oxygenated Tyrode' s solution at room temperature. The mucous layer was removed. The strips (about 2.0 mm×15.0 mm) of gastric antral circular and longitudinal smooth muscle were prepared by cutting along the vertical direction of the longer axis of the stomach and along muscle strips were placed in a chamber. One end of the strip was fixed on the lid of the chamber through glass claws, the other end was attached to an

isometric force transducer (TD-112S, JAPAN) to record the contraction. The chamber (2 ml volume) was constantly perfused with pre-oxygenated Tyrode's solution at 1 ml/min. The temperature was maintained at (37.0±0.5) ℃ by a water bath thermostat (WC/09-05, Chongqing, China). The muscle strips were incubated for at least 40 minutes before experiments. The samples of human stomach were provided by the Affiliated Hospital of College of Medicine, Yanbian University, (As the gastric sample was limited, the gastric antral of humans was used).

Cell preparation and electrophysiologic recording

Guinea pigs of either sex, weighing 250-350 g, were anaesthetised by a lethal dose of intravenous pentobarbital sodium (50 mg/kg). The antral part of the stomach was rapidly cut, then the muscosal layer was separated from the muscle layers. The longitudinal layer of muscle was then dissected from the other muscle layers using fine scissors, and then cut into small segments (1 mm×4 mm). These segments were kept in the modified Kraft-Bruhe (K-B) medium at 4 ℃ for 15 minutes. Then, they were incubated at 36 ℃ in 4 ml of digestion medium [Ca-free physiologic salt solution (Ca-free PSS)] containing 0.1 % collagenase II, 0.1 % dithioerythreitol, 0.15 % trypsin inhibitor and 0.2 % bovine serum albumin for 25-35 minutes. The softened muscle segments were transferred into the modified K-B medium, and the single cells were dispersed by gentle trituration with a wide-bore fire-polished glass pipette. Then, isolated gastric myocytes were kept in a modified K-B medium at 4 ℃ until they were ready for use.

Isolated cells were transferred to a 0.1 mL chamber on the stage of an inverted microscope (IX-70 Olympus, Japan) and allowed to settle for 10-15 minutes. Then the cells were continuously perfused with an isosmotic physiologic salt solution at a rate of 0.9-1.0 ml/min. A 8-channel perfusion system (L/M-sps-8, List Electronics, Germany) was used to exchange the solution. The $I_{K(ca)}$ was recorded using the conventional whole cell patch-clamp technique. Patch-clamp pipettes were made from borosilicate glass capillaries (GC 150T-7.5, Clark Electromedical Instruments, UK) using a two-stage puller (PP-83, Narishige, Japan). The resistance of patch pipette was 3-5 MΩ, when it was filled with pipette solution. Liquid junction potentials were cancelled prior to the seal formation. The whole-cell current was recorded with an Axopatch 1-D patch-clamp amplifier (Axon Instrument, USA), and data were filtered at 1 KHz. Command pulses, data acquisition and storage were applied by using the IBM-compatible 486-grade computer and pCLAMP 6.02 software. Spontaneously transient outward currents (STOCs) were recorded simultaneously by EPC-10-HEAKA amplifier (HEAKA Instrument, GERMAN). All experiments were performed at room temperature (20-25 ℃).

Drugs and solutions

Tyrode solution containing (mmol· L^{-1}) NaCl 147, KCl 4, $MgCl_2$· $6H_2O$ 1.05, $CaCl_2$· $2H_2O$ 0.42, Na_2PO_4. $2H_2O$ 1.81, and 5.5 mM glucose was used. Ca^{2+}-free PSS containing (mmol/L) NaCl 134.8, KCl 4.5, glucose 5, and N-[2-hydroxyethyl] piperazine-N-[2-ethanesulphonic acid] (HEPES) 10 was adjusted to pH 7.4 with Tris [hydroxymethyl] aminomethane (TRIZMA). Modified K-B solution containing (mmol/L) L-glutamate 50, KCl 50, taurine 20, KH_2PO_4 20, $MgCl_2$· $6H_2O$ 3, glucose 10, HEPES 10 and egtazic acid 0.5 was adjusted to pH 7.40 with KOH. PSS containing (mmol/L) NaCl 134.8, KCl 4.5, $MgCl_2$· $6H_2O$ 1, $CaCl_2$· $2H_2O$ 2, glucose 5, HEPES 10, sucrose 110, was adjusted to pH 7.4 with Tris. CsCl 99, HEPES 10, sucrose 90, were adjusted to pH 7.40 with Tris. The pipette solution recording $I_{K(ca)}$ contained (mmol· L^{-1}) potassium-aspartic acid 110, Mg-ATP 5, HEPES 5, $MgCl_2$· $6H_2O$ 1.0, KCl 20, egtazic acid 0.1, di-*tris*-creatine phoshate 2.5, disodium-creatine phosphate 2.5 and its pH was adjusted to 7.3 with KOH. Tetraethylammonium (TEA), C-type natriuretic peptide (CNP), Ly83583 and Zaparinast were made as stock solutions. All chemicals in this experiment were purchased from Sigma (USA).

Data analysis

All the data were expressed as means ± SD. Statistical significance was evaluated by a *t* test. Differences were considered to be significant when *P* value was less than 0.05.

RESULTS

Effect of CNP on spontaneous contraction of gastric antral circular smooth muscle

Different concentrations of CNP obviously inhibited spontaneous contraction in a dose-dependent manner and the inhibition percentage was 26.21 %±3.12 %, 52.41 %±4.21 % and 73.42 %±8.01 % (n=6) at 10^{-8} mol· L^{-1}, 10^{-7} mol· L^{-1} and 10^{-6} mol· L^{-1}, respectively (Figure 1).

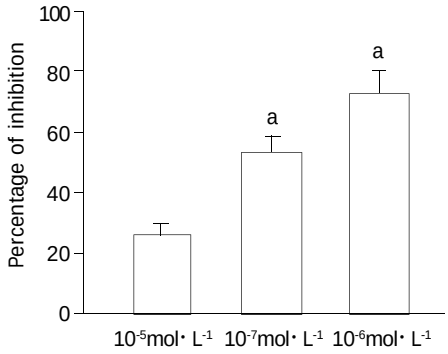

Figure 1 Effect of CNP on spontaneous contraction of gastric circular smooth muscle in a dose-dependent manner in guinea pigs. ^aP<0.01 *vs* 10^{-8} mol·L^{-1} group.

Effect of Ly83583 and Zaparinast on CNP-induced inhibition in gastric antral circular smooth muscle

To further investigate the mechanism of CNP-induced inhibition on spontaneous contraction, the effect of CNP on gastric motility was observed in the condition of administering Ly83583, a kind of inhibitor of guanylate cyclase, and Zaparinast as a phosphoesterase inhibitor to change production of cGMP. Ly83583 (10^{-7} mol· L^{-1}) markedly diminished the inhibitory effect of CNP on spontaneous contraction (P<0.05) (Figure 2), Zparinast (10^{-6}mol· L^{-1}) potentiated the inhibitory effect of CNP on spontaneous contraction (P<0.05)(Figure 3).

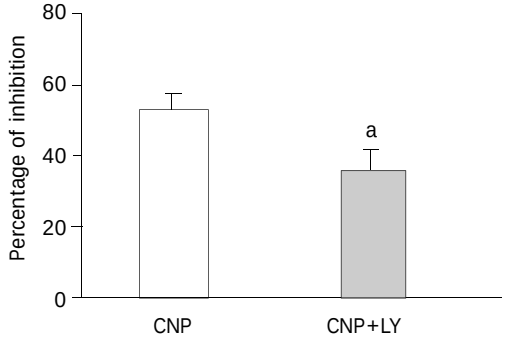

Figure 2 Effect of Ly83583 on CNP-induced inhibition in gastric circular smooth muscle of guinea pigs. ^aP<0.05 *vs* CNP group.

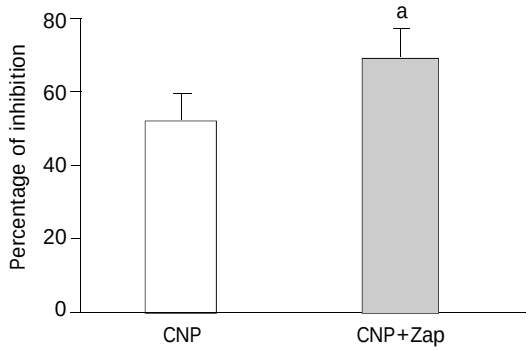

Figure 3 Effect of Zaparinast on CNP-induced inhibition in gastric circular smooth muscle of guinea pigs. [a]$P<0.05$ *vs* CNP group.

Effect of CNP on spontaneous contraction in the presence of TEA

To investigate the relationship between potassium channel and CNP-induced inhibition, the effect of TEA, a nonselective potassium channel blocker, on inhibition of gastic motility induced by CNP was observed. After muscle strips were pretreated with TEA (10 mol· L^{-1}), the inhibitory effect of CNP (10^{-7} mol· L^{-1}) on spontaneous contraction was significantly diminished (n=7) (Figure 4).

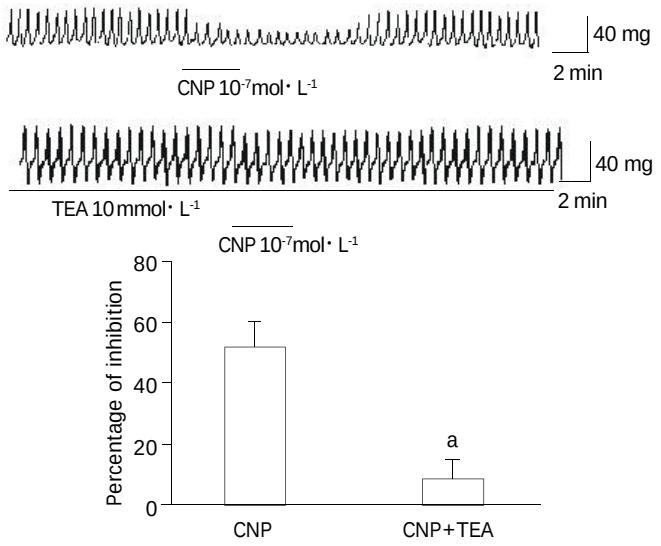

Figure 4 Effect of TEA on CNP-induced inhibition in gastric circular smooth muscle of guinea pigs. [a]$P<0.01$ *vs* CNP group.

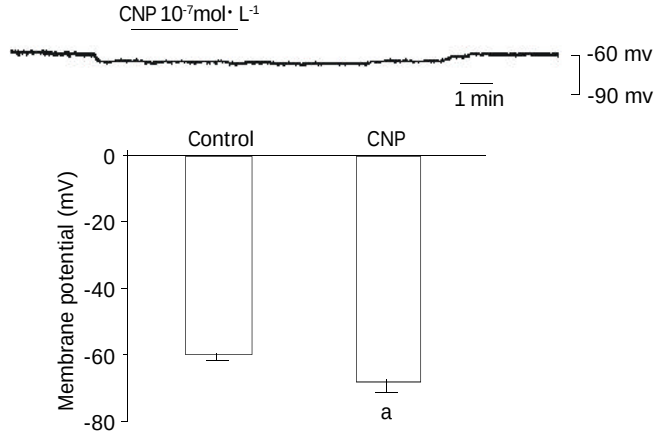

Figure 5 Effect of CNP on membrane potential of gastric circular myocytes in guinea pigs. [a]$P<0.05$ *vs* Control group.

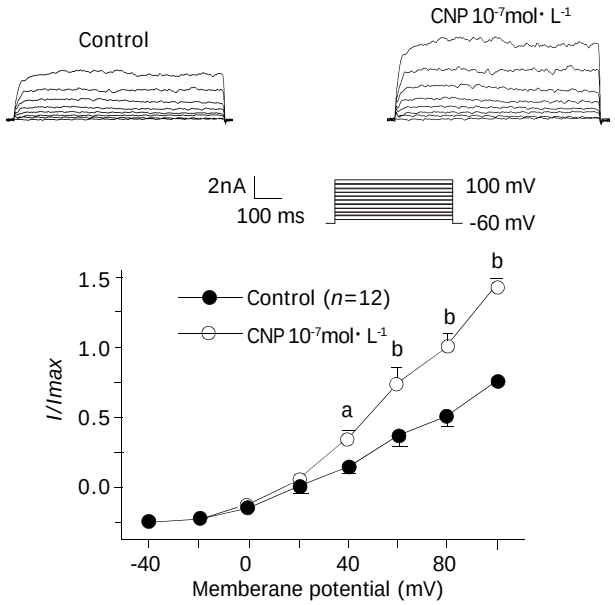

Figure 6 Effect of CNP on $I_{k(ca)}$ in gastric circular smooth muscle of guinea pigs. [a]$P<0.05$ *vs* Control group; [b]$P<0.01$ *vs* Control group.

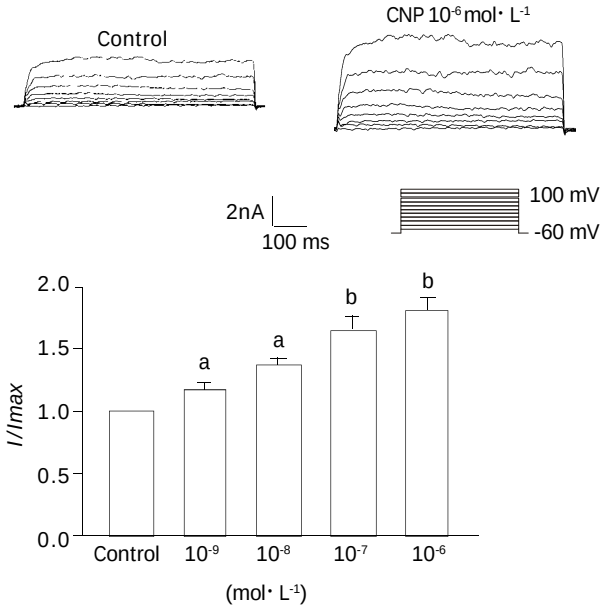

Figure 7 Dose-dependent manner of CNP calcium-activated potassium currents in gastric circular smooth muscle of guinea pigs. [a]$P<0.05$ *vs* Control group, [b]$P<0.01$ *vs* Control group.

Effect of CNP on membrane potential

To further investigate the mechanism of CNP-induced relaxation, the conventional whole cell patch-clamp technique was used. Membrane current was clamped and membrane potential was modulated to -60.0 mV, so that it was close to the resting potential of the gastric myocytes. After addtion of CNP(10^{-7} mol· L^{-1}), the membrane potential was hyperpolarized from -60.0 mV±2.0 mV to -68.3 mV±3.0 mV, and the amplitude of polarization was increased by 13.31 %±1.12 % (P<0.05) (Figure 5).

Effect of CNP on $I_{K(ca)}$

Under conventional whole cell patch clamp mode, the membrane potential was clamped at -60mV, and $I_{K(ca)}$ was elicited by step voltage command pulse from -40 mV to 100 mV for 400 ms with a 20 mV increment at 10 sec intervals.

CNP (Figure 6) (10^{-7} mol· L^{-1}) markedly increased $I_{K(ca)}$ and the increasing amplitude was 62.31 %±3.22 % at 60 mV. Different concentrations of CNP obviously increase $I_{K(ca)}$ in a dose-dependent manner, and the increasing percentage was 16.72 %±1.12 %, 37.51 %±2.32 %, 62.51 %±3.31 % and 82.32 %±3.71 % at 10^{-9} mol· L^{-1}, 10^{-8} mol· L^{-1},10^{-7} mol· L^{-1} and 10^{-6} mol· L^{-1} respectively at 60 mV (Figure 7). In conventional whole cell patch clamp mode, the holding potential was clamped at -20 mV, the spontaneously transient outward currents (STOCs) were recorded. CNP (10^{-7} mol· L^{-1}) also significantly increased STOCs (Figure 8).

Effect of cGMP on CNP-induced increase of $I_{K(ca)}$

The effect of Ly83583 and Zaparinast on CNP-induced increase of $I_{K(ca)}$ was observed. The percentage of CNP-induced increase was diminished from 64.24 %±3.32 % to 26.53 %±2.31 % at 60 mV after pretreated with Ly83583 (P<0.05) (Figure 9) at the same time, the percentage of CNP-induced increase was potentiated from 63.71 %±1.82 % to 81.13 %±2.21 % at 60 mV after pretreated with Zaparinast (P<0.05) (Figure 10).

Figure 8 Effect of CNPon STOCs in gastric circular smooth muscle of guinea pigs.

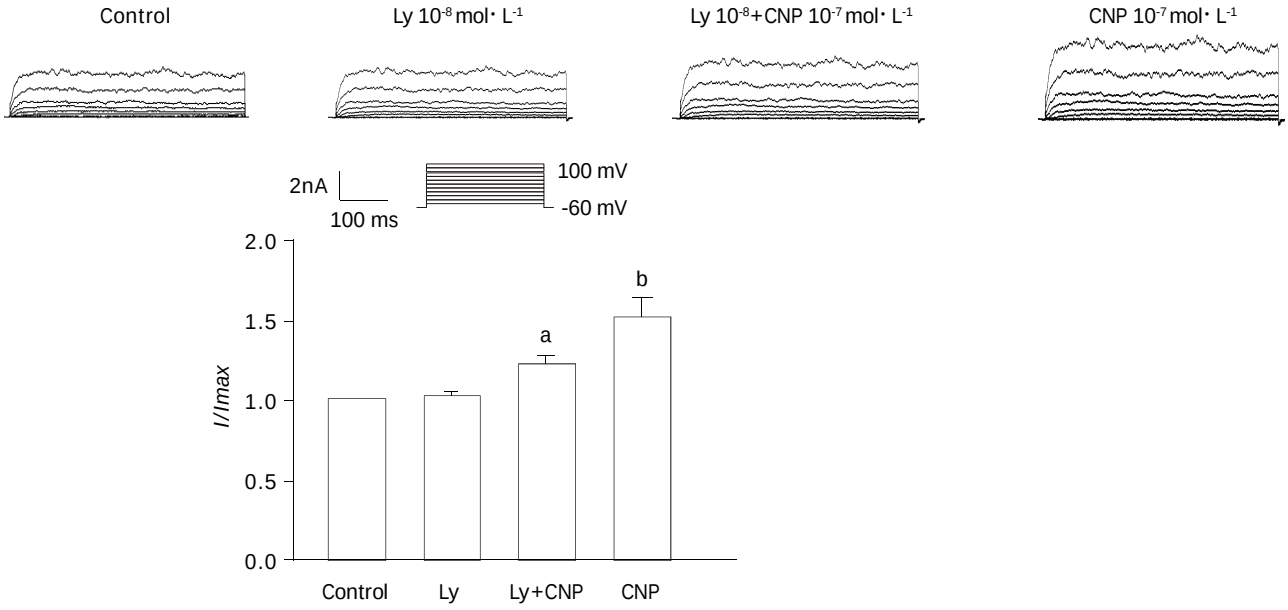

Figure 9 Effect of Ly83583 on CNP-induced increase of calcium-activated potassium currents in gastric circular smooth muscle of guinea pigs. [a]P<0.05 *vs* Ly group, [b]P<0.01 *vs* Ly+CNP group.

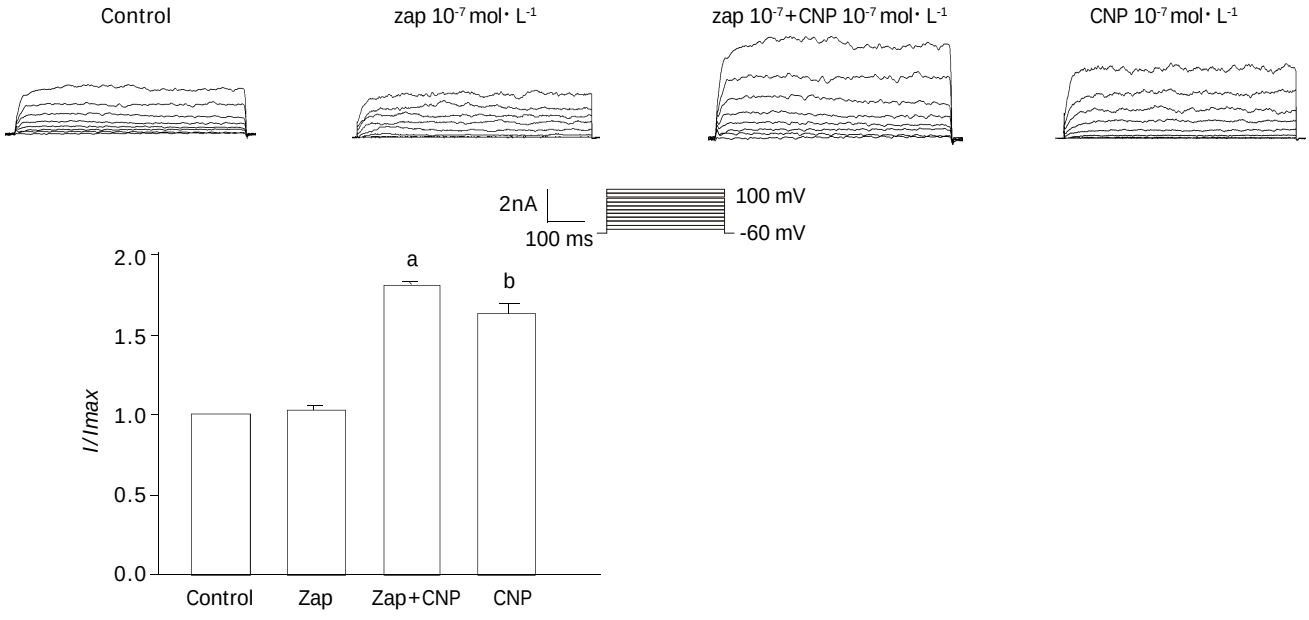

Figure 10 Effect of Zaparinast on CNP-induced increase of calcium-activated potassium currents in gastric circular smooth muscle of guinea pigs. [a]P<0.01 *vs* Zap group, [b]P<0.01 *vs* Zap+CNP group.

DISCUSSION

The present study indicated that CNP inhibited spontaneous contraction of the gastric antral smooth muscle in guinea pigs, and the inhibitory effect was markedly decreased by Ly83583 and potented by Zaparinast. TEA blocked CNP-induced inhibition. CNP hyperpolarized membrane potential and obviously increased $I_{K(ca)}$ in gastric circular myocytes in guinea pigs. CNP-induced increase of $I_{K(ca)}$ was partly blocked by Ly83583, but potentiated by Zaparinast.

Since Komatsu *et al*[14] demonstrated that CNP was distributed in the gastrointestinal tract of rats and humans, the study on the relationship between CNP and gastrointestinal function has recently become the hot topic. In the present study, CNP inhibited spontaneous contraction of gastric circular smooth muscle in guinea pigs. It was similar to many previous studies. Kim *et al*[15,16] indicated that CNP inhibited colonic motility of rabbits and both the frequency and the amplitude of basal motility of the oviduct in a dose-dependent manner. Our previous study also demonstrated that CNP inhibited spontaneous contraction of gastric circular smooth muscles in rats, guinea pigs and humans[8].

In this study, CNP-induced relaxation was mediated by cGMP pathway, since Ly83583 markedly diminished CNP-induced inhibition on spontaneous contraction, but Zaparinast obviously potentiated the effects in the gastric antral circular smooth muscle of guinea pigs. Many studies demonstrated that NP exerted a physiological function by cGMP pathway. Wellard *et al*[17] showed that atrial natriuretic peptides elevated cGMP levels in the primary cultures of rat ependymal cells. ANP and endothelin-1 (ET-1) might prevent renal dysfunction during the progression of congestive heart failure (CHF) through the cGMP pathway in dogs[18]. Tsuruda *et al*[19] demonstrated that BNP could control cardiac fibroblast function via cGMP pathway.

In our present study, TEA weakened the effect of CNP-induced inhibition on spontaneous contraction and CNP hyperpolarized membrane potential in gastric myocytes. It is well known that potassium channel has an intimate relationship with relaxation of smooth muscles. There were two kinds of potassium current, calcium-activated potassium current and delayed rectified potassium current in gastric antral smooth musle cells of guinea pigs[20,21]. This study demonstrated that CNP increased $I_{K(ca)}$ in a dose-dependent manner and CNP also increased STOCs. It could be concluded that potassium channel participates in CNP-induced relaxation. Many previous studies also reported that potassium channel was involved in NP-induced regulation of many physiological functions. Van der Zander *et al*[22] demonstrated that NO and calcium-activated potassium currents could regulate the effect of BNP-induced relaxation on vascular smooth muscles. In guinea pig sino-atrial (SA) node cells, ANP and cGMP increased the delayed rectified potassium current to exert certain physiological functions[23]. However, CNP relaxed the coronary arterial smooth muscle by activating of low conductance Ca^{2+}-activated K^+ channels, natriuretic peptide clearance receptors, and activity/regulation of phosphodiesterases in pigs[24].

NP can exert physiological functions by cGMP-PKG-ion channel pathway. Nakamura *et al*[25] indicated that ANP enhanced the level of cGMP to active cGMP-dependent protein kinase (PKG) to change the activity of inwardly rectifying K(+) channel. Nara *et al*[26] demenstrated that ANP increased $I_{K(ca)}$ by cGMP-PKG pathway in Xenopus oocytes. Our next step is to determine the relationship between CNP-induced increase of $I_{K(ca)}$ and cGMP-PKG pathway in gastric circular myocytes of guinea pigs.

In summary, CNP activated $I_{K(ca)}$ by cGMP pathway can hyperpolarize membrane potential,and gastric smooth muscle can be relaxed in guineapigs.

REFERENCES

1 **Lai FJ,** Hsieh MC, Hsin SC, Lin SR, Guh JY, Chen HC, Shin SJ. The cellular localization of increased atrial natriuretic peptide mRNA and immunoreactivity in diabetic rat kidneys. *J Histochem Cytochem* 2002; **50**: 1501-1508

2 **Cayli S,** Ustunel I, Celik-Ozenci C, Korgun ET, Demir R. Distribution patterns of PCNA and ANP in perinatal stages of the developing rat heart. *Acta Histochem* 2002; **104**: 271-277

3 **Zhao L,** Mason NA, Strange JW, Walker H, Wilkins MR. Beneficial effects of phosphodiesterase 5 inhibition in pulmonary hypertension are influenced by natriuretic Peptide activity. *Circulation* 2003; **107**: 234-237

4 **Peng N,** Chambless BD, Oparil S, Wyss JM**.** Alpha2A-adrenergic receptors mediate sympathoinhibitory responses to atrial natriuretic peptide in the mouse anterior hypothalamic nucleus. *Hypertension* 2003; **41**: 571-575

5 **Vuolteenaho O**, Arjamaa O, Vakkuri O, Maksniemi T, Nikkila LJ, Puurunen J, Ruskoaho H, Leppaluoto J. Atrial natriuretic peptide (ANP) in rat gastrointestinal tract. *FEBS Lett* 1988; **233**: 79-82

6 **Brockway PD**, Hardin JA, Gall DG. Intestinal secretory response to atrial natriuretic peptide during postnatal development in the rabbit. *Biol Neonate* 1996; **69**: 60-66

7 **Akiho H,** Chijiiwa Y, Okabe H, Harada N, Nawata H. Interaction between atrial natriuretic peptide and vasoactive intestinal peptide in guinea pig cecal smooth muscle. *Gastroenterology* 1995; **109**:1105-1112

8 **Guo HS**, Jin Z, Jin ZY, Li ZH, Cui YF, Wang ZY, Xu WX. Comparative study in the effect of C-type natriuretic peptide on gastric motility in various animals. *World J Gastroenterol* 2003; **9**: 547-552

9 **Guo HS,** Cui X, Cui YG, Kim SZ, Cho KW, Li ZL, Xu WX. Inhibitory effect of C-type natriuretic peptide on spontaneous contraction in gastric antral circular smooth muscle of rat. *Acta Pharmacol Sin* 2003 (in press)

10 **Carvajal JA,** Aguan K, Thompson LP, Buhimschi IA, Weiner CP. Natriuretic peptide-induced relaxation of myometrium from the pregnant guinea pig is not mediated by guanylate cyclase activation. *J Pharmacol Exp Ther* 2001; **297**: 181-188

11 **Mc Cann SM,** Gutkowska J, Antunes-Rodrigues J. Neuroendocrine control of body fluid homeostasis. *Braz J Med Biol Res* 2003; **36**: 165-181

12 **Carini R,** De Cesaris MG, Splendore R, Domenicotti C, Nitti MP, Pronzato MA, Albano E. Mechanisms of hepatocyte protection against hypoxic injury by atrial natriuretic peptide. *Hepatology* 2003; **37**: 277-285

13 **Kanwal S,** Elmquist BJ, Trachte GJ. Atrial natriuretic peptide inhibits evoked catecholamine release by altering sensitivity to calcium. *J Pharmacol Exp Ther* 1997; **283**: 426-433

14 **Komatsu Y,** Nakao K, Suga S, Ogawa Y, Mukoyama M, Arai H, Shirakami G, Hosoda K, Nakagawa O, Hama N. C-type natriuretic peptide (CNP) in rats and humans. *Endocrinology* 1991; **129**: 1104-1106

15 **Kim JH**, Jeon GJ, Kim SZ, Cho KW, Kim SH. C-type natriuretic peptide system in rabbit colon. *Peptides* 2001; **22**: 2061-2068

16 **Kim SH,** Lee KS, Lee SJ, Seul KH, Kim SZ, Cho KW. C-type natriuretic peptide system in rabbit oviduct. *Peptides* 2001; **22**: 1153-1159

17 **Wellard J,** Rapp M, Hamprecht B, Verleysdonk S. Atrial natriuretic peptides elevate cyclic GMP levels in primary cultures of rat ependymal cells. *Neurochem Res* 2003; **28**: 225-233

18 **Yamamoto T,** Wada A, Ohnishi M, Tsutamoto T, Fujii M, Matsumoto T, Takayama T, Wang X, Kurokawa K, Kinoshita M. Chronic administration of phosphodiesterase type 5 inhibitor suppresses renal production of endothelin-in dogs with congestive heart failure. *Clin Sci* 2002; **48**(Suppl 103): 258S-262S

19 **Tsuruda T,** Boerrigter G, Huntley BK, Noser JA, Cataliotti A, Costello-Boerrigter LC, Chen HH, Burnett JC Jr. Brain natriuretic Peptide is produced in cardiac fibroblasts and induces matrix metalloproteinases. *Circ Res* 2002; **91**: 1127-1134

20 **Li Y**, Xu WX, Li ZL. Effects of nitroprusside, 3-morpholino-sydnonimine, and spermine on calcium-sensitive potassium currents in gastric antral circular myocytes of guinea pig. *Acta Pharmacol Sin* 2000; **21**: 571-576

21 **Piao L**, Li Y, Li L, Xu WX. Increment of calcium-activated and delayed rectifier potassium current by hyposmotic swelling in gastric antral circular myocytes of guinea pig. *Acta Pharmacol Sin* 2001; **22**: 566-572

22 **Van der Zander K**, Houben AJ, Kroon AA, De Mey JG, Smits PA, de Leeuw PW. Nitric oxide and potassium channels are involved in brain natriuretic peptide induced vasodilatation in man. *J Hypertens* 2002; **20**: 493-499

23 **Shimizu K,** Shintani Y, Ding WG, Matsuura H, Bamba T. Potentiation of slow component of delayed rectifier K(+) current by cGMP via two distinct mechanisms: inhibition of phosphodiesterase 3 and activation of protein kinase G. *Br J Pharmacol* 2002; **137**: 127-137

24 **Barber DA,** Burnett JC Jr, Fitzpatrick LA, Sieck GC, Miller VM. Gender and relaxation to C-type natriuretic peptide in porcine coronary arteries. *J Cardiovasc Pharmacol* 1998; **32**: 5-11

25 **Nakamura K,** Hirano J, Itazawa S, Kubokawa M. Protein kinase G activates inwardly rectifying K(+) channel in cultured human proximal tubule cells. *Am J Physiol Renal Physiol* 2002; **283**: F784-791

26 **Nara M**, Dhulipala PDK, Ji GJ, Kamasani UR, Wang YX, Matalon S, Kotlikoff MI. Guanylyl cyclase stimulatory coupling to K_{Ca} channels. *Am J Physiol Cell Physiol* 2000; **279**: C1938-C1945

Edited by Zhang JZ and Wang XL

P.O.Box 2345, Beijing 100023,China
Fax: +86-10-85381893
E-mail: wjg@wjgnet.com www.wjgnet.com

World J Gastroenterol 2003;9(9):2060-2064
World Journal of Gastroenterology
 ISSN 1007-9327

• BASIC RESEARCH •

Morphological changes of cell proliferation and apoptosis in rat jejunal mucosa at different ages

Li Wang, Jian Li, Qing Li, Jian Zhang, Xiang-Lin Duan

Li Wang, Jian Li, Qing Li, Jian Zhang, Xiang-Lin Duan, Life Science College, Hebei Normal University, Shijiazhuang 050016, Hebei Province, China
Supported by the Natural Science Foundation of Hebei Province, No.303158; Education Department Foundation of Hebei Province, No.2002136
Correspondence to: Xiang-Lin Duan, Life Science College, Hebei Normal University, Shijiazhuang 050016, Hebei Province, China. duanxianglin@mail.hebtu.edu.cn
Telephone: +86-311-6269480 **Fax:** +86-311-5828784
Received: 2002-07-02 **Accepted:** 2002-07-12

Abstract

AIM: To study the changes of cell proliferation and apoptosis in rat jejunal epithelium at different ages.

METHODS: Cell proliferation and apoptosis of the jejunal mucosal and glandulous epithelia from birth to postnatal 12th month were observed using immunocytochemistry (ICC), and TUNEL method. The height of villus, the thickness of muscle layer and the number of goblet cells in jejunal mucosal and glandulous epithelia were measured by BeiHang analytic software and analyzed by STAT.

RESULTS: (1) Proliferating cell nuclear antigen (PCNA) positive cells of jejunal glandulous recess were found and increased in number from birth to the postnatal 3rd month. The number of PCNA positive cells peaked in the postnatal 3rd month, and decreased from then on. (2) The number of apoptotic cells also peaked in the postnatal 3rd month, showing a similar trend to that of the PCNA positive cells. (3) The height of jejunal villus increased after birth, peaked in the postnatal 3rd month and decreased from then on. The jejunal muscle layer became thicker in the postnatal 3rd week and the postnatal 12th month. The number of goblet cells of the jejunal mucosal and glandulous epithelia had a linear correlation with age.

CONCLUSION: (1) PCNA positive cells are distributed in the jejunal glandulous recess. (2) Apoptotic cell number peaks in the postnatal 3rd month, indicating that cell proliferation and apoptosis are developed with the formation of digestive metabolism as rat grows to maturity. (3) The thickness of jejunal muscle layer increases to a maximum in the postnatal 3rd week, which may be related to the change in diet from milk to solid food. (4) The number of goblet cells increases rapidly in the postnatal 3rd week, probably due to ingestion of solid food.

Wang L, Li J, Li Q, Zhang J, Duan XL. Morphological changes of cell proliferation and apoptosis in rat jejunal mucosa at different ages. *World J Gastroenterol* 2003; 9(9): 2060-2064
http://www.wjgnet.com/1007-9327/9/2060.asp

INTRODUCTION

The small intestine is the primary digestive apparatus of mammals, and nutrient absorption is ongoing mostly via intestinal epithelium. Mathan *et al* in 1976[1-4] observed the embryogenesis and postnatal change of rat duodenal villi using transmission electron microscope and scanning electron microscope respectively. Weinstein *et al*[5-7] described the ultrastructure and function of intestinal epithelial lining in 1981. In 1995, Gao *et al*[8-10] studied the epithelialization, expression pattern, and transformation of some enzymes of duodenum with histological methods. However, the status of proliferation and apoptotic changes in developing jejunal epithelial lining has not yet been elucidated. The present study was to provide a digestive physiological proof more directly in proliferation and apoptotic changes at four representative developmental stages in rats: birth, postnatal 3rd week, postnatal 3rd month, and postnatal 12th month.

MATERIALS AND METHODS

Materials

Sprague-Dawly rats (male, Grade II, Certificate *No* 04036, obtained from the Experimental Animal Center of Hebei Province) were divided into four groups: newborn (n=6), postnatal 3rd week (n=6), postnatal 3rd month (n=6) and postnatal 12th month (n=6). The rats were held for 12 hours without food. The mean weight was 5.6±0.3 g for newborn, 53.5±1.2 g for postnatal 3rd week, 390±0.9 g for postnatal 3rd month and 601.7±3.4 g for postnatal 12th month. The abdominal cavity was opened immediately after the rat was killed with ether. Several segments of jejunum (1-2 cm) were removed and placed immediately in a fixative consisting of 4 % paraformaldehyde and 0.01 mol/L phosphate buffered saline (PBS, pH7.4) (4 ℃, 12 h). The segments were used for TdT-mediated X-dUTP nick end labeling (TUNEL) examination and HE staining, and other segments were placed in a fixative consisting of Bouin's solution. Fixed jejunum segments were embedded in paraffin and continuously sliced up at 6 μm thickness and mounted onto glass slides covered with 3-aminopropyl-triethoxysilane (APES). They were dried at 37 ℃, and used for immunostaining of proliferating cell nuclear antigen (PCNA).

Reagents

Rabbit anti-rat PCNA antibody and SP kit were purchased from Beijing Zhongshan Biotechnology Company. TUNEL examination kit was purchased from Wuhan Boster Biological Technology Company.

HE staining

Several segments of jejunum were fixed in formalin and embedded in paraffin. Slides were cut and stained with hematoxylin and eosin according to routine methods.

Immunohistochemistry

Immunohistochemical staining for PCNA was performed using SP technique with following procedures. Mounted specimens were washed in 0.01 mol/L phosphate-buffered saline (PBS). Endogenous peroxidase was blocked by 0.3 % H_2O_2 in methanol for 25 min. Slides were washed with PBS followed by incubation in normal goat serum for 30 min at room temperature. The primary rabbit anti-rat PCNA antibody was

diluted 1:75 and applied to sections for 12 hours at 4 ℃. Slides were washed with PBS again and incubated with biotinylated secondary antibody for 60 min at 37 ℃. After rinsed in PBS, the slides were incubated with peroxidase-conjugated streptavidin for 60 min at 37 ℃. Colour reaction was performed by incubating the sections with diaminobenzidine-H_2O_2 for 5 min. The sections were counterstained with hematoxylin, dehydrated in gradient alcohol, and hyalinized in dimethylbenzene. Finally, the sections were mounted and observed under a microscope. PBS was used as a substitute for primary antibody as negative control.

TdT-mediated X-dUTP nick end labeling (TUNEL) examination technique

Mounted specimens were dewaxed and endogenous peroxidase was blocked by 3 % H_2O_2 in methanol for 10 min. After washed with water, 20 μl labeling buffer (1 μl TdT, 1 μl DIG-UTP, and 18 μl Labeling Buffer) was added to each section and incubated for 12 hours at 4 ℃. The sections were washed with 0.01 mol/L TBS and 50 μl blocking solution was added to each slide, followed by incubation for 30 min at room temperature. Biotinylated antidigoxin antibody was added to the slides for 30 min at 37 ℃. SABC was added for 40 min at 37 ℃ followed by washing with TBS. Then the specimens were incubated with diaminobenzidine-H_2O_2 for 5 min. After rinsed in tap water, the sections were counterstained with hematoxylin. Then they were dehydrated in gradient alcohol and hyalinized in dimethylbenzene. The sections were mounted and observed under a microscope. PBS was used as a substitute for primary antibody as negative control.

Data processing

The Northern image analyzing software was employed to analyze the stained area (the percentage of immunoreaction positive cells in total number of cells within a vision field). Three sections were selected from each experimental animal, and ten fields of vision from each section were inspected by statistical random sampling. The villus height was measured, the apoptotic cells under 16×40 double OLYMPUS microscope with testing resection and the number of goblet cells in unit area were counted[11]. The proliferation index was calculated. Under 15×10 double microscope, the thickness of muscle layer was measured according to the statistical random sampling with a micrometer, then the mean value was calculated. The values were expressed as $\bar{x}\pm s$. Statistical analysis was performed using the STAT software and analysis of variance was used as appropriate. $P<0.05$ was considered significant.

RESULTS

The number of jejunal mucosal goblet cells increased from birth to postnatal 3rd week and decreased from postnatal 3rd week to postnatal 3rd month, and then increased again after the postnatal 3rd month (Figure 1, Table 1). The number of

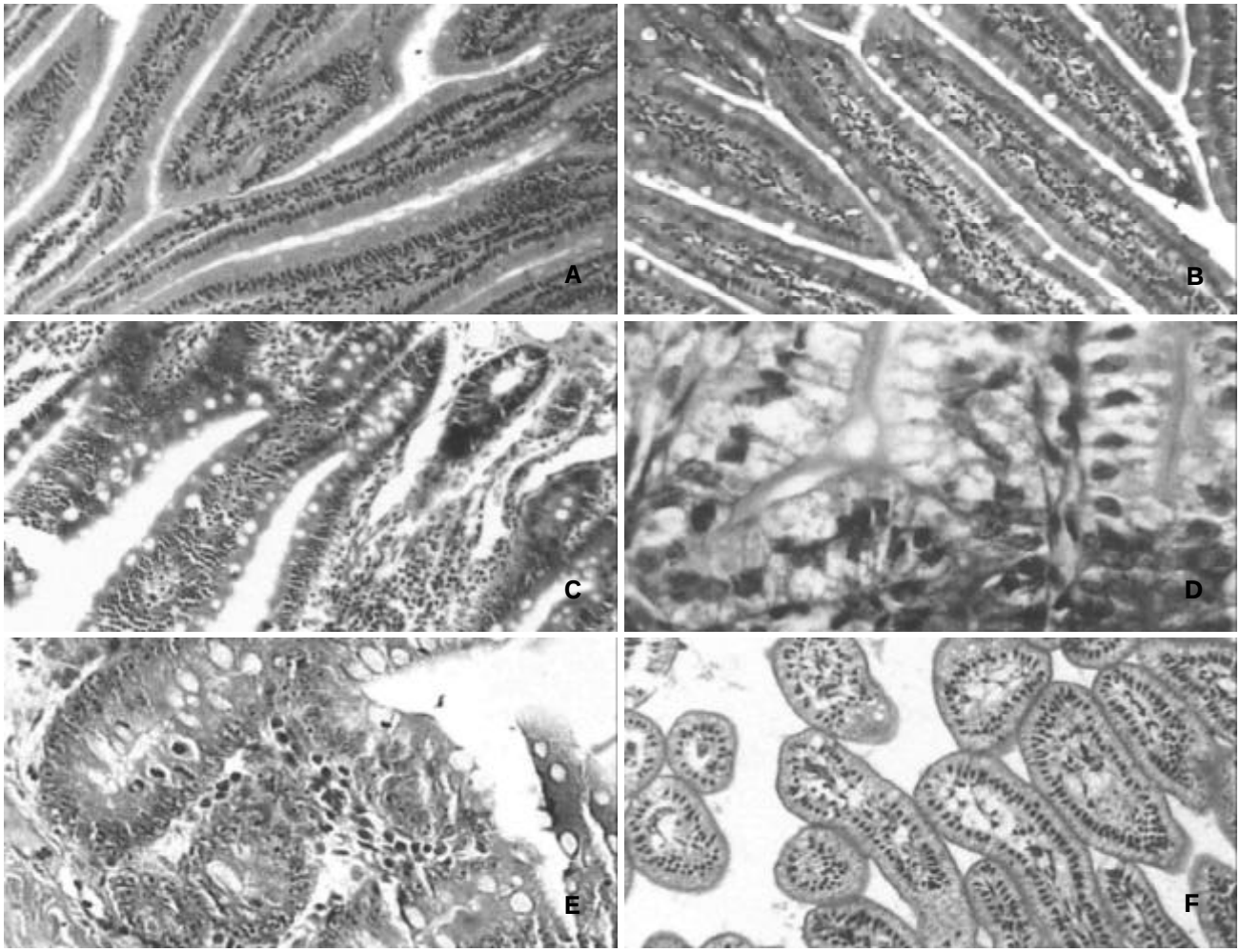

Figure 1 A: The number of goblet cells and the morphology of jejunal villi in the postnatal 3rd month ×100. B: The number of goblet cells in rat jejunal villi in the postnatal 3rd month ×100. C: The number of goblet cells and the morphology of jejunal villi in the postnatal 12th month ×100. D: There were few or no goblet cells in the jejunal glands of newborn rats ×400; E: The number of goblet cells in rat jejunal gland was much higher in the postnatal 12th month than in any other month ×400. F: The jejunal villi of newborn rats displayed ateliosis and were very small ×200.

glandulous epithelial goblet cells had a linear correlation with age (Figure 1), and there were significant differences between groups ($P<0.01$, Table 1). The height of jejunal villus increased from birth, peaked in the postnatal 3rd month and decreased from then on, and the villi were swollen in postnatal 12th month (Figure 1, Table 1). The thickness of jejunal muscle layer appeared crest on postnatal 3rd week and postnatal 12th month, the muscle fibers were quite dense in the postnatal 3rd month but very loose in the postnatal 3rd week (Table 1).

The immunostaining of PCNA positive cells was shown as light brown deposited in the nuclei. The PCNA positive cells in rat jejunum were mainly distributed in jejunal glandulous recess and proper lamina (Figure 2). The PCNA positive cells were shown to increase from birth to postnatal 3rd month, and decrease from then on (Figure 2, Table 2).

Table 2 Surface densities of PCNA-positive cells and the number of apoptotic cells at different stages ($\bar{x}\pm s$, $n=6$)

Age	Surface densities of PCNA-positive cells	The number of apoptotic cells
Newborn group	0±0	0±0
Postnatal 3rd week	0.022±0.012	9.71±2.43
Postnatal 3rd month	0.449±0.063[b]	38.83±7.41[b]
Postnatal 1 year	0.096±0.045[d]	11.36±3.14[d]

[b]$P<0.01$, *vs* Postnatal 3rd week. [d]$P<0.01$, *vs* Postnatal 3rd month.

The apoptotic cells were stained by TUNEL and positive cells were shown as dark brown in the nuclei. The apoptotic positive cells were mainly distributed in lamina propria (Figure 2). The number of apoptotic positive cells increased from newborn to postnatal 3rd month, and then decreased with aging. The pattern was similar to that of the PCNA positive cells (Figure 2, Table 2).

DISCUSSION

The goblet cell is a typical cell capable of excreting glycoprotein, containing a lot of spumous grume and granules of inhomogeneous electronic density. The jejunal glandulae of newborn rats could not develop but goblet cells can be seen in the villi. The number of goblet cells increased in the postnatal 3rd month, which might be related to the change in diet from milk to solid food. In the postnatal 12th month, the number of goblet cells increased again, and in this phase the increase of goblet cells led to the increase of mucus, which has the functions of lubricating mucosa and defending intestinal wall. The increasing change in the number of gerontic goblet cells might be a kind of protective mechanism against the weakening of excreting function of digestive gland in gerontic rat.

Cheng *et al*[12] considered that rat intestinal villi had perfectly developed on the 21st day of pregnancy, but there were only a few intestinal glands and few goblet cells. Our result was coincident with that of Cheng *et al*. We found that along with

Table 1 Developmental changes in cell type and morphology of rat villi after staining ($\bar{x}\pm s$, $n=6$)

Group	Number of villus goblet cells (entries/μm²)	Number of crypt goblet cells (entries/μm²)	Thickness of muscle layer (μm)	Villus height (μm)
Newborn group	4.89±2.67	0±0	32.0±15.71	315.20±43.74
Postnatal 3rd week	7.14±1.54[b]	4.47±1.10[b]	64.86±14.91[b]	532.75±53.36[b]
Postnatal 3rd month	4.44±1.11	5.27±0.93	56.34±15.41	629.64±48.22
Postnatal 1 year	9.31±1.50[d]	6.49±1.98	60.48±11.93	510.95±82.93[d]

[b]$P<0.01$, *vs* Newborn group. [d]$P<0.01$, *vs* Postnatal 3rd month.

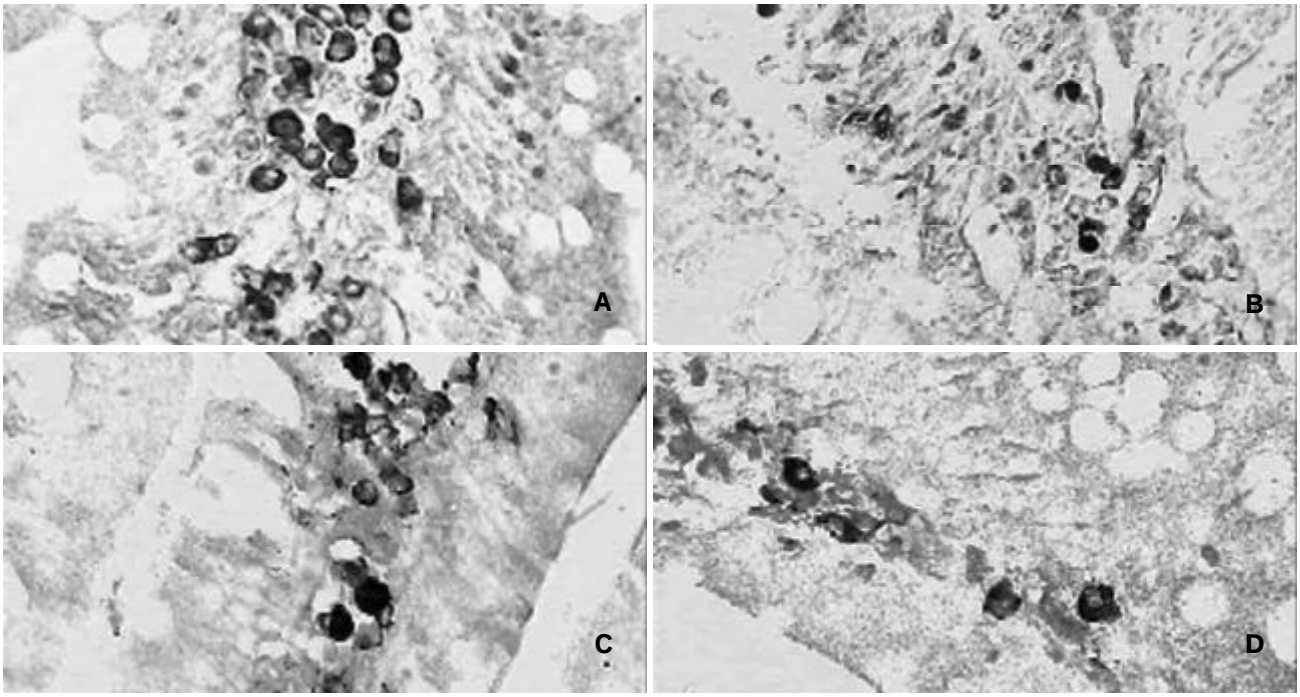

Figure 2 A: The expression of PCNA positive cells of the rat jejunum in the postnatal 3rd month ×400. B: The number of jejunal PCNA positive cells in the postnatal 12th month ×400. C: The expression of apoptotic positive cells of rat jejunum in the postnatal 3rd month ×400. D: The number of rat jejunal apoptotic positive cells in the postnatal 12th month ×400.

the development of intestinal glands the number of goblet cells in the intestinal gland gradually increased in the rat of postnatal 3rd week, postnatal 3rd month and postnatal 12th month, and this phenomenon might be corresponding to hearty digestive function in mature rats.

With the commence of sucking activity of newborn rat, the digestive tract starts its digestive activities. The newborn rat villi are very fine, and immature. In this period the intestinal digestive function is quite feeble, great molecule materials are assimilated via endocytosis with the help of lysosomes, thus the nutrients are absorbed. This absorptive manner only suits to the materials in milk[13]. Milk has balanced and all-sided nutrition, and contains many growth factors which are necessary to the development of the rat, so it can promote intestinal cells to develop[14]. To absorb various kinds of nutrients, gastrointestinal tract of rat develops rapidly and matures gradually to adapt to the digestive function[15]. In the postnatal 3rd week, villi become primarily matured. The muscle layer is quite thick, and the enteric digestive function of rat is boosted up. In this phase, endocytosis has weakened, and the rat can gradually digest food, and many absorptive mechanisms like glucide simple diffusing, solvent dragging, active ion transport and co-transport appear. In the postnatal 3rd month, villi heighten and peak, which increase the intestinal digestive areas. In this period, microvilli on the top of intestinal villus can be seen under an electron microscope, and they gather together to be known as brush border. Villi and microvilli increase the intestinal digestive area to 200 m^2 or more. There are capillary, lymphatic capillary, smooth muscle fiber and nerve net in intestinal villi, and one or more central small arteries and a central chyle vessel in each intestinal villus. The villus height increases with advancing age. The structures of capillary, lymphatic capillary, smooth muscle fiber and nerve net in intestinal villi are perfectly developed, in favor of substance countercurrent exchange in ascending and descending vessels of villi. At the same time, the muscle fiber relaxation and contraction and the pump function of central chyle vessels in villi help digestion. Besides, increase of muscle fibers which enhance the whip and rhythmic condensing movement is also helpful to digestion, and this period becomes the strongest phase of the digestive function. In the postnatal 12th month, there are effete changes like swelling and shortening of some villi, and the enteric digestive function slacks up, thus food is insufficiently digested in the enterocoelic cavity. The phenomenon of exocytosis manner assimilating large molecule substances appear again, maybe this manner is a kind of compensation for the digestion.

PCNA has a molecular weight of 36 kDa and is an assistant protein of DNA polymerase δ in terms of its physiological function. It can objectively reflect the proliferation degree of cells, and is a better proliferating marker of cells. PCNA immunostaining signal is almost completely disappeared in the nuclei. Positive substance takes on the form of dispersion or granule, or a combination of the two forms. The cell nuclei of strong positive cells are brown-yellow, nuclei of positive cells are yellow, the cell nuclei of feeble positive cells are buff. The proliferating bloom region of PCNA positive cells is distributed in jejunal glandulous recess, and the differentiation of positive cells on the top of villi is a sort of "ladder-like" movement[16-19]. The experiment showed that the proliferative index of PCNA positive cells in the recess increased from birth to postnatal 3rd month, and reached the crest in postnatal 3rd month, which made the cells in recess to be continuously hyperplastic. The proliferation index decreased at postnatal 12th month, indicating that the proliferation of cells becomes weak as the organism ages.

As the fastest renewing cells in the body, the cell cycle of small intestinal epithelia only exists for 12 h, and they also have apoptosis[20-23]. As early as the end of 19th century, the granules of epithelial cells in embryonic digestive tube under optical microscope were named "meconium corpuscles". Harmon *et al*[24-27] confirmed under the electron microscope that in fact meconium corpuscles were the apoptotic globules in digestive tract epithelia. Iwanaga *et al*[28-34] considered that macrophages in small intestinal proper lamina of adult rats could induce apoptosis of epithelia. It was observed in this experiment that the apoptotic cell number of intact jejunal villi of SD rats increased from birth to postnatal 3rd month and reached its peak in postnatal 3rd month, which may be indicated that when the rat grows up, cell proliferation and apoptosis activity became abundant with the buildup of body metabolism function. The metabolic level decreased in postnatal 12th month with the senescence of body, the number of apoptotic cells began to decline compared with that in the postnatal 3rd month.

REFERENCES

1 **Mathan M**, Moxey PC, Trier JS. Morphogenesis of fetal rat duodenal villi. *Am J Anat* 1976; **146**: 73-92

2 **Ono K**. Changes of the caecal villi during postnatal development in rats. *Cell Tissue Res* 1980; **208**: 253-259

3 **Atuma C**, Strugala V, Allen A, Holm L. The adherent gastrointestinal mucus gel layer: thickness and physical state *in vivo*. *Am J Physiol Gastrointest Liver Physiol* 2001; **280**: G922-G929

4 **Varedi M**, Greeley GH Jr, Herndon DN, Englander EW. A thermal injury-induced circulating factor(s) compromises intestinal cell morphology, proliferation, and migration. *Am J Physiol* 1999; **277**: G175-G182

5 **Weinstein L**, Edelstein SM, Madara JL, Falchuk KR, McManus BM, Trier JS. Intestinal cryptosporidiosis complicated by disseminated cytomegalovirus infection. *Gastroenterology* 1981; **81**: 584-591

6 **Pacha J.** Development of intestinal transport function in mammals. *Physiol Rev* 2000; **80**: 1633-1667

7 **Yeaman C**, Grindstaff KK, Nelson WJ. New perspectives on mechanisms involved in generating epithelial cell polarity. *Physiol Rev* 1999; **79**: 73-79

8 **Gao JG**, Wang SP, Xing SG. Histological and histochemical observation on the development and differentiation of the mouse duodenum. *Jiepao Xuebao* 1995; **26**: 425-430

9 **Ramalho-Santos M**, Melton DA, McMahon AP. Hedgehog signals regulate multiple aspects of gastrointestinal development. *Development* 2000; **127**: 2763-2772

10 **Plateroti M**, Freund JN, Leberquier C, Kedinger M. Mesenchyme-mediated effects of retinoic acid during rat intestinal development. *Journal Cell Science* 1997; **110**: 1227-1238

11 **Zheng FS**. The cell morphometry. Beijing: *Beijing Medical University and PUMC United Publishing House* 1990: 11

12 **Cheng D**, Chen AJ, Yin X, Xu YL, Zhu XX. Morphogenesis of Duodenal Villi in Rat. *Jiepao Xuebao* 1990; **21**: 437-440

13 **Cheng LZ**. Histology. 2nd Ed. Beijing: *The Peoples' Health Publishing House* 1993: 1106

14 **Li ZB**. Research progress in gut development of newborn. *Guowai Yixue Er Kexue Fence* 2000; **27**: 9-23

15 **Mubiru JN,** Xu RJ. Growth and development of the exocrine pancreas in newborn pigs: the effect of colostrum feeding. *Biol Neonate* 1997; **71**: 317-326

16 **Xie JX**, Gu Y, Zhao SM, Luo BG, Chen LL, Wu ZH, Zuo HT. Study on changes of apoptosis and expression of PCNA in atrophic intestinal mucosal epithelia. *Jiepaoxue Zazhi* 1999; **22**: 124-127

17 **Varedi M**, Chinery R, Greeley GH Jr, Herndon DN, Englander EW. Thermal injury effects on intestinal crypt cell proliferation and death are cell position dependent. *Am J Physiol Gastrointest Liver Physiol* 2001; **280**: G157-G163

18 **Jones BA**, Gores GJ. Physiology and pathophysiology of apoptosis in epithelial cells of the liver, pancreas, and intestine. *Am J Physiol* 1997; **273**: G1174-G1188

19 **Hall PA**, Coates PJ, Ansari B, Hopwood D. Regulation of cell number in the mammalian gastrointestinal tract: the importance of apoptosis. *Journal Cell Science* 1994; **107**: 3569-3577

20 **Iiboshi Y**, Nezu R, Kennedy M, Fujii M, Wasa M, Fukuzawa M, Kamata S, Takagi Y, Okada A. Total parenteral nutrition decreases luminal mucous gel and increased permeability small instestine. *J Parenter Enteral Nutr* 1994; 1**8**: 346-350
21 **Burrin DG**, Stoll B, Jiang R, Chang XY, Hartmann B, Holst JJ, Greeley GH Jr, Reeds PJ. Minimal enteral nutrient requirements for intestinal growth in neonatal piglets: how much is enough? *Am J Clin Nutr* 2000; **71**: 1603-1610
22 **Remillard RL**, Dudgeon DL, Yardley JH. Atrophied small intestinal responses of piglets to oral feedings of milk. *J Nutr* 1998; **128**: 2727S-2729S
23 **Jeppesen PB**, Mortensen PB. Intestinal failure defined by measurements of intestinal energy and wet weight absorption. *Gut* 2000; **46**: 701-706
24 **Harmon B**, Bell L, Williams L. An ultrastructural study on the "meconium corpuscle" in rat foetal intestinal epithelium with particular reference to apoptosis. *Anat Embryol* 1984; **169**: 119-124
25 **Jordinson M**, Goodlad RA, Brynes A, Bliss P, Ghatei MA, Bloom SR, Fitzgerald A, Grant G, Bardocz S, Pusztai A, Pignatelli M, Calam J. Gastrointestinal responses to a panel of lectins in rats maintained on total parenteral nutrition. *Am J Physiol* 1999; **276**: G1235-G1242
26 **Williams CL**, Bihm CC, Rosenfeld GC, Burks TF. Morphine tolerance and dependence in the rat intestine *in vivo*. *J Pharmacol Exp Ther* 1997; **280**: 656-663
27 **Haertel-Wiesmann M**, Liang YX, Fantl WJ, Williams LT. Regulation of cyclooxygenase-2 and periostin by Wnt-3 in mouse mammary epithelial cells. *J Biological Chemistry* 2000; **275**: 32046-32051
28 **Iwanaga T**, Hoshi O, Han H, Takahashi-Iwanaga H, Uchiyama Y, Fujita T. Lamina propria macrophages involved in cell death (apoptosis) of enterocytes in the small intestine of rats. *Arch Histol Cytol* 1994; **57**: 267-276
29 **Yamamoto A**, Tatsumi H, Maruyama M, Uchiyama T, Okada N, Fujita T. Modulation of intestinal permeability by nitric oxide donors: Implications in intestinal delivery of poorly absorbable drugs. *J Pharmacol Experimental Therapeutics* 2001; **296**: 84-90
30 **Noda T**, Iwakiri R, Fujimoto K, Matsuo S, Aw TY. Programmed cell death induced by ischemia-reperfusion in rat intestinal mucosa. *Am J Physiol* 1998; **274**: G270-G276
31 **Cowen T**, Johnson RJR, Soubeyre V, Santer RM. Restricted diet rescues rat enteric motor neurones from age related cell death. *Gut* 2000; **47**: 653-660
32 **Ikeda H**, Suzuki Y, Suzuki M, Koike M, Tamura J, Tong J, Nomura M, Itoh G. Apoptosis is a major mode of cell death caused by ischaemia and ischaemia / reperfusion injury to the rat intestinal epithelium. *Gut* 1998; **42**: 530-537
33 **Varedi M**, Chinery R, Greeley GH Jr, Herndon DN, Englander EW. Thermal injury effects on intestinal crypt cell proliferation and death are cell position dependent. *Am J Physiol Gastrointest Liver Physiol* 2001; **280**: G157-G163
34 **Nakamura K**, Bossy-Wetzel E, Burns K, Fadel MP, Lozyk M, Goping IS, Opas M, Bleackley RC, Green DR, Michalak M. Changes in endoplasmic reticulum luminal environment affect cell sensitivity to apoptosis. *The J Cell Biol* 2000; **150**: 731-740

Edited by Zhu LH and Wang XL

P.O.Box 2345, Beijing 100023,China
Fax: +86-10-85381893
E-mail: wjg@wjgnet.com www.wjgnet.com

World J Gastroenterol 2003;9(9):2065-2067
World Journal of Gastroenterology
 ISSN 1007-9327

• BASIC RESEARCH •

Effect of enterokinetic prucalopride on intestinal motility in fast rats

Hui-Bin Qi, Jin-Yan Luo, Xin Liu

Hui-Bin Qi, Jin-Yan Luo, Xin Liu, Department of Gastroenterology, Second Hospital of Xi' an Jiaotong University, Xi' an 710004, Shannxi Province, China
Correspondence to: Dr. Hui-Bin Qi, Department of Gastroenterology, Second Hospital of Xi' an Jiaotong University, Xi' an 710004, Shannxi Province, China. qihuibin123@hotmail.com
Telephone: +86-29-7583715 **Fax:** +86-29-7231758
Received: 2003-01-04 **Accepted:** 2003-02-18

Abstract

AIM: To evaluate the effects of prucalopride on intestinal prokinetic activity in fast rats and to provide experimental basis for clinical treatment of gastrointestinal motility diseases.

METHODS: Gastrointestinal propulsion rate was measured by the migration rate of activated charcoal, which reflexes gastrointestinal motility function. 120 Spraque-Dawley rats were randomly divided into four groups and received an intravenous injection of physiological saline (served as control), prucalopride 1 mg/kg, prucalopride 2 mg/kg and cisapride 1 mg/kg, respectively. The gastrointestinal propulsion rate was measured 1, 2 or 4 hours after intravenous injection of the drugs.

RESULTS: Significant accelerations of gastrointestinal propulsion rate in prucalopride 1 mg/kg and 2 mg/kg groups were found compared with control group at 2 and 4 hours (83.2 %±5.5 %, 81.7 %±8.5 % *vs* 70.5 %±9.2 %, $P<0.01$; 91.2 %±2.2 %, 91.3 %±3.9 % *vs* 86.8 %±2.6 %, $P<0.01$). The gastrointestinal propulsion rates at 1, 2 or 4 hours were faster in prucalopride 1 mg/kg and 2 mg/kg groups than in cisapride group (84.0 %±11.7 %, 77.1 %±11.9 % *vs* 66.3 %±13.6 %, $P<0.01$, $P<0.05$; 83.2 %±5.5 %, 81.7 %±8.5 % *vs* 75.4 %±5.9 %, $P<0.01$, $P<0.05$; 91.2 %±2.2 %, 91.3 %±3.9 % *vs* 88.6 %±3.5 %,$P<0.05$, $P<0.05$). No difference of gastrointestinal propulsion rate was found between prucalopride 1 mg/kg group and prucalopride 2 mg/kg group ($P>0.05$).

CONCLUSION: Prucalopride accelerates intestinal motility in fast rats, and has no dose dependent effect.

Qi HB, Luo JY, Liu X. Effect of enterokinetic prucalopride on intestinal motility in fast rats. *World J Gastroenterol* 2003; 9 (9): 2065-2067
http://www.wjgnet.com/1007-9327/9/2065.asp

INTRODUCTION

Prucalopride is the first representative of the novel class of benzofurans,and is a highly specific and selective 5-HT_4 receptor agonist. Prucalopride can exert effect on intestinal prokinetic activity in fast rats.

MATERIALS AND METHODS

Experimental animals

One hundred and twenty healthy male Sprague-Dawley (SD) rats weighing 200-250 g were purchased from the Experimental Animal Center of Xi' an Jiaotong University. The rats were housed in rat cages at 22-25 ℃ with free access to standard rat pellet food and water for 10 days. They were fasted for 48 hours with free access to water.

Chemicals

Prucalopride and cisapride were kindly provided by Janssen Research Foundation. Prucalopride was dissolved in sterile, and cisapride in 0.57 mol/L ascorbic acid. Activated charcoal was purchased from the Chemical Factory of the Forestry Science Institute of China. Arabic gum powder was purchased from the Third Chemical Factory of Tianjin. Diethyl ether was purchased from Xi' an Chemical Factory.

Experimental procedure

The rats were randomly divided into four groups. Each group had 30 rats. The first group served as control and received intravenous injection of physiological saline under ether anaesthesia. The second group and the third received intravenous injection of prucalopride 1 mg/kg and 2 mg/kg under ether anaesthesia, and the fourth group received intravenous injection of cisapride 1 mg/kg in the same way. They then received intragastric injection of 100 g/L activated charcoal suspension (10 mg/kg, 100 g/L activated charcoal and 100 g/L Arabic gum powder respectively) through a specially designed orogastric cannula introduced through the mouth. The animals were killed 1, 2 and 4 hours respectively after ether anesthesia by cervical dislocation and decapitation. They had a laparotomy and migration of activated charcoal from esophagus-stomach junction to the most distal point of migration, and were expressed as distance (cm) migration by the stain. At 1 hour after injection, the most distal point of migration was in the small intestine and gastrointestinal(GI) propulsion rate was expressed as: gastrointestinal propulsion rate =the migration distance of activated charcoal(cm)÷the distance from esophagus-stomach junction to ileocecal opening (cm)×100 %. At 2 hours after injection, the most distal point of migration was all in the distal small intestine or proximal colon and at 4 hour after injection, the most distal point of migration was in the colon. So gastrointestinal propulsion rate was expressed as: gastrointestinal propulsion rate =the migration distance of activated charcoal (cm)÷the distance from esophagus-stomach junction to large intestine terminal (cm)×100 %.

Statistical analysis

Data were expressed as $\bar{x}\pm s$. Statistical analyses used were unpaired *t* test. Statistical significance was taken as $P<0.05$.

RESULTS

One hour effect of prucalopride

At 1 hour after injection, the most distal point of migration was in the small intestine. Compared with control group, in prucalopride 1 mg/kg group and prucalopride 2 mg/kg group, GI propulsion rate had no difference ($P>0.05$). Prucalopride at a

dose of either 1 or 2 mg/kg had no significant effect on gastrointestinal motility. Compared with cisapride group, GI propulsion rate had differences in prucalopride 1 mg/kg group and prucalopride 2 mg/kg group ($P<0.01$, $P<0.05$, Table 1).

Table 1 One hour effect of prucalopride on intestinal motility in SD rats ($\bar{x}\pm s$, $n=10$)

Group	GI length (cm)	Migration of activated charcoal (cm)	GI propulsion rate (%)
Control	82.9±12.2	63.8±10.5	77.9±7.5
Prucalopride (1 mg/kg)	70.9±4.1	59.7±9.5	84.0±11.7[b]
Prucalopride (2 mg/kg)	73.8±11.7	57.0±12.8	77.1±11.9[a]
Cisapride (1 mg/kg)	78.1±10.7	52.2±14.4	66.3±13.6

[a]$P<0.05$, [b]$P<0.01$, *vs* cisapride.

Two hour effect of prucalopride

At 2 hours after injection, the most distal point of migration was in the distal small intestine or proximal colon. Compared with control group, GI propulsion rate had significant differences in prucalopride 1 mg/kg group and prucalopride 2 mg/kg group ($P<0.01$).

Prucalopride at a dose of either 1 or 2 mg/kg significantly increased GI propulsion, suggesting that prucalopride might enhance gastrointestinal motility. Compared with cisapride group, GI propulsion rate had differences in prucalopride 1 mg/kg group and prucalopride 2 mg/kg group ($P<0.01$, $P<0.05$,Table 2).

Table 2 Two hour effect of prucalopride on intestinal motility in SD rats ($\bar{x}\pm s$, $n=10$)

Group	GI length (cm)	Migration of activated charcoal (cm)	GI propulsion rate (%)
Control	91.9±11.8	63.9±3.8	70.5±9.2
Prucalopride (1 mg/kg)	87.1±8.5	72.6±10.0	83.2±5.5[bd]
Prucalopride (2 mg/kg)	100.1±12.2	81.9±14.0	81.7±8.5[ad]
Cisapride (1 mg/kg)	95.4±12.3	72.0±6.9	75.4±5.9

[a]$P<0.05$, [b]$P<0.01$, *vs* cisapride; [d]$P<0.01$, *vs* control.

Table 3 Four hour effect of prucalopride on intestinal motility in SD rats ($\bar{x}\pm s$, $n=10$)

Group	GI length (cm)	Migration of activated charcoal (cm)	GI propulsion rate (%)
Control	89.9±8.6	78.0±7.3	86.8±2.6
Prucalopride (1 mg/kg)	83.7±5.1	76.3±5.2	91.2±2.2[ad]
Prucalopride (2 mg/kg)	97.4±9.8	87.3±10.4	91.3±3.9[ad]
Cisapride (1 mg/kg)	99.5±12.7	88.1±13.7	88.6±3.5

[a]$P<0.05$, *vs* cisapride; [d]$P<0.01$, *vs* control.

Four hour effect of prucalopride

At 4 hours after injection, the most distal point of migration was in the colon. Compared with control group, GI propulsion rate had significant differences in prucalopride 1 mg/kg group and prucalopride 2 mg/kg group ($P<0.01$). Prucalopride at a dose of either 1 or 2 mg/kg significantly increased GI propulsion, suggesting that prucalopride might enhance gastrointestinal motility. Compared with cisapride group, GI propulsion rate had differences in prucalopride 1 mg/kg group and prucalopride 2 mg/kg group ($P<0.05$, Table 3).

Response to different doses of prucalopride

At 1, 2 and 4 hours after prucalopride injection, GI propulsion rate in prucalopride 1 mg/kg group was not different from that in prucalopride 2 mg/kg group ($P>0.05$, Table 1, 2 and 3). The effect of prucalopride was not clearly dose related.

DISCUSSION

Prucalopride (R093877) is a newly synthesized enterokinetic agent which is a benzofuran derivative with the chemical structure of 4-animo-5-chloro-2, 3-dihydro-*N*-[1(3-methoxypropyl)-4-piperidinyl]-7-benzofurancarboxamide monochloride. It is a highly specific and selective 5-HT_4 receptor agonist[1]. *In vitro* animal experiments have shown facilitation of cholinergic[2] and excitatory non-adrenergic,non-cholinergic (NANC) neurotransmission. It is the first compound known to enhance NANC transmission in colonic preparations of guinea pig. Since cholinergic neurons and NANC neurons are known to play an important part in physiological regulation of colonic motility, it is likely that constipation will be favourably influenced by compounds facilitating NANC excitatory neurotransmission. Prucalopride is a specific and selective for 5-HT_4 receptor and is devoid of affinity to M_3 cholinoceptors, $5HT_{2A}$ and $5HT_3$ receptors, and cholinesterases. *In vivo* canine colonic studies confirmed the selectivity of the effects on 5-HT_4 receptors, as the selective and potent 5-HT_4 antagonist completely prevented the effects of prucalopride. But some 5-HT_4 agonist prokinetics stimulate $5HT_{2A}$ and $5HT_3$ receptors. *In vivo* and *in vitro* studies have shown that prucalopride can facilitate gastric, small intestinal, and colonic motility[3-5].

This study in fast rats showed that prucalopride had no significant effects on GI propulsion rate at 1 hour after intravenous injection. However, it significantly increased GI propulsion rate at 2, 4 hour after intravenous injection, suggesting that prucalopride might enhance gastrointestinal motility in the distal small intestine and colon instead of the stomach and proximal small intestine. This is consistent with the observations of Emmanuel *et al* in healthy volunteers. Emmanuel showed that 1 mg and 2 mg of prucalopride shortened orocaecal transit and whole gut transit,and suggested that prucalopride accelerated upper gut and colonic transit. Orocaecal transit was measured by lactoluse-hydrogen breath test. Whole gut transit was measured by radio-opaque markers. Bouras *et al*[6] reported that gastrointestinal and colonic transits were measured by scintigraphic techniques in healthy humans, and a daily dose of 0.5, 1, 2, or 4 mg prucalopride accelerated colonic transit, partly by stimulating proximal colonic empting, but did not alter gastric or small bowel transit. Poen *et al*[7] reported that prucalopride was well tolerated by healthy subjects and had a markedly consistent effect on stool frequency and colonic transit. Prucalopride, given orally or intravenously, altered colonic motility in the fast conscious dog in a dose-dependent manner. It induced signicant migrating contractions, stimulated proximal colon and inhihibed contractile motility patterns of distal colon by stimulating 5-HT4 receptors[4,8]. It deserves further study in patients with constipation. The fact that prucalopride did not affect stomach and proximal small intestine in fast rats does not preclude its potential beneficial effects in pathological states such as delayed gastric emptying. For example, in an animal model for delayed gastric emptying, prucalopride accelerated gastric emptying. In humans, Emmanuel *et al* observed that prucalopride shortened orocaecal transit, while Bouras *et al* found that prucalopride did not alter gastric or small bowel transit. This discrepancy probably was resulted from differences in methods used to measure transit. In Emmanuel *et al* studies, lactoluse-hydrogen breath test of a liquid marker

could measure orocaecal transit, but could not differentiate effects on stomach or small intestine. Whole gut transit was measured by radio-opaque markers. In Bouras *et al* studies, a scintigraphic technique was used to measure gastrointestinal and colonic transit[6]. The effects of prucalopride on stomach or small intestine deserves further study. Patients with idiopathic constipation had postprandial sigmoid mortor activity[9]. Prolonged colonic motility was recorded in patients with slow transit constipation[10]. Slow transit constipation was common[11-16]. Laxatives are often ineffective in treating constipation. An alternative therapeutic approach is to target serotonin-4 receptors, which are involved in initiating peristalsis[17-30]. Some Chinese herbal medicines can promote gastrointestinal motility and be used to treat constipation[31,32].

The reason for the lack of a dose-response effect of prucalopride on gastrointestinal motility is unclear. Maybe the dose groups were too few and the extent of doses was too narrow. It should design more dose groups to deserve the dose related effects. The dose dependent effects on significant colonic migrating have been more clearly shown by intravenous injection than by oral administration of prucalopride in dogs. Briejer *et al* observed a sigmoid dose-response curve in a dose of 0.001 to 1.25 mg/kg, the linear part of the curve was between 0.02 and 0.31 mg/kg. But Bouras *et al* reported that in healthy humans, a daily dose of 0.5, 1, 2, or 4 mg prucalopride was almost equally effective, and lack of dose-response effects[6]. The lack of stronger effects of 2 mg over 1 mg in this study might be resulted from turning off the signal: mechanisms that attenuate signaling by G protein-coupled receptors, by which serotonin receptors are characterized. In futher study, we shall investigate the dose related effects of prucalopride in patients with constipation and slow colonic transit.

This study showed that prucalopride whether 1 mg/kg or 2 mg/kg doses accelerated greater gastrointestinal propulsion rate compared with cisapride 1 mg/kg dose.

In conclusion, prucalopride can accelerate intestinal motility in fast rats, and maybe hold a promising new class of treatment for chronic constipation.

REFERENCES

1 **Prins NH**, Akkermans LM, Lefebvre RA, Schuurkes JA. Characterization of the receptors involved in the 5-HT-induced excitation of canine antral longitudinal muscle. *Br J Pharmacol* 2001; **134**: 1351-1359

2 **Leclere PG**, Lefebvre RA. Presynaptic modulation of cholinergic neurotransmission in the human proximal stomach. *Br J Pharmacol* 2002; **135**: 135-142

3 **Prins NH**, van Der Grijn A, Lefebvre RA, Akkermans LM, Schuurkes JA. 5-HT(4) receptors mediating enhancement of contractility in canine stomach; an *in vitro* and *in vivo* study. *Br J Pharmacol* 2001; **132**: 1941-1947

4 **Briejer MR**, Prins NH, Schuurkes JA. Effects of the enterokinetic prucalopride (R093877) on colonic motility in fasted dogs. *Neurogastroenterol Motil* 2001; **13**: 465-472

5 **Jin JG**, Foxx-Orenstein AE, Grider JR. Propulsion in guinea pig colon induced by 5-hydroxytryptamine (HT) via 5-HT4 and 5-HT3 receptors. *J Pharmacol Exp Ther* 1999; **288**: 93-97

6 **Bouras EP**, Camilleri M, Burton DD, McKinzie S. Selective stimulation of colonic transit by the benzofuran 5HT4 agonist, prucalopride, in healthy humans. *Gut* 1999; **44**: 682-686

7 **Poen AC**, Felt-Bersma RJ, Van Dongen PA, Meuwissen SG. Effect of prucalopride, a new enterokinetic agent, on gastrointestinal transit and anorectal function in healthy volunteers. *Aliment Pharmacol Ther* 1999; **13**: 1493-1497

8 **Briejer MR**, Schuurkes JA, Sarna SK. Idiopathic constipation: too few stools and too little knowledge. *Trends Pharmacol Sci* 1999; **20**: 1-3

9 **Li FJ**, Zhou YY, Zhang XC, Shen SR. A postprandial manometric recording of sigmoid motor activity in patients with idiopathic colonic constipation. *Shijie Huaren Xiaohua Zazhi* 2002; **10**: 1232-1233

10 **Rao SS**, Sadeghi P, Batterson K, Beaty J. Altered periodic rectal motor activity: a mechanism for slow transit constipation. *Neurogastroenterol Motil* 2001; **13**: 591-598

11 **Zhang WW**, Li Y. Psychiatric and psychologic factors of functional gastrointestinal disorders. *Shijie Huaren Xiaohua Zazhi* 2002; **10**: 1324-1328

12 **Tian B**, Yang SL, Li YH, Duan QH, Chen GT, Li F, Ma SF. Pathological changes and clinical significance of colonic myenteric plexus in patients with slow transit constipation. *Shijie Huaren Xiaohua Zazhi* 2000; **8**: 1385-1388

13 **Yu DH**. Sugestions on surgical treatment of constipation. *Shijie Huaren Xiaohua Zazhi* 1999; **7**: 169-170

14 **Gao F**, Zhang SB, Zhang LY, Cai WQ, Tong WD, Li FZ, Li WH. Ultrastructural abnormalities of colonic myenteric plexus in patients with slow transit constipation. *Shijie Huaren Xiaohua Zazhi* 1999; **7**: 1049-1051

15 **Tomita R**, Tanjoh K, Fujisaki S, Ikeda T, Fukuzawa M. Regulation of the enteric nervous system in the colon of patients with slow transit constipation. *Hepatogastroenterology* 2002; **49**: 1540-1544

16 **Wald A**. Slow Transit Constipation. *Curr Treat Options Gastroenterol* 2002; **5**: 279-283

17 **Emmanuel AV**, Roy AJ, Nicholls TJ, Kamm MA. Prucalopride, a systemic enterokinetic, for the treatment of constipation. *Aliment Pharmacol Ther* 2002; **16**: 1347-1356

18 **Alaradi O**, Barkin JS. Irritable bowel syndrome: update on pathogenesis and management. *Med Princ Pract* 2002; **11**: 2-17

19 **Krogh K**, Jensen MB, Gandrup P, Laurberg S, Nilsson J, Kerstens R, De Pauw M. Efficacy and tolerability of prucalopride in patients with constipation due to spinal cord injury. *Scand J Gastroenterol* 2002; **37**: 431-436

20 **Sloots CE**, Poen AC, Kerstens R, Stevens M, De Pauw M, Van Oene JC, Meuwissen SG, Felt-Bersma RJ. Effects of prucalopride on colonic transit, anorectal function and bowel habits in patients with chronic constipation. *Aliment Pharmacol Ther* 2002; **16**: 759-767

21 **De Schryver AM**, Andriesse GI, Samsom M, Smout AJ, Gooszen HG, Akkermans LM. The effects of the specific 5HT(4) receptor agonist, prucalopride, on colonic motility in healthy volunteers. *Aliment Pharmacol Ther* 2002; **16**: 603-612

22 **Kamm MA**. Review article: the complexity of drug development for irritable bowel syndrome. *Aliment Pharmacol Ther* 2002; **16**: 343-351

23 **Boeckxstaens GE**, Bartelsman JF, Lauwers L, Tytgat GN. Treatment of GI dysmotility in scleroderma with the new enterokinetic agent prucalopride. *Am J Gastroenterol* 2002; **97**: 194-197

24 **Ahn J**, Ehrenpreis ED. Emerging treatments for irritable bowel syndrome. *Expert Opin Pharmacother* 2002; **3**: 9-21

25 **Talley NJ**. Serotoninergic neuroenteric modulators. *Lancet* 2001; **358**: 2061-2068

26 **Talley NJ**. Drug therapy options for patients with irritable bowel syndrome. *Am J Manag Care* 2001; **7**(8 Suppl): S261-S267

27 **De Ponti F**, Tonini M. Irritable bowel syndrome: new agents targeting serotonin receptor subtypes. *Drugs* 2001; **61**: 317-332

28 **De Schryver AM**, Samsom M. New developments in the treatment of irritable bowel syndrome. *Scand J Gastroenterol Suppl* 2000; **232**: 38-42

29 **Bouras EP**, Camilleri M, Burton DD, Thomforde G, McKinzie S, Zinsmeister AR. Prucalopride accelerates gastrointestinal and colonic transit in patients with constipation without a rectal evacuation disorder. *Gastroenterology* 2001; **120**: 354-360

30 **Scarpignato C**, Pelosini I. Management of irritable bowel syndrome: novel approaches to the pharmacology of gut motility. *Can J Gastroenterol* 1999; **13**(Suppl A): 50A-65A

31 **Zhu JZ**. New development of the gastrointestinal prokinetic agents. *Xin Xiaohua Bingxue Zazhi* 2001; **9**: 1439-1444

32 **Zhu JZ**, Yang GH, Leng ER, Chen DF. Gastrointestinal motility promoting action of traditional Chinese medicine. *Shijie Huaren Xiaohua Zazhi* 1999; **7**: 689-690

Edited by Yuan HT and Wang XL

P.O.Box 2345, Beijing 100023,China
Fax: +86-10-85381893
E-mail: wjg@wjgnet.com www.wjgnet.com

World J Gastroenterol 2003;9(9):2068-2072
World Journal of Gastroenterology
 ISSN 1007-9327

• BASIC RESEARCH •

Optical properties of human normal small intestine tissue determined by Kubelka-Munk method *in vitro*

Hua-Jiang Wei, Da Xing, Guo-Yong Wu, Ying Jin, Huai-Min Gu

Hua-Jiang Wei, Da Xing, Ying Jin, Huai-Min Gu, Institute of Laser Life Science, South China Normal University, Guangzhou, 510631, Guangdong Province, China
Hua-Jiang Wei, Department of Physics, Guangdong College of Pharmacy, Guangzhou, 510224, Guangdong Province, China
Guo-Yong Wu, Department of Surgery, the First Affiliated Hospital, Sun Yat-Sen Medical University, Guangzhou, 510080, Guangdong Province, China
Supported by the Special Funds of National Key Basic Research Project of China, No. 2002CCC0 0400 and the Team Project of Natural Science Foundation of Guangdong Province, No.015012
Correspondence to: Da Xing, Institute of Laser Life Science, South China Normal University, Shipai, Tianhe District, Guangzhou 510631, Guangdong Province, China. xingda@hsut.scnu.edu.cn
Telephone: +86-20-85210089 **Fax:** +86-20-85216052
Received: 2002-12-22 **Accepted:** 2003-03-26

Abstract

AIM: To study the optical properties of human normal small intestine tissue at 476.5 nm, 488 nm, 496.5 nm, 514.5 nm, 532 nm, 808 nm wavelengths of laser irradiation.

METHODS: A double-integrating-sphere system, the basic principle of measuring technology of light radiation, and an optical model of biological tissues were used in the study.

RESULTS: The results of measurement showed that there were no significant differences in the absorption coefficients of human normal small intestine tissue at 476.5 nm, 488 nm, 496.5 nm laser in the Kubelka-Munk two-flux model ($P>0.05$). The absorption coefficients of the tissue at 514.5 nm, 532 nm, 808 nm laser irradiation were obviously increased with the decrease of these wavelengths. The scattering coefficients of the tissue at 476.5 nm, 488 nm, 496.5 nm laser irradiation were increased with the decrease of these wavelengths. The scattering coefficients at 496.5 nm, 514.5 nm, 532 nm laser irradiation were obviously increased with the increase of these wavelengths. The scattering coefficient of the tissue at 532 nm laser irradiation was bigger than that at 808 nm. There were no significant differences in the total attenuation coefficient of the tissue at 476.5 nm and 488 nm laser irradiation ($P>0.05$). The total attenuation coefficient of the tissue at 488 nm, 496.5 nm, 514.5 nm, 532 nm, 808 nm laser irradiation was obviously increased with the decrease of these wavelengths, and their effective attenuation coefficient revealed the same trend. There were no significant differences among the forward scattered photon fluxe, backward scattered photon fluxe, and total scattered photon fluxe of the tissue at 476.5 nm, 488 nm, 496.5 nm laser irradiation. They were all obviously increased with attenuation of tissue thickness. The attenuations of forward and backward scattered photon fluxes, and the total scattered photon fluxe of the tissue at 514.5 nm laser irradiation were slower than those at 476.5 nm, 488 nm, 496.5 nm laser irradiation respectively. The attenuations of forward and backward scattered photon fluxes, and total scattered photon fluxes at 532 nm laser irradiation were obviously slower than those at 476.5 nm, 488 nm, 496.5 nm, 514.5 nm laser irradiation. The attenuations of forward and backward scattered photon fluxes, and total scattered photon fluxe at 808 nm laser irradiation were all obviously slower than those at 476.5 nm, 488 nm, 496.5 nm, 514.5 nm, 532 nm laser irradiation respectively.

CONCLUSION: There are significant differences in optical parameters of human normal small intestine tissue in the Kubelka-Munk two-flux model at six different wavelengths of laser radiation. The results would provide a new method of information analysis for clinical diagnosis.

Wei HJ, Xing D, Wu GY, Jin Y, Gu HM. Optical properties of human normal small intestine tissue determined by Kubelka-Munk method *in vitro*. *World J Gastroenterol* 2003; 9(9): 2068-2072
http://www.wjgnet.com/1007-9327/9/2068.asp

INTRODUCTION

Much effort is being made in the study of light propagation in tissues due to the development and wide use of lasers in surgery and therapy[1-3]. In particular, the effectiveness of photodynamic therapy (PDT) is greatly influenced by photosensitizer content and light distribution in the irradiated tissue[4-7], and an accurate evaluation of energy fluence in depth should allow an estimate of whether the whole tumor mass is properly irradiated[8,9]. Consequently, determination of tissue optical properties is important. Photons are absorbed and scattered when they come into contact with biological tissues[10]. The depolarization degree of different biological tissues at linearly polarized light is different. All these have a correlation with the components and structures of biological tissues and optical properties. Consequently, photons have already taken the information that has a close relationship with the components and structures of biological tissues since photons came into contact with biological tissues[11-13]. Biological tissues may be looked upon as turbid media from the point of view of tissue optics. The optical properties of biological tissues change with the characteristics of living organisms[14-17]. The typical optical properties are obtained by using solutions of the radiative transport equation that expresses the optical properties in terms of readily measurable quantities. These solutions are either exact or approximate and correspond to the direct or indirect methods. A double-integrating-sphere system, the basic principle of measuring technology of light radiation, an optical model of biological tissues were used in this experiment[18-21]. In our study, we detected the optical properties of human normal small intestine tissue at 476.5 nm, 488 nm, 496.5 nm, 514.5 nm, 532 nm, 808 nm wavelengths of laser irradiation, and analyzed the experimental results.

MATERIALS AND METHODS

The optical properties of tissues describe the three-dimensional propagation of radiation. Through modeling simplifications (i.e., Kubelka-Munk Two-Flux Theory) the radial propagation

is often reduced to a one-dimensional propagation of radiation. Kubelka-Munk two-flux theory was used to calculate the absorption coefficient A_{KM}, scattering coefficient S_{KM}, total attenuation coefficient E_t and effective attenuation coefficient E_{eff} of human normal small intestine tissue at six laser wavelengths by measuring reflection R, transmission T of diffuse irradiance on a slab of thickness d of the sample.

Kubelka-Munk two-flux theory

The Kubelka-Munk two-flux theory is applied to the thin slab of scattering material without sources, and its prime advantage as compared to more complicated models is that the scattering coefficient S_{KM} and absorption coefficient A_{KM} can be directly expressed in terms of the measured reflection R, transmission T, and thickness d of the sample[22]. Consequently, it has been widely applied. Its parameters are commonly used in the field of medical physics. It regards the scattering light as none but the forward scattered photon fluxes i(x) and backward scattered photon fluxes j(x) when incident light radiates in a slab of thickness X (cm) of the turbid media. The sum of the forward and backward scattered photon fluxes is equal to the total scattered photon fluxes I(x)[23]. The scattering and absorption coefficients exist[24]. The description of A_{KM} and S_{KM} as a function of R, T, and X are given by

$$A_{KM} = \left[\left(1 + R^2 + T^2\right)/2R - 1\right]S_{KM} \qquad (1)$$

$$S_{KM} = \frac{1}{Xb} In\left[\frac{1 - R/(a + b)}{T}\right] \qquad (2)$$

The description of total attenuation coefficients E_t and effective attenuation coefficients E_{eff} as a function of A_{KM} and S_{KM} are given by[25]

$$E_t = A_{KM} + S_{KM} \qquad (3)$$

$$S_{KM} = \frac{1}{Xb} In\left[\frac{1 - R/(a + b)}{T}\right] \qquad (4)$$

The human normal small intestine tissue was regarded as a slab of turbid medium of thickness X. Then, A_{KM}, S_{KM}, E_t, E_{eff} were respectively regarded as the absorption coefficients, scattering coefficients, total attenuation coefficients, effective attenuation coefficients of human normal small intestine tissue at laser irradiation.

Materials

Sample preparation The sample used in our experiments was obtained within 2 hours after human normal small intestine tissue resection from one subject. The sample was rinsed briefly in saline to remove excess surface blood, and peeled off surface fats. The sample was cut with scissors along its direction of axis and stored at -70 ℃ until the experiments. For the thin tissues, two-faces of sample were not cut by microtome in order to keep integrity of the sample. Because the area of a slice of sample cut by microtome was large, the cytoplasmic liquid exuded severely, which increased the excessive liquid on the surface of the sample. Consequently, the measured results were influenced. The tissue-sample holder was designed and made from a black piece of opacity that was rounded with scissors. The piece was drilled two holes, and its inside radius and outside radius were respectively equal to 6 mm and 12 mm, as shown in Figure 1. The sample was spread out on the tissue-sample holder and nipped. The sample area and thickness were respectively 16.1 mm×16.4 mm and 1.42×0.16 mm, and then it was put in the sample-pool of a double-integrating-sphere system to be measured. The whole experimental process took 4 hours, including sample preparation and taking the sample.

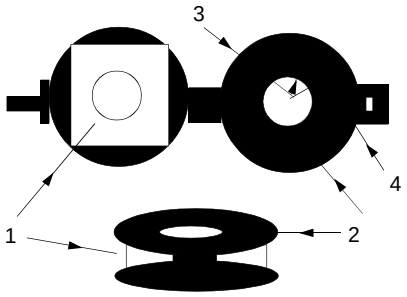

Figure 1 Exhibition map of the tissue- sample holder. 1. Tissue-sample, 2. Tissue- sample holder, 3. R_a=6 mm 4. R_b=12mm.

Methods

Measurement of diffuse reflectance and transmittance The double-integrating-sphere system was a traditional technique to obtain the diffuse reflectance and transmittance of a sample[26-28]. A double-integrating-sphere system shown in Figure 2 consisted of Ti: S ring laser (COHERENT, model 899-05), an argon ion laser (COHERENT, model: INNOVA 70), light attenuator, mirror, 2 mm pinhole, 6 mm pinhole, beam expander of 25 times, two integrating-spheres and two detectors and two optical traps (Anhui Institute of Optics and Fine Mechanics, Academia Sinica, China, model: F4). A Ti:S ring laser emitted at 532 nm and 808 nm wavelengths of laser. An argon ion laser emitted at 476.5 nm, 488 nm, 496.5 nm and 514.5 nm wavelengths of laser. The structures of the two integrating-spheres were the same, the diameter of the sphere was 0.05 m. The diameter of entrance and exit port of the integrating-spheres was equally 0.012 m. The laser beam was passed through two light attenuators, and reflected by the mirror. It was passed through a 2 mm pinhole, and expanded into a collimated laser beam by the beam expander of 25 times. It was passed through a 6 mm pinhole, and perpendicularly incident on the sample. The integrating-sphere I was only used to measure the diffuse reflectance R_d of the sample, not including the specularly reflected light of the sample. The optical trap backed of sample was used for light extinction, including the transmitted light and the diffusely transmitted light. The other optical trap backing the integrating-sphere II was used for light extinction, including all exiting light. The integrating-sphere II was only used to measure the diffuse Transmittance T_d of the sample, not including the collimatedly transmitted light. In this experiment, the diffuse reflectance and transmittance of the wall and the ektexine of the thin sample at 476.5 nm, 488 nm, 496.5 nm, 514.5 nm, 532 nm, 808 nm wavelengths of laser were measured.

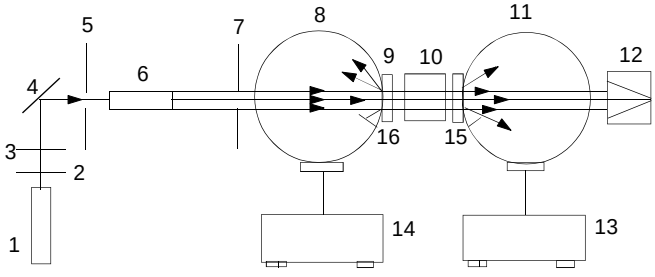

Figure 2 A double-integrating-sphere system was used to determine the optical properties of biological tissues. 1. Laser, 2. Attenuator, 3. Attenuator, 4. Mirror, 5. 2 mm pinhole, 6. Beam expander, 7. 6 mm pinhole, 8. Intergrating sphere I, 9. Sample, 10. Optical trap, 11. Intergrating sphere II, 12. Optical trap, 13. Detector system, 14. Detector system, 15. Baffle, 16. Baffle.

The measuring method of diffuse reflectance was the same as reported[24]. The diffuse reflectance of the sample was given by

$$R_d = \left(\frac{K_S}{K_P} \right) r \qquad (5)$$

where K_p is the diffuse reflection value of the standard target, K_s is the diffuse reflection value of the sample, ρ is the reflection coefficient of the standard target. The diffuse transmittance of the sample was given by

$$T_d = \frac{I_s}{I_0} \qquad (6)$$

where I_s is the diffuse transmission value of the sample, I_o is the total transmission value. Figure 3 shows the arrangement to measure the total transmission value. The half-angle subtended by this aperture from the sample was 3°, and the standard target was placed at the exit port of integrating-sphere II. The wall and ektexine of the sample were respectively radiated at laser and measured.

Measurement of specular reflectance and collimated transmittance

Figure 3 shows the arrangement and method to measure the specularly reflected light, collimated light and the total transmitted light. The half-angle subtended by this aperture from the sample was 3°, and the standard target was placed at the exit port of integrating-sphere II. The other was the same as Figure 2. The integrating-sphere I was used to measure the diffusely and specularly reflected light of the sample. The integrating-sphere II was used to measure the diffusely and collimatedly transmitted light of the sample, and the sum of the diffusely and collimatedly transmitted light of the sample was the totally transmitted light of the sample. The specular reflectance of the sample was given by

$$R_m = \left(\frac{K'_S}{K'_P} \right) r - R_d \qquad (7)$$

where K_p' is the diffuse reflection value of the standard target, K_s' is the diffuse reflection value of the sample, R_d is the diffuse reflectance of the sample, R_m is the specular reflectance of the sample. The collimated transmittance of the sample was given by

$$T_c = \frac{I'_s}{I'_0} - T_d \qquad (8)$$

where T_d is the diffuse transmittance of the sample, T_c is the collimated transmittance of the sample, I_s' is the diffuse transmission value of the sample, I_o' is the total transmission value.

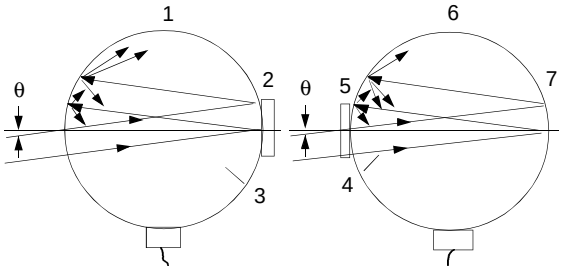

Figure 3 Measuring set of specular reflectance and collimated transmittance of biological tissues. 1. Intergrating sphere I 2. Sample 3. Baffle 4. Baffle 5. Sample 6. Intergrating sphere II 7. Standard reference plate θ=3°.

Statistical analysis

Experimental data were shown as mean and standard deviation (X±SD). The SPSS10 for Windows was used for statistical analysis. The difference between each group was analyzed by *t* test. Significant difference was set at $P<0.05$.

RESULTS

In this experiment, 476.5 nm, 488 nm, 496.5 nm, 514.5 nm, 532 nm, 808 nm wavelengths of laser radiation were respectively used for radiating the wall and ektexine of the thin sample. Each datum was the mean of at least ten measurements of human normal small intestine tissue, and each wavelength of laser in the same way. Each time the sample was measured, the position of incident light spot on the sample was changed. The data had very good repetition. There were no significant differences in the diffuse reflectance and transmittance, the specular reflectance and collimated transmittance of the wall and ektexine of the sample at each wavelength of laser radiation ($P>0.05$). Consequently, the measured results of the wall and ektexine of the sample at the same wavelength of laser radiation were estimated by arithmetical average.

Optical parameters of the tissue in Kubelka-Munk two-flux model

The absorption coefficients, scattering coefficients, total attenuation coefficients and effective attenuation coefficients of human normal small intestine tissue in Kubelka-Munk two-flux model at 476.5 nm, 488 nm, 496.5 nm, 514.5 nm, 532 nm, 808 nm wavelengths of laser radiation are given in Table 1 and shown in Figure 4.

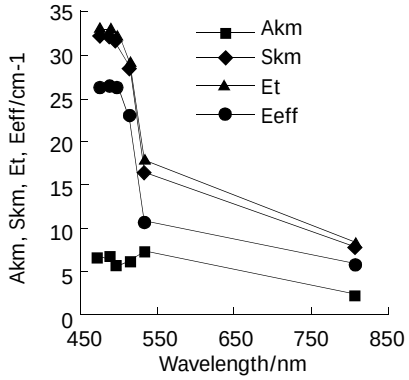

Figure 4 Broken line graphs of A_{KM}-λ, S_{KM}-λ, E_t-λ, S_{eff}-λ of human normal small intestine tissue.

Table 1 The absorption coefficients, scattering coefficients, total attenuation coefficients and effective attenuation coefficients of human normal small intestine tissue in Kubelka-Munk two-flux model at six different wavelengths of laser irradiation

λ / nm	A_{KM} / (cm^{-1})	S_{KM} / (cm^{-1})	E_t / (cm^{-1})	E_{eff} / (cm^{-1})
476.5	26.3±1.15	6.67±0.32	33.0±1.09	32.3±1.53
488	26.5±1.19	6.47±0.29	33.0±1.09	32.3±1.53
496.5	26.4±1.18	5.82±0.24	32.2±1.05	31.7±1.49
514.5	23.2±1.12	6.06±0.28	29.3±0.97	28.6±1.37
532	10.8±0.52	7.27±0.37	18.0±0.89	16.5±0.81
808	5.92±0.26	2.29±0.14	8.21±0.40	7.89±0.39

Light distribution of the tissue in Kubelka-Munk two-flux model along the tissue thickness

Light distribution of i(x), j(x), I(x) of human normal small intestine tissue in Kubelka-Munk two-flux model that changed with tissue thickness at six different wavelengths of laser radiation are shown in Figure 5. Light distribution was automatically created by using the experimental data in Table 1 and Mathcad2001 for Windows.

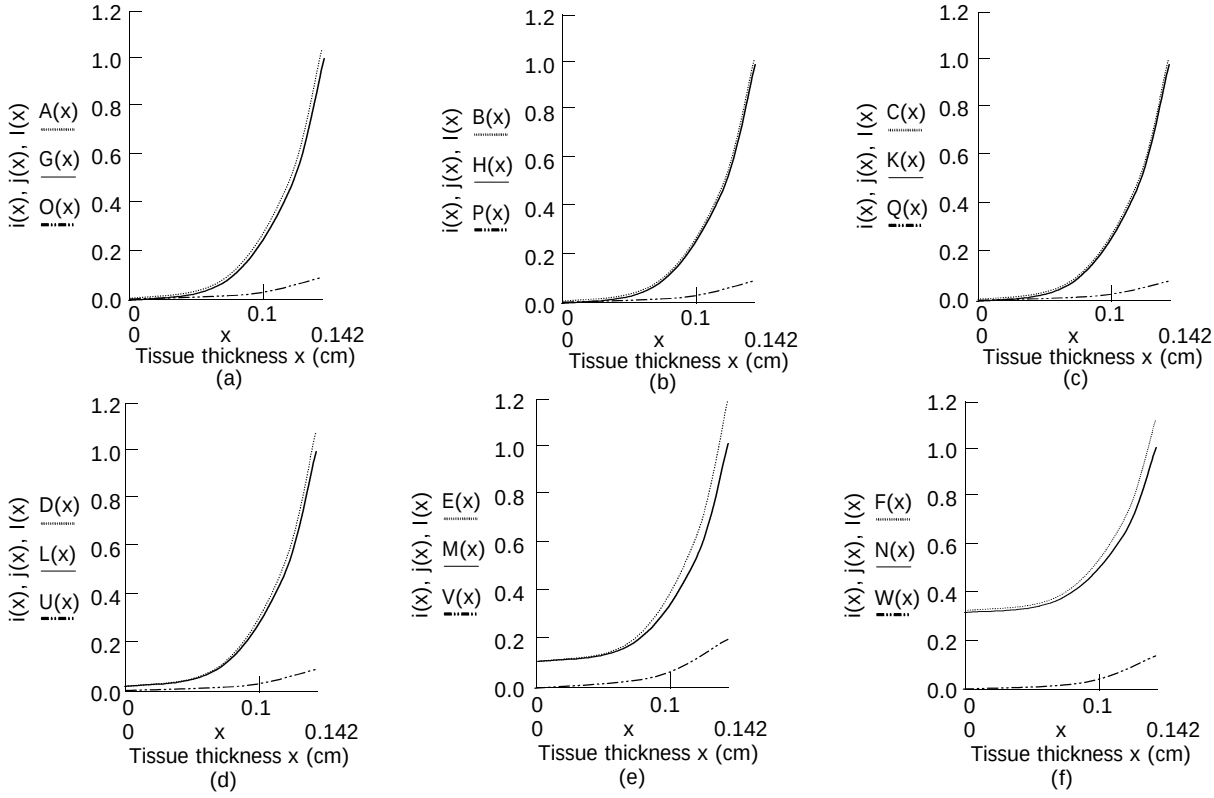

Figure 5 Light distribution of i(x), j(x), I(x) of human normal small intestine tissue in Kubelka-Munk two-flux model changed with tissue thickness at six different wavelengths of laser radiation. (a) A(x), G(x) and O(x) respectively represented the forward and backward, and the total scattered photon fluxes of the tissue at 476.5 nm laser irradiation. (b) B(x), H(x) and P(x) respectively represented the forward, backward and the total scattered photon fluxes of the tissue at 488 nm laser irradiation. (c) C(x), K(x) and Q(x) respectively represented the forward, backward and the total scattered photon fluxes of the tissue at 496.5 nm laser irradiation. (d) D(x), L(x) and U(x) respectively represented the forward, backward and the total scattered photon fluxes of the tissue at 514.5 nm laser irradiation. (e) E(x), M(x) and V(x) respectively represented the forward, backward and the total scattered photon fluxes of the tissue at 532 nm laser irradiation. (f) F(x), N(x) and W(x) respectively represented the forward, backward and the total scattered photon fluxes of the tissue at 808 nm laser irradiation.

The results showed that there were differences both in optics properties of the tissue at six different wavelengths of laser radiation in Kubelka-Munk two-flux model, and in light distribution of i(x), j(x), I(x) of the tissue in Kubelka-Munk two-flux model which changed with the tissue thickness at six different wavelengths of laser radiation.

DISCUSSION

Table 1 and Figure 4 show that there were no significant differences in the absorption coefficients of human normal small intestine tissue in Kubelka-Munk two-flux model at 476.5 nm, 488 nm, 496.5 nm laser radiation (P>0.05). The absorption coefficients of the tissue at 514.5 nm, 532 nm, 808 nm laser radiation obviously increased with decrease of these wavelengths. The scattering coefficients of the tissue at 476.5 nm, 488 nm, 496.5 nm laser radiation increased with decrease of these wavelengths. And the scattering coefficients of the tissue at 496.5 nm, 514.5 nm, 532 nm laser radiation obviously increased with increase of these wavelengths. The scattering coefficient of the tissue at 532 nm laser radiation was bigger than that of the tissue at 808 nm laser radiation. There were no significant differences in the total attenuation coefficients of the tissue at 476.5 nm and 488 nm laser radiation (P>0.05). The total attenuation coefficients of the tissue at 488 nm, 496.5 nm, 514.5 nm, 532 nm, 808 nm laser irradiation obviously increased with decrease of these wavelengths, and their effective attenuation coefficients revealed the same trend. It is suggested that the optical parameters of human tissues in Kubelka-Munk two-flux model can be measured by using the measuring technology of light radiation, and the optical parameters of human tissues with pathological changes and normal human tissues can be compared and analyzed. The results provide a new method of information analysis for clinical diagnosis. Figure 5 shows there were no obvious differences in the forward, backward and the total scattered photon fluxes of the tissue at 476.5 nm, 488 nm, 496.5 nm laser irradiation. All of them obviously increased with attenuation of the tissue thickness. Attenuations of the forward, backward and the total scattered photon fluxes of the tissue at 514.5 nm laser radiation were slightly slower than those at 476.5 nm, 488 nm, 496.5 nm laser radiation. And attenuations of the forward, backward, and the total scattered photon fluxes of the tissue at 532 nm laser radiation were obviously slower than those at 476.5 nm, 488 nm, 496.5 nm, 514.5 nm laser radiation. Attenuations of the forward, backward, and the total scattered photon fluxes of the tissue at 808 nm laser radiation were all obviously slower than those at 476.5 nm, 488 nm, 496.5 nm, 514.5 nm, 532 nm laser radiation. Consequently light attenuation of human normal small intestine tissue at six different wavelengths of laser radiation increased with decrease of these wavelengths, and the change of light attenuation of the tissue accorded completely with the changing rule of penetrability of biological tissues at light radiation of different wavelengths, namely the penetrability of biological tissues from visible light to Infrared light, a range of wavelengths from 400 nm to 900 nm, increased with the increase of wavelengths. It was obvious that penetrability of biological tissues at 808 nm laser was better than the other five wavelengths of laser radiation. 808 nm laser may be used to treat the deep disease

focus in organisms by photodynamic therapy[29-32]. The results of measurement provide useful references and data to laser therapy that is used in clinics, and help improve the effectiveness of photodynamic therapy[33-35].

REFERENCES

1 **Feng L**, Wu YL, Zhu Q, Zhong J. Argon plasma coagulator in the endoscopic treatment of 78 patients with gastrointestinal polyps. *Shijie Huaren Xiaohua Zazhi* 2000; **8**: 1336-1338
2 **Cheng YS**, Shang KZ. Gastrointestinal imageology in China: a 50 year evolution. *Shijie Huaren Xiaohua Zazhi* 2000; **8**: 1225-1232
3 **Feng L**, Wu YL, Zhong J, Zhu Q. Argon plasma coagulation in the endoscopic treatment of verrucosal gastritis. *Shijie Huaren Xiaohua Zazhi* 2000; **8**: 1332-1335
4 **Li CZ**, Cheng LF, Gu Y, Wang ZQ, Yang YS, Liu QS, Linghu EQ. Obliteration effect of photodynamic therapy on small veins: an experimental study. *Zhongguo Jiguang Yixue Zazhi* 2003; **12**: 5-8
5 **Wan XQ**, Wang CP, Cheng K, Li LL, Xu SZ, Li CS, Yang ZQ. Study on the killing effect of in vitro photodynamic therapy using delta-aminolevulinic acid on HEP-2 cells. *Zhongguo Jiguang Yixue Zazhi* 2000; **9**: 102-104
6 **Chen WH**, Yu JX, Yao JZ, Shen WD, Liu JF, Xu DY. Pharmacokinetic studies on hematoporphyrin monomethyl ether: A new promising drug for photodynamic therapy of tumors. *Zhongguo Jiguang Yixue Zazhi* 2000; **9**: 105-108
7 **Liu FG**, Gu Y, Fu QT, Pan YM, Li JH. Absorptive characteristics of HMME and HpD in chicken comb skin and vascular endothelial cells. *Zhongguo Jiguang Yixue Zazhi* 2001; **10**: 9-12
8 **Ritz JP**, Roggan A, Isbert C, Müller G, Buhr HJ, Germer CT. Optical properties of native and coagulated porcine liver tissue between 400 and 2400nm. *Lasers Surg Med* 2001; **29**: 205-212
9 **Qu J**, MacAulay C, Lam S, Palcic B. Optical properties of normal and carcinomatous bronchial tissue. *Appl Opt* 1994; **33**: 7397-7405
10 **Liu G**, Xing D, Wang HM, Wu J. Study of protein in human gallstones by fourier transform infrared spectroscopy and surface-enhanced Raman spectroscopy. *Guangxue Xuebao* 2002; **22**: 441-446
11 **Sankaran V**, Everett MJ, Maitland DJ, Walsh JT Jr. Comparison of polarized-light propagation in biological tissue and phantoms. *Opt Lett* 1999; **24**: 1044-1046
12 **Kim AD**, Ishimaru A. Optical diffusion of continuous-wave, pulsed, and density waves in scattering media and comparisons with radiative transfer. *Appl Opt* 1998; **37**: 5313-5319
13 **Li J**, Li SR, Cao JB, Gao G. Laser-induced fluorescence spectrum of colon cancer *in vivo*. *Shijie Huaren Xiaohua Zazhi* 1999; **7**: 164-165
14 **Liao XH**, Chen ZL, Tang JM, Luo YS. An experimental study on optical properties of rat viscera. *Jiguang Zazhi* 2002; **23**: 74
15 **Li BH**, Xie SS, Lu ZK. Time-resolved spectroscopy for human esophageal and breast tissues *in vitro*. *Guangdianzi Jiguang* 2002; **13**: 1071-1073
16 **Gorti S**, Tone H, Imokawa G. Triangulation method for determining capillary blood flow and physical characteristics of the skin. *Appl Opt* 1999; **38**: 4914-4929
17 **Van der Putten WJM**, Van Gemert MJC. A modelling approach to the detection of subcutaneous tumours by haematoporphyrin-derivative fluorescence. *Phys Med Biol* 1983; **28**: 639-645
18 **Chen R**, Xie SS, Chen YJ, Wang HP. Transmission properties of ray in blood in laser irradiation blood therapy. *Guangdianzi Jiguang* 2001; **12**: 1310-1312
19 **Wu GL**, Luo QM, Zeng SQ, Mu CP, Liu XD. Photon diffusion theory and its application in biomedicine. *Guangdianzi Jiguang* 2001; **12**: 323-328
20 **Cheng SY**, Huang JH, Lin WX, Zhang G, Huang XJ, Huang CH, Shen HY. Problems in measuring attenuation coefficient μt of blood by direct measurement method. *Guangzi Xuebao* 2001; **30**: 1045-1049
21 **Liu XL**, Zhang R, Bao HJ, Zhong JK. Study on the method for determination of tissue optical properties by time resolved reflectance. *Shengwu Wuli Xuebao* 2001; **17**: 209-215
22 **Vogel A**, Dlugos C, Nuffer R, Birngruber R. Optical properties of human sclera, and their consequences for transscleral laser applications. *Lasers Surg Med* 1991; **11**: 331-340
23 **Graaff R**, Aarnoudse JG, De Mul FFM, Jentink HW. Light propagation parameters for anisotropically scattering media based on a rigorous solution of the transport equation. *Appl Opt* 1989; **28**: 2273-2279
24 **Wei HJ**, Li XY, Wu GY, Liu XX, Wei DJ, Tan RC. Scattering and absorbing characteristics of human arteries and veins in Kubelka-Munk model at He-Ne laser *in vitro*. *Zhongguo Jiguang* 2001; **A28**: 573-576
25 **Seiyama A**, Chen SS, Kosaka H, Shiga T. Microspectroscopic measurement of the optical properties of rat liver in the visible region. *J Microscopy* 1994; **175**: 84-89
26 **Pickering JW**, Prahl SA, Van Wieringen N, Beek JF, Sterenborg HJCM, Van Gemert MJC. Double-integrating-sphere system for measuring the optical properties of tissue. *Appl Opt* 1993; **32**: 399-410
27 **Zhu D**, Luo QM, Zeng SQ, Ruan Y. Changes in the optical properties of slowly heated human whole blood and albumen. *Guangxue Xuebao* 2002; **22**: 369-373
28 **Zhu D**, Luo QM, Zeng SQ, Yin M, Ruan Y. Modified double-integrating-sphere system for measuring the optical properties of tissue. *Guangzi Xuebao* 2001; **30**: 1175-1181
29 **Deng XH**, Gu Y, Huang F, Liu FG, Zhu JG, Pan YM. Preliminary study of cytotoxic effect of HMME mediated photodynamic action on synovial cells of rheumatoid arthritis *in vitro*. *Zhongguo Jiguang Yixue Zazhi* 2001; **10**: 218-222
30 **Liu FG**, Gu Y, Liu HL, Fu QT, Zhu JG, Pan YM, Li JH. An experimental study on the comparison of photodynamic effects of hematoporphyrin monomethyl ether and hematoporphyrin derivative. *Zhongguo Jiguang Yixue Zazhi* 2001; **10**: 69-73
31 **Gu Y**, Liu FG, Wang K, Zhu JG, Liang J, Pan YM, Li JH. A clinic analysis of 1216 cases of port wine stain treated by photodynamic therapy. *Zhongguo Jiguang Yixue Zazhi* 2001; **10**: 86-89
32 **Zeng CY**, Huang P, Yang D, Yang SM, Chen F. A study on liver damage induced by photodynamic therapy. *Zhongguo Jiguang Yixue Zazhi* 2000; **9**: 141-145
33 **Zeng CY**, Yang D, Huang P, Zhang HJ, Chen J, Lu GR. Long-term follow-up results of 70 liver cancer cases received ultrasound guided percutaneous PDT. *Zhongguo Jiguang Yixue Zazhi* 2000; **9**: 146-149
34 **Tao R**, Gu Y, Liu FG, Zeng J, Zhang L, Pan YM. Mechanism of photosensitized reaction induced by hematoporphyrin monomethyl ether *in vitro*. *Zhongguo Jiguang Yixue Zazhi* 2002; **11**: 149-153
35 **Zhou SR**, Liu CY, Xu SZ, Xiong LY, Zhou XF. δ-ALA-PDT in treatment in BXSB lupus-prone mice: An experimental study. *Zhongguo Jiguang Yixue Zazhi* 2002; **11**: 154-156

Edited by Zhu LH and Wang XL

P.O.Box 2345, Beijing 100023,China
Fax: +86-10-85381893
E-mail: wjg@wjgnet.com www.wjgnet.com

World J Gastroenterol 2003;9(9):2073-2077
World Journal of Gastroenterology
 ISSN 1007-9327

• BASIC RESEARCH •

Involvement of ATM/ATR-p38 MAPK cascade in MNNG induced G1-S arrest

Ke-Qing Zhu, Suo-Jiang Zhang

Ke-Qing Zhu, Suo-Jiang Zhang, Department of Pathology, School of Medicine, Zhejiang University, Hangzhou 310031, Zhejiang Province, China
Supported by Natural Science Foundation of Zhejiang Province, No.29801
Correspondence to: Dr. Suo-Jiang Zhang, Department of Pathology, School of Medicine, Zhejiang University, Hangzhou 310031, Zhejiang Province, China. zhangsuojiang@yahoo.com
Telephone: +86-571-87217411
Received: 2003-02-26 **Accepted:** 2003-03-12

Abstract

AIM: To understand the effect of low concentration of N-methyl-N'-nitro-nitrosoguanidine (MNNG), which is a widely distributed environmental mutagen and carcinogen especially for human gastric cancer, on DNA damage and to study its possible pathway in regulating cell cycle arrest.

METHODS: The DNA damage effect was measured by Comet assay. A specific phospho-(Ser/Thr) ATM/ATR substrate antibody was used to detect the damage sensor by Western blot. p38 kinase activity was measured by direct kinase assay, and immunoprecipitation for the possible connection between ATM/ATR and p38 MAPK. Flow cytometry analysis and p38 MAPK specific inhibitor SB203580 were combined to detect the possible cell cycle arrest by p38 MAPK.

RESULTS: With the same low concentration MNNG exposure (0.2 μM 2.5 h), Comet assays indicated that strand breaks accumulated, Western blot and kinase assay showed ATM/ATR and p38 kinase activated, immunoprecipitation showed phospho-ATM/ATR substrate antibody combined with both p38 MAPK antibody and phospho-p38 MAPK antibody. p38 MAPK pathway was involved in the G1-S arrest.

CONCLUSION: Activation of ATM/ATR by MNNG induced DNA damage leads to activation of p38 MAPK, which involves in the G1 checkpoint in mammalian cells.

Zhu KQ, Zhang SJ. Involvement of ATM/ATR-p38 MAPK cascade in MNNG induced G1-S arrest. *World J Gastroenterol* 2003; 9 (9): 2073-2077
http://www.wjgnet.com/1007-9327/9/2073.asp

INTRODUCTION

Human beings are exposed to a multitude of carcinogens in their environment, and most cancers are considered to be chemically induced. Monofunctional alkylating agents like N-methyl-N'-nitro-Nitrosoguanidine (MNNG) are widely distributed environmental mutagens and carcinogens that, on activation, react with DNA and proteins and generate adducts. The main target of MNNG is believed to be chromosomal DNA damage, which in turn would provide the primary signal, triggering the DNA damage response that involves coordinate control of multiple signal transduction pathways[1-4]. MNNG is responsible for human gastric cancer, and thus MNNG-induced signal transduction should be most relevant to human gastric carcinogenesis. Since the concentration we used was close to the actual environment concentration, the results would be of much practical significance.

The complex network of DNA damage sensors, signal transmitters, and effectors (checkpoints) is evolved in all eukaryota[5]. The top level of sensors/transmitters in the signal transduction cascade that responds to DNA strand breaks is the members of the phosphatidylinositol 3-kinase family: ataxia-telangiectasia-mutated protein (ATM), ATM- and Rad3-related protein (ATR), and DNA-dependent protein kinase (DNA-PK)[6-8]. Recent findings indicate that ATM activation is not limited to the ionizing radiation-induced response and potentially plays an important role in response to DNA alkylation[9] .

Some evidences have shown that ATM-dependent p53 and c-Jun N-terminal kinase (JNK) pathways are linked to UVA-induced apoptosis. On the other hand, UVC-induced apoptosis occurs through ATR-dependent p53 phosphorylation as well as the JNK pathway[10]. Recently, other data suggest a model in which activation of ATM by gamma irradiation leads to the activation of MKK6, and p38 gamma, and is essential for the proper regulation of the G(2) checkpoint in mammalian cells. But there is no report about the effect of alkylating agents on the possible ATM/ATR-p38MAPK cascade[11].

Based on the above findings, we wanted to know whether low dose of MNNG could damage DNA, what possible function of DNA damage sensor ATM/ATR was in the damage reaction, what the relationship was between ATM/ATR and p38 MAPK, and what effect was on cell cycle.

MATERIALS AND METHODS

Cell culture and MNNG treatment

African green monkey kidney Vero cells cultivated as monolayer in DMEM with 10 % (v/v) heat inactivated fetal calf serum and 100 U/ml penicillin, 100 mg/ml streptomycin in a humidified 5 % CO2 incubator at 37 ℃. For MNNG treatment, the medium was replaced by serum-free DMEM containing 0.2 μmol/L MNNG with 0.2 % solvent DMSO in the medium for indicated period of time (2.5 h). Cells treated in the same way with 0.2 % (v/v) DMSO served as solvent control.

Comet assay

A base layer of 1.0 % agarose was placed on microscope slides and allowed to harden. 75 μl of 1 % low melting point agarose (37 ℃) diluted in deionized H_2O was mixed with 1.0×10^4 treated or untreated cells (5-10 μl in volume) and applied to the coated slide. A glass coverslip was then overlaid on the cell layer, and the agarose was allowed to solidify. The coverslip was then removed, and a third layer of low melting point agarose (75 μl) was added to the slide. Again, a coverslip was overlaid, and the agarose was allowed to solidify. After this, the coverslip was removed, and the slides were placed in a lysis solution (10 mM Tris, pH 10.0, 2.5 M NaCl, 100 mM EDTA, 1 % Triton X-100, 10 % Me_2SO) at 4 ℃ overnight.

The slides were then transferred to an electrophoresis apparatus containing an alkaline solution consisting of 300 mM NaOH and 1 mM EDTA. The slides remained in this solution for 1 h to promote DNA unwinding and were finally subjected to electric current (200 mA) for 1 h. Then the slides were removed, washed three times for 5 min in neutralizing buffer (0.4 M Tris-HCl, pH 7.5) at room temperature, and stained in 50 μl 20μg/ml dilution of EB. The stained nuclei were subsequently examined and photographed.

Western blotting

Protein bands in gels were transferred to nitrocellulose (NC) membranes for 90 min under 100 voltages. After that, all performances about the membranes including washing, primary antibody and horseradish peroxides (HRP) conjugated antibody interactions, enhanced chemiluminescence (ECL) and exposure to films were carried out according to the instruction manual provided by the manufacturer. Bands emerged on films were scanned with a scanning densitometer and quantitated with Kodak 1 D Analysis 2.0 software. Assuming the absorbance of band of DMSO control as 1, the ratio between band of MNNG treatment group and DMSO treatment group of the same kinase on the film was calculated by comparing the relative absorbances of these two bands.

Assay for p38MAPK activity

p38 kinase assay was carried out as described by the protocol of cell signaling technologies. In brief, the Vero cells were washed twice with ice-cold phosphate-buffered saline and exposed to 0.2 μmol/L MNNG for 2.5 h. Then, the cells were washed once with ice-cold phosphate-buffered saline and lysed in 500 μl of lysis buffer per sample (20 mmol/L Tris, pH 7.5, 150 mmol/L NaCl, 1 mmol/L EDTA, 1 mmol/L EGTA, 1 % Triton, 2.5 mmol/L sodium pyrophosphate, 1 mmol/L β-glycerophosphate, 1 mmol/L Na_3VO_4, 1 mg/ml leupeptin, 1 mmol/L PMSF). The lysates were sonicated and centrifuged and the supernatant (which contained 200 μg total protein) was incubated with an immobilized phospho-p38 kinase antibody (Thr 180/Tyr 182) with gentle shocking overnight at 4 ℃. The beads were washed twice with 500 ml of lysis buffer and twice with 500 μl of kinase buffer (25 mmol/L Tris, pH 7.5, 5 mmol/L β-glycerophosphate, 2 mmol/L DTT, 0.1 mmol/L Na_3VO_4, 10 mmol/L $MgCl_2$). The kinase reactions were carried out in the presence of 200 μmol/L ATP, and 2 μg of ATF-2 at 30 ℃ for 30 min. ATF-2 phosphorylation was selectively measured by Western immunoblotting using a chemiluminescent detection system and specific antibodies against phosphorylation of ATF-2 at Thr[71].

Immunoblot analysis

The cells were harvested by trypsinization, and the extracts were prepared by resuspending cell pellets in lysis buffer per sample (20 mmol/L Tris, pH 7.5, 150 mmol/L NaCl, 1 mmol/L EDTA, 1 mmol/L EGTA, 1 % Triton, 2.5 mmol/L sodium pyrophosphate, 1 mmol/L β-glycerophosphate, 1 mmol/L Na_3VO_4, 1 mg/ml leupeptin, 1 mmol/L PMSF). The lysates were sonicated and centrifuged and the supernatant (which contained 200 μg total protein) was incubated with a specific phospho-(Ser/Thr) ATM/ATR substrate antibody with gentle shocking overnight at 4 ℃. Followed by adding 20 μl protein A agarose at 4 ℃ 2 h, the lysates were centrifuged at 1 500×g for 1 min at room temperature. The bands were washed five times with 500 ml of lysis buffer. The protein concentrations were determined using the Bradford assay. Prior to electrophoresis, an appropriate volume of 20 μl 3×SDS sample buffer (150 mM Tris-HCl, pH 6.8, 10 % β-mercaptoethanol, 20 % glycerol, 3 % SDS, 0.01 % bromphenol blue, 0.01 % pyronin-Y) were boiled for 3 min, then it was subjected to SDS-PAGE on 10 % polyacrylamide gels and electrotransferred onto nitrocellulose membranes. The membranes were probed with antibodies against total p38MAPK, phospho-p38MAPK (cell signaling technology). Quantitation of immunoblot signals was performed by densitometry of exposed X-ray films.

Flow cytometry analysis

Was carried out according to the instruction manual provided by the manufacturer.

RESULTS

Accumulation of strand breaks indicated by Comet assays

After treatment with 0.2 μM MNNG 2.5 h, Comet assay (single cell gel electrophoresis, SCGE) showed significant Comet tail formation, similar to the positive control group (4NQO 2.5 mM 30 min). While the control group, both the DMSO treatment group and PBS treatment group, showed no Comet tail formation (Figure 1). Evidently even low concentration of MNNG (0.2 μM) could cause DNA strand broken.

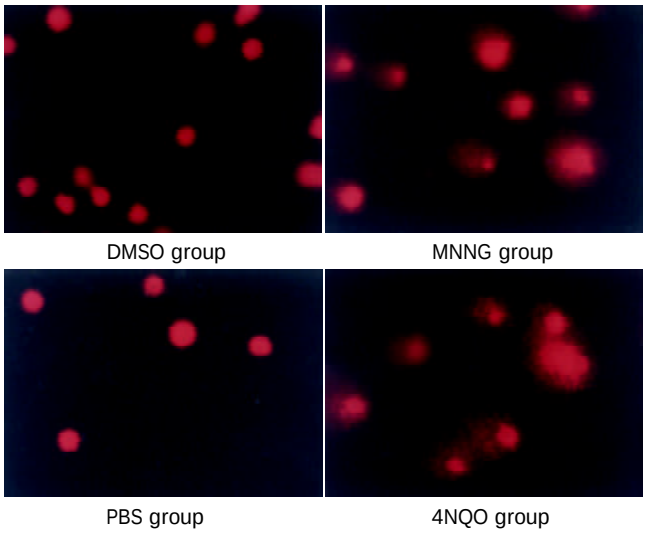

Figure 1 Comet assays indicated accumulation of strand breaks. With low concentration MNNG 0.2 μM 2.5 h treatment, SCGE showed significant comet tail formation, just like the positive control group (4NQO 2.5 mM 30 min). While the control group, both the DMSO treatment group and PBS treatment group, showed no comet tail formation.

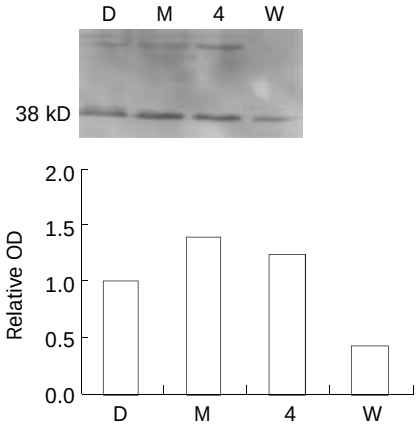

Figure 2 MNNG exposure activates ATM / ATR in Vero cells. Increased phosphorylation of ATM / ATR was observed after 0.2 μM MNNG 2.5 h exposure. One activated substrate molecular weight is about 38 Kda. Pretreatment with 100 μM

wortmannin abrogated the upregulation. Positive control 4-NQO 2.5 mM 30 minutes.

ATM/ATR activated by low concentration MNNG exposure

To test if ATM/ATR was activated in Vero cells following 0.2 μM MNNG exposure, we selected specific phospho-(Ser/Thr) ATM/ATR substrate antibody. We observed increased phosphorylation of ATM/ATR substrate after 2.5 h treatment. The molecular weight of one activated substrate was about 38 Kda. Pretreatment with 100 μM wortmannin abrogated the upregucation. Positive control 4-NQO 2.5 μM for 30 minutes showed similar activated band as the MNNG treatment group (Figure 2). ATM/ATR up-regulation/phosphorylation suggested that DNA strand breaks arising during the repair process activate ATM. These findings indicated that ATM activation was not limited to the ionizing radiation-induced response and potentially played an important role in response to DNA alkylation.

p38 kinase activated by MNNG treatment

Results showed the exposure to 0.2 μmol/L MNNG for 2.5 h, p38 kinase in Vero cells was activated by about 1.47 fold (Figure 3).

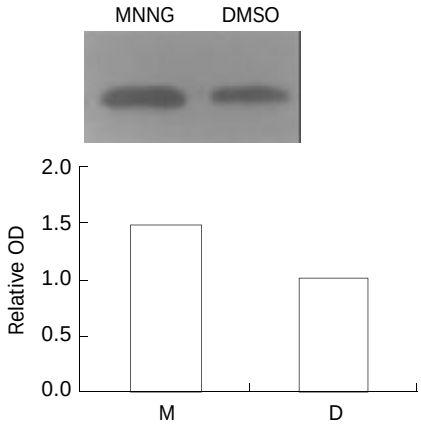

Figure 3 MNNG treatment activated p38 kinase. p38 kinase in Vero cells was activated by about 1.47 fold after the exposure to 0.2 μmol/L MNNG for 2.5 h.

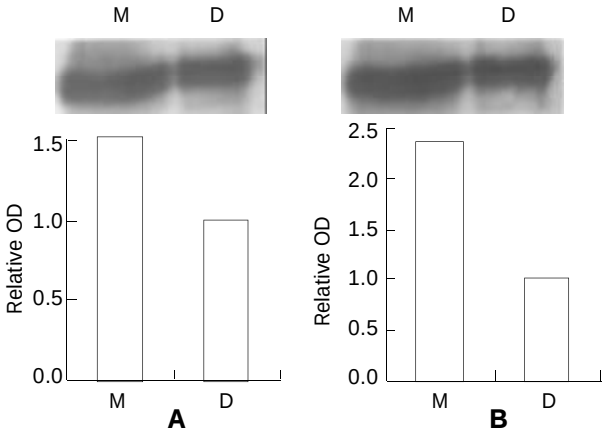

Figure 4 ATM/ATR-P38MAPK pathway is activated by MNNG. Immunoprecipitation showed phospho-ATM/ATR substrate antibody connected with both the p38 MAPK antibody and the phospho-p38MAPK antibody. The band of MNNG group is 1.78 fold (p38MAPK) and 2.37 fold (phospho-p38MAPK) stronger than DMSO group. Combined with the result that P38MAPK was activated by the same treatment, we conclude that ATM/ATR-P38MAPK pathway is activated by MNNG.

ATM/ATR-P38MAPK pathway activated by MNNG

With same treatment (0.2 μM MNNG 2.5 h), immunoprecipitation (IP) showed phospho-ATM/ATR substrate antibody combined with both p38 MAPK antibody and phospho-p38MAPK antibody. The band of MNNG group was 1.78 (p38MAPK) and 2.37 fold (phospho-p38MAPK) stronger than that of DMSO group (Figure 4). Combined with the result of P38MAPK activated by the same treatment, we concluded that ATM/ATR-P38MAPK pathway was activated by MNNG.

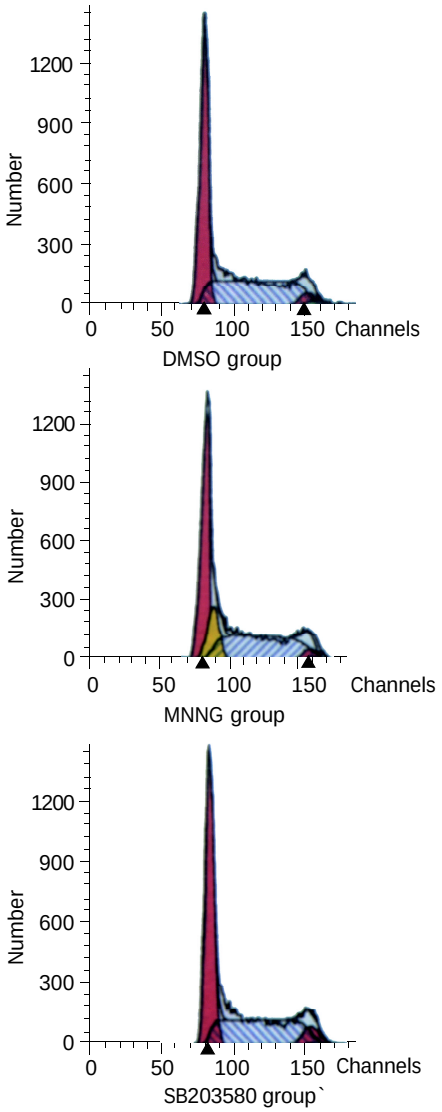

Figure 5 P38MAPK joined G1-S arrest. In the flow cytometry analysis work, it was found that the population of S phase of cell cycle in MNNG treatment group was decreased as compared with the controls (DMSO group). Pretreatment with p38MAPK specific inhibitor SB203580 for 1 h, the G1-S arrest disappeared after the same MNNG treatment.

Table 1 Cell cycle analysis by flow cytometer

Cell	Cell cycle phase fraction (%)		
	G_0-G_1	S	G_2-M
DMSO group	50.22	42.24	4.54
MNNG group	90.36	0.00	9.64
SB203580 group	51.78	41.79	6.43

P38MAPK involved in G1-S arrest

In the flow cytometry analysis (Figure 5), it was found that the population of S phase of cell cycle in MNNG treatment group was decreased as compared with the controls (DMSO group). Pretreatment with p38MAPK specific inhibitor SB203580 for 1

h, the G1-S arrest disappeared after the same MNNG treatment (Table 1). It implied that P38MAPK was involved in the G1-S arrest.

DISCUSSION

Genotoxic events activate a number of signaling pathways that serve, for example, to activate DNA repair mechanisms, halt cell cycle progression and/or trigger advancement into apoptosis. Although all genotoxins produce such general responses, the mechanisms governing response to divergent forms of DNA damage are potentially diverse themselves. γ-irradiation produces double and single strand breaks as well as numerous oxidative changes to bases and deoxyribose moieties, whereas MNNG alkylates (methylates) several nucleophilic centers in bases but does not directly induce strand breaks. MNNG exposure produces mutagenic and cytotoxic O^6-methylguanine (O^6MeG) adducts that can force O^6MeG-T mispairing following replication. In addition to O^6MeG, MNNG causes base alkylation at numerous nucleophilic centers within DNA, such as the N^3 position of adenine. The presence of such adducts triggers DNA glycosylases to generate apurinic/apyrimidinic sites during repair. Apurinic/apyrimidinic sites, in turn, activate an apurinic/apyrimidinic-specific endonuclease resulting in cleavage of DNA.

MNNG can activate JNK/SAPK in human 293 cells at concentrations as high as 70 μmol/L[12]. By our experience, MNNG at concentration of 20 μmol/L is enough to kill over 80 % Vero cells while at concentration of 0.2 μmol/L the highest nontargeted mutation frequency is induced without remarkable mortality[13]. Although it has been verified that with ultraviolet and high concentration of chemical DNA damaging agents, signal transduction is activated not only by damaged but also by undamaged DNA pathways. Insufficient knowledge has been obtained on details of cellular response to low concentration of chemicals especially MNNG. Comet assay (Single cell gel electrophoresis assay, SCGE) is a new and sensitive test for DNA damage studies[14-19]. In our study, with low concentration of MNNG 0.2 μM 2.5 h treatment, Comet assay showed significant Comet tail formation, indicating that strand breaks are accumulated. So even with very low concentration of 0.2 μM of MNNG, DNA strand can also be broken.

It is widely believed that it is the presence of broken DNA strands that activates the catalytic activity of ATM. The ATM gene is mutated in ataxia-telangiectasia, a pleiotropic autosomal recessive disorder characterized by progressive cerebellar degeneration, oculocutaneous telangiectasia, immunodeficiency, cancer predisposition, and an extreme sensitivity to ionizing radiation (IR). Cells derived from ataxia-telangiectasia patients exhibit chromosomal instability and a profound defect in all cellular responses to DNA double strand breaks (DSBs). ATM is a serine/threonine protein kinase that is located mainly in the cell nucleus. Upon infliction of DSBs, ATM mediates the rapid induction of numerous cellular responses that lead to damage repair, and activation of cell cycle checkpoints and other survival pathways[20,21]. To test if ATM/ATR was activated in Vero cells following 0.2 μM MNNG exposure, we selected specific phospho-(Ser/Thr) ATM/ATR substrate antibody. We observed increased phosphorylation of ATM/ATR substrate after 2.5 h treatment. The molecular weight of one activated substrate was about 38 Kda. Pretreatment with 100 μM wortmannin abrogated the upregulation while in positive control it showed similar activated bands as in the MNNG treatment group. ATM/ATR up-regulation/phosphorylation suggested that DNA strand breaks activated ATM/ATR. These findings also indicate that ATM activation is not limited to the ionizing radiation-induced response and potentially plays an important role in response to DNA alkylation.

Downstream targets of ATM/ATR kinase activity that partially delineate DNA damage-activated cell cycle checkpoint signaling pathways have been recently described. The best characterized checkpoint pathways involve p53, Chk1, Chk2, c-Abl, and BRCA1[22-28], but the participating signaling pathways are less clear[29,30]. The complex phenotype of AT cells suggests that it must have other cellular substrates as well[31,32]. Our Western blot result showed that the molecular weight of one activated phosphorylated ATM/ATR substrate was about 38Kda. To identify the possible substrates for ATM and the related kinases ATR, we selected immunoprecipitation test and found that phospho-ATM/ATR substrate antibody was connected with both p38 MAPK antibody and phospho-p38MAPK antibody. By *in vitro* kinase assays, with the same MNNG treatment, p38 MAPK was activated. Taken together, we conclude that ATM/ATR- P38MAPK pathway is activated by MNNG.

MAPKs (mitogen-activated protein kinase) are evolutionarily conserved enzymes connecting cell surface receptors to critical regulatory targets with in cells. MAPKs respond to chemical and physical stresses, thereby controlling cell survial and adaptation. It is becoming clear that MAPKs regulate almost all cellular processes, from gene expression to cell death[33-36]. Mammals express at least four distinctly regulated groups of MAPKs, extracellular signal related kinase (ERK)-1/2, C-Jun N-terminal kinase (JNK1/2/3), p38 MAPK and ERK5. Among MAPKs, both JNK/SAPK and p38MAPK play important roles in cellular stress signal transduction. The involvement of MAP kinases in cell cycle arrest has been studied in a number of organisms. Perhaps due to differences in substrate specificity and regulation among the MAP kinases, their roles in cell cycle regulation appear to be different. Activation of $p42^{MAPK}$ is required for the G_2/M transition in the maturation of Xenopus oocytes[37]. BMK1 (ERK5) was reported to be required for epidermal growth factor-induced progression through S phase[38]. p38α has been reported to be involved in Cdc42-induced G_1 arrest as well as the spindle assembly checkpoint[39,40]. In our experiment, treatment of Vero cells with SB203580, a selective inhibitor of the p38 MAPK pathway, effectively inhibited the G1-S arrest which could be induced by MNNG. These data support an important interplay between the p38 pathway and G_1 cell cycle checkpoint control.

In conclusion, low concentration of MNNG can damage DNA, activate ATM/ATR-p38MAPK cascade and induce G1-S arrest. To our knowledge, this is the first report about the involvement of the ATM/ATR-p38MAPK cascade in the G1-S arrest induced by monofunctional alkylating agent MNNG.

REFERENCES

1 **Schar P**. Spontaneous DNA damage, genome instability, and cancer-when DNA replication escapes control. *Cell* 2001; **104**: 329-332
2 **Lindahl T**, Wood RD. Quality control by DNA repair. *Science* 1999; **286**: 1897-1905
3 **Elledge SJ**. Cell cycle checkpoints: preventing an identity crisis. *Science* 1996; **274**: 1664-1672
4 **Hoeijmakers JH**. Genome maintenance mechanisms for preventing cancer. *Nature* 2001; **411**: 366-374
5 **Zhou BB**, Elledge SJ. The DNA damage response: putting checkpoints in perspective. *Nature* 2000; **408**: 433-439
6 **Khanna KK**, Jackson SP. DNA double-strand breaks: signaling, repair and the cancer connection. *Nat Genet* 2001; **27**: 247-254
7 **Abraham RT**. Cell cycle checkpoint signaling through the ATM and ATR kinases. *Genes Dev* 2001; **15**: 2177-2196
8 **Cortez D**, Guntuku S, Qin J, Elledge SJ. ATR and ATRIP: partners in checkpoint signaling. *Science* 2001; **294**: 1713-1716
9 **Adamson AW**, Kim WJ, Shangary S, Baskaran R, Brown KD. ATM is activated in response to N-methyl-N'-nitro-N-nitrosoguanidine-induced DNA alkylation. *J Biol Chem* 2002;

277: 38222-38229

10 **Zhang Y**, Ma WY, Kaji A, Bode AM, Dong Z. Requirement of ATM in UVA-induced signaling and apoptosis. *J Biol Chem* 2002; **277**: 3124-3131

11 **Wang X**, McGowan CH, Zhao M, He L, Downey JS, Fearns C, Wang Y, Huang S, Han J. Involvement of the MKK6-p38gamma cascade in gamma-radiation-induced cell cycle arrest. *Mol Cell Biol* 2000; **20**: 4543-4552

12 **Wilhelm D**, Bender K, Knebel A, Angel P. The level of intracellular glutathione is a key regulator for the induction of stress-activated signal transduction pathways including Jun N-terminal protein kinases and p38 kinase by alkylating agents. *Mol Cell Biol* 1997; **17**: 4792-4800

13 **Zhang XS**, Yu YN, Chen XR. Evidence for non targeted mutagenesis in a monkey kidney cell line and analysis of its sequence specificity using a shuttle-vector plasmid. *Mutat Res* 1994; **323**: 105-112

14 **Kassie F**, Parzefall W, Knasmuller S. Single cell gel electrophoresis assay: a new technique for human biomonitoring studies. *Mutat Res* 2000; **463**: 13-31

15 **Schreiber V**, Ame JC, Dolle P, Schultz I, Rinaldi B, Fraulob V, Menissier-de Murcia J, de Murcia G. Poly (ADP-ribose) polymerase-2 (PARP-2) is required for efficient base excision DNA repair in association with PARP-1 and XRCC1. *J Biol Chem* 2002; **277**: 23028-23036

16 **Heron-Milhavet L**, Karas M, Goldsmith CM, Baum BJ, LeRoith D. Insulin-like growth factor-I (IGF-I) receptor activation rescues UV-damaged cells through a p38 signaling pathway. Potential role of the IGF-I receptor in DNA repair. *J Biol Chem* 2001; **276**: 18185-18192

17 **Klaude M**, Eriksson S, Nygren J, Ahnstrom G. The comet assay: mechanisms and technical considerations. *Mutat Res* 1996; **363**: 89-96

18 **Fairbairn DW**, Olive PL, O'Neill KL. The comet assay: a comprehensive review. *Mutat Res* 1995; **339**: 37-59

19 **McKelvey-Martin VJ**, Green MH, Schmezer P, Pool-Zobel BL, De Meo MP, Collins A. The single cell gel electrophoresis assay (comet assay): a European review. *Mutat Res* 1993; **288**: 47-63

20 **Pandita TK**, Lieberman HB, Lim DS, Dhar S, Zheng W, Taya Y, Kastan MB. Ionizing radiation activates the ATM kinase throughout the cell cycle. *Oncogene* 2000; **19**: 1386-1391

21 **Khanna KK**. Cancer risk and the ATM gene: a continuing debate. *J Natl Cancer Inst* 2000; **92**: 795-802

22 **Caspari T**. How to activate p53. *Curr Biol* 2000; **10**: R315-317

23 **Turenne GA**, Paul P, Laflair L, Price BD. Activation of p53 transcriptional activity requires ATM's kinase domain and multiple N-terminal serine residues of p53. *Oncogene* 2001; **20**: 5100-5110

24 **Saito S**, Goodarzi AA, Higashimoto Y, Noda Y, Lees-Miller SP, Appella E, Anderson CW. ATM mediates phosphorylation at multiple p53 sites, including Ser (46), in response to ionizing radiation. *J Biol Chem* 2002; **277**: 12491-12494

25 **Ye R**, Bodero A, Zhou BB, Khanna KK, Lavin MF, Lees-Miller SP. The plant isoflavenoid genistein activates p53 and Chk2 in an ATM-dependent manner. *J Biol Chem* 2001; **276**: 4828-4833

26 **Kharbanda S**, Yuan ZM, Weichselbaum R, Kufe D. Etermination of cell fate by c-Abl activation in the response to DNA damage. *Oncogene* 1998; **17**: 3309-3318

27 **Abraham RT**. Cell cycle checkpoint signaling through the ATM and ATR kinases. *Genes Dev* 2001; **15**: 2177-2196

28 **Gatei M**, Scott SP, Filippovitch I, Soronika N, Lavin MF, Weber B, Khanna KK. Role for ATM in DNA damage-induced phosphorylation of BRCA1. *Cancer Res* 2000; **60**: 3299- 3304

29 **Durocher D**, Jackson SP. DNA-PK, ATM and ATR as sensors of DNA damage: variations on a theme? *Curr Opin Cell Biol* 2001; **13**: 225-231

30 **Shiloh Y**. ATM and ATR: networking cellular responses to DNA damage. *Curr Opin Genet Dev* 2001; **11**: 71-77

31 **Lavin MF**, Shiloh Y. The genetic defect in ataxia-telangiectasia. *Annu Rev Immunol* 1997; **15**: 177-202

32 **Kim ST**, Lim DS, Canman CE, Kastan MB. Substrate specificities and identification of putative substrates of ATM kinase family members. *J Biol Chem* 1999; **274**: 37538-37543

33 **Widmann C**, Gibson S, Jarpe MB, Johnson GL. Mitogen-activated protein kinase: conservation of a three-kinase module from yeast to human. *Physiol Rev* 1999; **79**: 143-180

34 **Schaeffer HJ**, Weber MJ. Mitogen-activated protein kinases: specific messages from ubiquitous messengers. *Mol Cell Biol* 1999; **19**: 2435-2444

35 **Chang L**, Karin M. Mammalian MAP kinase signalling cascades. *Nature* 2001; **410**: 37-40

36 **Johnson GL**, Lapadat R. Mitogen-activated protein kinase pathways mediated by ERK, JNK, and p38 protein kinases. *Science* 2002; **298**: 1911-1912

37 **Palmer A**, Gavin AC, Nebreda AR. A link between MAP kinase and p34(cdc2)/cyclin B during oocyte maturation: p90(rsk) phosphorylates and inactivates the p34(cdc2) inhibitory kinase Myt1. *EMBO J* 1998; **17**: 5037-5047

38 **Kato Y**, Tapping RI, Huang S, Watson MH, Ulevitch RJ, Lee JD. Bmk1/Erk5 is required for cell proliferation induced by epidermal growth factor. *Nature* 1998; **395**: 713-716

39 **Molnar A**, Theodoras AM, Zon LI, Kyriakis JM. Cdc42Hs, but not Rac1, inhibits serum-stimulated cell cycle progression at G1/S through a mechanism requiring p38/RK. *J Biol Chem* 1997; **272**: 13229-13235

40 **Takenaka K**, Moriguchi T, Nishida E. Activation of the protein kinase p38 in the spindle assembly checkpoint and mitotic arrest. *Science* 1998; **280**: 599-602

Edited by Zhu LH and Wang XL

P.O.Box 2345, Beijing 100023,China
Fax: +86-10-85381893
E-mail: wjg@wjgnet.com www.wjgnet.com

World J Gastroenterol 2003;9(9):2078-2082
World Journal of Gastroenterology
 ISSN 1007-9327

• BASIC RESEARCH •

Protein kinase C/ζ (*PRKCZ*) Gene is associated with type 2 diabetes in Han population of North China and analysis of its haplotypes

Yun-Feng Li, Hong-Xia Sun, Guo-Dong Wu, Wei-Nan Du, Jin Zuo, Yan Shen, Bo-Qin Qiang, Zhi-Jian Yao, Heng Wang, Wei Huang, Zhu Chen, Mo-Miao Xiong, Yan Meng, Fu-De Fang

Yun-Feng Li, Hong-Xia Sun, Guo-Dong Wu, Wei-Nan Du, Jin Zuo, Yan Meng, Fu-De Fang, National Laboratory of Medical Molecular Biology, Institute of Basic Medical Sciences, Chinese Academy of Medical Sciences & Peking Union Medical College, Beijing 100005, China
Yan Shen, Bo-Qin Qiang, Zhi-Jian Yao, Chinese National Human Genome Center at Beijing, Beijing, 100176, China
Wei Huang, Zhu Chen, Chinese National Human Genome Center at Shanghai, Shanghai, 201203, China
Heng Wang, Peking Union Hospital, Chinese Academy of Medical Sciences & Peking Union Medical College, Beijing, 100730, China
Mo-Miao Xiong, Human Genetics Center, Health Science Center, The University of Texas, Houston TX 77225, USA
Supported by the National Natural Science Foundation of China, No.39896200, No30170441, the National High Technology Research and Development Program, No.2001AA221161, No. 2002BA711A05, No.2002BA711A10-02. The National Program for Key Basic Research Projects, No.G1998051016, the Natural Science Foundation of Beijing, No.7002026
Correspondence to: Fu-De Fang and Yan Meng, National Laboratory of Medical Molecular Biology, Institute of Basic Medical Sciences, Chinese Academy of Medical Sciences & Peking Union Medical College, Beijing 100005, China. fangfd@public3.bta.net.cn, ymengsmile@yahoo.com
Telephone: +86-10-65253005 **Fax**: +86-10-65253005
Received: 2003-01-18 **Accepted:** 2003-03-03

Abstract

AIM: To identify the susceptible gene (s) for type 2 diabetes in the prevously mapped region, 1p36.33-p36.23, in Han population of North China using single nucleotide polymorphisms (SNPs) and to analyze the haplotypes of the gene (s) related to type 2 diabetes.

METHODS: Twenty three SNPs located in 10 candidate genes in the mapped region were chosen from public SNP domains with bioinformatic methods, and the single base extension (SBE) method was used to genotype the loci for 192 sporadic type 2 diabetes patients and 172 normal individuals, all with Han ethical origin, to perform this case-control study. The haplotypes with significant difference in the gene (s) were further analyzed.

RESULTS: Among the 23 SNPs, 8 were found to be common in Chinese Han population. Allele frequency of one SNP, rs436045 in the protein kinase C/ζgene (*PRKCZ*) was statistically different between the case and control groups ($P<0.05$). Furthermore, haplotypes at five SNP sites of *PRKCZ* gene were identified.

CONCLUSION: *PRKCZ* gene may be associated with type 2 diabetes in Han population in North China. The haplotypes at five SNP sites in this gene may be responsible for this association.

Li YF, Sun HX, Wu GD, Du WN, Zuo J, Shen Y, Qiang BQ, Yao ZJ, Wang H, Huang W, Chen Z, Xiong MM, Meng Y, Fang FD. Protein kinase C/ζ (*PRKCZ*) Gene is associated with type 2 diabetes in Han population of North China and analysis of its haplotypes. *World J Gastroenterol* 2003; 9(9): 2078-2082
http://www.wjgnet.com/1007-9327/9/2078.asp

INTRODUCTION

Type 2 diabetes is a highly heterogeneous multifactorial disease with both genetic and environmental determinants and an uncertain mode of inheritance. It is characterized by hyperglycaemia due to defects in insulin secretion and action[1]. Now there are 143 millions people with the disease and more than 15 millions diabetic patients in China. In addition, the prevalence of diabetes is still increasing. The belief that type 2 diabetes has strong genetic determinants is based on several lines of evidence, including the high concordance rate among MZ twins[2,3], the marked difference in disease rate between populations[4-6], and the close correspondence between admixture rate and disease prevalence in hybrid populations[7,8]. In addition, there are evidences for major gene (s) influencing diabetes or its specific clinical manifestations, such as glucose concentration, 2-h postprandial insulin level, and age at onset of diabetes[9-11]. However, the mode of inheritance of type 2 diabetes appears to be variable across populations, suggesting a complex genetic mechanism underlying the disease.

In our previous genome-wide screening, we detected the possible susceptibility gene loci located on chromosomes 1, 12, 18 and 20 in Han population of North China. The 4 regions on chromosome 1 (1p36, 1p31, 1q22, 1q42-43) showed strong evidences of linkage with type 2 diabetes. Interestingly, there are 5 serial makers in the p terminal region, 1p36.33-36.23, showed the linkage, which strongly suggests that there might be susceptible genes residing in this region[12].

In order to clone the susceptible genes in the 1p36.33-36.23 region, we conducted a linkage relative study by using single nucleotide polymorphism (SNP), and observed that three SNPs might be associated with the disease. One of these was the SNP rs43605 in protein kinase C/ζ (PRKCZ) gene, which showed a significantly different frequency between patients and normal controls, implying a possible association with the disease.

Then a set of SNPs located in the upstream and downstream from rs436045 in PRKCZ gene were selected to conduct a case-control study with the linkage disequilibrium (LD) analysis. The results suggested that five SNPs extending about 7kb were in the same haplotype block and there was a significant difference in their haplotype frequencies between case and control groups, which further proves that the PRKCZ gene is a susceptible gene for type 2 diabetes.

MATERIALS AND METHODS

Samples

One hundred and ninety two unrelated type 2 diabetes patients from North China together with 172 controls, matched both

for sex and age, were enrolled in a case-control study. The criteria for diagnosis of diabetes mellitus conformed to those of World Health Organization. Informed consent was obtained from each subject, and the study was performed with the approval of the Ethical Committee of Peking Union Hospital. Genomic DNA was isolated from the blood samples by conventional phenol and chloroform methods. Their final concentrations were all adjusted to 20 ng/μl.

SNP-searching in the 1p36.33-36.23 region

23 SNPs in 10 genes located in or near the 1p36.33-36.23 region were selected from the NCBI SNP database (www.ncbi.nlm.nih.gov/SNP) for genotyping. All these genes were either glucose metabolism-related or lipid metabolism- related or involved in signal transduction pathways.

Primer design

The Primer3.0 program (http://zeno.well.ox.ac.uk:8080/gitbin/primer3_www.cgi) was used to design three primers to every SNP site. One pair of primers was used to amplify the fragments including the SNP site from genomic DNA. The third primer was designed to carry out the single base extension (SBE) reaction[13], and this primer should be near the upstream of the SNP site, and could be used to anneal with the template. We then carried out a multiplex polymerase chain reaction (PCR). We designed eight different SBE primers according to different SNPs. The primers' lengths were 18, 22, 26, 30, 34, 38, 42 and 46 bp, respectively, with Tm between 60 ℃-80 ℃.

PCR and purification of the products

The touch-down PCR was carried out. The reaction system was 10 μl mixture containing 50 ng genomic DNA, 3 mmol/L Mg^{2+}, 0.3 mmol/L dNTP, 1 U AmpliTaq Gold. The reaction conditions were denaturation at 94 ℃ for 12 min, then 15 cycles of denaturation at 94 ℃ for 30 s, annealing at 63 ℃ for 30 s, extension at 72 ℃ for 40 s, with the annealing temperature being decreased 0.5 ℃ every cycle. After 15 cycles, the reaction conditions were denaturation at 94 ℃ for 30 s, annealing at 56 ℃ for 30 s, extension at 72 ℃ for 40 s, for 25 cycles, then extension at 72 ℃ for 10 min. The excess primers and dNTPs were removed by adding exonuclease I (1 U, USB, OHIO, USA) and calf intestine alkaline phosphatase (1.5 U, Boehringer Mannheim, Germany) to the PCR reaction mixture and incubating it at 37 ℃ for 1 hour, and then at 95 ℃ for 15 min to inactivate the enzymes.

SBE reaction and identification of genotypes

SBE reaction was carried out on the purified PCR products using SBE primer (100 nM), Joe-ddATP (30 nM), Fam-ddGTP (30 nM), Tamra-ddCTP (30 nM), Rox-ddUTP (150 nM) and Thermosequenase (1 U, Amersham Pharmacia, USA). The reaction conditions were denaturation at 95 ℃ for 30 s, annealing at 50 ℃ for 30 s, extension at 60 ℃ for 40 s, for a total of 35 cycles, followed by extension at 60 ℃ for 3 min.

One μl of SBE products in loading buffer (2 μl) was electrophoresed in the ABI377 sequencers. The length of the products was compared with differently colored luciferin marking a DNA complex with different lengths (i.e.19, 23, 27, 31, 35, 39, 43 and 47 bp). The SNP's genotype was determined by the color and length of each line. Then the PCR products were sequenced to check the SBE genotypes.

Statistical analysis

Hardy-Weinberg equilibrium[14] was tested for each genotyped locus. Using SPSS10.0 program, we compared the difference in allele frequency between cases and controls with χ^2 test.

SNP genotype in PRKCZ gene and haplotype analysis

The SNPs in PRKCZ gene were found from the NCBI SNP database according to gene name and 16 SNPs upstream and downstream of rs436045 were selected and genotyped. For SNP genotyping in *PRKCZ* gene and analysis of the haplotypes, the association analysis was carried out as follows: (1) Hardy-Weinberg equilibrium analysis; (2) The allele association analysis using SPSS10.0 program; (3) The linkage disequlibrium analysis and haplotype analysis were performed to find the haplotype related to type 2 diabetes. Genotyping results were chosen from the 24 normal controls to calculate the number of individuals with different haplotypes using the Phase program. The above results were transformed into a FASTA file analyzed using DnaSP3.5 program (http://www.bio.ub.es/~julio/DnaSP.html). The degree of linkage disequlibrium between each SNP pair (D' and r^2) and the minimum number of recombination events and their locations were calculated in order to determine the haplotype block structure of these loci. The number of haplotypes and the number of individuals with different haplotypes in each haplotype block in both case and control groups were calculated by the DnaSP3.5 program again to search for the disease-associated haplotypes.

RESULTS

Results of 23 SNPs in both case and control groups analyzed by SPSS program

Of the 23 candidate SNPs tested, one was failed to be amplified from genomic DNA (rs586965) and three were heterozydous in all the samples tested (rs5251, rs15431 and rs15854). We deduced that these three were false SNPs due to paralogous sequences. In the remaining 20 candidates, 7 SNPs were homozygous in all the samples (rs91350, ss91351, rs9117, rs5259, rs228691, rs228677 and rs170633), suggesting that they might not be true polymorphisms. Four SNPs (rs1801131, rs14311, rs5254 and rs609805) had minor allele frequencies of less than 15 % and thus were discarded. The remaining 8 SNPs (rs1801133, rs436045, rs228648, rs11740, rs262669, rs228669, rs170629 and rs161825) were genotyped in both case and control groups. Their minor allele frequencies ranged from 26.3 % to 43.16 % and all belonged to the transition type. All the SNPs were studied in the Hardy-Weinberg equilibrium. SPSS analysis showed that the allele frequency of one SNP, namely rs436045 in an intron of PRKCZ gene, was statistically different between case and control groups (Table 1).

Results of SNP genotype in PRKCZ gene and haplotype analysis

Sixteen SNPs in the upstream and downstream of rs436045 in PRKCZ gene were selected, and genotyped. Then the results were analyzed. (1) Hardy-Weinberg equilibrium analysis. (2) The allele frequencies analysis, χ^2 analysis showed the difference between the case and controls (Table 2). (3) Linkage disequlibrium analysis and haplotype analysis were used to find the haplotype related to type 2 diabetes.

To search for the disease-associated haplotypes, haplotypes were constructed by linkage disequlibrium mapping in the region. The results were analyzed using DnaSP3.5. The recombination analysis showed that the minimum number of recombination events was three and they were detected between [rs1878745, rs1467217], [rs1467217, rs1401126], [rs1401126, rs411021]. From the results, we believed that 10 SNPs from rs411021 to rs262642 in 13 loci were in the linkage disequlibrium. They were in the same haplotype block. Further analysis on the frequencies of haplotypes formed by alleles of the 10 loci in case and control groups showed that a more

significant difference existed in the frequencies of different haplotypes (Table 3). There were mainly 4 haplotypes in the control group, accounting for 98.3 % of the total, suggesting that these loci were in the same haplotype block. But there were many more different haplotypes with variable frequencies in the case group. Analysis using the DnaSP3.5 program showed that recombination events existed between [rs809912, rs262669], [rs262669, rs262662], [rs262662, rs381664], [rs381664, rs262650] and [rs262650, rs262642], suggesting that only rs411021, rs436045, rs427811, rs385039 and rs809912, were in the same haplotype block in the case group (Figure 1). The haplotypes containing these five loci were further analyzed in the two groups. The results showed that there were mainly two haplotypes and their frequencies were significantly different in the two groups (Table 4).

Table 1 SPSS analysis results of genotyped SNPs in case and control group

SNP		Allele				Total	*P* value	Frequency of allele
		C	T	A	G			
rs11740	Case	129	245			374	0.978	0.345
	Control	110	208			318		0.346
	Total	239	453			692		
rs161825	Case			216	140	356	0.917	0.393
	Control			176	116	292		0.397
	Total			392	256	648		
rs170629	Case	261	119			380	0.710	0.313
	Control	156	76			232		0.328
	Total	417	195			612		
rs228648	Case			113	297	410	0.029	0.276
	Control			111	205	316		0.351
	Total			224	502	726		
rs228669	Case	264	110			374	0.455	0.294
	Control	212	100			312		0.321
	Total	476	210			686		
rs262669	Case	269	129			398	0.639	0.324
	Control	207	107			314		0.341
	Total	476	236			712		
rs436045	Case	329	75			404	0.003	0.186
	Control	207	81			288		0.281
	Total	536	156			692		
rs1801133	Case			224	156	380	0.607	0.411
	Control			133	101	234		0.432
	Total			357	257	614		

Table 2 Statistical analysis of genotyped SNPs in *PRKCZ*

SNP name	Minor allele	Allele frequency (%)		*P* value	
		Case	Control	χ^2	T^2
rs1878745	G	48.2	53.3	0.213	0.219
rs1467217	G	45.9	53.0	0.049	0.041
rs1401136	A	10.7	15.3	0.302	0.268
rs411021	T	17.9	27.3	0.005	0.007
rs436045	A	18.6	28.1	0.003	0.005
rs427811	G	17.9	28.0	0.009	0.013
rs385039	G	16.7	27.3	0.003	0.005
rs809912	A	16.7	27.3	0.003	0.005
rs262669	T	28.0	31.9	0.199	0.209
rs262662	C	28.4	35.9	0.029	0.030
rs381664	C	17.9	27.3	0.005	0.007
rs262650	A	20.4	27.3	0.022	0.030
rs262642	T	17.8	24.1	0.066	0.036

Table 3 Difference in frequencies of haplotypes formed by alleles of the 10 loci in case and control groups

Haplotypes	Frequency (%)	
	Control	Case
CGTAGCTTGC	63.5	64.7
TAGGATCCAC	22.5	13.1
CGTAGTCTGC	7.8	6.2
TAGGATCCAT	4.5	2.9
CGTAGCCTGC	0.8	1.3
CGGAGTCTGC	0.4	0.7
CAGAGTCCAT	0.4	0
CGTAGCCTAC	0	2.9
CGTAGCTTGT	0	2.3
CGTAGTTTGC	0	2.3
CGTAGTCTAC	0	1.0
TAGGATTCGT	0	1.0
TAGAGTCCAC	0	0.3
CAGGATCCAT	0	0.3
CGGAGTTTGC	0	0.3
TAGGATTCGC	0	0.3
CGTAGTTCGC	0	0.3
TAGGATTTGT	0	0.3
TAGGACCCAT	0	0.3

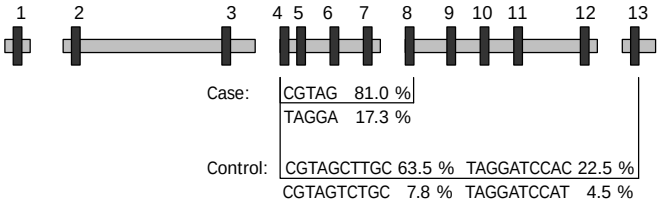

Figure 1 Haplotype block in PRKCZ gene in case and control groups. The black bars 1-13 represented the 13 SNP loci, namely rs1878745, rs1467217, rs1401136, rs411021, rs436045, rs427811, rs385039, rs809912, rs262669, rs262662, rs381664, rs262650 and rs262642, respectively.

The frequency of CGTAG haplotype was considerably increased and that of TAGGA haplotype decreased in the case group ($P<0.01$), with odds ratio (OR) of 1.652, suggesting that CGTAG and TAGGA might be disease-associated haplotypes (Table 4).

Table 4 Difference in frequencies of haplotypes formed by alleles of the 5 loci in case and control groups

Haplotype	Frequency (%)		*P* value	OR
	Control	Case		
CGTAG	72.1	81.0	0.007	1.652
TAGGA	27.0	17.3		
CGGAG	0.4	1.0		
CAGAG	0.4	0		
TAGAT	0	0.3		
CAGGA	0	0.3		

DISCUSSION

In our previous genome-wide screening, we detected the possible susceptible gene loci located on chromosomes 1, 12, 18 and 20 in Han people of North China. Especially, the four regions on chromosome 1 (1p36, 1p31, 1q22 and 1q42-43) showed evidences of linkage with type 2 diabetes[12]. Interestingly, five serial makers in the p terminal region, 1p36.33-36.23, showed the linkage, strongly suggesting that there may be susceptible

genes residing in this region. Eight SNPs from six genes in the region were genotyped for 192 unrelated type 2 diabetic patients and 172 normal controls. The results showed that one SNP (rs436045) in *PRKCZ* gene was statistically different, suggesting that the SNP may be associated with type 2 diabetes. So we suggested that *PRKCZ* might be a susceptible gene for type 2 diabetes.

Protein kinase C zeta (PRKCZ) is a member of the PKC family of serine/threonine kinases, which consists of at least 10 structurally related enzymes that have been implicated in a variety of cellular processes. *PRKCZ* gene belongs to the aPKC subfamily and is thought to function downstream of phosphatidylinositol 3-kinase (PI 3-kinase) in the insulin signal pathway and to contribute to the translocation of the protein encoded by *GLUT4*. The activated PRKCZ products can accelerate glucose transport during insulin action on rat skeletal muscle and adipocytes[15-18]. In addition, PRKCZ may participate in a negative feedback pathway by phosphorylating insulin receptor substrate-1 (IRS-1) and impairing its ability to activate phosphatidylinositol 3-kinase in response to insulin[19,20]. Insulin-stimulated glucose transport is defective in type 2 diabetes, and this defect is ameliorated by thiazolidinediones and lowering of blood glucose by chronic insulin therapy or short-term fasting. Rosiglitazone treatment, insulin treatment, and fasting can reverse the defects in PRKC-zeta/lambda activation by insulin in GK rat muscles and adipocytes and increase glucose transport in GK rat adipocytes, suggesting that insulin-sensitizing modalities may similarly improve defects in insulin-stimulated glucose transport at least partly by correcting defects in insulin-induced activation of PRKC-zeta/lambda[21]. The above may explain our results.

It is the essential prerequisite for localizing genes associated to disease on the base of the multitude to study linkage disequlibrium (LD) model in detail of the multitude. Now there are still some controversies on the LD capacity. The computer imitating[22] and the experience data[23] all showed that the LD would elongate several kilo basepair near some common SNP, while some other data showed that the LD would elongate more sometimes beyond 100 kilo basepairs[24-26]. Some new research data showed that the LDs would exist in the genomic DNA as the block structure, they would be broken up by the recombination spot[27-30]. Understanding the LD structure is very important for LD analysis, and for carrying out studies on disease-related mutations, population genetics, and the human genomes project. Haplotype blocks are very important for LD. Once a haplotype block is identified in some sequences, different alleles based on it can be selected for LD analysis. So, haplotype block is a very effective method to test the genomic DNA fragments associated with diseases.

Blocks are defined according to the genetic content, not according to how the information is produced and why it exists. Thus, there is no strictly limit in the definition of blocks, which may be different according to different aims. Now there are no very accurate methods to construct haplotype blocks. When we constructed the blocks, we classified a series of SNPs, which have a high linkage disequlibrium but have no recombination, into one block under the condition of the capacity of LD and the recombination spots for every two SNPs.

In order to further study PRKCZ associated with diseases, a set of SNPs located in the upstream and downstream from rs436045 in PRKCZ gene were selected to conduct a case-control study and LD analysis. The results showed that the frequencies of many sites' alleles were significantly different between case and control groups. LD analysis and recombination analysis were further carried out, and the results showed that there was a slight difference between case and control groups. The LD capacity was very high between rs411021 to rs262642 among about 50 kilobasepairs region, and the recombination frequency was very low, suggesting that these SNPs existed in one haplotype block. In cases, however, the LD capacity was very high only in five SNPs from rs411021 to rs809912, within the about 7 kilo basepaires region. The haplotypes containing these five loci were further analyzed in the two groups. The results showed that there were mainly two haplotypes with frequencies very different between the two groups. The frequency of CGTAG haplotype was significantly increased while that of TAGGA haplotype decreased in the case group ($P<0.01$), suggesting that CGTAG and TAGGA might be disease-associated haplotyps. In conclusion, *PRKCZ* gene may be associated with type 2 diabetes in Han population of North China. The haplotypes at five SNP sites in this gene may be responsible for this association.

REFERENCES

1 **DeFronzo RA**, Bonadonna RC, Ferrannini E. Pathogenesis of NIDDM. A balanced overview. *Diabetes Care* 1992; **15**: 318-368

2 **Barnett AH,** Leslie RD, Pyke DA. Chlorpropamide-alcohol flushing and proteinuria in non-insulin-dependent diabetics. *Diabetologia* 1981; **20**: 87-93

3 **Newman B,** Selby JV, King MC, Slemenda C, Fabsitz R, Friedman GD. Concordance for type 2 (non-insulin dependent) diabetes mellitus in male twins. *Diabetologia* 1987; **30**: 763-768

4 **Zimmet P**. Epidemiology of diabetes and its macrovascular manifestations in Pacific populations: the medical effects of social progress. *Diabetes Care* 1979; **2**: 144-153

5 **Diehl AK,** Stern MP. Special health problems of Mexican-Americans: obesity, gallbladder disease, diabetes mellitus, and cardiovascular disease. *Adv Intern Med* 1989; **34**: 73-96

6 **Mckeigue PM,** Shah B, Marmot MG. Relation of central obesity and insulin resistance with high diabetes prevalence and cardiovascular risk in South Asians. *Lancet* 1991; **337**: 382-386

7 **Brosseau JD,** Eelkema RC, Crawford AC, Abe TA. Diabetes among the three affiliated tribes: correlation with degree of Indian inheritance. *Am J Public Health* 1979; **69**: 1277-1278

8 **Knowler WC,** Williams RC, Pettitt DJ, Steinberg AG. Gm3; 5, 13, 14 and type 2 diabetes mellitus: an association in American Indians with genetic admixture. *Am J Hum Genet* 1988; **43**: 520-526

9 **Hanson RL,** Elston RC, Pettitt DJ, Bennett PH, Knowler WC. Segregation analysis of non-insulin-dependent diabetes mellitus in Pima Indians: evidence for a major-gene effect. *Am J Hum Genet* 1995; **57**: 160-170

10 **Mitchell BD,** Kammerer CM, O'Connell P, Harrison CR, Manire M, Shipman P, Moyer MP, Stern MP, Frazier ML. Evidence for linkage of postchallenge insulin levels with intestinal fatty acid-binding protein (FABP2) in Mexican-Americans. *Diabetes* 1995; **44**: 1046-1053

11 **Stern MP,** Mitchell BD, Blangero J, Reinhart L, Krammerer CM, Harrison CR, Shipman PA, O'Connell P, Frazier ML, MacCluer JW. Evidence for a major gene for type II diabetes and linkage analyses with selected candidate genes in Mexican-Americans. *Diabetes* 1996; **45**: 563-568

12 **Du W**, Sun H, Wang H, Qiang B, Shen Y, Yao Z, Gu J, Xiong M, Huang W, Chen Z, Zuo J, Hua X, Gao W, Sun Q, Fang F. Confirmation of susceptibility gene loci on chromosome 1 in Northern China Han families with type 2 diabetes. *Chin Med J* 2001; **114**: 876-878

13 **Lindblad-Toh K**, Winchester E, Daly MJ, Wang DG, Hirschhorn JN, Laviolette JP, Ardlie K, Reich DE, Robinson E, Sklar P, Shah N, Thomas D, Fan JB, Gingeras T, Warrington J, Patil N, Hudson TJ, Lander ES. Large-scale discovery and genotyping of single-nucleotide polymorphisms in the mouse. *Nat Genet* 2000; **24**: 381-386

14 **Cannings C**, Edwards AW. Expected genotypic frequencies in a small sample: deviation from Hardy-Weinberg equilibrium. *Am J Hum Genet* 1969; **21**: 245-247

15 **Standaert ML**, Galloway L, Karnam P, Bandyopadhyay G, Moscat J, Farese RV. Protein kinase C-ζ as a downstream effector of phosphatidylinositol 3-kinase during insulin stimulation in rat adipocytes potential role in glucose transport. *J Biol Chem* 1997; **272**: 30075-30082

16 **Standaert ML**, Bandyopadhyay G, Sajan MP, Cong L, Quon MJ,

Farese RV. Okadaic acid activates atypical protein kinase C (zeta/lambda) in rat and 3T3/L1 adipocytes. An apparent requirement for activation of Glut4 translocation and glucose transport. *J Biol Chem* 1999; **274**: 14074-14078

17 **Etgen GJ**, Valasek KM, Broderick CL, Miller AR. *In vivo* adenoviral delivery of recombinant human protein kinase C-ζ stimulates glucose transport activity in rat skeletal muscle. *J Biol Chem* 1999; **274**: 22139-22142

18 **Tremblay F,** Lavigne C, Jacques H, Marette A. Defective insulin-induced GLUT4 translocation in skeletal muscle of high fat-fed rats is associated with alterations in both Akt/protein kinase B and atypical protein kinase C(ζ/λ) activities. *Diabetes* 2001; **50**: 1901-1910

19 **Ravichandran LV**, Esposito DL, Chen J, Quon MJ. Protein kinase C-ζ phosphorylates insulin receptor substrate-1 and impairs its ability to activate phosphatidylinositol 3-kinase in response to insulin. *J Biol Chem* 2001; **276**: 3543-3549

20 **Liu YF**, Paz K, Herschkovitz A, Alt A, Tennenbaum T, Sampson SR, Ohba M, Kuroki T, LeRoith D, Zick Y. Insulin stimulates PKCζ-mediated phosphorylation of insulin receptor substrate-1 (IRS-1). A self-attenuated mechanism to negatively regulate the function of IRS proteins. *J Biol Chem* 2001; **276**: 14459-14465

21 **Kanoh Y**, Bandyopadhyay G, Sajan MP, Standaert ML, Farese RV. Rosiglitazone, insulin treatment, and fasting correct defective activation of protein kinase C-zeta/lambda by insulin in vastus lateralis muscles and adipocytes of diabetic rats. *Endocrinology* 2001; **142**: 1595-1605

22 **Kruglyak L**. Prospects for whole-genome linkage disequilibrium mapping of common disease genes. *Nat Genet* 1999; **22**: 139-144

23 **Dunning AM**, Durocher F, Healey CS, Teare MD, McBride SE, Carlomagno F, Xu CF, Dawson E, Rhodes S, Ueda S, Lai E, Luben RN, Van Rensburg EJ, Mannermaa A, Kataja V, Rennart G, Dunham I, Purvis I, Easton D, Ponder BA. The extent of linkage disequilibrium in four populations with distinct demographic histories. *Am J Hum Genet* 2000; **67**: 1544-1554

24 **Abecasis GR**, Noguchi E, Heinzmann A, Traherne JA, Bhattacharyya S, Leaves NI, Anderson GG, Zhang Y, Lench NJ, Carey A, Cardon LR, Moffatt MF, Cookson WO. Extent and distribution of linkage disequilibrium in three genomic regions. *Am J Hum Genet* 2001; **68**: 191-197

25 **Taillon-Miller P**, Bauer-Sardina I, Saccone NL, Putzel J, Laitinen T, Cao A, Kere J, Pilia G, Rice JP, Kwok PY.Juxtaposed regions of extensive and minimal linkage disequilibrium in human Xq25 and Xq28. *Nat Genet* 2000; 25: 324-328

26 **Collins A**, Lonjou C, Morton NE. Genetic epidemiology of single-nucleotide polymorphisms. *Proc Natl Acad Sci U S A* 1999; **96**: 15173-15177

27 **Goldstein DB**. Islands of linkage disequilibrium. *Nat Genet* 2001; **29**: 109-111

28 **Jeffreys AJ**, Kauppi L, Neumann R. Intensely punctate meiotic recombination in the class II region of the major histocompatibility complex. *Nat Genet* 2001; **29**: 217-222

29 **Johnson GC,** Esposito L, Barratt BJ, Smith AN, Heward J, Di Genova G, Ueda H, Cordell HJ, Eaves IA, Dudbridge F, Twells RC, Payne F, Hughes W, Nutland S, Stevens H, Carr P, Tuomilehto-Wolf E, Tuomilehto J, Gough SC, Clayton DG, Todd JA. Haplotype tagging for the identification of common disease genes. *Nat Genet* 2001; **29**: 233-237

30 **Rioux JD,** Daly MJ, Silverberg MS, Lindblad K, Steinhart H, Cohen Z, Delmonte T, Kocher K, Miller K, Guschwan S, Kulbokas EJ, O'Leary S, Winchester E, Dewar K, Green T, Stone V, Chow C, Cohen A, Langelier D, Lapointe G, Gaudet D, Faith J, Branco N, Bull SB, McLeod RS, Griffiths AM, Bitton A, Greenberg GR, Lander ES, Siminovitch KA, Hudson TJ. Genetic variation in the 5q31 cytokine gene cluster confers susceptibility to Crohn disease. *Nat Genet* 2001; **29**: 223-228

Edited by Xia HHX and Wang XL

P.O.Box 2345, Beijing 100023,China
Fax: +86-10-85381893
E-mail: wjg@wjgnet.com www.wjgnet.com

World J Gastroenterol 2003;9(9):2083-2087
World Journal of Gastroenterology
 ISSN 1007-9327

• BASIC RESEARCH •

Gene transfer and expression of enhanced green fluorescent protein in variant HT-29c cells

Min Wang, Lars Boenicke, Bradley D. Howard, Ilka Vogel, Holger Kalthoff

Min Wang, Department of Surgical Oncology, First Affiliated Hospital of Medical College, Zhejiang University, Hangzhou 310003, Zhejiang Province, China
Lars Boenicke, Bradley D. Howard, Ilka Vogel, Holger Kalthoff, Molecular Oncology Research Laboratory, Clinic for General and Thoracic Surgery, Christian-Albrechts-University, 24105 Kiel, Germany
Supported by the Scientific Research Foundation for Returned Overseas Chinese Scholars, Personnel Affairs Bureau of Zhejiang Province
Correspondence to: Dr. Min Wang, Department of Surgical Oncology, First Affiliated Hospital of Medical College, Zhejiang University, 79# Qingchun Road, Hangzhou 310003, Zhejiang Province, China. pfeng@mail.hz.zj.cn
Telephone: +86-571-7236880 **Fax:** +86-571-7236628
Received: 2003-01-18 **Accepted:** 2003-03-10

Abstract

AIM: To study the expression of enhanced green fluorescent protein (EGFP) gene in retrovirally transduced variant HT-29 cells.

METHODS: The retroviral vector p*rkat* EGFP/neo was constructed and transfected into the 293T cell using a standard calcium phosphate precipitation method. HT-29c cells (selected from HT-29 cells) were transduced by a retroviral vector encoding the GEFP gene. The fluorescence intensity of colorectal carcinoma HT-29c cells after transduced with the EGFP bearing retrovirus was visualized using fluorescence microscope and fluorescence activated cell sorter (FACS) analysis. Multiple biological behaviors of transduced cells such as the proliferating potential and the expression of various antigens were comparatively analyzed between untransduced and transduced cells *in vitro*. EGFP expression of the fresh tumor tissue was assessed *in vivo*.

RESULTS: After transduced, HT-29c cells displayed a stable and long-term EGFP expression under the nonselective conditions *in vitro*. After cells were successively cultured to passage 50 *in vitro*, EGFP expression was still at a high level. Their biological behaviors, such as expression of tumor antigens, proliferation rate and aggregation capability were not different compared to untransduced parental cells *in vitro*. In subcutaneous tumors, EGFP was stable and highly expressed.

CONCLUSION: An EGFP expressing retroviral vector was used to transduce HT-29c cells. The transduced cells show a stable and long-term EGFP expression *in vitro* and *in vivo*. These cells with EGFP are a valuable tool for *in vivo* research of tumor metastatic spread.

Wang M, Boenicke L, Howard BD, Vogel I, Kalthoff H. Gene transfer and expression of enhanced green fluorescent protein in variant HT-29c cells. *World J Gastroenterol* 2003; 9(9): 2083-2087
http://www.wjgnet.com/1007-9327/9/2083.asp

INTRODUCTION

The detection of tumor invasion and micrometastasis in fresh tissues is necessary for critical understanding of tumor progression and its control. The real-time visualization of tumor cells, micrometastasis and their progression during the course of the disease is not easy to study in current models of metastasis. The green fluorescent protein (GFP) from the jellyfish *Aequorea victoria* has attracted widespread interest and has become an important reporter gene since heterologous expression of the cloned gene was found to be able to generate striking green fluorescence[1,2]. GFP is a relatively small polypeptide consisting of 238 amino acid residues, and is able to produce green fluorescence when excited with a blue light. So far, it has been used as a reporter of gene expression, tracers of cell lineage, and fusion tags to monitor protein localization within living cells in a broad spectrum of model organisms[3]. No additional substrates are required to detect GFP and it can be monitored in living cells. But the sensitivity of wild type GFP is below that of standard reporter proteins, such as β-galactosidase, which utilizes enzymatic amplification. Wild type GFP exhibits lower fluorescence intensity which is hard to detect in several mammalian cells[4]. To improve the detection of GFP in transduced mammalian cells, a unique GFP variant, which contains a chromophore mutation making the protein 35 times brighter than wild type GFP, and is codon-optimized for high level expression in mammalian cells has been constructed[5,6]. These changes in the GFP coding sequence provide an enhanced GFP (EGFP) that greatly increases the sensitivity of the reporter protein[7, 8].

GFP has demonstrated its potential for use as a marker for gene expression in a variety of cell types[9,10]. Numerous studies have proven the usefulness of GFP as a reporter molecule in the setting of transient gene expression[11,12]. However, it remains unclear whether colorectal carcinoma cell lines are able to stably express and maintain high level of EGFP expression over many passages in the absence of selective growth conditions. In this study, we assessed the expression of colorectal carcinoma cells after transduced with EGFP gene, and evaluated their biological behaviors *in vitro*. Moreover, to develop an experimental animal model of colorectal carcinoma that improves the visualization of fresh tissue, we injected EGFP-expressing human colorectal carcinoma cells subcutaneously into rats. This model involves the stable transduction of HT-29c tumor cells *in vitro* with the EGFP gene that could be stably and highly expressed *in vivo*.

MATERIALS AND METHODS

Materials

Cell lines and cell culture HT-29 cell line, a gift of Dr. Dippold (Mainz, Germany), was established from a human colon adenocarcinoma with moderate differentiation, HT-29c with increased metastatic activity was a variant cell line after three cycles of selection of liver metastases from injected HT-29 cells[13]. All cell lines were grown in 75 cm^2 cluture flasks in RPMI-1640 medium supplemented with 10 % fetal bovine serum, 2 mM L-glutamine and 1 mM sodium pyruvate (Life

Technologies) in a humidified atmosphere of 5 % CO_2 and 95 % air at a 37 ℃ incubator (Heraeus, Germany).

Plasmids For subcloning the HSV-TK gene and modifying the restriction sites on the 5' and 3' ends, the pSP72 cloning vector was obtained from Promega Corp., Madison, WI. The gene coding for humanized EGFP of Aequorea victoria contained in the plasmid pEGFP-C was obtained from Clontech Laboratories (Heidelberg, Germany). prkat, a retroviral vector backbone derived from the Moloney murine leukemia virus (MMLV) was provided by Cell Genesys Corp. The expression vector for the vesicular stomatitis virus G protein, pCMV VSV-G, was generously provided by Dr. Ted Friedman.

Construction of retroviral vector General molecular biological cloning techniques and the necessary solutions used to generate this plasmid vector were found in standard protocols[14]. A 0.7 kb EcoR I/BamH I fragment containing the coding region of EGFP gene was isolated and ligated into the prkat to generate prkat EGFP/neo. In this construct, the MMLV long terminal repeat (LTR) controled the expression of EGFP gene and an internal IRES sequence drived the expression of the neomycin resistance marker.

Experimental animal Three-week-old male athymic Rowett nude rats (Hsd: RH-nu/nu) were obtained from Harlan/ Winkelmann (Borchen, Germany). All the rats were housed in cages with filter bonnet under special pathogen-free conditions in a laminar flow cabinet (EHRET, DIPL.-ING. W. EHRET GmbH, Germany) at constant temperature (24-26 ℃), humidity (40-50 %) and 12-hour light/12-hour dark cycle. The rats were fed on standard rat food (Altromin, Lage/Lippe, Germany) and water *ad libitum*. Operative equipments, all cages and bedding were autoclaved at 121 ℃ for 30 minutes. All animal manipulations were done aseptically in a transverse laminar flow hood (BDK, Luft-und Reinraumtechnik GmbH, Germany).

Methods

Production of retrovirus particles and transduction of HT-29c cells with rkat EGFP/neo retroviruses 1.5×10^6 293T cells were seeded onto 10 cm^2 Primaria™ dishes. The next day, fresh medium was added 4 hours prior to transduction. 10 μg of prkat EGFP/neo, 5 μg of prkat gag/pol and 5 μg pCMV-VSV were co-transfected into the 293T cells using a standard calcium phosphate precipitation method. 24 hours later fresh medium (DMEM high glucose with 10 % FCS plus 2 mM glutamine, 1 mM sodium pyruvate and 1X non essential amino acids) was added. 48 hours after the cells were washed, the supernatant containing VSV-G pseudotyped recombinant retroviruses was harvested from the plate and filtered using a 0.45 μm low protein binding Acrodisc™ filter (Gelman Sciences, Ann Arbor, MI). 3 ml of the retroviral supernatant was then added to a 6 cm^2 dish seeded with 1×10^5 HT-29c cells containing 8 μg/ml polybrene. 24 hours later, the transduced HT-29c cells were placed under geneticin (G418, Life Technologies) selection (700 μg/ml). After two weeks, individual clones were generated by limited dilution. 96 well plates were seeded using cell densities of 3, 5 and 10 cells per well. Within 3-4 weeks, 12 separate clones were generated and expanded into 6 well plates. To analyze the expression of EGFP in the individual clones, 5×10^5 cells from each clone were fixed in 2 % formaldehyde and the fixed cells were analyzed by FACS. The two clones with the most intense fluorescence, HT-29cEGFPclone #1 and #7 were selected and used for *in vitro* or *in vivo* studies.

Cell culture of transduced HT-29c cells HT-29cEGFP, HT-29cEGFPclone#1 and clone#7 cells were grown in supplemented RPMI-1640 medium. The cultures were incubated at 37 ℃ in a humidified atmosphere of 5 % CO_2. G418 was added to cell medium at a final concentration of 600 mg/ml from first till 15th passage for selection. After passage 15, the cells were grown in the absence of G418 and cells were passaged twice per week.

Microscopic and FACS analysis of EGFP expressing cells *in vitro* HT-29c EGFPclone#1 and clone#7 cells were seeded onto chamber slides. When cells grown in monolayer became confluent, the fluorescence of the cells were visualized with an Axioskop fluorescence microscope (Carl Zeiss, Germany) equipped with a FITC filter set (UV light exciter BP 546 nm, FT 580 nm, emitter LP 590 nm). Cultivated cells were harvested by trypsinization and were fixed in 0.4 ml 2 % formaldehyde. The fluorescence intensity of samples was analyzed using fluorescence activated cell sorter (FACS, Epics XL, Hamburg, Germany).

Comparative analysis of biological behavior between transduced and untransduced cell lines *in vitro* Growth rate determination: HT-29, HT-29c, HT-29c EGFPclone#1 and clone#7 cells were seeded in six-well plastic culture plates, in triplicate at a density of 1×10^5 in supplemented medium. The cells were harvested by trypsinization and counted every 24 hours using a hemocytometer. The test was repeated three times. The mean number of cells in each interval for each cell line was determined. The growth curve of each cell line was constructed. The doubling time of tumor cell growth was calculated from the cell growth curve over 5 days according to the formula: Doubling time=(T_2-T_1) In 2/(In N_2-In N_1), in which N_1 and N_2 are the number of tumor cells at time points of T_1 and T_2, respectively.

Three-dimensional spheroid culture of cell lines: Three-dimensional spheroid culture of HT-29c and HT-29cEGFPclone cells were performed as follows: six-well culture plates were pre-coated with 2 ml 1% (w/v) agarose gel/per well. The single-cell suspension containing 1×10^5 tumor cells in supplemented medium was seeded onto each well and incubated in a humidified 5 % CO_2 at a 37 ℃ incubator. Cell aggregation was monitored daily using a phase-contrast microscope (Carl Zeiss, Germany).

Expression of different antigens: Cells were seeded onto 10-well mask slides and incubated for 48 hours as described above. Cells on the slides were fixed in cold acetone (Merck, Darmstadt, Germany) for 5 minutes. Immunohistochemical staining (IHC) was performed using the standard ABC method with VECTASTAIN ABC-kit and monoclonal antibodies (mAbs) KL-1 (Keratin), IT-ks20.10 (Cytokeratin 20), C1P83 (CEA), CA19-9 (CA19-9), MiB-1 (Ki-67) and Do7 (p53). All mAbs were commercially available except for C1P83 which was provided by Prof. Kalthoff H. The percentage of positive tumor cells was determined by calculating 1 000 tumor cells in 5 random vision fields of one section under microcope.

EGFP expression of HT-29c cells *in vivo* All the rats were stabilized for one week in the laboratory before the experiments. 0.5 ml single-cell suspension containing 2×10^7 cells of HT-29cEGFPclone#7 was injected subcutaneously into both flanks of the rat. The rat was monitored daily. When the tumor reached 15 mm in diameter, the rat was killed. The fresh tumor tissues were sliced at 0.7-1.0 mm thickness and sliced at 60 μm cryosections, then observed directly under the fluorescence microscope.

Statistical analysis

Statistical analyses were performed using the *F* test.

RESULTS

Expression of EGFP in transduced HT-29c cells in vitro

HT-29c cells could be transduced by retroviral vector with EGFP and then selected in G418. Transduced HT-29c cells with EGFP (HT-29cEGFP, HT-29c EGFPclone#1 and clone#7)

were grown *in vitro* in G418 (600 μg/ml). Untransduced HT-29c cells did not survive in G418, suggesting all cells within the transduced pools contained at least one copy of a transcriptionally active neomycin phosphotransferase gene. Under fluorescence microscope, the selected neomycin-resistant HT-29cEGFP and HT-29cEGFPclone cells all displayed strong fluorescence (Figure 1). HT-29cEGFPclone cells exhibited stronger fluorescence than HT-29cEGFP cells, no significant difference was found between fluorescence levels of HT-29cEGFPclone#1 and clone#7 cells by FACS analysis (Table 1). After 8 weeks in culture, G418 was removed from the growth medium. The expression of EGFP fluorescence of HT-29cEGFP clone cells was still stable for over six months *in vitro*. No significant difference was found between passage 5 and passage 50 of HT-29cEGFPclone#1 in fluorescence intensity by FACS (Table 2).

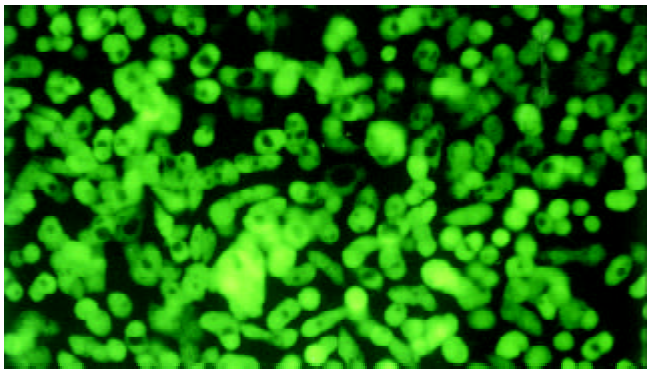

Figure 1 Stable high level of EGFP expression of transduced HT-29c EGFP clone cells *in vitro*. ×100.

Table 1 FACS analysis of EGFP expression in cell lines

Cell lines	Fluorescence intensity
HT-29c	2.5±0.9[a]
HT-29cEGFP pool	64.6±7.4[b]
HT-29cEGFPclone#1	206.5±39.9[c]
HT-29cEGFPclone#7	203.4±46.4[d]

The fluorescence intensity refers to fluorescence of 10 000 cells according to standard software supplied by the FACS cytometer manufacturer. a: $P<0.001$ *vs* b, c or d, respectively. b: $P<0.001$ *vs* c or d, c: $P=0.818$ *vs* d.

Table 2 EGFP expression in different passages of transduced HT-29c cells by FACS

Clone #1	Fluorescence intensity
Passage 5	217.8
Passage 17	198.1
Passage 31	193.4
Passage 40	212.1
Passage 50	208.8

Table 3 Doubling times of parental HT-29 cells and EGFP transduced HT-29 cells

Cell line	Doubling time (h)[a]
HT-29	25.3±5.5
HT-29c	26.0±3.3
HT-29cEGFPclone #1	26.3±4.7
HT-29cEGFPclone #7	27.7±5.3

a: *F* test $F=0.62$, $P>0.05$.

Comparison of biological behavior between untransduced and transduced cells in vitro

Comparison of cell proliferation rate The results indicated that there was no significant difference in the cell proliferation rates of parental cells and selected transfectants as determined by comparing their doubling time (Table 3).

Table 4 Phenotypical comparison of HT-29cells, HT-29c cells and EGFP transduced cells

mAb	Percentage of positive cells (%)		
	HT-29	T-29c	HT-29c EGFPclone
KL-1	100	100	100
IT- Ks20.10	100	100	100
C1 83	33.9	34.6	36.5
CA19-9	48.0	49.3	47.2
MiB-1	96.7	97.8	97.2
Do-7	96.8	97.1	98.3

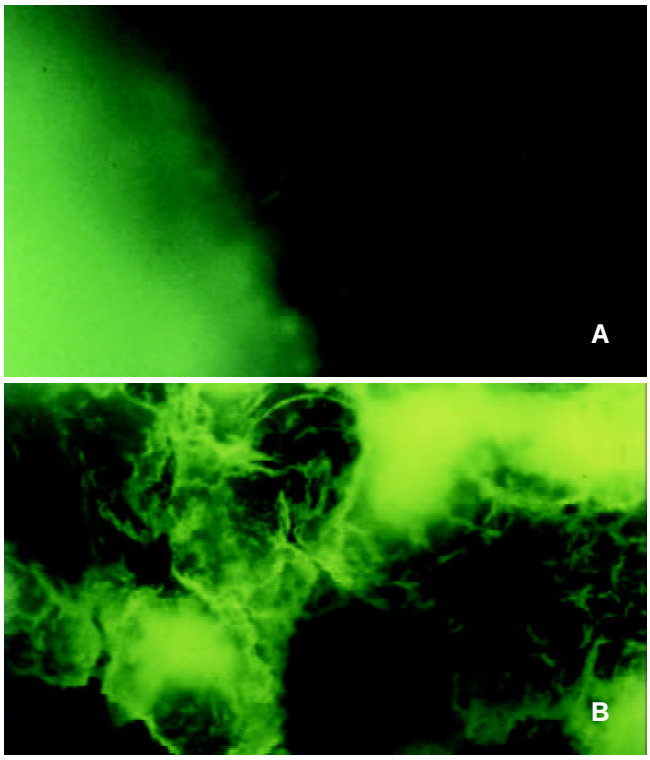

Figure 2 Stable high level of EGFP expressing s.c. tumor in nude rats formed from HT-29c EGFP clone#7 cells under fluorescence microscope (a: the tumor tissue was sliced at 0.8 mm, b: 60 μm cryosection). ×100.

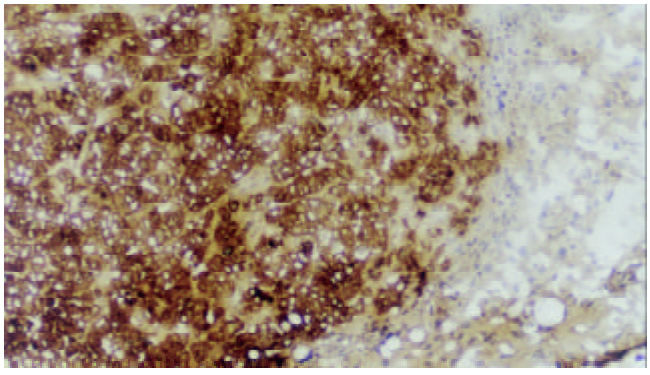

Figure 3 Immunostaining of the s.c. tumor with mAb KL-1 (c) ×100.

Comparison of aggregation potential To compare cell aggregation potential between untransfected and transfected cells *in vitro*, HT-29c and HT-29cEGFPclone cells were monitored under three dimensional culture conditions. At 4 hours after incubation, cell aggregation began. Most of the cell clumps were formed by 8-15 cells. The membranes of single cells in the clumps could be distinguished under phase-contrast microscope. At 24 hours after incubation, the cells aggregated together to form 1-3 larger elliptic cell spheroids in each cell line. The cell spheroids consisted of more than 100 cells. There were still several cell clumps formed by 10-30 cells besides a few larger cell spheroids. Moreover, a lot of cells remained as single cells. After incubation for 1 week, most of the cell clumps remained the same size as at 24 hours. No significant difference was observed in cell aggregation capability between untransduced and transduced cells *in vitro*.
Comparison of cell antigen expression by IHC The ratio of positive cells of antigen expression in HT-29, variant HT-29c and transfected HT-29cEGFPclone cells are shown in Table 4. No significant difference was observed in the positive ratios of HT-29, HT-29c and HT-29cEGFPclone cells.

EGFP expression in vivo

Five days after injection of HT-29cEGFPclone#7 cells, a rat s.c. tumor could be found. Two weeks after injection the rat was sacrificed. The rat had a s.c. tumor that ranged from 13.0-15.3 mm in diameter. The fresh tumor tissues were sliced at 0.7-1.0 mm and at 60 μm cryosections, then observed directly under fluorescence microscope. The tumor tissue displayed strong fluorescence (Figure 2), thereby demonstrating stable, high level EGFP expression *in vivo* during tumor growth. The rat s.c. tumor was also diagnosed by immunostaining with mAb KL-1 (Figure 3).

DISCUSSION

Previous studies have demonstrated the effectiveness and sensitivity of EGFP gene as a marker to visualize micrometastases in live tissue[15,16]. To use EGFP as a marker for *in vivo* experiments, it is necessary to establish very stable transfectants that can express EGFP constantly under nonselective conditions. In this study the retroviral vector expressing EGFP gene was transduced into HT-29c cells and the transduced cells were selected under G418. The present study showed HT-29cEGFPclone cells had stable and long-term EGFP expression under nonselective conditions *in vitro*. When passaged successively to passage 50 *in vitro*, EGFP expression was still high and stable.

The distinct metastatic potential of tumor cell is one of the most important factors in determining the outcome of metastasis. Many biological characteristics of tumor cells are associated with their metastatic ability such as proliferating potential, cell surface adhesion molecule expression, expression of oncogenes or tumor suppressor genes[17] and cell-cell junctions and active cell separation[18]. Spheroidal aggregates of malignant cells may serve as *in vitro* model of tumor microregions and of an early, avascular stage of tumor growth. The similarities between the original tumor and the respective spheroids include volume growth kinetics, cellular heterogeneity, e.g. induction of proliferation gradients and quiescence, differentiation characteristics, development of specific histological structures or expression of antigens[19]. Some research using cell aggregates has focused on mechanisms involved in the control of distribution, spread, invasion and metastasis of tumors[20]. Cellular heterogeneity, which is a general property of solid tumors may occur in multicellular spheroids rather than in conventional monolayer cultures. In the present study some biological behaviors were compared between transduced and parental cells *in vitro*. No differences were found in the expression of antigens. There was no difference in the cell proliferation rate determined by comparing their doubling times. And there was no difference in the cell aggregation capability either, which correlated with the metastatic potential.

In the present study, EGFP gene-transduced HT-29c cells were successfully used to visualize s.c. tumors in rat. The fresh tumor tissues could be analyzed directly under fluorescence microscope. The tumor tissue showed strong fluorescence, demonstrating stable, high level of EGFP expression *in vivo* during tumor growth. Other studies also demonstrated that EGFP gene transduced tumor cells were successfully used to visualize extensive peritoneal seeding[21], lung metastasis[22], skeletal metastasis[23] and bone metastasis[24,25], brain tumor[26,27] and liver metastasis[28]. Using EGFP fluorescence, diagnosis of tumor metastasis can be detected down to the single-cell level. This method has a higher resolution and is much more feasible than the traditional cumbersome pathological examination procedures, such as histology and immunohistochemistry. It is possible that when EGFP-expressing cells undergo apoptosis, they could be engulfed by macrophages. However, when EGFP-expressing cells die, they lose their fluorescence, such as in necrotic areas of tumors, suggesting that these macrophages will not interfere with the detection of metastases[29]. Studies have shown that EGFP transfectants should also be useful with new techniques such as intravital videomicroscopy, which previously involved labeling of tumor cells with dyes[30]. Flotte *et al*.[31] reported gene transfer and expression could be detected by a fluorescence video-endoscopy technique. This method could be used to reliably track transfer in living animals or patients. Other results also showed all intravital imaging, that is, imaging of an intact primary tumor in a living animal was carried out on the laser scanning confocal microscope using the whole-animal platform in animal models with EGFP-expressing tumor cells[32]. Recent studies showed whole-body optical imaging, in real time, of genetically EGFP-expressing tumor growth and metastases. The whole-body optical imaging system is external and noninvasive. It affords unprecedented continuous visual monitoring of malignant growth and spread within intact animals[33,34]. A major advantage of EGFP-expressing tumor cells is that they do not need any preparation and can be seen in fresh living tissues at the microscopic level, and it allows direct observations of metastasis in an intact orthotopically growing primary tumor in a living animal.

ACKNOWLEDGEMENT

We sincerely thank Dr. Zhu Kejian in the Department of Dermatology of the Second Affiliated Hospital of Medical College, Zhejiang University, Hangzhou, Zhejiang Province for performing the FACS analysis.

REFERENCES

1 **Prasher DC,** Eckenrode VK, Ward WW, Prendergast FG, Cormier JM. Primary structure of the Aequorea victoria green-fluorescent protein. *Gene* 1992; **111**: 229-233
2 **Chalfie M,** Tu Y, Euskirchen G, Ward WW, Prasher DC. Green fluorescent protein as a marker for gene expression. *Science* 1994; **263**: 802-805
3 **Cubitt AB,** Heim R, Adams SR, Boyd AE, Gross LA, Tsien RY. Understanding, improving and using green fluorescent proteins. *Trends Biochem Sci* 1995; **20**: 448-455
4 **Stearns T**. Green fluorescent protein. The green revolution. *Curr Biol* 1995; **5**: 262-264
5 **Heim R,** Cubitt AB, Tsien RY. Improved green fluorescence. *Nature* 1995; **373**: 663-664
6 **Zhang G,** Gurtu V, Kain RS. An enhanced green fluorescent pro-

tein allows sensitive detection of gene transfer in mammalian cells. *Biochem Biophys Res Commun* 1996; **227**: 707-711

7 **Kimata Y,** Iwaki M, Lim CR, Kohno K. A novel mutation which enhances the fluorescence of green fluorescent protein at high temperatures. *Biochem Biophys Res Commun* 1997; **232**: 69-73

8 **Cheng L,** Fu J, Tsukamoto A, Hawley RG. Use of green fluorescent protein variants to monitor gene transfer and expression in mammalian cells. *Nat Biotechnol* 1996; **14**: 606-609

9 **Wysocka A,** Krawczyk Z. Green fluorescent protein as a marker for monitoring activity of stress-inducible hsp70 rat gene promoter. *Mol Cell Biochem* 2000; **215**: 153-156

10 **D'Assoro AB,** Stivala F, Barrett S, Ferrigno G, Salisbury JL. GFP-centrin as a marker for centriole dynamics in the human breast cancer cell line MCF-7. *Ital J Anat Embryol* 2001; **106**(2 Suppl 1): 103-110

11 **Ahmed F,** Wyckoff J, Lin EY, Wang W, Wang Y, Hennighausen L, Miyazaki J, Jones J, Pollard JW, Condeelis JS, Segall JE. GFP expression in the mammary gland for imaging of mammary tumor cells in transgenic mice. *Cancer Res* 2002; **62**: 7166-7169

12 **Zhao H,** Hart LL, Keller U, Holth LT, Davie JR. Characterization of stably transfected fusion protein GFP-estrogen receptor –alpha in MCF-7 human breast cancer cells. *J Cell Biochem* 2002; **86**: 365-375

13 **Vogel I,** Shen Y, Soeth E, Juhl H, Kremer B, Kalthoff H, Henne-Bruns D. A human carcinoma model in athymic rats reflecting solid and disseminated colorectal metastases. *Langenbecks Arch Surg* 1998; **383**: 466-473

14 **Sambrook J,** Gething MJ. Protein structure. Chaperones, paperones. *Nature* 1989; **342**: 224-225

15 **Chishima T,** Miyagi Y, Wang X, Yamaoka H, Shimada H, Moossa AR, Hoffman RM. Cancer invasion and micrometastasis visualized in live tissue by green fluorescent protein expression. *Cancer Res* 1997; **57**: 2042-2047

16 **Shintani S,** Mihara M, Nakahara Y, Aida T, Tachikawa T, Hamakawa H. Lymph node metastasis of oral cancer visualized in live tissue by green fluorescent protein expression. *Oral Oncol* 2002; **38**: 664-669

17 **Takahashi Y,** Ellis LM, Wilson MR, Bucana CD, Kitadai Y, Fidler IJ. Progressive upregulation of metastasis-related genes in human colon cancer cells implanted into the cecum of nude mice. *Oncol Res* 1996; **8**: 163-169

18 **Guvakova MA,** Adams JC, Boettiger D. Functional role of alpha-actinin, PI 3-kinase and MEK1/2 in insulin-like growth factor I receptor kinase regulated motility of human breast carcinoma cells. *J Cell Sci* 2002; **115**(Pt 21): 4149-4165

19 **Mueller-Klieser W.** Multicellular spheroids. A review on cellular aggregates in cancer research. *J Cancer Res Clin Oncol* 1987; **113**: 101-122

20 **Grill J,** Lamfers ML, van Beusechem VW, Dirven CM, Pherai DS, Kater M, Van der Valk P, Vogels R, Vandertop WP, Pinedo HM, Curiel DT, Gerritsen WR. The organotypic multicellular spheroid is a relevant three-dimensional model to study adenovirus replication and penetration in human tumors *in vitro*. *Mol Ther* 2002; **6**: 609-614

21 **Fujiwara H,** Kubota T, Amaike H, Inada S, Takashima K, Atsuji K, Yoshimura M, Ueda Y, Hagiwara A, Yamagishi H. Functional analysis of peritoneal lymphoid tissues by GFP expression in mice-possible application for targeting gene therapy against peritoneal dissemination. *Gan To Kagaku Ryoho* 2002; **29**: 2322-2324

22 **Huang MS,** Wang TJ, Liang CL, Huang HM, Yang IC, Yi-Jan H, Hsiao M. Establishment of fluorescent lung carcinoma metastasis model and its real-time microscopic detection in SCID mice. *Clin Exp Metastasis* 2002; **19**: 359-368

23 **Yang M,** Hasegawa S, Jiang P, Wang X, Tan Y, Chishima T, Shimada H, Moossa AR, Hoffman RM. Widespread skeletal metastatic potential of human lung cancer revealed by green fluorescent protein expression. *Cancer Res* 1998; **58**: 4217-4221

24 **Yang M,** Jiang P, Sun FX, Hasegawa S, Baranov E, Chishima T, Shimada H, Moossa AR, Hoffman RM. A fluorescent orthotopic bone metastasis model of human prostate cancer. *Cancer Res* 1999; **59**: 781-786

25 **Peyruchaud O,** Winding B, Pecheur I, Serre CM, Delmas P, Clezardin P. Early detection of bone metastases in a murine model using fluorescent human breast cancer cells: application to the use of the bisphosphonate zoledronic acid in the treatment of osteolytic lesions. *J Bone Miner Res* 2001; **16**: 2027-2034

26 **Jung S,** Kim HW, Lee JH, Kang SS, Rhu HH, Jeong YI, Yang SY, Chung HY, Bae CS, Choi C, Shin BA, Kim KK, Ahn KY. Brain tumor invasion model system using organotypic brain-slice culture as an alternative to *in vivo* model. *J Cancer Res Clin Oncol* 2002; **128**: 469-476

27 **MacDonald TJ,** Tabrizi P, Shimada H, Zlokovic BV, Laug WE. Detection of brain tumor invasion and micrometastasis *in vivo* by expression of enhanced green fluorescent protein. *Neurosurgery* 1998; **43**: 1437-1442

28 **Li X,** Wang J, An Z, Yang M, Baranov E, Jiang P, Sun F, Moossa AR, Hoffman RM. Optically imageable metastatic model of human breast cancer. *Clin Exp Metastasis* 2002; **19**: 347-350

29 **Steff AM,** Fortin M, Arguin C, Hugo P. Detection of a decrease in green fluorescent protein fluorescence for the monitoring of cell death: an assay amenable to high-throughput screening technologies. *Cytometry* 2001; **45**: 237-243

30 **Chambers AF,** MacDonald IC, Schmidt EE, Koop S, Morris VL, Khokha R, Groom AC. Steps in tumor metastasis: new concepts from intravital videomicroscopy. *Cancer Metastasis Rev* 1995; **14**: 279-301

31 **Flotte TR,** Beck SE, Chesnut K, Potter M, Poirier A, Zolotukhin S. A fluorescence video-endoscopy technique for detection of gene transfer and expression. *Gene Ther* 1998; **5**: 166-173

32 **Farina KL,** Wyckoff JB, Rivera J, Lee H, Segall JE, Condeelis JS, Jones JG. Cell motility of tumor cells visualized in living intact primary tumors using green fluorescent protein. *Cancer Res* 1998; **58**: 2528-2532

33 **Yang M,** Baranov E, Jiang P, Sun FX, Li XM, Li L, Hasegawa S, Bouvet M, Al-Tuwaijri M, Chishima T, Shimada H, Moossa AR, Penman S, Hoffman RM. Whole-body optical imaging of green fluorescent protein-expressing tumors and metastases. *Proc Natl Acad Sci U S A* 2000; **97**: 1206-1211

34 **Bouvet M,** Wang J, Nardin SR, Nassirpour R, Yang M, Baranov E, Jiang P, Moossa AR, Hoffman RM. Real-time optical imaging of primary tumor growth and multiple metastatic events in a pancreatic cancer orthotopic model. *Cancer Res* 2002; **62**: 1534-1540

Edited by Zhu LH

P.O.Box 2345, Beijing 100023,China
Fax: +86-10-85381893
E-mail: wjg@wjgnet.com www.wjgnet.com

World J Gastroenterol 2003;9(9):2088-2091
World Journal of Gastroenterology
 ISSN 1007-9327

• CLINICAL RESEARCH •

Diagnostic value of endoscopic ultrasonography for gastrointestinal leiomyoma

Guo-Qiang Xu, Bing-Ling Zhang, You-Ming Li, Li-Hua Chen, Feng Ji, Wei-Xing Chen, Shu-Ping Cai

Guo-Qiang Xu, Bing-Ling Zhang, You-Ming Li, Li-Hua Chen, Feng Ji, Wei-Xing Chen, Shu-Ping Cai, Department of Gastroenterology, First Affiliated Hospital, School of Medicine, Zhejiang University, Hangzhou 310003, Zhejiang Province, China
Supported by the Initiative Fund of Ministry of Education for Returned Overseas Scholars, No. 491010-G50040
Correspondence to: Guo-Qiang Xu, Department of Gastroenterology, First Affiliated Hospital, School of Medicine, Zhejiang University, Hangzhou 310003, Zhejiang Province, China. xuguoqi@mail.hz.zj.cn
Telephone: +86-571-87236522 **Fax:** +86-571-87236611
Received: 2003-03-03 **Accepted:** 2003-05-16

Abstract

AIM: To investigate the clinical pathologic features of gastrointestinal leiomyoma and the diagnostic value of endoscopic ultrasonography (EUS) on gastrointestinal leiomyoma.

METHODS: A total of 106 patients with gastrointestinal leiomyoma diagnosed with EUS were studied. The location, size and layer origin of gastric and esophageal leiomyomas were analyzed and compared. The histological diagnosis of the resected specimens by endoscopy or surgery in some patients was compared with their results of EUS.

RESULTS: The majority of esophageal leiomyomas were located in the middle and lower part of the esophagus and their size was smaller than 1.0 cm, and 62.1 % of esophageal leiomyomas originated from the muscularis mucosae. Most of the gastric leiomyomas were located in the body and fundus of the stomach with a size of 1-2 cm. Almost all gastric leiomyomas (94.2 %) originated from the muscularis propria. The postoperative histological results of 54 patients treated by endoscopic resection or surgical excision were completely consistent with the preoperative diagnosis of EUS, and the diagnostic specificity of EUS to gastrointestinal leiomyoma was 94.7 %.

CONCLUSION: The size and layer origin of esophageal leiomyomas are different from that of gastric leiomyomas. Being safe and accurate, EUS is the best method not only for gastrointestinal leiomyoma diagnosis but also for the follow-up of patients.

Xu GQ, Zhang BL, Li YM, Chen LH, Ji F, Chen WX, Cai SP. Diagnostic value of endoscopic ultrasonography for gastrointestinal leiomyoma. *World J Gastroenterol* 2003; 9(9): 2088-2091
http://www.wjgnet.com/1007-9327/9/2088.asp

INTRODUCTION

With the development and popularization of endoscopic ultrasonography (EUS) in clinical diagnosis, great progress has been made in diagnosis and treatment of gastrointestinal leiomyoma[1-3]. We collected 106 patients with gastrointestinal leiomyoma diagnosed by EUS from the First Affiliated Hospital, School of Medicine, Zhejiang University, in China from August 2000 to September 2002. This report is to summarize and analyze the clinical pathologic features and results of diagnosis and treatment of gastrointestinal leiomyoma and to evaluate the clinical diagnostic value of EUS for gastrointestinal leiomyoma.

MATERIALS AND METHODS

Patients

The patients with submucosal protruding lesions in gastrointestine by conventional endoscopy were examinated by EUS. Before making EUS, physical examinations were performed. One hundred and six patients (63.8 %) were diagnosed having gastrointestinal leiomyoma by EUS among 166 patients with true submucosal lesions, their mean age was 51 years, ranging from 2 to 88 years. There were 52 men and 54 women. Including 66 cases of esophageal leiomyoma, 35 cases of gastric leiomyoma, 2 cases of duodenum leiomyoma and 3 cases of colon leiomyoma.

Instrument

Instruments of EUS included Fujino EG-410D double-cavity electronic gastroscope, Olympus CF-VL electronic colonoscope and Fujino SP-70 high-frequency echoprobe system. The frequency of probe is between 7.5 MHz to 20 MHz.

Methods

According to the information of the location and size of lesion in gastrointestine shown by the conventional endoscopy examination, we chose different frequency microprobes and examination methods (water-ballon method, water-soak method or water-pour method) to scan the lesion[4]. Then a diagnosis was made for the size, origin, invasion field and nature of the lesion. Some patients were treated by endoscopic resection or surgical excision after EUS, the postoperative histological results were compared with the preoperative diagnoses of EUS. In addition, a follow-up with EUS was made for a few patients without endoscopic or surgical resection because of different reasons.

RESULTS

Ninety-eight patients (92.5 %) showed no related symptoms and were found by conventional endoscopic examination occasionally among 106 patients with gastrointestinal leiomyoma diagnosed by EUS. Only 8 patients (7.5 %) had fixed symptoms, of them, 6 cases had esophageal leiomyoma and 2 cases had gastric leiomyoma. The size of tumor was > 2.0 cm, and major symptoms were dysphagia, feeling of foreign body, pain behind chest bone, upper abdominal indisposition, etc. The distribution, layer of origin, size and number of esophageal or gastric leiomyoma were summarized in Tables 1 and 2. The majority of esophageal leiomyoma were located in the middle and lower part of the esophagus, and their size was <1.0 cm, and 62.1 % of the esophageal leiomyomas originated from the muscularis mucosae. Most of the gastric

leiomyomas were located in the body and fundus of stomach, their size was 1-2 cm. Almost all gastric leiomyomas (94.2 %) originated from the muscularis propria. Duodenal leiomyomas in two patients were derived from the muscularis propria, being 0.5-0.8 cm in size. Colon leiomyomas in three patients were located in cecum, transverse colon and sigmoid colon, respectively. The lesions were originated from the muscularis propria, 1.1-1.6 cm in size. One hundred and one of 106 patients just had single leiomyoma. After EUS examination, 35 patients with leiomyoma originating from muscularis mucosa were treated with endoscopic resection (Figure 1A,B,C). The other group of 22 patients received surgical excision because their lesions appeared to be in the proper muscle layer. The size, number and layer-origin of the lesions in 57 patients treated with endoscopic or surgical resection were completely consistent with the preoperative diagnosis of EUS. However, postoperative histological results of only 3 patients were carcinoid, esophageal cyst gland hyperplasia and tubercle, respectively, which were not in agreement with the preoperative diagnosis of EUS. The diagnostic accuracy of EUS for leiomyoma was 94.1 % (54/57). The remaining 49 patients were not treated with endoscopic or surgical resection due to various reasons. They were observed and followed up. Fifteen of 49 patients were examined with EUS at three, six and twelve months later, the results of examination showed that the position, shape and structure of their lesions were unchanged. In our study, all the patients could well tolerate EUS without serious complications such as bleeding, perforation, shock and asphyxia except a few patients who felt disorder in throat, and abdominal distension. No complication occurred in 35 patients treated by endoscopic resection.

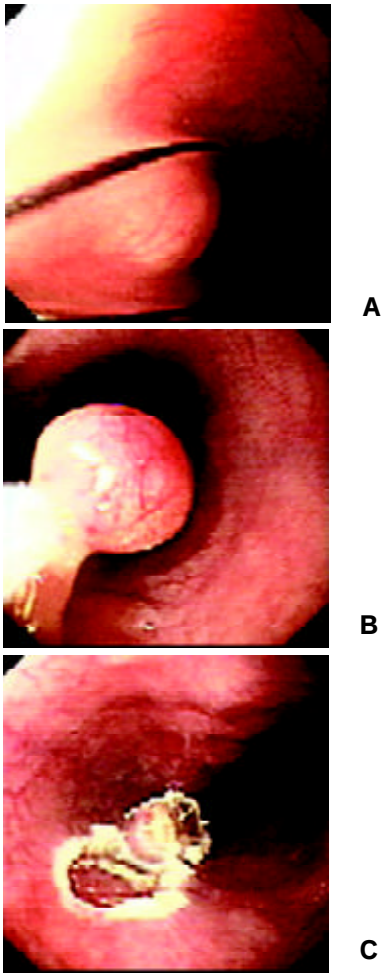

Figures 1 Endoscopic resection of esophgeal leiomyoma.

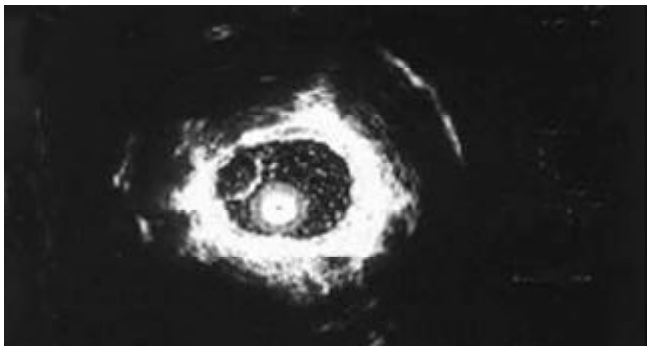

Figure 2 Esophageal leiomyoma, originating from muscularis mucosa.

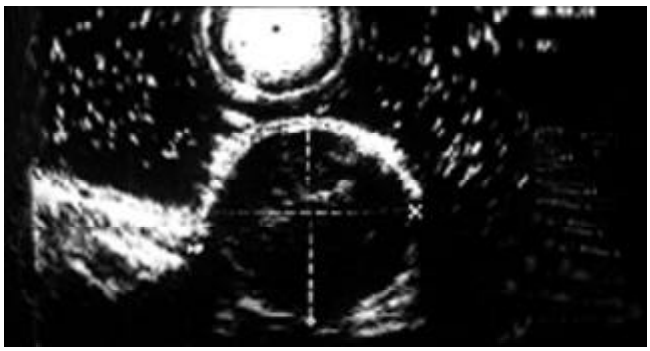

Figure 3 Gastric leiomyoma, originating from muscularis propria.

Table 1 Clinical pathological characteristics of gastric leiomyoma (*n*=35)

Location (*n*)	Origin (*n*)	Size (*n*)	Number (*n*)
Antumn (6)	Muscularis mucosae (3)	≤1.0 cm (4)	Single (34)
Body (11)	Muscularis propria (32)	>1.0,≤2.0 cm (20)	Multiple (1)
Fundus (11)		>2.0 cm (11)	
Cardia (7)			

Table 2 Clinical pathological characteristics of esophgeal leiomyoma (*n*=66)

Location (*n*)	Origin (*n*)	Size (*n*)	Number (*n*)
Upper part (11)	Muscularis mucosae (41)	≤1.0cm (32)	Single (62)
Middle part (28)	Muscularis propria (25)	>1.0, ≤2.0 cm (24)	Multiple (4)
Lower part (27)		>2.0 cm (10)	

DISCUSSION

Gastrointestinal leiomyoma is a common kind of benign submucosal tumor in gastrointestine[1,5], because it originates from muscularis mucosa or muscularis propria, the conventional endoscopy can not diagnose it accurately. Since EUS was used in clinical diagnosis, the diagnostic situation of gastrointestinal leiomyoma has changed greatly[6-9]. The five-layered structure of gastrointestinal wall can be shown clearly, and gastrointestinal leiomyoma presents homogeneous and hypoechoic lesion with clear margin, and the lesion is around the hyperechoic wrapping area under endosonography (Figures 2,3). According to these features of ultrasonography, leiomyoma is easy to be distinguished from hemoangioma, cyst and lipoma in digestive tract wall[10-15]. Thus we can define not only the nature of leiomyoma, but also its size, number and the layer of origin by EUS. Our clinical study showed that

gastrointestinal leiomyoma mainly occurred in esophagus and stomach. The incidence in duodenum and colon is markedly lower than that in esophagus and stomach. The partial reason of the lower incidence of colon leiomyoma may be that the number of patients undergoing colonoscopic examination was significantly less than that of gastroscopic examination (the ratio of gastroscopy to colonoscopy was 3:1 in this study). The incidence of esophageal leiomyoma was higher than that of stomach leiomyoma, the size and layer origin of esophageal leiomyoma were different from gastric leiomyoma. The reason is still unknown. Although leiomyoma was located in different positions of gastrointestine, almost all the patients (101/106) only had single lesion, which conformed with other reports[16,17]. With regard to the diagnosis of gastrointestinal leiomyoma, our clinical data indicated that most cases (92.5 %) were occasionally found by endoscopic examination, these patients showed no related symptoms and signs, and no positive change in blood examination. The diagnosis of leiomyoma mainly depends on EUS, which combines the function of endoscope and ultrasonic, by which we can not only inspect the surface shape of gastrointestinal lesion, but also gain the image of the layer of origin, the invasive scope and the structure of the lesion. According to the literature[18-20], the diagnostic specificity of EUS to gastrointestinal leiomyoma is superior to other imaging techniques such as B type ultrosonophy, gastrointestinal radiography and computed tomography. In our clinical study, the size, number and the layer of origin of the resected lesions were completely consistent with the diagnosis of EUS in 57 patients treated by endoscopic resection or surgical excision, The nature of the lesions in 54 of 57 patients was in agreement with the diagnosis of EUS, the diagnostic accuracy of EUS for leiomyoma was 94.7 %. Our study indicated that EUS had a very important diagnostic value for gastrointestinal leiomyoma[21]. However, we are still possible to make a mistake in the diagnosis of gastrointestinal leiomyoma, because the image of ultrasonophy of a few other lesions is the same as that of gastrointestinal leiomyoma, e.g, the gastrointestinal carcinoid and tubercle. For these diseases, we should depend on other clinical information to differentiate them. Furthermore, when EUS finds that the size of leiomyoma is bigger than 4 cm, or the surface of leiomyoma has erosion or ulceration, or internal echo being unhomogeneous, we should consider the possibility of leiomyosarcoma[22]. Presently, EUS is considered the best method for the diagnosis of submucosal lesion[7,8,23], Which can not only diagnose leiomyoma correctly, but also help us work out scientific and rational therapeutic strategies. EUS can clearly show the origin of gastrointestinal leiomyoma, either from the muscularis mucosae or the muscularis propria. Usually, leiomyoma originating from the muscularis mucosae can be treated by endoscopic resection[24-27], whereas leiomyoma originating from the proper muscle layer contraindicates endoscopic resection. Unwell-planned resection will bring about perforation of gastrointestine. Thirty-five patients with leiomyoma originating from muscularis mucosae were treated by endoscopic resection in our study. No complications such as bleeding, perforation occurred, showing that EUS has a very important value to the selection of therapeutic methods for gastrointestinal leiomyoma[28-31]. It makes the therapy of gastrointestinal leiomyoma more rational, safe and economic. In addition, for those patients with gastrointestinal leiomyoma who refused to receive or could not be treated by endoscopic resection or surgical excision, we followed up them by EUS periodically. The results showed that gastrointestinal leiomyoma grew slowly and showed no marked change in a short time. Thus, we can choose observation and follow-up for the patients with small lesions, and lesions originating from the muscularis propria, or the special position of lesion.

In conclusion, EUS is a safe and effective diagnostic method for gastrointestinal leiomyoma.

REFERENCES

1 **Chak A**. EUS in submucosal tumors. *Gastrointest Endosc* 2002; **56** (Suppl 4): S43-48

2 **Wang Y**, Sun Y, Liu Y, Li Y, Wang Z. Transesophageal intraluminal ultrasonography in diagnosis and differential diagnosis of esophageal leiomyoma. *Zhonghua Yixue Zazhi* 2002; **82**: 456-458

3 **Nomura N**, Goto H, Niwa Y, Arisawa T, Hirooka Y, Hayakawa T. Usefulness of contrast-enhanced EUS in the diagnosis of upper GI tract diseases. *Gastrointest Endosc* 1999; **50**: 555-560

4 **Xu GM**, Niu YL, Zou XP, Jin ZD, Li ZS. The diagnostic value of transendoscopic miniature ultrasonic probe for esophageal diseases. *Endoscopy* 1998; **30**(Suppl): A28-32

5 **Xu GQ**, Li YM, Chen WX, Ji F, Huang HD. Diagnostic value of transendoscopic miniature ultrasonic probes on esophageal and gastric submucosal lesions. *Zhonghua Chaosheng Yingxiangxue Zazhi* 2002; **11**: 188-189

6 **Shen EF**, Arnott ID, Plevris J, Penman ID. Endoscopic ultrasonography in the diagnosis and management of suspected upper gastrointestinal submucosal tumours. *Br J Surg* 2002; **89**: 231-235

7 **Gress F**, Schmitt C, Savides T, Faigel DO, Catalano M, Wassef W, Roubein L, Nickl N, Ciaccia D, Bhutani M, Hoffman B, Affronti J. Interobserver agreement for EUS in the evaluation and diagnosis of submucosal masses. *Gastrointest Endosc* 2001; **53**: 71-76

8 **Rosch T**, Kapfer B, Will U, Baronius W, Strobel M, Lorenz R, Ulm K. Accuracy of endoscopic ultrasonography in upper gastrointestinal submucosal lesions: a prospective multicenter study. *Scand J Gastroenterol* 2002; **37**: 856-862

9 **Kameyama H**, Niwa Y, Arisawa T, Goto H, Hayakawa T. Endoscopic ultrasonography in the diagnosis of submucosal lesions of the large intestine. *Gastrointest Endosc* 1997; **46**: 406-411

10 **Massari M**, De Simone M, Cioffi U, Gabrielli F, Boccasanta P, Bonavina L. Endoscopic ultrasonography in the evaluation of leiomyoma and extramucosal cysts of the esophagus. *Hepatogastroenterology* 1998; **45**: 938-943

11 **Varas Lorenzo MJ**, Maluenda MD, Pou JM, Abad R, Turro J, Espinos JC. The value of endoscopic ultrasonography in the study of submucosal tumors of the digestive tract. *Gastroenterol Hepatol* 1998; **21**: 121-124

12 **Araki K**, Ohno S, Egashira A, Saeki H, Kawaguchi H, Ikeda Y, Kitamura K, Sugimachi K. Esophageal hemangioma: a case report and review of the literature. *Hepatogastroenterology* 1999; **46**: 3148-3154

13 **Lu ZC**, Jing ZD. Submucosal tumors of the esophagus. Modern Intralumen Ultrasonics. *Beijing: Science Press* 2000: 174-182

14 **Buscarini E**, Stasi MD, Rossi S, Silva M, Giangregorio F, Adriano Z, Buscarini L. Endosonographic diagnosis of submucosal upper gastrointestinal tract lesions and large fold gastropathies by catheter ultrasound probe. *Gastrointest Endosc* 1999; **49**: 184-191

15 **Hizawa K**, Matsumoto T, Kouzuki T, Suekane H, Esaki M, Fujishima M. Cystic submucosal tumors in the gastrointestinal tract: endosonographic findings and endoscopic removal. *Endoscopy* 2000; **32**: 712-714

16 **Wang Y**, Sun Y, Liu Y, Li Y, Wang Z. Transesophageal intraluminal ultrasonography in diagnosis and differential diagnosis of esophageal leiomyoma. *Zhonghua Yixue Zazhi* 2002; **82**: 456-458

17 **Zou XP**. Gastric leiomyoma. Modern Intralumen Ultrasonics. *Beijing: Science Press* 2000: 202-205

18 **Koch J**, Halvorsen RA Jr, Levenson SD, Cello JP. Prospective comparison of catheter-based endoscopic sonography versus standard endoscopic sonography: evaluation of gastrointestinal-wall abnormalities and staging of gastrointestinal malignancies. *Clin Ultrasound* 2001; **29**: 117-124

19 **Catalano MF**. Endoscopic ultrasonography for esophageal and gastric mass lesions. *Gastroenterologist* 1997; **5**: 3-9

20 **Xu GQ**. Benign tumors of the esophagus. Modern Esopgagology. *Shanghai: Shanghai Science And Technique Press* 1999: 268-273

21 **Futagami K**, Hata J, Haruma K, Yamashita N, Yoshida S, Tanaka S, Chayama K. Extracorporeal ultrasound is an effective diagnostic alternative to endoscopic ultrasound for gastric submu-

cosal tumours. *Scand J Gastroenterol* 2001; **36**: 1222-1226
22 **Palazzo L**, Landi B, Cellier C, Cuillerier E, Roseau G, Barbier JP. Endosonographic features predictive of benign and malignant gastrointestinal stromal cell tumours. *Gut* 2000; **46**: 88-92
23 **Massari M**, Lattuada E, Zappa MA, Pieri G, Cioffi U, De Simone M, Segalin A, Bonavina L. Evaluation of leiomyoma of the esophagus with endoscopic ultrasonography. *Hepatogastroenterology* 1997; **44**: 727-731
24 **Kawamoto K**, Yamada Y, Furukawa N, Utsunomiya T, Haraguchi Y, Mizuguchi M, Oiwa T, Takano H, Masuda K. Endoscopic submucosal tumorectomy for gastrointestinal submucosal tumors restricted to the submucosa: a new form of endoscopic minimal surgery. *Gastrointest Endosc* 1997; **46**: 311-317
25 **Waxman I**, Saitoh Y, Raju GS, Watari J, Yokota K, Reeves AL, Kohgo Y. High-frequency probe EUS-assisted endoscopic mucosal resection: a therapeutic strategy for submucosal tumors of the GI tract. *Gastrointest Endosc* 2002; **55**: 44-49
26 **Waxman I**, Saitoh Y. Clinical outcome of endoscopic mucosal resection for superficial GI lesions and the role of high-frequency US probe sonography in an American population. *Gastrointest Endosc* 2000; **52**: 322-327
27 **Kajiyama T**, Sakai M, Torii A, Kishimoto H, Kin G, Uose S, Ueda S, Okuma M, Inoue K. Endoscopic aspiration lumpectomy of esophageal leiomyomas derived from the muscularis mucosae. *Am J Gastroenterol* 1995; **90**: 417-422
28 **Giovannini M**, Bernardini D, Moutardier V, Monges G, Houvenaeghel G, Seitz JF, Derlpero JR. Endoscopic mucosal resection (EMR): results and prognostic factors in 21 patients. *Endoscopy* 1999; **31**: 698-701
29 **Izumi Y**, Inoue H, Kawano T, Tani M, Tada M, Okabe S, Takeshita K, Endo M. Endosonography during endoscopic mucosal resection to enhance its safety: a new technique. *Surg Endosc* 1999; **13**: 358-360
30 **Takada N**, Higashino M, Osugi H, Tokuhara T, Kinoshita H. Utility of endoscopic ultrasonography in assessing the indications for endoscopic surgery of submucosal esophageal tumors. *Surg Endosc* 1999; **13**: 228-230
31 **Sun S**, Wang M, Sun S. Use of endoscopic ultrasound-guided injection in endoscopic resection of solid submucosal tumors. *Endoscopy* 2002; **34**: 82-85

Edited by Ma JY and Wang XL

P.O.Box 2345, Beijing 100023,China
Fax: +86-10-85381893
E-mail: wjg@wjgnet.com www.wjgnet.com

World J Gastroenterol 2003;9(9):2092-2095
World Journal of Gastroenterology
 ISSN 1007-9327

• CLINICAL RESEARCH •

Evaluation of liver functional reserve by combining D-sorbitol clearance rate and CT measured liver volume

Yi-Ming Li, Fan Lv, Xin Xu, Hong Ji, Wen-Tao Gao, Tuan-Jie Lei, Gui-Bing Ren, Zhi-Lan Bai, Qiang Li

Yi-Ming Li, Fan Lv, Xin Xu, Hong Ji, Wen-Tao Gao, Tuan-Jie Lei, Gui-Bing Ren, Zhi-Lan Bai, Qiang Li, General Surgery Department, the 2nd Affiliated Hospital of Xi' an Jiaotong University, Xi' an 710004, ShaanXi Province, China
Supported by Natural Science Foundation of Shaanxi Province, No. 99SM61
Correspondence to: Yi-Ming Li, General Surgery Department, the 2nd Hospital of Xi' an Jiaotong University, 710004, Xi' an, Shaanxi Province, China. liyiming@yahoo.com.cn
Telephone: +86-29-7276936-29246
Received: 2003-01-14 **Accepted:** 2003-03-10

Abstract

AIM: Our research attempted to evaluate the overall functional reserve of cirrhotic liver by combination of hepatic functional blood flow, liver volume, and Child-Pugh's classification, and to discuss its value of clinical application.

METHODS: Ninety two patients with portal hypertension due to hepatic cirrhosis were investigated. All had a history of haematemesis and hematochezia, esophageal and gastric fundus varices, splenomegaly and hypersplenia. A 2-year follow-up was routinely performed and no one was lost. Twenty two healthy volunteers were used as control group. Blood and urine samples were collected 4 times before and after intravenous D-sorbitol infusion. The hepatic clearance (CL_H) of D-sorbitol was then calculated according to enzymatic spectrophotometric method while the total blood flow (Q_{TOTAL}) and intrahepatic shunt (R_{INS}) were detected by multicolor Doppler ultrasound, and the liver volume was measured by spiral CT. Data were estimated by *t*-test, variance calculation and chi-squared test. The relationships between all these parameters and different groups were investigated according to Child-Pugh classification and postoperative complications respectively.

RESULTS: Steady blood concentration was achieved 120 mins after D-sorbitol intravenous infusion, which was (0.358±0.064) mmol· L^{-1} in cirrhotic group and (0.189±0.05) mmol· L^{-1} in control group (P<0.01). CL_H=(812.7±112.4) ml· min^{-1}, Q_{TOTAL}=(1280.6±131.4) ml· min^{-1}, and R_{INS}=(36.54±10.65) % in cirrhotic group and CL_H=(1248.3±210.5) ml· min^{-1}, Q_{TOTAL}= (1362.4±126.9) ml· min^{-1}, and R_{INS}=(8.37±3.32) % in control group (P<0.01). The liver volume of cirrhotic group was 1057±249 cm^3, 851±148 cm^3 and 663±77 cm^3 in Child A, B and C group respectively with significant difference (P<0.001). The average volume of cirrhotic liver in Child B, C group was significantly reduced in comparison with that in control group (P<0.001). The patient, whose liver volume decreased by 40 % with the CL_H below 600 ml· min^{-1}, would have a higher incidence of postoperative complications. There was no strict correspondent relationship between CL_H, liver volume and Child-Pugh's classification.

CONCLUSION: The hepatic clearance of D-sorbitol, CT measured liver volume can be reliably used for the evaluation of hepatic functional blood flow and liver metabolic volume. Combined with the Child-Pugh's classification, it could be very useful for further understanding the liver functional reserve, therefore help determine reasonable therapeutic plan, choose surgical procedures and operating time.

Li YM, Lv F, Xu X, Ji H, Gao WT, Lei TJ, Ren GB, Bai ZL, Li Q. Evaluation of liver functional reserve by combining D-sorbitol clearance rate and CT measured liver volume. *World J Gastroenterol* 2003; 9(9): 2092-2095
http://www.wjgnet.com/1007-9327/9/2092.asp

INTRODUCTION

Accurate evaluation of the hepatic functional reserve is very important in the development of hepatobiliary surgery. Hepatic functional reserve means the whole functions of all hepatic parenchyma cells, which depend on the interaction between relatively healthy hepatic cells and blood perfusion. Based on Child-Pugh' s classification, we have established a new method to evaluate the liver functional reserve by D-sorbitol clearance rate indicating hepatic functional blood flow and CT measured liver volume indicating normal hepatic metabolic volume.

MATERIALS AND METHODS

Materials

Ninety two patients with portal hypertension due to hepatic cirrhosis, were selected in our hospital from March 1999 to January 2001, including 57 males and 35 females aged between 20-66 years, with a mean age 43.5±11.8 years. All of them had a history of haematemesis and hematochezia, and moderate esophageal varices were found in 41 patients and severe ones in 51 patients by gastroscopy. Porta-azygous devascularization was applied to all patients and the pathological diagnosis was confirmed by biopsy during the surgical procedure. According to Child-Pugh' s classification, 36 cases were scored as A, 39 as B and 17 as C. A 2-year follow-up was routinely performed. The healthy control group consisted of 20 volunteers, 11 males and 9 females, who had no abnormality in CT scan and related history of liver disease.

The postoperative data of operative complications and hepatic functions were carefully recorded and a routine follow-up was given. There was no operative mortality, severe complications occurred in 31 cases because of liver function deterioration after the operation, including 13 cases of long standing jaundice, 7 hepatic coma, 13 severe ascites, and 6 recurring hemorrhage of upper GI tract.

Methods

Intravenous infusion of D-sorbitol and collection of blood and urine samples Controlled by the peristalsis pump, 5 % D-sorbitol solution was continuously infused intravenously for 3 hours at a rate of 1 ml· min^{-1} (a dose of 50 mg· min^{-1}). The

samples of blood (3 ml), urine and the volumes at the same time were collected and recorded once before infusion and 3 times at 120,150,180 min after infusion.

Determination of D-sorbitol concentration and calculation The enzymatic spectrophotometric method was used to determine the D-sorbitol concentration in blood and urine[1, 2]. The total D-sorbitol clearance rate (CL_{TOTAL}), renal D-sorbitol clearance rate (CL_{REN}) and liver D-sorbitol clearance rate (CL_H) were calculated according to the formula reported[3,4] as $CL_{TOTAL}=R \div Css$ and $CL_{REN}=U \div Css$. (R: D-sorbitol infusion rate; Css: homeostatic plasma concentration; U: average urinary excretion rate, ($C_{LH}=CL_{TOTAL}- C_{LREN}$).

Hepatic total blood flow (Q_{TOTAL}) and intrahepatic shunt rate (R_{INS}) and liver extraction rate (E) assay and calculation The angle between blood flow and Doppler ultrasound wave direction was controlled below 60 degrees, the mean blood flow rates of three main liver veins (left, middle, right hepatic vein) were carefully detected by ultrasonic equipment. Then, the accurate blood flow of each vein was calculated according to the formula as $Q=1/4\pi D^2\times 60\times V_{mean}$[5, 6], and their sum was the total blood flow (Q_{TOTAL}). The D-sorbitol hepatic clearance rate equaled to the liver functional blood flow (Q_{FUNC}), and $R_{INS}=(Q_{TOTAL}-Q_{FUNC})/Q_{TOTAL}$. According to Fick' s rule[7, 8], the hepatic extractive rate $E=CL_H/Q_{TOTAL}$.

Method for measuring liver volume change by CT Guided by the reported method[9], the cirrhotic liver volume was measured by CT (PQ6000), at the same time the expected "normal" liver volume of the patient was calculated according to the reported formula[10]. The volume change rate (R) was then calculated according to the formula : (CT measured LV-expected LV)/expected LV×100 %.

Statistical analysis

The relationship between liver functional blood flow, liver volume change rate, Child-Pugh' s classification, postoperative complication rate was investigated.Data were expressed as mean ±S. Statistical significance was estimated by *t*-test. The multiple means between various groups were estimated by variance calculation. The difference of percentage was estimated by chi-squared test.

RESULTS

Changes of D-sorbitol clearance index in two groups

Table 1 Indexes of D-sorbitol clearance (mean ±s)

Groups	*n*	Css (mmol·L^{-1})	R_{INS} (%)	$CL_H(Q_{FUNC})$ (ml·min^{-1})	E (%)	Q_{TOTAL} (ml·min^{-1})
Control	20	0.189±0.05	8.37±3.32	1248.3±210.5	91.6±6.5	1362.4±126.9
Cirrhotic	92	0.385±0.064[a]	36.54±10.65	812.7±112.4[a]	63.5±9.4[a]	1280.6±131.4

[a]P<0.01 in comparison between the two groups.

Table 1 shows that the D-sorbitol plasma concentration of each group could come to a stable level after continuous intravenous infusion for 120 minutes. The homeostatic plasma concentration of control group was (0.189±0.05) mmol· L^{-1}, and that of hepatic cirrhotic group was (0.358±0.064) mmol· L^{-1}. The difference between the two groups was significant (P<0.01). The total liver blood flow between the two groups had no significant difference. The D-sorbitol liver extraction rate and hepatic clearance rate decreased significantly while intrahepatic shunt flow increased significantly in the cirrhotic group. All reached statistical significance compared with that of the control group.

Relationship between Child-Pugh' s classification and D-sorbitol liver clearance rate and liver volume change rate

Table 2 Relationship between Child-Pugh' s classification and D-sorbitol liver clearance rate and liver volume change rate

Child-Pugh' s classification	*n*	CL_H (ml·min^{-1})	Q_{INS} (%)	Mean cirrhotic liver volume (cm^3)
A	36	995.8±174.8	22.2±4.2	1057±249
B	39	783.4±120.6[a]	38.8±7.3[a]	851±148[a]
C	17	548.6±32.8[b]	57.8±6.6[b]	663±77[b]

[b]P<0.01, [a]P<0.05 in comparison between the two groups.

Table 2 shows that there was a clear correlation between each Child-Pugh' s classification group and D-sorbitol liver clearance rate and liver volume,respectively. The higher the Child-Pugh' s classification degree, the lesser the liver functional blood flow, the more the intrahepatic shunt flow, and the smaller the mean liver volume. The difference had statistical significance between each group (P<0.05).

Table 3 Correlative relationship between hepatic D-sorbitol clearance rate and liver volume change rate and Child-Pugh' s classification

Child-Pugh' s classification	CL_H (mL·min^{-1})			Liver volume change rate		
	>800	600-800	<600	R≥-20 %	-40 %<R<-20 %	R ≤-40 %
A(case)	21	11	4	20	13	3
B(case)	8	24	7	9	26	4
C(case)	0	6	11	2	5	10

Table 3 shows in view of individual patient, there was not any complete correlation between the D-sorbitol liver clearance rate and liver volume change rate or liver function status in cirrhotic patients. Even in the same Child-Pugh' s classification group, the D-sorbitol clearance rate and liver volume change rate varied remarkably. It was found that a mild Child' s classified patient could have a low D-sorbitol clearance rate and a small liver volume, and *vice versa*.

Relationship between postoperative complications and D-sorbitol clearance rate and liver volume change rate

Table 4 shows that severe postoperative complications increased steadily as the D-sorbitol clearance rate and/or liver volume decreased. When the CL_H was below 600 /ml· min^{-1}, R below -40 %, the incidence of severe complications was higher than 70 % (P<0.05).

Table 4 Relationship between hepatic D-sorbitol clearance rate and liver volume change rate and postoperative complications

Postoperative complications	CL_H / mL·min^{-1}			Liver volume change rate		
	>800	600-800	<600	R≥-20 %	-40 %<R<-20 %	R ≤-40%
Case number	29	41	22	31	44	17
Complication cases	1	14	16	3	16	12
Rate (%)	3.4	34.2[a]	72.7[b]	9.7	36.4[a]	70.6[b]

[b]P<0.01, [a]P<0.05 in comparison between each groups.

Table 5 shows that 22 cases had a D-sorbitol clearance rate lower than 600/ml· min^{-1}. 8 of them had their liver volume change rate between -20 % and -40 %, 14 below -40 %, and the incidences of postoperative complications were 62.5 % (5/8), and 78.6 % (11/14), respectively.

Table 5 Correlation between hepatic D-sorbitol clearance rate and liver volume change rate and operation complications

CL_H(ml·min^{-1})	-40 %<R<-20 %			R≤ -40%		
	Number	Complication case	Complication rate	Number	Complication case	Complication rate
600-800	35	12	34.3(%)	3	1	33.3(%)
<600	8	5	62.5(%)	14	11	78.6(%)

DISCUSSION

It is essential in the surgical treatment of portal hypertension, to evaluate accurately the patient' s preoperative liver functional reserve and to make a reasonable peri-operative therapeutic plan in order to choose the best surgical procedures and to increase its efficacy. The Child-Pugh' s classification is still the most important method to determine the type and time of operation, and is widely accepted for the patients who are in stage I or II. But there are relatively high-risks for post-operative complications and mortality[11-13]. This is because the present classification cannot completely reflect the injured and whole hepatic function, besides the technical factors[14-16]. What condition would go worse with the operative burden is another factor that is difficult to tell. It is therefore necessary to find more objective criteria for the evaluation of hepatic functional reservation.

The liver inherent metabolic volume and blood flow determine its functions in most occasions, which also depend on the relative ratio and mutual influence of the two factors[17-20]. When cirrhosis and portal hypertension occur, necrosis of liver cells, hyperplasia of fibrous tissue, formation of pseudo lobules and abnormality of liver microcirculation will result in decrease of liver inherent metabolic volume, increase of anatomical and physiological intrahepatic shunt and change of their relevant ratio[21]. Therefore, measurement of liver inherent metabolic volume and functional blood flow can provide more information on the understanding of physiological changes and functional reserve of the cirrhotic liver, and help to make individualized and reasonable therapeutic decisions.

Liver functional blood flow is a part of total liver blood flow that enters the hepatic sinusoid involved in the metabolic process[1]. Currently it can only be measured by assay of its clearance rate. D-sorbitol is the first substance suitable for noninvasive evaluation of hepatic blood flow, and is widely used to observe the normal and pathologic perfusion of the liver outside China[22]. Molino, Susanne *et al*, reported that the normal liver had a very high D-sorbitol extraction rate of around 94 %, and CL_H could be used to represent the liver total blood flow (Q_{TOTAL}), and its variation could reflect the change of liver blood flow[8,23]. In our research, D-sorbitol clearance rate and color Doppler ultrasonography were used to study the liver blood flow. It was found that D-sorbitol plasma concentration of the healthy control group always came to homeostasis by continuously intravenous infusion after 120 minutes (0.189±0.05 mmol/l), CL_H was 1 248.3±210.5/ml.min^{-1}, Q_{TOTAL} was 1 362.4±126.9/ml· min^{-1} and the D-sorbitol extraction rate of the liver was 91.6±6.5 %. The D-sorbitol extraction rate decreased dramatically to 63.5±9.4 % in the cirrhotic group, which was statistically significant compared with that of control group (P<0.01). The CL_H, reflecting the liver functional blood flow[1,11,24], was 812.7±112.4/ml.min^{-1} significantly different from that of the control group (P<0.01). The R_{INS} was 8.37±3.32 % in control group and was 36.54±10.65 % in cirrhotic group (P<0.01). The intrahepatic shunt consisted of anatomical shunt and physiological shunt, and the latter had no help to hepatic function even passing through hepatic sinusoid[25]. Therefore, the combination of D-sorbitol clearance rate and color Doppler ultrasonography can show the liver functional blood flow and the conditions of intrahepatic shunt which are so meaningful for the evaluation of liver blood flow in the liver functional reserve before proper medication is given[26, 27]. Our conclusion is that D-sorbitol clearance rate can be widely used in clinical practice, which is safe, economical, practicable, and noninvasive.

The liver inherent metabolic volume and liver functional blood flow are complementary to each other, especially their matching. It is a mature and repeatable method to use CT in measuring liver volume[28-30]. Liver volume is considered as a liver function index as important as the Child-Pugh' s classification because it can partly represent the hepatic parenchyma cell volume[31-33]. Combining liver volume measured by CT scanning and an expected "normal" liver volume calculated according to a standard liver volume formula[8], the cirrhotic liver volume change rate has been measured quantitatively. The Child-Pugh' s liver function classification is a classic liver function index and is widely used in clinical practice. Our research results demonstrated that the indexes for liver inherent metabolic volume and liver functional blood flow could be used as a complement to Child-Pugh' s classification to gain overall and objective data of liver functional reserve. The CL_H, R_{INS} and liver volume change rate had some correlations with the Child-Pugh' s classification. The higher the Child-Pugh' s classification, was the less the liver functional blood flow existed, the more the intrahepatic shunt occurred, the smaller the liver volume was. This result is comparable with other reports[34, 35]. It was also found that variation of CL_H and liver volume change rate did not always correlate with each other even the Child-Pugh' s classification was the same. There was an overlap among different groups, indicating that a patient classified as Child A might have a smaller CL_H and liver volume than a patient classified as Child B or C. This may explain why some deadly complications such as severe ascites or hepatic coma might occur in Child-Pugh' s A patients but not in Child-Pugh' s B or C patients after operation. In conclusion, the functional blood flow and cirrhotic liver volume are two critical indexes which are complementary to Child-Pugh' s classification and can help the evaluation of the overall status of cirrhotic liver and the establishment of individualized therapeutic plan[17,18,30,31].

The CL_H and liver volume change rate had a close relationship with the postoperative complications in cirrhotic patients. The complication incidence increased as the CL_H or liver volume change rate decreased. The complication rate exceeded 70 % (P<0.05) when CL_H was below 600/ml.min^{-1} or R below 40 %. This can be explained by the theory that the liver can not stand anesthesia and operative risks when decreased metabolic volume and functional blood flow have already put the liver at the edge of collapse. The CL_H and liver volume change rate could be complementary to each other when postoperative complications were to be predicted. 22 cases had D-sorbitol clearance rate lower than 600/ml· min^{-1}. 8 of them had their liver volume change rate between -20 % and -40 %, 14 below -40 %. The incidence of postoperative complications was 62.5 % (5/8) and 78.6 % (11/14), respectively. Therefore, the Child-Pugh' s classification complemented by CL_H and liver volume change rate should be used to determine the surgical time and type. When the liver has a better functional blood flow with liver volume compensated, the portal-systemic shunt

or combination operation can be performed. When the functional blood flow and /or liver volume are decreased dramatically, the treatment of perioperative period should be strengthened to increase the tolerance of the cirrhotic liver, and porta-azygous devascularization would be more suitable. When CL_H <600/ml· min^{-1}, R<-40 %, conservative therapy should be recommended. If no improvement of these indexes is achieved after that, the patients should be considered as the end stage of liver cirrhosis and liver transplantation should be possibly considered.

REFERENCES

1 **Molino G**, Avagnina P, Belforte G, Bircher J. Assessment of the hepatic circulation in humans: new concepts based on evidence derived from a D-sorbitol clearance method. *J Lab Clin Med* 1998; **131**: 393-405

2 **Clemmesen JO**, Tygstrup N, Ott P. Hepatic plasma flow estimated according to Fick's principle in patients with hepatic encephalopathy: evaluation of indocyanine green and D-sorbitol as test substances. *Hepatology* 1998; **27**: 666-673

3 **Sinha V**, Brendel K, Mayersohn M. A simplified isolated perfused rat liver apparatus: characterization and measurement of extraction ratios of selected compounds. *Life Sci* 2000; **66**: 1795-1804

4 **Rosemurgy AS 2nd**, Norman JG, Goode SE. Does the direction of portal blood flow determine outcome with small-diameter prosthetic H-graft portacaval shunt? *Surgery* 1997; **121**: 95-101

5 **Fabbri A**, Magalotti D, Brizi M, Bianchi G, Zoli M, Marchesini G. Prostaglandin E1 infusion and functional hepatic flow in control subjects and in patients with cirrhosis. *Dig Dis Sci* 1999; **44**: 377-384

6 **Sugimoto H**, Kaneko T, Inoue S, Takeda S, Nakao A. Simultaneous Doppler measurement of portal venous peak velocity, hepatic arterial peak velocity, and splenic arterial pulsatility index for assessment of hepatic circulation. *Hepatogastroenterology* 2002; **49**: 793-797

7 **Le Couteur DG,** Hickey H, Harvey PJ, Gready J, Mclean AJ. Hepatic artery flow and propranolol metabolism in perfused cirrhotic rat liver. *J Pharmacol Exp Ther* 1999; **289**: 1553-1558

8 **Keiding S**, Engsted E, Ott P. Sorbitol as a test substance for measurement of liver plasma flow in humans. *Hepatology* 1998; **28**: 50-56

9 **Kayaalp C**, Arda K, Oto A, Oran M. Liver volume measurement by spiral CT: an *in vitro* study. *Clin Imaging* 2002; **26**: 122-124

10 **Urata K**, Hashikura Y, Ikegami T, Terada M, Kawasaki S. Standard liver volume in adults. *Transplant Proc* 2000; **32**: 2093-2094

11 **Ziser A**, Plevak DJ, Wiesner RH, Rakela J, Offord KP, Brown DL. Morbidity and mortality in cirrhotic patients undergoing anesthesia and surgery. *Anesthesiology* 1999; **90**: 42-53

12 **Rizvon MK,** Chou CL. Surgery in the patient with liver disease. *Med Clin North Am* 2003; **87**: 211-227

13 **Pisani Ceretti A**, Cordovana A, Pinto A, Spina GP. Surgery in the cirrhotic patient. Prognosis and risk factors. *Minerva Chir* 2000; **55**: 771-778

14 **Fan ST**. Methods and related drawbacks in the estimation of surgical risks in cirrhotic patients undergoing hepatectomy. *Hepatogastroenterology* 2002; **49**: 17-20

15 **Wu CC**, Yeh DC, Lin MC, Liu TJ, P'Eng FK. Improving operative safety for cirrhotic liver resection. *Br J Surg* 2001; **88**: 210-215

16 **Pagliaro L**. MELD: the end of Child-Pugh classification? *J Hepatol* 2002; **36**: 141-142

17 **Hashimoto M,** Watanabe G. Simultaneous measurement of effective hepatic blood flow and systemic circulation. *Hepatogastroenterology* 2000; **47**: 1669-1674

18 **Zipprich A**, Steudel N, Behrmann C, Meiss F, Sziegoleit U, Fleig WE, Kleber G. Functional significance of hepatic arterial flow reserve in patients with cirrhosis. *Hepatology* 2003; **37**: 385-392

19 **Shoup M**, Gonen M, D'Angelica M, Jarnagin WR, DeMatteo RP, Schwartz LH, Tuorto S, Blumgart LH, Fong Y. Volumetric analysis predicts hepatic dysfunction in patients undergoing major liver resection. *J Gastrointest Surg* 2003; **7**: 325-330

20 **Kwon AH**, Matsui Y, Ha-Kawa SK, Kamiyama Y. Functional hepatic volume measured by technetium-99m-galactosyl-human serum albumin liver scintigraphy: comparison between hepatocyte volume and liver volume by computed tomography. *Am J Gastroenterol* 2001; **96**: 541-546

21 **Blaker H**, Theuer D, Otto HF. Pathology of liver cirrhosis and portal hypertension. *Radiologe* 2001; **41**: 833-839

22 **Burggraaf J**, Schoemaker RC, Lentjes EG, Cohen AF. Sorbitol as a marker for drug-induced decreases of variable duration in liver blood flow in healthy volunteers. *Eur J Pharm Sci* 2000; **12**: 133-139

23 **Garello E**, Battista S, Bar F, Niro GA, Cappello N, Rizzetto M, Molino G. Evaluation of hepatic function in liver cirrhosis: clinical utility of galactose elimination capacity, hepatic clearance of D-sorbitol, and laboratory investigations. *Dig Dis Sci* 1999; **44**: 782-788

24 **Zoli M**, Magalotti D, Bianchi G, Ghigi G, Orlandini C, Grimaldi M, Marchesini G, Pisi E. Functional hepatic flow and Doppler-assessed total hepatic flow in control subjects and in patients with cirrhosis. *J Hepatol* 1995; **23**: 129-134

25 **Koranda P**, Myslivecek M, Erban J, Seidlova V, Husak V. Hepatic perfusion changes in patients with cirrhosis indices of hepatic arterial blood flow. *Clin Nucl Med* 1999; **24**: 507-510

26 **Kok T**, van der Jagt EJ, Haagsma EB, Bijleveld CM, Jansen PL, Boeve WJ. The value of Doppler ultrasound in cirrhosis and portal hypertension. *Scand J Gastroenterol Suppl* 1999; **230**: 82-88

27 **Piscaglia F**, Donati G, Serra C, Muratori R, Solmi L, Gaiani S, Gramantieri L, Bolondi L. Value of splanchnic Doppler ultrasound in the diagnosis of portal hypertension. *Ultrasound Med Biol* 2001; **27**: 893-899

28 **Imsamran W**, Leelawat K, Leelawat T, Subwongcharoen S, Ratanachu-ek T, Treepongkaruna SA. Simple technique in the measurement of liver volume. *J Med Assoc Thai* 2003; **86**: 151-156

29 **Usuki N,** Miyamoto T. Chronic hepatic disease: usefulness of serial CT examinations. *J Comput Assist Tomogr* 2002; **26**: 418-421

30 **Sandrasegaran K**, Kwo PW, Di Girolamo D, Stockberger SM Jr, Cummings OW, Kopecky KK. Measurement of liver volume using spiral CT and the curved line and cubic spline algorithms: reproducibility and interobserver variation. *Abdom Imaging* 1999; **24**: 61-65

31 **Lin XZ**, Sun YN, Liu YH, Sheu BS, Cheng BN, Chen CY, Tsai HM, Shen CL. Liver volume in patients with or without chronic liver diseases. *Hepatogastroenterology* 1998; **45**: 1069-1074

32 **Schiano TD**, Bodian C, Schwartz ME, Glajchen N, Min AD. Accuracy and significance of computed tomographic scan assessment of hepatic volume in patients undergoing liver transplantion. *Transplantation* 2000; **69**: 545-550

33 **Dunkelberg JC**, Feranchak AP, Fitz JG. Liver cell volume regulation: size matters. *Hepatology* 2001; **33**: 1349-1352

34 **Zhu JY**, Leng XS, Dong N, Qi GY, Du RY. Measurement of liver volume and its clinical significance in cirrhotic portal hypertensive patients. *World J Gastroenterol* 1999; **5**: 525-526

35 **Hoshida Y,** Shiratori Y, Koike Y, Obi S, Hamamura K, Teratani T, Shiina S, Omata M. Hepatic volumetry to predict adverse events in percutaneous ablation of hepatocellular carcinoma. *Hepatogastroenterology* 2002; **49:** 451-455

Edited by Xu JY, Zhu LH and Wang XL

P.O.Box 2345, Beijing 100023,China
Fax: +86-10-85381893
E-mail: wjg@wjgnet.com www.wjgnet.com

World J Gastroenterol 2003;9(9):2096-2099
World Journal of Gastroenterology
 ISSN 1007-9327

• CLINICAL RESEARCH •

Clinical effects of continuous high volume hemofiltration on severe acute pancreatitis complicated with multiple organ dysfunction syndrome

Hao Wang, Wei-Qin Li, Wei Zhou, Ning Li, Jie-Shou Li

Hao Wang, Wei Zhou, Wei-Qin Li, Ning Li, Jie-Shou Li, Department of Surgery, School of Medicine, Nanjing University, Nanjing 210002, Jiangsu Province, China
Supported by the Social Development Foundation of Jiangsu Province, No. BS2000051
Correspondence to: Dr. Hao Wang, Department of Surgery, Jinling Hospital, 305 East Zhongshan Road, Nanjing 210002, Jiangsu Province, China. wanghao_nju@sina.com
Telephone: +86-25-3685194 **Fax:** +86-25-4803956
Received: 2003-03-19 **Accepted:** 2003-04-11

Abstract

AIM: To investigate the efficiency of continuous high volume hemofiltration (HVHF) in the treatment of severe acute pancreatitis (SAP) complicated with multiple organ dysfunction syndrome (MODS).

METHODS: A total of 28 SAP patients with an average of 14.36±3.96 APACHE II score were involved. Diagnostic criteria for SAP standardized by the Chinese Medical Association and diagnostic criteria for MODS standardized by American College of Chest Physicians (ACCP) and Society of Critical Care Medicine (SCCM) were applied for inclusion. HVHF was started 6.0±6.1 (1-30) days after onset of the disease and sustained for at least 72 hours, AN69 hemofilter (1.2 m^2) was changed every 24 hours. The ultrafiltration rate during HVHF was 4 000 ml/h, blood flow rate was 250-300 ml/min, and the substitute fluid was infused with pre-dilution. Low molecular weight heparin was used for anticoagulation.

RESULTS: HVHF was well tolerated in all the patients, and lasted for 4.04±3.99 (3-24) days. 20 of the patients survived, 6 patients died and 2 of the patients quited for financial reason. The ICU mortality was 21.4 %. Body temperature, heart rate and breath rate decreased significantly after HVHF. APACHE II score was 14.4±3.9 before HVHF, and 9.9±4.3 after HVHF, which decreased significantly ($P<0.01$). Partial pressure of oxygen in arterial blood before HVHF was 68.5±19.5 mmHg, and increased significantly after HVHF, which was 91.9±25 mmHg ($P<0.01$). During HVHF the hemodynamics was stable, and serum potassium, sodium, chlorine, glucose and pH were at normal level.

CONCLUSION: HVHF is technically possible in SAP patients complicated with MODS. It does not appear to have detrimental effects and may have beneficial effects. Continuous HVHF, which seldom disturbs the hemodynamics and causes few side-effects, is expected to become a beneficial adjunct therapy for SAP complicated with MODS.

Wang H, Li WQ, Zhou W, Li N, Li JS. Clinical effects of continuous high volume hemofiltration on severe acute pancreatitis complicated with multiple organ dysfunction syndrome. *World J Gastroenterol* 2003; 9(9): 2096-2099

http://www.wjgnet.com/1007-9327/9/2096.asp

INTRODUCTION

Acute pancreatitis is an inflammatory process of the pancreas with multiple etiologies and a physiopathology that is still unclear. It has a nonspecific clinical presentation, varying from moderate to severe forms, including MODS. The latter is associated with SAP and evolves with high morbidity, mortality and costs[1,2]. MODS has become the primary cause of death in SAP. From Jan 1997 to May 2002, we accepted 283 patients involved in acute pancreatitis. 11 of 31 cases complicated with MODS died, accounting for 91.7 % of the death toll in acute pancreatitis.

Evidences accumulated over the last years demonstrate that many soluble inflammatory molecules of the systemic inflammatory (and anti-inflammatory) response syndrome (SIRS) can be removed by hemofiltration[3-5]. This has led to the hypothesis that hemofiltration could play a major role in sepsis therapy as immunomodulatory treatment, in addition to being a blood purification technique. Particular attention has been paid to HVHF to remove inflammatory molecules as compared to standard volume hemofiltration[6]. HVHF might be of more benefits for amelioration of severe SIRS or MODS, but the clinical feasibility and safety are noticeable. The present study was therefore to investigate the clinical efficacy of continuous HVHF on SAP complicated with MODS.

MATERIALS AND METHODS

Patient population

A total of 28 patients with SAP complicated with MODS, including 7 women and 21 men, with an average age of 51.43±12.96 years were admitted to the study. SAP was diagnosed according to the criteria of Chinese Medical Association for SAP (2001), and MODS was diagnosed according to the criteria of ACCP and SCCM for MODS (1992)[7]. All the patients had complications such as SIRS, systemic infection, shock, etc (Table 1). The average of APACHE II score was 14.36±3.96. SAP was caused by alcohol in 5 patients, hyperlipidemia in 3 patients, high fat diet in 3 patients and biliary disease in 17 patients. The CT scan on admission revealed that necrosis of the body of the pancreas was below 33 % in 6 patients, 33-67 % in 12 patients and 67-100 % in 10 patients. The average CT severity score was 8.5±1.4, and 9 patients were in grade B and 19 in grade C according to Balthazar CT grading criteria of SAP[8].

Conventional treatment for SAP

Seven patients had accepted surgical treatment in other hospitals before admission to our hospital due to severe complications. All the patients were allocated to ICU and underwent following conventional treatments such as fasting and fluid resuscitation, gastrointestinal decompression, drainage of pancreatic (or bile) duct, and abdominal cavity, oxygen therapy, in which 3 patients underwent mechanical ventilation by non-invasive method and 24 patients underwent mechanical ventilation by tracheotomy, gut cleaning (enema

by taking magnesium sulfate orally), somatostatin, prostaglandin E1, nutritional support (enteral nutrition), antibiotics. 12 patients underwent drainage of peripancreatic abscess and necrosis, and 5 patients who suffered from pancreatitis secondary to biliary disease underwent cholecystectomy.

Table 1 Incidence of complications before HVHF

Complications	Case	Incidence (%)
SIRS*	28	100
Systemic infection	10	35.7
ARDS*	20	71.4
Shock	14	50.0
Renal failure	7	25.0
Pancreatic encephalopathy	6	21.4
Bleeding in alimentary tract	12	42.8
Cardiac arrhythmia	4	14.3
Heart failure / pulmonary edema	2	7.1
Dysfunction of coagulation	4	14.3
Liver function failure	2	7.1
Fungal infection	7	25.0

SIRS: systemic inflammatory response syndrome; ARDS: acute respiratory distress syndrome.

HVHF technique

For vascular access, a double coaxial lumen 14-Fr catheter was inserted percutaneously either through the right internal jugular or the femoral vein using the Seldinger technique. A Baxter BM25 machine (Baxter, USA) was used for HVHF with a polyacrylonitrile AN69 hemofilter (1.2 m^2 surface area, 35-kD limit; Hospal, USA). Blood flow was set at 250-300 ml/min and ultrafiltrate flow at 4 000 ml/h, transmembrane pressure was maintained between 300-500 mmHg, and the substitute fluid was infused with pre-dilution. Low molecular weight heparin served as the anticoagulant, patient-activated clotting time was adjusted to 60-70 seconds, a strictly neutral balance was maintained using a digital balance system (Baxter). Elapsed time was expressed in hours from the beginning of HVHF as a T value. T_0 was the beginning of HVHF at zero hours, T_{24} was 24 hours after T0, *et al*. These values were recorded for each patient.

Clinical variables

Vital signs, including body temperature, breath rate, blood pressure and heart rate were recorded every half an hour. Blood samples were collected every 24 hours to observe blood cell count, serum amylase and electrolyte, hepatic and renal function, and arterial blood gas. The APACHE II score was applied to evaluate the state of the patients.

Statistical calculations

Results were expressed as mean ±SD and analyzed using pair-matching *t* test. The difference was considered significant at $P<0.05$.

RESULTS

Outcome

20 patients were cured and discharged from hospital, 6 patients died and 2 patients quit for financial reason. One patient died of pulmonary embolism secondary to the exfoliation of cardiac valve emboli, four of fungal sepsis and one of septic shock. The mortality rate was 21.4 %.

Clinical symptoms and signs

During HVHF the hemodynamics and mean arterial pressure (MAP) were stable, while body temperature, heart rate and breath rate decreased eventually after the beginning of HVHF with amelioration of the symptoms (Table 2). 6 patients suffering from pancreatic encephalopathy secondary to SAP were administrated with 50-100 mg chlorpromazine each day simultaneously, and state of awareness recovered during the procedure with amelioration of dysphoria and delirium. Three of four patients complicated with acute renal failure recovered after HVHF.

Table 2 Changes of vital signs after HVHF

	T_0	T_{24}	T_{48}	T_{72}	T_{96}	T_{120}
Case	28	28	28	28	28	28
BT (℃)	37.8±0.8	37.3±0.8[a]	37.2±0.7[a]	37.2±0.8[a]	37.3±0.9	37.5±0.9[b]
HR (bpm)	127±23	120±30	107±25[a]	101±24[a]	103±17[a]	102±21[a]
BR (tpm)	31±5	22±4[a]	21±5[a]	19±1[a]	20±1[a]	19±2[a]
MAP(kpa)	13.8±1.9	13.8±2.0	14.1±2.3	13.6±1.7	13.5±1.7	13.8±1.8

[a]$P<0.01$, *vs* T_0; [b]$P<0.05$, *vs* T_0; BT: body temperature (℃); HR: heart rate (beats per minute); BR: breath rate (times per minute); MAP: mean arterial pressure (kpa).

Severity and homeostasis

APACHE II score before HVHF was 14.4±3.9, and decreased significantly after HVHF, which was 9.9±4.3 ($P<0.01$, Table 3). Hyperkalemia in two patients and metabolic acidosis in eleven patients were redressed after 24 hours of HVHF. During HVHF the serum potassium, sodium, chlorine, glucose and pH were at normal level.

Table 3 Changes of laboratory parameters after HVHF

Index	Pre HVHF	Post HVHF
Case	28	28
APACHE II score	14.4±3.9	9.9±4.3[a]
PaO_2	68.5±19.5	91.9±25[a]
CRP	187±39	87.4±112
White cell count	15.5±5.8	14.9±6.9
Serum amylase	392±517	103±184[a]
Blood urea nitrogen	9.9±10.1	5.0±2.9[b]
Serum albumin	33.0±5.4	31.8±4.8

[a]$P<0.01$, *vs* pre-HVHF; [b]$P<0.05$, *vs* pre-HVHF.

Side-effects correlated with HVHF

Two patients got a high fever caused by infection of intravenous catheter, and recovered after the catheter was removed. Hypophosphatemia occurred in four patients and was redressed by transvenous recruit of compound phosphate solution. The drainage fluid of abdominal cavity of two patients who suffered from intraabdominal hemorrhage became bloody after the beginning of HVHF. Bleeding was controlled following reducing the administration of anticoagulant.

DISCUSSION

With patho-morphological, pathophysiological, biochemical, immunologic and real time imaging observations, adequate evidences have revealed that SAP is a systemic rather than a local critical condition[9]. Extensive peripancreatic necrosis of fat tissue in the omentum and retroperitoneum may induce a SIRS that extends beyond the pancreas. Hemorrhage is caused

by tissue necrosis or rupture of surrounding blood vessels[10]. Associated complications include sepsis, MODS, acute respiratory distress syndrome (ARDS), acute renal failure, disseminated intravascular coagulation (DIC), hypovolemic shock, and acute liver failure. MODS has become the primary cause of morbidity and mortality in SAP. Systemic lymphocyte activation (triggered by local release of mediators) causes the distant organ complications in SAP[11]. Utilizing proteolytic enzymes and toxicant, neutrophils injure the infiltrated vital organs, causing cellular damage and dysfunction of vital organs distant from the pancreas. Multiple organ failure in acute pancreatitis with septic complications can develop, at least in part, by proinflammatory cytokine release and neutrophil activation[12]. Recent studies have established the critical role played by inflammatory mediators such as TNFα, IL-1β, IL-6, IL-8, CINC/GROα, PAF, IL-10, C5a, ICAM-1 and substance P in acute pancreatitis and the resultant MODS[11-18]. Potentially, there is a therapeutic window between symptom onset and the development of distant organ damage, when anti-inflammatory therapy may be of use. Strategies have been used to target cytokines, such as cytokine antibody, transfection of human anti-inflammation gene and blood purification. Method targeting only one inflammatory mediator is far from combating with complicated cytokines network. Blood purification, such as plasmapheresis, hemadsorption, hemofiltration, can remove nonselective inflammatory mediators, which may make it possible to develop clinically effective anti-inflammatory therapy. Among them, hemofiltration is used widely in clinic.

In 1977, hemofiltration was applied in clinic for the first time to cure the over-hydrated patients resistant to diuretics[19]. Hemofiltration has been widely applied to patients with MODS as an artificial support such as an artificial kidney or an artificial liver[20,21]. Recent advances in medical engineering have made it possible to apply hemofiltration continuously (i.e., 24 hours a day, 7 days a week, if necessary) even to critically ill patients, such as MODS patients with renal and hepatic failure[22]. Continuous hemofiltration (CHF), especially continuous venovenous hemofiltration (CVVH), was developed as continuous renal replacement therapy (CRRT) for patients with severe conditions and has been widely performed mainly in critical care, taking the place of intermittent hemodialysis (IHD). The membrane pore size of a hemofilter used for CHF allows passage of substances ranging from 30 000 to 50 000 Daltons, and the method for solute removal in CHF employs the principle of convection, which is advantageous for removing middle- to high-molecular-weight substances[20]. Many inflammatory mediators, such as TNF, IL-1, IL-6, sIL-2R, IL-8, IL-2 and IL-10, can be removed by CHF for their molecular weights are under 50 000 Daltons[6]. Since 1990s, CHF has been employed in treatment of SIRS and MODS secondary to SAP. In 1999, Yekebas[23] performed experiments in pigs to investigate the effects of CHF on SAP. It was found that effective removal of tumor necrosis factor, phospholipase, and kinin by CHF significantly improved survival time. Animals that received prophylactic CHF had a longer survival period than those in which HVHF was started after clinical onset. Bellomo *et al*.[24] reported that CHF could remove cytokines from the circulation of septic patients.

There are a large amount of soluble inflammatory mediators in circulation in severe sepsis, so the low intensity therapy, such as standard CRRT at 1 000 ml/h of ultrafiltration rate, would be inadequate. For this reason, many investigators have long felt that if we wish to tackle blood purification therapy in sepsis, we need to move "renal dose" CRRT to "sepsis dose" CRRT. HVHF represents the logical response to these observations[6]. Rogiers *et al*[25] studied the effect of hemofiltration at various levels of intensity and varying times of intervention in dogs made septic by the infusion of endotoxin. The results suggested that, even at ultrafiltration rates of 3 000 ml/h (close to 7 000-8 000 ml/h in humans), one could achieve clinically important and beneficial hemodynamic effects. Lonnemann *et al*.[26] were able to demonstrate a beneficial effect of HVHF on macrophage function with restoration of the ability to produce TNF in response to exposure endotoxin. This is the first demonstration that HVHF has an effect on cell function. In the present study we have reported the effects of zero-balanced continuous HVHF on 28 patients suffering SAP complicated with MODS. Body temperature, heart rate, breath rate and APACHE II score decreased significantly and partial pressure of oxygen in arterial blood increased significantly after HVHF. During HVHF the hemodynamics parameters were stable, and serum electrolytes, glucose and pH were at normal level. This investigation established the fact that HVHF was well tolerated in SAP patients complicated with MODS and might be of potential benefits.

Furthermore, hemofiltration might be able to improve organ functions. The study performed by Roman Ullrich[27] demonstrated that high-volume CVVH improved arterial oxygenation and lung function in endotoxin-induced acute lung injury in pigs. This improvement in arterial oxygenation with CVVH might be due to the removal of interstitial edema, improvement in the microcirculation and uptake of oxygen by parenchymal cells, or it might be due to removal of humoral mediators that depressed oxygen uptake by parenchymal cells. The results clearly indicate that hemofiltration can effectively improve tissue oxygen metabolism. More and more evidences have shown that gut barrier dysfunction is related to multiorgan system failure in sepsis and immune dysregulation[28,29]. Gut endothelial barrier dysfunction probably plays a central role in the development of the complications of SAP[30,31]. Pancreatitis-induced hypovolemia due to endothelial barrier leakage and gut arteriovenous shunting could cause intestinal ischemia and reperfusion injury with concomitant gut barrier dysfunction[32-34]. Hemofiltration can improve the splanchnic vascular infusion, so we might conclude that hemofiltration is helpful to improve the gut barrier function. Improvement of the splanchnic vascular infusion could also decrease the content of endotoxin and the rate of intestinal bacterial translocation in SAP[35]. Moreover, hemofiltration might play an important role in maintaining the hydrate, electrolyte and acid-base balance and homeostasis, especially when renal function was injured.

In summary, HVHF is technically possible in patients suffering from SAP complicated with MODS. It does not appear to have detrimental effects and may have beneficial effects. Continuous HVHF, which seldom disturbs the hemodynamics and causes few side-effects, offers therapeutic options for SAP complicated with MODS. The mechanisms underlying HVHF in SAP are thus complex and yet not fully elucidated.

REFERENCES

1 **Beger HG**, Rau B, Mayer J, Pralle U. Natural course of acute pancreatitis. *World J Surg* 1997; **21**: 130-135

2 **Dugernier T**, Starkel P, Laterre PF, Reynaert MS. Severe acute pancreatitis: pathophysiologic mechanisms underlying pancreatic necrosis and remote organ damage. *Acta Gastroenterol Belg* 1996; **59**: 178-185

3 **Bellomo R**. Continuous hemofiltration as blood purification in sepsis. *New Horiz* 1995; **3**: 732-737

4 **Hoffmann JN**, Hartl WH, Deppisch R, Faist E, Jochum M, Inthorn D. Hemofiltration in human sepsis: evidence for elimination of immunomodulatory substances. *Kidney Int* 1995; **48**: 1563-1570

5 **Lonnemann G**, Linnenweber S, Burg M, Koch KM. Transfer of endogenous pyrogens across artificial membranes? *Kidney Int Suppl* 1998; **66**: S43-S46

6 **Bellomo R**, Baldwin I, Cole L, Ronco C. Preliminary experience with high-volume hemofiltration in human septic shock. *Kidney Int Suppl* 1998; **66**: S182-S185

7 **Bone RC**, Balk RA, Cerra FB, Dellinger RP, Fein AM, Knaus WA, Schein RM, Sibbald WJ. Definitions for sepsis and organ failure and guidelines for the use of innovative therapies in sepsis. The ACCP/SCCM Consensus Conference Committee. American College of Chest Physicians/Society of Critical Care Medicine. *Chest* 1992; **101**: 1644-1655

8 **Balthazar EJ**, Ranson JH, Naidich DP, Megibow AJ, Caccavale R, Cooper MM. Acute pancreatitis: prognostic value of CT. *Radiology* 1985; **156**: 767-772

9 **Wu XZ**. Therapy of acute severe pancreatitis awaits further improvement. *World J Gastroenterol* 1998; **4**: 285-286

10 **Krumberger JM**. Acute pancreatitis. *Crit Care Nurs Clin North Am* 1993; **5**: 185-202

11 **Mayer J**, Rau B, Gansauge F, Beger HG. Inflammatory mediators in human acute pancreatitis: clinical and pathophysiological implications. *Gut* 2000; **47**: 546-552

12 **Ogawa M**. Acute pancreatitis and cytokines: "second attack" by septic complication leads to organ failure. *Pancreas* 1998; **16**: 312-315

13 **Wu XN**. Current concept of pathogenesis of severe acute pancreatitis. *World J Gastroenterol* 2000; **6**: 32-36

14 **Wrobleski DM**, Barth MM, Oyen LJ. Necrotizing pancreatitis: pathophysiology, diagnosis, and acute care management. *AACN Clin Issues* 1999; **10**: 464-477

15 **Zhao H**, Chen JW, Zhou YK, Zhou XF, Li PY. Influence of platelet activating factor on expression of adhesion molecules in experimental pancreatitis. *World J Gastroenterol* 2003; **9**: 338-341

16 **Zhang Q**, Ni Q, Cai D, Zhang Y, Zhang N, Hou L. Mechanisms of multiple organ damages in acute necrotizing pancreatitis. *Chin Med J* 2001; **114**: 738-742

17 **Norman J**. The role of cytokines in the pathogenesis of acute pancreatitis. *Am J Surg* 1998; **175**: 76-83

18 **Bhatia M**, Brady M, Shokuhi S, Christmas S, Neoptolemos JP, Slavin J. Inflammatory mediators in acute pancreatitis. *J Pathol* 2000; **190**: 117-125

19 **Kramer P**, Wigger W, Rieger J, Matthaei D, Scheler F. Arteriovenous hemofiltration: a new and simple method for treatment of over-hydrated patients resistant to diuretics. *Klin Wochenschr* 1977; **55**: 1121-1122

20 **Grootendorst AF**, van Bommel EF. The role of hemofiltration in the critically-ill intensive care unit patient: present and future. *Blood Purif* 1993; **11**: 209-223

21 **Hirasawa H**, Sugai T, Ohtake Y, Oda S, Matsuda K, Kitamura N. Blood purification for prevention and treatment of multiple organ failure. *World J Surg* 1996; **20**: 482-486

22 **Van Bommel EF**, Leunissen KM, Weimar W. Continuous renal replacement therapy for critically ill patients: an update. *J Intensive Care Med* 1994; **9**: 265-280

23 **Yekebas EF**, Treede H, Knoefel WT, Bloechle C, Fink E, Izbicki JR. Influence of zero-balanced hemofiltration on the course of severe experimental pancreatitis in pigs. *Ann Surg* 1999; **229**: 514-522

24 **Bellomo R**, Tipping P, Boyce N. Continuous veno-venous hemofiltration with dialysis removes cytokines from the circulation of septic patients. *Crit Care Med* 1993; **21**: 522-526

25 **Rogiers P**, Zhang H, Smail N, Pauwels D, Vincent JL. Continuous venovenous hemofiltration improves cardiac performance by mechanisms other than tumor necrosis factor-alpha attenuation during endotoxic shock. *Crit Care Med* 1999; **27**: 1848-1855

26 **Lonnemann G**, Bechstein M, Linnenweber S, Burg M, Koch KM. Tumor necrosis factor-alpha during continuous high-flux hemodialysis in sepsis with acute renal failure. *Kidney Int Suppl* 1999; **72**: S84-S87

27 **Ullrich R**, Roeder G, Lorber C, Quezado ZM, Kneifel W, Gasser H, Schlag G, Redl H, Germann P. Continuous venovenous hemofiltration improves arterial oxygenation in endotoxin-induced lung injury in pigs. *Anesthesiology* 2001; **95**: 428-436

28 **Hirsh M**, Dyugovskaya L, Bashenko Y, Krausz MM. Reduced rate of bacterial translocation and improved variables of natural killer cell and T-cell activity in rats surviving controlled hemorrhagic shock and treated with hypertonic saline. *Crit Care Med* 2002; **30**: 861-867

29 **Zhu L**, Yang ZC, Li A, Cheng DC. Reduced gastric acid production in burn shock period and its significance in the prevention and treatment of acute gastric mucosal lesions. *World J Gastroenterol* 2000; **6**: 84-88

30 **Shi X**, Gao NR, Guo QM, Yang YJ, Huo MD, Hu HL, Friess H. Relationship between overexpression of NK-1R, NK-2R and intestinal mucosal damage in acute necrotizing pancreatitis. *World J Gastroenterol* 2003; **9**: 160-164

31 **Ammori BJ**. Role of the gut in the course of severe acute pancreatitis. *Pancreas* 2003; **26**: 122-129

32 **Kinnala PJ**, Kuttila KT, Gronroos JM, Havia TV, Nevalainen TJ, Niinikoski JH. Splanchnic and pancreatic tissue perfusion in experimental acute pancreatitis. *Scand J Gastroenterol* 2002; **37**: 845-849

33 **Andersson R**, Wang XD. Gut barrier dysfunction in experimental acute pancreatitis. *Ann Acad Med Singapore* 1999; **28**: 141-146

34 **Juvonen PO**, Tenhunen JJ, Heino AA, Merasto M, Paajanen HE, Alhava EM, Takala JA. Splanchnic tissue perfusion in acute experimental pancreatitis. *Scand J Gastroenterol* 1999; **34**: 308-314

35 **Qin RY**, Zou SQ, Wu ZD, Qiu FZ. Influence of splanchnic vascular infusion on the content of endotoxins in plasma and the translocation of intestinal bacteria in rats with acute hemorrhage necrosis pancreatitis. *World J Gastroenterol* 2000; **6**: 577-580

Edited by Zhu LH

P.O.Box 2345, Beijing 100023,China
Fax: +86-10-85381893
E-mail: wjg@wjgnet.com www.wjgnet.com

World J Gastroenterol 2003;9(9):2100-2104
World Journal of Gastroenterology
 ISSN 1007-9327

• CLINICAL RESEARCH •

Correlation of CT enhancement, tumor angiogenesis and pathologic grading of pancreatic carcinoma

Zhong-Qiu Wang, Jie-Shou Li, Guang-Ming Lu, Xin-Hua Zhang, Zi-Qian Chen, Kui Meng

Zhong-Qiu Wang, Guang-Ming Lu, Zi-Qian Chen, Department of Medical Imaging, Jinling Hospital, Medical School, Nanjing University, Nanjing 210002, Jiangsu Province, China
Jie-Shou Li, Department of General Surgery, Jinling Hospital, Medical School, Nanjing University, Nanjing 210002, Jiangsu Province, China
Xin-Hua Zhang, Kui Meng, Department of Pathology, Jinling Hospital, Medical School, Nanjing University, Nanjing 210002, Jiangsu Province, China
Correspondence to: Zhong-Qiu Wang, Department of Medical Imaging, Jinling Hospital, No 305 Zhongshan East Road, Nanjing 210002, Jiangsu Province, China. zhq2001us@yahoo.com
Telephone: +86-25-4801827 **Fax**: +86-25-4821929
Received: 2002-12-22 **Accepted:** 2003-02-13

Abstract

AIM: To study the correlation between pancreatic phase CT enhancement, intratumor microvessel density (MVD) and pathologic grading of pancreatic carcinoma and to evaluate the relationship between the degrees of CT enhancement and malignancy of pancreatic carcinoma.

METHODS: Thirty four patients with pancreatic carcinoma underwent CT scanning before resection. The enhancement degrees and forms of tumor were observed in pancreatic phase. The operative sample was stained with HE and CD34 marked by immunohistochemistry. MVD and histopathological grades of pancreatic carcinoma were examined. CT enhancement of the tumor, MVD counting in hot spot areas of neoplastic parenchymal cells and pathological grades of pancreatic carcinoma were comparatively analyzed.

RESULTS: Highly differentiated pancreatic adenocarcinoma was identified in 16 patients, moderately-differentiated tumor in 7 and poorly-differentiated in 11. Isodensity CT enhancement was demonstrated in 13 cases, slightly low density enhancement in 9, slightly low density enhancement with small cystic lesions in 9 and slightly low density enhancement with large cystic lesions in 3. The counting of MVD with CD34 marked by immunohistochemistry in hot spot areas of neoplastic parenchyma cells was small in 10 cases, medium in 16 and large in 8. The pathological grades correlated well with CT enhancement of the tumor (r=0.7857, P<0.001) and with MVD counting of tumor (r=0.3613, P<0.05). The CT enhancement of tumor correlated with MVD(r=0.6768, P<0.001).

CONCLUSION: There is an obvious and significant correlation between CT enhancement, pathological grades and MVD number in the hot spot areas of tumor. The extent of CT enhancement is inversely proportional to the malignant degree of pancreatic carcinoma, and to the MVD number in the hot spot areas of neoplastic parenchyma. The MVD in the hot spot areas of neoplastic parenchyma cells can also reflect the prognosis of the patients, and is directly proportional to the malignant degree of pancreatic carcinoma.

Wang ZQ, Li JS, Lu GM, Zhang XH, Chen ZQ, Meng K. Correlation of CT enhancement, tumor angiogenesis and pathologic grading of pancreatic carcinoma. *World J Gastroenterol* 2003; 9(9): 2100-2104
http://www.wjgnet.com/1007-9327/9/2100.asp

INTRODUCTION

Pancreatic carcinoma is a common malignant tumor. Patients with pancreatic carcinoma have a high mortality rate and short survival time[1-10]. The resection rate of the tumor is only 10-25 %[1,3,6,7]. Early diagnosis is of great clinical significance for pancreatic carcinoma. Some authors reported[11-17, 23-32] that tumor angiogenesis was closely correlated with the growth, metastasis and malignancy degree of the tumor. CT enhancement of pancreatic carcinoma in pancreatic phase, intratumor MVD and tumor malignancy degree were assessed in this article.

MATERIALS AND METHODS

Patients

Thirty four patients with pancreatic carcinoma (26 men, 8 women; age range 31-76 years, mean age 55.5 years) were evaluated retrospectively. All the patients underwent CT enhancement and surgery from June 1997 to May 2002. The tissue samples available were studied with CD34 marker by immunohistochemistry in our hospital.

CT scaning

Somatom plus spiral CT scanner (Siemens Company, Germany) and electron beam CT (EBCT) (Imatron Co, America.) were used. Before examination, the patients took 1 000 ml water containing a few iodinated contrast materials (Iodinated degree less than 5 %). The section thickness was usually 10 mm in liver and 5mm in pancreas. The scanning time was 1 s. Iodinated non-ionic contrast material? (iopamidol 300; Bracco, Milan, Italy) was injected at a rate of 2.5-3 ml/S for a total of 100 ml by a high pressure autoinjector. General scanning was done at first. CT enhancement was performed in the pancreatic phase, and the scanning time was 35 s after injection of the contrast agent.

Pathologic study

Tumor specimens obtained from resected pancreatic carcinoma were fixed with 10 % formalin and embedded in paraffin. The specimens were stained with hematoxylin-eosin. Four-micron-thick sections were mounted on silanized slides. The histopathologic grades of pancreatic carcinoma were observed by microscopy. The neoplastic parenchyma cells, fibrotic stroma, necrotic tissuse and residual pancreatic tissue were also examined. The sections were then incubated with mouse monoclonal antibody of CD34 for 24 h at room temperature. After being washed with phosphate-buffered solution (PBS), the sections were incubated with avidin-biotin-peroxidase complex (Histofine) for 30 min and washed once more with PBS. The sections were finally incubated with 3,3-

diaminobenzidine (Simplestain DAB; Nichirei). To assess the intratumor MVD, we used the counting methods of intratumor MVD reported by Weidenr[17] . We assessed delineated CD34-positive cells as microvessels (size 0.02-0.10). Stained vessels were counted in a ×200 microscopic field in hot spot areas of neoplastic parenchyma cells. To count the immunohistochemical anti-CD34 antibody stained vessels in hot spot areas of tumor parenchymal cells, the average MVDs were calculated in three hot spot areas. The tumor MVD was categorized into four grades: "+" the average number of MVD <10, "++" between 10 and 20, "+++" between 20 and 40, "++++" >40.

Statistical analysis

Methods of evaluating extent of CT enhancement The enhancement effects of pancreatic parenchymal tissue were the same in the pancreatic-phase and dual-phase enhanced scanning[18-20,33-36]. Therefore, the extent of CT enhancement of pancreatic carcinoma was only assessed in the pancreatic phase. The degree and form of the tumor in CT enhancement compared to normal pancreatic tissue could be classified as follows: I-isodense enhancement, indicating the degree of tumor CT enhancement was the same as that of the surrounding normal pancreatic tissues; II-slightly low density enhancement, indicating the degree of tumor CT enhancement was slightly lower than that of the surrounding normal pancreatic tissue, with few blood vessels in the tumor; III-slightly low density enhancement with small hypodense cystic lesions, indicating the tumor enhancement was the same as II, but with small cystic density regions in the tumor; IV-cystic low density lesion with slight enhancement of surrounding tumor tissue, indicating large necrotic lesions in the central area and slight enhancement in the surrounding tumor tissue.

Statistical methods The degree of CT enhancement of the tumor, pathological grading of pancreatic carcinoma and the average number of MVD in hot spot areas of neoplastic parenchymal cells were assessed by SPSS software. We used Spearman correlation test with two unpaired samples, a level of significance was set when P value <0.05.

RESULTS

The results of the patients' CT scanning, HE staining and immunohistochemistry were calculated. Well-differentiated pancreatic carcinoma was identified in 16 cases, one with solid cystic-papillary tumor. Moderately-differentiated pancreatic carcinoma was identified in 7, among which one was highly moderately-differentiated. Poorly differentiated pancreatic carcinoma was identified in 11, among which one was highly poorly-differentiated and 2 were moderately poorly-differentiated. The tumor was localized in pancreatic head in 19 cases, pancreatic head and body in 2, pancreatic body in 6, pancreatic body and tail in 1, pancreatic tail in 4, upper edge of pancreas with involvement of ligamentum hepatoduodenale in 1, pancreatic groove with involvement of second part of horizontal duodenum in 1. Immunohistochemical study of tumor specimens' showed MVD count in hot spot areas of tumor parenchymal cells was least in 10 cases, medium in 16 and most in 8. Its routine histopathological results, CT enhancement, MVD and pathological grading are shown in Tables 1 and 2 and Figures 1-4.

CT enhancement degree of tumor, pathological grading of pancreatic carcinoma and the average count of MVD in hot spot areas of neoplastic parenchyma cells were comparatively assessed by Spearman correlation test. The pathological grades correlated well with CT enhancement of tumor (r=0.7857, t=7.1851, P<0.001), and with MVD count of tumor(r=0.3613, t=2.1917, P<0.05).

Table 1 CT enhancement, pathologic grades and MVD number in hot spot areas of neoplastic parenchymal cells of pancreatic carcinoma

Pathologic grades	No of cases	CT enhancement degree of tumor				MVD in hot spot area in neoplastic parenchymal cells			
		I	II	III	IV	+	++	+++	++++
Well differentiated	16	12	3	1	0	8	5	3	0
Moderately differentiated	7	1	4	2	0	1	5	1	0
Poorly differentiated	11	0	2	6	3	1	6	4	0
Total	34	13	9	9	3	10	16	8	0

Table 2 CT enhancement degree in pancreatic phase and MVDs in hot spot areas of tumor parenchyma in pancreatic carcinoma

CT enhancement degree		MVDs in hot spot areas in tumor parenchyma			
Enhanced type	n	+	++	+++	++++
I	13	9	4	0	0
II	9	1	5	3	0
III	9	0	6	3	0
IV	3	0	1	2	0

There was a significant correlation between CT enhancement degree in pancreatic phase and MVDs in hot spot areas of neoplastic parenchyma in pancreatic carcinoma (r=0.6768, t=5.2006, P<0.001).

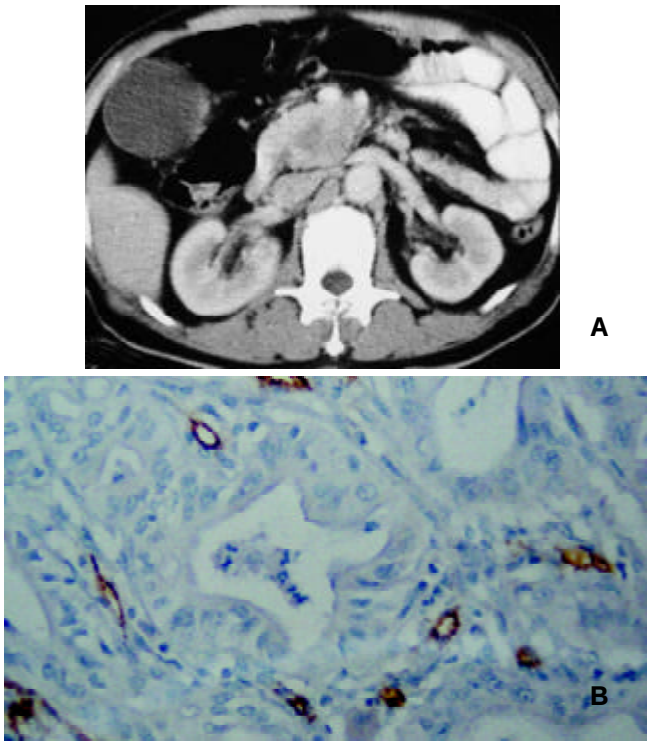

Figure 2 A 52-year-old man with moderately-differentiated pancreatic head carcinoma. A: Pancreatic-phase helical CT enhancement imaging 35 s after administration of contrast agent revealed that CT enhancement of mass in pancreatic head was slightly lower than that of normal pancreatic tissues. Scarce blood vessel area appeared in the central region of the mass; B: Showing immunohistochemical staining of anti-CD34 antibody (200×). CD34-positive cells were counted as microvessels (tan color), moderate MVDs in hot spot area of the neoplastic cells in moderately-differentiated pancreatic carcinoma.

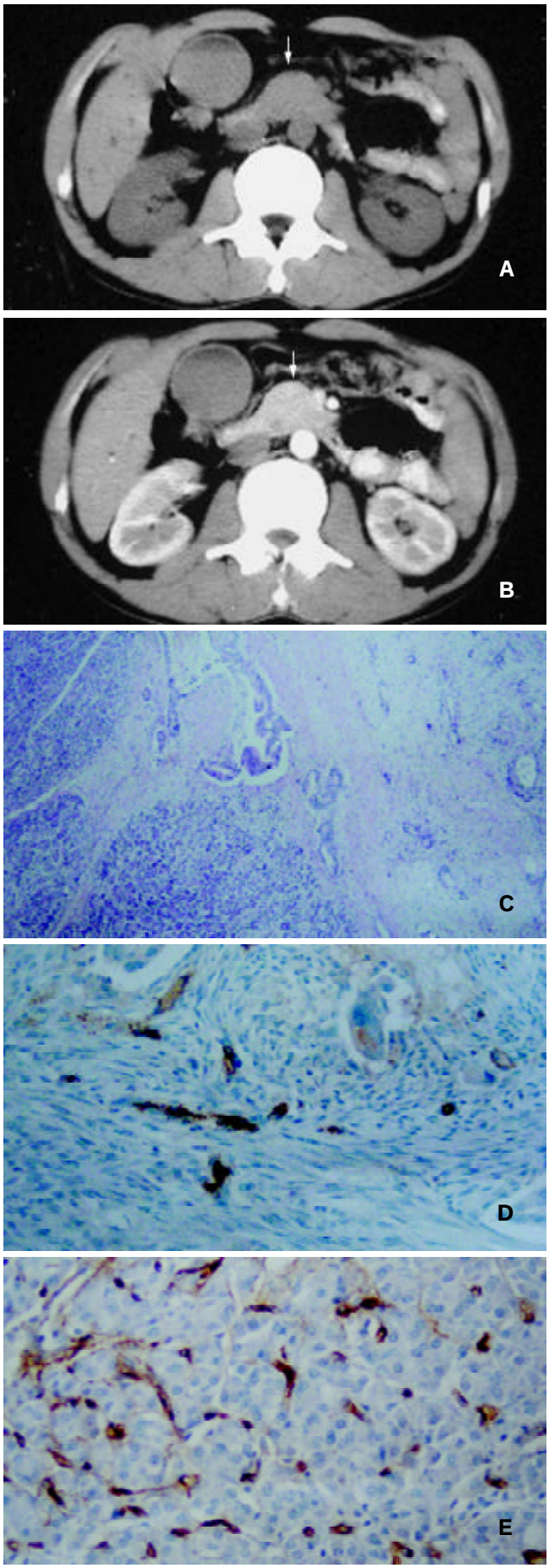

Figure 1 A 52-year-old man with well-differentiated pancreatic head carcinoma. A: EBCT imaging revealed that bulging pancreatic head (white arrow), density of mass in head and neck were the same as that of pancreatic body; B: EBCT enhancement imaging was 35 s after administration of contrast agent revealed that enhancement of mass in pancreatic head (white arrow) was the same as that of normal pancreatic tissue; C: Hematoxylin-eosin-stained specimen (100×) demonstrated the irregularity around tumor cell adeno-tubula structure and residual pancreatic tissue; D: Showing immunohistochemical staining of anti-CD34 antibody (200×). CD34-positive cells were counted as microvessels (tan color), MVDs in hot spot area of the neoplastic cells in well- differentiated pancreatic carcinomal; E: High MVDs of residual pancreatic tissue in well differentiated pancreatic carcinoma (200×).

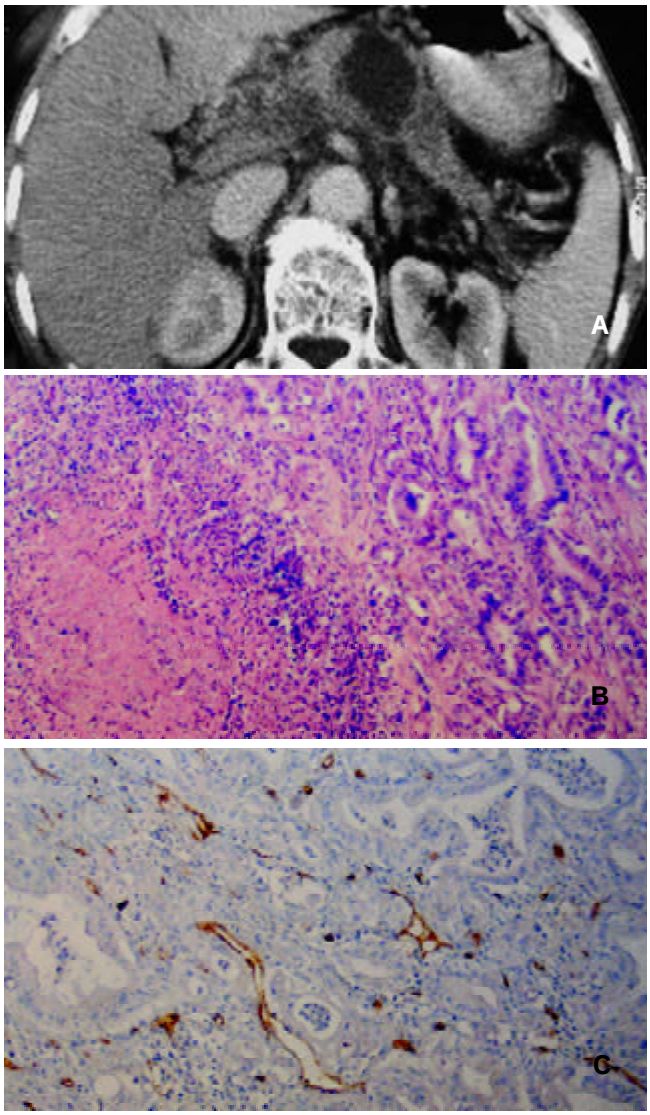

Figure 3 A 59-year-old man with poorly differentiated pancreatic body carcinoma. A: Helical CT enhancement imaging 35 s after administration of contrast agent revealed that pancreatic-phase CT enhancement of mass in pancreatic body was lower than that of surrunding normal pancreatic tissues. Necrotic tissue in the center of the mass was not enhanced. Tumor tissue around the necrotic tissue was slightly enhanced; B:Hematoxylin-eosin-stained specimen (100×) demonstrated massive necrosis and decreased residual pancreatic tissue; C: Showing immunohistochemical staining of anti-CD34 antibody (200×). CD34-positive cells were seen as microvessels (brown yellow color), more MVDs in hot spot area of the neoplastic cells in poorly-differentiated pancreatic carcinoma.

DISCUSSION

The grading of the tumor, its occurrence, progression and metastasis, were all dependent on tumor angiogenesis[13,17,23-25].

Tumor angiogenesis was first proposed by Folkman[11,13]. In recent years, study of intratumor angiogenesis has become a hot spot in neoplastic research[11-17,23-25]. Tumor angiogenesis mainly includes an increase of newly grown microvessels and their permeability change. Histopathology usually reflects an increase or decrease of intratumour MVDs. CT enhancement can also indirectly reflect the situation of intratumor angiogenesis because the enhancement degree of tumor is dependent upon the number of blood vessels within the tumor[12,21,22].

The result of our study showed that the pathological grades of pancreatic carcinoma and CT enhancement of the tumor were significantly correlated (r=0.7857, P<0.001). Table 1 shows isodensity in 75 % (12/16) of well-differentiated pancreatic cancer, 14.3 % (1/7) in moderately-differentiated, and 0 % (0/11) in poorly differentiated. Slightly low density or low density was 25 % (4/16) in well-differentiated tumour, 85.7 % (6/7) in moderately-differentiated tumour, 100 % (11/11) in poorly differentiated tumour. This indicated that the malignant degree of pancreatic carcinoma was inversely proportional to its CT enhancement degree, i.e., the higher the malignant degree, the lower the CT enhancement.

It is agreed that the pathological grades of pancreatic carcinoma are directly proportional to the number of intratumor MVD[21], but Table 2 shows that CT enhancement was inversely proportional to the number of MVD in hot spot areas of neoplastic parenchymal cells (P<0.001). The reason was that the microvessel and its tissue composition of pancreatic carcinoma were different from malignant tumors of other organs such as lung cancer and renal cancer. Pancreatic carcinoma has its own distinct characteristics, usually diffuse fibrosis[23]. Therefore, the CT enhancement is decided by the combination of the total number of intratumor MVD, the fibrous stroma and residual normal pancreatic tissue. A small number of tumor parenchymal cells, a medium number of fibrosis and a large number of residual normal pancreatic tissue constitute well-differentiated pancreatic carcinoma shown in its histopathology. The MVD of the residual pancreatic tissue stained CD34 by immunohistochemistry was abundant (Figure 1D), and the MVD in hot spot areas of neoplastic parenchymal cells was scarce in well-differentiated pancreatic cancer. So the total number of intratumor MVD was mainly decided by the number of MVD within the residual pancreatic tissue (Figure 1E). As we could see that the total number of MVD within the well-differentiated pancreatic cancer was almost the same as that of the surrounding normal pancreatic tissue, hence, the CT enhancement degree of well-differentiated pancreatic carcinoma in pancreatic phase was similar to that of the surrounding normal pancreatic tissue. Whereas in the moderately and poorly-differentiated pancreatic carcinoma, the volume of tumor parenchymal cells increased and the residual pancreatic tissue was relatively decreased. Therefore, CT enhancement degree in these pancreatic carcinoma was lower than that in the well-differentiated pancreatic carcinoma. One could see the scarce microvessel showed slightly-low density enhancement (Figure 2A). Some small cyst and large cystic or low density regions within the tumor were necrosis lesions (Figure 3A).

Linder and others belivered that MVD count of tumor cells was larger than that of the tumor matrix, the former was closely related to the degree of malignancy[23]. According to our data, the pathological grades of pancreatic carcinoma were to some extent correlated with the intratumor MVD count (P<0.05), but significantly correlated with the CT enhancement degree in the pancreatic-phase. This indicated that CT enhancement could effectively evaluate the malignant degree of pancreatic carcinoma before operation. However, pancreatic-phase CT enhancement of pancreatic carcinoma has its own particular features (Figure 4).

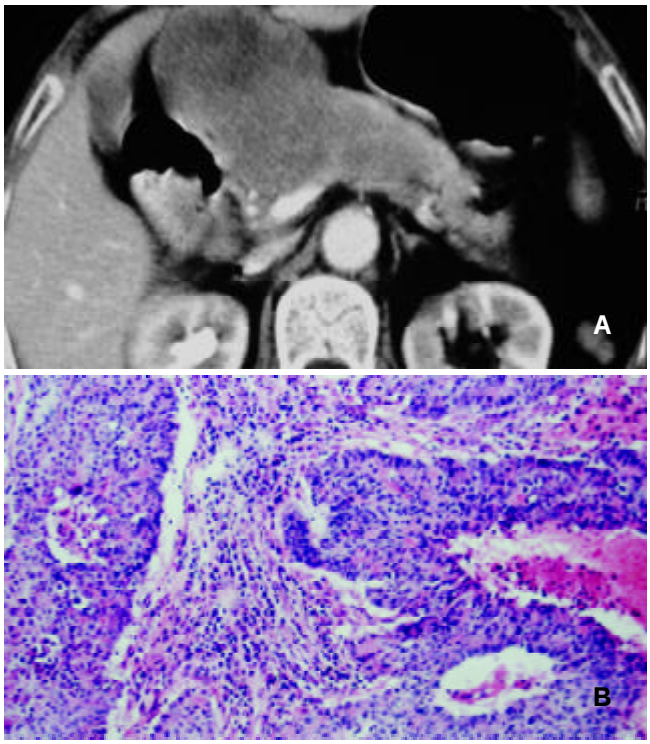

Figure 4 A 70-year-old woman with solid-cystic-papillary well-differentiated pancreatic carcinoma with involvement of ligamentum hepatoduodenale. A: Helical CT enhancement imaging 35 s after administration of contrast agent revealed that CT enhancement of mass was heterogenously slight low density with low density necrotic region; B: Hematoxylin-eosin-stained specimen (100×) demonstrated massive necrosis tissuse and irregular tubula structure in well-differentiated pancreatic carcinoma.

To sum up, if CT enhancement degree of pancreatic carcinoma is as high as that of the surrounding normal pancreatic tissues, it would reflect a high MVD in the residual pancreatic tissue and a small count of intratumoral MVD indicating pancreatic carcinoma is well-differentiated. If CT enhancement degree is slightly lower than that of the normal pancreatic tissue with a vessel voided area, with or without low-density cystic areas, it would reflect a moderately-differentiated pancreatic cancer. The appearance of heterogeneously slight-low density areas with a large low density necrotic lesion might reflect a highly malignant and poorly-differentiated pancreatic carcinoma.

ACKNOWLEDGEMENT

I wish to express our sincere and hearty thanks to Professor Li Jieshou, academician of the Chinese Academy of Engineering. We are deeply indebted to his careful and enlightening advice.

REFERENCES

1 **Ghaneh P**, Slavin J, Sutton R, Hartley M, Neoptolemos JP. Adjuvant therapy in pancreatic cancer. *World J Gastroenterol* 2001; **7**: 482-489
2 **Qin LX**. Chromosomal aberrations related to metastasis of human solid tumors. *World J Gastroenterol* 2002; **8:** 769-776
3 **Shankar A**, Russell RCG. Recent advances in the surgical treatment of pancreatic cancer. *World J Gastroenterol* 2001; **7**: 622-626
4 **Guo XZ**, Friess H, Shao XD, Liu MP, Xia YT, Xu JH, Buchler MW. KAI1 gene is differently expressed in papillary and pancreatic cancer: influence on metastasis. *World J Gastroenterol* 2000; **6**: 866-871
5 **Liu B**, Staren E, Iwamura T, Appert H, Howard J. Effects of Taxotere on invasive potential and multidrug resistance pheno-

type in pancreatic carcinoma cell line SUIT-2. *World J Gastroenterol* 2001; **7**: 143-148
6 **Fidler IJ.** Angiogenesis and cancer metastasis. *Cancer J* 2000; **6** (Suppl 2): 134-141
7 **Ruf W,** Mueller BM. Tissue factor in cancer angiogenesis and metastasis. *Curr Opin Hematol* 1996; **3**: 379-384
8 **Liu B**, Staren E, Iwamura T, Appert H, Howard J. Taxotere resistance in SUIT Taxotere resistance in pancreatic carcinoma cell line SUIT 2 and its sublines. *World J Gastroenterol* 2001; **7**: 855-859
9 **Zhou ZG**, Chen YD, Sun W, Chen Z. Pancreatic microcirculatory impairment in experimental acute pancreatitis in rats. *World J Gastroenterol* 2002; **8**: 933-936
10 **Demachi H**, Matsui O, Kobayashi S, Akakura Y, Konishi K, Tsuji M, Miwa A, Miyata S. Histological influence on contrast-enhanced CT of pancreatic ductal adenocarcinoma. *J Comput Assist Tomogr* 1997; **21**: 980-985
11 **Folkman J**. What is the evidence that tumors are angiogenesis dependent? *JNCI* 1990; **82**: 4-6
12 **Passe TJ**, Bluemke DA, Siegelman SS. Tumor angiogenesis: Tutorial on implications for imaging. *Radiology* 1997; **203**: 593-600
13 **Folkman J**. Fighting cancer by attacking its blood supply. *Sci Am* 1996; **275**: 150-154
14 **Hanahan D**, Folkman J. Patterns and emerging mechanisms of the angiogenic switch during tumorigenesis. *Cell* 1996; **86**: 353-364
15 **Jiang WG**, Puntis MC, Hallett MB. Molecular and cellular basis of cancer invasion and metastasis: implications for treatment. *Br J Surg* 1994; **81**: 1576-1590
16 **Boucher Y**, Leunig M, Jain RK. Tumor angiogensis and interstitial hypertension. *Cancer Res* 1996; **56**: 4264-4266
17 **Weidner N**. Intratumor microvessel density as a prognostic factor in cancer. *Am J Pathol* 1995; **147**: 9-19
18 **Boland GW**, O'Malley ME, Saez M, Fernandez-del-Castillo C, Warshaw AL, Mueller PR. Pancreatic-phase versus portal vein-phase helical CT of the pancreas: optimal temporal window for evaluation of pancreatic adenocarcinoma. *Am J Roentgenol* 1999; **172**: 605-608
19 **Sheridan MB**, Ward J, Guthrie JA, Spencer JA, Craven CM, Wilson D, Guillou PJ, Robinson PJ. Dynamic contrast-enhanced MR imaging and dual-phase helical CT in the preoperative assessment of suspected pancreatic cancer: a comparative study with receiver operating characteristic analysis. *Am J Roentgenol* 1999; **173**: 583-590
20 **McNulty NJ**, Francis IR, Platt JF, Cohan RH, Korobkin M, Gebremariam A. Multi-detector row helical CT of the pancreas: effect of contrast-enhanced multiphasic imaging on enhancement of the pancreas, peripancreatic vasculature, and pancreatic adenocarcinoma. *Radiology* 2001; **220**: 97-102
21 **Miles KA**. Tumour angiogenesis and its relation to contrast enhancement on computed tomography: a review. *Eur J Radiol* 1999**; 30**: 198-205
22 **Tateishi U**, Nishihara H, Watanabe S, Morikawa T, Abe K, Miyasaka K. Tumor angiogenesis and dynamic CT in lung adenocarcinoma: radiologic-pathologic correlation. *J Comput Assist Tomogr* 2001; **25**: 23-27
23 **Linder S**, Blasjo M, von-Rosen A, Parrado C, Falkmer UG, Falkmer S. Pattern of distribution and prognostic value of angiogenesis in pancreatic duct carcinoma: a semiquantitative immunohistochemical study of 45 patients. *Pancreas* 2001; **22**: 240-247
24 **Kasper HU**, Ebert M, Malfertheiner P, Rosesner A, Kirkpatrick CJ, Wolf HK. Expression of thrombospondin-1 in pancreatic carcinoma: correlation with microvessel density. *Virchows Arch* 2001; **438**: 116-120
25 **Hotz HG**, Reber HA, Hotz B, Sanghavi PC, Yu T, Foitzik T, Buhr HJ, Hines OJ. Angiogenesis inhibitor TNP-470 reduces human pancreatic cancer growth. *J Gastrointest Surg* 2001; **5**: 131-138
26 **Bruns CJ**, Harbison MT, Davis DW, Portera CA, Tsan R, McConkey DJ, Evans DB, Abbruzzese JL, Hicklin DJ, Radinsky R. Epidermal growth factor receptor blockade with C225 plus gemcitabine results in regression of human pancreatic carcinoma growing orthotopically in nude mice by antiangiogenic mechanisms. *Clin Cancer Res* 2000; **6**: 1936-1948
27 **Bruns CJ**, Solorzano CC, Harbison MT, Ozawa S, Tsan R, Fan D, Abbruzzese J, Traxler P, Buchdunger E, Radinsky R, Fidler IJ. Blockade of the epidermal growth factor receptor signaling by a novel tyrosine kinase inhibitor leads to apoptosis of endothelial cells and therapy of human pancreatic carcinoma. *Cancer Res* 2000; **60**: 2926-2935
28 **Seo Y**, Baba H, Fukuda T, Takashima M, Sugimachi K. High expression of vascular endothelial growth factor is associated with liver metastasis and a poor prognosis for patients with ductal pancreatic adenocarcinoma. *Cancer* 2000; **88**: 2239-2245
29 **Banerjee SK**, Zoubine MN, Mullick M, Weston AP, Cherian R, Campbell DR. Tumor angiogenesis in chronic pancreatitis and pancreatic adenocarcinoma: impact of K-ras mutations. *Pancreas* 2000; **20**: 248-255
30 **Fujimoto K**, Hosotani R, Wada M, Lee JU, Koshiba T, Miyamoto Y, Tsuji S, Nakajima S, Doi R, Imamura M. Expression of two angiogenic factors, vascular endothelial growth factor and platelet-derived endothelial cell growth factor in human pancreatic cancer, and its relationship to angiogenesis. *Eur J Cancer* 1998; **34**: 1439-1447
31 **Terris B**, Scoazec JY, Rubbia L, Bregeaud L, Pepper MS, Ruszniewski P, Belghiti J, Flejou J, Degott C. Expression of vascular endothelial growth factor in digestive neuroendocrine tumours. *Histopathology* 1998; **32**: 133-138
32 **Ikeda N**, Adachi M, Taki T, Huang C, Hashida H, Takabayashi A, Sho M, Nakajima Y, Kanehiro H, Hisanaga M, Nakano H, Miyake M. Prognostic significance of angiogenesis in human pancreatic cancer. *Br J Cancer* 1999; **79**: 1553-1563
33 **Coley SC**, Strickland NH, Walker JD, Williamson RC. Spiral CT and the pre-operative assessment of pancreatic adenocarcinoma. *Clin Radiol* 1997; **52**: 24-30
34 **Kaneko K**, Honda H, Hayashi T, Fukuya T, Ro T, Irie H, Masuda K. Helical CT evaluation of arterial invasion in pancreatic tumors: comparison with angiography. *Abdom Imaging* 1997; **22**: 204-207
35 **Furukawa H**, Iwata R, Moriyama N, Kosuge T. Selective intraarterial contrast-enhanced CT of pancreaticoduodenal tumors: early clinical experience in evaluating blood supply and detectability. *Am J Roentgenol* 2000; **175**: 91-97
36 **O'Malley ME**, Boland GW, Wood BJ, Fernandez-del-Castillo C, Warshaw AL, Mueller PR. Adenocarcinoma of the head of the pancreas: determination of surgical unresectability with thin-section pancreatic-phase helical CT. *Am J Roentgenol* 1999; **173**: 1513-1518

Edited by Wu XN and Wang XL

P.O.Box 2345, Beijing 100023,China
Fax: +86-10-85381893
E-mail: wjg@wjgnet.com www.wjgnet.com

World J Gastroenterol 2003;9(9):2105-2108
World Journal of Gastroenterology
 ISSN 1007-9327

• CLINICAL RESEARCH •

Clinical study on nutrition support in patients with severe acute pancreatitis

Gang Zhao, Chun-You Wang, Fang Wang, Jiong-Xin Xiong

Gang Zhao, Chun-You Wang, Jiong-Xin Xiong, Pancreatic Surgery Center, Union Hospital, Tongji Medical College, Huazhong University of Science and Technology, Wuhan 430022, Hubei Province, China
Fang Wang, Department of Pharmacology, Tongji Medical College, Huazhong University of Science and Technology, Wuhan 430030, Hubei Province, China
Correspondence to: Dr. Gang Zhao, Pancreatic Surgery Center, Union Hospital, Tongji Medical College, Huazhong University of Science and Technology, Wuhan 430022, Hubei Province, China. zhaogang1427@yahoo.com.cn
Telephone: +86-27-85726273
Received: 2003-03-20 **Accepted:** 2003-04-22

Abstract

AIM: To investigate the effect of nutritional support therapy on severe acute pancreatitis (SAP).

METHODS: A total of 96 patients with severe acute pancreatitis were divided randomly into control and treatment groups. The former group received total parenteral nutrition (TPN) via central venous infusion, while parenteral nutrition (PN) and enteral nutrition (EN) therapies were applied in different phases for the latter group. The nutrition status, acute phase responses, pancreas lesions, enteric mucosa penetrability and immune functions were monitored.

RESULTS: Body weight and prealbumin concentration were increased in treatment group, compared to those in the control group, but albumin concentration did not change significantly. Acute physiology and chronic health evaluation II (APACHE II) scores decreased after 7 d of treatment, whereas the scores of the control group decreased on the 11th day. Concentrations of tumor necrosis factor-α (TNF-α), interleukine-6 (IL-6) and serum C reactive protein (CRP) dropped earlier in the treatment group (on the 4th day) than that in the control group (on the 7th day). No difference was observed in pancreatic lesions between the control and treatment groups. Concentration of endotoxin and lactulose/manicol (L:M) ratio of urine did not change in treatment group, but those in the control group were elevated markedly. Compared with the treatment group, CD4:CD8 T cells ratio and immunoglobulin G (IgG) concentration in the control group decreased significantly.

CONCLUSION: Compared to TPN, the combined therapy of EN and PN could improve the nutrition status and moderate the acute phase response obviously. Moreover, the integrity of enteric mucosa and immune function were protected more effectively in treatment group than in the control one. On the other hand, EN did not simulate the excretion of pancreas and avoid exaggerating the inflammation of pancreas. Thus, appropriate application of PN and EN appears to be more effective for patients with SAP.

Zhao G, Wang CY, Wang F, Xiong JX. Clinical study on nutrition support in patients with severe acute pancreatitis. *World J Gastroenterol* 2003; 9(9): 2105-2108
http://www.wjgnet.com/1007-9327/9/2105.asp

INTRODUCTION

Severe acute pancreatitis (SAP) is characterized by a diffuse inflammatory process of the pancreas with variable involvement of adjacent tissues and dysfunction of remote organs[1]. The metabolic alterations of SAP are involved in a classical stress state, as proposed for sepsis, including hyperdynamic changes, hypermetabolism and hypercatabolism. Thus, artificial nutritional support should be a suitable treatment[2-4]. The clinical nutritional management of pancreatitis has changed from total parenteral nutrition (TPN) to enteral nutrition (EN). However, it remains to be clarified whether EN is the best approach or not[5-8]. The purpose of this observation was to evaluate different nutrition therapies for SAP.

MATERIALS AND METHODS

Patients

A total of 96 patients with SAP admitted to the Pancreatic Surgery Center of Union Hospital (Wuhan, China) between February 2000 and October 2002 were recruited to the randomized study. The severity of pancreatitis was defined according to the Atlanta classification system for acute pancreatitis. Criteria for this observation were the acute physiology and chronic health evaluation II (APACH II) score higher than 8, and no indication for operation temporarily[9, 10]. These patients consisted of 58 males and 38 females with a mean age of 47.8 years (range 24-68 years). After 48 hours of common management including active liquid resuscitation and organ function protection[11,12], the patients were divided randomly into control and treatment groups. No significant differences of male:female ratio (15.6:16.7) and average age (48.2 and 46.7) were found between the two groups.

Study protocol

The 41 patients in control group were commenced on TPN via central venous infusion. In the treatment group, PN and EN were carried out by three stages for 55 patients. At first, the patients of treatment group only received glutamine-supplemented PN. When the paralysis was relieved, EN and PN were applied at the same time. EN was administrated via a nasojejunal feeding tube under endoscopy or X-ray. Following the study period, the volume and speed of enteral feeding were adjusted depending on the individual tolerance. Deficiency of energy was compensated through glutamine-supplemented PN. At last, the enteric feeding reached approximately 2 000 ml in 5-7 d, and PN was ceased.

Nutrition formulas

Conventional TPN was based on an amino acid solution providing 0.25 g nitrogen/(kg· d) with lipid emulsion and glucose. Half of the non-protein calories were provided by lipid. The total calorie was 30 kcal/(kg· d) and the calorie to nitrogen ratio was 120:1 in each patient. Electrolytes, trace elements and vitamins were added to maintain requirements [13].

PN in treatment group was based on the same elements as TPN but with supplement of 0.22 g glutamine/kg. EN formula was Peptide-2000 (Nutricia, Holland) semi-elementary diet

(2.9 g nitrogen and 500 kcal non-protein calorie/500 ml), with supplement of glutamine tablets to increase the intake of glutamine[14,15].

Experimental protocols

Body weight, albumin and prealbumin concentrations were determined to evaluate the nutrition status once of a week. APACH II scores, serum C reactive protein (CRP), tumor necrosis factor-α (TNF-α) and interleukine-6 (IL-6) were quantified every three days to assess the acute phase response. Pancreatic and peripancreatic necrosis were detected by contrast-enhanced CT scan once a week. These results of CT scan were scored with a modified Balthazar scoring system. Permeability of gastrointestinal mucosa was evaluated by concentration of endotoxin and lactulose/manicol (L:M) ratio of urine. CD4:CD8 ratio of T cell and concentration of immunoglobulin G (IgG) were quantified to assess immunological function.

Statistical analysis

All data were expressed as the mean ± standard deviation. Student' s *t* test was used to analyze the difference. A value of $P<0.05$ was considered statistically significant.

RESULTS

Nutrition status

Compared to the control group, body weight and plasma prealbumin concentration were increased in the treatment group after two weeks of treatment ($P<0.05$), whereas plasma albumin concentration did not change (Table 1).

Table 1 Changes of body weight, plasma albumin and prealbumin concentrations in two groups

	1 d		7 d		14 d		21 d	
	Control	Treatment	Control	Treatment	Control	Treatment	Control	Treatment
Weight (kg)	66.5±13.4	65.7±13.1	56.9±13.1	55.4±13.5	55.7±12.9	60.4±13.4[a]	58.81±4.2	63.2±13.2[a]
Albumin (g/L)	38.7±5.2	38.8±3.9	33.4±4.1	33.8±3.7	35.2±4.3	36.5±2.9	37.3±4.5	38.7±5.1
Prealbumin(g/L)	12.6±3.2	12.7±5.2	8.4±2.9	11.1±2.2[a]	9.6±4.1	12.5±5.1[a]	11.9±6.1	12.7±5.9

[a]$P<0.05$ *vs* control.

Table 2 Changes of APACHE II scores and concentration of TNF-α, IL-6 and CRP in two groups

	1 d		4 d		7 d		11 d		15 d	
	Control	Treatment	Control	Treatment	Control	Treatment	Control	Treatment	Control	Treatment
APACH II	8.2±0.7	8.3±0.6	8.4±0.9	7.9±0.6[a]	7.1±0.8	5.7±0.7[a]	5.2±0.7	3.7±0.8[a]	1.6±0.4	1.5±0.5
TNF-α(pg/ml)	63.5±15.2	68.4±13.5	55.6±16.3	47.4±11.6[a]	43.9±9.7	34.2±7.6[a]	34.6±7.5	14.2±3.2[a]	16.5±9.6	15.4±5.3
IL-6(pg/ml)	43.3±11.4	46.7±12.4	39.8±9.2	31.4±8.5[a]	34.3±9.2	22.5±7.6[a]	13.2±58	21.7±9.4[a]	11.5±4.7	12.3±3.8
CRP(mg/L)	77.3±13.5	75.4±14.5	67.3±18.6	54.8±11.2[a]	54.3±9.6	41.2±8.5[a]	37.5±9.8	24.7±9.8[a]	21.3±8.6	19.7±6.4

[a]$P<0.05$ *vs* control.

Table 3 Changes of serum amylase, urine amylase and CT scores in two groups

	1 d		4 d		7 d		11 d		15 d	
	Control	Treatment	Control	Treatment	Control	Treatment	Control	Treatment	Control	Treatment
Serum amylase (IU)	672±83	640±79	869±96	821±87	621±69	585±72	432±47	445±39	124±27	135±31
Urine amylase (IU)	1327±324	1521±284	2227±357	2312±312	1413±315	1486±274	924±189	945±157	522±114	547±142
CT score	2.5±0.8	2.3±0.7			3.8±1.1	3.7±0.9			2.1±0.5	2.1±0.6

Table 4 Changes of endotoxin concentration and L:M ratio of urine in two groups

	1 d		7 d		15 d		21 d	
	Control	Treatment	Control	Treatment	Control	Treatment	Control	Treatment
Endotoxin (pg/ml)	–	–	5.9±1.1	2.4±0.7[a]	8.3±3.2	1.9±0.8[a]	8.4±1.6	1.7±0.6[a]
L:M	0.047±0.019	0.052±0.021	0.097±0.023	0.063±0.011[a]	0.143±0.046	0.061±0.027[a]	0.156±0.032	0.057±0.028[a]

[a]$P<0.05$ *vs* control.

Table 5 Changes of CD4:CD8 ratio and IgG concentration in two groups

	1 d		7 d		15 d		21 d	
	Control	Treatment	Control	Treatment	Control	Treatment	Control	Treatment
CD4:CD8	1.82±0.02	1.85±0.04	1.54±0.05	1.72±0.06[a]	1.64±0.07	1.82±0.04[a]	1.78±0.03	1.87±0.05[a]
IgG (mg/L)	12.3±1.7	11.8±1.1	9.8±0.9	11.4±0.7	10.8±0.6	11.8±0.7[a]	11.0±0.5	12.2±0.6[a]

[a]$P<0.05$ *vs* control.

Acute phase responses

APACH II scores decreased earlier in the treatment group (on the 4th day) than those in the control group (on the 7th day). Moreover, the concentration of serum CRP, TNF-α and IL-6 in treatment group decreased earlier too (Table 2).

Pancreas lesions

The concentrations of serum and urine amylase in both groups decreased on the 7th day, and there were no significant differences between these two groups. Similar changes were observed in the CT scores (Table 3).

Enteric mucosal permeability

Few endotoxins were detected in the treatment group on the 7th day, and the urine L:M ratio remained unchanged. Endotoxin concentration and urine L:M ratio in control group elevated gradually and were much higher than those in the treatment one ($P<0.05$) (Table 4).

Immune function

CD4:CD8 T cell ratio and serum IgG concentration did not change in the treatment group. In control group, CD4:CD8 T cell ratio and serum IgG concentration decreased continuously and were markedly lower than those in the treatment group ($P<0.05$) (Table 5).

DISCUSSION

Infected pancreatic necrosis is the most severe complication in patients with SAP. Its occurrence is associated with systemic inflammatory response syndrome (SIRS), sepsis, and multiple organ failure (MOF). Failure of intestinal barrier function is probably responsible for the occurrence of these phenomena[16-19]. Experimental models have shown that infection of necrotic pancreas is caused by translocated intestinal bacteria. Bacterial endotoxins and antigens invade the portal circulation and generate cytokines, causing multiple organ failure syndrome (MODS). Enteral feeding has been proved to be beneficial in burn patients and major trauma victims. Theoretically, EN should help preserve intestinal barrier function in patients with SAP[20-23].

It is worth considering which factors contribute to the failure of gut barrier function in acute pancreatitis. Some of these factors are consequences of the disturbance of peristalsis caused by paralysis and disturbance of perfusion caused by hypotension. The most important factor is the deficiency of oxygen and substrate supply for enteric mucosae. Atrophy and apoptosis of intestinal mucosae occur after several days of PN, and the permeability of intestinal wall increases[24-26]. The increased permeability of intestinal wall allows macromolecules, bacteria, endotoxins, and antigens to enter into the portal circulation and adjacent tissues. This invasion elicits an inflammatory response by stimulating the macrophages and neutrophil granulocytes and by inflammatory cytokines (IL-1, 2, and 6 and TNF). These inflammatory mediators may be responsible for the development of SIRS and MODS[27-29]. Our study indicated that inflammatory mediators (CRP, IL-6 and TNF-α) in the treatment group decreased earlier (on the 4th day) than those in the control group (on the 7th day). Similarly, APACH II scores in the treatment group declined earlier (on the 7th day) than those in the control group (on the 11th day). These results suggest that the combined therapy of EN and PN could avoid the excess production of inflammatory mediators, and then alleviate SIRS and acute phase response.

Glutamine is an amino acid rich in the plasma and intracellular free amino acid pool. It is essential for a wide variety of physiologic processes, in particular, the growth and function of enteric mucosae and immune cells including lymphocytes and macrophages[30-32]. In SAP, glutamine is in condition of excess utilization and endogenous glutamine production may not adequate. In our present study, glutamine was added into the elements of PN and EN. The results showed that endotoxin concentration and urine L:M ratio in the treatment group did not have any change, but elevated markedly in the control group. It was indicated that intestinal epithelial cells and immune cells received nutrients especially glutamine from the gut and reins in the treatment group. Furthermore, intestinal motility adjusted the secretion of enteral hormones and enhanced blood flow. Therefore, the combined therapy of PN and EN can prevent mucosae from atrophy and apoptosis effectively. Meanwhile, the results of CD4:CD8 ratio of T cells and serum IgG concentration indicated that the immune function in the treatment group was protected effectively. The combined therapy of PN and EN protected mucosal barrier and immune function, which could prevent the translocation of bacteria effectively.

Several investigations have emphasized that early EN should be beneficial to patients with SAP. However, too early EN or intragastric nutrition would increase the exocrine of pancreas, which aggravates pancreatitis. Our criteria for the enteral feeding are to alleviate the acute phase response, stabilize the organs function and limit the local necrosis tissue and exudates. Nutritional tube must be placed in the superior segment of jejunum, so enteric feeding will not increase the amount of pancreatic secretions[33, 34]. Because the gut failed to function in patients with SAP and the nutritional tube couldnot peristalsize, the tube should be pushed with endoscopy or under X-ray to the superior segment of the jejunum[35]. In this study, CT scores and the concentration of amylase indicated that EN did not simulate the excretion of pancreas, and thus could avoid exaggerating the inflammation of pancreas.

In summary, the results of our study provide evidences that combined therapy of EN and PN can significantly modulate acute phase response and improve the mucosal barrier and immune defense. Thus, appropriate application of PN and EN appears to be more effective for patients with SAP.

REFERENCES

1 **Zazzo JF**. Nutrition in acute pancreatitis. *Schweiz Med Wochenschr* 1999; **129**: 1617-1625
2 **Schneider H**, Boyle N, McCluckie A, Beal R, Atkinson S. Acute severe pancreatitis and multiple organ failure: total parenteral nutrition is still required in a proportion of patients. *Br J Surg* 2000; **87**: 362-373
3 **Lobo DN**, Memon MA, Allison SP, Rowlands BJ. Evolution of nutritional support in acute pancreatitis. *Br J Surg* 2000; **87**: 695-707
4 **Clancy TE**, Ashley SW. Current management of necrotizing pancreatitis. *Adv Surg* 2002; **36**: 103-121
5 **Everitt NJ**. Enteral nutrition is superior to parenteral nutrition in severe acute pancreatitis: results of a randomized prospective trial. *Br J Surg* 1998; **85**: 716
6 **Kale-Pradhan PB**, Elnabtity MH, Park NJ, Laus M. Enteral nutrition in patients with pancreatitis. *Pharmacotherap*. 1999; **19**: 1036-1041
7 **Sahin M**, Ozer S, Vatansev C, Akoz M, Vatansev H, Aksoy F, Dilsiz A, Yilmaz O, Karademir M, Aktan M. The impact of oral feeding on the severity of acute pancreatitis. *Am J Surg* 1999; **178**: 394-398
8 **Rao MP**, Mulleague L. Nutritional support in acute pancreatitis: the enteral vs parenteral dilemma. *Hosp Med* 2001; **62**: 580
9 **Ribeiro MD**, Paiva JA, Landeiro N, Duarte J. Patients with severe acute pancreatitis should be more often treated in an Intensive Care Department. *Rev Esp Enferm Dig* 2002; **94**: 523-532
10 **Chen QP**. Enteral nutrition and acute pancreatitis. *World J Gastroenterol* 2001; **7**: 185-192

11 **Mao EQ**, Tang YQ, Zhang SD. Effects of time interval for hemofiltration on the prognosis of severe acute pancreatitis. *World J Gastroenterol* 2003; **9**: 373-376
12 **Slavin J**, Ghaneh P, Sutton R, Hartley M, Rowlands P, Garvey C, Hughes M, Neoptolemos J. Management of necrotizing pancreatitis. *World J Gastroenterol* 2001; **7**: 476-481
13 **Abou-Assi S**, O'Keefe SJ. Nutrition support during acute pancreatitis. *Nutrition* 2002; **18**: 938-943
14 **Windsor AC**, Kanwar S, Li AG, Barnes E, Guthrie JA. Compared with parenteral nutrition, enteral feeding attenuates the acute phase response and improves disease severity in acute pancreatitis. *Gut* 1998; **42**: 431-435
15 **Ockenga J**, Borchert K, Rifai K, Manns MP, Bischoff SC. Effect of glutamine-enriched total parenteral nutrition in patients with acute pancreatitis. *Clin Nutr* 2002; **21**: 409-416
16 **Erstad BL**. Enteral nutrition support in acute pancreatitis. *Ann Pharmacother* 2000; **34**: 514-521
17 **Papapietro K**, Marin M, Diaz E, Watkins G, Berger Z, Rappoport J. Digestive refeeding in acute pancreatitis. When and how? *Rev Med Chil* 2001; **129**: 391-396
18 **Fang J**, DiSario JA. Nutritional management of acute pancreatitis. *Curr Gastroenterol Rep* 2002; **4**: 120-127
19 **Abou-Assi S**, Craig K, O'Keefe SJ. Hypocaloric jejunal feeding is better than total parenteral nutrition in acute pancreatitis: results of a randomized comparative study. *Am J Gastroenterol* 2002; **97**: 2255-2262
20 **Olah A**, Pardavi G, Belagyi T, Nagy A, Issekutz A, Mohamed GE. Early nasojejunal feeding in acute pancreatitis is associated with a lower complication rate. *Nutrition* 2002; **18**: 259-262
21 **Dejong CH**, Greve JW. Nutrition in patients with acute pancreatitis. *Curr Opin Crit Care* 2001; **7**: 251-256
22 **Kotani J**, Usami M, Nomura H, Iso A, Kasahara H, Kuroda Y, Oyanagi H, Saitoh Y. Enteral nutrition prevents bacterial translocation but does not improve survival during acute pancreatitis. *Arch Surg* 1999; **134**: 287-292
23 **Qin HL**, Su ZD, Hu LG, Ding ZX, Lin QT. Effect of early intrajejunal nutrition on pancreatic pathological features and gut barrier function in dogs with acute pancreatitis. *Clin Nutr* 2002; **21**: 469-473
24 **Imrie CW**, Carter CR, McKay CJ. Enteral and parenteral nutrition in acute pancreatitis. *Best Pract Res Clin Gastroenterol* 2002; **16**: 391-397
25 **McClave SA**, Dryden GW. Issues of nutritional support for the patient with acute pancreatitis. *Semin Gastrointest Dis* 2002; **13**: 154-160
26 **Qamruddin AO**. Preventing pancreatic infection in acute pancreatitis. *J Hosp Infect* 2000; **44**: 245-253
27 **Lehocky P**, Sarr MG. Early enteral feeding in severe acute pancreatitis: can it prevent secondary pancreatic (super) infection? *Dig Surg* 2000; **17**: 571-577
28 **Foitzik T**. Pancreatitis and nutrition. Significance of the gastrointestinal tract and nutrition for septic complications. *Zentralbl Chir* 2001; **126**: 4-9
29 **Hallay J**, Kovacs G, Szatmari K, Bako A, Szentkereszty Z. Early jejunal nutrition and changes in the immunological parameters of patients with acute pancreatitis. *Hepatogastroenterology* 2001; **48**: 1488-1492
30 **De Beaux AC**, O'Riordain MG, Ross JA. Glutamine-supplemented total parenteral nutrition reduces blood mononuclear cell interleukin-8 release in severe acute pancreatitis. *Nutrition* 1998; **14**: 261-265
31 **Foitzik T**, Stufler M, Hotz HG, Klinnert J. Glutamine stabilizes intestinal permeability and reduces pancreatic infection in acute experimental pancreatitis. *J Gastrointest Surg* 1997; **1**: 40-47
32 **Yu JC**, Jiang ZM, Li DM. Glutamine: a precursor of glutathione and its effect on liver. *World J Gastroenterol* 1999; **5**: 143-146
33 **Olah A**, Belagyi T, Issekutz A, Gamal ME, Bengmark S. Randomized clinical trial of specific lactobacillus and fibre supplement to early enteral nutrition in patients with acute pancreatitis. *Br J Surg* 2002; **89**: 1103-1107
34 **Foitzik T**. Pancreatitis and nutrition. Significance of the gastrointestinal tract and nutrition for septic complications. *Zentralbl Chir* 2001; **126**: 4-9
35 **Berger Z**, Papapietro K. Long nasojejunal feeding tube: endoscopic method for placing and its use for enteral nutrition in acute pancreatitis. *Rev Med Chil* 1999; **127**: 53-58

Edited by Su Q and Wang XL

P.O.Box 2345, Beijing 100023,China
Fax: +86-10-85381893
E-mail: wjg@wjgnet.com www.wjgnet.com

World J Gastroenterol 2003;9(9):2109-2113
World Journal of Gastroenterology
 ISSN 1007-9327

• CLINICAL RESEARCH •

Prospective study of biofeedback retraining in patients with chronic idiopathic functional constipation

Jun Wang, Mao-Hong Luo, Qing-Hui Qi, Zuo-Liang Dong

Jun Wang, Department of Colorectal Surgery, Tianjin Binjiang Hospital, Tianjin 300022, China
Mao-Hong Luo, Department of Public Health, Tianjin Medical University, Tianjin 300070, China
Qing-Hui Qi, Zuo-Liang Dong, Department of General Surgery, Tianjin Medical University Hospital, Tianjin 300050, China
Supported by the Natural Science Foundation of Tianjin Health Bureau, No. 99KY2D07
Correspondence to: Dr. Jun Wang, Department of Colorectal Surgery, Tianjin Binjiang Hospital, Tianjin 300022, China. chinahcc@vip.sina.com
Telephone: +86-22-27632249
Received: 2002-08-03 **Accepted:** 2002-10-18

Abstract

AIM: To determine the efficacy and long-term outcome of biofeedback treatment for chronic idiopathic constipation and to compare the efficacy of two modes of biofeedback (EMG-based and manometry-based biofeedback).

METHODS: Fifty consecutive contactable patients included 8 cases of slow transit constipation, 36 cases of anorectic outlet obstruction and 6 cases of mixed constipation. Two modes of biofeedback were used for these 50 patients, 30 of whom had EMG-based biofeedback, and 20 had manometry-based biofeedback. Before treatment, a consultation and physical examination were done for all the patients, related information such as bowel function and gut transit time was documented, psychological test (symptom checklist 90, SCL90) and anorectic physiological test and defecography were applied. After biofeedback management, all the patients were followed up. The Student's *t*-test, chi-squared test and Logistic regression were used for statistical analysis.

RESULTS: The period of following up ranged from 12 to 24 months (Median 18 months). 70 % of patients felt that biofeedback was helpful, and 62.5 % of patients with constipation were improved. Clinical manifestations including straining, abdominal pain, bloating, were relieved, and less oral laxative was used. Spontaneous bowel frequency and psychological state were improved significantly after treatment. Patients with slow and normal transit, and those with and without paradoxical contraction of the anal sphincter on straining, benefited equally from the treatment. The psychological status rather than anorectal test could predict outcome. The efficacy of the two modes of biofeedback was similar without side effects.

CONCLUSION: This study suggests that biofeedback has a long-term effect with no side effects, for the majority of patients with chronic idiopathic constipation unresponsive to traditional treatment. Pelvic floor abnormalities and transit time should not be the selection criteria for treatment.

Wang J, Luo MH, Qi QH, Dong ZL. Prospective study of biofeedback retraining in patients with chronic idiopathic functional constipation. *World J Gastroenterol* 2003; 9(9): 2109-2113
http://www.wjgnet.com/1007-9327/9/2109.asp

INTRODUCTION

Chronic constipation is a common and distressing complaint, which may be secondary to many diseases, or may also be of functional origin. In the United Stats, it is more common in blacks (17 %), women (18 %), elderly over 60 years (23 %), and in those who are inactive, low income, or poorly educated[1]. In Tianjin, China, 4.43 % of the general population had this complaint according to a study in 1994.

Chronic idiopathic functional constipation is a severe type of constipation and has poor response to the traditional management. Many such patients could not live without the use of laxatives, suppositories or enemas and experience major physical, social, and psychological impairments from the condition.

Biofeedback has been used for a long time to strengthen pelvic floor muscles in patients with fecal incontinence[2]. In recent years, biofeedback has been used for retraining of the pelvic floor with paradoxical sphincter contraction[3]. The reported results varied and the successful rate ranged from 0 to over 90 %[5,6]. Although most groups restricted the use of biofeedback to patients with normal transit and paradoxical pelvic floor contraction during straining[6-9], the technique has a wide therapeutic benefit.

Behavioral techniques were applied to patients with three kinds of constipation (pelvic floor dysfunction, slow transit, and mixed) in order to assess prospectively the effects of biofeedback, to evaluate factors that might be helpful in selecting patients or the optimal method of biofeedback, and to explore the mechanism of this treatment.

MATERIALS AND METHODS

Patients

From October 1998 to October 1999, 50 patients with chronic idiopathic functional constipation from Tianjin Binjiang hospital and Tianjin Medical University Hospital were offered biofeedback. The duration of constipation of the patients was more than 2 years. All the 50 patients failed to respond to first-line therapy, including dietary advice, bulk-forming agents, and use of laxatives. Operation was performed on 4 patients. There were 36 females and 14 males, their mean age was 52.6 years (range, 16-71), mean duration of constipation was 4.6 years (range, 2.5-30). Detailed information is shown in Table1.

Table 1 Common features of the patients

No. of cases	50 (36, female)
Average age	52.6 (10-71)years
Average history	4.6 (2.5-30)years
Average onset age	34 (1-60)years
Complaint in childhood	4
Average follow-up period	18 (12-28)months
Times of biofeedback treatment	1
Failed treatment prior to BF	
Normal traditional conservative treatment	50
Operation	4

All the patients had constipation as defined by the Rome II criteria, complaining of either decreased bowel frequency (less than three times per week), a sensation of incomplete emptying or a history of difficult evacuation on at least a quarter of occasions, or a need to strain. According to the criteria, we divided the patients into pelvic floor dysfunction (n=36), slow transit (n=8) and mixed (n=6). The algorithm for clinical approach in this study is showed in Figure 1.

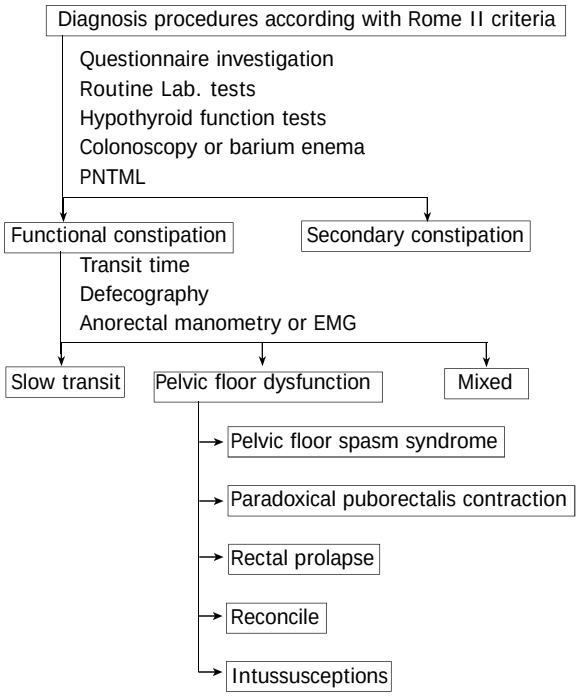

Figure 1 Algorithm for clinical approach.

Methods

Physical examination and thyroid function test were done to exclude constipation secondary to other causes. Moreover, an initial series of tests, including colonoscopy or barium enema failed to detect organic lesions in all patients. Patients were assessed clinically using a specially designed questionnaire that was filled out by a specialist, physician or a medically qualified researcher. The questionnaire included history of age at onset, bowel frequency, precipitation factors, use of laxatives, major and secondary syndromes, family history, urinary syndromes, gynecologic history, and other relevant diseases. A series of tests of colonic and pelvic floor functions were performed before and after biofeedback treatment as described below.

Whole gut transit study We used the method previously reported[10]. Patients ingested twenty radiologically distinguishable radio-opaque markers on day one, and no laxatives or enemas were allowed for five days. In women, the investigation was performed in the nonmenstrual phase. A single plain abdominal radiograph was taken 120 hours after ingesting of the markers. We interpreted more than 8(>40 percent) markers left in the colon as abnormal, which were divided into two kinds: slow transit of whole colon, slow transit of sigmoid colon and rectum.

Anorectal manometry We used an open-tip perfused catheter system (Medtronic Synectics Ltd). The catheter had a four-channel flexible probe with an outside diameter of 4.8 mm. Rectal sensory function to distension was assessed using an intrarectal balloon, according to previously published techniques. The initial sense, a sense of urgency, and the maximum tolerated volume were recorded. Rectal sensation to an electrical stimulus was also assessed using a bipolar electrode placed in the rectum 6 cm above the upper limit of the anal canal. The length of the anal canal was also measured. This technique had been previously validated. Manometric studies were performed with the patient lying on the left side.

Electromyography of the external sphincter muscle We used surface EMG electrode to measure the electromyographic activity of the anal sphincter as described by Abdullhakim and Gerger. The study was performed with the patient in the right lateral position. We repeatedly assessed the myoelectric activity during resting, squeezing, and straining. A reproducible increase in myoelectrical activity during straining was considered as the paradoxical puborectalis contraction.

Defecography Cinedefecography was a dynamic study of anorectal function, and was described before. Evacuation was started from the beginning of straining to completion of rectal emptying, and measured in seconds on a video counter. Subjective evaluation of rectal emptying was then undertaken to determine completeness and speed of evacuation. Prolonged (>35 seconds) emptying or incomplete emptying or both were considered as abnormal pelvic floor function. A rectocele that failed to empty the evacuation was considered as significant pelvic floor dysfunction. Paradoxical puborectalis contraction, rectal prolapse and intussusception were diagnosed with defecography.

Psychological questionnaire Symptom Checklist 90 (SCL-90) was used to evaluate the psychological state of patients[11]. Nine factors could be described, which were somatization, obsessive-compulsive, interpersonal sensitivity, depression, anxiety, hostility, photic anxiety, padanoid ideation and psychoticism. We could also get the general symptomatic index.

Telephone interview Each patient was interviewed over telephone by an investigator who had not been the patient's biofeedback therapist. Data were obtained using a questionnaire containing the same questions as those before treatment. Using these pretreatment and post-treatment data, an assessment was made regarding the age of constipation onset of the patient, and whether there were any precipitating factors, including vaginal delivery, hysterectomy, or other surgery. Bowel function before and after biofeedback, and at the time of interview was assessed, including use of bowel evacuants (oral laxatives, enemas, and suppositories), bowel frequency without laxatives, need of strain, need of dig with finger, and a sense of incomplete evacuation. Enquiries were also made about the presence and subjective severity of abdominal pain or bloating. To establish the possible subjective benefits of the treatment as a whole, in addition to the effect on constipation, benefit of biofeedback, improvement of constipation and compliance with practice of biofeedback techniques were asked.

Questionaire A special questionaire including listing symptoms and daily use of laxatives or enemas during and after treatment was designed, and was filled out by patients and was checked by doctors in charge.

Biofeedback therapy Patients were subjected to biofeedback twice per week for five sessions. All the patients were treated as outpatients. At the first session, the anatomy and physiology of the gut and the pelvic floor were explained to the patients using diagrams and their own tests results. The objectives of biofeedback therapy were carefully explained to the patients.

In the pressure-based training, we used the same four-lumen catheter as described above. The side holes were placed in the distal rectum and the anal canal, and the balloon attached to the tip of the catheter was used for training expulsion. During training, the catheter was inserted in the same way as during diagnostic studies, and the subjects were allowed to view the manometric recordings. They were instructed to look for changes in the pressure tracing, thereby visualizing the location and function of the pelvic floor muscles, with specific attention to the responses of the anal sphincter during squeezing and

straining. Patients were told that the sphincter should relax during expulsion of the rectal balloon at the urge threshold, indicated by a decrease in basal pressure, and they should learn how to relax the pelvic floor muscles and to push down slowly using their abdominal muscles. Straining and relaxing were repeated until a normal pattern of expulsion occurred. The exercise was repeated several times during an one-hour session.

For EMG feedback, the subjects were seated on a toilet-like chair. Disposable bilateral prenatal surface EMG electrodes were connected to the EMG recording device, which provided auditory and visual signals to aid the patient in observing muscle activity. Resting EMG was noted, then the subject recorded a squeeze, bore down as defecation and tried to relax the pelvic floor and to lower the straining records below the resting recording. Afterward, the patients were trained to expel the rectal balloon connected to a catheter on lateral position and were instructed to pratise expulsion of rectal contents and relax without straining at home.

Polygraf ID (Medtronic Synetics Ltd) was used in this study. The patients were consulted on normal defecography behavior and bowel habits, such as adjusting the number of visits to the toilet, amount of time spent, and posture in toilet. At each biofeedback session the therapist tried to have a good understanding and collaboration with patients. An attempt was made to get patients off laxatives, enemas, and suppositories. When the course of biofeedback was completed, the patients were encouraged to continue practicing the techniques.

Prognostic factors To determine whether certain patient characteristics may predict a response to biofeedback treatment, the patients who benefited from biofeedback were compared with those who did not. Parameters used for comparison were the objective findings of slow or normal transit, the presence or absence of pelvic floor paradoxical contraction on straining, the presence of previous psychological factors, and the compliance of practice the biofeedback at home after the treatment. Difference between EMG-based and Manometry-based biofeedback was compared.

Assessment of symptoms A questionnaire was used to assess the manifestation of patients, it detailed the number of bowel movements, failed attempts of bowel movement, the use of laxatives and enemas, presence of bloating, severity of abdominal pain (0=no pain, 1=mild pain, 2=moderate pain, 3=severe pain) for each day during one week. The score of one-week abdominal pain was calculated as the sum of seven consecutive daily scores of pain severity.

Patients were investigated with anorectal manometry, EMG, and the one-week bowel habit questionnaire before and after biofeedback retraining. After treatment and 6 months following treatment, a global assessment for the treatment was evaluated by patients through filling the questionnaire, including the degree of improvement of bowel movement.

Statistical methods Non-normal data were expressed as median and full range. Normal data were expressed as mean ±standard deviation. Student' s *t*-test was used to compare the treatment results, and the chi-square test was used for comparison of proportions. Prognostic factors were analyzed by logistic regression.

RESULTS

All the 50 patients agreed to participate in the study. Table 1 shows characteristics of the patients. The vast majority of patients were female. Each patient had only one course of biofeedback. Almost 10 % of the patients had experienced constipation since childhood. Almost all the patients believed they could not identify a precipitating factor of their constipation. One fifth of patients were recorded as having possible relevant psychological factors.

The median time of follow up was 18 months (12-28 months).

At the end of treatment, 31 of the 50 patients reported a subjectively overall improvement. The overall successful rate was 62 %, the successful rate was 72.2 % for patients with pelvic floor dysfunction constipation.

Table 3 shows the prevalence of symptoms in the study group. The most common findings were difficult evacuation, hard stools, distention or bloating and laxative dependence.

All the patients underwent both a transit study and physiological study, 8 had slow colonic transit, 36 showed pelvic floor dysfunction constipation, 6 had both slow transit and pelvic floor dysfunction (Table 2).

Two methods of biofeedback were applied in this study. We used EMG-based biofeedback for 30 patients, and manometry-based biofeedback for 20 patients.

Table 2 Symptoms Changes before and after Biofeedback (BE)

Symptoms	No. of patients before BF	No. of patients 10 days after BF	No. of patients 1 year after BF
Difficult evacuation	50	16[a]	13[a]
Hard stools	40	18[b]	16[b]
Loose stools at onset of abd. Pain	39	19(NS)	22(NS)
No sense of defecate in 1 week	35	20(NS)	16(NS)
Need for digitations	21	11(NS)	11(NS)
Sense of incomplete emptying	31	18(NS)	16(NS)
Distention or bloating	42	15[b]	13[b]
Laxative dependence	48	12(P<0.01)	14[a]
Need of enema	31	9[b]	9[b]
Perianal pain at defecation	30	16(NS)	11(NS)

[a]P<0.01 *vs* before BF, [b]P<0.05 *vs* before BF.

Table 3 Successful rate in patients with different types of constipation

Types	*n*	Successful rate (%)
Slow transit	8	3
Pelvic floor dysfunction	36	26 (72.2 %)
Paradoxical puborectalis contraction	20	16 (80 %)
Pelvic floor spasm syndrome	9	6 (66.7 %)
Intussusception	7	4 (55.6 %)
Mixed	6	2

Symptoms

At the end of treatment, 31 of 50 patients reported a subjectively overall improvement in their symptoms. The need for enema, difficult evacuation, hard stools, distention or bloating and use of laxatives were all significantly improved immediately after biofeedback or after a long-term follow up (Table 3). The proportion of patients with loose stools at onset of pain, no feeling to defecate, need for digitations, feeling of incomplete emptying and perianal pain at defecation were also reduced, but these did not reach statistical significance, probably due to the small number of patients with these symptoms.

Physiological investigations

Whole gut transit Before biofeedback: 14 of 50 constipated patients were identified as having slow transit. Of them, seven had marker retention predominantly in the rectosigmoid as defined by more than half of the excessively retained markers present in the rectosigmoid, the remaining 7 patients with slow transit had excessive marker retention throughout the colon.

After biofeedback: 5 of 14 slow transit constipation patients reported subjective improvement after biofeedback. 26 of 36 patients with normal transit reported a similar improvement. The difference between the two groups was not significant. Similarly, there was no difference between patients with slow and normal transit.

Among the 7 patients with slow transit, 3 patients with only rectosigmoid delay and 2 with slow transit were due to a more generalized holding up of markers, and reported a subjective improvement.

Defecography Before biofeedback: 42 of 50 constipated patients were identified as having pelvic floor dysfunction constipation. Of them, 22 were complicated with paradoxical puborectalis contraction, 7 with pelvic floor spasm syndrome, 9 with major intussusception.

After biofeedback: 28 of 42 patients reported a subjective improvement after biofeedback. Among them, 15 were complicated with paradoxical puborectalis contraction predominantly, 8 with pelvic floor spasm syndrome and 5 with intussusception. The difference in outcome between the three groups was not significant.

Anorectal manometry There were significant reductions in the index of "initial sense" and "average rest pressure" before and after biofeedback. On the other hand, there was no difference in other results concerning the type of biofeedback (Table 4).

Table 4 Changes of anorectal manometry index before and after BF

Manometry index	Volume before BF	Volume after BF	Statistic value
Anal canal(mmHg)			
Average rest pressure	49.7±7.7	19.4±10.1	$P<0.05$
Voluntary squeeze	112.5±18.5	164.4±40.6	NS
Rectum			
Initial sense(ml)	95.4±39.1	41.4±19.2	$P<0.05$
Maximum tolerable(ml)	195.7±42.5	412.6±235.3	NS
Compliance(ml/mmHg)	5.1±1.5	6.3±2.9	NS

Table 5 Prognostic factors (1 year after BF therapy)

Factors	Percent of success (31)	Percent of failure (19)	Statistic value
Gender			
Female (36)	22(72.8 %)	14(73.7 %)	NS
Male (14)	9(28.1 %)	5(26.3 %)	NS
Methods of BF			
EMG-based (30)	20(64.5 %)	10(52.6 %)	NS
Manometry-based(20)	11(36.1 %)	9(47.3 %)	NS
Types of constipation			
Slow transit(8)	3	5	
Pelvic floor dysfunction(36)	26(83.9 %)	10(52.6 %)	$P<0.05$
Mixed (6)	2	4	
Psychological state			
High-level group [a](25)	15 (49.43 %)	10(52.6 %)	NS
low-level group [a](25)	16 (51.6 %)	9(47.3 %)	NS

[a]Limitation to measure high and low group was half of total number.

Psychological state

The general symptomatic index was significantly reduced after biofeedback therapy (from 44.80±33.34 before BF to 24.05±20.62 after BF, $P<0.01$). All the factors were improved after BF, and except photic anxiety, all the factors had a significant difference between before and BF ($P<0.05$-0.01, Table 6).

Prognostic factors

No practice of biofeedback techniques after treatment was significantly associated with poor outcome immediately after biofeedback treatment (practised: 76 % in the success group versus 43 % in the failure group, $P<0.01$, χ^2 test), however, this difference at long-term follow up was no longer significant. Patients with slow transit gained more benefit than those with normal transit, but the number of patients with slow transit was too small to draw conclusion. Patients with normal pelvic floor contraction gained less benefit than those with abnormal one. Different methods of biofeedback did not predict outcome.

Table 6 Symptomatic factors index of SCL-90

Factors	Before BF	After BF
Somatization	0.5	0.2
Obsessive-compulsive	0.6	0.3
Interpersonal sensitivity	0.9	0.4
Depression	0.7	0.1
Anxiety	0.8	0.2
Hostility	0.7	0.3
Padanoid ideation	0.7	0.2
Psychoticism	0.5	0.2
Photic anxiety	0.1	0.1

DISCUSSION

This study showed that biofeedback was a successful treatment for patients with constipation unresponsive to other treatments. 62 % of patients reported a subjective improvement in long-term follow up. This was objectively supported by their decreased use of laxatives. Symptom improvement was related not only to bowel frequency, but also to symptoms such as bloating.

The biofeedback component was important. Similar training without biofeedback from the sphincter was not effective, as was shown in a recent study by Bleijenberg and Kuijpers[12]. They compared the efficacy of EMG biofeedback with that of retraining defecation using an intrarectal balloon only. In the former group, 8 of 11 patients improved as opposed to only 2 of 9 in the latter group. The efficacy of biofeedback over other treatments was also demonstrated by Loening-Baucke[13], who studied children with constipation and encopresis. Nineteen patients were treated with conventional therapy combined with EMG feedback, 7 months later, 77 % of the biofeedback-treated children improved as opposed to only 13 % of those treated conventionally.

Our selection of patients for biofeedback was based on international criteria for functional constipation-Roma II criteria. Organic lesions were excluded by colonoscopy or barium enema, as Hirschsprung's disease and megarectum by anorectal manometry. According to the criteria, the patients were divided into slow transit, pelvic floor dysfunction and mixed. Others had their own opinions on classification. Another type associated with irritable bowel syndrome (IBS) that was defined as combination of normal transit and normal pelvic floor function was reported, Pemberton reported 71.1 % of constipated patients (n=277) had IBS (n=197). Nyam reported 59.2 % (597) of 1009 patients belonged to this type. Glia A and Lindberg G found that 35 % of the constipated patients complained of constipation but had no detectable disturbance of anorectal or colonic function, and thought that the methods were too crude to detect clinically relevant disturbances of

colorectal function. The patients with normal transit constipation more often reported normal stool frequency, alternating diarrhea and constipation, urgent need for defecation, history of previous anorectal surgery, and looser stools at onset of pain. In the absence of a quantifiable abnormality, patients with normal-transit constipation previously diagnosed as IBS. Our data showed that the International Working Team criteria for IBS did not discriminate between different diagnostic groups. Further studies are needed to determine if a modification of the IBS criteria works well.

This prospective study shows that biofeedback is an effective behavioral treatment for chronic idiopathic constipation with slow transit and normal transit. Five of 14 patients with slow transit were normal by the end of treatment. This study has also shown that the changes in transit occurred in patients with excessive retained markers are distributed around the colon. The effect may relate to whole colon function or innervations and not just the distal large bowel. Treatment also significantly speed up transit in those with normal transit pretreatment, with 18 % reduction in the number of markers present on the follow up transit study.

For such a labor intensive treatment it is important to determine which patients are likely to respond to treatment. In our research, the gender of patients, and the type of constipation, physiological factors and the method of biofeedback could not predict response to treatment.

This study demonstrated that patients with idiopathic constipation had significantly greater psychological morbidity than age matched healthy controls. They had higher levels of depression, anxiety, psychoticism and hostility. This finding was partly reproduced in studies[14,15] which suggested that psychological factors influenced gut function via autonomic efferent neural pathways.

In the meantime, after biofeedback therapy, the general symptomatic index was significantly reduced, and except photic anxiety, all the factors fell down. So it is possible that the biofeedback therapy improved the psychological state.

The mechanism of action of biofeedback treatment is complicated. It was as effective in patients with slow transit as it was in those with paradoxical contraction, 82 % of those with paradoxical contraction and 50 % of those without paradoxical contraction reported subjective improvements after treatment. Previous studies showed that patients with and without animus, with both slow and normal transit benefited equally from biofeedback[16-18].

There are several mechanisms by which behavioral treatment may have altered gut function and blood flow. Cerebral autonomic control of the gut and its microcirculation may have been changed. Alternatively, it is possible that the observed increases in rectal mucosal blood flow are due to improvement in psychological or social functioning brought about by behavioral treatment.

ACKNOWLEDGMENTS

We are indebted to Drs. Shu-Ling Yuan, Ying-Chao Hu, and Zhang-Rong Jiang for assistance in performing the biofeedback treatment.

REFERENCES

1 **Corman M**. Colon and Rectal Surgery. 4th ed. U.S.A: *Lippincott-Raven Pubilishers* 1998: 368-400
2 **Ferrara A**, De Jesus S, Gallagher JT, Williamson PR, Larach SW, Pappas D, Mills J, Sepulveda JA. Time-related decay of the benefits of biofeedback therapy. *Tech Coloproctol* 2001; **5**: 131-135
3 **McKee RF,** McEnroe L, Anderson JH, Finlay IG. Identification of patients likely to benefit from biofeedback for outlet obstruction constipation. *Br J Surg* 1999; **86**: 355-359
4 **Bleijenberg G**, Kuijpers HC. Treatment of the spastic pelvic floor syndrome with biofeedback. *Dis Colon Rectum* 1987; **30**: 108-111
5 **Wiesel PH**, Dorta G, Cuypers P, Herranz M, Kreis ME, Schnegg JF, Jornod P. Patient satisfaction after biofeedback for constipation and pelvic floor dyssynergia. *Swiss Med Wkly* 2001; **131**: D152-D156
6 **Thompson WG**. Constipation: a physiological approach. *Can J Gastroenterol* 2000; **14**(Suppl): 155-162
7 **De Paepe H,** Renson C, Van Laecke E, Raws A, Vande Walle J, Hoebeke P**.** Pelvic-floor therapy and toilet training in young children with dysfunctional voiding and obstripation. *BJU Int* 2000; **85**: 889-893
8 **Brown SR**, Donati D, Seow-Choen F, Ho YH. Biofeedback avoids surgery in patients with slow-transit constipation: report of four cases. *Dis Colon Rectum* 2001; **44**: 737-739; discussion 739-740
9 **Nehra V,** Bruce BK, Rath-Harvey DM, Pemberton JH, Camilleri M. Psychological disorders in patients with evacuation disorders and constipation in a tertiary practice. *Am J Gastroenterol* 2000; **95**: 1755-1758
10 **Liu SX**, Zhang DW, Wu F, Xie RB, Zhang PD, Ma DW, Meng YC, Xiao KS, Tang HQ. The value of whole gut transit time to the diagnosis of constipation. *Zhongguo Yixue Zazhi* 1993; **73**: 75-77
11 **Huang XD**, Wang XL, Ma H. Rating Scales For Mental Health. 1st ed. Beijing: *Zhongguo Xiliweisheng Zazhishi Publishers* **1999**: 31-35
12 **Wiesel PH**, Norton C, Roy AJ, Storrie JB, Bowers J, Kamm MA. Gut focused behavioural treatment (biofeedback) for constipation and faecal incontinence in multiple sclerosis. *J Neurol Neurosurg Psychiatry* 2000; **69**: 240-243
13 **McGrath ML,** Mellon MW, Murphy L. Empirically supported treatments in pediatric psychology:constipation and encopresis. *J Pediatr psychol* 2000; **25**: 225-254
14 **Devroede G**, Girard G, Bouchoucha M, Roy T, Black R, Camerlain M, Pinard G, Schang JC, Arhan P. Idiopathic constipation by colonic dysfunction. Relationship with personality and anxiety. *Dig Dis Sci* 1989; **34**: 1428-1433
15 **Dailianas A,** Skandalis N, Rimikis MN, Koutsomanis D, Kardasi M, Archimandritis A. Pelvic floor study in patients with obstructive defecation: influence of biofeedback. *J Clin Gastroenterol* 2000; **30**: 176-180
16 **Emmanuel AV**, Kamm MA. Response to a behavioural treatment, biofeedback, in constipated patients is associated with improved gut transit and autonomic innervation. *Gut* 2001; **49**: 214-219
17 **Coulter ID**, Favreau JT, Hardy ML, Morton SC, Roth EA, Shekelle P. Biofeedback interventions for gastrointestinal conditions: a systematic review. *Altern Ther Health Med* 2002; **8**: 76-83
18 **Heymen S**, Wexner SD, Vickers D, Nogueras JJ, Weiss EG, Pikarsky AJ. Prospective, randomized trial comparing four biofeedback techniques for patients with constipation. *Dis Colon Rectum* 1999; **42**: 1388-1393

Edited by Ren SY and Wang XL

P.O.Box 2345, Beijing 100023,China
Fax: +86-10-85381893
E-mail: wjg@wjgnet.com www.wjgnet.com

World J Gastroenterol 2003;9(9):2114-2116
World Journal of Gastroenterology
 ISSN 1007-9327

• BRIEF REPORTS •

Studies on specific interaction of beta-2-glycoprotein I with HBsAg

Pu-Jun Gao, Yun-Feng Piao, Xiao-Dong Liu, Li-Ke Qu, Yang Shi, Xiao-Cong Wang, Han-Yi Yang

Pu-Jun Gao, Yun-Feng Piao, Yang Shi, Xiao-Cong Wang, Department of Digestion, 1st Hospital affiliated to Jilin University, Changchun 130021, Jilin Province, China
Xiao-Dong Liu, the Key Laboratory of Radiobiology, Ministry of Public Health, Jilin University, Changchun 130021, Jilin Province, China
Li-Ke Qu, Han-Yi Yang, Department of Biochemistry, School of Basic Medicine, Jilin University, Changchun 130021, Jilin Province, China
Supported by the National Natural Science Foundation of China, No.30070338
Correspondence to: Pu-Jun Gao, Department of Digestion, 1st Hospital affiliated to Jilin University, Changchun 130021, Jilin Province, China. pujun-gao@163.com
Telephone: +86-431-5612242
Received: 2002-11-05 **Accepted:** 2002-12-12

Abstract

AIM: To observe the binding activity of beta-2-glycoprotein I (β_2GPI) to hepatitis B surface antigen (HBsAg) and the possible roles of β_2GPI in hepatitis B virus (HBV) infection.

METHODS: The rationale of ELISA methods and ELISA-based research method and ligand-blotting technique were used to detect the specific interaction of β_2GPI with HBsAg.

RESULTS: With the increase of rHBsAg, the binding of β_2GPI to rHBsAg elevated, and these changes had statistic significance. When we added non- biotinlyated β_2GPI, the OD value significantly decreased though they still were positively relevant to rHBsAg, suggesting non- biotinlyated β_2GPI competed with biotinlyated β_2GPI to saturate the binding sites on rHBsAg. Meanwhile BSA was used as negative control to substitute for rHBsAg coating the plates. The results indicated no interaction between β_2GPI and BSA, suggesting the affinity of β_2GPI to rHBsAg was specific. The ligand blotling indicated that β_2GPI might bind to rHBsAg no matter whether it was under reduced condition or not.

CONCLUSION: The binding of β_2GPI to HBsAg suggests that β_2GPI may be a carrier of HBV and that β_2GPI may play important roles in HBV infection.

Gao PJ, Piao YF, Liu XD, Qu LK, Shi Y, Wang XC, Yang HY. Studies on specific interaction of beta-2-glycoprotein I with HBsAg. *World J Gastroenterol* 2003; 9(9): 2114-2116
http://www.wjgnet.com/1007-9327/9/2114.asp

INTRODUCTION

β_2GPI (beta-2-glycoproteinI) is a plasm glycoprotein circulating as a free protein and is associated to lipoproteins. This protein is also referred to as apolipoprotein H(Apo H). Human β_2GPI is a single-chain molecule consisting of 326 amino acid residues and 5 carbohydrate chain and has a molecule mass of approximately 55 kDa[1-3]. The amino acid sequences of β_2GPI in human, bovine, mouse, and rat appear to be highly conserved[4-6]. The protein contains 5 internal repeat unit of 60 amino acid residues, each with 2 internal disulfide bonds, known as Sushi domain[7].

Although quite a lot is known about the structure of β_2GPI, its biological function remains unclear. It is known that β_2GPI can bind to negatively charged substances such as DNA and heparin and negatively charged phospholipids etc *in vivo*[8,9], but the meaning of such interaction is still unclear. It is known that β_2GPI may serve as a major factor in clearing the plasma liposome[10] as well as an anticoagulant in blood[11]. β_2GPI may also modulate the function of kidney and placenta. The abnormality of plasma β_2GPI level has been shown to be associated with many diseases such as arterial and venous thrombosis, recurrent abortion and alcoholic liver disease[12,13]. In addition, it has been found that, in diabetes or atherosclerosis patients, the concentration of plasma β_2GPI increases and distribution of the protein among different types of lipoprotein is perturbed[14,15]. Recent research on β_2GPI has given a further impetus to the discovery that lipid- associated β_2GPI can bind to some pathogenic antigens or proteins such as HBV Dane particles, protein p18, p26, gp160 of HIV and so on[16], and perhaps hepatitis virus antigen[17,18]. These findings highlighted a potentially critical role of β_2GPI in the mechanism of hepatitis B, AIDS, and systemic lupus erythematosus, etc.

The lipid-binding and transportation functions are considered as a basic mechanism related to its physiological and pathogenic functions. It has been demonstrated by several labs that β_2GPI prefers to bind negatively charged phospholipids[9,19-21]. It was reported that β_2GPI could be removed from the membranes with a weakly acidic buffer and it was partly associated with chylomicrons and high-density lipoproteins, both of which were targeted to hepatocytes during the normal course of lipid metabolism[22]. In the present paper, the characteristics of β_2GPI interacting with HBsAg were further examined by several measurements. As a result, the standpoints that β_2GPI might participate in HBV infection were held out accordingly. Our results may also help to explain how β_2GPI facilitates HBV transportation, location and the important roles of β_2GPI in HBV infection.

MATERIALS AND METHODS

Reagents

TEMED, APS, PMSF, and aprotinin purchased from Sigma Chemical Co., acrylamide and biacrylamide purchased from Serva, human β_2GPI provided by Prof. Zhang GR from Jilin University, rHBsAg offered by Zhang HY from Jilin Institute of Family Plan, Hybond obtained from Amersham, SDS, NP-40, Coomasie brilliant blue obtained from Fluka (Finland). The other chemicals used were of analytical grade made in China.

ELISA-based determination of b_2GPI-rHBsAg interaction

rHBsAg was diluted into 0.125 μg/ml, 0.5 μg/ml and 2 μg/ml in 0.05 $NaHCO_3$ (pH 9.4) and added to 96-well plates respectively at 4 ℃ overnight (8 wells/group). Non-specific sites were blocked with PBS containing 1 % BSA for 1.5 h at 37 ℃. Plates were washed three times between the different incubation steps. Biotinylated β_2GPI was added to every well followed by adding HRP-Avidin and substrate consequentially. Simultaneously, 40 ng of non-labeled β_2GPI was added to

4well/group as a competitor. OPD was used to develop color and the intensity of color was quantified at 492 nm with Model 550 Microplate Reader (Bio-Rad). In addition, BSA was used as negative control (2 ug/ml, 1 ug/ml, 0.2 ug/ml), to observe its binding to β_2GPI.

SDS-PAGE and ligand blotting

The β_2GPI protein was performed by SDS-PAGE using the vertical electrophoritic apparatus (Bio-Rad) on 12 % acrylamide under reduced and non-reduced condition. The gels were stained with Coomassie brilliant blue to visualize the proteins. The proteins separated were transferred onto nitrocellulose using an electric transfer system at 50 V for 16 min, followed by immunoblot analysis employing biotinylated rHBsAg as a detecting probe and DAB as a developing system. The blotting buffer consisted of phosphate-buffered saline (10 mM phosphate, pH7.5, 138 mM NaCl, 2.7 mM KCl) containing 5 % dried skimmed milk powder and 1 % Tween 20 detergent (Sigma). Biotinylated rHBsAg was used at a dilution of 1/200 and HRP-avidin (Huamei Company), a dilution of 1/200. The density was analyzed with Luzex-F Image-analysis System.

Statistical analysis

Results from quantitative parameters were presented as mean ±SD and comparisons of which were performed using the Student' s *t* test.

RESULTS

ELISA-based determination of b_2GPI- rHBsAg interaction

rHBsAg was diluted into 0.125 μg/ml, 0.5 μg/ml and 2 μg/ml and used as capture antibody to coat the plates, then biotinlyated β_2GPI was added to interact with rHBsAg, simultaneously we used non- biotinlyated β_2GPI to observe the competitive binding interaction. The following figure indicated that with the increase of rHBsAg the binding of β_2GPIto rHBsAg elevated and these changes had statistic significance (*vs* 0.125 μg/ml group, $P<0.05$). When we added non- biotinlyated β_2GPI, the OD value significantly decreased though they still were positively relevant to rHBsAg, suggesting that non-biotinlyated β_2GPI competed with biotinlyated β_2GPI to saturate the binding sites on rHBsAg (Figure 1). Meanwhile BSA was used as negative control to substitute for rHBsAg coating the plates, the results indicated no interaction between β_2GPI and BSA, (Figure 2) suggesting the affinity of β_2GPI to rHBsAg was specific.

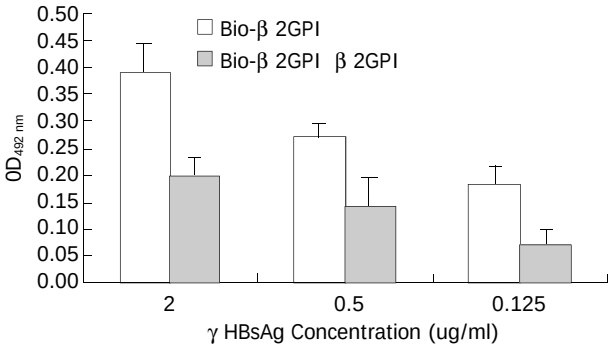

Figure 1 Comparative binding reaction of β_2GPI to rHBsAg by ELISA-based determination of protein interaction.

Binding of b_2GPI to rHBsAg observed by ligand blotting

The discrepancy between ligand blotting and Western blotting was that the former made use of ligand-receptor reaction, while the latter, the antigen-antibody interaction. The image showing -50 kDa protein bands in both lane 1 and lane 2 represented reduced (with DTT) and non-reduced (without DTT) condition, respectively (Figure 3). The results indicated that β_2GPI might bind to rHBsAg no matter whether it was under reduced condition or not, which manifested difference from that reported by Mehdi *et al*[17]. The subsequent digital scaning by Luzex-F Imager confirmed no quantitative changes in density between lane1 and lane 2.

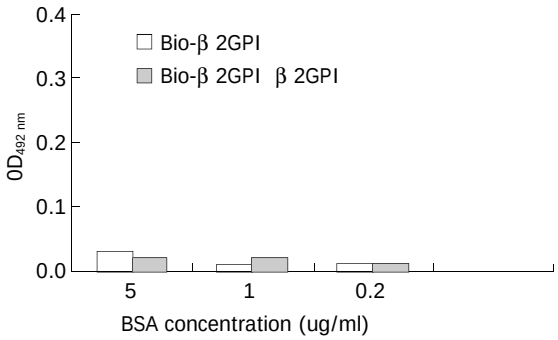

Figure 2 Comparative binding reaction of β_2GPI to BSA by ELISA-based determination of protein interaction.

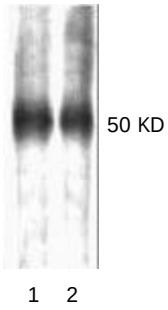

Figure 3 Reduced (lane1) and non-reduced (lane2) human β_2GPI (1 μg/lane) was separated with 12 % SDS-PAGE and applied to Hybond nitrocellous membrane, blocked with 5 % skimmed milk, then probed with biotinylated rHBsAg, color was developed with HRP-avidin in DAB solution. Single band at -50 kDa was observed, no significant diference in color density was observd, which was further confirmed by digital scaning.

DISCUSSION

Hepatitis B virus (HBV) is a member of the hepadnavirus family, which includes duck HBV, woodchuck hepatitis virus and ground squirrel hepatitis virus. These viruses are highly infectious for their host animals, targeting primarily, though not exclusively, the liver. Although many researches have been done, it is not clear which of these virus' components is in responsible for its attachment to a target cell[23]. As a step toward identifying the mechanism of HBV targeting hepatocytes, Haider Mehdi reported that a 50 kDa protein known as β_2GPI, which could be removed from the membranes with a weakly acidic buffer, might participate in the infection of HBV. Examination of human serum revealed that β_2GPI was a serum protein. Isolation of plasma lipoproteins revealed that β_2GPI was in part associated with chylomicrons and high-density lipoproteins, both of which are targeted to hepatocytes during the normal course of lipid metabolism[21]. In this study, we further examined the possible roles of β_2GPI in HBV infection. A ligand-blotting system was used to identify and partially characterize a rHBsAg-binding protein associated with hepatocyte membrane, plasma and lipoproteins. Immunoassay was performed to characterize the properties of rHBsAg binding to β_2GPI and to demonstrate the specificity of this

interaction.

β_2GPI is a glycoprotein with four N-linked carbohydrate chains[2,3] present at concentrations of approximately 200 μg/ml in serum[17]. The 326-residue mature protein is composed of a 61 amino acid motif repeated four times, followed by one longer, modified repeat. Each of the first four repeats contains four cysteines in conserved positions, at least one of which is critical for its rHBsAg-binding activity. This pattern of disulfide bonds is similar to the short consensus repeat units found in a family of approximately 20 proteins which includes many of the complement control proteins. It is interesting that the measles virus receptor, CD46[24,25] also belongs to this short consensus repeat family.

The work described in the present report was to reveal the possible roles of β_2GPI in HBV infection. As we have known that β_2GPI may target to hepatocytes in the form of chylomicrons and high-density lipoproteins. The result of the present paper suggested that β_2GPI might specifically bind to HBsAg no matter whether it was under reduced condition or not. We might well reckon that β_2GPI might contribute to transportation of HBV to hepatocytes as a kind of carrier. Since β_2GPI is associated with lipoproteins, particularly chylomicrons and HDL, it is possible that HBV binds to β_2GPI on the surface of these lipoprotein particles. In the bloodstream, chylomicrons are partially degraded by lipoprotein lipase, resulting in chylomicron remnants, which are taken up by hepatocytes. HDLs are also taken up by hepatocytes in the process of "reverse cholesterol transport". They may have been associated with the process of HBV infection. It is tempted to speculate that infectious HBV might bind to chylomicron or HDL particles by interacting with β_2GPI and be taken into hepatocytes as a "hitchhiker" along with these lipoproteins. Our results showed that β_2GP I might bind to rHBsAg no matter whether it was under reduced condition or not manifested difference from that reported by Mehdi *et al*[17]. In Mehdi experimental system, they used human serum to observe the relationship between β_2GPI and HBsAg, while we used purified β_2GPI. There might exist differences between the two kinds of β_2GPI sources in their first, second or third structure, which might lead to the differences of sensitivity to reduced-agents. Moreover, the genetic heterogeneity of β_2GPI could also cause mutations of sequences of some domains, which eventually affect the binding of β_2GPI to rHBsAg. Related issues should be further investigated.

To sum up, if HBV infection to hepatocytes involves β_2GPI on chylomicrons and /or HDL, it is a novel mechanism for virus attachment and entry.

REFERENCES

1 **Okkels H,** Rasmussen TE, Sanghera DK, Kamboh MI, Kristensen T. Structure of the human β_2-glycoprotein I (apolipoprotein H) gene. *Eur J Biochem* 1999; **259**: 435-440

2 **Mehdi H,** Nunn M, Steel DM, Whitehead AS, Perez M, Walker L, Peeples ME. Nucleotide sequence and expression of the human gene encoding apolipoprotein H (beta 2-glycoprotein I). *Gene* 1991; **108**: 293-298

3 **Steinkasserer A,** Estaller C, Weiss EH, Sim RB, Day AJ. Complete nucleotide and deduced amino acid sequence of human beta 2-glycoprotein I. *Biochem J* 1991; **277**(Pt 2): 387-391

4 **Kato H,** Enjyoji K. Amino acid sequence and location of the disulfide bonds in bovine beta 2 glycoprotein I: the presence of five Sushi domains. *Biochemistry* 1991; **30**: 11687-11694

5 **Bendixen E,** Halkier T, Magnusson S, Sottrup-Jensen L, Kristensen T. Complete primary structure of bovine beta 2-glycoprotein I: localization of the disulfide bridges. *Biochemistry* 1992; **31**: 3611-3617

6 **Cocca BA,** Seal SN, D'Agnillo P, Mueller YM, Katsikis PD, Rauch J, Weigert M, Radic MZ. Structural basis for autoantibody recognition of phosphatidylserine-beta 2 glycoprotein I and apoptotic cells. *Proc Natl Acad Sci U S A* 2001; **98**: 13826-13831

7 **Ichinose A,** Bottenus RE, Davie EW. Structure of transglutaminases. *J Biol Chem* 1990; **265**: 13411-13414

8 **Kochl S,** Fresser F, Lobentanz E, Baier G, Utermann G. Novel interaction of Apolipoprotein (a) with β2 glycoprotein I mediated by the Kringle IV domain. *Blood* 1997; **90**: 1482-1489

9 **Matsuda J,** Saitoh N, Gotih M, Gohchi K, Tsukamoto M, Syoji S, Miyake K, Yamanaka M. High prevalence of anti-phospholipid antibodies and anti-thyroglobulin antibody in patients with Hepatitis C virus infection treated with interferon-α. *Am J Gastroenterology* 1995; **90**: 1138-1141

10 **Chonn A,** Semple SC, Cullis PR. Beta 2-glycoprotein I is a major protein associated with very rapidly cleared liposomes *in vivo*, suggesting a significant role in the immune clearance of "Non-self" particles. *J Bio Chem* 1995; **270**: 25845-25849

11 **Brighton TA,** Hogg PJ, Dai YP, Murray BH, Chong BH, Chesterman CN. Beta 2-glycoprotein I in thrombosis: evidence for a role as a natural anticoagulant. *Br J Haematol* 1996; **93**: 185-194

12 **Shiozaki A,** Niiya K, Higuchi F, Tashiro S, Arai T, Izumi R, Sakuragawa N. Ellagic acid / phospholipid-induced coagulation and dextran sulfate-induced fibrinolytic activities in beta 2-glycoprotein I-depleted plasma. *Thromb Res* 1994; **76**: 199-210

13 **Rolla R,** Vay D, Mottaran E, Parodi M, Vidali M, Sartori M, Rigamonti C, Bellomo G, Albano E. Antiphospholipid antibodies associated with alcoholic liver disease specifically recognise oxidised phospholipids. *Gut* 2001; **49**: 852-859

14 **Mc Nally T,** Crook M, Mackie IJ, Isenberg DA, Machin SJ. Beta 2 glycoprotein-I antigen is increased in primary hyperlipidaemia. *Br J Haematol* 1994; **88**: 424-426

15 **Cassader M,** Ruiu G, Gambino R, Veglia F, Pagano G. Apolipoprotein H levels in diabetic subjects: correlation with cholesterol levels. *Metabolism* 1997; **46**: 522-525

16 **Stefas I,** Rucheton M, D'Angeac AD, Morel-Baccard C, Seigneurin JM, Zarski JP, Martin M, Cerutti M, Bossy JP, Misse D, Graafland H, Veas F. Hepatitis B virus Dane particles bind to human plasma apolipoprotein H. *Hepatology* 2001; **33**: 207-217

17 **Mehdi H,** Kaplan MJ, Anlar FY, Yang X, Bayer R, Sutherland K, Peeples ME. Hepatitis B virus surface antigen binds to apolipoprotein H. *J Virol* 1994; **68**: 2415-2424

18 **Neurath AR,** Strick N. The putative cell receptors for hepatitis B virus (HBV), annexin V, and apolipoprotein H, bind to lipid components of HBV. *Virology* 1994; **204**: 475-477

19 **Kertesz Z,** Yu BB, Steinkasserer A, Haupt H, Benham A, Sim RB. Characterization of binding of human beta 2-glycoprotein I to cardiolipin. *Biochem J* 1995; **310**(Pt 1): 315-321

20 **Ohkura N,** Hagihara Y, Yoshimura T, Goto Y, Kato H. Plasmin can reduce the function of human β_2-glycoprotein I by cleaving domain V into a nicked from. *Blood* 1998; **91**: 4173-4179

21 **Willems GM,** Janssen MP, Pelsers MM, Comfurius P, Galli M, Zwaal RF, Bevers EM. Role of divalency in the high-affinity binding of anticardiolipin antibody-beta 2-glycoprotein I complexes to lipid membranes. *Biochemistry* 1996; **35**: 13833-13842

22 **Mehdi H,** Naqvi A, Kamboh MI. A hydrophobic Sequence at position 313-316 (Leu-Ala-Phe-Trp) in the fifth domain of apolipoprotein H (β_2-glycoprotein I) is crucial for cardiolipin binding. *Eur J Biochem* 2000; **267**: 1770-1776

23 **Mehdi H,** Yang X, Peeples ME. An altered form of apolipoprotein H binds Hepatitis B virus surface antigen most efficiently. *Virology* 1996; **217**: 58-66

24 **Dorig RE,** Marcil A, Chopra A, Richardson CD. The human CD46 molecule is a receptor for measles virus. *Cell* 1993; **75**: 295-305

25 **Naniche D,** Varior-Krishnan G, Cervoni F, Wild TF, Rossi B, Rabourdin-Combe C, Gerlier D. Human membrane cofactor protein (CD46) acts as a cellular receptor for measles virus. *J Virol* 1993; **67**: 6025-6032

Edited by Zhao M and Wang XL

P.O.Box 2345, Beijing 100023,China
Fax: +86-10-85381893
E-mail: wjg@wjgnet.com www.wjgnet.com

World J Gastroenterol 2003;9(9):2117-2120
World Journal of Gastroenterology
 ISSN 1007-9327

• BRIEF REPORTS •

Inhibitory effect of all-trans retinoic acid on human hepatocellular carcinoma cell proliferation

Yun-Feng Piao, Yang Shi, Pu-Jun Gao

Yun-Feng Piao, Yang Shi, Pu-Jun Gao, Department of Gastroenterology, the First Hospital of Jilin University, Changchun, 130021, Jilin Province, China
Correspondence to: Dr. Yang Shi, Department of Gastroenterology, the First Hospital of Jilin University, No.1 Xinmin Road, Changchun, 130021, Jilin Province, China. shiyangwhy@163.com
Telephone: +86-431-5612242 **Fax:** +86-431-5612542
Received: 2002-11-14 **Accepted:** 2002-12-20

Abstract

AIM: To study the inhibitory effect of all-trans retinoic acid on human hepatocellular carcinoma cell line SMMC-7721 and to explore the mechanism of its effect.

METHODS: SMMC-7721 cells were divided into two groups, one treated with all-trans retinoic acid (ATRA) for 5 days and the other as a control group. Light microscope and electron microscope were used to observe the morphological changes. Telomerase activity was analyzed with silver-stained telomere repeated assay protocal (TRAP). Expression of Caspase-3 was demonstrated with western blot.

RESULTS: ATRA-treated cells showed differentiation features including small and pyknotic nuclei, densely stained chromatin and fewer microvilli. Besides, ATRA could inhibit the activity of telomerase, promote the expression of Caspase-3 and its activation.

CONCLUSION: Telomerase activity and Caspase-3 expression are changed in human hepatocellular carcinoma cell line SMMC-7721 treated with all-trans retinioc acid. The inhibition of telomerase activity and the activation of Caspase-3 may be the key steps through which ATRA inhibits the proliferation of SMMC-7721 cell line.

Piao YF, Shi Y, Gao PJ. Inhibitory effect of all-trans retinoic acid on human hepatocellular carcinoma cell proliferation. *World J Gastroenterol* 2003; 9(9): 2117-2120
http://www.wjgnet.com/1007-9327/9/2117.asp

INTRODUCTION

Several isomers have been found for retinoic acid (RA), an oxidative product of vitamin A, including all-trans retinoic acid (ATRA) and 9-cis retinoic acid (9C-RA). ATRA has been used successfully in treatment of acute promyelocytic leukemia and other hematologic diseases[1-3]. It can induce cellular differentiation of many malignant tumors and inhibit their growth[4-11]. Morphological and biological changes were also observed in the human hepatocellular carcinoma (HCC) cell line SMMC-7721, treated with ATRA[12,13], but the mechanism remains obscure. For this reason, the changes in telomerase activity and Caspase-3 expression induced by ATRA were analyzed in SMMC-7721 in this study.

MATERIALS AND METHODS

Cell culture

The hepatocellular carcinoma cell line SMMC-7721, was kindly provided by the Hematology Institute of the First Hospital of Norman Bethune University of Medical Sciences, and cultivated in Iscove' s modified Dulbecco' s medium (IMDM, Gibco) containing 10 % fetal bovine serum at 37 ℃ in an incubator with 5 % CO_2. During the exponential stage, ATRA was added to the medium (10^{-5} mmol/L). Cells growing in the ATRA-free medium were used as the control group.

Morphological observation

The ATRA-treated cells and the control cells were observed everyday. After 5 days, the cells were collected, stained and observed under the light microscope. About 10^7 cells were collected, washed with cold saline, and fixed with 4 % glutaral and 1 % osmium acid. After dehydration, embedding, sectioning and staining, the cells were observed under transmission electron microscope.

Activity of telomerase assayed by TRAP silver staining

About 2.5×10^5 cells were collected, washed and homogenized. The telomerase activity was detected using a TRAP kit following instructions of manufacturer (Beijing Tiangekangning biotech institute). The reaction system, containing 25 μl TRAP agent, 0.2 μl Taq enzyme and 1 μl cell extract, was incubated for 30 min at 25 ℃. Then 0.5 μl of primer was added and PCR was conducted for 30 cycles with denaturing at 94 ℃ for 30 s, annealing at 60 ℃ for 30 s, extending at 72 ℃ for 30 s. 15 μl PCR products was loaded onto a 9 % non-degenerative SDS gel, resolved through the SDS-PAGE, demonstrated by a reaction in 0.2 % silver nitrate for 15 min, and visualized by incubation in 30 g/L anhydrous sodium carbonate containing formaldehyde (1 ml/L). The activity of telomerase was indicated by the presence of a 6 bp-DNA ladder. The cell extracts inactivated by incubation at 75 ℃ for 10 min were used as the negative control.

Expression of Caspase-3 assayed by western blot

About 10^6 SMMC-7721 cells were harvested, washed, and lyzed in the 5 volumes extract buffer (5 mM Tris-Cl (pH8.0), 150 mM NaCl, 5 mM EDTA, 1 mM DTT, 100 μg/ml PMSF, 2 μg/ml aprotinin, 1 % NP-40) in the iced bath for 20 min. The supernatant was stored at -70 ℃. After protein quantification, 80 μg of the extraction was subjected to SDS-PAGE. Proteins resolved on the gel were transferred to a nitrocellulose filter (Amersham) in the buffer containing 48 mmol/L Tris, 39 mmol/L glycocol, 0.037 % SDS and 20 % methanol. After being blocked in phosphate buffer saline containing 5 % defatted milk, the blots were incubated with goat antibody against Caspase-3 (Santa Cruz). After being washed three times, the filter was incubated with HRP-labeled rabbit anti-goat immunoglobulin, and the reaction was visualized by incubation with a buffer containing DAB and H_2O_2.

RESULTS

Morphological changes

ATRA-treated cells appeared spindle-shaped, rather than polygon-shaped as under normal conditions. Their nuclei became smaller and pyknotic. The cytoplasma was also stained densely. Cell shrinkage, loss of microvilli, chromatin clumps and reduction of the nuclear/cytoplasmic ratio were noted under the electron microscope. The mitochondria proliferation, enlargement of Golgi complex, cytoplasmic vacuolation and glycogen accumulation, as well as lipofuscin and tonofilaments were also observed (Figure 1).

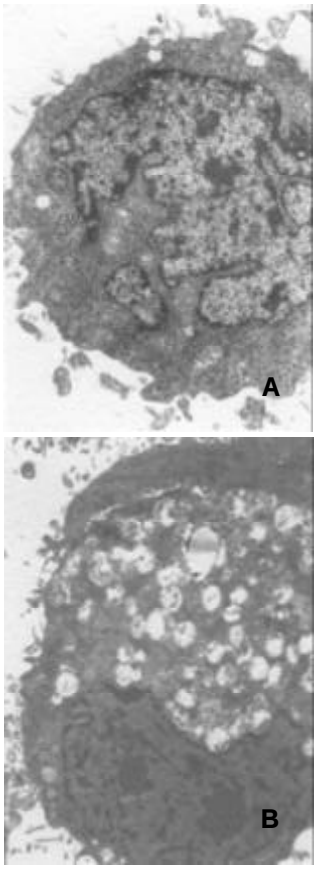

Figure 1 Morphology of SMMC-7721 observed under transmission electron microscope. Untreated-cells have many microvilli, and their nuclei have a great of incisure (A). ATRA-treated cells have smaller volume, fewer microvilli on the surface, densed chromatin and increased heterochromatin. With the plasma increased, the nuclear/cytoplasmic ratio decreased. The mitochondria also increased. The Golgi complex became bigger. More vacuole and glycogen were seen. There were also many lipofuscin and tonofilaments (B).

Activity of telomerase

The untreated cells showed a 6 bp ladder pattern, suggesting the active telomerase, so it served as the positive control. The negative control did not show the pattern, the samples were inactivated at 75 ℃. Similarly the ATRA-treated cells did not show the DNA ladder. We considered that ATRA could inhibit the telomerase activity (Figure 2).

Expression of Caspase-3

All the control groups showed a weak signal at the position of 32 kD, suggesting the presence of Caspase-3 expression at a low level. For the ATRA-treated cells, the 32 kD signal was shown to be strong. In addition, another signal at the position of 20 kD was detected. The latter represented the p20 subunit of Caspase-3, an active form of the molecule (Figure 3).

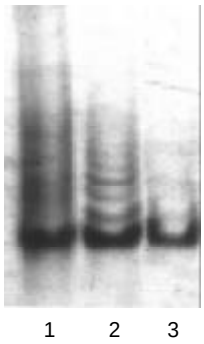

Figure 2 Telomerase activity of SMMC-7721. The untreated cells showed 6bp ladder pattern, suggesting the active telomerase. So it served as the positive control (Lane 2). The negative control did not show the DNA ladder because the sample was inactivated at 75 ℃ (Lane 3). The ATRA-treated cells showed no ladder as the negative control (Lane 1).

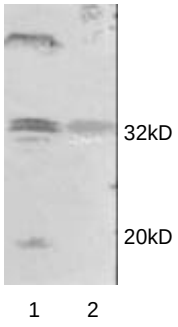

Figure 3 The expression of Caspase-3. All the control groups showed weak signals at the position of 32kD, suggesting the presence of Caspase-3 (Lane 2). For the ATRA-treated cells, the 32kD signal was shown to be stronger. In addition, another signal at the position of 20kD was detected. The latter represented the p20 subunit of Caspase-3, an active form of the molecule (Lane 1).

DISCUSSION

It is estimated that about 437 000 people die of HCC every year worldwide, and that their 5-year survival rate is below 3 %. It is believed that development of HCC is associated with many factors[14-18]. Several gene mutations have been proven to play some roles during this process[19]. Eukaryotic chromosomes are capped with repetitive telomere sequences that appear important for maintaining chromosomal integrity. In all normal somatic cells, each cycle of cell division and DNA replication results in the loss of 50-200 terminal nucleotides from each chromosome. This gradually results in instability of the chromosomes and cell death[20,21]. Telomerase is a type of reverse transcriptase being essential in many cases for telomere stability and cell proliferation, immortalization and transformation[22-35].

Recently, more than ten types of proteases with homology to ICE/CED-3 that is specific to aspartic acid have been found. The Caspase family plays key biological roles in inflammatory responses and in regulation of apoptosis of mammalian cells. Among them, Caspase-3 is known as a key protease whose activation can induce apoptosis of mammalian cells[36-42]. It lies in the upper stream of a series of cascade reactions. Therefore, it may be of some help to delineate Caspase-3 expression during the ATRA-associated cell differentiation and death for further understanding of its mechanism.

In the present study, a reduction of telomerase activity, upregulation of Caspase-3 expression and the activation of this molecule were linked to the ATRA-induced differentiation of

SMMC-7721 cells. A few mechanisms have been proposed for the growth inhibition of HCC cells by ATRA. For example, ATRA can inhibit telomerase activity and shorten telomere length of cancer cells and disrupt the stability of the chromosomes. Alternatively, Caspase may also be involved in this process. ATRA activates Caspase-3, stimulating a series of apoptotic signals and resulting in cell death. It is presumed that ATRA may directly or indirectly affect the function of Caspase-3 at the following three levels: 1) up-regulating the expression of Caspase-3; 2) indirectly acting on the upper stream regulator of Caspase-3; and 3) directly acting on Caspase-3 itself and promoting its activity. In conclusion, inactivation of telomerase and activation of Caspase-3 may be important pathways for the inhibition of HCC cell proliferation by ATRA.

REFERENCES

1 **Mologni L**, Marchesi E, Nielsen PE, Gambacorti-Passerini C. Inhibition of promyelocytic leukemia (PML)/retinoic acid receptor-α and PML expression in acute promyelocytic leukemia cells by anti-PML peptide nucleic acid. *Cancer Res* 2001; **61**: 5468-5473

2 **Ferrara FF**, Fazi F, Bianchini A, Padula F, Gelmetti V, Minuc S, Mancini M, Pelicci PG, Lo Coco F, Nervi C. Histone deacetylase-targeted treatment restores retinoic acid signaling and differentiation in acute myeloid leukemia. *Cancer Res* 2001; **61**: 2-7

3 **Manfredini R**, Trevisan F, Grande A, Tagliafico E, Montanari Lemoli R, Visani G, Tura S, Ferrari S. Induction of a functional vitamin D receptor in all-trans-retinoic acid-induced monocytic differentiation of M2-type leukemic blast cells. *Cancer Res* 1999; **59**: 3803-3811

4 **Chung J**, Liu C, Smith DE, Seitz HK, Russell RM, Wang XD. Restoration of retinoic acid concentration suppresses ethanol-enhanced c-Jun expression and hepatocyte proliferation in rat liver. *Carcinogenesis* 2001; **22**: 1213-1219

5 **Rexer BN**, Zheng WL, Ong DE. Retinoic acid biosynthesis by normal human breast epithelium is via aldehyde dehydrogenase 6, absent in MCF-7 cells. *Cancer Res* 2001; **61**: 7065-7070

6 **Sapi E**, Flick MB, Tartaro K, Kim S, Rakhlin Y, Rodov S, Kacinski BM. Effect of all-trans-retinoic acid on c-fms proto-oncogene [colony-stimulating factor 1 (CSF-1) receptor] expression and CSF-1- induced invasion and anchorage-independent growth of human breast carcinoma cells. *Cancer Res* 1999; **59**: 5578-5585

7 **Zhu WY**, Jones CS, Amin S, Matsukuma K, Haque M, Vuligonda V, Chandraratna RA, De Luca LM. Retinoic acid increases tyrosine phosphorylation of focal adhesion kinase and paxillin in MCF-7 human breast cancer cells. *Cancer Res* 1999; **59**: 85-90

8 **Miller WH Jr**. The emerging role of retinoids and retinoic acid metabolism blocking agents in the treatment of cancer. *Cancer* 1998; **83**: 1471-1482

9 **Kalemkerian GP**, Jiroutek M, Ettinger DS, Dorighi JA, Johnson DH, Mabry M. A phase II study of all-trans-retinoic acid plus cisplatin and etoposide in patients with extensive stage small cell lung carcinoma: an Eastern Cooperative Oncology Group Study. *Cancer* 1998; **83**: 1102-1108

10 **Hatoum A**, El-Sabban ME, Khoury J, Yuspa SH, Darwiche N. Overexpression of retinoic acid receptors alpha and gamma into neoplastic epidermal cells causes retinoic acid-induced growth arrest and apoptosis. *Carcinogenesis* 2001; **22**: 1955-1963

11 **Schneider SM**, Offterdinger M, Huber H, Grunt TW. Activation of retinoic acid receptor is sufficient for full induction of retinoid responses in SK-BR-3 and T47D human breast cancer cells. *Cancer Res* 2000; **60**: 5479-5487

12 **Ai ZW**, Cha XL, Ye JN, Chen HL. Reverse effect of retinoic acid on some cell membrane phenotype of human hepatocellular carcinoma cells. *Shengwu Huaxue yu Shengwu Wuli Xuebao* 1990; **22**: 147-150

13 **Ai ZW**, Cha XL, Liu Y, Chen HL. Reverse effect of retinoic acid on some cell plasma phenotype of human hepatocellular carcinoma cells. *Shengwu Huaxue yu Shengwu Wuli Xuebao* 1990; **22**: 135-139

14 **Hao MW**, Liang YR, Liu YF, Wu MY, Yang HX. Transcription factor EGR-1 inhibits growth of hepatocellular carcinoma and esophageal carcinoma cell lines. *World J Gastroenterol* 2002; **8**: 203-207

15 **Ogami M**, Ikura Y, Nishiguchi S, Kuroki T, Ueda M, Sakurai M. Quantitative analysis and in situ localization of human telomerase RNA in chronic liver disease and hepatocellular carcinoma. *Lab Invest* 1999; **79**: 15-26

16 **Kojima H**, Yokosuka O, Imazeki F, Saisho H, Omata M. Telomerase activity and telomere length in hepatocellular carcinoma and chronic liver disease. *Gastroenterology* 1997; **112**: 493-500

17 **Zhang G**, Long M, Wu ZZ, Yu WQ. Mechanical properties of hepatocellular carcinoma cells. *World J Gastroenterol* 2002; **8**: 243-246

18 **Wang X**, Liu FK, Li JS, Xu GX. Inhibitory effect of endostatin expressed by human liver carcinoma SMMC7721 on endothelial cell proliferation *in vitro*. *World J Gastroenterol* 2002; **8**: 253-257

19 **Ohno J**, Horio Y, Sekido Y, Hasegawa Y, Takahashi M, Nishlzawa J, Saito H, Ishikawa F, Shimokata K. Telomerase activation and p53 mutations in urethane-induced A/J mouse lung tumor development. *Carcinogenesis* 2001; **22**: 751-756

20 **Blackburn EH**. Structure and function of telomeres. *Nature* 1991; **350**; 569-573

21 **Figueroa R**, Lindenmaier H, Hergenhahn M, Nielsen KV, Boukamp P. Telomere erosion varies during *in vitro* aging of normal human fibroblasts from young and adult donors. *Cancer Res* 2000; **60**: 2770-2774

22 **Morin GB**. The human telomere terminal transferase enzyme is a ribonucleoprotein that synthesizes TTAGGG repeats. *Cell* 1989; **59**: 521-529

23 **Dahse R**, Fiedler W, Ernst G. Telomeres and telomerase: biological and clinical importance. *Clin Chem* 1997; **43**: 708-714

24 **Feng J**, Funk WD, Wang SS, Weinrich SL, Avilion AA, Chiu CP, Adams RR, Chang E, Allsopp RC, Yu J, Le S, West MD, Harley CB, Andrews WH, Greider C, Villeponteau B. The RNA component of human telomerase. *Science* 1995; **269**: 1236-1241

25 **Kim NW**, Piatyszek MA, Prowse KR, Harley CB, West MD, Ho PL, Coviello GM, Wright WE, Weinrich SL, Shay JW. Specific association of human telomerase activity with immortal cells and cancer. *Science* 1994; **266**: 2011-2015

26 **Toomey D**, Smyth G, Condron C, Kay E, Conroy R, Foley D, Hong C, Hogan B, Toner S, McCornick P, Broe P, Kelly C, Bouchier-Hayes D. Immune function, telomerase, and angiogenesis in patients with primary, operable nonsmall cell lung carcinoma: tumor size and lymph node status remain the most important prognostic features. *Cancer* 2001; **92**: 2648-2657

27 **Hytiroglou P**, Kotoula V, Thung SN, Tsokos M, Fiel MI, Papadimitriou CS. Telomerase activity in precancerous hepatic nodules. *Cancer* 1998; **82**: 1831-1838

28 **Kitamoto M**, Ide T. Telomerase activity in precancerous hepatic nodules. *Cancer* 1999; **85**: 245-248

29 **Nakashio R**, Kitamoto M, Tahara H, Nakanishi T, Ide T, Kajiyama G. Significance of telomerase activity in the diagnosis of small differentiated hepatocellular carcinoma. *Int J Cancer* 1997; **74**: 141-147

30 **Yan P**, Coindre JM, Benhattar J, Bosman FT, Guillou L. Telomerase activity and human telomerase reverse transcriptase mRNA expression in soft tissue tumors; correlation with grade, histology, and proliferative activity. *Cancer Res* 1999; **59**: 3166-3170

31 **Engelhardt M**, Mackenzie K, Drullinsky P, Silver RT, Moore MAS. Telomerase activity and telomere length in acute and chronic leukemia, pre- and post-ex vivo culture. *Cancer Res* 2000; **60**: 610-617

32 **Yan P**, Saraga EP, Bouzourene H, Bosman FT, Benhattar J. Expression of telomerase genes correlates with telomerase activity in human colorectal carcinogenesis. *J Pathol* 2001; **193**: 21-26

33 **Youssef N**, Paradis V, Ferlicot S, Bedossa P. *In situ* detection of telomerase enzymatic activity in human hepatocellular carcinogenesis. *J Pathol* 2001; **194**: 459-465

34 **Sato N**, Maehara N, Mizumoto K, Nagai E, Yasoshima T, Hirata K, Tanaka M. Telomerase activity of cultured human pancreatic carcinoma cell lines correlates with their potential for migration and invasion. *Cancer* 2001; **91**: 496-504

35 **Matthews P**, Jones CJ, Skinner J, Haughton M, de Micco C, Wynford-Thomas D. Telomerase activity and telomere length in

thyroid neoplasia: biological and clinical implications. *J Pathol* 2001; **194**: 183-193

36 **Nicholson DW**, Ali A, Thornberry NA, Vaillancourt JP, Ding CK, Gallant M, Gareau Y, Griffin PR, Labelle M, Lazebnik YA, Munday NA, RaJu SM, SmulsonME, Yamin TT, Yu VL, Miller DK. Identification and inhibition of the ICE/CED-3 protease necessary for mammalian apoptosis. *Nature* 1995; **376**: 37-43

37 **Wolf BB**, Green DR. Suicidal tendencies: apoptotic cell death by caspase family proteinases. *J Bio Chem* 1999; **274**: 20049-20052

38 **Marshman E**, Ottewell PD, Potten CS, Watson AJ. Caspase activation during spontaneous and radiation-induced apoptosis in the murine intestine. *J Pathol* 2001; **195**: 285-292

39 **Sane AT**, Bertand R. Caspase inhibition in camptothecin-treated U-937 cells is coupled with a shift from apoptosis to transient G_1 arrest followed by necrotic cell death. *Cancer Res* 1999; **59**: 3565-3569

40 **Mori M**, Terui Y, Tanaka M, Tomizuka H, Mishima Y, Ikeda M, Kasahara T, Uwai M, Ueda M, Inoue R, Itoh T, Yamada M, Hayasawa H, Furukawa Y, Ishizaka Y, Ozawa K, Hatake K. Antitumor effect of β2-microglobulin in leukemic cell-bearing mice via apoptosis-inducing activity: activation of caspase-3 and nuclear factor-kappaB. *Cancer Res* 2001; **61**: 4414-4417

41 **Jiang C**, Wang Z, Ganther H, Lu J. Caspases as key executors of methyl selenium-induced apoptosis (anoikis) of DU-145 prostate cancer cells. *Cancer Res* 2001; **61**: 3062-3070

42 **Shariat SF**, Desai S, Song W, Khan T, Zhao J, Nguyen C, Foster BA, Greenberg N, Spencer DM, Slawin KM. Adenovirus-mediated transfer of inducible caspases: a novel "death switch" gene therapeutic approach to prostate cancer. *Cancer Res* 2001; **61**: 2562-2571

Edited by Su Q

P.O.Box 2345, Beijing 100023,China
Fax: +86-10-85381893
E-mail: wjg@wjgnet.com www.wjgnet.com

World J Gastroenterol 2003;9(9):2121-2124
World Journal of Gastroenterology
 ISSN 1007-9327

• BRIEF REPORTS •

Efficacy of intra-tumor injection of Xiao-Zhi-Ling on transplanted hepatoma in rats

Yun Lu, Li-Qun Wu

Yun Lu, Li-Qun Wu, Department of Hepato-biliary Vascular Surgery, Medical College, Qingdao University, Qingdao 266003, Shandong Province, China
Correspondence to: Yun Lu, Department of Hepato-biliary Vascular Surgery, Medical College, Qingdao University, 16 Jiangsu Road, Qingdao 266003, Shandong Province, China. cloudylucn@yahoo.com.cn
Telephone: +86-532-2911369 **Fax:** +86-532-2911999
Received: 2003-03-02 **Accepted:** 2003-03-25

Abstract

AIM: To study the therapeutic effectiveness of intra-tumor injection of Xiao-Zhi-Ling(XZL) on transplanted hepatoma in rats.

METHODS: Sixty rats were divided into 3 groups (groups S, X and E), 20 in each. Different drugs were injected into the implanted hepatoma (Group S with 0.2 ml saline as control, group X with 0.2 ml XZL, group E with 0.2 ml ethanol). After 3 days and 8 days respectively, we detected the hepatoma volume (HV), the level of albumin, alanine aminotransferase (ALT), aspartate aminotransferase (AST) and alkaline phosphatase (ALP) in serum, and the expression of proliferating cell nuclear antigen (PCNA) in hepatoma.

RESULTS: The results were obtained after 3 days, the HVs in groups X and E were smaller than those in group S (group X *vs* S P=0.010*, group E *vs* S P=0.002*, P<0.05). The levels of ALT and AST in group S and X were lower than those in group E (ALT Group S *vs* E P=0.019*, group X *vs* E P=0.003*, P<0.05; AST group X *vs* E P=0.002*, P<0.05). The levels of ALP and PCNA labeling index in group X were lower than those in group S and E (ALP group X *vs* S P=0.000*, group X *vs* E P=0.000*. P<0.05; PCNA group X *vs* S P=0.008*, group X *vs* E P=0.048*, P<0.05). The levels of creatinine in group S were lower than those in group E (group S *vs* E P=0.017, P<0.05). The degree of tumor necrosis in group S was lower than those in groups X and E (group S *vs* X P=0.006*, group S *vs* E P=0.006*, P<0.05). After 8 days, the HVs in groups X and E were smaller than those in group S (group X *vs* S P=0.007*, group E *vs* S P=0.004*, P<0.05). The difference of HVs between groups X and E was not significant. The levels of albumin, ALT, AST and creatinine in group X were not higher than those in other groups, the levels of ALP and PCNA in group X were lower than those in groups S and E (ALP group X *vs* E P=0.006* P<0.05; PCNA group X *vs* S P=0.044*, group X *vs* E P=0.021*, P<0.05). The degree of tumor necrosis in group S was lower than that in groups X and E (group S *vs* X P=0.001*, group S *vs* E P=0.002*, P<0.05).

CONCLUSION: The therapeutic effectiveness of intra-tumor injection of XZL and ethanol on implanted hepatoma is obvious, but the toxicity of XZL on liver function is markedly lower than that of group E, at the same time XZL can inhibit the growth of tumor. XZL is relatively better and safer than ethanol in intra-tumor injection therapy.

Lu Y, Wu LQ. Efficacy of intra-tumor injection of Xiao-Zhi-Ling on transplanted hepatoma in rats. *World J Gastroenterol* 2003; 9(9): 2121-2124
http://www.wjgnet.com/1007-9327/9/2121.asp

INTRODUCTION

The resection rate of hepatocellular carcinoma (HCC) is only about 20 %. Percutaneous ethanol injection therapy (PEIT) and transcatheter arterial chemoembolization (TACE) can be used in patients who have lost the chance of surgical operation. Both could be used easily and widely. But to small HCC, they cannot treat it thoroughly. To huge HCC, repeated use can cause liver function failure and biliary tract injury, so the application in clinic is limited. Xiao-Zhi-Ling (XZL) is a traditional Chinese drug, it can cause vascular embolization and tissue fibrosis. In this research XZL was used in the treatment of implanted hepatoma in rats in order to find its therapeutic effectiveness.

MATERIALS AND METHODS

Tumor implantation

Walker-256 tumor cells were injected into the abdominal cavity of Wistar rats, tumor ascites were removed from the abdominal cavity 7 days later. After diluting them subcutaneous vaccination was given in right forefoot axillary fossa of healthy Wistar rats[1]. 8 days later we obtained the subcutaneous tumor which grew quickly, then cut it into pieces of 1×1×1 mm^3, put them into RPMI medium 1640[2,3]. A small subcapsular incision on the left lateral lobe of the liver of healthy Wistar rats was made. Tumor fragments were gently put into the pocket and abdominal wall was then closed. After that rats were maintained on the previous diet[4,5].

Experimental procedures

8 days after tumor cells were implanted, 60 rats were divided into 3 groups (groups S, X and E), 20 rats in each group. Different drugs were injected into the implanted hepatoma of each rat, group S with 0.2 ml saline as control, group X with 0.2 ml XZL (obtained from Ji-an Pharm Corp in Jilin province, China), group E with 0.2 ml ethanol.

After 3 days and 8 days respectively, 10 rats were sacrificed in each group at random. Tumors in the left lobe of liver were removed and fixed in 10 % formalin. The respective blood samples were centrifuged, then the level of albumin, alanine aminotransferase (ALT), aspartate aminotransferase (AST) and alkaline phosphatase (ALP) in serum were detected[6,7].

Immunohistochemistry analysis

The implanted liver tumor tissues were paraffin-embedded and sectioned, sections were made for standard histological detection using hematoxylin and eosin[8,9]. The expression of proliferating cell nuclear antigen (PCNA) in hepatoma was detected in each case[10,11].

Statistical analysis

The data were expressed as $\bar{x}\pm s$. Statistical differences were

analyzed by *t*-test, a value of $P<0.05$ was considered significant. The difference between groups was compared by LAD method.

RESULTS

Comparison of hepatoma volume (HV) between different groups (Table 1 and 2)

After 3 and 8 days, the HVs in group X and E were smaller than those in group S ($P<0.05$).

By the 3rd day, the differences of hepatoma volume between different groups were as follows: group S *vs* X $P=0.010$*, group S *vs* E $P=0.002$*, group X *vs* E $P=0.443$.

By the 8th day, the differences of hepatoma volume between different groups were as follows: group S *vs* X $P=0.007$*, group S *vs* E $P=0.004$*, group X *vs* E $P=0.771$.

Comparison of hepatoma necrosis between different groups

After 3 days the difference of hepatoma necrosis between groups X and S, and groups E and S was significant ($P<0.01$). After 8 days group S was significantly different from groups X and E. But there was no difference between groups X and E.

By the 3rd day, the differences of hepatoma necrosis between different groups were as follows: group S *vs* X $P=0.006$*, group S *vs* E $P=0.006$*, group X *vs* E $P=1.000$.

By the 8th day, the differences of hepatoma necrosis between different groups were as follows: group S *vs* X $P=0.001$*, group S *vs* E $P=0.002$*, group X *vs* E $P=0.690$.

Rate of tumor inhibition (RTI)

Tumor volume was calculated by the formula ($\pi/6\times$length$\times$width$\times$height). The rate of tumor inhibition (RTI) could be calculated by the formula: (volume of control group -volume of test group)/volume of control group$\times$100 %; 3 and 8 days after injecting drug, RTIs in groups X and E were 45.86 %, 57.73 % and 62.47 %, 68.24 %. MDDT stands for multiplication diameter time, which indicates the growth rate of tumor. Table 3 shows different growth rates in the 3 groups.

Table 3 MDDT of the tumor in groups S, X and E

Group	MD (3 days)	MD (8 days)	MDDT
Group S	4.56	9.62	4.51
Group X	4.6	6.74	10.75
Group E	3.54	6.5	5.9

Comparison of hepatic and renal function (Table 1 and 2)

Serum albumin After 3 and 8 days the level of serum albumin in group X was higher than those in groups S and E, but there was no statistical significance ($P=0.13$).

Serum ALT After 3 days, the level of serum ALT in groups S and X was lower than that in group E, there was statistical significance ($P<0.01$). After 8 days, the level of serum ALT showed no statistical difference among three groups ($P>0.05$). By the 3rd day, the differences between every two groups were as follows: group S *vs* X $P=0.309$, group S *vs* E $P=0.019$*, group X *vs* E $P=0.003$*.

Serum AST After 3 days, the level of serum AST showed statistical difference among three groups ($P<0.05$). After 8 days, the level of serum AST showed no statistical difference among three groups ($P>0.05$). By the 3rd day, the differences between every two groups were as follows: group S *vs* X $P=0.077$, group S *vs* E $P=0.067$, group X *vs* E $P=0.002$*.

Serum ALP After 3 days the level of serum ALP in group X was lower than those in groups S and E, there was statistical significance ($P<0.01$). After 8 days the level of serum ALP in group X was lower than that in group E, there was statistical significance ($P<0.01$). By the 3rd day, the differences between every two groups were as follows: group S *vs* X $P=0.000$*, group S *vs* E $P=0.649$, group X *vs* E $P=0.000$*. By the 8th day, the

Table 1 Change of the parameters 3 days after injection $\bar{x}\pm s$

Indexes	Saline	XZL	Ethanol	F	*P*
Tumor volume (mm^3)	48.02±14.01	26.00±5.41	20.30±12.66	8.356	0.005
Tumor necrosis (mm^3)	1.40±0.55	3.20±0.84	3.20±0.10	7.364	0.008
Albumin (g/L)	34.02±2.98	47.10±18.31	32.88±4.92	2.540	0.120
ALT (U/L)	96.80±28.45	75.60±17.87	150.60±43.05	7.520	0.008
AST (U/L)	305.00±117.72	209.00±47.89	404.00±45.50	7.778	0.007
ALP (U/L)	373.80±78.02	184.40±25.39	422.60±52.18	25.119	0.000
Creatinine (μmol/L)	34.60±1.95	38.60±1.82	39.80±4.38	4.228	0.041
PCNA	62.80±12.62	40.60±7.89	56.00±12.06	5.288	0.023

Table 2 Change of the parameters 8 days after injection $\bar{x}\pm s$

Indexes	Saline	XZL	Ethanol	F	*P*
Tumor Volume (mm^3)	464.62±212.00	174.38±109.46	147.58±60.17	7.658	0.007
Tumor Necrosis(mm^3)	1.60±0.89	3.8±0.45	3.6±0.89	12.333	0.001
Albumin (g/L)	33.68±5.66	36.88±5.78	30.01±2.67	2.447	0.128
ALT (U/L)	104.00±43.39	68.80±13.81	118.60±42.72	2.522	0.122
AST (U/L)	341.00±84.63	233.14±52.28	328.20±64.27	3.714	0.056
ALP (U/L)	237.40±80.63	250.80±75.24	474.0±148.15	7.767	0.007
Creatinine (μmol/L)	38.40±6.02	37.80±6.38	36.60±4.0	0.135	0.875
PCNA	56.20±8.67	41.40±10.00	58.80±12.10	4.063	0.045

differences between every two groups were as follows: group S *vs* X, *P*=0.846, group S *vs* E, *P*=0.004*, group X *vs* E, *P*=0.006*.

Serum creatinine After 3 days the level of serum creatinine in group E was higher than that in group S. There was statistical significance among three groups ($P<0.05$). After 8 days there was no statistical difference among three groups ($P>0.05$). By the 3rd day, the differences between every two groups were as follows: group S *vs* X *P*=0.054, group S *vs* E *P*=0.017*, group X *vs* E *P*=0.543.

PCNA expression in tumor tissue (Table 1 and 2)

After 3 and 8 days fine positive expression existed in the remnant tumor tissue in every group. PCNA labeling index among 3 groups was statistically different ($P<0.05$). PCNA labeling index in group X was lower than that in groups S and E, but there was no statistical significance between groups S and E ($P>0.05$). By the 3rd day, the differences between every two groups were as follows: group S *vs* X *P*=0.008*, group S *vs* E *P*=0.350, group X *vs* E *P*=0.048*. By the 8th day, the differences between every two groups were as follows: group S *vs* X *P*=0.044*, group S *vs* E *P*=0.700, group X *vs* E *P*=0.021*.

DISCUSSION

Primary liver carcinoma is one of the most popular malignancies in China, and its incidence has been increasing in recent years. The reported mortality of primary liver carcinoma in China is higher than that of other malignant tumors. Because of difficulty in early diagnosis, 75 % of the clinically diagnosed are large ones when the patients lose the opportunity of operation. Non-operation therapy becomes more and more important, and many basic researches have been done[12,13]. In some experiments, massive proliferation of donor-derived normal hepatocytes was observed in the liver of rats previously given retrorsine (RS). Suicide gene therapy based on ganciclovir (GCV) metabolism by transgene herpes simplex thymidine kinase (HSV-1 TK) has been used to selectively kill proliferating cells in hepatic tumor. Effect of Avemar and Avemar + vitamin C on hepatic tumor growth was observed in experimental animals. Through various experiments, some encouraging results have been reported[14,15]. In the nude mice hepatoma model, the antitumor effects of pDR2-TK/GCV system on tumor growth were evaluated. Through MTT method, they found that the pDR2-TK/GCV had cytotoxic effect and about 70 % SMMC-7721 cells were killed when GCV was at 1 000 umol/L. *In vivo* experiment showed that the tumor size in nude mice with transferred pDR2-TK gene was significantly smaller than that in control group. PEIT was used clinically, because this method of intra-tumor injection was easy, cheap and could be used repeatedly, it has been widely used. But both of these methods cannot treat the patients thoroughly. Repeated use can cause liver function failure and biliary tract injury. Therefore researches on drugs which can be used in intra-tumor injection therapy become more and more important. Some kinds of traditional Chinese drugs were purified and the immunosuppressive function was examined[16].

XZL is mainly composed of Wu-Bei-Zi extracts and alum, both of which have the function of astringing, antidiarrheal, hemostasis and antisepsis. The vascular vessels would astringe immediately after injection of XZL. Then inflammatory reaction and hyperplasia would occur in the local artery. Endoangiitis and intravascular coagulation would occur in arteries and veins. All the above finally lead to fibrinoid necrosis of local tissue. These changes perhaps are the reason why XZL has antineoplasitc activity.

From this research we conclude that the therapeutic effects of intra-tumor injection of XZL on implanted hepatoma is obvious. XZL can evidently inhibit the growth of tumor. The inhibition of XZL on implanted hepatoma is no better than that of PEIT according to statistical analyses. But in terms of MDDT, XZL is much better than PEIT, perhaps because the toxicity of XZL on liver function is markedly lower than that of ethanol.

Based on the results of liver and renal function, the toxicity of XZL on liver function is relatively less severe than that of ethanol. For patients with disorder of liver function, PEIT could not be used, we can try XZL instead. The dose of ethanol is very important in treatment, high-dose of ethanol can lead to liver function failure and systemic toxicity to the patient, but low-dose can not kill the edge cells of the tumor thoroughly. Many experiments have shown that high-dose therapy of common drugs can lead to hepatic function failure, but if low-dose of drug is given, tumor cells cannot be killed thoroughly, because the tumor cells are supplied by duplicated vessels (liver artery and portal vein) and grow rapidly than before[17]. The patients' prognosis could be influenced and the tumor perhaps would recur and metastasize quickly. So we could use XZL to resolve this problem. We can inject XZL into the edge of the tumor to kill the tumor cells, thus to improve the therapeutic effectiveness, reduce recurrence and metastases of the tumor. This study revealed that 3 and 8 days after injection of drug (saline, XZL and ethanol), fine positive expression of PCNA occurred in the remnant tumor tissue of every group. PCNA labeling index among 3 groups was significantly different. PCNA labeling index in Group X was lower than that in groups S and E ($P<0.05$), but there was no statistical significance between groups S and E ($P>0.05$). This result implies although injection of ethanol can lead to necrosis of tumor tissue, it cannot influence proliferation activity of the remnant tumor tissues. Intra-tumor injection of XZL into implanted hepatoma can reduce the expression of PCNA labeling index, suggesting XZL can inhibit the proliferation activity of tumor cells. This might be the reason why XZL has the antineoplasitc activity.

REFERENCES

1 **Thiery JP**, Blazsek I, Legras S, Marion S, Reynes M, Anjo A, Adam R, Misset JL. Hepatocellular carcinoma cell lines from diethylnitrosamine phenobarbital-treated rats. Characterization and sensitivity to endothall, a protein serine/threonine phosphatase-2A inhibitor. *Hepatology* 1999; **29**: 1406-1417

2 **Donner C**, Choi S, Komaromy M, Cooper AD. Accelerated lipoprotein uptake by transplantable hepatomas that express hepatic lipase. *J Lipid Res* 1998; **39**: 1805-1815

3 **Gaunitz F**, Heise K, Schumann R, Gebhardt R. Glucocorticoid induced expression of glutamine synthetase in hepatoma cells. *Biochem Biophys Res Commun* 2002; **296**: 1026-1032

4 **Schotman SN**, Schraa EO, Marquet RL, Zondervan PE, Ijzermans JN. Hepatocellular carcinoma and liver transplantation: an animal model. *Transpl Int* 1998; **11**(Suppl 1): S201-S205

5 **Saito N,** Mitsuhashi M, Hayashi T, Narumo C, Nagata H, Soyama K, Kameoka S, Harumiya S, Fujimoto D. Inhibition of hepatic metastasis in mice treated with cell-binding domain of human fibronectin and angiogenesis inhibitor TNP-470. *Int J Clin Oncol* 2001; **6**: 215-220

6 **Ostashkina NM,** Dubovaya TK, Koblyakov VA, Konovalova GG, Lankin VZ. Activity of detoxication enzymes in rat hepatoma 27 transplanted in different organs. *Bull Exp Biol Med* 2000; **130**: 1109-1112

7 **Wen L,** Grude P, Conti F, Honiger J, Capeau J, Nordlinger B, Weill B, Calmus Y. Suppression of humoral immunization against encapsulated xenogeneic hepatocytes and prolongation of their function by 2-week cyclosporine treatment in the rat. *Surgery* 2000; **127**: 301-308

8 **Li M,** Li H, Xiao L, Jiang Z, Li H, Mu J. Antitumor activity of the lysates prepared from anti-CD3 antibody activated killer cells. *Huaxi Yike Daxue Xuebao* 2000; **31**: 49-51

9 **Sawada S,** Murakami K, Yamaura T, Mitani N, Tsukada K,

Saiki I. Therapeutic and analysis model of intrahepatic metastasis reflects clinical behavior of hepatocellular carcinoma. *Jpn J Cancer Res* 2002; **93**: 190-197

10 **Gong Y,** Han C, Chen J. Effect of tea polyphenols and tea pigments on the inhibition of precancerous liver lesions in rats. *Nutr Cancer* 2000; **38**: 81-86

11 **Lin SB,** Wu LC, Huang SL, Hsu HL, Hsieh SH, Chi CW, Au LC. *In vitro* and *in vivo* suppression of growth of rat liver epithelial tumor cells by antisense oligonucleotide against protein kinase C-alpha. *J Hepatol* 2000; **33**: 601-608

12 **Laconi S**, Pani P, Pillai S, Pasciu D, Sarma DS, Laconi E. A growth-constrained environment drives tumor progression *in vivo*. *Proc Natl Acad Sci U S A* 2001; **98**: 7806-7811

13 **Hidvegi M**, Raso E, Tomoskozi-Farkas R, Paku S, Lapis K, Szende B. Effect of Avemar and Avemar + vitamin C on tumor growth and metastasis in experimental animals. *Anticancer Res* 1998; **18**: 2353-2358

14 **Ding Q**, Wu Z, Chen X, Musa AH, Hu J, Zhan Y. Gene therapy of HSV-TK transferred by the EBV based expression vector on experimental hepatocellular carcinoma. *J Tongji Med Univ* 2001; **21**: 122-125

15 **Wu W**, Deng R, Ou Y. Therapeutic efficacy of microsphere-entrapped curcuma aromatica oil infused via hepatic artery against transplanted hepatoma in rats. *Zhonghua Ganzangbing Zazhi* 2000; **8**: 24-26

16 **Wang J**, Xu R, Jin R, Chen Z, Fidler JM. Immunosuppressive activity of the Chinese medicinal plant Tripterygium wilfordii. II. Prolongation of hamster-to-rat cardiac xenograft survival by combination therapy with the PG27 extract and cyclosporine. *Transplantation* 2000; **70**: 456-464

17 **Bralet MP**, Pichard V, Ferry N. Demonstration of direct lineage between hepatocytes and hepatocellular carcinoma in diethylnitrosamine-treated rats. *Hepatology* 2002 ; **36**: 623-630

Edited by Zhu LH and Wang XL

P.O.Box 2345, Beijing 100023,China
Fax: +86-10-85381893
E-mail: wjg@wjgnet.com www.wjgnet.com

World J Gastroenterol 2003;9(9):2125-2127
World Journal of Gastroenterology
 ISSN 1007-9327

• BRIEF REPORTS •

Modifications in combined liver-small bowel transplantation in pigs

Feng Jiang, Zhen-Yu Yin, Xiao-Dong Ni, You-Sheng Li, Ning Li, Jie-Shou Li

Feng Jiang, Zhen-Yu Yin, Xiao-Dong Ni, Medical School of Nanjing University, Nanjing 210093, Jiangsu Province, China
You-Sheng Li, Ning Li, Jie-Shou Li, Research Institute of General Surgery, General Hospital of PLA, Nanjing Military Command, Nanjing 210002, Jiangsu Province, China
Supported by the Military Medical Research Found of China, No. 96M022, and by the Major Project of Nanjing Military Command, No.02Z001
Correspondence to: Dr. Ning Li, Research Institute of General Surgery, General Hospital of PLA, Nanjing Military Command, Nanjing 210002, Jiangsu Province, China. jiangfeng174@sohu.com
Telephone: +86-25-4824804 **Fax:** +86-25-4803956
Received: 2002-12-28 **Accepted:** 2003-02-11

Abstract

AIM: To introduce combined liver-small bowel transplantation in pigs.

METHODS: Eighteen transplantations in 36 large white pigs were performed. Three modifications in combined liver-small bowel transplantation model were applied: Veno-venous bypass was not used. Preservation of the donor duodenum and head of pancreas in continuity with the combined graft to avoid biliary reconstruction. The splenic vein of donor was anastomosed end-to-end with the portal vein of recipients by the formation of a "cuff".

RESULTS: Without immunosuppressive therapy, 72-hour survival rate of the transplanted animals was 72 % (13/18). Five of 18 pigs operated died of respiratory failure (3 cases) and bleeding during hepatectomy (2 cases). The longest survival time of animals was 6 days.

CONCLUSION: Our surgical modifications are feasible and reliable, which have made the transplantation in pigs simpler and less aggressive, and thus these can be used for preclinical study.

Jiang F, Yin ZY, Ni XD, Li YS, Li N, Li JS. Modifications in combined liver-small bowel transplantation in pigs. *World J Gastroenterol* 2003; 9(9): 2125-2127
http://www.wjgnet.com/1007-9327/9/2125.asp

INTRODUCTION

Despite intestinal transplantation technique for the treatment of irreversible failure of the intestine has been improved, clinical intestinal transplantation still remains at an experimental stage. Compared with other solid organ transplantations, attempts at human small bowel transplantation had disappointed results in terms of survival of patients and grafts[1-4]. Bowel transplant can also be performed as a part of a multivisceral graft[5]. Even though total parenteral nutrition (TPN) and home parenteral nutrition (HPN) allow many patients with intestinal failure to live with a high life quality, it has some severe and even fatal complications, such as catheter sepsis, severe cholestasis, and chronic secondary hepatopathy[6-8]. Many institutions have performed combined liver-small bowel transplantations in human and small animals, but few studies were conducted in large animals[9]. Pigs are one of the standard models for large animal transplantation due to the anatomic features. In order to improve clinical prognosis of liver-small bowel transplantation (LSBT), we investigated the modifications of the experimental model.

MATERIALS AND METHODS

Large white pigs weighing 25±5 kg were used for LSBT under general anesthesia[10]. Animals were fasted with free access to water for 24 hours prior to surgery. The size of donor pigs was the same as or smaller than that of recipients.

Donor operation

After vascular cannulation for venous and hemodynamic monitoring, the abdomen was entered at middle line xipho-pubic incision. After transection of transverse colon, the whole intestine tract was inspected thoroughly. Total colon including the ileocecal valve was transectioned. Hepato-gastric and spleno-gastric ligaments including splenic and left gastric arteries were ligated. The splenic vein was prepared for perfusion, and the ligaments around the liver were mobilized. Then the abdominal aorta was dissected from infrarenal aorta until one centimeter cranially to celiac axis. Lymphatic vessels were tied carefully to avoid lymphorrea after transplantation. And the vena cava was also dissected from infrarenal until suprahepatic cava. Before systemic heparinization, blood was drawn and saved for use in recipient operations. Before clamping the cranial aorta upper the celiac axis, the distal aorta was cannulated and 1.5 liter of UW solution was perfused through the infrarenal aorta and splenic venous *in situ* and venting from the supra diaphragm vena cava and infrarenal vena cava. To ameliorate cooling of the graft, the abdominal cavity was filled with cold saline and melting ice. Then the liver-small bowel was *en bloc* harvested in continuity with duodenum and pancreas.

Bench surgery

The *en block* liver-small bowel was preserved in cold UW solution with melting ice. The proximal aorta and the thoracic vena cava were ligated. The vascular pedicles for vascular anastomoses were prepared. Diaphragm veins were ligated and a continuous hemostatic suture was performed. The subtotal pancreas was transected, leaving the head and uncinate processing attached to the duodenum. The stump of the pancreas was stapled and then over-sewn with a continuous suture using 0/4 polypropylene.

Recipient operation

During the recipient operation, the end-tidal carbon dioxide, electrocardiogram and arterial, central vein, and pulmonary artery pressure were monitored.

The abdomen was accessed at a middle line xipho-pubic incision. Firstly a cystostomy was performed using a Foley's

catheter. The small bowel was resectioned except for short segments of proximal jejunum and distal ileum. The recipient' s infrarenal aorta and the vena cava were dissected and encircled for anastomosis. The hepatic hilum was transected with the portal vein preserved. Then hepatectomy was performed with preservation of hepatic part encircling the vena cava. In this period, transfusion was necessary. Three vascular anastomoses between the recipient and the donor were performed as followings: The recipient' s infrarenal vena cava side-to-end anastomosis with donor' s infrahepatic vena cava with continuous 4/0 polypropylene suture, the recipient' s infrarenal aorta side-to-end anastomosis with the donor' s infrarenal aorta with continuous 4/0 polypropylene suture, and the recipient' s distal portal vein end-to-end anastomosis with donor' s splenic vein by the formation of a "cuff". The gut continuity was established proximally between allograft jejunum and native jejunum and distally between allograft ileum and native ileum. A loop enterostomy was performed for endoscopies after transplantation. At last, a gastrostomy was performed to reduce the gastric pressure.

RESULTS

Mean operation time in the donor and recipient was 3.5 hours±10 minutes and 4.5 hours±15 minutes, respectively. During the recipient operation, there was no obvious hemodynamic alteration. Survival rate at 72 hours was 72 % (13/18). Three pigs died of respiratory failure and two of bleeding during hepatectomy. The longest survival time was 6 days without immunosuppression.

DISCUSSION

Multivisceral transplantation was firstly performed for the treatment of short bowel syndrome complicated with liver failure due to long-term hyperalimentation[11]. Starzl reported the first study in dogs in 1960s. Investigations with large animals have shown that multivisceral transplantation is a technically complicated procedure with high mortality[12]. We have been studying on improving surgical techniques of the transplantation for more than 6 months and performed 18 consecutive operations with three innovations.

Firstly, veno-venous bypass, necessary in the conventional experiments[9], was avoided, and thus made the operation simple and less aggressive. It also reduced the incidence of bleeding due to heparinization in operation. Considering the anatomic features of pigs, bleeding in hepatectomy in recipients is unavoidable. But based on our experiences in many preliminary operations, we could control this operative bleeding with the new techniques. In order to keep the recipient hemodynamicaly stable during this period, transfusion and solution were necessary. With this modification the duration of unhepatic period was also shortened.

Secondly, preservation of the donor duodenum and head of pancreas in continuity with the combined graft avoided the need for biliary reconstruction. The standard technique involved an obligatory reconstruction of the biliary system with a defunctionalized loop of proximal allograft jejunum[13]. Consequent limitations of this technique were biliary leaks, obstructions and strictions[14]. In our surgical technique, we eliminated hilar dissection, leaving the hepatoduodenal ligament undisturbed by including the intact duodenum and a rim of pancreatic tissue in the allograft. Apart from obviating biliary anastomotic complications and potential vascular torsion of the small bowel graft[14, 15], surgical modifications also made bench surgery simpler. This modification was applied in human transplantation with satisfaction[14,15]. Debera *et al*[15] reported that the remaining head of the pancreas on the combined liver-small bowel allograft was not associated with a high incidence of pancreatic complications.

The third modification was that the donor splenic vein was end-to-end anastomosed to the recipient' s distal portal vein by the formation of a "cuff". In the standard technique, the recipient' s portal vein was end-to-side anastomosed with the donor portal vein or supra mesenteric vein to avoid portal hypertension in native remnant viscera[9,15,16]. This innovation shortened the operation time, simplified the surgical procedure and also reduced venous stagnation of the allograft and native viscera.

Our technical refinements have made combined liver-small bowel transplantation in pigs simpler and less aggressive. And the technique of this model is feasible and can be used for preclinical study. However, animals experienced with this operation were faced with life threatening respiratory failure, infection, GVHD and rejection[17-27]. Much more work should be done to improve the outcomes of both experimental and clinical combined liver-small bowel transplantations.

REFERENCES

1 **Bramhall SR**, Minford E, Gunson B, Buckels JA. Liver transplantation in the UK. *World J Gastroenterol* 2001; **7**: 602-611
2 **Zhu XF**, Chen GH, He XS, Lu MQ, Wang GD, Cai CJ, Yang Y, Huang JF. Liver transplantation and artificial liver support in fulminant hepatic failure. *World J Gastroenterol* 2001; **7**: 566-568
3 **Grant D**. Intestinal transplantation: 1997 report of the international registry. Intestinal Transplant Registry. *Transplantation* 1999; **67**: 1061-1064
4 **Dionigi P**, Alessiani M, Ferrazi A. Irreversible intestinal failure, nutrition support, and small bowel transplantation. *Nutrition* 2001; **17**: 747-750
5 **Rossi G**, Gatti S, Reggiani P, Galmarini D, Privitera G, Velio P, Melada E, Romito R, Latham L, Vannelli A, Langer M, Codazzi D, Prato P, Fassati LR. Small bowel transplantation under oral immunosuppression: Experimental study in the pig. *Transplant Proc* 1997; **29**: 1816-1818
6 **Schraut WH**. Current status of small-bowel transplantation. *Gastroenterology* 1988; **94**: 525-538
7 **Pritchard TJ**, Kirkman RL. Small bowel transplantation. *World J Surg* 1985; **9**: 860-867
8 **Beath SV**, Needham SJ, Kelly DA, Booth IW, Raafat F, Buick RG, Buckels JA, Mayer AD. Clinical features and prognosis of children assessed for isolated small bowel or combined small bowel and liver transplantation. *J Pediatr Surg* 1997; **32**: 459-461
9 **Gatti S**, Rossi G, Albani AP, Reggiani P, Caccamo L, Gridelli B, Lucianetti A, Paone G, Campanati L, Melada E, Galmarini M, Orsenigo R, Armiraglio E, Andreoni P, Di Mauro P, Reali Forster C, Proietti D, Pifferi S, Doglia M, Fassati LR, Galmarini D. Orthotopic liver-small bowel allotransplantation-surgical technique in the pig. *Transplant Proc* 1994; **26**: 1627-1628
10 **Pirenne J**, Gruessner AC, Benedetti E, Troppmann C, Nakhleh RE, Uckun FM, Gruessner RW. Donor-specific unmodified bone marrow transfusion does not facilitate intestinal engraftment after bowel transplantation in a porcine model. *Surgery* 1997; **121**: 79-88
11 **Zhu Y**, Furukawa H, Nakamura K, Starzl TE, Todo S. Multivisceral allotransplantation in pigs. *Transplant Proc* 1996; **28**: 2725
12 **Mitsuoka S**, Tanaka N, Orita K. Comparison of patterns of rejection in multivisceral transplantation and abdominal organ cluster transplantation in pigs. *Transplant Proc* 1994; **26**: 2450-2454
13 **Grant D**, Wall W, Mimeault R, Zhong R, Ghent C, Garcia B, Stiller C, Duff J. Successful small-bowel/liver transplantation. *Lancet* 1990; **335**: 181-184
14 **Bueno J**, Abu-Elmagd K, Mazariegos G, Madariaga J, Fung J, Reyes J. Composite liver-small bowel allografts with preservation of donor duodenum and hepatic biliary system in children. *J Pediatr Surg* 2000; **35**: 291-296
15 **Sudan DL**, Iyer KR, Deroover A, Chinnakotla S, Fox IJ Jr, Shaw

BW Jr, Langnas AN. A new technique for combined liver/small intestinal transplantation. *Transplantation* 2001; **72**: 1846-1848

16 **Todo S**, Tzakis AG, Abu-Elmagd K, Reyes J, Fung JJ, Casavilla A, Nakamura K, Yagihashi A, Jain A, Murase N, Iwaki Y, Demetris AJ, Thiel DV, Starzl TE. Cadaveric small bowel and small bowel-liver transplantation in humans. *Transplantation* 1992; **53**: 369-376

17 **Gruessner RW**, Nakhleh RE, Harmon JV, Dunning M, Gruessner AC. Donor-specific portal blood transfusion in intestinal transplantation a prospective, preclincal large animal study. *Transplantation* 1998; **66**: 164-169

18 **Perego C**, Marelli O, Rossi G, Gatti S, Reggiani P, Orsenigo R, Galmarini D, Franco P. Orthotopic liver-small bowel transplantation in pigs: study of immunologic parameters during therapy with FK 506-based immunosuppressive regimens. *Transplant Proc* 1996; **28**: 2471-2473

19 **Abu-Elmagd K**, Todo S, Tzakis A, Furukawa H, Nour B, Reyes J, Nakamura K, Scotti-Foglieni C, El-Hammadi H, Kadry Z, Fung J, Demetris J, Starzl TE. Rejection of human intestinal allografts: alone or in combination with the liver. *Transplant Proc* 1994; **26**:1430-1431

20 **Cicalese L**, Sileri P, Asolati M, Rastellini C, Abcarian H, Benedetti E. Infectious complications of following living-related small bowel transplantation in adults. *Transplant Proc* 2001; **33**: 1554-1555

21 **Li YX**, Li JS, Li N. Improved technique of vascular anastomosis for small intestinal transplantation in rats. *World J Gastroenterol* 2000; **6**: 259-262

22 **Farmer DG**, Mc Diarmid SV, Smith C, Stribling R, Seu P, Ament MA, Vargas J, Yersiz H, Markmann JF, Ghobriel RM, Goss JA, Martin P, Busuttil RW. Experience with combined liver-small intestine transplantation at the vniversity of California, Los Angeles. *Transplant Proc* 1998; **30**: 2533-2534

23 **Goulet O**. Intestinal failure in children. *Transplant Proc* 1998; **30**: 2523-2525

24 **Cicalese L**, Sileri P, Green M, Abu-Elmagd K, Kocoshis S, Reyes J. Bacterial translocation in clinical intestinal transplantation. *Transplantation* 2001; **71**: 1414-1417

25 **Li YS**, Li JS, Li N, Jiang ZW, Zhao YZ, Li NY, Liu FN. Evaluation of various solutions for small bowel graft preservation. *World J Gastroenterol* 1998; **4**: 140-143

26 **Todo S**, Tzakis AG, Abu-Elmagd K, Reyes J, Nakamura K, Casavilla A, Selby R, Nour BM, Wright H, Fung JJ, Demetris AJ, Van-Thiel DH, Trarzl TE. Intestinal transplantation in composite visceral grafts or alone. *Ann Surg* 1992; **216**: 223-233

27 **Khan FA**, Kato T, Pinna AD, Berho M, Nery JR, Colombani P, Tzakis AG. Graft failure in two multivisceral transplant recipients secondary to necrotizing enterocolitis. *Transplant Proc* 2000; **32**: 1204-1205

Edited by Ren SY and Wang XL

P.O.Box 2345, Beijing 100023,China
Fax: +86-10-85381893
E-mail: wjg@wjgnet.com www.wjgnet.com

World J Gastroenterol 2003;9(9):2128-2131
World Journal of Gastroenterology
 ISSN 1007-9327

• BRIEF REPORTS •

Characterization of M2 antibodies in asymptomatic Chinese population

Xiao-Hua Jiang, Ren-Qian Zhong, Xiao-Yun Fan, Yin Hu, Feng An, Jian-Wen Sun, Xian-Tao Kong

Xiao-Hua Jiang, Jian-Wen Sun, Department of Laboratory Medicine, 85 Hospital of Chinese PLA, Shanghai 200052, China
Ren-Qian Zhong, Xian-Tao Kong, Clinical Immunology Center of PLA, Changzheng Hospital, Second Military Medical University, Shanghai 200003, China
Xiao-Yun Fan, Center of Liver Research, Nanjing Military Command, Shanghai 200052, China
Yin Hu, Shanghai University of Engineering Science, Shanghai 200335, China
Feng An, Department of Pathology, Zhongshan Medical University, Guangzhou 510080, Guangdong Province, China
Correspondence to: Dr. Xiao-Hua Jiang, Department of Laboratory Medicine, 85 Hospital of Chinese PLA, Huashan Road, Shanghai 200052, China. jhlulu@citiz.net
Telephone: +86-21-62528805 **Fax:** +86-21-33110236
Received: 2003-03-04 **Accepted:** 2003-04-05

Abstract

AIM: To investigate the presence of M2 antibodies specific for primary biliary cirrhosis (PBC) in asymptomatic Chinese and identify patients with early PBC.

METHODS: Enzyme-linked immunosorbent assay (ELISA) tests for M2 antibodies to recombinant protein were performed in 5 011 subjects (age range, 26-85 years; mean age: 45.81±15.02 years) who took an annual physical examination. M2-positive subjects were further analyzed for immunoglobulin (Ig) classes and subclasses of M2 antibodies. Clinical, biochemical and immunological data were obtained for M2-positive subjects. In addition, ultrasonography (US) or endoscopic retrograde cholangio-pancreatography (ERCP) was performed to exclude any disorders other than PBC.

RESULTS: M2 antibodies were detected in 8 (0.16 %) of the 5 011 subjects studied. Of the 8 subjects, 7 were female and 1 was male (age range: 40-74 years). An unexplained increase of serum alkaline phosphatase (ALP) and gamma glutamyl transpeptidase (γ-GT) values, often to striking levels, was detected in 4 M2-positive subjects, 3 of them accorded with the diagnostic criteria recommended by the American Association for the Study of Liver Diseases, even though they had no symptoms of PBC (such as fatigue, pruritus or jaundice). Liver biopsy was performed in two M2-positive subjects and the histology was compatible with PBC in both cases.

CONCLUSION: Our data, while not assessing the true prevalence of asymptomatic PBC in the general population, suggest that asymptomatic PBC is much more common in China than has been supposed.

Jiang XH, Zhong RQ, Fan XY, Hu Y, An F, Sun JW, Kong XT. Characterization of M2 antibodies in asymptomatic Chinese population. *World J Gastroenterol* 2003; 9(9): 2128-2131
http://www.wjgnet.com/1007-9327/9/2128.asp

INTRODUCTION

Primary biliary cirrhosis (PBC) is a chronic progressive cholestatic liver disease with autoimmune basis. Patients are typically females aged 35-65[1, 2]. Many patients with PBC have no specific symptoms, rather, they have unexplained liver function abnormalities. Progression occurs over years or decades. The end stage is an established biliary cirrhosis[1].

A hallmark feature of PBC is the presence of high titer antimitochondrial antibodies (AMA) in patients sera. AMA are divided into nine subgroups termed M1-M9 according to the autoantigens they recognize. It has been established that only those antibodies known as M2 are specific for PBC. M2 antibodies are detectable years or decades before the presence of clinical and histological features of PBC[3-7].

The major autoantigens recognized by M2 antibodies are members of the 2-oxo-acid dehydrogenase complex, including pyruvate dehydrogenase complex E2 (PDC-E2), branched chain 2-oxo-acid dehydrogenase complex E2 (BCOADC-E2) and 2-oxo-glutarate dehydrogenase complex E2 (OGDC-E2). The immunodominant epitopes of PDC-E2, BCOADC-E2 and OGDC-E2 have been mapped within the lipoyl domains. Antibodies to these corresponding autoantigens have been reported to appear in PBC patients with a positive rate of 95 %, 53-55 % and 39-88 % respectively[8-10]. Using the above three immunodominant lipoyl domains, 92-100 % of patients with PBC can be verified[9-12]. In contrast, there is no report that M2 are found in diseases other than PBC[13-18]. We have designed a triple hybrid clone, designated as BPO, that coexpresses the three immunodominant lipoyl domains of PDC-E2, BCOADC-E2 and OGDC-E2 from human sources. We established and then used clinically specific immunological methods with purified BPO to detect the M2 antibodies[19,20].

According to some research, there is a wide spread impression that the number of patients with PBC is on the rise, many of whom, thanks to the application of the immunological diagnostic methods, are diagnosed at a stage of asymptomatic PBC in recent years[21-23]. However, the M2-positive rate in Chinese general population has not yet been determined. In the present research, we investigated the prevalence of M2 antibodies which are specific for PBC in asymptomatic Chinese population and identified patients with early diseases.

MATERIALS AND METHODS

Establishment of the immunological method

Recombinant fusion protein fragments of human BCOADC-E2, PDC-E2, OGDC-E2 and the triple-expression hybrid clone (BPO) were expressed in *Escherichia coli*, and then purified with Ni-NTA affinity chromatography under denaturing conditions. Enzyme-linked immunosorbent assay (ELISA) method for detecting M2 antibodies was established using purified recombinant proteins. The cut-off O.D. value for positive ELISA was defined as 0.303[19,20].

Subjects

Sera were collected from subjects aged over 26 years who took an annual physical examination in 85 Hospital the Chinese PLA in Shanghai, China from January 1, 2000 to August 30, 2001. A total of 5 011 adults including 3 108 females and 1 903 males,

aged between 26-85, with a median age of 45.81±15.02 years were enrolled in this investigation. ELISA method was used for screening M2 antibodies. M2-positive sera were verified using the kit provided by the Euroimmun Research Center (Germany) which used purified porcine heart mitochondrial protein as antigen. Clinical, biochemical and immunological data were obtained for M2-positive persons. In addition, ultrasonography (US) or endoscopic retrograde cholangiopancreatography (ERCP) was performed to exclude any disorders other than PBC.

In 2000, the American Association for the Study of Liver Diseases (AASLD) recommended a guideline to aid the practicing physicians in diagnosing PBC: the diagnosis of PBC can be made with confidence in a patient with high-titer AMA (>1:40) and elevation of serum ALP and γ-GT in the absence of an alternative explanation (normal bile ducts on ultrasound)[24].

RESULTS

Immunology

Of the 5 011 subjects tested, 8 (0.16 %) had detectable titers of M2 antibodies using the ELISA containing the purified BPO. The reactivities were confirmed using the Euroimmun' s kit. Of the 8 M2-positive subjects, 7 were females and 1 was male (age range: 40-75 years). 6 M2-positive subjects were also AMA positive tested by indirect immunofluorescence (IIF) at a titer of >1:100. Antinuclear autoantibodies (ANA) were present in subjects 2, 5 and 8. Anti-smooth-muscle antibodies (SMA) were found in subject 5. Elevated IgM was found in 5 of 8, 4 had elevated IgG, and 2 had elevated IgA (Table 1). Of the 8 reactive sera, 2 recognized PDC-E2, 2 recognized BCOADC-E2, 2 recognized both PDC-E2 and BCOADC-E2, and 2 recognized BCOADC-E2 and OGDC-E2. Each positive serum was analyzed for the identification of the reactive classes and subclasses of Ig: 2/8 had detectable IgM antibodies against BCOADC-E2 and 3/8 against PDC-E2, 2/8 contained IgA antibodies to BCOADC-E2 and 1/8 against PDC-E2, 4/8 contained IgG antibodies to BCOADC-E2, 3/8 against PDC-E2 and 2/8 against OGDC-E2. The active IgG subclass of M2 antibodies were mostly in the IgG1 and IgG2 subclasses (Table 2).

Table 2 Class and subclass of reactive M2 antibodies

BCOADC-E2	PDC-E2	OGDC-E2
IgM 2/8[a]	3/8	0/8
IgA 2/8	1/8	0/8
IgG13/8	0/8	2/8
IgG21/8	2/8	0/8
IgG30/8	1/8	0/8
IgG40/8	0/8	0/8

[a]Positive samples/total samples.

Biochemistry

An unexplained increase of serum ALP and γ-GT values, often to striking levels, was detected in 4 subjects (subjects 4, 5, 6, 8). These subjects were previously unaware of the rise in serum ALP and γ-GT. The types of clinical conditions of these subjects (such as cardiac, respiratory diseases) did not explain their high serum ALP and γ-GT levels. Other aetiological studies for viral hepatitis, haemochromatosis, α_1 antitrypsin deficiency and Wilson' s disease were also excluded. Subjects 4, 5 and 6 accorded with the AASLD' s guideline, even though they had no symptoms of PBC (such as fatigue, pruritus or jaundice).

Histology

With written consent, a percutaneous liver biopsy was obtained in two patients (Patients 5 and 6). Biopsies were routinely examined by two different pathologists. Both biopsies showed the presence of lymphoid aggregates within the portal areas and were thought to be consistent with the diagnosis of PBC.

Table 1 Clinical and laboratory data of M2-positive subjects

	M2-positive subjects No.							
	1	2	3	4	5	6	7	8
Age (y)	52	42	40	62	47	67	53	74
Sex	F	F	F	F	F	F	F	M
Laboratory parameters								
AMA titer	1:160	1:640	Negative	1:1 000	1:640	1:100	1:640	Negative
M2 (O.D.)	0.544	0.578	0.583	0.602	0.655	0.673	0.987	2.157
M2 reactivity	P	B,P	B	B	B,O	B,O	P	B,P,
Other autoantibodies	Negative	ANA	Negative	Negative	ANA,SMA	Negative	Negative	ANA
IgG (g/l)	12.12	13.73	22.95	10.57	19.30	11.65	16.35	15.66
IgM (g/l)	2.37	4.32	4.17	4.78	3.98	2.80	2.73	9.52
IgA (g/l)	3.5	1.7	3.3	2.6	3.7	14.2	1.4	9.3
ALP (U/l)	86	110	81	465	302	125	97	796
γ-GT (U/l)	43	48	20	237	211	150	42	494
T-Bil (umol/l)	12	8	13	25	8	15	14	62
ALT (U/l)	24	36	24	55	56	61	33	65
AST (U/l)	28	35	30	22	42	35	37	47
Ultrasonography	Normal	Normal	Normal	Normal	Normal	Normal	Normal	Normal
ERCP	ND	ND	ND	ND	Normal	Normal	ND	Normal
Liver histology	ND	ND	ND	ND	Compatible	Compatible	ND	ND
Accorded with the AASLD's guideline	No	No	No	Yes	Yes	Yes	No	No

Upper limits of normal for IgG<15.5 g/L, IgM<2.8 g/L, IgA<4.0 g/L, ALP<112 U/L, γ-GT <54 U/L, T-Bil<21 umol/L, ALT<40 U/L, AST<40 U/L; T-Bil: total serum cholesterol; ND: not done.

Clinical data

Of these 8 subjects, three were considered to be healthy (Subjects 1, 4 and 5), subject 2 had thyroid disease, subject 3 had rheumatoid arthritis who had taken rifampicin for one year, subject 6 had hypertension and non-insulin-dependent diabetes, subject 7 had pain and effusion in her knees and ankles, and subject 9 had lung cancer. None of the 8 M2-positive persons had symptoms of liver diseases.

DISCUSSION

In this study, we took advantage of the recombinant protein: BPO to investigate the prevalence of M2 antibodies in asymptomatic Chinese population and identified patients with early diseases. We revealed 8 M2-positive cases in 5 011 subjects who took an annual physical examination. All these 8 M2-positive persons had no symptoms attributed to liver diseases. Three (Subjects 4, 5 and 6) of the 8 fulfilled the AASLD' s guideline. Liver biopsy was performed in subjects 5 and 6 and the histology was compatible with PBC in both cases.

One M2-positive subject (subject 8) had an unexplained increase of serum ALP, γ-GT levels asympatomatically, but AMA was negative using IIF method. According to the guideline recommended by AASLD in 2000 and the standards recommended by other researchers, AMA have long been used as an important marker for the diagnosis of PBC[21,23], but AMA is inferior to M2 in sensitivity and specificity. Among AMA, only M2 antibodies are specific for PBC. Other sub-types of AMA have been found in diverse conditions, including drug-induced disorders, cardiomyopathies, systemic lupus erythematosus, rheumatoid arthritis, tuberculosis, syphilis and hepatitis C. Using IIF, AMA cannot be sub-classified, indicating the nonspecific nature of AMA in diagnosis of PBC[25]. About 5-17 % of patients with liver biochemcal and histological features compatible with the diagnosis of PBC had no detectable AMA using IIF method. Autoimmune cholangitis (AIC) has been proposed as a better term for these patients[26-28]. In recent years, some researches have indicated that no difference was found between AMA-positive PBC and AIC, with respect to age, liver function tests, serum IgA, IgG and IgM, T-cell oligoclonality, laparoscopic features or pathologic stage(detection)[29-34], while the detection of M2 antibodies could be achieved by ELISA or Western-blot using recombinant antigen of PDC-E2, BCOADC-E2 and OGDC-E2[11,14,15,35]. Therefore, this subject should also be diagnosed as asymptomatic PBC.

In this research, we also found that 4 M2-positive subjects with normal liver biochemistry were women over 40 years old. Many studies indicated that the presence of AMA (M2 antibodies more accurately), the hallmark of PBC, preceded the clinical manifestations of the disease for many years. In 1986, Mitchison *et al*. reported 29 patients with AMA detected at a titer of at least 1:40 by IIF when screened for an autoimmune disease. None had any symptoms of a liver disease and all had normal liver biochemistry. An 18-year follow-up of this cohort revealed that 83 % developed persistent abnormal liver biochemistry and 76 % developed symptoms of PBC[3]. In 2001, Kisand *et al*. performed ELISA tests for antibodies to PDC-E2 in 1 961 persons, then identified 14 (0.71 %) asymptomatic persons with antibodies to PDC-E2. Eight of the 14 were followed-up. Three of the 8 persons with high levels of anti-PDC-E2 developed abnormal liver biochemical test results by the ninth year of follow-up[4]. Also in 2001, Koizumi *et al*. tested sera from 1 145 corporate workers who took an annual physical examination and evaluated the liver of AMA-positive subjects. AMA were detected in 5 of 1 145 (0.44 %) workers. AMA-positive people were all females aged over 40. All of the AMA-positive sera were also positive for M2 antibodies. Liver biopsy was performed in two M2-positive cases and the histology was compatible with PBC in both cases[5]. The authors of these studies concluded that, before the advent of any clinical or biochemical indications, individuals positive for M2 did have PBC.

In several autoimmune diseases, autoantibodies are detectable in the sera of patients several years before the onset of the disease. A better example is PBC. The appearance of M2 antibodies early in the course of the disease raises the possibility that they may precede and perhaps contribute to target organ damage. That M2 antibodies are present after transplantation in the presence of normal allograft histology is consistent with this suggestion. Recent evidences have shown that M2 antibodies to intracellular targets may act directly by penetrating the biliary epithelial cells, the target of PBC and interfering with cellular function[1,36].

According to James *et al*.[21], there is a widespread impression that the number of patients with PBC is increasing, although its prevalences vary widely. The prevalence of PBC rose from 201.9 per 10^6 in the adult population and 541.4 per 10^6 women over 40 in 1987 to 334.6 per 10^6 adults and 939.8 per 10^6 women over 40 in 1994 in northern England. Due to a lack of available diagnostic equipments, there are no reliable data relating to the epidemiology of PBC in China at present, and it is presumed that PBC is rare in China. However, we checked 10 patients with cirrhosis of liver hospitalized in January, February and April of 2000 whose serum immunological studies showed there was not any sign of viral infections, and the reason for their liver cirrhosis seemed unclear. But 7 of the 10 patients were found to be M2 positive by the detailed studies of the Euroimmun Research Center (Germany). In the past two years since we established the specific immunological methods for the diagnosis of PBC, over 300 patients have been assayed,125 of them have been determined to be M2-positive. Our recent research and related domestic reports in 2001 indicate PBC is probably not so rare in China as it was thought before[19,20,37].

The three major autoantigens of M2 antibodies, i.e, BCOADC-E2, PDC-E2 and OGDC-E2 have no cross-reactivity. The M2 antibodies in serum from a confirmed patient may be reactive with one or more of them. There does not appear to be any clinical correlation with the pattern of M2 reactivity. Consequently, the use of recombinant hybrid molecule offers a rapid, simple, and sensitive ELISA for the immunodiagnosis of PBC. AMA screening using standard IIF method in a population of several thousand patients is not possible because of the economic costs. On the contrary, our methodology allows the screening of a large series of population at a minimal cost. In summary, this is one of the first studies aimed at assessing the prevalence of asymptomatic PBC in a large sample of Chinese population. Our data suggest that asymptomatic PBC in a certain Chinese population is much more common than has been supposed.

REFERENCES

1 **Medina J**, Jones EA, Garcia Monzon C, Moreno Otero R. Immunopathogenesis of cholestatic autoimmune liver diseases. *Eur J Clin Invest* 2001; **31**: 64-71

2 **Heathcote EJ**. Evidence-based therapy of primary biliary cirrhosis. *Eur J Gastroenterol Hepatol* 1999; **11**: 607-615

3 **Metcalf JV**, Mitchison HC, Palmer JM, Jones DE, Bassendine MF, James OF. Natural history of early primary biliary cirrhosis. *Lancet* 1996; **348**: 1399-1402

4 **Kisand KE**, Metskula K, Kisand KV, Kivik T, Gershwin ME, Uibo R. The follow-up of asymptomatic persons with antibodies to pyruvate dehydrogenase in adult population samples. *J Gastroenterol* 2001; **36**: 248-254

5 **Koizumi H**, Onozuka Y, Shibata M, Sano K, Ooshima Y, Morizane

T, Ueno Y. Positive rate of anti-mitochondrial antibody in Japanese corporate workers. *Rinsho Byori* 2000; **48**: 966-970

6 **Turchany JM**, Uibo R, Kivik T, Van de Water J, Prindiville T, Coppel RL, Gershwin ME. A study of antimitochondrial antibodies in a random population in Estonia. *Am J Gastroenterol* 1997; **92**: 124-126

7 **Nakano T**, Inoue K, Hirohara J, Arita S, Higuchi K, Omata M, Toda G. Long-term prognosis of primary biliary cirrhosis (PBC) in Japan and analysis of the factors of stage progression in asymptomatic PBC (a-PBC). *Hepatol Res* 2002; **22**: 250-260

8 **Migliaccio C**, Van de Water J, Ansari AA, Kaplan MM, Coppel RL, Lam KS, Thompson RK, Stevenson F, Gershwin ME. Heterogeneous response of antimitochondrial autoantibodies and bile duct apical staining monoclonal antibodies to pyruvate dehydrogenase complex E_2: the molecule versus the mimic. *Hepatology* 2001; **33**: 792-801

9 **Kitami N**, Komada T, Ishii H, Shimizu H, Adachi H, Yamaguchi Y, Kitamura T, Oide H, Miyazaki A, Ishikawa M. Immunological study of anti-M_2 in antimitochondrial antibody-negative primary biliary cirrhosis. *Intern Med* 1995; **34**: 496-501

10 **Jones DE**. Autoantigens in primary biliary cirrhosis. *J Clin Pathol* 2000; **53**: 813-821

11 **Miyakawa H**, Tanaka A, Kikuchi K, Matsushita M, Kitazawa E, Kawaguchi N, Fujikawa H, Gershwin ME. Detection of antimitochondrial autoantibodies in immunofluorescent AMA-negative patients with primary biliary cirrhosis using recombinant autoantigens. *Hepatology* 2001; **34**: 243-248

12 **Kitami N,** Ishii H, Shimizu H, Adachi H, Komada T, Mikami H, Yokoi Y, Sato N. Immunoreactivity to M_2 proteins in antimitochondrial antibody-negative patients with primary biliary cirrhosis. *J Gastroenterol Hepatol* 1994; **9**: 7-12

13 **Miyakawa H**, Kikuchi K, Jong Hon K, Kawaguchi N, Yajima R, Ito Y, Maekubo H. High sensitivity of a novel ELISA for anti-M_2 in primary biliary cirrhosis. *J Gastroenterol* 2001; **36**: 33-38

14 **Miyakawa H**, Kawaguchi N, Kikuchi K, Fujikawa H, Kitazawa E, Matsushita M. Definition of antigen specificity for antimitochondrial proteins detected by Western blotting using native mitochondrial proteins in primary biliary cirrhosis. *Hepatol Res* 2001; **21**: 101-107

15 **Jensen WA**, Jois JA, Murphy P, De Giorgio J, Brown B, Rowley MJ, Mackay IR. Automated enzymatic mitochondrial antibody assay for the diagnosis of primary biliary cirrhosis. *Clin Chem Lab Med* 2000; **38**: 753-758

16 **Leung PS**, van de Water J, Coppel RL, Nakanuma Y, Munoz S, Gershwin ME. Molecular aspects and the pathological basis of primary biliary cirrhosis. *J Autoimmun* 1996; **9**: 119-128

17 **Strassburg CP**, Manns MP. Autoimmune tests in primary biliary cirrhosis. *Baillieres Best Pract Res Clin Gastroenterol* 2000; **14**: 585-599

18 **Quaranta S**, Shulman H, Ahmed A, Shoenfeld Y, Peter J, McDonald GB, Van de Water J, Coppel R, Ostlund C, Worman HJ, Rizzetto M, Tsuneyama K, Nakanuma Y, Ansari A, Locatelli F, Paganin S, Rosina F, Manns M, Gershwin ME. Autoantibodies in human chronic graft-versus-host disease after hematopoietic cell transplantation. *Clin Immunol* 1999; **91**: 106-116

19 **Jiang XH**, Zhong RQ, Fan LY, Hu Y, Li WW, Kong XT. Cloning and expression of a humanized M_2 triple autoantigen and its application in Chinese patients with primary biliary cirrhosis. *World J Gastroenterol* 2003; **9**: 1352-1355

20 **Jiang XH**, Zhong RQ, Tu XQ, Kong XT. Evaluation of measurement of M_2 autoantibodies using a humanized triple autoantigen in diagnosis of primary billiary cirrhosis. *Zhonghua Ganzangbing Zazhi* 2002; **10**: 341-343

21 **James OF**, Bhopal R, Howel D, Gray J, Burt AD, Metcalf JV. Primary biliary cirrhosis once rare, now common in the United Kingdom? *Hepatology* 1999; **30**: 390-394

22 **Metcalf J**, James O. The geoepidemiology of primary biliary cirrhosis. *Semin Liver Dis* 1997; **17**: 13-22

23 **Metcalf JV**, Bhopal RS, Gray J, Howel D, James OF. Incidence and prevalence of primary biliary cirrhosis in the city of Newcastle upon Tyne, England. *Int J Epidemiol* 1997; **26**: 830-836

24 **Heathcote EJ**. Management of primary biliary cirrhosis. The American Association for the Study of Liver Diseases practice guidelines. *Hepatology* 2000; **31**: 1005-1013

25 **Strassburg CP**, Jaeckel E, Manns MP. Anti-mitochondrial antibodies and other immunological tests in primary biliary cirrhosis. *Eur J Gastroenterol Hepatol* 1999; **11**: 595-601

26 **Michieletti P**, Wanless IR, Katz A, Scheuer PJ, Yeaman SJ, Bassendine MF, Palmer JM, Heathcote EJ. Antimitochondrial antibody negative primary biliary cirrhosis: a distinct syndrome of autoimmune cholangitis. *Gut* 1994; **35**: 260-265

27 **Lacerda MA**, Ludwig J, Dickson ER, Jorgensen RA, Lindor KD. Antimitochondrial antibody-negative primary biliary cirrhosis. *Am J Gastroenterol* 1995; **90**: 247-249

28 **Heathcote J**. Autoimmune cholangitis. *Gut* 1997; **40**: 440-442

29 **Ikuno N**, Scealy M, Davies JM, Whittingham SF, Omagari K, Mackay IR, Rowley MJ. A comparative study of antibody expressions in primary biliary cirrhosis and autoimmune cholangitis using phage display. *Hepatology* 2001; **34**: 478-486

30 **Kinoshita H**, Omagari K, Whittingham S, Kato Y, Ishibashi H, Sugi K, Yano M, Kohno S, Nakanuma Y, Penner E, Wesierska Gadek J, Reynoso Paz S, Gershwin ME, Anderson J, Jois JA, Mackay IR. Autoimmune cholangitis and primary biliary cirrhosis-an autoimmune enigma. *Liver* 1999; **19**: 122-128

31 **Invernizzi P**, Crosignani A, Battezzati PM, Covini G, De Valle G, Larghi A, Zuin M, Podda M. Comparison of the clinical features and clinical course of antimitochondrial antibody-positive and -negative primary biliary cirrhosis. *Hepatology* 1997; **25**: 1090-1095

32 **Kaserer K**, Exner M, Mosberger I, Penner E, Wrba F. Characterization of the inflammatory infiltrate in autoimmune cholangitis. A morphological and immunhistochemical study. *Virchows Arch* 1998; **432**: 217-222

33 **Mayo MJ**, Lipsky PE, Miller SN, Stastny P, Combes B. Similar T-cell oligoclonality in antimitochondrial antibody-positive and -negative primary biliary cirrhosis. *Dig Dis Sci* 2001; **46**: 345-351

34 **Fujioka S**, Yamamoto K, Okamoto R, Miyake M, Ujike K, Shimada N, Terada R, Miyake Y, Nakajima H, Piao CY, Iwasaki Y, Tanimizu M, Tsuji T. Laparoscopic features of primary biliary cirrhosis in AMA-positive and AMA-negative patients. *Endoscopy* 2002; **34**: 318-321

35 **Nakajima M**, Shimizu H, Miyazaki A, Watanabe S, Kitami N, Sato N. Detection of IgA, IgM, and IgG subclasses of anti-M_2 antibody by immunoblotting in autoimmune cholangitis: is autoimmune cholangitis an early stage of primary biliary cirrhosis? *J Gastroenterol* 1999; **34**: 607-612

36 **Nishio A**, Keeffe EB, Gershwin ME. Immunopathogenesis of primary biliary cirrhosis. *Semin Liver Dis* 2002; **22**: 291-302

37 **Zhang F**, Jia J, Wang B, Qian L, Yin S, Wang Y, Cui Y, You H, Ma H, Wang H, Zhang C. Clinical characteristics of primary biliary cirrhosis: a report of 45 cases. *Zhonghua Neike Zazhi* 2002; **41**: 163-167

Edited by Zhu LH and Wang XL

P.O.Box 2345, Beijing 100023,China
Fax: +86-10-85381893
E-mail: wjg@wjgnet.com www.wjgnet.com

World J Gastroenterol 2003;9(9):2132-2134
World Journal of Gastroenterology
 ISSN 1007-9327

• BRIEF REPORTS •

Ultrasonography guided percutaneous radiofrequency ablation for hepatic cavernous hemangioma

Yan Cui, Li-Yan Zhou, Man-Ku Dong, Ping Wang, Min Ji, Xiao-Ou Li, Chang-Wei Chen, Zi-Pei Liu, Yong-Jie Xu, Hong-Wen Zhang

Yan Cui, Li-Yan Zhou, Man-Ku Dong, Ping Wang, Min Ji, Xiao-Ou Li, Chang-Wei Chen, Zi-Pei Liu, Yong-Jie Xu, Hong-Wen Zhang, Department of Hepatobiliary Surgery, Beijing 306 Hospital, Chaoyang District, Beijing 100101, China
Correspondence to: Yan Cui, Director of Department of Hepatobiliary Surgery, Beijing 306 Hospital, 9 Anxiang Beili, Chaoyang District, Beijing 100101, China. cuiyan@public.fhnet.cn.net
Telephone: +86-10-66356138 **Fax:** +86-10-64876056
Received: 2003-05-10 **Accepted:** 2003-06-02

Abstract

AIM: Hepatic cavernous hemangioma (HCH) is the most common benign tumor of the liver and its management is still controversial. Recent success *in situ* radiofrequency ablation of hepatic malignancies has led us to consider using this technique in patients with HCH. This study was to assess the efficacy, safety, and complications of percutaneous radiofrequency ablation (PRFA) under ultrasonography guidance in patients with HCH.

METHODS: Twelve patients (four men and eight women, age ranged 33-56 years, mean age was 41.7 years) with 15 hepatic cavernous hemangiomas (2.5 cm to 9.5 cm) were treated using the RF-2000 generator and 10-needle LeVeen electrode percutaneously guided by B-ultrasound. Lesions larger than 3 cm were treated by multiple overlapping ablations that encompass the entire lesion as well as a rim of normal liver tissue (approximately 0.5 cm).

RESULTS: All the patients who received PRFA therapy had no severe pain, bleeding or bile leakage during and after the procedures. Nine to 34 months' follow-up (mean, 21 months) by ultrasound and/or spiral CT scan demonstrated that the ablated lesions in this group were shrunk remarkably, and the shrunken range was 38-79 % (mean, 67 % per 21 months). The contrast enhancement was disappeared within the tumor or at its periphery in all cases on spiral CT scans obtained 3 to 6 months after treatment.

CONCLUSION: The results of this study suggest that PRFA therapy is a mini-invasive, simple, safe, and effective method for the treatment of selected patients with HCH.

Cui Y, Zhou LY, Dong MK, Wang P, Ji M, Li XO, Chen CW, Liu ZP, Xu YJ, Zhang HW. Ultrasonography guided percutaneous radiofrequency ablation for hepatic cavernous hemangioma. *World J Gastroenterol* 2003; 9(9): 2132-2134
http://www.wjgnet.com/1007-9327/9/2132.asp

INTRODUCTION

Hepatic cavernous hemangioma (HCH) is the most common benign tumor of the liver, its incidence in necropsy series ranges from 0.4 % to 7.4 %. It occurs at all ages and affects women predominantly,the sex ratio is 1.5-6:1, and may increase in size with pregnancy or with administration of estrogens. The majority of HCHs are small, single and asymptomatic. About 20 % are large (>5 cm) and 10 % to 29 % are multiple[1-5]. The largest HCH reported in the literature was 63 cm×48.5 cm×40 cm in size and 18 kg in weight[5]. They are often discovered incidentally on routine abdominal ultrasonography or at the time of laparotomy and necropsy. The widespread use of ultrasound (US) and computerized topography (CT) scanning nowadays has made the diagnosis of HCH easier. HCHs usually become symptomatic as they reach a certain size. Abdominal pain or discomfort is the most common complaint. Rarely, large HCHs sequester and destroy platelets, causing symptomatic thrombocytopenia, known as Kasabach-Merritt syndrome. Occasionally, these vascular lesions rupture spontaneously, or with minimal trauma, and present as hemoperitoneum[1-6].

The management of HCHs is still controversial. *In situ* radiofrequency ablation (RFA) of hepatic malignant tumors[7-21] has led us to consider using this minimally invasive technique in patients with HCH. On the basis of our successful experience in controlling hepatic malignances, we applied the percutaneous RFA (PRFA) guided by B-US to the treatment of patients with HCH and the initial results were promising[22,23]. This article describes our preliminary experiences and evaluates the efficacy, safety, and complications of PRFA therapy for HCHs.

MATERIALS AND METHODS

The study was performed at the RFA center of our department with the approval from the hospital authority. Written informed consent was obtained from each patient prior to treatment.

Twelve consecutive patients with 15 cavernous hemangiomas of the liver were treated with PRFA from May 2000 to June 2002. There were four males and eight females. Age ranged from 33 to 56 years (mean, 41.7 years). Eleven patients had a single lesion (4.8 cm to 9.5 cm), and one patient had four lesions (2.5 cm to 7.0 cm). The tumors were located in the right lobe of the liver in nine patients, left lobe in five, and both lobes in one. Nine patients had discomforts in the right upper quadrant of abdomen, while the remaining three were asymptomatic. The definite histologic diagnosis of HCHs was established by means of enhanced spiral CT scan and B-US guided percutaneous biopsy with 16-gauge biopsy needles in all cases.

The patients were fasted for 4 hours and under conscious sedation and analgesia induced by administering promethazine hydrochloride 25 mg, pethidine hydrochloride 50 mg and morphine hydrochloride 10 mg intravenously. An intercostal or subcostal approach was selected according to the location of hemangiomas in the liver. Local anesthesia was achieved by using 5 ml to 8 ml of 1 % lidocaine. The 10-needle LeVeen electrode, which was connected to the RF-2000 generator (Radio Therapeutics Corp., Mountain View, CA, USA), was inserted percutaneously into and fully deployed within the target tumor under real-time B-US guidance. Grounding was achieved by attaching two dispersive pads on the thighs of patients. The power was set at 30 watts initially and increased by 10 watts per minute until 90 watts were delivered via the needle electrode. The tissue impedance was monitored

automatically by using circuitry incorporated within the generator and the treatment was stopped at roll off. The ablation overlaps were intended so as to destroy HCHs completely. For tumors larger than 3 cm in diameter, the tip of LeVeen needle electrode was readjusted repeatedly under real-time B-US guidance until the entire lesion as well as a rim of normal liver tissue (approximately 0.5 cm) were encompassed and destroyed. The vital signs of patients were monitored continuously during the procedure. The patients were allowed to have a light diet six hours after PRFA therapy. Prophylactic antibiotics and liver protectives were given intravenously for 2 to 3 days. To evaluate the response of hemangiomas to PRFA therapy, B-US and enhanced spiral CT scan were performed regularly by using the same parameters as used for the pretreatment examination. Tumor size was observed, and complete tumor necrosis was considered when no focal enhancement was seen within the tumor or at its periphery on spiral CT scans obtained 3 to 6 months after the treatment.

RESULTS

All treatments were technically successful. When the patients were treated under sedation and analgesia, they experienced a mild pain during the procedure, which disappeared immediately following cessation of PRFA. As radiofrequency energy was applied to the treatment probes, a hyperechoic focus was observed by B-US around the uninsulated portion of the electrodes, which was attributed to the tissue vaporization, microbubble formation and tissue necrotic coagulation. There was a single treatment session in one tumor which was 2.5 cm in diameter, and 2-7 treatment sessions in 14 tumors which were 4.8 cm to 9.5 cm in diameter. The duration of the treatment sessions was quite different from patient to patient, and even from lesion to lesion in the same patient. The average treatment duration was 39 minutes (8-125 minutes). The liver function study showed that serum aspartate aminotransferase (AST) and alanine aminotransferase (ALT) levels were increased two to three times above the baseline values, and normalized 2-5 days posttreatment. No change was observed in other serum element levels. No PRFA-related complications including bleeding or bile leakage occurred, and no repeated PRFA treatment was needed. The post-PRFA course was uneventful, and the patients were discharged on the third to fifth day postprocedure. The fact that the hospital stay was longer than that in Western countries was largely due to our local preferences and social reasons.

All the patients were followed up for 9 to 34 months (mean, 21 months). Nine patients' discomforts in the right upper quadrant of abdomen were ameliorated, the symptoms were significantly or completely controlled in 7 patients for a mean of 2 months (range 1-4 months). B-US and CT scan showed that the ablated lesions were swollen within 2 to 4 weeks after PRFA and started to shrink thereafter. The shrunk range was 38-79 % (mean, 67 % per 21 months). The contrast enhancement was disappeared within the tumor or at its periphery in all cases on spiral CT scans obtained 3 to 6 months after treatment.

DISCUSSION

Traditionally, surgical resection has been considered the choice of treatment for HCHs including those of symptomatic, larger than 10 cm in diameter, and manifested as Kasabach-Merritt syndrome. Steroid therapy and external radiation have provided relief for a few patients[1-5]. The transcatheter arterial embolization (TAE), an effective interventional therapy for hepatic malignancies, has also been advocated for the treatment of HCHs[24,25]. However, there are some differences of hepatic hemodynamics between hepatic malignancies and HCHs[26,27]. The value of TAE as well as its disadvantages have not been fully evaluated. Though TAE has the advantages of avoiding operative intervention and prolongation of hospitalization, TAE may result in disastrous consequences including complications of severe destructive biliary damages and ectopic embolizations[28-30].

Recent successes in local treatment of malignant tumors of the liver have led us to consider using the minimally invasive PRFA in patients with HCHs. In the procedure, the needle-electrode with an insulated shaft and an uninsulated distal tip is inserted directly into hepatic tumor through percutaneous approach under local anesthesia and conscious sedation by the guidance of ultrasonography. Energy is transferred from the uninsulated distal tip of the needle to the tissue as current rather than as direct heat. As the alternate current flows to the grounding pads, it agitates ions in the surrounding tissue of the needle tip, resulting in frictional heat exceeding 80-100 ℃. The local tissue is heated and dried, creating a 3.5 cm to 5.0 cm oval or spherical thermal coagulative necrosis. Thus the tumors are ablated and destroyed *in situ*. The dead cells are not removed, but they eventually shrink and become scar tissues[7-17].

On the basis of our successful experience in controlling hepatic malignances with PRFA therapy, we applied this technique to the treatment of HCHs with a considerable success, and our initial experience was reported in 2001[22, 23]. To our knowledge, this is the first publication on the use of percutaneous radiofrequency ablation therapy for hepatic cavernous hemangiomas. We observed that the patients who accepted PRFA recovered quickly, the ablated lesions were remarkably shrunk after treatment, and no minor or major complications occurred. PRFA has an additional advantage of being easily repeated, so large HCHs can be retreated and the benefits of it to HCHs are definite, which is quite different from the repeat PRFA for hepatic malignancies in which local tumor control is greatly influenced by its size[7-12]. In this group, we managed to adjust LeVeen needle electrode repeatedly under real-time B-US guidance, and large HCHs were completely ablated, and repeat treatment was not needed. Our study showed that this technique was safe and effective for the treatment of HCHs in selected patients. An important limitation of PRFA is related to location of HCHs, in which the near-hilum, near-gallbladder and submembranous HCHs should not be heated lest the tumor' s surrounding tissues or organs be damaged. The interference with the ribs, lung, and adjacent bowel may also affect the procedure.

It is well documented that HCHs should not be disturbed by attempts at biopsy or aspiration, lest serious bleeding occurs, so percutaneous biopsy is contraindicated[1-3]. But several studies have also shown that percutaneous fine needle biopsy with ultrasound guidance is safe for HCH diagnosis[31-35]. We performed percutaneous biopsy successfully in patients with HCHs unexpectedly in our early diagnostic liver biopsies. Along with the experience with recent practice of PRFA for hepatic malignances, we performed both B-US guided biopsy with 16-gauge biopsy needle and PRFA therapy with 15-gauge LeVeen electrode needle in patients with HCHs. There was no hemorrhage or other complications, indicating that both percutaneous biopsy and PRFA therapy under ultrasonography guidance can be performed safely for the diagnosis and treatment of HCHs.

In conclusion, the results of this study suggest that PRFA is a promising and minimally invasive technique for the treatment of HCHs. Long-term studies to assess the clinical outcome of PRFA for HCHs are ongoing. We believe that by virtue of its mini-invasion, effectiveness, simplicity, safety, and easy repeatability, PRFA therapy can be the choice of treatment for HCHs in selected patients.

REFERENCES

1 **Kew MC**. Tumors of the liver. In: Zakim D, Boyer TD, eds. Hepatology. A textbook of liver disease. *Philadelphia: W.B. Saunders Company* 1982:1048-1084
2 **Smith III RB**, Warren WD. The liver. In: Nardi GL, Zuidema GD, eds. Surgery. Essentials of clinical practice. Fourth edition. *Boston: Little, Brown and Company* 1982: 416-446
3 **Meyers WC**. Neoplasms of the liver. In: Sabiston DC, ed. Textbook of Surgery. The biological basis of modern surgical practice. Thirteenth edition. *Philadelphia: W.B.Saunders Company* 1986: 1079-1092
4 **Wu BW**, Wu MC, Zhang XH, Chen H, Yao XP, Yang JM, Yang GS. Surgical treatment for cavernous hemangiomas of the liver: 640 cases report. *Shijie Huaren Xiaohua Zazhi* 1997; **5**: 644
5 **Zhang XH**, Wu MC, Chen H. Cavernous hemangioma of the liver: clinical analysis of 21 cases. *Chin Med J* 1979; **92**: 61-66
6 **Chen ZY**, Qi QH, Dong ZL. Etiology and management of hem morrhage in spontaneous liver rupture: a report of 70 cases. *World J Gastroenterol* 2002; **8**:1063-1066
7 **Rossi S**, Di Stasi M, Buscarini E, Cavanna L, Quaretti P, Squassante E, Garbagnati F, Buscarini L. Percutaneous radiofrequency interstitial thermal ablation in the treatment of small hepatocellular carcinoma. *Cancer J Sci Am* 1995; **1**: 73-81
8 **Livraghi T**, Goldberg SN, Lazzaroni S, Meloni F, Solbiati L, Gazelle GS. Small hepatocellular carcinoma: treatment with radiofrequency ablation versus ethanol injection. *Radiology* 1999; **210**: 655-661
9 **Curley SA**, Izzo F, Delrio P, Ellis LM, Granchi J, Vallone P, Fiore F, Pignata S, Daniele B, Cremona F. Radiofrequency ablation of unresectable primary and metastatic hepatic malignancies: Results in 123 patients. *Ann Surg* 1999; **230**: 1-8
10 **Solbiati L**, Livraghi T, Goldberg SN, Ierace T, Meloni F, Dellanoce M, Cova L, Halpern EF, Gazelle GS. Percutaneous radio-frequency ablation of hepatic metastases from colorectal cancer: long-term results in 117 patients. *Radiology* 2001; **221**: 159-166
11 **Kuvshinoff BW**, Ota DM. Radiofrequency ablation of liver tumors: influence of technique and tumor size. *Surgery* 2002; **132**: 605-612
12 **Shiina S**, Teratani T, Obi S, Hamamura K, Koike Y, Omata M. Nonsurgical treatment of hepatocellular carcinoma: from percutaneous ethanol injection therapy and percutaneous microwave coagulation therapy to radiofrequency ablation. *Oncology* 2002; **62**(Suppl 1): 64-68
13 **Guo W**, Zhang ZS, Yuan AL. Treatment of liver malignant tumor by percutaneous radiofrequency thermal abation. *Shijie Huaren Xiaohua Zazhi* 2000; **8**: 208-210
14 **Wang CP**, Wang Y, Peng XJ, Hu DR. Radiofrequency ablation in treatment of liver neoplasms. *Shijie Huaren Xiaohua Zazhi* 2000; **8**: 323-324
15 **Zhu T**, Cao J, Chu HM. B-ultrasound guided multiple probe ablation of metastasis of liver: results in 40 patients. *Shijie Huaren Xiaohua Zazhi* 2001; **9**: 971-972
16 **Liu LX**, Jiang HC, Piao DX. Radiofrequence ablation of liver cancers. *World J Gastroenterol* 2002; **8**: 393-399
17 **Jiang HC**, Liu LX, Piao DX, Xu J, Zheng M, Zhu AL, Qi SY, Zhang WH, Wu LF. Clinical short-term results of radiofrequency ablation in liver cancers. *World J Gastroenterol* 2002; **8**: 624-630
18 **Rai R**. Radiofrequency ablation: A good regional therapy for liver cancer. *World J Gastroenterol* 2003; **9**: 192
19 **Liu LX**, Zhang WH, Jiang HC. Current treatment for liver metastases from colorectal cancer. *World J Gastroenterol* 2003; **9**: 193-200
20 **Tang ZY**. Progress in the treatment of hepatocellular carcinoma. *Shijie Huaren Xiaohua Zazhi* 2003; **11**: 249-254
21 **Zhou ZG**. Advance in minimally invasive surgery in 21st century. *Shijie Huaren Xiaohua Zazhi* 2002; **10**: 869-872
22 **Cui Y**, Zhou LY, Hou YJ, Lin J, Xu YJ, Wang P, Dong MK, Ji M, Liu ZP, Li XO, Xiao GS, Chen CW. Percutaneous radiofrequency ablation for hepatic cavernous hemangiomas. *Zhonghua Gandan Waike Zazhi* 2001; **7**: 665-666
23 **Xu YJ**, Liang HZ, Cui Y, Zhou LY, Hou YJ, Lin J. Real-time ultrasound guided radiofrequency ablation for hepatic cavernous hemangiomas. *Zhongguo Yixue Yingxiang Jishu* 2002; **18**: 1334
24 **Deutsch GS**, Yeh KA, Bates WB 3rd, Tannehill WB. Embolization for management of hepatic hemangiomas. *Am Surg* 2001; **67**: 159-164
25 **Srivastava DN**, Gandhi D, Seith A, Pande GK, Sahni P. Transcatheter arterial embolization in the treatment of symptomatic cavernous hemangiomas of the liver: a prospective study. *Abdom Imaging* 2001; **26**: 510-514
26 **Xie ZG**, Wang ZD. Blood supply of hepatic cavernous haemangioma and interventional treatment. *Xin Xiaohua Bingxue Zazhi* 1996; **4**: 46-48
27 **Ouyang Y**, Ouyang XH, Yu M, Gu SB. Frequency of arteriovenous shunts in hepatic cavernous hemangiomas in adults as seen on selective arteriography and postembolization radiography. *Cardiovasc Intervent Radiol* 2001; **24**: 161-167
28 **Wang X**, Zhong YX, Zhang LL, Huang YX, Wen QS, Chu YK, Zhang HX, Wang QL. Effect of IL-8 and ET-1 on secondary liver injury by hepatic arterial embolization in rabbits. *Shijie Huaren Xiaohua Zazhi* 2000; **8**: 413-416
29 **Huang ZQ**, Huang XQ. Changing patterns of traumatic bile duct injuries: a review of forty years experience. *World J Gastroenterol* 2002; **8**: 5-12
30 **Huang XQ**, Huang ZQ, Duan WD, Zhou NX, Feng YQ. Severe biliary complications after hepatic artery embolization. *World J Gastroenterol* 2002; **8**:119-123
31 **Solbiati L**, Livraghi T, De Pra L, Ierace T, Masciadri N, Ravetto C. Fine-needle biopsy of hepatic hemangioma with sonographic guidance. *Am J Roentgenol* 1985; **144**: 471-474
32 **Brambs HJ**, Spamer C, Volk B, Wimmer B, Koch H. Histological diagnosis of liver hemangiomas using ultrasound-guided fine needle biopsy. *Hepatogastroenterology* 1985; **32**: 284-287
33 **Caturelli E**, Rapaccini GL, Sabelli C, De Simone F, Fabiano A, Romagna-Manoja E, Anti M, Fedeli G. Ultrasound-guided fine-needle aspiration biopsy in the diagnosis of hepatic hemangioma. *Liver* 1986; **6**: 326-330
34 **Chen KW**, Zhu CB, Chen YM. Diagnosis of hepatic cavernous hemangiomas through repeated biopsies: case report. *Xin Xiaohua Bingxue Zazhi* 1997; **5**: 768
35 **Caturelli E**, Pompili M, Bartolucci F, Siena DA, Sperandeo M, Andriulli A, Bisceglia M. Hemangioma-like lesions in chronic liver disease: diagnostic evaluation in patients. *Radiology* 2001; **220**: 337-342

Edited by Zhang JZ and Wang XL

P.O.Box 2345, Beijing 100023,China
Fax: +86-10-85381893
E-mail: wjg@wjgnet.com www.wjgnet.com

World J Gastroenterol 2003;9(10):2135-2136
World Journal of Gastroenterology
 ISSN 1007-9327

• REVIEW •

Gastroesophageal reflux disease at the turn of *millennium*

Lee-Guan Lim, Khek-Yu Ho

Lee-Guan Lim, Khek-Yu Ho, Department of Medicine, National University Hospital, Singapore
Correspondence to: Associate Professor Khek-Yu Ho, MBBS (Syd Hons 1) MD FRACP FAMS, Department of Medicine, National University Hospital, Lower Kent Ridge Road, 119074 Singapore. mdchoky@nus.edu.sg
Telephone: +65-67724353 **Fax:** +65-67794112
Received: 2003-07-04 **Accepted:** 2003-07-14

Abstract

Gastroesophageal reflux disease (GERD) has been an area of active research in the Asia-Pacific region in the recent years. This article outlines some of the interesting research findings. It comprises three parts. The first part dealt with recent data on the changing epidemiology of GERD in Asia. The second part summarized published studies on the relationship between GERD and *Helicobacter pylori*, relevant to the Asia-Pacific region. The last part discussed some of the recent advances in the treatment of GERD.

Lim LG, Ho KY. Gastroesophageal reflux disease at the turn of *millennium*. *World J Gastroenterol* 2003; 9(10): 2135-2136
http://www.wjgnet.com/1007-9327/9/2135.asp

INTRODUCTION

Gastroesophageal reflux disease (GERD) has been an area of dynamic research in the Asia Pacific region in the last few years. This article outlines some of the interesting research findings.

CHANGING EPIDEMIOLOGY OF GERD IN THE ASIA PACIFIC REGION

There was little information on GERD in the Asia Pacific region until recently. A cross-sectional survey of randomly selected adults in Singapore provided evidence that reflux-type symptoms were uncommon in the Asian population in the early 90' s[1]. Of 700 persons evaluated, only 2 % reported having heartburn more than once a month. A similar study among a random sample of 5 000 adult residents in Shanghai and Beijing showed a point prevalence of symptomatic GERD of 6 %[2].

These prevalence rates were lower than those of Western populations. Endoscopic esophagitis was also less common among Asians than their Western counterparts. One of the evidences came from a comparative study of consecutive English patients and Singaporean patients seen for upper abdominal discomfort[3]. Reflux *esophagitis* was found in 25 % of the English patients and only 6 % of the Singaporean patients ($P<0.005$). The most important risk factor for *esophagitis* was race. An endoscopic study conducted among 16 606 patients in Southern China supported the Singaporean finding, showing a similarly low frequency of endoscopic esophagitis of 4 %[4]. It also showed that esophagitis, when present, was often mild with the vast majority of cases being Los Angeles grade A or B. Severe esophagitis and large hiatal hernia were rare in Asians.

In the past few years, there has been an increase in the frequency of GERD in Asia. In a re-survey[5] of community residents who were interviewed in an earlier study in 1994[1], there was a more than 4-fold increase in the frequency of heartburn. This trend could not be explained by genetic factors *per se*. It also did not appear to be related to lifestyle changes such as smoking, alcohol consumption, or changes in body weight. Among a consecutive series of 9 000 patients who had diagnostic esophagogastroduodenoscopy, the frequency of endoscopic *esophagitis* was also increasing ($P<0.001$) while that of duodenal ulcer was decreasing ($P<0.005$), from 1992 to 1999[6].

The lower frequency of GERD in Asian populations in the early 90' s was unlikely to be solely caused by the known extrinsic risk factors. Genetic factors were probably involved as Asians have a smaller parietal cell mass and a lower acid output compared with Caucasians. The lower prevalence of *hiatus hernia* and smaller body mass index in the Asian population might also have accounted for the lower prevalence of GERD in Asia[7]. The cause of the opposing time trend of GERD and duodenal ulcer disease in Asia was unclear but might be related to the declining rate of *Helicobacter pylori* (*H pylori*) infection, or lifestyle changes, such as increased dietary fat intake.

However, similarities exist in Asian and Western patients with GERD. Interestingly, pathogenic factors of reflux esophagitis in Asians were found to include lower esophageal sphincter competence, esophageal peristaltic contractility, and esophageal acid exposure[8], which were identical to results in Western studies. Elderly Chinese patients were found to have more severe gastroesophageal reflux and esophageal lesions compared with their younger counterparts[9].

GERD AND *HELICOBACTER PYLORI*

Although the relationship between *H pylori*, peptic ulcer disease and gastric malignancy is well established, the link between *H pylori* and GERD remains controversial.

In a systemic review of 20 studies[10], the prevalence of *H pylori* infection in subjects with GERD was significantly lower than that in those without GERD. Geographical location was a strong contributor to the heterogeneity between studies. Although the prevalence of *H pylori* in the general population was found to be higher in the East, patients from the Far East with reflux disease had a lower prevalence of *H pylori* infection than patients from Europe and North America.

Since associations do not prove causality, a more pertinent question is whether eradication of *H pylori* increases the risk of GERD. Hamada and colleagues[11] addressed this question by comparing the prevalence of new onset reflux *esophagitis* among 286 patients who underwent *H pylori* eradication therapy with that of 286 age- and disease-matched *H pylori*-positive controls who did not undergo eradication therapy. Within 3 years of follow-up, 18 % of those who had successful eradication of *H pylori* developed reflux *esophagitis* and this prevalence was higher than the 0.3 % recorded among those without therapy. Reflux esophagitis, when present was mild in most cases. The presence of *hiatal hernia* and severe corpus gastritis was closely related to the development of reflux esophagitis after *H pylori* eradication therapy. The data suggested that increased gastric acid secretion after *H pylori* eradication might only be one of the several factors responsible

for the increased risk of GERD following *H pylori* eradication. On the other hand, in a post hoc analysis of 8 prospective double blind US trials of *H pylori* therapy for patients with active duodenal ulcers or a history of duodenal ulcers[12], no difference was found in the likelihood of developing new GERD symptoms or *esophagitis* in individuals cured of *H pylori* infection compared with those with persistent infection. There was no association of *H pylori* eradication with worsening symptoms in those with preexisting GERD. The likelihood for patients who were successfully cured of their *H pylori* disease to experience a worsening of their GERD symptoms was less than that for those with persistent infection (odds ratio: 0.47, 95 % confidence interval: 0.24-0.91). However, this study had its limitations. Although the overall number of subjects included in the analysis was large, the numbers of patients in some of the subgroup analyses were small. In addition, follow-up was less than 2 months in 7 of the 8 studies included in the analysis. Nevertheless, this study suggested that *H pylori* eradication should not be withheld for fear of causing or worsening GERD. The findings in this study that patients with preexisting GERD were less likely to develop worse symptoms must not be taken to mean that patients with GERD improved after *H pylori* eradication. At present, the treatment of *H pylori* in patients with GERD remains controversial.

TREATMENT OF GERD

In a study investigating the healthcare-seeking behavior of Asian subjects with heartburn, the decision to medicate and to seek medical advice was linked to symptom severity, but not to ethnicity[13].

The mainstay of treatment for GERD is acid suppression. Proton pump inhibitors provide the most rapid symptomatic relief and the highest healing rates for *esophagitis*. Omeprazole, lansoprazole, pantoprazole, rabeprazole and esomeprazole had all been demonstrated to improve GERD symptoms and to heal *esophagitis*. Interestingly, antireflux therapy has been shown to decrease bronchial hyper-responsiveness and improve pulmonary function in asthmatic patients with GERD[14].

For patients with GERD who do not like the idea of taking long-term proton pump inhibitors, Nissen fundoplication, which was modified to the laparoscopic technique in 1991, is an option. However, its association with significant morbidity and its mortalilty rate of 0.2 % prompted the birth of innovative endoscopic techniques.

The Stretta procedure, which involves radiofrequency induction of localized thermal energy to lower *esophageal sphincter* or *cardia*, has been shown in a multicentre randomized double-blind sham-controlled trial[15] to improve heartburn symptom scores and physical quality of life scores. There was no bleeds, perforations or deaths in this study. Another technique, known as the gatekeeper system, has the unique advantage of allowing addition or removal of implants as necessary and was shown to improve symptoms and decrease requirement for anti-reflux medication[16]. A third option, transesophageal endoscopic plication, resulted in significant improvement in lower *esophageal sphincter* pressure and post-procedure 24-hour *esophageal* pH[17]. Finally, endoscopic implantation of inert materials such as Enteryx has been shown to improve symptom scores, quality of life and 24-hour *esophageal* pH, with reduction in the use of acid suppression 6 months after treatment[18].

REFERENCES

1 **Ho KY**, Kang JY, Seow A. Prevalence of gastrointestinal symptoms in a multi-racial Asian population, with particular reference to reflux-type symptoms. *Am J Gastroenterol* 1998; **93**: 1816-1822

2 **Pan GZ**, Xu GM, Ke MY, Han SM, Guo HP, Li ZS, Fang XC, Zou DW, Lu SC, Liu J. Epidemiological study of symptomatic gastroesophageal reflux disease in China: Beijing and Shanghai. *Chin J Dig Dis* 2000; **1**: 2-8

3 **Kang JY**, Ho KY. Different prevalences of reflux oesophagitis and hiatus hernia among dyspeptic patients in England and Singapore. *Eur J Gastroenterol Hepatol* 1999; **11**: 845-850

4 **Wong WM**, Lam SK, Hui WM, Lai KC, Chan CK, Hu WH, Xia HH, Hui CK, Yuen MF, Chan AO, Wong BC. Long-term prospective follow-up of endoscopic oesophagitis in southern Chinese - prevalence and spectrum of the disease. *Aliment Pharmacol Ther* 2002; **16**: 2037-2042

5 **Ho KY**, Lim LS, Goh WT, Lee JMJ. The prevalence of gastrooesophageal reflux has increased in Asia: A longitudinal study in the community. *J Gastro Hepatol* 2001; **16**(Suppl): A132

6 **Ho KY**, Gwee KA, Yeoh KG, Lim SG, Kang JY. Increasing frequency of reflux esophagitis in Asian patients. *Gastroenterology* 2000; **118**: A5704

7 **Ho KY.** Gastroesophageal reflux disease is uncommon in Asia: evidence and possible explanations. *World J Gastroenterol* 1999; **5**: 4-6

8 **Ho KY**, Kang JY. Reflux esophagitis patients in Singapore have motor and acid exposure abnormalities similar to patients in the Western hemisphere. *Am J Gastroenterol* 1999; **94**: 1186-1191

9 **Huang X**, Zhu HM, Deng CZ, Porro GB, Sangaletti O, Pace F. Gastroesophageal reflux: the features in elderly patients. *World J Gastroenterol* 1999; **5**: 421-423

10 **Raghunath A**, Pali A, Hungin S, Wooff D, Childs S. Prevalence of *Helicobacter pylori* in patients with gastro-oesophageal reflux disease: systematic review. *BMJ* 2003; **326**: 737

11 **Hamada H**, Haruma K, Mihara M, Kamada T, Yoshihara M, Sumii K, Kajiyama G, Kawanishi M. High incidence of reflux oesophagitis after eradication therapy for *Helicobacter pylori*: impacts of hiatal hernia and corpus gastritis**.** *Aliment Pharmacol Ther* 2000; **14**: 729-735

12 **Laine L**, Sugg J. Effect of *Helicobacter pylori* eradication on development of erosive esophagitis and gastroesophageal reflux disease symptoms: A post hoc analysis of eight double blind prospective studies. *Am J Gastroenterol* 2002; **97**: 2992-2997

13 **Ho KY**, Kang JY, Seow A. Patterns of consultation and treatment for heartburn: findings from a Singaporean community survey. *Aliment Pharmacol Ther* 1999; **13**: 1029-1033

14 **Jiang SP**, Liang RY, Zeng ZY, Liu QL, Liang YK, Li JG. Effects of antireflux treatment on bronchial hyper-responsiveness and lung function in asthmatic patients with gastroesophageal reflux disease. *World J Gastroenterol* 2003; **9**: 1123-1125

15 **Corley DA**, Katz P, Wo J, Stefan A, Patti m, Rothstein RI, Edmundowicz SA, Kline M, Mason R, Wolfe MM. Radiofrequency energy to the gastroesophageal junction for treatment of GERD (the Stretta procedure): A randomized sham-controlled multicentre clinical trial. *Gastrointest Endos* 2002; **55**: AB100

16 **Fockens P**, Bruno MJ, Hirsch DP, Lei A, Boeckxstaens GE, Tytgat GN. Endoscopic augmentation of the lower esophageal spincter: Pilot study of the gatekeeper reflux repair system in patients with GERD. *Gastrointest Endosc* 2002; **55**: AB257

17 **Swain CP**, Park P, Kjellin T, Gong F, Kadairkamanathan SS, Appleyard M. Endoscopic gastroplasty for gastroesophageal reflux disease. *Gut* 2002; **46**(Sppul): TH3

18 **Lehman GA**, Aisenberg J, Cohen LB, Deviere J, Ganz RA, Haber GB, Hagenmuller F, Johnson DA, Neuhaus H, Ortner MAE, Eters JH, Ponchon T, Rey JF, Hieston K, Silverman D, Visor J. Enteryx solution: A minimally invasive injectable treatment for GERD. International multicentre trial results. *Gastrointest Endosc* 2002; **55**: AB101

Edited by Xu XQ

P.O.Box 2345, Beijing 100023,China
Fax: +86-10-85381893
E-mail: wjg@wjgnet.com www.wjgnet.com

World J Gastroenterol 2003;9(10):2137-2139
World Journal of Gastroenterology
 ISSN 1007-9327

• REVIEW •

Helicobacter pylori infection and micronutrient deficiencies

Javed Yakoob, Wasim Jafri, Shahab Abid

Javed Yakoob, Wasim Jafri, Shahab Abid, Section of Gastroenterology, Department of Medicine, Aga Khan University Hospital, Stadium Road, Karachi, Pakistan
Correspondence to: Javed Yakoob, MBBS, PhD. Section of Gastroenterology, Department of Medicine, Agha Khan University Hospital, Stadium Road, Karachi-74800, Pakistan. yakoobjaved@hotmail.com
Telephone: +92-21-48594661 **Fax:** +92-21-4934294
Received: 2003-06-05 **Accepted:** 2003-08-19

Abstract

It is known that deficiencies of micronutrients due to infections increase morbidity and mortality. This phenomenon depicts itself conspicuously in developing countries. Deficiencies of iron, vitamins A, E, C, B12, *etc* are widely prevalent among populations living in the third world countries. *Helicobacter pylori* (*H pylori*) infection has a high prevalence throughout the world. Deficiencies of several micronutrients due to *H pylori* infection may be concomitantly present and vary from subtle sub-clinical states to severe clinical disorders. These essential trace elements/ micronutrients are involved in host defense mechanisms, maintaining epithelial cell integrity, glycoprotein synthesis, transport mechanisms, myocardial contractility, brain development, cholesterol and glucose metabolism. In this paper *H pylori* infection in associaed with various micronutrients deficiencies is briefly reviewed.

Yakoob J, Jafri W, Abid S. *Helicobacter pylori* infection and micronutrient deficiencies. *World J Gastroenterol* 2003; 9 (10): 2137-2139
http://www.wjgnet.com/1007-9327/9/2137.asp

INTRODUCTION

Helicobacter pylori (*H pylori*) is a gram negative, microaerophilic human pathogen which colonizes the gastric mucosa. Infection with *H pylori* leads to gastritis and is associated with the development of peptic ulcer disease, gastric carcinoma and lymphoma[1]. *H pylori* may be acquired at any age, and the infection persists for years once acquired. The age specific prevalence of *H pylori* infection is higher in developing countries and particularly in lower socioeconomic group[2]. In developing countries *H pylori* infection occurs early in life, and hypochlorhydria commonly seen in the malnourished predisposes them to repeated gastrointestinal infection, persistent diarrhea and malnutrition[3]. *H pylori* infection usually causes both acute and chronic inflammatory cell infiltration, leading to an increase in reactive oxygen species (ROS) which have been shown to accumulate in *H pylori* gastritis[4]. Excessive production of reactive oxygen metabolites (ROMs) by phagocytic cells is thought to contribute to mucosal lesions produced by *H pylori* infection. These are highly reactive compounds capable of combining with DNA in a number of potentially genotoxic ways[5]. Reactive oxygen species can react with the lipid-bilayers releasing peroxidation products such as malondialdehyde. These processes could lead to alterations in the structure of DNA facilitating mutations and carcinogenesis.

Nutrition is a critical determinant of the outcome of host microbe interactions through a modulation of the immune response. "Micronutrient" or "trace elements" are generally defined as constituting less than 0.01 % of body mass and are needed in much smaller amounts. Trace minerals and vitamins are essential for life and include iron (Fe), zinc (Zn), copper (Cu), nickel (Ni), *etc*. They act as essential cofactors of enzymes and as organizers of the molecular structures of the cell, e.g. mitochondria and its membrane. Deficiencies of micronutrients influence immune homeostasis and thus affect infection-related morbidity and mortality. Micronutrients like β carotene, vitamin C, selenium, copper and others are powerful antioxidants and have a significant impact on infection related morbidity in humans. Subclinical deficiencies are known to impair biological and immune functions in the host. Antioxidants play a part in gastric mucosal defense by protecting against damage caused by excessive oxygen derived free radicals. β-carotene and α-tocopherol are lipophilic and have been shown to suppress the oxidation induced by either lipophilic or hydrophilic radical species[6]. In addition, they could act as anti-carcinogens through their ability to prevent the formation of N-nitrosamines which are important in the development of gastric carcinoma[7]. These vitamins are the major oxidant scavengers in biomembranes in contrast to vitamin C, which is mainly responsible for scavenging free radicals in the aqueous phase. However, compensatory mechanisms may become defective while gastric inflammation develops from normal to chronic gastritis and finally to gastric atrophy/intestinal metaplasia, perhaps due to reduced infiltration of inflammatory cells, loss of gastric gland cells and increased ROM production.

IRON

Iron deficiency anemia affects all groups of the under privileged population in most developing countries. Iron is an essential growth factor for *H pylori*, which contains Fe in their outer membrane protein and a system for intracellular storage of iron, consisting of ferritin like molecules pfr and napA[8]. Patients with *H pylori* associated iron deficiency anemia (IDA) would have involvement of both antral and corporal mucosa when compared with controls (90 % *vs* 42.7 %; P=0.0001)[9]. Iron deficiency anemia associated with *H pylori* gastritis is characterized by a concomitant increase in median intragastric pH value >3 and lowering of intragastric concentrations of ascorbic acid. A significant percentage (43 %) of *H pylori* positive IDA patients presented atrophic changes in the gastric body, and the remaining had a superficial gastritis extended to the fundic mucosa, in contrast with *H pylori* positive controls[10]. *H pylori* eradication has also been shown to improve the absorption of other nutrients besides iron, and produce more rapid and complete clinical responses in patients with iron deficiency anemia[11].

COPPER

Copper is involved in the function of several enzymes. It is required for infant growth, host defense mechanisms, bone strength, red and white cell maturation, iron transport, *etc*. Acquired deficiency is mainly seen in infants. However, it has been diagnosed also in malnourished children and adults[12]. A

gene, copA, associated with copper transport, has been isolated from *H pylori* UA802. The adenosine triphosphatase-derived copper-transporting mechanism is employed by various *H pylori* strains[13]. As a cofactor in various redox enzymes and an essential trace metal required for the synthesis of metalloproteins, copper plays a role in the pathogenesis of *H pylori*. *H pylori* has a differential effect on some gastric mucosal scavenger enzymes of ROMs, namely mitochondrial and cytoplasmic superoxide dismutases reflected by a large increase in the cytokine inducible manganese superoxide dismutase and a decrease in the constitutive copper/zinc superoxide dismutase[14].

VITAMIN B12

The mechanisms of vitamin B12 malabsorption caused by *H pylori* infection are unclear but following are the possibilities: a) The diminished acid secretion in *H pylori* induced gastritis may lead to a failure of critical splitting of vitamin B12 from food binders and its subsequent transfer to R binder in the stomach. b) A secretory dysfunction of the intrinsic factor. c) Decreased secretion of ascorbic acid from the gastric mucosa and increased gastric pH[15,16]. Annibale *et al*, studied the prevalence of *H pylori* infection in pernicious anemia patients and have demonstrated that almost two thirds of pernicious anemia patients had evidence of *H pylori* but only those with an active *H pylori* infection had distinctively functional and histological features[17]. These findings support the hypothesis that *H pylori* infection could play a triggering role in a subgroup of pernicious anemia patients, and suggest the possibility that *H pylori* is involved in the early stages of PA that lead to severe corpus atrophy. The later progress of gastritis seems to be dependent on factors other than *H pylori*, most likely "autoimmune" mechanisms[18]. *H pylori* may also be involved in the pathogenesis of pernicious anemia via antigenic mimicry as antibodies directed against the H+, K+- adenosine-triphosphate protein that has been found in high numbers of patients with *H pylori* infection[19]. Food cobalamin malabsorption may occur without gastric atrophy or achlorhydria. Malabsorption can respond to antibiotics, but only in some patients[20].

VITAMIN A

Vitamin A has effects on important determinants of immune function and epithelial cell integrity such as gene expression, cellular proliferation and differentiation and also glycoprotein synthesis. Loss of integrity of the epithelial lining of mucus membranes in a vitamin A deficient state could explain its close association with increased susceptibility to infections particularly of gastrointestinal, respiratory and genitourinary tracts especially in children and pregnant women[21]. Even mild or subclinical vitamin A deficiency could induce keratinizing metaplasia of the epithelium and depletes goblet cells from mucosal linings thus causing xerosis of the membrane[22]. The xerotic surfaces form potential sites for increased bacterial adherence thus leading to bacterial colonization. The antimicrobial enzyme lysozyme depends on vitamin A for its synthesis. A decrease in T cell number with no change in proliferative activity has been demonstrated in children suffering from mild xerophthalmia due to vitamin A deficiency. *H pylori* infection and low β-carotene in plasma contribute to the increased risk of gastric atrophy, indicating that *H pylori* infection might be associated with low plasma β-carotene[23].

VITAMIN E

Vitamin E is composed of a group of compounds termed tocopherols and tocotrienols. α-tocopherol is the major active form in the human body, accounting for 95 % of vitamin E and is the most effective lipid soluble anti-oxidant in biomembranes. It acts as the major chain breaking antioxidant and is able to interfere with the propagation of lipid peroxidation. It plays an immune modulatory part and is capable of increasing natural killer cell activity. Concentrations of α-tocopherol in *H pylori* negative subjects were higher in the corpus than in the antrum or duodenum[6]. This distribution of α-tocopherol is reversed in the presence of antral *H pylori* infection. These findings may reflect a mobilization of antioxidant defenses to the sites of maximal inflammation in the stomach.

VITAMIN C

Vitamin C exists as ascorbic acid (AA) or dehydroascorbic acid. The stomach secretes ascorbic acid across the gastric mucosa into the gastric juice against a concentration gradient. Ascorbic acid is the reduced form of the vitamin and can act as a potent antioxidant, and is able to scavenge ROS in gastric mucosa. This has been proposed as one means by which it exerts an anti-carcinogenic effect. Ascorbic acid may also prevent formation of N-nitroso compounds in gastric juice by scavenging nitrite. It has been observed that diets poor in foods containing AA were associated with an increased risk of gastric cancer[24]. Wei-cheng *et al* showed that presence of *H pylori* infection at the baseline and smoking were strongly associated with progression to dysplasia or gastric cancer, whereas the risk of progression was decreased by 80 % among subjects with baseline ascorbic acid levels in the highest tertile compared with those in the lowest tertile[25]. A number of studies have demonstrated that gastric juice but not gastric mucosal AA levels were reduced in the presence of *H pylori* gastritis and that successful eradication restored the juice/plasma AA ratio[23, 26]. The lower plasma AA concentration in *H pylori* positive subjects could be due to reduced bioavailability, active secretion from plasma to gastric juice in attempts to restore the positive gastric juice/plasma ratio or both[27]. In some studies no difference was found in the gastric juice AA concentration between patients with antral-limited gastritis and *H pylori* negative healthy controls, while lower AA levels were observed in patients with gastric body involvement and increased pH[28]. These observations suggest that AA, which is very unstable in the presence of increased pH, is converted to the less active form of dehydroascorbic acid, in the presence of gastric damage extending to the corporal mucosa with consequent hypochlorhydria[29,30]. It has been demonstrated that eradication of *H pylori* could lead to a reduction in ROS activity in gastric mucosa[31]. Ascorbic acid has also been shown to inhibit *H pylori* urease activity and growth *in vitro*[32]. *H pylori* infection associated low gastric juice-ascorbic acid levels return to normal after successful eradication of the infection[33]. A study of antibiotic treatment failure showed that compliant patients in whom *H pylori* infection did not clear had lower baseline plasma and gastric juice vitamin C concentrations than patients whose infection was cleared[26].

In developing countries micronutrient deficiencies facilitated by *H pylori* infection are a clinical and public health problem. It is essential to define the precise extent of the problem. Several micro and macronutrient deficiencies could be concomitantly present in the population with several other deficits. They will require correction to achieve significant effects on the over all health of the population.

REFERENCES

1 **Huang JQ**, Sridhar S, Chen Y, Hunt RH. Meta-analysis of the relationship between *Helicobacter pylori* seropositivity and gastric cancer. *Gastroenterology* 1998; **114**: 1169-1179

2 **Graham DY**. *Helicobacter pylori*: its epidemiology and its role in duodenal ulcer disease. *J Gastroenterol Hepatol* 1991; **6**: 105-113

3 **Gilman RH**, Partanen R, Brown KH, Spira WM, Khanam S, Greenberg B, Bloom SR, Ali A. Decreased gastric acid secretion and bacterial colonization of the stomach in severely malnourished Bangladeshi children. *Gastroenterology* 1988; **94**: 1308-1314

4 **Farinati F**, Della Libera G, Cardin R, Molari A, Pelabani M, Rugg M, DiMario F, Naccarato R. Gastric antioxidant, nitrites and mucosal lipoperoxidation in chronic gastritis and *Helicobacter pylori* infection. *J Clin Gastroenterol* 1996; **22**: 275-281

5 **Guyton KZ**, Kensler TW. Oxidative mechanisms in carcinogenesis. *Br Med Bullet* 1993; **49**: 523-544

6 **Sies H**, Stahl W. Vitamin E and C, β-carotene and other carotenoids as antioxidants. *Am J Clin Nutr* 1995; **62**: 1315S-1321S

7 **Hwang H**, Dwyer J, Russel RM. *H pylori* infection, food preservation and gastric cancer risk: are there new roles for preventive factors? *Nutr Rev* 1994; **52**: 75-83

8 **Dundon WG**, Polenghi A, DelGuidice G, Rappuoli R, Montecucco C. Neutrophil-activating protein (HP-NAP) versus ferritin (Pfr): comparison of synthesis in *Helicobacter pylori*. *FEMS Microbiol Lett* 2001; **199**: 143-149

9 **Annibale B**, Capurso G, Delle Fava G. Consequences of *Helicobacter pylori* infection on the absorption of micronutrients. *Digest Liver Dis* 2002; **34**: S72-77

10 **Annibale B**, Capurso G, Lahner E, Passi S, Ricci R, Maggio F, Delle Fava G. Concomitant alterations in intragastric pH and ascorbic acid concentration in patients with *Helicobacter pylori* gastritis and associated iron deficiency anemia. *Gut* 2003; **52**: 496-501

11 **Annibale B**, Marignani M, Monarca B, Antonelli G, Marcheggiano A, Martino G, Mandelli F, Caprilli R, Delle Fave G. Reversal of Iron deficiency anemia after *Helicobacter pylori* eradication in patients with asymptomatic gastritis. *Ann Intern Med* 1999; **131**: 668-672

12 **Olivares M**, Uauy R. Copper as an essential nutrition. *Am J Clin Nutr* 1996; **63**: 791S-796S

13 **Ge Z**, Jiang Q, Taylor DE. Conservation and diversity of the *Helicobacter pylori* copper-transporting ATPase gene (copA) sequence among *Helicobacter species* and *Campylobacter* species detected by PCR and RFLP. *Helicobacter* 1996; **1**: 112-117

14 **Gotz JM**, Thio JL, Verspaget HW, Offerhaus GJ, Biemond I, Lamers CB, Veenendaal RA. Treatment of *Helicobacter pylori* infection favorably affects gastric mucosal superoxide dismutases. *Gut* 1997; **40**: 591-596

15 **Del Corral A**, Carmel R. Transfer of cobalamin from the cobalamin-binding protein of egg-yolk to R binder of human saliva and gastric juice. *Gastroenterology* 1990; **98**: 1460-1466

16 **Appelmelk BJ**, Simoons-Smit I, Negrrini R, Moran AP, Aspinall GO, Forte JG, DeVries T, Quan H, Verboom T, Maaskantt JJ, Ghiara P, Kuipers EJ, Bloemena E, Tadema TM, Townsend RR, Tyagarajan K, Crothers JM Jr, Monteiro MA, Savio A, De Graaff J. Potential role of molecular mimicry between *Helicobacter pylori* lipopolysaccharide and host Lewis blood group antigens in autoimmunity. *Infect Immun* 1996; **64**: 2031-2040

17 **Annibale B**, Lahner E, Bordi C, Martino G, Caruana P, Grossi C, Negrini R, Delle Fava G. Role of *Helicobacter pylori* infection in pernicious anemia. *Digest Liver Dis* 2000; **32**: 756-762

18 **Varis O**, Valle J, Siurala M. Is *Helicobacter pylori* involved in the pathogenesis of the gastritis characteristic of pernicious anemia? Comparison between pernicious anemia relatives and duodenal ulcer relatives. *Scand J Gastroenterol* 1993; **28**: 705-708

19 **Claeys D**, Faller G, Appelmelk BJ, Negrini R, Kirchner T. The gastric H^+K^+-ATPase is a major autoantigen in chronic *Helicobacter pylori* gastritis with body mucosa atrophy. *Gastroenterology* 1998; **115**: 340-347

20 **Cohen H**, Weinstein WM, Carmel R. Heterogeneity of gastric histology and function in food cobalamin malabsorption: absence of atrophic gastritis and achlorhydria in some patients with severe malabsorption. *Gut* 2000; **47**: 638-645

21 **Christian P**, Schulze K, Stolzfus RJ, West KP Jr. Hyporetinolemia, illness symptoms and acute phase protein response in pregnant women with and without night blindness. *Am J Clin Nutr* 1998; **67**: 1237-1243

22 **Reddy V**, Rao VM, Jyothi A, Reddy M. Conjunctival impression cytology for assessment of vitamin A status. *Am J Clin Nutr* 1989; **50**: 814-817

23 **Tsugane S**, Kabuto M, Imai H, Goy F, Tai Y, Hanaoka T, Sugano K, Watanabe S. *Helicobacter pylori*, dietary factors and atrophic gastritis in five Japanese populations with different gastric cancer mortality. *Cancer Causes Control* 1993; 4: 297-305

24 **Block G**. Epidemiologic evidence regarding vitamin C and cancer. *Am J Clin Nutr* 1991; **54**: S1310-S1314

25 **Weicheng Y**, Zhang L, Gail MH. Gastric dysplasia and gastric cancer *Helicobacter pylori*, serum vitamin C and other risk factors. *J Natl Cancer Instit* 2000; **92**: 1607-1611

26 **Ruiz B**, Rood JC, Fontham ETH, Malcom GT, Hunter FM, Sobhan M, Johnson WD, Correa P. Vitamin C concentration in gastric juice before and after anti- *Helicobacter pylori* treatment. *Am J Gastroenterol* 1994; **89**: 533-539

27 **Woodward M**, Tunstall-Pedoe H, McColl KEL. *Helicobacter pylori* infection reduces systematic availability of dietary vitamin C. *Eur J Gastroenterol Hepatol* 2001; **13**: 233-237

28 **Zhang ZW**, Patchett SE, Perrett D, Katelaris PH, Domizio P, Farthing MJG. The relationship between gastric vitamin C concentrations, mucosal histology and CagA seropositivity in the human stomach. *Gut* 1998; **43**: 322-326

29 **Sobala GM**, Schorah CJ, Shires S, Lynch DA, Gallacher B, Dixon MF, Axon AT. Effect of eradication of *Helicobacter pylori* on gastric juice ascorbic acid concentrations. *Gut* 1993; **34**: 1038-1041

30 **Waring AJ**, Drake IM, Schorah CJ, White KL, Lynch DA, Axon AT, Dixon MF. Ascorbic acid and total vitamin C concentrations in plasma gastric juice, and gastrointestinal mucosa: effects of gastritis and oral supplementation. *Gut* 1996; **38**: 171-176

31 **Goodman KJ**, Correa P, Tengana Aux HJ, Delany JP, Collazos T. Nutritional factors and *Helicobacter pylori* infection in Colombian children. *J Paedr Gastroentrol Nutr* 1997; **25**: 507-515

32 **Nilius M**, Bode G, Lehnhardt G, Malfertheiner P. *In vitro* inhibition of *Helicobacter pylori urease*: Biochemical and ultrastructural analysis. *Eur J Clin Invest* 1991; **21**: 551-557

33 **Phull PS**, Green CJ, Jacyna MR. A radical view of the stomach: The role of oxygen-derived free radical and anti-oxidants in gastroduodenal disease. *Eur J Gastroenterol Hepatol* 1995; **7**: 265-274

Edited by Wang XL

P.O.Box 2345, Beijing 100023,China
Fax: +86-10-85381893
E-mail: wjg@wjgnet.com www.wjgnet.com

World J Gastroenterol 2003;9(10):2140-2142
World Journal of Gastroenterology
 ISSN 1007-9327

• REVIEW •

Pathophysiological aspects of diverticular disease of colon and role of large bowel motility

Gabrio Bassotti, Fabio Chistolini, Antonio Morelli

Gabrio Bassotti, Fabio Chistolini, Antonio Morelli, Clinica di Gastroenterologia ed Epatologia, Dipartimento di Medicina Clinica e Sperimentale, Università di Perugia, Italy
Correspondence to: Dr. Gabrio Bassotti, Strada del Cimitero, 2/a, 06131 San Marco (Perugia), Italy. gabassot@tin.it
Telephone: +39-75-5847570 **Fax:** +39-75-5847570
Received: 2003-06-16 **Accepted:** 2003-07-14

Abstract

Colonic diverticular disease (diverticulosis) is one of the most common gastrointestinal disorders in Western countries. This disorder is strictly related to aging and fibre intake, and still bears a discrete amount of morbidity. Numerous etiological co-factors have to date been implicated in the pathogenesis of the disease, yet the supporting evidence is still far from absolute. The present review considers the pathophysiology of colonic diverticular disease, with a special emphasis on factors related to abnormal colonic motility.

Bassotti G, Chistolini F, Morelli A. Pathophysiological aspects of diverticular disease of colon and role of large bowel motility. *World J Gastroenterol* 2003; 9(10): 2140-2142
http://www.wjgnet.com/1007-9327/9/2140.asp

INTRODUCTION

Diverticular disease of the colon (diverticulosis) is the most common disease affecting the large bowel in the Western world[1]. This disease is correlated with the aging process and a low-fiber diet and bears a considerable amount of morbidity[2]. The continuous aging process of the population also leads to an increase of this disease.

It is commonly thought that an altered motility of the large bowel may have a major pathophysiological role, even though it is probable that multiple factors (anatomic features intrinsic to the colon, alterations in colonic wall with aging, dietary fiber, motor dysfunction, abnormal intraluminal pressures, and possibly genetic influences) interact in ill-defined relationships to play a greater or lesser role in the genesis of colonic diverticul[3,4].

This article will review the pathogenetic factors of colonic diverticular disease (diverticulosis), with an emphasis on those related to large bowel motility.

ANATOMIC FACTORS

Diverticul are usually found in the left (sigmoid, descending) colon on either mesenteric side of the antimesenteric teniae in Western countries[5], and occur at weak points in the circular muscle layer, where the blood vessels supply the mucosa[6], suggesting that increased intraluminal pressure might play a role in their formation. The presence of right-sided diverticula is conversely more frequently seen in Eastern populations[7]. An impaired structure of the colonic wall has been described in patients with diverticular disease. In fact, both *in vitro*[8] and *in vivo*[9] studies showed that these patients displayed an increased colonic compliance in the affected segments. This might be due to a pathological accentuation of the physiological differences among colonic segments[10], that has been ascribed to qualitative than quantitative changes in collagen[11], since the content of the latter remained unaltered, with respect to controls, in the entire colonic wall[12] and in the muscle layers[13]. However, the available studies measured colonic compliance by means of latex balloons that constitute a suboptimal method for this measurement. More precise studies with up to date systems (i.e., polyethylene bags, which intrinsic compliance is negligible) are needed. Colonic diverticula were also prevalent in young patients with connective tissue disease[14,15].

Previous studies showed that a consistent anatomic finding in colonic diverticular disease was the presence of thickening of the bowel wall muscle layers[16,17]. However, no evidence of hyperplasia or hypertrophy of the muscle cells has been found (although this finding has been challenged[18]). There is an enormous increase in elastin deposition in the teniae, that leads to shortening of this layer with thickening of the circular muscle layer and produces the concertina-like folds in the inner muscle layer[12,19]. This deformity (also called myochosis) would narrow the lumen, allowing muscle contractions to obliterate the lumen and divide the bowel into isolated segments[4].

Unfortunately, available neurophysiopathological data are remarkably few in colonic diverticulosis. A study investigating the myenteric plexus in such patients was unable to demonstrate any morphological abnormality[20]. Another more recent study showed that cholinergic nerves were dominant in the left-sided diverticular colon, and that a decreased action of non-adrenergic non-cholinergic nerves by nitric oxide might be related to the high intracolonic pressures by colonic segmentation observed in such portions of the viscus[21]. Moreover, *in vitro* cholinergic stimulation of colons of patients with diverticular disease yielded increased low frequency and uncoordinated smooth muscle contractions in response to acetylcholine, compared with controls[22].

AGING

Colonic diverticular disease showed a striking correlation with advancing age[23], and it was estimated that 50 % of the Western population approximately 70 years of age were affected[24], an important consequence of aging was that the properties of the colon wall changed with a decrease of the tensile strength[25]. The reason of this decrease is unknown, but it might be related to an increased cross-linking of collagen fibrils with age, which also became smaller, more numerous and more tightly packed in the left colon[9]. These changes seemed to be accentuated in diverticular disease[26]. Moreover, since elastin deposition continued throughout life in all layers of the colonic wall[27] (with predominance in the teniae in diverticular disease), the fibers lost some mechanical properties and became more distensible in diverticulosis[28].

DIET

There is substantial evidences that colonic diverticulosis was related to civilization, industrialization, and a Western lifestyle and diet[29]. Dietary factors, and in particular low fiber intake,

have been considered as main pathogenic factors[30,31], as also shown by the observations that populations moving from rural to urban environments displayed an increased prevalence of the disease[32], and that vegetarians had a lower incidence of diverticular disease of the colon[33]. In addition, an interesting observation in rats showed that the animals whose mothers were fed on a fiber-deficient diet had an increased incidence of colonic diverticulosis[34].

The "protective" action of dietary fiber would make the stools bulkier, thereby increasing the colon size and decreasing intraluminal pressures (since according to Laplace's law, the pressure required to distend the wall is the greatest where the radius is small)[35], and reducing colonic transit time[36]. These hypotheses have been indirectly confirmed by the observations that typical African diets yielded rapid colonic transit times, bulkier stools and no need to strain[37], whereas those of Europeans resulted in almost double colonic transit times[38] and firmer and more viscous stools that increased intraluminal pressures and the need to strain. Of course, other dietary factors are likely to play a role in this area, as shown by the fact that a Western-type diet was implicated in the increased proline intake from the gut, that led to elastosis of the sigmoid colon[39], and that the prevalence of right-sided diverticular disease displayeds a strongly positive association with past meat consumption frequency[40].

COLONIC MOTILITY

Abnormal intraluminal pressure and disordered colonic motility have been implicated as pathogenic factors in diverticulosis. The evidence for this belief (as discussed below) is far from absolute, however, there are several data suggesting that abnormal colonic motility may be considered as an important pathophysiologic mechanism. It is worth noting that most studies on colonic motility and myoelectrical activity were biased by poor patient selection, small numbers of patients recruited, heterogeneity of clinical conditions, recording techniques (only the rectosigmoid or even rectal motor activity was often obtained) and duration of recording periods (at best, less than two hours, whereas colonic motility displayed wide and important fluctuations around-the-clock[41]).

Concerning right-sided colonic diverticular disease, there is paucity of studies facing the motor aspects. Two investigations, featuring very brief recording periods, reported that patients with diverticulosis displayed higher motility indices with respect to controls, both basally and after pharmacologic stimulation[42, 43]. An increased motor activity was also observed in the segment with diverticula with respect to the non affected sigmoid colon.

Looking at studies in patients with "traditional" diverticulosis, most manometric investigations, as already stated, were carried out in the rectum and (at best) very distal sigmoid area. Therefore, it was possible that the portion of the viscus harboring diverticula might have not been studied at all. This might justify the fact that increased pressures were documented[44-47] or not found[48-51] with respect to controls and in response to pharmacological stimulation. Similar contrasting results were reported from myolectrical studies of the rectosigmoid area[52, 53]. However, more recent studies, carried out in the true sigmoid and descending colon (and, therefore, investigating colonic segments actually bearing diverticula) are available, which showed an increased motor activity in such patients (both symptomatic and asymptomatic) with respect to controls[54,55]. This abnormal motility was reduced following surgery[56]. More recently, we investigated colonic motility in patients with symptomatic uncomplicated diverticular disease, by means of a 24-hour manometric technique that allows studying most of the viscus, its daily fluctuations[57], and detection of the motor equivalents of mass movements, the so-called high-amplitude propagated contractions (HAPC)[58]. With respect to controls, patients with diverticulosis displayed a significantly overall increase of daily motor activity, except in the transverse colon (the segment not involved by diverticula), and of propulsive activity[59]. Interestingly, patients had several retropropagated HAPC (never observed in controls), and the motor activity of the affected segments, especially the sigmoid, was significantly higher than that of the unaffected ones (the transverse).

All the above observations seem to support a discrete role of colonic motility (with the probable concourse of other factors) as a pathophysiological mechanism in diverticular disease. Colonic motility is influenced by the aging process, as shown by the decrease of HAPC frequency with age, whereas segmental contractile activity increases[60]. Anatomical studies in experimental animal models showed that these changes might be related to aging of colonic smooth muscle[61].

The muscle thickening observed in affected bowel segments was thought to be obstructive, and to contribute to the delayed transit of feces[18]. Studies with intracolonic displacement tools suggested that an accentuation of segmentary motor activity (as observed in diverticular disease) might abolish oro-aboral progression of contents[62], thereby facilitating retropropulsion and drying of the semiliquid fecal matter. Moreover, reverse peristalsis, as observed in animal studies, might be a general response to distal obstruction associated with a narrowed terminal colon segment[63]. We have shown that a similar mechanism is present in diverticulosis, and this might have some pathophysiological relevance (for instance, a local nondominant pacemaker might take over in the "spastic" region, initiating an oral spreading of contractions along the less active proximal colonic segments).

CONCLUSIONS

Although many evidences suggest that colonic diverticular disease is related to low-residue diet, the scarce effectiveness of dietary manipulations[64] and the complex relationships with other factors, among which abnormal colonic motility might play an important role, still make this disease a fascinating pathophysiological puzzle. Further studies are needed to understand the intrinsic mechanisms better and possibly, to give us useful insights for a better and more targeted therapeutic approach.

REFERENCES

1 **Smith AN**. Diverticular disease of the colon. In Phillips SF, Pemberton JH, Shorter RG, eds. The large intestine: physiology, pathophysiology, and disease. *Raven Press, New York* 1991: 549-577

2 **Torsoli A**, Inoue M, Manousos O, Smith A, Van Steensel CJ. Diverticular disease of the colon: data relevant to management. *Gastroenterol Int* 1991; **4**: 3-20

3 **Simpson J**, Scholefield JH, Spiller RC. Pathogenesis of colonic diverticula. *Br J Surg* 2002; **89**: 546-554

4 **Simmang CL**, Shires GT. Diverticular disease of the colon. In Feldman M, Friedman LS, Sleisenger MH, eds. Sleisenger & Fordtran's gastrointestinal and liver disease, 7th edition. *Saunders, Philadelphia* 2002: 2100-2112

5 **Almy TP**, Howell DA. Diverticular disease of the colon. *N Engl J Med* 1980; **302**: 324-331

6 **Slack WW**. The anatomy, pathology, and some clinical features of diverticulitis of the colon. *Br J Surg* 1962; **50**: 185-190

7 **Chia JG**, Wilde CC, Ngoi SS, Goh PM, Ong CL. Trends of diverticular disease of the large bowel in a newly developed country. *Dis Colon Rectum* 1991; **34**: 498-501

8 **Smith AN**, Shepherd J, Eastwood MA. Pressure changes after balloon distension of the colon wall in diverticular disease. *Gut* 1981; **22**: 841-844

9 **Parks TG**. Rectal and colonic studies after resection of the sigmoid for diverticular disease. *Gut* 1970; **11**: 121-125
10 **Ford MJ**, Camilleri M, Wiste JA, Hanson RB. Differences in colonic tone and phasic response to a meal in the transverse and sigmoid human colon. *Gut* 1995; **37**: 264-269
11 **Bode MK**, Karttunen TJ, Makela J, Risteli L, Risteli J. Type I and III collagens in human colon cancer and diverticulosis. *Scand J Gastroenterol* 2000; **35**: 747-752
12 **Wess L**, Eastwood MA, Wess TJ, Busuttil A, Miller A. Cross linking of collagen is increased in colonic diverticulosis. *Gut* 1995; **37**: 91-94
13 **Whiteway J**, Morson BC. Elastosis in diverticular disease of the sigmoid colon. *Gut* 1985; **26**: 258-266
14 **Beighton PH**, Murdoch JL, Votteler T. Gastrointestinal complications of the Ehlers-Danlos Syndrome. *Gut* 1969; **10**: 1004-1008
15 **Eliashar R**, Eliashar R, Sichel JY, Biron A, Dano I. Multiple gastrointestinal complications in Marfan syndrome. *Postgrad Med J* 1998; **74**: 495-497
16 **Morson BC**. The muscular abnormality in diverticular disease of the sigmoid colon. *Br J Radiol* 1963; **36**: 385-392
17 **Hughes LE**. Postmortem survey of diverticular disease of the colon. II. The muscular abnormality of the sigmoid colon. *Gut* 1969; **10**: 344-351
18 **Raguse T**, Bubenzer J. Functional and morphological studies on diverticulosis of the large bowel. *Chir Forum Exp Klin Forsch* 1979; **3**: 138-143
19 **Whiteway J**, Morson BC. Pathology of the ageing – diverticular disease. *Clin Gastroenterol* 1985; **14**: 829-846
20 **Vuong NP**, Sezeur A, Balaton A, Malafosse M, Camilleri JP. Myenteric plexuses and colonic diverticulosis: results of a histological study. *Gastroenterol Clin Biol* 1985; **9**: 434-436
21 **Tomita R**, Fujisaki S, Tanjoh K, Fukuzawa M. Role of nitric oxide in the left-sided colon of patients with diverticular disease. *Hepatologastroenterology* 2000; **47**: 692-696
22 **Huizinga JD**, Waterfall WE, Stern HS. Abnormal response to cholinergic stimulation in the circular muscle layer of the human colon in diverticular disease. *Scand J Gastroenterol* 1999; **34**:363-368
23 **Cheskin LJ**, Bohlman M, Schuster MM. Diverticular disease of the elderly. *Gastroenterol Clin North Am* 1990; **19**: 391-403
24 **Manousos ON**, Truelove SC, Lumsden K. Prevalence of colonic diverticula and diverticulosis in general population of Oxford area. *Br Med J* 1967; **3**: 762-763
25 **Watters DA**, Smith AN, Eastwood MA, Anderson KC, Elton RA, Mugerwa JW. Mechanical properties of the colon: comparison of the features of the African and European colon *in vitro*. *Gut* 1985; **26**: 384-392
26 **Thomson HJ**, Busuttil A, Eastwood MA. Submucosal collagen changes in the normal colon and in diverticular disease. *Int J Colorectal Dis* 1987; **2**: 208-213
27 **Smith AN**. Colonic muscle in diverticular disease. *Clin Gastroenterol* 1986; **15**: 917-935
28 **Smith AN**, Shepherd J. The strength of the colon wall in diverticular disease. *Br J Surg* 1976; **63**: 666
29 **Mimura T**, Emanuel A, Kamm MA. Pathophysiology of diverticular disease. *Best Pract Res Clin Gastroenterol* 2002; **16**: 563-576
30 **Painter NS**, Burkitt DP. Diverticular disease of the colon: a deficiency disease of Western civilization. *BMJ* 1971; **2**: 450-454
31 **Mendeloff AI**. Thoughts on the epidemiology of diverticular disease. *Clin Gastroenterol* 1986; **15**: 855-877
32 **Segal I**, Solomon A, Hunt JA. Emergence of diverticular disease in the urban South African black. *Gastroenterology* 1977; **72**: 215-219
33 **Nair P**, Mayberry JF. Vegetarianism, dietary fibre and gastrointestinal disease. *Dig Dis* 1994; **12**: 177-185
34 **Wess L**, Eastwood M, Busuttil A, Edwards C, Miller A. An association between maternal diet and colonic diverticulosis in an animal model. *Gut* 1996; **39**: 423-427
35 **Painter NS**. The cause of diverticular disease of the colon, its symptoms and its complications. Review and hypothesis. *J R Coll Surg Edinb* 1985; **30**: 118-122
36 **Lupton JR**, Turner ND. Potential protective mechanisms of wheat bran fiber. *Am J Med* 1999; **106**: 24S-27S
37 **Walker AR**, Walker BF, Richardson BD. Bowel transit times in Bantu populations. *BMJ* 1970; **3**: 48-49
38 **Chaussade S**, Roche H, Khyari A, Couturier D, Guerre J. A new method for measuring colonic transit time. Description and validation. *Gastroenterol Clin Biol* 1986; **10**: 385-389
39 **Ludeman L**, Warren BF, Shepherd NA. The pathology of diverticular disease. *Best Pract Res Clin Gastroenterol* 2002; **16**: 543-562
40 **Lin OS**, Soon MS, Wu SS, Chen YY, Hwang KL, Triadafilopoulos G. Dietary habits and right-sided colonic diverticulosis. *Dis Colon Rectum* 2000; **43**: 1412-1418
41 **Narducci F**, Bassotti G, Gaburri M, Morelli A. Twenty four hour manometric recording of colonic motor activity in healthy man. *Gut* 1987; **28**: 17-25
42 **Sugihara K**, Muto T, Morioka Y. Motility study in right sided diverticular disease of the colon. *Gut* 1983; **24**: 1130-1134
43 **Sasaki D**, Kido A, Yoshida Y. An endoscopic method to study the relationship between bowel habit and motility of the ascending and sigmoid colon. *Gastrointest Endosc* 1986; **32**: 185-189
44 **Arfwidsson S**. Pathogenesis of multiple diverticula of the sigmoid colon in diverticular disease. *Acta Chir Scand* 1964; **342** (Suppl): 1-68
45 **Painter NS**, Truelove SC, Ardran GM. Segmentation and the localization of intraluminal pressures in the human colon, with special reference to the pathogenesis of colonic diverticula. *Gastroenterology* 1965; **49**: 169-177
46 **Parks TG**, Connell AM. Motility studies in diverticular disease of the colon. *Gut* 1969; **10**: 534-542
47 **Ritsema GH**, Thijn CJ, Smout AJ. Motility of the sigmoid in irritable bowel syndrome and colonic diverticulosis. *Ned Tijdschr Geneeskd* 1990; **134**: 1398-1401
48 **Weinreich J**, Andersen D. Intraluminal pressure in the sigmoid colon. II. Patients with sigmoid diverticula and related conditions. *Scand J Gastroenterol* 1976; **11**: 581-586
49 **Weinreich J**, Moller SH, Andersen D. Colonic haustral pattern in relation to pressure activity and presence of diverticula. *Scand J Gastroenterol* 1977; **12**: 857-864
50 **Leandro A**, Cecconello I, Habr-Gama A, de Olivereira e Silva A, Pontes JF. Gastrointestinal motility in normal subjects and patients with diverticulosis of the colon. *Arq Gastroenterol* 1984; **21**:157-163
51 **Viebig RG**, Pontes JF, Michelson NH. Electromanometry of the rectosigmoid in colonic diverticulosis. *Arq Gastroenterol* 1994; **31**: 135-144
52 **Kratzsch KH**. Results of electromyographic studies of the rectosigmoid. *Dtsch Z Verdau Stoffwechselkr* 1985; **45**: 45-51
53 **Suchowiecky M**, Clarke DD, Bhasker M, Perry RJ, Snape WJ Jr. Effect of secoverine on colonic myoelectric activity in diverticular disease of the colon. *Dig Dis Sci* 1987; **32**: 833-840
54 **Trotman IF**, Misiewicz JJ. Sigmoid motility in diverticular disease and the irritable bowel syndrome. *Gut* 1988; **29**: 218-222
55 **Cortesini C**, Pantalone D. Usefulness of colonic motility study in identifying patients at risk for complicated diverticular disease. *Dis Colon Rectum* 1991; **34**: 339-342
56 **Cortesini C**, Bruno L, Pantalone D. Motility effects of anterior resection of the rectum performed for diverticular disease. *Ital J Surg Sci* 1989; **19**: 369-373
57 **Bassotti G**, Crowell MD. Colon and rectum: normal function and clinical disorder. Manometry. In Schuster MM, Crowell MD, Koch KL, eds. Schuster Atlas of Gastrointestinal Motility in health and disease. Second Edition. *BC Decker Inc, Hamilton* 2002: 241-252
58 **Bassotti G**, Gaburri M. Manometric investigation of high-amplitude propagated contractile activity of the human colon. *Am J Physiol* 1988; **255**: G660-G664
59 **Bassotti G**, Battaglia E, Spinozzi F, Pelli MA, Tonini M. Twenty-four hour recordings of colonic motility in patients with diverticular disease. Evidence for abnormal motility and propulsive activity. *Dis Colon Rectum* 2001; **44**: 1814-1820
60 **Di Lorenzo C,** Flores AF, Hyman PE. Age related changes in colon motility. *J Pediatr* 1995; **127**: 593-596
61 **Butt WG**, Wang M, Kaufmann ST. Age-related changes in rat colon mechanics. *J Gastrointest Mot* 1993; **5**: 121-128
62 **Garcia-Olmo D**, Sanchez PC. Patterns of colonic motility as recorded by a sham fecaloma reveal differences among patients with idiopathic chronic constipation. *Dis Colon Rectum* 1998; **41**:480-489
63 **Brann L**, Wood JD. Motility of the large intestine of piebald-lethal mice. *Am J Dig Dis* 1976; **21**: 633-640
64 **Simpson J**, Spiller RC. Colonic diverticular disease. *Clin Evid* 2002; **7**: 398-405

Edited by Xu XQ and Wang XL

P.O.Box 2345, Beijing 100023,China
Fax: +86-10-85381893
E-mail: wjg@wjgnet.com www.wjgnet.com

World J Gastroenterol 2003;9(10):2143-2148
World Journal of Gastroenterology
 ISSN 1007-9327

• ESOPHAGEAL CANCER •

Separation and identification of differentially expressed nuclear matrix proteins between human esophageal immortalized and carcinomatous cell lines

Xing-Dong Xiong, En-Min Li, Li-Yan Xu, Hai-Bin Chen, Ling Chen, Wei-Jia Cai, Ya-Li Han, Zhong-Ying Shen, Yi Zeng

Xing-Dong Xiong, En-Min Li, Department of Biochemistry and Molecular Biology, Medical College, Shantou University, Shantou 515031, Guangdong Province, China
Xing-Dong Xiong, En-Min Li, Li-Yan Xu, Zhong-Ying Shen, Wei-Jia Cai, Institute of Oncologic Pathology, Medical College, Shantou University, Shantou 515031, Guangdong Province, China
Hai-Bin Chen, Department of Histology and Embryology, Medical College, Shantou University, Shantou 515031, Guangdong Province, China
Ling Chen, Molecular Biological Center, Medical College, Shantou University, Shantou 515031, Guangdong Province, China
Ya-Li Han, Department of Biology, Shantou University, Shantou 515031, Guangdong Province, China
Yi Zeng, Institute of Virology, Chinese Academy of Preventive Medicine, Beijing 100052, China
Supported by the National Natural Science Foundation of China, No. 39900069, No.30170428; Natural Science Foundation of Guangdong Province, No.990799, No.010431; College Natural Science Foundation of Guangdong province, No.200033; Medical Scientific Foundation of Guangdong Province, No.A2001419 and Research and Development Foundation of Shantou University, No.L0004, No.L00012
Correspondence to: Dr. En-Min Li, Department of Biochemistry and Molecular Biology, Medical College, Shantou University, 22 Xinling Road, Shantou 515031, Guangdong Province, China. nmli@stu.edu.cn
Telephone: +86-754-8532720 +86-754-8900847
Received: 2002-11-19 **Accepted:** 2003-03-11

Abstract

AIM: To separate and identify differentially expressed nuclear matrix proteins (NMPs) between the immortalized human esophageal epithelial cell line (SHEE) and the malignantly transformed esophageal carcinoma cell line (SHEEC), and to provide new ways for finding specific markers and the pathogenesis of esophageal carcinoma.

METHODS: SHEE and SHEEC cell lines were used to extract NMPs. The quality of NMPs was monitored by Western blot analysis including DNA topoisomerase IIα, proliferation cell nuclear antigen (PCNA) and histone. NMPs of SHEE and SHEEC were analyzed by two-dimensional electrophoresis (2-DE), silver staining and PDQuest6.2 image analysis software. Three spots in which the differentially expressed NMPs were more obvious, were selected and analyzed with matrix-assisted laser desorption/ionization time of flying mass spectrometry (MALDI- TOF-MS) and database search.

RESULTS: Western blot analysis revealed that DNA topoisomerase IIα and PCNA were detected, and the majority of histones were deleted in NMPs of SHEE and SHEEC. After 2-DE image analysis by PDQuest6.2 software, the 2-DE maps were detected with an average of 106±7.1 spots in SHEE and 132±5.0 spots in SHEEC. Most of them were matched one another (r=0.72), only 16 protein spots were found differing in intensity. Three NMPs including cytoskeletal tropomyosin, FK506-binding protein 6, similar to retinoblastoma binding protein 8 were preliminarily identified by MALDI- TOF-MS.

CONCLUSION: These differentially expressed NMPs may play an important role during malignant transformation from SHEE to SHEEC. Their separation and identification will contribute to searching for specific markers and probing into the pathogenesis of esophageal carcinoma.

Xiong XD, Li EM, Xu LY, Chen HB, Chen L, Cai WJ, Han YL, Shen ZY, Zeng Y. Separation and identification of differentially expressed nuclear matrix proteins between human esophageal immortalized and carcinomatous cell lines. *World J Gastroenterol* 2003; 9(10): 2143-2148
http://www.wjgnet.com/1007-9327/9/2143.asp

INTRODUCTION

Nuclear matrix (NM) represents the insoluble structural framework of nucleus which removes membrane lipid, soluble protein and chromatin. According to many investigations, nuclear matrix has been shown to play an important role not only in maintaining the structure of nucleus, but also in chromatin/chromosome construction, DNA replication, gene expression and regulation (RNA synthesis, RNA splicing and RNA transportation)[1]. Recently changes of the composition, structure and function of NMPs in the generation and development of tumors have been more and more concerned. Separation and identification of tumor associated NMPs have been a new way to search for tumor specific markers and to study tumor pathogenesis. Nowadays several tumor specific NMPs have been separated and identified from hepatocellular carcinoma[2], colon cancer[3] and prostate cancer[4], etc. Some of them (such as NMP22) have been applied to clinical diagnosis and therapy[5], but studies of the separation and identification of esophageal carcinoma specific NMPs have not been carried out.

Esophageal carcinoma is one of the most common malignant tumors in China[6-27]. In recent years, it has been increasingly concerned about the roles of human papilloma virus (HPV) in esophageal carcinogenesis[28-32]. In our previous work, we transfected human embryonic esophageal mucosal cells with HPV18 E6E7 genes, and established an immortalized epithelial cell line SHEE[33,34]. The SHEE cells were further exposed to the tumor promoter (12-O-tetradecanoyl-phorbol-13-acetate, TPA) to induce malignant transformation from which a human embryonic esophageal epithelial carcinoma cell line SHEEC was then established[35,36]. These studies not only provided the evidence for the close relationship between HPV and esophageal carcinogenesis, but also established a reliable model for studying the molecular mechanisms of esophageal carcinogenesis. In the present study, the differentially expressed NMPs between SHEE and SHEEC were investigated by Western blot, 2-DE and MALDI-TOF-MS, and three esophageal carcinoma associated NMPs were preliminarily identified. The separation and identification of these proteins may contribute to searching for specific markers and studying the pathogenesis of esophageal carcinoma.

MATERIALS AND METHODS

Cell culture

SHEE and SHEEC were cultured in MEM medium (Gibco) supplemented with 100 ml/L fetal bovine serum (100 u/ml penicillin, 100 u/ml streptomycin) and incubated at 37 ℃ in humidified atmosphere of 50 ml/L CO_2. Cells were harvested when they grew into a full monolayer and kept at -70 ℃ until use.

Extraction of NMPs

The method used was modified from Fey *et al*[37]. Cultured cells were extracted by cytoskeleton (CSK) buffer (100 mM KCl, 3 mM $MgCl_2$, 1 mM EGTA, 10 mM PIPES pH6.8, 300 mM sucrose, 0.5 % triton X-100, 1.2 mM PMSF) for 5 min at 4 ℃. After centrifugation at 650 g for 5 min, the supernatants contained cytoplasmic proteins. The pellets were resuspended in digestion buffer (same as CSK buffer except with 50 mM NaCl instead of KCl) containing 400 μg/ml DNase I and 100 μg/ml RNase A. Enzyme digestion was carried out for 20 min at room temperature and terminated by adding cold ammonium sulfate to a final concentration of 0.25 M. After centrifugation at 1 000 g for 10 min, the pellets were then solubilized in disassembly buffer (8 M urea, 20 mM Mes pH6.6, 0.1 mM $MgCl_2$, 1 mM EGTA, 1 % 2-mercaptoethanol, 1 mM PMSF) and dialyzed overnight at 4 ℃ against 1 000 volumes of assembly buffer (150 mM KCl, 5 mM $MgCl_2$, 0.125 mM EGTA, 25 mM imidazole hydrochloride pH7.1, 2 mM dithiothreitol, 0.2 mM PMSF). The samples were centrifuged at 200 000 g for 100 min. The protein concentration of supernatants containing NMPs was determined by Bradford method and then precipitated in 5 volumes of absolute ethanol. The dried pellets were resuspended in electrophoresis sample buffer. The sample aliquots were stored at -70 ℃ until use.

Western blot

The experimental procedures were referred to *Molecular cloning*[38]. Briefly, the proteins were separated by SDS-PAGE and then transferred onto nitrocellulose membranes. Nonspecific reactivity was blocked by incubation overnight at 4 ℃ in buffer (10 mM Tris-HCl pH7.5, 150 mM NaCl, 2 % Tween-20, 4 % bovine sreum albumin). The membrane was then incubated with primary antibody including mouse anti-human histone (Roche), mouse anti-human DNA topoisomerase IIα. (Roche) and mouse anti-human PCNA (Dako). The secondary antibody (Zymed) was used to detect bound primary antibody. Reactive protein was detected by Western blot luminol reagent (Santa Cruz) and exposed to X-films (Kodak). The X-films were scanned and analyzed with Kodak 1-D 3.5 software (Kodak).

Two-dimensional electrophoresis

To separate NMPs, the 2-DE procedures were referred to Xiong *et al*[39]. Briefly, 2-DE was carried out by using the Mini-PROTEAN II 2-D apparatus (Bio-Rad). 90 μg of the NMPs was mixed with the rehydration solution to a total volume of 125 μl. After rehydration, the isoelectric focusing (IEF) and equilibration, and the IPG strips (pH4-7, 7 cm) were placed on a 1.0 mm thick, 10 % SDS-PAGE gel. On electrophoresis, the SDS-PAGE gels were stained with PlusOne™ silver staining kit (Phamacia).

Image acquisition and analysis

Image scanning for the silver-stained 2-D gels was performed with EDAS290 digital camera system (Kodak) and image analysis with the PDQuest 6.2 software (Bio-Rad). To obtain reliable results, three gels were employed for each cell line. After the background subtraction, spot detection and match, one standard gel for each cell line was obtained. These standard gels were then matched to yield information about the spots of differentially expressed NMPs.

Protein identification by MALDI-TOF-MS

Three spots in which the differentially expressed protein was more obvious in each cell line were cut out from the gel. The gel pieces were treated by a series of steps including silver-removal, reduction, alkylation and in-gel digestion with trypsin. The peptide mass maps were generated by Applied Biosystems Voyager System 6192 MALDI-TOF-mass spectrometry (ABI, USA). Peptide masses were analyzed using the MS-Fit search program (http:// prospector.ucsf.edu/ucsfhtml4.0u/ msfit.htm).

RESULTS

Evaluation of NMPs quality

The NMPs extracted from SHEE and SHEEC were evaluated by Western blot, and the aim of evaluation was to monitor whether some NMPs were lost and whether other non-NMPs components were mixed. In recent years, many studies proved that DNA topoisomerase IIα and PCNA were the major components of NMPs[40,41], the existence of histone in nucleosome was the major soluble protein of nucleus. In our study, 170 kD DNA topoisomerase IIα was detected in the nuclear protein fraction of SHEE and SHEEC at the same position of NMPs fraction, but the density in NMPs fraction was weaker than that in the nuclear protein fraction (Figure 1). This agreed with other reports[40]. PCNA (36kD) was detected in the NMPs fraction of SHEE and SHEEC, and this showed PCNA was the major protein of NMPs (Figure 2). Moreover, histone was seen at 23 kD and 12-15 kD in the nuclear protein fraction (Mw of histone: H1:23 kD, H2A:14.5 kD, H2B: 13.8 kD, H3:15 kD, H4:11.8 kD) and almost no histone was detected at the same position of NMPs (Figure 3). This showed majority of histone was removed during extraction and there was almost no histone in the NMPs fraction of SHEE and SHEEC. According to these results, the NMPs fractions extracted from SHEE and SHEEC almost deleted the histone and retained the major NMPs components including DNA topoisomerase IIα and PCNA, so the NMPs were pure in high quality.

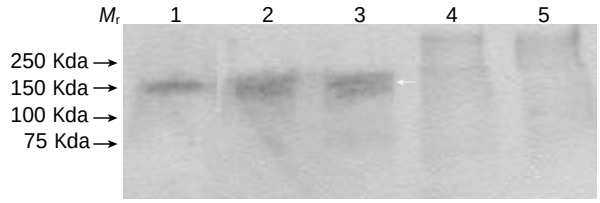

Figure 1 Western blot analysis of DNA topoisomerase IIα. Lane 1, nuclear matrix fraction of SHEE. Lane 2, total crude nuclear protein fraction of SHEEC. Lane 3, total crude nuclear protein fraction of SHEE. Lane 4, cytoplasmic protein fraction of SHEEC. Lane 5, cytoplasmic protein fraction of SHEE. M_r, molecular weight standard.

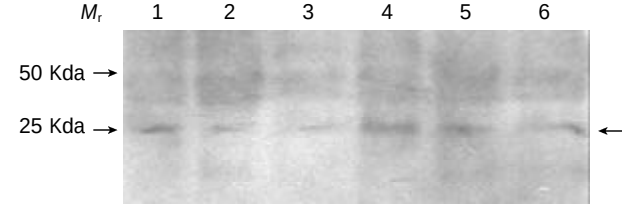

Figure 2 Western blot analysis of PCNA. Lane 1 to Lane 3, nuclear matrix fraction of SHEEC. Lane 4 to Lane 6, nuclear matrix protein of SHEE. M_r, molecular weight standard.

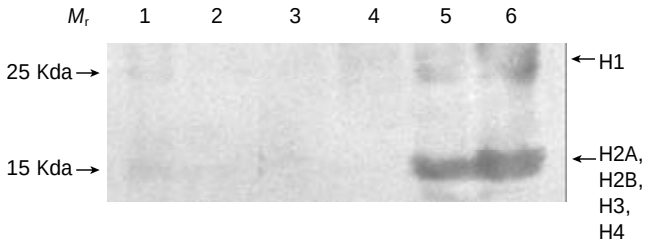

Figure 3 Western blot analysis of histone. Lane 1, nuclear matrix fraction of SHEEC. Lane 2, nuclear matrix protein of SHEE. Lane 3, cytoplasmic protein fraction of SHEEC. Lane 4, cytoplasmic protein fraction of SHEE. Lane 5, total crude nuclear protein fraction of SHEEC. Lane 6, total crude nuclear protein fraction of SHEE. *M*r, molecular weight standard.

2-D map and image analysis

To obtain a higher electrophoretic resolution, IPG strips (pH4-7) were selected to separate the NMPs of SHEE and SHEEC in our study because the p*I* range of NMPs was mainly in acid pH. Three pairs of gels from different batches of SHEE and SHEEC were analyzed by using the software PDQuest6.2. There were 106±7.1 and 132±5.0 protein spots observed in SHEE and SHEEC respectively. Most of them were matched one another (r=0.72), only 16 protein spots were found differing in intensity. These 16 protein spots belonged to 4 types. Namely A: one protein spot was detected in SHEE (No.2). B: Seven protein spots were detected only in SHEEC (No.3, 4, 9, 11, 12, 14, 16), C: One protein spot was expressed higher in SHEE (No.1), D: Seven protein spots were expressed higher in SHEEC (No.5, 6, 7, 8, 10, 13, 15). According to the standard molecular weight and pH gradient of IPG strips, the positions of these 16 protein spots were estimated with the software PDQuest6.2 (Table 1). Three protein spots (No.4, 14, 16) which belonged to type B and had a higher intensity were selected and analyzed with MALDI-TOF-MS (Figure 4).

MALDI-TOF-MS analysis and protein identification

These three protein spots (No.4, 14, 16) were cut out from the gels and analyzed with MALDI-TOF-MS. Peptide mass fingerprint (PMF) of each protein spot was then generated (Figure 5). By searching the NCBInr protein database with the MS-Fit search program, we identified these three proteins combined with the searching results. The characteristics of the protein, the number and intensity of peptide matching peak, the sequence coverage of matching peptide, as well as the theoretical and approximate values of M_r and p*I*, the identified protein names, accession numbers, as well as the sequence coverages, the theoretical M_r and p*I* values for each protein spot are listed in Table 2.

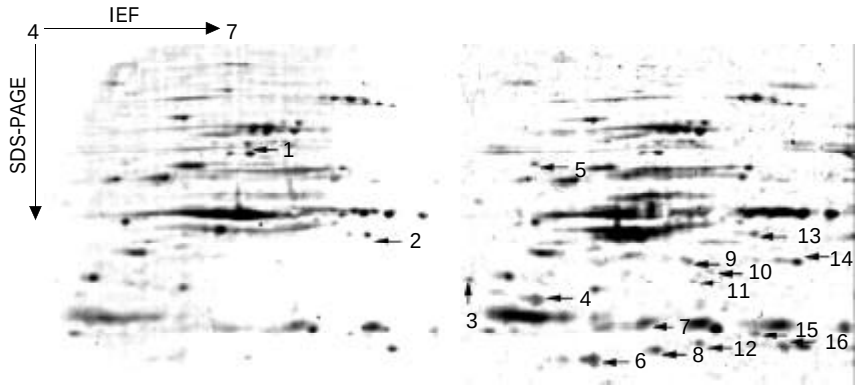

Figure 4 Differentially expressed NMP spots observed in SHEE (left) and SHEEC (right) two-dimensional gels (IPG dry strips: pH 4-7, 7 cm). The arrows show differentially expressed protein spots. Three protein spots (No.4, 14, 16) were selected and analyzed with MALDI-TOF-MS.

Table 1 Differentially expressed protein spots between SHEE and SHEEC

Spot No.	Type	Experimental M_r	Experimental p*I*	Spot No.	Type	Experimental M_r	Experimental p*I*
1	C	73.0	5.55	9	B	38.2	5.79
2	A	45.1	6.60	10	D	35.8	5.96
3	B	34.0	4.10	11	B	33.5	5.83
4	B	30.0	4.60	12	B	23.1	5.88
5	D	62.5	4.50	13	D	44.6	6.32
6	D	21.0	5.03	14	B	37.6	6.66
7	D	26.2	5.45	15	D	24.6	6.33
8	D	22.2	5.53	16	B	22.7	6.54

Table 2 Proteins identified by MALDI-TOF-MS

Spot No.	Accession No.(gi)	Theoretical M_r	Theoretical p*I*	Intensity matched	Length (aa)	Name of protein
4	37424	27975	4.8	44 %	239	Cytoskeletal tropomyosin
14	17149849	37227	6.9	29 %	327	FK506-binding protein 6
16	13647876	26775	5.7	54 %	230	Similar to retinoblastoma binding protein 8

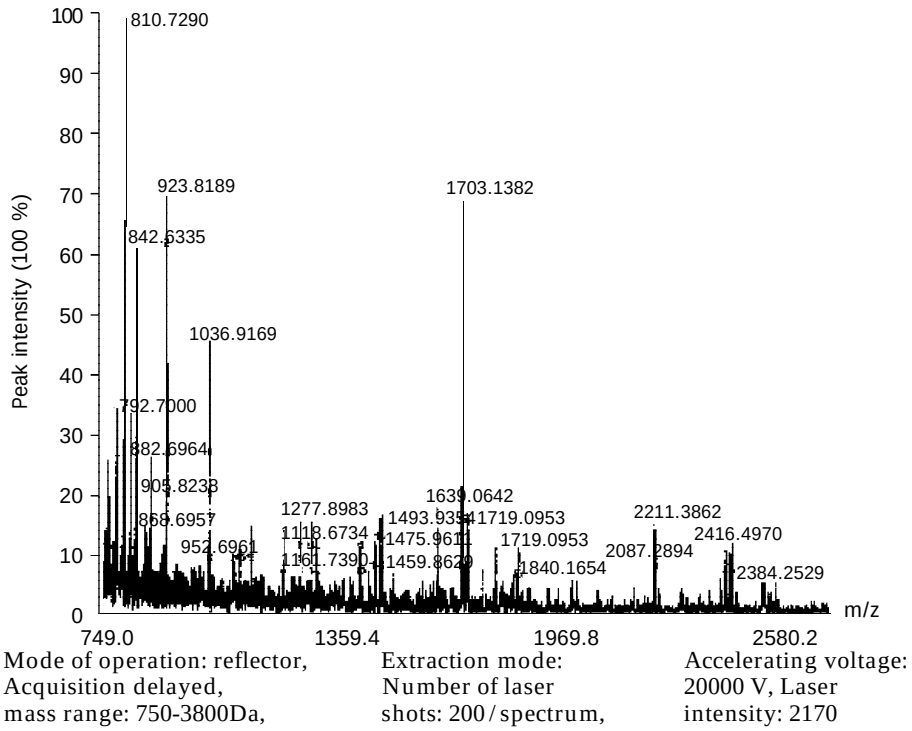

Figure 5 MALDI-TOF mass spectrum map of protein spot 16.

DISCUSSION

In the present study, we studied the differentially expressed NMPs extracted from SHEE and SHEEC by Western blot, 2-DE and MALDI-TOF-MS, and preliminarily identified three differentially expressed NMPs. According to their characteristics, these three proteins were connected with diseases such as colon carcinoma and myofibroblastic tumor, etc, but they were not related to esophageal carcinoma.

Cytoskeletal tropomyosin (tropomyosin 3, cytoskeletal (TPM3)) belongs to the tropomyosin family. There were at least 5 isoforms in tropomyosins including TPM1, TPM2, TPM3, TPM4, TPM5 which were produced by a tissue-specific alternative mRNA splicing mechanism[42]. The tropomyosins were a group of actin-binding proteins which served to mediate the effect of Ca^{2+} on the actin-myosin interaction[43]. Actin is one of the major components of NMPs. Owing to active cell division during the course of malignant transformation, cytoskeletal tropomyosin connected with actin in the nucleus becomes overexpressed. Zeng and his associates[44] found that tropomyosin was localized in the nuclear matrix and chromosome scaffold, and dispersively distributed in the interphase nuclei and metaphase chromosomes. Many studies have proved that cytoskeletal tropomyosin is related to the generation and development of tumors. Martin-Zanca and his associates[45] found the oncogene-Onc D (named later "trk" (tropomyosin(t)-receptor(r) -kinase(k)) in colon carcinoma. Sequence analysis for the oncogene Onc D found that it was generated by a somatic rearrangement of two genes, one of which coded for cytoskeletal tropomyosin (TPM3) and the other for a tyrosine-specific protein kinase. The amino end of TPM3 has been found to be fused with tyrosine protein kinase domain and has become a new oncogenic protein. These results indicate that cytoskeletal tropomyosin is related to the generation and development of colon carcinoma. Furthermore, Lawrence and his associates[46] reported that TPM3-ALK (anaplastic lymphoma kinase, ALK) and TPM4-ALK fusion genes occurred in inflammatory myofibroblastic tumors. In our study, cytoskeletal tropomyosin (TPM3) showed overexpression in the NMPs fraction of SHEEC cells, indicating that cytoskeletal tropomyosin as a oncoprotein might be related to esophageal carcinoma. But its characteristics and functions in esophageal carcinoma remain to be further studied.

FK506-binding protein 6 (FKBP6) is one member of FKBP family. The FKBP family proteins were those directly binding to the immunosuppressant drug FK506[47]. So far there are several FKBP family members, namely FKBP6, FKBP12, FKBP13, FKBP25 and FKBP52. These FKBP family members differ in their subcellular localization. FKBP12 and FKBP52 are localized in the cytosol, FKBP13 in the endoplasmic reticulum, and FKBP25 in the nucleus. Like other FKBP members, FKBP6 had some peptidyl-prolyl cis-trans isomerase activity and a drug binding site[48]. Owing to its possession of cis-trans isomerase activity, FKBPs are thought to be essential for protein folding during protein synthesis. FKBP6 gene is localized in chromosome 11 and consists of nine exons. Meng and his associates[49] found FKBP6 gene was deleted in Williams syndrome (WS), and this might contribute to certain defects such as hypercalcemia and growth delay in WS. In our study, FKBP6 was overexpressed in the NMPs fraction of SHEEC. This indicated that FKBP6 as an active NMP might play a role during malignant transformation of the immortalized human esophageal epithelial cells.

Similar to retinoblastoma binding protein 8 (STRBP8), it contains 230 amino acid residues. Its sequences are the same as residues 668-897 of retinoblastoma binding protein 8 (RBP8), and so it is named STRBP8. So far there are not any reports about the function of STRBP8. Moreover, RBP8 is localized in the nucleus. It might interact with some tumor suppressive factors including CtBP1, Rb1 and BRCA1, and was involved in transcription regulation and tumor suppression[50,51]. The interaction with CtBP1 requires a short amino acid motif PLDLS (residues 490-494) of RBP8, whereas the Rb1 tumor suppressor binding to a LXCXE motif is located within the N-terminal region of RBP8 (residues 153-157). Unlike RBP8, STRBP8 has no Rb1 binding motif (sequence LXCXE) and CtBP1 binding motif (sequence PLDLS). The results indicate that STRBP8 possibly loses the function of tumor suppression and on the contrary possesses carcinogenetic effect. The fact that STRBP8 was overexpressed in SHEEC in our study, showed that STRBP8 as a new oncoprotein might

be involved in the malignant transformation of SHEE.

Although three NMPs have been found to be associated with esophageal carcinoma in the present study, but whether they would become specific markers of esophageal carcinoma needs to be further studied. In addition, the generation and development of tumors are the extraordinary pathological complex phenomena, and the process of coordinated interaction and programed development of many proteins. It will help elucidate the process of tumor generation and development to study the network relationship of these tumor associated proteins. Therefore, the network functional relationship of these differentially expressed NMPs needs to be further studied.

REFERENCES

1 **Pederson T**. Thinking about a nuclear matrix. *J Mol Biol* 1998; **277**: 147-159
2 **Yoon GS**, Lee H, Jung Y, Yu E, Moon HB, Song K, Lee I. Nuclear matrix of calreticulin in hepatocellular carcinoma. *Cancer Res* 2000; **60**: 1117-1120
3 **Brunagel G**, Vietmeier BN, Bauer AJ, Schoen RE, Getzenberg RH. Identification of nuclear matrix protein alterations associated with human colon cancer. *Cancer Res* 2002; **62**: 2437-2442
4 **Lakshmanan Y**, Subong EN, Partin AW. Differential nuclear matrix protein expression in prostate cancers:correlation with pathologic stage. *J Urol* 1998; **159**: 1354-1358
5 **Oge O**, Atsu N, Kendi S, Ozen H. Evaluation of nuclear matrix protein 22 (NMP22) as a tumor marker in the detection of bladder cancer. *Int Urol Nephrol* 2001; **32**: 367-370
6 **Xiong XD**, Xu LY, Shen ZY, Cai WJ, Luo JM, Han YL, Li EM. Identification of differentially expressed proteins between human esophageal immortalized and carcinomatous cell lines by two-dimensional electrophoresis and MALDI-TOF-mass spectrometry. *World J Gastroenterol* 2002; **8**: 777-781
7 **Hou J**, Lin PZ, Chen ZF, Ding ZW, Li SS, Men FS, Guo LP, He YT, Qiao CY, Guo CL, Duan JP, Wen DG. Field population-based blocking treatment of esophageal epithelia dysplasia. *World J Gastroenterol* 2002; **8**: 418-422
8 **Hao MW**, Liang YR, Liu YF, Liu L, Wu MY, Yang HX. Transcription factor EGR-1 inhibits growth of hepatocellular carcinoma and esophageal carcinoma cells lines. *World J Gastroenterol* 2002; **8**: 203-207
9 **Shen ZY**, Shen WY, Chen MH, Shen J, Cai WJ, Zeng Y. Mitochondria, calcium and nitric oxide in the apoptotic pathway of esophageal carcinoma cells induced by As203. *Int J Mol Med* 2002; **9**: 385-390
10 **Xu M**, Jin YL, Fu J, Huang H, Chen SZ, Qu P, Tian HM, Liu ZY, Zhang W. The abnormal expression of retinoic acid receptor-β, p53 and Ki67 protein in normal, premalignant and malignant esophageal tissues. *World J Gastroenterol* 2002; **8**: 200-202
11 **Deng LY**, Zhang YH, Xu P, Yang SM, Yuan XB. Expression of IL 1β converting enzyme in 5-FU induced apoptosis in esophageal carcinoma cells. *World J Gastroenterol* 1999; **5**: 50-52
12 **Wang AH**, Sun CS, Li LS, Huang JY, Chen QS. Relationship of tobacco smoking, CYP1A1, GSTM1 gene polymorphism and esophageal cancer in Xi'an. *World J Gastroenterol* 2002; **8**: 49-53
13 **Shen ZY**, Xu LY, Li EM, Cai WJ, Chen MH, Shen J, Zeng Y. Telomere and telomerase in the initial stage of immortalization of esophageal epithelial cell. *World J Gastroenterol* 2002**; 8**: 357-362
14 **Shen ZY**, Shen WY, Chen MH, Shen J, Cai WJ, Yi Z. Nitric oxide and calcium ions in apoptotic esophageal carcinoma cells induced by arsenite. *World J Gastroenterol* 2002; **8**: 40-43
15 **Shen ZY**, Shen J, Li QS, Chen CY, Chen JY, Zeng Y. Morphological and functional changes of mitochondria in apoptotic esophageal carcinoma cells induced by arsenic trioxide. *World J Gastroenterol* 2002; **8**: 31-35
16 **Shen ZY**, Xu LY, Li C, Cai WJ, Shen J, Chen JY, Zeng Y. A comparative study of telomerase activity and malignant phenotype in multistage carcinogenesis of esophageal epithelial cells induced by human papillomavirus. *Int J Mol Med* 2001; **8**: 633-639
17 **Yu GQ**, Zhou Q, Ivan D, Gao SS, Zheng ZY, Zou JX, Li YX, Wang LD. Changes of p53 protein blood level in esophageal cancer patients and normal subjects from a high incidence area in Henan, China. *World J Gastroenterol* 1998; **4**: 365-366
18 **Li J**, Feng CW, Zhao ZG, Zhou Q, Wang LD. A preliminary study on ras protein expression in human esophageal cancer and precancerous lesions. *World J Gastroenterol* 2000; **6**: 278-280
19 **Liu XL**, Xiao B, Yu ZC, Guo JC, Zhao QC, Xu L, Shi YQ, Fan DM. Down-regulation of Hsp90 could change cell cycle distribution and increase drug sensitivity of tumor cells. *World J Gastroenterol* 1999; **5**: 199-208
20 **Zhang LJ**, Chen KN, Xu GW, Xing HP, Shi XT. Congenital expression of mdr-1 gene in tissues of carcinoma and its relation with pathomorphology and prognosis. *World J Gastroenterol* 1999; **5**: 53-56
21 **Gao SS**, Zhou Q, Li YX, Bai YM, Zheng ZY, Zou JX, Liu G, Fan ZM, Qi YJ, Zhao X, Wang LD. Comparative studies on epithelial lesions at gastric cardia and pyloric antrum in subjects from a high incidence area for esophageal cancer in Henan, China. *World J Gastroenterol* 1998; **4**: 332-333
22 **Shen ZY**, Tan LJ, Cai WJ, Shen J, Chen C, Tang XM, Zheng MH. Arsenic trioxide induces apoptosis of oesophageal carcinoma *in vitro*. *Int J Mol Med* 1999; **4**: 33-37
23 **Shen ZY**, Shen J, Cai WJ, Hong C, Zheng MH. The alteration of mitochondria is an early event of arsenic trioxide induced apoptosis in esophageal carcinoma cells. *Int J Mol Med* 2000; **5**: 155-158
24 **Gu ZP**, Wang YJ, Li JG, Zhou YA. VEGF165 antisense RNA suppresses oncogenic properties of human esophageal squamous cell carcinoma. *World J Gastroenterol* 2002; **8**: 44-48
25 **Su M**, Lu SM, Tian DP, Zhao H, Li XY, Li DR, Zheng ZC. Relationship between ABO blood groups and carcinoma of esophagus and cardia in Chaoshan inhabitants of China. *World J Gastroenterol* 2001; **7**: 657-661
26 **Wu MY**, Chen MH, Liang YR, Meng GZ, Yang HX, Zhuang CX. Experimental and clinicopathologic study on the relationship between transcription factor Egr-1 and esophageal carcinoma. *World J Gastroenterol* 2001; **7**: 490-495
27 **Xiao ZF**, Yang ZY, Zhou ZM, Yin WB, Gu XZ. Radiotherapy of double primary esophageal carcinoma. *World J Gastroenterol* 2000; **6**: 145-146
28 **Chen HB**, Chen L, Zhang JK, Shen ZY, Su ZJ, Cheng SB, Chew EC. Human papillomavirus 16 E6 is associated with the nuclear matrix of esophageal carcinoma cells. *World J Gastroenterol* 2001; **7**: 788-791
29 **Lavergne D**, de-Villiers EM. Papillomavirus in esophageal papillomas and carcinomas. *Int J Cancer* 1999; **80**: 681-684
30 **Xu LY**, Li EM, Xiong HQ, Cai WJ, Shen ZY. Study of neutrophil gelatinase associated lipocalin (NGAL) gene overexpression in the progression of malignant transformation of human immortalized esophageal epithelial cell. *Shengwu Huaxue Yu Shengwu Wuli Jinzhan* 2001; **28**: 839-843
31 **Ma QF**, Jiang H, Feng YQ, Wang XP, Zhou YA, Liu K, Jia ZL. Detection of human papillomavirus DNA in squamous cell carcinoma of the esophagus. *Shijie Huaren Xiaohua Zazhi* 2000; **8**: 1218-1224
32 **Zhang J**, Yan XJ, Yan QJ, Duan J, Hou Y, Su CZ. Cloning and expression of HPV16 L2 DNA from esophageal carcinoma in E. coli. *Shijie Huaren Xiaohua Zazhi* 2001; **9**: 273-278
33 **Shen ZY**, Xu LY, Chen XH, Cai WJ, Shen J, Chen JY, Huang TH, Zeng Y. The genetic events of HPV-immortalized esophageal epithelium cells. *Int J Mol Med* 2001; **8**: 537-542
34 **Shen ZY**, Cen S, Cai WJ, Teng ZP, Shen J, Hu Z, Zeng Y. Immortalization of human fetal esophageal epithelial cells induced by E6 and E7 genes of human papillomavirus 18. *Zhonghua Shiyan He Linchuang Bingduxue Zazhi* 1999; **13**: 121-124
35 **Shen ZY**, Cai WJ, Shen J, Xu JJ, Cen S, Teng ZP, Hu Z, Zeng Y. Human papilloma virus 18E6E7 in synergy with TPA induced malignant transformation of human embryonic esophageal epithelial cells. *Bingdu Xuebao* 1999; **15**: 1-5
36 **Shen Z**, Cen S, Shen J, Cai W, Xu J, Teng Z, Hu Z, Zeng Y. Study of immortalization and malignant transformation of human embryonic esophageal epithelial cells induced by HPV18 E6E7. *J Cancer Res Clin Oncol* 2000; **126**: 589-594
37 **Fey EG**, Penman S. Nuclear matrix proteins reflect cell type of origin in cultured human cells. *Proc Natl Acad Sci U S A* 1988; **85**: 121-125

38 **Sambrook J**, Fritsch EF, Maniatis T. *Molecular cloning A Laboratory Manual, 3th ed*. Jin DY, Li MF, trans-ed, Beijing, China: *Sci Pub* 1998: 888-898

39 **Xiong XD**, Xu LY, Shen ZY, Han M, Niu YD, Han YL, Li EM. An optimized protocol for two-dimensional gel electrophoresis. *Shantou Daxue Xuebao* 2002; **17**: 5-9

40 **Fernandes DJ**, Qiu J, Catapano CV. DNA topoisomerase II isozymes involved in anticancer drug action and resistance. *Adv Enzyme Regul* 1995; **35**: 265-281

41 **Balajee AS**, May A, Bohr VA. Fine structural analysis of DNA repair in mammalian cells. *Mutat Res* 1998; **404**: 3-11

42 **Reinach FC**, MacLeod AR. Tissue-specific expression of the human tropomyosin gene involved in the generation of the trk oncogene. *Nature* 1986; **322**: 648-650

43 **MacLeod AR**, Houlker C, Reinach FC, Talbot K. The mRNA and RNA-copy pseudogenes encoding TM30nm, a human cytoskeletal tropomyosin. *Nucleic Acids Res* 1986; **14**: 8413-8426

44 **Zeng XL**, Jiao MD, Xing M, Wang XG, Hao S. Tropomyosin is localized in the nuclear matrix and chromosome scaffold of Physarum polycephalum. *Cell Res* 1999; **9**: 61-69

45 **Martin-Zanca D**, Hughes SH, Barbacid M. A human oncogene formed by the fusion of truncated tropomyosin and protein tyrosine kinase sequences. *Nature* 1986; **319**: 743-748

46 **Lawrence B**, Perez-Atayde A, Hibbard MK, Rubin BP, Dal Cin P, Pinkus JL, Pinkus GS, Xiao S, Yi ES, Fletcher CD, Fletcher JA. TPM3-ALK and TPM4-ALK oncogenes in inflammatory myofibroblastic tumors. *Am J Pathol* 2000; **157**: 377-384

47 **Fruman DA**, Bierer BE, Benes JE, Burakoff SJ, Austen KF, Katz HR. The complex of FK506-binding protein 12 and FK506 inhibits calcineurin phosphatase activity and IgE activation-induced cytokine transcripts, but not exocytosis, in mouse mast cells. *J Immunol* 1995; **154**: 1846-1851

48 **Jin YJ**, Burakoff SJ. The 25-kDa FK506-binding protein is localized in the nucleus and associates with casein kinase II and nucleolin. *Proc Natl Acad Sci U S A* 1993; **90**: 7769-7773

49 **Meng X**, Lu X, Morris CA, Keating MT. A novel human gene FKBP6 is deleted in Williams syndrome. *Genomics* 1998; **52**: 130-137

50 **Schaeper U**, Subramanian T, Lim L, Boyd JM, Chinnadurai G. Interaction between a cellular protein that binds to the C-terminal region of adenovirus E1A (CtBP) and a novel cellular protein is disrupted by E1A through a conserved PLDLS motif. *J Biol Chem* 1998; **273**: 8549-8552

51 **Yu X**, Baer R. Nuclear localization and cell cycle-specific expression of CtIP, a protein that associates with the BRCA1 tumor suppressor. *J Biol Chem* 2000; **275**: 18541-18549

Edited by Wu XN and Wang XL

P.O.Box 2345, Beijing 100023,China
Fax: +86-10-85381893
E-mail: wjg@wjgnet.com www.wjgnet.com

World J Gastroenterol 2003;9(10):2149-2153
World Journal of Gastroenterology
 ISSN 1007-9327

• GASTRIC CANCER •

15d-PGJ$_2$ inhibits cell growth and induces apoptosis of MCG-803 human gastric cancer cell line

Yun-Xian Chen, Xue-Yun Zhong, Yan-Fang Qin, Wang Bing, Li-Zhen He

Yun-Xian Chen, Department of Hematology, the First Affiliated Hospital of Sun-Yat-Sen University, Guangzhou 510080, Guangdong Province, China
Xue-Yun Zhong, Yan-Fang Qin, Wang Bing, Li-Zhen He, Department of Pathology, Medical College, Jinan University, Guangzhou 510632, Guangdong Province, China
Supported by Science Fund of Guangdong Province, No. 015012, Science Fund of Guangzhou, 2001-Z-01-2 and the State 973 Projects, 2002ccc0400
Correspondence to: Dr. Xue-Yun Zhong, Department of Pathology, Medical College, Jinan University, Guangzhou 510632, Guangdong Province, China. tzxy@jnu.edu.cn
Telephone: +86-20-85220252
Received: 2003-04-08 **Accepted:** 2003-05-19

Abstract

AIM: To investigate the influence of peroxisome proliferator-activated receptor γ (PPARγ) ligand, 15-deoxy-△12, 14-prostaglandin J_2 (15dPGJ$_2$) on the proliferation and apoptosis of MCG-803 human gastric cancer cell lines.

METHODS: Cell proliferation was measured by ^{3}H-TdR assay. Apoptosis was determined by ELISA and TUNEL staining. Protein and mRNA level of bcl-2 family and COXs were measured by Western blotting and Northern blotting respectively. PGE_2 production was examined by RIA.

RESULTS: 15dPGJ$_2$ inhibited cell growth and induced apoptosis of MCG-803 cells. The COX-2 and bcl-2/bax ratios were decreased following 15dPGJ$_2$ treatment. The PGE_2 production in supernatants was also decreased. These changes were in a dose-dependent manner.

CONCLUSION: 15dPGJ$_2$ may be a useful therapeutic agent for the treatment of gastric cancer.

Chen YX, Zhong XY, Qin YF, Bing W, He LZ. 15d-PGJ$_2$ inhibits cell growth and induces apoptosis of MCG-803 human gastric cancer cell line. *World J Gastroenterol* 2003; 9(10): 2149-2153
http://www.wjgnet.com/1007-9327/9/2149.asp

INTRODUCTION

Peroxisome proliferator-activated receptor γ (PPARγ), a nuclear hormone receptor, provided a strong link between lipid metabolism and the regulation of gene transcription[1,2]. Recent studies showed that PPARγ was expressed at high levels in human colon cancer cells[3-5]. Ligand activation of PPARγ in human colon cancer cells caused a reduction of growth[3,4]. In contrast, two independent groups demonstrated that activation of PPARγ promoted the development of colon tumors in mice[6,7]. Thus the roles of PPARγ activation in the growth of colon tumors are controversial. In addition to colon cancer, PPARγ activation induced growth arrest in human liposarcoma, prostate cancer and breast cancer[8-10]. These results suggest that PPARγ activation may be implicated in the proliferation and apoptosis of malignant tumor cells.

Gastric cancer is the most common malignant tumor of gastrointestinal tract in the world. The survival rate in gastric cancer is poor. Although PPARγ expression has been studied in various epithelial cancer cell lines such as colon, prostate and breast, no information is available as to whether PPARγ is involved in the regulation of gastric cancer cell survival. In the present study, we investigated the effect of natural PPARγ ligand, 15dPGJ$_2$ on the growth and apoptosis of gastric cancer cell lines. We have further examined the role of bcl-2 family in the regulation of 15dPGJ$_2$-induced apoptosis. In addition, the change of cyclooxyenase (COXs) and the rate-limiting enzyme in the synthesis of prostaglandins (PGs) have been investigated in the process since COXs is recently considered as a promoter of human gastrointestinal cancer.

MATERIALS AND METHODS

Cell line and reagents

MCG-803 gastric cancer cell was kindly provided by Cancer Institute, Zhongshan University. Cells were maintained in RPMI-1640 medium and supplemented with 10 % new fetal bovine serum. Antibodies used in this study were obtained from Santa Cruz Biotech. The apoptosis ELISA kit and RIA kit were purchased from Sigma.

[^{3}H] Thymidine incorporation

Cells were planted in 96-well plates and grown for 24 h after they were serum starved for 48 h. They were treated with 15dPGJ$_2$ for 48 h and pulsed with 5 μCi of [^{3}H] thymidine for 4 h. We counted the radioactivity in Beckman L5 counter after washing the cells and stopping the reaction with 5 % trichloroacetic acid and solubilizing the cells in 0.5 % of 0.25 N sodium hydroxide. Each experiment was done in quadruplicates and repeated at least three times.

TUNEL

TUNEL assay was performed using the apoptosis detection system.15dPGJ$_2$ (0, 10, 30 μM) was added to the culture medium for 48 h. Cells were fixed with 4 % paraformaldehyde in PBS overnight at 4 ℃. The samples were washed three times in PBS and permeabilized by 0.2 % Triton X-100 in PBS for 15 min on ice. After washed twice, cells were equilibrated at room temperature for 15-30 min in equilibration buffer (200 mmol/L potassium cacodylate, 0.2 mmol/L dithiothreitol, 0.25 g· L^{-1} bovine serum albumin, and 2.5 mmol/L cobalt chloride in 25 mmol/L Tris-HCL, pH 6.6) and incubated in the presence of 5 μmol/L pluorescein-12-dUTP, 10 μmol/L dATP, 100 μmol/L ethylenediaminetetraacetic acid (EDTA), and terminal deoxynucleotidyl transferase at 37 ℃ for 1.5 h in dark. The tailing reaction was terminated by 2×standard saline citrate (SSC). The samples were washed three times in PBS and analyzed by fluorescence microscopy. At least 1000 cells were counted, and the percentage of TUNEL-positive cells was determined.

Detection of apoptotic DNA fragmentation

MCG-803 cells were grown in 96-well culture plates. The cells

were incubated with various doses of $15dPGJ_2$ for 24 h. Apoptotic DNA fragmentation was determined using a commercially available enzyme-linked immunosorbent assay (ELISA) kit from Sigma. This assay was based on a quantitative Sandwich enzyme-immunoassay directed against cytoplasmic histone-associated DNA fragments. Briefly, the cells were incubated in 200 μL lysis buffer provided with the kit, the lysates were centrifuged, and 20 μL supernatant containing cytoplasmic histone-associated DNA fragments were reacted overnight at 4 ℃ in streptavidin-coated microtitrator wells with 80 μL immunoreagent mixture containing biotinylated anti-histone antibody and peroxidase-conjugated anti-DNA antibody. After washED, the immunocomplex-bound peroxidase was probed with 2, 2' -azino-di [3-ethylbenzthiazoline sulfonate] for spectrophotometric detection at 405 nm.

RIA for PGE2

The amounts of immunoreactive PGE_2 in supernatants were determined by radioimmunoassay (RIA) using a commercially available RIA kit according to the manufacturer' s instructions. Briefly, to each polypropylene RIA tube were added 100 μL each of anti-PGE_2, ^{125}I-PGE_2 , and PGE_2 or the sample. Immune complexes were precipitated 24 h later with 1 ml of 16 % polyethylene glycol solution, and a gamma counter determined the radioactivity in the precipitate. There was no nonspecific interference of the assay by the components of the sample. Determinations were carried out in triplicate and the means and standard deviations were obtained.

Western blot analysis

The cells were lysed in lysis buffer containing 25 mM Hepes, 1.5 % Triton X-100, 1 % sodium deoxycholate, 0.1 % SDS, 0.5 M NaCl, 5 mM EDTA, 50 mM NaF, 0.1 mM sodium vanadate, 1 mM phenylmethylsulfonyl fluoride (PMSF), and 0.1 g/L eupeptic (pH7.8) at 4 ℃ with sonication. The lysates were centrifuged at 15 000×g for 15 min and the concentration of the protein in each lysate was determined with Coomassie brilliant blue G-250. Loading buffer (42 mM Tris-HCl, 10 % glycerol, 2.3 % SDS, 5 % 2-mercaptoethanol and 0.002 % bromophenol blue) was then added to each lysate, which was subsequently boiled for 3 min and then electrophoresed on a SDS-polyacrylamidel gel. Proteins were transferred to nitrocellulose and incubated respectively with antibodies against COX-1, COX-2, PPARγ, Bcl-2, bax, bcl-x_l and β-actin, and then with peroxidase-conjugated secondary antibodies. Detection was performed with enhanced chemiluminescence reagent.

Northern blot

Total mRNA was isolated and stored at -80 ℃ until use. The synthetic DNA oligonucleotide probes complemented to COX-1, COX-2, PPARγ, Bcl-2, bax, bcl-x_l and β-actin mRNA were labeled using terminal deoxynucleotidyltransferase [Boehringer]. Thirty mg of RNA per sample was separated on 1 % agarose-formaldehyde gels and transferred to nylon membranes. The blots were hybridized overnight at 42 ℃, washed in 0.2×SSC containing 0.1 % SDS at 50 ℃ for 10 min, and subjected to autoradiography.

Statistical analysis

Data were presented as the mean ± standard error of the mean, unless otherwise indicated. Multiple comparisons were made for significant differences using analysis of variance, followed by individual comparisons with the Bonferroni post-test. Comparisons between two groups were made with the Student *t* test. *A P*<0.05 was considered significant.

RESULTS

15dPGJ2 inhibited growth of MCG-803 cells

To evaluate the effect of $15dPGJ_2$ on the growth of MCG-803 cells, $15dPGJ_2$ (1,10,30 μM) was added to the culture medium for 48 h. Cell growth was determined by ^{3}H-dRT assay (Figure 1). $15dPGJ_2$ inhibited MCG-803 cell growth in a dose-dependent manner.

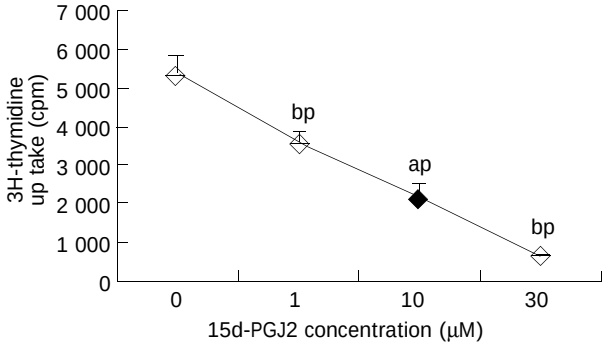

Figure 1 Effect of 15d-PGJ_2 on cell growth by H^3-TdR assay (48 h). MCG-803 cells were incubated with various concentrations of 15d-PGJ_2 for 48 h. The value is represented as mean±SEM (n=3). ^aP<0.05, ^bP<0.01 *versus* control group.

15dPGJ2 induced apoptosis in MCG-803 cells

There are several methods to evaluate apoptosis. In this study, we used ELISA and TUNEL to check for apoptosis of MCG-803 cells after 24 h treatment with $15dPGJ_2$. The percentage of TUNEL-positive cells increased from 13.7±1.5 % to 48.3±2.9 % (Table 1). The same results were obtained by ELISA. The effect of 15dPGJ2 at concentrations from 1 μmol/L to 30 μmol/L on DNA fragmentation in MCG-803 cells is shown in Figure 2. 15dPGJ2 was found to significantly induce DNA fragmentation after the onset of incubation and this effect was in a dose-dependent manner.

Table 1 TUNEL assay performed using apoptosis detection system

15d-PGJ_2 (μM)	Control	10	30
Percentage of TUNEL-positive cells	13.7±1.5 %	34.9±2.7 %^{bp}	48.3±2.9 %^{bp}

$15dPGJ_2$ (0, 10, 30 μM) was added to the culture medium for 48 h. The percentage of TUNEL-positive cells was determined. ^aP<0.05, ^bP<0.01 compared with respective controls. The value is represented as mean ±SEM (n=3). ^bP<0.01 *versus* corresponding control groups.

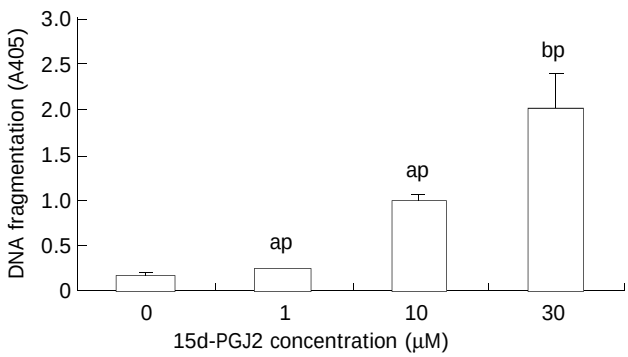

Figure 2 Effect of 15d-PGJ2 on DNA fragmentation in MCG-803 cells. Cytoplasmic histone-associated DNA fragments were determined using a commercial ELISA kit. Culture of MCG-803 cells for 24 h in the presence of 15d-PGJ2 resulted in dose

dependent DNA fragmentation. $^aP<0.05$, $^bP<0.01$ compared with the controls. The value is represented as mean±SEM (n=3).

PPAR mRNA and protein expression in MCG-803 cells increased by 15dPGJ2

Since 15dPGJ$_2$ is a potent PPAR agonist in the events leading to cell apoptosis, we have investigated its effects on the expression of PPARγ mRNA and protein. MCG-803 cells were treated with 15dPGJ$_2$ in the range of 1-30 μM for 6 h. Figure 4 shows that PPARγ mRNA expression was significantly increased in a dose-dependent manner. A Western blot analysis further showed that the mRNA levels encoding PPARγ upon treatment with 15dPGJ$_2$ could be related to the variation of the corresponding protein (Figure 3).

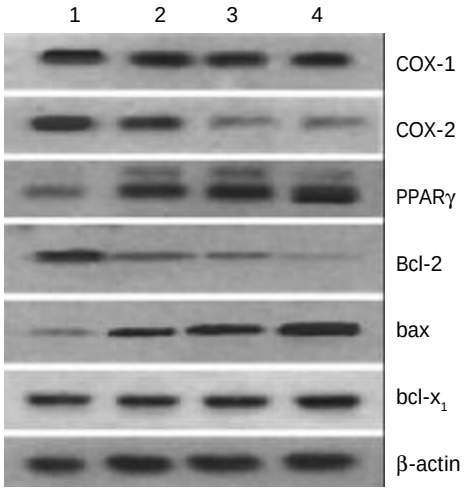

Figure 3 COX-1, COX-2, PPARγ, bcl-2, bax, and bcl-XL protein levels in MCG-803 cells treated with 15d-PGJ2. Cell lysates were collected and processed at 6 h. The whole cellular protein was electrophoresed in SDS-PAGE gel. Western blot was performed using antibodies against COX-1, COX-2, PPARγ,bcl-2, bax, bcl-XL. β-actin was used as a lane-loading control. (1) control, (2) 1 μM, (3) 10 μM, (4) 30 μM.

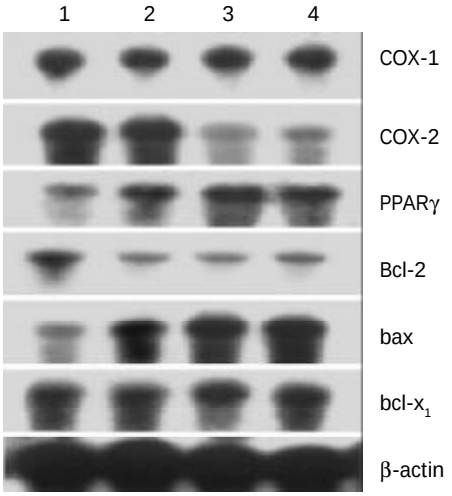

Figure 4 COX-1, COX-2, PPAR-γ, bcl-2, bax, bcl-XLmRNA levels in MCG-803 cells treated with 15d-PGJ2 for 6 h by Northern blot. (1) control, (2) 1 μM, (3) 10 μM, (4) 30 μM.

Effect of 15dPGJ2 on bcl-2, bcl-XL and bax expression in MCG-803 cells

To further elucidate the mechanism of 15dPGJ$_2$ induced apoptosis in MCG-803 cells, we evaluated the involvement of bcl-2 family in the apoptosis process by Western blot and Northern blot analysis. The protein and mRNA of bax were increased and bcl-2 decreased in a dose-dependent manner 6 h after 15dPGJ$_2$ treatment (Figures 3, 4). No change was observed in protein and mRNA expression of bcl-X$_L$ (Figures 3, 4).

Effect of 15dPGJ2 on COXs expression and PGE2 production in MCG-803 cells

To assess the role of COXs in 15dPGJ$_2$ induced apoptosis, we first examined the changes of COX-1 and COX-2 in MCG-803 cells treated with 15dPGJ$_2$. As shown in Figures 3 and 4, the COX-2 protein increased 6 h after 15dPGJ$_2$ treatment and no change was observed in protein expression of COX-1. In Northern blot analysis, similar results were obtained. The expression of COX-1 mRNA was not changed and COX-2 mRNA was not regulated by 15dPGJ$_2$ in dose dependent manners. We used specific RIA to measure the production of PGE$_2$ as COX$_s$ catalyzed the rate-limiting step in the biosynthesis of prostaglandins. Parallel to the inhibition of COX-2, decrease of PGE$_2$ was found in culture medium of HCG-803 cells stimulated by 15dPGJ$_2$ (Figure 5). These results further confirmed that COX-2, not COX-1 activity was changed by 15dPGJ$_2$.

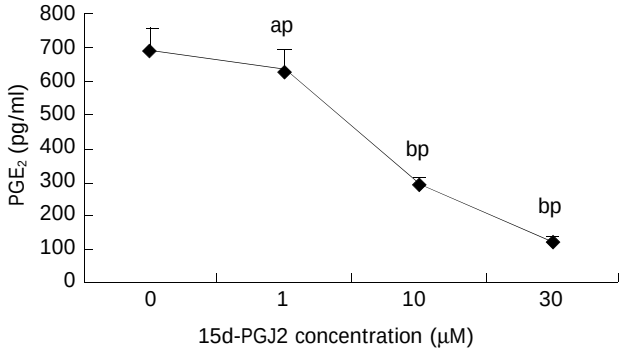

Figure 5 Effect of 15d-PGJ$_2$ on PGE2 production by RIA (24 h). MCG-803 cells were incubated at various concentrations of 15d-PGJ$_2$ for 24 h. The value is represented as mean ±SEM (n=3). $^aP<0.05$ and, $^bP<0.01$ *versus* corresponding control groups.

DISCUSSION

Peroxisome proliferator-activated receptor (PPAR) γ, a member of the steroid nuclear hormone receptor superfamily[11], has been known to trigger adipocyte differentiation and lipid storage by regulating the expression of genes critical for adipogenesis[12]. PPARγ functioned as a ligand-dependent transcription factor[13], which upon heterodimerization with the retinoid X receptor (RXR)[14], bound to specific response elements termed peroxisome proliferator response elements (PPRE). This in turn regulated the expression of target genes[15,16]. Activation of this receptor has been implicated in tumor promotion, cellular differentiation and apoptosis[17]. There are a number of naturally occurring agents that activate PPARγ. Some J-series prostaglandins have been found to bind to PPARγ in low micromolar range[18,19]. The PGD2 derivative, 15-deoxy-12, 14-PGJ2 (15d-PGJ2) was a high affinity ligand (*K*d=300 nM) that demonstrated anti-inflammatory[20,21] and anti-neoplastic activity[22].

The anti-neoplastic activity of PPARγ ligand prompted us to determine whether 15dPGJ$_2$ would trigger MCG-803 cells to undergo apoptosis. The results from Western blotting and Northern blotting have demonstrated that the PPARγ gene and protein expression were clearly observed in MCG-803 cells. 15dPGJ$_2$ stimulated the expression of PPARγ mRNA and its product. Coincubation of MCG-803 cells with 15dPGJ$_2$ potently inhibited cell growth and induced apoptosis in a dose-

related fashion. The dose-dependent suppression of cell growth in cancer cells was also reported after a number of synthetic PPARγ ligands such as thiazolidinediones (TZDs) and non-steroidal anti-inflammatory drugs (NSAIDs) treatment[9]. These results suggest that activation of the PPARγ pathway by $15dPGJ_2$ induces MCG-803 cells to undergo apoptosis.

In this study, the well-known important mediator of apoptosis, bcl-2 family was examined in MCG-803 cells treated with $15dPGJ_2$. In bcl-2 family, bcl-2 and bcl-X_L were anti-apoptotic, whereas bax, bad and bak were pro-apoptotic[23]. The ratio of anti-apoptotic factor to pro-apoptotic factor in the cells was assumed to be a critical mechanism in maintaining normal homeostasis. A higher concentration of bax compared with bcl-2 enhanced susceptibility to apoptosis. Nevertheless, the cell continued to survive if bcl-2 predominated over bax. One of the most significant problems in the treatment of cancer was the resistance of cancer cells to chemotherapy-induced apoptosis. Of gastric cancers, 72 % bcl-2 overexpression and 33-40 % bax frameshift mutation were observed[24-26]. A higher ratio of bcl/bax strongly blocked gastric cancer cell apoptosis by inhibiting cytochrome C release from mitochondria and Caspase-3 activation[27-31]. Our data indicated that $15dPGJ_2$ led to a dramatic decrease in bcl-2 and increase in bax. The bcl-X_L remained unchanged after $15dPGJ_2$. In addition, the decreased ratio of bcl/bax was detected prior to commencement of cell apoptosis after 6 h treatment. These results suggested a direct effect of PPAR pathway on bcl/bax expression. Therefore we concluded that the change of bcl-2 family might play a key role in $15dPGJ_2$-induced apoptosis in MCG-803 cells.

Cyclo-oyxgenase (COX) was the rate-limiting enzyme that catalyzed the initial step in biosynthesis of prostaglandins (PG) from arachidonic[32,33]. COX is encoded by two separate genes, COX-1 and COX-2, both of which participate in formation of a variety of eicosanoids. COX-1 is expressed constitutionally in most tissues and has been proposed to be a housekeeping gene involved in cytoprotection of gastric mucosa, vasodilation in the kidney, and control of platelet aggregation. In contrast, COX-2 is an inducible immediate early gene that is upregulated by various stimuli including mitogens, cytokines, growth factors, and tumor promoters. Accumulating evidence has shown that increased PGE_2 levels via overexpression of the inducible COX-2 isoform were important in the development of human cancer[34]. Previous studies have demonstrated that COX-2 expression was aberrantly increased in various human epithelial cancers, including those of colorectal[35,36], esophageal[37], gastric[38], lung[39] and bladder origin[40]. Data in this study also showed apparent COX-2 expression in MCG-803 cells. These findings suggest that cellular upregulation of COX-2 and PGE_2 may be a common mechanism in epithelial carcinogenesis.

In gastrointestinal system, it has been reported that COX-2 overexpression led to the inhibition of apoptosis or altered cell cycle kinetics in epithelial cells[41,42]. Numerous epidemiological studies suggested that non-steroidal anti-inflammatory drugs (NSAIDs) decreased incidence of gastrointestinal cancers and COX-2 was recognized as a major target of NSAIDs. Inhibition of COX-2 by NSAIDs or COX-2-specific inhibitors caused cell death in cancer cells[43-49], indicating that COX-2 was an important molecular target for prevention and treatment in gastrointestinal cancers. In this study, a crucial issue yet to be resolved was whether COX-2 inhibition played a role in the induction of apoptosis by $15dPGJ_2$ in human gastric carcinoma. We found decreased expression of COX-2 mRNA and protein as well as PGE_2 production in MCG-803 after $15dPGJ_2$ treatment. Our current study demonstrated that the decrease in COX-2 expression occurred prior to apoptosis, suggesting that down-regulation of COX-2 might be an upstream event of $15dPGJ_2$-induced apoptosis. These changes may imply that $15dPGJ_2$ interferes with the expression of COX-2 and PGE_2 production, thereby contributing to induced apoptosis in MCG-803 cells.

The premise is that COX-2 inhibitor has antitumor effect is based on the assumption that prostaglandins and other COX-2 generated downstream mediators promote tumor cell proliferation, survival, and angiogenesis in an autocrine and/or paracrine manner[50-53]. It was also reported that selective cyclo-oxygenase-2 inhibitor induced apoptosis and down-regulated bcl-2 expression in cancer cells[54]. Sheng H also found modulation of apoptosis and Bcl-2 expression by PGE_2 in human colon cancer cells[55]. However, Hsu AL reported that the cyclo-oxygenase-2 inhibitor celecoxib induced apoptosis by blocking Akt activation in human prostate cancer cells independent of Bcl-2[56]. In this study no data proved that Bcl-2 was one of the downstream mediators when COX-2 was inhibited by $15dPGJ_2$. The precise mechanisms on the molecular interaction of COX and bcl-2 expression in $15dPGJ_2$ induced gastric apoptosis should be established by more profound analysis.

In summary, our data demonstrate that 15dPGJ2 inhibited the growth of human gastric cancer cells (MCG803). It is proposed that the decrease of bcl-2/bax ratio and COX-2 be responsible for the apoptotic process in MCG803 cells. Furthermore, PPARγ ligand is a new strategic approach to provide new anticancer therapies.

REFERENCES

1 **Forman BM**, Chen J, Evans RM. Hypolipidemic drugs, polyunsaturated fatty acids, and eicosanoids are ligands for peroxisome proliferator-activated receptors alpha and delta. *Proc Natl Acad Sci* 1997; **94**: 4312-4317

2 **Kliewer SA**, Sundseth SS, Jones SA, Brown PJ, Wisely GB, Koble CS. Fatty acids and eicosanoids regulate gene expression through direct interactions with peroxisome proliferator-activated receptors alpha and gamma. *Proc Natl Acad Sci* 1997; **94**: 4318-4323

3 **Saffaf P**, Mueller E, Jones D, King F, DeAngelo DJ, Partridge JB, Holden SA, Chen LB, Singer S, Fletcher C, Spiegelman BM. Differentiation and reversal of malignant changes in colon cancer through PPARgamma. *Nature Med* 1998; **4**: 1046-1052

4 **Brockman JA**, Gupta RA, Dubois RN. Activation of PPARgamma leads to inhibition of anchorage-independent growth of human colorectal cancer cells. *Gastroenterology* 1998; **115**: 1049-1055

5 **Fajas L**, Auboeuf D, Raspe E, Schoonjans K, Lefebvre AM, Saladin R, Najib J, Laville M, Fruchart JC, Deeb S, Vidal-Puig A, Flier J, Briggs MR, Staels B, Vidal H, Auwerx J. The organization, promoter analysis, and expression of the human PPARgamma gene. *J Biol Chem* 1997; **272**: 18779-18789

6 **Lefebvre AM**, Chen I, Desreumaux P, Najib J, Fruchart JC, Geboes K, Briggs M, Heyman R, Auwerx J. Activation of the peroxisome proliferator-activated receptor g promotes the development of colon tumors in C57BL/6J-APCMin/+ mice. *Nature Med* 1998; **4**: 1053-1057

7 **Saez E**, Tontonoz P, Nelson MC, Alvarez JGA, Ming T, Baird SM, Thomazy VA, Evans RM. Activators of the nuclear receptor PPARgamma enhance colon polyp formation. *Nat Med* 1998; **4**: 1058-1061

8 **Tontonoz P**, Singer S, Forman BM, Sarraf P, Fletcher JA, Fletcher CD, Burn RP, Mueller E, Altiok S, Oppenheim H, Evans RM, Spiegelman BM. Terminal differentiation of human liposarcoma cells induced by ligands for peroxisome proliferator-activated receptor gamma and the retinoid X receptor. *Proc Natl Acad Sci U S A* 1997; **94**: 237-241

9 **Kubota T**, Koshizuka K, Willamson EA, Asou H, Said JW, Holden S, Miyoshi I, Koe•er HP. Ligand for peroxisome proliferator-activated receptor gamma (troglitazone) has potent antitumor effect against human prostate cancer both *in vitro* and *in vivo*. *Cancer Res* 1998; **58**: 3344-3352

10 **Elstner E**, Muller C, Koshizuka K, Williamson EA, Park D, Asou H, Shintaku P, Said JW, Heber D, Koe•er HP. Ligands for peroxisome proliferator-activated receptorgamma and retinoic acid

receptor inhibit growth and induce apoptosis of human breast cancer cells *in vitro* and in BNX mice. *Proc Natl Acad Sci U S A* 1998; **95**: 8806-8811

11 **Evans RM**. The steroid and thyroid hormone receptor superfamily. *Science* 1988; **240**: 889-895

12 **Spiegelman BM**. PPARgamma: adipogenic regulator and thiazolidinedione receptor. *Diabetes* 1998; **47**: 507–514

13 **Dreyer C**, Keller H, Mahfoudi A, Laudet V, Krey G, Wahli W. Positive regulation of the peroxisome beta-oxidation pathway by fatty acids through activation of peroxisome proliferator-activated receptors (PPAR). *Biol Cell* 1993; **77**: 67-76

14 **Kliewer SA**, Umesono K, Noonan D, Heyman R, Evans RM. Positive regulation of the peroxisome beta-oxidation pathway by fatty acids through activation of peroxisome proliferator-activated receptors (PPAR). *Nature* 1992; **358:** 771-774

15 **Lemberger T**, Desvergne B, Wahli W. Peroxisome proliferator-activated receptors: a nuclear receptor signaling pathway in lipid physiology. *Annu Rev Cell Dev Biol* 1996; **12**: 335–363

16 **Tugwood JD**, Issemann I, Anderson RG, Bundell KR, McPheat WL, Green S. The mouse peroxisome proliferator activated receptor recognizes a response element in the 5' flanking sequence of the rat acyl CoA oxidase gene. *EMBO J* 1992; **11**: 433-439

17 **Vanden Heuvel JP**. Peroxisome proliferator-activated receptors (PPARs) and carcinogenesis. *Toxicol Sci* 1999; **47**: 1-8

18 **Yu K**, Bayona W, Kaline CB, Harding HP, Ravera CP, McMahon G, Brown M, Lazar MA. Differential activation of peroxisome proliferator-activated receptors by eicosanoids. *J Biol Chem* 1995; **270**: 23975–23983

19 **Straus DS**, Glass CK. Cyclopentenone prostaglandins: new insights on biological activities and cellular targets. *Med Res Rev* 2001; **21**: 185-210

20 **Ricote M**, Li AC, Willson TM, Kelly CJ, Glass CK. The peroxisome proliferator-activated receptor g is a negative regulator of macrphage activation. *Nature* 1998; **391**: 79–82

21 **Jiang C**, Ting A, Seed B. PPARγ agonists inhibit production of monocyte inflammatory cytokines. *Nature* 1998; **391**: 82–86

22 **Ohta K**, Endo T, Haraguchi K, Hershman JM, Onaya T. Ligands for peroxisome proliferator-activated receptor-γ inhibit growth, and induce apoptosis of human papillary thyroid carcinoma cells. *J Clin Endocrinol Metab* 2001; **86**: 2170–2177

23 **Reed JC**. Mechanisms of Bcl-2 family protein function and dysfunction in health and disease. *Behring Inst Mitt* 1996; **97**: 72-100

24 **Susin SA**, Lorenzo HK, Zamzami N. Molecular characterization of mitochondrial apoptosis-inducing factor. *Nature* 1999; **397**: 441–446

25 **Lavoie JN**, Nguyen M, Marcellus RC, Brantou PE, Shore GC. E4orf4, a novel adenovirus death factor that induces p53-independent apoptosis by a pathway that is not inhibited by zVAD-fmk. *J Cell Biol* 1998; **140**: 637–645

26 **Schlapbach R**, Fontana A. Differential activity of bcl-2 and ICE enzyme family protease inhibitors on Fas and puromycin-induced apoptosis of glioma cells. Biochim. *Biophys. Acta* 1997; **1359**: 174–180

27 **Wolter KG**, Hsu YT, Smith CL, Nechushtan A, Xi XG, Youle RJ. Movement of Bax from the cytosol to mitochondria during apoptosis. *J Cell Biol* 1997; **139:** 1281–1292

28 **Rosse T**, Olivier R, Monney L, Rager M, Conus S, Fellay I, Jansen B, Borner C. Bcl-2 prolongs cell survival after Bax-induced release of cytochrome c. *Nature* 1998; **391**: 496–499

29 **Vaux DL**. CED-4-the third horseman of apoptosis. *Cell* 1997; **90**: 389–390

30 **Zou H**, Henzel WJ, Liu X, Lutschg A, Wang X. Apaf-1, a human protein homologous to C. elegans CED-4, participates in cytochrome c-dependent activation of caspase-3. *Cell* 1997; **90**: 405–413

31 **Pan G**, Humke EW, Dixit VM. Activation of caspases triggered by cytochrome c *in vitro*. *FEBS Lett* 1998; **426**: 151–154

32 **Dubois RN**, Abramson SB, Crofford L, Gupta RA, Simon LS, Van De, Putte LB. Cyclooxygenase in biology and disease. *FASEB J* 1998; **12**: 1063-1073

33 **Herschman HR**. Prostaglandin synthase 2. *Biochem Bioph Acta* 1996; **1299**: 125-140

34 **Taketo MM**. Cyclooxygenase-2 inhibitors in tumorigenesis (part II). *J Natl Cancer Inst* 1998; **90**: 1609-1620

35 **Eberhart CE**, Coffery RJ, Radhika A, Giardiello FM, Ferrenbach S, DuBois RN. Up-regulation of cyclooxygenase 2 gene expression in human colorectal adenomas and adenocarcinomas. *Gastroenterology* 1994; **107**: 1183-1188

36 **Hao X**, Bishop AE, Wallace M, Wang H, Willcocks TC, Maclouf J, Polak JM, Knight S, Talbot IC. Early expression of cyclo-oxygenase-2 during sporadic colorectal carcinogenesis. *J Pathol* 1999; **187**: 295-301

37 **Wilson KT**, Fu S, Ramanujam KS, Meltzer SJ. Increased expression of inducible nitric oxide synthase and cylooxygenase-2 in Barrett's esophagus and associated adenocarcinomas. *Cancer Res* 1998; **58**: 2929-2934

38 **Ristimaki A**, Honkanen N, Jankala H. Expression of cyclooxygenase-2 in human gastric carcinoma. *Cancer Res* 1997; **57**: 1276-1280

39 **Wolff H**, Ssukkonen K, Anttila S, Karjalainen A, Vainio H, Restimaki A. Expression of cyclooxygenase-2 in human lung carcinoma. *Cancer Res* 1998; **58**: 4997-5001

40 **Mohammed SI**, Knapp DW, Bostwick DG, Foster RS, Khan KN, Masferrer JL, Woerner BM, Snyder PW, Koki AT. Expression of cyclooxygenase-2 (COX-2) in human invasive transitional cell carcinoma (TCC) of the urinary bladder. *Cancer Res* 1999; **59**: 5647-5650

41 **Tsujii M**, DuBois RN. Alterations in celluar adhesion and apoptosis in epithelial cells overexpressing prostaglandin endoperoxide synthase 2. *Cell* 1995; **83**: 493-501

42 **DuBois RN**, Shao J, Tsujii M, Sheng H, Beauchamp RD. G1 delay in cells overexpressing prostaglandin endoperoxide synthase-2. *Cancer Res* 1996; **56**: 733-737

43 **Chan TA**, Morin PJ, Vogelstein B, Kinzler KW. Mechanisms underlying nonsteroidal anti-inflammatory drug-mediated apoptosis. *Proc Natl Acad Sci USA* 1998; **95**: 681-686

44 **Piazza GA**, Rahm AL, Krutzsch M, Sperl G, Paranka NS, Gross PH. Antineoplastic drugs sulindac sulfide and sulfone inhibit cell growth by inducing apoptosis. *Cancer Res* 1995; **55**: 3310-3116

45 **Hanif R**, Pittas A, Feng Y, Koutsos ML, Qiao L, Staiano-Coico L. Effects of nonsteroidal anti-inflammatory drugs on proliferation and on induction of apoptosis in colon cancer cells by a prostaglandin-independent pathway. *Biochem Pharmacol* 1996; **52**: 237-245

46 **Thompson HJ**, Jiang C, Lu J, Mehta RG, Piazza GA, Paranka NS. Sulfone metabolite of sulindac inhibits mammary carcinogenesis. *Cancer Res* 1997; **57**: 267-271

47 **Jones MK**, Wang H, Peskar BM, Levin E, Itani RM, Sarfeh IJ. Inhibition of angiogenesis by nonsteroidal anti-inflammatory drugs: insight into mechanisms and implications for cancer growth and ulcer healing. *Nat Med* 1999; **5**: 1418-1423

48 **Williams CS**, Tsujii M, Reese J, Dey SK, Dubois RN. Host cyclooxygenase-2 modulates carcinoma growth. *J Clin Invest* 2000; **105**: 1589-1594

49 **Zhang X**, Morham SG, Langenbach R, Young DA. Malignant transformation and antineoplastic actions of nonsteroidal anti-inflammatory drugs (NSAIDs) on cyclooxygenase-null embryo fibroblasts. *J Exp Med* 1999; **190**: 451-459

50 **Hla T**, Ristimaki A, Appleby S, Barriocanal JG. Cyclooxygenase gene expression in inflammation and angiogenesis. *Ann N Y Acad Sci* 1993; **696**: 197-204

51 **Taketo MM**. Cyclooxygenase-2 inhibitors in tumorigenesis (part 1). *J Natl Cancer Inst* 1998; **90**: 1529-1536

52 **Hla T**, Bishop-Bailey D, Liu CH, Schaefers HJ, Trifan OC. Cyclooxygenase-1 and –2 isoenzymes. *Inst J Biochem Cell Biol* 1999; **31**: 551-557

53 **Prescott SM**, Fitzpatrick FA. Cyclooxygenase-2 and carcinogenesis. *Biochim Biophys Acta* 2000; **1470**: M69-78

54 **Liu XH**, Yao S, Kirschenbaum A, Levine AC. NS398, a selective cyclooxygenase-2 inhibitor, induces apoptosis and down-regulates bcl-2 expression in LNCaP cells. *Cancer Res* 1998; **58**: 4245-4249

55 **Sheng H**, Shao J, Morrow JD, Beauchamp RD, DuBois RN. Modulation of apoptosis and Bcl-2 expression by prostaglandin E2 in human colon cancer cells. *Cancer Res* 1998; **58**: 362-366

56 **Hsu AL**, Ching TT, Wang DS, Song X, Rangnekar VM, Chen CS. The cyclooxygenase-2 inhibitor celecoxib induces apoptosis by block Akt activation in human prostate cancer cells independently of Bcl-2. *J Biol Chem* 2000; **275**: 11397-11403

Edited by Ma JY

P.O.Box 2345, Beijing 100023,China
Fax: +86-10-85381893
E-mail: wjg@wjgnet.com www.wjgnet.com

World J Gastroenterol 2003;9(10):2154-2159
World Journal of Gastroenterology
 ISSN 1007-9327

• GASTRIC CANCER •

Ets1 as a marker of malignant potential in gastric carcinoma

Yong Yu, Yi-Chu Zhang, Wen-Zhu Zhang, Li-Song Shen, Paul Hertzog, Trevor J Wilson, Da-Kang Xu

Yong Yu, Yi-Chu Zhang, Department of General Surgery, Xinhua Hospital, Shanghai Second Medical University, Shanghai 200092, China
Wen-Zhu Zhang, Department of Pathology, Xinhua Hospital, Shanghai Second Medical University, Shanghai 200092, China
Li-Song Shen, Laboratory Diagnostic Center, Shanghai Children's Medical Centre, Shanghai Second Medical University, Shanghai 200127, China
Paul Hertzog, Trevor J Wilson, Da-Kang Xu, Centre for Functional Genomics and Human Disease, Monash Institute of Reproduction and Development, Monash University, Vic 3168, Australia
Correspondence to: Da-Kang Xu, MD.PhD, Centre for Functional Genomics and Human Disease, Monash Institute of Reproduction and Development, Monash University, 27-31 Wright Street, Clayton, Vic 3168, Australia. dakangxu@med.monash.edu.au
Telephone: +61-3-9594-7229 **Fax:** +61-3-9594-7211
Received: 2003-06-30 **Accepted:** 2003-08-18

Abstract

AIM: Ets1 proto-oncogene is a transcription factor involved in the activation of several genes of tumor invasion and metastasis. We aimed to determine the relationship between the extent and intensity of Ets1 expression and patients' clinicopathological factors in gastric carcinoma.

METHODS: Immunohistochemical analysis was performed for gastric tumor paraffin-embedded sections, followed by image analysis.

RESULTS: Ets1 was not expressed in the normal gastric epithelium and its surrounding cells. The percentage of Ets1 expressing cells detected increased significantly in both epithelial tumor and stromal cells from high T classification, lymph node metastasis positive, clinical advanced-stage groups ($P<0.001$). The level of Ets1 staining in epithelial tumor cells also reflected the degree of cell differentiation. The percentage of epithelial and stromal cells expressing Ets1 was significantly correlated with the presence of lymph node metastasis ($P=0.014$ and $P<0.001$ respectively). Ets1 expression was not observed in tissue samples from patients with benign gastric ulcers.

CONCLUSION: Ets1 protein expression in epithelial tumor cells reflects the degree of differentiation, and the percentage of Ets1 positive tumor and stromal cells correlates with lymph node metastasis. Thus Ets1 is a valuable marker of malignant potential in terms of invasiveness and metastasis of gastric carcinoma. It is also possible that inhibition of Ets1 is a potential avenue for therapy in gastric cancer.

Yu Y, Zhang YC, Zhang WZ, Shen LS, Hertzog P, Wilson TJ, Xu DK. Ets1 as a marker of malignant potential in gastric carcinoma. *World J Gastroenterol* 2003; 9(10): 2154-2159
http://www.wjgnet.com/1007-9327/9/2154.asp

INTRODUCTION

Gastric cancer is a leading cause of cancer death in the world. The pathological stage of gastric cancer, including the depth of tumor penetration and the presence of metastases to lymph nodes or distal organs, remains the most important determinant in its prognosis. Usually, these parameters can be determined by microscopic examination of tissue sections from the primary neoplasm and lymph nodes. However, where only primary gastric carcinoma specimens are available for histopathological examination cannot always accurately predict metastasis and disease progression. Recently, from microarray gene expression profiling data[1], the occurrence and progression of cancer were suggested to be related to a series of genetic events affecting the structure and expression of a number of genes. These genes include potential oncogenes, tumor suppressors and those involved in angiogenesis and extracellular matrix (ECM) remodeling. The factors regulating these genes could thus be important markers for disease prognosis and potential therapeutic targets. Since most transcription factors are expressed at very low levels (-10 copies/cell), sensitive assays are required. One suitable approach is to use a specific antibody to detect these factors by immunohistochemical analysis. This allows analysis of the epithelial tumor cells and its surrounding stromal cells. In addition, this approach will enable further understanding of the molecular mechanisms of gastric carcinoma invasion and metastasis.

The Ets family of transcription factors is defined by a conserved DNA binding domain of approximately 85 amino acids. These proteins bind to specific purine-rich DNA sequences, with a core motif of GGAA/T, and have been shown to transcriptionally regulate a number of viral and cellular genes. Ets factors have been shown to be important in a number of biological processes, including cellular proliferation, differentiation, development, transformation, and apoptosis[2-6]. Indeed the Ets1 protein has recently been shown to regulate genes such as vascular endothelial growth factor(VEGF), urokinase plasminogen activator (uPA), matrix-metallopteases (MMPs) and integrin in a variety of cancer cell lines and tissues[7-12]. Many of these genes are involved in angiogenesis and extracellular matrix (ECM) remodeling, important events in the processes of cancer invasion and metastasis.

Microarray analysis from a number of epithelial tumor tissues or cell lines indicate that alterations in Ets1 expression are associated with lung carcinoma[13], breast carcinoma[14], pancreatic carcinoma[15], thyroid carcinoma[16] and oral squamous cell carcinoma[17]. However, it is not clear from these data which cells in the tumor expressed Ets1 or whether this expression was associated with invasive growth. Thus the purpose of this study was to analyze the relationship between Ets1 expression and the malignant behavior in gastric carcinoma, in particular to determine whether Ets1 may have a role in breaking through the muscularis mucosae by invasive tumors and metastasis. This will determine whether Ets1 has potential as a credible marker in predicting the metastatic potential of gastric cancer and assisting in elucidating its role in gastric carcinoma's malignant progression.

MATERIALS AND METHODS

Samples and patients

Since January 2001 to June 2002, we collected biopsies from 43 patients who underwent surgery for gastric neoplasia in the General Surgery Department of Xinhua Hospital, Shanghai Second Medical University. The data set for each patient

included sex, age, histological classification, clinical grade, depth of infiltration (T classification), presence of lymph node metastasis (N classification), distant metastasis (M classification), and clinical stage. Pathological assessments were determined by clinical pathologists according to WHO standards. T1 indicated infiltration of the *lamina propria* or submucosa, T2 infiltration of muscularis propria or the subserosa, T3 penetration of the serosa (visceral peritoneum), and T4 penetration of the serosa and infiltration of adjacent structures. Lymph node (N) classification was divided into no metastasis (N0) and metastasis in 1-6 (N1), 7-15 (N2) or >15 (N3) regional lymph nodes. M classification was M1 for presence or M0 for absence of distant metastasis. Clinical stage was determined by combination of these parameters as stage IA (T1N0M0), stage IB (T1N1M0), stage II (T1N2M0, T2N1M0 or T3N0M0), stage IIIA (T2N2M0, T3N1M0 or T4N0M0), stage IIIB (T3N2M0) and stage IV (TxN3M0, T4NxM0, TxNxM1). In addition, two samples of both benign gastric ulcer and breast cancer were used as controls.

Samples were fixed in formalin immediately after the operation and specially prepared for immunohistochemistry. Briefly, samples of no more than 2×1.5×0.2 cm were dehydrated at 4 ℃, and low temperature paraffin wax (<60 ℃) was used for embedding. 3 μm thick sections were de-waxed immediately before use with xylene (4 ℃) and rehydrated for immunohistochemistry.

Immunohistochemistry

Endogenous peroxidase activity was quenched with 3 % hydroperoxide followed by incubation with 1 % bovine serum albumin to block any nonspecific binding. Primary antibodies used were anti-human Ets1 monoclonal antibody (Transduction Laboratories, Lexington, KY), rabbit anti-human Ets1 polyclonal antibody (Santa Cruz Biotechnology, CA) or rabbit anti-human cytokeratin polyclonal antibody (DAKO, Copenhagen, Denmark). Amplification of the primary antibody reaction was achieved by incubation with an appropriate secondary antibody [Goat anti-Rabbit or anti-mouse IgG, Gene Tech] conjugated to peroxidase. The binding was visualized by DAB and the sections were counterstained with hematoxylin. All incubations and washing were performed at room temperature.

Image analysis

Intensities, percentages, and patterns of immunohistochemical staining for each sample slide were analyzed by KS4000 image analysis system (Zeiss Company, Germany) and recorded individually. For each sample, six representative images were collected at high magnification (×400). Image analysis determined the proportion of epithelial or stromal cells within the tumor expressing Ets1 and the percentage of cells with moderate and intense staining. The data were expressed as proportion of tumor.

Statistic analysis

The data were presented as the mean ± standard deviation (SD) for each group. Statistical analysis was performed using analysis of variance (ANOVA) and Mann-Whitney non-parametric test. Intergroup difference was evaluated by Fisher' s test. $P<0.01$ was considered statistically significant.

RESULTS

Patients characteristics

Samples were obtained from 41 patients, 30 males and 10 females. The age range was from 37 to 87. The 41 patients were diagnosed with malignant tumor. The histological classification included adenocarcinoma (30), signet ring cell carcinoma (6), undifferentiated carcinoma (4) and gastrointestinal stromal tumor (GIST) (1). The samples were divided into two groups according to their depth of infiltration (WHO classification): 15 of T1 or T2, and 25 of T3 or T4. Specimens were also divided according to histological grade: grade I (highly differentiated carcinoma) for 7 samples, grade II (moderately differentiated carcinoma) for 19 samples, grade III (poorly differentiated carcinoma) for 14 samples. 26/40 patients demonstrated lymph node metastasis and only one patient had known distant metastasis (liver).

Expression of Ets1 in gastric carcinoma

In our study, staining of Ets1 was observed in all malignant gastric tumor cells, including adenocarcinoma, signet ring cell adenocarcinoma and undifferentiated carcinoma, and the results are summarized in Table 1. Epithelial tumor cells stained for Ets1 were mainly in the nucleus and only rarely was staining observed in the cytoplasm (Figure 1A). No staining for Ets1 was observed in the non-neoplastic tissue or in tissues from a patient with benign gastric ulcer (Figure 1G). In contrast, antibodies to another Ets factor which is known to be epithelium-specific (Elf5), stained normal gastric epithelium, but lost its expression in gastric cancer (data not shown). Ets1 staining was also observed in newly formed blood vessel endothelial cells (Figure 1B) and interstitial cells in surrounding tissue (Figure 1C). Ets1 protein was localized in both cytoplasm and nucleus of the stromal cells. Furthermore intense staining for Ets1 was observed in invasive cells at the junction of normal tissue and malignant tissue (Figure 1D). Increased Ets1 protein expression observed by immunohistochemistry was confirmed by quantitation of Ets1mRNA levels by RT-PCR and Northern blot (data not shown). Immunohistochemistry of a breast cancer specimen also detected Ets1, but it was predominantly expressed in the cytoplasm (Figure 1E).

Relationship between percentage of Ets1 expressing cells and pathological assessment in gastric carcinoma

Age, sex and histological grade Statistical analysis determined that there was no significant correlation between the expressions of Ets1 in gastric cancer and age, sex or WHO histopathological classifications. Although there was a trend in proportions of Ets1 positively stained epithelial cells from 26.9 % in grade I, increasing to 39.5 % in grade II and 32.8 % in grade III (Table 1), there was no significant correlation ($P=0.366$). A similar trend was also observed for staining of tumor stromal cells ($P=0.486$).

Depth of infiltration (T) classification Considering the importance of breaking through muscularis mucosae, we compared the groups with tumors confined to the mucosa/submucosa (15 samples, T1 or T2) and those tumors which had penetrated the serosa (25 samples, T3 or T4). Our data demonstrated that Ets1 was detected in a higher proportion of both epithelial and stromal cells in tumors from patients with more advanced disease. For example, 17.2±12.0 % of tumor epithelial cells from T1 or T2 tumors were positive for Ets1, whereas 45.6±17.9 % were positive for T3 or T4 tumours ($P<0.001$, Table 1). The proportion of Ets1 expressing tumor stromal cells also significantly correlated with the presence of more advanced disease T classification ($P<0.05$).

Lymph node and distant metastasis Similarly, grouping of patients according to the presence (N123) or absence (N0) of lymph node metastasis showed an increase in Ets1 positive tumor epithelial cells from 24.1±17.4 % (N0) to 40.8±20.8 % (N123, $P<0.05$). In addition, the proportion of Ets1 expressing tumor stromal cells was also significantly higher in patients with lymph node metastasis ($P<0.001$). Only one patient in our samples had known distant metastasis, but Ets1 was detected in both epithelial and stromal cells in tumor sections from this patient (71 % and 61 % respectively).

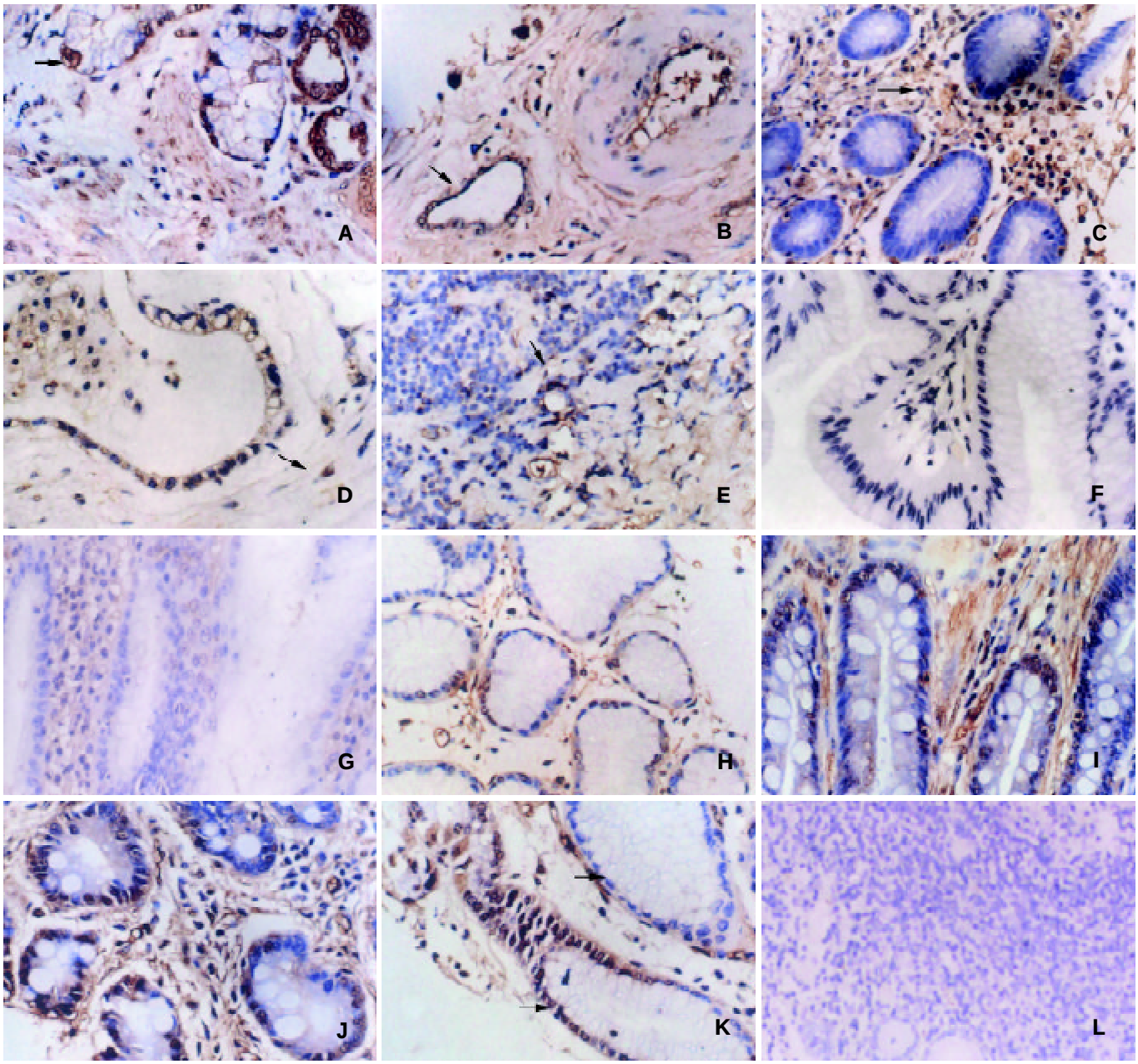

Figure 1 A: Ets1 immunohistochemical stain in gastric cancer cells. The arrowed cell is a typical Ets1 positively stained cell. The area of stain was mainly, located in the nucleus of epithelial tumor cells. Ets1 protein was localized in both cytoplasm and nucleus of the stromal cells. B: Ets1 expression in vascular endothelial cells. This was an example of pooly differentiated gastric adenocarcinoma. Ets1 was present in endothelial cells of blood vessels (arrowed). C: Ets1 is expressed in interstitial cells. Photomicrograph of a typical gastric carcinoma. Ets1 positive stromal cells were detected in the interstitial tissue. D: The expression of Ets1 in polarity. Image of gastric cancer cells infiltrating to the muscular layer. Intense staining of Ets1 was observed at the junction of the infiltrating tumor cells and the serosa. We termed it the polarity expression. E: Ets1 expression in breast carcinoma. Example of breast carcinoma, Ets1 positive cells arrowed. F: Ets1 negative control staining. G: Ets1 is not expressed in glandular cells of benign gastric ulcer. H-J: Ets1 expression in tissues with different histopathological grades. Section of grade I(H), grade II(I) and grade III(J) gastric cancer showing increased positive cells and intensity of Ets1 staining with advanced disease. K: Ets1 expression is high in undifferentiated tumor cell. The image contained well differentiated and poorly differentiated tumor tissues. The number of positive cells and the intensity of the Ets1 staining were increased in undifferentiated tumor cells. L: Ets1 is not expressed in GIST. Photomicrograph of gastrointestinal stromal tumor (GIST). No Ets1 positive cancer cells were observed. (A, H, I, J, K original magnification ×400), (B, C, D, E, F, G original magnification ×100), (L, original magnification ×50).

Clinical stage When the T, N and M classifications were combined into the WHO defined clinical stages, there was a significant correlation between Ets1 staining in epithelial and stromal cells with the presence of more advanced disease ($P<0.001$ and $P<0.005$ respectively).

Relationship between Ets1 levels and clinical disease

Our image analysis also enabled us to compare the signal intensity of Ets1 staining (Table 2-1,2), which reflected the levels of Ets1 (confirmed by RT-PCR, data not shown). When all the patients were considered together, the majority (24/40, 60 %) displayed moderate staining levels in tumor epithelial cells whereas 10/40 (25 %) displayed intense staining. Of these 10 patients with intense staining, however, 9 had tumors penetrating the mucosa (T3 or T4) and 8 had metastasis into the regional lymph nodes. The single patient with distant metastasis also displayed intense staining for Ets1. Similar high levels of Ets1 labelling were observed in stromal cells from

patients with advanced disease. In stromal cells 16/40 (40 %) displayed intense staining. These 16 patients with intense staining included a single patient with distant metastasis, while 11 of these 16 patients had tumors penetrating the mucosa (T3 or T4) and metastasis into the regional lymph nodes. Thus it appeared both the level of Ets1 and the proportion of positive cells were correlated with advanced gastric carcinoma.

Table 1 Ets1 expression in tumor and stromal cells

Factors	No.	Ets1 percentage[T] (mean±SD)	*P* value	Ets1 percentage[S] (mean±SD)	*P* value
Total patients	40	35.0±21.1		44.6±17.5	
Gender					
Male	30	38.0±22.5	0.115	45.2±17.3	0.704
Female	10	25.9±13.1		42.7±18.7	
Age					
>50	32	35.9±20.8	0.572	46.3±17.7	0.206
<50	8	31.1±23.3		37.5±15.7	
Histological classification (WHO)					
Ad	30	35.2±19.9	0.269	43.0±15.4	0.647
Srcc	6	43.3±26.4		49.3±15.2	
Uc	4	21.1±19.6		48.8±34.7	
Grade (WHO)					
I	7	26.9±26.7	0.366	37.3±18.3	0.486
II	19	39.5±19.7		45.7±11.6	
III	14	32.8±19.8		46.6±23.2	
T (tumor)					
T1,2	15	17.2±12.0	<0.001	35.3±17.7	0.008
T3,4	25	45.6±17.9		50.1±15.1	
N (lymph node)					
N0	14	24.1±17.4	0.014	32.4±13.8	0.001
N1,2,3	26	40.8±20.8		51.1±15.8	
M (metastasis)					
M0	39	34.0±20.5	<0.001	44.1±17.5	<0.001
M1	1	71		61	
Clinical stage					
I, II	18	21.8±15.2	<0.001	36.2±18.1	0.005
III, IV	22	45.7±19.2		51.4±13.9	

[T] refers to Ets1 expression in tumor cells [S] refers to Ets1 expression in stromal cells.

Table 2-1 Intensity of Ets1 staining in tumor cell and distribution of patients

Compartment	No.	Weak (+)	Moderate (++)	Intense (⩾+++)	*P* value
Tumor cells	40	6 (15 %)	24 (60 %)	10 (25 %)	
T classification					
T1,2	15	2 (13.3 %)	12 (80 %)	1 (6.7 %)	0.087
T3,4	25	4 (16 %)	12 (48 %)	9 (36 %)	
LN metastasis					
Negative	14	3 (21.4 %)	9 (64.3 %)	2 (14.3 %)	0.438
Positive	26	3 (11.5 %)	15 (57.7 %)	8 (30.8 %)	
Distant metastasis					
Negative	39	6 (15.4 %)	24 (61.5 %)	9 (23.1 %)	0.214
Positive	1	0 (0 %)	0 (0 %)	1 (100 %)	
Clinical stage					
Stage I,II	18	3 (16.7 %)	13 (72.2 %)	2 (11.1 %)	0.183
Stage III,IV	22	3 (13.6 %)	11 (50 %)	8 (36.4 %)	

Table 2-2 Intensity of Ets1 staining in stromal cell and distribution of patients

Compartment	No.	Weak (+)	Moderate (++)	Intense (⩾+++)	*P* value
Stromal cells	40	3 (7.5 %)	21 (52.5 %)	16 (40 %)	
T classification					
T1,2	15	3 (20 %)	7 (46.7 %)	5 (33.3 %)	0.066
T3,4	25	0 (0 %)	14 (56 %)	11 (44 %)	
LN metastasis*					
Negative	14	3 (21.4 %)	6 (42.9 %)	5 (35.7 %)	0.048
Positive	26	0 (0 %)	15 (57.7 %)	11 (42.3 %)	
Distant metastasis					
Negative	39	3 (7.7 %)	21 (53.8 %)	15 (38.5 %)	0.463
Positive	1	0 (0 %)	0 (0 %)	1 (100 %)	
Clinical stage					
Stage I,II	18	3 (16.7 %)	8 (44.4 %)	7 (38.9 %)	0.129
Stage III,IV	22	0 (0 %)	13 (59.1 %)	9 (40.9 %)	

DISCUSSION

Gastric cancer is the most frequent malignancy of the gastrointestinal tract in China and the second most common cause of cancer-related death in the world[18]. The prognosis of patients with gastric cancer has been improving owing to the progress in diagnostic techniques and treatment methods for gastric cancer, but peritoneal dissemination is the main cause of recurrence after curative resection of advanced cancer. The prognosis of gastric cancer which has invaded as far as the gastric serosa was still poor with a 5-year survival of less than 35 %[19]. Among these malignant characteristics of gastric cancer cells, metastasis to the peritoneum is an especially complex phenomenon, which requires the involvement of many different genes in multiple steps for tumor cells. Although many aspects of gastric cancer metastasis await further clarification, adhesion molecules, apoptosis-related genes, and others have been reported to play an important role in peritoneal dissemination of gastric cancers[20], but details of the mechanism involved remain unclear. Since Ets1 has been shown to regulate many genes involved in angiogenesis and extracellular matrix (ECM) remodeling, events important in cancer metastasis, we analyzed the relationship between Ets1 expression and the malignant behavior in gastric carcinoma. This demonstrated that Ets1 expression was related to the pathological stage of gastric cancer, including tumor infiltration and presence of metastases to lymph nodes or distal organs. These data are consistent with other studies that have shown significant correlation between Ets1 expression in tumor cells and the presence of lymph node metastasis. But our data also demonstrated that Ets1 expression in cancer associated stromal cells was significantly correlated with the presence of lymph node metastasis. The proportion of Ets1 expressing cells was also associated with metastasis kinetics, expression of Ets1 within a few epithelial tumor cells in early disease, then expression in stromal, endothelial and other cells in advanced malignant disease where cancer has broken through muscularis mucosae. This suggested that Ets1 had a specific role in the regulation of genes involved in gastric invasion and metastasis, rather than carcinogenesis[2,3] in gastric carcinoma. It also indicated that Ets1 was a promising marker of malignant potential and a potential avenue for therapeutic intervention in gastric cancer.

The level of Ets1 expression in epithelial tumor cells was correlated with the progression of disease, perhaps associated with the degree of cancer cell differentiation. In addition, Ets1 expressing cells were located at the invasive front of the tumor. This is consistent with previous observations that Ets1 was associated with branching morphogenesis and organ formation in embryos[21] and embryonic stem cell differentiation (Xu *et al*.,

unpublished data). Other cell types in gastric cancer, such as stromal cells, significantly increased Ets1 expression which was correlated with penetration through the muscularis mucosae and the presence of lymph node metastasis. These data are important observations since the key approach for advancing our treatment of gastric carcinoma is to clarify the mechanism of infiltration, especially for the first step, namely penetrating the muscularis mucosae. Previously, the interrelated elements concerned with gastric carcinoma' s penetration of the extracellular matrix (ECM), angiogenesis and the surrounding microenvironment have not been connected.

Increased expression of genes encoding enzymes involved in degradation of the extracellular matrix (ECM), such as MMP-1 (collagenase-1), MMP-3 (stromelysin-1), MMP-7 (matrilysin), and MMP-9 (type IV collagenase/gelatinase) has been identified in cancer from recent microarray data[22]. Hence, Ets1 is likely to contribute to tumor invasion and progression through activation of these enzymes. Indeed, expression of these ECM remodeling enzymes was detected concomitant with Ets1 mRNA in tumor cells and/or stroma cells.

Ets1 is also involved in angiogenesis, which is essential for tumor progression. In a non-vascularized tumor the growing tumor becomes hypoxic, thus the observation that Ets1 was induced by hypoxia via hypoxia-inducible factor-1 (HIF-1)[23] is important. VEGF and bFGF also induce Ets1 in endothelial cells. Ets1 was believed to confer an angiogenic phenotype to the endothelial cells through induction of the urokinase-type plasminogen activator (u-PA))[24-26] and MMPs, and also to regulate N-acetylglucosaminyl-transferase V (GnT-V), which has been associated with metastasis of tumors[27]. Thus the microenvironment of a growing tumor may induce Ets1 in tumor cells and/or stroma cells, which subsequently induces angiogenesis-related genes and ECM remodeling enzymes required for tissue invasion and metastasis. It is interesting to note that expression of Ets1 in both tumor and stroma was correlated with poor prognosis in human ovarian carcinoma[28].

Recent development in microarray technologies has resulted in extensive profiling of cancer and cancer metastases[29]. These approaches have generated a vast amount of new data to investigate the molecular mechanisms of cancer metastasis, however, many of these studies have not identified Ets1 as significantly increased. This is surprising given both our data and other data demonstrating increased Ets1 in lung carcinoma, breast carcinoma, pancreatic carcinoma, thyroid carcinoma, and oral squamous cell carcinoma[7-12]. We suggest that this anomaly is due to the sensitivity of microarray analysis, which is commonly used to detect genes with altered expression of more than 2 fold. As a transcription factor, 1-2 fold increased expression could have significant biological effects. It is interesting to note that one microarray study of gastric cancer cell lines reported that it did not find any transcription factor more than 2.0 fold upregulated from 20 k genes examined. However this study identified increased levels of defined Ets regulated genes, such as MMP and VEGF. It is also possible that mRNA status was not consistent with protein expression status or perhaps variation in cell types and Ets1 expression in the tumor sample concealed a more localized Ets1 increase. Thus we believe that our results from immunohistochemistry do not conflict with these microarray data.

In addition to the potential of Ets1 as a diagnostic marker, there is also potential for Ets1 as a potential therapeutic target for metastasis in gastric carcinogenesis. Since increased expression of Ets1 and subsequently its downstream target genes (MMPs, VEGF and HIF) contribute to invasiveness and metastasis of gastric carcinoma, inhibition of its expression is potentially therapeutic. Recently, we reported that inhibition of Ewing' s sarcoma associated EWS/FLI-1 transcription via sequence-specific transcriptional suppressor was sufficient to inhibit the transformed phenotype[30]. Thus specific inhibition of Ets1 function (or induction of Ets1) has potential for reducing metastasis in gastric carcinoma[31].

REFERENCES

1 **Hasegawa S**, Furukawa Y, Li M, Satoh S, Kato T, Watanabe T, Katagiri T, Tsunoda T, Yamaoka Y, Nakamura Y. Genome-wide analysis of gene expression in intestinal-type gastric cancers using a complementary DNA microarray representing 23,040 genes. *Cancer Res* 2002; **62**: 7012-7017

2 **Yordy JS**, Muise-Helmericks RC. Signal transduction and the Ets family of transcription factors. *Oncogene* 2000; **19**: 6503-6513

3 **Xu D**, Wilson TJ, Chan D, De Luca E, Zhou J, Hertzog PJ, Kola I. Ets1 is required for p53 transcriptional activity in UV-induced apoptosis in embryonic stem cells. *EMBO J* 2002; **21**: 4081-4093

4 **Wolvetang EJ**, Wilson TJ, Sanij E, Busciglio J, Hatzistavrou T, Seth A, Hertzog PJ, Kola I. ETS2 overexpression in transgenic models and in Down syndrome predisposes to apoptosis via the p53 pathway. *Hum Mol Genet* 2003; **12**: 247-255

5 **Li X**, Lu JY, Zhao LQ, Wang XQ, Liu GL, Liu Z, Zhou CN, Wu M, Liu ZH. Overexpression of ETS2 in human esophageal squamous cell carcinoma. *World J Gastroenterol* 2003; **9**: 205-208

6 **Zhou J**, Ng AY, Tymms MJ, Jermiin LS, Seth AK, Thomas RS, Kola I. A novel transcription factor, ELF5, belongs to the ELF subfamily of ETS genes and maps to human chromosome 11p13-15, a region subject to LOH and rearrangement in human carcinoma cell lines. *Oncogene* 1998; **17**: 2719-2732

7 **Baillat D**, Begue A, Stehelin D, Aumercier M. ETS-1 transcription factor binds cooperatively to the palindromic head to head ETS-binding sites of the stromelysin-1 promoter by counteracting autoinhibition. *J Biol Chem* 2002; **277**: 29386-29398

8 **Rutter JL**, Mitchell TI, Buttice G, Meyers J, Gusella JF, Ozelius LJ, Brinckerhoff CE. A single nucleotide polymorphism in the matrix metalloproteinase-1 promoter creates an Ets binding site and augments transcription. *Cancer Res* 1998; **58**: 5321-5325

9 **Nakada M**, Yamashita J, Okada Y, Sato H. Ets-1 positively regulates expression of urokinase-type plasminogen activator (uPA) and invasiveness of astrocytic tumors. *J Neuropathol Exp Neurol* 1999; **58**: 329-334

10 **Trojanowska M**. Ets factors and regulation of the extracellular matrix. *Oncogene* 2000; **19**: 6464-6471

11 **Liu Z**, Klominek J. Regulation of matrix metalloprotease activity in malignant mesothelioma cell lines by growth factors. *Thorax* 2003; **58**: 198-203

12 **Chung AS**, Yoon SO, Park SJ, Yun CH. Role of matrix metalloproteinases in tumor metastasis and angiogenesis. *J Biochem Mol Biol* 2003; **36**: 128-137

13 **Sasaki H** , Yukiue H, Moiriyama S, Kobayashi Y, Nakashima Y, Kaji M, Kiriyama M, Fukai I, Yamakawa Y, Fujii Y. Clinical significance of matrix metalloproteinase-1 and Ets-1 gene expression in patients with lung cancer. *J Surg Res* 2001; **101**: 242-247

14 **Span PN**, Manders P, Heuvel JJ, Thomas CM, Bosch RR, Beex LV, Sweep CG. Expression of the transcription factor Ets-1 is an independent t prognostic marker for relapse-free survival in breast cancer. *Oncogene* 2002; **21**: 8506-8509

15 **Ito T**, Nakayama T, Ito M, Naito S, Kanematsu T, Sekine I. Expression of the ets-1 proto-oncogene in human pancreatic carcinoma. *Mod Pathol* 1998; **11**: 209-215

16 **Nakayama T**, Ito M, Ohtsuru A, Naito S, Nakashima M, Sekine I. Expression of the ets-1 proto-oncogene inhuman thyroid tumor. *Mod Pahtol* 1999; **12**: 61-68

17 **Soni S**, Pande P, Shukla NK, Ralhan R. Coexpression of Ets-1 and p53 in oral carcinomas is associated with P-glycoprotein expression and poor prognosis. *J Cancer Res Clin Oncol* 2002; **128**: 336-342

18 **Pisani P**, Parkin DM, Bray F, Ferlay J. Estimates of the worldwide mortality from 25 cancers in 1990. *Int J Cancer* 1999; **83**: 18-29

19 **Shimada K**, Ajani JA. Adjuvant therapy for gastric carcinoma patients in the past years: a review of western and oriental trials. *Cancer* 1999; **86**: 1657-1668

20 **Tahara E**. Molecular aspects of invasion and metastasis of stomach cancer. *Verh Dtsch Ges Pathol* 2000; **84**: 43-49

21 **Kola I**, Brookes S, Green AR, Garber R, Tymms M, Papas TS, Seth A. The Ets1 transcription factor is widely expressed during murine embryo development and is associated with mesodermal cells involved in morphogenetic processes such as organ formation. *Proc Natl Acad Sci U S A* 1993; **90**: 7588-7592
22 **Kallioniemi OP**, Wagner U, Kononen J, Sauter G. Tissue microarray technology for high-throughput molecular profiling of cancer. *Hum Mol Genet* 2001; **10**: 657-662
23 **Oikawa M**, Abe M, Kurosawa H, Hida W, Shirato K, Sato Y. Hypoxia induces transcription factor ETS-1 via the activity of hypoxia-inducible factor-1. *Biochem Biophys Res Commun* 2001; **289**: 39-43
24 **Sato Y**, Teruyama K, Nakano T, Oda N, Abe M, Tanaka K, Iwasaka-Yagi C. Role of transcription factors in angiogenesis: Ets-1 promotes angiogenesis as well as endothelial apoptosis. *Ann N Y Acad Sci* 2001; **947**: 117-123
25 **Takai N**, Miyazaki T, Fujisawa K, Nasu K, Miyakawa I. Expression of c-Ets1 is associated with malignant potential in endometrial carcinoma. *Cancer* 2000; **89**: 2059-2067
26 **Behrens P**, Rothe M, Wellmann A, Krischler J, Wernert N. The Ets-1 transcription factor is up-regulated together with MMP 1 and MMP 9 in the stroma of pre-invasive breast cancer. *J Pathol* 2001; **194**: 43-50
27 **Ko JH**, Miyoshi E, Noda K, Ekuni A, Kang R, Ikeda Y, Taniguchi N. Regulation of the GnT-V promoter by transcription factor Ets-1 in various cancer cell lines. *J Biol Chem* 1999; **274**: 22941-22948
28 **Davidson B**, Reich R, Goldberg I, Gotlieb WH, Kopolovic J, Berner A, Ben Baruch G, Bryne M, Nesland JM. Ets-1 messenger RNA expression is a novel marker of poor survival in ovarian carcinoma. *Clin Cancer Res* 2001; **7**: 551-557
29 **Inoue H**, Matsuyama A, Mimori K, Ueo H, Mori M. Prognostic score of gastric cancer determined by cDNA microarray. *Clin Cancer Res* 2002; **8**: 3475-3479
30 **Chan D**, Wilson TJ, Xu D, Cowdery HE, Sanij E, Hertzog PJ, Kola I. Transformation induced by Ewing's sarcoma associated EWS/FLI-1 is suppressed by KRAB/FLI-1. *Br J Cancer* 2003; **88**: 137-145
31 **Shuey DJ**, McCallus DE, Giordano T. RNAi: gene-silencing in therapeutic intervention. *Drug Discov Today* 2002; **7**: 1040-1046

Edited by Wang XL

P.O.Box 2345, Beijing 100023,China
Fax: +86-10-85381893
E-mail: wjg@wjgnet.com www.wjgnet.com

World J Gastroenterol 2003;9(10):2160-2163
World Journal of Gastroenterology
 ISSN 1007-9327

• GASTRIC CANCER •

Expression of MTLC gene in gastric carcinoma

Guang-Bin Qiu, Li-Guo Gong, Dong-Mei Hao, Zhi-Hong Zhen, Kai-Lai Sun

Guang-Bin Qiu, Li-Guo Gong, Dong-Mei Hao, Zhi-Hong Zhen, Kai-Lai Sun, Department of Medical Genetics, China Medical University, Shenyang 110001, Liaoning Province, China
Supported by the National Natural Science Foundation of China, No.30171008; Funds of Educational Department, Liaoning Province, No. 20121034
Correspondence to: Kai-Lai Sun, Department of Medical Genetics, China Medical University, No.92 North 2nd Road, Heping District, Shenyang 110001, Liaoning Province, China. sunkailai@21cn.com
Telephone: +86-24-23256666-5325 **Fax:** +86-24-23265842
Received: 2003-03-12 **Accepted:** 2003-05-11

Abstract

AIM: To investigate the expression of c-myc target from laryngeal cancer cells (MTLC) gene in gastric carcinoma (GC) tissues and the effect of MTLC over-expression on gastric carcinoma cell line BGC823.

METHODS: RT-PCR was performed to determine the expression of MTLC mRNA in GC and matched control tissues. BGC823 cells were transfected with an expression vector pcDNA3.1-MTLC by liposome and screened by G418. Growth of cells expressing MTLC was observed daily by manual counting. Apoptotic cells were determined by TdT-mediated dUTP nick-end labeling (TUNEL) assay.

RESULTS: The expression of MTLC mRNAs was down-regulated in 9(60%) of 15 cases of GC tissues. The growth rates of the BGC823 cells expressing MTLC were indistinguishable from that of control cells. A marked acceleration of apoptosis was observed in MTLC-expressing cells.

CONCLUSION: MTLC was down-regulated in the majority of GC tissues and could promote apoptosis of GC cell lines, which suggests that MTLC may play an important role in the carcinogenesis of gastric carcinoma.

Qiu GB, Gong LG, Hao DM, Zhen ZH, Sun KL. Expression of MTLC gene in gastric carcinoma. *World J Gastroenterol* 2003; 9(10): 2160-2163
http://www.wjgnet.com/1007-9327/9/2160.asp

INTRODUCTION

Gastric carcinoma (GC) is one of the most common malignant tumors in the world[1,2]. Numerous data have shown that some genes such as p53, c-myc, bcl-2, COX-2 and PTEN[3-6] might be associated with the gastric carcinogenesis. However, the exact molecular mechanism underlying GC remains to be fully elucidated. Therefore, it is necessary to look for novel genes to obtain a thorough understanding about gastric carcinogenesis.

c-myc target from laryngeal cancer cells (MTLC) gene, a putative target of c-myc, was recently cloned in our laboratory (GenBank access number AF527367). MTLC was located in 6q25, a chromosome region involved in various kinds of cancers[7-11]. Previous studies have shown that its protein product expressed in nuclei and might take part in the regulation of cell cycle[12], suggesting that MTLC was potentially related to the carcinogenesis. In this study, we therefore performed RT-PCR and eukaryotic transfection to reveal the relationship between MTLC and GC.

MATERIALS AND METHODS

Tissues and cell line

All the gastric cancer and matched control tissues confirmed pathologically were obtained from the First Affiliated Hospital of China Medical University. Tumor tissues were dissected from the resected specimens. The normal tissue block was taken from the distal resection margin and was apart from cancer at least 1 cm. Gastric carcinoma cell line BGC823 was kept in our laboratory.

RT-PCR

Total RNAs were extracted from cancer tissues by TRIZOL reagents (GibcoBRL, Grand Island, NY, USA), and were reverse-transcripted to the first strand of cDNA using reverse transcriptase system (Promega, Madison, WI, USA). MTLC cDNA was amplified by PCR under the following condition: first at 95 ℃for 1 min, 30 cycles at 95 ℃for 30 s, at 60 ℃for 1 min, at 72 ℃for 1.5min, and finally at 72 ℃for 10 min. PCR primers consisted of the sequences of forward: 5-ATGGATCCCTGCACTGGCTGATGAGTGTGTA-3 and reverse: 5-GTAAGCTTGAACAGTGCCTTCACCCTCG AGGT-3. β-actin gene was used as internal control.

Construction of MTLC expression vector

MTLC segment amplified by PCR was ligated to pMD-18T vector (Takara, Dalian, China) by TA cloning. The recombinant was digested by *BamH I* and *EcoR I*, and then the target fragment was recollected and cloned into pcDNA3.1 vector (Invitrogen, Carlsbad, CA, USA). Both PCR product and the expression vector pcDNA3.1-MTLC were confirmed by sequencing to avoid mutation.

Transfection and screening of BGC823 cells

BGC823 cells in logarithmic phase were seeded in 35 mm plates and cultured with DMEM containing 10 % serum overnight. Cells were transfected with 1 μg expression vector or empty parental vector by Lipofectamin 2000 (Invitrogen, Carlsbad, CA, USA) and subsequently screened by G418 at a final concentration of 5 g/L after cultured for 24 h.

Observation of cell growth

Cells transfected by pcDNA3.1-MTLC or empty parental vector were plated in 35 mm plates at a concentration of 1×10^5 cells/plate with DMEM culture containing 10 % serum. Individual plates were trypsinized daily and the total number of viable cells per plate was determined by manual counting.

Detection of apoptosis

DeadEnd™ Fluorometric TUNEL System (Promega, Madison, WI, USA) was used to determine the apoptosis of cells. 1×10^5 cells transfected by pcDNA3.1-MTLC or empty parental vector were seeded into a plate with a poly-L-lysine-coated slide on its center and grown for 24 h in DMEM culture containing 10 % serum. The cells were then maintained for additional

18 h in serum-free culture and then detected according to the protocol provided by the manufacturer. The samples were stained with propidium iodide (PI) to make a red background and then observed under fluorescence microscope.

RESULTS

Expression of MTLC mRNA in GC tissues

RT-PCR was performed in 15 paired tissues to reveal the expression levels of MTLC mRNA. The result of electrophoresis showed that the PCR product was a single band on agar gel (Figure 1). MTLC was down-regulated in cancer tissues in 9(60 %) of 15 cases after normalization by comparing the band intensities with software UVP Gelworks ID advanced version 2.5 (Figure 1).

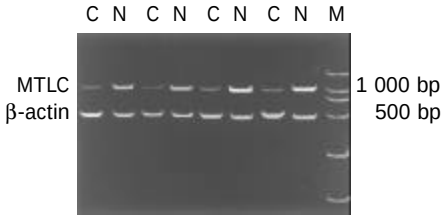

Figure 1 RT-PCR products were electrophoresed on 1 % agarose gel containing ethidium bromide. The level of β-actin was used as internal control. M: DL2000 DNA marker; C: gastric cancer tissue; N: adjacent normal gastric tissue.

Effects of MTLC expression on cell growth

One of the effects of c-myc on cells is to affect their growth properties. Therefore, we determined whether over-expression of MTLC could recapitulate this character. As seen in Figure 2, the growth rates of MTLC-expressing cells were indistinguishable from those of control cells transfected with the empty parental vector.

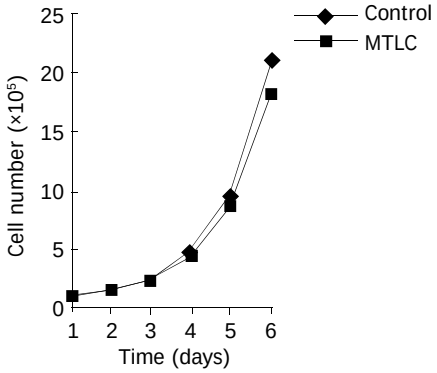

Figure 2 Cells were determined by manual counting daily. The data was analyzed by Microsoft Excel.

Promotion of apoptosis by MTLC

We studied the response of MTLC-expression BGC823 cell line to avoid its growth factors. Compared with the control

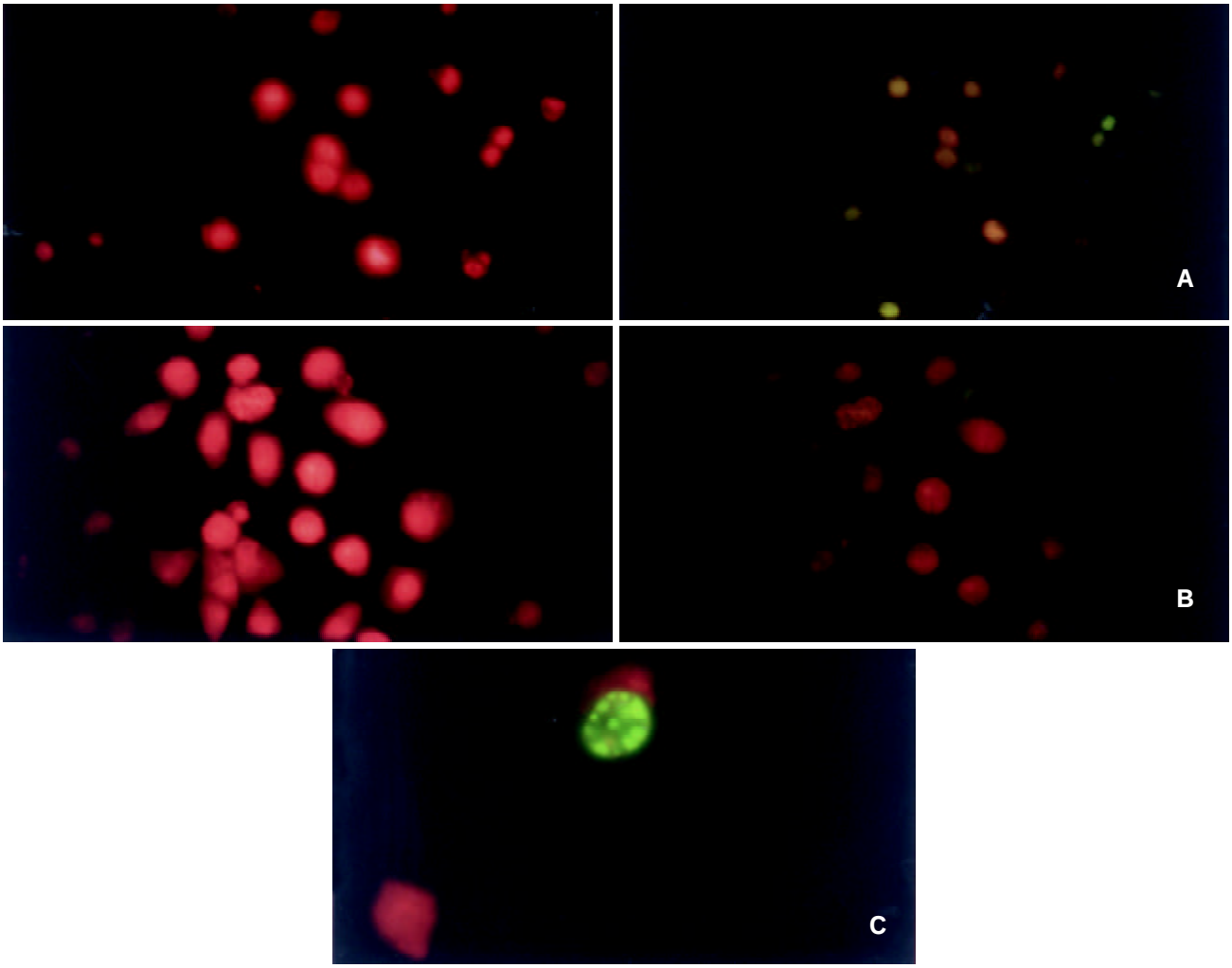

Figure 3 Apoptosis of cells were detected by TUNEL (TdT-mediated dUTP Nick-End Labeling) assay. Green fluorescence of fluorescein-12-dUTP was detected in apoptotic cells, whereas red fluorescence of PI was observed in all cells. Both signals in a same field were photographed respectively. A: MTLC-expressing cells (×400); B: control cells (×400). C: a single apoptotic cell (×1000).

cells, MTLC-expression cells showed a marked acceleration of apoptosis (Figure 3).

Table 1 Relative expressions of MTLC / β-actin in GC tissues and control tissues

Case No.	GC	Control	Ratio[a]
1	0.27	2.56	0.10
2	0.16	3.78	0.04
3	0.56	2.64	0.21
4	0.93	1.56	0.59
5	1.25	1.17	1.06
6	0.52	2.31	0.22
7	0.35	1.75	0.20
8	0.35	1.21	0.29
9	0.64	0.73	0.87
10	1.21	0.98	1.29
11	0.39	2.35	0.16
12	0.57	1.54	0.37
13	0.47	1.56	0.30
14	0.69	0.76	0.90
15	0.83	0.93	0.89

[a]The ratios less than 0.5 were defined as down-regulation.

DISCUSSION

MTLC is a novel gene cloned in our laboratory recently and has no known function. Previous studies showed that it was located in 6q25, a chromosome region involved in a variety of human malignancies, including gastric cancer. Analysis of the 5' flanking sequence also demonstrated two E-boxes on the promoter region of MTLC, suggesting that MTLC may be a target of oncogene c-myc. C-myc, a helix-loop-helix leucine zipper transcription factor, can exert considerable control over transformation, differentiation, apoptosis, and cell cycle progression through a number of target genes, including CAD[13], ODC[14,15], LDH-A[16,17], cyclin E[18], MrDb[19], telomerase/hTERT[20-25], rcl[26], IRP2[27], cdc25A[28], and JPO1[29]. It was also shown that c-myc could contribute to gastric carcinogenesis[30-36], but the exact mechanism is still not clear.

In this study, therefore, we detected the expression of MTLC mRNA in gastric cancer tissues and the effects of MTLC over-expression in gastric carcinoma cell line BGC823 to reveal the relationship between MTLC and gastric cancer. Results of RT-PCR showed that MTLC was down-regulated in 60 % (9/15) cases of gastric cancer tissues, a considerable frequency approximating to other genes suppressed in gastric cancer[37-40], suggesting that MTLC may play an important role in carcinogenesis. Furthermore, we performed gene transfection to reveal the possible function of MTLC in gastric carcinogenesis. MTLC did not affect cell growth but remarkably promoted apoptosis in response to growth factor deprivation, although we could not yet explain how this occurred. Over-expression of some other c-myc targets such as p21[41-45] and GADD45[46-51] has been reported to exhibit similar effects through p53 pathway. However, the mechanism of MTLC promoting GC cells apoptosis needs to be further studied. It is also necessary to verify the down-regulation of MTLC in GC tissues by detecting more samples with various types or clinical stages.

REFERENCES

1 **Parkin DM**. Global cancer statistics in the year 2000. *Lancet Oncol* 2001; **2:** 533-543

2 **Deng DJ.** Progress of gastric cancer etiology: N-nitrosamides 1999s. *World J Gastroenterol* 2000; **6:** 613-618

3 **Xu AG**, Li SG, Liu JH, Gan AH. Function of apoptosis and expression of the proteins Bcl-2, p53 and C-myc in the development of gastric cancer. *World J Gastroenterol* 2001; **7:** 403-406

4 **Xue YW**, Zhang QF, Zhu ZB, Wang Q, Fu SB. Expression of cyclooxygenase-2 and clinicopathologic features in human gastric adenocarcinoma. *World J Gastroenterol* 2003; **9:** 250-253

5 **Guo XL**, Wang LE, Du SY, Fan CL, Li L, Wang P, Yuan Y. Association of cyclooxygenase-2 expression with Hp-cagA infection in gastric cancer. *World J Gastroenterol* 2003; **9:** 246-249

6 **Yang L**, Kuang LG, Zheng HC, Li JY, Wu DY, Zhang SM, Xin Y. PTEN encoding product: a marker for tumorigenesis and progression of gastric carcinoma. *World J Gastroenterol* 2003; **9:** 35-39

7 **Wang VW**, Bell DA, Berkowitz RS, Mok SC. Whole genome amplification and high-throughput allelotyping identified five distinct deletion regions on chromosomes 5 and 6 in microdissected early-stage ovarian tumors. *Cancer Res* 2001; **61:** 4169-4174

8 **Rodriguez C**, Causse A, Ursule E, Theillet C. At least five regions of imbalance on 6q in breast tumors, combining losses and gains. *Genes Chromosomes Cancer* 2000; **27:** 76-84

9 **Stilgenbauer S**, Bullinger L, Benner A, Wildenberger K, Bentz M, Dohner K, Ho AD, Lichter P, Dohner H. Incidence and clinical significance of 6q deletions in B cell chronic lymphocytic leukemia. *Leukemia* 1999; **13:** 1331-1334

10 **Gao H,** Wang Q, Wang B, Yan C, Wang S, Wang B, Zhu J, Huang C, Fu S. Genescan analysis of non-small cell lung cancer in the long arm of chromosome 6. *Zhonghua Yixue Yichuanxue Zazhi* 2002; **19:** 14-16

11 **Acevedo CM**, Henriquez M, Emmert-Buck MR, Chuaqui RF. Loss of heterozygosity on chromosome arms 3p and 6q in microdissected adenocarcinomas of the uterine cervix and adenocarcinoma in situ. *Cancer* 2002; **94:** 793-802

12 **Qiu G**, Xu Z, Huang D, Gong L, Li C, Sun X, Sun K. Cloning and characterization of MTLC, a novel gene in 6q25. *Zhonghua Yixue Yichuanxue Zazhi* 2003; **20:** 94-97

13 **Boyd** KE, Farnham PJ. Myc versus USF: discrimination at the cad gene is determined by core promoter elements. *Mol Cell Biol* 1997; **17:** 2529-2537

14 **Bello-Fernandez** C, Packham G, Cleveland JL. The ornithine decarboxylase gene is a transcriptional target of c-Myc. *Proc Natl Acad Sci U S A* 1993; **90:** 7804-7808

15 **Wu S**, Pena A, Korcz A, Soprano DR, Soprano KJ. Overexpression of Mxi1 inhibits the induction of the human ornithine decarboxylase gene by the Myc / Max protein complex. *Oncogene* 1996; **12:** 621-629

16 **Shim H**, Dolde C, Lewis BC, Wu CS, Dang G, Jungmann RA, Dalla-Favera R, Dang CV. C-myc transactivation of LDH-A: Implications for tumor metabolism and growth. *Proc Natl Acad Sci U S A* 1997; **94:** 6658-6663

17 **Hubank M**, Schatz DG. Identifying differences in mRNA expression by representational difference analysis of cDNA. *Nucleic Acids Res* 1994; **22:** 5640-5648

18 **Perez-Roger** I, Solomon DL, Sewing A, Land H. Myc activation of cyclin E / Cdk2 kinase involves induction of cyclin E gene transcription and inhibition of p27(Kip1) binding to newly formed complexes. *Oncogene* 1997; **14:** 2373-2381

19 **Grandori C**, Mac J, Siebelt F, Ayer DE, Eisenman RN. Myc-Max heterodimers activate a DEAD box gene and interact with multiple E box-related sites *in vivo*. *EMBO J* 1996; **15:** 4344-4357

20 **Wang J**, Xie LY, Allan S, Beach D, Hannon GJ. Myc activates telomerase. *Genes Dev*1998; **12:** 1769-1774

21 **Greenberg RA**, O' Hagan RC, Deng H, Xiao Q, Hann SR, Adams RR, Lichtsteiner S, Chin L, Morin GB, DePinho RA. Telomerase reverse transcriptase gene is a direct target of c-Myc but is not functionally equivalent in cellular transformation. *Oncogene* 1999; **18:** 1219-1226

22 **Horikawa I**, Cable PL, Afshari C, Barrett JC. Cloning and characterization of the promoter region of human telomerase reverse transcriptase gene. *Cancer Res* 1999; **59:** 826-830

23 **Takakura M**, Kyo S, Kanaya T, Hirano H, Takeda J, Yutsudo M, Inoue M. Cloning of human telomerase catalytic subunit (hTERT) gene promoter and identification of proximal core promoter sequences essential for transcriptional activation in immortalized and cancer cells. *Cancer Res* 1999; **59:** 551-557

24 **Wick M**, Zubov D, Hagen G. Genomic organization and promoter characteriza- tion of the gene encoding the human

telomerase reverse transcriptase (hTERT). *Gene* 1999; **232:** 97-106
25 **Qiu GB**, He G, Gong LG, Zhao Z, Pan ZM, Tang YC, Sun KL. Cloning of hTERT cDNA fragment and application of anti-hTERT monoclonal antibody in mechanism of laryngeal carcinogenesis. *Yichuan Xuebao* 2003; **30:** 109-113
26 **Lewis BC**, Shim H, Li Q, Wu CS, Lee LA, Maity A, Dang CV. Identification of putative c-myc-responsive genes: characterization of rcl, a novel growth-related gene. *Mol Cell Biol* 1997; **17:** 4967-4978
27 **Wu KJ**, Polack A, Dalla-Favera R. Coordinated regulation of iron-controlling genes, H-ferritin and IRP2, by c-myc. *Science* 1999; **283:** 676-679
28 **Galaktionov K**, Chen X, Beach D. Cdc25 cell-cycle phosphatase as a target of c-myc. *Nature* 1996; **382:** 511-517
29 **Prescott JE**, Osthus RC, Lee LA, Lewis BC, Shim H, Barrett JF, Guo Q, Hawkins AL, Griffin CA, Dang CV. A novel c-myc-responsive gene, JPO1, participates in neoplastic transformation. *J Biol Chem* 2001; **276:** 48276-48284
30 **Yang Y**, Deng CS, Peng JZ, Wong BC, Lam SK, Xia HH. Effect of *Helicobacter pylori* on apoptosis and apoptosis related genes in gastric cancer cells. *Mol Pathol* 2003; **56:** 19-24
31 **Liu JR**, Chen BQ, Yang YM, Wang XL, Xue YB, Zheng YM, Liu RH. Effect of apoptosis on gastric adenocarcinoma cell line SGC-7901 induced by cis-9, trans-11-conjugated linoleic acid. *World J Gastroenterol* 2002; **8:** 999-1004
32 **Chen RC**, Su JH, Yang SM, Li J, Wang TJ, Zhou H. Effect of isoverbascoside, a phenylpropanoid glycoside antioxidant, on proliferation and differentiation of human gastric cancer cell. *Acta Pharmacol Sin* 2002; **23:** 997-1001
33 **Ishii HH**, Gobe GC, Pan W, Yoneyama J, Ebihara Y. Apoptosis and cell proliferation in the development of gastric carcinomas: associations with c-myc and p53 protein expression. *J Gastroenterol Hepatol* 2002; **17:** 966-972
34 **Kawanaka H**, Tomikawa M, Baatar D, Jones MK, Pai R, Szabo IL, Sugimachi K, Sarfeh IJ, Tarnawski AS. Despite activation of EGF-receptor-ERK signaling pathway, epithelial proliferation is impaired in portal hypertensive gastric mucosa: relevance of MKP-1, c-fos, c-myc, and cyclin D1 expression. *Life Sci* 2001; **69:** 3019-3033
35 **Hensel F**, Hermann R, Brandlein S, Krenn V, Schmausser B, Geis S, Muller-Hermelink HK, Vollmers HP. Regulation of the new coexpressed CD55 (decay-accelerating factor) receptor on stomach carcinoma cells involved in antibody SC-1-induced apoptosis. *Lab Invest* 2001; **81:** 1553-1563
36 **Ye YN**, Liu ES, Shin VY, Koo MW, Li Y, Wei EQ, Matsui H, Cho CH. A mechanistic study of proliferation induced by Angelica sinensis in a normal gastric epithelial cell line. *Biochem Pharmacol* 2001; **61:** 1439-1448
37 **Yoshikawa Y**, Mukai H, Hino F, Asada K, Kato I. Isolation of two novel genes, down-regulated in gastric cancer. *Jpn J Cancer Res* 2000; **91:** 459-463
38 **Liu DH**, Zhang XY, Fan DM, Huang YX, Zhang JS, Huang WQ, Zhang YQ, Huang QS, Ma WY, Chai YB, Jin M. Expression of vascular endothelial growth factor and its role in oncogenesis of human gastric carcinoma. *World J Gastroenterol* 2001; **7:** 500-505
39 **Rosivatz E**, Becker I, Specht K, Fricke E, Luber B, Busch R, Hofler H, Becker KF. Differential expression of the epithelial-mesenchymal transition regulators snail, SIP1, and twist in gastric cancer. *Am J Pathol* 2002; **161:** 1881-1891
40 **Zhang J**, Wang Y, Shou C, Xu G, Chen X, Wu J, Xie Y, Li J, So S, Jiafu J. Detection of Mycoplasma hyorhinis in gastric cancer using bio-chip technology. *Zhonghua Yixue Zazhi* 2002; **82:** 961-965
41 **Bearss DJ**, Lee RJ, Troyer DA, Pestell RG, Windle JJ. Differential effects of p21(WAF1/CIP1) deficiency on MMTV-ras and MMTV-myc mammary tumor properties. *Cancer Res* 2002; **62:** 2077-2084
42 **Horiguchi-Yamada** J, Fukumi S, Saito S, Nakayama R, Iwase S, Yamada H. DNA topoisomerase II inhibitor, etoposide, induces p21WAF1/CIP1 through down-regulation of c-myc in K562 cells. *Anticancer Res* 2002; **22:** 3827-3832
43 **Seoane J**, Le HV, Massague J. Myc suppression of the p21(Cip1) Cdk inhibitor influences the outcome of the p53 response to DNA damage. *Nature* 2002; **419:** 729-734
44 **Bergsmedh A**, Szeles A, Spetz AL, Holmgren L. Loss of the p21 (Cip1/Waf1) cyclin kinase inhibitor results in propagation of horizontally transferred DNA. *Cancer Res* 2002; **62:** 575-579
45 **Wu YL**, Sun B, Zhang XJ, Wang SN, He HY, Qiao MM, Zhong J, Xu JY. Growth inhibition and apoptosis induction of Sulindac on Human gastric cancer cells. *World J Gastroenterol* 2001; **7:** 796-800
46 **Conzen SD**, Gottlob K, Kandel ES, Khanduri P, Wagner AJ, O'Leary M, Hay N. Induction of cell cycle progression and acceleration of apoptosis are two separable functions of c-myc: transrepression correlates with acceleration of apoptosis. *Mol Cell Biol* 2000; **20:** 6008-6018
47 **Wang A**, Gu J, Judson-Kremer K, Powell KL, Mistry H, Simhambhatla P, Aldaz CM, Gaddis S, MacLeod MC. Response of human mammary epithelial cells to DNA damage induced by BPDE: involvement of novel regulatory pathways. *Carcinogenesis* 2003; **24:** 225-234
48 **Chen Z**, Clark S, Birkeland M, Sung CM, Lago A, Liu R, Kirkpatrick R, Johanson K, Winkler JD, Hu E. Induction and superinduction of growth arrest and DNA damage gene 45 (GADD45) alpha and beta messenger RNAs by histone deacetylase inhibitors trichostatin A (TSA) and butyrate in SW620 human colon carcinoma cells. *Cancer Lett* 2002; **188:** 127-140
49 **Vairapandi M**, Balliet AG, Hoffman B, Liebermann DA. GADD45b and GADD45g are cdc2/cyclinB1 kinase inhibitors with a role in S and G2/M cell cycle checkpoints induced by genotoxic stress. *J Cell Physiol* 2002; **192:** 327-338
50 **Uberti D**, Carsana T, Bernardi E, Rodella L, Grigolato P, Lanni C, Racchi M, Govoni S, Memo M. Selective impairment of p53-mediated cell death in fibroblasts from sporadic Alzheimer's disease patients. *J Cell Sci* 2002; **115**(Pt 15): 3131-3138
51 **Okura T**, Nakamura M, Takata Y, Watanabe S, Kitami Y, Hiwada K. Troglitazone induces apoptosis via the p53 and Gadd45 pathway in vascular smooth muscle cells. *Eur J Pharmacol* 2000; **407:** 227-235

Edited by Ma JY

P.O.Box 2345, Beijing 100023,China
Fax: +86-10-85381893
E-mail: wjg@wjgnet.com www.wjgnet.com

World J Gastroenterol 2003;9(10):2164-2168
World Journal of Gastroenterology
 ISSN 1007-9327

• GASTRIC CANCER •

Identification of antigens by monoclonal antibody PD4 and its expression in *Escherichia coli*

Jin-Ying Ning, Guo-Xun Sun, Su Huang, Hong Ma, Ping An, Lin Meng, Shu-Mei Song, Jian Wu, Cheng-Chao Shou

Jin-Ying Ning, Guo-Xun Sun, Su Huang, Hong Ma, Ping An, Lin Meng, Shu-Mei Song, Jian Wu, Cheng-Chao Shou, Department of Biochemistry and Molecular Biology, School of Oncology and Beijing Institute for Cancer Research, Peking University, Beijing 100034, China
Supported by Key Project of National Natural Science Foundation of China, No.30130190, Beijing Natural Science Foundation, No.7012007, Oncology Key Program and Cancer Center of Peking University
Correspondence to: Dr. Cheng-Chao Shou, Department of Biochemistry and Molecular Biology, School of Oncology and Beijing Institute for Cancer Research, Peking University, Beijing 100034, China. cshou9_@hotmail.com
Telephone: +86-10-66160960 **Fax:** +86-10-66175832
Received: 2003-06-04 **Accepted:** 2003-07-24

Abstract

AIM: To clone and express the antigen of monoclonal antibody (MAb) PD4 for further investigation of its function.

METHODS: MGC803 cDNA expression library was constructed and screened with PD4 as probes to clone the antigen. After failed in the library screening, immunoprecipitation and SDS-polyacrylamide gel electrophoresis were applied to purify the antigen for sequence analysis. The antigen coming from *Mycoplasma hyorhinis (M. hyorhinis)* was further confirmed with Western blot analysis by infecting *M. hyorhinis* -free HeLa cells and eliminating the *M. hyorhinis* from MGC803 cells. The full p37 gene was cloned by PCR and expressed successfully in *Escherichia coli* after site-directed mutations. Immunofluorescence assay was used to demonstrate if p37 protein could directly bind to gastric tumor cell AGS.

RESULTS: The cDNA library constructed with MGC803 cells was screened by MAb PD4 as probes. Unfortunately, the positive clones identified with MAb PD4 were also reacted with unrelated antibodies. Then, immunoprecipitation was performed and the purified antigen was identified to be a membrane protein of *Mycoplasma hyorhinis (M. hyorhinis*) by sequencing of N-terminal amino acid residues. The membrane protein was intensively verified with Western blot by eliminating *M. hyorhinis* from MGC803 cells and by infecting *M. hyorhinis*-free HeLa cells. The full p37 gene was cloned and expressed successfully in *Escherichia coli* after site-directed mutations. Immunofluorescence demonstrated that p37 protein could directly bind to gastric tumor cell AGS.

CONCLUSION: The antigen recognized by MAb PD4 is from *M. hyorhinis,* which suggests the actions involved in MAb PD4 is possibly mediated by p37 protein or *M. hyorhinis.* As p37 protein can bind directly to tumor cells, the pathogenic role of p37 involved in tumorigenesis justifies further investigation.

Ning JY, Sun GX, Huang S, Ma H, An P, Meng L, Song SM, Wu J, Shou CC. Identification of antigens by monoclonal antibody PD4 and its expression in *Escherichia coli*. *World J Gastroenterol* 2003; 9(10): 2164-2168
http://www.wjgnet.com/1007-9327/9/2164.asp

INTRODUCTION

Gastric cancer is common in China[1-14]. For decades, a goal of cancer researchers is to be able to immunize patients with their own tumor tissues or tumor associated antigens after surgical operation to stimulate their immune response. The benefits of this aim include host immune surveillance to eliminate the metastatic cells and prevent its relapse. Many tumor associated antigens defined by monoclonal antibodies have been successfully applied clinically in detecting different tumors[15,16]. However, only a few of the genes for these markers have been cloned[17,18], primarily because the epitopes usually are not protein or not linear in amino acid sequence.

MAb PD4 has been derived from mouse immunized with human gastric cell line MGC803 and could specially react with some tumor cells[19]. Our previous studies showed that MAb PD4 could induce apoptosis of MGC803 cells[20], inhibit both the growth of ras transformed cell line Rat3-3 and the tumorigenesis in nude mice[21], suggesting that the antigen recognized by MAb PD4 could be associated with cancerous development. Obviously the critical step in investigating the molecular mechanisms involved in the antigen is to isolate its cDNA.

As it was shown previously that PD4 worked well in Western blot in which the recognized protein was around 40 kilo-Dalton in molecular weight[21]. First, we screened the cDNA library constructed with MGC803 cells by MAb PD4 as probes. Unfortunately, the positive clones identified with MAb PD4 were reacted with unrelated antibodies. We tried with other different tumor expression cDNA libraries and also did not get any specific clones. Then, immunoprecipitation was performed and the target molecule was identified to be a membrane protein of *M. hyorhinis* by N-termial amino acid residues sequencing. The membrane protein was intensively verified with Western blot by eliminating *M. hyorhinis* from MGC803 cells and by infecting *M. hyorhinis*-free Hela cells. Therefore, the actions involved in MAb PD4 were possibly mediated by p37 protein or *M. hyorhinis.*

p37 is a membrane protein of *M. hyorhinis* located on the outside of the cell membrane. It contains 1209 nucleotides and encodes 403 amino acid residues[22]. An analysis of the protein sequence has revealed that p37 has a 41 % similarity to a periplasmic binding-protein-dependent transport system found in Gram-negative bacteria[22]. Thus, p37 is thought to be part of a high affinity transport system from *M. hyorhinis*. Also, there are lines of evidence indicating the linkage between p37 or *M. hyorhinis* and cancer[23-25]. For example, antibodies against p37 could inhibit the invasive potential of FS9 cells and cause malignant cells to revert to a more normal behavior.

In this study, we identified the antigen recognized by MAb PD4, which was previously considered as an antibody against cancer. The full gene encoding the antigen was cloned and expressed successfully in *Escherichia coli (E. coli)* after site-directed mutation of the seven codes tryptophan TGA into universal codes tryptophan TGG and demonstrated that p37 could bind directly to tumor cell AGS. Considering the association between p37 and tumor development and invasion, this work provides a basis for further investigation of the pathogenic role of p37 involved in *M. hyorhinis* infection.

MATERIALS AND METHODS

Cell culture and regents

Human gastric cancer cell lines MGC803 and AGS, human ovarian cancer cell line HeLa, expression plasmid pGEX-4T-1, *E. coli* BL21(DE3) and MAb PD4 were all kept in our laboratory. Site-directed mutation kit was purchased from Promega Corp. Anti-glutathione-S-transferase (GST) mouse antibody, goat anti-mouse antibody conjugated with tetramethyl rhodaine isothiacy-anate (TRITC), 3,3'-diaminobenzidine (DAB), isopropylthiogalactoside (IPTG) were from Sigma. All primers for PCR and site-directed mutation were synthesized by Sangon Corp. (Shanghai, China). Various restriction endonucleases were products of New England BioLabs (NEB). RPMI1640 and F12K medium were from GIBCO BRL. RNA extraction kit was from Invitrogen Corp.

cDNA library construction, screening and clone identification

mRNA purification and poly(A)+ mRNA enrichment were processed with a messenger RNA isolation kit (Strategene Corp.) from 5×10^7 MGC803 cells. A cDNA library was prepared and packaged with ZAP Express cDNA Gigapack III gold cloning kit (Strategene Corp.) according to the manufacture's instruction. The library quality was determined with its diversity and the average size of the inserted cDNA fragments. The non-amplified library was plated and transferred to nitrocellulose filters. Initial screening was performed with 1 $\mu g\cdot mL^{-1}$ MAb PD4 (diluted in phosphate-buffered saline containing 1 % bovine serum albumin). The filters were then washed in phosphate-buffered saline (PBS) and bound MAb PD4 was detected by alkaline phosphatase coupled to sheep anti-mouse antibodies followed by the mixture solution of nitro blue tetrazolium and bromochloroindolylphosphate. The positive bacteriophages were subcloned and the positive individual clones were checked with unrelated antibodies for its specificity.

Preparation of MGC803 cell membrane proteins

2×10^8 MGC803 cells were frozen and thawed repeatedly for 4-5 times in phosphate-buffered saline containing 1 $mmol\cdot L^{-1}$ PMSF, then centrifuged at 4 000×g for 30 min at 4 ℃. The supernatant was collected, centrifuged at 100 000×g for 1 h at 4 ℃. The precipitated membrane debris was suspended with 1-2 ml lysis buffer (20 mM Tris-HCl pH 7.5, 150 mM NaCl, 2 mM EDTA, 1 % NP-40, 5 % sodium deoxycholate, 1 mM PMSF, 2 $\mu g\cdot mL^{-1}$ aprotinin), shaken for 30 min at 4 ℃, then centrifuged at 100 000×g for 1 h at 4 ℃. The supernatant was analyzed by Western blot with MAb PD4.

Purification and identification of the antigen protein

The lysates from MGC803 cells were immunoprecipitated for overnight at 4 ℃ by MAb PD4 coupled with protein A-sepharose 4B beads (Sigma). The normal mouse IgG was used as control. The immunoprecipitated beads were washed three times with lysis buffer and subjected to 12 % SDS-polyacrylamide gel electrophoresis (SDS-PAGE). The gel-separated proteins were transferred onto PVDF membranes. A piece cut off from the membrane was used for Western blot with MAb PD4 and the left transferred membrane was stained with ponceau S. After the identification, the corresponding band with the Western blot was cut off and the sequence of N-terminal amino acid residues was performed in Life Science Center of Peking University.

Further identification of the antigen from mycoplasma infected cells

When *M. hyorhinis*-free HeLa cells grew to appropriate confluence, the conditional medium from cultured MGC803 cells, which reacted with MAb PD4, was added into the cultured HeLa cells system. After 72 h incubation, total proteins were extracted from HeLa cells with lysis buffer (1 % Triton X-100/PBS, 1 $mmol\cdot L^{-1}$ PMSF) and Western blot was performed with MAb PD4 as first antibody. Moreover, cultured MGC803 cells were treated with BM cyclin antibiotics for 3 weeks (Roche, Mannheim, Germany) which were recognized as the most effective against mycoplasma infection[26]. Then the total proteins of MGC803 cells were extracted, followed by Western blot as above.

Cloning, site-directed mutations and sequencing of p37 gene

3 mL supernatant from cultured MGC803 cells infected with *M. hyorhinis* was collected, centrifuged at 12 000×g for 5 min, rinsed once with PBS, dissolved in 30 μl ddH2O, then boiled for 5 min, centrifuged for 5 min at 10 000×g. 2 μl supernatant was used as the template for PCR to amplify p37 gene. Upstream primer 5'-aatcggatcc gaggtagcttttatgctc-3' (including *Bam*H I site) and downstream primer 5'-aaagaattctcatttaatggcttttt c-3' (including *Eco*R I site) were synthesized by Sangon Co. (Shanghai. China). The PCR program was consisted of 30 cycles at 94 ℃ for 1 min, at 48 ℃ for 1 min, at 72 ℃ for 90 s, and at 72 ℃ for 10 min for the final extension. The PCR product was inserted into a pBluescript vector after digestion with endonucleases *Bam*HI and *Eco*R I. The seven tryptophan TGA codes were mutated into universal codes tryptophan TGG using mutation vector pALTER-1 according to the instructions of the site-directed mutation kit (Promega) and verified by DNA sequencing. The 5' phosphated mutated primers were as follows: (1) 5'-p(A GGTCAATG**G**G ATAAAAGTA)-3', (2)5'-p(GCAAGTTG **G**ACTGATGA AAATC A TAAGTG**G**AATGGTAATG)-3', (3)5'-p (GGAATGATTTG**G**ATAAAAGGTAAT G)-3', (4)5'-p (AAAAAGCTTG**G**AATGATA AAGATTG**G**AATAC ATTTAGAAA TTTT)-3', (5)5'-p(GG T TCTTTTGCTTG**G**A CACATAAC A)-3'. The bold letters were changed from A.

Expression, purification and identification of GST-P37 fusion protein

The recombinant vector pGEX-4T-p37 was constructed through inserting the mutated p37 into plasmid pGEX-4T-1, then it was introduced into *E. coli* BL21(DE3). The transformed bacteria were induced with 0.1 mM IPTG to express the fusion protein at 30 ℃ overnight. Then the induced bacteria were collected and lysed by ultrasonocation. After centrifugation, the supernatant was incubated with glutathione-sepharose-4B and binding protein was eluted with elution buffer (50 mM Tris-HCl, pH 8.0, 15 mM reduced glutathione). The GST-p37 protein in elution buffer was tested by SDS-PAGE and identified by Western blot after concentrated with sucrose and dialyzed with PBS.

Binding assay with immunofluorescence microscopy

AGS cells were seeded into 6-well culture plates in F-12K medium and crept on cover slides for 24 h. Then the cells were washed twice by PBS. The GST-p37 and GST proteins (10 $\mu g\cdot mL^{-1}$) dissolved in serum-free F-12K medium were added respectively. After incubation for 1 h, cells were gently washed 3 times by PBS and fixed for 15 min with freshly prepared 4 % paraformaldehyde. Then the cells were washed twice by PBT buffer (PBS with 0.1 % bovine serum albumin and 0.01 % Tween 20) and blocked with 10 % normal goat serum for 1 h at 37 ℃. Anti-GST antibodies were added as the first antibody and incubated for 1 h at 37 ℃. After the cells were washed twice for 5 min each by PBT buffer, TRITC-conjugated goat anti-mouse IgG antibodies were used as secondary antibody to detect bound GST-p37 and GST

proteins. The cells were washed twice with PBT buffer and briefly rinsed with water before mounted onto slides for observation under fluorescence microscopy.

RESULTS

cDNA library construction, screening and identification

We obtained 2 μg poly(A)+ enriched mRNA for synthesizing the cDNA library. Double-stranded cDNA was generated by means of "nick-translation". *Eco*R I adapters were ligated to the double-stranded cDNA, which was then digested with *Xho*I and size selected. Only the cDNA molecules larger than 500 bp were collected and ligated into ZAP expression vectors. The diversity of the primary library was 1.2×10^6 pfu. The recombinant rate was 9/9, and the average size of cDNA inserts was about 1.5 kb. A total of 10^6 non-amplified library clones were screened with MAb PD4 and the positive clones were confirmed with unrelated antibodies as controls. Anyhow no specific positive clone reacted with MAb PD4 was obtained.

Purification of the antigen recognized by MAb PD4

First, the total membrane protein from MGC803 was analyzed by Western blot with MAb PD4, and a specific 40 kilo-Dalton band could be found (Figure 1A). Then immunoprecipitation was performed and the protein complex was subjected to 12 % SDS-PAGE. The gel-separated proteins were analyzed with Western blot, and the target band was cut off from the membrane (Figure 1B). The sequence of N-terminal amino acid residues revealed that 16 amino acid residues (CSNTGVVKQEDVSVSQ) were completely identical with protein p37 from *M. hyorhinis*, which suggested the antigen recognized by MAb PD4 was from mycoplasma, not from tumor cells, and the PD4 was a MAb against *M. hyorhinis.*

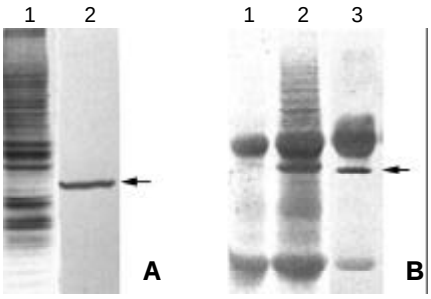

Figure 1 Purification of the antigen by MAb PD4. (A) 1. SDS-PAGE and Coomassie blue staining of the membrane proteins extracted from MGC803 cells; 2. Western blot analysis of the membrane proteins extracted from MGC803 with MAb PD4, the arrow indicating the target protein of MAb PD4. (B) 1. SDS-PAGE analysis of immunoprecipited protein complex bound with normal mouse IgG. (B) 2. SDS-PAGE analysis of immunoprecipited protein complex bound with MAb PD4. (B) 3. Western blot analysis of immunoprecipited protein complex bound with MAb PD4, arrow indicating the target protein of MAb PD4.

Further identification of the antigen with mycoplasma infected cells

If the antigen was really derived from *M. hyorhinis*, it should be transferred along with *M. hyorhinis* infection and also would disappear when the infected mycoplasma was cleared away from host cells. HeLa cells, which were mycoplasma-free and not reactive with PD4, were treated with conditional medium from *M. hyorhinis* infected cell MGC803. After 72 h treatment, the totally extracted cell protein could react with PD4 (Figure 2A). Meanwhile, the reacting band with PD4 disappeared after MGC803 cells were treated by BM cyclin antibiotics. This result indicated that the antigen of MAb PD4 was a protein from *M. hyorhinis.*

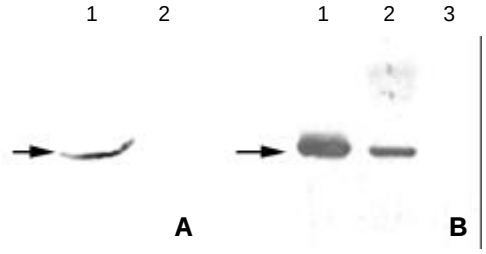

Figure 2 Further identification of the antigen from mycoplasma infection. (A) 1. Western blot analysis of the total protein from Hela cells with MAb PD4, which was treated with cultured MGC803 medium. (A) 2. Western blot analysis of the total protein from untreated HeLa cells with MAb PD4. (B) Western blot analysis of the total proteins from MGC803 cells treated with BM cyclin antibiotics differently. Lane 1: untreated, lane 2: treated for two weeks, and lane 3: treated for three weeks. As indicated by the arrow, the band reacted with MAb PD4 disappeared gradually following the treatment.

Cloning, expression and purification of GST-P37 protein

The results above suggested that the effect of MAb PD4 on tumor cells was mediated by p37 or *M. hyorhinis.* To investigate the molecular mechanisms of the effect, the gene p37 was cloned and mutated by site-directed mutagenesis successfully. After checked by DNA sequencing, the full length p37 was expressed as fusion protein GST-p37 and it could react with PD4 specifically by Western blot (Figure 3).

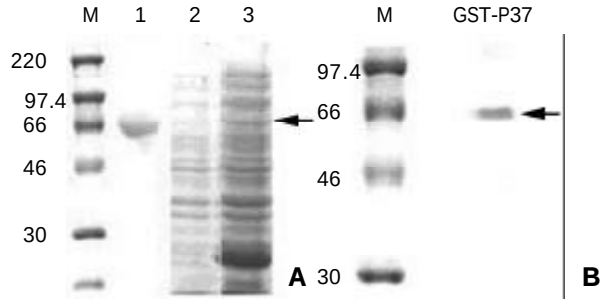

Figure 3 Analysis of GST-p37 with SDS-PAGE and Western blot. (A) Coomassie blue staining of the SDS-PAGE gel. M protein standards. lane 1: protein of BSA, lane 2: total proteins from un-induced bacteria, lane 3: total proteins from IPTG induced bacteria, the arrow indicating GST-p37 band. (B) Western blot analysis of purified protein with MAb PD4, the arrow indicating GST-p37 band.

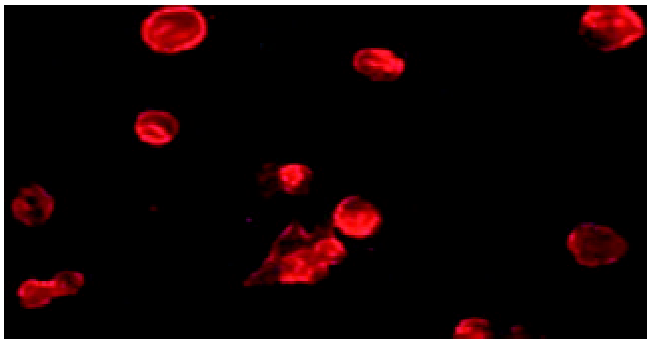

Figure 4 p37 binding AGS cells assay. Observation of the immunofluorecence under microscopy, which showed GST-p37 protein binding to AGS cells, whereas GST protein has no such binding ability (data not shown).

Binding assay

Because p37 is a dominant protein component of *M. hyorhinis* located on the outside of the cell membrane, we hypothesized that p37 was capable of mediating *M. hyorhinis* binding to host cells. In current study, we first demonstrated that p37 could directly bind to gastric cell line AGS (Figure 4), which provided the basis for further related investigation of p37.

DISCUSSION

Our study indicated that the antigen recognized by MAb PD4, which was derived from mice immunized with gastric tumor cell line MGC803, was a protein from *M. hyorhinis.* This result suggests that the actions of MAb PD4, which we showed before, are mediated possibly by p37 protein or *M. hyorhinis*. Mycoplasmas are a heterogeneous group of the smallest organisms capable of self-replication that can cause a wide variety of diseases in animals. Some mycoplasmas cause respiratory or urogenital diseases in humans[27,28], but others chronically colonize on respiratory and urogenital tracts without apparent clinical significance. There have been some discrete reports about the correlation between mycoplasma infection and cancer since last century. In 1960s, two studies reported that infection of mycoplasma (*M. orale* and one unspeciated) caused chromosomal changes[29]. Other researches in the 1980s reported that an arthropod spiroplasma could rapidly transform mouse and monkey cells[30]. However, investigating the possible association between mycoplasma infection and carcinogenesis did not become more active until Tsai *et al*. reported that continuous infection of *M. penetrans* or *M. fermentans* could lead to multiple stage of malignant transformation of murine embryonic C3H cells, accompanied by abnormal karyotypes and some oncogene upregulation[30, 31].

Also, there are documents indicating the linkage between p37 protein or *M. hyorhinis* and cancer. One is that elevated tumor invasion, as suggested by a leukocyte adherence inhibition (LAI) response, correlates with the presence of *M. hyorhinis* in patients with lung cancer, colon cancer, and breast cancer[32]. Furthermore, two independent research groups showed that p37 on the surface of FS9 mouse fibrosarcoma cells correlated with a highly invasive phenotype, as measured in an *in vitro* cellular invasion assay[22,23]. Antibodies against p37 inhibited the invasive potential of FS9 cells in the assay *in vitro*[23]. Using Abercrombie' s confronted explant assay, it was shown that antibodies against p37 caused malignant cells to revert to a more normal behavior[24]. More recently, p37 antibodies were reported to reduce the lung metastasis of colon cancer in nude mouse models[25]. These results, taken together, suggest that *M. hyorhinis* infection causes enhanced tumor invasion and correlates with tumorigenesis, and that p37 is an essential component of this phenomenon.

In order to further investigate the pathogenic role of p37 in *M. hyorhinis* infection, we cloned the full p37 gene and expressed it successfully in *E. coli*. Eighty percent of the expressed GST-p37 fusion protein was soluble at the inducing condition (IPTG 0.1 mM, 30 ℃ overnight). Western blot analysis indicated the expressed p37 protein was intact. As p37 is a dominant protein component of *M. hyorhinis* located on the outside of the cell membrane, we hypothesize that p37 may be capable of mediating *M. hyorhinis* binding to host cells. In the current study, we first demonstrated that p37 could directly bind to gastric cell line AGS, which provided the basis for further related investigation of p37.

M. hyorhinis contamination is very common in routine cell culture and mycoplasma may be more prone to stimulate immune response when mice are immunized with tumor cells infected with mycoplasma. Thus, the obtained monoclonal antibodies are possibly raised to mycoplasma, especially when the infected tumor cells are used as both immunogen and target cells for screening positive clones. This should draw more attention during preparing monoclonal antibodies. Interestingly, when we recently performed immunohistochemistry with PD4 to detect *M. hyorhinis* infection in paraffin embedded carcinoma tissues, the results indicated that positive rates in gastric carcinoma, esophageal cancer, colon carcinoma and lung cancer were around 50 %, but they were less than 25 % in other gastric diseases, such as chronic superficial gastritis, gastric ulcer and intestinal metaplasia[33]. Meanwhile, we have also isolated *M. hyorhinis* successfully from human gastric cancer tissues by direct culture (data not published). These results strongly suggest an association between mycoplasma infection and tumorigenesis. Undoubtedly, the molecular mechanism of p37 action on tumor cells needs to be intensively investigated.

REFERENCES

1 **Xue FB**, Xu YY, Wan Y, Pan BR, Ren J, Fan DM. Association of *H pylori* infection with gastric carcinoma: a Meta analysis. *World J Gastroenterol* 2001; **7**: 801-804

2 **Wu YL**, Sun B, Zhang XJ, Wang SN, He HY, Qiao MM, Zhong J, Xu JY. Growth inhibition and apoptosis induction of Sulindac on Human gastric cancer cells. *World J Gastroenterol* 2001; **7**: 796-800

3 **Cai L**, Yu SZ, Zhan ZF. Cytochrome P450 2E1 genetic polymorphism and gastric cancer in Changle, Fujian Province. *World J Gastroenterol* 2001; **7**: 792-795

4 **Xu CT**, Huang LT, Pan BR. Current gene therapy for stomach carcinoma. *World J Gastroenterol* 2001; **7**: 752-759

5 **Cai L**, Yu SZ, Zhang ZF. Glutathione S-transferases M1, T1 genotypes and the risk of gastric cancer: A case-control study. *World J Gastroenterol* 2001; **7**: 506-509

6 **Niu WX**, Qin XY, Liu H, Wang CP. Clinicopathological analysis of patients with gastric cancer in 1200 cases. *World J Gastroenterol* 2001; **7**: 281-284

7 **Miehlke S**, Kirsch C, Dragosics B, Gschwantler M, Oberhuber G, Antos D, Dite P, Luter J, Labenz J, Leodolter A, Malfertheiner P, Neubauer A, Ehninger G, Stolte M, Bayerdorffer E. *Helicobacter pylori* and gastric cancer: current status of the Austrian Czech German gastric cancer prevention trial (PRISMA Study). *World J Gastroenterol* 2001; **7**: 243-247

8 **Li XY**, Wei PK. Diagnosis of stomach cancer by serum tumor markers. *Shijie Huaren Xiaohua Zazhi* 2001; **9**: 568-570

9 **Gao HJ**, Yu LZ, Bai JF, Peng YS, Sun G, Zhao HL, Miu K, Lü XZ, Zhang XY, Zhao ZQ. Multiple genetic alterations and behavior of cellular biology in gastric cancer and other gastric mucosal lesions: *H pylori* infection, histological types and staging. *World J Gastroenterol* 2000; **6**: 848-854

10 **Cai L**, Yu SZ, Ye WM, Yi YN. Fish sauce and gastric cancer: an ecological study in Fujian Province, China. *World J Gastroenterol* 2000; **6**: 671-675

11 **Cai L**, Yu SZ, Zhang ZF. *Helicobacter pylori* infection and risk of gastric cancer in Changle County, Fujian Province, China. *World J Gastroenterol* 2000; **6**: 374-376

12 **Feng DY,** Chen RX, Peng Y, Zheng H, Yan YH. Effect of HCV NS-3 protein on P53 protein expression in hepatocarcinogenesis. *World J Gastroenterol* 1999; **5**: 45-46

13 **Qiao GB**, Han CL, Jiang RC, Sun CS, Wang Y, Wang YJ. Overexpression of P53 and its risk factors in esophageal cancer in urban areas of Xi'an. *World J Gastroenterol* 1998; **4**: 57-60

14 **Deng ZL**, Ma Y. Aflatoxin sufferer and *p53* gene mutation in hepatocellular carcinoma. *World J Gastroenterol* 1998; **4**: 28-29

15 **Devine PL**, McGuckin MA, Ward BG. Circulating mucins as tumor markers in ovarian cancer. *Anticancer Res* 1992; **12**: 709-718

16 **Kawa S**, Tokoo M, Hasebe O, Hayashi K, Imai H, Oguchi H, Kiyosawa K, Furuta S, Homma T. Comparative study of CA242 and CA19-9 for the diagnosis of pancreatic cancer. *Br J Cancer* 1994; **70**: 481-486

17 **Grimm T**, Johnson JP. A modified screening method for pcDNA-1 expression libraries which is applicable to both surface and intracellular antigens. Cloning of a colon carcinoma antigen. *J*

Immunol Methods 1995; **186**: 305-312

18 **Merlo GR**, Siddiqui J, Cropp CS, Liscia DS, Lidereau R, Callahan R, Kufe DW. Frequent alteration of the DF3 tumor-associated antigen gene in primary human breast carcinomas. *Cancer Res* 1989; **49**: 6966-6971

19 **Dong ZW**, Wei SM, Mu ZY. Monoclonal antibodies against human gastric cancer. *Zhonghua Zhongliu Zazhi* 1989; **1**: 1-6

20 **Xiao H**, Shou CC, Dong ZW. Induction of apoptosis in human gastric carcinoma cell line MGC803. *Zhonghua Zhongliu Zazhi* 1998; **1**: 91-95

21 **Yin WN**, Dong ZW, Deng GR. Study of the inhibitory effect of monoclonal antibody PD4 to Ha-ras transfected cell line Rat3-3. *Zhonghua Zhongliu Zazhi* 1991; **13**: 82-86

22 **Dudler R**, Schmidhauser C, Parish RW, Wettenhall RE, Schmidt TA. A mycoplasma high-affinity transport system and the *in vitro* invasiveness of mouse sarcoma cells. *The EMBO Journal* 1988; **7**: 3963-3970

23 **Steinemann C**, Fenner M, Binz H, Parish RW. Invasive behavior of mouse sarcoma cells is inhibited by blocking a 37,000-dalton plasma membrane glycoprotein with Fab Fragments. *Proc Natl Acad Sci U S A* 1984; **81**: 3747 -3750

24 **Schmidhauser C**, Dudler R, Schmidt T, Parish RW. A mycoplasmal protein influences tumour cell invasiveness and contact inhibition *in vitro*. *J Cell Sci* 1990; **95**: 499-506

25 **Ushio S**, Iwaki K, Taniai M, Ohta T, Fukuda S, Sugimura K, Kurimoto M. Metastasis -promoting activity of a novel molecule, Ag 243-5, derived from mycoplasma, and the complete nucleotide sequence. *Microbiol Immunol* 1995; **39**: 393-400

26 **Uphoff CC,** Drexler HG. Comparative antibiotic eradication of mycoplasma infections from continuous cell lines. *In Vitro Cell Dev Biol Anim* 2002; **38**: 86-89

27 **Loo VG**, Richardson S, Quinn P. Isolation of Mycoplasma pneumoniae from pleural fluid. *Diagn Microbiol Infect Dis* 1991; **14**: 443-445

28 **Taylor-Robinson D**. Genital mycoplasma infections. *Clin Lab Med* 1989; **9**: 501-523

29 **Paton GR**, Jacobs JP, Perkins FT. Chromosome changes in human diploid-cell cultures infected with Mycoplasma. *Nature* 1965; **207**: 43-45

30 **Tsai S**, Wear DJ, Shih JW, Lo SC. Mycoplasmas and oncogenesis: persistent infection and multistage malignant transformation. *Proc Natl Acad Sci U S A* 1995; **92**: 10197-10201

31 **Feng SH**, Tsai S, Rodriguez J, Lo SC. Mycoplasmal infections prevent apoptosis and induce malignant transformation of interleukin-3-dependent 32D Hematopoietic cells. *Molecular Cellular Biology* 1999; **19**: 7995-8002

32 **Ilantzis C**, Thomson DM, Michaelidou A, Benchimol S, Stanners CP. Identification of a human cancer related organ-specific neoantigen. *Microbiol Immunol* 1993; **37**: 119-128

33 **Huang S**, Li JY, Wu J, Meng L, Shou CC. Mycoplasma infections and different human carcinomas. *World J Gastroenterol* 2001; **7**: 266-269

Edited by Wang XL

P.O.Box 2345, Beijing 100023,China
Fax: +86-10-85381893
E-mail: wjg@wjgnet.com www.wjgnet.com

World J Gastroenterol 2003;9(10):2169-2173
World Journal of Gastroenterology
 ISSN 1007-9327

• LIVER CANCER •

Different approaches to caudate lobectomy with "curettage and aspiration" technique using a special instrument PMOD: A Report of 76 cases

Shu-You Peng, Jiang-Tao Li, Yi-Ping Mou, Ying-Bin Liu, Yu-Lian Wu, He-Qing Fang, Li-Ping Cao, Li Chen, Xiu-Jun Cai, Cheng-Hong Peng

Shu-You Peng, Jiang-Tao Li, Ying-Bin Liu, Yu-Lian Wu, He-Qing Fang, Li-Ping Cao, Li Chen, Xiu-Jun Cai, Cheng-Hong Peng, Department of Surgery, 2nd Affiliated Hospital, School of Medicine, Zhejiang University, Hangzhou 310009, Zhejiang Province, China
Yi-Ping Mou, Department of Surgery, Sir Run Run Shaw Hospital, School of Medicine, Zhejiang University, Hangzhou 310009, Zhejiang Province, China
Correspondence to: Shu-You Peng, Department of Surgery, 2nd Affiliated Hospital, School of Medicine, Zhejiang University. No 88 Jie Fang Road, Hangzhou 310009, Zhejiang Province, China sypeng@mail.hz.zj.cn
Telephone: +86-571-87783766 **Fax:** +86-571-87022776
Received: 2003-08-06 **Accepted:** 2003-09-17

Abstract

AIM: To study different approaches to caudate lobectomy with "curettage and aspiration" technique using Peng's multifunctional operative dissector (PMOD). The surgical procedure of isolated complete caudate lobectomy was specially discussed.

METHODS: In 76 cases of various types of caudate lobectomy, three approaches were used including left side approach, right side approach, and anterior approach. Among the 76 cases, isolated complete caudate lobectomy was carried out in 6 cases with transhepatic anterior approach. The surgical procedure consisted of mobilization of the total liver, ligation and separation of the short hepatic veins, splitting the liver parenchyma through the Cantlie's plane, ligation and division of the caudate portal triads from the hilum, dissection of the root of major hepatic veins, detachment of the caudate lobe from liver parenchyma.

RESULTS: The mean operative time was 285±51 min, the mean blood loss was 1 600 ml. No severe complications were observed. Among the 6 cases receiving isolated complete caudate lobectomy with transhepatic anterior approach, one case died 17 months after operation due to disease recurrence and liver failure, the other 5 cases have been alive without recurrence, with one longest survival of 49 months.

CONCLUSION: The choice of approach is essential to the success of caudate lobectomy. As PMOD and "curettage and aspiration" technique can delineate intrahepatic or extrahepatic vessels clearly, caudate lobe resection has become safer, easier and faster.

Peng SY, Li JT, Mou YP, Liu YB, Wu YL, Fang HQ, Cao LP, Chen L, Cai XJ, Peng CH. Different approaches to caudate lobectomy with "curettage and aspiration" technique using a special instrument PMOD: A Report of 76 cases. *World J Gastroenterol* 2003; 9(10): 2169-2173
http://www.wjgnet.com/1007-9327/9/2169.asp

INTRODUCTION

The caudate lobe of the liver is difficult to resect because it lies deep beneath the confluence of main hepatic veins and between porta hepatis and inferior vena cava[1]. Isolated or combined caudate lobectomy is the treatment of choice for a mass originating in caudate lobe or for hepatobiliary cancer invading the hepatic hilum. Among various types of caudate lobectomy, isolated complete resection of caudate lobe is technically the most difficult one. Anterior approach is considered to be a safe, potentially curative option for isolated resection of the entire caudate lobe, especially in the presence of cirrhosis, as we can spare innocent hepatic parenchyma using this approach[2,3]. With the use of a specially designed instrument-Peng's multifunctional operative dissector (PMOD), we developed a new surgical technique called "curettage and aspiration" technique with which transection of the liver parenchyma can be carried out in a nearly bloodless field[4]. Precise anatomy of caudate lobe can be achieved with this technique and instrument. Therefore isolated complete resection of caudate lobe has become easier and faster as the liver is split into two halves by anterior approach. From 1994 to June 2003, we performed 76 cases of various types of hepatectomy with caudate lobectomy, which included 6 isolated complete caudate lobectomies by anterior transhepatic approach. This review studied different approaches to caudate lobectomy especially the anterior transhepatic approach for isolated complete caudate lobectomy with "curettage and aspiration" technique using PMOD.

MATERIALS AND METHODS

Patients

Seventy-six cases were enrolled in the study. Various types of hepatectomy with caudate lobectomy were performed in 51 cases, isolated caudate lobectomy was performed in 25 cases. Forty-five cases had hepatocellular carcinoma (HCC) originating from or invading caudate lobe, 7 cases had benign tumors and stone of caudate lobe, 17 cases had cholangiocarcinoma, 7 cases had metastatic tumor in the liver (6 cases of colonic carcinoma, 1 case of adrenal carcinoma). These 6 patients received isolated complete caudate lobectomy by anterior approach. Among them, four were male and 2 female, their age ranged from 32 to 65 years (mean 52 years); five cases had HCC accompanied by cirrhosis, and one had hemoangioma.

Surgical procedures

In the majority of cases, a reversed L-shaped skin incision from xiphoid to the tip of the twelfth right rib was used, giving an excellent exposure, which was of vital importance for caudate lobectomy. The whole abdominal cavity was explored to rule out intra-abdominal metastasis.

The choice of approach is essential to the success of caudate lobectomy. Approaches are dependent largely on the size, location of the lesion and the severity of cirrhosis. In this series, four approaches were used for various types of

caudate lobectomy. Left side approach was suitable for small tumors situated in Spiegelian lobe or when caudate lobe was to be resected combined with the left liver. Left lateral segmentectomy, left hemi-hepatectomy or left trisegmentectomy was carried out before caudate lobe was exposed and resected. Right side approach was more suitable for tumor located in the caudate process or when the caudate lobe was resected together with the right liver, mostly right hemi-hepatectomy. The combined approach was a combination of the left side and right side approach. The caudate lobe might be approached mainly from the right or left side although dissection from both sides was necessary in many cases. Anterior transhepatic approach was suitable for cases when isolated complete resection of caudate lobe was indicated and innocent liver parenchyma should not be resected due to cirrhosis of the liver (Figure 1). The characteristics of this approach were that the liver was split through the interlobar plane into two halves, so as to fully expose the caudate lobe.

The anterior transhepatic approach included 7 steps. (1) The falciform ligament was separated up to the front of suprahepatic IVC, then the incision was turned to the right and left. The coronary ligaments, triangular ligaments and hepato-renal ligament were separated, respectively. The adrenal gland was detached from the liver, and hepatogastric ligament was completely separated. (2) The short hepatic veins (SHV) were dissected and ligated caudal cranially, three to five thick short hepatic veins were separated in this process (Figure 2). (3) Tapes were used to encircle the suprahepatic and infrahepatic IVC, respectively (Figure 3). (4) The interlobar plane was split and the anterior surface of the paracaval portion and the hilar plate were explored. (5) The ascending caudate portal triads were ligated and separated (Figure 4). (6) The caudate lobe was separated from the major hepatic veins (MHV) (Figure 5). (7) The caudate lobe was detached from the neighboring liver parenchyma. No large branches here needed to be ligated, the small vessels encountered could be cauterized with PMOD. Thus isolated complete caudate lobe was resected and two halves of the liver were sutured (Figure 6).

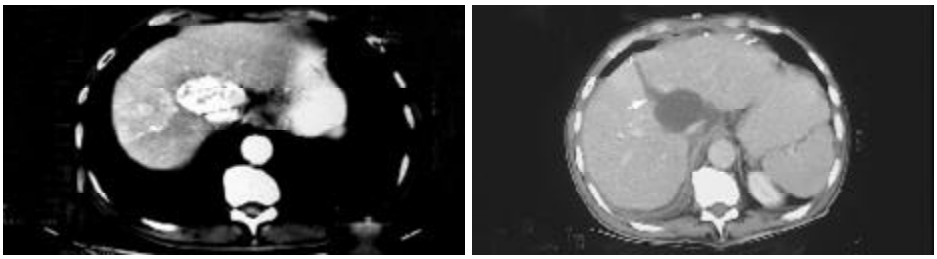

Figure 1 Pre-operative CT scan shows the tumor originating in caudate lobe, post-operative CT scan shows splitting line(arrow).

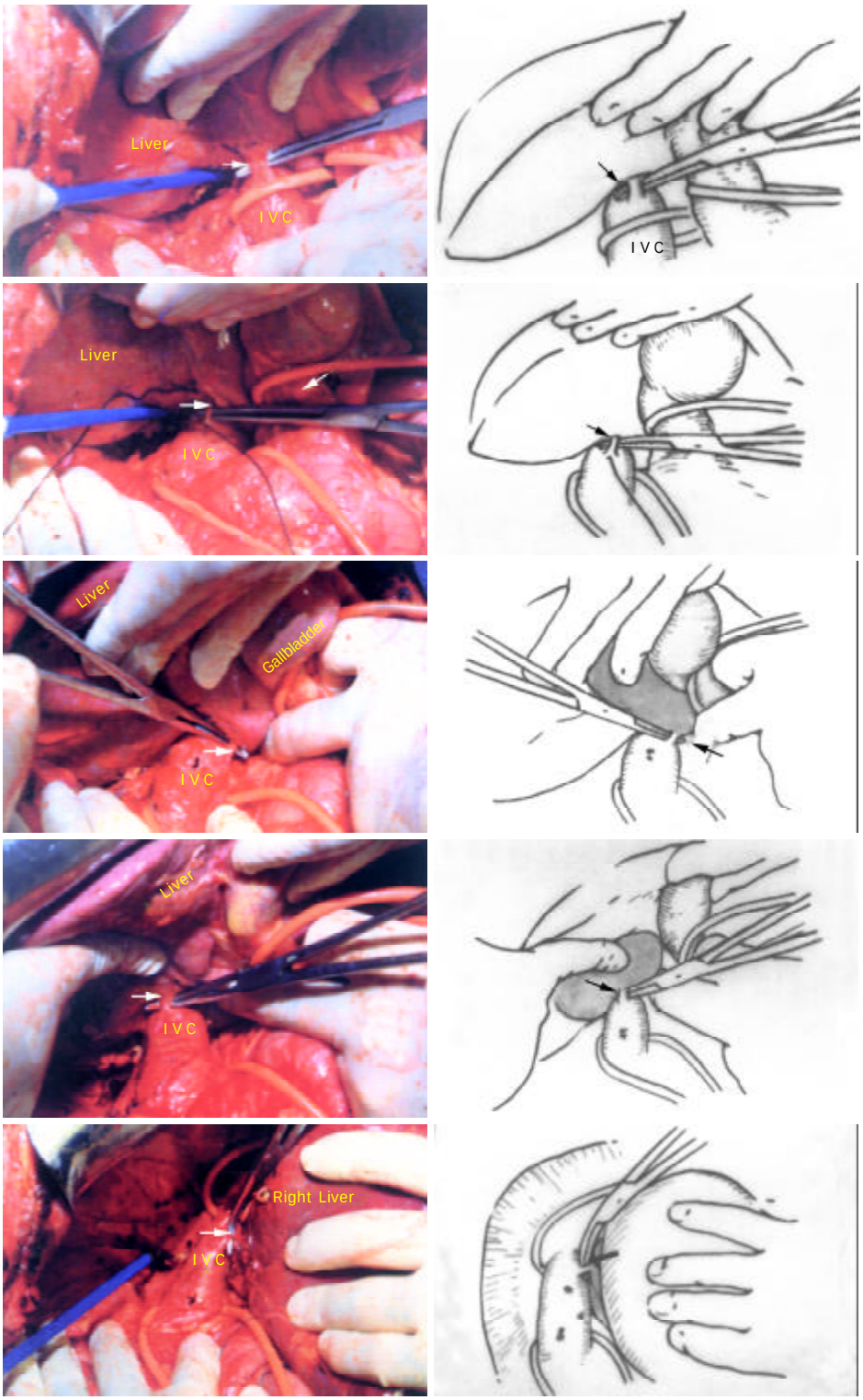

Figure 2 Five short hepatic veins ligated from caudal direction to cranial direction respestively (Arrow).

In this series, the mobilization of caudate lobe was from left side first in most of the cases. Bartlett *et al*. reported that the ligamentous attachment should be separated and the tip of caudate lobe was mobilized before separation of the caudate veins[5].

The liver parenchyma was transected by means of "curettage and aspiration" technique using PMOD with intermittent inflow occlusion at the hepatoduodenal ligament (Pringle's maneuver), the time limit was 10 min each time with reperfusion for 2 min. Total vascular exclusion was seldom necessary except that when the tumor involved IVC or major hepatic veins. PMOD is a special instrument, it has the functions of dissection, coagulation and aspiration separately or synchronously. As a result, the surgical field was nearly bloodless and the intrahepatic duct structures could be identified, isolated and treated individually.

RESULTS

Isolated or combined caudate lobectomy was successfully performed in 76 patients (Table 1). Isolated caudate lobectomy was performed in 25 cases. Of these 25 cases, isolated complete caudate lobectomy was performed in 19 cases, 6 cases (31.6 %,6/19) underwent complete resection by anterior transhepatic approach (Table 2). In these 6 cases, the size of tumor was from 3 cm to 8 cm, the mean operating time was 285±51 min, and the total occlusion time ranged from 50 to 110 min, the operative blood loss ranged from 500-3 000 ml (mean 1 600 ml).

No intraoperative death and signs of liver failure occurred in all the 6 cases, serum aspartate transaminase level recovered to normal range within one week postoperatively. One case had ascites because of liver cirrhosis, one case had right pleural effusion and was cured after aspiration two times. One case had bile leakage and was cured after two weeks' conservative treatment. Abdominal drains were placed in all the patients and removed within one week except the case with bile leakage.

All the 6 cases received a long-term follow-up. One case died in the 17th month postoperatively due to disease recurrence and liver failure, the other 5 cases have been alive without recurrence, with the longest survival of 49 months in 1 case.

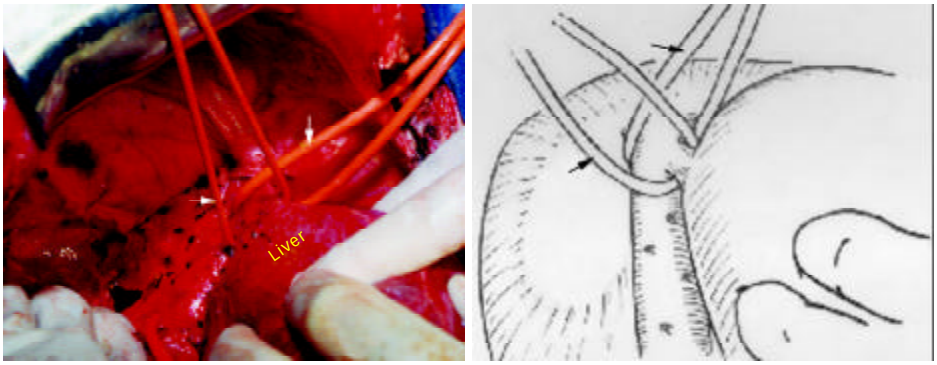

Figure 3 The suprahepatic inferior vena cava and right hepatic vein (RHV) dissected and encircled with tapes (thick arrow: RHV, thin arrow: suprahepatic IVC).

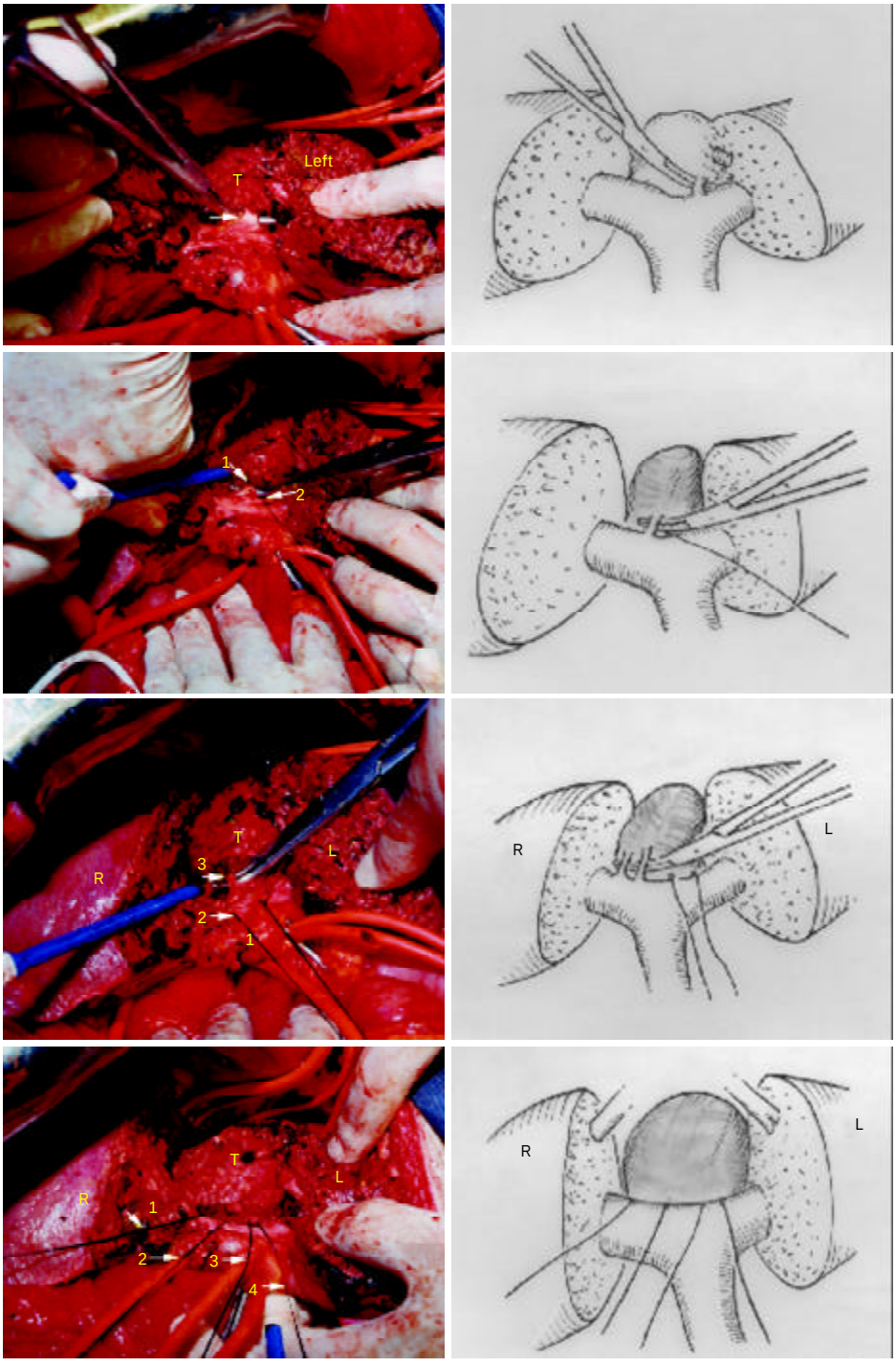

Figure 4 Four groups of portal triads to the caudate lobe(Arrow) were divided, the tumor was detached from the hilum.

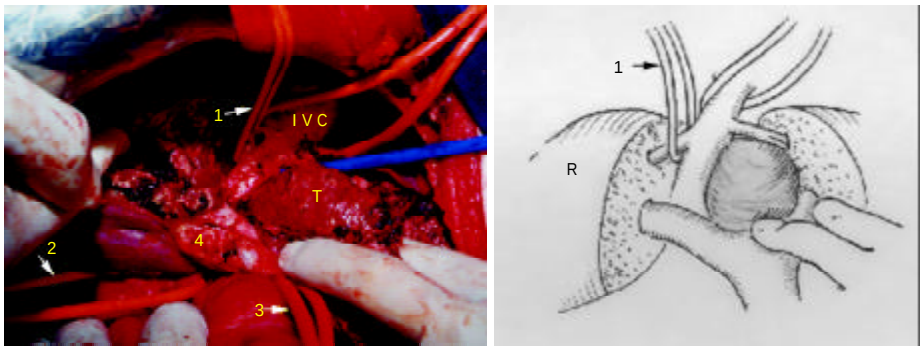

Figure 5 The tumor still attaches to MHV (1: tape across RHV, 2: tape across IVC, 3: tape across pedicle, 4: the portion of bifurcation, T: tumor).

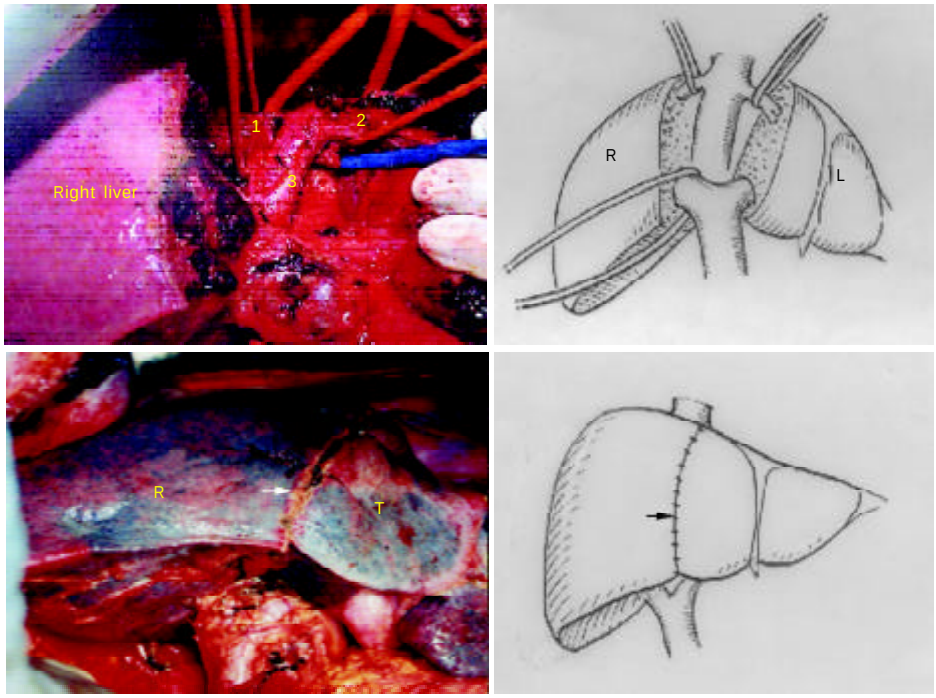

Figure 6 Completely resected tumor. Two halves of the liver were sutured. (1: RHV, 2: common trunk of MHV and LHV, 3:IVC, R: right liver, L: left liver, Arrow: interlobar plane, T: tumor).

Table 1 Resection procedures

Operation	No. of patients
Complete caudate lobectomy(49cases)	
Isolated	19 (total)
Anterior transhepatic approach	6
Other approaches	13
Combined	30 (total)
Right hepatectomy+S1(C)	13
Left hepatectomy+S1(C)	14
Extend left hepatectomy+S1(C)	2
VI segmentectomy+S1(C)+T colon	1
Partial caudate lobectomy(27 cases)	
Isolated	6 (total)
Combined	21 (total)
Left hepatectomy+S1(P)	5
Right hepatectomy+S1(P)	8
Right hepatectomy+S1(P)+adrenal gland	1
V segmentectomy +S1(P)	1
VI segmentectomy +S1(P)	4
VII segmentectomy +S1(P)	1
V+VI segmentectomy +S1(P)	1
Total	76

S1: caudate lobe, T Colon: transverse colon, P: partial, C:complete.

DISCUSSION

The caudate lobe is a single anatomic segment that is defined by the presence of portal venous and hepatic arterial branches, which supply the lobe, drain biliary ducts and hepatic veins[6]. Three parts make up the entire caudate lobe, namely, the usual caudate lobe (Spiegelian lobe), the caudate process, and the paracaval portion[7]. Partial or complete caudate lobectomy with major hepatectomy is often necessary for extirpation of the tumor. But in China, most liver cancers occur in cirrhotic liver. The poor liver function of our cases prevented us from performing a combined or preparatory resection of major segment or other liver segments for tumors situated only in the caudate lobe.

Caudate lobectomy is classified by complete and partial resection, it is also classified by isolated and combined resection. Therefore caudate lobectomy is generally composed of four types: isolated complete resection, combined complete resection, isolated partial resection and combined partial resection. To select an appropriate surgical approach is essential for resection of caudate lobe. In our experience, right side approach is suitable for the tumor confined in caudate process or for cases when hepatectomy is indicated for cancer involvement. Left side approach is suitable for the combined resection of the left liver overlying the caudate lobe or for tumor confined in Spiegelian lobe. Isolated complete caudate lobectomy without resection

of innocent parenchyma is sometimes performed by splitting the parenchyma through interlobar plane as anterior approach. In addition, central segmentectomy is also classified as anterior approach, anterior segmentectomy together with caudate lobectomy has been considered as an appropriate treatment for hilar cholangiocarcinoma without infiltration of the posterior hepatic branch[8,9].

Some of the isolated caudate lobectomies could be performed through both left side and right side approaches when the tumor was small, but when the tumor was large or IVC and/or major hepatic veins were compressed by the tumor, the above methods might not be appropriate due to the possibility of laceration of major hepatic veins. Under such circumstances, anterior transhepatic approach is the best choice for isolated complete caudate lobectomy. In 1992, Yamamoto *et al*. described a patient with cirrhosis and a 3×3 cm HCC in the paracaval portion of the caudate lobe for whom they performed isolated caudate lobectomy by splitting the cirrhotic liver into two halves. The anterior transhepatic approach could provide a safe strategic alternative for isolated complete caudate lobectomy[10]. The separation of hepatic parenchyma overlying the caudate lobe could expose the major hepatic veins and the hilar plate to direct view, facilitating control of venous bleeding and interruption of the ascending paracaval portal branches along the hilar plate. Usually it would be associated with a significant amount of blood loss. In this series, we used PMOD to transect the liver parenchyma by means of "curettage and aspiration" technique, all of the intrahepatic ducts could be identified and isolated before it was transected. Asahara *et al*. reported that the minor operative time and blood loss were 355 min and 1 100 ml[2]. Because PMOD could facilitate the transection of cirrhotic liver, the minor operation time and blood loss were 234 min and 500 ml respectively. In our series with "curettage and aspiration" technique, not only the blood loss was decreased obviously, but also no atrophy of the medial segment was observed on postoperative computed tomography. So the benefit exceeded the risk of splitting the medium hepatic plane. For selective caudate lobectomy, the most dangerous part is the parenchyma division of its anterosuperior portion, where the roots of major hepatic veins are running next to the line of dissection. Without an outflow occlusion, any inadvertently deep cleavage could result in sudden and massive hemorrhage from a hepatic vein. Although total vascular exclusion could limit blood loss from the hepatic venous system and decrease the risk of air embolism. Such a maneuver would result in hemodynamic instability in up to 40 %[11]. In our series, Tapes were used to encircle the suprahepatic and infrahepatic IVC for precautions. The author usually isolated the common trunk and the right hepatic vein to pre-place the tapes for controlling the three major hepatic veins. In case massive hemorrhage occurred from a hepatic vein, we could control the hepatic vein to substitute the total vascular exclusion. In addition, during hepatic transection, usually dissection was carried out along the section plane, but when large vessels were shown, curettage was proceeded in parenchyma in parallel with the vessels in deep cleavage plane by altering direction, so sudden and massive hemorrhage occurred rarely, and we could treat vessels in direct view even if there was hemorrhage. In fact, we did not use tapes in all the 6 cases.

The anterior transhepatic approach for isolated complete caudate lobectomy is a curative procedure for primary or metastatic hepatobiliary neoplasm originating from caudate lobe, especially in the presence of cirrhosis when the tumor is large and involves IVC and/or the major hepatic veins. As PMOD and "curettage and aspiration" technique can delineate intrahepatic or extra hepatic vessels clearly, caudate lobe resection has become safer, easier and faster.

ACKNOWLEDGMENT

We are deeply grateful to Professor Fang Zheng (Department of Anatomy, School of Medicine, Zhejiang University) for producing the figures of this paper.

REFERENCES

1 **Lucandri G**, Stipa F, Sapienza P, Ziparo V, Stipa S. Resection of the caudate lobe for hepatocellular carcinoma. *Eur J Surg* 1998; **164**: 395-398
2 **Asahara T**, Dohi K, Hino H, Nakahara H, Katayama K, Itamoto T, Ono E, Moriwaki K, Yuge O, Nakanishi T, Kitamoto M. Isolated caudate lobectomy by anterior approach for hepatocellular carcinoma originating in the paracaval portion of the caudate lobe. *J Hepatobiliary Pancreat Surg* 1998; **5**: 416-421
3 **Yamamoto J**, Kosuge T, Shimada K, Yamasaki S, Takayama T, Makuuchi M. Anterior transhepatic approach for isolated resection of the caudate lobe of the liver. *World J Surg* 1999; **23**: 97-101
4 **Peng S**, Mou Y, Peng C, Cai X, Jiang X, Li J. Resection of caudate lobe of liver: report of 26 cases. *Zhonghua Waike Zazhi* 1999; **37**: 12-13
5 **Bartlett D**, Fong Y, Blumgart LH. Complete resection of the caudate lobe of the liver: technique and results. *Br J Surg* 1996; **83**: 1076-1081
6 **Blumgart LH**, Fong Y. Surgery of the liver and biliary tract. 3rd ed. *Health Science Asia Elsevier Science* 2000: 1639
7 **Takayama T**, Makuuchi M. Segmental liver resections, present and future-caudate lobe resection for liver tumors. *Hepatogastroenterology* 1998; **45**: 20-23
8 **Shimada H**, Izumi T, Note M, Seki H, Nakagawara G. Anterior segmentectomy with caudate lobectomy for hilar cholangiocarcinoma. *Hepatogastroenterology* 1993; **40**: 61-64
9 **Nagino M**, Nimura Y, Kamiya J, Kanai M, Uesaka K, Hayakawa N, Yamamoto H, Kondo S, Nishio H. Segmental liver resections for hilar cholangiocarcinoma. *Hepatogastroenterology* 1998; **45**: 7-13
10 **Yamamoto J**, Takayama T, Kosuge T, Yoshida J, Shimada K, Yamasaki S, Hasegawa H. An isolated caudate lobectomy by the transhepatic approach for hepatocellular carcinoma in cirrhotic liver. *Surgery* 1992; **111**: 699-702
11 **Yanaga K**, Matsumata T, Hayashi H, Shimada M, Urata K, Sugimachi K. Isolated hepatic caudate lobectomy. *Surgery* 1994; **115**: 757-761

Edited by Wang XL and Zhu LH

P.O.Box 2345, Beijing 100023,China
Fax: +86-10-85381893
E-mail: wjg@wjgnet.com www.wjgnet.com

World J Gastroenterol 2003;9(10):2174-2177
World Journal of Gastroenterology
 ISSN 1007-9327

• LIVER CANCER •

Inhibitory effects of antisense RNA of HAb18G/CD147 on invasion of hepatocellular carcinoma cells *in vitro*

Yu Li, Peng Shang, Ai-Rong Qian, Li Wang, Yong Yang, Zhi-Nan Chen

Yu Li, Peng Shang, Ai-Rong Qian, Li Wang, Yong Yang, Zhi-Nan Chen, Department of Cell Biology, Fourth Military Medical University, Xi' an 710032, Shaanxi Province, China
Supported by National Natural Science Foundation of China, No. 39989002
Correspondence to: Dr. Zhi-Nan Chen, Department of Cell Biology, Fourth Military Medical University, Xi' an 710032, Shaanxi Province, China. chcerc2 @fmmu.edu.cn
Telephone: +86-29-3374547 **Fax:** +86-29-3293906
Received: 2003-05-11 **Accepted:** 2003-06-07

Abstract

AIM: To study the inhibitory effects of antisense RNA of HAb18G/CD147 on invasion of hepatocellular carcinoma (HCC) cells *in vitro*.

METHODS: Antisense RNA of HAb18G/CD147 vector PCI-asHAb18G was constructed by reversely inserting HAb18G/CD147 cDNA to eukaryotic expression vector PCI-neo. The HCC cell line HHCC was transfected by PCI-asHAb18G via cation liposome. Expression of HAb18G/CD147 of transfected cells selected by G418 (geneticin) was observed by immunohistochemical SP staining and FACS (fluorescence activated cell sorting). Gelatin zymography was used to determine the effect of PCI-asHAb18G on reducing secretions of MMP-2 and MMP-9 of the transfected cells. Boyden chamber was employed to test the invasion of HCC cells *in vitro*.

RESULTS: The construction of antisense RNA vector PCI-asHAb18G was verified correct by partial nucleotide sequencing and restricted endonuclease digestion. The expression of HAb18G/CD147 in transfected HHCC was inhibited by PCI-asHAb18G. Secretions of MMP-2 and MMP-9 of transfected HHCC were reduced and the invasion of transfected HHCC was inhibited compared to HHCC, respectively.

CONCLUSION: Invasion of HCC cells can be inhibited by antisense RNA of HAb18G/CD147. HAb18G/CD147 may be used as a potential target of drugs for anti-invasion and metastasis of HCC.

Li Y, Shang P, Qian AR, Wang L, Yang Y, Chen ZN. Inhibitory effects of antisense RNA of HAb18G/CD147 on invasion of hepatocellular carcinoma cells *in vitro*. *World J Gastroenterol* 2003; 9(10): 2174-2177
http://www.wjgnet.com/1007-9327/9/2174.asp

INTRODUCTION

Invasion and metastasis are malignant characteristies of HCC and the main mortal reason for patients[1,2]. In the invasive and metastatic process of malignant tumor, molecules existing in extracellular matrix (ECM) and receptors or ligands existing on the surfaces of tumor cells play critical roles[3,4]. HAb18G is such a molecule obtained by screening cDNA library with HAb18 specific monoclonal antibody (mAb) against HCC[5-7]. The gene sequence of HAb18G is homologous to that of CD147. CD147, also named extracelluar matrix metalloproteinase inducer (EMMPRIN), is originated from human lung cancer cell line LX-1, firstly found in human HCC tissue in our laboratory. Previous studies demonstrated that EMMPRIN, a member of the immunoglobulin superfamily, concentrated on the surfaces of most tumor cells, promoted invasion of tumor cells by stimulating stromal cells to produce elevated levels of several matrix metalloproteinase (MMPs)[8,9] which play very important roles in several aspects of tumor progression, including growth, invasion, metastasis, and angiogenesis[10-12]. To study the relationship between HAb18G/CD147 and metastasis of HCC, we constructed a vector of antisense RNA of HAb18G/CD147 and investigated its inhibitory effects on invasion of HCC cells *in vitro*.

MATERIALS AND METHODS

Plasmid, bacteria strain and cell line

Plasmid pBluescript ks(+/-)/HAb18G including full length cDNA of HAb18G/CD147 was constructed by our laboratory. Eukaryotic expressing vector PCI-neo was purchased from Promega. *E.Coli* strain JM109 was purchased from Huamei Co, Ltd. Human HCC cell line HHCC was purchased from Type Culture Collection of Chinese Academy of Sciences, Shanghai, China. Human embryo dermal fibroblast cell line (fb) was kindly presented by Dr. Han (Department of Plastic Surgery, Fourth Military Medical University).

Construction and identification of antisense vector

Full length cDNA fragment of HAb18G/CD147 was obtained from pBluescript ks(+/-)/HAb18G by cutting with *Xba*I and *Xho*I and inserted reversely into eukaryotic expressing vector PCI-neo by cutting with the same restriction endonucleases. The antisense vector of HAb18G/CD147, named as PCI-asHAb18G, was transformed into *E.coli* stain JM109 and identified by restricted endonuclease digestion and DNA sequences analysis by an automatic fluorescence sequenator using T_3 sequencing primer.

Cloning of cell transfected with antisense RNA vector

Empty vector PCI-neo and antisense vector PCI-asHAb18G were transfected into human HCC cell line HHCC via cation liposome Lipfectinamine^{2000} (Gibco) respectively. The two kinds of transfected cells were named as HHCC/neo and HHCC/asHAb18G respectively. All transfection procedures were performed according to the product manual. After two days of transfection, cells were selected by culture medium containing G418 (400 mg/L) for 4 weeks. The single clone was picked out by using limiting dilution method and cultured constantly in the culture medium containing G418 (100 mg/L).

Immunohistochemical staining of transfected cells

Transfected cells were plated on glass slides overnight, fixed with cold acetone, and stained with SP (streptomycin avidin-peroxidase) according to the manufacturer' s instructions.

Briefly, mAb HAb18 was used as primary antibody and the goat anti-mouse mAb coupled with biotin as secondary antibody followed by indirect immunohistochemical staining with the mixture of streptomycin-avidin peroxidase and its substrate DAB. HHCC/neo served as the control.

FACS analysis

HHCC/asHAb18G suspension was prepared by adding primary antibody and secondary antibody coupled with fluorescein into 10^8 cells per liter. Then the cells were fixed and analyzed by flow cytometer.

Gelatin zymography

Five experimental groups of cells were HHCC, fb, HHCC/neo+fb, HHCC/asHb18G +fb and HHCC+fb, which were plated into 100 mL culture flasks respectively. The ratio of HCC cells/fb cells was 1:1. After cultured in completed DMEM medium for 24 hours, all the groups of cells were washed three times with serum free DMEM and cultured for 2-3 days in DMEM with 20 mL/L bovine serum. Subsequently, the supernatants were collected and centrifuged to remove the cell debris. Proteins were precipitated with 800 g/L saturated $(NH_4)_2SO_4$. Precipitations were dissolved in 10 mmol/L Tris-HCl, pH 7.5 and dialyzed. Dialyzed samples were determined with SDS-PAGE that was modified in four points. Gelatin (Sigma) was added into the separating gel with 1.0 g/L, concentration of the stacking gel was 5 %, samples were not boiled and sample buffers did not contain DTT. After electrophoresis, the gel was washed with 0.1 mol/L NaCl and incubated for 24 hours at 37 ℃. Finally, the gel was dyed and decolorized.

Reconstituted basement membrane invasion detection

Matrigel (main component was type IV collagen, purchased from Cell-biology Department of Pecking University) was added onto the inner surface of Boyden chambers (Millipore) to form the reconstituted basement membrane. Three groups of cells were HHCC+fb, HHCC/asHAb18G+fb, HHCC/neo+fb (the ratio of HCC cells/fb cells was 1:1), which were added on the reconstituted basement membrane respectively. Then the chambers were put in the 24-well plates and cultured overnight. Cells infiltrated through the reconstituted basement membrane and appeared on the outer surfaces of the membrane were stained with HE. The numbers of the cells were counted under high-power microscope.

RESULTS

Construction and identification of PCI-asHAb18G

Two fragments were obtained by digesting HAb18G/CD147 antisense vector with *Xho*I and *Xba*I , one was human HAb18G/CD147 cDNA fragment about 1.7 kb and the other was 5.5 kb fragment. Two fragments of 1.1 kb and 6.1 kb were also obtained with *Sma*I digestion (both MCS of vector and 1.1 kb site of HAb18G/CD147 cDNA respectively have a *Sma*I site). The construction of the vector was verified correct by endonuclease digestion (Figure 1) and nucleotide sequencing. The vector was named as PCI-asHAb18G.

Immunohistochemical staining and FACS

HHCC/as HAb18G was negative, HHCC/neo and HHCC groups were positive (Figures 2-4). Average value of the fluorescence intensities of HHCC/asHAb18G cells was 5, and that of HHCC/neo cells was 500 (Figure 5).

Gelatin zymography and cell invasion

The secretions of MMP-9 and MMP-2 in the transfected cells HHCC/asHAb18G co-cultured with fb were inhibited compared to those in the HHCC/neo and intact HHCC. The cells of HHCC/asHAb18G infiltrated through the reconstituted basement membrane were less than those of HHCC/neo and intact HHCC (Figure 7).

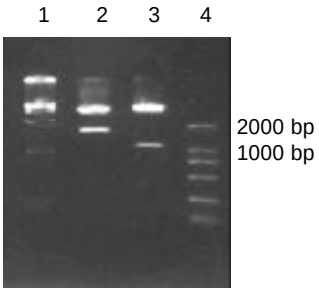

Figure 1 Restricted endonuclease analysis of recombinant plasmid PCI-asHAb18G. 1: DNA marker DL15000, 2: PCI-asHAb18G/*Xho*I+*Xba*I, 3: PCI-asHAb18G/*Sma*I, 4: DNA marker DL2000.

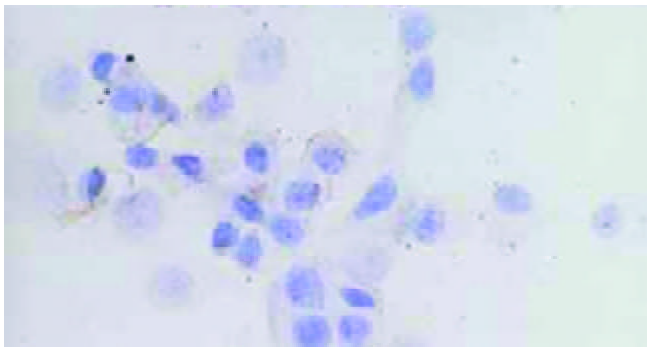

Figure 2 Negative staining of HAb18G/CD147 on membrane of HHCC/asHAb18G SP ×400.

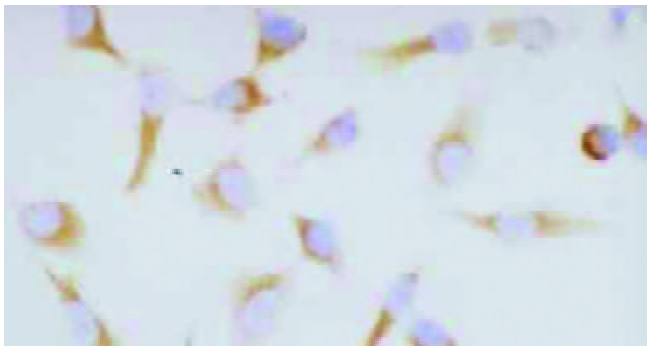

Figure 3 Positive staining of HAb18G/CD147 on membrane of HHCC/neo SP ×400.

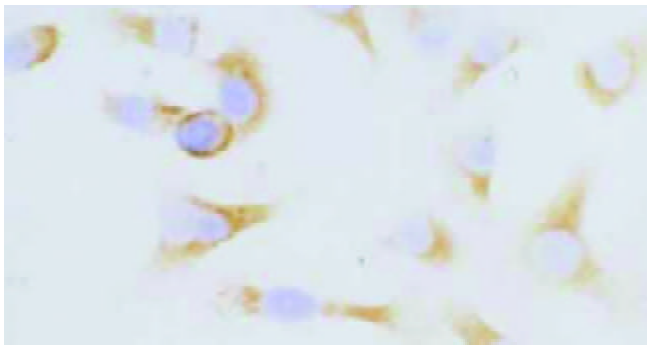

Figure 4 Positive staining of HAb18G/CD147 on membrane of HHCC SP ×400.

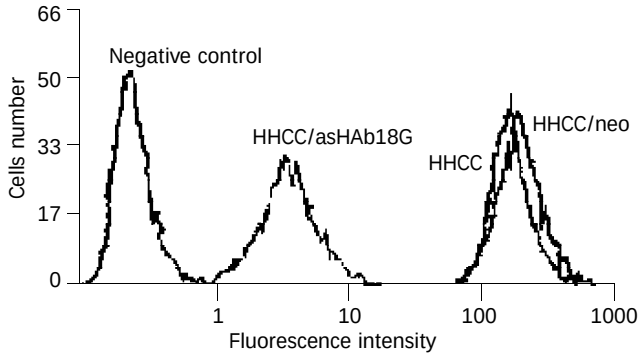

Figure 5 FACS analysis of expressions of HAb18G / CD147 in four kinds of cells.

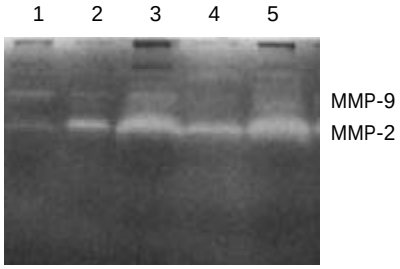

Figure 6 Gelatin zymography of secretions of MMP-2 and MMP-9 in five groups of cells. 1: fb, 2: HHCC, 3: HHCC / neo+fb, 4: HHCC / asHAb18G+fb, 5: HHCC+fb.

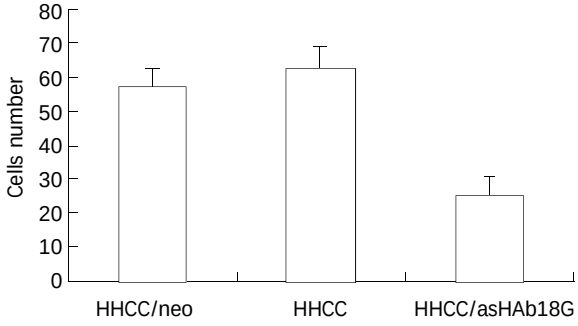

Figure 7 Inhibitory effects of antisense RNA on invasion of HHCC / asHAb18G.

DISCUSSION

Matrix metalloproteinases (MMPs) play an important part in tumor progression and tumor cell survival, with a positive correlation between MMP expression and the invasive and metastatic potential of malignant tumors, including colon, lung, head and neck, basal cell, breast, thyroid, prostate, ovarian, and gastric carcinomas. CD147 is a heavily glycosylated transmembrane glycoprotein containing two immunoglobulin superfamily domains, which induces MMPs production in the adjacent stromal cells. Some results implied that a CD147 counter-receptor might existed on the fb cell surface, but such a counter- receptor has not been identified[13]. Other studies[14] showed that CD147 also acted in an autocrine fashion to increase productions of MMPs and invasiveness in tumor cells themselves. CD147 enriched in HCC tissue was first reported by our laboratory and might be a potential target for anti-invasion and metastasis therapies. Our previous studies showed that HAb18G/CD147 was highly expressed in HCC tissues and lowly expressed in normal tissues. HAb18G/CD147, not only participated adhesion of cell-cell or cell-matrix but also enhanced metastatic potentials of human hepatoma cells by disrupting the regulation of store-operated Ca(2+) entry by NO/cGMP[15,16].

The principle of antisense technology is the sequence-specific binding of an antisense oligonucleotide to target mRNA, resulting in the prevention of gene translation. The specificity of hybridisation makes antisense treatment an attractive strategy selectively modulating the expression of genes involved in the pathogenesis of diseases. In 1998, the first antisense drug (fomivirsen) was approved by the US Food and Drugs Administration (FDA) for the treatment of cytomegalovirus-induced retinitis in patients with AIDS[17]. Now, several antisense oligonucleotides have been under clinical trials, including oligonucleotides targeting the mRNA of Bcl-2[18,19], protein-kinase-C alpha[20,21], RAF kinase[22,23], H-ras[24,25], C-myb [26], DNA methyltransferase[27] and RI-alpha regulatory subunit of protein kinase A (PKA)[28,29]. Antisense oligonucleotides are well tolerated and might have therapeutic activities.

Our experimental findings showed that the expression of HAb18G/CD147 on HCC cells transfected by PCI-asHAb18G was decreased by analysis of immunohistochemical staining and FACS. Gelatin zymography demonstrated that secretions of MMP-2 and MMP-9 of HHCC/asHAb18G were lower than those of HHCC/neo and HHCC. Matrigel invasion assay indicated that invasion of HHCC/asHAb18G cells was inhibited significantly. All of the results confirm that antisense RNA targeting HAb18G/CD147 mRNA interfered with translation and expression of HAb18G/CD147, weakened the productions of MMPs, and inhibited the invasion of HCC cells through reconstituted basement membrne *in vitro*.

We suggest that HAb18G/CD147 be used as a novel target for anti-hepatoma metastatic therapy. Intervention in HAb18G/CD147 function by agents, such as antisense RNA, may have potential therapeutic value in the prevention of hepatoma invasion and metastasis.

REFERENCES

1 **Li Y**, Tang ZY, Ye SL, Liu YK, Chen J, Xue Q, Chen J, Gao DM, Bao WH. Establishment of cell clones with different metastatic potential from the metastatic hepatocellular carcinoma cell line MHCC97. *World J Gastroenterol* 2001; **7**: 630-636

2 **Xiao CZ**, Dai YM, Yu HY, Wang JJ, Ni CR. Relationship between expression of CD44v6 and nm23-H1 and tumor invasion and metastasis in hepatocellular carcinoma. *World J Gastroenterol* 1998; **4**: 412-414

3 **Liu LX**, Jiang HC, Liu ZH, Zhou J, Zhang WH, Zhu AL, Wang XQ, Wu M. Integrin gene expression profiles of human hepatocellular carcinoma. *World J Gastroenterol* 2002; **8**: 631-637

4 **Su JM**, Gui L, Zhou YP, Zha XL. Expression of focal adhesion kinase and alpha5 and beta1 integrins in carcinomas and its clinical significance. *World J Gastroenterol* 2002; **8**: 613-618

5 **Lou C**, Chen ZN, Bian HJ, Li J, Zhou SB. Pharmacokinetics of radioimmunotherapeutic agent of direct labeling mAb 188Re-HAb18. *World J Gastroenterol* 2002; **8**: 69-73

6 **Yang LJ**, Sui YF, Chen ZN. Preparation and activity of conjugate of monoclonal antibody HAb18 against hepatoma F(ab')(2) fragment and staphylococcal enterotoxin A. *World J Gastroenterol* 2001; **7**: 216-221

7 **Bian HJ**, Chen ZN, Deng JL. Direct technetium-99m labeling of anti-hepatoma monoclonal antibody fragment: a radioimmunoconjugate for hepatocellular carcinoma imaging. *World J Gastroenterol* 2000; **6**: 348-352

8 **Kanekura T**, Chen X, Kanzaki T. Basigin (CD147) is expressed on melanoma cells and induces tumor cell invasion by stimulating production of matrix metalloproteinases by fibroblasts. *Int J Cancer* 2002; **99**: 520-528

9 **Bordador LC**, Li X, Toole B, Chen B, Regezi J, Zardi L, Hu Y. Ramos DM. Expression of emmprin by oral squamous cell carcinoma. *Int J Cancer* 2000; **85**: 347-352

10 **Hou L**, Li Y, Jia YH, Wang B, Xin Y, Ling MY, Lü S. Molecular mechanism about lymphogenous metastasis of hepatocarcinoma

cells in mice. *World J Gastroenterol* 2001; **7**: 532-536

11 **Roeb E**, Schleinkofer K, Kernebeck T, Potsch S, Jansen B, Behrmann I, Matern S, Grotzinger J. The matrix metalloproteinase 9 (mmp-9) hemopexin domain is a novel gelatin binding domain and acts as an antagonist. *J Biol Chem* 2002; **277**: 50326-50332

12 **Wang TN,** Albo D, Tuszynski GP. Fibroblasts promote breast cancer cell invasion by upregulating tumor matrix metalloproteinase-9 production. *Surgery* 2002; **132**: 220-225

13 **Guo HM**, Li RS, Zucker S, Bryan P. Toole EMMPRIN (CD147), an Inducer of matrix metalloproteinase synthesis, also binds interstitial collagenase to the tumor cell surface. *Cancer Research* 2000; **60**: 888-891

14 Sun JX, Hemler ME. Regulation of MMP-1 and MMP-2 production through CD147/extracellular matrix metalloproteinase inducer interactions. *Cancer Research* 2001; **61**: 2276-2281

15 **Jiang JL**, Yu MK, Chen ZN, Chan HC. cGMP-regulated store-operated calcium entry in human hepatoma cells. *Cell Biol Int* 2001; **25**: 993-995

16 **Jiang JL**, Zhou Q, Yu MK, Ho LS, Chen ZN, Chan HC. The involvement of HAb18G/CD147 in regulation of store-operated calcium entry and metastasis of human hepatoma cells. *J Biol Chem* 2001; **276**: 46870-46877

17 **Vitravene Study Group.** A randomized controlled clinical trial of intravitreous fomivirsen for treatment of newly diagnosed peripheral cytomegalovirus retinitis in patients with AIDS. *Am J Ophthalmol* 2002; **133**: 467-474

18 **Waters JS**, Webb A, Cunningham D, Clarke PA, Raynaud F, di Stefano F, Cotter FE. Phase I clinical and pharmacokinetic study of bcl-2 antisense oligonucleotide therapy in patients with non-Hodgkin's lymphoma. *J Clin Oncol* 2000; **18**: 1812-1823

19 **Marcucci G,** Byrd JC, Dai G, Klisovic MI, Kourlas PJ, Young DC, Cataland SR, Fisher DB, Lucas D, Chan KK, Porcu P, Lin ZP, Farag SF, Frankel SR, Zwiebel JA, Kraut EH, Balcerzak SP, Bloomfield CD, Grever MR, Caligiuri MA. Phase 1 and pharmacodynamic studies of G3139, a Bcl-2 antisense oligonucleotide, in combination with chemotherapy in refractory or relapsed acute leukemia. *Blood* 2003; **101**: 425-432

20 **Tolcher AW**, Reyno L, Venner PM, Ernst SD, Moore M, Geary RS, Chi K, Hall S, Walsh W, Dorr A, Eisenhauer E. A randomized phase II and pharmacokinetic study of the antisense oligonucleotides ISIS 3521 and ISIS 5132 in patients with hormone-refractory prostate cancer. *Clin Cancer Res* 2002; **8**: 2530-2535

21 **Cripps MC**, Figueredo AT, Oza AM, Taylor MJ, Fields AL, Holmlund JT, McIntosh LW, Geary RS, Eisenhauer EA. Phase II randomized study of ISIS 3521 and ISIS 5132 in patients with locally advanced or metastatic colorectal cancer: a National Cancer Institute of Canada clinical trials group study. *Clin Cancer Res* 2002; **8**: 2188-2192

22 **McPhillips F**, Mullen P, Monia BP, Ritchie AA, Dorr FA, Smyth JF, Langdon SP. Association of c-Raf expression with survival and its targeting with antisense oligonucleotides in ovarian *cancer*. *Br J Cancer* 2001; **85**: 1753-1758

23 **Coudert B,** Anthoney A, Fiedler W, Droz JP, Dieras V, Borner M, Smyth JF, Morant R, de Vries MJ, Roelvink M, Fumoleau P. European organization for research and treatment of cancer (EORTC). Phase II trial with ISIS 5132 in patients with small-cell (SCLC) and non-small cell (NSCLC) lung cancer. *Eur J Cancer* 2001; **37**: 2194-2198

24 **Adjei AA,** Dy GK, Erlichman C, Reid JM, Sloan JA, Pitot HC, Alberts SR, Goldberg RM, Hanson LJ, Atherton PJ, Watanabe T, Geary RS, Holmlund J, Dorr FA. Phase I trial of ISIS 2503, an antisense inhibitor of H-ras, in combination with gemcitabine in patients with advanced cancer. *Clin Cancer Res* 2003; **9**: 115-123

25 **Cunningham CC**, Holmlund JT, Geary RS, Kwoh TJ, Dorr A, Johnston JF, Monia B, Nemunaitis J. A phase I trial of H-ras antisense oligonucleotide ISIS 2503 administered as a continuous intravenous infusion in patients with advanced carcinoma. *Cancer* 2001; **92**: 1265-1271

26 **Luger SM**, O'Brien SG, Ratajczak J, Ratajczak MZ, Mick R, Stadtmauer EA, Nowell PC, Goldman JM, Gewirtz AM. Oligodeoxynucleotide-mediated inhibition of c-*myb* gene expression in autografted bone marrow: a pilot study. *Blood* 2002; **99**: 1150-1158

27 **Goffin J**, Eisenhauer E. DNA methyltransferase inhibitors-state of the art. *Ann Oncol* 2002; **13**: 1699-1716

28 **Wang H**, Hang J, Shi Z, Li M, Yu D, Kandimalla ER, Agrawal S, Zhang R. Antisense oligonucleotide targeted to RIalpha subunit of cAMP-dependent protein kinase (GEM231) enhances therapeutic effectiveness of cancer chemotherapeutic agent irinotecan in nude mice bearing human cancer xenografts: *in vivo* synergistic activity, pharmacokinetics and host toxicity. *Int J Oncol* 2002; **21**: 73-80

29 **Agrawal S**, Kandimalla ER, Yu D, Ball R, Lombardi G, Lucas T, Dexter DL, Hollister BA, Chen SF. GEM 231, a second-generation antisense agent complementary to protein kinase A RIalpha subunit, potentiates antitumor activity of irinotecan in human colon, pancreas, prostate and lung cancer xenografts. *Int J Oncol* 2002; **21**: 65-72

Edited by Zhu LH

P.O.Box 2345, Beijing 100023,China
Fax: +86-10-85381893
E-mail: wjg@wjgnet.com www.wjgnet.com

World J Gastroenterol 2003;9(10):2178-2181
World Journal of Gastroenterology
 ISSN 1007-9327

• LIVER CANCER •

Role of serum total sialic acid in differentiating cholangiocarcinoma from hepatocellular carcinoma

Prachya Kongtawelert, Pisit Tangkijvanich, Siriwan Ong-Chai, Yong Poovorawan

Prachya Kongtawelert, Siriwan Ong-Chai, Department of Biochemistry, Faculty of Medicine, Chiang Mai University, Chiang Mai, 50200 Thailand
Pisit Tangkijvanich, Department of Biochemistry, Faculty of Medicine, Chulalongkorn University, Bangkok, 10330 Thailand
Yong Poovorawan, Viral Hepatitis Research Unit, Department of Pediatrics, Faculty of Medicine, Chulalongkorn University, Bangkok, 10330 Thailand
Correspondence to: Dr. Yong Poovorawan, Viral Hepatitis Research Unit, Department of Pediatrics, Faculty of Medicine, Chulalongkorn University, Bangkok, 10330 Thailand. yong.p@chula.ac.th
Telephone: +662-256-4909 **Fax:** +662-256-4929
Received: 2003-06-04 **Accepted:** 2003-08-02

Abstract

AIM: This study was designed to evaluate the clinical application of serum total sialic acid (TSA) in the diagnosis of cholangiocarcinoma (CCA).

METHODS: Serum TSA was determined by periodate-resorcinol microassay in 69 patients with CCA, 59 patients with hepatocellular carcinoma (HCC), 37 patients with cirrhosis, 61 patients with chronic hepatitis and 50 healthy blood donors.

RESULTS: The mean serum TSA concentration in CCA (2.41±0.70 mmol/L) was significantly higher than those of HCC, cirrhosis, chronic hepatitis and healthy blood donors (1.41±0.37 mmol/L, 1.13±0.31 mmol/L, 1.16±0.26 mmol/L, and 1.10±0.14 mmol/L, respectively; $P<0.001$). Based on ROC curve analysis, a cut-off point of 1.75 mmol/L discriminated between CCA and HCC with a sensitivity, specificity and accuracy of 82.6 %, 83.1 %, and 82.8 %, respectively.

CONCLUSION: Based on our results, serum TSA would be a useful marker for the differential diagnosis of CCA from HCC.

Kongtawelert P, Tangkijvanich P, Ong-Chai S, Poovorawan Y. Role of serum total sialic acid in differentiating cholangiocarcinoma from hepatocellular carcinoma. *World J Gastroenterol* 2003; 9(10): 2178-2181
http://www.wjgnet.com/1007-9327/9/2178.asp

INTRODUCTION

Cholangiocarcinoma (CCA) constitutes a common primary liver cancer in Southeast Asia where the liver fluke, *Opisthorchis viverrini*, is endemic[1]. Most patients with CCA are diagnosed at advanced stages, therefore, treatment of the cancer is usually palliative and the prognosis is poor[2]. Currently, there is no ' gold standard' tumor marker for the diagnosis of CCA. This is particularly remarkable for early detection of the tumor itself, for screening of the high-risk groups, and for differentiating CCA from hepatocellular carcinoma (HCC), another primary liver cancer which is common in Southeast Asia and frequently associated with chronic hepatitis B or C[3]. Among the available serum tumor markers, the most commonly used is a high-molecular-weight glycolipid, carbohydrate antigen 19-9 (CA 19-9). CA 19-9, however, is not a sensitive or specific tumor marker for CCA. As a single diagnostic test, CA 19-9 increases in approximately 65 % of liver fluke-associated CCA[4]. Elevated concentrations of this marker have also been observed in patients with a variety of gastrointestinal cancers, as well as benign cholestasis and acute cholangitis[5]. As a result, a more sensitive and specific serum marker for the diagnosis of CCA is considered necessary.

Sialic acid, a class of important ketoses that contain nine carbon atoms, is an acetylated derivative of neuraminic acid (2-keto-5-amino-3, 5-dideoxy-D-nonulosonic acid)[6]. The unique structural features of this molecule, which includes a negative charge owing to a carboxyl group, enable it to play an important role in cellular functions, such as cell-to-cell recognition and transformation to malignancy[7]. Elevated levels of serum total sialic acid (TSA) have been reported in patients diagnosed with various cancers such as lymphoma, malignant melanoma, lung cancer and gastrointestinal cancers[8,9]. Recently, it has been shown that most patients with CCA have an elevated concentration of serum TSA, and determination of this marker yields high diagnostic values that differentiate between CCA and benign hepatobiliary diseases[10]. However, the diagnostic role of the serum marker in discriminating CCA from HCC has never been verified.

Therefore, the aim of this study was to use a simple technique (microassay) to determine the clinical application of serum TSA in the diagnosis of CCA by comparison with HCC and other chronic liver diseases including chronic hepatitis and cirrhosis.

MATERIALS AND METHODS

Subjects

Sera for the measurement of TSA levels were obtained from 5 groups of subjects who were attending King Chulalongkorn Memorial Hospital and Udonthani Hospital from January 1998 to July 1999.

Group 1 consisted of 50 adult healthy blood donors as control subjects.

Group 2 consisted of 61 patients with chronic hepatitis which was diagnosed based on histopathology.

Group 3 consisted of 37 patients with cirrhosis. The diagnosis of cirrhosis was based on histopathology and/or clinical features such as the presence of ascites, or esophageal varices.

Group 4 consisted of 59 patients with HCC. The diagnosis of HCC was based on histopathology and/or imaging techniques combined with serum alpha-fetoprotein levels above 400 ng/ml.

Group 5 comprised 69 patients with CCA. All patients in this group were residents of Thailand's northeastern provinces where *O. viverrini* was endemic. The peripheral type CCA was diagnosed based on liver tumor features detected by ultrasound/CT scan and confirmed by histology. Criteria for

diagnosis of the hilar type included findings of primary mass at the hilum and the evidence of bile duct dilatation on ultrasound/ CT scan and confirmed by characteristic features on cholangiography or histopathology.

All subjects were informed about the objective of the study, and subsequently provided their consent. Blood was obtained during investigation at the initial presentation, sera were separated by centrifugation and stored at -70 ℃ at Viral Hepatitis Research Unit until tested for TSA concentrations.

Measurement of serum TSA by periodate-resorcinol microassay

Serum TSA determination was performed as previously described[6], with some modifications. Briefly, 40 μL of samples or pure standard sialic acid solution (2-10 μg/well) was added to the wells of a 96-well microtiter plate. Then, 50 μL of 1.3 mM periodic acid (prepared from stock 0.32 M), was added to each well and mixed by shaking the plate for 5 minutes on a microplate shaker at room temperature. The plate was placed (floated) in an icebox for 60 minutes, then 100 μL of 0.6 g/dL of resorcinol reagent (prepared from stock 6 g/dL) was added and mixed by shaking as described above. The plate was covered with a glass and heated at 80 ℃ for 60 minutes in water bath, then it was removed and placed on the shaker for about 2 minutes mixing as well as cooling the contents down to room temperature. Then, 100 μL of 95 % tert-butyl alcohol was added to each well and mixed once again as described above. The absorbance at 620 nm was measured immediately by a microtiter plate reader.

The precision of the test was determined by analysis of an intra- and inter-assay coefficient variation (CV). The method described herein demonstrated an intra- and inter-assay CV of 0.79 % and 4.68 %, respectively. Furthermore, the recovery percentage of this assay was 94.25 %.

Statistical analysis

The data were expressed as mean values ± standard deviation. Statistical significance in the mean values was evaluated by the Student' s *t* test. Receiver-operating characteristic (ROC) curves were constructed to establish the diagnostic cut-off level of serum TSA in discriminating CCA from other groups. Sensitivity, specificity, positive and negative predictive values and diagnostic accuracy were calculated in accordance with standard methods. *P* value below 0.05 was considered statistically significant.

RESULTS

Comparison of the characteristics of the subjects in each group (Table 1) showed that the mean age of patients with CCA (60.2±12.6 years) was significantly higher than those with HCC and cirrhosis (53.0±12.0 and 50.0±13.3 years, respectively; P=0.001), chronic hepatitis and blood donors (42.0±13.0 and 34.6±10.3 years, respectively; P<0.001). There was no significant difference in the sex distribution in each group. Mean total bilirubin level was significantly higher in patients with CCA compared with those with HCC, cirrhosis and chronic hepatitis (P<0.05), whereas mean serum alkaline phosphatase was significantly higher in patients with CCA compared to those with cirrhosis and chronic hepatitis (P<0.05).

The distributions of serum TSA levels in each group are shown in Figure 1. The mean serum TSA concentration in patients with CCA (2.41±0.70 mmol/L) was significantly higher than that in those with HCC, cirrhosis, chronic hepatitis and blood donors (1.41±0.37 mmol/L, 1.13±0.31 mmol/L, 1.16±0.26 mmol/L, and 1.10±0.14 mmol/L, respectively; P<0.001). The mean concentration of serum TSA in patients with HCC was also significantly higher than that in those with cirrhosis, chronic hepatitis and blood donors (P=0.001). However, there was no significant difference in mean serum level of TSA among patients with cirrhosis, chronic hepatitis and blood donors.

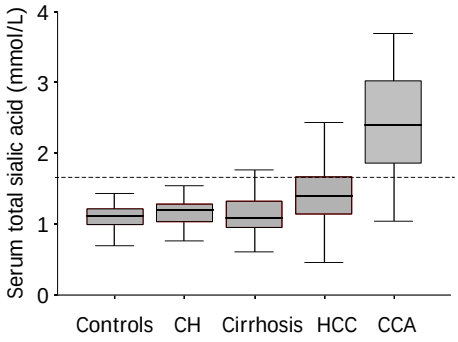

Figure 1 Serum total sialic acid (TSA) concentrations in each group. Cut-off value of serum TSA as a tumor marker was 1.75 mmol/L.

In order to discriminate CCA from HCC with an optimal accuracy, an analysis of the ROC curve was performed. As shown in Figure 2A, the area under the curve of CCA and HCC was 0.885 [95 % confidence interval (CI) 0.828-0.0.942]. This result indicated that approximately 89 % of randomly selected patients from the positive group (CCA) would have a higher TSA value than a patient randomly selected from the HCC group. Similarly, the area under the ROC curve of CCA and the other three groups (cirrhosis, chronic hepatitis and healthy controls) was 0.964 (95 % CI 0.938-0.0.989) (Figure 2B), indicating that approximately 96 % of patients with CCA would have a higher level of serum TSA than patients with cirrhosis, chronic hepatitis and healthy controls.

Based on the ROC curve analysis, a cut-off point of serum TSA concentration considered as the highest accuracy for diagnosing CCA was 1.75 mmol/L. At this concentration, the sensitivity, specificity and accuracy for differentiating CCA from HCC were 82.6 %, 83.1 %, and 82.8 %, respectively.

Table 1 Clinical characteristics of the subjects in this study

Group	No	Age (yr)	Sex (M/F)	TB (mg/dl)	ALT (IU/L)	Alb (g/l)	AP (IU/L)
Controls	50	34.6±10.3[a]	29/21	-	-	-	-
CH	61	42.0±13.0[a]	46/15	1.6±0.9[a]	98.1±72.9	3.8±0.3	201.5±106.2[a]
Cirrhosis	37	50.0±13.3[a]	26/11	2.5±1.3[a]	65.0±49.6	3.3±0.5	290.2±212.5[a]
HCC	59	53.0±12.0[a]	50/9	3.0±2.1[a]	79.9±46.1	3.4±0.3	612.9±393.7
CCA	69	60.2±12.6	46/23	7.5±7.6	71.4±68.7	3.4±0.5	894.3±850.2

Controls=healthy blood donors, CH=chronic hepatitis, HCC=hepatocellular carcinoma, CCA=cholangiocarcinoma. TB=total bilirubin, ALT=alanine aminotransferase, Alb=albumin, AP=alkaline phosphatase. Data were expressed as mean±standard deviation. Statistical analysis compared to CCA: [a]P<0.05.

Likewise, when compared to patients with cirrhosis, chronic hepatitis and healthy blood donors, the same cut-off level of serum TSA exhibited a sensitivity, specificity and accuracy for diagnosing CCA of 82.6 %, 86.0 %, and 84.8 %, respectively.

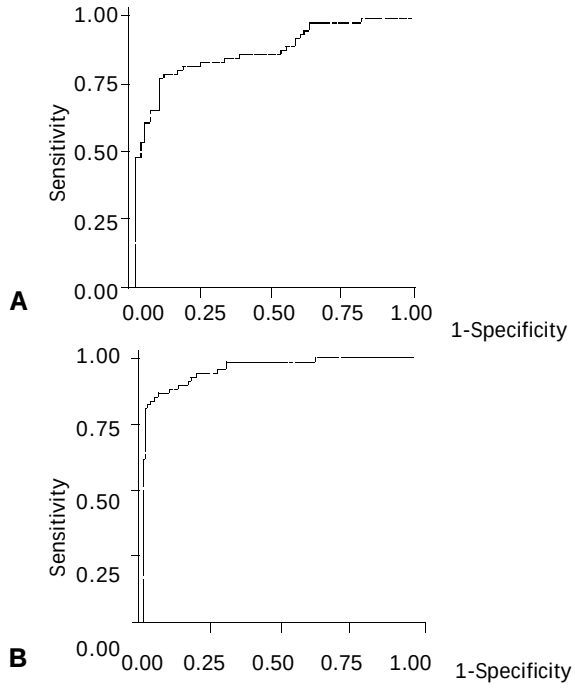

Figure 2 ROC curves of serum TSA in distinguishing CCA from other groups. A: CCA and HCC (the area under the curve was 0.885), B: CCA and cirrhosis, chronic hepatitis, blood donors (the area under the curve is 0.964).

DISCUSSION

Liver fluke-associated CCA is typically associated with its insidious onset of clinical manifestations, which frequently escapes detection until late stages. The clinical features of CCA appeared to differ according to the location of the tumor along the intrahepatic duct, whether in the hilum or periphery[11, 12]. The hilar type tends to present with progressive jaundice or ascending cholangitis due to tumor obstructtion in the confluence of the hepatic ducts, while the peripheral type usually presents with weight loss and progressive right upper quadrant pain caused by the expanding tumors. In areas where both liver flukes and chronic viral hepatitis are prevalent, it remains an essential problem to differentiate CCA from HCC. Although HCC is usually associated with cirrhosis, while conversely, CCA develops in a non-cirrhotic liver, the occurrence of CCA in cirrhosis has been increasingly recognized[13]. Moreover, approximately 10 % of patients with HCC presented with obstructive jaundice, a clinical feature that might imitate the hilar type of CCA[14]. Accordingly, a sensitive and specific serum marker of CCA would be considered as a valuable adjunct to non-invasive imaging for the diagnosis of the cancer.

Serum TSA has been reported as a diagnostic maker for patients with various cancers such as lymphoma, malignant melanoma, lung cancer and gastrointestinal cancers[8,9]. A variety of methods for the detection and estimation of free and glycosidically-bound sialic acids have been performed. These techniques could be broadly classified as colorimetric, fluorometric, enzymatic methods, as well as the highly sensitive high performance liquid chromatographic (HPLC) method[7]. Among these, the most widely used technique is the colorimetric method, which includes the Ehrlich method, the periodate-thiobabituric acid method, and the periodic-resorcinol assay. In this report, we employed a newly developed periodate-resorcinol micorassay that has several advantages over the conventional methods. These include use of smaller samples (5 μL), a larger number of samples simultaneously analyzed, and a greater speed in measuring absorbance by a microtiter plate spectrophotometer. Moreover, this method enables the direct transfer of data to a computer, or even an adaptation to an automated system.

In this study, we demonstrated that increased serum TSA concentration yielded a high sensitivity, specificity and accuracy for the diagnosis of CCA. Our data showed that the mean serum TSA level in patients with CCA was significantly increased compared to those with cirrhosis, chronic hepatitis and healthy controls ($P<0.001$). Notably, the mean concentration of serum TSA in patients with CCA was substantially higher than that in those with HCC ($P<0.001$). Based on the ROC curve analysis, a cut-off point of 1.75 mmol/L provided a satisfactorily high sensitivity, specificity and accuracy of above 80 % for the differential diagnosis of CCA from HCC. The data of the present study are in agreement with those previously reported which described an increase in serum TSA in patients with CCA[10,15]. Thus, serum TSA would be a useful marker, particularly in conjunction with radiological studies such as ultrasonography or CT scan, for the detection of CCA in patients presenting with clinical features of liver mass and jaundice.

The mechanisms underlying the substantial difference in levels of TSA between patients with CCA and HCC are unclear. One possible explanation is that, in certain cancers, increased activity of sialytransferase might lead to spontaneous shedding of aberrant sialic acid-containing cell surface glycoconjugates into the circulation[16]. Alternatively, since TSA has been well described as being associated with the acute-phase protein response[17], increased activity of serum or tissue sialidase in combination with inflammatory response could considerably elevate serum TSA levels in patients with CCA. Also, the difference between the ages of the CCA and HCC groups might be responsible for this discrepancy, since serum TSA concentration slightly increased with advancing age[18]. Nonetheless, the age-dependent difference between groups might not be sufficient to interfere with the discrimination of serum TSA values in our study. To confirm this observation, the group of age-matched patients with HCC should also be examined for serum TSA levels.

In conclusion, we have demonstrated that serum TSA concentrations, which were determined by a simple microassay, are significantly higher in patients with CCA than in those with HCC, cirrhosis, chronic hepatitis and blood donors. At a cut-off point of 1.75 mmol/L, this serum marker can yield a satisfactory accuracy for the differential diagnosis of CCA from HCC. Accordingly, the measurement of serum TSA level might be useful for the diagnosis of CCA, particularly in the regions where liver flukes are common.

ACKNOWLEDGEMENT

We would like to thank Venerable Dr. Mettanando Bhikkhu of Wat Nakprok, Bangkok, for editing the manuscript. This work was supported by grants from the National Research Council, Bangkok, the Center of Excellent Fund, Center of Excellence Viral Hepatitis Research Unit, Faculty of Medicine, Chulalongkorn University, the Thailand Research Fund, Senior Research Scholar (YP) and Junior Research Scholar (PK).

REFERENCES

1 **Parkin DM**, Srivatanakul P, Khlat M, Chenvidhya D, Chotiwan P, Insiripong S, L'Abbe KA, Wild CP. Liver cancer in Thailand. I. A case-control study of cholangiocarcinoma. *Int J Cancer* 1991; **48**: 323-328

2 **Watanapa P**. Cholangiocarcinoma in patients with opisthorchiasis. *Br J Surg* 1996; **83**: 1062-1064
3 **Tangkijvanich P**, Hirsch P, Theamboonlers A, Nuchprayoon I, Poovorawan Y. Association of hepatitis viruses with hepatocellular carcinoma in Thailand. *J Gastroenterol* 1999; **34**: 227-233
4 **Pungpak S**, Akai PS, Longenecker BM, Ho M, Befus AD, Bunnag D. Tumour markers in the detection of opisthorchiasis-associated cholangiocarcinoma. *Trans R Soc Trop Med Hyg* 1991; **85**: 277-279
5 **Duffy MJ**. CA 19-9 as a marker for gastrointestinal cancers: a review. *Ann Clin Biochem* 1998; **35**(Pt 3): 364-370
6 **Bhavanandan VP**, Sheykhnazari M. Adaptation of the periodate-resorcinol method for determination of sialic acids to a microassay using microtiter plate reader. *Anal Biochem* 1993; **213**: 438-440
7 **Narayanan S**. Sialic acid as a tumor marker. *Ann Clin Lab Sci* 1994; **24**: 376-384
8 **Kokoglu E**, Sonmez H, Uslu E, Uslu I. Sialic acid levels in various types of cancer. *Cancer Biochem Biophys* 1992; **13**: 57-64
9 **Polivkova J**, Vosmikova K, Horak L. Utilization of determining lipid-bound sialic acid for the diagnosis and further prognosis of cancer. *Neoplasma* 1992; **39**: 233-236
10 **Wongkham S**, Boonla C, Kongkham S, Wongkham C, Bhudhisawasdi V, Sripa B. Serum total sialic acid in cholangiocarcinoma patients: an ROC curve analysis. *Clin Biochem* 2001; **34**: 537-541
11 **Uttaravichien T,** Buddhisawasdi V. Experience of non-jaundiced cholangiocarcinoma. *Hepatogastroenterology* 1990; **37**: 608-611
12 **Kullavanijaya P**, Tangkijvanich P, Poovorawan Y. Current status of infection-related gastrointestinal and hepatobiliary diseases in Thailand. *Southeast Asian J Trop Med Public Health* 1999; **30**: 96-105
13 **Hui CK**, Yuen MF, Tso WK, Ng IO, Chan AO, Lai CL. Cholangiocarcinoma in liver cirrhosis. *J Gastroenterol Hepatol* 2003; **18**: 337-341
14 **Qin LX**, Tang ZY. Hepatocellular carcinoma with obstructive jaundice: diagnosis, treatment and prognosis. *World J Gastroenterol* 2003; **9**: 385-391
15 **Wongkham S**, Bhudhisawasdi V, Chau-in S, Boonla C, Muisuk K, Kongkham S, Wongkham C, Boonsiri P, Thuwajit P. Clinical significance of serum total sialic acid in cholangiocarcinoma. *Clin Chim Acta* 2003; **327**: 139-147
16 **Singhal A**, Hakomori S. Molecular changes in carbohydrate antigens associated with cancer. *Bioessays* 1990; **12**: 223-230
17 **Crook MA**, Treloar A, Haq M, Tutt P. Serum total sialic acid and acute phase proteins in elderly subjects. *Eur J Clin Chem Clin Biochem* 1994; **32**: 745-747
18 **Stefenelli N**, Klotz H, Engel A, Bauer P. Serum sialic acid in malignant tumors, bacterial infections, and chronic liver diseases. *J Cancer Res Clin Oncol* 1985; **109**: 55-59

Edited by Wang XL

P.O.Box 2345, Beijing 100023,China
Fax: +86-10-85381893
E-mail: wjg@wjgnet.com www.wjgnet.com

World J Gastroenterol 2003;9(10):2182-2185
World Journal of Gastroenterology
 ISSN 1007-9327

• LIVER CANCER •

Prevention of hepatocellular carcinoma in mice by IL-2 and B7-1 genes co-transfected liver cancer cell vaccines

Ning-Ling Ge, Sheng-Long Ye, Ning Zheng, Rui-Xia Sun, Yin-Kun Liu, Zhao-You Tang

Ning-Ling Ge, Sheng-Long Ye, Ning Zheng, Rui-Xia Sun, Yin-Kun Liu, Zhao-You Tang, Liver Cancer Institute of Zhongshan Hospital Affiliated to Fudan University, Shanghai 200032, China
Supported by the National Key Technologies Research and Development during the 9th Five-Year Plan period, Program of China, No. 96-906-01-20
Correspondence to: Dr. Sheng-Long Ye, Liver Cancer Institute of Zhongshan Hospital Affiliated to Fudan University, Shanghai 200032, China. slye@shmu.edu.cn
Telephone: +86-21-64041990 Ext 2150 **Fax:** +86-21-64037181
Received: 2003-05-12 **Accepted:** 2003-06-02

Abstract

AIM: To study the immunoprotective effect of liver cancer vaccine with co-transfected IL-2 and B7-1 genes on hepatocarcinogenesis in mice.

METHODS: The murine liver cancer cell line Hepal-6 was transfected with IL-2 and/or B7-1 gene via recombinant adenoviral vectors and the liver cancer vaccines were prepared. C57BL/6 mice were immunized with these vaccines and challenged with the parental Hepal-6 cells afterwards. The immunoprotection was investigated and the reactive T cell line was assayed.

RESULTS: The immunoprotection of the tumor vaccine was demonstrated. The effect of IL-2 and B7-1 genes co-transfected Hepal-6 liver cancer vaccine (Hep6-IL2/B7 vaccine) on the onset of tumor formation was the strongest. When attacked with wild Hepal-6 cells, the median survival period of the mice immunized with Hep6-IL2/B7 vaccine was the longest (68 days, χ^2=7.70-11.69, P<0.05) and the implanted tumor was the smallest (z =3.20-44.10, P<0.05). The effect of single IL-2 or B7-1 gene-transfected vaccine was next to the IL2/B7 gene co-transfected group, and the mean survival periods were 59 and 54 days, respectively. The mean survival periods of wild or enhanced green fluorescence protein gene modified vaccine immunized group were 51 and 48 days, respectively. The mice in control group all died within 38 days and the implanted tumor was the largest (z=3.20-40.21, P<0.05). The cellular immunofunction test and cytotoxicity study showed that the natural killer (NK) cell, lymphokine activated killer (LAK) cell and cytotoxic T lymphocyte (CTL) activities were significantly increased in mice immunized with the Hep6-IL2/B7 vaccine, (29.5±2.5 %, 65.0±2.9 %, 83.1±1.5 % respectively, compared with other groups, P<0.05).

CONCLUSION: The Hep6-IL2/B7 liver cancer vaccines can induce the mice to produce activated and specific CTL against the parental tumor cells, and demonstrate stronger effect on the hepatocarcinogenesis than single gene modified or the regular tumor vaccine. Therefore, the vaccines may become a novel potential therapy for recurrence and metastasis of HCC.

Ge NL, Ye SL, Zheng N, Sun RX, Liu YK, Tang ZY. Prevention of hepatocellular carcinoma in mice by IL-2 and B7-1 genes co-transfected liver cancer cell vaccines. *World J Gastroenterol* 2003; 9(10): 2182-2185
http://www.wjgnet.com/1007-9327/9/2182.asp

INTRODUCTION

Hepatocellular carcinoma (HCC) is the most common primary malignancy of liver in humans and the rate of incidence and mortality is very high in East Asia and China[1]. Though many approaches, such as surgical resection, transarterial chemoembolization (TACE), percutaneous ethanol injection (PEI), radiofrequency ablation (RFA), radiotherapy and liver transplantation were developed to treat it, and the effective and survival rates were increased, a large number of patients died from recurrence and metastasis[2-6].

Some studies showed immunogene modified tumor vaccines could induce effective specific active T cell immune response to prevent tumor recurrence and metastasis[7-10]. Also some reports demonstrated that specific active immunotherapy based on specific antitumor T cell immunity could be a potential modality for further improving the survival of HCC patients on preventing tumor recurrence and metastasis[11-14]. But HCC is poorly immunogenic. Poor or no immunogenicity and lack of costimulating molecules on the surface of tumor cells are some of the causes of most tumors including HCC[15].

The successful induction of an anti-tumor immune response has been reported in a number of tumor models including HCC animal models by using B7-1 (CD80) transfected tumor cells as a vaccine[16]. The rationale of B7-1 based immunotherapy is that T cells require both an antigen-specific signal delivered through the T-cell receptor and a co-stimulatory signal to be fully activated and proliferated, and secrete cytokines or generate cytotoxic T lymphocyte (CTL) to cytolyse tumor cells[17-19].

Interleukin 2 (IL-2) is a growth factor that stimulates the proliferation of cytotoxic T cells, helper T cells, natural killer (NK) cells, and lymphokine activated killer (LAK) cells, all of which can participate in the anti-tumor response[20-22]. Many HCC animal models demonstrated that local secretion of IL-2 abrogated the tumorigenicity of cytokine-producing tumor cells and inducing a long-lasting protective immune response against a subsequent tumor graft[23,24].

In this study, we compared the effect and immunological mechanism of mouse Hepal-6 liver cancer cell vaccine modified by IL-2 and/or B7-1 genes on protecting the C57BL/6 mice from challenge of wild parental Hepal-6 cells. The results provide some experimental evidences that gene modified tumor vaccine can prevent recurrence and metastasis of liver cancer.

MATERIALS AND METHODS

Cell lines

For the experiments, three tumor cell lines were used. Hepal-6 was a liver cancer cell line derived from C57BL/6 mice generously provided by Dr. Li-Xin Wei from Eastern Hepato-Biliary Surgery Hospital, Second Military Medical University,

Shanghai. P815 (NK cell resistant) and Yac-1 (NK cell sensitive) were leukemia cell lines derived from C57BL/6 mice and generous gifts from Prof. Xue-Tao Cao from Institute of Immunology, Second Military Medical University, Shanghai.

Mice

Female C57BL/6 mice, 6-8 weeks old (15-19 g), were purchased from the Animal Center of Chinese Academy of Sciences and housed in a specific-pathogen-free animal facility in Shanghai Medical University.

Replication-deficient recombinant adenoviral vectors

Recombinant adenoviruses carrying human IL-2 and B7-1 genes (AdVhIL-2 and AdVhB7-1) were obtained from Prof. Xue-Tao Cao. The control AdVEGFP (recombinant adenovirus carrying enhanced green fluorescence protein) was gifted from Dr. Gambotto from Pittsburgh University, USA.

Reagents

CD3-FITC, CD4-PE, CD8-PE and CD25-PE, monoclonal antibodies (mAbs) specific for murine CD3, CD4, CD8 and CD25 respectively,used for flow cytometry were purchased from Pharmingen Co. (USA). MTS kits used for cytolytic assay were purchased from Promega Co. (USA). CD80-FITC which was mAbs specific for human CD80 was purchased from Pharmingen Co. (USA). Human IL-2 ELISA Kits used to detect the active part p70 of IL-2 in solution were purchased from DIACLONE Co. (USA).

Preparation of gene modified Hepal-6 tumor cell vaccines

Hepal-6 cells were transfected with various recombinant adenoviruses according to the five protocols listed below, namely 200 pfu/cell AdhIL-2, 200 pfu/cell AdhB7-1, co-transfection of 200 pfu/cell AdhIL-2 and 200 pfu/cell AdhB7-1, 200 pfu/cell AdEGFP, and wild Hepal-6 cell not transfected with any gene. All of the modified Hepal-6 cells in the five groups were inactivated with mitomycin-C (80 ug/ml) to prepare tumor vaccines. These tumor vaccines were named as Hep6-IL2, Hep6-B7, Hep6-IL2B7, Hep6-EGFP and Hep6 tumor cell vaccines, respectively.

Immunization of C57BL/6 mice with various gene modified Hepal-6 tumor cell vaccines

The mice were divided into six groups with 6 mice in each. Five groups were injected 5×10^6 cell vaccines/mouse subcutaneously in the left scapula of those above 5 tumor cell vaccines, respectively. The sixth group was control group and the mice were injected culture medium. All the mice were injected twice a week.

Immunoprotection of tumor cell vaccines to mice

On the 7th day after the final immunization, the mice were injected 8×10^6/mouse of wild Hepal-6 cell subcutanously in right scapula. The mice were scored for tumor growth twice a week according to the tumor volume, and calculated as $V=L*W^2/2$ (L: length, W: width)[25]. The survival time of the mice was investigated.

Preparation of lymphocytes in spleens from mice immunized with gene modified Hepal-6 tumor cell vaccines

The mice in each group were killed by dislocating cervical vertebra on the 7th day after the final immunization, and the spleens were cut aseptically and minced into suspension of single splenocytes. Then the suspensions were centrifuged at 1 000 rpm for 5 min and RBCs in the splenocytes were lysed with sterile distilled water for 10 sec to get lymphocytes, and then the debris was filtered. The filtered cells were centrifuged, and the lymphocytes were harvested and maintained in 1 640 medium (GIBCO BRL, USA) containing 10 % FCS (HYCLONE, USA).

Immunostaining and FACS analysis

The freshly prepared spleocytes were analyzed by direct immunofluorescence staining with mAbs CD3-FITC, CD4-PE, CD8-PE and CD25-PE. Flow cytometry analysis was then performed with a FACScan (Becton Dickson Co.) in the Department of FACS, the Chinese Academy of Sciences.

Induction of the cytolytic activity of LAK cells and CTL from the lymphocytes

The harvested lymphocytes (2×10^6 cell/ml) were cultured in 1 640 containing 10 % FCS with rhIL-2 at 1 000 U/ml at 37 ℃ in a 5 % CO_2 incubator for 5 days and then cocultured with mitomycin Ctreated Hepal-6 cells (20:1 of responder to tumor cell ratio) in 1 640 containing 10 % FCS with rhIL-2 at 50 U/ml at 37 ℃ in a 5 % CO_2 incubator for 5-7 days.

In vitro cytolytic assay of NK, LAK cells, and CTL

MTS assay was employed to test the cytolytic activity of NK cell, LAK cell and CTL from stimulated lymphocytes. Target cells were Yac-1, P815 and Hepal-6 respectively and incubated with various lymphocytes at 37 ℃ in a 5 % CO_2 incubator for 2-4 hours at 100:1 of effector/target ratio. Assays were performed in triplicate wells. Cytolytic activity was calculated according to the formula provided by the MTS kits: cytolytic activity (%) =[(ODe-ODb)+(ODt-ODb)-(ODa- ODb)]×100 %/(ODt- ODb).

Statistical analysis

The data were analyzed with SAS 6.12 and STATA 6.0 software, and expressed as $\bar{x}\pm s$. The cytolytic activity of NK cell, LAK cell and CTL was determined by *t* test. The growth curves of tumor volume were analyzed with a generalized regression model and the mice survival period was analyzed with Log-Rank test.

RESULTS

In vivo immuno-protection by various tumor cell vaccines

After the immunized mice were challenged with wild Hepal-6 cells, the change of the tumor volume was assessed as is shown in Figure 1. The tumors grew progressively in Hep6-EGFP and Hep6 tumor vaccine immunized mice. The tumors in Hep6-IL2 and Hep6-B7 tumor vaccine immunized mice grew more slowly than those in Hep6-EGFP, Hep6 tumor vaccine immunized mice and the control. Compared with the above 5 groups of mice, the tumors in Hep6-IL2B7 tumor vaccine immunized mice grew most slowly and the tumor volume was the smallest (z=3.20-44.10, P<0.05) and about 50 % of the tumor disappeared 68 days after attacked by the wild Hepal-6 cell.

The survival periods of each group of mice were compared. The median survival time of Hep6, Hep6-EGFP, Hep6-B7 and Hep6-IL2 tumor vaccine immunized mice was 51, 48, 54 and 59 days, respectively and significantly longer than that of the control group (χ^2=10.61-23.81, P<0.05). The median survival period of the control mice was the shortest and all the mice died within 41 days. The median survival period of the Hep6-IL2B7 tumor vaccine immunized mice was significantly longer than that of other groups (χ^2=7.70-11.69, P<0.05) and all the mice in this group were alive for more than 68 days after attacked by the wild Hepal-6 cell.

Expression of B7-1 and IL-2 genes transduced Hepal-6 tumor vaccine

Flow cytometry analysis confirmed that the transfected tumor

vaccines Hep6-IL2B7 and Hep6-B7 expressed a higher level of CD80 (55.47 % and 59.11 %, respectively) than Hep6-IL2, Hep6 and Hep6-EGFP tumor vaccines (12.48 %, 11.87 %, and 7.93 %, respectively).

In the supernant of Hep6-B7, Hep6 and Hep6-EGFP tumor vaccines, no IL-2 was detected, while a high level IL-2 was detected in the supernant of Hep6-IL2 and Hep6-IL2B7 tumor vaccines (1 885 pg and 460 pg per $3*10^5$ cells, respectively).

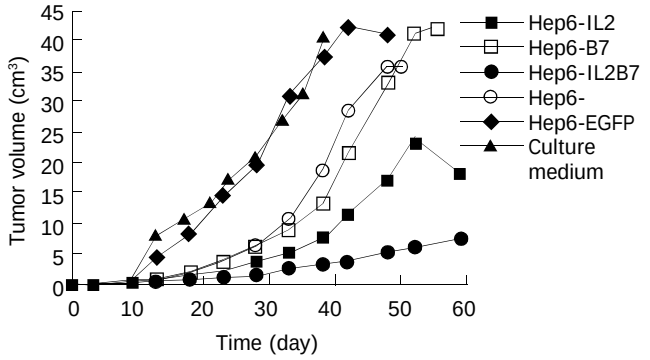

Figure 1 Change of tumor volumes after cancer vaccine immunization.

Flow cytometry analysis

The CD4/CD8 ratio in lymphocytes of the Hep6-IL2B7 tumor vaccine immunized mice was the lowest (0.91) among all the study groups and the CD25 positive rate was the highest (32.85 %). The CD4/CD8 ratios in lymphocytes of the Hep6-B7, Hep6-IL2 and Hep6 tumor vaccine immunized mice and normal mice were 1.02, 1.17, 1.24 and 1.31, respectively, while the CD25 positive rates were 28.62 %, 26.13 %, 19.32 % and 3.59 %, respectively.

Cytolytic assay of NK cell, LAK cell, CTL of spleen lymphocytes

The results are shown in Table 1. The cytolytic activities of the NK cells in each group of tumor vaccine immunized mice were all significantly higher than those in the normal mice (t=11.3-15.5, P<0.05) and it was the highest in the Hep6-IL2B7 group (29.5±2.5 %, t=10.4-15.5, P<0.05). The cytolytic activities of the LAK cells in Hep6-IL2 and Hep6-IL2B7 tumor vaccine immunized mice were significantly higher than those in the normal mice (60.9±1.7 %, 65.0±2.9 %, t=10.6-40.2, P<0.05). The cytolytic activities of the CTL induced by Hep6-IL2B7 tumor vaccine were significantly higher than those in other groups (83.1±1.5 %, t=13.7-53.3, P<0.05).

Table 1 The NK cell, LAK cell and CTL activities of each group mice against different target cells ($\bar{x}$±s %)

Effector cell	Target cell		
	Yac-1	p815	Hepal-6
Normal group	19.0±1.9	48.4±1.9[c]	29.9±1.3[e]
Hep6-IL2 cancer vaccine immunized group	32.5±2.7[a]	60.9±1.7	64.4±12.3[e]
Hep6-B7 cancer vaccine immunized group	17.0±1.7	47.7±1.2[c]	71.2±1.5[e]
Hep6-IL2B7 cancer vaccine immunized group	29.5±2.5[a]	65.0±2.9	83.1±1.5
Hep6 cancer vaccine immunized group	18.5±1.4	42.5±1.3[c]	52.8±1.2[e]

NK cell activities: [a]P<0.05 *vs* normal, Hep6-B7 and Hep6 cancer vaccine immunized group; LAK cell activities: [c]P<0.05 *vs* Hep6-IL2 and Hep6-IL2B7 cancer vaccine immunized group; CTL activities: [e]P<0.05 *vs* Hep6-IL2B7 cancer vaccine immunized group.

DISCUSSION

Hepatocellular carcinoma was poor immunogenicity partly because of poor antigen expression and lack of co-stimulatory molecules[26]. Though successful induction of anti-tumor immunity by means of B7-1 gene[11,14,16] or cytokine (IL-2, IL-4, IL-12, GM-CSF, IFN, and so on) gene[9,12-14,27] transfection has been reported in some HCC animal models, prevention of tumor recurrence and metastasis still needs to be improved.

Some animal experiments showed that IL-2 gene-modified tumor vaccine constantly secreted a relatively high level of IL-2 in local areas, induced local and systemical specific antitumor immuno-reactions and immuno-memory T cells in the body of the animals, prevented the challenge of the next parental tumor and decreased the recurrence rate[28-30]. Reports showed the locally secreted high level of IL-2 generated much less side effects than a systemically administered high dose of IL-2[31].

Double signal systems were needed in the process of inducing effective specific active antitumor T cell immune response[18]. B7-1 was an important co-stimulating molecule for tumor antigen presentation, and could provide the second signal system for T cell immune[11,32,33]. Tumors could escape from the immune surveillance of host when they were lack of it[17]. B7-1 gene-modified tumor vaccine could break the immuno-tolerance of the tumor to the host and induce effective specific antitumor immunology[32,34].

Some reports showed a single immunogene modified tumor vaccine could not induce very effective immune response because double signal systems were needed in the process[18,19] and multi-gene modified tumor vaccine could improve the immunogenicity of tumor vaccines in different ways and promote T cell immunity[18,19,35-39]. So in our experiment, we investigated the immunoprotection of single IL-2 or B7-1 gene or both IL-2 and B7-1 genes immunized mice HCC cell line Hepal-6 tumor vaccines.

In our experiment, the results showed Hepal-6 liver cancer cell line expressed a low level of B7-1 molecule and no IL-2 was secreted, and the tumorigenicity was 100 %. The vaccine prepared from wild Hepal-6 cells showed very weak protection against wild tumor cell attacking. The tumor vaccine modified with IL-2 or B7-1 gene induced a stronger immunoprotective effect than the wild vaccines, and could significantly improve the survival rate and median survival time. More excitingly, the immunoprotection induced by IL-2 and B7-1 genes co-transfected tumor cell vaccine was even better than that of either of the genes. These two genes improved the immunogenicity of the liver cancer cell vaccine synergically and induced the mice to generate stronger anti-tumor immunoreactions. The immunological analysis of spleno-lymphocytes from the mice showed that IL-2 and B7-1 genes co-transfected liver cancer cell vaccine induced lymphocytes to express a significantly higher CD25 positive level and a lower CD4/CD8 ratio. This result suggested the T cells were activated. The cytotoxic analysis showed after immunization with this vaccine, specific CTLs were induced in the mice.

The results in this mouse liver cancer model demonstrated that after immunization with IL-2 and B7-1 genes co-transfected liver cancer cell vaccine, more effective systemic anti-tumor cell immunoreactions could be induce in mice than that with either of the gene modified vaccines, and the induced immuno-memory reaction could protect against the challenge of the wild parental Hepal-6 cell. The results suggest that the co-transfected gene tumor vaccine can prevent recurrence and metastasis of liver cancer.

ACKNOWLEDGMENTS

We are grateful to Drs. Yan Zhao and Wei-Hua Bao for their advice and help in the study.

REFERENCES

1 **Pisani P,** Parkin DM, Bray F, Ferlay J. Estimates of the worldwide mortality from 25 cancers in 1990. *Int J Cancer* 1999; **83**: 18-29

2 **Tang ZY**. Hepatocellular carcinoma-cause, treatment and metastasis. *World J Gastroenterol* 2001; **7**: 445-454

3 **Hanazaki K,** Kajikawa S, Shimozawa N, Mihara M, Shimada K, Hiraguri M, Koide N, Adachi W, Amano J. Survival and recurrence after hepatic resection of 386 consecutive patients with hepatocellular carcinoma. *J Am Coll Surg* 2000; **191**: 381-388

4 **Takayama T,** Sekine T, Makuuchi M, Yamasaki S, Kosuge T, Yamamoto J, Shimada K, Sakamoto M, Hirohashi S, Ohashi Y, Kakizoe T. Adoptive immunotherapy to lower postsurgical recurrence rates of hepatocellular carcinoma: a randomized trial. *Lancet* 2000; **356**: 802-807

5 **Huang YH,** Wu JC, Lui WY, Chau GY, Tsay SH, Chiang JH, King KL, Huo TI, Chang FY, Lee SD. Prospective case-controlled trial of adjuvant chemotherapy after resection of hepatocellular carcinoma. *World J Surg* 2000; **24**: 551-555

6 **Poon RTP,** Fan ST, Wong J. Risk factors, prevention, and management of postoperative recurrence after resection of hepatocellular carcinoma. *Ann Surg* 2000; **232**: 10-24

7 **Natsume A,** Mizuno M, Ryuke Y, Yoshida J. Antitumor effect and cellular immunity activation by murine interferon-beta gene transfer against intracerebral glioma in mouse. *Gene Ther* 1999; **6**: 1626-1633

8 **Parmiani G,** Rodolfo M, Melani C. Immunological gene therapy with ex vivo gene-modified tumor cells: a critique and a reappraisal. *Hum Gene Ther* 2000; **11**: 1269-1275

9 **Arienti F**, Belli F, Napolitano F, Sule-Suso J, Mazzocchi A, Gallino GF, Cattelan A, Santantonio C, Rivoltini L, Melani C, Colombo MP, Cascinelli N, Maio M, Parmiani G, Sanantonio C. Vaccination of melanoma patients with interleukin 4 gene-transduced allogeneic melanoma cells. *Hum Gene Ther* 1999; **10**: 2907-2916

10 **Del Vecchio M**, Parmiani G. Cancer vaccination. *Forum* 1999; **9**: 239-256

11 **Li Z,** Sui Y, Jiang Y, Lei Z, Shang J, Zheng Y. Reconstruction of SEA-B7.1 double signals on human hepatocellular carcinoma cells and analysis of its immunological effect. *Biochem Biophys Res Commun* 2001; **288**: 454-461

12 **Yamashita YI,** Shimada M, Hasegawa H, Minagawa R, Rikimaru T, Hamatsu T, Tanaka S, Shirabe K, Miyazaki JI, Sugimachi K. Electroporation-mediated interleukin-12 gene therapy for hepatocellular carcinoma in the mice model. *Cancer Res* 2001; **61**: 1005-1012

13 **Barajas M,** Mazzolini G, Genove G, Bilbao R, Narvaiza I, Schmitz V, Sangro B, Melero I, Qian C, Prieto J. Gene therapy of orthotopic hepatocellular carcinoma in rats using adenovirus coding for interleukin 12. *Hepatology* 2001; **33**: 52-61

14 **Shi M,** Wang FS, Wu ZZ. Synergetic anticancer effect of combined quercetin and recombinant adenoviral vector expressing human wild-type p53, GM-CSF and B7-1 genes on hepatocellular carcinoma cells in vitro. *World J Gastroenterol* 2003; **9**: 73-78

15 **Dan Q**, Sanchez R, Delgado C, Wepsic HT, Morgan K, Chen Y, Jeffes EW, Lowell CA, Morgan TR, Jadus MR. Non-immunogenic murine hepatocellular carcinoma Hepa1-6 cells expressing the membrane form of macrophage colony stimulating factor are rejected *in vivo* and lead to CD8+ T-cell immunity against the parental tumor. *Mol Ther* 2001; **4**: 427-437

16 **Tatsumi T**, Takehara T, Kanto T, Kuzushita N, Ito A, Kasahara A, Sasaki Y, Hori M, Hayashi N. B7-1 (CD80)-gene transfer combined with interleukin-12 administration elicits protective and therapeutic immunity against mouse hepatocellular carcinoma. *Hepatology* 1999; **30:** 422-429

17 **Chen L**, McGowan P, Ashe S. Tumor immunogenicity determines the effect of co-stimulation by B7 on T-cell-mediated tumor immunity. *J Exp Med* 1994; **179**: 523-532

18 **Paul DB,** Barth RF, Yang W, Shen GH, Kim J, Triozzi PL. B7.1 expression by the weakly immunogenic F98 rat glioma does not enhance immunogenicity. *Gene Ther* 2000; **7**: 993-999

19 **Buggins AG,** Lea N, Gaken J, Darling D, Farzaneh F, Mufti GJ, Hirst WJ. Effect of costimulation and the microenvironment on antigen presentation by leukemic cells. *Blood* 1999; **94**: 3479-3490

20 **Heike Y,** Takahashi M, Ohira T, Naruse I, Hama S, Ohe Y, Kasai T, Fukumoto H, Olsen KJ, Podack EE, Saijo N. Genetic immunotherapy by intrapleural, intraperitoneal and subcutaneous injection of IL-2 gene-modified Lewis lung carcinoma cells. *Int J Cancer* 1997; **73**: 844-849

21 **Atkins MB**. Interleukin-2: clinical applications. *Semin Oncol* 2002; **29**: 12-17

22 **Herberman RB**. Cancer immunotherapy with natural killer cells. *Semin Oncol* 2002; **29**: 27-30

23 **Guarini A**, Riera L, Cignetti A, Montacchini L, Massaia M, Foa R. Transfer of the interleukin-2 gene into human cancer cells induces specific antitumor recognition and restores the expression of CD3 / T-cell receptor associated signal transduction molecules. *Blood* 1997; **89**: 212-218

24 **Kim JH**, Gong SJ, Yoo NC, Lee H, Shin DH, Uhm HD, Jeong SJ, Cho JY, Rha SY, Kim YS, Chung HC, Roh JK, Min JS, Kim BS. Effects of interleukin-2 transduction on the human hepatoma cell lines using retroviral vector. *Oncol Rep* 1999; **6**: 49-54

25 **Vanhaesebroeck B**, Mareel M, Van Roy F, Grooten J, Fiers W. Expression of the tumor necrosis factor gene in tumor cells correlates with reduced tumorigenicity and reduced invasiveness *in vivo*. *Cancer Res* 1991; **51**: 2229-2238

26 **Tatsumi T**, Takehara T, Katayama K, Mochizuki K, Yamamoto M, Kanto T, Sasaki Y, Kasahara A, Hayashi N. Expression of costimulatory molecules B7-1 (CD80) and B7-2 (CD86) on human hepatocellular carcinoma. *Hepatology* 1997; **5**: 1108-1114

27 **Qian SB,** Chen SS. Transduction of human hepatocellular carcinoma cells with human alpha-interferon gene via retroviral vector. *World J Gastroenterol* 1998; **4**: 210-213

28 **Hajkova R,** Indrova M, Jandlova T, Bubenik J, Reinis M. Interleukin 2 gene therapy of surgical minimal residual tumor disease: characterization of cytolytic effector cells from tumor progressore and regressors. *Folia Biol Praha* 1999; **45**: 227-231

29 **Mizuno H,** Yanoma S, Nishimura G, Hattori S, Ito T, Okudera K, Tsukuda M. Therapeutic efficiency of IL-2 gene transduced tumor vaccine for head and neck carcinoma. *Cancer Lett* 2000; **152**: 175-185

30 **Palmer K,** Moore J, Everard M, Harris JD, Rodgers S, Rees RC, Murray AK, Mascari R, Kirkwood J, Riches PG, Fisher C, Thomas JM, Harries M, Johnston SR, Collins MK, Gore ME. Gene therapy with autologous, interleukin 2-secreting tumor cells in patients with malignant melanoma. *Hum Gene Ther* 1999; **10**: 1261-1268

31 **Tagawa M.** Cytokine therapy for cancer. *Curr Pharm Des* 2000; **6**: 681-699

32 **Takahashi T,** Hirano N, Takahashi T, Chiba S, Yazaki Y, Hirai H. Immunogene therapy against mouse leukemia using B7 molecules. *Cancer Gene Ther* 2000; **7**: 144-150

33 **Yang G,** Mizuno MT, Hellstrom KE, Chen L. B7-negative versus B7-positive P815 tumor: differential requirements for priming of an antitumor immune response in lymph nodes. *J Immuno* 1997; **158**: 851-858

34 **Antonia SJ**, Extermann M, Flavell RA. Immunologic nonresponsiveness to tumors. *Crit Rev Oncog* 1998; **9**: 35-41

35 **Barnard AL,** Farzaneh F, Gaken J, Darling D. Local versus systemic interlukin-2: tumor formation by wild-type and B7-1-positive murine melanoma cells. *Cancer Gene Ther* 2000; **7**: 207-214

36 **Fujiwara H**, Yamauchi N, Sato Y, Sasaki K, Takahashi M, Okamoto T, Sato T, Iyama S, Koshita Y, Hirayama M, Yamagishi H, Niitsu Y. Synergistic suppressive effect of double transfection of tumor necrosis factor-alpha and interleukin 12 genes on tumorigenicity of Meth-A cells. *Jpn J Cancer Res* 2000; **91**: 1296-1302

37 **Hurwitz AA**, Townsend SE, Yu TF, Wallin JA, Allison JP. Enhancement of the anti-tumor immune response using a combination of interferon-gamma and B7 expression in an experimental mammary carcinoma. *Int J Cancer* 1998; **77**: 107-113

38 **Mazzocchi A,** Melani C, Rivoltini L, Castelli C, Del Vecchio M, Lombardo C, Colombo MP, Parmiani G. Simultaneous transduction of B7-1 and IL-2 genes into human melanoma cells to be used as vaccine: enhancement of stimulatory activity for autologous and allogeneic lymphocytes. *Cancer Immunol Immunother* 2001; **50**: 199-211

39 **Jang YJ,** Nam SY, Kim MS, Seong RH, Park YS, Chung YH, Chung HY. Simultaneous expression of allogenic class II MHC and B7.1 (CD80) molecules in A20 B-lymphoma cell line enhances tumor immunogenicity. *Mol Cells* 2002; **13**: 130-136

Edited by Zhang JZ and Wang XL

P.O.Box 2345, Beijing 100023,China
Fax: +86-10-85381893
E-mail: wjg@wjgnet.com www.wjgnet.com

World J Gastroenterol 2003;9(10):2186-2193
World Journal of Gastroenterology
 ISSN 1007-9327

• LIVER CANCER •

Oxidative DNA damage in peripheral leukocytes and its association with expression and polymorphisms of $hOGG_1$: A study of adolescents in a high risk region for hepatocellular carcinoma in China

Tao Peng, Han-Ming Shen, Zhi-Ming Liu, Lu-Nan Yan, Min-Hao Peng, Le-Qun Li, Ren-Xiang Liang, Zong-Liang Wei, Barry Halliwell, Choon Nam Ong

Tao Peng, Zhi-Ming Liu, Min-Hao Peng, Le-Qun Li, Department of Hepatobiliary Sugery, First Affiliated Hospital of Guangxi Medical University, Nanning, 530021, Guangxi Zhuang Autonomous Region, China
Han-Ming Shen, Choon Nam Ong, Department of Community, Occupational and Family Medicine, National University of Singapore, Singapore
Lu-Nan Yan, Department of General Surgery, First Affiliated Hospital of West China University of Medical Sciences, Chengdu, 610041, Sichuan Zhuang Autonomous Region, China
Ren-Xiang Liang, Zong-Liang Wei, Fusui Cancer Research Institute, Fusui County, 532100, Guangxi Province, China
Barry Halliwell, Department of Biochemistry, National University of Singapore, Singapore
Supported by the Guangxi Natural Sciences Grant, No.GKZ9912028 and No.GKJ0236030, Guangxi Educational Committee Grant, No. GZBH 2000-272, Guangxi Health Ministry Medicine Grant, No. Z2001087 and Singapore Science Grant, No.R-186-000-044-213
Correspondence to: Dr. Tao Peng, Department of Hepatobiliary Surgery, First Affiliated Hospital of Guangxi Medical University, Nanning, 530021, Guangxi Zhuang Autonomous Region, China. pengpang@hotmail.com
Telephone: +86-771-5352400
Received: 2003-07-12 **Accepted:** 2003-07-24

Abstract

AIM: To study the oxidative DNA damage to adolescents of hepatocellular carcinoma (HCC) families in Guangxi Zhuang Autonomous Region, China.

METHODS: Peripheral leukocytes' DNA 7, 8-dihydro-8-oxoguanine (8-oxoG) and repair enzyme $hOGG_1$ were quantified by flow-cytometry. $hOGG_1$-Cys326Ser single nucleotide polymorphism (SNP) was distinguished by polymerase chain reaction-single strand conformational polymorphism (PCR-SSCP) assay.

RESULTS: There was a positive correlation between 8-oxoG and repair enzyme $hOGG_1$ expression ($P<0.001$). HCC children ($n=21$) in Fusui county had a higher level of $hOGG_1$ ($P<0.01$) and a lower level of 8-oxoG ($P<0.05$) than the controls ($n=63$) in Nanning city. Children in Nanning exposed to passive-smoking had a higher $hOGG_1$ expression ($P<0.05$) than the non-exposers. 8-oxoG and $hOGG_1$ were negatively correlated with body mass index, while $hOGG_1$ was positively correlated with age. There was a peak of 8-oxoG level nearby the 12 year point. Individuals with the $hOGG_1$ 326Ser allele had a significantly marginal higher concentration of leukocyte 8-oxoG level than $hOGG_1$ 326Cys allele.

CONCLUSION: This is the first report using flow-cytometry to simultaneously quantify both the DNA oxidative damage and its repairing enzyme hOGG1. The results provide new insights towards a better understanding of the mechanisms of oxidative stress in a population highly susceptible to hepatocarcinogenesis.

Peng T, Shen HM, Liu ZM, Yan LN, Peng MH, Li LQ, Liang RX, Wei ZL, Halliwell B, Ong CN. Oxidative DNA damage in peripheral leukocytes and its association with expression and polymorphisms of $hOGG_1$: A study of adolescents in a high risk region for hepatocellular carcinoma in China. *World J Gastroenterol* 2003; 9(10): 2186-2193
http://www.wjgnet.com/1007-9327/9/2186.asp

INTRODUCTION

Reactive oxygen species (ROS) possess a high reactivity of a variety of biological molecules, among which, DNA is one of the most important targets[2]. Oxidative DNA damage, caused by either endogenous or exogenous source of ROS, has been linked to aging, chronic degenerative diseases, inflammatory diseases and cancers[3-6]. Among various types of DNA base modifications induced by ROS attack, 7,8-dihydro-8-oxoguanine (8-oxoG) has been the most widely studied and is considered as a key biomarker of oxidative DNA damage[7]. Leaving unrepaired, 8-oxoG is highly mutagenic because of its propensity to mispair with adenine during DNA replication, ultimately yielding GC to TA transversion[8].

To minimize 8-oxoG accumulation within genomes, this lesion is subjected to DNA repair primarily through the base excision repair pathway[9]. A key component of this pathway in eukaryotes is OGG_1, a DNA glycosylase/β-lyase that recognizes 8-oxoG opposite cytosine[10]. Inactivation of the OGG_1 gene generates a mutator phenotype characterized by GC-TA transversions in yeast[10]. Analysis of the human OGG_1 gene ($hOGG_1$) and its transcripts in normal and tumoral tissues has revealed alternative splicing, polymorphisms and somatic mutations[11]. The repair effectiveness of OGG_1 may be modulated by gene polymorphisms. A Cys326Ser substitution in exon 7 has been the most extensively studied. The Cys326 isoform is postulated to exhibit reduced 8-oxoG repair activity[12], increase susceptibility to squamous cell carcinoma of lung cancer[13,14], otolaryngeal cancer[15] and esophageal cancer[16], nevertheless, controversy still remains[17-21].

Dietary aflatoxin exposure[22,23] and hepatitis infection[24,25] are two well known risk factors in liver carcinogenesis, which involves ROS generation and oxidative DNA damage. A synergistic effect of aflatoxin B_1 (AFB_1) and hepatitis virus B (HBV) may be involved in the hepatocellular carcinoma (HCC) formation, and may be responsible for the predominance of one hotspot GC→TA transversion in the p53 gene of affected individuals[22,23].

HCC is the third most common cause of cancer death in China[26], and the main killer in a south-western province, Guangxi Zhuang Autonomous Region[27]. The age-standardized mortality of HCC for males and females in this province was 32.5/100 000 and 8.5/100 000, respectively[1], accounting for 50 % and 25 % of all the cancer deaths in this region in men and women, respectively[1]. Thus far, dietary AFB_1 exposure[28] and HBV infection[1] are the well documented risk factors

for the extraordinarily high prevalence of HCC in this area. Our earlier data[29,30] together with that of Stern *et al*[31] have highlighted a frequency of 36-73 % of p53-249 codon mutation in HCCs in this region, which is consistent with the notion that, the p53-249 hot-spot mutation is a fingerprint of AFB_1 contamination, and possibly synergistic with HBV infection in hepatocarcinogenesis[22].

In the present study, on the assumption that environmental carcinogens may impose oxidative stress on the residents living in Guangxi Zhuang Autonomous Region, we examined the level of 8-oxoG and $hOGG_1$ expression in leukocytes of a random sample of adolescents aged 4-18 in an area of Guangatxi exposed to a high level of aflatoxin and high risk of HCC, using a newly developed flow cytometry method. Furthermore, we examined the relationship between DNA damage and genetic polymorphisms of oxidative damage repair gene $hOGG_1$.

MATERIALS AND METHODS

Study subjects

This collaborative study by the Guangxi University and Fusui Cancer Institute was part of a community-based health survey in the Nanning region of Guangxi Zhuang Autonomous Region, conducted during April to June 2001. Based on the local cancer registry from 1974 to 1999, the HCC incidence rate in this region ranged from 32 to 97 per 100 000 for males and 4.27 to 17.32 per 100 000 for females, respectively. The aims of the study were explained in detail prior to the survey. From a total of 472 informed residents, 162 adults and 123 adolescents (60.4 % response rate) participated in on a voluntary basis.

After written consents were obtained from all the individuals or children' s parent/guidance. Ten-milliliter venous blood was collected with heparin as anticoagulant. Buffy-coat and plasma separated soon after collection, and kept in liquid-nitrogen during transportation, and stored at -80 ℃ till analysis. Body weight, height, age, gender, occupation, alcohol and smoking habit and family history of hepatitis infections were also recorded using a structured questionnaire approved by the Guangxi Medical University. Plasma of all subjects was screened to differentiate HBV, HCV, HDV, HEV and HGV infections. 25.6 % (73/285) subjects were positive of HV infection (63/HBV(+), 1/HBV&HCV(+), 1/HCV(+), 4/HBV&HDV(+), 2/HEV(+), 2/HBV&HGV(+)). These cases were excluded, in order to rule out the possibility of influence from hepatitis viruse infection[24,25]. Furthermore, subjects with known exposure to known environmental or occupational hazards (such as cigarette smoking, alcohol or pesticides), as well as those who were currently under medication or known to have a chronic illness were also excluded. Fifty-six boys and 28 of girls aged from 4 to 18 (mean±SD, 11.45±3.0 years) born and grown up in this region met the above mentioned criteria, and were selected for this investigation.

Determination of DNA 8-oxoguanine and $hOGG_1$ in leukocytes

Prior to the investigation, extensive experiments were conducted to optimize the antibody/probe titers and the amount of cells to be used for flow cytometry. It was found that reproducible data could be achieved with 40 μl-buffy coat (around $0.8\text{-}1.1\times10^6$ WBC). The buffy-coat was first transferred from -80 ℃ to 4 ℃, gently thawed for 4 h, and then shifted to room temperature till completely thawed. Forty micro liters buffy-coat were counted for leukocytes using a hemocytometer, and another 40 μl buffy-coat was transferred into an Eppendorf tube containing 1 ml of PBS with 1 % paraformaldehyde, stood on ice for 30 min. After washed twice with PBS, Cells were then fixed in ice-cool 70 % ethanol and kept at -20 ℃ till staining.

8-oxoG was stained by a Biotrin OxyDNA Assay Kit (Fluorescein isothiocyanate, FITC-conjugated probe, Biotrin Int. Ltd., Dublin, Ireland.) according to the manufacturer' s protocol with some minor modifications[32,33]. For $hOGG_1$ staining, first antibody (1st Ab, goat-anti-$hOGG_1$) was obtained from Santa Cruz Biotech, Inc (California, U.S.A.) (goat polyclonal antibody, against a peptide mapping at the amino terminus of OGG_1 of human origin, reacts with all OGG_1 splice variants of human origin). The second antibody (2nd Ab, R-phycoerythrin, PE-conjugated rabbit anti-goat IgG) was purchased from Sigma-Aldrich Inc., (St. Louis, MO, USA). Before staining, the cells were treated by Biotrin Blocking Solution at 37 ℃ for 60 min. After washed with Biotrin Washing Solution, the cells were first incubated with 1st Ab (goat-anti-$hOGG_1$, 1:100 in 3 % FBS/PBS), followed by a mixture of Biotrin 8-oxoG probe (FITC-conjugate, 1:10 dilution) and 2nd Ab (rabbit-anti-goat, PE conjugate, 1:400 dilution) in the Biotrin Washing Solution at 37 ℃ in the dark for 60 min per step. The cells were then re-suspended and quantified by a flow cytometer (Coulter Epics Elite Flow Cytometer, Coulter Corporation, Miami, USA), at 488 nm excitation and 525 nm (FITC), 578 nm (PE) emission, respectively. Blood from a healthy adult volunteer was included and served as an internal control. Data were analyzed using the WinMDI2.8 software (http: //facs.scripps.edu/software.html). 8-oxoG and $hOGG_1$ levels were determined as percentage of positive-staining-cells (oxoGP, $hOGG_1P$) and mean of relative fluorescence intensity (RFI for oxoGI, $hOGG_1I$) of 10 000 cells counted by the flow cytometer[34]. To eliminate possible batch-to-batch variations, all the samples were analyzed at the same batch by the same cytometer.

Genotyping of $hOGG_1$ Cys326Ser single nucleotide polymorphism (SNP)

PCR-SSCP analysis of $hOGG_1$ Cys326Ser SNP was modified from a technique described by Kohno *et al*[12]. DNA extracted from leukocytes using phenol-chloroform method was amplified by PCR. The primers used were 5' -actgt-cacta-gtctc-accag-3' (forward) and 5' -tgaat-tcgga-aggtg-cttgg-ggaat-3' (reverse) (Research Biolabs Pte., Ltd., Singapore). PCR polymerase and dNTP were from Finnzymes (ESPOO, Finland). Twenty-μl PCR reaction mixture contained 2 μl 10×PCR-buffer, 1.5 mM $MgCl_2$, 0.1 mM dNTP, 0.5 μM of each primer, 1 U Finnzyme polymerase and -100 ng of sample DNA. PCR reaction on a thermocycler (Biometra TGradient, Göttingen, Germany) began with pre-incubation at 94 ℃ for 5 min, followed by 30 cycles of denaturation at 94 ℃ for 30 s, annealing at 54 ℃ for 30 s, and elongation at 72 ℃ for 30 s. PCR products were diluted with 4 volumes of loading buffer (0.5×TBE, 0.05 % bromophenol blue, 0.05 % xylene cyanol, 20 mM methylmercury hydroxide), heat-denatured at 85 ℃ for 5 min and rapidly cooled on ice before loading. Twenty microliters of each sample were separated on 10 % non-denaturing polyacrylamide gels with or without 5 % glycerol. Electrophoresis was conducted at 200 V constant for 5 h at 4-5 ℃. Silver staining followed Forsberg *et al*[35]. Genotype of each band-pattern was confirmed by a subsequent sequencing in a commercial laboratory (Research Biolabs Pte., Ltd, Singapore) using BigDye™ Terminator kits on a ABI PRISM® 377-96 DNA Sequencer. A blank was inserted into each batch PCR to monitor PCR contamination, and for each sample, at least one independent repeat of PCR-SSCP assay was done.

Statistical analysis

All analyses were performed using the SPSS 10.0 program (Chicago, USA). Two cases were excluded from flow cytometry assays because of inadequate leukocytes. The frequency distributions of 8-oxoGP, 8-oxoGI, $hOGG_1P$ and $hOGG_1I$ skewed to the right while body mass index (BMI)

skewed to the left. In order to obtain acceptable fit to the normal distribution and stabilize the variance, 8-oxoGI, $hOGG_1I$ and BMI were log-transformed while 8-oxoGP and $hOGG_1P$ were transformed by the formula: log ((100+X)/(100-X)). Non-parameter Mann-Whitney test and one-way ANOVA were used to examine the influence of gender and $hOGG_1$ genotype on the four biomarkers, respectively. A partial correlation was calculated to examine the closeness of relationship between continuous variables (biomarkers, age and BMI). Multiple linear regressions were conducted to examine the influence of risk factors on the four biomarkers, respectively. A two-tailed *P* value <0.05 was considered significant.

RESULTS

Levels of 8-oxoG and $hOGG_1$

Figures 1a to 1d show the images of leukocytes stained for 8-oxoG and $hOGG_1$ under laser confocal microscope. The mean levels of the four biomarker parameters in male and female children are summarized in Table 1. The positive-staining cell percentage of 8-oxoG and $hOGG_1$ ranged between 45-99 % and 44-98 %, respectively. It was noted that the majority (>72 %) of cases had over 90 % positive-staining leukocytes for both 8-oxoG and $hOGG_1$. The data suggested that between male and female children, there was no significant difference in both 8-oxoG and $hOGG_1$ expressed either as percentage or fluorescent intensity.

Association between 8-oxoG, $hOGG_1$, age and BMI

Table 2 reveals that there were significant correlations between 8-oxoG level and $hOGG_1$ expression even after adjustment of age and BMI. Furthermore, a positive correlation was seen between age and $hOGG_1$ expression, either measured as percentage or intensity. In contrast, a negative correlation was noted between BMI and 8-oxoGP, and between BMI and $hOGG_1P$. These associations remained significant even when BMI or age was adjusted. These data suggested that age and BMI could independently influence the levels of oxidative damage and $hOGG_1$ gene expression.

Association between biomarkers and $hOGG_1$ Cys326Ser SNP

The median levels and 95 % confidence interval (95 % CI) of the four biomarker parameters of their respective $hOGG_1$ Cys326Ser SNP genotype are presented in Table 3. Children with $hOGG_1$ Cys326Ser heterozygote were found to have a higher level of 8-oxoG than those with Cys/Cys homozygote, although statistical significance was observed only in 8-oxoG intensity. Also, comparison of subgroup Cys/Cys *vs.* (Cys/Ser + Ser/Ser) revealed similar results (data not shown).

Multivariate analysis

To explore possible interactions of risk factors, a linear regression was then conducted for the four biomarkers, respectively (Table 4). Based on the multiple regression analysis against 8 variables, $hOGG_1$ expression level increased with aging, leaner children had a lower level of 8-oxoG, and $hOGG_1$ 326Ser allele had an increasing effect on 8-oxoG level while a reducing effect on $hOGG_1$ expression. However, the 8 factors listed in Table 4 explained only less than 50 % of the entire variations, suggesting that other oxygen radical-forming factors might be involved.

Table 1 Level of biomarkers in male and female children

	8-oxoGP (%)	8-oxoGI (RFI)	$hOGG_1$ (%)	$hOGG_1$ (RFI)	Double staining percentage (%)
Male (*n*=54)	94.55 (89.14, 94.16)[b]	61.74 (58.02, 73.57)	93.29 (88.39, 93.11)	110.50 (100.39, 125.07)	86.76 (81.10, 86.90)
Female (*n*=28)	94.98 (90.03, 95.17)	69.91 (60.28, 78.83)	91.78 (88.31, 92.86)	102.51 (85.39, 116.24)	87.10 (81.14, 87.79)
P[a]	0.469	0.323	0.577	0.225	0.822

A: Non-parameter Mann-Whitney Test, B: Data in cells presented as median (95 % confidence interval).

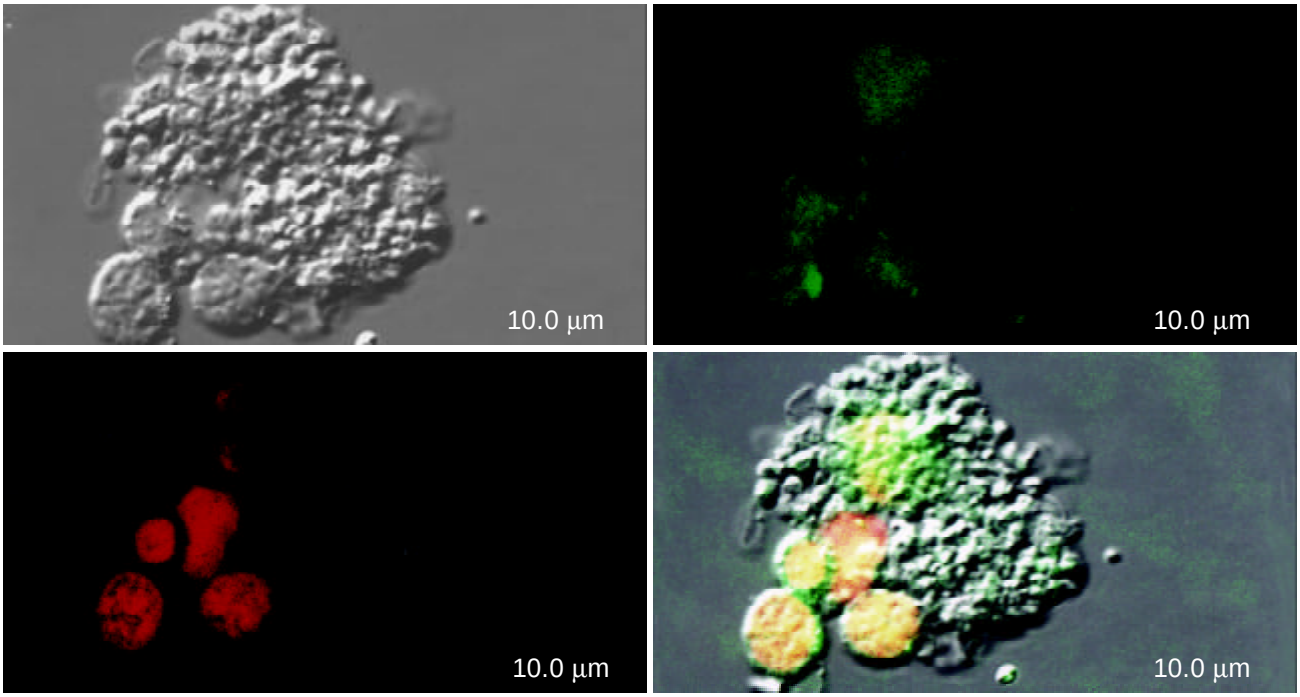

Figure 1 Representative images of leukocytes stained by 8-oxoG-FITC probes (green) and $hOGG_1$-PE complex (red) under laser confocal microscopy. The bottom-right figure demonstrated that some of the leukocytes were simultaneously stained with both FITC and PE complex.

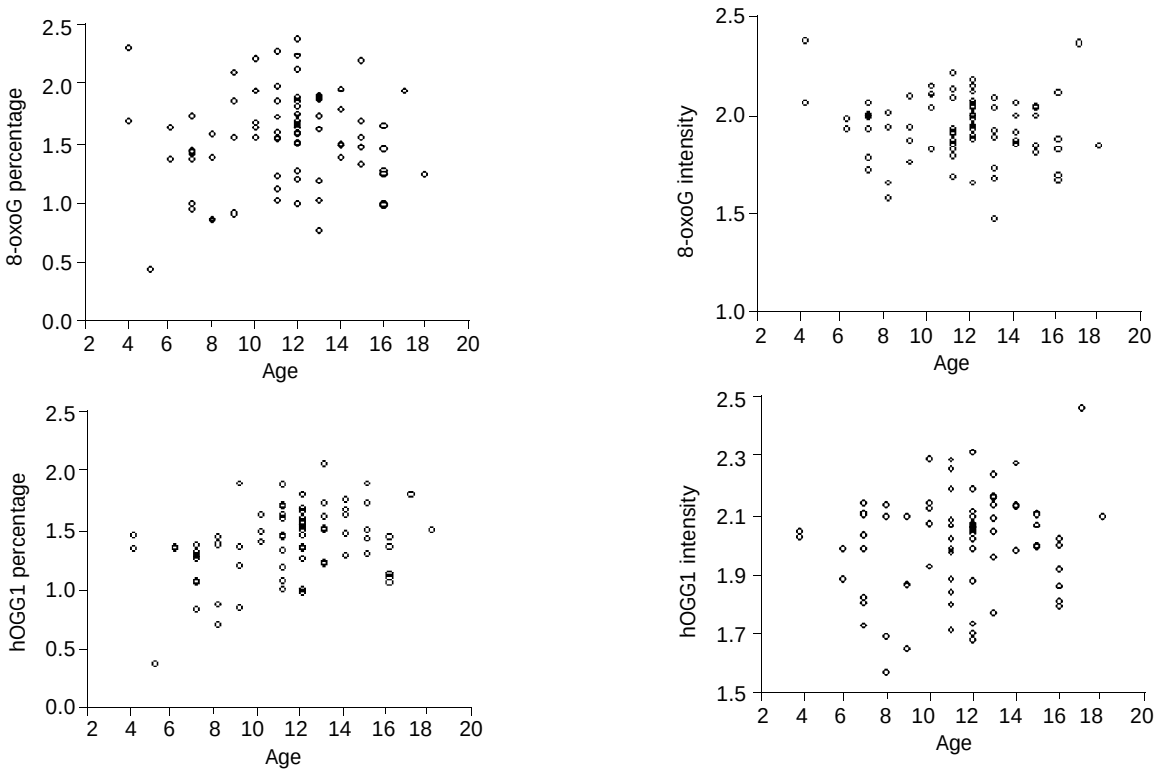

Figure 2 Scatters of age-biomarkers.

Table 2 Partial Correlation between biomarkers, age and BMI

	8-oxoGP (%)	8-oxoGI (RFI)	$hOGG_1P$ (%)	$hOGG_1I$ (RFI)	Double staining percentage (%)
8-oxoGP (%)[a]		0.6987 (0.000)[f]	0.8333 (0.000)[f]	0.5299 (0.000)[f]	0.9553(0.000)[f]
8-oxoGI (RFI)[a]			0.4843 (0.000)[f]	0.5155 (0.000)[f]	0.7075(0.000)[f]
$hOGG_1P$ (%)[a]				0.6727 (0.000)[f]	0.8482(0.000)[f]
$hOGG_1I$ (RFI)[a]					0.6528(0.000)[f]
Age[b]	0.1832 (0.102)	-0. 0326 (0.773)	0.3332 (0.002)[f]	0. 2316 (0.037)[e]	0.1655(0.140)
BMI[b]	-0.3339 (0.002)[f]	-0. 0983 (0.383)	-0. 3111 (0.005)[f]	-0. 0415 (0.713)	-0.2285(0.0040)[f]
Age[c]	0.2414(0.031)[e]	-0.0204 (0.858)	0.3954 (0.000)[f]	0.2390 (0.033)[e]	0.2015(0.073)
BMI[d]	-0.3663 (0.001)[f]	-0.0950 (0.402)	-0.3779 (0.001)[f]	-0.0735 (0.517)	-0.2552(0.022)[e]

A: Adjusted for (gender+age+BMI), B: Adjusted for gender; C:Adjusted for (gender+BMI), D: Adjusted for (gender+age), E: Correlation was significant at the 0.05 level, F: Correlation was significant at the 0.01 level, G: Data presented in cells were correlation coefficient (*P*).

Table 3 Association between biomarkers and $hOGG_1$-326 SNP (Oneway ANOVA)

	8-oxoGP (%)			8-oxoGI (RFI)			$hOGG_1P$ (%)			$hOGG_1I$ (RFI)		
	Median	*P* (LSD)		Median	*P* (LSD)		Median	*P* (LSD)		Median	*P* (LSD)	
	(95 % CI)	Cys / Ser	Ser / Ser	(95 % CI)	Cys / Ser	Ser / Ser	(95 % CI)	Cys / Ser	Ser / Ser	(95 % CI)	Cys / Ser	Ser / Ser
Cys / Cys	94.03	0.075	0.250	58.61	0.023[a]	0.252	93.37	0.633	0.699	116.72	0.714	0.329
(*n*=32)	(85.96, 93.78)			(50.01, 70.31)			(85.58, 93.45)			(94.94, 133.28)		
Cys / Ser	94.73		0.864	71.16		0.573	93.28		0.452	110.90		0.205
(*n*=37)	(91.48, 95.53)			(64.25, 80.99)			(90.26, 93.35)			(97.92, (123.07)		
Ser / Ser	94.98			58.73			91.80			94.93		
(*n*=13)	(88.98, 96.61)			(52.01, 84.67)			(87.18, 93.64)			(73.26, 106.82)		
(F) *P*		(1.751) 0.180			(2.741) 0.071			(0.312) 0.733			(0.821) 0.444	

[a]*P*<0.05.

Table 4 Multiple regression models of predictors on levels of oxidative DNA damage biomarkers

Predictors in the model	Double staining percentage (%)		8-oxoGP		8-oxoGI		$hOGG_1P$		$hOGG_1I$	
	Beta[b]	*P*	Beta	*P*	Beta	*P*	Beta	*P*	Beta	*P*
8-oxoGP							0.463		0.000[c]	
8-oxoGI	0.521	0.000[c]							131.226	0.000[c]
$hOGG_1P$			0.922	0.000[c]						
$hOGG_1I$	0.411	0.000[c]			6.591E-02	0.008[c]				
Age	0.090	0.201	-0.139	0.108	-0.075	0.426	2.532E-02	0.001[c]	3.069	0.018[c]
Gender	-0.027	0.693	-0.081	0.336	-0.106	0.253	0.058	0.474	0.104	0.262
BMI	-0.046	0.496	-0.055	0.511	-1.048E-02	0.050[c]	-0.053	0.516	0.037	0.696
$hOGG_1$ 326SNP	0.056	0.427	0.103	0.029[c]	2.370E-03	0.000[c]	-0.112	0.166	-15.684	0.006[c]
Constant	0.480	0.000	6.969E-02	0.705	1.601	0.000	0.401	0.001	-133.512	0.001
R^2(F)[d]	0.667 (79.227)[e]		0.470 (35.033)[e]		0.377 (15.729)[e]		0.509(40.875)[e]		0.386(16.369) [e]	

A: $hOGG_1$ 326SNP: Cys/Cys=1; Cys/Ser=2; Ser/Ser=3; B: Beta: standardized coefficient; C: Variables entered final equation (backward); D: R square of model (F value of ANOVA); E: ANOVA *P* value <0.01.

DISCUSSION

Population-based researches can provide new clues to etiology of a disease. The unique epidemiology of high mortality rate of HCC in Guangxi Zhuang Autonomous Region, China has provided an ideal population model for the study of oxidative DNA damage and corresponding repair mechanism[1]. Although aflatoxin exposure was not measured in the present study, our earlier reports and others have shown that the dietary intake of aflatoxin in the local residents was high[28,36]. Furthermore, it has been well established that AFB1 causes rapid ROS formation and leads to DNA oxidative damage, which plays a critical role in hepato-carcinogenesis[22]. The subjects of the present study came from a typical HCC high risk community. In order to rule out the possibility of influence from hepatitis virus infection and other potential environmental and occupational factors, such as pesticides, cigarette smoking and alcohol, we have limited the present study to 82 children under the age of 18 with no known liver diseases or other medical history.

Methodology of quantification for oxidative DNA damage

Immunohistochemistry-based approaches have been widely used for the quantification of DNA adducts in various tissues[37], as well as in *in-situ*[38,39] or urinary[40] 8-oxoG quantification. On the other hand, flow cytometry technology allows multi-parameter analyses of heterogeneous cell population, in which immunophenotyping of both surface and cytoplasmic antigens, DNA analysis and functional evaluations are combined. Subsets of cells can be identified and characterized by patterns of maturation antigens and staining intensity[41]. This report is the first study thus far utilizing flow cytometry for simultaneous quantification of both 8-oxoG and a high risk population of HCC as a model. Compared to the immuno-quantification of 8-oxoG using visualized counting of positive-staining cells, the flow cytometry approach we used, has the following advantages. The assessment is more objective compared to other methods as the scoring is not operator dependent, both the number of positive-staining cells and fluorochrome intensity could be quantified simultaneously, the sample required (-1×10^6 cells) is much less, compared to other traditional methods, and high-throughput (it can handle as many as 100 samples per batch, thus eliminating possible batch to batch variations).

Prior to the present investigation, attention was paid during the pilot study to standardize and validate the instrumentation and methodology. Factors such as specificity and performance of the reagents, staining intensity, spectral overlap, and instrument compensation were carefully evaluated[41]. The overall indication is that the flow cytometry determinations of 8-oxoG and $hOGG_1$ are of high reliability. The reproducibility is generally over 90 % with batch-to batch variation of less than 10 %. As for the actual samples from Guangxi, a substantial proportion of leukocytes was found to be positively-stained for both 8-oxoG and $hOGG_1$. These values are much higher compared to normal healthy subjects from Singapore of about 20 % to 40 % (Tao *et al*, unpublished data). Table 2 clearly demonstrates that there were significant correlations between 8-oxoG level and $hOGG_1$ expression, either expressed as percentage or chromophore intensity. Even after confounding factors such as age and BMI were adjusted, there were still significant associations between oxidative damage and $hOGG_1$ expression in leukocytes (Table 2). This finding supports that normal cells have certain defensive mechanism against ubiquitous oxidative DNA damage[9], and $hOGG_1$ works as a housekeeping gene, ubiquitously expressed during cell cycle[42].

Although inter-individual variations of $hOGG_1$ are genetically determined, the present data and several earlier studies suggest that its expression could be influenced by endogenous formation of ROS or environmental carcinogens. Increased 8-oxoG repair activity has been shown to increase in smoker's leukocytes[43] and in lung cells exposed to asbestos[44]. Quantitative assessment of hOGG1 expression in peripheral blood cells can provide information on exposure to environmental carcinogens[45]. The present study has clearly demonstrated that hOGG1 in leukocytes, expressed either in percentage or fluorescence intensity, can indicate the oxidative damage in an HCC high risk population, suggesting that $hOGG_1$ is a useful biomarker for monitoring oxidative stress, in addition to 8oxoG.

Gender and oxidative DNA damage

Based on the epidemiological data obtained earlier in other parts of China as well as in Guangxi Zhuang Autonomous Region, the occurrence of HCC is predominant in men, the ratio of male to female is 4-6:1[1]. However, in the present study, we did not observe any difference in either 8oxoG or $hOGG_1$ level between male and female children (Table 1). According to Loft *et al*.,

adult healthy men aged 40 to 60 excreted 29 % (10-48 %) more 8-oxoG in urine than women[46]. Nevertheless, DNA damage, measured as either percentage of DNA migrated in COMET tail[47] or 8-oxoG excretion in urine[48], was not associated with gender in other two adult populations. In healthy individuals, there was no difference in $hOGG_1$ activity due to gender by means of an 8-oxoG-containing oligonucleotide assay[17]. Since this was a children-based study, further evidences from adult subjects are required to elucidate the role of gender-related factors in hepatocarcinogenesis in this population.

Age, BMI and oxidative DNA damage

An inversed relationship between BMI and urinary excretion of 8-oxoG in adults has been documented[46,49], and was postulated to be due to a higher metabolic rate in lean persons[46]. In the present study, similarly, we observed a negative correlation between BMI and 8-oxoGP, and between BMI and $hOGG_1P$ (Table 2), which was consistent with that in previous reports. There was also a positive correlation between $hOGG_1$ level and age, which was not consistent with that of 8-oxoG (Figure 2, Table 2). This age-dependent increase of $hOGG_1$ in children has never been reported elsewhere. The results indicated that, the age-dependent increase of $hOGG_1$ level can not simply be explained by metabolic rate and BMI.

Using COMET assay to study DNA damage of children in Mexico City, Calderon-Garciduenas[50] showed that there was an age-dependent increase in the percentage of nasal cells with COMET tails >10 microns, implying a dose response relationship between exposure to environment pollutants and increase of age. Drury[51] in a preliminary study of 15 children observed an increase of mean 8-OHdG excretion in urine with postnatal age (r=0.80, P<0.0001). Nevertheless, the author argued that these changes could also be due to changes in the activity of the enzyme responsible for 8-OHdG excision. According to Bogdanov[52], however, neonates of 50-60 days had a higher 8-OHdG excretion in urine (13.39±0.082 ng/mg creatinine, n=150) than children aged 3-9 (4.62±0.091 ng/mg creatinine, n=32). So far no report about hOGG1 expression in children is available. Therefore it is not known whether this age-dependency is attributed to growth-related increase of metabolism or dietary increase (accumulation) of exposure to aflatoxin or other hazards, or both. Further studies with a larger population should be able to provide more insights in this preliminary observation.

$hOGG_1$-Cys326Ser SNP and oxidative DNA damage

DNA repair enzyme OGG1 is a DNA glycosylase/AP lyase that has been hypothesized to play an important role in preventing carcinogenesis by repairing oxidative damage to DNA. Specifically, it can efficiently repair 8-oxoG, a major base lesion produced by ROS and formed by endogenous metabolism or exposure to environmental oxidizing agents or genotoxic compounds[10]. In this study we have analyzed the variants of $hOGG_1$-Cys326Ser in 84 children and the results showed that the frequency of $hOGG_1$-Cys326 allele of 54.8 % was similar to that reported by Sugimura[13] and Takezaki[53] conducted in two other Chinese populations (54.5 % to 60.7 %). In the present investigation, individuals with the $hOGG_1$ 326Ser allele rather than $hOGG_1$ 326Cys allele, had a significantly higher concentration of leukocyte 8-oxoG level (Tables 3 and 4).

Kohn *et al*. first described a reduced repair activity of $hOGG_1$-Cys326 protein in a complementation assay system[12]. Nevertheless, this observation was not supported by another study using cell homogenates-cleavage system[17]. A recent study by Janssen *et al* found that DNA repair activity of OGG1 in human lymphocytes was not dependent on the Ser326Cys variants[17]. Paralleling to the results of functional studies, population studies on $hOGG_1$-326 polymorphism and cancer susceptibility thus far were also not conclusive[17-21]. It is however important to note that the proportion of homozygous Ser-Ser individuals is the highest in Melanesians (74.5 %), and German (57.1 %), lower in Australian Caucasians (40 %), Japanese (27.7 %) and even lower in Chinese (12 %)[13].

Since the 8-oxoG level measured in a tissue at time is an integration of a number of parameters including the level of ROS, tissue redox status, cellular antioxidant defense mechanism and DNA repair system[21], our data suggest that the role of $hOGG_1$ SNP, if any, in modulating 8-oxoG level of individuals, may be diluted by other confounders. On the other hand, it is believed that $hOGG_1$ may not be the only gene associated with oxidative damage. An alternative DNA oxidative damage repair pathway to minimize the effects of 8-oxoG in genomes has also been reported recently[54]. Carefully designed studies considering these confounders however, are obviously needed to verify this observation.

From the data obtained in this study, it is concluded that, oxidative damage is significantly correlated with the DNA damage repair enzyme $hOGG_1$, there are positive associations between oxidative damage, repair enzyme $hOGG_1$ and age, while there are reverse relationships between oxidative damage and body mass indexes, and polymorphism of $hOGG_1$ variant appears to influence 8-oxoG level in peripheral leukocytes, but only at a marginal strength. These findings provide some new insights into a better understanding of the complex etiology and molecular events that could lead to the development of HCC. Further study should take into consideration of both long term environment exposure and genetic susceptibility in a larger population.

ACKNOWLEDGEMENT

We are grateful to Prof. Chia SE and Dr. Dong F for their statistical advice and critical comments on the manuscript. We are also grateful to Ong HY and Ong YB for their technical support (Department of Community, Occupational and Family Medicine, National University of Singapore, Singapore.).

REFERENCES

1 **Yeh FS**, Mo CC, Luo S, Henderson BE, Tong MJ, Yu MC. A serological case-control study of primary hepatocellular carcinoma in Guangxi, China. *Cancer Res* 1985; **45**: 872-873
2 **Halliwell B**. Can oxidative DNA damage be used as a biomarker of cancer risk in humans? Problems, resolutions and preliminary results from nutritional supplementation studies. *Free Radic Res* 1998; **29**: 469-486
3 **Cerutti PA,** Trump BF. Inflammation and oxidative stress in carcinogenesis. *Cancer Cells* 1991; **3**: 1-7
4 **Ames BN**. Endogenous oxidative DNA damage, aging, and cancer. *Free Radic Res Commun* 1989; **7**: 121-128
5 **Halliwell B**. Effect of diet on cancer development: is oxidative DNA damage a biomarker?(1,2). *Free Radic Biol Med* 2002; **32**: 968-974
6 **De Flora S**, Izzotti A, Randerath K, Randerath E, Bartsch H, Nair J, Balansky R, van Schooten F, Degan P, Fronza G, Walsh D, Lewtas J. DNA adducts and chronic degenerative disease. Pathogenetic relevance and implications in preventive medicine. *Mutat Res* 1996; **366**: 197-238
7 **Kasai H**. Analysis of a form of oxidative DNA damage, 8-hydroxy-2'-deoxyguanosine, as a marker of cellular oxidative stress during carcinogenesis. *Mutat Res* 1997; **387**: 147-163
8 **Hazra TK**, Hill JW, Izumi T, Mitra S. Multiple DNA glycosylases for repair of 8-oxoguanine and their potential *in vivo* functions. *Prog Nucleic Acid Res Mol Biol* 2001; **68**: 193-205
9 **Brozmanova J**, Dudas A, Henriques JA. Repair of oxidative DNA damage-an important factor reducing cancer risk. Minireview. *Neoplasma* 2001; **48**: 85-93

10 **Bruner SD**, Norman DP, Verdine GL. Structural basis for recognition and repair of the endogenous mutagen 8-oxoguanine in DNA. *Nature* 2000; **403**: 859-866

11 **Boiteux S,** Radicella JP. Base excision repair of 8-hydroxyguanine protects DNA from endogenous oxidative stress. *Biochimie* 1999; **81**: 59-67

12 **Kohno T**, Shinmura K, Tosaka M, Tani M, Kim SR, Sugimura H, Nohmi T, Kasai H, Yokota J. Genetic polymorphisms and alternative splicing of the hOGG1 gene, that is involved in the repair of 8-hydroxyguanine in damaged DNA. *Oncogene* 1998; 16: 3219-3225

13 **Sugimura H**, KohnoT, Wakai K, Nagura K, Genka K, Igarashi H, Morris BJ, Baba S, Ohno Y, Gao C, Li Z, Wang J, Takezaki T, Tajima K, Varga T, Sawaguchi T, Lum JK, Martinson JJ, Tsugane S, Iwamasa T, Shinmura K, Yokota J. hOGG1 Ser326Cys polymorphism and lung cancer susceptibility. *Cancer Epidemiol Biomarkers Prev* 1999; **8**: 669-674

14 **Le Marchand L**, Donlon T, Lum-Jones A, Seifried A, Wilkens LR. Association of the hOGG1 Ser326Cys polymorphism with lung cancer risk. *Cancer Epidemiol Biomarkers Prev* 2002; **11**: 409-412

15 **Elahi A**, Zheng Z, Park J, Eyring K, McCaffrey T, Lazarus P. The human OGG1 DNA repair enzyme and its association with orolaryngeal cancer risk. *Carcinogenesis* 2002; **23**: 1229-1234

16 **Xing DY**, Tan W, Song N, Lin DX. Ser326Cys polymorphism in hOGG1 gene and risk of esophageal cancer in a Chinese population. *Int J Cancer* 2001; **95**: 140-143

17 **Janssen K**, Schlink K, Gotte W, Hippler B, Kaina B, Oesch F. DNA repair activity of 8-oxoguanine DNA glycosylase 1 (OGG1) in human lymphocytes is not dependent on genetic polymorphism Ser326/Cys326. *Mutat Res* 2001; **486**: 207-216

18 **Xu J**, Zheng SL, Turner A, Isaacs SD, Wiley KE, Hawkins GA, Chang BL, Bleecker ER, Walsh PC, Meyers DA, Isaacs WB. Associations between hOGG1 sequence variants and prostate cancer susceptibility. *Cancer Res* 2002; **62**: 2253-2257

19 **Wikman H**, Risch A, Klimek F, Schmezer P, Spiegelhalder B, Dienemann H, Kayser K, Schulz V, Drings P, Bartsch H. hOGG1 polymorphism and loss of heterozygosity (LOH): significance for lung cancer susceptibility in a Caucasian population. *Int J Cancer* 2000; **88**: 932-937

20 Hanaoka T, Sugimura H, Nagura K, Ihara M, Li XJ, Hamada GS, Nishimoto I, Kowalski LP, Yokota J, Tsugane S. hOGG1 exon7 polymorphism and gastric cancer in case-control studies of Japanese Brazilians and non-Japanese Brazilians. *Cancer Lett* 2001; **170**: 53-61

21 **Hardie LJ**, Briggs JA, Davidson LA, Allan JM, King RF, Williams GI, Wild CP. The effect of hOGG1 and glutathione peroxidase I genotypes and 3p chromosomal loss on 8-hydroxydeoxyguanosine levels in lung cancer. *Carcinogenesis* 2000; **21**: 167-172

22 **Shen HM,** Ong CN. Mutations of the p53 tumor suppressor gene and ras oncogenes in aflatoxin hepatocarcinogenesis. *Mutat Res* 1996; **366**: 23-44

23 **Smela ME**, Currier SS, Bailey EA, Essigmann JM. The chemistry and biology of aflatoxin B(1): from mutational spectrometry to carcinogenesis. *Carcinogenesis* 2001; **22**: 535-545

24 **Hagen TM**, Huang S, Curnutte J, Fowler P, Martinez V, Wehr CM, Ames BN, Chisari FV. Extensive oxidative DNA damage in hepatocytes of transgenic mice with chronic active hepatitis destined to develop hepatocellular carcinoma. *Proc Natl Acad Sci U S A* 1994; **91**: 12808-12812

25 **Moriya K**, Nakagawa K, Santa T, Shintani Y, Fujie H, Miyoshi H, Tsutsumi T, Miyazawa T, Ishibashi K, Horie T, Imai K, Todoroki T, Kimura S, Koike K. Oxidative stress in the absence of inflammation in a mouse model for hepatitis C virus-associated hepatocarcinogenesis. *Cancer Res* 2001; **61**: 4365-4370

26 **National Cancer Control Office**. Atlas of Cancer Mortality in The People's Republic of China. Nanjing Institute of Geography, *China Map Press Shanghai* 1979

27 **Huang TR**, Yu JH, Zhang ZHQ. Analysis on epidemic feature and secular trend of primary liver cancer in Guangxi. *Guangxi Medical J* 2000; **22**: 677-679

28 **Wang JS**, Huang T, Su J, Liang F, Wei Z, Liang Y, Luo H, Kuang SY, Qian GS, Sun G, He X, Kensler TW, Groopman JD. Hepatocellular Carcinoma and Aflatoxin Exposure in Zhuqing Village, Fusui County, People's Republic of China. *Cancer Epidemiol Biomarkers Prev* 2001; **10**: 143-146

29 **Peng T**, Li LQ, Lin JL, Lu YF, Wu S, Liang ST, Xiao Q, Liao QH. p53 gene 249codon mutation in recurrent hepatocellular carcinoma from Guangxi province. *Chinese J General Surgery* 2000; **15**: 17

30 **Deng Z**, Pan L, Ma Y. Sequence alterations in p53 gene of hepatocellular carcinoma from high aflatoxin risk area in Guangxi. *Zhonghua Zhongliu Zazhi* 1997; **19**: 18-21

31 **Stern MC**, Umbach DM, Yu MC, London SJ, Zhang ZQ, Taylor JA. Hepatitis B, aflatoxin B(1), and p53 codon 249 mutation in hepatocellular carcinomas from Guangxi, People's Republic of China, and a meta-analysis of existing studies. *Cancer Epidemiol Biomarkers Prev* 2001; **10**: 617-625

32 **Struthers L**, Patel R, Clark J, Thomas S. Direct detection of 8-oxodeoxyguanosine and 8-oxoguanine by avidin and its analogues. *Anal Biochem* 1998; **255**: 20-31

33 **Sattler U**, Calsou P, Boiteux S, Salles B. Detection of oxidative base DNA damage by a new biochemical assay. *Arch Biochem Biophys* 2000; **376**: 26-33

34 **Lenka N**, Lu ZJ, Sasse P, Hescheler J, Fleischmann BK. Quantitation and functional characterization of neural cells derived from ES cells using nestin enhancer-mediated targeting *in vitro*. *J Cell Sci* 2002; **115**: 1471-1485

35 **Forsberg L**, de Faire U, Morgenstern R. Low yield of polymorphisms from EST blast searching: analysis of genes related to oxidative stress and verification of the P197L polymorphism in GPX1. *Hum Mutat* 1999; **13**: 294-300

36 **Zhu JQ**, Zhang LS, Hu X, Xiao Y, Chen JS, Xu YC, Fremy J, Chu FS. Correlation of dietary aflatoxin B1 levels with excretion of aflatoxin M1 in human urine. *Cancer Res* 1987; **47**: 1848-1852

37 **Poirier MC**, Santella RM, Weston A. Carcinogen macromolecular adducts and their measurement. *Carcinogenesis* 2000; **21**: 353-359

38 **Kitada T**, Seki S, Iwai S, Yamada T, Sakaguchi H, Wakasa K. In situ detection of oxidative DNA damage, 8-hydroxydeoxyguanosine, in chronic human liver disease. *J Hepatol* 2001; **35**: 613-618

39 **Otani K**, Shimizu S, Chijiiwa K, Yamaguchi K, Noshiro H, Tanaka M. Immunohistochemical detection of 8-hydroxy-2'-deoxyguanosine in gallbladder epithelium of patients with pancreaticobiliary maljunction. *Eur J Gastroenterol Hepatol* 2001; **13**: 1363-1369

40 **Saito S**, Yamauchi H, Hasui Y, Kurashige J, Ochi H, Yoshida K. Quantitative determination of urinary 8-hydroxydeoxyguanosine (8-OH-dg) by using ELISA. *Res Commun Mol Pathol Pharmacol* 2000; **107**: 39-44

41 **Owens MA**, Vall HG, Hurley AA, Wormsley SB. Validation and quality control of immunophenotyping in clinical flow cytometry. *J Immunol Methods* 2000; **243**: 33-50

42 **Dhenaut A**, Boiteux S, Radicella JP. Characterization of the hOGG1 promoter and its expression during the cell cycle. *Mutat Res* 2000; **461**: 109-118

43 **Asami S**, Hirano T, Yamaguchi R, Tomioka Y, Itoh H, Kasai H. Increase of a type of oxidative DNA damage, 8-hydroxyguanine, and its repair activity in human leukocytes by cigarette smoking. *Cancer Res* 1996; **56**: 2546-2549

44 **Kim HN**, Morimoto Y, Tsuda T, Ootsuyama Y, Hirohashi M, Hirano T, Tanaka I, Lim Y, Yun IG, Kasai H. Changes in DNA 8-hydroxyguanine levels, 8-hydroxyguanine repair activity, and hOGG1 and hMTH1 mRNA expression in human lung alveolar epithelial cells induced by crocidolite asbestos. *Carcinogenesis* 2001; **22**: 265-269

45 **Hanaoka T**, Yamano Y, Hashimoto H, Kagawa J, Tsugane S. A preliminary evaluation of intra- and interindividual variations of hOGG1 messenger RNA levels in peripheral blood cells as determined by a real-time polymerase chain reaction technique. *Cancer Epidemiol Biomarkers Prev* 2000; **9**: 1255-1258

46 **Loft S**, Vistisen K, Ewertz M, Tjonneland A, Overvad K, Poulsen HE. Oxidative DNA damage estimated by 8-hydroxydeoxyguanosine excretion in humans: influence of smoking, gender and body mass index. *Carcinogenesis* 1992; **13**: 2241-2247

47 **Giovannelli L**, Saieva C, Masala G, Testa G, Salvini S, Pitozzi V, Riboli E, Dolara P, Palli D. Nutritional and lifestyle determinants of DNA oxidative damage: a study in a Mediterranean population. *Carcinogenesis* 2002; **23**: 1483-1489

48 **Witherell HL**, Hiatt RA, Replogle M, Parsonnet J. *Helicobacter pylori* infection and urinary excretion of 8-hydroxy-2-deoxyguanosine, an oxidative DNA adduct. *Cancer Epidemiol Biomarkers Prev* 1998; **7**: 91-96

49 **Kasai H**, Iwamoto-Tanaka N, Miyamoto T, Kawanami K, Kawanami S, Kido R, Ikeda M. Life style and urinary 8-hydroxydeoxyguanosine, a marker of oxidative dna damage: effects of exercise, working conditions, meat intake, body mass index, and smoking. *Jpn J Cancer Res* 2001; **92**: 9-15

50 **Calderon-Garciduenas L**, Wen-Wang L, Zhang YJ, Rodriguez-Alcaraz A, Osnaya N, Villarreal-Calderon A, Santella RM. 8-hydroxy-2'-deoxyguanosine, a major mutagenic oxidative DNA lesion, and DNA strand breaks in nasal respiratory epithelium of children exposed to urban pollution. *Environ Health Perspect* 1999; **107**: 469-474

51 **Drury JA**, Jeffers G, Cooke RW. Urinary 8-hydroxydeoxyguanosine in infants and children. *Free Radic Res* 1998; **28**: 423-428

52 **Bogdanov MB**, Beal MF, McCabe DR, Griffin RM, Matson WR. A carbon column-based liquid chromatography electrochemical approach to routine 8-hydroxy-2'-deoxyguanosine measurements in urine and other biologic matrices: a one-year evaluation of methods. *Free Radic Biol Med* 1999; **27**: 647-666

53 **Takezaki T**, Gao CM, Wu JZ, Li ZY, Wang JD, Ding JH, Liu YT, Hu X, Xu TL, Tajima K, Sugimura H. hOGG1 Ser (326) Cys polymorphism and modification by environmental factors of stomach cancer risk in Chinese. *Int J Cancer* 2002; **99**: 624-627

54 **Klungland A**, Rosewell I, Hollenbach S, Larsen E, Daly G, Epe B, Seeberg E, Lindahl T, Barnes DE. Accumulation of premutagenic DNA lesions in mice defective in removal of oxidative base damage. *Proc Natl Acad Sci U S A* 1999; **96**: 13300-13305

Edited by Wang XL

P.O.Box 2345, Beijing 100023,China
Fax: +86-10-85381893
E-mail: wjg@wjgnet.com www.wjgnet.com

World J Gastroenterol 2003;9(10):2194-2197
World Journal of Gastroenterology
 ISSN 1007-9327

• LIVER CANCER •

Total vascular exclusion technique for resection of hepatocellular carcinoma

Zhen-Yu Yin, Xiao-Ming Wang, Ren-Xiang Yu, Bai-Meng Zhang, Ke-Ke Yu, Ning Li, Jie-Shou Li

Zhen-Yu Yin, Ning Li, Jie-Shou Li, Institute of General Surgery, School of Medicine, Nanjing University, Nanjing 210093, Jiangsu Province, China
Zhen-Yu Yin, Xiao-Ming Wang, Ren-Xiang Yu, Bai-Meng Zhang, Ke-Ke Yu, Department of General Surgery, Zhongshan Hospital, Xiamen 361004, Fujian Province, China
Correspondence to: Zhen-Yu Yin, Department of General Surgery, Zhongshan Hospital, Xiamen 361004, Fujian Province, China. davidmd@sohu.com
Telephone: +86-592-2292045 **Fax:** +86-592-2212328
Received: 2003-05-13 **Accepted:** 2003-06-02

Abstract

AIM: To improve the low resection rate, poor prognosis and to control the massive hemorrhage during operation, total vascular exclusion (TVE) technique was used in hepatectomies of advanced and complicated hepatocellular carcinomas (HCCs).

METHODS: Five hundred and thirty patients with HCCs were admitted in our hospital. They were divided into TVE technique group (group A: n=78), Pringle maneuver method group (group B: n=176) and unresectable group (group C: n=276). The clinical, operative, pathological parameters and outcome of the patients were statistically evaluated.

RESULTS: Group A had a significantly higher resection rate than group B (accounting for 47.92 % and 33.21 % respectively). There was no significant difference in blood loss, blood transfusion and perioperative mortality between groups A and B. Both groups had the similar median disease free survival time (14.6 *vs* 16.3 months) and 1 year survival rate (92.9 % *vs* 95.5 %). The TVE group had a medial survival time of 40.5 months and its 5-year survival rate was 34.6 %.

CONCLUSION: As compared with Pringle maneuver method, the total vascular exclusion is a safe and effective technique to increase the total resection rate of advanced and complicated HCCs.

Yin ZY, Wang XM, Yu RX, Zhang BM, Yu KK, Li N, Li JS. Total vascular exclusion technique for resection of hepatocellular carcinoma. *World J Gastroenterol* 2003; 9(10): 2194-2197
http://www.wjgnet.com/1007-9327/9/2194.asp

INTRODUCTION

At present, operations including tumor resection and liver transplantation offer the only chance of cure for the patients with HCCs[1], and hepatectomy remains the normal choice when liver transplantation is not available. HCCs we met were mostly advanced with a low resection rate and had a high risk of lethal blood loss during operation as well as a high mortality after operation especially when the liver was affected by chronic hepatitis or cirrhosis[2-7]. To avoid excessive bleeding and blood transfusion, several methods to limit bleeding have been developed since hepatic portal clamping was successfully performed by Pringle in 1908, which led to the development of total vascular exclusion (TVE) of the liver by Heaney in 1966. Since then, Huguet and his colleagues have better characterized and widely advocated the use of TVE, which can greatly reduce the risk of massive hemorrhage and air embolism[8].

Pringle maneuver method is routinely used in hepatectomy to control blood loss during HCCs operation, TVE is there fore controversial. To the present, no study has documented its safety and efficacy as compared with Pringle maneuver method in resection of HCCs. This study was review our experiences with resection of HCCs by TVE and Pringle maneuver methods.

MATERIALS AND METHODS

Patients

From January 1994 to January 2002, 530 patients with HCCs were admitted in our hospital, they were divided into 3 groups. Group A: 78 patients with complicated HCCs underwent total vascular exclusive hepatectomies. Group B: 176 patients with HCCs underwent Pringle maneuver hepatectomies. Group C: 276 patients with unresectable HCCs underwent conservative treatments such as transhepatic artery embolization.

Diagnosis and vascular exclusion selection

HCCs were diagnosed by examinations such as serum tumor marker α-fetal protein, B-type ultrasound, plain or enhanced spiral computed tomography, magnetic resonance imaging before operation. The diagnosis was confirmed by pathologic examination after operation.

Pringle maneuver method was routinely used in the hepatectomy in our center, and the TVE was only used in advanced and complicated HCC patients such as massive tumors needing major hepatectomy, tumor closing or invading the major blood vessels of liver, tumor in the caudate lobe and multiple tumors.

Perioperative care and treatment

Preoperative care: A venous catheter was introduced one week before operation for routine parenteral nutrition to improve the patient' s liver function, nutritional status and coagulation condition. During perioperative care period, frozen plasma should be infused and blood transfusion must be strictly controlled. Blood loss and ascites production during the operation were balanced by infusing fresh frozen plasma. Intraoperative blood transfusion was given only if the hematocrit value was below 0.30. To prevent bleeding, hemostatic drugs such as fibrinogen and thrombinogen were always intravenously given. The main aim during the first few postoperative days was to restore the liver function and prevent hepatic failure. We used 20 % human albumin 100-200 ml/day to maintain the serum protein level. Glucose solution was given for the energy, and short-term antibiotics, histamine blockers were also administered. Appropriate oral intake was restored as soon as possible. The blood discharge from the drain was

carefully monitored. When bleeding exceeded 100 mL/h, an emergency laparotomy was performed. The patients were taken care of in an intensive care unit for the first 24 to 48 hrs with their the life signs inspected. Immediate postoperative treatments included hemostasis, prophylaxis antibiotic treatment and total parental nutritional support.

Operative technique

The surgical technique was described previously[2,8]. In general, a bilateral subcostal incision with or without an upward midline extension was used, and intraoperative ultrasound was routinely used to determine location of the tumor, or possible tumor modules in the contralateral lobe and the exact relationship between the tumor and the major liver blood vessels. In group A, all the hepatic ligaments were divided to allow complete mobilization of the liver and exposure of the whole retrohepatic vena cava. TVE was prepared by carefully dissecting the suprahepatic and infrahepatic vena cava, and right adrenal veins and accessory hepatic veins were ligated if necessary to allow complete venous control during clamping. Clamps were always applied in the following sequence: hepatoduodenal ligament, infrahepatic vena cava and suprahepatic vena cava. During transection of the liver, 5 min interval was always allowed in every 15-20 min TVE until the transection was over. After the resection was completed, the clamps were removed in reverse order of their application. Pringle maneuver method was applied in group B at the time of liver transection and consisted of cross-clamping the hepatoduodenal ligament until the liver transection was completed. If the time was more than 20 min, the clamp was released for about 5 min until the operation was completed. Hemostasis of the raw surface of the liver was assured by biological fibrin glue and exact suture. Closed drainage was routinely used before closure of the incision.

Data collection and analysis

All medical records of the patients of the three groups were reviewed retrospectively. Major hepatectomy was defined as resection of two or more liver segments according to Goldsmith and Woodburne, while minor hepatectomy was defined as resection of only one segment[2]. Tumor closing or invading the major liver blood vessels was defined as the distance between them which was less than 1 cm.

The values were expressed as median (range) and cases (percent). The overall survival after hepatic resection was calculated by the Kaplan-Meier method. Statistical evaluations were performed by using unpaired Student *t* test and chi-spuare analysis, and comparison was made by log rank analysis. Statistical significance was determined by a *P* value of less than 0.05. Calculations were made with SPSS computer software (Chicago, IL).

RESULTS

As shown in Table 1, the two groups (groups A and B) of patients were similar in terms of age, sex. Both groups had similar high HBV infectious rate. Although the operative time and blood exclusive time were long in TVE group, no significant difference was found in blood loss and blood transfusion between groups A and B. More major hepatectomies and caudate lobe hepatectomies were performed in group A than in group B.

The pathologic data are shown in Table 2. There was a significant difference in the size of tumors between groups A and B. From the data, the rate of tumor closing or invading the major liver blood vessels in group A was higher than that in group B. The patients with HCCs in group A had a higher probability in their advanced stage, about 70 % of the patients were TNM stage 3 or 4 in group A, while only about 32 % in group B. Although higher cirrhosis rate, multiple tumor possibility, more caudate lobe location and higher risk of tumor rupture were found during operation in group A than in group B, the possibilities of tumor free resection margin in the two groups were similar.

Table 1 General clinical data

Clinical parameters	Group A (*n*=78)	Group B (*n*=176)
Age (yr)	51.72 (36-71)	49.66 (14-74)
Male	69 (88.64 %)	147 (83.52 %)
HbsAg (+)	67 (85.89 %)	151 (85.79 %)
Child-Push grade		
Grade A	41 (52.54 %)[a]	124 (70.45 %)
Grade B	28 (35.90 %)[a]	38 (21.59 %)
Grade C	9 (11.53 %)	14 (8.0 %)
Total resection rate	47.92%(254 / 530)[a]	33.21 %(176 / 530)
Procedure time (min)	268 (150-325)[a]	178(128-356)
Blood exclusion time (min)	25.4 (12-55)[a]	14.2(8-28)
Blood loss (ml)	818 (250-2800)	725(180-2400)
Blood transfusion (ml)	690 (0-2400)	620 (0-2600)
Total hospital stay time (d)	29.4 (12-35)	19.8 (10-39)
Re-operation	11 (14.10 %)	16 (9.09 %)
Emergency operation	5 (6.41 %)	9 (5.11 %)
Local hepatectomy	12 (15.38 %)[a]	48 (27.28 %)
Minor hepatectomy	21 (26.92 %)[a]	96 (54.55 %)
Major hepatectomy	45 (57.69 %)[a]	32 (18.19 %)
Caudate lobe hepatectomy	4 (5.13 %)[a]	0 (0)

[a]*P*<0.05 *vs* statistically significant when compared with group B.

Table 2 Pathologic data

Clinical parameters	Group A (*n*=78)	Group B (*n*=176)
The mass		
Median diameter (cm)	11.58 (6.2-24.6)[a]	6.25 (1.8-12.7)
>or =5 cm	72 (92.30 %)[a]	118 (67.05 %)
>or =10 cm	53 (67.95 %)[a]	28 (15.90 %)
Close or invade vana cana	23 (29.49 %)[a]	17 (9.65 %)
Close or invade major hepatic vein	21 (26.92 %)[a]	13 (7.39 %)
Close or invade major bile duct	11 (14.10 %)[a]	8 (4.55 %)
Close or invade major port vein	32 (41.03 %)[a]	22 (12.5 %)
TNM tumor stage		
Stage 1	6 (7.69 %)[a]	49 (27.84 %)
Stage 2	12 (15.38 %)[a]	71 (40.34 %)
Stage 3	36 (46.15 %)[a]	32 (18.19 %)
Stage 4a	20 (25.64 %)[a]	22 (12.5 %)
Stage 4b	4 (5.13 %)[a]	2 (1.14 %)
Cirrhosis	59 (75.64 %)	120 (68.18 %)
Multiple tumor	8 (10.25 %)[a]	6 (3.41 %)
Caudate lobe tumor	4 (5.13 %)[a]	0 (0)
Tumor free resection margin	74 (94.87 %)	173 (98.3 %)
Tumor rupture during operation	11 (14.10 %)[a]	13 (7.39 %)

[a]*P*<0.05 *vs* statistically significant when compared with group B.

Bleeding was most common short-term complication after hepatectomy, but there was no significant difference between the two groups, accounting for 20.5 % and 16.48 %, respectively. Although the complications in group A including bile leakage, ascites, pleural effusion, jaundice, hepatic failure were significantly higher than those in group B, the reoperation

rate within 24 h after operation and perioperative mortality were similar in the two groups. The data are shown in Table 3.

The prognostic data are shown in Table 4. As compared with Pringle maneuver technique, the hepatectomy of TVE might lead to similar median disease-free survival time and short-term survival rate (92.3 % *vs* 95.5 % of one year survival rate, $P>0.05$). The median survival time and long-term survival rate in group A were significantly lower than those in group B, but obviously higher than those in group C. The results showed that the Pringle maneuver group had a higher incidence of remote metastasis than the other two groups.

Table 3 Postoperative complications

Clinical parameters	Group A	Group B
Bleeding	16 (20.51 %)	29 (16.48 %)
Bile leakage	6(7.69 %)[a]	8 (4.55 %)
Infection (including abscess)	12 (15.38 %)	23 (13.68)
Pleural effusion	31 (39.74 %)[a]	34 (19.32 %)
Reoperation within 24 h after operation	3 (3.85 %)	6 (3.40 %)
Ascites	16 (20.51 %)[a]	20 (11.36 %)
Jaundice	6 (7.69 %)[a]	5 (2.84 %)
Hepatic failure	6 (7.69 %)[a]	5 (2.84 %)
Total morbidity	40 (51.28 %)[a]	45 (25.57 %)
Perioperative mortality	2 (2.56 %)	5 (2.84 %)

[a]$P<0.05$ *vs* statistically significant when compared with group B.

Table 4 Outcome after hepatic resection

Clinical parameters	Group A	Group B	Group C
Median disease-free survival (m)	14.6 (8-25)	16.3 (9-37)	-
Median survival (m)	40.5 (28-52)	57.6 (33-84)	8.8 (5-31)
Cumulative survival rate			
1 year survival	92.3 %[b]	95.5 %[b]	29.9 %
3 year survival	51.3 %[ab]	69.6 %[b]	2.9 %
5 year survival	34.6 %[ab]	48.0 %[b]	0
Remote metastasis rate	16.27%[a]	23.9%[b]	14.8 %

[a]$P<0.05$ *vs* statistically significant when compared with group B; [b]$P<0.05$ *vs* statistically significant when compared with group C.

DISCUSSION

With the advances in surgical technique, the mortality rate of hepatectomy today is less than 5 %[2]. Despite of the satisfactory outcome of hepatectomy for HCC[9], hepatectomy of advanced and complicated HCC remains a major surgical challenge, especially when underlying liver cirrhosis is present[10-12]. HCC is mostly resulted from hepatitis virus infection and liver cirrhosis, and the conventional approach used in hepatcetomy will always lead to excessive bleeding and high risk of perioperative mortality[13,14]. Perioperative transfusion has been found to promote recurrence of HCC and to result in short disease-free and overall survivals[15], the highlight of surgery of advanced and complicated HCC is thus to prevent massive bleeding and blood transfusion in hepatectomies[2]. HCCs we met were always in their terminal stage with a diameter larger than 10 cm. Since the Pringle maneuver method does not prevent hepatic venous bleeding or air embolism, new ways of vascular exclusion has to be devised. The TVE technique has been widely accepted in resection of advanced and complicated HCCs since it was introduced by Heaney in 1966 and modified in clinical practice[3,7,8,16]. In general, the TVE technique is used predominantly for major resections or centrally placed lesions or in cases with blood vessels involved.

TVE technique means the total vascular block of the liver during hepatectomy. Though bleeding is decreased in the operation, the TVE technique will prolong the warm ischemia time of the liver, so we must emphasize its safety. Complications were noted in the total vascular exclusive group, which was regarded to be corresponded to the higher incidence of complex resections[17]. Berney and his colleagues showed that the risk factors for postoperative complications were the duration of surgery and the amount of blood transfused[3]. The frequency of perihepatic infected fluid collections has been reported to be 2 % to 20 %, biliary fistulas occurrence was up to 8 % of patients[18]. Brancatisano showed similar perioperative mortality (2.5 %) in radical major hepatic surgery by TVE but with a lower postoperative complication rate (about 46 %) than that of ours[19].

At present, it is generally accepted that liver resection performed under intermittent warm ischema is a safe and well-tolerated modality in patients with and without cirrhotic livers[20]. Huguet and others showed that hepatocytes could tolerate normothermic ischemia in excess of 1 hour, and ischemia up to 2 hour without major detrimental effects other than transient hepatic failure has never been reported[21,22]. Others suggested that the risks related to hemorrhage were of greater concern than those related to the time of ischemia. Thus, for advanced and complicated HCC, it is safer to continue vascular exclusion, within 1 h, until complete resection is achieved, rather than take the risk of significant bleeding for the sake of a shorter period of ischemia. A prospective randomized trial showed that the postoperative outcome of patients who underwent liver resection with Pringle maneuver method was better than that of those who underwent operation with other methods[2]. The results of our data showed that although the TVE group had a high hepatic failure rate and complication occurrence than the Pringle maneuver group, but the perioperative mortality was not significantly higher, suggesting that the hepatic failure and complication occurrence might be transient and recoverable.

Another major problem of TVE is the hemodynamic change during TVE. As reported before, hemodynamic tolerance to TVE was excellent in most patients[3], and we also found that the patients could adapt well and quickly to the haemodynamic changes observed after total vascular exclusion. On the bases of the reported complications of spinal cord ischemia, renal failure or aortic injury after routine aortic clamping[23] and the excellent hemodynamic tolerance obtained without aortic occlusion, we applied the modified TVE without aortic exclusion.

Advanced and complicated HCCs were formerly regarded as contraindications of operation for their high mortality and postoperative recurrent rate, the resection rate of advanced and complicated HCCs was extremely low. It was reported that the resection rate of HCCs was 12-28 %[18, 24,25]. After the use of TVE technique, the resection rate of HCCs increased remarkably, which was also confirmed in our retrospective analysis.

Untreated patiens with HCCs had a median survival time of 6 months, no 5-year survival has been reported. But the surgical treatment prolonged the median survival to 42 months and the 5-year survival to 32 % in some center[26]. Good results could be obtained through an aggressive surgical approach for patients with advanced and complicated HCCs, even for those with tumor thrombi in the portal trunk and vena cava invasion[27]. Comparatively, our perioperative mortality of the patients with advanced and complicated HCCs by TVE was similar to the hepatectomy by Pringle maneuver method and the 5-year survival rate of TVE group after resection was similar to others[28]. The shorter long-term survival rate and median survival time of complicated HCCs by TVE compared with

Pringle maneuver group might be resulted from their poorer conditions such as inflammatory activity, hepatic reserve and tumor characteristics, advanced TNM stage, higher possibility of introgenic tumor rupture, higher rate of metachronous and multicentric liver carcinogenesis[29-31]. However, the long-term survival rate and median survival time of the TVE group were remarkably higher than those of the unresectable group. By the way, the remote metastasis rate of the Pringle maneuver group was higher than that of the TVE group and unresectable group, and this result needs to be further studied. In addition, the potentially harmful effect on the metabolic function of hepatocytes should be mentioned in future study.

In summary, hepatectomy by TVE is a safe and effective technique in surgical treatment of advanced and complicated HCC as compared with Pringle maneuver technique. It can increase the resection rate of HCCs, reduce the massive bleeding during operation and increase the survival rate of advanced and complicated HCCs. This series of HCCs demonstrate that an aggressive policy of liver resection by TVE can be adopted as a feasible therapeutic option without excess mortality.

REFERENCES

1 **Wakabayashi H**, Yachida S, Maeba T, Maeta H. Indications for portal vein embolization combined with major hepatic resection for advanced-stage hepatocellular carcinomas. A preliminary clinical study. *Dig Surg* 2000; **17**: 587-594
2 **Man K**, Fan ST, Ng IO, Lo CM, Liu CL, Wong J. Prospective evaluation of Pringle maneuver in hepatectomy for liver tumors by a randomized study. *Ann Surg* 1997; **226**: 704-711
3 **Berney T**, Mentha G, Morel P. Total vascular exclusion of the liver for the resection of lesions in contact with the vena cava or the hepatic veins. *Br J Surg* 1998; **85**: 485-488
4 **Shimada M**, Matsumata T, Akazawa K, Kamakura T, Itasaka H, Sugimachi K, Nose Y. Estimation of risk of major complications after hepatic resection. *Am J Surg* 1994; **167**: 399-403
5 **Torzilli G**, Makuuchi M, Inoue K, Takayama T, Sakamoto Y, Sugawara Y, Kubota K, Zucchi A. No-mortality liver resection for hepatocellular carcinoma in cirrhotic and noncirrhotic patients: Is there a way? A prospective analysis of our approach. *Arch Surg* 1999; **134**: 984-992
6 **Rui JA**, Wang SB, Chen SG, Zhou L. Right trisectionectomy for primary liver cancer. *World J Gastroenterol* 2003; **9**: 706-709
7 **Qin LX**, Tang ZY. The prognostic significance of clinical and pathological features in hepatocellular carcinoma. *World J Gastroenterol* 2002; **8**: 193-199
8 **Huguet C,** Addario-Chieco P, Gavelli A, Arrigo E, Harb J, Clement RR. Technique of hepatic vascular exclusion for extensive liver resection. *Am J Surg* 1992; **163**: 602-605
9 **Makuuchi M**, Takayama T, Kubota K, Kimura W, Midorikawa Y, Miyagawa S, Kawasaki S. Hepatic resection for hepatocellular carcinoma- Japanese experience. *Hepatogastroenterology* 1998; **45**(Suppl 3): 1267-1274
10 **Capussotti L**, Polastri R. Operative risks of major hepatic resections. *Hepatogastroenterology* 1998; **45**: 184-190
11 **Farges O**, Malassagne B, Flejou JF, Balzan S, Sauvanet A, Belghiti J. Risk of major liver resection in patients with underlying chronic liver disease: a reappraisal. *Ann Surg* 1999; **229**: 210-215
12 **Tang ZY**. Hepatocellular carcinoma-cause, treatment and metastasis. *World J Gastroenterol* 2001; **7**: 445-454
13 **Liu CL**, Fan ST, Lo CM, Tung-Ping Poon R, Wong J. Anterior approach for major right hepatic resection for large hepatocellular carcinoma. *Ann Surg* 2000; **232**: 25-31
14 **Tjandra JJ**, Fan ST, Wong J. Peri-operative mortality in hepatic resection. *Aust Nz J Surg* 1991; **61**: 201-206
15 **Hanazaki K**, Kajikawa S, Shimozawa N, Shimada K, Hiraguri M, Koide N, Adachi W, Amano J. Hepatic resection for large hepatocellular carcinoma. *Am J Surg* 2001; **181**: 347-353
16 **Stephen MS**, Gallagher PJ, Sheil AG, Sheldon DM, Storey DW. Hepatic resection with vascular isolation and routine supraceliac aortic clamping. *AM J Surg* 1996; **171**: 351-355
17 **Buell JF**, Koffron A, Yoshida A, Hanaway M, Lo A, Layman R, Cronin DC, Posner MC, Millis JM. Is any method of vascular control superior in hepatic resection of metastatic cancers? Longmire clamping, pringle maneuver, and total vascular isolation. *Arch Surg* 2001; **136**: 569-575
18 **Fong Y**, Brennan MF, Brown K, Heffernan N, Blumgart LH. Drainage is unnecessary after elective liver resection. *Am J Surg* 1996: **171**: 158-162
19 **Brancatisano R**, Isia A, Habib N. Is radical hepatic surgery safe? *Am J Surg* 1998; **175**: 161-163
20 **Wu CC**, Hwang CR, Liu TJ, P'eng FK. Effects and limitations of prolonged intermittent ischaemia for hepatic resection of the cirrhotic liver. *Br J Surg* 1996; **83**: 121-124
21 **Huguet C**, Gavelli A, Chieco PA, Bona S, Harb J, Joseph JM, Jobard J, Gramaglia M, Lasserre M. Liver ischemia for hepatic resection: where is the limit? *Surgery* 1992; **111**: 251-259
22 **Hannoun L**, Borie D, Delva E, Jones D, Vaillant JC, Nordlinger B, Parc R. Liver resection with normothermic iscaemia exceeding 1 h. *Br J Surg* 1993; **80**: 1161-1165
23 **Emre S**, Schwartz ME, Katz E, Miller CM. Liver resection under total vascular isolation. Variations on a theme. *Ann Surg* 1993; **217**: 15-19
24 **Makuuchi M**, Mori T, Gunven P, Yamazaki S, Hasegawa H. Safety of hemihepatic vascular occlusion during resection of the liver. *Surg Gynecol Obstet* 1987; **164**: 155-158
25 **Hu RH**, Lee PH, Yu SC, Dai HC, Sheu JC, Lai MY, Hsu HC, Chen DS. Surgical resection for recurrent heapatocullar carcinoma: prognosis and analysis of risk factors. *Surgery* 1996; **120**: 23-29
26 **Nagorney DM**, van Heerden JA, Ilstrup DM, Adson MA. Primary hepatic malignancy: surgical management and determinants of survival. *Surgery* 1989; **106**: 740-748
27 **Madariaga JR**, Fung J, Gutierrez J, Bueno J, Iwatsuki S. Liver resection combined with excision of vena cava. *J Am Coll Surg* 2000; **191**: 244-250
28 **Buell JF**, Rosen S, Yoshida A, Labow D, Limsrichamrern S, Cronin DC, Bruce DS, Wen M, Michelassi F, Millis JM, Posner MC. Hepatic resection: effective treatment for primary and secondary tumors. *Surgery* 2000; **128**: 686-693
29 **Fan ST**. What patients can survive disease free after complete resection for hepatocellular carcinoma? A multivariate analysis. *Jpn J Clin Oncol* 2000; **30**: 75-81
30 **Sakon M**, Umeshita K, Nagano H, Eguchi H, Kishimoto S, Miyamoto A, Ohshima S, Dono K, Nakamori S, Gotoh M, Monden M. Clinical significance of hepatic resection in hepatocellular carcinoma: Analysis by disease-free survival curves. *Arch Surg* 2000; **135**: 1456-1459
31 **Hanazaki K**, Kajikawa S, Shimozawa N, Mihara M, Shimada K, Hiraguri M, Koide N, Adachi W, Amano J. A 15-year retrospective study of hepatic resection for stage IV-A hepatocellular carcinoma shows value in hepatitis B negative patients. *Am J Surg* 2002; **183**: 89-94

Edited by Wang XL

P.O.Box 2345, Beijing 100023,China
Fax: +86-10-85381893
E-mail: wjg@wjgnet.com www.wjgnet.com

World J Gastroenterol 2003;9(10):2198-2201
World Journal of Gastroenterology
 ISSN 1007-9327

• LIVER CANCER •

Role of multiphase scans by multirow-detector helical CT in detecting small hepatocellular carcinoma

Hong Zhao, Kang-Rong Zhou, Fu-Hua Yan

Hong Zhao, Department of Radiology, First Hospital, Shanxi Medical College, Taiyuan 030001, Shanxi Province, China
Kang-Rong Zhou, Fu-Hua Yan, Department of Radiology, Zhongshang Hospital, Fudan University, Shanghai 200032, China
Supported by the Ministry Public Health Programme, No.97030220
Correspondence to: Dr. Hong Zhao, Department of Radiology, First Hospital, Shanxi Medical College, Taiyuan 030001, Shanxi Province, China. zhaohongmd@sina.com
Telephone: +86-351-4044111 Ext 24781
Received: 2003-03-12 **Accepted:** 2003-04-14

Abstract

AIM: To evaluate the role of multiphasic scanning by multirow-detector helical CT (MDCT) in detecing small hypervascular hepatocellular carcinoma (SHCC).

METHODS: Multiphasic scanning was carried out in 75 patients with SHCC with Marconi MX8000 CT scanner. The early arterial phase (EAP), late arterial phase (LAP) and the portal venous phase (PVP) scans were started at 21 s, 34 s and 85 s respectively. The mean difference of CT values between tumor and liver parenchyma for each scanning phase was measured, and the sensitivity of detection of SHCC in each of these phases and in the combined phase was calculated and statistically analyzed.

RESULTS: The mean difference of CT values between tumor and liver parenchyma was significant in 71 lesions$\geqslant$1 cm in three phases (P<0.05). In 91 tumor foci, the detectability of SHCC was 45.1 %, 83.5 % and 92.3 % in EAP, LAP and double arterial phases (DAP), respectively. The early arterial phase plus the portal venous phase and the double arterial phase plus the portal venous phase were 94.5 %, 97.8 %, respectively. Whereas the detectability in LAP plus PVP and in DAP plus PVP had no statistical difference.

CONCLUSION: The utility of faster speed and thinner slice MDCT and multiphase scanning protocol can improve the detectability of hypervascular small hepatocellular carcinoma. Among which LAP is superior to EAP in depicting the lesions.

Zhao H, Zhou KR, Yan FH. Role of multiphase scans by multirow-detector helical CT in detecting small hepatocellular carcinoma. *World J Gastroenterol* 2003; 9(10): 2198-2201
http://www.wjgnet.com/1007-9327/9/2198.asp

INTRODUCTION

It has been recognized that the majority of hepatocellular carcinomas (HCC) are hypervascular. During the hepatic arterial phase (AP), hypervascular lesions will be greatly enhanced, and become iso- or hypodense in the portal venous phase (PVP), which is a sensitive and specific feature for diagnosing SHCC. A biphasic hepatic acquisition helical CT scanning technique has become a standard method for clinical diagnosis of SHCC. Some studies and clinical applications have shown that the arterial dominant phase using a single row detector helical CT (SDCT) is effective for detection of SHCC[1-6], but by using this kind of scanner, the scanning of the whole liver takes approximately 20 s with a great difference in scanning time from subdiaphragmatic region to the right lower border of the liver. So that, some lesions are not conspicuously enhanced within the time.

Recently, a new generation of MDCT has been used in clinical practice. The scanning time can be shortened to 0.5 s. If the four-detector array CT scanner is used, the entire hepatic acquisition can be accomplished in a very short period (4-8 s). Therefore, to makes use of the advantages of faster scanning speed of MDCT, we can create a double arterial phase (DAP) scanning technique and compare the detectability of SHCC in the early arterial phase (EAP), late arterial phase (LAP) and portal venous phase (PVP).

MATERIALS AND METHODS

Patients

From September 2001 to July 2002, 75 patients (67 men, 8 women, mean age 49 years) with 91 lesions were enrolled in this study. All the patients were proved or suspected to have SHCC who had undergone imaging diagnostics as US, SDCT or MRI. Among them, 40 cases were confirmed by surgical operation or biopsy, 11 recurred cases were postoperatively diagnosed, and the other 24 cases were diagnosed by clinical data, such as history of liver diseases, evaluation of serum AFP and other imaging modalities.

Methods

Multiphasic CT scans of liver were performed with Marconi MX8000 CT scanner using the following parameters, namely 0.5-0.75 s scanning time, 6.5 mm thick section, 23.3 mm/s table speed, 120 KVp and 200-250 mA.

Before examination, 800-1 000 ml water was taken as oral contrast. The whole liver scanning was followed by nonionic contrast enhancement with a dose of 1.5 ml/kg and an injection rate of 3 ml/s via the antecubital vein. Multiphase acquisition was performed with a scanning delay set for EAP, LAP and PVP at 21 s, 34 s and 85 s, respectively. Each of the whole liver scanning by cephalad-caudal orientation was completed in 4-8 s with breath held.

Imaging analysis

CT attenuations of 71/91 tumor foci with diameter$\geqslant$1 cm were measured in all images, and the difference in density of the tumor foci and surrounding hepatic parenchyma was calculated during the enhanced three phases.

Based on the enhancement and the comparison with adjacent liver parenchyma, the tumor foci were described as hyper-, iso- and hypoattenuation, only hyper- and hypoattenuation lesions could be detected and the number of tumor foci was recorded blindly by two radiologists.

Statistical analysis

The statistical analysis was done by SPSS10.0 software, Chi-square test and analysis of variance.

RESULTS

Among the ninety-one tumor foci identified on the images, 20 of them were less than 1 cm in diameter. The size of the other 71 lesions varied from 10 mm to 30 mm (mean 21.3 mm.) The maximum contrast of tumor-to-liver of the majority lesions during the late arterial phase is shown in Table 1. The difference of tumor-to-liver contrast among the EAP, LAP and PVP was statistically significant (P<0.05).

Table 1 Mean attenuation difference of tumor-to-liver in all phases

Scanning phases	No of SHCCs	X±SD
Noncontrast	71	15.75±7.0[a]
Early arterial phase	71	11.0±9.4[a]
Late arterial phase	71	20.2±14.7[a]
Portal venous phase	71	18.0±10.68

Note: The mean attenuation difference value of each phase was an absolute value. [a]P<0.05.

The sensitivity of tumor foci detection in each scanning phase is shown in Table 2.

Table 2 Sensitivity of SHCC detection for each scanning phase

Scanning phases	Sensitivity (%) (n=91)
EAP	45.1(41/91)
LAP	83.5(76/91)
DAP	92.3(84/91)
PVP	78.0(71/91)
EAP+PVP	84.6(77/91)
LAP+PVP	94.5(86/91)
EAP+LAP+PVP	97.8(89/91)

Table 2 shows that there was a significant difference in the sensitivity of SHCCs detection between EAP and LAP (45.1 % *vs* 83.5 %). Considering the importance of different phases, the sensitivity of the combined phase was 92.3 %, 94.5 %, and 97.8 % for DAP, LAP plus PVP and DAP plus PVP, respectively, which was higher than that of each phase. (Figures 1-3).

The comparison of detectability is shown in Table 3. The EAP had a lower sensitivity for SHCCs compared with others (P<0.05). A notably statistical significance was found in LAP plus PVP and EAP plus PVP (P<0.05), but no statistical significance was observed in LAP plus PVP and DAP plus PVP.

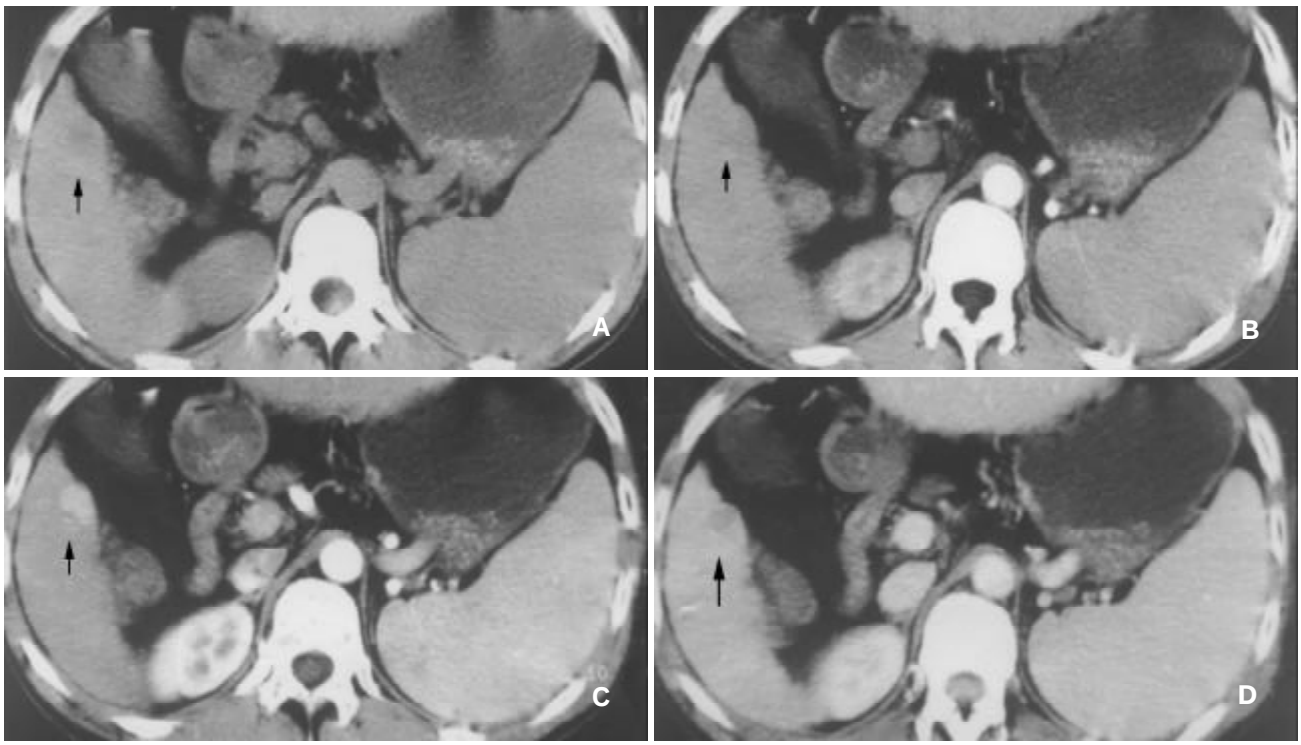

Figure 1 SHCC with size of 1.5 cm in diameter. A: Precontrast image shows hypoattenuating lesion. B:The early arterial phase image shows nonenhanced lesion. C: In the late arterial phase,the lesions enhanced. D: In the portal venous phase, the lesions enhanced dropped down.

Table 3 Comparison of X^2 value between each scanning phase

Scanning phases	LAP	ELAP	PVP	EAP+PVP	LAP+PVP	EAP+LAP+PVP
EAP	P<0.001[a]	P<0.0018	P<0.001[a]	P<0.001[a]	P<0.001[a]	P<0.001[a]
LAP		P=0.088	P=0.258	P=0.831	P=0.033[a]	P=0.006[a]
ELAP			P=0.088	P=0.135	P=0.669	P=0.285
PVP				P=0.200	P<0.001[a]	P<0.001[a]
EAP+PVP					P=0.053	P=0.010[a]
LAP+PVP						P=0.521

Note: All data represented the comparison between each scanning phase using McNemar Test. [a]P<0.05 was considered significant.

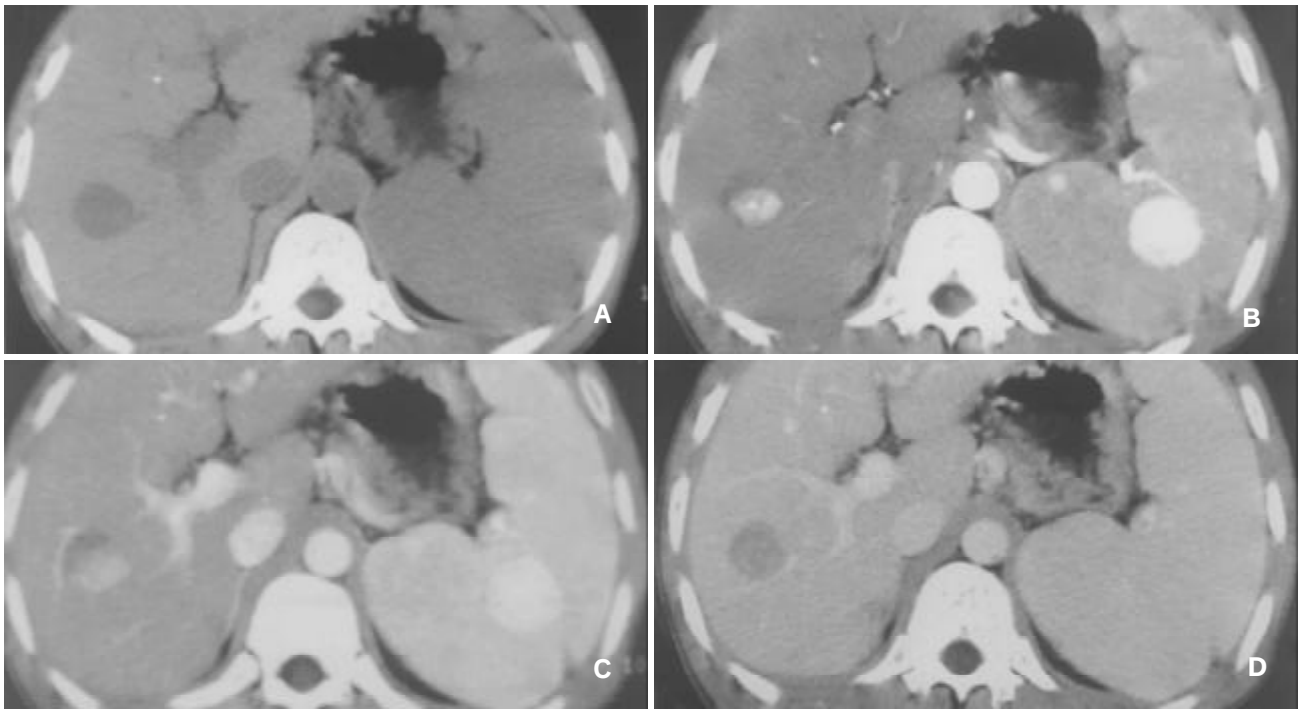

Figure 2 SHCC of 2.0 cm in diameter, A: Precontrast image shows hypoattenuating lesion. B: CT scan obtained at the same level as in the early arterial phase, Tumor intensely enhanced. C: In the late arterial phase, the lesions showed enhancement yet. D: In the portal venous phase, the lesions enhancement dropped down.

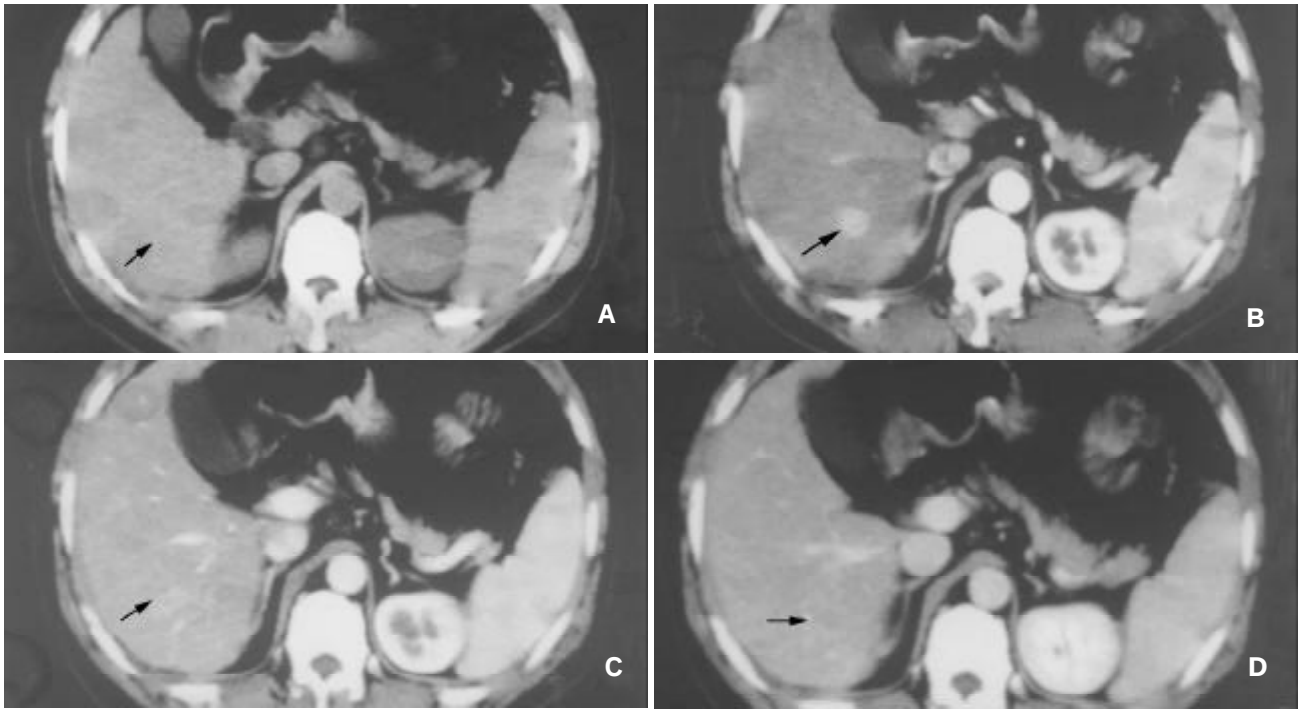

Figure 3 SHCC of 1.5 cm in diameter, A: Hypoattenuating lesion showed in plance image. B: CT scan obtained at the same level as in the early arterial phase, Tumor intensely enhanced. C: In the late arterial phase tumor becomes isodense (arrow). D: In the portal venous phase, the tumor turned to hypodense.

DISCUSSION

The biphasic acquisition helical CT scanning technique has become a standard method for the detection of suspected hypervascular hepatomas. But the single-row detector helical CT (SDCT) has a slow scanning speed (0.8-1 s) and acquires only one section of CT data with each rotation of the X-ray tube. The whole liver scanning using SDCT only takes 20-25 s. It is recognized that the liver has a dual blood supply, the duration of the virtual hepatic arterial phase equals the interval from the beginning of the contrast inflow into the liver from arteries to the beginning of the contrast inflow from the portal vein. It is so short that SDCT is impossible to cover the whole liver during the real hepatic arterial phase[1-6].

Application of MDCT technology in clinical practice has brought about a decisive breakthrough, which is an important milestone in helical CT technologic revolution. The major attribution of MDCT is faster Z-axis coverage speed and improves the longitudinal resolution. MDCT can acquire multiple sections of CT data with each rotation of the X-ray tube and scan the whole liver in 4-8 s, thus imaging of the whole liver can be completed

during the virtual arterial phase[7-13], even twice of the whole liver scanning can be accomplished during the virtual arterial phase. In our study the images in EAP showed intense enhancement of hepatic artery, and minimum enhancement of portal vein, and none of the hepatic parenchyma. The images in the late arterial phase demonstrated substantial portal vein, slight parenchyma enhancement, and no hepatic vein enhancement. The images in PVP showed hepatic veins enhancement, which were not yet enhanced during the early and late arterial phases[14-17].

Our previous studies[18] of continuously dynamic enhancement at the levels of hepatic artery, aorta and hepatic parenchyma, as well as at the level of SHCC foci showed that the arterial phase scanning was started at 16 s (12-22 s) and ended at 40 s. The mean duration of the arterial phase was 23 s. SHCCs were enhanced most markedly in the arterial phase. Due to its hypervascular nature , the mean peak time of the enhancement of SHCC foci was 45.4 s (31-56 s), and the maximum difference of the enhancement between tumor and liver parenchyma occurred at 36 s (28-48 s). Although SHCCs enhanced maximally at 45.4 s, the liver enhancement increased gradually and became quite obvious at that time. The conspicuity depended upon the enhancement difference of the tumor to the liver. Hence the optimally delayed scanning time should be the period when the maximum difference of enhancement occurred between tumor and liver and should not be at the peak time of the tumor enhancement[1,19,20]. This was the theoretical basis on which we set the EAP, LAP and PVP (or parenchyma phase) at 21 s, 34 s and 85 s, respectively. The delayed scanning time at different phases set up by us was in consistency with that reported by Murakami *et al*. They decided the delayed scanning timing for EAP (19.4s) using a mini bolus test, and for LAP (34.9 s), just a 5 s interscan delay after the end of the first pass scanning for table increment patients' movement and patients' respiration[15,16].

This study showed that SHCCs were enhanced during the arterial phase gradually and declined during the portal venous phase (Figure 1). But the mean enhancement difference was greater in LAP than that in EAP (P<0.05) (Table 1). We presume that this reflects the time interval for distribution of contrast-enhanced hepatic arterial blood into the tumor neovasculature and diffusion into the interstices of the tumor[15-22].

The results of our study showed that the sensitivity of detection of SHCC foci (n=91) was 45.1 % and 83.5 % for EAP and LAP. So the late arterial phase was very important for the detection of tumor foci. During the double arterial phase, it could reach 92.3 %, and was higher than that in the portal venous phase (P<0.05). This result indicated that the arterial phase was superior to the portal venous phase in the detectability of SHCCs and was similar to that reported by other authors using biphasic scanning of SDCT[15,16]. But the CT attenuation difference of enhancement of tumors and liver between LAP and EAP led to an extremely significant difference (P<0.001) in the detectability between LAP and EAP (83.5 % *vs* 45.1 %). Therefor, LAP is the best way for demonstrating SHCCs, which represents the advantage of triphasic scanning using MDCT. In addition, MDCT scans allow hepatic imaging with least image thickness and acquire the data in the early arterial phase, later arterial and portal venous phases and improve the sensitivity for depicting SHCC[15,16].

Since DAP combined with PVP had the highest detectability (97.8 %), but with no statistical difference when compared with LAP plus PVP (94.5 %). We consider the latter is more practical.

REFERENCES

1 **Baron RL**, Oliver JH 3rd, Dodd GD 3rd, Nalesnik M, Holbert BL, Carr B. Hepatocellular carcinoma: evaluation with biphasic, contrast-enhanced, helical CT. *Radiology* 1996; **199**: 505-511

2 **Oliver JH 3rd**, Baron RL, Federle MP, Rockette HE Jr. Detecting hepatocellular carcinoma: value of unenhanced or arterial phase CT imaging or both used in conjunction with conventional portal venous phase contrast-enhanced CT imaging. *Am J Roentgenol* 1996; **167**:71-77

3 **Oliver JH** 3rd, Baron RL. Helical biphasic contrast-enhanced CT of the liver: technique, indications, interpretation, and pitfalls. *Radiology* 1996; **201**: 1-14

4 **Oliver JH** 3rd, Baron RL, Federle MP, Jones BC, Sheng R. Hypervascular liver metastases: do unenhanced and hepatic arterial phase CT images effect tumor detection? *Radiology* 1997; **205**: 709-715

5 **Paulson EK**, McDermott VG, Keogan MT, Delong DM, Frederick MG, Nelson RC. Carcinoid metastases to the liver: role of triple-phase helical CT. *Radiology* 1998; **206**: 143-150

6 **Mitsuzaki K**, Yamashita Y, Ogata I, Nishiharu T, Urata J, Takahashi M. Multiple-phase helical CT of the liver for detecting small hepatomas in patients with liver cirrhosis: contrast-injection protocol and optimal timing. *Am J Roentgenol* 1996; **167**: 753-757

7 **Berland L**, Smith K. Multidetector-array CT: Once again, technology creates new opportunities. *Radiology* 1998; **209**: 327-329

8 **Lewis MA**. Multislice CT. Opportunities and challenges. *British J Radiol* 2001; **74**: 779-781

9 **Spielmann AL**, Nelson RC, Lowry CR, Johnson GA, Sundaramoothy G, Sheafor DH, Paulson EK. Liver: Single breath-hold dynamic subtraction CT with multi-detector row helical technology-feasibility study. *Radiology* 2002; **222**: 278-283

10 **Hu H**, He HD, Foley WD, Fox SH. Four multidetector-row helical CT: Image quality and volume coverage speed. *Radiology* 2000; **215**: 55-62

11 **Fuchs T**, Kachelrieb M, Kalender WA. Technical advances in multi-slice spiral CT. *European J Radiol* 2000; **36**: 69-73

12 **Hu H**. Multi-slice helical CT: Scan and reconstruction. *Med Phys* 1999; **26**: 5-18

13 **Tadafumi S**, Toshimasa M, Kazuhiro Y,Kazuhiro S, Isamu N. Helical CT of the liver with computer-assisted bolus-tracking technology: Scan delay of arterial phase scanning and effect of flow rates. *J Comput Assist Tomogr* 2000; **24**: 219-223

14 **Sandstede JJW**, Tschammler A, Beer M, Vogelsang C, Wittenberg G, Hahn D. Optimization of automatic blous tracking for timing of the arterial phase of helical liver CT. *Eur Radiol* 2001; **11**: 1396-1400

15 **Till BR**, Rupert PW, Florian G. Timing of the hepatic arterial phase during contrast-enhanced computed tomography of the liver: Assessment of normal values in 25 volunteers. *Invest Radiol* 2000; **35**: 486-492

16 **Foley WD**, Mallisee TA, Hohenwalter MD, Wilson CR, Quiroz FA, Taylor AJ. Multiphase hepatic CT with a multirow detector CT scanner. *AJR* 2000; **175**: 679-685

17 **Murakami T**, Kim T, Takamura M, Hori M, Takahashi S, Federle MP, Tsuda K, Osuga K, Kawata S, Nakamura H, Kudo M. Hypervascular hepatocellular carcinoma: Detection with double arterial phase multi-detector row helical CT[1]. *Radiology* 2001; **218**: 763-767

18 **Zhou KR**, Yan FH, Tu BW. Evaluation of the arterial phase of biphase enhanced SCT in the diagnosis of small HCC. *Chin J Hepatol* 1999; **7**: 135-137

19 **Ohashi I,** Hanafusa K, Yoshida T. Small hepatocellular carcinomas: two-phase dynamic incremental CT in detection and evaluation. *Radiology* 1993; **189**: 851-855

20 **Hollett MD**, Jeffrey RB Jr, Nino-Murcia M, Jorgensen MJ, Harris DP. Dual-phase helical CT of the liver: value of arterial phase scans in the detection of small (<or=1.5 cm) malignant hepatic neoplasms. *Am J Roentgenol* 1995; **164**: 897-884

21 **Ichikawa T**, Kitamura T, Nakajima H, Sou H, Tsukamoto T, Ikenaga S, Araki T. Hypervascular hepatocellular carcinoma: Can double arterial phase imaging with multidetector CT improve tumor depiction in the cirrhotic liver? *AJR* 2002; **179**: 751-758

22 **Larson RE**, Semelka RC, Bagley AS, Molina PL, Brown ED, Lee JKT. Hypervascular malignant liver lesions: comparison of various MR imaging pulse sequences and dynamic CT[1]. *Radiology* 1994; **192**: 393-399

Edited by Wu XN and Wang XL

P.O.Box 2345, Beijing 100023,China
Fax: +86-10-85381893
E-mail: wjg@wjgnet.com www.wjgnet.com

World J Gastroenterol 2003;9(10):2202-2206
World Journal of Gastroenterology
 ISSN 1007-9327

• COLORECTAL CANCER •

Expressing patterns of p16 and CDK4 correlated to prognosis in colorectal carcinoma

Po Zhao, Ying-Chuan Hu, Ian C. Talbot

Po Zhao, Department of Pathology, Chinese PLA General Hospital, Beijing 100853, Beijing, China and Academic Department of Pathology, St. Mark' s Hospital, Cancer Research UK, Colorectal Cancer Unit, Harrow, HA1 3UJ, London, UK
Ying-Chuan Hu, Department of Pathology, Huaxi Medical College, Sichuan University, Chengdu 610041, Sichuan Province, China
Ian C. Talbot, Academic Department of Pathology, St. Mark' s Hospital, Cancer Research UK, Colorectal Cancer Unit, Harrow, HA1 3UJ, London, UK
Correspondence to: Dr. Po Zhao, Department of Pathology, Chinese PLA General Hospital, 28 Fuxing Road, Beijing 100853, China. zhaopo@plagh.com.cn or Professor Ian C. Talbot, Academic Department of Pathology, St Mark' s Hospital, Cancer Research UK, Colorectal Cancer Unit, Watford Road, Harrow HA1 3UJ, London, UK. i.talbot@cancer.org.uk
Telephone: +86-10-66937954 **Fax:** +86-10-68181689
Received: 2003-03-02 **Accepted:** 2003-05-16

Abstract

AIM: To describe the correlation between innunostaining patterns of p16 and CDK4 and prognosis in colorectal carcinoma.

METHODS: Paraffin sections of 74 cases of colorectal carcinoma were analysed immunohistochemically for expression of p16 and CDK4 proteins.

RESULTS: Most carcinomas showed stronger p16 and CDK4 immunostaining in the cytoplasm than the adenomas or the adjacent normal mucosa. Strong immunostaining of p16 was a predictor for better prognosis whereas strong cytoplasmic immunostaining of CDK4 was a predictor for poor prognosis. Both p16 and CDK4 immunostainings were correlated with histological grade or Dukes' stage.

CONCLUSION: These results support the experimental evidence that interaction of expression of p16 and CDK4 may play an important role in the Rb/p16 pathway, and the expression paterns of CDK4 and p16 may be imperative in the development of colorectal carcinoma, thus becoming a new prognostic marker in colorectal cancer.

Zhao P, Hu YC, Talbot IC. Expressing patterns of p16 and CDK4 correlated to prognosis in colorectal carcinoma. *World J Gastroenterol* 2003; 9(10): 2202-2206
http://www.wjgnet.com/1007-9327/9/2202.asp

INTRODUCTION

p16 gene, an important tumor suppressor gene, regulates cell proliferation negatively through inhibition of the kinase activity of cyclin-dependent kinase 4/6 (CDK4/6), which promotes phosphorylation and therefore inactivation of a very important tumor suppressor product, the retinoblastoma (Rb) gene protein[1-4]. The Rb/p16 tumor-suppressor pathway is abrogated frequently in multiple types of human tumors, either through inactivation of Rb or p16 tumor-suppressor protein, or through overexpression of cyclin D1 or cyclin-dependent kinase 4 (CDK4) oncoproteins. But no deletion and only quite a low frequency of mutation on p16 gene have been found in colorectal cancer since this gene was identified in 1994[1,5]. CpG islands are areas rich in CpG dinucleotides, which are found within the promotors of about 60 % of human genes. These CpG islands normally lack DNA methylation, regardless of the expression status of the gene[6]. Methylation of promotor usually leads to irreversible inhibition of gene transcription[7]. It has become apparent that *de novo* methylation is an important alternate mechanism to code region mutation for inactivating tumor suppressor genes during neoplasia[8-11]. Herman *et al*.[9] previously reported that there was methylation of p16 gene in 40 % of primary colorectal cancers and 92 % of colorectal cancer cell lines, in which all the p16 genes were inactivited by Southern analysis. Gonzalez-Zulueta *et al*.[10] found the evidence of methylation of the 5' CpG island not only in cancer tissues but also in normal colonic tissues by the more sensitive PCR-based assay, in which methylation of p16 exon 1 was detected in 1 of 10 (10 %) colon carcinomas and methylation of p16 exon 2 was detected in 7 of 10 (70 %) colon cancers. It is interesting that in 50 % of the colon normal/tumor matched cases, p16 was methylated and not expressed in the normal tissues but unmethylated and highly expressed in the tumor tissues. It also suggested that methylation of exon 1, but not exon 2, of p16 was associated with transcriptional silencing although the CpG island in exon 2 of p16 underwent extensive *de novo* methylation in colorectal carcinoma. More recently, Ahuja *et al*.[12] found that 16 (34 %) of 47 colorectal cancers exhibited methylation in exon 1 of the p16 gene, which was associated with microsatellite instability. Transcriptional silencing of p16 gene could be due to either gene deletion or methylation in exon 1. In either event, there would be no expression product in the cells. Therefore, we used an immunohistochemical method to detect p16 protein level *in situ* and compared with its binding oncoprotein, CDK4, as a simple way to investigate their possible interaction in the development and prognosis of colorectal carcinoma. We also detected the mRNA levels of both p16 and CDK4 genes and checked the methylation status on the promoter region of p16 gene to confirm their expression results in immunocytochemistry.

MATERIALS AND METHODS

Colorectal carcinoma

Seventy-four cases of colorectal carcinoma were randomly and retrospectively selected from the files of the Academic Department of Pathology, St. Mark' s Hospital, London, UK and the Department of Pathology, the former West China University of Medical Sciences, China. Specimens obtained at surgery were routinely fixed in 10 % neutral formalin and embedded in paraffin. The clinical stage was determined according to the Dukes' stages A, B and C. The histological grade of tumors was also determined according to the WHO criteria as follows: grade I as well differentiated, grade II as moderately differentiated, and grade III as poorly differentiated. Follow-up data on 5-year survival rate in 32 cases were available for further analysis with variables.

Immunohistochemical staining

Immunohistochemical staining for p16 and CDK4 was performed according to the standard ABC method except that the pressure for cooking procedure was used for antigen retrieval pretreatment[13, 14]. Serial 4 μm thick sections were cut and dewaxed in xylene and rehydrated in a graded ethanol series. The sections were immersed in 3 % hydrogen peroxide in methanol for 15 minutes to block endogenous peroxidase activity. and rinsed in running water. After that, sections were immersed in boiling 1 mM EDTA-NaOH (pH 8.0) buffer in a pressure cooker. The pressure cooker was then sealed and brought to full pressure. The heating time was 2 minutes which began only when full pressure was reached. At 2 minutes, the cooker was depressured and cooled under running water. The lid was then removed, and the hot buffer was flushed out with cold water from a running tap. The cooled sections were washed twice in PBS before immunohistochemical staining, then immersed in 0.05 % avidin for 30 minutes to block any possible endogenous biotin exposed to heating. Prior to immunohistochemical staining, the sections were first incubated with 10 % horse serum for monoclonal antibody and 10 % goat serum for polyclonal antibody respectively for 15 minutes to block non-specific binding. The primary monoclonal mouse antibody against human p16 protein (Pierce, USA) and polyclonal rabbit antibody against human CDK4 protein (Santa Cruz Biotechnology, USA) were diluted in 200 with 0.01 M PBS (pH 7.2), respectively. Then the sections were allowed to react by the standard ABC method using a VECTASTAIN Elite PK-6100 kit (Vector Labratories, Inc., USA), as directed by the manufacturer. A previously known positive pancreatic carcinoma was used as a positive control. The primary antibody was replaced by 0.01 M PBS or 10 % serum as a negative control. Normal colon mucosal tissue was used as a normal control.

Evaluation of score

The slides were examined and data regarding staining positivity were recorded before the clinical outcome was available. When p16 or CDK4 protein expression was scored, both the extent and intensity of immunopositivity were considered, according to Hao *et al*[15]. The intensity of positivity was scored as follows: 0 as negative, 1 as weak, 2 as moderate, 3 as strong as normal liver. The extent of positivity was scored as follows: 0 <5, 1>5-25 %, 2>25-50 %, 3>50-75 %, and 4>75 % of the tumor cells in the respective lesions. The final score was determined by multiplying the intensity of positivity and the extent of positivity scores, yielding a range from 0 to 12. Scores 9-12 were defined as strong staining pattern (++), 5-8 as weak staining pattern (+), and 0-4 as markedly reduced or negative expression (-).

RNA extraction and RT-PCR

Total RNA was isolated from the frozen tissues of 10 paired normal and tumor samples using the total RNA isolation system (Promega) and treated with RNase-free DNase I (GeneHunter). Equal amount (0.2 μg) of total RNA from each sample was added into the access RT-PCR system (Promega) which carried on both cDNA syntheses by reverse transcription and PCR in a same tube with a total volume of 25 μl reaction solution according to the manufacturer' s directions. The primer pairs used to amplify p16 and CDK4 genes were as follows. The sequence of p16 sense primer was 5' -CCCGCTTTCGTAGTTTTCAT-3' and that of antisense primer was 5' -TTATTTGAGCTTTGGTTCTG-3' [16] and that of CDK4 sense primer was 5' -ATGGCTGCCACTCGATAT GAACCC-3' and antisense primer, 5' -GTACCAGAGCGT AACCACCACAGG-3' [17]. In addition, primers for glyceraldehyde 3-phosphate dehydrogenase (G3PDH) gene were used as an internal control to ensure the quality of the templet RNA and reagents in reactions. The sequence of sense primer was 5' -TGGTATCGTGGAAGGACTCATGAC-3' and antisense primer was 5' -ATGCCAGTGAGCTTCCCGTT CAGC-3' [16]. cDNA for each sample was synthesized at 48 ℃ for 45 min, followed by at 94 ℃ for 2 min to inactivate reverse transcriptase and was subjected to 40 cycles of amplification under the conditions described before[16,17] except for modified extension step during each cycle at 68 ℃ for 2 min according to the access RT-PCR system' s direction. Water controls, including primers and all reagents except for RNA in PCR reactions, were setup for potential DNA contamination.

Methylation-specific PCR

Samples from 24 cases of colorectal carcinoma with residual adenoma were selected for DNA extraction. DNA was extracted from these cases according to the conventional methods. The methylation status on the promoter region of p16 was assessed by methylation-specific PCR (MSP) as described previously[9] Genomic DNAs from the primary tumors were subjected to bisulfate modification using the CpGenome DNA modification kit (Intergen, New York, NY). Treatment of genomic DNA with sodium bisulfate converted unmethylated cytosines (but not methylated cytosines) to uracil, which was then converted to thymidine during the subsequent PCR step, yielding sequence differences between methylated DNA. PCR primers distinguishing these methylated and unmethylated DNA sequences were used. Primer sequences of p16 genes[9] for both the methylated and unmethylated forms were 5' -TTATTAGAGGGTGGGGCGGATCGC-3' /5' -GACCCCGAACCGCGACCGTAA-3' and 5' -TTATTAGAGGGTGGGGTGGATTGT-3' /5' -CAACCCCAAACCACAACCATAA-3' , with annealing temperature at 65 ℃ and at 60 ℃, and the expected PCR product sizes were 150 bp and 151 bp, respectively. For PCR amplification, 2 μl of bisulfate-modified DNA was added in a final volume of 25 μl PCR mixture containing 1×PCR buffer, $MgCl_2$, deoxynucleotide triphosphates, and primers (100 pmol each per reaction), and 1 unit of AmpiTaq Gold (Applied Biosystems, Branchburg, NJ). Amplification was performed at 95 ℃ for 12 min, 35 cycles at 95 ℃ for 1 min, the specific annealing temperature for both methylated and unmethylated at 65 ℃ and at 60 ℃ for 1 min, and at 72 ℃ for 1 min, followed by a final 7-min extension at 72 ℃. PCR products (15 μl) were loaded onto a 10 % nondenaturing polyacrylamide gel, stained with ethidium bromide after 2 hours of electrophoresis, visualized under UV illumination. MSP for all samples was repeated to confirm their methylation status.

Statistical analysis

Fisher' s exact test (two sided) and Pearson Chi square test for trends in proportions were used to assess the associations between Fhit expression and pathological indices. A $P<0.05$ was considered statistically significant.

RESULTS

The results are summarized in Tables 1-2.

The 5-year survival of the 32 patients according to the available data was significantly shorter in patients with Dukes' C tumors than in those with Dukes' A and B tumors ($P<0.01$).

p16 expression in colorectal carcinoma

In 61 patients in whom non-neoplastic mucosa was detected adjacent to the carcinoma, weak p16 expression was observed in the nuclei and moderate p16 expression only in the cytoplasm around nuclei. Most of the cytoplasm of goblet cells filled with

mucus was negative (Figures 1A, B). Of the 74 specimens examined, 73 (98.6 %) were p16-positive (Table 1). Expression of p16 was almost always observed in the cytoplasm but only sporadically in the nuclei. Of the p16 positive specimens, 53 showed a strong expression pattern and 20 a weak expression pattern (Figure 1C). Strong p16 expressions were detected in 15 (78.9 %) patients who survived more than 5 years, while weak p16 expressions were detected in 8 (61.5 %) patients who survived less than 5 years after operation (Table 1). The prognosis was significantly better in patients with tumors in strong expression pattern of p16 (P<0.001).

Table 1 Relationship between p16 expression and clinicopathological features

Clinicopathological features	No. of patients	p16 Immunostaining patterns		
		Strong	Weak	Negative
Dukes' stage				
A	23	16	7	0
B	22	16	6	0
C	29	21	7	1
Histological grade				
I	24	17	7	0
II	41	30	10	1
III	9	6	3	0
Total	74	53	20	1
5-year survival rate				
Alive	20	15	5	0
Dead	12	4	8	0
Total	32	19	13	0

CDK4 expression in colorectal carcinoma

In 49 of 61 non-neoplastic mucosaea adjacent to the carcinoma, CDK4 nuclear and cytoplasmic immunoreactivity was a little weaker than the p16 staining, but otherwise identical. The remaining 12 were negative. Expression of CDK4 was observed predominantly in the cytoplasm (Figure 1D). All the 74 specimens showed CDK4 expression (Table 2). Of the CDK-positive specimens, 33 showed a strong expressing pattern and 41 yielded a weak expressing pattern. Tumors with strong CDK4 expression were found in 4 (28.6 %) patients who had survived for more than 5 years after operation, whereas those with weak CDK4 expression were found only in 2 (11.1 %) patients who died within 5 years after operation. The prognosis was significantly poorers in patients with cancers in strong expression of CDK4 (P<0.001).

Table 2 Relationship between CDK4 expression and clinicopathological features

Clinicopathological features	No. of patients	CDK4 Immunostaining patterns		
		Strong	Weak	Negative
Dukes' stage				
A	23	9	14	0
B	22	10	12	0
C	29	14	15	0
Histological grade				
I	24	8	16	0
II	41	19	22	0
III	9	6	3	0
Total	74	33	41	0
5-year survival rate				
Alive	20	4	16	0
Dead	12	10	2	0
Total	32	14	18	0

Correlation between p16 and CDK4 expression

Of the 74 tumors with CDK4 expression (strong in 33, weak in 41), p16 expression was also found in all but one (strong in 53, weak in 20). There was a significantly reverse correlation between p16 and CDK4 expression patterns (P<0.001).

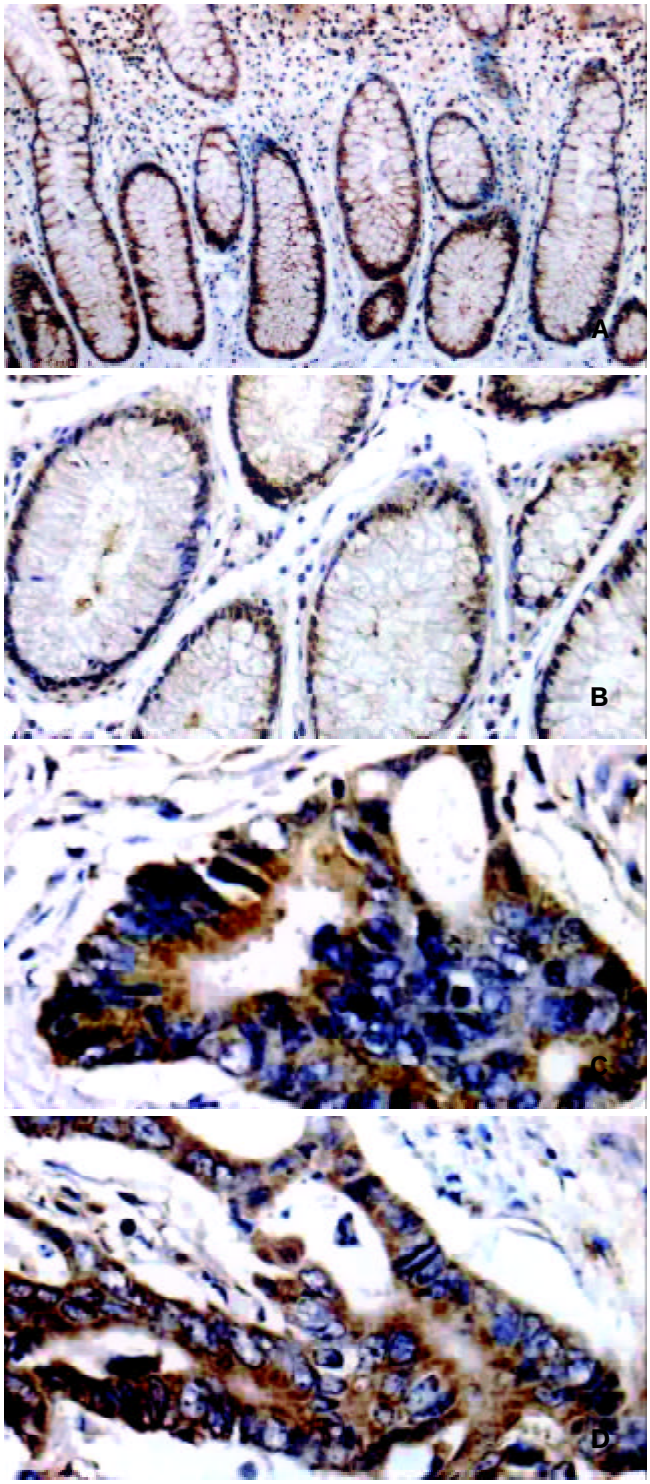

Figure 1 Expression patterns for p16 and CDK4 gene proteins. A, B: nuclear/cytoplasmic pattern of p16 protein in normal crypts (SP×100, 200), C: overexpression pattern of p16 in the cytoplasm of colon cancer cells (SP×400), D: overexpression pattern of CDK4 in the cytoplasm of colon cancer cells (SP×400).

Correlation between p16 or CDK4 expression and clinicopathological features

In our study, a significant correlation was found between p16 or CDK4 expression patterns and the tumor stage (P<0.001;

P<0.001) or the histological grade (*P*<0.001; *P*<0.001) (Tables 1, 2). The prognosis was significantly poorer in patients with weak p16 expression pattern (*P*<0.001), or with strong CDK4 expression pattern (*P*<0.001).

Results of RT-PCR and MSP

We investigated the mRNA expression of p16 and CDK4 genes in 10 frozen normal-tumor paired tissues. The results showed that the level of mRNA expressions of p16 (9/10) and CDK4 (10/10) of cancer tissues rose in accordence with that of proteins of p16 and CDK4 in immunostaining (Figures 2A, B). We also determined the frequency of promoter methylation of p16 gene by MSP-PCR, but the result showed no positively methylated signal in all the 24 cases of colorectal carcinoma with residual adenoma (Figure 2C).

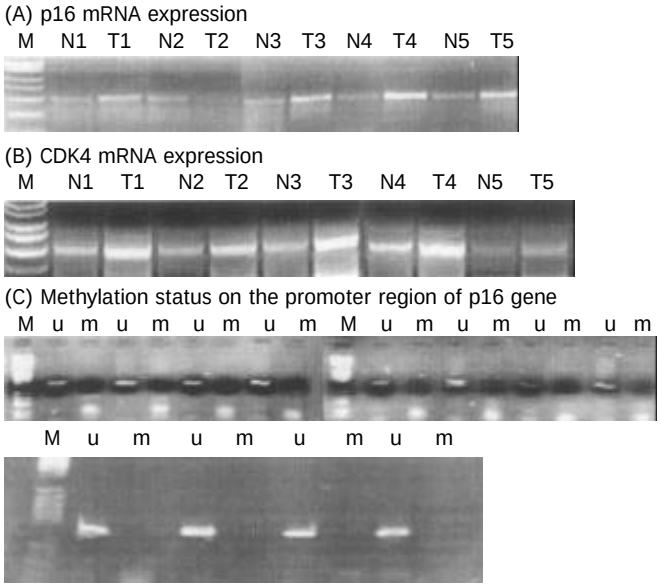

Figure 2 Results in p16 and CDK4 mRNA expressions as well as p16 gene methylation status on the promoter region. (A) and (B): mRNA levels of both p16 and CDK4 genes were elevated in colorectal carcinoma (T), compared with their matched normal (N) tissues. (C) There was no methylation detected on p16 promoter region in all 24 cases of cancer tissue with residue adenoma. u: unmethylated, m: methylated, M: molecular marker (PBR322 / Hae III).

DISCUSSION

Loss of expression of proteins such as p16 could occur as a consequence of either homozygous gene deletion or gene methylation. One aim of this study was to assess the extent to which both homozygous deletion and methylation on promoter region of p16 gene occurred with loss of gene expression in colorectal carcinoma. All carcinomas but one in this study showed the expression of p16 protein, confirmed not only by immunocytochemistry but also by RT-PCR and MSP, suggesting that loss of p16 gene expression is infrequent in primary colorectal carcinoma. The localization of p16 protein was similar to that of CDK4, almost always in the cytoplasm of adenocarcinoma cells. This indicates that the main site of interaction between p16 and CDK4 in adenocarcinoma cells is the cytoplasm. This contrasts with the localization of p16 protein in astrocytoma[18], in which nuclear expression is always more intense than any cytoplasmic expression. Based on these findings, our results indicate that CDK4 may contribute to phosphorylation of pRB, and to the loss of regulating function of p16 protein in nuclei, leading to the development of colorectal carcinoma. Induction of p16 overexpression would act as a brake at G1/S transition through pRB phosphorylation by CDK4 overexpression on the one hand, but predominant mislocation or only in cytoplasm might also imply the function of p16 in the nuclei, its ability to regulate transcriptions of other important genes related to proliferation and angiogenesis[19-21], was lost in colorectal carcinogenesis on the other hand.

The previous results[22-26] suggest that the deletion or mutational inactivity of both p16 and Rb proteins may be a rare event in cervical carcinogenesis. Moreover, overexpression of the p16 protein may be a useful diagnostic marker for cervical neoplastic lesions on routine laboratory screening. It was proposed that the expression of two viral oncogenes, E6 and E7, in epithelial stem cells be required to initiate and maintain cervical carcinogenesis and result in significant overexpression of the cellular p16 protein. Since this protein was not expressed in normal cervical squamous epithelia, screening for p16 over-expressing cells could specifically identify dysplastic lesions, and significantly reduced the inter-observer disagreement of the conventional cytological or histological tests. The similar results[28-30] have also been reported in prostate cancer, gastrointestinal stromal tumor and gastritis, in which overexpression of p16 in high grade prostate intraepithelial neoplasia (HGPIN) and cancer was correlated with, but independent of, pathological stage and was associated with early relapse in cancer patients treated with radical prostatectomy. Overexpression of p16 in HGPIN was also an independent predictor of disease relapse and increased the risk of recurrence 2.24-fold, providing the first evidence for a prognostic marker in HGPIN. The aberrant cytoplasmic expression as well as overexpression of p16 in colorectal carcinoma might be due to its binding to CDK4, CDK6 and some unknown proteins, thereby forming a larger volume of molecule which is uneasy to pass through the nuclear membrane. Nuclear expression of p16 would therefore imply extra unbound p16[5, 19], which might play other important roles in inhibiting transcription of genes related to tumor progression in the nuclei. For instance, VEGF for angiogenesis is besides or independent of binding CDK4/6[18-20]. It could be that CDK4 overexpression is an initial event, which is followed by a reactive overexpression of p16 in colorectal carcinoma, thus the oncoprotein function of CDK4 is inhibited to some extent by binding to p16. In our study, the histological grade, Dukes' stage and prognosis in colorectal carcinoma were closely related to p16 or CDK4 expression (*P*<0.001), respectively, suggesting that the expression of p16 or CDK4 protein may be a useful diagnostic and prognostic marker for colorectal neoplastic lesions. A more extended study is required to confirm the value of aberrant cytoplasmic expression or overexpression of p16 protein as a prognostic marker.

REFERENCES

1 **Kamb A,** Gruis NA, Weaver-Feldhaus J, Liu Q, Harshman K, Tavtigian SV, Stockert E, Day RS 3rd, Johnson BE, Skolnick MH. A cell cycle regulator potentially involved in genesis of many tumor types. *Science* 1994; **264:** 436-440

2 **Serrano M,** Hannon GJ, Beach D. A new regulatory motif in cell-cycle control causing specific inhibition of cyclin D / CDK4. *Nature* 1993; **366:** 704-707

3 **Marx J.** New tumor suppressor may rival p53. *Science* 1994; **264:** 344-345

4 **Nobori T,** Miura K, Wu DJ, Lois A, Takabayashi K, Carson DA. Deletions of the cyclin-dependent kinase-4 inhibitor gene in multiple human cancers. *Nature* 1994; **368:** 753-756

5 **Okamoto A,** Demetrick DJ, Spillare EA, Hagiwara K, Hussain SP, Bennett WP, Forrester K, Gerwin B, Serrano M, Beach DH, Harris CC. Mutations and altered expression of $p16^{INK4}$ in human cancer. *Proc Natl Acad Sci U S A* 1994; **91:** 11045-11049

6 **Bird AP.** CpG-rich islands and the function of DNA methylation. *Nature* 1986; **321:** 209-213

7 **Eden S,** Cedar H. Role of DNA methylation in the regulation of transcription. *Curr Opin Genet Dev* 1994; **4:** 255-259

8 **Sakai T,** Toguchida J, Ohtani N, Yandell DW, Rapaport JM, Dryja TD. Allele-specific hypermethylation of the retinoblastoma tumor-suppressor gene. *Am J Hum Genet* 1991; **48:** 880-888

9 **Herman JG,** Merlo A, Mao L, Lapidus RG, Issa JP, Davidson NE, Sidransky D, Baylin SB. Inactivation of the CDKN2/p16/MTS1 gene is frequently associated with aberrent DNA methylation in all common human cancers. *Cancer Res* 1995; **55:** 4525-4530

10 **Gonzalez-Zulueta M,** Bender CM, Yang AS, Nguyen T, Beart RW, Van Tornout JM, Jones PA. Methylation of the 5'CpG island of the p16/CDKN2 tumor suppressor gene in normal and transformed human tissues correlates with gene silencing. *Cancer Res* 1995; **55:** 4531-4535

11 **Herman JG,** Latif F, Weng Y, Lerman MI, Zbarl B, Liu S, Samib D, Duan DS, Gnarra JR, Linehan WM, Baylin SB. Silencing of the VHL tumor-suppressor gene by DNA methylation in renal carcinoma. *Proc Natl Acad Sci U S A* 1994; **91:** 9700-9704

12 **Ahuja N,** Mohan AL, Li Q, Stolker JM, Herman JG, Hamilton SR, Baylin SB, Issa JP. Association between CpG island methylation and microsatellite instability in colorectal cancer. *Cancer Res* 1997; **57:** 3370-3374

13 **Norton AJ,** Jordan S, Yeomans P. Brief, high-temperature heat denaturation (pressure cooking): a simple and effective method of antigen retrieval for routinely processed tissues. *J Pathol* 1994; **173:** 371-379

14 **Pileri SA,** Roncador G, Ceccarelli C, Piccioli M, Briskomatis A, Sabattini E, Ascani S, Santini D, Piccaluga PP, Leone O, Damiani S, Ercolessi C, Sandri F, Pieri F, Leoncini L, Falini B. Antigen retrieval techniques in immunohistochemistry: comparison of different methods. *J Pathol* 1997; **183:** 116-123

15 **Hao XP,** Willis JE, Pretlow TG, Rao JS, MacLennan GT, Talbot IC, Pretlow TP. Loss of fragile histidine triad expression in colorectal carcinomas and premalignant lesions. *Cancer Res* 2000; **60:** 18-21

16 **Chen YJ,** Shih LS, Chen YM. Quantitative analysis of CDKN2, p53 and retinoblastoma mRNA in human gastric carcinoma. *Int J Oncol* 1998; **13:** 249-254

17 **Ohtsuki F,** Yamamoto M, Nakagawa T, Tanizawa T, Wada H. Granulocyte-macrophage colony-stimulating factor abrogates transforming growth factor-b1-mediated cell cycle arrest by upregulating cyclin D2/Cdk6. *Br J Haematol* 1997; **98:** 520-527

18 **Rao LS,** Miller DC, Newcomb EW. Correlative immunohistochemistry and molecular genetic study of the inactivation of the $p16^{INK4A}$ genes in astrocytomas. *Diagn Mol Pathol* 1997; **6:** 115-122

19 **Emig R,** Magener A, Ehemann V, Meyer A, Stilgenbauer F, Volkmann M, Wallwiener D, Sinn HP. Aberrant cytoplasmic expression of the p16 protein in breast cancer is associated with accelerated tumour proliferation. *Br J Cancer* 1998; **78:** 1661-1668

20 **Harada H,** Nakagawa K, Iwata S, Saito M, Kumon Y, Sakaki S, Sato K, Hamada K. Restoration of wild-type p16 down-regulates vascular endothelial growth factor expression and inhibits angiogenesis in human gliomas. *Cancer Res* 1999; **59:** 3783-3789

21 **Bartkova J,** Lukas J, Guldberg P, Alsner J, Kirkin AF, Zeuthen J, Bartek J. The P16-cyclinD/Cdk4-PRb pathway as a functional unit frequently altered in melanoma pathogenesis. *Cancer Res* 1996; **56:** 5475-5483

22 **Klaes R,** Friedrich T, Spitkovsky D, Ridder R, Rudy W, Petry U, Dallenbach-Hellweg G, Schmidt D, von Knebel Doeberitz M. Overexpression of p16(INK4A) as a specific marker for dysplastic and neoplastic epithelial cells of the cervix uteri. *Int J Cancer* 2001; **92:** 276-284

23 **Klaes R,** Benner A, Friedrich T, Ridder R, Herrington S, Jenkins D, Kurman RJ, Schmidt D, Stoler M, von Knebel Doeberitz M. p16INK4a immunohistochemistry improves interobserver agreement in the diagnosis of cervical intraepithelial neoplasia. *Am J Surg Pathol* 2002; **26:** 1389-1399

24 **von Knebel Doeberitz M.** New molecular tools for efficient screening of cervical cancer. *Dis Markers* 2001; **17:** 123-128

25 **Sano T,** Oyama T, Kashiwabara K, Fukuda T, Nakajima T. Immunohistochemical overexpression of p16 protein associated with intact retinoblastoma protein expression in cervical cancer and cervical intraepithelial neoplasia. *Pathol Int* 1998; **48:** 580-585

26 **Negri G,** Egarter-Vigl E, Kasal A, Romano F, Haitel A, Mian C. p16INK4a is a useful marker for the diagnosis of adenocarcinoma of the cervix uteri and its precursors: an immunohistochemical study with immunocytochemical correlations. *Am J Surg Pathol* 2003; **27:** 187-193

27 **Mc Cluggage WG,** Jenkins D. p16 immunoreactivity may assist in the distinction between endometrial and endocervical adenocarcinoma. *Int J Gynecol Pathol* 2003; **22:** 231-235

28 **Henshall SM,** Quinn DI, Lee CS, Head DR, Golovsky D, Brenner PC, Delprado W, Stricker PD, Grygiel JJ, Sutherland RL. Overexpression of the cell cycle inhibitor p16INK4A in high-grade prostatic intraepithelial neoplasia predicts early relapse in prostate cancer patients. *Clin Cancer Res* 2001; **7:** 544-550

29 **Schneider-Stock R,** Boltze C, Lasota J, Miettinen M, Peters B, Pross M, Roessner A, Gunther T. High prognostic value of p16INK4 alterations in gastrointestinal stromal tumors. *J Clin Oncol* 2003; **21:** 1688-1697

30 **Shirin H,** Hibshoosh H, Kawabata Y, Weinstein IB, Moss SF. p16Ink4a is overexpressed in *H pylori*-associated gastritis and is correlated with increased epithelial apoptosis. *Helicobacter* 2003; **8:** 66-71

Edited by Ma JY and Wang XL

P.O.Box 2345, Beijing 100023,China
Fax: +86-10-85381893
E-mail: wjg@wjgnet.com www.wjgnet.com

World J Gastroenterol 2003;9(10):2207-2210
World Journal of Gastroenterology
 ISSN 1007-9327

• COLORECTAL CANCER •

Prognostic factors in 165 elderly colorectal cancer patients

Ke-Jun Nan, Hai-Xia Qin, Guang Yang

Ke-Jun Nan, Hai-Xia Qin, Department of Oncology, First Hospital of Xi' an Jiaotong University, Xi' an 710061, Shaanxi Province, China
Guang Yang, Medical College, Xi' an Jiaotong University, Xi' an 710061, Shaanxi Province, China
Correspondence to: Ke-Jun Nan, Department of Oncology, First Hospital of Xi' an Jiaotong University, 1 Jiankang Xilu, Xi' an 710061, Shaanxi Province, China. qinhaixia100925@sina.com.cn
Telephone: +86-29-5324086 **Fax:** +86-29-5324086
Received: 2003-06-28 **Accepted:** 2003-07-24

Abstract

AIM: To analyse the prognostic factors in 165 colorectal patients aged ⩾70.

METHODS: One hundred and sixty-five elderly patients with colorectal cancer diagnosed by histology were entered into the retrospective study between 1994 and 2001. Patients were given optimal operation alone, chemotherapy after operation, or chemotherapy alone according to tumor stage, histology, physical strength, and co-morbid problems. Survival rate was calculated by Kaplan-Meier method, and compared with meaningful variances by Log-rank method. Prognostic factors were analyzed by Cox regression.

RESULTS: The 1,2,3,4,5 year survival rate (all-cause mortality) was 87.76 %, 65.96 %, 52.05 %, 42.77 %, 40.51 %, respectively. The mean survival time was 41.89±2.33 months (95 % CI: 37.33-46.45 months), and the median survival time was 37 months. Univariate analysis showed that factors such as age, nodal metastasis, treatment method, Duke's stage, gross findings, kind of histology, and degree of differentiation had influences on the survival rate. Multivariate analysis showed that factors such as treatment method, Duke's stage, kind of histology and degree of differentiation were independent prognostic factors.

CONCLUSION: This study suggests that the prognosis of elderly colorectal cancer patients is influenced by several factors. Most of elderly patients can endure surgery and/or chemotherapy, and have a long-time survival and good quality of life.

Nan KJ, Qin HX, Yang G. Prognostic factors in 165 elderly colorectal cancer patients. *World J Gastroenterol* 2003; 9(10): 2207-2210
http://www.wjgnet.com/1007-9327/9/2207.asp

INTRODUCTION

Colorectal cancer (CRC) is one of the most common malignant tumors in the world[1-5]. In China it is the fifth of malignant tumor, and the third of alimentary tract malignant tumor[6, 7]. Its incidence rises with increasing age[8,9]. Currently, the majority of colon and rectum tumors arise in patients aged 70 and over. Improvements in public health, nutrition and the prevention and treatment measures have prolonged the life of elderly individuals. The average life expectancy of a 70-year-old man can be prolonged ten years and of a 70-year-old woman 15 years. As a result, there will be a rise in the prevalence of CRC in elderly patients in the coming decades. But the elderly always have some co-morbid problems, and their clinical, pathological characteristics are different from young patients, so how to rationally treat CRC cancer of the old becomes very important.

MATERIALS AND METHODS

Clinical data

There were 205 elderly colorectal patients (aged ⩾70) in the First Hospital of Xi' an Jiaotong University from 1994 to 2001, accounting for 12.1 % of the total colorectal cancer patients. One hundred and sixty-five cases were enrolled into the study that had full histology, clinical and follow-up records. There were 105 males, and 60 females (sex ratio was 1.75:1). All patients were aged from 70 to 91 (the median 74 years), and the mean age was 74.67±0.54 years. The latent period ranged from 1 day to 4.5 years, and the mean latent time was 6.21±0.69 months. One hundred and three tumors were located in colon, and 68 in rectum, respectively, including 3 simultaneous double-tumors and 3 different time double-tumors. In the 129 resection specimens, the dimension was smaller than 5 cm in 74 and ⩾5 cm in 55. Forty-six patients had adenomatous polyps simultaneously. One hundred and forty-five had co-morbidity, among them 73 had cardiovascular diseases, 24 respiratory tract disorders, and 17 cerebral vessel disorders, 16 diabetes mellitus, and 15 other diseases.

Treatment methods

Operation 118 Duke's A, B, C, D stage patients received curative resection, 27 received palliate resection, and 4 received only emergency surgery. 16 cases received no surgery because of their reluctance or bad status.

Chemotherapy Patients who conformed with the requirements were given chemotherapy: PS 0-2 with Duke's C or D or high risk Duke's B tumors (having any characteristic such as perforated or obstructed tumors, T4 tumors, poor differentiation in histology, extra-mural vascular invasion, or mucinous differentiation). They were given 5-Fu/CF+L-OHP every 21 days, L-OHP 80-100 mg· m^{-2} >2 h iv d_1, LV 200 mg· m^{-2}· d^{-1} 2 h iv d_{1-5}, 5-Fu 400 mg· m^{-2}· d^{-1} iv d_{1-5}. Forty-seven patients with Duke's B and C tumors had 197 cycles of chemotherapy. Patients with Duke's D tumor accepted 154 cycles of chemotherapy. Among them, 15 cases received post-operation chemotherapy, and 28 cases pure chemotherapy.

Statistical analysis

Kaplan-Meier method was used to calculate survival rate, and Log rank test was used in the univariate analysis. Cox regression Model was used in the multivariate analysis. The SPSS 10.0 for windows was used for all the statistical analyses.

RESULTS

General information

In this study, the 1, 2, 3, 4, 5 year survival rate (all-cause mortality) was 87.76 %, 65.96 %, 52.05 %, 42.77 %, 40.51 %, respectively. The mean survival time was 41.89±2.33 months (95 % CI: 37.33-46.45 months), and the median survival time

was 37 months. The mortality of surgery was 2.8 % (4/145), and death occurred due to perforation, pulmonary infection, and cachexia, respectively. The rate of chemotherapy side effect was 87.3 %, but besides 1 IV^0 diarrhea and 1 IV^0 myelosupression, all others were 0-III^0.

Univariate analysis

There were several risk factors by univariate analysis as shown in Table 1. But other factors had nothing to do with prognosis, such as gender, latent period, tumor size, co-morbid problems, precancerous lesion, and bloody stool.

Table 1 Results of univariate analysis

Variance	*n*	1 year survival rate (%)	3 year survival rate (%)	5 year survival rate (%)	*P* value
Age					0.0332
70-75	96	91.49	59.40	48.62	
75-91	69	82.58	41.79	28.84	
Treatment					
Curative resection+ chemotherapy	47	95.67	78.24	60.72	
Curative resection	71	95.65	62.62	55.01	
Palliate resection + chemotherapy	21	71.43	11.11	0	<0.005
Palliate resection	6	50.00	0	0	
Chemotherapy	16	75	0	0	
Emergency surgery	4	0	0	0	
Duke's stage					
A	8	100	75	37.5	
B	35	100	79.16	64.57	<0.005
C	72	97.16	70.55	56.05	
D	50	63.88	6.74	0	
Gross finding					
Ulcer form	66	92.40	64.88	53.52	
Projection form	57	92.88	58.86	49.15	<0.005
Infiltration form	6	100	50	33.33	
Type of histology					
Tubular adenoma	130	91.41	55.33	44.77	
Mucinous adenocarcinoma	23	73.91	29.12	23.29	0.0018
Other types	12	75.0	56.25	0	
Differentiation of tumor					
High	10	100	74.07	44.44	
Middle	123	95.87	57.84	47.55	<0.005
Low	32	52.78	22.62	14.14	
Nodular metastasis					
No	43	100	79.62	67.24	0.0008
Yes	122	83.52	42.69	31.21	

Table 2 Results of multivariate analysis for elderly colorectal cancer

Factors	Regression coefficient	Standard error	OR	OR 95 % CI		*P value*
				Lower	Upper	
Treatment method	2.028	0.356	7.603	3.782	15.284	0.000
Duke's stage	0.648	0.295	0.523	0.293	0.933	0.028
Type of histology	-0.824	0.248	0.439	0.270	0.713	0.003
Differentiation of tumor	-0.850	0.246	0.427	0.264	0.692	0.016

Value: resection + chemotherapy=0, resection only=1. Duke's A+B stage=0, Duke's C+D stage=1. Other type=0, tubular adenoma=1. Low differentiation=0, middle and high differentiation=1.

Multi-variate analysis

The factors associated with the risk of colorectal cancer at $P<0.05$ were furthered tested using backward stepwise conditional Cox regression. The final model consisted of the variables having a significant association with the risk of elderly colorectal cancer at $P<0.05$. The results are shown in Table 2.

DISCUSSION

Though the number of elderly CRC patients is increasing, study about their treatment is rare, especially in China. A number of factors may account for the reluctance to receive operation and chemotherapy in elderly CRC patients. For example, family members do not want them to accept operation and chemotherapy in their old age, co-morbid problems may complicate or even preclude operation and chemotherapy, elderly patients may be more susceptible to side-effects of operation and chemotherapy which may decrease their quality of life[10], studies on the efficacy and toxicity of chemotherapy in elderly group are limited[11,12].

Treatment method is the most important prognostic index of elderly CRC in this study. Univariate and multivariate analyses showed that operation combined with post-operation chemotherapy was superior to resection only and chemotherapy only. The curative resection rate of the 165 patients was 71.52 % (118/165), and the total resection rate was 87.88 % (145/165). Operation mortality rate was 2.8 %. So it is evident that age is not the contraindication for surgery[13,14]. Resection should still be the first choice of treatment for elderly colorectal patients[15]. Patients who can endure operation after pre-operation management should receive operation in order to decrease the tumor burden. But acute abdomen is frequent in elderly CRC patients, and emergency operation is frequent accordingly, so active peri-operation preparations are necessary[16,17], such as the selection of optimal anesthesia and operation method to make them more endurable to operation, carefully nursing and supporting to reduce the opportunity of complication. Suitable chemotherapy can prolong the life of advanced patients, and improve their quality of life[18]. In this study, the patients who received chemotherapy lived longer than those who only received operation, and there were no severe side effects. It is obvious that elderly patients can survive chemotherapy and have a long-time survival and good quality of life, if an optimal chemotherapy scheme is given[19-23]. Also, because most of CRC relapse or transfer in the following 3 years of operation, it is necessary to give patients adjuvant chemotherapy[24, 25]. As to the elderly patients, several factors must be taken into consideration when chemotherapy is given, such as suitable chemotherapy regimen with good efficiency and low side effects[26,27], the importance of the first cycle[28], liver and kidney function testing and blood cell calculation before every cycle with heart and lung function evaluated if necessary, active support simultaneously, less or no anti-HT3 used to decrease the rate of constipation, long-cycle and convenient scheme to decrease the in-patient time, and changing scheme when it is inefficient[29].

In this study, univariate and multivariate analyses showed that the patients aged 70-75 years had a longer survival than those aged 75-91 years, which conformed with the study that aging was a risk factor for prognosis[30]. The elder the patient the lower of sensitivity, so older patients are always diagnosed in their late stage, which significantly influences the treatment and prognosis. But another study showed that aging had nothing to do with prognosis[31].

Lymph nodular metastasis is a negative indicator of prognosis for elderly CRC patients[30,32-34]. When cancer cells stay in the celiac lymph node, it is probable that malignant cells have transferred to liver, lung, bone, etc, through lymph

circulation and blood circulation. At last patients may become fatigue, even die of target organ' s dysfunction. However, some researchers hold that lymph nodular metastasis is not correlated with prognosis[25].

Both univariate and multi-variate analyses showed that Duke' s stage was an important prognostic factor in this study[34]. The early the stage, the easy the treatment, and the better the long-survival. Duke' s A and some B stage patients did not need to receive chemotherapy at all, but their survival time was the best at all stages. While Duke' s C and D patients needed both operation and chemotherapy, but their prognosis was always poor. Precise pre-operation staging is beneficial to the optimal treatment, which has something to do with the prognosis[35,36]. So doctors must carefully and precisely evaluate the Duke' s stage before and during operation so as to give elderly CRC patients the optimal treatment.

Univariate analysis showed that gross finding was another prognostic factor[34]. In this study, ulcer patients had a longer survival than those with infiltration, which was similar to the result of L.Roncucci' s study[37]. Infiltration type and prominence type always result in intestinal obstruction, which makes the patients have to accept emergency operation. Also, both of them can make patients emaciation, which decreases the endurance to necessary treatment, because of dysfunction of digestion and absorbance. Furthermore, infiltration type always has a poor differentiation in histology.

Univariate and multi-variate analyses showed that histology type and differentiation influenced prognosis in this study[34, 38]. Tubular adenocarcinoma had a better prognosis than mucinous adenocarcinoma. The latter had a poorer differentiation, and this kind of cancer cells had a tendency to transfer to distant sites, which leads to a poor survival. However the high and middle differentiations had a better prognosis and quality of life[30, 39].

In conclusion there are several factors influencing the prognosis of elderly CRC patients. When selecting treatment method, doctors have to take PS, Duke' s stage, age, gross finding, histology type, differentiation, lymph node metastasis into consideration. Besides the clinical characteristics that influence the prognosis of elderly CRC patients, other molecular markers such as oncogene mutation, change of chromosome and vascular endothelial growth factor are also significant prognostic factors[40-46]. Searching for new biology markers and better treatment methods will be one part of the future study.

REFERENCES

1 **Zhang YL,** Zhang ZS, Wu BP, Zhou DY. Early diagnosis for colorectal cancer in China. *World J Gastroenterol* 2002; **8**: 21-25

2 **Thiis-Evensen E,** Hoff GS, Sauar J, Majak BM, Vatn MH. Flexible sigmoidoscopy or colonoscopy as a screening modality for colorectal adenomas in older age groups? Findings in a cohort of the normal population aged 63-72 years. *Gut* 1999; **45**: 834-839

3 **Li S,** Nie Z, Li N, Li J, Zhang P, Yang Z, Mu S, Du Y, Hu J, Yuan S, Qu H, Zhang T, Wang S, Dong E, Qi D. Colorectal cancer screening for the natural population of Beijing with sequential fecal occult blood test: a multicenter study. *Chin Med J* 2003; **116**: 200-202

4 **Repetto L,** Venturino A, Fratino L, Serraino D, Troisi G, Gianni W, Pietropaolo M. Geriatric oncology: a clinical approach to the older patient with cancer. *Eur J Cancer* 2003; **39**: 870-880

5 **Gatta G,** Faivre J, Capocaccia R, Ponz de Leon M. Survival of colorectal cancer patients in Europe during the period 1978-1989. *Eur J Cancer* 1998; **34**: 2176-2183

6 **Tang ZY.** Xiandai Zhongliuxue. 2ed. *ShangHai: ShangHai Medical University Press* 2000: 776

7 **Li L,** Lu F, Zhang S. Analyses of variation trend and short-term detection of Chinese malignant tumor mortality during twenty years. *Zhonghua Zhongliu Zazhi* 1997; **19**: 3-9

8 **Wymenga AN,** Slaets JP, Sleijfer DT. Treatment of cancer in old age, shortcomings and challenges. *Neth J Med* 2001; **59**: 259-266

9 **Franceschi S,** La Vecchia C. Cancer epidemiology in the elderly. *Crit Rev Oncol Hematol* 2001; **39**: 219-226

10 **De Marco MF,** Janssen-Heijnen ML, van der Heijden LH, Coebergh JW. Comorbidity and colorectal cancer according to subsite and stage: a population-based study. *Eur J Cancer* 2000; **36**: 95-99

11 Toxicity of fluorouracil in patients with advanced colorectal cancer: effect of administration schedule and prognostic factors. Meta-Analysis Group In Cancer. *J Clin Oncol* 1998; **16**: 3537-3541

12 **Daniele B,** Simmonds PD, Best LY, Ross PJ, Cunningham D. Should chemotherapy be used as a treatment of advanced colorectal carcinoma (ACC) in patients over 70 years of age? *Eur J Cancer* 1999; **35**: 1640-1649

13 Surgery for colorectal cancer in elderly patients: a systematic review. Colorectal Cancer Collaborative Group. *Lancet* 2000; **356**: 968-974

14 **Platell C,** Lim D, Tajudeen N, Tan JL, Wong K. Dose surgical sub-specialization influence survival in patients with colorectal cancer? *World J Gastroenterol* 2003; **9**: 961-964

15 **Smith JJ,** Lee J, Burke C, Contractor KB, Dawson PM. Major colorectal cancer resection should not be denied to the elderly. *Eur J Surg Oncol* 2002; **28**: 661-666

16 **Catena F,** Pasqualini E, Tonini V, Avanzolini A, Campione O. Emergency surgery of colorectal cancer in patients older than 80 years of age. *Ann Ital Chir* 2002; **73**: 173-177

17 **Catena F,** Pasqualini E, Tonini V, Avanzolini A, Campione O. Emergency surgery for patients with colorectal cancer over 90 years of age. *Hepatogastroenterology* 2002; **49**: 1538-1539

18 **Magne N,** Francois E, Broisin L, Guardiola E, Ramaioli A, Ferrero JM, Namer M. Palliative 5-fluorouracil-based chemotherapy for advanced colorectal cancer in the elderly: results of a 10-year experience. *Am J Clin Oncol* 2002; **25**: 126-130

19 **Liu LX,** Zhang WH, Jiang HC, Zhu AL, Wu LF, Qi SY, Piao DX. Arterial chemotherapy of 5-fluorouracil and mitomycin C in the treatment of liver metastases of colorectal cancer. *World J Gastroenterol* 2002; **8**: 663-667

20 **Romiti A,** Tonini G, Santini D, Di Seri M, Masciangelo R, Mezi S, Veri A, Santuari L, Vincenzi B, Brescia A, Marchei P, Frati L, Tomao S. Tolerability of Raltitrexed ('Tomudex') in elderly patients with colorectal cancer. *Anticancer Res* 2002; **22**: 3071-3076

21 **Mattioli R,** Lippe P, Recchia F, Massacesi C, Imperatori L, De Filippis S, Rosselli M, Gattafoni P, Casadei V, Consales D. Advanced colorectal cancer in elderly patients: tolerance and efficacy of leucovorin and fluorouracil bolus plus continuous infusion. *Anticancer Res* 2001; **21**: 489-492

22 **Kohne CH,** Grothey A, Bokemeyer C, Bontke N, Aapro M. Chemotherapy in elderly patients with colorectal cancer. *Ann Oncol* 2001; **12**: 435-442

23 **Feliu J,** Mel JR, Camps C, Escudero P, Aparicio J, Menendez D, Garcia Giron C, Rodriguez MR, Sanchez JJ, Gonzalez Baron M. Raltitrexed in the treatment of elderly patients with advanced colorectal cancer: an active and low toxicity regimen. *Eur J Cancer* 2002; **38**:1204-1211

24 **Cunningham D,** Haller D, Miles A. The effective management of colorectal cancer. 1st ed. *London: Aesculapius Medical Press* 2000: 75-81

25 **Allen PJ,** Kemeny N, Jarnagin W, DeMatteo R, Blumgart L, Fong Y. Importance of response to neoadjuvant chemotherapy in patients undergoing resection of synchronous colorectal liver metastases. *J Gastrointest Surg* 2003; **7**: 109-115

26 **Honecker F,** Wedding U, Kolb G, Bokemeyer C. Chemotherapy of colorectal cancer-which therapy is justified for elderly patients? *Onkologie* 2001; **24**: 87-94

27 **Cunningham D,** Zalcberg J, Maroun J, James R, Clarke S, Maughan TS, Vincent M, Schulz J, Gonzalez Baron M, Facchini T. Efficacy, tolerability and management of raltitrexed (Tomudex) monotherapy in patients with advanced colorectal cancer. a review of phase II/III trials. *Eur J Cancer* 2002; **38**: 478-486

28 **Tsalic M,** Bar-Sela G, Beny A, Visel B, Haim N. Severe toxicity related to the 5-fluorouracil/leucovorin combination (the Mayo Clinic regimen): a prospective study in colorectal cancer patients. *Am J Clin Oncol* 2003; **26**: 103-106

29 **Corsi DC,** Ciaparrone M, Zannoni G, Mancini M, Cassano A, Specchia M, Pozzo C, Martini M, Barone C. Predictive value of

thymidylate synthase expression in resected metastases of colorectal cancer. *Eur J Cancer* 2002; **38**: 527-534

30 **Tsigris C,** Karayiannakis AJ, Zbar A, Syrigos KN, Baibas N, Diamantis T, Alexiou D. Clinical significance of serum and urinary c-erbB-2 levels in colorectal cancer. *Cancer Lett* 2002; **184**: 215-222

31 **Maisey NR,** Norman A, Watson M, Allen MJ, Hill ME, Cunningham D. Baseline quality of life predicts survival in patients with advanced colorectal cancer. *Eur J Cancer* 2002; **38**: 1351-1357

32 **Stief CG,** Jonas U, Raab R. Long-term follow-up after surgery for advanced colorectal carcinoma involving the urogenital tract. *Eur Urol* 2002; **41**: 546-550

33 **Steup WH,** Moriya Y, van de Velde CJ. Patterns of lymphatic spread in rectal cancer. A topographical analysis on lymph node metastases. *Eur J Cancer* 2002; **38**: 911-918

34 **Wang JP,** Yang ZL, Wang L, Dong WG, Huang YH, Qin JZ, Zhan WH. Multi-variate regression analysis of clinicopathological characteristics and prognosis of colorectal cancer. *Zhonghua Zhongliu Zazhi* 2003; **25**: 59-61

35 **Walker J,** Quirke P. Prognosis and response to therapy in colorectal cancer. *Eur J Cancer* 2002; **38**: 880-886

36 **Gu J,** Ma ZL, Li Y, Li M, Xu GW. Angiography for diagnosis and treatment of colorectal cancer. *World J Gastroenterol* 2003; **9**: 288-290

37 **Roncucci L,** Fante R, Losi L, Di Gregorio C, Micheli A, Benatti P, Madenis N, Ganazzi D, Cassinadri MT, Lauriola P, Ponz de Leon M. Survival for colon and rectal cancer in a population-based cancer registry. *Eur J Cancer* 1996; **32A**: 295-302

38 **Galindo Gallego M,** Fernandez Acenero MJ, Sanz Ortega J, Aljama A. Vascular enumeration as a prognosticator for colorectal carcinoma. *Eur J Cancer* 2000; **36**: 55-60

39 **Massacesi C,** Norman A, Price T, Hill M, Ross P, Cunningham D. A clinical nomogram for predicting long-term survival in advanced colorectal cancer. *Eur J Cancer* 2000; **36**: 2044-2052

40 **Yi J,** Wang ZW, Cang H, Chen YY, Zhao R, Yu BM, Tang XM. p16 gene methylation in colorectal cancers associated with Duke's staging. *World J Gastroenterol* 2001; **7**: 722-725

41 **Weber JC,** Nakano H, Bachellier P, Oussoultzoglou E, Inoue K, Shimura H, Wolf P, Chenard-Neu MP, Jaeck D. Is a proliferation index of cancer cells a reliable prognostic factor after hepatectomy in patients with colorectal liver metastases? *Am J Surg* 2001; **182**: 81-88

42 **Lee JC,** Wang ST, Chow NH, Yang HB. Investigation of the prognostic value of coexpressed erbB family members for the survival of colorectal cancer patients after curative surgery. *Eur J Cancer* 2002; **38**: 1065-1071

43 **Bouzourene H,** Gervaz P, Cerottini JP, Benhattar J, Chaubert P, Saraga E, Pampallona S, Bosman FT, Givel JC. p53 and Ki-ras as prognostic factors for Dukes' stage B colorectal cancer. *Eur J Cancer* 2000; **36**: 1008-1015

44 **Zhou W,** Goodman SN, Galizia G, Lieto E, Ferraraccio F, Pignatelli C, Purdie CA, Piris J, Morris R, Harrison DJ, Paty PB, Culliford A, Romans KE, Montgomery EA, Choti MA, Kinzler KW, Vogelstein B. Counting alleles to predict recurrence of early-stage colorectal cancers. *Lancet* 2002; **359**: 219-225

45 **Lin LJ,** Zheng CQ, Jin Y, Ma Y, Jiang WG, Ma T. Expression of survivin protein in human colorectal carcinogenesis. *World J Gastroenterol* 2003; **9**: 974-977

46 **Zheng S,** Han MY, Xiao ZX, Peng JP, Dong Q. Clinical significance of vascular endothelial growth factor expression and neovascularization in colorectal carcinoma. *World J Gastroenterol* 2003; **9**: 1227-1230

Edited by Wang XL

P.O.Box 2345, Beijing 100023,China
Fax: +86-10-85381893
E-mail: wjg@wjgnet.com www.wjgnet.com

World J Gastroenterol 2003;9(10):2211-2215
World Journal of Gastroenterology
 ISSN 1007-9327

• VIRAL HEPATITIS •

Expression of ORF2 partial gene of hepatitis E virus in tomatoes and immunoactivity of expression products

Ying Ma, Shun-Quan Lin, Yi Gao, Mei Li, Wen-Xin Luo, Jun Zhang, Ning-Shao Xia

Ying Ma, Yi Gao, Wen-Xin Luo, Jun Zhang, Ning-Shao Xia, The Key Laboratory of the Ministry of Education for Cell Biology and Tumor Cell Engineering, Xiamen University, Xiamen 361005, Fujian Province, China
Ying Ma, Ministry of Education Key Laboratory for Marine Environmental Science, Center for Marine Environmental Science, Xiamen University, Xiamen 361005, Fujian Province, China
Shun-Quan Lin, College of Horticulture, South China Agricultural University, Guangzhou, 510642, Guangdong Province, China
Mei Li, Xiamen Overseas Chinese Subtropical Plant Introduction Garden, Xiamen 361002, Fujian Province, China
Supported by a grant from the Natural Science Foundation of Fujian Province, No. C9910004 and Xiamen Kaili Biologic Product Limited Company
Correspondence to: Ning-Shao Xia, The Key Laboratory of the Ministry of Education for Cell Biology and Tumor Cell Engineering, Xiamen University, Xiamen 361005, Fujian Province, China. nsxia@jingxian.xmu.edu.cn
Telephone: +86-592-2184110 **Fax:** +86-592-2184110
Received: 2003-03-12 **Accepted:** 2003-07-15

Abstract

AIM: To transfer hepatitis E virus (HEV) ORF2 partial gene to tomato plants, to investigate its expression in transformants and the immunoactivity of expression products, and to explore the feasibility of developing a new type of plant-derived HEV oral vaccine.

METHODS: Plant binary expression vector p1301E2, carrying a fragment of HEV open reading frame-2 (named HEV-E2), was constructed by linking the fragment to a constitutive CaMV35s promoter and nos terminator, then directly introduced into *Agrobacterium tumefaciens* EHA105. With leaf-disc method, tomato plants medicated by EHA105 were transformed and hygromycin-resistant plantlets were obtained in selective medium containing hygromycin. The presence and integration of foreign DNA in transgenic tomato genome were confirmed by Gus gene expression, PCR amplification and Southern dot blotting. The immunoactivity of recombinant protein extracted from transformed plants was examined by enzyme-linked immunosorbant assay (ELISA) using a monoclonal antibody specifically against HEV. ELISA was also used to estimate the recombinant protein content in leaves and fruits of the transformants.

RESULTS: Seven positive lines of HEV-E2-transgenic tomato plants confirmed by PCR and Southern blotting were obtained and the immunoactivity of recombinant protein could be detected in extracts of transformants. The expression levels of recombinant protein were 61.22 ng/g fresh weight in fruits and 6.37-47.9 ng/g fresh weight in leaves of the transformants.

CONCLUSION: HEV-E2 gene was correctly expressed in transgenic tomatoes and the recombinant antigen derived from them has normal immunoactivity. Transgenic tomatoes may hold a good promise for producing a new type of low-cost oral vaccine for hepatitis E virus.

Ma Y, Lin SQ, Gao Y, Li M, Luo WX, Zhang J, Xia NS. Expression of ORF2 partial gene of hepatitis E virus in tomatoes and immunoactivity of expression products. *World J Gastroenterol* 2003; 9(10): 2211-2215
http://www.wjgnet.com/1007-9327/9/2211.asp

INTRODUCTION

Research on using plants for expression and delivery of oral vaccine has attracted much academic attention and has become a hot spot of study since 1990 when Curtiss *et al*. first reported the expression of *Streptococcus mutans* surface protein antigen A(SpaA) in tobacco, and great progress has been made since then[1]. So far, more than 10 viral epitopes and subunits of bacterial toxins have been successfully expressed in plants, mainly including hepatitis B surface antigen (HBsAg)[2-9], *E.coli* heat-labile enterotoxin B subunit (LT-B)[10-15], cholera toxin B subunit (CT-B)[16], Norwalk virus capsid protein (NVCP)[17,18], rabies virus glycoprotein[19], *etc*. The involved plant receptors are mostly mode species: tobacco, potato, *etc*., some fruits and vegetables that can be consumed raw, tomato, banana, lettuce and lupine have also been attempted. Significant breakthrough has been achieved in increasing the expression of vaccine components in plants. At present, the plant-derived oral vaccines from potato for HBsAg and LT-B are undergoing clinical trials[13,14], but there has been no report about plant-derived oral vaccine for hepatitis E virus (HEV).

HEV is the major cause of acute, enteric non-A, non-B (NANB) hepatitis in the world, and large outbreaks occur primarily in underdeveloped countries. China is one of the high epidemic areas. The highest infection rate is in young adults (15-40 years). Although only 1 % to 3 % of non-pregnant patients with HEV infection progress to fatal fulminant hepatitis, the mortality can be as high as 20 % in pregnant patients[20]. There is neither effective antiviral drugs nor vaccine against HEV available for commercial use at present. Since HEV pathogen is difficult to culture, it is not easy to develop the live attenuated strains for vaccine. A promising approach is to develop recombinant subunit vaccines. Compared with gene engineering vaccine for hepatitis B, the study of hepatitis E recombinant vaccine was only a recent endeavor, but some progress has been made.

ORF2-encoded protein of HEV is the most promising subunit vaccine candidate because it possesses good antigenicity. So far, HEV ORF2 gene or its fragments have been expressed in prokaryote cells[21-24], insect cells[25], animal cells[26], and *Pichia pastoris*[27], *etc*., and the expression products possessed immunogenicity. HEV vaccine is about to undergo clinical trials[28].

Since hepatitis E occurs primarily in developing countries and impoverished regions with poor environmental sanitation, where administration of various medicinal vaccines may be hampered by the relatively high cost. Plant-derived hepatitis

E vaccine is a promising approach that may solve the problem because of its low cost for delivery and administration, and its safety for humans.

Tomato is a nutrition-rich fruit that can be consumed raw and easily transformed, so it is an ideal plant carrier for oral vaccine. In this paper we reported that a plant expression vector of HEV antigen gene was constructed and transformed into tomato plants with *Agrobacterium tumefaciens*, and its expression in plants and immunoactivity of the expression product were examined. This study would lay the foundation for further research on the development of a new type of plant-derived hepatitis E oral vaccine or other oral vaccines, and promote their practical application.

MATERIALS AND METHODS

Plant material

Tomato (*Lycopersium esculentum* CV. "XiuNu") seeds were purchased from Xiamen Nong-You Seed Co., Ltd.

Reagents, bacteria and plasmids

Restriction endonucleases and T4 DNA ligase were obtained from Promega Co. Hygromycin and X-gluc staining solution from Calbiochem-novabiochem Co. and Amres Co., respectively. Double antibody sandwich-ELISA kit was provided by Beijing Wantai Biological Pharmaceutical Co. *Agrobacterium tumefaciens* strain EHA105 was kindly presented by Professor Zhang Qi-fa, Huazhong Agricultural University. Plasmid pBPFΩ7 containing CaMV35s promoter and nos terminator, and plant binary plasmid pCAMBIA1301 containing hygromycin-resistant gene, kanamycin-resistant gene and Gus gene, were constructed and preserved in our laboratory.

Construction of plant binary expression vector

An 810 bp DNA fragment (named E2) of HEV ORF2 region, located between amino acid residue 394 and 604[23], was obtained by a PCR-based assembly from the patient' s serum and inserted into pBPFΩ7 between CaMV35S promoter and nos terminator at *Bam*HI/*Eco*RI site to form pBE2. The fragment containing "P35S+Ω+E2+Tnos" was isolated by gel extraction from plasmid pBE2 after *Pst*I restrictive digestion and then subcloned into plasmid pCAMBIA1301 that had been digested by the same restriction endonuclease to yield the reconstructed plant binary expression plasmid p1301E2 (Figure 1). Confirmed by restriction digestion, p1301E2 was directly introduced into *Agrobacterium tumefaciens* strain EHA105 by freeze-thaw method.

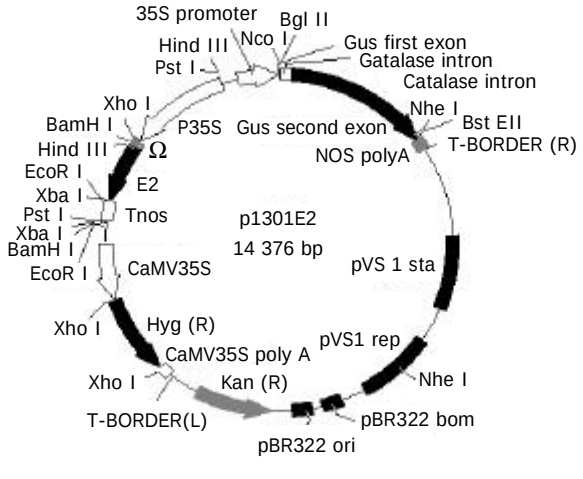

Figure 1 Structure of plasmid p1301E2.

Plant transformation and regeneration

Tomato was transformed through leaf discs mediated by *Agrobacterium tumefaciens* EHA105 with p1301E2. Shoots were generated from transformed callus after 3-4 weeks selected on medium containing 20 mg of hygromycin (Hyg) and 300 mg of cefotaxime per liter. The rooting was obtained in medium containing 20 mg of Hyg per liter, and the plantlets was transplanted to soil, and watered with 1/2 MS medium.

Analysis of Gus gene expression

Both transformed and untransformed tissues were cut from tomato plants, immerged into Gus reaction buffer (X-gluc staining solution) for 12 to 24 hours at 37 ℃, then bleached with absolute alcohol, observed and photographed under dissecting microscope.

Analysis of HEV-E2 gene integration

PCR amplification Genomic DNAs extracted from leaves of tomato plants by CTAB[29] were used as PCR templates. The forward primer HEFP and reverse primer HERP were: 5' -GGA TCC ATA TGC AGC TGT TCT ACT CTC GTC-3' and 5' -CTC GAG AAA TAA ACT ATA ACT CCC GA-3', respectively (synthesized by BioAsia Co., Shanghai). PCR reaction was performed using 50 ng of template DNA, 0.5 μM of each primer in a total volume of 30 μl. Cycling parameters were at 94 ℃ for 10 min, followed by 35 cycles at 94 ℃ for 50 s, at 57 ℃ for 50 s, and at 72 ℃ for 50 s, and a final extension at 72 ℃ for 7 min.

Southern dot blotting It was performed as reported previously[29].

Analysis of HEV-E2 gene expression

ELISA Total soluble proteins were extracted from leaf and fruit tissues as described[29], and HEV-E2 recombinant protein was detected by HEV enzyme-linked immunosorbant assay (ELISA) kit, the protocol and positive determination were performed according to the instructions supplied with the kit. The expression levels of HEV-E2 in transformants were quantified by ELISA. The extract of transformant was diluted several fold until it could reach the same OD value (measurement wavelength: 450 nm) as the standard HEV-E2 protein (1 ng/mg), then HEV-E2 expression levels in transformants could be calculated according to the sampling quantity, and diluting times.

RESULTS

Regeneration of transgenic tomato plants

The plasmids for expression of HEV-E2 in plants allowed morphogenesis of transformants on selective medium containing hygromycin. Through about 1 month of selection, 7 independent Hyg-resistant plantlets were obtained. These transformants bore fruits and the seeds were collected. The flowers and fruits of the transformants resembled those of wild-type tomato plants and the seeds were plump. Each fruit produced approximately 70 seeds. This demonstrated that the introduction of foreign gene into tomato plants did not influence the normal growth and development of the transformants (Figure 2).

Gus expression in transgenic plants

Untransformed tissues appeared colourless when stained with Gus reaction solution and bleached with absolute alcohol, whereas transformed tissues presented blue spots even after bleached with absolute alcohol, the spots were generally large in size, with a deep blue color (Figure 3). The results indicated that Gus gene was stably integrated into the genomic DNA of transformed tomatoes.

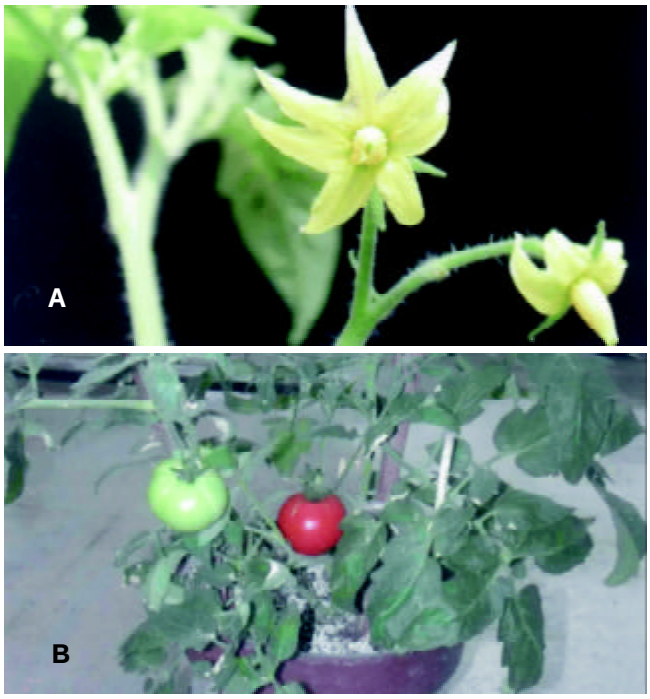

Figure 2 Transgenic plants in greenhouse. A: Flowers of transformants, B: Fruits of transformants.

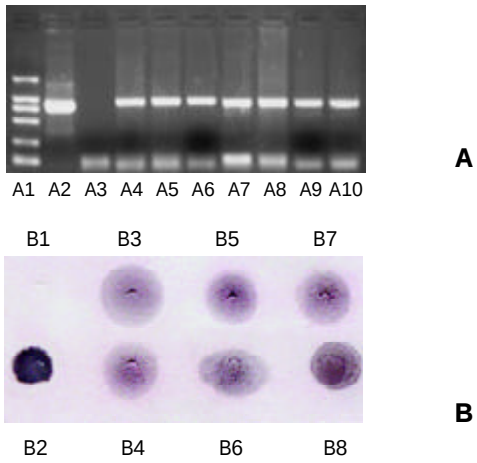

Figure 4 Analysis of HEV-E2 gene integration. A: PCR amplification of genomic DNA of tomato plants, B: Southern dot blotting of genomic DNA of tomato plants. A1: DL-2000 marker, A2: Positive control (p1301E2), A3: Total DNA of wild-type control plant, A4-A10: Total DNA of independent transformants. B1: Total DNA of wild-type control plant, B2: Positive control (p1301E2), B3-B8: Total DNA of independent transformants.

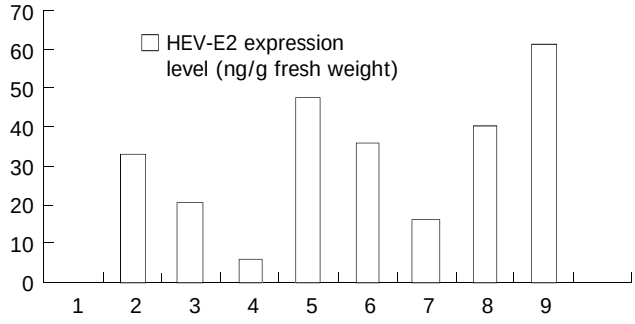

Figure 5 HEV-E2 expression levels in transgenic tomato plants. 1: Leaves of wild-type control plant, 2-8: Leaves of seven independent transformants, 9: The mixed flesh tissue of 3 independent transformant fruits.

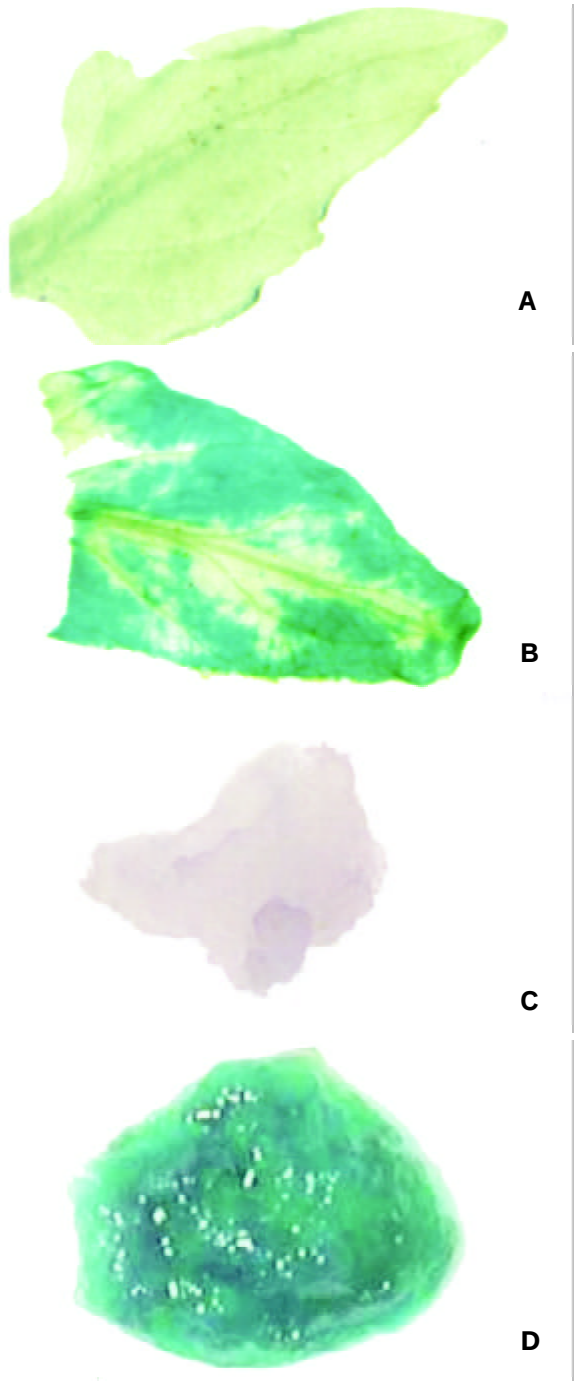

Figure 3 Analysis of Gus gene expression. A: Leaf of untransformed tomato plant, B: Leaf of transformed tomato plant, C: Flesh of untransformed tomato, D: Flesh of transformed tomato.

PCR amplification

The expected 810 bp fragments were amplified from 7 transformed lines of tomatoes, the length of the fragments was identical with that amplified from p1301E2 (positive control), whereas there was no PCR product in wild-type tomato plants (negative control). The results primarily verified that the target gene was integrated into the genomic DNA of transformed tomatoes (Figure 4A).

Southern dot blotting

To further verify the integration of foreign gene into tomato plants, the total genomic DNA of transformed tomatoes was hybridized by a DIG-labeled probe (encompassing the coding region of HEV-E2 gene) generated by PCR amplification from p1301E2 with HEFP and HERP primers, and all the

transformants gave the same hybridization spots as the positive control(p1301E2) did, whereas the untransformed plant showed no detectable hybridization signal (Figure 4B). Thus the results further confirmed that the target gene was integrated into the tomato plants.

Expression of HEV-E2 gene in transgenic tomato plants

The leaf extracts of 7 lines of transformants and the mixed fruit tissue extracts from 3 transformants were tested by ELISA for the presence of HEV-E2 expression products, and foreign protein could be detected in all of the examined samples. The reaction was specific because wild-type tomato showed no detectable expression products. The result demonstrated that HEV-E2 gene was expressed in transformed tissue. The expression level of HEV-E2 protein was lower as compared to HBsAg in transgenic tomatoes[8], the maximal expression level was only 47.9 ng/g fresh weight in leaves. The expression levels were different between different transformants and between different organs of the same plant, which indicated that the inserting site of foreign DNA into the plant genome was random. The expression in fruits (61.22 ng/g fresh weight) was higher than that in leaves, which was similar to that of HBsAg in transgenic tomatoes[8]. The higher expression of target protein in edible tissue mightbe helpful for producing oral vaccine.

DISCUSSION

The most striking advantage of using tomato as oral vaccine vector is that the plant-derived vaccine is cheap and tomato is a freshly-eaten fruit, which allows the target population to acquire immunity at the same time when they enjoy the delicious fruits. But accumulation of protein in tomato itself is low, the expression levels of foreign protein in it are much lower. This will make it difficult when administering the plant-derived vaccine. However, the expression of foreign protein in plants might be increased by several modifications, including the use of stronger promoters, the use of plant-derived leader sequences and signal peptide, and targeting the protein for retention in edible tissue and so on[1]. For example, Mason *et al*[2] increased the level of HBsAg 11 fold in transgenic tobacco by linking CaMV35S promoter to the tobacco etch virus (TEV) 5' leader sequence (acts as a translational enhancer). In 1998, Mason *et al*[12] increased the expression of LT-B in transgenic potatoes 3-14 times by designing and constructing a plant-optimized synthetic gene encoding LT-B. Tackaberry *et al*[30] reported the synthesis of recombinant glycoprotein B which expressed specifically in tobacco seeds, with expression level reaching 70-146 ng/mg extracted protein. Lauterslager *et al*[11] made a synthetic gene coding for LT-B and optimized it for expression specifically in potato tubers and accumulation in endoplasmic reticulum, which resulted in a high expression level about 13 μg/g fresh weight of LT-B in potato tubers. Besides, by using chloroplast expression system, Cosa *et al*[31] introduced foreign genes into the chromoplast genome, which enabled the foreign protein to accumulate at 46 % of the total soluble protein in leaves of transgenic plants. All these studies provided us successful experiences in improving expression level of HEV-E2 in transgenic tomatoes. In our study, we only inserted an enhancer Ω in the promoter, there were many reconstruction possibilities to achieve high expression. Currently we are engaged in researches on increasing expression level of foreign proteins, and the animal trials of oral immunization of mice with transgenic tomatoes expressing HEV-E2 are also in progress.

We have successfully introduced HEV-E2 gene into tomatoes and identified the expression protein. The expression product possessed HEV specific antigenicity in transgenic plants. Previous studies also demonstrated that plant-derived vaccines were safe and functional. It is cheap to produce and store, easy to deliver and administer, it has many advantages over other vaccines. Although this technology is not likely to produce great commercial value in the short term, the present advance in plant genetic engineering demonstrates that there is a tremendous potential to develop various low-cost recombinant vaccines by using plants.

REFERENCES

1 **Ma Y,** Zhang J, Lin SQ, Xia NS. Genetic Engineering vaccines produced by transgenic plants. *Xiamen Daxue Xuebao* 2001; **40:** S71-77

2 **Mason HS,** Lam DM, Arntzen CJ. Expression of hepatitis B surface antigen in transgenic plants. *Proc Natl Acad Sci U S A* 1992; **89:** 11745-11749

3 **Thanavala Y,** Yang YF, Lyons P, Mason HS, Arntzen C. Immunogenicity of transgenic plant-derived hepatitis B surface antigen. *Proc Natl Acad Sci U S A* 1995; **92:** 3358–3361

4 **Kong Q,** Richter L, Yang YF, Arntzen CJ, Mason HS, Thanavala Y. Oral immunization with hepatitis B surface antigen expressed in transgenic plants. *Proc Natl Acad Sci U S A* 2001; **98:** 11539–11544

5 **Kapusta J,** Modelska A, Figlerowicz M, Pniewski T, Letellier M, Lisowa O, Yusibov V, Koprowski H, Plucienniczak A, Legocki AB. Plant-derived edible vaccine against HBV. *FASEB J* 1999; **13:** 1796-1799

6 **Liu DH.** Plant as a system for production of pharmaceutical proteins. *Shengwu Jishu Tongbao* 1999; **4:** 1-5

7 **Zhao CH,** Wang R, Zhao CS, Wang GL, Tian B. Expression of human hepatitis B virus surface antigen gene with and without preS in transgenic tomato. *Nongye Shengwu Jishu Xuebao* 2000; **8:** 85-88

8 **Ma Y,** Lin SQ, Gao Y, Zhang J, Lu LX, Xia NS. Transformation of HBsAg (hepatitis B virus surface antigen) into tomato plants. *Fujian Nonglin Daxue Xuebao* 2002; **31:** 223-227

9 **Gao Y,** Ma Y, Li M, Cheng T, Li SW, Zhang J, Xia NS. Oral immunization of animals with transgenic cherry tomatillo expressing HBsAg. *World J Gastroenterol* 2003; **9:** 996-1002

10 **Haq TA,** Mason HS, Clements JD, Arntzen CJ. Oral immunization with a recombinant bacterial antigen produced in transgenic plants. *Science* 1995; **268:** 714–716

11 **Lauterslager TG,** Florack DE, van der Wal TJ, Molthoff JW, Langeveld JP, Bosch D, Boersma WJ, Hilgers LA. Oral immunization of naive and primed animals with transgenic potato tubers expressing LT-B. *Vaccine* 2001; **19:** 2749-2755

12 **Mason HS,** Haq TA, Clements JD, Artzen CJ. Edible vaccine protects mice against *Escherichia coli* heat-labile enterotoxin (LT): potatoes expressing a synthetic LT-B gene. *Vaccine* 1998; **16:** 1336–1343

13 **Tacket CO,** Mason HS, Losonsky G, Clements JD, Levine MM, Arntzen CJ. Immunogenicity in humans of a recombinant bacterial antigen delivered in a transgenic potato. *Nat Med* 1998; **4:** 607-609

14 **Tacket CO,** Reid RH, Boedeker EC, Losonsky G, Nataro JP, Bhagat H, Edelman R. Enteral immunization and challenge of volunteers given enterotoxigenic *E. coli* CFA / II encapsulated in biodegradable microspheres. *Vaccine* 1994; **12:** 1270-1274

15 **Streatfield SJ,** Jilka JM, Hood EE, Turner DD, Bailey MR, Mayor JM, Woodard SL, Beifuss KK, Horn ME, Delaney DE, Tizard IR, Howard JA. Plant-based vaccines: unique advantages. *Vaccine* 2001; **19:** 2742-2748

16 **Arakawa T,** Chong DK, Langridge WH. Efficacy of a food plant-based oral cholera toxin B subunit vaccine. *Nat Biotechnol* 1998; **16:** 292-297

17 **Mason HS,** Ball JM, Shi JJ, Jiang X, Estes MK, Arntzen CJ. Expression of Norwalk virus capsid protein in transgenic tobacco and potato and its oral immunogenicity in mice. *Proc Natl Acad Sci U S A* 1996; **93:** 5335-5340

18 **Tacket CO,** Mason HS, Losonsky G, Estes MK, Levine MM, Arntzen CJ. Human immune responses to a novel Norwalk virus vaccine delivered in transgenic potatoes. *J Infect Dis* 2000; **182:** 302-305

19 **McGarvey PB,** Hammond J, Dienelt MM, Hooper DC, Fu ZF,

Dietzschold B, Koprowski H, Michaels FH. Expression of the rabies virus glycoprotein in transgenic tomatoes. *Biotechnology* 1995; **13:** 1484-1487

20 **Skidmore S**. Overview of Hepatitis E Virus. *Curr Infect Dis Rep* 2002; **4**: 118-123

21 **Zhang M**, Zhao H, Jiang Y. Expression of hepatitis E virus structural gene in E. coli. *Zhonghua Shiyan He Linchuangbing Duxue Zazhi* 1999; **13**: 130-132

22 **Bi S,** Lu J, Jiang L, Huang G, Pan H, Jiang Y, Zhang M, Shen X. Preliminary evidence that a hepatitis E virus (HEV) ORF2 recombinant protein protects cynomolgus macaques against challenge with wild-type HEV. *Zhonghua Shiyan He Linchuangbing Duxue Zazhi* 2002; **16:** 31-32

23 **Li SW**, Zhang J, He ZQ, Ge SX, Gu Y, Lin J, Liu RS, Xia NS. The study of aggregate of the ORF2 peptide of hepatitis E virus expressed in Escherichia coli. *Shengwu Gongcheng Xuebao* 2002; **18**: 463-467

24 **Zhang M**, Yi Y, Zhan M, Liu C, Bi S. Expression of thermal stable, soluble hepatitis E virus recombinant antigen. *Zhonghua Shiyan He Linchuangbing Duxue Zazhi* 2002; **16**: 20-22

25 **Zhang M**, Emerson SU, Nguyen H, Engle R, Govindarajan S, Blackwelder WC, Gerin J, Purcell RH. Recombinant vaccine against hepatitis E: duration of protective immunity in rhesus macaques. *Vaccine* 2002; **20**: 3285-3291

26 **Jameel S,** Zafrullah M, Ozdener MH, Panda SK. Expression in animal cells and characterization of the hepatitis E virus structural proteins. *J Virol* 1996; **70:** 207-216

27 **Tong Y,** Zhan M, Lu J, Bai Y, Bi S. Immunogenicity of recombinant HEV ORF2 protein expressed in pichia pastoris. *Zhonghua Shiyan He Linchuangbing Duxue Zazhi* 2002; **16:** 23-26

28 **Ling X.** The development of hepatitis E vaccine in China. *Zhonghua Yixue Zazhi* 2001; **81:** 120

29 **Wang GL,** Fang HJ. Principle and technology of plant genetic engineering, 1st ed, Beijing: *Science Press* 1998

30 **Tackaberry ES,** Dudani AK, Prior F, Tocchi M, Sardana R, Altosaar I, Ganz PR. Development of biopharmaceuticals in plant expression systems: cloning, expression and immunological reactivity of human cytomegalovirus glycoprotein B (UL55) in seeds of transgenic tobacco. *Vaccine* 1999; **17:** 3020-3029

31 **De Cosa B,** Moar W, Lee SB, Miller M, Daniell H. Overex pression of the Bt Cry2Aa2 operon in chloroplasts leads to formation of insecticidal crystals. *Nat Biotechnol* 2001; **19:** 71-74

Edited by Zhu LH

P.O.Box 2345, Beijing 100023,China
Fax: +86-10-85381893
E-mail: wjg@wjgnet.com www.wjgnet.com

World J Gastroenterol 2003;9(10):2216-2220
World Journal of Gastroenterology
 ISSN 1007-9327

• VIRAL HEPATITIS •

Lethiferous effects of a recombinant vector carrying thymidine kinase suicide gene on 2.2.15 cells via a self-modulating mechanism

Quan-Cheng Kan, Zu-Jiang Yu, Yan-Chang Lei, Lian-Jie Hao, Dong-Liang Yang

Quan-Cheng Kan, Yan-Chang Lei, Lian-Jie Hao, Dong-Liang Yang, Division of Clinical Immunology, Tongji Hospital; Institute of Immunolgy, Tongji Medical College, Huazhong University of Science and Technology, Wuhan 430030, Hubei Province, China
Zu-Jiang Yu, Department of Infectious Diseases, First Affiliated Hospital of Zhengzhou University, Zhengzhou 450052, Henan Province, China
Supported by the State Key Basic Research Program of China (973 Program, No. 20014CB51008) and National Key R & D Program of China for the 10th Five-Year Plan Period (No. 2001BA705B05)
Correspondence to: Dr. Dong-Liang Yang, Division of Clinical Immunology, Tongji Hospital, Tongji Medical College, Huazhong University of Science and Technology, 1095# Jiefang Avenue, Wuhan 430030, Hubei Province, China. dlyang@tjh.tjmu.edu.cn
Telephone: +86-27-83662894
Received: 2003-07-18 **Accepted:** 2003-08-07

Abstract

AIM: To determine the lethiferous effects of a recombinant vector carrying thymidine kinase (TK) suicide gene on 2.2.15 cells and the possible self-modulating mechanism.

METHODS: A self-modulated expressive plasmid pcDNA3-SCITK was constructed by inserting the fragments carrying hepatitis B virus antisense-S (HBV-anti-S) gene, hepatitis C virus core (HCV-C) gene, internal ribosome entry site (IRES) element of HCV and TK gene into the eukaryotic vector pcDNA3, in which the expression of TK suicide gene was controlled by the HBV S gene transcription. 2.2.15 cells that carry the full HBV genome and stably express series of HBV antigen were transfected with $pcDNA_3$-SCITK or vector $pcDNA_3$-SCI which was used as the mock plasmid. The HepG2 cells transfected with $pcDNA_3$-SCITK were functioned as the negative control. All the transfected cells were incubated in DMEM medium supplemented with 10 μg/ml. of ganciclovir (GCV). The HBsAg levels in the supernatant of cell culture were detected by ELISA on the 1st, 3rd and 6th day post-transfection. Meanwhile, the morphology of tranfected cells was recorded by the photograph and the survival cell ratio was assessed by the trypan blue exclusion test on the 6th day post-transfection.

RESULTS: The structural accuracy of $pcDNA_3$-SCITK was confirmed by restriction endonuclease digestion, PCR with specific primers and DNA sequencing. The HBsAg levels in the supernatant of transfected 2.2.15 cell culture were significantly decreased on the 6th day post-transfection as compared with that of the mock control ($P<0.05$). The lethiferous effect of $pcDNA_3$-SCITK expression on 2.2.15 cells was initially noted on the 3rd day after transfection and aggravated on the 6th day post transfection, in which the majority of transfected 2.2.15 cells were observed shrunken, round in shape and even dead. With assessment by the trypan blue exclusion test, the survival cell ratio on the 6th day post transfection was 95 % in the negative control and only 11 % in the experimental group.

CONCLUSION: The results indicate that suicide gene expression of $pcDNA_3$-SCITK can only respond to HBV-S gene transcription, which may be potentially useful in the treatment of HBV infection and its related liver malignancies.

Kan QC, Yu ZJ, Lei YC, Hao LJ, Yang DL. Lethiferous effects of a recombinant vector carrying thymidine kinase suicide gene on 2.2.15 cells via a self-modulating mechanism. *World J Gastroenterol* 2003; 9(10): 2216-2220
http://www.wjgnet.com/1007-9327/9/2216.asp

INTRODUCTION

Despite the availability of efficient vaccines, chronic hepatitis B virus (HBV) infection remains a major public health problem worldwide[1-7]. The World Health Organization estimates that there are still 350 million chronic carriers of the virus who are at risk of developing chronic hepatitis, liver cirrhosis and hepatocellular carcinoma[8, 9]. This issue is also an important problem in China. The carrier rates of HBsAg are estimated to be as high as more than 10 % of Chinese population and a substantial proportion of liver cancer incidence is associated with chronic HBV infection[10-12]. Currently interferon-alpha (IFN-α), an immunomodulator, and two synthetic nucleoside analogues, lamivudine and adefovir dipivoxil, are the only licensed antiviral agents for the treatment of chronic HBV infection. However, this therapeutical modality is still problematic. In addition to the standard treatment endpoints being achievable only in approximately 20-30 % of those treated with either type of agents, interferon usually confers serious side effects, and lamivudine is associated with the occurrence of viral mutations and drug-resistant strains[13-17]. Thus, there is an urgent need for the development of more effective modalities to deal with HBV infection. As yet, several therapeutic protocols with molecular biological techniques have been tried in experimental studies of this disease in the last few years[1,18-25], although significant progress remains to be made in such kinds of explorations. In the present study, we tried to construct a recombinant vector carrying TK suicide gene and harboring a self-modulating property for gene therapy in an attempt to vanquish HBV infection in a fire-new strategy.

MATERIALS AND METHODS

Materials

Plasmid $pcDNA_3$-TK containing TK gene and $pcDNA_3$-S carrying HBV-S gene were maintained in our laboratory. Eukaryotic expression vector $pcDNA_3$ was from Invitrogen Company, Netherlands. Purification kit for PCR product was obtained from QIAGEN Company (Germany). Reverse transcriptase and PCR amplification system were purchased from Shenzhen Jingmei Company (China) and Expand PCR kit form Stratgene Company (USA). Taq and Pfu enzymes were purchased from Bio-Star Company (Canada). Restriction endonucleases such as EcoR I, BamH I and HinD III, T_4 DNA ligase and ELISA kit for detecting HBsAg were from Huamei Bioengineering Company (Luoyang,

China). All the PCR primers used in the study were synthesized by Takara Ltd (Dalian, China).

Preparation of gene fragments

The fragments of HCV-IRES element and core gene were obtained by RT-PCR. Total HCV RNA was extracted and purified from 100 μl samples of HCV-positive sera using a guanidium isothiocyanate-acid phenol extraction procedure (Jingmei Company, Shenzhen, China). Precipitated RNA was dissolved in 20 μl of diethyl pyrocarbonate-treated water and quantified by UV spectrum analysis. Specific cDNA for HCV IRES element and core gene were amplified respectively with RT-PCR kit by adding their corresponding primers according to the protocols of Reverse Transcription System (Jingmei Company, Shenzhen, China). The primers for the HCV IRES were sequenced as sense: 5' -GCGCGGATCCGGGCGACAC TCCACCATAG-3' (nucleotides [nt] 17 to 36) and antisense: 5' -GCGAATTCGTTTTTCTTTGAGGTTTAGGATTC-3' (nt 347 to 371). The primers for the HCV core gene were 5' -TAGGAATCCTGATGAGCACGAATCCTAAACCTC-3' (sense) and 5' -GCGCGGATCCTTAAGCGGAAGCTGGGA TG-3' (antisense). PCR was performed on the Real-time PCR apparatus (Roche, USA) with a program for 30 cycles at 42 ℃ for 45 min and at 94 ℃ for 5 min followed by at 92 ℃ for 30 s, at 55 ℃ for 30 s and at 72 ℃ for 30 s. After prepared by routine procedures, the PCR products were analyzed by agarose gel electrophoresis and stored at -20 ℃ until use.

The antisense fragment of HBV-S gene lack of initiating codon (ATG) was amplified with the PCR protocol using the oligonucleotide sequence 5' -GCGCGTGCAAGCTT ATAAAACGCCGCAGACACATC-3' (sense) and 5' -ATTCGTGCTCATCAGGATTCCTAGGACCCCTTC-3' (antisense) as primers, and $pcDNA_3$-S as the template. After an initial denaturation step was performed, PCR was carried out for 45 cycles at 95 ℃ for 15 s, at 70 ℃ for 5 s and at 72 ℃ for 15 s each cycle. The PCR products were identified by electrophoresis on an l % of agarose gel stained with ethidium bromide and stored at -20 ℃ until use.

TK gene segment was prepared by digestion of plasmid $pcDNA_3$-TK with EcoR I and purified with the routine procedures.

Construction of self-modulated expression vector

The construction scheme for the self-modulated expression vector that can respond to HBV infection and eliminate the infected hepatic cells is shown in Figure 1. Briefly, ligation of antisense fragment of HBV-S gene with HCV-C gene segment was performed by SOEing PCR[26-28], in which the sense sequence of HCV-C gene primer 5' -TAGGAATCCTGATGA GCACGAATCCTAAACCT**C**-3' and a truncated antisense sequence of HBV-S gene primer 5' -ATTCGTGCTCATCA GGATTCCTAGGACCCC-3' were used as primers. The major SOEing PCR round comprised of 30 cycles at 92 ℃ for 30 s, at 50 ℃ for 45 s and at 72 ℃ for 60 s each cycle, and a final extension at 72 ℃ for 10 min. The ligated PCR products were purified and analyzed by agarose gel electrophoresis and used to link with the HCV-IRES fragment by T_4 ligase after both segments were digested by BamH I. The resultant HBV antisense S-HCV C-HCV IRES (SCI) fragment was further amplified by PCR with the major round to be at 92 ℃ for 30 s, at 53 ℃ for 45 s and at 72 ℃ for 60 s for 30 cycles, and the final extension at 72 ℃ for 10 min, in which HBV-S gene sense primer, 5' -GCGCGTGCAAGCTTATAAAACGCC GCAGACACATC-3, and HCV-IRES antisense primer, 5' -GCGAATTCGTTTTTCTTTGAGGTTTAGGATTC-3' , were employed as primers. After digested by corresponding restriction endonucleases, the amplified HBV antisense S-HCV C-HCV IRES fragment was cloned into Hind III and EcoR I sites of $pcDNA_3$ to generate eukaryotic expression plasmid pcDNA3-SCI (Figure 1). In the same way, the expression plasmid $pcDNA_3$-SCITK was yielded by cloning TK fragment into EcoR I site of $pcDNA_3$-SCI. Both of the newly constructed plasmid were confirmed by restriction endonuclease digestion, PCR with specific primers and finally by DNA sequencing (Baosheng Company, Daliang, China).

Self-restricted expression of recombinant plasmid

HepG2 and its derived cell line 2.2.15 that carries the full HBV genome and can stably express series of HBV antigen were maintained in our laboratory. They were cultured in a modified Eagal' s essential medium (Sigima) supplemented with 100 $U \cdot ml^{-1}$ penicillin, 100 $U \cdot ml^{-1}$ streptomycin, and L-glutamine, nonessential amino acids and sodium bicarbonate

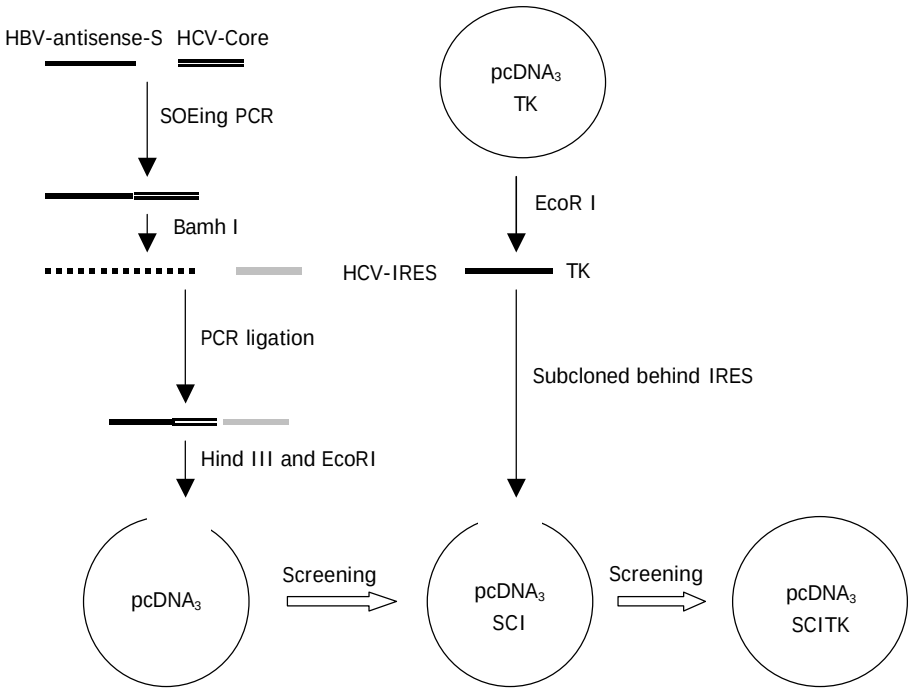

Figure 1 Construction scheme of recombinant plasmid $pcDNA_3$-SCITK.

in doses recommended by the China Type Culture Collection (Wuhan, China) at 37 ℃ in a humidified atmosphere containing 5 % of CO_2. One day prior to transfection, cells were transferred onto an 8-well plate and incubated in complete Dulbecco' s modified Eagle' s medium (DMEM) containing 10 % (v/v) fetal calf serum (FCS) and 10 μg/ml of ganciclovir. When the cells grew to 50-80 % confluence, they were transfected with $pcDNA_3$-SCITK or pcDNA3-SCI plasmid in a ratio of per 10^6 cells to 1 μg of plasmid DNA by LipofectAMINE transfection reagent following the manufacturer' s instructions. (Invitrogen Co. USA). 2.2.15 cells transfected with $pcDNA_3$-SCITK or $pcDNA_3$-SCI plasmids were designated as the experimental group or the mock group. The HepG2 cells transfected with $pcDNA_3$-SCITK plasmids were functioned as the negative control. All of the transfected cells were maintained in DMEM medium with 10 % (v/v) fetal calf serum (FCS) and 10 μg/ml of ganciclovir for at least 7 days. The HBsAg levels in the supernatant of cell culture were detected by ELISA on the 1st, 3rd and 6th day after transfection. Meanwhile, the morphology of transfected cells were recorded by the photograph and the survival cell ratio was assessed by the trypan blue exclusion test on the 6th day of posttransfection.

Statistical analysis

Experimental data were processed by analysis of variance and *t*-test for comparison between groups. Results were expressed as mean ± SE. $P<0.05$ was selected as the level of statistical significance.

RESULTS

Structural identification of constructed plasmids

The segment analysis of recombinant plasmid $pcDNA_3$-SCITK by restriction endonuclease digestion and PCR with specific primers demonstrated that the inserted gene sequences in the plasmid were completely consistent with that of the theoretical

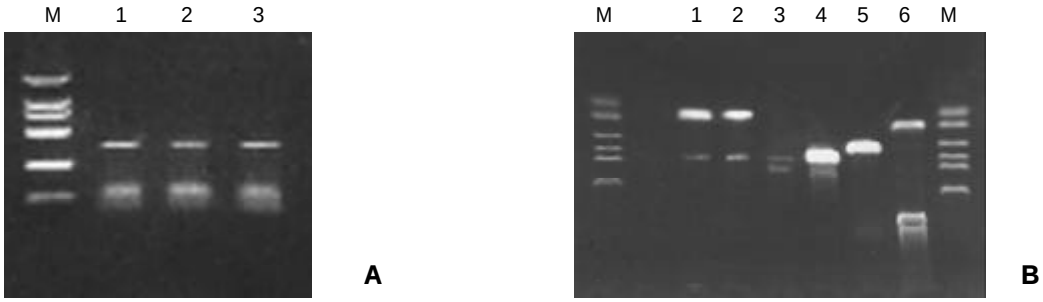

Figure 2 A: RT-PCR products of HCV IRES element. M: marker (2 kb), Lanes 1-3: HCV IRES element (330 bp). B. Component segment analysis of $pcDNA_3$-SCITK by agarose gel electrophoresis. M: marker (2 kb), Lanes 1-2: SCI-TK fragment demonstrated by PCR with HBV-S gene sense primer and TK antisense primer (5'-ACTTCCGTGGCTTCTTGCTG-3' (nt 150-170). Lane 3: SCI fragment verified by PCR with HBV-S gene sense primer and HCV IRES antisense primer. Lane 4: SI segment from the ligation of HBV-S and HCV-Core gene by SOEing PCR. Lane 5: RT-PCR product of HCV-Core gene. Lane 6: Partial antisense segment of HBV-S gene.

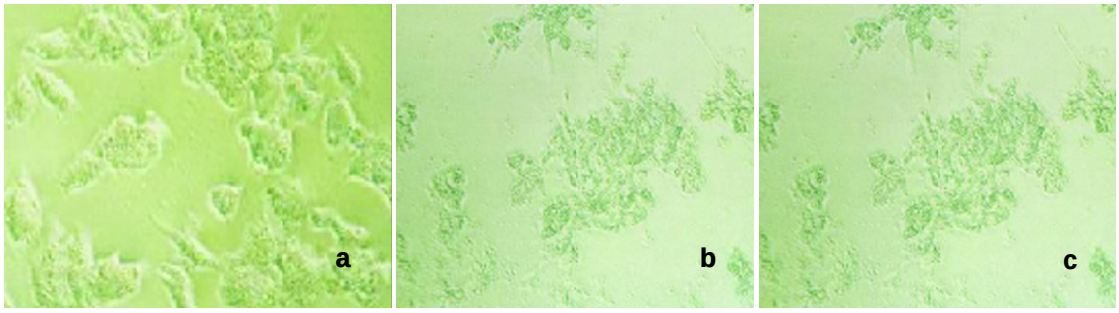

A. Experimental group.

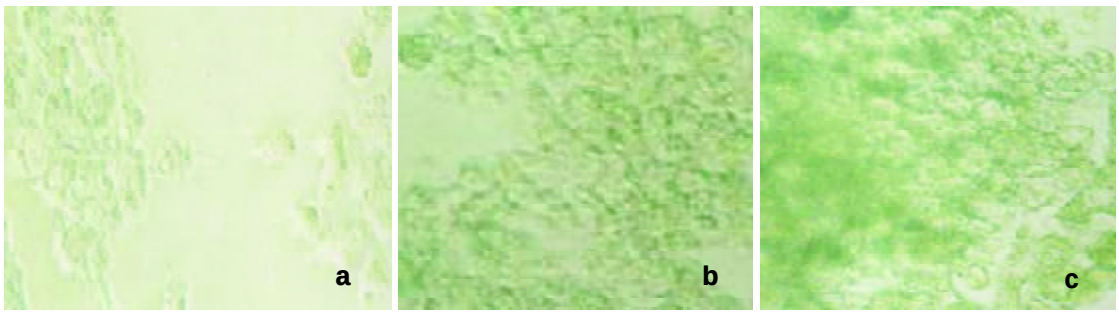

B. Negative control.

Figure 3 Effects of $pcDNA_3$-SCITK expression on morphological alterations of 2.2.15 and HepG2 cells. Photographs a, b and c in each group exhibited respectively the cell changes on the 1st, 3rd and 6th day post transfection. Lethiferous changes of 2.2.15 cells transfected with $pcDNA_3$-SCITK were noted initially on the 3rd day of posttransfection and aggravated on the 6th day after transfection, in which the majority of cells were observed shrunken, rounded in shape and even dead. However, the negative contrl HepG2 cells grew well.

calculations as shown in Figure 2, which were further confirmed by the DNA sequencing (data not shown).

Effects of pcDNA3-SCITK expression on HBV-infected cells

The expressive efficiency of TK protein by 2.2.15 cells transfected with pcDNA$_3$-SCITK was confirmed in our previous investigations (data to be published). In the present study, the effects of pcDNA$_3$-SCITK transfection on the expression of HBsAg by 2.2.15 cells was observed. The results showed that HBsAg in the supernatant of transfected 2.2.15 cell culture was significantly decreased on the 6th day post-transfection as compared with that of the mock group (P<0.05, Table 1).

Table 1 HBsAg expression in supernants of cell culture by experimental cells

Groups	OD Value		
	1st day	3rd day	6th day
Mock group	0.32±0.13	0.61±0.23	0.61±0.25
Experimental group	0.31±0.11	0.51±0.22	0.41±0.16[a]

[a]P<0.05 *vs* Blank control.

The lethiferous effect of pcDNA$_3$-SCITK expression on 2.2.15 cells was first noted on the 3rd day after transfection and aggravated on the 6th day posttransfection, in which the majority of transfected 2.2.15 cells were observed shrunken, round in shape and even dead (Figure 3). With assessment by the trypan blue exclusion test, the survival cell ratio on the 6th day posttransfection was 95 % in the negative control and only 11 % in the experimental group.

DISCUSSION

Chronic hepatitis B infection remains a major public health problem worldwide. Hepatitis B virus belongs to the family of hepadnaviruses that replicate their DNA genome via a reverse transcription pathway. The chronicity of infection in infected hepatocytes is maintained by the persistence of the viral covalently closed circular DNA. Traditionally, the strategy to combat chronic HBV infection depends mainly on the stimulation of specific antiviral immune response or on the inhibition of viral replication, or on both. However, it has been found that prolonged administration of therapeutic agents is often associated with the production of resistant mutants and serious side effects, as well as a control of viral replication rather than eradication. To further search for effective therapeutic modalities to deal with the chronic infection of HBV is therefore urgently needed to design a brand-new strategy to clear the causative virus.

Hepatitis C virus, a member of the Flaviviridae family and an enveloped virus with a single-stranded 9.6 kb RNA genome of positive polarity[29], utilizes a cap-independent mechanism to initiate translation on its genomic RNAs. This process could involve an internal ribosome entry sites (IRES) located in the 5' nontranslated RNA (5'-NTR), and both canonical and noncanonical translation initiation factors[30-32]. The former could be constructed in some of the bicistronic systems with a higher efficiency in the initiation of protein translation and has been used to construct recombinant vectors[33-36]. It has been recently found that HCV-C protein, another functional modulator localized both in cytoplasm and in perinuclear regions, could interact with IRES and down-regulate IRES-directed translation[37-42], which has been considered to be involved in the establishment or maintenance of the virus persistence[40-43]. Based on these observations, we hypothesized that a self-modulating mechanism by the interaction of HCV-C protein with IRES element was possible to be employed in gene therapy for the eradication of chronic HBV infection.

In the present study, we constructed a recombinant plasmid pcDNA3-SCITK by cloning HCV-C gene and IRES element, partial antisense sequence of HBV-S gene, and TK suicide gene into the eukaryotic expression vector pcDNA3, in which the expression of TK gene was driven in turn by human cytomegalovirus (CMV) promoter, HBV-anti-S and HCV core-IRES sequences. The prominent feature of this plasmid was the temperate expression of effector gene in transfected cells by a self-modulating mechanism. When HBV in the infected cells began to replicate, the transcribed mRNA of HBV-S gene could be combined with its counterpart produced by HBV-antisense-S gene in the recombinant plasmid to form a mRNA dimmer prior to the initiation codon AUG of HCV-C gene, which brought about a decreased expression of HCV-C protein. The consequently reduced HCV core protein-IRES combination could enhance the IRES element to promote the expression of TK suicide gene and further to cause a lethiferous effect on HBV infected cells. In contrast, the expression of effector gene TK was inhibited in non-infected cells because of the normal level of HCV-C protein expression and its normal combination with HCV-IRES element, which would not cause any damage to the healthy cells.

In order to identify the anti-HBV efficiency of pcDNA3-SCITK, 2.2.15 cells that carry the full HBV genome and can stably express series of HBV antigen were transfected with the plasmid. The results showed that HBsAg level in the supernatant of transfected 2.2.15 cell culture was significantly decreased on the 6th day post transfection as compared with that of the mock cells (Table 1). The lethiferous effect of pcDNA$_3$-SCITK expression on 2.2.15 cells was noted initially on the 3rd day after transfection and aggravated on the 6th day posttransfection, in which the majority of transfected 2.2.15 cells were observed shrunken, round in shape and even dead. However, the negative control HepG2 cells grew well (Figure 3). With assessment by the trypan blue exclusion test, the survival cell ratio on the 6th day post transfection was 95 % in the negative control and only 11 % in the experimental group. All these observations confirmed that plasmid pcDNA3-SCITK could exert a lethiferous effect on HBV infected cells via a self-modulating mechanism, which might also be served as a potential therapeutic strategy for the liver cancers derived from chronic HBV infection.

The limitation of the present study is the neglect of anti-HBV infection by preventing the pathogen from invading target cells or by interrupting the virus replication at the beginning of the disease. How to apply our present therapeutic strategy in combination with other treatment protocols to the eradication of chronic HBV infection is to be further investigated.

REFERENCES

1 **Xu R,** Cai K, Zheng D, Ma H, Xu S, Fan ST. Molecular therapeutics of HBV. *Curr Gene Ther* 2003; **3:** 341-355

2 **Morrissey DV,** Lee PA, Johnson DA, Overly SL, McSwiggen JA, Beigelman L, Mokler VR, Maloney L, Vargeese C, Bowman K, O'Brien JT, Shaffer CS, Conrad A, Schmid P, Morrey JD, Macejak DG, Pavco PA, Blatt LM. Characterization of nuclease-resistant ribozymes directed against hepatitis B virus RNA. *J Viral Hepat* 2002; **9:** 411-418

3 **Gumina G,** Song GY, Chu CK. Advances in antiviral agents for hepatitis B virus. *Antivir Chem Chemother* 2001; **12**(Suppl 1): 93-117

4 **Feng Y,** Kong YY, Wang Y, Qi GR. Intracellular inhibition of the replication of hepatitis B virus by hammerhead ribozymes. *J Gastroenterol Hepatol* 2001; **16:** 1125-1130

5 **Staschke KA,** Colacino JM. Drug discovery and development of antiviral agents for the treatment of chronic hepatitis B virus infection. *Prog Drug Res* 2001; **Spec No:** 111-183

6 **Harrison GL,** Murray-McIntosh R, Penny D. Hepatitis B virus genotypes: a South Pacific perspective. *Pac Health Dialog* 2001; **8:** 188-192
7 **Zoulim F.** Therapy of chronic hepatitis B virus infection: inhibition of the viral polymerase and other antiviral strategies. *Antiviral Res* 1999; **44:** 1-30
8 **Merle P,** Trepo C, Zoulim F. Current management strategies for hepatitis B in the elderly. *Drugs Aging* 2001; **18:** 725-735
9 **Bernardi M,** Biselli M, Gramenzi A. Chronic hepatitis B. Recent advances in diagnosis and treatment. *Recenti Prog Med* 2002; **93:** 397-402
10 **Fang JN,** Jin CJ, Cui LH, Quan ZY, Choi BY, Ki M, Park HB. A comparative study on serologic profiles of virus hepatitis B. *World J Gastroenterol* 2001; **7:** 107-110
11 **Rabe C,** Pilz T, Klostermann C, Berna M, Schild HH, Sauerbruch T, Caselmann WH. Clinical characteristics and outcome of a cohort of 101 patients with hepatocellular carcinoma. *World J Gastroenterol* 2001; **7:** 208-215
12 **Roussos A,** Goritsas C, Pappas T, Spanaki M, Papadaki P, Ferti A. Prevalence of hepatitis B and C markers among refugees in Athens. *World J Gastroenterol* 2003; **9:** 993-995
13 **Liaw YF.** Therapy of chronic hepatitis B: current challenges and opportunities. *J Viral Hepat* 2002; **9:** 393-399
14 **Chin R,** Locarnini S. Treatment of chronic hepatitis B: current challenges and future directions**.** *Rev Med Virol* 2003; **13:** 255-272
15 **Karayiannis P.** Hepatitis B virus: old, new and future approaches to antiviral treatment. *J Antimicrob Chemother* 2003; **51:** 761-785
16 **Raj V.** Treatment of hepatitis B. *Clin Cornerstone* 2001; **3:** 24-36
17 **Zoulim F,** Trepo C. New antiviral agents for the therapy of chronic hepatitis B virus infection. *Intervirology* 1999; **42:** 125-144
18 **Klein C,** Bock CT, Wedemeyer H, Wustefeld T, Locarnini S, Dienes HP, Kubicka S, Manns MP, Trautwein C. Inhibition of hepatitis B virus replication in vivo by nucleoside analogues and siRNA. *Gastroenterology* 2003; **125:** 9-18
19 **Wo JE,** Wu XL, Zhu HH, Zhou LF, Yao HP, Chen LW. DNAzymes in vitro inhibit the expression of hepatitis B virus genes. *Zhejiang Daxue Xuebao Yixueban* 2003; **32:** 112-115
20 **Tung FYT,** Bowen SW. Targeted inhibition of hepatitis B virus gene expression: a gene therapy approach. *Front Biosci* 1998; **3:** a11-a15
21 **Guha C,** Shah SJ, Ghosh SS, Lee SW, Roy-Chowdhury N, Roy-Chowdhury J. Molecular therapies for viral hepatitis. *Bio Drugs* 2003; **17:** 81-91
22 **Wu C,** Zeng Z, Wang Q. Experimental study of inhibition of hepatitis B by dual-target antisense RNA. *Zhonghua Yixue Zazhi* 2001; **81:** 605-608
23 **Robaczewska M,** Guerret S, Remy JS, Chemin I, Offensperger WB, Chevallier M, Behr JP, Podhajska AJ, Blum HE, Trepo C, Cova L. Inhibition of hepadnaviral replication by polyethylenimine-based intravenous delivery of antisense phosphodiester oligodeoxynucleotides to the liver. *Gene Ther* 2001; **8:** 874-881
24 **Feng Y,** Kong YY, Wang Y, Qi GR. Inhibition of hepatitis B virus by hammerhead ribozyme targeted to the poly (A) signal sequence in cultured cells. *Biol Chem* 2001; **382:** 655-660
25 **Zu Putlitz J,** Wieland S, Blum HE, Wands JR. Antisense RNA complementary to hepatitis B virus specifically inhibits viral replication. *Gastroenterology* 1998; **115:** 702-713
26 **Yang YS,** Watson WJ, Tucker PW, Capra JD. Construction of recombinant DNA by exonuclease recession. *Nucleic Acids Res* 1993; **21:** 1889-1893
27 **Horton RM.** *In vitro* recombination and mutagenesis of DNA. SOEing together tailor-made genes. *Methods Mol Biol* 1997; **67:** 141-149
28 **Horton RM.** PCR-mediated recombination and mutagenesis. SOEing together tailor-made genes. *Mol Biotechnol* 1995; **3:** 93-99
29 **Bartenschlager R,** Lohmann V. Replication of hepatitis C virus. *J Gen Virol* 2000; **81:** 1631-1648
30 **Reynolds JE,** Kaminski A, Kettinen HJ, Grace K, Clarke BE, Carroll AR, Rowlands DJ, Jackson RJ. Unique features of internal initiation of hepatitis C virus RNA translation. *EMBO J* 1995; **14:** 6010-6020
31 **Morgan RA,** Couture L, Elroy-Stein O, Ragheb J, Moss B, Anderson WF. Retroviral vectors containing putative internal ribosome entry sites: development of a polycistronic gene transfer system and applications to human gene therapy. *Nucleic Acids Res* 1992; **25:** 1293-1299
32 **Lu HH,** Wimmer E. Poliovirus chimeras replicating under the translational control of genetic elements of hepatitis C virus reveal unusual properties of the internal ribosomal entry site of hepatitis C virus. *Proc Natl Acad Sci* 1996; **93:** 1412-1417
33 **Urabe M,** Hasumi Y, Ogasawara Y, Matsushita T, Kamoshita N, Nomoto A, Colosi P, Kurtzman GJ, Tobita K, Ozawa K. A novel dicistronic AAV vector using a short IRES segment derived from hepatitis C virus genome. *Gene* 1997; **200:** 157-162
34 **Kruger M,** Beger C, Li QX, Welch PJ, Tritz R, Leavitt M, Barber JR, Wong-Staal F. Identification of eIF2Bgamma and eIF2gamma as cofactors of hepatitis C virus internal ribosome entry site-mediated translation using a functional genomics approach. *Proc Natl Acad Sci U S A* 2000; **97:** 8566-8571
35 **Zhang H,** Hanecak R, Brown-Driver V, Azad R, Conklin B, Fox MC, Anderson KP. Antisense oligonucleotide inhibition of hepatitis C virus (HCV) gene expression in livers of mice infected with an HCV-vaccinia virus recombinant. *Antimicrob Agents Chemother* 1999; **43:** 347-353
36 **Liang XS,** Lian JQ, Zhou YX, Nie QH, Hao CQ. A small yeast RNA inhibits HCV IRES mediated translation and inhibits replication of poliovirus *in vivo*. *World J Gastroenterol* 2003; **9:** 1008-1013
37 **Santolini E,** Migliaccio G, La Monica N. Biosynthesis of biochemical properties of the hepatitis C virus core protein. *J Virol* 1994; **68:** 3631-3641
38 **Yasui K,** Wakita T, Tsukiyama-Kohara K, Funahashi SI, Ichikawa M, Kajita T, Moradpour D, Wands JR, Kohara M. The native form and maturation process of hepatitis C virus core protein. *J Virol* 1998; **72:** 6048-6055
39 **Urabe M,** Hasumi Y, Ogasawara Y, Matsushita T, Kamoshita N, Nomoto A, Colosi P, Kurtzman GJ, Tobita K, Ozawa K. A novel discistronic AAV vector using a short IRES segment derived from hepatitis c virus genome. *Gene* 1997; **200:** 157-162
40 **Shimoike T,** Mimori S, Tani H, Matsuura Y, Miyamura T**.** Interaction of hepatitis c virus core protein with viral sense RNA and suppression of its translation. *J Virol* 1999; **73:** 9718-9725
41 **Zhang J,** Yamada O, Yoshida H, Iwai T, Araki H. Autogenous translational inhibition of core protein: implication for switch from translation to RNA replication in hepatitis C virus. *Virology* 2002; **293:** 141-150
42 **Li D,** Takyar ST, Lott WB, Gowans EJ. Amino acids 1-20 of the hepatitis C virus (HCV) core protein specifically inhibit HCV IRES-dependent translation in HepG2 cells, and inhibit both HCV IRES- and cap-dependent translation in HuH7 and CV-1 cells. *J Gen Virol* 2003; **84:** 815-825
43 **Yao ZQ,** Ray S, Eisen-Vandervelde A, Waggoner S, Hahn YS. Hepatitis C virus: immunosuppression by complement regulatory pathway. *Viral Immunol* 2001; **14:** 277-295

Edited by Wang XL

P.O.Box 2345, Beijing 100023,China
Fax: +86-10-85381893
E-mail: wjg@wjgnet.com www.wjgnet.com

World J Gastroenterol 2003;9(10):2221-2225
World Journal of Gastroenterology
 ISSN 1007-9327

• VIRAL HEPATITIS •

Association between HLA class II gene and susceptibility or resistance to chronic hepatitis B

Ye-Gui Jiang, Yu-Ming Wang, Tong-Hua Liu, Jun Liu

Ye-Gui Jiang, Yu-Ming Wang, Jun Liu, Institute of Infectious Diseases, Southwest Hospital, Third Military Medical University, Chongqing 400038, China
Tong-Hua Liu, Department of Pharmacy, Xinqiao Hospital, Third Military Medical University, Chongqing 400038, China
Correspondence to: Dr. Ye-Gui Jiang, Institute of Infectious Diseases, Southwest Hospital, Third Military Medical University, Chongqing 400038, China. jiangyegui@yahoo.com.cn
Telephone: +86-23-68754141 **Fax:** +86-23-68754479
Received: 2003-05-10 **Accepted:** 2003-06-19

Abstract

AIM: To investigate the association between the polymorphism of HLA-DRB1, -DQA1 and -DQB1 alleles and viral hepatitis B.

METHODS: HLA-DRB1, -DQA1 and -DQB1 alleles in 54 patients with chronic hepatitis B, 30 patients with acute hepatitis B and 106 normal control subjects were analyzed by using the polymerase chain reaction/sequence specific primer (PCR/SSP) technique.

RESULTS: The allele frequency of HLA-DRB1*0301 in the chronic hepatitis B group was markedly higher than that in the normal control group (17.31 % *vs* 5.67 %), there was a significant correlation between them (χ^2=12.3068, *Pc*=0.0074, RR=4.15). The allele frequency of HLA-DQA1*0501 in the chronic hepatitis B group was significantly higher than that in the normal control group (25.96 % *vs* 13.68 %), there was a significant correlation between them (χ^2=9.2002, *Pc*=0.0157, RR=2.87). The allele frequency of HLA-DQB1*0301 in the chronic hepatitis B group was notably higher than that in the normal control group (35.58 % *vs* 18.87 %), there was a significant correlation between them (χ^2=15.5938, *Pc*=0.0075, RR=4.07). The allele frequency of HLA-DRB1*1101/1104 in the chronic hepatitis B group was obviously lower than that in the normal control group (0.96 % *vs* 13.33 %), there was a significant correlation between them (χ^2=11.9206, *Pc*=0.0145, RR=18.55). The allele frequency of HLA-DQA1*0301 in the chronic hepatitis B group was remarkably lower than that in the normal control group (14.42 % *vs* 30 %), there was a significant correlation between them (χ^2=8.7396, *Pc*=0.0167, RR=0.35).

CONCLUSION: HLA-DRB1*0301, HLA-DQA1*0501 and HLA-DQB1*0301 are closely related with susceptibility to chronic hepatitis B, and HLA-DRB1*1101/1104 and HLA-DQA1*0301 are closely related with resistance to chronic hepatitis B. These findings suggest that host HLA class II gene is an important factor determining the outcome of HBV infection.

Jiang YG, Wang YM, Liu TH, Liu J. Association between HLA class II gene and susceptibility or resistance to chronic hepatitis B. *World J Gastroenterol* 2003; 9(10): 2221-2225
http://www.wjgnet.com/1007-9327/9/2221.asp

INTRODUCTION

The progression of hepatitis B virus (HBV) infection may be influenced by a number of factors including the viral genotype and the level of viremia, but these factors alone do not account for the variability in outcome. There is an increasing awareness that host factors are involved. A great deal of evidences suggest that both cellular and humoral immune responses are required for viral clearance[1-3]. Polymorphisms of human leukocyte antigen (HLA) influence immune responses. Variability in immune response is often associated with HLA polymorphism. HLA genotype of an individual may influence the progression of HBV infection. Patients who have successfully recovered from acute hepatitis B develop strong HLA classes I and II restricted T cell response, whereas these responses are weak or absent in patients with chronic hepatitis B[4, 5]. In the present study, we have analyzed the polymorphism of HLA-DRB1, -DQA1 and -DQB1 alleles in patients with chronic and acute hepatitis B and healthy controls using the polymerase chain reaction with sequence specific primers (PCR/SSP). This study aimed at investigating whether these alleles might be associated with susceptibility or resistance to chronic hepatitis B.

MATERIALS AND METHODS

Subjects

Fifty-two patients (43 males, 9 females, mean age: 33.46 years) with chronic hepatitis B and 30 patients (24 males, 6 females, mean age: 33.25 years) with acute hepatitis B, and 106 healthy blood donors (88 males, 18 females, mean age: 31.27 years) were included in this study. All the patients were from the Institute of Infectious Diseases, Southwest Hospital of Third Military Medical University. The diagnosis of all the cases was made according to the criteria established on the Viral Hepatitis Conference held in 2000. All the patients and controls were Chinese Han people without relatives from Chongqing. The subjects were divided into chronic hepatitis B group, acute hepatitis B group and healthy control group.

Primer synthesis and reagents

The polymorphisms of HLA-DRB1, -DQA1 and -DQB1 alleles were assessed by PCR/SSP technique. HLA-DRB1, -DQA1 and -DQB1 loci of specific PCR primers were designed by Olerup *et al*[6, 7], and synthesized by Shanghai Branch, Canadian Sangon Company. The primers amplifying human growth hormone gene (5' -primer: 5' -GCC TTC CCA ACC ATT CCC TTA-3' , 3' -primer: 5' -TCA CGG ATT TCT GTT GTG TTTC-3') were synthesized by Shanghai Branch, Canadian Sangon Company. Taq DNA polyenzyme and dNTP were purchased from Shanghai Branch, Canadian Sangon Company, pBR322/ Hand III marker and the ReadyPCR™ whole blood genomic DNA purification system were provided by Sino-American Biotechnology Company.

Methods

DNA extraction Genomic DNA was extracted from peripheral blood by using the Ready PCR™ whole blood genomic DNA purification system.

PCR amplification

A total amount of 25 μl PCR reaction solution contained 8 pmoles of each sequence specific primer (3.2 μl), 0.8 pmoles of each internal control primer (0.32 μl), 80-100 ng of genomic DNA (2 μl), 2.5 μl of 10×buffer, 25 mmol/L of $MgCl_2$ (2.5 μl), 10 mmol/L of dNTP (1 μl), 5 unit/μl of Taq polymerase (0.5 μl) and 13 μl of demonized H_2O. The PCR cycling parameters of HLA-DRB1 alleles were as follows: predenaturation at 94 ℃ for 5 min, denaturation at 94 ℃ for 50 s, annealing at 65 ℃ for 1 min, extension at 72 ℃ for 1 min, repetition for 30 cycles and final extension at 72 ℃ for 5 min. The PCR cycling parameters of HLA-DQA1 and -DQB1 alleles were as follows: predenaturation at 94 ℃ for 4 min, denaturation at 94 ℃ for 1 min, annealing at 65 ℃ for 1 min, extension at 72 ℃ for 1 min, repetition for 30 cycles and final extension at 72 ℃ for 2 min. In each PCR reaction a primer pair was included to amplify the human growth hormone gene, which functioned as an internal positive amplification control and gave rise to a 429 base pair fragment.

Detection of PCR products PCR products were loaded in 2 % agars gel containing 0.5 μg/ml of ethidium bromide, electrophoresed for 20 min at 15 V/cm, examined under ultraviolet light. The individual alleles were assigned for the specific pattern of appropriately sized bands.

Statistical analysis

Allele frequencies of HLA-DRB1, -DQA1 and -DQB1 were calculated by direct count. AF for the study group was compared with that for the control group using Chi-square (χ^2) test. The Fisher' s exact test was used when χ^2 value exceeded 3.84, the *P* values were corrected for the number of alleles (corrected *P*=*Pc*). Relative risk frequencies (RR) were calculated according to Wolf formula.

RESULTS

HLA-DRB1 alleles in patients with chronic and acute hepatitis B and healthy controls

The distribution of HLA-DRB1 alleles is shown in Table 1. The allele frequencies of HLA-DRB1*0301 in the chronic hepatitis B group (17.31 %) were markedly higher than those in the normal control group (5.67 %), there was a significant correlation between them (χ^2=12.3068, *Pc*=0.0074, RR=4.15). The allele frequencies of HLA-DRB1*1101/1104 in the chronic hepatitis B group (0.96 %) were significantly lower than those in the acute hepatitis B group (13.33 %), with significant correlation between them (χ^2=11.9206, *Pc*=0.0145, RR=18.55). The data of electrophoresis of HLA-DRB1 alleles amplification are shown in Figure 1.

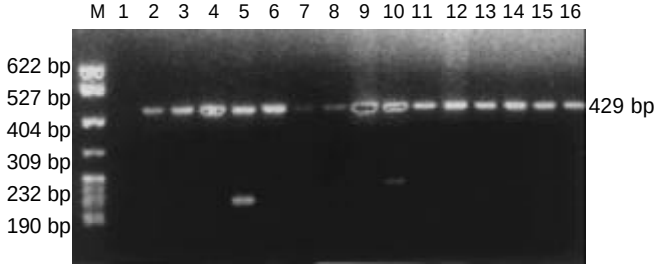

Figure 1 Electrophoresis of HLA-DRB1 alleles amplification by PCR/SSP. M: pBR322DNA/MSP I marker, 1: negative control, 2: 0101/0103, 3: 0301, 4: 0401/0411, 5: 0701/0702, 6: 0801/0804, 7: 0901, 8: 1001, 9: 1101/1104, 10: 1201/1202, 11: 1301/1302, 12: 1303/1304, 13: 1401,1404, 14: 1402,1403, 15: 1501/1502, 16: 1601/1602.

Table 1 Allele frequency of HLA-DRB1 in patients with chronic and acute hepatitis B and normal heathy individuals

HLA-DRB1 allele	Normal control (*n*=106)		Chronic hepatitis B (*n*=52)		Acute hepatitis B (*n*=30)	
	PN	AF	PN	AF	PN	AF
0101/0103	1	0.47	1	0.96	1	1.67
0301*	12	5.66	18	17.31	6	10.00
0401/0411	24	11.32	13	12.50	7	11.67
0701/0702	11	5.19	8	7.69	4	6.67
0801/0804	9	4.25	6	5.77	3	5.00
0901	32	15.09	16	15.39	8	13.33
1001	2	0.94	2	1.92	1	1.67
1101/1104**	13	6.13	1	0.96	8	13.33
1201/1202	34	16.04	15	14.42	8	13.33
1301/1302	4	1.89	1	0.96	1	1.67
1303/1304	1	0.47	1	0.96	1	1.67
1401,1404	14	6.60	6	5.77	4	6.67
1402,1403	0	0.00	0	0.00	0	0.00
1501/1502	34	16.04	11	10.58	5	8.33
1601/1602	13	6.13	2	1.92	1	1.67
Blank	8	3.77	3	2.89	2	3.33

PN: positive number, AF: allele frequency. *χ^2=12.3068, *Pc*=0.0074, RR=4.15. **χ^2=11.9206, *Pc*=0.0145, RR=18.55.

HLA-DQA1 alleles in patients with chronic and acute hepatitis B and healthy controls

The distribution of HLA-DQA1 alleles is shown in Table 2. The allele frequencies of HLA-DQA1*0501 in the chronic hepatitis B group (25.96 %) were markedly higher than those in the normal control group (13.68 %), there was a significant correlation between them (χ^2=9.2002, *Pc*=0.0157, RR=2.87). The allele frequencies of HLA-DQA1*0301 in the chronic hepatitis B group (14.42 %) was significantly lower than those in the acute hepatitis B group (30 %), there was a significant correlation between them (χ^2=7.6781, *Pc*=0.0388, RR=3.70). The data of electrophoresis of HLA-DQA1 alleles amplification are shown in Figure 2.

Table 2 Allele frequency of HLA-DQA1 in patients with chronic and acute hepatitis B and normal heathy individuals

HLA-DQA1 allele	Normal control (*n*=106)		Chronic hepatitis B (*n*=52)		Acute hepatitis B (*n*=30)	
	PN	AF	PN	AF	PN	AF
0101	17	8.02	9	8.65	4	6.67
0102	45	21.23	22	21.15	12	20.00
0103	9	4.25	5	4.81	2	3.33
0104	3	1.42	1	0.96	1	1.67
0201	7	3.30	3	2.88	1	1.67
0301*	57	26.89	15	14.42	18	30.00
0302	1	0.47	0	0.00	0	0.00
0401	2	0.49	1	0.96	1	1.67
0501**	29	13.68	27	25.96	10	16.67
0601	23	10.85	12	11.54	6	10.00
Blank	19	8.96	9	8.65	5	8.33

PN: positive number, AF: allele frequency. *χ^2=7.6781, *Pc*=0.0388, RR=3.70. **χ^2=9.2002, *Pc*=0.0157, RR=2.87.

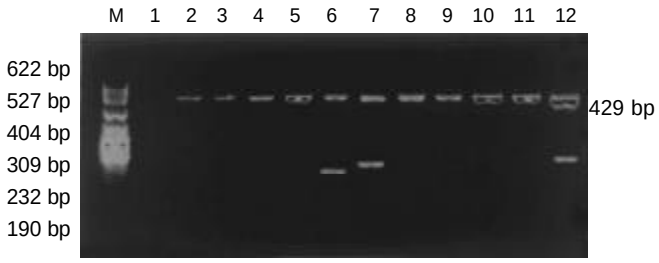

Figure 2 Electrophoresis of HLA-DQA1 alleles amplification by PCR/SSP. M: pBR322DNA/MSPImarker, 1: negative control, 2: 0101/0104, 3: 0101/0102/0104, 4: 0102/0103, 5: 0103, 6: 0201, 7: 0301, 8: 0302, 9: 0401, 10: 0501, 11: 0601, 12: A (when the amplification product was -DQA1*0104, "A" was negative. When the amplification product was non-DQA1*0104, "A"was positive.).

HLA-DQA1 alleles in patients with chronic and acute hepatitis B and healthy controls

The distribution of HLA-DQB1 alleles is shown in Table 3. The allele frequencies of HLA-DQB1*0301 allele in the chronic hepatitis B group (35.58 %) were markedly higher than those in the normal control group (18.87 %), there was a significant correlation between them (χ^2=15.5938, *Pc*=0.0075, RR=4.07). The data of electrophoresis of HLA-DQB1 alleles amplification are shown in Figure 3.

Table 3 Allele frequency of HLA-DQB1 in patients with chronic and acute hepatitis B and normal heathy individuals

HLA-DQB1 allele	Normal control (*n*=106)		Chronic hepatitis B (*n*=52)		Acute hepatitis B (*n*=30)	
	PN	AF	PN	AF	PN	AF
0201	23	10.85	10	9.62	6	10.00
0301*	40	18.87	37	35.58	16	26.67
0302	14	6.61	6	5.77	3	5.00
0303	35	16.51	15	14.42	10	16.67
0401	11	5.19	5	4.81	3	5.00
0402	2	0.94	1	0.96	1	1.67
0501	9	4.25	3	2.88	2	3.33
0502	20	9.43	7	6.73	3	5.00
0503	6	2.83	2	1.92	1	1.67
0601	20	9.43	7	6.73	7	11.67
0602	12	5.66	4	3.85	3	5.00
0603	5	2.36	2	1.92	1	1.67
0604	7	3.30	2	1.92	2	3.33
Blank	8	3.77	3	2.89	2	3.33

PN: positive number, AF: allele frequency. χ^2=15.5938, *Pc*=0.0075, RR=4.07.

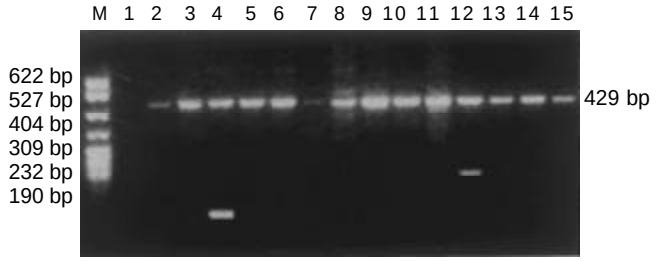

Figure 3 Electrophoresis of HLA-DQB1 alleles amplification by PCR/SSP. M: pBR322DNA/MSP I marker, 1: negative control, 2: 0201, 3: 0201/0302, 4: 0301, 5: 0302/0303, 6: 0303, 7: 0401, 8: 0402, 9: 0501, 10: 0502, 11: 0503, 12: 0601, 13: 0602, 14: 0603, 15: 0604.

DISCUSSION

Host and viral factors undoubtedly influence the clinical expression and behavior of chronic hepatitis B. Attempts to explain the clinical expression and the behavior of chronic hepatitis B by viral factors have shown the importance of viral genotypes and viraemia level for the clinical presentation. However, there remain large inconsistencies, and it is very likely that immune response to hepatitis B virus (HBV) of the host can modify disease outcome[8-10]. HLA is a critical genetic factor that determines individual variations of immune response. The ternary structure of HLA molecules and their roles in the control of immune response have been clearly elucidated. There are many reports about statistical associations between HLA and diseases. HLA gene contributes to the host response against HBV[11-28]. Individuals with different HLA types may differ in susceptibility or resistance to disease[29-35], and associations between HLA polymorphism and susceptibility or resistance to diseases have been identified.

Researches on the correlation between HLA and hepatitis B have been performed for many years. Traditional serological method was used in some investigations, but it has become obsolete and inaccurate. To have a better understanding of the disease, correlation between hepatitis B and HLA should be further studied using nucleotide-typing techniques. Therefore, in the present study, we examined the HLA-DRB1, -DQA1 and -DQB1 alleles by PCR/SSP technique in patients with hepatitis B in an attempt to investigate the association between the polymerase of HLA class II gene and hepatitis B. Fourteen HLA-DRB1 alleles, ten HLA-DQA1 alleles and thirteen HLA-DQB1 alleles were detected. The allele frequencies of HLA-DRB1, -DQA1 and -DQB1 in healthy individuals tallied with genetic characteristics of the Han people in southern region of China.

A previous study showed that the allele frequencies of HLA-B8, DR3, A30, DQA1*0501 in patients with chronic hepatitis B were markedly increased, suggesting that these alleles are associated with chronic hepatitis B[36]. Thio *et al*[37] found that HBV persistence was significantly associated with two class II alleles, DQA1*0501 (OR=2.6) and DQB1 *0301 (OR=3.9), the two-locus haplotype consisted of these same two alleles (OR=3) and the three-locus haplotype consisted of DQA1 *0501, DQB1 *0301 and DRB1 *1102 (OR=10.7). The study by Shen *et al* suggested that the susceptibility to chronic hepatitis B was strongly associated with HLA-DRB1*10 allele in northern Chinese patients[38]. In the present study, we found that the allele frequencies of HLA-DRB1*0301, -DQA1*0501 and -DQB1*0301 in the chronic hepatitis B group were markedly higher than those in the normal control group, there was a significant correlation between them (Tables 1, 2 and 3). These findings suggest that HLA-DRB1*0301, -DQA1*0501 and -DQB1*0301 are closely associated with the susceptibility to chronic hepatitis B, and may be the susceptible gene.

Cotrina *et al*[39] analyzed the HLA-DRB1 genotype in a series of patients with chronic hepatitis B and acute hepatitis B, which further confirmed that HLA-DRB1*1301 and -DRB1*1302 alleles were associated with the clearance of HBV infection and protected people against chronic hepatitis B. Diepolder *et al*[40] found that a strong virus-specific $CD4^+$ and $CD8^+$ T lymphocyte response to hepatitis B virus was associated with viral clearance, patients with acute hepatitis B carrying HLA-DR13 had a more vigorous $CD4^+$ T cell response to HBV core than patients not carrying HLA-DR13, suggesting that HLA-DR13 is associated with a self-limited course of HBV infection, and the beneficial effect of HLA-DR13 alleles on the outcome of HBV infection could be explained by a more vigorous HBV core-specific $CD4^+$ T cell response, which might be either due to a more proficient antigen presentation by HLA-

DR13 molecules themselves or due to a linked polymorphism in a neighboring immunoregulatory gene. In the present study, we found that the allele frequencies of HLA-DRB1*1101/1104 and HLA-DQA1*0301 in the chronic hepatitis B group were markedly lower than those in the acute hepatitis B group, there was a significant correlation between them (Tables 1 and 2). These findings suggest that HLA-DRB1*1101/1104 and -DQA1*0301 are closely associated with the resistance to chronic hepatitis B, and may be the resistant gene.

The results of the present study suggest that HLA-DRB1*0301, -DQA1*0501 and -DQB1*0301 may be the susceptible gene, and HLA-DRB1*1101/1104 and -DQA1*0301 may be the resistant genes to chronic hepatitis B, and that host HLA class II gene is an important factor determining the outcome of HBV infection, which will give some new clues to the study of pathogenesis of chronic hepatitis B.

REFERENCES

1 **Takayama T**, Sekine T, Makuuchi M, Yamasaki S, Kosuge T, Yamamoto J, Shimada K, Sakamoto M, Hirohashi S, Ohashi Y, Kakizoe T. Adoptive immunotherapy to lower postsurgical recurrence rates of hepatocellular carcinoma: a randomised trial. *Lancet* 2000; **356**: 802-807

2 **Chiari R**, Hames G, Stroobant V, Texier C, Maillere B, Boon T, Coulie PG. Identification of a tumor-specific shared antigen derived from an Eph receptor and presented to CD4 T cells on HLA class II molecules. *Cancer Res* 2000; **60**: 4855-4863

3 **Feinmesser M**, Sulkes A, Morgenstern S, Sulkes J, Stern S, Okon E. HLA-DR and beta 2 microglobulin expression in medullary and atypical medullary carcinoma of the breast: histopathologically similar but biologically distinct entities. *J Clin Pathol* 2000; **53**: 286-291

4 **Zhang SL**, Liu M, Zhu J, Chai NL. Predominant Th-2 immune response and chronic hepatitis B virus infection. *Shijie Huaren Xiaohua Zazh* 1999; **7**: 513-515

5 **Chen WN**, Oon CJ. Mutation "hot spot" in HLA class I- restricted T cell epitope on hepatitis B surface antigen in chronic carriers and hepatocellular carcinoma. *Biochem Biophys Commun* 1999; **262**: 757-761

6 **Olerup O**, Zetterquist H. HLA-DR typing by PCR amplification with sequence-specific primers (PCR-SSP) in 2 hours: an alternative to serological DR typing in clinical practice including donor-recipient matching in cadaveric transplantation. *Tissue Antigens* 1992; **39**: 225-235

7 **Olerup O**, Aldener A, Fogdell A. HLA-DQB1 and DQA1 typing by PCR amplification with sequence-specific primers (PCR-SSP) in 2 hours. *Tissue Antigens* 1993; **41**: 119-134

8 **Jiang YG**, Li QF, Mao Q, WangYM. Primary human fetal hepatocytes with HBV infection *in vitro*. *Shijie huaren Xiaohua Zazhi* 2000; **8**: 403-405

9 **Sing G**, Butterworth L, Chen X, Bryant A, Cooksley G. Composition of peripheral blood lymphocyte populations during different stages of chronic infection with hepatitis B virus. *J Viral Hepat* 1998; **5**: 83-93

10 **Cao T**, Meuleman P, Desombere I, Sallberg M, Leroux-Roels G. *In vivo* inhibition of anti-hepatitis B virus core antigen (HBcAg) immunoglobulin G production by HBcAg-specific CD4(+) Th1-type T-cell clones in a hu-PBL-NOD / SCID mouse modle. *J Virol* 2001; **75**: 11449-11456

11 **Du YP**, Deng CS, Lu DY, Huang MF, Guo SF, Hou W. The relation between HLA-DQA1 genes and genetic susceptibility to duodenal ulcer in Wuhan Hans. *World J Gastroenterol* 2000; **6**: 107-110

12 **Ding HL**, Cheng H, Fu ZZ, Deng QL, Yan T. The relationship of lmp2 and DR3 genes with susceptibility to type I diabetes mellitus in south China Han population. *World J Gastroenterol* 2000; **6**: 111-114

13 **Lin J**, Deng CS, Sun J, Zheng XG, Huang X, Zhou Y, Xiong P, Wang YP. HLA-DRB1 allele polymorphisms in genetic susceptibility to esophageal carcinoma. *World J Gastroenterol* 2003; **9**: 412-416

14 **Pu J**, Yang XS, Zhang YL, Pan LJ, Zhou DY. Expression of HLA-DR in epithelie around lymphofollicle of human gastrointestinal mucosa. *Shijie huaren Xiaohua Zazhi* 2000; **8**: 706-707

15 **Zhai SH**, Liu JB, Zhu P, Wang YH. CD54, CD80, CD86 and HLA-ABC expressions in liver cirrhosis and hepatocarcinoma. *Shijiehuaren Xiaohua Zazhi* 2000; **8**: 292-295

16 **Qu S**, Li QF, Deng YZ, Zhang JM, Zhang J. Cloning and expression of HLA-B7 gene. *World J Gastroenterol* 1999; **5**: 345-348

17 **Asti M**, Martinetti M, Zavaglia C, Cuccia MC, Gusberti L, Tinelli C, Cividini A, Bruno S, Salvaneschi L, Ideo G, Mondelli MU, Silini EM. Human leukocyte antigen class II and III alleles and severity of hepatitis C virus-related chronic liver disease. *Hepatology* 1999; **29**: 1272-1279

18 **Barrett S**, Ryan E, Crowe J. Association of the HLA-DRB1*01 allele with spontaneous viral clearance in an Irish cohort infected with hepatitis C virus via contaminated anti-D immunoglobulin. *J Hepatol* 1999; **30**: 979-983

19 **Lechmann M**, Schneider EM, Giers G, Kaiser R, Dumoulin FL, Sauerbruch T, Spengler U. Increased frequency of the HLA-DR15 (B1*15011) allele in German patients with self-limited hepatitis C virus infection. *Eur J Clin Invest* 1999; **29**: 337-343

20 **Mangia A**, Gentile R, Cascavilla I, Margaglione M, Villani MR, Stella F, Modola G, Agostiano V, Gaudiano C, Andriulli A. HLA class II favors clearance of HCV infection and progression of the chronic liver damage. *J Hepatol* 1999; **30**: 984-989

21 **Chang KM**, Gruener NH, Southwood S, Sidney J, Pape GR, Chisari FV, Sette A. Identification of HLA-A3 and –B7-restricted CTL response to hepatitis C virus in patients with acute and chronic hepatitis C. *J Immunol* 1999; **162**: 1156-1164

22 **Aaltonen L**, Partanen J, Auvinen E, Rihkanen H, Vaheri A. HLA-DQ alleles and human papillomavirus DNA in adult-onset laryngeal papillomatosis. *J Infect Dis* 1999; **179**: 682-685

23 **Harcourt G**, Hellier S, Bunce M, Satsangi J, Collier J, Chapman R, Phillips R, Klenerman P. Effect of HLA class II genotype on T helper lymphocyte responses and viral control in hepatitis C virus infection. *J Viral Hepat* 2001; **8**: 174-179

24 **Zhou HC**, Xu DZ, Wang XP, Zhang JX, Huang Y, Yan YP, Zhu Y, Jin BQ. Identification of the epitopes on HCV core protein recognized by HLA-A2 restricted cytotoxic T lymphocytes. *World J Gastroenterol* 2001; **7**: 583-586

25 **Ma X**, Qiu DK. Relationship between autoimmune hepatitis and HLA-DR4 and DRbeta allelic sequences in the third hypervariable region in Chinese. *World J Gastroenterol* 2001; **7**: 718-721

26 **Godkin A**, Jeanguet N, Thursz M, Openshaw P, Thomas H. Characterization of novel HLA-DR11-restricted HCV epitopes reveals both qualitative and quantitative differences in HCV-specific CD4+ T cell responses in chronically infected and non-viremic patients. *Eur J Immunol* 2001; **31**: 1438-1446

27 **Bosi I**, Ancora G, Mantovani W, Miniero R, Verucchi G, Attard L, Venturi V, Papa I, Sandri F, Dallacasa P, Salvioli GP. HLA DR13 and HCV vertical infection. *Pediatr Res* 2002; **51**: 746-749

28 **Hue S**, Cacoub P, Renou C, Halfon P, Thibault V, Charlotte F, Picon M, Rifflet H, Piette JC, Pol S, Caillat-Zucman S. Human leukocyte antigen class II alleles may contribute to the severity of hepatitis C virus-related liver disease. *J Infect Dis* 2002; **186**: 106-109

29 **Mc Dermott AB**, Cohen SB, Zuckerman JN, Madrigal JA. Human leukocyte antigens influence the immune response to a pre-S / S hepatitis B vaccine. *Vaccine* 1999; **17**: 330-339

30 **McDermott AB**, Madrigal JA, Sabin CA, Zuckerman JN, Cohen SB. The influence of host factors and immunogenetics on lymphocyte responses to Hepagene vaccination. *Vaccine* 1999; **17**: 1329-1337

31 **Wang FS**, Xing LH, Liu MX, Zhu CL, Liu HG, Wang HF, Lei ZY. Dysfunction of peripheral blood dendritic cells from patients with chronic hepatitis B virus infection. *World J Gastroenterol* 2001; **7**: 537-541

32 **Sobao Y**, Sugi K, Tomiyama H, Saito S, Fujiyama S, Morimoto M, Hasuike S, Tsubouchi H, Tanaka K, Takiguch M. Identification of hepatitis B virus-specific CTL epitopes presented by HLA-A*2402, the most common HLA class I allele in East Asia. *J Hepatol* 2001; **34**: 922-929

33 **Thimme R**, Chang KM, Pemberton J, Sette A, Chisari FV. De-

generate immunogenicity of an HLA-A2-restricted hepatitis B virus nucleocapsid cytotoxic T-lymphocyte epitope that is also presented by HLA-B51. *J Virol* 2001; **75**: 3984-3987

34 **Pellegris G**, Ravagnani F, Notti P, Fissi S, Lombardo C. B and C hepatitis viruses, HLA-DQ1 and -DR3 alleles and autoimmunity in patients with hepatocellular carcinoma. *J Hepatol* 2002; **36**: 521-526

35 **Desombere I**, Gijbels Y, Verwulgen A, Leroux-Roels G. Characterization of the T cell recognition of hepatitis B surface antigen (HBsAg) by good and poor responders to hepatitis B vaccines. *Clin Exp Immunol* 2000; **122**: 390-399

36 **Chen DF**, Kliem V, Endres W, Brunkhorst R, Tillmann HL, Koch KM, Manns MP, Stangel W. Relationship between human leukocyte antigen determinants and courses of hepatitis B virus infection in Caucasian patients with end-stage renal disease. *Scand J Gastroenterol* 1996; **31**: 1211-1215

37 **Thio CL**, Carrington M, Marti D, O'Brien SJ, Vlahov D, Nelson KE, Astemborski J, Thomas DL. Class II HLA alleles and hepatitis B virus persistence in African Americans. *J Infect Dis* 1999; **179**: 1004-1006

38 **Shen JJ**, Ji Y, Gu XL, Huang RJ, Sun YP. The association of HLA-DRB1*10 with chronic hepatitis B in Chinese patients. *Zhonghua Weishengwuxue He Mianyixue Zazhi* 1999; **19**: 58-59

39 **Cotrina M**, Buti M, Jardi R, Rodriguez-Frias F, Campins M, Esteban R, Guardia J. Study of HLA-II antigens in chronic hepatitis C and B and in acute hepatitis B. *Gastroenterol Hepatol* 1997; **20**: 115-118

40 **Diepolder HM**, Jung MC, Keller E, Schraut W, Gerlach JT, Gruner N, Zachoval R, Hoffmann RM, Schirren CA, Scholz S, Pape GR. A vigorous virus-specific CD4+ T cell response may contribute to the association of HLA-DR13 with viral clearance in hepatitis B. *Clin Exp Immunol* 1998; **113**: 244-251

Edited by Wang XL

P.O.Box 2345, Beijing 100023,China
Fax: +86-10-85381893
E-mail: wjg@wjgnet.com www.wjgnet.com

World J Gastroenterol 2003;9(10):2226-2231
World Journal of Gastroenterology
 ISSN 1007-9327

• VIRAL HEPATITIS •

No requirement of HCV 5'NCR for HCV-like particles assembly in insect cells

Wei Zhao, Guo-Yang Liao, Yan-Jun Jiang, Shu-De Jiang

Wei Zhao, Guo-Yang Liao, Yan-Jun Jiang, Shu-De Jiang, Laboratory of Vaccine Research, Institute of Medical Biology, Chinese Academy of Medical Sciences, Peking Union Medical College, Kunming 650118, Yunnan Province, China
Correspondence to: Shu-De Jiang, Laboratory of Vaccine Research, Institute of Medical Biology, Chinese Academy of Medical Sciences. 379 Jiaoling Road, Kunming 650118, Yunnan Province, China. jsd2000@163.net
Telephone: +86-871-8334330 **Fax:** +86-871-8334483
Received: 2003-08-05 **Accepted:** 2003-09-10

Abstract

AIM: To express all three HCV structural proteins in the presence or absence of HCV 5'NCR to investigate the requirement of 5'NCR for the assembly of HCV-like particles in insect cells.

METHODS: HCV structural protein encoding sequences CE1E2 and 5'NCR-CE1E2 were amplified with PCR. Recombinant baculovirus were constructed with recombinant DNA techniques. HCV structural proteins expressed in insect cells were analyzed by immunofluorescence and SDS-PAGE. Immunoprecipitation experiment of insect cell lysates with anti-E2 monoclonal antibody (MAb) was carried out and the immunoprecipitated proteins were subjected to SDS-PAGE and immunoblotting with anti-C, anti-E2 MAbs and HCV positive serum. The virus-like particles in insect cells were visualized by electron microscopy (EM). The HCV-like particles were purified by sucrose gradient centrifugation and identified by EM and immune aggregation EM.

RESULTS: The recombinant baculovirus reBV/CE1E2 containing HCV C, E1, E2 genes and reBV/CS containing the same structural protein genes plus 5'NCR were constructed. The insect cells infected with either reBV/CE1E2 or reBV/CS expressed HCV C, E1 and E2 proteins with a molecular weight of 20 kD, 35 kD and 66 kD respectively. The results of immunoprecipitation and the immunoblotting revealed the coimmunoprecipitation of C, E1, and E2 proteins, indicating the interaction of HCV structural proteins expressed in insect cells. Electron microscopy of insect cells infected with reBV/CE1E2 or reBV/CS demonstrated spherical particles (40 to 60 nm in diameter) similar to the HCV virions from sera or hepatic tissues of HCV infected humans. The HCV-like particles were partially purified by sucrose gradient centrifugation, and the purified VLPs showed immuno-reactivity with anti-HCV antibodies.

CONCLUSION: HCV 5'NCR is not required for the assembly of HCV-like particles in insect cells, HCV core and envelope proteins are sufficient for viral particle formation.

Zhao W, Liao GY, Jiang YJ, Jiang SD. No requirement of HCV 5'NCR for HCV-like particles assembly in insect cells. *World J Gastroenterol* 2003; 9(10): 2226-2231
http://www.wjgnet.com/1007-9327/9/2226.asp

INTRODUCTION

Hepatitis C virus (HCV) is the major causative agent of posttransfusion and sporadic non-A, non-B hepatitis. It is estimated that 170 million people worldwide are infected with HCV[1], more than 75 % of infected individuals develop a chronic infection, frequently with severe long-term pathologies such as cirrhosis and hepatocellular carcinoma[2]. Neither an effective treatment for chronic HCV infection nor a vaccine to prevent HCV infection is available at the present time.

HCV belongs to the genus *hepacivirus* of the *flaviviridae* family. Its genome is a 9.6-kb single-stranded RNA of positive polarity with a 5' noncoding region (5' NCR) that functions as an internal ribosome entry site, a single long open reading frame encoding a polyprotein of approximately 3 000 amino acids (aa) and a 3' NCR. This polyprotein is posttranslationally cleaved by host cell peptidases to yield structural proteins and by viral proteases, which generate nonstructural proteins. The three structural proteins, namely core (C) and envelope glycoproteins E1 and E2, are located within the amino-terminal region of the polyprotein. The nonstructural proteins (NS) 2 to 5B reside within the carboxyl-terminal part. By analogy with other *flaviviruses*, HCV virion is presumed to consist of a nucleocapsid or core protein and a viral genome coated by a lipid envelope containing glycoproteins E1 and E2. The study of HCV has been hampered by the low level of viral particles in infected individuals, the inability to propagate efficiently the virus in cultured cells, and the lack of a convenient animal model. Due to these obstacles, neither the structure of the virus nor the prerequisites for its assembly have been clearly defined. Synthesis of virus like particles (VLPs) in eukaryotic cells has opened up new possibilities for defining the structural requirements for viral particle assembly under natural intracellular conditions. In this way, by manipulating the sequence of the different proteins involved, it will be possible to define experimentally the essential morphogenic interactions required for the assembly process.

The assembly of VLPs has been reported for a number of viruses[3,4] with the most successful example of human *papillomavirus* (HPV). Baumert *et al*. have reported the recombinant *baculovirus* containing entire structural protein encoding sequences plus part of 5' NCR led to the expression and assembly of HCV-like particles in insect cells[5].

In the present study we reported the expression of HCV structural proteins in the presence or absence of HCV 5' NCR to investigate the requirement of 5' NCR for the assembly of HCV-like particles in insect cells.

MATERIALS AND METHODS

Cloning of cDNAs encoding HCV structural proteins

HCV cDNA was isolated from a HCV patient from Hebei Province, China, as previously described[6], and used as the amplifying template. cDNA fragments encoding HCV structural proteins were generated by PCR with the following primers: P1: 5'-ACAGATCTACCATGAGCACGAATCCTAAACC-3', P2: 5'-ACAGATCTACTCCACCATAGATCACTCCCC-3', P3: 5'-ATCAAGCTTACGCGTCTGCTAGTAGAAGGA-3',

P1 and P3, P2 and P3 were for CE1E2 and 5' NCR-CE1E2 respectively. A *Bgl*II site was introduced in P1 and P2 primers separately, a stop codon and a *Hin*dIII site were introduced in P3 primer. The correct sequences of CE1E2 and 5' NCR-CE1E2 were confirmed by DNA sequencing.

Baculovirus constructs and insect cell cultures

For the construction of recombinant *baculoviruses*, a Bac-to-Bac *baculovirus* expression system (Gibco-BRL/Life Technologies) was applied. The *Bgl*II-*Hin*dIII digestion products of PCR fragments were subcloned into *Bam*HI-*Hin*dIII site (multiple cloning site) of *baculovirus* donor plasmid pFastBacI. After identification by restriction digestion and PCR, each of the recombinant plasmids was used to transform DH10Bac. Through Tn7 transposon-mediated site-specific transposition foreign gene expression cassette was integrated into a *baculovirus* shuttle vector (bacmid). The size of inserts was confirmed by PCR with the pUC/M13 amplification primers, which were directed at sequences on either side of the mini-*att*Tn7 site in the bacmid. The recombinant bacmids were used for transfection of Sf9 cells (*Spodoptera frugiperda*). Recombinant *baculoviruses* were harvested thereafter and purified by plaque screening. The recombinant *baculoviruses* were verified by PCR with CE1E2 and 5' NCR-CE1E2 gene specific primers and amplified by subsequent rounds of Sf9 cell infection until a final titer of 5×10^7 PFU/ml was achieved. Detailed methods for *baculovirus* manipulation were referred to the instruction manual. Sf9 insect cells were maintained in spinner or monolayer cultures at 27 ℃ in Grace' s medium (Gibco-BRL/Life Technologies) supplemented with 10 % fetal bovine serum.

Protein expression assay

For all protein expression experiments, Sf9 cells in mid-log growth in monolayer cultures were infected with a multiplicity of infection (MOI) of 10. Infection of insect cells with non-recombinant *baculovirus* served as a negative control in all experiments. The expression of HCV structural proteins was analyzed at 72 h postinfection by immunofluorescence and SDS-PAGE. For immunofluorescence, cells were fixed with -20 ℃ acetone for 5 min. The primary antibody used was anti-HCV serum, and the secondary antibody was fluorescein isothiocyanate (FITC)-conjugated goat anti-human IgG antibody. Detailed methods were referred to Ausubel[7]. For SDS-PAGE, the cells were lysed by ultrasonic, the cell lysate was briefly centrifuged to remove cell debris and nuclei, and the supernatant was subjected to electrophoresis on a SDS-12 % polyacrylamide gel. Detailed methods were referred to Sambrook[8].

Immunoprecipitation and immunoblotting of HCV proteins

The Immunoprecipitation starter packthe (Amersham Pharmacia Biotech) was used for immunoprecipitation analysis, details of the experimental procedures were referred to the manufacturer' s protocols. Briefly, at 96 h postinfection, cells were lysed with RIPA buffer [50 mM Tris-HCl, 150 mM NaCl, 0.1 % Nonidet P-40 (NP-40), 5 mM EDTA (pH 7.5), 0.5 % sodium deoxycholate (DOC), 1 mM phenylmethylsulfonyl fluoride (PMSF)]. The cell lysate was cleared of cell debris and nuclei by low-speed centrifugation (15 min at 15 000×g and 4 ℃) and immunoprecipitated with anti-E2 monoclonal antibody (MAb). The immunoprecipitated proteins were analyzed by electrophoresis on a 12 % polyacrylamide gel. After gel transfer to polyvinylidene difluoride membranes, the blots were probed with anti-C, anti-E2 MAb, or anti-HCV serum followed by horseradish peroxidase (HRP)-conjugated goat anti-mouse (for anti-C and anti-E2 MAb) or anti-human (for serum) IgG antibody. Detailed methods for immunoblotting were referred to Sambrook[8].

Electron microscopy (EM) of VLPs in insect cells

A flask (25 cm^2) of infected cells (MOI=10, at 96 h postinfection) was harvested, washed in PBS and centrifuged at 1 000 r/min for 5 min. The cell pellets were fixed with 3.8 % glutaraldehyde in PBS for 24 h at 4 ℃. After fixation, the cells were washed three times in PBS (8 h each time) at 4 ℃ and post-fixed with 1 % osmium tetroxide for 2 h at 4 ℃. The samples were then dehydrated with acetone of a series of graded concentration, and embedded in 1:1 acetone-Epon 812 for 30 min at room temperature, further embedded in Epon 812 overnight at 37 ℃, and then polymerized for 24 h at 60 ℃. Ultrathin sections were cut with LKBIII ultramicrotome, mounted on copper grids, stained with uranyl acetate and lead citrate, washed, dried and finally examined under transmission electron microscope.

Purification of VLPs

Cells were harvested at 96 h postinfection, All purification steps were carried out on ice. Insect cells infected with reBV/CS or reBV/CE1E2 (approximately 5×10^7 cells, grown in suspension) were lysed in 50 mM Tris, 50 mM NaCl, 0.5 mM EDTA, 1 mM PMSF, 0.1 % NP-40. Sonication of the lysate was performed. The lysate was homogenized and subjected to low-speed centrifugation (15 min at 4 ℃ and 15 000×g), and the supernatant was pelleted over a 30 % (wt/vol) sucrose (in 20 mM Tris, 150 mM NaCl [pH 7.4]) cushion (6 h at 4 ℃ and 150 000×g). The pellet was resuspended in 50 mM Tris, 100 mM NaCl (pH 7.4), homogenized, and subjected to a second sucrose gradient centrifugation. The resuspended pellet was layered onto a 20 % to 60 % (wt/wt) sucrose (in 50 mM Tris, 100 mM NaCl [pH 7.4]) gradient and centrifuged for 22 h at 4 ℃ and 150 000×g. Fractions (0.5 ml) were collected from the top and analyzed by immunoblotting.

Electron microscopy and immune aggregation electron microscopy of purified VLPs

After the sucrose gradient centrifugation, VLPs were diluted in PBS (1:10), centrifuged for 2 h at 4 ℃ and 150 000×g, the pellet was resuspended in PBS. Anti-HCV serum (diluted 1:200 in PBS) was homogenized, incubated at 37 ℃ for 1 h, then stored at 4 ℃ overnight. Samples were centrifuged again for 1h at 4 ℃ and 150 000×g, the pellet was resuspended in PBS. Samples (3 ul) were absorbed on the surface of carbon-coated 300 mesh copper grids, and stained negatively with 2 % phosphotungustic acid for EM examination.

RESULTS

Construction and identification of recombinant baculoviruses

The fragment CE1E2 consisting of HCV C, E1, E2 encoding sequences and the fragment 5' NCR-CE1E2 containing the same structural protein genes plus 5' NCR were produced by PCR, with the size of 2 578 bp and 2 238 bp respectively (Figure 1). The correct sequences of CE1E2 and 5' NCR-CE1E2 were confirmed by DNA sequencing.

5' NCR-CE1E2 and CE1E2 were separately subcloned into *baculovirus* donor plasmid pFastBacI. The resulting recombinant plasmids pFB1-CS and pFB1-CE1E2 were verified (Figure 2) and used to transform DH10Bac. Through Tn7 transposon-mediated site-specific transposition foreign gene expression cassette was integrated into a *baculovirus* shuttle vector (bacmid). The result of PCR with M13/pUC forward and reverse primers indicted the correct insertion of 5' NCR-CE1E2 and CE1E2 fragments into bacmids (Figure 3),

and the resulting recombinant bacmids were named as bacmid/CS and bacmid/CE1E2 respectively. The non-recombinant bacmid was named as bacmid/0.

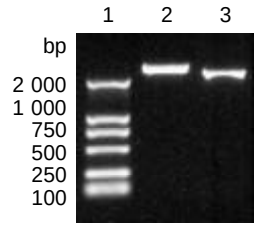

Figure 1 PCR products of HCV structural protein genes. Lane1: DNA molecular weight marker (DL-2000), lane2: 5' NCR-CE1E2, lane3: CE1E2.

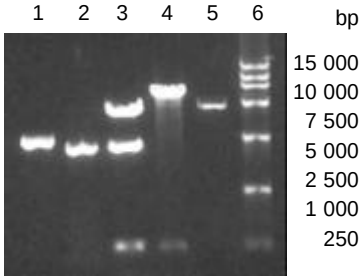

Figure 2 Confirmation of recombinant *baculovirus* donor plasmids. Lane1: PCR of pFB1-CS, lane 2: PCR of pFB1-CE1E2, lane 3: pFB1-CS digested by *Xho*I / *Hin*dIII, lane 4: pFB1-CE1E2 digested by *Xho*I / *Hin*dIII, lane 5: pFastBacI digested by *Bam*HI / *Hin*dIII, lane 6: DL-15000 marker.

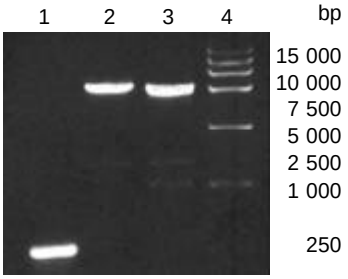

Figure 3 Confirmation of recombinant bacmids by PCR. Lane 1: bacmid / 0 control, lane 2: bacmid / CS, lane 3: bacimd / CE1E2, lane 4: DL-15000 marker.

Bacmid/CS and bacmid/CE1E2 were separately used to transfect Sf9 cells to generate recombinant *baculoviruses*, yielding reBV/CS and reBV/CE1E2, respectively. Bacmid/0 was used to generate non-recombinant *baculovirus* control, BV/Bac.

A large number of *baculoviruses* could be observed in nuclei of the Sf9 cells transfected with bacmid DNAs (Figure 4).

The recombinant *baculoviruses* reBV/CS and reBV/CE1E2 were confirmed by PCR with 5' NCR-CE1E2 and CE1E2 specific primers (Figure 5).

Immunofluorescence of HCV proteins

Either the recombinant *baculovirus* reBV/CS or reBV/CE1E2 directed the production of HCV structural proteins in insect cells, as demonstrated by immunofluorescence analysis of infected insect cells with anti-HCV antibodies (Figure 6). Immuno-staining was observed in the cells infected with recombinant *baculovirus* (Figures 6A and B). The anti-HCV antibodies used in this study did not display any cross-reactivity against insect cell or *baculovirus* proteins (Figure 6C).

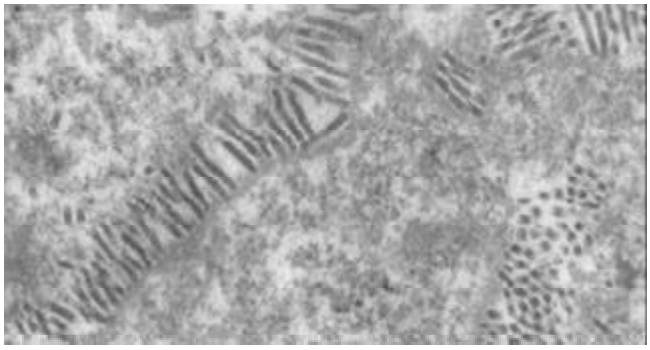

Figure 4 *Baculoviruses* in nuclei of Sf9 cells transfected with recombinant bacmid DNA (×25 000).

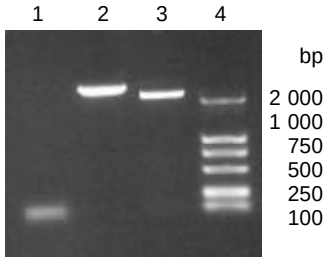

Figure 5 Confirmation of recombinant *baculoviruses* by PCR. Lane 1: BV / Bac control, lane 2: reBV / CS, lane 3: reBV / CE1E2, lane 4: DL-2000 marker.

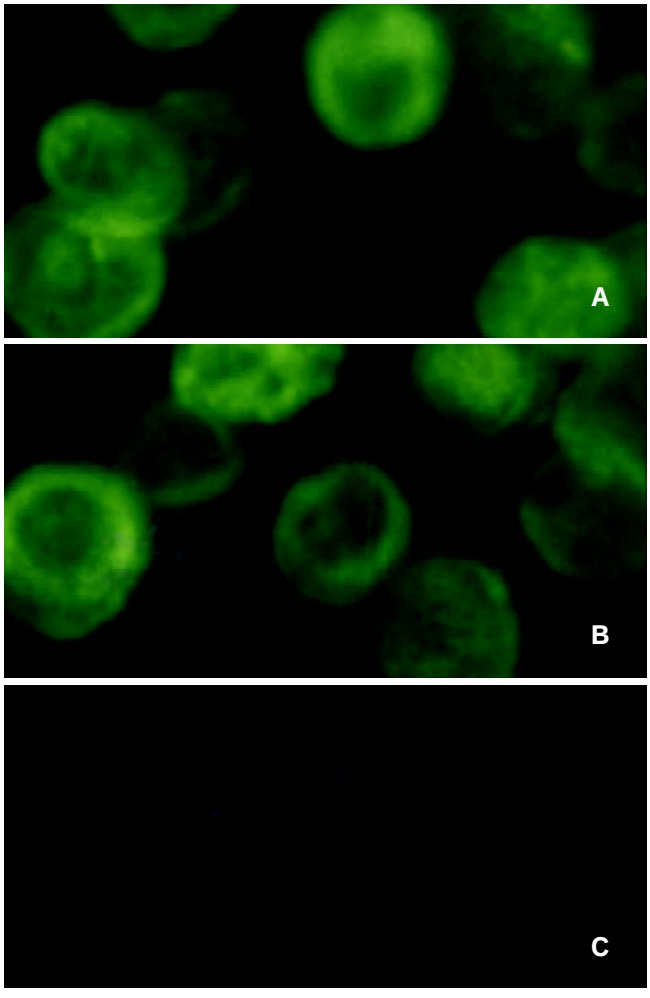

Figure 6 Immunofluorescence analysis of expression of HCV structural proteins in Sf9 cells. Sf9 cells infected with A: reBV / CS, B: reBV / CE1E2, C: control BV / Bac.

HCV structural proteins expressed in insect cells

SDS-PAGE analysis of lysates from Sf-9 cells infected with either reBV/CS or reBV/CE1E2 demonstrated 3 novel bands of the size of expected HCV E2, E1 and C proteins which were 66 kD, 35 kD and 20 kD respectively, which were not present in cells infected with non-recombinant *baculovirus* BV/Bac (Figure 7).

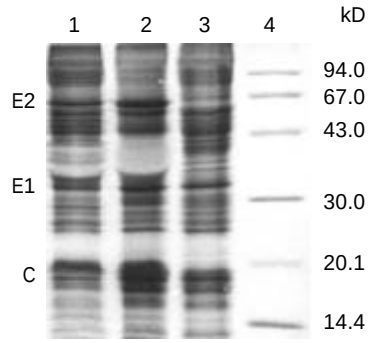

Figure 7 Identification of HCV structural proteins expressed in Sf9 cells by SDS-PAGE. Lanes 1-2: cells infected with reBV/CS and reBV/CE1E2 respectively, lane 3: control cells infected with BV/Bac, lane 4: molecular weight marker.

Coimmunoprecipitation of C and E1 with E2 protein

To further investigate the association of C, E1, and E2 proteins expressed in insect cells, cell extracts were immunoprecipitated with anti-E2 monoclonal antibody (MAb), and the precipitated proteins were separately probed with anti-C, anti-E2 MAb, or anti-HCV serum.

As shown in Figure 8, E2 protein was precipitated by anti-E2 MAb (Figure 8A), C protein could be detected in the immunoprecipitation complex when probed with anti-C MAb (Figure 8B), while C and E1 proteins could be detected together with E2 protein when probed with anti-HCV serum (Figure 8C). These results revealed the coimmunoprecipitation of C, E1 and E2 proteins.

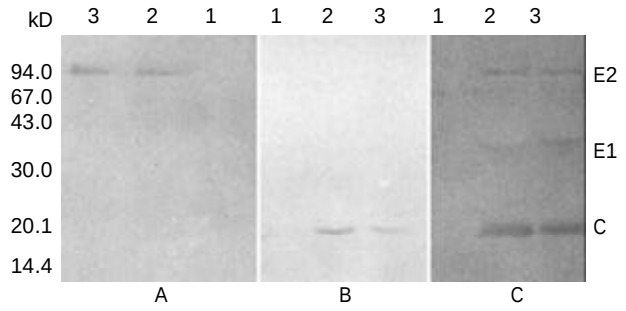

Figure 8 Immunoblotting of anti-E2 antibody immunoprecipitated proteins with anti-E2 mAb (A), anti-C mAb (B) and anti-HCV serum from HCV-infected patients (C). Lane 1: control BV/Bac, lane 2: reBV/CE1E2, lane 3: reBV/CS.

Electron microscopy of infected Sf9 cells

Transmission electron microscopy of the cells infected with either reBV/CS or reBV/CE1E2 revealed abundant virus-like particles in cytoplasm (Figures 9A and B). These particles (indicated by arrow "➡"), 40 to 60 nm in diameter, were polymorphic in appearance, many of them had unevenly distributed electron-dense structures suggestive of possible nucleocapsids. No such structures were observed in the control cells infected with BV/Bac (Figure 9C) in spite of the existence of abundant *baculoviruses* in the nuclei (indicated by arrow "▶").

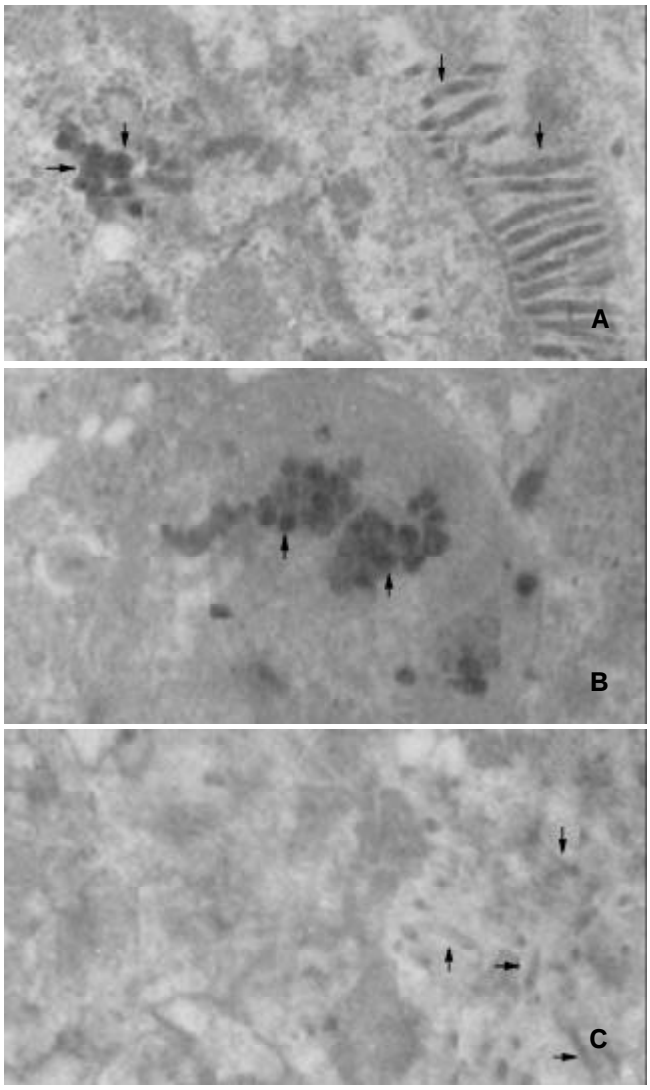

Figure 9 Electron micrographs of *baculovirus*-infected Sf9 cells (×25 000). Sf9 cells infected with A: reBV/CS, B: reBV/CE1E2, C: control BV/Bac.

Purification and identification of VLPs

VLPs were purified from large-scale cell cultures. The band corresponding to VLPs in sucrose gradient centrifugation was indicated in Figure 10. Portions of the VLPs were examined by EM which showed separate spherical particles similar to those seen in Sf9 cells infected with recombinant baculoviruses (Figures 11A and B), other portions of VLPs were examined by immune aggregation EM which revealed aggregated VLPs by anti-HCV serum (Figures 11C and D), indicating the immuno-reactivity of VLPs with anti-HCV antibodies.

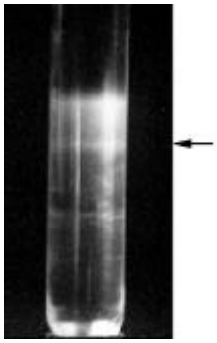

Figure 10 VLP band (indicated by arrow) in sucrose gradient centrifugation.

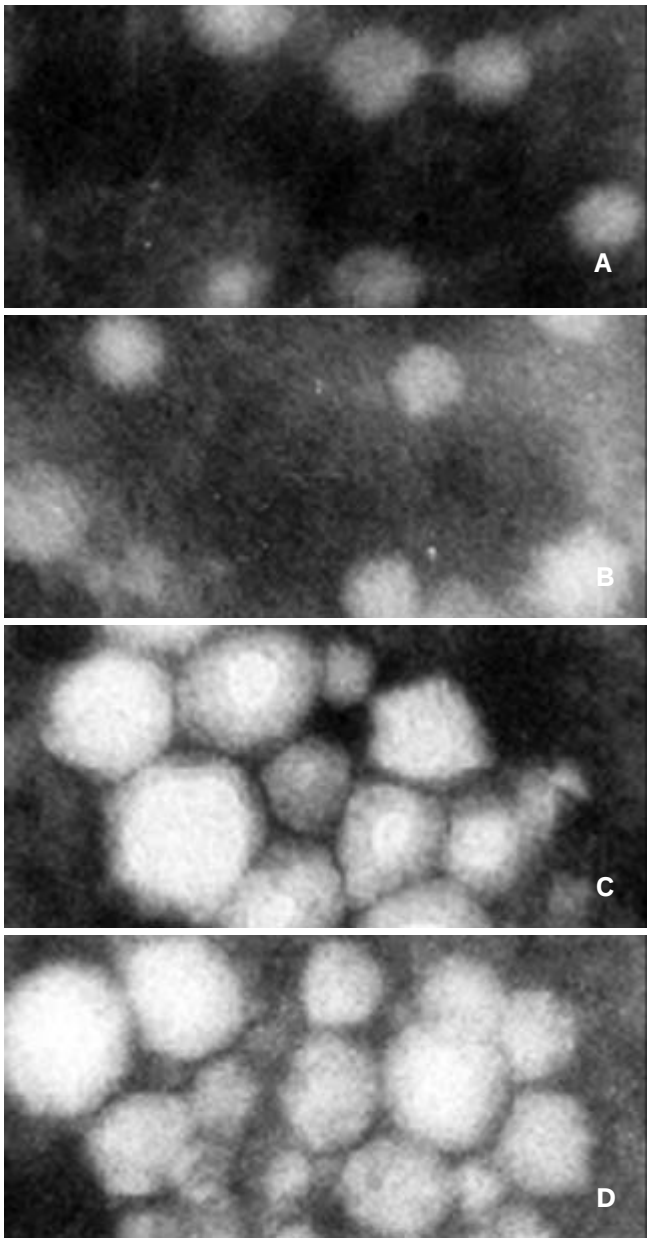

Figure 11 Electron microscopy and immune aggregation electron microscopy analysis of VLPs (negative staining). A and B (×100 000): VLPs isolated from Sf9 cells infected with reBV/CS and reBV/CE1E2, respectively. C and D (×150 000): Immune aggregation of VLPs from A and B with anti-HCV serum, respectively.

DISCUSSION

In this study, either in the presence or absence of HCV 5' NCR, the recombinant *baculovirus* (reBV/CS or reBV/CE1E2) efficiently expressed all the three HCV structural proteins, indicating the efficient cleavage of the polyproteins into individual proteins. The sizes of C, E1 and E2 proteins were 20 kD, 35 kD and 66 kD respectively, similar to those of HCV structural proteins expressed in mammalian cells[9], suggesting similar posttranslational processing of HCV structural proteins in insect and mammalian expression systems.

The interactions of HCV structural proteins expressed in insect cells were investigated by means of immunoprecipitation and immunoblotting. In addition to E2 protein, C and E1 proteins were also present in the immunoprecipitation complex (Figures 8B and C), indicating that C and E1 proteins were precipitated together with E2 protein by anti-E2 MAb. The result of immunoblotting of the immunoprecipitated proteins with anti-E2 MAb (Figure 8A) showed that the coimmunoprecipitation of the three structural proteins was not precipitated because there existed cross-reactivity between E2 MAb and C or E1 protein. So, we could conclude that the coimmunoprecipitation of C, E1 and E2 proteins was due to the association of the three structural proteins. These results extended the findings of previous studies which demonstrated interactions of E1 and E2 proteins[10] as well as C and E1 proteins[11], and provided immunological and biochemical evidences for the assembly of HCV structural proteins into VLPs in insect cells.

Detail ultrastructural features of HCV virions remain elusive since direct visualization of virus particles from infected serum and tissues has proven to be difficult. Filtration studies have estimated the virion particle size was 30 to 60 nm in diameter[12], Shimizu *et al*. detected VLPs with a diameter of approximately 50 nm in cytoplasm of the liver cells obtained during the acute phase of hepatitis C from a chimpanzee[13]. Kaito *et al*. reported visualization of 55 to 65 nm VLPs by immunogold electron microscopy with antibodies to HCV envelope protein[14]. Takahashi *et al*. observed by EM 55 nm VLPs in a gradient fraction when human plasma containing HCV was separated by potassium bromide density gradient centrifugation[15].

In our study, abundant spherical particles with the size of 40-60 nm in diameter were observed in the cytoplasm of Sf9 cells infected with either reBV/CS or reBV/CE1E2. Such particles could not be found in the cells infected with nonrecombinant *baculovirus* although the existence of abundant *baculoviruses* in the nuclei, indicating that VLPs in the infected cells were not correlated with the propagation of *baculovirus* in insect cells, but were resulted from the expression of HCV structural proteins in insect cells. Furthermore, VLPs isolated from recombinant *baculovirus* infected cells showed immuno-reactivity with anti-HCV antibodies, indicating that VLPs were derived from HCV proteins. Our data suggest that the morphology of HCV-like particles synthesized in insect cells is similar to the features described for HCV virions isolated from HCV-infected humans and chimpanzees. These results provided the morphological evidence for the assembly of HCV structural proteins into HCV-like particles.

In conclusion, either in the presence or absence of 5' NCR, the recombinant *baculovirus* containing HCV structural protein encoding sequences can direct the expression of correctly processed individual HCV structural proteins, which assemble into VLPs similar to HCV particles from sera or hepatic tissues of HCV infected humans or chimpanzees. HCV core and envelope proteins are sufficient for viral particle formation, 5' NCR is not required for the assembly of VLPs in insect cells.

REFERENCES

1 **Cohen J.** The scientific Challenge of hepatitis C. *Science* 1999; **285**: 26-30
2 **Shimotohno K.** Hepatitis C virus and its pathogenesis. *Semin Cancer Biol* 2000; **10**: 233-240
3 **Schiller JT,** Lowy DR. Papillomavirus-like particle based vaccines: cervical cancer and beyond. *Expert Opin Biol Ther* 2001; **1**: 571-581
4 **Latham T,** Galarza JM. Formation of wild-type and chimeric influenza virus-like particles following simultaneous expression of only four structural proteins. *J Virol* 2001; **75**: 6154-6165
5 **Baumert TF,** Ito S, Wong DT, Liang TJ. Hepatitis C virus structural proteins assemble into viruslike particles in insect cells. *J Virol* 1998; **72:** 3827-3836
6 **Bi SL,** Bai XH, Cong ME, Tian HW, Sun DG, Margolis HS, Liu CB. Primary Structure and Variation of Chinese Hepatitis C Virus Genome. *Bingdu Xuebao* 1993; **9**: 114-127

7 **Ausubel FM,** Brent R, Kingston RE, Moore DD, Seidman JG, Smith JA, Struhl K. Short Protocols in Molecular Biology. 3rd ed. *John Wiley Sons, Inc* 1995: 23-29

8 **Sambrook J,** Fritsch EF, Maniatis T. Molecular cloning, A Laboratory Manual. 2nd ed. *Cold Spring Harbor Laboratory Press* 1989: 620-665

9 **Moradpour D,** Wakita T, Wands JR, Blum HE. Tightly regulated expression of the entire hepatitis C virus structural region in continuous human cell lines. *Biochem Biophys Res Commun* 1998; **246**: 920-924

10 **Patel J,** Patel AH, McLauchlan J. Covalent interactions are not required to permit or stabilize the non-covalent association of hepatitis C virus glycoproteins E1 and E2. *J Gen Virol* 1999; **80** (Pt 7): 1681-1690

11 **Ma HC,** Ke CH, Hsieh TY, Lo SY. The first hydrophobic domain of the hepatitis C virus E1 protein is important for interaction with the capsid protein. *J Gen Virol* 2002; **83**(Pt 7): 3085-3092

12 **He LF,** Alling D, Popkin T, Shapiro M, Alter HJ, Purcell RH. Determining the size of non-A, non-B hepatitis virus by filtration. *J Infect Dis* 1987; **156**: 636-640

13 **Shimizu YK,** Feinstone SM, Kohara M, Purcell RH, Yoshikura H. Hepatitis C virus: detection of intracellular virus particles by electron microscopy. *Hepatology* 1996; **23**: 205-209

14 **Kaito M,** Watanabe S, Tsukiyama-Kohara K, Yamaguchi K, Kobayashi Y, Konishi M, Yokoi M, Ishida S, Suzuki S, Kohara M. Hepatitis C virus particle detected by immunoelectron microscopic study. *J Gen Virol* 1994; **75**(Pt 7): 1755-1760

15 **Takahashi K,** Kishimoto S, Yoshizawa H, Okamoto H, Yoshikawa A, Mishiro S. p26 protein and 33-nm particle associated with nucleocapsid of hepatitis C virus recovered from the circulation of infected hosts. *Virology* 1992; **191**: 431-434

Edited by Wang XL

P.O.Box 2345, Beijing 100023,China
Fax: +86-10-85381893
E-mail: wjg@wjgnet.com www.wjgnet.com

World J Gastroenterol 2003;9(10):2232-2235
World Journal of Gastroenterology
 ISSN 1007-9327

Interobserver variation in histopathological assessment of *Helicobacter pylori* gastritis

Ozlem Aydin, Reyhan Egilmez, Tuba Karabacak, Arzu Kanik

Ozlem Aydin, Reyhan Egilmez, Tuba Karabacak, Arzu Kanik, Department of Pathology and Biostatistics, Medical School, Mersin University, Mersin-Icel, Turkey
Correspondence to: Ozlem Aydin, M.D. Department of Pathology, Medical School, Mersin University, 33079 Mersin- Icel, Turkey. ozlemaydin66@hotmail.com
Telephone: +90-324-3374300/1192 **Fax:** +90-324-3374305
Received: 2003-07-04 **Accepted:** 2003-08-19

Abstract

AIM: Because the presence or absence of *H pylori* infection has important implications for therapeutic decisions based on histological assessment, the reproducibility of Sydney system is important. The study was designed to test the reproducibility of features of *Helicobacter pylori* gastritis, using the updated Sydney classification.

METHODS: Gastric biopsies of 40 randomly selected cases of *H pylori* gastritis were scored semiquantitatively by three pathologists. Variables analysed included chronic inflammation, inflammatory activity, atrophy, intestinal metaplasia, *H pylori*, surface epithelial damage. κ values below 0.5 represented poor, those between 0.5 and 0.75 good and values over 0.75 excellent interobserver agreement.

RESULTS: The best interobserver agreement (κ=0.62) was present for intestinal metaplasia. The agreement was the poorest for evaluating atrophy (κ=0.31).

CONCLUSION: Although the results of this study were in accordance with some previous studies, an excellent agreement could not be reached for any features of *H pylori* gastritis. This low degree of concordance is assumed to be due to the personal evaluation differences in grading the features, the lack of standardized diagnostic criteria, and the ignorance to reach a consensus about the methods to be used in grading the features of *H pylori* gastritis before initiating the study.

Aydin O, Egilmez R, Karabacak T, Kanik A. Interobserver variation in histopathological assessment of *Helicobacter pylori* gastritis. *World J Gastroenterol* 2003; 9(10): 2232-2235
http://www.wjgnet.com/1007-9327/9/2232.asp

INTRODUCTION

Although gastritis was first interpreted to be due to aging and lifelong exposure to various insults, it is now clear that the most common cause of this inflammatory condition is infection with *H pylori*[1]. It has been shown[2] that this organism is strongly associated with chronic active gastritis as well as gastric adenocarcinoma and MALToma.

The Sydney system for grading and classifying chronic gastritis was devised to provide a standardized approach to the histologic interpretation of gastric biopsies in 1990[3,4], and it was later updated in 1994[5,6]. Although it was reported that the Sydney systems' weakness was that it was used in complex descriptions rather than true diagnosis[7]. After the updating of the Sydney classification, several studies on interobserver variation for the assessment of *H pylori* gastritis have been reported[6,8-11]. The evaluation of interobserver agreement by using kappa (κ)-statistics has been accepted by pathologists for several years[9].

Although the histologic examination of gastric biopsy specimens is accepted as the gold standard[12,13] for the diagnosis of *H pylori* gastritis, it has not been demonstrated that histopathologic assessment is both accurate and reproducible[9].

The study was designed to test the reproducibility of the features of *H pylori* gastritis, using the updated Sydney classification by κ-statistics.

MATERIALS AND METHODS

Three pathologists participated in the study. One was a professor with primary interest in gastrointestinal pathology. The second was a 4th-year assistant professor in pathology. An other was an 18th-month pathology resident. The slides were examined independently, and also incombination with any clinical information by each of the pathologists.

Histologic evaluation

From 130 cases diagnosed as *H pylori* gastritis in our department (Department of Pathology, Medical School, Mersin University.) in a period of 17 months, 40 [22 (55.0 %) female, 18 (45.0 %) male] were randomly selected for study, their age ranged from 23 to 72 years, with a mean of 47.2. The specimens were excluded from the study because they were insufficient in mucosal thickness for proper assessment of atrophy and without surface epithelium before the selection. Slides were coded using a computer generated list of random numbers.

Biopsy samples from the antrum and body were formalin-fixed and paraffin-embedded and cut into 2-3 μm sections which were stained using hematoxylin and eosin (H&E), and alcien blue/PAS for intestinal metaplasia. Five H&E sections were examined for each case. The biopsies were scored semiquantitatively by three pathologists according to the updated Sydney classification[14].

The updated Sydney system has a scale of 0-3 for scoring the features of chronic gastritis[14]. In order to improve assessment of minor degrees of alteration, a detailed histopathological classification was used, which also provides numerical data for statistical analysis[15]. At first, each variable was divided into seven subcategories, resulting in a score on a scale of 0-6. But the κ values could not be calculated using this classification. The 6 subcategories (excluding 0, none) were then amalgamated by pairs (none, 0; mild, 1-2; moderate, 3-4; severe, 5-6), but the calculation of the κ values was again impossible for the majority of variations using this classification, and the calculated values were found to be low. So, we came to a conclusion that the agreement between pathologists could be improved when a different amalgamated 3-point scale classification was used for each variable (Table 1).

Table 1 Histologic features evaluated on each slide and score scale

Histologic features	Score	Grading
Chronic inflammation	0, none	0, none
	1, <10 cic*/HPF**	1-2-3, mild
	2, >10 cic/HPF	4-5-6, moderate to marked
	3, some areas with dense cic	
	4, diffuse infiltration with dens cic	
	5, nearly whole mucosa contains a dense cic	
	6, entire mucosa contains a dense cic infiltrate	
Inflammatory activity	0, none	0, none
	1, only one crypt involved/ biopsy	1-2, mild
	2, two crypts involved/ biopsy	3-4-5-6, moderate to marked
	3, many crypts (<25%) involved/ biopsy	
	4, 25-50% of crypts involved/ biopsy	
	5, >50% of crypts involved/ biopsy	
	6, all crypts involved	
Atrophy	0, none	0, none
	1, foci where a few gastric glands are lost or replaced by ie•	1-2, mild
	2, small areas in which gastric glands have disappeared or been replaced by ie	3-4-5-6, moderate to marked
	3, <25% of gastric glands lost or replaced by ie	
	4, 25-50% of gastric glands lost or replaced by ie	
	5, >50% of gastric glands lost or replaced by ie	
	6, only a few small areas of gastric glands remaining	
Intestinal metaplasia	0, none	0, none
	1, only one crypt replaced by ie	1-2-3, mild
	2, one focal area (1-4 crypts) in one of two biopsies	4-5-6, moderate to marked
	3, two separate foci	
	4, multipl foci in one or both biopsies	
	5,>50% of gastric epithelium diffusely replaced by ie	
	6, only a few small area of gastric epithelium are not replaced by ie	
H pylori	0, none	0, none
	1, *H pylori* found only in one place	1-2-3-4, mild
	2, only a few *H pylori* found	5-6, moderate to marked
	3, scattered *H pylori* found in separate areas/foci	
	4, numerous *H pylori* in separate areas/foci	
	5, nearly complete gastric surface covered by a layer of *H pylori*	
	6, continuous gastric surface coverage by a thick layer of *H pylori*	
Surface epithelial damage	0, none	0, none
	1, slight	1-2-3-4, mild
	2, mild deg♦ in the top of the epithelial cells	5-6, moderate to marked
	3, moderate deg with disorientation of the epithelial lining	
	4, indistinct cell borders at the surface of the epithelium	
	5, flattened epithelial cells with severe deg and enlarged nuclei	
	6, flattened to erosive epithelium of the entire surface	

*: Chronic inflammatory cells, **: High power field, •: Intestinal type epithelium, ♦: Degeneration.

Table 2 Kappa values and their 95 % confidence intervals between three pathologists for *H pylori* gastritis

Variable	Pairwise analysis between pathologists					
	1:2		1:3		2:3	
	Kappa	95 % CI	Kappa	95 % CI	Kappa	95 % CI
Chronic inflammation	0.49[a]	0.13-0.85	-0.34	NS	0.14	NS
Inflammatory activity	0.44[a]	0.13-0.71	-0.13	NS	-0.27	NS
Atrophy	0.31[a]	0.83-0.56	0.03	NS	0.14	NS
Intestinal metaplasia	0.51[a]	0.25-0.85	0.52[a]	0.20-0.80	0.62[a]	0.40-0.85
H pylori	0.40[a]	0.10-0.71	0.38[a]	0.06-0.71	0.56[a]	0.28-0.84
Surface epithelial damage	-0.01	NS	-	-	-	-

NS: Non-significant, 95 % CI: 95 % confidence interval, -: Kappa statistics could not be done because data table had less than two rows or columns; [a]$P<0.05$.

Statistical analysis

Interobserver agreement was analysed with the use of κ statistics (BMDP software: Cork, Ireland). The benchmarks suggested by Svanholm *et al*[16] were accepted. Values below 0.5 represented poor, those between 0.5 and 0.75 good and values over 0.75 excellent interobserver agreement. Only values greater than 0.5 were considered good enough for diagnostic reliability. Confidence interval was calculated for only statistically significant values.

RESULTS

κ values and their 95 % confidence intervals between three pathologists for *H pylori* gastritis are shown in Table 2. On

blinded review of the coded slides the best interobserver agreement (κ=0.62, CI: 0.40-0.85) was present for intestinal metaplasia. The good agreement was reached in the assessment of the grade of *H pylori*, with κ value of 0.56 (CI: 0.28-0.84). The interobserver agreement was the poorest for evaluating atrophy (κ=0.31, CI: 0.13-0.56). Following atrophy, the two variables with poor agreement were chronic inflammation (κ=0.49, CI: 0.13-0.85) and inflammatory activity (κ=0.44, CI: 0.13-0.71).

There was an agreement among the three observers for only evaluating intestinal metaplasia and the grade of *H pylori*. There was no interobserver agreement among the three pathologists for the assessment of surface epithelial damage. An excellent agreement could not be reached in any features of *H pylori* gastritis in our study.

DISCUSSION

Correct and reliable histological diagnosis of *H pylori* gastritis has a great influence on clinical practice as an indicator for therapy. Reliability in assessing intestinal metaplasia and atrophy in histological specimens was especially important because these changes were associated with an increased risk of gastric cancer[12,17-19]. Andrew *et al*[8] and Tepes *et al*[12] held that histopathology was a reliable diagnostic method for *H pylori* gastritis based on their results.

The best interobserver agreement was reached for intestinal metaplasia. The κ values were 0.51-0.62 (CI: 0.40-0.85). As in our study, others have also shown a good agreement for scoring intestinal metaplasia, with κ values varying from 0.54 (CI: 0.31-0.77) in the study by Tepes *et al*[12] to 0.73 in the study by Andrew *et al*[8]. However, our κ values were lower than those reported by Fiocca *et al*[20]; (κ=0.75-0.92). Although, the H&E stain has been the standard basis for recognition of intestinal metaplasia[21], we based our observations on the alcian blue/PAS in addition to H&E because of ease to identify the goblet cells.

In the present study, the grading of *H pylori* reached good reproducibility, with κ value of 0.56 (CI: 0.28-0.84). This result was consistent with the study of Fiocca *et al*[20] (κ=0.62), Andrew *et al*[8] (κ=0.74) and Tepes *et al*[12] (κ=0.43), but lower than the value reported by El-Zimaity *et al*[9] (κ=0.90). Our results have also confirmed that H&E was an adequate stain for the detection of *H pylori*. There was no need for an additional staining like Warthin-Starry to identify the organism.

The lack of explicit criteria for the diagnosis of normal gastric mucosa when mononuclear cells were present, made grading difficult[12]. Therefore, the κ value for assessment of the degree of chronic inflammation (κ=0.49, CI:0.13-0.85) using semiquantitative scoring was lower than that for intestinal metaplasia and for the grading of *H pylori* in the present study. Tepes *et al*[12], also found a κ value for chronic inflammation ranged from 0.39 to 0.53. Our result is also in accordance with those of Fiocca *et al*[20], who reported κ values ranging from 0.49 to 0.82 and Andrew *et al*[8] who reported κ value of 0.58.

The interobserver agreement was poor with κ value of 0.44 (CI: 0.13-0.71) for scoring neutrophil infiltration in gastric mucosa. This result was consistent with those of Tepes *et al*[12] (κ=0.28-0.41) and Andrew *et al*[8] (κ=0.69). But the interobserver agreements of the studies of El-Zimaity *et al*[9] (κ=0.80) and Fiocca *et al*[20] (κ=0.58-0.77) were better than ours. Inflammatory activity and *H pylori* infection were present together and when only neutrophils were discovered in the tissue specimen the pathologists should intensively search for some residual *H pylori*[22].

Recently, it has been shown in several studies that even experienced gastrointestinal pathologists had poor interobserver agreement over the assessment of gastric atrophy of *H pylori* gastritis[6,8-11]. In the present study, the interobserver agreement for the grade of atrophy was lower than that for the other gastritis features. As in our study (κ=0.31, CI:0.13-0.56), others have also shown the lowest agreement for scoring atrophy, with κ values varying from 0.42 in the study of Fiocca *et al*[20] to 0.51 in the study of Andrew *et al*[8]. Tepes *et al*[12] also found the lowest interobserver agreement for atrophy (κ=0.17-0.57). Although El-Zimaity *et al*[9] also found the poorest agreement for atrophy, with κ value ranged from 0.08 to 0.29, the agreement in our study for the evaluation of atrophy was still better.

Among the similar previous studies, the surface epithelial damage in *H pylori* gastritis has been evaluated in only the study of Chen *et al*[15]. They reached good to excellent reproducibility in grading this feature, with weighed κ values of 0.6 and 0.73. But there was no interobserver agreement between the three pathologists for the assessment of surface epithelial damage in our study. Although the Sydney classification has been used routinely, the surface epithelial damage in *H pylori* gastritis have not been evaluated in our department until the present study was designed. It is suggested that the reason of this disagreement may be the lack of our experience in evaluating epithelial damage.

The results of this study suggest that assessment of many histopathologic features of *H pylori* infection have a low degree of concordance. Interobserver variation has been rather high in this study as in some other studies[9,12,23]. This may be due to the discrepancies in the semiquantitative evaluation of the features of *H pylori* gastritis, or due to the observations of the pathologists. Essentially, a perfect agreement by pathologists was practically impossible because pathology results were based on subjective interpretation of different features and classification, and numerous studies on the reproducibility of histopathologic data have reached similar conclusion. Pathologists could usually agree in the presence or absence of a particular histological characteristic, but were seldom consistent when they estimated its degree[24-27].

In the present study, the best interobserver agreement was reached between the assistant professor and the pathology resident, suggesting that the scale of the score is more important than experiences.

Because of the level of agreement in the presence or absence of *H pylori* infection had important implications for therapeutic decisions based on histological assessment[8], reproducibility of Sydney system is important. The updated Sydney system for scoring *H pylori* gastritis is useful and reproducible, but it needs to be improved in the criteria for grading the histologic features[15]. The lack of standardized diagnostic criteria is likely to have contributed significantly to the poor interobserver agreement found in certain features such as atrophy[9] as in our study. More exact criteria will probably further improve the interobserver agreement in assessing the histologic features, but some interobserver variability will probably persist because of the subjectivity that has been part of all semiquantitative grading systems[12]. The point that where cases were reviewed and numerical parameters were established was the best strategy to improve diagnostic concordance between pathologists[28].

Although, the results of this study were in accordance with some previous studies, an excellent agreement could not be reached for any features of *H pylori* gastritis. In conclusion, this unexpectedly low degree of concordance is assumed to be due to the personal evaluation differences in grading the features, and the lack of the standardized diagnostic criteria, as well as the ignorance to reach a consensus about the methods to be used in grading the features of *H pylori* gastritis before initiating the study.

REFERENCES

1 **Soll AH**. Gastritis and *Helicobacter pylori*. In: Goldman L,

Bennett JC, eds. Cecil Textbook of Medicine, 21st ed. Philadelphia: *Saunders* 2000: 643-767
2 **Peterson WL**, Graham DY. *Helicobacter pylori*. In: Feldman M, Scharschmidt BF, Sleisenger MH, eds. Sleisenger&Fordtran's Gastrointestinal and Liver Disease. Pathophysiology (Diagnosis) Management, 6th ed. Philadelphia: *Saunders* 1998: 604-620
3 **Misiewice JJ**, Tytgat GNJ, Goodwin CS. The Sydney system: a new classification of gastritis. *J Hepatol Gastroenterol* 1991; **6**: 209-222
4 **Owen DA**. The Stomach. In: Sternberg SS, ed. Diagnostic Surgical Pathology. 3rd ed. Philadelphia: *Lippincott Williams Wilkins* 1999: 1311-1349
5 **Genta RM**, Dixon MF. The Sydney system revisited: the Houston international gastritis workshop. *Am J Gastroenterol* 1995; **90**: 1039-1041
6 **Genta RM**. *Helicobacter pylori*, inflammation, mucosal damage, and apoptosis: pathogenesis and definition of gastric atrophy. *Gastroenterology* 1997; **113**(Suppl): 551-555
7 **Fenoglio-Preiser CM**, Noffsinger AE, Stemmermann GN, Lantz PE, Listrom MB, Rilke FO. The Nonneoplastic Stomach. In: Fenoglio-Preiser CM, Noffsinger AE, Stemmermann GN, Lantz PE, Listrom MB, Rilke FO, eds. Gastrointestinal Pathology An Atlas and Text, 2nd ed. Philadelphia: *Lippincott-Raven* 1999: 153-237
8 **Andrew A**, Wyatt JI, Dixon MF. Observer variation in the assessment of chronic gastritis according to the Sydney system. *Histopathol* 1994; **25**: 317-322
9 **el-Zimaity HM**, Graham DY, al-Assi MT, Malaty H, Karttunen TJ, Graham DP, Huberman RM, Genta RM. Interobserver variation in the histopathological assessment of *Helicobacter pylori* gastritis. *Hum Pathol* 1996; **27**: 35-41
10 **Alhomsi MF**, Adeyemi EO. Grading *Helicobacter pylori* gastritis in dyspeptic patients. *Comp Immunol Microbiol Infect Dis* 1996; **19**: 147-154
11 **van Grieken NC**, Weiss MM, Meijer GA, Bloemena E, Lindeman J, Offerhaus GJ, Meuwissen SG, Baak JP, Kuipers EJ. Rapid quantitative assessment of gastric corpus atrophy in tissue sections. *J Clin Pathol* 2001; **54**: 63-69
12 **Tepes B**, Ferlan-Marolt V, Jutersek A, Kaucic B, Zaletel-Kragelj L. Interobserver agreement in the assessment of gastritis reversibility after *Helicobacter pylori* eradication. *Histopathology* 1999; **34**: 124-133
13 **Genta RM**. Pathology of *Helicobacter pylori* infection. In: Weinstein RS, ed. Advances in Pathology an Laboratory Medicine. *St. Louise, Mosby* 1994: 443-465
14 **Dixon MF**, Genta RM, Yardley JH, Correa P. Classification and grading of gastritis, the updated Sydney system. *Am J Surg Pathol* 1996; **20**: 1161-1181
15 **Chen XY**, Hulst RWM, Bruno MJ, van der Ende A, Xiao SD, Tytgat GN, Ten Kate FJ. Interobserver variation in the histopathological scoring of *Helicobacter pylori* related gastritis. *J Clin Pathol* 1999;**52**: 612-615
16 **Svanholm H**, Starklint H, Gundersen HJ, Fabricius J, Bartebo H, Olsen S. Reproducibility of histomorphologic diagnoses with special reference to kappa statistics. *APMIS* 1989; **97**: 689-698
17 **Correa P**. Human gastric carcinogenesis: a multistep and multifactorial process. First american cancer society award lecture on cancer epidemiology and prevention. *Cancer Res* 1992; **52**: 6735-6740
18 **Sipponen P**. Gastric cancer-a long term consequence of *Helicobacter pylori* infection? *Scand J Gastroenterol Suppl* 1994; **201**: 24-27
19 **Meining A**, Stolte M. Close correlation of intestinal metaplasia and corpus gastritis in patients infected with *Helicobacter pylori*. *Z Gastroenterol* 2002; **40**: 557-560
20 **Fiocca R**, Villani L, Cornaggia M. Interobserver variation in the assessment of *H pylori* gastritis [abstract]. *Gut* 1996; **Suppl 2**: A104-105
21 **Segura DI**, Montero C. Histochemical characterization of different types of intestinal metaplasia in gastric mucosa. *Cancer* 1983; **52**: 498-503
22 **Genta RM**, Lew GM, Graham DY. Changes in the gastric mucosa following eradication of *Helicobacter pylori*. *Mod Pathol* 1993; **6**: 281-289
23 **Landis JR**, Koch GG. The measurement of observer agreement for categorical data. *Biometrics* 1977; **33**: 159-174
24 **Riddell RH**, Goldman H, Ransohoff DF, Appelman HD, Fenoglio CM, Haggitt RC, Ahren C, Correa P, Hamilton SR, Morson BC, Sommers SC, Yardley JH. Displasia in inflammatory bowel disease: Standardized classification with provisional clinical application. *Hum Pathol* 1983; **14**: 931-968
25 **Reid BJ**, Haggitt RC, Rubin CE, Roth G, Surawicz CM, Van Belle G, Lewin K, Weinstein WM, Antonioli DA, Goldman H, Mac Donaid W, Owen D. Observer variation in the diagnosis of dysplasia in Barrett's esophagus. *Hum Pathol* 1988; **19**: 166-178
26 **Dawson A**, Ibrahim NB, Gibbs AR. Observer variation in the histopathological classification of thymoma: Correlation with prognosis. *J Clin Pathol* 1994; **47**: 519-523
27 **Sorensen JB**, Hirsch FR, Gazdar A, Olsen JE. Interobserver variability in histopathologic subtyping and grading of pulmonary adenocarcinoma. *Cancer* 1993; **71**: 2971-2976
28 **Guarner J**, Herrera-Goepfert R, Mohar A, Sanchez L, Halperin D, Ley C, Parsonnet J. Interobserver variability in application of the revised Sydney classification for gastritis. *Hum Pathol* 1999; **30**: 1431-1434

Edited by Wang XL

P.O.Box 2345, Beijing 100023,China
Fax: +86-10-85381893
E-mail: wjg@wjgnet.com www.wjgnet.com

World J Gastroenterol 2003;9(10):2236-2239
World Journal of Gastroenterology
 ISSN 1007-9327

Gastric polypoid lesions: Analysis of 150 endoscopic polypectomy specimens from 91 patients

Rasim Gencosmanoglu, Ebru Sen-Oran, Ozlem Kurtkaya-Yapicier, Erol Avsar, Aydin Sav, Nurdan Tozun

Rasim Gencosmanoglu, Ebru Sen-Oran, the Unit of Surgery, Institute of Gastroenterology, School of Medicine, Marmara University, Istanbul, Turkey
Ozlem Kurtkaya-Yapicier, Aydin Sav, Department of Pathology, School of Medicine, Marmara University, Istanbul, Turkey
Erol Avsar, Nurdan Tozun, the Unit of Gastroenterology, Institute of Gastroenterology, School of Medicine, Marmara University, Istanbul, Turkey
Correspondence to: Rasim Gencosmanoglu, M.D., Unit of Surgery, Institute of Gastroenterology, Marmara University,Basibuyuk, Maltepe, PK:53, TR-81532, Istanbul, Turkey. rgencosmanoglu@marmara.edu.tr
Telephone: +90-216-383-3057 **Fax:** +90-216-399-9912
Received: 2003-06-16 **Accepted:** 2003-08-02

Abstract

AIM: To analyze gastric polypoid lesions in our patient-population with respect to histopathologic features and demographic, clinical, and endoscopic characteristics of patients.

METHODS: Clinical records and histopathologic reports of patients with gastric polypoid lesions were analyzed retrospectively. All lesions had been totally removed by either endoscopic polypectomy or hot biopsy forceps. The histopathologic slides were re-evaluated by the same histopathologist.

RESULTS: One-hundred and fifty gastric polypoid lesions were identified in 91 patients. There were 53 (58 %) women and 38 (42 %) men with a median age of 53 (range, 31 to 82) years. The most frequent presenting symptom was dyspepsia that was observed in 35 (38.5 %) patients. Symptoms were mostly related to various associated gastric abnormalities such as chronic gastritis or *H pylori* infection rather than polypoid lesion itself. Polypoid lesions were commonly located in the antrum followed by cardia. Out of 150 lesions, 80 (53 %) had the largest dimensions less than or equal to 5 mm and only 7 were pedunculated. The frequencies of hyperplastic polyps, foveolar hyperplasia, and fundic gland polyps were 46 %, 18 %, and 14 % respectively. We also detected gastritis varioliformis in 12 specimens, lymphoid follicles in 9, 4 adenomatous polyps in 4, polypoid lesions with edematous mucosa in 4, inflammatory polyps in 3, and carcinoid tumor in 1. Adenomatous changes were observed within two hyperplastic polyps and low grade dysplasia in one adenoma. Histopathologic evaluation of the surrounding gastric mucosa demonstrated chronic gastritis in 72 (79 %) patients and *H pylori* infection in 45 (49 %).

CONCLUSION: Hyperplastic polyps are the most frequently encountered subtype of gastric polypoid lesions. They are usually associated with chronic gastritis or *H pylori* gastritis. Contrary to the previous belief, they may harbour adenomatous changes or dysplastic foci. Therefore, endoscopic polypectomy seems as a safe and fast procedure for both diagnosis and treatment of gastric polypoid lesions at the same session. In addition, edematous mucosa may appear misleadingly as a polypoid lesion in some instances and it can be ruled out only by histopathologic examination.

Gencosmanoglu R, Sen-Oran E, Kurtkaya-Yapicier O, Avsar E, Sav A, Tozun N. Gastric polypoid lesions: Analysis of 150 endoscopic polypectomy specimens from 91 patients. *World J Gastroenterol* 2003; 9(10): 2236-2239
http://www.wjgnet.com/1007-9327/9/2236.asp

INTRODUCTION

The frequency of gastric polyps is gradually increasing due to widespread use of endoscopic examinations[1,2]. Any discrete lesion protruding into the lumen of gastrointestinal (GI) tract appeared at endoscopy is called as "polypoid lesion"[3]. However, a polyp is defined as a proliferative or neoplastic lesion of gastrointestinal mucosal layer[3]. Although endoscopic appearances of some polyps may be diagnostic, the term "polyp" should not be used for every discrete protrusions identified at endoscopy unless histopathologically confirmed[4,5]. According to the classification suggested by Oberhuber and Stolte[4], gastric polypoid lesions are divided into five distinct groups: non-neoplastic polyps such as hyperplastic polyp, hamartomatous polyps such as Peutz-Jeghers polyps, heterotopic tissue polyps such as heterotopic pancreas, neoplastic polyps such as adenoma, and reactive polypoid lesions such as foveolar hyperplasia. In their series, hyperplastic polyps and fundic gland polyps are the two most common subtypes of gastric polypoid lesions[4].

In this study, the demographic, clinical, and endoscopic characteristics of patients with gastric polypoid lesions were presented. The histopathologic features of these lesions were also reported and their malignancy potential is discussed.

MATERIALS AND METHODS

Patients with gastric polypoid lesions detected by upper gastrointestinal endoscopy at the Institute of gastroenterology, Marmara University, between January 1998 and December 2002 were analyzed retrospectively. All gastroscopies were performed under sedation with intravenous midazolam and topical pharyngeal anesthesia with 10 % lidocaine. The location, shape, size, and surface appearance of each polypoid lesion were assessed. Polypoid lesions were totally removed either by endoscopic polypectomy with an attempt or by hot biopsy forceps with multiple attempts according to their size. In addition, multiple biopsies were collected from both antrum and incisura angularis for *Helicobacter pylori* (*H pylori*) urease test and from surrounding gastric mucosa to detect any associated histopathologic changes such as chronic gastritis, *H pylori* infection, or intestinal metaplasia. Endoscopic records were screened for any complication resulted from polypectomy.

An experienced pathologist (O. K-Y.) re-evaluated all the tissue samples to confirm the histopathologic subclassification of gastric polypoid lesions in our series according to the classification suggested by Oberhuber and Stolte[4].

RESULTS

Demographic features

One hundred and fifty gastric polypoid lesions were identified in 91 consecutive patients from 2 630 (3.4 %) upper GI endoscopies. There were 53 (58 %) women and 38 (42 %) men with slightly female predominance (1.4:1). The ages of patients ranged from 31 to 82 years with a median of 53.

Clinical features

The most frequent presenting symptom was dyspepsia (38.5 %) followed by epigastric pain (27.5 %), and anemia (11 %). Symptoms were usually related to the associated gastric abnormalities such as gastritis rather than polypoid lesion itself. Exceptionally, there was an antral hyperplastic polyp causing intermittent gastric outlet obstruction in one case in which the problem was solved with its removal by endoscopic polypectomy. The patient was symptom-free in the 8 months of follow-up.

Endoscopic features

Characteristics of the gastric polypoid lesions are shown in Table 1. Out of 150 gastric polypoid lesions, 61 (40.6 %) were located in the antrum followed by 40 (26.6 %) in cardia, 34 (22.6 %) in corpus, and 13 (8.6 %) in fundus. In two patients who had previously undergone partial gastrectomy, the lesions were detected around anastomoses (1.2 %). Only 7 out of 150 (4.6 %) lesions were pedunculated (Figure 1A), while the remainder was sessile.

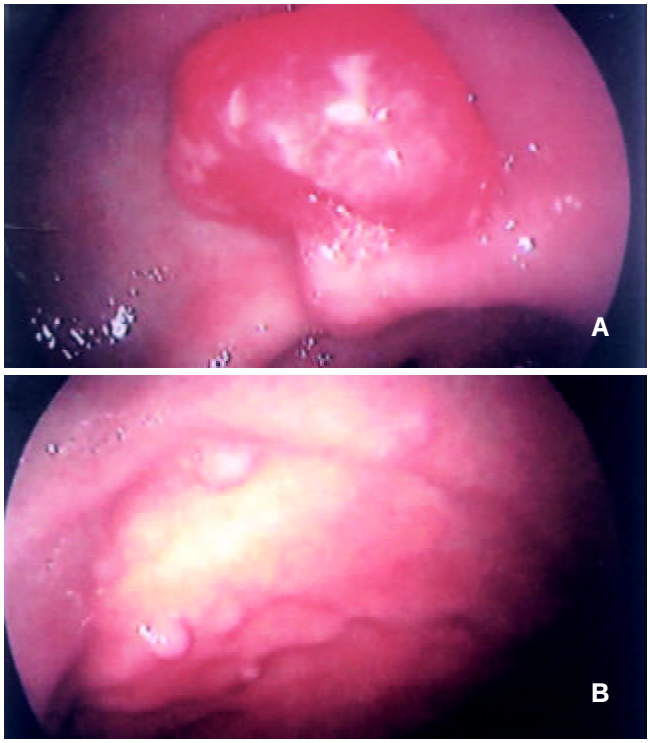

Figure 1 Endoscopic views of pedunculated gastric polyp (A) and multiple gastric polyps (B).

Eighty (53 %) gastric polypoid lesions with the largest dimensions less than or equal to 5 mm were totally removed by hot biopsy forceps. In the remainder, the largest dimension ranged from 6 to 30 mm and all lesions but one were excised by snare polypectomy. One lesion was initially evaluated by forceps biopsy because it was suspected to be a submucosal lesion. After a definite histopathologic diagnosis of carcinoid tumor was established in this patient, it was totally removed by snaring. Among 17 (11 %) polypoid lesions with surface erosion, 5 were larger than 10 mm. Multiple lesions were detected in 29 (32 %) patients (Figure 1B). No complication developed following the endoscopic procedure in any patient.

Table 1 Characteristics of gastric polypoid lesions

Characteristics	Number* (%)
Location	
Antrum	61 (40.7%)
Cardia	40 (26.7%)
Corpus	34 (22.7%)
Fundus	13 (8.7%)
Peri-anastomotic	2 (1.2%)
Shape	
Sessile	143 (95.3%)
Pedunculated	7 (4.7)
Size	
<5 mm	80 (53.4%)
5-10 mm	51 (34.0%)
10-20 mm	17 (11.4%)
20-30 mm	2 (1.2%)
Histologic subtypes	
Hyperplastic polyp	69 (46.0%)
Foveolar hyperplasia	27 (18.0%)
Fundic gland polyp	21 (14.0%)
Gastritis varioliformis	12 (8.0%)
Lymphoid follicles	9 (6.0%)
Adenoma	4 (2.7%)
Edematous mucosa	4 (2.7%)
Inflammatory polyp	3 (2.0%)
Carcinoid tumor	1 (0.6%)

*Number of lesions.

Histopathologic features of the lesions

The most frequently encountered histopathologic subtype of gastric polypoid lesions was hyperplastic polyp (Figure 2A) which was diagnosed in 46 % of the lesions, followed by foveolar hyperplasia (Figure 2B), fundic gland polyp (Figure 2C), and gastritis varioliformis (Table 2). Three of 43 patients with hyperplastic polyp had adenomas (Figure 2D) as well. Interestingly, the lesions ranging from 4 to 15 mm in diameter were observed as polypoid in 4 patients at endoscopy, but no pathologic changes except an edematous mucosa were determined in samples of endoscopic polypectomy. On the other hand, adenomatous changes were noted within two hyperplastic polyps. Out of 150 lesions, low grade dysplasia was found in one adenoma.

Table 2 Histopathologic features of surrounding gastric mucosa in patients with gastric polyp

Surrounding gastric mucosa	Type of Polyp			
	Hyperplastic	Fundic gland	Adenomatous	Inflammatory
Normal	10	3	1	-
Chronic gastritis	33	1	3	3
H pylori gastritis	19	1	1	1
Intestinal metaplasia	12	-	3	1

Evaluation of the surrounding gastric mucosa revealed that 72 (79 %) patients had chronic gastritis, 45 (49 %) associated *H pylori* infection, and 33 (36 %) intestinal metaplasia, while the remainder (21 %) had normal gastric mucosa (Table 2).

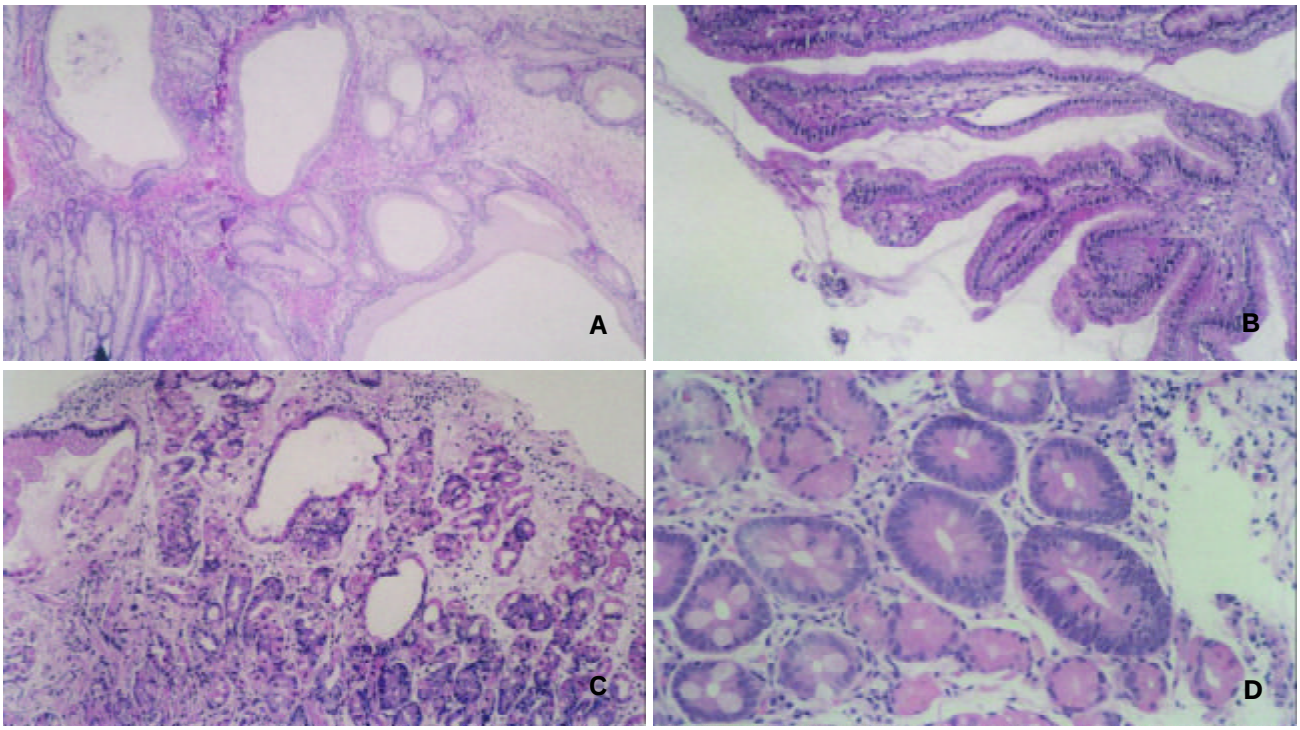

Figure 2 Microscopic pictures of gastric hyperplastic polyp, H&E, X40 (A), foveolar hyperplasia, H&E, X100 (B), fundic gland polyp, H&E, X100 (C), and tubular adenoma,H&E, X200 (D).

The average size of hyperplastic polyps was 8 mm in diameter. However, there was quite a large, hyperplastic polyp 30 mm in diameter, in one patient, and it caused gastric outlet obstruction by plugging the pyloric channel because of its antral location. They were preferentially located in the antrum (42 %) and out of 69 hyperplastic polyps, 5 (7 %) were pedunculated. Only fourteen patients (32 %) had multiple hyperplastic polyps, while all the fundic gland polyps were multiple. Coexistent gastric abnormalities such as chronic gastritis, *H pylori* infection, and intestinal metaplasia were determined in 33 (77 %), 19 (44 %), and 12 (28 %) patients, respectively.

DISCUSSION

The incidence of gastric polyps was 2 % in 2 630 patients who underwent upper GI endoscopic examination at our institution. Our rate was very similar to previously reported frequencies of 2-3 %[4]. However, the overall incidence of gastric polypoid lesions in our patient-population was 3.4 %. Gastric polyps were usually seen as small and sessile polypoid lesions at endoscopy in patients over 40 years old[6]. Although a vast majority of gastric polyps were asymptomatic, they might cause epigastric pain, gastrointestinal bleeding, and symptoms of gastric outlet obstruction[6-8]. The complication risk was generally related to polyp size. We detected only two polyps larger than 2 cm in diameter in our series. A relationship between the presenting symptom and the polyp itself was observed only in one lesion as detailed above. Our results support the fact that underlying gastric abnormalities are likely to be responsible factors for presenting symptoms in patients with gastric polyps.

While polypectomy was performed either endoscopically or surgically in the treatment of symptomatic gastric polyps, there were still no standardized guidelines concerning the management of asymptomatic ones[5,9]. Many endoscopists first took forceps biopsies from gastric polypoid lesions. After obtaining a definite histopathologic diagnosis, they performed polypectomy to these lesions[5]. However, forceps biopsies carried the risk of missing the neoplastic foci within polyp, since only a small portion of the lesion was sampled in this technique[10]. Seifert and Elster[11] compared histopathologic results of biopsy materials and polypectomy specimens of same lesions and showed a remarkable discrepancy between them in 70 % of cases. With this observation, the authors recommended to remove all gastric polyps larger than 5 mm in diameter by an experienced endoscopist[10,12]. In our study, all lesions except one, which was likely to be a submucosal lesion, were totally removed by either snare or hot biopsy forceps without any complication. Endoscopic polypectomy seems as a safe and fast procedure for both diagnosis and treatment of gastric polypoid lesions at the same session.

Some authors reported hyperplastic polyps or fundic gland polyps as the most frequently encountered subtypes of gastric polyps[13-16]. These lesions have previously been accepted as completely benign. However, some current studies showed that they might include adenomatous changes or dysplastic areas[4,7,13,17]. The reported frequencies of dysplastic foci within hyperplastic polyps showed a wide range (4-22 %)[18,19]. Hizawa[20] and Zea-Iriarte[21] found the incidence of malignancy in hyperplastic polyps was 2 % and 1.8 %, respectively. Since hyperplastic polyps were usually associated with chronic gastritis, particularly autoimmune gastritis and *H pylori* gastritis, patients with hyperplastic polyp had an increased risk of synchronous or metachronous adenocarcinomas elsewhere in the stomach[2,4,22]. In a series including 21 patients with hyperplastic polyps, chronic atrophic gastritis was found in all of them and *H pylori* gastritis in 16[16]. On the other hand, the rate of gastric cancer development in nonpolypoid mucosa was reported as 3.3 % in another study of 2 036 hyperplastic polyps[23]. In our series, the presence of chronic gastritis and *H pylori* gastritis was demonstrated in 76 % and in 45 % of hyperplastic polyps, respectively. In addition, two of 69 hyperplastic polyps contained adenomatous changes. These results support the suggestion of removing polypoid lesions instead of taking biopsy from them if feasible, when they are observed at endoscopy.

Gastric adenomas, similar to hyperplastic polyps, were usually detected in pathologically abnormal gastric mucosa

such as gastritis or intestinal metaplasia[13,16]. The malignant potential of gastric adenomas was related to their histologic features, size, shape, and surface appearance[24]. While malignancy risk of adenomas smaller than 2 cm in diameter ranged from 1 % to 5 %, it was higher than 50 % in larger ones[8]. The risk of gastric cancer in other parts of gastric mucosa in patients with adenoma varied between 8 % and 59 %[4]. Contrarily, fundic gland polyps were almost always associated with normal gastric mucosa and sometimes with long-term use of omeprazole[4,13]. They are divided into two different forms: sporadic form and syndromic form, which are associated with familial adenomatous polyposis (FAP) and attenuated variants. In a series including 319 fundic gland polyps from the John Hopkins Hospital, the FAP-associated polyps tended to include low grade dysplasia more than the sporadic ones (25 % *versus* 1 %)[25]. Furthermore, patients with fundic gland polyp might have an increased risk of harbouring a colorectal adenoma or carcinoma[4,23]. Nevertheless, prospective studies are necessary to ascertain whether fundic gland polyp is a sign for colorectal tumours or not. In our study, 75 % of patients with adenoma had chronic gastritis and intestinal metaplasia, whilst gastritis was detected solely in one patient with fundic gland polyps.

Foveolar hyperplasia was the second most common type of gastric polypoid lesions in our series. There is still a debate on whether foveolar hyperplasia is a precursor of hyperplastic polyps[4,23]. The most important distinction between the two lesions was based on the presence of neoplastic foci. Orlowska and associates[26] analyzed 751 hyperplastic lesions and did not find carcinoma in any of foveolar hyperplasia either by primer biopsy or at follow-up. It is wise to separate foveolar hyperplasia and hyperplastic polyp from each other as two distinct subtypes of foveolar hyperplastic lesions, since foveolar hyperplasia has no malignant potential.

We determined that four lesions with polypoid appearance at endoscopy were actually areas of edematous mucosa by histopathological examination. This observation showed that a lesion protruding into the gastric lumen might appear as polypoid lesion even it was not a true polyp. In order to prevent diagnostic confusion, the term "polyp" should be used after achieving exact histopathologic diagnosis as well-supported by the above instance.

In summary, hyperplastic polyp is the most frequently encountered subtype of gastric polypoid lesions. It is usually associated with chronic gastritis or *H pylori* gastritis. Hyperplastic polyps have been described as harmless lesions until recently. However, risk of their malignant transformation has been emphasized in the current literature. For this reason, endoscopic polypectomy seems to be a sensible diagnostic and therapeutic procedure of hyperplastic polyps when feasible. Finally, endoscopic surveillance in these patients may be recommended to exclude both possibility of recurrence and cancer development elsewhere in stomach.

ACKNOWLEDGEMENTS

The authors thank Dr. Ilgin Ozden for contributing to the redaction of this article.

REFERENCES

1 **Silverstein FE,** Tytgat GNJ. Stomach II: Tumors and polyps. In: Silverstein FE, Tytgat GNJ, eds. Gastrointestinal Endoscopy. 3rd ed. *London*: *Mosby* 1997: 147-180
2 **Dent TL,** Kukora JS, Buinewicz BR. Endoscopic screening and surveillance for gastrointestinal malignancy. *Surg Clin North Am* 1989; **69**: 1205-1225
3 **Crawford JM**. The gastrointestinal tract. In: Cotran RS, Kumar V, Robbins SL, eds. Pathologic Basis of Disease. 6th ed. *Philadelphia: W. B. Saunders Company* 1999: 775-843
4 **Oberhuber G**, Stolte M. Gastric polyps: an update of their pathology and biological significance. *Virchows Arch* 2000; **437**: 581-590
5 **Lau CF**, Hui PK, Mak KL, Wong AM, Yee KS, Loo CK, Lam KM. Gastric polypoid lesions-illustrative cases and literature review. *Am J Gastroenterol* 1998; **93**: 2559-2564
6 **Sebastian MW**. Benign tumors of stomach. In: Sabiston DC, ed. The biological basis of modern surgical practise. 15th ed. Philadelphia: *W.B. Saunders Company* 1997: 868-875
7 **Dean PG,** Davis PM, Nascimento AG, Farley DR. Hyperplastic gastric polyp causing progressive gastric outlet obstruction. *Mayo Clin Proc* 1998; **73**: 964-967
8 **Kumar A**, Quick CR, Carr-Locke DL. Prolapsing gastric polyp, an unusual cause of gastric outlet obstruction: a review of the pathology and management of gastric polyps. *Endoscopy* 1996;**28**: 452-455
9 **Kudis V,** Siegel E, Schilling D, Nusse T, Bohrer MH, Riemann JF. The hyperplastic gastric polyp-a praecancerosis. *Z Gastroenterol* 2002; **40**: 295-298
10 **Muehldorfer SM,** Stolte M, Martus P, Hahn EG, Ell C. Diagnostic accuracy of forceps biopsy versus polypectomy for gastric polyps: a prospective multicentre study. *Gut* 2002; **50**: 465-470
11 **Seifert E,** Elster K. Gastric polypectomy. *Am J Gastroenterol* 1975; **63**: 451-456
12 **Ginsberg GG**, Al-Kawas FH, Fleischer DE, Reilly HF, Benjamin SB. Gastric polyps: relationship of size and histology to cancer risk. *Am J Gastroenterol* 1996; **91**: 714-717
13 **Debongnie JC**. Gastric polyps. *Acta Gastroenterol Belg* 1999; **62**: 187-189
14 **Stolte M,** Sticht T, Eidt S, Ebert D, Finkenzeller G. Frequency, location, and age and sex distribution of various types of gastric polyp. *Endoscopy* 1994; **26**: 659-665
15 **Papa A**, Cammarota G, Tursi A, Montalto M, Cuoco L, Certo M, Fedeli G, Gasbarrini G. Histologic types and surveillance of gastric polyps: a seven year clinico-pathological study. *Hepatogastroenterology* 1998; **45**: 579-582
16 **Ljubicic N**, Kujundzic M, Roic G, Banic M, Cupic H, Doko M, Zovak M. Benign epithelial gastric polyps-frequency, location, and age and sex distribution. *Coll Antropol* 2002; **26**: 55-60
17 **Declich P,** Ambrosiani L, Grassini R, Tavani E, Bellone S, Bortoli A, Gozzini C, Prada A. Fundic gland polyps: a still elusive entity on the eve of the year 2000. *Pol J Pathol* 2000; **51**: 3-8
18 **Daibo M,** Itabashi M, Hirota T. Malignant trasformation of gastric hyperplastic polyps. *Am J Gastroenterol* 1990; **85**: 327-328
19 **Davaris P,** Petraki K, Archimandritis A, Haritopoulos N, Papacharalampous N. Mucosal hyperplastic polyps of the stomach. Do they have any potential to malignancy? *Pathol Res Pract* 1986; **181**: 385-389
20 **Hizawa K**, Fuchigami T, Iida M, Aoyagi K, Iwashita A, Daimaru Y, Fujishima M. Possible neoplastic transformation within gastric hyperplastic polyp. Application of endoscopic polypectomy. *Surg Endosc* 1995; **9**: 714-718
21 **Zea-Iriarte WL,** Sekine I, Itsuno M, Makiyama K, Naito S, Nakayama T, Nishisawa-Takano JE, Hattori T. Carcinoma in gastric hyperplastic polyps: a phenotypic study. *Dig Dis Sci* 1996; **41**: 377-386
22 **Abraham SC**, Singh VK, Yardley JH, Wu TT. Hyperplastic polyps of the stomach: associations with histologic patterns of gastritis and gastric atrophy. *Am J Surg Pathol* 2001; **25**: 500-507
23 **Stolte M.** Clinical consequences of the endoscopic diagnosis of gastric polyps. *Endoscopy* 1995; **27**: 32-37
24 **Park DI,** Rhee PL, Kim JE, Hyun JG, Kim YH, Son HJ, Kim JJ, Paik SW, Rhee JC, Choi KW, Oh YL. Risk factors suggesting malignant transformation of gastric adenoma: univariate and multivariate analysis. *Endoscopy* 2001; **33**: 501-506
25 **Wu TT**, Kornachi S, Rashid A, Yardley JH, Hamilton SR. Dysplasia and dysregulation of proliferation in foveolar and surface epithelia of fundic gland polyps from patients with familial adenomatous polyposis. *Am J Surg Pathol* 1998; **22**: 293-298
26 **Orlowska J,** Jarosz D, Pachlewski J, Butruk E. Malignant transformation of benign epithelial gastric polyps. *Am J Gastroenterol* 1995; **90**: 2152-2159

Edited by Wang XL

P.O.Box 2345, Beijing 100023,China
Fax: +86-10-85381893
E-mail: wjg@wjgnet.com www.wjgnet.com

World J Gastroenterol 2003;9(10):2240-2250
World Journal of Gastroenterology
 ISSN 1007-9327

Construction of expression systems for *flaA* and *flaB* genes of *Helicobacter pylori* and determination of immunoreactivity and antigenicity of recombinant proteins

Jie Yan, Shao-Hui Liang, Ya-Fei Mao, Li-Wei Li, Shu-Ping Li

Jie Yan, Ya-Fei Mao, Li-Wei Li, Shu-Ping Li, Department of Medical Microbiology and Parasitology, College of Medical Sciences, Zhejiang University, Hangzhou 310031, Zhejiang Province, China
Shao-Hui Liang, Department of Medical Microbiology and Parasitology, College of Medical Sciences, Zhejiang University, Hangzhou 310031, Zhejiang Province, China and Department of Parasitology, Wenzhou Medical College, Wenzhou 325027, Zhejiang Province, China
Supported by the Excellent Young Teacher Fund of Chinese Education Ministry and the General Research Plan of the Science and Technology Department of Zhejiang Province, No. 001110438
Correspondence to: Jie Yan, Department of Medical Microbiology and Parasitology, College of Medical Sciences, Zhejiang University, 353 Yan an Road, Hangzhou 310031, Zhejiang Province, China. yanchen@mail.hz.zj.cn
Telephone: +86-571-87217385 **Fax:** +86-571-87217044
Received: 2003-05-13 **Accepted:** 2003-06-02

Abstract

AIM: To clone flagellin genes A (*flaA*) and B (*flaB*) from a clinical strain of *Helicobacter pylori* (*H pylori*) and to construct prokaryotic expression systems of the genes and identify immunity of the fusion proteins.

METHODS: The *flaA* and *flaB* genes from a clinical *H pylori* isolate Y06 were amplified by high fidelity PCR. The nucleotide sequences of target DNA amplification fragments from the two genes were sequenced after T-A cloning. The recombinant expression vector *pET32a* inserted with *flaA* and *flaB* genes was constructed, respectively. The expressions of FlaA and FlaB fusion proteins in *E. coli* BL21DE3 induced by isopropylthio-β-D-galactoside (IPTG) at different concentrations were examined by SDS-PAGE. Western blot using commercial antibodies against whole cell of *H pylori* and immunodiffusion assay using self-prepared rabbit antiserum against FlaA (rFlaA) or FlaB (rFlaB) recombinant proteins were applied to the determination of the fusion proteins immunity. ELISA was used to detect the antibodies against rFlaA and rFlaB in sera of 125 *H pylori* infected patients and to examine rFlaA and rFlaB expression in 98 clinical isolates of *H pylori*, respectively.

RESULTS: In comparison with the reported corresponding sequences, the nucleotide sequence homologies of the cloned *flaA* and *flaB* genes were from 96.28-97.13 % and 96.31-97.73 %, and their putative amino acid sequence homologies were 99.61-99.80 % and 99.41-100 % for the two genes, respectively. The output of rFlaA and rFlaB expressed by *pET32a-flaA*-BL21DE3 and *pET32a-flaB*-BL21DE3 systems was as high as 40-50 % of the total bacterial proteins. Both rFlaA and rFlaB were able to combine with the commercial antibodies against whole cell of *H pylori* and to induce rabbits to produce specific antibodies with the same 1:2 immunodiffusion titers after the animals were immunized with the two recombinant proteins. Ninety-eight and zero point 4 and 92.80 % of the serum samples from 125 patients infected with *H pylori* were positive for rFlaA and rFlaB antibodies, respectively. One hundred percent and 98.98 % of the 98 tested isolates of *H pylori* were detectable for rFlaA and rFlaB epitopes, respectively.

CONCLUSION: Two prokaryotic expression systems with high efficiency of *H pylori flaA* and *flaB* genes were successfully established. The expressed rFlaA and rFlaB showed satisfactory immunoreactivity and antigenicity. High frequencies of FlaA and FlaB expression in different *H pylori* clinical strains and the general existence of specific antibodies against FlaA and FlaB in *H pylori* infected patients strongly indicate that FlaA and FlaB are excellent antigen candidates for developing *H pylori* vaccine.

Yan J, Liang SH, Mao YF, Li LW, Li SP. Construction of expression systems for *flaA* and *flaB* genes of *Helicobacter pylori* and determination of immunoreactivity and antigenicity of recombinant proteins. *World J Gastroenterol* 2003; 9(10): 2240-2250
http://www.wjgnet.com/1007-9327/9/2240.asp

INTRODUCTION

In China, chronic gastritis and peptic ulceration are two most common gastric diseases, and gastric cancer is one of the malignant tumors with high mortalities and morbidities[1-34]. *Helicobacter pylori* (*H pylori*), a microaerophilic, spiral and Gram-negative bacterium, is considered as a human-specific gastric pathogen that colonizes the stomach of at least half of the world population[35]. Most infected individuals are asymptomatic. However, in some subjects, the infection causes acute, chronic gastritis and peptic ulceration, and plays important roles in the development of peptic ulcer and gastric adenocarcinoma, mucosa-associated lymphoid tissue (MALT) lymphoma and primary gastric non-Hodgkin' s lymphoma[36-43]. This microorganism has been categorized as class I carcinogen by the World Health Organization[44], and direct evidence of carcinogenesis has been recently demonstrated in animal models[45, 46]. Immunization against the bacterium represents a cost-effective strategy to prevent *H pylori*-associated peptic ulcer diseases and to reduce the incidence of global gastric cancer[47]. Selection of antigenic targets is critical in design of *H pylori* vaccine. So far, no vaccine preventing *H pylori* infection has been commercially available. The majority of studies attempting to produce a vaccine have focused on urease enzyme, heat shock protein, and vacuolating cytotoxin[35, 48-50], but rarely on *H pylori* flagellin. *H pylori* flagellin is composed of two subunits, named as FlaA with 53KDa and FlaB with 54 KDa respectively. The flagellin plays a main role in motility and is necessary for colonization or persistence of *H pylori* infection[51]. The motility of *H pylori* is a virulent factor in the pathogenesis of gastric mucosal injury[52]. The data mentioned

above indicate that FlaA as well as FlaB may be used as antigen candidates for *H pylori* vaccine. Therefore, in this study, two prokaryotic vectors responsible for expressing recombinant FlaA (rFlaA) and FlaB (rFlaB) were constructed. Immunoreactivity and antigenicity of rFlaA and rFlaB were further examined. Furthermore, these two recombinant proteins were used for detecting specific antibodies in sera from *H pylori* infected patients, and rabbit anti-rFlaA and anti-rFlaB sera were prepared for examining the corresponding epitopes of *H pylori* clinical isolates. The results of this study may contribute to the development of *H pylori* vaccines.

MATERIALS AND METHODS

Materials

A clinical strain of *H pylori* was used in this study, which was provisionally named Y06, and well-characterized by the Department of Medical Microbiology and Parasitology, College of Medical Sciences, Zhejing University. A plasmid *pET32a* (Novagen) and an *E. coli* strain BL21DE3 (Novagen) were used as the expression vector and host cell, respectively. Primers for PCR amplification, the Pfu-Taq high fidelity PCR kit and restriction endonucleases were purchased from BioAsia (Shanghai, China). The T-A cloning kit and sequencing service were provided by BBST (Shanghai, China). Rabbit antiserum against the whole cell of *H pylori*, HRP-labeling sheep antisera against rabbit IgG and against human IgG were purchased from DAKO and Jackson ImmunoResearch, respectively. Agents used in isolation and identification of *H pylori* were purchased from Sigma and bioMérieux. Gastric biopsy specimens with positive *H pylori* isolation from 126 patients (86 males and 40 females, age range: from 6-78 years old, mean age: 40.5 years old) referred for gastroduodenoscopic examination in four different hospitals in Hangzhou were collected during the period between December 2001 and June 2002. Each of the patients gave a written informed content for this study. Of the 126 patients, 68 had chronic gastritis (CG, 48 superficial, 10 active and 10 atrophic), and the other 58 had peptic ulcer disease (PUD, 12 gastric ulcer, 40 duodenal ulcer and 6 gastric and duodenal ulcer). None of the patients had taken nonsteroidal anti-inflammatory drugs, antacids and antibiotics during the two weeks before seeking medical advice. At the same time, serum specimens were also collected from these patients.

Methods

Isolation and identification of *H pylori* Each gastric biopsy specimen was homogenized with a tissue grinder and then inoculated on Columbia agar plates supplemented with 8.0 % (V/V) sheep blood, 0.5 % (W/V) cyclodextrin, 5 mg/L trimethoprim, 10 mg/L vancomycin, 2 500 U/L cefsoludin and 2.5 mg/L amphotericin B. The plates were incubated at 37 ℃ under microaerobic conditions (5 % O_2, 10 % CO_2 and 85 % N_2) for 3 to 5 days. A bacterial isolate was identified as *H pylori* according to typical Gram staining morphology, biochemical tests positive for urease and oxidase, and agglutination with the commercial rabbit antibody against whole cell of the microbe. All of *H pylori* isolates were stored at -70 ℃ for ELISA.

Preparation of DNA template Genomic DNA of *H pylori* strain Y06 was extracted by the conventional phenol-chloroform method and DNase-free RNase treatment[52]. The obtained DNA was dissolved in TE buffer, and its concentration and purity were determined by ultraviolet spectrophotometry[52].

Polymerase chain reaction Oligonucleotide primers were designed to amplify the whole sequence of *flaA* and *flaB* genes from *H pylori* strain Y06 based on the published corresponding genomic sequences[53-56]. The sequence of *flaA* sense primer with an endonuclease site of *Eco*RV was 5' -CCG GATATCATGGCTTTTCAGGTCAA-3' . The sequence of *flaA* antisense primer with an endonuclease site of *Xho*I was 5' -CCGCTCGAGAAACTAAGTTAAAAGCC-3' . The sequence of *flaB* sense primer with an endonuclease site of *Eco*RI was 5' -CCGGAATTCATGAGTTTTAGGATAAA-3' . The sequence of *flaB* antisense primer with an endonuclease site of *Xho*I was 5' -CCGCTCGAGCTGTTATTGTAAAA GCC-3' . The total volume per PCR was 100 μl containing 2.5 mol· L^{-1} each dNTP, 500 nmol· L^{-1} each of the two primers, 15 mol· L^{-1} $MgCl_2$, 3.0 U Pfu-Taq polymerase, 100 ng DNA template and 1×PCR buffer (pH8.8). The parameters for PCR were at 94 ℃ for 5 min, ×1; at 94 ℃ for 30 s, at 52 ℃ for 30 s, at 72 ℃ for 90 s, ×10; at 94 ℃ for 30 s, at 52 ℃ for 30 s, at 72 ℃ for 100 s (10 s addition for the each of the following cycles), ×15; then at 72 ℃ for 10 min, ×1. The results of PCR were observed under UV light after electrophoresis in 15 g· L^{-1} agarose pre-stained with ethidium bromide. The expected sizes of target amplification fragments were 1 530 bp for *flaA* gene and 1 542 bp for *flaB* gene.

Cloning and sequencing The target amplification DNA fragments from *flaA* and *flaB* genes were respectively cloned into *pUCm*-T vectors (*pUCm*-T-*flaA* and *pUCm*-T-*flaB*) by using the T-A cloning kit according to the manufacturer' s instructions. The recombinant plasmids were amplified in an *E. coli* strain DH5α and then extracted by the Sambrook' s method[57]. A professional company (BBST) was responsible for nucleotide sequence analysis of the inserted fragments. Three strains of *E. coli* DH5α containing *pUCm*-T-*flaA*, *pUCm*-T-*flaB* and expression vector *pET32a* were amplified in BL medium, and the three plasmids were extracted, respectively[57]. These plasmids were digested with *Eco*RV and *Xho*I, *Eco*RI and *Xho*I, respectively. The *flaA* target fragment and *pET32a*, and the *flaB* fragment and *pET32a* were recovered and then ligased. The recombinant expression vectors *pET32a-flaA* and *pET32a-flaB* were respectively transformed into *E.coli* BL21DE3, and the expression systems were named as *pET32a-flaA*-BL21DE3 and pET32a-*flaB*-BL21DE3. The target fragments of *flaA* and *flaB* genes inserted in *pET32a* plasmid were sequenced again.

Expression and identification of fusion proteins *pET32a-flaA*-BL21DE3 and *pET32a-flaB*-BL21DE3 were rotatively cultured in LB medium at 37 ℃ induced by isopropylthio-β-D-galactoside (IPTG) at different concentrations of 1.0, 0.5 and 0.1 mmol· L^{-1}. The supernatant and precipitate were separated through centrifugation after the bacterial pallet was ultrasonically broken (300V, 5 s×3). The molecular weight and output of rFlaA and rFlaB were examined by SDS-PAGE. The two recombinant proteins were collected by Ni-NTA affinity chromatography. The commercial rabbit antiserum against whole cell of *H pylori* and HRP-labeling sheep antiserum against rabbit IgG were used as the first and second antibodies to determine the immunoreactivity of rFlaA and rFlaB by Western blot. Rabbits were immunized with rFlaA and rFlaB, respectively, for preparation of antisera. Immunodiffusion assay was applied to the determination of the antigenicity of rFlaA and rFlaB.

ELISA The specific antibodies against FlaA and FlaB in sera of the 126 patients infected with *H pylori* were detected by ELISA, by using rFlaA and rFlaB as antigens at the coated concentration of 20 μg/ml and a patient serum sample (1:400 dilution) as the first antibody and HRP-labeling sheep antibody against human IgG (1:4 000 dilution) as the second antibody. The result of ELISA for a patient' s serum sample was considered as positive if the optical density at 490 nm (OD_{490}) was over the mean plus 3 SD of five negative serum samples[58]. FlaA and FlaB expression in clinical isolates of *H pylori* was detected by ELISA using the ultrasonic supernatant of each *H pylori*

isolate (50 μg/ml) as a coated antigen, the self-prepared rabbit antisera against rFlaA and rFlaB (1:800 dilution in both) as the first antibody and HRP-labeling sheep antibody against rabbit IgG (1:3 000 dilution) as the second antibody. The result of ELISA for a *H pylori* ultrasonic supernatant sample was considered as positive if its OD_{490} value was over the mean plus 3 SD of five ultrasonic supernatant samples at the same protein concentration of *E. coli* ATCC 25922[58].

Date analysis The nucleotide sequences of the cloned *flaA* and *flaB* genes were compared for homology with the 3 published *flaA* gene sequences (NC000915, NC000921, X60746)[53-55] and the 4 published *flaB* gene sequences (NC000915, NC000921, L08907, AF479024)[53,54,56,59] by using a molecular biological analysis software.

RESULTS

PCR

Target fragments of *flaA* and *flaB* genes with expected sizes amplified from DNA template of *H pylori* stain Y06 are shown in Figure 1.

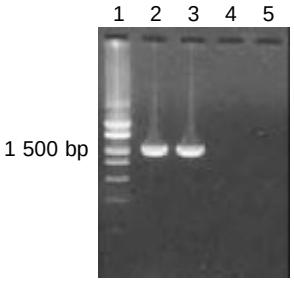

Figure 1 Target fragments of *flaA* and *flaB* genes amplified from *H pylori* strain Y06 DNA.

Nucleotide sequence analysis

The nucleotide sequences of *flaA* gene in *pUCm*-T-*flaA* and *pET32a-flaA* were completely the same and so as for *flaB* gene. The homologies of nucleotide and putative amino acid sequences of the cloned *flaA* gene compared with the published *flaA* sequences[53-55] were from 96.28 % to 97.13 % and from 99.61 % to 99.80 %, respectively (Figures 2 and 3). The homologies of nucleotide and putative amino acid sequences of the cloned *flaB* gene were 96.31-97.73 % and 99.41-100 %, compared with the published *flaB* sequences (Figures 4 and 5)[53,54,56,59].

Expression of target fusion proteins

IPTG at concentrations of 1.0, 0.5 and 0.1 mmol· L^{-1} efficiently induced the expression of rFlaA and rFlaB in *pET32a-flaA*-BL21DE3 and *pET32a-flaB*-BL21DE3 systems. The products of rFlaA and rFlaB were mainly presented in ultrasonic precipitates, and the output was 40-50 % of the total bacterial proteins (Figures 6 and 7).

Immunoreactivity and antigenicity of rFlaA and rFlaB

The commercial rabbit antibodies against the whole cell of *H pylori* combined with rFlaA and rFlaB as confirmed by Western blot (Figures 8 and 9). Both the titer of immunodiffusion assay between rFlaA and its rabbit antiserum, rFlaB and its rabbit antiserum was 1:2.

ELISA

Since the mean ±SD of OD_{490} values of the five negative serum samples were 0.338±0.036 for rFlaA and 0.102±0.051 for rFlaB in the detection of specific antibodies in patients' sera, the positive reference value was 0.446 for FlaA and 0.255 for FlaB. According to the reference values, 98.4 % (123/125, one serum sample was contaminated) of the tested patients' serum samples were positive for antibodies against rFlaA with an OD_{490} value range of 0.52-1.76, and 92.8 % (116/125) were positive for antibodies against rFlaB with an OD_{490} value range of 0.26-1.50. Since the mean ±SD of OD_{490} of the five negative bacterial controls was 0.200±0.046 for FlaA and 0.170±0.044 for FlaB in the detection of clinical *H pylori* isolates, the positive reference value was 0.338 for FlaA and 0.302 for FlaB. According to the reference values, 100 % (98/98) of the tested *H pylori* isolates were detectable for the epitope of rFlaA with an OD_{490} value range of 0.36-2.01 and 99 % (97/98) of the isolates were detectable for the epitope of rFlaB with an OD_{490} value range of 0.31-1.78.

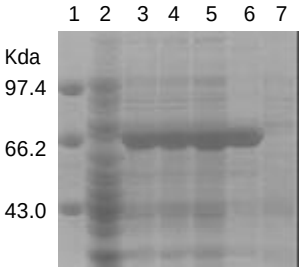

Figure 6 Expression of rFlaA induced by IPTG at different concentrations.

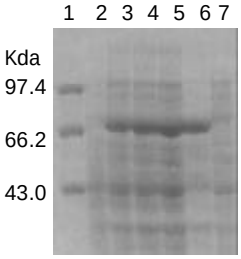

Figure 7 Expression of rFlaB induced by IPTG at different concentrations.

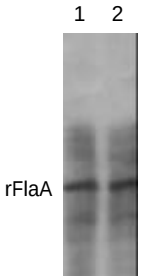

Figure 8 Western blot result of rabbit antibodies against whole cell of *H pylori* and rFlaA.

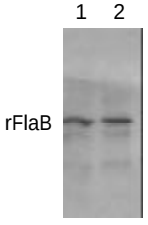

Figure 9 Western blot result of rabbit antibodies against whole cell of *H pylori* and rFlaB.

```
(1)1    ATGGCTTTTCAGGTCAATACAAATATCAATGCGATGAATGCGCATGTGCAATCCGCACTC
(2)1    ............................................................
(3)1    ...........................................................A....
(4)1    ............................................................

(1)61   ACTCAAAATGCGCTTAAAACTTCATTGGAGAGATTGAGTTCAGGTTTAAGGATTAATAAA
(2)61   ........C.....................C...........................
(3)61   ............................................................
(4)61   ........C..A..................C.....................C......

(1)121  GCGGCTGATGATGCATCAGGCATGACGGTGGCAGATTCTTTGCGTTCACAAGCGAGCAGT
(2)121  ...........C.....................G...........................
(3)121  ...........C.....................G...........................
(4)121  ...........C.....................G.............G............

(1)181  TTGGGTCAAGCGATTGCCAACACGAATGACGGCATGGGGATTATCCAAGTTGCGGATAAG
(2)181  ................................................G............
(3)181  ................................................G............
(4)181  ................................................G............

(1)241  GCTATGGATGAGCAGTTAAAAATCTTAGACACCGTTAAGGTTAAAGCGACTCAAGCGGCT
(2)241  ............................................................
(3)241  ............................................................
(4)241  ..............A.............................................

(1)301  CAAGACGGGCAAACTACGGAATCTCGTAAAGCGATTCAATCTGACATCGTTCGTTTGATT
(2)301  .....T...........A.....................................
(3)301  .....T.....................................................
(4)301  .....T.....................................................

(1)361  CAAGGTTTAGATAATATCGGTAACACGACTACTTATAACGGGCAAGCGTTATTGTCTGGT
(2)361  ...........C...........T.....................................
(3)361  ...........C...........T.....................................
(4)361  ........G.................A..G...............................

(1)421  CAATTCACTAACAAAGAATTCCAAGTAGGGGCTTATTCTAACCAAAGCATTAAGGCTTCT
(2)421  ........C.....................................................A......
(3)421  ................................................T............
(4)421  ............................................................

(1)481  ATCGGCTCTACCACTTCGGATAAAATCGGTCAGGTTCGTATCGCTACAGGCGCGTTAATC
(2)481  ..................C.................................T.........
(3)481  ..................C.....................................
(4)481  ..................C.....................................

(1)541  ACGGCTTCTGGGGATATTAGCTTGACTTTTAAACAAGTGGATGGCGTGAATGATGTAACT
(2)541  ..C........A.....................................
(3)541  ...........................................T................
(4)541  ............................................................

(1)601  TTAGAGAGCGTAAAAGTTTCTAGTTCAGCAGGCACGGGGATCGGTGTGTTAGCGGAAGTG
(2)601  ..................................A.....T..C........A......
(3)601  ..................C.................A.....T..C........A......
(4)601  ..................................A........C........A......

(1)661  ATTAACAAAAATTCTAACCGAACAGGGGTTAAAGCTTATGCGAGCGTTATCACCACGAGC
(2)661  ........G..C.............C........C.....................
(3)661  ..C.....................................................
(4)661  ..C..T.....C.....................................

(1)721  GATGTGGCGGTCCAATCAGGAAGTTTGAGTAATTTAACTTTAAATGGGATCCATTTGGGT
(2)721  ..............G.....................C...........T........G
(3)721  ..............G.....................C.....................C
(4)721  ..............G.....................C...........T.........

(1)781  AATATCGCAGATATTAAGAAAAATGACTCAGACGGAAGGTTAGTCGCAGCGATCAATGCG
```

```
(2)781  ......................C............C.A.....................
(3)781  ..........................................................
(4)781  ......................C...................................

(1)841  GTTACTTCAGAAACCGGCGTGGAAGCTTATACGGATCAAAAAGGGCGCTTGAATTTGCGC
(2)841  ..........................................................
(3)841  ................T.........................................
(4)841  ..C............T.........................................

(1)901  AGTATAGATGGTCGTGGGATTGAAATCAAAACCGATAGCGTCAGTAATGGGCCTAGTGCT
(2)901  ....................................T.....................
(3)901  ..................................C.....................
(4)901  ..................................C..........C........C...

(1)961  TTAACGATGGTCAATGGCGGTCAGGATTTAACAAAAGGTTCTACTAACTATGGGAGGCTT
(2)961  ..........T........................C..........C..A......
(3)961  ..................................C..........C..A......
(4)961  ..................................C..........C..A......

(1)1021 TCTCTCACACGCTTAGACGCTAAAAGCATCAATGTCGTTTCGGCTTCTGATTCGCAACAT
(2)1021 ......................G.........................C.........
(3)1021 ..........A..........G..........A.....A........C..A..G...
(4)1021 ..........A..........G.........................C..A..G...

(1)1081 TTAGGTTTCACAGCGATTGGTTTTGGGGAATCTCAAGTGGCAGAAACCACGGTGAATTTG
(2)1081 .....C....................................................
(3)1081 ..........................................................
(4)1081 .....C.....G..............................................

(1)1141 CGCGATGTTACTGGGAATTTTAACGCTAATGTCAAATCAGCCAGTGGCGCGAACTATAAC
(2)1141 ..........C.....................................T...........
(3)1141 ..........C..........................................
(4)1141 ..........................................................

(1)1201 GCCGTGATCGCTAGCGGTAACCAAAGCTTGGGATCTGGGGTTACAACCTTGAGAGGCGCG
(2)1201 .....C........T..C..T............................A.....T...
(3)1201 .....C........T..C..T............................A.........
(4)1201 ..................................................A.........

(1)1261 ATGGTGGTGATTGATATTGCGGAATCGGCGATGAAAATGTTGGATAAAGTCCGCTCTGAT
(2)1261 ..............C.....C..G..T.........................A......
(3)1261 ..................C..G..T.....................................
(4)1261 ..............C.....C.....A.....................................C

(1)1321 TTAGGTTCTGTGCAAAATCAAATGATTAGCACCGTGAATAACATCAGCATCACTCAAGTG
(2)1321 ..........................................................
(3)1321 ..........................................................
(4)1321 ..............................T...........................

(1)1381 AATGTTAAAGCGGCTGAGTCTCAAATCAGGGATGTGGATTTTGCTGAAGAGAGCGCGAAT
(2)1381 ................A.....................................
(3)1381 ................A.....................................
(4)1381 ................A.....................C...............

(1)1441 TTCAATAAAAACAATATTTTGGTGCAATCAGGCAGCTATGCGATGAGTCAAGCTAACACC
(2)1441 ..............C.......CA........T...................C......
(3)1441 ..............C.......C.............................C......
(4)1441 .....C........C.......C.............................C..T...

(1)1501 GTCCAACAAAATATCTTAAGGCTTTTAACTTAG
(2)1501 ..T..........................
(3)1501 ..T..........................
(4)1501 ..T..........................
```

Figure 2 Homologies of nucleotide sequence of cloned *H pylori flaA* gene with reported sequences. (1): the sequencing result of *H pylori* strain Y06 *flaA* gene; (2)-(4): the reported sequences from GenBank (No. NC000915, strain 26695; No. NC_000921, strain J99; No. X60746, strain 898-1). Underlined areas indicate the positions of primer sequences.

```
(1)1   MAFQVNTNINAMNAHVQSALTQNALKTSLERLSSGLRINKAADDASGMTVADSLRSQASS
(2)1   ............................................................
(3)1   ............................................................
(4)1   ................E...........................................

(1)61  LGQAIANTNDGMGIIQVADKAMDEQLKILDTVKVKATQAAQDGQTTESRKAIQSDIVRLI
(2)61  ............................................................
(3)61  ............................................................
(4)61  ............................................................

(1)121 QGLDNIGNTTTYNGQALLSGQFTNKEFQVGAYSNQSIKASIGSTTSDKIGQVRIATGALI
(2)121 ............................................................
(3)121 ............................................................
(4)121 ............................................................

(1)181 TASGDISLTFKQVDGVNDVTLESVKVSSSAGTGIGVLAEVINKNSNRTGVKAYASVITTS
(2)181 ............................................................
(3)181 ............................................................
(4)181 ............................................................

(1)241 DVAVQSGSLSNLTLNGIHLGNIADIKKNDSDGRLVAAINAVTSETGVEAYTDQKGRLNLR
(2)241 ............................................................
(3)241 ............................................................
(4)241 ............................................................

(1)301 SIDGRGIEIKTDSVSNGPSALTMVNGGQDLTKGSTNYGRLSLTRLDAKSINVVSASDSQH
(2)301 ............................................................
(3)301 ............................................................
(4)301 ............................................................

(1)361 LGFTAIGFGESQVAETTVNLRDVTGNFNANVKSASGANYNAVIASGNQSLGSGVTTLRGA
(2)361 ............................................................
(3)361 ............................................................
(4)361 ............................................................

(1)421 MVVIDIAESAMKMLDKVRSDLGSVQNQMISTVNNISITQVNVKAAESQIRDVDFAEESAN
(2)421 ............................................................
(3)421 ............................................................
(4)421 ............................................................

(1)481 FNKNNILVQSGSYAMSQANTVQQNILRLLT      510aa
(2)481 .......A......................
(3)481 .......A......................
(4)481 .......A......................
```

Figure 3 Homologies of putative amino acid sequence of *H pylori flaA* gene with reported sequences. (1): the sequencing result of cloned *H pylori* strain Y06 *flaA* gene; (2)-(4): the reported sequences from GenBank (No. NC000915, strain 26695; No. NC_000921, strain J99; No. X60746, strain 898-1).

```
(1)1    ATGAGTTTTAGGATAAATACCAATATCGCCGCTTTAACTTCTCATGCGGTAGGGGTTCAA
(2)1    ...........................................................
(3)1    ..........................................................G......
(4)1    ...........................................................
(5)1    ...........................................................

(1)61   AACAACAGAGACCTTTCAAGCTCGCTTGAAAAGTTAAGCTCAGGGCTTAGGATCAATAAG
(2)61   ...........................................................A
(3)61   ..........................................T..............A
(4)61   ...........................................................A
(5)61   ...........................................................A

(1)121  GCCGCTGACGATTCTAGTGGGATGGCGATCGCTGATAGCTTAAGGAGTCAAAGCGCGAAT
(2)121  ...........................................................
(3)121  ...........................................................
(4)121  ...........................................................
(5)121  ...........................................................
```

```
(1)181  TTAGGCCAGGCGATTCGCAACGCTAATGACGCTATTGGTATGGTTCAAACCGCTGATAAA
(2)181  ..G..T..A.....C........C.............................A......
(3)181  ..................................................................
(4)181  ..G..T..A.....C.....................................................
(5)181  ..G.....................................................................

(1)241  GCGATGGATGAGCAAATCAAAATCTTAGACACCATTAAAACCAAAGCCGTTCAAGCCGCT
(2)241  ..................................................................
(3)241  ..................................................................
(4)241  ..................................................................
(5)241  ..................................................................

(1)301  CAAGATGGGCAAACTTTAGAAAGCCGAAGAGCACTCCAGAGCGATATTCAAAGGTTGTTA
(2)301  ................................G.....................................
(3)301  ................................G.....................................
(4)301  ................................G.....................................
(5)301  ................................G.....................................

(1)361  GAAGAACTGGACAATATCGCTAACACCACAAGCTTTAACGGCCAACAAATGCTTTCAGGA
(2)361  ..................................................................
(3)361  ........A.....................................................
(4)361  ........A.....................................................
(5)361  ........A...........C.........................................

(1)421  AGTTTTTCTAACAAAGAATTTCAAATTGGCGCGTATTCTAACACCACGGTTAAAGCGTCT
(2)421  ..........................................G.....................
(3)421  ..................................................................
(4)421  ..................................................................
(5)421  ..........................................................G.......

(1)481  ATTGGCTCAACAAGCTCAGATAAGATTGGGCATGTGCGCATGGAAACCTCTTCTTTTAGC
(2)481  ...........G.....................................T.............
(3)481  ...........G..T..G.....A.......................T..A.........
(4)481  ...........G...........A..C...................T.............
(5)481  ...........G...........A.....................................

(1)541  GGTGAAGGCATGCTCGCTAGCGCGGCGG CGCAAAACTTGACTGAAGTGGGATTGAATTT
(2)541  ....C..................... A..............................
(3)541  ............................ ..............................
(4)541  ........................C.G...... ..........................
(5)541  ..C...................A.... ..............................

(1)600  CAAACAAGTCAATGGCGTGAACGATTATAAGATTGAAACCGTGCGCATTTCTACGAGCGC
(2)600  ......................T.....................................T..
(3)600  ......................T.....................................
(4)600  ......................T.....................................
(5)600  ......................T.................................A.....

(1)660  TGGCACTGGGATCGGAGCGTTAAGCGAAATCATCAATCGTTTTTCTAACACTTTAGGCGT
(2)660  ............T.....................................................
(3)660  C...........T..G.....................C...........C.......
(4)660  ......A.....T.....................................................
(5)660  ......A.....T..G...........G...........C...........C.......

(1)720  TAGGGCGTCTTATAATGTCATGGCTACCGGCGGCACTCCCGTGCAATCAGGAACTGTTAG
(2)720  ......T.....................................................
(3)720  ...A..A.................................T.............C..G..
(4)720  ..........................................A...............
(5)720  ......T........C.............T.....A..G.................G..

(1)780  GGAGCTTACCATTAATGGCGTAGAAATTGGGACCGTGAATGATGTGCATAAAAATGACGC
(2)780  ..................................................C.....
(3)780  A.............................A.....................C.....
(4)780  ..................................................C.....
(5)780  A..A..C.....................A.............G......C.....

(1)840  TGATGGGAGGTTGACTAATGCGATCAACTCCGTCAAAGACAGGACCGGCGTGGAAGCGAG
```

```
(2)840  .........A..........A.....................G..T..........
(3)840  ...C.................................TC.C.....T..........
(4)840  ...C................................................
(5)840  ...C..C..A..................................G.....A........

(1)900  CTTGGATATTCAAGGGCGCATTAATTTGCACTCCATTGACGGGCGTGCGATTTCTGTGCA
(2)900  ........................A.................C.............
(3)900  ....................................T.....C.............
(4)900  ....................................................C.............
(5)900  ....................................T.....C.............

(1)960  TGCAGCGAGCGCGAGCGGTCAGGTTTTTGGGGGAGGGAATTTTGCAGGGATTTCTGGGAC
(2)960  ............................................................
(3)960  ..........................................A.............
(4)960  .........T.................................A..............
(5)960  ..................C.........................................

(1)1020 ACAACATGCGGTTATTGGGCGCTTAACCTTGACCAGGACCGACGCTAGAGACATCATTGT
(2)1020 ...G.................................A.....................
(3)1020 ...G.............................T...................T..C..
(4)1020 ...G.....A.........................A.................T.....
(5)1020 ...G.........................A..T..A........C.....T........

(1)1080 GAGCGGTGTGAATTTTAGCCATGTGGGCTTTCATTCCGCTCAAGGGGTGGCAGAATACAC
(2)1080 ..............C.............................................
(3)1080 ............................................................
(4)1080 ............................................................
(5)1080 ............C.............................................

(1)1140 CGTGAATTTGAGAGCGGTTAGGGGCATTTTTGATGCGAATGTGGCTTCAGCAGCCGGAGC
(2)1140 ............................................................
(3)1140 ..........................................................G.........
(4)1140 ............................................................G..
(5)1140 ............G.............................................

(1)1200 GAACGCTAATGGCGCACAAGCGGAGACCAATTCTCAAGGTATAGGGGCTGGGGTAACAAG
(2)1200 ..............G.............................................
(3)1200 ..............G.............................A..C..A........
(4)1200 ....................T.................C....................
(5)1200 ..............G.............................................

(1)1260 CCTTAAAGGAGCGATGATTGTGATGGATATGGCGGACTCAGCGCGCACGCAATTAGACAA
(2)1260 .........G.....................A..T.................G.....
(3)1260 .........G.....................A..T.....................
(4)1260 .........G................C.........T.....................
(5)1260 .........G.........................T..T...................

(1)1320 GATCCGCTCGGATATGGGTTCGGTGCAAATGGAATTGGTTACAACCATTAATAATATTTC
(2)1320 ............................................................
(3)1320 ..........................................C........C........
(4)1320 ......A.....................................................
(5)1320 ..........................................C.................

(1)1380 TGTAACCCAAGTGAATGTTAAAGCGGCTGAATCTCAAATCAGAGATGTGGATTTTGCTGA
(2)1380 ............................................................
(3)1380 ......T.....................G.............C.............
(4)1380 ............................................................
(5)1380 ..............................................C.............

(1)1440 AGAAAGTGCGAACTTTTCTAAATACAATATTTTGGCGCAAAGCGGGAGTTTTGCTATGGC
(2)1440 ...G..C.....................................................
(3)1440 ...G..C.....................................................
(4)1440 ...G........................................................
(5)1440 ...G..C.....................................T...............

(1)1500 ACAAGCGAATGCGGTGCAACAAAATGTCTTAAGGCTTTTACAATAA
```

```
(2)1500 G.....................................
(3)1500 G.............................A.......
(4)1500 ..................G......................
(5)1500 G.................G......................
```

Figure 4 Homologies of nucleotide sequence of cloned *H pylori flaB* gene with reported sequences. (1) the sequencing result of *H pylori* strain Y06 *flaB* gene; (2)-(5): the reported sequences from GenBank (No. NC000915, strain 26695; No. NC_000921, strain J99; No. L08907, strain 85P; No. AF479024, strain CH-CTX1). Underlined areas indicate the positions of primer sequences.

```
(1)1   MSFRINTNIAALTSHAVGVQNNRDLSSSLEKLSSGLRINKAADDSSGMAIADSLRSQSAN
(2)1   ............................................................
(3)1   ............................................................
(4)1   ............................................................
(5)1   ............................................................

(1)61  LGQAIRNANDAIGMVQTADKAMDEQIKILDTIKTKAVQAAQDGQTLESRRALQSDIQRLL
(2)61  ............................................................
(3)61  ............................................................
(4)61  ............................................................
(5)61  ............................................................

(1)121 EELDNIANTTSFNGQQMLSGSFSNKEFQIGAYSNTTVKASIGSTSSDKIGHVRMETSSFS
(2)121 .................................A..........................
(3)121 ............................................................
(4)121 ............................................................
(5)121 ............................................................

(1)181 GEGMLASAAAQNLTEVGLNFKQVNGVNDYKIETVRISTSAGTGIGALSEIINRFSNTLGV
(2)181 .A..........................................................
(3)181 ............................................................
(4)181 .........GA.................................................
(5)181 ............................................................

(1)241 RASYNVMATGGTPVQSGTVRELTINGVEIGTVNDVHKNDADGRLTNAINSVKDRTGVEAS
(2)241 ............................................................
(3)241 ............................................................
(4)241 ............................................................
(5)241 .................................R..........................

(1)301 LDIQGRINLHSIDGRAISVHAASASGQVFGGGNFAGISGTQHAVIGRLTLTRTDARDIIV
(2)301 ............................................................
(3)301 ............................................................
(4)301 .................................T..........................
(5)301 ............................................................

(1)361 SGVNFSHVGFHSAQGVAEYTVNLRAVRGIFDANVASAAGANANGAQAETNSQGIGAGVTS
(2)361 ............................................................
(3)361 ............................................................
(4)361 ............................................................
(5)361 ............................................................

(1)421 LKGAMIVMDMADSARTQLDKIRSDMGSVQMELVTTINNISVTQVNVKAAESQIRDVDFAE
(2)421 ............................................................
(3)421 ............................................................
(4)421 ............................................................
(5)421 ............................................................

(1)481 ESANFSKYNILAQSGSFAMAQANAVQQNVLRLLQ    514aa
(2)481 ..............................
(3)481 ..............................
(4)481 ..............................
(5)481 ..............................
```

Figure 5 Homologies of putative amino acid sequences of *H pylori flaB* gene with reported sequences. (1): the sequencing result of *H pylori* strain Y06 *flaB* gene; (2)-(5): the reported sequences from GenBank (No. NC000915, strain 26695; No. NC_000921, strain J99; No. L08907, strain 85P; No. AF479024, strain CH-CTX1).

DISCUSSION

In the present study, *H pylori flaA* and *flaB* genes were detected in genomic DNA of almost all *H pylori* isolates, and their nucleotide and amino acid sequences were considerably conserved[53,54]. The FlaA and FlaB expressed by *H pylori* rendered the organism strong motility in mucous environment, induced IL-8 secretion and facilitated inflammation in gastric tissue[51,52]. Furthermore, we observed that serum antibodies against FlaA and FlaB were present in approximate 98.4 % and 92.8 % of *H pylori* infected patients, respectively, the rates were significantly higher than those of heat shock protein (68 %) and vacuolating cytotoxin (68 %)[60]. These data indicate that *flaA* and *flaB* genes express their products in majority of *H pylori* strains and efficiently induce specific antibodies, implying a brilliant potential for developing *H pylori* vaccine.

The *flaA* gene from *H pylori* strain Y06, cloned in this study, showed high homologies of nucleotide and putative amino acid sequences compared with the published corresponding sequences (Figures 2 and 3)[53-55]. Similarly, the homologies of nucleotide and putative amino acid sequences of the cloned *flaB* gene from *H pylori* strain Y06 were quite high when compared with the published corresponding sequences (Figures 4 and 5)[53,54,56-59]. The high conservation of nucleotide and putative amino acid sequences found in the cloned *flaA* and *flaB* genes were probably due to their expression products just as the structural peptides of *H pylori*.

In the present study, SDS-PAGE demonstrated that the constructed expression systems *pET32a-flaA*-BL21DE3 and *pET32a-flaB*-BL21DE3 were able to efficiently produce the target recombinant proteins. However, rFlaA and rFlaB were mainly presented with the form of inclusion body even if they were induced by IPTG at a lower concentration. The high output of rFlaA and rFlaB (40-50 %) was beneficial to the production of a possible *H pylori* vaccine.

The rabbit antiserum against the whole cell of *H pylori* recognizes and combined with rFlaA and rFlaB as confirmed by Western blot, indicated that the two recombinant proteins had a relatively high immunoreactivity. The immunodiffusion assay performed in this study demonstrated that rFlaA and rFlaB could efficiently induce rabbit to produce specific antibodies with a higher titer, which indicated that these two recombinant proteins exhibited favorable antigenicity.

All tested *H pylori* isolates (98/98) expressed FlaA while 99.0 % (97/98) of the tested isolates expressed FlaB, as detected by ELISA. Of the *H pylori* infected patients, 98.4 % (123/125) and 92.8 % (116/125) were seropositive for the specific antibodies against rFlaA and against rFlaB, respectively. The universal existence of FlaA and FlaB in *H pylori* strains and the efficient induction of specific antibodies against FlaA and FlaB in patients were the strong favorable evidences for using these two recombinant proteins as the potential antigens in the development of *H pylori* vaccine.

In conclusion, FlaA and FlaB are excellent and ideal antigens that can be potentially used for the development of *H pylori* vaccine, and the expression systems of FlaA and FlaB with a high efficiency has been successfully constructed.

ACKNOWLEDGEMENTS

We are grateful to the four hospitals in Hangzhou that provided gastric biopsies in this study, which help us to complete the research subject.

REFERENCES

1 **Ye GA**, Zhang WD, Liu LM, Shi L, Xu ZM, Chen Y, Zhou DY. *Helicobacter pylori vacA* gene polymorphism and chronic gastrosis. *Shijie Huaren Xiaohua Zazhi* 2001; **9**: 593-595

2 **Lu SY**, Pan XZ, Peng XW, Shi ZL. Effect of Hp infection on gastric epithelial cell kinetics in stomach diseases. *Shijie Huaren Xiaohua Zazhi* 1999; **7**: 760-762

3 **Zhang Z**, Yuan Y, Gao H, Dong M, Wang L, Gong YH. Apoptosis, proliferation and p53 gene expression of *H pylori* associated gastric epithelial lesions. *World J Gastroenterol* 2001; **7**: 779-782

4 **Lu XL**, Qian KD, Tang XQ, Zhu YL, Du Q. Detection of *H pylori* DNA in gastric epithelial cells by in situ hybridization. *World J Gastroenterol* 2002; **8**: 305-307

5 **Yao YL**, Xu B, Song YG, Zhang WD. Overexpression of cyclin E in Mongolian gerbil with *Helicobacter pylori*-induced gastric precancerosis. *World J Gastroenterol* 2002; **8**: 60-63

6 **Guo DL**, Dong M, Wang L, Sun LP, Yuan Y. Expression of gastric cancer-associated MG7 antigen in gastric cancer, precancerous lesions and *H pylori*-associated gastric diseases. *World J Gastroenterol* 2002; **8**: 1009-1013

7 **Peng ZS**, Liang ZC, Liu MC, Ouyang NT. Studies on gastric epithelial cell proliferation and apoptosis in Hp associated gastric ulcer. *Shijie Huaren Xiaohua Zazhi* 1999; **7**: 218-219

8 **Hiyama T**, Haruma K, Kitadai Y, Miyamoto M, Tanaka S, Yoshihara M, Sumii K, Shimamoto F, Kajiyama G. B-cell monoclonality in *Helicobacter pylori*-associated chronic atrophic gastritis. *Virchows Arch* 2001; **483**: 232-237

9 **Harry XH**. Association between *Helicobacter pylori* and gastric cancer: current knowledge and future research. *World J Gastroenterol* 1998; **4**: 93-96

10 **Quan J**, Fan XG. Progress in experimental research of *Helicobacter pylori* infection and gastric carcinoma. *Shijie Huaren Xiaohua Zazhi* 1999; **7**: 1068-1069

11 **Liu HF**, Liu WW, Fang DC. Study of the relationship between apoptosis and proliferation in gastric carcinoma and its precancerous lesion. *Shijie Huaren Xiaohua Zazhi* 1999; **7**: 649-651

12 **Zhu ZH**, Xia ZS, He SG. The effects of ATRA and 5-Fu on telomerase activity and cell growth of gastric cancer cells *in vitro*. *Shijie Huaren Xiaohua Zazhi* 2000; **8**: 669-673

13 **Tu SP**, Zhong J, Tan JH, Jiang XH, Qiao MM, Wu YX, Jiang SH. Induction of apoptosis by arsenic trioxide and hydroxy camptothecin in gastric cancer cells *in vitro*. *World J Gastroenterol* 2000; **6**: 532-539

14 **Cai L**, Yu SZ, Zhang ZF. *Helicobacter pylori* infection and risk of gastric cancer in changle county, Fujian Province, China. *World J Gastroenterol* 2000; **6**: 374-376

15 **Yao XX**, Yin L, Zhang JY, Bai WY, Li YM, Sun ZC. Htert expression and cellular immunity in gastric cancer and precancerosis. *Shijie Huaren Xiaohua Zazhi* 2001; **9**: 508-512

16 **Xu AG**, Li SG, Liu JH, Gan AH. Function of apoptosis and expression of the proteins *Bcl*-2, *p*53 and *C-myc* in the development of gastric cancer. *World J Gastroenterol* 2001; **7**: 403-406

17 **Wang X**, Lan M, Shi YQ, Lu J, Zhong YX, Wu HP, Zai HH, Ding J, Wu KC, Pan BR, Jin JP, Fan DM. Differential display of vincristine-resistance-related genes in gastric cancer SGC7901 cells. *World J Gastroenterol* 2002; **8**: 54-59

18 **Liu JR**, Li BX, Chen BQ, Han XH, Xue YB, Yang YM, Zheng YM, Liu RH. Effect of cis-9, trans-11-conjugated linoleic acid on cell cycle of gastric adenocarcinoma cell line (SGC-7901). *World J Gastroenterol* 2002; **8**: 224-229

19 **Cai L**, Yu SZ. A molecular epidemiologic study on gastric cancer in Changle, Fujian Province. *Shijie Huaren Xiaohua Zazhi* 1999; **7**: 652-655

20 **Gao GL**, Yang Y, Yang SF, Ren CW. Relationship between proliferation of vascular andothelial cells and gastric cancer. *Shijie Huaren Xiaohua Zazhi* 2000; **8**: 282-284

21 **Xue XC**, Fang GE, Hua JD. Gastric cancer and apoptosis. *Shijie Huaren Xiaohua Zazhi* 1999; **7**: 359-361

22 **Niu WX**, Qin XY, Liu H, Wang CP. Clinicopathological analysis of patients with gastric cancer in 1200 cases. *World J Gastroenterol* 2001; **7**: 281-284

23 **Li XY**, Wei PK. Diagnosis of stomach cancer by serum tumor markers. *Shijie Huaren Xiaohua Zazhi* 2001; **9**: 568-570

24 **Fang DC**, Yang SM, Zhou XD, Wang DX, Luo YH. Telomere erosion is independent of microsatellite instability but related to loss of heterozygosity in gastric cancer. *World J Gastroenterol* 2001; **7**: 522-526

25 **Morgner A**, Miehlke S, Stolte M, Neubauer A, Alpen B, Thiede C, Klann H, Hierlmeier FX, Ell C, Ehninger G, Bayerdorffer E.

Development of early gastric cancer 4 and 5 years after complete remission of *Helicobacter pylori* –associated gastric low-grade marginal zone B-cell lymphoma of MALT type. *World J Gastroenterol* 2001; **7**: 248-253

26 **Deng DJ**. Progress of gastric cancer etiology: N-nitrosamides in the 1999s. *World J Gastroenterol* 2000; **6**: 613-618

27 **Liu ZM**, Shou NH, Jiang XH. Expression of lung resistance protein in patients with gastric carcinoma and its clinical significance. *World J Gastroenterol* 2000; **6**: 433-434

28 **Guo CQ**, Wang YP, Liu GY, Ma SW, Ding GY, Li JC. Study on *Helicobacter pylori* infection and p53, c-erbB-2 gene expression in carcinogenesis of gastric mucosa. *Shijie Huaren Xiaohua Zazhi* 1999; **7**: 313-315

29 **Cai L**, Yu SZ, Ye WM, Yi YN. Fish sauce and gastric cancer: an ecological study in Fujian Province, China. *World J Gastroenterol* 2000; **6**: 671-675

30 **Xue FB**, Xu YY, Wan Y, Pan BR, Ren J, Fan DM. Association of *H pylori* infection with gastric carcinoma: a Meta analysis. *World J Gastroenterol* 2001; **7**: 801-804

31 **Wang RT**, Wang T, Chen K, Wang JY, Zhang JP, Lin SR, Zhu YM, Zhang WM, Cao YX, Zhu CW, Yu H, Cong YJ, Zheng S, Wu BQ. *Helicobacter pylori* infection and gastric cancer: evidence from a retrospective cohort study and nested case-control study in China. *World J Gastroenterol* 2002; **8**: 1103-1107

32 **Hua JS**. Effect of *Hp*: cell proliferation and apoptosis on stomach cancer. *Shijie Huaren Xiaohua Zazhi* 1999; **7**: 647-648

33 **Liu DH**, Zhang XY, Fan DM, Huang YX, Zhang JS, Huang WQ, Zhang YQ, Huang QS, Ma WY, Chai YB, Jin M. Expression of vascular endothelial growth factor and its role in oncogenesis of human gastric carcinoma. *World J Gastroenterol* 2001; **7**: 500-505

34 **Cao WX**, Ou JM, Fei XF, Zhu ZG, Yin HR, Yan M, Lin YZ. Methionine-dependence and combination chemotherapy on human gastric cancer cells *in vitro*. *World J Gastroenterol* 2002; **8**: 230-232

35 **Michetti P**, Kreiss C, Kotloff KL, Porta N, Blanco JL, Bachmann D, Herranz M, Saldinger PF, Corthesy-Theulaz I, Losonsky G, Nichols R, Simon J, Stolte M, Acherman S, Monath TP, Blum AL. Orla immunization with urease and Escherichia coli heat-labile enterotoxin is safe and immunogenic in *Helicobacter pylori*-infected adults. *Gastroenterology* 1999; **116**: 804-812

36 **Suganuma M**, Kurusu M, Okabe S, Sueoka N, Yoshida M, Wakatsuki Y, Fujiki H. *Helicobacter pylori* membrane protein 1: a new carcinogenic factor of *Helicobacter pylori*. *Cancer Res* 2001; **61**: 6356-6359

37 **Nakamura S**, Matsumoto T, Suekane H, Takeshita M, Hizawa K, Kawasaki M, Yao T, Tsuneyoshi M, Iida M, Fujishima M. Predictive value of endoscopic ultrasonography for regression of gastric low grade and high grade MALT lymphomas after eradication of *Helicobacter pylori*. *Gut* 2001; **48**: 454-460

38 **Uemura N**, Okamoto S, Yamamoto S, Matsumura N, Yamaguchi S, Yamakido M, Taniyama K, Sasaki N, Schlemper RJ. *Helicobacter pylori* infection and the development of gastric cancer. *N Engl J Med* 2001; **345**: 8298-8232

39 **Morgner A**, Miehlke S, Fischbach W, Schmitt W, Muller-Hermelink H, Greiner A, Thiede C, Schetelig J, Neubauer A, Stolte M, Ehninger G, Bayerdorffer E. Complete remission of primary high-grade B-cell gastric lymphoma after cure of *Helicobacter pylori* infection. *J Clin Oncol* 2001; **19**: 2041-2048

40 **Kate V**, Ananthakrishnan N, Badrinath S. Effect of *Helicobacter pylori* eradication on the ulcer recurrence rate after simple closure of perforated duodenal ulcer: retrospective and prospective randomized controlled studies. *Br J Surg* 2001; **88**: 1054-1058

41 **Zhuang XQ**, Lin SR. Progress in research on the relationship between *Hp* and stomach cancer. *Shijie Huaren Xiaohua Zazhi* 2000; **8**: 206-207

42 **Gao HJ**, Yu LZ, Bai JF, Peng YS, Sun G, Zhao HL, Miu K, Lü XZ, Zhang XY, Zhao ZQ. Multiple genetic alterations and behavior of cellular biology in gastric cancer and other gastric mucosal lesions: *H pylori* infection, histological types and staging. *World J Gastroenterol* 2000; **6**: 848-854

43 **Yao YL**, Zhang WD. Relation between *Helicobacter pylori* and gastric cancer. *Shijie Huaren Xiaohua Zazhi* 2001; **9**: 1045-1049

44 **Goto T**, Nishizono A, Fujioka T, Ikewaki J, Mifune K, Nasu M. Local secretory immunoglobulin A and postimmunization gastritis correlated with protection against *Helicobacter pylori* infection after oral vaccination of mice. *Infect Immun* 1999; **67**: 2531-2539

45 **Watanabe T**, Tada M, Nagai H, Sasaki S, Nakao M. *Helicobacter pylori* infection induces gastric cancer in Mongolian Gerbils. *Gastroenterology* 1998; **115**: 642-648

46 **Honda S**, Fujioka T, Tokieda M, Satoh R, Nishizono A, Nasu M. Development of *Helicobacter pylori*-induced gastric carcinoma in Mongolian Gerbils. *Cancer Res* 1998; **58**: 4255-4259

47 **Hatzifoti C**, Wren BW, Morrow WJ. *Helicobacter pylori* vaccine strategies-triggering a gut reaction. *Immuno Today* 2000; **21**: 615-619

48 **Kotloff KL**, Sztein MB, Wasserman SS, Losonsky GA, DiLorenzo SC, Walker RI. Safety and immunogenicity of oral inactivated whole-cell *Helicobacter pylori* vaccine with adjuvant among volunteers with or without subclinical infection. *Infect Immun* 2001; **69**: 3581-3590

49 **Dubois A**, Lee CK, Fiala N, Kleanthous H, Mehlman PT, Monath T. Immunization against natural *Helicobacter pylori* infection in nonhuman primates. *Infect Immune* 1998; **66**: 4340-4346

50 **Ikewaki J**, Nishizono A, Goto T, Fujioka T, Mifune K. Therapeutic oral vaccination induces mucosal immune response sufficient to eliminate long-term *Helicobacter pylori* infection. *Microbiol Immunol* 2000; **44**: 29-39

51 **Eaton KA**, Suerbaum S, Josenhans C, Krakowka S. Colonization of gnotobiotic piglets by *Helicobacter pylori* deficient in two flagellin genes. *Infect Immun* 1996; **64**: 2445-2448

52 **Watanabe S**, Takagi A, Tada U, Kabir AM, Koga Y, Kamiya S, Osaki T, Miwa T. Cytotoxicity and motility of *Helicobacter pylori*. *J Clin Gastroenterol* 1997; **25**(Suppl 1): S169-171

53 **Tomb JF**, White O, Kerlavage AR, Clayton RA, Sutton GG, Fleischmann RD, Ketchum KA, Klenk HP, Gill S, Dougherty BA, Nelson K, Quackenbush J, Zhou L, Kirkness EF, Peterson S, Loftus B, Richardson D, Dodson R, Khalak HG, Glodek A, McKenney K, Fitzegerald LM, Lee N, Adams MD, Venter JC, Hickey EK, Berg DE, Gocayne JD, Utterback TR, Peterson JD, Kelley JM, Karp PD, Smith HO, Fraser CM. The complete genome sequence of the gastric pathogen *Helicobacter pylori*. *Nature* 1997; **388**: 539-547

54 **Alm RA**, Ling SL, Moir DT, King BL, Brown ED, Doig PC, Smith DR, Noonan B, Guild BC, Dejonge BL, Carmel G, Tummino PJ, Caruso A, Uria-Nickelsen M, Mills DM, Lves C, Gibson R, Merberg D, Mills SD, Jiang Q, Taylor DE, Vovis GF, Trust TJ. Genomic-sequence comparison of two unrelated isolates of the human gastric pathogen *Helicobacter pylori*. *Nature* 1999; **397**: 176-180

55 **Leying H,** Suerbaum S, Geis G, Haas R. Cloning and genetic characterization of a *Helicobacter pylori* flagellin gene. *Mol Microbiol* 1992; **6**: 2863-2874

56 **Suerbaum S,** Josenhans C, Labigne A. Cloning and genetic characterization of the *Helicobacter pylori* and Helicobacter mustelae *flaB* flagellin genes and construction of *H pylori flaA*- and *flaB*-negative mutants by electroporation-mediated allelic exchange. *J Bacteriol* 1993; **175**: 3278-3288

57 **Sambrook J**, Fritsch E F, Maniatis T. Molecular Cloning, A Laboratory Manual [M]. 2nd edition. New York: *Cold Spring Harbor Laboratory Press* 1989: 1.21-1.52, 2.60-2.80, 7.3-7.35, 9.14-9.22

58 **Chen Y**, Wang JD, Shi L. *In vitro* study of the biological activities and immunogenicity of recombinant adhesion of *Helicobacter pylori* rHpaA. *Zhonghua Yixue Zazhi* 2001; **81**: 276-279

59 **Josenhans C,** Labigne A, Suerbaum S. Comparative ultrastructural and functional studies of *Helicobacter pylori* and *Helicobacter* mustelae flagellin mutants: both flagellin subunits, FlaA and FlaB, are necessary for full motility in *Helicobacter species*. *J Bacteriol* 1995; **177**: 3010-3020

60 **Opazo P**, Muller I, Rollan A, Valenzuela P, Yudelevich A, Garcia-de la Guarda R, Urra S, Venegas A. Serological response to *Helicobacter pylori* recombinant antigens in Chilean infected patients with duodenal ulcer, non-ulcer dyspepsia and gastric cancer. *APMIS* 1999; **107**: 1069-1078

Edited by Xia HHX and Wang XL

P.O.Box 2345, Beijing 100023,China
Fax: +86-10-85381893
E-mail: wjg@wjgnet.com www.wjgnet.com

World J Gastroenterol 2003;9(10):2251-2257
World Journal of Gastroenterology
 ISSN 1007-9327

Deletion of *Helicobacter pylori* vacuolating cytotoxin gene by introduction of directed mutagenesis

Jian-Ping Yuan, Tao Li, Xiao-Dong Shi, Bao-Yu Hu, Gui-Zhen Yang, Shan-Qing Tong, Xiao-Kui Guo

Jian-Ping Yuan, Tao Li, Xiao-Dong Shi, Bao-Yu Hu, Gui-Zhen Yang, Shan-Qing Tong, Xiao-Kui Guo, Department of Microbiology and Parasitology, Shanghai Second Medical University, Shanghai 200025, China
Supported by Ministry of Education Research Foundation for Returned Overseas Chinese Scholars Abroad (2001) 498
Correspondence to: Xiao-Kui Guo, Department of Microbiology and Parasitology, Shanghai Second Medical University, 280 Chongqingnan Road, Shanghai 200025, China. xkguo@shsmu.edu.cn
Telephone: +86-21-64671226 **Fax:** +86-21-64671226
Received: 2003-03-02 **Accepted:** 2003-05-16

Abstract

AIM: To construct a *vacA*-knockout *Helicobacter pylori* mutant strain, whose only difference from the wild strain is its disrupted *vacA* gene.

METHODS AND RESULTS: A clone containing kanamycin resistance gene used for homologous recombination was constructed in a directional cloning procedure into pBluescript II SK, and then transformed into *vacA*$^+$ *H pylori* by electroporation. Colonies growing on the selective media containing kanamycin were harvested for chromosomal DNA extraction, and the allelic exchange was determined by polymerase chain reactions and sequencing. Loss of vacuolating activity of the *vacA*-knockout strain was confirmed by examining the gastric cells co-cultured with cell-free supernatants from *H pylori* wild strain or the mutant.

CONCLUSION: We constructed a *vacA*-knockout strain of *H pylori* through direct mutagenesis, which creates an important precondition for the future research on virulence comparison with gene expression analysis.

Yuan JP, Li T, Shi XD, Hu BY, Yang GZ, Tong SQ, Guo XK. Deletion of *Helicobacter pylori* vacuolating cytotoxin gene by introduction of directed mutagenesis. *World J Gastroenterol* 2003; 9(10): 2251-2257

http://www.wjgnet.com/1007-9327/9/2251.asp

INTRODUCTION

Helicobacter pylori (*H pylori*) is a Gram-negative bacterium that colonizes the gastric mucosa of humans[1], and plays an important role in pathogenesis of chronic gastritis, peptic ulcers, gastric adenocarcinomas, and gastric mucosa-associated lymphoid tissue lymphomas[2-6]. Leunk *et al* first reported in 1988 that cell-free supernatants from *H pylori* broth cultures induced striking vacuolar degeneration when added to cultured eukaryotic cells[7]. Subsequently in 1992, this effect was disclosed to be caused by a secreted toxin VacA[8].

The gene encoding the vacuolating cytotoxin has been cloned from an *H pylori* isolate, and termed *vacA*[9]. Analysis of the nucleotide sequence of the *vacA* open reading frame (ORF) suggested that *vacA* encoded a 139-kDa protoxin that has three functional domains: a 33-amino-acid N-terminal signal sequence, a mature cytotoxin domain (approximately 87kDa), and a cleaved C-terminal domain (approximately 50kDa)[10,11]. VacA could induce vacuole formation from the cell cytosol, as determined by transfection of epithelial cells with a plasmid encoding the complete 95-kDa domain of VacA[12]. These vacuoles are acidic, and their membrane contains the vacuolar ATPase proton pump and the small GTP-binding protein rab7. Therefore, they have been suggested to arise from late compartments of the endocytic pathway[13].

Over the past decade, there has been considerable effort directing toward understanding the molecular mechanisms underlying VacA action. But till now, little is known about the mechanisms of vacuole formation and other effects of VacA. In this study, using the technique of direct mutagenesis to disrupt *vacA* gene, we constructed a *vacA*-knockout *H pylori* mutant strain for the further research on virulence comparison between the *H pylori* wild strain and the mutant.

MATERIALS AND METHODS

Bacterial strain and growth conditions

H pylori NCTC 11638 as a gift from Dr. Tong Shi (Shanghai Institute of Digestive Diseases) was cultured routinely on brain heart infusion (BHI) agar plates with 5 % sheep blood in an environment containing 6 % CO_2 at 37 ℃. For the preparation of cell-free supernatants from *H pylori* broth cultures, *H pylori* was cultured in BHI broth+10 % fetal bovine serum (FBS) in an environment containing 6 % CO_2 at 37 ℃ with agitation (200 rpm) for 48 h. The cultures were centrifuged (15 000 g, 30 min, 4 ℃) and filtrated with a 0.2 μm syringe filter.

Disruption of vacA gene

The strategy for disruption of *vacA* gene by direct mutagenesis is shown in Figure 1, and genetic techniques involved were described as follows.

DNA isolation To isolate chromosomal DNA, *H pylori* cells were lysed in lysis buffer (10 mM Tris· HCl, pH 8.0, 0.1 M EDTA, pH 8.0, 0.5 % (w/v) SDS, 20 μg/ml DNase free pancreatic RNase), and then, protease K (Sangon, Shanghai, China) was added in to a final concentration of 100 μg/ml. The lysate was incubated in a water bath at 50 ℃ for 3 h. Then, the solution was cooled to room temperature, and mixed with an equal volume of phenol equilibrated with 0.1 M Tris· HCl (pH 8.0). The two phases were separated by centrifugation at 5 000 g for 15 min at room temperature, and the aqueous phase was extracted with phenol twice again. Afterwards, 0.2 volume of 10 M ammonium acetate and 2 volume of ethanol were added to the aqueous phase. The precipitate was collected by centrifugation at 5 000 g for 2 min, washed twice with 70 % ethanol, and dissolved in an appropriate volume of TE buffer (pH8.0)[14].

Polymerase chain reactions (PCR) PCR was carried out in 100 μl volume containing 100 ng of genomic DNA, 1 U of Ex Taq (Takara), 50 pmol of each primer, and 10 nmol of each deoxynucleoside triphosphate in a standard buffer. Oligonucleotide primers (5'-CGTGGAAATCTTATTACT CTTAGC-3' and 5'-TGATGCTGACTAATGCTCCT-3')

were used to amplify a 1.7 kb product from *H pylori* NCTC 11 638. Primers for amplifying kanamycin resistance gene (*kanR*) and two fragments flanking *kanR*, *LA* and *RA*, were designed as shown in Table 1.

Gel purification and enzyme digestion PCR products were electrophoresed and excised from a 1 % agarose gel, purified using a Qiaquick gel extraction kit (Qiagen, Hilden, Germany), and digested with corresponding restriction enzymes (Promega, Madison, USA) depending on different restriction sites.

Cloning of different DNA fragments Purified PCR products for sequencing were cloned into *pGEM-T* vector (Promega). Fragments *kanR*, *LA*, and *RA* with different restriction sites on both sides were digested with corresponding endonucleases (Promega), and then cloned into *pBluescript SK* II digested with the same enzymes.

Sequencing Every clone was sequenced with the ABI DNA sequencer (Bioasia Biotechnology Company, Shanghai, China).

***H pylori* DNA transformation by electroporation** *H pylori* NCTC 11 638 cells were transformed with plasmid *pLKR* by electroporation, and kanamycin-resistant (*Km*^{r}) transformants were selected by a method similar to that described by Clayton *et al*[15]. Briefly, *H pylori* cultured on plates were scraped and suspended in 30 ml cold double-distilled water. Cells were harvested by centrifugation at 4 360 g at 4 ℃ for 5 min, and the pellet was suspended in 20 ml of cold 10 % glycerol. The cells were centrifuged once, and resuspended in 2 ml ice-cold 10 % glycerol. Plasmid DNA (1 μg in 5 μl TE buffer) was mixed with 0.2 ml cell suspension. The mixture was added to a prechilled (-20 ℃) 0.2 cm electroporation cuvet (Bio-Rad, Hercules, USA), and subjected to single-pulse electroporation of initial voltage 2.5 kV, 25 μF and 600Ω in parallel. The sample was transferred onto a cold plate and incubated for 12 h at 37 ℃. Then the cells were inoculated onto selective media with 30 μg/mL kanamycin, followed by incubation for 4 d to allow the growth of transformants.

Cell culture and detection of vacuole formation

Cells of gastric cancer cell line SGC7901 as a gift from Jie Yang (Department of Cell Biology, Shanghai Second Medical University) were grown in DMEM (GIBCO-BRL, Gaithersburg, USA) supplemented with 10 % FBS, 2 mmol/L glutamine, 100 U/mL penicillin, and 100 μg/mL streptomycin in a humidified 5 % CO_2 atmosphere. SGC7901 cells were co-cultured with cell-free supernatants from *H pylori* NCTC11638 wild strain or mutant strain for 12 h, and then observed by contrast microscopy.

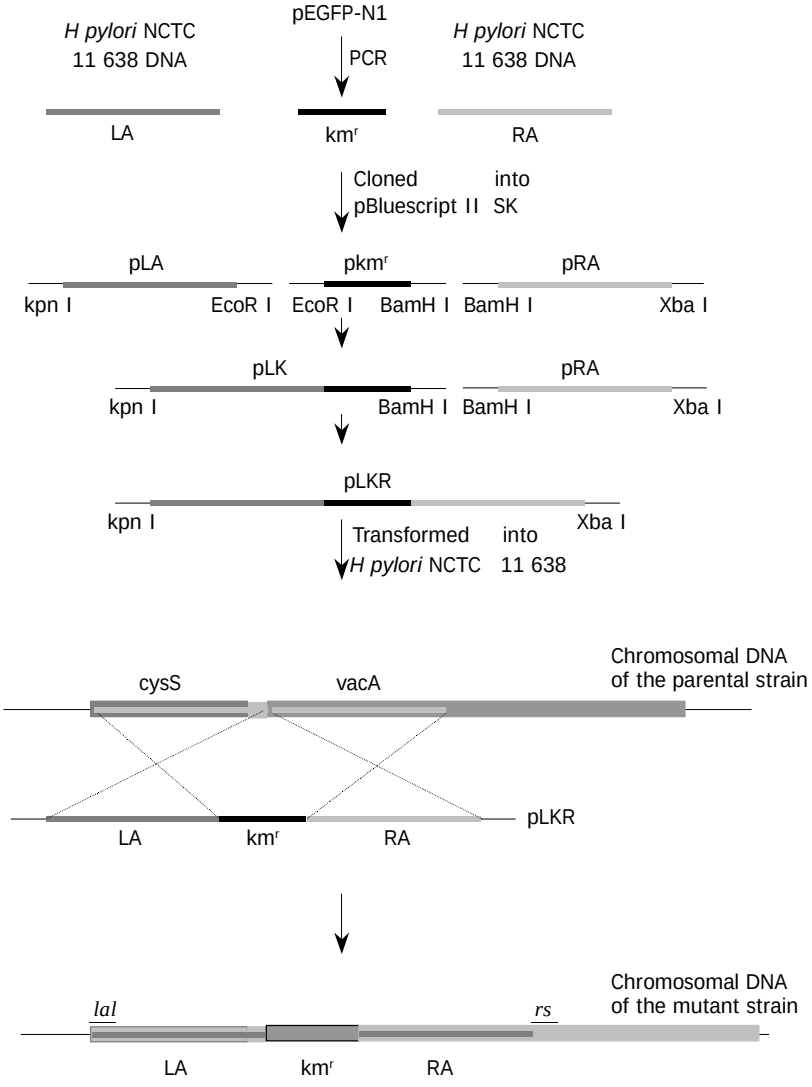

Figure 1 The strategy for disruption of *vacA* gene by directed mutagenesis. LA and RA were PCR-amplified from *H pylori* NCTC 11638 genomic DNA, and the kanamycin resistance gene, from pEGFP-N1. PCR products with different restriction sites on both sides were digested with corresponding endonucleases, and then cloned into pBluescript II SK digested with the same enzymes. Because there is an *EcoR* II site in RA, *pLA* and *pkm*^{r} were firstly joined together, resulting in *pLK*, which then was joined with *pRA*, resulting in *pLKR*. The plasmid *pLKR* was transformed into *H. pyloi* NCTC 11638, where the *Km*^{r} marked mutation was introduced into the genome by homologous recombination, resulting in the *vacA*$^-$Km^r mutant strain.

Table 1 Primers for amplifying *km*^{r}, LA and RA

Primer	Sequence (5' to 3')	Site	Coordinates
la1	GGGGTACCCTTTTGAGCCTTTAGTT	*Kpn* I	cysS bp36-54
la2	CGGAATTCTCCTTTCTTTTTGTAAAAC	*Eco*R I	HPU07145 bp382-400
km^r*1*	CGGAATTCATGATTGAACAAGATGGATTG	*Eco*R I	pEGFP-N1 bp 2629-2649
km^r*2*	CGGGATCCTCAGAAGAACTCGTCAAG	*Bam*H I	pEGFP-N1 bp3406-3423
ra1	CGGGATCCATCGCCCTCTGGTTTCTC	*Bam*H I	HPU07145 bp 437-454
ra2	GCTCTAGACACCCACTTGATTATTCACTCT	*Xba* I	HPU07145 bp 1786-1807

cysS *la1*

1 ATGTTTATTT ATGATACCAA ATTAAAACAA AAAGTCCCTT TTGAGCCTTT

51 AGTTGAAAAA AAGGCGAATA TTTATGTGTG CGGGCCTACG GTGTATGATG
101 ACGCTCATTT AGGGCATGCC AGGAGCGCGA TTGCTTTTGA TTTGTTAAGG
151 CGCACGCTTG AATTGAGCGG CTATGAAGTG GTGTTAGTAA GGAATTTCAC
201 GGATATTGAC GATAAAATCA TCAACAAAGC CTTAAAAGAA AACAAAAGCA
251 TTCAAGAATT AAGCAGCATT TACATTGAAT CTTACACGAG GGATTTAAAC
301 GCTTTGAACG TGAAAAAACC CAGCCTAGAG CCTAAAGCGA GCGAGTATTT
351 AGACGCTATG GTGGGCATGA TTGAAACGCT TTTAGAAAAA AATATCGCTT
401 ATCAGGTCTC TAATGGGGAT ATTTATTTAG ACACGAGCAA GGATAAAGAT
451 TACGGCTCTT TGAGCGTGCA TAATAGCAGT ATGGAATTTG GCCGTATTGG
501 TTTGGTGCAA GAAAAACGGC TTGAGCAGGA TTTTGTGCTA TGGAAAAGCT
551 ATAAGGGGGA TAATGATGTG GGTTTTGATA GCCCTTTAGG CAAAGGGCGC
601 CCTGGCTGGC ATATAGAATG CTCTAGCATG GTTTTTGAAA CTTTAGCACT
651 CGCTAACACC CCTTATCAAA TTGACATCCA TGCAGGCGGA GCGGATCTGT
701 TATTCCCCCA CCATGAAAAT GAAGCGTGCC AAACCCGTTG CACCTTTGGC
751 GTGGAGCTTG CTAAATACTG GATGCATAAT GGCTTTGTGA ATATCAACAA
801 CGAAAAAATG TCTAAAAGTT TAGGGAATAG CTTTTTTATT AAAGACGCCC
851 TGAAAAACTA TGATGGCGAG ATTTTGCGCA ATTATTTACT AGGGGTGCAT
901 TATCGCTCTG TTTTGAATTT CAATGAAGAA GACTTGTTAG TGAGTAAAAA
951 ACGCTTGGAT AAAATCTATC GTTTGAAACA GCGCGTTTTA GGGACTTTGG
1001 GAGGAATAAA TCCAAACTTT AAAAAAGAAA TTTTAGAGTG CATGCAAGAT
1051 GATTTAAACG TTTCTAAAGC GTTGAGCGTT TTAGAAAGCA TGCTTTCTTC
1101 TACGAATGAA AAACTGGATC AAAACCCCAA AAACAAGGCT TTGAAGGGCG
1151 AAATTTTAGC GAATTTGAAA TTCATAGAAG AACTGCTTGG TATTGGGTTT
1201 AAAGACCCTA GCGCGTATTT CCAGTTAGGC GTGAGCGAGA GCGAAAAACA
1251 AGAAATTGAA AACAAGATAG AAGAAAGAAA ACGCGCCAAA GAACAAAAAA
1301 TTTTTTTAAA AGCCGATAGC ATCAGAGAAG AACTTTTGAA ACAAAAAATC
1351 GCTTTGATGG ACACCCCACA AGGCACGATT TGGGAGAAGT TTTTTTAAAC
1401 GCCTCCAATT TTACCTTTTT ACACATTCTA GTAACAACCT TCAGCATTTT
1451 TGCTTTTTAA TCTTGTTAAG TTTTATGTTC ATTTACTTTA ATTTGATAAA

1501 AATTGAACAT TGGTTGTAGA TACTATATAT TTATAGCCTT AATCGTAAAT
-35 signal -10 signal

1551 GCAACAGAAA TTTTCTAGTC TAAAGTCGCA CCCTTTGTGC AAAAATCGTT

la2 km^r

1601 TTACAAAAAG AAAGGAGAAT TCATGATTGA ACAAGATGGA TTGCACGCAG
rbs

1651 GTTCTCCGGC CGCTTGGGTG GAGAGGCTAT TCGGCTATGA CTGGGCACAA
1701 CAGACAATCG GCTGCTCTGA TGCCGCCGTG TTCCGGCTGT CAGCGCAGGG

1751 GCGCCCGGTT CTTTTTGTCA AGACCGACCT GTCCGGTGCC CTGAATGAAC
1801 TGCAAGACGA GGCAGCGCGG CTATCGTGGC TGGCCACGAC GGGCGTTCCT
1851 TGCGCAGCTG TGCTCGACGT TGTCACTGAG GCGGGAAGGG ACTGGCTGCT
1901 ATTGGGCGAA GTGCCGGGGC AGGATCTCCT GTCATCTCAC CTTGCTCCTG
1951 CCGAGAAAGT ATCCATCATG GCTGATGCAA TGCGGCGGCT GCATACGCTT
2001 GATCCGGCTA CCTGCCCATT CGACCACCAA GCGAAACATC GCATCGAGCG
2051 AGCACGTACT CGGATGGAAG CCGGTCTTGT CGATCAGGAT GATCTGGACG
2101 AAGAGCATCA GGGGCTCGCG CCAGCCGAAC TGTTCGCCAG GCTCAAGGCG
2151 AGCATGCCCG ACGGCGAGGA TCTCGTCGTG ACCCATGGCG ATGCCTGCTT
2201 GCCGAATATC ATGGTGGAAA ATGGCCGCTT TTCTGGATTC ATCGACTGTG
2251 GCCGGCTGGG TGTGGCGGAC CGCTATCAGG ACATAGCGTT GGCTACCCGT
2301 GATATTGCTG AAGAGCTTGG CGGCGAATGG GCTGACCGCT TCCTCGTGCT
2351 TTACGGTATC GCCGCTCCCG ATTCGCAGCG CATCGCCTTC TATCGCCTTC
ra1
2401 TTGACGAGTT CTTCTGAGGA TCCATCGCCC TCTGGTTTCT CTCGCTTTAG

2451 TAGGAGCATT AGTCAGCATC ACACCGCAAC AAAGTCATGC CGCCTTTTTC
2501 ACAACCGTGA TCATTCCAGC CATTGTTGGG GGTATCGCTA CAGGCACCGC
2551 TGTAGGAACG GTCTCAGGGC TTCTTAGCTG GGGGCTCAAA CAAGCCGAAG
2601 AAGCCAATAA AACCCCAGAT AAACCCGATA AAGTTTGGCG CATTCAAGCA
2651 GGAAAAGGCT TTAATGAATT CCCTAACAAG GAATACGACT TATACAGATC
2701 CCTTTTATCC AGTAAGATTG ATGGAGGTTG GGATTGGGGG AATGCCGCTA
2751 GGCATTATTG GGTCAAAGGC GGGCAACAGA ATAAGCTTGA AGTGGATATG
2801 AAAGACGCTG TAGGGACTTA TACCTTATCA GGGCTTAGAA ACTTTACTGG
2851 TGGGGATTTA GATGTCAATA TGCAAAAAGC CACTTTACGC TTGGGCCAAT
2901 TCAATGGCAA TTCTTTTACA AGCTATAAGG ATAGTGCTGA TCGCACCACG
2951 AGAGTGGATT TCAACGCTAA AAATATCTCA ATTGATAATT TTGTAGAAAT
3001 CAACAATCGT GTGGGTTCTG GAGCCGGGAG GAAAGCCAGC TCTACGGTTT
3051 TGACTTTGCA AGCTTCAGAA GGGATCACTA GCGATAAAAA CGCTGAAATT
3101 TCTCTTTATG ATGGTGCCAC GCTCAATTTG GCTTCAAGCA GCGTTAAATT
3151 AATGGGTAAT GTGTGGATGG GCCGTTTGCA ATACGTGGGA GCGTATTTGG
3201 CCCCTTCATA CAGCACGATA AACACTTCAA AAGTAACAGG GGAAGTGAAT
3251 TTTAACCACC TCACTGTTGG CGATAAAAAC GCCGCTCAAG CGGGCATTAT
3301 CGCTAATAAA AAGACTAATA TTGGCACACT GGATTTGTGG CAAAGCGCCG
3351 GGTTAAACAT TATCGCTCCT CCAGAAGGTG GCTATAAGGA TAAACCCAAT
3401 AATACCCCTT CTCAAAGTGG TGCTAAAAAC GACAAAAATG AAAGCGCTAA
3451 AAACGACAAA CAAGAGAGCA GTCAAAATAA TAGTAACACT CAGGTCATTA
3501 ACCCACCCAA TAGTGCGCAA AAAACAGAAG TTCAACCCAC GCAAGTCATT
3551 GATGGGCCTT TTGCGGGCGG CAAAGACACG GTTGTCAATA TCAACCGCAT
3601 CAACACTAAC GCTGATGGCA CGATTAGAGT GGGAGGGTTT AAAGCTTCTC
3651 TTACCACCAA TGCGGCTCAT TTGCATATCG GCAAAGGCGG TGTCAATCTG
3701 TCCAATCAAG CGAGCGGGCG CTCTCTTATA GTGGAAAATC TAACTGGGAA
ra2
3751 TATCACCGTT GATGGGCCTT TAAGAGTGAA TAATCAAGTG GGTGGCTATG

rs
3801 CTTTGGCAGG ATCAAGCGC

Figure 2 Nucleotide sequence of cysS gene and the downstream sequence amplified from the *vacA*$^{-}$*Km*^{r} mutant *H pylori*. The 1 398 bp *cysS* ORF and the 795 bp *km*^{r} ORF are shown. Primers *la1*, *la2*, *ra1*, *ra2*, and *rs* for amplifying LA, RA, and ASm are indicated. -35 signal, -10 signal, and rbs of *vacA* gene serving km^{r} gene in the mutant strain are also shown.

RESULTS

Upstream sequence close to vacA *gene*

Genome of NCTC 11638 was not completely sequenced, and the upstream portion close to *vacA* gene going to be used in the mutagenesis technique was not published in GeneBank. Therefore, the upstream sequences close to *vacA* gene of 26695 and J99, whose genomes were completely sequenced and published, were aligned and searched for conservative sequences. Then a 1.7-kb product was PCR-amplified from *H pylori* NCTC11638 DNA and sequenced. The sequencing result showed the complete *cysS* (cysteinyl-tRNA synthetase) gene of NCTC 11638 (Figure 2).

Cloning of pLKR for transforming H pylori

As shown in Figure 1, LA which contains the *H pylori vacA* promoter and RA were amplified from genomic DNA of NCTC11638, while *kanR* gene which has no promoter was amplified from the plasmid *pEGFP-N1* (Clontech, Palo Alto, USA). PCR-products LA, *kanR* and RA, with restriction sites incorporated at the termini, were joined together in a directional cloning procedure into *pBluescript* II *SK*, resulting in *pLKR*.

Construction of vacA-knockout H pylori mutant strain

pLKR which is unable to replicate in *H pylori*, was introduced into *H pylori* NCTC11638 by electroporation. After 4 d of growth, five Km^r single colonies were isolated. To determine whether *vacA* had been disrupted in the transformed strains through allelic exchange, DNA isolated from *H pylori* NCTC11638 wild-type strain and the Km^r mutant strain were PCR-amplified with the primers *la1* and *rs* (5' -GCGCTTGATC CTGCCAAAGCATAGC-3') annealing to *H pylori* NCTC 11638 *vacA* at bp 1808 to 1832 flanking *ra2* (Figures 1 and 2). A 3.8-kb product consistent with the expected size was PCR-amplified from Km^r mutant strain, as compared with a 3.0-kb product amplified from wild strain (Figure 3), suggesting a substitution of Km^r gene for a short fragment of *vacA* gene by homologous recombination between plasmid and chromosomal sequences. The sequencing result of the 3.8-kb product confirmed the occurrence of allelic exchange (Figure 2).

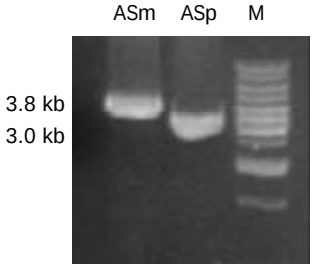

Figure 3 PCR amplification for the determination of homologous recombination in Km^r mutant strain. Genomic DNA of NCTC 11638 wild strain and Km^r mutant strain were respectively PCR-amplified for the fragments ASm and ASp using the primers *ra1* and *rs*. A single 3.8 kb product ASm was amplified from Km^r mutant strain as compared with the 3.0 kb product ASp amplified from the wild strain.

Characterization of vacA-knockout H pylori mutant

To determine the loss of vacuolating activity of the mutant strain, gastric cells SGC7901 were co-cultured with cell-free supernatants from *H pylori* NCTC11638 wild strain or mutant strain for 12 h, and then observed by contrast microscopy. Intracellular vacuoles developed in cells co-cultured with supernatant from the wild strain, while no vacuoles developed in cells co-cultured with supernatant from $vacA^-Km^r$ mutant strain (Figure 4).

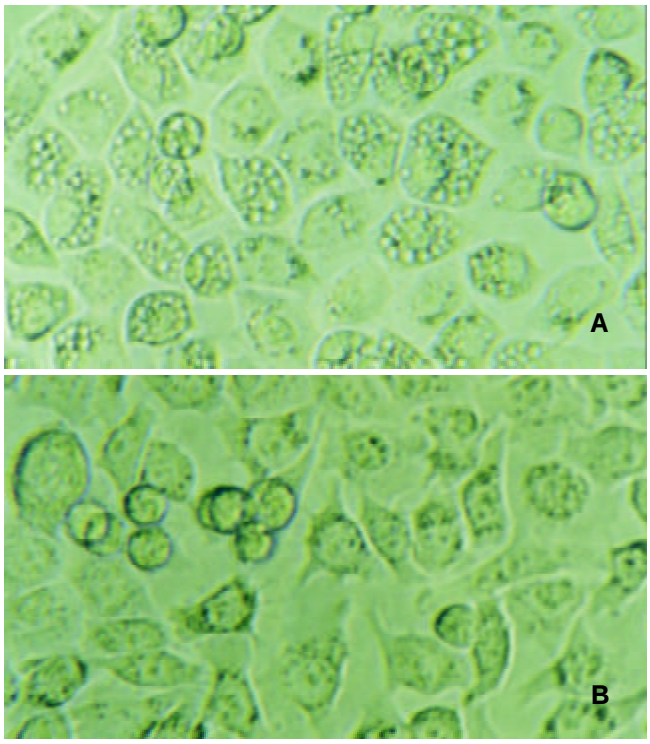

Figure 4 Gastric cancer cells SGC-7901 were co-cultured with the supernatant either from *Helicobacter pylori* NCTC 11638 or its *vacA*-knockout mutant strain. 12 h after the incubation, A: cells co-cultured with NCTC 11638 developed vacuoles in the cytosol; B: cells co-cultured with $vacA^-$ mutant strain developed no vacuoles at all.

DISCUSSION

VacA, produced by pathogenic strains of *H pylori*, was a major virulence factor in pathogenesis of gastroduodenal ulcers[8,16]. VacA induced the formation of membrane-delimited vacuoles in intoxicated cells[7], and showed many other effects on cellular functions and viability, such as causing mitochondrial depolarization[17], inducing apoptosis in gastric cells[18], affecting or interacting with various components of cytoskeleton to cause actin rearrangements[19], and even disorganizing microtubular network[20]. To study VacA machanism of action, we have tried to get purified VacA used as single virulence determinant, to study its effect on the expression profile of eukaryocyte. However, like Manetti *et al*[21], we did not successfully get the expressed VacA as a functional recombinant protein in *E. coli*, probably due to its incorrect fold. We have also considered letting VacA directly expressed in the cytosol to induce vacuole formation. In our experiments, vacuoles were induced in only 10 % of cells transfected with plasmids expressing VacA, because the efficiency of the transfection method was relatively low. In addition, when VacA acts outside the cells, the pathway by which it interacts with the cells is quite different from that when the protein is produced in the cytosol. Under natural conditions, association of VacA with the eukaryotic cell surface was the first step in the intoxication of cells[22]. The initial interaction of VacA with target cells was through high-affinity cell surface receptors, and this interaction was necessary for its biologic activity[23,24]. A 250 kDa receptor protein tyrosine phosphatase (RPTP) β served as a receptor for VacA on AZ521 cells, and another protein, p140, was also commonly detected in VacA-susceptible cells[25,26]. Increased binding of acid- or alkali-activated VacA to RPTPβ may alter its activity and possibly accelerates or inhibits dephosphorylation of tyrosine on cytosolic proteins. Moreover, VacA acting outside the cells

is a kind of exogenous antigen, having different pathways of processing and presentation from that of VacA expressed in the cytosol as an endogenous antigen. All of these processes may affect gene expression of the host cells.

Direct mutagenesis was probably the most useful technique for assessing the contribution to virulence of specific bacterial gene products[27]. In our study, *vacA* gene encoding vacuolating cytotoxin that has been identified by conventional biochemical means was disrupted by gene replacement. This technique requires a means for introducing DNA into the pathogen, as well as suitable selective markers and an inherent capacity for homologous recombination. In previous studies, the Km^r determinant often came from *Campylobacter coli*[28]. Here we introduced a simple method to get the Km^r gene from commercialized plasmids such as *pEGFP-N1*. Coding sequence of the gene without a promotor was PCR-amplified from *pEGFP-N1* and ligated downstream with the promotor of *H pylori vacA* gene. Upon insertion into chromosomal DNA of *H pylori* through homologous recombination, this gene could be efficiently transcribed because the *vacA* promoter was recognized by *H pylori* transcriptional machinery, introducing kanamycin resistance characteristics into *H pylori*. Due to the stop coden of Km^r, *vacA* would not be translated at all although most of the sequences still existed. The results of PCR and sequencing confirmed the occurrence of allelic exchange. Therefore, using the direct mutagenesis technique, we obtained the isogenic mutant strain of *H pylori*, which differed from the wild strain only in that the *vacA* gene was knocked out. Through co-culture of cell-free supernatants from the wild or mutant *H pylori* strain with gastric cells, loss of vacuolating activity of the *vacA*-knockout strain was confirmed. These results clearly show that VacA is an indispensable toxin secreted by *H pylori* for the induction of vacuole formation.

Such kind of technique has been used to yield $vacA^-$ mutant *H pylori*[9,28,29]. But no further experiment has been done to compare the virulence between the mutant and the parental strain. On the other hand, microarray analysis has been used in several studies to screen gene expression profiles in gastric epithelial cells induced by *H pylori*[30-32]. Our group has also analyzed different expression profiles of gastric cancer cells co-cultured with supernatants of $VacA^+$ or $VacA^-$ *H pylori* isolates. However, VacA has not been used as a single virulence determinant to stimulate host cells, thus one can not determine which virulent factors result in the alteration of the expression. In this study, we successfully constructed the $vacA^-$ mutant strain, using the direct mutagenesis technique, which creates an important precondition for the further research on virulence comparison with gene expression analysis.

REFERENCES

1 **Dunn BE**, Cohen H, Blaser MJ. *Helicobacter pylori*. *Clin Microbiol Rev* 1997; **10**: 720-741

2 **Marshall BJ**, Warren JR. Unidentified curved bacilli in the stomach of patients with gastritis and peptic ulceration. *Lancet* 1984; **1**: 1311-1315

3 **Graham DY**, Lew GM, Klein PD, Evans DG, Evans DJ Jr, Saeed ZA, Malaty HM. Effect of treatment of *Helicobacter pylori* infection on the long-term recurrence of gastric or duodenal ulcer. A randomized, controlled study. *Ann Intern Med* 1992; **116**: 705-708

4 **Parsonnet J**, Friedman GD, Vandersteen DP, Chang Y, Vogelman JH, Orentreich N, Sibley RK. *Helicobacter pylori* infection and the risk of gastric carcinoma. *N Engl J Med* 1991; **325**: 1127-1131

5 **Forman D**, Newell DG, Fullerton F, Yarnell JW, Stacey AR, Wald N, Sitas F. Association between infection with *Helicobacter pylori* and risk of gastric cancer: evidence from a prospective investigation. *BMJ* 1991; **302**: 1302-1305

6 **Xue FB**, Xu YY, Wan Y, Pan BR, Ren J, Fan DM. Association of *H pylori* infection with gastric carcinoma: a Meta analysis. *World J Gastroenterol* 2001; **7**: 801-804

7 **Leunk RD**, Johnson PT, David BC, Kraft WG, Morgan DR. Cytotoxic activity in broth-culture filtrates of *Campylobacter pylori*. *J Med Microbiol* 1988; **26**: 93-99

8 **Cover TL**, Blaser MJ. Purification and characterization of the vacuolating toxin from *Helicobacter pylori*. *J Biol Chem* 1992; **267**: 10570-10575

9 **Cover TL**, Tummuru MK, Cao P, Thompson SA, Blaser MJ. Divergence of genetic sequences for the vacuolating cytotoxin among *Helicobacter pylori* strains. *J Biol Chem* 1994; **269**: 10566-10573

10 **Schmitt W**, Haas R. Genetic analysis of the *Helicobacter pylori* vacuolating cytotoxin: structural similarities with the IgA protease type of exported protein. *Mol Microbiol* 1994; **12**: 307-319

11 **Hou P**, Tu ZX, Xu GM, Gong YF, Ji XH, Li ZS. *Helicobacter pylori vacA* genotypes and cagA status and their relationship to associated diseases. *World J Gastroenterol* 2000; **6**: 605-607

12 **De Bernard M**, Arico B, Papini E, Rizzuto R, Grandi G, Rappuoli R, Montecucco C. *Helicobacter pylori* toxin VacA induces vacuole formation by acting in the cell cytosol. *Mol Microbiol* 1997; **26**: 665-674

13 **Papini E**, de Bernard M, Milia E, Bugnoli M, Zerial M, Rappuoli R, Montecucco C. Cellular vacuole induced by *Helicobacter pylori* originate from late endosomal compartments. *Proc Natl Acad Sci U S A* 1994; **91**: 9720-9724

14 **Sambrook J,** Russell DW. Molecular Cloning-A Laboratory Manual. 3thed, Cold Spring Harbor, New York: *Cold Spring Harbor Laboratory Press* 2001; Vol 1: 6.4-6.11

15 **Clayton CL**, Mobley HLT. Methods in Molecular Medicine, *Helicobacter pylori* Protocols. 1sted. Totowa: *Humana Press Inc* 1997: 145-152

16 **Cover TL**. The vacuolating cytotoxin of *Helicobacter pylori*. *Mol Microbiol* 1997; **20**: 241-246

17 **Kimura M**, Goto S, Wada A, Yahiro K, Niidome T, Hatakeyama T, Aoyagi H, Hirayama T, Kondo T. Vacuolating cytotoxin purified from *Helicobacter pylori* causes mitochondrial damage in human gastric cells. *Microb Pathog* 1999; **26**: 45-52

18 Kuck D, Kolmerer B, Iking-Konert C, Krammer PH, Stremmel W, Rudi J. Vacuolating cytotoxin of *Helicobacter pylori* induces apoptosis in the human gastric epithelial cell line AGS. *Infect Immun* 2001; **69**: 5080-5087

19 **Ashorn M**, Cantet F, Mayo K, Megraud F. Cytoskeletal rearrangements induced by *Helicobacter pylori* strains in epithelial cell culture: possible role of the cytotoxin. *Dig Dis Sci* 2000; **45**: 1774-1780

20 **Pai R**, Cover TL, Tarnawski AS. *Helicobacter pylori* vacuolating cytotoxin (VacA) disorganizes the cytoskeletal architecture of gastric epithelial cells. *Biochem Biophys Res Commun* 1999; **262**: 245-250

21 **Manetti R**, Massari P, Burroni D, de Bernard M, Marchini A, Olivieri R, Papini E, Montecucco C, Rappuoli R, Telford JL. *Helicobacter pylori* cytotoxin: importance of native conformation for induction of neutralizing antibodies. *Infect Immun* 1995; **63**: 4476-4480

22 **Papini E**, Zoratti M, Cover TL. In search of the *Helicobacter pylori* VacA mechanism of action. *Toxicon* 2001; **39**: 1757-1767

23 **Garner JA**, Cover TL. Binding and internalization of the *Helicobacter pylori* vacuolating cytotoxin by epithelial cells. *Infect Immun* 1996; **64**: 4197-4203

24 **Massari P**, Manetti R, Burroni D, Nuti S, Norais N, Rappuoli R, Telford JL. Binding of the *Helicobacter pylori* vacuolating cytotoxin to target cells. *Infect Immun* 1998; **66**: 3981-3984

25 **Yahiro K**, Niidome T, Kimura M, Hatakeyama T, Aoyagi H, Kurazono H, Imagawa K, Wada A, Moss J, Hirayama T. Activation of *Helicobacter pylori* VacA toxin by alkaline or acid conditions increases its binding to a 250-kDa receptor protein-tyrosine phosphatase β. *J Biol Chem* 1999; **274**: 36693-36699

26 **Yahiro K**, Niidome T, Hatakeyama T, Aoyagi H, Kurazono H, Padilla PI, Wada A, Hirayama T. *Helicobacter pylori* vacuolating cytotoxin binds to the 140-kDa protein in human gastric cancer cell lines, AZ-521 and AGS. *Biochem Biophys Res Commun* 1997; **238**: 629-632

27 **Henderson B**, Wilson M, McNab R, Lax AJ. Cellular Microbiology: Bacteria-host interactions in health and disease. Hoboken: *John Wiley Sons Ltd* 1999: 163-188
28 **Copass M**, Grandi G, Rappuoli R. Introduction of unmarked mutations in the *Helicobacter pylori vacA* gene with a sucrose sensitivity marker. *Infect Immun* 1997; **65**: 1949-1952
29 **Burroni D**, Lupetti P, Pagliaccia C, Reyrat JM, Dallai R, Rappuoli R, Telford JL. Deletion of the major proteolytic site of the *Helicobacter pylori* cytotoxin does not influence toxin activity but favors assembly of the toxin into hexameric structures. *Infect Immun* 1998; **66**: 5547-5550
30 **Sepulveda AR**, Tao H, Carloni E, Sepulveda J, Graham DY, Peterson LE. Screening of gene expression profiles in gastric epithelial cells induced by *Helicobacter pylori* using microarray analysis. *Aliment Pharmacol Ther* 2002; **16**(Suppl 2): 145-157
31 **Cox JM**, Clayton CL, Tomita T, Wallace DM, Robinson PA, Crabtree JE. cDNA array analysis of *cag* pathogenicity island-associated *Helicobacter pylori* epithelial cell response genes. *Infect Immun* 2001; **69**: 6970-6980
32 **Maeda S**, Otsuka M, Hirata Y, Mitsuno Y, Yoshida H, Shiratori Y, Masuho Y, Muramatsu M, Seki N, Omata M. cDNA microarray analysis of *Helicobacter pylori*-mediated alteration of gene expression in gastric cancer cells. *Biochem Biophys Res Commun* 2001; **284**: 443-449

Edited by Xia HHX

P.O.Box 2345, Beijing 100023,China
Fax: +86-10-85381893
E-mail: wjg@wjgnet.com www.wjgnet.com

World J Gastroenterol 2003;9(10):2258-2260
World Journal of Gastroenterology
 ISSN 1007-9327

Distribution of *cagG* gene in *Helicobacter pylori* isolates from Chinese patients with different gastroduodenal diseases and its clinical and pathological significance

Can Xu, Zhao-Shen Li, Zhen-Xing Tu, Guo-Ming Xu, Yan-Fang Gong, Xiao-Hua Man

Can Xu, Zhao-Shen Li, Zhen-Xing Tu, Guo-Ming Xu, Yan-Fang Gong, Xiao-Hua Man, Department of Gastroenterology, Changhai Hospital, Second Military Medical University, Shanghai 200433, China
Supported by the National Natural Science Foundation of China, No. 30170427
Correspondence to: Dr. Can Xu, Department of Gastroenterology, Changhai Hospital, Second Military Medical University, Shanghai 200433, China. xucan9@hotmail.com
Telephone: +86-21-25070556 **Fax:** +86-21-25074635
Received: 2003-05-12 **Accepted:** 2003-06-12

Abstract

AIM: To determine the distribution of *cagG* gene of *Helicobacter pylori* (*H pylori*) isolates cultured from patients with various digestive diseases and its relationship with gastroduodenal diseases.

METHODS: *cagG* was amplified by polymerase chain reaction in 145 *H pylori* isolates cultured from patients with chronic gastritis (n=72), duodenal ulcer (n=48), gastric ulcer (n=17), or gastric and duodenal ulcer (n=8), and the relationship between *cagG* status and the grade of gastric mucosal inflammation was determined.

RESULTS: *cagG* was present in 91.7 % of the 145 *H pylori* isolates, with the rates were 90.3 %, 93.8 %, 88.2 % and 100.0 %, respectively, in those from patients with chronic gastritis, duodenal ulcer, gastric ulcer, and gastric and duodenal ulcer. There was no significant difference among the four groups (P>0.05). The average grade of gastric mucosal inflammation in the antrum and corpus was 1.819±0.325 and 1.768±0.312, respectively in *cagG* positive patients, whereas the average inflammation grade was 1.649±0.297, 1.598±0.278 respectively in *cagG* negative cases (P>0.05).

CONCLUSION: *cagG* gene of *H pylori* was quite conservative, and most *H pylori* strains in Chinese patients were *cagG* positive. *cagG* status was not related to clinical outcome or the degree of gastric mucosal inflammation. Therefore, *cagG* can not be used as a single marker for discrimination of *H pylori* strains with respect to a specific digestive disease.

Xu C, Li ZS, Tu ZX, Xu GM, Gong YF, Man XH. Distribution of *cagG* gene in *Helicobacter pylori* isolates from Chinese patients with different gastroduodenal diseases and its clinical and pathological significance. *World J Gastroenterol* 2003; 9(10): 2258-2260

http://www.wjgnet.com/1007-9327/9/2258.asp

INTRODUCTION

Helicobacter pylori is a well-recognized pathogen that chronically infects more than 50 % of the world population. *H pylori* is associated with the development of acute or chronic gastritis, peptic ulcer diseases, gastric adenocarcinoma and gastric mucosa-associated lymphoid tissue (MALT) lymphoma. Most infected subjects will remain asymptomatic throughout life with only about 20 % developing peptic ulcer diseases or gastric carcinoma[1-5]. What determines the outcome of an infection remains unclear. The reasons for these different outcomes of *H pylori* infection may be related to both bacterial factors and host responses. The major *H pylori* disease-associated genetic factor is the whole *cag* pathogenicity island (PAI), which contains 25 open reading frames and at least 30 genes. The *cag* PAI is associated with increased interleukin (IL)-8 production by gastric epithelial cells[6,7].

The cytotoxin-associated gene A (*cagA*) is located in the most downstream part of the *cag* PAI. The presence of this gene or its encoded protein, CagA, has been regarded as a marker for the *cag* PAI. Many clinical studies have demonstrated that *cagA* gene or CagA protein is associated with a more severe clinical outcome. CagA was reported to increase the risk of development of duodenal ulcer, atrophic gastritis and gastric adenocarcinoma. In contrast to the *cagA*-negative patients, gastric mucosal inflammation of *cagA*-positive patients was more severe[8-10]. *cagG* is located within the *cag* PAI upstream of *cagA*. The distribution of this gene in *H pylori* strains isolated from Chinese digestive patients and its relation with the gastroduodenal diseases remain unclear. In the present study, a set of specific primers were designed to detect the *cagG* gene in 145 clinical *H pylori* strains, and the relationship between *cagG* and different digestive diseases was determined.

MATERIALS AND METHODS

H pylori isolates

H pylori isolates obtained from 145 patients (80 males, 65 females, aged 18-69 years, mean age 42.5 years old) who underwent upper endoscopy in our department were included in this study. These patients were diagnosed endoscopically as chronic gastritis (n=72), duodenal ulcer (n=48), gastric ulcer (n=17), or gastric and duodenal ulcer (n=8). Informed consents were obtained from all patients. The standard strains CCUG17874 (NCTC11638) and Tx30a were kindly provided by the Italian IRIS Research Center.

H pylori culture

Two antral biopsy specimens taken during endoscopy were immediately cultured on the *H pylori* selective agar plates with 10 % defibrillated sheep blood and antibiotics (Merck Company, Germany) at 37 ℃ under microaerophilic conditions with 5 % O_2 10 % CO_2 and 85 % N_2 for 3-6 days. The colonies were identified as *H pylori* if Gram stain morphology and biochemical tests were positive for urease, oxidase and catalase. All stock cultures were preserved at -80 ℃ in Brucella broth with 20 % glycerol, and subcultured for genomic DNA extraction. The passage number of *H pylori* used in this study averaged six.

Histopathologic examination

Two biopsy specimens each taken from the gastric corpus and antrum endoscopically were used for histopathologic examination to grade the severity of gastritis after they were embedded in paraffin and stained with hematoxylin and eosin. The severity of gastritis (i.e. mononuclear cell and polymorphonuclear leukocyte infiltration) was evaluated, and graded on a scale of 0-3 (i.e. 0=no, 1=mild, 2=moderate, and 3=marked) according to the updated Sydney system[11].

Genomic DNA extraction

Subcultured *H pylori* cells were collected from the agar plates, then genomic DNA was extracted and purified from each *H pylori* isolate using cetyltrimethyl ammonium bromide (CTAB), phenol-chloroform-isoamyl alcohol, and ethanol precipitation.

Detection of cagG with polymerase chain reaction (PCR)

The primers to amplify *cagG* gene and give a 497 base pair (bp) product were designed based on the published gene sequence[12]. *cagG*F: 5' -GCCATGTTAACACCCCCTAG-3' , and *cagG*R:5' -TTAATGCGCTAGAATAGTGC-3' . PCR was performed in an Eppendorf thermal cycler using a PCR kit (Takara, Dalian, China) according to the manufacturer' s instructions. Briefly, the reaction was performed in a total volume of 50 μl containing 20 ng genomic DNA as a template and 200 μM each deoxynucleotide, 1.5U Taq polymerase, 0.4 μM each primer and PCR buffer. The PCR amplification program comprised at 95 ℃ for 5 min, then 35 cycles at 95 ℃ for 1 min, at 52 ℃ for 1 min and at 72 ℃ for 1 min, followed by at 72 ℃ for 7 min, then cooled at 4 ℃. The PCR products were analyzed on 1.5 % agarose gels with ethidium bromide. CCUG17874 was taken as a positive control, Tx30a as a negative control, and deionized water as a blank control.

Statistical analysis

The data were expressed as the mean ±SD. The *t* test and χ^2 test were used for statistical analysis. A *P* value <0.05 was considered to be statistically significant.

RESULTS

Amplification of cagG gene

After PCR amplification of the *cagG* gene, the products were electrophoresed on 1.5 % agarose gels, and stained with ethidium bromide. Under ultraviolet light, *cagG* appeared as a specific band with 497 bp (Figure 1).

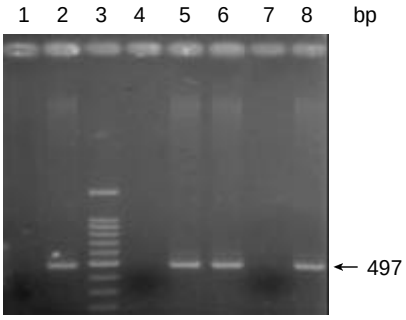

Figure 1 Electrophoresis of PCR products. Lane 3: 100 bp DNA Marker; Lanes 1, 2 and 4: controls: Tx30a, CCUG17874, and deionized water; Lanes 5, 6, 7 and 8: clinical *H pylori* isolates.

CagG status in H pylori isolates from patients with various diseases

H pylori cagG gene was detected in 91.7 % of the 145 isolates, the rate was 90.3 %, 93.8 %, 88.2 % and 100.0 % in patients with chronic gastritis, duodenal ulcer, gastric ulcer and gastric/duodenal ulcer, respectively (Table 1). There was no significant difference among the groups (*P*>0.05).

Table 1 *cagG* in *H pylori* isolates from patients with different gastroduodenal diseases

Group	Number	*cagG* positive	*cagG* negative	*cagG* positive rate (%)[a]
Chronic gastritis	72	65	7	90.3
Duodenal ulcer	48	45	3	93.8
Gastric ulcer	17	15	2	88.2
Gastric duodenal ulcer	8	8	0	100.0
Total	145	133	12	91.7

[a]*P*>0.05 between any two groups.

CagG status and gastric mucosal inflammation

The average grade of gastric mucosal inflammation in the antrum and corpus was 1.819±0.325 and 1.768±0.312 in *cagG* positive patients, respectively, whereas the average grade was 1.649±0.297, 1.598±0.278 in *cagG* negative group, respectively (*P*>0.05, both in the antrum and body).

DISCUSSION

H pylori infects human gastric mucosa which evokes a mucosal inflammatory response by neutrophil recruitment from the microcirculation. Persistent inflammation may lead to the development of digestive diseases such as chronic gastritis, peptic ulcer disease and gastric cancer. Although pathogenicity of *H pylori* infection is not well understood, there were several putative virulence factors that might contribute to mucosal damage by *H pylori* infection[13,14].

The *cag* PAI is an approximately 40-kb cluster of genes in *H pylori* chromosome, and a quite conservative entity. Many of *H pylori* strains had an intact *cag* PAI divided into two regions: *cag*I in downstream and *cag*II in upstream, and some with an insert sequence IS605 or IS606[15,16]. There were at least 14 and 16 open reading frames in *cag*I and *cag*II, several of which were virulence factors[17]. Several studies suggested that *cagA* gene could be used as a marker for *cag* PAI[16]. *cagG* is another gene in *cag*I region which is located upstream of *cagA* gene. The function of this gene is not well known. Recently, Hsu *et al*[17] reported that an intact *cag* PAI was identified in 95 % and 100 % of the strains that possessed *cagA* and *cagG* respectively, whereas the *cagA* and *cagG* genes were found in 100 % and 95 % of the strains containing a partial or complete set of *cag* PAI, indicating that *cagA* gene is not associated with a complete *cag* PAI in 5 % of the strains, and cannot be considered as an absolute marker for the presence of a complete set of *cag* PAI, but *cagG* gene may be a better indicator for the presence of an intact *cag* PAI.

Extensive studies of *cagA* gene indicated that CagA protein encoded by *cagA* gene was associated with severe clinical outcomes, such as peptic ulcer disease and gastric cancer. Therefore, it was considered as a main virulence factor of *H pylori*[16]. Some reports suggested that the presence of *cagE* gene within *cag*I might be related to more severe clinical outcomes. For example, Day *et al*[18] revealed that *H pylori* isolates containing *cagE* were associated with duodenal ulcer in Canadian children. Fallone *et al*[19] reported that *cagE*-positive isolates were more prevalent in Canadian adult patients with peptic ulcer or gastric cancer than in those with gastritis only. In the present study, we designed a set of primers to amplify *cagG* gene of 145 clinical *H pylori* isolates, and

determined the correlation of *cagG* status with endoscopic presentation, and histological findings. The results showed that *cagG* was present in 91.7 % *H pylori* isolates examined. 100 % of *H pylori* isolates from patients with gastric and duodenal ulcer were *cagG* positive, which was higher, but not statistically significant than that in other groups ($P>0.05$). Lack of difference in *cagG* positive rate might be due to patient selection or the relatively small number of patients with gastric and duodenal ulcer. Nevertheless, our study suggested that positive rate of *cagG* in *H pylori* was high and *cagG* was quite conservative in Chinese population, and that there was no difference in the frequencies of *cagG*-positive isolates among patients with gastritis, duodenal ulcer, gastric ulcer or gastric duodenal ulcer. Our results are supported by the study by Jenks *et al*[20] who demonstrated that no specific genes within the *cag* PAI could reliably predict the clinical outcome of *H pylori* infection in French patients, and also by Hsu *et al*[17] who concluded that any of the *cag* PAI genes such as *cagE* could not predict the clinical presentation in Korean patients.

Hsu *et al* reported that of the 120 clinical isolates from Korean patients with various gastrointestinal diseases, 86.7 % (104/120) were *cagG* positive[17]. Mizushima *et al*[21] used PCR and Southern blot to investigate the prevalence of *cagG* gene in 236 clinical *H pylori* isolates from Japanese patients, and found that *cagG* was present in 97 % of the isolates. These results were similar with ours. The same Japanese research group[21] further used flow cytometry to assay the ability of *H pylori* with or without *cagG* to adhere to KATOIII and ELISA to detect the IL-8 secreted from gastric epithelial cells induced by *H pylori*. They observed that in comparison with the *cagG*-positive strains, all *cagG*-deleted strains decreased adherence to KATOIII cells, and abolished IL-8 induction despite the presence of *cagE*, which was reported to be essential for IL-8 induction. *H pylori* genome is known to be diversified and may differ between geographic regions. However, there has no reports so far about *cagG* gene distribution in the Western countries.

Infection with *cagA* positive *H pylori* induces stronger gastric chemokine mRNA expression such as IL-8 in the antral mucosa, which may be relevant to the increased mucosal damage associated with *cagA* positive *H pylori* infection. The levels of the chemokines were correlated with cellular infiltration in the antrum and inflammation of the gastric mucosa[22,23]. We compared the severity of gastric mucosal inflammation in the antrum and corpus in *cagG*-positive and *cagG*-negative patients, and observed that, the average grade of inflammation was only slightly higher in *cagG*-positive group than that in *cagG* negative group both in the antrum and in the corpus ($P>0.05$). Therefore, the *cagG* status has no relation to the severity of gastritis.

In conclusion, *cagG* gene was quite conservative in clinical *H pylori* isolates from Chinese patients with different gastroduodenal diseases, since most *H pylori* isolates were *cagG* positive. There was no difference in the frequency of *cagG* -positive isolates among patients with different diseases. The *cagG* status was not related to gastric mucosal inflammation grade. Therefore, *cagG* cannot reliably predict the clinical and histological outcomes.

REFERENCES

1 **Kapadia CR**. Gastric atrophy, metaplasia, and dysplasia: a clinical perspective. *J Clin Gastroenterol* 2003; **36**: S29-36

2 **Matsuhisa TM**, Yamada NY, Kato SK, Matsukura NM. *Helicobacter pylori* infection, mucosal atrophy and intestinal metaplasia in Asian populations: a comparative study in age-, gender- and endoscopic diagnosis-matched subjects. *Helicobacter* 2003; **8**: 29-35

3 **Kelley JR**, Duggan JM. Gastric cancer epidemiology and risk factors. *J Clin Epidemiol* 2003; **56**: 1-9

4 **McColl KE**, El-Omar E. How does *H pylori* infection cause gastric cancer? *Keio J Med* 2002; **51**(Suppl): 53-56

5 **Sepulveda AR**, Graham DY. Role of *Helicobacter pylori* in gastric carcinogenesis. *Gastroenterol Clin North Am* 2002; **31**: 517-535

6 **Figura N**, Valassina M. *Helicobacter pylori* determinants of pathogenicity. *J Chemother* 1999; **11**: 591-600

7 **Megraud F**. Impact of *Helicobacter pylori* virulence on the outcome of gastroduodenal diseases: lessons from the microbiologist. *Dig Dis* 2001; **19**: 99-103

8 **Audibert C**, Burucoa C, Janvier B, Fauchere JL. Implication of the structure of the *Helicobacter pylori cag* pathogenicity island in induction of interleukin-8 secretion. *Infect Immun* 2001; **69**: 1625-1629

9 **Li CQ**, Pignatelli B, Ohshima H. Increased oxidative and nitrative stress in human stomach associated with *cagA+ Helicobacter pylori* infection and inflammation. *Dig Dis Sci* 2001; 46: 836-844

10 **Perez-Perez GI**, Peek RM, Legath AJ, Heine PR, Graff LB. The role of CagA status in gastric and extragastric complications of *Helicobacter pylori*. *J Physiol Pharmacol* 1999; **50**: 833-845

11 **Dixon MF**, Genta RM, Yardley JH, Correa P. Classification and grading of gastritis. The updated Sydney System. International Workshop on the Histopathology of Gastritis, Houston 1994. *Am J Surg Pathol* 1996; **20**: 1161-1181

12 **Yamaoka Y**, Kodama T, Kita M, Imanishi J, Kashima K, Graham DY. Relation between clinical presentation, *Helicobacter pylori* density, interleukin 1β and 8 production, and *cagA* status. *Gut* 1999; **45**: 804-811

13 **Suzuki H**, Masaoka T, Miyazawa M, Suzuki M, Miura S, Ishii H. Gastric mucosal response to *Helicobacter pylori*. *Keio J Med* 2002; **51**(Suppl): 40-44

14 **McGee DJ**, Mobley HL. Mechanisms of *Helicobacter pylori* infection: bacterial factors. *Curr Top Microbiol Immunol* 1999; **241**: 155-180

15 **Zhang M**, Zhang J, He L, Guo H, Yin Y, Zhou Z. Dissemination of insertion sequences IS605, IS606 among clinical isolates of *Helicobacter pylori* in China. *Zhonghua Liuxing Bingxue Zazhi* 2002; **23**: 366-369

16 **Owen RJ**, Peters TM, Varea R, Teare EL, Saverymuttu S. Molecular epidemiology of *Helicobacter pylori* in England: prevalence of *cag* pathogenicity island markers and IS605 presence in relation to patient age and severity of gastric disease. *FEMS Immunol Med Microbiol* 2001; **30**: 65-71

17 **Hsu PI**, Hwang IR, Cittelly D, Lai KH, El-Zimaity HM, Gutierrez O, Kim JG, Osato MS, Graham DY, Yamaoka Y. Clinical presentation in relation to diversity within the *Helicobacter pylori cag* pathogenicity island. *Am J Gastroenterol* 2002; **97**: 2231-2238

18 **Day AS**, Jones NL, Lynett JT, Jennings HA, Fallone CA, Beech R, Sherman PM. *cagE* is a virulence factor associated with *Helicobacter pylori*-induced duodenal ulceration in children. *J Infect Dis* 2000; **181**: 1370-1375

19 **Fallone CA**, Barkun AN, Gottke MU, Best LM, Loo VG, Veldhuyzen van Zanten S, Nguyen T, Lowe A, Fainsilber T, Kouri K, Beech R. Association of *Helicobacter pylori* genotype with gastroesophageal reflux disease and other upper gastrointestinal diseases. *Am J Gastroenterol* 2000; **95**: 659-669

20 **Jenks PJ,** Mégraud F, Labigne A. Clinical outcome after infection with *Helicobacter pylori* does not appear to be reliably predicted by the presence of any of the genes of the *cag* pathogenicity island. *Gut* 1998; **43**: 752–758

21 **Mizushima T**, Sugiyama T, Kobayashi T, Komatsu Y, Ishizuka J, Kato M, Asaka M. Decreased adherence of *cagG*-deleted *Helicobacter pylori* to gastric epithelial cells in Japanese clinical isolates. *Helicobacter* 2002; **7**: 22-29

22 **Shimoyama T**, Everett SM, Dixon MF, Axon AT, Crabtree JE. Chemokine mRNA expression in gastric mucosa is associated with *Helicobacter pylori cagA* positivity and severity of gastritis. *J Clin Pathol* 1998; **51**: 765-770

23 **Yamaoka Y**, Kita M, Kodama T, Sawai N, Tanahashi T, Kashima K, Imanishi J. Chemokines in the gastric mucosa in *Helicobacter pylori* infection. *Gut* 1998; **42**: 609-617

Edited by Xia HHX

P.O.Box 2345, Beijing 100023,China
Fax: +86-10-85381893
E-mail: wjg@wjgnet.com www.wjgnet.com

World J Gastroenterol 2003;9(10):2261-2265
World Journal of Gastroenterology
 ISSN 1007-9327

• BASIC RESEARCH •

Effect of oral epidermal growth factor on mucosal healing in rats with duodenal ulcer

Jane CJ Chao, Kuo-Yu Liu, Sheng-Hsuan Chen, Chia-Lang Fang, Chih-Wei Tsao

Jane CJ Chao, Kuo-Yu Liu, School of Nutrition and Health Sciences, Taipei Medical University, 110 Taiwan
Sheng-Hsuan Chen, Department of Gastroenterology, Taipei Medical University Hospital, 110 Taiwan
Chia-Lang Fang, Department of Pathology, Taipei Medical University, 110 Taiwan
Chih-Wei Tsao, Department of Surgery, National Defense Medical Center, Tri-Service General Hospital, 110 Taiwan
Supported by the National Council Science of Taiwan (grant NSC88-2314-B-038-008)
Correspondence to: Jane CJ Chao, School of Nutrition and Health Sciences, Taipei Medical University, 250 Wu Hsing Street, Taipei, 110 Taiwan. chenjui@tmu.edu.tw
Telephone: +886-2-2736-1661 #6551-6556 Ext. 117
Fax: +886-2-2737-3112
Received: 2003-06-28 **Accepted:** 2003-08-02

Abstract

AIM: To investigate the effect of epidermal growth factor (EGF) on mucosal healing in rats with duodenal ulcer.

METHODS: Male Sprague-Dawley rats were randomly divided into sham operation without EGF, sham operation with EGF, duodenal ulcer without EGF, or duodenal ulcer with EGF groups. Additionally, normal rats without operation served as the control group. Duodenal ulcer was induced in rats by 300 mL/L acetic acid. Rats with EGF were orally administered at a dose of 60 μg/kg/day in drinking water on the next day of operation (day 1). Healing of duodenal ulcer was detected by haematoxylin and eosin staining. Cell growth of damaged mucosa was determined by the contents of nucleic acids and proteins. The level of EGF in duodenal mucosa was measured by ELISA.

RESULTS: The pathological results showed that duodenal ulcer rats with EGF improved mucosal healing compared with those without EGF after day 5. Duodenal ulcer rats with EGF significantly increased duodenal DNA content compared with those without EGF on day 15 (6.44±0.54 mg/g *vs* 1.45±0.52 mg/g mucosa, $P<0.05$). Duodenal RNA and protein contents did not differ between duodenal ulcer rats with and without EGF during the experimental period. Sham operation and duodenal ulcer rats with EGF significantly increased duodenal mucosal EGF content compared with those without EGF on day 5 (76.0±13.7 ng/g *vs* 35.7±12.9 ng/g mucosa in sham operation rats, and 68.3±10.9 ng/g *vs* 28.3±9.2 ng/g mucosa in duodenal ulcer rats, $P<0.05$).

CONCLUSION: Oral EGF can promote mucosal healing of the rats with duodenal ulcer by stimulating mucosal proliferation accompanied by an increase in mucosal EGF content.

Chao JCJ, Liu KY, Chen SH, Fang CL, Tsao CW. Effect of oral epidermal growth factor on mucosal healing in rats with duodenal ulcer. *World J Gastroenterol* 2003; 9(10): 2261-2265
http://www.wjgnet.com/1007-9327/9/2261.asp

INTRODUCTION

Epidermal growth factor (EGF) is present in various body fluids and tissues, and is continuously secreted into the gastrointestinal lumen in humans by submandibular glands, mucous neck cells of the stomach, Brunner's glands of the duodenum, Paneth cells of the small intestine, and ulcer-associated cell lineage (a recently identified glandular structure induced at the sites of injury)[1-3]. EGF and EGF family of related peptides are involved as key constituents in the maintenance and repair of gastrointestinal mucosa[4]. There has been evidence that increases in the EGF receptor and EGF producing cells around acetic acid-induced gastric ulcer in rats, and a novel cell lineage in human mucosal ulceration secreting EGF adjacent to peptic ulcer[3,5]. The results suggest that EGF plays an important role in ulcer healing.

Previous studies showed that EGF administration regulated the healing of ulcers in rats[6,7] and humans[8]. Oral administration of EGF, given at 30 μg/kg/day in the drinking water for 25 or 50 days, promoted the healing of cysteamine HCl-induced duodenal ulcer in rats to the same extent as cimetidine, a H_2-receptor antagonist[6]. However, Kuwahara *et al*.[7] demonstrated human EGF, given orally twice daily at 30 and 100 μg/kg for 2 weeks or at 100 μg/kg for 4 weeks, had no effect on natural healing of acetic acid-induced gastric ulcer in rats. It has been controversial if orally administered EGF, a feasible and easy way in clinical therapy, is effective to promote the healing of duodenal ulcer. Therefore, the purpose of the study was to investigate the effect of orally administered EGF on the healing of intestinal mucosa and the content of EGF in acetic acid-induced duodenal ulcer rats.

MATERIALS AND METHODS

Animals and duodenal ulcer operation

Male Sprague-Dawley rats (-200 g) were purchased from the National Laboratory Animal Center (National Science Council, Taipei, Taiwan). The rats were housed in individual cages and had free access to food (powdered laboratory autoclavable rodent diet 5 010, PMI Nutrition International Inc., Brentwood, MO), except for the fasting period. The light cycle was 12 h and the room temperature was kept at 22-24 ℃. The rats were randomly divided into four operated groups: sham operation without EGF, sham operation with EGF, duodenal ulcer without EGF, and duodenal ulcer with EGF groups (n=10 on each sacrificed day, 6 rats for biological analysis, and 4 rats for pathological examination and photography). Additionally, normal rats (n=10) without operation served as the control group. Duodenal ulcer was induced in rats by acetic acid according to the modified method of Konturek *et al*[9]. Prior to operation, the rats were fasted overnight, anesthetized by intraperitoneal injection with 50 mg/kg body weight thiopental sodium (Abbott Australia Pty.Ltd., Kurnell, Australia), and the abdomen was then opened. A plastic tube (4.5 mm inner diameter) filled with 70 μL of 300 mL/L acetic acid was applied tightly to the surface of the duodenum for 10 sec. Due to different tolerance to acetic acid in various layers of the duodenum, it only caused immediate necrosis in the mucosal and submucosal

layers exactly within the area (4.5 mm diameter) of acetic acid application without penetration or perforation to the surrounding organs. Normal saline instead of 300 mL/L acetic acid was applied to sham operation rats. After operation, the rats were allowed to recover from anesthesia. The operated rats received only water on the day of operation (day 0), and were fed a normal chow diet *ad libitum* next day (day 1). Body weight, food intake, and water intake of the rats were routinely recorded. All protocols were conducted under the guidelines of Animal Care and Use Committee, Taipei Medical University.

Treatment and pathological observation

The next day after operation at approximately 15:00, the rats were orally administered recombinant human EGF (60 μg/kg body weight) (Biosource International, Camarillo, CA) in 35 mL (minimal intake during the adaptation period) sterile deionized drinking water, and remaining water was exactly recorded to determine actual intake of EGF. The rats without oral EGF were given the same amount of sterile deionized drinking water. The operated rats were killed on day 1 to identify the formation of duodenal ulcer, and on days 5 and 15 at 15:00 for pathological and biological analyses. The duodenum (5×5 mm) was excised, preserved in 10 % formaldehyde, and stained with haematoxylin and eosin. The diameter of ulcer size was measured in sectioned samples by microscopy. Coded mucosal specimens were evaluated under a light microscope at ×100 or ×200 magnification by a pathologist in a blinded fashion.

DNA, RNA, and protein in duodenal mucosa

The ulcer area of duodenal mucosa in duodenal ulcer rats and a similar area of intact duodenal mucosa in sham operation rats were excised. Duodenal mucosa was entirely scraped off, weighed, and immediately frozen at -80 ℃ for further analysis. DNA, RNA, and protein in duodenal mucosa were purified using a commercial TRIZOL reagent (Life Technologies, Inc., Rockville, MD) to evaluate mucosal growth[10]. Duodenal mucosa (0.2-0.5 g wet weight) was homogenized in 1 mL of TRIZOL reagent followed by the addition of 200 μL chloroform. After centrifugation, RNA remained exclusively in the aqueous phase, and DNA and protein were then recovered by sequential precipitation. RNA was precipitated with isopropanol. DNA was precipitated with ethanol from the interphase, and protein was precipitated with isopropanol from the organic phase after separation from DNA. DNA, RNA, and protein pellets were resuspended in 8 mmol/L NaOH, diethylpyrocarbonate-water, or 1 mol/L NaOH, respectively. DNA and RNA were quantitated spectrophotometrically at 260 nm. Protein content was determined spectrophotometrically at 690 nm by a Bio-Rad Dc protein assay kit (Bio-Rad Laboratories, Hercules, CA).

EGF in duodenal mucosa

Duodenal mucosal EGF content was measured by a commercial EGF immunoassay kit (Quantikine™, DEG00, Research and Diagnostics Systems, Inc., Minneapolis, MN)[11]. Duodenal mucosa (0.2-0.3 g wet weight) was homogenized with RD1 reagent. The mucosal homogenate (200 μL) was incubated with EGF antibody coated in a 96-well plate for 2 h at room temperature, washed 3 times with 400 μL wash buffer, and then incubated with 200 μL polyclonal EGF antibody conjugated to horseradish peroxidase for 2 h. After several washes, samples were incubated with 200 μL substrate (tetramethylbenzidine: H_2O_2=1:1) for 20 min. The reaction was terminated by 50 μL of 1 mol/L sulfuric acid. Mucosal EGF content was determined at 450 nm and corrected at 540 nm using an ELISA reader (Multiskan RC, Labsystems, Helsinki, Finland).

Statistical analysis

All values were expressed as mean ± SE. Data were analyzed by three-way ANOVA to determine the main effects of duodenal ulcer, oral EGF, and time using SAS 6.12 (SAS Institute, Cary, NC). *Post hoc* multiple comparisons between two groups were performed either by Fisher's least significant difference or Dunnett's test. Differences were considered significant at $P<0.05$.

RESULTS

Weight gain, EGF and food intake

Body weight of sham operation and duodenal ulcer rats with or without EGF on different sacrificed days is shown in Table 1. At the beginning of the experiment, body weight of the rats was similar in all operated groups and the control group (189.0±4.5 g). Body weight of sham operation and duodenal ulcer rats with or without EGF significantly increased ($P<0.05$) on day 15 compared with that of the control group on day 0 and the corresponding group on day 5. Oral EGF did not affect body weight.

Table 1 Body weight of sham operation and duodenal ulcer rats with or without oral EGF before operation and sacrifice

Group	Sham operation		Duodenal ulcer	
	- EGF	+ EGF	- EGF	+ EGF
	Body weight before operation (g)[2]			
Day 5	192.0±3.9	199.8±3.8	200.6±5.0	195.2±5.0
Day 15	192.4±4.8	198.9±4.2	194.9±4.7	195.9±6.0
	Body weight before sacrifice (g)[2]			
Day 5	203.6±4.0*	209.9±3.6*	208.1±4.7*	200.5±4.9
Day 15	271.4±5.5*†	279.8±7.7*†	267.1±7.7*†	278.8±5.3*†

[1]Data are mean ± SE (n=10). [2]Values were not significantly different ($P>0.05$) among different groups in each row by Fisher's least significant difference test. *Body weight was significantly different ($P<0.05$) from that in the control group (189.0±4.5 g, n=10) on day 0 by Dunnett's test. †$P<0.05$ compared with day 5 within the same group by Fisher's least significant difference test.

Table 2 EGF and food intake of sham operation and duodenal ulcer rats with or without oral EGF[1]

Group	Sham operation		Duodenal ulcer	
	- EGF	+ EGF	- EGF	+ EGF
	EGF intake (μg / kg / day)[2]			
Day 5	-[3]	59.9±3.8	-	57.8±0.4
Day 15	-	57.3±0.6	-	58.1±0.3
	Food intake before operation (g / day)[2]			
Day 5	24.5±1.1	25.2±0.8	26.5±0.5	25.4±0.9
Day 15	25.1±0.5	25.3±0.4	26.6±0.8	24.8±0.6
	Food intake before sacrifice (g / day)			
Day 5	27.9±4.3[a]	27.4±6.4[a]	24.2±3.6[a]	25.6±5.4[a]
Day 15	27.2±1.8[b]	26.7±1.0[b]	25.1±1.4[a]	25.2±1.8[ab]

[1]Data are mean ± SE (n=10). Values in a row not sharing a superscript letter were significantly different ($P<0.05$) by Fisher's least significant difference test. [2]Values were not significantly different ($P>0.05$) among different groups in each row and column by Fisher's least significant difference test. [3]Data were not measured.

Exact oral EGF intake of the rats was close to 60 μg/kg/day, and not significantly different between sham operation and duodenal ulcer groups, and between different days in the same group (Table 2). The initial food intake of the rats before

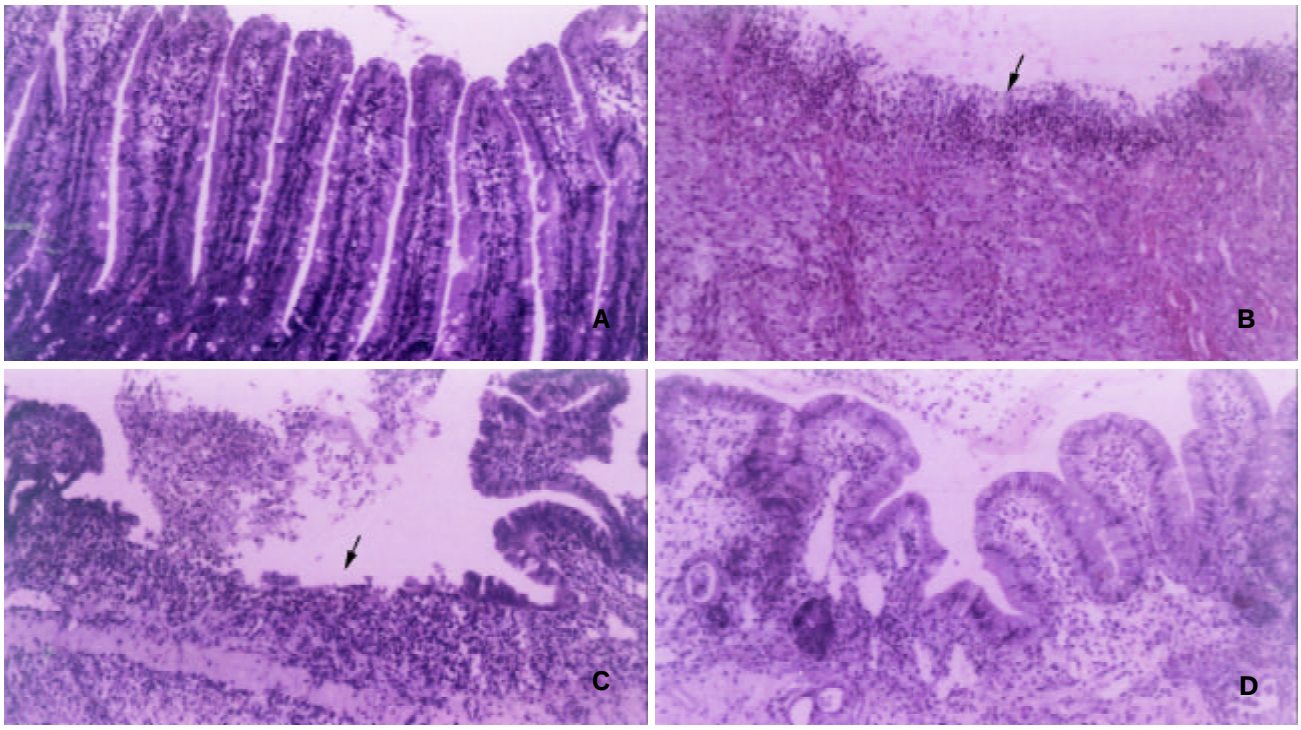

Figure 1 Representative micrographs of duodenal mucosa stained by haematoxylin and eosin were selected from 4 sectioned samples per group. A: control rats on day 0 (×200), B: duodenal ulcer rats without EGF on day 1 (×100), C: duodenal ulcer rats without EGF on day 5 (×100), D: duodenal ulcer rats with EGF on day 5 (×200). Arrow represents the discontinuous lining of the duodenal mucosa.

operation was similar to that in the control group (26.7±3.1 g/day), and not significantly different among the groups. On day 15, decreased food intake was only observed in duodenal ulcer rats without EGF compared with that in sham operation rats. Neither EGF nor time in sham operation or duodenal ulcer rats affected food intake.

Morphological appearance

To identify the formation and healing of duodenal ulcer in rats after operation, the morphological appearance magnified by ×100 or ×200 is shown in Figure 1. Compared with the control group (Figure 1A), duodenal ulcer rats on day 1 had the discontinuous lining of the mucosal and submucosal layers, and serious inflammation (Figure 1B). The mean diameter of ulcer damage was 2 mm. Sham operation rats had similar morphology as the control rats (data not shown). The morphology was not different between sham operation and the control rats on days 5 and 15. On day 5, the mean diameter of ulcer damage reduced to 1 mm in duodenal ulcer rats without EGF. Although some microvilli proliferated, but the discontinuous lining of the mucosal layer and inflammation were still observed in the ulcer area of duodenal ulcer rats without EGF (Figure 1C). Duodenal ulcer rats with EGF had obvious mucosal healing and proliferation (Figure 1D), and the mean diameter of ulcer damage was undetectable on day 5. On day 15, the morphology was not different between duodenal rats with and without EGF (data not shown).

DNA, RNA, and protein in duodenal mucosa

The results of mucosal DNA, RNA, and protein contents in the duodenum are shown in Table 3 to evaluate the growth of duodenal mucosa in rats after operation. Mucosal DNA content in the duodenum significantly increased (P<0.05) in sham operation rats without EGF (2.96±1.27 mg/g mucosa) and duodenal ulcer rats with EGF (6.44±0.54 mg/g mucosa) on day 15 compared with that in the control rats (0.86±0.06 mg/g mucosa) on day 0 and the corresponding group on day 5 (Table 3). Duodenal ulcer rats with EGF had higher duodenal DNA content (P<0.05) on day 15 compared with other groups. Three-way ANOVA showed both oral EGF and time significantly increased duodenal DNA content (P<0.05).

Mucosal RNA content in the duodenum did not change with EGF treatment and time in sham operation and duodenal ulcer rats (Table 3). However, duodenal ulcer significantly decreased mucosal RNA content (P<0.05). Duodenal ulcer rats had significantly lower RNA content (P<0.05) in duodenal mucosa on day 5 compared with the control rats (15.9±9.3 mg/g mucosa) on day 0. Sham operation rats with EGF had higher duodenal RNA content (P<0.05) than other operated groups on day 5. On day 15, duodenal RNA content did not differ among four operated groups.

Three-way ANOVA showed that oral EGF and time affected duodenal protein content (P<0.05). Duodenal protein content in sham operation rats without EGF significantly decreased (P<0.05) with time, but significantly increased (P<0.05) compared with that in the control group (25.1±1.4 mg/g mucosa) on day 0 and other operated groups on day 5 (Table 3). On day 15, duodenal protein content did not differ among four operated groups.

EGF in duodenal mucosa

Duodenal EGF content significantly increased (P<0.05) with time in sham operation rats without EGF, but significantly decreased (P<0.05) in duodenal ulcer rats with EGF (Table 4). Sham operation or duodenal ulcer rats with EGF significantly increased duodenal EGF content (P<0.05) compared with those without EGF on day 5. However, duodenal EGF content did not differ between sham operation and duodenal ulcer rats with or without EGF on day 5. On day 15, duodenal EGF content significantly decreased (P<0.05) in duodenal ulcer rats without EGF (12.9±3.9 ng/g mucosa) compared with that in the control rats (61.1±5.4 ng/g mucosa) on day 0 and sham operation rats without EGF (84.8±22.8 ng/g mucosa). However, duodenal EGF content did not differ between

sham operation or duodenal ulcer rats with and without EGF. Three-way ANOVA showed only duodenal ulcer significantly decreased mucosal EGF content ($P<0.05$).

Table 3 Duodenal mucosal DNA, RNA, and protein contents in sham operation and duodenal ulcer rats with or without oral EGF[1]

Group	Sham operation		Duodenal ulcer	
	-EGF	+EGF	-EGF	+EGF
	Duodenal mucosal DNA (mg/g mucosa)			
Day 5	1.06±0.20[a]	1.51±0.57[a]	1.31±0.45[a]	0.70±0.25[a]
Day 15	2.96±1.27[a*†]	1.77±0.64[a]	1.45±0.52[a]	6.44±0.54[b*†]
	Duodenal mucosal RNA (mg/g mucosa)			
Day 5	4.89±0.42[a]	7.10±0.20[b]	4.71±0.35[a*]	3.32±0.82[a*]
Day 15	5.24±1.60[a]	6.00±0.30[a]	5.38±0.44[a]	4.79±0.91[a]
	Duodenal mucosal protein (mg/g mucosa)			
Day 5	49.8±2.9[a*]	20.5±5.4[b]	22.7±2.8[b]	25.5±3.3[b]
Day 15	25.2±2.8[a†]	19.3±2.7[a]	24.3±1.6[a]	26.2±1.3[a]

[1]Data are mean ± SE (n=6). Values in a row not sharing a superscript letter were significantly different ($P<0.05$) by Fisher's least significant difference test. *The contents of DNA, RNA, and protein in duodenal mucosa were significantly different ($P<0.05$) from those in the control group (0.86±0.06 mg/g, 6.57±0.40 mg/g, 25.1±1.4 mg/g mucosa, n=6) on day 0 by Dunnett's test. †$P<0.05$ compared with day 5 within the same group by Fisher's least significant difference test.

Table 4 Duodenal mucosal EGF content in sham operation and duodenal ulcer rats with or without oral EGF[1]

Group	Sham operation		Duodenal ulcer	
	- EGF	+ EGF	- EGF	+ EGF
	Duodenal mucosal EGF (ng/g mucosa)			
Day 5	35.7±12.9[ab]	76.0±13.7[c]	28.3±9.2[a]	68.3±10.9[bc]
Day 15	84.8±22.8[a†]	47.5±19.3[ab]	12.9±3.9[b*]	28.3±10.5[b†]

[1]Data are mean ± SE (n=6). Values in a row not sharing a superscript letter were significantly different ($P<0.05$) by Fisher's least significant difference test. *The content of EGF in duodenal mucosa was significantly different ($P<0.05$) from that in the control group (61.1±5.4 ng/g mucosa, n=6) on day 0 by Dunnett's test. †$P<0.05$ compared with day 5 within the same group by Fisher's least significant difference test.

DISCUSSION

Duodenal ulcer *per se* and oral EGF at a dose of 60 μg/kg/day did not obviously affect body weight of the rats in this study. However, Majumdar[12] found administration of EGF (20 μg/kg/day, ip. injection) to undernourished weanling rats for 7 days significantly reversed the decreased weight of whole body, small intestine, and oxyntic gland in the stomach caused by undernutrition. Similar to the results of body weight, oral EGF did not affect food intake. Because food intake was similar, body weight of the rats did not differ among four operated groups.

From the pathological observation, the mean diameter of ulcer area was undetectable in duodenal ulcer rats with EGF on day 5, and the damaged mucosa apparently recovered. However, the damaged mucosa was still found in duodenal ulcer rats without EGF on day 5. The data revealed that oral EGF reversed the damaged mucosa of duodenal ulcer on day 5, but duodenal ulcer could be self-recovered after 15 days. The results for cell growth of duodenal ulcer evaluated by mucosal DNA, RNA, and protein levels in the duodenum showed that mucosal DNA content did not significantly increase in duodenal ulcer rats with EGF until day 15 compared with those without EGF. Although we only measured DNA, RNA, and protein contents in the ulcer area of duodenal mucosa in duodenal ulcer rats and a similar area of intact duodenal mucosa in sham operation rats, these levels could be overestimated due to mixed cell types while collecting the samples. According to the results of pathological observation, the healing of damaged mucosa obviously occurred after day 5 in duodenal ulcer rats with EGF. Mucosal DNA content could reflect cell proliferation or cell division, but not measure DNA synthesis in the real time. While the pathological observation in the healing of damaged mucosa included the overall results of both cell proliferation and DNA synthesis. Oral EGF did not affect mucosal RNA and protein contents in duodenal ulcer rats. The data suggested that oral EGF had hyperplastic rather than hypertrophic effect on duodenal mucosa in duodenal ulcer rats. Although oral EGF did not influence cell proliferation in sham operation rats, EGF supplementation might temporarily cause cell hypertrophy due to increased ratio of RNA to protein caused by an increase in RNA and a decrease in protein on day 5. However, a previous study[7] demonstrated that orally administered EGF twice daily at 30 and 100 μg/kg body weight for 2 weeks had no effect on ulcer area and healing rate in Donryu rats with gastric ulcer induced by a submucosal injection of 20 mL/L acetic acid into the antrum. Different strain of animals, method of ulcer induction, severity of ulcer, and duration of EGF treatment could cause different results.

Our data showed that sham operation and duodenal ulcer rats with EGF significantly elevated mucosal EGF to 2.1- and 2.4-fold, respectively, compared with those without EGF on day 5. However, mucosal EGF did not differ between sham operation and duodenal ulcer rats with or without EGF on day 5. The results indicated that exogenous EGF increased mucosal EGF in the duodenum of both sham operation and duodenal ulcer rats to the similar extent on day 5. Therefore, exogenous EGF could be directly uptaken by the mucosa, and increased mucosal EGF in the duodenum of sham operation and duodenal ulcer rats could be derived from both exogenous and endogenous EGF. Increased mucosal EGF in sham operation and duodenal ulcer rats with EGF reduced to the similar level as in those without EGF on day 15, probably because of the adaptation to exogenous EGF through down-regulation of endogenous EGF. The EGF receptor was localized in the apical membrane of the enterocytes of rat duodenum[13,14], therefore the hypertrophic and hyperplastic effect of EGF on the mucosa of sham operation and duodenal ulcer rats, respectively, in this study could be induced via the interaction with the EGF receptor. Whereas if and how exogenous EGF regulates endogenous production of EGF or the interaction with the EGF receptor in the gastrointestinal tract of sham operation or duodenal ulcer rats, a further study to measure EGF mRNA and EGF receptors in the duodenum is required.

Our study showed that oral EGF significantly increased EGF content in the duodenal mucosa on day 5, accompanied by grossly improved healing in duodenal ulcer rats after day 5, and followed by elevated mucosal DNA content on day 15. The data suggested that oral EGF improved mucosal healing in duodenal ulcer rats by increasing EGF content in the duodenal mucosa to accelerate cell proliferation. Although EGF could be cleaved to smaller, less active forms in acidic gastric juice, the proportion of intact EGF increased to about 60 % if the pH was maintained above 4[15], which allowed it to survive passage through the intestinal tract. After administration of ^{125}I-labeled EGF, reversed-phase HPLC identified >90 % and 46-51 % of C18-extracted radioactivity from gastric and

midjejunal luminal contents as intact ^{125}I-EGF, whereas <3 % of C18-extracted radioactivity in extracts of duodenal, jejunal, and ileal luminal contents was intact ^{125}I-EGF in adult mice[16]. The result indicated that EGF, given by oral administration, in the gut lumen, more or less, was still intact. Additionally, Tsujikawa *et al*[17] suggested that the luminal EGF might play a role only under tissue damage, where enhanced permeability allowed passage of luminal EGF to its receptor on the membranes. The mechanism for the healing effect of EGF on the damaged intestine is now uncertain. Most studies have focused on the mitogenic and antisecretory actions of EGF[6,9,18-21]. Konturek *et al*.[18] suggested that the mechanism for protective and ulcer healing effects of EGF involved the activation of ornithine decarboxylase, the key enzyme in the biosynthesis of polyamines, which play a crucial role in the growth-promoting action of EGF. Additionally, EGF administration (50 μg/kg) accelerated the healing of acetic acid-induced duodenal ulcer in rats via an increase in collagen proliferation and secretion without affecting gastric acid secretion[19]. A previous study[9] reported that subcutaneous injection of EGF increased duodenal DNA and RNA contents in rats with duodenal ulcer after 7-day treatment, but oral administration of EGF did not. In addition, they indicated that oral dose (10 μg/kg) of EGF had no influence on gastric secretion in rats with chronic gastroduodenal ulcer but subcutaneous injection of EGF (10 μg/kg) decreased gastric acid output by 59 % compared with the control rats without EGF administration. They suggested that the ulcer-healing effects of EGF were mediated by factors other than the inhibition of acid secretion, because oral EGF did not have any influence on gastric secretion. However, decreased gastric acid secretion in rats with chronic duodenal ulcer was observed after intravenous administration of EGF at a dose of 36 μg/kg but not at doses of 0.36 or 3.6 μg/kg[6]. Furthermore, EGF has been reported to inhibit gastric acid and stimulate duodenal bicarbonate secretion[20]. The physiological effect of EGF on acid secretion was mediated by induction of gastric H^+, K^+-ATPase gene expression[21,22].

In conclusion, oral administration of EGF (60 μg/kg/day) can increase EGF content in the duodenal mucosa and promote the healing of the rats with duodenal ulcer by its mitogenic action.

REFERENCES

1 **Marti U**, Burwen SJ, Jones AL. Biological effects of epidermal growth factor, with emphasis on the gastrointestinal tract and liver: an update. *Hepatology* 1989; **9**: 126-138

2 **Poulsen SS**, Nexo E, Olsen PS, Hess J, Kirkegaard P. Immunohistochemical localization of epidermal growth factor in rat and man. *Histochemistry* 1986; **85**: 389-394

3 **Wright NA**, Pike C, Elia G. Induction of a novel epidermal growth factor- secreting cell lineage by mucosal ulceration in human gastrointestinal stem cells. *Nature* 1990; **343**: 82-85

4 **Jones MK**, Tomikawa M, Mohajer B, Tarnawski AS. Gastrointestinal mucosal regeneration: role of growth factors. *Front Biosci* 1999; **4**: D303-309

5 **Konturek PC**, Bielanski W, Bobrzynski A, Hahn EG, Konturek SJ. Gastric mucosal expression and luminal release of growth factors in gastric carcinoma and duodenal ulcer patients before and after eradication of *Helicobacter pylori*. *J Physiol Pharmacol* 1997; **48**: 375-382

6 **Skov Olsen P**, Poulsen SS, Therkelsen K, Nexo E. Oral administration of synthetic human urogastrone promotes healing of chronic duodenal ulcers in rats. *Gastroenterology* 1986; **90**: 911-917

7 **Kuwahara Y**, Sunagawa Y, Imoto Y, Okabe S. Effects of orally administered human epidermal growth factor on natural and delayed healing of acetic acid-induced gastric ulcers in rats. *Jpn J Pharmacol* 1990; **52**: 164-166

8 **Palomino A**, Hernandez-Bernal F, Haedo W, Franco S, Mas JA, Fernandez JA, Soto G, Alonso A, Gonzalez T, Lopez-Saura P. A multicenter, randomized, double-blind clinical trial examining the effect of oral human recombinant epidermal growth factor on the healing of duodenal ulcers. *Scand J Gastroenterol* 2000; **35**: 1016-1022

9 **Konturek SJ**, Dembinski A, Warzecha Z, Brzozowski, Gregory H. Role of epidermal growth factor in healing of chronic gastroduodenal ulcers in rats. *Gastroenterology* 1988; **94**: 1300-1307

10 **Chomczynski P**. A reagent for the single-step simultaneous isolation of RNA, DNA and proteins from cell and tissue samples. *Biotechniques* 1993; **15**: 532-534, 536-537

11 **Sizemore N**, Dudeck RC, Barksdale CM, Nordblom GD, Mueller WT, McConnell P, Wright DS, Guglietta A, Kuo BS. Development and validation of two solid-phase enzyme immunoassays (ELISA) for quantitation of human epidermal growth factors (hEGFs). *Pharm Res* 1996; **13**: 1088-1094

12 **Majumdar AP**. Postnatal undernutrition: effect of epidermal growth factor on growth and function of the gastrointestinal tract in rats. *J Pediatr Gastroenterol Nutr* 1984; **3**: 618-625

13 **Montaner B**, Perez-Tomas R. Epidermal growth factor receptor (EGF-R) localization in the apical membrane of the enterocytes of rat duodenum. *Cell Biol Int* 1999; **23**: 475-479

14 **Montaner B**, Asbert M, Perez-Tomas R. Immunolocalization of transforming growth factor-alpha and epidermal growth factor receptor in the rat gastroduodenal area. *Dig Dis Sci* 1999; **44**: 1408-1416

15 **Playford RJ**, Marchbank T, Calnan DP, Calam J, Royston P, Batten JJ, Hansen HF. Epidermal growth factor is digested to smaller, less active forms in acidic gastric juice. *Gastroenterology* 1995; **108**: 92-101

16 **Rao RK**. Luminal processing of epidermal growth factor in mouse gastrointestinal tract *in vivo*. *Peptides* 1995; **16**: 505-513

17 **Tsujikawa T**, Itoh A, Yasuoka T, Fukunaga T, Satoh J, Uda K, Ihara T, Sasaki M, Fujiyama Y. Mucosal permeability regulates receptor binding of luminal epidermal growth factor in the adult rat intestine. *Int J Mol Med* 2003; **11**: 349-352

18 **Konturek JW**, Brzozowski T, Konturek SJ. Epidermal growth factor in protection, repair, and healing of gastroduodenal mucosa. *J Clin Gastroenterol* 1991; **13**(Suppl 1): S88-S97

19 **Perez Aisa A**, Sopena Biarge F, Arceiz Gonzalo E, Sainz Samitier R, Ortego Diez De Retana J, Lanas Arbeloa A. Effect of exogenous administration of platelet-derived growth factor and epidermal growth factor on duodenal ulcer healing in rats treated with indomethacin. *Gastroenterol Hepatol* 2002; **25**: 299-305

20 **Szabo S**, Vincze A. Growth factors in ulcer healing: lessons from recent studies. *J Physiol Paris* 2000; **94**: 77-81

21 **Kaise M**, Muraoka A, Yamada J, Yamada T. Epidermal growth factor induces H^+, K^+-ATPase alpha-subunit gene expression through an element homologous to the 3' half-site of the c-fos serum response element. *J Biol Chem* 1995; **270**: 18637-18642

22 **Kusayanagi S**, Takeuchi Y, Todisco A, Mitamura K. Extracellular signal-regulated protein kinases mediate H(+),K(+)-ATPase alpha-subunit gene expression. *Biochem Biophys Res Commun* 2002; **290**: 1289-1294

Edited by Wang XL

P.O.Box 2345, Beijing 100023,China
Fax: +86-10-85381893
E-mail: wjg@wjgnet.com www.wjgnet.com

World J Gastroenterol 2003;9(10):2266-2269
World Journal of Gastroenterology
 ISSN 1007-9327

• BASIC RESEARCH •

Role of oxygen free radicals in patients with acute pancreatitis

Byung Kyu Park, Jae Bock Chung, Jin Heon Lee, Jeong Hun Suh, Seung Woo Park, Si Young Song, Hyeyoung Kim, Kyung Hwan Kim, Jin Kyung Kang

Byung Kyu Park, Jae Bock Chung, Jin Heon Lee, Jeong Hun Suh, Seung Woo Park, Si Young Song, Jin Kyung Kang, Department of Internal Medicine, Institute of Gastroenterology, College of Medicine, Yonsei University, Seoul, Korea
Hyeyoung Kim, Kyung Hwan Kim, Department of Pharmacology, College of Medicine, Yonsei University, Seoul, Korea
Correspondence to: Jae Bock Chung, M.D. Department of Internal Medicine, College of Medicine, Yonsei University, 134 Shinchon-Dong, Seodaemun-ku, Seoul, 120-752 Korea. jbchung@yumc.yonsei.ac.kr
Telephone: +82-2-361-5427 **Fax:** +82-2-393-6884
Received: 2003-06-04 **Accepted:** 2003-08-02

Abstract

AIM: The generation of oxygen free radicals has been implicated in the pathogenesis of experimental pancreatitis. The aim of this study was to determine the role of oxygen free radicals in patients with acute pancreatitis.

METHODS: The plasma levels of C-reactive protein (CRP), lipid peroxide (LPO), myeloperoxidase (MPO) and superoxide dismutase (SOD) were measured in 13 patients with acute pancreatitis and 14 healthy volunteers.

RESULTS: Among the patients with acute pancreatitis, there were higher plasma levels of LPO and MPO and lower SOD activity in patients with severe pancreatitis than in those with mild pancreatitis. However, there was no significant difference in the serum marker of oxidative stress no matter what the etiology was. The LPO level was especially correlated with the concentration of serum CRP and CT severity index.

CONCLUSION: The oxygen free radicals may be closely associated with inflammatory process and the severity of acute pancreatitis. Especially, the concentration of plasma LPO is a meaningful index for determining the severity of the disease.

Park BK, Chung JB, Lee JH, Suh JH, Park SW, Song SY, Kim H, Kim KH, Kang JK. Role of oxygen free radicals in patients with acute pancreatitis. *World J Gastroenterol* 2003; 9(10): 2266-2269

http://www.wjgnet.com/1007-9327/9/2266.asp

INTRODUCTION

Oxygen free radicals are molecules produced continuously in cells by several mechanisms. The generation of oxygen free radicals is physiologic. In most circumstances, oxygen free radicals are neutralized immediately by enzymatic scavengers. However, when formation of oxygen free radicals overwhelms radical neutralization in cells, oxidative stress occurs. As they are very reactive, they react well with all biological substances such as proteins, polysaccharides and nucleic acids, resulting in tissue injury[1-3]. It has been suggested that oxygen free radicals are responsible for a wide variety of diseases or conditions[1,4-8].

Oxygen free radicals have been known to play an important role in the pathogenesis of pancreatitis of some experimental models[6-12]. Oxygen free radicals are involved in initiation of pancreatitis[11]. Also, it was reported that oxygen free radicals acted as important mediators of tissue damage in experimental acute pancreatitis[10]. Therapeutic effects of antioxidants and radical scavengers have been shown in experimental models of acute pancreatitis[11,13,14].

However, there is doubt that experimental models of acute pancreatitis will match clinically acute pancreatitis in humans. Although there were some data that reflected enhanced oxygen stress in patients with acute pancreatitis[15-17], the role of oxygen free radicals in patients with acute pancreatitis has not been well clarified.

Therefore, this study was conducted to evaluate the role of oxygen free radicals in human acute pancreatitis and to analyze the correlation between oxygen free radicals and the severity of acute pancreatitis.

MATERIALS AND METHODS

Patients

Thirteen patients admitted to Medical Center of Yonsei University with a diagnosis of acute pancreatitis were included in this study. The diagnosis was established on the basis of acute abdominal pain, at least 3-fold elevated levels of serum amylase and computed tomography (CT). All patients had no previous history of acute pancreatitis. Fourteen healthy subjects without previous medical history were enrolled as controls. The mean age was 53.6 years in patients and 32.5 years in control group. The male to female ratio was 11:2 in patients and 10:4 in control groups.

Measurement of oxygen free radicals

Peripheral blood samples were taken on recruitment. After the blood was centrifuged, the plasma was stored at -70 ℃ until analysis. The blood samples of control group underwent the same process. C-reactive protein was measured by the routine method. Serum lipid peroxide (LPO) and myeloperoxide (MPO) as markers of oxygen free radicals were measured. Also the activity of superoxide dismutase (SOD) that diminished in oxidative stress due to its role as enzymatic scavenger was measured.

Lipid peroxidation

LPO was analyzed by measuring the amount of thiobarbituric acid reactive substances (TBARS). It was preceded that the standard solution was prepared by diluting 1 000 nmol/ml tetraethoxy propane, which was made by mixing with tetraethoxy propane and tertiary distilled water. Tertiary distilled water was used as blank solution. Plasma, blank, and standard solution 200 μL, respectively, were mixed with 20 % acetic acid. TBARS resulted from the reaction with thiobarbituric acid (TBA) 400 μL, was detected as reading fluorescence at 535 nm emission. The result was compared with standard curve.

Myeloperoxidation

MPO was analyzed as a marker of neutrophil activation by

Bioxytech®MPO enzyme immunoassay kit (OXIS International Inc., Portland, USA). This assay detects the fluorescence of solution at 405 nm emission using sandwich enzyme-linked immunosorbent assay (ELISA) against biotin-labeled goat polyclonal anti-MPO.

Superoxide dismutase

SOD activity was measured by using Bioxytech® SOD-525™ assay kit (OXIS International Inc., Portland, USA). This assay detects the fluorescence of solution at 525 nm, based on the principle that autoxidation of tetracyclic cathechol accelerates in condition of SOD.

Other parameters

To determine the severity and prognosis of acute pancreatitis, the level of C-reactive protein (CRP) in serum was used for a single indicator, Ranson' s score for multiple indicator, and CT severity index[18] for morphological indicator. Atlanta classification[19] was used as a main determining index for the severity of acute pancreatitis.

Statistical analysis

We used chi-square test and independent sample *t*-test for comparison in each group. A *P* value less than 0.05 was considered significant.

RESULTS

Levels of oxygen free radicals

The mean plasma level of LPO was 21.9±26.5 nmol/ml in acute pancreatitis and 5.7±1.7 nmol/ml in control group (*P*=0.030). Also, the mean plasma level of MPO was 12.3±11.7 nmol/ml in acute pancreatitis and 2.7±1.2 nmol/ml in control group (*P*=0.005). Oxygen free radicals significantly increased more in acute pancreatitis patients than in control group. The mean level of SOD activity was 48.2±41.4 U/dl in acute pancreatitis patients and 100.4±20.2 U/dl in control group (*P*=0.002). The decrease of SOD activity was more prominent in acute pancreatitis than in control group (Table 1).

Table 1 Laboratory parameters in patients with acute pancreatitis and control group

Parameters	Control (*n*=14)	Acute pancreatitis (*n*=13)	*P*-value
Amylase (IU / dL)	141.9±179.3	393.3±243.1	0.005
LPO (nmol / mL)	5.7±1.7	21.9±26.5	0.030
MPO (nmol / mL)	2.7±1.2	12.3±11.7	0.005
SOD (U / dL)	100.4±20.2	48.2±41.4	0.002

Values are means ± SD, LPO = lipid peroxide, MPO = myeloperoxidase, SOD=superoxide dismutase.

Oxygen free radicals according to etiology of acute pancreatitis

The etiologies of acute pancreatitis were gallstone (*n*=5), alcohol (*n*=4), hyperlipidemia (*n*=1), and unexplained (*n*=3). Comparing gallstone pancreatitis patients with alcohol induced pancreatitis, the plasma levels of CRP, LPO, MPO, and SOD showed no significant differences between the two groups (Table 2).

Association with severity of acute pancreatitis

According to the Atlanta classification, acute pancreatitis was classified as mild in 8 patients and as severe in 5 patients based on their clinical manifestations. There were no differences of age and sex between the two groups (Table 3). The mean level of serum CRP in patients with severe pancreatitis was higher than the one in patients with mild pancreatitis (12.3±9.0 mg/dl *vs* 6.7±4.5 mg/dl, *P*=0.311). The mean level of SOD activity more markedly decreased in patients with severe pancreatitis than in patients with mild pancreatitis (27.3±15.4 U/dl *vs* 65.7±49.2 U/dl, *P*=0.130).

Table 2 Laboratory parameters according to etiology of acute pancreatitis

Paramerters	Gallstone group (*n*=5)	Alcohol group (*n*=4)	*P*-value
Age (years)	55.4±19.7	44.5±14.2	0.368
Amylase (IU / dL)	364.6±271.9	366.5±252.5	0.992
Lipase (IU / dL)	10 004.0±15873.2	6 035.8±8,265.2	0.646
CRP (mg / dL)	6.0±2.5	12.3±9.8	0.296
LPO (nmol / mL)	15.6±10.5	38.7±45.1	0.385
MPO (nmol / mL)	11.3±15.3	15.5±14.3	0.689
SOD (U / dL)	59.2±49.3	21.0±17.1	0.171

Values are means ±SD, LPO = lipid peroxide, MPO = myeloperoxidase, SOD = superoxide dismutase.

Table 3 Clinical characteristics of patients with acute pancreatitis classified according to Atlanta classification

	Mild group	Severe group
No. of cases	8	5
Age (years)	53.5±17.1	53.8±15.7
Sex (M:F)	7:1	5:1
Etiology		
Gallstone	2	3
Alcohol	2	2
Others*	4	0
No. of mortality	0	0

*One case was due to hyperlipidemia and 3 cases were idiopathic.

Table 4 Laboratory parameters in patients with mild and severe pancreatitis according to Atlanta classification

Parameters	Mild group (*n*=8)	Severe group (*n*=5)	*P*-value
Amylase (IU / dL)	374.7±252.4	423.0±253.1	0.745
Lipase (IU / dL)	10 082.8±12 565.6	30 008.0±3 314.9	0.167
CRP (mg / dL)	6.7±4.5	12.3±9.0	0.311
LPO (nmol / mL)	11.5±6.8	38.7±38.1	0.068
MPO (nmol / mL)	7.5±4.1	20.1±15.4	0.053
SOD (U / dL)	65.7±49.2	27.3±15.4	0.130
Ranson's score	1.4±0.7	2.8±1.9	0.177
CT severity index	2.0±1.1	5.8±3.1	0.008

Values are means ±SD, LPO = lipid peroxide, MPO = myeloperoxidase, SOD = superoxide dismutase.

The mean plasma levels of LPO and MPO were higher in patients with severe pancreatits than those in patients with mild pancreatitis (LPO: 38.7±38.1 nmol/ml *vs* 11.5±6.8 nmol/ml, *P*=0.068, MPO: 20.1±16.1 nmol/dl *vs* 7.5±4.1 nmol/dl, *P*=0.053). The significant difference was for CT severity index between the two groups (5.8±3.1 in severe pancreatitis, 2.0±1.1 in mild pancreatitis, *P*=0.008) (Table 4). To analyze the relationship between oxygen free radicals and CT severity index, serum CRP that is widely used as an index for severity of pancreatitis, plasma LPO showed a close correlation with CT severity index and serum CRP (r^2=0.373, and 0.675, *P*=0.027, and 0.001, respectively) (Figure 1). Plasma MPO showed a close correlation

with CT severity index but not with serum CRP (r^2=0.319 and 0.202, P=0.044 and 0.143, respectively) (Figure 2). But SOD activity showed no significant correlation with either CT severity index or serum CRP (r^2=0.026 and 0.307, P=0.638 and 0.096, respectively) (Figure 3). CT severity index was correlated with serum CRP and Ranson' s score (r^2=0.334 and 0.382, P=0.049 and 0.024, respectively).

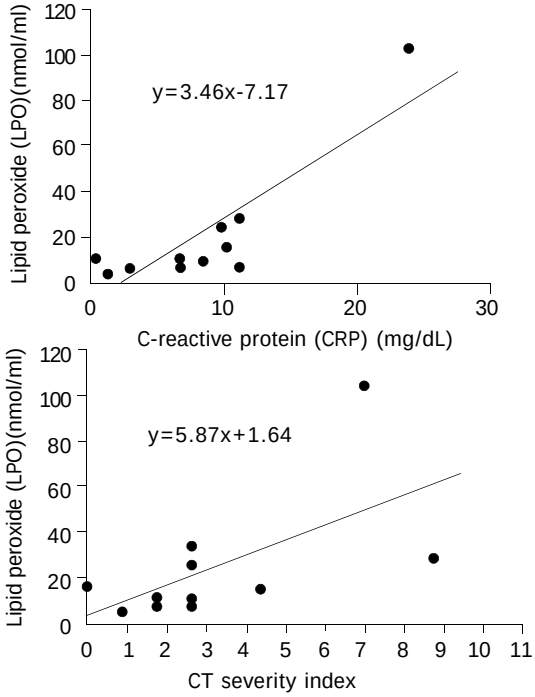

Figure 1 Relationships between serum levels of LPO and prognostic indices (CRP and CT severity index). There was a statistically significant correlation between LPO levels with CRP and CT severity index (γ2=0.675 and 0.373, P=0.001 and 0.027, respectively).

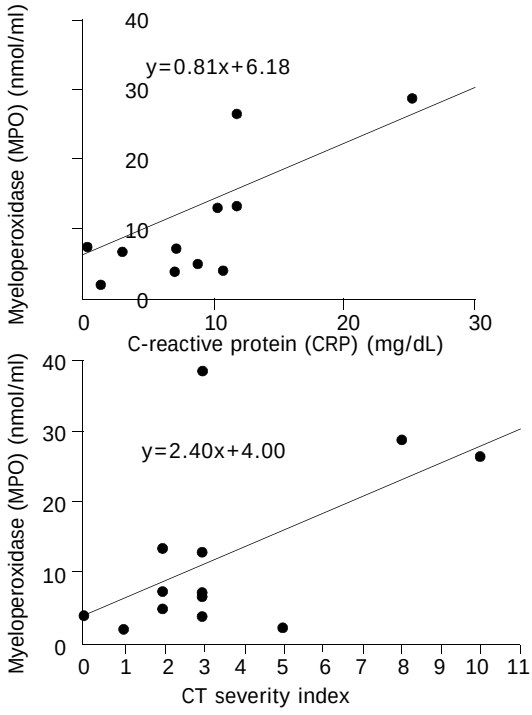

Figure 2 Relationships between serum levels of MPO and prognostic indices (CRP and CT severity index). There was no statistically significant correlation between MPO level and CRP (γ2=0.202, P=0.143). However, MPO level correlated positively and significantly with CT severity index (γ2=0.319, P=0.044).

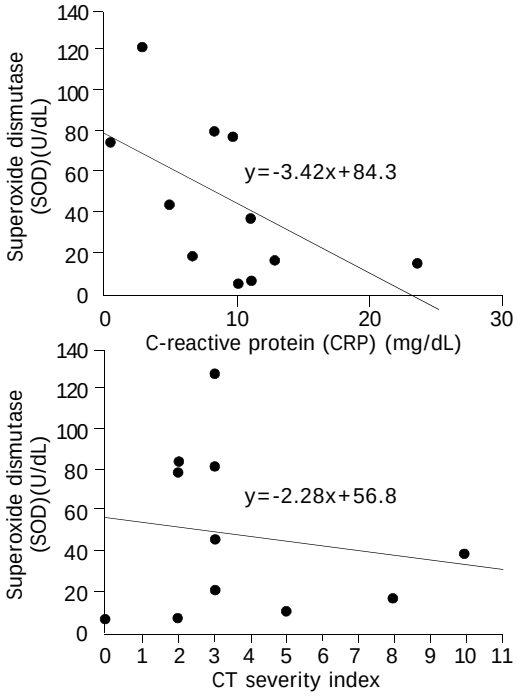

Figure 3 Relationships between serum enzymatic activity of SOD and prognostic indices (CRP and CT severity index). There was no statistically significant correlation between serum SOD concentrations and CRP and CT severity index (γ2=0.307 and 0.026, P=0.096 and 0.638, respectively).

DISCUSSION

Acute pancreatitis led to various degrees of interstitial edema, acinar cell damage, hemorrhage and necrosis[8]. Although the inflammation initiates in pancreas, the disease may lead to systemic multi-organ failure. Several factors (complement activation, cytokines, oxygen free radicals, ischemia, and autodigestion of pancreatic enzyme) have been known to be involved in the pathogenesis of acute pancreatitis. But the role of these factors remains still unclear. Among them, oxygen free radicals could damage extracellular tissue by degrading hyaluronic acid and collagen in the intercellular matrix and directly attack biological membrane through the peroxidation of structurally and functionally important lipids[20]. Furthermore, they could denature enzymes and other important proteins, and damage nucleic acid. In addition, they could indirectly trigger the accumulation of polymorphonulclear (PMN) leukocyte in the tissue. Activated PMN leukocytes could secrete various enzymes such as myeloperoxidase, protease, and elastase[21]. As a result, the inflammatory reaction accelerated. Also, oxygen free radicals could indirectly stimulate arachidonic acid metabolism with increased production of prostaglandins, thromboxane, and leukotrienes, and eventually could lead to microcircular derangement and cellular damage[2,15].

There are some reports concerning mechanisms of enhanced production of oxygen free radicals. Xanthine oxidase, PMN leukocyte, and cytochromes P-450 have been introduced as the source of oxygen free radicals[3,12]. However, the true sources of oxygen free radicals that are responsible for the pathogenesis of acute pancreatitis have not yet been identified. Since the first study by Sanfey *et al*[9], many studies have demonstrated the role of oxygen free radicals in the pathogenesis of acute pancreatitis in experimental models and patients. Oxygen free radicals have been known to mediate an important step in the initiation of acute pancreatitis[11]. But most results have been derived from experimental animal models in which acute pancreatitis was induced by stress, cerulein

injection, choline-deficient diet, or taurocholate injection into pancreatic duct. Only a few data have been derived from patients. Furthermore, there are many limitations on studying patients with acute pancreatitis in clinical settings.

Because of the nature of their high reactivity, oxygen free radicals are difficult to measure directly. Direct measurement of oxygen free radicals with electron spin resonance (ESR) technique was limited to *in vitro* studies due to short half time of free radicals and toxicity of compounds[22]. For these reasons, the alternative of measuring stable metabolites was met with broad acceptance. In most studies, measurements of the effects of radical reaction with biological substances (i.e., lipid peroxides and changes of glutathione metabolism) have replaced the assessment of oxygen free radicals.

In acute pancreatitis patients, increased production of lipid peroxidation, decreased level of vitamin C, and direct correlation between oxidative stress and severity of acute pancreatitis have been reported[15-17]. Equally, our results showed that plasma levels of LPO and MPO increased more in acute pancreatitis patients than in normal control group, and that increase of LPO and MPO was more prominent in severe pancreatitis than in mild pancreatitis, and that SOD activity, as a scavenger of oxygen free radical, was lower in acute pancreatitis patients than in normal control group. From these results, we can suggest that oxygen-derived free radicals play a pivotal role in the pathogenesis of acute pancreatitis in patients. In our study, it was probable that lipid peroxidation was correlated with severity of acute pancreatitis. There was a close correlation of lipid peroxidation with serum CRP and CT severity index. Therefore, there is some possibility that LPO could be a predictor of severity of acute pancreatitis. Similarly it was shown that lipid peroxidation was significantly increased in patients with septic shock[23]. In contrast, Abu-Zidan *et al*[16] have reported that lipid peroxidation was highly correlated with the severity of pancreatitis but not a good predictor of it. This discordance may be due to different method of measuring lipid peroxidation and study design.

In our study, the level of SOD activity, enzymatic scavenger, was significantly decreased in the plasma of patients with acute pancreatitis, and although not significant, it was related to the severity of acute pancreatitis. The effects of antioxidant, such as vitamins C and E, in experimental models have been reported[11,13,14]. However, the results have varied according to different models. Because in these most studies, antioxidant therapy was performed before acute pancreatitis was induced, the results were unlikely to be applied to clinical conditions. As well, the therapeutic effect of antioxidants and radical scavenger in patients has not been demonstrated yet.

There was no difference of oxygen free radicals between alcohol-induced pancreatitis and gallstone pancreatitis in our study. In many various experimental models and patients with acute pancreatitis, oxygen free radicals have been related to the disease[2,15,24,25]. Thus in our opinion, the role of oxygen free radicals may not be different no matter what the etiology of the disease is.

In conclusion, oxygen-derived free radicals may be closely associated with inflammatory process and the severity of acute pancreatitis, and the plasma level of LPO is a meaningful index for determining the severity of the disease.

REFERENCES

1 **Kerr ME**, Bender CM, Monti EJ. An introduction to oxygen free radicals. *Heart Lung* 1996; **25**: 200-209
2 **Schoenberg MH**, Birk D, Beger HG. Oxidative stress in acute and chronic pancreatitis. *Am J Clin Nutr* 1995; **62**: 1306S-1314S
3 **Schulz HU**, Niederau C, Klonowski-Stumpe H, Halangk W, Luthen R, Lippert H. Oxidative stress in acute pancreatitis. *Hepato-Gastroenterol* 1999; **46**: 2736-2750
4 **Janero DR**. Ischemic heart disease and antioxidants: mechanistic aspects of oxidative injury and its prevention. *Crit Rev Food Sci Nutr* 1995; **35**: 65-81
5 **Thomas MJ**. The role of free radicals and antioxidants: how do we know that they are working? *Crit Rev Food Sci Nutr* 1995; **35**: 21-39
6 **Correa P**. The role of antioxidants in gastric carcinogenesis. *Crit Rev Food Sci Nutr* 1995; **35**: 59-64
7 **Machlin LJ**. Critical assessment of the epidemiological data concerning the impact of antioxidant nutrients on cancer and cardiovascular disease. *Crit Rev Food Sci Nutr* 1995; **35**: 41-50
8 **Bulkley GB**. The role of oxygen free radicals in human disease processes. *Surgery* 1983; **94**: 407-411
9 **Sanfey H**, Bulkley GB, Cameron JL. The role of oxygen-derived free radicals in the pathogenesis of acute pancreatitis. *Am Surg* 1984; **200**: 405-413
10 **Rau B**, Poch B, Gansauge F, Bauer A, Nüssler AK, Nevalainen T, Schoenberg MH, Beger HG. Pathophysiologic role of oxygen free radicals in acute pancreatitis initiating event or mediator of tissue damage? *Ann Surg* 2000; **231**: 352-360
11 **Schoenberg MH**, Büchler M, Gaspar M, Stinner A, Younes M, Melzener I, Bültmann B, Beger HG. Oxygen free radicals in acute pancreatitis of the rat. *Gut* 1990; **31**: 1138-1143
12 **Sanfey H**, Bulkley GB, Cameron JL. The pathogenesis of acute pancreatitis the source and role of oxygen-derived free radicals in three different experimental models. *Ann Surg* 1985; **201**: 633-639
13 **Sarr MG**, Bulkley GB, Cameron JL. Temporal efficacy of allopurinol during the induction of pancreatitis in the ex *vivo* perfused canine pancreas. *Surgery* 1987; **101**: 342-346
14 **Shikata A**, Suganuma M, Marugami Y, Sakurai Y, Ochiai M, Kamei K, Funabiki T, Shinohara R. The role of oxyhen-derived free radicals and their scavengers in experimental acute pancreatitis. *Digestion* 1996; **57**: 264
15 **Tsai K**, Wang SS, Chen TS, Kong CW, Chang FY, Lee SD, Lu FJ. Oxidative stress: an important phenomenon with pathogenetic significance in the progression of acute pancreatitis. *Gut* 1998; **42**: 850-855
16 **Abu-Zidan FM**, Bonham MJD, Windsor JA. Severity of acute pancreatitis: a multivariate analysis of oxidative stress markers and modified Glasgow criteria. *Br J Surg* 2000; **87**: 1019-1023
17 **Bonham MJD**, Abu-Zidan FM, Simovic MO, Sluis KB, Wilkinson A, Winterbourn CC, Windsor JA. Early ascorbic acid depletion is related to the severity of acute pancreatitis. *Br J Surg* 1999; **86:** 1296-1301
18 **Balthazar EJ**, Robinson DL, Megibow AJ, Ranson JHC. Acute pancreatitis: value of CT in establishing prognosis'. *Radiology* 1990; **174**: 331-336
19 **Bradley EL**. A clinically based classification system for acute pancreatitis. *Arch Surg* 1993; **128**: 586-590
20 **Slater TF**. Free-radical mechanisms in tissue injury. *Biochem J* 1984; **222**: 1-15
21 **Babior BM**. Oxygen-dependent microbial killing by phagocytes. *N Engl J Med* 1978; **298**: 659-668
22 **Schoenberg MH**, Büchler M, Beger HG. Oxygen radicals in experimental acute pancreatitis. *Hepato-Gastroenterol* 1994; **41**: 313-319
23 **Goode HF**, Cowley HC, Walker BE, Howdle PD, Webster NR. Decreased antioxidant status and increased lipid peroxidation in patients with septic shock and secondary organ dysfunction. *Crit Care Med* 1995; **23**: 646-651
24 **Uden S**, Schofield D, Miller PF, Day JP, Bottiglieri T, Braganza JM. Antioxidant therapy for recurrent pancreatitis: biochemical profiles in a placebo-controlled trial. *Aliment Pharmacol Ther* 1992; **6**: 229-240
25 **Gut A**, Shiel N, Kay PM, Segal I, Braganza JM. Heightened free radical activity in blacks with chronic pancreatitis at Johannesburg, *South Africa*. *Clin Chim Acta* 1994; **230**: 189-199

Edited by Wang XL

P.O.Box 2345, Beijing 100023,China
Fax: +86-10-85381893
E-mail: wjg@wjgnet.com www.wjgnet.com

World J Gastroenterol 2003;9(10):2270-2273
World Journal of Gastroenterology
 ISSN 1007-9327

• BASIC RESEARCH •

Parenteral versus early intrajejunal nutrition: Effect on pancreatitic natural course, entero-hormones release and its efficacy on dogs with acute pancreatitis

Huan-Long Qin, Zhen-Dong Su, Lei-Guang Hu, Zai-Xian Ding, Qing-Tian Lin

Huan-Long Qin, Zhen-Dong Su, Lei-Guang Hu, Zai-Xian Ding, Qing-Tian Lin, Department of Surgery, Sixth People' s Hospital, Shanghai Jiaotong University Shanghai 200233, China
Supported by Shanghai Science Fund for the Morning Star Young Scholars, No.99QB14010
Correspondence to: Dr. Huan-Long Qin, Department of Surgery, Sixth People' s Hospital, Shanghai Jiaotong University Shanghai 200233, China. sshosp @public.sta.net.cn
Telephone: +86-21-64368920 **Fax:** +86-21-64368920
Received: 2003-05-11 **Accepted:** 2003-06-02

Abstract

AIM: To evaluate the effect of early intrajejunal nutrition (EIN) on the natural course, entero-hormone secretion and its efficacy on dogs with acute pancreatitis.

METHODS: An acute pancreatitis model was induced by injecting 1 ml/kg of combined solution (2.5 % sodium taurocholate and 8 000-10 000 BAEE units trypsin/ml) into the pancreas via pancreatic duct. Fifteen dogs were divided into parenteral nutrition (PN) group and EIN group. Two groups were isonitrogenous and isocaloric. EIN was used at postoperative 24 h. Serum glucose, calcium, amylase and lysosomal enzymes were determined before and 1, 4, 7 d after acute pancreatitis was induced. All the dogs were injected 50 uCi ^{125}I-BSA 4 h before sacrificed on the 7th day. The ^{125}I -BSA index of the pancreas/muscle, pancreas/blood, and pancreas pathology score (PPS) were determined. The peripheral plasma cholecystokinin (CCK), secretin (SEC) and gastrin were measured by ELISA and RIA, and was quantitative analysis of pancreatic juice and amylase, pancreatolipase and HCO_3^-, Cl^-, Na^+ and K^+ performed by an autochemical analyzer at 30, 60, 120 and 180 min after beginning PN or EIN on the first day.

RESULTS: There was no difference between two groups in the contents of serum calcium, amylase and lysosomal enzymes, ^{125}I-BSA index of pancreas/muscle and pancreas/blood and PPS. The contents of CCK and gastrin in EIN were higher than those in PN group at 60 and 120 min (P<0.05). The content of SEC post-infusion of nutrition solution was higher than that of pre-infusion of nutrition solution in both groups, and only at 60 min SEC in EIN group was higher than that in PN group. The content of gastrin in EIN was higher than that in PN group at 120 and 180 min (P<0.05). The changes of pancreatic juice, amylase, pancreatolipase and HCO_3^-, Cl^-, Na^+ and K^+ between two groups did not reach significantly statistical difference (P>0.05).

CONCLUSION: EIN does not stimulate entero-hormone and pancreatic juice secretion, and enzyme-protein synthesis and release. EIN has no effect on the natural course of acute pancreatitis.

Qin HL, Su ZD, Hu LG, Ding ZX, Lin QT. Parenteral versus early intrajejunal nutrition: Effect on pancreatitic natural course, entero-hormones release and its efficacy on dogs with acute pancreatitis. *World J Gastroenterol* 2003; 9(10): 2270-2273
http://www.wjgnet.com/1007-9327/9/2270.asp

INTRODUCTION

Total parenteral nutrition (TPN) has been the standard practice for providing exogenous nutrients to patients with acute pancreatitis in order to improve their nutritional status and to avoid pancreatic stimulation. However, TPN is associated with certain disadvantages. In particular, there is an increased risk of central catheter infection, severe hyperglycaemia, and other metabolic and electrolyte disturbances and a possible exacerbation of metabolic disturbances. TPN may also result in gut barrier function alterations due to increasing intestinal permeability[1-10].

Benefits from the use of total enteral nutrition (TEN) have been noted in a number of other diseases, such as burns, trauma, and sepsis. In comparison with TPN, use of TEN reduces nosocomical infection, multiple organ failure (MOF), and length of hospitalization[3,4]. The use of early enteral feeding for nutritional support in patients with acute pancreatitis has not been evaluated systematically. The commonly encountered problems of gastric atony and outlet obstruction have limited the successful delivery of enteral formulas to patients with severe acute pancreatitis. In addition, many surgeons hold scrupulously that the EIN may exacerbate the clinical pathological features, and lead to recurrence of symptoms and delayed complications to be cured[11-18]. However, these problems could be overcome if enteral nutrition is delivered to the distal ileum far away from the Treitz' s ligament, to avoid stimulation of the cephalic and gastric phase, and those effects are not so pronounced as nutrients are delivered directly into jejunum[3,9-13]. Therefore, it is necessary to investigate the efficiency of early intrajejunal nutrition on pancreatitic clinicopathological changes, entero- hormone release and its efficacy on dogs with acute pancreatitis.

MATERIALS AND METHODS

Animal model

A total of 22 dogs weighing 18-22 kg, were allowed *ad libitum* intake of water. After fasted for 12-14 hours, all the dogs were induced anesthesia by intramuscular injection of ketamine 10 ml/kg, and intravenous injection of sodium pentobarbital 30 mg/kg. Under sterile conditions, a middle laparotomy and a duodenotomy were performed. The duodenum papilla was found and a silastic catheter was inserted into pancreatic tube and fixed for collecting pancreatic juice. Acute pancreatitis model was induced by injecting 1 mg/kg of combined solution of 2.5 % sodium taurocholate and 8 000-10 000 BAEF units trypin/ml into pancreas via pancreatic duct with a pressure of 30 cmH_2O, and the common biliary duct was clamped. After the model

was established, the duodenum and abdomen were closed. A catheter via jejunostomy was set at 30 cm away from the Treitz' s ligament. The neck region of the dogs was shaved and prepared in a sterile manner for catheterization. A silastic catheter (1.0 mm inner diameter and 1.5 mm outer diameter) was inserted through the external jugular vein to reach the superior vena cava. The catheter was fixed to connect the infusion solution. Fifteen dogs with acute pancreatitis survived over 7 days, and the death rate was 32 % (7/22). The trial was approved by the Institutional Animal Committee.

Experimental groups and preparation of nutritional solution

Fifteen dogs having survived over 7 days with acute pancreatitis were randomly divided into PN group (n=7) and EIN group (n=8). The two groups were isocaloric and isonitrogenous. The PN solutions were consisted of 7 % Vamin (SSPC, 9.4 g/1 000 ml) and 20 % Intralipid (SSPC) and 50 % glucose (GS). Non-protein calorie was 50 kC (209.2 kJ/kg) and nitrogen was 0.3 g/kg/d. The total volume of solution infused was 70 ml/kg/d. Energy index supported with glucose and fat emulsion was 1∶1. Multivitamins and electrolytes were also contained in TPN solutions. The normal saline was infused by 250 ml/kg during operation time and 8 h postoperation, and then infused with 125±25 ml/kg. The nutrient solution was infused at a constant infusion rate by a pump (100-120 ml/h).

The EIN solution was Nutrison (Nutricia). At the 24th h after acute pancreatitis was induced, the jejunum through jejunostomy catheter was infused 250 ml Nutrison and 500 ml NS. At the 48th h after acute pancreatitis, 500 ml Nutrison and 250 ml NS were infused for 5 days. The infusion rate was controlled by a microcomputer-pump (Nutricia). During EIN supporting, the content with insufficient calories and nitrogen were supplemented by partial parenteral nutrition[3,16,18].

Laboratory tests, ^{125}I-BSA index and pancreatic pathology

Serum glucose, calcium, amylase and lysosomal enzymes (according to Kit' s indication) were determined before and 1, 4, 7 d after the occurrence of acute pancreatitis. All the dogs were injected 50 uCi ^{125}I-BSA 4 h before sacrificed on the seventh day. The ^{125}I-BSA volume in the pancreas (/g), muscle of the right leg (/g) and blood (/ml) were tested by a r-accounter radioimmunology analyzer. The ^{125}I -BSA index of the pancreas/muscle and pancreas/blood was measured. Fixed tissues of the pancreatic head, body, tail and the total pancreas were sectioned and the histological change was observed. Pancreatitic pathological scores (PPS) were taken by the extent of pancreas tissue edema, inflammation, hemorrhage and necrosis according to scores 1, 2, 3 and 4, and PPS of the different parts of the pancreas was determined.

Entero-hormone determination

Twenty-four hours after the occurrence of acute pancreatitis, serum was used to determine the CCK and SEC (Peninsula Laboration, Inc.USA), and gastrin (Beijing Furui Bioengineer Co.) at the same time before and 30, 60, 120 and 180 min after PN or EIN. The former two samples were measured by competitive ELISA. The serum gastrin was measured by competitive binding RIA. The serum amylase, pancreaolipase and pancreatic juice, electrolytes (HCO_3^-, Cl^-, Na^+ and K^+) were determined by a 1 600 full-automatic biochemical analyser.

Statistical analysis

These data were expressed as means ± SEM, and comparison between two groups was made using χ^2 analysis of variance. A P value less than 0.05 was considered statistically significant.

RESULTS

Changes of serum glucose, calcium, amylase and lysosomal enzymes

After the acute pancreatitis model was prepared, serum glucose level in PN group was higher as compared with that in EIN group during the whole experimental period. Serum calcium was markedly decreased after acute pancreatitis was induced, and there was no difference in the changes of serum calcium in the latter days between two groups. Serum amylase and lysosomal enzymes (LE) increased and gradually decreased later during the experimental period, there was no difference between two groups (P>0.05) (Table 1).

Table 1 Effect of different nutrition support methods on serum glucose, calcium amylase and lysosomal enzymes

Groups	Time	Glu (umol/L)	Ca (mmol/L)	Amylase (SU)	LE(U)
PN group	Pre-AP	4.0±0.5	2.50±0.10	328±96	22±10
	30 min	8.3±0.8[a]	2.42±0.11	636±100[a]	53±11
	1 d	9.7±0.7[a]	2.35±0.09	1 689±298[a]	68±17
	4 d	10.3±1.0[a]	2.36±0.13	1 150±416[a]	45±14
	7 d	9.80±1.1[a]	2.20±0.11	1 060±260[a]	47±13
EIN group	Pre-AP	4.7±0.8	2.34±0.16	400±110	26±9
	30 min	8.4±1.0[a]	2.39±0.11	734±164	64±17
	1 d	8.9±0.8[a]	2.31±0.09	1 289±439[b]	71±13
	4 d	6.7±1.0	2.34±0.15	1 215±416	50±19
	7 d	6.6±0.7	2.30±0.09	1 169±362	52±20

[a]P<0.05, *vs* pre-SAP, [b]P<0.05, *vs* PN group, Pre-AP: before acute pancreatitis.

^{125}I-BSA index and pancreatitic pathological scores

^{125}I-BSA index of pancreas/muscle and pancreas/blood in EIN group (4.22±0.18 cpm/g, 0.22±0.03 cpm/ml) and PN group (3.69±0.26 cpm/g, 0.17±0.02 cpm/ml) did not reach statistical difference (P>0.05). Pancreatitic pathological scores (PPS) of different parts including head, body, tail and total pancreas in EIN group (1.40±0.24, 2.3±0.20, 2.1±0.20, 1.9±0.23) and PN group (1.30±0.38, 2.4±0.22, 2.2±0.22, 1.9±0.06) also did not reach statistical difference (P>0.05).

Entero-hormone, pancreatic juice and their components analysis

CCK The content of CCK in EIN group was higher than that in PN group at 30 and 60 min (P<0.05). There was no difference before and after nutrition liquid infusion in PN group (Table 2).

Table 2 Changes of serum CCK at different times (ng/ml)

Group	0 min	30 min	60 min	120 min	180 min
PN group	0.24±0.02	0.17±0.01	0.23±0.01	0.23±0.02	0.33±0.03
EIN group	0.22±0.02	0.29±0.06[a]	0.33±0.05[a]	0.29±0.03[a]	0.31±0.05

[a]P<0.05 *vs* PN group.

Table 3 Changes of serum SEC at different times (ng/ml)

Group	0 min	30 min	60 min	120 min	180 min
PN group	0.33±0.03	0.65±0.14	0.74±0.17	0.61±0.20	0.56±0.23
EIN group	0.35±0.06	0.61±0.17	0.88±0.25[a]	0.64±0.13	0.61±0.25

[a]P<0.05 *vs* PN group.

SEC SEC after infusion of nutrition liquid was higher than that before infusion of nutrition liquid ($P<0.05$), but it did not reach statistical difference between two groups at 30, 120 and 180 min ($P>0.05$). SEC only at 60 min in EIN group was higher than that in PN group (Table 3).

Gastrin The changes of gastrin in the PN group did no reach statistical difference before and after nutrition liquid infusion. Gastrin in EIN group gradually increased, and was higher than that in PN group at 120 and 180 min ($P<0.05$) (Table 4).

Table 4 Changes of serum gastrin at different times (pg / ml)

Group	0 min	30 min	60 min	120 min	180 min
PN group	12.5±3.7	13.9±4.1	20.8±5.1	16.4±5.2	17.6±6.3
EIN group	12.2±3.2	14.4±4.6	20.7±5.5	24.2±6.3[a]	25.3±6.5[a]

[a]$P<0.05$ *vs* PN group.

Pancreatic secretion and its component analysis

The changes of pancreatic juice, amylase, pancreatolipase, HCO_3^-, Cl^-, Na^+ and K^+ did not reach statistical difference between two groups (Table 5).

Table 5 Changes of pancreatic juice, amylase, pancreatolipase, HCO_3^-, Cl^-, Na^+ and K^+

Component	PN group	EIN group
Pancreatic juice (ml)	6±1	9±3
Amylase (U / L)	6 717±540	7 121±670
pancreatolipase (U / L)	629±78	661±101
HCO_3^- (mmol / L)	17±3	22±4
Cl^-(mmol / L)	117±11	126±9
Na^+(mmol / L)	133±21	147±17
K^+(mmol / L)	4.1±1.0	5.7±1.4

DISCUSSION

Autodigestion of the pancreas is the main mechanism of acute pancreatitis. The conception of pancreatic rest stems from the belief that stimulation of pancreatic exocrine function in patients with acute pancreatitis releases large quantities of proteolytic enzymes that result in autodigestion of the inflammatory pancreas and peripancreatic tissues, causing a deterioration in the patient' s condition. The presence of food in the stomach and duodenum elicits gastropancreatic and duodenopancreatic reflexs that result in stimulation of pancreatic exocrine secretions. Therefore, traditionally, enteral nutrition could be adopted after parenteral nutrition support for over 2-3 weeks. That means to keep the pancreas in rest and rehabilitation for a long time. However, these effects are not so pronounced when nutrients are delivered directly into the jejunum[11-18].

Heidenhain in 1 875 first demonstrated the effect of vagal and entero- hormone stimulation on pancreatic secretion, in which hormones played a more important role than vagal stimulation. There were three classic phases, namely cephalic, gastric and intestinal phases of digestion that describe the response of the pancreas to a meal. The hormones served a major function in mediating pancreatic exocrine secretion[16,19]. Normally, during the cephalic and gastric phases, oral nutrients can stimulate the release of gastric acid, duodenum juice and pancreatic enzyme, and activation of proteins and peptide in the nutrients commences after the peptidase enters the duodenum, where mucosal enterokinase cleaves trypsinogen to trypsin, leaving trypsin to further activate the other peptidases, and then stimulates entero-hormones secretion such as cholecystokinin (CCK), secretin (SEC) and gastrin to increase pancreatic secretion. It is known that CCK and SEC are synthesized in the mucosal I and S cells of the crypts of Liberkuhn in the proximal small intestine and released in the presence of luminal acid and bile. The gastic G cell product, gastrin, which serves a major function to promote gastric acid release also serves as a weak stimulator of pancreatic enzyme secretion. CCK is one of the most important entro-hormones known to stimulate pancreatic enzyme secretion. Some authors also found that avoidance of cephalic, gastric and duodenual stimuli by jejunal tube feeding did not result in pancreatic stimulation. They concluded that bypassing the stomach, and minimizing acid secretion, played an important role in keeping the pancreas at rest[16,21,22].

Some authors[20-25] described an experience of early enteral nutrition in severe acute pancreatitis using nasoenteral feeding. No patients developed relapse, hypertri-glyceridaemia or abnormalities of liver function, indicating that jejunal feeding can be used safely in acute pancreatitis without reactivation of the inflammatory process[26-32]. Our experimental results showed that the changes of serum glucose, calcium, and amylase did not reach statistical difference between two groups. The serum lysosomal enzymes is believed to be the gold standard for reflecting the extent of pancreatic tissue necrosis and inflammation and more attention has been paid to them in international medicine. Once the pancreatic tissue necrosis stoped, the volume of systemic lysosomal enzymes discharging from pancreatitis tissue would be attenuated. Our results indicated that serum lysosomal enzymes was markedly increased after acute pancreatitis was induced, but did not reach statistical difference between two groups. In addition, the ^{125}I-BSA index of pancreas/muscle and pancreas/blood reflected the permeability of the pancreas microcirculation. If this ^{125}I-BSA index decreased, microvessal permeability would be improved. Once the ^{125}I- BSA index in pancreatic tissue increased, the microvessal permeability elevated and deteriorated pancreatitis. Our study showed that administration of EIN did not increase the content of serum lysosomal enzymes, and deteriorate the course of acute pancreatitis. As to the PPS in different parts of the pancreas, there was no difference between EIN group and PN group. Kalfarentzos *et al*[17], reported that EIN was well tolerated following acute pancreatitis, and was of comparable efficacy to PN. In fact, EIN did not deteriorate pancreatitic pathology, and might be safely adopted in dogs with acute pancreatitis[26-32].

Normally, it is known that secretion of CCK, SEC and gastrin is mainly located in the duodenum and jejunum. The number of CCK-produced cells is 11-30 per square millimeter both in duodenum and in proximal jejunum, and their amount is 52.5±8 pmol/g, and 26±5 pmol/g respectively; The number of pancreatic SEC-produced cells is >31 in duodenum, 1-10 in proximal jejunum per square millimeter respectively, and their amount is 73±7 pmol/g and 32±4 pmol/g. The number of gastrin CCK-produced cells is >31 in gastric antrum, 11-30 in duodenum and 1-10 in proximal jejunum per square millimeter respectively, and their amount is 2 342±14 pmol/g, 1 397±192 pmol/g, 190±24 pmol/g, respectively. Therefore, the secretory locations of entero-hormones are mostly in gastric antrum, duodenum and proximal jejunum, and less in the distal jejunum. Theoretically, if the nutrients were infused from proximal jejunum to distal jejunum, it would decrease stimulatory activation of pancreatic secretion to a minimum degree[16].

To further study the possibility of EIN stimulated entero-hormones and pancreatic juice release, we observed the effects of different nutrition support methods on the CCK, SEC, gastrin and pancreatic secretion and their components. Our results suggested that the serum CCK increased at 60 min after nutrient was infused in EIN group as compared with PN group.

It was interesting that SEC was elevated after nutrition infusion in both groups, but it was only higher at 60 min in EIN group than in PN group. The serum gastrin was gradually increased in EIN group at 120 and 180 min as compared with PN group. Based on pancreatic juice and its component analysis, our results suggested that the amount of pancreatic juice was higher in EIN than in PN group. But the changes of the amylase, pancreatolipase and electrolytes were not significant. The study suggested that EIN indeed stimulated entero- hormones secretion at some degrees, but did not increase enzyme-proetin and pancreatic juice secretion. The reason was not clear, maybe due to the fact that the pancreatic acinar cells swelling, hemorrhage and necrosis decreased the physiological efficiency of entero-hormones by altering the membrane receptor number and activity.

In recent years, effect of human EIN or oral feeding on the natural course and entero-hormones secretion was seldom reporte. It was well tolerable, feasible and desirable as TPN in the management of acute pancreatitis, but it failed to reveal any detrimental effect on the clinical pathologic features of AP, and increase pancreatic secretion. Therefore, EIN can contribute to the study of pancreatic natural course, and may play an important role in keeping the pancreas at rest, bypassing the stomach, and minimizing acid secretion.

REFERENCES

1 **Kalfarentzos FE**, Karavias DD, Karatzas TM, Alevizatos BA, Androulakis JA. Total parenteral nutrition in severe acute pancreatitis. *J Am Coll Nutr* 1991; **10**: 156-162

2 **Buchman AL**, Moukarzel AA, Bhutta S, Belle M, Ament ME, Eckhert CD, Hollander D, Gornbein J, Kopple JD, Vijayaroghavan SR. Parenteral nutrition is associated with intestinal morphologic and functional changes in humans. *JPEN* 1995; **19**: 453-460

3 **Qin HL**, Su ZD, Hu LG, Ding ZX, Lin QT. Effect of early intrajejunal nutrition on pancreatic pathological features and gut barrier function in dogs with acute pancreatitis. *Clin Nutr* 2002; **21**: 469-473

4 **Mitchell RM**, Byrne MF, Baillie J. Pancreatitis. *Lancet* 2003; **26**: 1447-1455

5 **Ammori BJ**. Gut barrier dysfunction in patients with acute pancreatitis. *J Hepatobiliary Pancreat Surg* 2002; **9**: 411-412

6 **McClave SA**, Greene LM, Snider HL, Makk LJ, Cheadle WG, Owens NA, Dukes LG, Goldsmith LJ. Comparison of the safety of early enteral vs parenteral nutrition in mild acute pancreatitis. *JPEN* 1997; **21**: 14-20

7 **Vison N**, Hecketsweiler P, Butel J, Bernier JJ. Effect of continuous jejunal perfusion of elemental and complex nutritional solutions on pancreatic enzyme secretion in human subjects. *Gut* 1978; **19**: 194-198

8 **Maillet P**. Enteral nutrition by alimentation jejunostomy in 11 cases of severe acute pancreatitis. In controversies in Acute pancreatitis. *Hollender LF(ed.). Beilin* 1982: P293

9 **Lobo DN**, Memon MA, Allison SP, Rowlands BJ. Evolution of nutritional support in acute pancreatitis. *Br J Surg* 2000; **87**: 695-707

10 **Windsor AC**, Kanwar S, Li AG, Barnes E, Guthrie JA, Spark JI, Welsh F, Guillou PJ, Reynolds JV. Compared with parenteral nutrition,enteral feeding attenuates the acute phase response and improves disease severity in acute pancreatitis. *Gut* 1998; **42**: 431-435

11 **Abou-Assi S**, Craig K, O'Keefe SJ. Hypocaloric jejunal feeding is better than total parenteral nutrition in acute pancreatitis: results of a randomized comparative study. *Am J Gastroenterol* 2002; **97**: 2255-2262

12 **Olah A**, Pardavi G, Belagyi T, Nagy A, Issekutz A, Mohamed GE. Early nasojejunal feeding in acute pancreatitis is associated with a lower complication rate. *Nutrition* 2002; **18**: 259-262

13 **Chen QP**. Enteral nutrition and acute pancreatitis. *WJG* 2001; **7**: 185-192

14 **Hallay J**, Kovacs G, Szatmari K, Szatmari K, Bako A, Szentkereszty Z, Lakos G, Sipka S, Sapy P. Early jejunal nutrition and changes in the immunological parameters of patients with acute pancreatitis. *Hepatogastroenterology* 2001; **48**: 1488-1492

15 **Eatock FC**, Brombacher GD, Steven A, Imrie CW, McKay CJ, Carter R. Nasogastric feeding in severe acute pancreatitis may be practical and safe. *Int J Pancreatol* 2000; **28**: 23-29

16 **Qin HL**, Su ZD, Hu LG, Ding ZX, Lin QT. Effect of early intrajejunal nutrition on secretion of entero-hormone and its efficiency in acute pancreatitic dogs. *Chang Wai Chang Nei Ying Yang* 2002; **9**: 193-195

17 **Kalfarentzos F**, Kehagias J, Mead N, Kokkinis K, Gogos CA. Enteral nutrition is superior to parenteral nutrition in severe acute pancreatitis:results of a randomized prospective trial. *Br J Surg* 1997; **84**: 1665-1669

18 **Qin HL**, Su ZD, Ding ZX, Lin QT. Effects of enteral nutrition on uptake of amino acid and enzyme-protein synthesis of pancreatic acinar cell in acute pancreatic dogs. *Zhonghua Waike Zazhi* 2003; **41**: 146-149

19 **Takacs T**, Hajnal F, Nemeth J, Lonovics J, Pap A. Stimulated gastrointestinal hormone release and gallbladder contraction during continuous jejunal feeding in patients with pancreatic pseudocyst is inhibited by octreotide. *Int J Pancreatol* 2000; **28**: 215-220

20 **MacFie J**. Enteral versus parenteral nutrition. *Br J Surg* 2000; **87**: 1121-1122

21 **Neoptolemos JP**, Raraty M, Finch M, Sutton R. Acute pancreatitis: the subatantial human and financial costs. *Gut* 1998; **42**: 886-891

22 **Al-Omran M**, Groof A, Wilke D. Enteral versus parenteral nutrition for acute pancreatitis. *Cochrane Database Syst Rev* 2003; **3**: CD002837

23 **Austrums E**, Pupelis G, Snippe K. Postoperative enteral stimulation by gut feeding improve outcomes in severe acute pancreatitis. *Nutrition* 2003; **19**: 487-491

24 **Powell JJ**, Murchison JT, Fearson KC, Ross JA, Siriwardena AK. Randomized controlled trial of the effect of early enteral nutrition on markers of the inflammatory response in predicted severe acute pancreatitis. *Br J Surg* 2000; **87**: 1375-1381

25 **McGregor CS**, Marshall JC. Enteral feeding in acute pancreatitis: just do it. *Curr Opin Crit Care* 2001; **7**: 89-91

26 **Sanabria A**. Randomized controlled trial of the effect of early enteral nutrition on markers of the inflammatory response in prevent severe acute pancreatitis. *Br J Surg* 2001; **88**: 728

27 **Eckerwall G**, Andersson R. Early enteral nutrition in severe acute pancreatitis:a providing nutrients, gut barrier protection, immunomodul or all of them? *Scand J Gastroenterol* 2001; **36**: 449-458

28 **Pupelis G**, Austrums E, Jansone A, Sprucs R, Wehbi H. Randomised trial of safety and efficacy of postoperative enteral feeding in patients with severe pancreatitis: preliminary report. *Eur J Surg* 2000; **166**: 383-387

29 **Sahin M**, Ozer S, Vatansev C, Akoz M, Vatansev H, Aksoy F, Dilsiz A, Yilmaz O, Karademir M, Aktan M. The impact of oral feeding on the severity of acute pancreatitis. *Am J Surg* 1999; **178**: 394-398

30 **Hamvas J**, Schwab R, Pap A. Jejunal feeding in necrotising acute pancreatitis- a restrospective study. *Acta Chir Hung* 1999; **38**: 177-185

31 **Tesinsky P**. Nutritional care of pancreatitis and its complication. *Curr Opin Clin Nutr Metab Care* 1999; **2**: 395-398

32 **Duerksen DR**, Bector S, Yaffe C, Parry DM. Does jejunal feeding with a polymeric immune-enhancing for increase pancreatic exocrine output as compared with TPN: case report. *Nutrition* 2000; **16**: 47-49

Edited by Zhang JZ and Wang XL

P.O.Box 2345, Beijing 100023,China
Fax: +86-10-85381893
E-mail: wjg@wjgnet.com www.wjgnet.com

World J Gastroenterol 2003;9(10):2274-2277
World Journal of Gastroenterology
 ISSN 1007-9327

• BASIC RESEARCH •

Protective effects of transplanted and mobilized bone marrow stem cells on mice with severe acute pancreatitis

Hui-Fei Cui, Zeng-Liang Bai

Hui-Fei Cui, Biochemical and Biotechnological Institute of Materia Medica, Pharmaceutical College of Shandong University, Jinan 250012, Shandong Province, China
Zeng-Liang Bai, College of Life Sciences, Shandong University, Jinan 250100, Shandong Province, China
Correspondence to: Hui-Fei Cui, Associate Professor, Biochemical and Biotechnological Institute of Materia Medica, Pharmaceutical College of Shandong University, Jinan 250012, Shandong Province, China. cuihuifei@sdu.edu.cn
Telephone: +86-531-8380288 **Fax:** +86-531-8380288
Received: 2003-09-01 **Accepted:** 2003-09-15

Abstract

AIM: To evaluate the protective effects of transplanted and mobilized bone marrow stem cells (BMSCs) on mice with severe acute pancreatitis (SAP) and to probe into their possible mechanisms.

METHODS: A mouse model of SAP induced by intraperitoneal injections of L-arginine was employed in the present study. Two hundred female Balb/c mice weighing 18-22 g were randomly assigned into 4 groups. Group A was the stem cell mobilized group treated by injection of granulocyte-colony stimulating factor (G-CSF) into mice for 4 days at a dose of 40 μg· kg^{-1}· d^{-1} before induction of SAP. Group B was the group of BMSCs transplantation, in which the mice were given the isolated BMSCs via the tail vein 4 days prior to induction of SAP. Group C served as the model control and only SAP was induced. The mice without induction of SAP in group D acted as the normal control. At the time of animal sacrifice at 24, 48 and 72 h after induction of SAP, blood samples were obtained and prepared to detect serum amylase, while the abdominal viscera were examined both grossly and microscopically for the observation of pathological changes.

RESULTS: The mortality of mice in the model control, groups A and B was 34 %, 8 % and 10 % respectively within 72 h after induction of SAP. The serum level of amylase in the model control was significantly increased at all time points after induction of SAP as compared with that of the normal control (P<0.05-0.01). When the mice were pretreated with BMSCs' transplantation or G-CSF injection, their serum level of amylase was significantly reduced at 48 h and 72 h after induction of SAP in comparison with that of the model control (P<0.05-0.01). In accordance with these observations, both gross and microscopic examinations revealed that the pathological changes of SAP in mice pretreated with BMSCs transplantation or G-CSF injection were considerably attenuated as compared with those in the model control at all observed time points.

CONCLUSION: Both transplanted allogenic and mobilized autologous BMSCs can protect mouse pancreas from severe damage in the process of SAP.

Cui HF, Bai ZL. Protective effects of transplanted and mobilized bone marrow stem cells on mice with severe acute pancreatitis. *World J Gastroenterol* 2003; 9(10): 2274-2277
http://www.wjgnet.com/1007-9327/9/2274.asp

INTRODUCTION

Severe acute pancreatitis (SAP) is a life-threatening disease with a mortality rate of 20 to 30 percent[1,2]. Despite recent improvements in our understanding of the disease process and the development of a range of supportive measures, today's treatment approaches for SAP are still less than ideal. It has been demonstrated recently that multipotent somatic stem cells in adult bone marrow can exhibit tremendous functional plasticity[3-9] and reprogram in a new environmental tissue niche to give rise to cell lineages specific for the new organ site. Stem cells from bone marrow, autologous or allogenic, have been used to treat myocardial infarction[10-13], hepatic disease[14-20], nervous system dysfunction[21-25] and severe autoimmune diseases[26, 27]. However, there have been fewer reports concerned about the treatment of SAP with BMSCs as yet. Since the two critical determinants, tissue damage and higher level of pluripotent cells, seem to be the prerequisite for the transdifferentiation of transplanted BMSCs and G-CSF has been proved to have a great potency in mobilizing both hematopoietic stem cell (HSC) and mesenchymal stem cells (MSCs) of bone marrow, we hypothesized that the transplanted allogenic BMSCs, as well as the autologous BMSCs mobilized by G-CSF would exert a protective role in the treatment of SAP. The present study is therefore designed to verify our hypothesis in attempt to develop new protocols for the improvement of SAP therapy.

MATERIALS AND METHODS

Animals and experimental protocol

Two hundred female Balb/c mice weighing 18-22 g were randomly assigned into 4 groups according to different treatment protocols with 50 mice each. Group A was the stem cell mobilized group treated by injection of sc G-CSF into mice for 4 days at a dose of 40 μg· kg^{-1}· d^{-1} before induction of SAP. Group B was the group of BMSCs transplantation, in which the mice were given BMSCs isolated from male mice bone marrow at a dose of 2×10^7 per mouse via tail vein 4 days prior to induction of SAP. Group C served as the model control and only SAP was induced. The mice in group D acted as the normal control treated only with an equal amount of saline as sc G-CSF in group A and without induction of SAP.

Mouse model of SAP was prepared in all animals except that in group D according to the scheme described elsewhere[28]. Briefly, the mice were fasted overnight but allowed to free access to water. The SAP inducer, a 20 g/L of L-arginine (Sigma) solution, was freshly prepared with saline just prior to use. In induction of SAP, the animals were injected intraperitoneally L-arginine solution at a dose of 2 g· kg^{-1} twice at an interval of 1 h.

The mice in groups A, B and C were sacrificed at 24, 48 and 72 h after induction of SAP. In the meanwhile, the mice in group D were killed at the corresponding time points. At the time of animal sacrifice, blood samples were obtained and prepared to

detect serum amylase, while the abdominal viscera were examined both grossly and microscopically for the observation of pathological changes.

Transplantation of primary BMSCs

Primary BMSCs to be transplanted to group B animals were isolated from donor male mice. The whole bone marrow cells were harvested by rinsing the thighbone and shankbone' s medullary cavities with cold DMEM (Gibco, Grand Island, NY) and then fractionated by density gradient centrifugation with lymphocytic separating medium. Mononuclear component, the constituent rich in BMSCs, was obtained from the interface after centrifugation at 2 500 r/min for 30 min. After repeatedly washed in cool D-Hanks solution, BMSCs were resuspended and adjusted to a cell density of 10^8/mL with the same solution. The transplantation of primary BMSCs into group B animals was performed via the tail vein injection at a dose of 0.2 ml cell suspension per mouse 4 days prior to induction of SAP.

The transplanted stem cells were identified at the end of the experiment (72 h post SAP induction) by examining the existence of Y chromosome Sry region in recipient female mice with a PCR scheme. Briefly, the female recipients were killed by cervical dislocation and DNA samples were extracted respectively from the pancreas, bone marrow, liver and spleen. The sequence of the sense primer was 5' -ATTTATGGTG TGGTCCCG-3' and that of the antisense primer was 5' -GCTGTAAAATGCCACTCC-3' . PCR consisted of an initial denaturation step at 96 ℃ for 6 min, followed by 35 cycles at 94 ℃ for 1 min, at 52 ℃ for 1 min and at 72 ℃ for 1 min each, and a final extension at 72 ℃ for 10 min. The resulting products were analyzed by electrophoresis on a 2 % agarose gel and stained with ethidium bromide. The expected size of amplified DNA fragment was 239 base pair.

Statistical analysis

All the data were expressed as $\bar{x}\pm s$. Comparisons between the means of different groups were performed using analysis of variance followed by Student' s *t*-test. $P<0.05$ was selected to be the level of statistical significance.

RESULTS

Animal mortality

The mortality of mice in the model control was 34 % within 72 h after induction of SAP, which was considerably decreased in the mices pretreated with BMSCs' transplantation or sc G-CSF injection. The mortality of mice in groups A and B was 8 % and 10 % respectively.

Table 1 Changes of serum amylase activity after SAP induction ($\bar{x}\pm s$, n=10)

Group	Serum amylase activity (μkat/L)		
	24 h	48 h	72 h
A	25.3±4.8	40.8±7.4[b,c]	27.6±6.2[a,c]
B	25.9±4.9	40.7±6.7[b,c]	27.3±6.3[a,c]
C	46.1±12.8[a]	78.4±15.8[b]	50.2±13.3[a]
D	17.2±6.2	16.9±2.7	19.0±3.4

[a]$P<0.05$, [b]$P<0.01$ *vs* group D; [c]$P<0.05$ *vs* group C.

Alterations of serum amylase

The serum level of amylase was significantly increased in the mice of model control at all time points after induction of SAP as compared with that of the normal control ($P<0.05$-0.01). When the mice were pretreated with BMSCs transplantation or G-CSF injection, their serum level of amylase was significantly reduced at 48 h and 72 h after induction of SAP as compared with that of the model control ($P<0.05$-0.01), although the amylase value was still significantly higher than that of the normal control ($P<0.05$, Table 1).

Pathological changes

Grossly, a typical appearance of SAP changes was observed in animals of the model control. These pathological changes were progressively aggravated after SAP induction and manifested in a time- dependent manner. Twenty-four hours after L-arginine injection, the pancreas was sprinkled with hemorrhagic spots and focal necrosis with a dark-color appearance. At the same time, a little bloody ascites was noted in the abdominal cavity. At 48 h, different sizes of more hemorrhagic and necrotic focus appeared on the pancreatic surface with the increment of bloody ascites. Seventy-two hours after induction SAP, the pancreatic necrosis and blood ascites were even more prominent with saponification of fatty tissue around. Massive necrosis of multiple organs such as the intestine, lungs and kidneys was found in the mice died from SAP (Figure 1).

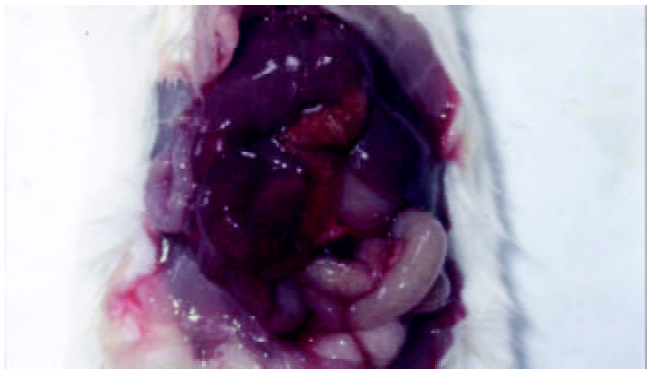

Figure 1 Gross appearance of abdominal cavity in SAP model control.

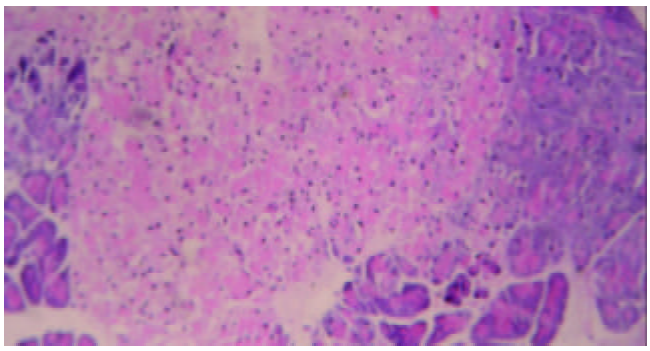

Figure 2 Pathological changes of pancreas at 24 h post SAP induction in mice of model control (HE, ×200).

Attenuated pathological lesions were noted both in group A and in group B mice, which were manifested mainly as minor pancreatic edema and congestion with less bloody or non-bloody ascites generated, no fat saponification and necrosis were observed.

In the microscopic examination, various degrees of pancreatic impairments were found in all mice injected with L-arginine. In mice of the model control, pancreatic congestion, interstitial edema, disorganized lobular architecture, as well as the focal hemorrhage and necrosis appeared at 24 h after induction of SAP, along with an obvious mesenchymal infiltration by inflammatory cells (Figure 2). The changes above were even more aggravated at 48 h and large areas of

coagulation necrosis occurred in the pancreatic parenchyma acompanied by the destroyed lobular architecture and massive inflammatory cell infiltration at the time of 72 h after induction of SAP (Figure 3).

In contrast, these pathological changes were obviously attenuated in mice pretreated with BMSCs' transplantation or G-CSF injection (Figures 4, 5). Most lobular architecture in these animals remained recognizable with alleviated hemorrhage, necrosis and infiltration of inflammatory cells, whereas some focal necrosis remained in the periphery of pancreas.

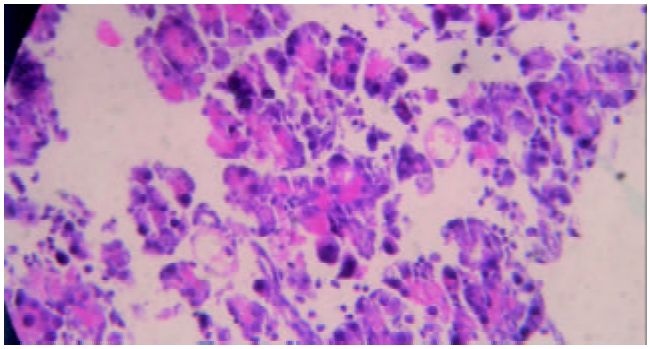

Figure 3 Pathological changes of pancreas at 72 h post SAP induction in mice of model control (HE, ×200).

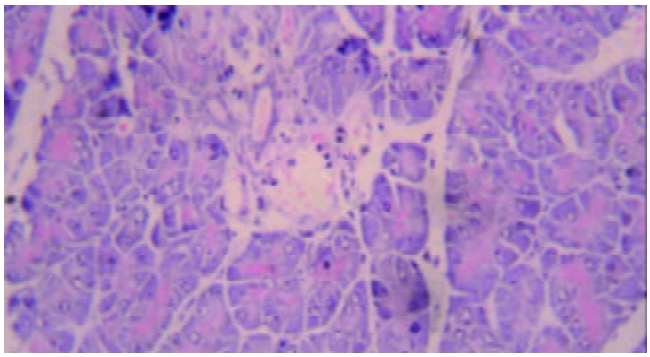

Figure 4 Microscopic changes of pancreas at 72 h after induction of SAP in mice pretreated with G-CSF (HE, ×200).

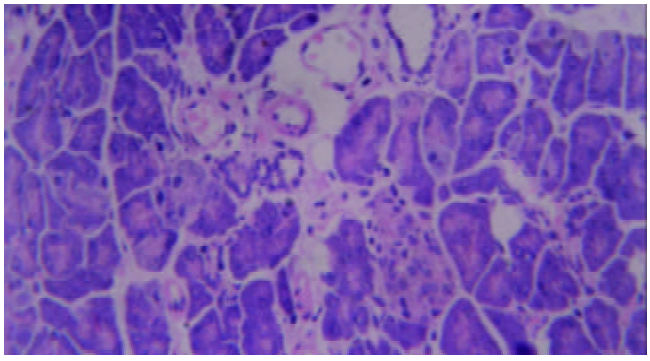

Figure 5 Microscopic changes of pancreas at 72 h post SAP induction in mice pretreated with BMSCs transplantation (HE, ×200).

Identification of transplanted BMSC

All sampled tissues from the pancreas, liver, spleen and bone marrow of the female recipients were demonstrated harboring a DNA fragment, 239 bp in length, of Y chromosome Sry region of donor mice, indicating that the engrafted BMSCs could migrate and survive in the impaired pancreas of SAP animals (Figure 6).

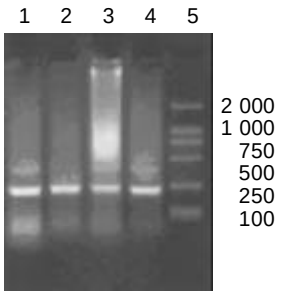

Figure 6 PCR products of Y chromosome Sry region gene existed in some organs of recipient female mice after male BMSCs transplantation demonstrated by agarose gel electrophoresis. Lane 1: pancreas, Lane 2: liver, Lane 3: liver, Lane 4: spleen, Lane 5: DNA marker.

DISCUSSION

The management of SAP has changed significantly over the past 20 years. In contrast to surgical intervention, there is now a strong tendency towards a more conservative therapy. The established treatment of SAP included aggressive fluid resuscitation, oxygen supplementation, prophylactic use of antibiotics, enteral feeding and intensive care support of any failing organ or system[29]. Nevertheless, the fact that these therapeutic modalities did not aim directly at the etiological factors made the treatment lack of specificity. Therefore, it remains a great challenge for the improvement of SAP therapy in the daily clinical practice. Recently, it has been shown that somatic stem cells were capable of regenerating injured tissue and improving the functions of involved organs[6,30-32], which might be used also as a new potential therapeutic modality for SAP treatment.

Bone marrow is an ideal source of stem cells. The multidirectional differentiation potential of BMSCs has been proved to be more than what we expected[32]. It has been reported that BMSCs could transdifferentiate into a variety of cell types derived from three embryonic layers such as endoblast-derived hepatic cells and lung alveolar epithelial cells, mesoblast-derived kidney and muscle cells, and ectoblast-derived neurons and epidermic cells. Furthermore, some authors have shown that bone marrow might serve as an extra-pancreatic hideout for the pancreatic stem cells[33,34] that contributed to the adult islet neogenesis. Transplantation with bone marrow cells has been used in several animal experiments for the treatment of types I and II diabetes mellitus, which has been achieved some promising results. All these facts indicate that BMSCs harbor a biological basis which can be used as an excellent candidate for SAP therapy.

In the present study, we observed the protective effects of BMSCs transplantation in a mouse model of SAP. It showed that a considerably reduced mortality and serum amylase activity, as well as obviously attenuated pancreatic pathological changes in the animals treated by transplantation of BMSCs or by injection of G-CSF, which presented a striking contrast to those of the model control. Regarding the mechanisms involved, these protective effects might be mediated by the rehabilitative action of BMSCs, which was partially supported by the existence of transplanted stem cells in the assaulted pancreas with a PCR scheme. The transplanted BMSCs might be ' tweaked' from the peripheral blood circulation to the injured tissues whenever SAP took place, where they exerted the function of pancreatic stem cells to regenerate the destroyed cells. As a result, gradual necrosis of impaired pancreas was effectively prevented. On the other hand, critical ill conditions such as SAP can usually caused serious injuries to multiple organs or systems, leading to a poor capability for the tissue repair. At

this time, transplanted stem cells in peripheral circulation were no doubt helpful for regeneration of injured tissues[38]. However, the direct evidence of BMSCs transdifferentiating to pancreatic cells should be further demonstrated by *in situ* hybridization and immuneohistochemistry.

An important phenomenon that deserved to note in the present study was the protective effects of autologous BMSCs mobilized by G-CSF injection in this model of SAP, whose efficiency was similar to that of alligeneic BMSCs transplantation. It implies that BMSCs, no matter autologous or allogenic, could get to and reside in the impaired tissue via blood circulation to repair the dysfunctional organs. Recently, Jensen and his associates[31] have shown that a normal physiological process of tissue regeneration and repair could be achieved by *in situ* mobilization of autologous stem cells from the bone marrow. Through the stimulation of normal stem cell migration, therapeutic benefits could be achieved with less invasive regimens than the removal and re-injection of stem cells. In this way, some obstacles in the allograft such as rejection and shortness of tissue donor supply would be also overcome easily. However, there were fewer BMSCs with weaker expansion and differentiation capacity in the peripheral circulation. Once mobilized by G-CSF, BMSCs in the peripheral circulation were estimated to be increased about 250 times higher than the baseline, along with an enhanced expansion and differentiation capacity. Thereby, autologous BMSCs transplantation could be performed safely and conveniently. Further research should be focused on the more efficient mobilization of autologous BMSCs to attract them to the injured region for tissue repair. This cell-restoring therapy may serve as a new modality in the future management of SAP and other serious diseases.

REFERENCES

1 **Ponette J,** Wilmer A. Update on the management of acute severe pancreatitis. *Acta Clin Belg* 2001; **56:** 135-145
2 **Bank S,** Singh P, Pooran N, Stark B. Evaluation of factors that have reduced mortality from acute pancreatitis over the past 20 years. *J Clin Gastroenterol* 2002; **35:** 50-60
3 **Anderson DJ**, Gage FH, Weissman IL. Can stem cells cross lineage boundaries? *Nat Med* 2001; **7**: 393-395
4 **Tao H,** Ma DD. Evidence for transdifferentiation of human bone marrow-derived stem cells: recent progress and controversies. *Pathology* 2003; **35:** 6-13
5 **Goodell MA.** Stem-cell "plasticity": befuddled by the muddle. *Curr Opin Hematol* 2003; **10:** 208-213
6 **Prockop DJ.** Further proof of the plasticity of adult stem cells and their role in tissue repair. *J Cell Biol* 2003; **160:** 807-809
7 **Zubair AC**, Silberstein L, Ritz J. Adult hematopoietic stem cell plasticity. *Transfusion* 2002; **42:** 1096-1101
8 **Avots A,** Harder F, Schmittwolf C, Petrovic S, Muller AM. Plasticity of hematopoietic stem cells and cellular memory. *Immunol Rev* 2002; **187:** 9-21
9 **Forbes SJ,** Vig P, Poulsom R, Wright NA, Alison MR. Adult stem cell plasticity: new pathways of tissue regeneration become visible. *Clin Sci* 2002; **103:** 355-369
10 **Jackson KA,** Majka SM, Wang H, Pocius J, Hartley CJ, Majesky MW, Entman ML, Michael LH, Hirschi KK, Goodell MA. Regeneration of ischemic cardiac muscle and vascular endothelium by adult stem cells. *J Clin Invest* 2001; **107**: 1395-1402
11 **Orlic D**, Kajstura J, Chimenti S, Jakoniuk I, Anderson SM, Li B, Pickel J, McKay R, Nadal-Ginard B, Bodine DM, Leri A, Anversa P. Bone marrow cells regenerate infracted myocardium. *Nature* 2001; **410**: 701-705
12 **Strauer BE**, Brehm M, Zeus T, Kostering M, Hernandez A, Sorg RV, Kogler G, Wernet P. Repair of infracted myocardium by auotologous intracoronary mononuclear bone marrow cells transplantation in humans. *Circulation* 2002; **106**: 1913-1918
13 **Kocher AA**, Schuster MD, Szabolcs MJ, Takuma S, Burkhoff D, Wang J, Homma S, Edwards NM, Itescu S. Neovascularization of ischemic myocardium by human bone-marrow-derived angioblast prevents cardiomyocyte apoptosis, reduces remodeling and improves cardiac function. *Nat Med* 2001; **7**: 430-436
14 **Lagasse E.** Purified hematopoietic stem cells can differentiate to hepatocytes *in vivo*. *Nature Med* 2000; **6**: 1229-1234
15 **Theise ND,** Badve S, Saxena R, Henegariu O, Sell S, Crawford JM, Krause DS. Derivation of hepatocyte from bone marrow cells in mice after radiation-induced myeloablation. *Hepatology* 2000; **31**: 235-240
16 **Theise ND**. Liver from bone marrow in human. *Hepatology* 2000; **32**: 11-16
17 **Okumoto K,** Saito T, Hattori E, Ito JI, Adachi T, Takeda T, Sugahara K, Watanabe H, Saito K, Togashi H, Kawata S. Differentiation of bone marrow cells into cells that express liver-specific genes *in vitro*: implication of the Notch signals in differentiation. *Biochem Biophys Res Commun* 2003; **304:** 691-695
18 **Petersen BE**, Bowen WC, Patrene KD, Mars WM, Sulivan AK, Murase N, Boggs SS, Greenberger JS, Goff JP. Bone marrow as a potential source of hepatic oval cells. *Science* 1999; **284:** 1168-1170
19 **Austin TW,** Lagasse E. Hepatic regeneration from hematopoietic stem cells. *Mech Dev* 2003; **120:** 131-135
20 **Gao ZH,** McAlister V, Williams G. Repopulation of liver endothelium by bone marrow-derived cells. *Lancet* 2001; **357:** 932-933
21 **Woodbury D**, Schwarz EJ, Prockop DJ, Black IB. Adult rat and human bone marrow stromal cells differentiate into neurons. *J Neurosci Res* 2000; **61**: 364-370
22 **Prockop DJ,** Azizi SA, Colter D, Digruolamo C, Kopen G, Phinney DG. Potential use of stem cells from bone marrow to repair the extracellular matrix and the central nervous system. *Biochem Soc Trans* 2000; **28**: 341-345
23 **Kopen G**, Prockop D, Phinney D. Marrow stromal cells migrate throughout forebrain and cerebellum, and they differentiate into astrocytes after injection into neonatal mouse brains. *Proc Natl Acad Sci U S A* 1999; **96:** 10711-10716
24 **Brazelton TR,** Rossi FM, Keshet GI, Blau HM. From marrow to brain: expression of neuronal phenotypes in adult mice. *Science* 2000; **290:** 1775-1779
25 **Hess DC,** Hill WD, Martin-Studdard A, Carroll J, Brailer J, Carothers J. Bone marrow as a source of endothelial cells and NeuN-expressing cells After stroke. *Stroke* 2002; **33**: 1362-1368
26 **Ikehara S.** Bone marrow transplantation: a new strategy for intractable diseases. *Drugs Today* 2002; **38**: 103-111
27 **Marmont AM**. Stem cell transplantation for severe autoimmune diseases: progress and problems. *Haematologica* 1998; **83:** 733-743
28 **Czako L**, Takacs T, Varga IS, Hai DQ, Tiszlavicz L, Hegyi P, Mandi Y, Matkovics B, Lonovics J. The pathogenesis of L-arginine-induced acute necrotizing pancreatitis: inflammatory mediators and endogenous cholecystokinin. *J Physiol Paris* 2000; **94**: 43-50
29 **Zulewski H,** Abraham EJ, Gerlach MJ, Gerlach MJ, Daniel PB, Moritz W, Muller B, Vallejo M, Thomas MK, Habener JF. Multipotential nestin-positive stem cells isolated from adult pancreatic islets differentiate ex vivo into pancreatic endocrine, exocrine, and hepatic phenotypes. *Diabetes* 2001; **50:** 521-533
30 **Poulsom R,** Alison MR, Forbes SJ, Wright NA. Adult stem cell plasticity. *J Pathol* 2002; **197**: 441-456
31 **Jensen GS**, Drapeau C. The use of in situ bone marrow stem cells for the treatment of various degenerative diseases. *Med Hypotheses* 2002; **59:** 422-428
32 **Krause DS,** Theise ND, Collector ML, Henegariu O, Hwang S, Gardner R, Neutzel S, Sharkis SJ. Multi-organ, multi-lineage engraftment by a single bone marrow-derived stem cell. *Cell* 2001; **105:** 369-377
33 **Ianus A,** Holz GG, Theise ND, Hussain MA. *In vivo* derivation of glucose-competent pancreatic endocrine cells from bone marrow without evidence of cell fusion. *J Clin Invest* 2003; **111**: 843-850
34 **Lee VM,** Stoffel M. Bone marrow: an extra-pancreatic hideout for the elusive pancreatic stem cell? *J Clin Invest* 2003; **111**: 799-801

Edited by Wang XL

P.O.Box 2345, Beijing 100023,China
Fax: +86-10-85381893
E-mail: wjg@wjgnet.com www.wjgnet.com

World J Gastroenterol 2003;9(10):2278-2283
World Journal of Gastroenterology
 ISSN 1007-9327

• BASIC RESEARCH •

Biomechanical properties of ileum after systemic treatment with epithelial growth factor

Jian Yang, Jing-Bo Zhao, Yan-Jun Zeng, Hans Gregersen

Jian Yang, Yan-Jun Zeng, Biomedical Engineering Center, Beijing Polytechnic University, Beijing,100022, China
Jian Yang, Jing-Bo Zhao, Hans Gregersen, Center for Sensory-Motor Interaction, Aalborg University and Department of Medicine M and Department of Surgery A, Aalborg Hospital, Denmark
Supported by Karen Elise Jensens Foundation and the Danish Technical Research Council
Correspondence to: Hans Gregersen, M.D.Sci., Center for Sensory-Motor Interaction, Aalborg University, Fredrik Bajers Vej 7D-3, DK-9200 Aalborg, Denmark. hag@smi.auc.dk
Telephone: +45-96358843 **Fax:** +45-98133060
Received: 2002-11-26 **Accepted:** 2003-02-26

Abstract

AIM: Systemic treatment with epidermal growth factor (EGF) leads to growth of all parts of the small intestine in normal functioning rats. In this study, we investigated the effect of this growth process on morphometric and biomechanical parameters of ileum.

METHODS: Rats were treated with EGF (150 μg· $kg^{-1}day^{-1}$) or placebo via osmotic minipumps for 2, 4, 7, and 14 days. A segment of ileum was removed. The morphology at no-load state and zero-stress state was measured and passive biomechanical properties were assessed using a biaxial test machine (combined inflation and axial stretching).

RESULTS: The ileum weight increased after EGF administration. After 4 days' EGF treatment, the wall thickness was increased. Significantly smaller inner perimeters were seen in 4 day and 7 day EGF treatment groups. The opening angle and residual strain began to increase after 7 days' EGF treatment. Wall stiffness, evaluated from the stress-strain curves, showed a continuous decrease in circumferential direction during the first 7 days' EGF treatment. The longitudinal stiffness increased during the first 7 days. The stress-strain curves for both circumferential and longitudinal direction tended to shift back to normal 14 days after starting EGF administration.

CONCLUSION: EGF can cause significant changes both in the morphology and in the passive mechanical properties of the rat ileum.

Yang J, Zhao JB, Zeng YJ, Gregersen H. Biomechanical properties of ileum after systemic treatment with epithelial growth factor. *World J Gastroenterol* 2003; 9(10): 2278-2283
http://www.wjgnet.com/1007-9327/9/2278.asp

INTRODUCTION

Epidermal growth factor (EGF) is a peptide growth factor belonging to the EGF family[1]. Throughout the last decade, the pharmacological potential of systemic treatment of EGF has been explored[2]. In the gastrointestinal tract, EGF causes growth, inhibits gastric acid secretion, and leads to changes in electric potentials, enzyme activity and transport of amino acids[3-6]. Due to the pronounced effects on intestinal mucosa, the therapeutic potential of systemic treatment of EGF has been explored in animal experiments. For example it has been shown that EGF accelerates adaptive growth of the small intestine in different species[7-10].

Only few studies have addressed the effect of systemic treatment of EGF on the normal small intestine. In a series of studies, we have examined its effect on the morphological and biomechanical properties of the small intestine. Vinter-Jensen, *et al*[11] used impedance planimetry to examine the tension-strain properties of the intestinal wall after EGF treatment and found that the circumferential wall stiffness decreased during EGF treatment. However, their study had limitations because the circumferential strain was referenced to the no-load state rather than to the zero-stress state and the mechanical properties were only studied for the circumferential direction.

The present study was to investigate the time-dependent effect of systemic treatment with EGF on the passive biomechanical properties of the small intestine. Segments obtained from the ileum were tested in a biaxial mechanical test machine that renders possible simultaneous inflation and longitudinal stretch. Stress and strain were computed and material constants were derived for the circumferential and longitudinal directions.

MATERIALS AND METHODS

Animals and study design

Thirty-four female Wistar rats (bred at the Department of Pathology, Aalborg Hospital Denmark) weighing 190-200 grams were included in this study. The animals were housed individually in cages on white special span wall bedding (temperature 21 ℃, humidity 55±5 %, dark/light cycle 12-h shift). They were fed on a standard laboratory diet. The study complied with Danish regulations for care and use of laboratory animals.

Twenty-two rats were allocated to four groups and treated for 2 (n=6), 4 (n=6), 7 (n=6), and 14 (n=4) days with human recombinant EGF (150 ug/kg/day, Upstate Biotechnology, New York, USA) using osmotic minipumps (ALZET 2001; ALZA, Palo Alto, California, USA). Twelve rats served as controls (n=3 for each time period). The body weights of both the control and EGF treated rats were measured at the beginning and the end of the study.

Collection of specimens

After treatment, the rats were anaesthetized (pentobarbital 50 mg· kg^{-1} intraperitoneally) and a midline laparotomy was performed. The calcium antagonist papaverine (60 mg· kg^{-1}) was injected into the lower thoracic aorta through a cannula (22 G/25 mm) in order to abolish any contractile activity in the gastrointestinal tract. A 5.5-cm-long segment from ileum was excised after the attainment of muscle relaxation (no visible contraction was observed). The residual contents in the lumen were gently cleared using saline and the *in vitro* weight and length of the segment were measured. Then the segment was placed in cold Krebs solution containing 6 % dextran aerated

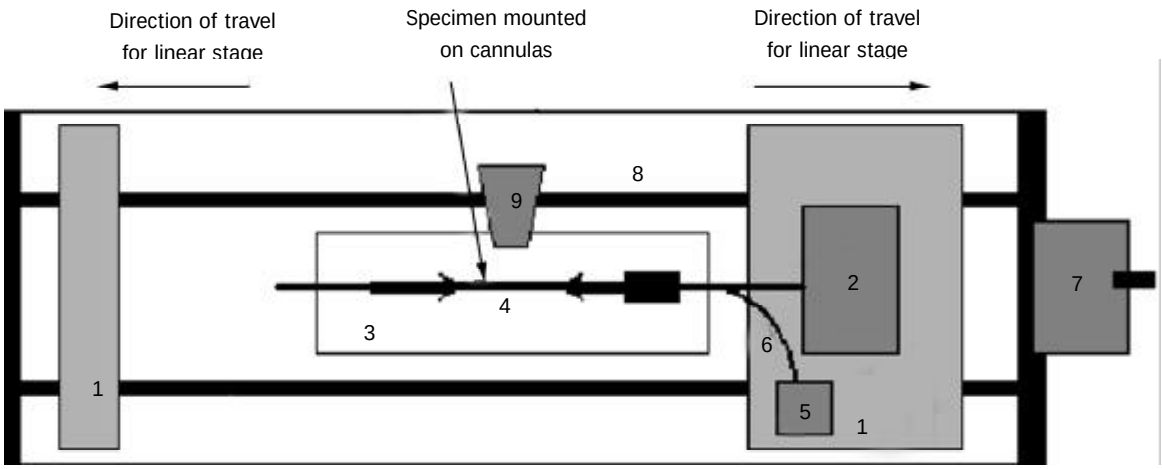

Figure 1 Legend, biaxial test machine setup. 1: Stage, 2: Force transducer, 3: Organ bath, 4: Specimen, 5: Pressure transducer, 6: Infusion channel, 7: Motor for linear stage, 8: Rails for linear stage, 9: Video camera.

with a gas mixture (95 % O_2 and 5 % CO_2, pH 7.4). Rings of 1-2 mm in length were cut at the edge of the tissue for no-load and zero-stress state measurements. The remaining part was used for the biaxial test.

Stress-strain experiment

The stress-strain test was conducted on the self-developed biaxial machine (Figure 1), which consists of the force and pressure transducers, the organ bath, motion stage and electronics. The specimen was bathed in the physiological Krebs solution. The two ends of the sample were tied with silk threads on the cannulas and the length between the threads was measured. The length *in vitro* was approximately 30 mm. Then the cannulas were mounted on the rods. The rod on the right side contained a T-connector for changing the pressure in the ileum. The rod on the right was also attached to a force transducer. The rods could be moved towards or apart from each other at controlled rates by two linear stages using a motor. The whole segment was photographed using a video camera (SONY CCD Camera, Japan) for later analysis of length and diameter.

In mechanical testing of living tissues, preconditioning was necessary to obtain repeatable results. This meant that after the specimen was installed in the test machine, the loading and unloading processes were repeated for a number of cycles until the stress-strain relationship became stabilized. The number of cycles required depended on the tissue and method of preparation. In these experiments, we preconditioned the ileum at 6 cm H_2O pressure, 4 stretch cycles to stretch ratio 1.25. The segment was then elongated to stretch ratios of 1.0, 1.08, 1.16, and 1.25. At each stretch level, we applied the pressure to the levels of 0, 2, 4, and 6 cm H_2O. The corresponding diameter and gauge length, displacement and axial force at each stress level were monitored.

Determination of no-load state and zero-stress state

The tissue rings were immersed separately in small organ baths containing the aerated Krebs solution. They were photographed in the no-load state and then cut radially on the anti-mesenteric side to obtain their zero-stress state (Figure 2). A 30-min-period was allowed for equilibration after the radial cut and the specimens were photographed again. The selection of this time period was based on pilot experiments.

Data analysis

Morphometric data were obtained from the digitalized images of the segments in the zero-stress, no-load and deformed states. The measurements were done using dedicated software (Sigmascan 4.0, Jandel Scientific, USA). The following data were measured from each specimen at the no-load and zero-stress states (illustrated in Figure 2), which were the circumferential length (*C*), the wall thickness (*h*), the wall area (*A*), and the opening angle at the zero-stress state (α). The subscripts *i*, *o*, *m*, *n*, *z* and *d* refered to the inner (mucosal) surface, outer (serosal) surface, the mid-wall, the no-load state, zero-stress state and deformed condition, respectively. The opening angle α was defined as the angle subtended by two radii drawn from the midpoint of the inner wall to the inner tips of two ends of the specimen. Furthermore, the outer diameter (*D*) and the length (L_d) were measured from the images of the deformed segments.

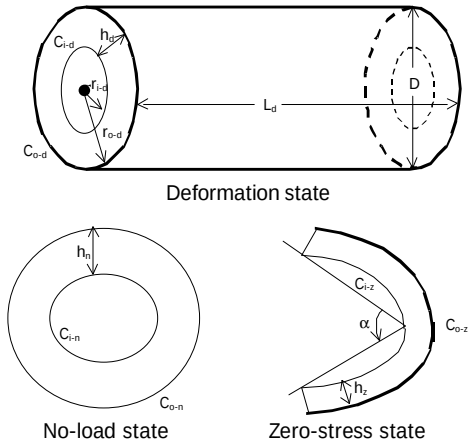

Figure 2 Legend, illustrations of intestinal small intestinal segment in the no-load, zero-stress and deformed states. C, h, α, denoted the circumference, thickness, and opening angle, respectively. The subscripts *n*, *z*, *d* denoted the no-load state, zero stress state and deformed state, respectively. The subscripts *i*, *o* referred to the inner (mucosal) surface, outer (serosal) surface, respectively.

The measured data were used for computation of the biomechanical parameters. Circumferential residual Green' s strain at the mucosal and serosal surface:

$$E_i = \frac{(\frac{C_{i-n}}{C_{i-z}})^2 - 1}{2} \quad \text{and} \quad E_o = \frac{(\frac{C_{o-n}}{C_{o-z}})^2 - 1}{2} \qquad (1)$$

The stress and strain of the intestine in the deformed state were determined under assumptions that the intestinal wall was thin and homogenous and the intestinal geometry was a circular

tube when pressurized. The circularity assumption had been verified in yet unpublished studies. The simplification we wished to make under the thin wall assumption was that the normal stress in the radial direction, s_{rr}, was negligible and that the stresses s_{qq}, and s_{ff} were approximately uniform throughout the wall thickness. Here r, q, f were polar coordinates in radial, circumferential and axial directions, respectively. The calculations were based on knowing the zero-state, no-load state dimensions, the outer diameters and lengths of the specimen at varying pressures, and assuming incompressibility of the intestinal wall. The longitudinal mid-wall stretch ratio, $l_{ff} = \frac{L_d}{L_n}$; the luminal radius, $r_{i-d} = \sqrt{r_{o-d}^2 - \frac{A_n}{p\, l_{ff}}}$; the wall thickness, $h_d = r_{o-d} - r_{i-d}$; the mucosal circumferential length, $C_{i-d} = 2p\, r_{i-d}$; the serosal circumferential length, $C_{o-d} = 2p\, r_{o-d}$; the mid-wall circumferential length, $C_{m-d} = \frac{C_{i-d} + C_{o-d}}{2}$; the mid-wall circumferential length at zero-stress state $C_{m-z} = \frac{C_{i-z} + C_{o-z}}{2}$, the circumferential stretch ratio, $l_{qq} = \frac{C_{m-d}}{C_{m-z}}$.

The longitudinal mid-wall stretch ratio was referenced to the no-load state because tissue strips were not cut for obtaining the zero-stress state in both directions. However, the longitudinal mid-wall length in rat intestine did not differ between the no-load and zero-stress states.

Kirchhoff ' s stress and Green' s strain at a given pressure were computed according to the following equations.

The circumferential and longitudinal Kirchhoff' s stress:

$$S_{qq} = \frac{\Delta \mathrm{Pr}_{i-d}}{(r_{o-d} - r_{i-d})\, l_{qq}^2}, \text{ and } S_{ff} = \frac{F + \Delta P p r_{i-d}^2}{p\, l_{ff}^2 (r_{o-d}{}^2 - r_{i-d}{}^2)} \quad (2)$$

Where ΔP was the transmural pressure difference, F was the force applied on the two ends of intestine.

The circumferential and longitudinal midwall Green' s strain:

$$E_{qq} = \frac{l_{qq}^2 - 1}{2}, \text{ and } \quad E_{ff} = \frac{l_{ff}^2 - 1}{2} \quad (3)$$

The stress and strain under each level of pressure and stretch ratio were calculated. In order to compare the stress-strain relationships among different EGF groups, one dimensional stress-strain curve was fitted, averaged and plotted: Circumferential stress-strain relationship (P=0 to P=6 cmH_2O (l_{ff}=1)) was fitted by the exponential equation: $strain = y_0 + k\exp(stress/t)$. Longitudinal stress-strain relationship (l_{ff}=1 to l_{ff}=1.25 (P=0 cmH_2O)) was fitted by another exponential equation because of different curve shapes, $stress = exp(a + b \times strain)$. Where y_0, k, and t, a, b were derived from the curve-fit regression done for each of segments. After fitting and averaging, the average curves with error bar could be obtained in different groups.

The exponential strain expression proposed by Fung[12] was applied to a set of test results on EGF treatment ileum. The stress and strain at a fixed stretch ratio of l_{ff}=1.16 and at varying pressure (P=0, 2, 4, 6 cmH_2O) were calculated and fitted to the function.

$$r_0 W^{(2)} = \frac{C}{2}\exp\left[a_1(E_{qq}^2 - E_{qq}^{*2}) + a_2(E_{ff}^2 - E_{ff}^{*2}) + 2a_4(E_{qq}E_{ff} - E_{qq}^* E_{ff}^*)\right] \quad (4)$$

where W was the strain energy per unit mass of the tissue, and r_0 was the mass density (mass per unit volume) in the initial zero-stress state. Then $r_0 W^{(2)}$ was the strain energy per unit volume of the tissue at zero-stress state for two dimensions.

From $S_{qq} = \frac{s_{qq}}{l_{qq}^2} = \frac{\partial(r_0 W^{(2)})}{\partial E_{qq}}$ and $S_{ff} = \frac{s_{ff}}{l_{ff}^2} = \frac{\partial(r_0 W^{(2)})}{\partial E_{ff}}$ (5)

We obtained $S_{qq} = C(a_1 E_{qq} + a_4 E_{ff})\exp[F(a,E)]$, and
$S_{ff} = C(a_4 E_{qq} + a_2 E_{ff})\exp[F(a,E)]$ (6)

Where

$$F(a,E) = a_1(E_{qq}^2 - E_{qq}^{*2}) + a_2(E_{ff}^2 - E_{ff}^{*2}) + 2a_4(E_{qq}E_{ff} - E_{qq}^* E_{ff}^*) \quad (7)$$

Where C (with units of stress,) and a_1, a_2, a_4 (dimensionless) were material constants, $E_{\theta\theta}{}^*$, $E_{\phi\phi}{}^*$ were strains corresponding to a selected pair of stresses $S_{\theta\theta}{}^*$, $S_{\phi\phi}{}^*$. The material constants were determined by a modified version of Marquardt' s nonlinear least-squares algorithm.

The meaning of the material constants was discussed in detail by Fung[12]. Constant a_1 would affect the curve for $S_{\theta\theta}$ *vs.* $E_{\theta\theta}$, the higher the a_1, the curve of $S_{\theta\theta}$ *vs.* $E_{\theta\theta}$ would leave the origin closer to the strain axis, and rise more rapidly, the more non-linear the curve was. Constant a_2 would affect the curve for $S_{\phi\phi}$ *vs.* $E_{\phi\phi}$ in a similar way. Constant a_4 specified the cross talk between the circumferential and longitudinal directions. The constant C fixed the scale on the stress axis. The larger the value of a_1, a_2 and a_4 was, the smaller C was[12].

Statistical analysis

Data were expressed as mean ±SEM. One-way analysis of variance was used to detect variations between treatment groups (Sigmastat 2.0™, Jandel Scientific, Germany). In case of significance (P<0.05), differences were tested between the control group and EGF-treated groups at 2, 4, 7, and 14 days treatment (Dunnet' s Test). If the normality test failed, Kruskal-Wallis one way analysis of variance on ranks was used instead.

RESULTS

Weight and morphological data

The total body weight did not change (Figure 3A). The ileum weight began to increase after 2 days' EGF treatment (Figure 3B). The wall thickness increased significantly after 4 days' EGF treatment, it did not change further (Figure 3C). A significantly larger wall area was observed in the 4 days' treatment group (Figure 3D). The luminal area did not change significantly (Figure 3E). However, a significantly smaller inner perimeter was observed in the 4 days, and 7 days' EGF treatment groups, but not in the 14 days' group (Figure 3F).

Zero-stress state data

The opening angle increased significantly after 7 days' EGF treatment and continued to increase up to 14 days (Figure 3G). The mucosal residual strain was compressive in all groups and decreased from 4 days of EGF treatment. The serosal residual strain was tensile with relatively higher values after 14 days of EGF treatment (Figure 3H).

Biomechanical data

The stress-strain relationships are shown in Figure 4. In circumferential direction, the curves representing 4 days and 7 days of EGF treatment were shifted to the right, whereas 14 days' EGF treatment curve shifted back towards normal. In longitudinal direction, the stress-strain curves representing 4 days and 7 days of EGF treatment were shifted to the left. Like the circumferential direction, the curves shifted towards normal after 14 days' EGF treatment.

The derived material constants a_1, a_2, a_4, and C from the strain energy function are illustrated in Table 1. Constant a_1 and a_2 having comparably smaller SEM values were therefore more stable than the other parameters. A significantly smaller a_1 value was found in the 7 days' and 14 days' EGF treatment groups and larger a_2 values were found in the 2 days' and 7 days' EGF treatment groups. This demonstrated that 7 days'

EGF treatment had the lowest circumferential stiffness and comparatively high longitudinal stiffness, and that the remodeling was most significant in the 7 days' EGF treatment group.

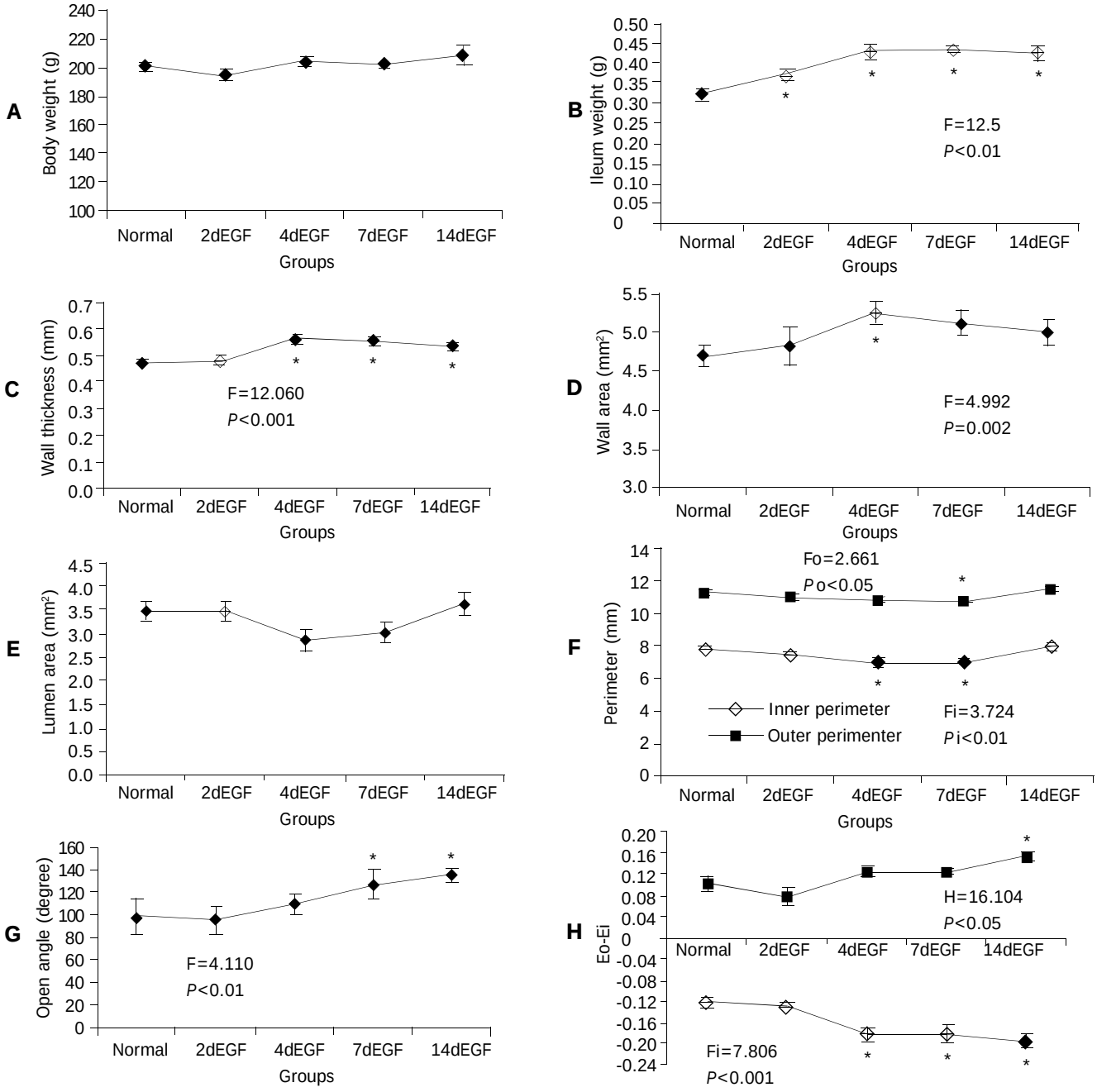

Figure 3 Legend, morphometric data of ileum in the no-load (A-F) and zero-stress states (G-H). *F* and *P* values were from one-way ANOVA for different treatment groups: If significant difference ($P<0.05$) was found using one-way ANOVA (marked with a), multiple comparisons with normal controls were done using Dunnet's test. Significantly different groups were marked with b.

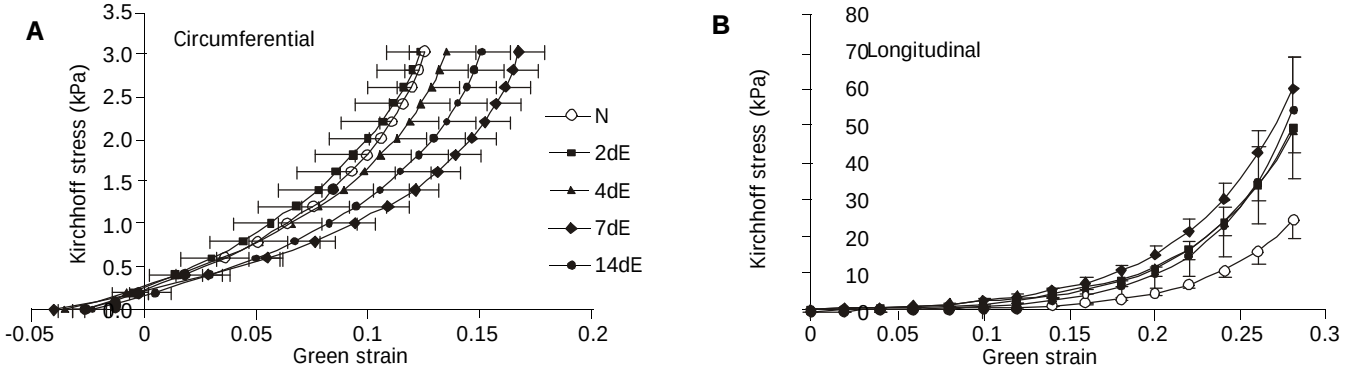

Figure 4 Legend, intestinal stress-strain curves in the EGF-treated and normal control groups. Translation of the stress-strain curve to the right in the coordinate system implied tissue softening (decreased stiffness) and *vice versa.*

Table 1 Material constants

	Normal	2dEGF	4dEGF	7dEGF	14dEGF
a_1[a]	25.42±1.91	18.19±2.80	19.32±3.91	11.57±2.04[b]	13.61±3.00[b]
a_2[a]	21.51±3.19	36.24±0.95[b]	24.90±3.72	34.74±5.17[b]	27.51±4.41
a_4	6.41±1.20	12.20±2.98	7.13±3.53	5.39±1.29	4.78±1.15
C (kPa)	1.13±0.18	1.30±0.27	2.32±0.97	1.75±0.30	1.02±0.12

A: One-way ANOVA result: $P<0.05$; B: Post analysis (Dunnet´s test) result: significantly different from normal control group ($P<0.05$).

DISCUSSION

The major findings in the present study were that EGF treatment induced time-dependent morphometric and biomechanical remodeling in the ileum. The ileum weight and wall thickness increased. The biomechanical changes were characterized by increased opening angle, inner and outer residual strains, decreased circumferential wall stiffness and increased longitudinal wall stiffness.

As the function of the GI tract is to a large degree mechanical, it has become increasingly popular to acquire biomechanical information on the GI tract[13-17]. However, many aspects of its biomechanical function are still largely left unexplored. Previous investigations were mainly conducted on uni-axial isolated strip experiments and balloon distension[18,19]. In the isolated strip studies, the structural integrity of the organ wall was not preserved and the strip was not necessarily in its zero-stress state at resting conditions since large residual strains existed in the GI tract[19]. In the balloon distension test, by means of impedance planimetry, the luminal cross-sectional area (CSA) could be measured. CSA as function of pressure provided important information on luminal dimensions during the loading but gave little information about material properties without further mechanical analysis. Furthermore, the tension-strain relationship was only computed for the circumferential direction and the strain was not referenced to the zero stress state[18].

The zero stress state of an organ is the state at which the organ is stress-free, meaning that all external and internal forces are removed. Vaishnav and Vossoughi[20] and Fung[21] independently reported respectively that the no-load state of a blood vessel was not the zero stress state. Recently, residual strains were demonstrated in the esophagus, small intestine, and large intestine[14-16, 22-28] and were found to be closely related to the growth and remodeling[24-30]. Hence the analysis of stress and strain begins with identification of the zero stress state.

This study was to explore how EGF affects geometric and biomechanical remodeling. EGF induced remodeling of the material structure, zero-stress state, and mechanical properties. The changes were quantified in terms of material constants in the constitutive equation. For computation of mechanical parameters we used video image techniques during loading and at no-load and zero-stress states. Assuming the intestine wall to be a membrane, biaxial experiments were done and a two- dimensional pseudostrain energy function was used to express the stress-strain relationship with reference to the zero-stress state. The use of pseudoelasticity to describe biological materials has been justified by Fung *et al*[12]. The vascular study by Liu and Fung[31] found that the zero stress state and the material constants changed with the development of diabetes.

Remodeling of the small intestine was evident after 4 days' EGF treatment with increased wall thickness and decreased luminal area. This was consistent with Vinter-Jensen' s study[11]. They demonstrated that EGF stimulated intestinal wall thickness growth before the surface area growth. According to the histology observation, the growth progress mainly involved the mucosa layer. The speed of growth began to decrease after 4 days' EGF treatment.

The small intestinal residual strains were negative at the mucosal layer and positive at the serosal layer. This implied that the mucosa was under compression in the no-load state and at physiological conditions in the low pressure range, whereas the muscle layers were in tension. As expected, both the residual strain and the opening angle increased in a time-dependent manner. The change of the opening angle was a result of non-uniform tissue remodeling of the organ wall. The opening angle increases when the inner layers had a higher growth rate than the outer layers or when the outer layer' atrophy was more severe than the inner layer[32]. In the present EGF study, the mucosa growth was much faster than that in the other layers, which resulted in the increased opening angle and residual strains. It has been demonstrated that residual stress reduces the stress concentration at the inner wall of the GI tract at no-load and homeostatic states[15, 16, 22]. The residual stress in the resting condition may also serve as a growth-regulation factor[33]. However, additional studies are needed to investigate whether the growth influences the residual stress distribution or *vice versa*.

The biaxial test showed that the wall stiffness changed in response to EGF treatment. After 7 days' EGF treatment, the wall stiffness decreased in circumferential direction and increased in longitudinal direction. The wall stiffness remodeled towards the normal state in both directions after 14 days' EGF treatment. In circumferential direction, the result was consistent with Vinter-Jensen' s report[11]. The different tendency of intestinal wall stiffness change in the two directions demonstrated that EGF-induced tissue remodeling was heterogeneous in the ileum. The elastic modulus of the intestine wall was closely related to the morphological wall composition and the stiffness was mainly dependent on the collagen in the submucosal layer[15, 34]. The submucosal layer did not remodel to the same degree as the mucosal layer. Therefore, the intestinal wall became softer in the circumferential direction after EGF treatment. At this point we could not explain the different remodeling in the two directions. A possible explanation is that the collagen orientation changed its direction during EGF treatment. This study did not intend to evaluate the collagen orientation angle, so this needs to be evaluated in future studies. Another noticeable result was that after 14 days' EGF treatment the curves shifted towards normal in both directions. We hypothesize that the pronounced proliferation of the intestine in the first week is due to direct stimulation by exogenous EGF. However, after one week, a negative feedback mechanism of the organ reduced the response to endogeneous EGF, resulting in reduced growth speed of the intestine. Finally, after two weeks, the remodeling might be determined by the stress in the tissue in accordance with the stress-growth law proposed by Fung[21].

ACKNOWLEDGEMENT

The recombinant EGF was a generous gift from Professor Esam Z. Dajani, International Drug Development Consultants Corporation, a Division of Mid Gulf U.S.A., Inc., Long Grove, Illinois, U.S.A.

REFERENCES

1 **Prigent SA**, Lemoine NR. The type 1 (EGFR-related) family of growth factor receptors and their ligands. *Prog Growth Factor Res* 1992; **4**: 1-24

2 **Vinter-Jensen L**. Pharmacological effects of epidermal growth factor (EGF) with focus on the urinary and gastrointestinal tracts. *APMIS* 1999; **93**(Suppl): 1-42

3 **Gregory H**. Isolation and structure of urogastrone and its relationship to epidermal growth factor. *Nature* 1975; **257**: 325-327

4 **Opleta-Madsen K**, Hardin J, Gall DG. Epidermal growth factor upregulates intestinal electrolyte and nutrient transport. *Am J Physiol* 1991; **260**(6Pt 1): 807-814

5 **Ghishan FK,** Kikuchi K, Riedel B. Epidermal growth factor upregulates intestinal Na+ / H+ exchange activity. *Proc Soc Exp Biol Med* 1992; **201**: 289-295

6 **Salloum RM**, Stevens BR, Schultz GS, Souba WW. Regulation of small intestinal glutamine transport by epidermal growth factor. *Surgery* 1993; **113**: 552-559

7 **Dunn JC**, Parungo CP, Fonkalsrud EW, McFadden DW, Ashley SW. Epidermal growth factor selectively enhances functional enterocyte adaptation after massive small bowel resection. *J Surg Res* 1997; **67**: 90-93

8 **Liu CD**, Rongione AJ, Shin MS, Ashley SW, McFadden DW. Epidermal growth factor improves intestinal adaptation during somatostatin administration *in vivo*. *J Surg Res* 1996; **63**: 163-168

9 **Rao R**, Porreca F. Epidermal growth factor protects mouse ildeal mucosa from Triton X-100-induced injury. *Eur J Pharmacol* 1996; **303**: 209-212

10 **Ulshen MH**, Raasch RH. Luminal epidermal growth factor preserves mucosal mass of small bowel in fasting rats. *Clin Sci* 1996; **90**: 427-431

11 **Vinter-Jensen L**, Duch BU, Petersen JA, Ryslev A, Gregersen H. Systemic treatment with epidermal growth factor in the rat. Biomechanical properties of the growing small intestine. *Regul Pept* 1996; **61**: 135-142

12 **Fung YC**, Fronek K, Patitucci P. Pseudoelasticity of arteries and the choice of mathematical expression. *Am J Physiol* 1979; **237**: H620-H631

13 **Gregersen H**, Giversen IM, Rasmussen LM, Tottrup A. Biomechanical wall properties and collagen content in the partially obstructed opossum esophagus. *Gastroenterology* 1992; **103**: 1547-1551

14 **Gregersen H**, Kassab G. Biomechanics of the gastrointestinal tract. *Neurogastroenterol Motil* 1996; **8**: 277-297

15 **Gregersen H**, Kassab GS, Pallencaoe E, Lee C, Chien S, Skalak R, Fung YC. Morphometry and strain distribution in guinea pig duodenum with reference to the zero-stress state. *Am J Physiol* 1997; **273**(4Pt 1): G865-G874

16 **Gregersen H**, Lee TC, Chien S, Skalak R, Fung YC. Strain Distribution in the layered wall of the esophagus. *J Biomech Eng* 1999; **121**: 442-448

17 **Orvar KB**, Gregersen H, Christensen J. Biomechanical characteristics of the human esophagus. *Dig Dis Sci* 1993; **38**: 197-205

18 **Gregersen H**, Vinter-Jensen L, Juhl CO, Dajani EZ. Impedance planimetric characterization of the distal oesophagus in the Goettingen minipig. *J Biomech* 1996; **29**: 63-68

19 **Tottrup A**, Forman A, Uldbjerg N, Funch-Jensen P, Andersson KE. Mechanical properties of isolated human esophageal smooth muscle. *Am J Physiol* 1990; **258**(3Pt 1): G338-G343

20 **Vaishnav RN**, Vossoughi J. Estimation of residual strains in aortic segments. In: Hall CW, eds. Biomedical engineering II. Recent Developments. *New York: Pergamon Press* 1983: 330-333

21 **Fung YC**. What principle governs the stress distribution in living organs? In: Fung YC, Fukada E, Junjian W, eds. Biomechanics in China, Japan and USA. *Science, Beijing, China* 1983: 1-13

22 **Gao C**, Zhao J, Gregersen H. Histomorphometry and strain distribution in pig duodenum with reference to the zero-stress state. *Dig Dis Sci* 2000; **45**: 1500-1508

23 **Lu X**, Gregersen H. Regional distribution of axial strain and circumferential residual strain in the layered rabbit oesophagus. *J Biomech* 2001; **34**: 225-233

24 **Dou Y**, Gregersen S, Zhao J, Zhuang F, Gregersen H. Effect of refeeding after starvation on biomechanical properties in rat small intestine. *Med Eng Phys* 2001; **23**: 557-566

25 **Dou Y**, Gregersen S, Zhao J, Zhuang F, Gregersen H. Morphometric and biomechanical intestinal remodeling induced by fasting in rats. *Dig Dis Sci* 2002; **47**: 1158-1168

26 **Dou Y**, Lu X, Zhao J, Gregersen H. Morphometric and biomechanical remodeling in the intestine after small bowel resection in the rat. *Neurogastroenterol Motil* 2002; **14**: 43-53

27 **Zhao J**, Sha H, Zhou S, Tong X, Zhuang FY, Gregersen H. Remodelling of zero-stress state of small intestine in streptozotocin-induced diabetic rats. Effect of Gliclazide. *Dig Liver Dis* 2002; **34**: 707-716

28 **Zhao JB**, Sha H, Zhuang FY, Gregersen H. Morphological properties and residual strain along the small intestine in rats. *World J Gastroenterol* 2002; **8**: 312-317

29 **Saini A**, Berry C, Greenwald S. Effect of age and sex on residual stress in the aorta. *J Vasc Res* 1995; **32**: 398-405

30 **Fung YC**, Liu SQ. Change of residual strains in arteries due to hypertrophy caused by aortic constriction. *Circ Res* 1989; **65**: 1340-1349

31 **Liu SQ**, Fung YC. Influence of STZ-induced diabetes on zero-stress states of rat pulmonary and systemic arteries. *Diabetes* 1992; **41**: 136-146

32 **Rodriguez EK**, Hoger A, McCulloch AD. Stress-dependent finite growth in soft elastic tissues. *J Biomech* 1994; **27**: 455-467

33 **Fung YC**, Liu SQ. Changes of zero-stress state of rat pulmonary arteries in hypoxic hypertension. *J Appl Physiol* 1991; **70**: 2455-2470

34 **Gregersen H**, Kassab GS, Fung YC. The zero-stress state of the gastrointestinal tract: biomechanical and functional implications. *Dig Dis Sci* 2000; **45**: 2271-2281

Edited by Wu XN and Wang XL

P.O.Box 2345, Beijing 100023,China
Fax: +86-10-85381893
E-mail: wjg@wjgnet.com www.wjgnet.com

World J Gastroenterol 2003;9(10):2284-2288
World Journal of Gastroenterology
 ISSN 1007-9327

• BASIC RESEARCH •

Effects of *Rheum tanguticum* polysaccharide on TNBS -induced colitis and CD4$^+$T cells in rats

Li Liu, Zhi-Peng Wang, Chang-Tai Xu, Bo-Rong Pan, Qi-Bing Mei, Yin Long, Jia-Yun Liu, Si-Yuan Zhou

Li Liu, Zhi-Peng Wang, Qi-Bing Mei, Si-Yuan Zhou, Department of Pharmacology, Fourth Military Medical University, Xi' an 710032, Shaanxi Province, China
Yin Long, Jia-Yun Liu, Department of Traditional Chinese Medicine, Fourth Military Medical University, Xi' an 710032, Shaanxi Province, China
Chang-Tai Xu, Editorial Department of Journal of Fourth Military Medical University, Xi' an 710032, Shaanxi Province, China
Bo-Rong Pan, Department of Oncology, Xijing Hospital, Fourth Military Medical University, Xi' an 710032, Shaanxi Province, China
Supported by the National Natural Science Foundation of China, No 30100239
Correspondence to: Qi-Bing Mei, Department of Pharmacology, Fourth Military Medical University, Xi' an 710032, Shaanxi Province, China. qbmei@hotmail.com
Telephone: +86-29-3374552 **Fax:** +86-29-3374552
Received: 2003-03-10 **Accepted:** 2003-06-19

Abstract

AIM: To study the effects of *Rheum tanguticum* polysaccharide$_{-1}$ (RTP$_{-1}$) on ulcerative colitis in rats induced by 2, 4, 6-trinitrophene sulphonic acid (TNBS) and their possible mechanism.

METHODS: RTP$_1$ (200 mg·kg^{-1}, ig) extracted from *Rheum tanguticum* Maxim. ex Regel was administrated to rats with colitis induced by TNBS for 5 d, 7 d, 10 d and 14 d, respectively. The effects of RTP$_1$ and dexamethasone (DX, 0.2 mg·kg^{-1}, ig) were contrastively investigated. The MPO level and SOD activity were determined by chromatometry. The expansion and protein expression of CD4$^+$T lymphocytes isolated from colon mucosae and mesenteric lymph nodes of colitis rats were performed by immunohistochemical analysis and Western-blot methods.

RESULTS: Treatments of RTP$_1$ (200 mg·kg^{-1}, ig) significantly reduced diarrhea, mortality, colon mass, ulcer areas and MPO level in colon mucosae on days 5, 7, 10 and 14 (5.2±1.4, 5.4±0.7, 5.2±1.8, $P<0.05$. 3.4±0.8, $P<0.01$. 16.1±12.1, $P<0.01$. 31.8±8.6, 17.7±5.3, 12.7±4.1, $P<0.05$). The effects of RTP$_1$ were similar to those noted above in DX group, but there were no immunosupressive effects of DX in RTP$_{-1}$ group, such as body mass loss, thymus and spleen atrophy. The decreased number and down-regulated protein levels of CD4$^+$T cells isolated from the colon of colitis rats treated with RTP$_1$ were found.

CONCLUSION: RTP$_1$ shows significantly protective effects but lower side effects on rats with colitis induced by TNBS. The mechanism may be due to the resistance to over expansion of CD4.

Liu L, Wang ZP, Xu CT, Pan BR, Mei QB, Long Y, Liu JY, Zhou SY. Effects of *Rheum tanguticum* polysaccharide on TNBS -induced colitis and CD4$^+$T cells in rats. *World J Gastroenterol* 2003; 9(10):2284-2288
http://www.wjgnet.com/1007-9327/9/2284.asp

INTRODUCTION

Inflammatory bowel diseases (IBD), including ulcerative colitis (UC) and Cron' s disease, are complex autoimmune diseases whose etiology and pathogenesis have not been fully elucidated. IBD is related with multiple etiologic theories such as genetics, immunology and environment[1,2]. In recent years, a study of animal models of IBD pathogenesis showed that immune imbalance led to the inflammation in the gastrointestinal tract[3]. A growing number of evidences support an important role for dysregulated CD4+T cells response to the antigens, such as enteric bacterial flora, as a common disease mechanism[4-6]. Previous studies have also demonstrated an increasing number of infiltrating CD4+T cells and anti-CD4 antibodies are thought to be effective[7-9]. The fact showed that an imbalance of excessive CD4/Th1 cell response or inadequate CD4/Th2 cells response was involved in experimental colitis[10]. These studies strongly suggest that immunomodulatory drugs have a bright future in IBD therapy, and CD4 could be a potential therapeutic target of colitis drug research[11]. Many biologic therapies are being evaluated for the treatment of chronic inflammatory bowel diseases[12-15]. However, during recent years, the mainstay therapies for IBD were anti-inflammatory drugs and glucocorticosteroids (GCS)[16,17]. The incidence of IBD is increasing in Asia[18,19], some traditional Chinese medicine therapies, such as moxibustion[20] and decoction, have shown significant therapeutic effectiveness on IBD. Rhubarb which has been used for gastrointestinal disease, is a main ingredient of some decoctions administrated to patients with IBD. Our previous data showed *Rheum tanguticum* polysaccharide (RTP) extracted from *Rheum tanguticum* Maxim. ex Regel, could significantly protect against acute hepatic injury and oxidation injury[21,22]. Although there is no evidence whether IBD patients can benefit from RTP, heparin exhibits significant effects on colitis[23,24] and some plant polysaccharides exhibit immune regulative effects[25,26]. Therefore, we administered RTP$_1$ to colitis rats and investigated its therapeutical effectiveness on colitis rats-induced by TNBS and the expansion and protein level of CD4$^+$ lymphocytes, which were the potential targets of colitis immunoregulatory therapy.

MATERIALS AND METHODS

Animal

Male Sprague-Dawley rats (220-250 g) obtained from the Animal Center of Fourth Military Medical University were fed on a standard laboratory diet and free to access tap water. The rats were kept in a room at a controlled temperature (22±1 ℃), humidity (65-70 %), and a 12:12-h light-dark cycle. Forty rats were randomly divided into four groups, namely normal, model, RTP (200 mg· kg^{-1}, ig) and dexamethasone (DX, 0.20 mg· kg^{-1}, ig) groups.

Materials

Sephacryl-S400 was from Pharmacia Biotech AB, dexamethasone (DX) and 2, 4, 6-trinetrophene sulphonic acid (TNBS) were purchased from Sigma, hexadecytrimethyl-ammonium was a product of Fluka. CD4 mAb was a product

of Immunotech Co. SABC immunehistochemical kits were purchased from Boshide Co. Electrophoresis apparatus was purchased from Bio-Rad.

Preparation of polysaccharide from Rheum tanguticum Maxim. ex Regel

Rhubarb, identified by professor Ren Yi Northwest University of china, was *Rheum tanguticum* Maxim.ex Regel. *Rheum tanguticum* polysaccharide (RTP) was extracted according to the methods described previously[27]. In brief, *Rheum tanguticum* Maxim (1 kg) was fragmented and boiled 3 times,8 hours each time with absolute ethanol for 24 hours to extract the components dissolved in ethanol. The residue was boiled for another three times (8 h each time) with water to extract polysaccharide. All the water extractions were finally pooled and mixed with a finally concentrated ethanol solution of 75 ml/L to precipitate the polysaccharide-enriched fractions. After proteins removed by freezing-thawing methods, crude *Rheum tanguticum* polysaccharide (RTP) was obtained by dialysis, concentration and lyophilization. In this study, the polysaccharide (uronic acid) content of RTP_1 was 97.4 % (27.5 %), and their molecular masses were 60 Kda-80 Kda , and $RTP_1$was administered orally to rats to study the effects and mechanism on colitis.

Induction of ulcerative colitis model in rats

Male Sprague-Dawley rats were fasted for 24 hours before experimentation but with free access to drinking tap water. Colitis model was produced as before[28] (*Gastroenterology* 1989;96:795-811). In brief, the rats (except rats in normal group) were lightly anesthetized with ether. A rubber catheter (OD 2 mm) was inserted rectally into the colon so that the tip was 8 cm proximal to the anus, approximately at the splenic flexure. TNBS dissolved in 40 mL/L in ethanol was instilled into the lumen of colon through the rubber catheter. Saline, RTP and DX were administrated 6 hours after induction of colitis model. The body weight was recorded during the experimental period. The rats were anesthetized with ether and killed by cervical dislocation on d5, d7, d10, d14, respectively. Each was 10 rats. The distal colon was removed and opened by a longitudinal incision, rinsed with saline, and weighed. Mucosal damage was assessed by measurement of ulcerative areas in colon mucosae by a single observer blinded to characteristics or treatment of the animals being studied. Colon samples were then excised, snap-frozen in liquid nitrogen, and stored at -80 ℃ for later assay of myloperoxidase (MPO) and superoxide dismutase (SOD). Additional samples were preserved in formaldehyde for histological and immunohistochemical analysis. Meantime, the spleen and thymus were removed and weighed.

Determination of biochemical marker

The activity of MPO and SOD was determined by chromatometry. In brief, the colon tissue was suspended in 5 g/L hexadecytrimethyl-ammonium (pH6.0, 50 mg of tissue per milliliter) for MPO level and suspended in PBS (pH 7.2, 100 mg per milliliter) for SOD level and then homogenized for 15 s by using a polytron generator in ice bathing. The MPO and SOD levels in colon tissue were determined by using the technique described as before (*Gastroenterology* 1984;84:1344).

Immunohistochemical analysis on $CD4^+$ lymphocyte

Immunohistochemical staining was performed on paraffin embedded sections by using biotinylated anti-CD4 mAb, and then operated according to the procedure for SBC immunohistochemiacal kit.

Western-blot analysis on $CD4^+$ lymphocyte

The rats with colitis induced by TNBS ethanol were killed by cervical dislocation. The lumenal lymphoid node was separated and homogenized in 1 ml lysis buffer in ice bathing for 10 min, then centrifuged at 11 000 g for 5 min at 4 ℃, and 30 μl suspension was moved to lodding buffer 15 ml. The samples were boiled for 10 min and subjected to electrophoresis on 120 g/L SDS-acrylamide gel. The gel was then electroblotted onto a ultrocellulose membrane, and detection of CD4 protein was conducted by using anti-CD4 mAb.

Statistical analysis

Results were expressed as mean ± standard deviation ($\bar{x}\pm s$). Differences between two groups were examined by Student' s *t*-test. A probability (*P* value) of less than 0.05 was considered statistically significant.

RESULTS

Effects of RTP_1 on rats with TNBS-induced colitis

Grossly visible colon wall thicking, inflammation, and ulcers were found in the animals that received TNBS in 400 mL/L ethanol. Treatments of RTP_1 (200 $mg \cdot kg^{-1}$ ig) significantly reduced diarrhea, mortality, colon mass and ulcer area. The effect of RTP_1 on colitis was similar to that in DX group (Figure 1, Table 1).

Table 1 Effects of RTP_1 (200 $mg \cdot kg^{-1}$, ig) on rats with TNBS -induced colitis (n=10, $\bar{x}\pm s$)

t / d	Colon mass index ($mg \cdot g^{-1}$)				Ulcerative area (%)			
	Normal	Model	RTP_1	DX	Normal	Model	RTP_1	DX
5	2.8±0.4	7.0±1.4[d]	5.2±1.4[a]	5.5±0.6[a]	0.0±0.0	35.7±12.9[d]	16.1±12.1[b]	26.2±4.1[a]
7		6.9±1.7[d]	5.4±0.7[a]	5.6±0.4[a]		44.5±12.0[d]	31.8±8.6[a]	35.7±2.4[a]
10		7.3±1.5[d]	5.2±1.8[a]	5.2±0.6[b]		27.5±13.7[d]	17.7±5.3[a]	22.1±4.9
14		5.4±0.9[d]	3.4±0.8[b]	4.1±0.3[b]		21.8±9.7[d]	12.7±4.1[a]	13.5±2.7[a]

[a]P<0.05, [b]P<0.01 *vs* Model; [d]P<0.01 *vs* Normal.

Table 2 Effects of RTP_1 on SOD and MPO activity of colon in rats with TNBS- induced colitis (n=10, $\bar{x}\pm s$)

t / d	SOD ($NU \cdot g^{-1}$)				MPO ($U \cdot g^{-1}$)			
	Normal	Model	RTP_1	DX	Normal	Model	RTP_1	DX
5	40.9±7.7	48.7±8.4[c]	69.1±16.1[b]	72.5±13.5[b]	0.09±0.02	9.7±3.2[d]	2.9±1.9[b]	4.8 ±1.0[d]
7		54.7±7.8[d]	66.0±6.8[b]	67.2±12.1[b]		7.7±1.5[d]	3.1±0.8[b]	6.1±1.1[e]
10		44.4±7.9	63.4±4.8[b]	60.1±5.4[b]		6.0 ±1.9[d]	4.3±0.9[a]	4.3±1.1[a]
14		38.8±5.7	60.7±10.5[b]	60.2±6.4 [b]		4.1±1.2[d]	1.8±0.5[b]	2.9±0.8[e]

[a]P<0.05, [b]P<0.01 *vs* Model. [c]P<0.05, [d]P<0.01 *vs* Normal. [e]P<0.01 *vs* RTP_1.

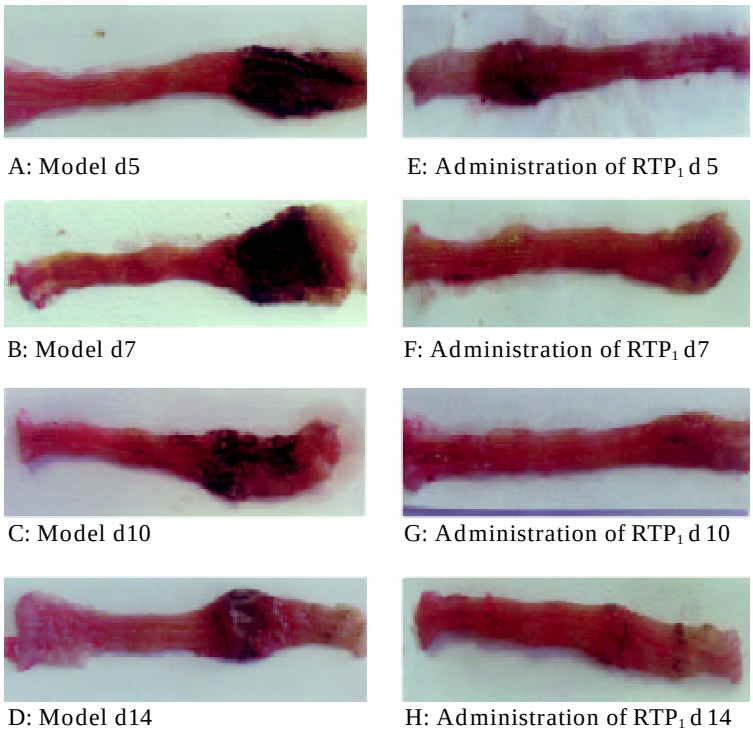

Figure 1 Photographs of rats colon. A-D. TNBS-induced colitis with gross enlargement of the colon and large ulcers. E-H. TNBS with RTP$_1$, smaller ulcer area and reduced colon mass.

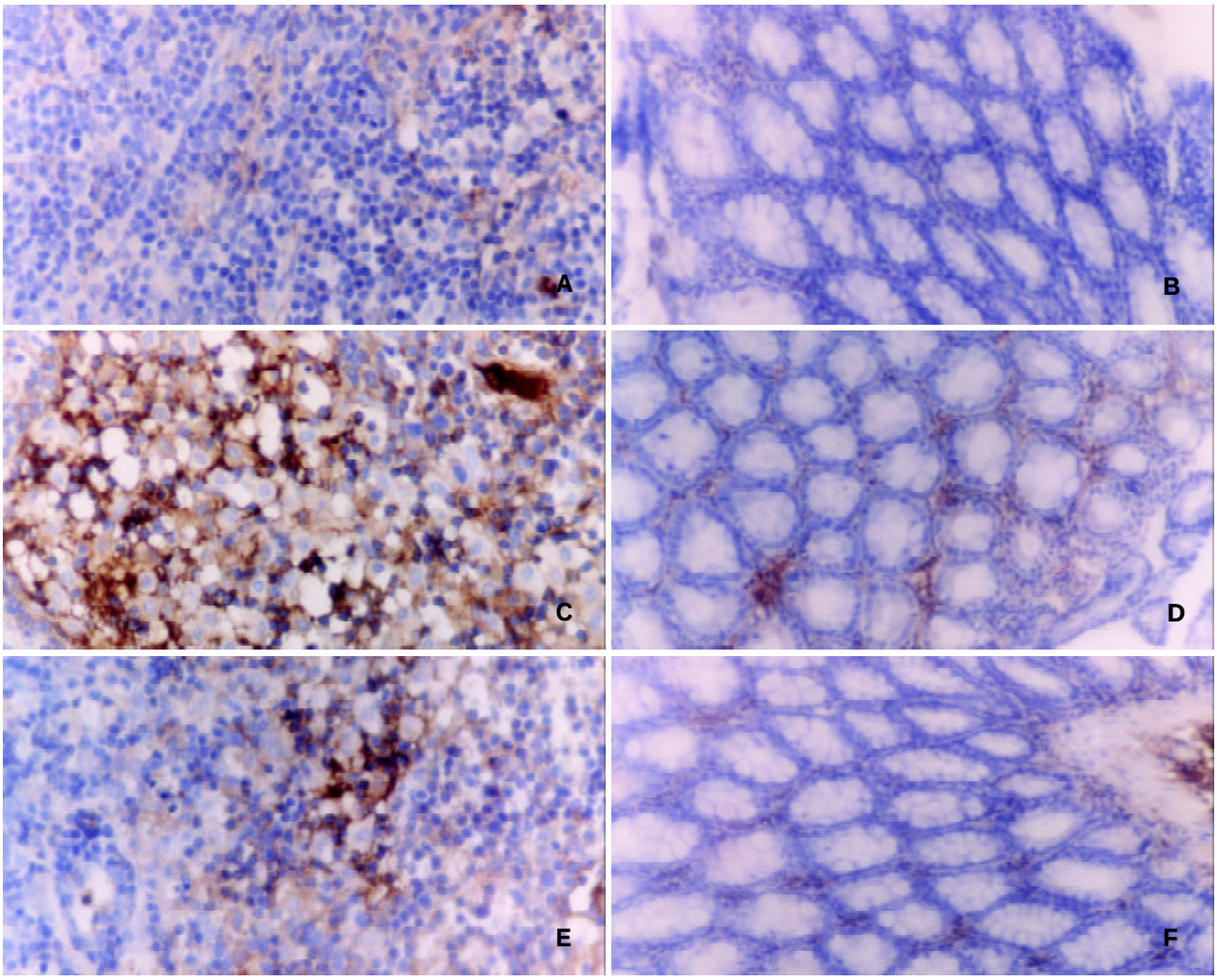

Figure 3 Immunohistochemical analysis on CD4$^+$ lymphocytes in mesenteric lymphoid nodes and colon tissues SABC×400. A, C, E: Mesenteric lymphoid nodes. B, D, F: Colon tissues.

Table 3 Effects of RTP_1 on thymus, spleen and body mass in rats with TNBS- induced colitis (n=10, $\bar{x}\pm s$)

t / d	Body mass (g)				Spleen index (mg·g^{-1})				Thymus index (mg·g^{-1})			
	Normal	Model	RTP_1	DX	Normal	Model	RTP_1	DX	Normal	Model	RTP_1	DX
5	242±16	210±26^{b}	235±32	215±27^{d}	2.3±0.4	3.2±0.4^{d}	3.0±0.4^{d}	3.0±0.6^{d}	2.4±0.03	0.9±0.3^{d}	1.2±0.5^{d}	0.7±0.2^{d}
7	255±23	223±39^{c}	243±24	196±21^{bde}		3.9±1.0^{d}	3.6±0.6^{d}	2.3±0.2		1.1±0.5^{d}	1.3±0.5^{d}	0.6±0.3^{bd}
10	277±29	252±27	267±38	176±33^{bde}		2.6±0.2^{c}	2.7±0.5	2.4±0.2		1.0±0.4^{d}	1.2±0.4^{d}	0.4±0.7^{bd}
14	278±30	258±22^{c}	272±31	165±31^{bde}		2.7±0.3^{c}	2.5±0.6	1.8±0.3^{bd}		1.2±0.3^{d}	1.4±0.2^{d}	0.02±0.01^{bd}

^{a}P<0.05, ^{b}P<0.01 *vs* Model; ^{c}P<0.05, ^{d}P<0.01 *vs* Normal; ^{e}P<0.05, ^{f}P<0.01 *vs* RTP_1.

Effects of RTP_1 on SOD and MPO of colon mucosa

The MPO activity and SOD level in TNBS-induced colitis rats were much higher than those in control. Treatments with RTP_1 (200 mg·kg^{-1} ig) significantly increased SOD activity, meanwhile, decreased MPO level in colon mucosae. The effects of DX on MPO and SOD activity of colon mucosae were similar to those of RTP_1 (Table 2).

Effects of RTP_1 on body weight, thymus and spleen index

During the inflammatory period, the rats with colitis showed marked body mass loss, thymus atrophy and spleen hypertrophy. Administration of RTP_1 (200 mg·kg^{-1}, ig) significantly prevented body mass loss. But the effects of DX showed farther body mass loss, thymus atrophy compared with control and RTP_1, suggesting severe immunosuppression occurred (Table 3).

Effects of RTP_1 on $CD4^+$T lymphocytes

Evidences indicated that $CD4^+$T cells played a key role in the pathogenesis of gastrointestinal tissue damage in ulcerative colitis. According to the results of immunohistochemical and Western-blot of $CD4^+$T lymphocytes isolated from colon tissues, there were a great increase of CD4 lymphocytes in the diseased colon and a significant decrease ofter the treatment with RTP_1 (200 mg·kg^{-1} ig). (Figures 2, 3).

Figure 2 Western-blot analysis of $CD4^+$T cells isolated from mesenteric lymphoid node. Left: Saline, Middle: RTP_1, Right: TNBS.

DISCUSSION

Some plant polysaccharides are known to posses immunorgulatory effects and wide bioactivities[29,30]. Rhubarb has traditionally been used as a folk remedy for gastrointestinal diseases for over two thousand years in China. We hypothesized that polysaccharide isolated from rhubarb might exhibit immune regulation on colitis rats. To test this hypothesis, we extracted polysaccharide from a breed of rhubarb, *Rheum tanguticum* Maxim. ex Regel., then administrated RTP to rats with colitis induced by TNBS. The results showed striking therapeutic effectiveness of RTP on the experimental colitis by attenuating the colon weight increase, decreasing the ulcer area formation, which resulted in a rapid recovery of animals from colitis induced by TNBS-enema. There was no significant difference between RTP and DX on colitis. Besides, RTP had no immunosuppressive side effects as DX.

Ulcerative colitis (UC) is considered to have a multifactorial etiology leading to intricate pathogenic mechanism that results in complex clinical manifestations. In recent years, the established animal models of immunology, genetics and biochemistry have promoted the study on pathogenic mechanism of UC[3]. The animal model of colitis induced by TNBS-enema, used in the present study, was considerated the characteristics as excessive Th1/$CD4^+$T lymphocytes response and similar to human IBD[31]. The TNBS-induced animal model, which was duplicated and cheap, was most commonly used to estimate the therapeutic effectiveness of colitis[3]. Therefore, this TNBS/ethanol-induced animal model may be suitable for investigate the therapeutic effectiveness and mechanism of RTP on colitis.

Colonic lesion and inflammation induced by TNBS-ethanol were accompanied by a drastic elevation of MPO activity in colonic tissues. This enzyme was used as an index of quantitative inflammation and a marker of neutrophil infiltration in the tissue (*Gastroenterology* 1989;96:795-811). In the present study, administration of RTP significantly attenuated the increase of colonic MPO activity, indicating its anti-inflammatory effect. SOD is an antioxidant enzyme that is cytoprotective in many tissues, because it scavenges the overproduced superoxide by stimulants. This study showed that the SOD activity in colonic tissue was significantly increased on days 5 and 7, but returned to normal level on days 10 and 14 after TNBS-enema. It is envisaged that the elevated SOD activity may be a protective reaction in the colonic tissue against the overproduction of superoxide during the early active phase of colonic inflammation. Administration of RTP markedly increased SOD activity after TNBS-enema and kept SOD at a higher level till 14 days. This result indicated that the therapeutic effectiveness of RTP on colitis might be at least in part, through its anti-oxidative effect. However, the underlying mechanisms of the therapeutic effectiveness of RTP need further studies. All these findings implicate that RTP has a very impressive therapeutic effectiveness on experimental colitis, and RTP may be the main component of *Rheum Rheum tanguticum* that is commonly used as a classic Chinese drug against inflammation in gut.

An increasing body of evidence suggests that inflammatory bowel disease (IBD) is due to abnormal function of regulatory T cells required for immunological homeostasis in gut-associated lymphoid tissue (GALT)[32]. CD4+T lymphocytes play an important role in the progressive and perpetuated inflammation of colitis[33,34]. In this study, RTP showed significant effects on resistance to the up-expression of $CD4^+$protein levels, suggesting that the mechanism of RTP on colitis is related to the modulation of $CD4^+$T cell dysfunction. $CD4^+$ T cells containing both $CD45RB^{high}$ and $CD45RB^{low}$ populations participatein as a pathogenic subset that in turn leads to inflammatory reactions selectively in the large intestine, indicating that UC can be cured by maintaining the balance between the two subunits of CD4 and the balance between the cytokines nets[35]. Therefore, $CD4^+$ T cell may be a new potential target of therapeutic drugs on UC patients.

REFERENCES

1 **Alstead E**. Fertility and pregnancy in inflammatory bowel disease. *World J Gastroenterol* 2001; **7**: 455-459

2 **Kirsner JB**. Historical origins of current IBD concepts. *World J Gastroenterol* 2001; **7**: 175-184
3 **Strober W**, Fuss IJ, Blumberg RS. The immunology of mucosal models of inflammation. *Annu Rev Immunol* 2002; **20**: 495-549
4 **Yoshida M**, Shirai Y, Watanabe T, Yamori M, Iwakura Y, Chiba T, Kita T, Wakatsuki Y. Differential localization of colitogenic Th1 and Th2 cells monospecific to a microflora-associated antigen in mice. *Gastroenterology* 2002; **123**: 1949-1961
5 **Elson CO**, Cong Y. Understanding immune-microbial homeostasis in intestine. *Immunol Res* 2002; **26**: 87-94
6 **Cong Y**, Brandwein SL, McCabe RP, Lazenby A, Birkenmeier EH, Sundberg JP, Elson CO. $CD4^+$ T cells reactive to enteric bacterial antigens in spontaneously colitic C3H / HeJBir mice: increased T helper cell type 1 response and ability to transfer disease. *J Exp Med* 1998; **187**: 855-864
7 **Monteleone I**, Vavassori P, Biancone L, Monteleone G, Pallone F. Immunoregulation in the gut: success and failures in human disease. *Gut* 2002; **50**(Suppl 3): III60-64
8 **Cottrez F**, Hurst SD, Coffman RL, Groux H. T regulatory cells 1 inhibit a Th2-specific response *in vivo*. *J Immunol* 2000; **165**: 4848-4853
9 **Dohi T**, Fujihashi K, Kiyono H, Elson CO, McGhee JR. Mice deficient in Th1- and Th2-type cytokines develop distinct forms of hapten-induced colitis. *Gastroenterology* 2000; **119**: 724-733
10 **Mizoguchi A**, Mizoguchi E, Saubermann LJ, Higaki K, Blumberg RS, Bhan AK. Limited CD4 T-cell diversity associated with colitis in T-cell receptor alpha mutant mice requires a T helper 2 environment. *Gastroenterology* 2000; **119**: 983-995
11 **Gad M,** Brimnes J, Claesson MH. $CD4^+$ T regulatory cells from the colonic lamina propria of normal mice inhibit proliferation of enterobacteria-reactive, disease-inducing Th1-cells from scid mice with colitis**.** *Clin Exp Immunol* 2003; **131**: 34-40
12 **Sandborn WJ**, Targan SR. Biologic therapy of inflammatory bowel disease. *Gastroenterology* 2002; **122**: 1592-1608
13 **Van Montfrans C**, Rodriguez Pena MS, Pronk I, Ten Kate FJ, Te Velde AA, Van Deventer SJ. Prevention of colitis by interleukin 10-transduced T lymphocytes in the SCID mice transfer model. *Gastroenterology* 2002; **123**: 1865-1876
14 **Singh B**, Read S, Asseman C, Malmstrom V, Mottet C, Stephens LA, Stepankova R, Tlaskalova H, Powrie F. Control of intestinal inflammation by regulatory T cells. *Immunol Rev* 2001; **182**: 190-200
15 **Rachmilewitz D**, Karmeli F, Takabayashi K, Hayashi T, Leider-Trejo L, Lee J, Leoni LM, Raz E. Immunostimulatory DNA ameliorates experimental and spontaneous murine colitis. *Gastroenterology* 2002; **122**: 1428-1441
16 **Xu CT**, Pan BR. Current medical therapy for ulcerative colitis. *World J Gastroenterol* 1999; **5**: 64-72
17 **Jani N**, Regueiro MD. Medical therapy for ulcerative colitis. *Gastroenterol Clin North Am* 2002; **31**: 147-166
18 **Jiang XL**, Cui HF. An analysis of 10218 ulcerative colitis cases in China. *World J Gastroenterol* 2002; **8**: 158-161
19 **Salupere R**. Inflammatory bowel disease in Estonia: a prospective epidemiologic study 1993-1998. *World J Gastroenterol* 2001; **7**: 387-388
20 **Wu HG**, Zhou LB, Shi DR, Liu SM, Liu HR, Zhang BM, Chen HP, Zhang LS. Morphological study on colonic ulcerative colitis treated by moxibustion. *World J Gastroenterol* 2000; **6**: 861-865
21 **Liu L**, Li BL, Mei QB. Effects of *tanguticum Maxim* polysaccharide on acute liver injury of mice. *Disi Junyi Daxue Xuebao* 1999; **20**: 549-551
22 **Liu L**, Mei QB, Zhou SY, Li BL. Effects of *tanguticum Maxim* polysaccharide on antioxidation of mice. *Disi Junyi Daxue Xuebao* 2001; **22**: 530-533
23 **Michell NP**, Lalor P, Langman MJ. Heparin therapy for ulcerative colitis? Effects and mechanisms. *Eur J Gastroenterol Hepatol* 2001; **13**: 449-456
24 **Cui HF**, Jiang XL. Treatment of corticosteroid-resistant ulcerative colitis with oral low molecular weight heparin. *World J Gastroenterology* 1999; **5**: 448-450
25 **Strickland FM**. Immune regulation by polysaccharide: implications for skin cancer. *J Photochem Photobiol B* 2001; **63**: 132-140
26 **Qiu Z**, Jones K, Wylie M, Jia Q, Orndorff S. Modified Aloe barbadensis polysaccharide with immunoregulatory activity. *Planta Med* 2000; **66**: 152-156
27 **Cho CH**, Mei QB, Shang P, Lee SS, So HL, Guo X , Li Y. Studyof the gastrointestineal protective effects of polysaccharides from Angelica sinensis in rats. *Planta Med* 2000; **66**: 348-351
28 **Zheng L**, Gao ZQ, Wang SX. A chronic ulcerative colitis model in rats. *World J Gastroenterol* 2000; **6**: 150-152
29 **Gomez-Flores R**, Calderon CL, Scheibel LW, Tamez-Guerra P, Rodriguez-Padilla C, Tamez-Guerra R, Weber RJ. Immuoenhancing properties of Plantago major leaf extract. *Phytother Res* 2000; **14**: 617-622
30 **Han SB,** Park SH, Lee KH, Lee CW, Lee SH, Kim HC, Kim YS, Lee HS, Kim HM. Polysaccharide isolated from the radix of Platycodon grandiflorum selectively activates B cells and macrophages but not T cells. *Int Immunopharmacol* 2001; **1**: 1969-1978
31 **Strober W**, Fuss IJ, Ehrhardt RO, Neurath M, Boirivant M, Ludviksson BR. Mucosal immunoregulation and inflammatory bowel disease: new insights from murine models of inflammation. *Scand J Immunol* 1998; **48**: 453-458
32 **Kweon MN**, Takahashi I, Yamamoto M, Jang MH, Suenobu N, Kiyono H. Development of antigen induced colitis in SCID mice reconstituted with spleen derived memory type $CD4^{(+)}$ $CD45RB^{(+)}$ T cells. *Gut* 2002; **50**: 299-306
33 **Leithäuser F**, Trobonjaca Z, Moller P, Reimann J. Clustering of colonic lamina propria $CD4^{(+)}$ T cells to subepithelial dendritic cell aggregates precedes the development of colitis in a murine adoptive transfer model. *Lab Invest* 2001; **81**: 1339-1349
34 **Xu D**, Liu H, Komai-Koma M, Campbell C, McSharry C, Alexander J, Liew FY. $CD4^{(+)}CD25^{(+)}$ regulatory T cells suppress differentiation and functions of Th1 and Th2 cells, leishmania major infection, and colitis in mice. *J Immunol* 2003; **170**:394-399
35 **Claesson MH**, Bregenholt S, Bonhagen K,Thoma S, Moller P, Grusby MJ, Leithauser F, Nissen MH, Reimann J. Colitis-inducing potency of $CD4^{(+)}$ T cells in immunodeficient, adoptive hosts depends on their state of activation, IL-12 responsiveness. *J Immunol* 1999; **162**: 3702-3710

Edited by Zhu L and Wang XL

P.O.Box 2345, Beijing 100023,China
Fax: +86-10-85381893
E-mail: wjg@wjgnet.com www.wjgnet.com

World J Gastroenterol 2003;9(10):2289-2292
World Journal of Gastroenterology
 ISSN 1007-9327

• BASIC RESEARCH •

Effect of ischemic preconditioning on P-selectin expression in hepatocytes of rats with cirrhotic ischemia-reperfusion injury

Xiang-Dong Cheng, Xian-Chuan Jiang, Yin-Bing Liu, Cheng-Hong Peng, Bin Xu, Shu-You Peng

Xiang-Dong Cheng, Department of Hepatobiliary Surgery, Zhejiang Cancer Hospital,Hangzhou 310022, Zhejiang Province, China
Xian-Chuan Jiang, Yin-Bing Liu, Cheng-Hong Peng, Bin Xu, Shu-You Peng, Department of Surgery, Second Affiliated Hospital of Zhejiang University, Hangzhou 310006, Zhejiang Province, China
Supported by Science and Technology Fund, Department of Health, Zhejiang Province, No.M-9810
Correspondence to: Xiang-Dong Cheng, Department of Hepatobiliary Surgery, Zhejiang Cancer Hospital, Hangzhou 310022, Zhejiang Province, China. chengxd516@sohu.com
Telephone: +86-571-88144401-507
Received: 2003-04-02 **Accepted:** 2003-05-17

Abstract

AIM: To investigate the effects and mechanisms of ischemic preconditioning (IPC) on the ischemia/reperfusion (I/R) injury of liver cirrhosis in rats and the effect of IPC on P-selectin expression in hepatocytes.

METHODS: Forty male SD rats with liver cirrhosis were randomly divided into sham operation group (SO group), ischemia/reperfusion group (I/R group), ischemic preconditioning group (IPC group), L-Arginine preconditioning group (APC group), L-NAME preconditioning group (NPC group), eight rats in each group. Hepatocellular viability was assessed by hepatic adenine nucleotide level and energy charge (EC) determined by HPLC, ALT, AST and LDH in serum measured by auto- biochemical analyzer and bile output. The expression of P-selectin in the liver tissue was analyzed by immunohistochemical technique. Leukocyte count in ischemic hepatic lobe was calculated.

RESULTS: At 120 min after reperfusion, the level of ATP and EC in IPC and APC groups was higher than that in I/R group significantly. The increases in AST, ALT and LDH were prevented in IPC and APC groups. The livers produced more bile in IPC group than in I/R group during 120 min after reperfusion (0.101±0.027 *versus* 0.066±0.027 ml/g liver, P=0.002). There was a significant difference between APC and I/R groups, (P=0.001). The leukocyte count in liver tissues significantly increased in I/R group as compared with SO group (P<0.05). The increase in the leukocyte count was prevented in IPC group. Administration of L-arginine resulted in the same effects as in IPC group. However, inhibition of NO synthesis (NPC group) held back the beneficial effects of preconditioning. Significant promotion of P-selectin expression in hepatocytes in the I/R group was observed compared with the SO group (P<0.01). IPC or L-arginine attenuated P-selectin expression remarkably (P<0.01). However, inhibition of NO synthesis enhanced P-selectin expression (P<0.01). The degree of P-selectin expression was positively correlated with the leukocyte counts infiltrating in liver (r=0.602, P=0.000).

CONCLUSION: IPC can attenuate the damage induced by I/R in cirrhotic liver and increase the ischemic tolerance of the rats with liver cirrhosis. IPC can abolish I/R induced leukocyte adhesion and infiltration by preventing post-ischemic P-selectin expression in the rats with liver cirrhosis via a NO-initiated pathway.

Cheng XD, Jiang XC, Liu YB, Peng CH, Xu B, Peng SY. Effect of ischemic preconditioning on P-selectin expression in hepatocytes of rats with cirrhotic ischemia-reperfusion injury. *World J Gastroenterol* 2003; 9(10):2289-2292
http://www.wjgnet.com/1007-9327/9/2289.asp

INTRODUCTION

Ischemic preconditioning (IPC) refers to a phenomenon in which a tissue is rendered resistant to the deleterious effects of prolonged ischemia and reperfusion (I/R) by prior exposure to a short period of vascular occlusion. This phenomenon was first demonstrated in the heart a decade ago[1] and has been the subject of intensive investigation ever since. Although it is clear that activation of adenosine receptors and protein kinase C (PKC) is critical to the development of the beneficial action of IPC, the downstream effectors in the signaling cascade initiated by IPC are uncertain. Akimisn *et al*[2] and Kubes *et al*[3] have demonstrated that IPC prevents intestinal and skeletal muscle I/R injury by inhibiting postischemic leukocyte-endothelial cell interaction. However, identification of the end effectors of the ant adhesive effects of IPC remains unclear. A likely candidate effector molecule that may be targeted by the signaling cascade initiated by IPC is P-selectin, because post-ischemic leukocyte rolling (and thus subsequent stationary adhesion and emigration) is critically dependent on the expression of P-selectin on venular endothelium[4]. IPC has been commonly studied in the heart, but few studies have been performed on cirrhotic liver IPC. This study was aimed to determine the effects and mechanisms of IPC on the I/R injury rats with liver cirrhosis and the effect of IPC on the expression of P-selectin.

MATERIALS AND METHODS

Reproduction of rat cirrhotic liver model

Sprague-Dawley (SD) Male rats initially weighing 200±20 g were used.

Subcutaneous injection of 60 % Ccl_4 (0.3 mg/kg) was made once every 4 days for 8 weeks and 5% ethanol was allowed for 60 days[5].

Operative procedure

At first, ligamentous attachments around the liver were dissected. The common bile duct was then cannulated and bile output was measured. Ischemia was induced in the median and left lateral hepatic lobes by clamping the corresponding hepatic arterial and portal vein, while the blood flowing to the other lobe was left intact. When the assigned period of warm ischemia was completed, the clamp was removed and the pedicles to the non-ischemic lobe were ligated[6].

Grouping of animals

Forty male SD rats with liver cirrhosis were divided into 5

groups randomly, eight rats in each group. Animals in sham Operation group (SO group) were subjected to anesthesia and laparotomy. Animals in ischemia/reperfusion group (I/R group) were subjected to 30 min of left and middle lobe hepatic ischemia, followed by 120 min of reperfusion. Animals in ischemic preconditioning group (IPC group) were same as I/R group, but subjected to 10 min of ischemia and 5 min of reperfusion prior to I/R. Animals in L-arginine preconditioning group (APC group) were same as IPC group, but treated with a continuous intravenous infusion of L-Arginine (10 mg/kg, portal vein) for 5 min before preconditioning. Animals in L-NAME preconditioning group (NPC group) were same as IPC group, but treated with a continuous intravenous infusion of L-NAME (10 mg/kg, portal vein) for 5 min before preconditioning.

The animals were killed after blood samples were collected from the inferior vena cava after 120 min of reperfusion. Liver samples were excised from the anterior edge of the median lobe before ischemia, after the induction of ischemia and 120 min after reperfusion respectively. The specimens were immersed in liquid nitrogen immediately after sampling to measure the tissue concentration of adenine nucleotides, adenosine 5'-triphosphate (ATP), adenosine 5'-diphosphate (ADP), adenosine 5'-monophosphate (AMP) and total adenosine nucleotide. At 120 min after reperfusion, livers were perfused and fixed *in situ* with 4 % para formaldehyde.

Energy metabolism

ATP and its metabolites, ADP and AMP in the liver tissue were assayed as follows. After the frozen tissue with a mortar and pestle was ground, the powder was mixed with 1 ml 6 % perchloric acid at 4 ℃. The mixture was centrifuged at 3 000 rpm for 10 min and the supernatant was stored at 4 ℃, then 0.5 ml 6 % perchloric acid was added to the precipitate and centrifuged in the same manner. The supernatant was neutralized with 3 mol/l potassium carbonate and centrifuged at 3 000 rpm for 10 min. The final supernatant was used as a sample for ATP and its metabolites. The tissue concentration of ATP and its metabolites was determined by high-performance liquid chromatography (HPLC). Energy charge (EC) was equal to (ATP+1/2ADP)/(ATP+ADP+AMP)[7].

Measurement of serum cytosolic enzymes

Serum alanine aminotransferase (ALT), aspartate aminotransferase (AST) and lactate dehydrogenase (LDH) were measured at 4 ℃ using commercially available kits (Horizon, American) by an auto-biochemistry analyzer.

Measurement of bile output

Bile output from the ischemic liver was measured through a choledochotomy tube placed in the common bile duct.

P-selectin expression in liver tissues

Immunohistochemical staining for P-selectin protein was performed using SP technique[8]. The immunostaining of P-selectin was visually classified into four groups: no staining present in any tumor cells (-), slight staining in most of the hepatocytes (+), most of the hepatocytes with moderate staining (++), and strong staining in most of the hepatocytes (+++). Two senior pathologists who did not know the clinicopathological data did the classification.

Histological examination

Liver samples were excised from the anterior edge of the median lobe 120 min after reperfusion. Small portions (0.5 cm×0.5 cm) were fixed immediately in 4 % buffered para formaldehyde (pH 7.2) and embedded in paraffin. These portions were cut into 4 μm thick sections and stained with hematoxylin and eosin (H & E). Leukocyte count in ischemic hepatic lobe could be calculated randomly under microscopy(×400).

Statistical analysis

The results were expressed as $\bar{x}\pm s$. The one-way NOVA and H test were used for statistical significance of differences between groups. Correlation analysis between two factors was made by Spearman method. $P<0.05$ was considered significant.

RESULTS

Change of ATP, ADP, AMP and EC levels in liver after ischemia and reperfusion

At 30 min of hepatic inflow occlusion, the ATP and EC levels in liver tissues were significantly decreased in I/R, IPC, APC and NPC groups ($P<0.05$). At 120 min after reperfusion, the ATP and EC levels in IPC and APC groups were significantly higher than those in I/R group ($P=0.000$, $P=0.001$). But there was no significant difference between NPC and I/R groups ($P>0.05$) (Table 1).

Change of ALT, AST and LDH in serum

Significant increases of ALT, AST and LDH levels in serum were observed in the group subjected to ischemia and reperfusion (I/R group) in comparison with the control group (SO group). When ischemia was preceded by 10 min of ischemia and 5 min of reperfusion (IPC), the increases of AST, ALT and LDH in serum were prevented ($P=0.000$). Administration of L-Arginine (APC group) resulted in the same effects on ALT, AST and LDH as above ($P=0.001$). However, infusion of L-NAME (NPC group) inhibited the beneficial effects of preconditioning (Table 2).

Results of bile output and leukocyte count in ischemic hepatic lobe

The livers produced more bile in IPC group than in I/R group during 120 min after reperfusion (0.101±0.027 *versus* 0.066±0.027 ml/g liver, $P=0.002$). There was a significant difference between APC and I/R, NPC and SO groups ($P=0.001$, $P=0.000$) respectively. However, there was no significant

Table 1 ATP, ADP, AMP and EC levels in liver after ischemia and reperfusion (U/L)

Groups	*n*	After ischemia				After reperfusion			
		ATP	ADP	AMP	EC	ATP	ADP	AMP	EC
SO	8	5.4±1.3	3.1±0.8	1.0±0.2	0.7±0.0	5.5±0.8	3.2±1.0	1.0±0.1	0.7±0.0
I/R	8	0.5±0.2[b]	2.3±0.6[a]	3.5±1.0[b]	0.3±0.0[b]	1.5±0.6[b]	2.3±1.2	2.6±1.3[a]	0.4±0.1[b]
IPC	8	0.5±0.1[b]	2.1±0.5[a]	3.6±1.5[b]	0.3±0.1[b]	4.1±1.6[ac]	2.3±0.8	1.9±0.9	0.6±0.1[ac]
APC	8	0.5±0.1[b]	2.2±0.5[a]	3.4±0.7[b]	0.3±0.0[b]	4.0±1.6[ac]	2.5±1.1	2.2±1.2[a]	0.6±0.1[ac]
NPC	8	0.5±0.2[b]	2.0±0.7[a]	3.3±0.6[b]	0.3±0.0[b]	2.3±1.6[b]	2.2±0.9[a]	3.2±1.1[b]	0.4±0.1[b]

[a]$P<0.05$, [b]$P<0.01$, *vs* SO group; [c]$P<0.01$, *vs* I/R group.

difference between NPC and I/R groups (P>0.05). The leukocyte counts in liver tissue showed a more significant increase in I/R group than in SO group (P=0.000). The increase in leukocytes count was inhibited in IPC group (P=0.028). Administration of L-arginine resulted in the same effects as in IPC group (P=0.020). However, inhibition of NO synthesis (NPC group) prevented the beneficial effects of preconditioning (P>0.05) (Table 3).

Table 2 Results of ALT, AST and LDH in serum after reperfusion (U/L)

Groups	Cases	ALT	AST	LDH
SO	8	300.5±159.2	551.1±84.7	4 612.3±1 042.8
I/R	8	2 218.8±825.3[a]	3 043.8±1 198.9[a]	13 762.5±5 371.9[a]
IPC	8	568.8±214.6[b]	1 315.0±958.9[b]	6 266.3±2 425.5[b]
APC	8	508.8±142.8[b]	1 108.8±637.2[b]	5 355.0±1 237.9[b]
NPC	8	2 091.3±684.6[a]	3 083.8±844.5[a]	11 361.3±4 211.8[a]

[a]P<0.01, *vs* SO group; [b]P<0.01, *vs* I/R group.

Table 3 Results of bile output and leukocyte count in ischemic hepatic lobe

Groups	Cases	Bile output (ml/g liver)	Leukocyte count (piece/HP)
SO	8	0.15±0.02	181.38±59.23
I/R	8	0.07±0.03[a]	442.38±94.10[a]
IPC	8	0.10±0.03[ab]	353.00±84.11b[a]
APC	8	0.10±0.02[ab]	347.75±51.53[ba]
NPC	8	0.07±0.01[a]	407.88±90.40[a]

[a]P<0.01, *vs* SO group; [b]P<0.05, *vs* I/R group.

Results of P-selectin expression in liver tissues

Significant promotion of P-selectin expression in hepatocytes in the I/R group was observed in comparison with the SO group (P=0.000). IPC or L-arginine attenuated P-selectin expression significantly (P=0.005). However, inhibition of NO synthesis enhanced the expression of P-selectin (P=0.001) (Table 4).

Table 4 Expression of P-selectin in liver tissues

Groups	Cases	Grade			Average rank
		(+)	(++)	(+++)	
SO	8	7	1	0	10.69
I/R	8	0	5	3	30.50[a]
IPC	8	5	3	0	15.06[b]
APC	8	4	4	0	17.25[b]
NPC	8	0	6	2	29.00[a]

[a]P<0.01, *vs* SO group; [b]P<0.05, *vs* I/R group.

Correlation between leukocytes infiltration and P-selectin expression in liver tissues

Leukocytes infiltration was significantly correlated with P-selectin expression in liver tissues. The degree of P-selectin expression was positively correlated with the counts of leukocyte infiltration in liver (r=0.602, P=0.000).

DISCUSSION

IPC is a unique phenomenon which attenuates organ injury caused by I/R. This is accomplished through a brief preceding episode of vascular occlusion which renders these tissues resistant to the deleterious effects of prolonged ischemia and reperfusion. The protective effects of IPC have been well documented in the previous studies involving different tissues and organs. These included cardicmuscle[1,9], skeletal muscle[2], small intestines[10] and more recently the liver[11]. Although the mechanism of IPC is still unclear up to now, several potential mediators (nitrogen monoxide, adenosine, oxide radical, bradykinin and so on) have been found to play different roles in different organs[11-14]. Adenosine and protein kinase C (PKC) were critical to the beneficial actions of IPC in the heart[15]. IPC-induced adenosine A_1-receptor stimulation during the period of preconditioning ischemia increased phospholipose C (PLC) activity, an event that is coupled by pertussis toxin-sensitive G proteins[12,13]. Activation of PLC induced the formation of diacylglycerol, which in turn promotes the translocation and activation of PKC. Activation of PKC stimulated the activation of ATP-sensitive potassium (Katp) channels, and the beneficial actions of IPC in the heart were induced[15], while adenosine stimulated NO production in IPC to protect against the injury associated with I/R in liver[16]. In the case of the cirrhotic liver, our work revealed that the ATP and EC levels in IPC group were higher than those in I/R group. There was significantly more bile produced by the livers in IPC group too. However, the increase of AST, ALT and LDH release was attenuated, when IPC was performed before ischemia. This fact shows the protective effect of IPC on preventing ischemia-reperfusion damage of cirrhotic liver. In addition, we found that L-arginine administration in hepatic ischemia reperfusion attenuated the injury in a manner similar to that of IPC. Accordingly, inhibition of NO synthesis abolished the beneficial effects of IPC. Thus, our data suggest that NO is one of the potential mediators of the protective effects of IPC.

Akimisn.[2] and Kubes[3] demonstrated that IPC prevented intestinal and skeletal muscle I/R injury by inhibiting postischemic leukocyte-endothelial cell interactions. These observations are important because they indicate that in addition to protecting against the deleterious effects of ischemia and reperfusion, IPC could induce cellular changes that also prevent leukocyte recruitment to ischemic tissues. This might limit the reperfusion component of I/R injury, which was primarily leukocyte dependent in the small intestine and other organs[17,18]. Thus, in addition to K^+-ATP channels, IPC appears to target effector molecules that modulate the inflammatory response to I/R. A likely candidate effector molecule that may be targeted by the signaling cascade initiated by IPC is P-selectin, for several researches have shown that I/R injury is a leukocyte-mediated event resulted from a cascade of acute phase reactants causing leukocyte-endothelial cell interactions. The interactions progressed from rolling to saltation to firm adhesion with subsequent tissue infiltration and organ injury[19-24]. The cascade of acute phase reactants was critically dependent on the expression of P-selectin on venular endothelium[4,25]. In our study, significant promotion of the expression of P-selectin in hepatocytes in the I/R group was observed in comparison with the SO group. IPC or L-arginine attenuated P-selectin expression significantly. However, inhibition of NO synthesis enhanced the expression of P-selectin. The increase in the leukocytes count was prevented in IPC group. Administration of L-arginine resulted in the same effects as in IPC group. In the mean time, there was a significant correlation between leukocytes infiltration and P-selectin expression in liver tissues. The degree of P-selectin expression was positively correlated with the counts of leukocyte infiltration in liver.

In summary, IPC can abolish I/R induced leukocyte adhesion and infiltration by preventing postischemic P-selectin expression in rats with liver cirrhosis via a NO-initiated pathway.

REFERENCES

1 **Murry CE**, Jennings RB, Reimer KA. Preconditioning with ischemia: a delay of lethal cell injury in ischemic myocardium. *Circulation* 1986; **74**: 1124-1136
2 **Akimitsu T**, Gute DC, Korthuis RJ. Ischemic preconditioning attenuates postischemic leukocyte adhesion and emigration. *Am J Physiol* 1996; **271**(5Pt 2): H2052-2059
3 **Kubes P**, Payne D, Ostrovsky L. Preconditioning and adenosine in I/R-induced leukocyte-endothelial cell interactions. *Am J Physiol* 1998; **274**(4Pt 2): H1230-H238
4 **Kurose I**, Anderson DC, Miyasaka M, Tamatani T, Paulson JC, Todd RF, Rusche JR, Granger DN. Molecular determinants of reperfusion-induced leukocyte adhesion and vascular protein leakage. *Circ Res* 1994; **74**: 336-343
5 **Wu MC**, Yang GS. Reproduction of cirrhotic liver of rat. *Zhonghua Shiyan Waike Zazhi* 1984; **1**: 145-147
6 **Canada AT**, Stein K, Martel D, Watkins WD. Biochemical appraisal of models for hepatic ischemic/reperfusion injury. *Circ Shock* 1992; **36**: 163-168
7 **Shimabukuro T**, Ymamoto Y, Kume M, Kimoto S, Okamoto R, Morimoto T, Yamaoka Y. Induction of heat shock response: effect on the rat liver with carbon tetrachloride-induced fibrosis from ischemia-reperfusion injury. *World J Surg* 1998; **22**: 464-469
8 **Wang D**, Shi JQ, Liu FX. Immunohistochemical detection of proliferating cell nuclear antigen carcinoma. *China Natl J New Gastroenterol* 1997; **3**: 101-103
9 **Yellon DM**, Alkhulaifi AM, Pugsley WB. Preconditioning the human myocardium. *Lancet* 1993; **342**: 276-277
10 **Jerome SN**, Akimitsu T, Gute DC, Korthuis RJ. Ischemic preconditioning attenuates capillary no-reflow induced by prolonged ischemia and reperfusion. *Am J Physiol* 1995; **268**(5Pt 2): H2063-2067
11 **Ferencz A**, Szanto Z, Borsiczky B, Kiss K, Kalmar-Nagy K, Szeberenyi J, Horvath PO, Roth E. The effects of preconditioning on the oxidative stress in small-bowel autotransplantation. *Surgery* 2002; **132**: 877-884
12 **Downey JM**, Cohen MV, Ytrehus K, Liu Y. Cellular mechanisms in ischemic preconditioning: the role of adenosine and protein kinase C. *Ann NY Acad Sci* 1994; **723**: 82-98
13 **Ishida T**, Yarimizu K, Gute DC, Korthuis RJ. Mechanisms of ischemic preconditioning. *Shock* 1997; **8**: 86-94
14 **Laude K,** Beauchamp P, Thuillez C, Richard V. Endothelial protective effects of preconditioning. *Cardiovasc Res* 2002; **55**: 466-473
15 **Gross GJ**, Fryer RM. Sarcolemmal versus mitochondrial ATP-sentitive K^+ channels and myocardial preconditioning. *Circ Res* 1999; **84**: 973-979
16 **Peralta C**, Hotter G, Closa D, Gelpi E, Bulbena O, Rosello-Catafau J. Protective effect of preconditioning on the injury associated to hepatic ischemia-reperfusion in the rat: role of nitric oxide and adenosine. *Hepatology* 1997; **25**: 934-937
17 **Granger DN**, Korthuis RJ. Physiologic mechanisms of postischemic tissue injury. *Annu Rev Physiol* 1995; **57**: 311-332
18 **Gute DC**, Ishida T, Yarimizu K, Korthuis RJ. Inflammatory responses to ischmia and reperfusion in skeletal muscle. *Mol Cell Biochem* 1998; **179**: 169-187
19 **Sanz MJ**, Johnston B, Issekutz A, Kubes P. Endothelin-1 causes P-selectin-dependent leukocyte rolling and adhesion within rat mesenteric microvessels. *Am J Physiol* 1999; **277**(5Pt 2): H1823-H1830
20 **Cotran RS**, Pober JS. Cytokine-endothelial interactions in inflammation, immunity, and vascular injury. *J Am Soc Nephrol* 1990; **1**: 225-235
21 **Bienvenu K**, Granger DN. Molecular determinants of shear rate-dependent leukocyte adhesion in postcapillary venules. *Am J Physiol* 1993; **264**(5Pt 2): H1504-H1508
22 **Springer TA**. Traffic signals for lymphocyte recirculation and leukocyte emigration: the multistep paradigm. *Cell* 1994; **76**: 301-314
23 **Jaeschke H,** Smith CW. Mechanisms of neutrophil-induced parenchymal cell injury. *J Leukoc Biol* 1997; **61**: 647-653
24 **Lefer AM**, Tsao PS, Lefer DJ, Ma XL. Role of endothelial dysfunction in the pathogenesis of reperfusion injury after myocardial ischemia. *FASEB J* 1991; **5**: 2029-2034
25 **Lefer DJ,** Flynn DM, Anderson DC, Buda AJ. Combined inhibition of P-selectin and ICAM-1 reduces myocardial injury following ischemia and reperfusion. *Am J Physiol* 1996; **271**(6Pt 2): H2421-H2429

Edited by Ma JY

P.O.Box 2345, Beijing 100023,China
Fax: +86-10-85381893
E-mail: wjg@wjgnet.com www.wjgnet.com

World J Gastroenterol 2003;9(10):2293-2299
World Journal of Gastroenterology
 ISSN 1007-9327

• CLINICAL RESEARCH •

Pan-enteric dysmotility, impaired quality of life and alexithymia in a large group of patients meeting *ROME* II criteria for irritable bowel syndrome

Piero Portincasa, Antonio Moschetta, Giuseppe Baldassarre, Donato F. Altomare, Giuseppe Palasciano

Piero Portincasa, Antonio Moschetta, Giuseppe Palasciano, Section of Internal Medicine, Department of Internal Medicine and Public Medicine (DIMIMP), University Medical School, Bari
Giuseppe Baldassarre, Division of Geriatrics, Hospital "*Miulli*", Acquaviva delle Fonti, Bari, Italy
Donato F. Altomare, Section of Surgery, Department of Emergency and Organ Transplant (DETO), University Medical School, Bari, Italy
Correspondence to: Piero Portincasa, MD, PhD, Chair Person of Semeiotica Medica-Section of Internal Medicine, Department of Internal and Public Medicine (DIMIMP), University of Bari Medical School-Policlinico-70124 Bari-Italy. p.portincasa@semeiotica.uniba.it
Telephone: +39-80-5478-227 **Fax:** +39-80-5478-232
Received: 2003-05-10 **Accepted:** 2003-08-02

Abstract

AIM: Psychological factors, altered motility and sensation disorders of the intestine can be variably associated with irritable bowel syndrome (IBS). Such aspects have not been investigated simultaneously. The aim of this paper was to evaluate gastrointestinal motility and symptoms, psychological spectrum and quality of life in a large group of IBS patients in southern Italy.

METHODS: One hundred IBS patients (F:M=73:27, age 48±2 years, mean±SE) fulfilling ROME II criteria matched with 100 healthy subjects (F:M=70:30, 45±2 years). Dyspepsia, bowel habit, alexithymia, psycho-affective profile and quality of life were assessed using specific questionnaires. Basally and postprandially, changes in gallbladder volumes and antral areas after liquid meal and orocaecal transit time (OCTT) were measured respectively by ultrasonography and H_2-breath test. Appetite, satiety, fullness, nausea, and epigastric pain/discomfort were monitored using visual-analogue scales.

RESULTS: Compared with controls, IBS patients had increased dyspepsia (score 12.6±0.7 *vs* 5.1±0.2, $P<0.0001$), weekly bowel movements (12.3±0.4 *vs* 5.5±0.2, $P<0.00001$, comparable stool shape), alexithymia (score 59.1±1.1 *vs* 40.5±1.0, $P=0.001$), poor quality of life and psycho-affective profile. IBS patients had normal gallbladder emptying, but delayed gastric emptying (T_{50}: 35.5±1.0 *vs* 26.1±0.6 min, $P=0.00001$) and OCTT (163.0±5.4 *vs* 96.6±1.8 min, $P=0.00001$). Fullness, nausea, and epigastric pain/discomfort were greater in IBS than in controls.

CONCLUSION: ROME II IBS patients have a pan-enteric dysmotility with frequent dyspepsia, associated with psychological morbidity and greatly impaired quality of life. The presence of alexithymia, a stable trait, is a novel finding of potential interest to detect subgroups of IBS patients with different patterns recoveed after therapy.

Portincasa P, Moschetta A, Baldassarre G, Altomare DF, Palasciano G. Pan-enteric dysmotility, impaired quality of life and alexithymia in a large group of patients meeting *ROME* II criteria for irritable bowel syndrome. *World J Gastroenterol* 2003; 9(10):2293-2299

http://www.wjgnet.com/1007-9327/9/2293.asp

INTRODUCTION

Irritable bowel syndrome (IBS) is a common, chronic biopsychological functional disorder of unknown aetiology, affecting 10-20 % of all individuals any one time. Psychological factors, altered motility and sensation disorders of the intestine can be variably associated[1]. Dysfunctions of the gastrointestinal tract in IBS appear as altered bowel function[2], associated with pain or discomfort, without organic disease[3-5]. Besides lowered visceral perception thresholds involving the rectum[6] and more proximal districts[7], motility defects seem to develop. Thus, IBS patients may complain of a constellation of both gastrointestinal and extra-intestinal symptoms[7], and a significant proportion of patients may have disordered perception[8,9] resulting in more readily feeling of normal intestinal contractions[10]. Psychological factors, such as abnormal illness attitute[11], may also play a role in the pathogenesis of IBS[5], with a significant impact on health-related quality of life (HRQOL)[12]. More recently, revised diagnostic criteria for IBS have been proposed (ROME II criteria)[4]. Moreover, sophisticated questionnaires are now available for studying both quality of life and specific psychological aspects like the alexithymia construct. The latter includes difficulties in identifying and describing feelings, impoverishment of fantasy life and excessive preoccupation with physical symptoms and external events[13].

Such aspects have not been investigated simultaneously in IBS patients. Therefore, the aim of the present study was to evaluate gastrointestinal motility and symptoms, psychological status, including alexithymia and HRQOL in a large group of IBS patients from a referral center in southern Italy.

MATERIALS AND METHODS

Subjects

A total number of 200 adult subjects were studied prospectively and divided into 2 cohorts: 100 consecutive patients with IBS (27 males and 73 females) and 100 healthy subjects (30 males and 70 females) with their age and body size matched. The two groups were also comparable for years of education (9.3±1.5 years and 9.6±1.3 years in healthy and IBS, respectively). The characteristics of patients are depicted in Table 1. There was no difference in sex ratio, age and body size. The percentage of non-coffee drinkers and smokers was greater in IBS than in healthy subjects ($0.02<P<0.03$). The IBS group was composed of out-patients, with a firm diagnosis through positive identification of the ROME II diagnostic criteria[4]. With the inclusion criteria used in this study, the specificity of IBS diagnosis was about 98 %[14,15]. Mean years since first diagnosis have been 5.9 years with bowel habit alternating between diarrhea and constipation, according to standardized criteria[4]. During the above mentioned period, patients had tried several -albeit poorly effective- therapeutic trials with the help of their family practices. All patients were symptomatic at the time of the study, and lower abdominal discomfort or pain was the main reason for seeking medical advice, and none was on specific therapy for IBS at the time of evaluation. There was no coexistent disease and all patients had normal haematology, biochemistry, urinalysis, together with a normal colonoscopy

or barium enema if aged over 50 years. Excluded were subjects if they had a history of gastrointestinal surgery. Female subjects were excluded if they were pregnant, breast feeding, or hysterectomised and were studied during the first phase of the menstrual cycle or while taking oestrogen/progesterone contraceptive medication. Drugs and cigarette smoking were not allowed for 48 hours prior to the study while alcohol and caffeine containing drinks were stopped 24 hours prior to the study. All subjects smoked less than 5 cigarettes per day and drank below the recommended safe alcohol limit (that is less than 21 units/week).

Because lactose maldigestion-intolerance and IBS may have almost identical symptoms[16], all patients were screened by lactose H_2-breath test, which was invariably negative. Healthy volunteers were recruited from staff members and with the help of local family practices. Laboratory investigations were normal (as above) in all healthy subjects and there was a negative toxicology for substances of abuse. All subjects gave informed consent to join the study which was approved by the Ethics Committee of Bari University Hospital.

Measures

Symptomatology was assessed by focusing on an estimate of the maximum degree of lower abdominal pain or discomfort, and abdominal bloating in the previous 12 months was assessed by visual analogue scales (VAS)[17]. The weekly frequency of bowel movements over a time span of one month was estimated by a self-assessed diary. A specific stool form scale was also used based on a semi-quantitative score[18]. To carefully characterise the association between IBS and functional dyspepsia[19], the presence and severity of dyspeptic symptoms were quantified in two ways: validated semiquantitative score[20]; and self-assessed VAS of upper gastrointestinal perception monitoring appetite, satiety, nausea, abdominal fullness and upper abdominal (epigastric) pain or discomfort[21]. In the latter case, scores were obtained at baseline (*i.e.* time 0) and at 15, 30, 45, 60, 90 and 120 min postprandially. The Middlesex Hospital Questionnaire (MHQ) symptom check list was used to investigate six symptoms: anxiety, phobic behavior, obsessive-compulsive behavior, somatization, depression, and hysteria[22]. Traits of alexithymia were assessed by the Toronto Alexithymia scale based on a 20-item scale (TAS-20)[23] with the validated Italian translation[24,25]. A final score $\geqslant$61 was considered positive for alexithymia, while a score ranging from 50 to 60 was "border line"[25]. The short form check list (SF-36) was used to assess HRQOL in the following 8 domains: general health, physical functioning, role-physical, role-emotion, social functioning, mental health, body pain, and vitality[26,27].

Motility studies

After an overnight fast, subjects attended the Functional Investigations Unit. Standard criteria recently reviewed by our group[28] were used to study gallbladder and gastric emptying by functional ultrasonography in response to a liquid test meal, consisting of 200 mL solution totalling 13 g (39 %) fat, 10 g (13 %) protein and 35 g (48 %) carbohydrates, calorie content 1 270 kJ, 365 mmol /L (*Nutridrink*®, Nutricia, Milano, Italy), which was consumed within 2 min. Gallbladder emptying was assessed by monitoring fasting and postmeal course of gallbladder volumes. Sagittal and transverse scans of the gallbladder at its largest dimension were obtained at 5-15 minute intervals over 2 hours. Gastric emptying was assessed by monitoring fasting and postmeal course of antral areas[17,29]. Oro-caecal transit time was measured simultaneously with ultrasonographic studies by hydrogen breath test using 10 g lactulose and collecting the breath with a portable equipment (EC60-Gastrolyzer, Bedfont, USA)[30].

Statistical analysis

All calculations were performed with the *NCSS 2001* statistical software (Kaysville, UT, USA, see http://www.ncss.com/). Results were given as mean ± standard error (SE). Differences in emptying curves were evaluated by two way *ANOVA* repeated-measures followed by Fisher's LSD multiple comparison test. Differences of means between healthy and IBS were evaluated using the Student's *t* test for unpaired data. Linear regression analysis was performed by the method of least square. The chi-square test was used to assess associations between categorical data. A two-tailed probability (*P*) value of less than 0.05 was considered statistically significant[31,32].

RESULTS

All subjects tolerated the tests well. Table 1 also shows that VAS scores for lower abdominal pain and bloating were significantly higher in IBS patients than in healthy subjects. Whereas the frequency of bowel movements was greater in IBS patients than in healthy subjects (12.3±0.4 *vs* 5.5±0.2 evacuations/wk, *P*=0.00001) (Figure 1A), stool form was similar (Buckley score: 3.9±0.1 *vs* 3.5±0.1 in patients and controls, respectively),(Figure 1B).

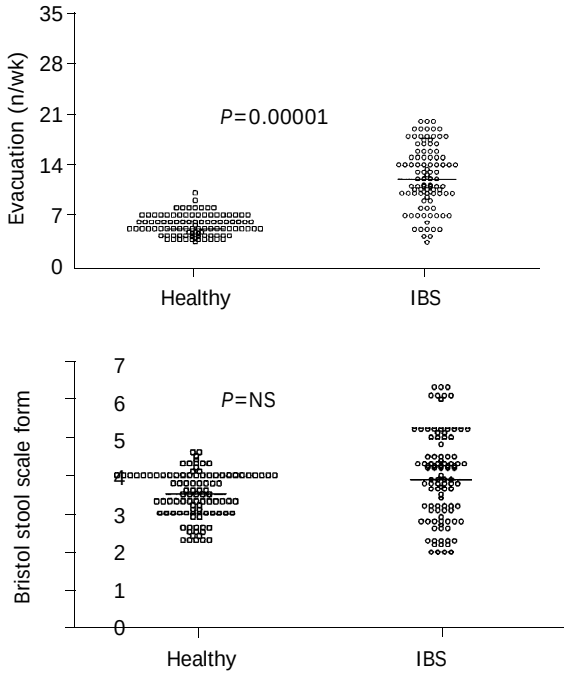

Figure 1 A: Significantly more bowel movements in IBS patients than in healthy subjects. B: Comparable score for stool form between IBS patients and healthy subjects. Results are expressed as individual data and median (horizontal line).

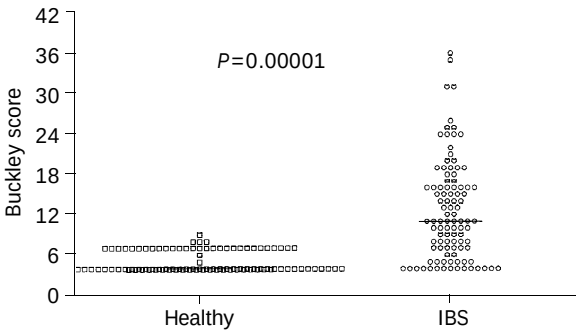

Figure 2 Significant dyspepsia in IBS patients compared with healthy subjects. Results are expressed as individual data and median.

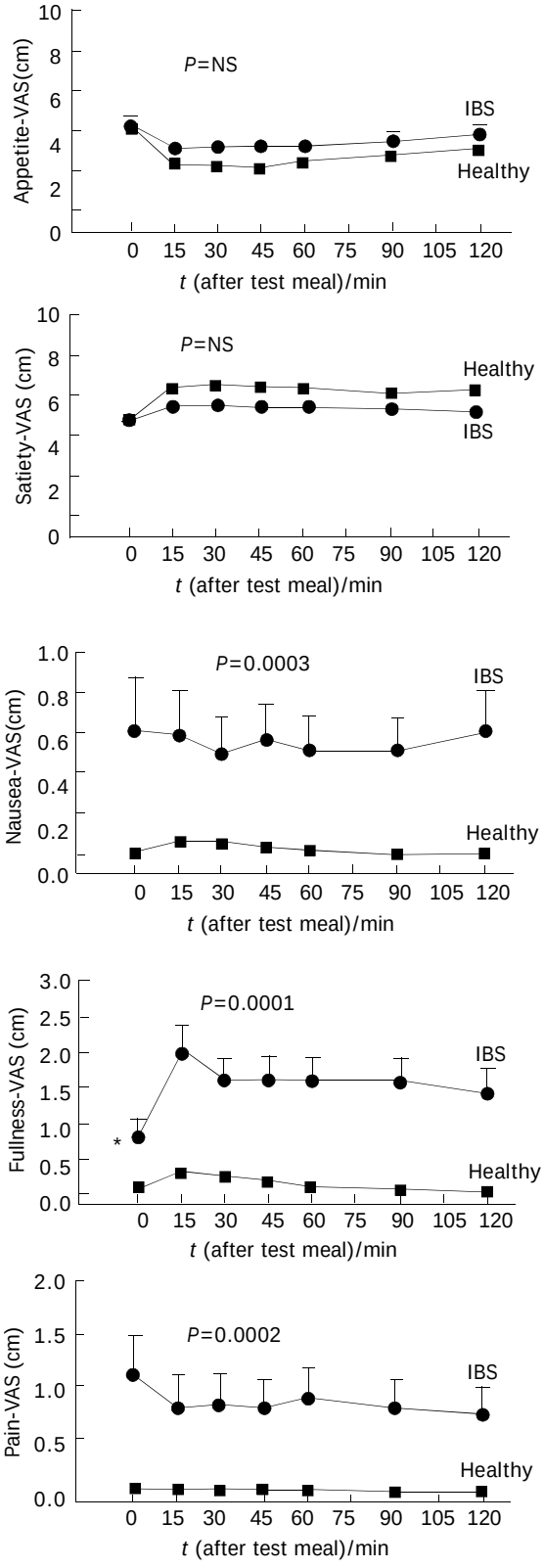

Figure 3 Time-course of visual analogue scale (VAS) for appetite, satiety, nausea, abdominal fullness and epigastric pain (or discomfort) in healthy subjects. On the X-axis time "0" is before ingestion of test meal. Asterisks indicate significant differences ($0.0001<P<0.001$) of IBS patients *vs* healthy subjects at baseline. Significant differences for nausea, fullness and epigastric pain / discomfort of IBS patients *vs* healthy subjects (area under curve).

Mean score of dyspepsia was greater in patients than in healthy subjects (12.6±0.7 *vs* 5.1±0.2, $P<0.0001$), an abnormal score was found in 75 % and 5 % of patients and healthy subjects, respectively ($P<0.0001$, Figure 2). As expected, the perception of satiety and appetite (both at fasting and as postprandial AUC) showed a strong negative correlation in IBS patients and healthy subjects ($0.91<r<0.92$, $P<0.0001$). There was no difference in appetite and satiety between IBS patients and healthy subjects (either at baseline and postprandially), By contrast, the AUC during 120 min was invariably greater in IBS than in control subjects for nausea (58.0±14.1 *vs*3.9±1.0, $P=0.002$), fullness (133.5±26.1 *vs* 17.1±1.9, $P=0.00002$) and pain/discomfort (75.1±24.2 *vs* 2.5±0.6, $P=0.002$). Time-dependent profiles for these scores are depicted in Figure 3.

Table 1 Patient characteristics in study group (mean ± SE)

	IBS	Healthy	*P**
No of subjects	100	100	
Female: Male ratio	73:27	70:30	NS
Age (yr)	48±2	45±2	NS
BMI (Kg / m^2)	23.5±0.4	22.9±0.3	NS
Coffee-drinkers No (%)			
None	43 (43%)	24 (24%)	0.03°
<1 per day	9 (9%)	22 (22%)°	
1-5 per day	48 (48%)	54 (54%)°	
Smokers No (%)	30 (30%)	15 (15%)	0.02°
Lower abdominal pain (VAS, cm)	5.8±0.1	0.04±0.01	0.0001
Abdominal bloating (VAS, cm)	6.2±0.1	0.1±0.02	0.0001

*Student's *t* test or χ^2 for comparison of proportions, VAS=visual analogue scale.

Results from the MHQ questionnaire are given in Figure 4A which shows that IBS patients had significantly higher scores for anxiety, somatization, phobia and depression than healthy subjects. Results from the TAS 20 questionnaire on alexithymia are given in Figure 4B which shows a significantly increased score in IBS patients (59.1±1.1) compared to healthy subjects (40.5±1.0). An abnormal (*i.e.*>61) score for alexithymia was found in 43 % of patients and in 2 % of healthy subjects. Mean scores of SF-36 are reported in Figure 5 which shows that HRQOL was significantly poorer for all domains in IBS patients compared with healthy subjects. There was no difference between IBS patients and healthy subjects with respect to gallbladder motility, *i.e.* fasting and postprandial volumes and half-emptying times (Table 2). Concerning gastric motility, the mean cross-sectional antral areas at fasting and immediately after the test meal were comparable between IBS patients and healthy subjects (Table 2). However, postprandial minimal antral areas were significantly larger and half-emptying time longer in IBS than in healthy subjects (Table 2, Figure 6). With respect to OCTT, basal levels of H_2 were invariably <10 p.p.m. in all subjects (*i.e.* absence of bacterial overgrowth) and did not differ between IBS patients and healthy subjects. OCTT, however, was increased by 62 % in IBS patients compared to healthy subjects (Table 2) with scattered distribution depicted in Figure 7. A value of OCTT above 130 min, representing the upper limit of normal (mean+2SDs), was found in 70 % of patients and in 2 % of healthy subjects ($P=0.000001$).

Overall, the score of dyspepsia was positively correlated with OCTT ($r=0.38$, $P=0.0001$) but not with gastric emptying speed. Also, the dyspepsia score was negatively correlated with all domains of HRQOL ($-0.34< r <-0.43$, $P<0.001$), while there was a positive correlation with somatization ($r=0.32$, $P=0.001$), anxiety ($r=0.29$, $P=0.002$) and alexithymia ($r=0.47$, $P=0.00001$). Frequency of bowel movements increased with anxiety ($r=0.39$,

P=0.00001), somatization (*r*=0.34, *P*=0.0004) and alexithymia (*r*=0.52, *P*=0.000001).

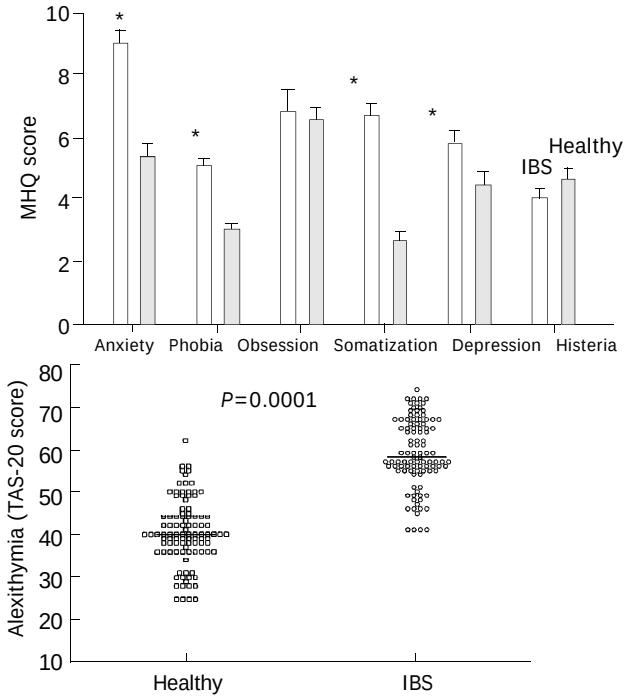

Figure 4 A: Scores of psychological disorders (mean ± SE, *0.0009<*P*<0.04). B: Scores of alexithymia (individual data and median) in IBS patients and healthy subjects.

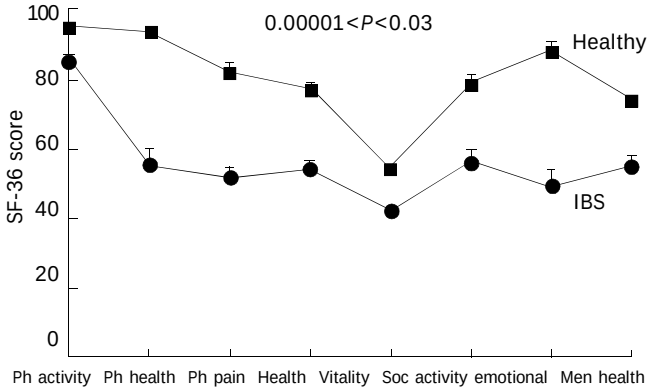

Figure 5 Profiles of health-related quality of life-HRQOL (SF-36 questionnaire) for IBS patients and healthy subjects. Data are mean±SE. Significantly poorer HRQOL for all 8 scales in IBS patients compared with healthy subjects. Legend: Ph, physical; soc, social.

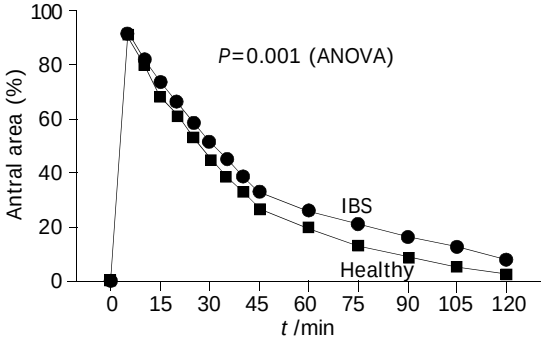

Figure 6 Time-course of gastric emptying in IBS patients and healthy subjects after ingestion of 200 mL of standard liquid meal. Symbols indicate mean (SE is very small and not visible at each time-point). IBS patients had impaired emptying with larger postprandial antral areas (expressed as % of basal area) than healthy subjects. See also Table 2 for half-emptying time differences.

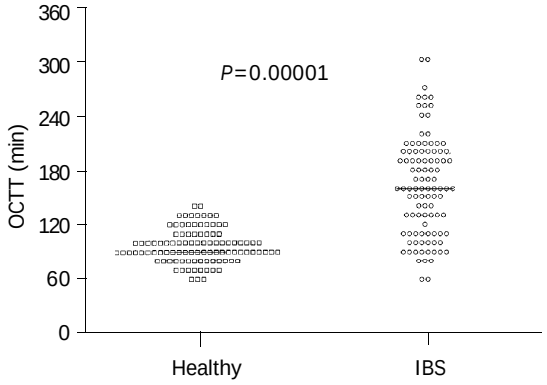

Figure 7 Significant delay of orocaecal transit time (OCTT) in IBS patients compared with healthy subjects. Results are expressed as individual data and median.

Table 2 Motility indices in study group (mean ± SE)

	IBS	Healthy	*P**
No of subjects	100	100	
Gallbladder (volume)			
Fasting (mL)	21.4±1.0	22.0±0.9	NS
Postprandial residual, mL (%)	5.3±0.6 (23.4±1.2)	5.7±0.3 (25.7±0.9)	NS
T_{50} (min.)	20.1±0.9	21.4±0.6	NS
Stomach (antral area)			
Fasting (cm^2)	3.1±0.1	3.4±0.1	NS
Postprandial maximal (cm^2)	10.4±0.2	11.8±0.2	0.001
Postprandial minimal (%)	6.1±1.0	2.8±0.5	0.02
T_{50} (min.)	35.5±1.0	26.1±0.6	0.00001
Small bowel			
Orocaecal transit time (min.)	161.9±5.5	96.6±1.8	0.00001

*Student's *t* test, OCTT=orocaecal transit time, NS=not significant. Indices of gallbladder motility: fasting volume (mean of 3 measurements at -15, -5 and 0 min before test meal, expressed in mL), residual volume (minimum volume measured postprandially, in mL) and half-emptying time (T_{50}, time to achieve 50 % decrease of fasting volume). Indices of stomach emptying: fasting antral area (mean of 3 measurements at –15, -5 and 0 min before test meal, expressed in cm^2), maximal antral area at 2 min postmeal in cm^2, minimal postprandial antral area during the 2-hour observation period (expressed in %, normalized to maximal area after subtracting basal areas: i.e. $100x(A_t-a)/(A_2-a)$, where A_t=postprandial area at any given time; a=basal area; A_2=area at 2 min postprandially[37]) and half-emptying time (T_{50}).

DISCUSSION

We used an integrated approach in a large group of IBS patients to investigate gastrointestinal motility patterns in relation to symptoms, quality of life and psychological comorbidity. We believe that the present study may offer a fairly representative picture of IBS characteristics in southern Italy. The ROME II criteria[4] were chosen because they perform well in the clinic and they have greater simplicity than other less recent criteria[1]. Due to the setting where the study was performed (*i.e.* a tertiary referral center), caution must be expressed in interpreting our results, for at least two reasons. Firstly, only a minority of IBS patients were thought to consult physicians[33] and secondly,

characteristics of patients seen in a third referral center miqht differ from those of patients referred to primary or secondary care[25,34]. Nevertheless, IBS patients had multiple and simultaneous gastrointestinal motility defects involving stomach and intestine at a different extent, and were associated with diffuse gastrointestinal symptoms, abnormal psychological status, including alexythimia, and poor quality of life.

Ultrasonography was chosen as a non-invasive and validated technique to assess both gallbladder[35,36] and gastric emptying[17,29,37-40] simultaneously[28]. The protocol we employed, moreover, was further informative due to the simultaneous assessment of small bowel transit by H_2-breath test. Such a novel combined procedure allows a one-day (and time-saving) test for studying upper gastrointestinal motility in a clinical setting.

Despite "normal" feeling of appetite and satiety, IBS patients had strikingly abnormal upper gastrointestinal perception for nausea, fullness, epigastric pain/discomfort, both at fasting and postprandially. This was also the case in gastrectomized patients[21], Thus, ingestion of 200 mL of a moderately caloric, isosmotic test meal might prove useful in identifying groups of patients with dyspepsia, as also proposed in different clinical settings[41]. About 30 % of IBS patients included in this study had delayed gastric emptying, as was found in other gastrointestinal functional disorders such as dyspepsia and slow transit constipation[30,42]. Although this study was primarily focusing on patients with lower abdominal symptoms for IBS, we found that the score for dyspepsia was abnormal in about two-thirds of patients, as was also reported by Agreus *et al.* in the Swedish population[43]. Taken together, these findings suggest that dyspepsia and IBS are closely related and develop as a *continuum*[19]. No close correlation existed between delayed gastric emptying and dyspepsia. Indeed, gastric emptying was defective only in a subgroup of dyspeptic patients and this also seemed to be the case in IBS patients. Moreover, both symptoms or gastric half emptying times were poor predictors of gastrointestinal dysmotility in functional dyspepsia[44]. Also, dyspeptic symptoms might originate from an altered fundic receptive relaxation (not measured in the present study) and/ or from disorders of other organs, including duodenum under acidic stress[45].

At variance with an early study in a scant number of IBS patients[46], we found no gross evidence for impaired gallbladder motility. Differences in selection criteria might partly explain the variability. CCK played a key role in postprandial gallbladder contraction, and abnormal sensitivity of the gallbladder smooth muscle to exogenous CCK has been reported in IBS[47]. Apparently, the defect was absent postprandially, since either a high-fat[47] or a low-fat (this study) liquid meal yielded similar gallbladder contractions. Whether or not the trend we showed of faster refilling in IBS points to an abnormality of the smooth muscle in the digestive tract[47], remains to be established. Impaired gallbladder motility has been found in a subgroup of patients with functional dyspepsia[42] and delayed transit constipation[30]. Disturbed motilin and CCK release might be a potential cause of intestinal dysmotility in IBS[48].

This study also showed that OCTT was delayed in IBS. Changes in phase II and phase III components of the migrating motor complex suggested that both local (*i.e.* enteric) and central mechanisms might operate to produce intestinal dysmotility[49]. Delayed OCTT could be independent of colonic transit (as seen in patients with functional dyspepsia[42]) or might be associated with delayed colonic transit (as seen in patients with functional constipation[30]). Although accelerated small bowel and colonic transit have been reported in diarrhea-predominant IBS[50], a similar conclusion could not be drawn from this study, since patients alternated between diarrhea and constipation in their history. IBS patients had rather increased bowel habits, despite delayed OCTT. This finding pointed to a diffuse impairment of visceral sensitivity and perception, involving not only the rectum[6], but also the colon or even more proximal districts such as small bowel and stomach[7,51]. Abnormal motor patterns in the small bowel might be associated with symptoms in patients with IBS (*e.g.* clustered jejunal contractions and propagated giant ileal contractions during abdominal colic[52]). It must be stressed, however, that no motor abnormality in either small or large intestine was pathognomonic for IBS[53]. Whether or not delayed OCTT in IBS could contribute to accumulation of gas in the intestine[54,55] and/or abnormal colonic fermentation in the colon[56], remains to be determined. Interestingly, we found delayed OCTT with increased bowel movements in chronic alcoholic patients during abstinence, associated with dysfunction of autonomic nervous system[57]. This possibility deserves further attention, since a form of subclinical autonomic neuropathy might predispose to a diffuse disorder of smooth muscle,which was suggestive for the multi-organic involvement of the gastrointestinal tract[7].

It is known that visceral hyperalgesia in IBS could exacerbate symptoms due to lactose maldigestion[58]. A recent study found that 24 % of previously diagnosed IBS patients had lactose intolerance[16], this was not the case in the present study where lactose maldigestion or intolerance was an exclusion criterion. It is still controversial whether or not a subset of patients with IBS might be positive for coeliac disease[59,60]. Since the recent British Society of Gastroenterology guidelines estimated that routine antiendomysial antibodies would reveal only 1-2 % of abnormalities[3], systematic screening for coeliac disease in this study was not believed to be cost-effective and was not performed.

It is believed that up to 60 % of IBS patients seen at referral centers might have psychological morbidity[5,61-64]. An abnormal psychological profile in IBS patients emerged also from the present study. Psychological disturbances could influence aspects of bowel habit[1,65]. We found increased bowel movements to be associated with anxiety, somatisation and also with alexithymia. Alexithymia construct is one of the four syndromes in the Diagnostic Criteria for Psychosomatic Research[34]. A stronger positive association was reported between alexithymia and somatoform rather than chronic somatic disorders[25,66,67]. In the present study we employed TAS-20, the most validated questionnaire available so far[23] and found significant alexithymia in over 40 % of IBS patients (increasing to about 80 % if patients with border-line scores were included). These results are in line with those from another although smaller study conducted in a closed geographical area, investigating alexithymia in patients with IBS and other functional gastrointestinal disorders[25]. The finding may have at least two practical implications. Firstly, whether IBS patients are first seen in a gastroenterological or psychiatric setting might determine if patients are classified as suffering mainly from IBS or somatoform disturbances, respectively. Secondly, as alexithymia is seen as a stable feature, it might act as an important prognostic factor related to treatment outcomes in subgroups of IBS patients. If the IBS patients were seen within the broader spectrum of functional gastrointestinal diseases, our findings pointed to an association between alexithymia and tendency to negative affectivity[25,67].

IBS patients showed a significantly poorer HRQOL than healthy subjects. This finding was in accordance with previous studies[12,61] and pointed to related problems, namely absenteeism, the social indirect costs and, ultimately, the need for appropriate treatment of IBS patients. Interestingly, both IBS patients and healthy subjects in this setting had a HRQOL profile remarkably

similar to that derived from subjects across different cultures in the USA and UK[12]. This finding underscored the internal consistency of HRQOL questionnaires. Taken together, our findings confirmed that although IBS was not a life-threatening condition, it could lead to significant impairment of quality of life, at least in the subgroup of patients seen in a tertiary referral center.

In conclusion, these data show that IBS patients have a pan-enteric dysmotility with frequent dyspepsia, associated with psychological morbidity and greatly impaired quality of life. The presence of alexithymia, a stable trait, is a novel finding of potential interest to detect subgroups of IBS patients with different patterns of recovery after therapy.

REFERENCES

1 **Camilleri M**, Heading RC, Thompson WG. Consensus report: clinical perspectives, mechanisms, diagnosis and management of irritable bowel syndrome. *Aliment Pharmacol Ther* 2002; **16**: 1407-1430
2 **Camilleri M**. Motor function in irritable bowel syndrome. *Can J Gastroenterol* 1999;**13**(Suppl A): 8A-11A
3 **Jones J**, Boorman J, Cann P, Forbes A, Gomborone J, Heaton K, Hungin P, Kumar D, Libby G, Spiller R, Read N, Silk D, Whorwell P. British Society of Gastroenterology guidelines for the management of the irritable bowel syndrome. *Gut* 2000; **47**(Suppl 2): II1-19
4 **Thompson WG**, Longstreth GF, Drossman DA, Heaton KW, Irvine EJ, Muller-Lissner SA. Functional bowel disorders and functional abdominal pain. *Gut* 1999; **45**(Suppl 2): II43-II47
5 **Horwitz BJ**, Fisher RS. The irritable bowel syndrome. *N Engl J Med* 2001; **344**: 1846-1850
6 **Mertz H**, Naliboff B, Munakata J, Niazi N, Mayer EA. Altered rectal perception is a biological marker of patients with irritable bowel syndrome. *Gastroenterology* 1995; **109**: 40-52
7 **Whorwell PJ**, McCallum M, Creed FH, Roberts CT. Non-colonic features of irritable bowel syndrome. *Gut* 1986; **27**: 37-40
8 **Houghton LA**, Whorwell PJ. Opening the doors of perception in the irritable bowel syndrome. *Gut* 1997; **41**: 567-568
9 **Azpiroz F**. Hypersensitivity in functional gastrointestinal disorders. *Gut* 2002;**51**(Suppl 1): i25-i28
10 **Naliboff BD**, Munakata J, Fullerton S, Gracely RH, Kodner A, Harraf F, Mayer EA. Evidence for two distinct perceptual alterations in irritable bowel syndrome. *Gut* 1997; **41**: 505-512
11 **Gomborone J**, Dewsnap P, Libby G, Farthing M. Abnormal illness attitudes in patients with irritable bowel syndrome. *J Psychosom Res* 1995; **39**: 227-230
12 **Hahn BA**, Yan S, Strassels S. Impact of irritable bowel syndrome on quality of life and resource use in the United States and United Kingdom. *Digestion* 1999; **60**: 77-81
13 **Kosturek A**, Gregory RJ, Sousou AJ, Trief P. Alexithymia and somatic amplification in chronic pain. *Psychosomatics* 1998; **39**: 399-404
14 **Kruis W**, Thieme C, Weinzierl M, Schussler P, Holl J, Paulus W. A diagnostic score for the irritable bowel syndrome. Its value in the exclusion of organic disease. *Gastroenterology* 1984; **87**: 1-7
15 **Vanner SJ**, Depew WT, Paterson WG, DaCosta LR, Groll AG, Simon JB, Djurfeldt M. Predictive value of the Rome criteria for diagnosing the irritable bowel syndrome. *Am J Gastroenterol* 1999; **94**: 2912-2917
16 **Bohmer CJ**, Tuynman HA. The effect of a lactose-restricted diet in patients with a positive lactose tolerance test, earlier diagnosed as irritable bowel syndrome: a 5-year follow-up study. *Eur J Gastroenterol Hepatol* 2001; **13**: 941-944
17 **Hveem K**, Jones KL, Chatterton BE, Horowitz M. Scintigraphic measurement of gastric emptying and ultrasonographic assessment of antral area: relation to appetite. *Gut* 1996; **38**: 816-821
18 **O'Donnell MR**, Virjee J, Heaton KW. Detection of pseudo diarrhoea by simple assessment of intestinal transit rate. *Br Med J* 1990; **300**: 439-440
19 **Talley NJ**, Fett SL, Zinsmeister AR, Melton LJ, III. Gastrointestinal tract symptoms and self-reported abuse: a population- based study. *Gastroenterology* 1994; **107**: 1040-1049
20 **Buckley MJ**, Scanlon C, McGurgan P, O'Morain C. A validated dyspepsia symptom score. *Ital J Gastroenterol Hepatol* 1997; **29**: 495-500
21 **Portincasa P**, Altomare DF, Moschetta A, Baldassarre G, Di Ciaula A, Venneman NG, Rinaldi M, Vendemiale G, Memeo V, vanBerge-Henegouwen GP, Palasciano G. The effect of acute oral erythromycin on gallbladder motility and on upper gastrointestinal symptoms in gastrectomized patients with and without gallstones: a randomized, placebo-controlled ultrasonographic study. *Am J Gastroenterol* 2000; **95**: 3444-3451
22 **Crown S**, Crisp AH. A short clinical diagnostic self-rating scale for psychoneurotic patients. The Middlesex Hospital Questionnaire (M.H.Q.). *Br J Psychiatry* 1966; **112**: 917-923
23 **Taylor GJ**, Ryan D, Bagby RM. Toward the development of a new self-report alexithymia scale. *Psychother Psychosom* 1985; **44**: 191-199
24 **Bressi C**, Taylor G, Parker J, Bressi S, Brambilla V, Aguglia E, Allegranti I, Bongiorno A, Giberti F, Bucca M, Todarello O, Callegari C, Vender S, Gala C, Invernizzi G. Cross validation of the factor structure of the 20-item Toronto Alexithymia Scale: an Italian multicenter study. *J Psychosom Res* 1996; **41**: 551-559
25 **Porcelli P**, Taylor GJ, Bagby RM, De Carne M. Alexithymia and functional gastrointestinal disorders. A comparison with inflammatory bowel disease. *Psychother Psychosom* 1999; **68**: 263-269
26 **Ware JE**, Snow KK, Kosinski M. SF-36 health survey. Manual and interpretation guide. Boston: The Health Institute: *New England Medical Center* 1993
27 **Stewart AL**, Greenfield S, Hays RD, Wells K, Rogers WH, Berry SD, McGlynn EA, Ware JE Jr. Functional status and well-being of patients with chronic conditions. Results from the Medical Outcomes Study. *JAMA* 1989; **262**: 907-913
28 **Portincasa P**, Colecchia A, Di Ciaula A, Larocca A, Muraca M, Palasciano G, Roda E, Festi D. Standards for diagnosis of gastrointestinal motility disorders. Ultrasonography. *Dig Liver Dis* 2000; **32**: 160-172
29 **Bolondi L**, Bortolotti MSV, Calleti T, Gaiani S, Labo' G. Measurement of gastric emptying by real-time ultrasonography. *Gastroenterology* 1985; **89**: 752-759
30 **Altomare DF**, Portincasa P, Rinaldi M, Di Ciaula A, Martinelli E, Amoruso AC, Palasciano G, Memeo V. Slow-transit constipation: a solitary symptom of a systemic gastrointestinal disease. *Dis Colon Rectum* 1999; **42**: 231-240
31 **Armitage P**, Berry G. Statistical methods in medical research. 3rd ed. Oxford: *Blackwell Science Ltd* 1994
32 **Dawson B**, Trapp RG. Basic & Clinical Biostatistics. 3rd ed. New York: *McGraw-Hill* 2001
33 **Jones R**, Lydeard S. Irritable bowel syndrome in the general population. *BMJ* 1992; **304**: 87-90
34 **Porcelli P**, De Carne M, Fava GA. Assessing somatization in functional gastrointestinal disorders: integration of different criteria. *Psychother Psychosom* 2000; **69**: 198-204
35 **Everson GT**, Braverman DZ, Johnson ML, Kern F Jr. A critical evaluation of real-time ultrasonography for the study of gallbladder volume and contraction. *Gastroenterology* 1980; **79**: 40-46
36 **Portincasa P**, Di Ciaula A, Baldassarre G, Palmieri VO, Gentile A, Cimmino A, Palasciano G. Gallbladder motor function in gallstone patients: sonographic and *in vitro* studies on the role of gallstones, smooth muscle function and gallbladder wall inflammation. *J Hepatol* 1994; **21**: 430-440
37 **Wedmann B**, Schmidt G, Wegener M, Coenen C, Ricken D, Althoff J. Effects of age and gender on fat-induced gallbladder contraction and gastric emptying of a caloric liquid meal: a sonographic study. *Am J Gastroenterol* 1991; **86**: 1765-1770
38 **Ricci R**, Bontempo I, Corazziari E, La Bella A, Torsoli A. Real-time ultrasonography of the gastric antrum. *Gut* 1993; **34**: 173-176
39 **Bergmann JF**, Chassany O, Petit A, Triki R, Caulin C, Segrestaa JM. Correlation between echographic gastric emptying and appetite: influence of psyllium. *Gut* 1992; **33**: 1042-1043
40 **Darwiche G**, Almer LO, Bjorgell O, Cederholm C, Nilsson P. Measurement of gastric emptying by standardized real-time ultrasonography in healthy subjects and diabetic patients. *J Ultrasound Med* 1999; **18**: 673-682
41 **Strid H**, Norstrom M, Sjoberg J, Simren M, Svedlund J, Abrahamsson H, Bjornsson ES. Impact of sex and psychological factors on the water loading test in functional dyspepsia. *Scand J*

Gastroenterol 2001; **36**: 725-730
42 **Portincasa P**, Moschetta A, Venneman NG, Palasciano G. Gastrointestinal motility in patients with chronic functional dyspepsia. *Dig Liver Dis (Ital J Gastroenterol) 30 (Suppl. II), A111* 1998
43 **Agreus L**, Svardsudd K, Nyren O, Tibblin G. Irritable bowel syndrome and dyspepsia in the general population: overlap and lack of stability over time. *Gastroenterology* 1995; **109**: 671-680
44 **Wilmer A**, Van Cutsem E, Andrioli A, Tack J, Coremans G, Janssens J. Ambulatory gastrojejunal manometry in severe motility-like dyspepsia: lack of correlation between dysmotility, symptoms, and gastric emptying. *Gut* 1998; **42**: 235-242
45 **Samsom M**, Verhagen MA, vanBerge Henegouwen GP, Smout AJ. Abnormal clearance of exogenous acid and increased acid sensitivity of the proximal duodenum in dyspeptic patients. *Gastroenterology* 1999; **116**: 515-520
46 **Braverman DZ**. Gallbladder contraction in patients with irritable bowel syndrome. *Isr J Med Sci* 1987; **23**: 181-184
47 **Kellow JE**, Miller LJ, Phillips SF, Zinsmeister AR, Charboneau JW. Altered sensitivity of the gallbladder to cholecystokinin octapeptide in irritable bowel syndrome. *Am J Physiol* 1987; **253**: G650-G655
48 **Sjolund K**, Ekman R, Lindgren S, Rehfeld JF. Disturbed motilin and cholecystokinin relese in the irritable bowel syndrome. *Scand J Gastroenterol* 1996; **31**: 1110-1114
49 **Kellow JE**, Eckersley GM, Jones M. Enteric and central contributions to intestinal dysmotility in irritable bowel syndrome. *Dig Dis Sci* 1992; **37**: 168-174
50 **Vassallo M**, Camilleri M, Phillips SF, Brown ML, Chapman NJ, Thomforde GM. Transit through the proximal colon influences stool weight in the irritable bowel syndrome. *Gastroenterology* 1992; **102**: 102-108
51 **Kellow JE**, Phillips SF. Functional disorders of the small intestine. In: Snape WJJ, editor. Pathogenesis of functional bowel disorders. New York: *Plenum Publ Corp* 1989: 171-198
52 **Stivland T**, Camilleri M, Vassallo M, Proano M, Rath D, Brown M, Thomforde G, Pemberton J, Phillips S. Scintigraphic measurement of regional gut transit in idiopathic constipation. *Gastroenterology* 1991; **101**: 107-115
53 **Kellow JE**, Phillips SF. Altered small bowel motility in irritable bowel syndrome is correlated with symptoms. *Gastroenterology* 1987; **92**: 1885-1893
54 **Whorwell PJ**. The problem of gas in irritable bowel syndrome. *Am J Gastroenterol* 2000; **95**: 1618-1619
55 **Serra J**, Azpiroz F, Malagelada JR. Impaired transit and tolerance of intestinal gas in the irritable bowel syndrome. *Gut* 2001; **48**: 14-19
56 **King TS**, Elia M, Hunter JO. Abnormal colonic fermentation in irritable bowel syndrome. *Lancet* 1998; **352**: 1187-1189
57 **Portincasa P**, Moschetta A, Radicione T, Pugliese S, Castore A, Salerno MT, Palasciano G. Coexistence of diffuse gastrointestinal dysmotility, dyspepsia and autonomic dysfunction in chronic alcoholism. *Gastroenterology* 2001; **120**(Suppl1): A1496
58 **Tolliver BA**, Jackson MS, Jackson KL, Barnett ED, Chastang JF, DiPalma JA. Does lactose maldigestion really play a role in the irritable bowel? *J Clin Gastroenterol* 1996; **23**: 15-17
59 **Sanders DS**, Carter MJ, Hurlstone DP, Pearce A, Ward AM, McAlindon ME, Lobo AJ. Association of adult coeliac disease with irritable bowel syndrome: a case-control study in patients fulfilling ROME II criteria referred to secondary care. *Lancet* 2001; **358**:1504-1508
60 **Hamm LR**, Sorrells SC, Harding JP, Northcutt AR, Heath AT, Kapke GF, Hunt CM, Mangel AW. Additional investigations fail to alter the diagnosis of irritable bowel syndrome in subjects fulfilling the Rome criteria. *Am J Gastroenterol* 1999; **94**: 1279-1282
61 **Whitehead WE**, Burnett CK, Cook EW, III, Taub E. Impact of irritable bowel syndrome on quality of life. *Dig Dis Sci* 1996; **41**: 2248-2253
62 **Drossman DA**, McKee DC, Sandler RS, Mitchell CM, Cramer EM, Lowman BC, Burger AL. Psychosocial factors in the irritable bowel syndrome. A multivariate study of patients and nonpatients with irritable bowel syndrome. *Gastroenterology* 1988; **95**: 701-708
63 **Fullwood A**, Drossman DA. The relationship of psychiatric illness with gastrointestinal disease. *Annu Rev Med* 1995; **46**: 483-496
64 **Whitehead WE**, Bosmajian L, Zonderman AB, Costa PT Jr, Schuster MM. Symptoms of psychologic distress associated with irritable bowel syndrome. Comparison of community and medical clinic samples. *Gastroenterology* 1988; **95**: 709-714
65 **Gorard DA**, Gomborone JE, Libby JW, Farthing MJ. Intestinal transit in anxiety and depression. *Gut* 1996; **39**: 551-555
66 **Bagby RM**, Taylor GJ, Parker JD. Construct validity of the Toronto Alexithymia Scale. *Psychother Psychosom* 1988; **50**: 29-34
67 **Taylor GJ**, Parker JD, Bagby RM, Acklin MW. Alexithymia and somatic complaints in psychiatric out-patients. *J Psychosom Res* 1992; **36**: 417-424

Edited by Wang XL

P.O.Box 2345, Beijing 100023,China
Fax: +86-10-85381893
E-mail: wjg@wjgnet.com www.wjgnet.com

World J Gastroenterol 2003;9(10):2300-2307
World Journal of Gastroenterology
 ISSN 1007-9327

• CLINICAL RESEARCH •

Association of extraintestinal manifestations of inflammatory bowel disease in a province of western Hungary with disease phenotype: Results of a 25-year follow-up study

Laszlo Lakatos, Tunde Pandur, Gyula David, Zsuzsanna Balogh, Pal Kuronya, Arpad Tollas, Peter Laszlo Lakatos

Laszlo Lakatos, Tunde Pandur, Gyula David, 1st Department of Medicine, Csolnoky F. Province Hospital, Veszprem
Zsuzsanna Balogh, Department of Medicine, Grof Eszterhazy Hospital, Papa
Pal Kuronya, Department of Infectious Diseases, Magyar Imre Hospital, Ajka
Arpad Tollas, Department of Medicine, Municipal Hospital, Varpalota
Peter Laszlo Lakatos, 1st Department of Medicine, Semmelweis University, Budapest, Hungary
Correspondence to: Laszlo Lakatos, MD, 1st Department of Medicine, Csolnoky F. Province Hospital, Korhaz u.1, Veszprem, H-8200 Hungary. laklaci@hotmail.com
Telephone: +36-20-911-9339 **Fax:** +36-1-313-0250
Received: 2003-06-21 **Accepted:** 2003-08-02

Abstract

AIM: IBD is a systemic disease associated with a large number of extraintestinal manifestations (EIMs). Our aim was to determine the prevalence of EIMs in a large IBD cohort in Veszprem Province in a 25-year follow-up study.

METHODS: Eight hundred and seventy-three IBD patients were enrolled (ulcerative colitis/UC/: 619, m/f: 317/302, mean age at presentation: 38.3 years, average disease duration: 11.2 years; Crohn's disease/CD/: 254, m/f: 125/129, mean age at presentation: 32.5 years, average disease duration: 9.2 years). Intestinal, extraintestinal signs and laboratory tests were monitored regularly. Any alteration suggesting an EIMs was investigated by a specialist.

RESULTS: A total of 21.3 % of patients with IBD had EIM (UC: 15.0 %, CD: 36.6 %). Age at presentation did not affect the likelihood of EIM. Prevalence of EIMs was higher in women and in CD, ocular complications and primary sclerosing cholangitis (PSC) were more frequent in UC. In UC there was an increased tendency of EIM in patients with a more extensive disease. Joint complications were more frequent in CD (22.4 % *vs* UC 10.2 %, $P<0.01$). In UC positive family history increased the risk of joint complications (OR:3.63). In CD the frequency of type-1 peripheral arthritis was increased in patients with penetrating disease ($P=0.028$). PSC was present in 1.6 % in UC and 0.8 % in CD. Dermatological complications were present in 3.8 % in UC and 10.2 % in CD, the rate of ocular complications was around 3 % in both diseases. Rare complications were glomerulonephritis, autoimmune hemolytic anaemia and celiac disease.

CONCLUSION: Prevalence of EIM in Hungarian IBD patients is in concordance with data from Western countries. The high number of EIM supports a role for complex follow-up in these patients.

Lakatos L, Pandur T, David G, Balogh Z, Kuronya P, Tollas A, Lakatos PL. Association of extraintestinal manifestations of inflammatory bowel disease in a province of western Hungary with disease phenotype: Results of a 25-year follow-up study. *World J Gastroenterol* 2003; 9(10):2300-2307
http://www.wjgnet.com/1007-9327/9/2300.asp

INTRODUCTION

Ulcerative colitis (UC) and Crohn' s disease (CD) are chronic inflammatory diseases of undetermined origin. Inflammatory bowel disease (IBD) is a multifactorial polygenic disease with probable genetic heterogeneity. In this hypothesis, the disease may develop in a genetically predisposed host as a consequence of altered mucosal barrier and disregulated immune response to environmental, in particular enteric antigens, resulting in continuous immune-mediated inflammation[1-4]. IBD predominantly affects the gastrointestinal system but it is associated with a large number of extraintestinal manifestations (EIMs)[5]. Some disorders parallel the activity of the bowel disease but for a number of these conditions, their courses run independently of the course of the intestinal disease[6,7]. Furthermore, there has been some variance in the literature as to whether these EIMs are more associated with CD or UC. In the classical study of Greenstein *et al*.[8] EIMs were classified as colitis associated, small bowel associated and none specific manifestations.

EIMs contribute significantly to morbidity and mortality. Defining specific associations of immune mediated diseases in extraintestinal sites and IBD may be helpful in the better understanding of the pathogenesis of IBD.

The pathogenesis of EIMs is also multifactorial. The role of genetic factors is supported by family and candidate (e.g. certain HLA) gene studies[9-11]. The role of humoral immunity is supported by the higher prevalence of autoantibodies in the presence of EIMs, especially pANCA in primary sclerosing cholangitis (PSC). The immunological and clinical connections between these diseases and IBD have never been fully elucidated.

In this study we aimed to define the prevalence of EIMs in a 25-year follow up study in Hungarian IBD patients. We sought to determine if any of the EIMs was more likely associated with CD or UC, with male or female gender in a follow-up study. Possible associations between EIMs and location and disease behaviour were also investigated.

MATERIALS AND METHODS

Eight hundred and seventy-three IBD patients followed-up at the Out- and Inpatient Gastroenterology Units of the Csolnoky F. Province Hospital in Veszprem Province were enrolled. This hospital is the secondary referral center for IBD patients in the province.

The data of the 619 UC patients (male/female: 317/302) are summarized in Table 1. The age at presentation varied between 9 and 80 years (average: 38.3 years). Average disease duration was 11.2 years (1-56 years). The location of UC according to the known greatest extent was proctitis in 117,

left sided colitis in 304 (including 171 patients with proctosigmoiditis), subtotal (98) and pancolitis (100) in 198 cases. Two hundred and fifty-four CD patients were included (125 males, 129 females). Average age at presentation was 32.5 years (12-80 years). According to the Vienna classification 192 patients were classified as A1, while 62 as A2. Disease duration was 9.2 years (1-40 years). Location of CD was ileal (L1) in 60, colonic (L2) in 81 and ileocolonic (L3) in 113 cases. Patients with upper GI manifestation had lower GI disease as well and they were classified according to their lower GI disease. According to the disease behavior 83 of our CD patients were defined as non-stricturing non-penetrating, 62 as stricturing and 105 as penetrating. Fifty-eight patients of the 95 penetrating cases had parallel strictures. Patients with indeterminate colitis were excluded.

Table 1 Clinical data of IBD patients

	Ulcerative colitis	Crohn's disease
Number of patients	619	254
Male / female	317 / 302	125 / 129
Mean age at diagnosis	38.3 yrs (9-80 yrs)	32.5 yrs (12-80 yrs)
Location	Proctitis: 117	L1: 60
	Left sided colitis: 304	L2: 81
	Pancolitis: 198	L3: 113
Behaviour of CD	-	B1: 87
		B2: 62
		B3: 105

In Crohn's disease (CD). Location: L1: terminal ileum, L2: colonic, L3: ileocolonic, behaviour: B1: non stricturing-non penetrating, B2: stricturing, B3: penetrating.

Patients in remission were followed-up twice per year. Patients who relapsed were followed-up or hospitalised according to the actual disease activity. Special interest was dedicated to the presence of EIM. Screening of EIMs was not performed, therefore the number of EIMs may have been underestimated. Routine follow-up consisted of assessment of patient's complaints, physical examination and laboratory testing.

Any alteration suggesting an EIMs was investigated by a specialist. In this study we did not assess the association between disease activity and the presence of EIM. Major EIMs studied in this report were axial and peripheral arthropathies (including ankylosing spondylitis), aseptic femoral head necrosis, primary sclerosing cholangitis (PSC), small duct cholangitis, autoimmune hepatitis, erythema nodosum, pyoderma gangrenosum, chronic urticaria, acute anterior uveitis, iritis, episcleritis, conjunctivitis, autoimmune hemolytic anaemia (AIHA), immune thrombocytopenic purpura (ITP), celiac disease, myositis, and glomerulonephritis.

Joint involvements were classified as peripheral and/or axial arthropathies. Peripheral arthropathies were divided into two subgroups according to the classification of Orchard *et al*[13]. Type-1 arthritis is an acute self-limiting pauciarticular (less than 5 joints) arthropathy typically affecting large joints. It is associated with other EIMs and its course parallels with the activity of the bowel disease. In contrast, type 2 arthritis is a chronic bilateral, symmetrical polyarticular arthropathy affecting five or more small joints. Its course runs independently of the course of the intestinal disease. Axial arthropathies are divided into sacroileitis and ankylosing spondylitis (SPA). Its incidence is 20-times higher than that in the normal population[14]. Rheumatologists investigated sacroileitis and ankylosing spondylitis cases. Laboratory testing (rheumatoid factor), X-ray and since 1997 MRI examinations were done.

Patients with elevated liver function tests (LFT, aminotransferases, cholestatic enzymes) were followed-up more cautiously. In patients with chronic or progressive elevation of enzyme levels liver biopsy and/or endoscopic retrograde cholangiopancreatography (ERCP) examination was done if patient gave informed consent. The diagnosis of PSC was based on elevated liver function tests, ERCP and consistent histology findings. Small duct PSC was diagnosed if histology suggested PSC, but ERCP could not verify the diagnosis[15,16]. Cholelithiasis, cirrhosis and focal nodular hyperplasia (FNH) were excluded from hepatobiliary manifestations.

In patients with verified thrombosis, blood samples were examined for hypercoagulability including in almost all cases analysis of plasminogen, proteins C and S activity and factor V Leiden mutation.

Patients with glomerulonephritis were followed-up by nephrologists as well. Diagnosis was based on clinical and chemical data and congruent histology findings. Ureteral obstruction was diagnosed by cystoscopy and urography, CT or MRI. If the alteration suggested fistulae in the urinary tract, cytography was also performed.

Statistical analysis

For statistical comparison of the data, Statistica 6.0 (Statsoft Inc, USA) was used. Normality was tested by Shapiro-Wilk's W test. χ^2 test with Yates correction was used to compare groups and odds ratios were calculated.

RESULTS

The prevalence of major (joint, hepatobiliary, ocular and cutaneous) and all EIMs determined in this study are shown in Table 2. Major EIMs were apparent more frequently in CD than in UC (36.6 % *vs* 15.0 %, $P<0.001$). EIMs were more frequent in patients with a disease duration for more than 10 years in both CD (22.1 % *vs* 48.9 %, $P=0.003$) and UC (22.1 % *vs* 10.4 %, $P<0.001$).

Table 2 Prevalence of extraintestinal manifestations (EIM) in IBD

	Total *n* (%)	Disease duration	
		⩽ 10 yrs *n* (%)	> 10 yrs *n* (%)
IBD	873	511	352
Major EIMs	186 (21.3)	86 (16.8)	102 (30.0)
All EIM signs	547 (62.7)	278 (54.4)	269 (76.4)
Ulcerative colitis	619	357	262
Major EIMs	93 (15.0)	37 (10.4)	58 (22.1)
All EIM signs	360 (58.2)	167 (46.8)	193 (73.7)
Crohn's disease	254	164	90
Major EIMs	93 (36.6)	49 (29.9)	44 (48.9)
All EIM signs	187 (73.6)	111 (67.7)	76 (84.4)

The prevalence of EIMs was higher in CD except ocular complications and PSC ($P<0.001$ for joint, hepatobiliary and cutaneous manifestations, Tables 3 and 4). In general, EIMs were more frequent in women except hepatobiliary manifestations and arthropathies in UC patients.

All major EIMs were more prevalent in more extensive UC (Table 5). There was a tendency of increased frequency of joint manifestations in CD patients with colonic involvement (L2 and L3: 23.7 %) compared to patients with only ileal disease (18.3 %, P=NS, Table 5). The prevalences of hepatobiliary, ocular and cutaneous manifestations were not different according to disease location.

Table 3 Age at presentation and prevalence of major extraintestinal manifestations in patients with IBD

	A1 *n* (%)	A2 *n* (%)
UC (*n*: 619)	369	250
Joint	32 (8.7)	20 (8.0)
Hepatobiliary	49 (13.3)	28 (11.2)
Cutaneous	17 (4.6)	7 (2.8)
Ocular	11 (3.0)	8 (3.0)
CD (*n*: 254)	192	62
Joint	48 (25.0)	9 (14.5)
Hepatobiliary	48 (25.0)	9 (14.5)
Cutaneous	20 (10.4)	6 (9.7)
Ocular	5 (2.6)	3 (4.8)

A1: age at presentation <40 yrs, A2: age at presentation ⩾40 yrs.

Table 4A Familial IBD and association with extraintestinal manifestations

	Total	First degree relative	Second degree relative
Ulcerative colitis	24/619 (3.9 %)	18 (14 UC+4 CD) (2.9 %)	6 (5 UC+1 CD) (1.0%)
Crohn's disease	31/254 (12.2 %)	20 (3 UC+17 CD) (7.9%)	11 (2 UC+9 CD) (4.3%)

Table 4B Familial IBD and association with extraintestinal manifestations

	Ulcerative colitis	Familial IBD
Number of patients	619	24
Joint	52 (8.4 %)	6 (25.0 %)
Hepatobiliary	77 (12.4 %)	3 (12.5 %)
Cutaneous	24 (3.9 %)	1 (4.2 %)
Ocular	19 (3.0 %)	2 (8.3 %)
	Crohn's disease	Familial IBD
Number of patients	254	31
Joint	57 (22.4 %)	11 (35.5 %)
Hepatobiliary	57 (22.4 %)	4 (12.9 %)
Cutaneous	26 (10.2 %)	2 (6.5 %)
Ocular	8 (3.1%)	0

Table 5 Prevalence of extraintestinal manifestations in ulcerative colitis and Crohn's disease according to location and disease behaviour

	Joint *n* (%)	Hepatobiliary *n* (%)	Cutaneous *n* (%)	Ocular *n* (%)
Location		Ulcerative colitis		
Proctitis (*n*=117)	5 (4.3)	9 (7.7)	1 (0.9)	1 (0.9)
Left sided colitis (*n*=304)	14 (4.6)	32 (15.7)	8 (2.6)	7 (2.3)
Pancolitis (*n*=198)	33 (16.7)	36 (18.2)	15 (7.6)	12 (6.1)
Location		Crohn's disease		
L1 (*n*=60)	11 (18.3)	14 (23.3)	6 (10.0)	2 (3.3)
L2 (*n*=81)	17 (21.0)	17 (21.0)	10 (12.3)	3 (3.7)
L3 (*n*=113)	29 (25.7)	26 (23.0)	10 (8.8)	3 (2.7)
Behaviour				
B1 (*n*=87)	13 (14.9)	22 (25.3)	11 (12.6)	1 (1.1)
B2 (*n*=62)	16 (25.8)	11 (17.7)	5 (8.1)	0
B3 (*n*=105)	28 (27.6)	24 (22.9)	10 (9.5)	7 (6.7)

Age at presentation (A1: <40 years, A2: =40 years) did slightly affect the prevalence of EIMs (Table 3). Joint manifestations were more prevalent in CD patients with earlier disease onset (OR: 1.96, 95 % CI: 1.01-4.21). The same tendency was observed for cutaneous manifestations.

Familial disease was seen in 3.9 % of patients with UC and 12.2 % of patients with CD (Tables 4A-B). Joint manifestations were more frequent in UC patients with familial disease (OR: 3.63, 95 % CI: 1.43-9.31) than without. The same tendency was seen in UC patients (OR: 1.9, 95 % CI: 0.87-4.14) and ocular manifestations were found in familial UC cases.

Table 6A Joint manifestations in IBD patients

	Total *n* (%)	Axial arthritis *n* (%)	Type-1 arthritis *n* (%)	Type-2 arthritis *n* (%)
Ulcerative colitis				
Total (*n*=619)	52 (8.4)	20 (3.2)	17 (2.7)	13 (2.1)
Male (*n*=317)	24 (7.6)	10 (3.2)	7 (2.2)	7 (2.2)
Female (*n*=302)	28 (9.3)*	10 (3.4)	10 (3.3)	6 (2.0)
Crohn's disease				
Total (*n*=254)	57 (22.4)	26 (10.2)	29 (11.4)	8 (3.1)
Male (*n*=125)	23 (18.4)	11 (8.8)	12 (9.6)	3 (2.4)
Female (*n*=129)	34 (26.4)	15 (11.6)	17 (13.2)	5 (3.9)

*Two female patients with ulcerative colitis had rheumatoid arthritis.

Table 6B Joint manifestations in IBD according to location and disease behaviour

	Total *n* (%)	Axial arthritis *n* (%)	Type-1 arthritis *n* (%)	Type-2 arthritis *n* (%)
Location		Ulcerative colitis		
Proctitis (*n*=117)	5 (4.3)*	1 (0.9)	2 (1.8)	1 (0.9)
Left sided colitis (*n*=304)	14 (4.6)	4 (1.3)	5 (1.6)	5 (1.6)
Pancolitis (*n*=198)	33 (16.7)*	15 (7.6)	10 (5.0)	7 (3.5)
Location		Crohn's disease		
L1 (*n*=60)	11 (18.3)	5 (8.3)	4 (6.7)	2 (3.3)
L2 (*n*=81)	17 (21.0)	7 (8.6)	10 (12.3)	3 (3.7)
L3 (*n*=113)	29 (25.7)	14 (12.4)	15 (13.3)	3 (2.7)
Behaviour				
B1 (*n*=87)	13 (14.9)	8 (9.2)	5 (5.7)	2 (2.3)
B2 (*n*=62)	16 (25.8)	8 (12.9)	6 (9.7)	3 (4.8)
B3 (*n*=105)	28 (27.6)	10 (9.5)	18 (17.1)	3 (2.9)

*One patient with proctitis and one with pancolitis had rheumatoid athritis.

Joint manifestations were more frequent in CD than in UC ($P<0.001$, Tables 6A-B.). There was a tendency of increased frequency of joint manifestations in women with CD (26.4 % *vs* 18.4 %, OR: 1.58, 95 % CI: 0.87-2.87). Axial arthritis (10.2 % *vs* 3.2 %, $P=0.0001$) and type 1(11.4 % *vs* 2.7 %, $P=0.0001$) arthritis were more frequent in CD, with equal prevalence of type-2 arthritis. In UC joint manifestations were almost three-fold more frequent in patients with pancolitis compared to proctitis and left sided colitis cases ($P<0.002$ for both, Table 5). In CD a tendency of increased frequency of joint manifestations was observed in patients with colonic involvement (L2 and L3: 23.7 %) or stricturing/penetrating disease (26.3 %) compared to patients with ileal only disease (18.3 %) or non-stricturing non-penetrating disease behavior

(14.9 %, Table 6B). An increased frequency of type 1 arthritis was observed in patients with penetrating compared to non-stricturing non-penetrating disease (P=0.028), the same tendency was observed in patients with or without colonic involvement. Type-1 arthritis affected more frequently the joints of the lower extremities (most frequently the knee and ankle), while type-2 arthritis was more common in the joints of the upper extremities.

Hepatobiliary manifestations are summerised in Table 7. PSC was diagnosed in 10 patients with UC and only 2 patients with CD. Small duct PSC was diagnosed in 8 and 6 cases, respectively. Non-alcoholic fatty liver disease (NAFLD) or non-alcoholic steatohepatitis (NASH) was diagnosed in 9.4 % of UC patients and 19.3 % of CD patients (P<0.0001). These patients had unexplained abnormal liver function tests (viral hepatitis, autoimmune, drug or alcohol induced disease, extrahepatic obstruction excluded). Liver biopsy was performed in 22/107 cases, which identified NAFLD or NASH in almost all cases. US proved hepatomegaly in 13/107 (12.1 %). Progression to cirrhosis was not observed in these patients during follow-up.

Table 7 Hepatobiliary manifestations in IBD patients

	Total *n* (%)	PSC *n* (%)	Small duct PSC *n* (%)	NAFLD / NASH *n* (%)
Ulcerative colitis				
Total (*n*=619)	77* (12.4)	10 (1.6)	8 (1.3)	58 (9.4)
Male (*n*=317)	39 (12.3)	3 (1.0)	6 (1.9)	30 (9.5)
Female (*n*=302)	38* (12.6)	7 (2.3)	2 (0.7)	28 (9.3)
Crohn's disease				
Total (*n*=254)	57 (22.4)	2 (0.8)	6 (2.4)	49 (19.3)
Male (*n*=125)	27 (21.6)	2 (1.6)	6 (4.8)	19 (15.2)
Female (*n*=129)	30 (23.3)	0	0	30 (23.3)

*One female patient had autoimmune hepatitis. NAFLD: non-alcoholic fatty liver disease, NASH: non-alcoholic steatohepatitis.

Cutaneous manifestations were seen in 10.2 % of the patients with CD and 3.9 % of the patients with UC (Tables 8A-B). Cutaneous manifestations were more common in women in both UC (male/female: 5.0 %/2.8 %) and CD (13.2 %/7.2 %, OR: 1.95, 95 % CI: 0.85-4.48). Erythema nodosum and pyoderma gangrenosum were the most frequent manifestations. In UC cutaneous manifestations were more frequent in more extensive disease (7.6 % in pancolitis *vs* 2.1 % in proctitis or left sided colitis, P=0.002).

Ocular manifestations were apparent in approximately 3.0 % of UC and CD patients (Table 9). The prevalence was more frequent in women in both UC (P=0.009, OR: 4.37, 95 % CI: 1.51-12.6) and CD (OR:3.0, 95 % CI=0.67-8). Conjunctivitis, acute anterior uveitis and scleritis were the most frequent manifestations. Ocular manifestations developed mostly during the early years of the disease. In UC more than half of the patients with ocular complication had pancolitis (6.1 % in pancolitis *vs* 1.9 % in left sided colitis or proctitis, P=0.01).

Iron deficiency anaemia was seen in 35.8 % of CD patients and in one fourth of UC patients (Tables 10A-C). It was more frequent in women in UC (32.1 % *vs* 19.6 %, P<0.001, OR=1.95, 95 % CI: 1.35-2.81). Chronic anaemia was more frequent in patients with CD (9.6 % *vs* 17.7 %, P<0.001). The prevalence of macrocytic anaemia was around 4 % in both diseases. It was also observed more frequently in patients with ileocolonic disease than without it (P=0.03). The same tendency was observed according to disease behaviour; chronic anaemia tended to be more frequent in patients with stricturing or penetrating disease (P=0.06, Table 10C). AIHA developed in four UC patients.

Table 8A Cutaneous manifestations in patients with ulcerative colitis (*n*=619)

	Total *n* (%)	Male *n* (%)	Female *n* (%)
Erythema nodosum	8 (1.3)	2 (0.6)	6 (2.0)
Pyoderma gangrenosum	3 (0.5)	1 (0.3)	2 (0.6)
Chronic urticaria	6 (1.0)	2 (0.6)	4 (1.3)
Psoriasis	3 (0.5)	2 (0.6)	1 (0.3)
Aphthous stomatitis	3 (0.5)	1 (0.3)	2 (0.6)
Herpes zoster	2 (0.3)	1 (0.3)	1 (0.3)
Cellulitis	2 (0.3)	0	2 (0.6)
Recurrent dermatitis	2 (0.3)	1 (0.3)	1 (0.3)
Lichen ruber planus	1 (0.2)	1 (0.3)	0
Total	24 (3.9)	9 (2.8)	15 (5.0)

Table 8B Cutaneous manifestations in patients with Crohn's disese (*n*=254)

	Total *n* (%)	Male *n* (%)	Female *n* (%)
Erythema nodosum	14 (5.5)	4 (3.1)	10 (7.8)
Pyoderma gangrenosum	4 (1.6)	3 (2.4)	1 (0.8)
Erythema exsudativum multiforme	2 (0.8)	1 (0.8)	1 (0.8)
Erythroderma	2 (0.8)	1 (0.8)	1 (0.8)
Stevens Johnson syndrome	1 (0.4)	0	1 (0.8)
Psoriasis	1 (0.4)	0	1 (0.8)
Eczema	1 (0.4)	0	1 (0.8)
Recurrent dermatitis	1 (0.4)	0	1 (0.8)
Total	26 (10.2)	9 (7.2)	17 (13.2)

Table 9 Ocular manifestations in IBD patients

	Total *n* (%)	Anterior uveitis *n* (%)	Conjunctivitis *n* (%)	Scleritis *n* (%)
Ulcerative colitis				
Total (*n*=619)	20* (3.2)	6 (1.0)	9 (1.5)	4 (0.7)
Male (*n*=317)	4 (1.3)	1 (0.3)	3 (1.0)	1 (0.3)
Female (*n*=302)	16 (5.3)	5 (1.7)	6 (2.0)	3 (1.0)
Crohn's disease				
Total (*n*=254)	8 (3.1)	4 (1.6)	4 (1.6)	1 (0.4)
Male (*n*=125)	2 (1.6)	1 (0.8)	0	1 (0.8)
Female (*n*=129)	6 (4.7)	3 (2.3)	4 (3.1)	0

*One orbital pseudotumor was observed in a young female UC patient.

Table 10A Hematological manifestations in patients with ulcerative colitis

	Total *n* (%)	Male *n* (%)	Female *n* (%)
Iron deficieny anaemia	159 (25.9)	62 (19.6)	97 (32.1)
Chronic anaemia	59 (9.6)	34 (10.7)	25 (8.3)
Macrocytic anaemia	24 (3.9)	15 (4.7)	9 (3.0)
AIHA	4 (0.6)	2 (0.6)	2 (0.6)
Non-Hodgkin lymphoma	1 (0.2)	1 (0.3)	0
CML	1 (0.2)	1 (0.3)	0
Chronic myeloproliferative disease	1 (0.2)	0	1 (0.3)
Leukemoid reaction	1 (0.2)	0	1 (0.3)
Methaemoglobinaemia	1 (0.2)	0	1 (0.3)
Total	260 (42.0)	90 (28.4)	170 (56.3)

AIHA: autoimmune hemolytic anaemia, CML: chronic myeloid leukaemia.

Table 10B Hematological manifestations in patients with Crohn's disease

	Total *n* (%)	Male *n* (%)	Female *n* (%)
Iron deficieny anaemia	91 (35.8)	40 (32.0)	51 (39.5)
Chronic anaemia	45 (17.7)	23 (18.4)	22 (17.1)
Macrocytic anaemia	11 (4.3)	6 (4.8)	5 (3.9)
Chronic myeloproliferative disease	1 (0.4)	0	1 (0.8)
Leukopenia	1 (0.4)	0	1 (0.8)
ITP	1 (0.4)	0	1 (0.8)
Total	150 (59.1)	69 (55.2)	81 (62.8)

ITP: immune thrombocytopenic purpura

Table 10C Association between hematological complications and location and disease behaviour in Crohn's disease patients

	Iron deficieny anaemia *n* (%)	Chronic anaemia *n* (%)	Macrocytic anaemia *n* (%)
Location			
L1 (*n*=60)	17 (28.3)	9 (15.0)	3 (5.0)
L2 (*n*=81)	22 (27.2)	9 (11.1)	2 (2.5)
L3 (*n*=113)	42 (37.2)	27 (23.9)	6 (5.3)
Behaviour			
B1 (*n*=87)	27 (31.0)	10 (11.4)	2 (2.3)
B2 (*n*=62)	23 (37.1)	12 (19.4)	3 (4.8)
B3 (*n*=105)	41 (39.0)	23 (21.9)	6 (5.7)

Thromboembolic complication was observed in 11 CD and 8 UC patients (Table 11.). Male predominance was observed in UC, while it was more frequent in women with CD, 1/15 (6.3 %) patient was positive for factor V Leiden mutation.

4.5 % of all IBD patients had multiple major extraintestinal diseases, three-fold more frequent in patients with CD than in patients with UC (9.1 % *vs* 3.1 %, $P<0.001$, Table 12.). Rare complications are summarized in Table 13. A relatively high number of glomerulonephritis was worth mentioning.

Table 11 Thromboembolic complications in patients with IBD

	Ulcerative colitis	Crohn's disease
Number of patients (%)	11/619 (1.8)	8/254 (3.1)
Male/female	9/2	2/6
Location	Proctitis: 0	L1: 3
	Left sided colitis: 6	L2: 1
	Pancolitis: 5	L3: 4
Behaviour of CD	-	B1: 0
		B2: 2
		B3: 6
Place of thromboembolism		
Lower extremity thrombosis	8	4
Pulmonary embolism	1	0
Lower extremity thrombosis complicated by pulmonary embolism	2	3
Splenic vein thrombosis	0	1

Table 12 Prevalence of multiple extraintestinal diseases

	Total *n*	Ulcerative colitis *n*	Crohn's disease *n*
Two	27	14	13
Three	14	5	9
Four	1	0	1
Total	42/873 (4.5%)	19/619 (3.1%)	23/254 (9.3%)

Table 13 Extraintestinal manifestations in IBD affecting other organ systems

	Total *n* (%)	Ulcerative colitis *n* (%)	Crohn's disease *n* (%)
Glomerulonephritis	3 (0.4)	1 (0.2)	2 (0.8)
Asthma bronchiale	7 (0.8)	4 (0.6)	3 (1.2)
Chronic pancreatitis	4 (0.5)	3 (0.5)	1 (0.4)
Acute pancreatitis	2 (0.2)	1 (0.2)	1 (0.4)
Celiac disease	2 (0.2)	1 (0.2)	1 (0.4)
Thyreoiditis	2 (0.2)	2 (0.3)	0
SLE	2 (0.2)	1 (0.2)	1 (0.4)

SLE: systemic lupus erythematodes.

DISCUSSION

It is difficult to define the true prevalence of EIMs in IBD. If one was counting only major EIMs with common immunogenetic background the prevalence was about 20-25 %[1,5,8,17,18]. However, if all possible secondary systemic effects and/or complications of therapy are also included, then almost all patients will have "extra-intestinal manifestations". Prevalence may vary depending on the actual geographic area, IBD population, location and duration of the disease, medication and diagnostic accuracy.

Only few large cohort follow-up data are available on the prevalence of EIMs in IBD. The study of Greenstein *et al*. was one of the first reports[8]. Farmer *et al*.[19] reported a prevalence of 16.7 % during a 13-year follow-up study. EIMs were more prevalent in patients with colonic involvement or previous operations. In the Swedish epidemiology study Monsen *et al*.[20] excluded arthralgia, stomatitis and episcleritis from the EIMs. More recently, Jiang and Cui[21] analyzed the data of 10218 ulcerative colitis cases in China. The frequency of EIMs was 6.1 %, however no further data were available about the type of EIM. Bernstein *et al*.[22] investigated the prevalence of five "major" EIMs (iritis/uveis, PSC, pyoderma gangrenosum, erythema nodosum and ankylosing spondylitis) with the help of the University of Manitoba IBD Database in IBD patients with a disease history of at least 10 years. They found a single EIM prevalence of 6.2 %, which was one of the lowest rates reported. However, peripheral arthropathies were excluded from their study. There is undoubtedly a debate with the diagnosis of peripheral arthopathy, as it is sometimes difficult to distinguish arthropathy from arthralgia, especially in retrospective studies. In contrast, it is one of the most typical EIMs, observed in a high frequency of the patients. Excluding peripheral arthropathy from EIMs in one study and including it in another make the data difficult to compare. The reported overall EIM prevalence of 21.3 % in our study is in concordance with previous studies. The overall prevalence of EIMs was higher in patients with a longer disease history, but age at presentation did not affect the prevalence of EIMs.

There were gender predilections. EIMs were more frequent in femal pateints compared to males, which may support the hypothesis that autoimmune diseases are more common in female subjects.

The role of genetic factors has been implicated in the pathogenesis of IBD and EIMs[8-11]. In our study we investigated the familial occurrence in IBD. Positive family history was four times more frequent in CD compared to UC. The frequencies of joint and ocular manifestations were higher in patients with familial UC. Others have suggested high concordance of the occurrence of EIMs in affected siblings with IBD[23].

Previous studies have suggested multiple extraintestinal diseases[8,22] with certain genetic associations[10,23]. We found multiple extraintestinal diseases in 4.5 % of IBD patients, more

common in patients with CD. The most frequent associations were co-existing ocular, cutaneous and joint (type 1 arthritis) manifestations. The Canadian study reported multiple extraintestinl disease in only 0.3 % of all patients[22], however the rate of multiple EIMs was comparable to our results in most studies[17, 19].

Relation of EIMs with type, location and behaviour of IBD

Type of IBD Overall EIMs were more frequent in patients with CD than in patients with UC, in concordance with previous studies[8,24] with the exception of ocular manifestations and PSC. These two EIMs were equally prevalent in CD and UC (both occurred approximately in 3 % of the patiens) in concordance with previous data[10,16,25].

Location of IBD In UC EIMs were thought to be more prevalent in extensive disease[5], but there were some contradiction in the literature[13]. In our study the rate of EIMs increased with the increasing extent of the disease. In CD it was generally accepted, that some EIMs were associated with colonic (e.g. peripheral arthropathy) others with small bowel (e.g. cholelithiasis) location[8,19]. We also found that type-1 arthritis was twice as frequent in patients with colonic or ileocolonic disease compared to patients with only ileal disease. The difference was smaller compared to patients with axial arthritis and disappeared in patients type 2 arthritis. The prevalences of cutaneous, ocular and hepatobiliary manifestations were not associated with location.

Behaviour of CD We did not find data in the literature about the relation of EIMs and the behaviour of CD, according to the Vienna classification. Earlier studies have suggested that EIMs tended to associate with perianal (=penetrating) disease[26]. We found a higher rate of joint complications in stricturing and penetrating disease than in non-stricturing non penetrating form. All but one ocular disease developed in patients with penetrating disease, but the rate of other complications was similar in the three groups.

Extraintestinal manifestations according to affected organs

Arthritis is the most common EIM in IBD IBD related arthropaties were originally classified as axial and peripheral arthritides. Orchard *et al*. subdivided the peripheral disease into type 1 (large joint, pauciarticular, parallels with the course of IBD) and type-2 (small joint, polyarticular, the course independent of IBD) arthritides[13]. In our study joint manifestations were more frequently seen in patients with CD, first of all with the higher prevalence of axial and type-1 arthritis in these patients. Type-1 arthritis was more frequent in patients with stenosing and penetrating disease compared to patients with non-stenosing non-penetrating disease behaviour. In patients with penetrating disease bacterial infections could explain the high prevalence, the reason for the high prevalence in patients with stenosing disease is not clear, perhaps it has a genetic background.

Hepatobiliary complications PSC was diagnosed in 1.6 % in UC and even more infrequently in CD. When small duct PSC was included, the overall prevalence was 2.9-3.2 % in both diseases, in concordance with the majority of previous reports (2.4-11 %)[15,16,27]. PSC was a precancerosus condition with increased risk for cholangiocarcinoma and colorectal cancer[28]. In this study 3 patients with PSC and one patient with small duct cholangitis developed colorectal cancer and one PSC patient developed cholangiocarcinoma, which supports a role for more intensive follow-up in these subgroups of patients.

The cause of elevated LFT was found to be steatosis and/or steatohepatitis, reported in 6.3 % in UC and in 4 % in CD in previous studies[29,30]. An Italian study found that 12 % of the 474 asymptomatic IBD patients had hepatobiliary disease[31]. In non-selected or operated UC patients the prevalence of steatosis could be as high as 15-45 %[16,32,33]. In our study the rate of NAFLD was twice as high in CD than in UC, otherwise our data are in concordance with the data of previous studies. Several cutaneous diseases were diagnosed, 14 were classified as EIM. Cutaneous manifestations were more frequent in CD and in female patients. The prevalence of erythema nodosum and pyoderma gangrenosum was in the range previously reported[10,34,35] with very few psoriasis cases.

Ocular complications were equally frequent in both diseases with increased prevalence in women. Anterior uveitis was found at a frequency as previously reported[8,10,22]. We found one orbital pseudotumour in a young woman with severe ulcerative pancolitis. Ocular manifestations occurred mostly in the early few years after diagnosis. Pancolitis patients with UC were more liable to develop ocular manifestations compared to other locations. Ocular manifestations did frequently occur together with other (joint or cutaneous) extraintestinal diseases.

Haematological complications Iron deficiency anaemia is the most frequent hematological manifestation. In most of the cases its course ran parallel to the course of the intestinal disease. "Chronic anaemia" that occurs in inflammatory conditions and tumours was mostly apparent in severe, refractory cases and resolved only slowly after remission. Macrocytic anaemia was more frequent in patients with ileal and penetrating/stricturing disease than in patients with colonic involvement or non-stricturing non-penetrating disease. It was less frequent since preventive folate supplementation has been introduced in patients receiving sulfasalazine treatment.

Autoimmune haemolytic anaemia (AIHA) rarely complicates IBD, the reported prevalence rates were between 0.2 % and 1.7 %. Our observed rate (0.6 %) correlated with the previous data. In concordance with other studies AIHA occurred in patients with extensive colitis. In most of the cases AIHA could be treated successfully with steroids and/or immunosuppressive drugs[36]. In our study one patient required splenectomy, and in another case haemolysis subsided only after colectomy.

Increased risk of lymphoma has been reported in IBD, especially in patients receiving immunosupressives, but data were conflicting[37,38]. Our data do not support the notion of increased risk in these patients. In our series one 76-year old male UC patient with left sided colitis developed a high grade B-cell lymphoma in the rectum, but he did not receive immunosuppressive therapy. ITP might be true EIM, methaemoglobinaemia was associated with high dose sulfasalazine treatment, leukaemoid reaction was seen in a fulminant relapse.

Hypercoagulability was thought to be involved in the pathogenesis of IBD[39-41], and increased risk of thromboembolic complications (1-6 %) has been reported in IBD[42]. The prevalence of prothrombotic inherited and/or acquired coagulation abnormalities in patients with IBD remains controversial. Genetic thrombophilia with deficiencies in some coagulation inhibitors (antithrombin, proteins C and S), acquired thrombophilia due to inflammation, antiphospholipid syndrome and mutations of factor V Leiden and recently other genes involved in thrombogenesis (prothrombin mutation 20210A or factor V fV4070G polymorphism) have been described[39,43]. The most common cause of hypercoagulability status in Europe is resistance to activated protein C (APC). Resistance to APC and mutations that cause APC resistance (mainly factor V Leiden) have been of particular interest[42,43]. Some studies reported increased frequency of Leiden mutation in IBD[42], however others found that Leiden mutation was associated with thromboembolism with (14.3 %) or without IBD (15.5 %) but not with IBD (0 % and controls 3.6 %) itself [39,44]. In our study Leiden mutation was infrequent in IBD patients with thrombosis. The frequency was the same

that as observed in normal Hungarian population without thrombosis (5.26 %)[45]. Most thromboembolic episodes developed in the lower extremities, in some patient with pulmonary embolism as a complication. Thrombosis of the splenic vein occurred in one young female CD patient with ileocolonic disease.

Other EIMs Glomerulonephritis is a rare complication in IBD. Only case reports could be found in the literature[46]. Deposition of immune-complexes is thought to be involved in the pathogenesis. Finding 3 patients (1 UC and 2 CD) in this series was an unexpected high number. Histology revealed IgA nephropathy, membranous glomerulonephritis and focal glomerulosclerosis. Ductal changes suggesting chronic pancreatitis were common in IBD[47]. Our two pancreatitis cases developed in patients taking azathioprine.

In conclusion, in IBD a variety of EIMs may occur during the course of the disease affecting several organ systems. In Hungarian IBD patients, major EIMs develop in concordance with previous European data in approximately one fifth of the patients. The high number of EIMs supports a role for complex follow-up in these patients.

ACKNOWLEDGEMENT

Dr. Zsuzsanna Erdelyi, Dr. Agnes Horvath, Dr Gabor Mester (Veszprem), Dr. Sandor Meszaros (Ajka), Dr. Csaba Molnar (Ajka), Dr. Mihály Balogh (Papa) and Dr. Istvan Szipocs for help in data collection and to Gabriella Demenyi for technical assistance.

REFERENCES

1 **Podolsky DK**. Inflammatory bowel disease. *NEJM* 2002; **347**: 417-428
2 **Farrell RJ**, Peppercorn MA. Ulcerative colitis. *Lancet* 2002; **359**: 331-340
3 **Lakatos L**. Immunology of inflammatory bowel diseases. *Acta Physiol Hung* 2000; **87**: 355-372
4 **Fiocchi C**. Inflammatory bowel disease: etiology and pathogenesis. *Gastroenterology* 1998; **115**: 182-205
5 **Weiss A**, Mayer L. Extraintestinal manifestations of inflammatory bowel disease. In: Allan RN, Rhodes JM, Hanauer SB, eds. Inflammatory bowel diseases. *Churchill Livingstone, New York* 1997: 623-636
6 **Lamers CB**. Treatment of extraintestinal complications of ulcerative colitis. *Eur J Gastroenterol Hepatol* 1997; **9**: 850-853
7 **Ljung T**, Staun M, Grove O, Fausa O, Vatn MH, Hellstrom PM. Pyoderma gangrenosum associated with Crohn disease: effect of TNF-alpha blokade with infliximab. *Scand J Gastroenterol* 2002; **37**: 1108-1110
8 **Greenstein AJ**, Janowitz HD, Sachar DB. The extra-intestinal complications of Crohn's disease and ulcerative colitis: a study of 700 patients. *Medicine* 1976; **55**: 401-412
9 **Orchard TR**. Arthritis associated with inflammatory bowel disease. In: Bayless TM, Hanauer SB, eds. Advanced therapy of inflammatory bowel disease. *Decker inc., Hamilton* 2001: 279-282
10 **Orchard TR**, Chua CN, Ahmad T, Cheng H, Welsh KI, Jewell DP. Uveitis and erythema nodosum in inflammatory bowel disease: clinical features and the role of HLA genes. *Gastroenterology* 2002; **123**: 714-718
11 **Roussomoustakaki M**, Satsangi J, Welsh K, Louis E, Fanning G, Targan S, Landers C, Jewell DP. Genetic markers may predict disease behavior in patients with ulcerative colitis. *Gastroenterology* 1997; **112**: 1845-1853
12 **D'Arienzo A**, Manguso F, Scarpa R, Astarita C, D'Armiento FP, Bennato R, Gargano D, Sanges M, Mazzacca G. Ulcerative colitis, seronegative spondyloarthropathies and allergic diseases: the search for a link. *Scand J Gastroenterol* 2002; **37**: 1156-1163
13 **Orchard TR**, Wordsworth BP, Jewell DP. Peripheral arthropathies in inflammaroty bowel disease: their articular distribution and natural history. *Gut* 1998; **42**: 387-391
14 **Russell AS**. Arthritis, inflammatory bowel disease and histocompatibility antigens. *Ann Int Med* 1977; **86**: 820-821
15 **Lee YM**, Kaplan MM. Management of primary sclerosing cholangitis. *Am J Gastroenterol* 2002; **97**: 528-534
16 **Heikius B**, Niemela S, Lehtola J, Karttunen T, Lahde S. Hepatobiliary and coexisting pancreatic duct abnormalities in patients with inflammatory bowel disease. *Scand J Gastroenterol* 1997; **32**: 153-161
17 **Rankin GB**, Watts HD, Melnyk CS, Kelley ML Jr. The National Cooperative Crohn's Disease Study: Extraintestinal manifestations and perianal complications. *Gastroenterology* 1979; **77**: 914-920
18 **Rankin GB**. Extraintestinal and systecim manifestations of inflammatory bowel disease. *Med Clin North Am* 1990; **74**: 39-50
19 **Farmer RG**, Whelan G, Fazio VW. Long-term follow-up of patients with Crohn's disease. *Gastroenterology* 1985; 88: 1818-1825
20 **Monsen U**, Sorstad J, Hellers G, Johannson C. Extracolonic diagnoses in ulcerative colitis: an epidemiological study. *Am J Gastroenterol* 1990; **85**: 711-716
21 **Jiang XL**, Cui HF. An analysis of 10218 ulcerative colitis cases in China. *World J Gastroenterol* 2002; **8**: 158-161
22 **Bernstein CN**, Blanchard JF, Rawsthorne P, Yu N. The prevalence of extraintestinal diseases in inflammatory bowel disease: A population-based study. *Am J Gastroenterol* 2001; **96**: 1116-1122
23 **Satsangi J**, Grootscholten C, Holt H, Jewell DP. Clinical patterns of familial inflammatory bowel disease. *Gut* 1996; **38**: 738-741
24 **Danzi JT**. Extraintestinal manifestations of idiopathic inflammatory bowel disease. *Arch Int Med* 1988; **148**: 297-302
25 **Lee YM**, Kaplan MM. Management of primary sclerosing cholangitis. *Am J Gastroenterol* 2002; **97**: 528-534
26 **Rankin GB**. Extraintestinal and systemic manifestations of inflammatory bowel disease. *Med Clin North Am* 1990; **74**: 39-50
27 **Olsson R**, Danielsson A, Jarnerot G, Lindstrom E, Loof L, Rolny P, Ryden BO, Tysk C, Wallerstedt S. Prevalence of primery sclerosing cholangitis in patients with ulcerative cholitis. *Gastroenterology* 1991; **100**: 1319-1323
28 **Loftus EV**, Sandborn WJ, Tremaine WJ, Mahoney DW, Zinsmeister AR, Offord KP, Melton LJ 3rd. Risk of colorectal neoplasa in patients with primary sclerosing cholangitis. *Gastroenterology* 1996; **110**: 432-440
29 **Perrett AD**, Higgins G, Johnston HH, Massarella G, Truelove SC, Wrigth R. The liver in ulcerative colitis. *Q J Med* 1971; **40**: 211-238
30 **Perrett AD**, Higgins G, Johnston HH, Massarella G, Truelove SC, Wrigth R. The liver in Crohn's disease. *Q J Med* 1971; **40**: 187-209
31 **Riegler G**, D'Inca R, Sturniolo C, Corrao G, Blancho CDV, Di Leo V, Carratu R, Ingrosso M, Pelli MA, Morini S, Valpiani D, Cantarini D, Usai P, Papi C, Caprilli R. Hepatobiliary alterations in patients with inflammatory bowel disease: A multicenter study. *Scand J Gastroenterol* 1998; **33**: 93-98
32 **Broome U**, Glaumann H, Hultcrantz R. Liver histology and follow-up of 68 patients with ulcerative colitis and normal liver function tests. *Gut* 1990; **31**: 468-472
33 **Mattila J**, Aitola P, Matikainen M. Liver lesions found at colectomy in ulcerative colitis: correlation between histological findings and biochemical parameters. *J Clin Pathol* 1994; **47**: 1019-1021
34 **Noussari HC**, Provost TT, Anhalt GJ. Cutaneous manifestations of inflammatory bowel disease. In: Bayless TM, Hanauer SB, eds. Advanced therapy of inflammatory bowel disease. *Decker inc, Hamilton* 2001: 271-274
35 **Tromm A**, May D, Almus E, Voigt E, Greving I, Schwegler U, Griga T. Cutaneous manifestations in inflammatory bowel disease. *Z Gastroenterol* 2001; **39**: 137-144
36 **Giannadaki E**, Potamianos S, Poussomoustakaki M, Kyriakou D, Fragkiadakis N, Manousos ON. Autoimmune hemolytic anemia and positive Coombs test associated with ulcerative colitis. *Am J Gastroenterol* 1997; **92**: 1872-1874
37 **Lewis JD**, Bilker WB, Brensinger C, Deren JJ, Vaughn DJ, Strom BL. Inflammatory bowel disease is not associated with an increased risk of lymphoma. *Gastroenterology* 2001; **121**: 1080-1087

38 **Lewis JD**, Schwartz JS, Lichtenstein GR. Azathioprine for maintenance of remission in Crohn's disease: benefits outweigh the risk of lymphoma. *Gastroenterology* 2000; **118**: 1018-1024
39 **Guedon C**, Le Cam-Duchez V, Lalaude O, Menard JF, Lerebours E, Borg JY. Prothrombotic inherited abnormalities other than factor V Leiden mutation do not play a role in inflammatory bowel disease. *Am J Gastroenterol* 2001; **96**: 1448-1454
40 **Meucci G**, Pareti F, Vecchi M, Saibeni S, Bressi C, de Franchis R. Serum von Willebrand factor levels in patients with inflammatory bowel disease are related to systemic inflammation. *Scand J Gastroenterol* 1999; **34**: 287-290
41 **Collins CE**, Cahill MR, Newland AC, Rampton DS. Platelets circulate in an activated state in inflammatory bowel disease. *Gastroenterology* 1994; **106**: 840-845
42 **Liebman HA**, Kashani N, Sutherland D, McGehee W, Kam AL. The factor V Leiden mutation increases the risk of venous thrombosis in patients with inflammatory bowel disease. *Gastroenterology* 1998; **115**: 830-834
43 **Haslam N**, Standen GR, Probert CS. An investigation of the association of the factor V Leiden mutation and inflammatory bowel disease. *Eur J Gastroenterol Hepatol* 1999; **11**: 1289-1291
44 **Grip O**, Svensson PJ, Lindgren S. Inflammatory bowel disease promotes venous thrombosis earlier in life. *Scand J Gastroenterol* 2000; **35**: 619-623
45 **Nagy Z**, Nagy A, Karadi O, Figler M, Rumi G Jr, Suto G, Vincze A, Par A, Mozsik G. Prevalence of the factor V Leiden mutation in human inflammatory bowel disease with different activity. *J Physiol Paris* 2001; **95**: 483-487
46 **Pardi DS**, Tremaine WJ, Sandborn WJ, McCarthy JT. Renal and urologic complications of inflammatory bowel disease. *Am J Gastroenterol* 1998; **93**: 504-514
47 **Barthet M**, Hastier P, Bernard JP, Bordes G, Frederick J, Allio S, Mambrini P, Saint-Paul MC, Delmont JP, Salducci J, Grimaud JC, Sahel J. Chronic pancreatitis and inflammatory bowel disease: true or coincidental association? *Am J Gastroenterol* 1999; **94**: 2141-2148

Edited by Wang XL

P.O.Box 2345, Beijing 100023,China
Fax: +86-10-85381893
E-mail: wjg@wjgnet.com www.wjgnet.com

World J Gastroenterol 2003;9(10):2308-2312
World Journal of Gastroenterology
 ISSN 1007-9327

• CLINICAL RESEARCH •

Seroreactivity against *Saccharomyces cerevisiae* in patients with Crohn's disease and celiac disease

Zsolt Barta, István Csípõ, Gábor G. Szabó, Gyula Szegedi

Zsolt Barta, István Csí põ, Gábor G. Szabó, Gyula Szegedi, 3rd Department of Medicine, University of Debrecen, Móricz Zs. Krt. 22. 4004 Debrecen, Hungary
Correspondence to: Zsolt Barta, M.D., 3rd Department of Medicine, University of Debrecen, Móricz Zs. Krt.22. 4004 Debrecen, Hungary. mailto:barta@iiibel.dote.hu
Telephone: +36-52-453-337 **Fax:** +36-52-414-969
Received: 2003-03-12 **Accepted:** 2003-05-09

Abstract

AIM: To explore whether there was anti-*Saccharomyces cerevisiae* antibodies (ASCA) positivity in our patients with biopsy-confirmed celiac disease.

METHODS: A cohort of patients with inflammatory bowel diseases (42 patients with Crohn's disease and 10 patients with ulcerative colitis) and gluten sensitive enteropathy (16 patients) from Debrecen, Hungary were enrolled in the study. The diagnosis was made using the formally accepted criteria. Perinuclear antineutrophil cytoplasmic antibodies (pANCA) and *anti-Saccharomyces cerevisiae* antibodies (ASCA), *antiendomysium* antibodies (EMA), antigliadin antibodies (AGA) and anti human tissue transglutaminase antibodies (tTGA) were investigated.

RESULTS: The results showed that ASCA positivity occurred not only in Crohn's disease but also in Celiac disease and in these cases both the IgG and IgA type antibodies were proved.

CONCLUSION: It is conceivable that ASCA positivity correlates with the (auto-) immune inflammation of small intestines and it is a specific marker of Crohn's disease.

Barta Z, Csípõ I, Szabó GG, Szegedi G. Seroreactivity against *Saccharomyces cerevisiae* in patients with Crohn's disease and celiac disease. *World J Gastroenterol* 2003; 9(10):2308-2312
http://www.wjgnet.com/1007-9327/9/2308.asp

INTRODUCTION

Gluten-sensitive enteropathy (GSE) or, as it is more commonly called, celiac disease, is an immune-mediated enteropathic condition (specified as an autoimmune inflammatory disease of the small intestine) that is precipitated by the ingestion of gluten, a component of wheat protein, in genetically susceptible persons. Exclusion of dietary gluten results in healing of the *mucosa*, resolution of the malabsorptive state, and reversal of most, if not all, effects of celiac disease. GSE commonly manifests as "silent" celiac disease (i.e., minimal or no symptoms). Histological examination and serologic tests for antibodies against *endomysium*, transglutaminase, and gliadin identify most patients with the disease[1].

Crohn's disease (CD) and ulcerative colitis (UC) are both classified under the medical rubric of inflammatory bowel disease (IBD). It is currently accepted that the term "IBD" does not encompass just two diseases (CD or UC), but rather a group of diseases, triggered and perpetuated by a variety of diverse genetic, environmental, and immunologic factors that share similar clinical manifestations. They cause life-impaired symptoms, necessitate long-term dependence on powerful drugs, and often result in debilitating surgery and even death. Although the etiology of UC and CD remains unclear, in addition to genetic and other environmental factors (food allergens, *etc*.), microorganisms have been discussed as possibly playing an important role. The gastrointestinal (GI) tract has direct contact with the environment and therefore forms a very important protective barrier within the human's organism. The *gut mucosa* has to stop foreign materials, such as bacteria or antigens, from entering the body and also prevent excessive loss of "body material" into the lumen. If the mucosal barrier is broken, an influx of luminal antigens may result in the perpetuation of intestinal inflammation by chronically stimulating resident and recruited immunocompetent cells of the *lamina propria*. Bacteria present within the intestinal lumen or in the intestinal wall are important in the development of mucosal inflammation. Recent reports in the literature do not suggest that a specific persistent infection causes IBD (i.e. the repeatedly blamed *Mycobacterium paratuberculosis avium*), but indicate that enteric pathogens could cause initial onset of IBD and are associated with reactivation of quiescent disease. CD patients may have a heterogeneous serological response to specific bacteria and bacterial related antigens. The serologic responses seen in CD patients include antibodies to *Saccharomyces cerevisiae, Mycobacteria, Bacteriodes, Listeria,* and *E. coli*. Many of the specific organisms have been proposed to directly or indirectly contribute to the pathogenesis of CD. Despite their self-limited character, these infections initiate a cascade of inflammatory events leading to chronic, relapsing disease in a genetically susceptible host ("hit-and-run" hypothesis). So, epidemiological and microbiologic studies suggest that enteropathogenic microorganisms play a substantial role in the clinical initiation and relapses of IBD. Thus microbiologic screening might be helpful in patients with flares of IBD for optimal medical treatment and as many bacteria cannot be cultured, culture-independent techniques are expected to be of great help in identifying microorganisms in IBD. With more comprehensive knowledge of the intestinal microflora and how the latter interacts with the host's immune system, it may be possible to define specific microbial substances in specific patients that are either present or absent from the normal flora to cause disease. The diagnoses of CD, UC and GSE are based on clinical features and the results of barium X-rays, endoscopy, mucosal biopsy histology, and in some cases operative findings and resected bowel pathology and histology. Serologic disease markers are accepted in GSE but unambiguously in IBD. Serologic tests that could serve as an adjunct to these invasive and expensive diagnostic studies, or possibly replace them, would have clinical utility[2-5]. Antibodies have attracted much interest for the study of the immune response in inflammatory bowel disease (IBD) and are also used as a tool for phenotyping. Antibodies to baker's yeast and brewer's yeast (anti-*Saccharomyces cerevisiae* antibodies or ASCA) directed against cell wall oligomannoside epitopes have been proposed as a serological marker for CD[6,7].

They have a sensitivity of 60 % and a specificity of 80-95 % for differentiating CD from controls[8]. One small study also reported the production of ASCA by a fraction of unaffected relatives of Crohn's patients. The role of ASCA's in CD is completely unknown, but one hypothesis links them to increased intestinal permeability. 50-60 % of patients with CD exhibit an activity-related increase in intestinal permeability, and this increase might be predictive for relapse. A variable proportion of healthy first-degree relatives of CD patients also have abnormal permeability of the small intestine, which lead some authors to postulate a primary defect of the tight junctions as etiologic factor in CD. Increased exposure of the epithelium to common food antigens such as yeasts due to a break in the epithelial barrier may then result in an antibody response. The effect of dietary yeast (*Saccharomyces cerevisiae*) on the activity of stable CD disease was assessed in patients. The patients' mean CD activity index (CDAI) while taking baker's yeast was significantly greater than that during yeast exclusion and patients with elevated yeast antibodies tended to develop a higher CDAI while receiving baker's yeast. These results suggest that dietary yeast may affect the activity of CD[9]. Antinuclear cytoplasmic antibodies (ANCA) with a perinuclear staining pattern have been proposed as a serologic marker for UC. pANCA's were found in 60-70 % of patients with UC. There is no clear association of pANCA with severity of disease but it is predictive of pouchitis after restorative proctocolectomy with ileoanal pouch anastomosis[10]. pANCA's are also found in 15-20 % of patients with CD. These patients present diffuse left-sided colitis with symptoms such as rectal bleeding, urgency, and mucus discharge and this phenotype is labeled "UC-like CD".

Saccharomyces cerevisiae (SC) is "ubiquitous" yeast and occurs in diverse places in naturally on plants and in the ground. Mankind used in the past and use now yeast for making miscellaneous foods (i.e. beer, bread) so we can come into contact with it principally with our consumed food products and beverages. It is generally accepted that SC is not a pathogen, but it has been suggested that in case of *fungemia* with SC (in patients with damaged/defective immune system) various organs can be affected and injured. The titer of pANCA does not change with the activity of the disease, does not depend on the therapy or the surgical intervention and but persists after resection of the affected part of the bowels. Similarly, the titer of the ASCA is stable irrespective of the activity of the disease and the drug-therapy. ASCA titers correlated with small bowel involvement and occurred particularly in cases of young adults with CD.

The aim of the study was to determine the prevalence of serological markers for GSE and IBD in patients with celiac disease (16 patients), UC (10 patients) and Crohn's disease (42 patients) and to correlate the presence with the characteristics of these diseases.

MATERIALS AND METHODS

Patients

The entire cohort of patients with IBD (42 patients with CD and 10 patients with UC) and GSE (16 patients) from Debrecen, Hungary were enrolled in the study. Adult patients of both sexes were included. The diagnosis of CD, UC or GSE was made using the formally accepted criteria. The medical records for these patients have previously been reviewed by investigators and abstracted for patient characteristics. The blood samples for the study were collected between January 2000 and March 2000. Their sera were separated and stored at -70 ℃. Determination of serum values was performed by individuals blinded to the clinical data for the patients in our Regional Immunology Laboratory.

Specific antibody measurement

Gliadin Glia-test from Diagnosticum Rt.(Budapest, Hungary) was warmed up to room temperature and the dilution of the diluents solution and the buffer solution was dispensed. For the measurement of specific IgG and IgA, the samples were diluted 1:500 (v/v). Micro standardization strips were incubated with one hundred microlitres of washing buffer, negative control, IgA positive control, IgG positive control, and the samples from the patients, for 30 min at 37 ℃. After the incubation, the plate was washed three times with a Labsystems ELISA washer (Beverly, MA). Both of the anti-IgG and anti-IgA conjugate were diluted 1:200 in diluents solution (100 μL per well divided). Wells were again incubated for 30 min at 37 ℃ and washed three times with two hundred microlitres of washing buffer. Next step was incubation with 100 μL of TM B substrate buffer (protected from light) at room temperature for 30 min. Reaction was stopped with 50 μL 4N sulphuric acid per well. Optical density (OD) was determined at 450 nm. All chemical reagents were reagent grade, from Sigma unless otherwise stated.

Transglutaminase Greiner plates (N° 655180) were incubated with transglutaminase, dissolved in PBS at 10 μg per milliliters, 50 μL per well, 16 hours at +4 ℃. Binding sites were blocked by incubating with two hundred microlitres per well of 1 % (w/v) bovine serum albumin (BSA) in PBS for 2 hours at 37 ℃. 100 μL per well of each sample as incubated at room temperature for 2 hours. (For the measurement, the serum samples were diluted 1:100) Anti-human IgA/HRPO conjugate, diluted 1:4 000 (v/v) in diluents solution (1 % BSA-PBS) were incubated (100 μL per well) for 1 hour at room temperature. The color reaction was developed by adding a solution (containing 12.5 ml citrate-phosphate buffer pH 5.0, 4.25 mg OPD, 5 μL of 30 % H_2O_2). The enzymatic reaction was stopped after 15 min with 50 μL per well of 4N H_2SO_4. Optical density (OD) was determined at 492 nm. After each incubation step, wells were washed two times with PBS containing 0.05 % (v/v) Tween 20 (PBS-T) during 10 minutes. Each sample was analyzed in duplicate. All chemical reagents were reagent grade, from Sigma unless otherwise stated.

Endomysium Indirect immunofluorescent method was developed in our laboratory. The substrate (umbilical cord) was incubated in PBS with sera (diluted 1:10 in diluent), washed twice with PBS for 10 min, then incubated with anti-human IgA/FITC and IgG/FITC, washed twice with PBS for 10 min. The preparates were coated with a mixture of glycerin/PBS (1:1) and covered with cover plate. Evaluation was interpreted with fluorescent microscopy. All chemical reagents were reagent grade, from Sigma.

ASCA IgG and IgA Medizym® ASCA IgA is an enzyme immunoassay for the quantitative determination of IgA antibodies to *Saccharomyces cerevisiae* in human serum. Autoantibodies of the diluted patient samples and calibrators reacted with mannan (cell surface component of baker's yeast) immobilized on the solid phase of a microtiter plate. Following an incubation period of 60 min at 37 ℃, unbound serum components are removed by a washing step. The bound antibodies react specifically with anti-human-IgA-antibodies conjugated to horseradish peroxidase (HRPO). Within the incubation period of 30 min at 37 ℃, excessive conjugate was separated from the solid-phase immune complexes by the following washing step. Horseradish peroxidase converted the colorless substrate solution of 3, 3', 5, 5' -tetramethylbenzidine (TMB) added into a blue product. This enzyme reaction was stopped by dispensing an acidic solution (H_2SO_4) into the wells after 10 min at room temperature turning the solution from blue to yellow. The optical density (OD) of the solution at 450 nm was directly proportional to the amount of specific antibodies bound. The standard curve was established by

plotting the concentrations of the antibodies of the standards (x-axis) and their corresponding OD values (y-axis) were measured. The concentration of antibodies of the specimen was directly read off the standard curve.

ANCA The presence of ANCA was first screened by means of a fixed neutrophil enzyme-linked immunosorbent assay (ELISA). Methanol-fixed neutrophils were incubated with control and coded sera at 1:100 dilutions. Neutrophil-bound antibody was labeled by alkaline phosphatase-conjugated goat antihuman IgG. After the addition of p-nitrophenol, specific absorbance was measured at 405 nm. The cutoff for positivity was determined by positive controls from well-defined patients with UC. Indirect immunofluorescent staining was then performed on ANCA ELISA-positive samples to determine whether a predominantly perinuclear (pANCA) or cytoplasmic (cANCA) staining pattern was present. Methanol-fixed neutrophils on glass slides were incubated with the coded sera samples (1:20 dilution). Specific binding was visualized by fluorescence microscopy after the addition of fluorescein-labeled antihuman IgG. The specificity of the perinuclear staining pattern in UC was finally confirmed by its disappearance after DNase treatment of the neutrophils. Results were considered positive when both the ANCA titers were above the cutoff and the indirect immunofluorescence revealed a perinuclear binding of ANCA that disappeared after DNase treatment.

Statistical analysis

The relations were concluded from the evidences with statistical methods and summarized them in tables. Data was presented as percentages or mean values ± standard deviation (SD). The statistical package used in data interpretation (the two-tailed Student's *t*-test, Pierce regression coefficient assay) was Statistica for Windows software (StatSoft, Inc., OK, U.S.A.).

RESULTS

Results are summarized in (Tables 1-3, Figures 1-4). Twenty-seven patients with CD had only colonic localization (27/42), terminal ileitis was in 7 cases (7/42). Both the small and large bowels were affected in 8 cases (8/42). IgG type ASCA was found in 9 patients (1 colitis, 4 ileitis, 4 duodenitis-ileitis-colitis). IgA type ASCA was positive only in the patients with terminal ileitis (6/10) and in the patients with the duodenitis-ileitis-colitis type CD (10/15). The 27 patients with only colonic localization (27/42) had no IgA type ASCA positivity (Figures 1-2). All together, we detected that the increased IgG and IgA type ASCA titers, were mainly in patients with small bowel type CD (with the exception of one patient with colitis-type form with only IgG type ASCA) and celiac disease (Figure 3-4). IgG and IgA ASCA progressed together. IgA type ASCA values were between 0.35-938.19 U/ml (positive $\geqslant$20 U/ml). The prevalence of ASCA in patients with celiac disease outlined a possible role of anti-*Saccharomyces cerevisiae* antibodies in GSE. These findings outlined a noticeable startling resemblance, suggesting a possible kind of connection between CD and GSE.

Table 1 ASCA positive patients in different diseases of bowels

	ASCA IgG+	ASCA IgA+	ASCA IgG+IgA+	IgG *vs* IgA corr.*(r)*
All patients (*n*=68)	5	4	10	0.75
Crohn's disease (*n*=42)	1	2	8	0.81
Ulcerative colitis (*n*=10)	2	1	0	-0.01
Celiac disease (*n*=16)	2	1	2	0.50
Controls (*n*=20)	0	0	0	-0.18

Notes: It is clear that there was no ASCA positivity in the controls. ASCA positivity was common in patients with Crohn's disease. The ASCA IgG- and IgA-type seropositivity was concomitant.

Table 2 ASCA positive patients with different forms of Crohn's disease

Affected section of the bowels	ASCA IgG+	ASCA IgA+	ASCA IgG+IgA+
Only the colon (*n*=27)	1	0	0
Large and small bowels both (*n*=8)	0	0	4
Only small bowels (*n*=7)	0	2	4
Small bowel together (*n*=15)	0	2	8

Notes: Both the IgA and IgG type ASCA associated to the small bowels. $P<0.0004$, ASCA IgG+ *vs* small bowels; $P<0.0001$ ASCA IgA+ *vs* small bowels.

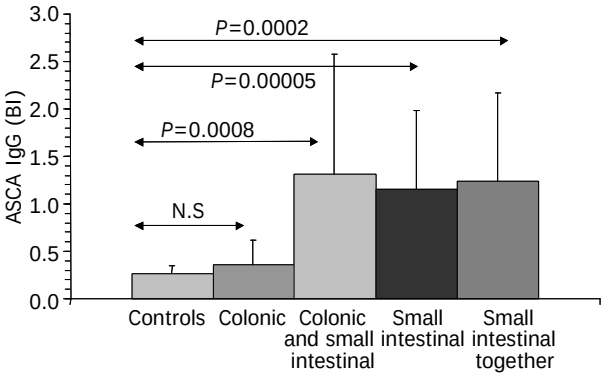

Figure 1 ASCA IgG values in Crohn's disease.

Table 3 Summary of ASCA positive cases with Crohn's disease

Case:	ASCA IgG	ASCA IgA	ASCA IgG+IgA	Age (years)	Sex	Affected sections of gastrointestinal tract
1.		+		19	Female	Terminal ileum
2.			+	46	Male	Terminal ileum
3.			+	37	Male	Terminal ileum
4.			+	38	Female	Terminal ileum
5.	+			50	Female	Colon
6.			+	29	Male	From the duodenum to the rectum
7.		+		40	Female	Terminal ileum
8.			+	24	Male	Terminal ileum + colon
9.			+	49	Female	From the duodenum to the rectum
10.			+	41	Female	Terminal ileum
11.			+	27	Male	Terminal ileum + colon

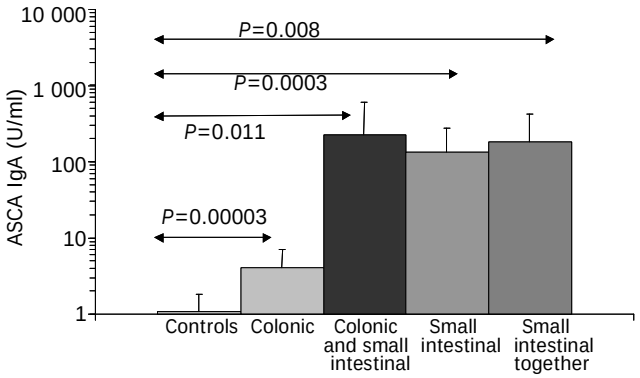

Figure 2 ASCA IgA values in Crohn's disease.

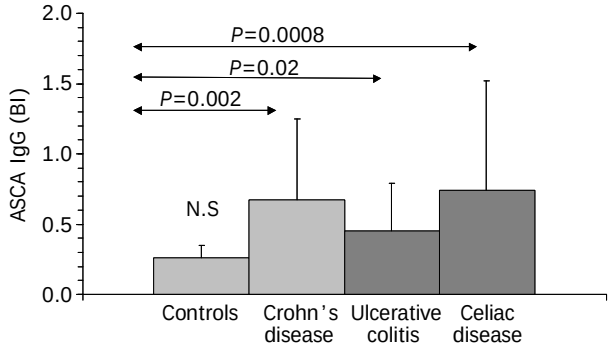

Figure 3 ASCA IgG values in inflammatory diseases of intestines.

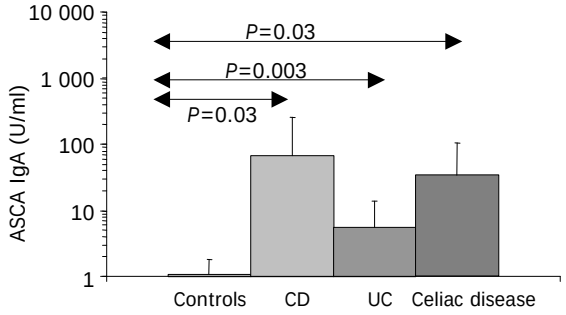

Figure 4 ASCA IgA values in inflammatory diseases of intestines. [The IgA type ASCA values are between 0.35-938.19 U / ml (positive: IgA ⩾20 U / ml).]

DISCUSSION

Both celiac disease and Crohn' s disease are characterized by the presence of distinct (auto) antibodies. Based upon our results, theoretically and practically it is thinkable that ASCA positivity is not only a specific marker of Crohn' s disease but correlates with the (auto-) immune inflammation of the small intestines How does it happen?

Macrophages can produce proinflammatory cytokines (i.e. TNF-α) with direct and indirect microbicide activity. Several cell-wall components of *Candida albicans* were investigated in relation with the TNF-alfa secretion of macrophages and confirmed that they all had beta-1,2-oligomannoside[11,12]. The incubation with purified oligomannoside activated macrophages and they secreted TNF-alfa (in dose and molecule-size dependently) *in vitro* and *in vivo*[13,14]. Similar observations were demonstrated with *Saccharomyces cerevisiae*: the oligomannose structures influenced per interaction the cytokine network[15-17]. It is conceivable that miscellaneous *fungus*-oligosaccharides (their signal function in phytopathology is well-known) could play a key role in the regulation of human infections[18]. Oligomannosids of *Saccharomyces cerevisiae* with modification by ASCA can change their immunopathogenicity and trigger a process that results in specific inflammation such as CD.

The human gastrointestinal tract possesses a complex ecosystem, the components of which are multifaceted and metabolically diverse. Although the presence of intestinal microflora certainly contributes to the maintenance of human health, intestinal mucosa has the task, among others, of preventing the passage of commensal microflora and occasional pathogens to other compartments. To carry out such a function, the mucosa has to behave as a physical barrier but it also has to play an active role. Oral tolerance (OT) consists of the oral administration of antigens that could alter the response of the immune system[19]. This is a form of peripheral immune tolerance in which mature lymphocytes in the peripheral lymphoid tissues are rendered non functional or hyporesponsive by prior oral administration of antigens. The mechanisms by which OT is mediated include deletion or anergy and active cellular suppression. The primary factor determining which form of tolerance will be developed after oral administration of antigen is its dosage. Thus, it is thought that low doses of antigen can induce the generation of active suppression, *via* regulatory T cells in the gut-associated lymphoid tissue (GALT), which then migrate to the systemic immune system. These regulatory T cells produce down-regulatory cytokines such as IL-4, IL-10 and TGF-β in a Th2 /Th3 cytokine pattern. Conversely, high dose of antigen favors anergy or clonal deletion. The phenomenon in which regulatory cells, as generated by oral tolerance, are primed in an antigen specific manner, but act in the respective microenvironment in a non-antigen specific manner is called bystander suppression. This phenomenon is of particular interest and can explain the use of oral/mucosal tolerance in T cell mediated autoimmune diseases such as rheumatoid arthritis and some diseases in which the autoantigen remains unknown or where there are reactivities to multiple autoantigens. T helper type 1 (Th1) lymphocytes secrete interleukin (IL)-2, interferon-γ and lymphotoxin-α, and stimulate type 1 immunity, which is characterized by intense phagocytic activity. Conversely, Th2 cells secrete IL-4, IL-5, IL-9, IL-10 and IL-13, and stimulate type 2 immunity, which is characterized by high antibody titers. Type 1 and type 2 immunity are not strictly synonymous with cell-mediated and humoral immunity, because Th1 cells also stimulate moderate levels of antibody production, whereas Th2 cells actively suppress phagocytosis. For most infections caused by large eukaryotic pathogens, type 1 immunity is protective, whereas type 2 responses assist with the resolution of cell-mediated inflammation. Severe systemic stress, immunosuppression, or overwhelming microbial inoculation causes the immune system to mount a type 2 response to an infection normally controlled by type 1 immunity. Macrophages also play a crucial role in the mucosal network as they must perform a number of diverse cellular functions that allow them to kill invading micro-organisms and neoplastic cells as well as produce growth factors involved in wound healing. Macrophages that develop these diverse functions arise from a common precursor. By a process of selective adaptation, the common precursor monocyte/ macrophage differentiates into a distinctive macrophage with a different and specific phenotype, characterized by the expression of a specific set of gene products. The local environment plays a critical role in shaping or directing the pattern or pathway of macrophage differentiation: one pathway was believed to play a role in wound repair and characterized by the induction of insulin-like growth factor-1 (IGF-I) and a second pathway was involved in macrophage cytocidal activation and characterized

by the induction of the inducible form of nitric oxide synthase (iNOS)[20,21].

IBDs are a group of diseases due to chronic inflammation of the gastrointestinal tract, but without proved etiology. IBD appears to be resulted from a dysregulated immune response with contributions from environmental, genetic, and bacterial factors. In the last decades, our understanding of the pathogenesis of IBD has greatly expanded but a better insight is needed into the environmental agents responsible for either initiation or perpetuation of IBD. The increasing attention given to the ecosystem of the gut may help define the antigens responsible for immune reactivity and provide opportunities toward application of antigen-specific therapeutic interventions such as induction of tolerance. Further investigation into probiotic agents and their mechanisms is especially appealing as a way to provide alternative therapies to decrease the inflammatory response. Antibodies to an oligomannose epitope of *Saccharomyces cerevisiae* demonstrated in 60-70 % of the patients with Crohn' s disease. The origin and clinicopathological role of ASCA have not been clarified. The sporadic information about ASCA positivity in patients suffering from gluten sensitive enteropathy in the literature suggests another occurrence.

We examined the ASCA' s occurrence in our patients and compared it with the clinical picture of the Crohn' s disease. The results supported the theory that ASCA positivity correlated with small intestinal Crohn' s disease and in these cases both IgG and IgA type antibodies were proved. The relatively high incidence of ASCA in GSE was unexplained but indicated further surveys to elucidate it as it was definitely more than accidental[22]. The antibodies in the sera of the analyzed ASCA positive cases proved a systemic immune response against *Saccharomyces cerevisiae* and suggested the end of the oral tolerance against the yeast' s antigens. The diet restriction (elemental diet, total parenteral nutrition, and fecal diversion) may ameliorate the status of the patients with Crohn' s disease. It can also be speculated that the yeast-free diet as a part of the therapy for the ASCA positive patients can be reasonable, moreover the permanent "forbidding" of the yeast can be an acceptable alternative in case of getting well.

REFERENCES

1 **Scoglio R,** Di Pasquale G, Pagano G, Lucanto MC, Magazzu G, Sferlazzas C. Is intestinal biopsy always needed for diagnosis of celiac disease? *Am J Gastroenterol* 2003; **98**: 1325-1331

2 **Barnes RM,** Allan S, Taylor-Robinson CH, Finn R, Johnson PM. Serum antibodies reactive with Saccharomyces cerevisiae in inflammatory bowel disease: is IgA antibody a marker for Crohn's disease? *Int Arch Allergy Appl Immunol* 1990; **92**: 9-15

3 **Falchuk KR**, Isselbacher KJ. Circulating antibodies to bovine albumin in ulcerative colitis and Crohn's disease. Characterization of the antibody response. *Gastroenterology* 1976; **70**: 5-8

4 **Hoffenberg EJ**, Fidanza S, Sauaia A. Serologic testing for inflammatory bowel disease. *J Pediatr* 1999; **134**: 447-452

5 **Knoflach P**, Park BH, Cunningham R, Weiser MM, Albini B. Serum antibodies to cow's milk proteins in ulcerative colitis and Crohn's disease. *Gastroenterology* 1987; **92**: 479-485

6 **Main J**, McKenzie H, Yeaman GR. Antibody to Saccharomyces cerevisiae (bakers yeats) in Crohndisease. *BMJ* 1988; **297**: 1105-1106

7 **Giaffer MH**, Clark A, Holdsworth CD. Antibodies to Saccharomyces cerevisiae in patients with Crohns disease and their possible pathogenic importance. *Gut* 1992; **33**: 1071-1075

8 **Quinton JF,** Sendid B, Reumaux D, Duthilleul P, Cortot A, Grandbastien B, Charrier G, Targan SR, Colombel JF, Poulain D. Anti-Saccharomyces cerevisiae mannan antibodies combined with antineutrophil cytoplasmic autoantibodies in inflammatory bowel disease: prevalence and diagnostic role. *Gut* 1998; **42**: 788-791

9 **Barclay GR,** McKenzie H, Pennington J, Parratt D, Pennington CR. The effect of Dietary Yeast on the Activity of Stable Chronic Crohn's Disease. *Scand J Gastroenterol* 1992; **27**: 196-200

10 **Vidrich A,** Lee J, James E, Cobb L, Targan S. Segregation of pANCA antigenic recognition by DNase treatment of neutrophils: ulcerative colitis, type I autoimmune hepatitis, and primary sclerosing cholangitis. *J Clin Immunol* 1995; **15**: 293-299

11 **Domer J**, Elkins K, Ennist D, Baker P. Modulation of immune responses by surface polysaccharides of Candida albicans. *Rev Infect Dis* 1988; **10**: S419-422

12 **Trinel PA,** Plancke Y, Gerold P, Jouault T, Delplace F, Schwarz RT, Strecker G, Poulain D. The Candida albicans phospholipomannan is a family of glycolipids presenting phosphoinositolmannosides with long linear chains of beta-1, 2-linked mannose residues. *J Biol Chem* 1999; **274**: 30520-30526

13 **Janusz MJ,** Austen KF, Czop JK. Isolation of a yeast heptaglucoside that inhibits monocyte phagocytosis of zymosan particles. *J Immunology* 1989; **142**: 959-965

14 **Jouault T,** Lepage G, Bernigaud A, Trinel PA, Fradin C, Wieruszeski JM, Strecker G, Poulain D. Beta-1,2 linked oligomannosides from Candida albicans act as signals for tumor necrosis factor alpha production. *Infect Immun* 1995; **63**: 2378-2381

15 **Heelan BT**, Allan S, Barnes RMR. Identification of a 200-kDa glycoprotein antigen of Saccharomyces cerevisiae. *Immunol Letters* 1991; **28:** 181-186

16 **Sander U,** Kunze I, Broker M, Kunze G. Humoral immune response to a 200-kDa glycoprotein antigen of Saccharomyces cerevisiae is common in man. *Immunology Letters* 1998; **61**: 113-117

17 **Sendid B,** Colombel JF, Jacquinot PM, Faille C, Fruit J, Cortot A, Lucidarme D, Camus D, Poulain D. Specific antibody response to oligomannosidic epitopes in Crohns disease. *Clin Diagn Lab Immunol* 1996; **2**: 219-226

18 **Ryan C.** Oligosaccharide signals: From plant defense to parasite offense. *Proc Natl Acad Sci U S A* 1994; **91**: 1-2

19 **Strobel S**, Mowat AM. Immune responses to dietary antigens: oral tolerance. *Immunol Today* 1998; **19**: 173-181

20 **Spellberg B**, Edwards JE. Type 1/Type 2 immunity in infectious diseases. *Clin Infect Dis* 2001; **32**: 76-102

21 **Winston BW**, Krein PM, Mowat C, Huang Y. Cytokine-induced macrophage differentiation: a tale of 2 genes. *Clin Invest Med* 1999; **22**: 236-255

22 **Damoiseaux JG,** Bouten B, Linders AM, Austen J, Roozendaal C, Russel MG, Forget PP, Tervaert JW. Diagnostic value of anti-Saccharomyces cerevisiae and antineutrophil cytoplasmic antibodies for inflammatory bowel disease: high prevalence in patients with celiac disease. *Clin Immunol* 2002; **22**: 281-288

Edited by Xu XQ and Wang XL

P.O.Box 2345, Beijing 100023,China
Fax: +86-10-85381893
E-mail: wjg@wjgnet.com www.wjgnet.com

World J Gastroenterol 2003;9(10):2313-1316
World Journal of Gastroenterology
 ISSN 1007-9327

• CLINICAL RESEARCH •

Clinical utility, safety and tolerability of capsule endoscopy in urban Southeast Asian population

Tiing-Leong Ang, Kwong-Ming Fock, Tay-Meng Ng, Eng-Kiong Teo, Yi-Lyn Tan

Tiing-Leong Ang, Kwong-Ming Fock, Tay-Meng Ng, Eng-Kiong Teo, Yi-Lyn Tan, Division of Gastroenterology, Changi General Hospital, Singapore
Correspondence to: Dr. Ang Tiing Leong, Division of Gastroenterology, Department of Medicine, Changi General Hospital, 2 Simei Street 3, 529889 Singapore. tiing_leong_ang@cgh.com.sg
Telephone: +65-67888833 **Fax:** +65-67816202
Received: 2003-07-17 **Accepted:** 2003-08-02

Abstract

AIM: Capsule endoscopy has demonstrated its clinical utility in the evaluation of small bowel pathology in several Western studies. In this prospective study, we aimed to determine the clinical utility, safety and tolerability of capsule endoscopy in the evaluation of suspected small bowel disease in an urban Southeast Asian population.

METHODS: We used the given (M2A) capsule endoscopy system in 16 consecutive patients with suspected small bowel pathology. In 9 patients the indication was obscure gastrointestinal bleeding, while in 6 patients it was to determine the extent of small bowel involvement in Crohn's disease. One patient underwent capsule endoscopy for evaluation of chronic abdominal pain. Patient's tolerability to the procedure was evaluated by standardized questionnaires and all patients were reviewed at one week to ensure that the capsule had been excreted without any adverse events.

RESULTS: Abnormal findings were present in 8 patients (50 %). The cause of obscure gastrointestinal bleeding was determined in 5 out of 9 patients. Findings included 2 cases of angiodysplasia, 2 cases of jejunal ulcers and 1 case of both angiodysplasia and jejunal ulcer. One patient had small bowel erosions and foci of erythema of doubtful significance. Ileal lesions were diagnosed in 2 out of 6 patients with Crohn's disease. Capsule endoscopy was well tolerated by all patients. One patient with Crohn's disease had a complication of capsule retention due to terminal ileum stricture. The capsule eventually passed out spontaneously after 1 month.

CONCLUSION: Our study, which represented the first Asian series, further confirms the diagnostic utility, safety and tolerability of wireless capsule endoscopy.

Ang TL, Fock KM, Ng TM, Teo EK, Tan YL. Clinical utility, safety and tolerability of capsule endoscopy in urban Southeast Asian population. *World J Gastroenterol* 2003; 9(10):2313-2316
http://www.wjgnet.com/1007-9327/9/2313.asp

INTRODUCTION

Small bowel imaging is important in the evaluation of obscure gastrointestinal bleeding[1], inflammatory disease of the small bowel[2] and tumours. The main methods of small bowel imaging have been either enteroscopy or small bowel barium studies in the evaluation of luminal pathology. Angiography is a diagnostic option in the context of suspected small intestinal bleeding. Push enteroscopy allows examination of only 80 to 120 cm of the small bowel beyond the ligament of Treitz, while intra-operative enteroscopy requires general anesthesia and laparotomy. Small bowel series and enteroclysis have limited sensitivity, and in particular, could not detect flat lesions such as angiodysplasia[3].

Wireless capsule endoscopy was first reported by Iddan *et al*[4] in 2000, and it represents a major advancement in the imaging of the small intestine. It is able to capture video-images of the mucosal surface of the entire length of the small intestine directly, and has been reported to be virtually pain-free since it is essentially propelled forward through the gastrointestinal tract by peristalsis, without the need for any air-insufflation.

Thus far all published data on the use of capsule endoscopy have been from Western countries, with only 2 case reports on its use from India. One was a case of ileal angiodysplasia[5] while another was that of small intestine tuberculosis[6].

In this prospective study, we aimed to determine the clinical utility, safety and tolerability of capsule endoscopy in the evaluation of suspected small bowel disease in an urban Southeast Asian population.

MATERIALS AND METHODS

Study population

Consecutive patients with suspected small bowel pathology seen at the Division of Gastroenterology, Changi General Hospital, Singapore, were recruited. Indications for capsule endoscopy included obscure gastrointestinal bleeding, assessment of extent of small intestine involvement in Crohn's disease, evaluation of chronic abdominal pain and assessment for small bowel pathology in the presence of malabsorption. Patients with the following conditions were excluded from the study: pregnant subjects, suspected small bowel obstruction, presence of cardiac pacemaker, subjects expected to undergo MRI examination before elimination of capsule and subjects with swallowing difficulty. The study was approved by the Hospital Ethics Committee. Informed consent was obtained from all patients before commencement of the study.

Given diagnostic imaging system

The given diagnostic imaging system is comprised of the 26 mm by 11 mm M2A® capsule which contains a miniscule color video-camera equipped with a localization feature, a data recorder which is a portable, battery operated external receiving/recording unit that receives data transmitted by the capsule and subsequently allows data downloading, the Rapid® Workstation, a modified personal computer which has been designed for storage, processing and presentation of captured images as well as generation of reports. The technical details have previously been described in an earlier paper[7].

M2A® capsule ingestion, data capture and follow-up

After a 12-hour fast, subjects underwent capsule examination with the M2A®capsule according to the standard procedure. Briefly it involved attaching 8 sensory arrays to the abdomen

based on a standard template. These arrays were then attached to the portable battery powered data recorder. The capsule was swallowed and subjects were advised that fluids were allowed after 2 hours and light snack after 4 hours. Subjects were then allowed to go home. After 8 hours, the subject returned and the equipment was removed and the data were downloaded into the Rapid® Workstation and the images were analyzed using the proprietary software. The subjects were asked to look for the capsule in the feces. They were also reviewed again at 1 week for any complications and to ensure that the capsule had passed out. If excretion of the capsule was not noticed by the subject, an abdominal X-ray would be done.

Assessment of tolerability and complications

All subjects were asked about tolerability of the procedure in the following areas using a standardised questionnaire, which included ease of swallowing, pain or discomfort experienced during the procedure, pain or discomfort experienced after the procedure, overall tolerability of the procedure, and overall convenience of the procedure. The subjects were also evaluated at one week after procedure for any adverse events such as pain, nausea,vomiting and capsule impaction or retention.

Capsule image interpretation

Two gastroenterologists (Drs Tay-Meng Ng and Tiing-Leong Ang) reviewed the capsule images independently and reported on the findings. Questionable findings were discussed. Positive findings were defined as detected abnormalities that were potentially related to the presenting problem.

RESULTS

Demographics

During the period from mid February to May 2003, 16 consecutive patients with suspected small bowel pathology and no contraindication to capsule endoscopy were recruited. Their mean age was 55.6 years (range: 19 to 82 years) with a male to female ratio of 9:7. Table 1 summarizes the patient profile, indication for capsule endoscopy and the results of the study.

Nine patients had obscure gastrointestinal bleeding, having presented with anaemia and melaena. All underwent both gastroscopy and colonoscopy. These investigations did not reveal significant pathology that could have accounted for the bleeding. Push enteroscopy was done in 2 of these patients, and small bowel series were done in another 4. Apart from small bowel diverticula seen on small bowel series in one patient, the rest of the small bowel imaging were normal.

Six patients were diagnosed to have Crohn' s disease on the basis of characteristic clinical, endoscopic and histologic features. Capsule endoscopy was performed to determine the extent of small bowel involvement in these patients.

One patient had a problem of recurrent abdominal pain and capsule endoscopy was performed to exclude any small intestine pathology after previous endoscopies did not reveal any significant lesions.

Findings in capsule endoscopy

Among the 9 patients with obscure gastrointestinal bleeding, capsule endoscopy was able to diagnose a clinically significant pathology in 5 of them (55.6 %). Two patients had jejunal ulcers (Figure 1). Two patients had angiodysplasia while the last patient had both angiodysplasia and jejunal ulcer. It was felt that the jejunal ulcers could have been related to NSAID usage. A sixth patient had the finding of small bowel erosions and foci of erythema, but the authors felt that these lesions could not have accounted for the gastrointestinal bleeding. Among the 6 patients with Crohn' s disease, capsule endoscopy revealed small bowel pathology in 2 cases. One patient had multiple ileal ulcers and strictures (Figure 2) while the other had erythema in the terminal ileum. These abnormalities were not detected by small bowel barium studies done prior to capsule endoscopy. Overall, abnormalities were present in 50 % (8/16) of the subjects.

Patient tolerability and complications

All the patients rated the procedure as comfortable and very convenient. Despite the size of the capsule being larger than most tablets, all the patients described swallowing as very easy. There was no complaint of pain or discomfort during or after the procedure. However, 2 of the patients commented on the weight of the portable recorder/battery pack.

The capsule was excreted in all the patients without any ill effects. One patient had retention of capsule beyond one week without developing any obstructive symptoms. It took 31 days before the capsule was noted to have passed out spontaneously. This was the patient with Crohn' s disease who had ileal ulcer and stricture. In fact, an attempt was made to retrieve it endoscopically at one week but it was unsuccessful. It was then decided to follow up the patient and wait for spontaneous passage of the capsule as he had remained asymptomatic

Table 1 Patient characteristics and results of capsule endoscopy

SN.	Age / sex	Indication for capsule endoscopy	Results of capsule endoscopy
1	66 / male	Extent of small bowel involvement in Crohn's disease	Erythema in terminal ileum
2	30 / male	Extent of small bowel involvement in Crohn's disease	Edematous small bowel
3	62 / female	Obscure gastrointestinal blood loss	Small bowel angiodysplasia
4	39 / male	Extent of small bowel involvement in Crohn's disease	Ulcers and strictures in ileum
5	28 / male	Extent of small bowel involvement in Crohn's disease	Normal small bowel
6	74 / female	Extent of small bowel involvement in Crohn's disease	Gastric erosions; normal small bowel
7	62 / male	Obscure gastrointestinal blood loss	Gastric erosion; normal small bowel
8	69 / male	Obscure gastrointestinal blood loss	Jejunal ulcer; small bowel angiodysplasia
9	59 / female	Obscure gastrointestinal blood loss	Mild gastritis and duodenitis; normal small bowel
10	82 / female	Obscure gastrointestinal blood loss	Gastritis; small bowel angiodysplasia
11	54 / female	Extent of small bowel involvement in Crohn's disease	Normal small bowel
12	69 / male	Evaluation for small intestine pathology in context of chronic abdominal pain	Normal small bowel
13	71 / female	Obscure gastrointestinal blood loss	Jejunal ulcer
14	66 / female	Obscure gastrointestinal blood loss	Bleeding jejunal ulcer
15	46 / male	Obscure gastrointestinal blood loss	Normal small bowel
16	19 / male	Obscure gastrointestinal blood loss	Small bowel erosions and foci of erythema

throughout, rather then subject him to surgery. For the remaining 15 patients, the capsule was excreted within a week, six of these patients actually did not notice the passage of the capsule, but an abdominal X-ray done at one week proved that the capsule had not been retained.

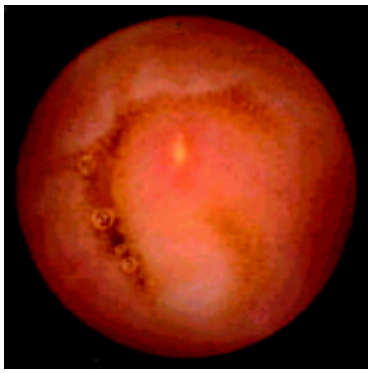

Figure 1 A case of jejunal ulcer due to NSAIDS.

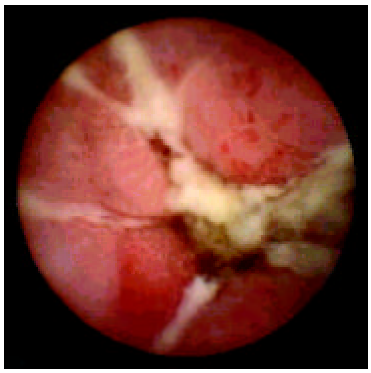

Figure 2 Terminal ileum ulcer and stricture in a patient with Crohn's disease.

DISCUSSION

Our study, which represented the first Asian series, further confirmed the diagnostic utility, safety and tolerability of wireless capsule endoscopy. In our series, it was able to reveal significant small intestine pathology in 43.8 % (7/16) of the patients. In particular, for obscure gastrointestinal bleeding, it was able to reveal the cause in 55.6 % of the patients. It was remarkably well tolerated, and apart from one patient with delayed capsule excretion, there were no complications. This complication highlighted the need to be vigilant towards the possibility of intestinal obstruction when considering the use of capsule endoscopy.

In a prospective study of 20 patients, Costamagna *et al*[7] confirmed the superiority of capsule endoscopy over small bowel radiographs in the diagnosis of suspected small bowel disease. Capsule endoscopy was able to detect abnormalities in 17 out of 20 patients, compared to 3 out of 20 using barium studies. Similarly, Scapa[8] in another prospective study found that among 35 patients with suspected small intestine pathology but normal small bowel series, capsule endoscopy was able to detect clinically significant small intestine pathology in 63 % of (22/35) patients.

For the evaluation of obscure gastrointestinal bleeding, our results were comparable to other published data. Scapa[8] was able to find a source of bleeding in 75 % (15/20) of his patients with obscure gastrointestinal bleeding. Lewis[9] had a positive yield of 55 % (11/20) in the evaluation of obscure gastrointestinal bleeding with capsule endoscopy. Ell[10] detected a definite source in 66 % of his patients.

For the diagnosis of Crohn's disease, Fireman[11], Eliakim[12] and Herrerias[13] have demonstrated the clinical utility of capsule endoscopy in diagnosis as well as in assessment of the extent of disease. It was particularly relevant where conventional endoscopic and radiological techniques have not identified pathological findings but clinical suspicion based on symptoms and laboratory tests was strong. In our series, only 33 % of the patients with Crohn's disease had abnormal findings on capsule endoscopy. This probably simply reflected the actual prevalence of small bowel involvement in our series, rather than under-diagnosis, since alternative imagings, such as barium studies when done, did not reveal any small bowel lesions either. In addition it was recognized that about 1/3 of patients with Crohn's disease had ileocolic disease, about 1/3 had colonic disease and about 1/3 had small bowel disease[14]. An important point to note was that one patient actually had ileal stricture that led to delayed excretion of the capsule. In this case, the presence of small bowel stricture was not suspected, as the patient did not have any clinical evidence of small bowel obstruction. It is therefore suggested that if Crohn's disease is a diagnostic consideration, then small bowel series or enema should precede the use of capsule endoscopy in order to minimize the risk of capsule retention. It is also worth noting that despite the stricture, the capsule was able to pass out without any ill effect after 31 days. Therefore in the absence of any signs or symptoms of capsule impaction or obstruction, a conservative approach may be adopted, with the use of high dose steroid to reduce the inflammation and oedema so as to facilitate the passage of the capsule, as occurred in this patient with Crohn's stricture.

Possible complications and limitations exist with any procedure, and capsule endoscopy is no exception, in spite of the high diagnostic yield. The key complication is that of capsule retention proximal to a stricture, and a 5 % retention rate has been reported, with the need for surgery in less than 1 % of patients[15]. Another concern is delayed passage of capsule due to slow transit time, resulting in capsule recording terminating before it has passed to the caecum, and hence incomplete data acquisition. Other limitations included difficulty in determining the exact site of the abnormality in the small bowel, inability to take tissue biopsy, problem of visual clarity due to intestinal fluids and long viewing time of the video, which could take up to 2 hours[7]. It is also costly, with the estimated cost of each capsule being greater than the cost of undergoing colonoscopy in the Singapore context. Thus it is likely that its use would remain selective, being reserved for situations when endoscopy or other imaging modalities have failed to achieve a definite diagnosis. These would include the investigation of obscure gastrointestinal bleeding, and in the context where clinical suspicion for Crohn's disease is strong but the results of all other tests have been equivocal.

In conclusion, our study affirms the diagnostic utility and safety of capsule endoscopy in clinical practice. It has the promise to become a leading method in the evaluation of small bowel pathology, but limitations and the issue of cost need to be addressed.

ACKNOWLEDGEMENT

Servicom Medical (Singapore) Pte Ltd: For provision of M2A®Capsules (Given Imaging Limited, Yoqneam, Israel)) for the study.

REFERENCES

1 **Zuckerman GR**, Prakash C, Askin MP, Lewis BS. AGA technical review on the evaluation and management of occult and obscure gastrointestinal bleeding. *Gastroenterology* 2000; **118**: 201-221

2 **Gay GJ**, Delmotte JS. Enteroscopy in small intestinal inflammatory diseases. *Gastrointest Endosc Clin North Am* 1999; **9**: 115-123
3 **Nolan DJ**, Traill ZC. The current role of the barium examination of the small intestine. *Clin Radiol* 1997; **52**: 809-820
4 **Iddan G**, Meron G, Glukhovsky A, Swain P. Wireless capsule endoscopy. *Nature* 2000; **405**: 417
5 **Nagral A**, Nisar P, Nagral S. Capsule endoscopy diagnosis of ileal angiodysplasia. *Indian J Gastroenterol* 2003; **22**: 64-65
6 **Reddy DN**, Sriram PV, Rao GV. Capsule endoscopy appearances of small bowel tuberculosis. *Endoscopy* 2003; **35**: 99
7 **Costamagna G**, Shah SK, Riccioni ME. A prospective trial comparing small bowel radiographs and video capsule endoscopy for suspected small bowel disease. *Gastroenterology* 2002; **123**: 999-1005
8 **Scapa E**, Jacob H, Lewkowicz S. Initial experience of wireless capsule endoscopy for evaluating occult gastrointestinal bleeding and suspected small bowel pathology. *Am J Gastroenterol* 2002; **97**: 2776-2779
9 **Lewis BS**, Swain P. Capsule endoscopy in the evaluation of patients with suspected small intestinal bleeding: results of a pilot study. *Gastrointest Endosc* 2002; **56**: 349-353
10 **Ell C**, Remke S, May A. The first prospective controlled trial comparing wireless capsule endoscopy with push enteroscopy in chronic gastrointeastinal bleeding. *Endoscopy* 2002; **34**: 685-689
11 **Fireman Z**, Mahajna E, Broide E. Diagnosing small bowel Crohn's disease with wireless capsule endoscopy. *Gut* 2003; **52**: 390-392
12 **Eliakim R**, Fischer D, Suissa A. Wireless capsule endoscopy is a superior diagnostic tool in comparision to barium follow-through and computerized tomography in patients with suspected Crohn's disease. *Eur J Gastroenterol Hepatol* 2003; **15**: 363-367
13 **Carucci LR**, Levine MS. Radiographic imaging of inflammatory bowel disease. *Gastroenterol Clin N Am* 2002; **31**: 93-117
14 **Herrerias JM**, Caunedo A, Rodriguez-Tellez M. Capsule endoscopy in patients with suspected Crohn's disease and negative endoscopy. *Endoscopy* 2003; **35**: 564-568
15 **Cave DR**. Wireless video capsule endoscopy. *Clinical Perspectives Gastroenterol* 2002; **5**: 203-207

Edited by Wang XL

P.O.Box 2345, Beijing 100023,China
Fax: +86-10-85381893
E-mail: wjg@wjgnet.com www.wjgnet.com

World J Gastroenterol 2003;9(10):2317-2321
World Journal of Gastroenterology
 ISSN 1007-9327

• CLINICAL RESEARCH •

Budd-Chiari syndrome: Diagnosis with three-dimensional contrast-enhanced magnetic resonance angiography

Jiang Lin, Xiao-Hai Chen, Kang-Rong Zhou, Zu-Wang Chen, Jian-Hua Wang, Zhi-Ping Yan, Ping Wang

Jiang Lin, Xiao-Hai Chen, Kang-Rong Zhou, Zu-Wang Chen, Jian-Hua Wang, Zhi-Ping Yan, Ping Wang, Department of Radiology, Affiliated Zhongshan Hospital, Fudan University, Shanghai 200032, China
Correspondence to: Dr. Jiang Lin, Department of Radiology, Affiliated Zhongshan Hospital, Fudan University, Shanghai 200032, China. linjiang@zshospital.net
Telephone: +86-21-64041990 Ext 2463 **Fax:** +86-21-64038472
Received: 2003-04-02 **Accepted:** 2003-05-11

Abstract

AIM: To evaluate the role of three-dimensional contrast-enhanced magnetic resonance angiography (3D CE MRA) in the diagnosis of Budd-Chiari syndrome (BCS).

METHODS: Twenty-three patients with BCS underwent 3D CE MRA examination, in which 13 cases were secondary to either hepatocellular carcinoma (11 cases), right adrenal carcinoma (1 case) or thrombophlebitis (1 case) and 10 suffered from primary BCS. The patency of the inferior vena cava (IVC), hepatic and portal veins as well as the presence of intra- and extrahepatic collaterals, liver parenchymal abnormalities and porto-systemic varices were evaluated. Inferior vena cavography was performed in 10 cases. The diagnosis of IVC obstruction by 3D CE MRA was compared with that demonstrated by inferior vena cavography.

RESULTS: The major features of BCS could be clearly displayed on 3D CE MRA. Positive hepatic venous signs included tumor thrombosis (9 cases), tumor compression (2 cases), nonvisualization (4 cases) and focal stenosis (2 cases). Positive IVC findings were noted as severe stenosis or occlusion (10 cases), tumor invasion (2 cases), thrombosis (3 cases), thrombophlebitis (1 case) and septum formation (3 cases). Intrahepatic collaterals were shown in 9 patients, 2 of them with "spider web" sign. The displayed extrahepatic collaterals included dilated azygos and hemi-azygos veins (13 cases) and left renal-inferior phrenic-pericardiophrenic veins (2 cases). The occlusion of the left intrahepatic portal veins was found in 2 cases. Porto-systemic varices were detected in 10 patients. Liver parenchymal abnormalities displayed by 3D CE MRA were enlargement of the caudate lobe (7 cases), heterogenous enhancement (18 cases) and complicated tumors (13 cases). Compared with the inferior vena cavography performed in 10 cases, the accuracy of 3D CE MRA was 100 % in the diagnosis of IVC obstruction.

CONCLUSION: 3D CE MRA can display the major features of BCS and provide an accurate diagnosis.

Lin J, Chen XH, Zhou KR, Chen ZW, Wang JH, Yan ZP, Wang P. Budd-Chiari syndrome: Diagnosis with three-dimensional contrast-enhanced magnetic resonance angiography. *World J Gastroenterol* 2003; 9(10):2317-2321
http://www.wjgnet.com/1007-9327/9/2317.asp

INTRODUCTION

Budd-Chiari syndrome (BCS) is a rare disease caused by the obstruction of the hepatic venous outflow or the inferior vena cava (IVC) above the hepatic vein[1]. It often occurs secondary to intrinsic vascular thrombosis, hepatic tumor invasion/compression, or associates with an idiopathic obstructing membrane[1,2]. The clinical signs of ascites, abdominal pain and hepatomegaly are the typical triad of BCS. Since these signs are nonspecific, the clinical diagnosis of this syndrome is difficult. Conventionally, X-ray angiography and/or liver biopsy are used to confirm the diagnosis of BCS with the limitation of invasiveness. Ultrasound (US), computed tomography (CT) and magnetic resonance imaging (MRI) are the noninvasive imaging techniques currently used in the evaluation of the patency of hepatic veins, IVC and portal vein. However, some limitations are also existed in each of these modalities[2-7].

Three-dimensional contrast-enhanced magnetic resonance angiography (3D CE MRA) is a new technique and widely used in the imaging of the arterial system, portal venous system and central venous system[8-16]. However, to our knowledge, few studies have been reported so far concerning its use in the diagnosis of BCS[17]. Therefore, this study was conducted to evaluate the usefulness of this technique in the imaging of BCS and to present various findings of BCS demonstrated on 3D CE MRA.

MATERIALS AND METHODS

Patients

Twenty-three patients with BCS underwent 3D CE MRA. There were 20 men and 3 women ranging from 26 to 56 years of age (average age 38 years). In 11 patients, BCS was secondary to the invasion and occlusion of the hepatic vein and/or IVC by hepatocellular carcinoma (HCC). In 1 patient, BCS was resulted from tumor invasion of IVC by right adrenal carcinoma. In 1 patient, IVC obstruction was due to superior extension of pelvic thrombophlebitis. The above 13 patients were considered to be secondary BCS. Ten patients had primary BCS with an unknown origin. The diagnosis of BCS was confirmed by inferior vena cavography in 10 cases, percutaneous liver biopsy in 2 cases, and surgery in 5 cases. The diagnosis of the remaining 6 cases was confirmed by combined color Doppler sonography and contrast-enhanced CT.

3D CE MRA examination

All scans were performed using a 1.5T MR imager (Signa, General Electric Medical Systems, Milwaukee, WI.) and a body coil. After the localizing images were obtained, a breathhold T1-weighted fast multiplanar spoiled gradient-echo (FMPSPGR) sequence (repetition time/echo time, 150/4.2 msec; flip angle, 90°; field of view, 360 mm; matrix, 128×256; 18 slices; slice thickness, 7.0 mm; gap, 3.0 mm; one signal acquired) and a respiratory-triggered T2-weighted fast spin-echo sequence (repetition time/echo time, 2800-4200/80 msec; echo train length 8-12, field of view, 360 mm; matrix, 128×256; 18 slices; slice thickness, 7.0 mm; gap, 3.0 mm; 2 signals

acquired) were performed in the liver. For 3D CE MRA, a breath-hold 3D fast spoiled gradient-echo sequence (repetition time/echo time, 5.2-10.2/1.2-1.9 msec; flip angle, 30° or 45°; field of view, 360-480 mm; matrix, 128×256; imaging volume, 75-168 mm; number of partitions, 24-30; one signal acquired; and acquisition time, 19-28 sec) was used.

With T1-weighted and T2-weighted images as reference, the imaging volume of 3D CE MRA was acquired in a coronal plane to cover the hepatic veins, IVC, portal veins and collateral vessels. The imaging volume was determined by a radiologist depending on each patient´s abnormalities, liver size and ability of breathholding.

A gadolinium chelate called gadopentetate-dimeglumine (Magnevist; Schering AG, Berlin, Germany) was used as a contrast material for all examinations, with a concentration of 0.15 mmol per kilogram of body weight. In all cases the contrast material was injected by an experienced MR technician through an antecubital vein with an injection rate of approximately 3 ml/sec. In 2 patients, however, due to poor visualization of IVC after injection of the contrast material into an arm vein, the study was repeated and the contrast agent was injected via a pedal vein for assessment of IVC. Scanning was commenced immediately after the injection and repeated three times with a 6-second delay between each acquisition for patient' s breathing. The first acquisition was the imaging of the arterial phase, the second acquisition was the portal venous phase for demonstration of the portal vein and IVC, while the third acquisition coincided with the image of the late venous phase for visualization of the hepatic veins. Source images of each acquisition were reviewed first, and then these images were reconstructed on a workstation (Advantage windows workstation, General Electric Medical Systems, Milwaukee, WI) to produce projectional images like X-ray angiography. Both maximum intensity projection (MIP) and multiplanar reconstruction (MPR) techniques were employed to analyze the acquired image.

Image analysis

3D CE MRA images were reviewed together by two radiologists unaware of the patients' clinical statuses and other imaging findings. The patency of the hepatic veins, IVC and portal veins was assessed. The presence of intra- and extrahepatic collaterals, liver parenchymal abnormalities and porto-systemic varices were also noted. Inferior vena cavography was performed in 10 cases. The diagnosis of IVC obstruction by 3D CE MRA was compared with that demonstrated by inferior vena cavography.

RESULTS

3D CE MRA findings

Hepatic veins 3D CE MRA demonstrated tumor thrombosis of two or three hepatic veins in each of the 9 patients with HCC (Figure 1). The right and middle hepatic veins were severely compressed and distorted by HCC in 2 patients. Nonvisualization of hepatic veins occurred in 4 patients with primary BCS. Focal stenosis of the right and middle hepatic veins near the caval confluence was detected in 2 patients with primary BCS (Figure 2).

IVC Severe stenosis or occlusion of the IVC was found in 10 patients (Figure 3), 3 of them were associated with the external compression or direct invasion of IVC by HCC. Tumor thrombosis was found in 3 cases with HCC (Figure 1). Direct invasion of IVC by right adrenal tumor was observed in 1 case. Thrombosis of IVC was shown in 1 patient with pelvic thrombophlebitis. A septum or obstructing membrane was demonstrated in the IVC in 3 patients (Figure 4). Localized dilatation of the distal IVC and renal veins were shown in 2 cases with IVC obstruction. In 10 patients with inferior vena cavography, the site and extent of IVC obstruction and distribution of collaterals presented by 3D CE MRA were in agreement with those by cavography (Figure 3). The accuracy of 3D CE MRA was 100 % in the diagnosis of IVC obstruction.

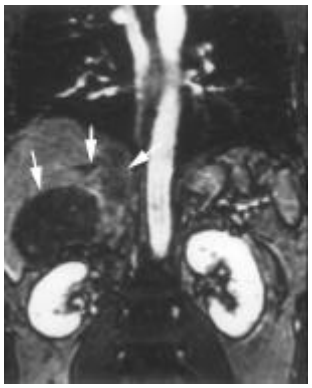

Figure 1 Source image of three-dimensional contrast-enhanced magnetic resonance angiography shows tumor thrombosis of the right hepatic vein (short arrow) and inferior vena cava (long arrow). A hypointense hepatocellular carcinoma (arrowhead) is shown simultaneously.

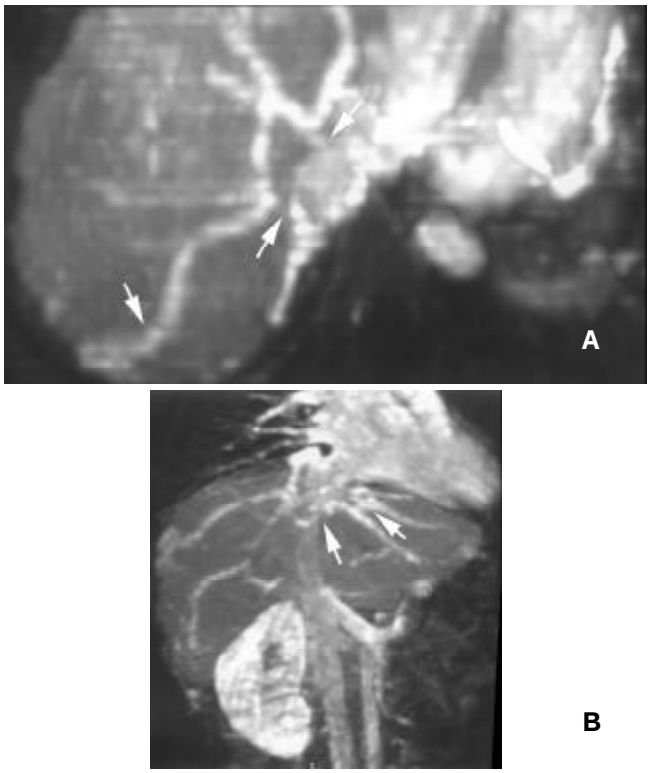

Figure 2 A: Axial reconstruction of three-dimensional contrast-enhanced magnetic resonance angiography demonstrates focal stenosis of right and middle hepatic veins (arrow heads). Intrahepatic collateral between right hepatic vein and subcapsular vein is also demonstrated (arrow). B: Coronal reconstruction reveals fine collaterals between hepatic veins (arrows), resembling a "spider web".

Intra-and extrahepatic collaterals 3D CE MRA revealed fine venous collaterals between the right hepatic veins and subcapsular veins, and between the right, middle and left hepatic veins in 2 patients with focal hepatic vein stenosis, appearing as the typical "spider web" sign (Figure 2B). Large and tortuous veins between enlarged right inferior accessory hepatic veins and right main hepatic veins were identified in 3

patients with IVC occlusion (Figure 3B). Various extrahepatic collaterals were found in the abdominal wall, peritoneal and retroperitoneal areas. Prominent azygos and hemiazygos veins were demonstrated in 13 patients. The left renal-inferior phrenic-pericardiophrenic collaterals were displayed in 2 patients (Figure 5).

Portal veins and porto-systemic varices The portal veins were found patent in all observed patients except 2 whose left intrahepatic portal veins were occluded (Figure 6). Gastroesophageal/esophageal varices and spontaneous splenorenal shunts were identified in 8 and 2 patients respectively.

Liver parenchyma An enlarged caudate lobe was found in 7 patients. Heterogenous liver enhancement was observed in 18 cases (Figure 6). HCC, which showed hyperintensity in arterial phase and hypointensity in portal venous phase, was found in 13 patients (Figure 1). In 2 of them, the tumor was developed after the primary BCS formation, because these two patients underwent long-term follow-up studies and the initial imaging findings indicated no intrahepatic tumors.

Figure 3 A: Source image depicts occlusion of the inferior vena cava(arrowhead). B: Maximum intensity projection of three-dimensional contrast-enhanced magnetic resonance angiography depicts tortuous intrahepatic collaterals (arrows) between right inferior accessory hepatic vein and right main hepatic vein. C: Inferior vena cavography confirms the occlusion of the inferior vena cava (arrowhead) and the intrahepatic collaterals (arrow).

Figure 4 Three-dimensional contrast-enhanced magnetic resonance angiography identifies a septum (arrowheads) in the inferior vena cava.

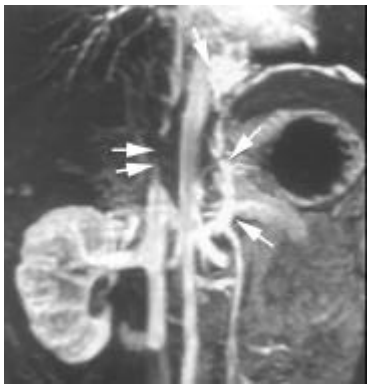

Figure 5 Three-dimensional contrast-enhanced magnetic resonance angiography detects occlusion of the inferior vena cava(white arrowheads), prominent left renal-inferior phrenic-pericardiophrenic collaterals (arrows) and esophageal varix (black arrowhead).

Figure 6 Three-dimensional contrast-enhanced magnetic resonance angiography demonstrates occlusion of the left portal vein (arrowhead) and heterogeneous enhancement pattern of the liver (arrows).

DISCUSSION

BCS is difficult to be diagnosed clinically. However, accurate and early diagnosis is important for its treatment. Radiologic assessment is an important step for its diagnosis. Diagnosis by US was noninvasive, relatively inexpensive and readily available, but its accuracy was limited by operator' s experience, poor acoustic window, inaccessible anatomic structure and body forms[1,3,7]. Contrast-enhanced CT was readily available too, but it used ionizing radiation and required intravenous administration of a large amount of iodinated contrast material with the risk of

nephrotoxicity and possible allergic reactions[1,5,6]. X-ray angiography was the reference criteria for the evaluation of BCS, due to its superb spatial resolution[1,3], but it was invasive and uncomfortable. Like CT, it also involved radiation and use of iodinated contrast material. Disadvantages also included high cost, requirement of operator' s expertise (especially for hepatic venography), and associated complications such as hemorrhage. MRI and non-enhanced magnetic resonance angiography (MRA) with time-of-flight (TOF) and phase-contrast (PC) techniques were other non-invasive means for demonstrating the hepatic venous system, but were limited by long acquisition time, motion and flow artifacts, and saturation effects[2,4,18-21].

3D CE MRA is a recently developed, non-invasive, fast and easy to be performed technique, which is capable of depicting vascular anatomy in multiple projections. It involves no radiation. With this technique, the imaging of the hepatic veins, IVC and portal veins is accomplished with only one injection of contrast material and short breath holding. It requires only a peripheral venous injection of a small amount of gadolinium, which is much safer than iodine-based contrast material. By using gadolinium to shorten the T1 value of the blood, it overcomes flow artifacts and saturation effects in TOF and PC. Moreover, it permits assessment of liver parenchyma and extravascular abnormalities during investigation of the vascular system[12,15,17]. So 3D CE MRA has many advantages over the currently more conventional methods for imaging the BCS.

According to our study, 3D CE MRA was able to demonstrate the patency of the hepatic veins, IVC and portal veins. It could show intra- and extrahepatic collaterals as well as porto-systemic varices caused by cirrhosis. 3D CE MRA could distinguish extravascular compression from intravascular thrombosis, detect liver abnormalities and evaluate the extent of the disease. By means of only one examination, 3D CE MRA provided all these crucial information for accurate diagnosis of BCS and for possible surgical or interventional managements, such as porto-caval shunt, liver transplantation, transjugular intrahepatic porto-systemic shunt (TIPSS), percutaneous transluminal angioplasty (PTA) and stent placement[22-27].

Among 13 patients of secondary BCS, tumor thrombosis, external compression and direct invasion of hepatic veins and/or IVC by tumors were the main causes of this disease. Through demonstration of intra- and extrahepatic disorders and the involved blood vessels, 3D CE MRA could disclose the etiology of BCS. For patients with primary BCS, nonvisualization, focal stenosis of the hepatic veins, occlusion or a septum formed in IVC were the most common findings on 3D CE MRA, as have been reported by Miller *et al*[5] with CT and MRI techniques. Compared with vena cavography, 3D CE MRA was 100 % accurate in diagnosis of IVC obstruction. On the basis of this study and Erden' s report[17], 3D CE MRA could replace inferior vena cavography for diagnosing IVC obstruction.

3D CE MRA could evaluate the intra- and extrahepatic collateral pathways. Identification of intrahepatic collateral veins is highly suggestive of BCS[6,17,28]. The intrahepatic collateral veins divert blood away from the stenotic or occluded hepatic vein and into a patent hepatic vein or a systemic vein. According to Cho' s report[6], intrahepatic collaterals were poorly defined on contrast-enhanced CT. In this study, 3D CE MRA found these collateral veins in 2 patients with stenosis of the hepatic veins. On 3D CE MRA, they were identified either by typical "spider web" sign or by large connecting veins between accessory and main hepatic veins. The dilated azygos and hemiazygos veins were the most commonly collateralized extrahepatic routes shown in this study. The infrequent left renal-inferior phrenic-pericardiophrenic collaterals were also seen on 3D CE MRA.

Our study indicated that a strong point of 3D CE MRA was to display the portal venous system simultaneously with hepatic veins and IVC. Obstruction or increased pressure in hepatic veins resulted in portal hypertension and portal flow stasis, which might further cause porto-systemic varices and portal vein thrombosis. Complications of portal hypertension were fatal in more than 50 % of BCS patients[27]. Thus the accurate delineation of the abnormalities of the portal vein, and the anatomic relationship between portal vein, hepatic veins and IVC were very important, particularly when preparing the treatment with porto-caval shunt or TIPSS[22-24,27]. In this study, 3D CE MRA showed the ability to provide all these relevant information.

Hypertrophy of the caudate lobe was found on 3D CE MRA. This was related to independent blood supply and drainage of this lobe. Heterogeneous enhancement pattern observed by 3D CE MRA has been already known from studies on contrast-enhanced CT[1]. It reflected the hemodynamic disturbance in the liver with BCS. 3D CE MRA found 2 patients with primary BCS developed HCC during a long-term follow-up period. The development of HCC in patients with chronic BCS has been reported in the literature[29]. According to that report, many factors, such as chronic viral infection or cirrhosis might play a role in the development of this malignancy.

Our study had two limitations. Firstly, a detailed comparison between 3D CE MRA and X-ray angiography was not performed, because none of our patients underwent hepatic venography and only some had inferior vena cavography. But 3D CE MRA could demonstrate various findings of BCS, which might provide clues to the correct diagnosis. Secondly, the opacification of IVC, after injection of contrast material into an arm vein, was inadequate in 2 patients with severe cirrhosis, portal hypertension and edema. We speculated this was due to the dilution of the contrast material in the porto-systemic collaterals, enlarged spleens and increased extracellular fluid. In these circumstances, the IVC could be enhanced properly by injecting contrast material into a pedal vein.

In conclusion, 3D CE MRA can display various features of BCS and provide an accurate diagnosis.

REFERENCES

1 **Stanley P**. Budd-Chiari syndrome. *Radiology* 1989; **170**(3Pt 1): 625-627

2 **Kane R**, Eustace S. Diagnosis of Budd-Chiari syndrome: comparison between sonography and MR angiography. *Radiology* 1995; **195**: 117-121

3 **Millener P**, Grant EG, Rose S, Duerinckx A, Schiller VL, Tessler FN, Perrella RR, Ragavendra N. Color Doppler imaging findings in patients with Budd-Chiari syndrome: correlation with venographic findings. *Am J Roentgenol* 1993; **161**: 307-312

4 **Soyer P**, Rabenandrasana A, Barge J, Laissy JP, Zeitoun G, Hay JM, Levesque M. MRI of Budd-Chiari syndrome. *Abdom Imaging* 1994; **19**: 325-329

5 **Miller WJ**, Federle MP, Straub WH, Davis PL. Budd-Chiari syndrome: imaging with pathologic correlation. *Abdom Imaging* 1993; **18**: 329-335

6 **Cho OK**, Koo JH, Kim YS, Rhim HC, Koh BH, Seo HS. Collateral pathways in Budd-Chiari syndrome: CT and venographic correlation. *Am J Roentgenol* 1996; **167**: 1163-1167

7 **Ralls PW**, Johnson MB, Radin DR, Boswell WD Jr, Lee KP, Halls JM. Budd-Chiari syndrome: detection with color Doppler sonography. *Am J Roentgenol* 1992; **159**: 113-116

8 **Leung DA**, Mckinnon GC, Davis CP, Pfammater T, Krestin GP, Debatin JF. Breath-hold, contrast-enhanced, three-dimensional MR angiography. *Radiology* 1996; **200**: 569-571

9 **Kopka L**, Rodenwaldt J, Vosshenrich R, Fischer U, Renner B, Lorf T, Graessner J, Ringe B, Grabbe E. Hepatic blood supply: comparison of optimized dual phase contrast-enhanced three-dimen-

sional MR angiography and digital subtraction angiography. *Radiology* 1999; **211**: 51-58
10 **Zeh H**, Choyke PL, Alexander HR, Bartlett D, Libutti SK, Chang R, Summers RM. Gadolinium-enhanced 3D MRA prior to isolated hepatic perfusion for metastases. *J Comput Assist Tomogr* 1999; **23**: 664-669
11 **Glockner JF**, Forauer AR, Solomon H, Varma CR, Perman WH. Three-dimensional gadolinium-enhanced MR angiography of vascular complications after liver transplantation. *Am J Roentgenol* 2000; **174**: 1447-1453
12 **Hawighorst H**, Schoenberg SO, Knopp MV, Essig M, Miltner P, van Kaick G. Hepatic lesions: morphologic and functional characterization with multiphase breath-hold 3D gadolinium-enhanced MR angiography-initial results. *Radiology* 1999; **210**: 89-96
13 **Saddik D**, Frazer C, Robins P, Reed W, Davis S. Gadolinium-enhanced three-dimensional MR portal venography. *Am J Roentgenol* 1999; **172**: 413-417
14 **Laissy JP**, Trillaud H, Douek P. MR angiography: noninvasive vascular imaging of the abdomen. *Abdom Imaging* 2002; **27**: 488-506
15 **Thornton MJ**, Ryan R, Varghese JC, Farrell MA, Lucey B, Lee MJ. A three-dimensional gadolinium-enhanced MR venography technique for imaging central veins. *Am J Roentgenol* 1999; **173**: 999-1003
16 **Shinde TS**, Lee VS, Rofsky NM, Krinsky GA, Weinreb JC. Three-dimensional gadolinium-enhanced MR venographic evaluation of patency of central veins in the throrax: initial experience. *Radiology* 1999; **213**: 555-560
17 **Erden A**, Erden I, Krayalcin S, Yurdaydin C. Budd-Chiari syndrome: evaluation with multiphase contrast-enhanced three-dimensional MR angiography. *Am J Roentgenol* 2002; **179**: 1287-1292
18 **Colletti PM**, Christopher TO, Terk MR, Boswell MD. Magnetic resonance of the inferior vena cava. *Magn reson imaging* 1992; **10**: 177-185
19 **Ruehm SG**. MR venography. *Eur Radiol* 2003; **13**: 229-230
20 **Butty S**, Hagspiel KD, Leung DA, Angle JF, Spinosa DJ, Matsumoto AH. Body MR venography. *Radiol Clin North Am* 2002; **40**: 899-919
21 **Mohiaddin RH**, Wann SL, Underwood R, Firmin DN, Rees S, Longmore DB. Vena caval flow: assessment with cine MR velocity mapping. *Radiology* 1990; **177**: 537-541
22 **Slakey DP**, Klein AS, Venbrux AC, Cameron JL. Budd-Chiari syndrome: current management options. *Ann Surg* 2001; **233**: 522-527
23 **Perello A**, Garcia-Pagan JC, Gilabert R, Suarez Y, Moitinho E, Cervantes F, Reverter JC, Escorsell A, Bosch J, Rodes J. TIPS is a useful long-term derivative therapy for patients with Budd-Chiari syndrome uncontrolled by medical therapy. *Hepatology* 2002; **35**: 132-139
24 **Schepke M**, Sauerbruch T. Transjugular portosystemic stent shunt in treatment of liver diseasse. *World J Gastroenterol* 2001; **7**: 170-174
25 **Pelage JP**, Denys A, Valla D, Sibert A, Sauvanet A, Belghiti J, Menu Y. Budd-Chiari syndrome due to prothrombotic disorder: mid-term patency and efficacy of endovascular stents. *Eur Radiol* 2003; **13**: 286-293
26 **Suhocki PV**, Trotter JF. Percutaneous hepatic vein reconstruction for Budd-Chiari syndrome. *Am J Roentgenol* 1998; **171**: 189-191
27 **Blum U**, Rossle M, Haag K, Ochs A, Blum HE, Hauenstein KH, Astinet F, Langer M. Budd-Chiari syndrome: technical, hemodynamic, and clinical results of treatment with transjugular intrahepatic portosystemic shunt. *Radiology* 1995; **197**: 805-811
28 **Naganuma H**, Ishida H, Konno K, Komatsuda T, Hamashima Y, Ishida J, Masamune O. Intrahepatic venous collaterals. *Abdom Imaging* 1998; **23**: 166-171
29 **Vilgrain V**, Lewin M, Vons C, Denys A, Valla D, Flejou JF, Belghiti J, Menu Y. Hepatic nodules in Budd-Chiari syndrome: imaging features. *Radiology* 1999; **210**: 443-450

Edited by Zhu L

P.O.Box 2345, Beijing 100023,China
Fax: +86-10-85381893
E-mail: wjg@wjgnet.com www.wjgnet.com

World J Gastroenterol 2003;9(10):2322-2324
World Journal of Gastroenterology
 ISSN 1007-9327

• BRIEF REPORTS •

Healthy ranges of serum alanine aminotransferase levels in Iranian blood donors

Mehdi Mohamadnejad, Akram Pourshams, Reza Malekzadeh, Ashraf Mohamadkhani, Afsaneh Rajabiani, Ali Ali Asgari, Seyed Meysam Alimohamadi, Hadi Razjooyan, Mansooreh Mamar-Abadi

Mehdi Mohamadnejad, Akram Pourshams, Reza Malekzadeh, Ashraf Mohamadkhani, Ali Ali Asgari, Seyed Meysam Alimohamadi, Hadi Razjooyan, Mansooreh Mamar-Abadi, Digestive Disease Research Center, Tehran University of Medical Sciences, Tehran, Iran
Afsaneh Rajabiani, Department of Pathology, School of Medicine, Tehran University of Medical Sciences, Tehran, Iran
Correspondence to: Reza Malekzadeh, Digestive Disease Research Center, Tehran University of Medical Sciences, Shariati Hospital, North Kargar Avenue Tehran 14114, Iran. malek@ams.ac.ir
Telephone: +98-21-8012992 **Fax:** +98-21-2253635
Received: 2003-05-13 **Accepted:** 2003-07-20

Abstract

AIM: The healthy ranges for serum alanine aminotransferase (ALT) levels are less well studied. The aim of this study was to define the upper limit of normal (ULN) for serum ALT levels, and to assess factors associated with serum ALT activity in apparently healthy blood donors.

METHODS: A total of 1 939 blood donors were included. ALT measurements were performed for all cases using the same laboratory method. Healthy ranges for ALT levels were computed from the population at the lowest risk for liver disease. Univariate and multivariate analyses were performed to evaluate associations between clinical factors and ALT levels.

RESULTS: Serum ALT activity was independently associated with body mass index (BMI) and male gender, but not associated with age. Association of ALT with BMI was more prominent in males than in females. Upper limit of normal for non-overweight women (BMI of less than 25) was 34 U/L, and for non-overweight men was 40 U/L.

CONCLUSION: Serum ALT is strongly associated with sex and BMI. The normal range of ALT should be defined for male and female separately.

Mohamadnejad M, Pourshams A, Malekzadeh R, Mohamadkhani A, Rajabiani A, Asgari AA, Alimohamadi SM, Razjooyan H, Mamar-Abadi M. Healthy ranges of serum alanine aminotransferase levels in Iranian blood donors. *World J Gastroenterol* 2003; 9(10):2322-2324
http://www.wjgnet.com/1007-9327/9/2322.asp

INTRODUCTION

Elevation of aminotransferase level is an important and common finding in different types of parenchymal liver disease. Measurement of serum ALT is one of the most important tests for detection of patients with viral hepatitis or non-alcoholic steatohepatitis (NASH), and the exact definition of upper normal levels of serum ALT activity is an initial and critical step in different screening and follow up studies for chronic liver diseases. Current upper limits of normal for ALT level are set on average, at 40 U/L. This normal range was set in the 1950s and has changed a little since then[1]. Several studies have recently questioned whether previously established values to define normal ALT range are accurate and have suggested that the upper limit of normal should be assessed more accurately and revised accordingly[2,3].

There is no study regarding normal level of ALT in Iranian healthy adults at low risk for chronic liver diseases. This information, in addition to daily clinical practice, is specially important and necessary for different research studies of chronic liver diseases in Iran. The aim of this study was to assess the normal value of ALT in a population at low risk for subclinical chronic liver diseases in the capital city of Tehran and to investigate factors associated with abnormal ALT in this population.

MATERIALS AND METHODS

Study population

From March 2001 through April 2002, 1 959 apparently healthy blood donors at Tehran Blood Donation Center were randomly recruited into the study. The participants were part of a study for identifying the causes of elevated serum ALT level. After explanation about the objectives of the study and possible necessity for further blood test and follow up, a written informed consent was obtained, and a clinical questionnaire with emphasis on psychosocial and medical history to exclude subjects who were considered the high risk group for blood born infections was completed by a physician interviewer, and serum samples were collected from all consenting subjects. Our study was in accordance with the ethical standards for human experimentation and approved by the Ethical Committee of the Digestive Disease Research Center, Tehran University of Medical Sciences. Body weight and height of all subjects were measured and history of alcohol and drug use was taken.

Laboratory methods

Blood samples were centrifuged within 30 minutes of collection. The biochemistry and virologic tests including hepatitis B s antigen (HBsAg), and hepatitis C virus antibody (HCV Ab), and rapid plasma regain test, and HIV Ab were measured. All tests were performed at Digestive Disease Research Center, Tehran University of Medical Sciences, Tehran, Iran. Analyses of serum ALT levels were performed by using the Hitachi 704 autoanalyser, Tokyo, Japan. The upper limit of normal introduced by manufacturer was 40 U/L for both men and women. Body mass index (BMI) was calculated by dividing the weight (in kg) and the squared height (in meter). We considered a BMI of 24.9 kg/m^2 as the upper limit for healthy weight[5].

Definitions of ULN ALT value

Seven methods were used to compare their impact. Method 1: 95th percentile of ALT distribution regardless of the sex. Method 2: 95 th percentile of ALT distribution after separating males and

females. Method 3: a common threshold of 40 IU/L for both males and females proposed by the manufacturer. Method 4: 95th percentile after separating subjects with body mass index (BMI) under the median which was 27.12. Method 5: 95th percentile after separating subjects with body mass index (BMI) under 25 -a threshold proposed for separating abnormal and normal weight-[5]. Method 6: 95th percentile of ALT distribution stratified according to BMI (<25) and sex. Method 7: 95th percentile of ALT distribution in each age decade after separating males and females.

Statistical analysis

Statistical analyses were performed by using the SPSS, version 10.1, software package (SPSS, Inc., Chicago, IL). The 50th (median), and 95th percentiles for ALT level were calculated on the basis of the empirical distribution of the data. We set the upper limit for healthy ALT level to the 95 th percentile, as is commonly done for distribution of a continuous variable in the normal population. The univariate associations between factors and ALT expressed in decimal logarithm were assessed by Pearson's correlation coefficient for quantitative factors and by the Student's *t* test for qualitative factors. Multivariate analyses were used to identify factors independently associated with ALT: linear regression, and logistic regression. *P* values less than 0.05 were considered statistically significant.

RESULTS

Twenty persons were excluded because of positive HBsAg (10 persons), positive HCV Ab (9 persons), or use of alcohol more than 20 grams daily (1 person). Four persons also consumed less than 20 grams per day of alcohol who were included into the study. Thus a total of 1 939 persons (1 451 males, and 488 females) were included. The characteristics of tested individuals are given in Table 1. Except one subject who took drugs containing female sex hormones, no body had a history of regular drug usage.

Table 1 Characteristics of 1 939 Blood Donors

Factor	Mean	SE
Age (yr)	37.4	0.26
Weight (kg)	79	0.3
Height (cm)	169.96	0.19
BMI (kg/cm^2)	27.35	0.09
ALT (U/L)	19.87	0.27

Abbreviations: SE: Standard error of the mean.

Table 2 Correlation of serum ALT with quantitative clinical factors

Factor	Number	Pearson correlation	*P* value
BMI	1939	0.125	<0.001
Weight	1939	0.17	<0.001
Height	1939	0.096	<0.001
Age	1939	0.027	0.23

Table 3 Serum ALT according to sex, and BMI (lower or higher than 25)

Variable	Count	Mean	SD	*P* Value
Female	488	16.4	8.8	<0.001
Male	1 451	21	12.3	
All subjects with BMI <25	563	17.9	10.4	<0.001
All subjects with BMI ⩾25	1 376	20.7	12.1	
Men with BMI <25	391	19.1	10.8	<0.001
Men with BMI ⩾25	1 060	21.7	12.8	
Women with BMI <25	172	15.2	8.8	0.025
Women with BMI ⩾25	316	17	8.7	

Abbreviation: SD: Standard deviation.

Table 4 Prevalence among blood donors with normal and abnormal ALT according to the six definitions

Subjects	Method 1: 95th percentile of ALT distribution without stratification	Method 2: 95th percentile of ALT distribution stratified according to sex	Method 3: 40 IU/L for both male and female	Method 4: 95th percentile of ALT distribution stratified according to BMI (<27.1)	Method 5: 95th percentile of ALT distribution stratified according to BMI (<25)	Method 6: 95th percentile of ALT distribution stratified according to BMI (<25) and sex
Males	1451	1451	1451	1451	1451	1451
Threshold	40	45	40	39 for BMI⩾27.1	39 for BMI <25	40 for BMI <25
				41/ 721	20/ 391	16/391
				45 for BMI>27.1	43 for BMI ⩾25	46 for BMI⩾25
				40/ 730	65/1060	48/1060
Normal (%)	1 363 (94%)	1378 (95%)	1363 (94%)	1370 (94. 5%)	1366 (94.1%)	1 387 (95. 6%)
Abnormal (%)	88 (6%)	73 (5%)	88 (6%)	81 (5. 5%)	85 (5. 9%)	64 (4.4%)
Females	488	488	488	488	488	488
Threshold	40	34	40	39 for BMI⩾27.1	39 for BMI <25	34 for BMI <25
				6/249	4/ 172	8/172
				45 for BMI >27.1	43 for BMI ⩾25	34 for BMI⩾25
				2/ 239	2/ 316	15/316
Normal (%)	481 (98. 6%)	464 (95%)	481 (98. 6%)	480 (98.4%)	482 (98.8%)	465 (95. 3%)
Abnormal (%)	7 (1.4%)	24 (5%)	7 (1.4%)	8 (1. 6%)	6 (1. 2%)	23 (4.7%)
All donors	1939	1939	1939	1939	1939	1939
Threshold	40	45 for female	40	39 for BMI ⩾27.1	39 for BMI <25	Male: 40 for BMI<25
		34 for male		45 for BMI>27.1	43 for BMI⩾25	46 for BMI⩾25
						Female: 34 for BMI<25
						34 for BMI⩾25

Correlation between factors and ALT

ALT was significantly correlated with BMI, weight, and height, but was not correlated with age (Table 2).

For qualitative factors (Table 3), ALT was higher in males than in females, and ⩾25 than BMI<25 in persons with BMI. Association of ALT with BMI was more prominent in men (P<0.001) than in women (P=0.025).

Linear regression analysis showed that ALT was independently associated with male sex (Regression coefficient: 4.633, 95 % CI: 3.459-5.808, P<0.0001), and BMI (Regression coefficient: 0.362, 95 % CI: 0.237-0.487, P<0.0001), but not with height, weight, and age.

Also, logistic regression analysis showed that men were 4.57 times more likely to have elevated ALT (ALT>40) than women (95 % CI, 2.1-9.96, P=0.0001). BMI was also independently associated with elevated ALT (OR: 1.07, 95 % CI: 1.03-1.13, P=0.004). Age, height, and weight were not found to be related to elevated ALT.

Different definitions of abnormal ALT

The thresholds corresponding to the first six methods to the definition of abnormal ALT are given in Table 4. The threshold to the definition of abnormal ALT according to method 7 is demonstrated in Figure 1.

The threshold for ULN ALT varied from 34 U/L (methods 2 and 6 for females) to 46 U/L (method 6 for males with BMI>25).

The overall median ALT level for the entire study sample was 17 U/L, and the level across the 95th percentile was 40 U/L. In the 1 451 male participants, the median serum ALT level was 18 U/L, and the ALT levels across the 95 th percentile was 45 U/L. The median and 95th percentiles of ALT level in women were 14 U/L and 34 U/L, respectively. When we considered the population at the lowest risk for liver diseases (persons with negative viral markers, use of alcohol less than 20 g/d, normal BMI, and absence of concurrent medication use), the threshold for abnormal ALT was 40 U/L for men, and 34 U/L for women.

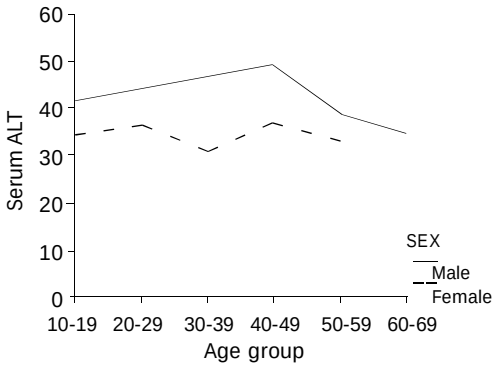

Figure 1 95th percentile of ALT distribution in each age decade after separating males and females. Note that males over age 70 (41 subjects), and females over age 60 (8 subjects) were omitted from the chart, because of a small number of them.

DISCUSSION

This study has identified the factors associated with ALT variability, and determined the thresholds for ALT according to different definitions of ULN ALT. This study further emphasized the findings of previous studies regarding the strong correlation of ALT with sex and BMI[2,3]. This has probably reflected the association between liver steatosis and obesity. The correlation between abnormal ALT and BMI was stronger in men than in women. Additionally, the 95th percentile of ALT in females with BMI <25 was equal to females with BMI ⩾25. This may be due to the fact that the waist to hip ratio (WHR) is higher in men than in women, and non-alcoholic fatty liver disease (NAFLD) is associated with central obesity and higher WHR[5]. WHR was correlated with visceral adipose tissue, which provided a greater supply of potentially hepatotoxic fatty acids to the liver[6].

Our study had some limitations. The study population were apparently healthy blood donors. They could have other unknown factors associated with ALT and they might not exactly reflect the normal general population. Second, the estimation of alcohol consumption was based only on the interview data and might be inaccurate. Third, we could not measure some paraclinical factors associated with ALT such as serum glucose, triglyceride and cholesterol[2,5].

The ULN ALT may differ from different nations and populations and may be influenced by mean BMI and alcohol usage in different societies.

The 95th percentile of ALT in overweight and obese persons may be too high to be defined as the threshold for healthy ranges of ALT. We suggest that even in overweight and obese persons healthy ranges of ALT should be defined as in non-overweight persons (40 U/L and 34 U/L in men and in women respectively). Since higher values may be due to liver steatosis which occurs more frequently in obese persons, and thus may be abnormal. Adjustment of ALT for sex but not for BMI has also been proposed previously[1]. It seems necessary to repeat this type of investigations in a population based sample and in different ethnic and nationals in order to check whether the impact of sex and BMI remain consistent and if it is proved to be so, then the laboratories should set different ranges of ALT for male and female independently.

In conclusion, this study has demonstrated a strong impact of sex and BMI on serum ALT level. Furthermore, if these findings are proved by other studies, then the normal range of ALT according to sex should be defined. This is particularly helpful in follow up and therapy of patients with chronic hepatitis and designing research protocols.

REFERENCES

1 **Kaplan MM**. Alanine Aminotransferase Levels: What's Normal? *Ann Intern Med* 2002; **137**: 49-51

2 **Prati D**, Taioli E, Zanella A, Della Torre E, Butelli S, Del Vecchio E, Vianello L, Zanuso F, Mozzi F, Milani S, Conte D, Colombo M, Sirchia G. Updated definitions of healthy ranges for serum alanine aminotransferase levels. *Ann Intern Med* 2002; **137**: 1-9

3 **Piton A**, Poynard T, Imbert-Bismut F, Khalil L, Delattre J, Pelissier E, Pelissier E, Sansonetti N, Opolon P. Factors associated with serum alanine transaminase activity in healthy subjects: consequences for the definition of normal values, for selection of blood donors, and for patients with chronic hepatitis C. *Hepatology* 1998; **27**: 1213-1219

4 **Willett WC**, Dietz WH, Colditz GA. Guidelines for healthy weight. *N Engl J Med* 1999; **341**: 427-434

5 **Ruhl CE**, Everhart JE. Determinants of the association of overweight with elevated serum alanine aminotransferase activity in the United States. *Gastroenterology* 2003; **124**: 71-79

6 **Falck-Ytter Y**, Younossi ZM, Marchesini G, McCullough AJ. Clinical features and natural history of nonalcoholic steatosis syndromes. *Semin Liver Dis* 2001; **21**: 17-26

Edited by Wang XL

P.O.Box 2345, Beijing 100023,China
Fax: +86-10-85381893
E-mail: wjg@wjgnet.com www.wjgnet.com

World J Gastroenterol 2003;9(10):2325-2327
World Journal of Gastroenterology
 ISSN 1007-9327

• BRIEF REPORTS •

Adrenomedullin in cirrhotic and non-cirrhotic portal hypertension

V Tahan, E Avsar, C Karaca, E Uslu, F Eren, S Aydin, H Uzun, HO Hamzaoglu, F Besisik, C Kalayci, A Okten, N Tozun

V Tahan, E Avsar, F Eren, HO Hamzaoglu, C Kalayci, N Tozun, Gastroenterology Institute, Marmara University
C Karaca, F Besisik, A Okten, Gastroenterology Department' Medical Faculty, Istanbul University
E Uslu, S Aydin, H Uzun, Biochemistry Department, Cerrahpasa Medical Faculty, Istanbul University
Correspondence to: Dr. Veysel Tahan, Alemdag Cad. Yanyol Rifat Bey Sokak Ugur Apt. No=27/19 Kısıklı, Üsküdar, Istanbul/Turkey.
veytahan@yahoo.com
Telephone: +90-532-3629602
Received: 2003-06-04 **Accepted:** 2003-08-02

Abstract

AIM: Adrenomedullin (ADM) is a potent vasodilator peptide. ADM and nitric oxide (NO) are produced in vascular endothelial cells. Increased ADM level has been linked to hyperdynamic circulation and arterial vasodilatation in cirrhotic portal hypertension (CPH). The role of ADM in non-cirrhotic portal hypertension (NCPH) is unknown. plasma ADM levels were studied in patients with NCPH, compensated and decompensated cirrhosis in order to determine its contribution to portal hypertension (PH) in these groups.

METHODS: There were 4 groups of subjects. Group 1 consisted of 27 patients (F/M: 12/15) with NCPH due to portal and/or splenic vein thrombosis (mean age: 41±12 years), group 2 consisted of 14 patients (F/M: 6/8) with compensated (Child-Pugh A) cirrhosis (mean age: 46±4), group 3 consisted of 16 patients (F/M: 6/10) with decompensated (Child-Pugh C) cirrhosis (mean age: 47±12). Fourteen healthy subjects (F/M: 6/8) (mean age: 44±8) were used as controls in Group 4. ADM level was measured by ELISA. NO was determined as nitrite/nitrate level by chemoluminescence.

RESULTS: ADM level in Group 1 (236±61.4 pg/mL) was significantly higher than that in group 2 (108.4±28.3 pg/mL) and group 4 (84.1±31.5 pg/mL) (both $P<0.0001$) but was lower than that in Group3 (324±93.7 pg/mL) ($P=0.002$). NO level in group 1 (27±1.4 μmol/L) was significantly higher than that in group 2 (19.8±2.8 μmol/L) and group 4 (16.9±1.6 μmol/L) but was lower than that in Group 3 (39±3.6 μmol/L) (for all three $P<0.0001$). A strong correlation was observed between ADM and NO levels ($r=0.827$, $P<0.0001$).

CONCLUSION: Adrenomedullin and NO levels were high in both non-cirrhotic and cirrhotic portal hypertension and were closely correlated, Adrenomedullin and NO levels increased proportionally with the severity of cirrhosis, and were significantly higher than those in patients with NCPH. Portal hypertension plays an important role in the increase of ADM and NO. Parenchymal damage in cirrhosis may contribute to the increase in these parameters.

Tahan V, Avsar E, Karaca C, Uslu E, Eren F, Aydin S, Uzun H, Hamzaoglu HO, Besisik F, Kalayci C, Okten A, Tozun N. Adrenomedullin in cirrhotic and non-cirrhotic portal hypertension. *World J Gastroenterol* 2003; 9(10):2325-2327
http://www.wjgnet.com/1007-9327/9/2325.asp

INTRODUCTION

Portal hypertension (PH) is a clinical condition characterized by specific hemodynamic abnormalities such as low arterial pressure, high cardiac output, over activity of vasoconstrictor systems and marked decrease in total systemic vascular resistance. Arterial vasodilatation and activation of several vasoactive and neurohumoral systems may play a key role in pathogenesis of sodium and water retention and ascites formation in cirrhosis[1,2]. These changes have been attributed to increased production of vasodilator substances[2,3]. Adrenomedullin (ADM) and nitric oxide (NO) are considered as essential mediators of hyperdynamic state. NO, a potent vasodilator substance synthesized from L-arginin by NO synthase, is increased in cirrhotic patients and experimental models of cirrhosis[3,4]. Specific NO inhibitors have been shown to counteract vasodilatation and hyperdynamic circulation in these groups[4,5]. In addition, circulating levels of potent vasodilating peptides (substance P, CGRP), pulsatile blood flow, and shear stress could contribute to the up regulation of endothelial NO-synthase (e-NOS)[3,6].

ADM is a potent endogenous vasorelaxing factor that was originally isolated from the extracts of human pheochromocytoma[7]. ADM is expressed in adrenal gland, lungs, kidneys, smooth muscle vascular endothelial cells, and splanchnic organs[3,8]. ADM level is increased after stimulation with bacterial endotoxin and cytokines[9]. The renal effects of ADM and part of its cardiovascular effects seem to be mediated by NO[10,11]. Previous studies reported that increased ADM level in cirrhotic patients occurred via increased production or decreased clearance of this substance, the elevation was more prominent in decompensated cirrhotic patients with marked PH[2,4,12,13]. Although ADM level is known to be increased in cirrhotic PH (CPH), there are no data concerning its level in non-cirrhotic PH (NCPH).

To our knowledge this is the first study determining plasma ADM concentrations in NCPH patients. We also aimed to compare the results within the group of compensated and decompensated cirrhotic patients (Child-Pugh A & C) and healthy subjects in order to estimate the contribution of cirrhosis and PH either separately or concomitantly to the elevation of ADM and NO level.

We compared ADM levels in the patients with compensated or decompensated cirrhosis and also in healthy subjects in order to determine whether portal hypertension or cirrhosis led to elevation in ADM and NO levels.

MATERIALS AND METHODS

Patients

Our study included patients with NCPH, cirrhosis and healthy subjects as control. Cirrhosis was due to hepatitis C infection in all-cirrhotic cases, while in all cases of NCPH the origin was extrahepatic portal venous thrombosis. group 1 included 27 patients (F/M: 12/15 with NCPH due to portal and/or splenic vein thrombosis (mean age: 41±12 years), Group 2 consisted of 14(F/M: 6/8) compensated (Child-Pugh A) cirrhotic patients (mean age: 46±4), group 3 included 16 (F/M: 6/10) decompensated cirrhotic (Child-Pugh C) patients (mean age: 47±12), and group 4 consisted of 14 (F/M: 6/8) healthy subjects (mean age: 44±8) taken as controls.

The diagnosis of PH and cirrhosis was established on the basis of clinical, biochemical and ultrasonographic findings and/or liver biopsy. Patients with active or recent gastrointestinal bleeding, bacterial infection, severe hepatic encephalopathy, cardiopulmonary disease and portal vein thrombosis within the previous ten days were excluded.

Study protocol

All patients and controls received restricted sodium diet (70 mmol/day) for at least 5 days before the study. Diuretics, beta-blockers and other cardioactive drugs were withheld during the 10-day period before the study. At 8.00 a.m. on the day of study, blood samples were drawn after the patients were fasted overnight and then waited for 45 min in supine position. This study was performed in accordance with the Declaration of Helsinki. A written informed consent was obtained from each patient and control subject participating in the study.

Biochemical analysis

Nitric oxide heparinized whole blood was obtained by venipuncture, centrifuged (3 000 rpm, 10 minutes, 0-40 C). Plasma concentration of NO was studied by chemoluminescence method using commercially available colorimetric assay (Roche, Cat No 1746081)[14].

Adrenomedullin

Blood samples for ADM were collected into the vacutainer tubes, which contained EDTA. Blood was transferred from the vacutainer tubes to centrifuge tubes containing aprotinin (0.6 TIU/ml of blood) and gently rocked for several times to inhibit the activity of proteinases. Blood was centrifuged at 1 600 G for 15 min at 4 ℃. Plasma ADM concentration was measured by enzyme immunoassay (Phoenix Pharmaceuticals Inc. Harbor Boulevard, Belmont, California 94002) after extraction through the Sep-pak C-18 column supplied by the manufacturer[15,16].

Plasma in both parameters was immediately frozen and stored at -80 ℃ until assayed.

Statistical analysis

All results were expressed as mean ± standard deviation. Comparisons between the groups were performed by Kruskal-Wallis variance analysis and a *P*- value <0.05 was accepted as statistically significant.

RESULTS

ADM level in Group 1 (236±61.4 pg/mL) was significantly higher than that in Group 2 (108.4±28.3 pg/mL) and Group 4 (84.1±31.5 pg/mL) (both $P<0.0001$) but was lower than that in Group 3 (324±93.7 pg/mL)($P=0.002$) (Figure 1).

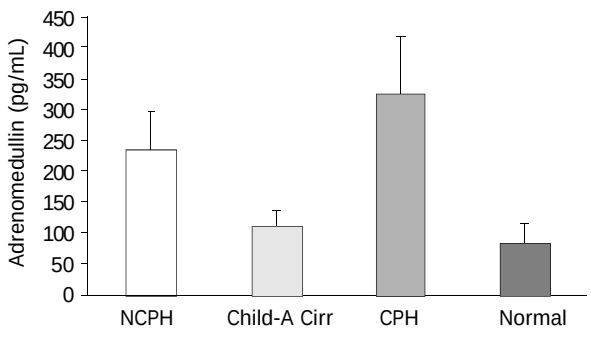

Figure 1 Adrenomedullin levels in various groups. NCPH: Non-cirrhotic portal hypertension, Cirr: Cirrhosis, CPH: Cirrhotic portal hypertension, Normal: Healthy subjects. NCPH *vs* Child-Pugh A Cirr: $P<0.0001$, NCPH *vs* Healthy Subjets: $P<0.0001$, NCPH *vs* Child-Pugh C CPH: $P=0.002$.

Nitrite/nitrate level in Group 1 (27±1.4 μmol/L) was significantly higher than that in Group 2 (19.8±2.8 μmol/L) and Group 4 (16.9±1.6 μmol/L) but was lower than that in Group 3 (39±3.6 μmol/L) ($P<0.0001$ for all three) (Figure 2). A significant correlation was observed between ADM and NO levels ($r=0.827$, $P<0.0001$) (Figure 3).

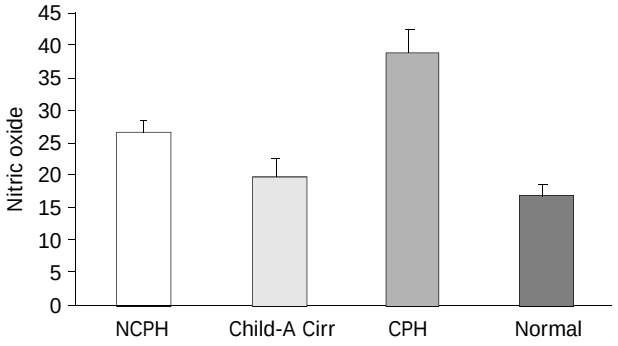

Figure 2 Nitric oxide levels in various groups. NCPH: Non-cirrhotic portal hypertension, Cirr: Cirrhosis, CPH: Cirrhotic portal hypertension, Normal: Healthy subjects. NCPH *vs* Child-Pugh A Cirr: $P<0.0001$, NCPH *vs* Healthy Subjets: $P<0.0001$, NCPH *vs* Child-Pugh CCPH: $P<0.0001$.

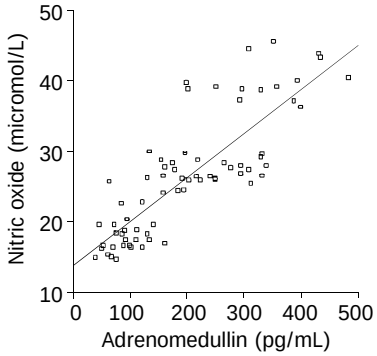

Figure 3 Correlation between nitric oxide and adrenomedullin A significant correlation was observed between two vasoactive agents ($r=0.827$, $P<0.0001$).

DISCUSSION

Our study demonstrated increased plasma ADM and NO concentrations in both CPH and NCPH patients, the level of ADM was the highest in the CPH group. Increased ADM level was strongly associated with PH and plasma volume expansion[10,11]. In our series, ADM level was not different between compensated cirrhotic patients and controls but higher in both groups of patients with CPH and NCPH, evidencing the role of PH in the increase of ADM.

Cirrhotic patients showed hemodynamic abnormalities such as arterial hypotension, increased cardiac output and reduced systemic vascular resistance. These changes have been attributed to peripheral vasodilatation. The reduction in the effective blood volume, and the subsequent activation of renin-angiotensin-aldosterone system (RAAS) and sympathetic nervous system initiated renal sodium and water retention and ultimately led to ascites formation[11]. Furthermore, excessive production of endogenous vasodilatators played an important role in peripheral vasodilatation. ADM and NO are well known mediators in the pathophysiology of PH. ADM is a potent vasodilatator and natriuretic peptide[4]. ADM concentration was positively correlated with plasma renin activity and aldosterone, which are indicators of RAAS activity[1]. ADM had an indirect effect on hyperdynamic circulation. It might play a role in the

mechanism of initiation of peripheral vasodilatation counterbalanced by the activation of RAAS and sympathetic nervous system and followed by renin and aldosterone increase. Previous studies reported that concentrations of ADM similar to those found in patients with ascites had vasodilatatory effect in the rat mesenteric circulation[2,12]. In addition, administration of ADM to anesthetized rat caused arterial hypotension, increased cardiac output and reduced systemic vascular resistance similar to the circulatory changes observed in cirrhosis[13]. All these changes may account for increased ADM level in patients with ascites and may also be seen in non-cirrhotic PH.

Cytokines were incriminated as to contribute to increased ADM levels via increased levels of TNF-α, interleukin-6 and bacterial endotoxin in advanced liver cirrhosis[18,19]. These factors are the result of parenchymal damage, which is known to stimulate the production of ADM by vascular smooth muscle and endothelial cells. However, a previous study reported that TNF-α and interleukin-6 levels showed very weak correlations with ADM levels[4]. In our study ADM level in CPH patients was significantly higher than that in NCPH patients. We conclude that cytokines are not completely responsible for the significant increase of ADM level in liver cirrhosis but they may contribute to this change.

Increased hepatic outflow resistance is the initial cause of CPH. It stimulates endothelial shear stress. Previous studies reported that ADM mRNA expression in endothelial cells was markedly increased by shear stress[20]. Thus ADM could be increased by the shear stress secondary to hyperdynamic circulation. ADM may also be produced in excess as an outcome of the volume expansion. Increased ADM level was found in cirrhotic chronic renal failure patients[2]. An increased ADM production to balance plasma volume overload might be an additional mechanism accounting for elevated ADM plasma concentration in patients with chronic renal disease.

NO is an important mediator of the hemodynamic alterations of liver cirrhosis. In our study ADM levels correlated with serum nitrite and nitrate levels. It was probably due to the fact that elevated NO levels in patients with advanced liver cirrhosis might further stimulate the production of NO and aggravate the vasodilatation in a vicious cycle[9,10].

In our study, ADM and NO levels in NCPH and advanced cirrhosis were higher than those in healthy controls and compensated cirrhotics. Likewise ADM and NO levels in CPH were higher than those in NCPH. Increased ADM level was closely correlated with NO level.

In conclusion, the results of our study suggest that portal hypertension *per se* is an independent factor for the elevation of ADM and NO in both cirrhotic and non-cirrhotic portal hypertension. Parenchymal destruction at various stages in cirrhosis may further contribute to the effects of these potent vasodilators and lead to a vicious cycle.

REFERENCES

1 **Groszmann RJ.** Hyperdynamic circulation of liver disease 40 years later: pathophysiology and clinical consequences. *Hepatology* 1994; **20**: 1359-1363

2 **Guevara M,** Gines P, Jimenez W, Sort P, Fernandez-Esparrach G, Escorsell A, Bataller R, Bosch J, Arroyo V, Rivera F, Rodes J. Increased adrenomedullin levels in cirrhosis: relationship with hemodynamic abnormalities and vasoconstrictor systems. *Gastroenterology* 1998; **114**: 336-343

3 **Fernandez-Rodriguez CM,** Prada IR, Prieto J, Montuenga LM, Elssasser T, Quiroga J, Moreiras M, Andrade A, Cuttitta F. Circulating adrenomedullin in cirrhosis: relationship to hyperdynamic circulation. *J Hepatol* 1998; **29**: 250-256

4 **Genesca J**, Gonzalez A, Catalan R, Segura R, Martinez M, Esteban R, Groszmann RJ, Guardia J. Adrenomedullin, a vasodilator peptide implicated in hemodynamic alterations of liver cirrhosis: relationship to nitric oxide. *Dig Dis Sci* 1999; **44**: 372-376

5 **Pizcueta P,** Pique JM, Fernandez M, Bosch J, Rodes J, Whittle BJ, Moncada S. Modulation of the hyperdynamic circulation of cirrhotic rats by nitric oxide inhibition. *Gastroenterology* 1992; **103**: 1909-1915

6 **Fernandez-Rodriguez CM**, Prieto J, Quiroga J, Zozoya JM, Andrade A, Nunez M, Sangro B, Penas J. Plasma levels of substance P in liver cirrhosis: relationship to the activation of vasopressor systems and urinary sodium excretion. *Hepatology* 1995; **21**: 35-40

7 **Kitamura K,** Kangawa K, Kawamoto M, Ichiki Y, Nakamura S, Matsuo H, Eto T. Adrenomedullin: a novel hypotensive peptide isolated from human pheochromocytoma. *Biochem Biophys Res Commun* 1993; **192**: 553-560

8 **Ichiki Y**, Kitamura K, Kangawa K, Kawamoto M, Matsuo H, Eto T. Distribution and characterization of immunoreactive adrenomedullin in human tissue and plasma. *FEBS Lett* 1994; **338**: 6-10

9 **Sugo S,** Minamino N, Shoji H, Kangawa K, Kitamura K, Eto T, Matsuo H. Interleukin-1, tumor necrosis factor and lipopolysaccharide additively stimulate production of adrenomedullin in vascular smooth muscle cells. *Biochem Biophys Res Commun* 1995; **207**: 25-32

10 **Ishimitsu T,** Nishikimi T, Saito Y, Kitamura K, Eto T, Kangawa K, Matsuo H, Omae T, Matsuoka H. Plasma levels of adrenomedullin, a newly identified hypotensive peptide, in patients with hypertension and renal failure. *J Clin Invest* 1994; **94**: 2158-2161

11 **Jougasaki M,** Rodeheffer RJ, Redfield MM, Yamamoto K, Wei CM, McKinley LJ, Burnett JC Jr. Cardiac secretion of adrenomedullin in human heart failure. *J Clin Invest* 1996; **97**: 2370-2376

12 **Fabrega E,** Casafont F, Crespo J, de la Pena J, San Miguel G, de las Heras G, Garcia-Unzueta MT, Amado JA, Pons-Romero F. Plasma adrenomedullin levels in patients with hepatic cirrhosis. *Am J Gastroenterol* 1997; **92**: 1901-1904

13 **Kojima H,** Tsujimoto T, Uemura M, Takaya A, Okamoto S, Ueda S, Nishio K, Miyamoto S, Kubo A, Minamino N, Kangawa K, Matsuo H, Fukui H. Significance of increased plasma adrenomedullin concentration in patients with cirrhosis. *J Hepatol* 1998; **28**: 840-846

14 **Green LC,** Wagner DA, Glogowski J, Skipper PL, Wishnok JS, Tannenbaum SR. Analysis of nitrate, nitrite, and [15N]nitrate in biological fluids. *Anal Biochem* 1982; **126**: 131-138

15 **Porstmann T**, Kiessig ST. Enzyme immunoassay techniques. An overview. *J Immunol Methods* 1992; **150**: 5-21

16 **Avrameas S**. Amplification systems in immunoenzymatic techniques. *J Immunol Methods* 1992; **150**: 23-32

17 **Schrier RW,** Arroyo V, Bernardi M, Epstein M, Henriksen JH, Rodes J. Peripheral arterial vasodilation hypothesis: a proposal for the initiation of renal sodium and water retention in cirrhosis. *Hepatology* 1988; **8**: 1151-1157

18 **Guarner C,** Soriano G, Tomas A, Bulbena O, Novella MT, Balanzo J, Vilardell F, Mourelle M, Moncada S. Increased serum nitrite and nitrate levels in patients with cirrhosis: relationship to endotoxemia. *Hepatology* 1993; **18**: 1139-1143

19 **Khoruts A,** Stahnke L, McClain CJ, Logan G, Allen JI. Circulating tumor necrosis factor, interleukin-1 and interleukin-6 concentrations in chronic alcoholic patients. *Hepatology* 1991; **13**: 267-276

20 **Chun TH,** Itoh H, Ogawa Y, Tamura N, Takaya K, Igaki T, Yamashita J, Doi K, Inoue M, Masatsugu K, Korenaga R, Ando J, Nakao K. Shear stress augments expression of C-type natriuretic peptide and adrenomedullin. *Hypertension* 1997; **29**: 1296-1302

Edited by Wang XL

P.O.Box 2345, Beijing 100023,China
Fax: +86-10-85381893
E-mail: wjg@wjgnet.com www.wjgnet.com

World J Gastroenterol 2003;9(10):2328-2331
World Journal of Gastroenterology
 ISSN 1007-9327

• BRIEF REPORTS •

Candida esophagitis: Risk factors in non-HIV population in Pakistan

Javed Yakoob, Wasim Jafri, Shahab Abid, Nadeem Jafri, Muhammad Islam, Saeed Hamid, Hasnain A Shah, Akbar S Hussainy

Javed Yakoob, Wasim Jafri, Shahab Abid, Nadeem Jafri, Muhammad Islam, Saeed Hamid, Hasnain A Shah, Akbar S Hussainy, Section of Gastroenterology, Department of Medicine and Pathology, Agha Khan University Hospital, Karachi, Pakistan
Correspondence to: Dr. Javed Yakoob, MBBS, PhD. Section of Gastroenterology, Department of Medicine, Agha Khan University Hospital, Stadium Road, Karachi-74800, Pakistan. yakoobjaved@hotmail.com
Telephone: +92-21-48594661 **Fax:** +92-21-4934294
Received: 2003-06-05 **Accepted:** 2003-08-19

Abstract

AIM: *Candida* esophagitis is a frequent infection in immunocompromised patients. This study was designed to determine its characteristics in non- human immune deficiency virus (HIV) infected patients attending a teaching hospital.

METHODS: Clinical records of all patients coded by international classification of diseases 9th revision with clinical modifications' (ICD-9-CM), with *candida* esophagitis diagnosed by esophagogastroduodenoscopy (EGD) and histopathology over a period of 5 years were studied.

RESULTS: Fifty-one patients (27 males, 24 females, range 21-77 years old and mean age 52.9 years) fulfilled the criteria (0.34 % of the EGD). The common predisposing factors were carcinoma (OR 3.87, CI 1.00-14.99) and diabetes mellitus (OR 4.39, CI 1.34-14.42). The frequent clinical symptoms were retrosternal discomfort, dysphagia and epigastric abdominal pain with endoscopic appearance of scattered mucosal plaques. Another endoscopic lesion was associated with *candida* esophagitis in 15 % patients.

CONCLUSION: Carcinomas, diabetes mellitus, corticosteroid and antibiotic therapy are major risk factors for *candida* esophagitis in Pakistan. It is an easily managed complication that responds to treatment with nystatin.

Yakoob J, Jafri W, Abid S, Jafri N, Islam M, Hamid S, Shah HA, Hussainy AS. *Candida* esophagitis: Risk factors in non-HIV population in Pakistan. *World J Gastroenterol* 2003; 9(10): 2328-2331
http://www.wjgnet.com/1007-9327/9/2328.asp

INTRODUCTION

Infective esophagitis is a rare disease, affecting mostly immunocompromised patients. *Candida* esophagitis is one of the most common opportunistic infections in patients with impaired immunity and the most common cause of esophageal disease in patients with acquired immune deficiency syndrome (AIDS)[1]. It also occurs in debilitated patients who have received broad-spectrum antibiotics, steroids and immunosuppressants. With the advent of transplantation and AIDS, esophageal infection is now a common medical problem[2]. The common infections involving immunocompromised non-human immunodeficiency virus (HIV) infected patients include *candida* and viral diseases such as *cytomegalovirus* (*CMV*) and *herpes simplex virus* (*HSV*)[2]. Immunocompromised patients who develop esophageal symptoms need to undergo endoscopy to rule out *candida* esophagitis. It is well recognized that *candida* esophagitis may coexist with other esophageal disorders in these patients[3]. The occurrence of multiple simultaneous processes makes definitive endoscopic examination important[4]. Several studies have been carried out in the west for *candida* esophagitis but it has not been studied before in Pakistan. Incidence of AIDS and HIV prevalence are still very low in Pakistan[5]. The purpose of our study was to assess the risk factors associated with *candida* esophagitis in our patients who came from an area with a low incidence of AIDS.

MATERIALS AND METHODS

Patients

The study was conducted at Agha Khan University Hospital (AKUH) in Karachi, a private Academic Medical Center that offers state of the art medical facilities and is used as a referral center for patients from all over the country for expert opinion and treatment. Karachi is a southern port and the largest metropolitan city in Pakistan with a population of over 11 million. In August 2002 we carried out a retrospective analysis of medical records of all the patients who attended endoscopy unit of gastrointestinal section at the AKUH from January 1997-December 2001 and were diagnosed as *candida* esophagitis. These patients had undergone endoscopy for symptoms arising from the upper gastrointestinal tract over this period and were diagnosed on the basis of endoscopy and histopathology as *candida* esophagitis. Clinical symptoms at the time of presentation, diagnosis, drug treatment dosage and duration preceding the symptoms such as nystatin suspension or fluconazole, past history of oral candidiasis, candida esophagitis, neutrophil and lymphocyte counts from complete blood picture, random blood glucose, hepatitis B, C and HIV serology were noted. A lymphocyte count was described as low when it was less than 1.5×10^9 per liter[6]. All endoscopic examinations were performed by staff-members of our hospital's gastroenterology section, using an Olympus videoscope GIF x Q 140. *Candida* esophagitis was diagnosed when characteristic *candidal* plaques were endoscopically identified and pathological confirmation of yeast forms typical for *candida* was found in association with an active esophagitis. Case patients were labeled as group A and the control group as group B which consisted of those patients without a diagnosis of *candida* esophagitis and in whom an endoscopic examination was performed immediately before and after every case patient was examined endoscopically (2 controls per case). Therefore, *candida* esophagitis cases and controls were evaluated by the same medical team using the same diagnostic criteria.

Endoscopy

To describe the severity of *candida* esophagitis both in AIDS[7,8] and in non-AIDS populations, a grading scale was described by Kodsi *et al*[9] or a modification thereof has been

used[10]. *Candida* esophagitis was graded as the following: Grade 1 as scattered mucosal plaques involving less than 50 % of the esophageal mucosa, grade 2 as mucosal plaques involving more than 50 % esophageal mucosa, grade 3 as confluent plaque material circumferentially coating at least 50 % of the esophageal mucosa but without luminal impingement, grade 4 as circumferential plaque mat coating at least 50 % of the esophageal mucosa with luminal impingement despite air insufflations. In most cases, an ulcer could be readily distinguished endoscopically by the marked hyperemia and granularity of the ulcer base from the surrounding *candida* esophagitis.

Histopathology

At the time of endoscopy, routine biopsies were performed on all endoscopic abnormalities. At least 2 biopsies were performed on each esophageal lesion with standard biopsy forceps. All tissue specimens were submitted for routine histopathology, and stained with hematoxylin-eosin (H-E) and periodic acid-Schiff stains (PAS). In the presence of ulcer tissue, immuno-histochemical staining for *CMV* and *HSV* was performed using previously described technique to confirm infection[3]. An ulcer was considered secondary to *candida* esophagitis alone when it was found endoscopically and histopathologically. Fungal organisms compatible with *candida* were seen in the superficial epithelium, there was an absence of viral cytopathic effect histopathologically, no clinical or endoscopic evidence of gastroesophageal reflex disease or drug-induced esophagitis existed.

Statistical analysis

Results were expressed as mean ± standard deviation, median range for all continuous variables (e.g., age) and number (percentage) for categorical data (e.g., gender, diabetes mellitus, steroids, etc) were provided. Univariate analysis was performed using the independent sample *t*-test, Pearson Chi-square test and Fisher exact test when ever appropriate. A *P* value <0.05 was considered as statistically significant. All *P* values were two sided. Statistical interpretation of data was performed using the computerized software programme SPSS version 10.0.

RESULTS

Patients

During the study period, 15 000 upper endoscopies were performed in our endoscopy unit. Fifty-one patients were diagnosed with *candida* esophagitis on the basis of endoscopic and histopathologic criteria. The age, sex and percentage of inpatients are given in Table 1.

Risk factors

The common risk factors for candida esophagitis were carcinoma (OR 8.05, 95 % CI 1.91-47.1 and *P*=0.001), uncontrolled diabetes mellitus (OR 7.34, 95 % CI 2.26-27.5 and *P*=0.001), corticosteroid therapy (OR 6.67, 95 % CI 2.20-22.3 and *P*=0.001) and antibiotics (OR 4.56, 95 % CI 1.14-21.5 and *P*=0.02) (Table 2).

Clinical feature

The clinical details are given in Table 1. The clinical symptoms in group A were retrosternal discomfort in 39.2 % (20/51) patients, of these 6/20 were associated with dysphagia and 3/20 with epigastric pain. Dysphagia was present in 25.4 % (13/51) and epigastric symptoms in 35.2 % (18/51) with only 9/18 describing it as an epigastric pain (Table 1). In control group B, retrosternal discomfort was described in 30.3 % (31/102), dysphagia in 19.6 % (20/102) and epigastric symptoms in 50 % (51/102). These patients responded well to treatment with nystatin or fluconazole, 84.3 % (43/51) and 15.7 % (8/51), respectively (Table 1).

Table 1 Details of patients presenting with *candida* esophagitis and controls

	Cases *n*=51	Control *n*=102
Sex		
Male	27 (53)	58 (57)
Female	24 (47)	44 (43)
Age in years (yrs)		
Range:	21-77	19-74
Mean ±SD	52.9±14.6	50.08±12.64
No: % of In-patients	34 (64)	58 (54)
Risk factors for *candida* esophagitis		
Steroid therapy	15 (29.4 %)	6 (5.8 %)
Diabetes mellitus type 1 and 2	14 (27.4 %)	5 (4.9 %)
Carcinoma (e.g. breast, gastric, esophagus)	10 (19.6 %)	3 (2.9 %)
Broad spectrum antibiotics	8 (15.6 %)	4 (3.9 %)
Chronic liver disease	2 (3.9 %)	6 (5.8 %)
Tuberculosis	2 (3.9 %)	1 (0.9 %)
Ischemic heart disease	-	26 (25.4 %)
Peptic ulcer disease	-	26 (25.4 %)
Hypertension	-	20 (19.6 %)
Chronic anemia	-	2 (1.9 %)
Arthritis	-	1 (0.9 %)
Primary Infertility	-	1 (0.9 %)
Osteoporosis	-	1 (0.9 %)
Clinical symptoms		
Retrosternal discomfort	20 (39.3 %)	31 (30.3 %)
Dysphagia	13 (25.4 %)	20 (19.7 %)
Epigastric symptoms	18 (35.3 %)	51 (50 %)
Endoscopic grading		
Grade 1	9	
Grade 2	19	
Grade 3	10	
Grade 4	13	
Treatment		
Nystatin	84.3 % (43/51)	
Fluconazole	15.7 % (8/51)	

Results were expressed as number and percentage, mean ± standard deviation (SD).

Polymorphonuclear leucocyte and lymphocyte counts

All of our patients had polymorphonuclear leucocyte count within the normal range, while 33.3 % (17/51) had lymphocyte count below the normal range. These patients were mostly those who were on steroid or antibiotics therapy (Table 3).

Endoscopy finding

The endoscopic appearance of plaques varied in color from yellow to white. With increasing severity, scattered mucosal plaques coalesced circumferentially coating the mucosal surface and impinged into the esophageal lumen. In group A, 9 patients had localized disease, 5 patients had disease more prominent in the distal esophagus than in proximal esophagus, while it involved middle esophagus and middle to distal esophagus equally in 4 patients (Table 1). Esophageal ulceration was noted endoscopically and histopathologically in 3.9 % (2/51). In these patients, ulcer was believed to be secondary to *candida* esophagitis alone, as other etiologies of esophageal ulceration were excluded by testing for *CMV*, *HSV* and *HIV* by serology and immuno-histochemistry. In 15.6 % (8/51) of group ‘ A’ patients, associated endoscopic findings included 7.8 % (4/51) with antral gastritis, 1.9 % (1/51) with gastric ulcer, 5.8 % (3/51) with duodenitis. In control group B

esophageal disease was found in 35.3 % (36/102) cases, gastric disease in 38.3 % (39/102) cases, and duodenal pathology was seen in 26.4 % (27/102) cases.

Correlation of clinical symptoms and endoscopic feature

There was no correlation between clinical symptoms and endoscopic findings.

Hepatitis B, C and HIV serology

HIV serology was negative for hepatitis B, and 9.8 % (5/51) were positive for hepatitis C virus.

Histopathology

Histopathology revealed varying degrees of hyperplastic squamous mucosa with moderate-severe degree of acute-chronic inflammation in the surface epithelium. Mucosal surface was covered with desquamated epithelium and inflammatory necrotic slough. Superficial colonies of *candida* organism showed non-branching hyphae. In cases of ulcerative esophagitis, intact and focally ulcerated mucosa revealed moderate-severe inflammation, basal cell hyperplasia with non-septate fungal hyphae.

Table 2 Results of univariate analysis of potential risk factors for acquisition of *candida* esophagitis

Variable	No. of cases (%)	No. of control (%)	Odd ratio (95% CI)	*P* value
Carcinoma	10 (19.6 %)	3 (2.9 %)	8.05 (1.91-47.1)	0.001
Diabetes mellitus	14 (27.4 %)	5 (4.9 %)	7.34 (2.26-27.5)	0.001
Prior use of steroid	15 (29.4 %)	6 (5.8 %)	6.67 (2.20-22.3)	0.001
Prior use of antibiotics	8 (15.6 %)	4 (3.9%)	4.55 (1.14-21.5)	0.02

Table 3 Distribution of low lymphocyte counts in patients presenting with *candida* esophagitis

Association	Cases (*n*=17)
Steroids	6
Antibiotics	6
Malignancy	3
Diabetes mellitus	1
Chronic liver disease	1

DISCUSSION

Our study is the first attempt to evaluate the risk factors and endoscopic manifestations of *candida* esophagitis in Pakistan, an area where AIDS is not endemic. All of our patients diagnosed with *candida* esophagitis did not have oral thrush. This was similar to a study by Bonacini *et al* in which 110 HIV positive patients with esophageal symptoms, 38 % of those without oral thrush had *candida* esophagitis[11]. In this study, the patients had oral, intravenous and nebulizer steroid treatment in varying durations and doses of therapy. Steroid levels were not measured on admission. However, steroid therapy was associated with lymphopenia and 33.3 % of our patients presented with a low lymphocyte count[12]. Diabetic patients complicated with *candida* esophagitis had uncontrolled diabetes at the time of presentation, irrespective of its type. Malignancies beside other mechanisms were also associated with esophageal stasis due to mechanical obstruction that predisposes to *candida* esophagitis[13]. However, esophageal obstruction was not a feature in our cases of *candida* esophagitis associated with malignancies. A high frequency of bacterial or mycotic infections has been reported in HCV-associated membranoproliferative glomerulonephritis and diabetes mellitus due to acquired defects of polymorphonuclear leukocyte (PMN) functions[14,15]. In HIV seropositive cases, coexistent *candida* esophagitis and tuberculosis have been frequently described [16], but in non-HIV immunosuppressed patients, there were few reports of active pulmonary or intestinal tuberculosis associated with *candida* esophagitis[17].

Epigastric pain has been known to be associated with *candida* infection[18]. In our study, no correlation was found between the symptoms and the endoscopy grade score similar to another study[19]. At endoscopy, the presence of classic whitish exudates or plaques should predict candidiasis in at least 90 % of cases, although viral infection occasionally might cause a similar appearance[11]. We found that *candida* esophagitis resulted in typical endoscopic appearances and both characteristic and uniform histopathologic findings. These *candida* esophagitis patients were treated with either nystatin 5 ml QDS/fluconazole 100 mg a day by mouth for 5 days. None of these candida esophagitis patients was found to be resistant to this treatment. As treatment with fluconazole was expensive, fewer patients were prescribed this medication. Culture for identifying *candida* species was not carried out, as it would have added cost to the management of disease. The limitation of our study included a small number of patients and a retrospective design. There were few patients with risk factors in the control group B as their stable disease did not predispose them to *candida* esophagitis (Table 1).

The implications of our study are that in Pakistan *candida* esophagitis is associated with chronic diseases and those on treatment with corticosteroids and antibiotics are predisposed to it. Patients on these medications need to be monitored and reviewed frequently. *Candida* esophagitis should be considered early in patients who have been on steroids and antibiotic treatment and presented with upper gastro-intestinal symptoms. Oral candidiasis does not accompany candida esophagitis. Our study showed that *candida* esophagitis by itself was an easily managed complication. In conclusion, *candida* esophagitis in Pakistan is more common due to chronic diseases, corticosteroid and antibiotic therapy which impaires the immune system rather than as an AIDS-defining disease. It occurs in the absence of local obstructive lesions and responds to treatment with nystatin and fluconazole.

REFERENCES

1 **Laine L**, Boncini M. Esophageal disease in human immunodeficiency virus infection. *Arch Intern Med* 1994; **154**: 1577-1582
2 **Wilcox CM**, Karowe MW. Esophageal infections: etiology, diagnosis and management. *Gastroenterology* 1994; **2**: 188-206
3 **Schwartz DA**, Wilcox CM. Atypical cytomegalovirus inclusions in gastrointestinal biopsy specimens from patients with the acquired immunodeficiency syndrome: diagnostic role of in situ nucleic acid hybridization. *Hum Pathol* 1992; **23**: 1019-1026
4 **Connolly GM**, Hawkins D, Harcourt-Webster JN, Parsons PA, Husain OA, Gazzard G. Esophageal symptoms, their causes, treatment and prognosis in patients with the acquired immunodeficiency syndrome. *Gut* 1989; **30**: 1033-1039
5 **Hyder AA**, Khan OA. HIV / AIDS in Pakistan: the context and magnitude of an emerging threat. *J Epidemiol Community Health* 1998; **52**: 579-585
6 **Bagby GC**. Disorders of neutrophil production. In: Bennet JC, Plum F, eds. Cecil Text book of Medicine. *WB Saunders* 1996: 908-915
7 **Laine L**, Dretler RH, Conteas CN, Tuazon C, Koster FM, Sattler F, Squires K, Islam MZ. Fluconazole compared with ketoconazole for the treatment of candida esophagitis in AIDS. A randomized trial. *Ann Intern Med* 1992; **117**: 655-660
8 **Porro GB**, Parente F, Cernuschi M. The diagnosis of esophageal candidiasis in patients with acquired immune deficiency syndrome: Is endoscopy always necessary? *American J Gastroenterol* 1989; **84**: 143-146

9 **Kodsi BE**, Wickremesinghe PC, Kozinn PJ, Iswara K, Goldberg PK. Candida esophagitis: A prospective study of 27 cases. *Gastroenterology* 1976; **71**: 715-719
10 **Wilcox CM**, Schwartz DA. Endoscopic-pathologic correlates of candida esophagitis in acquired immunodeficiency syndrome. *Dig Dis Sci* 1996; **41**: 1337-1345
11 **Boncini M**, Young T, Laine L. The causes of esophageal symptoms in human immunedeficiency virus infection: a prospective study of 110 patients. *Arch Intern Med* 1991; **151**: 1567-1572
12 **Demir G**, Derman U, Berkarda B. Haematological effects of pulse steroid therapy. *Int J Clin Pharmacol Res* 1994; **14**: 101-106
13 **Rigas B**, Spiro HM. Clincal Gastroenterology. *McGraw Hill* 1995: 12-15
14 **Mazzaro C**, Panarello G, Tesio F, Santini G, Crovatto M, Mazzi G, Zorat F, Tulissi P, Pussini E, Baracetti S, Campanacci L, Pozzato G. Hepatitis C Virus risk: a HCV related syndrome. *J Intern Med* 2000; **247**: 535-545
15 **Jirillo E**, Greco B, Caradonna L, Satalino R, Pugliese V, Cozzolongo R, Cuppone R, Manghisi OG. Evaluation of cellular immune responses and soluble mediators in patients with cHCV infection. *Immunopharmacol Immunotoxicol* 1995; **17**: 347-364
16 **George J**, Hamide A, Das AK, Amarnath SK, Rao RS. Clinical and laboratory profile of sixty patients with AIDS: a South Indian study. *Southeast Asian J Trop Med Public Health* 1996; **27**: 686-691
17 **Hirasaki S**. Active intestinal tuberculosis with esophageal *candidiasis* due to idiopathic CD (+) T-lymphocytopenia in an elderly woman. *J Gastroenterol* 2000; **35**: 47-51
18 **Alexander JA**, Brouillette DE, Chien MC, YooYK, Tarter RE, Gavaler JS, Van Thiel DH. Infectious esophagitis following liver and renal transplantation. *Dig Dis Sci* 1988; **33**: 1121-1126
19 **Rodriquez Hernandez H**, Reyes Gutierrez E, Elizondo Rivera J. Esophageal candidiasis in AIDS, Clinical, endoscopic and histopathologic analysis of 19 cases. *Rev Invest Clin* 1991; **43**: 124-127

Edited by Wang XL

P.O.Box 2345, Beijing 100023,China
Fax: +86-10-85381893
E-mail: wjg@wjgnet.com www.wjgnet.com

World J Gastroenterol 2003;9(10):2332-2334
World Journal of Gastroenterology
 ISSN 1007-9327

• BRIEF REPORTS •

Serum malondialdehyde level in patients infected with *Ascaris lumbricoides*

Eser Kilic, Süleyman Yazar, Recep Saraymen, Hatice Ozbilge

Eser Kilic, Recep Saraymen, Department of Biochemistry and Clinical Biochemistry, Medical Faculty, Erciyes University, Kayseri-Turkey
Süleyman Yazar, Department of Parasitology, Medical Faculty, Erciyes University, Kayseri-Turkey
Hatice Ozbilge, Department of Microbiology, Medical Faculty, Harran University,[a] anl1urfa-Turkey
Correspondence to: Eser Kilic, Department of Biochemistry Medical Faculty, Erciyes, University, 38039 Kayseri-Turkeyemail. kiliceser@hotmail.com
Received: 2003-07-12 **Accepted:** 2003-08-20

Abstract

AIM: The aim of the study was to investigate the changes of serum malondialdehyde level, i.e; the oxidative stress hypothesis in patients infected with *Ascaris lumbricoides*.

METHODS: Serum malondialdehyde activity was measured in 43 patients who were positive for intestinal parasite of *Ascaris lumbricoides*. Scores were obtained for the positives and their age-and sex-matched 60 *Ascaris lumbricoides* negative healthy controls.

RESULTS: The difference between malondialdehyde levels of patients infected with *Ascaris lumbricoides* and control group was statistically significant both for females ($P<0.05$) and for males ($P<0.05$). In the patient and control groups, no correlation was found between age and malondialdehyde levels ($P>0.05$) both in females and in males. In addition, no significant correlation could be found between malondialdehyde levels of both females and males for patients and control groups ($P>0.05$).

CONCLUSION: Malondialdehyde levels clearly increase in patients infected with *Ascaris lumbricoides*.

Kilic E,Yazar S, Saraymen R, Ozbilge H. Serum malondialdehyde level in patients infected with *Ascaris lumbricoides*. *World J Gastroenterol* 2003; 9(10): 2332-2334
http://www.wjgnet.com/1007-9327/9/2332.asp

INTRODUCTION

Ascaris lumbricoides (A. lumbricoides) is one of the largest nematode (roundworm) parasitizing the human intestine[1-5]. It is estimated that 25 % of the world' s population was infected with this nematode[4]. The adult worms live in the small intestine and eggs are passed in the feces. A single female can produce up to 200 000 eggs each day. About two weeks after passage in the feces the eggs contain an infective larval or juvenile stage, and humans are infected when they ingest such infective eggs. The eggs hatch in the small intestine, the juvenile penetrates the small intestine and enters the circulatory system, and eventually the juvenile worm enters the lungs. In the lungs the juvenile worm leaves the circulatory system and enters the air passages of the lungs. The juvenile worm then migrates up the air passages into the pharynx where it is swallowed, and once in the small intestine the juvenile grows into an adult worm.Why *Ascaris lumbricoides* undergoes such a migration through the body to only end up where it started is unknown.Such a migration is not unique to *Ascaris lumbricoides*, as its close relatives undergo a similar migration in the bodies of their hosts[1-3,5].

Ascaris lumbricoides infections in humans can cause significant pathology.Infection with ascarids is called ascariasis. The migration of the larvae through the lungs causes the blood vessels of the lungs to hemorrhage, and there is an inflammatory response accompanied by edema. The resulting accumulation of fluids in the lungs results in "ascaris pneumonia", and this can be fatal[1,3,5,6]. The large size of the adult worms also presents problems, especially if the worms physically block the gastrointestinal tract. *Ascaris lumbricoides* is notorious for its reputation to migrate within the small intestine, and when a large worm begins to migrate there is not much that can stop it. Instances have been reported in which *Ascaris lumbricoides* has migrated into and blocked the bile or pancreatic duct or in which the worms have penetrated the small intestine resulting in acute (and fatal) peritonitis. *Ascaris lumbricoides* seems to be especially sensitive to anesthetics, and numerous cases have been documented where patients in surgical recovery rooms have had worms migrating from the small intestine, through the stomach, and out the patient' s nose or mouth[1-3,5].

Infections are diagnosed by finding the typical eggs in the patient' s feces, on occasion the larval or adult worms are found in the feces, or especially for *Ascaris lumbricoides*, in the throat, mouth, or nose[1]. This infection may self-cure after the larvae have matured into adults or may require anthelmintic treatment. In severe cases, surgical removal may be necessary. Allergic symptoms (especially but not exclusively of the asthmatic sort) are common in long-lasting infections or upon reinfection in ascariasis[1,3,7]. Eggs of *Ascaris lumbricoides*. have been detected on fresh vegetables[2,3,5]. This infection is cosmopolitan, but ascariasis is more common in North America and in Europe. Relative infection rates on other continents are not available[3,4].

Lipid peroxidation is a well-established mechanism of cellular injury in human, and is used as an indicator of oxidative stress in cells and tissues. Lipid peroxides derived from polyunsaturated fatty acids, are unstable and can decompose to form a complex series of compounds. These include reactive carbonyl compound, which is the most abundant malondialdehyde (MDA). Therefore, measurement of malondialdehyde is widely used as an indicator of lipid peroxidation. Increased levels of lipid peroxidation products have been associated with a variety of chronic diseases in both humans and model systems[8-10]. The aim of this study was to test the hypothesis of decreased activity of defense system protecting tissues from free radical damage in patients with *A. lumbricoides* by measuring the level of MDA (an end-product of lipid peroxidation) in serum samples.

MATERIALS AND METHODS

Patients

We assayed MDA activities of 103 subjects aged between 12-44 years (48 males and 55 females). None of them was smoker,

and had any known pathologies and taking steroids or medications such as iron for anemia at the time of sampling. Serum samples for control group were obtained from healthy people who came to the different departments of Medical Faculty Erciyes University, for regular check-up and students or employees of the University. All subjects weer fasted after midnight before blood collection the next morning. 43 patients and 60 controls were examined in this study. The mean age of the patient group, which consisted of 21 men and 22 women were 25±13 years and 27±13 years, respectively. The mean age of the control group, which included 27 men and 33 women were 30±14 years and 29±12 years respectively. Wet mount preparations in 0.9 % NaCl, diluted Lugol's iodine and flotation technique in saturated saline solution were used for the detection of intestinal parasites.

Assay

All venous blood samples taken between 8 and 9 a.m. after 8 h of fasting were collected in polystyrene tubes and vacutainers containing heparin. The tubes were centrifuged at 500×g for 15 min. Sera were then removed and stored at -20 ℃ until analysis. Serum MDA levels were measured by the double heating method[11,12]. The principle of the method was based on the spectrophotometric measurement of the color occurred during the reaction to thiobarbituric acid with MDA. Concentration of thiobarbituric acid reactive substances (TBARS) was calculated by the absorbance coefficient of malondialdehyde-thiobarbituric acid complex and expressed in nmol/ml.

Statistical analysis

Statistical analysis was performed with SPSS software package (Version 11.0 for Windows). The data were expressed as mean ± standard deviation (SD). For comparison of two groups of continuous variables, independent sample *t*-test was used. A probability value of $P<0.05$ indicated a statistically significant difference.

RESULTS

Malondialdehyde scores are given in Table 1.

Table 1 MDA levels of patients infected with *A. lumbricoides* and control group

Patients	Age(year)	MDA levels (nmol/ml)
Female (22)	27±13	0.67±0.16
Male (21)	25±13	0.62±0.11
Controls	Age(year)	MDA levels (nmol/ml)
Female (33)	29±12	0.21±0.15
Male (27)	30±14	0.22±0.14

The difference between MDA levels of patients and control group was statistically significant both for females ($P<0.05$) and males ($P<0.05$), (Table 1). In the patient and control groups, no correlation was found between age and MDA levels ($P>0.05$) both in females and in males. In addition, no significant correlation could be found between MDA levels of both females and males for patients and control group ($P>0.05$).

DISCUSSION

This present study was aimed to evaluate and characterize the relationship between intestinal parasite infection of *ascariasis*, which can cause pathology and oxidative stress mechanism as a mediator of tissue damage concurrent with ascariasis infection.

Ascariasis is the most common human worm infection. Human can become infected after touching mouth with hands contaminated with eggs from soil or other contaminated surfaces. Infection has occurred worldwide and has been most common in tropical and subtropical areas where sanitation and hygiene were poor[1-3,5]. Children are infected more often than adults. Estimates suggest that 1 in 4 of the world's population, or more than 1 billion people, are infected with the intestinal roundworm *A. lumbricoides*. In Europe, infection was common, but the most common in rural areas of the southeast[3-5].

Although *Ascaris lumbricoides* has only a single host and it is found in the small intestine, its life cycle is far from simple. It has been suggested that from an evolutionary perspective that *Ascaris lumbricoides* originally had two hosts and has secondarily lost its intermediate host[1-3,5-7]. Although most people have no symptoms, symptoms can be broken down into 2 categories: early (larval migration, 4-16 days after egg ingestion) fever, cough and wheezing and late (mechanical effects, 6-8 weeks after ingestion). All symptoms resulted from mechanical irritation include; vague abdominal complaints (i.e, cramping, nausea, vomiting), small bowel obstruction (mostly in children), pancreatitis (secondary to worm migration), cholecystitis (secondary to worm migration), appendicitis (less common, secondary to worm migration). Secondary complications could arise with *Ascaris lumbricoides* infections because sometimes when the worms were undergoing this migration they appeared to get lost and started wandering through other organs such as the brain, bile duct, pancreas or appendix[1-3,5,7].

Ascaris lumbricoides proteins are very immunogenic and people can become very sensitive to the worm and have strong allergic reactions. The parasite could be treated very easily with drugs such as mebendazole or pyrantel pamoate[1,3,5,13,14]. However, reinfections frequently occur if other control measures are not taken. This is a particular problem where night soil is used as a fertilizer.

Oxidative stress as a mediator of tissue damage concurrent with *A. lumbricoides* infection was investigated. This was the first study to characterize the relationship between *A. lumbricoides*, (may cause no symptoms however, some complains of cramping, nausea, vomiting, small bowel obstruction, pancreatitis, cholecystitis, appendicitis can be seen) and MDA (lipid peroxidation), which is a well-established mechanism of cellular injury in human, and is used as an indicator of oxidative stress in cells and tissues.

Levels of MDA were significantly increased in patients infected with *A. lumbricoides*. The results of our study strongly suggested that one of the main reasons for high MDA levels in patients infected with *A.lumbricoides* could be decreased activity of defense system protecting tissues from free radical damage. However, in the patients and control groups, no correlation was found between age and MDA levels both in females and in males. In addition, no significant correlation could be found between MDA levels of both females and males for *A. lumbricoides* infected and control groups. These results for patients infected with *A. lumbricoides* could possibly be explained as that with high MDA activity in all ages.

As it is known that lipid peroxidation is a free radical-related process that in biologic systems may occur under enzymatic control, e.g., for the generation of lipid-derived inflammatory mediators, or nonenzymatically. This latter form was associated mostly with cellular damage as a result of oxidative stress, which also involved cellular antioxidants in this process[10]. The high infection/control ratio of MDA concentration and the significant correlation strongly indicate the occurrence of oxidative stress and lipid peroxidation as a mechanism of tissue damage in cases of *A.lumbricoides* infection.

REFERENCES

1 **Crompton DW**. Ascaris and ascariasis. *Adv Parasitol* 2001; **48**:

285-375
2 **Goncalves ML**, Araujo A, Ferreira LF. Human intestinal parasites in the past: new findings and a review. *Mem Inst Oswaldo Cruz* 2003; **98**: 103-118
3 **O'Lorcain P**, Holland CV. The public health importance of Ascaris lumbricoides. *Parasitology* 2000; **121**: 51-71
4 **Hall A**, Holland C. Geographical variation in Ascaris lumbricoides fecundity and its implications for helminth control. *Parasitol Today* 2000; **16**: 540-544
5 **Sarinas PS**, Chitkara RK. Ascariasis and hookworm. *Semin Respir Infect* 1997; **12**: 130-137
6 **Geiger SM**, Massara CL, Bethony J, Soboslay PT, Carvalho OS, Correa-Oliveira R. Cellular responses and cytokine profiles in Ascaris lumbricoides and Trichuris trichiura infected patients. *Parasite Immunol* 2002; **24**: 499-509
7 **Palmer LJ**, Celedon JC, Weiss ST, Wang B, Fang Z, Xu X. Ascaris lumbricoides infection is associated with increased risk of childhood asthma and atopy in rural China. *Am J Respir Crit Care Med* 2002; **165**: 1489-1493
8 **Draper HH**, Hadley M. A review of recent studies on the metabolism of exogenous and endogenous malondialdehyde. *Xenobiotica* 1990; **20**: 901-907
9 **Nayak DU**, Karmen C, Frishman WH, Vakili BA. Antioxidant vitamins and enzymatic and synthetic oxygen-derived free radical scavengers in the prevention and treatment of cardiovascular disease. *Heart Dis* 2001; **3**: 28-45
10 **Romero FJ**, Bosch-Morell F, Romero MJ, Jareno EJ, Romero B, Marin N, Roma J. Lipid peroxidation products and antioxidants in human disease. *Environ Health Perspect* 1998; **106**: 1229-1234
11 **Stocks J**, Dormandy TL. The autoxidation of human red cell. Lipids induced by hydrogen peroxide. *Br J Haematol* 1971; **20**: 95-111
12 **Jain SK**. Evidence for membrane lipid peroxidation during the invivo aging of human erythrocytes. *Biochem Biophys Acta* 1998; **937**: 205-210
13 **Montresor A**, Awasthi S, Crompton DW. Use of benzimidazoles in children younger than 24 months for the treatment of soil-transmitted helminthiasis. *Acta Trop* 2003; **86**: 223-32S
14 **Georgiev V**. Pharmacotherapy of ascariasis. *Expert Opin Pharmacother* 2001; **2**: 223-239

Edited by Wang XL

P.O.Box 2345, Beijing 100023,China
Fax: +86-10-85381893
E-mail: wjg@wjgnet.com www.wjgnet.com

World J Gastroenterol 2003;9(10):2335-2337
World Journal of Gastroenterology
 ISSN 1007-9327

• BRIEF REPORTS •

Problems in screening colorectal cancer in the elderly

Davidoviæ M. Mladen, Milosevic P. Dragoslav, Zdravkovic Sanja, Bojic Bozidar, Djurica Snezana

Davidovic M. Mladen, Milosevic P. Dragoslav, Zdravkovic Sanja, Bojic Bozidar, Djurica Snezana, Center of Geriatric Medicine, 11050 Beograd, Rifata Burdzevica 31, Yugoslavia
Correspondence to: Davidoviæ M. Mladen, at Center, 11050 Beograd, Rifata, Burdževiæa 31, Yugoslavia. davidovi@EUnet.yu
Telephone: +381-11-417094 **Fax:** +381-11-765731
Received: 2003-05-11 **Accepted:** 2003-06-20

Abstract

AIM: To explore the problems in the screening of colorectal carcinoma in the elderly.

METHODS: Three models of colorectal cancer prevention were examined: standard screening, active check-up of suspected cases and summons to have endoscopic check-up for previously diagnosed colorectal polyps. The study was performed among three groups of elderly individuals: Group 1 (167 cases), hospitalized asymptomatic individuals without symptoms in large intestines. Group 2 (612 cases): old individuals at home for the aged, out of which 32 showed symptoms of colon disorders; Group 3 (44 cases): elderly people with diagnosed polyps. As a result of 1788 rectosigmoidoscopies, we identified 61 individuals with polyps, out of which 44 patients were over 65 years old. However, only 9 of these 44 individuals agreed to have the endoscopy performed again.

RESULTS: One cancer and 13 polyps were detected in Group 1, and two polyps in Group 2. However, it should be noted that only eleven individuals from Group 2 agreed to have the endoscopy. In Group 3, there were no relapses of the polyps among the nine individuals who came back for the endoscopy.

CONCLUSION: Poor understanding of the screening procedures is one of the greatest problems in early detection of the cancer in the aged. Paradoxically, the cooperation is better with hospitalized patients, than with "successfully old" persons.

Mladen DM, Dragoslav MP, Sanja Z, Bozidar B, Snezana D. Problems in screening colorectal cancer in the elderly. *World J Gastroenterol* 2003; 9(10): 2335-2337
http://www.wjgnet.com/1007-9327/9/2335.asp

INTRODUCTION

Incidence of colorectal cancer in the world has increased over the past few decades, which is in turn, the cause for the increased importance of the screening for colorectal *carcinoma* (CRC). The incidence of colorectal cancer increases with age and doubles every ten years after the age of 40. In USA, the incidence of CRC is 35/100 000 population, thus one from 20 people will suffer from CRC during their life. High incidence of CRC has been recorded in Western European countries, which stands opposed to the numbers from the Far-East countries and Africa where the incidence is low, i.e. Nigeria has the incidence of 3.4/100 000. The average colorectal cancer age-adjusted death rates in Serbia from 1971 to1996 were 11.2/100 000 for men, and 8.3/100 000 for women[1].

Colorectal cancer screening includes fecal occult blood tests (FOBT), sigmoidoscopy, air-contrast *barium enema* examination and colonoscopy. These methods are recommended for persons in moderate risk, but its merits and limitations are still under investigation. Persons at high risk, i.e. family history of hereditary non-polyposis CRC, patients with ulcerous colitis, should be screened by colonoscopy. Screening method can surely have a positive effect on the survival rate of CRC. Since survival rate of CRC correlates to the anatomical spread of tumor, as well as to the surgical treatment at the right time, rectosigmoidoscopy can prevent and disclose the earliest stages of distal colon *carcinoma*.

Colonoscopy is certainly the "gold standard" for colorectal examination, but it is not most commonly accepted due to costs, bowel preparation, sedation and perforation risks (1/2 000 examinations). It is the most efficient method for detecting adenomas and probably has greater significance in the detection of the advanced tumor than other screening methods.

In carrying out our project on screening rectosigmoidoscopy, we found two kinds of problems. Like in all screening projects, one was the motivation of the participants (both the researchers and especially the subjects). The other problem was related to, what was in the developed countries called the cost/benefit issue, and in the under-developed countries was simply the issue of cost, which was extra high.

In the recent "American Cancer Society Guidelines for the Early Detection of Cancer"[2], the prevalence of screening procedure in American adult population was 19.0 % for FOBT, and 32.3 % for colonoscopy or sigmoidoscopy. Chinese author Wan J[3] claimed that multimorbidity was noted in 87 % of the investigated elder cases and the incidence of complication was only 0.05 %.

MATERIALS AND METHODS

Patients

The study was performed among three groups of elderly (from 65 to 80 yr, mean age 74.37) individuals: Group 1 had 167 hospitalized asymptomatic individuals without any symptoms in the large intestine, Group 2 consisted of 612 old individuals at home for the aged, out of which 32 had symptoms of colon disorders and Group 3 consisted of 44 individuals with polyps. Group 3 resulted from 1788 rectosigmoidoscopies, among which 61 individuals with polyps were found. 44 of these individuals were over the age of 65, and only 9 agreed to come back for a check-up of endoscopy.

Endoscopy

In our study, screening rectosigmoidoscopy was used with the purpose of assessing the importance of the rectoscopic examination for the early diagnosis and prevention of colorectal cancer. Rectosigmoidoscopy was performed with OLYMPUS endoscope after colon cleaning which was usually with SENNA.

Grouping

We selected three groups of elderly persons. The first one was the group of asymptomatic individuals (regarding digestive

tract) hospitalized at our institute. The answer to the screening was optimal, however it was difficult to obtain such results in the majority of the old population. The second trial was more selective. We included in our endoscopy proposition only the persons with digestive disorders. This selection was based on and followed the assessment procedure in home for the aged. There was a very low percentage of agreement to the endoscopy. Finally, Group 3 was reselected from the elderly persons with previously diagnosed colon polyps, and invited for a control endoscopy. Only 25 % of the group was available for the control rectosigmoidoscopy.

RESULTS

Three models of colorectal cancer prevention were examined: standard screening, active check-up of suspected cases and summons to endoscopic check-up for previously diagnosed colorectal polyps.

Group 1 consisted of hospitalized asymptomatic persons (without symptoms in large intestines).

The second trial (Group 2)was more selective. We included only the persons with digestive disorders in our endoscopy proposition, after the assessment procedure in home for the aged.

Group 3 consisted of the patients who already had polyps of the *rectum* removed and had never reported for endoscopic follow up although advised to do so. All the subjects were summoned by phone and letter.

Table 1 Data of three groups

Number of investigated cases	Selection criteria	Results
167	Hospitalized asymptomatic	1 cancer and 13 polyps
612 (32 with symptoms of colon disorders), 11 agreed to have the endoscopy	Home for the aged	2 polyps
1788 rectosigmoidoscopies (61 polyps) 44 older than 65 y 9 agreed on the endoscopy	With previous diagnosis of colon polyp	0 relapses of polyps

DISCUSSION

As colorectal tumor represents a considerable medical problem in the elderly, early detection of adenomatous polyps, as the precursors of intestinal *carcinomas*, is increasingly important and relevant to geriatricians.

The incidence of colorectal cancer increases with age, and approximately half of patients who develop it die from it. The possibility of developing cancer during the lifetime is approximately 5-6 %. Those that belong to the risk groups are more in a position to get this disease. In all cases, however, early diagnosis is decisive.

Sigmoidoscopy studies showed that regarding the possibility of CRC development, people older than 65 years were equaled in the incidence with patients having an *adenoma* of distal colon for more than 90 % CRC cases were diagnosed after the age of 55 and the peak of incidence of sigmoidoscopically discovered *adenomas* was before 70 years old.

The reason for lack of improvement in survival is that in most cases of CRC the disease has already been at an advanced stage by the time of diagnosis. Therefore, the main goal of screening is to discover CRC at the early stage when successful radical treatment is possible. Screening is an examination in asymptomatic individuals for CRC.

The American Cancer Society' s (ACS) Colorectal Cancer Advisory Group recommends FOBT once a year for people older than 50, rectosigmoidoscopy every 5 years, *barium enema* every 5 years and colonoscopy every 10 year[4].

According to WHO, screening tests must be sensitive, specific, applicable in the asymptomatic population and it must aim at lowering morbidity and mortality rate. Although rectosigmoidoscopy has certain disadvantages (such as being invasive, unpleasant and expensive compared to FOBT), it is more reliable than other screening tests in that it is highly sensitive (no false negative results even for lesions less than 5 mm in diameter) and the lesion can be removed during the screening examination.

In almost all patients with CRC, preceding lesions were asymptomatic *adenoma*. Therefore, it is of great importance to locate and remove *adenoma* before the development of *dysplasia* and the following malignant alterations, which, at the same time, represents secondary prevention of colorectal cancer. This is also obvious in British National Polyp Study from 1993, which showed 90 % decline of CC incidence in a group of 1500 patients who underwent polypectomy and were followed up for 6-8 years[5].

There are different problems regarding colorectal screening in old age: (1) The problem of performing screening or not seems that consensus was reached that different panel group and association have agreed that the answer was YES[7-15,17]; (2) Recently there were more references that supported colonoscopy as a choice[11,12,16,17]; (3) Are there any age limits for the colorectal screening procedure? There were two opposed opinions: No limits, or regarding biological age, and individual limit as consequence of the personal expected survival, on average, 75 to 80 y[19]; (4) What about national programs, accepted by the national authority supported by health funds? There were no such data[11]; (5) Regarding cost/ benefits ratio, it is rational to invest in screening procedure. Developing countries are between high standards and low economies. With minute financial support, the choice is to modify screening method, to reduce the number of investigated persons, or to quit the program of prevention; (6) It seemed very important to have influence on public opinions regarding screening procedure[15,16 ,19].

The authors do not have any doubts about the justification of the screening procedure, so an attempt should be made to find a solution for active prevention. However, in developing countries which have fewer technological and financial options, better choice, and the only choice for prevention must be a less costly one. The relation of cost and benefit is principally dependent on the economic possibilities of a country' s health service, within which the priorities of a health system play an especially meaningful role.

Further, the selection of hospitalized patients with other diagnosis is not statistically proper for screening of rectosigmoidoscopy. Hypothetically, optimal way to find patients for screening is to start from the homes for the aged or with the patients with colon symptoms that are treated at their homes. This is the best way to find patients when it is not possible to perform massive screening. Periodical checkup of the patients with polyipectomy is necessary.

Judging by the commentary[6], the idea on a prior questionnaire in active search for persons with high risk of contracting (developing) colon malignome is not recommended. In the same article, the recommendation of USA on compulsory screening of persons over 50 is adjusted to the needs of UK service. If the choice is either screening an insignificantly small population or absolute impossibility of screening or just screening of the high-risk group, including those actively detected after the questionnaire, it is highly probable that the latter solution is the one that should be chosen.

Results of our investigation showed that the main problem in the prevention of cancer was the extent of acceptance of

this method by the elderly patients. Screening methods for hospitalized patients (Group 1) were necessary, since they were already motivated for medical treatment. However, the screening method had the lowest acceptance among the old persons from the homes for the aged. A very small number of patients were going for endoscopic checkups. Those patients usually conducted controls on repeated doctor' s invitations.

REFERENCES

1 **Gajic-Veljanoski O**, Jarebinski M, Jovicevic-Bekic A, Pekmezovic T. Analysis of mortality in cancer of the large intestine in a cohort group in Serbia from 1971 to 1996. *Srp Arh Celok Lek* 2002; **130**: 173-177

2 **Smith RA,** Cokkinides V, von Eschenbach AC, Levin B, Cohen C, Runowicz CD, Sener S**.** American cancer society guidelines for the early detection of cancer. *CA Cancer J Clin* 2002; **52**: 8-22

3 **Wan J,** Zhang ZQ, Zhu C, Wang MW, Zhao DH, Fu YH, Zhang JP, Wang YH, Wu BY. Colonoscopic screening and follow-up for colorectal cancer in the elderly. *World J Gastroenterol* 2002; **8**: 267-269

4 **Levin B,** Brooks D, Smith RA, Stone A. Emerging technologies in screening for colorectal cancer: CT colonography, immunochemical fecal occult blood tests, and stool screening using molecular markers. *CA Cancer J Clin* 2003; **53**: 44-55

5 **Atkin W**. Implementing screening for colorectal cancer. *BMJ* 1999; **319**: 1212-1213

6 **Scholefield JH**. ABC of colorectal cancer Screening. *BMJ* 2000; **321**: 1004-1006

7 **Steele RJC,** Parker R, Patnick J, Warner J, Fraser C, Mowat NAG, Wilson J, Alexander FE, Paterson JG. A demonstration pilot trial for colorectal cancer screening in the United Kingdom: a new concept in the introduction of healthcare strategies. *J Med Screen* 2001; **8:** 197-203

8 **Martyres R**, St John DJ, Irving FH, Wyman K. Colorectal cancer screening in general practice. A survey of current practice and attitudes in Victoria. *Aust Fam Physician* 1999; **28**: 755-758

9 **Lieberman DA**, Weiss DG, Bond JH, Ahnen DJ, Garewal H, Chejfec G. Use of colonoscopy to screen asymptomatic adults for colorectal cancer. Veterans Affairs Cooperative Study Group 380. *N Engl J Med* 2000; **343**: 162-168

10 **Rossos PG**, Yeung E. Screening for colorectal cancer in older adults. *Geriatrics aging* 2002;**5/ 3**:16-18 http: / / www.geriatricsandaging. com

11 **Anderson J**. Clinical practice guidelines: Review of the recommendations for colorectal screening. *Geriatrics* 2000; **55**: 67-73

12 **Sonnenberg A**, Delc F, Inadomi JM. Cost-effectiveness of colonoscopy in screening for colorectal cancer. *Ann Intern Med* 2000; **133**: 573-584

13 **O'Connor AM,** Stacey D, Rovner D, Holmes-Rovner M, Tetroe J, Llewellyn-Thomas H, Entwistle V, Rostom A, Fiset V, Barry M, Jones J. Decision aids for people facing health treatment or screening decisions (Cochrane Review)**.** *The Cochrane Libary, Issue* 2001. http: / / www.medlib.com

14 **Lieberman DA,** Weiss DG, Bond JH. Use of colonoscopy to screen asymptomatic adults for colorectal cancer. *N Engl J Med* 2000; **343**: 162-168

15 **Lieberman DA**, Harford WV, Ahnen D J, Provenzale D, Sontag SJ, Schnell TG, Chejfec G, Campbell DR, Durbin TE. One-time screening for colorectal cancer with combined fecal occult-blood testing and examination of the distal colon. *N Engl J Med* 2001; **345**: 555-560

16 **Wilson LS**, Lightwood J. Model of estimated rates of colorectal cancer from polyp growth by year of surveillance. *J Med Scr* 2001; **8**: 187-196

17 **Mayor S**. Single flexible sigmoidoscopy screening could help prevent colorectal cancer. *BMJ* 2002; **324**: 934

18 **Wardle J**, Taylor T, Sutton S, Atkin W. Does publicity about cancer screening raise fear of cancer?Randomised trial of the psychological effect of information about cancer screening. *BMJ* 1999; **319:** 1037-1038

19 **Smith RA**, Cokkinides V, Eyre HJ. American Cancer Society. American Cancer Society guidelines for the early detection of cancer, 2003. *CA Cancer J Clin* 2003; **53**: 27-43

20 **Early DS**. Colorectal Cancer Screening: An overview of available methods and current recommendations. *South Med J* 1999; **92**: 258-265

21 **Frame PS.** Implementing clinical preventive medicine: time to fish or cut bait. *J Am Board Fam Pract* 2000; **13**: 84-85

22 **Spencer MP**. Screening colonoscopy. *Medscape Gastroenterol* 2000; **2** http: **//**www.medscape.com

23 **Slattery ML**, Edwards SL, Ma KN, Friedman GD. Colon cancer screening, lifestyle, and risk of colon cancer. *Cancer Causes Control* 2000; **11**: 555-563

24 **Saltzstein SL**, Behling CA. 5- and 10-year survival in cancer patients aged 90 and older: A study of 37,318 patients from SEER. *J Surg Oncol* 2002; **81**: 113-116

25 **Huang X**, Zhu HM, Deng CZ, Porro GB, Sangaletti O, Pace F. Gastroesophageal reflux: the features in elderly patients. *World J Gastroenterol* 1999; **5**: 421-423

Edited by Xu XQ and Wang XL

P.O.Box 2345, Beijing 100023,China
Fax: +86-10-85381893
E-mail: wjg@wjgnet.com www.wjgnet.com

World J Gastroenterol 2003;9(10):2338-2340
World Journal of Gastroenterology
 ISSN 1007-9327

• BRIEF REPORTS •

Significant factors associated with fatal outcome in emergency open surgery for perforated peptic ulcer

Mario Testini, Piero Portincasa, Giuseppe Piccinni, Germana Lissidini, Fabio Pellegrini, Luigi Greco

Mario Testini, Giuseppe Piccinni, Germana Lissidini, Section of General Surgery and Vascular Surgery and Clinical Oncology, Department of Applications in Surgery of Innovative Technologies (DACTI), University Medical School, Bari, Italy
Piero Portincasa, Section of Internal Medicine, Department of Internal Medicine and Public Medicine (DIMIMP), University Medical School, Bari, Italy
Fabio Pellegrini, Department of Clinical Pharmacology and Epidemiology, Pharmacological Research Institute, Consortium "Mario Negri" South, Maria Imbaro (L' Aquila), Italy
Luigi Greco, Section of General Surgery, Department of Emergency and Organ Transplantations (DETO), University Medical School, Bari, Italy
This paper is dedicated to the memory of Prof. Francesco Paccione, Head of the Department of Surgery who died prematurely in 1996.
Correspondence to: Mario Testini, MD, Sezione Chirurgia Generale, Vascolare ed Oncologia Clinica, Dipartimento per le Applicazioni in Chirurgia delle Tecnologie Innovative (D.A.C.T.I.). Università degli Studi di Bari. mario.testini@tin.it
Telephone: +39-80-5592882 **Fax:** +39-80-5478759
Received: 2003-05-13 **Accepted:** 2003-08-02

Abstract

AIM: To evaluate the main factors associated with mortality in patients undergoing surgery for perforated peptic ulcer referred to an academic department of general surgery in a large southern Italian city.

METHODS: One hundred and forty-nine consecutive patients (M:F ratio=110:39, mean age 52 yrs, range 16-95) with peptic ulcer disease were investigated for clinical history (including age, sex, previous history of peptic ulcer, associated diseases, delayed abdominal surgery, ulcer site, operation type, shock on admission, postoperative general complications, and intra-abdominal and/or wound infections), serum analyses and radiological findings.

RESULTS: The overall mortality rate was 4.0 %. Among all factors, an age above 65 years, one or more associated diseases, delayed abdominal surgery, shock on admission, postoperative abdominal complications and/or wound infections, were significantly associated (χ^2) with increased mortality in patients undergoing surgery ($0.0001<P<0.03$).

CONCLUSION: Factors such as concomitant diseases, shock on admission, delayed surgery, and postoperative abdominal and wound infections are significantly associated with fatal outcomes and need careful evaluation within the general workup of patients admitted for perforated peptic ulcer.

Testini M, Portincasa P, Piccinni G, Lissidini G, Pellegrini F, Greco L. Significant factors associated with fatal outcome in emergency open surgery for perforated peptic ulcer. *World J Gastroenterol* 2003; 9(10): 2338-2340
http://www.wjgnet.com/1007-9327/9/2338.asp

INTRODUCTION

There has been a marked decrease in elective surgery for peptic ulcer disease (PUD) following introduction of medical therapies including H_2-receptor antagonists, and more recently proton pump inhibitors with or without antibiotics for *H pylori* eradication. By contrast, the number of acute complications *e.g.* ulcer perforation and bleeding requiring emergency surgery, have remained quantitatively constant[1,2]. Peptic ulcer perforation is a serious complication which affects almost 10 % of PUD patients. Overall, PUD accounts for more than 70 % of mortality associated with the disease[3,4]. Several potential predicting factors for perforation have been evaluated in the literature, including use of ulcerogenic drugs (*e.g.* steroids, NSAIDs, immunosuppressive agents, *etc*.), and the development of an acute, rather than chronic peptic ulcer[5-8].

In this paper, we studied the main factors associated with mortality in a large number of patients undergoing surgery for perforated peptic ulcers (PPU) in a large referral academic hospital in southern Italy.

MATERIALS AND METHODS

Patients

The study population comprised 149 consecutive patients with an established intra-operative final diagnosis of PUD referred for emergency surgery to the 1st Department of General Surgery of the University of Bari. Bari is the main city of a province of about 1 500 000 inhabitants in the south-eastern coast of Italy. During a time spanning from 1988 to 1997 all patients were treated exclusively by open surgical approach, as agreed by all staff members. Since then, additional patients have been treated also by laparoscopy for PPU, but due to the scant number of cases, they were not included in the present analysis. Overall, there were 39 females and 110 males (mean age 52 years, range 16-95). The diagnosis of gastrointestinal ulcers was based on clinical features, blood tests, routine laboratory tests, and radiological findings (*i.e.* plain abdominal X-ray in all cases and abdominal CT scan in 87 % of patients). Invariably, the definitive diagnosis of PPU was obtained at surgery. The time between presumed perforation and surgery was considered delayed if longer than 12 h. The following factors were analysed: age >65 years, sex, previous ulcer history, associated medical diseases, delayed operation, site of ulcer, type of operation, shock on admission, postoperative general complications, postoperative intra-abdominal and/or wound infections.

Surgical procedure

An open surgical approach was performed leading to a non definitive operation (*i.e.* ulcer excision and suture with or without pyloroplasty) in 120 patients (80.5 %) and to definitive operations (*i.e.* Billroth II resection) in 29 patients (19.5 %). The decision to perform one or the other type of surgery depended on several known factors including location and extent of lesions, feasibility of a safe non-definitive surgery, presence or absence of anaesthesiological risk factors, and surgeon' s attitude. No truncal or selective vagotomies were performed. All operations were performed by the same surgical staff whose colleagues were well trained in gastrointestinal surgery.

Statistical analysis

All calculations were performed with the *NCSS 2001* statistical software (Kaysville, UT, USA). The chi-square test was used to compare proportions. A two-tailed probability (*P*) value of less than 0.05 was considered statistically significant[9,10].

RESULTS

The time between perforation and surgery was delayed in 51 patients (34.2 %), 79 patients (53.0 %) had associated diseases which are listed in Table 1. Cardiovascular, chronic obstructive pulmonary diseases and diabetes mellitus were the most frequently (over 65 %) associated conditions. A previous history of PUD was found in 53 (35.6 %) patients and 9 (6.0 %) were shocked on admission. Gastric and duodenal ulcers were perforated in 23 (15.4 %) and 126 (84.6 %) patients, respectively.

Table 1 Associated diseases in study group

Cardiovascular disease	27
Diabetes mellitus	20
Chronic obstructive pulmonary disease	19
Impaired liver function	8
Renal failure	7
Coagulation disorders	6
Cerebrovascular disease	4
Neurological disease (others)	3
Malignancy	2
Thyroid disease	1
Gallstones	1
Acute pancreatitis	1
Total	99

Types of postoperative complications are reported in Table 2. The most frequent events were due to general, rather than abdominal complications or wound infections.

Table 2 Postoperative complications

General	
Cardiac	7
Respiratory	7
Sepsis	7
Renal	5
Mental disorders	2
Ictus	1
Deep venous thrombosis	1
Total	30
Abdominal	
Abscess	6
Bleeding	2
Stenosis	2
Total	10
Wound infections	8
Total	48

The analysis of factors associated with mortality is depicted in Table 3. Of the 149 patients, 6 died yielding an overall mortality rate of 4.0 %. The presence of one or more associated diseases, delay in surgical approach, shock on admission, postoperative abdominal complications (6 dehiscence/abscess, 2 bleedings, 2 stenosis) and the postoperative wound infections were all significantly ($0.0001<P<0.04$) associated with increased mortality in patients undergoing surgery for PPU. By contrast, age, sex, previous history and site of peptic ulcer, type of surgical treatment and the development of postoperative general complications were not associated with increased mortality.

Table 3 Analysis of factors associated with mortality in 149 patients undergoing surgery for perforated peptic ulcer

	n	Mortality (%)	*P* value
Male:Female	110:39	3.6 *vs.* 5.1	NS
Age (<65: >65 years)	63:86	1.6 *vs.* 5.8	NS
Previous ulcer history (yes:no)	53:96	5.7 *vs.* 3.1	NS
Associated disease (yes:no)	79:70	7.6 *vs.* 0.0	0.02
Delayed operations (yes:no)	41:108	9.8 *vs.* 1.9	0.04
Site (duodenal:gastric)	126:23	3.1 *vs.* 8.7	NS
Operation type (non definitive:definitive)	120:29	2.5 *vs.* 10.3	NS
Shock on admission (yes : no)*	9:140	55.6 *vs.* 0.7	0.0001
Postop. general complications (yes:no)	30:119	6.7 *vs.* 3.4	NS
Postop. abdominal complications (yes:no)*	10:139	50.0 *vs.* 0.7	0.0001
Postoperative wound infections (yes:no)*	8:141	37.5 *vs.* 2.1	0.0001

Data analyzed by χ^2 test and *Fisher's exact test.

DISCUSSION

Several factors might contribute to increased postoperative mortality in patients with PPU. Perforation has been found to be a major complication of PUD with a mortality rate ranging from 6 % to 31 %[6-8, 11-20].

Age of patients with PPU has been gradually increasing over the last years[21-23]. In this series, an age >65 years tended to be associated with increased mortality. This finding is in line with other studies in which older patients frequently had associated diseases, or they were more on NSAIDs treatment[8,16,22]. It should be also noted that the mean age of patients from this series was considerably lower than that from patients included in different studies. Thus, such differences might account for the markedly lower overall mortality rate (4.0 %), as compared to other series[6-8, 11-20].

In accord with others[19, 23], we could not find that male sex was associated with a greater mortality rate. Also, there was no significant difference in mortality rate between gastric or duodenal ulcer and in patients with or without previous ulcer history. Apparently, these findings were at variance with those from two other studies[13, 24] reporting a higher mortality rate in gastric peptic ulcer than in duodenal peptic ulcer and in acute peptic ulcer than in chronic peptic ulcer. Such apparent discrepancies might be explained by the characteristics of patients included in the study, and/or by different age or different surgical procedures[16,18].

This study confirmed the previous observations[5,8,15,25-28] that shock on admission and delayed operation were both associated with a greater mortality rate.

Despite the fact that surgery remains the choice of treatment for PPU, the type of procedure in emergency is still debated. In some series definitive surgery had lower rates of recurrence and mortality than non definitive surgery[16,18,19,29,30]. Otherwise, non-definitive surgery was more frequently performed in patients admitted with more risk factors than definitive surgery, and this might explain the higher mortality rate of such studies. Moreover, diffusion of the laparoscopic approach to PPU with less surgical trauma and less metabolic and physiological disturbances, has determined an increase of non definitive surgical procedures performed by simple closures[3,20,22,31]. In the present study, there was no difference in mortality rate between definitive (*i.e.* Billroth II resection) or non-definitive (*i.e.* ulcer excision and suture with or without pyloroplasty)

surgical procedure.

It has been reported that mortality rate increased progressively with increasing numbers of risk factors[6,8]. Indeed, the mortality rate was 0 % and 7.6 % in the group of patients without and with associated diseases, respectively. In the present study cardiovascular, chronic obstructive pulmonary diseases and diabetes mellitus were the most frequent concomitant diseases. Besides, 6 patients developing a postoperative abscess had a previous history of chronic obstructive pulmonary disease. A possible explanation for such an outcome could be the reduced tissue oxygenation resulting in damage of post-surgical wound healing process. This possibility was supported by recent studies from our group at the intestinal level in both experimental and clinical conditions[32-36].

We also observed that in patients developing postoperative abdominal complications (*i.e.* 6 abscesses, 2 bleedings, and 2 stenosis) and wound infections, the mortality rate was significantly higher (P=0.0001) than those without abdominal complications. We would like to explain that such a striking difference was due to the development of a generalized sepsis in the group of patients with intra-abdominal abscess. Indeed, 83.3 % (*i.e.* 5/6) of patients with dehiscence and abdominal abscess, died in the postoperative period, otherwise, in this group with postoperative complications, the appearance of stenosis or bleeding was not associated with a higher mortality rate. In our experience the presence of wound infection appeared to be a predictive factor for mortality. A careful analysis of the 3 patients who died of wound infection, however, revealed that the cause of exitus was septicaemia complicating an abdominal abscess. By contrast, postoperative general complications did not influence the prognosis of patients with PPU.

In conclusion, concomitant diseases, shock on admission, delayed surgery, and postoperative abdominal and wound infections are factors significantly associated with fatal outcomes in patients undergoing emergency surgery for perforated peptic ulcer. Older age tends to fulfill a similar trend. Thus, such factors need to be carefully taken into account during the general workup of patients admitted for PPU.

REFERENCES

1 **Christensen A**, Bousfield R, Christiansen J. Incidence of perforated and bleeding peptic ulcers before and after the introduction of H2-receptor antagonist. *Ann Surg* 1988; **207**: 4-6
2 **Bliss DW**, Stabile BE. The impact of ulcerogenic drugs on surgery for the treatment of peptic ulcer disease. *Arch Surg* 1991; **126**: 609-612
3 **Lau WL**, Leung KL, Kwong KH, Davey IC, Robertson C, Dawson JJ, Chung SC, Li AK. A randomised study comparing laparoscopic versus open repair of perforated peptic ulcer using suture or sutureless technique. *Ann Surg* 1996; **224**: 131-138
4 **Svanes C**, Salvesen H, Stangeland L, Svanes K, Soreide O. Perforated peptic ulcer over 56 year. Time trends in patients and disease characteristics. *Gut* 1993; **34**: 1666-1671
5 **Boey J**, Wong J, Ong GB. A prospective study of operative risk factors in perforated duodenal ulcers. *Ann Surg* 1982; **195**: 265-269
6 **Boey J**, Choi SKY, Alagaratnam TT, Poon A. Risk stratification in perforated duodenal ulcers. *Ann Surg* 1987; **205**: 22-26
7 **Boey J**, Wong J. Perforated duodenal ulcers. *World J Surg* 1987; **11**: 319-324
8 **Evans JP**, Smith R. Predicting poor outcome in perforated peptic ulcer disease. *Aust N Z J Surg* 1997; **67**: 792-795
9 **Armitage P**, Berry G. Statistical methods in medical research. *Blackwell Scientific Publ* 1994
10 **Dawson B**, Trapp RG. Basic & Clinical Biostatistics. New York: *McGraw-Hill* 2001
11 **Gunshefsky L**, Flancbaum L, Brolin R, Frankel A. Changing pattern in perforated peptic ulcer disease. *Am Surg* 1990; **56**: 270-274
12 **Greiser WB**, Bruner BW, Shamoun JM, Jurkovich GJ, Ferrara JJ. Factors affecting mortality in patients operated upon for complications of peptic ulcer disease. *Am Surg* 1989; **55**: 7-11
13 **Hodnett RM**, Gonzalez F, Lee WC, Nance FC, Deboisblanc R. The need for definitive therapy in the management of the perforated gastric ulcers. Review of 202 cases. *Ann Surg* 1989; **209**: 36-39
14 **Horowitz J**, Kukora JS, Ritchie WP Jr. All perforated ulcers are not alike. *Ann Surg* 1989; **209**: 693-697
15 **Irvin TT**. Mortalità and perforated peptic ulcer: a case for risk stratification in elederly patients. *Br J Surg* 1989; **76**: 215-218
16 **Suter M**. Surgical treatment of perforated peptic ulcer. Is there a need for a change? *Acta Chir Belg* 1993; **93**: 83-87
17 **Lee FY**, Leung KL, Lai BS, Ng SS, Dexter S, Lau WY. Predicting mortality and morbidity of patients operated on for perforated peptic ulcers. *Arch Surg* 2001; **139**: 90-94
18 **Blomgren LGM**. Perforated peptic ulcer: long-term results after simple closure in the elderly. *World J Surg* 1997; **21**: 412-415
19 **Sillakivi T**, Lang A, Tein A, Peetsalu A. Evaluation of risk factors for mortality in surgically treated perforated peptic ulcer. *Hepatogastroenterology* 2000; **47**: 1765-1768
20 **Michelet I**, Agresta F. Perforated peptic ulcer: laparoscopic approach. *Eur J Surg* 2000; **166**: 405-408
21 **Svanes C**, Salvesen H, Stangeland L, Svanes K, Soreide O. Perforated peptic ulcer over 56 years. Time trend in patients and disease characteristics. *Gut* 1993; **34**: 1666-1671
22 **Cocks JR**. Perforated peptic ulcer - the changing scene. *Dig Dis* 1992; **10**: 10-16
23 **Walt R**, Katschinski B, Logan R, Ashley J, Langman M. Rising frequency of ulcer perforation in elderly people in the United Kingdom. *Lancet* 1986; **3**: 489
24 **McGee GS**, Sawyers JL. Perforated gastric ulcers. *Arch Surg* 1987; **122**: 555-561
25 **Hamby LS**, Zweng TN, Strodel WE. Perforated gastric and duodenal ulcer: an analysis of prognostic factors. *Am Surg* 1993; **59**: 319-324
26 **Mattingly SS**, Ram MD, Griffin WO Jr. Factors influencing morbidity and mortality in perforated duodenal ulcer. *Am Surg* 1980; **46**: 61-66
27 **McIntosh JH**, Berman K, Holliday FM, Byth K, Chapman R, Piper DW. Some factors associated with mortality in perforated peptic ulcer: a case control study. *J Gastroenterol Hepatol* 1996; **11**: 82-87
28 **Wakayama T**, Ishizaki Y, Mitsusada M, Takahashi S, Wada T, Fukushima Y, Hattori H, Okuyama T, Funatsu H. Risk factors influencing the short-term results of gastroduodenal perforation. *Surg Today* 1994; **24**: 681-687
29 **Jordan PH**, Thornby J. Perforated pyloroduodenal ulcers. Long-term results with omental patch closure and parietal cell vagotomy. *Ann Surg* 1995; **221**: 479-488
30 **Robles R**, Parrilla P, Lujan JA, Torralba JA, Cifuentes J, Liron R, Pinero A. Short note: long-term follow-up of bilateral truncal vagotomy and pyloroplasty for perforated duodenal ulcer. *Br J Surg* 1995; **82**: 665
31 **Matsuda M**, Nishiyama M, Hanai T, Saeki K, Watanabe T. Laparoscopic omental patch repair for perforated peptic ulcer. *Ann Surg* 1995; **221**: 336-240
32 **Testini M**, Scacco S, Loiotila L, Regina G, Vergari R, Papa F, Paccione F. Comparison of oxidative phosphorilation in the small vs. large bowel anastomosis. *Eur Surg Res* 1998; **30**: 1-7
33 **Testini M**, Piccinni G. Wound healing of intestinal anastomosis after digestive surgery under septic condition. *World J Surg* 1999; **23**: 1315-1316
34 **Testini M**, Margari A, Amoruso M, Lissidini G, Bonomo GM. Le deiscenze nelle anastomosi colo-rettali: fattori di rischio. *Ann Ital Chir* 2000; **71**: 433-440
35 **Testini M**, Piccinni G, Amoruso M, Di Venere B, Nicolardi V, Bonomo GM. Chronic obtructive pulmonary disease and failure of large bowel anastomosis. *It J Coloproctol* 2000; **3**: 91-94
36 **Testini M**, Portincasa P, Scacco S, Piccinni G, Minerva F, Lissidini G, Papa F, Loiotila L, Bonomo GM, Palasciano G. Contractility *in vitro* and mitochondrial response in small and large anastomosed rabbit bowel. *World J Surg* 2002; **26**: 493-498

Edited by Wang XL

P.O.Box 2345, Beijing 100023,China
Fax: +86-10-85381893
E-mail: wjg@wjgnet.com www.wjgnet.com

World J Gastroenterol 2003;9(10):2341-2343
World Journal of Gastroenterology
 ISSN 1007-9327

• BRIEF REPORTS •

Effect of resveratrol on cell cycle proteins in murine transplantable liver cancer

Liang Yu, Zhong-Jie Sun, Sheng-Li Wu, Cheng-En Pan

Liang Yu, Zhong-Jie Sun, Sheng-Li Wu, Cheng-En Pan, Department of Hepatobiliary Surgery, First Hospital of Xi' an Jiaotong University, Xi' an 710061, Shaanxi Province, China
Supported by Traditional Chinese Medicine Bureau Foundation of Shaanxi Province, No. 2001-035
Correspondence to: Dr. Liang Yu, Department of Hepatobiliary Surgery, First Hospital of Xi' an Jiaotong University, Xi' an 710061, Shaanxi Province, China. yuliang@163.com
Telephone: +86-29-5324009
Received: 2002-11-11 **Accepted:** 2002-12-25

Abstract

AIM: To study the antitumour activity of resveratrol and its effect on the expression of cell cycle proteins including cyclin D1, cyclin B1 and p34cdc2 in transplanted liver cancer of murine.

METHODS: Murine transplanted hepatoma H22 model was used to evaluate the *in vivo* antitumor activity of resveratrol. Following abdominal administration of resveratrol, the change in tumour size was recorded and the protein expression of cyclin D1, cyclin B1 and p34cdc2 in the tumor and adjacent noncancerous liver tissues were measured by immunohistochemistry.

RESULTS: Following treatment of H22 tumour bearing mice with resveratrol at 10 or 15 mg/kg bodyweight for 10 days, the growth of murine transplantable liver cancer was inhibited by 36.3 % or 49.3 %, respectively. The inhibitory effect was significant compared to that in control group ($P<0.05$). The level of expression of cyclin B1 and p34cdc2 protein was decreased in the transplantable murine hepatoma 22 treated with resveratrol whereas the expression of cyclin D1 protein did not change.

CONCLUSION: Resveratrol exhibits anti-tumour activities on murine hepatoma H22. The underlying anti-tumour mechanism of resveratrol might involve the inhibition of the cell cycle progression by decreasing the expression of cyclinB1 and p34cdc2 protein.

Yu L, Sun ZJ, Wu SL, Pan CE. Effect of resveratrol on cell cycle proteins in murine transplantable liver cancer. *World J Gastroenterol* 2003; 9(10): 2341-2343
http://www.wjgnet.com/1007-9327/9/2341.asp

INTRODUCTION

Resveratrol (3,4,5-trihydroxy-trans-stilbene) is a kind of phytoalexin found in root extract of the weed polygonum cuaspidatum and in grape skins as well as red wine. Studies have demonstrated that resveratrol can alter the synthesis and secretion of lipids and lipoproteins by liver cells, block human platelet aggregation and inhibit the synthesis of pro-aggregatory and proinflammtory eicosanoids by platelets and neutrophils[1-5]. Moreover, some reports have shown that resveratrol is a potential chemopreventive agent of cancer and it can prevent tumor growth and metastasis in human lung carcinoma, pancreatic cancer, prostate cancer, bronchial epithelioma cancer and breast cancer models[6-10]. The present investigation evaluated the potency of resveratrol on tumour cell growth and proliferation and on expression of cell cycle proteins in a transplantable murine hepatoma 22 model.

MATERIALS AND METHODS

Materials

Resveratrol was purchased from Sigma Co (USA). The resveratrol was dissolved and sterilized in dimethyl sulfoxide (DMSO) first and then diluted to the required working concentration in RPMI-1640 (Gibco, USA) containing 10 % calf serum (SiJiQing Co, Hangzhou, China). MS-110cdk1/p34cdc2 Ab-1 0.1 ml, MS-210 cyclin D1/bcl-1 Ab-1 0.1 ml, MS-338 cyclin B1 Ab-1 0.1 ml were purchased from Santa Cruz Co (USA). S-P ultra sensitive immunostaining kit was purchased from Maixin Biotechnology Developing Co (Fuzhou, China). Mouse hepatocellular carcinoma cell line H22 was kindly supplied by Cheng Wei (Center of Molecular Biology, First Affiliated Hospital, Xi' an Jiaotong University). Balb/c mice were purchased from the Animal Center of Xi' an Jiaotong University.

Methods

Suppressive effect of resveratrol on transplanted liver cancer of mouse H22 cells were first subcultured in RPMI 1640 containing 10 % fetal bovine serum. Then the cells were washed twice and resuspended in RPMI 1640 culture medium (1×10^8/ml). About 0.2 ml cell solution (including 2×10^7 cells) was taken and injected into the right groin of 5 Balb/c mice. After 14 days, when tumors of 3-5 mm in diameter formed in the right groin of these mice, they were taken out and sheared into small pieces of 1 mm^3 under sterile condition. Forty Balb/c mice were anesthetized by using coelio-injection of pentobarbitone (70 mg/Kg) and laparotomy was performed. Under sterile condition their middle lobes of liver were punctured to form a 3 mm-long sinus tract and a small piece of tumor tissue was put into each sinus tract. Then these mice were divided into 4 groups randomly: one control group and 3 experimental groups. The experimental groups were designed to be injected with resveratrol (dissolved in DMSO and diluted to the working concentration of 25 mM in RPMI-1640 containing 10 % calf serum) at 5, 10 or 15 mg/kg body weight while the control group was designed to be given the same volume of the solution as for experimental group but absent of resveratrol. Twenty-four hours following liver tumour transplantation, each mouse was injected corresponding dosage of resveratrol into its abdominal cavity once a day for 10 days. These mice were then sacrificed on the following day after the last injection. After the maximum diameter and transverse length of tumour were measured, the hepatocellular carcinoma tissues and adjacent noncancerous liver tissues were sampled and fixed in 10 % formalin.

Measurement of tumour volume The tumour volume was

calculated using formula V=1/2 (maximum diameter x transverse length^2). The suppressive rate of tumour growth was calculated as [(mean V of tumour in control group - mean V of tumour in experimental group)/mean V of tumour in control group]×100 %.

Determination of protein expression of cyclin D1, cyclin B1 and p34cdc2 in murine transplantable liver cancer tissue

The tumour tissues and adjacent noncancerous liver tissues taken from therapeutic group (resveratrol in 10 mg/kg) and control group were 10 % formalin-fixed, paraffin-embedded and cut into 4 μm thick sections for staining. PBS of 0.01 mol· L^{-1} was used to substitute for primary antibody for negative control while a breast cancerous tissue expressing cyclin D1 and a tonsil tissue expressing cyclin B1 and cdk1/p34cdc2 were used for positive controls. The working concentration of each antibody was cyclin B1 (1:100), cyclin D1 (1:40) and cdk1/p34cdc2 (1:70), respectively. The staining procedures used were as described in S-P immunostaining kit. The sections were examined twice on different days by the same pathologist and the distribution of positively stained cells for each protein was evaluated semi-quantitatively by calculating the percentage of positive cells in nonoverlaping microscopic fields. The protein expression was then scored arbitrarily as "-" <5 % positive cells, "+" 5-50 % positive cells, "++" >50 % positive cells. χ^2 test was used to evaluate the statistical significance of the difference between experimental and control groups.

RESULTS

Suppressive effect of resveratrol on murine transplantable liver cancer

Except 2 Balb/c mice (one in control group and one in 15 mg/kg resveratrol therapeutic group), all the mice inoculated with hepatocarcinoma cell line H22 were successively transplanted with liver cancer. After treatment of the tumour bearing mice with 5, 10 or 15 mg/kg resveratrol for 10 days, the tumour size was reduced from 134 mm^3±40 mm^3 in control group to 105 mm^3±14mm^3, 85 mm^3±22mm^3 and 68 mm^3±17mm^3 in experimental groups, resulting in an inhibition rate of tumour growth of 21.6 %, 36.3 % and 49.3 %, respectively. The inhibition effect in the latter 2 therapeutic groups was significant compared with that in control group (all P<0.05) (Table 1).

Table 1 The suppressing effect of resveratrol on murine transplanted liver tissue

	Dose (mg/kg)	No. of mice (begin/end)	Tumour size (mm^3, $\bar{x}$±s)	GIR (%)
Control group	0	10/9	134±40	
Resveratrol	5.0	10/10	105±14[a]	21.6
	10.0	10/10	85±22[b]	36.3
	15.0	10/9	68±17[b]	49.3

[a]P>0.05, [b]P<0.01, *vs* control.

Effect of resveratrol on expression of cyclin D1, cyclin B1 and p34cdc2 in murine liver cancer tissue

Cyclin D1 immunoreactivity was observed in the nucleolus of tumour cell, cyclin B1 immunoreactivity and p34cdc2 immunoreactivity were observed in the cytoplasm of tumour cell. The expression level of cyclin D1, cyclin B1 and p34cdc2 in transplanted liver cancer tissue was significantly higher than that of adjacent noncancerous liver tissues in control group (All P<0.05) (Tables 2-4). Following treatment with resveratrol, a depressed expression of cyclin B (77.8 % *vs* 30.0 %, P<0.05) and p34cdc2 protein (88.9 % *vs* 40.0 %, P<0.05) was observed, but the expression of cyclin D1 protein (66.7 % *vs* 60.0 %, P>0.05) did not change.

Table 2 Effect of resveratrol on the expression of cyclin D1 in murine liver tumor and adjacent noncancerous liver tissues

	No. of mice	Cyclin D1			Positive rate (%) (+, ++)
		-	+	++	
Noncancerous tissues	9	9	0	0	0
Control group	9	3	2	4	66.7[a]
Therapeutic group	10	4	3	3	60.0[b]

[a]P<0.01, *vs* noncancerous tissues; [b]P>0.05, *vs* control.

Table 3 Effect of resveratrol on the expression of cyclin B1 in murine liver tumor and adjacent noncancerous liver tissues

	No. of mice	CyclinB1			Positive rate (%) (+,++)
		-	+	++	
Noncancerous tissues	9	7	1	1	22.2
Control group	9	2	2	5	77.8[a]
Therapeutic group	10	7	2	1	30.0[b]

[a]P<0.05, *vs* noncancerous tissues; [b]P<0.05, *vs* control.

Table 4 Effect of resveratrol on the expression of p34cdc2 in murine liver tumor and adjacent noncancerous liver tissues

	No. of mice	p34cdc2			Positive rate (%) (+,++)
		-	+	++	
Noncancerous tissues	9	7	2	0	22.2
Control group	9	1	3	5	88.9[a]
Therapeutic group	10	6	3	1	40.0[b]

[a]P<0.01, *vs* noncancerous tissues; [b]P<0.05, *vs* control.

DISCUSSION

In 1997 Park *et al*, showed that resveratrol inhibited tumorigenesis in a mouse skin cancer model[11]. Since then, many studies have shown that resveratrol has suppressive effects on tumour cells in human lung carcinoma, prostate cancer, bronchial epithelioma and breast cancer models[12-14]. The ability of resveratrol to inhibit cellular events associated with tumour initiation, promotion, and progression might be attributed to its anticyclooxygenase activity (COX-1), inducing apoptosis of tumour cells, antagonizing mutation, antioxidation and anti-free radicals activity and its effect on cell cycle[15,16].

Recent studies have shown that many drugs exhibited their anti-tumour activity by interfering cell cycles. The cell cycle regulators have thus become a new target in drug discovery research. Of the 3 cell cycle regulators of cyclins, CDKs, and CKIs which have been found, CDKs is the core of the modulation network, which is positively regulated by cyclins and negatively by CKIs. Cyclin D1, a member of cyclins family, modulates mainly G1/S stage transition. Under normal conditions, the amount of cyclin D1 is invariable in G1 stage and its overexpression will lead to cells passing through G1/S without control, which is considered to be associated with carcinogenesis. Cyclin B1 is related mainly to the completion of M stage. CDC2 (CDK1) gene, a modulating core of G2/M inspect point, codes for p34cdc2 protein. The p34cdc2 combines with cyclin B1 to form MPF which plays an important role in the process from G2 stage to M stage. Studies have shown that cyclin B1-CDC2 was in activated state in many tumour cell lines no matter what the state of DNA was. Even

though cells had DNA damage, they could still enter the cleavage stage. Therefore, p34cdc2 and cyclinB1 were also associated with carcinogenesis[17].

In the present investigation, resveratrol was administered into murine abdomen and its potency on growth and proliferation of H22-innoculated tumour was evaluated by measuring the size of hepatoma and examining the expression of cell cycle proteins. The tumour size was found to be reduced by each dosage of 5, 10 or 15 mg/kg of resveratrol for 10 days. When the higher dosage of resveratrol was applied, the tumour size was significantly reduced, the inhibition rate of tumour growth by 10 or 15 mg/kg reached to 36.3 % and 49.3 %, respectively (P<0.01). We also found the protein expression of cyclin D1, cyclin B1 and p34cdc2 in murine transplanted liver cancer tissue was significantly higher than that in adjacent noncancerous liver tissues, suggesting that the overexpression of these cell cycle proteins may play a role in the onset and development of carcinoma. Compared with control group, a depressed expression of cyclin B1 and p34cdc2 protein was observed in the transplantable murine hepatoma following treatment with resveratrol, suggesting that the anti-tumor mechanism of resveratrol may be to prevent mitosis of tumor cells by suppressing the protein expression of cyclin B1and p34cdc2, and thus, interfering with the process of tumor cells from S stage to G2/M stage.

In short, the data presented in this paper suggest that resveratrol has an apparent antitumour activity, and blocking of S stage of tumour cells may be the underlying mechanism. The demonstration of modulating effect of resveratrol on cell cycle should provide certain theoretical basis for further study of resveratrol and other cell cycle interfering agents.

REFERENCES

1 **Afaq F**, Adhami VM, Ahmad N. Prevention of short-term ultraviolet B radiation-mediated damages by resveratrol in SKH-1 hairless mice small star, filled. *Toxicol Appl Pharmacol* 2003; **186**: 28-37

2 **Fremont L**. Biological effects of resveratrol. *Life Sci* 2000; **66**: 663-673

3 **Sato M**, Ray PS, Maulik G, Maulik N, Engelman RM, Bertelli AA, Bertelli A, Das DK. Myocardial protection with red wine extract. *J Cardiovasc Pharmacol* 2000; **35**: 263-268

4 **Roemer K**, Mahyar-Roemer M. The basis for the chemopreventive action of resveratrol. *Drugs Today* 2002; **38**: 571-580

5 **Zou JG**, Wang ZR, Huang YZ, Cao KJ, Wu JM. Effect of red wine and wine polyphenol resveratrol on endothelial function in hypercholesterolemic rabbits. *Int J Mol Med* 2003; **11**: 317-320

6 **Kimura Y**, Okuda H. Resveratrol isolated from Polygonum cuspidatum root prevents tumor growth and metastasis to lung and tumor-induced neovascularization in Lewis lung carcinoma-bearing mice. *J Nutr* 2001; **131**: 1844-1849

7 **Narayanan BA**, Narayanan NK, Re GG, Nixon DW. Differential expression of genes induced by resveratrol in LNCaP cells: P53-mediated molecular targets. *Int J Cancer* 2003; **104**: 204-212

8 **Ding XZ**, Adrian TE. Resveratrol inhibits proliferation and induces apoptosis in human pancreatic cancer cells. *Pancreas* 2002; **25**: e71-76

9 **Kuo PL**, Chiang LC, Lin CC. Resveratrol- induced apoptosis is mediated by p53-dependent pathway in Hep G2 cells. *Life Sci* 2002; **72**: 23-34

10 **Banerjee S**, Bueso-Ramos C, Aggarwal BB. Suppression of 7,12-dimethylbenz(a)anthracene-induced mammary carcinogenesis in rats by resveratrol: role of nuclear factor-kappaB, cyclooxygenase 2, and matrix metalloprotease 9. *Cancer Res* 2002; **62**: 4945-4954

11 **Park JW**, Choi YJ, Jang MA, Lee YS, Jun DY, Suh SI, Baek WK, Suh MH, Jin IN, Kwon TK. Chemopreventive agent resveratrol, a natural product derived from grapes, reversibly inhibits progression through S and G2 phases of the cell cycle in U937 cells. *Cancer Lett* 2001; **163**: 43-49

12 **Mollerup S**, Ovrebo S, Haugen A. Lung carcinogenesis: resveratrol modulates the expression of genes involved in the metabolism of PAH in human bronchial epithelial cells. *Int J Cancer* 2001; **92**: 18-25

13 **Kozuki Y**, Miura Y, Yagasaki K. Resveratrol suppresses hepatoma cell invasion independently of its anti-proliferative action. *Cancer Lett* 2001; **167**: 151-156

14 **Rodrigue CM**, Arous N, Bachir D, Smith-Ravin J, Romeo PH, Galacteros F, Garel MC. Resveratrol, a natural dietary phytoalexin, possesses similar properties to hydroxyurea towards erythroid differentiation. *Br J Haematol* 2001; **113**: 500-507

15 **Young J**, Barker M, Fraser L, Walsh MD, Spring K, Biden KG, Hopper JL, Leggett BA, Jass JR. Mutation searching in colorectal cancer studies: experience with a denaturing high-pressure liquid chromatography system for exon-by-exon scanning of tumour suppressor genes. *Pathology* 2002; **34**: 529-533

16 **Takahashi M**, Shimomoto T, Miyajima K, Iizuka S, Watanabe T, Yoshida M, Kurokawa Y, Maekawa A. Promotion, but not progression, effects of tamoxifen on uterine carcinogenesis in mice initiated with N-ethyl-N'-nitro-N-nitrosoguanidine. *Carcinogenesis* 2002; **23**: 1549-1555

17 **Pommier Y**, Kohn KW. Cell cycle and checkpoints in oncology: new therapeutic targets. *Med Sci* 2003; **19**: 173-186

Edited by Liu HX and Wang XL

P.O.Box 2345, Beijing 100023,China
Fax: +86-10-85381893
E-mail: wjg@wjgnet.com www.wjgnet.com

World J Gastroenterol 2003;9(10):2344-2347
World Journal of Gastroenterology
 ISSN 1007-9327

• BRIEF REPORTS •

Rapid and high throughput detection of HBV YMDD mutants with fluorescence polarization

Yui-Jie Bai, Jin-Rong Zhao, Guan-Ting Lv, Wen-Hong Zhang, Yan Wang, Xiao-Jun Yan

Yui-Jie Bai, Jin-Rong Zhao, Guan-Ting Lv, Wen-Hong Zhang, Yan Wang, Xiao-Jun Yan, Institute of Genetic Diagnosis, Fourth Military Medical University, Xi' an 710032, Shannxi Province, China
Supported by Shen Zhen Syno Gene Digital Co. Ltd
Correspondence to: Dr. Yu-Jie Bai, Institute of Genetic Diagnosis, Fourth Military Medical University, Xi' an 710032, Shannxi province, China. yujiebai@163.com
Telephone: +86-29-3216587 **Fax:** +86-29-3285729
Received: 2003-04-09 **Accepted:** 2003-05-19

Abstract

AIM: To develop a simple and rapid detection of HBV gene variants and prediction of lamivudine-resistance in patients.

METHODS: Initially, plasmids harboring the wild-type or mutant HBV DNA fragments were used in a model system. The technique was then applied to clinical samples for an analysis of YMDD mutations. The sera were extracted from chronic hepatitis patients who had received lamivudine treatment for more than one year. P region gene of HBV was amplified by polymerase chain reaction. The excess primers and dNTPs in PCR products were removed by cleaning-up reagents. Template-directed dye-terminator incorporation reaction was performed and R110 or TAMRA labeled acyclo-terminator was added on the 3' end of TDI-primer specifically. Fluorescence polarization value was measured with Victor 2 multilabel counter and the genotypes of HBV were analyzed.

RESULTS: The YMDD genotypes in recombined positive plasmid and 56 serum samples of HBV infected patients were analyzed by using our TDI-FP method and the specificity and sensitivity were confirmed by DNA sequencing. Five of 56 serum samples showed YVDD phenotype (9 %), including 1 YMDD and YVDD mixed infection. Four of 56 showed YIDD phenotype (7.1 %).

CONCLUSION: This is a simple, rapid, low cost and high throughput assay to detect HBV polymerase gene variants and suitable for large-scale screening and prediction of the lamivudine-resistance in clinical samples.

Bai YJ, Zhao JR, Lv GT, Zhang WH, Wang Y, Yan XJ. Rapid and high throughput detection of HBV YMDD mutants with fluorescence polarization. *World J Gastroenterol* 2003; 9(10): 2344-2347
http://www.wjgnet.com/1007-9327/9/2344.asp

INTRODUCTION

Hepatitis virus B (HBV) is the causative agent of acute and chronic hepatitis. Approximately 400 million people worldwide are chronically infected with HBV. There are 170 million people infected in China[1,2]. HBV infection can lead to cirrhosis and primary hepatocellular carcinoma[3-5]. To date, interferon alfa and lamivudine are the only two agents approved for chronic hepatitis[6-10]. Because interferon alfa shows significant dose-dependent side effects, lamivudine has emerged as the first therapeutic agent[11-13]. Chinese patients are immunotolerant to interferon alfa because of acquisition of the disease during early childhood. The efficacy of interferon alfa in Chinese is lower than in white patients[14]. However, the efficacy of lamivudine is equal in Chinese and white patients.

Lamivudine is an antiviral nucleoside analogue. It can inhibit HBV reverse transcriptase activity and also act as a viral DNA chain terminator[15]. It is an inactive form before activated in hepatocytes by addition of phosphate group[2]. Lamivudine has two pathways of viral suppression. First, the active triphosphate metabolite is incorporated into newly synthesized HBV DNA to stop the chain extension. Second, it inhibits HBV reverse transcriptase. Its clinical use has resulted in HBeAg seroconversion and undetectable HBV DNA[16]. Unlike some nucleoside analogues, lamivudine is well tolerated and has an excellent safety profile. It has little or no effect on bone marrow, hepatocytes, kidney, or muscle tissues. However, long-term lamivudine treatment has led to emergence of HBV variants resistant to lamivudine therapy in some patients. The major sites of mutation are situated in the highly conserved motif, tyrosine (Y), methionine (M), aspartate (D), aspartate (D) (YMDD), of the catalytic (C) domain of the reverse transcriptase. Mutations consist of an amino acid substitution from M to either valine (A739G, $Met_{552} \rightarrow Val_{552}$) or isoleucine (G741T, $Met_{552} \rightarrow Ile_{552}$). Those mutations at the YMDD motif could render HBV resistant to lamivudine[17].

Fluorescence polarization assay (FPA) is a well established method used to analyze associations and dissociations between molecules in solution. This technique relates the change in the molecular size of a fluorophore to a change in the fluorescence polarization value (mp unit). The value changes indicate molecular associations or dissociations, so that FPA have been used to examine the interactions between molecules, such as protein-protein interactions, DNA-protein interaction and DNA-DNA hybridization.

Based on the FP detection method and the combined template-directed dye-terminator incorporation technique, a novel SNP (single nucleotide polymorphism) detection system (TDI-FP) has been developed[18]. It relies on the ability of AcycloPol™, a novel mutant thermostable polymerase from the Archeon family, to extend accurately an annealed probe by a single dye-terminator that is complementary to the opposite strand. It performs an assay to determine the base at a SNP site with many advantages over the other methods, such as homogeneity, low cost, high accuracy, high throughput and ready adaptation to automation. This method has been used to genotyping and SNP detections but has not, to our knowledge, been used to microbial mutant analysis yet.

Routine detection of HBV YMDD mutation after lamivudine treatment will be required to increase the efficacy. In this study, we undertook such a study using TDI-FP to detect the YMDD variants using mutagenesis plasmids and serum samples of 56 patients. This new method is a rapid, accurate and high throughout method to analyses the YMDD mutations**.** It will be a very useful tool for the clinical diagnosis and monitor of the lamivudine resistance.

MATERIALS AND METHODS

Instrumentation

Fluorescence polarization values were determined with the VICTOR2 multilabel counter (Perkin-Elmer, USA). The excitation and emission wavelengths were 544 nm and 595 nm for R110 and 485 nm and 535 nm for TAMRA, respectively. The samples were measured in 384 well PCR plates (MSP-3862 MJ Research, USA).

Reagents

Taq DNA polymerase, DNA extractor kit were obtained from Hua-mei Bio-tech Co., LTD. AcycloPrime™-FP detection kit (including AcycloPol™, AcycloTeminators™ labeled with R110 and TAMRA, shrimp alkaline phosphatase, exonuclease I) was product of Perkin-Elmer Co., Ltd.

Oligonucleotides

A set of PCR primers was designed to amplify the P region of HBV gene including the YMDD motif encoding sequences. 2 TDI-primers were also designed to encompass 17-21 bp 5' (A739Gtdi, sense) or 3' (G741T, antisense) to the nucleotide adjacent to the mutation sites using DNAStar software. 3 sets of primers for the site-directed mutagenesis were also designed using DNAStar software. All the primers, whose sequences are shown in Table 1, were synthesized using 391 DNA synthesizer (Perkin-Elmer, USA) by Bao Tai Ke Biotech Co.

Site-directed mutagenesis

The site-directed HBV YMDD mutants were made using Takara MutanBEST Kit by TaKaRa Biotechnology Co., Ltd. The A719G mutation was created using primers A739G*for* and A739G*rev*. The G741T mutation was created using primers G741T*for* and G741T*rev*. The A739G/G741T double mutants were made using primers diMut*for* and diMut*rev* with the plasmid pMD/HBV as a template respectively. (All the sequences of primers are shown in Table 1). The mutagenesis was detected according to the manufacture' s manual and verified by DNA sequencing.

Table 1 Primer sequences

Primer	Sequence
PCR*for*	5'-GCACTTGTATTCCCATCCCATCAT-3'
PCR*rev*	5'-GTATACCCAAAGACAAAAGAA-3'
739*tdi*	5'-CACTGTTTAGCTTTCAGTTAT-3'
741*tdi*	5'-CCCAATACCACATCATC-3'
A719G*for*	5'-CTTTCAGTTATGTGGATGATGTGGTA 3'
A719G*rev*	5' -CCAGACAGTGGGGGAAAGC 3'
G741T*for*	5'-CTTTCAGTTATATTGATGATGTGGTA 3'
G741T*rev*	5'- CCAGACAGTGGGGGAAAGC 3'
diMut*for*	5'-CTTTCAGTTATGTTGATGATGTGGTA 3'
diMut*rev*	5' -CCAGACAGTGGGGGAAAGC 3'

DNA samples

Venous blood (1 ml) was obtained from 56 patients with HBV chronic hepatitis B in Tangdu Hospital and Second Hospital of Jiaotong University, Xi' an.

Amplification of P region of HBV gene

PCR amplification was performed in a total volume of 50 μL, containing 1.5U Taq polymerase, PCR buffer, 0.1 mmol/L dNTPs, 1 μL of DNA sample (10 ng plasmid DNA or 100 ng genome DNA), 100 nmol/L PCR*for* and PCR*rev* primer each. The amplification procedure consisted of an initial denaturation and enzyme activation step at 94 ℃ for 5 min, followed by 40 cycles containing denaturation at 94 ℃ for 30 s, annealing at 56 ℃ for 30 s and extension at 72 ℃ for 1 min. After a final extension step at 72 ℃ for 10 minutes, the reactions were cooled to 4 ℃ until further use. The PCR reaction was carried out in a Touchgene gradient termal cycler (TECHNE Co. USA). In order to evaluate the amplification, each 5 μL of PCR products was separated on a 20 g/L agarose gel in 0.5× TBE buffer. The products were visualized and photographed under ultraviolet (UV) light.

Fluorescence polarization detection

Following PCR amplification, 2 μL clean-up reagent (including shrimp alkaline phosphatase and exonuclease I and reaction buffer) was added into 5 μL of PCR product and incubated at 37 ℃ for 60 min to remove unincorporated dNTPs and free primers. The enzymes were then heat-inactivated at 80 ℃ for 30 min.

TDI-FP was performed according to the protocol supplied by the manufacturer (Perkin-Elmer Life Sciences, Inc, USA). The reaction system consisted of 13 μL of AcycloPrime-FP mixture (containing 0.05 μL of AcycloPol™ polymerase, 2 μL of 10× reaction buffer, 1 μL of Acyclo-Terminator Mix, 0.5 μL mutant detection primer and 9.45 μL of water) and 7 μL of amplified and processed target DNA. After an initial denaturation at 95 ℃ for 2 min, 25 cycles at 95 ℃ for 15 sec and at 55 ℃ for 30 s were performed on a black 384-well PCR plate (MSP-3862, MJ Research). The fluorescence polarization values were measured on the 384-well plate using Victor2 multilabel counter directly.

RESULTS

PCR amplification

The PCR products were analyzed by agarose gel electrophoresis (Figure 1). A single band corresponding to a molecular size of 200 bp was detected, which was in concordance with expectation.

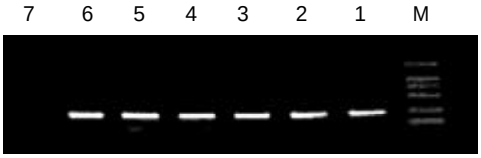

Figure 1 Electrophoretic analysis of PCR products. 1: plasmid pMD / HBV-A739G as PCR template, 2-6: serum samples as PCR template, 7: water as template (negative control), M: DNA molecular weight marker.

TDI-FP assay

Following PCR amplification, excess primers and dNTPs were removed. In the TDI extension reaction, 729*tdi* primer and dye-terminators mix (R110-acyGTP/ TAMRA-acyATP) were used to detect the A739G mutation (Figure 2). 741*tdi* primer and R110-acyCTP/TAMRA- acyATP) were used to detect the G741T mutation. The dye-terminator was incorporated and the TDI-primer was extended by one base complementary to the specific mutation site. The fluorescence intensity was measured using Victor 2 multilabel counter and the FP value was calculated by the instrument software automatically. The graph was created from an Excel workbook and the cluster of AcycloPrime-FP data was obtained by plotting the TAMRA polarization *vs* the R110 polarization. The FP reading of the samples was clustered into four distinct groups (Figure 3). As expected, for HBV YVDD samples, the values for R110-acyGTP were high and the values for TAMRA-acyATP were low, reflecting incorporation of the R110-acyGTP but not

TAMRA-acyATP. The genotypes were represented by the cluster in the lower left. Conversely, the YMDD genotypes appeared in the upper right. YMDD and YVDD double mutations or mixed infection samples appeared in the upper right. Negative controls were in the lower left cluster (Figure 3). For the G741T detection, the YIDD samples appeared in the upper left, YMDD samples in the lower right and the negative control in the lower left.

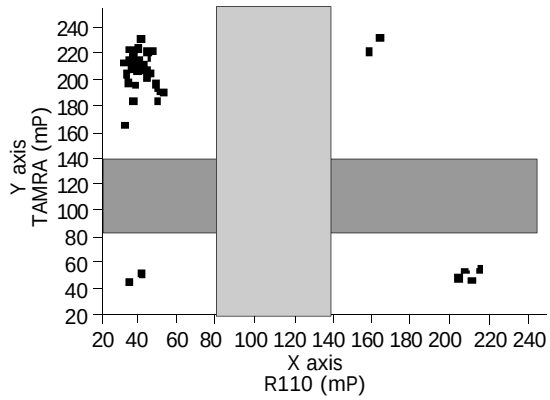

Figure 3 TDI-FP analysis data of YMDD mutation.

Detection of YMDD mutation in clinical samples

To evaluate the utility and accuracy of the TDI-FP in clinical samples, 56 serum samples from patients with chronic hepatitis B were analyzed. Among the sera analyzed, the wild-type YMDD variant was detected in 46 (82 %), the YVDD variant in 5 (8.9 %) and the YIDD in 4 (7.1 %). In one patient (1.8 %), both YMDD and YVDD variants were detected, which might reflect a mixed infection.

DISCUSSION

As reported before, the major drawback to the therapy of lamivudine is the emergence of drug-resistance due to the HBV DNA mutations. The patients who have lamivudine resistant HBV variants infection are more likely to develop more severe liver damage than those who do not have drug-resistant mutants. The mutation at YMDD (YMDD→YVDD or YMDD →YIDD) is considered to be the major lamivudine-resistance related variants. DNA sequencing is considered as the ideal method for characterizing DNA mutants, but it can not be afforded by most laboratories, especially clinical laboratories due to the cost and equipment requirement. Type-specific PCR, PCR-RLFP and PCR-SSCP have been used to detect HBV YMDD mutants. However, all the methods have drawbacks, e.g. lack of accuracy, difficulty in determining the mutation sites exactly or detecting mixed infection[19].

We reported here, for the first time, the successful application of the TDI-FP to detect the HBV YMDD mutation in hepatitis B patients. As a homogenous assay, the FP value reflected the total sum of free and incorporated dye-terminators. Two major factors affecting the result were faced: (1) The concentration of the first PCR product in TDI extension was too high or too low, which would create misincorporation or lower incorporation of dye-terminators, (2) the excess primers

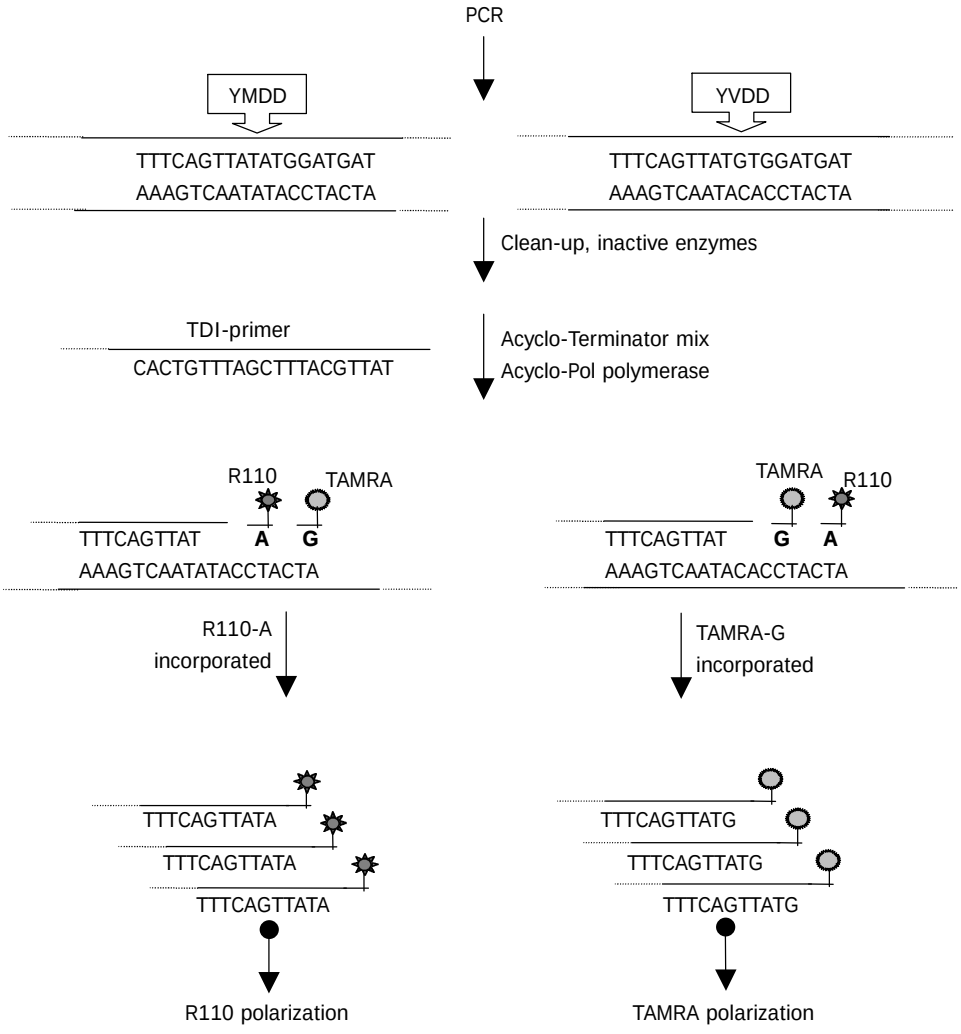

Figure 2 The scheme of TDI assay of YMDD.

in the first PCR product might lead to misincorporation, while excess dNTPs would interfere the dye-terminator incorporation competitively. We increased the number of thermal cycles to 40-45 to ensure that all PCR components were exhausted and adjusted to the concentration of dNTPs and primer in PCR reaction, which were lower than standard PCR protocol. We also prolonged the digestion time from 30 min to 60 min to completely remove the dNTPs and primers. At the same time, to get best TDI-FP performance, forward and reverse TDI primers were used and compared in our study (data not shown). The predicted reaction conditions (annealing temperature and $MgCl_2$) were tested on several nonessential DNA samples to optimize the system.

DNA diagnostic tests will no doubt be applied more and more in clinical rather than in research laboratories. The main advantages of our technique over the other methods for scoring DNA variation, are high accuracy, high throughput and easy to adaptation automatic. It will improve the analysis and prediction of drug-resistance in clinic.

REFERENCES

1 **Yan JC**, Ma JY, Pan BR, Ma LS. The study of chronic hepatitis B in China. *Shijie Huaren Xiaohua Zazhi* 2001; **9**: 611-616

2 S**u Q**, Fu Y, Liu YF, Zhang W, Liu J, Wang CM. Laminin induces the expression of cytokeratin 19 in hepatocellular carcinoma cells growing in culture. *World J Gastroenterol* 2003; **9**: 921-929

3 **Cao XY**, Liu J, Lian ZR, Clayton M, Hu JL, Zhu MH, Fan DM, Feitelson M. Differentially expressed genes in hepatocellular carcinoma induced by woodchuck hepatitis B virus in mice. *World J Gastroenterol* 2001; **7**: 575-578

4 **Huang YX**, Wu GH. The relationship between hepatitis B and hepatocellular carcinoma. *Shijie Huaren Xiaohua Zazhi* 2001; **9**: 682-685

5 **Wang FS**, Xing LH, Liu MX, Zhu CL, Liu HG, Wang HF, Lei ZY. Dysfunction of peripheral blood dendritic cells from patients with chronic hepatitis B virus infection. *World J Gastroenterol* 2001; **7**: 537-541

6 **Han HL**, Lang ZW. Changes in serum and histology of patients with chronic hepatitis B after interferon alpha-2b treatment. *World J Gastroenterol* 2003; **9**: 117-121

7 **Lai YC**, Hu RT, Yang SS, Wu CH. Coinfection of TT virus and response to interferon therapy in patitents with chronic hepatitis B or C. *World J Gastroenterol* 2002; **8**: 567-570

8 **Zhuang L**, You J, Tang BZ, Ding SY, Yan KH, Peng D, Zhang YM, Zhang L. Preliminary results of Thymosin-α1 versus interferon-a-treatment in patients with HBeAg negative and serum HBV DNA positive chronic hepatitis B. *World J Gastroenterol* 2001; **7**: 407-410

9 **You J**, Zhuang L, Tang BZ, Yang WB, Ding SY, Li W, Wu RX, Zhang HL, Zhang YM, Yan SM, Zhang L. A randomized controlled clinical trial on the treatment of Thymosin α1 versus interferon-α in patients with hepatitis B. *World J Gastroenterol* 2001; **7**: 411-414

10 **Cheng ML**, Wu YY, Huang KF, Luo TY, Ding YS, Lu YY, Liu RC, Wu J. Clinical study on the treatment of liver fibrosis due to hepatitis B by IFN-alpha(1) and traditional medicine preparation. *World J Gastroenterol* 1999; **5**: 267-269

11 **Zoulim F**. A preliminary benefit-risk assessment of lamivudine for the treatment of chronic hepatitis B virus infection. *Drug Saf* 2002; **25**: 497-510

12 **Yang SS**, Hsu CT, Hu JT, Lai YC, Wu CH. Lamivudine does not increase the efficacy of interferon in the treatment of mutant type chronic viral hepatitis B. *World J Gastroenterol* 2002; **8**: 868-871

13 **Han T**, Qian SC, Chen Y, Xiao SX, Wang FM, Han ZC, Lu HM. Treatment of 198 patients with chronic hepatitis B with lamivudine and Yi –Gan-Jian. *Shijie Huaren Xiaohua Zazhi* 2002; **10**: 1236-1237

14 **Lai CL**, Dienstag J, Schiff E, Leung NW, Atkins M, Hunt C, Brown N, Woessner M, Boehme R, Condreay L. Prevalence and clinical correlates of YMDD variants during lamivudine therapy for patients with chronic hepatitis B. *Clin Infect Dis* 2003; **36**: 687-696

15 **Cao H**, Tao P. Anti-hepatitis B virus effects of lamivudine and other five drugs *in vitro*. *Zhonghua Yixue Zazhi* 2001; **81**: 1004-1007

16 **Dienstag JL**, Schiff ER, Wright TL, Perrillo RP, Hann HW, Goodman Z, Crowther L, Condreay LD, Woessner M, Rubin M, Brown NA. Lamivudine as initial treatment for chronic hepatitis B in the United States. *N Engl J Med* 1999; **341**: 1256-1263

17 **Li G**, Shu X, Ma HH, Chen W, Chen WS, Chen Q Jiang YS, Yao JL. Detection of HBV, HCV and HBV YMDD mutants by DNA microarray. *Shijie Huaren Xiaohua Zazhi* 2003; **11**: 178-181

18 **Hsu TM**, Chen X, Duan S, Miller RD, Kwok PY. Universal SNP genotyping assay with fluorescence polarization detection. *Biotechniques* 2001; **31**: 560-568

19 **Jardi R,** Buti M, Rodriguez-Frias F, Cotrina M, Costa X, Pascual C, Esteban R, Guardia J. Rapid detection of lamivudine-resistant hepatitis B virus polymerase gene variants. *J Virol Methods* 1999; **83**: 181–187

Edited by Zhang JZ and Wang XL

P.O.Box 2345, Beijing 100023,China
Fax: +86-10-85381893
E-mail: wjg@wjgnet.com www.wjgnet.com

World J Gastroenterol 2003;9(10):2348-2349
World Journal of Gastroenterology
 ISSN 1007-9327

• BRIEF REPORTS •

Ultrasonography in predicting and screening liver cirrhosis in children: A preliminary study

Jia-An Zhu, Bing Hu

Jia-An Zhu, Bing Hu, Department of Ultrasound in Medicine, Affiliated Sixth People' s Hospital, Shanghai Jiaotong University, Shanghai 200233, China
Correspondence to: Dr. Zhu Jia-An, Department of Ultrasound in Medicine, Shanghai Sixth People' s Hospital, 600 Yishan Road, Shanghai 200233, China. zhujiaan@tom.com
Telephone: +86-21-64369181-8751
Received: 2003-05-13 **Accepted:** 2003-06-02

Abstract

AIM: To evaluate the value of ultrasonography in predicting and screening liver cirrhosis in children.

METHODS: Twenty-eight children with liver cirrhosis of various etiologies were examined by routine ultrasonography. A percutaneous liver biopsy guided by ultrasound was also performed on each patient, and the results of liver biopsy and ultrasonography were compared.

RESULTS: When compared with the biopsy results, ultrasonography in combination of clinical and laboratory findings gave accurate diagnoses of children liver cirrhosis. Although ultrasound imaging of children with liver cirrhosis revealed abnormal characteristics, these images were not specific to this disease, thus reinforcing the necessity of ultrasound-guided liver biopsy in the diagnosis of children liver cirrhosis.

CONCLUSION: Ultrasonography is reliable in the diagnosis of children liver cirrhosis, and its usefulness should be stressed in the screening and follow-up of high-risk pediatric patients.

Zhu JA, Hu B. Ultrasonography in predicting and screening liver cirrhosis in children: A preliminary study. *World J Gastroenterol* 2003; 9(10): 2348-2349
http://www.wjgnet.com/1007-9327/9/2348.asp

INTRODUCTION

Cirrhosis of the liver is a morphological entity, and it has been assumed to be an end-stage condition of all chronic active liver diseases. There are many types of liver cirrhosis, including posthepatitic, alcoholic and mixed types of cirrhosis, and congestive, biliary and parasitic cirrhosis, etc. The etiological factors underlying this disease, as well as its morbidity, have been shown to be different in different geographical regions[1-8]. It should be mentioned that morphological changes are different in liver cirrhosis, which include the structural changes not only in the parenchymal disorganizations, but also in the stromal vascular changes in the cirrhotic process[9,10]. It has been widely accepted that ultrasonography is a useful diagnostic procedure for advanced liver cirrhosis. However, liver cirrhosis of children and its applicable techniques are usually different from those of adults. Several types of the cirrhosis resulted from metabolic diseases including glycogen storage disease and hepatolenticular degeneration are rare in adults. In children, the onset of cirrhosis is often occult. Children cirrhosis lacks the early typical clinical symptoms as seen in adult patients, thus contributing to its frequent misdiagnosis[11]. Unfortunately, reports on children cirrhosis are few. To determine if ultrasonography could be of clinical value in predicting the etiology of children cirrhosis, we performed this test in 28 children whose cirrhosis was confirmed by histopathology.

MATERIALS AND METHODS

Patients

We studied 45 children with clinically and ultrasonically suspected cirrhosis of the liver. Only 28 children (23 males and 5 females) aged from 11 months to 12 years (mean 7.9 years) who had a definite biopsy were included in this study. The other 17 children who had no biopsy were excluded.

All the patients were regularly evaluated by clinical assessment, biochemical tests, ultrasound study, and liver biopsy when clinically indicated. Among them, six had chronic hepatitis, and two lived in areas with a high prevalence of *Schistosoma mansoni* while the other 20 had no known etiology. In eight cases, their mothers were positive for HbsAg, among these cases three had hepatitisB. In three cases, their fathers were positive for HbsAg, among these cases one had hepatitisB. In two cases, both parents were positive for HbsAg. Seventeen patients came to hospital because of indigestion or abdominal bloating, four because of diarrhoea, and one each because of dyspneic respiration, bellyache, or jaundice. One patient was identified during routine physical examination.

Sonography

Ultrasonography was performed by conventional techniques with a high-resolution, real-time scanner (Sonoline AC) equipped with 5 MHz and 7 MHz rectilinear array or convex scan probes combined with a puncture guider. Liver size was assessed according to routine methods (transverse and longitudinal sections, relationship between the hepatic border and the right kidney). The contour of the liver (smooth and nodular) was observed. The ultrasound patterns of the liver (nonspecific hepatomegaly, homogeneously increased echogenicity, heterogeneously increased echogenicity, and nodular liver) were observed. The presence of ascites, signs of portal hypertension, and splenomegaly were also recorded.

Ultrasound guided biopsy was performed on all the patients, each biopsy was subsequently examined immunohistochemically.

RESULTS

The diagnosis of children cirrhosis was confirmed in the 28 cases by histopathology, and liver cirrhosis was classified into six groups: post-hepatitis B, biliary disease, congestive disease, schistosomiasis, glycogen storage disease and hepatolenticular degeneration cirrhosis according to the results from biopsy (Table 1).

Among the patients, most were post hepatitis B, accounting for 67.9 % (Table 1). The ultrasound patterns of post-hepatitis B cirrhosis were similar in appearance to the adult disease, with increased parenchymal echo, coarsened echo texture,

irregularities on the liver surface, abnormalities of the intrahepatic biliary tree and splenomegaly. Because the etiology of liver cirrhosis was multifactorial, each particular patient might have a different pathogenesis and different hepatic ultrasound changes. Sonography revealed intrahepatic cholangiectasis in three children with cholestasic cirrhosis. One case of congestive cirrhosis showed an enlargement of the venae hepaticae and inferior vena cava, and almost no change in the inner diameter of the vessels during respiratory movement. In two cases of schistosomiasis cirrhosis, who lived in an epidemic region for *Schistosoma mansoni*, a grid pattern was observed. By sonography, two patients with glycogen storage disease and one hepatolenticular degeneration showed relatively characteristic ultrasound patterns. The echo patterns of liver parenchyma of glycogen storage disease were found to have coarsened echo texture, but the surface of their livers appeared smooth. The pattern of hepatolenticular degeneration showed a coarsened parenchymal echo, with a normal distribution, and the route of the intrahepatic biliary duct was not altered.

Table 1 Diagnosis of children with cirrhosis

Classification	<2 years	2-7 years	8-12 years	Total	%
Post hepatitis B cirrhosis	1	2	16	19	67.9
Biliary cirrhosis		1	2	3	10.7
Congestive cirrhosis			1	1	3.6
Schistosomiasis cirrhosis			2	2	7.1
Glycogen storage disease		1	1	2	7.1
Hepatolenticular degeneration			1	1	3.6
Total	1	4	23	28	100

DISCUSSION

The value of ultrasonography in diagnosing cirrhosis of the liver has been recognized clinically[12-14]. By observing the press extents of the surface of the left hepatic septum in front of the inferior vena cava, real time ultrasound could directly determine the degree of cirrhosis. Estimating the condition of esophageal varices by detecting portal hypertension was important in differentiating the source of gastrointestinal hemorrhage[14]. Because the child liver was smaller in size, we obtained high-resolution ultrasound images by using high frequency probes (5 MHz and 7 MHz).

Our results showed that the echo pattern revealed by ultrasound in combination of the patient' s medical history, could be useful in the diagnosis of children liver cirrhosis and prediction of its the etiology. Then, physicians could select appropriate subsequent diagnostic methods to confirm the diagnosis. Since ultrasound does not allow for the specificity of imaging, we suggest that percutaneous liver biopsy guided by ultrasound should be performed when possible, in order to provide the most accurate method for clinical diagnosis. Ultrasonic scans could localize areas for biopsy away from major vessels and the gall bladder.

Most children with chronic hepatitis have no history of acute hepatitis. Chronic hepatitis has few clinical symptoms and most children patients cannot be diagnosed early in the course of their disease. Thus, by the time they do present the symptoms, the disease is well advanced, and their prognosis is poor. Of the 28 children described here, only six had a previous history of hepatitis. More than half of them came to hospital because of indigestion and abdominal bloating. One patient was misdiagnosed as having biliary ascarid, and was not diagnosed as cirrhosis until bleeding of the digestive tract was observed following ineffective antihelminthic treatment. One child with chronic diarrhoea was found to have complications of ascites. Children cirrhosis was thus easily misdiagnosed. For this reason, if a child manifests symptoms associated with cirrhosis, such as hypodynamia, poor appetite, nausea, vomiting, diarrhea, and intense stomach pains, an ultrasound examination and correlated clinical examination should be performed.

Of the 28 children in this study, 19 (67.9 %) had post-hepatitis B cirrhosis. China is a country with a high prevalence of hepatitis B infection. Perinatal infection is recognized as the predominant mode of transmission of the virus, resulting in many carriers of HbsAg. Infection occurred predominantly at or after birth by maternal-infant transmission, and might even occur as early as the oosperm stage[15]. Embryos infected in the uterus have been reported to develop cirrhosis. Thus the children' s parents who are positive for HbsAg or have a history of hepatitis B infection should be examined by ultrasound and correlated clinical tests at regular intervals. This may lead to an early detection of children liver cirrhosis.

In conclusion, ultrasonography can accurately reveal morphological characteristics and predict the etiologic factors underlying children liver cirrhosis. This technique can be used to screen high-risk groups and allows for early treatment.

REFERENCES

1 **Imperial JC**. Natural history of chronic hepatitis B and C. *J Gastroenterol Hepatol* 1999; **14**(Suppl): 1-5
2 **Noble JA**, Caces MF, Steffens RA, Stinson FS. Cirrhosis hospitalization and mortality trends, 1970-87. *Public Health Rep* 1993; **108**: 192-197
3 **Jorke D**, Reinhardt M. Contributions to the epidemiology of liver cirrhosis and chronic hepatitis. *Dtsch Z Verdau Stoffwechselkr* 1982; **42**: 129-137
4 **Haraszti A**, Vadnay I, Toth K, Baranyai T. Importance of environmental factors for the development of liver cirrhosis. *Zentralbl Allg Pathol* 1983; **128**: 411-423
5 **Li H**, Li RC, Liao SS, Gong J, Zeng XJ, Li YP. Long-term effectiveness of infant low-dose hepatitis B vaccine immunization in Zhuang Minority Area in China. *World J Gastroenterol* 1999; **5**: 122-124
6 **Wu J**, Cheng ML, Zhang GH, Zhai RW, Huang NH, Li CX, Luo TY, Lu S, Yu ZQ, Yao YM, Zhang YY, Ren LZ, Ye L, Li L, Zhang HN. Epidemiological and histopathological study of relevance of Guizhou Maotai liquor and liver diseases. *World J Gastroenterol* 2002; **8**: 571-574
7 **Roussos A**, Goritsas C, Pappas T, Spanaki M, Papadaki P, Ferti A. Prevalence of hepatitis B and C markers among refugees in Athens. *World J Gastroenterol* 2003; **9**: 993-995
8 **Harbin WP**, Robert NJ, Ferrucci JT Jr. Diagnosis of cirrhosis based on regional changes in hepatic morphology: a radiological and pathological analysis. *Radiology* 1980; **135**: 273-283
9 **Okudaira M**, Atari E, Oubu M. Liver cirrhosis, its definition and classification-from a morbid anatomical point of view. *Nippon Rinsho* 1994; **52**: 5-10
10 **Kamegaya K.** Definition and classification of liver cirrhosis. *Nippon Rinsho* 1994; **52**: 11-18
11 **Peter L**, Dadhich SK, Yachha SK. Clinical and laboratory differentiation of cirrhosis and extrahepatic portal venous obstruction in children. *J Gastroenterol Hepatol* 2003; **18**: 185-189
12 **Ohta M**, Hashizume M, Kawanaka H, Akazawa K, Tomikawa M, Higashi H, Kishihara F, Tanoue K, Sugimachi K. Prognostic significance of hepatic vein waveform by Doppler ultrasonography in cirrhotic patients with portal hypertension. *Am J Gastroenterol* 1995; **90**: 1853-1857
13 **Chou YH**, Chiou HJ, Tiu CM, Chiou SY, Lee SD, Hung GS, Wu SC, Kuo BI, Lee RC, Chiang JH, Chang T, Yu C. Duplex Doppler ultrasound of hepatic Schistosomiasis japonica: a study of 47 patients. *Am J Trop Med Hyg* 2003; **68**: 18-23
14 **Gorg C**, Riera-Knorrenschild J, Dietrich J. Pictorial review: Colour Doppler ultrasound flow patterns in the portal venous system. *Br J Radiol* 2002; **75**: 919-929
15 **Gu CH**. New development of Lemology(No 2). 1st ed. *Chongqing*: *Science Technol Press* 1990: 105

Edited by Zhang JZ and Wang XL

P.O.Box 2345, Beijing 100023,China
Fax: +86-10-85381893
E-mail: wjg@wjgnet.com www.wjgnet.com

World J Gastroenterol 2003;9(10):2350-2352
World Journal of Gastroenterology
 ISSN 1007-9327

• BRIEF REPORTS •

Experimental study of diode-laser induced thermocoagulation on hepatic tissue with scanner fiber tip

De-Fei Hong, Shu-You Peng, Song-Ying Li, Li-Min Tong

De-Fei Hong, Shu-You Peng, Department of General Surgery, Sir Run Run Shaw Hospital, Zhejiang University, Hangzhou 310016, Zhejiang Province, China
Song-Ying Li, Department of Pathology, Medical College of Zhejiang University, Hangzhou 310006, Zhejiang Province, China
Li-Min Tong, Department of Physics, State Key Laboratory of Silicon Marterial, Zhejiang University, Hangzhou 310027, Zhejiang Province, China
Supported by the Youth Science Foundation of National 863 Laser Technique
Correspondence to: De-Fei Hong, Department of General Surgery, Sir Run Run Shaw Hospital, Zhejiang University, Hangzhou 310016, Zhejiang Province, China. hongdefi@mail.hz.zj.cn
Telephone: 13605700656
Received: 2002-12-22 **Accepted:** 2003-02-13

Abstract

AIM: To explore a safe, efficient, and cost-effective technique for local thermo-ablation of hepatic tumors.

METHODS: The livers of 16 healthy rabbits were thermocoagulated by diode-laser with a hand-made scanner fiber tip, 6 w for 10 min. At the same time, the temperature was measured at 5 and 10 mm from the laser tip. Liver function 7 days post-thermocoagulation was compared to pre-thermocoagulation. Pathological changes were also studied 1 month after laser thermocoagulation.

RESULTS: All the rabbits lived and the temperature of hepatic tissues at 0 mm, 5 mm, 10 mm from laser tip reached 96.39±3.97 ℃, 60.79±6.21 ℃, 46.10±4.58 ℃, respectively after 10 min thermocoagulation. There was no significant change in liver function. The hepatic thermocoagulated necrosis and the surrounding fibrosis was 26.0 mm in diameter. Light microscopy observation revealed no surviving cells in the coagulated area.

CONCLUSION: Hepatic tissue can be locally ablated safely and effectively by diode-laser with scanner fiber tip, and this technique may be a new method to treat hepatic tumors.

Hong DF, Peng SY, Li SY, Tong LM. Experimental study of diode-laser induced thermocoagulation on hepatic tissue with scanner fiber tip. *World J Gastroenterol* 2003; 9(10): 2350-2352
http://www.wjgnet.com/1007-9327/9/2350.asp

INTRODUCTION

In recent years, thermo-ablation of liver cancer has received increasing attention. Generally this can be achieved by radio-frequency (RF) or Nd: YAG laser. Several factors have prevented these techniques from gaining widespread use including availability and cost, in addition to some uncertainty about their therapeutic effectiveness. With these concerns in mind, it is appropriate to consider a new technique for thermo-ablation that we believe is safe, stable, convenient and cost effective. Semiconductor taper-scattered light for thermo-ablation of liver tissue in an experimental model is advanced as such a technique with details presented as follows.

MATERIALS AND METHODS

Material and apparatus

Hand-made semiconductor taper-scattered laser therapeutic system (HTLTS) has a wavelength of 810±10 nm. The working tip is 10 mm long and 1 mm in diameter. Power utilization was 6 w and after dispersion output power was at 2.1 w with an exposure time of 10 min. Sixteen adult rabbits were obtained from the Animal Laboratory of Zhejiang University, weighing 2 to 3 kg.

Methods

Intravenous anesthesia was administered via ear vein using 2 % sodium pentothal. The abdomen was entered with a midline incision and right or left lobes of the liver were exposed. A 18G PTC needle was introduced into the liver and through it, the laser tip was advanced into the liver tissue before turning on the power for the laser. Care was taken to advance the laser tip fully into the liver tissue. Power input was 6 w and 2.1w after dispersion.

For temperature measurement during laser application, a nickel-chrome-nickel thermocouple 300 μm in diameter was placed intrahepatically at 5 and 10 mm from the laser tip. Temperature was continuously measured during application. After thermocoagulation the abdomen was closed with silk suture. Liver function was measured before surgery and 7 days afterwards. One month after irradiation the rabbits were sacrificed and the liver specimen was fixed in formaldehyde. Multiple sections were taken from the ablative and surrounding area in the verticle plane of the optical fiber. After H&E staining the sections were examined grossly and microscopically with particular attention to the diameter of the coagulated area. Liver function data were analyzed using the *t*- test with the "SAS" software.

RESULTS

The temperature variation is shown in Table 1. Note that two of the rabbits were irradiated for only six minutes because of carbonization of tissue at the center of the optical fiber.

Table 1 The temperature variation

Time (Seconds)	Temperature (℃)		
	0 mm	5 mm	10 mm
0	34.00±0.00	34.00±0.00	34.00±0.00
120		55.70±4.81	40.50±1.47
240		58.75±5.65	43.30±2.54
360		60.26±5.52	45.00±2.67
480		59.89±6.65	46.10±3.87
600	96.39±3.97	60.79±6.21	46.10±4.58

Liver function changes are shown in Table 2.

Table 2 Liver function changes

	Pre-coagulation	7 days after coagulation	*P*
ALT(IU / L)	67.78±24.98	77.11±49.79	>0.05
AST(IU / L)	87.22±58.82	66.55±44.75	>0.05
TBIL(mg / dl)	1.84±1.79	1.21±0.51	>0.05
ALB(g / L)	17.90±3.98	14.77±2.79	>0.05
TP (g / L)	66.54±13.95	59.40±9.55	>0.05

All rabbits were alive after the procedure. When the animals were sacrificed after one month the livers were cut in the vertical plane of the optical fiber and the gray coagulated necrotic tissue was measured. Gross evaluation demonstrated a diameter of 23 mm with a perimeter zone of 3 mm (Figure 1). Under light microscopy the central zone of coagulation necrosis was followed by a layer showing inflammatory cell infiltration and finally the layer of fibrosis, the last two were 0.5 mm and 2.4 mm, respectively.

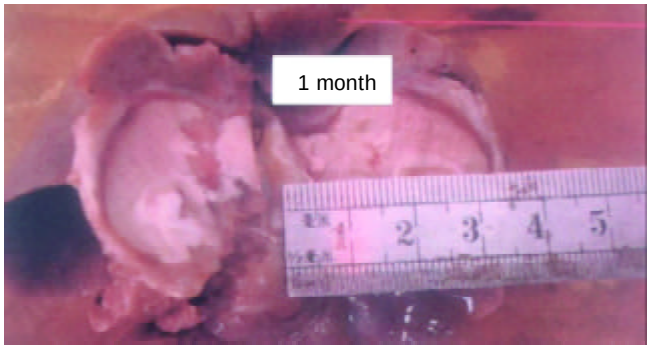

Figure 1 The necrotic center with surrounding fibrosis (HE).

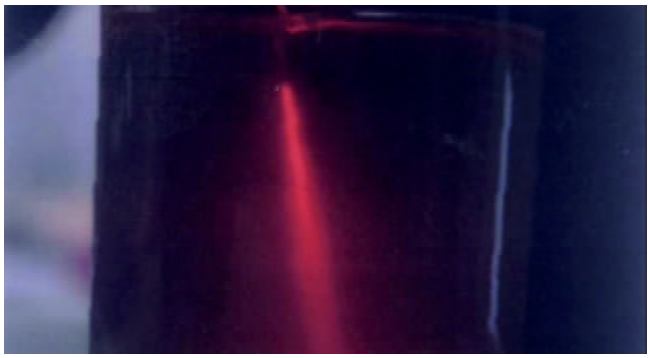

Figure 2 High density linear laser energy from fiber.

Figure 3 Low density up-tip taper scattered laser energy after conversion.

DISCUSSION

Currently the optimal treatment for liver cancer is surgical excision with curative intent. However, because of the frequency of coexistent cirrhosis and the difficulty of early detection, only 25 to 30 percent of newly diagnosed patients with primary or metastatic liver cancer undergo potential curative resection and the recurrence rate is at least 50 %[1-2]. This means many patients are not even candidates for a surgical procedure and have little chance even for palliation, which has led to increasing interest in alternatives such as thermo-ablative procedures including radio-frequency, Nd:YAG laser and microwave. However, limited benefit, high cost and difficulties in technical application have limited the usefulness of these modalities as well[3-6].

The basis for laser thermo-ablation is that light energy can be absorbed by tissues after its conversion into heat, resulting in deep penetration with therapeutic destruction of tumor tissues. The temperature and therefore the extent of destruction are controlled by the intensity and duration of the energy transmitted. This has already been shown effective using Nd: YAG laser as the energy source. However high cost and difficulties in use have restricted its application in this setting[6-9]. More recently, semi-conductor focused laser energy has come to the forefront due to decreased cost, stable-performance, durability and ease of use. In addition it does not require water cooling equipment[7,8]. In this report, we have examined a similar process using semiconductor taper-scattered light. We have shown 1064 nm Nd:YAG and 800-900 nm semiconductor laser light both exhibit deep penetration in tissue. Dong[10] has shown normal liver cells necrotize in one minute with a temperature of 54 ℃ and immediately with a temperature of 60 ℃. In addition he has shown liver carcinoma cells are more sensitive than normal cells if the temperature is less than 130 ℃. We also know penetration of laser energy is significantly reduced by vaporization and carbonization of tissues. Obviously, to enlarge the treatment area and avoid injury to adjacent areas it is necessary to elevate the temperature of the treatment area but not so high as to cause vaporization and carbonization. It is our opinion that semiconductor taper-scattered laser light may be superior to other systems in this regard. HTLTS can convert high density linear laser energy into up-tip taper scattered laser light which is lower in energy and density as shown in Figure 2 and Figure 3. In effect it can increase the power of laser light equipment, enlarge the treatment area, shorten the duration of application and avoid injury to important areas adjacent to the treatment area such as major hepatic vessels. Specifically, the power is only 6 watts and after scatter only 2.1 W. Ten minutes after thermocoagulation the temperature at the center of the optical fiber is 96.39±3.97 ℃ and 10 mm from the center the temperature is 46.1±4.58 ℃. One month after the procedure the diameter of necrosis was 26 mm and there was no viable tissue in this area. HTLTS is more efficient than Nd:YAG or semiconductor focused laser light. In the study by Ping Liang[5] Nd:YAG provided only 15 mm necrosis using 2 to 6 W energy after 15 to 40 min application. Fan[7] demonstrated only 7-13 mm necrosis with semiconductor focused laser energy from a British laser using 2 W and 2800-8400 J respectively. Injury beyond the intended area is less likely since it is not necessary to place the tip of the instrument exactly in the center of the lesion and this makes the procedure also applicable for more superficial lesions. The optical fiber can be separated from the tissue with the catheter thus avoiding contamination from the blood and the length of the fiber tip can be altered to fit the diameter of the tumor. Furthermore, the optical fiber can be sterilized and reused, the fiber is flexible, allowing access to areas one side or the other of the primary objective. Overall,

HTLTS is more convenient, economical and effective than the currently available ablative procedures.

In regards to the effect of HTLTS on hepatic carcinoma or metastatic lesions, we have shown greater penetration than in normal tissue. For example, the penetration of YAG (wavelength 670 nm) in normal liver tissue, liver sclerosis, HCC, and metastatic lesions is 0.75 mm, 0.97 mm, 1.43 mm and 2.78 mm, respectively[11]. HCC is also more sensitive to thermal ablation than normal tissue. Again HTLTS is more effective and efficient than the other methods. HTLTS can also be applied to the clinical area easily. The fiber is passed into the intended tissue through a 18G paracentesis needle guided by B-ultrasound. The length of the fiber tip can be adjusted according to the size of the target tissue. Special techniques are also available to utilize more than one fiber at a time to improve the resulting effect according to the exact size and location of the target tissue.

In conclusion, we believe that the foregoing report indicates HTLTS may be the best technique yet devised for thermo-ablation of hepatic lesions.

REFERENCES

1 **Cance WG,** Stwart AK, Menck HR. The national cancer data base report on treatment patterns for hepatocellular carcinoma: improved of surgically resected patiens, 1985-1986. *Cancer* 2000; **88**: 912-920

2 **Wu MC,** Chen H, Sheng F. Surgical treatment of primary liver cancer: report of 5524 cases. *Zhonghua Waike Zazhi* 2001; **39**: 25-28

3 **Curley SA,** Lzzo F, Delrio P, Ellis LM, Granchi J, Vall Fiore F, Pignata S, Daniele B, Cremona F. Radiofrequency ablation of unresectable primary and metastatic hepatic malignancies: results in 123 patients. *Ann Surg* 1999; **230**: 1-8

4 **Ohmoto K,** Miyake I, Tsuduki M, Shibata N, Takesue M, Kunieda T, Ohno S, Kuboki M, Yamamoto S. Percutaneous Microwave coagulation therapy for unresectable hepatocellular carcinoma. *Hepatogastroenterology* 1999; **46**: 2894-2900

5 **Liang P,** Dong BW, Gu Y, Li JH, Yu XN, Su L, Zhang Y. Effect of Nd:YAG laser coagulation on hepatic tissue and its application to hepatic cancer. *Zhonghua Liliao Zazhi* 1999; **22**: 158-160

6 **Heisterkamp J,** Van Hillegersberg R, Ijzermans JN. Interstitial laser coagulation for hepatic tumor. *Br J Surg* 1999; **86**: 293-304

7 **Fan XH,** Shen TZ, Lu W, Gong DX. Laser ablation of liver malignant tumor. *Zhongguo Yixue Jishuanji Chengxiang Zazhi* 2000; **6**: 404-407

8 **Devaux BC,** Roux FX, Nataf F, Turak B. Cioloca C. High-power diode laser in neurosurgery: clinical experience in 30 cases. *Surg Neurol* 1998; **50**: 33-40

9 **Zhang ZX,** Jiang DZ. Laser-Tissue Interactions: Foundaments and Application. 1st ed. *Xi'an*: *Xian Jiaotong University Publishing House* 1999: 64-65

10 **Dong BW,** Liang P, Yu XL, Zeng XQ, Wang PJ, Su L, Wang H, Li S. Sonographically guided microwave coagulation treatment of liver cancer: an experimental and clinical study. *Am J Roentgenol* 1998; **171**: 449-454

11 **Li DJ,** Hu ZS. Tumor thermotherapy. 1st ed. *Henan: Henan Medical University Publishing House* 1995: 186-187

Edited by Pang LH

P.O.Box 2345, Beijing 100023,China
Fax: +86-10-85381893
E-mail: wjg@wjgnet.com www.wjgnet.com

World J Gastroenterol 2003;9(10):2353-2355
World Journal of Gastroenterology
 ISSN 1007-9327

• BRIEF REPORTS •

Is a low dose of hepatitis B vaccine enough for a rapid vaccination scheme?

Ru-Xiang Wang, Greet Boland, Ying Guo, Shao-Ping Lei, Chang-Hong Yang, Juan Chen, Jie Tian, Jin-Ying Wen, Ke-Hong Du, Jan van Hattum, Gijsbert C. de Gast

Ru-Xiang Wang, Ying Guo, Juan Chen, Shenyang Center for Disease Control and Prevention, Shenyang 110031, Liaoning Province, China
Greet Boland, Jan van Hattum, Department of Gastroenterology, University Hospital Utrecht, Netherlands
Shao-Ping Lei, Hospital of Institute of Shenyang Electricity Power, Shenyang 110031, Liaoning Province, China
Chang-Hong Yang, Dongling District Anti-epidemic Station, Dongling District, Shenyang 110031, Liaoning Province, China
Jie Tian, Shenyang No.4 Hospital, Shenyang 110031, Liaoning Province, China
Jin-Ying Wen, Shenyang 606 Hospital, Shenyang 110031, Liaoning Province, China
Ke-Hong Du, Shenzhen Kangtai Biological Products Company, Shenzhen 518000, Guangdong Province, China
Gijsbert C. de Gast, Netherlands Cancer Institute, Amsterdam, Netherlands
Correspondence to: Dr. Ru-Xiang Wang, Shenyang Center for Disease Control and Prevention, 37 Qishanzhong Road, Huanggu District, Shenyang 110031, China. rxwtxh@pub.sy.ln.cn
Telephone: +86-24-86853243 **Fax:** +86-24-86863778
Received: 2003-04-12 **Accepted:** 2003-06-11

Abstract

AIM: To determine whether or not a low dose of HB vaccine can be effectively used in the rapid vaccination.

METHODS: Rapid vaccination (0, 1, 2 months) with low dose (5 μg) or routine dose (10 μg) HB vaccine was studied in 250 subjects (130 school children and 120 university students). Serum from all the participants was tested for HBsAg, anti-HBs and anti-HBc at 1, 3 and 7 months after the first dose of vaccination and all subjects were serum HBV marks negative before the vaccination. Non-responders to a complete initial vaccination from university students were given an additional vaccination with 10 μg of HB vaccine and their serum anti-HBs was tested again one month later.

RESULTS: One month after the third dose of vaccination (third month) sero-conversion rates and geometric mean titer (GMTs) were significantly ($P<0.01$) higher in the routine dose (resp. 89 % and 106.8) than in the low dose group (resp. 72 % and 59.5). Sero-conversion rates and GMTs were maintained stable for another 4 months in both groups. After an additional vaccination to non-responders with 10 μg HB vaccine, 17/23 subjects (13/15 from those vaccinated with 5 μg vaccine and 4/8 from those vaccinated with 10 μg vaccine) became anti-HBs positive, yielding similar sero-conversion rates for both dose groups.

CONCLUSION: Higher sero-conversion rates and GMTs were reached in those vaccinated with 10 μg HB vaccine than in those vaccinated with 5 μg HB vaccine after a complete vaccination with a 0, 1, 2 month scheme. But the subjects vaccinated with 5 μg vaccine can also reach the similar sero-conversion rate after an additional vaccination.

Wang RX, Boland G, Guo Y, Lei SP, Yang CH, Chen J, Tian J, Wen JY, Du KH, van Hattum J, de Gast GC. Is a low dose of hepatitis B vaccine enough for a rapid vaccination scheme? *World J Gastroenterol* 2003; 9(10): 2353-2355
http://www.wjgnet.com/1007-9327/9/2353.asp

INTRODUCTION

Although hepatitis B vaccine has been available for 20 years, hepatitis B nowadays remains prevalent in the world, especially in a majority of the developing countries. In China, 5 μg of vaccine (Merck) has been used in the HB vaccination for several years and acquired acceptable results. The long-term effectiveness of low-dose HB vaccine immunization in the infancy has been observed, but that in school children or adults remains to be determined. It is known that protective anti- HBs antibody titers can generally be reached in 80-90 % of individuals vaccinated with 10 μg vaccine according to a 0,1, 6 month vaccination scheme. Considering of the relative length of the current HB vaccination scheme and the availability of low dose HB vaccine in the market, it seemed, therefore, worthwhile to test a routine dose (10 μg) vaccination in a rapid scheme (0, 1, 2 months) compared to a low dose (5 μg) vaccination. We here report that significantly higher sero-conversion rates and GMTs are reached in those vaccinated with a 10 μg dose vaccination than those vaccinated with 5 μg dose vaccination after 3 months from the initial dose. School children and university students showed no significant differences apart from a more rapid response in school children.

MATERIALS AND METHODS

Two hundred and fifty subjects (130 school children aged 8-10 years old and 120 university students aged 18-20 years old) with negative HB marks (HBsAg, anti-HBs, anti- HBc) were included in the study. One hundred and thirty subjects (72 school children and 58 university students) nominated as low dose group and were vaccinated with 5 μg HB vaccine, 120 subjects (55 school children and 65 university students) named as routine dose group received 10 μg HB vaccine (5 μg dose x 2) respectively according to a 0, 1, 2 month vaccination scheme. All non-responding university students after a complete initial vaccination series were given a fourth dose with 10 μg HB vaccine at the 8th month. All injections were given intramuscularly at the site of deltoid muscle. The HB vaccine used in this study is 5 μg yeast recombinant HB vaccine (Lot no: 2990104-1, from Merck), provided by Kangtai Biological Pharmaceutical Company, China.

Blood samples that were collected from all vaccinees for three times performed were used to detect serum anti-HBs (Ausab EIA, No 642841 M401) at month 1, 3 and 7 after the first dose of vaccination respectively. The third month serum specimen from all non responders after the initial vaccination was tested for HBsAg and anti-HBc by ELISA (Lizon Kit, China) in order to make sure that they are real no-responders to HB vaccine and not HBV carriers. Those with negative tests

received a fourth dose of vaccine at 8th month after vaccination and were again tested for serum anti- HBs one month later.

RESULTS

128/130 subjects in low dose group were tested for serum anti-HBs levels one month after the first dose of vaccination and only 114 subjects were available for the test one month after the third vaccination. The anti-HBs sero-conversion rate and GMT in this group was 71.9 % and 9.5 respectively (Table 1). 116/120 subjects in the routine group were tested for anti-HBs levels one month after the first dose of vaccination and only 110 subjects were available for the test one month after the third dose of vaccination. A significantly higher anti-HBs sero-conversion rate (89.1 %, $P<0.01$) and GMT (106.8, $P<0.01$) in routine dose group were observed after the third dose of vaccination compared with that in low dose group. At the seventh month the sero-conversion rate and GMT persisted at similar level to that after the second dose of vaccination.

Table 1 Serum conversion rate and GMT induced by low and routine dose of vaccines

Dose of vaccine	Time after first injection	*n*	Sero- conversion rate (%)	GMT
5 μg	1st time	128	12.5	
	2nd time	114	71.9	59.5
	3rd time	113	69.9	58.5
10 μg	1st time	116	19 .0	
	2nd time	110	89.1[b]	106.8
	3rd time	98	91.8[b]	94.6

[b]$P<0.01$ *vs.* 5 μg group.

Twenty three non-responding university students (15 vaccinated with 5 μg vaccine and 8 with 10 μg vaccine) were given a fourth dose of 10 μg HB vaccine after completion of the initial vaccination. Of these individuals, 13/15 non-responders in the low dose group and 4/8 non-responders in the routine dose group responded with anti-HBs one month after the additional dose. As a result of this additional vaccination, serum conversion rate in the low dose group was nearly similar to that in the routine dose group (95.2 % *vs* 92.9 %, Figure 1).

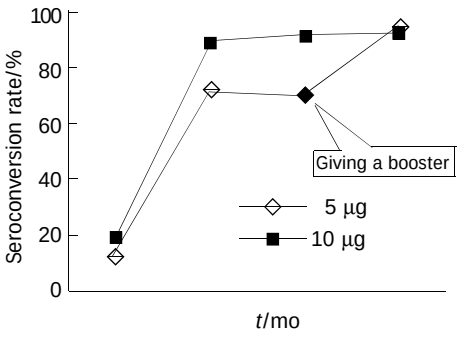

Figure 1 Seroconversion rate before and after a booster.

DISCUSSION

Since the introduction of hepatitis B vaccination in the early 1980s, the safety and immunogenicity of the plasma-derived and yeast-derived hepatitis B vaccines have been well demonstrated[1-12]. However, the disease remains a global problem. The failure of obtaining a complete 3 doses HB vaccination due to the length of the scheme probably contributes to the current prevalence of hepatitis B in the developing countries. Clearly, the protection against hepatitis B could be improved if a shorter vaccination regimen of achieving protective anti-HBs levels in >90 % of vaccinees was available. Our results clearly showed that with a rapid vaccination scheme (0, 1, 2 months) using 10 μg HB vaccine, serum anti-HBs levels can be induced, while it can not be reached by using 5 μg of HB vaccine. The similar results were also reported previously by Carlsson *et al*[13] who vaccinated some medical staff and compared the effects of intramuscular (I m, 20 μg.) vaccination with the low-dose intradermal (i d, 2 μg) vaccination on their early sero-conversion rates according to a 0, 4, 8 week scheme or to an accelerated 0, 2, 6 week scheme. He concluded that when a rapid protection against hepatitis B virus (HBV) infection was needed, such as the post-exposure prophylaxis, low-dose i.d. vaccination schedule could not be used.

A study on evaluating the potential for developing rapid seroprotection was performed by Young *et al*[14], beneficial results of a one month/two dose regimen with a novel triple antigen vaccine (Hepacare) have been achieved[14]. These results confirmed that an accelerated vaccination could be achieved with appropriate vaccinating protocols.

Low-dose vaccination has been proposed as a cost-saving strategy to implement mass vaccination of neonates with HB vaccine world-wide, particularly in developing countries. In a previous study, Shokri F compared the effectiveness of three doses of recombinant HB vaccine (Heberbiovac) in three different doses, among three groups of healthy Iranian neonates. His results showed that there were no significant differences in sero-protection rate and GMTs between the 10 and 5 μg dose recipients. Both parameters, however, were significantly lower in neonates vaccinated with a 2.5 μg vaccine dose[12]. Leroux-Roels G observed the immunogenicity and reactogenicity profiles of different doses of Engerix-B(R) (10 microg hepatitis B surface antigen) and Recombivax (R) (5 microg hepatitis B surface antigen), on a 0, 1, 6 month schedule in healthy adolescents. One month following the third dose of vaccination, seroprotection rates of Engerix-B and Recombivax vaccination were similar but the geometric mean titer was significantly higher in those vaccinated with Engerix-B than that with Recombivax[15]. Similar results were also reported that higher immunogenicity is usually related with higher vaccine dosages, especially in older adult population[13-18]. Our results showed that a higher dose (10 μg) of vaccine can induce much higher sero- conversion rate and higher GMTs compared with the reduced dose (5 μg) vaccination whereas the GMTs can be sustained for at least 5 months in both groups after the primary vaccination.

In most studies on immunocompetent subjects, 5 % to 10 % vaccinees failed to respond to HB vaccination. The possible reasons for lack of adequate antibody response have been well reported[16-22]. In order to confirm if the reduced dose of HB vaccination could cause a higher rate of non- or hypo-response to HB vaccine, we gave all non-responders an additional dose after the initial HB vaccination scheme and one month later, the majority of them converted into anti-HBs positive. The final sero-conversion rates of non-responders in low dose group and routine dose group were 95.2 % and 92.9 % respectively, showing that it is rather a hyporesponse to a lower dose of HB vaccine than a non-response as found earlier [23-31]. Based on the results, we conclude that it is better for adults to choose 10 μg HB vaccine, especially when a rapid vaccination program is needed.

REFERENCES

1 **Kojouharova M**, Teoharov P, Bahtchevanova T, Maeva I, Eginlian

A, Deneva M. Safety and immunogenicity of a yeast-derived recombinant hepatitis B vaccine in Bulgarian newborns. *Infection* 2001; **29**: 342-344

2 **Liao SS**, Li RC, Li H, Yang JY, Zeng XJ, Gong J, Wang SS, Li YP, Zhang KL. Long-term efficacy of plasma-derived hepatitis B vaccine among Chinese children: a 12-year follow-up study. *World J Gastroenterol* 1999; **5**: 165-166

3 **Li H**, Li RC, Liao SS, Yang JY, Zeng XJ, Wang SS. Persistence of hepatitis B vaccine immune protection and response to hepatitis B booster immunization. *World J Gastroenterol* 1998; **4**: 493-496

4 **Rendi-Wagner P**, Kundi M, Stemberger H, Wiedermann G, Holzmann H, Hofer M, Wiesinger K, Kollaritsch H. Antibody-response to three recombinant hepatitis B vaccines: comparative evaluation of multicenter travel-clinic based experience. *Vaccine* 2001; **19**: 2055-2060

5 **Ozaki T**, Mochizuki H, Ichikawa Y, Fukuzawa Y, Yoshida S, Morimoto M. Persistence of hepatitis B surface antibody levels after vaccination with a recombinant hepatitis B vaccine: a 3-year follow-up study. *J Oral Sci* 2000; **42**: 147-150

6 **Jain A**, Mathur US, Jandwani P, Gupta RK, Kumar V, Kar P. A multicentric evaluation of recombinant DNA hepatitis B vaccine of Cuban origin. *Trop Gastroenterol* 2000; **21**: 14-17

7 **Al-Faleh FZ**, Al-Jeffri M, Ramia S, Al-Rashed R, Arif M, Rezeig M, Al-Toraif I, Bakhsh M, Mishkkhas A, Makki O, Al-Freihi H, Mirdad S, AlJuma A, Yasin T, Al-Swailem A, Ayoola A. Seroepidemiology of hepatitis B virus infection in Saudi children 8 years after a mass hepatitis B vaccination programme. *J Infect* 1999; **38**: 167-170

8 **Li H**, Li RC, Liao SS, Gong J, Zeng XJ, Li YP. Long-term effectiveness of infant low dose hepatitis B vaccine immunization in Zhuang Minority Area in China. *World J Gastroenterol* 1999; **5:** 122-124

9 **Liu HB**, Meng ZD, Ma JC, Han CQ, Zhang YL, Xing ZC, Zhang YW, Liu YZ, Cao HL. A 12 year cohort study on the efficacy of plasma-derived hepatitis B vaccine in rural newborns. *World J Gastroenterol* 2000; **6**: 381-383

10 **Li H**, Wang L, Wang SS, Gong J, Zeng XJ, Li RC, Nong Y, Huang YK, Chen XR, Huang ZN. Research on optimal immunization strategies for hepatitis B in different endemic areas in China. *World J Gastroenterol* 2000; **6**: 392-394

11 **Zeng XJ**, Yang GH, Liao SS, Chen AP, Tan J, Huang ZJ, Li H. Survey of coverage, strategy and cost of hepatitis B vaccination in rural and urban areas of China. *World J Gastroenterol* 1999; **5**: 320-323

12 **Shokri F**, Jafarzadeh A. High seroprotection rate induced by low doses of a recombinant hepatitis B vaccine in healthy Iranian neonates. *Vaccine* 2001; **19**: 4544-4548

13 **Carlsson T**, Struve J, Sonnerborg A, Weiland O. The anti-HBs response after 2 different accelerated intradermal and intramuscular schemes for hepatitis B vaccination. *Scand J Infect Dis* 1999; **31**: 93-95

14 **Young MD**, Rosenthal MH, Dickson B, Du W, Maddrey WC. A multi-center controlled study of rapid hepatitis B vaccination using a novel triple antigen recombinant vaccine. *Vaccine* 2001; **19**: 3437-3443

15 **Leroux-Roels G**, Abraham B, Fourneau M, De Clercq N, Safary A. A comparison of two commercial recombinant vaccines for hepatitis B in adolescents. *Vaccine* 2000; **19**: 937-942

16 **Treadwell TL**, Keeffe EB, Lake J, Read A, Friedman LS, Goldman IS, Howell CD, DeMedina M, Schiff ER, Jensen DM. Immunogenicity of two recombinant hepatitis B vaccines in older individuals. *Am J Med* 1993; **95**: 584-588

17 **de Rave S**, Heijtink RA, Bakker-Bendik M, Boot J, Schalm SW. Immunogenicity of standard and low dose vaccination using yeast-derived recombinant hepatitis B surface antigen in elderly volunteers. *Vaccine* 1994; **12**: 532-534

18 **Bennett RG**, Powers DC, Remsburg RE, Scheve A, Clements ML. Hepatitis B virus vaccination for older adults. *J Am Geriatr Soc* 1996; **44**: 699-703

19 **Yucesoy B**, Sleijffers A, Kashon M, Garssen J, de Gruijl FR, Boland GJ, van Hattum J, Simeonova PP, Luster MI, van Loveren H. IL-1beta gene polymorphisms influence hepatitis B vaccination. *Vaccine* 2002; **20**: 3193-3196

20 **Jabaaij L**, van Hattum J, Vingerhoets JJ, Oostveen FG, Duivenvoorden HJ, Ballieux RE. Modulation of immune response to rDNA hepatitis B vaccination by psychological stress. *J Psychosom Res* 1996; **41**: 129-137

21 **Sleijffers A**, Yucesoy B, Kashon M, Garssen J, De Gruijl FR, Boland GJ, Van Hattum J, Luster MI, Van Loveren H. Cytokine polymorphisms play a role in susceptibility to ultraviolet B-induced modulation of immune responses after hepatitis B vaccination. *J Immunol* 2003; **170**: 3423-3428

22 **Goldwater PN**. Randomized, comparative trial of 20 micrograms vs 40 micrograms Engerix B vaccine in hepatitis B vaccine non-responders. *Vaccine* 1997; **15**: 353-356

23 **Wismans P**, van Hattum J, Stelling T, Poel J, de Gast GC. Effect of supplementary vaccination in healthy non-responders to Hepatitis B vaccination. *Hepatogastroenterol* 1988; **35**: 78-79

24 **Wismans P**, van Hattum J, Mudde GC, Endeman HJ, Poel J, de Gast GC. Is booster injection with hepatitis B vaccine necessary in healthy responders? *J Hepatol* 1988; **8**: 236-240

25 **Zaruba K**, Grob PJ, Bolla K. Thymopentin as adjuvant therapy to hepatitis B vaccination in formerly non-or hyporesponding hemodialysis patients. *Surv Immunol Res* 1985; **4**: S102-S106

26 **Maruyama N**, Sata M, Ishii K, Atono Y, Ono K, Matuda T, Suzuki H, Muraoka H, Nakano H, Hino K. Hepatitis B vaccination in alcoholics. *Kansenshogaku Zasshi* 1989; **63**: 27-34

27 **Fabrizi F**, Andrulli S, Bacchini G, Corti M, Locatelli F. Intradermal versus intramuscular hepatitis b re-vaccination in non-responsive chronic dialysis patients: a prospective randomized study with cost-effectiveness evaluation. *Nephrol Dial Transplant* 1997; **12**: 1204-1211

28 **Hollinger FB**. Factors Influencing the Immune Response to Hepatitis B Vaccine, booster dose guidelines and vaccine protocol recommendations. *Am J Med* 1989; **87**: 3A-36S

29 **Erensoy S,** Bilgic A, Arda B, Ozer O. Low-dose intramuscular hepatitis B vaccination in medical students: 4-year follow-up. *Infection* 2002; **30**: 303-305

30 **Huang LM**, Chiang BL, Lee CY, Lee PI, Chi WK, Chang MH. Long-term response to hepatitis B vaccination and response to booster in children born to mothers with hepatitis B e antigen. *Hepatology* 1999; **29**: 954-959

31 **Clemens R**, Sanger R, Kruppenbacher J, Hobel W, Stanbury W, Bock HL, Jilg W. Booster immunization of low- and non-responders after a standard three dose hepatitis B vaccine schedule-results of a post-marketing surveillance. *Vaccine* 1997; **15**: 349-352

Edited by Wang XL

P.O.Box 2345, Beijing 100023,China
Fax: +86-10-85381893
E-mail: wjg@wjgnet.com www.wjgnet.com

World J Gastroenterol 2003;9(10):2356-2358
World Journal of Gastroenterology
 ISSN 1007-9327

• BRIEF REPORTS •

Role of activation-induced cell death in pathogenesis of patients with chronic hepatitis B

Chun-Sheng Hou, Gui-Qiang Wang, Shu-Lan Lu, Bei Yue, Ming-Rong Li, Xiao-Yan Wang, Jian-Wu Yu

Shu-Lan Lu, Bei Yue, Ming-Rong Li, Xiao-Yan Wang, Jian-Wu Yu, Department of Infectious Diseases, The 2nd Affiliated Hospital, Harbin Medical University, Harbin 150086, Heilongjiang Province, China
Chun-Sheng Hou, Jining Infectious Diseases Hospital, Jining 272031, Shandong Province, China
Gui-Qiang Wang, Department of Infectious Diseases, The First Affiliated Hospital, Beijing Medical University, Beijing 100034, China
Supported by the National Natural Science Foundation of China, No. 39570655
Correspondence to: Dr. Chun-Sheng Hou, Jining Infectious Diseases Hospital, Jining 272031, Shandong Province, China. cshou2000@sina.com
Telephone: +86-537-2032536
Received: 2003-03-05 **Accepted:** 2003-06-19

Abstract

AIM: To study and compare the difference of activation-induced cell death (AICD) in peripheral blood T-lymphocytes (PBL-Ts) from patients with chronic hepatitis B (CHB) and the normal people *in vitro*, and to explore the role of AICD in chronic hepatitis B virus (HBV) infection and the pathogenesis of CHB.

METHODS: Twenty-five patients and fourteen healthy people were selected for isolation of PBL-Ts. During cultivation, anti-CD3 mAb, PMA and ionomycin were used for AICD of PBL-Ts. AICD ratio of PBL-Ts was detected with TdT-mediated dUTP nick end labeling and assessed by flow cytometry.

RESULTS: When induced with anti-CD3, PMA and ionomycin *in vitro*, AICD ratio of PBL-Ts from CHB patients was significantly higher than that from healthy control (17.24±1.21 *vs*. 6.63±1.00, $P<0.01$) and that from CHB patients without induction (17.24±1.21 *vs*. 9.88±1.36, $P<0.01$). There was a similar AICD ratio of PBL-Ts between induction group and without induction group, but no difference was found before and after induction in healthy control. The density of INF-γ in culture media of induction groups of CHB was lower than that of other groups ($P<0.01$). There was no difference between these groups in density of IL-10 ($P>0.05$).

CONCLUSION: When induced during cultivation *in vitro*, PBL-Ts from CHB have AICD very commonly. This phenomenon has a potentially important relation with pathogenesis of CHB and chronicity of HBV infection.

Hou CS, Wang GQ, Lu SL, Yue B, Li MR, Wang XY, Yu JW. Role of activation-induced cell death in pathogenesis of patients with chronic hepatitis B. *World J Gastroenterol* 2003; 9(10): 2356-2358
http://www.wjgnet.com/1007-9327/9/2356.asp

INTRODUCTION

Currently, the exact pathogenesis of chronic hepatitis B (CHB) and the reason of chronic hepatitis B virus (HBV) infection are still not completely understood. Activation-induced cell death (AICD) is related with lymphocytes decrease and functional defect. This phenomenon can cause decrease of immune clearance. Alloreactive T cells can effectively be depleted from allogeneic T cells by induction of AICD to prevent graft-versus-host disease[1]. AICD is essential for the function, growth and differentiation of T-lymphocytes[2]. This may be an important reason of persistent infection of HBV. AICD in peripheral blood T-lymphocytes (PBL-Ts) of CHB *in vivo* has been approved by some reports, but does AICD occur more easily in PBL-Ts of CHB than in those of healthy control? In order to explore the role of AICD in chronic HBV infection, we studied and contrasted the difference of AICD in PBL-Ts from patients with CHB and from normal people *in vitro*.

MATERIALS AND METHODS

Patients

Twenty-five patients (17 men, 8 women, aged 19-49, mean age 35.6 years) with CHB between March 2000 and April 2001 were selected from the Second Affiliated Hospital of Harbin Medical University. The diagnoses of all the patients were in accord with the Fifth National Conference on the Diagnostic Criteria of Virus Hepatitis (Beijing, 1995). And 14 healthy persons were selected as control.

PBL-Ts isolation

10 mL peripheral blood was taken and heparin was added for anticoagulation. After equivalent Ficoll-Paque (from Amersham-Pharmacia, USA) was gently added, peripheral blood monocytes (PBMCs) were isolated by density gradient centrifugation (600 g, 20 min). Then PBL-Ts were purified with negative selection technique using immune-magnetic beads as follow. After PBMC was washed, mouse-anti-human anti-CD_{14}, anti-CD_{16}, anti-CD_{19} (2 μg· mL^{-1}, DAKO Company, Denmark) were added and incubated for 30 min at 0 ℃, centrifuged for removing the uncombined antibody. Then goat-anti-mouse CD3 mAb coating with magnetic beads (1 cell *vs.* 30 beads, Promega Company, USA) was added and incubated for 30 min at 0 ℃. B cells, NK cells and monocytes were all linked with immune-magnetic beads and absorbed by magnetic stock (DAKO Company, Denmark). After the liquor was gently extracted by centrifugation, PBL-Ts were purified. The viability (95 %) of the cells was confirmed by trypan blue staining. When detected by flow cytometry, the purity of PBL-Ts was over 97 %.

Cultivation and AICD induction of PBL-Ts in vitro

After washed 3 times with PBS, 2×10^6· mL^{-1} PBL-Ts were added to a 24 well plate (NENC Company, USA) for cultivation. The samples were divided into treatment group and control group. The culture medium was RPMI1640 (GIBCO Company, USA) containing 10 % calf blood serum (BANDIN TECH Company, China), penicillin (100 U· mL^{-1}, BANDIN TECH Company, China) and streptomycin (100 U· mL^{-1}, BANDIN TECH Company, China). The wells of treatment group were pre-coated with anti-CD_3 mAb (5 μg· mL^{-1}, DAKO

Company, Denmark). Phorbol 12-myrisate 13-acetate (PMA) (50 ng· mL^{-1}, Sigma Company, USA) and ionomycin (50 ng· mL^{-1}, Sigma Company, USA) were added to the culture medium[3]. The culture medium of control group did not contain CD_3, PMA and ionomycin. The liquid of culture medium was adjusted to 1 mL. After cultured for 14 h (37 ℃, 5 % CO_2), PBL-Ts were harvested for AICD detection.

Observation by fluorescence microscope

Some PBL-Ts were put on the carry sheet glass, dried naturally and fixed by 4 % formaldehydum polymerisatum. Then, all the cells were stained with TdT-mediated dUTP nick end labeling (TUNEL, procedure according to clarification of the kit) (Promega Company, USA). The positive cells of TUNEL staining were detected by fluorescence microscope (BG-12, Olympass, Japan).

Flow cytometry detection

1×10^6 PBL-Ts were washed, fixed by1 % formaldehydum polymerisatum, stayed overnight in 70 % ethanol (-20 ℃) and stained with TUNEL for apoptosis detection (procedure according to clarification of the kit). The apoptotic ratio of PBL-Ts was detected by a flow cytometer (Fort, B-D Company, USA).

Cytokine detection

100 μl supernatant of medium was collected respectively from each group after cultured for 14 h and frozen in -20 ℃ refrigerator for detection. The contents of IFN-γ and IL-10 were detected by using an ELISA kit. The parallel sample was set up for each sample. The OD450 value of each sample was measured with an enzyme label meter (550 model, Bio-RAD Program, USA), and then the content of each sample was converted according to the standard curve.

Statistical analysis

The data were presented as $\bar{x}\pm s$. ANOVA was used to compare the means.

RESULTS

Observation by fluorescence microscope

The apoptotic PBL-Ts presented DNA breakage. The breakage DNA could be linked by fluorescence labeling dUTP when TUNEL staining was adopted. The apoptotic cells took on kelly fluorescence under fluorescence microscope (Figure 1). This was named positive TUNEL staining. The plasm of PBL-Ts with AICD took on red fluorescence and the nuclei took on kelly fluorescence when TUNEL and PI double staining were adopted. But the cells without AICD only took on red fluorescence (Figure 2). The positive cells of TUNEL staining in PBL-Ts of CHB (with and without anti-CD3mAb, PMA and ionomycin) were more excessive than that of healthy control.

Results of flow cytometry detection

After cultivated for 14 h with induction, the PBL-Ts of CHB patients displayed distinct apoptosis. Apoptosis was also found in groups without anti-CD3 and other inductions, but their apoptotic ratio was lower. There was a similar AICD ratio of PBL-Ts between induction group and healthy control without induction. AICD ratio of PBL-Ts from CHB patients (with or without induction) was significantly higher than that from healthy control (Table 1).

Results of cytokine detection

Activated T lymphocytes may produce plentiful endogenous cytokine. Th_1 mainly produces IFN-γ, IL-2 and TNF-α. But Th_2 mainly produces IL-4, IL-5, IL-6, IL-10, etc. Cytokine IFN-γ, IL-10 were detected in this test. In all groups, the density of INF-γ in culture media of healthy control with induction group was the highest, and the patient in groups with induction was the lowest. But there was no difference among these groups in density of IL-10 (Table 2).

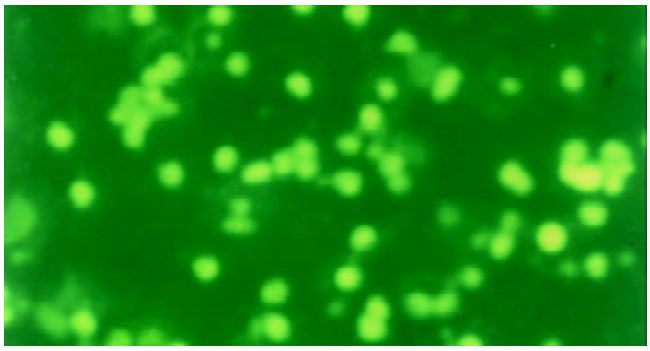

Figure 1 PBL-T with AICD took on kelly fluorescence and the cell without AICD did not take on any fluorescence (TUNEL staining, 200×, fluorescence microscope).

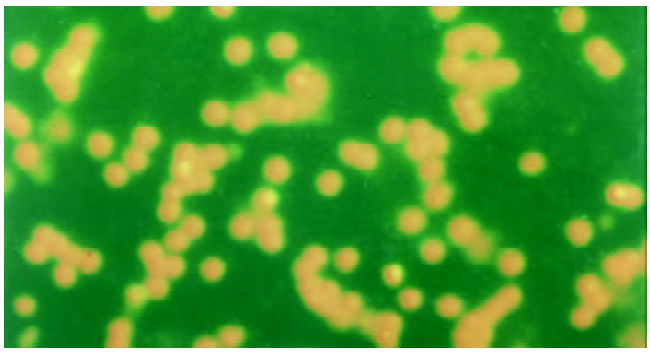

Figure 2 The plasm of PBL-T with AICD took on red fluorescence and the nucleus took on kelly fluorescence. But the cell without AICD only took on red fluorescence (TUNEL and PI double staining, fluorescence microscope, 200×).

Table 1 AICD ratio of each group ($\bar{x}\pm s$)

Group	*n*	AICD Ratio (%)
Patient with induction	26	$17.24\pm1.21^{a,b,c}$
Patient without induction	26	9.88 ± 1.36^{b}
Healthy control with induction	15	6.63 ± 1.00^{c}
Healthy control without induction	15	6.44±1.01

$^aP<0.01$ (F=164.34) *vs*. other groups; $^bP<0.01$ (F=660.45) *vs*. healthy control groups; $^cP<0.01$ (F=326.37) *vs*. without induction groups.

Table 2 The density of IFN-γ and IL-10 from medium of each group ($x\pm s$, pg·mL^{-1})

Group	*n*	IFN-γ	IL-10
Patient with induction	26	$728.32\pm149.59^{a,b,c}$	175.75 ± 34.65^{d}
Patient without induction	26	$1\,313.35\pm403.98^{b}$	74.48±37.21
Healthy control with induction	15	$2\,255.18\pm465.56^{c}$	188.86±66.26
Healthy control without induction	15	2 379.22±465.33	190.58±46.65

$^aP<0.01$ (F=7.37) *vs*. other three groups; $^bP<0.01$ (F=232.94) *vs*. healthy control groups; $^cP<0.01$ (F=25.90) *vs*. groups without induction; $^dP>0.05$ (F=0.02) *vs*. other three groups.

DISCUSSION

Chronic HBV infection is mainly related to the immune function of patients. In a large degree, immune tolerance, especially neonatal immune tolerance, results in persistence of chronic HBV infection. Because naive T cells are sensitive to Fas-mediated AICD and more easily deleted by Ag restimulation than primed T cells[4]. AICD of PBL-Ts plays a key role in central and peripheral immune tolerance[5,6]. AICD is one kind of apoptosis of reactivated lymphocytes when these lymphocytes are induced by activation signals (especially by complex of TCR/CD_3). Ashwell and his colleagues first detected the AICD phenomenon in 1987 when they studied T lymphocyte hybrid tumors. AICD plays an important role in the negative selection of T lymphocytes in thymus, peripheral elimination and clearance of T lymphocytes that have already cleaned the foreign antigens. Therefore, AICD is an important mechanism in maintaining immunoregulation and achieving immune system homeostasis[6,7]. If one' s AICD mechanism is disordered (up-regulation or down-regulation), immune tolerance or autoimmune disease would occur.

In this experiment, AICD of PBL-Ts was successfully induced using anti-CD3 mAb, PMA and ionomycin. The responses of PBL-Ts from CHB and healthy control were different. The results indicated that when induced with anti-CD3, PMA and ionomycin *in vitro*, AICD ratio of PBL-Ts from CHB patients was significantly higher than that from healthy control and that from CHB patients without induction. But there was a similar AICD ratio of PBL-Ts between induction group and healthy control without induction. The results imply that AICD exists in PBL-Ts of CHB and causes decrease of T lymphocytes especially Th_1 cells and functional defect. Specific immune response aiming directly at HBV should not occur. Finally, immunology tolerance to HBV would occur. Ji *et al* using staphylococcus aureus enterotoxin B and rHBcAg proved that AICD of PBMCs in patients would lead to persistent infection of HBV[8].

Reduction of deferent cytokines in culture medium implies apoptosis of deferent subtype T lymphocytes, because the types of cytokine secreted by Th1 and Th2 are different. The detection results revealed that the density of INF-γ in culture media of induction groups from CHB was lower than that of other groups ($P<0.01$). There was no difference between these groups in density of IL-10 ($P>0.05$). These results imply AICD cells are mainly Th1 cells.

After infection of HBV, the virus elimination depends on specific cell immunity of the body. Mostly, specific cell immunity responses are induced by Th1 lymphocytes, but humoral immunity responses are induced by Th2 type lymphocytes. The sensitivity of the two types of T lymphocytes is not equal. The occurrence of AICD is easily induced by Th1 but not Th2 when induced by Anti-CD3 and corresponding antigen[9-11]. Fan *et al* have proved that enhanced Th2 responses are present in chronic HCV infection, and this should be responsible for the persistent HCV infection[12-14]. So, if specific PBL-Ts of CHB are reactivated by HBV antigens, AICD would occur mostly in Th1 type lymphocytes. Thus, specific cell immunity response aiming directly at HBV would be defective, and HBV permanent infection would occur. However, it would be a possible method to surmount immune tolerance and to clean HBV of CHB patients that we have managed to block the apoptosis of activated T lymphocytes[6,15] and raise the amount of specific T lymphocytes.

ACKNOWLEDGEMENT

We are grateful to professor Hu-Lun Li (Harbin Medical University), Fang Liu, Wei Liu, Jin-Bai Guo, Shu-Yun Zhang, the staff members of Department of Infectious Diseases (the 2nd Affiliated Hospital, Harbin Medical University), Qin-Huan Wang (the First Affiliated Hospital, Beijing Medical University), Xue-Hai Zhang, Jin-Jian Bi (Jining Infectious Diseases Hospital) for their excellent technical assistant.

REFERENCES

1 **Hartwig UF**, Robbers M, Wickenhauser C, Huber C. Murine acute graft-versus-host disease can be prevented by depletion of alloreactive T lymphocytes using activation-induced cell death. *Blood* 2002; **99:** 3041-3049
2 **Baumann S**, Krueger A, Kirchhoff S, Krammer PH. Regulation of T cell apoptosis during the immune response. *Curr Mol Med* 2002; **2:** 257-272
3 **Kottilil S**, Bowmer MI, Trahey J, Howley C, Gamberg J, Grant MD. Fas/FasL-independent activation-induced cell death of T lymphocytes from HIV-infected individuals occurs without DNA fragmentation. *Cell Immunol* 2001; **214:** 1-11
4 **Inaba M**, Kurasawa K, Mamura M, Kumano K, Saito Y, Iwamoto I. Primed T cells are more resistant to Fas-mediated activation-induced cell death than naive T cells. *J Immunol* 1999; **163:** 1315-1320
5 **Hamad AR**, Schneck JP. Antigen-induced T cell death is regulated by CD4 expression. *Int Rev Immunol* 2001; **20:** 535-546
6 **Tanimoto Y**, Kizaki H. Proteasome inhibitors block Ras/ERK signaling pathway resulting in the down regulation of Fas ligand expression during activation-induced cell death in T cells. *J Biochem* 2002; **131:** 319-326
7 **Maher S**, Toomey D, Condron C, Bouchier-Hayes D. Activation-induced cell death: the controversial role of Fas and Fas ligand in immune privilege and tumour counterattack. *Immunol Cell Biol* 2002; **80:** 131-137
8 **Ji W**, Wang HF, Feng CQ. Activation-induced cell death in peripheral blood mononuclear cells (PBMCs) from patients with chronic hepatitis B may be related to abnormal production of interleukin 12 and 10. *J Viral Hepat* 2001; **8:** 30-33
9 **Varadhachary AS**, Peter ME, Perdow SN, Krammer PH, Salgame P. Selective up-regulation of phosphatidylinositol 3'-kinase activity in Th2 cells inhibits caspase-8 cleavage at the death-inducing complex: a mechanism for Th2 resistance from Fas-mediated apoptosis. *J Immunol* 1999; **163:** 4772-4779
10 **Gorak-Stolinska P**, Truman JP, Kemeny DM, Noble A. Activation-induced cell death of human T-cell subsets is mediated by Fas and granzyme B but is independent of TNF-alpha. *J Leukoc Biol* 2001; **70:** 756-766
11 **Roozendaal R**, Vellenga E, de Jong MA, Traanberg KF, Postma DS, de Monchy JG, Kauffman HF. Resistance of activated human Th2 cells to NO-induced apoptosis is mediated by gamma-glutamyltranspeptidase. *Int Immunol* 2001; **13:** 519-528
12 **Fan XG**, Liu WE, Li CZ, Wang ZC, Lou LX, Tan DM, Hu GM. Determination of serum cytokines in individuals with HCV infection. *Zhonghua Shiyan He Linchuangbing Duxue Zazhi* 2000; **14:** 145-147
13 **Fan XG**, Tang FQ, Yi H, Liu WE, Houghton M, Hu GL. Effect of IL-12 on T-cell immune responses in patients with chronic HCV infection. *APMIS* 2000; **108:** 531-538
14 **Fan XG**, Liu WE, Li CZ, Wang ZC, Luo LX, Tan DM, Hu GL, Zhang Z. Circulating Th1 and Th2 cytokines in patients with hepatitis C virus infection. *Mediators Inflamm* 1998; **7:** 295-297
15 **Da Rocha Dias S**, Rudd CE. CTLA-4 blockade of antigen-induced cell death. *Blood* 2001; **97:** 1134-1137

Edited by Wang XL

P.O.Box 2345, Beijing 100023,China
Fax: +86-10-85381893
E-mail: wjg@wjgnet.com www.wjgnet.com

World J Gastroenterol 2003;9(10):2359-2361
World Journal of Gastroenterology
 ISSN 1007-9327

• BRIEF REPORTS •

Temporary partially-covered metal stent insertion in benign esophageal stricture

Ying-Sheng Cheng, Ming-Hua Li, Wei-Xiong Chen, Ni-Wei Chen, Qi-Xin Zhuang, Ke-Zhong Shang

Ying-Sheng Cheng, Ming-Hua Li, Qi-Xin Zhuang, Ke-Zhong Shang, Department of Radiology, Sixth People' s Hospital, Shanghai Jiaotong University, Shanghai 200233, China
Wei-Xiong Chen, Ni-Wei Chen, Department of Gastroenterology, Sixth People' s Hospital, Shanghai Jiaotong University, Shanghai 200233, China
Supported by the National Key Medical Research and Development Program of China during the 9th Five-year Plan Period (No.96-907-03-04), Shanghai Nature Science Funds (No.02Z1314073), Shanghai Medical Development Funds (No.00419)
Correspondence to: Dr. Ying-Sheng Cheng, Department of Radiology, Sixth People' s Hospital, Shanghai Jiaotong University, Shanghai 200233, China. chengys@sh163.net
Telephone: +86-21-64368920 **Fax:** +86-21-64701361
Received: 2003-05-13 **Accepted:** 2003-06-02

Abstract

AIM: To study the therapeutic efficacy of temporary partially-covered metal stent insertion on benign esophageal stricture.

METHODS: Temporary partially-covered metal stent was inserted in 83 patients with benign esophageal stricture. All the patients had various dysphagia scores.

RESULTS: Insertion of 85 temporary partially-covered metal stents was performed successfully in 83 patients with benign esophageal stricture and dysphagia was effectively remitted in all the 83 cases. The dysphagia score was 3.20±0.63 (mean±SD) and 0.68±0.31 before and after stent insertion, and 0.86±0.48 after stent removal. The mean diameter of the strictured esophageal lumen was 3.37±1.23 mm and 25.77±3.89 mm before and after stent insertion, and 16.15±2.96 mm after stent removal. Follow-up time was from 1 week to 96 months (mean 54.26±12.75 months). The complications were chest pain (n=37) after stent insertion, and bleeding (n=12) and reflux (n=13) after stent removal.

CONCLUSION: Temporary partially-covered metal stent insertion is one of the best methods for treatment of benign esophageal stricture.

Cheng YS, Li MH, Chen WX, Chen NW, Zhuang QX, Shang KZ. Temporary partially-covered metal stent insertion in benign esophageal stricture. *World J Gastroenterol* 2003; 9(10): 2359-2361

http://www.wjgnet.com/1007-9327/9/2359.asp

INTRODUCTION

Benign esophageal stricture is a common complication in esophageal diseases. Balloon catheter dilation under X-ray was previously the most common treatment for benign esophageal stricture. Its short-term curative efficacy is good, but it does not last long. The development in stenting techniques has led to the increased application of stents in benign esophageal stricture. However, because of the relatively high incidence of complications and the difficulty of handling those complications, it is preferable to use stents with discretion. Here we report our experiences in using temporary partially-covered metal stent insertion in 83 patients with benign esophageal stricture.

MATERIALS AND METHODS

Materials

Eighty-three patients (48 males, 35 females, age 18-82 years) came to our clinic due to dysphagia. A dysphagia score was assessed by the quality of swallowing[1,2]. Grade 0 is for normal swallowing, grade 1 for swallowing most solid food, grade 2 for swallowing semisolids, grade 3 for swallowing liquid food only, and grade 4 for complete dysphagia. The dysphagia score of the 83 patients was 3.20±0.63 (mean±SD), and the causes of stricture were achalasia of cardia (n=70), anastomotic stenosis (n=5), sclerotic stricture due to ingestion of corrosive agents (n=3) and simple sclerosis stricture after radiation therapy for esophageal carcinoma (n=5). The diagnoses were made by an upper gastrointestinal contrast examination using barium-meal radiography and gastroscopic assessment. The mean diameter of the strictured esophageal lumen was 3.37±1.23 mm in the 83 patients with partially-covered metal stent insertion.

Methods

The preparation before stent insertion involved ensuring an empty stomach for at least 4 hours, testing of the bleeding and clotting times, and intramuscular injection of ataractics before interventional procedure. The stent made from nitinol (a nonmagnetic Ni-Ti alloy) by Chinese manufacturers (Zhiye Medical Instruments Corporation, Changzhou, China, and Youyan Yijin Advanced Materials Co.Ltd, Beijing, China) has a length of 4-12 cm and a diameter of 16-30 cm. Its surface is covered with silica gel. The savary conical silica-gel dilator has a diameter of 0.5-2 cm, and contrast medium.

The patients were placed in a sitting position or lying on the side during the stent-placement operation, and false teeth were removed and dental pads were placed. A 260-cm-long exchange guidewire was inserted into the stomach. Along with the guidewire, the nitinol stent was installed in the propeller. After the propeller was pushed to the stricture segment, the mantle annular tube was retracted, after which the stent would automatically expand. After stent expansion, barium-meal radiography was routinely used to examine the stent position and the dilated stricture. Three to seven days after stent deployment, 500-1 000 ml of ice-cold water was poured into the side hole of a gastroscope. A protractor was then used to loosen the stent from its surroundings and was then connected to the stent orifice. The stent orifice shrank when we contracted the protractor, and then the stent was removed along with the gastroscope. After that, a gastroscope was again inserted to examine bleeding and mucosa tearing membranes. The patients were allowed to consume cold food for the first 2 days after interventional procedure, and resumed a normal diet afterwards. Within 1 week, barium-meal examination was used to observe the intraluminal patency and swallowing function.

one-month, 6-months, and 1-year follow-ups were recommended.

RESULTS

We inserted 85 temporary partially-covered metal stents in 83 patients with esophageal stricture, which were removed 3-7 days later. The placement and removal of stents were successful in 100 % of cases. Immediately after placing the stent, we performed an esophageal contrast examination, which confirmed good stricture patency. The mean diameter of the esophageal lumen was 25.77±3.89 mm after stent insertion, and 16.15±2.96 mm after stent removal. The dysphagia score was 0.68±0.31 after stent insertion, and 0.86±0.48 after stent removal. The mean follow-up time was 54.26±12.75 months (range 1 week-96 months). The complications immediately after stent insertion were chest pain (37 cases). After stent removal, 12 cases had a small amount of bleeding and 13 had reflux. All these complications were managed effectively. Temporary partially-covered metal stent insertion and removal were obviously effective on the esophageal stricture and dysphagia.

DISCUSSION

The short-term effect of balloon dilation on esophageal benign stricture was good, but its mid-term and long-term curative effect was not ideal. In 1990 Domschke *et al*[1] first reported an expandable stent used in malignant esophageal strictures. Since then different types of stent have been developed and applied to the gastrointestinal system[2]. In 1993 Cwikiel *et al*[3] reported the application of silica-gel-covered stent in benign esophageal strictures. The covering of the stent was found to be effective against recurrence of esophageal stricture[4-39]. Because covered stents would migrate, they have not been widely used for some time. However, patients with uncovered stents exhibited more complications such as reflux, stricture recurrence (hyperplasia of granulation tissue), and pain. There is no effective way to manage these complications, which impacts on the long-term curative effect. The worse thing for cases was that another surgical operation was sometimes required to resect the stricture section and the stent placed previously. In order to solve these problems, we used temporary partially-covered metal stent insertion in benign esophageal stricture[40]. The follow-up time was approximately 8 years. The curative effect was long-lasting, dysphagia was clearly palliated, and complications were reduced and easy to manage. Temporary partially-covered metal stent insertion was effective on benign esophageal stricture. Our follow-up investigations revealed that the mid-term and long-term curative effect of temporary stent insertion was better than that of balloon dilation and permanently uncovered or antireflux covered or partially-covered metal stent[41-48]. Our results demonstrated that it was unnecessary to perform graded diameter increment in such stents, unlike when dilating the balloon catheter. Its necessity could be decided based on the follow-up data. After stent insertion, the complications of pain and reflux due to dilating the esophageal stricture by the stent were mainly caused by the chronic tissue tearing of the layer of esophageal muscle and the damage to the original anatomy of the stomach cardia. The stent continued to expand until it reached to body temperature. Since this took 16-24 hours, the tearing of the esophageal muscle tissue was relatively regular and comparatively less scar tissue was formed. Therefore, the recurrence of stricture was low, unlike in balloon dilation which caused acute and irregular tearing on the layer of esophageal muscle, and a corresponding high recurrence of stricture. This is one reason why the method of temporary partially-covered metal stent insertion in benign esophageal stricture is better than that of balloon dilation. We used uncovered stents in patients with benign esophageal strictures in order to reduce the occurrence rate of stent migration. After stent placement, dilation was excellent and dysphagia disappeared, thus achieving the goal of treatment. However, it was accompanied by new problems such as gastroesophageal reflux and recurrence of stricture (hyperplasia of granulation tissue). The reflux could be treated with drugs, but this took a long time. Recurrence of stricture could be reduced by heat cauterization under gastroscope, but it could easily reccur. When we used antireflux covered stent, compications of gastroesophageal reflux and hyperplasia of granulation tissue were not found, but many unexpected results occurred. Comparative studies and experimental research are recommended to further explore the recurrence mechanisms. Further research and development of new stents that are biodegraded by esophageal organism within 2 months after insertion would improve their curative effect, and provide a new therapeutic method for benign esophageal stricture[49]. With further developments in molecular biology, application of gene therapy in the treatment of benign esophageal stricture is expected.

REFERENCES

1 **Domschke W**, Foerster EC, Matek W, Rodl W. Self-expanding mesh stent for esophageal cancer stenosis. *Endoscopy* 1990; **22**: 134-136

2 **Song HY,** Choi KC, Kwon HC, Yang DH, Cho BH, Lee ST. Esophageal strictures: treatment with a new design of modified Gianturco stent, Work in progress. *Radiology* 1992; **184**: 729-734

3 **Cwikiel W,** Willen R, Stridbeck H, Lillo-Gil R, von Holstein CS. Self-expanding stent in the treatment of benign esophageal strictures: experimental study in pigs and presentation of clinical cases. *Radiology* 1993; **187**: 667-671

4 **Song HY,** Do YS, Han YM, Sung KB, Choi EK, Sohn KH, Kim HR, Kim SH, Min YI. Covered, expandable esophageal metallic stent tubes: experiences in 119 patients. *Radiology* 1994; **193**: 689-695

5 **Foster DR.** Use of a Strecker oesophageal stent in the treatment of benign oesophageal stricture. *Australas Radiol* 1995; **39**: 399-400

6 **Strecker EP**, Boos I, Vetter S, Strohm M, Domschke S. Nitinol esophageal stents: new designs and clinical indications. *Cardiovasc Intervent Radiol* 1996; **19**: 15-20

7 **Vanderburgh L,** Ho CS. Nonvascular stents. *Prog Cardiovasc Dis* 1996; **39**: 187-200

8 **Moores DW,** Ilves R. Treatment of esophageal obstruction with covered, self-expanding esophageal Wallstents. *Ann Thorac Surg* 1996; **62**: 963-967

9 **Heindel W,** Gossmann A, Fischbach R, Michel O, Lackner K. Treatment of a ruptured anastomotic esophageal stricture following bougienage with a Dacron-covered nitinol stent. *Cardiovasc Intervent Radiol* 1996; **19**: 431-434

10 **Fry SW,** Fleischer DE. Management of a refractory benign esophageal stricture with a new biodegradable stent. *Gastrointest Endosc* 1997; **45**: 179-182

11 **Song HY,** Park SI, Do YS, Yoon HK, Sung KB, Sohn KH, Min YI. Expandable metallic stent placement in patients with benign esophageal strictures: results of long-term follow-up. *Radiology* 1997; **203**: 131-136

12 **Song HY,** Park SI, Jung HY, Kim SB, Kim JH, Huh SJ, Kim TH, Kim YK, Park S, Yoon HK, Sung KB, Min YI. Benign and malignant esophageal strictures: treatment with a polyurethane-covered retrievable expandable metallic stent. *Radiology* 1997; **203**: 747-752

13 **Foster DR.** Self-expandable oesophageal stents in the management of benign peptic oesophageal strictures in the elderly. *Br J Clin Pract* 1997; **51**: 199

14 **Tan BS,** Kennedy C, Morgan R, Owen W, Adam A. Using uncovered metallic endoprostheses to treat recurrent benign esophageal strictures. *Am J Roentgenol* 1997; **169**: 1281-1284

15 **Hramiec JE,** O'Shea MA, Quinlan RM. Expandable metallic esophageal stents in benign disease: a cause for concern. *Surg Laparosc Endosc* 1998; **8**: 40-43

16 **Miller LS,** Jackson W, McCray W, Chung CY. Benign nonpeptic esophageal strictures. Diagnosis and treatment.*Gastrointest Endosc Clin N Am* 1998; **8**: 329-355

17 **Sheikh RA,** Trudeau WL. Expandable metallic stent placement in patients with benign esophageal strictures: results of long-term follow-up. *Gastrointest Endosc* 1998; **48**: 227-229

18 **Wengrower D**, Fiorini A, Valero J, Waldbaum C, Chopita N, Landoni N, Judchack S, Goldin E. EsophaCoil: long-term results in 81 patients. *Gastrointest Endosc* 1998; **48**: 376-382

19 **Cowling MG,** Adam A. Radiological management of oesophageal strictures. *Hosp Med* 1998; **59**: 693-697

20 **Kang SG,** Song HY, Lim MK, Yoon HK, Goo DE, Sung KB. Esophageal rupture during balloon dilation of strictures of benign or malignant causes: prevalence and clinical importance. *Radiology* 1998; **209**: 741-746

21 **Monda LA.** Diagnosis and treatment of esophageal strictures. *Radiol Technol* 1999; **70**: 361-372

22 **Vakil N,** Gross U, Bethge N. Human tissue responses to metal stents. *Gastrointest Endosc Clin N Am* 1999; **9**: 359-365

23 **Sandha GS,** Marcon NE. Expandable metal stents for benign esophageal obstruction. *Gastrointest Endosc Clin N Am* 1999; **9**: 437-446

24 **Boulis NM,** Armstrong WS, Chandler WF, Orringer MB. Epidural abscess: a delayed complication of esophageal stenting for benign stricture. *Ann Thorac Surg* 1999; **68**: 568-570

25 **Pajarinen J**, Ristkari SK, Mokka RE. A report of three cases with an oesophageal perforation treated with a coated self-expanding stent. *Ann Chir Gynaecol* 1999; **88**: 332-334

26 **Cowling MG.** Stenting in the oesophagus.*Hosp Med* 2000; **61**: 33-36

27 **Fiorini A,** Fleischer D, Valero J, Israeli E, Wengrower D, Goldin E.Self-expandable metal coil stents in the treatment of benign esophageal strictures refractory to conventional therapy: a case series. *Gastrointest Endosc* 2000; **52**: 259-262

28 **Chen JS,** Luh SP, Lee F, Tsai CI, Lee JM, Lee YC. Use of esophagectomy to treat recurrent hyperplastic tissue obstruction caused by multiple metallic stent insertion for corrosive stricture. *Endoscopy* 2000; **32**: 542-545

29 **Macdonald S,** Edwards RD, Moss JG. Patient tolerance of cervical esophageal metallic stents. *J Vasc Interv Radiol* 2000; **11**: 891-898

30 **Lee JG,** Hsu R, Leung JW. Are self-expanding metal mesh stents useful in the treatment of benign esophageal stenoses and fistulas? An experience of four cases. *Am J Gastroenterol* 2000; **95**: 1920-1925

31 **Song HY,** Jung HY, Park SI, Kim SB, Lee DH, Kang SG, Il Min Y. Covered retrievable expandable nitinol stents in patients with benign esophageal strictures: initial experience. *Radiology* 2000; **217**: 551-557

32 **Cordero JA Jr,** Moores DW. Self-expanding esophageal metallic stents in the treatment of esophageal obstruction. *Am Surg* 2000; **66**: 956-959

33 **Morgan R,** Adam A. Use of metallic stents and balloons in the esophagus and gastrointestinal tract. *J Vasc Interv Radiol* 2001; **12**: 283-297

34 **Ackroyd R**, Watson DI, Devitt PG, Jamieson GG. Expandable metallic stents should not be used in the treatment of benign esophageal strictures. *J Gastroenterol Hepatol* 2001; **16**: 484-487

35 **Catnach S,** Barrison I. Self-expanding metal stents for the treatment of benign esophageal strictures. *Gastrointest Endosc* 2001; **54**: 140

36 **McManus K**, Khan I, McGuigan J. Self-expanding oesophageal stents: strategies for re-intervention. *Endoscopy* 2001; **33**: 601-604

37 **Power C,** Rynne M, O'Gorman T, Maguire D, McAnena OJ. An unusual complication following intubation of a benign oesophageal stricture. *Endoscopy* 2001; **33**: 642

38 **Lee SH.** The role of oesophageal stenting in the non-surgical management of oesophageal strictures. *Br J Radiol* 2001; **74**: 891-900

39 **Dormann AJ,** Deppe H, Wigginghaus B. Self-expanding metallic stents for continuous dilatation of benign stenoses in gastrointestinal tract - first results of long-term follow-up in interim stent application in pyloric and colonic obstructions. *Z Gastroenterol* 2001; **39**: 957-960

40 **Chen WX,** Cheng YS, Yang RJ, Li MH, Zhuang QX, Chen NW, Xu JR, Shang KZ. Interventional therapy of achalasia with temporary metal internal stent dilatation and its intermediate and long term follow-up. *Shijie Huaren Xiaohua Zazhi* 2000; **8**: 896-899

41 **Moses FM,** Wong RK. Stents for Esophageal Disease. *Curr Treat Options Gastroenterol* 2002; **5**: 63-71

42 **Wang YG,** Tio TL, Soehendra N. Endoscopic dilation of esophageal stricture without fluoroscopy is safe and effective. *World J Gastroenterol* 2002; **8**: 766-768

43 **Profili S,** Meloni GB, Feo CF, Pischedda A, Bozzo C, Ginesu GC, Canalis GC. Self-expandable metal stents in the management of cervical oesophageal and/or hypopharyngeal strictures. *Clin Radiol* 2002; **57**: 1028-1033

44 **Therasse E,** Oliva VL, Lafontaine E, Perreault P, Giroux MF, Soulez G. Balloon dilation and stent placement for esophageal lesions: indications, methods, and results. *Radiographics* 2003; **23**: 89-105

45 **Petruzziello L**, Costamagna G. Stenting in esophageal strictures. *Dig Dis* 2002; **20**: 154-166

46 **Cheng YS,** Yang RJ, Li MH, Shang KZ, Chen WX, Chen NW, Chu YD, Zhuang QX. Interventional procedure for benign or malignant stricture or obstruction of upper gastrointestinal tract. *Shijie Huaren Xiaohua Zazhi* 2000; **8**: 1354-1360

47 **Chen WX,** Cheng YS, Yang RJ, Li MH, Shang KZ, Zhuang QX, Chen NW. Metal stent dilation in the treatment of benign esophageal stricture by interventional procedure:a follow-up study. *Shijie Huaren Xiaohua Zazhi* 2002; **10**: 333-336

48 **Cheng YS,** Shang KZ. Interventional therapy in dysphagia. *Shijie Huaren Xiaohua Zazhi* 2002; **10**: 1312-1314

49 **Fry SW,** Fleischer DE. Management of a refractory benign esophageal stricture with a new biodegradable stent. *Gastrointest Endosc* 1997; **45**: 179-182

Edited by Zhang JZ and Wang XL

P.O.Box 2345, Beijing 100023,China
Fax: +86-10-85381893
E-mail: wjg@wjgnet.com www.wjgnet.com

World J Gastroenterol 2003;9(10):2362-2365
World Journal of Gastroenterology
 ISSN 1007-9327

• BRIEF REPORTS •

Antiproliferative effect of octreotide on gastric cancer cells mediated by inhibition of Akt/PKB and telomerase

Shan Gao, Bao-Ping Yu, Yan Li, Wei-Guo Dong, He-Sheng Luo

Shan Gao, Bao-Ping Yu, Wei-Guo Dong, He-Sheng Luo, Department of Gastroenterology, Renmin Hospital of Wuhan University, Wuhan 430060, Hubei Province, China
Yan Li, Department of Clinical Laboratory, Renmin Hospital of Wuhan University, Wuhan 430060, Hubei Province, China
Correspondence to: Dr. Bao-Ping Yu, Department of Gastroenterology, Renmin Hospital of Wuhan University, Wuhan 430060, Hubei Province, China. yubaoping62@yahoo.com.cn
Telephone: +86-27-88075814
Received: 2003-03-20 **Accepted:** 2003-04-14

Abstract

AIM: To investigate the antiproliferative effect of octreotide, a long-acting analogue of somatostatin, on gastric cancer cell line SGC7901 and its possible molecular mechanisms.

METHODS: Gastric cancer cell line SGC7901 employed in the study was treated with 0.008, 0.04, 0.2, 1, 5 and 25 $\mu g \cdot ml^{-1}$ of octreotide respectively for 24 h to evaluate the antiproliferative effect of somatostatin analog on the tumor cells by MTT assay method. To elucidate the underlying mechanism, the cells were exposed to 1 $\mu g \cdot ml^{-1}$ of octreotide for 0, 12, 24 and 48 h, when their Akt/PKB and telomerase activities were respectively determined using PCR-ELSIA and nonradioactive protein kinase assay protocols. The same experimental procedures were also performed in the control cells that were treated with corresponding vehicles instead of somatostatin analog.

RESULTS: After exposed to octreotide for 24 h at the concentrations of more than 1 $\mu g \cdot ml^{-1}$, SGC7901 cells exhibited a dose-dependent inhibition of growth with the inhibiting rate to be as high as 34.66 % when 25 $\mu g \cdot ml^{-1}$ of octreotide was applied. The Akt/PKB and telomerase activity of SGC7901 cells was significantly inhibited when the cells were exposed to 1 $\mu g \cdot ml^{-1}$ of octreotide for 12, 24 and 48 h compared with that of their control counterparts ($P<0.01$), both of which exhibited in a time-dependent manner.

CONCLUSION: The antiproliferative effect of octreotide on SGC7901 cells might be mediated by the inhibition of Akt/PKB and telomerase.

Gao S, Yu BP, Li Y, Dong WG, Luo HS. Antiproliferative effect of octreotide on gastric cancer cells mediated by inhibition of Akt/PKB and telomerase. *World J Gastroenterol* 2003; 9(10): 2362-2365

http://www.wjgnet.com/1007-9327/9/2362.asp

INTRODUCTION

Gastric cancer continues to be one of the most common malignancies in human worldwide[1-4]. In China, its average rate of annual mortality is estimated to be as high as 16 per 100 000 population that accounts for the leading cause of death among malignant tumors[5-7]. Due to the limited efficacy and considerable toxicity of conventional chemotherapy, some novel cytotoxic and noncytotoxic agents such as certain dietary substances, natural hormones and synthetic compounds have been proposed to stop or reverse the process of carcinogenesis[8], in which increasing attention has been paid to somatostatin and its analogs that have been reported to exert antineoplastic effects in a wide range of tumor types such as carcinoid, osteosarcoma, leukemia, and cancers of thyroid, breast, lung, liver, pancreas, colon, as well as gastric carcinomas[9-19]. However, detailed mechanisms underlying the antineoplastic actions of somatostatin and its analogs that remain to be clarified have limited the therapeutic efficacy of these agents in the treatment of clinical malignancies[20, 21].

Recent advances in molecular biological science have revealed that some molecules such as telomerase and protein kinase B or Akt (PKB/Akt) are involved in the process of carcinogenesis. Telomerase is an enzyme that replaces repetitive (TTAGGG)n sequences on the ends of chromosomes that would otherwise be lost during successive cell divisions. Its activation is closely linked to the attainment of cellular immortality and considered to be an important step in tumorigenesis[22-26]. Another molecule PKB/Akt, a serine/threonine kinase, has also recently been a focus of intense research. It appears that Akt/PKB lies in the crossroads of multiple cellular signaling pathways and acts as a transducer of many functions initiated by growth factor receptors. It is particularly important that Akt/PKB can mediate cell survival and serve as a critical factor in the genesis of malignancies[27-30]. Thus, an investigation to clarify how the antiproliferative effects on these couple of molecules might be helpful in elucidating antineoplastic mechanisms of somatostatin analogs, which is no doubt of both theoretical and practical importance.

MATERIALS AND METHODS

Materials

Human gastric cancer cell line SGC7901 was obtained from Shanghai Institute of Cell Biology, Chinese Academy of Sciences. Somatostatin analogue octreotide was provided by Sandoz Corp, RPMI1640 and fetal bovine serum (FBS) were from Gibco. 3-(4,5-dimethyl thiazol-2- yl)-2, 5-diphenyl tetrazolium bromide (MTT), telomerase TRAP PCR-ELISIA kit and Akt/PKB kinase assay kit were purchased from Sigma, Roche Molecular Biochemicals and CST respectively. Microtiter plate reader was made by Digiscan, Austria ASYS Hitech.

Cell culture

SGC7901 cells were maintained in flasks with RPMI-1640 supplemented with 10 % heat- inactivated FBS, 100 $U \cdot ml^{-1}$ penicillin, 100 $U \cdot ml^{-1}$ streptomycin and 20 mM sodium bicarbonate at 37 ℃ in a humidified atmosphere containing 5 % of CO_2. The culture medium change was performed every 3 days.

MTT assay

A MTT assay was conducted to determine the cell proliferation. In brief, SGC-7901 cells were seeded at $5\times10^3 \cdot$ $wells^{-1}$ in a 96-

well plate and incubated in 200 μl of culture medium overnight. Then the cells were made quiescent by serum deprivation and treated with 0.008, 0.04, 0.2, 1, 5, 25 $\mu g \cdot ml^{-1}$ of octreotide respectively as the different observatory groups. The cells treated with equal amount of normal saline instead of octreotide served as the control. After cultivated for 24 h, 20 μl of stock MTT solution (2.5 $mg \cdot ml^{-1}$) was added to cells for each well which were further incubated at 37 ℃ for 4 hours. The culture medium was carefully removed followed by adding of 150 μl of DMSO to each well and vibrating culture well for 10 min. The absorbance of samples was measured at a wavelength of 490 nm with a microtiter plate reader. The negative control was conducted using only cell-free culture medium and each assay was performed in triplicate. The inhibiting rate of cell growth was expressed as (A-B)/A×100 %, where A is the absorbance value from the controls and B is that from the experimental cells.

Immunoprecipitation kinase assay

Akt/PKB activity was examined by the immunoprecipitation kinase assay. Briefly, 5×10^5 of SGC7901 cells were seeded in a 25-cm^2 flask and cultured for 3 days. When being confluent at 70 %, cells nominated as group A were incubated in serum-free RPMI-1640 for 24 h and then treated with 1 $\mu g \cdot ml^{-1}$ octreotide for further cultivation of 0-, 12-, 24- and 48-h respectively. Same procedures were also performed in group B cells that served as the control except being treated with equal volume of normal saline instead of octreotide. Confluent cells were washed three times in cold PBS, then lysed in buffer containing 20 $mmol \cdot L^{-1}$ Tris-HCl (pH 7.5), l50 $mmol \cdot L^{-1}$ NaCl, 1 % Triton X-l00, 1 $mmol \cdot L^{-1}$ EDTA, 1 $mmol \cdot L^{-1}$ EGTA, 2.5 $mmol \cdot L^{-1}$ sodium pyrophosphate, 1 $mmol \cdot L^{-1}$ β-glycerophosphate, 1 $mmol \cdot L^{-1}$ Na_3VO_4, 1 $\mu g \cdot ml^{-1}$ leupeptin and 1 $mmol \cdot L^{-1}$ phenyl-methyl-sulfonyl fluoride (PMSF) for 10 min at 4 ℃. Samples were microcentrifuged for 10 min and 200 μl of the cell lysate was incubated with 20 μl of resuspended immobilized Akt antibody slurry at 4 ℃ for 2 h to immunoprecipitate Akt/PKB, the latter was next used to phosphorylate a specific substrate, GSK-3 fusion protein (Ser21/9). That is, 1 μg of GSK-3 fusion protein was incubated with immunoprecipitated Akt/PKB in the presence of ATP for 30 min at 30 ℃ followed by adding 20 μl of 3×SDS sample buffer to terminate the reaction. Samples were then boiled for 5 min, separated by 12 % SDS-PAGE and transferred onto nitrocellulose membrane. Nonspecific reactivity was blocked by 5 % fat-free milk in TBST (10 mM Tris-HCl, pH7.5, l50 mM NaCl, 0.05 % Tween 20) for 1 h. The membrane was incubated with a 1:1 000 dilution of phospho-GSK-3 α/β antibody for 2 h, then with HRP-conjugated anti-rabbit (1:2 000) and anti-biotin antibody (1:1 000) for 1 h at room temperature. Finally, reactive protein was revealed by incubating with 10 ml of LumiGLO for 1 min and exposed to x-ray film for 1-2 min at room temperature.

Determination of telomerase activity

The telomerase activity was determined by using TRAP-ELSIA. 5×10^5 of SGC7901 cells were seeded in a 25-cm^2 flask and cultured for 3 days. When being confluent at 70 %, cells nominated as group A were incubated in serum-free RPMI-1640 for 24 h and then treated with 1 $\mu g \cdot ml^{-1}$ octreotide for further cultivation of 0-, 12-, 24- and 48-h respectively. Same procedures were also performed in group B cells that served as the control except being treated with equal volume of DMSO instead of octreotide. Confluent cells were harvested and centrifuged at 3 000 g for 10 min at 4 ℃. After resuspended, 5×10^3 cells were lysed in an Eppendorf tube, whose extract was next used to amplify telomeric repeat. The telomerase activity was determined with PCR-ELISA according to the manufacturer' s protocol. Sample absorbance was measured with a microtiter plate reader at the wavelength of 450/690 nm within 30 min after addition of the stop reagent.

Statistical analysis

Experimental data were analyzed by ANOVA and Student' s *t* test for multiple comparisons between groups. The data were finally expressed as mean ± standard error of the mean. *P* value less than 0.05 was considered statistically significant.

RESULTS

Antiproliferative effect of octreotide on SGC7901 cells

When exposed to octreotide for 24 h at the concentration of more than 1 $\mu g \cdot ml^{-1}$, SGC7901 cells exhibited a dose-dependent inhibition of growth with the inhibiting rate to be as high as 34.66 % when 25 $\mu g \cdot ml^{-1}$ of octreotide was applied (Table 1).

Table 1 Antiproliferative effect of octreotide on SGC7901 cells

Octreotide (μg / ml)	OD_{490}	IR (%)
Control	0.528±0.032	/
25	0.345±0.041	34.66[b]
5	0.436±0.022	21.21[b]
1	0.465±0.019	11.93[a]
0.2	0.493±0.008	6.63
0.04	0.510±0.031	3.41
0.008	0.504±0.065	0.76

[a]*P*<0.05, [b]*P*<0.01 *vs* control.

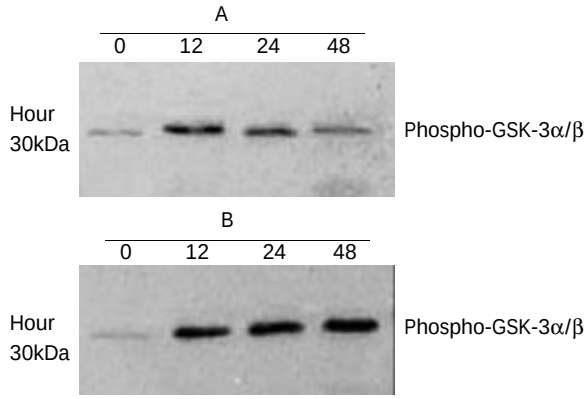

Figure 1 Inhibitory effects of octreotide on Akt / PkB activity in SGC7901 cells. The Akt / PKB activity in group A SGC7901 cells was significantly inhibited after the cells were exposed to 1 $\mu g \cdot ml^{-1}$ of octreotide for 12, 24 and 48 h compared with that of their control counterparts (Figure 1B), which manifested in a time-dependent manner as shown in Figure 1A.

Inhibition of Akt/PKB activity

The Akt/PKB activity in group A SGC7901 cells was significantly inhibited after the cells were exposed to 1 $\mu g \cdot ml^{-1}$ of octreotide for 12, 24 and 48 h compared with that of their control counterparts (Figure 1B), which exhibited in a time-dependent manner as shown in Figure 1A.

Inhibition of telomerase activity

Just like that of the Akt/PKB, the telomerase activity in group A SGC7901 cells was also significantly inhibited after the cells were exposed to 1 $\mu g \cdot ml^{-1}$ of octreotide for 12, 24 and 48 h compared with that of their control counterparts (*P*<0.01), which exhibited in a time- dependent manner as shown in Figure 2A.

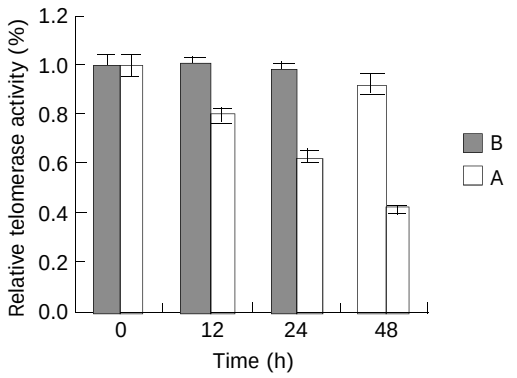

Figure 2 Inhibitory effects of octreotide on telomerase activity in SGC7901 cells. The telomerase activity in group A SGC7901 cells was significantly inhibited after the cells were exposed to 1 μg· ml^{-1} of octreotide for 12, 24 and 48 h compared with that of their control counterparts (P<0.01), which exhibited in a time-dependent manner as shown in Figure 2A.

DISCUSSION

Over the past decade, impressive antineoplastic effects of somatostatin and its analogs have been reported in plenty of tumor models and cancer cell types[9-19]. A more recent research has further provided considerable information regarding the mechanisms underlying the antiproliferative and apoptosis-inducing actions of these compounds. These included both "direct" mechanisms that were the sequellae of binding of somatostatin analogs to their corresponding receptors present on neoplastic cells and "indirect" mechanisms that might be the result of reduced or inhibited secretion of growth-promoting hormones and growth factors that stimulated the growth of various types of malignancies[21,31-33]. Apart from these discoveries, some biological actions such as the inhibition of angiogenesis and the negative influence on the immune system were also considered to be the important factors contributing to the antineoplastic effects of somatostatin analogs[21, 34], which therefore suggested that the latter might be involved in an even wider mechanism.

In the present study, we observed the inhibitory effects of octreotide on gastric cancer SGC7901cells, as well as on the activities of Akt/PKB and telomerase. As to our knowledge, it is one of the fewer reports in recent years that concerned about this subject. It revealed that after exposed to octreotide for 24 h at the concentration of more than 1 μg· ml^{-1}, SGC7901 cells exhibited a dose-dependent inhibition of growth with the inhibiting rate to be as high as 34.66 % when 25 μg· ml^{-1} of octreotide was applied. Furthermore, in a previous study, we also noted that this inhibitory action could not be abrogated by supplementing 10 % FBS to the cultured cells, which only prolonged the time course of cell death (data to be published). It indicated the mitogenic action provided by serum growth factors in the culture medium could be overcome by octreotide. Akt/PKB and telomerase are the enzymes that have recently been considered to be closely related to carcinogenesis[22-30]. Whether the activation of Akt/PKB was one of the critical factors in cell to determine either a survival or an apoptotic message was conducted on the signal passway[35]. Amplification of genes encoding Akt/PKB isoforms has been found in several types of human cancers[36]. In addition, Akt/PKB has been reported to promote tumor progression and invasiveness by enhancing angiogenesis[28]. So far as the telomerase is concerned, its activity has been detected in over 90 % of human cancers[37-41], In gastric cancer, telomerase was activated very early in the process of this disease[42], which suggested the activation of telomerase might be also a determining factor contributing to the tumorigenesis. The relationship between Akt/PKB and telomerase has also been noted by Kang and his coworkers[43] with the founding that Akt kinase enhanced human telomerase activity through phosphorylation of hTERT subunit as one of its substrate proteins in SK-MEL28 cells. In the present study, we found that both activities of Akt/PKB and telomerase in SGC7901 cells were significantly inhibited after the cells were exposed to 1 μg· ml^{-1} of octreotide for 12, 24 and 48 h compared with that of their control counterparts. Based on these findings, it can be concluded that the antiproliferative effects of somatostatin analogs on SGC7901 cells might be mediated at least in part via a mechanism of inhibition of Akt/PKB and then telomerase. Our further study should aim at elucidating the components on the signal conduction passway in up and downstreams of these events.

REFERENCES

1 **Newnham A,** Quinn MJ, Babb P, Kang JY, Majeed A. Trends in oesophageal and gastric cancer incidence, mortality and survival in England and Wales 1971-1998 / 1999. *Aliment Pharmacol Ther* 2003; **17:** 655-664
2 **Mathers CD,** Shibuya K, Boschi-Pinto C, Lopez AD, Murray CJ. Global and regional estimates of cancer mortality and incidence by site: I. Application of regional cancer survival model to estimate cancer mortality distribution by site. *BMC Cancer* 2002; **2:** 36
3 **Le Vu B,** de Vathaire F, de Vathaire CC, Paofaite J, Roda L, Soubiran G, Lhoumeau F, Laudon F. Cancer incidence in French Polynesia 1985-1995. *Trop Med Int Health* 2000; **5:** 722-731
4 **Mohandas KM,** Jagannath P. Epidemiology of digestive tract cancers in India. VI. Projected burden in the new millennium and the need for primary prevention. *Indian J Gastroenterol* 2000; **19:** 74-78
5 **Sun X,** Mu R, Zhou Y, Dai X, Qiao Y, Zhang S, Huangfu X, Sun J, Li L, Lu F. 1990-1992 mortality of stomach cancer in China. *Zhonghua Zhongliu Zazhi* 2002; **24:** 4-8
6 **Xue FB**, Xu YY, Wan Y, Pan BR, Ren J, Fan DM. Association of *H. pylori* infection with gastric carcinoma: a Meta analysis. *World J Gastroenterol* 2001; **7**: 801-804
7 **Cao WX,** Ou JM, Fei XF, Zhu ZG, Yin HR, Yan M, Lin YZ. Methionine-dependence and combination chemotherapy on human gastric cancer cells *in vitro*. *World J Gastroenterol* 2002; **8:** 230-232
8 **Morse MA**, Stoner GD. Cancer chemoprevention: principles and prospects. *Carcinogenesis* 1993; **14**: 1737-1746
9 **Scarpignato C,** Pelosini I. Somatostatin analogs for cancer treatment and diagnosis: an overview. *Chemotherapy* 2001; **47**(Suppl 2): 1-29
10 **Kinova S,** Duris I, Kratochvilova E, Ondrejka P, Payer J. Carcinoid tumors-somatostatine in the diagnosis and therapy. *Bratisl Lek Listy* 2002; **103:** 108-112
11 **Ain KB,** Taylor KD, Tofiq S, Venkataraman G. Somatostatin receptor subtype expression in human thyroid and thyroid carcinoma cell lines. *J Clin Endocrinol Metab* 1997; **82:** 1857-1862
12 **Khanna C**, Prehn J, Hayden D, Cassaday RD, Caylor J, Jacob S, Bose SM, Hong SH, Hewitt SM, Helman LJ. A randomized controlled trial of octreotide pamoate long-acting release and carboplatin versus carboplatin alone in dogs with naturally occurring osteosarcoma: evaluation of insulin-like growth factor suppression and chemotherapy. *Clin Cancer Res* 2002; **8**: 2406-2412
13 **Marschke RF Jr,** Grill JP, Sloan JA, Wender DB, Levitt R, Mailliard JA, Gerstner JB, Ghosh C, Morton RF, Jett JR. Phase II study of high-dose somatostatin analogue in patients either previously treated or untreated who have extensive-stage small cell lung cancer. *Am J Clin Oncol* 1999; **22:** 15-17
14 **Setyono-Han B,** Henkelman MS, Foekens JA, Klijn GM. Direct inhibitory effects of somatostatin (analogues) on the growth of human breast cancer cells. *Cancer Res* 1987; **47:** 1566-1570
15 **Wang XB,** Wang X, Zhang NZ. Inhibition of somatostatin analog Octreotide on human gastric cell MKN45 growth *in vitro*. *Shijie Huaren Xiaohua Zazhi* 2002; **10:** 40-42
16 **Gencosmanoglu R,** Bugra D, Bulut T, Yamaner S, Cevikbas U, Bilir A. The inhibitory effect of octreotide on experimental colorectal carcinogenesis. *Surg Today* 2002; **32:** 249-256

17 **Lee JU,** Hosotani R, Wada M, Doi R, Koshiba T, Fujimoto K, Miyamoto Y, Tsuji S, Nakajima S, Hirohashi M, Uehara T, Arano Y, Fujii N, Imamura M. Antiproliferative activity induced by the somatostatin analogue, TT-232, in human pancreatic cancer cells. *Eur J Cancer* 2002; **38:** 1526-1534

18 **Giannetti N,** Enjalbert A, Krantic S. Somatostatin analog SMS 201995 inhibits proliferation in human leukemia T-cell line: relevance of the adenylyl cyclase stimulation. *J Cell Biochem* 2000; **78:** 666-673

19 **Yuen MF,** Poon RT, Lai CL, Fan ST, Lo CM, Wong KW, Wong WM, Wong BC. A randomized placebo-controlled study of long-acting octreotide for the treatment of advanced hepatocellular carcinoma. *Hepatology* 2002; **36:** 687-691

20 **Jenkins SA,** Kynaston HG, Davies ND, Baxter JN, Nott DM. Somatostatin analogs in oncology: a look to the future. *Chemotherapy* 2001; **47**(Suppl 2): 162-196

21 **Froidevaux S,** Eberle AN. Somatostatin analogs and radiopeptides in cancer therapy. *Biopolymers* 2002; **66:** 161-183

22 **Watanabe N.** Telomerase, cell immortality and cancer. *Hokkaido Igaku Zasshi* 2001; **76:** 127-132

23 **Yang SM,** Fang DC, Luo YH, Lu R, Battle PD, Liu WW. Alterations of telomerase activity and terminal restriction fragment in gastric cancer and its premalignant lesions. *J Gastroenterol Hepatol* 2001; **16:** 876-882

24 **Zhan WH,** Ma JP, Peng JS, Gao JS, Cai SR, Wang JP, Zheng ZQ, Wang L. Telomerase activity in gastric cancer and its clinical implications. *World J Gastroenterol* 1999; **5:** 316-319

25 **Miyachi K,** Fujita M, Tanaka N, Sasaki K, Sunagawa M. Correlation between telomerase activity and telomeric-repeat binding factors in gastric cancer. *J Exp Clin Cancer Res* 2002; **21:** 269-275

26 **Nowak J,** Januszkiewicz D, Lewandowski K, Nowicka-Kujawska K, Pernak M, Rembowska J, Nowak T, Wysocki J. Activity and expression of human telomerase in normal and malignant cells in gastric and colon cancer patients. *Eur J Gastroenterol Hepatol* 2003; **15:** 75-80

27 **Semba S,** Moriya T, Kimura W, Yamakawa M. Phosphorylated Akt / PKB controls cell growth and apoptosis in intraductal papillary-mucinous tumor and invasive ductal adenocarcinoma of the pancreas. *Pancreas* 2003; **26:** 250-257

28 **Lee SH,** Kim HS, Park WS, Kim SY, Lee KY, Kim SH, Lee JY, Yoo NJ. Non-small cell lung cancers frequently express phosphorylated Akt; an immunohistochemical study. *APMIS* 2002; **110:** 587-592

29 **Lawlor MA,** Alessi DR. PKB / Akt: a key mediator of cell proliferation, survival and insulin responses? *J Cell Sci* 2001; **114** (Pt 16): 2903-2910

30 **Nicholson KM,** Anderson NG. The protein kinase B / Akt signalling pathway in human malignancy. *Cell Signal* 2002; **14:** 381-395

31 **Hocker M,** Wiedenmann B. Therapeutic and diagnostic implications of the somatostatin system in gastroenteropancreatic neuroendocrine tumour disease. *Ital J Gastroenterol Hepatol* 1999; **31** (Suppl 2): S139- S142

32 **Bousquet C,** Puente E, Buscail L, Vaysse N, Susini C. Antiproliferative effect of somatostatin and analogs. *Chemotherapy* 2001; **47**(Suppl 2): 30-39

33 **Zalatnai A,** Pogany V. Somatostatin analogs in the treatment of pancreatic cancer: utopia or feasible alternative? *Orv Hetil* 2000; **141:** 2333-2338

34 **Wang C,** Tang C. Inhibition of human gastric cancer metastasis by ocreotide *in vitro* and *in vivo*. *Zhonghua Yixue Zazhi* 2002; **82:** 19-22

35 **Itoh N,** Semba S, Ito M, Takeda H, Kawata S, Yamakawa M. Phosphorylation of Akt / PKB is required for suppression of cancer cell apoptosis and tumor progression in human colorectal carcinoma. *Cancer* 2002; **94:** 3127-3134

36 **Hill MM,** Hemmings BA. Inhibition of protein kinase B / Akt. Implications for cancer therapy. *Pharmacol Ther* 2002; **93:** 243-251

37 **Hao ZM,** Luo JY, Cheng J, Wang QY, Yang GX. Design of a ribozyme targeting human telomerase reverse transcriptase and cloning of it's gene. *World J Gastroenterol* 2003; **9:** 104-107

38 **Kim NW,** Piatyszek MA, Prowse KR, Harley CB, West MD, Ho PL, Coviello GM, Wright WE, Weinrich SL, Shay JW. Specific association of human telomerase activity with immortal cells and cancer. *Science* 1994; **266:** 2011-2015

39 **Feng RH,** Zhu ZG, Li JF, Liu BY, Yan M, Yin HR, Lin YZ. Inhibition of human telomerase in MKN-45 cell line by antisense hTR expression vector induces cell apoptosis and growth arrest. *World J Gastroenterol* 2002; **8:** 436-440

40 **Yakoob J,** Hu GL, Fan XG, Zhang Z. Telomere, telomerase and digestive cancer. *World J Gastroenterol* 1999; **5:** 334-337

41 **Tatsumoto N,** Hiyama E, Murakami Y, Imamura Y, Shay JW, Matsuura Y, Yokoyama T. High telomerase activity is an independent prognostic indicator of poor outcome in colorectal cancer. *Clin Cancer Res* 2000; **6:** 2696-2701

42 **Hiyama E,** Yokoyama T, Tatsumoto N, Hiyama K, Imamura Y, Murakami Y, Kodama T, Piatyszek MA, Shay JW, Matsuura Y. Telomerase activity in gastric cancer. *Cancer Res* 1995; **55:** 3258-3262

43 **Kang SS,** Kwon T, Kwon DY, Do SI. Akt protein kinase enhances human telomerase activity through phosphorylation of telomerase reverse transcriptase subunit. *J Biol Chem* 1999; **274:** 13085-13090

Edited by Zhu L and Wang XL

P.O.Box 2345, Beijing 100023,China
Fax: +86-10-85381893
E-mail: wjg@wjgnet.com www.wjgnet.com

World J Gastroenterol 2003;9(10):2366-2369
World Journal of Gastroenterology
 ISSN 1007-9327

• BRIEF REPORTS •

Molecule action mechanisms of NM-3 on human gastric cancer SGC-7901 cells *in vivo* or *in vitro*

Jin-Shui Zhu, Bo Shen, Jin-Lian Chen, Guo-Qiang Chen, Xiao-Hu Yu, Hua-Fang Yu, Zu-Ming Zhu

Jin-Shui Zhu, Bo Shen, Jin-Lian Chen, Guo-Qiang Chen, Xiao-Hu Yu, Hua-Fang Yu, Zu-Ming Zhu, Affiliated Sixth People' s Hospital, Shanghai Jiaotong University, Shanghai 200233, China
Guo-Qiang Chen, Shanghai Experimental Animal Center, Chinese Academy of Sciences, Shanghai 200233, China
Supported by Shanghai Natural Science Foundation, No.02ZB14072
Correspondence to: Jin-Shui Zhu, Department of Gastroenterology, Affiliated Sixth People' s Hospital, Shanghai Jiaotong University, Shanghai 200233, China. zhujs1803@hotmail.com
Telephone: +86-21-64369181 Exit 8351 **Fax:** +86-21-54778507
Received: 2003-05-12 **Accepted:** 2003-06-02

Abstract

AIM: To study the molecule action mechanisms of NM-3 on the growth of human gastric cancer SGC-7901 cells *in vivo* or *in vitro*.

METHODS: SGC-7901 from human non-differentiated gastric cancer cell line was cultured with NM-3 at 100 mg/ml for 24 h. We observed its inhibitory rate and the density of micro-vascular growth in grafted mice with human gastric cancer SGC-7901. The apoptosis of human gastric cancer SGC-7901 was revealed in NM-3 treatment group by using terminal deoxynucleotidyl transferase-mediated deoxyuridine triphosphate-fluorescene nick end labeling (TUNEL) method and flow cytometry analysis.

RESULTS: The growth of SGC-7901 cells was markedly inhibited compared with control growp, which was smaller than that in normal saline control group (4.17 g±0.22 g *vs* 9.45 g±1.38 g, $P<0.01$). The level of apoptosis of human gastric cell line SGC-7901 was obviously increased in NM-3 treatment group at 1 mg.L^{-1} for 24 h. NM-3 inducing apoptotic index in NM-3 plus carboplatin group was 3.5 times that of carboplatin control group (TUNEL: 27.98±6.12 % *vs* 12.94±2.12 %, FACScan: 26.86±5.69 % *vs* 11.86±1.09 %, $P<0.01$). Western blot analysis showed that the apoptotic index of human gastric cancer was elevated for 12, 24 and 36 h with an evident time-effect relationship in groups at 100 mg.L^{-1}. NM-3 enhanced the inhibitive effects and sensitivity of chemotherapy for human gastric cancer in nude mice. These results suggested that NM-3 played a key inhibitive role in the growth of grafted human gastric cancer in nude mice.

CONCLUSION: NM-3 can inhibit the growth of human gastric cancer cell line SGC-7901, and enhance the sensitivity of carboplatin on SGC-7901 and induced its apoptosis.

ZhuJS, Shen B, Chen JL, Chen GQ, Yu XH, Yu HF, Zhu ZM. Molecule action mechanisms of NM-3 on human gastric cancer SGC-7901 cells *in vivo* or *in vitro*. *World J Gastroenterol* 2003; 9(10):2366-2369
http://www.wjgnet.com/1007-9327/9/2366.asp

INTRODUCTION

Apoptosis plays a key role in the proliferation and turnover of malignant tumor cells. It has been known that its extent is often enhanced in gastric cancer by some anti-cancer drugs, such as chemotherapeutic drugs, hormones or immune agents, micro-vascular growth inhibitors have been proved to have some inhibitory effects on maligant tumors,especially on gastric tumors. But it has not been clear whether NM-3 is a micro-vascular inhibitive agent for solid tumor growth[1-3], it might suppress gastric cancer cell proliferation and cause tumor cell loss and nuclear condensation *in vitro*. Up to date, NM-3 is considered as the newest micro-vasular inhabitor[1-4]. Combined with carboplatin, it can soften hard lumps and dissolve phlegm, enhance apoptosis of human gastric cancer xenografts in nude mice. On the other hand, NM-3 can enhance the sensitivity of chemotherapeutic drugs on human gastric cancer. Based on previous studies, NM-3 exerts its effects on solid tumor growth by promoting apoptosis of human gastric cancer cell SGC-7901 and increasing the suppressive effects of carboplatin.

MATERIALS AND METHODS

Materials

A human gastric cancer cell line SGC-7901 grafted onto nude mice was used as the animal model, the age of these 60 mice was 6-7 weeks old female balb/c-nu/nu mice (weight 18-22 g) and a human gastric cancer cell line SGC-7901 was obtained from Shanghai Tumor Institute (No: 01842). The animals were subcutaneously xerografted under abdominal skin with the SGC-7901 cell line. The tumor transplantation procedure was described previously. The animal model and SGC-7901 cell line were obtained from Shanghai Experimental Animal Centre, Chinese Academy of Sciences.

NM-3 was composed of 2-c8-hydroxy-6-methoxy-1-oxo-1 h-2-benzopyran-3-yd, concentrantion of NM-3 was 100 mg· L^{-1}, the concentration of carboplatin was 100 mg· L^{-1}.

Methods

Experimental schedule: After grafting, these nude mice were randomly divided into 3 groups: control group and two experimental groups assigned to receive NM-3 or carboplatin respectly. Each experimental mouse in two experimental groups was given a 0.5 ml dose of NM-3 drug via intra-abdominal injection or gastric perfusion (empty control group) once every three days over a 40-day period beginning at 1st day after being xerografted. The control animals received normal saline according to the same schedule by gastric perfusion. The animals were killed 41 days after being xerografted.

In our study, NM-3 induced gastric cancer cell apoptosis, and enhanced the chemotherapeutic sensitivity of human gastric cancer cell line SGC-7901 on carboplatin *in vitro*. Apoptosis induced by NM-3 needed further investigation.

Therapeutic effects on human gastric cancer cell growth were assessed. Tumor size was measured twice a week by multiplying two perpendicular diameter and tumor weight was determined immediately by electron balance after the animals were killed. Apoptotic cells and apoptotic index were

determined by the terminal deoxynucleotidyl transferase-mediated deoxy-uridine triphosphate-fluorescene nick end labeling (TUNEL) method and flow cytometry analysis. Morphological atterations were observed with electron microscope.

Flow cytometry analysis: Propidium iodide (PI) staining was used for flow cytometric detection of apoptosis. 1×10^6 cells from each of the samples were treated with RNase and stained with PI.The apoptotic cells labled by DNA strand were measured with a flow cytometer (FACS Calibur,Becton Dickinson,U.S.A).The data from 1×10^6 cells/sample were collected,stored,and analyzed using CELLQUES' T and MODFITLT for macV1.01 software[4-12].

Statistical analysis

The results were expressed as $\bar{x}\pm s$, Student' s *t* test was used. *P* value <0.05 was concidered significantly.

RESULTS

NM-3 inhibited growth of micro-vascular of tumor in nude mice with human gastric cancer SGC-7901

NM-3 group decreased signicantly the neo-microvascular density (1.17±0.05 mm^3) of gastric cancer tumor implanted onto nude mice was significantly decreased in NM-3 group compared with that in saline group (5.37±1.12 mm^3) and carboplatin group (4.72±1.18 mm^3, $P>0.05$). The micro-vascular density in NM-3 combinated with carboplatin group (1.18±0.05 mm^3) was not significantly different from that in NM-3 group ($P>0.05$, Table 1).

Table 1 Growth of neo-microvascular around gastric tumor supressed by NM-3 ($\bar{x}\pm s$)

Treatment	*n*	Density (mm^3)
Carboplatin	10	4.72±1.18[a]
NM-3 plus carboplatin	10	1.18±0.05[b]
Saline	10	5.37±1.72

[a]$P>0.05$, [b]$P<0.01$ *vs t* test in saline control group.

NM-3 enhanced sensitivity of carboplatin on human gastric cancer induced by apoptosis of human gastric cancer cell in vitro or in vivo

The apoptotic indix (AI) of SGC-7901 induced by carboplatin was enhanced in NM-3 group. The apoptotic indix (TUNEL: 27.98±6.12 %, FACScan: 26.86±5.69 %) was markedly increasd in that of carboplatin group by using either TUNEL method or flow cytometry analysis compared with the carboplatin group (TUNEL: 12.94±2.12 %, $P<0.01$; FACScan: 11.86±1.09 %, $P<0.01$). The apoptotic indix in NM-3 group (TUNEL: 16.47±4.13 % FACScan: 15.97±1.49 %) was higher than that in normal saline group (TUNEL 1.83±0.12 %, $P<0.01$; FACScan: 1.06±0.09 %, $P<0.01$, Table 2).

Table 2 Apoptotic indix (AI) of human gastric cancer line SGC-7901 enhanced by NM-3 *in vitro* ($\bar{x}\pm s$)

Treatment	*n*	AI (TUNEL)%	AI (FACScan) %
NM-3	10	16.47±4.13[b]	15.97±2.49[b]
Carboplatin	10	12.94±2.12[b]	11.86±1.09[b]
NM-3 plus carboplatin	10	27.98±6.12[b]	26.86±5.69[b]
Saline	10	1.83±0.12	1.06±0.09

[a]$P>0.05$, [b]$P<0.01$ *vs t* test, in saline control group.

NM-3 effected on growth of xerografted human gastric cancer cell line SGC-7901 in nude mice

The tumor weight of nude mice in NM-3 group (4.17±0.22 g) was obviously lower than that in normal saline controls (9.45±0.38 g), the tumor size of the prior group (0.68 g±0.07cm^3, $P<0.05$) was smaller than that in normal saline control group (8.94±1.46 cm^3). The tumor weight and size of nude mice in NM-3 combinated with carboplatin group were 2.78±0.18 g and 0.34±0.02 cm^3 respectively. However, those in NM-3 group were not significantly different compared with carboplatin group (4.46±0.23 g, 0.71±0.08 cm^3) 7 weeks later. Tumor growth was (size and weight) markedly inhibited by treatment with NM-3 ($P<0.01$). The tumor inhibitory rate of single NM-3 on tumors was 67.7 %, that in NM-3 combinated with carboplatin group was up to 98.7 % (Table3).

Table 3 Growth of xerografted human gastric tumor affected by NM-3 in nude mice ($\bar{x}\pm s$)

Treatment	*n*	Weight (g)	Size (cm^3)
NM-3	10	4.17±0.22[a]	0.68±0.07[a]
Carboplatin	10	4.46±0.23[a]	0.71±0.08[a]
NM-3 plus carboplatin	10	2.78±0.18[b]	0.34±0.02[b]
Saline	10	9.45±1.38	8.94±1.46

[a]$P<0.05$, [b]$P<0.01$ *vs t* test, in saline control group.

DISCUSSION

Gastric cancer remains one of the most common causes of cancer-related death in the world. At present, gastric cancer is still diagnosed at its advanced stage in most patients throughout the world. Even with curative resection, they remain at a high risk of relapse[13-32]. Thus, there is a great need for effective adjuvant therapy for patients with gastric cancer. Our previous clinic paired comparative studies suggested that NM-3 had therapeutic effects on advanced gastric cancer. It could increase the surviving period of the patients, improve the life quality and increase the metastasis and recurrence after operation because of its lower toxic side-effect compared with intravenous chemical therapy[33-47]. Up to date, the effect of NM-3 on human gastric cancer has not been reported in the world. So we thought it is worth to make a further research on its anti-cancer mechanisms.

Gastric cancer is not only a disease with abnormal cell proliferation and differentiation, but also a disease with abnormal apoptosis. Enhanced apoptosis in human gastric cancer cells could be observed after treatmemt with 5-fluorouracil, cisplatin, arsenous oxide, *etc*. These data suggest that it is a therapeutic method for patients with gastric cancer to induce apoptosis of cancer cells[64]. The present study indicated that tumor growth was significantly inhibited by treatment with carboplatin or NM-3. The results obtained by TUNEL method and cytometry analysis suggested that gastric cancer cells were suppressed *in vivo*, NM-3 was related to the induction of apoptosis of human gastric cancer cell line SGC-7901. These data suggest that NM-3 can inhibit gastric cell proliferation. So inhibition of gastric cancer induced by NM-3 is also related to the suppression of its proliferation.

Apoptosis is a complex and active cellular process, whereby individual cells are triggered to undergo self-destruction in a manner that would neither injures neghiboring cells nor elicites any inflammatory reation. Various triggering factors initiate corresponding proteo-lysis cascade reaction depending on mitochondrion or APO 1\FAS\CD95 receptors mediate apoptotic pathways. There are oncogenes and tumor suppressor gene products in the regulation and execution of apoptosis.

It has been proved[14-22] that p53, Rb, myc, ras, raf, play important roles in apoptosis and are thus named the guardians of genomes[23-44]. They monitor the state of DNA and cell cycle is blocked in case of DNA damage. This takes place through the induction of CIP/Swaf/p21. In the absence of phosphorylated active cyclin-dependent kinases, the cell cycle remains inactive (unphosphorylated).

This leads to activation of DNA repair machinery. If DNA repair fails, p53 will take over again and trigger apoptosis in a process that involves upregulation of the apoptosis-inducing bax and down-regulation of the apoptotic bal-2[45-60]. We also detected apoptosis-inhibiting member of the bcl-2 family[61-64]: bcl-2 mRNA. The interaction between NM-3 and gastric cancer cell SGC-7901 induced its apoptosis of gastric cancer cells, but further *in vivo or in vitro* studies are needed.

REFERENCES

1 **Richardson M,** Gunawan J, Hatton MW, Seidlitz E, Hirte HW, Singh G. Malignant ascites fluid (MAF), including ovarian-cancer-associated MAF, contains angiostatin and other factor(s) which inhibit angiogenesis.*Gynecol Oncol* 2002; **86:** 279-287

2 **Basaki Y,** Chikahisa L, Aoyagi K, Miyadera K, Yonekura K, Hashimoto A, Okabe S, Wierzba K, Yamada Y. Gamma-Hydroxybutyric acid and 5-fluorouracil, metabolites of UFT, inhibit the angiogenesis induced by vascular endothelial growth factor. *Angiogenesis* 2001; **4:** 163-173

3 **Yamamoto S**, Yasui W, Kitadai Y, Yokozaki H, Haruma K, Kajiyama G, Tahara E. Expression of vascular endothelial growth factor in human gastric carcinomas. *Pathol Int* 1998; **48:** 499-506

4 **Li C**, Guo B, Bernabeu C, Kumar S. Angiogenesis in breast cancer: The role of transforming growth factor beta and CD105. *Microsc Res Tech* 2001; **52:** 437-449

5 **Zhai Y,** Yu J, Iruela-Arispe L, Huang WQ, Wang Z, Hayes AJ, Lu J, Jiang G, Rojas L, Lippman ME, Ni J, Yu GL, Li LY. Inhibition of angiogenesis and breast cancer xenograft tumor growth by VEGI, a novel cytokine of the TNF superfamily. *Int J Cancer* 1999; **82:** 131-136

6 **Masood R**, McGarvey ME, Zheng T, Cai J, Arora N, Smith DL, Sloane N, Gill PS. Antineoplastic urinary protein inhibits Kaposi's sarcoma and angiogenesis *in vitro* and *in vivo*. *Blood* 1999; **93:** 1038-1044

7 **Zhai Y,** Ni J, Jiang GW, Lu J, Xing L, Lincoln C, Carter KC, Janat F, Kozak D, Xu S, Rojas L, Aggarwal BB, Ruben S, Li LY, Gentz R, Yu GL. VEGI, a novel cytokine of the tumor necrosis factor family, is an angiogenesis inhibitor that suppresses the growth of colon carcinomas *in vivo*. *FASEB J* 1999; **13:** 181-189

8 **Tsunemi T,** Nagoya S, Kaya M, Kawaguchi S, Wada T, Yamashita T, Ishii S. Postoperative progression of pulmonary metastasis in osteosarcoma. *Clin Orthop* 2003; **407:** 159-166

9 **Thomas JP,** Arzoomanian RZ, Alberti D, Marnocha R, Lee F, Friedl A, Tutsch K, Dresen A, Geiger P, Pluda J, Fogler W, Schiller JH, Wilding G. Phase I pharmacokinetic and pharmacodynamic study of recombinant human endostatin in patients with advanced solid tumors. *J Clin Oncol* 2003; **21:** 223-231

10 **Anderson KC.** Moving disease biology from the laboratory to the clinic. *Semin Oncol* 2002; **29:** 17-20

11 **Folkman J**. Role of angiogenesis in tumor growth and metastasis. *Semin Oncol* 2002; **29:** 15-18

12 **Ferrara N.** Role of vascular endothelial growth factor in physiologic and pathologic angiogenesis: therapeutic implications. *Semin Oncol* 2002; **29:** 10-14

13 **Jain RK**. Tumor angiogenesis and accessibility: role of vascular endothelial growth factor. *Semin Oncol* 2002; **29:** 3-9

14 **Gee MS**, Procopio WN, Makonnen S, Feldman MD, Yeilding NM, Lee WM. Tumor vessel development and maturation impose limits on the effectiveness of anti-vascular therapy. *Am J Pathol* 2003; **162:** 183-193

15 **Koyanagi S,** Tanigawa N, Nakagawa H, Soeda S, Shimeno H. Oversulfation of fucoidan enhances its anti-angiogenic and antitumor activities. *Biochem Pharmacol* 2003; **65:** 173-179

16 **Buchler P**, Reber HA, Buchler M, Shrinkante S, Buchler MW, Friess H, Semenza GL, Hines OJ. Hypoxia-inducible factor 1 regulates vascular endothelial growth factor expression in human pancreatic cancer. *Pancreas* 2003; **26:** 56-64

17 **Chlenski A,** Liu S, Crawford SE, Volpert OV, DeVries GH, Evangelista A, Yang Q, Salwen HR, Farrer R, Bray J, Cohn SL. SPARC is a key Schwannian-derived inhibitor controlling neuroblastoma tumor angiogenesis.*Cancer Res* 2002; **62:** 7357-7363

18 **Davis PD**, Dougherty GJ, Blakey DC, Galbraith SM, Tozer GM, Holder AL, Naylor MA, Nolan J, Stratford MR, Chaplin DJ, Hill SA. ZD6126: a novel vascular-targeting agent that causes selective destruction of tumor vasculature. *Cancer Res* 2002; **62:** 7247-7253

19 **Cline EI**, Bicciato S, DiBello C, Lingen MW. Prediction of *in vivo* synergistic activity of antiangiogenic compounds by gene expression profiling. *Cancer Res* 2002; **62:** 7143-7148

20 **Giguere CM**, Bauman NM, Smith RJ. New treatment options for lymphangioma in infants and children. *Ann Otol Rhinol Laryngol* 2002; **111:** 1066-1075

21 **Manley PW**, Furet P, Bold G, Bruggen J, Mestan J, Meyer T, Schnell CR, Wood J, Haberey M, Huth A, Kruger M, Menrad A, Ottow E, Seidelmann D, Siemeister G, Thierauch KH. Anthranilic acid amides: a novel class of antiangiogenic VEGF receptor kinase inhibitors. *J Med Chem* 2002; **45:** 5687-5693

22 **Ranieri G**, Gasparini G. Angiogenesis and angiogenesis inhibitors: a new potential anticancer therapeutic strategy.*Curr Drug Targets Immune Endocr Metabol Disord* 2001; **1:** 241-253

23 **Lewy-Trenda I**. [Neoplasms and angiogenesis]. *Pol Merkuriusz Lek* 2002; **13:** 225-228

24 **Yoo GH**, Piechocki MP, Ensley JF, Nguyen T, Oliver J, Meng H, Kewson D, Shibuya TY, Lonardo F, Tainsky MA. Docetaxel induced gene expression patterns in head and neck squamous cell carcinoma using cDNA microarray and PowerBlot. *Clin Cancer Res* 2002; **8:** 3910-3921

25 **Lenzi R,** Rosenblum M, Verschraegen C, Kudelka AP, Kavanagh JJ, Hicks ME, Lang EA, Nash MA, Levy LB, Garcia ME, Platsoucas CD, Abbruzzese JL, Freedman RS. Phase I study of intraperitoneal recombinant human interleukin 12 in patients with Mullerian carcinoma, gastrointestinal primary malignancies, and mesothelioma. *Clin Cancer Res* 2002; **8:** 3686-3695

26 **Casassus P,** Caillat-Vigneron N, Martin A, Simon J, Gallais V, Beaudry P, Eclache V, Laroche L, Lortholary P, Raphael M, Guillevin L, Lortholary O. Treatment of adult systemic mastocytosis with interferon-alpha: results of a multicentre phase II trial on 20 patients. *Br J Haematol* 2002; **119:** 1090-1107

27 **Hata-Sugi N**, Kawase-Kageyama R, Wakabayashi T. Characterization of rat aortic fragment within collagen gel as an angiogenesis model; capillary morphology may reflect the action mechanisms of angiogenesis inhibitors. *Biol Pharm Bul* 2002; **25:** 446-451

28 **Matsunaga T,** Weihrauch DW, Moniz MC, Tessmer J, Warltier DC, Chilian WM. Angiostatin inhibits coronary angiogenesis during impaired production of nitric oxide. *Circulation* 2002; **105:** 2185-2191

29 **Chew LJ**, Pan H, Yu J, Tian S, Huang WQ, Zhang JY, Pang S, Li LY. A novel secreted splice variant of vascular endothelial cell growth inhibitor. *FASEB J* 2002; **16:** 742-744

30 **Kalmes A,** Daum G, Clowes AW. EGFR transactivation in the regulation of SMC function. *Ann N Y Acad Sci* 2001; **947:** 42-54

31 **Yu J**, Tian S, Metheny-Barlow L, Chew LJ, Hayes AJ, Pan H, Yu GL, Li LY. Modulation of endothelial cell growth arrest and apoptosis by vascular endothelial growth inhibitor. *Circ Res* 2001; **89:** 1161-1167

32 **Wong ST,** Baker LP, Trinh K, Hetman M, Suzuki LA, Storm DR, Bornfeldt KE. Adenylyl cyclase 3 mediates prostaglandin E(2)-induced growth inhibition in arterial smooth muscle cells. *J Biol Chem* 2001; **276:** 34206-34212

33 **Stepan H,** Leitner E, Bader M, Walther T. Organ-specific mRNA distribution of C-type natriuretic peptide in neonatal and adult mice. *Regul Pept* 2000; **95:** 81-85

34 **Damon DH.** Adrenoceptor-mediated modulation of endothelial-dependent vascular smooth muscle growth. *J Auton Pharmacol* 2000; **20**: 47-54

35 **Veyssier-Belot C**, Cacoub P. Role of endothelial and smooth muscle cells in the physiopathology and treatment management of pulmonary hypertension. *Cardiovasc Res* 1999; **44:** 274-282

36 **Hishikawa K**, Oemar BS, Tanner FC, Nakaki T, Fujii T, Luscher TF. Overexpression of connective tissue growth factor gene induces apoptosis in human aortic smooth muscle cells. *Circula-*

tion 1999; **100:** 2108-2112
37 **Shukunami C**, Iyama K, Inoue H, Hiraki Y. Spatiotemporal pattern of the mouse chondromodulin-I gene expression and its regulatory role in vascular invasion into cartilage during endochondral bone formation. *Int J Dev Biol* 1999; **43:** 39-49
38 **Nakano N**, Higashiyama S, Takashima S, Tsuruoka N, Klagsbrun M,Taniguchi N. Purification and characterization of a novel vascular endothelial cell growth inhibitor secreted by macrophage-like U-937 cells. *J Biochem* 1999; **125:** 368-374
39 **Masood R,** McGarvey ME, Zheng T, Cai J, Arora N, Smith DL, Sloane N, Gill PS. Antineoplastic urinary protein inhibits Kaposi's sarcoma and angiogenesis *in vitro* and *in vivo*. *Blood* 1999; **93:** 1038-1044
40 **Zhai Y**, Ni J, Jiang GW, Lu J, Xing L, Lincoln C, Carter KC, Janat F, Kozak D, Xu S, Rojas L, Aggarwal BB, Ruben S, Li LY, Gentz R, Yu GL. VEGI, a novel cytokine of the tumor necrosis factor family, is an angiogenesis inhibitor that suppresses the growth of colon carcinomas *in vivo*. *FASEB J* 1999; **13:** 181-189
41 **Van Rees BP**, Caspers E, Zur Hausen A, Van Den Brule A, Drillenburg P, Weterman MA, Offerhaus GJ. Different pattern of allelic loss in Epstein-Barr virus-positive gastric cancer with emphasis on the p53 tumor suppressor pathway. *Am J Pathol* 2002; **161:** 1207-1213
42 **Hiyama T**, Tanaka S, Kitadai Y, Ito M, Sumii M, Yoshihara M, Shimamoto F, Haruma K, Chayama K. p53 Codon 72 polymorphism in gastric cancer susceptibility in patients with *Helicobacter pylori*-associated chronic gastritis. *Int J Cancer* 2002; **100:** 304-308
43 **Murakami K**, Fujioka T, Kodama M, Honda S, Okimoto T, Oda T, Nishizono A, Sato R, Kubota T, Kagawa J, Nasu M. Analysis of p53 mutations and *Helicobacter pylori* infection in human and animal models. *J Gastroenterol* 2002; **37:** 1-5
44 **Chang MS**, Kim HS, Kim CW, Kim YI, Lan Lee B, Kim WH. Epstein-Barr virus, p53 protein, and microsatellite instability in the adenoma-carcinoma sequence of the stomach. *Hum Pathol* 2002; **33:** 415-420
45 **Moritani S,** Sugihara H, Kushima R, Hattori T. Different roles of p53 between Epstein-Barr virus-positive and -negative gastric carcinomas of matched histology. *Virchows Arch* 2002; **440**: 367-375
46 **Shigeishi H**, Yokozaki H, Oue N, Kuniyasu H, Kondo T, Ishikawa T, Yasui W. Increased expression of CHK2 in human gastric carcinomas harboring p53 mutations. *Int J Cancer* 2002; **99:** 58-62
47 **Kubicka S**, Claas C, Staab S, Kuhnel F, Zender L, Trautwein C, Wagner S, Rudolph KL, Manns M. p53 mutation pattern and expression of c-erbB2 and c-met in gastric cancer: relation to histological subtypes, *Helicobacter pylori* infection, and prognosis. *Dig Dis Sci* 2002; **47:** 114-121
48 **Fox JG,** Sheppard BJ, Dangler CA, Whary MT, Ihrig M, Wang TC. Germ-line p53-targeted disruption inhibits helicobacter-induced premalignant lesions and invasive gastric carcinoma through down-regulation of Th1 proinflammatory responses. *Cancer Res* 2002; **62:** 696-702
49 **Iwamatsu H,** Nishikura K, Watanabe H, Ajioka Y, Hashidate H, Kashimura H, Asakura H. Heterogeneity of p53 mutational status in the superficial spreading type of early gastric carcinoma. *Gastric Cancer* 2001; **4:** 20-26
50 **Jenkins GJ**, Morgan C, Baxter JN, Parry EM, Parry JM. The detection of mutations induced in vitro in the human p53 gene by hydrogen peroxide with the restriction site mutation (RSM)assay. *Mutat Res* 2001; **498:** 135-144
51 **Li HL**, Chen DD, Li XH, Zhang HW, Lu YQ, Ye CL, Ren XD.Changes of NF-kB, p53, Bcl-2 and caspase in apoptosis induced by JTE-522 in human gastric adenocarcinoma cell line AGS cells: role of reactive oxygen species. *World J Gastroenterol* 2002; **8:** 431-435
52 **Satomi D**, Takiguchi N, Koda K, Oda K, Suzuki H, Yasutomi J, Ishikura H, Miyazaki M. Apoptosis and apoptosis-associated gene products related to the response to neoadjuvant chemotherapy for gastric cancer. *Int J Oncol* 2002; **20:** 1167-1171
53 **Wu YL**, Sun B, Zhang XJ, Wang SN, He HY, Qiao MM, Zhong J, Xu JY. Growth inhibition and apoptosis induction of Sulindac on Human gastric cancer cells. *World J Gastroenterol* 2001; **7:** 796-800
54 **Wang J,** Chi DS, Kalin GB, Sosinski C, Miller LE, Burja I, Thomas E. *Helicobacter pylori* infection and oncogene expressions in gastric carcinoma and its precursor lesions. *Dig Dis Sci* 2002; **47:** 107-113
55 **Zhang TC**, Cao EH, Qin JF. Opposite biological effects of arsenic trioxide and arsacetin involve a different regulation of signaling in human gastric cancer MGC-803 cells. *Pharmacology* 2002; **64:** 160-168
56 **Monden N**, Abe S, Hishikawa Y, Yoshimura H, Kinugasa S, Dhar DK, Tachibana M, Nagasue N. The role of P-glycoprotein in human gastric cancer xenografts in response to chemotherapy. *Int J Surg Investig* 1999; **1:** 3-10
57 **Wacheck V**, Heere-Ress E, Halaschek-Wiener J, Lucas T, Meyer H, Eichler HG, Jansen B. Bcl-2 antisense oligonucleotides chemosensitize human gastric cancer in a SCID mouse xenotransplantation model. *J Mol Med* 2001; **79:** 587-593
58 **Enomoto A**, Esumi M, Yamashita K, Takagi K, Takano S, Iwai S. Abnormal nucleotide repeat sequence in the TGF-betaRII gene in hepatocellular carcinoma and in uninvolved liver tissue. *J Pathol* 2001; **195:** 349-354
59 **Shyu RY**, Lin DY, Reichert U, Jiang SY. Synthetic retinoid CD437 induces cell-dependent cycle arrest by differential regulation of cell cycle associated proteins. *Anticancer Res* 2002; **22:** 2757-2764
60 **Li Y,** Lu YY. Isolation of diallyl trisulfide inducible differentially expressed genes in human astric cancer cells by modified cDNA representational difference analysis. *DNA Cell Biol* 2002; **21:** 771-780
61 **Potthoff A**, Ledig S, Martin J, Jandl O, Cornberg M, Obst B, Beil W, Manns MP, Wagner S. Significance of the caspase family in *Helicobacter pylori* induced gastric epithelial apoptosis.*Helicobacter* 2002; **7:** 367-377
62 **Nitti D**, Belluco C, Mammano E, Marchet A, Ambrosi A, Mencarelli R, Segato P, Lise M. Low level of p27(Kip1) protein expression in gastric adenocarcinoma is associated with disease progression and poor outcome. *J Surg Oncol* 2002; **81:** 167-175
63 **Chen Y,** Wu Q, Song SY, Su WJ. Activation of JNK by TPA promotes apoptosis via PKC pathway in gastric cancer cells. *World J Gastroenterol* 2002; **8:** 1014-1018
64 **Liu JR**, Chen BQ, Yang YM, Wang XL, Xue YB, Zheng YM, Liu RH. Effect of apoptosis on gastric adenocarcinoma cell line SGC-7901 induced by cis-9, trans-11-conjugated linoleic acid. *World J Gastroenterol* 2002; **8:** 999-1004

Edited by Wang XL

P.O.Box 2345, Beijing 100023,China
Fax: +86-10-85381893
E-mail: wjg@wjgnet.com www.wjgnet.com

World J Gastroenterol 2003;9(10):2370-2373
World Journal of Gastroenterology
 ISSN 1007-9327

• BRIEF REPORTS •

Selection and evaluation of three interventional procedures for achalasia based on long-term follow-up

Ying-Sheng Cheng, Ming-Hua Li, Wei-Xiong Chen, Ni-Wei Chen, Qi-Xin Zhuang, Ke-Zhong Shang

Ying-Sheng Cheng, Ming-Hua Li, Qi-Xin Zhuang, Ke-Zhong Shang, Department of Radiology, Sixth People' s Hospital, Shanghai Jiaotong University, Shanghai 200233, China
Wei-Xiong Chen, Ni-Wei Chen, Department of Gastroenterology, Sixth People' s Hospital, Shanghai Jiaotong University, Shanghai 200233, China
Supported by the National Key Medical Research and Development Program of China during the 9th Five-year Plan Period (No.96-907-03-04), Shanghai Nature Science Funds (No.02Z1314073), Shanghai Medical Development Funds (No.00419)
Correspondence to: Dr. Ying-Sheng Cheng, Department of Radiology, Sixth People' s Hospital, Shanghai Jiaotong University, Shanghai 200233, China. chengys@sh163.net
Telephone: +86-21-64368920 **Fax:** +86-21-64701361
Received: 2003-05-13 **Accepted:** 2003-06-02

Abstract

AIM: To determine the best method out of the three types of interventional procedure for achalasia based on a long-term follow-up.

METHODS: The study cohort was comprised of 133 patients of achalasia. Among them, 60 patients were treated under fluoroscopy with pneumatic dilation (group A), 8 patients with permanent uncovered or antireflux covered metal stent dilation (group B), and 65 patients with temporary partially covered metal stent dilation (group C).

RESULTS: One hundred and thirty dilations were performed on the 60 patients of group A (mean 2.2 times per case). The mean diameter of the strictured cardia was 3.3±2.1 mm before dilation and 10.6±3.8 mm after dilation. The mean dysphagia score was 2.7±1.4 before dilation and 0.9±0.3 after dilation. Complications in group A were chest pain (n=30), reflux (n=16), and bleeding (n=6). Thirty-six patients (60 %) in group A exhibited dysphagia relapse during a 12-month follow-up, and 45 patients (90 %) out of 50 exhibited dysphagia relapse during a 36-month follow-up. Five uncovered and 3 antireflux covered expandable metal stents were permanently placed in the 8 patients of group B. The mean diameter of the strictured cardia was 3.4±1.9 mm before dilation and 19.5±1.1 mm after dilation. The mean dysphagia score was 2.6±1.3 before dilation and 0.4±0.1 after dilation. Complications in group B were chest pain (n=6), reflux (n=5), bleeding (n=3), and hyperplasia of granulation tissue (n=3). Four patients (50 %) in group B exhibited dysphagia relapse during a 12-month follow-up, and 2 case (66.7 %) out of 3 patients exhibited dysphagia relapse during a 36-month follow-up. Sixty-five partially covered expandable metal stents were temporarily placed in the 65 patients of group C and withdrawn after 3-7 days via gastroscopy. The mean diameter of the strictured cardia was 3.3±2.3 mm before dilation and 18.9±3.5 mm after dilation. The mean dysphagia score was 2.4±1.3 before dilation and 0.5±0.2 after dilation. Complications in group C were chest pain (n=26), reflux (n=13), and bleeding (n=8). 6 patients (9.2 %) out of 65 exhibited dysphagia relapse during a 12-month follow-up, and 8 patients (14.5 %) out of 55 exhibited dysphagia relapse during a 36-month follow-up. All the stents were inserted and withdrawn successfully. The follow-up in groups A-C lasted 12-96 months.

CONCLUSION: Temporary partially covered metal stent dilation is one of the best methods with interventional procedure for achalasia in terms of long-term follow-up.

Cheng YS, Li MH, Chen WX, Chen NW, Zhuang QX, Shang KZ. Selection and evaluation of three interventional procedures for achalasia based on long-term follow-up. *World J Gastroenterol* 2003; 9(10):2370-2373
http://www.wjgnet.com/1007-9327/9/2370.asp

INTRODUCTION

Achalasia is the most common primary motility disorder of the esophagus. Three interventional procedures are used clinically for achalasia, namely pneumatic dilation, permanent metal stent dilation, and temporary metal stent dilation. These methods provide excellent immediate therapeutic efficacy, but their long-term results are unknow[1,2]. Therefore, we formulated several treatment plans for patients with achalasia from July 1994 to May 2002 and evaluated them in terms of long-term follow-up.

MATERIALS AND METHODS

Materials

The subjects were 133 patients (77 males, 56 females; aged 12-84 years, mean 48.3 years) with symptoms of dysphagia. A dysphagia score was assessed by the quality of swallowing[1,2]: grade 0 for normal swallowing, grade 1 for swallowing most solid food, grade 2 for swallowing semisolids, grade 3 for swallowing liquid food, and grade 4 for complete dysphagia. Based on different methods of interventional procedure, the patients were divided into three groups as follows. In 60 patients with pneumatic dilation (group A), the mean dysphagia score was 2.7±1.4, and the mean diameter of the narrowest region of the cardia was 3.3±2.1 mm. In 8 patients with permanent uncovered or antireflux covered metal stent dilation (group B), the mean dysphagia score was 2.6±1.3, and the mean diameter of the narrowest region of the cardia was 3.4±1.9 mm. In 65 patients with temporary partially covered metal internal stent dilation (group C), the mean dysphagia score was 2.4±1.3, and the mean diameter of the narrowest region of the cardia was 3.1±2.3 mm. The course of disease in all the patients was 1-10 years (mean 5.4±4.4 years). All the patients were examined by barium-meal radiography of the upper digestive tract and gastroscope or esophageal intracavity manometric method.

Methods

Preoperative preparation involved an empty stomach for at least 4 hours and examination of the bleeding and clotting times. The device used was an SY dumbbell-like catheter (manufactured in Jinan, Shandong, China). The metal stent

for achalasia was a nitinol stent (developed by Zhiye Medical Equipment Research Institute, Changzhou, China, and Youyan Yijin Advanced Materials Co.Ltd, Beijing, China). Uncovered and antireflux covered metal stents were used in group B, partially covered metal stents were used in group C. The body of partially covered stents was covered with intracavity silica gel. The areas within 2 cm of both ends of partially covered stents were not covered. Stents were 6-10 cm in length and 16-30 mm in diameter.

The patients in which pneumatic dilation was used were placed in lying on the side or sitting position. Topical anesthesia of the pharynx was administered before the procedure. A guidewire was inserted through the mouth and passed through the stricture section under fluoroscopy. A catheter with a diameter of 28 mm was passed through the region of achalasia of the esophagus via the guidewire, which aligned the center of saccule with the most strictured point. The saccule was injected using an injector with dilated contrast medium or gas. Under fluoroscopy, and according to the pain reaction of the patient, pressurization was applied to gradually dilation of the saccule. The back of saccule was dumbbell-shaped. When further pressurization flattened the surface of saccule or when the pressure did not change as pressurization was applied, pressurization was suspended and the piston was closed off. The pressure of saccule was maintained for 5-30 min, after which the piston was released. After the pressure of saccule had been reduced for 5 min, pressurization was again applied. Typically each treatment involved 3-5 dilations, after which the catheter was withdrawn. The second and third treatments with graded pneumatic dilation were carried out using dilators with diameters of 30 mm and 32 mm, respectively, in some of the patients every 2 weeks until clinical symptoms disappeared and the patients returned to a nomal diet.

When stents were placed in groups B and C, the sites of thoracic vertebra and spine were determined by barium-meal radiography to facilitate the stent placement. Patients were placed in a sitting position or lying on the side, and false teeth were removed and a teeth bracket was mounted. A 260-cm-long exchange guidewire was firstly led into the stomach. The stent was installed on the propeller whose front end was covered with sterilized liquid paraffin. Guided by the guidewire, the propeller on which the stent was mounted was moved through the segment with lesions. Under fluoroscopic control, the outer sheath was slowly withdrawn and the stent expanded under its own tension. After a stent was placed, esophageal radiography was performed to observe the patency of the esophagus. In group C, 500-1 000 ml of ice-cold water was injected 3-7 days after stent placement via a bioptic hole under gastroscope, which caused the stent to retract and reduce its diameter. Bioptic pliers were then used to withdraw the stent with the help of a gastroscope. Gastroscopy was performed again to detect complications, such as bleeding, mucosa tearing, and esophageal perforation. The patients returned to the ward and consumed cold drinks and snacks for 2 days before returning to a normal diet. It was preferable for patients to eat solid food since the natural expansion of food reduced retraction of the esophagus.

The criteria for therapeutic efficacy were as follows: the diameter of the narrowest region of the esophagus before and after dilation, and the dysphagia score before and after dilation. Postoperative treatment of pneumatic dilation, barium-meal radiography of the esophagus was performed immediately after interventional procedure to check the esophagus patency and perforation and submucous hematomas. Patients drank fluids for 2 h after interventional procedure and were treated with antibiotics, antacid drugs, and analgesics. In groups B and C, after stent placement, barium-meal radiography was used to observe the patency of the esophagus. Patients ate semisolid food on the day after interventional procedure and were treated with antibiotics and antacid drugs. In group C, esophageal radiography was performed within 1 week after stent removal to observe the patency of the esophagus. The follow-up time was 1 month, 6 months, 1 year and 3 years by telephone or clinic visit.

All the data were expressed as the mean±SD, and the paired *t*-test was used for statistical comparisons before and after interventional procedure within a group.

RESULTS

The 60 patients in group A involved 130 dilations (mean 2.2 times per case), of which 29 patients had three graded dilations of increasing diameter, 12 patients had two graded dilations of increasing diameter, and 19 patients had one dilation. In 8 patients of group B, 5 uncovered and 3 antireflux covered stents were successfully placed. In group C, 65 partially covered stents were placed and removed under gastroscope guidance 3-7 days after intervertional procedure. The success rate of stent placement and removal was 100 %. The differences in the cardia diameter before and after the three methods of interventional procedure and the dysphagia scores (Table 1) were statistically significant ($P<0.01$). The incidence of complications in the three interventional procedures is presented in Table 2 and the rate of dysphagia recurrence during follow-up is shown in Table 3. The follow-up period for the three interventional procedures was 12-96 months.

Table 1 Diameter of the narrowest cardia region before and after treatment with three interventional procedures, and dysphagia score

Group	Diameter of cardia before and after treatment (mm)		Dysphagia score before and after treatment (grade)	
A	3.2±2.1	10.6±3.8[b]	2.7±1.4	0.9±0.3[b]
B	3.4±1.9	19.5±1.1[b]	2.6±1.3	0.4±0.1[b]
C	3.1±2.3	18.9±3.5[b]	2.4±1.3	0.5±0.2[b]

[b]$P<0.01$ *vs* before and after treatment.

Table 2 Incidence of complications following treatment with three interventional procedures (%)

Group	Pain (*n*)	Reflux (*n*)	Bleeding (*n*)	Hyperplasia of granulation tissue (*n*)
A	50.0 %(30/60)	26.7 %(16/60)	10.0 %(6/60)	-
B	62.5 %(5/8)	62.5 %(5/8)	37.5 %(3/8)	37.5 %(3/8)
C	40.0 %(26/65)	20.0 %(13/65)	12.3 %(8/65)	-

Table 3 Relapse rate of dysphagia during follow-up

Group	Follow-up >12 months			Follow-up >36 months		
	Follow-up (*n*)	Relapse of dysphagia (*n*)	Relapse rate (%)	Follow-up (*n*)	Relapse of dysphagia (*n*)	Relapse rate (%)
A	60	36	60%	50	45	90 %
B	8	4	50%	3	2	66.7 %
C	65	6	9.2%	55	8	14.5 %

DISCUSSION

Techniques of interventional procedures

The techniques used to treat achalasia, such as surgery, bougienage, pneumatic dilation, botulinum toxin injection, permanently uncovered or antireflux covered metal stent dilation and temporary partially covered metal stent dilation, had advantages and drawbacks[1-5]. Bougienage is now uncommon since it has poor therapeutic efficacy and many complications. The use of surgery is declining due to the associated large lesion, a high risk, and high recurrence rate. Pneumatic dilation was first introduced in the plasty of hematostenosis, as its reliable therapeutic efficacy led to its gradual application to other plasty operations. Remarkable results were achieved when it was used in benign gastrointestinal strictures, and later it was widely used in the nonsurgical treatment of achalasia, exhibiting remarkable therapeutic efficacy. Many authors[6-15] have reported that graded dilation is better than single dilation in therapeutic efficacy, and our experience has confirmed this. Botulinum toxin injection in achalasia had a short term therapentic efficacy, dysphagia was relapsed witnin 6 months.

Permanent metal stent dilation is primarily used in the treatment of malignant gastrointestinal stricture and obstruction, and exhibits remarkable palliative therapeutic efficacy. Cwikiel *et al*[1] reported an experimental and clinical study of the treatment of benign esophageal stricture with expandable metal stents. We used uncovered stents in five patients with achalasia in order to reduce the occurrence rate of stent migration. After stent placement, dilation was excellent and dysphagia disappeared, thus achieving the goal of treatment. However, it was accompanied by new problems such as gastroesophageal reflux, recurrence of stricture (hyperplasia of granulation tissue). The reflux could be treated with drugs, but this took a long time. Recurrence of stricture could be reduced by heat cauterization under gastroscope, but it could easily reccur. So we used antireflux covered stent, compication of gastroesophageal reflux and hyperplasia of granulation tissue were not found, but many unexpected results occurred. These difficulties led to the use of a temporary partially covered metal stent dilation. Clinicians and patients have gradually accepted and now prefer to use temporary partially covered metal stent dilation due to its fewer complications and excellent therapeutic efficacy[16-22].

Long-term follow-up

Dysphagia recurred in 60 % of the patients at a 12-month follow-up, and in 90 % of the patients at a 36-months follow-up, demonstrating that pneumatic dilation of achalasia has excellent immediate therapeutic efficacy but its long-term therapeutic efficacy is poor[23-44]. Firstly, this was associated with the diameter of the saccule. Kadakia *et al*[10] suggested that the saccule diameter in pneumatic dilation should be 35-45 mm, but the incidence of complications was very high (e.g., 15 % had esophageal perforation). We used saccules with diameters of 28-32 mm in order to reduce the incidence of serious complications, but their long-term therapeutic efficacy was not satisfactory. Secondly, the therapeutic efficacy was associated with the frequency of dilation. One dilation did not produce excellent therapeutic efficacy, since it was affected by various factors. For example, whether the saccule was correctly located, whether pressure applied to the saccule reached the stipulated index, and variations in the anatomy of the cardia. It was suggested that three graded dilations should be used to achieve the treatment goal. Thirdly, the therapeutic efficacy was associated with the course of the disease. If this was very short, the cardiac muscularis was not fleshy and elastic. If this was very long, the cardiac muscularis was fleshy and not elastic. We used permanently uncovered stent dilation in five patients with achalasia and achieved excellent immediate therapeutic efficacy, but its long-term therapeutic efficacy was poor. This was mainly due to the frequent occurrence of serious gastroesophageal reflux and hyperplasia of granulation tissue. After a 12-month follow-up the stent could not be removed in three patients, and hence we had to resect and reconstruct the esophageal cardia. Therefore, permanently uncovered metal stent dilation was unsuitable for patients with achalasia[45-48]. Temporary partially covered metal stent dilation had excellent immediate and long-term therapeutic efficacy. First, the design of the stent coincided with the specific physiological structure of the cardia and the specific pathological manifestations of achalasia. The epicardia is a part of the expanded esophagus and the lower cardiac part is a very large gastric cavity. If a stent is not well designed, it will lose its therapeutic efficacy, and moreover, the rate of stent migrations will increase. To avoid these problems, we designed a special stent for achalasia. The stent was partially covered with a membrane covering the inner wall of the stent but not covering the area within 2 cm of the stent outlet. The upper outlet of the stent was a large horn, which increased the stability of the stent but made it difficult to extract. Second, the diameter of the stents used in this group was 20-30 mm. By expanding the stent, the cardia could be returned nearly to the maximum diameter of the normally dilated esophageal lumen. The most appropriate stent diameter was that which could expand the cardia stricture while not cause gastroesophageal reflux. This needs to be investigated further. Thirdly, the internal metal stent expansion procedure took a long time, and the stent was placed for 3-7 days. Why the therapeutic efficacy of temporary partially covered stent dilation was better than that of pneumatic dilation? We considered that this was mainly due to the stent expansion which caused chronic tearing of the cardia muscularis. The stent gradually expanded with body temperature, taking 12-24 h to reach 36 ℃, for it to reach the expected diameter. Therefore, the cardia muscularis was torn regularly with relatively few scars formed and a very low incidence of restenosis when it was repaired. In pneumatic dilation the tearing of cardia muscularis was acute and irregular with many scars formed when it was repaired. Therefore, restenosis was common and the long-term therapeutic efficacy was poor. This might explain why the therapeutic efficacy of temporary partially covered metal stent dilation was better in the treatment of achalasia than that of pneumatic dilation.

Developments in biologically degradable stents for the esophagus which are degraded within 2 months, would provide the advantages of a long retention time without the need for stent removal. This would provide another interventional procedure for patients with achalasia. We compared three methods of interventional procedure for patients with achalasia and took the following factors into consideration such as extent of lesion, incidence of complications, therapeutic efficacy, and degree of patient acceptance. We found that in the treatment of benign gastrointestinal stricture, the use of temporary partially covered metal internal stent dilation was preferred due to its superior long-term therapeutic efficacy.

REFERENCES

1 **Cwikiel W,** Willen R, Stridbeck H, Liool-Gil R, Von Holstein CS. Self-expanding stent in the treatment of benign esophageal stricture:experimental study in pigs and presentation of clinical cases. *Radiology* 1993; **187**: 667-671

2 **Song HY,** Park SI, Do YS, Yoon HK, Sung KB, Sohn KH, Min YI. Expandable metallic stent placement in patients with benign esophageal strictures: results of long-term follow-up. *Radiology* 1997; **203**: 131-136

3 **Kadakia SC,** Wong RK. Graded pneumatic dilation using Rigiflex achalsia dilators in patients with primary esophageal achalasia.

Am J Gastroenterol 1993; **88**: 34-38
4 **Vaezi MF,** Richter JE. Current therapies for achalasia: comparison and efficacy. *J Clin Gastroenterol* 1998; **27**: 21-35
5 **Peracchia A,** Bonavina L.Achalasia: dilation, injection or surgery? *Can J Gastroenterol* 2000; **14**: 441-443
6 **Hoogerwerf WA,** Pasricha PJ. Achalasia: treatment options revisited. *Can J Gastroenterol* 2000; **14**: 406-409
7 **Massey BT.** Management of idiopathic achalasia: short-term and long-term outcomes. *Curr Gastroenterol Rep* 2000; **2**: 196-200
8 **Scarpignato C.** New therapeutic modalities for benign oesophageal disease: an overview. *Dig Liver Dis* 2001; **33**: 260-265
9 **Urbach DR,** Hansen PD, Khajanchee YS, Swanstrom LL.A decision analysis of the optimal initial approach to achalasia: laparoscopic Heller myotomy with partial fundoplication, thoracoscopic Heller myotomy, pneumatic dilatation, or botulinum toxin injection. *J Gastrointest Surg* 2001; **5**: 192-205
10 **Kadakia SC,** Wong RK. Pneumatic balloon dilation for esophageal achalasia. *Gastrointest Endosc Clin N Am* 2001; **11**: 325-346
11 **Bittinger M,** Wienbeck M. Pneumatic dilation in achalasia. *Can J Gastroenterol* 2001; **15**: 195-199
12 **Da Silveira EB,** Rogers AI. Achalasia: a review of therapeutic options and outcomes. *Compr Ther* 2002; **28**: 15-22
13 **Trifan A,** Stanciu C. Treatment of achalasia: an update. *Rev Med Chir Soc Med Nat Iasi* 2000; **104**: 11-13
14 **Chen WX,** Cheng YS, Yang RJ, Li MH, Zhuang QX, Chen NW, Xu JR, Shang KZ. Interventional therapy of achalasia with temporary metal internal stent dilatation and its intermediate and long term follow-up. *Shijie Huaren Xiaohua Zazhi* 2000; **8**: 896-899
15 **Cheng YS,** Yang RJ, Li MH, Shang KZ, Chen WX, Chen NW, Chu YD, Zhuang QX. Interventional procedure for benign or malignant stricture or obstruction of upper gastrointestinal tract. *Shijie Huaren Xiaohua Zazhi* 2000; **8**: 1354-1360
16 **Chen WX,** Cheng YS, Yang RJ, Li MH, Shang KZ, Zhuang QX, Chen NW. Metal stent dilation in the treatment of benign esophageal stricture by interventional procedure:a follow-up study. *Shijie Huaren Xiaohua Zazhi* 2002; **10**: 333-336
17 **Bansal R,** Nostrant TT, Scheiman JM, Koshy S, Barnett JL, Elta GH, Chey WD. Intrasphincteric botulinum toxin versus pneumatic balloon dilation for treatment of primary achalasia. *J Clin Gastroenterol* 2003; **36**: 209-214
18 **Scatton O,** Gaudric M, Massault PP, Chaussade S, Houssin D, Dousset B. Conservative management of esophageal perforation after pneumatic dilatation for achalasia. *Gastroenterol Clin Biol* 2002; **26**: 883-887
19 **Khan AA,** Shah SW, Alam A, Butt AK, Shafqat F. Efficacy of Rigiflex balloon dilatation in 12 children with achalasia: a 6-month prospective study showing weight gain and symptomatic improvement. *Dis Esophagus* 2002; **15**: 167-170
20 **Sabharwal T,** Cowling M, Dussek J, Owen W, Adam A. Balloon dilation for achalasia of the cardia: experience in 76 patients. *Radiology* 2002; **224**: 719-724
21 **O'Connor JB,** Singer ME, Imperiale TF, Vaezi MF, Richter JE. The cost-effectiveness of treatment strategies for achalasia. *Dig Dis Sci* 2002; **47**: 1516-1525
22 **West RL,** Hirsch DP, Bartelsman JF, de Borst J, Ferwerda G, Tytgat GN, Boeckxstaens GE. Long term results of pneumatic dilation in achalasia followed for more than 5 years. *Am J Gastroenterol* 2002; **97**: 1346-1351
23 **Upadhyaya M**, Fataar S, Sajwany MJ. Achalasia of the cardia: experience with hydrostatic balloon dilatation in children. *Pediatr Radiol* 2002; **32**: 409-412
24 **Vaezi MF,** Baker ME, Achkar E, Richter JE. Timed barium oesophagram: better predictor of long term success after pneumatic dilation in achalasia than symptom assessment. *Gut* 2002; **50**: 765-770
25 **Penagini R,** Cantu P, Mangano M, Colombo P, Bianchi PA. Long-term effects of pneumatic dilatation on symptoms and lower oesophageal sphincter pressure in achalasia. *Scand J Gastroenterol* 2002; **37**: 380-384
26 **Babu R,** Grier D, Cusick E, Spicer RD. Pneumatic dilatation for childhood achalasia. *Pediatr Surg Int* 2001; **17**: 505-507
27 **Becker K,** Biesenbach S, Erckenbrecht JF, Frieling T. Effect of balloon compliance on symptomatic success of pneumatic dilation in achalasia patients. *Z Gastroenterol* 2001; **39**: 831-836
28 **Diener U,** Patti MG, Molena D, Tamburini A, Fisichella PM, Whang K, Way LW. Laparoscopic Heller myotomy relieves dysphagia in patients with achalasia and low LES pressure following pneumatic dilatation. *Surg Endosc* 2001; **15**: 687-690
29 **Swift GL,** Smith PM, McKirdy HC, Lowndes RH. Vector volume analysis of the lower esophageal sphincter in achalasia and the effect of balloon dilation. *Dis Esophagus* 2001; **14**: 54-56
30 **Hep A,** Dolina J, Dite P, Plottova Z, Valek V, Kala Z, Prasek J. Restoration of propulsive peristalsis of the esophagus in achalasia. *Hepatogastroenterology* 2000; **47**: 1203-1204
31 **Hunt DR,** Wills VL, Weis B, Jorgensen JO, DeCarle DJ, Coo IJ. Management of esophageal perforation after pneumatic dilation for achalasia. *J Gastrointest Surg* 2000; **4**: 411-415
32 **Morino M,** Rebecchi F. Pneumatic dilatation and laparoscopic cardiomyotomy in the management of achalasia. *Surg Endosc* 2000; **14**: 870-871
33 **Rajput S,** Nandwani SK, Phadke AY, Bhandarkar PV, Abraham P, Tilve GH.Predictors of response to pneumatic dilatation in achalasia cardia. *Indian J Gastroenterol* 2000; **19**: 126-129
34 **Hamza AF,** Awad HA, Hussein O. Cardiac achalasia in children. Dilatation or surgery? *Eur J Pediatr Surg* 1999; **9**: 299-302
35 **Ponce J,** Juan M, Garrigues V, Pascual S, Berenguer J. Efficacy and safety of cardiomyotomy in patients with achalasia after failure of pneumatic dilatation. *Dig Dis Sci* 1999; **44**: 2277-2282
36 **Gideon RM,** Castell DO, Yarze J. Prospective randomized comparison of pneumatic dilatation technique in patients with idiopathic achalasia. *Dig Dis Sci* 1999; **44**: 1853-1857
37 **Singh V,** Duseja A, Kumar A, Kumar P, Rai HS, Singh K. Balloon dilatation in achalasia cardia. *Trop Gastroenterol* 1999; **20**: 68-69
38 **Khan AA,** Shah SW, Alam A, Butt AK, Shafqat F, Castell DO. Massively dilated esophagus in achalasia: response to pneumatic balloon dilation. *Am J Gastroenterol* 1999; **94**: 2363-2366
39 **Vaezi MF,** Baker ME, Richter JE. Assessment of esophageal emptying post-pneumatic dilation: use of the timed barium esophagram. *Am J Gastroenterol* 1999; **94**: 1802-1807
40 **Metman EH,** Lagasse JP, d'Alteroche L, Picon L, Scotto B, Barbieux JP. Risk factors for immediate complications after progressive pneumatic dilation for achalasia. *Am J Gastroenterol* 1999; **94**: 1179-1185
41 **Lisy J**, Hetkova M, Snajdauf J, Vyhnanek M, Tuma S. Long-term outcomes of balloon dilation of esophageal strictures in children. *Acad Radiol* 1998; **5**: 832-835
42 **Katz PO,** Gilbert J, Castell DO. Pneumatic dilatation is effective long-term treatment for achalasia. *Dig Dis Sci* 1998; **43**: 1973-1977
43 **Khan AA,** Shah SW, Alam A, Butt AK, Shafqat F, Castell DO. Pneumatic balloon dilation in achalasia: a prospective comparison of balloon distention time. *Am J Gastroenterol* 1998; **93**: 1064-1067
44 **Mukherjee S,** Kaplan DS, Parasher G, Sipple MS. Expandable metal stents in achalasia-is there a role? *Am J Gastroenterol* 2000; **95**: 2185-2188
45 **Lee JG,** Hsu R, Leung JW. Are self-expanding metal mesh stents useful in the treatment of benign esophageal stenoses and fistulas? An experience of four cases. *Am J Gastroenterol* 2000; **95**: 1920-1925
46 **De Palma GD,** Catanzano C. Removable self-expanding metal stents: a pilot study for treatment of achalasia of the esophagus. *Endoscopy* 1998; **30**: S95-96
47 **Mukherjee S,** Kaplan DS, Parasher G, Sipple MS. Expandable metal stents in achalasia–is there a role? *Am J Gastroenterol* 2000; **95**: 2185-2188
48 **De Palma GD**, Iovino P, Masone S, Persico M, Persico G. Self-expanding metal stents for endoscopic treatment of esophageal achalasia unresponsive to conventional treatments. Long-term results in eight patients. *Endoscopy* 2001; **33**: 1027-1030

Edited by Zhang JZ and Wang XL

P.O.Box 2345, Beijing 100023,China
Fax: +86-10-85381893
E-mail: wjg@wjgnet.com www.wjgnet.com

World J Gastroenterol 2003;9(10):2374-2376
World Journal of Gastroenterology
 ISSN 1007-9327

• BRIEF REPORTS •

Effects of glycine on plasma and liver tissue changes of TNF-α, ET-1 and nitric oxide contents in rats with obstructive jaundice

He-Qing Fang, Ying-Bin Liu, Hai-Jun Li, Shu-You Peng, Yu-Lian Wu, Bin Xu, Jian-Wei Wang, Jiang-Tao Li, Xin-Bao Wang

He-Qing Fang, Ying-Bin Liu, Hai-Jun Li, Shu-You Peng, Yu-Lian Wu, Bin Xu, Jian-Wei Wang, Jiang-Tao Li, Xin-Bao Wang, Department of General Surgery, Second Affiliated Hospital, Medical College of Zhejiang University, Hangzhou 310009, Zhejiang Province, China
Correspondence to: Dr. Ying-Bin Liu, Department of General Surgery, Second Affiliated Hospital, Medical College of Zhejiang University, Hangzhou 310009, Zhejiang Province, China. laoniulyb@163.com
Telephone: +86-571-87783585
Received: 2003-06-05 **Accepted:** 2003-07-22

Abstract

AIM: To evaluate the effect of glycine on plasma and liver tissue changes of tumor necrosis factor-α (TNF-α), endothelin-1 (ET-1) and nitric oxide (NO) contents in rats with obstructive jaundice.

METHODS: Ninety healthy Wistar rats of both sexes weighing 275±25 g were randomly divided into sham-operated, bile duct-ligated, and bile duct-ligated plus glycine-treated groups, the latter was performed with 5 % glycine solution substituting for tap water drunk *ad libium* for 5 days before and 6 days after operation. Blood and liver tissue were sampled at the time of sacrifice on the 8th day post operation. Plasma total bilirubin, endotoxin, levels, as well as TNF-α, ET-1 and NO contents in liver tissue were determined.

RESULTS: Plasma endotoxin and total bilirubin levels were significantly higher in both bile duct-ligated and bile duct-ligated plus glycine-treated rats than in sham-operated animals (P=0.000613, 0.00921 and 0.00737, 0.00841 respectively), whereas they did not display any statistically significant difference between the former groups (P=0.417 and 0.374 respectively). Likewise, TNF-α, ET-1 and NO contents in both plasma and liver tissue were significantly increased in both bile duct-ligated and bile duct-ligated plus glycine-treated rats compared with sham-operated animals (P=0.00813, 0.00793, 0.00671, 0.00804, 0.00872, and 0.00947 in plasma and 0.00531, 0.00785, 0.00912, 0.00981 and 0.00635 in liver tissue respectively). However, these inflammatory mediators in both plasma and liver tissue were significantly reduced in bile duct-ligated rats fed on 5 % glycine solution compared with that without (P=0.00953, 0.00891, 0.0795, 0.00867, 0.0697 and 0.00907 in plasma and liver tissue respectively).

CONCLUSION: Reduction of TNF-α, ET-1 and NO contents in plasma and liver tissue of rats fed on glycine may be helpful to alleviate pathological lesions in obstructive jaundice.

Fang HQ, Liu YB, Li HJ, Peng SY, Wu YL, Xu B, Wang JW, Li JT, Wang XB. Effects of glycine on plasma and liver tissue changes of TNF-α, ET-1 and nitric oxide contents in rats with obstructive jaundice. *World J Gastroenterol* 2003; 9(10):2374-2376
http://www.wjgnet.com/1007-9327/9/2374.asp

INTRODUCTION

Endotoxemia is one of the major causes that can lead to complicated pathophysiologic alterations in the process of obstructive jaundice. Current research has demonstrated that severe endotoxemia in obstructive jaundice could activate immunocompetent cells such as monocytes, macrophages and endothelial cells to produce a variety of cytokines that could contribute to an uncontrollable inflammatory cascade causing multiple organ dysfunction (MODS) or even death[1-3]. Among these cytokines, TNF-α, ET-1 and NO have been considered to be the main effectors in endotoxemia[4-10]. It is also worthy to note that glycine could provide an effective protection against endotoxemia that has been recently published in several repots[11-15]. The present study, therefore, was conducted with the aim to evaluate the effect of glycine on the plasma and liver tissue changes of TNF-α, ET-1 and nitric oxide contents in rats with obstructive jaundice.

MATERIALS AND METHODS

Animal model and experimental protocol

Ninety healthy Wistar rats of both sexes weighing 275±25 g were employed in the study. According to the experimental protocol, the animals were randomly divided into Group A in which the rats were performed a sham operation, Group B in which the rats were operated merely to ligate the common bile duct and Group C in which the rats were treated with both the ligation of common bile duct and a glycine regimen. Before operation, all animals were allowed access to standard rat chow and water *ad libium* for 5 days except that the rats in Group C drank 5 % glycine solution (provided by Shanghai Institute of Biological Products Research) instead of water[2]. After a 12-h fasting period, the animals were weighed and anesthetized with 1 % pentobarbitale sodium (30 mg/kg, ip) and their common bile duct was exposed and ligated to form a complete obstruction of the extrahepatic bile duct except that the common bile duct in rats of Group A was only exposed following laparotomy. When recovered for a period of 24 h, the rats were fed on their corresponding regimens for another 6 days. Rat venous blood was sampled and liver was removed surgically at the time of sacrifice on the 8th day post operation under anesthesia. Blood samples were prepared respectively according to the procedures for determinating different variables and the resulting plasma was stored at -70 ℃ until use. The liver was perfused via a cannula inserted into the portal vein with sterile normal saline to remove residual blood, and then prepared into 10 % tissue homogenate with 1.0 mol· L^{-1} acetic acid and centrifuged at 3 000×g for 40 min. The supernatant was stored at -70 ℃ until analysis.

Measurements

For determination of plasma endotoxin level, 1 ml of blood sample was collected in a pyrogen-free heparinized tube and centrifuged at 500×g for 5 min. The resulting plasma was analyzed with the limulus-amoebocyte-lysate test (LAL) kit according to the protocol of its manufacturer (Shanghai Yihua Medical Science & Technology Ltd.). The endotoxin

concentration was finally expressed as Eu/ml.

Measurement of ET-1 level was performed using 1 ml of blood samples that was collected in a test tube containing 15 μl of 10 % disodium edentate and 20 μl of aprotinin, and centrifuged at 3 000×g for 10 min at 4 ℃. The resulting plasma and liver homogenate were determined with ET-1 radioimmunoassay kit following the protocol of Research Institute of Radioimmunotechnology, General Hospital of PLA. Heparinised blood samples were collected in a separator tube and spun at 4 000 g for 10 min for detection of plasma bilirubin and TNF-α. To measure TNF-α, the resulting plasma and liver homogenate were analysed with a radioimmunoassay kit according to the instructions supplied by Research Institute of Radioimmunotechnology, General Hospital of PLA. Plasma bilirubin was determined with an automatic multifunction-biochemical analyzer.

Measurement of NO_2^-/NO_3^- content two ml of heparinised blood samples was incubated at 37 ℃ for 1 h and then centrifuged at 2 000×g for 5 min. The resulting plasma and liver homogenate were determined with a NO_2^-/NO_3^- assay kit following the procedures of Research Institute of Radioimmunotechnology, General Hospital of PLA.

Statistical analysis

Experimental data were processed by analysis of variance and *t*-tests for comparison between groups. Results were expressed as mean ± SE. $P<0.05$ was selected as the level of significance.

RESULTS

Poor appetite and jaundice were observed in rats of Groups B and C on the 2nd day after operation, the jaundice was more apparent on the ear and tail end skin. The dilation of proximal bile duct at the site of ligation, deep-brown-coloured liver and significantly elevated plasma total bilirubin (P=0.00921 and 0.00841 in Groups B and C respectively as compared to Group A) were also noted in these animals at the time of sacrifice on the 8nd day post operation. Animals in Group A did not exhibit obvious abnormalities. But there was no significant difference of plasma total bilirubin between rats in Groups B and C (P=0.374).

Plasma endotoxin levels in rats of Groups B and C were significantly increased compared with that in rats of Group A (P=0.000613 and 0.00737 respectively). However, It did not exhibit significant difference between rats in Groups B and C (P=0.417).

Plasma levels of TNF-α, ET-1 and NO in Group B rats were significantly elevated compared with that in Group A rats (P=0.00813, 0.00793 and 0.00671 respectively), which were significantly improved when the rats were fed on 5 % glycine solution as shown in Table 1 (P=0.00953, 0.00891 and 0.0795). The data for TNF-α, ET-1 and NO levels in liver tissue are shown in Table 2. In accordance with their plasma counterparts, significant reduction of these variables was found in bile duct-ligated rats fed on 5 % glycine solution (0.00867, 0.0697 and 0.00907).

DISCUSSION

Obstructive jaundice is associated with an increased incidence of postoperative complications such as infection, systemic inflammatory response, and even multiple organ failure due to metabolic and hemodynamic disorders, as well as depressed immune function. Current studies have revealed that endotoxemia was one of the major causes leading to high morbidity and mortality in patients with obstructive jaundice[1-3]. Therefore, the therapeutic strategy aimed at reducing plasma endotoxin level and interrupting its biological activities has become a focus of great concern[4].

It has been found that endotoxin could stimulate monocytes and macrophages to produce a variety of cytokines, because the elevated intracellular Ca^{2+} concentration in these cells was resulted from the activation of Ca^{2+} channel by endotoxin[11,12]. It has also been noted that glycine, a nonessential amino acid, could exert protective effects on animals in multiple morbid conditions by minimizing oxidative stress, as well as toxic eicosanoid cytokine production[11,13] Ding *et al*[14,15] demonstrated that the biological effects of endotoxin could be significantly inhibited by glycine via a mechanism of blocking TNF-α production in immunocompetent cells, the latter could play a critical role in the pathogenesis of endotoxin lesions[4-7]. ET and NO, although as the intense vasoconstrictor and vasodilator respectively, were also pleiotropic factors involveded in endotoxin-mediated pathological processes with endotoxin and TNF-α as their potent releasing irritants[3,8-10]. The present study demonstrated that severe endotoxemia could be observed in obstructive jaundice, and the TNF-α, ET and NO contents in plasma and liver tissue were all significantly increased in bile duct-ligated rats.

Persistent severe endotoxemia in obstructive jaundice could stimulate not only Kupffer cells to release TNF-α to insult directly parenchymal cells of the kidney and liver[3,16-18], but also other immunocompetent cells to produce excessive amount of ET-1 and NO[8] to aggravate the disturbance of splanchnic circulation leading to decreased oxygen delivery, and ultimately multiple organ dysfunction syndrome (MODS).

Table 1 Plasma levels of bilirubin, endotoxin, TNF-α, ET-1 and NO_2^-/NO_3^- in different groups of rats ($\bar{x}\pm s$, n=30)

Group	Bilirubin (μmol/L)	Endotoxin (Eu/ml)	TNF-α (pg/ml)	ET-1 (pg/ml)	NO_2^-/NO_3^- (μmol/L)
A	5.80±1.65	5.98±1.00	61.37±3.08	88.79±7.56	5.51±0.44
B	45.45±6.69[a]	11.65±1.57[a]	352.52±20.65[a]	183.24±34.01[a]	12.06±0.62[a]
C	43.18±6.53[a]	11.27±1.30[a]	158.63±7.07[ab]	120.68±10.99[ab]	8.55±0.40[ab]

[a]$P<0.01$ *vs* group A, [b]$P<0.01$ *vs* group B.

Table 2 Levels of TNF-α, ET-1 and NO_2^-/NO_3^- in liver tissues of different groups of rats ($\bar{x}\pm s$)

Group	Samples	TNF-α (pg/ml)	ET-1 (pg/ml)	NO_2^-/NO_3^- (μmol/L)
A	10	43.51±2.58	43.18±4.47	2.15±0.18
B	10	298.46±18.74[a]	124.56±11.67[a]	10.53±0.87[a]
C	10	113.45±6.67[ab]	81.49±7.39[ab]	7.23±0.34[ab]

[a]$P<0.01$ *vs* group A, [b]$P<0.01$ *vs* group B.

Besides, NO itself is also a highly active free radical and can convert further into NO_2^- and peroxynitrite. The more vigorous oxidants could result in cell injury[9]. Although glycine could reduce the plasma and liver tissue endotoxin level in our study, it did prevent TNF-α, ET-1 and NO from excessive production, which might be beneficial to alleviate the organ injury in obstructive jaundice. However, TNF-α, ET-1 and NO levels in both plasma and liver tissue remained elevated to some extent in rats fed on glycine as rats compared with sham-operated rats. To elucidate the mechanism underlying this phenomenon is thus the purpose of our further studies.

REFERENCES

1 **Greig JD,** Krukowski ZH, Matheson NA. Surgical morbidity and mortality in one hundred and twenty-nine patients with obstructive jaundice. *Br J Surg* 1988; **75**: 216–219

2 **Reynolds JV,** Murchan P, Leonard N, Clarke P, Keane FB, Tanner WA. Gut barrier failure in experimental obstructive jaundice. *J Surg Res* 1996; **62**: 11-16

3 **Inan M,** Sayek I, Tel BC, Sahin-Erdemli I. Role of endotoxin and nitric oxide in the pathogenesis of renal failure in obstructive jaundice. *Br J Surg* 1997; **84:** 943-947

4 **Sheen-Chen SM**, Chen HS, Ho HT, Chen WJ, Sheen CC, Eng HL. Effect of bile acid replacement on endotoxin-induced tumor necrosis factor-alpha production in obstructive jaundice. *World J Surg* 2002; **26**: 448-450

5 **Heller J**, Sogni P, Barriere E, Tazi KA, Chauvelot-Moachon L, Guimont MC, Bories PN, Poirel O, Moreau R, Lebrec D. Effects of lipopolysaccharide on TNF-alpha production, hepatic NOS2 activity, and hepatic toxicity in rats with cirrhosis. *J Hepatol* 2000; **33**: 376-381

6 **O'Neil S,** Hunt J, Filkins J, Gamelli R. Obstructive jaundice in rats results in exaggerated hepatic production of tumor necrosis factor-alpha and systemic and tissue tumor necrosis factor-alpha levels after endotoxin. *Surgery* 1997; **122**: 281-286

7 **Kennedy JA,** Lewis H, Clements WD, Kirk SJ, Campbell G, Halliday MI, Rowlands BJ. Kupffer cell blockade, tumour necrosis factor secretion and survival following endotoxin challenge in experimental biliary obstruction. *Br J Surg* 1999; **86**: 1410-1414

8 **Liu BH**, Xiao N, Chen HS, Zhou JH. Dynamic alteration and interaction of endothelin-1and nitric oxide levels in the plasma or the liver during endotoxemia. *Zhonghua Chuangshang Zazhi* 2001; **17:** 166-168

9 **Wang D**, Zhu JY, Leng XS, Li S, Wang FS, Du RY. The detection of nitric oxide synthase(NOS) *in liver* tissue from cirrhotic patients with portal hypertension and their clinicopathological significance. *Zhonghua Putong Waike Zazhi* 1999; **14:** 31-33

10 **Sarac AM,** Aktan AO, Moini H, Bilsel S, Scapa E. Role of endothelin in obstructive jaundice. *Dig Dis Sci* 1999; **44**: 356-363

11 **Ikejima K,** Iimuro Y, Forman DT, Thurman RG. A diet containing glycine improves survival in endotoxin shock in the rat. *Am J physiol* 1996; **271**(1Pt 1): G97-103

12 **Portoles MT**, Arahuetes RM, Pagani R. Intracellular calcium alterations and free radical formation evaluated by flow cytometry in endotoxin-treated rat liver Kupffer and endothelial cells. *Eur J Cell Biol* 1994; **65**: 200-205

13 **Wheeler MD**, Thurman RG. Production of superoxide and TNF-alpha from alveolar macrophages is blunted by glycine. *Am J Physiol* 1999; **277**(5Pt 1): L952-959

14 **Ding Y,** Lu DX, Sun W, Zhang SM, Li CJ. Observation on the effect of Gly on the TNF and IL-1 production of monocytes stimulated by ET. *Zhongguo Yiaolixue Tongbao* 1999; **15:** 184-185

15 **Sun W,** Lu DX, Ding Y, Li CJ. Effects of glycine on the combining rate of endotoxin to monocytes and endotoxic configuration. *Zhongguo Bingli Shengli Zazhi* 1998; **14:** 359-362

16 **Tomioka M**, Iinuma H, Okinaga K. Impaired Kupffer cell function and effect of immunotherapy in obstructive jaundice. *J Surg Res* 2000; **92**: 276-282

17 **Ding JW**, Andersson R, Soltesz V, Willen R, Bengmark S. Obstructive jaundice impairs reticuloendothelial function and promotes bacterial translocation in the rat. *J Surg Res* 1994; **57**: 238-245

18 **Sheen-Chen SM**, Chau P, Harris HW. Obstructive jaundice alters Kupffer cell function independent of bacterial translocation. *J Surg Res* 1998; **80**: 205-209

Edited by Zhu L and Wang XL

P.O.Box 2345, Beijing 100023,China
Fax: +86-10-85381893
E-mail: wjg@wjgnet.com www.wjgnet.com

World J Gastroenterol 2003;9(10):2377-2378
World Journal of Gastroenterology
 ISSN 1007-9327

• CASE REPORT •

Potentially fatal haemobilia due to inappropriate use of an expanding biliary stent

Rakesh Rai, John Rose, Derek Manas

Rakesh Rai, Derek Manas, Hepatobiliary Surgery and Liver Transplant Unit, Freeman Hospital, Newcastle, UK
John Rose, Department of Interventional Radiology, Freeman Hospital, Newcastle, UK
Correspondence to: Mr. Rakesh Rai, Flat-2, 108 St. Georges Terrace, Jesmond, Newcastle, NE22DP, UK. rai2000@hotmail.com
Telephone: +44-191-2818326
Received: 2003-05-12 **Accepted:** 2003-08-19

Abstract

AIM: To highlight the fatal complication caused by expanding biliary stents and the importance of avoiding use of expanding stent in potentially curable diseases.

METHODS: Arteriobiliary fistula is an uncommon cause of haemobilia. We describe a case of right hepatic artery pseudoaneurysm causing arteriobiliary fistula and presenting as severe malena and cholangitis, in a patient with a mesh metal biliary stent. The patient had lymphoma causing bile duct obstruction.

RESULTS: Gastroduodenoscopy failed to establish the exact source of bleeding and hepatic artery angiography and selective embolisation of the pseudo aneurysm successfully controlled the bleeding.

CONCLUSION: Bleeding from the pseudo aneurysm of the hepatic artery can be fatal. Mesh metal stents in biliary tree can cause this complication as demonstrated in this case. So mesh metal stent insertion should be avoided in potentially benign or in curable conditions. Difficulty in diagnosis and management is discussed along with the review of the literature.

Rai R, Rose J, Manas D. Potentially fatal haemobilia due to inappropriate use of an expanding biliary stent. *World J Gastroenterol* 2003; 9(10):2377-2378
http://www.wjgnet.com/1007-9327/9/2377.asp

INTRODUCTION

With increasing surgical and radiological intervention in the liver and biliary tree, incidence of haemobilia is on the rise. The mesh metal stent insertion can cause haemobilia as described. Thus inappropriate use of mesh metal stents in potentially curable diseases should be avoided.

The diagnosis of haemobilia may be difficult to establish and the bleeding may be fatal. Pseudoaneurysm of the right hepatic artery is an uncommon cause of haemobilia. A proper facility for radiological and surgical intervention is important to achieve success in control of bleeding.

The presentation and management of a case of haemobilia in a patient with mesh metal stent is described.

CASE REPORT

A 47-year-old lady was referred as an emergency from another hospital with recurrent cholangitis and severe malena.

Two years previously she had presented in the referring hospital with an abdominal mass, vomiting and obstructive jaundice. Further investigation including computed tomography (CT) scan of the abdomen was inconclusive. A laparotomy was carried out which revealed a large nodular mass in the abdomen causing gastric outlet obstruction and compression at the porta hepatis. It was not possible to resect this mass and because there were extensive small bowel adhesions, an enteric or biliary surgical bypass was not considered a safe option. A sample from the lesion was taken for histology.

Postoperatively the patient underwent percutaneous placement of a self expanding mesh metal stent in her bile duct to relieve the jaundice. Histology suggested the presence of a non-Hodgkin' s lymphoma. Radiotherapy and chemotherapy were commenced, which produced a very good response. The patient was asymptomatic for 6 months and during that time a repeated CT scan showed no evidence of intra-abdominal diseases. Six months later the patient presented with obstructive jaundice and ultrasound examination suggested occlusion of the metal stent. On endoscopy the metal stent was protruding into the duodenum, which was associated with duodenal ulceration. A plastic stent was inserted through the metal stent at ERCP.

After a few months the patient developed further cholangitis and had severe malena leading to referral to our unit.

On arrival the patient had symptoms and signs suggestive of cholangitis. The patient was pale and required blood transfusion and was started on antibiotics for cholangitis. After resuscitation, endoscopy examination showed ulcerations in the 2nd part of duodenum adjacent to the metal stent but no active bleeding. On the 2nd day the patient developed more severe malena and it necessitated laparotomy to control the bleeding. At laparotomy there was an inflammatory mass around the porta, and the common bile duct was adherent to the hepatic artery and portal vein. During dissection the common bile duct was entered inadvertently and the blocked plastic stent was therefore removed. As soon as the plastic stent came out, profuse bleeding occurred inside the common bile duct. The source of this bleeding was unclear. As it was impossible to control the bleeding coming from the bile duct urgent on table, hepatic angiography was performed via the right femoral artery. It showed a pseudo-aneurysm of the right hepatic artery which had ruptured into the common bile duct. A successful embolisation of the right hepatic artery aneurysm was carried out. A t-tube was placed in the common bile duct. Within 24 hours of surgery, percutaneous drainage of the obstructed biliary tree was achieved with an external-internal drain. The patient recovered from surgery with no further malena. The biliary drain was internalised using a plastic stent, T- tube was removed prior to discharge.

Over the fourteen months since laparotomy and embolisation of the right hepatic artery pseudo-aneurysm, the patient has been asymptomatic, the biliary drain has remained patent and a recent CT scan showed no evidence of residual lymphoma.

DISCUSSION

Haemobilia is an uncommon cause of gastrointestinal bleeding

and currently the most common cause of haemobilia in the Western world is as a consequence of percutaneous liver procedures. In a recent review of 222 cases of haemobilia, 147 were iatrogenic in aetiology following hepatobiliary intervention[1]. The origins of haemobilia might be diverse and included the cystic artery, anomalous hepatic artery, and hepatic artery to portal vein fistulas[2,3]. One of the reported causes of haemobilia was pseudoaneurysm of the hepatic artery, and the most common causes of this include laparoscopic cholecystectomy, exploration of the bile duct and other surgical biliary procedures.

Aneurismal disease of the hepatic artery from any cause is rare. Different authors have identified 21 % to 44 % of all splanchnic artery aneurysms as occurring in the hepatic artery[4,5]. Causes included arteriosclerosis (30-50 %), medial degeneration (25 %), trauma (20 %), mycotic infection (10 %), and congenital disorders (15 %)[3]. Eighty percent of hepatic artery aneurysms are extra hepatic and 20 % are intrahepatic. Extra hepatic aneurysms are distributed in the common hepatic artery (60 %), the right hepatic artery (30 %), the left hepatic artery (5 %), and rarely, in both (4 %).

In the present case, the severe bleeding on table was precipitated by removal of the plastic stent from the bile duct. The inflammation surrounding the bile duct and the presence of adhesions between the metal stent and the hepatic artery may have contributed to the formation of the pseudo-aneurysm of the right hepatic artery which was adherent to the metal stent. The previous episodes of malena probably indicated intermittent bleeding from the pseudoaneurysm, which was partially occluded by the plastic stent.

Thus mesh metal stent insertion can lead to this fatal complication. The most important aspect of this case is that the mesh metal stent was inserted before the response to radiotherapy and chemotherapy. The patient had no evidence of residual lymph node after therapy. Thus a long term mesh metal stent was unnecessary and could have been avoided.

The best treatment option for an occluded metal stent is not clear. The options are placement of a new coaxial metal stent, mechanical cleaning of the blocked stent or coaxial insertion of a plastic stent[6]. In a multicentric study of treatment of an occluded mesh metal stent due to tumour overgrowth, all the three methods were found to be equally effective but insertion of a plastic stent within a mesh metal stent appeared to be the most cost effective method[6].

Diagnosing haemobilia can be difficult. Haemobilia can present as upper or lower GI bleeding and the first investigation should be upper gastrointestinal tract endoscopy. If blood is seen coming from the ampulla of Vater, haemobilia is the likely cause of bleeding. But as few as 12 percent of these endoscopies might be diagnostic[7]. Due to intermittent bleeding from the biliary tree the source of bleeding may not be apparent. In a series of 29 patients with haemobilia, 22 patients had a normal endoscopy[8]. In our case as well the bleeding was not seen coming from the ampulla of Vater at the time of endoscopy and in the presence of duodenal ulceration due to the protruding metal stent, the cause of gastrointestinal bleeding was presumed to be duodenal ulcerations.

The choice of further investigation has varied over the years. Goodnight and Blaisdell[9] in 1981 recommended computed tomography (CT) and then angiography. But now angiography is recognised as the investigation of choice after gastrointestinal endoscopy, as it can be diagnostic as well as therapeutic.

Angiography could be expected to detect a vascular abnormality in over 90 % of cases of significant haemobilia[1]. Angiography can not only demonstrate pseudo-aneurysm of the arteries but also demonstrate arterio-biliary and arterio-portal fistulas.

Once the diagnosis of haemobilia is established, the aim is to stop the bleeding. It is important to correct any coagulopathy if present. The bleeding might stop on conservative treatment depending on the cause of bleeding. In a recent review of 171 cases of haemobilia, 73 (43 %) patients required only conservative treatment[1]. In case of continued bleeding, transarterial embolisation has been shown to be successful in 80 % to 100 % of cases[10-14]. Since the reported morbidity and mortality rates of transhepatic arterial embolisation (TAE) were lower than surgery[14], angiographic embolisation should be attempted first. The relative contraindication of arterial embolisation is hepatic sepsis, and in case of portal vein obstruction, arterial embolisation can cause hepatic necrosis.

Surgery is indicated if embolisation has failed or in case of hepatic sepsis. Adequate drainage of the biliary tree by endoscopic, percutaneous route or by surgery is important.

In conclusion, mesh metal stent insertion in the biliary tree can lead to fatal haemobilia. The diagnosis and management of haemobilia can be difficult and need an experienced multi-disciplinary team - mainly hepatobiliary surgeons, endoscopists and interventional radiologists. To avoid this complication unnecessary use of a mesh metal biliary stent in potentially curable diseases should be avoided.

REFERENCES

1 **Green MH**, Duell RM, Johnson CD, Jamieson NV. Haemobilia. *Br J Surg* 2001; **88**: 773-786

2 **Strickland SK**, Khoury MB, Kiproff PM, Raves JJ. Cystic artery pseudoaneurysm: a rare cause of hemobilia. *Cardiovasc Intervent Radiol* 1991; **14**: 183-184

3 **Fagan EA**, Allison DJ, Chadwick VS, Hodgson HJ. Treatment of haemobilia by selective arterial embolisation. *Gut* 1980; **21**: 541-544

4 **Salam TA**, Lumsden AB, Martin LG, Smith RB. Nonoperative management of visceral aneurysms and pseudoaneurysms. *Am J Surg* 1992; **164**: 215-219

5 **Miani S**, Arpesani A, Giorgetti PL, Rampoldi V, Giordanengo F, Ruberti U. Splanchnic artery aneurysms. *J Cardiovasc Surg* 1993; **34**: 221-228

6 Tham TCK, Carr-Locke DL, Vandervoort J, Wong RCK, Lichtenstein DR, Van Dam JV, Ruymann F, Chow S, Bosco JJ, Qaseem T, Howell D, Pleskow D, Vannerman W, Libby ED. Management of occluded biliary Wallstents. *Gut* 1998; **42**: 703-707

7 **Counihan TC**, Islam S, Swanson RS. Acute cholecystitis resulting from hemobilia after tru-cut biopsy: a case report and brief review of the literature. *Am Surg* 1996; **62**: 757-758

8 **Moodley J**, Singh B, Lalloo S, Pershad S, Robbs JV. Non-operative management of haemobilia. *Br J Surg* 2001; **88**: 1073-1076

9 **Goodnight JE** Jr, Blaisdell FW. Hemobilia. *Surg Clin North Am* 1981; **61**: 973-979

10 L'Hermine C, Ernst O, Delemazure O, Sergent G. Arterial complications of percutaneous transhepatic biliary drainage. *Cardiovasc Intervent Radiol* 1996; **19**: 160-164

11 **Horak D**, Guseinov E, Adamyan A, Titova M, Danilov M, Trostenyuk N, Voronkova O, Gumargalieva K. Poly (2-hydroxyethyl methacrylate) particles for management of hemorrhage of complicated origin: treatment of hemobilia. *J Biomed Mater Res* 1996; **33**: 193-197

12 **Dousset B**, Sauvanet A, Bardou M, Legmann P, Vilgrain V, Belghiti J. Selective surgical indications for iatrogenic hemobilia. *Surgery* 1997; **121**: 37-41

13 **Yoshida J**, Donahue PE, Nyhus LM. Hemobilia: review of recent experience with a worldwide problem. *Am J Gastroenterol* 1987; **82**: 448-453

14 **Richardson A**, Simmons K, Gutmann J, Little JM. Hepatic haemobilia: non-operative management in eight cases. *Aust N Z J Surg* 1985; **55**: 447-451

Edited by Wang XL and Zhu LH

P.O.Box 2345, Beijing 100023,China
Fax: +86-10-85381893
E-mail: wjg@wjgnet.com www.wjgnet.com

World J Gastroenterol 2003;9(10):2379-2381
World Journal of Gastroenterology
 ISSN 1007-9327

• CASE REPORT •

Liver cell adenoma with malignant transformation: A case report

Masahiro Ito, Makoto Sasaki, Chun Yang Wen, Masahiro Nakashima, Toshihito Ueki, Hiromi Ishibashi, Michitami Yano, Masayoshi Kage, Masamichi Kojiro

Masahiro Ito, Department of Pathology, National Nagasaki Medical Center, Omura, Japan
Makoto Sasaki, Department of Surgery, National Nagasaki Medical Center, Omura, Japan
Chun Yang Wen, Masahiro Nakashima, Atomic Bomb Disease Institute, Nagasaki University School of Medicine, Nagasaki, Japan
Toshihito Ueki, Hiromi Ishibashi, Michitami Yano, Clinical Research Center, National Nagasaki Medical Center, Omura, Japan
Masayoshi Kage, Masamichi Kojiro, Department of Pathology, Kurume University School of Medicine, Kurume, Japan
Correspondence to: Masahiro Ito, Director, Department of Pathology, National Nagasaki Medical Center 2-1001-1 Kubara, Omura City, Nagasaki 856-856 Japan. itohm@nmc.hosp.go.jp
Received: 2003-07-17 **Accepted:** 2003-08-02

Abstract

A 57-year-old woman was referred to our hospital because of a liver mass detected by computed tomography. She had taken oral contraceptives for only one month at the age of thirty. Physical examination revealed no abnormalities, and laboratory data, including hepatic function tests, were within the normal range, with the exception of elevated levels of those serum proteins induced by the absence of vitamin K or by raised levels of the antagonist (PIVKA)-II (3 502 AU/ml). Abdominal ultrasonography revealed a hyperechoic mass measuring 10×10 cm in the left posterior segment of the liver. Because hepatocellular carcinoma could not be completely excluded, this mass was resected. The tumor consisted of sheets of uniform cells with clear cytoplasm, perinuclear eosinophilic granules and round nuclei. These histological findings were consistent with liver cell adenoma. Background hepatic tissue appeared normal. After resection of the tumor, serum PIVKA-II fell to within the normal range. An area of hepatocellular carcinoma (HCC) with a mid-trabecular pattern was immunohistochemically found, which was positive for PIVKA-II. Sinusoidal endothelial cells were CD34-positive, containing scattered PIVKA-II positive cells. This tumor was therefore finally diagnosed as liver cell adenoma with focal malignant transformation to HCC.

Ito M, Sasaki M, Wen CY, Nakashima M, Ueki T, Ishibashi H, Yano M, Kage M, Kojiro M. Liver cell adenoma with malignant transformation: A case report. *World J Gastroenterol* 2003; 9(10):2379-2381
http://www.wjgnet.com/1007-9327/9/2379.asp

INTRODUCTION

Liver cell adenoma (LCA) is a benign neoplasm composed of cells that closely resemble normal hepatocytes. The lesion arises in normal liver. LCA typically develops in the setting of a hormonal or metabolic abnormality which stimulates hepatocyte proliferation. Exogenous steroid hormone ingestion is undoubtedly the most common such stimulus. Hence, oral contraceptive steroids are the cause of most LCAs[1] although some cases are related to glycogen storage diseases. LCA is still uncommon in countries where oral contraceptives are not used[2-4]. Although the incidence is very low, LCA has been reported in men, children, and women not taking oral contraceptives.

We report here a case of LCA with transformation to hepatocellular carcinoma (HCC) in a woman who had received oral contraceptives for only one month 30 years before.

CASE REPORT

A 57-year-old woman attended hospital because of slight abdominal fullness. She was referred to our hospital because of a liver mass detected by abdominal CT in June 2001. Computed tomography revealed a single mass at the left hepatic lobe measuring 10×10×8 cm. Her past history was unremarkable and she had no history of drug or alcohol abuse. At the age of thirty she had taken oral contraceptives for one month. Physical examination revealed no hepatomegaly or other abnormalities. The results of urinalysis and peripheral blood analysis were normal. Biochemical findings for blood, i.e. AST, ALT, LDH, γ-GTP, cholinesterase, total bilirubin, and total protein, were also normal. Hepatitis B surface (HBs) antigen, anti-HBs antibody, and anti-hepatitis C virus antibody were negative. Although serum protein induced by the absence of vitamin K, or by increased antagonist-II (PIVKA-II) levels, was elevated, serum alpha fetoprotein levels were normal (18 ng/ml). On June 11, PIVKA-II was 234 μAU/ml and increased rapidly to 3 503 μAU/ml on July 19. Levels of other tumor markers, i.e., CEA and CA 19-9 were all within normal limits.

Abdominal ultrasonography revealed a highly echoic lesion, measuring 10×9 cm in the left posterior segment of the liver. Computed tomography of the abdomen confirmed a large low-density mass, measuring 10.5×8.5 cm in size. Celiac angiography demonstrated a large hypervascular mass (Figure 1). On CT angiography, the mass lesion was enhanced heterogeneously during the early phase, and a sharply demarcated tumor stain was noted during the late phase. This abnormal lesion of the liver was also detected as iso-intensity on T1-weighted and hyper- and hypo-intensity on T2-weighted magnetic resonance imaging (MRI). Therefore, a left lobectomy of the liver was performed under the clinical diagnosis of HCC, in August 2001. After resection of the tumor, serum PIVKA-II fell to the normal level.

The surrounding liver tissue revealed no fibrosis or cirrhosis. The tumor was solitary and spherical, and measured 10×10×8 cm (Figure 2A). On the cut surface, the tumor was firm and well encapsulated. The color varied from yellow-white to reddish brown. There were irregular scars and a variegated appearance with hemorrhage. Microscopically, tumor cells were of uniform size but larger and paler than non-tumor hepatocytes in the surrounding tissue, and arranged in small sheets and cords with an occasional acinar pattern (Figure 2B). Background hepatic tissue looked to be normal. Tumor cell cytoplasm was clear and hydropic with eosinophilic granules around the nucleus in each cell. PAS staining revealed abundant accumulation of glycogen in the cytoplasm. The nuclei of tumor cells were uniform and regular, and mitosis was not seen. Thin-walled vascular channels were scattered throughout the tumor. Peliosis hepatic-like sinusoidal dilatation and hemorrhage were present especially in the central part of the tumor (Figure 2C). Portal tracts were absent throughout the tumor. These histological findings indicated LCA, but not simple LCA because of the following

features. Distinct areas with a mid-trabecular pattern were evident (Figure 2D). Reticulin fibers were well represented in each sheet, and most cell plates were of two-cell thickness. However, three or more cell plates were present in some hypercellular areas. Pseudoglandular structures were not encountered. Immunohistochemistry revealed that PIVKA-II (18B7, Eisai Co. Ltd.; Tokyo) was positive both in the adenoma cells and in mid-trabecular areas (Figure 3A). CD34 (Nichirei, Tokyo, Japan) was positive throughout the endothelial cells of the tumor (Figure 3B). Ki-67 (Dako) was positive sporadically in mid-trabecular area and tumor cells with enlarged nuclei. AFP (Dako, Demark), P53 (DO-7, Dako), estrogen receptor (Novocastra, Newcastle, UK), and progesterone receptor (Novocastra) were all negative throughout.

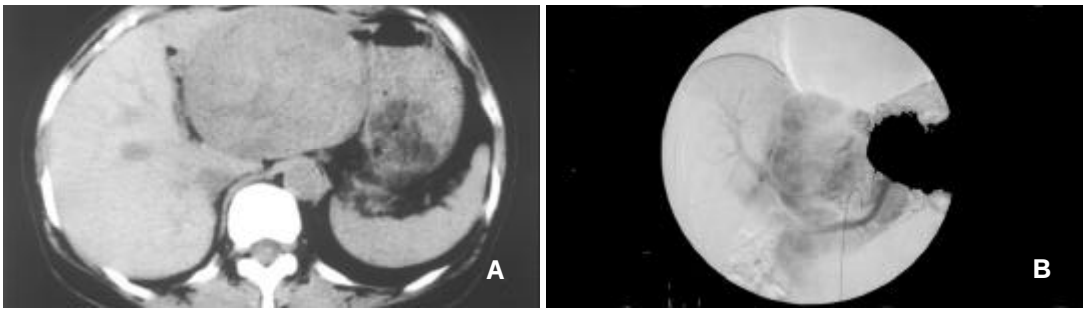

Figure 1 A: Computed tomography revealing a large tumor in the left lobe. B: Celiac angiography during the arterial phase, showing a large hypervascular lesion.

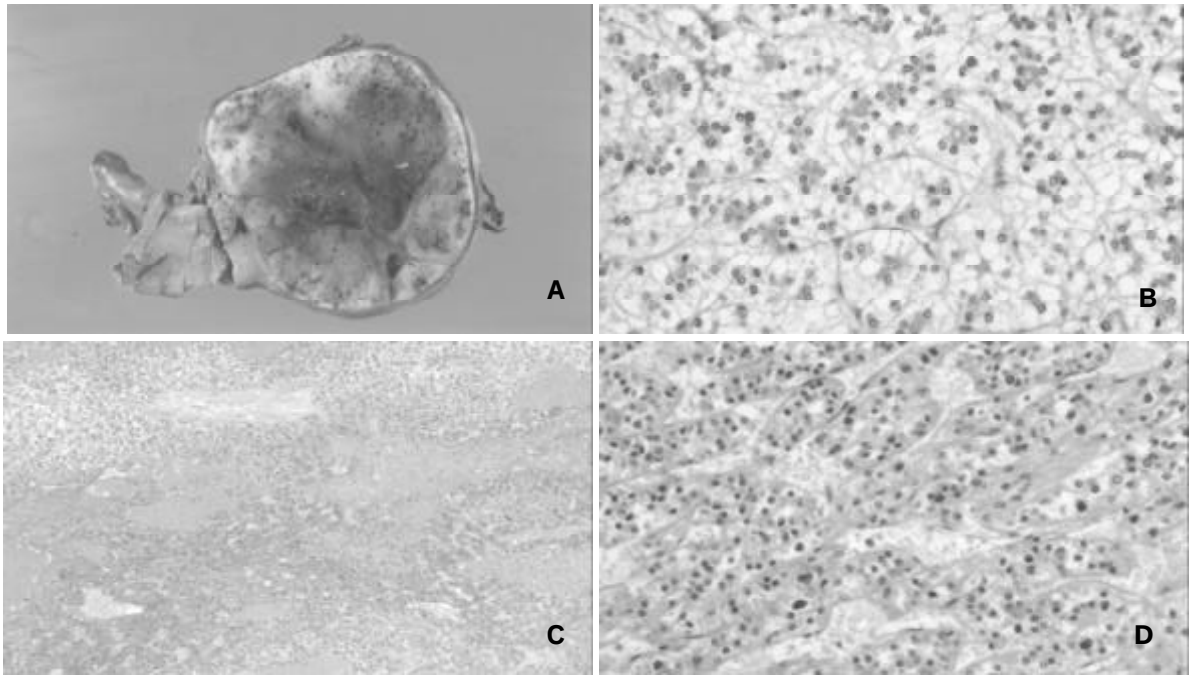

Figure 2 A: Macroscopic appearance of resected tumor. The tumor was incompletely encapsulated by thin fibrous tissues, and its cut surface was tan-yellowish. Hemorrhage was observed inside part of the tumor. B: Microscopic appearance of tumor. Tumor cells were relatively uniform and had clear eosinophilic cytoplasm with small round nuclei. C: Trabecular structures were sporadically encountered in association with hemorrhage. D: The tumor cells were arranged predominantly in a thin trabecular pattern with moderate nuclear atypia.

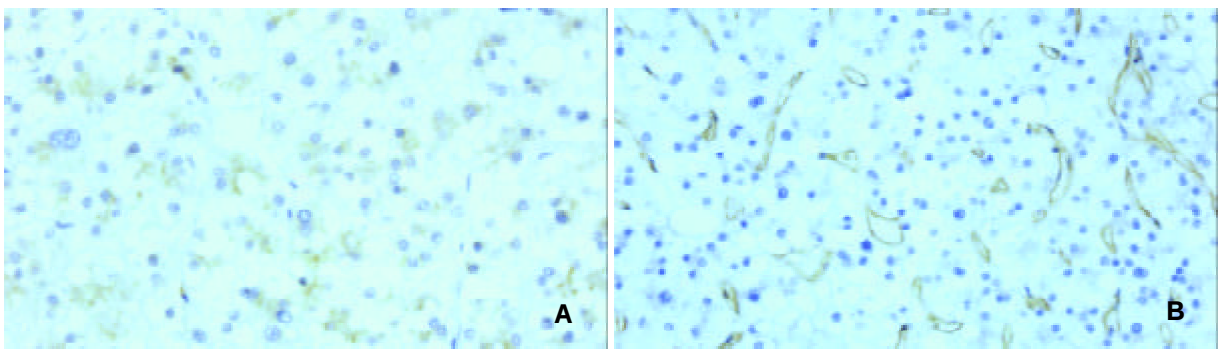

Figure 3 Immunohistochemistry. A: PIVKA-II. B: CD34. PIVKA-II was positive in the tumor cells with or without nuclear atypism and trabecular structure (A). CD34 was expressed diffusely in the sinusoidal endothelial cells (B).

DISCUSSION

Oral contraceptive steroids are the cause of most LCAs, as demonstrated by epidemiological case-control studies conducted in the 1970's[5]. The tumor is nearly always found in women aged 15 to 45, with an incidence estimated to be 3 to 4 per 100 000 long-term contraceptive steroid users per year. An incidence of only 1 per million occurs in non-users or women with less than 2 years' exposure to contraceptive steroids. The risk increases with the duration of contraceptive steroid use and with the potency of the preparation. The present case was not related to oral contraceptives although she had a very short period of oral contraceptive use about 30 years before.

Malignant transformation of LCAs is rare, because most are resected on discovery. However, there were a few well documented cases of hepatocellular carcinoma arising in unresected solitary and multiple adenomas[6-8]. This might represent an adenoma-carcinoma progression sequence in hepatocellular neoplasia, similar to that seen in colon cancer[9]. Intratumoral hemorrhage and intraperitoneal tumoral rupture occasionally occurred in LCA, so that surgical excision has been usually advised for LCA to prevent the risk of rupture and hemorrhage, and malignant transformation[10].

Distinguishing LCA from well-differentiated HCC by histopathology is a difficult task in small biopsies and occasionally even in resected tumor specimens. LCA can be differentiated clinically from HCC on the basis of tumor marker abnormalities, such as AFP and PIVKA-II. Gene analysis is one of the useful methods distinguishing these tumors, although it is not practical in ordinary diagnostic procedure. Multiple chromosomal aberrations detected by CGH, including gains or losses in one or more of six chromosomes (*1q, 4q, 8p, 8q, 16p*, and *17p*) have been reported in hepatocellular carcinomas, but not in LCAs[11]. The detection of frequent aberrations supported a diagnosis of carcinoma and made LCA unlikely, as consistently reported by several investigators[12,13].

LCA has a small but not negligible risk of malignant transformation into HCC. LCAs are rare tumors which may be difficult to differentiate from well differentiated HCCs. In the present case the key finding of malignant transformation into HCC was the presence of an irregular mid-trabecular growth pattern as determined histologically. p53 and Ki-67 are useful markers for differentiation of LCA from HCC. p53 protein was detected in the nuclei of tumor cells of 8.5 % to 44 % of HCC. In contrast, immunostaining of p53 was seen in none of the focal nodular hyperplasias examined, and also in none of the LCAs. In addition, mutant p53 expression in HCC was positively correlated with tumor grade[14,15]. Ki-67, assessed using the monoclonal antibody MIB-1, is expressed in the nuclei of cells of HCC, but not in adenoma cells. The nuclei of LCAs are typically uniform and regular, the nuclear/cytoplasmic ratio is normal, and mitosis is not seen. In the present case, p53 was negative throughout the tumor, even in the areas with a trabecular growth pattern that was the key finding of malignant transformation. Ki-67 was sporadically positive in mid-trabecular area and relatively large nuclei, but not many as conventional HCC.

In contrast to the results of Ki-67 and p53 staining, those of CD34 and PIVKA-II supported malignant transformation. CD34 was reported to show diffuse staining of a large number of sinusoids in HCC in contrast to LCA where the staining was focal or identified only marginal sinusoids[16]. However, consideration should be given to the possibility of LCA and focal nodular hyperplasia, which could also exhibit significantly diffuse CD34 reactivity[17]. PIVKA-II levels were elevated in most patients with HCC. Although LCAs with elevated serum levels of PIVKA-II have been sporadically reported, these were relatively low. Diffuse positive reactions of CD34 on sinusoid endothelial cells in the area of suspicious HCC and marked increase of PIVKA-II (3 503 mAU/ml), as seen in the present case, might indicate malignant transformation. The evaluation of a hepatic nodule is a very common clinical problem. Identification of malignant features remains, at times, inconsistent and controversial, and the distinction of HCC from dysplastic nodule can be difficult. Establishment of diagnostic standards for malignant features should be expected. Finally, this case was reviewed by four Western experts, and was diagnosed as LCA with malignant transformation to HCC (personal communication).

REFERENCES

1 **Edmondson HA**, Hendeson B, Benton B. Liver-cell adenomas associated with use of oral contraceptives. *N Engl J Med* 1976; **294**: 470-472

2 **Alshak NS**, Cocjin J, Podesta L, van de Velde R, Makowka L, Rosenthal P, Geller SA. Hepatocellular adenoma in glycogen storage disease type IV. *Arch Pathol Lab Med* 1994; **118**: 88-91

3 **Kerlin P**, Davis GL, McGill DB, Weiland LH, Adson MA, Sheedy PF 2nd. Hepatic adenoma and focal nodular hyperplasia: clinical, pathologic, and radiologic features. *Gastroenterology* 1983; **84**: 994-1002

4 **Wheeler DA**, Edmondson HA, Reynolds TB. Spontaneous liver cell adenoma in children. *Am J Clin Pathol* 1986; **85**: 6-12

5 **Rooks JB**, Ory HW, Ishak KG, Strauss LT, Greenspan JR, Hill AP**,** Tyler CW Jr. Epidemiology of hepatocellular adenoma. The role of oral contraceptive use. *JAMA* 1979; **242**: 644-648

6 **Foster JH**, Berman MM. The malignant transformation of liver cell adenomas. *Arch Surg* 1994; **129**: 712-717

7 **Janes CH**, McGrill DB, Ludwig J, Krom RA. Liver cell adenoma at the age of 3 years and transplantation 19 years later after development of carcinoma: a case report. *Hepatology* 1993; **17**: 583-585

8 **Scott FR**, El-Refaie A, More L, Scheuer PJ, Dhillon AP. Hepatocellular carcinoma in an adenoma: value of Q Bend 10 immunostaining in diagnosis of liver cell carcinoma. *Histopathology* 1996; **28**: 472-474

9 **Gordon SC**, Reddy KR, Livingstone S, Jeffers LJ, Schiff ER. Resolution of a contraceptive-steroid-induced hepatic adenoma with subsequent evolution into hepatocellular carcinoma. *Ann Intern Med* 1986:**105**: 547-549

10 **Closset J**, Veys I, Peny MO, Braude P, Van Gansbeke D, Lambilliotte JP, Gelin M. Retrospective analysis of 29 patients surgically treated for hepatocellular adenoma or focal nodular hyperplasia. *Hepatogastroenterology* 2000; **47:** 1382-1384

11 **Wilkens L**, Bredt M, Flemming P, Becker T, Klempnauer J, Kreipe HH. Differentiation of liver cell adenomas from well-differentiated hepatocellular carcinomas by comparative genomic hybridization. *J Pathol* 2001; **193**: 476-482

12 **Wilkens L**, Bredt M, Flemming P, Schwarze Y, Becker T, Mengel M, von Wasielewski R, Klempnauer J, Kreipe H. Diagnostic impact of fluorescence in situ hybridization in the differentiation of hepatocellular adenoma and well-differentiated hepatocellular carcinoma. *J Mol Diagn* 2001; **3**: 68-73

13 **Nolte M**, Werner M, Nasarek A, Bektas H, von Wasielewski R, Klempnauer J, Georgii A. Expression of proliferation associated antigens and detection of numerical chromosome aberrations in primary human liver tumours: relevance to tumour characteristics and prognosis. *J Clin Pathol* 1998; **51**: 47-51

14 **Schaff Z**, Sarosi I, Hsia CC, Kiss A, Tabor E. p53 in malignant and benign liver lesions. *Eur J Cancer* 1995; **31A**: 1847-1850

15 **Ojanguren I**, Ariza A, Castella EM, Fernandez-Vasalo A, Mate JL, Navas-Palacios JJ. p53 immunoreactivity in hepatocellular adenoma, focal nodular hyperplasia, cirrhosis and hepatocellular carcinoma. *Histopathology* 1995; **26**: 63-68

16 **Dhillon AP**, Colombari R, Savage K, Scheuer PJ. An immunohistochemical study of the blood vessels with primary hepatocellular tumours. *Liver* 1992; **12**: 311-318

17 **Kong CS**, Appenzeller M, Ferrell LD. Utility of CD34 reactivity in evaluating focal nodular hepatocellular lesions sampled by fine needle aspiration biopsy. *Acta Cytol* 2000; **44**: 218-222

Edited by Wang XL

P.O.Box 2345, Beijing 100023,China
Fax: +86-10-85381893
E-mail: wjg@wjgnet.com www.wjgnet.com

World J Gastroenterol 2003;9(10):2382-2384
World Journal of Gastroenterology
 ISSN 1007-9327

• CASE REPORT •

Massive gastrointestinal tubercolsis in a young patient without immunosupression

Yasar Settbas, Murat Alper, Yusuf Akcan, Yesim Gurbuz, Sükrü Oksuz

Yasar Settbas, Resident, A.I.B.U. Duzce Medical Faculty, Department of Internal Medicine, Duzce, Turkey
Murat Alper, Assistant professor, A.I.B.U. Duzce Medical Faculty, Department of Pathology, Duzce, Turkey
Yusuf Akcan, Assistant professor, A.I.B.U. Duzce Medical Faculty, Department of Internal Medicine, Duzce, Turkey
Yesim Gurbuz, Assistant professor, Kocaeli University Medical Faculty, Department of Pathology, Duzce, Turkey
Sükrü Oksuz, Resident, A.I.B.U. Duzce Medical Faculty, Department of Microbiology
Correspondence to: Yasar Settbas, M.D., Abant Izzet Baysal University Duzce Medical Faculty Department of internal Medicine, 14450, Konuralp, Duzce, Turkey. ysertbas@hotmail.com
Telephone: +90-380-5414107 **Fax**: +90-380-5414105
Received: 2002-10-17 **Accepted:** 2002-11-09

Abstract

Although the lung is the major site for *Mycobacterium tuberculosis* infection, gastrointestinal involvement can be present as part of multiorgan disease process or, less commenly, can be seen as primary gastrointestinal tuberculosis. In the cases where the culture is negative, it can be difficult to differantiate tuberculosis from Crohn's disease based on both the clinical and histological features. When side effects of classic antimycobacteria are encountered, we can initially add ciprofloxacin to the treatment of tuberculosis. We reported a case of 19-yr-old patient, who was treated as Crohn's disease and worsen. We began to tuberculosis treatment, and the patient improved clinically and histologically. The main point in this case is that widespread involvement of gastrointestinal tract can be brought about by non resistant strains of *Mycobacterium tuberculosis* even in immunocompetent patients.

Settbas Y, Alper M, Akcan Y, Gurbuz Y, Oksuz S. Massive gastrointestinal tubercolsis in a young patient without immunosupression. *World J Gastroenterol* 2003; 9(10):2382-2384
http://www.wjgnet.com/1007-9327/9/2382.asp

INTRODUCTION

Mycobacterium tuberculosis is the primary cause of tuberculosis, infects one third of world' s population and causes the most deaths per year of any infectious agents. It is found primarily in devoloping countries, where poor sanitation contributes to its spread. Although pulmonary manifestations predominate in most tuberculosis cases, gastrointestinal involvement may be present as a part of multiorgan disease process or, less commonly as primary gastrointestinal tuberculosis. Gastrointestinal tuberculosis is usually caused by *Mycobacterium tuberculosis* but may also be caused by *Mycobacterium bovis*. Prior to AIDS epidemic, it was seen most commonly in immune competent persons with untreated advanced pulmonary disease[1]. Today, it is most commonly observed in association with immunosupression and, in one series, more than 40 % of patients with gastrointestinal tuberculosis had AIDS[2]. Other groups at highest risk include those who abuse alcohol, injection drug users, those who take chronic steroids, elderly persons. Here, we described a case of gastrointestinal tuberculosis with diffuse involvement of esophagus, stomach, ileum and colon, who did not possess any known immunosuppressive state in his history (Diabetes mellitus, alcohol abuse, protein calori malabsorbtion, AIDS).

CASE REPORT

A 19 year old male patient presented to the outpatient department with complaints of dispepsia and nausea for two years. Recently, vomiting after meals made the patient fear of eating. He first recieved anti ulcer medication with the diagnosis of peptic ulcer in another center. Since his complaints continued, endoscopic and colonoscopic examinations were performed and several biopsies were obtained. A diagnosis of Crohn' s disease was made at the same center. Lansaprazol 30 mg, mesalazine (500 mg *p.o. t.i.d*), hydrocortisone 10 mg/kg/day were begun. Despite the treatment regimen, no response to mesalazine and hydrocortizone was seen and since his complaints increased, he was admitted to our center with abdominal pain, anorexia, nausea, fatigue, weigth loss (15 kg/6 month). There were no pathologic findings on his chest x-ray. Ultrasound examination of the abdomen revealed unremarkable findings, except some degree of cahexia and apathetic appereance. Laboratory data included hemoglobin 11.5 g/dL, erythrocyte sedimentation rate 10 mm/hr, alanin aminotransferase 30 U/L, aspartat aminotransferase 40 U/L, total protein 4.1 g/dL, albumin 2 g/dL white blood cell count 6 600, platelet count 314 000, HBsAg (-), AntiHBsAg(-), Anti-HCVAg(-), HIV(-) and PPD levels 7 mm. Physical examination did not find any abnormal findings. He had no history of any disease which practically can cause diabetes mellitus, alcoholism and renal insufficiency, which are associated with immunodefficiency.

Endoscopy and colonoscopy were performed due to these complaints in our institution. Endoscopy revealed hyperemia with granulomatous lesions at the lower third of the esophagus. A granular appereance was seen along small curvature of the corpus. Antrum had extensive hyperdmia. Additionally granulomas were seen at bulbar and the second part of duodenum. Subsequently biopsies were obtained from all described areas. A histopathological examination revealed existance of granuloma in the esophagus, stomach and small intestine with caseous necrosis in the stomach (Figures 1-3). Although ileal biopsy revealed edematous *lamina propria* with increase of inflammatory cells, there was a granulation at the ileal biopsy which was done 3 months before the treatment of Crohn' s disease started at another center (Figure 4).

Under the light microscopy of these findings, gastrointestinal tuberculosis was concluded and treated with anti tuberculosis treatment of isoniazid 200 mg/day, rifampicin 450 mg/day, morfazinamid 1 g/day and ethambutol 500 mg/day. During the follow up of the first and second month, retrobulber neuritis and peripheral neuritis were seen as the side effects of ethambutol and isoniazid respectively. At the second month of the treatment, morfazinamid was also stopped. Ciproxin 500 mg two times a day with the combination of rifampicin 450 mg/day was given. A significant improvement in clinical

situation of the patient was observed. He gained 25 kg during the theraphy and got 60 kg. The patient recieved anti tuberculosis treatment for 12 months. Check up endoscopy at the end of treatment revealed normal findings with no granulation and caseous necrosis.

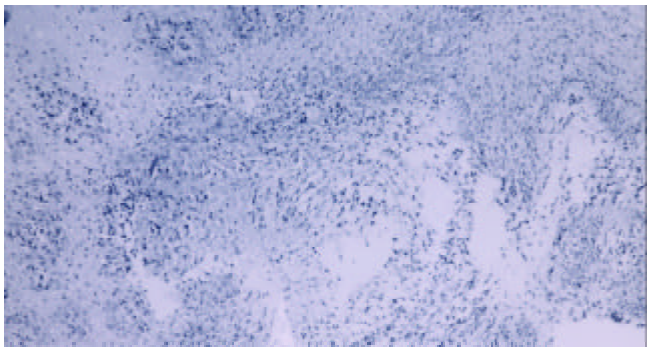

Figure 1 Granulomatous structures of esophagus (H & E×100).

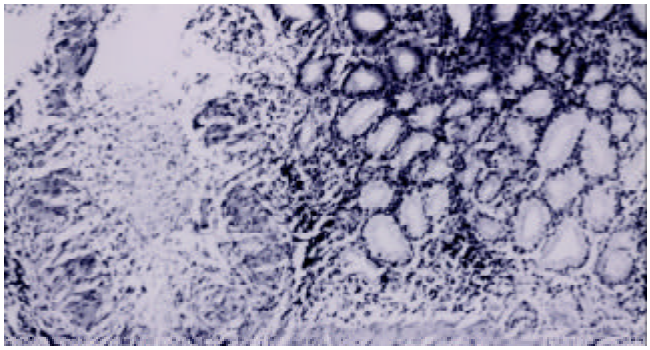

Figure 2 Granulomatous structures and caseous necrosis in the mucosa of stomach (H & E×100).

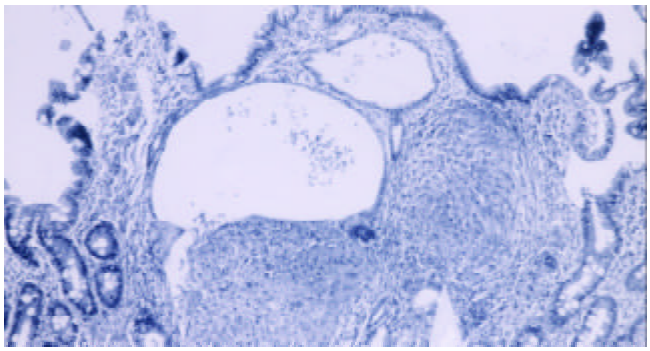

Figure 3 Granulomatous structures in the mucosa of small intestine (H & E×100).

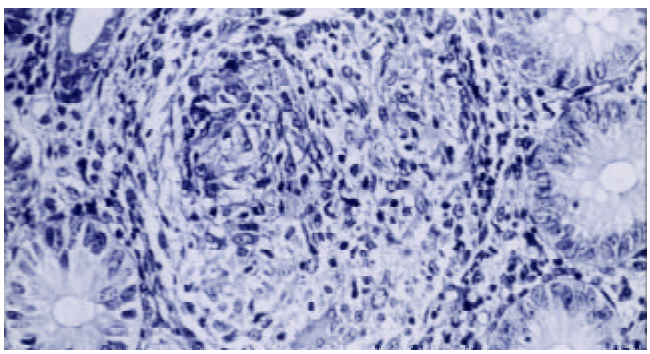

Figure 4 Granulomatous structures between glands of colon mucosa (H & E×310).

DISCUSSION

The diagnosis of gastrointestinal tuberrculosis is always difficult. We must keep in mind the possibility of patients with abdominal pain, even without concomitent lung involvement[2,3]. Tuberculosis may affect any part of gastrointestinal tract, but it most commonly involves the terminal ileum and ileocaecal region, as Crohn' s disease did[4]. However it is rare to see the involvement of all parts of the gastrointestinal tract. Therefore, our case is intresting as almost the whole gastrointestinal tract has been affected.

The symptoms of gastrointestinal tuberculosis are nonspecific, and in the absence of pulmonary tuberculosis the diagnosis may be difficult. The most common symptom associated with gastrointestinal tuberculosis is abdominal pain. Other symptoms included diarrhea, fever, anorexia, weight loss, constipation, and hemorrhage[5].

A presumptive diagnosis can be made in the presence of known active pulmonary tuberculosis and based on the clinical and radiological findings in the bowel. Definitive diagnosis is essentially made by histology, with Ziehl-Neelsen staining for acid fast *bacilli* and culture. Colonoscopy and endoscopy of gastrointestinal system are the most useful nonoperative diagnostic tools. A combination of histology and culture can establish the diagnosis up to 80 % of the patients. Altough more expensive PCR of biopsy specimens may facilitate diagnosis since it has higher sensitivity and specifity than routine culture, and results could be obtained in 48 hours instead of weeks[6]. The detection of anti-cord antibodies has recently been shown to facilitate the diagnosis of intestinal tuberculosis from Crohn' s disease[7]. However, the cases, which have negative results of culture and PCR can be seen and the diagnosis is achieved throuh histological assesment and response to antituberculosis treatment. Sometimes we could see the cases that had culture and PCR negative results were diagnosed histologically and recovered by tuberculosis tretment[8]. In our case, we established the diagnosis of tuberculosis by the presence of caseation and granulomatous lesions suggestive of tuberculosis, and essentially by the occurence of dramatic clinical improvement.

The lesions of gastrointestinal tuberculosis have clinically been divided into an acute ulcerative stage and chronic hypertrophic stage of the disease that is characterized by granulomas and extensive fibrosis. Ulcers are typically irregular with a necrotic base, which may extend to perforation. *Fistulae* and anorectal lesions may occur. These features are non-specific, and can also be seen in Crohn' s disease. In contrast, distinguishing histological features of granulomas in intestinal tuberculosis from Crohn' s disease have been described. Caseation, if present, strongly suggests tuberculosis. However central acute necrosis of granulomas may also be seen occasionally in Crohn' s disease.

Tuberculosis should always be considered in the differential diagnosis of patients with obscure abdominal symptoms. Other entities, which are commonly misdiagnosed are Crohn' s disease, lymhoma, carcinoma, diverticular diseases, appendicities and other infections of gastrointestinal tract. Ulcers were more typically linear, and granulomas, when they were found had no caseation necrosis or organisms[9,10].

The prognosis of gastrointestinal tuberculosis depends primarily on the imuune status of the apropriate theraphy in a timely manner. In untreated HIV-infected patients, the disease progresses rapidly and is almost always fatal. If there is suspicious tuberculosis as histologically, treatment should beginn without waiting the result of the culture. The regimen of choice in most of the cases is isoniazid 3 to 5 mg/kg, rifampin 10 mg/kg, pyraazinamid 20-25 mg/kg and ethambutol 15 mg/kg all given once daily. In resistant cases ciprofloxacin can be used. However in our case because of the side affects of

ethambutol and isoniazid, ciprofloxacin was given[11]. After a while of treatment histologic and clinical response was seen. It could be thought that ciprofloxacin could also be used in the treatment of Crohn' s disease[12]. Since the disease was worsen with the use of steroids, it should be thought that the effect of ciprofloxacin was against the tuberculosis.

This case report illustrates that the diagnosis of colonic tuberculosis requires a high index of suspicion. In cases where there is any doubt about the the diagnosis of Crohn' s disease, and even if the histology of colonic biopsies suggests Crohn' s disease, corticosteroids should be withheld due to disastrous results such as dissemination of tuberculosis. On the other hand, if the information not available to differentiate Crohn' s disease from tuberculosis, therapeutic trial of tuberculosis is justified because it whould not aggravate Crohn' s disease. In the cases of side affects of the drugs in tuberculosis, ciprofloxacin can be preferred in the combination with anti-mycobacterials which have no side affects. Tuberculosis of gastrointestinal tract can mostly be seen in immune compromised individuals such as HIV (+) individuals, alcoholic and chronic steroids users,but can also be seen in immunocompatible peoples. Although it' s mostly seen in the ileocecal region of gastrointestinal tract,it must be kept in mind that it can be widespreadly disseminated as in our case.

REFERENCES

1 **Pettengell KE**, Larsen C, Garb M, Mayet FG, Simjee AE, Piri D. Gastrointestinal tuberculosis in patients with pulmonary tuberculosis. *Q J Med* 1990; **74**: 303-308

2 **Shafer RW**, Kim DS, Weiss JP, Quale JM. Extrapulmonary tuberculosis in patients with human immunodeficiency virus infection. *Medicine* 1991; **70**: 384-397

3 **Perez del Rio MJ**, Fesno Forcelledo M, Diaz Iglesias JM, Veiga Gonzalez M, Alveraz Prida E, Ablanedo Ablanedo P, Herrero Zapatero A. Intestinal Tuberculosis, a difficult suspected diagnosis. *An Med Interna* 1999; **16**: 469-472

4 **Brizi MG**, Celi G, Scaldazza AV, Barbaro B. Diagnostic imaging of abdominal tuberculosis: gastrointestinal tract, peritoneum, lymph nodes. *Rays* 1998; **23**: 115-125

5 **Bouma BJ**, Tygata KM, Shipper HG, Kager PA. Be aware of abdominal tuberculosis. *Neth J Med* 1997; **51**: 119-122

6 **Gan H**, Ouyang Q, Bu H, Li S, Chen D, Li G, Yang X. Value of polymerase chain reaction assay in diagnosis of gastrointestinal tuberculosis and differentiation from Crohn's disease. *Chin Med J* 1995; **108**: 215-220

7 **Kashima K**, Oka S, Tabata A. Detection of anti-cord factor antibodies in intestinal tuberculosis for its differential diagnosis from Crohn's disease and ulcerative colitis. *Dig Dis Sci* 1995; **40**: 2630-2640

8 **Artu P**, Lavergne-Slove, Joly F, Bitoun A, Ramboud JC, Bouhnik Y. Isolated jejunal tuberculosis mimicking Crohn disease. Diagnosis by push video enteroscopy. *Gastroenterol Clin Biol Biol* 1999; **23**: 1086-1089

9 **Jakubowski A**, Elwood RK, Enarson DA. Clinical features of abdominal tuberculosis. *J Infect Dis* 1988; **158**: 687-692

10 **Tabrisky J**, Lindstran RR, Peters R, Lachman RS. Tuberculous enteritis, Review of a protean disease. *Am J Gastroenterol* 1975; **63**: 49-57

11 **Berning SE**. The role of fluoroquinolones in tuberculosis today. *Drugs* 2001; **61**: 9-18

12 **Peppercorn MA**. Is there a role for antibiotics as primary therapy in Crohn's ileitis? *J Clin Gastroenterol* 1993; **17**: 235-237

Edited by Xu XQ and Wang XL

P.O.Box 2345, Beijing 100023,China
Fax: +86-10-85381893
E-mail: wjg@wjgnet.com www.wjgnet.com

World J Gastroenterol 2003;9(11):2385-2389
World Journal of Gastroenterology
 ISSN 1007-9327

• REVIEW •

Gut in diseases: Physiological elements and their clinical significance

Lian-An Ding, Jie-Shou Li

Lian-An Ding, Department of General Surgery, Affiliated Hospital of Medical School, Qingdao University, Qingdao 266003, Shandong Province, China
Jie-Shou Li, Institute of General Surgery, Clinical Medical College of Nanjing University, Nanjing 210002, Jiangsu Province, China
Correspondence to: Lian-An Ding, Male, Associate Professor of Medical School, Qingdao University, 16 Jiangsu Road, Qingdao 266003, Shandong Province, China. dlahaolq@hotmail.com
Telephone: +86-532-5646006 **Fax:** +86-532-2911840
Received: 2003-03-05 **Accepted:** 2003-06-02

Abstract

The intestinal barrier function of GI tract is very important in the body except for the function of digestion and absorption. The functional status of gut barrier basically reflects the stress severity when body suffers from trauma and various stimulations. Many harmful factors such as drugs, illnesses, trauma and burns can damage the gut barrier, which can lead to the barrier dysfunction and bacterial/endotoxin translocation. The paper discusses and reviews the concepts, anatomy, pathophysiology of gut barrier and its clinical relations.

Ding LA, Li JS. Gut in diseases: Physiological elements and their clinical significance. *World J Gastroenterol* 2003; 9(11): 2385-2389

http://www.wjgnet.com/1007-9327/9/2385.asp

INTRODUCTION

The gut has long been thought to be quiescent or inactive during illnesses. It has not been paid much attention and not protected just like other organs such as the heart, lung, and kidney in ICU patients. It is generally considered that biochemical metabolism of the body takes place mainly in the liver. Developments in studying technology and advances in surgical skills have led to a better understanding of nutrients metabolism, anatomic architecture and physiological functions of the gut. Gastrointestinal (GI) tract has functions not only to digest and absorb nutrients, but also to modulate systemic immunity and to prevent enteric bacterial/endotoxin' s invasion, so-called gut barrier function. Functional status of the gut sometimes determines the patients' prognosis and recovery from diseases. Some traditional managements are not beneficial or completely harmful to intestinal barrier capability, and aggravate the primary diseases the body suffers. There is a practical significance to further study the physiological functions of GI tract. An overall understanding of the mechanisms of pathophysiological changes of the gut in illness would make us take measurable treatments to patients clinically. This review deals with a series of new concepts and advances in research of intestinal barrier that might be helpful to clinicians.

INTESTINAL BARRIER AND RELATED CONCEPTS

Intestinal barrier function

The definition of intestinal barrier function means that the gut can prevent the harmful materials in intestinal lumen such as bacteria and endotoxin from entering other aseptic organs, tissues and blood circulation through intestinal mucous membrane. The gut barrier is chiefly composed of three components: mucous epithelia, intestinal flora, and secreting immunoglobulin and gut associated lymphatic tissues (GALT)[1], namely the ecological barrier (normal inhabitant flora within intestine), mechanical barrier (mucous epithelia) and immune barrier (or secreting IgA, miscellaneous immune cells including intraepithelial lymphocytes and macrophages, neutrophils, natural killer cells underlying the mucous membrane, Payer' s nodes and mesenteric lymph node). Among them mucous epithelium is the most important one that establishes a mechanical barrier between the lumen and blood circulation. The gut barrier in general term means this structural epithelia[2-5].

Architecture of intestinal barrier

There are two pathways for materials in the lumen when entering into the blood circulation through mucous membrane. One is the transcellular route, the other is the paracellular route, which occupies 5 % of the total intestinal surface area. These two configurations are the main constituents of epithelial barrier[3,6]. It is considered that there are dispersively nonpolarized holes which are full of water and have a radius of 0.3-0.8 nm on the top of villous cells and a tight-junction of 0.95 nm in radius between villous cells. Substances with different sizes of radius get across intestinal epithelia through transcellular or paracellular way when entering into the body. Molecules smaller than 0.3-0.8 nm in radius could enter into the mucous membrane through these holes. Molecules bigger than those such as disaccharides (lactulose and cellobiose etc) and ^{51}Cr-EDTA seem to enter into epithelia through paracellular tight-junctions. Based on this mechanism the intestinal permeability is measured by combining the smaller (such as monosaccharide) and bigger molecules (such as disaccharide) clinically and experimentally[3,6,7]. The two accesses are influenced by alterations of absorbing intestinal area. Substanecs absorbed by the intestine would reduce after atrophy of villi or bowel resection[3, 5-7].

Bacterial translocation

Bacteria come into aseptic tissues from the bowel lumen through mucosal barrier and colonize in tissues such as mesenteric lymph node, liver, spleen and blood. This process is called bacterial translocation (BT). Studies in experimental rodents showed that translocated bacteria seen most oftenly within intact epithelial cells were *Candida*, *E. coli*, *Proteus mirabilis*, *Enterococcus faecalis* and so on, whereas *E. coli* was common and anaerobes and fungi were rare in human beings[1,8]. Endotoxin could pass through bowel wall into the body easier than bacteria in the lumen[9].

Mechanisms of intestinal barrier damage

Hunger, malnutrition and longer parenteral nutrition could cause intestinal mucosa atrophy and impair the mechanical bowel barrier[1,3,10,11]. Shock, ischemia/reperfusion damage, endotoxin of bacteria are the factors that lead to deterioration of intestinal barrier[4,12]. It was found that changes in

prostaglandin and related enzymes-Ca^{++} and cAMP system within cells affected significantly the structure of gut barrier. Non-steroid anti-inflammatory drugs (NSAIDs) could destroy the system and increase the intestinal permeability. Thus it caused bacteria/endotoxin translocating from intestinal lumen into blood circulation and other aseptic tissues, and sepsis would ensue[2,6]. Because of the increments of intestinal permeability, a series of alterations occurred, such as edema of tissues underlaid mucous membrane, microvasculature compression, stasis of blood circulation and thrombosis in microvasculature system. These patho-physiological changes impaired the microvasculature underlaid mucosa and aggravated further the damage of mucosal barrier[2]. Animal experiments showed that treatment with non-steroid anti-inflammatory drugs in aseptic rats did not cause impairment of intestinal mucous membrane. The clinical symptoms were remitted evidently by treatment with metronidazol to human bowel lesions caused by NSAIDs[13]. Managements with antibiotics in rats (it decreased the bacteria load within the intestine) also prevented NSAIDs from inducing intestine inflammation. In addition, the method of fasting for reducing bacterial antigen in alimentary tract could counteract inflammatory intestinal lesions that caused by NSAIDs either[2,14]. Studies showed that factors causing alterations in hormones secreted by mucous enterocytes and changes of related enzymatic system caused damage of intestinal barrier, and the enteric bacteria and endotoxin reinforced the damage. Prabhu *et al*[15] concluded from researches in rats that surgical stress in the small intestine caused structural and functional alterations in the brush border membrane (BBM) through oxidative stress which could affect gut barrier integrity and the generation of arachidonic acid, might mediate distal organ dysfunction. Activation of phospholipase A2 during the process was considered as a pivotal step. Other investigations discovered that the increment of intestinal permeability was mainly due to the relaxation of the tight-junction between intestinal epithelial cells, indicating that there are close connections between changes in tight-junction and cytoskeleton. Any drugs or chemical materials that could impact on cytoskeleton such as lipopolysaccharide, growth factors, cytokines, and hormones, would affect the intestinal permeability[16].

Nitric oxide and intestinal barrier

Nadler *et al*[12] considered that various insults working on human body could cause overexpression of inducible nitric oxide synthase (iNOS) and hence a redundant production of nitrix oxide (NO) occurred. This higher concentration of NO could lead to deposition of protein salts of nitrite-peroxide (and nitric-peroxide) on mitochondrial membrane, impair mitochondrial membrane potential (or permeability) or decrease ATP production. It would destroy the cellular respiratory function and aggravate cellular apoptosis, thus resulting in a breakage in mucous epithelial continuity and "bare area". Bacteria entering through the "bare area", so-called bacterial translocation takes place. A number of researches have shown that endotoxin increases NO over-production with intestinal barrier damages[17-20]. Our animal experiments confirmed this finding (data not published).

Gut is a central organ for surgical stress

The gut has long been thought to be quiescent or inactive during illnesses[29]. A large number of animal experiments and clinical investigations have suggested that functional changes in gastrointestinal mucous mumbrane occur during illness. Bacteria and endotoxin within the lumen enter into the other aseptic tissues and blood circulation through disordered functional and/or disorganized structural mucous epithelia, which influence greatly on occurrence, progress and transformation of illnesses[1-4,6,10-12,21-30]. In recent decades based on large amounts of animal experiments and clinical investigations, a series of new functions concerning gut metabolism and nutrition, intestinal barrier and immunity function, have been recognized. Following the elucidation on mechanisms of systemic inflammatory response syndrome (SIRS) and multiple-organ dysfunction syndrome (MODS)[4,11,29,31-37], the action of the gut as a central organ for surgical stress has also been put forward[29,30,32,35]. It is now known that the gastrointestinal tract contains about 50 % of reticular endothelia and other immune cells, and occupies about 80 % of the total humoral immunity of a human body. It is therefore the largest immune organ of the body[32-35]. Various insults such as trauma, burn, infection, shock, ischemia/reperfusion, irradiation therapy, chemical therapeutical medicines, and SIRS, could directly or indirectly cause an overgrowth of bacteria in bowel and lead to deterioration of intestinal barrier. Hence translocation of enteric bacteria and/or endotoxin, SIRS, sepsis and even MODS ensue[8,38-40], suggesting that the function of the gut in illness determines the patient' s prognosis[38, 41]. Based on this theory and clinical practice above, Wilmore *et al* put forward that gut was a reservoir of pathogens in illness and a central organ for surgical stress[29, 41]. This has been accepted by most scholars[8,38].

EVALUATION OF GUT BARRIER

There are many ways for measuring intestinal barrier function, but no one is perfect. Three regular approaches are often used to measure the function of gut barrier. The first is to examine the morphologies of mucous membrane such as thickness of mucosa, depth of crypts, architecture of villi, proliferating cellular nuclear antigen (PCNA) and intraepithelial lymphocytes (IELs). The second is to test translocation of bacteria/endotoxin, or bacteria growth and endotoxin concentration in mesenteric lymph node (MLN), liver, spleen, portal vein and/or systemic circulation. The third is to measure intestinal permeability[5,6], which is often carried out by using some labeling substances in experimental and clinical researches. Such substances could be water-soluble, nontoxic, and freely permeated through numerous small ' water pores' in the cell membranes of mucosal enterocytes. There is few or no such substances in body tissues that could not be metabolized. They should be excreted rapidly in an easily measured form. The substances matching with conditions mentioned above are lactulose, mannitol, ^{51}Cr-EDTA, PEG400 and inulin[2,6,42]. The approches that are most frequently used to examine intestinal permeability are the two-sugar test, or lactulose/mannitol test. There are two pathways for the subtances to get across the bowel mucous membrane, transcellular (through plasma membrane of enterocyte in the tip) and paracellular (the tight-junction between cells) routes. Smaller molecular substances (such as monosaccharide) pass through enterocytes by transcellular route, whereas bigger molecules (such as disaccharide) get across enterocytes by paracellular pathway. Thus, the increase of small intestinal permeability reflects the "leakeage degree" of mucous enterocytes [2,5-7].

DISEASES AND FACTORS CAUSING GUT BARRIER DYSFUNCTION

Any insults that lead to an overgrowth of enteric bacteria, an impairment of immune defence function and a damage to mechanical barrier of the gut would result in disorders of the intestinal barrier, and bacteria/endotoxin translocation would ensue[1,4,6,10,11,27]. Followings are the causes that lead to an increase of intestinal permeability.

Infection
This includes intestinal and intraperitoneal infections[38] and infections out of the intestinal tract (such as pneumonia)[43].

Parenteral nutrition
The issue has been confirmed by many animal experiments and clinical researches[10,11,21,25,44,45]. The reason is that 70 % of nutrients are absorbed directly from gut lumen, whereas only 30 % is provided by arterial blood supply[1]. Thus parenteral nutrition makes intestinal mucous membrane in a hunger state and leads to gut mucosa atrophy.

Mulnutrition
Mulnutrition could cause atrophy of intestinal mucosa, an insufficiency of protein synthesis and deficiency of body immunity. These would impair the gut barrier[3-27,28,32,34].

Overgrowth of enteric bacteria
Drugs or infection caused by some pathogens could lead to the overgrowth of intestinal bacteria and hence injures the gut barrier[8,27,39,45, 46].

Endotoxin
Endotoxin could increase NO production in the body and lead to impairment of intestinal barrier function[27,46,47]. Our animal experiments were in accordance with this (not shown).

Surgical stress
Various injuries such as burn/scald[10], organ transplantation (reperfusion injury), surgery and trauma[48-50], haemorrhagic shock and many other insults that lead to SIRS, would bring about an increment of intestinal permeability and damage of gut barrier[4,21].

Drugs
Oral administration of castor oil would cause a physical damage of intestinal mucous membrane in mice. Diabetes mellitus induced by streptozotocin in mice caused an overgrowth of enteric bacteria and an immunity injury of the body. Cyclo-oxygenase inhibitors of prostglandin such as mezolin can block production of prostacyclin in bowel mucous membrane, which increases the permeability of mucous epithelium and bacterial translocation[2,14]. It can also bring about intestinal pathological changes[13,51]. Immunosupressive agents such as chemotherapy drugs, anti-transplant rejection drugs[4,52], and antiacids can destroy gut mucosal barrier[53].

Multiple illnesses
Various abdominal diseases could cause an increase of intestinal permeability. One of these is inflammatory bowel disease (IBD)[2,9,42]. Others are intestinal obstruction, biliary block[4,9], leukemia, endotoxemia, parenteral and enteral nutrition[1, 4,10,11].

Physical injury
It includes radioactive intestinal damage[54].

AGENTS DECREASING INTESTINAL PERMEABILITY
Enteral nutrition could alleviate intestinal atrophy of mucous membrane during stress and could lower gut permeability, improve mucosal immunity. These have been confirmed by experiments and clinical practices[11,37]. Treatments with some special nutrients or immune-modulating drugs for patients with parenteral nutrition could also ameliorate intestinal barrier function[2,3,21].

Glutamine
Except for nutrient digestion and absorption, one of the functions of intestinal mucosa is to prevent enteric bacteria and endotoxin from entering into other parts and blood circulation of the body. It is now considered that gut barrier dysfunction is an important cause for infectious complications when patients suffer from hyper-metabolism after surgery and trauma[1,4,10,27,29,31]. It is still unclear what pathological mechanisms lead to gut barrier failure. It is taken for granted that two important factors causing intestinal barrier failure are the damage of intestinal blood supply and the lack of nutrient support[21]. It has been discovered from animal models and septic patients that the state is associated with insufficiency of perfusion (including disorders of microcirculation) and lack of essential nutrients (including glutamine) in their mucosa[2, 21]. Except for antimicrobial therapy of selective decontamination aiming at getting rid of enteric pathogens, it has been carried out to protect gut barrier function from being injured or have been injured in patients threatened by enterogenous infection. A promising approach is to use glutamine parenterally, which is an essential nutrient for the gut in stress and decreases sharply in illness. A series of experiments and clinical researches showed that nutritional support supplemented with glutamine could improve gut barrier function and enhence the body immunity[8,10,21,32,34,42,44,55-58].

Glutamine exerts its effects on the body in many ways. It supplies fuels for mucous enterocytes and strengthens the barrier structure of the gut on the one hand, and increases secretion of IgA by regulating IL-4 and IL-10 on the other hand, thus preventing enteric bacteria from adhesion to intestinal mucosa and subsequent bacterial translocation[59].

Arginine
Arginine influences the body immune system extensively. First, it is the precursor of polyamines and nucleic acids, which are essential for cell hyperplasia and differentiation. Second, it can produce hydroxyproline through metabolism to promote collagenation. Third, it can stimulate different human cells to secrete hormones such as growth hormone, glycagon, insulin-like growth factor 1 and insulin etc., which have various effects on the immune reactions of the body. In addition, arginine is also a precursor of nitric oxide, an important immune molecule[32,44], and has functions to kill bacteria, protect or impair intestinal barrier[32,44,60,61]. Some scholars reported that arginine could alleviate the secondary damage of gut barrier[62,63], whereas others held a completely different opinion, which had also confirmative evidences[50, 64]. Further investigations on the effects and mechanisms of arginine on the body are needed.

Recombinant human growth hormone (rhGH)
Growth hormone has many biological functions[22,44,64-66]. It could decrease intestinal permeability and improve gut barrier function in illness[39,58,69-71]. Possible mechanism of this may be that it promotes hyperplasia of intestinal epithelia[72], or enhances the mechanical barrier of mucous membrane.

Insulin-like growth factor-(IGF-I)
The main effects of IGF-I on the body are basically the same as rhGH[73, 74]. It promotes hyperplasia of mucous membrane of the intestine, and increase the uptake and utilization of glutamine by the bowel when in sepsis[70].

Nucleic acid
Kishibuchi *et al*[75] observed the alterations of cellular ultrastructure under electronic microscope, variations of intestinal permeability and changes of protease in bowel

mucous membrane, which showed that intestinal barrier function was significantly improved.

Others

Epidermal growth factors (EGF) have positive effects on the proliferation of mucous epithelia[76].

REFERENCES

1 **MacFie J**. Enteral versus parenteral nutrition: the significance of bacterial translocation and gut-barrier function. *Nutrition* 2000; **16**: 606-611
2 **Mohajer B**, Ma TY. Eicosanoids and the small intestine. *Prostaglandins Other Lipid Mediat* 2000; **61**: 125-143
3 **Van Der Hulst RR**, Von Meyenfeldt MF, Van Kreel BK, Thunnissen FB, Brummer RJ, Arends JW, Soeters PB. Gut permeability, intestinal morphology, and nutritional depletion. *Nutrition* 1998; **14**: 1-6
4 **Berg RD**. Bacterial translocation from the gastrointestinal tract. *Trends in Microbiol* 1995; **3**: 149-154
5 **Daugherty AL**, Mrsny RJ. Regulation of the intestinal epithelial paracellular barrier. *Pharm Sci Technol Today* 1999; **2**: 281-287
6 **Travis S**, Menzies I. Intestinal permeability: functional assessment and significance. *Clin Sci* 1992; **82**: 471-488
7 **Bijlsma PB**, Peeters RA, Groot JA, Dekker PR, Taminiau JA, Van Der Meer R. Differential *in vivo* and *in vitro* intestinal permeability to lactulose and mannitol in animals and humans: a hypothesis. *Gastroenterology* 1995; **108**: 687-696
8 **MacFie J,** O'Boyle C, Mitchell CJ, Buckley PM, Johnstone D, Sudworth P. Gut origin of sepsis: a prospective study investigating associations between bacterial translocation, gastric microflora, and septic morbidity. *Gut* 1999; **45**: 223-228
9 **Van Deventer SJ**, ten Cate JW, Tytgat GN. Intestinal endotoxemia. Clinical significance. *Gastroenterology* 1988; **94**: 825-831
10 **Sugiura T**, Tashiro T, Yamamori H, Takagi K, Hayashi N, Itabashi T, Toyoda Y, Sano W, Nitta H, Hirano J, Nakajima N, Ito I. Effects of total parenteral nutrition on endotoxin translocation and extent of the stress response in burned rats. *Nutrition* 1999; **15**: 570-575
11 **Kompan L**, Kremzar B, Gadzijev E, Prosek M. Effects of early enteral nutrition on intestinal prmeability and the development of multiple organ failure after multiple injury. *Intensive Care Med* 1999; **25**: 157-161
12 **Nadler EP,** Ford HR. Regulation of bacterial translocation by nitric oxide. *Pediatr Surg Int* 2000; **16**: 165-168
13 **Bjarnason I**, Hayllar J, Smethurst P, Price A, Gumpel MJ. Metronidazole reduces intestinal inflammation and blood loss in nonsteroidal anti-inflammatory drug induced enteropathy. *Gut* 1992; **33**: 1204-1208
14 **Robert A**, Asano T. Resistance of germ freerats to indomethacin-induced intestinal lesions. *Prostaglandins* 1977; **14**: 331-341
15 **Prabhu R**, Anup R, Balasubramanian KA. Surgical stress induces phospholipid degradation in the intestinal brush border membrane. *J Surg Res* 2000; **94**: 178-184
16 **Gasbarrini G**, Montalto M. Structure and function of tight junctions. Role in intestinal barrier. *Ital J Gastroenterol Hepatol* 1999; **31**: 481-488
17 **Dickinson E**, Tuncer R, Nadler E, Boyle P, Alber S, Watkins S, Ford H. NOX, a novel nitric oxide scavenger, reduces bacterial translocation in rats after endotoxin challenge. *Am J Physiol* 1999; **277**(6 Pt1): G1281-1287
18 **Unno N**, Wang H, Menconi MJ, Tytgat SH, Larkin V, Smith M, Morin MJ, Chavez A, Hodin RA, Fink MP. inhibition of inducible nitric oxide synthase ameliorates endotoxin-induced gut mucosal barrier dysfunction in rats. *Gastroenterology* 1997; **113**: 1246-1257
19 **Mishima S**, Xu D, Deitch EA. Increase in endotoxin-induced mucosal permeability is related to increased nitric oxide synthase activity using the Ussing chamber. *Crit Care Med* 1999; **27**: 880-886
20 **Forsythe RM**, Xu DZ, Lu Q, Deitch EA. Lipopolysaccharide-induced enterocyte-derived nitric oxide induces intestinal monolayer permeability in an autocrine fashion. *Shock* 2002; **17**: 180-184
21 **Foitzik T**, Kruschewski M, Kroesen AJ, Hotz HG, Eibl G, Buhr HJ. Does glutamine reduce bacterial translocation? A study in two animal models with impaired gut barrier. *Int J Colorectal Dis* 1999; **14**: 143-149
22 **Eizaguirre I**, Aldazabal P, Barrena MJ, Garcia-Arenzana JM, Ariz C, Candelas S, Tovar JA. Effect of growth hormone on bacterial translocation in experimental short-bowel syndrome. *Pediatr Surg Int* 1999; **15**: 160-163
23 **O'Boyle CJ**, MacFie J, Dave K, Sagar PS, Poon P, Mitchell CJ. Alterations in intestinal barrier function do not predispose to translocation of enteric bacteria in gastroenterologic patients. *Nutrition* 1998; **14**: 358-362
24 **Heys SD**, Ashkanani F. Glutamine. *Br J Surg* 1999; **86**: 289-290
25 **Pierro A**, van Saene HK, Donnell SC, Hughes J, Ewan C, Nunn AJ, Lloyd DA. Microbial translocation in neonates and infants receiving long-term parenteral nutrition. *Arch Surg* 1996; **131**: 176-179
26 **O'Dwyer ST**, Michie HR, Ziegler TR, Revhaug A, Smith RJ, Wilmore DW. A single dose of endotoxin increases intestinal permeability in healthy humans. *Arch Surg* 1988; **123**: 1459-1464
27 **Deith EA**, Ma WJ, Ma L, Berg RD, Specian RD. Protein malnutrition predisposes to inflammatory-induced gut-origin septic states. *Ann Surg* 1990; **211**: 560-567
28 **Welsh FK**, Farmery SM, MacLennan K, Sheridan MB, Barclay GR, Guillou PJ, Reynolds JV. Gut barrier function in malnourished patients. *Gut* 1998; **42**: 396-401
29 **Wilmore DW**, Smith RJ, O'Dwyer ST, Jacobs DO, Ziegler TR, Wang XD. The gut: a central organ after surgical stress. *Surgery* 1988; **104**: 917-923
30 **Marshall JC**, Christou NV, Meakins JL. Immunomodulation by altered gastrointestinal tract flora. The effects of orally administered, killed Staphylococcus epidermidis, Candida, and pseudomonas on systemic immune responses. *Arch Surg* 1988; **123**: 1465-1469
31 **Bengmark S**, Gianotti L. Nutritional support to prevent and treat multiple organ failure. *World J Surg* 1996; **20**: 474-481
32 **Hulswe KW**, Van Acker BA, von Meyenfeldt MF, Soeters PB. Nutritional depletion and dietary manipulation: effects on the immune response. *World J Surg* 1999; **23**: 536-544
33 **Goris RJ**, te Boekhorst TP, Nuytinck JK, Gimbrere JS. Multiple-organ failure. Generalized autodestructive inflammation? *Arch Surg* 1985; **120**: 1109-1115
34 **McCauley R**, Kong SE, Heel K, Hall JC. The role of glutaminase in the small intestine. *Int J Biochem Cell Biol* 1999; **31**: 405-413
35 **Brandtzaeg P**, Halstensen TS, Kett K, Krajci P, Kvale D, Rognum TO, Scott H, Sollid LM. Immunobiology and immunopathology of human gut mucosa: humoral immunity and intraepithelial lymphocytes. *Gastroenterology* 1989; **97:** 1562-1584
36 **Alverdy J**, Stern E, Poticha S, Baunoch D, Adrian T. Cholecystokinin modulates mucosal immunoglobulin A function. *Surgery* 1997; **122**: 386-393
37 **Keith Hanna M**, Zarzaur BL Jr, Fukatsu K, Chance DeWitt R, Renegar KB, Sherrell C, Wu Y, Kudsk KA. Individual neuropeptides regulate gut-associated lymphoid tissue integrity, intestinal immunoglobulin A levels, and respiratory antibacterial immunity. *J Parenter Enteral Nutr* 2000; **24**: 261-269
38 **Marshall JC**, Christou NV, Meakins JL. Small-bowel bacterial overgrowth and systemic immunosuppression in experimental peritonitis. *Surgery* 1988; **104**: 404-411
39 **Fukushima R**, Saito H, Inoue T, Fukatsu K, Inaba T, Han I, Furukawa S, Lin MT, Muto T. Prophylactic treatment with growth hormone and insulin-like growth factor I improve systemic bacterial clearance and survival in a murine model of burn-induced gut-derived sepsis. *Burns* 1999; **25**: 425-430
40 **Swank GM**, Deitch EA. Role of the gut in multiple organ failure: bacterial translocation and permeability changes. *World J Surg* 1996; **20**: 411-417
41 **Carrico CJ**, Meakins JL, Marshall JC, Fry D, Maier RV. Multiple-Organ-Failure Syndrome. *Arch Surg* 1986; **121**: 196-208
42 **Juby LD**, Rothwell J, Axon AT. Lactulose/mannitol test: an ideal screen for celiac disease. *Gastroenterology* 1989; **96**: 79-85
43 **Yu P**, Martin CM. Increased gut permeability and bacterial translocation in *Pseudomonas* pneumonia-induced sepsis. *Crit Care Med* 2000; **28**: 2573-2577
44 **Ziegler TR**, Leader LM, Jonas CR, Griffith DP. Adjunctive therapies in nutritional support. *Nutrition* 1997; **13** (9 Suppl): 64S-72S
45 **Pappo I**, Polacheck I, Zmora O, Feigin E, Freund HR. Altered

gut barrier function to candida during parenteral nutrition. *Nutrition* 1994; **10:** 151-154

46 **Mishima S**, Xu D, Lu Q, Deitch EA. Bacterial translocation is inhibited in inducible nitric oxide synthase knockout mice after endotoxin challenge but not in a model of bacterial overgrowth. *Arch Surg* 1997; **132**: 1190-1195

47 **Steinberg S**, Flynn W, Kelly K, Bitzer L, Sharma P, Gutierrez C, Baxter J, Lalka D, Sands A, Van Liew J, Hassett J, Price R, Beam T, Flint L. Development of a bacteria-independent model of the multiple organ failure syndrome. *Arch Surg* 1989; **124:** 1390-1395

48 **Reynolds JV**, Kanwar S, Welsh FK, Windsor AC, Murchan P, Barclay GR, Guillou PJ. Does the route of feeding modify gut barrier function and clinical outcome in patients after major upper gastrointestinal surgery? *J Parenter Enteral Nutr* 1997; **21**: 196-201

49 **Anup R**, Aprana V, Pulimood A, Balasubramanian KA. Surgical stress and the small intestine: Role of oxygen free radicals. *Surgery* 1999; **125**: 560-569

50 **Baue AE**. The role of the gut in the development of multiple organ dysfunction in cardiothoracic patients. *Ann Thorac Surg* 1993; **55**: 822-829

51 **Allison MC**, Howatson AG, Torrance CJ, Lee FD, Russell RI. Gastrointestinal damage associated with the use of nonsteroidal antiinflammatory drugs. *N Engl J Med* 1992; **327**: 749-754

52 **Nakamaru M**, Masubuchi Y, Narimatsu S, Awazu S, Horie T. Evaluation of damaged small intestine of mouse following methotrexate administration. *Cancer Chemother Pharmacol* 1998; **41**: 98-102

53 **Basaran UN,** Celayir S, Eray N, Ozturk R, Senyuz OF. The effect of an H_2-receptor antagonist on small-bowel colonization and bacterial translocation in newborn rats. *Pediatr Surg Int* 1998; **13**: 118-120

54 **Vazquez I**, Gomez-de-Segura IA, Grande AG, Escribano A, Gonz áez-Gancedo P, Gomez A, Diez R, De Miguel E. Protective effect of enriched diet plus growth hormone administration on radiation-induced intestinal injury and on its evolutionary pattern in the rat. *Dig Dis Sci* 1999; **44**: 2350-2358

55 **Van Der Hulst RR**, Van Kreel BK, Von Meyenfeldt MF, Brummer RJ, Arends JW, Deutz NE, Soeters PB. Glutamine and the preservation of gut integrity. *Lancet* 1993; **341**: 1363-1365

56 **Burke DJ**, Alverdy JC, Aoys E, Moss GS. Glutamine-supplemented total parenteral nutrition improves gut immune function. *Arch Surg* 1989; **124**: 1396-1399

57 **Li JY**, Lu Y, Hu S, Sun D, Yao YM. Preventive effect of glutamine on intestinal barrier dysfunction induced by severe trauma. *World J Gastroenterol* 2002; **8**: 168-171

58 **Gu Y**, Wu ZH. The anabolic effects of recombinant human growth hormone and glutamine on parenterally fed, short bowel rats. *World J Gastroenterol* 2002; **8**: 752-757

59 **Kudsk KA**, Wu Y, Fukatsu K, Zarzaur BL, Johnson CD, Wang R, Hanna MK. Glutamine-enriched total parenteral nutrition maintains intestinal interleukin-4 and mucosal immunoglobulin A levels. *J Parenter Enteral Nutr* 2000; **24**: 270-275

60 **Moncada S**, Higgs EA. Endogenous nitric oxide: physiology, pathology and clinical relevance. *Eur J Clil Inves* 1991; **21**: 361-374

61 **Nadler EP**, Ford HR. Regulation of bacterial translocation by nitric oxide. *Pediatr Surg Int* 2000; **16**: 165-168

62 **Hutcheson IR**, Whittle BJ, Boughton-Smith NK. Role of nitric oxide in maintaining vascular integrity in endotoxin-induced acute intestinal damage in the rat. *Br J Pharmacol* 1990; **101**: 815-820

63 **Brooks EC**, Mahr NN, Radisavljevic Z, Jacobson ED, Terada LS. Nitric oxide attenuates and xanthine oxidase exaggerates lung damage-induced gut injury. *Am J Physioly* 1997; **272**(4Pt1): G845-852

64 **Mishima S**, Xu D, Deitch EA. Increase in endotoxin-induced mucosal permeability is related to increased nitric oxide synthase activity using the Ussing chamber. *Crit Care Med* 1999; **27**: 880-886

65 **Tritos NA**, Mantzoros CS. Recombinant human growth hormone: old and novel uses. *Am J Med* 1998; **105**: 44-57

66 **Inoue Y**, Copeland EM, Souba WW. Growth hormone enhances amino acid uptake by the human small intestine. *Ann Surg* 1994; **219**: 715-724

67 **Byrne TA**, Morrissey TB, Nattakom TV, Ziegler TR, Wilmore DW. Growth hormone, glutamine, and a modified diet enhance nutrient absorption in patients with severe short bowel syndrome. *J Parenter Enteral Nutr* 1995; **19**: 296-302

68 **Zhou X,** Li YX, Li N, Li JS. Effect of bowel rehabilitative therapy on structural adaptation of remnant small intestine: animal experiment. *World J Gastroenterol* 2001; **7**: 66-73

69 **Scopa CD**, Koureleas S, Tsamandas AC, Spiliopoulou I, Alexandrides T, Filos KS, Vagianos CE. Beneficial effects of growth hormone and insulin-like growth factor I on intestinal bacterial translocation, endotoxemia, and apoptosis in experimentally jaundiced rats. *J Am Coll Surge* 2000; **190**: 423-431

70 **Balteskard L,** Unneberg K, Mjaaland M, Jenssen TG, Revhaug A. Growth hormone and insulinlike growth factor 1 promote intestinal uptake and hepatic release of glutamine in sepsis. *Ann Surg* 1998; **228**: 131-139

71 **Chen K**, Nezu R, Inoue M, Wasa M, Iiboshi Y, Fukuzawa M, Kamata S, Takagi Y, Okada A. Beneficial effects of growth hormone combined with parenteral nutrition in the management of inflammatory bowel desease: An experimental study. *Surgery* 1997; **14**: 212-218

72 **Zhou X**, Li N, Li JS. Growth hormone stimulates remnant small bowel epithelial cell proliferation. *World J Gastroenterol* 2000; **6**: 909-913

73 **Huang KF**, Chung HD, Herndon DN. Insulinlike growth factor 1 (IGF-1) reduces gut atrophy and bacterial translocation after severe burn injury. *Arch Surg* 1993; **128**: 47-53

74 **Chen K**, Okuma T, Okamura K, Tabira Y, Kaneko H, Miyauchi Y. Insulin-like growth factor-I prevents gur atrophy and maintains intestinal integrity in septic rats. *J Parenter Enteral Nutr* 1995; **19**: 119-124

75 **Kishibuchi M**, Tsujinaka T, Yano M, Morimoto T, Iijima S, Ogawa A, Shiozaki H, Monden M. Effects of nucleosides and a nucleotide mixture on gut mucosal barrier function on parenteral nutrition in rats. *J Parenter Enteral Nutr* 1997; **21**: 104-111

76 **Chen DL**, Wang WZ, Wang JY. Epidermal growth factor prevents gut atrophy and maintains intestinal integrity in rats with acute pancreatitis. *World J Gastroenterol* 2000; **6**: 762-765

Edited by Zhang JZ and Wang XL

P.O.Box 2345, Beijing 100023,China
Fax: +86-10-85381893
E-mail: wjg@wjgnet.com www.wjgnet.com

World J Gastroenterol 2003;9(11):2390-2394
World Journal of Gastroenterology
 ISSN 1007-9327

• REVIEW •

Gene therapy for gastric cancer: A review

Chao Zhang, Zhan-Kui Liu

Chao Zhang, Zhan-Kui Liu, Department of General Surgery, Southwest Hospital, Third Military Medical University, Gaotan Yan, Chongqing 400038, China
Correspondence to: Dr. Chao Zhang, M.D. Department of General Surgery, Southwest Hospital, Third Military Medical University, Gaotan Yan, Chongqing 400038, China. meizhang6688@yahoo.com.cn
Telephone: +86-23-68773074
Received: 2002-10-05 **Accepted:** 2003-04-11

Abstract

Gastric cancer is common in China, and its early diagnosis and treatment are difficult. In recent years great progress has been achieved in gene therapy, and a wide array of gene therapy systems for gastric cancer has been investigated. The present article deals with the general principles of gene therapy and then focuses on how these principles may be applied to gastric cancer.

Zhang C, Liu ZK. Gene therapy for gastric cancer: A review. *World J Gastroenterol* 2003; 9(11): 2390-2394
http://www.wjgnet.com/1007-9327/9/2390.asp

INTRODUCTION

Enormous progress has been seen in molecular genetics over the past few decades. It has given us insights at the molecular level, into vital progresses in living organisms, such as embryonic development, growth regulation, differentiation, pathogenesis and carcinogenesis. Insights into the mechanism of pathologic progresses such as developmental disorders and carcinogenesis, have stimulated efforts to develop therapeutic approaches to prevent or correct these processes. Techniques to directly change the genetic information of a cell have greatly improved expectations of the therapeutic potential of genetic manipulation. These developments have raised hopes that diseases appearing to be incurable can soon be cured. Especially for cancer such as gastric cancer, which is common in China. It is well established that most cancers result from a series of accumulated, acquired genetic lesions in somatic cells that are faithfully reproduced until a malignant clone is created, which is ultimately able to destroy the host. Gene therapy has emerged as a new method of therapeutic and possibly preventive intervention against cancer at the level of cellular gene expression[1-14]. Generally speaking, gene therapy can be defined as the introduction and expression of an exogenous gene into human cells for therapeutic benefit, and is conventionally restricted to human diseases associated with single gene defects[15].

In oncology, it can be defined as the introduction of DNA into cells (either neoplastic or normal) in order to shrink or eliminate a malignant tumor. This may be achieved by means of directly inducing malignant cell death, modulating immune response to tumors or reversing the malignant process by correcting genetic abnormalities. It may also be possible to enhance a tumor's responsiveness to conventional treatments such as chemotherapy and radiotherapy, and to protect normal tissue by introduction of genetic materials that confers resistance to the toxic effects of such treatment[16, 17]. A number of strategies have been developed to accomplish cancer gene therapy. These approaches included cytotoxic gene therapy, antisense therapy, and immunotherapy[18-22]. However, despite progress in the field, wide clinical applications and success have not been achieved[23,24]. As with all forms of gene therapy in cancer, the main problems to overcome will be optimizing delivery in order to maximize the proportion of successfully transduced cancer cells, In treatment of human malignant tumours, several obstacles explain the limitations of currently available treatments for achieving definitive cures in most cases of advanced disease. There are some problems in gene therapy. A combination of new chemotherapy drugs, higher doses of drugs, novel cytokines, improved regimens of radiotherapy, and more sophisticated surgery can achieve incremental improvements in cancer treatment. But these therapies do not address critical biological obstacles, and thus, probably will not bring about the much-needed radical advances in the implementation and results of cancer treatment. In contrast, gene therapy offers the potential for overcoming some of these fundamental barriers.

APPROACHES TO GENE THERAPY

Vector

One of the major problems in gene therapy is difficulty in delivering appropriate nucleic acid sequences to target cells. Various strategies have been evolved, which can be essentially divided into two types. One use viral vectors while the other uses non-viral vectors.

Viruses vector The main viruses which have been studied as potential vectors for transducing genes into cancer cells are retrovirus and adenovirus. Retroviruses are single-stranded RNA viruses, and after deletion of one or more structural genes, a foreign gene can be incorporated forming a "recombinant" retrovirus. This could then be used to infect a cell so that it integrates into the host cell's genome which then expresses viral genes as well as the "therapeutic" gene[25,26]. Adenoviruses consist of a core containing double-stranded DNA surrounded by a protein capsid. When an adenovirus vector is created, E1 genes are deleted in order to render the virus incapable of replication, thereby obviating the risk of transforming healthy host cells[27]. Adenoviruses have a greater potential than retroviruses in that they have a higher efficiency of infection and it is possible to incorporate larger segments of DNA. Weber *et al*[28] thought that oncoretrovirus-based vector was a safe and reliable vector system that could achieve permanent integration of delivered transgenes. Successful application of these vectors for gene therapy has proven difficult due to their relatively low transduction efficiency. However, cumulative improvements in methodology have recently yielded promising clinical results. Furthermore, significant improvements in basic retrovirus vector technology now can revitalize the field. But they do induce antiviral immune responses that may compromise the ability to treat an immunocompetent host on more than one occasions. Other viruses which have been used in this context include herpes virus, vaccinia virus and adenovirus-associated virus. Pieroni *et al*[29] found the use of baculovirus vectors for gene expression in mammalian cells was in continuous expansion. These vectors do not replicate in mammalian cells, do not cause a cytopathic effect upon

infection and are able to carry large DNA inserts. Baculovirus vectors have been shown to transduce various cell types *in vitro* and *in vivo* with significant efficiency leading to stable gene expression. This review focuses on recent the developments in baculovirus vector that highlight its potential use for new gene therapy strategies. Okada *et al*[30]. have done something about adeno-associated viral vector-mediated gene therapy for ischemia-induced neuronal death.

Non-viral vector The most widely studied non-viral vector is liposome. Liposome is a positively charged lipid membrane which can be complexed with DNA, and fusion of liposome-DNA complex with a negatively charged membrane leads to transfer of DNA into cells. Lasic *et al*[31] reviewed stabilized liposomes in cancer therapy and gene delivery. Unfortunately, the efficiency of gene transduction using liposomes was currently much lower than that achieved by viral vectors[32].

Other approach

Another approach is to use direct injection of plasmid DNA, but this technique can only transfect cells immediately adjacent to the injection site so that only a small number of cells can be treated[33].Vanden *et al*[34] found that oncoretroviral vectors and lentiviral vectors offered the potential for long-term gene expression by virtue of their stable chromosomal integration and lack of viral gene expression. Gomez *et al*[35]analyzed conditionally replicative adenoviral vectors. Liu *et al*[19] described that the successful transformation of C. sporogenes, a clostridial strain with the highest reported tumor colonization efficiency, with *E. coli* cytosine deaminase (CD) gene and showed that systemically injected spores of these bacteria expressed CD only in the tumor.

It is hoped, however, that by complexing adenovirus and plasmid DNA with protein ligands which bind to specific receptors, enhanced gene transfer into specific cellular targets might be achieved[36]. An example of this is the argenine-glycine-aspartic acid motif that targets integrin receptors[37]. Aside from different approaches to introducing genetic material into cells, gene therapy can be classified according to the different end results. The main aims in this respect are gene replacement, antisense therapy, cytotoxic gene therapy, immunotherapy and drug resistance transfer.

Cytotoxic gene therapy

One of the most promising strategies for gene therapy against various types of cancer is the introduction of a suicide gene, which is transduction of a gene that transforms a non- toxic "pro-drug" into a toxic substance. One approach to this general concept is the transfer of the gene for HSV thymidine kinase (HSV-tk), as this phosphorylates nucleoside analogues such as acyclovir and ganciclovir which are then incorporated into DNA as it replicates[38]. Floeth *et al*[39] analyzed the mechanisms of the "bystander effect" in VPC-mediated HSV-Tk/GCV gene therapy. Thus, these compounds are only toxic to cells expressing HSV-tk, although the bystander effect has also been noted in this type of gene therapy[40]. This is presumably due to release of toxic metabolites produced by the prodrug-activating enzymes which then kill surrounding non-transduced cells. A similar type of cytotoxic gene therapy involves an adenovirus carrying cDNA for cytosine deaminase enzyme of *E.coli* and prodrug 5-fluorocytosine. The prodrug is given orally and converted to 5-fluorouracil in the cells containing cytosine deaminase[41,42].

Antisense therapy

When oligonucleotides bind to their complementary RNA or DNA, they prevent translation or transcription, respectively. This process, known as "anti-sense", is a theoretically attractive method for inactivating oncogenes which are overexpressed in tumors[43,44]. Tang *et al*[45] amplified the 200 VEGF cDNA fragment and inserted it into human U6 gene cassette in the reverse orientation transcribing small antisense RNA which could specifically interact with VEGF165 and VEGF121 mRNA. Their conclusion was expression of antisense VEGF RNA in SMMC-7721 cells could decrease tumorigenicity and antisense-VEGF gene therapy might be an adjuvant treatment for hepatoma. Like gene replacement therapy, however, it would seem that all cells in tumors would have to be transduced, and oligonucleotides would have to last long enough to down-regulate the appropriate genes. Nonetheless, this approach did seem to be effective in certain animal models[46-48]. Kumai *et al*[49] investigated the effect of antisense oligodeoxynucleotides (AS ODN) against tyrosine hydroxylase (TH) on hypertension and sympathetic nervous system activity in spontaneously hypertensive rats (SHR). Systolic blood pressure (SBP) in SHR treated with TH AS ODN (50, 200 mg/rat, i.v.) was significantly lower than that in control SHR. Epinephrine and norepinephrine levels, TH activity, and TH protein levels in adrenal medulla of SHR were reduced concomitantly with TH AS ODN treatment-induced changes in SBP. In contrast, TH AS ODN (200 mg/rat) had no effect on SBP in Wistar-Kyoto rats (WKY), though catecholamine levels, TH activity, and TH protein levels were significantly decreased. These findings suggest that peripheral systemic injection of TH AS ODN may be effective as hypotensive therapy in SHR. Marchand *et al*[50] found the use of miniosmotic pumps, phosphate-buffered saline, VEGF, or VEGF combined with AS-Flk-1, AS-Flt-1, or AS-scrambled oligonucleotides were released in mouse testis for 14 days. VEGF (1, 2.5, and 5 mg) increased the formation of new capillary blood vessels by 236 %, 246 %, and 287 %, respectively. The combination of AS-Flk-1 or AS-Flt-1 (200 mg) to VEGF (2.5 mg) reduced by 87 % and 85 % of new blood vessel formation, respectively, and the expression of their corresponding proteins. These data demonstrate the therapeutical potential of AS-Flk-1 or AS-Flt-1 to prevent VEGF-mediated angiogenesis *in vivo*.

Immunotherapy

The main principle of genetic immunotherapy is to improve the host' s immune response to a particular tumor. One approach is to employ intramuscular injection of DNA which encodes a tumor-associated antigen such as CEA either directly or in form of a viral vaccine[51]. Cheng *et al*[52] have developed a new strategy to enhance nucleic acid vaccine potency by linking VP22, a herpes simplex virus type 1 (HSV-1) tegument protein, to a model antigen. This strategy facilitated the spread of linked E7 antigen to neighboring cells. In their study, they created a recombinant Sindbis virus (SIN)-based replicon particle encoding VP22 linked to a model tumor antigen, human papillomavirus type 16 (HPV-16) E7, using a stable SIN PCL. The linkage of VP22 to E7 in these SIN replicon particles resulted in a significant increase in the number of E7-specific CD8(+) T cell precursors and a strong antitumor effect against E7-expressing tumors in vaccinated C57BL/6 mice relative to wild-type E7 SIN replicon particles. Furthermore, a head-to-head comparison of VP22-E7-containing naked DNA, naked RNA replicons, or RNA replicon particle vaccines indicated that SINrep5-VP22/E7 replicon particles generated the most potent therapeutic antitumor effect. By leading to an active immune response, this was thought to be more effective than passive immunisation using specific antibodies against the antigen in question. Another way was to enhance immunity by using genes for cytokines such as interleukins (IL) which could recruit and stimulate appropriate effector cells[53,54]. Nishioka *et al*[55] have done something about genetic modification of dendritic cells and its application to cancer

immunotherapy. Although the results in the experimental systems were promising, the clinical application of gene-modified DCs had several problems such as the standardization of methods of manipulation and gene-transduction of DCs. Approaches to solve them require further studies. Takemura *et al*[56] have previously produced an anti-MUC1 x anti-CD3 diabody (Mx3 diabody) in an Escherichia coli (*E. coli*) expression system, other approaches have been found, for instance, Vonderheide *et al*[57] applied telomerase as a universal tumor-associated antigen. Schadendorf *et al*[58] reviewed the use of histamine in cancer immunotherapy.

APPLICATION OF GNEE THERAPY FOR GASTRIC CANCER

p53 gene

About 60 % of human gastric cancers carry point mutations of p53 gene, and because of its central role,this nuclear protein is believed to play a role in the regulation of cellular response to DNA damage. Wild-type p53 replacement therapy is an attractive concept in this disease. The responses of human gastric cancer cell lines to recombinant adenovirus encoding wild-type p53 gene have been analysed *in vitro* and *in vivo*[59]. In that study, growth inhibition was observed in cell lines expressing p53 mutations, but not in lines with wild-type p53. Furthermore, the mechanism of cell killing was found to be apoptosis. Thus, it seems that p53 replacement therapy has potential as a therapeutic strategy for human gastric cancer.

Antisense therapy

Antisense therapy has also been used in gastric cancer cell line. Proliferating cell nuclear antigen (PCNA) has been shown to stimulate DNA synthesis by DNA polymerase delta, and to be strongly expressed by gastric cancer cells with a high proliferative activity. Antisense oligonucleotides specific for PCNA mRNA have been shown to inhibit the growth of all gastric cancer cell lines tested, whereas random sequence oligonucleotides had no effect.

Cytotoxic gene therapy

Gastrointestinal cancer is the most important clinical target of gene therapy. Suicide gene therapy with herpes simplex virus type 1 thymidine kinase (HSV-TK) gene, has been shown to exert antitumor efficacy in various cancer models *in vitro*. A modificiation of this approach has been madee to insert carcinoembryonic antigen (CEA) promoter into the viral vector to increase the efficiency of transfection of HSV-tk into cells expressing CEA. When compared with transduction of HSV-tk with a ubiquitous promoter, the use of CEA promoter enhanced the killing effect of ganciclovir in CEA producing cells. While in colorectal cancer, about 40 % of gastric cancer expressed CEA, and CEA producing gastric cancer cell lines were susceptible to this treatment. Okino *et al*[60] described the sequential histopathological changes after suicide gene therapy of N-methyl-N' -nitro-N-nitrosoguanidine (MNNG)-induced gastric cancer in rats. Gastric tumors were induced by MNNG in 38/73 (52 %) of Wistar strain rats. The suicide gene therapy group (14 rats) was subjected to *in situ* gene transfer with a recombinant adenovirus vector carrying the HSV-TK gene driven by CAG promoter (Ad.CAGHSV-TK) in gastric tumor, followed by the antiviral drug ganciclovir (GCV). They observed the histopathological changes at various times after HSV-TK/GCV gene therapy, groups of animals were sacrificed at 3, 8, and 30 days after gene transfer. Apoptosis in gastric tumors was detected by the TUNEL method to assess the efficacy of HSV-TK/GCV gene therapy, and it was markable in the 8- and 30-day treatment groups compared to the sham operation controls (P<0.001). Various histopathological changes, degeneration of cancer tissue and fibrosis after necrosis and apoptosis were significantly greater in the 30-day treatment group. The HSV-TK gene was detectable in peripheral blood by PCR until 30 days after gene transfer. These results might be useful in devising a method of suicide gene therapy for humans.

Other forms of cytotoxic gene therapy which have been used with success in gastric cancer cell lines include transfection of E.coli phosphoribosyltransferase (UPRT) which could catalyse the synthesis of UMP from uracil and 5-phosphoribosyl-alpha-1-diphosphate, thereby sensitising the cell to 5-fluorouracil (5-FU). This has been shown to enhance the cell killing effect of 5-FU in gastric cell lines both *in vitro* and *in vivo*. Shimizu *et al*[61] have generated a recombinant adenovirus encoding the UP gene (AxCA.UP) which has been applied in gastric cancer gene therapy to sensitize cancer cells to lower concentrations of 5-FU.

Immunotherapy

Genetic immunotherapy is another area of active research, and work with severe combined immunodeficiency (SCID) mice given human peripheral lymphocytes and autologous human tumour cells from patients with gastric cancer has yielded interesting results. In one study, administration of an adenovirus vector expressing IL-6 cDNA-induced CD8+cytotoxic T-lymphocytes specific for tumour cells from the precursor human T-lymphocytes *in vivo*, inhibited growth and metastasis of autologous human tumours. In another study, SCID mice reconstituted with peripheral blood cells containing CD34+cells were inoculated with human gastric cancer cell lines transduced with cytokine genes including IL-2 and IL-6. It was found that the tumourigenicity of IL-2 producing tumour cells was significantly reduced in the CD34+ reconstituted but not in the non-reconstituted mice, whereas transduction of IL-6 did not affect tumourigenicity, irrespective of the reconstitution status of the mice. This system could provide a model for investigating the utility of transfecting tumours with individual cytokines. Yu *et al*[62] described the bioactivity of MG7 scFv for its application as a targeting mediator in gene therapy of gastric cancer. Two positive recombinant phage clones have been found to contain the exogenous scFv gene. ELISA showed that MG7 scFv had a strong antigen-binding affinity. Immunodotting assay showed that transfected E.coli HB2151 could successfully produce soluble MG7scFv with a high yield via induction by IPTG. The molecular mass of MG7 scFv was 30 kDa by Western blot. DNA sequencing demonstrated that VH and VL genes of MG7 scFv were 363 bp and 321 bp, respectively.

PROSPECT

With development of the genomic research, more and more individual patients have benefited from the revolution so far. Thus, despite a paucity of clinical information, gene therapy for gastric cancer is on the horizon. As with all forms of gene therapy in cancer, the main problems are to optimize delivery in order to maximize the proportion of successfully transduced cancer cells, and to choose the most appropriate targets for an individual tumor. There is no doubt that human cancers are heterogeneous in terms of genetic abnormality, and a better understanding of the mutational spectrum associated with a cancer type along with the ability to obtain mutation profiles for individual tumors is an important step to successful gene replacement and antisense therapy[63-68].

One factor critical to successful human gene therapy is the development of efficient gene delivery systems. Although numerous vector systems for gene transfer have been developed, a perfect vector system has not yet been constructed. Difficulties of *in vivo* gene transfer appear to be due to

resistance of living cells to invasion by foreign materials and interference of cellular functions. We should analyze what barriers in tissues affect *in vivo* gene transfection and focus on how to solve these problems for gene therapy[68-71].

REFERENCES

1 **Wadhwa PD**, Zielske SP, Roth JC, Ballas CB, Bowman JE, Gerson SL. Cancer gene therapy: scientific basis. *Annu Rev Med* 2002; **53**: 437-452
2 **Otsu M**, Wada T, Candotti F. Gene therapy for primary immune deficiencies. *Curr Opin Allergy Clin Immunol* 2001; **1**: 497-501
3 **Cupp CL**, Bloom DC. Gene therapy, electroporation, and the future of wound-healing therapies. *Facial Plast Surg* 2002; **18**: 53-57
4 **Yamaoka T**. Gene therapy for diabetes mellitus. *Curr Mol Med* 2001; **1**: 325-327
5 **Seto M**, Yamazaki T, Sonsda J, Matsumine A, Shinto Y, Uchida A. Suppression of tumor growth and pulmonary metastasis in murine osteosarcoma using gene therapy. *Oncol Rep* 2002; **9**: 337-340
6 **Englemann C**, Heslan JM, Fabre M, Lagarde JP, Klatzmann D, Panis Y. Importance, mechanisms and limitations of the distant bystander effect in cancer gene therapy of experimental liver tumors. *Cancer Lett* 2002; **179**: 59-69
7 **Okada Y**, Okada N, Nakagawa S, Mizuguchi H, Kanehira M, Nishino N, Takahashi K, Mizuno N, Hayakawa T, Mayumi T. Fiber-mutant technique can augment gene transduction efficacy and anti-tumor effects against established murine melanoma by cytokine-gene therapy using adenovirus vectors. *Cancer Lett* 2002; **177**: 57-63
8 **Ruiz J**, Mazzolini G, Sangro B, Qian C, Prieto J. Gene therapy of hepatocellular carcinoma. *Dig Dis* 2001; **19**: 324-332
9 **Li S**, Zhang X, Xia X. Regression of tumor growth and induction of long-term antitumor memory by interleukin 12 electro-gene therapy. *J Natl Cancer Inst* 2002; **94**: 762-768
10 **Manninen HI**, Makinen K. Gene therapy techniques for peripheral arterial disease. *Cardiovasc Intervent Radiol* 2002; **25**: 98-108
11 **Adachi O**, Nakano A, Sato O, Kawamoto S, Tahara H, Toyoda N, Yamato E, Matsumori A, Tabayashi K, Miyazaki J. Gene transfer of Fc-fusion cytokine by *in vivo* electroporation: application to gene therapy for viral myocarditis. *Gene Ther* 2002; **9**: 577-582
12 **Johnson-Saliba M**, Jans DA. Gene therapy: optimising DNA delivery to the nucleus. *Curr Drug Targets* 2001; **2**: 371-399
13 **Baum BJ**, Kok M, Tran SD, Yamano S. The impact of gene therapy on dentistry: a revisiting after six years. *J Am Dent Assoc* 2002; **133**: 35-44
14 **Havlik R**, Jiao LR, Nicholls J, Jensen SL, Habib NA. Gene therapy for liver metastases. *Semin Oncol* 2002; **29**: 202-208
15 **Li Y**, Okegawa T, Lombardi DP, Frenkel EP, Hsieh JT. Enhanced transgene expression in androgen independent prostate cancer gene therapy by taxane chemotherapeutic agents. *J Urol* 2002; **167**: 339-346
16 **Rieger PT**. The role of oncology nurses in gene therapy. *Lancet Oncol* 2001; **2**: 233-238
17 **Ohana P**, Bibi O, Matouk I, Levy C, Birman T, Ariel I, SchneiderY, Ayesh S, Giladi H, Laster M, De Groot N, Hochberg A. Use of H19 regulatory sequences for targeted gene therapy in cancer. *Int J Cancer* 2002; **98**: 645-650
18 **Huh WK**, Barnes MN, Kelley FJ, Alvarez RD. Gene therapy. *Cancer Treat Res* 2002; **107**: 133-157
19 **Liu SC**, Minton NP, Giaccia AJ, Brown JM. Anticancer efficacy of systemically delivered anaerobic bacteria as gene therapy vectors targeting tumor hypoxia / necrosis. *Gene Ther* 2002; **9**: 291-296
20 **Kaneko S**, Tamaoki T. Gene therapy vectors harboring AFP regulatory sequences. Preparation of an adenoviral vector. *Mol Biotechnol* 2001; **19**: 323-330
21 **Mc CF**. Cancer gene therapy: fringe or cutting edge? *Nature Rev Cancer* 2001; **1**: 130-141
22 **Chang LJ**, He J. Retroviral vectors for gene therapy of AIDS and cancer. *Curr Opin Mol Ther* 2001; **3**: 468-475
23 **Richardson PD**, Augustin LB, Kren BT, Steer CJ. Gene repair and transposon-mediated gene therapy. *Stem Cells* 2002; **20**: 105-118
24 **Xu AG**, Li SG, Liu JH, Gan AH. Function of apoptosis and expression of proteins Bcl-2, p53 and C-myc in the development of gastric cancer. *World J Gastroenterol* 2001; **7**: 403-406
25 **Roth JA**, Cristiano RJ. Gene therapy for cancer: what have we done and where are we going? *J Nat Cancer Inst* 1997; **89:** 21-39
26 **Brenner MK.** Genetic marking and manipulation of hematopoietic progenitor cells using retroviral vectors. *Immunomethod*s 1994; **5**: 204-210
27 **Mitani K,** Graham FL, Caskey CT. Transduction of human bone marrow by adenoviral vector. *Hum Gene Ther* 1994; **5**: 941-948
28 **Weber E**, Anderson WF, Kasahara N. Recent advances in retrovirus vector-mediated gene therapy: teaching an old vector new tricks. *Curr Opin Mol Ther* 2001; **3**: 439-453
29 **Pieroni L**, La Monica N. Towards the use of baculovirus as a gene therapy vector. *Curr Opin Mol Ther* 2001; **3**: 464-467
30 **Okada T**, Sakai T, Murata T, Kako K, Sakamoto K, Ohtomi M, Katsura T, Ishida N. Promoter analysis for daily expression of Drosophila timeless gene. *Biochem Biophys Res Commun* 2001; **283**: 577-582
31 **Lasic DD**, Vallner JJ, Working PK. Sterically stabilized liposomes in cancer therapy and gene delivery. *Curr Opin Mol Ther* 1999; **1**: 177-185
32 **Manthorpe M**, Cornefert-Jensen F, Hartikka J, Felgner J, Rundell A, Margalith M, Dwarki V. Gene therapy by intrmuscular injection of plasmid DNA: studies on firefly luciferase gene expression in mice. *Human Gene Therapy* 1993; **4**: 419-431
33 **Michael SI**, Curiel DT. Strategies to achieve targeted gene delivery via the receptor-mediated endocytosis pathway. *Gene Ther* 1994; **1**: 223-232
34 **Vanden Driessche T**, Naldini L, Collen D, Chuah MK. Oncoretroviral and lentiviral vector-mediated gene therapy. *Methods Enzymol* 2002; **346**: 573-579
35 **Gomez NJ**, Curiel DT. Conditionally replicative adenoviral vectors for cancer gene therapy. *Lancet Oncol* 2000; **1**: 148-158
36 **Simko V**, Michael S. Effect of ursodeoxycholic acid on *in vivo* and in vitro toxic liver injury in rats. *Aliment Pharmacol Ther* 1994; **8:** 315-322
37 **Hart SL**, Knight AM, Harbottle RP, Mistry A, Hunger HD, Cutler DF, Williamson R, Coutelle C. Cell binding and internalization by filamentous phage displaying a cyclic Arg-Gly-Asp-containing peptide. *J Bio Chem* 1994; **269**: 12468-12474
38 **Moolten FL**. Tumour chemosensitivity conferred by inserted herpes thymidine kinase genes: paradigm for a prospective cancer control strategy. *Cancer Research* 1986; **46**: 5276-5281
39 **Floeth FW**, Shand N, Bojar H, Prisack HB, Felsberg J, Neuen-Jacob E, Aulich A, Burger KJ, Bock WJ, Weber F. Local inflammation and devascularization-*in vivo* mechanisms of the "bystander effect" in VPC-mediated HSV-Tk / GCV gene therapy for human malignant glioma. *Cancer Gene Ther* 2001; **8**: 843-851
40 **Freeman SM**, Abboud CN, Whartenby KA, Packman CH, Koeplin DS, Moolten FL, Abraham GN. The "bystander effect": tumour regression when a fraction of the tumor mass is genetically modified. *Cancer Research* 1993; **53**: 5274-5283
41 **Huber BE**, Austin EA, Good SS, Knick VC, Tibbels S, Richards CA. *In vivo* antitumor activity of 5-fluorocytosine on human colorectal carcinoma cells genetically modified to express cytosine deaminase. *Cancer Research* 1993;**53**: 4619-4626
42 **Crystal RG,** Hirschowitz E, Lieberman M, Daly J, Kazam E, Henschke C, Yankelevitz D, Kemeny N< Silverstein R, Ohwada A, Russ T, Mastrangeli A, Sanders A, Cooke J, Harvey BG. Phase 1 study of direct administration of a replication deficient adenovirus vector containing the E. coli cytosine deaminase gene to metastatic colon carcinoma of the liver in association with the oral administration of the pro-drug 5-fluorocytosine. *Human Gene Therapy* 1997; **8**: 985-1001
43 **Milligan JF**, Matteucci MD, Martin JC. Current concepts in antisense drug design. *J Med Chem* 1993; **36**: 1923-1937
44 **Chen L**. Antibody gene therapy: old wine in a new bottle. *Nat Med* 2002; **8**: 333-334
45 **Tang YC**, Li Y, Qian GX. Reduction of tumorigenicity of SMMC-7721 hepatoma cells by vascular endothelial growth factor antisense gene therapy. *World J Gastroenterol* 2001; **7**: 22-27
46 **Sacco MG**, Barbieri O, Piccini D, Noviello E, Zoppe M, Zucchi I, Frattini A, Villa A, Vezzoni P. *In vitro* and *in vivo* antisense-me-

diated growth inhibition of a mammary adenocarcinoma from MMTV-neu transgenic mice. *Gene Therapy* 1998; **5**: 388-393

47 **Wagner RW.** Gene inhibition using antisense oligodeoxynucleotides. *Nature* 1994; **372**: 333-335

48 **Cotter FE**, Johnson P, Hall P, Pocock C, Al Mahdi N, Cowell JK, Morgan G. Antisense oligonucleotides suppress B-cell lymphoma growth in a SCID-hu mouse model. *Oncogene* 1994; **9**: 3049-3055

49 **Kumai T**, Tateishi T, Tanaka M, Watanabe M, Shimizu H, Kobayashi S. Tyrosine hydroxylase antisense gene therapy causes hypotensive effects in the spontaneously hypertensive rats. *J Hypertens* 2001; **19**: 1769-1773

50 **Marchand GS**, Noiseux N, Tanguay JF, Sirois MG. Blockade of *in vivo* VEGF-mediated angiogenesis by antisense gene therapy: role of Flk-1 and Flt-1 receptors. *Am J Physiol Heart Circ Physiol* 2002; **282**: H194-204

51 **Tsang KY**, Zaremba S, Nieroda CA, Zhu MZ, Hamilton JM, Scholm J. Generation of human cytotoxic T cells specific for human carcinoembryonic antigen epitopes from patients immunised with recombinant vaccinia-CEA vaccine. *J Nat Cancer Inst* 1995; **87**: 982-990

52 **Cheng WF**, Hung CF, Hsu KF, Chai CY, He L, Polo JM, Slater LA, Ling M, Wu TC. Cancer immunotherapy using Sindbis virus replicon particles encoding a VP22-antigen fusion. *Hum Gene Ther* 2002; **13**: 553-568

53 **Wei MX**, Tamiya T, Hurford JR, Boviatsis EJ, Tepper RI, Chiacca EA. Enhancement of interleukin-4-mediated tumour regression in athymic mice by in situ retroviral gene transfer. *Human Gene Therapy* 1995; **6**: 437-443

54 **Steele RJ**, Thompson AM, Hall PA, Lane DP. The p53 tumour suppressor gene. *British J Surgery* 1998; **85**: 1460-1467

55 **Nishioka Y**, Hua W, Nishimura N, Sone S. Genetic modification of dendritic cells and its application for cancer immunotherapy. *J Med Invest* 2002; **49**: 7-17

56 **Takemura S**, Kudo T, Asano R, Suzuki M, Tsumoto K, Sakurai N, Katayose Y, Kodama H, Yoshida H, Ebara S, Saeki H, Imai K, Matsuno S, Kumagai I. A mutated superantigen SEA D227A fusion diabody specific to MUC1 and CD3 in targeted cancer immunotherapy for bile duct carcinoma. *Cancee Immunol Immunother* 2002; **51**: 33-44

57 **Vonderheide RH**. Telomerase as a universal tumor-associated antigen for cancer immunotherapy. *Oncogene* 2002; **21**: 674-679

58 **Schadendorf D**. The use of histamine in cancer immunotherapy. *J Invest Dermatol* 2002; **118**: 560-561

59 **Ohashi M**, Kanai F, Ueno H, Tanaka T, Tateishi K, Kawakami T, Koike Y, Ikenoue T, Shiratori Y, Hamada H, Omata M. Adenovirus mediated p53 tumour suppressor gene therapy for human gastric cancer cells *in vitro* and *in vivo*. *Gut* 1999; **44**: 366-371

60 **Okino T**, Onda M, Matsukura N, Inada KI, Tatematsu M, Suzuki S, Shimada T. Sequential histopathological changes *in vivo* after suicide gene therapy of gastric cancer induced by N-methyl-N'-nitro-N-nitrosoguanidine in rats. *Jpn J Cancer Res* 2001; **92**: 673-679

61 **Shimizu T**, Shimada H, Ochiai T, Hamada H. Enhanced growth suppression in esophageal carcinoma cells using adenovirus-mediated fusion gene transfer (uracil phosphoribosyl transferase and herpes simplex virus thymidine kinase). *Cancer Gene Ther* 2001; **8**: 512-521

62 **Yu ZC**, Ding J, Pan BR, Fan DM, Zhang XY. Expression and bioactivity identification of soluble MG7 scFv. *World J Gastroenterol* 2002; **8**: 99-102

63 **Robbins PD**, Evans CH, Chernajovsky Y. Gene therapy for arthritis. *Gene Ther* 2003; **10**: 902-911

64 **Baker D**, Hankey DJ. Gene therapy in autoimmune, demyelinating disease of the central nervous system. *Gene Ther* 2003; **10**: 844-853

65 **Thomas CE**, Ehrhardt A, Kay MA. Progress and problems with the use of viral vectors for gene therapy. *Nat Rev Genet* 2003; **4**: 346-358

66 **Bagley J**, Iacomini J. Gene Therapy Progress and Prospects: Gene therapy in organ transplantation. *Gene Ther* 2003; **10**: 605-711

67 **Guarini S.** New gene therapy for the treatment of burn wounds. *Crit Care Med* 2003; **31**: 1280-1281

68 **Kaneda Y**. Gene therapy: a battle against biological barriers. *Curr Mol Med* 2001; **1**: 493-499

69 **Denny WA**. Prodrugs for gene-firected rnzyme-prodrug therapy (suicide gene therapy). *J Biomed Biotechnol* 2003; **2003**:48-70

70 **Scholl SM**, Michaelis S, McDermott R. Gene Therapy Applications to Cancer Treatment. *J Biomed Biotechnol* 2003; **2003**: 35-47

71 **Lundstrom K**. Latest development in viral vectors for gene therapy. *Trends Biotechnol* 2003; **21**: 117-122

Edited by Zhu LH and Wang XL

P.O.Box 2345, Beijing 100023,China
Fax: +86-10-85381893
E-mail: wjg@wjgnet.com www.wjgnet.com

World J Gastroenterol 2003;9(11):2395-2399
World Journal of Gastroenterology
 ISSN 1007-9327

• ESOPHAGEAL CANCER •

Correlation between expression of human telomerase subunits and telomerase activity in esophageal squamous cell carcinoma

Chun Li, Ming-Yao Wu, Ying-Rui Liang, Xian-Ying Wu

Chun Li, Ming-Yao Wu, Xian-Ying Wu, Department of Pathology, Medical College, Shantou University, Shantou 515031, Guangdong Province, China
Ying-Rui Liang, Department of Pathology, Foshan First People' s Hospital, Foshan 528000, Guangdong Province, China
Supported by the Medical Science Research Foundation of Guangdong Province, No.A2001413
Correspondence to: Dr. Chun Li, Department of Pathology, Medical College, Shantou University, Shantou, 515031 Guangdong Province, China. chli@stu.edu.cn
Telephone: +86-754-8900486
Received: 2003-05-12 **Accepted:** 2003-06-27

Abstract

AIM: To investigate telomerase activity and hTERT, TP-1 expression and their relationships in esophageal squamous cell carcinoma (ESCC).

METHODS: Telomerase activity was measured in 60 ESCC tissues using telomeric repeat amplification protocol (TRAP) assay by silver staining. *In situ* hybridization was used for detecting hTERT and TP-1mRNA.

RESULTS: The telomerase activity was detected in 83.3 % of ESCC tissues. The difference of telomerase activity was significant between well and poorly cancer differentiated lesions ($P<0.05$). The positive rate of telomerase activity was higher in patients with lymphatic metastasis than in patients without lymphatic metastasis. In cancer tissues hTERT mRNA expression was 75 % and TP-1 mRNA expression was 71.7 %. The expression of hTERT, TP-1 mRNA in well and poorly differentiated carcinoma was not significant. The expression of hTERT mRNA was correlated with telomerase activity, but TP-1 mRNA expression was not correlated with it.

CONCLUSION: Telomerase activity and hTERT, TP-1 mRNA expression are up-regulated in ESCC. Telomerase activity in ESCC is correlated with lymphatic metastasis and cancer differentiation. Telomerase activity may be used as a prognostic marker in ESCC. hTERT mRNA expression is correlated with telomerase activity. Enhanced hTERT mRNA expression may initially comprehend the telomerase activity level, but it is less sensitive than TRAP assay.

Li C, Wu MY, Liang YR, Wu XY. Correlation between expression of human telomerase subunits and telomerase activity in esophageal squamous cell carcinoma. *World J Gastroenterol* 2003; 9(11): 2395-2399
http://www.wjgnet.com/1007-9327/9/2395.asp

INTRODUCTION

Repetitive telomere sequences are present at the ends of eukaryotic chromosomes that protect the ends from damage and rearrangement. Progressive shortening of telomeric sequences is associated with cell division owing to the end replication involved in DNA replication. Telomerase is a special type of reverse transcriptase that stabilizes the telomeric ends of chomosome by adding TTAGGG repeats onto the chromosome ends. In humans, telomerase is composed of at least two components. hTR containing the template for reverse transcription[1], and telomerase associated proteins. Telomerase associated protein consists of hTP-1[2,3] and human telomerase reverse transcriptase (hTERT). hTERT is thought to be a enzyme' s catalytic subunit. In human, telomerase was active during embryonic development, and it was active in adult germ-line tissues, immortal cell[4,5] and most malignant tumors[6,7]. We have reported that telomerase activities were high both in esophageal squamous cell carcinoma (ESCC) and in their preneoplasia lesions[8]. This study was to examine telomerase activity, expression of hTERT mRNA, and hTP-1 mRNA in ESCC tissues and to analyze the relationship between teolmerase activity and its associated proteins.

MATERIALS AND METHODS

Materials

Esophageal squamous cell carcinoma tissues from 60 patients (40 men and 20 female, aged from 34 to 70 years) undergone surgical resection in Tumor Hospital of Medical College Shantou University from 1999 to 2001 were analyzed. All fresh tissues were taken immediately after operation and stored at -70 ℃.

TRAP-silver staining for telomerase activity

We used $TRAP_{EZE}$ telomerase detection kit (Intergen Company). After addition of 10-20 μl telomerase assay lysis buffer (1×CHAPS), the cells were lysed on ice. The lysate was incubated on ice for 30 min and then centrifuged at 12 000 r/min for 20 min at 4 ℃. The supernatant was collected and the protein concentration was determined by standard procedures (BCA protein assay). A volume of 0.6 μg protein equivalent was added to 48 μl reaction solution containing TRAP buffer, dNTP Mix, TS primer, RP primer, K_1 primer and 2 units Taq polymerase. PCR condition was 33 cycles at 94 ℃ for 30 s, at 59 ℃ for 30 s. PCR products were loaded and run on 12.5 % non-denaturing polyacrylamide gel. After electrophoresis, the gel was stained with silver.

In situ hybridization for hTERT and TP-1 mRNA expression

Samples were frozen and serially cut into 5 μm thick sections. One section was stained by hematoxylin and eosin (HE) for microscopic examination. Another was detected for hTERT and TP-1 mRNA expression. Expression of hTERT mRNA and hTP-1 mRNA was detected by digoxigenin-labeked gene probe which form a commercial kit (Boster Company, China) according to the manufacturer' s instructions. The hTERT oligonucleotides probes were 5' -AGTCA GGCTG GGCCT CAGAGAGCTG AGTAG GAAGG-3' , 5' -GCATG TACGG CTGGA GGTCT GTCAA GGTAG AGACG-3' , and 5' -AGCCA AGGTT CCAGG CAGCT CACTG ACCCT-3' . The hTP-1 oligonucleotides probes were 5' -ATATC TGAGT

GGGTA GATAC ATGCT GATGT-3', 5'-GTCAG ATAGA CCAAG ACAGT GCGGC CTGGC CTGGC-3', and 5'-AGCCA AGGTT CCAGG CAGCT CACTG ACCCT-3'. The positive expression showed brown staining signals in cytoplasm. The positive cancer cells constituted more than 75 % of all cancer cells on the section were defined as a score of 3+ (strong), about 25-75 % of positive cells had a score of 2+ (moderate), and less than 25 % had a score of 1+ (weak). The score of - (negative) had no positive cancer cell.

Controls

TRAP telomerase activity analysis: Esophageal cancer cell line EC109 was used as positive telomerase control, which was identified to be telomerase positive by our laboratory. Negative control was to perform a $TRAP_{EZE}$ kit assay with 1×CHAPS lysis buffer substituted for the cell extract. Heat-treatment of each sample by incubating at 85 ℃ for 20 minutes prior to $TRAP_{EZE}$ kit assay to inactivate telomerase served as a heat inactivation control. The $TRAP_{EZE}$ primer Mix contains internal control, which produce a 36 bp band (S-IC) in every lane to monitor PCR inhibition. If the extract with telomerase activity, a ladder of products with 6 bp increment starting at 50 bp nucleotide and a 36 bp internal control band could be seen. If the extract was telomerase negative, there was only a 36 bp internal control band (S-IC) (Figure1).

In situ hybridization: Positive control section was provided with the kit. Negative control included using incubation solution instead of the probe or the sections digested with ribonucleases (RNase) (10 mg· L^{-1}) before hTERT or hTP-1 detection.

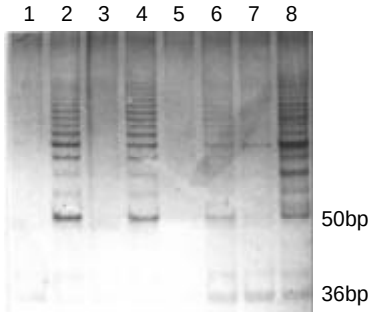

Figure 1 Carcinoma telomerase activity detected by TRAP-silver assay and separated on a 12.5 % polyacrylamide gel. Lane 1: primer-dimer/PCR contamination control, Lane 2: telomerase positive control, Lanes 4, 6 and 8: telomerase positive samples, Lanes 3, 5 and 7: heat-treated controls.

Statistical analysis

Statistical significance was tested using rectified chi-square test and exact method.

RESULTS

Relationship between telomerase activity and cancer differentiation

Histopathologically, the study population (n=60) was divided into 3 categories according to cancer differentiation as follows: grade I (n=15), grade II (n=33), and grade III (n=12). In 60 cases of esophageal SCC, telomerase activity was detected in 50 cases. The positive rate was 83.3 %. As showed in Table 1, the positive rates of telomerase activity were low in grade I and progressively increased from grade I to grade III. The significant difference of telomerase activity rate was found between grade I and grade II (χ^2=4.597, P<0.05), while, there was no significant differences between grade II and grade III (χ^2=0.263, P>0.05).

Table 1 Relationship between differentiation degree and telomerase activity in 60 cases of ESCC

Tumor stage	Sample (n)	Positive (n)	Prositive rate (%)	P value
I	15	9	60	
II	33	30	90.9	P<0.05
III	12	11	91.6	

Relationship between telomerase activity and lymphatic metastasis

There were 41 patients with lymph node metastasis out of the 60 patients. Telomerase activity rates were higher in patients with lymphatic metastasis (90.2 %) than in those without (63.2 %) (Table 2), and this difference was significant (χ^2=4.68, P<0.05).

Table 2 Relationship between telomerase activity and lymphatic metastasis

Sample (n)	Lymphatic metastasis	Telomerase activity		P value
		+	-	
41	+	37	4	P<0.05
19	-	12	7	

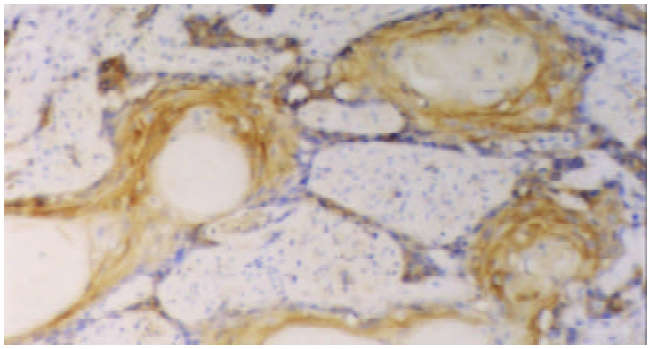

Figure 2 Esophageal squamous cell carcinoma (grade I). expression of hTERT mRNA was limited to the basaloid cell nests (40×).

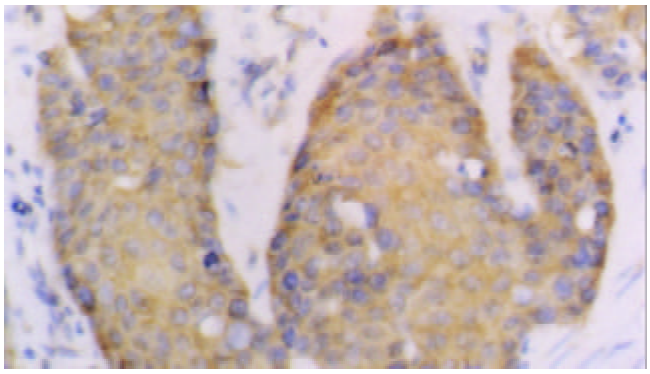

Figure 3 Poorly-differentiated esophageal squamous cell carcinoma. The expression of TP-1 mRNA was diffuse in cancer cells (40×).

Expression of hTERT and hTP-1 mRNA in esophageal squamous cell cacinoma

The positive rates of hTERT and hTP-1 mRNA expression were 75 % and 71.7 % respectively. The expression of hTERT and hTP-1 in well-differentiated carcinoma was limited to the basaloid cell nests (Figure 2). In the poorly-differentiated carcinoma, most tumor cells showed diffuse or occasionally

Table 3 Intensity of hTERT and hTP-1 mRNA expression in esophageal carcinoma tissues

Tumor stage	hTERT						*P* value	hTP-1					*P* value
	n	-	+	++	+++	Positive rate (%)		-	+	++	+++	Positive rate (%)	
I	15	7	4	3	1	53.3		7	5	3	0	53.3	
II	33	6	7	11	9	81.8	*P*>0.05	8	6	12	7	75.8	*P*>0.05
III	12	2	2	4	4	83.3		2	2	5	3	83.3	

Table 4 Relationship between hTERT, hTP-1 expression and telomerase activity

Telomerase activity	hTERT		*P* value	TP-1		*P* value
	+	-		+	-	
+	41	9	*P*<0.05	38	12	*P*>0.05
-	4	6		5	5	

focal expression (Figure 3). As showed in Table 3, the positive intensity and the positive rate of hTERT and hTP-1 expression progressively increased from grade I to grade III, but no significant differences existed between them (hTERT: χ^2=4.95, *P*>0.05; TP-1: χ^2=3.49, *P*>0.05).

Relationship between hTERT, hTP-1 expression and telomerase activity

Relationship between hTERT and hTP-1 expression and telomerase activity are summarized in Table 4. By statistical analyses, the expression of hTERT mRNA was correlated with telomerase activity (χ^2=5.76, *P*<0.05), but the expression of hTP-1 mRNA was no correlated with telomerase activity (χ^2=1.64, *P*>0.05).

DISCUSSION

Telomerase is a ribonucleoprotein reverse transcriptase that utilizes its own RNA template for the addition of telomeric sequences to chromosomal ends in order to maintain telomeric length. *In vivo* and *in vitro* studies suggested that telomerase was associated with cellular immortality and malignance, indicating that activation of telomerase might play an important role in tumorigenesis and immortalization. Telomerase activation has been demonstrated in many types of human tumors, including tumors in breast[9], nasopharynx[10,11], stomach[12-14], prostate[15], urinary bladder[16], skin[17], cervix[18], lung[19,20] and brain[21]. Some scientists suggested that telomerase activity was a diagnostic and prognostic marker for malignant tumors[22,23]. Previous research suggested that the positive rate of telomerase activity in esophageal carcinoma was 79-87 %, but there were different conclusions regarding the relationship between telomerase activity and cancer differentiation in esophageal cacinoma. Asai *et al*[24] reported that well-differentiated cancer had higher detectable telomerase activity, but Ikeguchi *et al*[25] found the opposite result. Zhao *et al*[26] concluded that telomerase activity had no correlation with cancer differentiation. Our present study results suggested that the detectable rate of telomerase activity was gradually increased from well-differentiated carcinoma to poorly-differentiated one. The difference between grade I and grade II was significant, while the difference between grade II and grade III was not significant. This result gave more evidences that telomerase activity was correlated with differentiation in esophageal SCC. The presence of telomerase activity in esophageal SCC with lymphatic metastasis suggested that the telomerase activity in patients with lymphatic metastasis was higher than that in patients without lymphatic metastasis.

Collins *et al*[27,28] first purified tetrahymena telomease protein p80. The p80 components could be specifically cross-linked to telomerase RNA. Then, the mammalian (mouse and human) homology of p80 was found, and termed telomerase-associated protein 1 (TP-1)[29]. The sequence of TP-1 showed most homology to tetrahymena p80. *In vitro* experiments suggested that TP-1 interacted specifically with telomerase RNA and that TP-1 was associated with telomerase activity. However, expression of TP-1 did not reflect the level of telomerase activity[30-32]. In the present study, we found that TP-1 expression was high in esophageal squamous cell carcinoma, but it was not correlated with telomerase activity. The specific mechanism by which the protein participated in telomerase function has not been defined.

Two related proteins, Est2p from the yeast *Saccharomyces cerevisiae* and p123 from the ciliate Euplotes aediculatus, have been identified as the catalytic subunits of telomerase in their respective species[33-36]. Est2 was first identified as a gene required for telomere maintenance in yeast[37] and was essential for telomerase activity. Then, a human gene, hEST2/hTERT (human telomerase reverse transcriptase), sharing significant sequence similarity with telomerase catalytic subunit genes of lower eukaryotes was cloned and the protein was identified[38]. Studies suggested that hTERT expression was correlated with telomerase activity. The expression of hTERT was up-regulated concomitantly with the activation of telomerase during the immortalization of cultured cells and down-regulated during *in vivo* cellular differentiation[39]. *In vitro*, changes in the sequence of hTERT amino acid might reduce telomerase activity, and transfer of hTERT into normal human cell might resurrect telomease[40]. Designing a ribozyme targeting hTERT also reduced telomerase activity[41]. However, some studies revealed that the levels of hTERT expression and detectable telomerase activity were not concomitant[42-48]. The present experiment suggested that hTERT mRNA expression was correlated with telomeras activity in esophageal SCC. But we found that the positive rate of hTERT mRNA expression was lower than detectable telomerase activity. The positive intensity and the positive rate of hTERT expression were progressively increased from grade I to grade III, but the differences between them was not significant. In 50 detectable telomerase activity cases, just 41 cases expressed hTERT mRNA, 9 cases had negatively expression of hTERT mRNA. There were 4 hTERT positive cases without detectable telomerase activity. It indicated that hTERT gene expression was an important factor to resurrect telomease, but not the only one. There was a possibility that other mechanisms were intervened to modulate telomerase activity. The reasons why the tissue had expression of hTERT mRNA without detectable telomerase activity are not clear. Following might be the explanations. Posttranscriptional modification of telomerase subunits would modulate telomerase activity, and there were some inhibitors in telomerase extract solution to reduce its activity. Using *in situ* hybiridization assay detected hTERT

expression might initially comprehend telomerase activity level. However, the result of hTERT expression and detectable telomerase activity were not identical. It was less sensitive than TRAP assay.

In summary, detectable telomerase activity and telomerase subunit expression are high in esophageal squamous cell carcinoma. Telomerase activity is related to tumor differentiation and lymphatic metastasis, which may provide a new marker for evaluating the prognosis of patients with esophageal SCC. Expression of hTERT mRNA is correlated with telomerase activity, but the expression of TP-1 mRNA is not correlated with telomerase activity.

REFERENCES

1 **Feng J**, Funk WD, Wang SS, Weinrich SL, Avilion AA, Chiu CP, Adams RR, Chang E, Allsopp RC, Yu J. The RNA component of human telomerase. *Science* 1995; **269:** 1236-1241

2 **Nakayama J**, Saito M, Nakamura H, Matsuura A, Ishikawa F. TLP1: a gene encoding a protein component of mammalian telomerase is a novel member of WD repeats family. *Cell* 1997; **88:** 875-884

3 **Harrington L**, Mcphail T, Mar V, Zhou W, Oulton R, Bass MB, Arruda I, Robinson MO. A mammalian telomerase-associated protein. *Science* 1997; **275:** 973-977

4 **Shen ZY,** Xu LY, Chen MH, Shen J, Cai WJ, Zeng Y. Progressive transformation of immortalized esophageal epithelial cells. *World J Gastroenterol* 2002; **8:** 976-981

5 **Shen ZY**, Xu LY, Li EM, Cai WJ, Chen MH, Shen J, Zeng Y. Telomere and telomerase in the initial stage of immortalization of esophageal epithelial cell. *World J Gastroenterol* 2002; **8:** 357-362

6 **Kim NW**, Piatyszek MA, Prowse KR, Harley CB, West MD, Ho PL, Coviello GM, Wright WE, Weinrich SL, Shay JW. Specific association of human telomerase activity with immortal cells and cancer. *Science* 1994; **266:** 2011-2015

7 **Hiyama E**, Hiyama K. Clinical utility of telomerase in cancer. *Oncogene* 2002; **21:** 643-649

8 **Li C**, Liang YR, Wu MY, Xu LY, Cai WJ. Telomerase activity analysis of esophageal carcinoma using microdissection-TRAP assay. *Chinese Med J* 2002; **115:** 1405-1408

9 **Hiyama E**, Gollahon L, Kataoka T, Kuroi, K, Yokoyama T, Gazdar AF, Hiyama K, Piatyszek MA, Shay JW. Telomerase activity in human breast tumors. *J Natl Cancer Inst* 1996; **88:** 116-122

10 **Cheng RY**, Yuen PW, Nicholls JM, Zheng Z, Wei W, Sham JS, Yang XH, Cao L, Huang DP, Tsao SW. Telomerase activation in nasopharyngeal carcinomas. *Br J Cancer* 1998; **77:** 456-460

11 **Tsao SW**, Zhang DK, Cheng RY, Wan TS. Telomerase activation in human cancers. *Chin Med J (Engl)* 1998; **111:** 745-750

12 **Hiyama E**, Yokoyama T, Tatsumoto N, Hiyama K, Imamura Y, Murakami Y, Kodama T, Piatyszek MA, Shay JW, Matsuura Y. Telomerase activity in gastric cancer. *Cancer Res* 1995; **55:** 3258-3262

13 **Yakoob J**, Hu GL, Fan XG, Zhang Z. Telomere, telomerase and digestive cancer. *World J Gastroenterol* 1999; **5:** 334-337

14 **Zhan WH**, Ma JP, Peng JS, Gao JS, Cai SR, Wang JP, Zheng ZQ, Wang L. Telomerase activity in gastric cancer and its clinical implications. *World J Gastroenterol* 1999; **5:** 316-319

15 **Sommerfeld HJ**, Meeker AK, Piatyszek MA, Bova GS, Shay JW, Coffey DS. Telomerase activity: a prevalemt marker of malignant human prostate tissue. *Cancer Res* 1996; **56:** 218-222

16 **Lin Y**, Miyamoto H, Fujinami K, Uemura H, Hosaka M, Iwasaki Y, Kubota Y. Telomerase activity in human bladder cancer. *Clin Cancer Res* 1996; **2:** 929-932

17 **Taylor RS**, Ramirez RD, Ogoshi M, Chaffins M, Piatyszek MA, Shay JW. Detection of telomerase activity in malignant and nonmalignant skin conditions. *J Invest Dermatol* 1996; **106:** 759-765

18 **Zhang DK**, Ngan HY, Cheng RY, Cheung AN, Liu SS, Tsao SW. Clinical significance of telomerase activation and telomeric restriction fragment (TRF) in cervical cancer. *Eur J Cancer* 1999; **35:** 154-160

19 **Wu TC,** Lin P, Hsu CP, Huang YJ, Chen CY, Chung WC, Lee H, Ko JL. Loss of telomerase activity may be a potential favorable prognostic marker in lung carcinomas. *Lung Cancer* 2003; **41:** 163-169

20 **Hiyama K**, Hiyama E, Ishioka S, Yamakido M, Inai K, Gazdar AF, Piatyszek MA, Shay JW. Telomerase activity in small-cell and non-small-cell lung cancers. *J Natl Cancer Inst* 1995; **87:** 895-902

21 **Sano T**, Asai A, Mishima K, Fujimaki T, Kirino T. Telomerase activity in 144 brain tumours. *Br J Cancer* 1998; **77:** 1633-1637

22 **Zhang YL**, Zhang ZS, Wu BP, Zhou DY. Early diagnosis for colorectal cancer in China. *World J Gastroenterol* 2002; **8:** 21-25

23 **Qin LX**, Tang ZY. The prognostic molecular markers in hepatocellular carcinoma. *World J Gastroenterol* 2002; **8:** 385-392

24 **Asai A**, Kiyozuka Y, Yoshida R, Fujii T, Hioki K, Tsubura A. Telomere length, telomerase activity and telomerase RNA expression in human esophageal cancer cells: correlation with cell proliferation, differentiation and chemosensitivity to anticancer drugs. *Anticancer Res* 1998; **18:** 1465-1472

25 **Ikeguchi M**, Kaibara N. Telomerase activity in esophageal squamous cell carcinoma and in normal esophageal epithelium adjacent to carcinoma. *Nippon Rinsho* 1998; **56:** 1176-1180

26 **Zhao CF**, Chen CL. Detection of telomerase activity in tumor tissues from patients with esophageal carcinoma. *Chin J Cancer* 2000; **19:** 131-133

27 **Collins K,** Kobayashi R, Greider CW. Purification of Tetrahymena telomerase and cloning of genes encoding the two protein components of the enzyme. *Cell* 1995; **81:** 677-686

28 **Kickhoefer VA**, Stephen AG, Harrington L, Robinson MO, Rome LH. Vaults and telomerase share a common subunit, TEP1. *J Biol Chem* 1999; **274:** 32712-32717

29 **Harrington L,** Mcphail T, Mar V, Zhou W, Oulton R, Bass MB, Arruda I, Robinson MO. A mammalian telomerase-associated protein. *Science* 1997; **275:** 973-977

30 **Harrington L**, Zhou W, McPhail T, Oulton R, Yeung DS, Mar V, Bass MB, Robinson MO. Human telomerase contains evolutionarily conserved catalytic and structural subunits. *Genes Dev* 1997; **11:** 3109-3115

31 **Nakayama J,** Saito M, Nakamura H, Matsuura A, Ishikawa F. TLP1: a gene encoding a protein component of mammalian telomerase is a novel member of WD repeats family. *Cell* 1997; **88:** 875-884

32 **Saito T**, Matsuda Y, Suzuki T, Hayashi A, Yuan X, Saito M, Nakayama J, Hori T, Ishikawa F. Comparative gene mapping of the human and mouse TEP1 genes, which encode one protein component of telomerases. *Genomics* 1997; **46:** 46-50

33 **Counter CM,** Meyerson M, Eaton EN, Weinberg RA. The catalytic subunit of yeast telomerase. *Proc Natl Acad Sci U S A* 1997; **94:** 9202-9207

34 **Lingner J**, Cech TR, Hughes TR, Lundblad V. Three Ever Shorter Telomere (EST) genes are dispensable for *in vitro* yeast telomerase activity. *Proc Natl Acad Sci U S A* 1997; **94:** 11190-11195

35 **Nakamura TM**, Morin GB, Chapman KB, Weinrich SL, Andrews WH, Lingner J, Harley CB, Cech TR. Telomerase catalytic subunit homologs from fission yeast and human. *Science* 1997; **277:** 955-959

36 **Lingner J,** Hughes TR, Shevchenko A, Mann M, Lundblad V, Cech TR. Reverse transcriptase motifs in the catalytic subunit of telomerase. *Science* 1997; **276:** 561-567

37 **Lendvay TS**, Morris DK, Sah J, Balasubramanian B, Lundblad V. Senescence mutants of Saccharomyces cerevisiae with a defect in telomere replication identify three additional EST genes. *Genetics* 1996; **144:** 1399-1412

38 **Meyerson M**, Counter CM, Eaton EN, Ellisen LW, Steiner P, Caddle SD, Ziaugra L, Beijersbergen RL, Davidoff MJ, Liu Q, Bacchetti S, Haber DA, Weinberg RA. hEST2 the putative human telomerase catalytic subunit gene, is up-regulated in tumor cells and during immortalization. *Cell* 1997; **90:** 785-795

39 **Counter CM**, Meyerson M, Eaton EN, Ellisen LW, Caddle SD, Haber DA, Weinberg RA. Telomerase activity is restored in human cells by ectopic expression of hTERT (hEST2), the catalytic subunit of telomerase. *Oncogene* 1998; **16:** 1217-1222

40 **Ramakrishnan S**, Eppenberger U, Mueller H, Shinkai Y, Narayanan R. Expression profile of the putative catalytic subunit of the telomerase gene. *Cancer Res* 1998; **58:** 622-625

41 **Hao ZM,** Luo JY, Cheng J, Wang QY, Yang GX. Design of a

ribozyme targeting human telomerase reverse transcriptase and cloning of it's gene. *World J Gastroenterol* 2003; **9:** 104-107

42 **Ulaner GA**, Hu JF, Vu TH, Giudice LC, Hoffman AR. Telomerase activity in human development is regulated by human telomerase reverse transcriptase (hTERT) transcription and by alternate splicing of hTERT transcripts. *Cancer Res* 1998; **58**: 4168-4172

43 **Liu K,** Schoonmaker MM, Levine BL, June CH, Hodes RJ, Weng NP. Constitutive and regulated expression of telomerase reverse transcriptase (hTERT) in human lymphocytes. *Proc Natl Acad Sci U S A* 1999; **96:** 5147-5152

44 **Hara T,** Noma T, Yamashiro Y, Naito K, Nakazawa A. Quantitative analysis of telomerase activity and telomerase reverse transcriptase expression in renal cell carcinoma. *Urol Res* 2001; **29:** 1-6

45 **Kameshima H,** Yagihashi A, Yajima T, Kobayashi D, Hirata K, Watanabe N. Expression of telomerase-associated genes: reflection of telomerase activity in gastric cancer. *World J Surg* 2001; **25:** 285-289

46 **Zhang RG,** Guo LX, Wang XW, Xie H. Telomerase inhibition and telomere loss in BEL-7404 human hepatoma cells treated with doxorubicin. *World J Gastroenterol* 2002; **8:** 827-831

47 **Yajima T,** Yagihashi A, Kameshima H, Kobayashi D, Hirata K, Watanabe N. Telomerase reverse transcriptase and telomeric-repeat binding factor protein 1 as regulators of telomerase activity in pancreatic cancer cells. *Br J Cancer* 2001; **85:** 752-757

48 **Tominaga T,** Kashimura H, Suzuki K, Nakahara A, Tanaka N, Noguchi M, Itabashi M, Ohkawa J. Telomerase activity and expression of human telomerase catalytic subunit gene in esophageal tissues. *J Gastroenterol* 2002; **37:** 418-427

Edited by Zhang JZ and Wang XL

P.O.Box 2345, Beijing 100023,China
Fax: +86-10-85381893
E-mail: wjg@wjgnet.com www.wjgnet.com

World J Gastroenterol 2003;9(11):2400-2403
World Journal of Gastroenterology
 ISSN 1007-9327

• ESOPHAGEAL CANCER •

Epidemiology of gastroenterologic cancer in Henan Province, China

Jian-Bang Lu, Xi-Bin Sun, Di-Xin Dai, Shi-Kuan Zhu, Qiu-Ling Chang, Shu-Zheng Liu, Wen-Jie Duan

Jian-Bang Lu, Xi-Bin Sun, Qiu-Ling Chang, Wen-Jie Duan, Henan Cancer Research Institute, Zhengzhou 450003, Henan Province, China
Di-Xin Dai, Shi-Kuan Zhu, Shu-Zheng Liu, Henan Tumor Hospital, Zhengzhou 450003, Henan Province, China
Supported by the National Medical Science and Technique Foundation of China during the 9th Five-Year Plan Period, No.96-906-01-01 and Science Research Fund of Henan Province, No. 971200101
Correspondence to: Dr. Jian-Bang Lu, Department of Epidemiology, Henan Cancer Research Institute, Dongming Road 127, Zhengzhou 450003, Henna Province, China. hncjbl@sohu.com
Telephone: +86-371-5962654
Received: 2002-07-23 **Accepted:** 2002-10-17

Abstract

AIM: To estimate the mortality rates of gastroenterologic cancers for the period between 1974 and 1999, in Henan Province, China and its epidemiologic features.

METHODS: Information on death of patients with cancer was provided by the county-city registries. Population data were provided by the local police bureau. All the deaths of cancer registered were classified according to the three-digit rubric of the ICD-9. Cancer mortality rates reported herein were age-adjusted, using the world population as standard and weighted piecewise linear regression analysis.

RESULTS: Total cancer age-adjusted mortality rates were 195.91 per 100 000 for males and 124.36 per 100 000 for females between 1996 and 1998. During the period of 1974-1999, a remarkable decrease took place in esophageal carcinoma, stomach cancer remained essentially stable and liver cancer, a moderate increase. Colorectal cancer was slightly increased over the last two decades.

CONCLUSION: The population-based cancer registry can give an accurate picture of cancer in Henan Province, by providing a set of analyses of selected cancer mortality data as a source of reference for researchers in cancer, public health and health care services.

Lu JB, Sun XB, Dai DX, Zhu SK, Chang QL, Liu SZ, Duan WJ. Epidemiology of gastroenterologic cancer in Henan Province, China. *World J Gastroenterol* 2003; 9(11): 2400-2403
http://www.wjgnet.com/1007-9327/9/2400.asp

INTRODUCTION

China is one of the countries with the highest esophageal cancer and gastric cancer risk over the past century which is still the leading cause of deaths worldwide[1-9]. The aim of this study was to estimate the mortality of digestive tract cancers in Henan Province.

Promotion of cancer control programs requires accurate data on cancer incidence and mortality from population-based registries. In 1977, we reviewed all causes of death between 1974 and 1976 retrospectly and enlisted the participation in this survey of the 15 cancer registries from 1983 to 1999 in Henan Province which was inhabited with about 9 million people, one-tenth of the province's total population. The geographical locations of these units are shown in Figure 1.

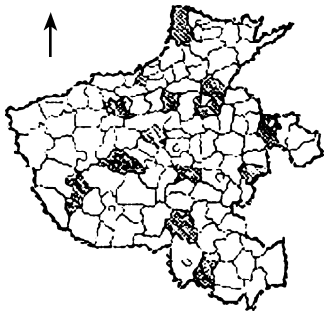

Figure 1 Geographical locations of the participating county and city registries of Henan Province, China.

MATERIALS AND METHODS

Information on death of patients with cancer was provided by the county-city registries, that consisted of the rural doctors and the local hospital doctors. Information was requested on demographic factors such as place of residence, age, sex, date of birth, and primary site of cancer as well as different diagnostic methods used such as radiology, cytology, and histology. Population data were provided by the local police bureau, consisting of the total population and the age-sex structure at the end of each year in each site studied.

All cancer deaths registered were classified according to the three-digit rubric of the ICD-9[10]. To facilitate comparison on an international basis, cancer mortality rates reported herein were age-adjusted, using the world population as standard. The direct standardization method was used to calculate various age groups from 5-years to 80 years and older. Cancer mortality trends from 1974 to 1999 were determined for more than 4 anatomic sites in males and females using weighted piecewise linear regression analysis.

RESULTS

The total cancer age-adjusted mortality rates were 193.68 per 100 000 for males and 133.29 per 100 000 for females in 1974-1976, and 218.29 per 100 000 and 125.52 per 100 000 in 1986-1988, and 195.91 per 100 000 and 124.36 per 100 000 in 1996-1998, respectively, accounting for 13.12 % for males and 10.71 % for females in 1974-1976, and 19.78 % and 15.82 % in 1986-1988, and 22.37 % and 17.25 % in 1996-1998, respectively of all cancer deaths. The major cancers diagnosed in Henan Province among males and femals are presented in Table 1. The main cancers in men included esophagus, stomach, liver and lung cancers, and the main cancers in women included esophagus, stomach, liver, lung, cervical and breast cancers. In general in Henan Province, men had higher mortality rates than women.

Table 1 Estimated cancer mortality rates[1] for males and females in Henan Province based on 15 selected registries

Site[2]	Years	Male		Female	
		ADM[1]	%	ADM[1]	%
All sites	1974-76	193.68	100.00	133.29	100.00
(140-208)	1986-88	218.29	100.00	125.52	100.00
	1996-98	195.91	100.00	124.36	100.00
Esophagus	1974-76	70.06	45.62	36.34	36.65
(150)	1986-88	67.78	31.04	35.99	32.14
	1996-98	43.77	25.70	25.73	24.19
Stomach	1974-76	36.02	19.89	19.79	15.01
(151)	1986-88	63.45	30.39	31.90	24.97
	1996-98	51.56	26.85	31.71	24.19
Colon / rectum	1974-76	6.47	3.92	6.14	4.48
(153-154)	1986-88	6.33	3.36	6.23	4.83
	1996-98	7.89	4.12	8.41	5.04
Liver (155)	1974-76	17.54	11.53	8.21	7.70
	1986-88	26.63	14.96	11.48	10.93
	1996-98	32.02	16.37	16.16	14.58

1: Age-adjusted mortality, standardized using world standard population. 2: Numbers in parentheses are ICD-9.

Table 2 illustrates urban-rural comparisons for selected cancer deaths from 1983 -1985 and 1997 in Henan Province, which included 12 counties and three cities. In Henan Province, rural areas had higher cancer mortality rates than urban areas, except for liver cancer in males.

Table 2 Urban and rural differences in mortality rates[1] of cancer from selected sites in Henan Province, China (1980's and 1990's)

Site[2]	Sex	Urban area		Rural area	
		1983-85	1997	1983-85	1997
All sites	M	170.09	149.52	208.80	190.34
(140-208)	F	99.89	52.83	126.99	103.07
Esophagus	M	78.74	12.10	87.63	50.03
(150)	F	45.62	5.48	57.29	25.58
Stomach	M	35.13	21.01	54.06	49.66
(151)	F	17.35	4.05	31.86	23.52
Colon / Rectum	M	8.10	8.92	6.38	9.17
(153-154)	F	5.48	2.36	4.36	4.81
Liver (155)	M	30.47	38.48	23.40	36.10
	F	11.11	9.43	11.28	17.06

1: Age-adjusted mortality, standardized using world standard population. 2: Numbers in parentheses are ICD- 9.

Cancer mortality rates at all sites did not change over the past two decades (Figure 2). During the period of 1974 -1999, marked changes took place in Henan Province in cancer mortality rates at certain sites. Esophageal carcinoma markedly declined, esophageal cancer mortality rates decreased over the period studied for males from approximately 70 per 100 000 in 1974-1976 to 43 per 100 000 in 1996-1998, and for females from approximately 36 per 100 000 to 25 per 100 000, respectively (Figure 3). Stomach cancer remained essentially stable (Figure 4), liver cancer have markedly increased (Figure 5). Colorectal cancer was the fifth most frequently diagnosed cancer in Henan Province. Men were diagnosed with this cancer slightly more frequently than women. Mortality rates for colorectal cancer have slightly increased over the last two decades (Table 1).

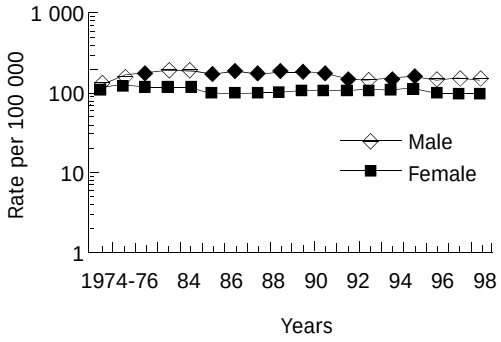

Figure 2 Total cancer mortality in Henan Province, China,1974-1999.

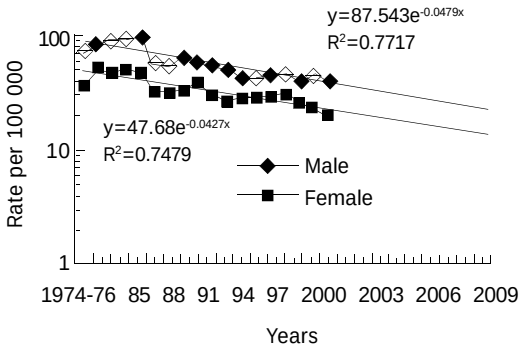

Figure 3 Age-adjusted mortality of esophageal cancer in Henan Province, China, 1974-1999.

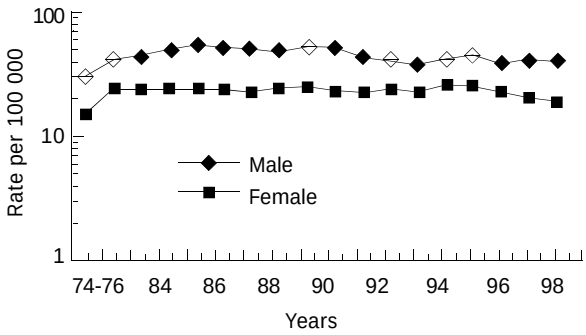

Figure 4 Age-adjusted mortality of stomach cancer in Henan Province, China, 1974-1999.

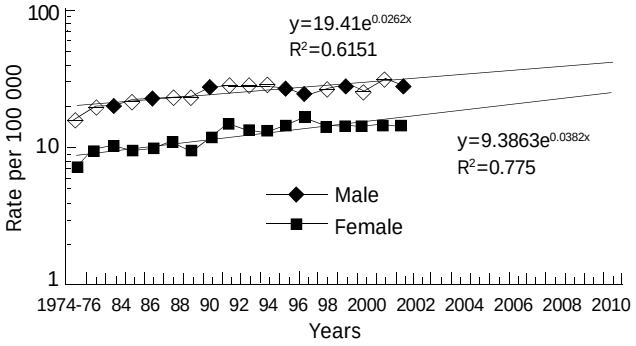

Figure 5 Age-adjusted mortality of liver cancer in Henan Province, China, 1974-1999.

DISCUSSION

Generally, genetic factors, per se, do not produce marked mortality changes over a short period of time, unless a specific

genetic factor present in the population interacts with a newly introduced agent in the environment. Thus marked changes in mortality rates, either increased or decreased, usually indicate that a new environmental agent has been introduced into or removed from the population in question. Compared with many other countries[11-18], all cancer mortality in Henan Province varied slightly over the past 25 years. Although mortality rates varied widely in specific cancers, cancers of the esophagus, stomach, liver and lung accounted for over 86 % of all cancer deaths in Henan Province. Cervical cancer and breast cancer made up 81 % of deaths in women. In general in Henan Province, men had higher mortality rates than women, and rural areas had higher mortality rates than urban areas, except for lung cancer.

Cancer mortality rates at all sites have been associated with many factors, including diet and nutrition[19-23], occupational exposure to toxic chemicals, tobacco and alcohol use, and certain viruses[24-31]. We found that lower socio-economic status, environmental pollution around the residential areas, lampblack in rooms, lower body mass index (BMI), more pickled food intake, cigarette smoking, alcohol drinking, mental-trauma and depression were risk factors of esophageal cancer. It also showed that the subjects having histories of upper digestive tract operation, dysplasia of esophagus and family histories of carcinoma had markedly increased risks for developing esophageal cancer[32]. Over the last 20 years, the dietary change occurred in Linzhou which was associated with the incidence and mortality decrease of esophageal cancer in the past ten years[33,34]. Cancer mortality rates at all sites remained essentially stable for males during the period studied, from approximately 193 per 100 000 in 1974-1976 to 195 per 100 000 in 1996-1998. Cancer mortality rates of females decreased over the last two decades from 133.29 per 100 000 in 1974-1976 to 124.36 per 100 000 in 1996-1998.

At the time of this study, esophageal cancer mortality rates decreased over the period studied for males, from approximately 70 per 100 000 in 1974-1976 to 43 per 100 000 in 1996-1998, and for females, from 36 per 100 000 in 1974-1976 to 24 per 100 000 in 1996-1998. Stomach cancer mortality rates did not change substantially during the period studied. Inversely, gastric cancer incidence and mortality rates showed a consistent decline in recent decades world-wide[12-15,21,22,35]. Liver cancer mortality rates for males markedly increased over the last two decades, from 17 per 100 000 in 1974-1976 to 32 per 100 000 in 1996-1998, for females from 8 per 100 000 in 1974-1976 to 16 per 100 000 in 1996-1998. Primary liver carcinoma (PLC) incidence and death rates in Australia increased in the past two decades[36]. Based on selected cancer registries around the world, developing countries have experienced PLC increases in incidence wherease developed countries have experienced declines[37].

The data analyzed in this report were age-adjusted using world standard population and stratified for sex and places. In temporary variation, the patterns presented were descriptive in nature. Secular trend in esophageal cancer and live cancer for both sexes in 1974-2010 with regression was used for spatial analysis.

At the end of the 20th century, cancer was the second leading cause of death in Henan Province. In the new century cancer will be the number one killer in Chinese.

Future cancer control research must aim to reduce cancer risk, incidence and mortality, and improve the quality of life[38].

CONCLUSIONS

The role of population-based cancer registry is to collect the data which give an accurate picture of cancer in a population, in order to understand and control the impact of cancer on that population. The cancer registry data can also be used to plan medical facilities and requirements needed for cancer control.

ACKNOWLEDGEMENTS

We thank the doctors from the 15 counties and cities for their assistance in data collection.

REFERENCES

1 **Ke L.** Mortality and incidence trends from esophagus cancer in selected geographic areas of China circa 1970-90. *Int J Cancer* 2002; **102**: 271-274
2 **Zhang W,** An F, Lin H. A case-control study on the risk factors of esophageal cancer in Jieyang City of Guangdong in China. *Zhonghua Liuxing Bingxue Zazhi* 2001; **22**: 442-445
3 **Botterweck AA,** Schouten LJ, Volovics A, Dorant E, van Den Brandt P. Trends in incidence of adenocarcinoma of the oesophagus and gastric cardia in ten European countries. *Int J Epidemiol* 2000; **29**: 645-654
4 **Desoubeaux N,** Le Prieur A, Launoy G, Maurel J, Lefevre H, Guillois JM, Gignoux M. Recent time trends in cancer of the oesophagus and gastric cardia in the region of Calvados in France, 1978-1995; a population based study. *Eur J Cancer Prev* 1999**; 8**: 479-486
5 **Adanja B,** Gledovic Z, Pekmezovic T, Vlajinac H, Jarebinski M, Zivaljevic V, Pavlovic M. Mortality trends of malignant tumours of digestive organ in Belgrade, Yugoslavia, 1975-1997. *Dig Liver Dis* 2000; **32**: 386-391
6 **Wijnhoven BP**, Louwman MW, Tilanus HW, Goebergh JW. Increased incidence of adenocarcinomas at the gastro-oesophageal junction in Dutch males since the 1990s. *Eur J Gastroenterol Hepatol* 2002; **14**: 115-122
7 **Blaser MJ,** Saito D. Trends in reported adenocarcinomas of the oesophagus and gastric cardia in Japan. *Eur J Gastroenterol Hepatol* 2002; **14**: 107-113
8 **Hansen S,** Wiig JN, Giercksky KE, Tretli S. Esophageal and gastric carcinoma in Norway 1958-1992: incidence time trend variability according to morphological subtypes and organ subsites. *Int J Cancer* 1997; **71**: 340-344
9 **Wolfgarten E,** Rosendahl U, Nowroth T, Leers J, Metzger R, Holscher AH, Bollschweiler E. Coincidence of nutritional habits and esophageal cancer in Germany. *Onkologie* 2001; **24**: 546-551
10 **World Health Organization**: International classification of diseases (ICD-9); 1 st ed. *Geneva: WHO* 1976
11 **Coleman MP,** Esteve J, Damiecki P, Arslan A, Renaard H. Trends in cancer incidence and mortality. *Lyon IARC Scientific Publications* 1993
12 **Newnham A,** Quinn MJ, Babb P, Kang JY, Majeed A. Trends in oesophageal and gastric cancer incidence, mortality and survival in England and Wales 1971-1998 / 1999. *Aliment Pharmacol Ther* 2003; **17**: 655-664
13 **Ruiz Ramos M,** Nieto Garcia MA, Mayoral Cortes JM. Mortality caused by cancer in Andalusia: trends and geographic distribution. *Aten Primaria* 2001; **28**: 634-641
14 **Corella D,** Guillen M. Dietary habits and epidemiolgy of gastric carcinoma. *Hepatogastroenterology* 2001; **48**: 1537-1543
15 **Gaudi I,** Kasler M. The course of cancer mortality in Hungary between 1975-2001. *Magy Onkol* 2002; **46**: 291-295
16 **Terry MB,** Gaudet MM, Gammon MD. The epidemiology of gastric cancer. *Sem in Radiat Oncol* 2002; **12**: 111-127
17 **Brooks-Brunn JA.** Esophageal cancer: an overview. *Medsurg Nurs* 2000; **9**: 248-254
18 **Bae JM,** Jung KM, Won YJ. Estimation of cancer deaths in Korea for the upcoming years. *J Korean Med Sci* 2002; **17**: 611-615
19 **Harvard Center for Cancer Prevention, Harvard School of Public Health**. Harvard report on cancer prevention. Volume 1. Causes of human cancer. *Cancer Causes Control* 1996; **7**: 3-59
20 **Palli D**, Russo A, Decarli A. Dietary patterns, nutrient intake and gastric cancer in a high-risk area of Italy. *Cancer Causes Control* 2001; **12**: 163-172
21 **Brown LM,** Devesa SS. Epidemiologic trends in esophageal and gastric cancer in United States. *Surg Oncol Clin N Am* 2002; **11**:

235-256
22 **Holtmann G**. Reflux disease: the disorder of the third millennium. *Eur J Gastroenterol Hepatol* 2001; **13**(Suppl 1): S5-11
23 **Mayne ST,** Navarro SA. Diet, obesity and reflux in the etiology of adenocarcinomas of the esophagus and gastric cardia in humans. *J Nutr* 2002; **132**(11Suppl): 3467S-3470S
24 Waste-mnnagement Education & Research Consortium (WERC), Collegge of Engineering, New Mexico State University (NMSU). *Cancer incidence rates in Eddy and Lea counties New Mexico* 1970-1994. 1998
25 **Tomeo CA**, Colditz GA, Willett WC, Giovannucci E, Platz E, Rockhill B, Dart H, Huneter DJ. Harvard report on cancer prevention Volume 3. Prevention of colon cancer in the United States. *Cancer Causes Control* 1999; **10**:167-180
26 **Colditz GA**, Atwood KA, Emmons RR, Nonson WC, Willett D, Trichopoulos Hunter DJ. Harvard report on cancer prevention. Volume 4. Harvard cancer risk index. *Cancer Causes Control* 2000; **11**: 477-488
27 **Bulbulyan MA,** Iiychova SA, Zahm SH, Astashevsky SV, Zaridze DG. Cancer mortality among women in the Russian printing industry. *Am J Ind Med* 1999; **36**: 166-171
28 **Tovar-Guzman VJ,** Barquera S, Lopez-Antunano FJ. Mortality trends in cancer attributable to tobacco in Mexico. *Salud Publica Mex* 2002; **44**(Suppl 1): S20-28
29 **Yu MC,** Yuan JM, Govindarajan S, Ross RK. Epidemiology of hepatocellular carcinoma. *Can J Gastroenterol* 2000; **14**: 703-709
30 **Cacoub P,** Geffray L, Rosenthal E, Perronne C, Veyssier P, Raguin G. Mortality among human immunodeficiency virus-infected patients with cirrhosis or hepatocellular carcinoma due to hepatitis C virus in Frence Departments of Internal Medicine / Infections Diseases, in 1995 and 1997. *Clin Infect Dis* 2001; **32**: 1207-1214
31 **El-Serag HB.** Epidemiology of hepatocellular carcinoma. *Clin Liver Dis* 2001; **5**: 87-107
32 **Lu JB**, Lian SY, Sun XB, Zhang ZX, Dai DX, Li BY, Cheng LP, Wei JR, Duan WJ. A case-control study on the risk factors of esophageal cancer in Linzhou. *Zhouhua Liuxingbingxue Zazhi* 2000; **21**: 434-436
33 **Lu JB**, Lian SY, Sun XB, Zhang ZX, Dai DX, Li BY, Cheng LP, Wei JR, Duan WJ. Dietary changes and the trends in morbidity and mortality on esophageal cancer in Linzhou. *Zhongguo Gonggong Weisheng* 2001; **17**: 60-61
34 **Lu JB**, Sun XB, Dai DX, Lian SY, Chang QL, Liu SZ, Li BY. Prevalence trends of esophageal cancer in Henan in 1974-1999. *Zhongliu Fangzhi Zazhi* 2002; **9**: 118-120
35 **Parkin DM**, Whelan SL, Ferlay J, Young J, eds. Cancer incidence In Five Continents, *IARC Scientific Publications* No.**143**. Lyon: International Agency for Research on Cancer, 1997
36 **Law MG,** Roberts SK, Dore GJ, Kaldor JM. Primary hepatocellular carcinoma in Australia, 1978-1997: increasing incidence and mortality. *Med J Aust* 2000; **173**: 403-405
37 **McGlynn KA,** Tsao L, Hsing AM, Devesa SS, Praumeni JF Jr. International trends and patterns of primary liver cancer. *Int J Cancer* 2001; **94**: 290-296
38 **Barbara K**. Rimer. Cancer control research 2001. *Cancer Causes Control* 2000; **11**: 257-270

Edited by Ma JY and Wang XL

P.O.Box 2345, Beijing 100023,China
Fax: +86-10-85381893
E-mail: wjg@wjgnet.com www.wjgnet.com

World J Gastroenterol 2003;9(11):2404-2408
World Journal of Gastroenterology
 ISSN 1007-9327

• ESOPHAGEAL CANCER •

Inhibition of adenovirus-mediated p27kip1 gene on growth of esophageal carcinoma cell strain

Qing-Ming Wu, Jie-Ping Yu, Qiang Tong, Xiao-Hu Wang, Guo-Jian Xie

Qing-Ming Wu, Jie-Ping Yu, Department of Gastroenterology, Renmin Hospital of Wuhan University, Wuhan 430060, Hubei Province, China
Qiang Tong, Xiao-Hu Wang, Guo-Jian Xie, Department of Gastroenterology, Taihe Hospital of Yunyang Medical College, Shiyan 442000, Hubei Province, China
Correspondence to: Dr. Qing-Ming Wu, Department of Gastroenterology, Taihe Hospital of Yunyang Medical College, 29 Renmin Road, Shiyan 442000, Hubei Province, China. wuhe9224@sina.com
Telephone: +86-719-8801431 **Fax:** +86-719-8883809
Received: 2003-03-04 **Accepted:** 2003-06-02

Abstract

AIM: To investigate the inhibition of p27kip1 gene on the growth of esophageal carcinoma cell strain (EC9706).

METHODS: Recombinant adenovirus Ad-p27kip1 was constructed and transfected into esophageal carcinoma cell EC-9706, and its effect on p27kip1 expression, the growth of esophageal carcinoma cell, DNA replication, protein synthesis, cell multiplication and apoptosis were explored by means of cell growth count, ^{3}H-TdR, ^{3}H-Leucine incorporation, flow cytometry, DNA fragment analysis and TUNEL.

RESULTS: Recombinant adenovirus Ad-p27kip1 was successfully constructed with a virus titer of 1.24×10^{12} pfu/ml. p27kip protein expression increased markedly after EC-9706 transfection, while incorporation quantity of ^{3}H-TdR and ^{3}H-Leucine decreased significantly. The growth of esophageal carcinoma cell was inhibited obviously. Testing of flow cytometry displayed a typical apoptosis peak, and DNA gel electrophoresis showed a typical apoptosis ladder. TUNEL showed the apoptosis rate of Ad-p27kip1 group and control group to be 37.3 % and 1.26 % ($P<0.001$) respectively.

CONCLUSION: Ad-p27kip1 can inhibit the growth and multiplication of esophageal carcinoma cells and induce apoptosis. Therefore, enhanced p27kip1 expression may be a new way to treat esophageal carcinoma.

Wu QM, Yu JP, Tong Q, Wang XH, Xie GJ. Inhibition of adenovirus-mediated p27kip1 gene on growth of esophageal carcinoma cell strain. *World J Gastroenterol* 2003; 9(11): 2404-2408
http://www.wjgnet.com/1007-9327/9/2404.asp

INTRODUCTION

As a kind of thermostable cell cycle inhibitive protein, p27 (mol. wt=27 KD) can inhibit CDK activity and consequently regulate cell cycle negatively when combined with CyclinE-CDK2 or CyclinE-CDK4[1]. The expression level and activity of p27 protein are associated with the formation of tumor. p27 protein quantity in tumor is markedly lower than that in normal cells level and its content is also closely related to the degree of differentiation, action of molecular biology and prognosis of tumor[2-7]. In the present study, we aim to give a tentative answer to whether enhanced expression of p27 protein inhibit the growth of cancer cell?

MATERIALS AND METHODS

Materials

Reagent p27kip1SP reagent was obtained from Beijing Zhongshan Biology Company. Endoenzyme, KpnI, BamHI and T4 DNA ligase were purchased from Huamei Biological Engineering Company. DMEM, RPMI1640, Lipofectamine were purchased from GIBCO/BRL Company. Low melting-temperature agarose and X-gal were obtained from Promega Company. CsCl was from Sigma Company. And high-grade neogenetic bovine serum from Hangzhou Sijiqing Biological Engineering Material Co. Ltd. p27kiplcDNA and adenovirus PCR primer were designed and synthesized by Saibaisheng Biological Company. And tryPsase from Shanghai Biological Products Company. ^{3}H-TDR and ^{3}H-Leucine were provided by Beijing Atomic Power Research Institute. DNA-PREPTMLPR and DNA-PREPTMstain were obtained from America Beckman Coulter Company.

Plasmid, strain, adenovirus and cell line PCMV5p27kip1 was presented by Dr. Wang Gang, Urinary Surgery Research Institute of the First Hospital of Beijing Medical University. PAACCMVPLPA and PJM17 were presented by academician Wu Zhuze, No. 2 Research Institute of Military Academy of Medical Science. DH 5a was presented by Dr. Peng Xu, Endocardial Department of the First Hospital of Beijing Medical University. Recombinant adenovirus was constructed by Molecular Biology Laboratory of Taihe Hospital. 293 cell was Hek cell line transferred from the gene of adenovirus E1 region, esophageal carcinoma cell strain EC9706 was presented by professor Wang Mingrong, China Academy of Medical Sciences.

Methods

Construction of adenovirus shuttle plasmid carrying p27kip1 Double enzyme cut was performed on pCMV5 p27kip1 and pACCMVPLPA with KpnI and BamHI respectively, and the fragments were separated at low melting-temperature agarose gel electrophoresis. The recovered p27kiplcDNA and adenovirus fragments were connected overnight with T_4DNA ligase at 4 ℃ by directional clone, and then transferred into receptive colibacillus DH_{5a}. From the selection of colonial amplification, a small quantity of plasmid was extracted and double cut with KpnI and BamHI. The presence of 690 bp and 8 800 bp in agarose gel after electrophoresis indicated that p27kip1cDNA had been inserted into adenovirus shuttle vector, hence successful construction of adenovirus shuttle plasmid pAd-p27kip1 carrying p27kip1.

Transfection of 293 cell by Lipofectamine-mediated pAd-p27kip1 and pJM17, and preparation of adenovirus recombinant Ad-p27kip1 (1) 293 cell was inoculated in a 9 cm plat, cultured in an incubator at 37 ℃ and 5 % CO_2, and transfected at 80 % fusion. (2) DNA-lipofectamine compound was dripped in an Eppendorf tube. Plasmid pAd-p27kip1 and pJM17 were diluted in 1 ml DMEM culture fluid, and revolved

for 1 s, then lipofectamine suspension was added uniformly. It was kept at room temperature for 30 minutes. (3) DNA-lipofectamine compound was dripped in culture flasks, and cultured in an incubator at 37 ℃ and 5 % CO_2. 0.5 % agarose was added for covering (0.5 % agarose contains 1×DMEM, 10 % Fcs), and cultured in an incubator with 37 ℃ and 5 % CO_2 after its coagulation, then pathological changes of 293 cell were observed.

PCR appraisal of recombinant adenovirus Ad-p27kip1[8] From 293 cell undergone pathologic changes after common transfection, culture supernate 100 μl was drawn, form which cell chip was removed centrifugally, and DNA was extracted and precipitated, then PCR amplification was performed on this DNA model. Primers 1 and 2 were used for amplifying p27kip1 gene, primer 3 and primer 4 for amplifying adenovirus skeleton gene fragments. The product of PCR amplification was appraised with 0.8 % agarose through electrophoresis, and held to be recombinant adenovirus Ad-p27kip1 containing human p27kip1 if gene fragments of 275 bp and 860 bp were both amplified. The sequence of primers was as follows.

Primer 1: 5' CCTAGAGGGCAAAGTACGAGTA 3'
Primer 2: 5' GAAGAATCGTCGGTTGCAGGTCGCT 3'
Primer 3: 5' TCGTTTCTCAGCAAGCTGTTG 3'
Primer 4: 5' CAATCTGAACTCAAAGCGTGG 3'

Amplification, purification and titer of recombinant adenovirus Ad-p27kip1 Recombinant adenovirus supernate 500 ul was added to 293 cell with 80 % fusion, and cultured in an incubator at 37 ℃ and 5 % CO_2. Ultracentrifugation in CsCl gradient and purification were performed on the adenovirus supernate by Graham method[8]. Then purified virus fluid 100 ul, 10 % SDS 20 ul, PBS 880 ul were taken to test light absorption value of OD_{260}nm and OD_{280} nm of the DNA of virus gene group, and accordingly to calculate the grannule quantity and purity of the virus. $1OD_{260}=10^{12}$pfu/ml, $OD_{260}/OD_{280}>1.3$ showed the purity was fairly high, virus titer pfu/ml=A260 ×dilution×10^{12}.

Transduction efficiency test of adenovirus Recombinant adenovirus Ad-LacZ was used to infect cells of esophageal carcinoma EC-9706 respectively by MOI 25, 50, 100 and 200. When X-gal was dyed, the cells dyed blue under microscope were positive cells expressed by LacZ gene, then the percentage of the cells dyed blue was calculated.

Influence of Ad-p27kip1 on growth curve of esophageal carcinoma cell $1×10^4$/ml cell suspension was made of the cultured esophageal carcinoma cells (5 % FcsRPMI1640) after digestion and collection. The cells of esophageal carcinoma were inoculated in 4 pieces of culture boards with 24 holes/piece according to the quantity of 1 ml/hole, cultured for 24 h. When in 40-50 % fusion, cells were rinsed with RPMI1640, and went on culture for 24 h for synchronization. The test was divided into three groups: experimental group: Ad-p27kip1, negative control groups: Ad-LacZ ,blank group: free-virus.The test groups were infected with the cells of esophageal carcinoma (RPMI1640) for 2 h with 100 MOI, during which the culture fluid was shaken every 15 min, and two hours later exchanged with 5 % Fcs RPMI1640 for culture. Prior to the transfection of esophageal carcinoma cells by virus, three holes were taken as cell count to obtain the average value, afterwards daily cell count was collected for 4 days, and the changes of growth curve of esophageal carcinoma cell were recorded.

Incorporation test of ^{3}H-TdR and ^{3}H-leucine As described above, the experimental group and control group were cultured for 3 h with 5 % Fcs RPMI1640, and then for 12 h with free-Fcs RPMI1640. Each group was added 1 μ Ci ^{3}H-TdR or ^{3}H-leucine, which was rinsed with PBS at the 24th, 48th and 72th hour and fixed with methyl alcohol for 10 min and absolute ethyl alcohol for 10 min. Finally, 0.1M NaOH 200 μl was added. 200 μl of each was taken after blowing, and mixed in 5 ml scintillation liquid for overnight. On the following day, the CPM of ^{3}H was tested, three times for each group with three wells.

Change of p27 protein expression of cell of esophageal carcinoma p27 protein expression of the three groups was detected by immunohistochemical SP method.

FCM detection after occurrence Ad-p27kip1 effect on esophageal carcinoma cell After 48 h effect, cells from the three groups were collected, centrifugated under digestion (1 000 rpm, 5 min). PBS was added for regulating the cell density to 10^6/ml with supernates removed. 100 ul cell suspension was put in a preparatory tube, and mixed with DNA-PREPTMLPR 200 ul. Half a minute later DNA-PREPTM stain reagent (PI staining) 2 ml was added for mixing. After staying static for half an hour, cell cycle and apoptosis were detected with FCM, and processed by SYSTEM II TM software from Coulter Company.

Apoptosis detected with DNA fragment analysis and TUENL method From the experimental group after the above-mentioned effect, genome DNA was extracted regularly. DNA fragment was analyzed by agarose gel electrophoresis. At the same time, apoptosis was detected by TUNEL method, and contrasted with that in the blank group.

RESULTS

Construction of pAd-p27kip1 shuttle plasmid

Double enzyme cutting was performed on pCMV5p27kip1 and pACCMVpLpA with KpnI and BamHI, then 690 bp fragment and 8 800 bp fragment were collected respectively at low melting-temprature agarose gel electrophoresis, for the production of plasmid pAd-p27kip1 with coupled reaction. Through transformation, amplification and extraction of colibacillus, enzyme cutting appraisal were conducted to approve that pAd-p27kip1 contained p27kip1 and adenovirus carrier skeleton (Figure 1).

Figure 1 pAd-p27kip1 appraisal 1 200 bp ladder Marker: 200, 400, 600, 800, 1 000, 1 200, 1 400, 1 600, 1 800, 2 000 bp. 2, pCMV5p27kip1 (kpnI+BamHI): 690 bp segment. 3, pAd-p27kip1(kpnI+BamHI): 690 bp and 8 800 bp segment. 4, pACCMVPLPA (kpnI+BamHI): 8 800 bp segment. 5, Hind III marker: 2 027, 2 322, 4 361, 6 557, 9 416, 23 130 bp.

Construction, amplification, purification, titer test of Ad-p27kip1 and PCR appraisal

When contransfected with the above synthesized pAd-p27kip1 and pJM17, 293 cells underwent pathologic changes and floated as in grape clusters, which suggested that Ad-p27kip1 was produced through homologous recombinant, ultracentrifugation in CsCl gradient and purification. Spectrophotometer detection showed that the virus titer was $1.24×10^{12}$ pfu/ml, $OD_{260}/OD_{280}>1.3$, which suggested that both the virus titer and the purity were fairly high. The extracted Ad-p27kip1 adenovirus DNA underwent PCR amplification for a contrast between PCMV5p27kip1 and pACCMVpLpA, with 275 bp and 860 bp as the amplification products (Figure 2).

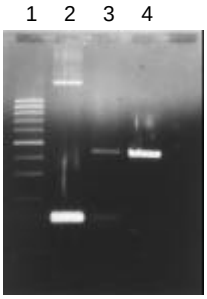

Figure 2 Ad-p27kip1 PCR appraisal 1 200 bp ladder Marker: 200, 400, 600, 800, 1 000, 1 200, 1 400, 1 600, 1 800, 2 000 bp, 2, pCMV5p27kip1model, 275 bp gene segament, 3, Ad-p27kip1 model: 275 bp and 860 bp gene segament, 4, PAVVMVPLPA model, 860 bp gene segament.

Transfection efficiency of recombinant adenovirus

Cells of esophageal carcinoma were infected with Ad-LacZ by MOI 25, 50, 100, 200 respectively, then stained with X-gal 48 h later. The transfection efficiency (%) was found to be 90, 100, 100, 100 respectively. It was concluded that 100 % transduction efficiency could be achieved with MOI $\geqslant$50, hence MOI 100 should be adopted for EC-9706 in the fellowing experiments.

Growth curve of esophageal carcinoma cell

Cell growth curve showed that the count of cancer cell in the experimental group declined over time, reached the bottom on the fourth day, but in Ad-Lacz group and blank group, it was just the opposite (Figure 3).

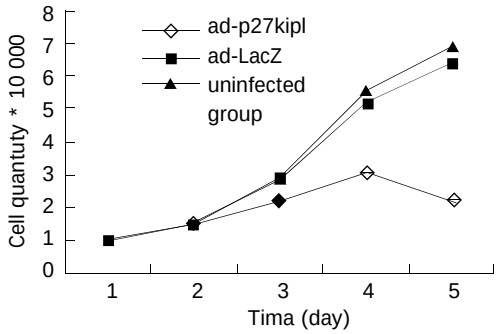

Figure 3 Growth curve of cell of esophageal carcinoma.

Table 1 ^{3}H-TdR incorporation quantity ($\bar{x}\pm s$ CPM / Well)

Group	2nd day	3rd day	4th day
Ad-p27kip1	2 013.42±84.38[a]	1 546.54±104.14[a]	244.22±39.62[a]
Ad-LacZ	3 316.81±96.37[b]	3 574.21±68.58[b]	4 451.38±154.67[b]
Blank	3 564.34±72.82	3 685.72±122.23	4 468.65±237.36

[a]P<0.001 *vs* Blank group, [b]P>0.05 Ad-LacZ group *vs* Blank group.

Table 2 Incorporation quantity of ^{3}H-Leucine ($\bar{x}\pm s$ CPM / Well)

Group	2nd day	3rd day	4th day
Ad-p27kip1	595.16±57.06[a]	422.82±45.81[a]	267.58±37.56[a]
Ad-LacZ	886.47±48.47[b]	915.44±93.58[b]	1 139.46±89.24[b]
Blank	895.21±967.52	967.52±78.35	1 243.95±06.72

[a]P<0.001 *vs* Blank group, [b]P>0.05 Ad-LacZ group *vs* Blank group.

Effect of Ad-p27kip1 on incorporation quantity of esophageal carcinoma cells ^{3}H-TdR and ^{3}H-leuine

The incorporation quantity of experimental group was markedly lower than that of the control group (P<0.001), declined over time as against the rise in Ad-LacZ group and blank group. There was no statistical difference (Table 1 and Table 2) between them.

Influence of Ad-p27kip1 on p27 expression of esophageal carcinoma cell

Immunocytochemical staining after virus transfection of esophageal carcinoma cells for 24 h showed that p27 expression increased clearly in experimental group, whereas there was not any change in control group (Figure 4 and 5).

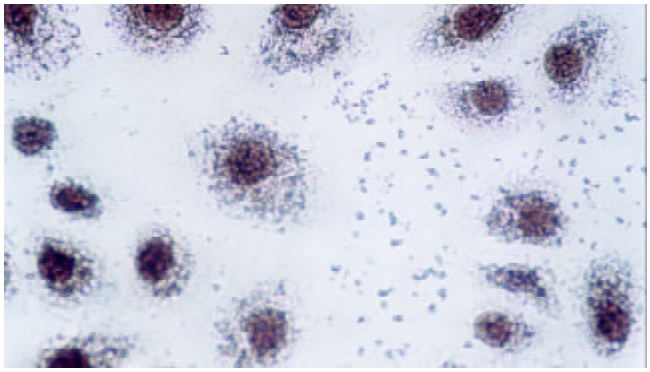

Figure 4 p27kip1 overexpression in transfection group ×200.

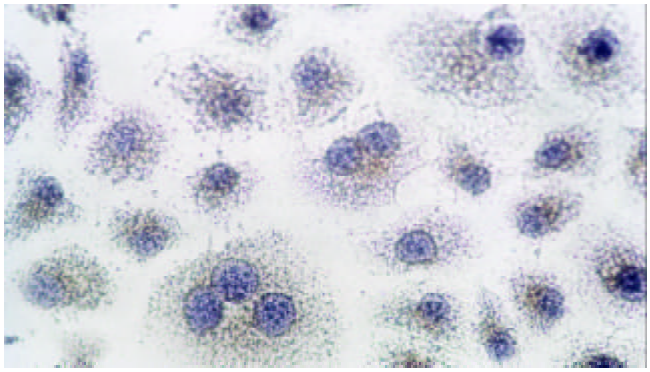

Figure 5 p27 negative expression in control group ×200.

Induction and quantitative detection of apoptosis esophageal carcinoma cells by Ad-p27kip1

Forty-eight hours after Ad-p27kip1, Ad-Lacz and blank management for EC-9706 cell, FCM determination showed that apoptotic cells took on an obvious apoptosis peak prior to G0/G1 peak. The apoptosis value of Ad-p27kip1, Ad-LacZ and blank group was 32.7 %, 5.72 % and 0.05 % respectively. Ad-p27kip1 group had the highest rate of apoptosis whereas blank group had the lowest rate.

Influence of Ad-p27kip on cell cycle of esophageal carcinoma

Cell cycle from FCM is listed in Table 3. In Ad-LacZ and blank control group, G1/G0 stage ratio decreased gradually whereas S stage increased, which indicated a rapidly changing G1/G0→S procedure and active cell multiplication. However, in the experimental group, G1/G0 stage ratio was fairly high and S stage decreased. There was a significant difference from control group (P<0.05). Cell cycle arrested G1 and inhibited cell multiplication.

Table 3 Effect of Ad-p27 on EC9706 cell cycle through fluid cell meter

Group	Distribution of cell cycle (%)		
	G0/G1	S	G2/M
Blank	40.39±3.86	49.61±4.27	13.10±1.03
Ad-LacZ	44.17±2.63	39.56±3.39	16.27±2.85
Ad-p27kip1	66.52±5.48[a,b]	21.15±3.26[a,b]	12.33±2.72

[a]P<0.05 *vs* Blank group, [b]P<0.05 *vs* Ad-LacZ group.

Analysis of DNA fragment

After cell EC-9706 was processed by Ad-p27kip1, gel electrophoresis of genome DNA displayed a clear ladder band, but no ladder band was found in contrasting group (Figure 6).

Figure 6 DNA fragment analysis 1 200 bp ladder marker: 200, 400, 600, 800, 1 000, 1 200, 1 400, 1 600, 1 800, 2 000 bp. 2, Ad-p27kip1group: 2 μg. 3, Ad-p27kip1group: 1 μg. 4. Blank group.

Detection of cell apoptosis by TUNEL Method

If brownish yellow color of karyon was found with TUNEL, it showed positive apoptosis, and no color was negative. The apoptosis rate of Ad-p27kip1 group and control group was 37.3 % and 1.26 % respectively, and there was obvious difference X^2 testing (P<0.01).

DISCUSSION

Advances in cellular biology of tumor and molecular biology have found that the occurrence of esophageal carcinoma is a comprehensive pathologic process with multifunction, multistage and multigene variations. Activation of various oncogenes and inactivation of anti-oncogene may be the major factors for normal epithelial canceration. Genetic treatment aimed to import objective genes into gene mutation or lost cells with the use of gene engineering technology, and to have functional expression replacing the original genes in order to recover the functions and effects of original genes and correct genetic distortion or genetic loss resulted from cellular developmental disturbance and realize the treatment[9]. p53, p21, Egr-1, FHIT, VEGF, E2F-1and hIFN-beta have been used as target genes in the treatment of esophagus carcinoma both *in vivo* and *in vitro*, and certain efficacy has been obtained[10-18]. Currently the analysis on esophagus carcinoma treatment through gene recombinant adenovirus p53 has entered the clinical stage[19], which will provide a bright future for tumor treatment.

P27 as candidate objective gene for tumor genetic treatment.

The key to genetic treatment is the correct selection of exogenous objective genes, its import into target cells and steady expression. Koguchi[20] used adenovirus carrier to pack p27 gene to transfect astrocytes, and found its overexpression inhibited multiplication activity of astrocytes. Katner[21] used adenovirus carrier containing p27kiplcDNA to transfect human 786-0 renal carcinoma cells, and found that the cell with p27kip1 overexpression lost the growth features of tumor cells, and that CDK activity of transfected cells was inhibited obviously, and that the multiplication time was extended. Patel[22] used p27kip gene to transfect human tumor cell line AV-W9 to induce cell death.The study of p27 gene in human breast cancer cells[23], neuroblastoma cells[24], prostate carcinoma cells[25]and lymphoma[26] showed the similar results, suggesting that p27 gene could be used as an objective gene for genetic treatment of tumor.

Construction of recombinant adenovirus carrier Ad-p27kip1 and its influence on p27 expression

Adenovirus carrier is of small pathogenicity and low genetic toxicity. With its wide host range, adenovirus can infect not only duplicated cells or cleavage cells, but also resting cells. Its huge package volume allows the insertion of 7.5kb exogenic gene fragment without any active carcinogene or insertion mutation within non-integral host chromosome. The virus can reach a high titer and 100 % infection rate through reproduction and purification. With its stable properties and safety for the human, it was considered as a gene conversion carrier of highly efficient expression[27] and most promising for genetic treatment[28].

Ad-p27kip1 constructed in the present study is a kind of replication of E1-deleted adenovirus vector. pJM17, the adenovirus skeleton with E1 region removed, can produce homologous recombinant with shuttle plasmids for producing infective adenovirus. Gene in E1 region is needed for adenovirus duplication, which requires that the duplication of intact adenovirus should be carried out in cell transfected by gene of E1 region. But since 293 cell is the right packaging cell for the transfection, replication of defective adenovirus has only one opportunity for infection in target cell without any duplication ability to fulfil the functions of adenovirus carrier, avoid damage of adenovirus itself to target cells and reach gene conversion.

Ad-p27kip1 containing human p27kip1 can positively connect p27kip1cDNA to CMV promoter of adenovirus. And as appraised by PCR amplification, p27 expression increased markedly after transfection of esophageal carcinoma cell. Contrasting adenovirus Ad-LacZ used in our study achieved 100 % induction efficiency with MOI=50. Ad-p27kip1 virus titer was 1.24×10^{12} pfu/ml, OD_{260}/OD_{280}>1.3, virus titer and purity were fairly high. This suggests that high expression of p27 after transfection is related to high induction efficiency and high purity, it can meet the demands of genetic treatment.

Inhibition of Ad-p27kip1 on growth of esophageal carcinoma

Studies demonstrated that declination of p27kip1 expression was an early event of esophageal carcinoma genesis, and also an independent prognostic factor of esophageal carcinoma[29-32]. We imported human p27kip1 gene into esophageal carcinoma cell EC9706 and analyzed its biological properties through cell growth curve, ^{3}H-TdR and ^{3}H-Leucine incorporation experiment, FCM and DNA fragment analysis. We found that esophageal carcinoma cell displayed G1 stage block after import of the gene, and that p27 inhibited cell multiplication of esophageal carcinoma obviously, and that from G1 stage to S stage, the self-multiplication ability of the control cell decreased, and the apoptosis rate increased to 32.7 %, a significant difference (P<0.01) compared with that of control group and Ad-LacZ group. It may be concluded p27kip1 gene is an important gene for occurrence of esophageal carcinoma, decreased p27 expression may be a major factor to cell differentiation and death disturbance, while increased of p27 expression can promote

cell death of esophageal carcinoma, which offers a new perspective on treating esophageal carcinoma.

REFERENCES

1 **Polyak K,** Kato JY, Solomon MJ, Sherr CJ, Massague J, Roberts JM, Koff A. p27kip1, a cyclin-Cdk inhibitor,links transforming growth factor-β and contact inhibiton to cell cycle arrest. *Genes Dev* 1994; **8**: 9-22

2 **Harada K**, Supriatno Yoshida H, Sato M. Low p27Kip1 expression is associated with poor prognosis in oral squamous cell carcinoma. *Anticancer Res* 2002; **22**: 2985-2989

3 **Chen AJ**, Meng QH, Long B, Yang GL. Relationship between p27 expression and prognosis of colorectal carcinoma. *Ai Zheng* 2002; **21**: 1075-1077

4 **Myung N**, Kim MR, Chung IP, Kim H, Jang JJ. Loss of p16 and p27 is associated with progression of human gastric cancer. *Cancer Lett* 2000; **153**: 129-136

5 **Lacoste-Collin L**, Gomez-Brouchet A, Escourrou G, Delisle MB, Levade T, Uro-Coste E. Expression of p27(Kip1) in bladder cancers: immunohistochemical study and prognostic value in a series of 95 cases. *Cancer Lett* 2002; **186**: 115-120

6 **Schwerer MJ**, Sailer A, Kraft K, Maier H. Cell proliferation and p27Kip1 expression in endophytic schneiderian papillomas. *Laryngoscope* 2002; **112**: 852-857

7 **Cesinaro AM**, Migaldi M, Corrado S, Maiorana A. Expression of p27kip1 in basal cell carcinomas and trichoepitheliomas. *Am J Dermatopathol* 2002; **24**: 313-318

8 **Zhang X**, Liu S, Liang C, Yang H. Adenovirus-mediated Rb gene transfect for head and neck cancer. *Huaxi Yike Daxue Xuebao* 2001; **32**: 194-195

9 **Roth JA**, Cristiano RJ. Gene therapy for cancer: what have we done and where are we going? *J Nat Cancer Inst* 1997; **89**: 21-39

10 **Matsubara H**, Maeda T, Gunji Y, Koide Y, Asano T, Ochiai T, Sakiyama S, Tagawa M. Combinatory anti-tumor effects of electroporation-mediated chemotherapy and wild-type p53 gene transfer to human esophageal cancer cells. *Int J Oncol* 2001; **18**: 825-829

11 **Shimada H**, Shimizu T, Ochiai T, Liu TL, Sashiyama H, Nakamura A, Matsubara H, Gunji Y, Kobayashi S, Tagawa M, Sakiyama S, Hiwasa T. Preclinical study of adenoviral p53 gene therapy for esophageal cancer. *Surg Today* 2001; **31**: 597-604

12 **Fujii T**, Tanaka Y, Tanaka T, Matono S, Sueyoshi S, Fujita H, Shirouzu K, Kato S, Yamana H. Experimental gene therapy using p21/WAF1 gene in esophageal squamous cell carcinoma-adenovirus infection and gene gun technology. *Gan To Kagaku Ryoho* 2001; **28**: 1651-1654

13 **Wu MY**, Chen MH, Liang YR, Meng GZ, Yang HX, Zhuang CX. Experimental and clinicopathologic study on the relationship between transcription factor Egr-1 and esophageal carcinoma. *World J Gastroenterol* 2001; **7**: 490-495

14 **Ishii H**, Dumon KR, Vecchione A, Trapasso F, Mimori K, Alder H, Mori M, Sozzi G, Baffa R, Huebner K, Croce CM. Effect of adenoviral transduction of the fragile histidine triad gene into esophageal cancer cells. *Cancer Res* 2001; **61**: 1578-1584

15 **Gu ZP**, Wang YJ, Li JG, Zhou YA. VEGF165 antisense RNA suppresses oncogenic properties of human esophageal squamous cell carcinoma. *World J Gastroenterol* 2002; **8**: 44-48

16 **Yang HL**, Dong YB, Elliott MJ, Liu TJ, McMasters KM. Caspase activation and changes in Bcl-2 family member protein expression associated with E2F-1-mediated apoptosis in human esophageal cancer cells. *Clin Cancer Res* 2000; **6**: 1579-1589

17 **Guo WZ**, Ran YL, Liu J, Yu L, Sun LX, Yang ZH. Enhancement by hypoxia of antisense VEGF(165) gene expression in esophageal cancer cells. *Shengwu Huaxue Yushengwu Wuli Xuebao (Shanghai)* 2002; **34**: 625-629

18 **Tsunoo H**, Komura S, Ohishi N, Yajima H, Akiyama S, Kasai Y, Ito K, Nakao A, Yagi K. Effect of transfection with human interferon-beta gene entrapped in cationic multilamellar liposomes in combination with 5-fluorouracil on the growth of human esophageal cancer cells *in vitro*. *Anticancer Res* 2002; **22**: 1537-1543

19 **Shimada H**, Matsubara H, Ochiai T. Gene therapy for esophageal cancer. *Nippon Geka Gakkai Zasshi* 2002; **103**: 371-375

20 **Koguchi K**, Nakatsuji Y, Nakayama K, Sakoda S. Modulation of astrocyte proliferation by cyclin-dependent kinase inhibitor p27 (Kip1). *Glia* 2002; **37**: 93-104

21 **Katner AL**, Gootam P, Hoang QB, Gnarra JR, Rayford W. A recombinant adenovirus expressing p27(Kip1) induces cell cycle arrest and apoptosis in human 786-0 renal carcinoma cells. *J Urol* 2002; **168**: 766-773

22 **Patel SD**, Tran AC, Ge Y, Moskalenko M, Tsui L, Banik G, Tom W, Scott M, Chen L, Van Roey M, Rivkin M, Mendez M, Gyuris J, McArthur JG. The p53-independent tumoricidal activity of an adenoviral vector encoding a p27-p16 fusion tumor suppressor gene. *Mol Ther* 2000; **2**: 161-169

23 **Craig C**, Wersto R, Kim M, Ohri E, Li Z, Katayose D, Lee SJ, Trepel J, Cowan K, Seth P. A recombinant adenovirus expressing p27Kip1 induces cell cycle arrest and loss of cyclin-Cdk activity in human breast cancer cells. *Oncogene* 1997; **14**: 2283-2289

24 **Matsuo T**, Seth P, Thiele CJ. Increased expression of p27Kip1 arrests neuroblastoma cell growth. *Med Pediatr Oncol* 2001; **36**: 97-99

25 **Katner AL**, Hoang QB, Gootam P, Jaruga E, Ma Q, Gnarra J, Rayford W. Induction of cell cycle arrest and apoptosis in human prostate carcinoma cells by a recombinant adenovirus expressing p27(Kip1). *Prostate* 2002; **53**: 77-87

26 **Turturro F**, Seth P. Prolonged adenovirus-mediated expression of p27(kip1) unveils unexpected effects of this protein on the phenotype of SUDHL-1 cells derived from t(2;5)-anaplastic large cell lymphoma. *Leuk Res* 2003; **27**: 329-335

27 **Zhang WW**. Development and application of adenoviral vectors for gene therapy of cancer. *Cancer Gene Ther* 1999; **6**: 113-138

28 **Tseng JF**, Farnebo FA, Kisker O, Becker CM, Kuo CJ, Folkman J, Mulligan RC. Adenovirus-mediated delivery of a soluble form of the VEGF receptor Flk1 delays the growth of murine and human pancreatic adenocarcinoma in mice. *Surgery* 2002; **132**: 857-865

29 **Yasunaga M**, Tabira Y, Nakano K, Iida S, Ichimaru N, Nagamoto N, Sakaguchi T. Accelerated growth signals and low tumor-infiltrating lymphocyte levels predict poor outcome in T4 esophageal squamous cell carcinoma. *Ann Thorac Surg* 2000;**70**: 1634-1640

30 **Shamma A**, Doki Y, Tsujinaka T, Shiozaki H, Inoue M, Yano M, Kawanishi K, Monden M. Loss of p27(KIP1) expression predicts poor prognosis in patients with esophageal squamous cell carcinoma. *Oncology* 2000; **58**: 152-158

31 **Shibata H**, Matsubara O, Wakiyama H, Tanaka S. The role of cyclin-dependent kinase inhibitor p27 in squamous cell carcinoma of the esophagus. *Pathol Res Pract* 2001; **197**: 157-164

32 **Taniere P**, Martel-Planche G, Saurin JC, Lombard-Bohas C, Berger F, Scoazec JY, Hainaut P. TP53 mutations, amplification of P63 and expression of cell cycle proteins in squamous cell carcinoma of the oesophagus from a low incidence area in Western Europe. *Br J Cancer* 2001; **85**: 721-726

Edited by Bo XN and Wang XL

P.O.Box 2345, Beijing 100023,China
Fax: +86-10-85381893
E-mail: wjg@wjgnet.com www.wjgnet.com

World J Gastroenterol 2003;9(11):2409-2412
World Journal of Gastroenterology
 ISSN 1007-9327

Flow cytometric analysis of DNA, telomerase content and multi-gene expression in esophageal epithelial dysplasia

Lian-Fu Zuo, Pei-Zhong Lin, Fing-Ying Qi, Jian-Wen Guo, Jiang-Hui Liu

Lian-Fu Zuo, Jian-Wen Guo, Jiang-Hui Liu, Hebei Provincial Tumor Institute, Shijiazhuang 050011, Hebei Province, China
Pei-Zhong Lin, Department of Pathology, Tumor Institute, Chinese Academy of Medical Sciences, Beijing 100021,China
Feng-Ying Qi, Department of Pathology, Hebei Medical University, Shijiazhuang 050017, Hebei Province,China
Supported by the National Key Technologies Research and Development Program of China during the 9th Five-year Plan Period, No.96-906-01-02
Correspondence to: Lian-Fu Zuo, Hebei Provincial Tumor Institute, Shijiazhuang 050011, Hebei Province, China. zuolianfu@sina.com
Telephone: +86-311-6033511 **Fax**: +86-311-6077634
Received: 2003-05-10 **Accepted:** 2003-06-19

Abstract

AIM: To investigate the alteration of molecular events and the early carcinogenesis mechanism of esophageal epithelial cells in the high incidence area of esophageal cancer.

METHODS: Esophageal epithelial cells of esophageal cancer patients were collected from the high incidence area in China. Content of DNA and telomerase as well as multi-gene expressions such as p^{53}, p^{21} and cyclin D_1 in esophageal precancer cells were quantitatively analysed by flow cytometry (FCM) with indirect immunofluorescence technique and DNA propidium iodide fluorescence staining.

RESULTS: FCM analysis results showed the DNA content increased significantly and the heteroploid rate was 87.9 % in occurred carcinogenesis. P^{53} protein accumulation and ras p^{21} increase were seen in the early carcinogenesis of the esophagus. The positive rate of p^{53} and ras p^{21} was 100 % (5/5, 4/4 respectively) in the cancer group. Telomerase and oncogene cyclin D_1 were over- expressed in all of the cancer patients.

CONCLUSION: Increased DNA content and heteroploid rate, accumulation of p53 protein, and over-expression of p21, telomerase and cyclin D_1 proteins were early molecular events during the development of esophageal cancer.

Zuo LF, Lin PZ, Qi FY, Guo JW, Liu JH. Flow cytometric analysis of DNA, telomerase content and multi-gene expression in esophageal epithelial dysplasia. *World J Gastroenterol* 2003; 9 (11): 2409-2412
http://www.wjgnet.com/1007-9327/9/2409.asp

INTRODUCTION

Esophageal cancer is one of the most common malignant tumors, and many studies have been made on it[1-3]. Former studies focused primarily on precancerous lesions and carcinogenesis of esophagus. But early carcinogenesis of esophageal cancer is unclear. In the present study, we investigated the DNA, telomerase content and P^{53}, ras P^{21} and cyclin D_1 multi-gene product of exfoliated cell samples from Cixian County, a high incidence area of esophageal cancer in Hebei Province of China with flow cytometry. It may provide a theoretic basis for under standing the carcinogenesis of esophageal epithelial cells and early diagnosis of esophageal cancer.

MATERIALS AND METHODS

Specimen collection

All samples were collected from Cixian County, a high incidence area of esophageal cancer, Hebei Province, China. One thousand nine hundred and sixteen cases of exfoliated cell specimens of esophagus were obtained with a mesh saccule. The exfoliated cell sample in each case was divided into two parts. One part was used for smear preparation on slides with papanicolaou stain for cytologic diagnosis, another part was used for preparation of a single cell suspension for flow cytometry analysis.

Specimen preparation for FCM DNA analysis

Exfoliated cells from 1916 cases for DNA analysis were obtained as follows. The exfoliated cells were washed out from the saccule with 0.9 % NaCl solution, centrifuged and fixed in 70 % ethanol. Before DNA analysis the cell samples were washed off 70 % ethanol in 0.9 % NaCl solution. Cell suspension (1×10^6 cells/ml) was centrifuged (5 min, 1 000 r/min) and washed twice with 0.9 % NaCl solution. After centrifugation the cells were stained in one million of propidium iodid (PI) solution (PI 50 μg/ml with triton-x-100 and RNase) for 30 minutes and filtered through a 47 μm nylon mesh to remove cellular fragments and clusters. Chicken red blood cells were added to the sample before stained as an internal standard for calibration of the FCM instrument.

The antibodies for immunofluorescence detection of telomerase, P^{53}, P^{21} and cyclin D1 protein were described as below: (1) Monoclonal antibody (MoAb) P^{53} was a mouse antibody against human P^{53} protein (Clone PAB1801, Oncogene Science, Inc. U S. working concentration 1:100). (2) MoAb P^{21} was a mouse antibody against human pan-ras P^{21} protein (Clone F-132, Santa Cruz, US, working concentration 1:100). (3) MoAb cyclin D1 was a mouse antibody against human cyclin D1 protein (Clone DCS-6, Santa Cruz, US, working concentration 1:100). (4) Telomerase was rabbit antibody against human telomerase associated protein (TP1) polyclonal antibody (Clone C-20, Stanta Cruz, US, working concentration 1:50). (5) The second antibody was used with FITC-conjugated goat anti-mouse/anti-rabbit IgG (Tackson Immunoresearch Laboratories Inc, code number 115-095-003/115095, working concentration 1:100).

Labeling method

The sample fluorescence staining was performed using indirect immunofluorescence labeling method. Samples from 100 cases were randomly selected for each antibody labeling. Each sample (10^6 cells/ml) was washed twice with PBS and incubated in water-bath for 30-min at 37 ℃ with 100 μl antibody (p53, p21, cyclin D1, telomerase). The samples were then washed twice with PBS and incubated in water-bath for 30 min at 37 ℃ with 100 μl of the second antibody of FITC-conjugated goat anti-mouse/rabbit IgG. The cell suspension

was washed, and resuspended in l.0 ml PBS, filtered through a 47 μm nylon mesh, analyzed by flow cytometry, before the samples were analyzed.

Three control samples were used. One sample was used as negative control with PBS replacing the first/second antibody. Another sample was used as positive isotype control with only the first antibody incubated. The remaining sample was incubated only with the second fluorescence antibody as positive isotype control.

Flow cytometry measurement of DNA and immunofluoresence

The stained samples were analyzed in a FACS 420 flow cytometer (FACS 420 Fluorescence Activated Cell Sorting, Becton. Dickinson, Sunnyvale. California, U S A). The light source was a 2w argon ion laser using a wave-length of 488 nm. The working power was 300 mw. Single parameter was measured respectively in DNA (with a liner mode) and each protein (with a Log mode). Usually, 10 000 cells for each sample were analyzed. The analytic data were processed with a HP-300 consort 300 computer. The coefficient of variation (CV)of the instrument was adjusted within 5 % using PI staining chicken red blood cells.

Measured data analysis

DNA ploid analysis DNA content was presented as the DNA index (DI), DI=G0/1 peak average channel value in experimental sample DNA histogram / G0/1 peak average channel value in normal cell sample DNA histogram. DNA ploids were judged according to DI value. The normal epithelial cells in each sample were used as internal standard reference cell for diploid DNA value, DI in diploid cell was 1.0. A diploid DNA histogram was defined as DI=1.0±2 cv. An aneuploid DNA histogram was defined as DI≠1.0±2 cv.

Cell cycle analysis DNA cell cycle was analyzed using a software of DNA histogram distribution (sum of broadened retangled model). The phases in G0/1.S.G2M were calculated according to DNA content distribution histogram. The proliferation index (PI) was used to present cell proliferation activity PI(%)=S+G2M/G0/1+S+G2M.

Quantitative analysis of P^{53}, rasP^{21}, cyclin D1 and telomerase expression Fluorescence index (FI) was used to describe P^{53}, P^{21}, cyclin D1 and telomerase expression. Following FI calculated formulation: FI=average fluorescence intensity of sample protein expression - average fluorescence intensity of isotype control/average fluorescence intensity of normal control. The sample was considered positive when FI was above 1.0.

Statistical analyses

Chi- square test and *t* test were used for statistical analysis of the results. The study was double blind with a group of cytologists making cytologic diagnosis, while another group performed DNA analysis.

RESULTS

Cytologic diagnosis

The cytologic observation showed that among the 1 916 cases of exfoliated cell smears, 217 were normal, 306 were mild dysplasia, 952 were moderate dysplasia, 349 were severe dysplasia and 92 were esophageal cancer.

Relationship between DI and cytologic diagnosis

The FCM DI value and corresponding cytologic diagnosis of 1916 samples are presented in Table 1. Table 1 shows that cellular DNA content was closely related to epithelial changes in esophagus. DI increased as the grade of dysplasia increased. Significant differences in DI were found in the mild, moderate and severe dysplasia groups. There was no significant difference in DI between the normal and mild dysplasia groups.

Table 1 Relationship between cellular DNA content and cytologic diagnosis

Cellular diagnosis	No.of cases	DI value ($\bar{x}$±s)	*P* value (*t* test)
Normal	217	1.01±0.06	>0.2
Mild dysplasia	306	1.03±0.10	<0.01
Moderte dysplasia	952	1.06±0.27	<0.01
Severe dysplasia	349	1.09±0.14	<0.01
Cancer	92	1.24±0.18	<0.01

Relationship between DNA ploid and cytologic diagnosis

The results of DNA ploid status in different cytologic groups of exfoliated esophageal cells are shown in Table 2, which shows that 21 cases in normal group were DNA heteroploid, but none became cancerous in follow-up. Thus, DNA heteroploidy in normal group was defined as false heteroploid. The rate of DNA heteroploid in dysplasia increased as the dysplasia lesion progressed. The difference in DNA heteroploid among three dysplasia groups was statistically significant (P<0.01).

Relationship between PI value and cytologic diagnosis

The results of cell cycle analysis showed that cell proliferation activity was closely related to epithelial changes in esophagus, PI value was 13.8±4.3 % in normal group, 16.4±2.5 % in mild dysplasia group, 17.9±4.1 % in moderate dysplasia group, 19.8±2.9 % in severe dysplasia group, 24.6±4.2 % in cancer group, respectively. PI value increased as dysplasia lesion progressed. The difference in PI value between normal group and the three dysplasia groups had a statistical significance (P<0.05).

Table 2 Relationship between DNA ploid and cytologic diagnosis

Cellular diagnosis	No.of cases	DNA ploidy pattern		Rate of heteroploid (%)	*P* value x^2 test
		diploid	heteroploid		
Normal	217	196	21	9.7	>0.05
Mild dysplasia	306	280	26	8.5	>0.01
Moderate dysplasia	952	791	161	16.9	<0.01
Severe dysplasia	349	229	120	34.4	<0.01
Cancer	92	20	72	78.3	<0.01

Relationship between P^{53}, P^{21} protein expression and cytologic grade

The results of P^{53}, P^{21} protein expression are shown in Table 3.

Table 3 Expression of P^{53}, P^{21} in various lesions of esophageal epithelial cells

Cytological group	No.of cases	P^{53} FI ($\bar{x}$±s)	P^{53+}cases (%)	P^{21} FI ($\bar{x}$±s)	P^{21+} cases (%)
Normal	10	1.00±0.11	0	1.00±0.19	0
Mild dysplasia	24	1.10±0.15	5 (20.8 %)	1.09±0.21	6 (25.0 %)
Severe dysplasia	61	1.36±0.32	34 (54.8 %)	1.34±0.35	35 (57.4 %)
Cancer	5	2.28±0.20	5 (100 %)	1.82±0.24	5 (100 %)

Expression of P^{53} and ras P^{21} in Table 3 showed that FI value increased as the grade of cytologic diagnosis of the esophageal epithelia increased. The differences in FI values among the normal, mild and severe dysplasia and cancer groups were statistically significant (P<0.01). The positive

rate of P^{53} and ras P^{21} expression among the four groups of esophageal epithelial lesion was also statistically significant ($P<0.01$).

Correlation of cyclin D1 and telomerase associated protein (TP1) expression with cytologic diagnosis grading

Table 4 Results of cyclin D1 and TP1 expression in various lesions of esophageal epithelia

Cytologic diagnosis	No.of cases	Cyclin D1, FI ($\bar{x}\pm s$)	Cyclin D_1^+ cases	TP FI ($\bar{x}\pm s$)	TP_1^+ cases
Normal	7	1.00±0.07	0	0.99±0.07	0
Mild dysplasia	11	0.97±0.12	1 (9.1 %)	1.22±0.15	7 (63.6 %)
Severe dysplasia	76	1.21±0.22	45 (59.2 %)	1.33±0.27	64 (84.2 %)
Cancer	6	1.84±0.18	6 (100 %)	1.70±0.15	6 (100 %)

Table 4 contains the cyclin D1 and TP1 expression data from 100 cases of esophageal epithelial lesion. The results showed that the cyclin D1 and TP1 protein expression level was correlated with cytologic diagnosis grading. FI values of cyclin D1 in normal group were not significantly different from that in mild esophageal dysplasia group. But FI values of TP1 between normal group and mild dysplasia group were significantly different ($P<0.05$).

The difference in FI value of cyclin D1 and TP1 among the mild, severe dysplasia and cancer groups was markedly significant ($P<0.01$), and the positive rate of cyclin D1 and TP1 protein expression among the four groups was also significantly different ($P<0.01$).

DISCUSSION

The results of this study showed that alteration of multiple molecular events occurred during esophageal epithelial carcinogenesis.

In this study, we found that the increased DI value was correlated with the precancerous lesion progression. Cellular DNA content and DNA ploid status were closely related to the severity of epithelial dysplasia. The rate of FCM DNA heteroploid increased significantly in the transition of dysplasia from mild to severe. Thus it is clear that cellular DNA content could reflect the pathologic changes in the epithelium of esophagus[4]. DNA content increase and DNA heteroploidy were the very important early signals of carcinogenesis[3,4].

Detection of FCM DNA heteroploidy might provide early cancerous information, before the morphologic evidence of cancer occurred[3,4]. It has been proved in previous studies that proliferation index (PI) is an indicator to reflect cell proliferation activity. In our study, the cell proliferation activity was closely related to the dysplasia degree of esophagus. PI was 16.4 % in mild dysplasia group, 17.9 % in moderate dysplasia group, 19.8 % in severe dysplasia group. The results proved that the rate and speed in cell proliferation were obviously increased during esophageal epithelial carcinogenesis.

In carcinogenesis, the precancerous cell lesion resulted in not only abnormal DNA change but also abnormal change in multiple genes and its product expression[3-14]. Previous studies demonstrated that lots of genetic alteration existed in esophageal precancer cells. P^{53} mutation in tumor-suppressor gene and ras P^{21} activated in tumor gene were revealed to be early molecular events during esophageal carcinogenesis[5,9,10,16]. In our studies, expression of P^{53} and P^{21} protein varied with dysplasia degree, FI value increased significantly from mild to severe dysplasia. Overexpression of P^{53} and P^{21} was closely related to early stages of esophageal carcinogenesis. The studies by Yasuda' s group also revealed that P^{53} mutation was a key molecular event in esophageal carcinogenesis[6]. The expression of P^{53} protein in our study accumulated at early stages of esophageal carcinogenesis.

The ras gene in normal cells possesses an important effect on cell growth and proliferation. The ras gene activation can speed up cell proliferation and malignant transformation. Overexpression of ras gene (P^{21}) occurred frequently in precancerous lesion of esophagus[15]. In our studies, expression of ras P^{21} varied with dysplasia degree. FI of ras P^{21} expression was significant among the normal, mild, severe dysplasia and cancer groups ($P<0.01$). It is suggested that ras P^{21} overexpression may be an important factor during esophageal epithelial carcinogenesis, and ras P^{21} may be a valuable marker at the early stages of carcinogenesis.

Recent studies have indicated that cyclin D1 is an oncogene which is related to the regulation of cell cycle[17-21]. The cyclin D1 gene product is a key protein which makes cells enter into proliferation condition, and cyclin D1 and CDK4 are composed of a complex which could functionally inhibit tumor suppressor gene P^{16} and Rb activity[23], thus promoting the cell proliferation ability. Many cells could enter into proliferation stage from G1 to S,G2M phase, so that excessive cell proliferation could cause carcinogenesis[19,23]. In this study, the expression of cyclin D1 protein increased in severe degree of esophageal epithelial dysplasia. The results indicate that overexpression of cyclin D1 plays an important role during esophageal carcinogenesis. An increase in cyclin D1 might result in an oncogene[22-25].

Recently, it has become a new research target of telomerase activity and its relation to carcinogenesis. It has been demonstrated that telomerase activity is increased in esophageal carcinoma. Telomerase activity could be used as an early stage marker of esophageal epithelial carcinogenesis[25-27]. Telomerase quantitative analysis of esophageal precancerous lesion has not been reported. In this study, telomerase content in esophageal epithelial dysplasia cells was quantitatively analyzed by flow cytometry. The results showed that telomerase content obviously increased in severe dysplasia group and cancer group. The positive rate of telomerase expression was 83.1 % in severe dysplasia group and 100 % in cancer group. Overexpression of telomerase might be an important factor and early molecular event to monitor the patients with high-risk of precancerous lesion during esophageal epithelial carcinogenesis[28-31]. Therefore, quantitative detection of telomerase content might be an early diagnostic method for esophageal cancer[27]. It is suggested that inhibition of telomerase activity might be a new therapy for cancer[29-31].

In summary, the DNA content, P^{53}, ras P^{21}, cyclin D1 and telomerase content showed significant changes during esophageal epithelial carcinogenesis, they could also become biomarkers to identify precancerous lesions in high-risk population at high incidence areas of esophageal cancer. These results indicate that combined analysis of multiple parameters can greatly increase the accuracy of early identification of esophageal cancer in the high risk population.

REFERENCES

1 **Moreto M**. Diagnosis of esophagogastric tumors. *Endoscopy* 2001; **33**: 1-7

2 **Bektas A**, Yasa MH, Kuzu I, Dogan I, Unal S, Ormeci N. Flow cytometric DNA analysis and immunohistochemical P^{53}, PCNA and histopathologic study in primary achalasia: preliminary results. *Hepatogastroenterology* 2001; **48**: 408-412

3 **Ma P**, Song M, Ren CS. Significance of P^{27} expressio and DNA contents in esophagus carcinoma. *Shiyong Aizheng Zazhi* 2001; **16**: 262-263

4 **Zuo LF**, Ling PZ, Qi FY, Wang JX, Ding ZW, Guo JW, Liu JH. Flow cytometric DNA analyses of epithelial dysplasia of the esophagus. *Analyt Quant Cytol Histol* 2000; **22**: 175-177

5 **Zhu MH**. Research advance and significance in biologic function of P^{53}. *Zhonghuan Binglixue Zazhi* 2000; **29**: 60-62

6 **Jin YL**, Zhang W, Liu BQ, Wang HP, Han SK, Han ST, Qu P, Li M, Ding ZW, Lin PZ. Abnormal expression of P^{53} Ki67, and iNOS in human esophageal carci moma in situ and pre-maligrant lesions. *Zhonghua Zhongliu Zazhi* 2001; **23**: 129-132

7 **Zuo LF**, Qi FY, Zhang LX, Lin PZ, Liu JH, Guo JW. The role of tumor suppressor gene P^{53} and cell-cycle relatedgene produces in the carcinogenesis of esophageal epithelia. *Zhonghua Xin Yixue* 2003; **4**: 1345-1347

8 **Yasuda M**, Kuwano H, Watanabe M, Toh Y, Ohno S, Suqimachi K. P^{53} expression in squamous dysplasia associated with carcinoma of the oesophagus: evidence for field carcinogenesis. *Br J Cancer* 2000; **83**: 1033-1038

9 **Geboes K**, Van Eyken P. The diagnosis of dysplasia and malignancy in Barrett's oesophagus. *Histophathology* 2000; **37**: 99-107

10 **Shimada Y**, Imamura M, Watanbae G, Uchida S, Harada H, Makino T, Kano M. Prognositic factors of oesophageal squamous cell carcinoma from the perspective of molecular biology. *Br J Cancer* 1999; **80**: 1281-1288

11 **Zhan XM**, Wang GX, Sun CW, Wang JY, Li L. Expression of P16, P21, P53 and cyclin D1, and their significance in esophageal carcinoma.*Shiyong Aizheng Zazhi* 2001; **16**: 36-38

12 **Itoshima T**, Fujiwara T, Waku T, Shao J, Kataoka M, Yarbrough WG, Liu TJ, Roth JA, Tanaka N, Kodama M. Induction of apoptosis in human esophageal cancer cells by sequential transfer of the wild-type P53and E2F-1 genes: involvement of P53 accumulation via ARF-mediated MDM2 down-regulation. *Clin Cancer Res* 2000; **6**: 2851-2859

13 **Kato H**, Yoshikawa M, Fukai Y, Tajima K, Masuda N, Tsukada K, Kuwano H, Nakajima T. An immunohistochemical study of P16. PRb. P21 and P53 proteins in human esophageal cancers. *Anticancer Res* 2000; **20**: 345-349

14 **Xu M**, Jin YL, Fu J, Huang H, Chen SZ, Qu P, Tian HM, Liu ZY, Zhang W. The abnormal expression of retinoic acid receptor-β, P53 and Ki 67 protein in normal, premalignant and malignant esophageal tissues .*World J Gastroenterol* 2002; **8**: 200-202

15 **Galiana C**, Fusco A, Martel N, Nishihira T, Hirohashi S, Yamasaki H. Possible role of activated ras genes in human esophageal carcinogenesis. *Int J Cancer* 1993; **54**: 978-982

16 **Qiao GB**, Han CL, Jiang RC, Sun CS, Wang Y, Wang YJ. Overexpression of P53 and its risk factors in esophageal cancer in urban areas of Xi'an. *World J Gastroenterol* 1998; **4**: 57-60

17 **Ikeda G**, Isaji S, Chandra B, Watanbe M, Kawarada Y. Prognostic significance of biologic factors in squamous cell carcinoma of the esophagus. *Cancer* 1999; **86**: 1396-1405

18 **Shinohara M**, Aoki T, Sato S, Takagi Y, Osaka Y, Koyanagi Y, Hatooka S, Shinoda M. Cell-cycle regulated factors in esophageal cancer. *Dis Esophagus* 2002; **15**: 149-154

19 **Ohbu M**, Kobayashi N, Okayasu I. Expression of cell cycle regulatory proteins in the multistep process of oesophageal carcinogenesis: stepwise over-expression of cyclin E and P53, reduction of P21(WAF1 / CIP1) and dysregulation of cyclin D1 and P27 (KIP1) . *Histopathology* 2001; **39**: 589-596

20 **Saeki H**, Ohno S, Miyazaki M, Araki K, Egashira A, Kawaguchi H, Watanabe M, Morita M, Sugimachi K. P53 protein accumulation in multiple oesophageal squamous cell carcinoma: Relationship to risk factors. *Oncology* 2002; **62**: 175-179

21 **Fujii S,** Tominaga O, Nagawa H, Tsuno N, Nita ME, Tsuruo T, Muto T. Quantitative analysis of the cyclin expression in human esophageal cancer cell lines. *J Exp clin Cancer Res* 1998; **17**: 491-496

22 **Shamma A**, Doki Y, Shiozaki H, Tsujinaka T, Yamamoto M, Inoue M, Yano M, Monden M. Cyclin D1 overexpression in esophageal dysplasia:a possible biomarker for carcinogenesis of esophageal squamous cell Carcinoma. *Int J Oncol* 2000; **16**: 261-266

23 **Liu SX**, Zuo LF, Zhang JY, Guo JW, Liu JH, Li YM. The expression of Rb, P21 and cyclin D1 in 41 esophageal cancers. *Zhonghua Xin Yixue* 2002; **3**: 97-99

24 **Toyoda H**, Nakamura T, Shinoda M, Suzuki T, Hatooka S, Kobayashi S, Ohashi K, Seto M, Shiku H, Nakamura S. Cyclin D1 expression is useful as a prognostic indicator for advanced esophageal Carcinomas bu not for superficial tumors. *Dig Dis Sci* 2000; **45**: 864-869

25 **Zhang LX**, Qi FY, Zuo LF, Lin PZ, Guo JW, Liu JH. The expression of $P^{16,}$ cyclin D1 and DNA content analysis in the carcinogenesis of esophageal epithelial cells. *Zhonghua Xin Yixue* 2001; **2**: 1-3

26 **Wu MY**, Wu XY, Zhuang CX. The expression of human telomerase reverse transcriptase in esophageal squamous cell carcinoma and paracancerous esophageal epithelium. *Shiyong Aizheng Zazhi* 2003; **18**: 132-134

27 **Zhang LX**, Qi FY, Zuo LF, Lin PZ, Guo JW, Liu JH. The quantitative analysis of telomerase and DNA ploid in the carcinogenesis of esophageal epithelium. *Zhonghua Xin Yixue* 2001; **2**: 193-195

28 **Shen ZY**, Xu LY, Li EM, Cai WJ, Chen MH, Shen J, Zeng Y. Telomere and telomerase in the initial stage of immortalization of esophageal epithelial cell. *World J Gastroenterol* 2002; **8**: 357-362

29 **Koyanagi K**, Ozawa S, Ando N, Takeuchi H, Ueda M, Kitajima M. Clinical significance of telomerase activity in the non cancerous epithelial region of oesophageal squamous cell carcinoma. *Br J Surg* 1999; **86**: 674-679

30 **Koyanagi K**, Ozawa S, Ando N, Mukai M, Kitagawa Y, Ueda M, Kitajima M. Telomerase activity as an indicator of malignany potential in iodine-nonreactive lesion of the esophagus. *Cancer* 2000; **88**: 1524-1529

31 **Rudolph P**, Schubert C, Tamm S, Heidorm K, Hauschild A, Michalska I, Majewski S, Krupp G, Jablonska S, Parwaresch R. Telomerase activity in melanocytic lesions: A potential marker of tumor biology. *Am J Path* 2000; **156**: 1425-1432

Edited by Wang XL and Zhu LH

P.O.Box 2345, Beijing 100023,China
Fax: +86-10-85381893
E-mail: wjg@wjgnet.com www.wjgnet.com

World J Gastroenterol 2003;9(11):2413-2418
World Journal of Gastroenterology
 ISSN 1007-9327

• GASTRIC CANCER •

Roles of PLC-g2 and PKCa in TPA-induced apoptosis of gastric cancer cells

Bing Zhang, Qiao Wu, Xiao-Feng Ye, Su Liu, Xiao-Feng Lin, Mu-Chuan Chen

Bing Zhang, Qiao Wu, Xiao-Feng Ye, Su Liu, Xiao-Feng Lin, Mu-Chuan Chen, Key Laboratory of the Ministry of Education for Cell Biology and Tumor Cell Engineering, School of Life Sciences, Xiamen University, Xiamen 361005, Fujian Province, China
Bing Zhang, Medical school, Xiamen University, Xiamen 361005, Fujian Province, China
Supported by the National Natural Science Foundation of China (No. 30170477), the National Outstanding Youth Science Foundation of China (No.39825502), and the Natural Science Foundation of Fujian Province (C0110004)
Correspondence to: Dr. Qiao Wu, Key Laboratory of the Ministry of Education for Cell Biology and Tumor Cell Engineering, School of Life Sciences, Xiamen University, Xiamen 361005, Fujian Province, China. xgwu@xmu.edu.cn
Telephone: +86-592-2182542 **Fax:** +86-592-2086630
Received: 2003-05-13 **Accepted:** 2003-06-27

Abstract

AIM: To investigate the roles of PLCγ2 and PKCα in TPA-induced apoptosis of gastric cancer cells.

METHODS: Human gastric cancer cell line MGC80-3 was used. Protein expression levels of PLCγ2 and PKCα were detected by Western blot. Protein localization of PLCγ2 and PKCα was shown by immunofluoscence analysis under laser-scanning confocal microscope. Apoptotic morphology was observed by DAPI fluorescence staining, and apoptotic index was counted among 1 000 cells randomly.

RESULTS: Treatment of gastric cancer cells MGC80-3 with TPA not only up-regulated expression of PLC-γ2 protein, but also induced PLC-γ2 translocation from the cytoplasm to the nucleus. However, this process was not directly associated with apoptosis induction. Further investigation showed that PKCa translocation from the cytoplasm to the nucleus was correlated with initiation of apoptosis. To explore the inevitable linkage between PLC-γ2 and PKCα during apoptosis induction, PLC inhibitor U73122 was used to block PLC-γ2 translocation, in which neither stimulating PKCα translocation nor inducing apoptosis occurred in MGC80-3 cells. However, when U73122-treated cells were exposed to TPA, not only PLC-γ2, but also PKCα was redistributed. On the other hand, when cells were treated with PKC inhibitor alone, PLC-γ2 protein was still located in the cytoplasm. However, redistribution of PLC-γ2 protein occurred in the presence of TPA, no matter whether PKC inhibitor existed or not.

CONCLUSION: PLC-γ2 translocation is critical in transmitting TPA signal to its downstream molecule PKCα. As an effector, PKCα directly promotes apoptosis of MGC80-3 cells. Therefore, protein translocation of PLCγ2 and PKCα is critical event in the process of apoptosis induction.

Zhang B, Wu Q, Ye XF, Liu S, Lin XF, Chen MC. Roles of PLC-γ2 and PKCα in TPA-induced apoptosis of gastric cancer cells. *World J Gastroenterol* 2003; 9(11): 2413-2418
http://www.wjgnet.com/1007-9327/9/2413.asp

INTRODUCTION

Once binding to the cell surface receptors, many extracellular signaling molecules could elicit intracellular responses by activating inositol phospholipid-specific phopholipase C (PLC)[1,2]. Activated PLC could catalyze the hydrolysis of phosphatidylinositol 4,5-biphosphate (PIP_2) to diacylglycerol (DAG) and inositol 1, 4, 5-triphosphate (IP_3). DAG and IP3 are second messengers, the former could function to activate protein kinase C (PKC), and the latter could stimulate release of Ca^{2+} from internal stores[1,3-5]. This bifurcating pathway constitutes the cornerstone of a transmembrane signal transduction mechanism that was known to regulate a large array of cellular processes[5-9].

Ten types of PLC isoform have been divided into three types, β, γ and δ[4-6,10,11]. One PLC isoform, PLC-γ, is a substrate of epidermal growth factor (EGF) receptor, and its catalytic activity could be stimulated by tyrosine phosphorylation[12]. PLC-γ has been implicated in mitogenic signaling by platelet-derived growth factor (PDGF) receptor. Through the pleiotropic actions of IP_3 and DAG, PLC-γ could participate in regulation of cell proliferation and differentiation[13]. PLC-γ overexpression could favor cell survival in response to acute oxidative stress[14,15]. In rat pheochromocytoma PC12 cells, overexpression of PLC-γ could inhibit apoptosis induced by short wave length ultraviolet radiation[16].

Protein kinase C (PKC) could play a variety of regulatory roles in proliferation, differentiation, apoptosis, gene expression, membrane transportation, and signal transduction[17-19]. There have been at least 11 distinct PKC isoforms[20]. In many tissues, both PKC activation and Ca2+ mobilization could act synergistically to evoke some cellular responses[21-24]. For example, activation of PKC and increase in Ca^{2+} were the "on" signals for T-cell activation[27,28]. By contrast, this PKC activator could also act as a negative regulator of T-cell activation[27,28]. Thus, PKC activation in T-cells has bidirectional effects on the cellular activation process.

Several evidences suggest that activation of PKC could attenuate receptor-coupled PLC activity in certain types of cell, providing a negative feedback signal to limit the magnitude and duration of receptor signaling[3,5]. Although such a regulatory mechanism has not been fully understood, it is possible that the targets might include receptors, G protein, PTK, protein tyrosine phosphatase and PLC itself[5]. Phosphorylation of Thr-654 of the EGF receptor by PKC reduced the ability of the receptor tyrosine kinase to phosphorylate PLC-γ, thereby preventing PLC-γ activation[29]. A decrease in the extent of tyrosine phosphorylation of PLC-γ has also been proved to be the mechanism by which the PKC activator, TPA and cAMP could attenuate the PIP2 hydrolysis induced by TCR[30]. Thus, interaction between PLC-γ and PKC is related to PLC-γ phosphorylation.

To date, little is known about the molecular event of PLC-γ translocation, and the functional consequences of PLC-γ in response to extracellular signal stimulation. It is generally accepted that PLC-γ localizes and functions in cytosol. EGF or PDGF treatment of cells could induce translocation of PLC-γ1 from a predominantly cytosolic localization to membrane

fraction[31], showing a preliminary clue that the function of PLC-γ may be in relation with its intracellular changes. In this study, we found that 12-O-tetradecanoylphorbol-1, 3-acetate (TPA) not only up-regulated the expression level of PLC-γ2, but also induced PLC-γ2 translocation from the cytoplasm to the nucleus in gastric cancer cells MGC80-3. In addition, according to our previous studies concerning the critical role of PKC-associated signaling pathway in promoting apoptosis of gastric cancer cell[32], we hypothesized that PLC-γ2 may play an important role in transmitting TPA signal to PKCα, which finally lead to apoptosis induction in gastric cancer cells. This notion may provide a novel strategy for exploring the cross-talk between PLC-γ2 and PKCα in apoptosis.

MATERIALS AND METHODS

Cell line and culture condition

Human gastric cancer cell line, MGC80-3 was established by Cancer Research Center, Xiamen University[33]. The cells were maintained in RPMI-1640 medium, supplemented with 10 % FCS, 1 mmol/L glutamine, and 100 U/ml penicillin.

Western blot analysis[34]

The cells were harvested, and suspended in RIPA buffer (10 mmol/L Tris (pH7.4), 150 mmol/L NaCl, 1 % Triton X-100, 1 % deoxycholic acid, 0.1 % SDS, 5 mmol/L EDTA (pH8.0), 1 mmol/L PMSF). Protein concentration was determined using the Bio-Rad protein assay system according to the manufacturer' s instructions (Bio-Rad Hereules, CA). 50 μg protein was subjected to SDS-PAGE and transferred to nitrocellulose membrane for Western blot analysis. The membrane was subsequently blocked with 5 % dry milk in TBS-T and then immunnoblotted with the responding antibody. Binding was detected by using the ECL kit (Pierce) according to the manufacturer' s instructions.

Apoptosis analysis[32]

The cells were trypsinized, and washed in PBS. The harvested cells were fixed in 3.7 % paraformaldehyde on ice, washed in PBS and stained with 50 μg/ml of 4, 6-diamidino-2-phenylindole (DAPI, Sigma) containing 100 μg/ml of DNase-free RNase A per ml. The cells were observed under fluorescence microscope. Apoptotic cells were counted among 1 000 cells randomly. The apoptotic index was the mean of three independent experiments.

Immunofluorescence analysis[35]

The cells were cultured on a cover glass overnight. After washed in PBS, the cells were fixed in 4 % paraformaldehyde. To display PLC-γ2 or PKCα protein, the cells were incubated first with anti-PLC-γ2 or anti-PKCα antibody (Santa Cruz), and then reacted with their corresponding FITC-conjugated anti-IgG (Pharmingen) as secondary antibodies. To visualize the nuclei, the cells were stained with propidium iodine (PI, 50 μg/ml) containing 100 μg of DNase-free RNase A per ml. Fluorescent image was observed under laser-scanning confocal microscope (Bio-Rad MRC-1024ES).

RESULTS

Expression and translocation of PLC-g2 in response to TPA

To determine the effect of TPA on PLC-γ2 protein expression, Western blot analysis was carried out. As shown in Figure 1A, PLC-γ2 protein was normally expressed in MGC80-3 cells. When exposed to TPA for different time, expression level of PLC-γ2 protein was increased in a time-dependent manner (Figure 1A), implying that PLC-γ2 might play a role in response to TPA. To examine whether redistribution of PLC-γ2 protein also occurred in response to TPA, immunofluorescent localization of PLC-γ2 protein was conducted and observed by laser-scanning confocal microscope. The result illustrated that in intact MGC80-3 cells, PLC-γ2 protein was more abundant in cytoplasm, and formed a much brighter circle a round the nuclear membrane (Figure 1B). After treatment of TPA for different time, PLC-γ2 protein was translocated from the cytoplasm to the nucleus by degrees (Figure 1B). To further confirm this translocation, cytoplasmic and nuclear protein fractions were prepared, and expression level of PLC-γ2 protein was analyzed by Western blot. Figure 1C shows that PLC-γ2 protein in intact cells mainly appears in the cytoplasmic fraction, and only a trace amount in the nuclear fraction. However, TPA-treatment changed the proportion of PLC-γ2 protein between the two fractions and such a change was time-dependent. After 48 hr TPA treatment, PLC-γ2 protein could only be detected in the nuclear fraction (Figure 1C). Clearly, this result was in accordance with that of Figure 1B, indicating that transloation of PLC-γ2 protein by TPA occurred in MGC80-3 cells.

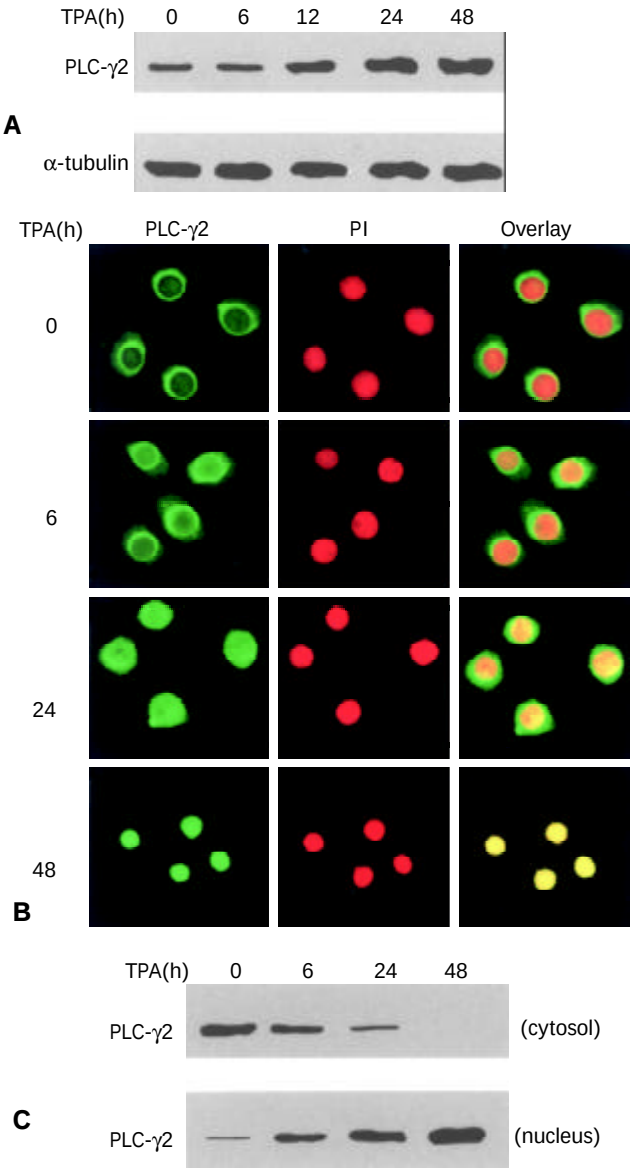

Figure 1 Expression and redistribution of PLC-γ2 in response to TPA. A: Effect of TPA on PLC-γ2 protein expression. Cells were treated with TPA (100 ng/ml) for indicated time, and expression level of PLC-γ2 protein was analyzed by Western blot. α-tubulin was used as a control to quantify the amount of

protein used in each lane. B: Translocation of PLC-γ2 in response to TPA. Cells were treated with TPA for indicated time, then immunostained with corresponding antibodies or dye as described in Materials and Methods. The fluorescent images were observed under laser-scanning confocal microscope. C: Redistribution of PLC-γ2 protein in response to TPA. The nuclear and cytosolic fractions were prepared as described in Materials and Methods.

PLC-γ2 expression was not required for apoptosis induction by TPA

Since TPA could induce apoptosis in many types of cancer cell lines[32,35-37], it would be interesting to know whether activation of PLC-γ2 was a necessary link for apoptosis induction by TPA. A PLC-specific inhibitor U73122[38] was thus used upon gastric cancer cells. Prior to be stimulated with TPA, U73122 partially repressed the expression level of PLC-γ2 protein (Figure 2A). In the presence of U73122, TPA-induced increase of PLC-γ2 expression was also blocked. Even after TPA treatment was prolonged for 48 hr, the expression level of PLC-γ2 was always lower than the control or TPA treatment alone (Figure 2A). In parallel, apoptosis of MGC80-3 cells was examined by DAPI staining. When the cells were treated with TPA alone, apoptotic cells became smaller, the nuclei became condensed and fragmented with bright chromatins. Importantly, an increased apoptotic index was clearly shown with the extension of TPA treatment (Figure2B: TPA). However, no such a change was observed in cells treated with U73122 alone (Figure 2B: U73122). By contrast, when cells pretreated with U73122, followed by TPA stimulation, many apoptotic cells were still seen, which not only showed morphological changes similar to those treated with TPA alone, but also had an increased apoptotic index with the extension of TPA treatment (Figure 2B: U73122+TPA). Therefore, these results showed that additional expression of PLC-γ2 protein was not required for TPA-induced apoptosis in MGC80-3 cells.

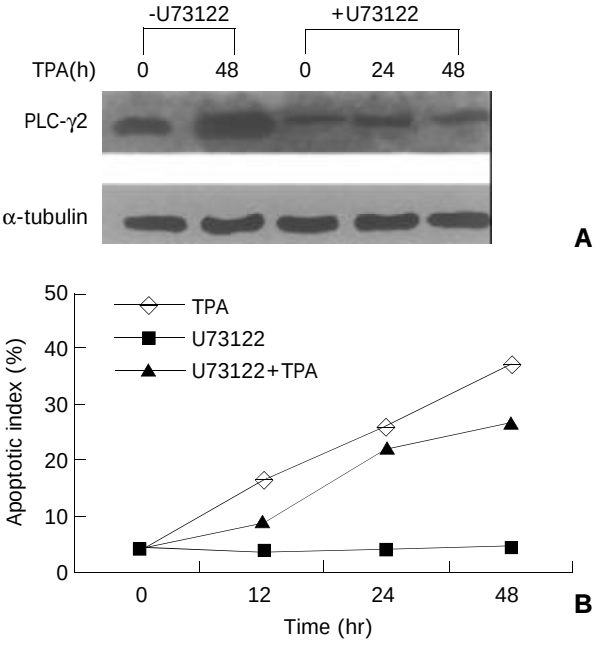

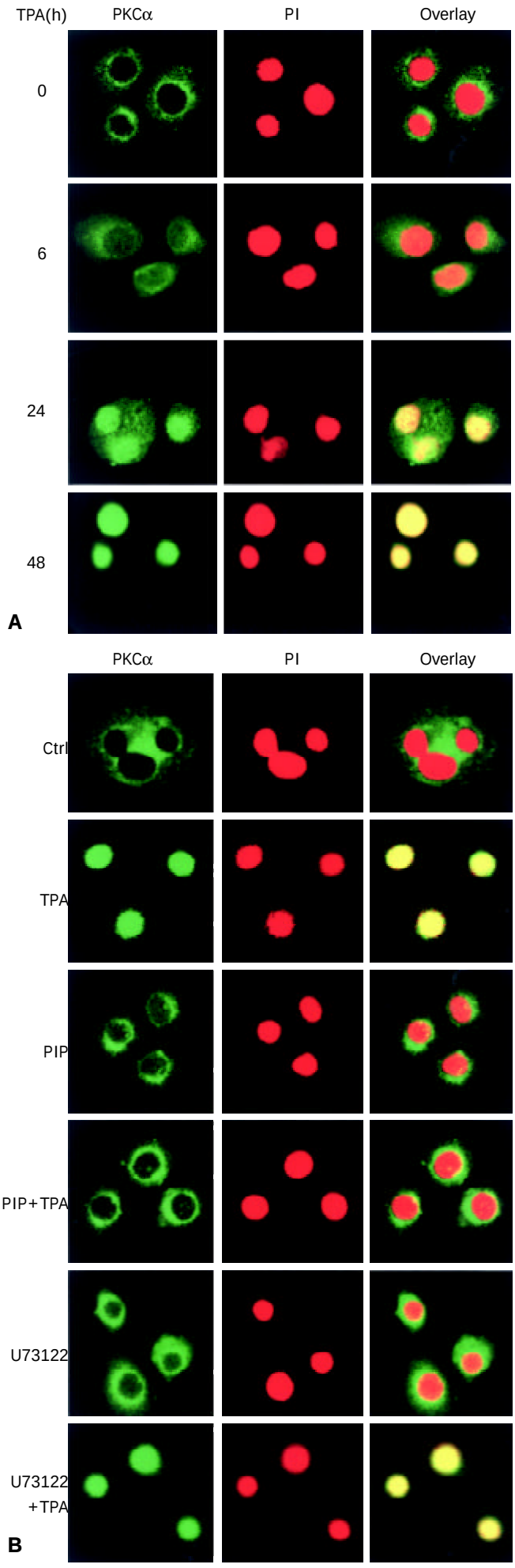

Figure 2 Effect of PLC-γ2 protein expression on apoptosis inducted by TPA. A: Effect of PLC-specific inhibitor U73122 on PLC-γ2 protein expression detected by Western blot. Cells were pretreated with or without U73122 (10^{-3} mmol/L) for 3 hr, and followed by TPA for indicated time. B: Analysis of apoptotic index. Cells were pretreated with or without U73122 for 3 hr, and then exposed to TPA for indicated time. Apoptotic cells were counted among 1 000 cells randomly.

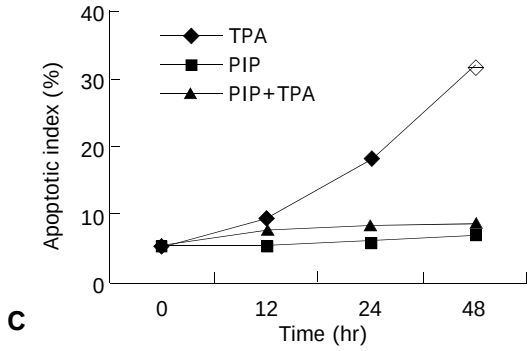

Figure 3 Translocation of PKCα protein in the process of apoptosis induced by TPA. A: Redistribution of PKCα protein. Cells were treated with TPA for indicated time, then immunostained with corresponding antibodies or dye as described in Materials and Methods. The images were observed under laser-scanning confocal microscope. B: Effects of various inhibitors, including PKC-specific inhibitor (PIP., 12 μmol/L) and PLC-specific inhibitor (U73122), on redistribution of PKCα. The detecting method was the same as described in Figure 3A. C: Analysis of apoptotic index. The method was similar as in Figure 2B.

PKCα translocation was directly associated with induction of apoptosis by TPA

The consequent question was that since TPA could induce rapid expression of PLC-γ2 protein which seemed to be not critical in TPA-induced apoptosis in MGC80-3 cells, then, what was the role of rapidly expressed PLC-γ2 protein in TPA-induced event? As PKC was a downstream molecule of PLC[3,4], it was inferred that PLC-γ2 might indirectly play its final effect through the downstream PKC signaling pathway in relation to TPA-induced apoptosis. To test this possibility, the effects of TPA on PKCα were investigated. Firstly, the expression of PKCα protein was determined by Western blot analysis. The result showed that PKCα was intrinsically expressed in MGC80-3 cells, but its expression was not changeable by TPA (data not shown). Secondly, the possible TPA-induced translocation of PKC in MGC80-3 cells was observed. PKCα protein was shown to localize in cytoplasm (Figure 3A). However, TPA treatment stimulated the translocation of PKCα protein from cytoplasm to nucleus in a time-dependent manner. After 48 hr of TPA treatment, cellular PKCα protein was completely translocated into the nucleus, showing a unique yellow color (Figure 3A). Finally, to investigate the behavior of PKCα translocation, PKC-specific inhibitor, a PKC inhibitor peptide(PIP)[39], was used. As expected, PKC inhibitor peptide could not induce PKCα protein translocated to the nucleus (Figure 3B, PIP.), even plus TPA for 48 hr it no longer initiated PKCα protein translocation (Figure 3B, PIP+TPA).

Since TPA could regulate redistribution, but not expression of PKCα protein, it would be attractive to ask whether redistribution of PKCα was in action in TPA-induced apoptosis. The results showed that TPA could no longer induce apoptosis when translocation of PKCα was blocked by PKC inhibitor peptide. Even though these cells were subsequently treated by TPA for 48 hr, the apoptotic index was obviously reduced reduced as compared with the TPA treatment alone (Figure 3C), suggesting that translocation of PKCα protein into the nucleus might be intrinsic in the mechanism of TPA-induced apoptosis.

PKCα was a downstream factor of PLC-γ2

It was then necessary to probe into the intrinsic mechanism of whether there was some inevitable linkage between PLC-γ2 and PKCα in the process of TPA-induced apoptosis. Since enhanced expression of PLCγ2 protein was not required for apoptosis induction (Figure 2), we therefore focused on the translocation behavior of PLC-γ2 with regard to the TPA-induced apoptosis effect. Out of our expectation, when cells were pre-treated with PLC-specific inhibitor U73122 for 3 hr alone, both PLC-γ2 and PKCα proteins did not redistribute (Figures 3B and 4A, U73122). However, when cells were exposing to TPA for 48 hr, not only PLC-γ2 protein but also PKCα protein were translocated into the nucleus (Figures 3B and 4A, U73122+TPA), although expression level of PKCα protein was not changed (Figure 4B). Together with the results in Figure 2, it was suggested that PLC-γ2 might function in passing TPA message to its downstream molecule PKCα in gastric cancer cells.

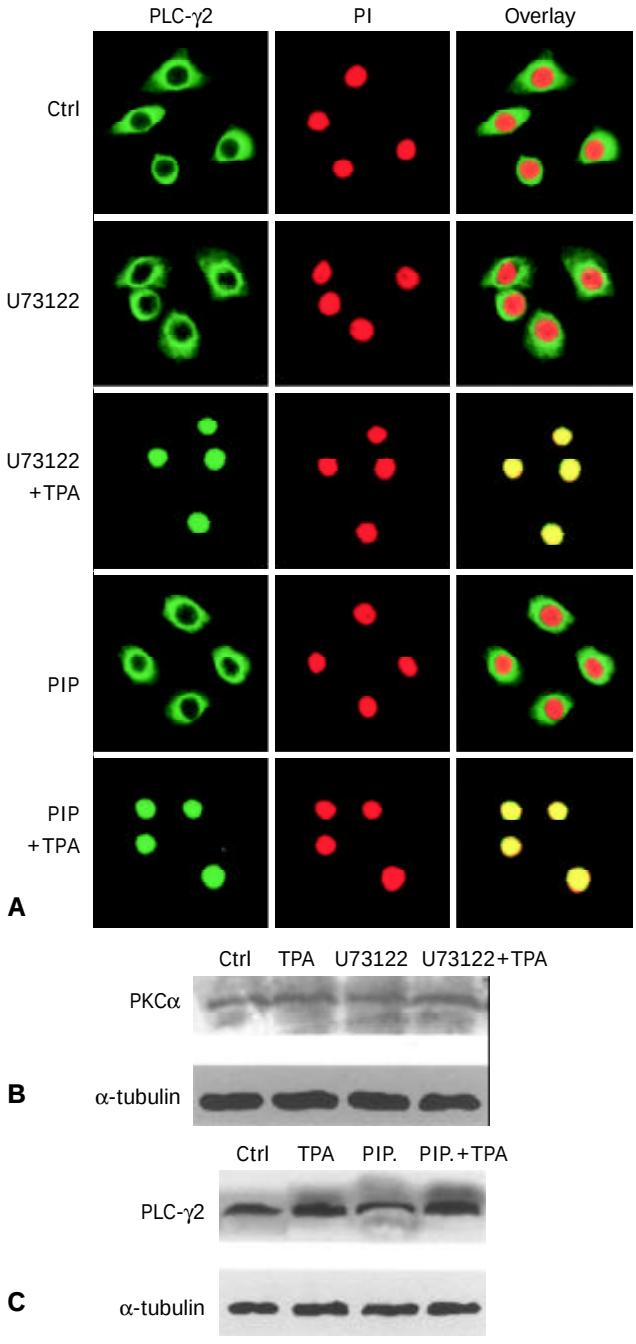

Figure 4 Correlation between PLC-γ2 and PKCα in their redistribution. A: Effects of PKC- and PLC-specific inhibitors on PLC-γs redistribution. The Method was as described in Figure 3B. B: Effects of PKC- and PLC-specific inhibitors on PKCα expression detected by Western blot. C: Effects of PKC- and PLC-specific inhibitors on PLC-γ2 expression.

On the other hand, PKC-specific inhibitor was also used to test its role in the expression of PLC-γ2 protein. When cells were treated with PKC inhibitor peptide (PIP) for 2 hr, PLC-γ2 protein was still located in the cytoplasm (Figure 4A, PIP). However, followed by TPA treatment for 48 hr, translocation of PLC-γ2 protein into the nucleus was not blocked by this inhibitor (Figure 4A: PIP+TPA). Similar result was observed in Western blot analysis, in which the expression level of PLC-γ2 protein was enhanced by TPA, no matter whether PKC inhibitor existed or not (Figure 4C). Taken together, all these findings above convincingly indicated that PKC inhibitor-induced inhibition of PKCα protein (mainly its translocation) and TPA-induced PLC-γ2 protein expression and translocation were two separate events. It also suggested that induction of PLC-γ2 protein translocation was a critical event in signal transmission between TPA and PKCα.

DISCUSSION

PLC-γ has been reported to be activated and up-regulated in response to external signals[13,15,40-44]. Most of these previous studies focused on PLC-γ2 phosphorylation and the relevant growth factor receptor(s), but its physiologic function and signaling pathway were rarely concerned. In the present study, we found that the enhanced expression of PLC-γ2 by TPA was not directly correlated to apoptosis induction. PLC-γ exerted its influence on intracellular process largely through the initiation of second messengers IP3 and DAG, and the subsequent Ca^{2+} mobilization and PKC activation. More importantly, these PLC-γ-induced chain reactions could be stimulated by some external stimuli[40,41]. Taking this fact into account, we therefore turned to investigate the possible regulatory mechanism of PLC-γ2 not correlated with its expression level.

PLC-specific inhibitor U73122 alone could partially suppress the expression of PLC-γ2 protein, but not induce apoptosis in MGC80-3 cells. However, TPA could still induce apoptosis in U73122-pretreated MGC80-3 cells, even though the expression of PLC-γ2 was in its supressed state, indicating that up-regulation of PLCγ2 expression was not required for apoptosis induced by TPA. However, TPA-induced apoptosis in MGC80-3 cells depended on PKCα protein translocation from cytoplasm into nucleus. When translocation of PKCα protein was blocked by its specific inhibitor PKC inhibitor peptide, the apoptosis decreased dramatically even in the presence of TPA. Therefore, these evidences strongly suggest that PLC-γ2 and PKCα can exert distinct effects in response to TPA, and regulation of PKCα protein translocation is closely associated with apoptosis induction.

We have indicated that TPA could promote PLC-γ2 translocation from cytoplasm to nucleus in a time-dependent manner, so it is interesting to figure out why PLC-γ2 is regulated (particularly its translocation) in response to TPA, and what the underlying functional implication is. Recently, some important evidences revealed that PLC-γ2 was critical for transmission of the B-cell antigen receptor complex (BCR)-dependent signals that led to the nuclear translocation of NF-κB[45], and PLC-γ1 was important for transducing survival signals against the cytotoxic effect of oxidant exposure[15]. These studies strongly imply that PLC-γ is capable of transducting signal, leading to translocation of its downstream molecule. To clarify whether TPA-induced apoptosis via PKC pathway was correlated with PLC-γ2, we investigated the effect of PLC-γ2 protein translocation on promoting PKCa translocation and initiating apoptosis. PLC-inhibitor U73122 alone could block the expression of PLC-γ2, but did not initiate the translocation of PLC-γ2 protein and induce PKCα expression, in which neither PKCα translocation nor apoptotic process could be detected. It is thus conceivable that PKCα translocation and cell apoptosis induced by TPA are PLC-γ2 translocation dependent in gastric cancer cells. Furthermore, our present study strongly supports the view that protein redistribution is an important event, which is critical for the function of protein.

Some literatures pointed out that down regulation of surface receptor expression represented an obvious mechanism by which PKC might block PLC activation[29,30]. For example, in Jurkat T cells, activation of PKC by PKC-stimulating agonists resulted in a decrease in its tyrosine phosphorylation, which was responsible for the apparently decreased PLC activity[5]. By contrast, in the present study, the relation between PLC-γ2 and PKCα seemed to be inter-dependent and synergistic. Our results showed a definite linkage between PLC-γ2 and PKCα translocation, and the synergistic effect of PLC-γ2 and PKCα in the initiation of apoptosis in MGC80-3 cells induced by TPA. In addition, the fact that pretreatment of cells with PKC inhibitor did not affect PLC-γ2 activation and translocation by TPA was consistent with the observation in which pretreatment of 293 cells for 30 min with PKC inhibitor Gö6976 did not stimulate PLC activation by EGF[46], demonstrating that PKC is a downstream molecule of PLCγ pathway. Taken together, PLC-γ2 functions in signal transmission to initiate TPA-induced apoptosis via PKCα pathway.

In summary, PLC-γ2 and its downstream molecule PKCα are essential for initiating TPA-induced apoptosis in gastric cancer cells. Translocation of PLC-γ2 and PKCα proteins is critical events in the process of apoptosis. In the cross-talk between TPA, PLC-γ2 and PKCα, PLCγ2 receives TPA message, then transmits it to PKCα. PKCα functions as an effector, directly promoting apoptosis of MGC80-3 cells. This is a novel concept for PLC-γ2 and PKCα functions, which will help us to get further insights into the relationship between PLC-γ2/PKCα and the subsequent cellular events.

REFERENCES

1 **Rana RS**, Hokin LE. Role of phosphoinositides in transmembrane signaling. *Physiol Rev* 1990; **70**: 115-164
2 **Majerus PW**. Inositol phosphate biochemistry. *Annu Rev Biochem* 1992; **61**: 225-250
3 **Rhee SG**, Bae YS. Regulation of phosphoinositide-specific phospholipase C isozymes. *J Biol Chem* 1997; **272**: 15045-15048
4 **Noh DY**, Shin SL, Rhee SG. Phosphoinositide-specific phospholipase C and mitogenic signaling. *Biochim Biophys Acta* 1995; **1242**: 99-113
5 **Rhee SG**, Choi KD. Regulation of inositol ignalingids-specific phospholipase C Isozymes. *J Biol Chem* 1992; **267**: 12393-12396
6 **Berridge MJ**. Inositol trisphosphate and calcium signaling. *Nature* 1993; **361**: 315-325
7 **Nishizuka Y**. Protein kinase C and lipid signaling for sustained cellular responses. *FASEB J* 1995; **9**: 484-496
8 **Berridge MJ**. Neuronal calcium signaling. *Neuron* 1998; **21**: 13-26
9 **Ji QS**, Winnier GE, Niswender KD, Horstman D, Wisdom R, Magnuson MA, Carpenter G. Essential role of the tyrosine kinase substrate phospholipase C-γ1 in mammalian growth and development. *Proc Natl Acad Sci U S A* 1997; **94**: 2999-3003
10 **Cockcroft S**, Thomas GMH. Inositol-lipid-specific phospholipase C isoenzymes and their differential regulation by receptors. *Biochem J* 1992; **288**: 1-14
11 **Lee SB**, Rhee SG. Significance of PIP2 hydrolysis and regulation of phospholipase C isozymes. *Curr Opin Cell Biol* 1995; **7:** 183-189
12 **Nishibe S**, Wahl MI, Wedegaertner PB, Kim JW, Rhee SG, Carpenter G, Kim KJW. Selectivity of phospholipase C phosphorylation by the epidermal growth factor receptor, the insulin receptor, and their cytoplasmic domains. *Proc Natl Acad Sci U S A* 1990; **87**: 424-428
13 **Kayali AG**, Eichhorn J, Haruta T, Morris AJ, Nelson JG, Vollenweider P, Olefsky JM, Webster NJG. Association of the insulin receptor with phospholipase C-γ(PLC-γ1) in 3T3-L1 adipocytes suggests a role for PLCr in metabolic signaling by

insulin. *J Biol Chem* 1998; **273**: 13808-13818
14 **Lee YH**, Kim SY, Kim JR, Yoh KT, Baek SH, Kim MJ, Ryu SH, Suh PG, Kim JH. Overexpression of phospholipase C beta-1 protects NIH3T3 cells from oxidative stress-induced cell death. *Life Sci* 2000; **67**: 827-837
15 **Wang XT**, McCullough KD, Wang XJ, Carpenter G, Holbrook NJ. Oxidative stress-induced phospholipase C-γ1 activation enhances cell survival. *J Biol Chem* 2001; **276**: 28364-28371
16 **Lee YH**, Kim S, Kim J, Young KK, Kim MJ, Ryu SIL, Suh P. Overexpression of phospholipase C-gamma1 suppresses UVC-induced apoptosis through inhibition of c-fos accumulation and c-Jun N-terminal kinase activation in PC12 cells. *Biochim Biophys Acta* 1999; **1440**: 235-243
17 **Han Y**, Han ZY, Zhou XM, Shi R, Zheng Y, Shi YQ, Miao JY, Pan BR, Fan DM. Expression and function of classical protein kinase C isoenzymes in gastric cancer cell line and its drug-resistant sublines. *World J Gastroenterol* 2002; **8**: 441-445
18 **Chen Y**, Wu Q, Song SY, Su WJ. Activation of JNK by TPA promotes apoptosis via PKC pathway in gastric cancer cells. *World J Gastroenterol* 2002; **8**: 1014-1018
19 **Joanne G**, Harald M, Walter K, Frederic Mushinski J. Immunocytochemical localization of eight protein kinase C isozymes overexpressed in NIH 3T3 fibroblasts. Isoform-specific association with microfilaments, Golgi, endoplasmic reticulum, and nuclear and cell membranes. *J Biol Chem* 1995; **270**: 9991-10001
20 **Shao RG**, Cao CX, Pommier Y. Activation of PKCa downstream from caspases during apoptosis induced by 7-hydroxystaurosporine or the topoisomerase inhibitors, camptothecin and etoposide, in human myeloid leukemia HL-60 cells. *J Biol Chem* 1997; **272**: 31321-31325
21 **Nishizuka Y**. Turnover of inositol phospholipids and signal transduction. *Science* 1984; **225**: 1365-1370
22 **Majerus PW**, Connolly TM, Dickmyn H, Ross TS, Bross TE, Ishii H, Bansal VS, Wilson DB. The Metabolism of phosphoinositide-derived messenger molecules. *Science* 1986; **234**: 1519-1526
23 **Isokov N**, Mally MI, Scholz W, Altman A. T-lymphocyte activation: the role of protein kinase C and the bifurcating inositol phospholipid signal transduction pathway. *Immunol Rev* 1987; **95**: 89-111
24 **Kaibuchi K**, Takai Y, Nishizuka Y. Protein kinase C and calcium ion in mitogenic response of macrophage- depleted human peripheral lymphocytes. *J Biol Chem* 1985; **260**: 1366-1369
25 **Albert F**, Hua C, Truneh A, Pierres M, Schmitt-Verhulst AM. Distinction between antigen receptor and IL2 receptor triggering events in the activation of alloreactive T cell clones with calcium ionophore and phorbol ester. *J Immunol* 1985; **134**: 3649-3655
26 **Isakov N**, Altman A. Human T lymphocyte activation by tumor promoters: role of protein kinase C. *J Immunol* 1987; **138**: 3100-3107
27 **Abraham RT**, Ho SN, Harna TJ, Rusovick KM, McKean D. Inhibition of T-cell antigen receptor-mediated transmembrane signaling by protein kinase C activation. *Mol Cell Biol* 1988; **8**: 5448-5458
28 **Mills GB**, May C, Hill M, Ebanks R, Roifman C, Mellors A, Gelfand EW. Physiologic activation of protein kinase C limits IL-2 secretion. *J Immunol* 1989; **142**: 1995-2003
29 **Decker SJ,** Ellis C, Pawson T, Velu T. Effects of substitution of threonine 654 of the epidermal growth factor receptor on epidermal growth factor-mediated activation of phospholipase C. *J Biol Chem* 1990; **265**: 7009-7015
30 **Park DJ**, Min HK, Rhee SG. Inhibition of CD3-linked phospholipase C by phorbol ester and by camp is associated with decreased phosphotyrosine and increased phosphoserine contents of PLC-1. *J Biol Chem* 1992; **267**: 1496-1501
31 **Todderud G**, Wahl MI, Rhee SG, Carpenter G. Stimulastion of phospholipase C-gamma 1 memebrane association by epidermal growth factor. *Science* 1990; **249**: 296-299
32 **Wu Q**, Liu S, Ding L, Ye XF, Su WJ. PKCα translocation from mitochondria to nucleus is closely related to induction of apoptosis in gastric cancer cells. *Science In China* 2002; **45:** 237-244
33 **Wang KH**. An in vitro cell line (MGc80-3) of a pooly differentiated mucoid adenocarcinoma of human stomach. *Shiyan Shengwu Xiebao* 1983; **16**: 257-267
34 **Wu Q,** Chen ZM, Su WJ. Growth inhibition of gastric cancer cells by all-trans retinoic acid through arresting cell cycle progression. *Chinese Med J* 2001; **114**: 958-961
35 **Wu Q**, Liu S, Ye XF, Huang ZW, Su WJ. Dual roles of Nur77 in selective regulation of apoptosis and cell cycle by TPA and ATRA in gastric cancer cells. *Carcinogenesis* 2002; **21**: 1583-1592
36 **Champelovier P**, Richard MJ, Seigneurin D. Autocrine regulation of TPA-induced apoptosis in monoblastic cell-line U-937: role for TNF-alpha, MnSOD and IL-6. *Anticancer Res* 2000; **20**: 451-458
37 Li Y, Bhuiyan M, Mohammad RM, Sarkar FH. Induction of apoptosis in breast cancer cells by TPA. *Oncogene* 1998; **17**: 2915-2920
38 **Bleasdale JE,** Bundy GL, Bunting S, Filzpatrick FA, Huff RM, Sun FF, Pike JE. Inhibition of phospholipase C dependent processes by U-73122. *Adv Prostaglandin Thromboxane Leukot Res* 1989; **19**: 590-593
39 **House C**, Kemp BE. Protein kinase C contains a pseudosubstrate prototope in its regulatory domain. *Science* 1987; **238**: 1726-1728
40 **Mclaughlin AP**, De Vries GW. Role of PLC gamma and Ca(2+) in VEGF- and FGF-induced choroidal andothelial cell proliferation. *Am J Physiol Cell Physiol* 2001; **281**: 1448-1456
41 **Doong H**, Prise J, Kim YS, Gasbarre C, Probst J, Liotta LA, Blanchette J, Rizzo K, Kohn E. CAIR-1/BAG-3 forms an EGF-regulated ternary complex with phospholipase C-gamma and Hsp70/Hsc70. *Oncogene* 2000; **19**: 4385-4395
42 **Jilek F**, Huttelova R, Petr J, Holubova M, Rozinek J. Activation of pig oocytes using calcium ionophore: effect of protein synthesis inhibitor cycloheximide. *Anim Reprod Sci* 2000; **63**: 101-111
43 **Kurosaki T**, Maeda A, Ishiai M, Hashioto A, Inabe K, Takata M. Regulation of the phospholipase C-gamma2 pathway in B cells. *Immunol Rev* 2000; **176**: 19-29
44 **Carpenter G**, Ji Q. Phospholipase C-gamma as a signal-transducing element. *Exp Cell Res* 1999; **253**: 15-24
45 **Petro JB**, Khant WN. Phospholipase C-γ2 Couples Bruton's Tyrosine Kinase to the NF-κB Signaling Pathway in B Lymphocytes. *J Biol Chem* 2001; **276**: 1715-1719
46 **Schmidt M,** Frings M, Mono ML, Guo Y, Oude Weernink PA, Evellin S, Han L, Jakobs KH. G Protein-coupled Receptor-induced Sensitization of Phospholipase C Stimulation by Receptor Tyrosine Kinases. *J Biol Chem* 2000; **275**: 32603-32610

Edited by Zhang JZ and Wang XL

P.O.Box 2345, Beijing 100023,China
Fax: +86-10-85381893
E-mail: wjg@wjgnet.com www.wjgnet.com

World J Gastroenterol 2003;9(11):2419-2423
World Journal of Gastroenterology
 ISSN 1007-9327

• GASTRIC CANCER •

Construction and analysis of SSH cDNA library of human vascular endothelial cells related to gastrocarcinoma

Yong-Bo Liu, Zhao-Xia Wei, Li Li, Hang-Sheng Li, Hui Chen, Xiao-Wen Li

Yong-Bo Liu, Hui Chen, Xiao-Wen Li, Department of Cell Biology and Medical Genetics, Medical College of Zhengzhou University, Zhengzhou, 450052, Henan Province, China
Zhao-Xia Wei, Department of Anatomy, Henan Medical College for Enterprise Employees, Zhengzhou 450003, Henan Province, China
Li Li, Department of Cardiovascular Disease, People' Hospital of Henan Province, Zhengzhou 450003, Henan Province, China
Hang-Sheng Li, Department of Gynecology and Obstetrics, Henan Medical College for Enterprise Employees, Zhengzhou 450003, Henan Province, China
Correspondence to: Yong-Bo Liu, Department of Cell Biology and Medical Genetics, Medical College of Zhengzhou University, Zhengzhou, 450052, Henan Province, China. liuyb415@163.net
Telephone: +86-371-6974324
Received: 2003-05-11 **Accepted:** 2003-06-04

Abstract

AIM: To construct subtracted cDNA libraries of human vascular endothelial cells (VECs) related to gastrocarcinoma using suppression substractive hybridization (SSH) and to analyze cDNA libraries of gastrocarcinoma and VECs in Cancer Gene Anatomy Project (CGAP) database.

METHODS: Human VECs related to gastric adenocarcinoma and corresponding normal tissue were separated by magnetic beads coupled with antibody CD31 (Dynabeads CD31). A few amount of total RNA were synthesized and amplified by SMART™ PCR cDNA Synthesis Kit. Then, using SSH and T/A cloning techniques, cDNA fragments of differentially expressed genes in human VECs of gastric adenocarcinoma were inserted into JM109 bacteria. One hundred positive bacteria clones were randomly picked and identified by colony PCR method. To analyze cDNA libraries of gastrocarcinoma and VECs in CGAP database, the tools of Library Finder, cDNA xProfiler, Digital GENE Expression Displayer (DGED), and Digital Differential Display (DDD) were used.

RESULTS: Forward and reverse subtraction cDNA libraries of human VECs related to gastrocarcinoma were constructed successfully with SSH and T/A cloning techniques. Analysis of CGAP database indicated that no appropriate library of VECs related to carcinoma was constructed.

CONCLUSION: Construction of subtraction cDNA libraries of human VECs related to gastrocarcinoma was successful and necessary, which laid a foundation for screening and cloning new and specific genes of VECs related to gastrocarcinoma.

Liu YB, Wei ZX, Li L, Li HS, Chen H, Li XW. Construction and analysis of SSH cDNA library of human vascular endothelial cells related to gastrocarcinoma. *World J Gastroenterol* 2003; 9(11): 2419-2423
http://www.wjgnet.com/1007-9327/9/2419.asp

INTRODUCTION

The microvascular system is indispensable throughout the full life span of an organism. Malformation and / or malfunction of VECs contribute to numerous human pathologies including various congenital abnormalities, arteriosclerosis, benign tumors, and cancer. Angiogenesis, the development of new blood vessels by sprouting from the preexisting vasculature, plays an important role in a number of physiological and pathological processes. Stimulated growth or strengthening of so-called collateral vascular branches might circumvent areas with obstructed blood flow in the case of stroke or coronary heart disease. On the other hand, there is substantial evidence suggesting that inhibition of tumor vascular rise might slow down, stop or eventually even reverse tumor growth and could thus become an important part of cancer therapy. The growth of micro vessel accompanying tumor development has, in particular, aroused greater interest and helped improve our understanding of the central role of Vices. Suppression subtractive hybridization (SSH), a PCR-based coda subtracted method, is an important method to reach this aim[1-4]. Because it still needs a lot of initiating RNA, bulk tissues (normal and cancerous) instead of individual cells are routinely used in the analysis. In recent two years, many articles have been publicized employing this method using various tissues[5,6] or cell lines[7,8]. However, bulk tissue contains many different cell types, which will burden the latter work for identifying special genes, and cell lines are different from cells *in vivo* especially for disease cells. With the introduction of Laser Capture Microdissection (LCM), the quantity and purity of RNA from either malignant or benign individual cells invariably yield more reliable and comprehensive experimental results[9-12]. But cell selection and extraction by LCM is currently a manual process, and at most only a few thousand cells can be extracted in an amount of time necessary to limit RNA degradation, and the machine is too expensive for average laboratory. Gastrocarcinoma, one of the most common human malignant tumors, ranks worldwide as the first leading cause of cancer-related mortality. A great deal of articles have been publicized about differentially expressed genes in normal and tumor gastric tissues[13-15]. Some researchers used cells separated from tissues digested with collagenase or cultured cells as material[16-18]. However, with cell culture even primary cell culture, the expressed gene map may change a lot. Likewise, in cells treated with collagenase at 37 ℃ for 30 minutes for separating the target cells from tissue, the specially expressed genes may lose before disposal or new genes may appear after disposal. The Cancer Gene Anatomy Project (CGAP) database of the National Cancer Institute has thousands of expressed sequences, derived from diverse normal and tumor cDNA libraries, but has no appropriate VECs cDNA library related to tumor. The aim of the present study was to select all genes specially expressed in VECs related to gastrocarcinoma rather than in normal gastric tissue. Using VECs mechanically separated by Dynabeads CD31 as materials without collagenase and culture, we built a cDNA library through SSH method, thus paved the way for further research on changes of VECs in gastrocarcinoma.

MATERIALS AND METHODS

Materials

The resected specimens about 2 cm^3 from gastric adenocarcinoma

confirmed pathologically and from normal gastric tissues 7 cm away from the edge of the adenocarcinoma in same patients who were admitted to Henan Provincial Hospital were put into RNA protecting solution (RNAlater™, Ambion Company) after being rinsed with PBS immediately after resection.

Methods

Separation of ECs with Dynabeads CD31 About 1 cm^3 of tissue cut from tissues stabilized by RNA*later* was put into a mortar with a little RNA*later* RNA Stabilization Reagent, and then was scissored and ground with scissors and pestle. To make cell suspension, 1 ml RNA*later* RNA Stabilization Reagent was added to it, then filtered through a sterile 80-μm-nylon filter. 25 μl washed Dynabeads®CD31 beads were added to the suspension for 30 minutes at 2-8 ℃. For identification, slide was made with one drop of this mixture and stained with hematoxylin and eosin (H&E). Then bead-bound cells were separated in a magnetic device (Dynal MPC®).

Isolation of total RNA

Rnaeasy Mini Kit and Rnase-Free Dnase set (QIAGEN Company) were used to extract the total RNA from bead-bound cells. RNA purified by Rnaeasy Column was analyzed for integrity and size by formaldehyde agarose gel electrophoresis and quantification and purity of RNA by OD value.

Synthesis, amplification and purification of cDNA

About 100 ng total RNA was used to synthesize the first strand of cDNA with SMART™ PCR cDNA Synthesis Kit (Clontech Company), then amplified by LD-PCR with 15, 18, 21, 24, 27 cycles separately and analyzed through 1.2 % agarose gel electrophoresis in order to get the perfect cycle number with which we harvested a suitable amount rather than a superfluous one to build the library. Placental total RNA was performed as control. CHROMA SPIN-100 Column was used to purify the cDNA.

Digestion with RsaI and purification of digested products

SampleI, cDNA from VECs of gastrocarcinoma, and sample II, cDNA from VECs of normal stomach tissue, and sample III, cDNA from VECs of placental tissue were treated with enzyme RsaI respectively. From each sample, 10-μl solutions was taken before digestion and 1 h, 3 h and 3.5 h after digestion, and 1.2 % agarose gel electrophoresis was performed for identification of digestion efficiency. Digested products were purified by QIAquick PCR purification Kit (QIAGEN Company), and subsequently concentrated to 6.7 μl by ethanol precipitation method.

Isolation of specially expressed cDNA fragments

Based on the instructions of Clontech PCR-Select™ cDNA Subtraction Kit, sample I and sample II were used as test 1 and driver 1, correspondingly sample II and sample I were used as test 2 and driver 2. Mixture of sample III and ω×174/Hae III DNA was treated as test 3, correspondingly sample III alone was performed as driver 3. Each sample test was divided into two parts, and each part was ligated separately with Adaptor 1 and Adaptor 2, and then hybridized with the corresponding sample driver. The mixture of two parts was hybridized with corresponding sample driver again. The fragments with both Adaptor 1 and Adaptor 2, namely specially expressed cDNA fragments in sample test rather than in sample driver, were amplified by nested PCR. Adeptors possessed outside primer and inside primer. So forward and reverse subtraction fragments were obtained. Subtraction efficiency was checked by G3PDH, a housekeeping gene, according to PCR cycles needed in subtracted sample and unsubtracted sample, with which the gene could be observed on agarose/EtBr gel.

Purification of subtraction fragments

QIAquick PCR Purification Kit was utilized to purify the subtraction fragments.

Clone and screening of subtraction fragments

1 μl, 2 μl, 3 μl PCR fragments of subtraction and non-subtraction and 2 μl control DNA were respectively taken to ligate with 1 μl pGEM-T easy Vector. 10-μl ligation reaction solutions were transformed into 150 μl competent cells JM109. Background control was set up by pGEM-T easy Vector without any insert, and transformation control was also set up by an uncut plasmid pGEM@-5Zf (+) Vector. The transformation culture was plated on petri dishes containing LB/ampicillin/IPTG/X-Gal, and then screened white colony for inset fragment.

Identification of positive recombination of vector

Select 100 white colonies separately from forward and reverse library and replant 5 ml LB/Amp solution. Then it was shaken at 37 ℃ overnight. Take 1 μg culture solution as model and Nested Primer 1 and Nested Primer 2R to amplify the insert and test it by electrophoresis.

Storage of library

Select white colonies separately from forward and reverse library and inoculate 5 ml LB/Amp solution. Then it was shaken at 37 ℃ overnight. Add 700 μl culture solution into 1.5 ml EP tube containing 50 % glycerin and keep it at -80 ℃.

Analysis of related library

cDNA library of stomach cancer tissue, normal stomach tissue and vascular endothelial cell were analyzed using GLS, cDNA xProfiler, DDD, DGED and Library Finder in Cancer Genome Anatomy Project (CGAP). dbEST was categorized using the GLS tool of CGAP. We considered precancer libraries as cancer libraries. All of the cDNA libraries were categorized according to tissue type (tissue origin), tissue histology (cancerous, normal, or fetal), and the library preparation method (microdissected, bulk, cell line, or flow cytometric sorted).

RESULTS

Through Dynabeads®CD31, about 8×10^6 endothelial cells were obtained with almost 100 % purity. Slides were made and stained with H&E (Figure 1).

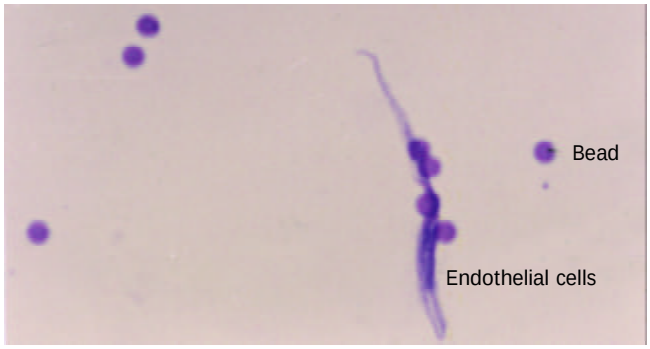

Figure 1 Endothelial cell attached with several beads.

The amount of RNA extracted from stomach cancer and normal stomach tissue was respectively 1.0 μg and 0.85 μg with OD_{260}/OD_{280} ratio 2.10 and 1.96. By formaldehyde agarose gel electrophoresis, the integrity and size were analyzed and clear bands of 18s and 28s were seen (Figure 2).

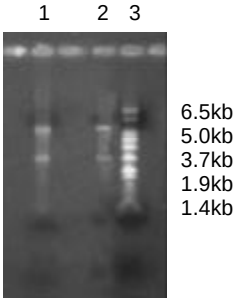

Figure 2 Lane 1, total RNA of stomach cancer. Lane 2, total RNA of normal stomach tissue. Lane 3, marker.

Figure 3 Lanes 1, 2, 3 demonstrate 21, 24, 27 PCR cycles of cDNA products of stomach cancer tissue. Lanes 4, 5, 6 demonstrate 21, 24, 27 PCR cycles of cDNA products of normal stomach tissue. Lanes 7, 8, 9 demonstrate 15, 18, 21 PCR cycles of cDNA products of placental tissue. Lane 10, marker.

Synthesis and amplification of cDNA

The first strands of cDNA have been amplified by LD-PCR with different cycles: 15, 18, 21, 24, and 27. The products could be viewed on 2 % agarose gel electrophoresis (Figure 3). For both normal tissue and cancer tissue, a total of 27 cycles were performed, respectively, and for placental tissue, totally 18 cycles were performed.

Analysis of RsaI digestion efficiency

cDNA, before digestion with *RsaI*, appeared as a smear of 0.5-10 kb on 1 % agarose gel electrophoresis, and after digestion the average cDNA size was smaller (0.1-2 kb) (Figure 4).

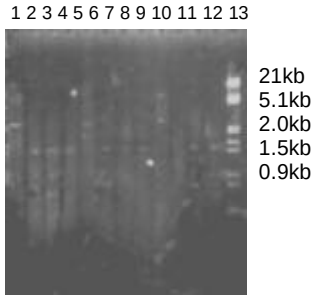

Figure 4 Lanes 1, 2, 3, 4: sampleI. Lanes 5, 6, 7, 8: sampleII. Lanes 9, 10, 11, 12: sample III. Lane 13, marker. Lanes 1, 5, 9: cDNA undigested. Lanes 2, 6, 10: cDNA digested for 1 h. Lanes 3, 7, 11: cDNA digested for 3 h. Lanes 4, 8, 12: cDNA digested for 3.5 h.

Analysis of ligation efficiency

That the intensity ratio of PCR products determined by G3PD primer 3' and Adaptor primer 1 to PCR products determined by G3PD primer 3' and 5' was over 1:4 on 2.0 % agarose/EB gel showed that ligation efficiency was above 25 % (Figure 5).

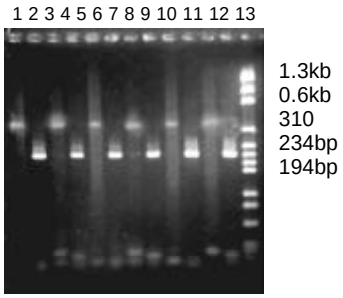

Figure 5 Lanes 1, 2, 3, 4 : sampleI. Lanes 5, 6, 7, 8: sample II. Lanes 9, 10, 11, 12: sample III. Lane 13, marker. Lanes 1, 5, 9: PCR products using cDNA ligated Adaptor 1 as model, and G3PDH 3' primer and PCR Primer 1. Lanes 2, 6, 10: PCR products using cDNA ligated Adaptor 1 as model, and G3PDH 3'primer and G3PDH 5'primer; Lanes 3, 7, 11: PCR products using cDNA ligated Adaptor 2 as model, and G3PDH 3' primer and primer 1. Lanes 4, 8, 12: PCR products using cDNA ligatefd Adaptor 2 as model, and G3PDH 3' primer and G3PDH 5' primer.

Analysis of differentially expressed cDNA with nest PCR

The second hybridization products were amplified by outside primers. The products presented unclear smear on 2 % agarose/EB gel. After second PCR with inside primers, several bands could be seen clearly among the smears. Based on the manual, the experiment was successful (Figure 6).

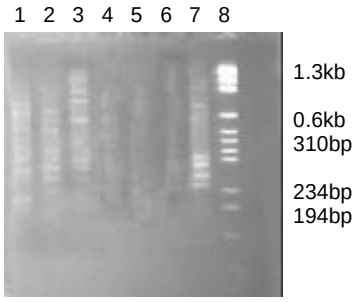

Figure 6 Lanes 1, 2, 3 indicated subtracted samples I, II, III. Lanes 4, 5, 6 indicated unsubtracted sample I, II, III. Lane 7 showed the subtracted control provided by the kit. Lane 8: Marker.

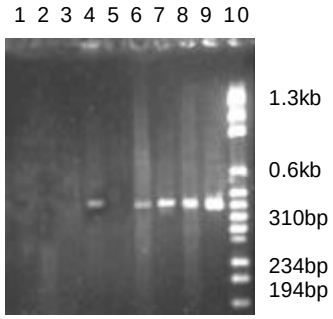

Figure 7 Lanes 1, 2, 3, 4 indicated the subtracted sample I was amplified by PCR wth different cycles: 18, 23, 28, 33. Lanes 6, 7, 8, 9 indicated the unsubtracted sample I was amplified by PCR wth different cycles: 18, 23, 28, 33. Lane 10: Marker.

PCR analysis of subtraction efficiency

After PCR amplification, the housekeeping gene G3PDHs appeared at 18 cycles in unsubtraction samples and at 33 cycles in subtraction samples. This result indicated that G3PDHs expressed in both parts have been greatly decreased

through the subtraction method. If five cycles corresponded roughly to 20-fold cDNA enrichment, G3PDHs would have been decreased almost 300 times. It implied that other genes expressed in both tissues have been reduced the same fold and the specially expressed genes in the test sample were selected (Figure 7).

Screening transformants for inserts

720 white colonies were observed on two petri dishes of positive control with 7 % presence ratio of blue colony. Two white colonies were observed on one petri dish of background control with 15 blue colonies. On one petri dish of transformation control, 160 white colonies without blue colony were observed. 992 white colonies appeared on 5 petri dishes of forward subtraction, and 890 white colonies appeared on 5 petri dishes of reverse subtraction. 60 white colonies were selected from forward and reverse subtractions, and amplified with nested Primer 1 and nested Primer 2R. 54 and 50 fragments ranged from 100 bp to 1 000 bp were selected from the corresponding forward and reverse subtraction libraries.

Analysis of CGAP database

dbEST was categorized using the GLS tool of the CGAP. All of the cDNA libraries were categorized according to tissue type (tissue origin), tissue histology (cancerous, normal, or fetal), and the library preparation method (microdissected, bulk, cell line, or flow cytometric sorted). Among 319 stomach cDNA libraries, all 73 libraries of normal stomach were from bulk tissues instead of cells and none was established by SSH method except those without label. Among the 245-cDNA libraries of stomach cancer, 28 originated from cell lines with 9 libraries built by SSH, and none of the other 217 libraries originating from tissue was built by SSH. All 15 vascular cDNA libraries came from normal tissue or cell line or cultured cells, and SSH method was not used. And appropriate VECs related to tumor have not been built into cDNA library. Among the libraries derived from cell lines, two derived from umbilical vein endothelium, one derived from aortic endothelium, another one came from endothelial cells of foreskin through primary culture of dermal microvascular endothelial cells. Among the 11 non-cell line libraries, 6 were from aorta, 2 umbilical veins, 1 unlabeled vein; another two were from choroidal plexus and basilar artery.

DISCUSSION

Bio-behavior such as growth and metastasis of cancer is closely related with proliferation of microvessel. Newborn capillaries of cancer differ from normal ones in growth process or distribution. For instance, VECs of breast cancer can grow 50 times faster than VEC in normal tissue[19] and vascular endothelial growth factors (VEGFs) play an important role in tumor angiogenesis[20,21], and their over- expression is closely related to clinical staging, lymph node metastasis and recurrence of gastric carcinoma[22]. So increasing attention has been paid to VECs[23].

Differentially expressed genes between the corresponding normal and cancer tissue can help us understand the molecular basis of malignancy and potentially serve as biomarkers or prognostic markers of malignancy. The identification and characterization of human genes expressed exclusively or preferentially in microvascular system of tumor will hopefully shed light on the mechanisms of tumor development and provide useful genetic markers for screening, diagnosis, prognosis, therapeutic monitoring and development of therapeutic vaccines. There are many techniques that aim at producing an inventory of differential transcripts between two populations of mRNAs. High-throughput gene expression techniques (microarrays, genechips) to identify cancer-specific genes are becoming available[24-26], however, the technology is not cost effective for average laboratories. SSH method allows identifying overexpressed genes (designated forward +SSH) but also underexpressed genes (designated reverse -SSH) by exchanging the driver and tester populations during the procedure (Clontech, Palo Alto, USA). Since this technique was established by Diatchenko, many new genes have been separated from almost all tissues, such as renal cell cancer, lung cancer, liver cancer[27-30], etc.

The CGAP database of the National Cancer Institute has thousands of expressed sequences, both known and novel, in the form of expressed sequence tags (ESTs). These ESTs derive from diverse normal and tumor cDNA libraries. In CGAP database, there are 8 221 libraries from various tissues. Among these libraries, 54 libraries are based on SSH method, and 69 material samples are prepared through microdissection. Among those 54 libraries with SSH method, none of the material sample has been prepared through microdissection.

CGAP also offers different data-mining tools: tools of the GLS, the cDNA xProfiler, the DDD, and the DGED. With these tools and database in CGAP, differently expressed genes can be predicted too[31-33]. Using DGED tool to compare normal stomach libraries and cancer libraries, 117 differently expressed genes can be found. But endothelial cells related to cancer have no appropriate library that can be matched and compared. So cDNA library of endothelial cells related to cancer needs to be built, and the more the better, just like prostate libraries.

TO separate VECs from microvessel, tissues were usually treated with collagenase at 37 ℃ for 30 minutes according to present common techniques, and magnetic beads coupled with monoclonal antibody CD31(Dynabeads CD31) have also been used[34,35]. VECs separated by monoclonal antibody have been identified without change[36]. Instead of using collagenase and cell culture, we separated VECs with Dynalbeads CD31 after mechanically grinding tissue and filtering through a sterile 80-μm-nylon filter. In this way, we obtained about 10^6 VECs, from which 1 μg total RNA was harvested. Although the amount of the cells was limited and even some cells were connected by fibers, they were relatively pure. The process of separating VECs from tissue with Danalbeads CD31 lasted almost 1 h, as a result RNAlater, solution-inhibiting degradation of RNA, has been used to substitute PBS required by the Danalbeads CD31 Kit. Because the amount was far from 1-2 mg total RNA required by SSH method, Smart cDNA Synthesis Kit was introduced to synthesize and amplify cDNA from the relatively few RNA, which requires only 50 ng total RNA. In the process of amplification, after the first 15 cycles, for each three more cycles, a little sample was taken and tested in order to get suitable copies of cDNA, as more copies would add burden to later screening work.

In performing SSH, each step was operated exactly according to the manual of the kit and the results were verified correct before each following step. G3PDH was used to identify the forward and reverse subtractions. On agarose/EB gel, appearance of G3PDH band was 15 PCR cycles later in subtraction sample than in unsubtraction sample. It implied the amount of G3PDH decreased 300 times by subtraction technique. Finally, with T/A technique, subtracted PCR products were ligated to T vector and transformed into bacteria JM109. So, both the forward subtraction cDNA library containing cDNA fragments only expressed in VECs of stomach cancer but not normal stomach tissue, and the reverse subtraction cDNA library containing cDNA fragments not expressed in VECs of stomach cancer tissue but normal stomach tissue were built up successfully, which was a good beginning for researching into new genes of VECs related to gastrocarcinoma and gene therapy of gastrocarcinoma.

ACKNOWLEDGEMENT

We thank Dr. Xu ZF, Dr. Pan Wi, Dr. Wang XL, from the Life Science Academy of Zhongshan University; and Mr. Zhang QX, Mr. Ding Y, Mr. Jin H, from the Histological Department of Medical College of Zhengzhou University.

REFERENCES

1 **Diatchenko L**, Lau YF, Campbell AP, Chenchik A, Moqadam F, Huang B, Lukyanov S, Lukyanov K, Gurskaya N, Sverdlov ED, Siebert PD. Suppression subtractive hybridization: a method for generating differentially regulated or tissue-specific cDNA probes and libraries. *Proc Natl Acad Sci U S A* 1996; **93**: 6025-6030

2 **Diatchenko L**, Lukyanov S, Lau YF, Siebert PD. Suppression subtractive hybridization: a versatile method for identifying differentially expressed genes. *Methods Enzymol* 1999; **303**: 349-380

3 **Ji W**, Wright MB, Cai L, Flament A, Lindpaintner K. Efficacy of SSH PCR in isolating differentially expressed genes. *BMC Genomics* 2002; **3**: 12

4 **Wang X**, Feuerstein GZ. Suppression subtractive hybridisation: application in the discovery of novel pharmacological targets. *Pharmacogenomics* 2000; **1**: 101-108

5 **Villalva C**, Trempat P, Zenou RC, Delsol G, Brousset P. Gene expression profiling by suppression subtractive hybridization (SSH): a example for its application to the study of lymphomas. *Bull Cancer* 2001; **88**: 315-319

6 **Li YJ**, Tian F, Chen ZC, Guan YJ, He CM, Yang XM, Xie DH. Isolation and Identification of cDNA Sequences Differentially Expressed in Laryngeal Carcinoma. *Shengwu Huaxue Yu Shengwu WuLi Xuebao* 2000; **32:** 153-157

7 **Eleveld-Trancikova D**, Kudela P, Majerciak V, Regendova M, Zelnik V, Pastorek J, Pastorekova S, Bizik J. Suppression subtractive hybridisation to isolate differentially expressed genes involved in invasiveness of melanoma cell line cultured under different conditions. *Int J Oncol* 2002; **20**: 501-508

8 **Langley RR**, Ramirez KM, Tsan RZ, Van Arsdall M, Nilsson MB, Fidler IJ. Tissue-specific Microvascular Endothelial Cell Lines from H-2K (b)-tsA58 Mice for Studies of Angiogenesis and Metastasis. *Cancer Res* 2003; **63:** 2971-2976

9 **Fend F**, Emmert-Buck MR, Chuaqui R, Cole K, Lee J, Liotta LA, Raffeld M. Immuno-LCM: laser capture microdissection of immunostained frozen sections for mRNA analysis. *Am J Pathol* 1999; **154**: 61-66

10 **Kerk NM**, Ceserani T, Tausta SL, Sussex IM, Nelson TM. Laser capture microdissection of cells from plant tissues. *Plant Physiol* 2003; **132:** 27-35

11 **Pedersen TX**, Leethanakul C, Patel V, Mitola D, Lund LR, Dano K, Johnsen M, Gutkind JS, Bugge TH. Laser capture microdissection-based *in vivo* genomic profiling of wound keratinocytes identifies similarities and differences to squamous cell carcinoma. *Oncogene* 2003; **22:** 3964-3976

12 **Yim SH,** Ward JM, Dragan Y, Yamada A, Scacheri PC, Kimura S, Gonzalez FJ. Microarray analysis using amplified mRNA from laser capture microdissection of microscopic hepatocellular precancerous lesions and frozen hepatocellular carcinomas reveals unique and consistent gene expression profiles. *Toxicol Pathol* 2003; **31**: 295-303

13 **Mori M**, Mimori K, Yoshikawa Y, Shibuta K, Utsunomiya T, Sadanaga N, Tanaka F, Matsuyama A, Inoue H, Sugimachi K. Analysis of the gene-expression profile regarding the progression of human gastric carcinoma. *Surgery* 2002; **131**(Suppl 1): S39-47

14 **Jung MH**, Kim SC, Jeon GA, Kim SH, Kim Y, Choi KS, Park SI, Joe MK, Kimm K. Identification of differentially expressed genes in normal and tumor human gastric tissue. *Genomics* 2000; **69**: 281-286

15 **Yoshikawa Y,** Mukai H, Hino F, Asada K, Kato I. Isolation of two novel genes, down-regulated in gastric cancer. *Jpn J Cancer Res* 2000; **91**: 459-463

16 **Su N,** Yan H**,** Li YP. Isolation, purification, identification and gene transfer of microvascular endothelial cells. *Xibao Shengwuxue Zazhi* 2000; **22**: 94-98

17 **Muczynski KA,** Ekle DM, Coder DM, Anderson SK. Normal human kidney HLA-DR-expressing renal microvascular endothelial cells: characterization, isolation, and regulation of MHC class II expression. *J Am Soc Nephrol* 2003; **14:** 1336-1348

18 **Stier S,** Totzke G, Grunewald E, Neuhaus T, Fronhoffs S, Sachinidis A, Vetter H, Schulze-Osthoff K, Ko Y. Identification of syntenin and other TNF-inducible genes in human umbilical arterial endothelial cells by suppression subtractive hybridization. *FEBS Lett* 2000; **467**: 299-304

19 **Jin HM,** Li XT. Neovascularization and disease. *Zhongguo Weixunhuan* 2001; **5**: 173-177

20 **Liu DH**, Zhang XY, Fan DM, Huang YX, Zhang JS, Huang WQ, Zhang YQ, Huang QS, Ma WY, Chai YB, Jin M. Expression of vascular endothelial growth factor and its role in oncogenesis of human gastric carcinoma. *World J Gastroenterol* 2001; **7**: 500-505

21 **Tao HQ**, Lin YZ, Wang RN. Significance of vascular endothelial growth factor messenger RNA expression in gastric cancer. *World J Gastroenterol* 1998; **4:** 10-13

22 **Konno H**, Baba M, Tanaka T, Kamiya K, Ota M, Oba K, Shoji A, Kaneko T, Nakamura S. Overexpression of vascular endothelial growth factor is responsible for the hematogenous recurrence of early-stage gastric carcinoma. *Eur Surg Res* 2000; **32**: 177-181

23 **Liu C**, Zhang L, Shao ZM, Beatty P, Sartippour M, Lane TF, Barsky SH, Livingston E, Nguyen M. Identification of a novel endothelial-derived gene EG-1. *Biochem Biophys Res Commun* 2002; **290**: 602-612

24 **Khan J**, Bittner ML, Saal LH, Teichmann U, Azorsa DO, Gooden GC, Pavan WJ, Trent JM, Meltzer PS. cDNA microarrays detect activation of a myogenic transcription program by the PAX3-FKHR fusion oncogene. *Proc Natl Acad Sci U S A* 1999; **23:** 13264-13269

25 **Elek J**, Park KH, Narayanan R. Microarray-based expression profiling in prostate tumors. *In Vivo* 2000; **14**: 173-182

26 **Wikman H,** Kettunen E, Seppanen JK, Karjalainen A, Hollmen J, Anttila S, Knuutila S. Identification of differentially expressed genes in pulmonary adenocarcinoma by using cDNA array. *Oncogene* 2002; **21**: 5804-5813

27 **Pitzer C,** Stassar M, Zoller M. Identification of renal-cell-carcinoma-related cDNA clones by suppression subtractive hybridization. *J Cancer Res Clin Oncol* 1999; **125:** 487-492

28 **Ai JK**, Huang X, Wang YJ, Bai Y, Lu YQ, Ye XJ, Xin DQ, Na YQ, Zhang ZW, Guo YL. Screening of novel genes differentially expressed in human renal cell carcinoma by suppression subtractive hybridization. *Ai Zheng* 2002; **21:** 1065-1069

29 **Zhang L**, Cilley RE, Chinoy MR. Suppression subtractive hybridization to identify gene expressions in variant and classic small cell lung cancer cell lines. *J Surg Res* 2000; **93:** 108-119

30 **Li J**, Han B, Huang G, Qian G, Liang P, Yang T, Chen J. Screening and identification for cDNA of differentially expressed genes in human primary hepatocellular carcinoma. *Zhonghua Yixue Yichuanxue Zazhi* 2003; **20:** 49-52

31 **Schmitt AO**, Specht T, Beckmann G, Dahl E, Pilarsky CP, Hinzmann B, Rosenthal A. Exhaustive mining of EST libraries for genes differentially expressed in normal and tumour tissues. *Nucleic Acids Res* 1999; **27**: 4251-4260

32 **Scheurle D**, De Young MP, Binninger DM, Page H, Jahanzeb M, Narayanan R. Cancer gene discovery using digital differential display. *Cancer Res* 2000; **60**: 4037-4043

33 **Asmann YW**, Kosari F, Wang K, Cheville JC, Vasmatzis G. Identification of differentially expressed genes in normal and malignant prostate by electronic profiling of expressed sequence tags. *Cancer Res* 2002; **62**: 3308-3314

34 **Zhou H**, Xu GW, Sheng ML, Tang J. Construction of human vascular endothelial cell database. *Shengwu Huaxue Zazhi* 1993; **9**: 507-509

35 **Van Leeuwen EB,** Molema G, de Jong KP, van Luyn MJ, Dijk F, Slooff MJ, Ruiters MH, van der Meer J. One-Step Method for Endothelial cell isolation from large human blood vessels using fibrin glue. *Lab Invest* 2000; **80**: 987-989

36 **Su X**, Sorenson CM, Sheibani N. Isolation and characterization of murine retinal endothelial cells. *Mol Vis* 2003; **9**: 171-178

Edited by Zhu LH

P.O.Box 2345, Beijing 100023,China
Fax: +86-10-85381893
E-mail: wjg@wjgnet.com www.wjgnet.com

World J Gastroenterol 2003;9(11):2424-2427
World Journal of Gastroenterology
 ISSN 1007-9327

• GASTRIC CANCER •

Therapeutic mechanism of ginkgo biloba exocarp polysaccharides on gastric cancer

Ai-Hua Xu, Hua-Sheng Chen, Bu-Chan Sun, Xiao-Ren Xiang, Yun-Fei Chu, Fan Zhai, Ling-Chang Jia

Ai-Hua Xu, Hua-Sheng Chen, Bu-Chan Sun, Medical College, Yangzhou University, Yangzhou 225001, Jiangsu Province, China
Xiao-Ren Xiang, Nanjing University of Traditional Chinese Medicine, Nanjing 210029, Jiangsu Province, China
Yun-Fei Chu, The First People Hospital of Yangzhou, Yangzhou 225002, Jiangsu Province, China
Fan Zhai, Ling-Chang Jia, Jiangsu Provincial Subei People Hospital, Yangzhou 225001, Jiangsu Province, China
Supported by the Society Development Foundation of Jiangsu Province, No. BS 2000086
Correspondence to: Ai-Hua Xu, Medical College, Yangzhou University, Yangzhou 225001, Jiangsu Province, China. yzxih@21cn.com
Telephone: +86-514-7310741 **Fax:** +86-514-7341733
Received: 2003-05-13 **Accepted:** 2003-06-02

Abstract

AIM: To study the therapeutic mechanism of Ginkgo biloba exocarp polysaccharides (GBEP) on gastric cancer.

METHODS: Thirty patients with gastric cancer were treated with oral GBEP capsules. The area of tumors was measured by electron gastroscope before and after treatment, then the inhibitory and effective rates were calculated. The ultrastructures of tumor cells were examined by transmissional electron microscope. Cell culture, MTT, flow cytometry were performed to observe proliferation, apoptosis and changes of relevant gene expression of human gastric cancer SGC-7901 cells.

RESULTS: Compared with the statement before treatment, GBEP capsules could reduce the area of tumors, and the effective rate was 73.4 %. Ultrastructural changes of the cells indicated that GBEP could induce apoptosis and differentiation in tumor cells of patients with gastric cancer. GBEP could inhibit the growth of human gastric cancer SGC-7901 cells following 24-72 h treatment *in vitro* at 10-320 mg/L, which was dose- and time-dependent. GBEP was able to elevate the apoptosis rate and expression of c-fos gene, but reduce the expression of c-myc and bcl-2 genes also in a dose-dependent manner.

CONCLUSION: The therapeutic mechanism of GBEP on human gastric cancer may relate to its effects on the expression of c-myc, bcl-2 and c-fos genes, which can inhibit proliferation and induce apoptosis and differentiation of tumor cells.

Xu AH, Chen HS, Sun BC, Xiang XR, Chu YF, Zhai F, Jia LC. Therapeutic mechanism of ginkgo biloba exocarp polysaccharides on gastric cancer. *World J Gastroenterol* 2003; 9(11): 2424-2427
http://www.wjgnet.com/1007-9327/9/2424.asp

INTRODUCTION

Ginkgo biloba exocarp polysaccharide (GBEP) is polysaccharides isolated from ginkgo biloba exocarp. Many studies showed that GBEP was able to inhibit tumors and enhance immune function of tumor bearing mice. Clinical studies showed that GBEP had certain therapeutic effects but few toxic side-effects on patients with tumors, and had good prospects in clinical application[1-4]. This study was to investigate the therapeutic effect and mechanism of GBEP on human gastric cancer.

MATERIALS AND METHODS

Patients

A total of 30 patients with gastric adenocarcinoma (20 males aged from 28 to 81 years old, 10 females aged from 52 to 75 years old) were all ascertained by the pathological examination in Jiangsu Provincial Subei People Hospital or the First People Hospital of Yangzhou, China. Their Karnofsky scores were all above 60. All the patients did not receive any other anti-tumor treatments recently.

Cell line

Human gastric cancer cells (SGC-7901) purchased from Department of Cellular and Molecular Biology, Shanghai Institute of Biochemistry and Cell Biology Academia Sinica, were sub-cultured every 2 or 3 days.

Reagents

GBEP was extracted from exocarp of ripe ginkgo biloba. The content of polysaccharides was higher than 80 %. RPMI 1640 was from GibcoBRL(Maryland, USA). MTT and trypsin (1:250) were from Sigma (ST. Louis, USA). Monoclonal mouse anti-human c-myc and bcl-2 were purchased from Antibody Diagnostica Inc., USA. Monoclonal rabbit anti-human c-fos was from Santa Cruz (Santa Cruz, USA).

Methods

Influence of GBEP on gastric carcinoma patients GBEP capsules are composed of GBEP dry powder and a certain proportion of excipient, and 0.25 g per capsule. Each patient with gastric carcinoma was treated with oral GBEP capsule, 2 pills each time, twice a day, for over 30 d. Changes of tumor size were measured by electron gastroscope. The inhibitory rates (IR) were calculated according to the formula: IR=(tumor area before treatment - tumor area after treatment) ÷ tumor area before treatment×100 %, which is used in the assessment of therapeutic effects. The assessment followed the clinical assessment standards for solid tumors made by WHO, which are classified as complete response (CR), partial response (PR), stable disease (SD) or no change (NC), and progressive disease (PD). The effective rate equals CR plus PR. At the meantime tumor biopsies were obtained for ultrastructural examination by transmissional electron microscope (HV-300). Images captured by transmissional electron microscope were analysed, and the nucleocytoplasmic ratio as well as the surface density of heterochromatin in the tumor cells were calculated before and after treatment.

MTT experiment SGC-7901 cells growing exponentially were digested by 0.25 % trypsin for 1-2 minutes, then washed in Hanks' balanced salt solution (HBSS) for 2 times, and RPMI

1640 containing 10 % new born bovine serum medium was added to adjust the cell density to 1×10^8 cells/L. After addition of the final cell suspensions of 100 μl/well, 96-well plates were put into an incubator containing 5 % CO_2, and incubated at 37 ℃ for 24 hours. Then, 100 μl RPMI 1640 containing different concentrations of GBEP was added to each well. Each concentration had 3 wells, and the control was added with 100 μl RPMI 1640. They were cultured for 24 hours, 48 hours and/or 72 hours. Fresh medium was changed per 24 hours, and GBEP was added. Four hours before the end of culture, 10 μl MTT (the final concentration was 5 g/L) was added, and cultured for 4 hours. Optical density (OD) values for each well were measured at 570 nm with the enzyme linked immunosorbent assay meter[5,6]. The inhibitory rates were calculated according to the formula: IR=[1-(the mean of treated group)/(the mean of control group)]×100 %.

Measurement of cell apoptosis SGC-7901 cells growing exponentially were digested with 0.25 % trypsin for 1-2 minutes. After that, the cells were washed 2 times with PBS buffer (pH 7.2), counted and mixed with RPMI 1640 containing 10 % new born bovine serum to create a final cell density of 2×10^8 cells/L. Four ml final cell suspension was added into each culture bottle, and cultured for 24 h in the condition of 5 % CO_2, at 37 ℃. Then the culture bottles were randomly mixed with different concentrations of GBEP or a positive control drug adriamycin. The negative control group was mixed with an equal volume of RPMI 1640. Then, all the culture bottles were cultured for another 48 h. After that, they were digested and washed. At last they were fixed with alcohol and kept at 4 ℃. The tumor cells were fixed with alcohol and kept in citrate buffer for at least 1 hour after washed in PBS to create a final cell density of 1×10^9 cells/L, they were then centrifuged and mixed with 1 800 μl solution A (trypsinization solution). After 10 minutes, they were mixed with 1 500 μl solution B (RNASE) for 20 minutes, then mixed with 1 500 μl solution C (PI) and filtered by a nylon net after 15 minutes. Finally, the apoptotic rate of the cells was examined.

Analysis of protein content Cell culture was carried out as previously described. The SGC-7901 cells were centrifuged (2 000 ω/minute for 5 minutes) after washed in PBS, mixed with monoclonal mouse anti-human c-myc, or bcl-2, or rabbit anti-human c-fos, and kept at 4 ℃ for 45 minutes. The cells were washed in PBS and mixed with sheep anti-mouse or sheep anti-rabbit IgG and kept at 4 ℃ for another 45 minutes. After washed in PBS and centrifugation, the cells were mixed with 300 μl PBS in sediment and the rate of positive protein for c-myc, bcl-2 and c-fos gene was measured by flow cytometry.

RESULTS

Effect of GBEP capsules on gastric cancer cells

Compared with that before treatment, the tumor area was apparently reduced, which was further proved by electron gastroscopy, and the inhibitory rate of GBEP on tumors was 53.5 %. According to the standards proposed by WHO for the short-term therapeutic effectiveness of solid tumors, there were 2 cases of CR (6.7 %), 20 PR (66.7 %), 5 SD (16.7 %), 3 PD (10 %) in the 30 cases, and the total effective rate was 73.4 %. Images captured by transmissional electron microscope showed that most of the cancer cells had sufficient euchromatins but deficient heterochromatins in the nuclei, the cancer cells had sufficient free ribosomes and deficient glycogens in the cytoplasm before treatment. After treatment with GBEP, most of the cancer cells had sufficient heterochromatins in the nuclei. Some cancer cells became pyknosis. Heterochromatin margination was seen in some of the cancer cells (in the course of apoptosis). Some euchromatins were dissolved, mitochondria were swollen, and rough endoplasmic reticulum was dilated. The results of image analysis showed that nucleocytoplasmic ratio in most of the cancer cells was reduced, surface density of heterochromatin was increased. Influence of GBEP capsules on the tumor area of gastric cancer, on the tumor cells' nucleocytoplasmic ratio and the surface density are shown in Figure 1.

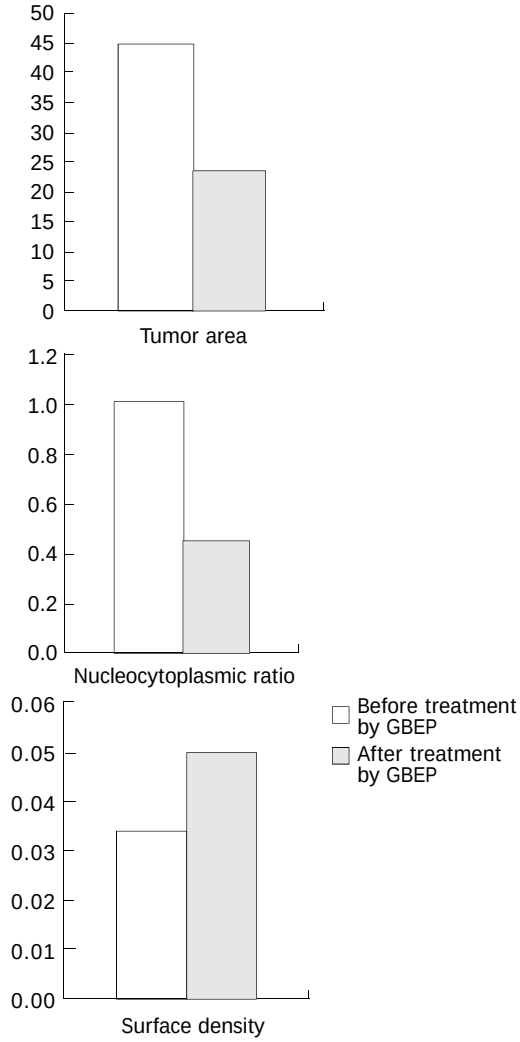

Figure 1 Influence of GBEP capsules on tumor area of gastric cancer, and on tumor cells' nucleocytoplasmic ratio and surface density.

Inhibition of GBEP on human gastric cancer SGC-7901 cells

GBEP could inhibit SGC-7901 cell proliferation following 24-72 hours treatment *in vitro* at 10-320 mg/L. Compared with the control group, the inhibition of SGC-7901 cell proliferation by GBEP was dose- and time-dependent ($P<0.01$) (Figure 2).

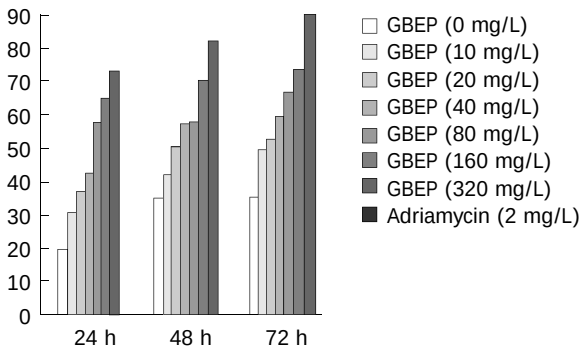

Figure 2 Inhibition of GBEP on human gastric cancer SGC-7901 cell proliferation *in vitro*.

Effects of GBEP on human gastric cancer SGC-7901 cell apoptosis

DNA contents of human gastric cancer SGC-7901 cells were analysed by flow cytometry. The results showed that GBEP could induce apoptosis in SGC-7901 cells at a certain degree (Figure 3).

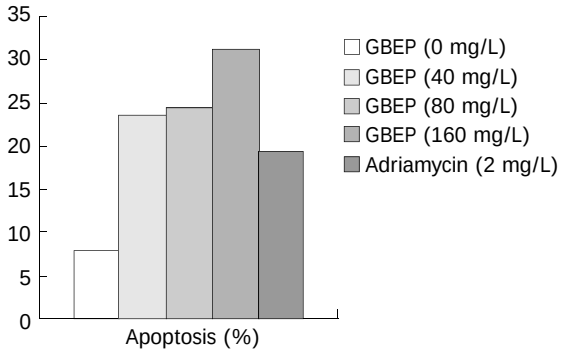

Figure 3 Effects of GBEP on human gastric cancer SGC-7901 cell apoptosis.

Effect of GBEP on expression of c-myc, bcl-2 and c-fos genes in SGC-7901 cells

Protein contents of human gastric cancer SGC-7901 cells were analysed by flow cytometry. The results showed that GBEP could inhibit the expression of c-myc and bcl-2 genes, but enhance the expression of c-fos in SGC-7901 cells (Table 1).

Table 1 Effect of GBEP on expression of c-myc, bcl-2 and c-fos genes in SGC-7901 cells

Group	Dose (mg/L)	Rate of positive protein sign (%)		
		c-myc	bcl-2	c-fos
RPMI 1640	-	22.05	19.35	12.68
GBEP	40	20.33	15.29	17.35
GBEP	80	12.50	11.74	24.96
GBEP	160	7.34	7.17	45.26
Adriamycin	2	9.67	9.31	68.01

DISCUSSION

Gastric cancer is one of the most common malignant tumors in China. Surgical treatment is the main therapy of it. Anti-tumor drugs still play an important role in comprehensive therapy. Now cytotoxic compounds remain the main part of the chemotherapy drugs. The main defects of the cytotoxic compounds are the poor therapeutic effects on solid tumors, higher toxic side-effects and easy occurrence of drug resistance. Many Chinese drugs can enhance the immune function of the body. When used in the treatment, they showed less toxic side-effects but lower inhibitory rate on tumors.

Polysaccharides are big molecules linked by monosaccharides. The sugar-chain of polysaccharides can regulate cell proliferation, differentiation, growth and aging. They showed definite therapeutic effectiveness in anti-tumor therapy, and the ability to enhance body' s immune function, as well as a lower toxic side-effect[7-10]. For example, mushroom polysaccharides have already been used as a drug to regulate the organism reaction in clinical therapy and to prevent tumors in Japan. Umbellate pore fungus polysaccharides which were developed and used in clinical therapy in China, could reduce side-effects of chemotherapy and enhance the effects of chemotherapy against tumors.

We performed this clinical experiment by treating 30 gastric cancer patients with oral GBEP capsules. The images captured by electron gastroscope showed the average inhibitory rate of its capsules on gastric tumor was 53.5 %. The effective rate was 73.4 %. It indicated that GBEP had good clinical therapeutic effectiveness on gastric cancer.

Apoptosis is an active cellular process whereby individual cells are triggered to undergo self-destruction. Recent studies showed apoptosis played a main role in the prevention and treatment of tumors[11-13]. Anti-tumor effect of many chemotherapy drugs could induce apoptosis in tumor cells[14,15]. Cell apoptosis was regulated by genes[16,17]. We have known that apoptosis regulators can be divided into two kinds, namely apoptosis-inducing genes and apoptosis-inhibitory genes. Up-regulation of apoptosis-inducing gene expression could elevate the sensitivity of cells to factors or signals inducing apoptosis, and trigger apoptosis in this way. Up-regulation of apoptosis-inhibitory gene expression could reduce the sensitivity of cells to factors or signals inducing apoptosis, and apoptosis could be inhibited or delayed in this way. Bcl-2 was an important apoptosis-inhibitory gene[18-20], it included a nucleus molecule that can block cell apoptosis, prolong cell lives, accelerate DNA repairing, and thus promoting tumor genesis and development. So it could down-regulate cell apoptosis[21-25]. This clinical study and examination of cellular ultrastructures showed clues of apoptosis induced by GBEP in human gastric cancer cells. Using techniques of cell culture *in vitro* and flow cytometry, the contents of DNA and protein of human gastric cancer SGC-7901 cells were analysed. The results showed GBEP could increase SGC-7901 cell apoptosis rate, down-regulate bcl-2 at concentrations of 40-160 mg/L. It indicated that one of the therapeutic mechanisms of GBEP on gastric cancers might be that it induced tumor cell apoptosis. It also indicated that bcl-2 was involved in this process.

Malignant cells are similar to undifferentiated embryonic cells in morphology, function and metabolism. When tissue changes into malignancy, many phenotypes of the cells go back to the embryonic cell phenotypes, which is called de-differentiation or retro-differentiation. Malignant cells can be induced to differentiate towards normal cells in the presence of differentiation-inducer. Many malignant cells can approach to normal cells, even transform into normal cells completely, which is called re-differentiation or reversion. Change of cells from normal to malignancy is a break of the balance between proliferation and differentiation. Uncontrollable proliferation and de-differentiation are the characteristics of most malignant tumors. Differentiation-inducers can decelerate proliferation, enhance differentiation, thus creating a new normal balance. Like apoptosis, proliferation and differentiation are regulated by genes. C-myc is an important gene involved in the control of cell proliferation, and could up-regulate cell cycle progression, and induce cell proliferation[26-29]. C-fos gene is considered as an early response gene, and its expression level was in proportion to the differentiation degree of gastric cancer[30-32]. This clinical study and results of the cell ultrastructural examination showed clues of apoptosis induced by GBEP in human gastric cancer cells. The results of MTT experiment *in vitro* showed GBEP could inhibit the proliferation of human gastric cancer SGC-7901 cells. The results measured by flow cytometry showed GBEP could down-regulate the expression of c-myc gene and up-regulate the expression of c-fos in SGC-7901 cells at the concentrations of 40-160 mg/L. It indicates that inhibition on cell proliferation and inducement on cell differentiation might be involved in the therapeutic mechanism of GBEP on gastric cancer. C-myc and c-fos genes might contribute to the regulation of proliferation and differentiation.

ACKNOWLEDGMENTS

We are very grateful to Drs. Huo-Ying Shi, Li-Ming Yuan

and Wei-Dong Zhou, Center of Electroscope, Yangzhou University, and Mei-Zao Le, Department of Pathology, Bayi Hospital, Nanjing, China for their technical assistance in ultrastructural analysis; Drs. Zhi-Jiang Wu, Lü-Rong Men, Department of Cellular and Molecular Biology, Shanghai Institute of Biochemistry and Cell Biology, Academica Sinica for their technical assistance in flow cytometry.

REFERENCES

1 **Xu AH,** Chen HS, Xiang XR, Gu WR, Zhang HQ. The suppressive effects of ginkgo biloba exocarp polysaccharides (GBEP) on tumor in mice. *Zhongyao Iaoli yu Linchuang* 1996; **12**: 24-26
2 **Chen HS**, Xu AH, Wang Y, Wang Q, Wang XL. Influence of ginkgo biloba exocarp polysaccharides (GBEP) on interleukin-2 (IL-2) activity and solubility interleukin-2 receptor (sIL-2R) level in mice under lower immune function. *Zhongyao Yaoli yu Linchuang* 2001; **17:** 17-19
3 **Zhai F,** Chen HS. Clinical observation on effects of ginkgo biloba exocarp polysaccharides (GBEP) in Treatment of 84 Cases in cancer of middle-late stage. *Liaoning Zhongyi Zazhi* 2002; **29:** 564
4 **Xu A,** Chen H, Wang L, Wang Q. Influence of Ginkgo biloba L. exocarp polysaccharides on serum superoxide dismutase activity and malondialdehyde level in mice under different states. *Zhongguo Zhongyao Zazhi* 1998; **23:** 746-747
5 **Mosmann T.** Rapid colorimetric assay for cellular growth and survival: appli- cation to proliferation and cytotoxicity assays. *J Immunol Methods* 1983; **65:** 55-63
6 **Wu Q,** Chen Z, Su W. Mechanism of inhibition on activator protein-1 activity by all-trans retinoic acid in gastric cancer cells. *Chin Med J* 2000; **113:** 972-976
7 **Liu C,** Gao P, Qian J, Yan W. Immunological study on the antitumor effects of fungus polysaccharides compounds. *Wei Sheng Yan Jiu* 2000; **29:** 178-180
8 **Wang Z,** Wang Y, Huang Z, Zhong S, Wu Y, Yu L. Study on antitumor effect and mechanism of aloe polysaccharides. *Zhong Yao Cai* 2001; **24:** 350-353
9 **Kodama N,** Komuta K, Sakai N, Nanba H. Effects of D-Fraction, a polysaccharide from Grifola frondosa on tumor growth involve activation of NK cells. *Biol Pharm Bull* 2002; **25:** 1647-1650
10 **Lu X,** Su M, Li Y, Zeng L, Liu X, Li J, Zheng B, Wang S. Effect of Acanthopanax giraldii Harms Var. Hispidus Hoo polysaccharides on the human gastric cancer cell line SGC-7901 and its possible mechanism. *Chin Med J* 2002; **115:** 716-721
11 **Yan J,** Xu YH. Tributyrin inhibits human gastric cancer SGC-7901 cell growth by inducing apoptosis and DNA synthesis arrest. *World J Gastroenterol* 2003; **9:** 660-664
12 **Su M,** Dai M, Lu X, Li H, Liu J. Effect of traditional Chinese medicine compounds aining on the expression of apoptosis inducing genes of human gastric cancer cell. *Zhong Yao Cai* 2002; **25:** 563-566
13 **Gao F,** Yi J, Shi GY, Li H, Shi XG, Tang XM. The sensitivity of digestive tract tumor cells to As2O3 is associated with the inherent cellular level of reactive oxygen species. *World J Gastroenterol* 2002; **8:** 36-39
14 **Kimura H,** Konishi K, Kaji M, Maeda K, Yabushita K, Tsuji M, Ogino H, Satomura Y, Unoura M, Miwa A. Apoptosis, cell proliferation and expression of oncogenes in gastric carcinomas induced by preoperative administration of 5-fluorouracil. *Oncol Rep* 2000; **7:** 971-976
15 **Sugamura K,** Makino M, Shirai H, Kimura O, Maeta M, Itoh H, Kaibara N. Enhanced induction of apoptosis of human gastric carcinoma cells after preoperative treatment with 5-fluorouracil. *Cancer* 1997; **79:** 12-17
16 **Masutani M,** Suzuki J, Matsuda T, Dochin A, Sadaoka K, Nomura A, Ohira K, Takahashi K, Yamazaki K, Dosaka-Akita H, Nishimura M, Kawakami Y. Increased apoptosis associated with depressed type of early intestinal gastric cancer. *Jpn J Cancer Res* 2001; **92:** 1214-1219
17 **Zhao AG,** Zhao HL, Jin XJ, Yang JK, Tang LD. Effects of Chinese jianpi herbs on cell apoptosis and related gene expression in human gastric cancer grafted onto nude mice. *World J Gastroenterol* 2002; **8:** 792-796
18 **Cao J,** Qiao Y, Min J. Bcl-2 anti-sense oligonucleotide sensitizes Fas-mediated apoptosis of gastric cancer cells. *Zhonghua Zhongliu Zazhi* 2000; **22:** 466-468
19 **Zhou HB,** Zhu JR. Paclitaxel induces apoptosis in human gastric carcinoma cells. *World J Gastroenterol* 2003; **9:** 442-445
20 **Wu YL,** Sun B, Zhang XJ, Wang SN, He HY, Qiao MM, Zhong J, Xu JY. Growth inhibition and apoptosis induction of Sulindac on Human gastric cancer cells. *World J Gastroenterol* 2001; **7:** 796-800
21 **Hofler H,** Becker KF. Molecular mechanisms of carcinogenesis in gastric cancer. *Recent Results Cancer Res* 2003; **162:** 65-72
22 **Dixon D,** Flake GP, Moore AB, He H, Haseman JK, Risinger JI, Lancaster JM, Berchuck A, Barrett JC, Robboy SJ. Cell proliferation and apoptosis in human uterine leiomyomas and myometria. *Virchows Arch* 2002; **441:** 53-62
23 **Wang NS,** Unkila MT, Reineks EZ, Distelhorst CW. Transient expression of wild-type or mitochondrially targeted Bcl-2 induces apoptosis, whereas transient expression of endoplasmic eticulum-targeted Bcl-2 is protective against Bax-induced cell death. *Biol Chem* 2001; **276:** 44117-44128
24 **Li JQ,** Chen RC, Cai KX, Ye ZY. Apoptosis of human gastric cancer cell induced by photochemical riboflavin. *Ai Zheng* 2003; **22:** 253-256
25 **Liu S,** Wu Q, Ye XF, Cai JH, Huang ZW, Su WJ. Induction of apoptosis by TPA and VP-16 is through translocation of TR3. *World J Gastroenterol* 2002; **8:** 446-450
26 **Chen JP,** Lin C, Xu CP, Zhang XY, Fu M, Deng YP, Wei Y, Wu M. Molecular therapy with recombinant antisense c-myc adenovirus for human gastric carcinoma cells *in vitro* and *in vivo*. *J Gastroenterol Hepatol* 2001; **16:** 22-28
27 **Liu HL,** Lo CR, Jones BE, Pradhan Z, Srinivasan A, Valentino KL, Stockert RJ, Czaja MJ. Inhibition of c-Myc expression sensitizes hepatocytes to tumor necrosis factor-induced apoptosis and Necrosis. *Biol Chem* 2000; **275:** 40155-40162
28 **Zhu GH,** Wong BC, Eggo MC, Ching CK, Yuen ST, Chan EY, Lai KC, Lam SK. Non-steroidal anti-inflammatory drug-induced apoptosis in gastric cancer cells is blocked by protein kinase C activation through inhibition of c-myc. *Br J Cancer* 1999; **79:** 393-400
29 **Ishii HH,** Gobe GC, Pan W, Yoneyama J, Ebihara Y. Apoptosis and cell proliferation in the development of gastric carcinomas: associations with c-myc and p53 protein expression. *J Gastroenterol Hepatol* 2002; **17:** 966-972
30 **Tsuji M,** Funahashi S, Takigawa M, Seiki M, Fujii K, Yoshida T. Expression of c-fos gene inhibits proteoglycan synthesis in transfected chondrocyte. *FEBS Lett* 1996; **381:** 222-226
31 **Ito N,** Hirose M, Takahashi S. Cell proliferation and forestomach carcinogenesis. *Environ Health Perspect* 1993; **101**(Suppl 5): 107-110
32 **Kane S**, Prentice MA, Mariano JM, Cuttitta F, Jakowlew SB. Differential induction of early response genes by adrenomedullin and transforming growth factor-beta1 in human lung cancer cells. *Anticancer Res* 2002; **22:** 1433-1444

Edited by Zhang JZ and Wang XL

P.O.Box 2345, Beijing 100023,China
Fax: +86-10-85381893
E-mail: wjg@wjgnet.com www.wjgnet.com

World J Gastroenterol 2003;9(11):2428-2432
World Journal of Gastroenterology
 ISSN 1007-9327

• LIVER CANCER •

Segregation analysis of hepatocellular carcinoma in a moderately high-incidence area of East China

Ru-Lin Cai, Wei Meng, Hong-Yan Lu, Wen-Yao Lin, Feng Jiang, Fu-Min Shen

Ru-Lin Cai, Wei Meng, Feng Jiang, Fu-Min Shen, Department of Epidemiology, School of Public Health, Fudan University, Shanghai 200032, China
Hong-Yan Lu, Wen-Yao Lin, Haimen City Anti-epidemic Station, Haimen 226100, Jiangsu Province, China
Supported by the National Natural Science Foundation of China, No. 39930160
Correspondence to: Dr. Wei Meng, Department of Epidemiology, School of Public Health, Fudan University, Shanghai 200032, China. wmeng@shmu.edu.cn
Telephone: +86-21-54237767 or 7710
Received: 2002-12-28 **Accepted:** 2003-02-19

Abstract

AIM: To explore the mode of inheritance of hepatocellular carcinoma (HCC) in a moderately high-incidence area of East China.

METHODS: A pedigree survey was conducted in 210 families (3315 individuals) ascertained through 210 HCC probands in Haimen, Jiangsu Province. Simple segregation analysis was conducted using SEGRANB software. The probability of ascertainment (p), segregation ratio (p), and the proportion of sporadic cases (x) were estimated. Complex segregation analysis was performed using the REGTL program of S.A.G.E. Models were fitted on the data of 3212 individuals that allowed for personal HBsAg status and variable age of onset in REGTL program.

RESULTS: The estimate of segregation ratio was 0.191 by SEGRANB. The probability of ascertainment was 0.0266, and the proportion of sporadic cases was 0.465. The results of complex segregation analysis showed that Mendelian autosomal recessive inheritance of a major gene that influenced the age of onset distribution of HCC, provided the best fit to the data. In the best-fitting recessive model, the frequency of the disease allele was 0.11138. HBsAg seropositive status would significantly increase the risk of developing HCC.

CONCLUSION: These results suggest that at least one major gene is involved in the genetic predisposition to develop HCC at an earlier age of onset. The seropositive HBsAg status can significantly increase the risk of developing HCC, which provides strong support for the interaction between genetic and environmental risk factors.

Cai RL, Meng W, Lu HY, Lin WY, Jiang F, Shen FM. Segregation analysis of hepatocellular carcinoma in a moderately high-incidence area of East China. *World J Gastroenterol* 2003; 9 (11): 2428-2432
http://www.wjgnet.com/1007-9327/9/2428.asp

INTRODUCTION

Hepatocellular carcinoma (HCC) is one of the most common types of malignant tumor in the world, the estimated number of new cases worldwide annually is over 500 000[1], ranking third in cause of cancer deaths in China. An estimated 26 000 deaths are from HCC annually worldwide, among which about 40 % are in China[2]. Classical epidemiological studies have shown that certain risk factors are associated with HCC, though the odds ratios (ORs) vary considerably from study to study[3-5]. On a worldwide basis, chronic infection with hepatitis B virus (HBV) appears to be the most important risk factor for HCC. About 80 % of the patients of HCC in China are seropositive for hepatitis B surface antigen (HBsAg)[6]. An IARC working group in 1993 found that the evidence for a causal association of HBV with HCC was pretty strong. HCC is common in cirrhotic patients when cirrhosis is secondary to chronic viral hepatitis[1]. In addition to viral factors, environmental exposures and genetic susceptibility are clearly involved. Dietary aflatoxin exposure is an important codeterminant of HCC risk in Africa and parts of Asia[7]. Aflatoxins together with chronic hepatitis B virus (HBV) infection contribute to the high incidence of hepatocellular carcinoma in developing countries[8-10]. Contaminated drinking water and chemical carcinogens are also associated with the development of HCC[3].

Many familial clusterings of HCC have been reported[11,12]. The prevalence of HCC among the first-degree relatives is significantly higher than that among the second-degree and third-degree relatives, which suggests that genetic mechanisms may be responsible for familial HCC. Haimen city is a HCC high-incidence area of East China, however, only a few studies have been performed to explore the genetic mode of HCC in this area. Consequently, in this study, data of 210 pedigrees ascertained through HCC probands were collected and segregation analysis of HCC was performed.

MATERIALS AND METHODS

Materials and data collection

Probands were 210 HCC patients from an eight-year follow-up of a 90 000-person Haimen City cohort. All the patients were pathologically diagnosed in hospitals of counties and cities. Information on four-generation pedigrees was obtained for 210 families. Data on 3 315 individuals in the 210 families were collected primarily by face-to-face interviews or by checking the medical records and according to the recall of their relatives if the proband patients were dead. Data on 3 212 individuals (97 %) were used to fit models in the REGTL program of S.A.G.E. The remaining individuals were excluded because of little information available.

Family history interview and data management

A family history of HCC was collected as part of an interview to gather information on the medical history of probands and their relatives. The questionnaire included questions on age, occupation, tobacco use, drinking water source by decades (60 s, 70 s, 80 s, 90 s), staple food consumption by decades, result of HBsAg test, history of chronic hepatitis B, history of other chronic diseases, family history of HCC and relationship of family member with HCC to proband cases.

All the questionnaires were reviewed and checked for quality control. Pedigree information database was developed using Epi-Info v5.0.

Statistical methods

Simple segregation analysis by SEGRANB program In SEGRANB, models were fitted to the data and maximum likelihood scores of parameters were estimated. Hypothesis tests were performed to determine which set of parameter was most consistent with the observed data. The involved parameters were probability of ascertainment (p) (the probability for a patient to be identified as a proband), segregation ratio (p), and the proportion of sporadic cases (x). S is the sibship size, r is the total number of the affected siblings and a is the total number of the probands. The function for the probability of ascertainment is:

$$P(a \mid a>0;\ r, \pi) = \frac{\binom{r}{a} p^{a}(1-p)^{r-a}}{\left[1-(1-p)^{r}\right]}$$

The function for the estimate of the segregation ratio in the pedigrees with more than one patient is:

$$P(r>1) = \frac{\binom{s}{r} p^{r} q^{s-r}\left[1-(1-p)^{r}\right]}{1-(1-pp)^{s}-psq^{s-1}}$$

The functions for estimate of p and x are:

$$P(r=1) = \frac{spp\left[x+(1+x)\ q^{s-1}\right]}{xspp+(1+x)\left[1-(1-pp)^{s}\right]}$$

$$P(r>1) = \frac{(1-x)\binom{s}{r} p^{r}(1-p)^{s-r}\left[1-(1-p)^{r}\right]}{sppx+(1-x)\left[1-(1-pp)^{s}\right]}$$

U_{π},U_{p}, and U_{x} are the maximum likelihood scores for p, p and x, respectively. If the value of U was negative, the initial estimated value of the parameter should be reduced to fit the observed data, and vice versa.

Complex segregation analysis using REGTL program of S.A.G.E. (Statistical analysis for genetic epidemiology, v3.1. Case Western Reserve University, Cleveland, OH) The REGTL program of S.A.G.E. (1997) (release 3.1) under a Window' s 9x operating system was used to perform complex segregation analysis. This program uses maximum-likelihood methods to estimate parameters of mathematical models of disease occurrence in families. It assumes that under a class A regressive model, a censored trait, such as age of onset to a disease or of the disease susceptibilities, follows a logistic distribution. Sibs are dependent on one another only because of common parentage. Mendelian inheritance, if present, is presumed to be through a single autosomal locus with two alleles, A and B, A being associated with the affected state. The "type" was used to describe the discrete factors that affect a person' s phenotype. The same concept was denoted as "ousiotype". Genotypes are the special case of types, or ousiotypes, that transmit to offspring in Mendelian fashion. Thus we should use the term "type" to allow for any kind of discrete transmission, whether Mendelian or not. Two general models can be assumed. In model 1, the segregation of a possible major locus is allowed for by letting the baseline and age coefficient parameters of the age of onset distribution, but not the susceptibility, depends on an unobserved qualitative factor u=AA, AB, BB. Susceptibility depends solely on randomly distributed environmental characteristics of the population studied. In model 2, type is presumed to influence susceptibility to the affected state, but not the parameters of the age-at-onset distribution, and groups of individuals of different types have the same mean age at onset. Analysis was performed under the model 1 in this study. HCC was represented by a dichotomous variable y, in which y=1 for affected and 0 for unaffected. The following parameters were estimated: type frequencies Ψ_{u} (u=AA, AB, BB. If the type frequencies are in Hardy-Weinberg equilibrium proportions, then they are defined in terms of q_{A}=frequency of allele A), transmission probabilities τ_{u} (the probability that a parent of type u transmits allele A to an offspring, under Mendelian transmission, τ_{AA}=1, τ_{AB}=0.5, τ_{BB}=0), baseline parameter β which can be sex-dependent and/or type-dependent, covariate coefficient ζ_{HbsAg} which is coded 1 if the individual is HBsAg positive and is coded 0 if negative or 9 if unknown. Thus, the coefficient ζ_{HBsAg} is the change in the logit (the risk of HCC) according to the HBsAg status, age adjustment coefficient α, and susceptibility parameter γ which can be sex-dependent. Susceptibility is the probability that an individual is susceptible.

To correct for ascertainment bias, the likelihood of each pedigree is conditioned on the proband' s HCC status by age at exam or death and his or her actual age of onset. This assumes single ascertainment, which is a reasonable approximation since only 1 (0.5 %) of 210 families has more than one patient eligible to be a proband. Under single ascertainment, the probability that any one family will be ascertained is small and proportional to the number of affected children in the family.

As the process of parameter estimate is complex and time consuming when complex models are fitted, a program written in Perl program was used to facilitate the estimate of the initial value of parameters. This program was used to generate random values for the initial estimate of parameters and to call modules in the REGTL program of the S.A.G.E. package to perform segregation analysis. For each model, thirty converged results were saved, among which the best-fitted result of each model was chosen.

Under the model 1, six hypotheses were tested against the likelihood of a general (unrestricted) model, in which all parameters were unrestricted and allowed to fit the empirical data. Thus this general model would give the best fit to the data. The six hypotheses of transmission are as follows: major gene type, Mendelian dominant, Mendelian recessive, Mendelian additive, purely environmental effect and no transmission. Twice the differences between the natural log likelihood (InL) for the data under the hypothesis of interest and that under the unrestricted model is in accordance with χ^{2} distribution, thus it is used to assess the degree of departure from expectation statistically. The degree of freedom (df) for the χ^{2} statistic is given by the differences in the number of estimated parameters between the hypothesis and the unrestricted model. If one or more parameters are fixed at a bound at the end of the estimation process, a range of the df and P values are given when appropriate. A non-significant χ^{2} indicates that the hypothetical model cannot be rejected. When covariates and major gene effects are considered simultaneously, the number of potential hypothesis tests is large and the natural hierarchy of the models may not be clear. In this case, models can also be compared with use of Akaike' s (1974) information criterion (AIC), which is defined as AIC= -2lnL+2×(Number of parameters estimated). A lower value of AIC represents a better fitting model.

RESULTS

Distribution of HCC and HBsAg status among relatives

Of 3 315 individuals in the 210 extended pedigrees, 330 (10.0 %)

including probands were affected with HCC. The distribution of HCC and HBsAg status among the relatives is summarized in Table 1. Among the first-degree relatives, the prevalence of HCC was 6.6 % (100/1511). Among the second-degree relatives, it was 2.1 % (20/945). The prevalence of HCC was 23.1 % (30/130) among the HBsAg positive first-degree relatives, it was 19.2 (5/26) among the HBsAg positive second-degree relative. As shown in Table 2, among the fathers of the probands, the

Table 1 HBsAg status of HCC cases among first-degree and second-degree relatives

HBsAg status	First-degree relatives		Second-degree relatives	
	No. of relatives	No. (%) of HCC	No. of relatives	No. (%) of HCC
+	130	30 (23.1 %)	26	5 (19.2 %)
-	1104	47 (4.3 %)	711	4 (0.6 %)
Unknown	277	23 (8.3 %)	208	11 (5.3 %)
Total	1511	100 (6.6 %)	945	20 (2.1 %)

Table 2 Distribution of HCC among the relatives of 210 probands

Characteristic	Relatives						
	Father	Mother	Brother	Sister	Son	Daughter	Spouse
No. (%) of HCC	11 (5.5 %)	14 (7.0 %)	59 (16.1 %)	15 (5.0 %)	1 (0.5 %)	0 (0 %)	2 (1.0 %)
Total	200	199	366	298	221	227	202

Table 3 Distribution of probands and affected siblings among families

Number of affected siblings	1	2	3	4	4	5
Number of probands in family	1	1	1	1	2	1
Number of families	162	32	7	7	1	1

Table 4 Maximum likelihood estimates of parameters of segregation models for HCC by SEGRANB

π	p	x	U_π	U_p	U_x	χ^2_π	χ^2_p	χ^2_x	$\bar{\pi}$	$\bar{p}$	$\bar{x}$	P value
0.026 556	0.50	0.00	116.922	-929.338	2482.747	1 069.75	1 074.303	1 712.618	9.176	-0.655 98	0.689 81	<0.05
0.026 556	0.25	0.00	50.272	-530.853	230.405	134.657	134.794	144.777	2.705	-0.003 92	0.628 36	<0.05
0.026 556	0.20	0.60	-7.363	50.253	-34.966	4.140	4.069	4.090	-0.536	0.280 97	0.483 03	<0.05
0.026 556	0.280 97	0.483	8.856	-41.824	36.699	3.566	3.806	3.817	0.429	0.189 96	0.587 05	<0.05
0.026 556	0.189 96	0.483	-0.055	0.200	0.464	0.097	0.098	0.09	-0.055	0.200 11	0.463 91	>0.05
0.026 556	0.189 96	0.464	-0.054	0.559	0.007	1.976E-04	3.118E-04	2.146E-07	0.029	0.190 52	0.463 94	>0.05
0.026 556	0.190 52	0.464	0.013	-0.003	0.276	1.097E-05	8.709E-09	3.252E-04	0.027	0.190 52	0.465 08	>0.05
0.026 6	0.190 52	0.465	-0.054	0.529	0.016	1.909E-04	2.822E-04	1.064E-06	0.030	0.191 06	0.465 07	>0.05
0.026 6	0.191	0.465	0.005	0.059	0.244	1.517E-06	3.486E-06	2.505E-04	0.027	0.191 06	0.466 03	>0.05

π, p and x: initially estimated values for π, p and x, respectively. U_π, U_p and U_x: maximum likelihood scores for π, p and x, respectively. χ^2_π, χ^2_p and χ^2_x: χ^2 of the estimated π, p and x, respectively. $\bar{\pi}$, $\bar{p}$, and $\bar{x}$: corrected value for π, p and x, respectively.

Table 5 Complex segregation analysis on HCC among the 210 extended pedigrees (SAGE-REGTL, model 1)

Parameter[a]	Hypothesis						
	Mendelian						
	Dominant	Recessive	Additive	Major gene	Environmental	No transmission	General
qA	0.003 04	0.111 38	0.114 51	0.879 64	0.022 29	0[b]	0.008 61
τAA	1.0[b]	1.0[b]	1.0[b]	1.0[b]	1.0[c]	0[b]	1.0[c]
τAB	0.5[b]	0.5[b]	0.5[b]	0.5[b]	1.0[c]	0[b]	0.0[c]
τBB	0[b]	0[b]	0[b]	0[b]	1.0[c]	0[b]	1.0[c]
βAA	-5.748 96	-6.862 19	-7.300 81	-13.664 08	-7.274 45	-6.744 03	-9.222 95
βAB	-5.748 96[d]	-14.229 74	-14.452 92	-22.641 40	-4.142 30	-6.744 03[d]	-6.194 60
βBB	-11.625 77	-14.229 74[d]	-21.605 02	-6.835 46	-9.940 49	-6.744 03[d]	-20.472 73
α	0.100 39	0.123 35	0.128 67	0.123 85	0.074 99	0.057 10	0.084 64
γ	0.721 25	1.000[c]	0.869 15	1.000[c]	0.899 22	1.000[c]	1.000[c]
ζHBsAg	0.931 55	1.363 80	1.840 08	1.202 00	2.723 39	2.708 74	1.475 35
-2lnL	831.079 18	799.687 16	805.170 10	798.206 61	822.204 67	842.795 94	803.246 35
AIC	843.079 18	811.687 16	817.170 10	812.206 61	838.204 67	850.795 94	825.246 35
χ^2	27.832 83	3.559 19	1.923 75	5.039 74	18.958 32	39.549 59	-
df[e]	1-5	2-5	1-5	1-4	2-3	4-7	-
P value	P<0.001	P>0.1	P>0.1	0.01<P<0.03	P<0.001	P<0.001	-

a: See Materials and Methods for definitions of the parameters. b: Parameter was fixed at this value and estimation was not carried out. c: Parameter estimate reached its bound. d: Parameter was constrained to equal the preceding one and was not estimated. e: Range in degrees of freedom was given since parameters in models reached their bounds.

prevalence of HCC was 5.5 % (11/200). Among siblings, it was 11.1 % (74/664) (16.1 % for brothers, 5.0 % for sisters). Among offsprings, it was 0.2 % (1/448), and among spouses of the probands, it was 1.0 % (2/202).

Parameter estimate in simple segregation analysis by SEGRANB software

The distribution of probands and their affected siblings among the 210 families is shown in Table 3. There was one family with two patients eligible to be a proband. The best fitted probability of ascertainment p was 0.026556, U_p was 6.500244×10^{-3}, χ^2 was 2.848217×10^{-8}. The estimated sets of parameters are shown in Table 4. The best fitted probability of ascertainment p was 0.0266, the segregation ratio p was 0.191, and the proportion of sporadic cases x was 0.465.

Results of complex segregation analysis by REGTL program of S.A.G.E.

Of the 210 families, 48 (22.9 %) had two or more HCC patients. The mean age at onset was 50 (range 21-83). Complex segregation analyses were performed by REGTL under model 1 that did not include regressive familial effects in the models and in which age at onset and susceptibility were not sex-dependent. One environmental covariate, HBsAg status, as a dichotomous variable was included in the models.

In Table 5, the best fitted parameter estimates for general and hypothetical models were reported. As a result, the Mendelian recessive and additive (codominant) hypotheses were not rejected (P>0.1) and the major gene model was marginally not rejected (0.01<P<0.03). All other models were rejected at a 0.001 significance level. According to AIC, Mendelian recessive inheritance was the best-fitted hypothesis, but the AICs for recessive (811.68716) and major gene (812.20661) models were very close. The recessive model suggested that approximately 11.1 % of the population could be expected to carry the candidate gene (or gene pattern). The coefficient of the covariate HBsAg was positive. If its standard deviation is to do the Wald' s test, we got $|\beta_{HBsAg}|/|S_{HBsAg}|$=1.36380/0.40661=3.354>1.96, P<0.05, which suggested that HBsAg seropositive status would increase the risk of developing HCC.

DISCUSSION

In this study, we explored the inheritance mode of HCC in the 210 extended pedigrees in Haimen City by simple and complex segregation analyses. This study used SEGRANB software and REGTL program of S.A.G.E. analyzing a population-based family data set to investigate the presence of a major gene effect for HCC. In simple segregation analysis procedure, as the estimate of segregation ratio p could be substantially affected by the estimated value of the probability of ascertainment p [13,14], especially on complex traits, therefore p was calculated using maximum likelihood method by SEGRANB program in this study. The estimated value of p was 0.0266, which suggested a single ascertainment for this study. Then the segregation ratio and the proportion of sporadic cases were also estimated by maximum likelihood method using SEGRANB. The best-fitted parameter set is shown in Table 4. The segregation ratio was 0.191 and the proportion of sporadic cases was 0.465 for this data, which suggested that HCC did not follow a mono-gene inheritance pattern in this population and environmental factors appeared to influence the development of HCC since 46.5 % of the cases were sporadic.

Due to the modest sample size and relatively high proportion of missed information for the elder generations of the probands in the studied pedigrees, gender and familial residual effects were not estimated simultaneously with other parameters of the corresponding models in complex segregation analysis. The results showed that although both the recessive and additive (codominant) hypotheses could not be rejected, Mendelian autosomal recessive inheritance of a major gene that influenced baseline and age of onset of HCC provided the best fit to the data. The estimated gene frequency under the recessive hypothesis was 0.11138. The result in this study was consistent with the result of an earlier complex segregation analysis by Shen *et al*. (1991) using the POINTER program in which an autosomal recessive major gene yielding lifetime risk of PHC (primary hepatocellular carcinoma) was suggested. In this study, the information of serum HBsAg status for relatives was obtained through the questionnaire and sometimes the report of laboratory test was unavailable. Although this situation could cause miss of information for many individuals in analysis, which might ruin the statistical power, the significance of seropositive HBsAg effect could still be observed. It strongly suggested that chronic HBV infection was a risk factor in developing HCC in this population.

The ultimate test of the utility of segregation analysis is whether the resulting models can be used in linkage analysis to identify disease-susceptibility loci. Although the recessive hypothesis provided the best fit to the data, segregation analysis had its limitation that it could not distinguish the effect of a single locus that underlied a trait from the effects of two or more independently acting loci with similar transmission patterns[15]. Thus, more than one gene, with different penetrances and modes of inheritance, may be involved. Even under oligogenic inheritance, the parameters derived from a single locus segregation analysis can provide power for detecting the susceptibility loci. Many studies have been performed to search for susceptibility genes for HCC[16-29], and several novel genes have been suggested to play a role in HCC development[30-32]. The HCC mortality differs in different areas in China and there are some environmental factors (e.g. local economic status, geographical factors, habit of food consumption and viral infection) that might differ in different areas. With the same environmental exposures, HCC occurrence differs a great deal from family to family, which is typified by the existence of highly aggregated "cancer families". It is hard to say which factor (environmental or genetic) is more important. All can play important roles in the etiology of HCC. The mutation of HCC gene (s) may act as a trigger for HCC onset, or people with the gene (s) may tend to be more susceptible to HCC under the influence of certain environmental risk factors.

In conclusion, our study showed that a Mendelian autosomal recessive major gene might play an important role in the etiology of HCC in a moderately high-incidence area of East China. This study provides some modeling parameters of HCC (in this area) for further linkage studies. The identification of the putative gene detected by the study is warranted.

ACKNOWLEDGEMENTS

This work was supported in part by the National Natural Science Foundation of China (No: 39930160). Some of the results in this paper were obtained by using the program package S.A.G.E., which was supported by a U.S. Public Health Service Resource Grant (1 P41 RR03655) from the National Center for Research Resources. Prof. Fu-Min Shen donated the version of the program package S.A.G.E. used in this study. We thank Dr. Yin Hu of the NCI Center for Bio-informatics for his help on compiling Perl script and on tackling some technical problems.

REFERENCES

1 **Montalto G,** Cervello M, Giannitrapani L, Dantona F, Terranova A, Castagnetta LA. Epidemiology, risk factors, and natural history of hepatocellular carcinoma. *Ann N Y Acad Sci* 2002; **963**: 13-20

2 **Zhao ZT,** Jia CX. Epidemiology of liver cancer. In: Liu Q, Wang WQ, eds. Cancer. *Beijing: People's Health Press* 2000: 221-239

3 **Evans AA,** Chen G, Ross EA, Shen FM, Lin WY, London WT. Eight-year follow-up of the 90000-person Haimen City cohort: I. Hepatocellular carcinoma mortality, risk factors, and gender differences. *Cancer Epidemiol Biomarkers Prev 2002*; **11**: 369-376

4 **Yoshizawa H.** Hepatocellular carcinoma associated with hepatitis C virus infection in Japan: projection to other countries in the foreseeable future. *Oncology* 2002; **62**(Suppl 1): 8-17

5 **Donato MF,** Arosio E, Del Ninno E, Ronchi G, Lampertico P, Morabito A, Balestrieri MR, Colombo M. High rates of hepatocellular carcinoma in cirrhotic patients with high liver cell proliferative activity. *Hepatology* 2001; **34**: 523-528

6 **Wang YL,** Zhou HG, Gu GW. Advances in liver cancer research. *Shanghai: Shanghai Science and Technology Literature Press* 1999: 13-27

7 **Ming L,** Thorgeirsson SS, Gail MH, Lu P, Harris CC, Wang N, Shao Y, Wu Z, Liu G, Wang X, Sun Z. Dominant role of hepatitis B virus and cofactor role of aflatoxin in hepatocarcinogenesis in Qidong, China. *Hepatology* 2002; **36**: 1214-1220

8 **Wild CP,** Yin F, Turner PC, Chemin I, Chapot B, Mendy M, Whittle H, Kirk GD, Hall AJ. Environmental and genetic determinants of aflatoxin-albumin adducts in the Gambia. *Int J Cancer* 2000; **86**: 1-7

9 **Chen SY,** Chen CJ, Tsai WY, Ahsan H, Liu TY, Lin JT, Santella RM. Associations of plasma aflatoxin B1-albumin adduct level with plasma selenium level and genetic polymorphisms of glutathione S-transferase M1 and T1. *Nutr Cancer* 2000; **38**: 179-185

10 **Wang JS,** Huang T, Su J, Liang F, Wei Z, Liang Y, Luo H, Kuang SY, Qian GS, Sun G, He X, Kensler TW, Groopman JD. Hepatocellular carcinoma and aflatoxin exposure in Zhuqing Village, Fusui County, People's Republic of China. *Cancer Epidemiol Biomarkers Prev* 2001; **10**: 143-146

11 **Tai DI,** Changchien CS, Hung CS, Chen CJ. Replication of hepatitis B virus in first-degree relatives of patients with hepatocellular carcinoma. *Am J Trop Med Hyg* 1999; **61**: 716-719

12 **Yu MW,** Chang HC, Liaw YF, Lin SM, Lee SD, Liu CJ, Chen PJ, Hsiao TJ, Lee PH, Chen CJ. Familial risk of hepatocellular carcinoma among chronic hepatitis B carriers and their relatives. *J National Cancer Institute* 2000; **92**: 1159-1164

13 **Tai JJ,** Hsiao CK. Effects of implicit parameters in segregation analysis. *Hum Hered* 2001; **51**: 192-198

14 **Haghighi F,** Hodge SE. Likelihood formulation of parent-of–origin effects on segregation analysis, including ascertainment. *Am J Hum Genet* 2002; **70**: 142-156

15 **Jarvik GP.** Complex segregation analyses: Uses and limitations. *Am J Hum Genet* 1998; **63**: 942-946

16 **Tufan NL,** Lian Z, Liu J, Pan J, Arbuthnot P, Kew M, Clayton MM, Zhu M, Feitelson MA. Hepatitis Bx antigen stimulates expression of a novel cellular gene, URG4, that promotes hepatocellular growth and survival. *Neoplasia* 2002; **4**: 355-368

17 **Yu MW,** Yang YC, Yang SY, Chang HC, Liaw YF, Lin SM, Liu CJ, Lee SD, Lin CL, Chen PJ, Lin SC, Chen CJ. Androgen receptor exon 1 CAG repeat length and risk of hepatocellular carcinoma in women. *Hepatology* 2002; **36**: 156-163

18 **Kinoshita M,** Miyata M. Underexpression of mRNA in human hepatocellular carcinoma focusing on eight loci. *Hepatology* 2002; **36**: 433-438

19 **Fu XY,** Wang HY, Tan L, Liu SQ, Cao HF, Wu MC. Overexpression of *p*28 / gankyrin in human hepatocellular carcinoma and its clinical significance. *World J Gastroenterol* 2002; **8**: 638-643

20 **Ito Y,** Miyoshi E, Takeda T, Nagano H, Sakon M, Noda K, Tsujimoto M, Monden M, Matsuura N. Linkage of elevated ets-2 expression to hepatocarcinogenesis. *Anticancer Res* 2002; **22**: 2385-2389

21 **Nakau M,** Miyoshi H, Seldin MF, Imamura M, Oshima M, Taketo MM. Hepatocellular carcinoma caused by loss of heterozygosity in Lkb1 gene knockout mice. *Cancer Res* 2002; **62**: 4549-4553

22 **Wei Y,** Van Nhieu JT, Prigent S, Srivatanakul P, Tiollais P, Buendia MA. Altered expression of E-cadherin in hepatocellular carcinoma: correlations with genetic alterations, beta-catenin expression, and clinical features. *Hepatology* 2002; **36**: 692-701

23 **Chiao PJ,** Na R, Niu J, Sclabas GM, Dong Q, Curley SA. Role of Rel / NF-kappaB transcription factors in apoptosis of human hepatocellular carcinoma cells. *Cancer* 2002; **95**: 1696-1705

24 **Jiang Y,** Zhou XD, Liu YK, Wu X, Huang XW. Association of hTcf-4 gene expression and mutation with clinicopathological characteristics of hepatocellular carcinoma. *World J Gastroenterol* 2002; **8**: 804-807

25 **Ikeguchi M,** Hirooka Y, Kaibara N. Quantitative analysis of apoptosis-related gene expression in hepatocellular carcinoma. *Cancer* 2002; **95**: 1938-1945

26 **Gao CJ,** Guo LL, Guo Y, Cao CA. Relationship between hepatitis C virus infection and expression of apoptosis-related gene bcl-2, bax and ICH-1 in hepatocellular carcinoma tissues. *Diyi Junyi Daxue Xuebao* 2002; **22**: 797-799

27 **Levy L,** Renard CA, Wei Y, Buendia MA. Genetic alterations and oncogenic pathways in hepatocellular carcinoma. *Ann N Y Acad Sci* 2002; **963**: 21-36

28 **Wang Y,** Wu MC, Sham JS, Tai LS, Fang Y, Wu WQ, Xie D, Guan XY. Different expression of hepatitis B surface antigen between hepatocellular carcinoma and its surrounding liver tissue, studied using a tissue microarray. *J Pathol* 2002; **197**: 610-616

29 **Joo M,** Kang YK, Kim MR, Lee HK, Jang JJ. Cyclin D1 overexpression in hepatocellular carcinoma. *Liver* 2001; **21**: 89-95

30 **Kohno H,** Nagasue N, Rahman MA. COX-2 - a target for preventing hepatic carcinoma? *Expert Opin Ther Targets* 2002; **6**: 483-490

31 **Zeng JZ,** Wang HY, Chen ZJ, Ullrich A, Wu MC. Molecular cloning and characterization of a novel gene which is highly expressed in hepatocellular carcinoma. *Oncogene* 2002; **21**: 4932-4943

32 **Harada H,** Nagai H, Ezura Y, Yokota T, Ohsawa I, Yamaguchi K, Ohue C, Tsuneizumi M, Mikami I, Terada Y, Yabe A, Emi M. Down-regulation of a novel gene, DRLM, in human liver malignancy from 4q22 that encodes a NAP-like protein. *Gene* 2002; **296**: 171

Edited by Wu XN and Wang XL

P.O.Box 2345, Beijing 100023,China
Fax: +86-10-85381893
E-mail: wjg@wjgnet.com www.wjgnet.com

World J Gastroenterol 2003;9(11):2433-2440
World Journal of Gastroenterology
 ISSN 1007-9327

• LIVER CANCER •

Expression of TNF-related apoptosis-inducing Ligand receptors and antitumor tumor effects of TNF-related apoptosis-inducing Ligand in human hepatocellular carcinoma

Xiao-Ping Chen, Song-Qing He, Hai-Ping Wang, Yong-Zhong Zhao, Wan-Guang Zhang

Xiao-Ping Chen, Song-Qing He, Hai-Ping Wang, Yong-Zhong Zhao, Wan-Guang Zhang, Hepatic Surgery Center, Affiliated Tongji Hospital, Tongji Medical College,Huazhong University of Science and Technology,Wuhan,430030, China
Supported by the major Foundation of Ministry of Public Health, No.2001-2003
Correspondence to: Xiao-Ping Chen, MD, Professor & Director, Hepatic Surgery Center, Tongji Hospital, Tongji Medical College, Huazhong University of Science and Technology, Wuhan 430030, Hubei Province, China. chenxp_53@sina.com
Telephone: +86-27-83662599 **Fax:** +86-27-83646605
Received: 2002-10-21 **Accepted:** 2002-11-20

Abstract

AIM: To investigate the expression of TNF-related apoptosis -inducing Ligand (TRAIL) receptors and antitumor effects of TRAIL in hepatocellular carcinoma (HCC).

METHODS: Expression of TRAIL receptors was determined in 60 HCC tissues, 20 normal liver samples and two HCC cell lines (HepG2 and SMMC-7721). The effects of TRAIL on promoting apoptosis in HCC cell lines were analyzed after the cells were exposed to the recombinant TRAIL protein, as well as transfected with TRAIL-expression construct. *In vivo* effects of TRAIL on tumor growth were investigated by using nude mice HCC model of hepG2.

RESULTS: Both death receptors were expressed in all HCC tissues and normal hepatic samples. In contrast, 54 HCC tissues did not express DcR1 and 25 did not express DcR2. But both DcR were detectable in all of the normal liver tissues. The expression patterns of DR and DcR in HCC samples (higher DR expression level and lower DcR expression level) were quite different from those in normal tissue. DR5, DR4, and DcR2 expressed in both cell lines, while no DcR1 expression was detected. Recombinant TRAIL alone was found to have a slight activity as it killed a maximum of 15 % of HCC cells within 24 h. Transfection of the TRAIL cDNA failed to induce extensive apoptosis in HCC lines. *In vivo* administration of TRAIL gene could not inhibit tumor growth in nude mice HCC model. However, chemotherapeutic agents or anticancer cytokines dramatically augmented TRAIL-induced apoptosis in HCC cell lines.

CONCLUSION: Loss of DcR (especially DcR1) in HCC may contribute to antitumor effects of TRAIL to HCC.HCC is insensitive towards TRAIL-mediated apoptosis, suggesting that the presence of mediators can inhibit the TRAIL cell-death-inducing pathway in HCC. TRAIL and chemotherapeutic agents or anticancer cytokines combination may be a novel strategy for the treatment of HCC.

Chen XP, He SQ, Wang HP, Zhao YZ, Zhang WG. Expression of TNF-related apoptosis-inducing Ligand receptors and antitumor tumor effects of TNF-related apoptosis-inducing Ligand in human hepatocellular carcinoma. *World J Gastroenterol* 2003; 9(11): 2433-2440
http://www.wjgnet.com/1007-9327/9/2433.asp

INTRODUCTION

Apoptosis, the process of programmed cell death, is a fundamental mechanism in developmental and homeostatic maintenance of complex biological systems. Maladjustment or disturbance in apoptotic process will result in transformation and provide a growth advantage to transformed cells. Members of the tumor necrosis factor (TNF) superfamily contribute to a variety of cell biological functions, including cellular activation, proliferation and death, by interaction with their corresponding receptors[1-3]. TNF and fasL have been focused on because of they can induce tumor cells apoptosis, whereas TNF and fas ligand were unlikely to provide useful target neoplastic elimination of tumors cells for two reasons. One is that many tumor cells are resistant to FasL or TNF-mediated cell death, as shown in the present studies, the other is that systemical administeration of TNF and FasL is limited by their acute cytotoxic effects on normal tissues *in vivo*, thereby limiting their widespread use in the treatment of cancer[4-7].

TNF-related apoptosis-inducing ligand (TRAIL), another TNF superfamily member, is a promising cancer therapeutic agent[8]. TRAIL appears to specifically kill transformed cells, and spare most normal cells[9]. TRAIL induces apoptotic death on binding to either of two proapoptosic TRAIL receptors, DR5 or DR4.Normal cells are believed to be resistant to TRAIL because of expressing higher levels of TRAIL decoy receptors DcR1 or DcR2 on their cell surface.

A recent study reported that chemotherapeutic agents could augment TRAIL-induced apoptosis in human hepatocellular carcinoma cell lines, indicating that TRAIL may have therapeutic potential in the treatment of human HCC[28]. In the present study, we investigated the expression of TRAIL receptors and antitumor effects of TRAIL in human HCC, in order to find an effective treatment of HCC.

MATERIALS AND METHODS

HCC and control liver Tissues

Sixty surgically resected specimens employed in this study were obtained from patients with HCC who had undergone potentially curative tumor resection at the Hepatic Surgery Center, Tongji Hospital during January, 2000-December, 2000. All HCC tissues were pathologically confirmed. Tweenty normal liver samples obtained from patients with benign tumor were used as control at the same time. We obtained informed consent from all patients. Resected tissues were frozen immediately at -70 ℃. All cases were selected on the basis of availability of frozen materials for study and in the absence of extensive tumor necrosis. Materials were composed of 5 cases of grade I, 23 cases of grade II, 27 cases of grade III and 5 cases of grade IV according to TNM system (1987). The tumor

lesions analyzed here including 35 poor differentiations, 15 moderate differentiations and 10 well differentiations. There were 53 males and 7 females, and the age was from 18 to 75 years with an average of 45.8 years (s, 13.5 years), HBsAg positive 55 and negative 5. Routinely processed 4 % paraformaldehyde-fixed, paraffin-embedded blocks containing principal tumor were selected. Serial sections of 5 μm thickness were prepared from the cut surface of blocks at the maximum cross-section of tumor.

Cell lines and cell culture

Human HCC cell lines (HepG2, SMMC-7721), Jurkat T-cell line and human colangiocarcinma cell line QBC939 were purchased from ATCC. Cells were cultured in DMEM supplemented with 1 % penicillin/streptomycin and 10 % heat-inactivated fetal calf serum in a 5 % CO_2 incubator at 37 ℃.

Detection of TRAIL-R

The expression of TRAILR1, TRAILR2, TRAILR3 and TRAILR4 in HCC cell lines and human HCC tissues was detected by *in situ* hybridization. Digoxigenin-labeled antisense and sense TRAILR probes were purchased from Boster Biotechnology Inc. *In situ* mRNA expressions were performed according to the manufacturer' s protocol. Deparaffinized, rehydrated tissue sections (5 μM) on silane-coated slides were permeabilized by incubation in proteinase 75 (20 μg/ml) for 30 min at 37 ℃ and acetylated in PBS containing 0.25 % acetic anhydride and 0.1 M triethanolamine for 10 min at room temperature. Prehybridization was carried out in 50 % formamide, 4×SSC, 1×Denhardt' s solution, 125 μg/ml tRNA, and 100 μg/ml freshly denatured salmon sperm DNA for 2-4 h at 42 ℃. Hybridization was performed using prehybridization solution containing denatured TRAILR antisense or sense probes (50 ng/slide) for 36 h at 42 ℃ and followed by washes at 52 ℃ with different solutions (2×SSC and 50 % formamide, 30 min; 1×SSC and 50 % formamide, 30 min; 0.5×SSC and 50 % formamide, 30 min). After that, the sections were incubated in turn in buffer 1 [150 mM NaCl and 100 mM Tris-HCl (pH 7.5)] containing 5 % BSA and 0.3 % Triton X-100 for 30 min and in horseradish peroxidase-conjugated antidigoxigenin antibody diluted 1:500 with buffer 1 containing 5 % BSA and 0.3 % Triton X-100 for 2 h at room temperature. After washed in buffer 1, the sections were immersed briefly in buffer 2 [100 mM NaCl, 50 mM $MgCl_2$, and 100 mM Tris-HCl (pH 9.5)] and incubated in buffer 2 containing 0.025 % diaminobenzidine and 0.02 % H_2O_2 for 15 min at 4 ℃. Finally, the sections were immersed in 10 mM Tris-HCl, 1 mM EDTA buffer (pH 8.0), rinsed in water, and mounted with glycerol mountant.

In vitro effects of TRAIL on cellular apoptosis of HCC

HCC cells were seeded into 96-well microtiter plates with 5×10^3 cells per well and cultured in DMEM supplemented with 10 % fetal calf serum at 37 ℃ under a humidified atmosphere of 5 % CO_2 for 24 h when the cells were in the exponential phase of growth. After treated with TRAIL at the indicated concentration (1, 10, 100, 1 000 ng/ml), the cell viability was assessed with MTT method and the absorbance was measured at 490 nm with a microtiter plate reader. Cell death was estimated with the following formula.

% specific death=A(untreated cells)-A(treated cells)/A (untreated cells)×100.

Results were derived form 3 individual experiments. Each experimental condition was repeated at least in sextuplicate wells for each experiment. We used the same method to detect the effects of TRAIL on Jurkat T-cell line and human colangiocarcinma cell line QBC939.

Construction of TRAIL expression plasmids

The sequence corresponding to the C-terminus extracellular region of 114-281 amino acid (aa) of TRAIL was amplified by PCR, and subcloned into the EcoRV/EcoRI site of expression vector pIRES-EGFP. Following DNA plasmid transfection with superfect reagent for 72 hours, cells were evaluated for apoptosis. The expression of cellular TRAIL protein was verified with Western blot. Briefly, cells were collected by centrifugation at 2 000 g for 10 minutes, cells lysed with lyse cell solution (50 mmol/L Tris-cl, 150 mmol/L NaCl, 0.02 % sodium azide, 0.1 % SDS, 100 ug/ml PMSF, 1 μg/ml aprotinin, 1 % NP-40, 0.5 % deoxysodium cholate), protein in the supernants was separated by 12 % SDS-PAGE and transferred by electroblotting to nitrocellulose membranes. The membranes were blocked by TBST (TBS-Tween) with 5 % non-fat milk, and then incubated with primary antibody (anti-hTRAILmAb) in TBST with 5 % non-fat milk overnight. Proteins were detected with horseradish peroxidase-conjucated secondary antibody and performed chemiluminscence according to the manufacturer' s instructions. MTT assay was used to measure cell viability. The tumor cells were infected with pIRES-EGFP-null as a control.

Flow cytometry

Collected cells were washed with PBS, fixed in 70 % ethanol, digested with RNase A (10 mg/L) in PBS for 30 min and then stained with propidium iodide (PI), and analyzed on a FACScan.

Gene therapy of experimental nude mice subcutaneous hepatocellular carcinoma by direct intratumoral injection of TRAIL gene

5×10^6 HepG2 cells were inoculated subcutaneously into the back of nude mice. One cm tumors were formed in nude mice about ten days after inoculation. Plasmid carrying TRAIL gene was delivered into the tumor by intra-tumor injection (n=10). pIRES-EGFP-null injection as a control (n=10). RT-PCR was adopted to examine the expression of TRAIL gene in tumor. The expression of TRAIL protein was detected by Western blotting. The anti-tumor effect of gene therapy was evaluated according to the sizes of tumors for 4 weeks. Therapeutic effects of TRAIL gene on experimental cholangiocarcinoma induced in nude mice were detected using the same method.

Treatment of HCC cell lines in combination with TRAIL and IFN-γ, IL-2 or chemotherapy drug

HCC cells exposed to IL-2 (different concentrations) combined with recombinant TRAIL protein (50 ng/ml) for 72 h were compared with treatment of TRAIL alone. In the same time, the effect of TRAIL in combination with IFN-γ or chemotherapy drugs (such as mitomycin, 5-fluorouracil) was investigated. Cell viability was examined by MTT assay.

Statistical analysis of data

Quantitative comparisons were performed by Student t test or the chi-square and Fisher exact tests. All statistical analyses were performed using SAS software. Statistical significance was set at 0.05.

RESULTS

Expression of TRAIL-R in HCC cell lines and tissues

DR5 and DR4 were present in all HCC tissue as well as normal hepatic tissues. In contrast, 54 tumors did not express DcR1 and 25 tumors did not express DcR2, but DcR1 and DcR2 were detected in all of the normal liver tissues. The expression patterns of DR and DcR in HCC samples (higher DR expression

level and lower DcR expression level) were quite different from those in normal tissue. DR5, DR4, and DcR2 were expressed, but DcR1 did not express in both cell lines. Expression of TRAIL-R was located mainly in the cytoplasm (Figure 1).

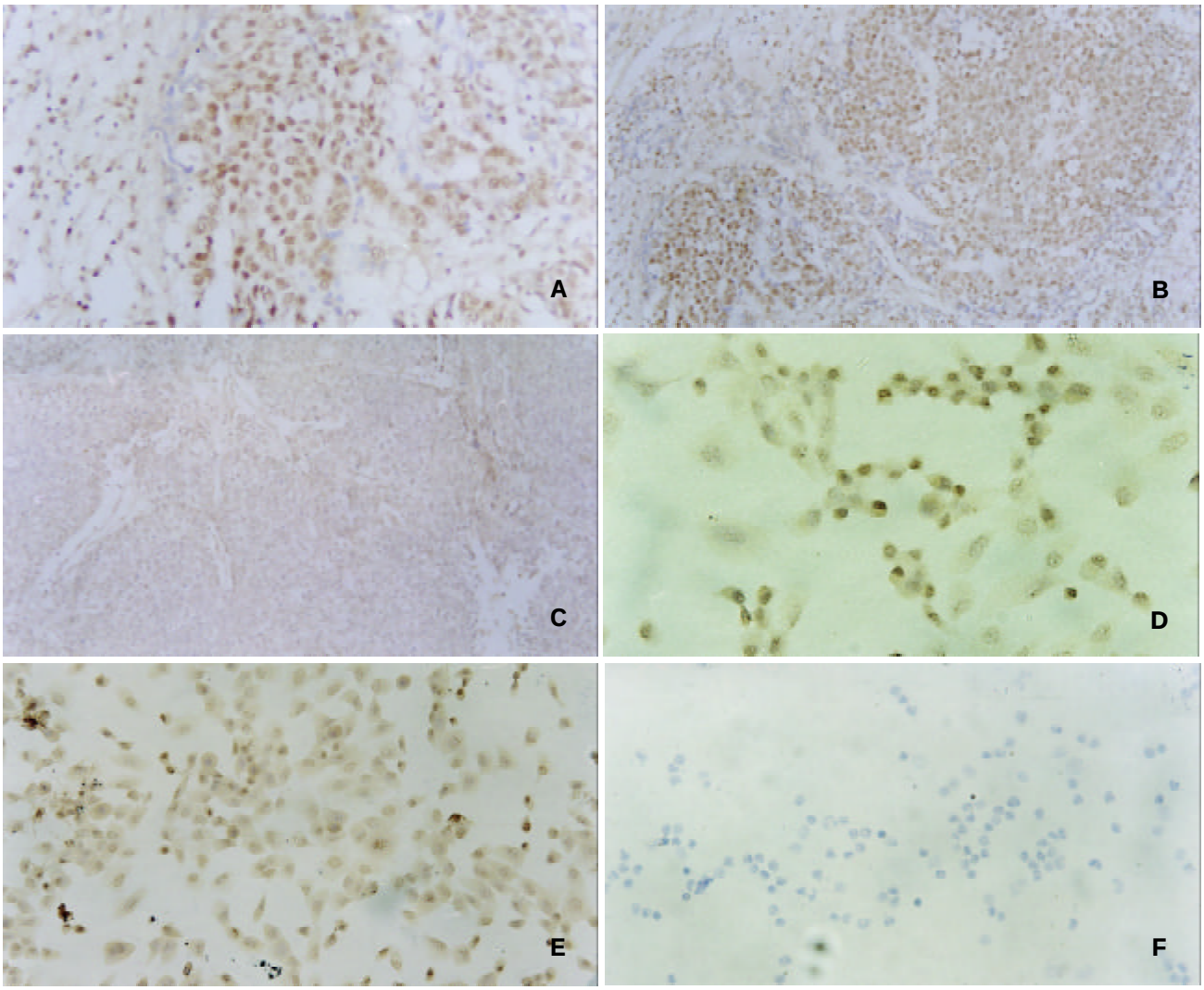

Figure 1 Expression of TRAILR in human HCC tissues and HCC cell lines by *in situ* hybridization. Stronger expression of DR5 (A and D) and DR4 (B and E) as well as negative expression of DcR1 C and F) in both human HCC tissues and HCC cell lines. Note that TRAIL-R staining was found mainly in the cytoplasm and membrane.

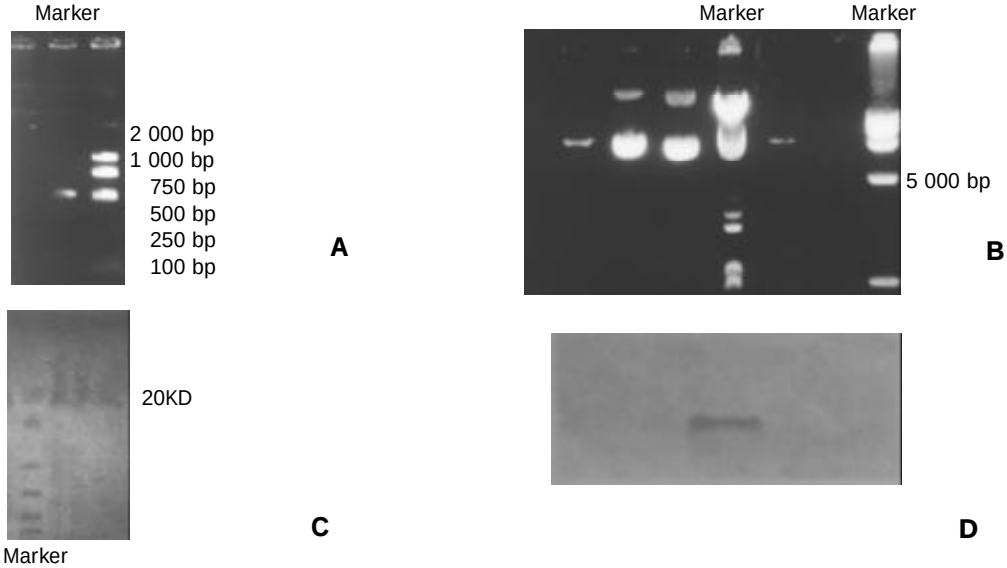

Figure 2 Construction of pIRES-EGFP-TRAIL. A: the C-terminus extracellular region of 114-281 amino acid (aa) was amplified by PCR, including EcoRV / EcoRI at two end, 523 bp. B: TRAIL expression plasmids pIRES-EGFP-TRAIL. C: The cellular proteins were separated by SDS-PAGE. D: Western blot identified expression of TRAIL, negative expression of TRAIL in control.

Production of TRAIL protein

TRAIL expression was assayed by Western blotting as shown, a 19.6 KD band sTRAIL monomers. In contrast, no corresponding bands were present in the negative control. These results demonstrated that the transfection of pIRES-EGFP-TRAIL resulted in transgene expression in human liver cancer cell lines (Figure 2).

Resistance of human HCC cells to both TRAIL and pIRES-EGFP-TRAIL transfection

TRAIL protein alone failed to induce significant apoptosis in both HCC cell lines, even at a dose up to 100 ng/ml, it killed only about 10 % of HCC cells within 24 h, compared with 70 % of Jurkat cells and about 50 % of cholangiocarcinoma cell line QBC939. Production of TRAIL following pIRES-EGFP-TRAIL transfection also failed to lead to tumor cell death. HCC cell lines were adequately transfected with pIRES-EGFP-TRAIL. Minimal cell death of HepG2 cells was observed upon infection with pIRES-EGFP-TRAIL. Analysis of TRAIL protein production by Western blot revealed detectable levels in HepG2 cell lysed by 6h post infection, with levels increasing over the entire time course. These results demonstrated that tumor cells infected with pIRES-EGFP-TRAIL could produce TRAIL protein, however failed to lead to their extensive death (Figure 3).

Effects of gene therapy on experimental hepatocellular caricinoma

Direct intra-tumor injection of pIRES-EGFP carrying TRAIL gene was performed on experimental hepatocellular caricinoma induced in nude mice. RT-PCR was adopted to examine the expression of TRAIL gene in nude mice tumor,the anti-tumoral

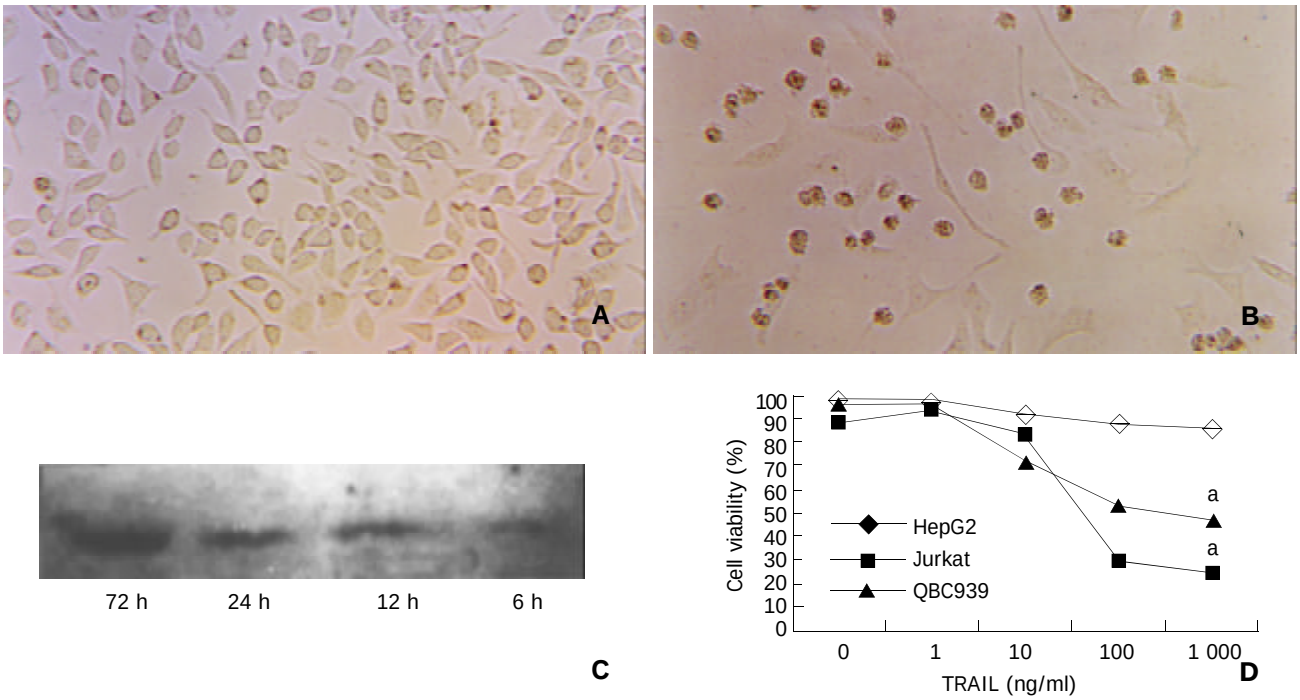

Figure 3 Determination of the percentage of cell viability by *in vitro* administration of recombinant TRAIL.A: Normal HepG2 shapes. B: HepG2 shaped treatment with TRAIL (100 ng / ml, 24 h). C: Western blot analyzed expression of TRAIL protein transfected with pIRES-EGFP-TRAIL (6 h, 12 h, 24 h 72 h). D:Survival of tumor cells treatment with TRAIL, detected by MTT. Each value represents the mean of the three wells. For clarity, SD bars are omitted from the graph, but are less than 5 % for all data points. Experiments were performed at least three separate times with similar results. [a]: Compared with hepG2, statistical significant (P<0.05). The results similar to HepG2 were obtained in SMMC-7721.

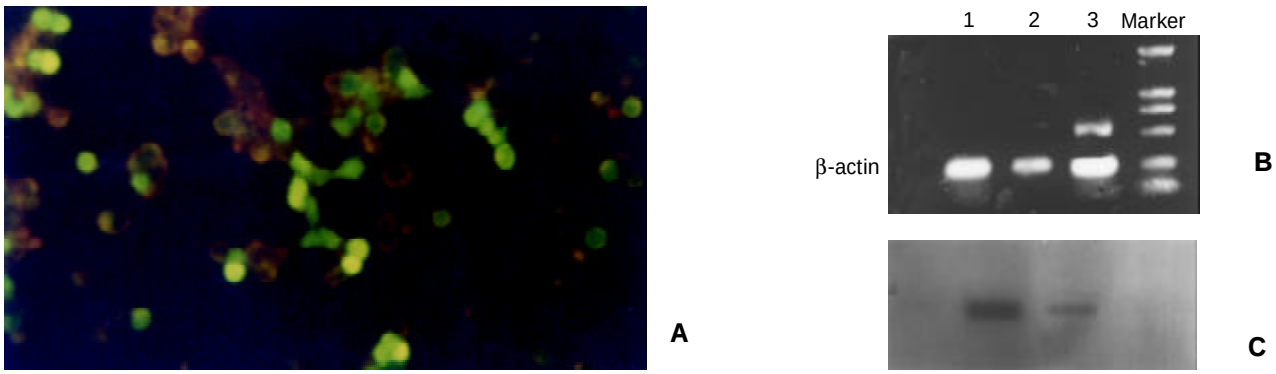

Figure 4 Transfection of pIRES-EGFP-TRAIL *in vitro* and *in vivo*. A: Transfected efficiency observed with fluorescence microscope (*in vitro*). B: The expression of TRAIL gene in nude mice tumor was all relatively strong (*in vivo*). (1), the expression of TRAIL gene in tissue near the tumor was weak (2) and that in normal liver tissue was negative after transfection of TRAIL gene (3). C: TRAIL protein production was determined by Western blot analysis. (a) Nude mice HCC tissue, (b) Adjacent tissue and (c) Normal tissue.

effect of gene therapy was evaluated according to the sizes of the tumors (as shown by Figure 4). Ten days after transfection of TRAIL gene, the expression of TRAIL gene in nude mice tumor was relatively strong, the expression of TRAIL transgene in tissue near the tumor was weaker and that in normal liver tissue was negative.

However, the tumor sizes were slightly less than those in control group (as shown in Table 1). TRAIL gene intra-tumor injection could lead to effective gene delivery and gene expression but had limited effect on experimental HCC in nude mice.

Table 1 Antitumor effects of pIRES-EGFP-TRAIL transfection on tumor growth in nude mice (tumor size $\bar{x}\pm s$, cm)

Target cell	pIRES-EGFP-TRAIL (n=10)	pIRES-EGFP-null (n=10)	P
HepG2	1.05±0.39	1.30±0.27	0.174
QBC939	0.85±0.23	0.32±0.15	0.023

Synergistic induction of apoptosis by combination of TRAIL and chemotherapeutic drugs

We incubated HCC cells with mitomycin (0.001 mg/ml) or 5-fluorouracil (5-Fu) (0.025 mg/ml) in combination with TRAIL (50 ng/ml). Cell viability was examined after 24-72 h. Cytoxicity of the combination of TRAIL and chemotherapeutic agents was compared with either agent alone (Figure 5). Sensitization of HCC cells to TRAIL-inducing apoptosis was independent of p53 status because both HepG2 and SMMC-7721 were similarly sensitized to TRAIL in combination with chemotherapeutic agents, and transfection of p53 could not enhance the sensitivity of SMMC-7721 to TRAIL-inducing apoptosis. The results demonstrated TRAIL could decrease the threshold of some chemotherapeutic drugs 50-100 folds.

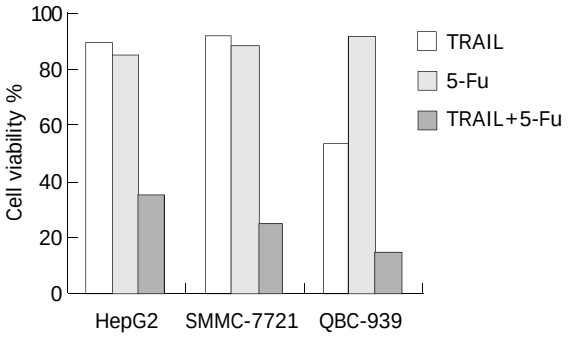

Figure 5 Cell viability of tumor cells incubated with TRAIL in combination with 5-Fu. Cell viability is shown as the percentage of viable cells relative to control cell after 24 h of incubation with TRAIL (50 ng/ml), 5-Fu (0.025 mg/ml) or both. SD bars are less than 5 % for all data points and omitted.

Low dose of interleukin-2 enhanced TRAIL-inducing apoptosis in HCC cells

HCC cells were cultured in the presence of TRAIL or TRAIL plus IL-2 or IFN-γ. Cultures were examined by phase contrast light microscopy at 6, 12, 24, 48, and 72 h. A rounded cytopathic effect was detectable in HCC cell cultures in the presence of TRAIL plus low dose IL-2 after 12 h, but was more prominent after 24 h. Extensive cell death was apparent in HCC cell cultures treated with TRAIL plus IL-2 at 48-72 h. To quantitate the extent of cell death, we measured cell viability treated with IL-2, TRAIL, or IL-2 and TRAIL using MTT. In contrast, HCC cultures treated with IL-2 alone appeared healthy throughout the experiment. Importantly, the death-inducing synergistic effects of TRAIL in combination with IL-2 were not specific to HCC cells, but also induced other tumor cells death (such as cholangiocarcinoma cell line QBC939, data not shown). These data indicated that TRAIL in combination with low dose IL-2 could induce cell death in HCC cells cultures *in vitro*. To our surprise, Low dose of IL-2 significantly enhanced TRAIL-inducing apoptosis in HCC cells after 48-72 h, but high dose of IL-2 only had a weaker role.

To delineate that TRAIL and IL-2 specifically killed HCC cells and spared normal liver cells, we cultured primary normal liver cells and normal fetal liver cell line L02 in the presence of TRAIL and IL-2 for 48 or 72 h. We subsequently determined whether they were undergoing apoptosis. By contrast to HCC cells, normal cells cultured in the presence of TRAIL and IL-2 exhibited no signs of apoptosis. These data indicated that TRAIL in combination with IL-2 could selectively induce apoptosis of HCC cells but not normal liver cells. Furthermore, we obtained similar synergistic results with combination of TRAIL and IFN-γ.

Apoptosis detection by FACScan

Cell death might occue through apoptosis or necrosis. Here, we found that TRAIL could kill HCC cells through apoptosis by FACScan (Figure 6).

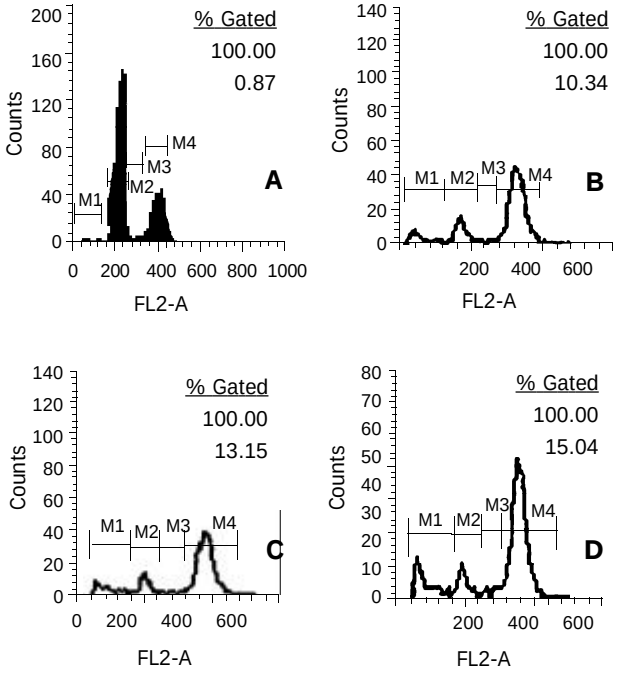

Figure 6 Apoptosis of HepG2 after treatment with TRAIL.A: HepG2 without treatment. B, C, D: HepG2 treatment with TRAIL for 24 h (B, 10 ng/ml. C, 100 ng/ml. D, 1 000 ng/ml). Compared to A P<0.05.

DISCUSSION

To selectively kill target tumor cells and spare normal tissues are one of the ultimate goals of cancer research. TRAIL, a type II transmembrane protein, was initially identified based on the homology of its extracellular domain with FasL, TNF and lymphotoxin-α[8]. TRAIL transcripts have been detected in the adult spleen, thymus, lung, prostate, ovary, small intestine, peripheral blood lymphocytes, colon, heart, placenta, skeletal muscle, and kidney, but not in the adult liver, brain, and testis. Receptors that bind to TRAIL include death receptor (DR) 4/TRAILR1[10], DR5/KILLER/TRAILR2/TRICK2[11-16], decoy receptor (DcR) 1/TRAILR3/TRID (TRAIL without an extracellular domain)/LIT (Lymphocyte Inhibitor of TRAIL)[12-15,19], DcR2/TRAILR4/TRUDD (TRAIL receptor

with a truncated death domain)[19-21] and a soluble receptor called osteoprotegerin (OPG)[22]. DR4, DR5, DcR1, and DcR2 have been shown to bind TRAIL with similar affinities. However, only two of the TRAIL receptors, DR4 and DR5, contain functional death domains and are capable of inducing apoptosis. DcR1, DcR2 are highly expressed in normal tissues, but have substantially lower expression in malignant cells, indicating a low cytotoxic effect in normal tissues. In contrast, DR4 and DR5 are expressed in malignant cells as well as in normal tissues. Despite having multiple receptors, TRAIL can selectively target tumor cells to undergo apoptosis while leaving normal cells unaffected. The selectivity of TRAIL-induced apoptosis has been demonstrated by systemic administration of TRAIL, which reduces tumor growth *in vivo*, without the severe toxic effects often seen in TNF or FasL treated mice. A relatively large number of tumor cell lines, such as leukemia, lymphoma, myeloma, melanoma, breast cancer, colon carcinoma, cholangiocarcinoma or thyroid carcinoma, are sensitive to cytotoxic effects of TRAIL, indicating that TRAIL may be a powerful selective cancer therapeutic [8,21-31].

However, the potential utility and safety of systemic administration of TRAIL have been recently questioned because results showed sensitivity of human but not monkey or mouse hepatocytes to a polyhisidine-tagged recombinant soluble form of TRAIL (amino acids 114-281,114-281TRAIL. his)[32]. Fortunately, another study showed that the toxicity of histidine-tagged TRAIL to human hepatocytes *in vitro* had aberrant biochemical properties, i.e., loss of zinc with the formation of intersubunit disulfide bonds. When this reagent was replaced by a nontagged soluble TRAIL zinc-replete TRAIL (114-281.TRAIL.rs), normal liver cell cytotoxicity was not observed[33-35].

Another potential drawback of TRAIL therapy was that not all cancer cells were sensitive to TRAIL. The regulation of TRAIL signaling is extremely complex, the mechanisms of TRAIL-resistance remain unclear. It has been suggested that the reason why some cells are susceptible to TRAIL while others appear to be resistant lies in the endogenous presence of the non-death-signaling TRAILR[35]. However, examination of various tumor cell types has shown that basal expression of TRAILR did not correlate with susceptibility to TRAIL[36,37]. Alternatively, the presence or absence of intracellular inhibitors of apoptosis such as the cellular inhibitor of caspase 8/FLICE-inhibitory protein (cFLIP) might be important[38-44], and in some circumstances, cFLIP expression did correlate with the susceptibility of tumor cells to TRAIL[37]. It has been found that NF-κB activation also protected cells against TRAIL-induced apoptosis[19]. Taken together, previous studies indicated that TRAIL resistance to apoptosis might be cell-type specific requiring up-regulation or down-regulation of one of the TRAIL receptors, assembly of different receptors, involvement of decoy receptors, and functions of intracellular inhibitors or intracellular anti-apoptotic/survival pathways working in concert. There is long way to clarify TRAIL-resistance mechanisms. How to reverse TRAIL-resistance is also an important topic before TRAIL is developed into an effective anticancer drug. Therefore, as the first step we detected the assembly of different receptors in HCC.

In the present study, both DR were present in all HCC tissue as well as in normal hepatic tissues derived from surgically resected margins of benign tumor. In contrast, 54 HCC tumors did not express DcR1 and 25 HCC tumors did not express DcR2. Both DcR were detectable in all of the normal liver tissues. High expression of DR and low or no expression of DcR in HCC tissue differed from low expression of DR and high expression of DcR in normal hepatic tissues. DR5, DR4, and DcR2 were expressed in both cell lines examined, but DcR1 did not express in both cell lines. Although expressed detectable TRAIL-R1 and -R2, both HCC cell lines showed strong resistance to TRAIL-induced apoptosis. Recombinant TRAIL (100 ng/ml) alone was found to have a slight activity as it killed about 10 % of HCC cells within 24 h compared with over 70 % of Jurkat cells and about 50 % of human cholangiocarcinoma cell line QBC939. Transfection of TRAIL cDNA also failed to induce extensive apoptosis in HCC lines. *In vivo* administration of TRAIL gene could not inhibit tumor growth in nude mice HCC model. These results suggest that some possibly endogenous suppressors of TRAIL-mediated apoptosis might exist in HCC cells. Certainly, components for TRAIL-induced apoptosis existed in these cell lines, and resistance to apoptosis in HCC was more likely mediated by intracellular signaling events than by alternations in receptor expression or the presence of decoy receptors. The mechanisms of TRAIL resistance in HCC should be identified in order to reverse TRAIL resistance.

The pharmacokinetic profile of soluble TRAIL indicated that after iv injection the majority of protein was cleared within 5 hours. Increasing in *vivo* t1/2 of soluble TRAIL or developing an alternative means of delivery may increase the relative tumoricidal activity of TRAIL. Identification of alternate methods to deliver TRAIL to the tumor site is also critical for further developing and testing anti-tumor activity of TRAIL *in vivo*. The results in our work described the production of an expression vector engineered to carry the gene for TRAIL. Shortly after cell tranfection, TRAIL protein was detected, rapidly leading to the induction of apoptosis in TRAIL-sensitive tumor cells (such as cholangiocarcinoma cell line QBC939, data not shown) *in vitro*, indicating the potential of using TRAIL gene and local expression of TRAIL to destroy TRAIL-sensitive tumor cells *in vivo*. As for TRAIL resistant tumor cells, effective treatment would be attached by new therapy strategies such as combining gene therapy.

How to reverse TRAIL-resistance is an important topic before TRAIL is developed into an effective anticancer drug. Consistent with several previous reports, our results showed that chemotherapeutic agents significantly sensitized HCC cell lines to TRAIL-induced apoptosis. TRAIL could decrease the threshold of some chemotherapeutic drugs 50-100 flods. The mechanism of overcoming tumor resistance to TRAIL-induced apoptosis by chemotherapeutic agents must be reserved for further investigation. Therefore, our results also showed that cytokines that compose part of the arsenal of the immune system against tumors might alter HCC sensitivities to TRAIL, For example, a subtoxic level of interlukin-2 could overcome the resistance of HCC cells. No significant apoptosis was induced in cells pretreated with IL-2 alone even at 10 000 unit/ml, and TRAIL (50 ng/ml) induced 10 % cell death after 24 h treatment. However, HCC cells treated with IL-2 (50 unit/ml) in combination with TRAIL (50 ng/ml) were killed about 50 % at 48 h, indicating that IL-2 could sensitize HCC cells to TRAIL-induced apoptosis. The effect of IL-2 which enhanced TRAIL-mediated apoptosis was not dose-depent, low dose IL-2 had a stronger sensitizing effect while high dose IL-2 had a weaker role. HCC cells could become sensitive to TRAIL-mediated cell death after treatment IFN-γ, too. The possible explanations for these effects are that IFN-γ could induce TRAIL expression, up-regulate DR and Caspase 8, significantly decrease NF-κB-activation, and prevent IAP2[45-48]. These findings have therapeutic implications because resistance to apoptosis in HCC cells may be dramatically overcome by agents used in combination.

In summary, TRAILR expression is prevalent in HCC and there is a different expression of receptor types in HCC cells compared with normal hepatic tissue. HCC cells are insensitive

to TRAIL-mediated apoptosis, suggesting the presence of mediators can inhibit the TRAIL-inducing apoptosis pathway in HCC and has a limited therapeutic role for TRAIL as a single agent in HCC. However, TRAIL-based tumor therapy in combination with chemotherapeutic agents or anticancer cytokines might be a powerful treatment for HCC.

REFERENCES

1 **Ashkenazi A**, Dixit VM. Apoptosis control by death and decoy receptors. *Curr Opin Cell Biol* 1999; **11**: 255-260
2 **Cosman D**. A family of ligands for the TNF receptor superfamily. *Stem Cells* 1994; **12**: 440-455
3 **Smith CA**, Farrah T, Goodwin RG. The TNF receptor superfamily of cellular and viral proteins: activation, costimulation, and death. *Cell* 1994; **76**: 959-962
4 **Havell EA**, Fiers W, North RJ. The antitumor function of tumor necrosis factor (TNF). I.Therapeutic action of TNF against an established murine sarcoma is indirect, immunologically dependent and limited by severe toxicity. *J Exp Med* 1988; **167**: 1067-1085
5 **Bird GL**, Sheron N, Goka AK, Alexander GL, Williams RS. Increased plasma tumor necrosis factor in severe alcoholic hepatitis. *Ann Intern Med* 1990; **112**: 917-920
6 **Schilling PJ**, Murray JL, Markowitz AB. Novel tumor necrosis factor toxic effects. Pulmonary hemorrhage and severe hepatic dysfunction. *Cancer* 1992; **69**: 256-260
7 **Ogasawara J**, Watanabe-Fukunaga R, Adachi M, Matsuzawa A, Kasugai T, Kitamura Y, Itoh N, Suda T, Nagata S. Lethal effect of the anti-Fas antibody in mice. *Nature* 1993; **364**: 806-809
8 **Wiley SR**, Schooley K, Smolak PJ, Din WS, Huang CP, Nicholl JK, Sutherland GR, Smith TD, Rauch C, Smith CA. Identification and characterization of a new member of the TNF family that induces apoptosis. *Immunity* 1995; **3**: 673-682
9 **Sheridan JP**, Marsters SA, Pitti RM, Gurney A, Skubatch M, Baldwin D, Ramakrishnan L, Gray CL, Baker K, Wood WI, Goddard AD, Godowski P, Ashkenazi A. Control of TRAIL-induced apoptosis by a family of signaling and decoy receptors. *Science* 1997; **277**: 818-821
10 **Pan G**, O'Rourke K, Chinnaiyan AM, Gentz R, Ebner R, Ni J, Dixit VM. The receptor for the cytotoxic ligand TRAIL. *Science* 1997; **276**: 111-113
11 **Walczak H**, Degli-Esposti MA, Johnson RS, Smolak PJ, Waugh JY, Boiani N, Timour MS, Gerhart MJ, Schooley KA, Smith CA, Goodwin RG, Rauch CT. TRAIL-R2: a novel apoptosis-mediating receptor for TRAIL. *EMBO J* 1997; **16**: 5386-5397
12 **Pan G**, Ni J, Wei YF, Yu G, Gentz R, Dixit VW. An antagonist decoy receptor and a death domain-containing receptor for TRAIL. *Science* 1997; **277**: 815-818
13 **Screaton GR**, Monkolsapaya J, Xu XN, Cowper AE, McMichael A, Bell JI. TRICK2, a new alternatively spliced receptor that transduces the cytotoxic signal from TRAIL. *Curr Biol* 1997; **7**: 693-696
14 **Schneider P**, Bodmer JL, Thome M, Hofmann K, Holler N, Tschopp J. Characterization of two receptors for TRAIL. *FEBS Lett* 1997; **416**: 329-334
15 **MacFarlane M**, Ahmad M, Srinivasula SM, Fernandes-Alnemri T, Cohen GM, Alnemri ES. Dentification and molecular cloning of two novel receptors for the cytotoxic ligand TRAIL. *J Biol Chem* 1997; **272**: 25417-25420
16 **Sheridan JP**, Marsters SA, Pitti RM, Gurney A, Skubatch M, Baldwin D, Ramakrishnan L, Gray CL, Baker K, Wood WI, Goddard AD, Godowski P, Ashkenazi A. Control of TRAIL-induced apoptosis by a family of signaling and decoy receptors. *Science* 1997; **277**: 818-821
17 **Miller LK**. The role of caspase family of cysteine proteases in apoptosis. Semin. *Immunol* 1997; **9**: 35
18 **Degli-Esposti MA**, Smolak PJ, Walczak H, Waugh J, Huang CP, DuBose RF, Goodwin RG, Smith CA. Cloning and characterization of TRAIL-R3, a novel member of the emerging TRAIL receptor family. *J Exp Med* 1997; **186**: 1165-1170
19 **Degli-Esposti MA**, Dougall WC, Smolak PJ, Waugh JY, Smith CA, Goodwin RG. The novel receptor TRAIL-R4 induces NF-κB and protects against TRAIL-mediated apoptosis, yet retains an incomplete death domain. *Immunity* 1997; **7**: 813-820
20 **Marsters SA,** Sheridan JP, Pitti RM, Huang A, Skubatch M, Baldwin D, Yuan J, Gurney A, Goddard AD, Godowski P, Ashkenazi A. A novel receptor for Apo2L/TRAIL contains a truncated death domain. *Curr Biol* 1997; **7**: 1003-1006
21 **Pan G**, Ni J, Yu G, Wei YF, Dixit VM. TRUNDD, a new member of the TRAIL receptor family that antagonizes TRAIL signaling. *FEBS Lett* 1998; **424**: 41-45
22 **Emery JG**, McDonnell P, Burke MB, Deen KC, Lyn S, Silverman C, Dul E, Appelbaum ER, Eichman C, DiPrinzio R, Dodds RA, James IE, Rosenberg M, Lee JC, Young PR. Ostroprotegerin is a receptor for the cytotoxic ligand TRAIL. *J Biol Chem* 1998; **273**: 14363-14367
23 **Keane MM**, Ettenberg SA, Nau MM, Russell EK, Lipkowitz S. Chemotherapy augments TRAIL-induced apoptosis in breast cell lines. *Cancer Res* 1999; **59**: 734-741
24 **Gibson SB**, Oyer R, Spalding AC, Anderson SM, Johnson GL. Increased expression of death receptors 4 and 5 synergizes the apoptosis response to combined treatment with eptoposide and TRAIL. *Mol Cell Biol* 2000; **20**: 205-212
25 **Gliniak B**, Le T. Tumor necrosis factor-related apoptosis-inducing ligand's antitumor activity *in vivo* is enhanced by the chemotherapeutic agent CPT-11. *Cancer Res* 1999; **59**: 6153-6158
26 **Gong B**, Almasan A. Apo2 ligand/TNF-related apoptosis-inducing ligand and death receptor 5 mediate the apoptotic signaling induced by ionizing radiation in leukemic cells. *Cancer Res* 2000; **60**: 5754-5760
27 **Tanaka S**, Sugimachi K, Shirabe K, Shimada M, Wands JR. Expression and antitumor effects of TRAIL in human cholangiocarcinoma. *Hepatology* 2000; **32**: 523-527
28 **Yamanaka T**, Shiraki K, Sugimoto K, Ito T, Fujikawa K, Ito M, Takase K, Moriyama M, Nakano T, Suzuki A. Chemotherapeutic agents augment TRAIL-induced apoptosis in human hepatocellular carcinoma cell lines. *Hepatology* 2000; **32**: 482-490
29 **Ahmad M**, Shi Y. TRAIL-induced apoptosis of thyroid cancer cells: potential for therapeutic intervention. *Oncogene* 2000; **19**: 3363-3371
30 **Mitsiades N**, Poulaki V, Tseleni-Balafouta S, Koutras DA, Stamenkovic I. Thyroid carcinoma cells are resistant to FAS-mediated apoptosis but sensitive tumor necrosis factor-related apoptosis-inducing ligand. *Cancer Res* 2000; **60**: 4122-4129
31 **Walczak H**, Miller RE, Ariail K, Gliniak B, Griffith TS, Kubin M, Chin W, Jones J, Woodward A, Le T, Smith C, Smolak P, Goodwin RG, Rauch CT, Schuh JC, Lynch DH. Tumoricidal activity of tumor necrosis factor–related apoptosis-inducing ligand *in vivo. Nat Med* 1999; **5**: 157-163
32 **Jo M**, Kim TH, Seol DW, Esplen JE, Dorko K, Billiar TR, Strom SC. Apoptosis induced in normal human hepatocytes by tumor necrosis factor-related apoptosis-inducing ligand. *Nat Med* 2000; **6**: 564-567
33 **Nicholson DW**. From bench to clinic with apoptosis-based therapeutic agents. *Nature* 2000; **407**: 810-816
34 **Lawrence D**, Shahrokh Z, Marsters S, Achilles K, Shih D, Mounho B, Hillan K, Totpal K, DeForge L, Schow P, Hooley J, Sherwood S, Pai R, Leung S, Khan L, Gliniak B, Bussiere J, Smith CA, Strom SS, Kelley S, Fox JA, Thomas D, Ashkenazi A. Differential hepatocyte toxicity of recombinant Apo2L/TRAIL versions. *Nat Med* 2001; **7**: 383-385
35 **Gura T,** How TR. AIL kills cancer cells, but not normal cells. *Science* 1997; **277**: 768
36 **Griffith TS**, Rauch CT, Smolak PJ, Waugh JY, Boiani N, Lynch DH, Smith CA, Goodwin RG, Kubin MZ. Functional analysis of TRAIL receptors using monoclonal antibodies. *J Immunol* 1999; **162**: 2597-2605
37 **Griffith TS**, Chin WA, Jackson GC, Lynch DH, Kubin MZ. Intracellular regulation of TRAIL-induced apoptosis in human melanoma cells. *J Immunol* 1998; **161**: 2833-2840
38 **Irmler M**, Thome M, Hahne M, Schneider P, Hofmann K, Steiner V, Bodmer JL, Schroter M, Burns K, Mattmann C. Inhibition of death receptor signals by cellular FLIP. *Nature* 1997; **388**: 190-195
39 **Kischkel FC**, Lawrence DA, Chuntharapai A, Schow P, Kim KJ, Ashkenazi A. Apo2L/TRAIL-dependent recruitment of endogenous FADD and caspase-8 to death receptors 4 and 5. *Immunity* 2000; **12**: 611-620

40 **Sprick MR**, Weigand MA, Rieser E, Rauch CT, Juo P, Blenis J, Krammer PH, Walczak H. FADD/MORT1 and caspase-8 are recruited to TRAIL receptors 1 and 2 and are essential for apoptosis mediated by TRAIL receptor 2. *Immunity* 2000; **12**: 599-609

41 **Kim IK**, Chung CW, Woo HN, Hong GS, Nagata S, Jung YK. Reconstitution of caspase-8 sensitizes JB6 cells to TRAIL. *Biochem Biophys Res Commun* 2000; **277**: 311-316

42 **Grotzer MA**, Eggert A, Zuzak TJ, Janss AJ, Marwaha S, Wiewrodt BR, Ikegaki N, Brodeur GM, Phillips PC. Resistance to TRAIL-induced apoptosis in primitive neuroectodermal brain tumor cells correlates with a loss of caspase-8 expression. *Oncogene* 2000; **19**: 4604-4610

43 **Peter ME**. The TRAIL DISCussion: It is FADD and caspase-8. *Cell Death Differ* 2000; **7**: 759-760

44 **Hopkins-Donaldson S**, Bodmer JL, Bourloud KB, Brognara CB, Tschopp J, Gross N. Loss of caspase-8 expression in highly malignant human neuroblastoma cells correlates with resistance to tumor necrosis factor-related apoptosis-inducing ligand-induced apoptosis. *Cancer Res* 2000; **60**: 4315-4319

45 **Shin EC**, Ahn JM, Kim CH, Choi Y, Ahn YS, Kim H, Kim SJ, Park JH. IFN-gamma induces cell death in human hepatoma cells through a RAIL/death receptor-mediated apoptotic pathway. *Int J Cancer* 2001; **93**: 262-268

46 **Langaas V**, Shahzidi S, Johnsen JI, Smedsrod B, Sveinbjornsson B. Interferon-gamma modulates TRAIL-mediated apoptosis in human colon carcinoma cells. *Anticancer Res* 2001; **21**: 3733-3738

47 **Park SY**, Billiar TR, Seol DW. IFN-gamma inhibition of TRAIL-induced IAP-2 upregulation, a possible mechanism of IFN-gamma-enhanced TRAIL-induced apoptosis. *Biochem Biophys Res Commun* 2002; **291**: 233-236

48 **Qin JZ**, Bacon P, Chaturvedi V, Nickoloff BJ. Role of NF-kappaB activity in apoptotic response of keratinocytes mediated by interferon-gamma, tumor necrosis factor-alpha, and tumor-necrosis-factor-related apoptosis-inducing ligand. *J Invest Dermatol* 2001; **117**: 898-907

Edited by Zhu L and Wang XL

P.O.Box 2345, Beijing 100023,China
Fax: +86-10-85381893
E-mail: wjg@wjgnet.com www.wjgnet.com

World J Gastroenterol 2003;9(11):2441-2444
World Journal of Gastroenterology
 ISSN 1007-9327

• LIVER CANCER •

Serum from rabbit orally administered cobra venom inhibits growth of implanted hepatocellular carcinoma cells in mice

Peng Sun, Xian-Da Ren, Hai-Wei Zhang, Xiao-Hong Li, Shao-Hui Cai, Kai-He Ye, Xiao-Kun Li

Peng Sun, Xian-Da Ren, Xiao-Hong Li, Shao-Hui Cai, Department of Clinical Pharmacology, Pharmacy College, Jinan University, Guangzhou 510632, Guangdong Province, China
Hai-Wei Zhang, Department of Pathology, Medical College, Jinan University, Guangzhou 510632, Guangdong Province, China
Kai-He Ye, Department of Pharmacology, Pharmacy College, Jinan University, Guangzhou 510632, Guangdong Province, China
Xiao-Kun Li, Biopharmaceutical R&D Center of Jinan University, Guangzhou 510632, Guangdong Province, China
Supported by the Overseas Chinese Affairs Office of the State Council Foundation, No. 98-33
Correspondence to: Xiao-Kun Li, Biopharmaceutical R&D Center of Jinan University, Guangzhou 510632, Guangdong Province, China. xiaokunli@163.net
Telephone: +86-20-8556-5109
Received: 2003-03-19 **Accepted:** 2003-06-07

Abstract

AIM: To investigate the inhibitory effect of serum preparation from rabbits orally administered cobra venom (SRCV) on implanted hepatocellular carcinoma (HCC) cells in mice.

METHODS: An HCC cell line, HepA, was injected into mice to prepare implanted tumors. The animals (n=30) were divided randomly into SRCV, 5-fluorouracil (5-FU), and distilled water (control) groups. From the second day after transplantation, 20 mg/kg 5-FU was administered intraperitoneally once a day for 9 days. SRCV (1 000 mg/kg) or distilled water (0.2 mL) was given by gastrogavage. Tumor growth inhibition was described by the inhibitory rate (IR). Apoptosis was detected by transmission electron microscopy (TEM), flow cytometry (FCM), and terminal deoxynucleotidyl transferase-mediated dUTP-biotin nick end labeling (TUNEL). Student's t-test was performed for statistical analysis.

RESULTS: The tumor growth was inhibited markedly by SRCV treatment compared to that in the control group (P<0.01). The treatment resulted in a significant increase in the apoptotic rate of cancer cells by the factors of 10.5±2.4 % and 20.65±3.2 % as demonstrated through TUNEL and FCM assays, respectively (P<0.01). The apoptotic cells were also identified by characteristic ultrastructural features.

CONCLUSION: SRCV can inhibit the growth of implanted HepA cells in mice, and the apoptosis rate appears to elevate during the process.

Sun P, Ren XD, Zhang HW, Li XH, Cai SH, Ye KH, Li XK. Serum from rabbit orally administered cobra venom inhibits growth of implanted hepatocellular carcinoma cells in mice. *World J Gastroenterol* 2003; 9(11): 2441-2444
http://www.wjgnet.com/1007-9327/9/2441.asp

INTRODUCTION

Snake venoms are complex mixtures of pharmacologically active polypeptides, some are of potential therapeutic value for embolism, cancer and other severe human disorders. Several snake venoms and their components have been demonstrated to be able to inhibit tumor growth and to induce apoptosis of neoplastic cells *in vitro* and *in vivo*[1-7]. We prepared a serum preparation from rabbits administered cobra venom (SRCV)[8]. Our *in vitro* studies have shown its growth-inhibitory and apoptosis-inducing effects of SRCV on cancer cells[9]. In the present study, we observed its effects *in vivo* using implanted hepatocellular carcinoma (HCC) cell line HepA in mice.

MATERIALS AND METHODS

Drugs and reagents

5-FU was purchased from Nantong Pharmaceutical Co (Cat. No. 001121; Nantong, Jiangsu, China). SRCV was prepared as described previously[8]. Briefly, the rabbits were given oral Chinese cobra (*Naja naja atra*) venom 45 mg/kg (Guangzhou Research Institute of Snake Venom, Guangzhou, Guangdong, China) once a day for 3 days. Serum was collected from the rabbits at 4 h after the last administration, then heated in a water bath for 30 min at 56 ℃, frozen at -20 ℃, lyophilized using a vacuum drier and stored at 4 ℃.

Animals

Female Kunming mice (18-22 g, No. 26-2002A002) were supplied from the Medical Animal Center of Guangdong Province. All animals were fed on basic diet and water. The cell line HepA was provided by the Cancer Institute of Sun Yet-Sen University.

Experimental schedule

As described previously[10,11], HepA cells, 2×10^7/mL, were injected subcutaneously into mice, 200 μL for each. Thirty Kunming mice with implanted HepA tumor were divided randomly into SRCV-, 5-FU-treated groups and control group. From the second day after the implantation, 20 mg/kg 5-FU was administered intraperitoneally once a day for 9 days. SRCV (1 000 mg/kg) or distilled water (0.2 mL, control group) was given by gastrogavage. The mice were sacrificed at 24 h after the last administration. The tumors were isolated and weighed immediately in order to calculate the inhibitory rate (IR) according to the formula: IR of tumor (%)=(1-tumor weight in test groups/mean tumor weight in control group)×100 %. Then, the tumors were fixed and used for transmission electron microscopy (TEM), flow cytometry (FCM) and terminal deoxynucleotidyl transferase-mediated dUTP-biotin nick end labeling (TUNEL). All of the tests were repeated twice.

Morphological analysis of apoptosis

Dissected tumor samples were fixed with 2.5 % glutaraldehyde for 1 h. After washed three times in a buffer, the samples were post-fixed in 1 % OsO_4 in a cacodylate buffer for 1 h, then dehydrated in graded ethanol and embedded in epoxy resin (Agar 100). Thin sections (70 nm) were stained with uranyl acetate and reynolds lead citrate and examined at 75 kV in an electron microscope (JEM-100CX 11/T). Morphological changes in the nuclear chromatin of cells undergoing apoptosis were detected by TEM.

Flow cytometry analysis

Cell apoptotic rate was quantitatively determined by flow cytometry. The percentage of cells with a sub-G1 DNA content was taken as the fraction of apoptotic cell population[12,13]. According to the procedure described previously[14-16], tumor tissues were sliced at a thickness of 400-500 μm, then the slices were gently pulverized using a mortar and pestle in phosphate-buffered saline (PBS) (pH7.2). The cell suspension was infiltrated through 200 and 350 μm meshes to remove residues. The cells were collected by centrifugation at 2 000 rpm for 10 min. The cell suspension was fixed in 70 % ice-cold ethanol in PBS, and stored at -20 ℃. Prior to analysis, the cells were washed and resuspended in PBS, then incubated with 10 mg/mL RNase A for 3-5 min and 50 μg/mL propidium iodide (PI) at 4 ℃ for 30 min in a dark chamber. The apoptotic cells having DNA strand breaks that had been labeled were detected by a flow cytometer (FACSCan, Becton Dickinson, San Jose, California, USA).

TUNEL reaction

An ApopTag plus peroxidase *in situ* apoptosis detection kit (Intergen Co Ltd., Burlington, Massachusetts, USA) was used to visualize the cells with DNA fragmentation. The procedure was performed following instructions of the manufacturer and in reference of the previous observations[17-19]. Briefly, 4-μm thick sections were dewaxed and hydrated, treated with 20 μg/mL proteinase K for 15 min at 37 ℃, equilibrated in a buffer for 5 min at room temperature, and incubated in a buffer containing terminal deoxynucleotidyl transferase (TdT) enzyme for 1 h in a humidified chamber at 37 ℃. The reaction was demonstrated by incubation with anti-digoxigenin-peroxidase for 30 min in a humidified chamber at room temperature and visualized in a buffer containing diaminobenzidine (DAB).

The positive cells were identified, counted and analyzed based on morphological characteristics of apoptotic cells as previously described[17]. Under the light microscope, apoptotic cells manifested as brownish staining in the nuclei. Non-necrotic zone was selected in the tissue section and images were randomly selected. At least 1000 tumor cells were counted, and the percentage of TUNEL-positive cells was determined.

Statistical analysis

The data shown were mean values of 8-10 samples and expressed as mean ± standard deviations. Student' s *t*-test was performed for statistical analysis. A *P* value less than 0.05 was considered statistically significant.

RESULTS

Anti-tumor effect of SRCV on implanted HepA tumor

In two separate experiments, the IRs were 30.4 % and 35.8 % after treatment with SRCV. The data, listed in Table 1, demonstrated the inhibitory effect of SRCV treatment on implanted HepA tumor growth, though it was not as strong as that of 5-FU.

Apoptosis - inducing effect of SRCV in mice with implanted HepA tumor

The apoptosis-inducing effect of SRCV was confirmed by electron microscopy. Compared with control group (Figure 1A), morphological changes indicative of apoptosis included cell shrinkage, nuclear chromatin condensation and peripheral shift of condensed chromatin to nuclear membrane or formation of crescent. In addition, the nuclear membrane was intact and there was little or no swelling of mitochondria or other organelles (Figure 1B).

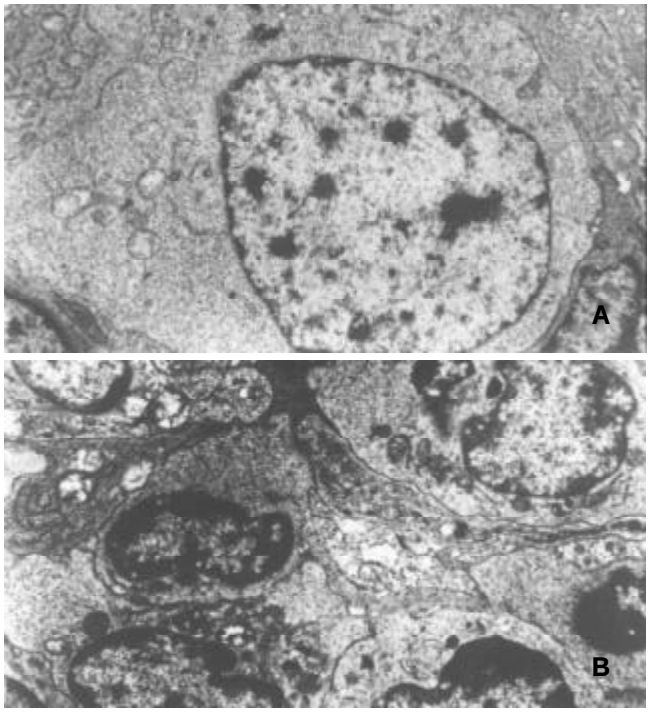

Figure 1 Morphological changes characteristic of apoptotic cells under transmission electron microscope in implanted tumors after treatment with SRCV. A: The normal tumor cells in distilled water control group (×5000). B: The apoptotic cells in SRCV group (×5000).

Table 2 Apoptotic rates (AR) of implanted tumor in SRCV treated mice determined by TUNEL and FCM methods (n=8, $\bar{x}\pm s$)

Groups	Mean apoptotic rate ± SEM (%)	
	TUNEL	FCM
SRCV	10.50±2.42[b]	20.65±3.2[b]
Control group	1.67±1.3	2.28±1.54

[b]P<0.01 *vs* control group.

The apoptosis-inducing effect of SRCV was further confirmed by FCM and TUNEL. After treatment with SRCV, the apoptotic rate was significantly increased in the SRCV group compared with the control group (Table 2). In TUNEL

Table 1 Anti-tumor effect of CVSR on implanted HepA tumors in mice (n=10, $\bar{x}\pm s$)

Group	Dose	Tumor weight/(g)		Inhibition rate (%)	
		First	Twice	First	Twice
SRCV	1 000 mg/kg	1.14±0.28[a]	1.14±0.13[a]	30.35±17.07	35.83±7.11
5-FU	20 mg/kg	0.78±0.14[a]	0.99±0.22[a]	52.57±8.56	44.39±10.5
Control	0.2 ml	1.63±0.26	1.78±0.47		

[a]P<0.01 *vs* control group.

assay, induction of apoptosis was represented by an increase in DNA fragments detected by a peroxidase reaction (Figure 2A), and the apoptotic cells in control tumors were scarcely scattered (Figure 2B).

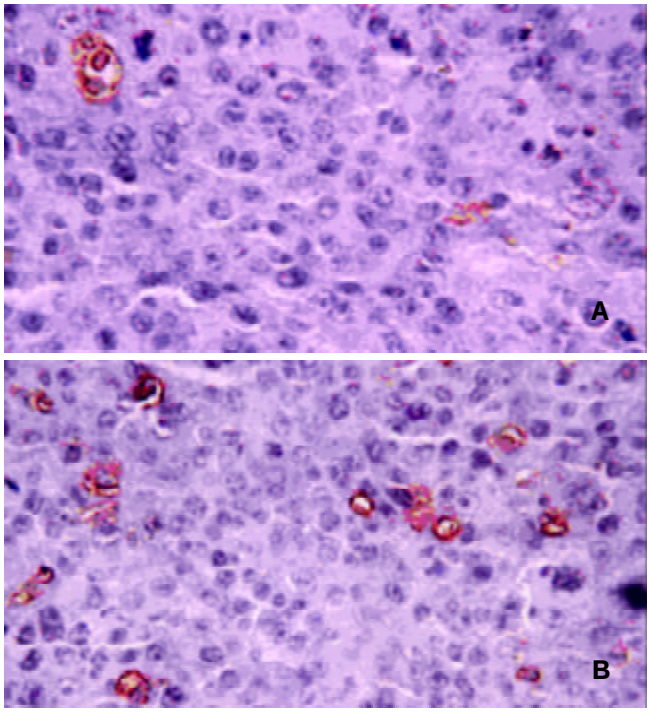

Figure 2 Apoptotic cells of implanted HepA tumors in SRCV treated mice detected by TUNEL assay. A: control group (× 400), B: SRCV 1 000 mg / kg group (×400).

DISCUSSION

Snake venoms have inhibitory effects on the growth of a variety of tumors *in vitro* and *in vivo*[20,21]. Markland *et al*. found that contortrostatin (CN), a homodimeric disintegrin from southern copperhead venom, inhibited dissemination ovarian cancer in a nude mouse model[22]. According to Da Silva *et al*., *Bothrops jararaca* venom (BjV) had anti-tumor effects on Ehrlich ascites tumor (EAT) cells in *vivo* and *in vitro*[23].

Snake venom was also shown to induce apoptosis in tumors. Apoptosis, in contrast to necrosis, was an active process of gene-directed cellular suicide[24]. It has been clear that apoptosis is often upregulated in tumor by many anticancer drugs[25-32].

Since Araki *et al*. first described that hemorrhagic snake venoms induced apoptosis in vascular endothelial cells (VEC)[33], data have been accumulated rapidly about apoptosis-inducing action of various snake venoms and their active components. In 1994, Strizhkov *et al*. reported that both neurotoxin II (NT II) from venom of *Naja naja oxiana* and 20-30 kDa proteins partially purified from pig brain (NTlm) cross-reacting with antibodies to NT II were cytotoxic to L929 and K562 tumor cells at concentrations of 10^{-6}-10^{-8} M, and induced apoptosis in L929 and K562 cells *in vitro*[34]. After that, L-amino acid oxidase (LAO) was found to induce apoptosis in human embryonic kidney cell line 293T[35] and human monocyte line MM6[36]. Recently, Araki *et al*.[37] and Masuda *et al*[38] associated integrins with vascular apoptosis-inducing protein 1 (VAP1)-induced apoptosis. Data from Zhao *et al*. indicated that snake venom secreted phospholipase A_2 ($sPLA_2$) induced apoptosis in Mv1Lu cells in a dose- and time-dependent manner, and was associated with a rapid increase in intracellular ceramide level[39].

The clinical trial using snake venom and their active components have succeeded in cancer therapies, but its application was confined to the auxiliary treatment of patients in the late stage[40,41]. Its toxic and side effects were unavoidable. Great efforts have been made[42-45], but the problem remains unresolved. So a long-standing goal in snake venom therapy of cancer is to find a stable, low toxic, highly effective chemotherapeutic agent that selectively targets tumor cells. Based on this idea, we prepared the SRCV agent[8].

In our previous studies, the anti-tumor activity and apoptosis-inducing effect of SRCV were shown *in vitro* using HepG-2, HL-60 and human lung adenocarcinoma cell line, and no cytotoxicity was observed on human fetal lung fibroblast cells[46-48]. The results presented herein demonstrate that SRCV has inhibitory and apoptosis-inducing effects on implanted HepA tumors. Further studies are needed to identify the active components of SRCV and to elucidate their underlying mechanism.

REFERENCES

1 **Souza DH**, Eugenio LM, Fletcher JE, Jiang MS, Garratt RC, Oliva G, Selistre-de-Araujo HS. Isolation and structural characterization of a cytotoxic L-amino acid oxidase from Agkistrodon contortrix laticinctus snake venom: preliminary crystallographic data. *Arch Biochem Biophys* 1999; **368**: 285-290
2 **Du XY**, Clemetson KJ. Snake venom L-amino acid oxidases. *Toxicon* 2002; **40**: 659-665
3 **Correa MC Jr**, Maria DA, Moura-da-Silva AM, Pizzocaro KF, Ruiz IR. Inhibition of melanoma cells tumorigenicity by the snake venom toxin jararhagin. *Toxicon* 2002; **40**: 739-748
4 **Della Morte R**, Squillacioti C, Garbi C, Derkinderen P, Belisario MA, Girault JA, Di Natale P, Nitsch L, Staiano N. Echistatin inhibits pp125FAK autophosphorylation, paxillin phosphorylation and pp125FAK-paxillin interaction in fibronectin-adherent melanoma cells. *Eur J Biochem* 2000; **267**: 5047-5054
5 **Zhou Q**, Nakada MT, Brooks PC, Swenson SD, Ritter MR, Argounova S, Arnold C, Markland FS. Contortrostatin, a homodimeric disintegrin, binds to integrin alphavbeta 5. *Biochem Biophys Res Commun* 2000; **267**: 350-355
6 **Kang IC,** Lee YD, Kim DS. A novel disintegrin salmosin inhibits tumor angiogenesis. *Cancer Res* 1999; **59**: 3754-3760
7 **Abe Y**, Shimoyama Y, Munakata H, Ito J, Nagata N, Ohtsuki K. Characterization of an apoptosis-inducing factor in Habu snake venom as a glycyrrhizin (GL)-binding protein potently inhibited by GL *in vitro*. *Biol Pharm Bull* 1998; **21**: 924-927
8 **Sun P,** Xu C, Ren XD, Liu JJ, Li XH. Acute toxicity test of three Cobra Venom preparation and their inhibitory effect on transplanted hepatoma in mice. *Jinan Daxue Xuebao* 2002; **23**: 1-4
9 **Luo YR**, Ye CL, Ren XD, Li HL, Zhong L. Inhibition of proliferation and apoptosis in HL60 cells induced by cobra venom serum. *Zhongguo Yaolixue Tongbao* 2002; **18**: 291-293
10 **Wang W**, Qin SK, Chen BA, Chen HY. Experimental study on antitumor effect of arsenic trioxide in combination with cisplatin or doxorubicin on hepatocellular carcinoma. *World J Gastroenterol* 2001; **7**: 702-705
11 **Bi WX**, Xu SD, Zhang PH, Kong F. Antitumoral activity of low density lipoprotein-aclacinomycin complex in mice bearing H (22) tumor. *World J Gastroenterol* 2000; **6**: 140-142
12 **Ryan KM**, Ernst MK, Rice NR, Vousden KH. Role of NF-kappaB in p53-mediated programmed cell death. *Nature* 2000; **404**: 892-897
13 **Chun YJ**, Park IC, Park MJ, Woo SH, Hong SI, Chung HY, Kim TH, Lee YS, Rhee CH, Lee SJ. Enhancement of radiation response in human cervical cancer cells *in vitro* and *in vivo* by arsenic trioxide (As2O3). *FEBS Lett* 2002; **519**: 195-200
14 **Lin SB**, Wu LC, Huang SL, Hsu HL, Hsieh SH, Chi CW, Au LC. *In vitro* and *in vivo* suppression of growth of rat liver epithelial tumor cells by antisense oligonucleotide against protein kinase C-alpha. *J Hepatol* 2000; **33**: 601-608
15 **Hou L**, Li Y, Jia YH, Wang B, Xin Y, Ling MY, Lu S. Molecular mechanism about lymphogenous metastasis of hepatocarcinoma cells in mice. *World J Gastroenterol* 2001; **7**: 532-536
16 **Tian G**, Yu JP, Luo HS, Yu BP, Yue H, Li JY, Mei Q. Effect of nimesulide on proliferation and apoptosis of human hepatoma

SMMC-7721 cells. *World J Gastroenterol* 2002; **8**: 483-487
17 **Cui RT**, Cai G, Yin ZB, Cheng Y, Yang QH, Tian T. Transretinoic acid inhibits rats gastric epithelial dysplasia induced by N-methyl-N-nitro-N-nitrosoguanidine: influences on cell apoptosis and expression of its regulatory genes. *World J Gastroenterol* 2001; **7**: 394-398
18 **Barnett KT**, Fokum FD, Malafa MP. Vitamin E succinate inhibits colon cancer liver metastases. *J Surg Res* 2002; **106**: 292-298
19 **Zhang XL**, Liu L, Jiang HQ. Salvia miltiorrhiza monomer IH764-3 induces hepatic stellate cell apoptosis via caspase-3 activation. *World J Gastroenterol* 2002; **8**: 515-519
20 **Zhou Q**, Sherwin RP, Parrish C, Richters V, Groshen SG, Tsao-Wei D, Markland FS. Contortrostatin, a dimeric disintegrin from Agkistrodon contortrix, inhibits breast cancer progression. *Breast Cancer Res Treat* 2000; **61**: 249-260
21 **Yeh CH**, Peng HC, Yang RS, Huang TF. Rhodostomin, a snake venom disintegrin, inhibits angiogenesis elicited by basic fibroblast growth factor and suppresses tumor growth by a selective alpha(v)beta(3) blockade of endothelial cells. *Mol Pharmacol* 2001; **59**: 1333-1342
22 **Markland FS**, Shieh K, Zhou Q, Golubkov V, Sherwin RP, Richters V, Sposto R. A novel snake venom disintegrin that inhibits human ovarian cancer dissemination and angiogenesis in an orthotopic nude mouse model. *Haemostasis* 2001; **31**: 183-191
23 **Da Silva RJ,** da Silva MG, Vilela LC, Fecchio D. Antitumor effect of Bothrops jararaca venom. *Mediators Inflamm* 2002; **11**: 99-104
24 **Yu CL**, Tsai MH. Fetal fetuin selectively induces apoptosis in cancer cell lines and shows anti-cancer activity in tumor animal models. *Cancer Lett* 2001; **166**: 173-184
25 **Wu K**, Zhao Y, Liu BH, Li Y, Liu F, Guo J, Yu WP. RRR-alpha-tocopheryl succinate inhibits human gastric cancer SGC-7901 cell growth by inducing apoptosis and DNA synthesis arrest. *World J Gastroenterol* 2002; **8**: 26-30
26 **Panichakul T**, Wanun T, Reutrakul V, Sirisinha S. Synergistic cytotoxicity and apoptosis induced in human cholangiocarcinoma cell lines by a combined treatment with tumor necrosis factor-alpha (TNF-alpha) and triptolide. *Asian Pac J Allergy Immunol* 2002; **20**: 167-173
27 **Zhang XL**, Liu L, Jiang HQ. Salvia miltiorrhiza monomer IH764-3 induces hepatic stellate cell apoptosis via caspase-3 activation. *World J Gastroenterol* 2002; **8**: 515-519
28 **Sun ZX**, Ma QW, Zhao TD, Wei YL, Wang GS, Li JS. Apoptosis induced by norcantharidin in human tumor cells. *World J Gastroenterol* 2000; **6**: 263-265
29 **Zhang C**, Gong Y, Ma H, An C, Chen D, Chen ZL. Reactive oxygen species involved in trichosanthin-induced apoptosis of human choriocarcinoma cells. *Biochem J* 2001; **355**(Pt3): 653-661
30 **Wang ZM**, Hu J, Zhou D, Xu ZY, Panasci LC, Chen ZP. Trichostatin A inhibits proliferation and induces expressin of p21WAF and p27 in human brain tumor cell lines. *Ai Zheng* 2002; **21**: 1100-1105
31 **Zhao AG**, Zhao HL, Jin XJ, Yang JK, Tang LD. Effects of Chinese Jianpi herbs on cell apoptosis and related gene expression in human gastric cancer grafted onto nude mice. *World J Gastroenterol* 2002; **8**: 792-796
32 **Tu SP**, Zhong J, Tan JH, Jiang XH, Qiao MM, Wu YX, Jiang SH. Induction of apoptosis by arsenic trioxide and hydroxy camptothecin in gastriccancer cells *in vitro*. *World J Gastroenterol* 2000; **6**: 532-539
33 **Du XY**, Clemetson KJ. Snake venom L-amino acid oxidases. *Toxicon* 2002; **40**: 659-665
34 **Strizhkov BN,** Blishchenko EY, Satpaev DK, Karelin AA. Both neurotoxin II from venom of naja naja oxiana and its endogenous analogue induce apoptosis in tumor cells. *FEBS Lett* 1994; **340**: 22-24
35 **Torii S**, Yamane K, Mashima T, Haga N, Yamamoto K, Fox JW, Naito M, Tsuruo T. Molecular cloning and functional analysis of apoxin I, a snake venom-derived apoptosis-inducing factor with L-amino acid oxidase activity. *Biochemistry* 2000; **39**: 3197-3205
36 **Ali SA**, Stoeva S, Abbasi A, Alam JM, Kayed R, Faigle M, Neumeister B, Voelter W. Isolation, structural, and functional characterization of an apoptosis-inducing L-amino acid oxidase from leaf-nosed viper (Eristocophis macmahoni) snake venom. *Arch Biochem Biophys* 2000; **384**: 216-226
37 **Araki S,** Masuda S, Maeda H, Ying MJ, Hayashi H. Involvement of specific integrins in apoptosis induced by vascular apoptosis-inducing protein 1. *Toxicon* 2002; **40**: 535-542
38 **Masuda S**, Ohta T, Kaji K, Fox JW, Hayashi H, Araki S. cDNA cloning and characterization of vascular apoptosis-inducing protein 1. *Biochem Biophys Res Commun* 2000; **278**: 197-204
39 **Zhao S**, Du XY, Chai MQ, Chen JS, Zhou YC, Song JG. Secretory phospholipase A(2) induces apoptosis via a mechanism involving ceramide generation. *Biochim Biophys Acta* 2002; **1581**: 75-88
40 **Cura JE**, Blanzaco DP, Brisson C, Cura MA, Cabrol R, Larrateguy L, Mendez C, Sechi JC, Silveira JS, Theiller E, de Roodt AR, Vidal JC. Phase I and pharmacokinetics study of crotoxin (cytotoxic PLA(2), NSC-624244) in patients with advanced cancer. *Clin Cancer Res* 2002; **8**: 1033-1041
41 **Costa LA**, Miles HA, Diez RA, Araujo CE, Coni Molina CM, Cervellino JC. Phase I study of VRCTC-310, a purified phospholipase A2 purified from snake venom, in patients with refractory cancer: safety and pharmacokinetic data. *Anticancer Drugs* 1997; **8**: 829-834
42 **Fu Q**, Gowda DC. Carbohydrate-directed conjugation of cobra venom factor to antibody by selective derivatization of the terminal galactose residues. *Bioconjug Chem* 2001; **12**: 271-279
43 **Wang XM**, Huang SJ. The selective cytotoxicity of cobra venom factor immunoconjugate on cultured human nasopharyngeal carcinoma cell line. *Hum Exp Toxicol* 1999; **18**: 71-76
44 **Schmitmeier S**, Markland FS, Chen TC. Anti-invasive effect of contortrostatin, a snake venom disintegrin, and TNF-alpha on malignant glioma cells. *Anticancer Res* 2000; **20**: 4227-4233
45 **Juhl H,** Petrella EC, Cheung NK, Bredehorst R, Vogel CW. Additive cytotoxicity of different monoclonal antibody-cobra venom factor conjugates for human neuroblastoma cells. *Immunobiology* 1997; **197**: 444-459
46 **Li HL**, Ren XD, Luo YR, Ye CL, Zhang HW. Effect of serum preparation derived from rabbits after the gastrolavage with Naja naja atra venom on human lung adenocarcinoma cell line. *Jinan Daxue Xuebao* 2001; **22**: 1-5
47 **Li HL**, Ren XD, Luo YR, Ye CL, Zhang HW. Effect of the oral administration with serum preparation of Naja naja atra venom on apoptosis in HepG2 cells. *Zhongguo Binglishengli Zazhi* 2002; **18**: 199-200
48 **Li HL**, Sun P, Ren XD, Luo YR, Ye CL, Zhang HW. A antihepatocarcinoma activity of the oral serum preparation of Naja naja atra venom. *Health Science J Macao* 2002; **2**: 59-61

Edited by Su Q and Wang XL

P.O.Box 2345, Beijing 100023,China
Fax: +86-10-85381893
E-mail: wjg@wjgnet.com www.wjgnet.com

World J Gastroenterol 2003;9(11):2445-2449
World Journal of Gastroenterology
 ISSN 1007-9327

• LIVER CANCER •

Influence of transarterial chemoembolization on angiogenesis and expression of vascular endothelial growth factor and basic fibroblast growth factor in rat with Walker-256 transplanted hepatoma: An experimental study

Xin Li, Gan-Sheng Feng, Chuan-Sheng Zheng, Chen-Kai Zhuo, Xi Liu

Xin Li, Gan-Sheng Feng, Chuan-Sheng Zheng, Chen-Kai Zhuo, Xi Liu, Department of Interventional Radiology, Union Hospital, Tongji Medical College, Huazhong University of Science and Technology, Wuhan 430022, Hubei Province, China
Supported by the National Natural Science Foundation of China, No.39770839
Correspondence to: Dr. Xin Li, Department of Radiology, Union Hospital, Tongji Medical College, Huazhong University of Science and Technology, Wuhan 430022, Hubei Province, China. wxyao2001@yahoo.com.cn
Telephone: +86-27-85726432
Received: 2003-03-02 **Accepted:** 2003-05-11

Abstract

AIM: After transarterial chemoembolization (TACE), the residual cancer cells are under extensive hypoxic or even anoxic environment. Hypoxia can lead to adaptive responses. For example, angiogenesis will help these cells survive. In this study, we examined the effect of TACE on angiogenesis and expression of vascular endothelial growth factor (VEGF) and basic fibroblast growth factor (b-FGF) and to assess their relevance to Walker-256 transplanted hepatoma.

METHODS: Male Wistar rats were inoculated with Walker-256 tumor in the left lobe of liver. Angiography and transarterial chemoembolization were performed at d14 after transplantation. Sixty rats bearing walker-256 transplanted hepatoma were randomly divided into control group, arterial infusion group and TACE group. Each group consisted of twenty rats. Normal saline, 5-Fu, 5-Fu and lipiodol were infused through hepatic artery respectively. Two weeks after the infusion, staining of factor VIII, VEGF and b-FGF was performed by immunohistochemistry method in routine paraffin-embeded sections. Microvessel density (MVD) was counted in endothelial cells with positive factor VIII. Their expression levels were analyzed in conjunction with the pathologic features.

RESULTS: While a smaller tumor volume was found in TACE group (F=37.818, P<0.001), no statistical differences between MVD and expression of VEGF and b-FGF were found among the 3 groups. MVD of the control group, chemotherapy group and chemoemoblization group was 80.84±24.24, 83.05±20.29 and 85.20±23.91 (F=0.193, P=0.873), respectively. The positive expression of VEGF and b-FGF was 75 %, 75 %, 85 % (χ^2=0.449, P=0.799) and 30 %, 25 %, 30 % (χ^2=0.141, P=0.922), respectively. Statistical analysis revealed a positive correlation between the expression of VEGF and MVD (r=0.552, P<0.001).

CONCLUSION: There has been little influence of lipiodol chemoembolization on the formation of tumor angiogenesis, but the development of neovascularization and expression of VEGF play important roles in establishment of collateral circulation and reconstruction of blood supply of residual cancer tissue.

Li X, Feng GS, Zheng CS, Zhuo CK, Liu X. Influence of transarterial chemoembolization on angiogenesis and expression of vascular endothelial growth factor and basic fibroblast growth factor in rat with Walker-256 transplanted hepatoma: An experimental study. *World J Gastroenterol* 2003; 9(11): 2445-2449
http://www.wjgnet.com/1007-9327/9/2445.asp

INTRODUCTION

Transarterial chemoembolization (TACE) has been widely practiced in the treatment of unresectable hepatocellular carcinoma (HCC)[1-5], but long-term TACE therapy was as yet unsatisfactory[6-8]. Histopathologic examination showed although TACE could induce significant necrosis, yet complete tumor necrosis was rare, the residual tumor cells remained viable in the peripheral region, which may play an important role in local recurrence or as a source of metastasis affecting the long-term efficacy of TACE[9-11].

Tissue in hypoxic environment is common in both experimental and human solid tumor[12]. Hypoxia cells have reduced metabolic rate, reduced transcription and translation, even cell cycle arrest. Hypoxia can inhibit cell division or even lead to cell death[13]. But body compensatory reaction can also lead to a wide range of responses including angiogenesis, anti-apoptosis gene expression and changes in metabolic rate at both systemic and cellular levels[14,15]. After TACE, the tumor cells are under extremely hypoxic or even anoxic environment. It is possible that some adaptive responses to hypoxia will help these cells survive, but to our knowledge, studies regarding these are very few.

Recent studies revealed that TACE might enhance the expression of VEGF in meningiomas[16,17]. In the study of hepatoma, TACE could enhance the expression of VEGF[18-21], but not the MVD level[22] or expression of b-FGF[19,22]. All these studies were retrospective.

Walker-256 transplanted hepatoma is a useful model for the study of cancer therapy[20,23,24]. In hepatic arteriography, the tumor is usually hypervascular and receives its blood supply almost exclusively from hepatic artery just as that seen in human HCC[23]. Our study was designed to observe the influence of TACE on the *expression of angiogenesis, VEGF and b-FGF and to assess their relevance to Walker-256 transplanted hepatoma.

MATERIALS AND METHODS

Walker-256 tumor inoculation into the rat livers

Walker-256 carcinoma cells (Cell Preserve Center, Wuhan University, Wuhan, P.R.China) were inoculated subcutaneously

in intact rats. Male Wistar rats (200-250 g) were anesthetized with pentobarbital sodium (30 mg/kg ip), then the tumor was inoculated as described in our previous study[23]. Walker-256 carcinoma cells were inoculated into the subcapsular parenchyma of the left lobe of liver.

Experimental methods

Fourteen days after transplantion, a second laparotomy was performed. A 0.6 mm polyethylene catheter was inserted into the gastroduodenal artery and fixed by a suture. The common hepatic artery and right hepatic artery were temporarily ligated during injection of the drugs. In this study, sixty rats were randomly divided into three groups, twenty rats each group (Table 1).

Table 1 Drug administration in the three groups

Group	Drug administration
Control	0.3 ml normal saline
Arterial infusion (AI group)	5-fluorouracil (5-FU) 20mg/kg
Transarterial chemoembolization (TACE group)	lipiodol ultra-fluis (Andre Guerbet Laboratories, Aulnay-Sous-Bios, France) 0.5ml/kg and 5-Fu 20mg/kg

Tumor volume and degree of tumor necrosis

MR images were performed on 1.5-Tesla system (Siemens Vision, Siemens, Germany) supplemented with a cervical coil. T1-weighted (TR/TE, 450/12 msec) and T2-weighted (TR/TE, 2 800/96 msec) transverse SE images (slice thickness 2 mm) were obtained by acquisition times of 7:25 min and 6:16 min, respectively.

The tumor volume was determined by MR measurements of the largest and smallest diameters and calculated according to the following formula: Tumor volume (mm^3)=largest diameter (mm)×[smallest diameter (mm)]^2/2.

Fourteen days after TACE, hepatoma specimens were obtained and fixed in 10 % formalin for 12 hours, then embedded in paraffin according to routine procedures. The histological sections were stained with hematoxylin-eosin (HE) for observation under light microscopy and measurement of the extent of tumor necrosis.

Immunohistochemistry

Immunohistochemistry was performed in sections from a selected block of each specimen. 5-μm thick sections mounted on 3-aminopropyltrietoxysilane-coated slides were dewaxed in xylene and rehydrated at graded concentrations of alcohol. Endogenous peroxide was blocked with 0.6 %H_2O_2 for 20 min. Then the sections were pretreated in a microwave oven in citrate buffer for 15 min at 95 ℃. Thereafter, the slides were processed according to the standard methods with ABC kit. The primary antibody used was polyclonal antibody of von-Willebrand factor at dilution of 1:100, polyclonal antibodies to VEGF and b-FGF at dilution of 1:50. All these antibodies were from Santa Cruz Biotechnology; Santa Cruz, Calif USA. Diaminobenzine was used for the coloration development. Negative controls were generated by substituting the primary antibody with distilled water.

Determination of MVD

The tumors were frequently inhomogeneous in their microvessel density. For determination of MVD, the five most vascular areas within a section were chosen and counted under a light microscope with a 200-fold magnification as described by Weidner[25]. A brownstain structure clearly separated from the adjacent microvessels was regarded as a single countable microvessel. The average count was recorded as MVD for each case.

Determination of VEGF and b-FGF expression

The counting of VEGF and b-FGF immunoreactive cells was made by scanning and scoring of five high-power fields using ×400 magnification. Positive VEGF and b-FGF were recognized as intensely stained in tumor cell cytoplasm.

The expression of VEGF was semi-quantitatively evaluated as follows. Those having positive staining less than 5 % were regarded as -, between 5 % and 15 % as +, between 15 % and 50 % as 2+, and greater than 50 % as 3+. The b-FGF immunostaining was evaluated by a qualitative method as follows. Positive staining less than 10 % was regarded as negative, greater than 10 % as positive.

Statistical analysis

Statistical analysis was carried out by SPSS packed program. Variance tests, chi-square tests, Mann-Whitney test and linear regression test were used. P value <0.05 based on a two-tailed test was considered statistically significant.

RESULTS

Histopathology findings in tumor

Hematoxylin-eosin (H&E) stained sections of the liver specimens showed poorly-differentiated carcinomas, which were apparently spherical or ovoid in shape. The tumor cells were arranged irregularly with hyperchromatosis, polymorphism and numerous mitoses. The mass was sharply demarcated from the surrounding normal parenchyma, its capsule was thin and composed of collagen fibers caused by tumor compression. The tumor showed inhomogeneous hypervascularization consisting mainly of small arteries and capillaries. Satellite nodules or portal vein tumor thrombus could be seen in some rats.

In TACE group, examination of the sections showed extensive central necrosis of the tumor in all cases. The central necrosis enlarged to moderate (16/20) or severe degree (4/20). Intra-tumoral hemorrhage or bile stases were seen in some, but the tumor cells tended to remain viable at the periphery of the nodules 2 weeks after embolization therapy. We also found thick fibrous capsules with chronic inflammatory and cells infiltration. Various degrees of degeneration and necrosis were seen in normal hepatic parenchyma adjacent to the tumor. In the control and AI groups, the interior of the tumor had many viable tumor cells with spotty and scattered necrosis, the capsules were thin and composed of collagen fibers. Tumor volume and tumor growth rate before and after therapy are listed in Table 2.

Table 2 Tumor volumes and tumor growth rate before and after therapy ($\bar{x}\pm s$)

Group	Tumor volume (mm^3)		Tumor growth rate(%)
	Before therapy	2 weeks after therapy	
Control	195.6±65.9	963.6±214.8	459.2±52.7
AI	218.9±48.7	868.9±179.8	412.2±18.9
TACE	210.2±59.2	356.5±78.4	173.4±20.4
F value	0.272	37.818	197.932
P value	0.764	<0.001	<0.001

Microvessel counts

The von Willebrand Factor (Factor-VIII) antibody gave an intense staining of the vascular endothelial cells (Figure 1). A substantial inhomogeneity in microvessel counts was found

Table 3 MVD counts, expression of VEGF and b-FGF in each group

Group	*n*	MVD ($\bar{x}$±*s*)	VEGF					b-FGF	
			0	+	++	+++	Mean	0	
Control	20	80.80±20.94	5	8	5	2	1.2	14	6
AI	20	83.55±18.26	5	7	6	2	1.25	15	5
TACE	20	85.20±23.91	3	9	5	3	1.4	14	6
Statistic value		*F*=0.193			χ^2=0.449			χ^2=0.141	
P value		*P*=0.873			*P*=0.799			*P*=0.922	

in different areas in the same section. In TACE group, the positive factor VIII cells were found focusing in the newly formed tumor. The MVD of each group is shown in Table 3.

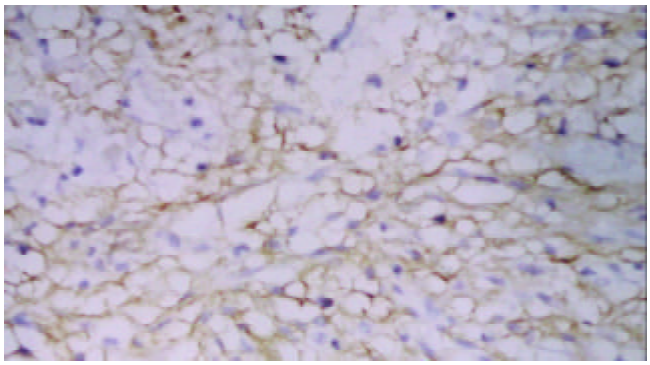

Figure 1 Positive factor-VIII endothelial cells in tumor nest (SABC ×100).

VEGF protein expression and its correlation with MVD

Immunohistochemical staining of VEGF showed strong immunoreactivity in tumor cells and vascular endothelial cells within the tumor tissues (Figure 2). In contrast, non-neoplastic hepatocytes showed weak staining. The staining of VEGF was inhomogeneous. In the sections after TACE, at the tumor nests, boundary of necrotic and non-necrotic area and pericapsular area, VEGF positive tumor cells were relatively easy seen. The expression of VEGF in each group is shown in Table 3.

Linear regression analysis showed a clear correlation between tumor MVD and VEGF protein expression (r=0.452, P<0.01). The MVD counts in negative and positive VEGF groups were 67.86±11.66 and 87.36±22.97 (per high power field), respectively (Table 4).

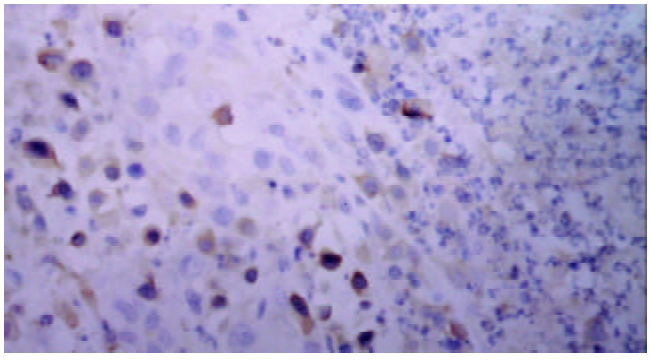

Figure 2 Positive VEGF cells in newly formed tumor nest after TACE (SABC ×200).

b-FGF protein expression and its correlation with MVD

b-FGF protein was identified sporadically in tumor tissues. No statistical differences were found between these groups (P=0.922) (Table 3). There was no correlation between b-FGF and MVD counts (r=0.036, P=0.786).

Table 4 MVD count in negative and positive VEGF groups after TACE

Expression of VEGF	*n*	MVD (per high power field) ($\bar{x}$±*s*)
Negative group	13	67.86±11.66
Positive group	47	87.36±22.97
T value		2.543
P value		0.014

DISCUSSION

Angiogenesis is an inherent property of tumor. It is important in its development and progression. Among many solid tumors, the degree of tumor angiogenesis was closely related to its biological behaviors, which reflect its ability for infiltration, recurrence and metastasis[26-30]. Intratumoral microvessel density (MVD) is commonly used to assess angiogenic activity. Defining and measuring MVD in the residual tumor cells after TACE might help judge the blood supply of residual tumor tissue and prognosticate the activity of these cells to a certain extent indirectly[31].

TACE could hardly abolish tumor blood supply. The possible causes included: incomplete embolization or partial recanalization of the artery, presence of intrahepatic porto-arterial shunt, formation of collateral circulation, and opening of potential communicating vessels[9,32,33]. The present study suggested that neovascularization and expression of VEGF might be another important factor. At the newly formed tumor nests, abundant factor VIII and positive VEGF cells could be found, and slight necrosis was seen in regions that had abundant neovasculature. These suggest that neovascularization plays an important role in the formation of collateral circulation, and relatively abundant blood supply will help tumor cells escape from the damage by TACE and increase the opportunity of survival.

Some authors considered that TACE might increase the chance of tumor recurrence or metastasis[20,34,35], which might be related to hypoxia caused by TACE and increased level of angiogenesis due to hypoxia[36-38]. The present study showed that MVD of TACE group was slightly higher than that of the control group and AI group, but no statistical difference was found, suggesting that TACE would not increase the level of tumor angiogenesis. Although the exact mechanism is currently unclear, we consider the possible explanation would be that the tumor cells were in an extreme hypoxia or even anoxia environment for a longer duration after TACE, which resulted in extensive necrosis and apoptosis of timorous and endothelial cells and decrease of secretion of angiogenic factor and weakening of the paracrine effect.

The intratumoral distribution of tumor neovasculature was inhomogeneous after embolization therapy. The newly formed blood vessels were less in the center of tumor but much more in the periphery and subcapsular area. This phenomenon might be related to the characteristics of tumor blood supply. Although blood supply of the tumor mainly came from hepatic artery, the peripheral area also received portal blood. There

were potential collateral circulations both between the artery-portal veins and between the lobular arteries. After TACE, the portal blood supply increased with opening of collateral circulation, the blood supply of the peripheral region of the tumor restored more easily.

A balance between angiogenic and angiostatic factors regulates the angiogenesis. These factors may be produced either by tumor cells or host cells. The most commonly studied angiogenic factors were VEGF and b-FGF. VEGF could stimulate endothelia cells to proliferate, migrate, and alter their patterns of gene expression, increase microvascular hyperpermeability, extravasate plasma proteins into extravascular space and induce plasma-derived matrix[39,40]. VEGF played a key role in tumoral angiogenesis, it could induce neovascularization and was considered to be crucial in tumor biology[41,42]. b-FGF had synergistic effects with VEGF[43].

In the present study, the expression of VEGF was slightly higher in TACE group than in the control and AI groups, but no statistical difference was found. There was a significant correlation between MVD and VEGF expression. MVD counts in positive VEGF group were much higher than in negative VEGF group. At the newly formed tumor nests, the boundary of necrotic and non-necrotic area and the subcapsular area, positive VEGF tumor cells were more abundant and this was consistent with the distribution of neovasculature. Taken together, the results in the current study strongly suggested that VEGF played a key role in the formation of tumor neovasculature after TACE.

In conclusion, the influence of lipiodol chemoembolization on formation of tumor angiogenesis is relatively limited, but the development of neovascularization and expression of VEGF play important roles in establishing collateral circulation and reconstructing blood supply of residual cancer tissue.

REFERENCES

1 **Rose DM**, Chapman WC, Brockenbrough AT, Wright JK, Rose AT, Meranze S, Mazer M, Blair T, Blanke CD, Debelak JP, Pinson CW. Transcatheter arterial chemoembolization as primary treatment for hepatocellular carcinoma. *Am J Surg* 1999; **177**: 405-410

2 **Zhang Z**, Liu Q, He J, Yang J, Yang G, Wu M. The effect of preoperative transcatheter hepatic arterial chemoembolization on disease-free survival after hepatectomy for hepatocellular carcinoma. *Cancer* 2000; **89**: 2606-2612

3 **Poyanli A**, Rozanes I, Acunas B, Sencer S. Palliative treatment of hepatocellular carcinoma by chemoembolization. *Acta Radio* 2001; **42**: 602-607

4 **Chen MS**, Li JQ, Zhang YQ, Lu LX, Zhang WZ, Yuan YF, Guo YP, Lin XJ, Li GH. High-dose iodized oil transcatheter arterial chemoembolization for patients with large hepatocellular carcinoma. *World J Gastroenterol* 2002; **8**: 74-78

5 **Saccheri S**, Lovaria A, Sangiovanni A, Nicolini A, De Fazio C, Ronchi G, Fasani P, Del Ninno E, Colombo M. Segmental transcatheter arterial chemoembolization treatment in patients with cirrhosis and inoperable hepatocellular carcinomas. *J Vasc Interv Radiol* 2002; **13**: 995-999

6 **Llad inverted question marko L,** Virgili J, Figueras J, Valls C, Dominguez J, Rafecas A, Torras J, Fabregat J, Guardiola J, Jaurrieta E. A prognostic index of the survival of patients with unresectable hepatocellular carcinoma after transcatheter arterial chemoembolization. *Cancer* 2000; **88**: 50-57

7 **Ueno K**, Miyazono N, Inoue H, Nishida H, Kanetsuki I, Nakajo M. Transcatheter arterial chemoembolization therapy using iodized oil for patients with unresectable hepatocellular carcinoma: evaluation of three kinds of regimens and analysis of prognostic factors. *Cancer* 2000; **88**: 1574-1581

8 **Chan AO**, Yuen MF, Hui CK, Tso WK, Lai CL. A prospective study regarding the complications of transcatheter intraarterial lipiodol chemoembolization in patients with hepatocellular carcinoma. *Cancer* 2002; **94**: 1747-1752

9 **Higuchi T**, Kikuchi M, Okazaki M. Hepatocellular carcinoma after transcatheter hepatic arterial embolization. *Cance* 1994; **73**: 2260-2267

10 **Lin Z**, Ren Z, Xia J. Appraisal of postoperative transcatheter arterial chemoembolization (TACE) for prevention and treatment of hepatocellular carcinoma recurrence. *Zhonghua Zhongliu Zazhi* 2000; **22**: 315-317

11 **Lee JK**, Chung YH, Song BC, Shin JW, Choi WB, Yang SH, Yoon HK, Sung KB, Lee YS, Suh DJ. Recurrences of hepatocellular carcinoma following initial remission by transcatheter arterial chemoembolization. *J Gastroenterol Hepatol* 2002; **17**: 52-58

12 **Harrington EA**, Fanidi A, Evan GI. Oncogenes and cell death. *Curr Opin Genet Dev* 1994; **4**: 120-129

13 **Schmaltz C**, Hardenbergh PH, Wells A, Fisher DE. Regulation of proliferation-survival decisions during tumor cell hypoxic. *Mol Cell Biol* 1998; **18**: 2845-2854

14 **Semenza GL**, Roth PH, Fang HM, Wang GL. Transcriptional regulation of genes encoding glycolytic enzymes by hypoxia-inducible factor 1. *J Biol Chem* 1994; **269**: 23757-23763

15 **Hockel M**, Schlenger K, Aral B, Mitze M, Schaffer U, Vaupel P. Association between tumor hypoxic and malignant progression in advanced cancer of the uterine cervix. *Cancer Res* 1996; **56**: 4509-4515

16 **Jensen RL**, Soleau S, Bhayani MK, Christiansen D. Expression of hypoxic inducible factor-1 alpha and correlation with preoperative embolization of meningiomas. *J Neurosurg* 2002; **97**: 658-667

17 **Park K**, Kim JH, Nam DH, Lee JI, Kim JS, Hong SC, Shin HJ, Eoh W, Park K. Vascular endothelial growth factor expression under ischemic stress in human meningiomas. *Neurosci Lett* 2000; **283**: 45-48

18 **An FQ**, Matsuda M, Fujii H, Matsumoto Y. Expression of vascular endothelial growth factor in surgical specimens of hepatocellular carcinoma. *J Cancer Res Clin Oncol* 2000; **126**: 153-160

19 **Shao G**, Wang J, Zhou K, Yan Z. Intratumoral microvessel density and expression of vascular endothelial growth factor in hepatocellular carcinoma after chemoembolization. *Zhonghua Ganzangbing Zazhi* 2002; **10**: 170-173

20 **Guo WJ**, Li J, Ling WL, Bai YR, Zhang WZ, Cheng YF, Gu WH, Zhuang JY. Influence of hepatic arterial blockage on blood perfusion and VEGF, MMP-1 expression of implanted liver cancer in rats. *World J Gastroenterol* 2002; **8**: 476-479

21 **Miyazaki M**, Shimoda T, Itoh H. Enhancement of cytotoxicity of doxorubicin by verapamil in the hepatic artery infusion for liver tumors in rats. *Cancer* 1993; **72**: 349-354

22 **Shao G**, Wang J, Zhou K, Yan Z. Intratumoral microvessel density and expression of vascular endothelial growth factor in hepatocellular carcinoma after chemoembolization. *Zhonghua Ganzangbing Zazh* 2002; **10**: 170-173

23 **Li X**, Zheng CS, Feng GS, Zhuo CK, Zhao JG, Liu X. An implantable rat liver tumor model for experimental transarterial chemoembolization therapy and its imaging features. *World J Gastroenterol* 2002; **8**: 1035-1039

24 **Yang R**, Rescorla FJ, Reilly CR, Faught PR, Sanghvi NT, Lumeng L, Franklin TD, Grosfeld JL. A reproducible rat liver cancer model for experimental therapy: introducing a technique of intrahepatic tumor implantation. *J Surg Res* 1992; **52**: 193-198

25 **Weidner N**, Carroll PR, Flax J, Blumenfeld W, Folkman J. Tumor angiogenesis correlates with metastasis in invasive prostate carcinoma. *Am J Pathol* 1993; **143**: 401-409

26 **Folkman J**. Role of angiogenesis in tumor growth and metastasis. *Semin Oncol* 2002; **29**: 15-18

27 **Takeda A**, Stoeltzing O, Ahmad SA, Reinmuth N, Liu W, Parikh A, Fan F, Akagi M, Ellis LM. Role of angiogenesis in the development and growth of liver metastasis. *Ann Surg Oncol* 2002; **9**: 610-616

28 **Koide N**, Nishio A, Hiraguri M, Shimada K, Shimozawa N, Hanazaki K, Kajikawa S, Adachi W, Amano J. Cell proliferation, apoptosis and angiogenesis in gastric cancer and its hepatic metastases. *Hepatogastroenterology* 2002; **49**: 869-873

29 **Qin LX**, Tang ZY. The prognostic molecular markers in hepatocellular carcinoma. *World J Gastroenterol* 2002; **8**: 385-392

30 **Skobe M**, Rockwell P, Goldstein N, Vosseler S, Fusenig NE. Halting angiogenesis suppresses carcinoma cell invasion. *Nature Med* 1997; **11**: 1222-1227

31 **Hasan J**, Byers R, Jayson GC. Intra-tumoral microvessel density

in human solid tumours. *Br J Cancer* 2002; **86**: 1566-1577
32 **Matsui O**, Kawamura I, Takashima T. Occurrence of an intrahepatic porto-arterial shunt after hepatic artery embolization with Gelfoam powder in rats and rabbits. *Acta Radiol Diagn* 1986; 27: 119-122
33 **Demachi H**, Matsui O, Takashima T. Scanning electron microscopy of intrahepatic microvasculature casts following experimental hepatic artery embolization. *Cardiovasc Intervent Radiol* 1991; **14**: 158-162
34 **Liou TC**, Shih SC, Kao CR, Chou SY, Lin SC, Wang HY. Pulmonary metastasis of hepatocellular carcinoma associated with transarterial chemoembolization. *J Hepatol* 1995; **23**: 563-568
35 **Hanazaki K**, Kajikawa S, Shimozawa N, Mihara M, Shimada K, Hiraguri M, Koide N, Adachi W, Amano J. Survival and recurrence after hepatic resection of 386 consecutive patients with hepatocellular carcinoma. *J Am Coll Surg* 2000; **191**: 381-388
36 **Shweiki D**, Itin A, Soffer D, Keshet E. Vascular endothelial growth factor induced by hypoxic may mediate hypoxic-initiated angiogenesis. *Nature* 1992; **359**: 843-845
37 **Hockel M**, Vaupel P. Biological consequences of tumor hypoxic. *Semin Oncol* 2001; **28**: 36-41
38 **Giatromanolaki A**, Harris AL. Tumor hypoxic, hypoxic signaling pathways and hypoxic inducible factor expression in human cancer. *Anticancer Res* 2001; **21**: 4317-4324
39 **Dvorak HF**, Brown L, Detmar M, Dvorak AM. Vascular permeability factor/vascular endothelial growth factor, microvascular hyperpermeability, and angiogenesis. *Am J Pathol* 1995; **146**: 1029-1039
40 **Dvorak HF**. Vascular permeability factor/vascular endothelial growth factor: a critical cytokine in tumor angiogenesis and a potential target for diagnosis and therapy. *J Clin Oncol* 2002; **20**: 4368-4380
41 **Park YN**, Boros P, Zhang DY, Sheiner P, Kim-Schluger L, Thung SN. Increased expression of vascular endothelial growth factor and angiogenesis in the early stage of multistep hepatoarcinogenesis. *Arch Pathol Lab Med* 2000; **124**: 1061-1065
42 **O'Byrne KJ**, Dalgleish AG, Browning MJ, Steward WP, Harris AL. The relationship between angiogenesis and the immune responses in carcinogenesis and the progression of malignant disease. *Eur J Cancer* 2000; **36**: 151-169
43 **Asahara T**, Bauters C, Zheng LP, Takeshita S, Bunting S, Ferrara N, Symes JF, Isner JM. Synergistic effect of vascular endothelial growth factor and basic fibroblast growth factor on angiogenesis *in vivo*. *Circulation* 1995; **92**: II365-371

Edited by Wu XN and WangXL

P.O.Box 2345, Beijing 100023,China
Fax: +86-10-85381893
E-mail: wjg@wjgnet.com www.wjgnet.com

World J Gastroenterol 2003;9(11):2450-2454
World Journal of Gastroenterology
 ISSN 1007-9327

• LIVER CANCER •

Expression of p27, cyclin E and cyclin A in hepatocellular carcinoma and its clinical significance

Qi Zhou, Qiang He, Li-Jian Liang

Qi Zhou, Qiang He, Li-Jian Liang, Department of Hepatobilliary Surgery, the First Affiliated Hospital of Sun Yat-Sen University, Guangzhou 510080, Guandong Province, China
Correspondence to: Professor Li-Jian Liang, Department of Hepatobilliary Surgery, the First Affiliated Hospital of Sun Yat-Sen University, Guangzhou 510080, Guandong Province, China. lianglj@medmail.com.cn
Telephone: +86-20-87755766-8096 **Fax:** +86-20-87755766-8663
Received: 2003-05-13 **Accepted:** 2003-06-02

Abstract

AIM: To investigate the expression of p*27*, cyclin E and cyclin A in hepatocellular carcinoma (HCC) and its potential clinical significance.

METHODS: Expression of p27, cyclin E and cyclin A in 45 HCC specimens and 30 adjacent noncancerous lesions obtained from 45 patients during surgery was examined by immunohistochemical SABC assay. The diameter of tumor ranged from 1 cm to 19 cm (d≤5 cm, 9 samples; 5 cm<d≤ 10 cm, 19 samples; d>10 cm, 17 samples). The tumors were graded according to the criteria described by Edmondson-Steiner: well-differentiated HCC group (Grade I+II), 26 samples; poorly-differentiated HCC group (Grade III+IV), 19 samples. According to the clinical-pathologic features, 19 samples were poorly encapsulated, 15 samples had portal invasion of cancer, 11 samples had extrahepatic metastasis, and 12 samples had intrahepatic metastasis. All of the samples were classified as the invasive and metastatic group, while the remaining was classified as the non-invasive and non- metastatic group.

RESULTS: The average labeling index (LI) of p27 in HCC lesions was significantly higher than that in adjacent noncancerous lesions (45.87±14.21 *vs* 33.77±12.92, t=3.745, P<0.001). The LI of p27 was associated with differentiation, invasiveness and metastasis of the tumors (34.46±12.29 *vs* 52.80±11.36, t=5.17; 41.42±12.86 *vs* 51.44±14.10, t=2.48; P<0.05). Cyclin E was overexpressed in 16 cases (35.6 %) while cyclin A was overexpressed in 21 cases (46.7 %) in HCC lesions. No overexpression of cyclin E or cyclin A could be observed in adjacent non-carcinoma lesions and normal liver tissues. The overexpressions of cyclin E and cyclin A were correlated with differentiation, tumor thrombus, invasiveness and metastasis (P<0.05). Expression of cyclin E was significantly correlated with expression of cyclin A (r=0.329, P<0.05). The LI of p27 was significantly decreased in cyclin E, cyclin A positive groups (40.33±11.91 *vs* 49.50±13.76, t=3.05; 38.86±11.19 *vs* 52.57±12.62, t=3.89; P<0.05).

CONCLUSION: p27, cyclin E, cyclin A play cooperative roles in HCC tumorigenesis, differentiation, invasiveness and metastasis. Detection of their expression may be helpful in prediction of tumor progression.

Zhou Q, He Q, Liang LJ. Expression of p27, cyclin E and cyclin A in hepatocellular carcinoma and its clinical significance. *World J Gastroenterol* 2003; 9(11): 2450-2454
http://www.wjgnet.com/1007-9327/9/2450.asp

INTRODUCTION

Hepatocellular carcinoma is one of the most common malignant tumors in China and has poor prognosis due to its high incidence of recurrence and metastasis. Recent studies on HCC have been focused on tumorigenesis, progression, invasiveness as well as novel strategy of therapeutics.

It has been implicated that the activity of cell proliferation is directly associated with tumorigenesis, progression and invasiveness. Therefore estimation of cell proliferative activity is important in prediction of the biological aggressiveness of tumor cells. The regulatory molecules of cell cycle are parameters for the prediction of cell proliferative activity[1]. Cell cycle progression is controlled by protein complexes such as cyclins, cyclin dependent kinases (CDKs) and cyclin dependent kinase inhibitors (CDKIs). The sequential activation and subsequent inactivation of cyclin-CDK complexes govern the progression of eukaryatic cells throughout cell cycle[2]. In cell cycle, the period from the late G1 to S phase is the most important restriction point for cell proliferation. Whether cells pass the G1/S restriction point determines the continuity of cell proliferation[3]. The most direct protein at G1/S point is retinoblastoma protein (pRb)[4]. Phosphorylated pRb can bind to transcription factor (E2F) that regulates cell cycle by activation of DNA synthesis. Both cyclin E and cyclin A play important roles in G1/S restriction point[5,6]. Cyclin E dramatically increases from the late G1 phase to the early S phase[5] which binds to CDK2 and phosphorylates pRb. When cell enters S phase, cyclin E and cyclin A-CDK2 complex cooperate continuously for the phosphorylation of pRb until the end of M phase[6]. As one of CDKIs, p27 can prevent pRb from phosphorylation and arrest the cell cycle at G1 phase[7]. Cyclin E and cyclin A are direct substrates of p27. Recent researches have shown that the activity of p27 protein can be up-regulated by multiple tumorigenesis related factors such as transforming growth factor β[8], interferon[9] and cAMP[10]. The expression of p27 has been implicated in the tumorigenesis of many kinds of tumors[11-15]. However, little is known about the association between cyclins and hepatocellular carcinoma. In the present study, we detected the expression of p27, cyclin E and cyclin A in 45 HCC samples and 30 adjacent noncancerous lesions by immunohistochemical assay to elucidate their correlation with tumorigenesis, progression and metastasis of HCC.

MATERIALS AND METHODS

Data of patients

From 1998 to 1999, 45 HCC specimens and 30 adjacent noncancerous lesions were obtained from 45 patients with HCC during surgery in our hospital. A senior pathologist made the final diagnosis on the basis of histological examination. No patient had received radioactive therapy, chemotherapy,

transcatheter arterial chemoembolization or immunotherapy before operation. There were 36 (80 %) males and 9 (20 %) females, aged from 30 to 65 with an average age of 45±11. A total of 30 (66.67 %) patients had AFP levels over 400 ng/ml, 32 (71.1 %) patients were HbsAg positive. The diameter of tumor in this group ranged from 1 cm to 19 cm (less than 5 cm in 9 samples, 5 cm to 10 cm in 19 samples, more than 10 cm in 17 samples). These tumors were graded based on the criteria of Edmondson-Steiner (Grade I+II in 26 samples, grade III+IV in 19 samples). According to the clinical-pathologic features, 19 specimens had no or little capsule, 12 samples had portal vein invasion of the tumors, 11 samples had extrahepatic metastasis and 12 samples had intrahepatic metastasis. The criteria for invasiveness or metastasis of tumor were the tumor tissue with no or poor capsule, or portal vein invasion, or intrahepatic or extrahepatic metastasis[16]. Twenty-five cases (55.56 %) were defined as invasive/metastatic group.

Tissue sampling

Fresh surgical tissue samples were fixed immediately in formaldehyde solution for 12-24 h and paraffin-embedded for immunohistochemical assay.

Immunohistochemical assay

Immunohistochemical study was performed using avidin-biotin-complex method. Briefly, 4 μm slices of tissue section were deparaffinized and rehydrated. Endogenous peroxidase activity was blocked with 0.3 % hydrogen peroxide for 10 min. Sections were then incubated with 0.03 mol/L citrate buffer (pH=6.0) and heated in microwave oven for 10 min. After three times of rinsing with phosphate-buffered saline (PBS) (pH=7.4), the slides were incubated with 10 % normal goat serum at room temperature for 20 min to block the nonspecific reaction, and incubated overnight with primary antibody (p27 monoclonal antibody 1:50, cyclin E polyclonal antibody 1:50 and cyclin A polyclonal antibody 1:100) at 4 ℃. After rinsed in PBS, they were incubated with second antibody (1:100) for 30 min at room temperature, and reacted with the avidin-biotin peroxidase complex at a concentration of 1:100 for 30 min after washed in PBS. The peroxidase reaction was visualized by incubating the section with 0.01 % 3,3'-diaminobenzidine tetrahydrochloride and hydrogen peroxide mixture. The slides were counterstained with hematoxylin. In negative control, primary antibody was replaced by normal mouse serum.

Immunohistochemical evaluation

The protein reaction (p27, cyclin E or cyclin A) was considered as positive when nuclei showed staining signals. At least 500 *p*27 positive cells from at least 5 randomly selected fields (×400) were counted[17]. When the positive rate for each protein of carcinoma cells was over 5 %, overexpression of cyclin E and cyclin A was defined according to the report[18,19].

Statistical analyses

The correlation of *p*27, cyclin E or cyclin A with carcinogenesis, differentiation, invasion and metastasis of HCC was analyzed with SPSS8.0 software. The χ^2 test and Student *t* test were employed for analyses, *P* value less than 0.05 was regarded as statistically significant.

RESULTS

*p*27 was expressed both in HCC and in adjacent noncancerous lesions (Figures 1,2). The average LI of p27 in HCC lesions was significantly higher than that in adjacent noncancerous lesions (45.87±14.21 *vs* 33.77±12.92, *P*<0.001). The LI of p27 was associated with differentiation, tumor size, invasiveness and metastasis of HCC (*P*<0.05). No correlation was found between the LI of p27 and the number of cancer foci (Table 1).

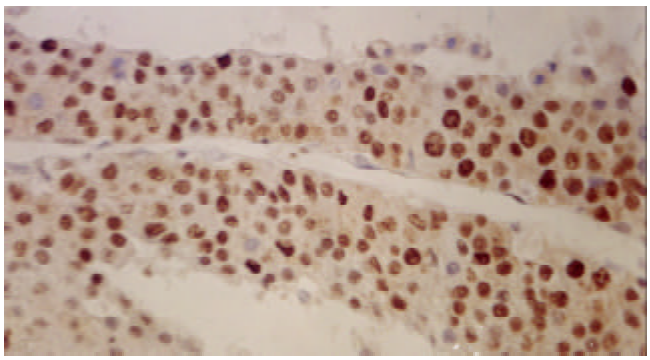

Figure 1 Nuclear staining of p27 protein in HCC (SABC, 400×).

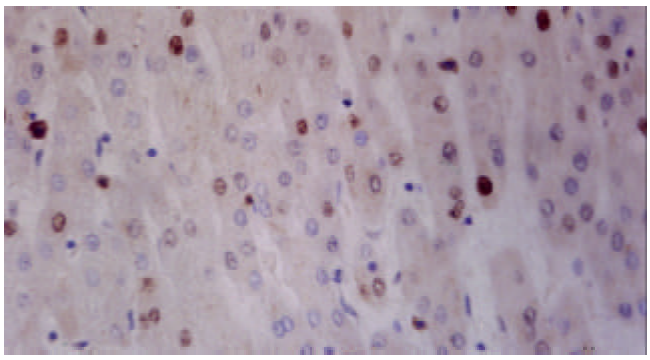

Figure 2 Nuclear staining of p27 protein in adjacent noncancerous lesions (SABC, 400×).

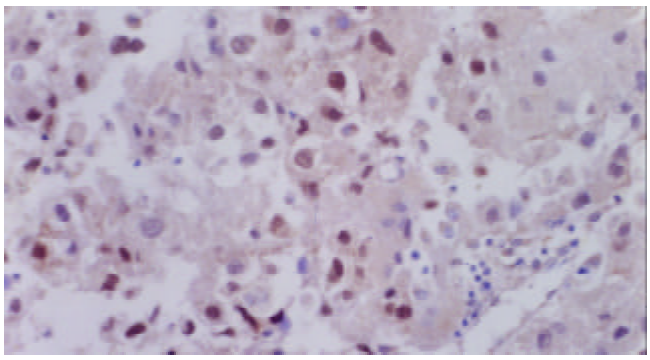

Figure 3 Nuclear staining of cyclin E protein in HCC (SABC, 400×).

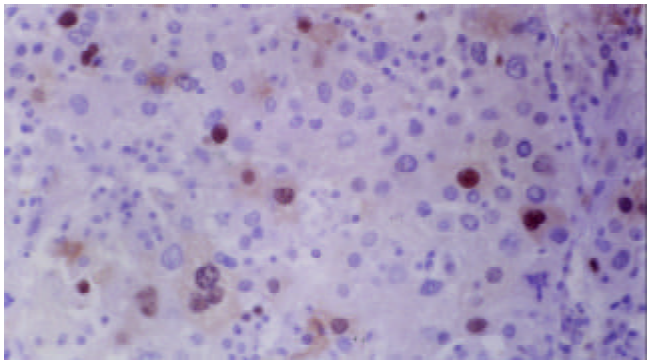

Figure 4 Nuclear staining of cyclin A protein in HCC (SABC, 400×).

Table 1 Expression of p27 and pathological features ($\bar{x}\pm s$)

Groups		*n*	p27 LI($\bar{x}\pm s$)		*P*
Histological grade	I+II	26	52.80±11.36	*t*=5.17	<0.001
	III+IV	19	34.46±12.29		
Tumor size (d)	≤5 cm	9	53.28±15.17	*F*=5.934	<0.005
	5 cm<d≤10 cm	19	49.50±10.96		
	>10 cm	17	37.59±13.12		
Envelope	Full	26	48.82±13.35	*t*=1.76	>0.05
	Rupture	19	41.54±14.15		
Tumor thrombi	+	13	36.83±12.74	*t*=2.77	<0.01
	-	32	49.16±13.41		
Metastasis	Positive	11	35.52±11.70	*t*=3.02	<0.05
	Negative	34	49.22±13.43		
Number	<2	33	47.65±15.08	*t*=1.41	>0.05
	≥2	12	40.98±10.52		
Non-invasive and non- metastatic group		20	51.44±14.10	*t*=2.48	<0.02
Invasive and metastatic group		25	41.42±12.86		

Table 2 Expression of cyclin E, cyclin A and pathological features

Group		*n*	Cyclin E		Cyclin A	
			+	χ^2 / *P*	+	χ^2 / *P*
Histological grade	I+II	26	5 (19.23 %)	7.16 / <0.05	8 (30.77 %)	6.25 / <0.05
	III+IV	19	11 (57.89 %)		13 (68.42 %)	
Tumor size (d)	≤5 cm	9	1 (11.11 %)	1.58 / >0.05	5 (55.56 %)	1.29 / >0.05
	5<d≤10 cm	19	7 (36.84 %)		7 (36.84 %)	
	>10 cm	17	8 (47.06 %)		9 (52.94 %)	
Envelope	Full	26	7 (26.92 %)	2.00 / >0.05	10(38.46 %)	1.67 / >0.05
	Rupture	19	9 (47.37 %)		11 (57.89 %)	
Tumor thrombi	+	13	8 (61.54 %)	5.38 / <0.01	10 (76.92 %)	6.72 / <0.01
	-	32	8 (25.00 %)		11 (34.38 %)	
Metastasis	Positive	11	6 (54.55 %)	1.32 / >0.05	9 (81.82 %)	7.23 / <0.01
	Negative	34	10 (29.41 %)		12 (35.29 %)	
Number	<2	33	9 (27.28 %)	2.47 / >0.05	12 (36.36 %)	5.76 / <0.05
	≥2	12	7 (58.33 %)		9 (75.00 %)	
Non-invasive and non- metastatic group			4 (20.00 %)	3.86 / <0.05	4 (20.00 %)	9.95 / <0.01
Invasive and metastatic group			12 (48.00 %)		17 (68.00 %)	

The overexpression of cyclin E and cyclin A could be exclusively seen in HCC (Figures 3,4), the overexpression rate was 35.6 %(16/45) for cyclin E and 46.7 %(21/45) for cyclin A. The overexpression of cyclin E and cyclin A was associated with differentiation, invasiveness and metastasis of HCC (P<0.05). No correlation could be found between the LI of p27 and the tumor size (P>0.05)(Table 2).

The LI of p27 decreased significantly both in cyclin E and in cyclin A overexpressed tissues (40.33±11.91 *vs* 49.50±13.76, 38.86±11.19 *vs* 52.57±12.62, P<0.05). The overexpression of cyclin E was significantly correlated with that of cyclin A (P<0.05, r=0.329), (Table 3).

Table 3 Relationship between expressions of cyclin E and cyclin A

		Cyclin A		*P*
		+	-	
cyclin E	+	11	5	<0.05
	-	10	19	

DISCUSSION

Uncontrollable proliferation is the property of tumor cells. Cell proliferation activity involves in tumorigenesis and progression, and is one of the prominent parameters in evaluating the biological aggressiveness of carcinoma.

As one of the major CDK inhibitors, p27 can arrest cell cycle by blocking phosphorylation of pRB. Its substrate is G1 cyclins such as cyclin E and cyclin A. Low p27 protein levels were found in aggressive stomach[11], lung[12], prostate[13], breast[14] and pituitary[15] cancers, suggesting that p27 might suppress the progression of tumor[20].

Our data showed that the LI of p27 was higher in HCC than in adjacent noncancerous tissues, and the expression of p27 was mainly localized in nuclei. This might suggest that p27 works as a positive regulator in tumorigenesis of HCC. Two possible mechanisms could be involved. First, p27 might be regulated by self-stabilization. It has been demonstrated[21] that expression of p27 was regulated primarily at the posttranscriptional level and its mRNA level was stable throughout the cell cycle. When cells are stimulated by

mitogen, p27 protein undergoes rapid degradation via the ubiquitin-proteasome pathway. However, this proteolysis was dramatically reduced in resting cells[22]. Thus, increased expression of p27 in some tumors may be resulted from self-stable regulating mechanism by which increased expression of cyclins attenuates the activity of the proteasome pathway for p27, and then causes an increased expression of free p27 protein that can counteract the increased cyclins in tumorigenesis. Second, gene mutation may also be responsible for this situation. Recent studies have revealed a gene deletion and polymorphism in primary breast cancer and leukemia[23,24]. Whether increased expression of p27 in HCC is caused by mutant protein remains to be elucidated.

In the present study, the expression of p27 was decreased in cases with biologically aggressive phenotypes such as poor differentiation, metastasis and invasiveness. It has been reported that cultured tumor cells expressed more p27 as they grew from single layer to tri-dimension and cell contact inhibition could be suppressed by p27 antisense oligonucleotide[25]. All these suggested that decreased expression of p27 was related with tumor progression and could be used as a potential prediction factor for HCC.

Although many researchers focused on the role of cyclin E and cyclin A in cell cycle in tumor cells[26,27], few studies have ever addressed on the aspect of HCC. Our data showed that cyclin E and cyclin A proteins were exclusively expressed in HCC but not in adjacent noncarcinous lesions. The expression of cyclin E and cyclin A was mainly localized in nuclei, suggesting that overexpression of cyclin E and cyclin A could promote cell cycle and cell proliferation, and therefore was associated with tumorigenesis. Cyclin E expressed in cytoplasm of tumor cell may be caused by increased synthesis, decreased degradation and failure to transportation. Our data also showed that overexpression rate of cyclin E and cyclin A was associated with low histological grade of tumors with high expression rate in poorly differentiated tumors, suggesting the overexpression of cyclin E and cyclin A was associated with poor differentiation. Overexpression of cyclin E was correlated with formation of tumor thrombi, while overexpression of cyclin A was associated with tumor thrombi, metastasis and satellite lesions. Thus overexpression of cyclin E and cyclin A is linked to tumor invasiveness and metastasis potency, suggesting a poor prognosis for patients with overexpression of cyclin E and cyclin A. Patients with cyclin E overexpression had a four-year survival rate[28] and overexpression of cyclin A had a positive relationship with the amount of cells at S-phase and a reverse correlation with the four-year survival rate[18]. Our data were partially similar to these findings. Unfortunately, we were unable to evaluate the correlation of overexpression of cyclin E and cyclin A with the prognosis due to incomplete follow-up data of the patients.

p27 suppresses cyclin/CDK complexes mainly by binding itself to cyclins. It has been reported that p27 could bind to CDK2 and played an inhibitory role in regenerating liver[29]. Zerfass-Thome[30] reported that p27 arrested cell cycle by blocking transactivation of cyclin-A gene which is dependent on cyclin-E gene expression, suggesting a mechanism of interaction among p27, cyclin E and cyclin A. The lower p27 LI in positive cyclin E and cyclin A group in our study might be resulted from the interaction of cyclin-CDK complexes that can suppress its expression. And expression of cyclin E had a positive relationship with expression of cyclin A. These suggest that p27, cyclin E and cyclin A play cooperatively important roles in tumorigenesis, differentiation, aggressiveness and metastasis of HCC.

Although a lot of studies on cyclins/CDKI have been done, many questions remain to be answered. It has been reported that proliferative tumor cells *in vitro* could be arrested in G1 phase by using antibody IgM against cyclin E and cyclin A in culture[31]. Other studies *in vivo* showed that invasiveness of tumor could be dramatically suppressed by down-regulation of G1 and S phase proteins[32]. It seems that cyclins may become potential targets for tumor therapy in the near future. Further studies are needed to elucidate the mechanism of interaction among cyclins and the pathway of regulation before they can finally be used as a novel strategy for prediction of prognosis and therapeutics of HCC.

REFERENCES

1 **Sheer CJ**. Cancer cell cycles. *Science* 1996; **274**: 1672-1678
2 **Draetta GF**, Mammalian G. Cyclins. *Curr Opin Cell Biol* 1994; **6:** 842-846
3 **Hartwell LA**, Weinnert TA. Checkpoints: control that ensure the order of cell cycle events. *Science* 1989; **246**: 629-634
4 **Toyoshima H,** Hunter T. p27, a novel inhibitor of G1 Cyclin dependent kinase protein kinase activity is related to p21. *Cell* 1994; **78**: 67-71
5 **Wimmel A,** Lucibello FC, Sewing A, Adolph S, Muller R. Wimmel A. Inducible acceleration of G1 Progression through tetra cycline-regulated expression of human cyclin E. *Oncogene* 1994; **9**: 995-997
6 **Pagano M,** Pepperkok R, Verde F, Ansorge W, Draetta G. Pagano M. Cyclin A is required at two points in the human cell cycle. *EMBO J* 1992; **11**: 961-967
7 **Hengst T**, Reed SI. Translational control of p27kip1 accumulation during the cell cycle. *Science* 1996; **271**: 1861-1864
8 **Polyak K,** Kato JY, Solomon MJ, Sherr CJ, Massague J, Roberts JM, Koff A. p27kipl, a Cyclin dependent kinase inhibitor, links transforming growth factor-β and contact inhibition to cell cycle arrest. *Genes Dev* 1994; **8**: 9-17
9 **Harvat BL**, Seth P, Jetten AM. The role of p27kip1 in gamma interferon mediated growth arrest of mammary epithelial cells and related defects in mammary carcinoma cell. *Oncogene* 1997; **372**: 570-573
10 **Kato JY,** Matsuoka M, Polyak K, Massague J, Sherr CJ. Cyclin AMP induce G1 phase arrest mediated by an inhibitor (p27kip1) of Cyclin dependent kinase 4 activation. *Cell* 1994; **79**: 487-495
11 **Ohtani M,** Isozaki H, Fujii K, Nomura E, Niki M, Mabuchi H, Nishiguchi K, Toyoda M, Ishibashi T, Tanigawa N. Impact of the expression of Cyclin dependent kinase inhibitor p27kip1 and apoptosis in tumor cells on the overall survival of the patients with non-early stage of gastric carcinomas. *Cancer* 1999; **85**: 1711-1718
12 **Esposito V,** Baldi A, De Luca A, Groger AM, Loda M, Giordano GG, Caputi M, Baldi F, Pagano M, Giordano A. Prognostic role of Cyclin dependent kinase inhibitor p27 in non-small cell lung cancer. *Cancer Res* 1997; **57**: 3381-3385
13 **Tsihlias J,** Kapusta LR, DeBoer G, Morava-Protzner I, Zbieranowski I, Bhattacharya N, Catzavelos GC, Klotz LH, Slingerland JM. Loss of Cyclin dependent kinase inhibitor p27kip1 is a novel prognostic factor in located human prostate adenocarcinoma. *Cancer Res* 1998; **58**: 542-548
14 **Tan P,** Cady B, Wanner M, Worland P, Cukor B, Magi-Galluzzi C, Lavin P, Draetta G, Pagano M, Loda M. The cell cycle inhibitor p27 is an independent prognostic marker in small (Ta, Tb) invasive breast carcinomas. *Cancer Res* 1997; **57**: 1259-1268
15 **Takeuchi S,** Koeffler HP, Hinton DR, Miyoshi I, Melmed S, Shimon I. Mutation and expression analysis of the Cyclin dependent kinase inhibitor gene p27kip1 in pituitary tumors. *J Endocrinol* 1998; **157**: 337-342
16 **Yao M**, Zhou XD, Liu YK,Tang ZY. E-cadherin expression in invasive hepatocellular carcinoma. *Zhonghua Xiaohua Zazhi* 1998; **18**: 31-33
17 **Ito Y,** Matsuura N, Sakon M, Miyoshi E, Noda K, Takeda T, Umeshita K, Nagano H, Nakamori S, Dono K, Tsujimoto M, Nakahara M, Nakao K, Taniguchi N, Monden M. Expression and prognostic roles of the G1-Smodulators in hepatocellular carcinoma: p27 independently predicts the recurrence. *Hepatology* 1999; **30:** 90-99
18 **Volm M,** Koomagi R, Mattern J, Stammler G. Cyclin A is associated with an unfavourable outcome in patient with non-small-cell lung carcinomas. *Br J Cancer* 1997; **75**: 1774-1778

19 **Peng SY,** Chou SP, Hsu HC. Association of down-regulation of Cyclin D and of overexpression of cyclin E with p53 mutation, high tumor grade and poor prognosis in hepatocellular carcinoma. *J Hepatol* 1998; **29**: 281-289
20 **Sgambato A**, Cittadini A, Faraglia B, Weinstein IB. Multiple functions of p27kip1 and its alterations in tumor cell: A review. *J Cell Physio* 2000; **183**: 18-27
21 **Asessandrini A**, Chiaur OS, Pagano M. Regulation of the Cyclin dependent kinase inhibitor p27kip1 by degradation and phosphrylation. *Leukemia* 1997; **11:** 342-345
22 **Pagano M,** Tam SW, Theodoras AM, Beer-Romero P, Del Sal G, Chau V, Yew PR, Draetta GF, Rolfe M. Role of the ubiquitin – proteasome pathway in regulating abundance of the Cyclin dependent kinase inhibitor p27. *Science* 1995; **269**: 682-691
23 **Ferrando AA,** Balbin M, Pendas AM, Vizoso F, Velasco G, Lopez-Otin C. Mutational analysis of the human Cyclin dependent kinase inhibitor p27kip1 in primary breast carcinomas. *Hum Genet* 1996; **97**: 91-94
24 **Morosetti R**, Kawamata N, Gombart AF. Alternation of the p27kip1 gene in non-Hodgkin's lymphomas and adult T-cell leukemia lymphoma. *Blood* 1995; **86**: 1924-1930
25 **Levenberg S,** Yarden A, Kam Z, Geiger B. p27 is involved in N-cadherin mediated contact inhibition of cell growth and S-phase entry. *Oncogene* 1999; **18**: 869-876
26 **Donnellan R**, Chetty R. Cyclin E in human cancers. *FASEB J* 1999; **13**: 773-780
27 **Huntunem RL**, Blomquist CP, Bohling TO. Expression of cyclin A in soft tissue sarcomas correlates with tumor aggressiveness. *Cancer Res* 1999; **59**: 2885-2892
28 **Ohashi R,** Gao C, Miyazaki M, Hamazaki K, Tsuji T, Inoue Y, Uemura T, Hirai R, Shimizu N, Namba M. Enhanced expression of cyclin E and cyclin A in human hepatocellular carcinomas. *Anticancer Res* 2001; **21**: 657-662
29 **Fero ML,** Randel E, Gurley KE, Roberts JM, Kemp CJ. The murine gene p27 is haplo-inufficent for tumor suppression. *Nature* 1998; **396**: 177-180
30 **Zerfass-Thome K,** Schulze A, Zwerschke W, Vogt B, Helin K, Bartek J, Henglein B, Jansen-Durr P. p27kip1 blocks Cyclin-E dependent transactivation of Cyclin-A gene expression. *Mol Cell Biol* 1997; **17**: 407-415
31 **Marches R,** Schenermann RH, Uhr TW. Cancer dormancy: role of Cyclin-dependent kinase inhibitors in induction of cell cycle arrest mediated via memberane IgM. *Cancer Res* 1998; **58**: 691-697
32 **Pascale RM,** Simile MM, De Miglio MR, Muroni MR, Calvisi DF, Asara G, Casabona D, Frau M, Seddaiu MA, Feo F. Cell cycle deregulation in liver lesions of rats with and without genetic predisposition to hepatocarcinogenesis. *Hepatology* 2002; **35**: 1341-1350

Edited by Ren SY and Wang XL

P.O.Box 2345, Beijing 100023,China
Fax: +86-10-85381893
E-mail: wjg@wjgnet.com www.wjgnet.com

World J Gastroenterol 2003;9(11):2455-2459
World Journal of Gastroenterology
 ISSN 1007-9327

• LIVER CANCER •

Study on hepatocelluar carcinoma-associated hepatic arteriovenous shunt using multidetector CT

Ming-Yue Luo, Hong Shan, Zai-Bo Jiang, Lu-Fang Li, Hui-Qing Huang

Ming-Yue Luo, Hong Shan, Zai-Bo Jiang, Lu-Fang Li, Hui-Qing Huang, Department of Radiology, the Third Affiliated Hospital, Sun Yat-Sen University, Guangzhou 510630, Guangdong Province, China
Correspondence to: Dr. Ming-Yue Luo, Department of Radiology, the Third Affiliated Hospital, Sun Yat-Sen University, Guangzhou 510630, Guangdong Province, China. myluo@yahoo.com.cn
Telephone: +86-20-85516867 Ext 3108 **Fax:** +86-20-87536401
Received: 2003-05-10 **Accepted:** 2003-06-02

Abstract

AIM: To investigate multidetector CT (MDCT) findings of hepatocelluar carcinoma (HCC)- associated hepatic arteriovenous shunt (HAVS) and to evaluate their clinical significance.

METHODS: Thin-slice and dynamic enhancement MDCT of HAVS was performed on 56 patients with HCC. MDCT findings, including those of portal veins, hepatic veins, superior mesenteric veins, splenic veins, HCC foci, liver parenchyma without HCC foci, spleens, and thromboses in portal veins and hepatic veins, were all confirmed by digital subtract angiography and analyzed.

RESULTS: MDCT demonstrated earlier enhancement of main portal trunks and/or the first order branches than that of superior mesenteric veins or splenic veins (n=31). One patient had strong early enhancement of left hepatic vein with thromboses in left hepatic vein and upper part of inferior vena cava and 1 patient had transient patchy enhancement peripheral to HCC foci in late hepatic arterial phase among them. It demonstrated stronger opacification of main portal trunks and/or the first order branches than that of superior mesenteric veins or splenic veins (n=18), and earlier enhancement of the second order and smaller branches of portal veins than that of main portal trunks (n=4), stronger opacification of the second order and smaller branches of portal veins than that of main portal trunks (n=3), with transient patchy enhancement (n=3) or wedge-shaped enhancement (n=4) peripheral to HCC foci in late hepatic arterial phase. Enhancement degree of HCC foci was all decreased. As for 49 patients with severe or moderate shunts, enhancement degree of liver parenchyma without HCC foci was increased with heterogeneous density, but enhancement degree of spleens was decreased. There were thromboses in main portal trunks and/or the first order branches in 32 patients.

CONCLUSION: The main MDCT findings of HCC-associated HAVS are earlier enhancement and stronger opacification of portal veins and/or hepatic veins. Understanding of these findings will contribute to the diagnosis and prognosis of the disease and improve therapy for the patients.

Luo MY, Shan H, Jiang ZB, Li LF, Huang HQ. Study on hepatocelluar carcinoma-associated hepatic arteriovenous shunt using multidetector CT. *World J Gastroenterol* 2003; 9(11): 2455-2459
http://www.wjgnet.com/1007-9327/9/2455.asp

INTRODUCTION

Hepatic arteriovenous shunt (HAVS) is the communication between hepatic artery or its branches and portal vein or hepatic vein, forming hepatic artery portal venous shunt (HAPVS) or hepatic artery hepatic venous shunt (HAHVS) respectively. Hepatocelluar carcinoma (HCC) is the most common condition associated with HAVS because of its easy invasion of portal vein and hepatic vein. HAVS could result in direct blood flow between hepatic artery and portal vein or hepatic vein, which may cause severe portal hypertension and consequently, splenomegaly, ascites, and esophagogastric varices and bleeding, accelerating intrahepatic dissemination and extrahepatic metastasis of carcinoma cells[1,2]. Understanding of CT findings of HCC-associated HAVS is of significant clinical implications. Multidetector CT (MDCT) could contribute to the diagnosis of HAVS associated with HCC due to its fast scanning and improved image resolution and quality[3]. The purpose of this study was to examine MDCT findings of HCC-associated HAVS and to evaluate their clinical significance.

MATERIALS AND METHODS

Clinical data

Fifty-six patients (49 men and 7 women, range 29-73 years, mean age 49.8 years) with HCC-associated HAVS were included in the present study. The diagnosis of HCC was based on the results of percutaneous needle biopsy (n=5) or laboratory testings, including elevated serum alpha-fetoprotein level, in combination with imaging appearance and follow-up images (n=51) according to the diagnostic criteria for HCC formulated by Chinese National Association of Anticancer Committee.

MDCT

MDCT scanning was performed with a LightSpeed QX/i MDCT scanner (General Electronic Medical System, Milwaukee, USA). Multidetector row helical technique was applied to the scanning in cranial to caudal direction. Plain scanning of the liver was carried out first. This was followed by enhancement scanning of 2.5 mm axial section performed at 15 seconds, 25 seconds and 65 seconds after injection of contrast media for early hepatic arterial phase, late hepatic arterial phase and portal venous phase image acquisition respectively. A total of 100 ml contrast medium (Ultravist 300, Schering Pharmacy, Guangzhou, China; or Iopamiro 300, Bracco S.P.A., Milano, Italy) was administered to each patient, with a power injector at a rate of 3.5 ml.sec^{-1} through a catheter placed in the peripheral vein of the antecubital fossa.

Digital subtract angiography (DSA)

DSA was performed using a TOSHIBA Digital 1000 MAX (Toshiba Corporation, Tokyo, Japan) within 2 weeks of MDCT examination. A catheter was introduced via the right femoral artery by the Seldinger technique. The celiac (6 patients) or selective hepatic (50 patients) DSA was carried out with a catheter placed in the celiac trunk or in the proper hepatic artery and 40 ml Ultravist 300 (Schering Pharmacy, Guangzhou, China)

or Iopamiro 300 (Bracco S.P.A., Milano, Italy) was injected with a power injector at a rate of 5.0 ml.sec^{-1}. Serial anterior-posterior images were obtained at 1 every 2 seconds for the first 8 seconds and a slower rate thereafter.

Diagnostic criterion for HAVS

Diagnostic criteria for HAPVS[4] were the earlier enhancement of main portal trunk and/or its first order branches than that of superior mesenteric vein or splenic vein, or stronger opacification of main portal trunk and/or its first order branches than that of superior mesenteric vein or splenic vein; or earlier enhancement of the second order and smaller branches of portal veins than that of main portal trunk, or stronger opacification of the second order and smaller branches of portal veins than that of main portal trunk. Diagnostic criteria for HAHVS were the earlier enhancement and stronger opacification of hepatic vein, approaching the density of enhanced aorta. The diagnosis of HAVS based on MDCT was confirmed by DSA.

Determination of shunting types and degrees of HAVS

According to the location of shunting, HAVS was divided into three types. The central HAVS was the shunting located in porta hepatis with earlier enhancement of main portal trunk and/or the first order branches, or hepatic veins at early hepatic arterial phase. The peripheral HAVS was the shunting located in peripheral liver parenchyma with earlier enhancement of the second order and smaller branches of portal vein, and transient patchy or wedge-shaped enhancement peripheral to HCC foci at late hepatic arterial phase. The mixed HAVS showed both central and peripheral HAVS.

According to the time of appearance of HAVS on images, HAVS was divided into three degrees. The severe HAVS showed opacification of main portal trunk and/or the first order branches, or hepatic veins, with enhancement of hepatic arterial and its branches at early hepatic arterial phase, without enhancement or with early enhancement of HCC foci. The moderate HAVS showed opacification of main portal trunk and/or the first order branches, or hepatic veins, with middle or late enhancement of HCC foci at late hepatic arterial phase. The mild HAVS showed opacification of the second order and smaller branches of portal veins at late hepatic arterial phase, with transient patchy or wedge-shaped enhancement peripheral to HCC foci.

Image analysis

Image analysis included examination of the shunting types and degrees of HAVS with or without thromboses in portal veins and/or hepatic veins; locations, gross pathologic patterns and enhancement of HCC; enhancement of liver parenchyma without HCC foci, spleens, superior mesenteric veins and splenic veins.

RESULTS

Earlier enhancement and stronger opacification of portal veins and hepatic veins

Earlier enhancement and stronger opacification of portal veins and hepatic veins were the major MDCT findings of HAVS. Their relations with shunting types and degrees of HAVS are shown in Table 1.

There was transient patchy (n=3, Figure 1) or wedge-shaped (n=4, Figure 2) enhancement peripheral to HCC foci at late hepatic arterial phase in patients with mild and peripheral HAVS, in addition to earlier enhancement of the second order and smaller branches of portal veins than that of main portal trunks, or stronger opacification of the second order and smaller branches of portal veins than that of main portal trunks.

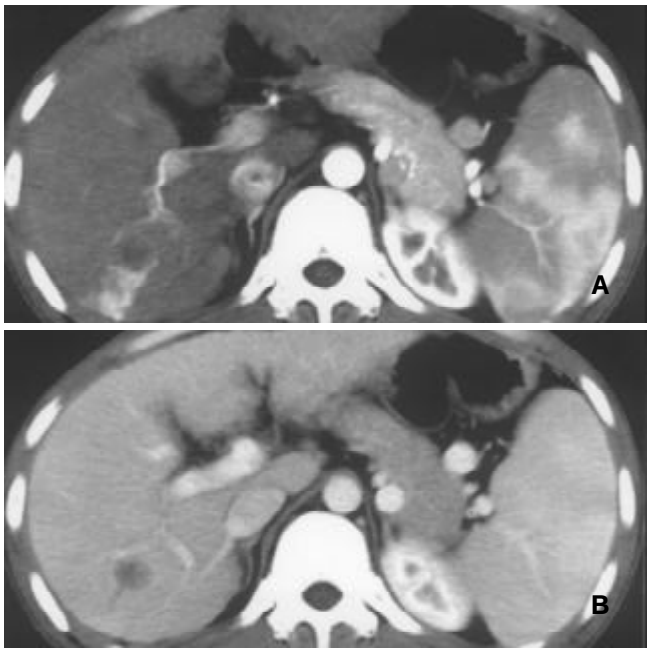

Figure 1 Nodular pattern of HCC with mild and peripheral HAVS. Transient patchy enhancement lateral to HCC foci at late hepatic arterial phase (A), becoming isoattenuation at portal vein phase (B).

Table 1 MDCT findings of earlier enhancement and stronger opacification of portal veins and hepatic veins and their relations with shunting types and degrees of HAVS

MDCT findings	Shunting patterns			Shunting degrees		
	Central	Peripheral	Mixed	Severe	Moderate	Mild
Earlier enhancement of MPT and / or the first order branches than that of SMV or SV	30	0	1[a]	31	0	0
Stronger opacification of MPT and / or the first order branches than that of SMV or SV	18	0	0	11	7	0
Earlier enhancement of the second order and smaller branches of PV than that of MPT	0	4	0	0	0	4
Stronger opacification of the second order and smaller branches of PV than that of MPT	0	3	0	0	0	3
Earlier enhancement and stronger opacification of HV, approaching density of enhanced aorta	1[b]	0	0	1[b]	0	0

a: mixed HAPVS, with transient patchy enhancement peripheral to HCC foci at late hepatic arterial phase at the same time. b: HAHVS+HAPVS, combined with earlier enhancement of main portal trunk and the first order branches than that of superior mesenteric vein. MPT=main portal trunk, SMV=superior mesenteric vein, SV=splenic vein, HV=hepatic vein.

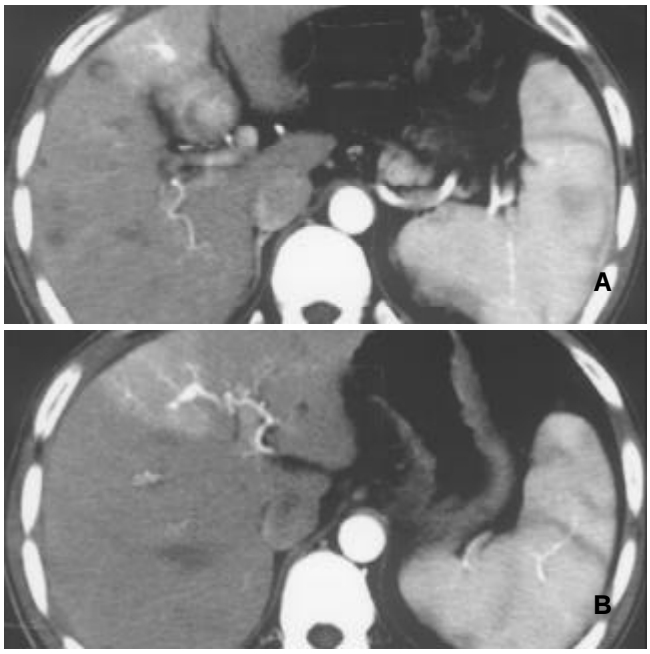

Figure 2 Nodular pattern of HCC accompanied by mild and peripheral HAVS. Stronger opacification of the third order portal vein branches than that of main portal trunk at late hepatic arterial phase with transient wedge-shaped enhancement lateral to HCC foci (A, B).

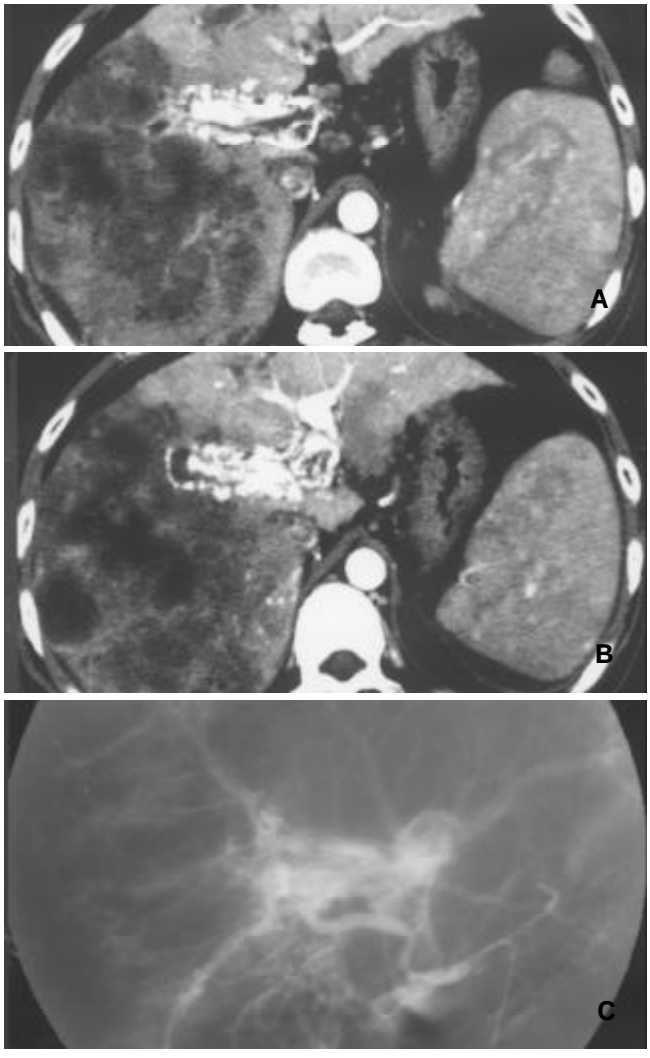

Figure 3 Massive and nodular pattern of HCC associated with severe and central HAVS. Earlier enhancement and stronger opacification of main portal trunk and the left and right first order branches with thromboses in them were shown. Enhancement degree of HCC foci was decreased, and enhancement degree of liver parenchyma without HCC foci was increased with heterogeneous density (A and B). DSA finding of the same patient (C).

Thromboses in portal veins and hepatic veins

Thromboses in portal veins and hepatic veins were seen in all cases of central HAVS. Thirty-two patients had thromboses in portal veins, including 18 patients with thromboses in main portal trunks and the first order branches (Figure 3), 11 patients with thromboses in the right first order branches and 3 patients with thromboses in the left first order branches. One patient with mixed HAVS had thromboses in the left hepatic vein and upper part of inferior vena cava.

Location, gross pathologic pattern and enhancement of HCC

HCC was located in different parts of liver parenchyma. Of the 49 patients with severe or moderate HAVS, 40 had foci adjacent to porta hepatis and 1 patient had foci nearby the secondary porta hepatis. Gross pathologic patterns included massive pattern (n=17), nodular pattern (n=11), massive and nodular pattern (n=23) and diffuse pattern (n=5). The enhancement of HCC foci was all decreased.

Enhancement of liver parenchyma without HCC foci and spleens

Liver parenchyma without HCC foci showed transient patchy (n=3) or wedge-shaped (n=4) enhancement peripheral to HCC foci at late hepatic arterial phase in 7 patients with mild and peripheral HAVS. In the 49 patients with severe or moderate and central HAVS, the enhancement degree of liver parenchyma without HCC foci was increased and heterogeneous, and enhancement degree of the spleen was all decreased (Figure 4).

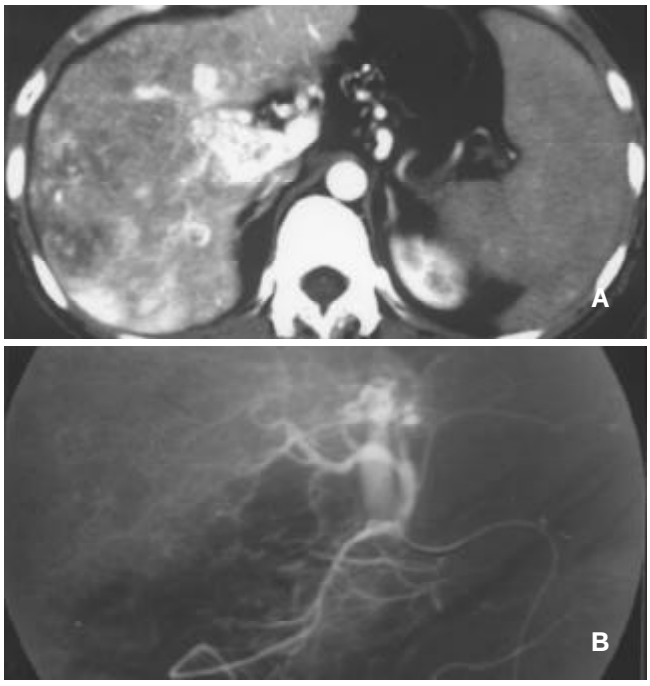

Figure 4 Massive pattern of HCC complicated with severe, central and slight, peripheral HAVS. Earlier enhancement and stronger opacification of main portal trunk with small thromboses in it were seen, with patchy enhancement internal and lateral to HCC foci. Enhancement degrees of HCC foci and spleen were decreased, enhancement degree of liver parenchyma without HCC foci was increased with heterogeneous density (A). DSA finding of the same patient (B).

DISCUSSION

Mechanism of formation of HAVS associated with HCC and MDCT findings

The formation of HAVS might be attributed to complex anatomy and various pathological conditions. Anatomically, hepatic artery and portal vein respectively branch and converge into hepatic sinuses, followed by entering into central vein and hepatic veins before into system circulation. Hence, there were abundant anastomoses between hepatic artery and portal vein[5, 6]. The pathological conditions may include followings. With continued progression of HCC adjacent to porta hepatis, it might directly invade and destroy portal veins and/or hepatic veins, forming tumor thromboses in them or growing along the venous wall. The tumor thromboses are vascularized by arterial network nourished by hepatic artery branches around the vein and are growing up. The enlarged and dilated hepatic artery branches might become the main supplying arteries of the tumor thromboses and their blood flow might enter directly into portal veins and/or hepatic veins which act as the efferent vessels, resulting in transvasal HAVS. In our serial, HCC foci of 40 patients were adjacent to porta hepatis and 1 patient adjacent to the secondary porta hepatis with apparent invasion of main portal trunks and/or the first order branches or hepatic veins. Irregular, tortuous and dilated arterial networks were seen around the porta hepatis or the secondary porta hepatis, which were confirmed by DSA as the supplying arteries of HAVS. The direct invasion and destruction of main portal trunks and/or the first order branches, or hepatic veins, were the main causes of transvasal HAVS. It was specially the case for HCC in internal left hepatic lobe where HAVS might occur even if HCC focus was small. The transvasal HAVS had severe shunts shown as an earlier enhancement of main portal trunks and/or the first order branches, or hepatic veins than that of superior mesenteric veins or splenic veins at early hepatic arterial phase (n=31), or as stronger opacification of main portal trunks and/or the first order branches than that of superior mesenteric veins or splenic veins (n=11), but livers and spleens were ischemia due to "stolen blood" by HAVS. HCC might thus show no or little enhancement, and enhancement of the spleen decreased.

Blood flow of portal veins might be obstructed due to compression of the first order branches of portal vein by HCC or carcinoma thromboses in the first order branches of portal vein. The compensative hyperplasia of vessel plexus around larger biliary ducts in the central part of liver might result in opening of hepatopetal collateral vessels and formation of transplexal HAPVS. In our study, 7 patients with moderate shunts manifested as stronger opacification of main portal trunks and/or the first order branches than that of superior mesenteric veins or splenic veins at late hepatic arterial phase with MDCT.

Compression and invasion of branches of hepatic veins by HCC might obstruct hepatic veins and cause hypertension of hepatic sinuses. The portal veins might thus become their efferent vessels and receive blood supply of hepatic arteries directly when pressure of hepatic sinuses was higher than that of portal veins, resulting in transsinusoidal HAPVS. Subsequently, functional blood flow of portal veins in this area decreased and blood flow of hepatic arteries increased as a compensation, aggravating transsinusoidal HAPVS[6]. In addition, because tumor vessel had no muscular layer and its capability of regulating blood flow by systolic function of vessel wall was poor, the normal branches of hepatic arteries around HCC would preferably take in compensatively increased hepatic arterial blood due to obstruct of hepatic veins, resulting in further intensifying of transsinusoidal HAPVS. On MDCT, it had mild shunts shown as an earlier enhancement of the second order and smaller branches of portal veins than that of main portal trunks (n=4), or stronger opacification of the second order and smaller branches of portal veins than that of main portal trunks (n=3) at late hepatic arterial phase, with transient patchy or wedge-shaped enhancement peripheral to HCC foci. In our series, 7 cases of peripheral HAPVS and 1 case of mixed HAPVS showed these findings.

Diagnosis and differential diagnosis of HCC- associated HAVS

It could be seen from above analyses that there seemed no much difficulty in diagnosis of severe or moderate and central HAVS associated with HCC. However, mild HAVS and peripheral HAVS should be differentiated from hepatic perfusion abnormalities of physiological conditions and other pathological causes[7-14].

Hepatic perfusion abnormalities caused by physiological conditions such as origin variety of segment or subsegment hepatic artery, aberrant biliary bladder vein or gastric vein were only shown as local transient hepatic parenchyma hyperattenuation at hepatic arterial phase with no abnormality at portal vein phase and no HCC foci[15]. HAPVS in hepatic hemangioma manifested as a wedge-shaped or irregular homogenous hyperattenuation in the liver parenchyma adjacent to the tumor at hepatic arterial phase, becoming isoattenuation or slight hyperattenuation, and hemangioma itself tending to show rapid enhancement at portal vein phase, specially for hemangioma of 2-3 cm in diameter or less[16-18]. Hepatic adenoma and focal nodular hyperplasia appeared as homogenous enhancement at hepatic arterial phase, being hypoattenuation at delayed time phase. Abnormal perfusion in cirrhotic liver had the typical wedge-shaped and homogeneous appearance with or without internal linear branching structures at hepatic arterial phase, returning to isoattenuation or slight hyperattenuation at portal vein phase[5]. The site of abnormal perfusion associated with thrombosis in portal vein was conformed to respective portal vein distribution. Hepatic metastasis with abundant blood supply, liver infection, Budd-Chiari syndrome, changes after transjugular intrahepatic portosystemic shunt (TIPS), HAVS following liver biopsy, abnormal perfusion resulted from acute biliary bladder inflammation and acute pancreas inflammation all had their own MDCT features. With the help of clinical materials, they could be differentiated from mild and peripheral HAVS[5,19-26].

Clinical significance of diagnosis of HCC- associated HAVS by MDCT

Diagnosis of HAVS was mainly based on transcatheter hepatic angiography (including DSA) in the past. However, a proportion of patients could not undergo transcatheter hepatic angiography due to restriction of equipment conditions and technology, cost and invasive examination etc., resulting in missed diagnosis of HAVS and loss of treatment opportunity[24, 27].

MDCT is a breakthrough in medical imaging examination technology. Equipped with a multidetector array, MDCT can perform multislice data acquisition simultaneously, which greatly reduces the time of volume scanning. In addition, image quality is improved due to increased image resolution and clarity. MDCT could therefore offer thin-slice and dynamic enhancement scanning of liver at early hepatic arterial phase, late hepatic arterial phase and portal venous phase and provide a convenient, fast and noninvasive new technology for examination of HAVS associated with HCC[3, 28].

Clinically, correct interpretation of MDCT findings of HCC-associated HAVS could assist in making right diagnosis and prognosis and working out effective therapeutic strategy. Forty-nine patients with severe or moderate and central HAVS in our series underwent transcatheter supplying artery embolism of HAVS under the guidance of MDCT information and their esophagogastric varix bleeding, ascites and stubborn diarrhea were all brought under control timely. Moreover, MDCT

provides a new technology for the study of mechanism of HAVS formation. With MDCT, shunting locations, types and degrees of HAVS can be determined, and mechanism of HAVS formation can be estimated. These may form the basis for comprehensive therapy of HCC and embolism of HAVS. Our study suggested that transvasal, transplexal and transsinusoidal HAVS might be the causes of severe, moderate and mild HAVS respectively, and enlarged and dilated nourishing artery manifested as irregular arterial network, originating from proximal proper hepatic artery, might be the main supplying artery of severe and central HAVS. Therefore, in embolism of HAVS, superselective embolism of nourishing artery rather than hepatic artery trunk was performed. If HAVS was supplied by many arteries, they should be embolized respectively. In addition, embolism agent should arrive at the end of nourishing artery to achieve permanent embolism and reduce the possibility of recanalization and recurrence of HAVS[29-33]. Our above-mentioned forty-nine patients with severe or moderate and central HAVS were all completely embolized by absolute ethanol combined with spring steel coil via 4.0F catheter or 3.0F microcatheter superselective embolism without recanalization and recurrence of HAVS by follow-up MDCT examinations.

In conclusion, our study investigated the complex MDCT findings of HAVS associated with HCC. The classification of shunting degrees into severe, moderate and mild shunts according to appearing time of HAVS at early or late hepatic arterial phase can contribute to the diagnosis and treatment of patients. It is also noted that transvasal, transplexal, transsinusoidal HAVS may be behind the formation of severe, moderate and mild HAVS respectively.

REFERENCES

1 **Tang ZY**. Hepatocellular carcinoma-cause, treatment and metastasis. *World J Gastroenterol* 2001; **7**: 445-454
2 **Guo WP**, Zhang HX, Wang ZM, Wang YQ, Ni DH, Li WX, Guan Y. DSA analysis of hepatic arteriovenous fistula concurrent with hepatic cancer and its clinical significance. *World J Gastroenterol* 2000; **6**: 872-876
3 **Mortele KJ**, McTavish J, Ros PR. Current techniques of computed tomography. Helical CT, multidetector CT, and 3D reconstruction. *Clin Liver Dis* 2002; **6**: 29-52
4 **Chen JH**, Chai JW, Huang CL, Hung HC, Shen WC, Lee SK. Proximal arterioportal shunting associated with hepatocellular carcinoma: features revealed by dynamic helical CT. *Am J Roentgenol* 1999; **172**: 403-407
5 **Kim TK**, Choi BI, Han JK, Chung JW, Park JH, Han MC. Nontumorous arterioportal shunt mimicking hypervascular tumor in cirrhotic liver: two-phase spiral CT findings. *Radiology* 1998; **208**: 597-603
6 **Nagino M**, Nimura Y, Kamiya J, Kanai M, Hayakawa N, Yamamoto H. Immediate increase in arterial blood flow in embolized hepatic segments after portal vein embolization: CT demonstration. *Am J Roentgenol* 1998; **171**: 1037-1039
7 **Luo TY**, Shi B, Li YM, Lu FJ, Yuan SW, Yan M, Wu JQ. A study on the transient hepatic abnormal enhancement in the hepatic arterial phase during dynamic contrast-enhanced spiral CT. *Zhonghua Fangshexue Zazhi* 2003; **37**: 258-263
8 **Quiroga S**, Sebastia C, Pallisa E, Castella E, Perez-Lafuente M, Alvarez-Castells A. Improved diagnosis of hepatic perfusion disorders: value of hepatic arterial phase imaging during helical CT. *Radiographics* 2001; **21**: 65-81
9 **Gryspeerdt S**, Van Hoe L, Marchal G, Baert AL. Evaluation of hepatic perfusion disorders with double-phase spiral CT. *Radiographics* 1997; **17**: 337-348
10 **Choi BI**, Lee KH, Han JK, Lee JM. Hepatic arterioportal shunts: dynamic CT and MR features. *Korean J Radiol* 2002; **3**: 1-15
11 **Park CM**, Cha SH, Kim DH, Choi JA, Cha IH, Kim YH, Chung KB, Suh WH. Hepatic arterioportal shunts not directly related to hepatocellular carcinoma: findings on CT during hepatic arteriography, CT arterial portography and dual phase spiral CT. *Clin Radiol* 2000; **55**: 465-470
12 **Chen WP,** Chen JH, Hwang JI, Tsai JW, Chen JS, Hung SW, Su YG, Lee SK. Spectrum of transient hepatic attenuation differences in biphasic helical CT. *Am J Roentgenol* 1999; **172:** 419-424
13 **Li L**, Wu PH, Mo YX, Lin HG, Zheng L, Li JQ, Lu LX, Ruan CM, Chen L. CT arterial portography and CT hepatic arteriography in detection of micro liver cancer. *World J Gastroenterol* 1999; **5**: 225-227
14 **Li L**, Wu PH, Lin HG, Li JQ, Mo YX, Zheng L, Lu LX, Ruan CM, Chen L. Findings of non-pathologic perfusion defects by CT arterial portography and non-pathologic enhancement of CT hepatic arteriography. *World J Gastroenterol* 1998; **4**: 513-515
15 **Yoon KH**, Matsui O, Kadoya M, Yoshigawa J, Gabata T, Arai K. Pseudolesion in segments II and III of the liver on CT during arterial portography caused by aberrant right gastric venous drainage. *J Comput Assist Tomogr* 1999; **23:** 306-309
16 **Kim KW**, Kim TK, Han JK, Kim AY, Lee HJ, Choi BI. Hepatic hemangiomas with arterioportal shunt: findings at two-phase CT. *Radiology* 2001; **219**: 707-711
17 **Vilgrain V**, Boulos L, Vullierme MP, Denys A, Terris B, Menu Y. Imaging of atypical hemangiomas of the liver with pathologic correlation. *Radiographics* 2000; **20**: 379-397
18 **Naganuma H**, Ishida H, Konno K, Hamashima Y, Komatsuda T, Ishida J, Masamune O. Hepatic hemangioma with arterioportal shunts. *Abdom Imaging* 1999; **24**: 42-46
19 **Yamasaki M,** Furukawa A, Murata K, Morita R. Transient hepatic attenuation difference (THAD) in patients without neoplasm: frequency, shape, distribution, and causes. *Radiat Med* 1999; **17**: 91-96
20 **Lee WK**, Stuckey S. Arterioportal fistula following liver biopsy demonstrated by lipiodol computed tomography. *Clin Radiol* 2000; **55**: 489-491
21 **Sato M**, Ishida H, Konno K, Komatsuda T, Hamashima Y, Naganuma H, Ohyama Y. Longstanding arterioportal fistula after laparoscopic liver biopsy. *Abdom Imaging* 1999; **24**: 383-385
22 **Lim JH**, Lee SJ, Lee WJ, Lim HK, Choo SW, Choo IW. Iodized oil retention due to postbiopsy arterioportal shunt: a false positive lesion in the investigation of hepatocellular carcinoma. *Abdom Imaging* 1999; **24**: 165-170
23 **Thampanitchawong P**, Piratvisuth T. Liver biopsy: complications and risk factors. *World J Gastroenterol* 1999; **5**: 301-304
24 **Chen JH**, Chen WP, Huang CL, Shen WC. Dynamic helical CT as a novel technique for diagnosing hepatic perfusion disorders. *Hepatogastroenterology* 1999; **46**: 303-307
25 **Quiroga S**, Sebastia MC, Moreiras M, Pallisa E, Rius JM, Alvarez-Castells A. Intrahepatic arterioportal shunt: helical CT findings. *Eur Radiol* 1999; **9**: 1126-1130
26 **Arita T**, Matsunaga N, Takano K, Hara A, Fujita T, Honjo K. Hepatic perfusion abnormalities in acute pancreatitis: CT appearance and clinical importance. *Abdom Imaging* 1999; **24**: 157-162
27 **Chen JH**, Huang CL, Hwang JI, Lee SK, Shen WC. Dynamic helical biphasic CT emerges as a potential tool for the diagnosis of proximal arterioportal shunting. *Hepatogastroenterology* 1999; **46**: 1791-1797
28 **Takahashi S**, Murakami T, Takamura M, Kim T, Hori M, Narumi Y, Nakamura H, Kudo M. Multi-detector row helical CT angiography of hepatic vessels: depiction with dual-arterial phase acquisition during single breath hold. *Radiology* 2002; **222**: 81-88
29 **Guan SH**, Dan H, Jiang ZB, Huang MS, Zhu KS, Li ZR, Meng XC. Transmicrocatheter local injection of ethanol to treat hepatocellular carcinoma with high flow arteriovenous shunts. *Zhonghua Fangshexue Zazhi* 2002; **36**: 997-1000
30 **Luo PF**, Chen XM, Zhang LM, Zhou ZJ, Fu L, Wei ZH. The management of arteriovenous shunting in hepatocellular carcinoma. *Zhonghua Fangshexue Zazhi* 2002; **36**: 114-117
31 **Fan J**, Wu ZQ, Tang ZY, Zhou J, Qiu SJ, Ma ZC, Zhou XD, Ye SL. Multimodality treatment in hepatocellular carcinoma patients with tumor thrombi in portal vein. *World J Gastroenterol* 2001; **7**: 28-32
32 **Li L**, Wu PH, Li JQ, Zhang WZ, Lin HG, Zhang YQ. Segmental transcatheter arterial embolization for primary hepatocellular carcinoma. *World J Gastroenterol* 1998; **4**: 511-512
33 **Fan J**, Ten GJ, He SC, Guo JH, Yang DP, Wang GY. Arterial chemoembolization for hepatocellular carcinoma. *World J Gastroenterol* 1998; **4**: 33-37

Edited by Liu HX and Wang XL

P.O.Box 2345, Beijing 100023,China
Fax: +86-10-85381893
E-mail: wjg@wjgnet.com www.wjgnet.com

World J Gastroenterol 2003;9(11):2464-2468
World Journal of Gastroenterology
 ISSN 1007-9327

• COLORECTAL CANCER •

Investigation of Epstein-barr virus in Chinese colorectal tumors

Huan-Xin Liu, Yan-Qing Ding, Xin Li, Kai-Tai Yao

Huan-Xin Liu, Yan-Qing Ding, Xin Li, Kai-Tai Yao, Department of Pathology, the First Military Medical University, Guangzhou 510515, Guangdong Province, China
Correspondence to: Dr. Yan-Qing Ding, Department of Pathology, the First Military Medical University, Guangzhou 510515 Guangdong Province, China. dyq@fimmu.edu.cn
Telephone: +86-20-61642148 **Fax:** +86-20-61642148
Received: 2002-10-09 **Accepted:** 2002-11-09

Abstract

AIM: To elucidate the association of Epstein-Barr virus (EBV) with colorectal tumors and to demonstrate whether infection of EBV existed in different stages of colorectal tumors involves in the carcinogenesis.

METHODS: One hundred and thirty paraffin-embedded tissues of colorectal tumors were classified into 5 groups: 26 adenomas, 23 adenomas complicated with dysplasia, 22 adenomas complicated with carcinomatous, 36 colon carcinoma and 23 HNPCC, were examined by PCR, IHC and ISH, respectively.

RESULTS: EBV DNA was detected by PCR in 26 cases out of the 130 specimens, including 5 cases of adenomas, 5 adenomas complicated with dysplasia, 5 adenomas complicated with carcinomatous, 7 colorectal carcinoma and 4 HNPCC. IHC detection showed the expression of LMP1 in 7 cases, including 1 adenoma, 1 adenoma with dysplasia, 1 HNPPC, 2 adenomas complicated with carcinomatous, and 2 colorectal carcinomas. The expression of EBER1 detected by ISH was positive in 6 cases, including 1 adenoma with dysplasia, 2 adenomas complicated with carcinomatous and 3 colorectal carcinomas. There were no significant differences among the results of PCR, IHC and ISH in the 5 groups. In all cases of HNPCC, none of the tumor cells showed positive signals of EBER1, but some EBV-positive tumor infiltrating lymphocytes were found in 2 of 23 cases.

CONCLUSION: Our results showed that infection of EBV exists in human colorectal tumors, which indicates that EBV may be involved in the carcinogenesis of colorectal tumors but does not play an important role. The mechanisms need to be clarified further.

Liu HX, Ding YQ, Li X, Yao KT. Investigation of Epstein-barr virus in Chinese colorectal tumors. *World J Gastroenterol* 2003; 9(11): 2464-2468
http://www.wjgnet.com/1007-9327/9/2464.asp

INTRODUCTION

Epstein-Barr virus (EBV) is a ubiquitous herpes virus that infects and establishes a persistent infection in the host. Clinically, its primary infection ranges from a mild self-limited illness in children to infectious mononucleosis in adolescents and adults[1,2]. EBV is associated with a number of human malignancies,including Burkitt lymphoma and nasopharyngeal carcinoma,etc. Recently, involvement of EBV has been demonstrated in gastric carcinoma. Detection rates of EBV in gastric carcinomas varied in different studies from 4 % to 18 %[5-15]. Although there are many similar features in histology and pathogenesis between gastric and colorectal carcinoma, there have been few papers about the relationship of EBV with colorectal cancers. However, a great deal of evidences support an etiologic role of EBV in carconogenesis in patients with EBV-positive gastric carcinomas[16,17,20]. In this study, we investigated the presence of EBV in 130 cases of colorectal tumors, including colorectal adenomas, adenomas complicated with dysplasia, adenomas complicated with carcinomatous, colorectal cancer and hereditary non-polyposis colorectal cancer (HNPCC) using immunohistochemical demonstration (IHC), polymerase chain reaction (PCR) and *in situ* hybridization (ISH).

MATERIALS AND METHODS

Tissue specimens

Surgical specimens for EBV detection were collected from 129 patients with colorectal tumors from February, 1998 to February, 2002. All cases were diagnosed by the Department of Pathology, NanFang Hospital, First Military Medical University. All specimens were formalin-fixed and paraffin-embedded. The age and sex of the patients among the five groups were similar (ANOVA analysis, $P>0.05$). As positive controls, Hodgkin' s disease and nasopharyngeal carcinoma specimens confirmed as EBV positive were used in every staining batch.

Immunohistochemitry

The monoclonal antibody LMP1 (DAKO) was used. Immunohistochemitry was performed on paraffin sections. Four-micrometer-thick specimens sectioned from a paraffin-embedded block were dewaxed in xylene and rehydrated in serially graded ethanol (100 %, 95 %), then treated with 0.28 % iodic acid for 60 sec,horse serum and first antibody for 10 minutes at 37 ℃, S-P-second antibody for 10 minutes at 37 ℃, S-P-third antibody for 10 minutes at 37 ℃, then detection was performed using the avidin-biotin-peroxidase complex technique and DAB (diaminobenzidine). A section of Hodgkin' s disease lymph node was used as an external positive control, while negative controls were obtained by replacing the primary antibody with nomal mouse serum.

Polymerase chain reaction

DNA was extracted from formalin-fixed and paraffin-embedded tissues. Two 5 μm thick rections were cut from each block, the samples were suspended in 50-150 μl of extraction buffer containing 100-300 μg/ml of proteinase K(Sigma, Missouri,USA), 50 mM tris-hydrochloric acid (ph8.5), 1 mM EDTA (PH8.0), and 0.5 % Tween20. After incubation for 36 h at 55 ℃, the samples were heated at 100 ℃ for 10 min. The primers corresponding to the 409 base pair region of the EBV BamHI W fragment, were synthesized based on the DNA sequences of GenBank (from www.icnet.uk/bmm) (primer: 1,5' -TCGCGTTGCTAGGCCACCTT-3' ; 2, 5' -CTTGGATGGCGGAGTCAGCG-3'), the PCR reaction mixture contained 1 μl model-DNA, 2.5 μl of 10×PCR buffer (mg^{2+}free), 1.5 μl of 25 mM$MgCl_2$, 2 μl of 2.5M dNTP mixture, 1 μl of 10 pmol/μl primer, and 1 μl of 1 Unit/ μl Taq polymerase

(HuaMei Biotech,China) in a final volume of 25 μl. After an initial incubation for 5 min at 94 ℃, the samples were subjected to 34 amplification cycles (at 94 ℃ for 45 s, at 55 ℃ for 45s and at 72 ℃ for 45 s). After the last cycle, the samples were held at 72 ℃ for 5 min.

In situ hybridization

Oligonucleotide probes used to detect EBER-1 were designed by our reseach group using Primer5.0 software, then synthesized and labeled with Dig by Bioasia Biotech, ShangHai. Each probe was labeled with 2 Dig. The method of *in situ* hybridization was described in the manual of BOSD Biotech. Four-micrometer-thick specimens sectioned from a paraffin-embedded block were dewaxed in xylene and rehydrated in serially graded ethanol (100 %, 95 %), then digested with pepsin (3 %) for 5-10 min at 30 ℃ and hybridized for 14 hours at 40 ℃. The slides were washed with 2×SSC for 5 min×2, 0.5×SSC for 15 min,0.2×SSC for 15 min at 37 ℃, then blocked with BSA at 37 ℃ for 30 min after trickled with biotin-rabbit antibodies to Dig at 37 ℃ for 60 min, slides were washed with 0.5M PBS for 5 min×4, then added SABC at 37 ℃ for 20 min and biotin- peroxidase at 37 ℃ for 20 min. At last, the slides were wished with 0.5M PBS for 5 min×4, stained with DAB for 10 min and counter-stained with hematein for 8 min. Two cases of nasopharyngeal carcinoma known to contain EBV were routinely used as positive controls, two slides treated without probe were used as negative controls.

Statistical analysis

Difference in proportions among the groups was calculated by Pearson χ^2 test using the spss 8.0 statistical software program (SPSS inc, Chicago, il). *P* values <0.5 were considered statistically significant.

RESULTS

The results of LMP1 immunohistochemistry (IHC) are shown in Table1. The positive-signals were localized over the cytoplasm of tumor cells. The cases which exhibited LMP1 staining in more than 10 % of the tumor cell cytoplasm were considered to be LMP1-positive (Figures1-4). A section of Hodgkin' s disease lymph node was used as an external positive control, while negative controls were obtained by replacing the primary antibody with normal mouse serum.IHC revealed that 7 of the 130 cases of colorectal tumors showed LMP1 signals, whereas non-carcinomatous colorectal mucosa was negative for LMP1.

Table 1 Results of immunohistochemistry

Group	*n*	EBV-positive	Positive rate (%)
Adenoma	26	1	3.8
Adenoma with dysplasia	23	1	4.3
Carcinomatous adenoma	22	2	9.1
Colorectal carcinoma	36	3	8.3
HNPCC	23	0	0
Total	130	7	5.4

χ^2 test, $\chi^2=0.0403<\chi^2_{0.05,4}=9.49$, $P>0.05$.

EBV DNA was amplified by PCR using the primers flanking the site of BamHI W fragment in 26 of 130 colorectal tumor tissues,including 5 cases of adenoma-group, 5 cases of adenomas complicated with dysplasia group, 5 cases of carcinomatous adenoma group, 7 cases of colorectal cancer and 4 cases of hereditary non-polyposis colorectal cancer (HNPCC) (Table 2 and Figue 5).

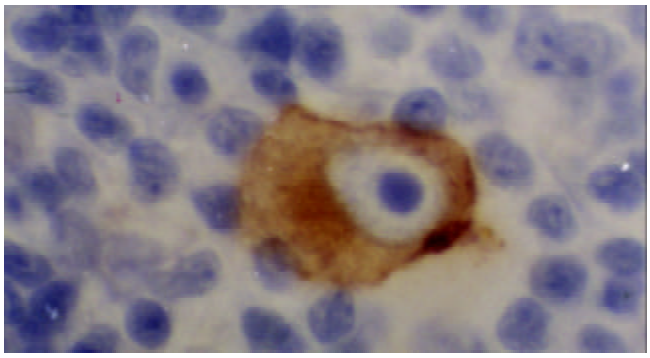

Figure 1 Positive-control of LMP1 from lymphoma of Hodgkin' disease. The cytoplasm of R-S cell showed clear positive signal.

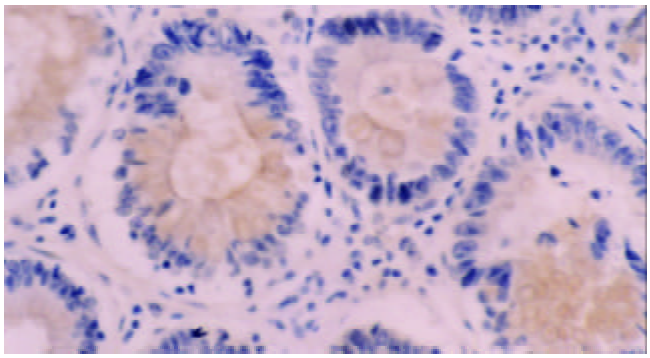

Figure 2 Immunohistochemical staining with anti-LMP1 antibody of adenoma specimen with dysplasia. The positive signals were localized at cytoplasm and membranes.

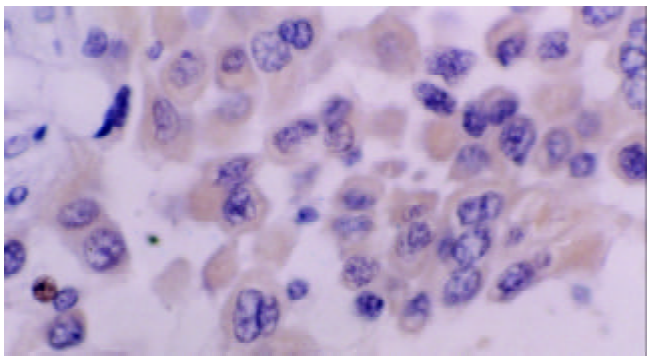

Figure 3 Immunohistochemical staining with anti-LMP1 antibody of colorectal carcinoma cells. The positive signals were localized at cytoplasm. But no clear positive signals localized at membranes.

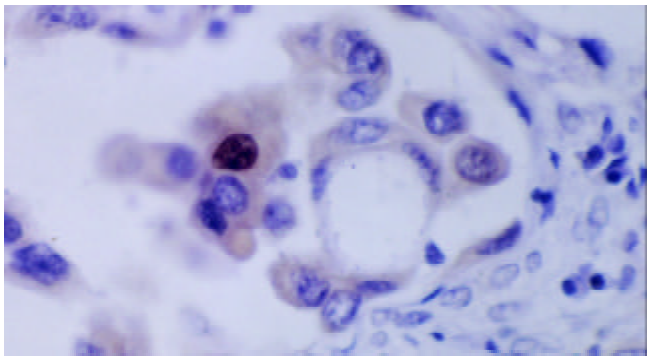

Figure 4 Metastatic colorectal carcinoma cells in lymphatic. The cytoplasm of neoplasm cells showed LMP1 positive, the nucleic showed positive signals too.

Table 2 Results of PCR

Group	*n*	EBV-positive	Positive rate (%)
Adenoma	26	5	19.2
Adenomas with dysplasia	23	5	21.7
Carcinomatous adenoma	22	5	22.7
Colorectal carcinoma	36	7	19.4
HNPCC	23	4	17.4
Total	130	26	20.0

χ^2 test, $\chi^2=2.725<\chi^2_{0.05,4}=9.49$, $P>0.05$.

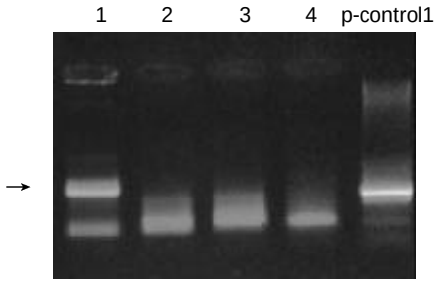

Figure 5 The electrophoresis photo of PCR. Arrow points to the positive lane.

The result of EBER *in situ* hybridization was similar to that of IHC, the signals of EBER were localized over the nuclei of most tumor cells (Figures 6-9), only the signal of EBER within the tumor nuclei was considered as a positive case. 6 of 130 cases showed EBER signals, and 5 cases that showed LMP1 signals were EBER positive (Table3). All cases with LMP1-positive and all cases with EBER-positive were PCR positive.

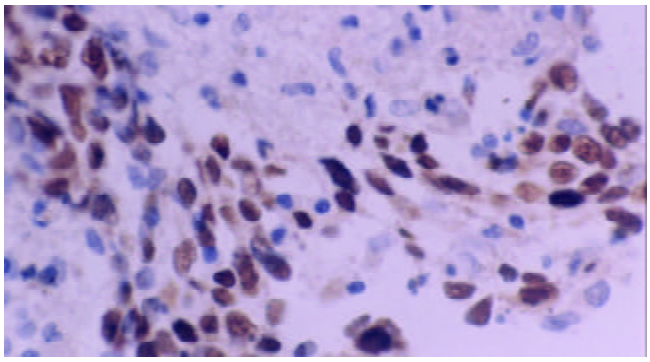

Figure 6 Positive control of EBER1 from a NPC specimen. Clear and strong hybridization signals (yellow nuclear grains) were shown in nuclei of the tumor cells. DAB and hematoxylin counterstaining,×200.

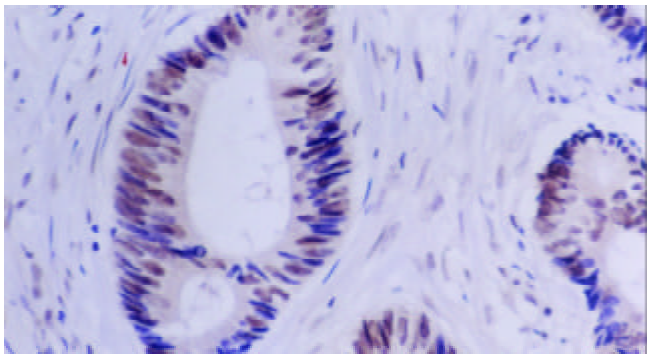

Figure 7 *In situ* hybridization with EBER1 (from an carcinomatous adenoma). Positive signals were shown in nuclei of the tumor cells. DAB and hematoxylin counterstaining, ×200.

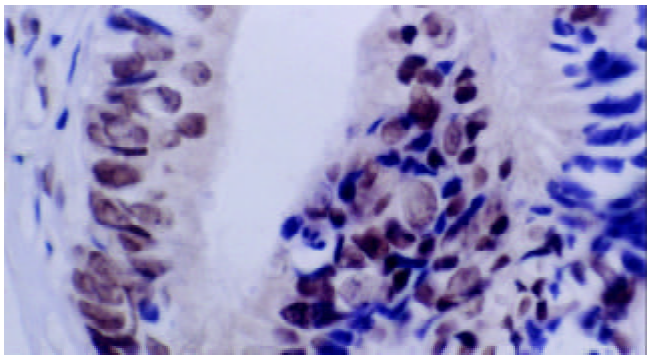

Figure 8 *In situ* hybridization with EBER1 (from a colorectal carcinoma). Clear and strong hybridization signals were shown in nuclei of the tumor cells. DAB and hematoxylin counterstaining, ×400

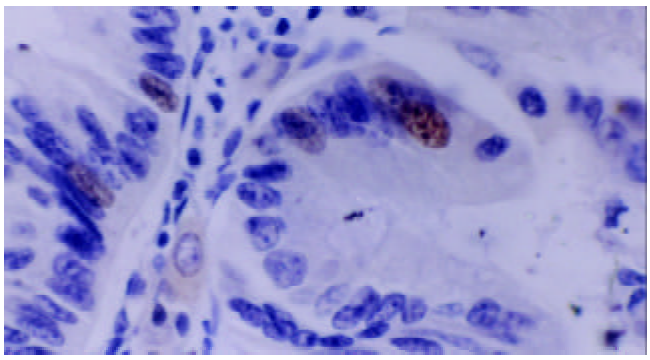

Figure 9 *In situ* hybridization with EBER1 (from a colorectal carcinoma, too). Interspersed positive signals were shown in neoplasm cells. DAB and hematoxylin counterstaining, ×400.

Table 3 Results of EBER-ISH

Group	*n*	EBV-positive	Positive rate (%)
Adenoma	26	0	0
Adenomas with dysplasia	23	1	4.3
Carcinomatous adenoma	22	2	9.1
Colorectal carcinoma	36	3	8.3
HNPCC	23	0	0
Total	130	6	4.6

χ^2 test, $\chi^2=5.39$, $P>0.05$.

DISCUSSION

The relationship between EBV and gastric carcinoma has been testified by Shibata, Tokunaga, Oda and Cho[13-15,19,24]. Throughout the world, EBV is detected in the tissues of about 10 % of gastric carcinoma cases[4]. Though colorectal epithelium is similar to that of gastric, and colorectal carcinoma is similar to gastric carcinoma, too, the association of EBV and colorectal tumors remains controversial. Yuen *et al*[22] investigated for the presence of EBV in 74 cases of gastric adenocarcinoma and 36 cases of colorectal adenocarcinoma from Chinese patients by *in situ* hybridization (ISH) using an antisense EBER probe, but none of the colorectal carcinomas showed a positive signal. Kijima *et al*[21] demonstrated the association of Epstein-Barr virus (EBV) with primary epithelial neoplasm in the south part of Kyushu, Japan, they found that there were no positive signals in 102 cases of colorectal cancer using EBER *in situ* hybridization. Cho *et al*[24] reported the same result that EBV was not associated with colorectal tumors. However, Yanai *et al*[23] found that EBV was detected in 63.6 % of Crohn's disease cases and 60 % of ulcerative colitis

cases using *in situ* hybridization for EBV-encoded small RNA1 (EBER-1), indicating that EBV infection may be related to IBD colonic diseases. Ioachim *et al*[26] studied 15 cases of primary anorectal lymphoma in AIDS patients and compared them with 4 cases of anorectal lymphoma unrelated to AIDS. In the AIDS-associated anorectal lymphomas, the presence of Epstein-Barr virus (EBV) in a latent form was demonstrated by an abundance of Epstein-Barr-encoded RNA (EBER) in 14 of 15 cases and latent membrane protein (LMP) in 4 cases, suggesting EBV may be associated to this kind of anorectal lymphomas. Samaha *et al*[25]and Kon *et al*[29] reported that lymphoepithelioma-like carcinoma of rectum was probably related to EBV, Ruschoff *et al*[27] used polymerase chain reaction test to examine the EBV DNA in 3 cases out of 20 differentiated colorectal adenocarcinomas. Though the positive signals restricted to the peritumor lymphoid infiltrate as shown by *in situ* hybridization, all of these findings suggest that EBV may associate to colorectal tumors. Moreover, Kim *et al*[30] investigated for the presence of EBV in 20 cases of colorectal adenocarcinomas and found 2 cases were EBER-positive. As a similarity, Grinstein *et al*[28] results suggested that EBV was not restricted to lymphoepithelioma-like carcinomas but might play an oncogenic role in frequent epithelial cancers, including colorectal cancers, and possibly also in hyperplasias and certain dysplasias preceding carcinomas.

In the current study, we analyzed 130 cases of colorectal tumors for the presence of EBV using immunohistochemistry, polymerase chain reaction and *in situ* hybridization. EBV was detected by each method, but the positive rates were different with different methods. Among the three methods, *in situ* hybridization was considered as the golden standard[3], nevertheless, we found 6 cases of colorectal tumors were EBER-positive. In our study, 1 case of adenoma complicated with dysplasia showed positive signals for EBER. This finding was different from the observation of Kijima *et al*, Yuen *et al* and Cho *et al*[21,22,24]. Moreover, detection of EBV in 1 case of dysplastic adenoma suggested that EBV infection occurred in the dysplastic phase before the occurrence of colorectal carcinoma, further indicating that EBV may play a role in tumor progression.

In all the EBV-assciated carcinomas,the virus was detected in the neoplasm cells but not in the nomal colorectal epithelium using ISH and IHC. However, we found much more positive-cases using PCR technique. In our study, 19 cases of PCR-positive colorectal tumors showed IHC negative and 20 cases showed EBER-negative. This could be interpreted as colorectal tumors with lymphoid stroma because the possibility of false positives using the PCR technique should be included[17]. Furthermore, reactive lymphocytes might possibly be contaminated during the micro dissection of a tumor portion and might become PCR-positive for EBV[16]. This supports the hypothesis that EBER *in situ* hybridization without further PCR method is enough to facilitate the detection of EBV within cancer cells. But Glaser *et al*[32] found that EBV EBER-1 transcript was not commonly expressed in breast cancer, based on a broadly representative case series. Therefore, in order to clarify the infection of EBV, more than one kind of methods should be used. Gulley *et al*[3] thought that new molecular tests combined with traditional serological or histochemical assays were helpful for diagnosis and monitoring of EBV-related diseases, PCR and IHC test were indispensable to the diagnosis of EBV associated diseases.

Our findings showed that in all EBV-positive colorectal tumors, male was preponderance. Other researchers, such as Chang *et al*[9], Oda *et al*[14] and Tokunaga *et al*[16] found the same results in the study of relationship between EBV and gastric carcinoma, the mechanism needs to be clarified further. Human cancer tissues are infiltrated by tumor-infiltrating lymphocytes (TILs), which have been considered a manifestation of a host immune response to cancer cells[22], the role of EBV-positive TILs in carcinoma remains unclear. Our data suggest that regardless of the site, the chances for epithelial cells to be exposed to EBV are similar in the gastrointestinal tract, because it is believed that EBV-carrying lymphocytes are a reservoir of EBV and may transfer EBV to the epithelial cells. Therefore, whether EBV plays an etiologic role in the carcinigenesis of this tissues is probably dependent on the infectability of epithelial cell interaction after infection.

Our data showed no significant differences in the frequency of EBV using PCR, IHC or ISH among adenoma, adenomas complicated with dysplasia, carcinomatous adenomas, colorectal cancer and hereditary non-polyposis colorectal cancer (HNPCC). The low frequency of EBV in HNPCC might be explained by different histological types of carcinoma, and the susceptibility to EBV of HNPCC might be lower than the other four groups. Our findings suggest that EBV does exist in colorectal tumor tissues in South China population, and the frequency of EBV positive colorectal tumors in Guangzhou, South China, where NPC is the most common in the world, may be higher than that in other parts of China. These findings agree with Hao *et al*[11] and Qiu *et al*[12]. Corvalan *et al*[18] thought that Epstein-Barr virus associated gastric carcinoma(EBVaGC) was linked to regional, ethnic, location of carcinoma in the organism and the histology type of tumors.

In conclusion, the present study has shown that EBV may play an etiologic role in the carcinogenesis of these tissues. But our data showed a very low frequency of EBV in these colorectal tumors, indicating that EBV does not play a major role in the etiology of colorectal carcinoma, and the carcinogenesis mechanism needs to be further elucidated.

REFERENCES

1 **Chow VT**. Cancer and viruses. *Ann Acad Med Singapore* 1993; **22**: 163-169

2 **Liebowitz D**. Pathogenesis of Epstein-Barr virus in McCance DJ (ed): Human Tumor Viruses. Washington, DC. *ASM Press* 1998; **24**: 175-179

3 **Gulley ML**. Molecular diagnosis of Epstein-Barr virus-related diseases. *J Mol Diagn* 2001; **3**: 1-10

4 **Takada K**. Epstein-Barr virus and gastric carcinoma. *Mol Pathol* 2000; **53**: 255-261

5 **Hsieh LL**, Lin PJ, Chen TC, Ou JT. Frequency of Epstein-Barr virus-associated gastric adenocarcinoma in Taiwan. *Cancer Lett* 1998; **129**: 125-129

6 **Gurtsevich VE**, Galetskii SA, Nered SN, Novikova EV, Iakovleva LS, Land ChE, Davydov MI, Klimenkov AA, Petrovichev NN, Tokunaga M. Detection and characterization of gastric carcinoma associated with epstein-barr herpes virus. *Vestn Ross Akad Med Nauk* 1999; **3**: 56-59

7 **Galetsky SA**, Tsvetnov VV, Land CE, Afanasieva TA, Petrovichev NN, Gurtsevitch VE, Tokunaga M.Epstein-Barr-virus-associated gastric cancer in Russia. *Int J Cancer* 1997; **73**: 786-789

8 **Chang MS**, Lee HS, Kim CW, Kim YI, Kim WH. Clinicopathologic characteristics of Epstein-Barr virus-incorporated gastric cancers in Korea. *Pathol Res Pract* 2001; **197**: 395-400

9 **Chang MS**, Kim WH, Kim CW, Kim YI. Epstein-Barr virus in gastric carcinomas with lymphoid stroma**.** *Histopathology* 2000; **37**: 309-315

10 **Koriyama C,** Akiba S, Iriya K, Yamaguti T, Hamada GS, Itoh T, Eizuru Y, Aikou T, Watanabe S, Tsugane S, Tokunaga M. Epstein-Barr virus-associated gastric carcinoma in Japanese Brazilians and non-Japanese Brazilians in Sao Paulo. *Jpn J Cancer Res* 2001; **92**: 911-917

11 **Hao Z,** Koriyama C, Akiba S, Li J, Luo X, Itoh T, Eizuru Y, Zou J. The Epstein-Barr virus-associated gastric carcinoma in Southern and Northern China. *Oncol Rep* 2002; **9**: 1293-1298

12 **Qiu K,** Tomita Y, Hashimoto M, Ohsawa M, Kawano K, Wu DM, Aozasa K. Epstein-Barr virus in gastric carcinoma in Suzhou,

China and Osaka, Japan: association with clinico-pathologic factors and HLA-subtype. *Int J Cancer* 1997; **71**: 155-158

13 **Shibata D,** Hawes D, Stemmermann GN, Weiss LM. Epstein-Barr virus-associated gastric adenocarcinoma among Japanese Americans in Hawaii. *Cancer Epidemiol Biomarkers Prev* 1993; **2**: 213-217

14 **Oda K,** Tamaru J, Takenouchi T, Mikata A, Nunomura M, Saitoh N, Sarashina H, Nakajima N. Association of Epstein-Barr virus with gastric carcinoma with lymphoid stroma. *Am J Pathol* 1993; **143**: 1063-1071

15 **Shibata D,** Weiss LM. Epstein-Barr virus-associated gastric adenocarcinoma. *Am J Pathol* 1992; **140**: 769-774

16 **Tokunaga M,** Land CE, Uemura Y, Tokudome T, Tanaka S, Sato E. Epstein-Barr virus in gastriccarcinoma. *Am J Pathol* 1993; **143**: 1250-1255

17 **Nakamura S,** Ueki T, Yao T, Ueyama T, Tsuneyoshi M. Epstein-Barr virus in gastric carcinoma with lymphoid stroma. Special reference to its detection by the polymerase chain reaction and in situ hybridization in 99 tumors, including a morphologic analysis. *Cancer* 1994; **73**: 2239-2249

18 **Corvalan A,** Koriyama C, Akiba S, Eizuru Y, Backhouse C, Palma M, Argandona J, Tokunaga M. Epstein-Barr virus in gastric carcinoma is associated with location in the cardia and with a diffuse histology: a study in one area of Chile. *Int J Cancer* 2001; **94**: 527-530

19 **Tokunaga M,** Uemura Y, Tokudome T, Ishidate T, Masuda H, Okazaki E, Kaneko K, Naoe S, Ito M, Okamura A. Epstein-Barr virus related gastric cancer in Japan: a molecular patho-epidemiological study. *Acta Pathol Jpn* 1993; **43**: 574-581

20 **Takano Y,** Kato Y, Saegusa M, Mori S, Shiota M, Masuda M, Mikami T, Okayasu I. The role of the Epstein-Barr virus in the oncogenesis of EBV(+) gastric carcinomas. *Virchows Arch* 1999; **434**: 17-22

21 **Kijima Y,** Hokita S, Takao S, Baba M, Natsugoe S, Yoshinaka H, Aridome K, Otsuji T, Itoh T, Tokunaga M, Eizuru Y, Aikou T. Epstein-Barr virus involvement is mainly restricted to lymphoepithelial type of gastric carcinoma among various epithelial neoplasms. *J Med Virol* 2001; **64**: 513-518

22 **Yuen ST,** Chung LP, Leung SY, Luk IS, Chan SY, Ho J. *In situ* detection of Epstein-Barr virus in gastric and colorectal adenocarcinomas. *Am J surg Pathol* 1994; **18**: 1158-1163

23 **Yanai H,** Shimizu N, Nagasaki S, Mitani N, Okita K. Epstein-Barr virus infection of the colon with inflammatory bowel disease. *Am J Gastroenterol* 1999; **94**: 1582-1586

24 **Cho YJ,** Chang MS, Park SH, Kim HS, Kim WH. *In situ* hybridization of Epstein-Barr virus in tumor cells and tumor-infiltrating lymphocytes of the gastrointestinal tract. *Hum Pathol* 2001; **32**: 297-301

25 **Samaha S,** Tawfik O, Horvat R, Bhatia P. Lymphoepithelioma-like carcinoma of the colon: report of a case with histologic, immunohistochemical, and molecular studies for Epstein-Barr virus. *Dis Colon Rectum* 1998; **41**: 925-928

26 **Ioachim HL,** Antonescu C, Giancotti F, Dorsett B, Weinstein MA. EBV-associated anorectal lymphomas in patients with acquired immune deficiency syndrome. *Am J Surg Pathol* 1997; **21**: 997-1006

27 **Ruschoff J,** Dietmaier W, Luttges J, Seitz G, Bocker T, Zirngibl H, Schlegel J, Schackert HK, Jauch KW, Hofstaedter F. Poorly differentiated colonic adenocarcinoma, medullary type: clinical, phenotypic, and molecular characteristics. *Am J Pathol* 1997; **150**: 1815-1825

28 **Grinstein S,** Preciado MV, Gattuso P, Chabay PA, Warren WH, De Matteo E, Gould VE. Demonstration of Epstein-Barr virus in carcinomas of various sites. *Cancer Res* 2002; **62**: 4876-4878

29 **Kon S,** Kasai K, Tsuzuki N, Nishibe M, Kitagawa T, Nishibe T, Sato N. Lymphoepithelioma-like carcinoma of rectum: possible relation with EBV. *Pathol Res Pract* 2001; **197**: 577-582

30 **Kim YS,** Paik SR, Kim HK, Yeom BW, Kim I, Lee D. Epstein-Barr virus and CD21 expression in gastrointestinal tumors. *Pathol Res Pract* 1998; **194**: 705-711

31 **Vilor M,** Tsutsumi Y. Localization of Epstein-Barr virus genome in lymphoid cells in poorly differentiated adenocarcinoma with lymphoid stroma of the colon. *Pathol Int* 1995; **45**: 695-697

32 **Glaser SL,** Ambinder RF, DiGiuseppe JA, Horn-Ross PL, Hsu JL. Absence of Epstein-Barr virus EBER-1 transcripts in an epidemiologically diverse group of breast cancers. *Int J Cancer* 1998; **75**: 555-558

Edited by Zhao M and Wang XL

P.O.Box 2345, Beijing 100023,China
Fax: +86-10-85381893
E-mail: wjg@wjgnet.com www.wjgnet.com

World J Gastroenterol 2003;9(11):2469-2473
World Journal of Gastroenterology
 ISSN 1007-9327

• COLORECTAL CANCER •

Lack of inhibitory effects of Lactic acid bacteria on 1,2-dimethylhydrazine-induced colon tumors in rats

Wei Li, Chong-Bi Li

Wei Li, Department of Obstetrics and Gynecology, First People's Hospital of Hangzhou, Hangzhou 310006, Zhejiang Province, China
Chong-Bi Li, Department of Biology, College of Zhaoqing, Duanzhou-Qu, Zhaoqing 526000, Guangdong Province, China
Correspondence to: Dr. Wei Li, Department of Obstetrics and Gynecology, First People's Hospital of Hangzhou, 261 Wansha-lu, Shangcheng-Qu, Hangzhou 310006, Zhejiang Province, China. lwmyj@hotmail.com
Telephone: +86-571-87065701-4331 **Fax**: +86-571-87914773
Received: 2003-03-05 **Accepted:** 2003-04-01

Abstract

AIM: A myriad of healthful effects has been attributed to the probiotic lactic acid bacteria, perhaps the most controversial issue remains that of anticancer activity. This study was aimed at investigating the putative anti-cancer effects of lactic acid bacteria strains on the progression of colon tumor in 1,2-dimethylhydrazine (DMH)-treated animals.

METHODS: The strain of lactic acid bacteria used in this study was lactic acid bacteria NZ9000 that conformed to the characteristics of plasmid free. Sixty male Wistar rats were given subcutaneous injections of DMH at a dose of 40 mg/kg body wt or saline once a week for 10 weeks. The rats were divided into 6 experimental groups. After the last DMH injection, animals in groups 1 and 4 were gavaged with 1 ml of lactic acid bacteria at a dose of 5×10^9 per day or vehicle until sacrifice at the end of week 22 or week 52. Animals in groups 1-3 were killed at the end of week 22 for histopathological examination. The whole period of experimental observation was 52 weeks.

RESULTS: By the end of 22nd week, final average body weights of the rats treated with DMH alone and all animals receiving lactic acid bacteria were significantly decreased compared with the vehicle control ($P<0.05$). No differences in tumor incidence, multiplicity, dimensions and stage in the colonic mucosa were observed among the groups. At week 52, the survival rate of the rats administered lactic acid bacteria was lower than that of the rats treated with DMH that were fed on control fluids of non-*lactococcus lactis*. The mean survival time of lactic acid bacteria-treated animals was 39 weeks.

CONCLUSION: These results indicate that lactic acid bacteria lacks inhibitory effects on the progression of colon tumor in DMH-treated animals, and does not support the hypothesis that alteration of colonic flora may exert an influence on the progression of colon tumor.

Li W, Li CB. Lack of inhibitory effects of Lactic acid bacteria on 1,2-dimethylhydrazine-induced colon tumors in rats. *World J Gastroenterol* 2003; 9(11): 2469-2473
http://www.wjgnet.com/1007-9327/9/2469.asp

INTRODUCTION

Epidemiological studies have provided evidences that the morbidity of colon cancer is influenced by diet. Several studies of humans and experimental animals suggested that the influence of diet was mediated by altering the metabolic activity of intestinal bacterial flora[1,2]. Some of these enteric bacteria are beneficial to the host and have been shown to exert antimutagenic and anticarcinogenic properties[3-5]. By definition, probiotic bacteria can beneficially affect the host by improving its intestinal microbial balance. Bacterial flora that ferment the dairy products (e.g. lactic acid bacteria) might be used for cancer chemoprevention[4].

Lactobacilli are one of the dominant species in the small intestine, and these micro-organisms presumably affect metabolic reactions occurring in this part of the gastrointestinal tract. Some metabolites of lactic bacteria, such as lactic acid and enzymes, have been reported to have some chemotherapeutic value[6]. Furthermore, several studies have also shown that consumption of *bifidobacteria* reduces colon cancer risk in carcinogen-treated animals, suggesting that consumption of certain bacteria has a beneficial effect on the balance of colon *bacteria*[7,8]. Although a myriad of healthful effects have been attributed to the probiotic lactic acid *bacteria*, perhaps the most controversial issue is its anticancer activity. How dietary components, including lactic acid *bacteria*, interact with genes contributes to tumor development?

An autochthonous colon cancer model is useful to evaluate the clinical therapeutic efficacy of drugs for colorectal cancer[9,10]. The experimental carcinogen DMH has been used in the study of the effect of diet in experimental animals[1,11]. As the DMH model is known to closely parallel the human disease in term of disease presentation, gross and microscopic pathology[12], it is anticipated that DMH-induced colon tumor in rats would respond to chemotherapeutic drugs used in man[13]. Although clinical use of 5-fluorouracil (5-FU) derivatives was tested in the DMH model, few studies on the effect of lactic acid bacteria on chemically induced colon tumor progression have been reported.

Supplementation of diet with components possessing antimutagenic and anticarcinogenic properties might result in a significant decrease of tumor frequency. A number of studies indicate that administration of *bifidobacteria* or lactobacilli alone or in combination with fermentable carbohydrate(defined as a prebiotic) can alter colonic microflora populations and decrease the development of early preneoplastic lesions and tumors. This study was aimed at investigating the putative anti-cancer effects of lactic acid bacteria strains on the progression of colon tumor in DMH-treated animals.

MATERIALS AND METHODS

Materials

Animals and chemicals Male Wistar rats at 5 weeks of age were obtained (Department of Animals, Chinese Academy of Medical Sciences, Beijing, China) and housed in plastic cages with wood chips for bedding in an animal room with a 12 h light/dark cycle at 22±2 ℃ and 44 %±5 % relative humidity. The rats were fed on the basal diet. Water was available *ad libitum*, and body weight and food consumption were measured weekly

during the experiments. DMH was purchased from Tokyo Kasei Co. (Tokyo, Japan).

Methods

Treatment protocol The experimental design is shown in Figure 1. One week after acclimatization, sixty rats of 6-week-old were randomly divided into six groups (10 rats/group). Animals in Groups 1 and 4 were given subcutaneous injections of DMH dissolved in normal saline solution (40 mg/kg body wt) once a week for 10 weeks. Rats in groups 2 and 5 were injected 0.9 % normal saline (vehicle) at the same time. After the last DMH treatment, the animals in groups 1 and 4 were additionally gavaged with 1 ml of lactic acid bacteria at a dose of 5×10^9 per day for 12 weeks or until they were dead. Groups 2 and 5 were gavaged with 1 ml of protective reagents per day (the vehicle control). Groups 3 and 6 served as a carcinogen control. The course of treatments differed slightly from each experiment. All surviving animals were sacrificed under ether anesthesia at week 22 (Groups 1-3) and at the end of experiment (Groups 4-6), respectively. The whole period of experimental observation was 52 weeks.

Tissue processing All animals were autopsied. The colons were removed, flushed with saline, opened along the longitudinal median axis. Macroscopically, the number of tumors in each colon was counted. Tumor width (*W*) and length (*L*) were measured with calipers. Tumor volume (*TV*) was determined according to the following formula: $TV=(L\times W^2)/2$[14]. After the gross pathologic changes (number, dimensions and distribution of the tumors) were recorded, the colons were fixed flat between pieces of filter paper in 10 % phosphate-buffered formalin. The liver and kidneys were removed and weighed. Other major organs (stomach, small intestine, spleen, lungs and lymph nodes) were also excised and fixed in 10 % phosphate-buffered formalin solution. Afterward, all tissues were embedded in paraffin and used for sectioning. After the sections were stained with routine hematoxylin and eosin, the colons were divided into proximal, intermediate, and distal segments and examined for histopathological analysis.

Tumor staging Animals with DMH-induced colon cancer characteristically developed multiple tumors and each tumor was at a different histological stage[15]. Consequently, for the purpose of this experiment, animals were staged (Duke's stage) with reference to a single index tumor, defined as the largest macroscopically and histologically identifiable colon tumor.

Preparation of lactococcus lactis The strain of *L. lactis* used in this study was lactic acid bacteria NZ9000 that conformed to the characteristics of plasmid free. The strain was obtained from French Academy of Agricultural Sciences. All cloning steps were done with *E.coli* Top10. *E. coli* was grown on Luria-Bertani (LB) medium and incubated at 37 ℃ under aeration. *L.lactis* was grown without shaking on M17 medium in which 1 %(wt/vol.) glucose was added (M17-Glu) and incubated at 30 ℃. When appropriate, antibiotics was added to the culture medium. For lactic acid bacteria strains, chloramphenicol was used at a final concentration of 10 ug/ml. Ampicillin was supplied at a concentration of 100 ug/ml in the case of *E.coli*. In the experiments, the lactic acid bacteria was induced with nisin as follows. An overnight culture of lactic acid bacteria was transferred into a fresh medium at a dilution of 1:50. After 3-4 h of incubation, 1 ng/ml of nisin (Sigma) was added to the culture, which was incubated for 3-4 h. For *L.lactis*, nisin induction was performed as described previously[16].

After incubation, lactic acid bacteria was concentrated to 5×10^9 cells/ml in PBS buffer (pH 7.0). This concentration would be used as an oral dosage for a rat. PBS buffer (pH 7.0) was used as a liquid protecting solution for lactic acid bacteria. The preparations were preserved at 4 ℃ for a week.

Statistical analysis

Statistical analyses were completed with SPSS 9.0 (Statistical Package for the Social Science). The significance of differences between the average values of the groups was analyzed using Cochran's two-tailed Student's *t*-test. The significance of differences in lesion incidences between the groups was assessed by chi-square test. Rat mortality was analysed by the Log Rank method of Peto *et al*[17].

RESULTS

All rats in groups1-3 and 5 survived to the final termination and maintained a relatively healthy appearance throughout the experiment. No signs of severe toxicity or diarrhea were observed in all animals given lactic acid bacteria. No tumors were found in vehicle-treated animals fed on the protective reagents. By the end of 22nd week, final average body weights of the rats treated with DMH alone and all animals receiving lactic acid bacteria were significantly decreased compared with the vehicle control ($P<0.05$). Relative liver and kidney weights

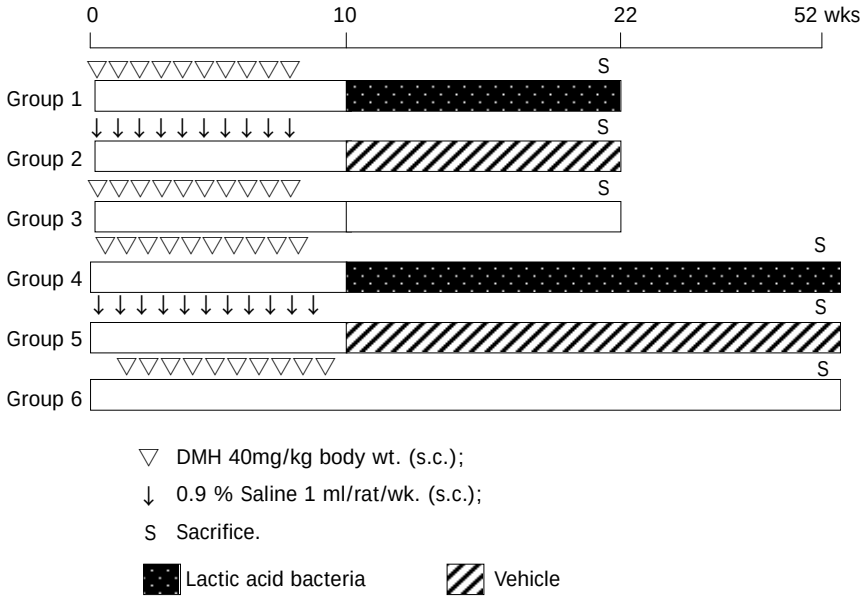

Figure 1 Experimental design.

Table 1 Average final body weight, relative liver and kidney weights, and food consumption data (22wk)

Group	Treatment	No. of rats	Final body Wt, (g)	Relative liver Wt, (g)	Relative kidney Wt, (g)	Average food consumption (g/rat/day)
1	DMH+ lactic acid	10	389.6±44.1[e]	2.92±0.24	0.54±0.06	19.45
2	Saline+ vehicle	10	439.5±39.3	3.09±0.35	0.56±0.12	20.07
3	DMH	10	383.5±19.2[e]	3.10±0.40	0.55±0.07	18.48

a: Values are means ±SD, DMH, 1, 2-dimethylhydrazine, b: Statistical significance: [e]$P<0.05$, Student's *t*-test, *vs* Group 2. c: Kidney weight values are totals for both kidneys.

Table 2 Colon tumor incidence, classification, multiplicity, tumor volume and stage in rats treated with DMH followed or not by lactic acid bacteria (22wk)[a]

Treatment	Incidence *n*(%)	Total no. tumors	Adenoma No (%)	Carcinoma *in situ* No (%)	Carcinoma No (%)	Multiplicity[b] No.	Tumor volume mm^3	Duke's stage[c] A	B	C
DMH+ lactic acid	9 (90)	28	12 (43)	8 (28.5)	8 (28.5)	3.11±2.00	1.64±1.92	0	2	1
DMH	10 (100)	40	27 (67.5)	3 (7.5)	10 (25)	4.00±2.96	4.31±4.56	0	0	3

a: Values are means ±SD. b: No. of tumors/tumor-bearing rat. c: No. of rats with carcinoma were allocated to one of three tumor stages.

and food consumption were not significantly differ among the groups (shown in Table 1). Macroscopically, the distribution of colon tumors was predominantly observed in the proximal and middle colon at the end of 22nd week, there were no significant differences among the groups (data not shown). Histo-pathological examinations of adenocarcinomas in the proximal and middle colon showed that all were invasive through the *muscularis mucosa* and moderately differentiated.

Histo-pathological findings are summarized in Table 2. Colon epithelial lesions were divided into adenoma, carcinoma *in situ* and carcinoma. At the end of 22nd week, the incidence of colon tumor was not significantly affected by lactic acid bacteria. The mean tumor incidence per tumor-bearing rat was 3.11 in group 1 and 4.00 in group 3. Tumor volume was decreased in rats receiving lactic acid bacteria, however, the differences were also not significant compared with DMH- treated group. On the other hand, there was no significant difference in the incidence of metastasis (Duke's stage) between the animals treated with DMH alone and those received lactic acid bacteria.

At the termination, the survival rate of rats in groups 4-6 is shown in Figure 2. None of the rats received *L. lactis* survived the full duration of the experiment, while the DMH-treated rats had a 20 % survival rate. However, the survival rats were sacrificed and macroscopically visible metastases were found in their lungs and livers. There was no significant differene in the survival rate between the lactic acid bacteria treated rats and DMH treated rats. All rats in Group 5 (the vehicle control) survived. The mean survival in lactic acid bacteria-treated animals was 39 weeks.

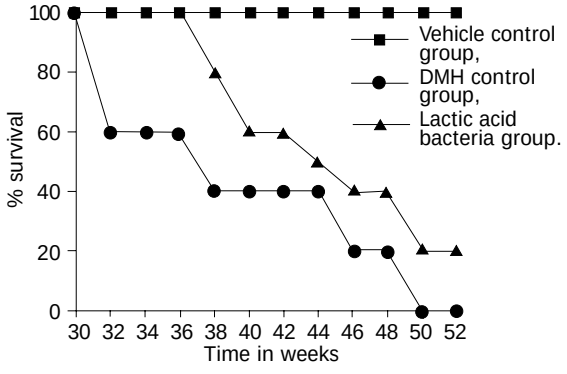

Figure 2 Survival rate of rats injected DMH followed or not by lactic acid bacteria and normal saline.

DISCUSSION

Oral administration of lactic acid bacteria has been shown to effectively reduce DNA damage in animals induced by chemical carcinogens, especially the damage of gastric and colonic mucosa in rats[7]. Certain strains of lactic acid bacteria have also been found to be able to prevent putative preneoplastic lesions induced by carcinogens and have antitumor activity[18,19]. However, findings of in current study do not support the suggestion that addition of lactic acid bacteria may protect against the progression of DMH-induced colon tumor in rats.

The exact change in tumor size or survival of the animals may be crucial for sensitivity determination of anticancer drugs. In this regard, our experimental results seem to be not ideal. The present data did not show any inhibitory effect of lactic acid bacteria on the dimension, multiplicity and invasion of colon tumors. By the end of 22nd week, although there was a reduction in colon tumor volume in animals received lactic acid bacteria, this difference was not statistically significant. The Duke's staging system for human colorectal cancer provides accurate prognostic information. In other words, animals with less advanced diseases (stage A) can survive significantly longer than those with more advanced diseases (stage B and C), irrespective of treatment. In the present study, there was no significant difference in the incidence of metastases at necropsy in lactic acid bacteria-treated and untreated animals. Moreover, the survival rate of rats received lactic acid bacteria was lower than that of rats treated with DMH that were fed on non-lactic acid bacteria. The lower survival rate of rats administered *L. lactis* suggested that lactic acid bacteria had no protective role in decreasing DMH-induced mortality. Whether lactic acid bacteria has some promoting role in the progression of colon tumor is not clear.

In fact, the data from experimental studies indicated that ingestion of certain lactic cultures or their fermented dairy products could reduce the risk of certain types of cancer and inhibit tumor growth[20-22]. The animal experiments did indicate that feeding certain lactic cultures or fermented milk not only suppressed the incidence of DMH-induced colon carcinogenesis but also increased the survival rate of rats with chemically induced colon cancer[23]. These lactic cultures have been shown to possess antimutagenic properties[24], and the probiotic was given during the initiation and promotion phases. However, the antimutagenic activity of lactic acid-producing bacteria was suspected to reside in cell wall[25], as lactic acid itself had no antimutagenic effects[26]. In a previous study, the findings failed

to demonstrate that *bifidobacteria* or *lactobacilli* administration alter colonic microflora had effects on the host[27], and no significant effect was observed when probiotic was given after the promotion phase. In the present study, the lower survival rate of the lactic acid bacteria group (Figure 2) suggested that lactic acid bacteria had no protective role in decreasing DMH-induced mortality. The observed results in survival rats might be due to the fact that lactic acid bacteria can not decrease faecal enzymes involved in formation of carcinogenesis. In addition, our studies failed to show a significant reduction in total number of colon tumors in rats. We believe that this indicates lactic acid bacteria lacks effects on colon cancer in rats. At present, the results from epidemiological studies do not appear to support the results from experimental studies of lactobacilli or lactic acid bacteria on colon cancer prevention or treatment. The reason for this is unclear but might be explained by differences in bacterial strains. The precise mechanisms by which lactic acid *bacteria* may inhibit colon cancer are presently unknown. However, many antitumor activities attributed to lactic cultures have been suggested to involve an enhanced immune response. Therefore, more work needs to be done to identify the specific strains and their antitumor effects and the mechanisms underlying these effects.

Human cancer-nude mice subcutaneous xenograft system as a sensitivity test for chemotherapeutic drugs was studied[28], but it has not been established that the system is a predictive model for screening anticancer drugs. Recently, investigators have been giving greater attention to more rigorous experimental endpoints, such as tumor regression[29-31]. In this respect, autochthonous colon cancer in rats may be suitable to disease oriented *in vivo* screening. DMH-induced rat colon tumor model might be a valuable for new therapeutic agents[9,10]. The fact that clinically used drugs such as 5FU could inhibit the growth of DMH-induced colon tumors and prolong the survival of their rodent hosts suggested a parallel in tumor sensitivity[13]. Therefore, colon tumors induced by DMH at present were the most popular models used in experimental oncology to study various aspects of the morphology, pathogenesis, prevention and treatment of colorectal cancer[9-13]. The animal model described in this study was a truly adjuvant model since the rats developed primary colon tumors *in situ*, which resembled the histopathologic features of human colon tumors. Moreover, DMH decreased animal body weight at the end of week 22, but had no effect on food intake, probably due to its aggressive effect on the mucosa and carcinogenicity.

In the present study, two possible reasons for the failure to alter rat colon tumor were put forward. One was that *L. lactis* lacked inhibitory effects because the initiation of DMH was too strong in our study. The other was that the dose of *L. lactis* might be inadequate to significantly alter colonic flora. It is clear that an optimal condition must be met for each inhibitor to be used for animal and possibly for human cancer prevention and treatment. Otherwise, the same substance, it might enhance the processes of growth of tumor instead of inhibiting. Therefore, it will be extremely difficult, to devise an optimal diet because of the wide variety of cancer inhibitors and enhancers present in human diet.

In conclusion, this study did not find any inhibitory effect in experimental colon tumor progression by addition of lactic acid bacteria after the promotion stage of carcinogenesis and thus does not support the hypothesis that alteration of colonic flora may exert an influence on the progression of DMH-induced colon tumor.

ACKNOWLEDGMENTS

Authors are very grateful to Prof. Shoji Fukushima, Department of Pathology, Osaka City Medical School (Japan) for valuable discussion and comments, and Prof. Yanfeng Zhong, Department of Pathology, Beijing University Medical School for histopathological examination.

REFERENCES

1 **Balansky R**, Gyosheva B, Ganchev G, Mircheva Z, Minakova S, Georgiev G. Inhibitory effects of freeze-dried milk fermented by selected Lactobacillus bulgaricus strains on carcinogenesis induced by 1,2-dimethylhydrazine in rats and by diethylnitrosamine in hamsters. *Cancer lett* 1999; **147**: 125-137

2 **Femia AP,** Luceri C, Dolara P, Giannini A, Biggeri A, Salvadori M, Clune Y, Collins KJ, Paglierani M, Caderni G. Antitumorigenic activity of the prebiotic inulin enriched with oligofructose in combination with the probiotics Lactobacillus rhamnosus and Bifidobacterium lactis on azoxymethane-induced colon carcinogenesis in rats. *Carcinogenesis* 2002; **23**: 1953-1960

3 **Renner HW**, Munzner R. The possible role of probiotics as dietary antimutagen. *Mutat Res* 1991; **262**: 239-245

4 **Lidbeck A,** Nord CE, Gustafsson JA, Refter J. Lactobacilli, anticarcinogenic activities and human intestinal microflora. *Eur J Cancer Prev* 1992; **1**: 341-353

5 **Vorob'eva LI,** Abilev SK. Antimutagenic properties of bacteria: a review. *Prikl Biokhim Mikrobiol* 2002; **38**: 115-127

6 **Shahani KM**, Chandan RC. Nutritional and healthful aspects of cultured and culture-containing dairy foods. *J Dairy Sci* 1979; **62**: 1685-1694

7 **Pool-Zobel BL**, Neudecker C, Domizlaff I, Ji S, Schillinger U, Rumney C, Moretti M, Vilarini I, Scassellati-Sforzolini R, Rowland I. Lactobacillus- and Bifidobacterium-mediated antigenotoxicity in the colon of rats. *Nutr Cancer* 1996; **26**: 365-380

8 **Singh J**, Rivenson A, Tomita M, Shimamura S, Ishibashi N, Reddy BS. Bifidobacterium longum, a lactic acid-producing intestinal bacterium inhibits colon cancer and modulates the intermediate biomarkers of colon carcinogenesis. *Carcinogenesis* 1997; **18**: 833-841

9 **Tsunoda A**, Shibusawa M, Tsunoda Y, Nakao K, Yasuda N, Kusano M. A model for sensitivity determination of anticancer agents against chemically-induced colon cancer in rats. *Anticancer Res* 1994; **14**: 2637-2642

10 **Tsunoda A**, Shibusawa M, Tsunoda Y, Yokoyama N, Nakao K, Kusano M, Nomura N, Nagayama S, Takechi T. Antitumor effect of S-1 on DMH induced colon cancer in rats. *Anticancer Res* 1998; **18**: 1137-1141

11 **Li W**, Wanibuchi H, Salim EI, Wei M, Yamamoto S, Nishino H, Fukushima S. Inhibition by ginseng of 1,2- dimethylhydrazine induction of aberrant crypt foci in the rat colon. *Nutr Cancer* 2000; **36**: 66-73

12 **LaMont JT**, O'Gorman TA. Experimental colon cancer. *Gastroenterology* 1978; **75**: 1157-1169

13 **Danzi M,** Lewin MR, Cruse JP, Clark CG. Combination chemotherapy with 5-fluorouracil (5FU) and 1,3-bis (2-chloro-ethyl)-1-nitrosourea (BCNU) prolongs survival of rats with dimethylhydrazine-induced colon cancer. *Gut* 1983; **24**: 1041-1047

14 **Yoon SS,** Eto H, Lin CM, Nakamura H, Pawlik TM, Song SU, Tanabe KK. Mouse endostatin inhibits the formation of lung and liver metastases. *Cancer Res* 1999; **59**: 6251-6256

15 **Pozharisski KM**. Morphology and morphogenesis of experimental epithelial tumours of the intestine. *J Natl Cancer Inst* 1975; **54**: 1115-1135

16 **De Ruyter PG,** Kuipers OP, Beerthuyzen MM, van Alen-Boerrigter I, de Vos WM. Functional analysis of promoters in the nisin gene cluster of Lactoccus lactis. *J Bacteriol* 1996; **178**: 3434-3439

17 **Peto R**, Pike MC, Armitage P, Breslow NE, Cox DR, Howard SV, Mantel N, McPherson K, Peto J, Smith PG. Design and analysis of randomized clinical trials requiring prolonged observation of each patient II analysis and examples. *Br J Cancer* 1977; **35**: 1-39

18 **Kelkar SM**, Shenoy MA, Kaklij GS. Antitumor activity of lactic acid bacteria on a solid fibrosarcoma, sarcoma-180 and Ehrlich ascites carcinoma. *Cancer Lett* 1988; **42**: 73-77

19 **Goldin BR**, Gualtieri LJ, Moore RP. The effect of Lactobacillus GG on the initiation and promotion of DMH-induced intestinal tumors in the rat. *Nutr Cancer* 1996; **25**: 197-204

20 **Bolognani F,** Rumney CJ, Pool-Zobel BL, Rowland IR. Effect of lactobacilli, bifidobacteria and inulin on the formation of aberrant crypt foci in rats. *Eur J Nutr* 2001; **40**: 293-300
21 **Gallaher DD,** Khil J. The effect of synbiotics on colon carcinogenesis in rats. *J Nutr* 1999; **129**(7Suppl): 1483S-1487S
22 **Reddy BS.** Possible mechanisms by which pro- and prebiotics influence colon carcinogenesis and tumor growth. *J Nutr* 1999; **129**(7Suppl): 1478S-1482S
23 **Shackelford LA**, Rao DR, Chawan CB, Pulusani SR. Effect of feeding fermented milk on the incidence of chemically-induced colon tumors in rats. *Nutr Cancer* 1983; **5**: 159-164
24 **Renner HW**, Munzner R. The possible role of probiotics as dietary antimutagen. *Mutat Res* 1991; **262**: 239-245
25 **Tejada-Simon MV,** Pestka JJ. Proinflammatory cytokine and nitric oxide induction in murine macrophages by cell wall and cytoplasmic extracts of lactic acid bacteria. *J Food Prot* 1999; **62**: 1435-1444
26 **Morita T**, Takeda K, Okumura K. Evaluation of clastogenicity of formic acid, acetic acid and lactic acid on cultured mammalian cells. *Mutat Res* 1990; **240**: 195-202
27 **Nielsen OH**, Jorgensen S, Pedersen K, Justesen T. Microbiological evaluation of jejunal aspirates and fecal samples after oral administration of bifidobacteria and lactic acid bacteria. *J Appl Bacteriol* 1994; **76**; 469-474
28 **Boven E**, Winograd B, Berger DP, Dumont MP, Braakhuis BJ, Fodstad O, Langdon S, Fiebig HH. Phase II preclinical drug screening in human tumor xenografts: a first European multicenter collaborative study. *Cancer Res* 1992; **52**: 5940-5947
29 **Gadducci A,** Viacava P, Cosio S, Fanelli G, Fanucchi A, Cecchetti D, Cristofani R, Genazzani AR. Intratumoral microvessel density, response to chemotherapy and clinical outcome of patients with advanced ovarian carcinoma. *Anticancer Res* 2003; **23:** 549-556
30 **Snyder C,** Harlan L, Knopf K, Potosky A, Kaplan R. Patterns of Care for the Treatment of Bladder Cancer. *J Urol* 2003; **169:** 1697-1701
31 **Raghavan D.** Progress in the chemotherapy of metastatic cancer of the urinary tract. *Cancer* 2003; **97**(8 Suppl): 2050-2055

Edited by Zhao M and Wang XL

P.O.Box 2345, Beijing 100023,China
Fax: +86-10-85381893
E-mail: wjg@wjgnet.com www.wjgnet.com

World J Gastroenterol 2003;9(11):2474-2479
World Journal of Gastroenterology
 ISSN 1007-9327

• VIRAL HEPATITIS •

Establishment of a cell-based assay system for hepatitis C virus serine protease and its primary applications

Hong-Xia Mao, Shui-Yun Lan, Yun-Wen Hu, Li Xiang, Zheng-Hong Yuan

Hong-Xia Mao, Shui-Yun Lan, Yun-Wen Hu, Li Xiang, Zheng-Hong Yuan, Key Laboratory of Medical Molecular Virology, Shanghai Medical College, Fudan University, Shanghai 200032, China
Supported by the National Natural Science Foundation of China, No. 39870010, No. 39825501, the Shanghai Scientific Development Foundation, No. 00QMH1404 and the State 973 Program of China, No. G1999054105
Correspondence to: Zheng-Hong Yuan, Key Laboratory of Medical Molecular Virology, Shanghai Medical College, Fudan University, 138 Yi Xue Yuan Road, Shanghai 200032, China. zhyuan@shmu.edu.cn
Telephone: +86-21-64161928 **Fax:** +86-21-64227201
Received: 2003-03-10 **Accepted:** 2003-06-12

Abstract

AIM: To establish an efficient, sensitive, cell-based assay system for NS3 serine protease in an effort to study further the property of hepatitis C virus (HCV) and develop new antiviral agents.

METHODS: We constructed pCI-neo-NS3/4A-SEAP chimeric plasmid, in which the secreted alkaline phosphatase (SEAP) was fused in-frame to the downstream of NS4A/4B cleavage site. The protease activity of NS3 was reflected by the activity of SEAP in the culture media of transient or stable expression cells. Stably expressing cell lines were obtained by G418 selection. Pefabloc SC, a potent irreversible serine protease inhibitor, was used to treat the stably expressing cell lines to assess the system for screening NS3 inhibitors. To compare the activity of serine proteases from 1b and 1a, two chimeric clones were constructed and introduced into both transient and stable expression systems.

RESULTS: The SEAP activity in the culture media could be detected in both transient and stable expression systems, and was apparently decreased after Pefabloc SC treatment. In both transient and stable systems, NS3/4A-SEAP chimeric gene from HCV genotype 1b produced higher SEAP activity in the culture media than that from 1a.

CONCLUSION: The cell-based system is efficient and sensitive enough for detection and comparison of NS3 protease activity, and screening of anti-NS3 inhibitors. The functional difference between NS3/4A from 1a and 1b subtypes revealed by this system provides a clue for further investigations.

Mao HX, Lan SY, Hu YW, Xiang L, Yuan ZH. Establishment of a cell-based assay system for hepatitis C virus serine protease and its primary applications. *World J Gastroenterol* 2003; 9 (11): 2474-2479

http://www.wjgnet.com/1007-9327/9/2474.asp

INTRODUCTION

The infection of hepatitis C virus (HCV) is associated with a high frequency of chronic hepatitis (up to 80 %), which often progresses to liver cirrhosis and hepatocellular carcinoma (up to 20 %)[1]. Until now, there has been no vaccine against HCV and the most efficacious pharmacological treatment, a combined therapy of interferon alpha and ribavirin, which could lead to sustained remission only in a minority of cases[2,3]. Considerable efforts have been therefore undertaken to develop specific antiviral agents.

HCV is a positive-sense, single-stranded RNA virus and belongs to the flaviviridae family. Its genome is about 9.6 kb in length and encodes the structural proteins C, E1, E2, and the non-structural proteins NS2, NS3, NS4A, NS4B, NS5A and NS5B, which are released by action of both host cell and virally encoded proteases[4,5]. The N-terminal domain of the NS3 protein contains a serine protease, belonging to the chymotrypsin family[6], which is responsible for the proteolytic cleavage at the NS3/4A, NS4A/NS4B, NS4B/NS5A and NS5A/5B junctions of the viral polyprotein[4]. The NS3 thus plays a pivotal role in the viral maturation and replication. It is also known to affect normal cellular functions, such as cell proliferation and cell death, suggesting its involvement either direct or indirect in HCV hepatocarcinogenesis[7-9]. Therefore, the NS3 protease has become one of the most attractive targets for the development of HCV specific antiviral agent.

To establish an efficient, sensitive, cell-based assay system for NS3 serine protease in an effort to study further the property of HCV and develop new antiviral agents, we first constructed the pCI-neo-NS3/4A-SEAP chimeric plasmid, in which the secreted alkaline phosphatase (SEAP) gene was fused in-frame to the downstream of NS4A/4B cleavage site. The protease activity of NS3 was reflected by the activity of SEAP in the culture media of transient or stably expressing cells. Stably expressing cell lines were obtained by G418 selection. To explore the possibility of applying this system to the screening of NS3 inhibitors, Pefabloc SC, a potent irreversible serine protease inhibitor, was then used to treat the stably expressing cell lines. After that, we investigated the difference of serine protease activity between HCV genotype 1b and 1a by constructing two pCI-neo-NS3/4A-SEAP chimeric clones and studying them in both transient and stable expression systems.

MATERIALS AND METHODS

Cloning of HCV NS3/4A and SEAP genes

To amplify NS3/4A region (HCV 1b) using PCR from a near-full length HCV cDNA (from a patient with 1b genotype), two pairs of primers were used: NS3/4A5' , 5' -CCG GAA TTC ATG GCC CCC ATC ACA GCC TAT-3' (nucleotides [nt] 3 420-3 437), and NS3/4A3' , 5' -CAGT CTC GAG GAG GTG TGA GGC GCA-3' (nucleotides [nt] 5 472-5 486); NS3/4A (TGA)3' , 5' - CCG CTC GAG *TCA* GCA CTC CTC CAT CTC ATC-3' (nucleotides [nt] 5 457-5 474, with stop codon, as negative control). RNS3/4A (HCV 1a) was amplified with primer RNS3/4A5' , 5' -AT GAA TTC ATG GCG CCC ATC ACG GCG TAC-3' (nucleotides [nt] 3 420-3 437) and primer RNS3/4A3' , 5' -GCC AAG CTT TAA GTG CTG AGA GCA-3' (nucleotides [nt] 5 472-5 486) from p90/HCV FL-long pU (AF009606) (a generous gift from Professor Charle M Rice from the Center for the Study of Hepatitis C, Rockefellor

University). SEAP fragment was obtained by PCR with two pairs of primers: SEAP(XhoI)5' , 5' -AT CTC GAG ATG CTG CTG CTG CTG CTG CTG-3' (nucleotides [nt] 54-74), SEAP (HindIII)5' , 5' -AT AAG CTT ATG CTG CTG CTG CTG CTG CTG CTG-3' (nucleotides [nt] 54-77), and SEAP3' , 5' -AT GCGGCCGC TCA GGG AGC AGT GGC CGT C-3' (nucleotides [nt] 1 628-1 647) from pCMV-SEAP (generously provided by Professor Byan R.Cullen of the Medical Center, Duke University).

Construction of pCI-neo-NS3/4A-SEAP

The NS3/4A fragment from HCV 1b genotype and digested with *Eco*RI and *Xho*I, was ligated into *Eco*RI/*Not*I site of pCI-neo vector (Stratagene) with the SEAP fragment digested with *Xho*I and *Not*I to generate pCI-neo-NS3/4A-SEAP. The HCV 1a RNS3/4A fragment digested with *Eco*RI and *Hind* III and the SEAP fragment digested with *Hind* III and *Not* I were ligated into *Eco*RI/*Not* I site of pCI-neo vector to generate pCI-neo-RNS3/4A-SEAP. The schematic diagram is shown in Figure 1. The *Eco*RI/*Xho* I fragment from the pET28a-NS3/4A(TGA) was ligated into *Eco*RI/*Sal* I site of pCI-neo vector and the clone was named as pCI-neo-NS3/4A(TGA).

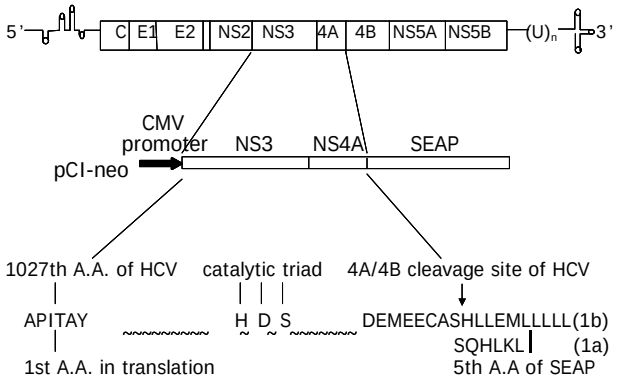

Figure 1 Schematic diagram of the pCI-neo-NS3/4A-SEAP and pCI-neo-RNS3/4A-SEAP expression vectors. The SEAP gene, which has N-terminal signal sequence, was fused in-frame to the HCV sequence encoding the full-length NS3 proteins followed by the NS4A cofactor. Amino acid sequences of (R)NS3/4A and SEAP in the fusion regions are shown by capitalized, bold characters. The cleavage site between NS4A and NS4B is indicated by arrow. HDS is the catalytic triad of NS3 protease.

Cell culture and transfection

HepG2 cells or Cos7 cells were cultured in Dulbecco's modified Eagle's medium (DMEM) with penicillin (100 U/ml) and streptomycin (100 μg/ml), supplemented with 10 % fetal calf serum. Recombinant plasmid DNA used for transfection was extracted and purified with the Qiagen Midiprep kits. DNA (5 μg) was used to transfect HepG2 or Cos7 cells in 6-well NUNC multidish by the calcium phosphate precipitation method as reported previously[10]. Duplicate dishes were used for all samples, and 3 μg of reporter plasmid pcDNA3.1-CAT expressing chloramphenicol acetyltransferase (CAT) was cotransfected as an internal control to normalize the transfection efficiency among dishes. Forty-eight hours after transfection, culture media and cells were collected separately to monitor the secretion of SEAP in the supernatant and NS3 protease expression in transfected cells. pCI-neo-NS3/4A (TGA) was used as a mock transfection control. Transfection experiments were repeated twice on separate days.

Colorimetric assay for SEAP

The SEAP activity of the culture media was measured at 48 h after transfection by performing a colorimetric assay according to the author's recommendation[11]. Briefly, 20 μl heat-treated (at 65 ℃ for 5 min) medium was adjusted to 1×SEAP assay buffer (1.0 M diethanolamine pH9.8, 0.5 mM $MgCl_2$, 10 mM L-homoarginine) in a final volume of 200 μl and prewarmed to 37 ℃ for 10 min in a 96-well flat-bottom culture dish. Twenty μl of prewarmed 120 mM *p*-nitrophenylphosphate dissolved in SEAP assay buffer was then added with mixing. The A_{405} of the reaction mixture was read in a BIO-RAD (Benchmark) microplate reader at 5-min intervals. The change in absorbance was plotted and the maximum linear reaction rate determined. The SEAP activity was expressed in milliunits (mU) per ml. One mu equals an increase of 0.04 A_{405} units per min. Each SEAP assay was performed in triplicate.

Establishment of NS3/4A-SEAP stable expression system

Two different cell lines of Cos7 and HepG2 cells were transfected with the plasmid pCI-neo-NS3/4A-SEAP, pCI-neo-RNS3/4A-SEAP or pCI-neo-NS3/4A (TGA), respectively by calcium phosphate precipitation method mentioned above. At 48 h after transfection, the cells were subcultured and selected with the 600 mg/l of G418. After 3 weeks of selection, the colonies were picked up and amplified in the presence of 200 mg/l G418.

Inhibition of HCV protease activity by Pefabloc SC

Cos7 cell lines (1b and 1a type) were seeded into a 6-well NUNC multidish at a density of 10^5 cells/ml in 3 ml medium and cultured overnight at 37 ℃ in a 50 ml· L^{-1} CO_2 incubator. The overnight culture media were changed with fresh one containing Pefabloc SC at the concentration of 0.1 mM, 0.2 mM, 0.4 mM, 0.5 mM, or 0.6 mM. The cells without Pefabloc SC treatment were set as control. After 24 hours, the media were collected for the colorimetric assay for SEAP activity. Effect of Pefabloc SC on the viability of Cos7 stable cells was evaluated by the alamarBlue™ assay (Biosource International Corp.)[12]. Alamar Blue was added in an amount equal to 10 % of the culture volume and after 2 hours of incubation at 37 ℃, the panels were read spectrofluorometrically (excitation, 544 nm; emission, 590 nm) by Ascent FL. The experiment was performed twice and each sample was detected in duplicate.

Northern blot analysis of NS3/4A expression in transfected cells

Total RNA was extracted using GIBCO-BRL TRIZOL Reagent (Cat No. 15596 Gibco Life Tech) according to the instructions of manufacturers. It was digested with RNase free DNase (Promega) to wipe off the transfected plasmid DNA. After electrophoresis in a 1 % agarose gel, 10 μg total RNA was blotted onto a positively charged Nylon membrane (Roche). HCV NS3/4A (100 ng of PCR products, 1a and 1b respectively) and random primers were used to prepare the [^{32}P] dCTP labled probes for hybridization. The signals were detected by autoradiography and scanned with densitometry for semiquantification of the intensity of signals. The corresponding intensity of β-actin signals was used as controls.

Western blot analysis of NS3/4A expression in transfected cells

To assess the expression levels of the HCV NS3/4A of two HCV genotypes in the transfected HepG2 or Cos7, Western blot analysis was conducted as described[13] with some modifications. Briefly, cells were lysed in 200 μl TSA buffer (50 mM Tris-HCl, 140 mM NaCl, 5 ml· L^{-1} NP40, 1 mM PMSF, 1 mM DTT). Ten μl aliquot was subjected to 7.5 % SDS-PAGE eletrophoresis. The separated proteins were transferred to nitrocellulose membrane in transfer buffer (20 mM Tris-HCl, 190 mM Glycine, 200 ml· L^{-1} methanol, pH 8.3) using Mini Trans-blot transfer system (Bio-Rad) at 100V for 1 h. The membrane was blocked with 50 mg· L^{-1} nonfat dried milk in

PBST (Tris-buffered saline containing 0.5 ml· L^{-1} Tween-20) and then incubated with mouse anti-NS3 multiclonal antibody. After three washes in PBST, the membrane was incubated with peroxidase-conjugated goat anti-mouse second antibody (A90-131P, BETHYL Co.). The blot was incubated with TMB substrate to reveal the antigen bands. Cellular protein La (a phosphoprotein, 47 KD, present at proximately 2×10^7 molecules per cell) was used as a quantificational control. The expression levels of the NS3 of two HCV isolates were compared by the semi-quantification of scanned intensity of antigen bands.

RESULTS

Transient expression of NS3/4A-SEAP

The plasmids pCI-neo-NS3/4A-SEAP, pCI-neo-NS3/4A (TGA) and pCMV-SEAP were transfected into HepG2 or Cos7 cells by calcium phosphate method and the SEAP activity of the culture media was measured at 48 h after transfection. As expected, in HepG2 cells, the pCMV-SEAP produced SEAP activity about 30.16±3.46 mu/ml, while pCI-neo-NS3/4A (TGA) produced 0.34±0.48 mu/ml, which is almost the background level (Figure 2). The culture media from cells transfected with pCI-neo-NS3/4A-SEAP showed a SEAP activity of about 12.05±1.25 mu/ml. Similar results were obtained in Cos7 cells (data not shown). The processing of fusion proteins expressed in transfected cells was examined by immunoblotting with anti-HCV human sera and mouse derived multiple-clonal sera. Processed NS3 protein of 70KD was detected (Figure 6). The results indicate that, depending on the cleavage activity of the NS3 protease, the SEAP could be cleaved and secreted into the extracellular media.

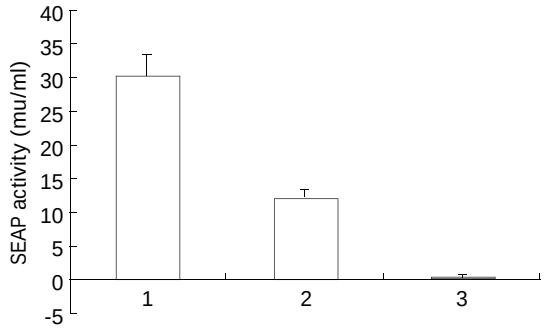

Figure 2 SEAP activity in the media of the transfected HepG2 cells. Lane 1: pCMV-SEAP, Lane 2: pCI-neo-NS3/4A-SEAP, Lane 3: pCI-neo-NS3/4A(TGA)(as negative control).

Stable expression of NS3/4A-SEAP

To establish the NS3/4A-SEAP assay system in stable expression cells, HepG2 and Cos7 cells transfected with the pCI-neo-NS3/4A-SEAP were selected for stable expression ones. During 600 mg/l G418 selection, most transfected HepG2 or Cos7 cells died out after 4 changes of media and the selected colonies were picked up and amplified in the presence of 200 mg/l G418. Results of SEAP assay showed that all selected stably expressing cell lines produced SEAP in their supernatant. However, the media from Cos7-derived stably expressing cell lines showed higher SEAP activity than those from HepG2-derived cell lines. Initially, the two kinds of stably expressing cell lines did not show any significant differences. Then, the HepG2-derived cell lines appeared to lose supernatant SEAP activity, depending on the passages and showed finally, very low SEAP activity (data not shown) while selected cell lines derived from Cos7 appeared to express high levels of SEAP during continuous passages over 4 months.

Comparison of protease activity of NS3/4A from HCV 1a and 1b two subtypes in both transient and stable expression systems

To compare the activity of serine proteases from HCV subtype 1b and 1a, two chimeric clones were constructed and studied in both transient and stable expression systems. Results of SEAP assay showed that, in transient expression system, the Cos7 cells transfected with the pCI-neo-NS3/4A(1b)-SEAP produced higher supernatant SEAP activity (37.49±3.06 mu/ml) than those transfected with pCI-neo-RNS3/4A(1a)-SEAP (3.48±0.15 mu/ml). The overall assay results were similar in HepG2 cells with pCI-neo-NS3/4A(1b)-SEAP at 11.82±0.92 mu/ml and pCI-neo-RNS3/4A(1a)-SEAP at 2.49±0.67 mu/ml. The above results indicated that cells transfected with pCI-neo-NS3/4A-SEAP from HCV 1b isolate produced 5-10 folds higher supernatant SEAP activity than those transfected with pCI-neo-RNS3/4A-SEAP from HCV 1a isolate (Figure 3). Consistently, the 1b derived stable cell lines also produced higher SEAP activity in media (39.11±2.97 mu/ml, 25.36±1.41 mu/ml) than those derived from 1a (6.92±0.56 mu/ml, 7.85±0.57 mu/ml, Figure 4).

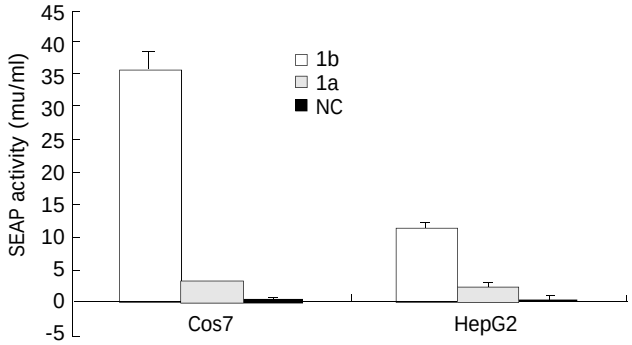

Figure 3 SEAP activity in the media of the transfected HepG2 and Cos7 cells. 1b: pCI-neo-NS3/4A-SEAP; 1a: pCI-neo-RNS3/4A-SEAP; NC: pCI-neo-NS3/4A(TGA)(as negative control).

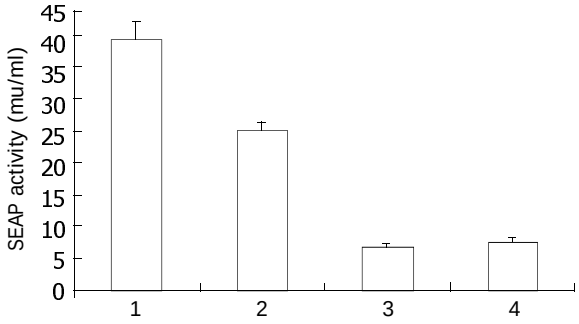

Figure 4 SEAP activity in the media of Cos7-derived stably expressing cell lines. Lane 1, 2: 1b type stable expression cell lines; Lane 3, 4: 1a type stable expression cell lines.

Northern blot analysis of NS3/4A mRNA level in transfected cells

To compare the amounts of NS3/4A mRNAs in transfected HepG2 and Cos7 cells, Northern blotting was carried out using the isotope-labeled DNA probes corresponding to NS3/4A regions of 1b and 1a. The NS3/4A specific signals could be detected in both HepG2 and Cos7 cells transfected with pCI-neo-NS3/4A-SEAP(1b), pCI-neo-NS3/4A(TGA), or pCI-neo-RNS3/4A-SEAP(1a) respectively. The hybridization signals of NS3/4A mRNA were similar between conspecific cells transfected with 1b or 1a constructs as the ratio of signal densities of NS3/4A to β-actin in pCI-neo-NS3/4A-SEAP(1b),

pCI-neo-NS3/4A(TGA) and pCI-neo-RNS3/4A-SEAP(1a) transfected cells were similar (2 066/2 360/2 400 in transfected Cos7 cells and 0.8/0.6/0.7 in transfected HepG2 cells) (Figure 5).

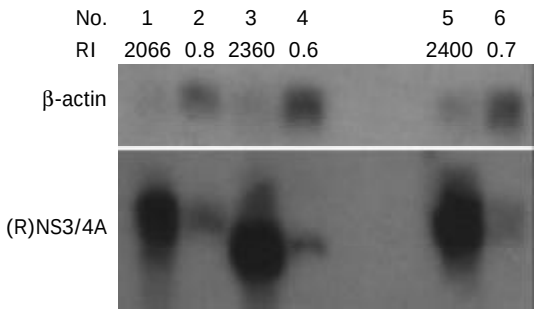

Figure 5 Northern blot analysis of NS3/4A mRNA level in transfected Cos7 cells (Lane 1, 3, 5) and HepG2 cells (Lane 2, 4, 6). Lane 1, 2 pCI-neo-NS3/4A-SEAP (1b type); Lane 3, 4 pCI-neo-NS3/4A (TGA) (control); Lane 5, 6 pCI-neo-RNS3/4A-SEAP (1a type); Intensity of hybridization signal was measured by densitometry, and the relative intensities of NS3/4A signal to β-actin are indicated below the lane No.

Western blot analysis of NS3 protein level in transfected cells

To compare the levels of NS3 proteins in transfected cells, Western blotting was carried out to detect the HCV protease expression with mouse anti-NS3 antibody. The expression levels of the NS3 were compared by the semiquantification of bands detected by immunoblotting. The relative intensities (RI) of NS3 to cellular protein La are indicated in Figure 6. The results showed that NS3 level expressed by pCI-neo-NS3/4A-SEAP (1b) was similar to the one expressed by pCI-neo-RNS3/4A-SEAP (1a) (3/3 in transfected Cos7 cells and 1/1 in transfected HepG2 cells) in transfected cells (Figure 6).

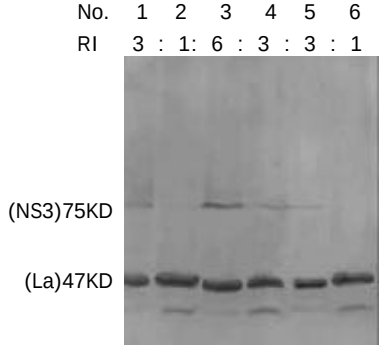

Figure 6 Western blot analysis of NS3 protein level in transfected Cos7 cells (Lane1, 3, 5) and HepG2 cells (Lane 2, 4, 6). Lane 1, 2 pCI-neo-NS3/4A-SEAP (1b type), Lane 3, 4 pCI-neo-NS3/4A(TGA) (control), Lane 5, 6 pCI-neo-RNS3/4A-SEAP (1a type). Intensity of hybridization signal was measured by densitometry, and the relative intensities (RI) of NS3 to cellular protein La in samples are indicated.

Inhibition of protease activity of NS3/4A by Pefabloc SC

Pefabloc SC, a serine protease inhibitor was added into the media of Cos7-derived stable expression cells at the concentration of 0.1 mM, 0.2 mM, 0.4 mM, 0.5 mM, or 0.6 mM. After 24 hours, the media were collected for the colorimetric assay of SEAP activity. The effect of Pefabloc SC on the viability of stable expression cells was evaluated by the alamarBlue™ assay. Results showed that, although the Pefabloc SC was relatively toxic to cells, it had some specific inhibitory effect on the protease activity of NS3/4A as the secretion of SEAP, which was dependent on the active HCV protease, was decreased more than the metabolic activity of the cells after treatment, and it was 60-70 % when the treated cells still kept almost 100 % metabolic activity (Figure 7).

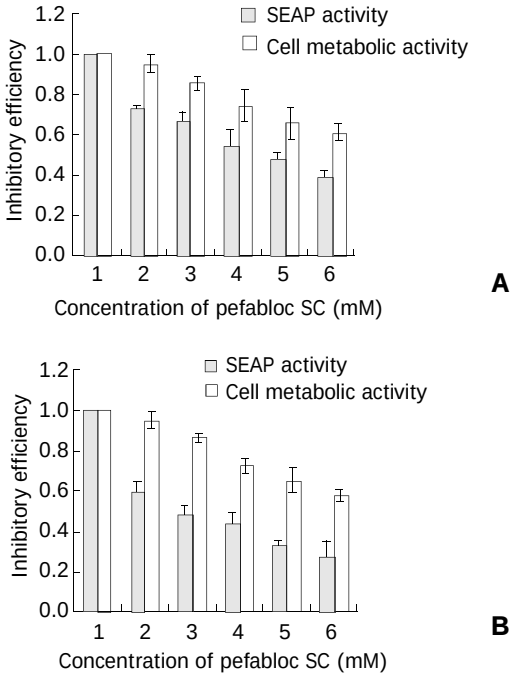

Figure 7 SEAP activity and viability of Cos7 stable cells treated with Pefabloc SC. The SEAP activity and viability of cells were measured with colorimetric and alamar Blue™ assay according to manufactures' recommendations. Each assay was performed in triplicate. A: 1b type stable expression cell lines, B: 1a type stable expression cell lines. 1: no treatment, 2: 0.1 mM, 3: 0.2 mM, 4: 0.4 mM, 5: 0.5 mM, 6: 0.6 mM.

DISCUSSION

It has been reported that the cleavage activity of NS3 could be detected by *in vitro* transcription/translation and transient expression experiments[14-16], or using purified active NS3 protease[17,18]. But they are known to be difficult to apply for screening specific NS3 inhibitors at large scale. Another problem has to be considered referring to the rather featureless substrate binding pocket of NS3[19], which may make the development of specific inhibitors rather difficult. Alternative *in vivo* assay systems for NS3 protease, which can differentiate the inhibitors' effects on NS3 protease and cellular metabolic activity (including cellular serine-type protease), will accelerate the screening of specific inhibitors. Several chimeric viral replication systems had been developed to screen HCV inhibitors in tissue culture[20,21]. These systems have some disadvantages regarding instability of chimeric viruses and difficulty in evaluating the inhibition quantitatively. Comparably, our cell-based NS3/4A-SEAP expression system is safe, easy to handle and the report gene of SEAP can be sensitively and quantitatively measured continuously without killing cells[11].

In the scheme of pCI-neo-NS3/4A-SEAP constructs, the NS4A/SEAP junction has the sequence DEMEEC ↓ ASHL (HCV 1b subtype)[22] or DEMEEC ↓ SQHL (HCV 1a subtype) which contains NS4A/4B cleavage site. The rationale for this system was based on the assumption that the secretion of SEAP protein into the culture media depends on the cleavage between NS4A protein and SEAP protein by HCV NS3 protease. The unusual substrate specificity, which is quite distinct from cellular serine-type proteases, makes it possible for the system to generate inhibitors with a high degree of selectivity[23,24]. To make the system more suitable for the screening of NS3

inhibitors, we also established the stably expressing cell lines. During the screening, the inhibitor could be introduced into the stable cells by transfection or simply adding in culture media[25] according to their own characteristics.

In the process of establishing both transient and stable expression systems, we found that Cos7-derived cells always showed higher SEAP activity in media than HepG2-derived ones. It is consistent with the previous report that Cos7 cells and other cell lines expressing the SV40 large T-antigen, have been of great benefit to the transfection studies using transient expression vectors containing the SV40 origin of replication, as these cells yield plasmid replication to a high copy number[26]. In addition, we also observed that the two kinds of cell lines initially did not show any significant differences in cell growth and morphology, but depending on the passages, the HepG2-derived cell lines appeared to lose SEAP activity and finally showed very low SEAP activity (data not shown). However, the Cos7-derived cell lines appeared to express high levels of SEAP activity during continuous passages even after 4 months. It is likely that the expression of active protease is relatively toxic in some cells, leading to selection of cells with low protease activity in the process of G418 selection and passage[22].

When this assay system was used to compare the activity of HCV serine proteases from different genotypes (1b and 1a), the cells transfected with 1b type plasmid DNA showed 5-10 folds higher SEAP activity in culture media than those with 1a type one in transient system. And there were no significant differences in protein and mRNA levels of NS3/4A between them in either transiently transfected Cos7 or HepG2 cells. The results indicated that the cleavage efficiency of 1b type NS3 protease was 5-10 folds higher than that of 1a type. Consistently, we observed similar results in the stable expression system. Since the NS3 serine protease activity is required for cleavages at the downstream 3/4A, 4A/4B, 4B/5A, 5A/5B sites, its cleavage efficiency will affect the assembly of functional HCV RNA replication complex, viral particle maturation and host-virus interaction. It has been reported that the success in establishing efficient HCV replication depended on the particular genotype 1b consensus cDNA clone studied[27]. Whether the higher protease activity of 1b subtype NS3 contributes to the above phenomenon is worthy of further investigations. The availability of replication system[27-29] will promote such studies.

In this study, the cell-based system was also successfully used to evaluate the inhibition effect of Pefabloc SC on the NS3 protease *in vivo*. Pefabloc SC[30] is one of the most potent inhibitors of the class of sulfonyl fluorides like phenylmethylsulfonylfluoride (PMSF). It has been widely used to inhibit all kinds of serine proteases (including HCV NS3)[31,32]. It was reported that 8mM of Pefabloc SC showed strong effects on NS3-4A junction in a trans-cleavage assay system[33]. Due to its toxicity to cells, the concentrations of Pefabloc SC used in our system were only from 0.1 mM to 0.6 mM. However, results here still showed that it had some specific inhibitory effect on the protease activity of the HCVNS3/4A as the secretion of SEAP, which depended on the active HCV protease, was decreased more than the metabolic activity of the cells after treatment (Figure 6). As shown in Figure 6, when the cells treated with 0.1 mM Pefabloc SC still kept near 100 % metabolic activity, the SEAP activity in culture media had decreased to 60-70 %. These data reflected the sensitivity of our system and its practicability for the detection and comparison of NS3 protease activity and the screening anti-NS3 inhibitors.

In summary, we reported the establishment of the cell-based NS3/4A-SEAP expression system in both transiently transfected and stable cell lines. It was further applied to the evaluation of Pefabolc SC, a known protease inhibitor and the comparison of activities of NS3 protease from 1a, 1b genotypes. It could be concluded that this cell-based system is efficient and sensitive enough for the detection and comparison of NS3 protease activity and the screening of anti-NS3 inhibitors. The functional difference between NS3/4A from 1a and 1b subtypes revealed by this system provides a clue for further investigations.

REFERENCES

1 **Saito I**, Miyamura T, Ohbayashi A, Harada H, Katayama T, Kikuchi S, Watanabe Y, Koi S, Onji M, Ohta Y. Hepatitis C virus infection is associated with the development of hepatocellular carcinoma. *Proc Natl Acad Sci U S A* 1990; **87**: 6547-6549

2 **Saracco G**, Ciancio A, Olivero A, Smedile A, Roffi L, Croce G, Colletta C, Cariti G, Andreoni M, Biglino A, Calleri G, Maggi G, Tappero GF, Orsi PG, Terreni N, Macor A, Di Napoli A, Rinaldi E, Ciccone G, Rizzetto M. A randomized 4-arm multicenter study of interferon alfa-2b plus ribavirin in the treatment of patients with chronic hepatitis C not responding to interferon alone. *Hepatology* 2001; **34**: 133-138

3 **Kronenberger B**, Ruster B, Elez R, Weber S, Piiper A, Lee JH, Roth WK, Zeuzem S. Interferon alfa down-regulates CD81 in patients with chronic hepatitis C. *Hepatology* 2001; **33**: 1518-1526

4 **Neddermann P**, Tomei L, Steinkuhler C, Gallinari P, Tramontano A, De Francesco R. The nonstructural proteins of the hepatitis C virus: structure and functions. *Biol Chem* 1997; **378**: 469-476

5 **Bartenschlager R**. The NS3/4A proteinase of the hepatitis C virus: unravelling structure and function of an unusual enzyme and a prime target for antiviral therapy. *J Viral Hepat* 1999; **6**: 165-181

6 **Lesk AM**, Fordham WD. Conservation and variability in the structures of serine proteinases of the chymotrypsin family. *J Mol Biol* 1996; **258**: 501-537

7 **Sakamuro D**, Furukawa T, Takegami T. Hepatitis C virus nonstructural protein NS3 transforms NIH 3T3 cells. *J Virol* 1995; **69**: 3893-3896

8 **Zemel R**, Gerechet S, Greif H, Bachmatove L, Birk Y, Golan-Goldhirsh A, Kunin M, Berdichevsky Y, Benhar I, Tur-Kaspa R. Cell transformation induced by hepatitis C virus NS3 serine protease. *J Viral Hepat* 2001; **8**: 96-102

9 **Fujita T**, Ishido S, Muramatsu S, Itoh M, Hotta H. Suppression of actinomycin D-induced apoptosis by the NS3 protein of hepatitis C virus. *Biochem Biophys Res Commun* 1996; **229**: 825-831

10 **Lin X,** Yuan ZH, Wu L, Ding JP, Wen YM. A single amino acid in the reverse transcriptase domain of hepatitis B virus affects virus replication efficiency. *J Virol* 2001; **75**: 11827-11833

11 **Berger J**, Hauber J, Hauber R, Geiger R, Cullen BR. Secreted placental alkaline phosphatase: a powerful new quantitative indicator of gene expression in eukaryotic cells. *Gene* 1988; **66**: 1-10

12 **Nakayama GR**, Caton MC, Nova MP, Parandoosh Z. Assessment of the Alamar Blue assay for cellular growth and viability *in vitro*. *J Immunol Methods* 1997; **204**: 205-208

13 **Kong WH**, Zheng G, Lu JN, Tso JK. Temperature dependent expression of cdc2 and cyclin B1 spermatogenic cells during spermatogenesis. *Cell Res* 2000; **10**: 289-302

14 **Du GX**, Hou LH, Guan RB, Tong YG, Wang HT. Establishment of a simple assay *in vitro* for hepatitis C virus NS3 serine protease based on recombinant substrate and single-chain protease. *World J Gastroenterol* 2002; **8**: 1088-1093

15 **Kolykhalov AA**, Agapov EV, Rice CM. Specificity of the hepatitis C virus NS3 serine protease: effects of substitutions at the 3/4A, 4A/4B, 4B/5A, and 5A/5B cleavage sites on polyprotein processing. *J Virol* 1994; **68**: 7525-7533

16 **Bartenschlager R**, Ahlborn-Laake L, Yasargil K, Mous J, Jacobsen H. Substrate determinants for cleavage in cis and in trans by the hepatitis C virus NS3 proteinase. *J Virol* 1995; **69**: 198-205

17 **Bianchi E**, Steinkuhler C, Taliani M, Urbani A, Francesco RD, Pessi A. Synthetic depsipeptide substrates for the assay of human hepatitis C virus protease. *Anal Biochem* 1996; **237**: 239-244

18 **Steinkuhler C**, Urbani A, Tomei L, Biasiol G, Sardana M, Bianchi E, Pessi A, De Francesco R. Activity of purified hepatitis C virus protease NS3 on peptide substrates. *J Virol* 1996; **70**: 6694-6700

19 **Pizzi E**, Tramontano A, Tomei L, La Monica N, Failla C, Sardana

M, Wood T, De Francesco R. Molecular model of the specificity pocket of the hepatitis C virus protease: Implications for substrate recognition. *Proc Natl Acad Sci U S A* 1994; **91**: 888-892

20 **Hahm B**, Back SH, Lee TG, Wimmer E, Jang SK. Generation of a novel poliovirus with a requirement of the hepatitis C virus protease NS3 activity. *Virology* 1996; **226**: 318-326

21 **Cho YG**, Moon HS, Sung YC. Construction of hepatitis C-SIN virus recombinants with replicative dependency on hepatitis C virus serine protease activity. *J Virol Methods* 1997; **65**: 201-207

22 **Cho YG,** Yang SH, Sung YC. *In vivo* assay for hepatitis C viral serine protease activity using a secreted protein. *J Virol Methods* 1998; **72**: 109-115

23 **Grakoui A**, McCourt DW, Wychowski C, Feinstone SM, Rice CM. Characterization of the hepatitis C virus-encoded serine proteinase: Determination of proteinase-dependent polyprotein cleavage sites. *J Virol* 1993; **67**: 2832-2843

24 **Komoda Y**, Hijikata M, Sato S, Asabe S, Kimura K, Shimotohno K. Substrate requirements of hepatitis C virus serine proteinase for intermolecular polypeptide cleavage in Echerichia coli. *J Virol* 1994; **68**: 7351-7357

25 **Heintges** T, Encke J, zu Putlitz J, Wands JR. Inhibition of hepatitis C virus NS3 function by antisense oligodeoxynucleotides and protease inhibitor. *J Med Virol* 2001; **65**: 671-680

26 **Harvey TJ**, Macnaughton TB, Gowans EJ. The development and characterisation of a SV40 T-antigen positive cell line of human hepatic origin. *J Virol Methods* 1997; **65**: 67-74

27 **Lohmann V**, Korner F, Koch J, Herian U, Theilmann L, Bartenschlager R. Replication of subgenomic hepatitis C virus RNAs in a hepatoma cell line. *Science* 1999; **285**: 110-113

28 **Blight KJ**, Kolykhalov AA, Rice CM. Efficient initiation of HCV RNA replication in cell culture. *Science* 2000; **290**: 1972-1974

29 **Guo JT**, Bichko VV, Seeger C. Effect of alpha interferon on the hepatitis C virus replicon. *J Virol* 2001; **75**: 8516-8523

30 **Dentan C**, Tselepis AD, Chapman MJ, Ninio E. Pefabloc, 4-[2-aminoethyl]benzenesulfonyl fluoride, is a new, potent nontoxic and irreversible inhibitor of PAF-degrading acetylhydrolase. *Biochim Biophys Acta* 1996; **1299**: 353-357

31 **Angelloz-Nicoud P**, Harel L, Binoux M. Recombinant human insulin-like growth factor (IGF) binding protein-3 stimulates prostate carcinoma cell proliferation via an IGF-dependent mechanism. Role of serine proteases. *Growth Regul* 1996; **6**: 130-136

32 **Hiramatsu N**, Ichikawa N, Fukada H, Fujita T, Sullivan CV, Hara A. Identification and characterization of proteases involved in specific proteolysis of vitellogenin and yolk proteins in salmonids. *J Exp Zool* 2002; **292**: 11-25

33 **Hahm B**, Han DS, Back SH, Song OK, Cho MJ, Kim CJ, Shimotohno K, Jang SK. NS3-4A of hepatitis C virus is a chymotrypsin-like protease. *J Virol* 1995; **69**: 2534-2539

Edited by Ma JY

P.O.Box 2345, Beijing 100023,China
Fax: +86-10-85381893
E-mail: wjg@wjgnet.com www.wjgnet.com

World J Gastroenterol 2003;9(11):2480-2483
World Journal of Gastroenterology
 ISSN 1007-9327

Oxymatrine therapy for chronic hepatitis B: A randomized double-blind and placebo-controlled multi-center trial

Lun-Gen Lu, Min-De Zeng, Yi-Min Mao, Ji-Qiang Li, Mo-Bin Wan, Cheng-Zhong Li, Cheng-Wei Chen, Qing-Chun Fu, Ji-Yao Wang, Wei-Min She, Xiong Cai, Jun Ye, Xia-Qiu Zhou, Hui Wang, Shan-Ming Wu, Mei-Fang Tang, Jin-Shui Zhu, Wei-Xiong Chen, Hui-Quan Zhang

Lun-Gen Lu, Min-De Zeng, Yi-Min Mao, Ji-Qiang Li, Shanghai Institute of Digestive Disease, Renji Hospital,Shanghai Second Medical University, Shanghai 200001, China
Mo-Bin Wan, Cheng-Zhong Li, Changhai Hospital, Second Military Medical University, Shanghai 200433, China
Cheng-Wei Chen, Qing-Chun Fu, Liver Disease Research Center, Nanjing Military Command, Shanghai 200233, China
Ji-Yao Wang, Wei-Min She, Zhongshan Hospital,Fudan University, Shanghai 200032, China
Xiong Cai, Changzheng Hospital, Second Military Medical University, Shanghai 200003, China
Jun Ye, Shanghai Putuo District Central Hospital, Shanghai 200062, China
Xia-Qiu Zhou, Hui Wang, Ruijin Hospital,Shanghai Second Medical University, Shanghai 200025, China
Shan-Ming Wu, Mei-Fang Tang, Shanghai General Hospital of Infectious Diseases, Shanghai 200083, China
Jin-Shui Zhu, Wei-Xiong Chen, Shanghai No.6 People' s Hospital, Shanghai 200230, China
Hui-Quan Zhang, Shanghai Shibei Hospital, Shanghai 200073, China
Supported by the Key Project of Shanghai Medical Development Foundation (NO: 99ZDI001) and grants from 1999 Foundation of Chinese Liver Diseases Association for Yong Scholars
Correspondence to: Lun-Gen Lu, MD, Shanghai Institute of Digestive Disease, Renji Hospital, Shanghai Second Medical University, Shanghai 200001, China. lulungen@online.sh.cn
Telephone: +86-21-33070834 **Fax:** +86-21-63364118
Received: 2003-05-13 **Accepted:** 2003-06-19

Abstract

AIM: To evaluate the efficacy and safety of capsule oxymatrine in the treatment of chronic hepatitis B.

METHODS: A randomised double-blind and placebo-controlled multicenter trial was conducted. Injection of oxymatrine was used as positive-control drug. A total of 216 patients with chronic hepatitis B entered the study for 24 weeks, of them 108 received capsule oxymatrine, 36 received injection of oxymatrine, and 72 received placebo. After and before the treatment, clinical symptoms, liver function, serum hepatitis B virus markers, and adverse drug reaction were observed.

RESULTS: Among the 216 patients, six were dropped off, and 11 inconsistent with the standard were excluded. Therefore, the efficacy and safety of oxymatrine in patients were analysed. In the capsule treated patients, 76.47 % became normal in ALT level, 38.61 % and 31.91 % became negative both in HBV DNA and in HBeAg. In the injection treated patients, 83.33 % became normal in ALT level, 43.33 % and 39.29 % became negative both in HBV DNA and in HBeAg. In the placebo treated patients, 40.00 % became normal in ALT level, 7.46 % and 6.45 % became negative both in HBV DNA and in HBeAg. The rates of complete response and partial response were 24.51 % and 57.84 % in the capsule treated patients, and 33.33 % and 50.00 % in the injection treated patients, and 2.99 % and 41.79 % in the placebo treated patients, respectively. There was no significance between the two groups of patients, but both were significantly higher than the placebo. The adverse drug reaction rates of the capsule, injection and placebo were 7.77 %, 6.67 % and 8.82 %, respectively. There was no statistically significant difference among them.

CONCLUSION: Oxymatrine is an effective and safe agent for the treatment of chronic hepatitis B.

Lu LG, Zeng MD, Mao YM, Li JQ, Wan MB, Li CZ, Chen CW, Fu QC, Wang JY, She WM, Cai X, Ye J, Zhou XQ, Wang H, Wu SM, Tang MF, Zhu JS, Chen WX, Zhang HQ. Oxymatrine therapy for chronic hepatitis B: A randomized double-blind and placebo-controlled multi- center trial. *World J Gastroenterol* 2003; 9 (11): 2480-2483

http://www.wjgnet.com/1007-9327/9/2480.asp

INTRODUCTION

Oxymatrine is a kind of alkaloid extracted from a Chinese herb *Sophora alopecuraides L.*[1]. Basic and clinical researches suggested that oxymatrine had the following pharmacological effects such as anti-virus, protecting hepatocytes, anti-hepatic fibrosis, immune regulation, etc[2-7]. In particular, wide attention was paid to its inhibitory effect on hepatitis B virus (HBV) in recent years. Oxymatrine has been proved to have distinct anti-virus effect in the treatment of chronic hepatitis B (CHB)[8-11]. But no information is available about the therapeutic efficacy and safety of oxymatrine capsule treated CHB. In this paper, we evaluated the therapeutic efficacy and safety of oxymatrine (kurorinone) capsule in the treatment of CHB based on a randomized multi-centre, double-blind and placebo-controlled clinical trial.

MATERIALS AND METHODS

Research design

This study was a clinical trial characterized by multi-centre, randomization, double blinding and placebo-control, which was fulfilled by Renji Hospital of Shanghai Second Medical University, Zhongshan Hospital of Fudan University, Changhai Hospital of Second Military Medical University.

Selection of subjects

Enrolled criteria: Age: 18-65 years old, regardless of sex, positiveness of serum HBsAg and HBV DNA for at least 6 months before enrolling, positiveness of serum HBeAg for at least 6 months before enrolling, abnormal serum value of alanine transaminase (ALT) twice or more with a value 1.2 times greater than normal upper limit and a duration more than 8 weeks between two tests within 6 months before enrolling, the serum

level of ALT was more than normal upper limit when screening, total serum bilirubin (TB) level less than or equal to 85.5 μmol/L, non-history of administrating antiviral and immunoregulating drugs, signing in the informed consent form, promising not to receive other drugs in clinical trial and systemic anti-viral agents, cytotoxic agents, hormone, immunoregulators, drugs capable of reducing serum enzyme activity and bilirubin level and Chinese traditional medicines, etc.

Exclusion criteria Patients with positive laboratory test of HIV, positiveness of serum anti-HCV and/or HCV RNA, uncompensable liver diseases, suggestive of autoimmune diseases with antinuclear antibody (ANA) titer greater than a 1:160 dilution, abnormality of serum creatinine with a value of 1.5 times greater than normal, concurrence of other associated severe diseases which might affect the present treatment, hypersensitive to oxymatrine capsule, women with pregnancy and during breast-feeding period.

Treatment procedures and drugs

A total of 216 selected patients were randomly divided into 3 groups: 108 in capsule oxymatrine group, 36 in injection oxymatrine group and 72 in placebo group. Both capsule oxymatrine and injection oxymatrine were provided by Ningxia Pharmaceutic Institute, Ningxia, China (Batch numbers 990426 and 990325, respectively). The magnitude, colour, shape and taste of the vacant placebo capsule were consistent with capsule oxymatrine. Capsule oxymatrine group: 300 mg oxymatrine capsules orally 3 times a day. Injection oxymatrine group: 400 mg intramuscularly once a day. Placebo group: 3 tablets, three times a day. Treatment course of the 3 groups was 24 weeks. After completion of selection and assessment, qualified subjects were allocated randomly into capsule oxymatrine group, injection oxymatrine group and placebo group for a treatment course of 24 weeks according to the treatment code based on stratified randomization.

Observing indexes and assessment

Clinical manifestations Weakness, pain in hepatic region, jaundice, hepatomegaly, splenomegaly, etc.

Liver function indexes Serum levels of total protein, albumin, ratio of albumin and globulin, ALT, aspartate aminotransferase (AST), γ-glutamyl transpeptidase (GGT), total bilirubin (TB), direct bilirubin (DB) and alkaline phosphatase (ALP).

Detection of serum markers of HBV HBV DNA was measured by dot blotting assay. HBsAg, anti-HBsAg, anti-HBc, HBeAg and anti-HBe were measured by Abbott kit before the treatment, 12 and 24 weeks after the treatment.

Analysis of blood and urine All parameters including electrolytes and renal function were measured before the treatment, 12 and 24 weeks after the treatment.

Assessment criteria of therapeutic effect and safety

Mainly evaluated indexes were negatively converting rate of serum HBV DNA and HbeAg, and the normalization rate of serum ALT. The assessment criteria of therapeutic effect were as follow. Complete response: negative conversion of HBeAg and HBV DNA, and normalization of serum ALT. Partial response: negative conversion of HBeAg and HBV DNA or normalization of serum ALT. Nonresponse: the effect didn' t reach the above criteria. Any abnormal clinical manifestations and laboratory tests occurred during the treatment were recorded and filled in a report form of side effects in time whether they were associated with drugs for trial or not.

Statistical analysis

Statistical analysis of the data was performed with SAS 6.12 software kit.

RESULTS

Number of subjects

A total of 216 patients were enrolled in the study, of them 108 in capsule oxymatrine group, 36 in injection oxymatrine group, and 72 in placebo control group. Twelve cases withdrew, and the withdrawal rate was 2.78 %. Eleven cases were excluded for not conforming selection criteria, and the excluding rate was 5.09 %. One hundred and ninety-nine cases entered statistical analysis of therapeutic effect included 102 cases in capsule oxymatrine group, 30 cases in injection oxymatrine group, and 67 cases in placebo control group.

General state of patients in three groups before treatment

Before treatment, the following data were similar among three groups (P>0.05, respectively), including sex, age, duration of hepatitis, abnormality of serum ALT and AST 2-fold higher than normal elevation, etc. There were no significant differences among three groups in symptoms and signs before treatment (P>0.05).

Negative conversion of serum virus markers

Negative conversion rate of serum HBsAg in capsule oxymatrine group, injection oxymatrine group and placebo group was 1.98 %, 3.33 %, and 0.00 %, respectively (Table 1). There were no obvious differences among 3 groups (P=0.269). The negative conversion rate of HBV DNA was 38.61 %, 43.33 % and 7.46 % respectively in the above groups. There were obvious differences between capsule oxymatrine group and placebo group or between injection oxymatrine group and placebo group (P=0.001), but there were no significant difference between capsule oxymatrine group and injection oxymatrine group (P=0.643). The negative conversion rate of serum HBeAg was 31.91 %, 39.29 % and 6.45 % respectively in the above groups. There was an obvious difference between capsule oxymatrine group and placebo group or between injection oxymatrine group and placebo group (P=0.001), but no significant difference between capsule oxymatrine group and injection oxymatrine group (P=0.469).

Normalization rate of serum ALT

The normalization rate of serum ALT in capsule oxymatrine group, injection oxymatrine group and placebo group was 76.47 %, 83.33 % and 40.00 %, respectively. There was an obvious difference between capsule oxymatrine group and placebo group or between injection oxymatrine group and placebo group (P=0.001, Table 2), but no significant difference between capsule oxymatrine group and injection oxymatrine group (P=0.425).

Comparison of therapeutic effect among 3 groups of chronic hepatitis B

The complete and partial response rates were 24.51 % and 57.84 % in capsule oxymatrine group, 33.33 % and 50.00 % in injection oxymatrine group, 2.99 % and 41.79 % in placebo group. There was an with obvious difference between capsule oxymatrine group and placebo group or between injection oxymatrine group and placebo group (P=0.001, Table 3), but no significant difference between capsule oxymatrine group and injection oxymatrine group (P=0.4589).

Adverse effects

In this study, 8 patients had adverse effects in capsule oxymatrine group with an incidence of 7.77 %, 2 patients in injection oxymatrine group with an incidence of 6.67 %, and 6 patients in placebo group with an incidence of 8.82 %. The difference among 3 groups had no statistical significance

Table 1 Negative conversion rates of serum HBsAg and comparison among capsule oxymatrine group, injection oxymatrine group and placebo group

Index	Group	Positive number	Number of negative conversion	Negative conversion rate (%)	Comparison among 3 groups	
					χ^2	*P* value
HBsAg	Capsule	101	2	1.98		
	Injection	30	1	3.33		0.269
	Placebo	67	0	0.00		
HBV DNA	Capsule	101	39	38.61		
	Injection	30	13	43.33	22.716	0.001
	Placebo	67	5	7.46		
HBeAg	Capsule	94	30	31.91		
	Injection	28	11	39.29	17.042	0.001
	Placebo	62	4	6.45		

The comparison of negative conversion rates of serum HBsAg, HBV DNA and HBeAg was performed with chi-square test, statistic was χ^2.

Table 2 Normalization rate of serum ALT and comparison among capsule oxymatrine group, injection oxymatrine group and placebo group

Group	Number of ALT abnormality before treatment	Number of ALT normalization after treatment	Normalization rate (%)	Comparison among 3 groups	
				χ^2	*P* value
Capsule	102	78	76.47		
Injection	30	25	83.33	28.352	0.001
Placebo	65	26	40.00		

The comparison of ALT normalization rate was performed with chi-square test, statistic was χ^2.

Table 3 Comparison of therapeutic effect among 3 groups with chronic hepatitis B

Group	Complete response	Partial response	Non-response	Comparison among 3 groups	
				χ^2	*P* value
Capusle (*n*=102)	25 (24.51 %)	59 (57.84 %)	18 (17.65 %)		
Injection (*n*=30)	10 (33.33 %)	15 (50.00 %)	5 (16.67 %)	35.957	0.0001
Placebo (*n*=67)	2 (2.99 %)	28 (41.79 %)	37(55.22 %)		

The comparison of therapeutic effect among 3 groups was performed with K-W test, statistic was χ^2.

(*P*=0.931). The adverse effects were mild or moderate and mainly manifested as symptoms of upper alimentary tract, rash, bad taste. No severe adverse effect occurred. The statistical analysis of adverse effects included 2 cases withdrawn because of side effects.

DISCUSSION

Hepatitis B virus is a DNA virus that produces both acute and chronic infections of the liver in humans. It has been estimated that over 300 million people worldwide are chronically infected with HBV and that over 250 000 people would die each year due to HBV-associated complications of cirrhosis and primary hepatocellular carcinoma[12-18]. For many years, alpha interferon has been the only approved therapy for chronic HBV infection in most countries. Interferon was effective in 30-40 % of patients, and it must be given by injection and was frequently associated with fever and influenza-like symptoms[19-23]. Recently, lamivudine was approved for the treatment of chronic HBV infection in many regions of the world. Although convenient and well-tolerated, lamivudine' s efficacy rate was similar to interferon and prolonged administration of lamivudine was associated with development of resistance[24-30]. New agents, such as adefovir dipivoxil, offered a promise either alone or in combination with lamivudine in the treatment of individuals who were ' treatment naï ve' have developed lamivudine resistance[31-33]. Up to date, no specific therapy is available for chronic hepatitis B. The following factors may be associated with its pathogenesis such as virulence of HBV strains, number of infected hepatocytes and host immune response, antiviral agents, immunomodulators and drugs might be capable of improving liver function[12-15,34-41].

Traditional Chinese medicine has been widely used for the treatment of liver disease in China[11]. Oxymatrine extracted from *Sophora alopecuraides L.* has been shown to have a remarkable HBV suppressing effect with 40 % serum conversion rate for HBeAg and HBV DNA, similar to that of alpha interferon[8,9,11]. Experiment *in vitro* indicated that oxymatrine had an inhibitory role in the secretion of HBsAg and HBeAg by 2.2.15 cell line transfected with HBV DNA and the inhibitory rates increased gradually following increased oxymatrine concentration and the extension of effect time within a definite range[42]. *In vivo* study of HBV transgenic mouse showed that when mice were injected intraperitoneally oxymatrine at 100 mg/kg, 200 mg/kg and 300 mg/kg once a day for 30 days, the quantity of HBsAg and HBeAg in the liver decreased obviously compared with control group, and there was no significant difference among 3 doses[10]. Clinical research suggested that the normalization rates of serum ALT and TB, and the negative conversion rates of serum HBsAg and HBV DNA were similar to alpha interferon when oxymatrine was applied to treatment of chronic hepatitis B. The results in

present study were similar to the therapeutic effect of interferon in the treatment of chronic hepatitis B at home and abroad[9,11,17,43], indicating that capsule oxymatrine is an effective and safe agent for treatment of chronic hepatitis B.

REFERENCES

1 **Lai JP**, He XW, Jiang Y, Chen F. Preparative separation and determination of matrine from the Chinese medicinal plant Sophora flavescens Ait by molecularly imprinted solid-phase extraction. *Anal Bioanal Chem* 2003; **375**: 264-269
2 **Liu J**, Manheimer E, Tsutani K, Gluud C. Medicinal herbs for hepatitis C virus infection: a Cochrane hepatobiliary systematic review of randomized trials. *Am J Gastroenterol* 2003; **98**: 538-544
3 **Dong Y**, Xi H, Yu Y, Wang Q, Jiang K, Li L. Effects of oxymatrine on the serum levels of T helper cell 1 and 2 cytokines and the expression of the S gene in hepatitis B virus S gene transgenic mice: a study on the anti-hepatitis B virus mechanism of oxymatrine. *J Gastroenterol Hepatol* 2002; **17**: 1299-1306
4 **Xiang X**, Wang G, Cai X, Li Y. Effect of oxymatrine on murine fulminant hepatitis and hepatocyte apoptosis. *Chin Med J* 2002; **115**: 593-596
5 **Yang W**, Zeng M, Fan Z, Mao Y, Song Y, Jia Y, Lu L, Chen CW, Peng YS, Zhu HY. Prophylactic and therapeutic effect of oxymatrine on D-galactosamine-induced rat liver fibrosis. *Zhonghua Ganzangbing Zazhi* 2002; **10**: 193-196
6 **Chen Y**, Li J, Zeng M, Lu L, Qu D, Mao Y, Fan Z, Hua J. The inhibitory effect of oxymatrine on hepatitis C virus *in vitro*. *Zhonghua Ganzangbing Zazhi* 2001; **9**(Suppl):12-14
7 **Li J**, Li C, Zeng M. Preliminary study on therapeutic effect of oxymatrine in treating patients with chronic hepatitis C. *Zhongguo Zhongxiyi Jiehe Zazhi* 1998; **18**: 227-229
8 **Chen YX**, Mao BY, Jiang JH. Relationship between serum load of HBV-DNA and therapeutic effect of oxymatrine in patients with chronic hepatitis B. *Zhongguo Zhongxiyi Jiehe Zazhi* 2002; **22**: 335-336
9 **Yu YY**, Wang QH, Zhu LM, Zhang QB, Xu DZ, Guo YB, Wang CQ, Guo SH, Zhou XQ, Zhang LX. A clinical research on oxymatrine for the treatment of chronic hepatitis B. *Zhonghua Ganzangbing Zazhi* 2002; **10**: 280-281
10 **Chen XS**, Wang GJ, Cai X, Yu HY, Hu YP. Inhibition of hepatitis B virus by oxymatrine *in vivo*. *World J Gastroenterol* 2001; **7**: 49-52
11 **Wang BE**. Treatment of chronic liver diseases with traditional Chinese medicine. *J Gastroenterol Hepatol* 2000; **15**(Suppl): E67-70
12 **Lok AS**, Heathcote EJ, Hoofnagle JH. Management of hepatitis B: 2000-summary of a workshop. *Gastroenterology* 2001; **120**: 1828-1853
13 **Gow PJ**, Mutimer D. Treatment of chronic hepatitis. *BMJ* 2001; **323**: 1164-1167
14 **Arguedas MR**, Fallon MB. Prevention in liver disease. *Am J Med Sci* 2001; **321**: 145-151
15 **Maddrey WC**. Update in hepatology. *Ann Intern Med* 2001; **134**: 216-223
16 **Ryder SD**, Beckingham IJ. ABC of diseases of liver, pancreas, and biliary system: Chronic viral hepatitis. *BMJ* 2001; **322**: 219-221
17 **Pramoolsinsup C**. Management of viral hepatitis B. *J Gastroenterol Hepatol* 2002; **17**(Suppl): S125-145
18 **Yuen MF**, Lai CL. Treatment of chronic hepatitis B. *Lancet Infect Dis* 2001; **1**: 232-241
19 **Feld J**, Locarnini S. Antiviral therapy for hepatitis B virus infections: new targets and technical challenges. *J Clin Virol* 2002; **25**: 267-283
20 **Rivkina A**, Rybalov S. Chronic hepatitis B: current and future treatment options. *Pharmacotherapy* 2002; **22**: 721-737
21 **Wai CT**, Lok AS. Treatment of hepatitis B. *J Gastroenterol* 2002; **37**: 771-778
22 **Schalm S**, De Man R, Janssen H. Combination and newer therapies for chronic hepatitis B. *J Gastroenterol Hepatol* 2002; **17** (Suppl 3): S338-S341
23 **Karayiannis P**. Hepatitis B virus: old, new and future approaches to antiviral treatment. *J Antimicrob Chemother* 2003; **51**: 761-785
24 **Marcellin P**. Advances in therapy for chronic hepatitis B. *Semin Liver Dis* 2002; **22**(Suppl 1): 33-36
25 **Zoulim F**. Assessing hepatitis B virus resistance *in vitro* and molecular mechanisms of nucleoside resistance. *Semin Liver Dis* 2002; **22**(Suppl 1): 23-31
26 **Papatheodoridis GV**, Dimou E, Papadimitropoulos V. Nucleoside analogues for chronic hepatitis B: antiviral efficacy and viral resistance. *Am J Gastroenterol* 2002; **97**: 1618-1628
27 **Bozdayi AM**, Uzunalimoglu O, Turkyilmaz AR, Aslan N, Sezgin O, Sahin T, Bozdayi G, Cinar K, Pai SB, Pai R, Bozkaya H, Karayalcin S, Yurdaydin C, Schinazi RF. YSDD: a novel mutation in HBV DNA polymerase confers clinical resistance to lamivudine. *J Viral Hepat* 2003; **10**: 256-265
28 **Torresi J**, Locarnini S. Antiviral chemotherapy for the treatment of hepatitis B virus infections. *Gastroenterology* 2000; **118**(2 Suppl 1): S83-103
29 **Doo E**, Liang TJ. Molecular anatomy and pathophysiologic implications of drug resistance in hepatitis B virus infection. *Gastroenterology* 2001; **120**: 1000-1008
30 **Zollner B**, Petersen J, Schroter M, Laufs R, Schoder V, Feucht HH. 20-fold increase in risk of lamivudine resistance in hepatitis B virus subtype adw. *Lancet* 2001; **357**: 934-935
31 **Pessoa MG**, Wright TL. Update on clinical trials in the treatment of hepatitis B. *J Gastroenterol Hepatol* 1999; **14**(Suppl): S6-11
32 **Galan MV**, Boyce D, Gordon SC. Current pharmacotherapy for hepatitis B infection. *Expert Opin Pharmacother* 2001; **2**: 1289-1298
33 **Marcellin P**, Chang TT, Lim SG, Tong MJ, Sievert W, Shiffman ML, Jeffers L, Goodman Z, Wulfsohn MS, Xiong S, Fry J, Brosgart CL. Adefovir dipivoxil for the treatment of hepatitis B e antigen-positive chronic hepatitis B. *N Engl J Med* 2003; **348**: 808-816
34 **Rich JD**, Ching CG, Lally MA, Gaitanis MM, Schwartzapfel B, Charuvastra A, Beckwith CG, Flanigan TP. A review of the case for hepatitis B vaccination of high-risk adults. *Am J Med* 2003; **114**: 316-318
35 **Shaw T**, Bowden S, Locarnini S. Chemotherapy for hepatitis B: new treatment options necessitate reappraisal of traditional endpoints. *Gastroenterology* 2002; **123**: 2135-2140
36 **Yao N**, Hong Z, Lau JY. Application of structural biology tools in the study of viral hepatitis and the design of antiviral therapy. *Gastroenterology* 2002; **123**: 1350-1363
37 **Chin R**, Locarnini S. Treatment of chronic hepatitis B: current challenges and future directions. *Rev Med Virol* 2003; **13**: 255-272
38 **Liaw YF**. Therapy of chronic hepatitis B: current challenges and opportunities. *J Viral Hepat* 2002; **9**: 393-399
39 **Lau GK**, Carman WF, Locarnini SA, Okuda K, Lu ZM, Williams R, Lam SK. Treatment of chronic hepatitis B virus infection: an Asia-Pacific perspective. *J Gastroenterol Hepatol* 1999; **14**: 3-12
40 **Farrell GC**. Clinical potential of emerging new agents in hepatitis B. *Drugs* 2000; **60**: 701-710
41 **Zoulim F**, Trepo C. New antiviral agents for the therapy of chronic hepatitis B virus infection. *Intervirology* 1999; **42**: 125-144
42 **Zeng Z**, Wang GJ, Si CW. Basic and clinical study of oxymatrime on HBV infection. *J Gastroenterol Hepatol* 1999; **14**(Suppl): A295-297
43 **Chen C**, Guo SM, Liu B. A randomized controlled trial of kurorinone versus interferon-alpha2a treatment in patients with chronic hepatitis B. *J Viral Hepat* 2000; **7**: 225-229

Edited by Zhang JZ and Wang XL

P.O.Box 2345, Beijing 100023,China
Fax: +86-10-85381893
E-mail: wjg@wjgnet.com www.wjgnet.com

World J Gastroenterol 2003;9(11):2484-2489
World Journal of Gastroenterology
 ISSN 1007-9327

• VIRAL HEPATITIS •

Liver fibrosis in chronic viral hepatitis: An ultrasonographic study

Rong-Qin Zheng, Qing-Hui Wang, Ming-De Lu, Shi-Bin Xie, Jie Ren, Zhong-Zhen Su, Yin-Ke Cai, Ji-Lu Yao

Rong-Qin Zheng, Qing-Hui Wang, Jie Ren, Department of Ultrasound, Third Affiliated Hospital, Sun Yat-Sen University, Guangzhou 510630, Guangdong Province, China
Ming-De Lu, Department of Ultrasound, First Affiliated Hospital, Sun Yat-Sen University, Guangzhou 510089, Guangdong Province, China
Shi-Bin Xie, Jie Ren, Zhong-Zhen Su, Yin-Ke Cai, Ji-Lu Yao, Department of Infectious Diseases, Third Affiliated Hospital, Sun Yat-Sen University, Guangzhou 510630, Guangdong Province, China
Supported by the Medical Science Foundation of Guangdong Province, No. A1999198
Correspondence to: Rong-Qin Zheng, Ph.D., Department of Ultrasound, Third Affiliated Hospital, Sun Yat-Sen University, Guangzhou 510630, Guangdong Province, China. zhengrongqin@hotmail.com
Telephone: +86-20-85516867-3030 **Fax:** +86-20-87536401
Received: 2002-08-03 **Accepted:** 2002-08-31

Abstract

AIM: To select valuable ultrasonographic predictors for the evaluation of hepatic inflammation and fibrosis degree in chronic hepatitis, and to study the value of ultrasonography in the evaluation of liver fibrosis and compensated liver cirrhosis in comparison with serology and histology.

METHODS: Forty-four ultrasonographic variables were analyzed and screened using color Doppler ultrasound system in 225 patients with chronic viral hepatitis and compensated liver cirrhosis. The valuable ultrasonographic predictors were selected on the basis of a comparison with histopathological findings. The value of ultrasonography and serology in the evaluation of liver fibrosis degree and the diagnosis of compensated liver cirrhosis was also studied and compared. Meanwhile, the influencing factors on ultrasonographic diagnosis of compensated liver cirrhosis were also analyzed.

RESULTS: By statistical analysis, the maximum velocity of portal vein and the degree of gall-bladder wall smoothness were selected as the valuable predictors for the inflammation grade (G), while liver surface, hepatic parenchymal echo pattern, and the wall thickness of gall-bladder were selected as the valuable predictors for the fibrosis stage (S). Three S-related independent ultrasonographyic predictors and three routine serum fibrosis markers (HA, HPCIII and CIV) were used to discriminate variables for the comparison of ultrasonography with serology. The diagnostic accuracy of ultrasonography in moderate fibrosis was higher than that of serology ($P<0.01$), while there were no significant differences in the general diagnostic accuracy of fibrosis as well as between mild and severe fibrosis ($P<0.05$). There were no significant differences between ultrasonography and serology in the diagnosis of compensated liver cirrhosis. However, the diagnostic accuracy of ultrasonography was higher in inactive liver cirrhosis and lower in active cirrhosis than that of serology (both $P<0.05$). False positive and false negative results where found when the diagnosis of compensated liver cirrhosis was made by ultrasonography.

CONCLUSION: There are different ultrasonographic predictors for the evaluation of hepatic inflammation grade and fibrosis stage of chronic hepatitis. Both ultrasonography and serology have their own advantages and disadvantages in the evaluation of liver fibrosis and compensated liver cirrhosis. Combined application of the two methods is hopeful to improve the diagnostic accuracy.

Zheng RQ, Wang QH, Lu MD, Xie SB, Ren J, Su ZZ, Cai YK, Yao JL. Liver fibrosis in chronic viral hepatitis: An ultrasonographic study. *World J Gastroenterol* 2003; 9(11): 2484-2489
http://www.wjgnet.com/1007-9327/9/2484.asp

INTRODUCTION

Viral hepatitis is one of the most common and prevalent infectious diseases in China. It was found that 25-40 % of the patients with chronic viral hepatitis would become liver cirrhosis or even hepatocellular carcinoma[1,2]. Prompt and effective treatment could postpone or interrupt the development of chronic hepatitis into liver cirrhosis. Accurate estimation of the disease severity is helpful for the evaluation of the therapeutic effect and the prognosis of the disease. At present, there are three ways for this purpose, namely histology, serology and imaging. Liver histological diagnosis based on needle biopsy is the gold standard to evaluate the degree of hepatic inflammation and fibrosis. However, liver biopsy can not be performed routinely at clinical settings becouse of its invasiveness. In addition, it is well known that liver parenchymal damage in chronic hepatitis and cirrhosis is not uniform. Sample errors were commonly encountered[3-5]. Serological examination is a non-invasive routine method. However, serological markers of fibrosis with high specificity have not been available yet in addition to the lack of organ specificity of these markers[6-8]. Imging technologies such as ultrasonography, computed tomography, magnetic resonance imaging could provide useful information on the morphological changes of the liver, and are important in the evaluation of chronic liver diseases[9-15]. Among them, ultrasonography has become the most common and valuable method because of its low cost, easy performance and high acceptability by the patient. It could provide not only valuable information on the morphological changes of the liver but also liver hemodynamics by color Doppler flow imaging[16-19].

It was reported that evaluating liver morphology and hemodynamics in patients with cirrhosis and portal hypertension had an important value for the estimation of the disease severity and prognosis[17-21]. As the disease progresses from chronic hepatitis to cirrhosis, a variety of intra- and extrahepatic abnormalities would occur. Using multiple ultrasonographic variables to evaluate morphological and hemodynamic changes of the liver, gallbladder and the spleen could be expected to reveal these abnormalites and improve the diagnostic ability of ultrasound[15,22,23].

In this study, 44 ultrasonographyic variables were analyzed and screened using color Doppler ultrasoud system in 225 patients with chronic viral hepatitis and compensated liver cirrhosis. The results were compared with histological findings based on the assessment criteria of the imflammation grade and fibrosis stage for chronic hepatitis, which were proposed

by the academic meeting of Chinese Medical Association on epidemic and parasitosis in 1995 (95-Protocol)[24]. The valuable predictors were selected by statistical analysis. The value of ultrasonography in the evaluation of fibrosis and compensated liver cirrhosis was investigated and compared with serology.

MATERIALS AND METHODS

Patients selected

Two hundred and twenty-five patients with chronic viral hepatitis and compensated liver cirrhosis were treated in our hospital from 1996 to 1999. Among them, 199 were males and 26 were females, their average age was 30.5 years (range from 10 to 57 years). The pathogenic diagnoses were: hepatitis B in 208 patients, hepatitis C in 10 patients, coinfection of hepatitis B and C in 3 patients, coinfection of hepatitis B and E in 2 patients, hepatitis B plus A and hepatitis B plus D in 1 patient, respectively. Clinical diagnoses were mild chronic hepatitis in 78 patients, moderate chronic hepatitis in 114 patients, severe chronic hepatitis in 12 patients, and cirrhosis in 21 patients. No clinical manifestations of decompensated liver cirrhosis were found in all the patients.

Fifty-one healthy volunteers were examined as a control group. There were 26 males and 25 females, their average age was 27.8 years (range from 18 to 76 years). Serological and biochemical tests were normal.

Ultrasonographic examination

Using Esaote AU4 color Doppler system with 3.5-5.0 MHz curved probe, ultrasonographic examination was performed for the patients fasted for about 8 hours 12-24 hours after liver biopsy. First, sonographic findings of the liver, spleen and gallbladder, such as size, form, surface, internal echo, and diameter of vessels were observed and measured. Second, blood flow parameters of the hepatic and splenic vessels were measured by color Doppler flow imaging with the patient holding his/her breath at the end of a quiet breathing. Sample volume was adjusted slightly smaller than the diameter of vessels, and the sample angle was less than 60 degrees. Doppler spectrum with 3-5 stable heart cycles was selected for the measurement, which was performed at least two times and the average value was used.

Forty-four ultrasonographyic variables were analyzed, including the largest oblige diameter (RL_{OD}) and anterior-posterior diameter (RL_{AP}) of the right liver lobe, longitudinal diameter and anterior-posterior diameter of the left liver lobe (LL_L, LL_{AP}), the caudate liver lobe (CL_L, CL_{AP}), the ratio of CL_L/LL_L, transverse diameter (SP_T) and longitudinal diameter (SP_L) of the spleen, liver surface (L_{sur}) and hepatic parenchymal echo pattern (L_E), size (GB_{siz}) and wall thickness (GB_T) of the gall-bladder, degree of gall-bladder wall smoothness (GB_{sm}), complication of gall-bladder stone (GB_{st}) and gall-bladder pulypus (GB_P), umbilical vein patent (U); diameter of the main portal vein trunk (PV_D), right portal vein (RPV_D) and left portal vein (LPV_D); maximum and mean blood flow velocity of the main portal vein trunk (PV_{max},PV_{mea}), right portal vein (RPV_D, RPV_{max}) and left portal vein (LPV_{max}, LPV_{mea}), blood flow volume of the main portal vein trunk (PV_F), right portal vein (RPV_F) and left portal vein (LPV_F); congestive index of the portal vein (CI); diameter (HV_D) and Doppler waveform (HV_W) of the hepatic vein; diameter (HA_D), peak systolic blood flow velocity (HA_S), blood flow volume (HA_F) and resistant index (HARI) of the hepatic artery; diameter (SPA_D), peak systolic blood flow velocity (SPA_S), blood flow volume (SPA_F), and resistant index (SPARI) of the splenic artery; diameter (SPV_D) and maximum blood flow velocity (SPV_{max}) of the splenic vein, and the ratio of SPV_F/PV_F.

The measurements and evaluation of the parameters referred to the methods described in the literature[1,4-6]. Liver surface and the degree of gall-bladder wall smoothness were classified into 3 grades, namely smooth, less smooth and rough. Hepatic parenchymal echo patterns were classified into 5 grades according to the distribution and echogenicity of the parenchymal echo texture as the renal parenchymal echo was used as the contrast.

Examination of serum fibrosis markers

One hundred and ninety-seven cases underwent ultrasonographic and serologic examinations successively. Among them, 48 had compensated cirrhosis, and the rest had chronic hepatitis. The serum fibrosis markers including hyalurionic acid (HA), human procollagen III(HPCIII) and collagen type IV(CIV) were tested using radioimmunological method. The normal ranges were HA(57±27 ng/L), HPCIII($\leqslant$120 μg/L)and CIV (38.22±11.88 μg/L)

Histological study

All the patients underwent liver biopsy. The tissue sections were stained with HE and reticular fibers respectively. Histological study was performed according to the 95-Protocol[24], in which inflammation grade (G) and fibrosis stage (S) were classified from G1 to G4, and S0 to S4, respectively, based on the various degrees of inflammation or fibrosis. Furthermore, G1-2, G3 and G4 were defined as mild, moderate and severe inflammation, respectively, while S0-2, S3 and S4 were defined as mild, moderate and severe fibrosis, respectively. S4 also meant early or definite cirrhosis.

Quantitative assessment of liver fibrosis

Quantitative assessment of liver fibrosis was performed in 107 liver specimens with reticular fiber stain using an imagine analysis system (KONTRON IBAS2.5, German). The images were amplified by 400 times. Fibrosis degree was expressed as the ratio of fibrous area to the section area. Three to five fields of vision were selected randomly at the peripheral and center of the section for the average value of the ratio.

Statistical analysis

SPSS 9.0 software was used for this study. Numerical variables were described as mean ±standard deviation. For the comparison of means in different groups, univariate analysis and Student-Newman-Keuls test were used. While for the categorical variables, non-parameter analysis and χ^2 test were used for the comparison. A P value less than 0.05 was considered statistically significant. Spearman' s rank correlation coefficient was used for the correlation analysis. As for the selection of useful variables from categorical and numerical data, stepwise discriminant analysis and multiple linear regression analysis were used, respectively.

RESULTS

Screening for valuable ultrasonographic predictors

Histological diagnosis of the case group is shown in Table 1.

Table 1 Histological results in case group

Inflammation grade (G)	No. subjects	Fibrosis stage (S)	No. subjects
0	0	0	7
1	31	1	54
2	85	2	66
3	85	3	52
4	24	4	46
Total	225		225

According to univariate analysis, there were 21 variables with significant difference (P<0.05) among groups classified by the inflammation grade. While there were 19 variables with significant difference (P<0.05) among groups classified by the fibrosis stage (Tables 2 and 3). When stepwise correlation analysis was used, 20 variables were correlated with G (P<0.01), and 18 variables were correlated with S (P<0.01).

Table 2 Univariate analysis of quantitative variables

Variables	Grouped by G		Grouped by S	
	F value	*P* value	F value	*P* value
PV_{max}	29.17	<0 .001	19.38	<0.001
GB_T	24.03	<0.001	14.60	<0.001
PV_D	20.43	<0.001	18.07	<0.001
PV_{mea}	18.69	<0.001	11.28	<0.001
HV_D	16.88	<0.001	20.21	<0.001
RPV_{max}	14.24	<0.001	7.18	<0.001
SP_L	11.57	<0.001	14.87	<0.001
SPV_D	9.47	<0.001	12.76	<0.001
SP_T	9.28	<0.001	11.18	<0.001
CI	5.22	<0.01	3.96	<0.01
RPV_D	5.30	<0.01	3.43	<0.01
LL_L	2.99	<0.05	3.41	<0.05
SPV_F	2.72	<0.05	4.97	<0.01
SPA_D	4.20	<0.01	2.29	>0.05

Table 3 Non-parametric analysis of categorical variables

Variables	Grouped by G		Grouped by S	
	χ^2 value	*P* value	χ^2 value	*P* value
L_E	50.17	<0.001	91.34	<0.001
GB_{siz}	22.18	<0.001	21.00	<0.001
HV_W	22.14	<0.001	33.34	<0.001
GB_{sm}	20.07	<0.001	78.99	<0.001
L_{sur}	18.31	<0.001	66.92	<0.001
U	13.66	<0.01	32.07	<0.001
GB_{st}	8.45	<0.05	6.06	>0.05

The correlation coefficient between the quantitative analysis results of liver fibrosis and S was 0.76 (P<0.001). The correlation coefficient between G and S was 0.75 (P<0.001).

Twenty-two ultrasonographic variables associated with G and 19 variables associated with S were selected on the basis of univariate and correlation analysis results (Table 4), and used as the preliminary valuable variables for further analysis. When compared between case group and control group, there were significant differences in these selected variables (P<0.05).

Table 4 Ultrasonographic variables with significant correlation with G and S

	Ultrasonographic variables
Associated with G (22 items)	GB_{sm}, PV_{max}, GB_T, L_E, PV_D, HV_D, PV_{mea}, RPV_{max}, SP_L, SP_T, SPV_D, HV_W, GB_{siz}, L_{sur}, CI, RPV_D, RPV_{mea}, U, LL_L, GB_{st}, SPV_F and SPA_D
Associated with S (19 items)	GB_T, $L_{E,,}$, GB_{sm}, PV_D, PV_{max}, L_{sur}, HV_D, PV_{mea}, RPV_{max}, SP_L, SP_T, SPV_D, HV_W, GB_{siz}, CI, U, LL_L, SPV_F and RPV_D

Stepwise discriminant analysis was used for further selection of valuable predictors. GB_{sm}, PV_{max} were finally selected as independent predictors which were significantly correlated to G, while the independent predictors of L_E, GB_T and L_{sur} were significantly correlated to S.

Comparison of ultrasonography and serology in evaluation of fibrosis degree and diagnosis of compensated cirrhosis

Evaluation of fibrosis degree Liver fibrosis was divided into mild, moderate and severe fibrosis on the basis of fibrosis stage according to the 95-Protocol. The case distribution was mild fibrosis in 127 patients, moderate fibrosis in 52 patients, and severe fibrosis in 46 patients.

Three independent ultrasonographyic predictors associated with S (L_E, GB_T, L_{sur}) and three serum fibrosis markers (HA, HPCIII and CIV) were taken as discriminating variables for the comparison.

The correlation coefficients of L_E, GB_T and L_{sur} were 0.63, 0.58 and 0.5, respectively (P<0.001). While the correlation coefficients of HA, HPCIII and CIV were 0.60, 0.46 and 0.50, respectively (P<0.001).

The comparison between ultrasonographic variables and serologic fibrosis markers for the evaluation of fibrosis degree is shown in Table 5.

Table 5 Diagnostic accuracy of ultrasonography and serology for the evaluation of fibrosis degrees (%)

	Mild fibrosis	Moderate fibrosis	Severe fibrosis
Serology	79.5	19.1[b]	66.7
Ultrasonography	74.5	46.8[b]	62.5

[b]P<0.01 serology *vs* ultrasonography.

The diagnostic accuracy of ultrasonography and serology was higher in mild liver fibrosis than in severe and moderate liver fibrosis. There were no significant differences between ultrasonography and serology in the general diagnostic accuracy of fibrosis and diagnostic accuracy of mild and severe fibrosis (P>0.05). However, the diagnostic accuracy of ultrasonography in moderate fibrosis was higher than that of serology (P<0.01).

Diagnosis of compensated cirrhosis

Among the 48 patients with compensated cirrhosis, 46 patients had hepatitis-related cirrhosis, and 2 patients had cholestatic cirrhosis. The fibrosis stage of all these patients was S4. All of them had no symptoms of decompensated cirrhosis.

The diagnostic accuracy of ultrasonography for compensated cirrhosis was 80.7 %, while that of serology was 79.7 %. There was no significant difference between them. However, ultrasonography had a lower sensitivity (62.5 % *vs* 72.9 %) and a higher specificity (86.6 % *vs* 81.9 %) compared with serology (P<0.05).

According to the 95-Protocol, it would be regarded as active cirrhosis when G>2 and S=4, while it was regarded as inactive cirrhosis when G⩽2 and S=4. In our patient group, there were 41 patients with active cirrhosis and 7 patients with inactive cirrhosis. Among the 7 patients with inactive cirrhosis, the clinical diagnoses were mild chronic hepatitis in 3 patients, moderate chronic hepatitis in 2 patients, and liver cirrhosis in 2 patients.

For the evaluation of inactive liver cirrhosis, the diagnostic accuracy of ultrasonography was higher than that of serology (100 % *vs* 42.9 %, P<0.05). However, the diagnostic accuracy of ultrasonography was lower than that of serology in active cirrhosis (56.1 % *vs* 78.0 %, P<0.05).

Ultrasonographic, histological and clinical figures of compensated cirrhosis with false positive and false negative results on ultrasonography

False negative results of cirrhosis on ultrasonography Eighteen patients who were predicted as mild or moderate

fibrosis by ultrasonography were finally diagnosed as cirrhosis by histology. Among them, 9 patients were diagnosed as moderate chronic hepatitis, 5 patients as severe chronic hepatitis and 4 patients as liver cirrhosis according to their clinical manifestations.

The ultrasonographic features were coarse and homogenous hepatic parenchymal echo patterns (Figure 1). All of these patients had active liver cirrhosis with fine and sparse fibrotic septa (Figure 2) or small and uniform pseudolobular nodules on histology. Serologic tests showed that liver dysfunction was evident. The serum level of fibrosis markers in these patients increased obviously (HA: 408.06±219.26, HPC3: 217.78±84.96, and IVC: 210.28±181.88).

Figure 1 Active cirrhosis. Ultrasonography showed that the hepatic parenchymal echo became coarse and dot-shaped, and the distribution was still homogenous.

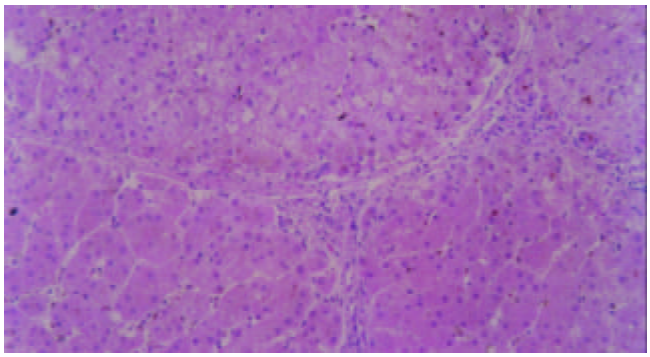

Figure 2 Active cirrhosis. Small and sparse fibroitc septa were shown on histology. (HE stain ×100).

Figure 3 Chronic viral hepatitis. On ultrasonography, the hepatic parenchymal echo became coarse and heterogeneous with speckled hyper- and hypoechoic areas.

False positive results of cirrhosis on ultrasonography

Twenty patients who were predicted as liver cirrhosis by ultrsonography were finally diagnosed as mild (n=6) and moderate (n=14) fibrosis by histology. Among them, 3 patients were diagnosed as mild chronic hepatitis, 12 patients as moderate chronic hepatitis, 1 patient as severe chronic hepatitis and 4 patients as liver cirrhosis according to their clinical manifestations.

The ultrasonographic and histological features were as follows. Hepatic parenchymal echo patterns became coarse and heterogeneous with speckled hyper- and hypoechoic areas (Figure 3), the correspondent histological findings were fatty degeneration foci heterogeneously distributed within the sections in addition to the inflammation and fibrosis changes (Figure 4), and changes of liver cirrhosis were not found. Hepatic parenchymal echoes were strip-shaped and coarse (Figure 5), the correspondent histology showed wide and compact fibrotic septa (Figure 6), lobular generation was not evident.

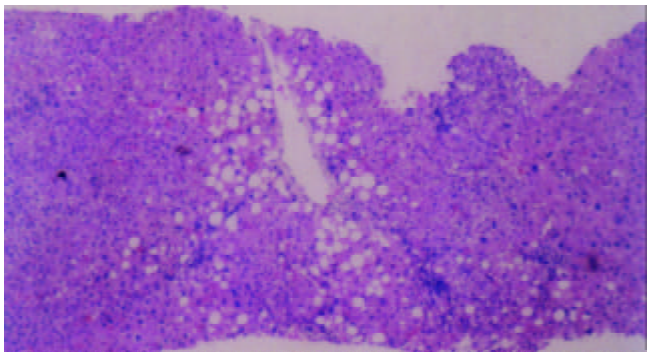

Figure 4 Chronic viral hepatitis. On histology, focal fatty degeneration foci were shown. (HE stain, ×40).

Figure 5 Chronic viral hepatitis. Ultrasonography showed the hepatic parenchymal echo to be strip-shaped and coarse.

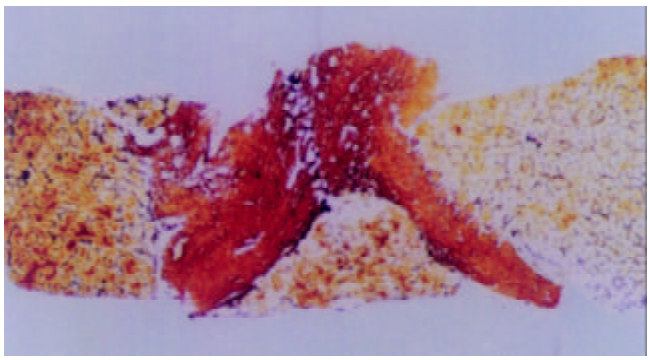

Figure 6 Chronic viral hepatitis. Wide and compact fibrotic septum was shown histologically. (Reticular fiber stain, ×40).

DISCUSSION

Among the multiple ultrasonographic parameters, PV_{max} and

GB_{sm} were selected as the independent predictors for the evaluation of fibrosis stage, while L_E, L_{sur} and GB_T were the independent predictors for the evaluation of inflammation grade. The results of this study showed that the portal venous velocity decreased and the wall of gallbladder became rough with the progress of fibrosis stage. While as the aggravation of inflammation grade, the liver parenchymal echo became coarse and heterogeneous, liver surface was rough and irregular, and the gallbladder wall became thick.

The decrease of portal venous velocity might relate to the increase of portal venous resistance. It was reported that patients with acute hepatitis and fulminant hepatitis developed portal hypertension with the aggravation of hepatic inflammation degrees[25,26].

There have been only a few reports about the relationship between the hemodynamic changes of portal vein and the histological changes in chronic hepatitis[22,27]. Aube *et al*[22] considered that the decrease of portal venous velocity was closely correlated with the histological degree of fibrosis. Our investigation showed that the decrease of portal venous velocity was significantly correlated not only with fibrosis stage but also with inflammation grade. The difference in the histological evaluating protocol used, and the difference in the sample size might partially account for the discrepancy.

The development of liver fibrosis into cirrhosis is a gradient course. There are non-specific findings on imaging. However, as the progresses of liver fibrosis reached to a certain degree, the liver pathological changes would become obvious. The acoustic interfaces would increase and the acoustic impedance between fibrotic tissue and other hepatic tissues would become large. On ultrasonography, the echo pattern of liver parenchymal would become coarse and echogenic, and the liver surface would become irregular. In this sense, the ultrasonographic features of liver parenchymal echo and liver surface would directly reflect the fibrotic changes in chronic hepatitis and liver cirrhosis, and thus playing an important role in the evaluation of fibrosis degree.

There is a close relationship between biliary system and the liver in histogenesis, anatomy and function. Viral hepatitis is often associated with biliary disorders. It was reported that abnormal ultrasonographic findings of the gallbladder such as wall thickening and double-edge sign, and abnormal size of the gallbladder and gallbladder stones were frequent in patients with hepatitis and liver cirrhosis[28-31]. The mechanism underlying the gallbladder disorders in viral hepatitis is still unclear. Some factors have been considered to be related with it[31,32] such as direct invasiveness of hepatitis virus, secondary infections, immunity injury, and edema of the gallbladder wall due to portal hypertension, circumfluence obstruction of the gallbladder vein, ete.

Ultrasonography and serology are both non-invasive methods in the evaluation of liver fibrosis and cirrhosis. However, their viewing aspects are different. The former is given priority to the reflection of morphological changes, while the latter reflects the function and metabolic changes. The knowledge about what are the similarities and differences between them in evaluating the liver fibrosis degree and diagnosis of cirrhosis is rarely known at present.

In our investigation, three independent ultrasonographic predictors correlated with fibrosis stage were chosen and compared with three serologic variables. Results showed that the correlation coefficients of ultrasonographic variables were similar to those of serological variables. There was the same tendency that the diagnostic accuracy of mild liver fibrosis was higher than that of moderate and severe fibrosis in both ultrasonography and serology, and the diagnostic accuracy of moderate liver cirrhosis was higher in ultrasonography. There were no significant differences between ultrasonography and serology in evaluating mild and severe liver fibrosis.

Referring to the diagnosis of compensated liver cirrhosis, there was no significant difference between ultrasonography and serology. However, the diagnostic sensitivity of ultrasonography was lower than that of serology, but its diagnostic specificity was higher than that of serology. It suggested that serological results should be mainly consulted for the early detection of pathological changes, while for the sake of exceptional diagnosis of cirrhosis, doctors had better to consult the results of ultrasonography in clinical practice.

Although the general diagnostic accuracy of compensated liver cirrhosis by ultrasonography and serology was similar, they were different in evaluating active and inactive stage cirrhosis. Results in our study showed that the diagnostic accuracy of ultrasonography for evaluating active stage cirrhosis was lower than that of serology with a high possibility of false-positive results, while the diagnostic accuracy for evaluating inactive stage cirrhosis was higher by ultrasonography than by serology. This difference might reflect the different features of the two modalities.

The serum fibrosis markers might reflect the activity of liver fibrosis and cirrhosis. When there was extensive inflammation in the liver, the level of serum fibrosis markers would raise with the active aggradation and degradation of the extracellular stroma. However, even if there was extensive fibrosis in the inactive stage cirrhosis, the level of serum fibrosis markers would be normal without active aggradation of the extracellular stroma[7]. Our results also illuminated that the level of serum fibrosis variables was distinctly higher in active stage cirrhosis than in inactive stage cirrhosis. Ultrasonography reflected the morphological changes of liver fibrosis and cirrhosis. When the accumulation of tissue morphological changes reached a certain degree, ultrasonography could depict these changes to a certain extent even if it was in the inactive fibrosis stage. Nevertheless, for the active fibrosis course at the level of cell and molecule, ultrasonography might fail to detect these fine morphological changes, and thus could not accurately evaluate the state of the disease.

It was inferred from our investigation that it was important to combine the two modalities for the evaluation of liver fibrosis and cirrhosis in clinical practice. When the level of serum fibrosis markers was normal, and the liver function damage was mild, liver cirrhosis should not be easily excluded with the distinct findings of cirrhosis showed by ultrasonography. The inactive stage cirrhosis might be possible at this situation. While the level of serum fibrosis markers rose obviously, and the liver function damage was severe, diagnosis of active stage cirrhosis should be considered with a long history of hepatitis viral infection even if there were no typical findings of cirrhosis on ultrasonography.

These results indicated that ultrasonography and serology both had their own advantages and disadvantages in the evaluation of liver fibrosis and liver cirrhosis.

The limitation of our investigation was that the case number of inactive stage cirrhosis was small. It was only a preliminary study and should be conducted more profoundly with a large sample size.

Ultrasonography is valuable in the evaluation of liver cirrhosis because of its low cost, easy performance, and high acceptability by the patients. However it is not a specific method and the diagnostic accuracy is still to be improved. Several factors could affect the diagnostic accuracy such as extra- and intraobserver variability, technical level of the operator, interference of obesity, ascites and intestinal gas, and modulation of the apparatus.

False positive and negative results might appear when diagnosis of compensated liver cirrhosis was made by ultrasonography. In patients with active stage liver cirrhosis,

ultrasonography could not depict the abnormalities caused by histological changes such as fine and sparse fibrotic septa or small and uniform pseudolobular nodules, thus false negative diagnosis might be made. However, high level of serum fibrotic markers might be valuable for the accurate diagnosis.

In some patients with a relative long history of chronic hepatitis, liver active inflammation and inactive phase occurred by turns, which made the pathological changes of the liver more complicated. The changes such as focal fatty degeneration or wide and compact fibrotic septa might cause coarse and heterogeneous parenchyma echo patterns in the liver, leading to a false positive diagnosis of liver cirrhosis on ultrasonography. The possible mechanisms might be assumed as follows. The acoustic interfaces between different liver tissues changed and the scatters increased because of focal fatty degeneration of the liver cells, thus causing focal echo attenuation and heterogeneous parenchyma echo patterns in the liver. When the fibrotic septa became wide and compact, the acoustic interfaces also became large and the acoustic impedance increased, causing coarse parenchyma echo patterns in the liver.

Hepatic pathological changes are often heterogeneous in patients with chronic hepatitis and liver cirrhosis. Sampling errors are liable. Gaiani *et al*[23] reported that thirty-two patients considered as liver cirrhosis by ultrasonography were identified as chronic hepatitis by histology. However, eight of these patients showed clinical manifestations of decompensated cirrhosis in the follow-up for half a year later. It indicated that ultrasonography could make up the deficiency of histology in the diagnosis of liver cirrhosis in certain situations.

In summary, there are different ultrasonographic predictors for the evaluation of hepatic inflammation grade and fibrosis stage of chronic hepatitis. Both ultrasonography and serology have their own advantages and disadvantages in the evaluation of liver fibrosis and compensated liver cirrhosis. False positive and negative results may occur in the diagnosis of compensated liver cirrhosis by ultrasonography. Combined application of ultrasonography and serology can contribute to the improvement in their diagnostic accuracy.

REFERENCES

1 **Wang BE**. Liver fibrosis: diagnosis and evaluation of disease severity. *Zhonghua Ganzangbing Zazhi* 1998; **6**: 193-194
2 **Yang XB**, Huang ZM, Wang JH. The drug therapy of liver fibrosis. *Shijie Huaren Xiaohua Zazhi* 2002; **10**: 956-957
3 **Cui DL**, Yao XX. Serum test of liver fibrosis. *Shijie Huaren Xiaohua Zazhi* 2000; **8**: 683-684
4 **Yao SK**, Yin F. The early diagnosis of liver fibrosis. *Shijie Huaren Xiaohua Zazhi* 2000; **8**: 681-683
5 **Maharaj B**, Maharaj RJ, Leary WP, Cooppan RM, Naran AD, Pirie D, Pudifin DJ. Sampling variability and its influence on the diagnostic yield of percutaneous needle biopsy of the liver. *Lancet* 1986; **1**: 523-525
6 **Bai WY**, Yao XX, Feng LY. Researching of liver fibrosis: status in quo. *Shijie Huaren Xiaohua Zazhi* 2000; **8**: 1267-1268
7 **Luo KX**. Serodiagnosis of liver fibrosis. *Linchuang Gandanbing Zazhi* 1996; **12**: 1-2
8 **Jing B**, Li YB. Diagnostic strategy for liver fibrosis. *Zhonghua Xiaohua Zazhi* 1997; **17**: 170-172
9 **Harisinghani MG**, Hahn PF. Computed tomography and magnetic resonance imaging evaluation of liver cancer. *Gastroenterol Clin North Am* 2002; **31**: 759-776
10 **Martin DR**. Magnetic resonance imaging of diffuse liver diseases. *Top Magn Reson Imaging* 2002; **13**: 151-163
11 **Kim MJ**, Mitchell DG, Ito K, Kim JH, Pasqualin D, Rubin R. Hepatic iron deposition on magnetic resonance imaging: correlation with inflammatory activity. *J Comput Assist Tomogr* 2002; **26**: 988-993
12 **Hung CH**, Lu SN, Wang JH, Lee CM, Chen TM, Tung HD, Chen CH, Huang WS, Changchien CS. Correlation between ultrasonographic and pathologic diagnoses of hepatitis B and C virus-related cirrhosis. *J Gastroenterol* 2003; **38**: 153-157
13 **Colli A**, Fraquelli M, Andreoletti M, Marino B, Zuccoli E, Conte D. Severe liver fibrosis or cirrhosis: accuracy of US for detection-analysis of 300 cases. *Radiology* 2003; **227**: 89-94
14 **Filly RA**, Reddy SG, Nalbandian AB, Lu Y, Callen PW. Sonographic evaluation of liver nodularity: Inspection of deep versus superficial surfaces of the liver. *J Clin Ultrasound* 2002; **30**: 399-407
15 **Xu Y**, Wang B, Cao H. An ultrasound scoring system for the diagnosis of liver fibrosis and cirrhosis. *Chin Med J* 1999; **112**: 1125-1128
16 **Tchelepi H**, Ralls PW, Radin R, Grant E. Sonography of diffuse liver disease. *J Ultrasound Med* 2002; **21**: 1023-1032
17 **Martinez-Noguera A**, Montserrat E, Torrubia S, Villalba J. Doppler in hepatic cirrhosis and chronic hepatitis. *Semin Ultrasound CT MR* 2002; **23**: 19-36
18 **Arda K**, Ofelli M, Calikoglu U, Olcer T, Cumhur T. Hepatic vein Doppler waveform changes in early stage (Child-Pugh A) chronic parenchymal liver disease. *J Clin Ultrasound* 1997; **25**: 15-19
19 **Gorka W**, al Mulla A, al Sebayel M, Altraif I, Gorka TS. Qualitative hepatic venous Doppler sonography versus portal flowmetry in predicting the severity of esophageal varices in hepatitis C cirrhosis. *Am J Roentgenol* 1997; **169**: 511-515
20 **Li XH**, Wang L, Fang YW, Lu YK. Color Doppler evaluation for the hemodynamics of portal hypertension in liver cirrhosis. *Shijie Huaren Xiaohua Zazhi* 1999; **7**: 453-454
21 **Ohta M**, Hashizume M, Kawanaka H, Akazawa K, Tomikawa M, Higashi H, Kishihara F, Tanoue K, Sugimachi K. Prognostic significance of hepatic vein waveform by Doppler ultrasonography in cirrhotic patients with portal hypertension. *Am J Gastroenterol* 1995; **90**: 1853-1857
22 **Aube C**, Oberti F, Korali N, Namour MA, Loisel D, Tanguy JY, Valsesia E, Pilette C, Rousselet MC, Bedossa P, Rifflet H, Maiga MY, Penneau-Fontbonne D, Caron C, Cales P. Ultrasonographic diagnosis of hepatic fibrosis or cirrhosis. *J Hepatol* 1999; **30**: 472-478
23 **Gaiani S**, Gramantieri L, Venturoli N, Piscaglia F, Siringo S, D'Errico A, Zironi G, Grigioni W, Bolondi L. What is the criterion for differentiating chronic hepatitis from compensated cirrhosis? A prospective study comparing ultrasonography and percutaneous liver biopsy. *J Hepatol* 1997; **27**: 979-985
24 **The academic meeting of Chinese Medical Association on Epidemic and Parasitosis in Beijing**. The protocol for the prevention and treatment of viral hepatitis. *Zhonghua Chuanranbing Zazhi* 1995; **13**: 241-247
25 **Yang SS**, Wu CH, Chen TK, Lee CL, Lai YC, Chen DS. Portal blood flow in acute hepatitis with and without ascites: a non-invasive measurement using an ultrasonic Doppler. *J Gastroenterol Hepatol* 1995; **10**: 36-41
26 **Tai DI**, Changchien CS, Chen CJ, Huang CS, Lo SK, Kuo CH. Changes in portal venous hemodynamics in patients with severe acute hepatitis over one year. *J Clin Ultrasound* 2000; **28**: 83-88
27 **Koda M**, Murawaki Y, Kawasaki H, Ikawa S. Portal velocity and portal blood flow in patients with chronic viral hepatitis: relation to histological liver fibrosis. *Hepatogastroenterology* 1996; **43**: 199-202
28 **Wang TF**, Hwang SJ, Lee EY, Tsai YT, Lin HC, Li CP, Cheng HM, Liu HJ, Wang SS, Lee SD. Gall-bladder wall thickening in patients with liver cirrhosis. *J Gastroenterol Hepatol* 1997; **12**: 445-449
29 **Dogra R**, Singh J, Sharma MP. Enterically transmitted non-A, non-B hepatitis mimicking acute cholecystitis. *Am J Gastroenterol* 1995; **90**: 764-766
30 **Portincasa P**, Moschetta A, Di Ciaula A, Palmieri VO, Milella M, Pastore G, Palasciano G. Changes of gallbladder and gastric dynamics in patients with acute hepatitis A. *Eur J Clin Invest* 2001; **31**: 617-622
31 **Xiao SS**. Ultrasonigraphic abnormalities of gallbladder in patients with viral hepatitis and liver cirrhosis: clinical significance. *Weichangbingxue He Ganbingxue Zazhi* 1996; **5**: 77-79
32 **Yan FM**, Chen AS, Hao F, Zhao XP, Gu CH, Zhao LB, Yang DL, Hao LJ. Hepatitis C virus may infect extrahepatic tissues in patients with hepatitis C. *World J Gastroenterol* 2000; **6**: 805-811

Edited by Zhang JZ and Wang XL

P.O.Box 2345, Beijing 100023,China
Fax: +86-10-85381893
E-mail: wjg@wjgnet.com www.wjgnet.com

World J Gastroenterol 2003;9(11):2490-2496
World Journal of Gastroenterology
 ISSN 1007-9327

• VIRAL HEPATITIS •

Diagnostic value of platelet derived growth factor-BB, transforming growth factor-b_1, matrix metalloproteinase-1, and tissue inhibitor of matrix metalloproteinase-1 in serum and peripheral blood mononuclear cells for hepatic fibrosis

Bin-Bin Zhang, Wei-Min Cai, Hong-Lei Weng, Zhong-Rong Hu, Jun Lu, Min Zheng, Rong-Hua Liu

Bin-Bin Zhang, Wei-Min Cai, Hong-Lei Weng, Zhong-Rong Hu, Jun Lu, Min Zheng, Rong-Hua Liu, Institute of Infectious Diseases, First Affiliated Hospital, School of Medicine, Zhejiang University, Hangzhou 310003, Zhejiang Province, China
Correspondence to: Professor Wei-Min Cai, Institute of Infectious Diseases, First Affiliated Hospital, School of Medicine, Zhejiang University, Hangzhou 310003, Zhejiang Province, China. zbb-2051@163.com
Telephone: +86-571-87236580
Received: 2003-03-20 **Accepted:** 2003-04-14

Abstract

AIM: Noninvasive diagnosis of hepatic fibrosis has become the focus because of the limited biopsy, especially in the surveillance of treatment and in screening hepatic fibrosis. Recently, regulatory elements involved in liver fibrosis, such as platelet derived growth factor-BB (PDGF-BB), transforming growth factor-β_1 (TGF-β_1), matrix metalloproteinase-1 (MMP-1), and tissue inhibitor of matrix metalloproteinase-1 (TIMP-1), have been studied extensively. To determine whether these factors or enzymes could be used as the indices for the diagnosis of hepatic fibrosis, we investigated them by means of receiver operating characteristic (ROC) curve.

METHODS: Serum samples from sixty patients with chronic viral hepatitis B and twenty healthy blood donors were assayed to determine the level of PDGF-BB, TGF-β_1, MMP-1, and TIMP-1 with ELISA, and HA, PCIII, C-IV, and LN level with RIA. The message RNA (mRNA) expression of TIMP-1 and MMP-1 in peripheral blood mononuclear cells (PBMCs) was detected by RT-PCR and Northern blot hybridization. Liver biopsy was performed in all patients. The biopsy samples were histopathologically examined. The trial was double-blind controlled.

RESULTS: The serum level of PDGF-BB, TIMP-1, the ratio of TIMP-1 and MMP-1 (TIMP-1/MMP-1), mRNA expression of TIMP-1 (TIMP-1mRNA), and the ratio of TIMP-1mRNA and MMP-1mRNA (TIMP-1mRNA/MMP-1mRNA) in patients was significantly higher than those in the healthy blood donors (t=2.514-11.435, P=0.000-0.016). The serum level of PDGF-BB, TIMP-1, TIMP-1/MMP-1, and TIMP-1mRNA was positively correlated with fibrosis stage and inflammation grade (r=0.239-0.565, P=0.000-0.033), while the serum level of MMP-1 was negatively correlated with fibrosis stage and inflammation grade, and TIMP-1mRNA/MMP-1mRNA was positively correlated with inflammation grade. Through the analysis by ROC curve, serum PDGF-BB was the most valuable marker, and its sensitivity was the highest among the nine indices. The markers with the highest specificity were TIMP-1mRNA and TIMP-1mRNA/MMP-1mRNA in PBMCs. The area under the curve (AUC) of PDGF-BB, TIMP-1mRNA, TIMP-1mRNA/MMP-1mRNA, TIMP-1/MMP-1, HA, PCIII, TIMP-1, C-IV, and LN was 0.985, 0.876, 0.792, 0.748, 0.728, 0.727, 0.726, 0.583, and 0.463, respectively. The sensitivity and the specificity in the parallel test was 99.0 % and 95.0 % when serum PDGF-BB, TIMP-1mRNA and TIMP-1mRNA/MMP-1mRNA was detected simultaneously.

CONCLUSION: Serum level of PDGF-BB, TIMP-1mRNA, TIMP-1mRNA/MMP-1mRNA in PBMCs, and serum level of TIMP-1 and TIMP-1/MMP-1 can be used as the indices for the diagnosis of hepatic fibrosis, but the former three are more useful. The combination of serum PDGF-BB, TIMP-1mRNA and TIMP-1mRNA/MMP-1mRNA in PBMCs is even more efficient in screening liver fibrosis.

Zhang BB, Cai WM, Weng HL, Hu ZR, Lu J, Zheng M, Liu RH. Diagnostic value of platelet derived growth factor-BB, transforming growth factor-β_1, matrix metalloproteinase-1, and tissue inhibitor of matrix metalloproteinase-1 in serum and peripheral blood mononuclear cells for hepatic fibrosis. *World J Gastroenterol* 2003; 9(11): 2490-2496
http://www.wjgnet.com/1007-9327/9/2490.asp

INTRODUCTION

Fibrosis is the leading cause of morbidity and mortality in hepatic diseases. More attention has been paid to its mechanism, diagnosis and treatment. The proper and rapid treatment depends on the accurate and simple diagnosis. Noninvasive diagnosis of hepatic fibrosis has become the focus because of the limited biopsy, especially in the surveillance of treatment and in screening hepatic fibrosis. Recently, regulatory factors involved in the mechanism of liver fibrosis such as PDGF-BB, TGF-β_1, interstitial enzyme, MMP-1 and its inhibitor, TIMP-1, have been studied extensively[1-14]. To find out whether these factors or enzymes could be used as the indices for diagnosis of liver fibrosis, protein level and mRNA expression were studied in sixty patients with chronic viral hepatitis B and twenty healthy blood donors. At the same time, these markers were compared with liver biopsy results and the routine serum markers (HA, PCIII, C-IV and LN) to identify their values in clinical practice via ROC curve and the combination test.

MATERIALS AND METHODS

Subjects

During the Sixth National Conference on Infectious and Parasitic Diseases in 2000, the Protocol of Prevention and Treatment for Viral Hepatitis (abbreviated as "2000 Criteria")[15] was modified. According to the "2000 Criteria", 60 patients with typical presentations of chronic hepatitis were included. Among them, 54 were men with an average age of 34.9±8.1 years, 6 were women with an average age of 36.6±1.0 years. Twenty-eight and thirty-two patients showed moderate and severe

degree of the disease, respectively. The patients' histories were mainly collected from the First Affiliated Hospital, School of Medicine, Zhejiang University and several other hospitals in Zhejiang Province between July 1998 and September 1999. All were positive in HBV markers without other viral infections or disorders except liver disease. The diagnosis was made by liver biopsy according to the "2000 Criteria". The normal control group included 20 healthy blood donors selected according to the random number table.

Histology

Biopsy samples of the liver >1 cm in length were fixed in 10 % neutralized formaldehyde, embedded in paraffin and stained with hematoxylin and eosin. The reticulin and Masson trichrome techniques were used specially for staining fibrous tissue components. Histological assessment of the liver for the division of fibrosis stage and inflammation grade, expressed as S1 to S4 and G1 to G4, was performed according to the "2000 Criteria".

Determination of serum level of PDGF-BB, TGFb_1, TIMP-1, MMP-1, HA, PCIII, C-IV, and LN

Serum specimens were stored at -20 ℃. The serum level of PDGF-BB, TGF-β_1, TIMP-1 and MMP-1 was assayed by ELISA. The kits of PDGF-BB and TGF-β_1 were provided by the American Genzyme Corporation, the American AND Corporation, respectively. The kits of TIMP-1 and MMP-1 were provided by the American ChemCon Corporation. The serum level of HA, PCIII, C-IV and LN was determined by RIA. The kits of HA, C-IV and LN were provided by Shanghai Navy Medical Institute. The PCIII kit was provided by Chongqing Tumor Institute. Assays were done following the manufacturers' manual.

Determiantion of TIMP-1mRNA and MMP-1mRNA in PBMCs

Total RNA extraction PBMCs were separated by Ficoll (GiBco. Life Technologies Inc) and the total RNA was extracted by Trizol reagent (GiBco. Life Technologies Inc).

Northern blot hybridization Total RNA 20 μg was denatured and undergone electrophoresis with 1 % agarose containing 2.2 mol/L formaldehyde and was transferred onto nitrocellulose membrane, which was dried at 80 ℃ for two hours. The filters were prehybridized at 68 ℃ for 1 hour in the solution containing 6×standard saline citrate (SSC), 5×Denhardt' s solution, 0.5×sodium dodecyl sulfate (SDS), and 100 mg/L salmon sperm DNA. The denatured probes were added into the solution for hybridization at 68 ℃ overnight. The filters were washed for three times, and then autoradiographed at -70 ℃.

RT-PCR Total RNA 1 μg and primer Oligo (dT) were used for reverse transcription (Promega). 5 μl reverse transcription template was used for amplification through PCR. The primers are MMP-1: 5' CTTCAGTGGTGATGTTCAGC3', 5' CATCGATATGCTTCAACGTTC3', 412 bp, TIMP-1: 5' GGAGTCCAGCAGACCACCTTA3', 5' -TGGGACACAG GTGCATGCCCTGCT-3', 110 bp. The amplified sequence length of β-actin is 224 bp. The PCR products were through 1.5 % (w/v) agarose gel electrophoresis and analyzed by gel imaging system.

Statistical analysis

Results were expressed as mean ± standard deviation ($\bar{x}\pm s$). *t* test and Spearman rank-correlation test were used. The results were considered statistically significant at $P<0.05$. Evaluation of the diagnostic test was made via ROC curve.

RESULTS

Comparison of serum level of PDGF-BB, TGF-b_1, TIMP-1, MMP-1 and TIMP-1/MMP-1 between patients and healthy blood donors

The serum level of PDGF-BB, TIMP-1 and TIMP-1/MMP-1 in 60 patients was significantly higher than that in the normal control group with an increase of 2.52, 0.5 and 1.67 fold, respectively. However, there was no difference in the serum level of MMP-1 and TGF-β_1 between patients and normal controls (Table 1). The serum level of MMP-1 was further studied. A declining tendency along the increase of fibrosis stage, inflammation grade and severity of the hepatic disease was observed while a significant difference appeared only between the patients in S4, G4 or with severe diseases and blood donors (Table 2). Moreover, it was also different between patients in S4 and those in S2 (Table 2). As to the serum level of TGF-β_1, there was no difference between patients and normal controls, even no significant difference among patients with the increase of fibrosis stage, inflammation grade and severity of the disease (Table 2).

Table 2 Comparison of the serum level of MMP-1 and TGF-β_1 between patients at different fibrosis stages, inflammation grades, and with different severities of the disease and the healthy controls ($\bar{x}\pm s$)

Group (*n*)	MMP-1(μg/L)	TGF-β_1(μg/L)
Controls (20)	7.98±3.13	26.28±16.69
S2(16)	6.34±2.96	31.66±18.01
S3(31)	6.80±5.34	34.19±26.23
S4(13)	3.93±2.93[ac]	25.16±20.90
G2(2)	7.66±0.36	18.25±6.01
G3(28)	6.41±4.91	31.89±21.61
G4(30)	5.61±4.15[a]	32.14±25.25
Mild disease (28)	6.56±3.66	34.39±24.43
Severe disease (32)	5.61±5.05	29.08±21.97

There was a statistically significant difference as compared with the control group [a]$P<0.05$, and a statistically significant difference as compared with S2 group [c]$P<0.05$.

Comparison of TIMP-1mRNA, MMP-1mRNA and TIMP-1mRNA/MMP-1mRNA in PBMCs between patients and healthy controls

As shown in Table 3, TIMP-1mRNA and TIMP-1mRNA/MMP-1mRNA were significantly elevated in patients than those in healthy controls with an increase of 1.6 and 1.79 fold, respectively. However, no difference was found in MMP-1mRNA expression between patients and healthy controls.

Table 1 Comparison of the serum level of PDGF-BB, TGF-β1, TIMP-1, MMP-1 and TIMP-1/MMP-1 between patients and healthy blood donors ($\bar{x}\pm s$)

Group (*n*)	PDGF-BB (ng/L)	TGF-β_1(μg/L)	TIMP-1(μg/L)	MMP-1(μg/L)	TIMP-1/MMP-1
Patients	67.75±30.08[b]	31.41±23.22	258.87±77.75[a]	6.05±4.44	83.66±100.36[b]
Controls	19.85±10.28	26.28±16.69	205.80±35.66	7.98±3.13	31.95±20.03
t	11.435	0.912	2.646	-1.79	3.176
P	0.000	0.365	0.01	0.077	0.002

There was a statistically significant difference as compared with the control group [a]$P<0.05$, [b]$P<0.01$.

Table 3 Comparison of TIMP-1mRNA, MMP-1mRNA and TIMP-1mRNA / MMP-1mRNA in PBMCs between patients and healthy controls ($\bar{x}\pm s$)

Group (n)	TIMP-1mRNA	MMP-1mRNA	TIMP-1mRNA / MMP-1mRNA
Patients (60)	1.05±0.69[b]	0.39±0.36	4.77±3.78[a]
Controls (20)	0.40±0.19	0.24±0.11	1.71±0.89
t	2.934	0.741	2.514
P	0.005	0.462	0.016

There was a statistically significant difference compared with the control group [a]P<0.05, [b]P<0.01.

Table 4 Relationship between serum level of PDGF-BB, TGF-β1, TIMP-1, MMP-1 and TIMP-1 / MMP-1, TIMP-1mRNA, MMP-1mRNA and TIMP-1mRNA / MMP-1mRNA and fibrosis stage and inflammation grade

Index	Fibrosis stage r	P	Inflammation grade r	P
TIMP-1	0.239[a]	0.033	0.261[a]	0.019
MMP-1	-0.333[b]	0.003	-0.266[a]	0.017
TIMP-1 / MMP-1	0.405[b]	0.000	0.340[b]	0.002
PDGF-BB	0.565[b]	0.000	0.534[b]	0.000
TGF-β1	-0.041	0.718	0.039	0.733
TIMP-1mRNA	0.366[b]	0.009	0.391[a]	0.015
TIMP-1mRNA / MMP-1mRNA	0.340	0.071	0.497[b]	0.006
MMP-1mRNA	0.091	0.582	0.001	0.995

[a]P<0.05, [b]P<0.01, compared with r_s threshold value.

Table 5 ROC curve analysis of nine indices

Index	AUC	P	Cut-off point	Sensitivity (%)	Specificity (%)	YI
PDGF-BB	0.985	0.000	≥40.50 ng / L	90.0	95.0	0.850
TIMP-1mRNA	0.876	0.000	≥0.79	73.7	100	0.737
TIMP-1mRNA / MMP-1mRNA	0.792	0.005	≥3.20	65.8	100	0.658
TIMP-1 / MMP-1	0.748	0.001	≥34.69	70.0	75.0	0.450
HA	0.728	0.003	≥145.20 μg / L	62.0	87.5	0.497
PCIII	0.727	0.004	≥137.40 mg / L	59.2	81.2	0.404
TIMP-1	0.726	0.003	≥254.00 μg / L	46.7	95.0	0.417
CIV	0.583	0.287	≥74.20 mg / L	55.1	68.7	0.238
LN	0.463	0.636	≥156.65 μg / L	37.8	75.0	0.128

YI (Youden Index)=sensitivity+specificity-1.

Table 6 Parameters of the combined diagnosis in the parallel test

Combined indices	Sensitivity (%)	Specificity (%)
TIMP-1mRNA+TIMP-1mRNA / MMP-1mRNA+PDGF-BB	99.0	95.0
PDGF-BB+TIMP-1mRNA+HA	99.0	83.1
TIMP-1mRNA+TIMP-1mRNA / MMP-1mRNA+PDGF-BB+HA	99.6	83.1
PDGF-BB+TIMP-1mRNA / MMP-1mRNA+HA	98.7	83.1
PDGF-BB+TIMP-1mRNA	97.4	95.0
TIMP-1mRNA+TIMP-1mRNA / MMP-1mRNA+HA	97.0	87.5
PDGF-BB+TIMP-1mRNA / MMP-1mRNA	96.6	95.0
PDGF-BB+HA	96.0	83.1
TIMP-1mRNA+TIMP-1mRNA / MMP-1mRNA	91.0	100
TIMP-1mRNA+HA	90.0	87.5
TIMP-1mRNA / MMP-1mRNA+HA	87.0	87.5

Table 7 Parameters of the combined diagnosis in the serial test

Combined indices	Sensitivity (%)	Specificity (%)
PDGF-BB+TIMP-1mRNA	66.3	100
PDGF-BB+TIMP-1mRNA / MMP-1mRNA	59.2	100
PDGF-BB+HA	56.0	99.4
TIMP-1mRNA+TIMP-1mRNA / MMP-1mRNA	48.5	100
TIMP-1mRNA+HA	45.7	100
PDGF-BB+TIMP-1mRNA+HA	41.1	100
TIMP-1mRNA / MMP-1mRNA+HA	40.8	100
TIMP-1mRNA+TIMP-1mRNA / MMP-1mRNA+PDGF-BB	40.4	100
PDGF-BB+TIMP-1mRNA / MMP-1mRNA+HA	36.7	100
TIMP-1mRNA+TIMP-1mRNA / MMP-1mRNA+HA	30.1	100
TIMP-1mRNA+TIMP-1mRNA / MMP-1mRNA+PDGF-BB+HA	27.1	100

Relationship between serum level of PDGF-BB, TGF-b_1,TIMP-1, MMP-1 and TIMP-1/MMP-1, TIMP-1mRNA, MMP-1mRNA and TIMP-1mRNA/MMP-1mRNA in PBMCs and fibrosis stage and inflammation grade

The serum level of PDGF-BB, TIMP-1, TIMP-1/MMP-1 and TIMP-1mRNA in PBMCs was positively correlated with fibrosis stage and inflammation grade, while the serum level of PDGF-BB had a stronger correlation than the other three indices. The serum level of MMP-1 was negatively correlated with fibrosis stage and inflammation grade. TIMP-1mRNA/MMP-1mRNA was positively correlated with inflammation grade. However, the serum level of TGF-β_1 and MMP-1mRNA was correlated with neither fibrosis stage nor inflammation grade.

Diagnostic value of serum level of PDGF-BB, TIMP-1, TIMP-1/MMP-1, MMP-1, HA, PCIII, CIV, LN and TIMP-1mRNA and TIMP-1mRNA/MMP-1mRNA in PBMCs

Table 5 shows that serum level of PDGF-BB, TIMP-1, TIMP-1/MMP-1, HA and PCIII, and TIMP-1mRNA and TIMP-1mRNA/MMP-1mRNA in PBMCs could be used to diagnose hepatic fibrosis. Among them, the serum level of PDGF-BB was most useful for its AUC and YI were close to 1, followed by TIMP-1mRNA and TIMP-1mRNA/MMP-1mRNA in PBMCs. Furthermore, the serum level of PDGF-BB was most sensitive, and the next was TIMP-1mRNA and TIMP-1mRNA/MMP-1mRNA in PBMCs. TIMP-1mRNA and TIMP-1mRNA/MMP-1mRNA in PBMCs were most specific, followed by the serum level of PDGF-BB and TIMP-1. When both the sensitivity and the specificity were taken into consideration, serum PDGF-BB, serum HA, TIMP-1mRNA and TIMP-1mRNA/MMP-1mRNA were the relatively efficient indices.

Diagnostic value of the single index combination

When both the sensitivity and the specificity needed to be taken into account, we could combine the following four indices, namely serum PDGF-BB, serum HA, TIMP-1mRNA/MMP-1mRNA and TIMP-1mRNA in PBMCs. Table 6 indicates that the combination of serum level of PDGF-BB, TIMP-1mRNA and TIMP-1mRNA/MMP-1mRNA in PBMCs was more useful in the parallel test. However, no efficient combination in the serial test was observed (Table 7).

DISCUSSION

Hepatic fibrosis is characterized by imbalanced deposition and degradation of extracellular matrix (ECM). Many factors are involved in the process. Thus, it is difficult to evaluate the fibroproliferative activity. Liver biopsy is still regarded as the gold standard for the diagnosis of fibrosis, but even elaborated scores of histological activity are limited to evaluate the prognosis in the individual case. Moreover, it is not convenient, to some degree, to use it as a routine method for the diagnosis, evaluation and supervision of the disease in clinical practice. Unfortunately, there have been no established noninvasive markers or tests for the diagnosis of hepatic fibrosis. Therefore, it is essential to explore the noninvasive and reliable indices for assessing the progress of liver fibrosis. Previously, we revealed the diagnostic value of ultrasonography on assessing liver fibrosis resulted from Schistosomiasis japonica[16], but sometimes we could not distinguish benign fatty infiltration from fibrosis, because both of their echogenicities appeared increased or diffuse. Detection of the biochemical indices in serum has been the focus in the filed of hepatic fibrosis. At present, the serum indices revealing the progress of hepatic fibrosis mainly include two kinds, reflecting deposition and degradation. Previously, more attention was paid to the factors reflecting the deposition or metabolism of ECM, and the serum level of HA, PCIII, PIIIP, CIVand LNwas studied. Zheng *et al*[17,18] confirmed the clinical value of the serum fibrosis indices (HA, PCIII, CIVand LN) through comparing them with the histological reports performed on liver fibrosis patients resulted from chronic hepatitis B. Furthermore, the serum level of HA was considered to be the most sensitive among the four indices, this result was also reported by others[19,20]. However, the four indices did not fully reflect the histological changes and were often influenced by other factors, moreover, in some chronic hepatitis B cases, they did not correspond to the biopsy results[21]. Thus, it is important and necessary to explore new and more reliable indices. With the mechanism of hepatic fibrosis elucidated further, the focus has been the elements involved in the degradation of ECM such as MMP-1[14,22,23] and TIMP-1[24-27] and the regulatory factors such as PDGF-BB and TGF-β_1 whose vital roles in hepatic fibrosis have been confirmed.

To establish the noninvasive index, the first step was to observe whether it demonstrated a difference between patients and normal controls. In our study, we compared the serum level of PDGF-BB, TIMP-1, MMP-1, TIMP-1/MMP-1 and TGF-β_1 between 60 fibrosis patients and 20 healthy blood donors. The serum level of PDGF-BB, TIMP-1 and TIMP-1/MMP-1 in patients was significantly elevated than that in healthy controls. However, the serum level of MMP-1 demonstrated a declining tendency with the severity of liver fibrosis, inflammation and the disease condition although the difference between two groups existed only when the patients were in S4, G4 or with severe hepatitis. This result indicted that the abnormal serum MMP-1 did not appear until the patients were in the advanced fibrosis. With regard to TGF-β_1 serum level, it was not different from that of the control group with the progress of liver fibrosis, inflammation and the severity of the disease, showing that serum TGF-β_1 may not be sensitive as a diagnostic index. Similar results were also reported. Daniluk *et al*[28] found that serum level of TGF-β_1 in alcohol-related liver cirrhosis was similar to that in controls. Oberti *et al*[29] detected several indices of chronic hepatitis patients, including HA, PT, GGT, alph2 macroglobulin, PIIIP, LN and TGF-β_1. They found that HA and PT were significant in cirrhosis. In fact, TGF-β_1 is secreted from cells in the manner of the complex formed by TGF-β_1 and its binding protein. However, pre TGF-β_1 can be activated to its active form only after its binding protein is released. This does not mean that TGF-β_1 may play a role freely once it is released into blood, for its corresponding receptors still block it. There are a lot of studies about the correlation of plasma TGF-β_1 with chronic hepatitis, liver fibrosis or cirrhosis[30,31]. But, in general, analysis of plasma level is fraught with difficulties related to contamination of the sample by TGF-β from platelets. Moreover, the plasmin in the plasma may increase the amount of TGF-β_1 through opening the LAP-TGF-β_1 complex. Clearance of TGF-β is also complicated. It binds locally at sites of injury to ECM and generally to vascular endothelium, it may be sequestered by soluble proteins, and can also undergo renal excretion or be taken up by hepatocytes. These modes of sequestration or clearance may vary at different circumstances. Thus, increase in plasma TGF-β may not reflect pericellular concentrations at the injury site, and due to this reason, plasma TGF-β is unlikely to be diagnostically useful[32,35]. But Kobayashi *et al*[36] found that serum TGF-β_1 could be used as an accurate indicator of progressive fibrogenesis in postoperative biliary atresia patients. The reason for the disagreement may be the different criteria for the division of liver fibrosis.

Correlation analysis was carried out to elucidate the cause leading to the difference in some indices between patients and normal controls. We found that the serum level of PDGF-BB,

TIMP-1 and TIMP-1/MMP-1 was positively correlated with fibrosis stage and inflammation grade while the serum level of MMP-1 was inversely correlated with fibrosis stage and inflammation grade. The data indicated that histological changes could directly result in the higher level of serum PDGF-BB, serum TIMP-1 and TIMP-1/MMP-1 in patients and could explain the declining tendency appearing in the comparison between each group of patients and the controls as well. Serum level of TGF-β_1 was not correlated with fibrosis stage or inflammation grade. This may confirm that detection of serum TGF-β_1 was not reliable in clinical practice.

It has been reported that mRNA levels of TIMP and MMP and corresponding proteins were related to liver fibrosis or cirrhosis. Chen *et al*[37] studied the collagen metabolism of liver fibrosis at transcription level in rabbits infected by Schistosomiasis japonica, and found that mRNA levels of MMP-1 and MMP-9 declined almost to the normal level at the later stage of fibrosis. Yata *et al*[38] found that mRNA expression of hepatic TIMP-1 increased in hepatic fibrosis. Lichtinghagen *et al*[27] investigated the mRNA levels of hepatic TIMP-1, 2, 3 and MMP-2, 7, 9 in 29 chronic active hepatitis C patients (CAH) and 7 cirrhosis patients resulted from hepatitis C virus, and found that none of mRNA levels was significantly different between CAH patients with and without fibrosis, while MMP-2, MMP-7, and TIMP-1 provided the best discrimination between cirrhosis and pre-cirrhotic stages. Lichtinghagen *et al*[39] found that mRNA expression of MMP-2, MMP-9 and TIMP in peripheral blood cells had no correlation with the circulating concentrations of these proteins, which indicated that detection of MMP mRNA and TIMP mRNA in peripheral blood cells may also give us important information about liver fibrosis. Boker *et al*[40] reported that TIMP-1 could be detected in lymphocytes and granulocytes. To determine whether TIMP-1mRNA and MMP-1mRNA in PBMCs could be used as the diagnostic markers, we detected them and TIMP-1mRNA/MMP-1mRNA, and compared these indices between patients and the healthy blood donators. The results demonstrated that TIMP-1mRNA, TIMP-1mRNA/MMP-1mRNA significantly increased while no change in mRNA expression of MMP-1 was observed. Correlation analysis revealed that TIMP-1mRNA was positively correlated with fibrosis stage and inflammation grade, while TIMP-1mRNA/MMP-1mRNA was only positively correlated with inflammation grade. No relationship was found between MMP-1mRNA and fibrosis stage or inflammation grade. With regard to MMP-1mRNA in PBMCs, no statistical difference may attribute to the higher standard deviation among individual values. Other factors influencing mRNA expression may also involve. Therefore, it could be more useful to detect TIMP-1mRNA in PBMCs for evaluating liver fibrosis.

As there was a difference in the serum level of PDGF-BB, TIMP-1, TIMP-1/MMP-1, MMP-1, TIMP-1mRNA and TIMP-1mRNA/MMP-1mRNA in PBMCs between patients and the normal controls, we wanted to know whether these indices could be used for diagnosis, and if they could, the following problem was whether they were more valuable than those four routine serum markers (HA, PCIII, CIV, LN). AUC and YI of the serum level of PDGF-BB were the closest to 1 through ROC curve. This revealed that the diagnostic value of serum level of PDGF-BB was the highest among nine indices (Table 5). Although TGF-β_1 as the main fibrogenic mediator mediates HSC activation and transformation, additional growth factors like PDGF become important in the later stage of HSC transformation. That means PDGF is vital in the progress of liver fibrosis. PDGF has been proved to be the main stimulator of HSC proliferation, migration and the strong mitogen for HSCs. Among the three subunits-AA, AB and BB, PDGF-BB is the vital cytokine for the signaling pathway in HSC and other cells[41-44]. In recent years, studies have not been adequately performed on the serum level of PDGF-BB for assessing liver fibrosis. Our results indicated that detection of the serum level of PDGF-BB had profound significance. TIMP-1mRNA and TIMP-1mRNA/MMP-1mRNA in PBMCs was inferior to serum PDGF-BB. The diagnostic value of serum level of HA, PCIII, TIMP-1 and TIMP-1/MMP-1 is similar, for their AUC are closer, but detection of serum level of HA and TIMP-1/MMP-1 was more applicable if we evaluated them according to YI. Researchers have studied TIMPs from hepatic tissues, serum level to mRNA expression, revealing the important relationship of TIMPs with fibrosis stage or inflammation grade. But it is still unclear whether the serum level of TIMP-1 and TIMP-1mRNA in PBMCs can be used as the markers for the diagnosis of liver fibrosis. If they can, are they superior or inferior to other established markers[45-47]? Our results demonstrated that TIMP-1mRNA was more sensitive than TIMP-1. Some studies[26,39] have revealed the role of the ratio of MMPs and TIMPs such as MMP-1/TIMP-1, MMP-2/TIMP-1, but did not report whether the ratio could be used for the diagnosis of liver fibrosis. We observed that both TIMP-1mRNA/MMP-1mRNA in PBMCs and TIMP-1/MMP-1 in serum could be used for the diagnosis of hepatic fibrosis. However, the former was superior to the latter. The data suggested that we should take both the protein level and mRNA expression into account to explore the noninvasive markers. The value of the serum level of CIV and LN was relatively low. In fact, their AUC values were 0.5 for their *P* values were above 0.05. The roles of serum MMPs in liver fibrosis had been studied[22,47]. Murawaki *et al*[22] found that the serum MMP-1 test was superior to the serum PIIINP test in assessing liver necroinflammation, and thought that the serum MMP-1 test might be useful clinically to differentiate active from inactive types of hepatitis in patients with chronic viral hepatitis, but they did not elucidate whether serum MMP-1 could be more efficient than other indices for assessing liver fibrosis. We evaluated the diagnostic value of MMP-1 for pre-cirrhosis and severe inflammation as there was a difference between patients in S4 or G4 and the normal controls. But the results revealed that the serum level of MMP-1 was of no use for assessing liver fibrosis and evaluating the severity of inflammation. However, our results revealed the declining tendency of the serum MMP-1 with the progress of hepatic fibrosis. The problem is worth further investigating.

The diagnostic value, the sensitivity and the specificity should be taken together, when an index is evaluated for the diagnosis of liver fibrosis. ROC curve analysis revealed that the sensitivity and the specificity of one index were not desirable. Thus, to overcome the limitation of the single index, combination test should be used. There are two kinds of combination test in clinical practice. One is the parallel test and the other is the serial test. The former is often used to screening diseases because it focuses on improving the sensitivity and decreasing the missing incidence. The latter is used to confirm the diagnosis. Table 6 showed that indices in the parallel test were more sensitive than one index. Furthermore, its specificity was also improved. These results revealed that the parallel test was beneficial to screening hepatic fibrosis because hepatic fibrosis continue to progress even though the pathogen have been eliminated. Table 7 showed that the specificity was improved, while the sensitivity was evidently decreased. The data demonstrated that the combination of serum PDGF-BB, HA, TIMP-1mRNA, and TIMP-1mRNA/MMP-1mRNA in PBMCs was clinically limited. However, the specificity of each kind of the combination in the serial test reached close to 100 %, indicating that the diagnostic value of any kind of combination was important and could provide the key information for doctors once some abnormal

results appeared.

In conclusion, we think that serum PDGF-BB, TIMP-1, TIMP-1/MMP-1, TIMP-1mRNA and TIMP-1mRNA/MMP-1mRNA in PBMCs may be used to diagnose hepatic fibrosis. Among them, serum PDGF-BB, TIMP-1mRNA and TIMP-1mRNA/MMP-1mRNA are more sensitive and could be used in clinical practice. The combination of serum PDGF-BB, TIMP-1mRNA and TIMP-1mRNA/MMP-1mRNA in PBMCs is more efficient in screening liver fibrosis. However, the ideal combination for confirming the diagnosis need to be further explored.

REFERENCES

1 **Yuan N**, Wang P, Wang X, Wang Z. Expression and significance of platelet derived growth factor and its receptor in liver tissues of patients with liver fibrosis. *Zhonghua Ganzangbing Zazhi* 2002; **10**: 58-60

2 **Weiner JA**, Chen A, Davis BH. Platelet-derived growth factor is a principal inductive factormodulating mannose 6-phosphate / insulin-like growth factor-II receptorgene expression via a distal E-box in activated hepatic stellate cells. *Biochem J* 2000; **345**(Pt2): 225-231

3 **Kinnman N**, Hultcrantz R, Barbu V, Rey C, Wendum D, Poupon R, Housset C. PDGF-mediated chemoattraction of hepatic stellate cells by bile duct segments in cholestatic liver injury. *Lab Invest* 2000; **80**: 697-707

4 **Benedetti A**, Di Sario A, Casini A, Ridolfi F, Bendia E, Pigini P, Tonnini C, D'Ambrosio L, Feliciangeli G, Macarri G, Svegliati-Baroni G. Inhibition of the NA(+) / H(+)exchanger reduces rat hepatic stellate cell activity and liver fibrosis: an *in vitro* and *in vivo* study. *Gastroenterology* 2001; **120**: 545-556

5 **Issa R,** Williams E, Trim N, Kendall T, Arthur MJ, Reichen J, Benyon RC, Iredale JP. Apoptosis of hepatic stellate cells: involvement in resolution of biliary fibrosis and regulation by soluble growth factors. *Gut* 2001; **48**: 548-557

6 **Huang YX**, Zhang GX, Lu MS, Fan GR, Chen NL, Wu GH. Increased expression of transforming growth factor-β1 in hepatocellular carcinoma. *Shijie Huaren Xiaohua Zazhi* 1999; **7**: 150-152

7 **Wang GY**, Cai WM, Weng HL, Chen F. Changes and significance of TGF-beta1 and IFN- gamma in experimental liver fibrosis. *Zhejiang Yixue Zazhi* 1999; **21**: 469-471

8 **Liu F**, Wang XM, Liu JX, Wei MX. Relationship between serum TGF-β1 of chronic hepatitis B and hepatic tissue pathology and hepatic fibrosis quantity. *ShijieHuaren Xiaohua Zazhi* 2000; **8**: 528-531

9 **Yan JC**, Chen WB, Ma Y, Tian RX, Ding TL, Xu CJ. Relationship between transforming growth factor beta-1 and vascular diseases in hepatitis B. *Shijie Huaren Xiaohua Zazhi* 2001; **9**: 751-754

10 **Dudas J**, Kovalszky I, Gallai M, Nagy JO, Schaff Z, Knittel T, Mehde M, Neubauer K, Szalay F, Ramadori G. Expression of decorin, transforming growth factor-beta1, tissue inhibitor metalloproteinase 1 and 2, and type IV collagenases in chronic hepatitis. *Am J Clin Pathol* 2001; **115**: 725-735

11 **Knittel T**, Mehde M, Grundmann A, Saile B, Scharf JG, Ramadori G. Expression of matrix metalloproteinases and their inhibitors during hepatic tissue repair in the rat. *Histochem Cell Biol* 2000; **113**: 443-453

12 **Mitsuda A**, Suou T, Ikuta Y, Kawasaki H. Changes in serum tissue inhibitor of matrix metalloproteinase-1 after interferon alpha treatment in chronic hepatitis C. *J Hepatol* 2000; **32**: 666-672

13 **Watanabe T,** Niioka M, Hozawa S, Kameyama K, Hayashi T, Arai M, Ishikawa A, Maruyama K, Okazaki I. Gene expression of interstitial collagenase in both progressive and recovery phase of rat liver fibrosis induced by carbon tetrachloride. *J Hepatol* 2000; **33**: 224-235

14 **Yang C**, Hu G, Tan D. Effects of MMP-1 expressing plasmid on rat liver fibrosis. *Zhonghua Ganzangbing Zazhi* 1999; **7**: 230-232

15 **Society of Infectious Disease and Parasitic Disease, CMA.** Criteria on the prevention and treatment for virus hepatitis. *Zhonghua Neike Zazhi* 2001; **40**: 62-68

16 **Cai WM**, Chen F, Zhao JK, Liu RH. The practical value of ultrasound examination in schistosomiasis japonica. *Chin Med J* 2000; **113**

17 **Zheng M**, Cai W, Weng H, Liu R. Determination of serum fibrosis indexes in patients with chronic hepatitis and its significance. *Chin Med J* 2003; **116**: 346-349

18 **Zheng M**, Cai WM, Weng HL, Liu RH. ROC curves in evaluation of serum fibrosis indices for hepatic fibrosis. *World J Gastroenterol* 2002; **8**: 1073-1076

19 **Li C**, Wan M, Zeng M, Su B, He Q, Lu L, Mao Y. A preliminary study of the combination of noninvasive parameters in the diagnosis of liver fibrosis. *Zhonghua Ganzangbing Zazhi* 2001; **9**: 261-263

20 **Tran A**, Hastier P, Barjoan EM, Demuth N, Pradier C, Saint-Paul MC, Guzman-Granier E, Chevallier P, Tran C, Longo F, Schneider S, Piche T, Hebuterne X, Benzaken S, Rampal P. Non invasive prediction of severe fibrosis in patients with alcoholic liver disease. *Gastroenterol Clin Biol* 2000; **24**: 626-630

21 **Cai WM**, Tao J, Weng HL, Liu RH. Study on the influence factors of the serum fibrosis markers. *Zhonghua Ganzangbing Zazhi* 2003; **11**: 23-25

22 **Murawaki Y**, Ikuta Y, Idobe Y, Kawasaki H. Serum matrix metalloproteinase-1 in patients with chronic viral hepatitis. *J Gastroenterol Hepatol* 1999; **14**: 138-145

23 **Okazaki I**, WatanabeT, Hozawa S, Niioka M, Arai M, Maruyama K. Reversibility of hepatic fibrosis: from the first report of collagenase in the liver to the possibility of gene therapy for recovery. *Keio J Med* 2001; **50**: 58-65

24 **Yoshiji H,** Kuriyama S, Miyamoto Y, Thorgeirsson UP, Gomez DE, Kawata M, Yoshii J Ikenaka Y, Noguchi R, Tsujinoue H, Nakatani T, Thorgeirsson SS, Fukui H. Tissue inhibitor of metalloproteinases-1 promotes liver fibrosis development in a transgenic mouse model. *Hepatology* 2000; **32**: 1248-1254

25 **Vaillant B,** Chiaramonte MG, Cheever AW, Soloway PD, Wynn TA. Regulation of hepatic fibrosis and extracellular matrix genes by the th response: new insight into the role of tissue inhibitors of matrix metalloproteinases. *J Immunol* 2001; **167**: 7017-7026

26 **Ninomiya T**, Yoon S, Nagano H, Kumon Y, Seo Y, Kasuga M, Yano Y, Nakaji M, Hayashi Y. Significance of serum matrix metalloproteinases and their inhibitors on the antifibrogenetic effect of interferon –alfa in chronic hepatitis C patients. *Intervirology* 2001; **44**: 227-231

27 **Lichtinghagen R**, Michels D, Haberkorn CI, Arndt B, Bahr M, Flemming P, Manns MP, Boeker KH. Matrix metalloproteinase (MMP)-2, MMP-7, and tissue inhibitor of metalloproteinase-1 are closely related to the fibroproliferative process in the liver during chronic hepatitis C. *J Hepatol* 2001; **34**: 239-247

28 **Daniluk J**, Szuster-Ciesielska A, Drabko J, Kandefer-Szerszen M. Serum cytokine levels in alcohol-related liver cirrhosis. *Alcohol* 2001; **23**: 29-34

29 **Oberti F**, Valsesia E, Pilette C, Rousselet MC, Bedossa P, Aube C, Gallois Y, Rifflet H, Maiga MY, Penneau-Fontbonne D, Cales P. Noninvasive diagnosis of hepatic fibrosis or cirrhosis. *Gastroenterology* 1997; **113**: 1609-1616

30 **Tsushima H**, Kawata S, Tamura S, Ito N, Shirai Y, Kiso S, Doi Y, Yamada A, Oshikawa O, Matsuzawa Y. Reduced plasma transforming growth factor-beta1 levels in patients with chronic hepatitis C after interferon-alpha therapy: association with regression of hepatic fibrosis. *J Hepatol* 1999; **30**: 1-7

31 **Flisiak R**, Pytel-Krolczuk B, Prokopowicz D. Circulating transforming growth factor beta (1) as an indicator of hepatic function impairment in liver cirrhosis. *Cytokine* 2000; **12**: 677-681

32 **Matsuzaki K**, Date M, Furukawa F, Tahashi Y, Matsushita M, Sakitani K, Yamashiki N, Seki T, Saito H, Nishizawa M, Fujisawa J, Inoue K. Autocrine stimulatory mechanism by transforming growth factor beta in human hepatocellular carcinoma. *Cancer Res* 2000; **60**: 1394-1402

33 **Shah M**, Revis D, Herrick S, Baillie R, Thorgeirson S, Ferguson M, Roberts A. Role of elevated plasma transforming growth facotor-beta1 levels in wound healing. *Am J Pathol* 1999; **154**: 1115-1124

34 **Okuno M**, Akita K, Moriwaki H, Kawada N, Ikeda K, Kaneda K, Suzuki Y, Kojima S. Prevention of rat hepatic fibrosis by the protease inhibitor, camostat mesilate, via reduced generation of active TGF-beta. *Gastroenterology* 2001; **120**: 1784-1800

35 **Breitkopf K**, Lahme B, Tag CG, Gressner AM. Expression and matrix deposition of latent transforming growth factor beta binding proteins in normal and fibrotic rat liver and transdifferentiating hepatic stellate cells in culture. *Hepatology* 2001; **33**: 387-396

36 **Kobayashi H**, Horikoshi K, Yamataka A, Lane GJ, Furuhata A, Sueyoshi N, Miyano T. Are stable postoperative biliary atresia patients really stable? *Pediatr Surg Int* 2001; **17**: 104-107
37 **Chen F,** Cai W, Chen Z, Chen X, Liu R. Dynamic changes in the collagen metabolism of liver fibrosis at the transcription level in rabbits with Schistosomiasis japonica. *Chin Med J* 2002; **115**: 1637-1640
38 **Yata Y**, Takahara T, Furui K, Zhang LP, Jin B, Watanabe A. Spatial distribution of tissue inhibitor of metalloproteinase-1 mRNA in chronic liver disease. *J Hepatol* 1999; **30**: 425-432
39 **Lichtinghagen R**, Huegel O, Seifert T, Haberkorn CI, Michels D, Flemming P, Bahr M, Boeker KH. Expression of matrix metalloproteinase-2 and -9 and their inhibitors in peripheral blood cells of patients with chronic hepatitis C. *Clin Chem* 2000; **46**: 183-192
40 **Boker KH,** Pehle B, Steinmetz C, Breitenstein K, Bahr M, Lichtinghagen R. Tissue inhibitors of metalloproteinases in liver and serum / plasma in chronic active hepatitis C and HCV-induced cirrhosis. *Hepatogastroenterology* 2000; **47**: 812-819
41 **Ikeda K**, Wakahara T, Wang YQ, Kadoya H, Kawada N, Kaneda K. *In vitro* migratory potential of rat quiescent hepatic stellate cells and its augmentation by cell activation. *Hepatology* 1999; **29**: 1760-1767
42 **Powell DW**, Mifflin RC, Valentich JD, Crowe SE, Saada JI, West AB. Myofibroblasts. II. Intestinal subepithelial myofibroblasts. *Am J Physiol* 1999; **277**(2 Pt1): C183-201
43 **Wang SN**, Hirschberg R. Growth factor ultrafiltration in experimental diabetic nephropathy contributes to interstitial fibrosis. *Am J Physiol Renal Physiol* 2000; **278**: F554-560
44 **Lohmann CH**, Schwartz Z, Niederauer GG, Carnes DL Jr, Dean DD, Boyan BD. Pretreatment with platelet derived growth factor-BB modulates the ability of costochondral resting zone chondrocytes incorporated into PLA / PGA scaffolds to form new cartilage *in vivo*. *Biomaterials* 2000; **21**: 49-61
45 **Murawaki Y,** Ikuta Y, Kawasaki H. Clinical usefulness of serum tissue inhibitor of metalloproteinases (TIMP)-2 assay in patients with chronic liver disease in comparison with serum TIMP-1. *Clin Chim Acta* 1999; **281**: 109-120
46 **Walsh KM,** Timms P, Campbell S, MacSween RN, Morris AJ. Plasma levels of matrix metalloproteinase-2 (MMP-2) and tissue inhibitors of metalloproteinases-1 and -2 (TIMP-1 and TIMP-2) as noninvasive markers of liver disease in chronic hepatitis C: comparison using ROC analysis. *Dig Dis Sci* 1999; **44**: 624-630
47 **Nie QH,** Cheng YQ, Xie YM, Zhou YX, Bai XG, Cao YZ. Methodologic research on TIMP-1, TIMP-2 detection as a new diagnostic index for hepatic fibrosis and its significance. *World J Gastroenterol* 2002; **8**: 282-287

Edited by Ma JY and Wang XL

P.O.Box 2345, Beijing 100023,China
Fax: +86-10-85381893
E-mail: wjg@wjgnet.com www.wjgnet.com

World J Gastroenterol 2003;9(11):2497-2500
World Journal of Gastroenterology
 ISSN 1007-9327

Influence factors of serum fibrosis markers in liver fibrosis

Jun Tao, Hui-Qin Peng, Wei-Min Cai, Feng-Qin Dong, Hong-Lei Weng, Rong-Hua Liu

Jun Tao, Hui-Qin Peng, Wei-Min Cai, Feng-Qin Dong, Hong-Lei Weng, Rong-Hua Liu, Institute of Infectious Diseases, First Affiliated Hospital, School of Medicine, Zhejiang University, Hangzhou 310003 Zhejiang Province, China
Correspondence to: Dr. Jun Tao, Institute of Infectious Diseases, First Affiliated Hospital, School of Medicine, Zhejiang University, Hangzhou 310003 Zhejiang Province, China. taojun20001@163.com
Telephone: +86-571-87236580 **Fax:** +86-571-87068731
Received: 2003-05-12 **Accepted:** 2003-06-02

Abstract

AIM: To analyze the factors which influence the serum levels of hyaluronic acid (HA), type III pro-collagen (PCIII), laminin (LN) and type IV collagen (C-IV) in liver fibrosis.

METHODS: The serum specimens from 141 chronic hepatitis patients were assayed for fibrosis indexes including HA, PCIII, LN and C-IV with radioimmunoassay (RIA) and liver function indexes by an automatic biochemistry analyzer. The patients were then divided into consistent group and inconsistent group. The patients' clinical manifestations were recorded, routine blood pictures were done by a blood counter and analyzer (AC-900). Liver biopsy specimens were examined path-morphologically. The inner diameters of portal vein, splenic vein and thickness of spleen were all measured by ultrasonography.

RESULTS: Sixteen patients (14.16 %) had serum fibrosis indexes inconsistent with histological stage of their hepatic fibrosis. Their serum fibrosis indexes did not correlate with the stage of hepatic fibrosis ($P>0.05$), but were positively correlated with the grade of inflammation ($\chi^2=12.07$, $P<0.05$). At the same time, serum albumin (ALB) and the ratio of albumin and globulin (A/G) were significantly increased ($t=3.06$, $P<0.01$), ($t=3.70$, $P<0.01$). Serum levels of glutamic-pyruvic transaminase (ALT), glutamic-oxaloacetic transaminase (AST), γ-glutamyl transferase (GGT) and globulin (GLB) were all significantly decreased ($t=2.45$, $P<0.05$), ($t=2.33$, $P<0.05$), ($t=2.08$, $P<0.05$), ($t=3.03$, $P<0.01$). Weary degree also decreased more obviously ($\chi^2=7.52$, $P<0.05$), but other clinical manifestations, routine blood indexes, serum levels of alkaline phosphatase (AKP), total bilirubin (TBIL), total protein (TP), width of main portal vein, width of splenic vein and thickness of spleen had no significant change ($P>0.05$).

CONCLUSION: Serum fibrosis indexes can be influenced by the grade of inflammation, some liver function indexes and clinical manifestations. Comprehensive analysis is necessary for its proper interpretation.

Tao J, Peng HQ, Cai WM, Dong FQ, Weng HL, Liu RH. Influence factors of serum fibrosis markers in liver fibrosis. *World J Gastroenterol* 2003; 9(11): 2497-2500
http://www.wjgnet.com/1007-9327/9/2497.asp

INTRODUCTION

Many chronic injuries can lead to fibrosis of liver[1-11]. Hepatic fibrosis is resulted from the loss of normal liver cell function due to disorganized over-accumulation of extra-cellular matrix (ECM) components in the liver[12-17]. It is clear that the increased production and degradation of ECM components are responsible for the altered ECM metabolism. Liver biopsy has traditionally been the standard method for assessing hepatic fibrosis, but the procedure is invasive in nature and has complications though with a low incidence. So its popularity is somewhat hindered. Reports showed that serum fibrosis indexes, including HA, PCIII, LN, C-IV and others, could reflect the activity of hepatic fibrosis to some extent[18-27]. Mean ± SD has always been used to express the standard for hepatic fibrosis. We have explored the clinical significance of the four serum fibrosis indexes by detecting them in 2 600 patients with chronic hepatitis including 280 patients undertaken biopsy[28,29]. At same time, patients whose four serum fibrosis indexes were not consistent with the degree of hepatic fibrosis were found, so we selected these patients to analyze what factors might influence the four serum fibrosis indexes (HA, PCIII, LN and C-IV) in diagnosing liver fibrosis.

MATERIALS AND METHODS

Subjects

During the Sixth National Conference for Infectious and Parasitic Diseases, the protocol of prevention and treatment for virus hepatitis was modified in 2000 (abbreviated as "2000 criteria")[30]. One hundred and forty-one patients had typical presentations of chronic hepatitis, 121 were males and 20 females. There were mild, moderate and severe degrees of the disease in the group. Case histories were mainly collected from the First Affiliated Hospital, School of Medicine, Zhejiang University. Some were from other hospitals in Zhejiang Province between July, 1998 and May, 2000. The age ranged from 18 to 62 years, the average age was 38.75±14.53. Weary Degree: 0: did not feel weary; 1: could join routine activities, but felt weary; 2: could join light work, but felt weary; 3: could not work, felt weary while moving. The disease course was from one to 30 years.

Clinical manifestations

Total volume of food taken by the patient every day, length of liver and spleen under costal margin were recorded. The criteria of clinical manifestations were as following: (1). Weary degree: as stated above. (2). Degree of abdominal distension: 0: did not feel abdominal distension; 1: felt abdominal distension while taking food or abdominal distension usually; 2: felt abdominal distension while taking a little food, but can endure; 3: felt abdominal distension, did not want to take food, felt abdominal distension while taking food, can not endure. (3). Secret anguish degree: 0: did not feel secret anguish; 1: felt secret anguish, but could take food; 2: felt secret anguish, could endure; 3: felt secret anguish, could not endure, needed medication.

Histology

The needles (18G) were purchased from Angiomed Corporation in German. The length of liver biopsy specimen exceeded 1 cm. Biopsy fragments of the livers were fixed in 10 % neutralized formaldehyde, embedded in paraffin, and then stained with hematoxylin and eosin. Reticulum fibrosis

stain and Sirius red method were used specially for staining fibrous tissue components. Histological assessment of the liver was done according to Wang' s report[31], and staging of fibrosis was divided into four, expressed as S1 to S4 according to the "2000 criteria"[30]. S0 showed no fibrosis. S1 showed expansion in portal tract areas with fibrosis. S2 showed fibrosis around portal tract areas with formation of fibrosis segregation while maintain lobular structure. S3 showed formation of fibrosis segregation and disorder of lobular structure without hepatic cirrhosis, and S4 showed early stage or confirmed cirrhosis.

Determination of serum fibrosis tests and liver function indexes

The serum specimens from 141 chronic hepatitis patients were stored at -20 ℃. Assay of the levels of serum HA, PCIII, C-IV and LN was done by RIA. The kits of HA, C-IV and LN were provided by the Shanghai Navy Medical Institute. The kit of PCIII was supplied by the Chongqing Tumor Institute. The procedures were performed according to the user' s manual. The assay of liver function indexes was measured by an automatic biochemistry analyzer, these indexes included total bilirubin (TBIL), gliutamic-pyruvic transaminase (ALT), glutamic-oxaloacetic transaminase (AST), γ glutamyl-transferase (GGT), alkaline phosphatase (AKP), total protein (TP), albumin (ALB), globulin (GLB) and the ratio of albumin and globulin (A/G).

Determination of routine blood indexes

Blood samples were drawn from the veins and treated with EDTA-K_2 (the concentration was 1.5 mg/ml). WBC, RBC and platelet were determined by a blood cell counter and analyzer (AC-900).

Ultrasonic examination

All patients were forbidden to take water and food for eight hours before examination. Inner diameters of the portal vein, splenic vein and thickness of the spleen were measured, all the procedures were performed by the same physician.

Definition of patients whose serum fibrosis indexes were inconsistent with histologic staging of their hepatic fibrosis

All patients were divided into two groups. If in S≥2 group, all four serum fibrosis indexes were less than or equal to the mean value of that in S1 group, these patients would then be classified as inconsistent group. On the contrary, they would be classified as the consistent group. There was also inconsistency in a single index, that meant staging belonged to S≥2, but the index was less than or equal to the mean of that in S1 group.

Statistical analysis

Results were expressed as mean ± standard deviation ($\bar{x}\pm s$) and *t* test was done when necessary, nonparametric one-way ANOVA was used for nonparametric data, all tests were done by SPSS 10.0 statistical program and considered statistically significant at $P<0.05$.

RESULTS

Inconsistency between each serum fibrosis index and stage of hepatic fibrosis

When hepatic fibrosis was in stage 1, the mean of HA was 187.23 ng/ml, LN was 144.68 ng/ml, PCIII was 151.42 μg/L, and C-IV was 74.26 μg/L. One hundred and thirteen patients were found in hepatic fibrosis stage II or more than that, 33 cases were inconsistent with staging of hepatic fibrosis for HA. More cases were inconsistent for C-IV, 43 cases were inconsistent with staging of hepatic fibrosis for LN (Table 1).

Table 1 Inconsistency between each serum fibrosis index and stage of hepatic fibrosis

Stage (S)	*n*	HA	C-IV	PCIII	LN
S2	30	13	14	16	17
S3	31	9	10	10	11
S4	52	11	12	13	15
Total	113	33 (29.20%)	36(31.86%)	39(34.51%)	43 (38.05%)

Distribution of patients whose four serum fibrosis indexes were inconsistent with stage of hepatic fibrosis

Among 113 patients, 16 (14.16 %) were in inconsistent group and 97(85.84 %) in consistent group, no significant difference was found in staging of hepatic fibrosis between two groups ($P>0.05$), (Table 2).

Table 2 Staging comparison between two groups

Groups	Stage of hepatic fibrosis		
	S2	S3	S4
Consistent group	24	27	46
Inconsistent group	6	4	6

$\chi^2=1.18$, $P>0.05$.

Inflammation grading of patients in inconsistent group

Table 3 shows that inflammation grade was mainly G2 in inconsistent group, while mainly G3 and G4 in consistent group. The difference was significant between two groups ($P<0.05$).

Table 3 Comparison of inflammation grade between two groups

Groups	Inflammation grade			
	G1	G2	G3	G4
Consistent group	5	17	49	26
Inconsistent group	1	9	4	2

$\chi^2=12.07$, $P<0.05$.

Clinical manifestations in inconsistent group

Table 4 and table 5 show no patient whose degree of weary, abdominal distension and secret anguish exceeded 2 in consistent group. There was no patient whose degree of weary, abdominal distension and secret anguish exceeded 1 in inconsistent group. The daily food volume of the patients increased slightly, the palpable length of liver and spleen decreased slightly. The difference was not significant between two groups ($P>0.05$) except weary degree ($P<0.05$).

Table 4 Comparison of clinical manifestations between two groups

Groups	Weary degree			Abdominal distension degree			Secret anguish degree		
	0	1	2	0	1	2	0	1	2
Consistent group	39	41	17	72	24	1	86	8	3
Inconsistent group	12[a]	4	0	14	2	0	16	0	0

$\chi^2=7.52$, $P<0.05$.

Table 5 Comparison of clinical manifestations between two groups ($\bar{x}\pm s$)

Groups	*n*	Volume of food(g)	Length of liver (cm)	Length of spleen(cm)
Consistent group	97	427.11±194.15	0.31±0.63	0.53±0.85
Inconsistent group	16	456.25±160.08	0.28±0.55	0.34±0.60

Change of routine blood indexes in inconsistent group

No significant difference was found in WBC, RBC and PLT between two groups (P>0.05), (Table 6).

Table 6 Comparison of routine blood tests between two groups ($\bar{x}\pm s$)

Groups	*n*	WBC	RBC	PLT
Consistent group	97	5.07±1.12	4.61±0.52	116.52±34.14
Inconsistent group	16	4.90±1.24	4.64±0.57	117.00±26.38

Change of liver function tests in inconsistent group

Serum ALT, AST, GGT and GLB decreased obviously in inconsistent group (P<0.05) or (P<0.01), ALB and A/G increased evidently (P<0.01), but AKP, TBIL and TP did not change significantly (P>0.05), (Table 7).

Table 7 Comparison of liver function tests between two groups ($\bar{x}\pm s$)

Groups	*n*	TBIL (μmol/L)	TP (g/L)	ALB (g/L)	GLB (g/L)	A/G
Consistent group	97	18.19±8.51	74.60±6.75	42.34±4.81	32.13±5.18	1.35±0.28
Inconsistent group	16	16.35±6.41	74.31±4.36	46.19±3.61[b]	28.05±3.47[b]	1.63±0.26[b]

[b]P<0.01 *vs* consistent group

Groups	*n*	ALT(U/L)	AST(U/L)	GGT(U/L)	AKP(U/L)
Consistent group	97	89.28±64.25	66.10±42.30	86.26±70.36	91.65±34.95
Inconsistent group	16	49.31±26.75[a]	40.83±22.40[a]	48.99±29.96[a]	85.25±30.60

[a]P<0.05 *vs* consistent group.

Results of ultrasonic examination in inconsistent group

Table 8 shows no significant difference in width of main portal vein, splenic vein and thickness of spleen between two groups (P>0.05).

Table 8 Comparison of ultrasonic examination between two groups (cm, $\bar{x}\pm s$)

Groups	*n*	Width of main portal vein	Width of splenic vein	Thickness of spleen
Consistent group	97	1.20±0.13	0.74±0.12	4.02±0.64
Inconsistent group	16	1.23±0.12	0.77±0.13	4.09±0.62

DISCUSSION

The basic pathological changes of chronic liver disease are inflammation and fibrosis, so they were analysed respectively in pathological diagnosis in recent year. Many semi quantitative score systems, such as Chevallier's criterion, Scheuer's criterion were developed[31-33], so chronic liver disease has been recognized more accurately and profoundly. Staging of liver fibrosis can help us to recognize the development of chronic liver disease. Serum indexes such as HA, PCIII, LN and C-IV which reflect the stage of liver fibrosis have been paid much attention to by many scholars[34-36] HA, PCIII, LN and C-IV were mainly produced by hepatic stellate cells[35,36]. HA and PCIII were absorbed and degraded by endothelial cells of hepatic sinusoids[37,38]. When liver fibrosis takes place, the phenotypes of the membrane of endothelial cells of hepatic sinusoids change, their absorption is blocked, the contents of serum HA, PCIII increase to some degree. LN and C-IV reflected basement membrane transformation and had some relation to portal hypertension[39,40]. Many scholars agreed the four serum fibrosis indexes had values in the serodiagnosis of hepatic fibrosis, including the diagnostic value of each serum fibrosis index and combination of several indexes[20,29]. When these indexes were applied to clinical diagnosis, we found some of them were inconsistent with pathological diagnosis. Even with a high stage of hepatic fibrosis, the four serum fibrosis indexes could still be around normal range. So we think it is necessary to find the influencing factors of this phenomenon.

Our results showed the rate of inconsistency between the four serum fibrosis indexes and stage of hepatic fibrosis was 14.16 % in the patients with chronic hepatitis. Table 1 shows the rate of inconsistency of serum HA was 29.21 %, C-IV 31.86 %, PCIII 34.51 % and LN 38.05 %. The rate of consistency between serum HA and stage of hepatic fibrosis was highest, followed by C-IV. This suggests that among the four serum fibrosis indexes, HA is the most ideal index for diagnosing hepatic fibrosis. This was consistent with the results of our previous study on the relationship between serum fibrosis indexes and liver histological changes[41], and was also consistent with other reports in the literature[42]. Stage distribution of hepatic fibrosis in inconsistent patients had no significant difference from that of consistent group. This indicates that inconsistency between the four serum fibrosis indexes and stage of hepatic fibrosis has no relationship with the staging. By further study we found inflammation grade of inconsistent patients was lower than that of consistent group. This suggests that the four serum fibrosis indexes are influenced by inflammation grade. In the patients with chronic hepatitis when their stage of hepatic fibrosis is at high level, such as S3 or S4, and inflammation grade is at low level, it is possible that the four serum fibrosis indexes can be inconsistent with stage of hepatic fibrosis. This could be found in patients with advanced stage of schistosomiasis japonica having severe liver fibrosis, but almost no inflammation or decompensation of hepatic function. In addition, it was also suggested that these four serum fibrosis indexes could be lowered by anti-inflammation treatment in patients with chronic hepatitis. As to clinical manifestations, weary degree of inconsistent patients decreased more obviously than that in consistent group. Other profiles had no obvious change. In liver function tests, we found serum ALT, AST, GGT and GLB of inconsistent patients were decreased more obviously, while serum ALB and A/G increased more evidently, serum AKP, TP and TBIL had no significant change. All these suggest that changes of weary degree, serum ALT, AST, GGT, GLB, ALB and A/G were affected by inflammation grade. So they should be taken into account when we assess the diagnostic value of the four serum fibrosis indexes for stage of hepatic fibrosis. At the same time, change of liver function indexes is more sensitive than clinical manifestations. So even without any clinical symptoms, patients should be checked regularly by liver function tests. In clinical practice, width of main portal vein, splenic vein and thickness of the spleen are usually used to determine whether the pressure of main portal vein is increased or not. Table 7 shows they had no significant change, indicating that these patients' condition did not reach the stage of liver cirrhosis.

We conclude that serum fibrosis indexes can only reflect abnormal metabolism of ECM. They are non-specific biochemical markers, when they are used in the diagnosis of hepatic fibrosis, other diseases should be ruled out. They should not be called hepatic fibrosis markers, serum fibrosis indexes should be the appropriate term. Our study indicates the influencing factors include hepatic inflammatory activity, weary degree and some liver function tests. The activity of inflammation is determined by pathological diagnosis of liver biopsy. So in clinical practice, we should put liver function, case history and clinical manifestations all into consideration in assessment of the diagnostic value of these four fibrosis indexes in the staging of hepatic fibrosis. While assessing therapeutic efficacy of anti-fibrosis drugs, we can also not

depend only on these four fibrosis indexes, a comprehensive analysis is necessary. Further studies on new indexes are needed to better understand the pathological changes of liver.

REFERENCES

1 **Friedman SL**. Molecular mechanisms of hepatic fibrosis and principles of therapy. *J Gastroenterol* 1997; **32**: 424-430
2 **Du LJ**, Tang WX, Dan ZL, Zhang WY, Li SB. Protective effect of Ganyanping on CCl-4 induced liver fibrosis in rats. *Huaren Xiaohua Zazhi* 1998; **6**: 21-22
3 **Yan JC**, Ma Y, Chen WB, Shen XH. Dynamic observation on liver fibrosis and cirrhosis of hepatitis B. *Huaren Xiaohua Zazhi* 1998; **6**: 699-702
4 **Peng YZ**, Huang QT, Yan SN, Deng B, Hu JJ. Effect of RNA against hepatic fibrosis in rabbits infected with Schistosomiasis japonica. *Zhongguo Jishengchongxue Yu Jishengchongbing Zazhi* 1998; **16**: 214-218
5 **Piscaglia F**, Gaiani S, Gramantieri L, Zironi G, Siringo S, Bolondi L. Superior mesenteric artery impedance in chronic liver disease: relationship with disease severity and portal circulation. *Am J Gastroenterol* 1998; **93**: 1925-1930
6 **Assy N**, Paizi M, Gaitini D,Baruch Y, Spira G. Clinical implication of VEGF serum levels in cirrhotic patients with or without portal hypertension. *World J Gastroenterol* 1999; **5**: 296-300
7 **Liu F**, Liu JX, Cao ZC, Li BS, Zhao CY, Kong L, Zhen Z. Relationship between TGF-β1, serum indexes of liver fibrosis and hepatic tissue pathology in patients with chronic liver diseases. *Shijie Huaren Xiaohua Zazhi* 1999; **7**: 519-521
8 **Yao SK**, Yin F. Diagnosis and treatment of hepatic fibrosis. *Shijie Huaren Xiaohua Zazhi* 2000; **8**: 681-683
9 **Bai WY**, Yao XX, Feng LY. The situation of hepatic fibrosis research. *Shijie Huaren Xiaohua Zazhi* 2000; **8**: 1267-1268
10 **Lin H**, Lü M, Zhang YX, Wang BY, Fu BY. Induction of a rat model of alcoholic liver diseases. *Shijie Huaren Xiaohua Zazhi* 2001; **9**: 24-28
11 **Chen WX**, Li YM, Yu CH, Cai WM, Zheng M, Chen F. Quantitatively analysis of transforming growth factor beta 1 mRNA in patients with alcoholic liver disease. *World J Gastroenterol* 2002; **8**: 379-381
12 **Cai WM**, Chen Z, Chen F, Zhou C, Liu RH, Wang JX. Changes of ultrasonography and two serum biochemical indices for hepatic fibrosis in schistosomiasis japonica patients one year after praziquantel treatment. *Chin Med J (Engl)* 1997; **110**: 797-800
13 **Bissell DM**. Hepatic fibrosis as wound repair: a progress report. *J Gastroenterol* 1998; **33**: 295-302
14 **Sun DL**, Sun SQ, Li TZ, Lu XL. Serologic study on extracellular matrix metabolism in patients with viral liver cirrhosis. *Shijie Huaren Xiaohua Zazhi* 1999; **7**: 55-56
15 **Apte MV**, Haber PS, Darby SJ, Rodgers SC, McCaughan GW, Korsten MA, Pirola RC, Wilson JS. Pancreatic stellate cells are activated by proinflammatory cytokines: implications for pancreatic fibrogenesis. *Gut* 1999; **44**: 534-541
16 **Ueki N**, Taguchi T, Takahashi M, Adachi M, Ohkawa T, Amuro Y, Hada T, Higashino K. Inhibition of hyaluronan synthesis by vesnarinone in cultured human myofibroblasts. *Biochim Biophys Acta* 2000; **1495**: 160-167
17 **Li C**, Wan M, Zeng M, Su B, He Q, Lu L, Mao Y. A preliminary study of the combination of noninvasive parameters in the diagnosis of liver fibrosis. *Zhonghua Ganzangbing Zazhi* 2001; **9**: 261-263
18 **Wang X**, Chen YX, Xu CF, Zhao GN, Huang YX, Wang QL. Relationship between tumor necrosis factor-α and liver fibrosis. *World J Gastroenterol* 1998; **4**: 18
19 **Guechot J**, Serfaty L, Bonnand AM, Chazouilleres O, Poupon RE, Poupon R. Prognostic value of serum hyaluronan in patients with compensated HCV cirrhosis. *J Hepatol* 2000; **32**: 447-452
20 **Luo R**, Yang S, Xie J, Zhao Z, He Y, Yao J. Diagnostic value of five serum markers for liver fibrosis. *Zhonghua Ganzangbing Zazhi* 2001; **9**: 148-150
21 **Lu X**, Liu CH, Xu GF, Chen WH, Liu P. Successive observation of laminin and collagen IV hepatic sinusoid during the formation of the liver fibrosis in rats. *Shijie Huaren Xiaohua Zazhi* 2001; **9**: 260-262
22 **Shen M**, Qiu DK, Chen Y, Xiong WJ. Effects of recombinant augmenter of liver regeneration protein, danshen and oxymatrine on rat fibroblasts. *Shijie Huaren Xiaohua Zazhi* 2001; **9**: 1129-1133
23 **He Y**, Wang JB, Wang YM. The diagnosis development of hepatic fibrosis with chronic hepatitis. *Shijie Huaren Xiaohua Zazhi* 2001; **9**: 1305-1309
24 **Leroy V**, De Traversay C, Barnoud R, Hartmann JD, Baud M, Ouzan D, Zarski JP. Changes in histological lesions and serum fibrogenesis markers in chronic hepatitis C patients non-responders to interferon alpha. *J Hepatol* 2001; **35**: 120-126
25 **Xie S**, Zheng R, Peng X, Gao Z. Accurate diagnosis of stage of hepatic fibrosis by measuring levels of serum hyaluronic acid, procollagen type III, and collagen type IV. *Zhonghua Ganzangbing Zazhi* 2001; **9**: 334-336
26 **Cai WM**, Chen F, Zhao JK, Liu RH. The practical value of ultrasomel examination in schistosomiasis japonica. *Zhonghua Yixue Zazhi* 2000: **113**
27 **Zhang BB**, Cai WM, Weng HL, Hu ZR, Lu J, Zheng M, Liu RH. Diagnostic value of platelet derived growth factor-BB, transforming growth factor-β1, matrix metalloproteinase-1 and tissue inhibitor of matrix metalloproteinase-1 in serum and peripheral blood mononucleocytes for hepatic fibrosis. *World J Gastroenterol* 2003; **9**: (in press)
28 **Zheng M**, Cai W, Weng H, Liu R. Determination of serum fibrosis indexes in patients with chronic hepatitis and its significance. *Chin Med J (Engl)* 2003; **116**: 346-349
29 **Zheng M**, Cai WM, Weng HL, Liu RH. ROC curves in evaluation of serum fibrosis indices for hepatic fibrosis. *World J Gastroenterol* 2002; **8**: 1073-1076
30 Chinese Society of Infectious disease and Parasitology and Chinese Society of Hepatology of Chinese medical association. The programme of prevention and cure for viral hepatitis. *Zhonghua Ganzangbing Zazhi* 2000; **8**: 324-329
31 **Wang TL**, Liu X, Zhou YP, He JW, Zhang J, Li NZ, Duan ZP, Wang BE. A semiquantitative scoring system for evaluation of hepatic inflammation and fibrosis in chronic viral hepatitis. *Zhonghua Ganzangbing Zazhi* 1998; **6**: 195-197
32 **Scheuer PJ**. Classification of chronic viral hepatitis: a need for reassessment. *J Hepatol* 1991; **13**: 372-374
33 **Chevallier M**, Guerret S, Chossegros P, Gerard F, Grimaud JA. A histological semiquantitative scoring system for evaluation of hepatic fibrosis in needle liver biopsy specimens: comparison with morphometric studies. *Hepatology* 1994; **20**: 349-355
34 **Li BS**, Wang J, Zhen YJ, Liu JX, Wei MX, Sun SQ, Wang SQ. Experimental study on serum fibrosis markers and liver tissue pathology and hepatic fibrosis in immuno-damaged rats. *Shijie Huaren Xiaohua Zazhi* 1999; **7**: 1031-1034
35 **Oberti F**, Valsesia E, Pilette C, Rousselet MC, Bedossa P, Aube C, Gallois Y, Rifflet H, Maiga MY, Peaneau-Fontbonne D, Cales P. Noninvasive diagnosis of hepatic fibrosis or cirrhosis. *Gastroenterology* 1997; **113**: 1609-1616
36 **Xie S**, Yao J, Zheng S, Yao C, Zheng R. The relationship between the levels of serum fibrosis marks and morphometric quantitative measurement of hepatic histological fibrosis. *Zhonghua Ganzangbing Zazhi* 2000; **8**: 203-205
37 **Tamaki S**, Ueno T, Torimura T, Sata M, Tanikawa K. Evaluation of hyaluronic acid binding ability of hepatic sinusoidal endothelial cells in rats with liver cirrhosis. *Gastroenterology* 1996; **111**: 1049-1057
38 **Nanji AA**, Tahan SR, Khwaja S, Yacoub LK, Sadrzadeh SM. Elevated plasma levels of hyaluronic acid indicate endothelial cell dysfunction in the initial stages of alcoholic liver disease in the rat. *J Hepatol* 1996; **24**: 368-374
39 **Li L**, Yao ZM, Yu T. Influence of BOL on hyaluronic acid, laminin and hyperplasia in hepatofibrotic rats. *World J Gastroenterol* 2001; **7**: 872-875
40 **Cui DL**, Yao XX. Serum diagnosis of hepatic fibrosis. *Shijie Huaren Xiaohua Zazhi* 2000; **8**: 683-684
41 **Cai W**, Zheng M, Weng H, Liu RH. Determination and significance of serum markers for fibrosis in patients with chronic hepatitis. *Zhonghua Neike Zazhi* 2001; **40**: 448-451
42 **Gu S**, Zhang H, Zhang L. Relationship between serum fibrosis markers and fibrosis quantitative analysis of liver tissue. *Zhonghua Ganzangbing Zazhi* 1999; **7**: 199-200

Edited by Xu JY and Wang XL

P.O.Box 2345, Beijing 100023,China
Fax: +86-10-85381893
E-mail: wjg@wjgnet.com www.wjgnet.com

World J Gastroenterol 2003;9(11):2501-2504
World Journal of Gastroenterology
 ISSN 1007-9327

Detection of serum anti-*Helicobacter pylori* immunoglobulin G in patients with different digestive malignant tumors

Ke-Xia Wang, Xue-Feng Wang, Jiang-Long Peng, Yu-Bao Cui, Jian Wang, Chao-Pin Li

Ke-Xia Wang, Xue-Feng Wang, Jiang-Long Peng, Yu-Bao Cui, Jian Wang, Chao-Pin Li, School of Medicine, Anhui University of Science and Technology, Huainan, 232001, Anhui Province, China
Supported by Natural Science Foundation of the Education Department of Anhui Province, China, No.2003kj111
Correspondence to: Dr. Chao-Pin Li, Department of Etiology and Immunology, School of Medicine, Anhui University of Science and Technology,Huainan, 232001, Anhui Province, China. cpli@aust.edu.cn
Telephone: +86-554-6658770 **Fax:** +86-554-6662469
Received: 2003-03-02 **Accepted:** 2003-06-04

Abstract

AIM: To investigate the seroprevalence of *Helicobacter pylori* infection in patients with different digestive malignant tumors.

METHODS: Enzyme linked immunosorbent assay (ELISA) was used to detect serum anti-*Helicobacter pylori* IgG antibody in 374 patients with different digestive malignant tumors and 310 healthy subjects (normal control group).

RESULTS: The seroprevalence of *Helicobacter pylori* infection was 61.50 %(230/374) and 46.77 % (145/310), respectively, in patients with digestive tumors and normal controls ($P<0.05$). The seroprevalence was 52.38 % (33/63), 86.60 % (84/97), 83.14 % (84/101), 45.24 (19/42), 51.13 % (18/35) and 44.44 % (16/36), respectively in patients with carcinomas of esophagus, stomach, duodenum, rectum, colon and liver ($P<0.01$). In patients with intestinal and diffuse type gastric cancers, the seroprevalence was 93.75 % (60/64) and 72.73 % (24/33), respectively ($P<0.05$). In patients with gastric antral and cardiac cancers, the seroprevalence was 96.43 % (54/56) and 73.17 % (30/41), respectively ($P<0.05$). In patients with ulcerous and proliferous type duodenal cancers, the seroprevalence of *H pylori* infection was 91.04 % (61/67) and 52.27 % (23/44), respectively ($P<0.05$). In patients with duodenal bulb and descending cancers, the seroprevalence was 94.20 % (65/69) and 45.20 % (19/42), respectively ($P<0.05$).

CONCLUSION: *H pylori* infection is associated with occurrence and development of gastric and duodenal carcinomas. Furthermore, it is also associated with histological type and locations of gastric and duodenal carcinomas.

Wang KX, Wang XF, Peng JL, Cui YB, Wang J, Li CP. Detection of serum anti-*Helicobacter pylori* immunoglobulin G in patients with different digestive malignant tumors. *World J Gastroenterol* 2003; 9(11): 2501-2504
http://www.wjgnet.com/1007-9327/9/2501.asp

INTRODUCTION

Helicobacter pylori is a gram-negative, spiral-shaped, microaerophilic bacterium that colonizes gastric epithelium of humans[1-4]. Clinical and epidemiological studies have shown a close association between *H pylori* and gastric cancer[5-10]. However, the relationship between *H pylori* and other digestive tumors has not been clarified. In order to investigate the relationship between *H pylori* infection and different digestive cancers, we detected serum anti-*H pylori* IgG in 374 patients with different digestive cancers and 310 healthy subjects, using an enzyme linked immunosorbent assay -(ELISA).

MATERIALS AND METHODS

Materials

Populations A total of 374 patients with different digestive cancers were involved in this study, including 63 esophagus carcinomas, 97 gastric cancers (64 of intestinal type and 33 of diffuse type, and 56 in gastric antrum and 41 in the cardia as displayed under gastroscopy), 101 duodenal carcinomas (67 of ulcerous type and 44 of proliferous type, and 65 in the bulb and 42 in the descending part of duodenum as manifested under gastroscopy), 42 rectal cancers, 35 carcinomas of colon, 36 liver cancers. There were 240 males and 134 females, aged from 23 to 71 years old. At the same time, 310 healthy subjects were recruited as a control group. There was no difference in age and gender between the two groups.

Reagents and instruments The test kit for *H pylori*-IgG was provided by Bioseed Company (USA, batch Hillbough CA 94010). The enzyme-labeling meter was SLT-Spectra-I type (Bio-rad, USA).

Methods

Blood samples were collected from all patients and the control group for the detection of anti-*H pylori* IgG.

Detection of anti-*H pylori* IgG In order to eliminate possibly disrupted other proteins, each sample was diluted at 1:100 and detected in duplicate according to the manufacturer's instructions. A series of standard samples with concentrations of 0, 5, 10, 20, 35 and 70 units/ml were added in corresponding reactive wells. When the reaction was stopped, the optical density (OD) values were tested within 10 min at light wavelength 450nm. To measure the concentrations of anti-*H pylori*-IgG in the serum samples, a standardized curve of each board was mapped with the concentrations of standard samples as the abscissa, and OD values of the two correspondent parallel wells as the ordinate. The average OD value of each sample in the two parallel wells above 12 units/ml was regarded to be positive, otherwise to be negative.

Statistical analysis Data analysis was conducted with χ^2 test.

RESULTS

Detection of serum anti-H pylori IgG in patients with different digestive cancers

The positive rates of anti-*H pylori* IgG in patients with digestive cancers and healthy subjects were 61.50 % (230/374) and 46.77 % (145/310), respectively, which were significantly different ($P<0.01$). The positive rates were 52.38 % (33/63), 86.60 % (84/97), 83.14 % (84/101), 45.24 % (19/42), 51.13 % (18/35) and 44.44 % (16/36), respectively, in patients with esophageal carcinoma, gastric cancer, duodenal carcinoma,

rectal cancer, colon carcinoma and liver cancer. There was a significant difference (P<0.01). The detailed results are shown in Table 1.

Table 1 Positive rates of *H pylori*-IgG in patients with different peptic cancers

	n	Anti-*H pylori* IgG	
		-	+ (%)
Normal group	310	165	145 (46.77)[a]
Cancer group	374	144	230 (61.50)[a]
Esophagus carcinoma	63	30	33 (52.38)[b]
Gastric cancer	97	13	84 (86.60)[b]
duodenal Carcinoma	101	17	84 (83.17)[b]
Rectal cancer	42	23	19 (45.24)[b]
Carcinoma of colon	35	17	18 (51.43)[b]
Liver cancer	36	20	16 (44.44)[b]

[a]P<0.01, χ^2=14.8; [b]P<0.01, χ^2=58.69.

Serum anti-H pylori IgG in patients with gastric cancer

The positive rates of anti-*H pylori* IgG in intestinal and diffuse type gastric cancer were 93.75 % (60/64) and 72.73 % (24/33), respectively (P<0.05).In addition, the positive rates in gastric antrum and cardia were 96.43% (54/56) and 73.17% (30/41) (P<0.05). The detailed results are shown in Table 2.

Table 2 Positive rates of anti-*H pylori* IgG in patients with gastric cancer of different types and at different locations

Group	*n*	*H pylori*-IgG	
		Positive	Positive rates (%)
Gastric cancer	97	84	86.60
Intestinal type	64	60	93.75[c]
Diffuse type	33	24	72.73[c]
Gastric antrum	56	54	96.43[d]
Gastric cardiac	41	30	73.17[d]

[c]P<0.05, χ^2=8.29; [d]P<0.05, χ^2=11.03.

Serum anti-H pylori IgG in patients with duodenal carcinoma

The positive rates of anti-*H pylori* IgG in patients with ulcerous and proliferous type duodenal carcinoma were 91.04 % (61/67) and 52.27 % (23/44) (P<0.05). In addition, the positive rates of *H pylori*-IgG in the bulb and descending part of duodenum were 94.20 % (65/69) and 45.20 % (19/42), (P<0.05). The detailed results are shown in Table 3.

Table 3 Positive rates of *H pylori*-IgG in patients with duodenal carcinoma of different types and at different locations

Group	*n*	*H pylori*-IgG	
		Positive	Positive rates (%)
Duodenal carcinoma	101	84	83.17
Ulcerous type	67	61	91.04[e]
Proliferous type	44	23	52.27[e]
Bulb of duodenum	69	65	94.20[f]
Descending part	42	19	45.20[f]

[e]P<0.05, χ^2=19.74; [f]P<0.05, χ^2=28.97.

DISCUSSION

H pylori is one of the common bacteria causing chronic infection, infects more than 50 % of the human population, causes chronic gastritis and plays an important role in the pathogenesis of gastroduodenal ulceration. *H pylori* has also been suggested to be involved in the genesis of adenocarcinoma and MALT lymphoma of the stomach[11-13]. It is believed that *H pylori* infection might result in the release of various bacterial and host dependent cytotoxic substances including ammonia, platelet activating factor, cytotoxins and lipopolysaccharide as well as cytokines such as interleukins (IL)-1-12, tumor necrosis factor alpha (TNF-alpha) and reactive oxygen species[14-20], tissue damage and gastro-duodenal disease[21-25]. In 1994, the World Health Organization and International Agency for Research on Cancer (IARC) classified it as a class I carcinogen[26-28]. In this study sera from 374 patients with digestive cancers and 310 healthy controls were tested for *H pylori* using a specific IgG ELISA. The results showed that the positive rate of anti-*H pylori* IgG was 61.50 % in the patients, which was significantly greater than that (46.77 %) in the control group (P<0.01). This finding indicated that patients with digestive cancers were more susceptible to infection by *H pylori* than healthy subjects, which might be related to a lower immunity in these patients. Furthermore, there was a significant difference in the positive rate among patients with cancers of esophageal, stomach, duodenum, rectum, colon and liver. This observation indicated that the prevalence of *H pylori* infection in patients with different digestive cancers was different, which was significantly higher in gastric and duodenal carcinomas than in other digestive cancers. All of these results were concordant with those previously reported[29-34].

In this study, the infection rate was 86.60 % (84/97) in patients with gastric cancer, with a rate of 96.43 % in antral cancer and 93.75 % in intestinal type cancer. We postulate that *H pylori* infection plays an important role in carcinomatous changes in gastric antrum, and is an important pathogenic factor causing intestinal type gastric cancer. This notion is consistent with previous literatures[35-39]. The histological process of intestinal type gastric cancer has been described as normal gastric mucosa→superficial chronic gastritis→atrophic gastritis→intestinal metaplasia→atypical hyperplasia→gastric cancer[40]. After long-term infection of *H pylori* in gastric mucosa, secretion of gastric acid could be reduced, flora in intestinal tract might survive and breed in stomach, and some bacteria recovering nitrate salts might form N-nitroso compounds that are important carcinogens. Moreover, *H pylori* leads to a decrease of vitamin C, which is a strong antioxidant and protective factor in gastric juice, preventing against the occurrence of gastric cancer. As a result, the levels of reactive oxygen and free radicals would increase, and direct DNA damage would incur. Thus, the chances of gene mutation would increase, and further accelerate the development of gastric cancer[41,42].

At present, the definite etiological factors of duodenal carcinoma are not clear, although many studies have suggested that some cholic acids like deoxycholic acid and its degradation products be related to the occurrence and development of duodenal carcinoma. Additionally, ulcerous and genetic factors have been considered to be associated with duodenal carcinoma. Stromberg *et al* found that the levels of several cytokines, such as interleukin-8 (IL-8), transforming growth factor beta (TGF-beta) and gamma interferon (IFN-gamma), were significantly lower in duodenal ulcer (DU) patients than in asymptomatic carriers (AS) and uninfected individuals. Then it was suggested that a number of cytokines might be important for the mucosal host defense against *H pylori* and a down-regulated immune response would play a role in the development of duodenal ulcers[43]. Colonizing in gastric antrum, *H pylori* can destroy the inhibitory feedback adjustment of gastrin release, which results in increased acid load in

duodenum, raises the risk of impairment of duodenal mucous membrane and thus convering of duodenal mucosa to gastric metaplasia. The metaplastic epithelium could provide a site where *H pylori* colonize, and cause duodenitis that was pre-ulcer status of DU and formed ulcer in the end[44]. In addition, some studies have suggested that the development of DU is related to *H pylori* density in patients. There was a tendency of higher *H pylori* density when the degree of deformity of the duodenal bulb increased[45]. The results of our study showed that 83.17 % of the patients with duodenal carcinoma were infected by *H pylori*, with the rate being 91.04 % in ulcerous type and 94.20 % in the bulb carcinoma. Therefore, we conclude that *H pylori* infection is associated with the development of duodenal carcinoma, especially with ulcerous type and in duodenal bulb.

ACKNOWLEDGEMENTS

We thank Department of Pathology, Benbu Medical College, Department of Oncology, Huainan First Miner' s Hospital and Department of Oncology, Huainan Second Miner' s Hospital, as well as Department of Oncology, Huainan Third Miner' s Hospital for sample collection.

REFERENCES

1 **Oyedeji KS,** Smith SI, Arigbabu AO, Coker AO, Ndububa DA, Agbakwuru EA, Atoyebi OA. Use of direct Gram strain of stomach biopsy as a rapid screening method for detection of *Helicobacter pylori* from peptic ulcer and gastritis patients. *J Basic Microbiol* 2002; **42**: 121-125

2 **Nguyen TN**, Barkun AN, Fallone CA. Host determinants of *Helicobacter pylori* infection and its clinical outcome. *Helicobacter* 1999; **4**: 185-197

3 **Brigic E**, Hodzic L, Zildzic M. *Helicobacter pylori* and gastroduodenal disease in our patients: 2-year experience. *Med Arh* 2000; **54**: 313-316

4 **Zawilak A**, Zakrzewska-Czerwinska J. Organization of the *Helicobacter pylori* genome. *Postepy Hig Med Dosw* 2001; **55**: 355-367

5 **Vandeplas Y.** *Helicobacter pylori* infection. *World J Gastroenterol* 2000; **6**: 20-31

6 **McNamara D**, O' Morain C. *Helicobacter pylori* and gastric cancer. *Ital J Gastroenterol Hepatol* 1998; **30**: 294-298

7 **Pineros DM,** Riveros SC, Marin JD**,** Ricardo O, Diaz OO. *Helicobacter pylori* in gastric cancer and peptic ulcer disease in a Colombian population. Strain heterogeneity and antibody profiles. *Helicobacter* 2001; **6:** 199-206

8 **Tanida N,** Sakagami T, Nakamura Y, Kawaua A, Hikasa Y, Shimoyama T. *Helicobacter pylori* and gastric cancer. *Nippon Geka Gakkai Zasshi* 1996; **97**: 257-262

9 **Hirai M,** Azuma T, Ito S, Kato T, Kohli Y, Fujiki N. High prevalence of neutralizing activity to *Helicobacter pylori* cytotoxin in serum of gastric-carcinoma patients. *Int J Cancer* 1994; **56**: 56-60

10 **Queiroz DM,** Mendes EN, Rocha GA, Oliveira AM, Oliveira CA, Cabral MM, Nogueira AM, Souza AF. Serological and direct diagnosis of *Helicobacter pylori* in gastric carcinoma: a case-control study. *J Med Microbiol* 1999; **48**: 501-506

11 **Nakajima N,** Kuwayama H, Ito Y, Iwasaki A, Arakawa Y. *Helicobacter pylori*, neutrophils, interleukins, and gastric epithelial proliferation. *J Clin Gastroenterol* 1997; **25**: 198-202

12 **Satoh K,** Sugano K. Causal relationship between *Helicobacter pylori* infection and upper gastroduodenal diseases. *Nippon Rinsho* 2001; **59**: 239-245

13 **Muller S,** Seifert E, Stolte M. Simultaneous MALT-type lymphoma and early adenocarcinoma of the stomach associated with *Helicobacter pylori* gastritis. *Z Gastroenterol* 1999; **37**: 153-157

14 **Ramirez Ramos AA.** *Helicobacter pylori*. *Rev Gastroenterol Peru* 2001; **21**: 99-101

15 **Yoshimura N**, Suzuki Y, Saito Y. Suppression of *Helicobacter pylori*-induced interleukin-8 production in gastric cancer cell lines by an anti-ulcer drug, geranylgeranylacetone. *J Gastroenterol Hepatol* 2002; **17**: 1153-1160

16 **Stassi G,** Arena A, Speranza A, Iannello D, Mastroeni P. Different modulation by live or killed *Helicobacter pylori* on cytokine production from peripheral blood mononuclear cells. *New Microbiol* 2002; **25**: 247-252

17 **Ji KY,** Hu FL. Progress on *Helicobacter pylori* and cytokine. *Shijie Huaren Xiaohua Zazhi* 2002; **10**: 503-508

18 **Walker MM.** Cyclooxygenase-2 expression in early gastric cancer, intestinal metaplasia and *Helicobacter pylori* infection. *Eur J Gastroenterol Hepatol* 2002; **14**: 347-349

19 **Konturek PC,** Konturek SJ, Bielanski W, Karczewska E, Pierzchalski P, Duda A, Starzynska T, Marlicz K, Popiela T, Hartwich A, Hahn EG. Role of gastrin in gastric cancerogenesis in *Helicobacter pylori* infected humans. *J Physiol Pharmacol* 1999; **50**: 857-873

20 **Han FC**, Yan XJ, Su CZ. Expression of the CagA gene of *H pylori* and application of its product. *World J Gastroenterol* 2000; **6**: 122-124

21 **Recavarren Ascencios R**, Recavarren Arce S. Chronic atrophic gastritis: pathogenic mechanisms due to cellular hypersensitivity. *Rev Gastroenterol Peru* 2002; **22**: 199-205

22 **Al- Muhtaseb MH,** Abu-Khalaf AM, Aughsteen AA. Ultrastructural study of the gastric mucosa and *Helicobacer pylori* in duodenal ulcer patients. *Saudi Med J* 2000; **21**: 569-573

23 **Zhang ZW**, Farthing MJ. Molecular mechanisms of *H pylori* associated gastric carcinogenesis. *World J Gastroenterol* 1999; **5**: 369-374

24 **Naito Y,** Yoshikawa T. Molecular and celluar mechanisms involved in *Helicobacter pylori*-induced inflammation and oxidative stress (1,2). *Free Radic Biol Med* 2002; **33**: 323-326

25 **Allen LA.** Intracellular niches for extracellular bacteria: lessons from *Helicobacter pylori*. *J Leukoc Biol* 1999; **66**: 753-756

26 **Xue FB,** Xu YY, Wan Y, Pan BR, Ren J, Fan DM. Association of *H pylori* infection with gastric carcinoma: a Meta analysis. *World J Gastroenterol* 2001; **7**: 801-804

27 **Palatka K,** Altorjay I, Szakall S, Gyorffy A, Udvardy M. Detection of *Helicobacter pylori* in tissue samples of stomach cancer. *Orv Hetil* 1999; **140**: 1985-1989

28 **Miehlke S,** Kirsch C, Dragosics B, Gschwantler M, Oberhuber G, Antos D, Dite P, Lauter J, Labenz J, Leodolter A, Malfertheiner P, Neubauer A, Ehninger G, Stolte M, Bayerdorffer E. *Helicobacter pylori* and gastric cancer: current status of the Austrain Czech German gastric cancer prevention trial (PRISMA Study). *World J Gastroenterol* 2001; **7**: 243-247

29 **Lan J,** Xiong YY, Lin YX, Wang BC, Gong LL, Xu HS, Guo GS. *Helicobacter pylori* infection generated gastric cancer through p53-Rb tumor-suppressor system mutation and telomerase reactivation. *World J Gastroenterol* 2003; **9**: 54-58

30 **Wu AH,** Crabtree JE, Bernstein L, Hawtin P, Cockburn M, Tseng CC, Forman D. Role of *Helicobacter pylori* CagA+ strains and risk of adenocarcinoma of the stomach and esophagus. *Int J Cancer* 2003; **103**: 815-821

31 **Kuniyasu H,** Yasui W, Yokozaki H, Tahara E. *Helicobacter pylori* infection and carcinogenesis of the stomach. *Langebecks Arch Surg* 2000; **385**: 69-74

32 **Meining A,** Bayerdorffer E, Muller P, Miehlke S, Lehn N, Holzel D, Hatz R, Stolte M. Gastric carcinoma risk index in patients infected with *Helicobacter pylori*. *Virchows Arch* 1998; **432**: 311-314

33 **Kuipers EJ**, Gracia-Casanova M, Pena AS, Pals G, Van Kamp G, Kok A, Kurz-pohlmann E, Pels NF, Meuwissen SG. *Helicobacter pylori* serology in patients with gastric carcinoma. *Scand J Gastroenterol* 1993; **28**: 433-437

34 **Rudelli A**, Vialette G, Brazier F, Seurat PL, Capron D, Dupas JL. *Helicobacter pylori* and gastroduodenal lesions in 547 symptomatic young adults. *Gastroenterol Clin Biol* 1996; **20**: 367-373

35 **Farinati F**, Valiante F, Germana B, Della Libera G, Baffa R, Rugge M, Plebani M, Vianello F, Di Mario F, Naccarato R. Prevalence of *Helicobacter pylori* infection in patients with precancerous changes and gastric cancer. *Eur J Cancer Prev* 1993; **2**: 321-326

36 **Meining AG**, Bayerdorffer E, Stolte M. *Helicobacter pylori* gastritis of the gastric cancer phenotype in relative of gastric carcinoma patients. *Eur J Gastroenterol Hepatol* 1999; **11**: 712-720

37 **El-Zimaity HM,** Ota H, Graham DY, Akamatsu T, Katsuyama T.

Patterns of gastric atrophy in intestinal type gastric carcinoma. *Cancer* 2002; **94**: 1428-1436

38 **Vasilenko IV**, Surgai NN, Sidorova ID. Modifications of gastric mucosa in diffuse and intestinal cancer. *Arkh Patol* 2001; **63**: 26-30

39 **Xia HH,** Kalantar JS, Talley NJ, Wyatt JM, Adams S, Chueng K, Mitchell HM. Antral-type mucosa in the gastric incisura, body, and fundus (antralization): a link between *Helicobacter pylori* infection and intestinal metaplasia. *Am J Gastroenterol* 2000; **95**: 114-121

40 **Meining A,** Morgner A, Miehlke S, Bayerdorffer E, Stolte M. Atrophy-metaplasia-dysplasia-carcinoma sequence in the stomach: a reality or merely an hypothesis? *Best Pract Res Clin Gastroeterol* 2001; **15**: 983-998

41 **Xia HH**, Talley NJ. Apoptosis in gastric epithelium induced by *Helicobacter pylori* infection: implications in gastric carcinogenesis. *Am J Gastroenterol* 2001; **96**: 16-26

42 **Pignatelli B,** Bancel B, Esteve J, Malaveille C, Calmels S, Correa P, Patricot LM, Laval M, Lyandrat N, Ohshima H. Inducible nitric oxide synthase, anti-oxidant enzymes and *Helicobacter pylori* infection in gastritis and gastric precancerous lesion in humans. *Eur J Cancer Prev* 1998; **7**: 439-447

43 **Kuipers EJ**, Thijs JC, Feston HP. The prevalence of *Helicobacter pylori* in peptic ulcer disease. *Aliment Pharmacol Ther* 1995; **9**: 59-69

44 **Olbe L,** Hamlet A, Dalenback J, Fandriks L. A mechanism by which *Helicobacter pylori* infection of the antrum contributes to the development of duodenal ulcer. *Gastroenterology* 1996; **110**: 1386-1394

45 **Lai YC,** Wang TH, Liao CC, Huang SH, Wu CH, Yang SS, Lee CL, Chen TK. Correlation between the degree of duodenal bulbar deformity and the density of *Helicobacter pylori* infection in patients with active duodenal ulcers. *J Formos Med Assoc* 2002; **101**: 263-267

Edited by Xia HHX and Wang XL

P.O.Box 2345, Beijing 100023,China
Fax: +86-10-85381893
E-mail: wjg@wjgnet.com www.wjgnet.com

World J Gastroenterol 2003;9(11):2505-2508
World Journal of Gastroenterology
 ISSN 1007-9327

• BASIC RESEARCH •

Effect of tetramethylpyrazine on exocrine pancreatic and bile secretion

Wen-Chao Zhao, Jin-Xia Zhu, Ning Tang, Yu-Lin Gou, Dewi Kenneth Rowlands, Yiu-Wa Chung, Ying Xing, Hsiao-Chang Chan

Yu-Lin Gou, Dewi Kenneth Rowlands, Yiu-Wa Chung, Hsiao-Chang Chan, Epithelial Cell Biology Research Center, Department of Physiology, Faculty of Medicine, The Chinese University of Hong Kong, Shatin, Hong Kong
Wen-Chao Zhao, Jin-Xia Zhu, Ning Tang, Ying Xing, Department of Physiology, Medical School, Zhengzhou University, Zhengzhou 450052, Henan, Province China
Supported by Innovation and Technology Funds of Hong Kong and strategic Program of the Chinese University of Hong Kong
Correspondence to: Professor Hsiao-Chang Chan, Epithelial Cell Biology Research Center, The Department of Physiology, Faculty of Medicine, The Chinese University of Hong Kong, Shatin, NT, Hong Kong, SAR, China. hsiaochan@cuhk.edu.hk
Telephone: +852-2609-6839 **Fax**: +852-2603-5022
Received: 2003-05-11 **Accepted:** 2003-08-19

Abstract

AIM: To investigate the effect of tetramethylpyrazine (ligustrazine, TMP) on the secretion of exocrine pancreas (and biliary).

METHODS: In *in vivo* study, we investigated the effect of TMP on the secretion of pancreatic-bile juice (PBJ) in rats. Using human pancreatic duct cell line, CAPAN-1, combined with the short-circuit current (I_{SC}) technique we further studied the effect of TMP on the pancreatic anion secretion.

RESULTS: Administration of TMP (80 mg/kg, ip) significantly increased the secretion of PBJ ($P<0.05$), but the pH of PBJ and the secretion of pancreatic protein were not significantly affected. Basolateral addition of TMP produced a dose-dependent increase in I_{SC} (EC_{50}=1.56 mmol/L), which contained a fast transient I_{SC} response followed by a slow decay. Apical application of Cl^- channel blockers, DPC (1 mmol/L), decreased the response by about 67.1 % ($P<0.001$), whereas amiloride (100 μmol/L), a epithelial sodium channel blockers, had no effect. Removal of extracellular HCO_3^- abolished TMP-induced increase in I_{SC} by about 74.4 % ($P<0.001$), but the removal of external Cl^- did not. Pretreatment with phosphodiesterase inhibitor, IBMX(0.5 mmol/L), decreased the TMP-induced I_{SC} by 91 % ($P<0.001$).

CONCLUSION: TMP could stimulate the secretion of PBJ, especially pancreatic ductal HCO_3^- secretion via cAMP or cGMP-dependent pathway. It need further study to investigate the roles of cAMP or cGMP in the effect of TMP on the secretion of exocrine pancreas.

Zhao WC, Zhu JX, Tang N, Gou YL, Rowlands DK, Chung YW, Xing Y, Chan HC. Effect of tetramethylpyrazine on exocrine pancreatic and bile secretion. *World J Gastroenterol* 2003; 9 (11): 2505-2508
http://www.wjgnet.com/1007-9327/9/2505.asp

INTRODUCTION

Tetramethylpyrazine (TMP, $C_8H_{12}N_2$, molecular mass 136.20 u, also known as ligustrazine) is an active alkaloid contained in the rhizome of *Chuanxiong*[1]. TMP has been widely used for the treatment of patients with cardiovascular and cerebrovascular diseases[1-5]. Its proposed pharmacological actions include antagonizing calcium mobilization[6], inhibiting platelet aggregation[7] and increasing intracellular cAMP level by inhibiting phosphodiesterase activity[8]. Recently it has been reported that TMP has antioxidant effect, reducing free radical generation[9,10] and decreasing nitric oxide production[11,12]. However, the effect of TMP on the pancreatic exocrine secretion are unknown. Since TMP is known to activate cAMP, it may act similarly to secretin, a physiological regulator of pancreatic secretion by elevating intracellular cAMP to act on pancreatic epithelial CFTR, which is a cAMP/cGMP-regulated Cl^- channel[13,14] and involved in pancreatic HCO_3^- secretion. In the present study, we investigated the effect of TMP on the secretion of pancreatic-bile juice (PBJ), which includes both pancreatic protein and HCO_3^-. We also undertook the present study using the short-circuit current (I_{SC}) technique to investigate TMP effect on HCO_3^- secretion by human pancreatic duct cell line, CAPAN-1, which retains most of the properties of pancreatic duct cells[15,16].

MATERIALS AND METHODS

Materials

Hydrochloride tetramethylpyrazine was purchased from the First Chengdu pharmaceutical Factory (Chengdu, China). RPMI 1640 medium and fetal bovine serum, trypsin-EDTA were supplied by Gibco Laboratories (New York). Hanks' balanced salt solution (HBSS), diphenylamine-2, 2'-dicarboxylic acid (DPC), glucose, calcium gluconate, N-2-hydroxethypiperazine-N'-2-ethanessulfonic acid (HEPES), sodium bicarbonate, DMEG, penicillin-streptomycin (P/S) and Bradford reagent were supplied by Sigma Chemical (St.Louis, MO). Calcium chloride, magnesium sulfate, potassium chloride, sodium chloride, were obtained from Merck (Darmstadt, Germany). Potassium gluconate and sodium gluconate were from BDH Chemicals (Poole, England). Tris was from Amersham Biosciences (Stockholm, Sweden).

Methods

Animal preparation Animal experimentation was conducted according to institutional guidelines. Adult male Sprague-Dawley rats, weighing 220-280 g, were housed under controlled temperature (23 ℃) and fasted for 12 h with free access to water before surgery. Midline abdominal incisions were made under xylazine and ketamine anesthesia (13 and 87 mg /kg body weight, respectively, im), followed by insertion of a polyethylene tube into the proximal duodenum for diversion of PBJ to the duodenum. A pancreatic duct cannula was made by inserting a polyethylene tube at the junction between the pancreatic duct and the duodenal wall for collection of PBJ[17-19].

Collection and measurement of exocrine pancreatic-bile secretions The animals were divided into two groups randomly: TMP group (TMP 80 mg/kg, ip. pH 2.3) and control

group (9 g/L NaCl solution, ip. pH 2.3). After a 30-minute stabilization period, pancreatic-bile secretions were collected every 15 minutes for 90 minutes. The volume was measured by a 1mL syringe and the pH value of PBJ was determined by a pH analyzer. 10 μL of PBJ was taken and diluted for pancreatic protein determination using spectra MAX 250 and Brandford reagent. The remaining undiluted PBJ was pumped into the duodenum via the duodenal cannula during the next collection period. Administrations were given after 2-time collections (30 minutes) and the second 15-minute-secretion was the basal PBJ secretion.

Cell culture Experiments were performed on the human pancreatic duct cell line, CAPAN-1 at a passage of 50-58. Cells were grown in RPMI 1640 medium with 200 mL/L fetal bovine serum and 10 g/L penicillin-streptomycin (P/S) as described previously[20,21]. Briefly, a volume of 0.2 mL of the cell suspension (1.5×10^9/L) was plated onto each permeable support, which was made of a millipore filter and a silicon ring with a confined area of 0.45 cm^2, floating on culture medium and incubated at 37 ℃ with 50 mL/L CO_2 and 950 mL/L O_2 for 7-8 days. The cells were used for I_{SC} once the monolayers reached confluence.

Short-circuit current measurement The basic principles of the short-circuit current experiments performed in the present study were the same as previously described[20,21]. Monolayers grown on permeable supports were clamped vertically between two halves of the Ussing chamber and bathed in Krebs-Henseleit (K-H) solutions with following compositions (mmol/L): NaCl, 117; KCl, 4.7; $MgSO_4$, 1.2; KH_2PO_4, 1.2; $NaHCO_3$, 24.8; $CaCl_2$, 2.56; Glucose, 11.1; with an osmalarity of 285 gassed with 950 mL/L O_2 and 50 mL/L CO_2. In some experiments, gluconate was used to replace Cl^-. For HCO_3^--free solution, HEPES and Tris were used and the solution was gassed in air. All the electrodes were connected to the voltage-current clamp amplifier. The signal output from the amplifier was the I_{SC} measured and recorded online by chart recorders. A 0.1 mV voltage pulse was applied intermittently across the epithelium and the transepithelial resistance was calculated from the corresponding current changes.

Statistical analysis

The data were collected and analyzed by SPSS statistical package 10.0. The results were expressed as $\bar{x}\pm S_{\bar{x}}$. Comparisons between groups of data were carried out using Student' s paired or unpaired *t*-test. Comparisons in one group of data were carried out using One-way ANOVA. A *P*-value less than 0.05 was considered to be statistically significant. EC_{50} values were determined by non-linear regression by GraphPad Prism software.

RESULTS

Effect of TMP on secretion of PBJ

Table 1 shows the volume of pancreatic-bile juice (PBJ) collected at different time points before and after intraperitoneal administration of TMP or 9 mL/L NaCl (control). Compared with the basal secretion, the PBJ secretion in TMP treated rats was increased by 7.0 % ($P<0.05$), 22.3 % ($P<0.001$), 14.3 % ($P<0.01$), 18.2 % ($P<0.01$) and 14.2 % ($P<0.01$) at 15, 30, 45, 60 and 75minutes, respectively ($n=13$) (Figure 1). However, the same treatment with of 9 mL/L NaCl solution did not produce significant effect ($n=12$) (Figure1). Protein content in PBJ and pH of PBJ were shown to have no differences between TMP-treated and control groups (data not shown).

Effect of TMP on CAPAN-1 cell line

The CAPAN-1 monolayer clamped in Ussing chambers bathing with normal K-HS (Cl^-/HCO_3^--containing) exhibited a potential difference of 0.52±0.04 mV, basal I_{SC} of 5.70±0.53 μA/cm^2 and transmembrane resistance of 93.6±4.5 Ωcm^2 ($n=77$). In Cl^--free ($n=9$) and HCO_3^--free ($n=9$) K-H solution, the transepithelial potential difference was 0.62±0.15 mV and 0.86±0.28 mV and the basal I_{SC} was 1.90±0.50 μA/cm^2 and 3.98±1.32 μA/cm^2, respectively, and the resistance of the monolayers were 208.6±33.6 Ωcm^2 and 161.8±25.6 Ωcm^2.

Table 1 Volume of secretion of pancreatic bile juice ($\bar{x}\pm S_{\bar{x}}$, μL)

	Groups	TMP $n=13$	Control $n=12$
	Basal	372.3±22.2	342.5±15.8
	15 min	398.5±23.3	326.7±1.74
After	30 min	455.4±18. 8	344.2±14.5
administration	45 min	425.4±19.8	331.7±17.5
	60 min	440.0±25.8	357.5±18.8
	75 min	425.0±25.2	342.5±18.2

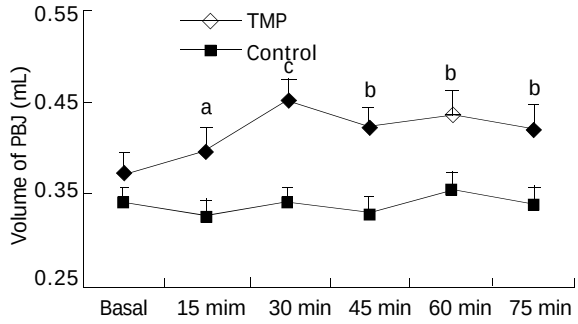

Figure 1 Effect of TMP on Volume of pancreatic-bile juice secretion. The volume of pancreatic-bile juice secretion collected before (basal) and 15, 30, 45, 60 and 75 minutes after intraperitoneal administration of TMP (80 mg/kg) and 9 mL/L NaCl in rats. The results were expressed as $\bar{x}\pm S_{\bar{x}}$. $^aP<0.05$, $^bP<0.01$, $^cP<0.001$, as compared to basal values.

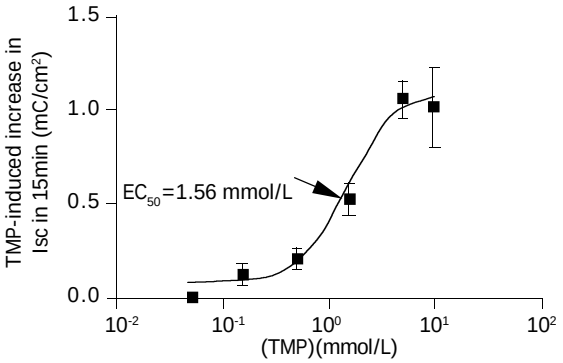

Figure 2 Concentration-response curve for TMP-induced I_{SC} in CAPAN-1 cells. Different concentrations of TMP were added to basalateral side. Each data point was obtained from at least 4 individual experiments. Arrow shows EC_{50}.

Basolateral addition of TMP (0.05, 0.15, 0.5, 1.5, 5 and 10 mmol/L) produced a dose-dependent increase in I_{SC}. EC_{50} was about 1.56 mmol/L (Figure 2). TMP (5 mmol/L)-induced I_{SC} increase was biphasic: a fast transient peak followed by a slow decay. The total transported charges for 15 minutes (the area under the curve of the TMP-induced I_{SC} response) were about 1.06±0.99 mC/cm^2 ($n=27$, Figure 3.A and C). TMP-induced current increase was inhibited by 67.1 % after apical pretreatment of 1 mmol/L DPC, a non-specific Cl^- channel blockers ($n=8$, $P<0.001$) (Figure 3.B and C). However apical application of epithelial sodium channel blockers, amiloride

(100 μmol/L) did not affect the TMP-produced response (n=3, Figure 3.C). After the removal of external HCO_3^-, TMP-induced I_{SC} was blocked by 74.4 % (n=9, P<0.001) (Figure 3. D), but the removal of external Cl^- did not reduce but increase the TMP-induced I_{SC} (n=8, P<0.05) (Figure 3.D). Pretreatment of phosphodiesterase inhibitor, IBMX (0.5 mmol/L) for 15 minutes decreased the TMP-induced I_{SC} by 91 % (n=4, P<0.001) (Figure 4.A and B).

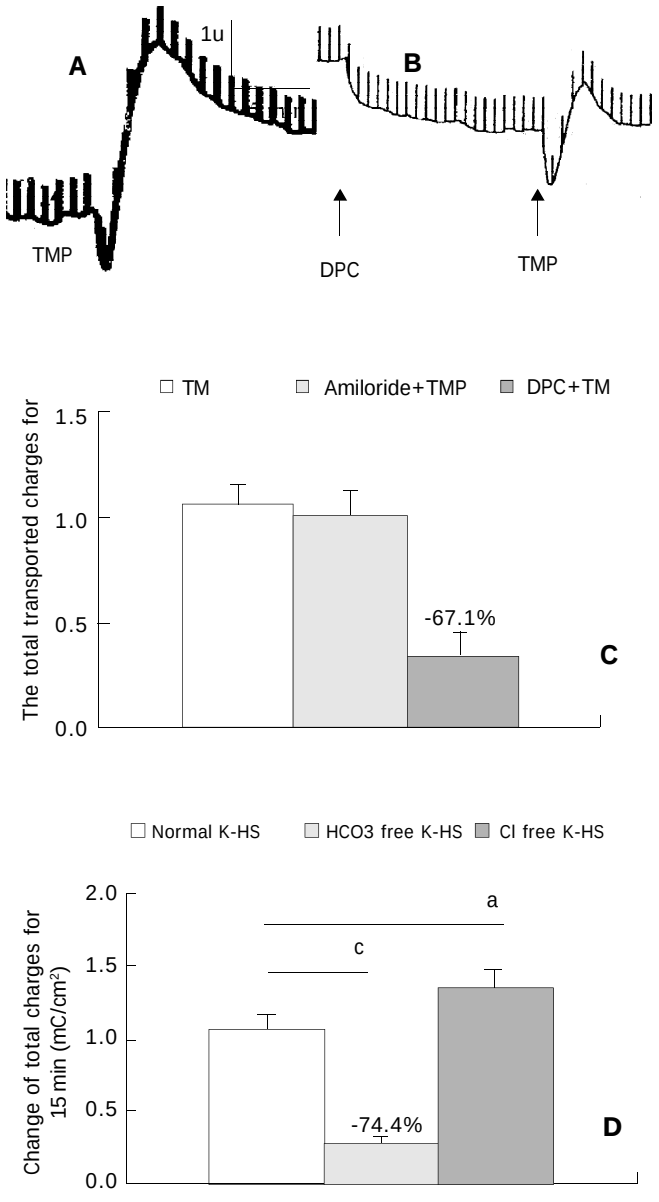

Figure 3 TMP-induced HCO_3^- secretion in CAPAN-1 cells. Comparison of TMP (5 mmoL/L)-induced I_{SC} (mC/cm²) obtained in control (A, C), pretreatment with DPC (1 mmoL/L) (B, C), Amiloride 100 umoL/L (C), HCO_3^--free solution (D), Cl^--free solution (D), Values are $\bar{x}\pm S_{\bar{x}}$, ^aP<0.05, ^cP<0.001.

DISCUSSION

While TMP has been widely used clinically for treating cardiovascular disorders and cerebrovascular diseases[1-5], little is known about its effect on pancreatic secretion. In the present study, intraperitoneal application of TMP increased secretion of pancreatic-bile juice (PBJ), but the protein content and pH value were not affected. It is known that PBJ consists of both bile and pancreatic juice, the volume of the basal secretion (or agonist induced) of pancreatic juice is normally very low, only about 9-18 μL in 15 minutes in rat[17,18], as compared to that of

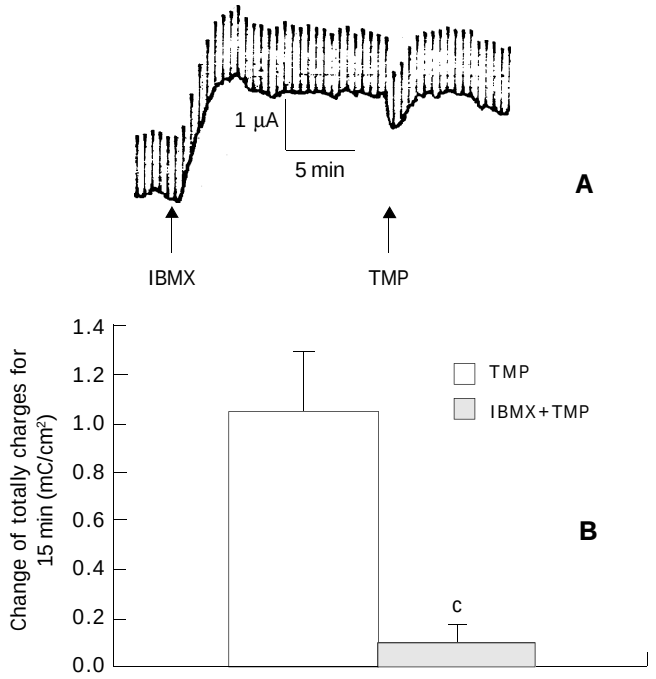

Figure 4 Pretreatment with IBMX decreased TMP–induced I_{SC} by 91 %. Values are $\bar{x}\pm s$, ^cP<0.001.

the liver. Although TMP increased the secretion of PBJ by 26-83 μL in 15 minutes, it was difficult to assess the contribution to exocrine pancreatic secretion from our experiments *in vivo*. Therefore, CAPAN-1 cell line was used to further demonstrate the effect of TMP on the pancreatic secretion. Our data suggested that TMP could directly stimulate HCO_3^- secretion in human pancreatic duct cells.

According to the HCO_3^- secretory model[22], the intracellular HCO_3^- was accumulated from the tissue fluid via the basolateral membrane[23-25] and mainly secreted by a Cl^-/HCO_3^- exchanger[26,27] and/or directly via cAMP/cGMP-dependent Cl^- channel (CFTR)[13,26,28]. Recently, it was reported that CFTR could also secrete HCO_3^- as Cl^-/HCO_3^- exchanger[29,30]. The TMP- increased I_{SC} in CAPAN-1 could be blocked by Cl^- channel blockers, as well as phosphodiesterase inhibitors, which were known to increase cAMP and cGMP, and abolished by removal of extracellular HCO_3^-, suggesting that TMP can stimulate pancreatic HCO_3^- secretion via CFTR since it has been shown to be activated by both cAMP and cGMP. The TMP-induced increase in the volume of PBJ observed in the rats could be due to an increase in pancreatic HCO_3^- secretion, as well as bile secretion, leading to enhanced water secretion. However, the inability of TMP to increase the pH of PBJ appeared to contradict to its observed effect on the increase in HCO_3^- secretion. This could be explained by two possible reasons. One is that the mechanism of HCO_3^- secretion in human pancreatic duct cells was different from that in rats since the HCO_3^- concentration of pancreatic juice in rats was only 70 mmol/L while in human was 145 mmol/L[22]. The other is that the HCO_3^- secreted by the pancreas might be diluted by bile juice and thus having less prominent effect on pH. It is interesting to note that TMP could stimulate HCO_3^- secretion that could be inhibited by extracellular Cl^- as evidenced by the increase in the TMP-induced I_{SC} observed in the absence of extracellular Cl^-. However, the mechanism for the observed inhibition of HCO_3^- secretion by extracellular Cl^- remains to be elucidated.

In conclusion, the present *in vivo* and *in vitro* results suggest that TMP can promote the secretion of PBJ in rats and HCO_3^- secretion in human pancreatic duct cells, which may be beneficial to improving digestive function.

REFERENCES

1 **Zheng HZ**, Dong ZH, Yu J. Chuanxiong in: Zhongyao XiandaiYanjiu Yu Yingyong. 1st Ed. *Beijing: Xueyuan Publisher* 1997: 629-682

2 **Liu LS,** Chen MQ, Zeng GY, Zhou BF. A forty-year study on hypertension. *Zhongguo Yixue Kexue Yuan Xuebao* 2002; **24**: 401-408

3 **Cai Y,** Ren M, Yang R. Observation on curative effect of acute ischemic cerebrovascular disease treated with different dosage of ligustrazine. *Zhongguo Zhongxiyi Jiehe Zazhi* 2000; **20**: 747-749

4 **Liao F**. Herbs of activating blood circulation to remove blood stasis. *Clin Hemorheol Microcirc* 2000; **23**: 127-131

5 **Huang RJ**, Liao CX, Chen DZ. Effect of tetramethylpyrazine on endothelin, von Willebrand factor and thromboxane A2 during cardiopulmonary bypass in patients of congenital heart disease with pulmonary hypertension. *Zhongguo Zhongxiyi Jiehe Zazhi* 2003; **23**: 268-271

6 **Zou LY**, Hao XM, Zhang GQ, Zhang M, Guo JH, Liu TF. Effect of tetramethyl pyrazine on L-type calcium channel in rat ventricular myocytes. *Can J Physiol Pharmacol* 2001; **79**: 621-626

7 **Sheu JR**, Kan YC, Hung WC, Lin CH, Yen MH. The antiplatelet activity of tetramethylpyrazine is mediated through activation of NO synthase. *Life Sci* 2000; **67**: 937-947

8 **Lin CI**, Wu SL, Tao PL, Chen HM, Wei J. The role of cyclic AMP and phosphodiesterase activity in the mechanism of action of tetramethylpyrazine on human and dog cardiac and dog coronary arterial tissues. *J Pharm Pharmacol* 1993; **45**: 963-966

9 **Pei L**, Wang J. Protective effect of tetramethylpyrazine on red blood cells during autotransfusion. *Zhonghua Yixue Zazhi* 2002; **82**: 322-324

10 **Shih YH**, Wu SL, Chiou WF, Ku HH, Ko TL, Fu YS. Protective effects of tetramethylpyrazine on kainate-induced excitotoxicity in hippocampal culture. *Neuroreport* 2002; **13**: 515-519

11 **Zhang Z**, Wei T, Hou J, Li G, Yu S, Xin W. Tetramethylpyrazine scavenges superoxide anion and decreases nitric oxide production in human polymorphonuclear leukocytes. *Life Sci* 2003; **72**: 2465-2472

12 **Wu CC**, Liao MH, Chen SJ, Yen MH. Tetramethylpyradizine prevents inducible NO synthase expression and improves survival in rodent models of endotoxic shock. *Naunyn Schmiedebergs Arch Pharmacol* 1999; **360**: 435-444

13 **Kulaksiz H**, Schmid A, Honscheid M, Eissele R, Klempnauer J, Cetin Y. Guanylin in the human pancreas: a novel luminocrine regulatory pathway of electrolyte secretion via cGMP and CFTR in the ductal system. *Histochem Cell Biol* 2001; **115**: 131-145

14 **Gray M**, O'Reilly C, Winpenny J, Argent B. Anion interactions with CFTR and consequences for HCO3- transport in secretory epithelia. *J Korean Med Sci* 2000; **15**(Suppl): S12-15

15 **Shumaker H**, Amlal H, Frizzell R, Ulrich CD 2nd, Soleimani M. CFTR drives Na+-nHCO-3 cotransport in pancreatic duct cells: a basis for defective HCO-3 secretion in CF. *Am J Physiol* 1999; **276**(1Pt1): C16-25

16 **Lohi H**, Kujala M, Kerkela E, Saarialho-Kere U, Kestila M, Kere J. Mapping of five new putative anion transporter genes in human and characterization of SLC26A6, a candidate gene for pancreatic anion exchanger. *Genomics* 2000; **70**: 102-112

17 **Li JP**, Chang TM, Chey WY. Roles of 5-HT receptors in the release and action of secretin on pancreatic secretion in rats. *Am J Physiol Gastrointest Liver Physiol* 2001; **280**: G595-602

18 **Li JP**, Lee KY, Chang TM, Chey WY. MEK inhibits secretin release and pancreatic secretion: roles of secretin-releasing peptide and somatostatin. *Am J Physiol Gastrointest Liver Physiol* 2001; **280**: G890-896

19 **Li Y**, Wu XY, Zhu JX, Owyang C. Intestinal serotonin acts as paracrine substance to mediate pancreatic secretion stimulated by luminal factors. *Am J Physiol Gastrointest Liver Physiol* 2001; **281**: G916-923

20 **Zhu JX**, Lo PS, Zhao WC, Tang N, Zhou Q, Rowlands DK, Gou YL, Chung YW, Chan HC. Bak Foong Pills stimulate anion secretion across normal and cystic fibrosis pancreatic duct epithelia. *Cell Biol Int* 2002; **26**: 1011-1018

21 **Cheng HS,** Wong WS, Chan KT, Wang XF, Wang ZD, Chan HC. Modulation of Ca2+-dependent anion secretion by protein kinase C in normal and cystic fibrosis pancreatic duct cells. *Biochim Biophys Acta* 1999; **1418**: 31-38

22 **Sohma Y**, Gray MA, Imai Y, Argent BE. HCO3- transport in a mathematical model of the pancreatic ductal epithelium. *J Membr Biol* 2000; **176**: 77-100

23 **Satoh H**, Moriyama N, Hara C, Yamada H, Horita S, Kunimi M, Tsukamoto K, Iso-O N, Inatomi J, Kawakami H, Kudo A, Endou H, Igarashi T, Goto A, Fujita T, Seki G. Localization of Na+-HCO-3 cotransporter (NBC-1) variants in rat and human pancreas. *Am J Physiol Cell Physiol* 2003; **284**: C729-737

24 **Marino CR**, Jeanes V, Boron WF, Schmitt BM. Expression and distribution of the Na^+-HCO_3^- cotransporter in human pancreas. *Am J Physiol* 1999; **277**(2 Pt1): G487-494

25 **Ishiguro H**, Naruse S, San Roman JI, Case M, Steward MC. Pancreatic Ductal Bicarbonate Secretion: Past, Present and future. *JOP* 2001; **2**(4 Suppl): 192-197

26 **Sohma Y**, Gray MA, Imai Y, Argent BE. 150 mM HCO3(-)-how does the pancreas do it? Clues from computer modelling of the duct cell. *JOP* 2001; **2**(4 Suppl): 198-202

27 **Novak I**. Keeping up with bicarbonate. *J Physiol* 2000; **528** (Pt2): 235

28 **Ishiguro H**, Naruse S, Kitagawa M, Mabuchi T, Kondo T, Hayakawa T, Case RM, Steward MC. Chloride transport in microperfused interlobular ducts isolated from guinea-pig pancreas. *J Physiol* 2002; **539**(Pt1): 175-189

29 **Choi JY**, Muallem D, Kiselyov K, Lee MG, Thomas PJ, Muallem S. Aberrant CFTR-dependent HCO3- transport in mutations associated with cystic fibrosis. *Nature* 2001; **410**: 94-97

30 **Choi JY**, Lee MG, Ko S, Muallem S. Cl(-)-dependent HCO3- transport by cystic fibrosis transmembrane conductance regulator. *JOP* 2001; **2**(4 Suppl): 243-246

Edited by Wang XL

P.O.Box 2345, Beijing 100023,China
Fax: +86-10-85381893
E-mail: wjg@wjgnet.com www.wjgnet.com

World J Gastroenterol 2003;9(11):2509-2512
World Journal of Gastroenterology
 ISSN 1007-9327

• BASIC RESEARCH •

Interleukin-10 modified dendritic cells induce allo-hyporesponsiveness and prolong small intestine allograft survival

Min Zhu, Ming-Fa Wei, Fang Liu, Hui-Fen Shi, Guo Wang

Min Zhu, Ming-Fa Wei, Hui-Fen Shi, Guo Wang, Department of Pediatric Surgery, Tongji Hospital, Tongji Medical College, Huazhong University of Science and Technology, Wuhan 430030, Hubei Province, China
Fang Liu, Department of Burns, Wuhan Third People' s Hospital, Wuhan 430060, Hubei Province, China
Correspondence to: Min Zhu, Institute of Organ Transplantation, Tongji Hospital, Tongji Medical College, Huazhong University of Science and Technology, Wuhan 430030, Hubei Province, China. eming43@hotmail.com
Telephone: +86-27-83663152 **Fax:** +86-27-83662892
Received: 2003-04-04 **Accepted:** 2003-05-19

Abstract

AIM: To investigate whether IL-10-transduced dendritic cells (DCs) could induce tolerogenicity and prolong allograft survival in rat intestinal transplantation.

METHODS: Spleen-derived DCs were prepared and genetically modified by hIL-10 gene. The level of IL-10 expression was quantitated by ELISA. DC function was assessed by MTT in mixed leukocyte reaction. Allogeneic T-cell apoptosis was examined by flow cytometric analysis. Seven days before heterotopic intestinal transplantation, 2×10^6 donor-derived IL-10-DC were injected intravenously, then transplantation was performed between SD donor and Wistar recipient.

RESULTS: Compared with untransduced DC, IL-10-DC could suppress allogeneic mixed leukocyte reaction (MLR). The inhibitory effect was the most striking with the stimulator/effector (S/E) ratio of 1:10. The inhibition rate was 33.25 %, 41.19 % ($P<0.01$) and 22.92 % with the S/E ratio of 1:1, 1:10 and 1:50 respectively. At 48 hours and 72 hours by flow cytometry counting, apoptotic T cells responded to IL-10-DC in MLR were 13.8 % and 30.1 %, while untransduced group did not undergo significant apoptosis ($P<0.05$). IL-10-DC pretreated recipients had a moderate survival prolongation with a mean allograft survival of 19.8 days ($P<0.01$), compared with 7.3±2.4 days in control group and 8.3±2.9 days in untransduced DC group. Rejection occurred in the control group within three days. The difference between untreated DC group and control group was not significant.

CONCLUSION: IL-10-DC can induce allogenic T-cell hyporesponsiveness *in vitro* and apoptosis may be involved in it. IL-10-DC pretreatment can prolong intestinal allograft survival in the recipient.

Zhu M, Wei MF, Liu F, Shi HF, Wang G. Interleukin-10 modified dendritic cells induce allo-hyporesponsiveness and prolong small intestine allograft survival. *World J Gastroenterol* 2003; 9(11): 2509-2512
http://www.wjgnet.com/1007-9327/9/2509.asp

INTRODUCTION

Dendritic cells (DCs) play critical roles in the initiation and modulation of immune responses and may determine the balance between tolerance and immunity[1-3]. Evidence has demonstrated that immunosuppressive cytokines modified DCs favour the induction of alloantigen-specific T cells anergy and prolong allograft survival. To date, there have been only a few reports of genetic manipulation of DCs for therapeutic application in organ transplantation. Retroviral and adenoviral gene transfer methods, for example, have been used to express immunosuppressive molecules such as vIL-10, TGF-β by DC[4,5]. In the present study, we demonstrated the feasibility of liposome transduction of DC to express hIL-10. In addition, we tested the *in vivo* ability of IL-10-DC to prevent small bowel graft rejection in rat intestinal transplantation model.

MATERIALS AND METHODS

Animals

Healthy adult Sprague-Dawley (SD) and Wistar-Furth rats, weighing 200-250 g, were used as donors and recipients, respectively. They were obtained from the Experimental Animal Center of Tongji Medical College, Huazhong University of Science and Technology.

DC propagation and transfection

Splenocyte suspensions from SD rats were prepared in RPMI1640 complete medium (Gibco/BRL), supplemented with 10 % v/v heat-inactivated fetal calf serum (Hyclone) in the presence of granulocyte-macrophage colony-stimulating factor (GM-CSF, 10 ng/ml, R&D) and IL-4 (10 ng/ml, R&D). Cultures were fed every 3 days by complete medium exchange including cytokines. After 6-8 days of culturing, when the adherent cells presented with primitive dendrites observed under electronic microscope, DC was propagated successfully. pcDNA3/hIL-10 vector encoding human IL-10 cDNA sequence was transfected to DC by the liposome method using the Lipofectamin 2000 kit (Gibco/BRL) according to the manufacturer' s instructions and the vector without insert was also transduced as a control. After 10-14 days in selective medium, DCs were then selected for geneticin-resistant colonies.

ELISA

The supernatant from transfected DCs was assayed for IL-10 expression by ELISA kit(Genzyme). The clone that gave the maximum ELISA reading was chosen for use in *in vivo* and *in vitro* experiments.

Mixed leukocyte reaction (MLR)

The ability of transduced DC to stimulate naive allogeneic T cells, assayed by using MTT (Sigma) method, was determined by MLR. Various numbers (2×10^3-2×10^5/well) of DC and IL-10-DC, pretreated with mitomycin C (25 μg/ml, Amresco), were cocultured with allogenic T-cells from Wistar rats as responders (2×10^5/well) at a ratio of 1:1, 1:10 and 1:50 for 72 hours in 0.2 ml RPMI-1640 complete medium in a 96-well U-bottomed microtiter plate. The results monitored by a microtiter plate reader (Bio-Rad, Tokyo, Japan) at 570 nm, were expressed as inhibition rate and calculated according to

the following equation: inhibition rate=1-(mean OD_{570nm} value of experiment group/mean OD_{570nm} value of control group)×100.

Flow cytometric analysis

At the indicated time point, supernatant cells were washed twice in cold PBS and then resuspended in 1×binding buffer at a concentration of 1×10^6 cells/ml. One hundred μl of the solution (1×10^5cells) was transferred to a 5 ml culture tube, then 5 μl of FITC-Annexin V and 10 μl of propidium iodide (Gibco/BRL) were added. The cells were gently vortexed and incubated for 15 min at room temperature in the dark and subjected to FACS. Those cells with negative propidium iodide staining and positive annexin V staining were considered as the proportion of cells actively undergoing apoptosis.

Experimental group and intestinal transplantation

All rats were randomized into three groups and each group had six pairs of rats. These groups were treated with a single intravenous injection of IL-10-DCs (2×10^6), untransduced DCs (2×10^6) or empty plasmid through tail vein seven days before intestinal transplantation. Operation procedures were performed under ether anesthesia. The small intestine was transplanted according to the modified procedure described by Monchik *et al*[6]. In brief, after an overnight fast, a 10-cm segment of proximal jejunum or distal ileum, including the superior mysenteric artery and vein, was removed from the donor after ligation of small mysenteric vessel branches and intravascular irrigation with cold heparinized saline solution. The graft was kept in 4 ℃ cold Ringer's solution until transplantation. The recipient abdomen was opened and the graft was reperfused by end-to-side anastomosis of the superior mesenteric artery and vein to the recipient's abdominal aorta and inferior vena cava under operative microscope, respectively. Both ends of the graft were then exteriorized through the right abdominal wall as stomas, isolating the segment from the recipient's native gastrointestinal tract. Death due to technical failure that occurred within 72 hours of operation was excluded from the study.

Histological examination

The rats were sacrificed and used for histological examination when recipients showed clinical signs of rejection[7,8]. After fixed in 10 % buffered formalin, embedded in paraffin, samples were stained with hematoxylin and eosin and examined by light microscope. Three samples were obtained at the time of donor operation and used as normal group for histological study.

Statistical analysis

All data were expressed as mean ± standard deviation. Statistical analyses were performed using Student's *t* test. Probability values of less than 0.05 were considered significant.

RESULTS

IL-10-DCs induced allospecific T cell hyporesponsiveness

We examined the responses of naï ve allospecific T cells to IL-10-DCs. As shown in Figure 1, IL-10-DCs could suppress allogeneic MLR compared with that of untransduced DCs. The latter were potent stimulators of allogeneic T-cell proliferation. The inhibitory effect was most striking with the stimulator / effector (S/E) ratio of 1:10. The inhibition rates were 33.25 %, 41.19 % and 22.92 % with the S/E ratio of 1:1, 1:10 and 1:50 respectively (Figure 1).

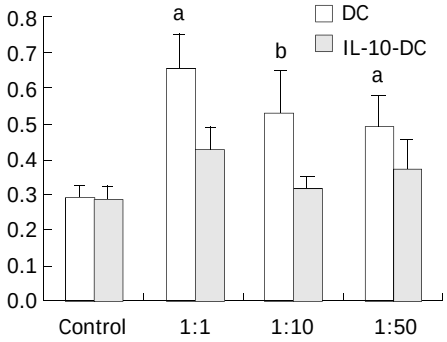

Figure 1 Inhibitory effect of IL-10-DC on allogenic T cell proliferation. [a]$P<0.05$, [b]$P<0.01$, *vs* DC group.

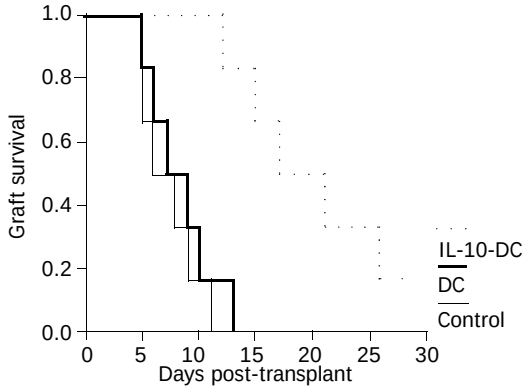

Figure 3 Survival (%) of recipient small intestines from control group (n=6), untransduced DC group (n=6) and IL-10-DC group (n=6).

Apoptosis assay by flow cytometric analysis

Supernatant T cells cocultured with IL-10-DCs in MLR underwent apoptosis. At 48 hours and 72 hours by flow cytometry counting apoptotic T cells were 13.8 % and 30.1 % with the S/E ratio of 1:10, but control group did not undergo significant apoptosis ($P<0.05$) (Figure 2).

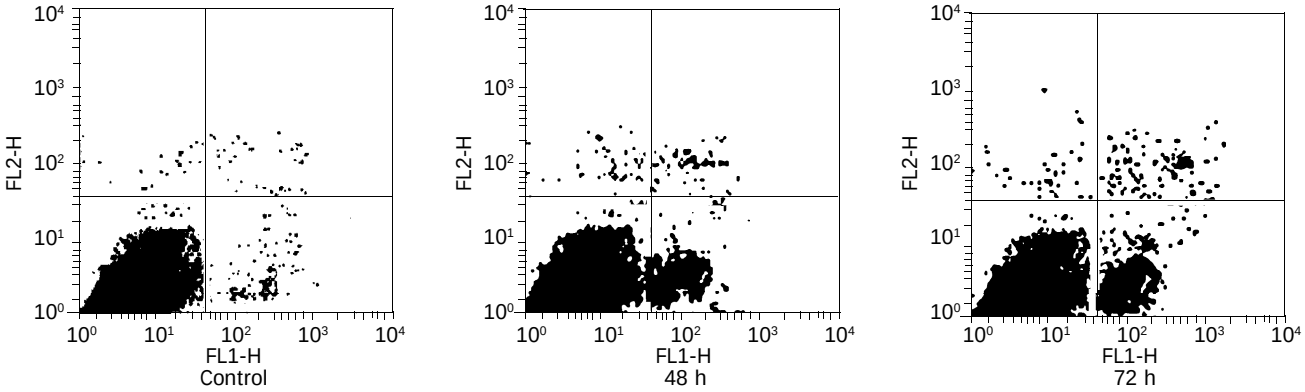

Figure 2 Flow cytometric analysis for apoptotic T cells induced by IL-10-DC.

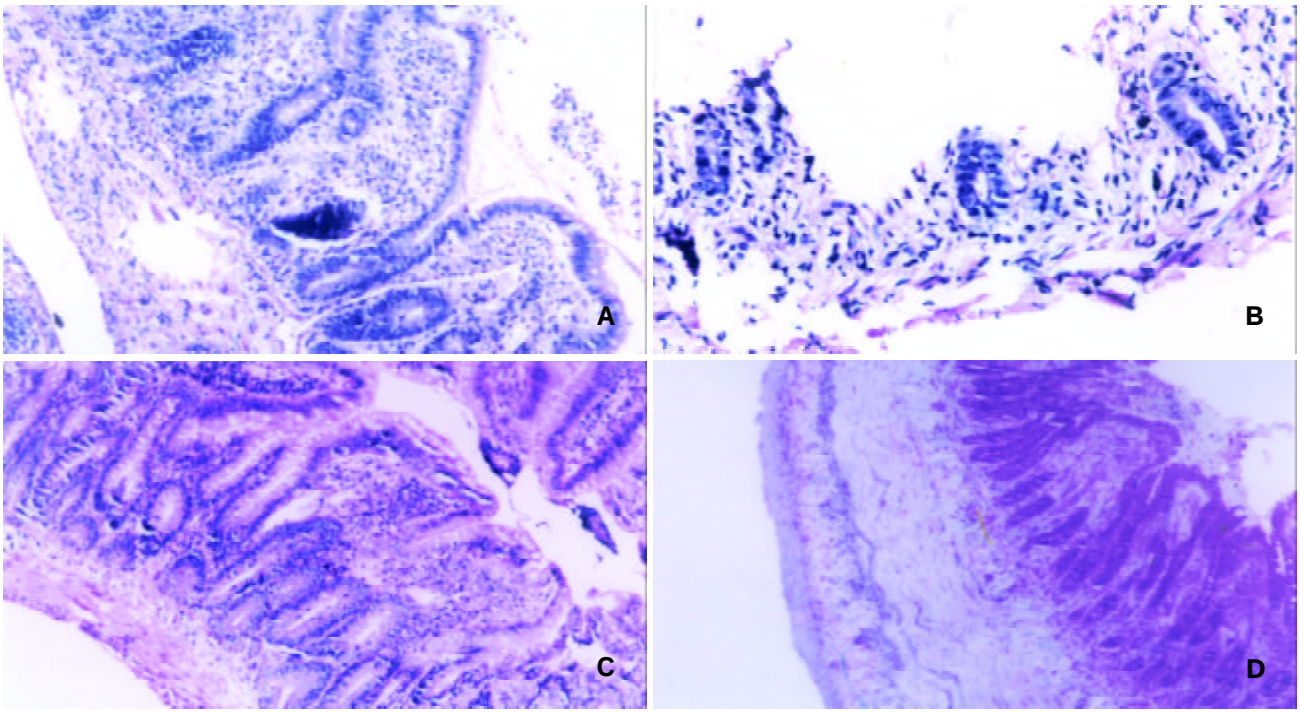

Figure 4 Histological comparison of allografts between control group rats and IL-10-DC pretreated rats. Control group showed acute rejection sign on POD 3 (A) and mucosal sloughing and necrosis and destruction of normal glandular architecture on POD 7(B). IL-10-DC group demonstrated mild lymphocyte infiltration and blunting of villi with edema on POD 7 (C) and fibroblastic proliferation extending from the submucosa to the lamina muscularis (D). (hematoxylin-erosin staining, ×200).

Allograft survival and histological evaluation

Untransduced DCs pretreatment did not affect allograft survival and the recipients pretreated with IL-10-DCs had a moderate allograft prolongation. Mean allograft survival in IL-10-DCs group was 19.8±6.3 days (P<0.01), compared with 7.3±2.4 days in control group and 8.3±2.9 days in untransduced DCs group (Figure 3). Although untreated recipient on postoperative day (POD) 3 showed acute rejection with blunted villi, the number of goblet cells was decreased and a large amount of inflammatory cell infiltration occurred in lamina propria mucosa, the grafts treated with IL-10-DCs demonstrated normal intestinal mucosa negative for rejection on POD 5 and mild lymphocyte infiltration and blunting of villi with edema on POD 7(Figure 4).

DISCUSSION

Despite improvements in the posttransplantation immunosuppressive therapeutic regimens, the management of allograft rejection has been still dependent on the use of nonspecific immunosuppressive agents[9], which could prevent the host from complications, such as infections and lymphoproliferative disorders[10,11]. In this regard, the successful induction of donor-specific immune tolerance remains a major challenge in organ transplantation. However, the lymphoid-rich small intestinal allograft might differ from such lymphoid-poor organs as the heart and kidney, making tolerance induction a particularly troublesome approach specific to this organ[12-14]. An approach to modify donor-derived DC in order to induce an immunological hyporesponsive state in the recipient has been attractive as a potential strategy in transplantation as it would theoretically let the possibility of donor-specific tolerance come true[15,16].

IL-10 has been regarded as an immunosuppressive cytokine because of its ability to down-regulate the synthesis of a broad spectrum of proinflammatory cytokines by DCs, monocytes or macrophages, and to inhibit allogeneic proliferative responses *in vitro*[17-19]. It is for these reasons that IL-10 has been considered as a potential means in the induction of tolerance. In the immature state, DC could express low levels of CD80, CD86 and co-stimulatory molecules that are essential for the amplification of immune response to foreign peptides[16,20-22]. IL-10 has been shown to block DC maturation *in vitro*[23,24]. Our approach was therefore to investigate strategies that might delay maturation of DC to prolong their immature phenotype. In our studies we found that these IL-10-DCs were less stimulatory in the MLR compared with untransduced DCs. One of the major mechanisms by which IL-10 inhibited DC antigen presenting function was to down-regulate MHC class II and costimulatory molecule expression on DC[25].

Our data confirmed that IL-10-DC could inhibit the proliferation of allogeneic T cells and induce these cell apoptosis, which may be related to the prolonged survival of graft. It has been accepted that the initiation of T-cell responses to grafted tissues requires two distinct signals[26-28]. The essential signal is the engagement of T cell receptors (TCR) to antigen peptide in the content of major histocompatibility complex molecules on antigen presenting cells. Other costimulatory receptor-ligand interactions between T cell and APC are needed. Signals through the TCR alone could lead to allospecific T-cell anergy or apoptosis[29]. Schartz[30] has demonstrated that lack of second signal would result in increased amounts of a negative regulatory factor, Nil-2a, in anergic human T cells. This factor has been shown to suppress IL-2 nuclear transcription factors of AP-1 and NF-κB. NF-κB could inhibit apoptosis by induction or up-regulation expression of anti-apoptotic gene such as Bcl-2. Therefore, the suppression of NF-κB activation could give rise to decreased IL-2 expression and T cell apoptosis[31,32].

Our studies were consistent with previous studies, perhaps not surprisingly, showing that IL-10-DC could exert tolerogenic effects on organ transplantation[25, 33]. In IL-10-DC group, median intestine allograft survival time was 19.8±6.3 days. Compared with control group (7.3±2.4 days) and untransduced DC group (8.3±2.9 days), the survival time was 2.5-fold longer. There are two possible explanations for the lack of long- term

survival in our study. One is that IL-10-DC might not survive long enough to induce a permanent state of tolerance. Long-term survival of IL-10-DC *in vivo* would be particularly important if apoptosis induction of allogeneic T cells was a major mechanism of allograft survival. The other, as far as long-term tolerance is concerned, is that the level of expression of IL-10 by IL-10-DC was still not high enough to affect the recipient immune modulation for all alloreactive T cells, though the level of IL-10 expression was higher than that in normal condition. For intestine, considering its high immunogenicity, it would be necessary to enhance gene transfer efficiency and transgene expression level[34].

In conclusion, these studies demonstrate the feasibility of immunosuppressive gene delivery system. We believe that this highly targeted method of inducing tolerogenicity of donor derived DC may reduce the need for recipient nonspecific immunosuppression and play an important role in clinical strategies of tolerance induction.

REFERENCES

1 **Steinman RM**. The dendritic cell system and its role in immunogenicity. *Annu Rev Immunol* 1991; **9**: 271-296
2 **Thomson AW**, Lu L. Dendritic cells as regulators of immune reactivity: implications for transplantation. *Transplantation* 1999; **68**: 1-8
3 **Brocker T**, Riedinger M, Karjalainen K. Targeted expression of major histocompatibility complex [MHC] class II molecules demonstrates that dendritic cells can induce negative but not positive selection of thymocytes *in vivo*. *J Exp Med* 1997; **185**: 541-550
4 **Takayama T**, Kaneko K, Morelli AE, Li W, Tahara H, Thomson AW. Retroviral delivery of transforming growth factor-beta1 to myeloid dendritic cells: inhibition of T-cell priming ability and influence on allograft survival. *Transplantation* 2002; **74**: 112-119
5 **Takayama T**, Nishioka Y, Lu L, Lotze MT, Tahara H, Thomson AW. Retroviral delivery of viral interleukin-10 into myeloid dendritic cells markedly inhibits their allostimulatory activity and promotes the induction of T-cell hyporesponsiveness. *Transplantation* 1998; **66**: 1567-1574
6 **Monchik GJ**, Russell PS. Transplantation of small bowel in the rat: technical and immunological considerations. *Surgery* 1971; **70**: 693-702
7 **Grover R**, Lear PA, Ingham Clark CL, Pockley AG, Wood RF. Method for diagnosing rejection in small bowel transplantation. *Br J Surg* 1993; **80**: 1024-1026
8 **Tzakis AG**, Thompson JF. Current status of diagnosis of small bowel rejection. *Pediatr Transplant* 1998; **2**: 87-88
9 **Sher LS**. Immunosuppression. *Curr Opin Organ Transplant* 2001; **6**: 311
10 **Ghanekar A**, Grant D. Small bowel transplantation. *Curr Opin Crit Care* 2001; **7**: 133-137
11 **De Bruin RW**, Heineman E, Marquet RL. Small bowel transplantation: an overview. *Transpl Int* 1994; **7**: 47-61
12 **Tam PKH**, Guo WH. Intestinal transplantation: Current Status. *Asian J Surg* 1999; **22**: 146-151
13 **Abu-Elmagd K**, Bond G. The current status and future outlook of intestinal transplantation. *Minerva Chir* 2002; **57**: 543-560
14 **Adams DH**. Immunologic aspects of small bowel transplantation. *Transplant Proc* 1998; **30**: 2557-2559
15 **Luke PP**, Thomson AW. Blockade of costimulatory molecules on dendritic cells: implications for tolerance induction. *Transplant Proc* 2001; **33**: 507-508
16 **Banchereau J**, Steinman RM. Dendritic cells and the control of immunity. *Nature* 1998; **392**: 245-252
17 **Akdis CA**, Blaser K. Mechanisms of interleukin-10-mediated immune suppression. *Immunology* 2001; **103**: 131-136
18 **De Fazio SR**, Gozzo JJ. Role of graft interleukin-10 expression in the tolerogenicity of neonatal skin allografts. *Transplantation* 2000; **70**: 1371-1377
19 **Moore KW**, de Waal Malefyt R, Coffman RL, O'Garra A. Interleukin-10 and the interleukin-10 receptor. *Annu Rev Immunol* 2001; **19**: 683-765
20 **Ni K**, O'Neill HC. The role of dendritic cells in T cell activation. *Immunol Cell Biol* 1997; **75**: 223-230
21 **Lee WC**, Jeng LB, Chiang YJ, Wang HC, Huang CC. Dendritic cell progenitors prolong allograft survival through T-helper 2 deviation of the Th1/Th2 paradigm. *Transplant Proc* 2000; **32**: 2076-2077
22 **DePaz HA**, Oluwole OO, Adeyeri AO, Witkowski P, Jin MX, Hardy MA, Oluwole SF. Immature rat myeloid dendritic cells generated in low-dose granulocyte macrophage-colony stimulating factor prolong donor-specific rat cardiac allograft survival. *Transplantation* 2003; **75**: 521-528
23 **Steinbrink K**, Wolfl M, Jonuleit H, Knop J, Enk AH. Induction of tolerance by IL-10-treated dendritic cells. *J Immunol* 1997; **159**: 4772-4780
24 **De Smedt T**, Van Mechelen M, De Becker G, Urbain J, Leo O, Moser M. Effect of interleukin-10 on dendritic cell maturation and function. *Eur J Immunol* 1997**; 27**: 1229-1235
25 **Coates PT**, Krishnan R, Kireta S, Johnston J, Russ GR. Human myeloid dendritic cells transduced with an adenoviral interleukin-10 gene construct inhibit human skin graft rejection in humanized NOD-scid chimeric mice. *Gene Ther* 2001; **8**: 1224-1233
26 **McCoy KD**, Le Gros G. The role of CTLA-4 in the regulation of T cell immune responses. *Immunol Cell Biol* 1999; **77**: 1-10
27 **Greenfield EA**, Nguyen KA, Kuchroo VK. CD28/B7 costimulation: a review. *Crit Rev Immunol* 1998; **18**: 389-418
28 **Kishimoto K**. The role of CD154-CD40 versus CD28-B7 costimulatory pathways in regulationg allogeneic Th1 and Th2 responses *in vivo*. *J Clin Inve* 2000; **106**: 63-72
29 **Jenkins MK**, Chen CA, Jung G, Mueller DL, Schwartz RH. Inhibition of antigen-specific proliferation of type 1 murine T cell clones after stimulation with immobilized anti-CD3 monoclonal antibody. *J Immunol* 1990; **144**: 16-22
30 **Schwartz RH**. Models of T cell anergy: Is there a common molecular mechanism? *J Exp Med* 1996; **184**: 1-5
31 **Ballard DW**. Molecular mechanisms in lymphocyte activation and growth. *Immunol Res* 2001; **23**: 157-166
32 **Prasad AS**, Bao B, Beck FW, Sarkar FH. Zinc enhances the expression of interleukin-2 and interleukin-2 receptors in HUT-78 cells by way of NF-kappaB activation. *J Lab Clin Med* 2002; **140**: 272-289
33 **Hong YS**, Laks H, Cui G, Chong T, Sen L. Localized immunosuppression in the cardiac allograft induced by a new liposome-mediated IL-10 gene therapy. *J Heart Lung Transplant* 2002; **21**: 1188-1200
34 **Gojo S**, Yamamoto S, Patience C, LeGuern C, Cooper DK. Gene therapy-its potential in surgery. *Ann R Coll Surg Engl* 2002; **84**: 297-301

Edited by Zhu LH and Wang XL

P.O.Box 2345, Beijing 100023,China
Fax: +86-10-85381893
E-mail: wjg@wjgnet.com www.wjgnet.com

World J Gastroenterol 2003;9(11):2513-2518
World Journal of Gastroenterology
 ISSN 1007-9327

• BASIC RESEARCH •

Effect of NF-κB and p38 MAPK in activated monocytes/macrophages on pro-inflammatory cytokines of rats with acute pancreatitis

Hong-Shan Liu, Cheng-En Pan, Qing-Guang Liu, Wei Yang, Xue-Min Liu

Hong-Shan Liu, Cheng-En Pan, Qing-Guang Liu, Wei Yang, Xue-Min Liu, Department of Hepatobiliary Surgery, First Affiliated Hospital, Xi' an Jiaotong University, Xi' an 710061, Shaanxi Province, China

Correspondence to: Dr. Hong-Shan Liu, Department of Hepatobiliary Surgery, First Affiliated Hospital, Xi' an Jiaotong University, Xi' an 710061, Shaanxi Province, China. doctorliuqi@yahoo.com.cn
Telephone: +86-29-5324009 **Fax:** +86-29-5324009
Received: 2003-04-05 **Accepted:** 2003-05-11

Abstract

AIM: Proinflammatory cytokines TNF-α and IL-6 play a main role in acute pancreatitis (AP). Cytokine biosynthesis runs through two major signaling pathways at the level of proteins: nuclear transcription factor-κB (NF-κB) and p38 mitogen-activated protein kinase (p38 MAPK). The aim of the study was to investigate the effect of NF-κB and p38 MAPK in activated monocytes/macrophages on cytokines of rats with acute pancreastitis.

METHODS: Taurocholate (3 % and 5 %) at doses of 1 mL/kg was administered into the biliopancreatic duct of male Sprague-Dawley (SD) rats to reduce acute edematous pancreariris (AEP) and acute necrotizing pancreatitis (ANP). Pancreatic tissues were prepared immediately after death. At this point, blood was obtained for determination of serum amylase and pro-inflammatory TNF-α and IL-6. Activated monocytes/macrophages were captured from blood and so were ascites. NF-κB and p38 MAPK in activated monocytes/macrophages were measured by immunohistochemistry method. Pancreatic tissue samples were prepared for routine light microscopy, using hematoxylin and eosin (HE) staining.

RESULTS: The serum levels of amylase were 3 056.00±1 232.35 IU/L and 4 865.12±890.34 IU/L at 3 and 6 hours in ANP group, which were significantly higher than those (3 056.00±1 232.35 IU/L and 3 187.17±821.16 IU/L) ($P<0.05$, respectively) in AEP group. In ascites the levels were 3.32±1.01 g and 3.76±1.12 g at 3 and 6 hours in ANP group, which were significantly higher than those (1.43±1.02 g and 2.56±1.21 g) ($P<0.05$, respectively) in AEP group. The serum levels of TNF-α were 54.27±23.48 pg/ml and 67.83±22.02 pg/ml in AEP group and 64.28±20.79 pg/ml and 106.59±43.71 pg/ml in ANP group, and the serum levels of IL-6 were 428.12±140.30 pg/ml and 420.13±139.40 pg/ml in AEP group and 1 600.32±309.78 pg/ml and 2 203.76±640.85 pg/ml in ANP group, which were far significantly higher than those in sham group ($P<0.001$, respectively). The serum level of TNF-α 6 hours after establishment of the studied model and that of IL-6 at 3 and 6 hours in ANP group were significantly higher than those in AEP ($P<0.05$, $P<0.001$, $P<0.05$). In ANP group, the levels of serum TNF-α and IL-6 6 hours after establishment of the studied model were significantly higher than those 3 hours after establishment of studied model ($P<0.05$, $P<0.05$, respectively). Three and 6 hours after establishment of the model, typical pathological changes of AEP and ANP were found, such as large numbers of inflammatory cells, edema, hemorrhage, necrosis, large amount of ascites. In AEP, NF-κB and p38 MAPK in activated monocytes/macrophages were moderately found at 3 and 6 hours after introduction of the model. However, in ANP, the expression of NF-κB and p38 MAPK in activated monocytes/macrophages was upregulated evidently at 3 and 6 hours after introduction of the model, reaching their highest levels at 6 hours after introduction of the model, which were consistent with the levels of TNF-α and IL-6.

CONCLUSION: Cytokine TNF-α and IL-6 play a main role in acute pancreatitis, expression of NF-κB and p38 MAPK in activated monocytes/macrophages might play a major role in cytokine transcription and biosynthesis.

Liu HS, Pan CE, Liu QG, Yang W, Liu XM. Effect of NF-κB and p38 MAPK in activated monocytes/macrophages on pro-inflammatory cytokines of rats with acute pancreatitis. *World J Gastroenterol* 2003; 9(11): 2513-2518
http://www.wjgnet.com/1007-9327/9/2513.asp

INTRODUCTION

The etiology of acute pancreatitis (AP) is mostly alcoholic or gallstone. Whatever the etiologic factors are, once the disease is initiated by an early molecular mechanism (which is still controversial) in or around acinar cells, a host inflammatory response is evoked in the pancreas. This locally limited inflammation is then manifested and amplified by the actions of diverse inflammatory mediators, such as cytokines (tumor necrosis factor-α (TNF-α), interleukin-1(IL-1) and interleukin-6(IL-6)), reactive oxygen species, proteolytic enzymes, lipids, as well as gaseous mediators, resulting in the induction of systemic inflammatory response syndrome (SIRS)[1-3]. Although SIRS is principally considered to be the normal host response to the insults, sustained or exaggerated SIRS, followed by the development of multiple organ dysfunction syndrome (MODS), is ultimately responsible for most pancreatitis- associated mortality and morbidity. Thus, the most distinctive feature of AP could be defined as its propensity to propagate locally limited inflammation into SIRS, and subsequently into MODS[4,5].

In AP, the very early phenomena that appear to occur are monocytes and neutrophils in the circulation migrating into the pancreatic interstitial space, mainly mediated by adhesion molecules on leukocytes[6,7]. These infiltrating cells accelerate further production and secretion of cytokines, as well as other inflammatory mediators. As a result, leukocytes in the circulation, as well as endothelial cells, in the pancreas and specific distant organs such as the lung, liver and spleen, are activated, eliciting further microcirculatory derangements, such as increased vascular permeability and accelerated leukocyte transmigration. The contribution of cytokines during this cascade of events has been increasingly apparent in the past decade, as indicated by several clinical and experimental studies exhibiting increased levels of cytokines in plasma, lymph, and ascites,as well as enhanced activitity of circulating leukocytes. Of the

various kinds of inflammatory mediators, TNF-α and IL-1 are regarded as most prominent "first-line" cytokines[8-10]. IL-6 is well known to be the primary inducer of acute-phase response. Therefore, IL-6 was recently reported to be the best prognostic parameter of pulmonary failure[11]. IL-6, IL-8 and TNF-α can be synthesized by monocytes/macrophages, neutrophils, endothelial cells, and even pancreatic duct cells.

Recent experimental studies appeared to have shed some light on the intracellular signaling pathway in the inflammatory cascade in AP. For example, recent evidence strongly suggested the crucial role of NF-κB in the initiation of AP, not only in pancreatic acinar cells and monocytes/macrophages but also in specific distant organs, such as the lung. NF-κB is able to mediate a variety of inflammatory mediators involved in AP, including cytokines and adhesion molecules, as well as specific inducible isoform of nitric oxide synthase enzymes[12-21]. Additionally, recent evidence has also shown the contribution of p38 MAP kinase to the mechanism underlying cytokine expression in pancreatic acinar cells and monocytes/ macrophages. An *in-vitro* experiment showed that cytokine expression of acinar cells was mediated by two separate signal pathways, i.e, NF-κB and p38 MAP kinase. of which p38 MAP kinase is now suggested to play a major role[22-27]. The definitive role of these intracellular signaling cascades may lead to new designs for cytokine modulation therapy.

This study was to investigate the effect of NF-κB and p38 MAPK in activated monocytes/macrophages on pro-inflammatory cytokines of mice with acute pancreatitis and to explore the biosynthesis mechanism of pro-inflammatory cytokines TNF-α and IL-6.

MATERIALS AND METHODS

Materials

Sixty pathogen-free male Sprague-Dawley (SD) rats (Animal Center, Xi' an Jiaotong University), weighing 250-300 g, were used in this experiment. The animals were kept at a constant room temperature of 25 ℃ with a 12-hour light-dark cycle, and were allowed free access to water. The animals were housed in the animal facility for at least seven days prior to use in order to stabilize their intestinal flora. All procedures including the rats receiving a very small amount of methoxyflurane for induction and pentobarbital intra-peritoneal injection (50 mg/kg) for anesthesia were performed under sterile conditions. SD rats were divided into subgroups of pancreatitis and controls. Taurocholate (3 % and 5 %, Sigma) at doses of 1 mL/kg was administered into the biliopancreatic duct of the rats to establish acute edematous pancreatitis (AEP) and acute necrotizing pancreatitis (ANP). In the sham group, the mice were only operated but not infused anything. All values reported were from animals killed at defined time points. During experiments the rats were closely observed, and pancreas tissues were prepared immediately after death. At this point, blood was obtained for determination of serum amylase and TNF-α and IL-6. The activated monocytes/ macrophages were captured from blood and ascites respectively.

Macroscopic assessment of the pancreas

Necrosis, hemorrhage and edema of the pancreas were each graded from 0 to 3 as follows: (a) necrosis: no necrosis =0, isolated necrotic lesion (<5 % of the pancreas)=1, necrotic areas 5-25 %=2, necrotic areas >25 % and partial destruction of the organ=3; (b) hemorrhage: not evident=0, single focal hemorrhage=1, multiple disseminated hemorrhagic dots=2, massive confluent hemorrhage=3; (c) edema: normal size=0, enlargement of the pancreas=1, recognizable accumulated fluid in the tissue=2, massive swelling and fluid accumulation=3. The scores of these parameters were summed, and the highest possible total score for an individual rat was 9[28].

Microscopic assessment of the pancreas

Pancreas tissue samples were prepared for routine light microscopy, using hematoxylin and eosin (HE) staining and examined by a pathologist who was unaware of the source of specimens. HE-stained pancreas sections were observed with a standard light microscope to evaluate morphologic alterations following AP.

Pancreatic water contents

The wet weight-dry weight ratio of the pancreas was obtained after about 200 mg of freshly prepared pancreatic tissue was dried for 20 h at 105 ℃.

Amylase assay

Amylase activity in plasma was determined using the a-amylase EPS assay purchased from Roche (Sigma) at 37 ℃.

Serum of TNF-α and IL-6

Blood was collected and centrifuged (3 000 rpm/min, for 5 min). The serum was captured and stored at -30 ℃. The pro-inflammatory TNF-α and IL-6 were measured by enzyme-linked immunosorbent assay (ELISA).

NF-κB and p38 MAPK in activated monocytes/macrophages

The activated monocytes/macrophages were captured from blood and ascites, respectively. They were separated and pasted for 12 hours in 10 % calf serum of 1640. NF-κB and p38 MAPK in activated monocyte/macrophage were measured by immunohistochemistry method (S-ABC). In brief, endogenous peroxidases were blocked for 15 min with methanol-H_2O_2, and after several washes unspecific-binding sites were blocked for 2 h with 3 % normal horse serum. Samples were then incubated overnight in a humidified chamber at 4 ℃ with the primary antibody against NF-κB and p38 MAPK(Sigma) diluted 1:200. This was followed by biotinylated goat anti-mouse antibody diluted 1:200 for 1 h, and the avidin-biotin complex (ABC kit, Vector Laboratories) (1:100) for 1 h. The reaction was developed with 0.05 % diaminobenzidine and 0.03 % H_2O_2. Negative controls were carried out by omission of the primary antibody in the overnight incubation. Several sections were counterstained with hematoxylin.

Statistical analysis

The values were expressed as the mean ±standard error (SEM). The data were analyzed for statistical significance using Student' s *t* test. There were six animals in each group at each time point. As the values in some data sets were not normally distributed or exhibited unequal standard deviations, the nonparametric Wilcoxon rank sum test was used to test for statistical differences between groups. In all instances $P<0.05$ was considered to be significant.

RESULTS

Amylase assay and ascites

The serum levels of AMS and ascites in AEP and ANP groups were significantly higher than those in sham group ($P<0.01$). The serum levels of AMS and ascites at 3 and 6 hours after the establishment of the studied model in ANP group were significantly higher than that in AEP ($P<0.05$). In ANP group, the levels of serum AMS and ascites 6 hours after the establishment of the studied model were not significantly higher than those 3 hours after the establishment of the studied model ($P>0.05$) (Table 1).

Table 1 Levels of AMS and ascites of AEP and ANP($\bar{x}\pm s$)

Group	AMS (IU/L)		Ascites (g)	
	3 h	6 h	3 h	6 h
Sham	792.80±265.08	793.8 0±265.08	0	0
AEP	3 056.00±1232.35[b]	3 187.17±821.16[b]	1.43±1.02[b]	2.56±1.21[b]
ANP	4 345.30±1005.77[ab]	4 865.12±890.34[ab]	3.32±1.01[ab]	3.76±1.12[ab]

[b]P<0.01 *vs* sham, [a]P<0.05 *vs* AEP.

Pancreatic water contents

The extent of pancreatic edema was determined as the wet weight/dry weight ratio of the tissue, and the macroscopic appearance of the pancreas was evaluated by a score (Table 2). In pancreatitis both parameters were significantly increased compared to the control (P<0.05).

Table 2 Macrocopic appearance and edema of pancreas in AEP and ANP (at 6 hours after of model)

	n	Sham	AEP	ANP
Score	0.2	1.1	6.9[a]	6.3[ac]
ww/dw	4.3	5.3	7.1[a]	8.2[ac]

The macroscopic appearance of the pancreas was scored. For an individual rat the highest possible score was 9. Pancreatic water content was estimated as the wet weight/dry weight ratio (ww/dw) of the tissue. N: untreated animals, anesthesia omitted; S: sham operations. [a]P<0.05 compared to the untreated group; [c]P<0.05 compared to the control group at 6 hours after induction of model.

Serum levels of TNF-α and IL-6

The serum levels of TNF-α and IL-6 in AEP and ANP groups were far significantly higher than those in sham group (P<0.001). The serum levels of TNF-α and IL-6 6 hours after establishment of the model in ANP group were significantly higher than those in AEP (P<0.05, P<0.001, P<0.05). In ANP group, the levels of serum TNF-α and IL-6 6 hours after establishment of the studied model were significantly higher than those 3 hours after establishment of the studied model (P<0.05) (Table 3).

Table 3 Serum levels of TNF-α and IL-6 in AEP and ANP ($\bar{x}\pm s$)

Group	TNF-α (pg/ml)		IL-6 (pg/ml)	
	3 h	6 h	3 h	6 h
Sham	4.13±2.5	55.87±3.79	100.79±53.89	151.04±91.79
AEP	54.27±23.48[b]	67.83±22.02[b]	428.12±140.30[b]	420.13±139.40[b]
ANP	64.28±20.79[b]	106.59±43.71[abc]	1 600.32±309.78[ab]	2 203.76±640.85[abc]

[b]P<0.001 *vs* sham group; [a]P<0.05 or 0.001 *vs* AEP group; [c]P<0.05 *vs* 3 h group.

Morphological examination

After induction of the AEP and ANP models, the pancreas showed mild edema and congestion. Three and 6 hours after introduction of the model, typical pathological changes of AEP and ANP were found, such as large numbers of inflammatory cells, edema, hemorrhage, necrosis, large amount of ascites (Table 1).

NF-κB and p38 MAPK in activated monocytes/macrophages

The expression of NF-κB and p38 MAPK in activated monocytes/macrophages at 3 and 6 hours was assessed by immunohistochemistry. In AEP, mild expression of NF-κB and p38 MAPK in activated monocytes/macrophages was found 3 and 6 hours after introduction of the model. However, in ANP, the expression of NF-κB and p38 MAPK in activated monocytes/macrophages was upregulated evidently 3 and 6 hours after introduction of the model, reaching their highest levels at 6 hours after introduction of the model (Figures 1,2,3 and 4).

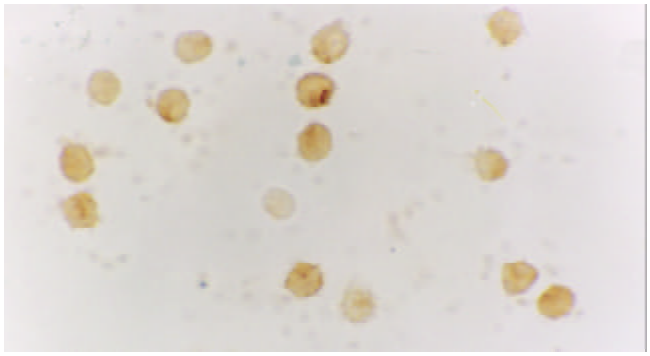

Figure 1 Moderate expression of NF-κB in the cytoplasm/nucleolus of monocytes in AEP (6 hours) 10×100.

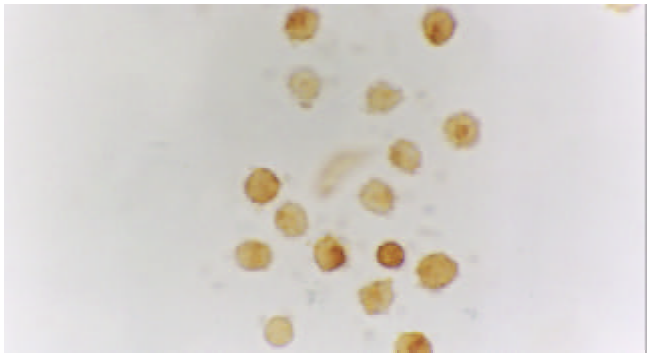

Figure 2 Strong expression of NF-κB in the cytoplasm/nucleolus of monocytes in ANP (6 hours) 10×100.

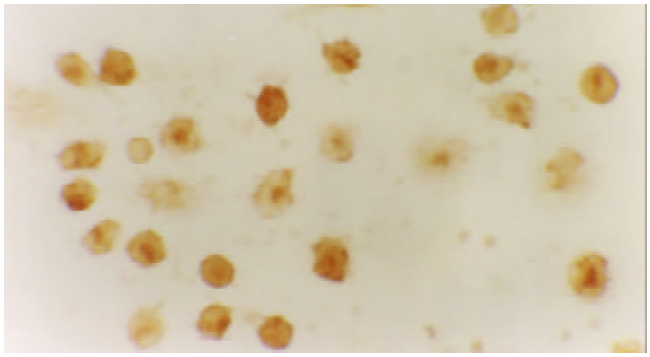

Figure 3 Moderate expression of p38MAPK in the cytoplasm/nucleolus of monocytes in AEP (6 hours) 10×100.

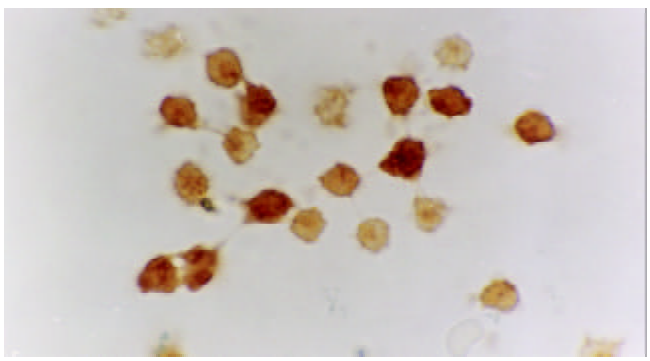

Figure 4 Strong expression of p38MAPK in the cytoplasm/nucleolus of monocytes in ANP (6 hours) 10×100.

DISCUSSION

The clinical manifestations of AP vary significantly from mild to lethal, severity of the disease is largely determined by the actions of various kinds of inflammatory mediators, including cytokines, reactive oxygen species, proteolytic enzymes, and lipids, as well as gaseous mediators. Despite increasing knowledge implicating the involvement of cytokines in the progression of AP, no clinical trials pertaining to cytokine modulation have been performed so far. Progress in intensive care technologies has contributed to the improvement of mortality and morbidity rates in severe AP in the past decade. However, it appears to be reasonable for clinicians to "line up their sights" on the modulation of cytokines as a direct treatment.

Pro-inflammatory cytokines played a main role in acute pancreatitis and complications due to acute pancreatitis[29,30]. Failure of different organ systems is a frequent problem in severe acute pancreatitis. The majority of fatalities in patients with severe acute pancreatitis are associated with the failure of at least one or more organ systems. Organ failure in severe acute pancreatitis has to be regarded as part of the inflammatory response following the liberation of activated enzymes from the pancreas. The mediators involved in this process include IL-1, TNF-α, IL-6, platelet activating factor, and IL-8. Of the various kinds of inflammatory mediators, TNF-α and IL-1 are regarded as the most prominent "first-line" cytokines. The primary involvement of TNF-α was demonstrated by elevation of TNF-α levels in rat severe AP models. This was confirmed by subsequent TNF-α antagonism experiments, using anti-TNF-α antibodies or a recombinant dimeric form of p55 TNF receptor. Similarly, the concurrent blockade of cytokines showed no additional benefit in the amelioration of pancreatic injury, however, it attenuated the systemic response, as indicated by reduced IL-6 levels and decreased mortality rates. With few exceptions, most studies carried out with the purpose of blocking proximal cytokines, such as TNF-α, IL-1 or IL-6, during the progression of AP showed favorable results in experimental settings. However, neither TNF-α nor IL-1 has a causative role in the initiation of AP. For example, exposure of isolated acinar cells to TNF-α and IL-1 *in vitro* did not induce either intracellular zymogen activation or release of enzymes. In addition, these cytokines were not able to induce either biological or histological evidence of pancreatitis by *in-situ* perfusion of isolated human pancreas[31].

As to the primary site of cytokine production, infiltrating macrophages in the pancreas and ascites are suggested to be the initial cellular origins of TNF-α. In a mouse cerulein AP model, the expression of TNF-α messenger RNA within the inflamed pancreas was observed as early as 30 min after the induction of AP, and was followed by elevation of intrapancreatic and serum TNF-α levels. In addition, neutrophils that have migrated into the inflamed pancreas appear to be equally involved in the production of TNF-α, IL-6 and IL-1. The production of these cytokines was subsequently observed in specific distant organs, such as the lungs, liver, and spleen. In particular, production of TNF-α and IL-1 in the lung was known to be closely associated with the development of adult respiratory distress syndrome (ARDS), which was the major cause of early death in patients with SAP[32].

IL-6 is well known to be the primary inducer of acute-phase response, while its level in circulation during AP reaches the maximum value 24-48 h before the maximal C-reactive protein level is reached. Therefore, IL-6 has been recently reported to be the best prognostic parameter of pulmonary failure. IL-6 is synthesized by monocytes/macrophages, neutrophils, endothelial cells, and even pancreatic duct cells. It is able to stimulate neutrophil chemotaxis and release of enzymes, thereby leading to tissue destruction when overproduced. In clinical settings, some authors have reported elevated IL-6 levels in AP patients, particularly in those with complications. This observation has been supported by *in-vitro* studies, using isolated blood monocytes from patients with AP, in which systemic complications were found to be closely associated with enhanced secretion of IL-6 and IL-8 from the cells. Based on an increasing body of evidence, both IL-6 and IL-8 are now considered to be early and excellent predictors of patient outcome, and are widely used as secondary end points in clinical trails[33].

Recent experimental studies have shed some light on the intracellular signaling pathway in the inflammatory cascade in AP. For example, recent evidence strongly suggested the crucial role of NF-κB in the initiation of AP, not only in pancreatic acinar cells, monocytes/macrophages and neutrophils, but also in specific distant organs such as the lung. NF-κB is able to mediate a variety of inflammatory mediators involved in AP, including cytokines and adhesion molecules, as well as specific enzymes. NF-κB plays a key role in the transcriptional regulation of adhesion molecules, enzymes and cytokines involved in acute inflammatory diseases. NF-κB is a key transcription factor for the expression of various proinflammatory molecules such as chemokines, cytokines, and adhesion molecules. This notion has recently been verified by adenoviral-mediated gene transfer of an active subunit, RelA/p65, into acinar cells delivered through an injection into the rat pancreatic duct. The overexpressed RelA/p65 protein trans-activated NF-κB and induced pancreatic inflammation, a pathological state very similar to acute pancreatitis. In addition to the importance of NF-κB in the pathogenesis of acute pancreatitis, it was also reported that NF-κB activation in macrophages was a key event both in the development of generalized complications during severe acute pancreatitis and as a cause of the high mortality in this condition. Studies also showed that glucocorticoids were one of the most potent inhibitors of NF-κB, which might be attributable to the inhibition of this key transcription factor both in acinar cells and in inflammatory cells such as monocytes/macrophages. It is known that the mechanism of the inhibition of NF-κB by corticosteroids is multifactorial. One is via the induction of IκBa, the inhibitor molecule of NF-κB, which can form a complex with NF-κB in the cytoplasm, inhibiting the translocation of NF-κB into the nucleus, where it enhances the transcriptional activation of various proinflammatory genes. The other is a cross-coupling mechanism of inhibition between activated glucocorticoid receptors and activated NF-κB. Because the activation of NF-κB is an early event in the pathogenetic mechanism of acute pancreatitis, it is reasonable that in most studies corticosteroids showed beneficial effects on acute pancreatitis[34].

Moreover, inflammatory mediators released during acute diseases activate multiple intracellular signalling cascades including the MAPK signal transduction pathway, which plays a significant role in the recruitment of leukocytes to sites of inflammation. Stimulation of leukocytes by pro-inflammatory cytokines is known to result in activation of MAPK isoform p38. However, the functional consequences of p38 MAPK activation during leukocyte recruitment, including adhesion, migration and effector functions such as oxidative burst and degranulation, are only just beginning to be elucidated. Recently, p38 MAPK has been implicated in the activation of NF-κB. Several groups have demonstrated that p38 MAPK-specific inhibitor SB203580 potently attenuated NF-κB-dependent transcription. However, phosphorylation of NF-κB subunits, nuclear translocation and DNA binding to NF-κB were not affected by this p38 inhibitor. This suggests that NF-κB and p38 MAPK are activated by separate effector pathways, which might converge further downstream in the cell nucleus.

So recent experimental studies have shed some light on the intracellular signaling pathway in the inflammatory cascade. Cytokine transcription and biosynthesis bifurcate into two major signaling pathways at the level of proteins. One runs through the NF-κB inducing kinase route, which regulates phosphorylation of inhibitory-kb (IκB) protein, the cytosolic inhibitor of NF-κB which allows NF-κB complex to translocate to the nucleus and promotes gene expression. The other is mediated through p38MAPK pathway and makes p38MAPK phosphorylated and activated[35].

So in recent years, much effort has been focused on delineating intracellular signaling cascades in inflammatory pathways. The intracellular signaling pathways used by leukocytes in response to pro-inflammatory stimuli have only begun to be unravelled. Much attention has been given to MAPK superfamily owing to their activation by pro-inflammatory cytokines IL-6 and TNF-α, which play a central role during inflammatory responses and in inflammatory diseases.

In this study, it showed that retrograde infusion of sodium taurocholate into the pancreatic duct resulted in an increase of amylase activity and ascites 3 and 6 hours after pancreatitis. The levels of serum AMS and ascites in AEP and ANP groups were far significantly higher than those in sham group (P<0.01). The serum levels of TNF-α and IL-6 in AEP and ANP groups were far significantly higher than those in sham group (P<0.001). The serum level of TNF-α of the studied model and the serum level of IL-6 3 and 6 hours in ANP group were significantly higher than that in AEP (P<0.05, P<0.001, P<0.05). In ANP group, the levels of serum TNF-α and IL-6 6 hours after establishment of the studied model were significantly higher than those 3 hours after establishment of the studied model (P<0.05, P<0.05).

After induction of AEP and ANP models, pancreas showed mild edema and congestion. Three and 6 hours after introduction of the model, typical pathological changes of AEP and ANP were found, such as large numbers of inflammatory cell, edema, hemorrhage, necrosis, large amount of ascites.

The expression of NF-κB and p38 MAPK in activated monocytes/macrophages at 3 and 6 hours after pancreatitis was assessed by immunohistochemistry. In AEP, moderate expression of NF-κB in activated monocytes/macrophages was found 3 and 6 hours after introduction of the model. However, in ANP, the expression of NF-κB and p38 MAPK in activated monocytes/macrophages were upregulated evidently 3 and 6 hours after introduction of the model, reaching their highest levels 6 hours after introduction of the model. So the expression of NF-κB and p38 MAPK in activated monocytes/macrophages at 3 and 6 hours assessed by immunohistochemistry was consistent with the increase of pro-inflammatory cytokines TNF-α and IL-6.

Thus, increased understanding of the signal transduction pathways involved in the regulation of cytokine production and cytokine signaling in inflammatory cells has opened the door for the discovery of novel therapeutics for treating a variety of inflammatory diseases in which cytokine production or signaling is implicated. The availability of potent and selective inhibitors of such signaling pathways also provides a means to further dissect the pathways to increase our understanding about the complex events underlying a particular immune mediated event at the cellular and molecular level. NF-κB and p38 MAPK are the most studied signaling molecules in this regard and their relevance to such disease states has been established primarily through the use of inhibitors. Indeed, selective inhibition of NF-κB and p38 MAP kinase inhibitors has demonstrated efficacy in a variety of animal models[36-40]. Specific p38 inhibitors and selective inhibition of NF-κB aimed at reducing the production of inflammatory mediators are now being developed, and might in the future provide more effective treatment for inflammatory diseases. At present, it may be too early to take an optimistic view of therapeutic cytokine modulation in AP. There are many obstacles to overcome. However, direct therapy by cytokine modulation sounds very attractive to clinicians.

REFERENCES

1 **Morrison CP,** Teague BD, Court FG, Wemyss-Holden SA, Metcalfe MS, Dennison AR, Maddern GJ. Experimental studies of serum cytokine concentration following pancreatic electrolytic ablation. *Med Sci Monit* 2003; **9**: 43-46

2 **Zhang Q,** Ni Q, Cai D, Zhang Y, Zhang N, Hou L.Mechanisms of multiple organ damages in acute necrotizing pancreatitis. *Chin Med J (Engl)* 2001; **114:** 738-742

3 **Makhija R,** Kingsnorth AN. Cytokine storm in acute pancreatitis. *J Hepatobiliary Pancreat Surg* 2002; **9:** 401-410

4 **Bhatia M,** Neoptolemos JP, Slavin J. Inflammatory mediators as therapeutic targets in acute pancreatitis. *Curr Opin Investig Drugs* 2001; **2:** 496-501

5 **Wereszczynska-Siemiatkowska U,** Dabrowski A, Siemiatkowski A, Mroczko B, Laszewicz W, Gabryelewicz A. Serum profiles of E-selectin, interleukin-10, and interleukin-6 and oxidative stress parameters in patients with acute pancreatitis and nonpancreatic acute abdominal pain. *Pancreas* 2003; **26:** 144-152

6 **Lundberg AH,** Granger N, Russell J, Callicutt S, Gaber LW, Kotb M, Sabek O, Gaber AO. Quantitative measurement of P-and E-selectin adhesion molecules in acute pancreatitis: correlation with distant organ injury. *Ann Surg* 2000; **231:** 213–222

7 **Qin RY,** Zou SQ,Wu ZD. Experimental research on production and uptake sites of TNF-α in rat with acute hemorrhagic necrotic pancreatitis. *World J Gastroenterol* 1998; **4:** 144-146

8 **Shimada M,** Andoh A, Hata K, Tasaki K, Araki Y, Fujiyama Y, Bamba T. IL-6 secretion by human pancreatic periacinar myofibroblasts in response to inflammatory mediators. *J Immunol* 2002; **168:** 861-868

9 **Riche FC,** Cholley BP, Laisne MJ, Vicaut E, Panis YH, Lajeunie EJ, Boudiaf M, Valleur PD. Inflammatory cytokines, C reactive protein, and procalcitonin as early predictors of necrosis infection in acute necrotizing pancreatitis. *Surgery* 2003; **133:** 257-262

10 **Coelho AM,** Machado MC, Cunha JE, Sampietre SN, Abdo EE. Influence of pancreatic enzyme content on experimental acute pancreatitis. *Pancreas* 2003; **26:** 230-234

11 **Mayer J,** Rau B, Gansauge F, Beger HG. Inflammatory mediators in human acute pancreatitis: clinical and pathophysiological implications. *Gut* 2000; **47:** 546–552

12 **Jaffray C,** Yang J, Carter G, Mendez C, Norman J. Pancreatic elastase activates pulmonary nuclear factor kappa B and inhibitory kappa B, mimicking pancreatitis-associated adult respiratory distress syndrome. *Surgery* 2000; **128:** 225-231

13 **Kim H,** Seo JY, Kim KH. NF-kappaB and cytokines in pancreatic acinar cells. *J Korean Med Sci* 2000; **15**(Suppl): S53-S54

14 **Blanchard JA,** Barve S, Joshi-Barve S, Talwalker R, Gates LK Jr. Cytokine production by CAPAN-1 and CAPAN-2 cell lines. *Dig Dis Sci* 2000; **45:** 927-932

15 **Frossard JL,** Pastor CM, Hadengue A. Effect of hyperthermia on NF-kappaB binding activity in cerulein-induced acute pancreatitis. *J Physiol Gastrointest Liver Physiol* 2001; **280:** G1157-1162

16 **Blanchard JA,** Barve S, Joshi-Barve S, Talwalker R, Gates LK Jr. Antioxidants inhibit cytokine production and suppress NF-kappaB activation in CAPAN-1 and CAPAN-2 cell lines. *Dig Dis Sci* 2001; **46:** 2768-2772

17 **Tando Y,** Algul H, Schneider G, Weber CK, Weidenbach H, Adler G, Schmid RM. Induction of IkappaB-kinase by cholecystokinin is mediated by trypsinogen activation in rat pancreatic lobules. *Digestion* 2002; **66:** 237-245

18 **Algul H,** Tando Y, Schneider G, Weidenbach H, Adler G, Schmid RM. Acute Experimental Pancreatitis and NF-kappaB/Rel Activation. *Pancreatology* 2002; **2:** 503-509

19 **Murr MM,** Yang J, Fier A, Kaylor P, Mastorides S, Norman JG. Pancreatic elastase induces liver injury by activating cytokine production within Kupffer cells via nuclear factor-Kappa B. *J Gastrointest Surg* 2002; **6:** 474-480

20 **Rakonczay Z,** Jarmay K, Kaszaki J, Mandi Y, Duda E, Hegyi P,

Boros I, Lonovics J, Takacs T. NF-kappaB activation is detrimental in arginine-induced acute pancreatitis. *Free Radic Biol Med* 2003; **34:** 696-709

21 **Altavilla D,** Famulari C, Passaniti M, Campo GM, Macri A, Seminara P, Marini H, Calo M, Santamaria LB, Bono D, Venuti FS, Mioni C, Leone S, Guarini S, Squadrito F. Lipid peroxidation inhibition reduces NF-kappaB activation and attenuates cerulein-induced pancreatitis. *Free Radic Res* 2003; **37:** 425-435

22 **Blinman TA,** Gukovsky I, Mouria M, Zaninovic V, Livingston E, Pandol SJ, Gukovskaya AS. Activation of pancreatic acinar cells on isolation from tissue: cytokine upregulation via p38 MAP kinase. *Am J Physiol Cell Physiol* 2000; **279:** 1993-2003

23 **Chen X,** Ji B, Han B, Ernst SA, Simeone D, Logsdon CD. NF-kappaB activation in pancreas induces pancreatic and systemic inflammatory response. *Gastroenterology* 2002; **122:** 448-457

24 **Murr MM,** Yang J, Fier A, Gallagher SF, Carter G, Gower WR Jr, Norman JG. Regulation of Kupffer cell TNF gene expression during experimental acute pancreatitis: the role of p38-MAPK, ERK1/2, SAPK/JNK, and NF-kappaB. *J Gastrointest Surg* 2003; **7:** 20-25

25 **Masamune A,** Kikuta K, Satoh M, Satoh A, Shimosegawa T. Alcohol activates activator protein-1 and mitogen-activated protein kinases in rat pancreatic stellate cells. *J Pharmacol Exp Ther* 2002; **302:** 36-42

26 **Fleischer F,** Dabew R, Goke B, Wagner AC. Stress kinase inhibition modulates acute experimental pancreatitis. *World J Gastroenterol* 2001; **7:** 259-265

27 **Dabrowski A,** Boguslowicz C, Dabrowska M, Tribillo I, Gabryelewicz A. Reactive oxygen species activate mitogen-activated protein kinases in pancreatic acinar cells. *Pancreas* 2000; **21:** 376-384

28 **Gilgenast O,** Brandt-Nedelev B, Wiswedel I, Lippert H, Halangk W, Reinheckel T. Differential oxidative injury in extrapancreatic tissues during experimental pancreatitis modification of lung proteins by 4-hydroxynonenal. *Dig Dis Sci* 2001; **46:** 932-937

29 **Osman MO,** Gesser B, Mortensen JT, Matsushima K, Jensen SL, Larsen CG. Profiles of pro-inflammatory cytokines in the serum of rabbits after experimentally induced acute pancreatitis. *Cytokine* 2002; **17:** 53-59

30 **Bidarkundi GK,** Wig JD, Bhatnagar A, Majumdar S. Clinical relevance of intracellular cytokines IL-6 and IL-12 in acute pancreatitis, and correlation with APACHE III score. *Br J Biomed Sci* 2002; **59:** 85-89

31 **Yamauchi J,** Shibuya K, Sunamura M, Arai K, Shimamura H, Motoi F, Takeda K, Matsuno S. Cytokine modulation in acute pancreatitis. *J Hepatobiliary Pancreat Surg* 2001; **8:** 195-203

32 **Denham W,** Yang J, Norman J. Evidence for an unknown component of pancreatic ascites that induces adult respiratory distress syndrome through an interleukin-1 and tumor necrosis factor-dependent mechanism. *Surgery* 1997; **122:** 295–301

33 **Powell JJ,** Murchison JT, Fearon KC, Ross JA, Siriwardena AK. Randomized controlled trial of the effect of early enteral nutrition on markers of the inflammatory response in predicted severe acute pancreatitis. *Br J Surg* 2000; **87:** 1375-1381

34 **Takaoka K,** Kataoka K, Sakagami J. The effect of steroid pulse therapy in the development of acute pancreatitis induced by closed duodenal loop in rats. *J Gastroenterol* 2002; **37:** 537–542

35 **Haddad JJ.** The involvement of L-gamma-glutamyl-L-cysteinyl-glycine (glutathione/GSH) in the mechanism of redox signaling mediating MAPK(p38)-dependent regulation of pro-inflammatory cytokine production. *Biochem Pharmacol* 2002; **63:** 305-320

36 **Ethridge RT,** Hashimoto K, Chung DH, Ehlers RA, Rajaraman S, Evers BM. Selective inhibition of NF-kappaB attenuates the severity of cerulein-induced acute pancreatitis. *J Am Coll Surg* 2002; **195:** 497-505

37 **Legos JJ,** McLaughlin B, Skaper SD, Strijbos PJ, Parsons AA, Aizenman E, Herin GA, Barone FC, Erhardt JA. The selective p38 inhibitor SB-239063 protects primary neurons from mild to moderate excitotoxic injury. *European J Pharmacol* 2002; **447:** 37- 42

38 **Elenitoba-Johnson KS,** Jenson SD, Abbott RT, Palais RA, Bohling SD, Lin Z, Tripp S, Shami PJ, Wang LY, Coupland RW, Buckstein R, Perez-Ordonez B, Perkins SL, Dube ID, Lim MS. Involvement of multiple signaling pathways in follicular lymphoma trans formation: p38-mitogen- activated protein kinase as a target for therapy. *Proc Natl Acad Sci* 2003; **10:** 1073-1082

39 **El Bekay R,** Alvarez M, Alba G, Chacon P, Vega A, Martin-Nieto J, Jimenez J, Monteseirin J, Pintado E, Bedoya FJ, Sobrino F. Oxidative stress is a critical mediator of the angiotensin II signal in human neutrophils: involvement of map kinases, calcineurin, and the transcription factor NF-kappaB. *Blood* 2003; **10:** 1464-1476

40 **Torres M.** Mitogen-activated protein kinase pathways in redox signaling. *Front Biosci* 2003; **8:** 369-391

Edited by Zhu LH and Wang XL

P.O.Box 2345, Beijing 100023,China
Fax: +86-10-85381893
E-mail: wjg@wjgnet.com www.wjgnet.com

World J Gastroenterol 2003;9(11):2519-2522
World Journal of Gastroenterology
 ISSN 1007-9327

• BASIC RESEARCH •

Influence of Kupffer cells on hepatic signal transduction as demonstrated by second messengers and nuclear transcription factors

Hong Ding, Jie-An Huang, Jing Tong, Xin Yu, Jie-Ping Yu

Hong Ding, Jing Tong, Xin Yu, Department of Pharmacology, College of Pharmacy, Wuhan University, Wuhan 430072, Hubei Province, China
Jie-An Huang, Department of Internal Medicine, the First Affiliated Hospital of Guangxi Medical University, Nanning 530021, Guangxi Zhuang Autonomous Region, China
Jie-Ping Yu, Department of Internal Medicine, the First Affiliated Hospital of School of Medicine, Wuhan University, Wuhan 430064, Hubei Province, China
Supported by the Chen Guang Project of Wuhan, No.20005004038, and the Natural Science Foundation of Hubei Province, No. 2001ABB160
Correspondence to: Dr. Hong Ding, Wuhan University College of Pharmacy, Wuhan 430072, Hubei Province, China. dinghong2000@263.net.cn
Telephone: +86-27-87682339 **Fax:** +86-27-87682339
Received: 2003-03-03 **Accepted:** 2003-04-11

Abstract

AIM: To understand the influence of Kupffer cell (KC) on signal transduction pathways in the liver.

METHODS: To decrease selectively the number and function of KC, Kunming mice were ip injected with a single dose of gadolinium chloride ($GdCl_3$, 20 mg·kg^{-1}), the time-effect relationship assessment was performed after 1 d, 3 d and 6 d. sALT, sGST, liver glycogen content, phagocytic index, and expression of CD68 were assessed as the indexes of hepatotoxicity and functions of KC respectively, and morphology of KC was observed with transmission electron microscopy. Furthermore, cAMP, PGE_2 level, nitric oxide(NO) content, and mRNA expression of NFkappaBp65, Erk1, STAT1 were examined.

RESULTS: $GdCl_3$ could selectively cause apoptosis of KC and obvious reduction of KC's activity, but no hepatotoxicity was observed. One day after KC blockade, NO, PGE_2, cAMP contents in the liver were reduced 21.0 %, 6.94-fold, 8.3 %, respectively, and mRNA expression of NFkappaBp65 was decreased 3.0-fold. The change tendency of NO, PGE_2, and cAMP contents and mRNA expression of NFkappaBp65 were concomitant with recovery of the functions of KC. The contents of NO, PEG2, cAMP were increased when the functions of KC was recovered. However, all of the changes could not return to the normal level except NO content after 6 d $Gdcl_3$ treatment. No obvious changes were found in STAT1 and Erk1 mRNA expression in the present study.

CONCLUSION: Hepatic NO, PGE2, cAMP level and mRNA expression of NFkappaBp65 are closely related with the status of KC. It suggests that KC may play an important role in the cell to cell signal transduction in the liver.

Ding H, Huang JA, Tong J, Yu X, Yu JP. Influence of Kupffer cells on hepatic signal transduction as demonstrated by second messengers and nuclear transcription factors. *World J Gastroenterol* 2003; 9(11): 2519-2522
http://www.wjgnet.com/1007-9327/9/2519.asp

INTRODUCTION

Kupffer cells (KCs) account for a major portion of the tissue macrophages and play an important role in the defense mechanisms of the body[1]. KCs are involved in the pathogenesis of chemically mediated liver injury through release of biologically active mediators that promote the pathogenic process[2]. KCs can synthesize and release a variety of immunomodulating and inflammatory mediators such as oxygen-derived free radicals, nitric oxide, lipid mediators, and cytokines, etc. There are certain points to be elucidated that KCs involve in the pathophysiologic response of liver injury[3]. And now, many new functions have been found. KCs can reverse liver fibrosis and are critical for the progression of alcoholic injury[3,4]. Abolishment of KCs sensitization could prevent alcoholic liver injury[5]. KCs are major contributors to cytokine production in hepatic ischemia/reperfusion[6] and play a stimulatory role in liver regeneration[7]. Up to now, few studies about the influence of KCs on signal transduction in the liver have been reported. NO, PGE_2, cAMP are important second messengers transmitting and magnifying messages to modulate gene expression. NFkappaB, STAT, Erk are important nuclear transcription factors, which are involved in the regulation of cell proliferation and differentiation[8,9]. To understand the effect of KCs on the second messengers and nuclear transcription factors is of great importance in studying the mechanism of liver diseases. $Gdcl_3$, as an inhibitor of KCs, is often used as a tool for studying the role of KC[10]. Kupffer cell toxicant $GdCl_3$ prevents stellate cell activation and the development of fibrosis[11]. The present study was designed to clarify the effect of KC on signal transduction pathway in the liver following $GdCl_3$-induced KC blockade.

MATERIALS AND METHODS

Reagents

Gadolinium chloride ($GdCl_3$), collagenase IV, Indian ink were purchased from Sigma, USA. NO, PGE_2 detection kits were obtained from Bangding Biotechnology Co., Ltd. cAMP detection kit was obtained from Shanghai College of Chinese Traditional Medicine. CD68 immunohistochemical kit and NFkappaBp65, STAT1, Erk1 *in situ* hybridization kit were purchased from Wuhan Boster Biological Technology Co., Ltd. Other reagents were all of A.R.

Animal treatment

Kunming ♂ mice (aged 4-6 wk), weighing 22±3 g were obtained from the Experimental Animal Center of School of Medicine, Wuhan University. The animals were fed on a standard diet in pellets, and allowed free access to water. The mice were randomly distributed to control group, $GdCl_3$-1d

Table 1 Influence of $GdCl_3$ on hepatic function and activity of KCs in mice (n=8, $\bar{x}\pm s$)

Group	sALT ($mmol\cdot min^{-1}\cdot L^{-1}$)	sGST ($\mu mol\cdot min^{-1}\cdot L^{-1}$)	Liver glycogen ($\mu mol\cdot mg^{-1}\cdot pro^{-1}$)	Phagocytic activity(α)	Expression of CD68 (relative O.D.)
Control	2.4±0.3	15.2±2.2	4.9±0.9	9.7±0.7	0.131±0.018
$GdCl_3$-1d	2.6±0.9	14.9±1.9	5.4±1.4	5.2±0.4[b]	0.065±0.010[b]
$GdCl_3$-3d	2.6±1.0	16.5±3.1	5.8±1.1	6.0±1.1[a]	0.084±0.015[b]
$GdCl_3$-6d	2.6±1.4	15.7±2.3	5.0±0.2	6.8±1.3[a]	0.108±0.014[b]

[a]P<0.05, [b]P<0.01 *vs* control.

group, $GdCl_3$-3d group, $GdCl_3$-6d group, in which the mice received ip injection of a single dose of 20 $mg\cdot kg^{-1}$ of $GdCl_3$, and were sacrificed after administration of $GdCl_3$ for 1 d, 3 d, 6 d, respectively.

Test for phagocytic function

14 % Indian ink (10 $ml\cdot kg^{-1}$) was injected into the mice tail vein. After 1 min and 5 min, 20 μl blood was obtained from the orbital vein of the mice and added into 2 ml of 0.1 % Na_2CO_3 solution. Absorbance (OD) at 600 nm was read, and the phagocytic activity (α) of KCs was calculated as described[12].

Biochemical assay

Twenty-five percent liver homogenate was prepared, the glycogen content was quantified by an enzymatic reaction as previously described[13]. NO content was measured by Griess reaction[14]. PGE_2 and cAMP concentration were determined by radioimmunoassay, and the radioactivity of the samples was measured with a P△CK△RD CA-2000 liquid scintillation spectrometer[15]. The protein content of liver homogenate was determined by Lowry[16].

In situ hybridization and immunohistochemistry methods

The livers were briefly washed in cold 0.1 M phosphate buffer containing 0.1 % DEPC and then fixed in cold 4 % formaldehyde (in 0.1 M phosphate buffer, pH7.4), paraffin-embedded sections in 5-6 μm thickness were cut and placed onto aminopropyltriethoxysilane-coated glass slides. The expression of CD68 was determined by i*n situ* hybridization with DIG detection system kit. The anti-sense sequence of the probe was 5' -AAGCT TGGCC CAAGC CACCT TGGTT TTAGA-3' for Erk1 (extracellular signal-regulated kinase), 5' -CAGGT TGTCT GTGGT CTGAA GTCTA GAAGG-3' for STAT1 (signal transducers and activators of transcription), 5' -AGTTG ATGTC CGCAA TGGAG GTCTT-3' for NF-kBp65 (nuclear factor kappa B p65).

Image analysis of immunohistochemistry and in situ hybridization

Microscopic images through an interference filter (Nikon, Tokyo, Japan) were transferred to the processor (HPIAS image analysis system, Wuhan Tongji Medical University). Average absorbances in defined areas of the sections were measured, relative optical density(OD) was used to evaluate expression level.

Liver cells isolation and transmission electron-microscopic study

Liver cells were isolated as described[17]. In brief, after washed in D-Hanks, liver tissue was digested with 0.075 % collagenase for 30 min. The resulting suspension was passed through 70 μm gaze and then 1 g of sediment was generated after 10 min. Hepatocytes were fixed in 2.5 % glutaraldehyde in 0.1 $mol\cdot L^{-1}$ phosphate buffer, transmission electron- microscope was used to observe the morphology of KCs.

Statistical analysis

The data were presented as $\bar{x}\pm s$, and statistical analysis was performed with Student's t-test.

RESULTS

Effect of $GdCl_3$ on sALT, sGST, liver glycogen and activity of KCs

After administration of $GdCl_3$, no changes in sALT, sGST level and liver glycogen content were observed. Liver expression of CD68 (specific surface antigen of macrophage) and phagocytic activity (α) obviously reduced 102 %, 86 % respectively after 1 d of $GdCl_3$ treatment, then the function of KCs was gradually recovered. However they could not return to the normal level after 6 d of $GdCl_3$ treatment.

Electron microscopic study

The characteristics of apoptosis (the membrane of KCs was integrate, chromatin in the nucleus presented uneven distribution and was close to nuclear measure) were observed after treatment of $GdCl_3$ (Figure 1).

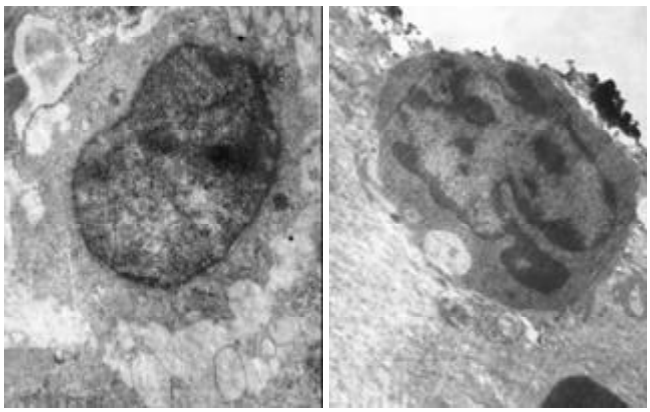

Figure 1 Influence of $GdCl_3$ on morphology of KCs under EM.

Effect on NO, PGE_2, cAMP content

After 1 d of $GdCl_3$ treatment, NO, PGE_2, cAMP contents were reduced 21.0 %, 6.94-fold, 8.3 %, respectively, and then they were gradually recovered. However, PGE_2 and cAMP contents could not return to the normal level after 6 d of treatment.

Table 2 Influence of $GdCl_3$ on NO, PGE_2, cAMP contents in liver (n=8 mice, $\bar{x}\pm s$)

Group	NO content ($pmol\cdot mg^{-1}\cdot pro^{-1}$.)	PGE_2 content ($pg\cdot mg^{-1}\cdot pro^{-1}$.)	cAMP content ($pmol\cdot mg^{-1}\cdot pro^{-1}$.)
Control	2.5±0.4	6.8±1.8	0.157±0.031
$GdCl_3$-1d	2.1±0.3[a]	0.9±0.2[b]	0.145±0.027[a]
$GdCl_3$-3d	2.0±0.3[a]	2.5±1.3[b]	0.131±0.010[a]
$GdCl_3$-6d	2.2±0.3	5.0±2.6[a]	0.133±0.010[a]

[a]P<0.05, [b]P<0.01 *vs* control.

Effect on NFkappaB, STAT1 and Erk1 mRNA expression

The time course of alteration of NFkappaB, STAT1 and Erk1 mRNA expressions after administration of 20 mg· kg^{-1} $GdCl_3$ showed that NFkappaB mRNA expression was decreased (3-fold) after administration of $GdCl_3$ for 1 d, then it was gradually recovered, but did not return to the normal level after 6 d of treament. No obvious influence on STAT1, Erk1 mRNA expressions was observed (Figure 2).

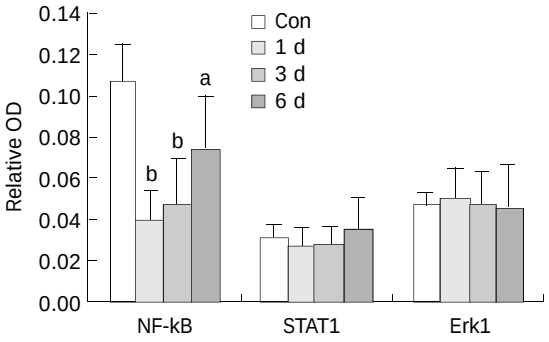

Figure 2 Time course of alteration of NFkappaB, STAT1 and Erk1 mRNA expressions after administration of 20 mg· kg^{-1} $GdCl_3$ (n=6, $\bar{x}\pm s$). $^aP<0.05$, $^bP<0.01$ *vs* control.

DISCUSSION

In the present study, ip injection of a single dose of $GdCl_3$ could selectively cause apoptosis of KCs, but did not induce hepatotoxicity. Therefore, it can be used as a tool for studying the role of KCs.

KCs are the phagocytic macrophages in the liver. NO, PGE_2, and cAMP could transmit and magnify extracellular messages to cells through a cascade system to regulate gene expression and cell proliferation and differentiation[18]. NO, PGE_2, and cAMP had different functions in hepatoprotection and hepatic injury. NO from KCs could induce membrane barrier dysfunction in liver sinusoid[19]. But according to Abou-Elella *et al*, the exacerbation of hepatocyte death by KCs was not related to NO[20]. Hsu *et al*, sproposed that KCs be the major source of induction of inducible NO synthase(iNOS) activity and NO production have a beneficial role in hepatic IR injury and the constitutive isoforms of NOS play a hepatoprotective role in hepatic injury[21-23]. The protective function of NO against hepatic injury might lie in that it could reduce tissue oxygenation[24]. PGE_2 derived from KCs increased cAMP, which caused triglyceride accumulation in the liver and fatty liver[3]. Increase of cAMP levels in KCs occurred during the late stage of polymicrobial sepsis, and might contribute to the depression of macrophage phagocytic function[25]. The current study showed that NO, PGE_2, and cAMP contents in the liver were reduced following KC blockade, and recovered following the functional recovery of KCs. It suggests that Kupffer cells may mediate signaling of second messengers in the liver. Moreover, in the present experiment, the hepatic function did not change following the alterations of NO, PGE_2, and cAMP content, the reasons remain to be researched.

It has widely been accepted that NFkappaB activation plays an important role in the pathophysiology of inflammatory disorders[26]. NFkappaB is an essential component of TNF proliferative pathway and TNF-induced changes in IL-6 mRNA, STAT3, and c-myc mRNA are dependent on NFkappaB activation[27]. NFkappaB activation may be important in "switching off" the cytokine cascade during acute pancreatitis[28]. The current study showed that mRNA expression of NFkappaB in the liver was down-regulated after KC blockade, suggesting that KCs may play an important role in mediating liver diseases and inflammatory disorders via changes of the signal transduction pathway in the liver.

In this experiment, STAT1 and Erk1 mRNA expressions were not affected by $GdCl_3$. STAT1 played a harmful role in Con A-mediated hepatitis, whereas STAT3 protected against liver injury[29]. Inhibition of STAT1 activation without reduction of STAT1 protein level might be one of the factors that are involved in the cAMP-dependent stellate cell growth arrest[30]. In this study, we only examined the expression of STAT1 mRNA, the relationship between STAT1 and hepatic injury needs to be further studied.

REFERENCES

1 **Fukumura D,** Yonei Y, Kurose I, Saito H, Ohishi T, Higuchi H, Miura S, Kato S, Kimura H, Ebinuma H, Ishi H. Role of nitric oxide in Kupffer cell-mediated hepatoma cell cytotoxicity *in vitro* and ex vivo. *Hepatology* 1996; **24**: 141-149

2 **Luckey SW**, Petersen DR. Activation of Kupffer cells during the course of carbon tetrachloride-induced liver injury and fibrosis in rats. *Exp Mol Pathol* 2001; **3**: 226-240

3 **Enomoto N**, Ikejima K, Yamashina S, Enomoto A, Nishiura T, Nishimura T, Brenner DA, Schemmer P, Bradford BU, Rivera CA, Zhong Z, Thurman RG. Kupffer cell-derived prostaglandin E(2) is involved in alcohol-induced fat accumulation in rat liver. *AM J Physiol Gastrointest Liver Physio* 2000; **279**: G100-106

4 **Sakaida I**, Hironaka K, Terai S, Okita K. Gadolinium chloride reverses dimethylnitrosamine (DMN)-induced rat liver fibrosis with increased matrix metalloproteinases (MMPs) of Kupffer cells. *Life Sci* 2003; **8**: 943-959

5 **Enomoto N**, Takei Y, Hirose M, Ikejima K, Miwa H, Kitamura T, Sato N. Thalidomide prevents alcoholic liver injury in rats through suppression of Kupffer cell sensitization and TNF-alpha production. *Gastroenterology* 2002; **1**: 291-300

6 **Mosher B**, Dean R, Harkema J, Remick D, Palma J, Crockett E. Inhibition of Kupffer cells reduced CXC chemokine production and liver injury. *J Surg Res* 2001; **2:** 201-210

7 **Takeishi T**, Hirano K, Kobayashi T, Hasegawa G, Hatakeyama K, Naito M. The role of Kupffer cells in liver regeneration. *Arch Histol Cytol* 1999; **5**: 413-422

8 **Liu DY**, Gorrod JW. Effects of cAMP-dependent protein kinase and ATP on N1oxidation of 9-benzyladenine by animal hepatic microsomes. *Life Sci* 2000; **66**: 77-88

9 **Wheeler MD**, Kono H, Rusyn I, Arteel GE, McCarty D, Jude Samulski R, Thurman RG. Chronic ethanol increases adeno-associated viral transgene expression in rat liver via oxidant and NFkappaB-dependent mechanisms. *Hepatology* 2000; **32**: 1050-1059

10 **Neyrinck A**, Eeckhoudt SL, Meunier CJ, Pampfer S, Taper HS, Brtnrrvl RK. Modulation of paracetamol metabolism by Kupffer cells; A study on rat liver slices. *Lif Sci* 1999; **65**: 2851-2859

11 **Rivera CA**, Bradford BU, Hunt KJ, Adachi Y, Schrum LW, Koop DR, Burchardt ER, Rippe RA, Thurman RG. Attenuation of CCl (4)-induced hepatic fibrosis by GdCl(3) treatment or dietary glycine. *Am J Physiol Gastrointest Liver Physiol* 2001; **1**: G200-207

12 **Joseph B,** Malhi H, Bhargava KK, Palestro CJ, McCuskey RS, Gupta S. Kupffer cells participate in early clearance of syngeneic hepatocytes transplanted in the rat liver. *Gastroenterology* 2002; **5**: 1677-1685

13 **Jaime RP**, Rosa G, Inmaculada A, Jose MS. Prenatal alcohol exposure affects galactosyltransferase activity and glycoconjugates in the Golgi apparatus of fetal rat hepatocytes. *Hepatology* 1997; **25**: 343-350

14 **Bartholomew B**. A rapid method for the assay of nitrate in urine using the nitrate reductase enzyme of Escherichia cilli. *Food Chem Toxicol* 1984; **22**: 543-551

15 **Hahn PY**, Yoo P, Ba ZF, Chaudry IH, Wang P. Upregulation of Kupffer cell beta-adrenoceptors and cAMP levels during the late stage of sepsis. *Biochim Biophys Acta* 1998; **1404**: 377-384

16 **Lowry OH**, Rosebrough NJ, Farr AL, Randall RJ. Protein measurement with the Folin phenol reagent. *J Biol Chem* 1951; **193**: 265-275

17 **Giorgio N**, Federica M, Giuseppe M, Claudio C, Anna C. Action of chronic CCl4 on the retinol and dolichol content of rat liver paren-

chymal and non-parenchymal cells. *Lif Sci* 2000; **67**: 2293-2304
18 **O'Dell TJ**. Test of the roles of two diffusible substances in long-term potentiation, evidence for nitric oxide as a possible early retrograde messenger. *Proc Natl Acad Sci U S A* 1991; **88**: 11285-11289
19 **Fukumura D**, Yonei Y, Kurose I, Saito H, Ohishi T, Higuchi H, Miura S, Kato S, Kimura H, Ebinuma H, Ishi H. Role in nitric oxide in Kupffer cell-mediated hepatoma cell cytotoxicity *in vitro* and *ex vivo*. *Hepatology* 1996; **1**: 141-149
20 **Abou-Elella AM**, Siendones E, Padillo J, Montero JL, De la Mata M, Relat JM. Tumour necrosis factor-alpha and nitric oxide mediate apoptosis by D-galactosamine in a primary culture of rat hepatocytes: exacerbation of cell death by cocultured Kupffer cells. *Can J Gastroenterol* 2002; **11**: 791-799
21 **Hsu CM**, Wang JS, Liu CH, Chen LW. Kupffer cells protect liver from ischemia-reperfusion injury by an inducible nitric oxide synthase-dependent mechanism. *Shock* 2002; **4**: 280-285
22 **Liu TH**, Robinson EK, Helmer KS, West SD, Castaneda AA, Chang L, Mercer DW. Does upregulation of inducible nitric oxide synthase play a role in hepatic injury? *Shock* 2002; **6**: 549-554
23 **Rhee JE**, Jung SE, Shin SD, Suh GJ, Noh DY, Youn YK, Oh SK, Choe KJ. The effects of antioxidants and nitric oxide modulators on hepatic ischemic-reperfusion injury in rats. *J Korean Med Sci* 2002; **4**: 502-506
24 **Koti RS**, Seifalian AM, McBride AG, Yang W, Davidson BR. The relationship of hepatic tissue oxygenation with nitric oxide metabolism in ischemic preconditioning of the liver. *FASEB J* 2002; **12**: 1654-1656
25 **Hahn PY**, Yoo P, Ba ZF, Chaudry IH, Wang P. Upregulation of Kupffer cell beta-adrenoceptors and cAMP levels during the late stage of sepsis. *Biochim Biophys Acta* 1998; **3**: 377-384
26 **Renard P**, Raes M. The proinflammatory transcription factor NFkappaB: a potential target for novel therapeutical strategies. *Cell Biol Toxicol* 1999; **15**: 341-344
27 **Kirillova I**, Chaisson M, Fausto N. Tumor necrosis factor induces DNA replication in hepatic cells through nuclear factor kappaB activation. *Cell Growth Differ* 1999; **12**: 819-828
28 **Murr MM**, Yang J, Fier A, Gallagher SF, Carter G, Gower WR Jr, Norman JG. Regulation of Kupffer cell TNF gene expression during experimental acute pancreatitis: the role of p38-MAPK, ERK1/2, SAPK/JNK, and NF-kappaB. *J Gastrointest Surg* 2003; **1**: 20-25
29 **Hong F**, Jaruga B, Kim WH, Radaeva S, El-Assal ON, Tian Z, Nguyen VA, Gao B. Opposing roles of STAT1 and STAT3 in T cell-mediated hepatitis: regulation by SOCS. *J Clin Invest* 2002; **10**: 1503-1513
30 **Kawada N**, Uoya M, Seki S, Kuroki T, Kobayashi K. Regulation by cAMP of STAT1 activation in hepatic stellate cells. *Biochem Biophys Res Commun* 1997; **2**: 464-469

Edited by Zhu LH and Wang XL

P.O.Box 2345, Beijing 100023,China
Fax: +86-10-85381893
E-mail: wjg@wjgnet.com www.wjgnet.com

World J Gastroenterol 2003;9(11):2523-2527
World Journal of Gastroenterology
 ISSN 1007-9327

• BASIC RESEARCH •

Gene and protein expressions of p28^{GANK} in rat with liver regeneration

Jian-Min Qin, Xiao-Yong Fu, Shen-Jing Li, Shu-Qin Liu, Jin-Zhang Zeng, Xiu-Hua Qiu, Meng-Chao Wu, Hong-Yang Wang

Jian-Min Qin, Xiao-Yong Fu, Shen-Jing Li, Shu-Qin Liu, Jin-Zhang Zeng, Xiu-Hua Qiu, Meng-Chao Wu, Hong-Yang Wang, International Co-operation Laboratory on Signal Transduction, Eastern Hepatobiliary Surgery Institute, Second Military Medical University, Shanghai, 200438, China
Correspondence to: Dr. Hong-Yang Wang, International Co-operation Laboratory on Signal Transduction, Eastern Hepatobiliary Surgery Institute, Second Military Medical University, Shanghai, 200438, China. hywangk@online.sh.cn
Telephone: +86-21-25070846 **Fax:** +86-21-65566851
Received: 2002-12-22 **Accepted:** 2003-02-11

Abstract

AIM: To observe the gene and protein expression changes of p28^{GANK} in regenerating liver tissues, and to reveal the biological function of p28^{GANK} on the regulation of liver regeneration.

METHODS: One hundred and thirty two adult male Sprague-Dawley rats were selected, weighing 200-250 g, and divided randomly into sham operation (SO) group and partial hepatectomy (PH) group. Each group had eleven time points: 0, 2, 6, 12, 24, 30, 48, 72, 120, 168 and 240 h, six rats were in each time point. The rats were undergone 70 % PH under methoxyflurane anesthesia by resection of the anterior and left lateral lobes of the liver. SO was conducted by laparotomy plus slight mobilization of the liver without resection. Liver specimens were collected at the indicated time points after PH or SO. The expression level of p28^{GANK} mRNA was determined by Northern blot as well as at protein level via immunohistochemical staining. The expressions of p28^{GANK} mRNA in these tissues were analyzed by imaging analysis system of FLA-2000 FUJIFILM and one way analysis of variance. The protein expressions of p28^{GANK} in these tissues were analyzed with Fromowitz' method and Rank sum test.

RESULTS: The expression of p28^{GANK} mRNA in the regenerating liver tissues possessed two transcripts, which were 1.5 kb and 1.0 kb. There was a significantly different expression patterns of p28^{GANK} mRNA between SO and PH groups (P<0.01). The expression of p28^{GANK} mRNA increased 2 h after PH, the peak time was 72 h (SO group: 163.83±1.4720; PH group: 510.5±17.0499, P<0.01). There was a significant difference in the 1.5 kb transcript, which decreased gradually after 72 hours. The protein expression of p28^{GANK} was mainly in the cytoplasm of regenerating hepatocytes, and increased near the central region 24 h after PH, and became strongly positive at 48 h (+++, *vs* the other time points P<0.05), but decreased 72 h after PH.

CONCLUSION: The expression of p28^{GANK} mRNA increases in the early stage of rat liver regeneration, the protein expression of p28^{GANK} is mainly in the cytoplasm of regenerating liver cells. It suggests that the gene of p28^{GANK} may be an important regulatory and controlled factor involved in hepatocyte proliferation during liver regeneration.

Qin JM, Fu XY, Li SJ, Liu SQ, Zeng JZ, Qiu XH, Wu MC, Wang HY. Gene and protein expressions of p28^{GANK} in rat with liver regeneration. *World J Gastroenterol* 2003; 9(11): 2523-2527
http://www.wjgnet.com/1007-9327/9/2523.asp

INTRODUCTION

Liver regeneration after 70 % partial hepatectomy in an adult rat involves initiation of proliferation of the remaining parenchymal cells and is a useful model for studying signaling molecules and other factors involved in cell proliferation. Cell proliferation begins very early during liver regeneration, peaking at 24 hours, followed by proliferating biliary epithelium at 48 hours, and kupffer cells and stellate cells at 72 hours. The proliferation of sinusoidal endothelial cells was peaked at 96 hours. Through its regenerative ability, the liver provides a model system for *in vivo* study of cell proliferation events following reentry into the cells cycle from the quiescent G_0 phase. The damage caused by surgical resection or treatment with toxins results in a cascade of growth factors and cytokines to restore the liver mass to its original size[1-6]. The residual hepatic parenchymal cells and nonparenchymal cells can proliferate and differentiate through the action of some cytokines, hormones and growth factors. When liver regeneration is induced by partial hepatectomy or inflammation, the cell cycle can transit from G_0 phase to G_1 phase, enter into the preparing stage of division and proliferation, and then into S phase, G_2 phase and M phase in turn. The late G_1 phase contains a restriction point (R point), which has a selective division function and decides cell entry into S phase or reverse to G_0 phase. The hepatic parenchymal and nonparenchymal cells can reconstitute the hepatic volume when they proliferate to some extent, and the liver regenerating response can be terminated by some factors[1,7,8], but the mechanisms of initiation and termination of liver regeneration have not been eventually clarified and need further study. Recently, a novel gene named *gankyrin* was cloned and identified from human hepatocellular carcinoma[9]. The *gankyrin* gene sequence is identical to one subunit of 26S proteasome named *p28* which was firstly cloned from human cDNA library by comparing a subunit amino acid of purified bovine erythrocyte PA700 complex (also defined as 19S complex) with protein structure of human protein cDNA library databases. The product of *gankyrin* or *p28* gene (p28^{GANK} protein) was an oncoprotein consisting of six conservative ankyrin repeats. The mRNA and protein level of p28^{GANK} increased substantially in hepatocellular carcinomatous tissues, compared with levels in the respective non-cancerous portion of the resected livers, but the increase was not related to the grade or stage of the cancer. The finding that the increase occurred regardless of the staging or grading of cancer indicates that p28^{GANK} may be involved in an early and essential step of liver carcinogenesis. However, the liver regeneration is involved in hepatocyte division, proliferation and termination. It is unclear whether p28^{GANK} can participate in hepatocyte proliferation. This study was intended to disclose the biological function of p28^{GANK} by establishing a liver regeneration rat

model and determining the expression of p28^{GANK} mRNA and protein levels.

MATERIALS AND METHODS

Experimental animal

One hundred and thirty two adult male Sprague-Dawley rats were obtained from the Experimental Animal Center of the Second Military Medical University, weighing from 200-250 g, and were randomly divided into sham operation (SO) group and partial hepatectomy (PH) group. Each group had eleven time points: 0, 2, 6, 12, 24, 30, 48, 72, 120, 168 and 240 h, six rats in each time point. The rats were housed in a room at 21 ℃ under a 12 -hour light/dark cycle and given tap water and commercial rat chow. The animals were acclimatized to the laboratory conditions for 1 week prior to the experiments.

Establishment of liver regenerating model

The rats were undergone 70 % PH under methoxyflurane anesthesia by resection of the anterior and left lateral lobes of the liver[10]. SO was undertaken only by laparotomy plus slight mobilization of the liver without resection. The rats were injected intraabdominally with 0.5-1 ml normal saline for fluid resuscitation after operation. Liver specimens were collected at 0, 2, 6, 12, 24, 30, 48, 72, 120, 168 and 240 h after PH or SO. The liver specimens obtained were snap frozen in liquid nitrogen. Total RNA was extracted using the guanidine isothiocyanate and phenol-chloroform method and aliquots of RNA samples were stored at -85 ℃ until use. The remaining liver was fixed in 4 % formaldehyde polymerisatum, embedded in paraffin and then sectioned for histological examination and analysis of protein expression.

Cloning of rat p28^{GANK} cDNA

The rat p28^{GANK} cDNA was cloned from rat placenta based on the GenBank (Rattus novegicus mRNA for p28^{GANK} homologue: AB022014), sense (11 bp-30 bp, G1): 5' -GTGTGTCTAACCTAATGGTC-3' , anti-sense (643bp-662 bp, G2): 5' -TTGAGTATTAACCCCAGGCC-3' . The segment length was 651 bp. The primers were synthesized by Sangon Company, Shanghai, P.R.China. Briefly, 5 μg of total RNA extracted from rat placenta served as template to synthesize the first strand cDNA. Polymerase chain reaction system was consisted of 1×buffer, 1.5 mM $MgCl_2$, 200 μM dNTPs, 0.5 μM of the oligonucleotide primers specific for rat p28^{GANK} gene, 1 μl of the first strand cDNA synthesized as described above, and 1.25 units of Taq DNA polymerase. Amplification was undertaken by initial denaturation at 94 ℃ for 4 min, followed by 30 reaction cycles (for 50 s at 94 ℃, for 50 s at 53 ℃, and for 60 s at 72 ℃) and a final cycle at 72 ℃ for 10 min. The PCR product with an expected size of 651 bp fractionated on a 2 % agarose gel was purified with QIAQUICK gel extract kit (QIAGEN, Germany) and subcloned into PMD18 vector[11], and then sequenced and compared. The synthetic segment was verified the same sequence as the GenBank.

Northern blot analysis

Rat p28^{GANK} cDNA released from PMD18 vector was labeled with α-^{32}P-dCTP using Promega-gene labeling system (Promega, USA) according to the protocol of the manufacturer[12]. 90 μg of total RNAs was separated on a 1 % formaldehyde/agarose gel by electropherosis, transferred to nitrocellulose and hybridized with α-^{32}P-labeled p28^{GANK} cDNA[13]. The hybridized nitrocellulose filters were exposed to X-ray film at -80 ℃ for 2 weeks. The developed signals were assayed for p28^{GANK} mRNA expression level after normalizion with 18S rRNA as internal standard using FujiFilm image gauge V3.3 analysis software (FujiFilm, Japan).

Immunohistochemistry

Immunohistochemical assay was performed as described by the manufacturer using SP kit (Dako Reagent, Denmark). Briefly, the rat liver sections of four-micrometer were deparaffnized, followed by blockage of endogenous peroxidase activity and restoration of the interested antigens. The sections were then subjected to incubation with purified primary polyclonal antibody (1:50 dilution, obtained from signal transduction laboratory, Shanghai, China) against p28^{GANK} protein at 4 ℃ overnight and with horseradish peroxidase-biotinylated anti-rabbit IgG at 37 ℃ for 30 min. The sections were finally incubated with benzidine and counterstained with hematoxylin for examination. The experiment was performed on control sections with omission of the primary antibody in the same way. The expression of p28^{GANK} was analyzed comprehensively by the staining extent and range referring to Fromowitz standard[14]. 5 visual fields were observed randomly, 100 cells were counted in each visual field. The average number of stained cells in 5 visual fields was regarded as the percent ratio of positively stained cells in each section. Positive range score: 0, 0-5 %; 1, 6-25 %; 2, 26-50 %; 3, 51-75 %; 4, >75 %. Positive extent score: 0, no staining; 1, light yellow; 2, brown; 3, dark brown. Judged by positive range score plus positive extent score: <2, negative (-); 2-3, slight positive (+); 4-5, moderately positive (++); 6-7, strongly positive (+++).

Statistical analysis

The expression level of p28^{GANK} mRNA detected by Northern Blot was presented as mean ± SD. ANOVA software (SPSS 8.0) was used to analyze the difference in mRNA level between the groups and Rank sum test for p28^{GANK} protein assay in immunohistochemical study. *P* values less than 0.05 were considered as having significant difference.

RESULTS

The expression of p28^{GANK} mRNA in regenerating liver tissues possessed two transcripts, which were 1.5 kb and 1.0 kb respectively. There was a significant difference between SO and PH groups ($P<0.01$). The expression of p28^{GANK} mRNA increased 2 h after PH, the peak time was at 72 h (SO group: 163.83±1.4720; PH group: 510.5±17.0499, $P<0.01$). There was a significant difference in the 1.5 kb transcript, which decreased gradually after 72 hours (Figures 1-2).

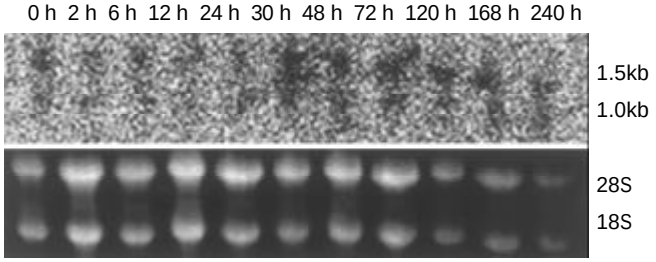

Figure 1 Northern blot of p28^{GANK} mRNA in rat regenerating liver tissues showed two transcripts of 1.5 kb and 1.0 kb. Expression level of p28^{GANK} mRNA increased 2h after PH, and reached the peak level at 72 h. More significant variation was found for 1.5 kb transcript.

The protein expression of p28^{GANK} was mainly in the cytoplasm of regenerating hepatocytes, and became increased near the central region 24 h after PH. The strongly positive expression was observed at 48 h (+++, *vs* the other time points, $P<0.05$), which decreased 72 h after PH (Figure 3).

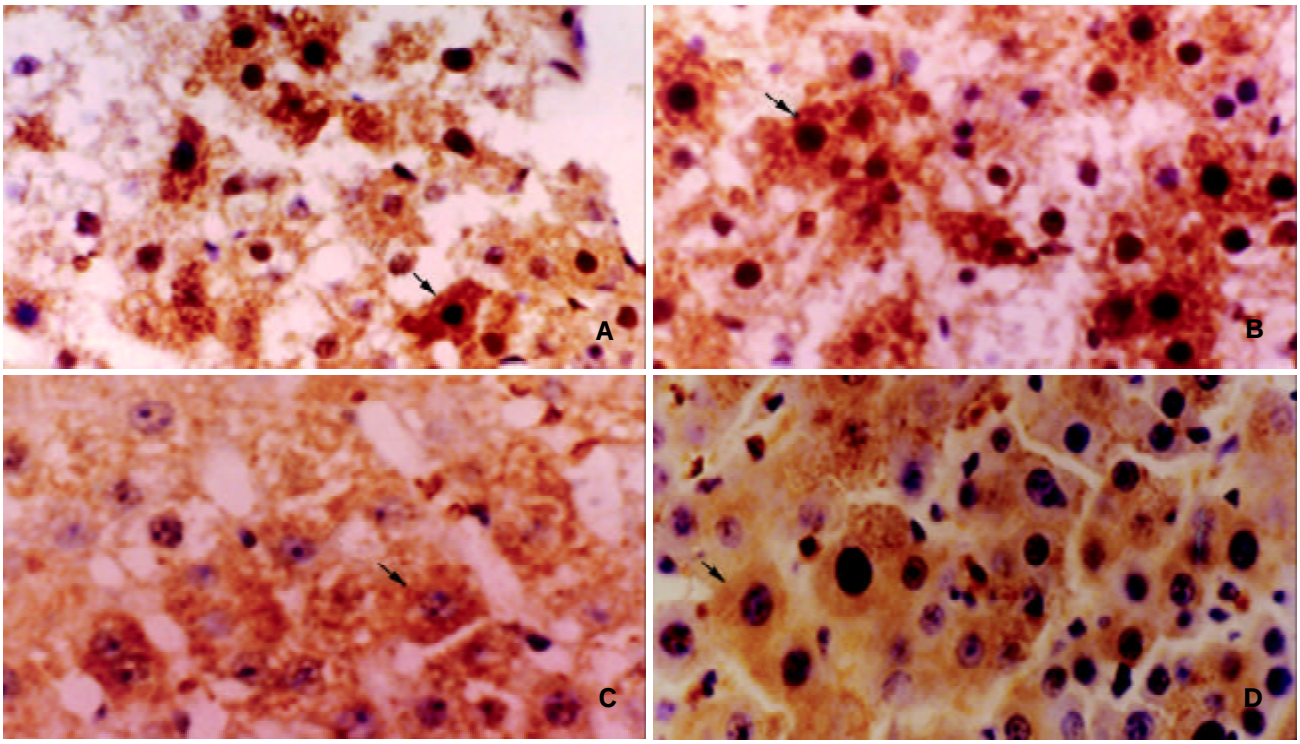

Figure 3 The expression of p28^{GANK} protein in regenerating liver tissues was examined by immunohistochemistry. A: Local brown expression of p28^{GANK} in the cytoplasm and nucleus of regenerating hepatocyte near central region 24 h after PH. IHC×400. B: Diffuse brown expression of p28^{GANK} in the cytoplasm and nucleus of regenerating hepatocyte 48 h after PH. IHC×400. C: Regional light yellow expression of p28^{GANK} in cytoplasm of regenerating hepatocyte 72 h after PH. IHC×400. D: Dispersed light yellow expression of p28^{GANK} in cytoplasm of regenerating hepatocyte 120 h after PH. IHC×400.

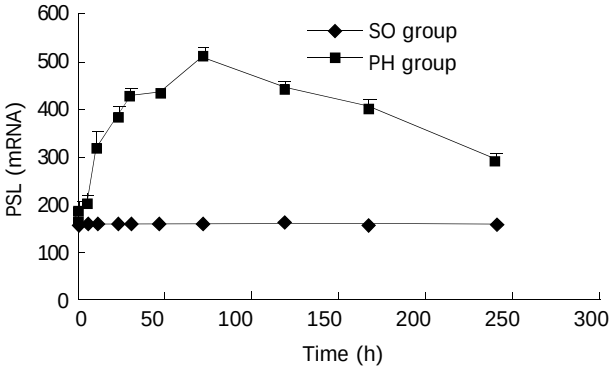

Figure 2 No significant difference of the expression of p28^{GANK} mRNA was seen in the SO group. In the PH group, the expression increased in 1.5 kb transcript 2 h after PH. The peak time was at 72 h, but gradually decreased after 72 hours.

DISCUSSION

Hepatocytes proliferate firstly according to the cascade response induced by growth factors and cytokines after hepatectomy or toxin damage. The first peak of DNA synthesis in hepatocytes occurs at about 24 hours, with a smaller peak between 36 and 48 hours. The restoration of the original number of hepatocytes theoretically requires 1.66 proliferative cycles among the residual hepatocytes. Most of the hepatocytes (95 % in the young and 75 % in very old rats) in the residual lobes participate in one or two proliferative events. The hepatocytes begin to proliferate early, the peak time is at 24 hours. Then biliary epithelial cells proliferate, the peak time is at 48 hours. Then the Kupffer cells and stellate cells proliferate and the proliferative peak is at 72 hours. The proliferative peak of sinusoidal endothelial cells is at 96 hours. Thus these cell proliferations result in restoration of the original volume[3,15]. Hepatocyte proliferation starts in the periportal zone, and then proceeds to the pericentral zone at 36 to 48 hours. The other cells of the liver enter into DNA synthesis about 24 hours after the hepatocytes proliferation, with a peak of DNA synthesis at 48 hours or later. The changes in the extracellular matrix after PH are undetectable until approximately 24 h post-PH. The hepatocytes begin to replicate in the periportal zones without corresponding increases in matrix within 3 days. The periportal areas consist of hepatocyte clusters of 10-14 cells without intervening sinusoids or matrix, as the wave of hepatocyte replication proceeds from periportal to pericentral regions of the lobule. The formation of cell clusters follows, the hepatocyte mitotic activity significantly decreases 4 days post-PH[16-20]. Liver regeneration is a complicated regulatory process, the volume and function of the liver restore after several periods. Many studies focus on the early factors associated with liver regeneration recently and on the important roles of these factors permitting the hepatocytes entering into cell division cycles. Activations of transcription factors (NF-kB and STAT3), immediately early protooncogenes (C-fos, C-myc, C-jun) and proinflammatory factors (TNF-α and IL-6) constitute the early responses to PH congenerically. The early changes play an important role in promoting the hepatocytes into cell cycles induced by hepatocytic reduction. Recruitment of early factors may be a part of ubiquitous response to stress protection and antiapoptosis of the liver, but it is unclear why the late downstream signal dissociates similar to the early response and certain time difference of cell proliferation process and atrophy or maintenance of liver size[21-24].

p28^{GANK} is a novel gene cloned and identified from human hepatocellular carcinoma and is identical to one of the PA700 non-ATPase subunits, a 700 kD multi-subunit regulatory complex of human 26S proteasome. p28^{GANK} contains six conservative ankyrin repeats, which suggests it may contribute to 26S proteasome interaction with other proteins, and its effect in hepatocellular carcinoma may be related to ubiquitin-

proteasome pathway which is often the target of cancer-related deregulation, and is involved in the processes such as oncogenic transformation, tumor progression, escape from immune surveillance and drug resistance[25-29]. The mRNA and protein levels of $p28^{GANK}$ was increased in cancerous tissues of hepatocellular carcinoma, and the increase was more substantial than that of non-cancerous tissues and was not related to the grading or staging of the tumors, indicating that $p28^{GANK}$ plays an early and crucial role in liver carcinogenesis. Moreover, the population doubling times in $p28^{GANK}$-transfected mouse NIH/3T3 cells were 18-20 hours, the control cells were 22-25 hours. All cells transfected with $p28^{GANK}$ formed colonies in soft agar, whereas the control cell did not. In homozygous nude mice, inoculation of all positive clones overexpressing $p28^{GANK}$ produced tumors within 30 days, in contrast, none of nude mice inoculated with control clone developed tumors. These results demonstrated that $p28^{GANK}$ remarkably promoted cell proliferation and was an oncogene. $p28^{GANK}$ had the retinoblastoma (RB_1)-binding motif LxCxE, resulted in an increased amount of the hyperphosphorylated form of RB_1, and accelerated the degradation of RB_1, activated the E2F transcription factors of nuclear partners of RB_1 by increasing the phosphorylation of RB_1, and induced the growth and oncogenity of anchoring independent cells. RB_1 exerts its growth-inhibitory effects in part by binding to and inhibiting essential regulatory proteins, including members of the E_2F family of transcription factors. E_2F is selectively associated with hypophosphorylated RB_1. Inactivation of RB_1 by phosphorylation, mutation or binding to viral oncoprotein seems to release E2F from an inhibitory complex, enabling it to promote the transcription of genes necessary for progression into late G_1 and S phases. $p28^{GANK}$ could bind to S6ATPase of the 26S proteasome and RB_1, increase E_2F activity and destabilize RB_1. It was demonstrated that $p28^{GANK}$ was a cellular protooncogene whose functions were more similar to those of the viral oncoprotein E_7 and related to protein degradation by 26S proteasome. Furthermore, ubiquitin-proteasome pathway played an important role in regulating cell growth and oncogenic transformation[9,30-34].

$p28^{GANK}$, as a positive cell proliferation regulatory factor, could promote cell proliferating process. We found that the expression of $p28^{GANK}$ mRNA was not significantly different at indicated times in control liver tissues during liver regeneration, but the expression of $p28^{GANK}$ mRNA possessed two transcripts in regenerating liver tissues after 70 % PH, about 1.5 kb and 1.0 kb. The mRNA level of $p28^{GANK}$ increased at 2 h, with a peak time at 72 h, but decreased gradually after 72 h, especially in the 1.5 kb transcript. The protein expression of $p28^{GANK}$ was mainly in the cytoplasm of the regenerating hepatocytes, strongly positive local expression of $p28^{GANK}$ in the cytoplasm and nucleus of regenerating hepatocyte near the central region at 24 h after 70 % PH, strongly positive diffuse expression of $p28^{GANK}$ in the cytoplasm and nucleus of regenerating hepatocyte at 48 h, and the expression of $p28^{GANK}$ decreased gradually at 72 h. These demonstrated the mRNA and protein levels of $p28^{GANK}$ occurred a curved changes, because three mitotic replicative waves occurred from 18 to 72 h, the two peak times occurred at 24 h and 36-38 h. Moreover, the two peak times of DNA synthesis occurred at 24 h and 36-48 h. All these suggest that $p28^{GANK}$ might be involved in the whole process of hepatocyte proliferation and the expression of $p28^{GANK}$ restores to its basic level with the termination of liver regeneration. It is necessary to be studied further whether it is the effect of $p28^{GANK}$ on hepatocyte proliferation through S6ATPase-$p28^{GANK}$-Rb-E2F1 pathway or through other pathways during liver regeneration and interaction with positive or negative cytokines, protooncogenes and anti-oncogenes associated with liver regeneration.

REFERENCES

1 **Stolz DB**, Mars WM, Petersen BE, Kim TH, Michalopoulos GK. Growth factor signal transduction immediately after two-thirds partial hepatectomy in the rat. *Cancer Res* 1999; **59**: 3954-3960

2 **Panis Y**, Lomri N, Emond JC. Early gene expression associated with regeneration is intact after massive hepatectomy in rats. *J Surg Res* 1998; **79**: 103-108

3 **Michalopoulos GK**, DeFrances MC. Liver regeneration. *Science* 1997; **276**: 60-66

4 **Widmann JJ**, Fahimi HD. Proliferation of mononuclear phagocytes (kupffer cells) and endothelial cells in regenerating rat liver. Alight and electron microscopic cytochemical study. *Am J Pathol* 1975; **80**: 349-366

5 **Tanaka Y**, Mak KM, Lieber CS. Immunohistochemical detection of proliferating lipocytes in regenerating rat liver. *J Pathol* 1990; **160**: 129-134

6 **Cressman DE**, Greenbaum LE, DeAngelis RA, Ciliberto G, Furth EE, Poli V, Taub R. Liver failure and defective hepatocyte regeneration in interleukin-6 –deficient mice. *Science* 1996; **274**: 1379-1383

7 **Taub R**. Blocking NF-kappa B in the liver:the good and bad news. *Hepatology* 1998; **27**: 1445-1456

8 **Brenner DA**. Signal transduction during liver regeneration. *J Gastroenterol Hepatol* 1998; **13**(Suppl): S93-S95

9 **Higashitsuji H**, Itoh K, Nagao T, Dawson S, Nonoguchi K, Kido T, Mayer RJ, Arii S, Fujita J. Reduced stability of retinoblastoma protein by gankyrin, an oncogenic ankyrin-repeat protein overexpressed in hepatomas. *Nature Med* 2000; **1**: 96-99

10 **Higgins GM**, Anderson RM. Experimental pathology of liver: restoration of liver of the white rat following partial surgical removal. *Arch Patho* 1931; **12**: 186-189

11 **Sambrook J**, Fritsh EF, Maniatis T. Molecular cloning, A Laboratory manual, 2 nd ed, New York, *Cold Spring Harbor Laboratory Press* 1989: 55

12 **Sambrook J**, Fritsh EF, Maniatis T. Molecular cloning, A Laboratory manual, 2 nd ed, New York, *Cold Spring Harbor Laboratory Press* 1989: 502

13 **Sambrook J**, Fritsh EF, Maniatis T. Molecular cloning, A Laboratory manual, 2 nd ed, New York, *Cold Spring Harbor Laboratory Press* 1989: 363

14 **Fromowitz FB**, Voila MV, Chao S, Oravez S, Mishriki Y, Finkel G, Grimson R, Lundy J. Ras P21 expression in the progression of breast cancer. *Hum Pathol* 1987; **18**: 1268-1275

15 **Della Fazia MA**, Pettirossi V, Ayroldi E, Riccardi C, Magni MV, Servillo G. Differential expression of CD44 isoforms during liver regeneration in rats. *J Hepatol* 2001; **34**: 555-561

16 **Gressner AM**. Cytokines and cellular crosstalk involved in the activation of fat-storing cells. *J Hepatol* 1995; **22**: 28-36

17 **Diehl AM**, Rai RM. Regulation of signal transduction during liver regeneration. *FASEB J* 1996; **10**: 215-227

18 **Block GD**, Locker J, Bowen WC, Petersen BE, Katyal S, Strom SC, Riley T, Howard TA, Michalopoulos GK. Population expansion, clonal growth, and specific differentiation patterns in primary cultures of hepatocytes induced by HGF/SF, EGF and TGF alpha in a chemically defined (HGM) medium. *J Cell Biol* 1996; **132**:1133-1149

19 **Sargent LM**, Sanderson ND, Thorgeirsson SS. Ploidy and karyotypic alterations associated with early events in the development of hepatocarcinogenesis in transgenic mice harboring c-myc and transforming growth factor alpha transgenes. *Cancer Res* 1996; **56**: 2137-2142

20 **Rana B**, Mischoulon D, Xie Y, Bucher NL, Farmer SR. Cell-extracellular matrix interactions can regulate the switch between growth and differentiation in rat hepatocytes: reciprocal expression of C/EBPα and immediate-early growth response transcription factors. *Mol Cell Biol* 1994; **14**: 5858-5869

21 **Fausto N**, Laird AD, Webber EM. Role of growth factors and cytokines in hepatic regeneration. *FASEB J* 1995; **9**: 1527-1536

22 **Yamada Y**, Kirillova I, Peschon JJ, Fausto N. Initiation of liver growth by tumor necrosis factor: Deficient liver regeneration in mice lacking type I tumor necrosis factor receptor. *Proc Natl Acad Sci U S A* 1997; **94**: 1441-1446

23 **Plumpe J**, Malek NP, Bock CT, Rakemann T, Manns MP, Trautwein C. NF-κB determines between apoptosis and proliferation in hepatocytes during liver regeneration. *Am J Physiol*

Gastrointest Liver Physiol 2000; **278**: G173-G183
24 **Leu JI**, Crissey MA, Leu JP, Ciliberto G, Taub R. Interleukin-6-induced STAT3 and AP-1 amplify hepatocyte nuclear factor-1 – mediated transactivation of hepatic genes, an adaptive response to liver injury. *Mol Cell Biol* 2001; **21**: 414-424
25 **DeMartino GN**, Moomaw CR, Zagnitko OP, Proske RJ, Chu-Ping M, Afendis SJ, Swaffield JC, Slaughter CA. PA700, an ATP-dependent activator of the 20 S proteasome, is an ATPase containing multiple members of nucleotide-binding protein family. *J Biol Chem* 1994; **269**: 20878-20884
26 **Hori T**, Kato S, Saeki M, DeMartino GN, Slaughter CA, Takeuchi J, Toh-e A, Tanaka K. cDNA cloning and functional analysis of P28-(Nas6p) and P40.5(Nas7p), two novel regulatory subunits of the 26S proteasome. *Gene* 1998; **216**: 113-122
27 **Baumeister W**, Walz J, Zühi F, Seemuller E. The proteasome: paradigm of a self-compartmentalizing protease. *Cell* 1998; **92**:367-380
28 **Venkataramani R**, Swaminathan K, Marmorstein R. Crystal structure of the CDK4/6 inhibitory protein p18INK4c provides insights into ankyrin-like repeat structure/function and tumor-derived p16INK4 mutations. *Nat Struct Biol* 1998; **5**: 74-81
29 **Ciechanover A**, Laszlo A, Bercovich B, Stancovski I, Alkalay I, Ben-Neriah Y, Orian A. The ubiquitin-mediated proteolytic system: involvement of molecular chaperones, degradation of oncoproteins, and activation of transcriptional regulators. *Cold Spring Harb Symp Quant Biol* 1995; **60**: 491-501
30 **Spataro V**, Norbury C, Harris AL. The ubiquitin-proteasome pathway in cancer. *Br J Cance* 1998; **77**: 448-455
31 **Nevins JR**, Leone G, Degregori J, Jakoi L. Role of the Rb/E_2F pathway in cell growth control. *J cell physiol* 1997; **173**: 233-236
32 **Weinberg RA**. The retinoblastoma protein and cell cycle control. *Cell* 1995; **81**: 323-330
33 **Park TJ**, Kim HS, Byun KH, Jang JJ, Lee YS, Lim IK. Sequential changes in hepatocarcinogenesis induced by diethynitrosamine plus thioacetamide in Fischer 344 rats: induction of gankyrin expression on liver fibrosis, pRB degradation in cirrhosis, and methylation of P16(ink4A) exon 1 in hepatocellular carcinoma. *Mol Carcinog* 2001; **30**: 138-150
34 **Fu XY**, Wang HY, Tan L, Liu SQ, Cao HF, Wu MC. Overexpression of p28/gankyrin in human hepatocellular carcinoma and its clinical significance. *World J Gastroenterol* 2002; **8**: 638-643

Edited by Wu XN and Wang XL

P.O.Box 2345, Beijing 100023,China
Fax: +86-10-85381893
E-mail: wjg@wjgnet.com www.wjgnet.com

World J Gastroenterol 2003;9(11):2528-2532
World Journal of Gastroenterology
 ISSN 1007-9327

• BASIC RESEARCH •

Changes of CD8+CD28- T regulatory cells in rat model of colitis induced by 2,4-dinitrofluorobenzene

Wen-Bin Xiao, Yu-Lan Liu

Wen-Bin Xiao, Department of Gastroenterology, Peking University People' s Hospital, Beijing 100044, China
Yu-Lan Liu, Department of Gastroenterology, Peking University People' s Hospital, Beijing 100044, China
Supported by the National Natural Science Foundation of China, No. 30240051
Correspondence to: Dr. Yu-Lan Liu, Department of Gastroenterology, Peking University People' s Hospital, Beijing 100044, China. lanhong@public.bta.net.cn
Telephone: +86-10-68314422 Ext 5448 **Fax:** +86-10-68318386
Received: 2003-03-12 **Accepted:** 2003-06-27

Abstract

AIM: To determine the changes of CD8+ T subsets especially CD8+CD28- T regulatory cells in rat model of experimental colitis induced by 2,4-dinitrofluorobenzene (DNFB).

METHODS: The rat model of experimental colitis was induced by enema with DNFB. Ten days later, colonic intraepithelial and splenic lymphocytes were isolated from colitis animals (n=16) and controls (n=8). The proportion of CD8+ T cells, CD8+CD28+ T cells and CD8+CD28- T regulatory cells were determined by flow cytometry.

RESULTS: The model of experimental colitis was successfully established by DNFB that was demonstrated by bloody diarrhea, weight loss and colonic histopathology. The proportion of CD8+ T cells in either splenic or colonic intraepithelial lymphocytes was not significantly different between colitis animals and controls (spleen: 34.6±7.24 % *vs* 33.5±9.41 %, colon: 14.0±8.93 % *vs* 18.0±4.06 %, P>0.05). But CD8+CD28- T regulatory cells from colitis animals were significantly more than those from controls (spleen: 11.3±2.26 % *vs* 5.64±1.01 %, colon: 6.50±5.37 % *vs* 1.07±0.65 %, P<0.05). In contrast, CD8+CD28+ T cells from colitis animals were less than those from controls (spleen: 23.3±6.14 % *vs* 27.8±9.70 %, P=0.06; colon: 7.52±4.18 % *vs* 16.9±4.07 %, P<0.05). The proportion of CD8+CD28- T regulatory cells in splenic and colon intraepithelial CD8+ T cells from colitis animals was higher than that from controls (spleen: 33.3±5.49 % *vs* 18.4±7.26 %, colon: 46.0±14.3 % *vs* 6.10±3.72 %, P<0.005).

CONCLUSION: Experimental colitis of rats can be induced by DNFB with simplicity and good reproducibility. The proportion of CD8+CD28- T regulatory cells in rats with experimental colitis is increased, which may be associated with the pathogenesis of colitis.

Xiao WB, Liu YL. Changes of CD8+CD28- T regulatory cells in rat model of colitis induced by 2,4-dinitrofluorobenzene. *World J Gastroenterol* 2003; 9(11): 2528-2532
http://www.wjgnet.com/1007-9327/9/2528.asp

INTRODUCTION

It is well known that immune system was involved in the pathogenesis of inflammatory bowel disease(IBD)[1-4]. Several extraintestinal autoimmune phenomena are accompanying IBD and immunosuppressive agents could alleviate the disease. Abnormalities in T-cell mediated immunity have also been noted in these patients[5]. But the exact mechanism remains to be clarified. The changes in T-cell subsets were controversial in the literature and should be deeply explored[6]. Although CD8+ T cells represent a major T-cell subset, there is little information available regarding the role of CD8+ T cells in the pathogenesis of colitis. CD8+ T cells specific for an epithelial cell-derived antigen have been shown to induce intestinal inflammation. It is possible that, like CD4+ T cells, functionally distinct CD8+ T-cell subsets may coexist. Thus we discussed the changes of CD8+ T-cell subsets in experimental colitis.

Another important part of ongoing studies of IBD was to use animal model to replicate some of the clinical features of this disease entity and to explore the mechanisms of IBD[7]. One of the important lessons learned from experimental models has been that recognition of the role of T regulatory cells plays in chronic intestinal inflammation. The ability of T cells to regulate colitis was first shown by studies of Powrie *et al*, who demonstrated that OX-22^{low} T cells could suppress the colitis induced by transfer of CD4+OX22^{high} T cells[8]. In the subsequent studies, several types of regulatory T cells have been identified. The Tr1 cells were initially reported to produce IL-10 and regulate the development of colitis in CD45RB model[9]. The effectiveness of immunosuppressive drugs in IBD may be partly related to the fact that Tr1 cells can be also generated in the presence of dexamethasone and vitamin D3. CD4+CD25+ T regulatory cells also have been demonstrated to prevent colitis in the CD45RB model[10]. A recent human study also showed that CD8+ CD28- T cells activated by the interaction with intestinal epithelial cells through gp-180 possessed a regulatory activity[11], which perhaps played important roles in the pathogenesis of colitis. However, until now there is no study reported about the roles of CD8+CD28- T regulatory cells in colitis.

In previous studies, several models of experimental colitis have been described such as TNBS, DDS, DNCB and CD45RB T-cell infusion. 2,4-dinitrofluorobenzene (DNFB) - inducing experimental colitis in mice was demonstrated to be a suitable cell-immune model[12-14]. Thus we have established the same model in rats to explore the changes in CD8+ T cell subsets especially CD8+CD28- T regulatory cells and their possible roles in the pathogenesis of DNFB-induced experimental colitis.

MATERIALS AND METHODS

Animals

Specific pathogen-free Sprague-Dawley male rats weighing 250-300 g were kept in standard laboratory conditions (room temperature of 22 ℃ with a controlled 12-hour light-dark cycle and free access to animal chow and water). Animal care was in compliance with guidelines from the Peking University Health Science Center Policy on Animal Care and Use. The rats were allowed to adapt to our laboratory environment for

one week before the onset of the experiment.

Reagents

DNFB was purchased from Acros Organics (NJ, USA), olive oil and acetone from Sigma Chemical Co. (St. Louis, Missouri, USA). Mouse anti-rat PE-conjugated-CD8b mAb (clone 341, Mouse IgG1) and FITC-conjugated-CD28 mAb (clone JJ319, Mouse IgG1) were from Serotec (Oxford, UK). Isotype control PE-conjugated mouse IgG1 and FITC-conjugated mouse IgG1 were from BD Pharmingen (San Diego, CA). RPMI 1640 and FCS were obtained from Gibco BRL (Gaithersburg, MD).

Induction of colitis

The animals in the experimental group (n=16) were pretreated with two sensitizing doses of 1 ml of 0.5 % w/v DNFB solution by rubbing the substance on previously shaved abdominal skin, 96 and 72 h before challenge[5]. The DNFB solution was prepared by diluting the original DNFB preparation with 4:1 acetone and olive oil. Freshly prepared solutions were used for each application. All the animals in the experimental group received a rectal enema with 0.4 ml of 0.2 % w/v DNFB solution in acetone and olive oil into the lumen of the colon by means of an 8-cm plastic catheter with an outer diameter of 0.9 mm, attached to a 1-ml syringe. Rectal enemas were administered under light ether anesthesia. The animals in the control group (n=8) received a rectal enema with 0.9 % w/v saline only.

Histology

Animals were killed on day 10 after the challenge enema. The entire colon was dissected, opened longitudinally, washed in ice-cold PBS. The ratio of colon / body weight was calculated, which has been shown to be a marker of colonic inflammation[15].

Macroscopic damage was assessed, according to a previously established score as follows[16]: 0: no ulcer and no inflammation, 1: no ulcer and local hyperemia, 2: ulceration without hyperemia, 3: ulceration and inflammation at one site only, 4: two or more sites of ulceration and inflammation, 5: ulceration extending more than 2 cm, 6-10: increment of 1 for each centimeter of ulceration greater than 2.

Randomized tissue samples from the site of DNFB application were subsequently excised for histology. Paraffin sections were stained with haematoxylin and eosin. Microscopic damage was quantified by image analysis of stained sections in a blinded fashion as follows[17]: 0: No evidence of inflammation. 1: Low level of lymphocyte infiltration seen in $\leqslant$10 % high power field and no structural changes observed. 2: Moderate lymphocyte infiltration seen in 10-25 % high power field and crypt elongation, bowel wall thickening that did not extend beyond the mucosal layer and no evidence of ulceration. 3: High level of lymphocyte infiltration seen in 25-50 % high power field, high vascular density, and thickening of the bowel wall that extended beyond the mucosal layer. 4: Marked degree of lymphocyte infiltration seen in $\geqslant$50 % high power field, high vascular density, crypt elongation with distortion and transmural bowel wall thickening with ulceration.

Isolation of lymphocytes

Splenocytes were isolated by conventional methods. Red blood cells were removed from spleen cell suspensions by using a standard lymphocyte gradient (Chemical Co, Shanghai, China). Intestinal intraepithelial lymphocytes were isolated according to a previously published method[18]. An average of 2-4×10^6 intraepithelial lymphocytes was yielded per colon.

Flow cytometry

A total of 1×10^6 spleen or intraepithelial lymphocytes were prepared in 100 μl and anti-CD8b and anti-CD28 mAb were added to the cell suspension. The cells were incubated at 4 ℃ for 30 min, and then the cells were washed two times with PBS/10 % v/v FCS. The cells were finally resuspended in 250 μl PBS containing 2 % w/v paraformaldehyde and then analyzed using a FACSCalibur with CellQuest software (BD Biosciences, San Jose, CA). 10 000 gated events were acquired for analysis. Isotype control was done according to the manufacturer.

Statistical analysis

Results were expressed as means ± standard deviation (SD). Comparison of results between groups was performed by unpaired t test. A probability (P) value <0.05 was considered as significant.

RESULTS

General findings

One day post-enema, diarrhea, hematochezia and reduced activity were observed in all experimental animals, but not in controls. Ten days later, the body weights of experimental animals were significantly lower than those of controls (P<0.05, as shown in Figure 1). The body weight of experimental animals decreased to the lowest on day 2 (92.8±5.0 % compared with pretreatment *vs* 106.4±1.4 % in controls, P<0.05). One rat died of colonic necrosis on the second day after DNFB enema.

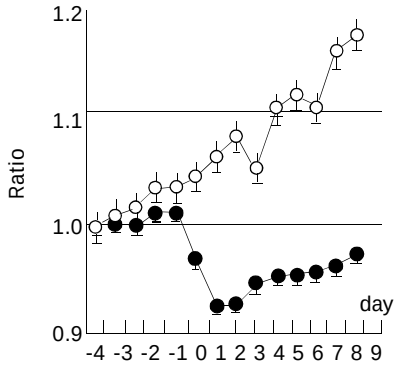

Figure 1 Body weight of experimental animals was significantly lower than that of controls (P<0.01), ○ controls, ● colitis.

Colon inflammation

The ratio of colon/body weight in experimental animals was two times more than that in controls (0.015±0.004 *vs* 0.007±0.002, P<0.05). Oedema, hemorrhage, superficial ulcerations, and necrosis were observed in the colon of experimental animals. Moreover, macroscopical characteritics of chronic phase such as adhesions, thickening of the colonic segments with narrowing of the lumen and prestenotic dilatation, atrophy and even with megacolon formation, were obviously in experimental animals but not in controls. Microscopically, active inflammatory process was characterized by mononuclear infiltration, fibrosis, smooth-muscle hypertrophy and lymphoid hyperplasia (as shown in Figure 2 left). Both the macroscopical and microscopical damage scores in experimental animals were higher than those in controls (macroscopical: 5.2±1.4 *vs* 1.4±0.6, P<0.0001; microscopical: 3.3±0.5 *vs* 1.2±0.5, P<0.0001, Figure 2 right).

Splenic CD8+ T-cell subsets

There was no difference in the proportion of CD8+ T cells between experimental animals and controls. However, CD8+CD28- T regulatory cells of experimental animals were significantly more than controls (as shown in Figure 3). Even

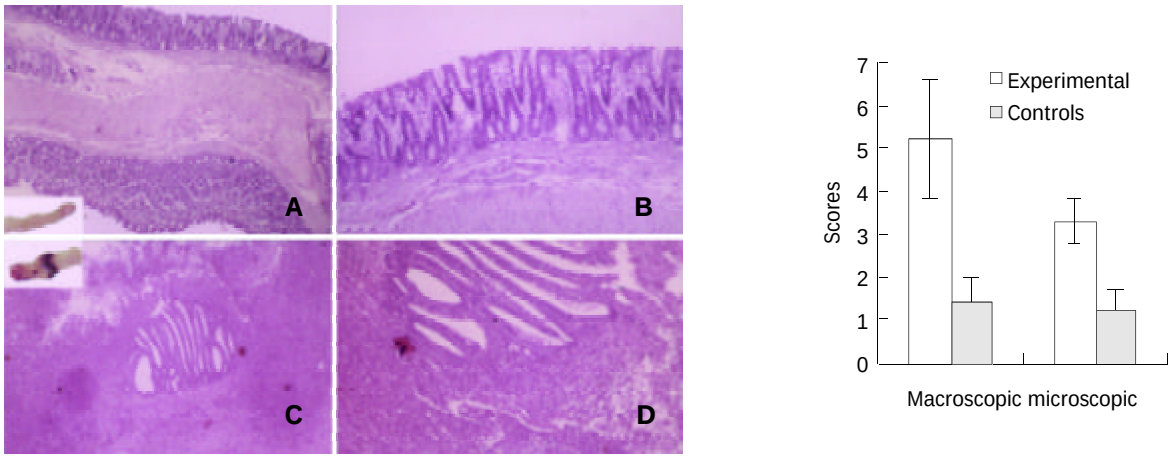

Figure 2 Left: Colon histological manifestation of experimental animals (C: 4×10, upper left is colon; D: 10×10) compared with controls (A: 4×10, lower left is colon; B: 10×10) (haematoxylin and eosin). Right: Macroscopical and microscopical damage scores in experimental animals are higher than those in controls.

Figure 3 Flow cytometry shows the proportion of CD8+CD28- T regulatory cells was 12.4 % in experimental animals (right) and 4.9 % in controls (left).

though it was not significantly, CD8+CD28+ T cells of experimental animals were less than controls. In CD8+ T cells pool, the proportion of CD8+CD28- T regulatory cells of experimental animals was also significantly higher than that of controls (as shown in Table 1).

Table 1 Splenic CD8+ T-cell subsets of experimental animals and controls on day 10 after enema

	Experimental colitis (%, *n*=16)	Control (%, *n*=8)	*P* value
CD8+CD28-T	11.3±2.26	5.64±1.01	0.0001
CD8+CD28+T	23.3±6.14	27.8±9.70	0.41
CD8+T	34.6±7.24	33.5±9.41	0.83
CD8+CD28-T/CD8+T	33.3±5.49	18.4±7.26	0.003

Table 2 Intraepithelial CD8+ T-cell subsets of experimental animals and controls on day 10 after enema

	Experimental colitis (%, *n*=16)	Control (%, *n*=8)	*P* value
CD8+CD28-T	6.50±5.37	1.07±0.65	0.049
CD8+CD28+T	7.52±3.16	16.9±4.07	0.004
CD8+T	14.0±6.83	18.0±4.06	0.38
CD8+CD28-T/CD8+T	46.0±14.3	6.10±3.72	0.0001

Intraepithelial CD8+ T-cell subsets

There was no difference in the proportion of CD8+ T cells between experimental animals and controls. However, CD8+CD28- T regulatory cells of experimental animals were significantly more than those of controls, and CD8+CD28+ T cells of experimental animals were significantly less than those of controls. In CD8+ T cells pool, the proportion of CD8+CD28- T regulatory cells of experimental animals was also significantly higher than that of controls (as shown in Table 2).

DISCUSSION

DNFB, a highly reactive compound with hapten characteristics, could bind to and covalently modify cell surface proteins, changing their antigenic conformation and their immunogenecity. T lymphocytes could recognize and lyse hapten-modified autologous cells quite efficiently in presensitized animals[19]. Thus DNFB was capable of inducing a delay-type hypersensitivity reaction when applied to the skin or to the intestinal mucosa[20]. In addition, DNFB was more reactive in protein modification than DNCB[21,22]. This is a possible explanation for DNFB causing the lesions, more pronounced in both acute phase and chronic phase than in previously described models induced by DNCB. In 1992, Banic *et al.* demonstrated that experimental colitis of mice was induced by DNFB, mimicking inflammatory bowel disease by the intestinal histopathological and extraintestinal manifestations[12-14]. It also responded well to glucorticosteroid and cyclosporine A, resembling TNBS-induced colitis[23,24]. Because of its simplicity and reproducibility this model represents a suitable preparation for investigating pathogenetic mechanisms of IBD especially that involves cellular immunity. We further explored this model in rats as the first time and the results were consistent with Banic *et al*. All morphologic changes in experimental group were similar to the changes characteristically observed in IBD in humans. Thus

experimental colitis model of rats induced by DNFB could be used to study the pathogenesis of IBD.

There is increasing evidence that IBD is a kind of autoimmune diseases. IBD could be envisioned as an imbalance between proinflammatory and anti-inflammatory cytokines[1-4]. It is suspected that changes in certain cytokines could be a result of changes in proportion or function of certain T-cell subsets. In a series study of Jewell *et al*, however, no difference was found in CD4+ and CD8+ T cells of peripheral blood and colonic mucosa between IBD and healthy controls[25-27]. Regretfully, subsets of CD4+ and CD8+ T cells were not further studied. Several studies demonstrated that T cells from IBD patients or experimental colitis model had diminished response to mitogen stimuli[28-30], and it could be recovered partially by exogenous IL-2[5]. The exact mechanism still remains unknown, but the roles of T regulatory cells should be considered[31,32]. Roman *et al*. found that CD4+CD45RO+ T cells were significantly expanded in Crohn' s disease but not in healthy controls[5], and CD4+ T regulatory cells were contained in CD4+CD45RO+ T cells[33]. The role of CD4+ T regulatory cells in pathogenesis of colitis has been studied in detail by Powrie *et al*[8]. To our knowledge, however, few studies have explored the roles of CD8+ T cells especially CD8+CD28- T regulatory cells in pathogenesis of colitis. Our study showed that the proportion of CD8+ T cells of spleen and colonic mucosa in experimental animals was not different from that in controls, which is consistent with previous findings. But we further found that there was increasing population of CD8+CD28- T regulatory cells in experimental animals compared to controls, and decreasing population of CD8+CD28+ T cells at the same time. These results have not been reported before.

CD8+ T cells comprise cells that are in different states of differentiation and under the control of complex homeostatic processes. In a number of situations such as chronic inflammatory conditions, infectious diseases, ageing, immunodeficiency, iron overload, heavy alcohol intake and transplantation, major phenotypic changes, usually associated with an increase in CD8+CD28- T cells, took place[34]. CD8+CD28- T cells are characterized by functional features of suppression. CD8+CD28- T cells could suppress alloreactive immune responses in an antigen-specific, major histocompatibility complex (MHC)-restricted manner[35].

The emergence of expanded CD8+CD28- T-cell clones has been ascribed to extensively continuous or repeated antigenic stimulation leading to immune exhaustion, as suggested by the accumulation of such cells in patients with human immunodeficiency virus (HIV) infection and autoimmune disease. Although the nature of the signals that give origin to this T-cell subset is uncertain, growing evidence argues for the existence of an interplay between epithelial cells, molecules with the MHC-class I fold and CD8+ T cells. By stimulation of antigen especially intestinal epithelial cells, CD8+CD28+ T cells can further differentiate into CD8+CD28- T regulatory cells, which was a kind of ending-stage cell and could suppress the proliferation of lymphocytes[11]. Stimulated by DNFB hapten-antigen, it is possible that CD8+CD28+ T cells differentiate into CD8+CD28- T regulatory cells. Thus the changes of CD8+ T cell pools mentioned above can be explained. We suspect that the increase of CD8+CD28- T regulatory cells is a feedback to autoimmune disease and it could explain diminished response to mitogen stimuli of T cells in IBD. Further study is urgently needed to explore the function of CD8+CD28- T regulatory cells and its exact role in the pathogenesis of IBD.

REFERENCES

1 **Fiocchi C**. Inflammatory bowel disease: etiology and pathogenesis. *Gastroenterology* 1998; **115**: 182-205

2 **Podolsky DK**. Inflammatory bowel disease. *N Engl J Med* 2002; **347**: 417-429

3 **Grimm MC**. Inflammatory bowel disease and inflammatory molecules: chickens, eggs and therapeutic targets. *J Gastroenterol Hepatol* 2002; **17**: 935-937

4 **Plevy S**. The immunology of inflammatory bowel disease. *Gastroenterol Clin North Am* 2002; **31**: 77-92

5 **Roman LI**, Manzano L, De La Hera A, Abreu L, Rossi I, Alvarez-Mon M. Expanded CD4+CD45RO+phenotype and defective proliferative response in T lymphocytes from patients with Crohn's disease. *Gastroenterology* 1996; **110**: 1008-1019

6 **Hoang P**, Senju M, Lowes JR, Jewell DP. Phenotypic characterization of isolated intraepithelial lymphocytes in patients with ulcerative colitis and normal controls. *Dig Dis Sci* 1992; **37**: 1725-1728

7 **Elson CO**, Sartor RB, Tennyson GS, Riddell RH. Experimental models of inflammatory bowel disease. *Gastroenterology* 1995; **109**: 1344-1367

8 **Powrie F**, Mason D. OX-22high CD4+ T cells induce wasting disease with multiple organ pathology: prevention by the OX-22low subset. *J Exp Med* 1990; **172**: 1701-1708

9 **Groux H**, O'Garra A, Bigler M, Rouleau M, Antonenko S, de Vries JE, Roncarolo MG. A CD4+ T cell subset inhibits antigen-specific T-cell responses and prevents colitis. *Nature* 1997; **389**: 737-742

10 **Read S**, Malmstrom V, Powrie F. Cytotoxic T lymphocyteassociated antigen 4 plays an essential role in the function of CD25+CD4+regulatory cells that control intestinal inflammation. *J Exp Med* 2000; **192**: 295–302

11 **Allez M**, Brimnes J, Dotan I, Mayer L. Expansion of CD8+ T cells with regulatory function after interaction with intestinal epithelial cells. *Gastroenterology* 2002; **123**: 1516-1526

12 **Brkic T**, Banic M, Anic B, Grabarevic Z, Rotkvic I, Artukovic B, Duvnjak M, Sikiric P, Troskot B, Hernandez DE. A model of inflammatory bowel disease induced by 2,4-dinitrofluorobenzene in previously sensitized BALB-c mice. *Scand J Gastroenterol* 1992; **27**: 184-188

13 **Anic B**, Brkic T, Banic M, Heinzl R, Dohoczky C, Smud D, Rotkvic I, Buljevac M. Histopathologic features of T-cell mediated colonic injury induced with 2,4-dinitrofluorobenzene in BALB/c mice. *Acta Med Croatica* 1997; **51**: 11-14

14 **Banic M**, Anic B, Brkic T. Animal models of inflammatory bowel disease. *Acta Med Croatica* 1997; **51**: 37-40

15 **Rolandelli RH**, Saul SH, Settle RG, Jacobs DO, Trerotola SO, Rombeau JL. Comparison of parenteral nutrition and enteral feeding with pectin in experimental colitis in the rat. *Am J Clin Nutr* 1988; **47**: 715-721

16 **Wallace JL**, Keenan CM. An orally active inhibitor of leukotriene synthesis accelerates healing in a rat model of colitis. *Am J Physiol* 1990; **258**(4 Pt1): G527-534

17 **Neurath MF**, Fuss I, Kelsall BL, Stuber E, Strober W. Antibodies to interleukin 12 abrogate established experimental colitis in mice. *J Exp Med* 1995; **182**: 1281-1290

18 **Davies MD**, Parrott DM. Preparation and purification of lymphocytes from the epithelium and lamina propria of murine small intestine. *Gut* 1981; **22**: 481-488

19 **Miller SD**. Suppressor T cell circuits in contact sensitivity. II. Induction and characterization of an efferent-acting, antigen-specific, H-2-restricted, monoclonal T cell hybrid-derived suppressor factor specific for DNFB contact hypersensitivity. *J Immunol* 1984; **133**: 3112-3120

20 **Hirashima M**, Sakata K, Tashiro K, Yoshimura T, Hayashi H. Dexamethasone suppresses concanavalin A-induced production of chemotactic lymphokines by releasing a soluble factor from splenic T lymphocytes. *Immunology* 1985; **54**: 533-540

21 **Rabin BS**, Rogers SJ. A cell-mediated immune model of inflammatory bowel disease in the rabbit. *Gastroenterology* 1978; **75**: 29-33

22 **Glick ME**, Falchuk ZM. Dinitrochlorobenzene-induced colitis in the guinea-pig: studies of colonic lamina propria lymphocytes. *Gut* 1981; **22**: 120-125

23 **Banic M**, Brkic T, Anic B, Rotkvic I, Grabarevic Z, Duvnjak M, Troskot B, Mihatov S. Effect of methylprednisolone on small bowel, spleen and liver changes in a murine model of inflammatory bowel disease. *Aliment Pharmacol Ther* 1993; **7**: 201-206

24 **Banic M**, Anic B, Brkic T, Ljubicic N, Plesko S, Dohoczky C, Erceg D, Petrovecki M, Stipancic I, Rotkvic I. Effect of

cyclosporine in a murine model of experimental colitis. *Dig Dis Sci* 2002; **47**: 1362-1368

25 **Selby WS**, Jewell DP. T lymphocyte subsets in inflammatory bowel disease: peripheral blood. *Gut* 1983; **24**: 99-105

26 **Selby WS**, Janossy G, Bofill M, Jewell DP. Intestinal lymphocyte subpopulations in inflammatory bowel disease: an analysis by immunohistological and cell isolation techniques. *Gut* 1984; **25**: 32-40

27 **Senju M**, Wu KC, Mahida YR, Jewell DP. Two-color immunofluorescence and flow cytometric analysis of lamina propria lymphocyte subsets in ulcerative colitis and Crohn's disease. *Dig Dis Sci* 1991; **36**: 1453-1458

28 **Davidsen B**, Kristensen E. Lymphocyte subpopulations, lymphoblast transformation activity, and concanavalin A-induced suppressor activity in patients with ulcerative colitis and Crohn's disease. *Scand J Gastroenterol* 1987; **22**: 785-790

29 **Manzano L**, Alvarez-Mon M, Vargas JA, Giron JA, Abreu L, Fernandez-Corugedo A, Roman LI, Albarran F, Durantez A. Deficient interleukin 2 dependent proliferation pathway in T lymphocytes from active and inactive ulcerative colitis patients. *Gut* 1994; **35**: 955-960

30 **Perez-Machado MA**, Espinosa LM, de la Madrigal EJ, Abreu L, Lorente GM, Alvarez-Mon M. Impaired mitogenic response of peripheral blood T cells in ulcerative colitis is not due to apoptosis. *Dig Dis Sci* 1999; **44**: 2530-2537

31 **Ilan Y**, Weksler-Zangen S, Ben-Horin S, Diment J, Sauter B, Rabbani E, Engelhardt D, Chowdhury NR, Chowdhury JR, Goldin E. Treatment of experimental colitis by oral tolerance induction: a central role for suppressor lymphocytes. *Am J Gastroenterol* 2000; **95**: 966-973

32 **Hoang P**, Dalton HR, Jewell DP. Human colonic intra-epithelial lymphocytes are suppressor cells. *Clin Exp Immunol* 1991; **85**: 498-503

33 **Singh B**, Read S, Asseman C, Malmstrom V, Mottet C, Stephens LA, Stepankova R, Tlaskalova H, Powrie F. Control of intestinal inflammation by regulatory T cells. *Immunol Rev* 2001; **182**: 190-200

34 **Arosa FA**. CD8+CD28- T cells: certainties and uncertainties of a prevalent human T-cell subset. *Immunol Cell Biol* 2002; **80**: 1-13

35 **Chang CC**, Ciubotariu R, Manavalan JS, Yuan J, Colovai AI, Piazza F, Lederman S, Colonna M, Cortesini R, Dalla-Favera R, Suciu-Foca N. Tolerization of dendritic cells by T(S) cells: the crucial role of inhibitory receptors ILT3 and ILT4. *Nat Immunol* 2002; **3**: 237-243

Edited by Zhu L and Wang XL

P.O.Box 2345, Beijing 100023,China
Fax: +86-10-85381893
E-mail: wjg@wjgnet.com www.wjgnet.com

World J Gastroenterol 2003;9(11):2533-2538
World Journal of Gastroenterology
 ISSN 1007-9327

• BASIC RESEARCH •

Ameliorative effects of sodium ferulate on experimental colitis and their mechanisms in rats

Wei-Guo Dong, Shao-Ping Liu, Bao-Ping Yu, Dong-Fang Wu, He-Sheng Luo, Jie-Ping Yu

Wei-Guo Dong, Shao-Ping Liu, Bao-Ping Yu, He-Sheng Luo, Jie-Ping Yu, Department of Gastroenterology, Renmin Hospital of Wuhan University, 238 Jiefang Road, Wuhan 430060, Hubei Province, China
Dong-Fang Wu, Department of Pharmacy, Renmin Hospital of Wuhan University, 238 Jie-fang Road, Wuhan 430060, Hubei Province, China
Supported by key Project in Scientific and Technological Researches of Hubei Province, No. 2001AA308B
Correspondence to: Professor Wei-Guo Dong, Renmin Hospital of Wuhan University, 238 Jiefang Road, Wuhan 430060, Hubei Province, China. dongwg@public.wh.hb.cn
Telephone: +86-27-88054511
Received: 2003-05-13 **Accepted:** 2003-06-02

Abstract

AIM: To investigate the ameliorative effects of sodium ferulate (SF) on acetic acid-induced colitis and their mechanisms in rats.

METHODS: The colitis model of Sprague-Dawley rats was induced by intracolon enema with 8 % (V/V) of acetic acid. The experimental animals were randomly divided into model control, 5-aminosalicylic acid therapy group and three dose of SF therapy groups. The 5 groups were treated intracolonically with normal saline, 5-aminosalicylic acid (100 mg·kg^{-1}), and SF at the doses of 200, 400 and 800 mg·kg^{-1} respectively and daily (8: 00 am) for 7 days 24 h following the induction of colitis. A normal control group of rats clystered with normal saline instead of acetic acid was also included in the study. Pathological changes of the colonic mucosa were evaluated by the colon mucosa damage index (CMDI) and the histopathological score (HS). The insulted colonic mucosa was sampled for a variety of determinations at the end of experiment when the animals were sacrificed by decapitation. Colonic activities of myeloperoxidase (MPO) and superoxide dismutase (SOD), and levels of malondialdehyde (MDA) and nitric oxide (NO) were assayed with ultraviolet spectrophotometry. Colonic contents of prostaglandin E_2 (PGE_2) and thromboxane B_2 (TXB_2) were determined by radioimmunoassay. The expressions of inducible nitric oxide synthase (iNOS), cyclo-oxygenase-2 (COX-2) and nuclear factor kappa B (NF-κB) p65 proteins in the colonic tissue were detected with immunohistochemistry.

RESULTS: Enhanced colonic mucosal injury, inflammatory response and oxidative stress were observed in the animals clystered with acetic acid, which manifested as the significant increase of CMDI, HS, MPO activities, MDA and NO levels, PGE_2 and TXB_2 contents, as well as the expressions of iNOS, COX-2 and NF-κB p65 proteins in the colonic mucosa, although the colonic SOD activity was significantly decreased compared with the normal control (CMDI: 2.9±0.6 *vs* 0.0±0.0; HS: 4.3±0.9 *vs* 0.7±1.1; MPO: 98.1±26.9 *vs* 24.8±11.5; MDA: 57.53±12.36 *vs* 9.21±3.85; NO: 0.331±0.092 *vs* 0.176±0.045; PGE_2: 186.2±96.2 *vs* 42.8±32.8; TXB_2: 34.26±13.51 *vs* 8.83±3.75; iNOS: 0.365±0.026 *vs* 0.053±0.015; COX-2: 0.296±0.028 *vs* 0.034±0.013; NF-κB p65: 0.314±0.026 *vs* 0.039±0.012; SOD: 28.33±1.17 *vs* 36.14±1.91; P<0.01). However, these parameters were found to be significantly ameliorated in rats treated locally with SF at the given dose protocols, especially at 400 mg·kg^{-1}and 800 mg·kg^{-1} doses (CMDI: 1.8±0.8, 1.6±0.9; HS: 3.3±0.9, 3.1±1.0; MPO: 63.8±30.5, 36.2±14.2; MDA: 41.84±10.62, 37.34±8.58; NO: 0.247±0.042; 0.216±0.033; PGE_2: 77.2±26.9, 58.4±23.9;TXB_2: 18.07±14.83; 15.52±8.62; iNOS:0.175±0.018, 0.106±0.019; COX-2: 0.064±0.018, 0.056±0.014; NF-κBp65: 0.215±0.019, 0.189±0.016; SOD: 32.15±4.26, 33.24±3.69; P<0.05-0.01). Moreover, a therapeutic dose protocol of 800 mg·kg^{-1} SF was observed as effective as 100 mg·kg^{-1} of 5-ASA in the amelioration of colonic mucosal injury as evaluated by CMDI and HS.

CONCLUSION: Administration of SF intracolonically may have significant therapeutic effects on the rat model of colitis induced by acetic acid enema, which was probably due to the mechanism of antioxidation, inhibition of arachidonic acid metabolism and NF-κB expression.

Dong WG, Liu SP, Yu BP, Wu DF, Luo HS, Yu JP. Ameliorative effects of sodium ferulate on experimental colitis and their mechanisms in rats. *World J Gastroenterol* 2003; 9(11): 2533-2538
http://www.wjgnet.com/1007-9327/9/2533.asp

INTRODUCTION

Inflammatory bowel disease (IBD) is a collection of chronic idiopathic inflammatory disorders of the intestine and/or colon. Although the pathophysiology of these disorders is not known with certainty, a growing body of experimental and clinical data suggested that this kind of chronic gut inflammation might be resulted from a maladjusted immune response to certain bacterial antigens[1-3]. This uncontrolled immune system activation results in a sustained overproduction of cytokines, eicosanoids, oxygen and nitrogen reactive species, which has been thought to be the major causative factors leading to intestinal and/or colonic injury and dysfunction in inflammatory bowel disease.

Based on this hypothesis, current therapeutic strategy for IBD has therefore focused on the use of anti-inflammatory agents, aminosalicylates and corticosteroids[1,4-9]. However, some notable limitations are found existing in the management of IBD patients and meanwhile some patients are refractory to these therapies. Long term use of glucocorticoids, for example, although effective in suppressing active inflammation, was associated with high rates of relapse and unacceptable toxicity[10-12]. On the other hand, 6-mercaptopurine and its prodrug azathioprine are effective in inducing and maintaining remission, however, a significant number of patients were resistant or intolerant to thiopurines[10]. All these suggest that seeking for more preferable drugs harboring better therapeutic results and less side-effects for the treatment of patients with IBD is urgently necessary.

Sodium ferulate (SF) is one of the effective components of Radix Angelica sinensis. Many researches have revealed that

SF possesses plenty of beneficial pharmacological effects such as inhibiting the production of inflammatory mediators, improving endothelial function, relieving oxidative stress and safe in use[13-18]. We presumed that SF might be a possible candidate to be used for the treatment of IBD, which to our knowledge has not been investigated in previous studies. The present study was therefore conducted to confirm our hypothesis with an effort to demonstrate the therapeutic effects of sodium ferulate on experimental colonitis.

MATERIALS AND METHODS

Animals

Healthy Sprague-Dawley rats of both sexes, weighing 250±30 g, from the Animal Center, Academy of Hubei preventive medical sciences were employed in the present study. The animals were fed on standard rat chow, allowed access to tap water *ad libitum* and acclimatized to the surroundings for one week prior to the experiments. The study protocol was in accordance with the guideline for animal research and was approved by the Ethical and Research Committee of the hospital.

Reagents

Acetic acid was obtained from Wuhan Chemical Corp. SF injection was provided by Pharmaceutical Factory of Zhongnan Hospital, Wuhan University (Lot. 20011219). 5-aminosalicylic acid (5-ASA) was purchased from Guoyi Pharmaceutical Ltd (Lot. 20029477). Polyclonal rabbit anti-rat-iNOS, COX-2 and NF-κB P65 were from Santa Cruz Company. S-P kits were obtained from Beijing Zhongshan Biological Technology CO Ltd. PGE_2 and TXB_2 radioimmunoassay kits were provided by Radioimmunity Institute of PLA General Hospital. MPO, SOD, MDA, NO detection kits were purchased from Nanjing Jiancheng Bioengineering Institute. Other reagents used in the present study were all of analytical grade.

Experimental protocol

The preparation of rat model of colitis was described in the literature[19,20]. Briefly, after rats were anesthetized with ether, a flexible plastic catheter with an outer diameter of 2 mm were inserted rectally into the colon with the aim to place the catheter tip at 8 cm proximal to the anus. Twenty seconds following enema with 2 ml of 8 % (V/V) acetic acid through the catheter, colon lumen was rinsed twice with 5 ml of normal saline. The experimental animals were randomly divided into normal control, model control, 5-aminosalicylic acid therapy and three dose SF therapy groups, and treated intracolonically with normal saline, normal saline, 5-aminosalicylic acid (100 mg· kg^{-1}), and SF 200, 400 and 800 mg· kg^{-1} respectively and daily (8: 00 am) for 7 days 24 h following the induction of colitis. Then the colon mucosa damage index (CMDI) and the histopathological score (HS) were evaluated and the colon mucosa was sampled for a variety of determinations and observations after the animals were sacrificed by decapitation.

Assessment of CMDI and HS

The colon segment taken from 10 cm proximal to anus of the sacrificed rats was excised longitudinally, rinsed by saline buffer and fixed on a wax block. CMDI and HS were assessed respectively by two independent researchers. The scoring formula for assessment of CMDI was reported in previous literature[20]. That is, 0: normal mucosa, no damage on the mucosal surface; 1: mild hyperemia and edema, no erosion or ulcer on the mucosal surface; 2: moderate hyperemia and edema, erosion appearing on the mucosal surface; 3: severe hyperemia and edema, necrosis and ulcer appearing on the mucosal surface with the major ulcerative area extending less than 1 cm; 4: severe hyperemia and edema, necrosis and ulcer appearing on the mucosal surface with the major ulcerative area extending more than 1 cm. For histopathological examination, the colonic samples were fixed in 4 % neutral buffered paraformaldehyde overnight and 4-μm thick sections were routinely prepared and stained with haematoxylin and eosin. The colonic pathological changes were observed and evaluated by two independent researchers with a modified histopathological score formula[19] as: (1) Infiltration of acute inflammatory cells: 0, without; 1, mild; 2, severe. (2) Infiltration of chronic inflammatory cells: 0, without; 1, mild; 2, severe. (3) Fibrin deposition: 0, negative; 1, positive. (4) Submucosal edema: 0, without; 1, focal; 2, diffuse. (5) Necrosis of epithelial cells: 0, without; 1, focal; 2, diffuse. (6) Mucosal ulcer: 0, negative; 1, positive.

Determination of colonic MPO, SOD activities and MDA, NO contents

For determination of colonic MPO activity, the sampled tissues were homogenized (50 g· L^{-1}) in 50 mmol· L^{-1} ice-cold potassium phosphate buffer (pH 6.0) containing 0.5 % of hexadecyltrimethylammoninm bromide. The homogenate was frozen and thawed thrice, then centrifuged at 4 000 rpm for 20 min at 4 ℃. The MPO activity in the supernatant was measured by the assay kit according to its provider' s instructions. The colonic samples for the determination of SOD activity, MDA and NO contents were homogenized in ice-cold PBS (pH 7.4) and centrifuged at 3 000 rpm for 10 min at 4 ℃. The resulting supernatant was stored at 20 ℃ until analysis with corresponding assay kits according to the manufacturer' s guide.

Measurement of colonic PGE_2 and TXB_2 level

Colonic specimens used for the assay of arachidonic acid metabolites were prepared according to the protocol by Raab *et al*[21] and Taniguchi *et al*[22], and their levels of PGE_2 and TXB_2 were measured by using the corresponding radioimmunoassay kits following the manufacturer' s instructions.

Detection of colonic iNOS, COX-2 and NF-κB p65 expression

The immunohistochemical methods for formalin-fixed and paraffin-embedded sections were described previously[23]. The determinations of colonic iNOS, COX-2 and NF-κB p65 expression were all performed with S-P technique following the recommendations of assay kit providers. Briefly, polyclonal rabbit anti-rat-iNOS, COX-2 and NF-κB p65 were diluted with PBS to 1:150, 1:120, 1:200 respectively and used as the primary antibody in the corresponding detections. For each of these determinations, dewaxed sections were incubated first with the primary antibody overnight at 4 ℃ after antigen retrieval. The binding of antibodies to their antigenic sites in the tissue sections was further amplified with biotinylated goat anti-rabbit antibody and followed by reaction with 3, 3' -diaminobenzidine. Sections prepared by substituting PBS for the primary antibody served as the negative control. iNOS, COX-2 or NF-κB p65 negatively expressed cells manifested as blue-stained nuclei while the positive cells as brown or dark brown cytoplasm and/or cell membrane. Expressions of these target proteins were semiquantitated respectively with automatic image analyzer (Nikon, Japan) and HPIAS-2000 image analyzing program, in which the average value of positive cell' s absorbance (A) in ten randomly selected high power fields (400×) for each section was used for the comparison of the target protein expressions.

Statistical analysis

Experimental results were expressed as $\bar{x}$±s. Statistical comparisons between groups were made by ANOVA followed

by Student's *t* test. *P* value less than 0.05 was considered statistically significant.

RESULTS

Inflammatory changes of the colonic mucosa

CMDI, HS and MPO activities were the main parameters for evaluating the degree of colonic inflammation in inflammatory bowel disease. Compared with the normal control, these parameters were all significantly increased in the colonic mucosa of the model control induced by acetic acid ($P<0.01$). After the model rats were treated with SF (400, 800 mg· kg^{-1}) or 5-ASA (100 mg· kg^{-1}) as described in the experimental protocol, these elevated parameters were significantly ameliorated ($P<0.05$ or 0.01) as shown in Table 1, in which a therapeutic dose protocol of 800 mg· kg^{-1} SF was observed as effective as 100 mg· kg^{-1} 5-ASA in the treatment of this rat model of colitis.

Table 1 Effects of sodium ferulate on CMDI, HS and MPO activity in the colon tissue of acetic acid-induced rats colitis (n=8, $\bar{x}\pm s$)

Group	Dose (mg·kg^{-1})	CMDI	HS	MPO (U·g^{-1})
Normal	-	0.0±0.0	0.7±1.1	24.8±11.5
Model	-	2.9±0.6^{d}	4.3±0.9^{d}	98.1±26.9^{d}
5-ASA	100	1.6±0.9^{b}	3.4±0.5^{a}	29.6±10.8^{b}
SF	200	2.0±0.8^{a}	3.6±1.2	79.5±38.4
SF	400	1.8±0.8^{b}	3.3±0.9^{a}	63.8±30.5^{a}
SF	800	1.6±0.9^{b}	3.1±1.0^{a}	36.2±14.2^{b}

$^{a}P<0.05$, $^{b}P<0.01$ *vs* model group; $^{d}P<0.01$ *vs* normal group.

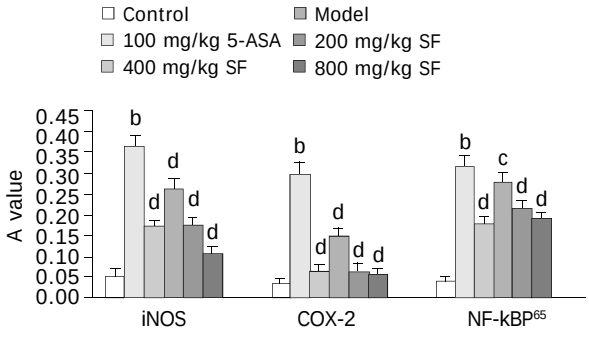

Figure 1 Effects of SF on the expressions of iNOS, COX-2 and NF-κB P65 in the colonic tissue of rats colitis induced by acetic acid (n=8, $\bar{x}\pm s$). $^{b}P<0.01$, *vs* control group; $^{c}P<0.05$, $^{d}P<0.01$, *vs* model group.

Colonic oxidative alterations

Prominent oxidative stress in colonic mucosa was induced by enema of acetic acid in the model controls as shown by the significant elevation of colonic MDA and NO contents and decrease of colonic SOD activities (Table 2). These oxidative abnormalities in colonic mucosa were obviously ameliorated by the treatment with SF at the dose protocols of 200, 400, 800 mg· kg^{-1}, which manifested as the significant reduction of colonic MDA content and the increase of SOD activity compared with the model control rats ($P<0.05$-0.01). Furthermore, a significant improvement for the elevated colonic NO content was also noted in animals treated with SF at the dose protocol of 400 or 800 mg· kg^{-1} ($P<0.05$-0.01) as shown in Table 2.

Effects of SF on the colonic PGE_2, TXB_2 levels

After the rats were insulted by enema of acetic acid, their colonic contents of PGE_2 and TXB_2 were significantly increased compared with the normal control ($P<0.01$). A significant amelioration of PGE_2 contents was observed in animals treated with SF at all dose protocols ($P<0.05$-0.01). However, significant reduction of colonic TXB_2 contents compared with the model control was only seen in rats treated with SF at the dose protocol of 400 and 800 mg· kg^{-1} ($P<0.05$-0.01) as shown in Table 3.

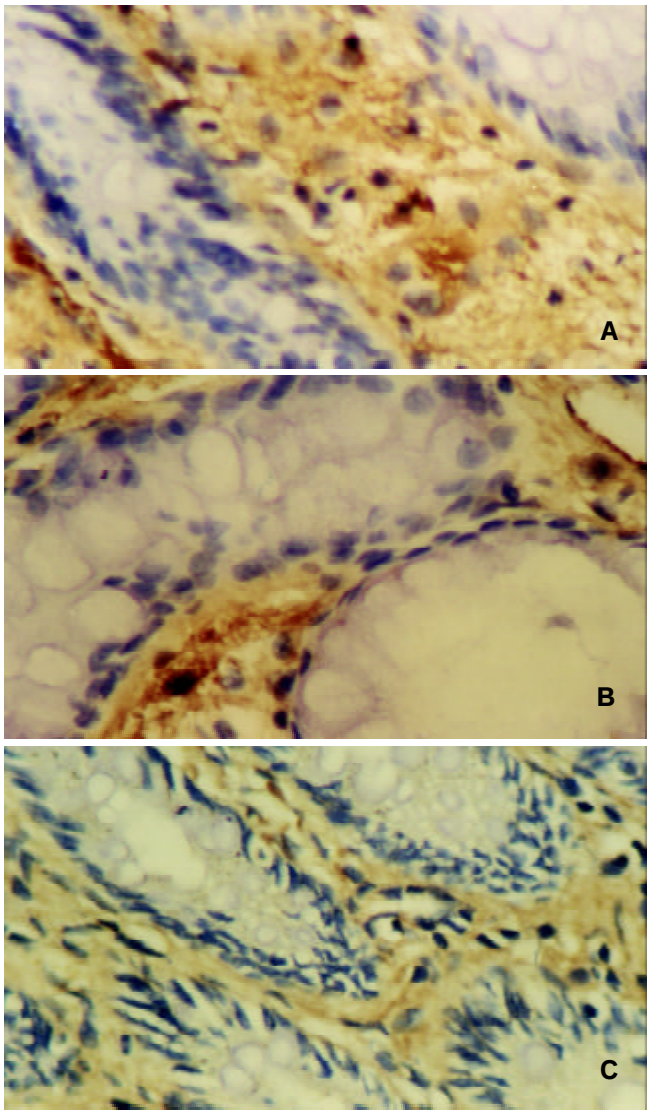

Figure 2 Expressions of iNOS (A), COX-2 (B) and NF-κB p65 (C) in the inflammatory areas of colonic tissue from rats with colitis induced by acetic acid enema, respectively. The strongly positive signal were found. SP stain ×400.

Table 2 Effects of sodium ferulate on SOD activity, MDA and NO contents in the colon tissue of acetic acid-induced rats colitis (n=8, $\bar{x}\pm s$)

Group	Dose (mg·kg^{-1})	SOD (kU·g^{-1})	MDA (nmol·g^{-1})	NO (nmol·g^{-1})
Normal	-	36.14±1.91	9.21±3.85	176±45
Model	-	28.33±1.17^{d}	57.53±12.36^{d}	331±92^{d}
5-ASA	100	32.74±3.52^{b}	31.85±11.72^{b}	244±51^{a}
SF	200	31.63±3.83^{a}	43.25±13.47^{a}	256±54
SF	400	32.15±4.26^{a}	41.84±10.62^{a}	247±42^{a}
SF	800	33.24±3.69^{b}	37.34±8.58^{b}	216±33^{b}

$^{a}P<0.05$, $^{b}P<0.01$, *vs* model group; $^{d}P<0.01$ *vs* normal group.

Table 3 Effects of sodium ferulate on the content of PGE_2 and TXB_2 in the colon tissue of acetic acid-induced rats colitis (n=8, $\bar{x}\pm s$)

Group	Dose ($mg\cdot kg^{-1}$)	PGE_2($ng\cdot g^{-1}$)	TXB_2($ng\cdot g^{-1}$)
Normal	-	42.8±32.8	8.83±3.75
Model	-	186.2±96.2[d]	34.26±13.51[d]
5-ASA	100	67.0±37.7[b]	18.53±14.26[a]
SF	200	90.7±52.3[a]	23.21±12.46
SF	400	77.2±26.9[b]	18.07±14.83[a]
SF	800	58.4±23.9[b]	15.52±8.62[b]

[a] $P < 0.05$, [b] $P < 0.01$ *vs* model group; [d] $P < 0.01$ *vs* normal group.

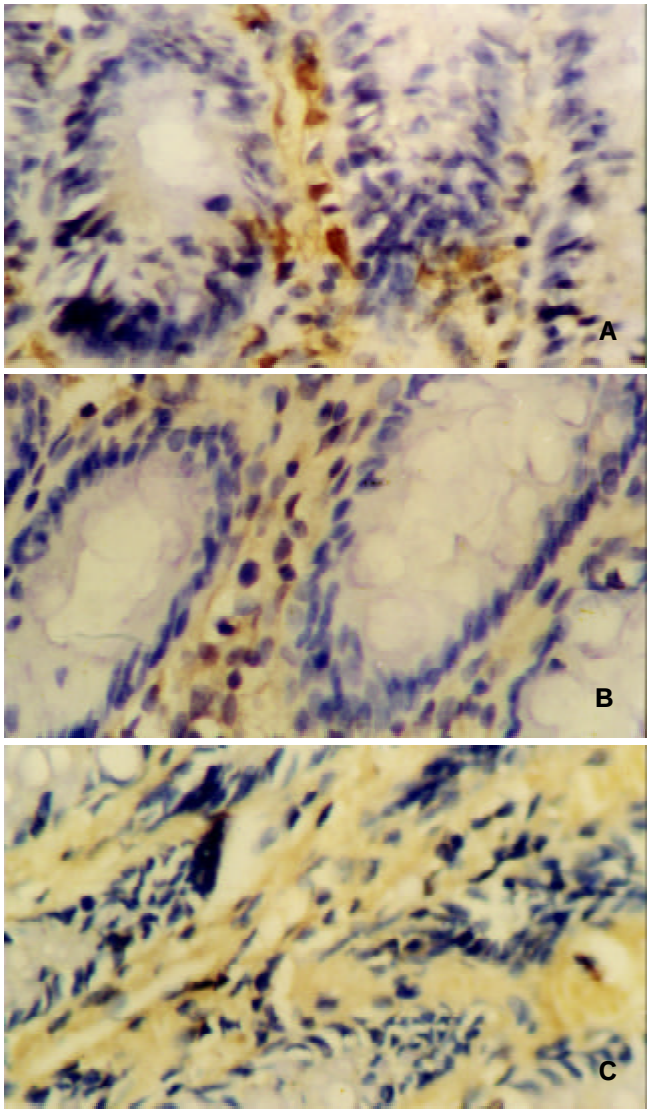

Figure 3 Expressions of iNOS (A), COX-2 (B) and NF-κB p65 (C) were significantly decreaed in the colonic tissue from rats with colitis induced by acetic acid enema after treasted with 800 $mg\cdot kg^{-1}$ ASP, respectively. The weakly positive staining could be found. SP stain ×400.

SF reduces the expression of colonic NOS, COX-2 and NF-κB p65

As shown in Figure 1, 2 and 3, the expressions of colonic NOS, COX-2 and NF-κB p65 proteins were observed to be significantly increased in animals clystered with acetic acid compared with the normal controls (P<0.01), which were ameliorated significantly in a dose-dependent manner as the animals treated with SF at the given doses (P<0.05-0.01).

DISCUSSION

Induction of colitis by acetic acid (AA) in rats is the classical method to produce an experimental model of inflammatory bowel disease (IBD). Several major causative factors in the initiation of human IBD such as exorbitant oxidative stress, enhanced vasopermeability, prolonged neutrophils infiltration and increased production of inflammatory mediators were all involved in the induction of this animal model[19,20,24]. It is therefore acknowledged nowadays that this experimental model is suitable for the investigation of IBD pathogenesis and evaluation the therapeutic agents of this disease.

In the present study, we employed this rat model to make sure whether or not the ameliorative effects of SF on the experimental colitis existed as assessed by CMDI, HS and MPO activities that were usually regarded as the main parameters to evaluate the severity of colonic inflammation in inflammatory bowel disease[19,20]. Compared with the normal control, these parameters were all significantly increased in the colonic mucosa of the model control animals induced by acetic acid (P<0.01). However, these elevated parameters were significantly ameliorated (P<0.05 or 0.01) as shown in Table 1 after the model rats were treated with SF (400, 800 $mg\cdot kg^{-1}$) or 5-ASA (100 $mg\cdot kg^{-1}$) as described in the experimental protocol, in which a therapeutic dose protocol of 800 $mg\cdot kg^{-1}$ SF was observed as effective as 100 $mg\cdot kg^{-1}$ 5-ASA in the treatment of this rat model of colitis. The results confirmed our previous speculation and strongly suggested that SF might serve as an alternative modality for the treatment of inflammatory bowel disease.

Although the pathogenesis is not known with certainty, some hypotheses have been proposed as the major causative factors contributing to inflammatory bowel disease. A large number of studies have revealed that the increase of oxidative stress and iNOS activity was a notable feature of IBD, which resulted in a pathological cascade of free radical reactions and further yielding more oxidative free radicals such as peroxynitrite ($ONOO^-$) to impair the structure and function of cells[2,25-27]. Meanwhile, excessive NO could dilate vasculature and enhance vasopermeability, as well as inactivate the activity of antioxidases such as SOD, CAT, and GSH-Px by means of reacting with hydrosulfide group (-SH) in the enzymes. Some oxidants have been known to modulate the expression of a variety of genes that are involved in the immune and inflammatory responses, which lead to the apoptosis of intestinal epithelial cells, cascades of inflammatory response and the disruption of integrity and function of the intestinal mucosa[28-30].

Abnormal metabolism of arachidonic acid is another vital factor in the IBD pathogenesis. As the crucial synthetase in the arachidonic acid metabolic pathway, COX-2 could be activated to produce excessive PGE_2 and TXB_2, two important inflammatory mediators, in the inflammatory bowel disease, which contribute to the bowel hyperemia, edema and even dysfunction. In addition, TXB_2 could also induce platelet aggregation, vasoconstriction and microthrombosis, aggravating the inflammatory reaction[31-35]. Administration of either COX-2 or thromboxane synthase inhibitors has been shown to be useful for the treatment of IBD[32-34].

Recently, plenty of literatures reported that NF-κB played a critical role in the early transcriptional changes of various immunoregulatory genes[28, 36], whose activation and increased expression have been demonstrated to be involved in the pathogenesis of inflammatory bowel disease[37]. Activated NF-κB could promote the production of various inflammatory factors, chemotaxins, cytokines, and adhesive factors, and the expression of iNOS and COX-2, which interact further with each other and lead to an uncontrollable cascade of inflammatory response[38-41]. NF-κB could also activate anti-apoptotic genes

including TNF receptor related genes (TRAF1, TRAF2), Bcl-2 homologens (A1/Bfl-1, IEX-1L), and repress the apoptosis of some inflammatory cells such as neutrophils and activated macrophages, thereby elongating and worsening tissue inflammatory injury[42-45]. In the NF-κB family, p65 is the major functional subunit, and an antisense oligonucleotide to NF-kappa B p65 has been shown to ameliorate inflammation even after induction of colitis[1].

To elucidate the mechanisms underlying the therapeutic effects of SF on this rat model of colitis, we observed simultaneously the changes of these oxidative and inflammatory variables mentioned above in the colonic tissue after SF therapy. The results revealed that the SOD activity, MDA and NO levels, PGE_2 and TXB_2 contents, as well as the expressions of iNOS, COX-2 and NF-κB p65 proteins in the colonic mucosa were significantly ameliorated in the rats treated locally with SF at the given dose protocols, especially at the 400 mg· kg^{-1} and 800 mg· kg^{-1} doses, compared with that in model control animals (P<0.05-0.01). Taken together, these observations suggest the anti-oxidative stress and anti-inflammatory response are the fundamentals of SF action in the therapy of IBD, although the ameliorating effects of SF might be involved in other multiple mechanisms.

In summary, the results of this study show that intracolonic treatment with SF at 400 mg· kg^{-1} and 800 mg· kg^{-1} dose protocols can ameliorate the pathological changes of experimental colitis in rats, which suggests that SF may serve as an effective therapeutic agent for the treatment of IBD.

REFERENCES

1 **Hibi T,** Inoue N, Ogata H, Naganuma M. Introduction and overview: recent advances in the immunotherapy of inflammatory bowel disease. *J Gastroenterol* 2003; **38**(Suppl 15): 36-42

2 **Pavlick KP,** Laroux FS, Fuseler J, Wolf RE, Gray L, Hoffman J, Grisham MB. Role of reactive metabolites of oxygen and nitrogen in inflammatory bowel disease. *Free Radic Biol Med* 2002; **33:** 311-322

3 **Lakatos L.** Immunology of inflammatory bowel diseases. *Acta Physiol Hung* 2000; **87:** 355-372

4 **Travis S.** Recent advances in immunomodulation in the treatment of inflammatory bowel disease. *Eur J Gastroenterol Hepatol* 2003; **15**: 215-218

5 **Tuvlin JA,** Kane SV. Novel therapies in the treatment of ulcerative colitis. *Expert Opin Investig Drugs* 2003; **12:** 483-490

6 **Goh J,** O'Morain CA. Nutrition and adult inflammatory bowel disease. *Aliment Pharmacol Ther* 2003; **17:** 307-320

7 **Hanauer SB.** Update on medical management of inflammatory bowel disease: ulcerative colitis. *Rev Gastroenterol Disord* 2001; **1:** 169-176

8 **Kane SV.** Novel therapies in the treatment of ulcerative colitis. *Expert Opin Investig Drugs* 2001; **10:** 1223-1229

9 **Das KM,** Farag SA. Current medical therapy of inflammatory bowel disease. *World J Gastroenterol* 2000; **6:** 483-489

10 **Schroder O,** Stein J. Low dose methotrexate in inflammatory bowel disease: current status and future directions. *Am J Gastroenterol* 2003; **98:** 530-537

11 **Holtmann MH,** Galle PR, Neurath MF. Immunotherapeutic approaches to inflammatory bowel diseases. *Expert Opin Biol Ther* 2001; **1:** 455-466

12 **Rampton DS.** Management of difficult inflammatory bowel disease: where are we now? *World J Gastroenterol* 2000; **6:** 315-323

13 **Kikuzaki H,** Hisamoto M, Hirose K, Akiyama K, Taniguchi H. Antioxidant properties of ferulic acid and its related compounds. *J Agric Food Chem* 2002; **50:** 2161-2168

14 **Ogiwara T,** Satoh K, Kadoma Y, Murakami Y, Unten S, Atsumi T, Sakagami H, Fujisawa S. Radical scavenging activity and cytotoxicity of ferulic acid. *Anticancer Res* 2002; **22:** 2711-2717

15 **Zhang ZH,** Yu SZ, Li GS, Zhao BT. Influence of sodium ferulate on human netrophil-derived oxygen metabolites. *Zhongguo Yaolixue Tongbao* 2001; **17:** 515-517

16 **Li YQ,** Zhang JS, Cai HW. Influence of sodium ferulate on MDA, SOD, ET and NO during myocardial ischemia and reperfusion injury. *Zhonghua Mazuixue Zazhi* 1998; **18:** 688-690

17 **Xu LN,** Yu WG, Tian JY, Liu QY. Effect of sodium ferulate on arachidonic acid metabolism. *Yaoxue Xuebao* 1990; **25:** 412-416

18 **Wang Z,** Gao YH, Huang RS, Zhu GQ. Sodium ferulate is an inhibitor of thromboxane A_2 synthetase. *Zhongguo Yaoli Xuebao* 1988; **9:** 430-433

19 **Millar AD,** Rampton DS, Chander CL, Claxson AW, Blades S, Coumbe A, Panetta J, Morris CJ, Blake DR. Evaluating the antioxidant potential of new treatments for inflammatory bowel disease using a rat model of colitis. *Gut* 1996; **39:** 407-415

20 **Deng CH,** Xia B, Chen DJ, Zhou Y, Gong TT, Guao ZQ. The mucosa protective effects of superoxide dismutase on rats colitis induced by acetic acid. *Zhongguo Bingli Shengli Zazhi* 1994; **10:** 23-25

21 **Raab Y,** Sundberg C, Hallgren R, Kuntson L, Gerdin B. Mucosal synthesis and release of prostaglandin E_2 from activated eosinophils and macrophages in ulcerative colitis. *Am J Gastroenterol* 1995; **90:** 614-620

22 **Taniguchi T,** Tsukada H, Nakamura H, Kodama M, Fukuda K, Tominaga M, Seino Y. Effects of a thromboxane A_2, receptor antagonist in an animal model of inflammatory bowel disease. *Digestion* 1997; **58:** 476-478

23 **Linnoila RI,** Jensen SM, Steinberg SM, Mulshine JL, Eggleston JC, Gazdar AF. Peripheral airway cell marker expression in non-small cell lung carcinoma. Association with distinct clinicopathologic features. *Am J Clin Pathol* 1992; **97:** 233-243

24 **Li L,** Wang ZL, Ke JT, Zhang M, Shao JF, Zhong CN. Select animal models for experimental colitis model. *Shijie Huaren Xiaohua Zazhi* 2001; **9:** 584-585

25 **Krieglstein CF,** Cerwinka WH, Laroux FS, Salter JW, Russell JM, Schuermann G, Grisham MB, Ross CR, Granger DN. Regulation of murine intestinal inflammation by reactive metabolites of oxygen and nitrogen: divergent roles of superoxide and nitric oxide. *J Exp Med* 2001; **194:** 1207-1218

26 **Zhou JF,** Cai D, Zhu YG, Yang JL, Peng CH, Yu YH. A study on relationship of nitric oxide, oxidation, peroxidation, lipoperoxidation with chronic chole-cystitis. *World J Gastroenterol* 2000; **6:** 501-507

27 **Wang QG,** He LY, Chen YW, Hu SL. Enzymohistochemical study on burn effect on rat intestinal NOS. *World J Gastroenterol* 2000; **6:** 421-423

28 **Jourd'heuil D,** Morise Z, Conner EM, Grisham MB. Oxidants, transcription factors, and intestinal inflammation. *J Clin Gastroenterol* 1997; **25**(Suppl 1): S61-S72

29 **Banan A,** Fields JZ, Zhang Y, Keshavarzian A. iNOS upregulation mediates oxidant-induced disruption of F-actin and barrier of intestinal monolayers. *Am J Physiol Gastrointest Liver Physiol* 2001; **280:** G1234-G1246

30 **Huycke MM,** Abrams V, Moore DR. Enterococcus faecalis produces extracelluar superoxide and hydrogen peroxide that damages colonic epithelial cell DNA. *Carcinogenesis* 2002; **23:** 529-536

31 **McCowen KC,** Ling PR, Bistrian BR. Arachidonic acid concentrations in patients with Crohn disease. *Am J Clin Nutr* 2000; **71:** 1008

32 **Carty E,** Macey M, McCartney SA, Rampton DS. Ridogrel, a dual thromboxane synthase inhibitor and receptor antagonist: anti-inflammatory profile in inflammatory bowel disease. *Aliment Pharmacol Ther* 2000; **14:** 807-817

33 **Karmeli F,** Cohen P, Rachmilewitz D. Cyclo-oxyenase-2 inhibitors ameliorate the severity of experimental colitis in rats. *Eur J Gastroenterol Hepatol* 2000; **12:** 223-231

34 **Kankuri E,** Vaali K, Korpela R, Paakkari I, Vapaatalo H, Moilanen E. Effects of a COX-2 preferential agent nimesulide on TNBS-induced acute inflammation in the gut. *Inflammation* 2001; **25:** 301-310

35 **Wu JX,** Xu JY, Yuan YZ. Effect of emodin and sandostatin on metabolism of eicosanoids in acute necrotizing pancreatitis. *World J Gastroenterol* 2000; **6:** 293-294

36 **Shi XZ,** Lindholm PF, Sarna SK. NF-kappa B activation by oxi-

dative stress and inflammation suppresses contractility in colonic circular smooth muscle cells. *Gastroenterology* 2003; **124:** 1369-1380

37 **Gan H,** Ouyang Q, Chen Y, Xia Q. Activation of nuclear factor-kappaB and effects of anti-inflammatory treatment thereon in intestinal mucosa of patients with ulcerative colitis. *Zhonghua Yixue Zazhi* 2002; **82:** 384-388

38 **Surh YJ,** Chun KS, Cha HH, Han SS, Keum YS, Park KK, Lee SS. Molecular mechanisms underlying chemopreventive activities of anti-inflammatory phytochemicals: down-regulation of COX-2 and iNOS through suppression of NF- kappa B activation. *Mutat Res* 2001; **480-481:** 243-268

39 **Yamamoto Y,** Gaynor RB. Therapeutic potential of inhibition of the NF-kappaB pathway in the treatment of inflammation and cancer. *J Clin Invest* 2001; **107:** 135-142

40 **Jobin C,** Sartor RB. NF-kappaB signaling proteins as therapeutic targets for inflammatory bowel diseases. *Inflamm Bowel Dis* 2000; **6:** 206-213

41 **Wulczyn FG,** Krappmann D, Scheidereit C. The NF-κB/Rel and IkB gene families: mediators of immune response and inflammation. *J Mol Med* 1996; **74:** 749-769

42 **Sahnoun Z,** Jamoussi K, Zeghal KM. Free radicals and antioxidants: physiology, human pathology and therapeutic aspects (part II). *Therapie* 1998; **53:** 315-339

43 **Petranka J,** Wright G, Forbes RA, Murphy E. Elevated calcium in preneoplastic cells activates NF-kappa B and confers resistance to apoptosis. *J Biol Chem* 2001; **276:** 37102-37108

44 **Potoka DA,** Upperman JS, Nadler EP, Wong CT, Zhou X, Zhang XR, Ford HR. NF-kappa B inhibition enhances peroxynitrite-induced enterocyte apoptosis. *J Surg Res* 2002; **106:** 7-14

45 **Teresa Bengoechea-Alonso M,** Pelacho B, Oses-Prieto JA, Santiago E, Lopez-Moratalla N, Lopez-Zabalza MJ. Regulation of NF-kappa B activation by protein phosphatase 2B and NO, via protein kinase A activity, in human monocytes. *Nitric Oxide* 2003; **8:** 65-74

Edited by Zhu L and Wang XL

P.O.Box 2345, Beijing 100023,China
Fax: +86-10-85381893
E-mail: wjg@wjgnet.com www.wjgnet.com

World J Gastroenterol 2003;9(11):2539-2543
World Journal of Gastroenterology
 ISSN 1007-9327

• BASIC RESEARCH •

Purification and characterization of 33.5 kDa vesicular protein in human bile

Jian-Bin Xiang, Duan Cai, Bao-Jin Ma, Xi-Liang Cha, Li-Ying Wang, Han-Qing Mo, Yan-Ling Zhang

Jian-Bin Xiang, Duan Cai, Bao-Jin Ma, Yan-Ling Zhang, Department of General Surgery, Huashan Hospital, Fudan University, Shanghai 200040, China
Xi-Liang Cha, Li-Ying Wang, Han-Qing Mo, Department of Biochemistry, Fudan University, Shanghai 200032, China
Supported by the National Natural Science Foundation of China, No.30070737
Correspondence to: Jian-Bin Xiang, Department of General Surgery, Huashan Hospital, Fudan University, Shanghai 200040, China. xjbzhw@yahoo.com.cn
Telephone: +86-21-62489999-6484 **Fax:** +86-21-62489743
Received: 2003-05-11 **Accepted:** 2003-06-07

Abstract

AIM: The present study was undertaken to purify and partially characterize the 33.5-kilodalton (33.5 kDa) vesicular protein in human bile and to explore the possible molecular mechanisms of the initial crystal nucleation process.

METHODS: The 33.5 kDa vesicular protein was isolated by ultracentrifugation and further purified by sodium dodecyl sulfate-polyacrylamide gel electrophoresis (SDS-PAGE) under nonreducing conditions. The purified 33.5 kDa vesicular protein was subjected to N-terminal amino acid sequencing and amino acid analysis. Cholesterol crystallization activity was detected by cholesterol crystal growth assay. The sugar chain of the 33.5 kDa vesicular protein was analyzed by dot-immunobinding assay of lectin coupled to a peroxidase (HRP-DSA, HRP-ConA, HRP-WGA) and was deglycosylated using two different enzymatic approaches (*N*-deglycosylation and *O*-deglycosylation) to determine the molecular weight of the protein component, the type of linkage between polypeptide and carbohydrate components.

RESULTS: The 33.5 kDa vesicular protein with complicated glycan was an extensively glycosylated (37.3 %) monomer and these sugar chains strongly bound to DSA, but did not bind to ConA. Amino acid sequencing indicated that the protein was unique. The 33.5 kDa vesicular protein exhibited potent cholesterol crystallization promoting activity *in vitro* with derived crystal growth curve indices It, Ig, Ic presented as 0.57, 1.52, and 1.63 respectively. Both enzymatic proteolysis and *N*-deglycosylation of the protein removed all activity.

CONCLUSION: These data suggest the 33.5 kDa vesicular protein may be responsible for the pathogenesis of cholesterol gallstone disease, and the sugar chains play an important role in pro-nucleating process.

Xiang JB, Cai D, Ma BJ, Cha XL, Wang LY, Mo HQ, Zhang YL. Purification and characterization of 33.5 kDa vesicular protein in human bile. *World J Gastroenterol* 2003; 9(11): 2539-2543
http://www.wjgnet.com/1007-9327/9/2539.asp

INTRODUCTION

Cholesterol nucleation process represents a critical step in the cholesterol gallstone formation. Cholesterol pro-nucleating and anti-nucleating proteins can accelerate or retard the rate of cholesterol crystallization in supersaturated bile, and thus may play important roles in cholesterol crystallization[1-3]. From 1988, both inhibitors and promoters of cholesterol crystallization have been isolated from human bile and characterized[4-7]. The major cholesterol crystallization promoting activity was localized at the concanavalin A-binding fraction of biliary glycoproteins (CABG). These proteins include mucin[8], immunoglobulins[9-11], α_1-acid protein[12], aminopeptidase N[4], low-density protein-lipid complex[5,13], and some unidentified proteins such as 70 kDa[14] and 200 kDa[15] pro-nucleating glycoproteins. Abei *et al*[16] provided comparative data regarding the relative potency of these different glycoprotein promoters and found that α_1-acid protein accounted for the greatest portion (33 %) of the net biliary Con A-bound promoting activity derived from currently defined and well-identified glycoproteins. But still more than 60 % of total Con A-bound promoting activity remains unaccounted for. It was speculated that there was still some other more important proteins involved in cholesterol nucleation process.

Lecithin vesicles are the primary cholesterol carriers in bile supersaturated with cholesterol and have been shown to play an important role in the nucleation of cholesterol. This nucleation takes place after aggregation and fusion of cholesterol-rich biliary vesicles, a process modulated by biliary proteins. Miquel *et al*[17] found a potent cholesterol pro-nucleating activity in purified biliary vesicles. Further study demonstrated that this activity was related with specific vesicular proteins including immunoglobulins IgA, IgG and IgM[18].

In this study, a novel 33.5 kDa vesicular protein obtained from human gallbladder bile of cholesterol gallstone patients was isolated, purified and partially characterized. We attempted to determine whether pro-nucleating activity occurred in the 33.5 kDa vesicular protein and to detect whether the protein was lectin-specific. Our results showed that the 33.5 kDa vesicular protein exhibited potent pro-nucleating activity *in vitro*, which depends on intact structure of peptide and sugar chain, and especially bound DSA lectin.

MATERIALS AND METHODS

Materials

Sodium salts of taurocholic(STC) and taurodeoxycholic (STDC) greater than 99 % purity, cholesterol(CH), egg lecithin and Tween 20 were obtained from Fluka Company. Metrizamide, nitrocellulose sheets, and all the chemicals for SDS-PAGE were obtained from Sigma Chemical Co. Datura stramonium agglutinin (DSA), wheat germ agglutinin (WGA), concanavalin A(Con A), peroxidase(HRP), and Sephadex G150 were also from Sigma Chemical Co. Periodic acid($NaIO_4$) was purchased from Wako Pure Chemical. *N*-glycosidase F, endo-α-N-acetyl-galactosaminidase, neuraminidase, and *Pronase K* were purchased from Boehringer Mannheim Corp., Germany, and 0.22 μm micropore filters were obtained from Millipore Corp., Bedford, MA. USA.

Methods

Patients and bile collection All patients gave written informed consent to participate in the study, which was approved by the ethical committee. Gallbladder bile was obtained from three patients by directly puncturing the gallbladder with a sterile 19G needle at cholecystectomy for cholelithiasis. The bile (20 ml) was immediately transported to the laboratory and stored at -80 ℃ until processed.

Protein purification procedure Pooled bile specimens were separated on a molecular sieving chromatography column (BioGel A-5m, 5×100 cm), eluted with 10 mmol/L Tris-HCl buffer to remove soluble mucin glycoprotein. The main fraction was centrifuged at 10 000 rev/min for 10 minutes at room temperature. The upper fraction was filtered through 0.22 μm micropore filters, and metrizamide (13 % w/v) was directly dissolved in the elution and centrifuged at 45 000 rev/min for 3.5 h at 10 ℃ in a Vti-50 vertical rotor (Beckman Instruments Inc., USA). The top opalescent vesicular fraction was collected by tube puncturing and loaded on SDS-PAGE under nonreducing conditions. The 33.5 kDa vesicular protein lane was resected according to the protein marker position and dialyzed in Tris-HCl buffer and concentrated as Ma *et al*[19] described.

SDS-PAGE SDS-PAGE(5-12 %) was developed in a buffer system described by Laemmli[20]. Aliquots (100 μl) of protein and bile samples were resolubilized with a sample buffer (60 mmol/L Tris-HCl, 2 % SDS, 10 % glycerol, pH 6.8). On completion of the electrophoretic run, gels were fixed in a 50 % methanol, 10 % acidic acid solution for 6 h and stained with Coomassie blue.

Preparation of lectin-HRP conjugate The lectin-HRP conjugate of DSA-HRP, WGA-HRP and Con A-HRP was made according to Guo *et al*[21]. Briefly, 5 mg HRP was dissolved in 0.5 ml distilled water, then added with 0.5 ml 60 mmol/L $NaIO_4$ and kept at 4 ℃ for 30 minutes. Five mg lectin such as DSA, WGA and Con A was mixed with HRP and 0.1 mol/L α-methyl mannose for Con A, and N-acetylglucosamine for DSA and WGA was added to protect the glycan binding site of the lectin. The reaction mixture was dialyzed in 50 mmol/L carbonate buffer (pH 9.5) and centrifuged at 4 000 rev/min for 10 minutes. The supernatant was removed and the pellet was dissolved and dialyzed in sodium phosphate buffer (20 mmol/L, pH 7.4).

Lectin affinity staining Five, 10, 15 μg/ml of purified 33.5 kDa vesicular proteins were blotted to nitrocellulose membrane respectively. The membrane was blocked with 1 % BSA overnight at 37 ℃. Subsequent incubation of the membrane with 1:500 peroxidase-labeled Datura stramonium agglutinin (DSA), wheat germ agglutinin (WGA), concanavalin A(Con A) in the same solution was followed by washing three times in the TTBS buffer (0.05 % Tween 20, 0.1 mol/L Tris-HCl, pH7.5) and chemiluminescent detection.

Amino acid analysis The purified 33.5 kDa vesicular protein was hydrolyzed for 16 hours at 115 ℃ in 6 N HCl/0.2 % phenol containing norleucine as an internal standard. After incubation, samples were dried and redissolved in 100 μl of NaS sample dilution buffer (Beckman Instruments Inc., USA) and run on a Beckman model 7300 Amino Acid Analyzer.

Amino acid sequencing The amino-terminal sequences of the 33.5 kDa vesicular protein were subjected to N-terminal amino acid sequencing with an automated sequencer (model 477A: Protein Sequencer, Applied Biosystems). Determined sequences were compared with those well-identified glycoproteins in the Pub-Med NCBI human gene bank database.

Enzymatic deglycosylation The 33.5 kDa vesicular protein was treated with *N*-glycanase enzyme according to supplier's specifications based on the work of Elder and Plummer *et al*[22,23]. Five hundred μg 33.5 kDa vesicular protein boiled for 5 minutes was diluted with 0.1 mmol/L sodium phosphate buffer, pH 8.6, 10 mmol/L 1, 10-phenanthroline, and then mixed with 10 U *N*-glycanase, and the reaction mixture was incubated for 24 h at 37 ℃. The molecular weight of deglycosylated polypeptide backbone was then detected using SDS-PADE.

In the *O*-deglycosylation study, the vesicular protein was diluted with 10 mmol/L calcium acetate, 20 mmol/L sodium cacodylate buffer (pH 7.0) and was incubated with 10 U/ml of neuraminidase for 12 h at 37 ℃. This was followed by further incubation with 2 U/ml of endo-α-N-acetyl-galactosaminidase for 12 h at 37 ℃. Finally, the mixture was examined using SDS-PAGE.

Proteolysis studies One hundred μg of 33.5 kDa vesicular protein was dissolved in 50 μl ammonium bicarbonate (25 mmol/L, pH 11), and then incubated with 1.5 U *Pronase K* for 24 h at 37 ℃. After incubation, the sample was concentrated and loaded on SDS-PAGE.

Cholesterol crystal growth assay Supersaturated model bile was prepared with a cholesterol saturation index of 1.4, a total lipid concentration of 125 g/L, and a bile acid/phospholipid ratio of 4.4. This model bile was made as Busch *et al*[24,25] described. In brief, this lipid mixture was evaporated to dryness, lyophilized, and then resolubilized with 20 mmol/L Tris-HCl/150 mmol/L NaCl (TBS), pH 7.4 at 55 ℃. After filtration (0.22 μm), 25 μl of this model bile mixed with 50 μg protein or its enzymatic samples was diluted with 475 μl TBS/10 mmol/L STDC solution. After 20 minutes, absorbance at a single wavelength within the visible range (700 nm) was sequentially measured. The cholesterol crystal growth curves of the supersaturated model bile without (control) and with (experimental) protein samples were thus generated for each sample. The three growth curve parameters were derived: growth index Ig=maximal slope of experimental curve/maximal slope of control, crystal index Ic=final crystal concentration of experimental/final crystal concentration of control, time index It=onset time of experimental/onset time of control.

Statistical analysis

The cholesterol crystal growth curves were compared by using analysis of variance (ANOVA) at each time to determine whether difference existed between the study groups. When the ANOVA was statistically significant ($P<0.05$), the Dunnett's multiple comparison procedure was made to compare each of the study groups to the control group.

RESULTS

Purification and identification of novel 33.5 kDa glycoprotein

The bile was divided into three fractions after ultracentrifugation (Figure 1). The top opalescent vesicular fraction was collected by tube puncture and the targeted vesicular protein was further separated by SDS-PAGE. The protein profile from three different gallstone patients with Coomassie blue staining is shown in Figure 2. The protein marker is shown at lane 1 and a single band of 33.5 kDa protein at lanes 2-4 on SDS-PAGE was stained under nonreducing condition. Amino acid analysis of the purified glycoprotein showed that the protein was composed of 153 amino acid residues of which almost one third were the following amino acids: glutamine/glutamic acid and asparagines/aspartic acid (Table 1). N-amino-terminal sequencing of the protein showed H_2N-Asp-Asn-Ser-Gln-His-Arg-Tyr-Val-Phe-Ile, which was different from α_1-acid protein, Ig, aminopeptidase N and phospholipase C. Lectin staining showed higher affinity for *Datura stramonium agglutinin* (DSA) than for wheat germ agglutinin (WGA) and concanavalin A(Con A)(Figure 3). *N*- deglycosylation studies showed disappearance of the original 33.5 kDa protein and the presence of a new 21kDa band on SDS-PAGE (Figure 4), indicating

the protein was heavily glycosylated (37.3 %) and the connection mode between polypeptide and carbohydrate components was *N*-linkage. Proteolysis studies showed the protein was sensitive to *Pronase K* digestion.

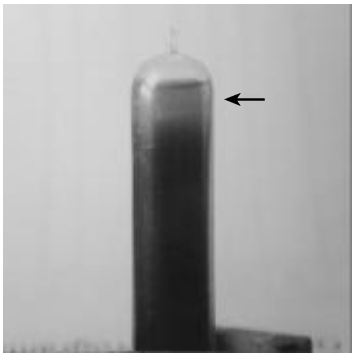

Figure 1 Pretreated bile centrifuged at 45 000 rev/min and divided into three fractions. Horizontal arrows indicate the vesicular phase bile.

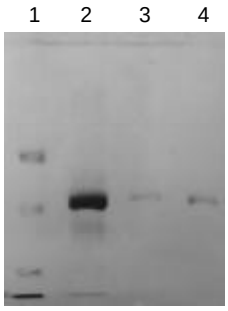

Figure 2 Purified 33.5 kDa vesicular proteins from three different bile samples run on SDS-PAGE. Lane 1: protein marker, Lanes 2-4: the 33.5 kDa vesicular protein.

Table 1 Amino acid composition of 33.5 kDa vesicular protein

Amino acid	nmol/total protein	No. of residues/mol protein
Asp/Asn	6.761	19
Thr	4.488	13
Ser	1.589	5
Glu/Gln	10.434	30
Gly	2.242	6
Ala	2.864	8
Val	2.501	7
Ile	3.226	9
Leu	4.782	14
Tyr	1.937	6
Phe	2.966	8
Lys	4.777	14
His	0.840	2
Arg	2.645	8
Pro	1.411	4
NH_2	11.297	32
Total	64.76	153

Cholesterol crystal growth assay

Figure 5 depicts the promoting effect of 33.5 kDa vesicular protein on cholesterol crystal growth curve at the concentration of 100 μg/ml. The protein strongly promoted cholesterol crystallization, accelerated the onset and increased the total quantity of crystal plates with derived crystal growth curve indices It, Ig, Ic presented as 0.57, 1.52, 1.63 respectively. But no promoting activity was detected in the same supersaturated model bile after incubation with *N*-glycanase enzyme or complete protein degradation (Table 2).

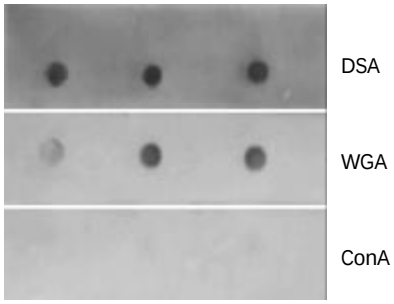

Figure 3 Lectin affinity staining with DSA, WGA, Con A labeled with peroxidase. The 33.5 kDa vesicular protein was strongly connected with DSA, and weakly bound to WGA, but did not react with Con A.

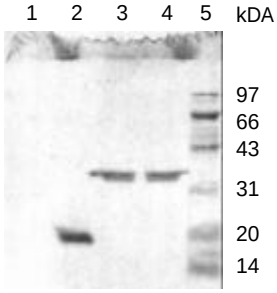

Figure 4 SDS-PAGE (reduced condition) of the 33.5 kDa vesicular protein after *N*-deglycosylation, *O*-deglycosylation and proteolysis. Complete disappearance was observed after incubation with *Pronase K* at lane 1. A single 21 kDa band was stained after treated with *N*-glycanase at lane 2, but no change of the protein after enzymatic *O*-deglycosylation at lane 3. The band of lane 4 and lane 5 represented the 33.5 kDa vesicular protein and protein marker respectively.

Table 2 Effect of 33.5 kDa vesicular protein on activity indices of cholesterol crystallization (100 μg/ml)

	It	Ig	Ic	*P* value
Purified 33.5 kDa protein	0.57	1.52	1.63	<0.05[a]
+ *N*-deglycosylation	1.08	1.01	0.98	<0.05[b]
+ *O*-deglycosylation	0.58	1.61	1.54	<0.05[a]
+ Proteolysis	1.12	0.87	0.99	<0.05[b]

a: compared with control, b: compared with 33.5 kDa vesicular protein group.

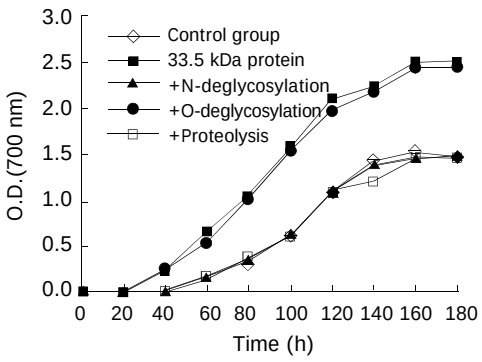

Figure 5 Promoting effect of 33.5 kDa vesicular protein and its enzymatic products on cholesterol crystal growth curves in model bile (TL=125 g/L, BA/PL=4.4, CSI=1.4). All curves are given as the mean ±SD, n=4. P<0.05 *vs* control at each time.

DISCUSSION

Since the first report of the presence of pro-nucleating activity in cholesterol patient' s bile by Burnstein *et al*[26], many groups have tried to purify and identify the active protein-related components[16,17,25,27,28]. Of particular interest are the presence and role of concanavalin A-binding fraction of biliary glycoproteins (CABG), which have a potent cholesterol crystallization-promoting activity. Proteins thought to explain this activity included α_1-acid protein[12], immunoglobulins[9-11], aminopeptidase N[4,6], and a pronase resistant carcinoembryonic antigen-related cell adhesion molecule 1 most recently described by Jirsa *et al*[29], and some unidentified proteins such as 200 kDa pro-nucleating glycoprotein[15]. But still most of the activity has not been identified[30]. In this study we purified and characterized a novel promoting-nucleation glycoprotein with molecular weight of 33.5 kDa in vesicular bile of cholesterol gallstone patients. In 1992, Miquel *et al*[17] isolated and purified human vesicles with potent cholesterol-nucleation-promoting activity, and found that this protein-related activity belonged to immunoglobulins. Although they were from the same vesicular bile, the difference between the immunoglobulin family of glycoprotein and the 33.5 kDa vesicular protein was obvious. We took considerable care to rule out the possibility that the present glycoprotein shared similar features with the immunoglobulins. First, the potent cholesterol-nucleation-promoting vesicular protein had a strong activity of accelerating the onset and increasing the total quantity of crystals appearance and was unique to have a high affinity for *Datura stramonium agglutinin* (DSA), and did not bind to *concanavalin A* (Con A). This was different from the previously described promoting-nucleation glycoprotein. Amino acid sequencing study further demonstrated that the 33.5 kDa vesicular protein with N-amino-terminal sequencing of H_2N-Asp-Asn-Ser-Gln-His-Arg-Tyr-Val-Phe-Ile, was a novel glycoprotein from vesicular bile.

In additional experiments, the 33.5 kDa vesicular protein could not only accelerate onset of nucleation, but also induce rapid cholesterol crystallization growth. We speculate the factor identified in this study may play an important role in the initial stage of the gallstone formation. To study the underlying mechanism and pathophysiological significance of the peptide and carbohydrate moiety, the 33.5 kDa vesicular protein was treated with glycanase enzyme and p*ronase* respectively. Incubation with *N*-glycanase resulted in disappearance of the original 33.5-kilodalton band and presence of a strong 21-kilodalton band on SDS-PAGE, and no cholesterol crystallization promoting activity of 33.5 kDa vesicular protein was detected in supersaturated model bile. It suggested that the sugar chain might be responsible for the promoting-nucleation activity. This striking characteristic of the vesicular protein was very similar to α_1-acid protein. Abei *et al*[12] reported that α_1-acid protein was 37 % glycosylated with mannose, sialic acid content, and some other multiple antennae and the carbohydrate moiety were essential to the promoting activity of glycoprotein. In addition, vesicular glycoprotein was completely degradated and no promoting activity existed after proteolytic digestion.

In conclusion, our results indicate that, the 33.5 kDa vesicular protein with complicated glycan and high affinity for DSA, is a novel and unique pro-nucleating glycoprotein, which exhibits potent cholesterol crystallization promoting activity *in vitro*. However, further studies are needed to evaluate the predictive value, concentration, relative potency and origin of the 33.5 kDa vesicular protein before we can ascertain its specific role in the pathogenesis of cholesterol gallstone disease.

ACKNOWLEDGMENTS

The skillful technical assistance of Dr. Chuan Xin Huang and Dr. Jia Da Li is gratefully acknowledged.

REFERENCES

1 **Miquel JF**, Van Der Putten J, Pimentel F, Mok KS, Groen AK. Increased activity in the biliary Con A-binding fraction accounts for the difference in crystallization behavior in bile from Chilean gallstone patients compared with Dutch gallstone patients. *Hepatology* 2001; **33**: 328-332
2 **Nunes DP**, Afdhal NH, Offner GD. A recombinant bovine gallbladder mucin polypeptide binds biliary lipids and accelerates cholesterol crystal appearance time. *Gastoenterology* 1999; **116**: 936-942
3 **Luk AS**, Kaler EW, Lee SP. Protein lipid interaction in bile: effects of biliary proteins on the stability of cholesterol-lecithin vesicles. *Biochim Biophys Acta* 1998; **1390**: 282-292
4 **Groen AK**, Noordam C, Drapers JA, Egbers P, Jansen PL, Tytgat GN. Isolation of a potent cholesterol nucleation-promoting activity from human gallbladder bile: role in the pathogenesis of gallstone disease. *Hepatology* 1990; **11**: 525-533
5 **Zijlstra AI**, Offner GD, Afdhal NH, van Overveld M, Tytgat GN, Groen AK. The pronase resistance of cholesterol-nucleating glycoproteins in human bile. *Gastroenterology* 1996; **110**: 1926-1935
6 **Nunez L**, Amigo L, Mingrone G, Rigotti A, Puglielli L, Raddatz A, Pimentel F, Greco AV, Gonzalez S, Garrido J, Miquel JF, Nervi F. Biliary aminopeptidase-N and the cholesterol crystalliszation defect in cholelithiasis. *Gut* 1995; **37**: 422-426
7 **Groen AK**, Stout JP, Drapers JA, Hoek FJ, Grijm R, Tytgat GN. Cholesterol nucleation-influencing activity in T-tube bile. *Hepatology* 1988; **8**: 347-352
8 **Gallinger S**, Taylor RD, Harvey PR, Petrunka CN, Strasberg SM. Effect of mucous glycoprotein on nucleation time of human bile. *Gastoenterology* 1985; **89**: 648-658
9 **Harvey PR**, Upadhya GA, Strasberg SM. Immunoglobulins as nucleating proteins in the gallbladder bile of patients with cholesterol gallstones. *J Biol Chem* 1991; **266**: 13996-14003
10 **Upadhya GA**, Harvey PR, Strasberg SM. Effect of human biliary immunoglobulins on the nucleation of cholesterol. *J Biol Chem* 1993; **268**: 5193-5200
11 **Busch N**, Lammert F, Matern S. Biliary secretory immunoglobulin A is a major constituent of the new group of cholesterol crystal-binding proteins. *Gastroenterology* 1998; **115**: 129-138
12 **Abei M**, Kawczak P, Nuutinen H, Langnas A, Svanvik J, Holzbach RT. Isolation and characterization of a cholesterol crystallization promoter from human bile. *Gastroenterology* 1993; **104**: 539-548
13 **De Bruijn MA**, Mok KS, Nibbering CP, Out T, Van Marle J, Stellaard F, Tytgat GN, Groen AK. Characterization of the cholesterol crystallization-promoting low-density particle isolated from human bile. *Gastroenterology* 1996; **110**: 1936-1944
14 **Jiao W**, Zhang YL, Cai D, Wu SQ. Isolation, purification and the characteristics of 70kDa pronucleation glycoprotein in the bile. *Zhonghua Waike Zazhi* 1994; **32**: 271-274
15 **Li F**, Cai D, Mo HQ, Zhang YL. The ELISA for the 200kDa glycoprotein in bile. *Zhonghua Xiaohua Zazhi* 1997; **17**: 333-335
16 **Abei M**, Schwarzendrube J, Nuutinen H, Broughan TA, Kawczak P, Williams C, Holzbach RT. Cholesterol crystallization-promoters in human bile: comparative potencies of immunoglobulins, α_1-acid glycoprotein, phospholipase C, and aminopeptidase N1. *J Lipid Res* 1993; **34**: 1141-1148
17 **Miquel JF**, Rigotti A, Rojas E, Brandan E, Nervi F. Isolation and purification of human biliary vesicles with potent cholesterol-nucleation-promoting activity. *Clin Sci* 1992; **82**: 175-180
18 **Miquel JF**, Nunez L, Rigotti A, Amigo L, Brandan E, Nervi F. Isolation and partial characterization of cholesterol pronucleating hydrophobic glycoproteins associated to native biliary vesicles. *FEBS Lett* 1993; **318**: 45-49
19 **Ma BJ**, Cai D, Zhang QH, Zhang YL. The potent cholesterol-nucleation activity of human biliary vesicles. *Zhonghua Gandan Waike Zazhi* 1998; **4**: 104-106
20 **Laemmli UK**. Cleavage of structural proteins during the assembly of the head of bacteriophage T_4. *Nature* 1970; **227**: 680-685
21 **Guo CX**, Guo XQ. Introducing a simple, rapid, and effective method of labeling antibody with peroxidase using periodic acid. *Shanghai Mianyixue Zazhi* 1983; **2**: 97-100
22 **Elder JH**, Alexander S. Endo-β-N-acetylglucosaminidase F:

endoglycosidase from Flavobacterium meningosepticum that cleaves both high-mannose and complex glycoproteins. *Proc Natl Acad Sci U S A* 1982; **79**: 4540-4544

23 **Plummer TH Jr**, Phelan AW, Tarentino AL. Detection and quantification of peptide-N^4-(N-acetyl-beta-glucosaminyl) asparagine amidases. *Eur J Bioche* 1987; **163**: 167-173

24 **Busch N**, Tokumo H, Holzbach RT. A sensitive method for determination of cholesterol growth using model solutions of supersaturated bile. *J Lipid Res* 1990; **31**: 1903-1909

25 **Busch N**, Matiuck N, Sahlin S, Pillay SP, Holzbach RT. Inhibition and promotion of cholesterol crystallization by protein fractions from normal human gallbladder bile. *J Lipid Res* 1991; **32**: 695-702

26 **Burnstein MJ**, Ilson RG, Petrunka CN, Taylor RD, Strasberg SM. Evidence for a potent nucleating factor in gallbladder bile of patients with cholesterol gallstones. *Gastroenterology* 1983; **85**: 801-807

27 **Chen YQ**, Zhang YL, Cai D, Hua TF, Huang JQ, Zhong CS. The actions of nucleating proteins in vesicle aggregation and fusion: a preliminary study. *Zhonghua Waike Zazhi* 1997; **35**: 181-185

28 **Afdhal NH**, Niu N, Gantz D, Small DM, Smith BF. Bovine gallbladder mucin accelerates cholesterol monohydrate crystal growth in model bile. *Gastroenterology* 1993; **104**: 1515-1523

29 **Jirsa M**, Muchova L, Draberova L, Draber P, Smid F, Kuroki M, Marecek Z, Groen AK. Carcinoembryonic antigen-related cell adhesion molecule 1 is the 85-kilodalton pronase-resistant biliary glycoprotein in the cholesterol crystallization promoting low density protein-lipid complex. *Hepatology* 2001; **34**: 1075-1082

30 **De Bruijn MA**, Mok KS, Out T, Tytgat GN, Groen AK. Immunoglobulins and α_1-acid glycoprotein do not contribute to the cholesterol crystallization-promoting effect of Concanavalin A-binding biliary protein. *Hepatology* 1994; **20**: 626-632

Edited by Zhu LH and Wang XL

P.O.Box 2345, Beijing 100023,China
Fax: +86-10-85381893
E-mail: wjg@wjgnet.com www.wjgnet.com

World J Gastroenterol 2003;9(11):2544-2547
World Journal of Gastroenterology
 ISSN 1007-9327

• BASIC RESEARCH •

Heat shock protein 90 is responsible for hyperdynamic circulation in portal hypertensive rats

Jian-Hua Ai, Zhen Yang, Fa-Zu Qiu, Tong Zhu

Jian-Hua Ai, Zhen Yang, Fa-Zu Qiu, Center for Hepatic Surgery, Tongji Hospital, Tongji Medical College, Huazhong Science and Technological University Wuhan 430030, Hubei Province, China
Tong Zhu, Institute of Organ Transplantation, Tongji Hospital, Tongji Medical College, Huazhong Science and Technological University, Wuhan 430030, Hubei Province, China
Supported by the National Natural Science Foundation of China, No.30170920
Correspondence to: Dr. Jian-Hua Ai, International Cooperation Laboratory on Signal Transduction, Eastern Hepatobiliary Surgery Institute, Second Military Medical University, Shanghai 200438, China. aijh_2000@yahoo.com
Telephone: +86-21-25070846
Received: 2003-05-10 **Accepted:** 2003-06-04

Abstract

AIM: To examine the participation of HSP90 in portal hypertensive rat mesentery *in vitro*.

METHODS: Immunohistochemistry and Western-blot were used to examine the expression of HSP90 in mesenteric vasculature. HSP90 mRNA was detected by RT-PCR, and the role of HSP90 in hyperdynamic circulation was examined by *in vitro* mesenteric perfusion studies.

RESULTS: HSP90 was overexpressed in endothelium of mesentery vasculature in animals with experimental portal hypertension induced by partial portal vein ligation (PVL) compared with normal animals. Geldanamycin (GA), a special inhibitor of HSP90 signaling, attenuated ACh-dependent vasodilation but did not affect vasodilation in response to sodium nitroprusside in normal rats. In PVL animals, the perfused mesentery was hyporesponsive to vasoconstrictor methoxamine. GA significantly potentiated methoxamine-induced vasoconstrictor after PVL.

CONCLUSION: HSP90 plays a key role in NO-dependent hyperdynamic circulation in portal hypertension and provides a novel method for future treatment of portal hypertension.

Ai JH, Yang Z, Qiu FZ, Zhu T. Heat shock protein 90 is responsible for hyperdynamic circulation in portal hypertensive rats. *World J Gastroenterol* 2003; 9(11): 2544-2547
http://www.wjgnet.com/1007-9327/9/2544.asp

INTRODUCTION

Cirrhosis of the liver, which usually develops as a long-term consequence of viral hepatitis or alcohol abuse, is a major cause of morbidity and mortality worldwide. The principal pathophysiologic feature of cirrhosis is an increase in portal pressure initiated by an increase in outflow resistance to the portal circulation. However, advanced cirrhosis was also associated with mesenteric arteriolar vasodilation[1], which contributes to portal hypertension and variceal hemorrhage by increasing portal inflow. It has been well established that portal hypertension was not a purely mechanical phenomenon[2]. There have been a large body of experimental evidences that demonstrated increased synthesis of nitric oxide (NO) in animal models of cirrhosis. Aortic cAMP, a surrogate marker of NO synthesis, was significantly elevated in CCl_4-induced cirrhosis rats compared to controls and the highest levels were observed in those with ascites[3]. Similar evidences also existed for elevated NOS activity in animal models of portal hypertension induced by partial vein ligation[4]. NO and endothelin-1-dependent increases in intrahepatic resistance in conjunction with vasodilation of splanchnic arterioles raised portal pressure and flow, thereby contributing to the vascular component of portal hypertension[5]. Indeed, the importance of splanchnic vasodilation in this process was highlighted by clinical utility of nonselective beta-blockers and octreotide, both of which could reduce splanchnic vasodilation and portal venous inflow[6]. However, cirrhotic vasculature was highly resistant to conventional vasopressors[7], and attempts to correct the hyperdynamic circulation in cirrhosis by antagonism of putative endogenous vasodilator mediators have been unsuccessful so far[8,9]. Pressure and resistance changes in perfused mesenteric vasculature occurred, in part through NO-dependent mechanisms, and in experimental portal hypertension this vascular bed demonstrated a hyporeactivity to vasoconstrictors such as methoxamine (MTX), mainly due to excessive endothelium-derived NO production[10,11].

NO is derived from L-arginine by the enzymatic action of NOS. Two isoforms of NOS have been shown to exist in the vasculature, one is a constitutively expressed and calcium-calmodulin-dependent isoform (eNOS)[12], the other is an inducible and calcium-independent isoform (iNOS)[13]. Indirect evidences for eNOS as the main source of elevated NO from studies showed that endothelial denudation could normalize vascular levels of NO[14] and reverses the hyporeactivity to vasoconstrictors[15,16] in cirrhotic rats. Several studies now suggested that eNOS was the major enzymatic source of NO overproduction[17-20] in vascular endothelium in cirrhosis. However, the molecular mechanism is still unknown. 90 kD heat shock protein (HSP90) has been found to be a molecular chaperon, and a constitutive homodimer, its main intersubunit contacted within COOH-terminal 190 residues[21]. The highly conserved 25 kD NH_2 - terminal domain of HSP90 is the binding site for geldanamycin (GA), a representative of ansamycin drugs, which specially targets HSP90[22]. HSP90 mediates the conformational regulation of a wide range of client proteins involved in signal transduction, cell proliferation and apoptosis. The recently demonstrated importance of HSP90 as an intermediate in the signaling cascades leading to activation of eNOS[23] suggested the possibility of a contributory role of this pathway in NO-dependent mesenteric vascular responses and excessive NO production in experimental portal hypertension.

The goals of this study were to examine HSP90 expression and localization in rat mesenteric microvasculature, to determine whether GA inhibited mesenteric vasodilation, and to test whether GA reversed the hyporeactivity to vasoconstrictors detected in mesenteric vasculature of portal hypertensive animals.

MATERIALS AND METHODS

Animals and reagents

Male Sprague-Dawley rats (Tongji Hospital Laboratories) weighing 250-300 g were used for experiments. Animal experiments and tissue harvesting were performed in accordance with the animal care guidelines of the institution. GA was dissolved in DMSO, and the final concentration of DMSO used in experiments was <0.006 %. MTX, ACh, and sodium nitroprusside (SNP) obtained from Sigma Chemical, were dissolved in distilled water and prepared daily.

Induction of portal hypertension

Prehepatic portal hypertension was provoked by partial portal vein ligation (PVL) as previously described[24]. In brief, rats were anesthetized, and after laparotomy, the portal vein was isolated and a stenosis created by placing a single ligature of 3-0 silk around both the portal vein and a 20-gauge blunt-tipped needle. The needle was then removed from the ligature, creating a calibrated constriction of the portal vein. In sham-operated (SO) rats, the portal vein was isolated but not ligated. Studies were performed in 24 hours fasted rats 21 days after PVL.

Immunohistochemistry

Mesenteric tissue was perfusion fixed *in situ* with 4 % paraformaldehyde, postfixed in sucrose, and embedded in OCT[25]. Frozen tissue sections were incubated overnight with HSP90 MAb, and a secondary incubation was performed with horse anti-mouse IgG for 30 min. Sections were developed with amino ethylcarbazole. Negative controls were incubated with appropriate serum substituted for the primary antibody.

RNA isolation and reverse transcriptase and polymerase chain reaction (RT-PCR)

Mesenteric tissue was harvested by dissecting and removing the highly vascular tissue situated between the mesenteric lymph nodes and small intestine. Mesenteric specimens from SO and PVL rats were immediately frozen in liquid nitrogen, then homogenated with Tripure isolation reagent to isolate total RNA. The RNA concentration in each sample was determined spectrophotometrically, and the quality of each RNA preparation was documented by visualization of 18S and 28S ribosomal bands after electrophoresis through a 1 % agarose gel. Total RNA samples were subjected to reverse transcription with Oligo-dt used as a template-primer. First strand synthesis was carried out for 1 hour at 37 ℃ in 25 μl of a reaction mixture containing 200 U M-MLV, 1 X reaction buffer, 0.5 mmol/L dNTP, 10 mmol/L DTT, 20 U RNAsin ribonuclease inhibitor and 0.25 -μg oligo-dT. The PCR primer sequences were as follow: HSP90 sense 5' GTCTGGGTATCGGAAAGCAAG3', antisense 5' CTGAGGGTTGGGGATGATGTC 3'. PCR assays contained 0.5 U Taq DNA polymerase, 0.5 μmmol/L of each oligonucleotide primer, 0.2 mmol/L dNTP, 1 X reaction buffer, 1.5 mmol/L MgCl in a final volume of 50 μl. 25 cycles were performed at 95 ℃ for 1 min, at 55 ℃ for 1 min, and at 72 ℃ for 2 min. PCR products were analyzed by electrophoresis in TAE buffer with ethidium bromide stained with (0.5 mmol/L) 2 % agarose gel. Each band was selected and used to measure the number of photons emitted.

Western blotting

Mesenteric sections were weighed and homogenized in 10 volumes of ice-cold 1 % NP-40 in 50 mM Tris (pH 8.8) buffer. The homogenates were centrifuged, and the supernatants were transferred into sterile tubes. Fifteen-microgram of protein aliquots of each sample, as determined by the Coomassie blue method, was resolved on 15 % SDS-polyacrylamide gels and transferred onto nitrocellulose membranes. The membranes were blocked with BSA before being incubated with primary antibody overnight at 4 ℃, and rinsed and then incubated for 1 h with peroxidase-conjugated secondary antibody. Immunoreactive proteins were visualized using the enhanced chemiluminescence system.

In vitro mesenteric perfusion

In vitro mesenteric perfusion was performed 14 days after PVL or after sham surgery, using the method described by McGregor and Sieber with some modifications[26]. In brief, the superior mesenteric artery (SMA) was cannulated with a PE-60 catheter and blood was removed by perfusion with 15 ml of warm Krebs solution. The gut was dissected at the mesenteric border, and the SMA with its adjoining mesenteric tissue was placed in a 37 ℃ water-jacketed container. The preparation was continuously perfused in a nonrecirculating system at a fixed rate of 4 ml/min throughout the course of the experiment with Krebs solution. Perfusion pressure was continuously monitored using a strain gauge transducer on a sidearm proximal to the perfusing cannula. The initial preparation was allowed to stabilize for 30 min, after which vehicle was infused for 15 min. Immediately after infusion of vehicle, concentration-response curves were examined in response to MTX infusion (30 and 100 μM). When a stable baseline was maintained in response to 100 μM MTX, responses to ACh boluses (0.1 ml) were examined (1 and 10 μg). All compounds were allowed to wash out over the next 50 min, after which GA was infused (3 μg/ml) for 15 min. Responses to MTX and ACh were repeated as described above. Additional experiments were performed after endothelial denudation. The denudation was achieved by combined treatment with cholic acid and distilled water as previously described[27]. In brief, after cannulation of the SMA and gentle flushing with 10 ml of warmed Krebs solution to eliminate blood, the mesentery was perfused with 1.5 ml of 0.5 % cholic acid for 10 s followed by 15 ml of warmed Krebs solution. The preparation was then transferred to a 37 ℃ water-jacketed container and perfused with warmed, oxygenated Krebs solution for 10 min. After the mesenteric vasculature was relaxed, warmed distilled water was perfused for 10 min. After a 45-min stabilization period, vehicle or alternatively GA was perfused for 15 min. Immediately after pretreatment with vehicle or GA, an infusion of 100 μM MTX was begun. When a stable baseline was maintained in response to 100 μM MTX, concentration-response curves to 0.1-ml SNP boluses (0.001-10 μg) were examined. Additional experiments were also performed in sham and PVL mesenteric vessels in response to GA preinfusion using MTX doses that allowed equivalent levels of constriction in response to preinfusion of vehicle. Equivalent constriction was achieved with 10 and 30 μM MTX in sham and PVL mesentery, respectively.

Statistics

All data were expressed as means ± SE. Statistical analysis was performed using paired and unpaired Student's *t*-tests as well as ANOVA where appropriate.

RESULTS

Expression and localization of HSP90 in mesenteric vasculature

The expression of HSP90 was significantly enhanced in PVL animals compared with SO and normal animals by Western blot and by RT-PCR (Figures 1A and B). The immunohistochemistry showed that HSP90 staining was not only found in vascular endothelium but also in mesenteric smooth cells (Figure 1C).

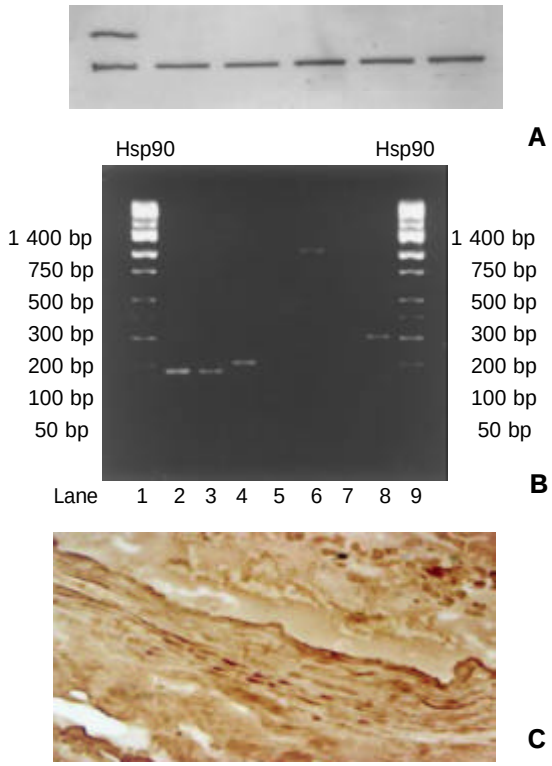

Figure 1 A: Expression of HSP90 by Western blot in PVL anima, B: Expression of HSP90 mRNA in PVL animals, C: Immunohistochemistry showed that HSP90 staining was not only found in vascular endothelium but also in mesenteric smooth cells.

GA potentiated mesenteric vascular responses to MTX in portal hypertensive animals

In response to 100 μM MTX, GA significantly potentiated the increase in perfusion pressure in portal hypertensive animals (Figure 2) (P<0.05, GA vs. vehicle) but not in sham animals. This result suggested that HSP90 was responsible for the hyporesponsness in portal hypertensive rats, thus playing a key role in hemodynamic dysfunction of portal hypertensive animals.

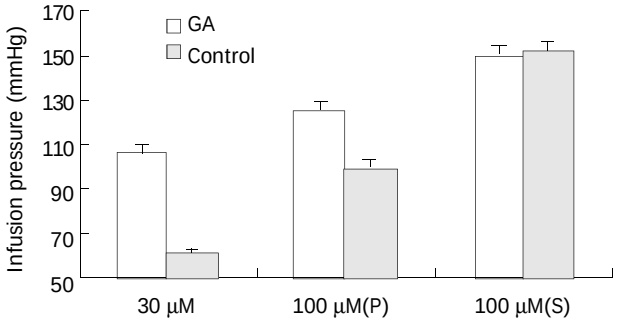

Figure 2 GA potentiates increase of perfusion pressure in portal hypertensive animals.

GA attenuated ACh-dependent vasorelaxation of the normally isolated and perfused rat mesentery but did not affect vasodilation in response to sodium nitroprusside

In this preparation, ACh induced vasorelaxation in a dose-dependent manner after preconstriction of the circulation with MTX. Mesenteric vasorelaxation in response to ACh (1 and 10 μg) was significantly attenuated after preinfusion of GA (3 μg/ml) compared with preinfusion of vehicle (Figure 3) (P<0.05, vehicle vs. GA; n=5). After endothelial denudation, pretreatment with GA did not affect vasodilation in response to SNP (n=6), indicating that the effects of GA were dependent on the endothelium and that GA did not directly affect soluble guanylate cyclase or other smooth muscle cell machinery required for NO-dependent vasodilation. These results showed that HSP90 was an important modulator in vasodilation of mesenteric vasculature.

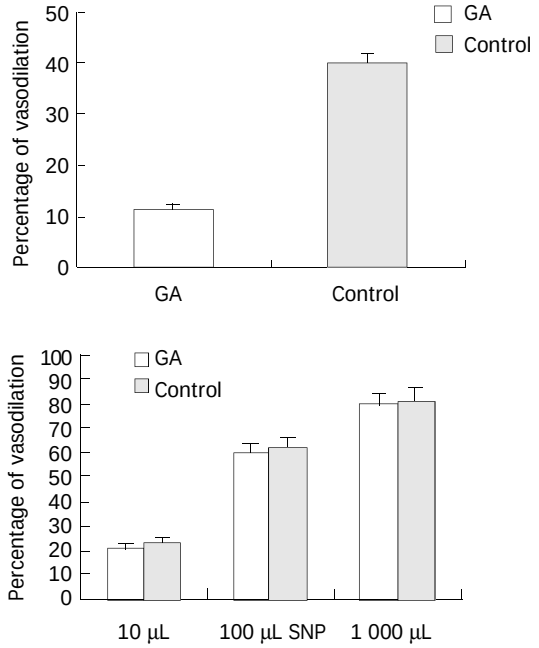

Figure 3 A: GA attenuates Ach dependent vasodilation. B: GA does not affect vasodilation in response to SNP.

DISCUSSION

This study suggested that HSP90 was overexpressed in the endothelium of mesenteric vasculature in PVL induced animals compared with SO and normal animals. Moreover, in PVL animals, the perfused mesentery was hyporesponsive to the vasoconstrictor methoxamine. GA, a special inhibitor of HSP90 signaling, significantly potentiated methoxamine-induced vasoconstrictor after PVL. It thus indicated a mechanism linking protein-protein interactions with vascular manifestations observed in portal hypertension.

HSP90, an ATP-dependent chaperon[28], facilitated the folding and stabilization of cellular proteins, and played a key role in cellular signal transduction networks. The highly conserved 25 kD NH_2-terminal domain of HSP90 was the binding site for ATP and GA[22], and crystallography has shown that GA occupied the nucleotide-binding cleft within the NH_2-terminal domain[28], which thereby has been used as a specific reagent to probe the importance of HSP90 in cellular pathways. An *in vivo* requirement for HSP90 has been established for some steroid hormone receptors[29], several serine/threonine kinases such as pp60/v-src and RAF[30,31] and disparate proteins such as NOS and calcineurin[23,32]. The present study demonstrated that GA also blocked vascular responses mediated by eNOS, without influencing the direct vasodilatory effects of SNP. These data, in conjunction with the above evidences for the specificity of GA, suggested that HSP90 participated in vasodilation of mesentery vasculature as a regulator of endothelial cell signal transduction, leading to eNOS activation and vasorelaxation.

Vessel homeostasis is maintained by a balance of vasoactive substances and hemodynamic forces, including shear stress which mediates vascular responses in part through modulation of eNOS. Two isoforms of NOS have been shown to exist in the vasculature, one is a constitutively expressed and calcium-calmodulin-dependent isoform (eNOS)[12], the other is an

inducible and calcium-independent isoform (iNOS)[13]. Several studies suggested that eNOS was the major enzymatic source of NO overproduction[17-20] in the vascular endothelium in cirrhosis. Our study found that the effects of GA were dependent on the endothelium and that GA did not directly affect soluble guanylate cyclase or other smooth muscle cell machinery required for NO-dependent vasodilation. These studies, in conjunction with the recent demonstration that activation of eNOS was facilitated through HSP90 signaling[23], suggested that eNOS activation in the portal hypertensive vasculature might be linked to a signaling pathway depending on HSP90. Thus we put forward the hypothesis that HSP90 signaling pathway potentiates the activity of eNOS, which results in NO overproduction and thereby induces hyperdynamic circulation in portal hypertension. However, the inability of GA to completely reverse the hyporesponsiveness to MTX in portal hypertensive mesentery suggested that other regulatory pathways for NOS activation in portal hypertension were also involved. In addition, it is possible that a small part of NO derived from iNOS might also contribute to hyperdynamic circulation in portal hypertensive vessels.

In summary, this study suggested that HSP90 played a key role in the NO-dependent hyporeactivity observed in portal hypertension. This interaction likely served to mediate NO-dependent responses in the perfused mesenteric vasculature. Taken together, the present study indicates that HSP90 is responsible for hyperdynamic circulation in portal hypertension, and pharmacological inhibition of the signal system may provide a novel target for future treatment of portal hypertensive complications such as ascites and fatal variceal bleeding.

REFERENCES

1 **Piscaglia F**, Zironi G, Gaiani S, Ferlito M, Rapezzi C, Siringo S, Gaia C, Gramantieri L, Bolondi L. Relationship between splanchnic, peripheral and cardiac haemodynamics in liver cirrhosis of different degrees of severity. *Eur J Gastroenterol Hepatol* 1997; **9:** 799-804

2 **Bhathal PS**, Grossman HJ. Reduction of the increased portal vascular resistance of the isolated perfused cirrhotic rat liver by vasodilators. *J Hepatol* 1985; **1:** 325-337

3 **Niederberger M**, Gines P, Tsai P, Martin PY, Morris K, Weigert A, McMurtry I, Schrier RW. Increased aortic cyclic guanosine monophosphate concentration in experimental cirrhosis in rats: evidence for a role of nitric oxide in the pathogenesis of arterial vasodilation in cirrhosis. *Hepatology* 1995; **21**: 1625-1631

4 **Cahill PA**, Redmond EM, Hodges R, Zhang S, Sitzmann JV. Increased endothelial nitric oxide synthase activity in the hyperemic vessels of portal hypertensive rats. *J Hepatol* 1996; **25**: 370-378

5 **Rockey D**. The cellular pathogenesis of portal hypertension: stellate cell contractility, endothelin, and nitric oxide. *Hepatology* 1997; **25**: 2-5

6 **Rodriguez-Perez F**, Groszmann R. Pharmacologic treatment of portal hypertension. *Gastroenterol Clin North Am* 1992; **21**: 15-40

7 **Wiest R**, Das S, Cadelina G, Garcia-Tsao G, Milstien S, Groszmann RJ. Bacterial translocation in cirrhotic rats stimulates eNOS-derived NO production and impairs mesenteric vascular contractility. *J Clin Invest* 1999; **104**: 1223-1233

8 **Trager K**, Matejovic M, Zulke C, Vlatten A, Vogt J, Wachter U, Altherr J, Brinkmann A, Jauch KW, Georgieff M, Radermacher P. Hepatic O_2 exchange and liver energy metabolism in hyperdynamic porcine endotoxemia: effects of iloprost. *Intensive Care Med* 2000; **26**: 1531-1539

9 **Laffi G**, La Villa G, Pinzani M, Marra F, Gentilini P. Arachidonic acid derivatives and renal function in liver cirrhosis. *Semin Nephrol* 1997; **17**: 530-548

10 **Sieber CC**, Groszmann RJ. *In vitro* hyporeactivity to methoxamine in portal hypertensive rats: reversal by nitric oxide blockade. *Am J Physiol* 1992; **262** (6Pt1): G996-G1001

11 **Sieber CC**, Groszmann RJ. Nitric oxide mediates hyporeactivity to vasopressors in mesenteric vessels of portal hypertensive rats. *Gastroenterology* 1992: **103**: 235-239

12 **Feron O**. Intracellular localization and activation of endothelial nitric oxide synthase. *Curr Opin Nephrol Hypertens* 1999; **8**: 55-59

13 **Kubes P**. Inducible nitric oxide synthase: a little bit of good in all of us. *Gut* 2000; **47**: 6-9

14 **Ros J**, Jimenez W, Lamas S, Claria J, Arroyo V, Rivera F, Rodes J. Nitric oxide production in arterial vessels of cirrhotic rats. *Hepatology* 1995; **21**: 554-560

15 **Castro A**, Jimenez W, Claria J, Ros J, Martinez JM, Bosch M, Arroyo V, Piulats J, Rivera F, Rodes J. Impaired responsiveness to angiotensin II in experimental cirrhosis: role of nitric oxide. *Hepatology* 1993; **18**: 367-372

16 **Weigert AL**, Martin PY, Niederberger M, Higa EM, McMurtry IF, Gines P, Schrier RW. Endothelium-dependent vascular hyporesponsiveness without detection of nitric oxide synthase induction in aortas of cirrhotic rats. *Hepatology* 1995; **22**: 1856-1862

17 **Wiest R**, Shah V, Sessa WC, Groszmann RJ. NO overproduction by eNOS precedes hyperdynamic splanchnic circulation in portal hypertensive rats. *Am J Physiol* 1999; **276**(4 Pt 1): G1043-G1051

18 **Gadano AC**, Sogni P, Yang S, Cailmail S, Moreau R, Nepveux P, Couturier D, Lebrec D. Endothelial calcium-calmodulin dependent nitric oxide synthase in the *in vitro* vascular hyporeactivity of portal hypertensive rats. *J Hepatol* 1997; **26**: 678-686

19 **Martin PY**, Xu DL, Niederberger M, Weigert A, Tsai P, St John J, Gines P, Schrier RW. Upregulation of endothelial constitutive NOS: a major role in the increased NO production in cirrhotic rats. *Am J Physiol* 1996; **270**(3 Pt 2): F494-F499

20 **Hori N**, Wiest R, Groszmann RJ. Enhanced release of nitric oxide in response to changes in flow and shear stress in the superior mesenteric arteries of portal hypertensive rats. *Hepatology* 1998; **28**: 1467-1473

21 **Nemoto T**, Ohara-Nemoto Y, Ota M, Takagi T, Yokoyama K. Mechanism of dimer formation of the 90-kDa heat-shock protein. *Eur J Biochem* 1995; **233**: 1-8

22 **Whitesell L**, Mimnaugh EG, De Costa B, Myers CE, Neckers LM. Inhibition of heat shock protein HSP90-pp60v-src heteroprotein complex formation by benzoquinone ansamycins: essential role for stress proteins in oncogenic transformation. *Proc Natl Acad Sci U S A* 1994; **91**: 8324-8328

23 **Garcia-Cardena** G, Fan R, Shah V, Sorrentino R, Cirino G, Papapetropoulos A, Sessa WC. Dynamic activation of endothelial nitric oxide synthase by Hsp90. *Nature* 1998; **392**: 821-824

24 **Chojkier M**, Groszmann RJ. Measurement of portal-systemic shunting in the rat by using gamma-labelled microspheres. *Am J Physiol* 1981; **240**: G371-G375

25 **Rudic RD**, Shesely EG, Maeda N, Smithies O, Segal SS, Sessa WC. Direct evidence for the importance of endothelium-derived nitric oxide in vascular remodeling. *J Clin Invest* 1998; **101**: 731-736

26 **Sieber CC**, Lopez-Talavera JC, Groszmann RJ. Role of nitric oxide in the *in vitro* splanchnic vascular hyporeactivity in ascitic cirrhotic rats. *Gastroenterology* 1993; **104**: 1750-1754

27 **Atucha NM**, Shah V, Garcia-Cardena G, Sessa WE, Groszmann RJ. Role of endothelium in the abnormal response of mesenteric vessels in rats with portal hypertension and liver cirrhosis. *Gastroenterology* 1996; **111**: 1627-1632

28 **Obermann WM**, Sondermann H, Russo AA, Pavletich NP, Hartl FU. *In vivo* function of HSP90 is dependent on ATP binding and ATP hydrolysis. *J Cell Biol* 1998; **143**: 901-910

29 **Picard D**, Khursheed B, Garabedian MJ, Fortin MG, Lindquist S, Yamamoto KR. Reduced levels of HSP90 compromise steroid receptor action *in vivo*. *Nature* 1990; **348**: 166-168

30 **Whitesell L**, Mimnaugh EG, De Costa B, Myers CE, Neckers LM. Inhibition of heat shock protein HSP90-pp60v-src heteroprotein complex formation by benzoquinone ansamycins: essential role for stress proteins in oncogenic transformation. *Proc Natl Acad Sci U S A* 1994; **91**: 8324-8328

31 **Van der Straten** A, Rommel C, Dickson B, Hafen E. The heat shock protein 83(HSP83) is required for Raf-mediated signaling in *Drosophila*. *EMBO J* 1997; **16**: 1961-1969

32 **Imai J**, Yahara I. Role of HSP90 in salt stress tolerance via stabilization and regulation of calcineurin. *Mol Cell Biol* 2000; **20**: 9262-9270

Edited by Zhang JZ and Wang XL

P.O.Box 2345, Beijing 100023,China
Fax: +86-10-85381893
E-mail: wjg@wjgnet.com www.wjgnet.com

World J Gastroenterol 2003;9(11):2548-2551
World Journal of Gastroenterology
 ISSN 1007-9327

• CLINICAL RESEARCH •

Expression and mutation of c-kit gene in gastrointestinal stromal tumors

Fei Feng, Xiao-Hong Liu, Qiang Xie, Wei-Qiang Liu, Cheng-Guang Bai, Da-Lie Ma

Fei Feng, Xiao-Hong Liu, Qiang Xie, Wei-Qiang Liu, Cheng-Guang Bai, Da-Lie Ma, Department of Pathology, Changhai Hospital, Second Military Medical University, Shanghai 200433, China
Supported by the National Natural Science Foundation of China, No.30070743
Correspondence to: Dr. Da-Lie Ma, Department of Pathology, Changhai Hospital, 174 Changhai Road, Shanghai 200433, China. gzff0524@21cn.com
Telephone: +86-21-25070660-808
Received: 2003-05-10 **Accepted:** 2003-06-07

Abstract

AIM: To investigate the expression and mutation of c-kit gene and its correlation with the clinical pathology and prognosis of gastrointestinal stromal tumors (GISTs).

METHODS: A total of 94 cases of GISTs, 10 leiomyomas and 2 schwannomas were studied for the expression of KIT by immunohistochemistry. The c-kit gene mutations in exon 11 of these specimens were detected by PCR-SSCP technique.

RESULTS: Of the 94 cases of GISTs, 91 (96.8 %) expressed the KIT protein. Leiomyomas and schwannomas were negative for KIT. The c-kit gene mutations of exon 11 were found in 38 out of the 94 cases of GISTs (40.4 %). The mutations involved point mutations (Val560-Asp, Ile563-Met), del 557-559 and 579ins12. No mutations were detectable in benign GISTs, leiomyomas or schwannomas. The patients with mutation-positive GISTs showed more frequent recurrences, invasion and metastasis in adjacent tissues than those with mutation-negative ones.

CONCLUSION: KIT is a useful marker for diagnosis of GISTs. Mutation of the c-kit gene may play a significant role in the pathogenesis of GISTs and may be associated with poor prognosis in patients with GISTs.

Feng F, Liu XH, Xie Q, Liu WQ, Bai CG, Ma DL. Expression and mutation of c-kit gene in gastrointestinal stromal tumors. *World J Gastroenterol* 2003; 9(11): 2548-2551
http://www.wjgnet.com/1007-9327/9/2548.asp

INTRODUCTION

Gastrointestinal stromal tumors (GISTs) are the most common mesenchymal tumors of the human gastrointestinal tract that may occur in the entire gastrointestinal tract[1-4]. In recent years, much attention has focused on GISTs. Studies have shown that GISTs strongly express the KIT protein[1,5,6], a type III tyrosine-kinase receptor encoded by the c-kit proto-oncogene[7,8]. The c-kit gene located in the long arm of chromosome 4, is the cellular homologue of oncogene v-kit of the HZ4 feline sarcoma virus[9]. KIT, which is structurally related to the receptors for platelet-derived growth factor and colony-stimulating factor, consists of an extracellular domain, a transmembrane domain, a juxtamembrane domain and a kinase domain with an insert that splits the kinase domain[10]. KIT and its ligand, stem cell factor (SCF), are known to play crucial roles in the development of germ cells, melanocytes, mast cells and interstitial cells of Cajal[11].

Recently, activated c-kit mutations have been identified in GISTs. Most mutations were detected in the juxtamembrane domain (Lys-550 to Val-560)[1,12-14]. These mutations were related to a poorer prognosis. The purpose of this study was to examine the KIT expression and characterize the range of c-kit mutations in GISTs, and to evaluate the significance between c-kit mutations and prognostic factors.

MATERIALS AND METHODS

Patients

Ninety-four cases of GISTs (62 male, 32 female) diagnosed at Changhai Hospital with a median age of 53 years (ranging from 5-77) were included in the study between January 1991 and December 2002. Forty-six tumors were located in the stomach, thirty-two in the small bowel, ten in the large intestine, three in the esophagus and three in the omentum and mesentery. We used Lewin's determination to separate benign from malignant lesions[15]. Sixty-seven cases of GISTs were malignant and 27 were benign. Of the patients in the malignant group, ten received reoperation due to recurrences, distant metastasis was found in 6 patients at the time of surgery, four to the liver and two to both the liver and peritoneum. The remaining patients were free of distant metastasis. One patient with liver metastasis died after operation. Twelve control tumors were also analyzed, including 10 leiomyomas and 2 schwannomas.

Immunohistochemistry

A rabbit polyclonal antibody against human KIT and an EnVision kit were purchased from DAKO. Immunohistochemistry was performed using the two-step technique. All specimens were fixed in 10 % buffered formalin and embedded in paraffin. Four-μm thick sections were cut from the tissue blocks. The sections were deparaffinized and rehydrated, then treated using a microwave epitope retrieval technique with citrate buffer, pH 6.0 at 85 ℃ for 3 min. After cooled at room temperature, the sections were washed in PBS (0.01M, pH7.2) and incubated with the antibody against c-kit (1:100) at room temperature for 1 hour. After washed in PBS, the sections were incubated with the EnVision compound at room temperature for 30 min. Staining was developed by immersing slides in 0.05 % DAB with 0.33 % hydrogen peroxide. All slides were counterstained with haematoxylin, dehydrated and mounted. PBS substituted for the primary antibody was used as the negative control.

DNA Extraction

DNA was extracted from formalin-fixed, paraffin-embedded tissues using standard methods with proteinase K digested and phenol/chloroform purified.

PCR-SSCP

Exon 11 of the c-kit gene was amplified by PCR using the following oligonucleotide primer pairs: sense primer 5'-

AACTCAGCCTGTTTCTGG-3' and antisense primer 5'-GATCTATTTTTCCCTTTCTC-3'. PCR was carried out with the following conditions: 50 μl total reaction volume, with 5 μl template, 5 μl of each oligonucleotide primer, 10 μl dNTP, 10 μl ddH_2O, 2 μl Taq polymerase, 8 μl Mg^{2+} and 5 μl 10×PCR buffer. Cycling conditions were as follows: an initial penetration at 95 ℃ for 4 min, 38 cycles each at 94 ℃ for 1 min, at 56 ℃ for 1 min, at 72 ℃ for 1 min, followed by one cycle at 72 ℃ for 10 min. PCR products were visualized by gel electrophoresis in 1.7 g/L agarose. Then the PCR products were subjected to 8 % non-denaturation polyacrylamide gel electrophoresis (aer: bis=49:1) with 5 % glycerin and silver nitrate staining.

DNA sequencing

PCR products that showed abnormal gel shift by PCR-SSCP were selected for sequencing after cloned into PMD18-T vector. The sequencing procedures were performed by Sangon Co., Shanghai.

Statistical methods

The data were analyzed with χ^2 test.

RESULTS

Immunohistochemistry

Immunohistochemical analyses revealed strong and diffuse KIT expression in 91 out of the 94 cases of GISTs. The positive signals were localized in cytoplasm and membrane (Figures 1 and 2). Ninety-seven percent of malignant GISTs and ninety-six percent of benign GISTs were KIT positive. Compared with the benign group, some malignant GISTs showed weaker and focal positivity. There was no significant difference in the expression of KIT between benign and malignant GISTs (P>0.05). Leiomyomas and schwannomas were negative for KIT.

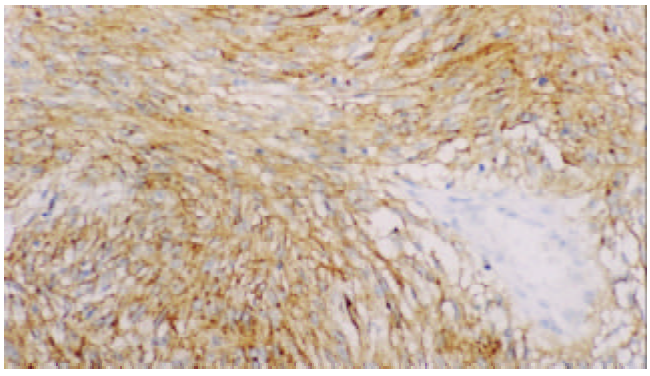

Figure 1 KIT staining in cytoplasm and membrane of GISTs (spindle type)×200.

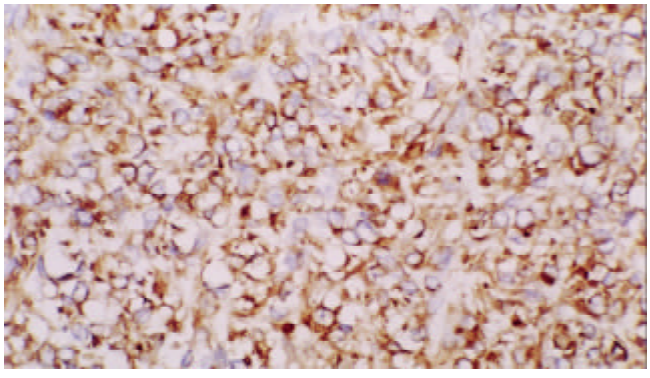

Figure 2 KIT staining in cytoplasm and membrane of GISTs (epithelioid type)×200.

Evaluation of mutations in exon 11 of c-kit gene

Analysis of PCR-SSCP showed abnormal gel shifts in 38 out of the 67 (56.7 %) malignant GISTs. No mutant bands were observed in benign GISTs, as well as in leiomyomas and schwannomas. Sequencing of 6 mutant bands revealed three types of mutations. One case showed point mutations (Val560-Asp and Ile563-Met), one case a 6-bp deletion involving codons 557 to 559, one case a 12-bp insertion at the codon 579 (Figure 3).

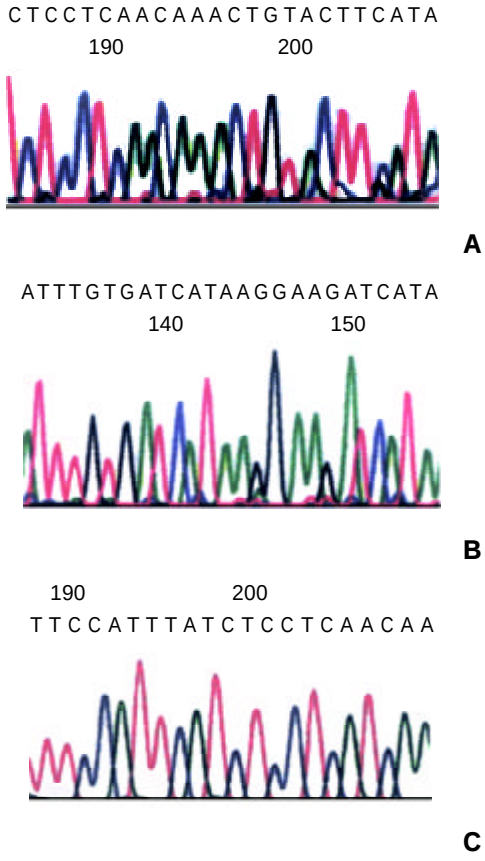

Figure 3 Sequence of the exon 11 of c-kit from the mutant bands obtained from the GISTs. A: 6-bp deletion involving codons 557 and 559 (GGAAGG), B: 12-bp insertion at codon 579 (CTTCCTTATGAT), C: two point mutations (Val 560-Asp, Ile 563-Met).

Correlation of c-kit mutations with clinicopathological parameters

Of the 38 cases of GISTs with c-kit mutations, six developed distant metastasis, eight had local recurrences and one died of liver metastasis. Only two recurrences were found in the remaining 56 cases of GISTs without c-kit mutations.

DISCUSSION

It has been reported that GISTs are strongly and nearly consistent KIT positive and mutations of the c-kit gene were observed in GISTs. In this study, we examined the sequences and expression of c-kit in the spectrum of GISTs, including benign and malignant variants from different sites. The expression and mutations of the c-kit gene were also evaluated in leiomyomas and schwannomas.

As this study has shown, 96.8 % (91/94) GISTs strongly and diffusely expressed KIT irrespective of tumor location, histologic subtype and grade. Neither age nor sex was significantly correlated with the expression levels of KIT. The findings were in agreement with the previous studies[16-18]. No

expression of KIT was found in leiomyomas and schwannomas. These results verified that KIT was a sensitive diagnostic marker for GISTs, but it could not be used as a prognostic index[19,20].

Recently, mutations of the c-kit gene were observed in GISTs. Most mutations were located at the juxtamembrane domain encoded by exon 11, especially between codons 550-560. Mutations of exon 11 were observed in 40.4 % (38/94) of GISTs in our study, and other group observed mutations of exon 11 in 57 %, 42 % and 21 % of GISTs[6,13,21]. The difference in mutation rates appeared to be due to the proportion of malignant GISTs, as suggested by our data and the previous reports. Some studies have shown that the mutant types including insertions or duplications, in addition to deletions and point mutations. These were consistent with our results. DNA sequencing showed that point mutations, deletions and insertions were found in our six GISTs and the range of the c-kit mutations was not only between codons 550-560 but also at codon 579. Although 96.8 % of GISTs expressed KIT, only 40.4 % of GISTs showed mutations in the juxtamembrane region of the c-kit gene. This indicated that some KIT-positive GISTs could occur without mutation of the c-kit gene or with mutations other than exon 11 of the c-kit gene. There was another possibility that some mutations of the NF-1 gene might result in the occurrence of KIT-positive GISTs[1,16,22]. Moreover, the mutations of exons 9, 13, 17, 14 and 15 in GISTs have been identified in recent years[23-25]. But mutations in these exons were found to be few compared with in exon 11[26,27]. These observations demonstrate that multiple mutations of c-kit, irrespective of domain-extracellular, juxtamembrane or kinase, are crucial tumorigenic events in GISTs.

Since c-kit mutations are commonly found in GISTs, how these mutations lead to kinase activation is a field of active investigation. KIT participates in complex networks of signal cascade proteins, and some of these proteins regulate KIT activation in positive or negative manners. Under normal conditions, KIT activation occurs when the receptor is bound to its ligand, a stem cell factor. Ligand-mediated KIT activation triggered various cell-signaling cascades that regulate cell behavior[28,29]. The c-kit mutations of these domains resulted in activation of kinase by allowing ligand-independent receptor dimerization[30-32]. In other words, the mutations in GISTs lead to structural changes of KIT oncoproteins that favor receptor oligomerization and cross-phosphorylation, even in the absence of ligand binding. Because activation of KIT is a ubiquitous oncogenic pathway in most GISTs and important to the growth of GISTs, it has become possible that patients with GISTs can be treated with STI571, a KIT tyrosine kinase inhibitor. STI571 is a 2-phenylaminopyrimidine that selectively inhibits protooncogenic and oncogenic forms of the ABL, PDGFR and c-kit tyrosine kinases[33,34]. STI571 has a potent activity against GIST cells grown *in vitro* and the majority of patients with malignant GIST have shown a benefit to treatment with STI571 in recent clinical trials[35-37].

Finally, we compared clinical outcome between the mutation-positive and negative GISTs, and found more frequent recurrences and poorer prognosis were related with mutation-positive GISTs. In our study, 6 out of the 38 patients with mutation-positive GISTs developed distant metastasis, 8 had local recurrences and 1 died of GIST, whereas only 2 out of the 56 patients with mutation-negative GISTs had recurrences. These findings are consistent with some other previous results[1,6,13,38,39], and indicate that the c-kit mutations seem to be related to poorer prognosis. But there is an opposite opinion recently. The results showed that these mutations occurred very early in the course of GISTs development and were of little prognostic importance in GISTs[40]. And now cytogenetic abnormalities have been detected in GISTs[41-43]. These findings suggest that molecular alterations and c-kit mutations are likely to be involved in determining the biologic behaviors of both benign and malignant GISTs.

Considering these findings, we conclude that most GISTs strongly and diffusely express KIT protein, and KIT is a useful and sensitive marker for diagnosis of GISTs. C-kit mutation is undoubtedly a pivotal event in GISTs and may be associated with poor prognosis. Evaluation of KIT mutation may have both prognostic and therapeutic significances as the new tyrosine kinase inhibitor (STI571) treatments are available. The correlation between c-kit mutations and clinical behaviors is far more complex than initially appreciated, and further studies are needed.

REFERENCES

1 **Hirota S,** Isozaki K, Moriyama Y, Hashimoto K, Nishida T, Ishiguro S, Kawano K, Hanada M, Kurata A, Takeda M, Muhammad Tunio G, Matsuzawa Y, Kanakura Y, Shinomura Y, Kitamura Y. Gain-of-function mutations of c-kit in human gastrointestinal stromal tumors. *Science* 1998; **279:** 577-580

2 **Miettinen M,** Monihan JM, Sarlomo-Rikala M, Kovatich AJ, Carr NJ, Emory TS, Sobin LH. Gastrointestinal stromal tumors / smooth muscle tumors (GISTs) primary in the omentum and mesentery: clinicopathologic and immunohistochemical study of 26 cases. *Am J Surg Pathol* 1999; **23:** 1109-1118

3 **Shibata Y,** Ueda T, Seki H, Yagihashi N. Gastrointestinal stromal tumour of the rectum. *Eur J Gastroenterol Hepatol* 2001; **13:** 283-286

4 **Miettinen M,** Sobin LH. Gastrointestinal stromal tumors in the appendix: a clinicopathologic and immunohistochemical study of four cases. *Am J Surg Pathol* 2001; **25:** 1433-1437

5 **Sarlomo-Rikala M,** Kovatich AJ, Barusevicius A, Miettinen M. CD117: a sensitive marker for gastrointestinal stromal tumors that is more specific than CD34. *Mod Pathol* 1998; **11:** 728-734

6 **Taniguchi M,** Nishida T, Hirota S, Isozaki K, Ito T, Nomura T, Matsuda H, Kitamura Y. Effect of c-kit mutation on prognosis of gastrointestinal stromal tumors. *Cancer Res* 1999; **59:** 4297-4300

7 **Chabot B,** Stephenson DA, Chapman VM, Besmer P, Bernstein A. The proto-oncogene c-kit encoding a transmembrane tyrosine kinase receptor maps to the mouse W locus. *Nature* 1988; **335:** 88-89

8 **Geissler EN,** Ryan MA, Housman DE. The dominant-white spotting (w) locus of the mouse encodes the c-kit proto-oncogene. *Cell* 1988; **55:** 185-192

9 **Majumder S,** Brown K, Qiu FH, Besmer P. C-kit Protein, a transmembrane kinase: identification in tissues and characterization. *Mol Cell Biol* 1988; **8:** 4896- 4903

10 **Hirota S.** Gastrointestinal stromal tumors: their origin and cause. *Int J Clin Oncol* 2001; **6:** 1-5

11 **Huizinga JD,** Thuneberg L, Klusppel M, Malysz J, Mikkelsen HB, Bernstein A. W / kit gene required for interstitial cells of Cajal and for intestinal pacemaker activity. *Nature* 1995; **373:** 347-349

12 **Nakahara M,** Isozaki K, Hirota S, Miyagawa J, Hase-Sawada N, Taniguchi M, Nishida T, Kanayama S, Kitamura Y, Shinomura Y, Matsuzawa Y. A novel gain-of-function mutation of c-kit gene in gastrointestinal stromal tumors. *Gastroenterology* 1998; **115:** 1090-1095

13 **Lasota J,** Jasinski M, Sarlomo-Rikala M, Miettinen M. Mutations in exon 11 of c-Kit occur preferentially in malignant versus benign gastrointestinal stromal tumors and do not occur in leiomyomas or leiomyosarcomas. *Am J Pathol* 1999; **154:** 53-60

14 **Miettinen M,** Lasota J. Gastrointestinal stromal tumors-definition, clinical, histological, immunohistochemical, and molecular genetic features and differential diagnosis. *Virchows Arch* 2001; **438:** 1-12

15 **Lewin KJ,** Riddell RH, Weinstein WM. Gastrointestinal pathology and its clinical implications.1 st ed. *New York: Igaku-shoin* 1992: 284-341

16 **Kindblom LG,** Remotti HE, Aldenborg F, Meis-Kindblom JM. Gastrointestinal pacemaker cell tumor (GIPACT): gastrointestinal stromal tumors show phenotypic characteristics of the interstitial cells of Cajal. *Am J Pathol* 1998; **152:** 1259-1269

17 **Sircar K,** Hewlett BR, Huizinga JD, Chorneyko K, Berezin I, Riddell RH. Interstitial cells of Cajal as precursors for gastrointestinal stromal tumors. *Am J Surg Pathol* 1999; **23:** 377-389

18 **Miettinen M,** Sarlomo-Rikala M, Lasota J. Gastrointestinal stromal tumors: recent advances in understanding of their biology. *Hum Pathol* 1999; **30:** 1213-1220

19 **Hasegawa T,** Matsuno Y, Shimoda T, Hirohashi S. Gastrointestinal stromal tumor: consistent CD117 immunostaining for diagnosis, and prognostic classification based on tumor size and MIB-1 grade. *Hum Pathol* 2002; **33:** 669-676

20 **Fletcher CD,** Berman JJ, Corless C, Gorstein F, Lasota J, Longley BJ, Miettinen M, O'Leary TJ, Remotti H, Rubin BP, Shmookler B, Sobin LH, Weiss SW. Diagnosis of gastrointestinal stromal tumors: A consensus approach. *Hum Pathol* 2002; **33:** 459-465

21 **Moskaluk CA,** Tian Q, Marshall CR, Rumpel CA, Franquemont DW, Frierson HF Jr. Mutations of c-kit JM domain are found in a minority of human gastrointestinal stromal tumors. *Oncogene* 1999; **18:** 1897-1902

22 **Ishida T,** Wada I, Horiuchi H, Oka T, Machinami R. Multiple small intestinal stromal tumors with skeinoid fibers in association with neurofibromatosis 1 (von Recklinghausen's disease). *Pathol Int* 1996; **46:** 689-695

23 **Lux ML,** Rubin BP, Biase TL, Chen CJ, Maclure T, Demetri G, Xiao S, Singer S, Fletcher CD, Fletcher JA. KIT extracellular and kinase domain mutations in gastrointestinal stromal tumors. *Am J Pathol* 2000; **156:** 791-795

24 **Andersson J,** Sjogren H, Meis-Kindblom JM, Stenman G, Aman P, Kindblom LG. The complexity of KIT gene mutations and chromosome rearrangements and their clinical correlation in gastrointestinal stromal (pacemaker cell) tumors. *Am J Pathol* 2002; **160:** 15-22

25 **Rubin BP,** Singer S, Tsao C, Duensing A, Lux ML, Ruiz R, Hibbard MK, Chen CJ, Xiao S, Tuveson DA, Demetri GD, Fletcher CD, Fletcher JA. KIT activation is a ubiquitous feature of gastrointestinal stromal tumors. *Cancer Res* 2001; **61:** 8118-8121

26 **Lasota J,** Wozniak A, Sarlomo-Rikala M, Rys J, Kordek R, Nassar A, Sobin LH, Miettinen M. Mutations in exon 9 and 13 of KIT gene are rare events in gastrointestinal stromal tumors. A study of 200 cases. *Am J Pathol* 2000; **157:** 1091-1095

27 **Hirota S,** Nishida T, Isozaki K, Taniguchi M, Nakamura J, Okazaki T, Kitamura Y. Gain-of-function mutation at the extracellular domain of KIT in gastrointestinal stromal tumors. *J Pathol* 2001; **193:** 505-510

28 **Linnekin D.** Early signaling pathways activated by c-Kit in hematopoietic cells. *Int J Biochem Cell Biol* 1999; **31:** 1053-1074

29 **Taylor ML,** Metcalfe DD. Kit signal transduction. *Hematol Oncol Clin North Am* 2000; **14:** 517-535

30 **Ma Y,** Cunningham ME, Wang X, Ghosh I, Regan L, Longley BJ. Inhibition of spontaneous receptor phosphorylation by residues in a putative alpha-helix in the KIT intracellular juxtamembrane region. *J Biol Chem* 1999; **274:** 13399-13402

31 **Isozaki K,** Terris B, Belghiti J, Schiffmann S, Hirota S, Vanderwinden JM. Germline-activating mutation in the kinase domain of KIT gene in familial gastrointestinal stromal tumors. *Am J Pathol* 2000; **157:** 1581-1585

32 **Heinrich MC,** Rubin BP, Longley BJ, Fletcher JA. Biology and genetic aspects of gastrointestinal stromal tumors: KIT activation and cytogenetic alterations. *Hum Pathol* 2002; **33:** 484-495

33 **Schindler T,** Bornmann W, Pellicena P, Miller WT, Clarkson B, Kuriyan J. Structural mechanism for STI-571 inhibition of abelson tyrosine kinase. *Science* 2000; **289:** 1938-1942

34 **Heinrich MC,** Blanke CD, Druker BJ, Corless CL. Inhibition of KIT tyrosine kinase activity: a novel molecular approach to the treatment of KIT-positive malignancies. *J Clin Oncol* 2002; **20:** 1692-1703

35 **Tuveson DA,** Willis NA, Jacks T, Griffin JD, Singer S, Fletcher CD, Fletcher JA, Demetri GD. STI571 inactivation of the gastrointestinal stromal tumor c-KIT oncoprotein:biological and clinical implications. *Oncogene* 2001; **20:** 5054-5058

36 **Joensuu H,** Roberts PJ, Sarlomo-Rikala M, Andersson LC, Tervahartiala P, Tuveson D, Silberman S, Capdeville R, Dimitrijevic S, Druker B, Demetri GD. Effect of the tyrosine kinase inhibitor STI571 in a patient with a metastatic gastrointestinal stromal tumor. *N Engl J Med* 2001; **344:** 1052-1056

37 **Van Oosterom AT,** Judson I, Verweij J, Stroobants S, Donato di Paola E, Dimitrijevic S, Martens M, Webb A, Sciot R, Van Glabbeke M, Silberman S, Nielsen OS. Safty and efficacy of imatinib (STI571) in metastatic gastrointestinal stromal tumors: a phase I study. *Lancet* 2001; **358:** 1421-1423

38 **Ernst SI,** Hubbs AE, Przygodzki RM, Emory TS, Sobin LH, O'Leary TJ. KIT mutation portends poor prognosis in gastrointestinal stromal/smooth muscle tumors. *Lab Invest* 1998; **78:** 1633-1636

39 **Miettinen M,** El-Rifai W, H L Sobin L, Lasota J. Evaluation of malignancy and prognosis of gastrointestinal stromal tumors: a review. *Hum Pathol* 2002; **33:** 478-483

40 **Corless CL,** McGreevey L, Haley A, Town A, Heinrich MC. KIT mutations are common in incidental gastrointestinal stromal tumors one centimeter or less in size. *Am J Pathol* 2002; **160:** 1567-1572

41 **El-Rifai W,** Sarlomo-Rikala M, Miettinen M, Knuutila S, Andersson LC. DNA copy number losses in chromosome 14: an early change in gastrointestinal stromal tumors. *Cancer Res* 1996; **56:** 3230-3233

42 **O'Leary T,** Ernst S, Przygodzki R, Emory T, Sobin L. Loss of heterozygosity at 1p36 predicts poor prognosis in gastrointestinal stromal/smooth muscle tumors. *Lab Invest* 1999; **79:** 1461-1467

43 **Gunawan B,** Bergmann F, Hoer J, Langer C, Schumpelick V, Becker H, Fuzesi L. Biological and clinical significance of cytogenetic abnormalities in low-risk and high-risk gastrointestinal stromal tumors. *Hum Pathol* 2002; **33:** 316-321

Edited by Zhang JZ and Wang XL

P.O.Box 2345, Beijing 100023,China
Fax: +86-10-85381893
E-mail: wjg@wjgnet.com www.wjgnet.com

World J Gastroenterol 2003;9(11):2552-2556
World Journal of Gastroenterology
 ISSN 1007-9327

• CLINICAL RESEARCH •

Endoscopic patterns of gastric mucosa and its clinicopathological significance

Jian-Min Yang, Lei Chen, Yu-Lin Fan, Xiang-Hong Li, Xin Yu, Dian-Chun Fang

Jian-Min Yang, Lei Chen, Yu-Lin Fan, Xiang-Hong Li, Xin Yu, Dian-Chun Fang, Gastroenterology Research Center, Southwest Hospital, Third Military Medical University, Chongqing 400038, China
Correspondence to: Dr. Jian-Min Yang, Gastroenterology Research Center, Southwest Hospital, Third Military Medical University, Chongqing 400038, China. jianminyang@hotmail.com
Telephone: +86-23-68754678
Received: 2003-04-12 **Accepted:** 2003-05-19

Abstract

AIM: To explore the correlation of magnifying endoscopic patterns and histopathology, *Helicobacter pylori (H pylori)* infection of the gastric mucosa.

METHODS: Gastric mucosal patterns in 140 patients with chronic gastritis were studied using Olympus GIF-Q240Z magnifying endoscope. Histopathological examination, rapid urease test and Warrthin-Starry staining were taken with biopsy samples from the magnified sites of stomach. The magnifying endoscopic patterns were compared with histopathological results and *H pylori* detection.

RESULTS: The pit patterns of gastric mucosa were classified as types A (round spot), B (short rod), C (branched), D (reticular) and E (villus). The detection rate of chronic atrophic gastritis (CAG) by magnifying endoscopy was 94.3 % (33/35), which was significantly higher than that by routine endoscopy (22.9 %, 8/35) ($P<0.01$). The pit patterns of 31 cases of intestinal metaplasia (IM) appeared as type E in 18 cases (58.1 %), type D in 8 cases (25.8 %) and type C in 5 cases (16.1 %). Fourteen out of 18 patients (77.8 %) with complete type (type I) of IM appeared as type E of pit patterns, whereas only 4 of 13 (30.8 %) patients with incomplete type (types II and III) of IM appeared as type E ($P<0.05$). Collecting venules in the anterior of lower part of gastric corpus were subgrouped into types R (regular), I (irregular) and D (disappeared). *H pylori* infection was found in 12.2 %(9/74), 60 %(9/15) and 84.3 %(43/51) cases in these types respectively. *H pylori* infection rate in type R was significantly lower than that in other two types ($P<0.01$).

CONCLUSION: Magnifying endoscopy may have an obvious value in diagnosing chronic atrophic gastritis, intestinal metaplasia and *H pylori* infection.

Yang JM, Chen L, Fan YL, Li XH, Yu X, Fang DC. Endoscopic patterns of gastric mucosa and its clinicopathological significance. *World J Gastroenterol* 2003; 9(11): 2552-2556
http://www.wjgnet.com/1007-9327/9/2552.asp

INTRODUCTION

Recently, magnifying endoscope has been used clinically for its developments in amplifying power, definition and operational capability. Lots of international studies on clinical application of magnifying endoscope especially from Japan have been reported, but most of them were focused on colon and esophagus, only a few of them on gastric mucosa have been published[1-28]. These studies implicate that classification of superficial mucosal appearances defined by magnifying endoscopy can reflect not only histological features but also mucin phenotypes. Magnifying endoscopy is helpful for more correctly distinguishing hyperplastic lesions from adenomatous and cancerous lesions, and for improving detection of early flat and depressed cancer. More interestingly, according to Japanese data, magnifying endoscopy could also be used to predict invasive depth and lymph node metastasis of cancer[6,16]. Up to now only a few studies on the field have been reported in China[29-33]. In this article, we reported our study on correlation of magnifying endoscopic patterns and histopathology, *Helicobacter pylori (H pylori)* infection of gastric mucosa in 140 patients with chronic gastritis to understand the value of magnifying endoscopy in diagnosing the minute lesions of gastric mucosa.

MATERIALS AND METHODS

Subjects

Subjects were 140 out-patients and in-patients (male: 68, female: 72, age range: 18-77 years old, average age: 50.6) with chronic superficial gastritis (CSG, $n=105$) and chronic atrophic gastritis (CAG, $n=35$) during June-August, 2002. All the patients had gastrointestinal symptoms such as abdominal distention, abdominalgia, belch and hyperhydrochloria.

Magnifying endoscope

New model of electronic magnifying endoscope GIF Q-240Z (Olympus Optical Co., Ltd., Tokyo, Japan) was used. It could be used to perform routine endoscopy (observation at standard magnification) as well as to magnify the image 80 times (in 14-inch monitor) as large as the original size through manual adjustment of the focal length.

Endoscopy

Magnifying endoscopy was performed by senior endoscopists and the real time static and successive images were recorded by computer image and text reporting system and video tape recorder. In order to inhibit gastrointestinal peristalsis, 10 mg of anisodaminum (654-2) and 5-10 mg of diazepamum were injected intramuscularly at 10 minutes pre-endoscopy. Routine endoscopy was performed first, and if necessary, dilution of dimethyl silicone oil was used to flush off the foam and mucus, then the appearance of gastric pits in the antrum, angel, corpus and fundus, and collecting venules in the anterior of lower part of gastric corpus were observed so that the patterns of gastric pits and collecting venules could be decided.

Histological examination

One piece of tissue in the greater curvature of gastric antrum was extracted for rapid urease test using RUT kit (Kedi Technology Co., LTD, Zhuhai, China). Two biopsies from the magnified sites in gastric antrum and corpus were performed for hematoxylin-eosin (HE) and Warrthin-Starry staining. Rapid urease test and Warrthin-Starry staining were used for

H pylori detection[34,35]. According to the national standard of China, *H pylori* infection was established after positive results were confirmed by both rapid urease test and Warrthin-Starry staining[35]. HE staining was performed for routine histopathological examination. Inflammatory levels were graded as mild, moderate and severe types according to the infiltration depth of <1/3, 1/3-2/3 and >2/3 of inflammatory cells in the mucous layer and CAG was graded as mild, moderate and severe types according to the decreased levels of <1/3, 1/3-2/3 and >2/3 of the intrinsic glands[35]. At the same time, mucus histochemical stainings of AB/PAS for distinguishing acid mucus from neutral mucus and AF/AB for distinguishing sulphomucins from sialomucins were performed on the samples with IM confirmed by histopathological examination. According to the histological structures and properties of mucus excreted by cells, IM was classified into type I (complete type), type II (incomplete small intestinal type) and type III (incomplete colonic type)[36].

Statistical analysis

Chi-square test was applied and *P* values less than 0.05 were considered significant.

RESULTS

Pit patterns and pathohistological findings

Classification of gastric pits Based on the analysis of recorded static and successive images and refered to Guelrud' s study on mucosal patterns of Barrett' s esophagus with enhanced magnification endoscopy[18], we classified gastric pits into the following five fundamental types: type A, round-spot-like, distributing only in the gastric corpus and fundus with basically normal histology; type B, short-rod-like, with deeper pits, branches and curvatures fewer than those in type C, mainly distributing in the gastric antrum without obvious lesions such as inflammation; type C, with elongated and tortuous pits with obviously increased branches and curvatures, connected to present branch-like form, seen in mucosa with pathological changes as inflammation, edema and IM; type D, with reticular pits, seen in areas with more severe inflammation, edema and IM, also found in mucosa around erosion and ulcers; and type E, with villus-like pits, or with finger-like tubers, similar to enteral villus-like changes, seen only in the areas with IM (Figure 1). Overlappings and crossings of gastric pits might be present except the above five fundamental patterns. For example, a combination of type A and type B of gastric pits was frequently presented in the gastric angle.

In types B, C, D and E, moderate and severe inflammations were seen in 18.6 %(26/140), 85.1 %(40/47), 100 %(13/13) and 88.9 %(16/18) cases respectively. The inflammatory levels in types C, D and E were significantly higher than those in type B ($P<0.01$).

Features of atrophic gastritis under magnifying endoscope Under routine endoscope, changes of rough mucosa, unflat granules, increased white areas, exposure of submucous vessels could be seen in CAG[35]. Generally, theses changes could be

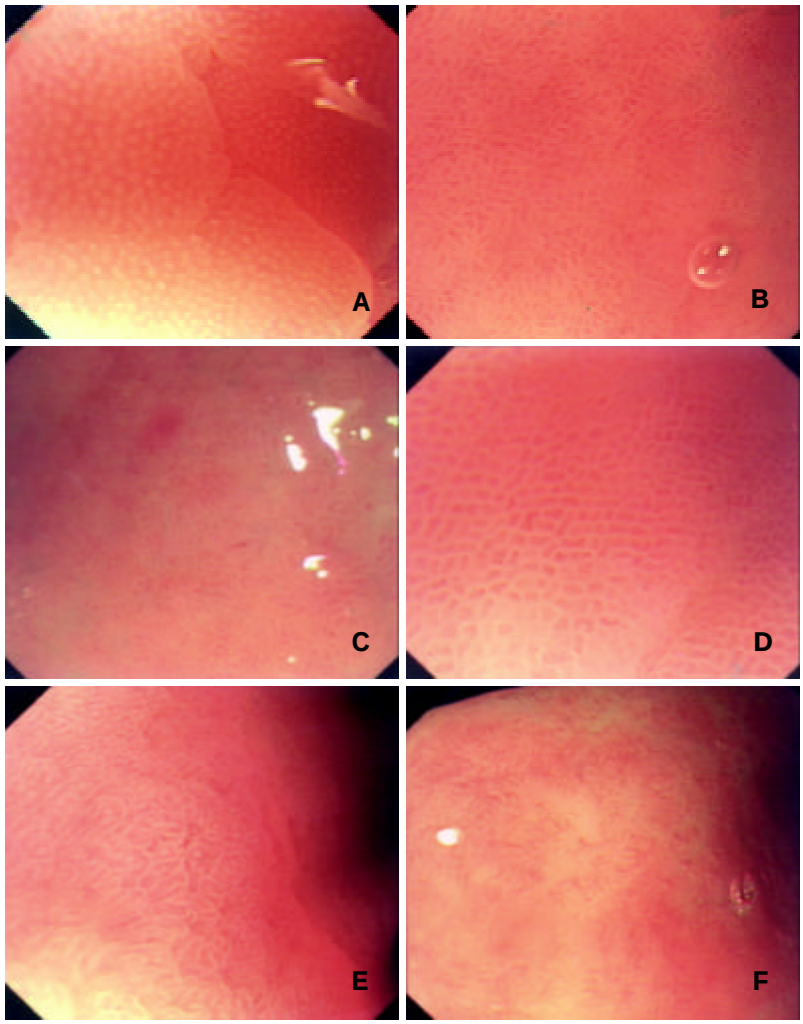

Figure 1 Pit patterns of gastric mucosa under magnifying endoscope. A: Type A: Gastric pits appeared as round spot, B: Type B: Gastric pits appeared as short rod, C: Type C: Gastric pits appeared as branched, D: Type D: Gastric pits appeared as reticular, E: Type E: Gastric pits appeared as villus, F: CAG: Decrease and disappearance of gastric pits.

more easily found in severe CAG, but it was hard to identify them in mild CAG. However, under magnifying endoscope, remarkably characteristic changes of CAG could be seen. With a comparatively low magnifying power, obvious red-white mucosa and increased white areas could be identified. When with enhanced magnifying power, disordered structures, decrease in quantity and even disappearance of pits as scar-like change could be observed in white areas (Figure 1-F).

Thirty-five patients with different grades of gastric mucous atrophy were confirmed by pathological examination in 140 patients, in which 27 in gastric antrum, 5 in gastric angle, 3 in gastric corpus, 16 with mild atrophy, 7 with moderate atrophy and 12 with severe atrophy. By routine endoscopy, only 8 patients (2 with moderate atrophy, 6 with severe atrophy), but by magnifying endoscopy, CAG-related changes were found in 33 patients (14 with mild atrophy, 7 with moderate atrophy, 12 with severe atrophy). The detection rates of atrophic gastritis by routine endoscopy and magnifying endoscopy were 22.9 %(8/35) and 94.3 %(33/35) respectively and significant difference was found by comparison of the two kinds of endoscopy (P<0.01).

Features of intestinal metaplasia under magnifying endoscope It was reported that characteristic changes such as light yellow or ivory-white nodosity-like, fishscale-like and diffusing granule-like appearances of IM in gastric mucosa could be found under routine endoscopy[37]. In this study, by analysis of magnifying endoscopy images of 31 patients with IM, we found that there were mainly three patterns of gastric pits in IM mucosal areas: type C (5 cases), type D (8cases) and type E (18cases). Particularly, very high specificity was found in type E. IM was confirmed pathologically in all the samples of 18 patients with type E. After classification of all the samples with IM by mucous histochemical staining, a certain relation was found between the patterns of gastric pits and classification of IM mucin phenotypes, as was shown in Table 1. Fourteen out of 18 patients (77.8 %) with complete type (type I) of IM appeared as type E of pit patterns, whereas only 4 of 13 (30.8 %) patients with incomplete type (types II and III) of IM appeared as the same type of pit patterns (P<0.05).

Table 1 Relation between IM pit patterns and IM mucin phenotypes

Pit patterns	Cases	Type I IM	Type II IM	Type III IM
Type C	5	2	3	0
Type D	8	2	5	1
Type E	18	14	3	1
Total	31	18	11	2

Architecture of collecting venules and H pylori infection

With reference to Yagi's literature[26], we classified the architecture of collecting venules into the following three types: type R (regular type) with diameter of minor venules being 0.4-0.5 mm and regular spider-like and jellyfish-like arrangement, type I (irregular type) in which decrease in quantity of collecting venules could be unclearly found with irregular arrangement, and type D (disappeared) in which collecting venules could not be found under magnifying endoscope (Figure 2).

When the patients in which positive *H pylori* was confirmed by both rapid urease test and Warrthin-Starry staining were regarded as being infected by *H pylori*, the *H pylori* infection rates in the patients with regular (R), irregular (I) and disappeared (D) types of collecting venules were 12.2 %, 60 % and 84.3 %, respectively. Statistical analysis revealed that *H pylori* infection rates in the patients with types D and I were markedly higher than those in patients with type R (P<0.01), but there was no significance between type I and type D (P>0.05). A comparison of different types of collecting venules by the corresponding rapid urease test and by Warrthin-Starry staining is shown in Table 2.

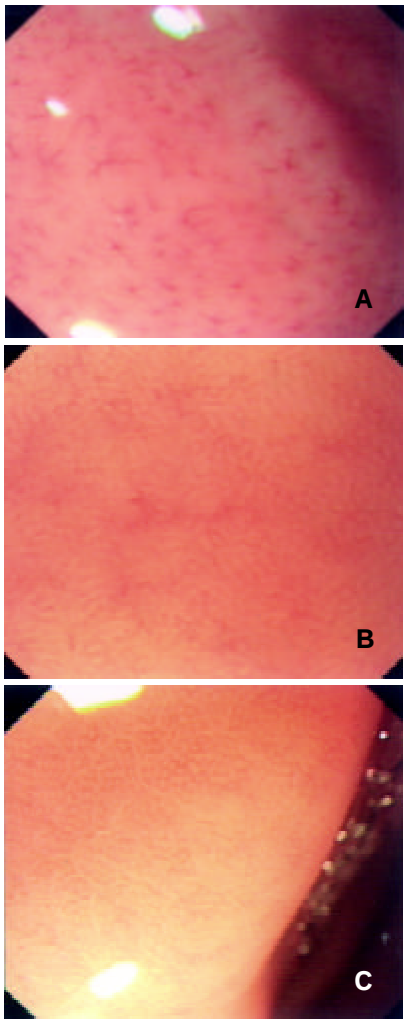

Figure 2 Architecture of collecting venules under magnifying endoscope. A: Type R: Regular spider-like arrangement of collecting venules, B: Type I: Unclear irregular arrangement of collecting venules, C: Type D: Disappearance of collecting venules.

Table 2 Relation of different architectures of collecting venules and *H pylori* infection

Collecting venules	Cases	Rapid urease test (+)	W-S staining (+)	Both methods(+)
Type R	74	9(12.2 %)	13(17.6 %)	9(12.2 %)
Type I	15	11(73.3 %)	9(60 %)	9 (60 %)
Type D	51	43(84.3 %)	45(86.3 %)	43(84.3 %)

DISCUSSION

The pit patterns observed on the mucosal surface are considered to reflect the arrangement and structure of surface epithelia, morphology, number, distribution, and function of glands, mucosal edema and inflammation, and vascular morphology, arrangement, number and distribution. The basic units of the microstructures on the surface of gastric mucosa are countless gastric pits that form gastric areas separated by minor gastric grooves (also called interval grooves). As the openings of glands, gastric pits are the first to have changes of the structures due to gastric mucosal lesions. Magnifying endoscope can be

used to observe the minute architecture of gastric pits because it has the similar magnifying power to that of stereomicroscope.

In this research, we studied the correlation of magnifying endoscopic patterns and histopathology, *Helicobacter pylori* infection of the gastric mucosa in 140 patients with chronic gastritis. There has been no widely accepted standard to the classification of gastric pits under magnifying endoscope, so the classification method, we used, was based on the analysis of our recorded static and successive images by magnifying endoscopy in the 140 patients and referred to Guelrud' s study on mucosal patterns of Barrett' s esophagus with enhanced magnification endoscopy[18]. Type A and type B represented the manifestation of normal gastric pits in gastric corpus and antrum, which concerned the distribution of gastric glands. Single tabular glands with short and fine neck were found in the gastric corpus and fundus, so gastric pits were presented with round spots as the openings of the gastric glands. Glands in frontal area of pyloric ostium and in gastric antrum were of multi-branches and curvatures and 3-5 glands often shared the same opening in one pit, thus the pits in frontal area of pyloric ostium and gastric antrum were short rod-like and deeper and longer than those of type A. Types C and D were formed by the enlargement, elongation, tortuosity of pits and connection of pits due to the pathological changes as inflammation and edema but type E might be the characteristic changes of intestinal metaplasia. Studies by Endo *et al.* of the mucosa with intestinal metaplasia in Barret esophagus in gastric cardia also revealed that villus-like pits were the characteristic change due to intestinal metaplasia[15].

Gastric mucosal atrophy could be identified by routine endoscopy usually when it was at more severe grade. Under magnifying endoscopy, disordered structures, deficiency and even disappearance of gastric pits were of high detection rate and accuracy for atrophic gastritis. As to mild and moderated grades of atrophy, the diagnostic sensitivity by magnifying endoscopy was higher than that by routine endoscopy. The decrease and disappearance of gastric pits due to atrophy were different from mucosal defect due to erosion in which there usually smooth-edged pits belonging to types C and D.

It was reported that characteristic changes such as light yellow or ivory-white nodosity-like, fishscale-like and diffusing granule-like appearances of intestinal metaplsia in gastric mucosa could be found under routine endoscopy[37]. The intestinal metaplasia could be classified into complete and incomplete types according to the histological structures and the properties of mucus excreted by cells[36]. In our study, the pit patterns of 31 patients with intestinal metaplasia appeared as type E in 18 (58.1 %), type D in 8 (25.8 %) and type C in 5 (16.1 %). Fourteen out of 18 patients (77.8 %) with complete type (type I) of intestinal metaplasia appeared as villus-like and finger-like changes (type E) of pit patterns, whereas only 4 out of 13 (30.8 %) patients with incomplete type (types II and III) of intestinal metaplasia appeared as the same type of pit patterns ($P<0.05$), suggesting type E of gastric pits was the result of characteristic change of complete intestinal metaplasia. In addition, our study also reveals that pits of incomplete intestinal metaplasia mainly belonged to types C and D (9/13, 69.2 %). Nevertheless, the above studies were still at preliminary stage with a small number of samples and further studies should be conducted to draw the final conclusion.

Collecting venules are tiny venules in gastric mucosa directly connected with capillary vessels. A few reports have been made on the architecture of collecting venules in gastric mucosa by magnifying endoscopy in which it was regarded as having certain specificity and feasibility to detect *Helicobacter pylori* infection[25,26]. It has also been verified by our study that *Helicobacter pylori* infection rate of patients with type R collecting venules was significantly lower than that with types I and D, suggesting that magnifying endoscopy was of high value in the diagnosis of *Helicobacter pylori* infection in gastric mucosa. As to the causes leading to the changes of collecting venules when *Helicobacter pylori* infection occurs, it has been reported that they were found in types I and D, in which remarkable increase of infiltration of neutrophils and monocytes was found and the architecture of collecting venules might be affected by edema of mucosa due to *Helicobacter pylori* infection[25,26]. However, further studies of the precise mechanism should be conducted because there are some other causes resulting in edema of mucosa.

In conclusion, it is a novel topic in the field of digestive endoscopy to diagnose minute lesions in gastric mucosa by magnifying endoscopy. Our preliminary study has shown that magnifying endoscopy is of high value in the diagnosis of gastric mucosal atrophy, intestinal metaplasia and *Helicobacter pylori* infection. However, the pit patterns of gastric mucosa, particularly those under magnifying chromoendoscopy are very complicated and there has been no widely accepted standard on the classification. Therefore, further studies are suggested on the clinicopathological significance of different patterns of gastric pits, particularly the characteristic changes of gastric pits and microvessels of intramucosal gastric carcinomas.

REFERENCES

1 **Makin GB**, Breen DJ, Monson JR. The impact of new technology on surgery for colorectal cancer. *World J Gastroenterol* 2001; **7**: 612-621

2 **Peitz U**, Malfertheiner P. Chromoendoscopy: from a research tool to clinical progress. *Dig Dis* 2002; **20**: 111-119

3 **Tamura S**, Furuya Y, Tadokoro T, Higashidani Y, Yokoyama Y, Araki K, Onishi S. Pit pattern and three-dimensional configuration of isolated crypts from the patients with colorectal neoplasm. *J Gastroenterol* 2002; **37**: 798-806

4 **Tonooka T**, Sano Y, Fujii T, Kato S, Yoshino T, Fu KI, Hironaka S, Ochiai A, Yoshida S. Adenocarcinoma in solitary large hyperplastic polyp diagnosed by magnifying colonoscope: report of a case. *Dis Colon Rectum* 2002; **45**: 1407-1411

5 **Morita T**, Tamura S, Miyazaki J, Higashidani Y, Onishi S. Evaluation of endoscopic and histopathological features of serrated adenoma of the colon. *Endoscopy* 2001; **33**: 761-765

6 **Matsumoto T,** Hizawa K, Esaki M, Kurahara K, Mizuno M, Hirakawa K, Yao T, Iida M. Comparison of EUS and magnifying colonoscopy for assessment of small colorectal cancers. *Gastrointest Endosc* 2002; **56**: 354-360

7 **Hurlstone DP**, Fujii T, Lobo AJ. Early detection of colorectal cancer using high-magnification chromoscopic colonoscopy. *Br J Surg* 2002; **89**: 272-282

8 **Tung SY**, Wu CS, Su MY. Magnifying colonoscopy in differentiating neoplastic from nonneoplastic colorectal lesions. *Am J Gastroenterol* 2001; **96**: 2628-2632

9 **Kato S**, Fujii T, Koba I, Sano Y, Fu KI, Parra-Blanco A, Tajiri H, Yoshida S, Rembacken B. Assessment of colorectal lesions using magnifying colonoscopy and mucosal dye spraying: can significant lesions be distinguished? *Endoscopy* 2001; **33**: 306-310

10 **Bruno MJ.** Magnification endoscopy, high resolution endoscopy, and chromoscopy; towards a better optical diagnosis. *Gut* 2003; **52**(Suppl 4): iv7-11

11 **Kudo S**, Kashida H, Tamura T, Kogure E, Imai Y, Yamano H, Hart AR. Colonoscopic diagnosis and management of nonpolypoid early colorectal cancer. *World J Surg* 2000; **24**: 1081-1090

12 **Nagata S**, Tanaka S, Haruma K, Yoshihara M, Sumii K, Kajiyama G, Shimamoto F. Pit pattern diagnosis of early colorectal carcinoma by magnifying colonoscopy: clinical and histological implications. *Int J Oncol* 2000; **16**: 927-934

13 **Inoue H**. Magnification endoscopy in the esophagus and stomach. *Digestive Endoscopy* 2001; **13**(Suppl): S40-S41

14 **Sharma P**, Weston AP, Topalovski M, Cherian R, Bhattacharyya A, Sampliner RE. Magnification chromoendoscopy for the detection of intestinal metaplasia and dysplasia in Barrett's oesophagus. *Gut* 2003; **52**: 24-27

15 **Endo T**, Awakawa T, Takahashi H, Arimura Y, Itoh F, Yamashita K, Sasaki S, Yamamoto H, Tang X, Imai K. Classification of Barrett's epithelium by magnifying endoscopy. *Gastrointest Endosc* 2002; **55**: 641-647
16 **Kumagai Y**, Inoue H, Nagai K, Kawano T, Iwai T. Magnifying endoscopy, stereoscopic microscopy, and the microvascular architecture of superficial esophageal carcinoma. *Endoscopy* 2002; **34**: 369-375
17 **Guelrud M**, Herrera I, Essenfeld H, Castro J, Antonioli DA. Intestinal metaplasia of the gastric cardia: A prospective study with enhanced magnification endoscopy. *Am J Gastroenterol* 2002; **97**: 584-589
18 **Guelrud M**, Herrera I, Essenfeld H, Castro J. Enhanced magnification endoscopy: a new technique to identify specialized intestinal metaplasia in Barrett's esophagus. *Gastrointest Endosc* 2001; **53**: 559-565
19 **Yao K**, Oishi T. Microgastroscopic findings of mucosal microvascular architecture as visualized by magnifying endoscopy. *Digestive Endoscopy* 2001; **13**(Suppl): S27-S33
20 **Tajiri H,** Matsuda K, Fujisaki J. What can see with the endoscope? Present status and future perspectives. *Digestive Endoscopy* 2002; **14**: 131-137
21 **Miwa H,** Sato N. Shed light again on magnifying endoscopy for diagnosis of early gastric cancer. *Digestive Endoscopy* 2001; **13**: 127-128
22 **Niwa Y,** Goto H, Ohmiya N, Ohtsuka Y, Ando N. Magnifying endoscopy for the diagnosis of early gastric cancer. *Digestive Endoscopy* 2002; **14**(Suppl): S70-S71
23 **Tajiri H**, Doi T, Endo H, Nishina T, Terao T, Hyodo I, Matsuda K, Yagi K. Routine endoscopy using a magnifying endoscope for gastric cancer diagnosis. *Endoscopy* 2002; **34**: 772-777
24 **Yao K**, Oishi T, Matsui T, Yao T, Iwashita A. Novel magnified endoscopic findings of microvascular architecture in intramucosal gastric cancer. *Gastrointest Endosc* 2002; **56**: 279-284
25 **Yagi K,** Nakamura A, Sekine A. Comparison between magnifying endoscopy and histological, culture and urease test findings from the gastric mucosa of the corpus. *Endoscopy* 2002; **34**: 376-381
26 **Yagi K,** Nakamura A, Sekine A. Characteristic endoscopic and magnified endoscopic findings in the normal stomach without *Helicobacter pylori* infection. *J Gastroenterol Hepatol* 2002; **17**: 39-45
27 **Cales P,** Oberti F, Delmotte JS, Basle M, Casa C, Arnaud JP. Gastric mucosal surface in cirrhosis evaluated by magnifying endoscopy and scanning electronic microscopy. *Endoscopy* 2000; **32**: 614-623
28 **Fujiya M,** Saitoh Y, Nomura M, Maemoto A, Fujiya K, Watari J, Ashida T, Ayabe T, Obara T, Kohgo Y. Minute findings by magnifying colonoscopy are useful for the evaluation of ulcerative colitis. *Gastrointest Endosc* 2002; **56**: 535-542
29 **Jiang B.** Chromoendoscopy and high-magnification colonoscopy in early detection of colorectal cancer. *Diyi Junyi Daxue Xuebao* 2002; **22**: 385-387
30 **Shi HX,** Wu YL. Distinguishing colorectal minute lesions by high-resolution video endoscope with indigo carmine dye spray. *Zhonghua Xiaohua Neijing Zazhi* 1999; **16**: 135-137
31 **Li ZX**, Zhang XR, An DL, Chen FL, Gong JZ. Diagnosis and treatment of early colorectal cancer. *Zhonghua Waike Zazhi* 2000; **38**: 352-354
32 **Yu YZ,** Wang QH, Yu ZL. The gastric mucosal features of *Helicobacter pylori* associated gastritis evaluated by high-resolution magnifying endoscopy. *Zhonghua Xiaohua Neijing Zazhi* 2002; **19**: 274-277
33 **Chen X,** Cen R, Xu FX, Xia J, Luo C, Cheng FL. Pathological analysis with new magnifying endoscopic classification of the gastric mucosal pattern. *Zhongguo Neijing Zazhi* 2002; **8**: 37-38
34 **Gao HJ**, Yu LZ, Bai JF, Peng YS, Sun G, Zhao HL, Miu K, Lu XZ, Zhang XY, Zhao ZQ. Multiple genetic alterations and behavior of cellular biology in gastric cancer and other gastric mucosal lesions: *H pylori* infection, histological types and staging. *World J Gastroenterol* 2000; **6**: 848-854
35 **Chinese Society of Gastroenteroloy, Chinese Medical Association**. Common opinions on chronic gastritis of China. *Zhonghua Xiaohua Zazhi* 2000; **20**: 199-201
36 **Liu YQ**, Zhao H, Ning T, Ke Y, Li JY. Expression of 1A6 gene and its correlation with intestinal gastric carcinoma. *World J Gastroenterol* 2003; **9**: 238-241
37 **Zhou LY**, Li JH, Lin SR, Jin Z, Ding SG, Huang XP, Xia ZW. Endoscopic diagnosis of intestinal metaplasia in gastric mucosa. *Zhonghua Xiaohua Neijing Zazhi* 2001; **18**: 84-86

Edited by Xia HHX and Wang XL

P.O.Box 2345, Beijing 100023,China
Fax: +86-10-85381893
E-mail: wjg@wjgnet.com www.wjgnet.com

World J Gastroenterol 2003;9(11):2557-2560
World Journal of Gastroenterology
 ISSN 1007-9327

• CLINICAL RESEARCH •

Regional variations in mortality rates of pancreatic cancer in China: Results from 1990-1992 national mortality survey

Ke-Xin Chen, Peizhong Peter Wang, Si-Wei Zhang, Lian-Di Li, Feng-Zhu Lu, Xi-Shan Hao

Ke-Xin Chen, Xi-Shan Hao, Tianjin Cancer Institute and Hospital, Tianjin Medical University, Tianjin, 300060, China
Peizhong Peter Wang, Department of Community Health, University of Toronto, Canada
Si-Wei Zhang, Lian-Di Li, Feng-Zhu Lu, Office of Cancer Prevention and Control in China, Beijing, 100021, China
Supported by the National Medical Science and Technology Foundation during the 8th Five-Year Plan Period, No. 85-914-01-07
Correspondence to: Dr. Ke-Xin Chen, Department of Epidemiology, Tianjin Cancer Institute and Hospital, Huanhu Xi Road, Ti Yuanbei, He Xi District, Tianjin, 300060, China. chenkexin@21cn.com
Telephone: +86-22-23359929 Ext 226 **Fax:** +86-22-23359984
Received: 2003-05-10 **Accepted:** 2003-06-04

Abstract

AIM: To examine the regional variations in mortality rates of pancreatic cancer in China.

METHODS: Aggregated mortality data of pancreatic cancer were extracted from the 1990-1992 national death of all causes and its mortality survey in China. Age specific and standardized mortality rates were calculated at both national and provincial levels with selected characteristics including sex and residence status.

RESULTS: Mortality of pancreatic cancer ranked the ninth and accounted for 1.38 percent of the total malignancy deaths. The crude and age standardized mortality rates of pancreatic cancer in China in the period of 1990-1992 were 1.48/100 000 and 1.30/100 000, respectively. Substantial regional variations in mortality rates across China were observed with adjusted mortality rates ranging from 0.43/100 000 to 3.70/100 000 with an extremal value of 8.7. Urban residents had significant higher pancreatic mortality than rural residents.

CONCLUSION: The findings of this study show different mortality rates of this disease and highlight the importance of further investigation on factors, which might contribute to the observed epidemiological patterns.

Chen KX, Wang PP, Zhang SW, Li LD, Lu FZ, Hao XS. Regional variations in mortality rates of pancreatic cancer in China: Results from 1990-1992 national mortality survey. *World J Gastroenterol* 2003; 9(11): 2557-2560
http://www.wjgnet.com/1007-9327/9/2557.asp

INTRODUCTION

Pancreatic cancer is a relatively common malignant disease in the world, both its incidence and mortality rate are ranked in the first ten cancers[1,2]. Especially in recent years, a gradually increased tendency of the disease has been found[3-6]. About 200 000 new cases of pancreatic cancer are reported worldwide annually. Despite the overall improvement in cancer diagnosis and treatment in the past half century, there has been little change in the survival of pancreatic cancer patients. The reported worldwide annual incidence accounts for 2 % of all malignant tumors and is associated with about 196 000 deaths from the disease[7-11]. Though pancreatic cancer is relatively uncommon in China, but it still accounts for substantial cancer related deaths because of its dismal survival rate. Thus, the mortality rate of this disease serves as a mirror for its incidence. Notwithstanding previous studies in China have shown that there were significant geographic variations for several cancer sites, such as liver and esophagus, little is known for pancreatic cancer[12-14]. As the causes of pancreatic cancer are largely unknown, epidemiological studies on regional mortality rate variations may shed light on seeking possible modifiable factors associated with this disease.

MATERIALS AND METHODS

Data source

1990-1992 national mortality survey As China does not have a centralized vital statistics system and cancer registration, national level information on disease specific mortality is often based on periodic national mortality surveys (NMS), the first of which was initiated in the early 1970s. Its purpose was to generate nationally representative estimates of mortality due to various health conditions, such as cancer, heart disease and stroke. The more recent one was conducted between 1990 and 1992 with the primary focus on malignant tumors, which was the data source for this study.

Briefly, the 1990-1992 NMS was a two-stage stratified probability survey. At the first stage, each of the 22 provinces, 5 autonomous regions, and 3 municipatities directly administrated cities under the Central Government (Beijing, Shanghai, and Tianjin) represented one of 30 strata. For the ease of the presentation, we referred to the 30 strata as "areas". The second stratum was formed at county or district level according to the cancer mortality levels (2-3 levels from low to high) from the previous survey. Thus, the primary sampling unit for this survey was county or district (for Beijing, Shanghai and Tianjin). Overall, the sample size for this survey was designed to cover 10 % of all deaths or 242 million baseline person years during the study period. Detailed information can be found from the National Mortality Survey Manual. With respect to pancreatic cancer, samples from 8 of the first level strata did not have sufficient number of cases to generate meaningful estimates, thus the mortality estimates were only applicable to 22 of the first level strata. Specifically, the 22 areas were Beijing, Tianjin, Hebei, Shanxi, Neimeng, Liaoning, Jilin, Heilongjiang, Shanghai, Jiangsu, Anhui, Jiangxi, Fujian, Henan, Hunan, Hainan, Guangxi, Sichuan, Yunnan, Guizhou, Gansu, and Ningxia.

Case assessment and baseline population All death certificates were retrieved from the local death registration offices for the sampled counties or districts. Local neighborhood representatives were also interviewed to further verify each deceased person for possible misreporting and discover deaths not reflected at death registration offices. Causes of deaths obtained from death certificates were checked with clinical records. When clinical records were missing or

not available, possible diagnoses were solicited from the medical professionals who had once treated the case. Each reported cause of death was further converted into 3-digit ICD-9 codes and pancreatic cancer was determined for ICD-9 157. Age-sex specific population data for each surveyed county or district were derived from interpolation using the data from the two most recent censuses conducted in 1982 and 1990.

Statistical analysis

Both crude and age-sex adjusted mortality rates were calculated both at provincial and national levels. In order to make the estimates comparable to reported mortality data from other populations, two standard populations were used: the 1980 Chinese population and the world standard population. The extremal quotient (EQ) was used to quantify regional variation[15]. The EQ is the ratio of the mortality from area with the highest level relative to the area with the lowest level. Age standardised mortality rates from each individual area (defined by resident status) were derived and compared with the corresponding national mean and median using the 1990-1992 NMS. In addition to assessing differences in mortality rate among areas and national levels, we also juxtaposed pancreatic cancer with other leading cancers, such as lung and breast cancers in terms of their relative ranking.

RESULTS

In total, pancreatic cancer deaths were identified from the 181 primary sampling units (counties or districts), among which 54 and 127 were considered as urban and rural respectively.

Table 1 displays the crude and standardized mortality rates of pancreatic cancer. As shown in this table, the crude and Chinese population adjusted mortality rates were 1.29 and 1.08 per 100 000 person-year during the study period.

Table 1 Selected indices derived from pancreatic cancer mortality (1/100 000) in China, 1990-1992

	Crude rate	ASMR1	ASMR2	Mortality proportion to all cancer death (%)
Total	1.48	1.30	1.74	1.38
Male	1.65	1.52	2.03	1.25
Female	1.29	1.08	1.46	1.62

ASMR: Age adjusted mortality rate, 1=the Chinese population in 1980, 2=world population.

Table 2 compares the mortality of pancreatic cancer with other leading cancers in terms of standardized rates, mortality proportion, and relative ranking. Overall, the mortality of pancreatic cancer ranked the 9th and accounted for 1.38 % of total cancer deaths after colon cancer.

While pancreatic cancer could occur at any age, its mortality varied greatly among different age groups. The mortality remained low and did not increase until age 45, there was a steep increase in both males and females from age 45 to age 75 before it reached a plateau around 75. There seemed to be a mortality drop in males after age 75. Pancreatic cancer mortality rates were apparently higher in males than in females, with the ratio 1.4:1.

Regional comparisons (Table 3) suggested that a substantial variation in pancreatic cancer mortality across the 22 regions and standardized mortality rates varied from the lowest 0.47/100 000 person-year in Hunan Province to the highest 3.73/100 000 person year in Shanghai with an extremal quotient of 8.76. Using the national average level as a standard, eight provinces had a rate higher than average and they were Shanghai, Tianjin, Liaoning, Heilongjiang, Jiangsu, Jilin, Beijing, and Ningxia. However, there was little variation in terms of mortality, sex ratios varying between 1.07 and 2.3, most of the values were around 1.5.

Table 3 Distribution of pancreatic cancer mortality in 22 provinces, cities, and autonomous regions in 1990-1992

Regions	Males		Females		Total		M/F
	CR	ASR	CR	ASR	CR	ASR	ratio
Hunan	0.57	0.54	0.36	0.32	0.47	0.43	1.69
Guangxi	0.73	0.73	0.40	0.36	0.58	0.55	2.03
Hainan	0.86	0.76	0.47	0.48	0.67	0.65	1.58
Gansu	0.85	0.87	0.46	0.49	0.66	0.69	1.78
Guizhou	0.97	0.99	0.52	0.51	0.75	0.76	1.94
Jiangxi	0.89	0.92	0.62	0.62	0.76	0.78	1.48
Henan	0.99	0.98	0.68	0.60	0.84	0.78	1.63
Sichuan	1.07	0.99	0.76	0.63	0.92	0.79	1.57
Fujian	1.32	1.36	0.69	0.60	1.01	0.96	**2.27**
Neimenggu	1.72	1.16	0.84	0.81	1.31	0.99	1.43
Shanxi	1.34	1.21	1.02	0.89	1.19	1.04	1.36
Yunnan	1.38	1.24	0.99	0.87	1.19	1.05	1.43
Hebei	1.49	1.37	0.95	0.81	1.23	1.08	1.69
Anhui	1.50	1.44	1.20	0.96	1.36	1.20	1.50
Ningxia	1.85	1.68	1.17	1.06	1.52	1.38	1.58
Beijing	3.21	2.28	1.97	1.25	2.59	1.75	1.82
Jilin	2.07	1.98	1.80	1.85	1.94	1.91	**1.07**
Jiangsu	3.29	2.62	3.29	2.20	3.29	2.40	1.19
Heilongjiang	2.52	2.57	2.26	2.38	2.40	2.47	1.08
Liaoning	3.71	3.16	2.76	2.38	3.24	2.78	1.33
Tianjin	5.68	3.80	4.53	2.91	5.10	3.34	1.31
Shanghai	7.55	**4.22**	6.87	**3.26**	7.21	**3.70**	1.29

Table 2 Age-standardized mortality rates and proportion of major malignant cancers in China

Type of tumor	Males			Females			Total		
	ASR	P(%)	Rank	ASR	P (%)	Rank	ASR	P (%)	Rank
Stomach	30.78	25.10	1	14.52	21.80	1	22.51	23.93	1
Liver	25.73	21.42	2	9.55	14.00	3	17.75	18.74	2
Esophagus	20.22	16.45	4	10.32	15.50	2	15.15	16.11	4
Lung	21.68	17.73	3	9.03	13.46	4	15.23	16.18	3
Rectum	3.60	2.94	5	2.55	3.80	7	3.06	3.29	5
Leukemia	3.46	2.67	6	2.86	3.70	8	3.16	3.04	6
Breast				2.93	4.24	6			
Brain& nervous system	2.01	1.63	7	1.48	2.02	9	1.74	1.77	7
Cervix	-	-	-	3.16	4.62	5	-	-	
Colon	1.49	1.21	9	1.19	1.80	10	1.34	1.43	8
Pancreas	1.52	1.25	8	1.08	1.62	11	1.30	1.38	9
Total	122.35	100.00		67.61	100.00		94.58	100.00	

These comparisons further indicated that urban residents had a significant higher mortality than their rural counterparts. These differences existed in both males and females (Table 4, Figure1) across age groups.

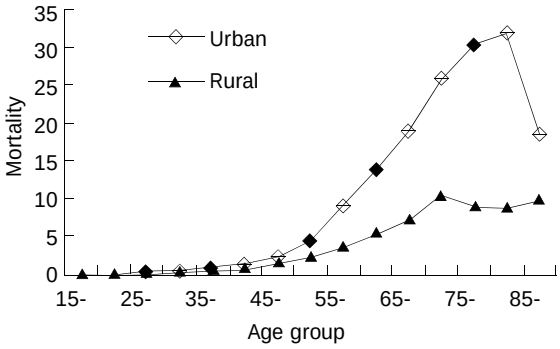

Figure 1 Comparison of age-specific mortality of pancreatic cancer between urban and rural areas, 1990-1992

Table 4 Comparison of pancreatic cancer mortality between urban and rural areas in China, 1990-1992

Region	Sex	CR	ASR
Total	Urban	2.83	2.27
	Rural	1.05	0.95
	U/R ratio	2.67	2.39
Male	Urban	3.16	2.68
	Rural	1.17	1.11
	U/R ratio	2.70	2.41
Female	Urban	2.47	21.89
	Rural	0.92	0.80
	U/R ratio	2.68	2.36

DISCUSSION

In this study, we described some epidemiological characteristics of pancreatic cancer using the most recent Chinese mortality survey data. Compared with other previous studies in China, the age standardized mortality rates from this study appeared to be higher than those reported previously. This may suggest that the mortality rate of pancreatic cancer is increasing.

Ecological studies[16-24] found as shown in Figures 2-3 that the mortality of pancreatic cancer seemed to be correlated with the level of economic development. Developed countries, such as Japan and the United States[25-29] had a higher pancreatic cancer mortality than that of less developed countries, such as some African countries[30-33]. China is a big country with unbalanced economic development and diverse lifestyles. The economic developmental gaps between urban and rural areas seen in China are greater than those in the developed countries. Findings from this study suggest substantial regional variations in the mortality rates of pancreatic cancer and in general, economically more developed regions have higher mortality rates than that of less developed regions. For example, Beijing, Shanghai, and Tianjin shared the 3 highest mortality rates. Thus, results from this study are in accord with previous observations.

The use of a population based national representative sample in the present study was unique in its reliability. Also, in this study most death certificates were crossly validated and consequently the reported causes of death were more believable. Furthermore, as all studied areas used uniform standards, the mortality rate estimates across areas had a good comparability. However, there were also limitations associated with this study. First, all information used in this study was derived from the survey, thus the case assessment method could not be compared with clinical diagnosis. Second, since this survey did not collect life style information (such as smoking and diet) for the deceased subjects, we were restricted from further exploring the impact of potential risk factors on this condition. Lastly, only aggregated data were available to the authors, we were unable to calculate the variances for the estimated mortality rates. As a result, we could only provide point estimates without 95 % confidence intervals.

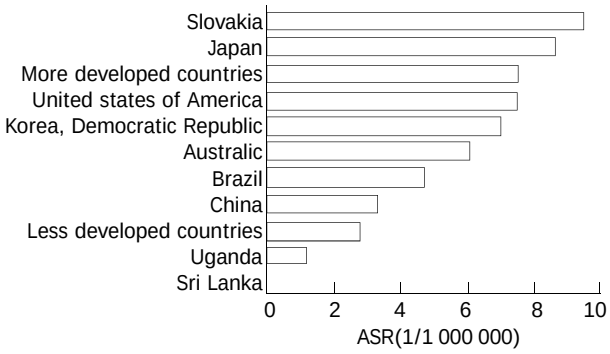

Figure 2 World pancreatic cancer mortality in different countries (male).

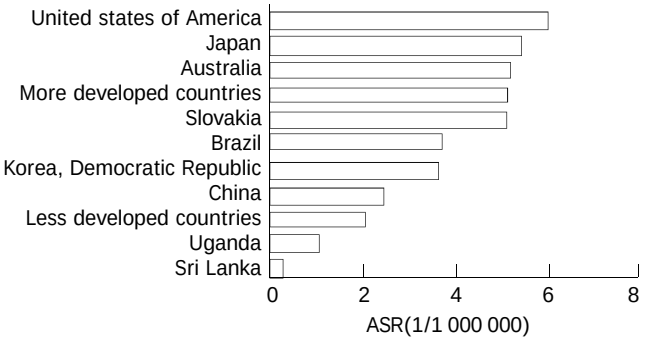

Figure 3 World pancreatic cancer mortality in different countries (female).

In conclusion, we have demonstrated a substantial variation in pancreatic cancer mortality rates across the Mainland China. The results reported in this study beg for answers to the observed differences. As pancreatic cancer is a fast growing disease associated with high fatality, more in-depth epidemiological studies on identifying modifiable risk factors are warranted.

ACKNOWLEGEMENTS

We are grateful to all medical workers from 22 provinces (cities, districts) in China for our data collection and preparation. We want to thank Tianjin Cancer Institute and Hospital for its financial support.

REFERENCES

1 **Levi F**, Lucchini F, Negri E, Boyle P, La Vecchia C. Mortality from major cancer sites in the European Union, 1955-1998. *Ann Oncol* 2003; **14**: 490-495

2 **Remontet L**, Esteve J, Bouvier AM, Grosclaude P, Launoy G, Menegoz F, Exbrayat C, Tretare B, Carli PM, Guizard AV, Troussard X, Bercelli P, Colonna M, Halna JM, Hedelin G, Mace-Lesec'h J, Peng J, Buemi A, Velten M, Jougla E, Arveux P, Le Bodic L, Michel E, Sauvage M, Schvartz C, Faivre J. Cancer incidence and mortality in France over the period 1978-2000. *Rev Epidemiol Sante Publique* 2003; **51**(1Pt 1): 3-30

3 **Fernandez E**, La Vecchia C, Porta M, Negri E, Lucchini F, Levi F. Trends in pancreatic cancer mortality in Europe, 1955-1989. *Int J Cancer* 1994; **57**: 786-792

4 **Vutuc C**, Waldhoer T, Haidinger G. Impact of non-invasive imaging techniques on the trend of pancreatic cancer mortality in Austria. *Wien Med Wochenschr* 1996; **146**: 258-260

5 **Lin RS**, Lee WC. Mortality trends of pancreatic cancer: an affluent type of cancer in Taiwan. *J Formos Med Assoc* 1992; **91**: 1148-1153

6 **Yang CY**, Chiu HF, Cheng MF, Tsai SS, Hung CF, Tseng YT. Pancreatic cancer mortality and total hardness levels in Taiwan's drinking water. *J Toxicol Environ Health A* 1999; **56**: 361-369

7 **Bakkevold KE**, Kambestad B. Morbidity and mortality after radical and palliative pancreatic cancer surgery. Risk factors influencing the short-term results. *Ann Surg* 1993; **217**: 356-368

8 **Riggs JE**. Longitudinal Gompertzian analysis of pancreatic cancer mortality in the U.S., 1962-1987: distinguishing between competitive and environmental influences upon evolving mortality patterns. *Mech Ageing Dev* 1991; **61**: 197-208

9 **Binstock M**, Krakow D, Stamler J, Reiff J, Persky V, Liu K, Moss D. Coffee and pancreatic cancer: an analysis of international mortality data. *Am J Epidemiol* 1983; **118**: 630-640

10 **Calle EE**, Murphy TK, Rodriguez C, Thun MJ, Heath CW Jr. Diabetes mellitus and pancreatic cancer mortality in a prospective cohort of United States adults. *Cancer Causes Control* 1998; **9**: 403-410

11 **Pickle LW**, Gottlieb MS. Pancreatic cancer mortality in Louisiana. *Am J Public Health* 1980; **70**: 256-259

12 **Boffetta P**, Burstyn I, Partanen T, Kromhout H, Svane O, Langard S, Jarvholm B, Frentzel-Beyme R, Kauppinen T, Stucker I, Shaham J, Heederik D, Ahrens W, Bergdahl IA, Cenee S, Ferro G, Heikkila P, Hooiveld M, Johansen C, Randem BG, Schill W. Cancer mortality among European asphalt workers: an international epidemiological study. II. Exposure to bitumen fume and other agents. *Am J Ind Med* 2003; **43**: 28-39

13 **Gapstur SM**, Gann PH, Lowe W, Liu K, Colangelo L, Dyer A. Abnormal glucose metabolism and pancreatic cancer mortality. *Jama* 2000; **283**: 2552-2558

14 **Ghadirian P**, Thouez JP, PetitClerc C. International comparisons of nutrition and mortality from pancreatic cancer. *Cancer Detect Prev* 1991; **15**: 357-362

15 **Neoptolemos JP**, Russell RC, Bramhall S, Theis B. Low mortality following resection for pancreatic and periampullary tumours in 1026 patients: UK survey of specialist pancreatic units. UK Pancreatic Cancer Group. *Br J Surg* 1997; **84**: 1370-1376

16 **Ghadirian P**, Lynch HT, Krewski D. Epidemiology of pancreatic cancer: an overview. *Cancer Detect Prev* 2003; **27**: 87-93

17 **Coughlin SS**, Calle EE, Patel AV, Thun MJ. Predictors of pancreatic cancer mortality among a large cohort of United States adults. *Cancer Causes Control* 2000; **11**: 915-923

18 **Imaizumi Y**. Longitudinal Gompertzian analysis of mortality from pancreatic cancer in Japan, 1955-1993. *Mech Ageing Dev* 1996; **90**: 163-181

19 **Bardin JA**, Eisen EA, Tolbert PE, Hallock MF, Hammond SK, Woskie SR, Smith TJ, Monson RR. Mortality studies of machining fluid exposure in the automobile industry. V: A case-control study of pancreatic cancer. *Am J Ind Med* 1997; **32**: 240-247

20 **Clary T**, Ritz B. Pancreatic cancer mortality and organochlorine pesticide exposure in California, 1989-1996. *Am J Ind Med* 2003; **43**: 306-313

21 **Inoue M**, Tajima K, Takezaki T, Hamajima N, Hirose K, Ito H, Tominaga S. Epidemiology of pancreatic cancer in Japan: a nested case-control study from the Hospital-based Epidemiologic Research Program at Aichi Cancer Center (HERPACC). *Int J Epidemiol* 2003; **32**: 257-262

22 **Kauppinen T**, Heikkila P, Partanen T, Virtanen SV, Pukkala E, Ylostalo P, Burstyn I, Ferro G, Boffetta P. Mortality and cancer incidence of workers in Finnish road paving companies. *Am J Ind Med* 2003; **43**: 49-57

23 **Mohan AK**, Hauptmann M, Freedman DM, Ron E, Matanoski GM, Lubin JH, Alexander BH, Boice JD Jr, Doody MM, Linet MS. Cancer and other causes of mortality among radiologic technologists in the United States. *Int J Cancer* 2003; **103**: 259-267

24 **Konner J**, O'Reilly E. Pancreatic cancer: epidemiology, genetics, and approaches to screening. *Oncology (Huntingt)* 2002; **16**: 1615-1622, 1631-1632

25 **Lee WC** , Lin RS. Age-period-cohort analysis of pancreatic cancer mortality in Taiwan, 1971-1986. *Int J Epidemiol* 1990; **19**: 839-847

26 **Mulder I**, Hoogenveen RT, van Genugten ML, Lankisch PG, Lowenfels AB, de Hollander AE, Bueno-de-Mesquita HB. Smoking cessation would substantially reduce the future incidence of pancreatic cancer in the European Union. *Eur J Gastroenterol Hepatol* 2002; **14**: 1343-1353

27 **Newnham A**, Quinn MJ, Babb P, Kang JY, Majeed A. Trends in oesophageal and gastric cancer incidence, mortality and survival in England and Wales 1971-1998 / 1999. *Aliment Pharmacol Ther* 2003; **17**: 655-664

28 **Lee IM**, Sesso HD, Oguma Y, Paffenbarger RS Jr. Physical activity, body weight, and pancreatic cancer mortality. *Br J Cancer* 2003; **88**: 679-683

29 **Zervos EE**, Norman JG, Gower WR, Franz MG, Rosemurgy AS. Matrix metalloproteinase inhibition attenuates human pancreatic cancer growth *in vitro* and decreases mortality and tumorigenesis *in vivo*. *J Surg Res* 1997; **69**: 667-671

30 **Muirhead CR**, Bingham D, Haylock RG, O'Hagan JA, Goodill AA, Berridge GL, English MA, Hunter N, Kendall GM. Follow up of mortality and incidence of cancer 1952-98 in men from the UK who participated in the UK's atmospheric nuclear weapon tests and experimental programmes. *Occup Environ Med* 2003; **60**: 165-172

31 **Corella Piquer D**, Cortina Greus P, Coltell Simon O. Nutritional factors and geographic differences in pancreatic cancer mortality in Spain. *Rev Sanid Hig Publica* 1994; **68**: 361-376

32 **Olsen GW**, Lacy SE, Bodner KM, Chau M, Arceneaux TG, Cartmill JB, Ramlow JM,Boswell JM. Mortality from pancreatic and lymphopoietic cancer among workers in ethylene and propylene chlorohydrin production. *Occup Environ Med* 1997; **54**: 592-598

33 **Pasquali C**, Sperti C, Filipponi C, Pedrazzoli S. Epidemiology of pancreatic cancer in Northeastern Italy: incidence, resectability rate, hospital stay, costs and survival (1990-1992). *Dig Liver Dis* 2002; **34**: 723-731

Edited by Xu JY and Wang XL

P.O.Box 2345, Beijing 100023,China
Fax: +86-10-85381893
E-mail: wjg@wjgnet.com www.wjgnet.com

World J Gastroenterol 2003;9(11):2561-2564
World Journal of Gastroenterology
 ISSN 1007-9327

• CLINICAL RESEARCH •

Intensity modulated radiation therapy and chemotherapy for locally advanced pancreatic cancer: Results of feasibility study

Yong-Rui Bai, Guo-Hua Wu, Wei-Jian Guo, Xu-Dong Wu, Yuan Yao, Yin Chen, Ren-Hua Zhou, Dong-Qin Lu

Yong-Rui Bai, Guo-Hua Wu, Xu-Dong Wu, Yuan Yao, Yin Chen, Ren-Hua Zhou, Dong-Qin Lu, Department of Radiation Oncology, Xinhua Hospital of Shanghai Second Medical University, Shanghai 200092, China
Wei-Jian Guo, Department of Oncology, Xinhua Hospital of Shanghai Second Medical University, Shanghai 200092, China
Supported by Health Bureau of Shanghai City, No. 00436
Correspondence to: Dr. Yong-Rui Bai, Department of Radiation Oncology, Xinhua Hospital of Shanghai Second Medical University, Shanghai 200092, China. baiyongrui@online.sh.cn
Telephone: +86-21-65790000 **Fax:** +86-21-65030840
Received: 2003-06-16 **Accepted:** 2003-07-24

Abstract

AIM: To explore whether intensity modulated radiation therapy (IMRT) in combination with chemotherapy could increase radiation dose to gross tumor volume without severe acute radiation related toxicity by decreasing the dose to the surrounding normal tissue in patients with locally advanced pancreatic cancer.

METHODS: Twenty-one patients with locally advanced pancreatic cancer were evaluated in this clinical trial. Patients would receive the dose of IMRT from 21Gy to 30Gy in 7 to 10 fractions within two weeks after conventional radiotherapy of 30Gy in 15 fractions over 3 weeks. The total escalation tumor dose would be 51, 54, 57, 60Gy, respectively. 5-fluororacil (5-FU) or gemcitabine was given concurrently with radiotherapy during the treatment course.

RESULTS: Sixteen patients who had completed the radiotherapy plan with doses of 51Gy (3 cases), 54Gy (3 cases), 57Gy (3 cases) and 60Gy (7 cases) were included for evaluation. The median levels of CA19-9 prior to and after radiotherapy were 716 U/ml and 255 U/ml respectively ($P<0.001$) in 13 patients who demonstrated high levels of CA19-9 before radiotherapy. Fourteen patients who suffered from pain could reduce at least 1/3-1/2 amount of analgesic intake and 5 among these patients got complete relief of pain. Ten patients improved in Karnofsky performance status (KPS). The median follow-up period was 8 months and one-year survival rate was 35 %. No patient suffered more than grade III acute toxicities induced by radiotherapy.

CONCLUSION: Sixty Gy in 25 fractions over 5 weeks with late course IMRT technique combined with concurrent 5-FU chemotherapy can provide a definitely palliative benefit with tolerable acute radiation related toxicity for patients with advanced pancreatic cancer.

Bai YR, Wu GH, Guo WJ, Wu XD, Yao Y, Chen Y, Zhou RH, Lu DQ. Intensity modulated radiation therapy and chemotherapy for locally advanced pancreatic cancer: Results of feasibility study. *World J Gastroenterol* 2003; 9(11): 2561-2564
http://www.wjgnet.com/1007-9327/9/2561.asp

INTRODUCTION

The incidence of pancreatic carcinoma has been continuously increasing worldwide in recent years. The incidence in Shanghai of China has increased to 9.6 per 100 000 for males and 9.2 per 100 000 for females. Most patients have locally advanced unresectable disease at the time of initial diagnosis because of lacking clinical symptoms and signs. Without treatment intervention, the mean time of survival was approximately 4 to 6 months[1]. Although surgery was considered to be the only curative treatment method, there were only 10-20 % patients who had resectable tumors suitable for radical resection and 30-85 % patients would have local recurrences[2].

At present, there are no satisfactory treatment modalities for patients with advanced pancreatic carcinoma. Adenocarcinoma of pancreas is a disease characterized by resistance to cytotoxic therapy including chemotherapy and radiotherapy. Treatment response of systemic chemotherapy is relatively poor with only 20 % response rate, which would last only a short time and most of the treatment effects are partial response. Meanwhile, the conventional radiation dose to gross tumor volume is not large enough to cure patients with pancreatic carcinoma because of the limited tolerant dose to the surrounding normal tissues such as gastrointestinal tract and kidneys. Many studies have shown that the local control and survival would be maximized if patients with pancreatic carcinoma were treated by surgery combined with chemoradiation therapy[3-6]. There were full laboratory and clinical evidences of potent radiosensitizing properties and significant systemic activity of 5-fluorouracil (5-FU) and/or gemcitabine (GEM) used in combination with radiothetapy in pancreatic carcinoma[7-12].

In addition, since 1990' s, radiation treatment equipments and related techniques have been developed dramatically. Especially, more attention has been paid to intensity modulated radiation therapy (IMRT), which is an approach with the aid of modern computer treatment planning system to conformal radiation therapy that conforms a high dose to the target (tumor) volume while restricting dose to the surrounding sensitive structures, and encouraging results have been achieved in clinical trials in head and neck carcinoma and thoracic carcinoma.

However, conventional radiotherapy can not give a higher dose needed to eradicate pancreatic carcinoma cells which are moderately sensitive to radiation due to the dose limited tissues adjacent to pancreas. In general, the dose adopted in conventional radiotherapy was approximately or less than 50Gy in 25 fractions over 5 weeks[5,11,12]. But the optimal dose of IMRT to treat patients with pancreatic carcinoma has not been established, especially in combination with chemotherapies such as 5-FU or GEM.

In this study, we reported our experience in the combination of IMRT and chemotherapy with 5-FU or GEM in a group of patients with locally advanced nonresectable pancreatic carcinoma. Our goal was to determine the feasibility of this treatment modality by evaluating the acute radiation toxicity and the treatment efficacy in this dose escalating trial. A second

purpose was to determine the palliation of symptoms, response rate and survival in this group of patients.

MATERIALS AND METHODS

Eligibility

From November 2001 to December 2002, patients with histologically proved pancreatic adenocarcinoma were enrolled into this study. Eligible patients included those with locally unresectable disease due to vascular invasion or extensive regional adenopathy, partial resection or local recurrence after operation. Patients with known metastasis to distant organs, ascites, Karnofsky performance status less than 70 were excluded. Required laboratory parameters included white blood cell count $\geqslant 4\times10^9$/L, platelet count $\geqslant 100\times10^9$/L, creatinine $\leqslant 264$ μmol/L. Patients with biliary or gastroduodenal obstruction must have had prior drainage before radiotherapy and chemotherapy were started. A complete history and physical examination were performed in all patients prior to scheduled treatment. Height, weight, performance status, tumor stage and serum level of tumor markers including carbohydrate antigen (CA) 19-9 were recorded. Required examinations for staging studies included a chest radiograph and abdominal computed tomographic (CT) scan or magnetic resonance image (MRI) scan, abdominal type B ultrosound and sometimes bone isotopic examination. All patients were required to sign a written informed consent according to national and institutional guidelines.

Radiotherapy

Patients were CT simulated and treated in the supine position with their arms overhead. In order to make it easier to define tumor target volume from the stomach and duodenum, 300 ml of oral CT contrast with 2 % gastrografin solution was administered respectively one hour and half an hour before starting CT simulation scan with ACQsim spiral CT. For immobilization, a customed thermoplastic cast extending from the mid-thoracic spine to the mid-pelvis was made. Each patient was scanned from the upper dome of the right diaphragm (approximately at the level of T9-T10) to the bottom of the L4 vertebral body. The patient was imaged with overlapping CT slices that were 5 mm thick at 3 mm intervals. Center of CT scanning was marked on the thermoplastic cast. The gross tumor volume (GTV) and the surrounding critical structures of concern including the liver, kidneys, stomach, small intestine and spinal cord were defined after the data of CT scan were sent to the workstation of ACQsim (version 4.3) CT simulation software system. GTV represents tumor in the pancreas, the surrounding tissue infiltrated and adjacent lymph node metastasis. The clinical target volume (CTV) includes GTV plus any microscopic extension of disease that is suspected around GTV. The planning target volume (PTV) represents CTV plus any additional margins that are required to compensate for daily setup variations. Isocenter coordinate of radiotherapy was marked on the thermoplastic cast with the help of a laser mark system. Cadplan treatment plan system using Helios reverse treatment planning software was adopted to optimize the dose distribution after the images of CT scan and digitally reconstructed radiographs were transmitted. Then, the treatment data were sent to Varian 2100C/D accelerator by Varis network. Port films were taken at the first time and once every week of treatment to verify the radiation position.

Radiotherapy was divided into two phases. Conventional radiotherapy was delivered to a total of 30Gy in 15 fractions of 2Gy per fraction to the initial fields including the primary tumor plus the regional peripancreatic, celiac, and porta hepatis lymph nodes at the first phase. IMRT was given at the second phase and GTV was covered by the 95 % prescribed isodose curve. The dose of IMRT ranged from 21Gy to 30Gy in 7-10 fractions of 3Gy per fraction. The total dose escalation levels were 51Gy, 54Gy, 57Gy and 60Gy respectively. Three patients were needed for each dose level. Dose-limiting toxicity (DLT) from radiotherapy was defined as grade IV hematologic toxicity or grade III nonhematologic toxicity according to common toxicity criteria (CTC, 2.0 version). Dose escalation continued to the next dose level if no patients suffered from DLT. Two or more instances of DLT among 3 patients occurred in the preceding dose level would declare it as the maximum tolerant dose (MTD). Another 3 patients would be needed for observation if one of them had DLT at a certain dose escalation level. If no one had DLT in these additional 3 patients, dose escalation would continue. However, if one patient developed DLT among the added 3 patients, the preceded dose level would be the MTD. In this study, the maximum escalation dose level was 60Gy.

Chemotherapy

Gemcitabine (GM), 150 mg/d, was administered daily prior to radiotherapy on weeks 1, 3, 5, or 5-fluorouracil (5-FU), 250 mg/d, was given every week from Monday to Friday during the days of whole radiotherapy course.

Toxicity and response evaluation

Toxicity was evaluated according to common toxicity criteria: version 2.0 (CTC 2.0)[13]. Hematologic parameters were assessed weekly, and all other adverse reactions were evaluated during the course of radiotherapy. Analgesic intake and weight were recorded at initial consultation and weekly during radiation therapy. Karnofsky performance status (KPS) was estimated prior to radiotherapy and recorded as it was improved, stable, or deteriorated after treatment. Weight change was classified as weight gain/loss if there was a weight increase/decrease $\geqslant$5 % over baseline value, otherwise it was classified as stable. Pain control was recorded when it was improved/deteriorated if there was a $\geqslant$50 % increase/decrease respectively in the daily intake of equivalent analgesic dose at least lasting for 4 weeks. The clinical response index was defined as a sustained improvement in at least one parameter (among three factors as KPS, weight and pain control) without the other two factors worsening for more than 4 weeks. Tumor volume response was assessed based on the tumor size pre- and postradiation CT scans. A complete response (CR) was defined as the disappearance of all clinical evidences of tumor without appearance of new lesions for more than 4 weeks. A partial response (PR) required a 50 % decrement in the maximal perpendicular tumor measurements, with no new lesion appearance for at least 4 weeks. No change (NC) was defined as less than 50 % reduction and less than 25 % increase of measurable tumor lesions. Progressive disease (PD) was defined as more than 25 % increase of measurable tumor lesions or new lesion developed. Response rate included the patients with CR and PR. Survival rate was calculated by the method of Kaplan Meier with the statistic software SPSS (version 9.0).

RESULTS

Dose escalation

Twenty-one patients were enrolled in this clinical study, 15 were unresectable as a result of major vascular invasion, 2 patients had partial tumor resected and other 4 patients had local recurrence at the primary site. Twelve were males and 9 females, and the median age of all patients was 64 years (range: 46-72 years).

Among these twenty-one patients, the primary lesions were

located at the head of 13 patients, at the body or tail of pancreas in 8 patients. Sixteen out of 21 patients completed the whole course of radiotherapy. The number of patients treated with different dose levels of 51Gy, 54Gy, 57Gy, 60Gy were 3, 3, 3 and 7 cases respectively. Dose volume histogram demonstrated that the median percentage of volume of small intestine received 80 % and 90 % of the prescribed dose was 10 % and 6 % respectively. Five out of 21 patients gave up the plan of radiotherapy because 4 patients had hepatic metastasis or ascites and another one had high fever, grade IV hematologic toxicity at the time of administration of GEM with a dose of 200 mg for the second time.

Clinical benefit

Sixteen patients were analyzed. CA19-9 levels prior to radiotherapy were elevated in 13 patients with a median value of 716 U/ml. At the end of radiotherapy, the levels of CA19-9 decreased significantly with a median value of 255 U/ml (P<0.001). Compared with that before radiotherapy, the value of CA19-9 decreased more than half after radiation treatment in 10/13 patients. Fourteen out of 16 patients suffered from pain at the start of chemoradiation had a decrease of oral analgesic consumption at the end of radiotherapy by more than 1/3 of the total amount before treatment. Ten out of 14 patients had a reduction of analgesic consumption more than 50 % and 5 patients were virtually painless. KPS was improved in 10/16 patients while 4 patients deteriorated during treatment, the other 2 patients remained unchanged. Only one patient (1/16) gained weight $\geqslant$5 % during treatment and maintained it for more than four weeks. Nine patients suffered from weight loss in excess of 5 % of their pretreatmeant weight. The other 6 patients remained stable in weight during the treatment. In total, seven patients were improved in at least one parameter of KPS, analgesic consumption or weight without simultaneous deterioration of any other parameters. So the clinical benefit ratio was 33 % (7/21). If the 5 patients who did not complete the radiation schedule were excluded, the benefit ratio increased to 44 % (7/16).

Radiological examination and survival rate

CT scanning after completion of radiotherapy demonstrated that no patient acquired CR, 5 out of 16 patients attained PR. Therefore, the response rate was 31 %. The median follow-up time was 8 months (range 3-17 months). One-year survival rate was 35 %.

Toxicity

No patient had radiation-induced acute reactions such as nausea, vomiting, diarrhea of greater than grade II. Among the six patients (6/21) who received chemotherapy with GEM as radiosensitizer, 3 patients had grade II neutropenia, 1 patients had grade IV neutropenia, and one patient had grade IV hematologic toxicities of neutropenia, thrombocytopenia and anemia. The latter was excluded from the dose escalation study. For patients receiving 5-FU as a radiosensitizer, only 3 patients had grade II neutropenia and two other patients had grade II abnormal liver function. All of them were able to complete the radiotherapy schedule with the support of some medication.

DISCUSSION

Locally advanced, surgically unresectable pancreatic carcinoma is a highly lethal disease. Its one-year survival rate is less than 10 %. Since diagnosis is usually made too late in the course of development of the disease to the chance of radical surgical resection, most patients experience progressive symptoms of pain, jaundice, weight loss, nausea, vomiting, or anorexia. An effective locoregional treatment would be the only chance for such patients. GEM and 5-FU have been studied in clinical trials by Radiation Therapy Oncology Group (RTOG) as radiation sensitizers in pancreatic cancer[14,15]. Studies of 5-FU and radiation have demonstrated that 5-FU was an effective radiation sensitizer by inhibiting tumor cell DNA synthesis. Gemcitabine (GEM) is also a radiosensitizer. It requires intracellular phosphorylation resulting in accumulation of difluorodeoxycytidine triphosphate (dFdCTP). dFdCTP competed with deoxycytidine triphosphate (dCTP) for incorporation into DNA and subsequently inhibited DNA synthesis and decreased intracellular deoxynucleoside triphosphate pools by curbing ribonucleotide reductase[14,15]. Both 5-FU and GEM have significant radiosensitization effect on tumor cells in which DNA band breakage induced by radiation is more difficult to be repaired. The severe toxicity reported by Crane *et al*[16] was significantly higher in patients treated with gemcitabine-based chemoradiation than in those treated with 5-FU-based chemoradiation, in which 12 out of 53 patients (23 %) treated with gemcitabine and one out of 61 patients (2 %) treated with 5-FU suffered from severe acute toxicity (P<0.001). But in a phase II trial of protracted 5-fluorouracil (200 mg/m^2/day) with concurrent radiotherapy, grade III or worse toxicity was observed in 20 % (4/20) patients[17]. In this study, among the 6 patients who were given GEM as a radiosensitizer with a dose of 200 mg/d on weeks 1, 3, 5, grade IV hematologic toxicities were found in two (33 %) patients. However, no one had acute toxicity greater than grade III in patients receiving 5-FU as a radiosensitizer. Therefore, in our study, 5-FU was the only drug used as a radiosensitizer at the later period of all cases. Boz *et al*[8] reported that it was relatively safe to use 5-FU through a central venous catheter at a dose of 300 mg/m^2/d, 7 d/wk, from the first day of external beam radiotherapy throughout the entire course of radiation treatment. In our study, only 5 patients who received 5-FU had grade II acute reaction and it was considered safe to combine the treatment with radiotherapy. No patient had radiotherapy induced severe acute reactions that interrupted the completion of radiotherapy.

Most cases in our study were patients with locally advanced unresectable pancreatic carcinoma. The aim of this study was to find the optimal maximum dose of external beam radiation using IMRT technique, which would not result in severe acute reaction induced by radiotherapy while improving the life quality and prolonging the survival as long as possible. Among the patients who received a total dose of 60Gy, no one suffered from dose-limiting toxicities resulted from radiotherapy. However, the dose greater than 60Gy was not given because of the possible occurrence of severe late toxicities due to radiation to normal tissue. Therefore, this study did not acquire the MTD of radiotherapy. Normalized with conventional dose 2Gy per fraction, the biological equivalent dose of 60Gy with IMRT technique for the early response tissues and the late response tissues were 62.2Gy and 66Gy respectively (for early response tissue: α/β=10Gy, for late response tissue: α/β=3Gy). Consequently, this study suggested that the IMRT adopted in this trial surely could improve the biological dose to tumor volume. The analysis of dose volume histogram (DVH) showed that the median volume of small intestine receiving 80 % and 90 % prescribed dose was 10 % and 6 % respectively. Moreover, late complications of gastrointestinal tract such as intestinal perforation, hemorrhage and obstruction were not found during follow-up. But we were not sure that patients given total dosage of 60Gy would not have severe complications in the future even the expected survival was relatively short. Therefore, our maximum escalation dose was limited to 60Gy. The tolerance of the patients were quite good in terms of normal tissue acute toxicities induced by radiation

when 30Gy was given in 10 fractions with IMRT technique (PTV margin was 5 mm from GTV) in addition to the conventional dose of 30Gy over 15 fractions.

A recent study by Crane *et al*[16] demonstrated that weekly administration of GEM combined with radiation led to 1-year survival rate of 42 % and median survival duration of 11 months. The response rate and 1-year survival rate of this series were 31 % and 35 % respectively. The difference between our results compared with that in literature may be due to discrepancy of patient' s selection. Up to now, no randomized prospective study in patients with pancreatic carcinoma compared the toxicities in gemcitabine-based *versus* 5-FU-based chemoradiation. Although the case number in our present study was relatively small, the primary results of our study indicated that the tolerance to 5-FU based chemoradiotherapy was much better than GEM based chemoradiotherapy.

In conclusion, for locally unresectable or recurrent pancreatic disease, this dose escalation clinical trial demonstrates that the dose level of 60Gy in 25 fractions over 5 weeks with IMRT technique combined with concurrent 5-FU is effective in improving survival, decreasing pain and the level of CA19-9 and promoting clinical benefit index without radiation-induced severe acute toxicities. Long term treatment effects and late toxicities remain to be evaluated.

REFERENCES

1 **Shankar A**, Russell RC. Recent advances in the surgical treatment of pancreatic cancer. *World J Gastroenterol* 2001; **7:** 622-626

2 **Ghaneh P**, Slavin J, Sutton R, Hartley M, Neoptolemos JP. Adjuvant therapy in pancreatic cancer. *World J Gastroenterol* 2001; **7:** 482-489

3 **Shinchi H**, Takao S, Noma H, Matsuo Y, Mataki Y, Mori S, Aikou T. Length and quality of survival after external-beam radiotherapy with concurrent continuous 5-fluorouracil infusion for locally unresectable pancreatic cancer. *Int J Radiat Oncol Biol Phys* 2002; **53:** 146-150

4 **Fisher BJ,** Perera FE, Kocha W, Tomiak A, Taylor M, Vincent M, Bauman GS. Analysis of the clinical benefit of 5-fluorouracil and radiation treatment in locally advanced pancreatic cancer. *Int J Radiat Oncol Biol Phys* 1999; **45:** 291-295

5 **Kornek GV,** Potter R, Selzer E, Schratter A, Ulrich-Pur H, Rogy M, Kraus G, Scheithauer W. Combined radiochemotherapy of locally advanced unresectable pancreatic adenocarcinoma with mitomycin C plus 24-hour continuous infusional gemcitabine. *Int J Radiat Oncol Biol Phys* 2001; **49:** 665-671

6 **Andre T,** Balosso J, Louvet C, Hannoun L, Houry S, Huguier M, Colonna M, Lotz JP, De Gramont A, Bellaiche A, Parc R, Touboul E, Izrael V. Combined radiotherapy and chemotherapy (cisplatin and 5-fluorouracil) as palliative treatment for localized unresectable or adjuvant treatment for resected pancreatic adenocarcinoma: results of a feasibility study. *Int J Radiat Oncol Biol Phys* 2000; **46:** 903-911

7 **Symon Z,** Davis M, McGinn CJ, Zalupski MM, Lawrence TS. Concurrent chemoradiotherapy with gemcitabine and cisplatin for pancreatic cancer: from the laboratory to the clinic. *Int J Radiat Oncol Biol Phys* 2002; **53:** 140-145

8 **Boz G,** De Paoli A, Innocente R, Rossi C, Tosolini G, Pederzoli P, Talamini R, Trovo MG. Radiotherapy and continuous infusion 5-fluorouracil in patients with nonresectable pancreatic carcinoma. *Int J Radiat Oncol Biol Phys* 2001; **51:** 736–740

9 **Yavuz AA,** Aydin F, Yavuz MN, Ilis E, Ozdemir F. Radiation therapy and concurrent fixed dose amifostine with escalating doses of twice-weekly gemcitabine in advanced pancreatic cancer. *Int J Radiat Oncol Biol Phys* 2001; **51:** 974-981

10 **Rich TA.** Chemoradiation for pancreatic and biliary cancer: current status of RTOG studies. *Ann Oncol* 1999; **10**(Suppl 4): 231-233

11 **Katz A**, Hanlon A, Lanciano R, Hoffman J, Coia L. Prognostic value of CA19-9 levels in patients with carcinoma of the pancreas treated with radiotherapy. *Int J Radiat Oncol Biol Phys* 1998; **41:** 393-396

12 **Tokuuye K**, Sumi M, Kagami Y, Murayama S, Ikeda H, Ikeda M, Okusaka T, Ueno H, Okada S. Small-field radiotherapy in combination with concomitant chemotherapy for locally advanced pancreatic carcinoma. *Radiother Oncol* 2003; **67:** 327-330

13 **Trotti A,** Byhardt R, Stetz J, Gwede C, Corn B, Fu K, Gunderson L, McCormick B, Morrisintegral M, Rich T, Shipley W, Curran W. Common toxicity criteria: version 2.0. An improved reference for grading the acute effects of cancer treatment: impact on radiotherapy. *Int J Radiat Oncol Biol Phys* 2000; **47:** 13-47

14 **Safran H,** Dipetrillo T, Iannitti D, Quirk D, Akerman P, Cruff D, Cioffi W, Shah S, Ramdin N, Rich T. Gemcitabine, paclitaxel, and radiation for locally advanced pancreatic cancer: a phase I trial. *Int J Radiat Oncol Biol Phys* 2002; **54:** 137-141

15 **Burris HA 3rd**, Moore MJ, Andersen J, Green MR, Rothenberg ML, Modiano MR, Cripps MC, Portenoy RK, Storniolo AM, Tarassoff P, Nelson R, Dorr FA, Stephens CD, Von Hoff DD. Improvements in survival and clinical benefit with gemcitabine as first-line therapy for patients with advanced pancreas cancer: a randomized trial. *J Clin Oncol* 1997; **15:** 2403-2413

16 **Crane CH,** Abbruzzese JL, Evans DB, Wolff RA, Ballo MT, Delclos M, Milas L, Mason K, Charnsangavej C, Pisters PW, Lee JE, Lenzi R, Vauthey JN, Wong AB, Phan T, Nguyen Q, Janjan NA. Is the therapeutic index better with gemcitabine-based chemoradiation than with 5-fluorouracil-based chemoradiation in locally advanced pancreatic cancer? *Int J Radiat Oncol Biol Phys* 2002; **52:** 1293-1302

17 **Ishii H**, Okada S, Tokuuye K, Nose H, Okusaka T, Yoshimori M, Nagahama H, Sumi M, Kagami Y, Ikeda H. Protracted 5-fluorouracil infusion with concurrent radiotherapy as a treatment for locally advanced pancreatic carcinoma. *Cancer* 1997; **79:** 1516-1520

Edited by Xu JY and Wang XL

P.O.Box 2345, Beijing 100023,China
Fax: +86-10-85381893
E-mail: wjg@wjgnet.com www.wjgnet.com

World J Gastroenterol 2003;9(11):2565-2569
World Journal of Gastroenterology
 ISSN 1007-9327

• CLINICAL RESEARCH •

Therapeutic efficacy of high-dose vitamin C on acute pancreatitis and its potential mechanisms

Wei-Dong Du, Zu-Rong Yuan, Jian Sun, Jian-Xiong Tang, Ai-Qun Cheng, Da-Ming Shen, Chun-Jin Huang, Xiao-Hua Song, Xiao-Feng Yu, Song-Bai Zheng

Wei-Dong Du, Zu-Rong Yuan, Jian Sun, Jian-Xiong Tang, Ai-Qun Cheng, Da-Ming Shen, Xiao-Hua Song, Chun-Jin Huang, Department of Surgery, Huadong Hospital, Shanghai 200040, China
Xiao-Feng Yu, Song-Bai Zheng, Department of Digestive Internal Medicine, Huadong Hospital, Shanghai 200040, China
Correspondence to: Dr. Wei-Dong Du, Department of Surgery, Huadong Hospital, No. 221, Yanan Xilu, Shanghai 200040, China. duzhuyi@sh163.net
Telephone: +86-21-62483180 **Fax:** +86-21-62483180
Received: 2002-12-22 **Accepted:** 2003-02-16

Abstract

AIM: To observe the therapeutic efficacy of high-dose Vitamin C (Vit. C) on acute pancreatitis (AP), and to explore its potential mechanisms.

METHODS: Eghty-four AP patients were divided into treatment group and control group, 40 healthy subjects were taken as a normal group. In the treatment group, Vit. C (10 g/day) was given intravenously for 5 days, whereas in the control group, Vit. C (1 g/day) was given intravenously for 5 days. Symptoms, physical signs, duration of hospitalization, complications and mortality rate were monitored. Meanwhile, serum amylase, urine amylase and leukocyte counts were also determined. The concentration of plasma vitamin C (P-VC), plasma lipid peroxide (P-LPO), plasma vitamin E (P-VE), plasma β-carotene (P-β-CAR), whole blood glutathione (WB-GSH) and the activity of erythrocyte surperoxide dimutase (E-SOD) and erythrocyte catalase (E-CAT) as well as T lymphocyte phenotype were measured by spectrophotometry in the normal group and before and after treatment with Vit. C in the treatment and the control group.

RESULTS: Compared with the normal group, the average values of P-VC, P-VE, P-β-CAR, WB-GSH and the activity of E-SOD and E-CAT in AP patients were significantly decreased and the average value of P-LPO was significantly increased, especially in severe acute pancreatitis (SAP) patients (P <0.05. P-VC, P =0.045; P-VE, P =0.038; P =0.041; P-β-CAR, P =0.046; WB-GSH, P =0.039; E-SOD, P =0.019; E-CAT, P =0.020; P-LPO, P =0.038). Compared with the normal group, CD_3 and CD_4 positive cells in AP patients were significantly decreased. The ratio of CD_4/CD_8 and CD_4 positive cells were decreased, especially in SAP patients (P<0.05. CD_4/CD_8, P =0.041; CD_4, P =0.019). Fever and vomiting disappeared, and leukocyte counts and amylase in urine and blood become normal quicker in the treatment group than in the control group. Moreover, patients in treatment group also had a higher cure rate, a lower complication rate and a shorter in-ward days compared with those in he control group. After treatment, the average value of P-VC was significantly higher and the values of SIL-2R, TNF-α, IL-6 and IL-8 were significantly lower in the treatment group than in the control group (P<0.05 P-VC, P =0.045; SIL-2R, P =0.012; TNF-α, P =0.030; IL-6, P =0.015; and IL-8, P =0.043). In addition, the ratio of CD_4/CD_8 and CD4 positive cells in the patients of treatment group were significantly higher than that of the control group after treatment (P<0.05. CD_4/CD_8, P =0.039; CD_4, P =0.024).

CONCLUSION: High-dose vitamin C has therapeutic efficacy on acute pancreatitis. The potential mechanisms include promotion of anti-oxidizing ability of AP patients, blocking of lipid peroxidation in the plasma and improvement of cellular immune function.

Du WD, Yuan ZR, Sun J, Tang JX, Cheng AQ, Shen DM, Huang CJ, Song XH, Yu XF, Zheng SB. Therapeutic efficacy of high-dose vitamin C on acute pancreatitis and its potential mechanisms. *World J Gastroenterol* 2003; 9(11): 2565-2569
http://www.wjgnet.com/1007-9327/9/2565.asp

INTRODUCTION

In the occurrence and progress of acute pancreatitis (AP), system inflammatory response syndrome (SIRS) often appears as a complication, and may result in pyemia and multiple organ dysfunction (MODS), and death may be the last consequence[1,2]. Many investigations have made it clear that over-activation of leucocytes and their cytokines, the imbalance between release and clearance of free radicals and other pathophysiological changes play important roles in this progress[3-5]. The prognosis of AP patients has a close correlation with infection and pyemia, whereas the occurrence and progress of infection and pyemia also have a correlation with the changes of host immune function[6]. It has been confirmed that vitamin C is an important antioxidant which protects the body from damage of inflammation[7,8], and high-dose vitamin C can improve the immune function[9]. In the present, randomized control study, we observed the clinical efficacy on a high-dose of vitamin C (10 g/day, intravenously) on AP and also monitored its influence on plasma vitamin C (P-VC), plasma lipid peroxide (P-LPO) and other biochemical and immunological markers in order to explore its underlying mechanisms.

MATERIALS AND METHODS

Patients

Based on the AP diagnostic criteria worked out by the Pancreatic Surgery Subgroup of Chinese Medical Association, we selected 84 cases of AP patients. They included 53 males and 31 females, and were aged from 25 to 71 (mean ± SD, 42±13) years. Patients with serious diseases in main visceral organs such as the heart, brain, liver and kidney, peptic ulcer disease, diabetes mellitus, auto-immune diseases ,and tumors were excluded. According to the classification criteria (2nd edition 1996), 70 patients were mild AP (MAP) cases, 14 patients were severe (SAP) cases. Forty healthy volunteers (male 26, female 14, age 28-66 (47±14) years old) were included in the study as a normal group. There was no

significant difference in age and gender between AP patients and healthy volunteers (P>0.05).

Methods

Treatment regimen the routine therapy was used in both treatment and control groups, which consisted of pancreatic excretion inhibition, anti-spasm, analgesia, maintenance of the water-electrolyte balance, prevention and cure of infection and other complications, and if necessary, fasting and gastrointestinal decompression. The patients were randomly divided into two groups. In the treatment group (n=40), vitamin C (10 g/day) was given intravenously for 5 days, while in the control group (n=44), vitamin C (1 g/day) was given intravenously for 5 days. There was no significant difference in age (40±12 *vs*. 43±14 years old), gender (M/F, 25/15 *vs*. 28/16) and disease severity (MAP/SAP, 33/7 *vs*. 37/7) between the treatment and control groups (all P>0.05).

Detection of clinical, biochemical and immunological markers Symptoms such as abdominal pain, fever, vomiting, and hospitalization duration were monitored. Serum amylase, urine amylase, leukocyte counts, concentrations of plasma vitamin c (P-VC), plasma lipid peroxide (P-LPO), plasma vitamin E (P-VE), plasma β-carotene (P-β-CAR), whole blood glutathione (WB-GSH) and the activity of erythrocyte surperoxide dimutase (E-SOD), erythrocyte catalase (E-CAT), serum interleukin-2 receptor (SIL-2R), tumor necrosis factor-alpha (TNF-α), IL-6, IL-8 and complement reaction protein (CRP), as well as T lymphocyte phenotypes CD_3, CD_4, and CD_8 were measured. P-VC and P-VE (μmol/L) were measured by spectrometry using ferrocyanide. P-LPO (μmol/L) was measured by spectrometry using sulfbarbitone. P-β-CAR (μmol/L) was measured with alcohol-petroleum ether spectrometer. WB-GSH (mmol/L) was measured by spectrometry using disulfhydry-dinitrobenzoic acid. E-SOD (U/g*Hb) was measured by spectrometry using pyrocatechol. E-CAT (K/g*Hb) was measured by spectrometryusing oxydol-acetic diachromic acid potassium. SIL-2R, TNF-α, IL-6 and IL-8 (pmol/L) were measured by enzyme-linked immunosorbent assays (ELISA). All reagents were supplied by the Roche Company (Swiss). CRP (mg/L) was measured by the quick immune extinction spectrometry. T-lymphocytephenotypes (%) were determined by spectrometry using anti-AKP monoclonal antibody AKP.

Clinically, cure of the disease was defined if symptoms such as abdominal pain, vomiting and fever disappeared, serum amylase, urine amylase and leukocyte counts returned to normal, and imaging examinations showed no abnormality. Improvement of the disease was defined if symptoms relieved or disappeared, and laboratory examinations showed almost normal results. The disease was defined to be unchanged if symptoms, physical signs and laboratory examinations had remained unchanged since hospitalization, and to be deteriorated if patient' s condition was getting worse, with occurrence of severe complications and death.

Statistics analysis

All the data were expressed as mean ± SD, when appropriate. SPSS 10.0 statistical package was used for statistical analysis. T-test and χ^2-test were used for the analysis, and P<0.05 was regarded as statistically significant.

RESULTS

Comparison of the results between patients and healthy volunteers

As shown in tables 1, 2 and 3, the serum levels of SIL-2R, TNF-α, IL-6, IL-8 and CRP in AP patients were much higher than those in healthy volunteers (P<0.05 or P<0.01). The average contents of P-VC, P-VE, P-β-CAR, WB-GSH, E-SOD and E-CAT were significantly lower, while the level of P-LPO was significantly higher in patients than in healthy volunteers. More importantly, all the above variables were higher in SAP patients than in MAP patients (P<0.05). The percentage of CD_3 and CD_4 positive cells in AP cases was significantly lower in AP patients compared to the healthy group (both P<0.05), CD_4 and the ratio of CD_4/CD_8 were much lower in SAP patients than in healthy group (both P<0.05).

Table 1 Comparison of cytokines between patients and healthy volunteers

	Patients (n=84)	Healthy volunteers (n=40)	P
SIL-2R (pmol/L)	213.42±54.68	72.34±23.17	<0.01
TNF-α (pmol/L)	3.67±1.01	0.58±0.15	<0.01
IL-6 (pmol/L)	92.43±25.67	29.57±11.64	<0.01
IL-8 (pmol/L)	267.58±121.88	60.49±25.35	<0.01
CRP (mg/L)	18.30±7.35	8.34±4.17	<0.01

Table 2 Comparison of oxidation and anti-oxidation levels between patients and healthy volunteers

	Patients (n=84)		Healthy volunteers (n=40)
	MAP (n=70)	SAP (n=14)	
P-VC(μmol/L)	32.56±6.73	43.51±2.15	55.12±13.24
P-VE(μmol/L)	19.21±1.75	13.26±3.14	24.01±5.28
P-LPO(μmol/L)	12.95±3.91	15.41±2.15	11.21±2.76
P-β-CAR(μmol/L)	1.38±0.25	0.94±0.11	1.61±0.23
WB-GSH(mmol/L)	1.08±0.27	0.70±0.33	1.21±0.21
E-SOD(U/g*Hb)	1 804.42±100.14	1 495.27±152.87	2 084.39±191.53
E-CAT(K/g*Hb)	221.54±20.47	174.76±34.56	280.42±77.26

Comparison between patients and healthy volunteers and between mild acute panceatitis (MAP) and severe acute panceatitis (SAP), all P<0.05.

Table 3 Comparison of cellular immunity between patients and healthy volunteers ($\bar{x}$±s)

	MAP (n=70)	SAP (n=14)	Healthy group (n=40)
CD_3(%)	46.73±10.15	45.23±12.24[a]	57.65±10.28
CD_4(%)	34.27±9.52[a]	23.65±7.53[ab]	43.23±7.65
CD_8(%)	22.32±7.29	27.18±4.56	26.18±4.79
CD_4/CD_8	1.84±0.78	0.80±0.67[ab]	2.13±0.66

[a]P<0.05 *vs* healthy volunteers, [b]P<0.05 *vs* MAP.

Table 4 Comparison of clinical symptoms and laboratory examinations between treatment and control groups ($\bar{x}$±s, h)

	Treatment group (n=40)	Control group (n=44)	P
Disappearance of fever	65.75±14.26	89.71±16.25	<0.05
Release of abdominal pain	23.43±5.66	25.31±6.37	>0.05
Disappearance of abdominal pain	55.23±10.08	54.23±11.73	>0.05
Disappearance of vomiting	43.19±12.65	51.67±10.93	<0.05
Normalization of serum amylase	79.14±19.64	91.45±10.45	<0.05
Normalization of urine amylase	100.22±19.22	122.38±13.56	<0.05
Normalization of leucocyte counts	69.59±15.41	81.34±14.05	<0.05

Table 5 Comparison of clinical efficacy between treatment and control groups (day, %)

	Case	Cure	Improvement	No change	Deterioration	Hospitalization
Treatment group	40	30 (75.00)	4(10.00)	4 (10.00)	2 (5.00)	9.34±4.24
Control group	44	18 (40.91)	10(22.73)	6 (13.64)	6 (13.64)	13.45±3.21
P		<0.05	<0.05	<0.05	<0.05	<0.05

Table 6 Comparison of cytokines between treatment and control groups before and after therapy ($\bar{x}\pm s$)

	Treatment group (*n*=40)		Control group (*n*=44)	
	Before therapy	After therapy	Before therapy	After therapy
SIL-2R (pmol/L)	221.67±87.30	118.37±43.68[a]	196.52±63.28	178.84±30.56
TNF-α (pmol/L)	3.65±1.25	1.52±0.78[b]	3.99±1.34	2.46±1.04
IL-6 (pmol/L)	95.58±18.64	39.53±10.36[b]	89.22±12.03	59.83±9.48
IL-8 (pmol/L)	273.49±88.50	127.35±49.86[a]	261.47±64.97	198.31±28.50
CRP (mg/L)	19.19±9.37	8.70±4.65	17.56±5.62	9.42±5.84

Before therapy: $P>0.05$ for each index in the two group. After therapy: [a]$P<0.05$, [b]$P<0.01$ *vs* treatment and control groups.

Table 7 Comparison of oxidation and anti-oxidation between treatment and control groups before and after therapy

	Treatment group (*n*=40)		Control group (*n*=44)	
	Before therapy	After therapy	Before therapy	After therapy
P-VC(μmol/L)	41.54±2.91	53.25±10.11[a]	41.78±1.96	45.21±9.25[1)]
P-VE(μmol/L)	18.47±3.45	19.97±4.26[b]	18.67±2.13	19.24±2.46[2)]
P-LPO(μmol/L)	13.53±2.12	11.54±1.45[a]	13.68±2.31	12.98±2.75[1)]
P-β-CAR(μmol/L)	1.25±0.17	1.37±0.71[b]	1.28±0.21	1.34±0.65[2)]
WB-GSH(mmol/L)	0.97±0.18	1.39±0.41[a]	0.98±0.21	1.04±0.35[1)]
E-SOD(U/g*Hb)	1 749.01±50.55	1 997.42±145.33[1)]	1 726.28±71.37	1 807.22±120.21[1)]
E-CAT(K/g*Hb)	217.34±19.51	269.52±65.32[1)]	220.18±20.14	239.17±70.15[1)]

Before therapy: each index in the two group, $P>0.05$. After therapy: [a]$P<0.05$, [b]$P<0.01$ *vs* treatment and control groups.

Comparison of results between treatment and control groups

As shown in in tables 4 and 5, except for abdominal pain, all symptoms disappeared and serum and urine amylase normalized at a much faster speed in the treatment group than in control group (all $P<0.05$). The treatment group had a higher cure rate and lower deterioration rate than the control group 5 days after therapy (both $P<0.05$).

Comparison of cytokines between treatment and control groups before and after therapy

There was no significant difference in the levels of SIL-2R, TNF-α, IL-6, IL-8 and CRP between the two groups before treatment (all $P>0.05$) (Table 6). However, the levels of cytokines decreased significantly 5 days after therapy in both groups ($P<0.05$), although they were still higher compared with the healthy group. The contents of SIL-2R, TNF-α, IL-6 and IL-8 were significantly lower in the treatment group than in the control group (all $P<0.05$) 5 days after therapy. The CRP level was lower compared with the control group, but the difference was not statistically significant ($P>0.05$, Table 6).

Comparison of oxidation and anti-oxidation levels between treatment and control groups before and after therapy

No notable difference in levels of P-VC, P-VE, P-LPO, P-β-CAR, WB-GSH, E-SOD and E-CAT was observed between the two groups ($P>0.05$) before treatment (Table 7). The average concentration of P-VC, WB-GSH, E-SOD and E-CAT was elevated significantly and P-LPO level was decreased in treatment group 5 days after therapy compared with the control group (all $P<0.05$, Table 7). The contents of P-VE and P-β-CAR had no remarkable difference between the two groups ($P>0.05$).

Comparison of cellular immunity between MAP cases in treatment and control groups before and after therapy

There was no significant difference in CD_3, CD_4 CD_8 and the ratio of CD_4/CD_8 between the MAP patients in the two groups before treatment (Table 8). The mean count of CD_3 and CD_4 and the ratio of CD_4/CD_8 were higher 5 days after treatment than those before treatment in both groups (all $P<0.05$). As far as the comparison of the CD_3 and CD_4 positive cells and the ratio of CD_4/ CD_8 between these two group was concerned, the levels in the former group were slightly higher than that in the latter group ($P>0.05$, Table 8).

Table 8 Immunity change before and after therapy in MAP cases of two groups ($\bar{x}\pm s$)

	Treatment group (*n*=33)		Control group (*n*=37)	
	Before therapy	After therapy	Before therapy	After therapy
CD_3(%)	45.99±9.75	52.34±6.87	47.48±10.35	50.18±7.10
CD_4(%)	36.43±8.56	38.79±7.65	36.01±9.47	37.25±6.92
CD_8(%)	21.98±6.85	20.46±3.53	22.45±7.11	21.33±4.88
CD_4/CD_8	1.88±0.64	1.97±0.74	1.75±0.76	1.85±0.43

Before therapy: $P>0.05$ *vs* the two groups. After therapy: $P>0.05$ *vs* the two groups.

Comparison of cellular immunity between SAP cases treatment and control groups before and after therapy

There was no significant difference in CD_3, CD_4 CD_8 and the ratio of CD_4/CD_8 between the MAP patients in the two groups before treatment (Table 9). The mean count of CD_3 and CD_4 and the ratio of CD_4/CD_8 were higher 5 days after treatment than those before treatment in both groups (all $P<0.05$).

Moreover, the CD_3 and CD_4 positive cells and the ratio of CD_4/CD_8 were remarkably higher in the treatment group than in the control group (all $P<0.05$).

Table 9 Immunity changes in SAP cases of two groups before and after therapy ($\bar{x}\pm s$)

	Treatment group (n=7)		Control group (n=7)	
	Before therapy	After therapy	Before therapy	After therapy
P-VC(μmol/L)	31.93±7.21	49.27±10.12[a]	32.89±2.17	38.17±9.41[a]
CD_3(%)	45.65±11.18	51.39±7.17	44.90±10.47	47.45±10.72
CD_4(%)	22.48±6.35	36.93±8.51[a]	23.85±7.52	25.67±7.57[a]
CD_8(%)	23.32±6.43	23.64±5.50	26.84±5.92	22.58±6.74
CD_4/CD_8	0.85±0.23	1.41±0.47[a]	0.86±0.45	1.17±0.52[a]

Before therapy: $P>0.05$ *vs* the two groups. After therapy: [a]$P<0.05$ *vs* the two groups.

DISCUSSION

Many free radicals are produced in body metabolic procedure. It is estimated that oxygen-derived free radicals account for 95 %. They are cleaned by antioxidants and antioxidases rapidly, and thus the production and clearance keep a homeostasis in normal conditions. Free radicals could exert physiological functions to some degree, such as taking part in biosynthesis, detoxification and microorganism clearance[10,11]. However, overdose free radicals could lead to tissue and cell injuries in pathologic conditions through different approaches[12]: (1) Free radicals attacked bio-membrane, which led to unsaturated fatty acid lipid peroxidation (LPO) and affected the function of membrane of cells and cell organelle. (2) Free radicals might destroy the major enzymes and other molecules, making them lose their functions. (3) Free radicals might disturb the synthesis and replication of DNA. (4) LPO could produce more toxic substances and free radicals. Usually the free radicals produced in metabolism can be cleared by the defence system of anti-oxidation. This system is mainly composed of anti-oxidases and antioxidants. These materials catch and clear the excessive free radicals, prevent the chain reaction of a serial of free radicals from pathologic acceleration and keep the homeostasis of antioxidation from imbalance. Vit. C, Vit. E and β-CAR were the most important anti-oxidases and antioxidants, and played an important role in anti-infection[7-9].

The occurrence and development of acute pancreatitis were related to the disturbance in release and clearance of free radicals, which resulted in the imbalance between oxidation and anti-oxidation[13]. Many studies have indicated that excessive free radicals could lead to tissue and cellular injury in pathological conditions[11]. Free radicals took part in the edema of AP, and probably in the necrosis process[13]. When AP happened, vitamin C was depleted at first by reacting with superoxide, anion hydroperoxide anion and hydroxylperoxide anion, and then by forming vitamin C free radicals to prevent DNA and membrane lipid from damage[14]. The concentration of vitamin C in AP cases decreased to various extents[15], reached the lowest level in the first 1-5 days of the disease course, and the vitamin C level correlated with the severity of the disease[16]. The output of free radicals was increased, and peroxidation reaction was reinforced, therefore a large amount of vitamin C, vitamin E, β-CAR, WB-GSH, E-SOD and E-CAT were depleted so that they could hardly prevent pancreas and other organs from damage caused by lipid peroxidation. Furthermore, the elevation of cytokines is a frequent phenomenon and the extention was closely associated with the severity of AP[17]. The reason why MAP developed into SAP was a chain and amplification reaction (so-called waterfall effect) of inflammatory agents that led to SIRS and MODS[18]. Therefore, the serum levels of cytokines SIL-2R, TNF-α, IL-6, IL-8 and CRP could be regarded as the biomarkers of therapeutic efficacy[19].

Recent studies have shown that the prognosis of AP is closely associated with infection and pyemia. At the same time, the occurrence, development and conversion of infection and pyemia were intimately associated with the changes of immune function[20,21]. Because histamine, bradykinin and many other cytokines produced in AP progression could inhibit the immune function in AP cases, especially in those with SAP, the injuries of immune function took place. Theses injuries included decreased proliferation of T cells, especially Th cells, decreased IL-2 level, reduced monocytes in peripheral blood and increased prostaglandin E2 from monocytes[22-24]. Our study indicated that cellular immune function damage took place in AP patients. The percentage of CD_3 and CD_4 positive lymphocytes was higher in treatment group than in control group after treatment, while that of CD_4 positive lymphocytes and the ratio of CD_4/CD_8 were lower in SAP than in MAP[25]. CD_4 positive T-lymphocytes could excrete IL-2, which stimulated the silent T-lymphocytes to express IL-2 receptor, and thus IL-2 conjugated its receptor, leading to a series of immune reactions and increased DNA synthesis[26]. Therefore, the decrease of CD_4 positive T-lymphocytes certainly influenced the body immune function and resistibility, and the susceptibility to infection increase[27].

We found that the average concentration of P-VC, P-VE, β-CAR, WB-GSH, E-SOD and E-CAT was significantly lower while P-LPO level was significantly higher in AP patients than in healthy volunteers. All these indicate that free radical reaction and lipid peroxidation, and disturbance can speed up free radical elimination and anti-oxidation. We also found that high-dose of vitamin C at early stage could contribute to the improvement of the levels of P-VC, P-VE, WB-GSH, E-SOD and E-CAT, which took part in eliminating injurious free radicals and protecting cells from damage by the free radicals. Simultaneously, the P-LPO level was lower in treatment group than in control group, further confirming the preventive effect of high-dose vitamin C against lipid peroxidation. It was also revealed that there was no significant difference in CD4/CD8 ratio between the MAP patients and the control group. The possible reason is that the immune system of MAP cases has not been seriously impaired, so that the immune adjusting mechanism is able to adjust the CD_8 cells to keep the CD_4/CD_8 ratio at a normal level. However, in SAP patients this mechanism was seriously impaired and could no longer keep the CD_4/CD_8 ratio. Vitamin C could improve the immune function by increasing CD_3, CD_4 and the CD_4/CD_8 ratio, and decreasing CD_8[28], elevating transformation efficiency of lymphocytes, stimulating the production of IL-1, IL-2, IL-6 and other cytokines, and reinforcing cell-mediated immune reaction parameters[29]. In the present study, the percentage of CD4 positive lymphocytes and CD_4/CD_8 ratio in SAP cases were much lower compared with the healthy volunteers, but these indices were significantly higher than those of control group after high-dose vitamin C application. These findings indicate that severe cellular immune defection exists in SAP cases. However, high-dose vitamin C can not only eliminate free radicals and reduce the damage of lipid peroxidation, but also improve the cellular immune function in SAP patients, and thus is useful in reducing the incidence and mortality of pyemia and MODS. SIL-2R, TNF-α, IL-6, IL-8 and CRP concentrations in AP patients were significantly higher than those in healthy volunteers. However, SIL-2R, TNF-α, IL-6 and IL-8 levels decreased significantly after high-dose of vitamin C application, and were significantly lower than those in the control group. It took a shorter time to cure or improve

the clinical symptoms (fever, abdominal pain and vomiting) and to normalize serum amylase, urine amylase and leukocyte counts in patients taking high dose of vitamin C, compared with those taking low dose of vitamin C. Thus, the therapeutic efficacy of high dose of vitamin C was much better than that of low dose of vitamin C. Therefore, we conclude that high-dose vitamin C has therapeutic efficacy on acute pancreatitis. The potential mechanisms include promotion of anti-oxidizing ability of AP patients, blocking of lipid peroxidation in the plasma, and improvement of cellular immune function.

REFERENCES

1 **Huis M**, Balija M, Lojna-Funtak I, Stulhofer M. Acute pancreatitis in the Zabok General Hospital. *Acta Med Croatica* 2001; **55**: 81-85

2 **Hirota M,** Nozawa F, Okabe A, Shibata M, Beppu T, Shimada S, Egami H, Yamaguchi Y, Ikei S, Okajima T, Okamoto K, Ogawa M. Relationship between plasma cytokine concentration and multiple organ failure in patients with acute pancreatitis. *Pancreas* 2000; **21**: 141-146

3 **Schulz HU,** Niederau C, Klonowski-Stumpe H, Halangk W, Luthen R, Lippert H. Oxidative stress in acute pancreatitis. *Hepatogastroenterology* 1999; **46**: 2736-2750

4 **Chen CC**, Wang SS, Lee FY, Chang FY, Lee SD. Proinflammatory cytokines in early assessment of the prognosis of acute pancreatitis. *Am J Gastroenterol* 1999; **94**: 213-218

5 **Tsai K,** Wang SS, Chen TS, Kong CW, Chang FY, Lee SD, Lu FJ. Oxidative stress: animportant phenomenon with pathogenetic significance in the progression of acute pancreatitis. *Gut* 1998; **42**: 850-855

6 **Lankisch PG,** Mahlke R, Blum T, Bruns A, Bruns D, Maisonneuve P, Lowenfels AB. Hemoconcentration: an early marker of severe and/or necrotizing pancreatitis? Acritical appraisal. *Am J Gastroenterol* 2001; **96**: 2081-2085

7 **Scott P,** Bruce C, Schofield D, Shiel N, Braganza JM, McCloy RF. Vitamin C status in patients with acute pancreatitis. *Br J Surg* 1993; **80:** 750-754

8 **Bonham MJ,** Abu-Zidan FM, Simovic MO, Sluis KB, Wilkinson A, Winterbourn CC, Windsor JA. Early ascorbic acid depletion is related to the severity of acute pancreatitis. *Br J Surg* 1999; **86:** 1296-1301

9 **Cartmell MT,** Kingsnorth AN. Acute pancreatitis. *Hosp Med* 2000; **61:** 382-385

10 **Braganza JM,** Scott P, Bilton D, Schofield D, Chaloner C, Shiel N, Hunt LP, Bottiglieri T. Evidence for early oxidative stress in acute pancreatitis. Clues for correction. *Int J Pancreatol* 1995; **17:** 69-81

11 **Wereszczynska-Siemiatkowska,** Dabrowski A, Jedynak M, Gabryelewicz A. Oxidative stress as an early prognostic factor in acute pancreatitis (AP): its correlation with serum phospholipase A2 (PLA2) and plasma polymorphonuclear elastase (PMN-E) in different-severity forms of human AP. *Pancreas* 1998; **17:** 163-168

12 **Kruse P,** Anderson ME, Loft S. Minor role of oxidative stress during intermediate phase of acute pancreatitis in rats. *Free Radic Biol Med* 2001; **30**: 309-317

13 **Jurkowska G,** Rydzewska G, Gabryelewicz A, Dzieciol J. The role of nitric oxide in caerulein-induced acute pancreatitis and the recovery process after inflammatory damage. *Eur J Gastroenterol Hepatol* 1999; **11:** 1019-1026

14 **Abu-Zidan FM,** Bonham MJ, Windsor JA. Severity of acute pancreatitis: a multivariate analysis of oxidative stress markers and modified Glasgow criteria. *Br J Surg* 2000; **87:** 1019-1023

15 **Sweiry JH,** Shibuya I, Asada N, Niwa K, Doolabh K, Habara Y, Kanno T, Mann GE. Acute oxidative stress modulates secretion and repetitive $Ca2^{+}$ spiking in rat exocrine pancreas.*Biochim Biophys Acta* 1999; **1454:** 19-30

16 **Simovic MO,** Bonham MJ, Abu-Zidan FM, Windsor JA. Manganese superoxide dismutase: a marker of ischemia-reperfusion injury in acute pancreatitis? *Pancreas* 1997; **15:** 78-82

17 **Mayer J,** Rau B, Gansauge F, Beger HG. Inflammatory mediators in human acute pancreatitis: clinical and pathophysiological implications. *Gut* 2000; **47:** 546-552

18 **Lipsett PA.** Serum cytokines, proteins, and receptors in acute pancreatitis: mediators, markers, or more of the same? *Crit Care Med* 2001; **29:** 1642-1644

19 **Brivet FG,** Emilie D, Galanaud P. Pro- and anti-inflammatory cytokines during acute severe pancreatitis: an early and sustained response, although unpredictable of death. Parisian Study Group on Acute Pancreatitis. *Crit Care Med* 1999; **27:** 749-755

20 **Kouris GJ,** Liu Q, Rossi H, Djuricin G, Gattuso P, Nathan C, Weinstein RA, Prinz RA. The effect of glucagon-like peptide 2 on intestinal permeability and bacterial translocation in acute necrotizing pancreatitis. *Am J Surg* 2001; **181:** 571-575

21 **Yekebas EF,** Eisenberger CF, Ohnesorge H, Saalmuller A, Elsner HA, Engelhardt M, Gillesen A, Meins J, The M, Strate T, Busch C, Knoefel WT, Bloechle C, Izbicki JR. Attenuation of sepsis-related immunoparalysis by continuous veno-venous hemofiltration in experimental porcine pancreatitis. *Crit Care Med* 2001; **29:** 1423-1430

22 **Bhatnagar A,** Wig JD, Majumdar S. Expression of activation, adhesion molecules and intracellular cytokines in acute pancreatitis. *Immunol Lett* 2001; **77:** 133-141

23 **Powell JJ,** Siriwardena AK, Fearon KC, Ross JA. Endothelial-derived selectins in the development of organ dysfunction in acute pancreatitis. *Crit Care Med* 2001; **29:** 567-572

24 **Berney T,** Gasche Y, Robert J, Jenny A, Mensi N, Grau G, Vermeulen B, Morel P. Serum profiles of interleukin-6, interleukin-8, and interleukin-10 in patients with severe and mild acute pancreatitis. *Pancreas* 1999; **18:** 371-377

25 **Inagaki T,** Hoshino M, Hayakawa T, Ohara H, Yamada T, Yamada H, Iida M, Nakazawa T, Ogasawara T, Uchida A, Hasegawa C, Miyaji M, Takeuchi T. Interleukin-6 is a useful marker for early prediction of the severity of acute pancreatitis. *Pancreas* 1997; **14**: 1-8

26 **Powell JJ,** Fearon KC, Siriwardena AK, Ross JA. Evidence against a role for polymorphisms at tumor necrosis factor, interleukin-1 and interleukin-1 receptor antagonist gene loci in the regulation of disease severity in acute pancreatitis. *Surgery* 2001; **129:** 633-640

27 **Cook JW,** Karakozis S, Kim D, Provido H, Gongora E, Kirkpatrick JR. Interleukin-10 attenuates proinflammatory cytokine production and improves survival in lethal pancreatitis. *Am Surg* 2001; **67:** 237-241

28 **Hartwig W,** Jimenez RE, Fernandez-del Castillo C, Kelliher A, Jones R, Warshaw AL. Expression of the adhesion molecules Mac-1 and L-selectin on neutrophils in acute pancreatitis is protease- and complement-dependent. *Ann Surg* 2001; **233:** 371-378

29 **Mandi Y,** Farkas G, Takacs T, Boda K, Lonovics J. Diagnostic relevance of procalcitonin, IL-6, and sICAM-1 in the prediction of infected necrosis in acute pancreatitis. *Int J Pancreatol* 2000; **28:** 41-49

Edited by Xa HHX and Wang XL

P.O.Box 2345, Beijing 100023,China
Fax: +86-10-85381893
E-mail: wjg@wjgnet.com www.wjgnet.com

World J Gastroenterol 2003;9(11):2570-2573
World Journal of Gastroenterology
 ISSN 1007-9327

• CLINICAL RESEARCH •

Organ failure associated with severe acute pancreatitis

Ai-Jun Zhu, Jing-Sen Shi, Xue-Jun Sun

Ai-Jun Zhu, Jing-Sen Shi, Xue-Jun Sun, Department of General surgery, The First Hospital of Xi' an Jiaotong University, Xi' an 710061, Shaanxi Province, China
Correspondence to: Dr. Ai-Jun Zhu, Department of General surgery, The First Hospital of Xi' an Jiaotong University, No.1 Jiankang Lu, Xi' an 710061, Shaanxi Province, China. zhaj_1023@163.com
Telephone: +86-29-5323527
Received: 2003-03-20 **Accepted:** 2003-04-11

Abstract

AIM: To investigate the relationship between severe acute pancreatitis (SAP) and organ failure.

METHODS: Clinical data of 74 cases of SAP from Jan. 1993 to Dec. 2002 were retrospectively reviewed, and the relationship between organ failure and age, gender, etiology, extent of necrosis, infection of necrosis and mortality was analyzed.

RESULTS: A total of 47 patients (63.5 %) showed organ failure, 20 patients (27.0 %) multiple organ failure, whereas 27 patients (36.5 %) with dysfunction of a single organ system. Pulmonary failure was the most common organ dysfunction (23.0 %) among single organ failures. There were no significant differences in age, gender and gallstone pancreatitis among patients with or without organ failure ($P>0.05$). The incidence of organ failure in infected necrosis was not higher compared with sterile necrosis, and patients with increased amount of necrosis did not have an increased prevalence of organ failure ($P>0.05$). Patients with organ failure had a higher mortality rate compared with those without organ failure ($P<0.05$). The death of SAP was associated with multiple organ failure ($P<0.005$), pulmonary failure ($P<0.005$), cardiovascular dysfunction ($P<0.05$) and gastrointestinal dysfunction ($P<0.05$).

CONCLUSION: Organ failure is common in patients with SAP, and patients with multiple organ failure and pulmonary failure have a higher mortality rate. Prevention and active treatment of organ failure can improve the outcome of patients with SAP.

Zhu AJ, Shi JS, Sun XJ. Organ failure associated with severe acute pancreatitis. *World J Gastroenterol* 2003; 9(11): 2570-2573
http://www.wjgnet.com/1007-9327/9/2570.asp

INTRODUCTION

Severe acute pancreatitis (SAP), as a common acute abdomen, is characterized by complicated causes, lots of morbidities, difficulties in the treatment, and high mortality[1-8]. The natural course of SAP progresses in two phases. The first 14 days are characterized by systemic inflammatory response syndrome resulted from the release of inflammatory mediators. In patients with SAP, organ failure is common and often occurs in the absence of infection. The second phase, beginning approximately 2 weeks after the onset of the disease, is dominated by sepsis-related complications resulted from infection of pancreatic necrosis. This is associated with multiple systemic complications, such as pulmonary, renal, and cardiovascular failure[9-18]. Despite considerable improvements in understanding of the pathophysiologic mechanisms and management of these patients, mortality of SAP remains between 15-50 %[19-22]. Organ failure is a severe complication of SAP and death occurs usually only in patients with SAP and is commonly associated with failure of at least one organ system[23-25]. From Jan. 1993 to Dec. 2002, a total of 74 patients with a diagnosis of SAP were admitted to Department of Hepatobiliary Surgery, the First Hospital of Xi' an Jiaotong University, 12 patients died in hospital. The aim of this study was to analyze the relationship between extent of necrosis, pancreatic infection, hospital death due to organ failure.

MATERIALS AND METHODS

Patients

From Jan. 1993 to Dec. 2002, a total of 74 patients with a diagnosis of SAP were admitted to Department of Hepatobiliary Surgery, the First Hospital of Xi' an Jiaotong University. Pancreatic necrosis was defined by findings on CT scan or in operation. There were 40 men and 34 women with a ratio of 1.18:1, the average age of the patients was 49.3 years (range 14-94). The presence of infected necrosis was determined by bacterial culture of CT or ultrasonography-guided percutaneous aspiration and pancreatic tissues debrided at surgery. Organ failure was defined according to the Criteria of Clinical Diagnosis and Classification System for Acute Pancreatitis (the second project, 1996, Pancreatic Surgery Association of CMA)[26]. Causes of SAP were identified as gallstone and non-gallstone. Initial management of these patients included bowel rest, gastric secretions, intravenous fluid resuscitation, suppression of pancreatic external secretion, and use of prophylactic antibiotics. The indication for surgical treatment was difined in the following instances, such as infection of necrosis, pancreatic abscesses, cholangitis, obstructive jaundice and pseudocyst formation for a long time.

Methods

The patients were divided into two groups according to patients with or without organ failure within 2 weeks after admission. The differences of age, gender, gallstone pancreatitis, APACHE II scores, and mortality were analyzed. According to the results of CT scan and findings in operation, the extent of pancreatic necrosis was estimated to be (1) <33 %, (2) 33-50 %, (3) >50 %. The relationship of organ failure to the extent of pancreatic necrosis and infection of necrosis was analyzed. Finally, the relationship between multiple organ failure and specific single organ failure with infected necrosis and mortality was evaluated.

Statistics

Continuous data were evaluated by *t* test, and categorized data were analyzed by Chi-square test. Significance was defined by $P<0.05$.

RESULTS

There were no significant differences in age, sex, gallstone

pancreatitis. Mortality and APACHE II scores were significantly higher in patients with organ failure than in those without organ failure (P<0.05 and P<0.001, respectively) (Table 1).

Table 1 Characteristics of 74 patients with or without organ failure

	Organ failure (n=47)	No organ failure (n=27)	Sig.
Age (Y)	48±15	49±15	NS
Gender (M/F)	26/21	14/13	NS
Etiology			
Gallstones	21	11	NS
Non-gallstones	26	16	
APACHE II scores	29±7	23±3	<0.001
Mortality (%)	12/47(25.5)	0	<0.05

Among the 74 patients, 20 patients (27.0 %) showed multiple organ failure (maximum 5 organ systems) and 9 of them died, 27 patients showed single organ failure. In patients suffering from single organ failure, 17 patients (23.0 %) had pulmonary failure and 3 patients (17.6 %) died, 7 patients showed hepatic failure and 3 patients showed gastrointestinal failure, but none of these patients died. No patient in this group was accompanied by cardiovascular failure, renal failure, or neurologic failure (Table 2).

Table 2 Number of patients with organ failure in 74 patients

Organ failure	Morbidity(%)	Mortality(%)
Multiple organ failure	20(27.0 %)	9(45 %)
Specific single organ failure		
Pulmonary failure	17(23.0 %)	3(17.6 %)
Renal failure	0	0
Cardiovascular failure	0	0
Hepatic failure	7(9.4 %)	0
Neurologic failure	0	0
Gastrointestinal failure	3(4.1 %)	0

As for the frequency of different specific single organ failure, pulmonary failure occurred in 45.9 % (34/74), renal failure in 16.2 % (12/74), cardiovascular failure in 17.6 % (13/74), hepatic failure in 18.9 % (14/74), neurologic failure in 5.4 % (4/74) and gastrointestinal failure in 10.8 % (8/74) (Table 3).

Table 3 Frequency of organ failure in 74 patients

Organ failure	No. organ failure	Frequency (%)
Multiple organ failure	20	27.0
Pulmonary failure	34	45.9
Renal failure	12	16.2
Cardiovascular failure	13	17.6
Hepatic failure	14	18.9
Neurologic failure	4	5.4
Gastrointestinal failure	8	10.8

No relationship was found between organ failure to the extent of necrosis and infected necrosis (Tables 4, 5). No difference was found between patients with infected necrosis and those with sterile necrosis in the development of multiple organ failure and specific organ failure (Table 6). Nevertheless patients died in hospital had a significantly higher incidence rate of multiple organ failure, pulmonary failure, cardiovascular failure and gastrointestinal failure compared with survivors (Table 7).

Table 4 Relationship between infected versus sterile necrosis and organ failure in 74 patients

	Organ failure (%)	No. organ failure (%)
Sterile necrosis	31(66.0)	16(34.0)
Infected necrosis	16(59.3)	11(40.7)

Note: χ^2=0.3320, P>0.05.

Table 5 Relationship between amount of necrosis and organ failure in 74 patients

Amount of necrosis (%)	Organ failure (n=47)	No. organ failure (n=27)
<33 %	21(55.3 %)	17(44.7 %)
33-50 %	11(64.7 %)	6(35.3 %)
>50 %	15(78.9 %)	4(21.1 %)

Note: χ^2=3.0784, P>0.05.

Table 6 Relationship between infected versus sterile necrosis and single organ failure in 74 patients

Organ failure (%)	Sterile necrosis (n=47)	Infected necrosis (n=27)	χ^2	Sig.
Multiple organ failure	13(27.7 %)	7(25.9 %)	0.0261	NS
Pulmonary failure	24(51.1 %)	10(37.0 %)	1.3585	NS
Renal failure	6(12.8 %)	6(22.2 %)	1.1287	NS
Cardiovascular failure	10(21.3 %)	3(11.1 %)	1.2237	NS
Hepatic failure	7(14.9 %)	7(25.9 %)	1.3607	NS
Neurologic failure	4(8.5 %)	0		NS[a]
Gastrointestinal failure	4(8.5 %)	4(14.8 %)	0.7068	NS

a: Fisher's exact probabilities test.

Table 7 Relationship between hospital death and organ failure in 74 patients

Organ failure	Survivor (n=62)	Nonsurvivor (n=12)	χ^2	P value
Multiple organ failure	11(17.7 %)	9(75 %)	16.7130	<0.005
Pulmonary failure	22(35.5 %)	12(100 %)	16.8501	<0.005
Renal failure	8(12.9 %)	4(33.3 %)	1.7680	NS
Cardiovascular failure	8(12.9 %)	5(41.7 %)	3.9295	<0.05
Hepatic failure	11(17.7 %)	3(25 %)	0.0342	NS
Neurologic failure	0	4(33.3 %)		NS[a]
Gastrointestinal failure	4(6.5 %)	4(33.3 %)	5.0050	<0.05

a: Fisher's exact probabilities test.

DISCUSSION

Most of SAP mortality is associated with organ failure. In the early courses, organ failure is resulted from inflammatory mediator released by systemic inflammatory response syndrome even if in the absence of infection. In the septic phase, organ failure occurs because of sepsis, so organ failure is common in SAP. Previous study showed that in SAP, organ failure occurred in 72-90.3 %, single organ failure in 24.7-37 %, multiple organ failure in 35-65.6 %. Among the single organ failures, pulmonary failure was the most commonly organ failure (39.1-63 %), followed by cardiovascular failure (23-37.7 %), hepatic failure (20.7 %), renal failure (8.5-13 %)[27,28]. The present data showed that organ failure occurred in 63.5 % (47/74), multiple organ failure in 27.0 % (20/74), single organ failure in 36.5 % (27/74) (Table 2). No relationship existed between organ failure and age, sex, gallstone pancreatitis,

but the severity (APACHE II scores) and mortality were significantly higher in patients with organ failure than in those without organ failure (Table 1). Pulmonary failure was the most common single organ failure (23.0 %, 17/74) in SAP. The mortality rate in patients with single pulmonary failure was 17.6 % (3/17), followed by hepatic and gastrointestinal failure. No patient in this group was accompanied by single renal failure, or cardiovascular organ failure, or encephalic failure (Table 2). Among all the organ failures, pulmonary failure was the most frequent organ failure (45.9 %), the second was multiple organ failure (Table 3).

Conflicting results about the relation between extent of necrosis, infected necrosis and organ failure have been reported[28-31]. The present study demonstrated that although the incidence of organ failure in sterile necrosis was slightly higher than that in infected necrosis (66.0 % *vs* 59.3 %), there was no difference in the prevalence of organ failure in sterile necrosis compared with infected necrosis (Table 4). The incidence of organ failure increased with increased extent of necrosis, but patients with increased amounts of necrosis did not have increased prevalence of organ failure (Table 5).

As to the relation between specific single organ failure and sterile and infected necrosis, previous study showed that the incidence of pulmonary failure was increased in infected necrosis compared with sterile necrosis, and there was no difference in the prevalence of renal failure, cardiovascular failure in infected necrosis compared with sterile necrosis[31]. Our study showed that there was no difference in the prevalence of specific single organ failure in infected necrosis compared with sterile necrosis (Table 6).

The mortality rate was 30 % in patients with multiple organ failure, and was 8 % in those with single organ failure[31]. Our data showed the mortality rate was 45 % (9/20) in patients with multiple organ failure, and was 11 % (3/27) in those with single organ failure (Table 2). Halonen *et al*[32] compared multiple organ dysfunction (MOD) score, sequential organ failure assessment (SOFA) score, and logistic organ dysfunction (LOD) score in predicting hospital mortality rates of 178 SAP patients. The results demonstrated that three different multiple organ dysfunction scores showed good accuracy and were comparable with APACHE II in predicting hospital mortality. In multiple logistic regression analysis, only hepatic, renal, and cardiovascular failures were independent risk factors for hospital mortality. Our study revealed that non survivors had a significantly higher morbidity of multiple organ failure, pulmonary failure, cardiovascular failure and gastrointestinal failure compared with survivors, there was no difference in the morbidity of renal failure, hepatic failure and neurologic failure in nonsurvivors and survivors (Table 7). The results demonstrated that the hospital mortality of SAP was associated with multiple organ failure, pulmonary failure, cardiovascular failure and gastrointestinal failure. Therefore, prophylactic and active treatment of these organ failures are very important in the treatment of SAP. Recently, hemoconcentration (hematocrit $\geqslant$44 % and/or failure of admission hematocrit to decrease at approximately 24 hours)[33,34], plasma concentrations of sTNF-Rs[35], activated polymorphonuclear leucocytes-elastase (PMN-E) and IL-6[36] have been reported as early markers for organ failure and necrotic pancreatitis. Patients coincident with this standard should be treated with strong fluid resuscitation and closely monitored in intensive care units, and new approaches have to be found to counteract these severe complications.

REFERENCES

1 **Wu XN**. Management of severe acute pancreatitis. *World J Gastroenterol* 1998; **4:** 90-91

2 **Qin RY,** Zou SQ, Wu ZD, Qiu FZ. Experimental research on production and uptake sites of TNFα in rats with acute hemorrhagic necrotic pancreatitis. *World J Gastroenterol* 1998; **4:** 144-146

3 **Zhao LG,** Wu XX, Han EK, Chen YL, Chen C, Xu DQ. Protective effect of YHI and HHI-I against experimental acute pancreatitis in rabbits. *World J Gastroenterol* 1998; **4:** 256-259

4 **Robert JH,** Frossard JL, Mermillod B, Soravia C, Mensi N, Roth M, Rohner A, Hadengue A, Morel P. Early prediction of acute pancreatitis: prospective study comparing computed tomography scans, Ranson, Glascow, Acute Physiology and Chronic Health Evaluation II scores, and various serum markers. *World J Surg* 2002; **26:** 612-619

5 **Wu XN.** Treatment revisited and factors affecting prognosis of severe acute pancreatitis. *World J Gastroenterol* 2000; **6:** 633-635

6 **Chen DL,** Wang WZ, Wang JY. Epidermal growth factor prevents gut atrophy and maintains intestinal integrity in rats with acute pancreatitis. *World J Gastroenterol* 2000; **6:** 762-765

7 **Mao EQ,** Tang YQ, Zhang SD. Effects of time interval for hemofiltration on the prognosis of severe acute pancreatitis. *World J Gastroenterol* 2003; **9:** 373-376

8 **Zhou ZG,** Chen YD, Sun W, Chen Z. Pancreatic microcirculatory impairment in experimental acute pancreatitis in rats. *World J Gastroenterol* 2002; **8:** 933-936

9 **Norman J.** The role of cytokines in the pathogenesis of acute pancreatitis. *Am J Surg* 1998; **175:** 76-83

10 **Yi Y,** Gao NR, Li ZL. Protective effects of ulinostatin on acute lung injury induced by acute necrotizing pancreatitis in rats. *Shijie Huaren Xiaohua Zazhi* 2002; **10**: 558-561

11 **Knoefel WT,** Kollias N, Warshaw AL, Waldner H, Nishioka NS, Rattner DW. Pancreatic microcirculatory changes in experimental pancreatitis of graded severity in the rat. *Surgery* 1994; **116:** 904-913

12 **He L,** Chen SF, Cao XH, Zhang LD, Pan LL, Zhou Z. Changes of serum level of IL-15, IL-18 and sTNF-1R in patients with acute pancreatitis. *Shijie Huaren Xiaohua Zazhi* 2003; **11:** 57-60

13 **Schmid SW,** Uhl W, Friess H, Malfertheiner P, Buchler MW. The role of infection in acute pancreatitis. *Gut* 1999; **45:** 311-316

14 **Berger HG,** Rau B, Mayer J, Pralle U. Natural course of acute pancreatitis. *World J Surg* 1997; **21:** 130-135

15 **Wu XZ.** Therapy of acute severe pancreatitis awaits further improvement. *World J Gastroenterol* 1998; **4:** 285-286

16 **Wu XN.** Current concept of pathogenesis of severe acute pancreatitis. *World J Gastroenterol* 2000; **6:** 32-36

17 **Slavin J,** Ghaneh P, Sutton R, Hartley M, Rowlands P, Garvey C, Hughes M, Neoptolemos J. Management of necrotizing pancreatitis. *World J Gastroenterol* 2001; **7:** 476-481

18 **Isenmann R,** Rau B, Berger HG. Early severe acute pancreatitis: characteristics of a new subgroup. *Pancreas* 2001; **22:** 274-278

19 **Abu-Zidan FM,** Bonham MJ, Windsor JA. Severity of acute pancreatitis:a multivariate analysis of oxidative stress markers and modified Glasgow criteria. *Br J Surg* 2000; **87:** 1019–1023

20 **Luo Y,** Yuan CX, Peng YL, Wei PL, Zhang ZD, Jiang JM, Dai L, Hu YK. Can ultrasound predict the severity of acute pancreatitis early by observing acute fluid collection? *World J Gastroenterol* 2001; **7:** 293-295

21 **Pezzilli R,** Mancini F. Assessment of severity of acute pancreatitis: a comparison between old and most recent modalities used to evaluate this perennial problem. *World J Gastroenterol* 1999; **5:** 283-285

22 **Shi X,** Gao NR, Guo QM, Yang YJ, Huo MD, Hu HL, Friess H. Relationship between overexpression of NK-1R, NK-2R and intestinal mucosal damage in acute necrotizing pancreatitis. *World J Gastroenterol* 2003; **9:** 160-164

23 **Baron TH,** Morgan DE. Acute necrotizing pancreatitis. *N Engl J Med* 1999; **340:** 1412-1417

24 **Yuan YZ,** Gong ZH, Lou KX, Tu SP, Zhai ZK, Xu JY. Involvement of apoptosis of alveolar epithelial cells in acute pancreatitis-associated lung injury. *World J Gastroenterol* 2000; **6:** 920-924

25 **Blum T,** Maisonneuve P, Lowenfels AB, Lankisch PG. Fatal outcome in acute pancreatitis: its occurrence and early prediction. *Pancreatology* 2001; **1:** 237-241

26 **Pancreatic Surgery Association of CMA.** The Criteria of Clinical Diagnosis and Classification System for Acute Pancreatitis (the second project, 1996,). *Zhonghua Waike Zazhi* 1997;

35: 773-775

27 **Buchler MW,** Gloor B, Muller CA, Friess H, Seiler CA, Uhl W. Acute necrotizing pancreatitis: Treatment strategy according to the status of infection. *Ann Surg* 2000; **232:** 619-626

28 **Gotzinger P,** Sautner T, Kriwanek S, Beckerhinn P, Barlan M, Armbruster C, Wamser P, Fugger R. Surgical treatment for severe acute pancreatitis: extent and surgical control of necrosis determine outcome. *World J Surg* 2002; **26:** 474-478

29 **Lankisch PG,** Pflichthofer D, Lehnick D. No strict correlation between necrosis and organ failure in acute pancreatitis. *Pancreas* 2000; **20:** 319-322

30 **Tenner S,** Sica G, Hughes M, Noordhoek E, Feng S, Zinner M, Banks PA. Relationship of necrosis to organ failure in severe acute pancreatitis. *Gastroenterology* 1997; **133:** 899-903

31 **Isenmann R,** Rau B, Beger HG. Bacterial infection and extent of necrosis are determinants of organ failure in patients with acute necrotizing pancreatitis. *Br J Surg* 1999; **86:** 1020-1024

32 **Halonen KI,** Pettila V, Leppaniemi AK, Kemppainen EA, Puolakkainen PA, Haapiainen RK. Multiple organ dysfunction associated with severe acute pancreatitis. *Crit Care Med* 2002; **30:** 1274-1279

33 **Brown A,** Orav J, Banks PA. Hemoconcentration is an early marker for organ failure and necrotizing pancreatitis. *Pancreas* 2000; **20:** 367-372

34 **Jiang CQ**, Ai ZL, Liu ZS, He YM, Sun Q, Xu R, Fan LF. Hemoconcentration as an early risk factor for severe acute pancreatitis. *Zhongguo Shiyong Waike Zazhi* 2001; **21:** 666-667

35 **Hirota M,** Nozawa F, Okabe A, Shibata M, Beppu T, Shimada S, Egami H, Yamaguchi Y, Ikei S, Okajima T, Okamoto K, Ogawa M. Relationship between plasma cytokine concentration and multiple organ failure in patients with acute pancreatitis. *Pancreas* 2000; **21**: 141-146

36 **Ikei S,** Ogawa M, Yamaguchi Y. Blood concentrations of polymorphonuclear leucocyte elastase and interleukin-6 are indicators for the occurrence of multiple organ failures at the early stage of acute pancreatitis. *J Gastroenterol Hepatol* 1998; **13:** 1274-1283

Edited by Zhao M and Wang XL

P.O.Box 2345, Beijing 100023,China
Fax: +86-10-85381893
E-mail: wjg@wjgnet.com www.wjgnet.com

World J Gastroenterol 2003;9(11):2574-2578
World Journal of Gastroenterology
 ISSN 1007-9327

• CLINICAL RESEARCH •

Grading and staging of hepatic fibrosis, and its relationship with noninvasive diagnostic parameters

Lun-Gen Lu, Min-De Zeng, Mo-Bin Wan, Cheng-Zhong Li, Yi-Min Mao, Ji-Qiang Li, De-Kai Qiu, Ai-Ping Cao, Jun Ye, Xiong Cai, Cheng-Wei Chen, Ji-Yao Wang, Shan-Ming Wu, Jin-Shui Zhu, Xia-Qiu Zhou

Lun-Gen Lu, Min-De Zeng, Yi-Min Mao, Ji-Qiang Li, De-Kai Qiu, Ai-Ping Cao, Shanghai Institute of Digestive Disease, Renji Hospital, Shanghai Second Medical University, Shanghai 200001, China
Mo-Bin Wan, Cheng-Zhong Li, Department of Infectious Diseases, Changhai Hospital, Shanghai 200433, China
Jun Ye, Department of Infectious Diseases, Putou District Central Hospital, Shanghai 200062, China
Xiong Cai, Department of Infectious Diseases, Changzheng Hospital, Shanghai 200003, China
Cheng-Wei Chen, Shanghai Liver Diseases Research Center, Nanjing Military Command, Shanghai 200233, China
Ji-Yao Wang, Department of Gastroenterology, Zhongshan Hospital, Shanghai 200032, China
Shan-Ming Wu, Shanghai Infectious Hospital, Shanghai 200085, China
Jin-Shui Zhu, Department of Gastroenterology, Shanghai NO.6 Hospital, Shanghai 200233, China
Xia-Qiu Zhou, Department of Infectious Diseases, Ruijin Hospital, Shanghai 200025, China
Supported by the Key Project of Shanghai Medical Development Foundation, No.99ZDI001
Correspondence to: Lun-Gen Lu, MD, Shanghai Institute of Digestive Disease, Renji Hospital, Shanghai Second Medical University, Shanghai 200001, China. lulungen@online.sh.cn
Telephone: +86-21-33070834 **Fax:**+86-21-63364118
Received: 2003-04-02 **Accepted:** 2003-06-19

Abstract

AIM: To explore the grade and stage of pathology and the relationship between grading and staging of hepatic fibrosis and noninvasive diagnostic parameters.

METHODS: Inflammatory activity and fibrosis of consecutive liver biopsies from 200 patients with chronic liver disease were determined according to the Diagnostic Criteria of Chronic Hepatitis in China, 1995. A comparative analysis was made in these patients comparing serum markers, Doppler ultrasonography, CT and/or MR imaging with the findings of liver biopsy.

RESULTS: With increase of inflammatory activity, the degree of fibrosis also rose. There was a close correlation between liver fibrosis and inflammatory activity. AST, GGT, albumin, albumin/globulin, ALP, AFP, hyaluronic acid, N-terminal procollagen III(P III NP), collagen type IV(Col IV), tissue inhibitors of metalloproteinases-1(TIMP-1), alpha-2-macroglobulin, natural killer cells(NK), some parameters of Doppler ultrasonography, CT and/or MR imaging were all related to the degree of inflammatory activity. GGT, albumin, albumin/globulin, ALP, AFP, hyaluronic acid, Col IV, TIMP-1, alpha-2- macroglobulin, transforming growth factor-beta 1(TGFβ1), NK, some parameters of Doppler ultrasonography, CT and/or MR imaging were all related to the staging of fibrosis. By regression analysis, the parameters used in combination to differentiate the presence or absence of fibrosis were age, GGT, the parameter of blood flow of portal vein per minute, the maximum oblique diameter of right liver by B ultrasound, the wavy hepatic surface contour by CT and/or MR. The sensitivity, specificity and accuracy of the above parameters were 80.36 %, 86.67 %, and 81.10 %, respectively.

CONCLUSION: There is close correlation between liver fibrosis and inflammatory activity. The grading and staging of liver fibrosis are related to serum markers, Doppler ultrasonography, CT and/or MR imaging. The combination of the above mentioned noninvasive parameters are quite sensitive and specific in the diagnosis of hepatic fibrosis.

Lu LG, Zeng MD, Wan MB, Li CZ, Mao YM, Li JQ, Qiu DK, Cao AP, Ye J, Cai X, Chen CW, Wang JY, Wu SM, Zhu JS, Zhou XQ. Grading and staging of hepatic fibrosis, and its relationship with noninvasive diagnostic parameters. *World J Gastroenterol* 2003; 9(11): 2574-2578

http://www.wjgnet.com/1007-9327/9/2574.asp

INTRODUCTION

Hepatic fibrosis has been a common response to chronic liver injury and might result in potentially lethal sequelae[1-3]. In chronic liver diseases, determination of stage and activity of the fibrotic process and evaluation of anti-fibrotic treatment required accurate variables, the commonly so-called ' fibrotic markers' [4-11]. Since the value of laboratory test to diagnose liver fibrosis was limited, biopsy has been still the golden criterion of the diagnosis of liver fibrosis and cirrhosis at present[12,13]. But it is an invasive diagnostic method, so its application and further propagation are somewhat limited. Searching for a noninvasive diagnostic approach is an interesting subject both at home and abroad. Although some parameters have been found to have important values in iconography and laboratory tests, they are still far from satisfactory. So it is of great realistic value to explore a credible, specific, and noninvasive diagnostic parameter of liver fibrosis for the prevention and treatment of chronic liver disease[14-28]. Therefore, on the basis of histology of chronic liver diseases, this study was designed to explore the relationship between the grade and stage of pathology, and noninvasive diagnostic parameters. We hoped that we could provide the basis for the noninvasive diagnosis of liver fibrosis, so as to improve the prevention and treatment of liver fibrosis.

MATERIALS AND METHODS

Selection of patients

The study was organized and carried out by Shanghai Cooperative Group of Hepatic Fibrosis Project. The Cooperaitive Group was led by Renji Hospital and Changhai Hospital in Shanghai. Cases collected by the Cooperative Group were 37 from Changhai Hospital, 36 from Renji Hospital, 30 from Putuo District Central Hospital, 22 from Shanghai Liver Disease Center of Nanjing Military Command, 20 from Changzheng Hospital, 14 from Zhongshan Hospital,

11 from Huashan Hospital, 9 from Shibei Hospital, 8 from Shanghai No.6 Hospital, 6 from Shanghai Infectious Disease Hospital, 3 from Ruijin Hospital, 3 from Shanghai No.9 hospital, and 1 from Shanghai No.1 hospital. A total of 200 patients were collected between July and October in 1999 according to both clinical and pathological criteria. There were 156 males and 44 females with an average age of 34 years (range 15-60).

Histological examination

One week after admission, all patients underwent liver puncture biopsy under the guide of B type ultrasound with the 14G Quick-cut needle (8-Light Company, Japan) or Menghini needle. The length of liver specimen was more than 1 cm. The samples were fixed with 10 % formaldehyde, paraffin slides were made and stained with hematoxylin-eosin, reticular fiber and collagen fiber according to the grading and staging of Diagnostic Criteria of Chronic Hepatitis in China in 1995[29]. Eleven patients were graded and staged for inflammatory activity and liver fibrosis. Three pathologists read the slide independently. The results were checked with Kappa test by statistical experts. It was shown that the coherence of grading and staging of hepatitis fibrosis was excellent. The pathological diagnosis of liver biopsy was finally made by the Department of Pathology , Medical Collage of Fudan University.

Laboratory tests

Blood and urine routine tests: α-fetoprotein(AFP) and prothrombin time were examined by the Cooperative Units.

Serum biochemical tests: Total bilirubin, indirect bilirubin, alanine aminotransferase (ALT), aspartate aminotransferase (AST), AST/ALT, γ-glutamyl transpeptidase(GGT), alkaline phosphatase(ALP), albumin, albumin/globulin, blood urea nitrogen(BUN), creatinine(Cr), triglyceride, cholersterol, high density lipoprotein and low density lipoprotein were all measured by Shanghai Institute of Digestive Disease.

Markers of hepatitis virus and immunological parameter: HBsAg, Anti-HBs, HBeAg, Anti-HBe, Anti-HBc, HBV- DNA, Anti-HCV, HCV- RNA, $CD3^+$, $CD4^+$, $CD8^+$, natural killer cell (NKC), interleukin-2 (IL-2), and interferon-γ (IFN-γ) were detected by Shanghai Institute of Digestive Disease.

Related liver fibrosis markers: α-2-macroglobulin(α-MA), transferrin, apolipoproteinA1, hyaluronic acid (HA), laminin, N-terminal procollagen III(PIIINP), 7S collagen IV (7S-IV), and transforming growth factor-β1(TGF-β1) were detected by the Clinical Immunology Center of Changzheng Hospital in Shanghai.

Tissue inhibitor of metalloproteinase-1(TIMP-1) were assayed by Shanghai Hongqiao Medical Reagent Institute.

B ultrasound examination

All B ultrasound examinations of the patients were carried out in Shanghai Institute of Digestive Disease. The patients had empty stomach for 14 hours before examination. Two skillful doctors performed the examination with color Doppler ultrasonic instrument(HDI 5000). The results were saved in compact disk, three experts judged the examination results and made the final reports.

CT and/or MR imaging

All CT and/or MR examinations were performed by Ruijin Hospital, Changzheng Hospital, Changhai Hospital, Zhongshan Hospital, and Shanghai No.6 Hospital in the Cooperative Group. CT scanners with PQ-2000 and/or PQ-5000 (Picker Company), Plus-s (Siemens Company), Hispeed Adv (GE Company), and MR scanners with Cyroscan T10-NT (Philips Company),Vision Plus and Magnetron Impact (Siemens Company) were used.

Statistical analysis

All the data were analyzed with SAS software by Statistical Department in Shanghai Second Medical University.

RESULTS

Histological examinations

It was revealed that there was a significantly positive correlation between the inflammatory activity and the staging of liver fibrosis. With increase of inflammatory activity, liver fibrosis became more serious (Table 1).

Table 1 Pathological diagnostic results of 200 liver biopsy samples

Staging of fibrosis	Grading of inflammation					value	
	1	2	3	4	Total	χ^2-value	*P*-value
0	18	2	0	0	20	278.3	1E-04
1	42	22	0	0	64		
2	6	33	26	0	64		
3	9	2	19	4	25		
4	0	0	3	23	26		
Total	66	59	48	27	200		

Laboratory examinations

Relationship between serum biochemical parameters and the grading of inflammation: Only serum biochemical parameters related to liver inflammation are listed in Table 2.

Table 2 Relationship between serum biochemical parameters and grading of inflammation

Parameter	Comparision among groups of inflammation grading					
	1-2	1-3	1-4	2-3	2-4	3-4
RBC			b		b	b
PLT			b		b	b
AST		b	b	a	b	
GGT	a	b	b	b	b	
Albumin			b		b	b
Albumin / globulin			b		b	b
ALP			b		b	
AFP	b	b	b	b	b	b
HA	b	b	b	b	b	b
PIIINP			b		b	
7S-IV		a	b	a	b	
TIMP-1		a	a			
α-MA			b		a	
NK			b		a	a
IgG			b		b	b
IgG+IgA+IgM			b		b	b

$^aP<0.05$, $^bP<0.01$.

Relationship between serum biochemical parameters and staging of liver fibrosis: Only the serum biochemical parameters related to liver fibrosis are listed in Table 3.

B ultrasound examinations

Comparison between parameters of ultrasonic 2-D and color Doppler flow image and the groups of inflammation grading: Only the parameters of ultrasonic 2-D and color Doppler flow image related with the groups of inflammation grading are listed in Table 4.

Comparison between parameters of ultrasonic 2-D and color Doppler flow image and groups of liver fibrosis staging: Only the parameters of ultrasonic 2-D and color Doppler flow image related with the groups of liver fibrosis staging are listed in Table 5.

CT and/or MR imaging examination

Among the 200 patients who received liver biopsy, 192 patients had CT and/or MR imaging examintion. Twenty cases (10.4 %) received both CT and MR imaging examination, 92cases (47.9 %) received only CT examination, 80 cases (41.7 %)

Table 3 Relationship between serum biochemical parameters and staging of liver fibrosis

Parameter	Comparision among groups of liver fibrosis staging									
	0-1	0-2	0-3	0-4	1-2	1-3	1-4	2-3	2-4	3-4
RBC				a			a		a	a
GGT		b	b	b	b	b	b			
Albumin				b			b		b	b
Albumin / globulin				b			b		b	b
ALP				b			a			
AFP			b	b		b	b		b	
HA		b	b	b	b	b	b		b	b
7S-IV				a			a		a	
TIMP-1			a	b		a	a			
α-MA				a			b		a	
TGFβ-1	a	a	a	a						
IgG				b			b		b	b
IgG+IgA+IgM				b			b		b	b

[a]$P<0.05$, [b]$P<0.01$.

Table 4 Comparison between parameters of ultrasonic 2-D and color Doppler flow image and groups of inflammation grading

Parameter	Comparision among groups of inflammation grading					
	1-2	1-3	1-4	2-3	2-4	3-4
Inner diameter of left portal vein		a				
Inner diameter of middle liver vein			a		a	
Inner diameter of right liver vein			b		a	
Thickness of gallbladder wall		a	b	a	b	
Shape of gallbladder			b		b	
Vertical diameter of spleen		a	b	a	b	a
Thickness of spleen		a	b	a	b	
Diameter of spleen vein			b		a	
Thickening of the light dots in liver substance			b		b	
Movement degree along with breath			b		a	
Movement degree along with heart beat			b		a	
Blood stream velocity in constriction phase of liver artery		a				
Blood stream velocity in dilation phase of liver artery			a			

[a]$P<0.05$, [b]$P<0.01$.

Table 5 Comparison between parameters of ultrasonic 2-D and color Doppler flow image and groups of liver fibrosis staging

Parameter	Comparision among groups of liver fibrosis staging									
	0-1	0-2	0-3	0-4	1-2	1-3	1-4	2-3	2-4	3-4
Thickness of liver capsule				a						
Maximum oblique diameter of right liver	a	b	b	b						
Tube diameter of portal vein trunk		a		a						
Inner diameter of left portal vein	a	b	b	a						
Inner diameter of right portal vein	a	a	a	a						
Thickness of gallbladder wall				b			b		a	a
Shape of gallblader				b			a		a	a
Diameter of splenic vein				b			a			a
Vertical diameter of spleen			a	b			b		a	
Thickness of spleen				a						
Thickening of the light dots in liver substance		a		b			a			
Movement degree along with breath				b			a			
Movement degree along with heart beat									b	a
Parameter of blood flow of portal vein per minute	a	a	a	a						

[a]$P<0.05$, [b]$P<0.01$.

received only MR examination.

The results demonstrated that the longitudinal diameter of the left lobe, volume index, the wavy hepatic surface contour, liver crack widening, size of the gallbladder, thickening of the gallbladder wall, changes like little bursa of peri-gallbladder tube, to and fro diameter of the spleen, and thickness of the spleen were all correlated with the grading of inflammation. The wavy hepatic surface contour, changes like little bursa of peri-gallbladder tube, and the to and fro diameter of the spleen were correlated with the staging of liver fibrosis.

DISCUSSION

At present, the diagnosis of liver fibrosis still depends on pathological examination of liver puncture tissue. Since the procedure is invasive, its application and extensive use in clinical practice are still limited. So great attention has been paid to search for and clinical study of a non-invasive diagnostic parameter for liver fibrosis[15,27,28]. It would not only speed up the study of basic medical theory about liver disease, but also be of value[1,3].

In 1995, a new pathological classification method was carried out in our country[29]. The criteria were established respective to distinguish inflammation from liver fibrosis by grading and staging. Both of them have quantified parameters, which are convenient for statistical analysis. Following these criteria, we compared pathological classification with some non-invasive parameters (serologic and imaging parameters), so as to evaluate the value and significance of different parameters in reflecting pathological changes. In the liver puncture tissue of 200 patients with chronic hepatitis, there was a significant positive correlation between inflammatory activity and staging of liver fibrosis. With the increase of inflammatory activity, liver fibrosis became more serious.

In serology, RBC, PLT, AST, GGT, albumin, albumin/globulin, ALP, AFP, HA, PIIINP, 7S-IV, TIMP-1, α2-MA, NK, *etc*. had a relationship with inflammatory activity, but GGT, albumin, albumin/globulin, ALP, AFP, HA, 7S-IV, and α2-MA had a relationship with liver fibrosis. So these latter parameters might be used as the parameters of liver fibrosis[5,10,30-34]. With the development of inflammation and fibrosis, the level of HA and 7S-IV rose gradually in different inflammatory grading and liver fibrosis staging. In pathological diagnosis, Stage 1 and Stage 2 indicated mild fibrosis, Stage 3 and Stage 4 indicated severe fibrosis. The accuracy, specificity and sensitivity of HA were 82.9 %, 93 %, and 56 %, respectively. The accuracy, specificity and sensitivity of 7S-IV were 72.4 %, 94.3 %, and 18 %, respectively. To some extent, PIIINP might reflect mild and severe changes of inflammation, but it might not reflect the fibrotic changes. This study revealed that laminin had no diagnostic value either in inflammation or in fibrotic changes. It was found that the level of TGFβ1 and TIMP-1 increased more significantly in inflammation and early stage of fibrosis, indicating that they could reflect the changes of liver inflammation and fibrosis[35-38]. In this study, PIIINP, laminin, transferrin, and apoproteinA1 which were known to have significant diagnostic value, were not confirmed. So, we should do more work to probe into their diagnostic significance. In the following study, we would increase the number of cases to further study the diagnostic value of the related parameters in liver fibrosis and evaluate the efficacy of anti-fibrotic drugs, so as to provide a sound basis for the reasonable combined use of the different parameters, and to improve the specificity, accuracy and sensitivity of noninvasive diagnostic tests for liver fibrosis[3,15,19,28].

With the development of modern medical imaging techniques, ultrasound, CT and MR would be widely used. These methods could significantly improve the diagnosis and differential diagnosis of liver disease[17,18,20-26]. In this study, ultrasound examination indicated that the thickness of liver capsule, maximum oblique diameter of right liver, tube diameter of portal vein trunk, diameter of left portal vein, diameter of right portal vein, thickness of gallbladder wall, thickness of spleen, diameter of splenic vein, parameter of blood stream quantity per minute in portal vein, light dot shape, and shape of gallbladder were correlated with the staging of liver fibrosis. CT and/or MR imaging only revealed that the volume of spleen was correlated with liver fibrosis. The results demonstrated that B ultrasound had more value than CT and/or MR imaging in the diagnosis of liver fibrosis. This of course needs further study. It should be noted that factors such as individual variation, nature of the instrument used, patient' s condition at the time of examination and difference of the performer' s skill might affect the evaluation of the result[21-24]. At the same time, we should carry out quantitative and/or semi-quantitative research on ultrasonic two-dimensional imaging and Doppler blood stream, so as to increase the sensitivity, specificity and accuracy of the diagnostic parameters.

REFERENCES

1 **Botta F**, Giannini E, Romagnoli P, Fasoli A, Malfatti F, Chiarbonello B, Testa E, Risso D, Colla G, Testa R. MELD scoring system is useful for predicting prognosis in patients with liver cirrhosis and is correlated with residual liver function: a European study. *Gut* 2003; **52**: 134-139

2 **Yang C**, Zeisberg M, Mosterman B, Sudhakar A, Yerramalla U, Holthaus K, Xu L, Eng F, Afdhal N, Kalluri R. Liver fibrosis: insights into migration of hepatic stellate cells in response to extracellular matrix and growth factors. *Gastroenterology* 2003; **124**: 147-159

3 **Oberti F**, Valsesia E, Pilette C, Rousselet MC, Bedossa P, Aube C, Gallois Y, Rifflet H, Maiga MY, Penneau-Fontbonne D, Cales P. Noninvasive diagnosis of hepatic fibrosis or cirrhosis. *Gastroenterology* 1997; **113**: 1609-1116

4 **Guechot J**, Serfaty L, Bonnand AM, Chazouilleres O, Poupon RE, Poupon R. Prognostic value of serum hyaluronan in patients with compensated HCV cirrhosis. *J Hepatol* 2000; **32**: 447-452

5 **Hayasaka A**, Saisho H. Serum markers as tools to monitor liver fibrosis. *Digestion* 1998; **59**: 381-384

6 **Ninomiya T**, Yoon S, Hayashi Y, Sugano M, Kumon Y, Seo Y, Shimizu K, Kasuga M. Clinical significance of serum hyaluronic acid as a fibrosis marker in chronic hepatitis C patients treated with interferon-alpha: histological evaluation by a modified histological activity index scoring system. *J Gastroenterol Hepatol* 1998; **13**: 68-74

7 **George DK**, Ramm GA, Walker NI, Powell LW, Crawford DH. Elevated serum type IV collagen: a sensitive indicator of the presence of cirrhosis in haemochromatosis. *J Hepatol* 1999; **31**: 47-52

8 **Murawaki Y**, Koda M, Okamoto K, Mimura K, Kawasaki H. Diagnostic value of serum type IV collagen test in comparison with platelet count for predicting the fibrotic stage in patients with chronic hepatitis C. *J Gastroenterol Hepatol* 2001; **16**: 777-781

9 **Wang T**, Wang B, Liu X. Correlation of serum markers with fibrosis staging in chronic viral hepatitis. *Zhonghua Binglixue Zazhi* 1998; **27**: 185-190

10 **Zheng M**, Cai W, Weng H, Liu R. Determination of serum fibrosis indexes in patients with chronic hepatitis and its significance. *Chin Med J* 2003; **116**: 346-349

11 **McHutchison JG**, Blatt LM, de Medina M, Craig JR, Conrad A, Schiff ER, Tong MJ. Measurement of serum hyaluronic acid in patients with chronic hepatitis C and its relationship to liver histology. Consensus Interferon Study Group. *J Gastroenterol Hepatol* 2000; **15**: 945-951

12 **Gabrielli GB**, Capra F, Casaril M, Squarzoni S, Tognella P, Dagradi R, De Maria E, Colombari R, Corrocher R, De Sandre G. Serum laminin and type III procollagen in chronic hepatitis C. Diagnostic value in the assessment of disease activity and fibrosis. *Clin Chim Acta* 1997; **265**: 21-31

13 **Castera L**, Hartmann DJ, Chapel F, Guettier C, Mall F, Lons T, Richardet JP, Grimbert S, Morassi O, Beaugrand M, Trinchet JC.

Serum laminin and type IV collagen are accurate markers of histologically severe alcoholic hepatitis in patients with cirrhosis. *J Hepatol* 2000; **32**: 412-418

14 **Stickel F**, Urbaschek R, Schuppan D, Poeschl G, Oesterling C, Conradt C, McCuskey RS, Simanowski UA, Seitz HK. Serum collagen type VI and XIV and hyaluronic acid as early indicators for altered connective tissue turnover in alcoholic liver disease. *Dig Dis Sci* 2001; **46**: 2025-2032

15 **Pilette C**, Rousselet MC, Bedossa P, Chappard D, Oberti F, Rifflet H, Maiga MY, Gallois Y, Cales P. Histopathological evaluation of liver fibrosis: quantitative image analysis vs semi-quantitative scores. Comparison with serum markers. *J Hepatol* 1998; **28**: 439-446

16 **Persico M**, Palmentieri B, Vecchione R, Torella R, De SI. Diagnosis of chronic liver disease: reproducibility and validation of liver biopsy. *Am J Gastroenterol* 2002; **97**: 491-492

17 **Wachsberg RH**, Bahramipour P, Sofocleous CT, Barone A. Hepatofugal flow in the portal venous system: pathophysiology, imaging findings, and diagnostic pitfalls. *Radiographics* 2002; **22**: 123-140

18 **Colli A**, Fraquelli M, Andreoletti M, Marino B, Zuccoli E, Conte D. Severe liver fibrosis or cirrhosis: accuracy of US for detection-analysis of 300 cases. *Radiology* 2003; **227**: 89-94

19 **Tran A**, Hastier P, Barjoan EM, Demuth N, Pradier C, Saint-Paul MC, Guzman-Granier E, Chevallier P, Tran C, Longo F, Schneider S, Piche T, Hebuterne X, Benzaken S, Rampal P. Non invasive prediction of severe fibrosis in patients with alcoholic liver disease. *Gastroenterol Clin Biol* 2000; **24**: 626-630

20 **Aube C**, Oberti F, Korali N, Namour MA, Loisel D, Tanguy JY, Valsesia E, Pilette C, Rousselet MC, Bedossa P, Rifflet H, Maiga MY, Penneau-Fontbonne D, Caron C, Cales P. Ultrasonographic diagnosis of hepatic fibrosis or cirrhosis. *J Hepatol* 1999; **30**: 472-478

21 **Murakami T**, Mochizuki K, Nakamura H. Imaging evaluation of the cirrhotic liver. *Semin Liver Dis* 2001; **21**: 213-224

22 **Laghi A**, Iannaccone R, Catalano C, Carbone I, Ferrari R, Mangiapane F, Passariello R. Multiphase multislice spiral CT for liver assessment: optimization in cirrhotic patients. *Radiol Med* 2002; **103**: 188-195

23 **Bernatik T**, Strobel D, Hahn EG, Becker D. Doppler measurements: a surrogate marker of liver fibrosis? *Eur J Gastroenterol Hepatol* 2002; **14**: 383-387

24 **Martinez-Noguera A**, Montserrat E, Torrubia S, Villalba J.Doppler in hepatic cirrhosis and chronic hepatitis. *Semin Ultrasound CT MR* 2002; **23**: 19-36

25 **Kok T**, van der Jagt EJ, Haagsma EB, Bijleveld CM, Jansen PL, Boeve WJ. The value of Doppler ultrasound in cirrhosis and portal hypertension. *Scand J Gastroenterol Suppl* 1999; **230**: 82-88

26 **Lonjedo E**, Ripolles T. Vascular imaging and interventional procedures in hepatic cirrhosis. *Semin Ultrasound CT MR* 2002; **23**: 130-140

27 **Thabut D**, Simon M, Myers RP, Messous D, Thibault V, Imbert-Bismut F, Poynard T. Noninvasive prediction of fibrosis in patients with chronic hepatitis C. *Hepatology* 2003; **37**: 1220-1221

28 **Myers RP**, Ratziu V, Imbert-Bismut F, Charlotte F, Poynard T. Biochemical markers of liver fibrosis: a comparison with historical features in patients with chronic hepatitis C. *Am J Gastroenterol* 2002; **97**: 2419-2425

29 Prevention and treatment projects of virus hepatitis (tryout). *Chin J Intern Med* 1995; **34**: 788-791

30 **Flisiak R**, Maxwell P, Prokopowicz D, Timms PM, Panasiuk A. Plasma tissue inhibitor of metalloproteinases-1 and transforming growth factor beta 1-possible non-invasive biomarkers of hepatic fibrosis in patients with chronic B and C hepatitis. *Hepatogastroenterology* 2002; **49**: 1369-1372

31 **Murawaki Y**, Nishimura Y, Ikuta Y, Idobe Y, Kitamura Y, Kawasaki H. Plasma transforming growth factor-beta 1 concentrations in patients with chronic viral hepatitis. *J Gastroenterol Hepatol* 1998; **13**: 680-684

32 **Walsh KM**, Timms P, Campbell S, MacSween RN, Morris AJ. Plasma levels of matrix metalloproteinase-2 (MMP-2) and tissue inhibitors of metalloproteinases -1 and -2 (TIMP-1 and TIMP-2) as noninvasive markers of liver disease in chronic hepatitis C: comparison using ROC analysis. *Dig Dis Sci* 1999; **44**: 624-630

33 **Kanzler S**, Baumann M, Schirmacher P, Dries V, Bayer E, Gerken G, Dienes HP, Lohse AW. Prediction of progressive liver fibrosis in hepatitis C infection by serum and tissue levels of transforming growth factor-beta. *J Viral Hepat* 2001; **8**: 430-437

34 **Pohl A**, Behling C, Oliver D, Kilani M, Monson P, Hassanein T. Serum aminotransferase levels and platelet counts as predictors of degree of fibrosis in chronic hepatitis C virus infection.*Am J Gastroenterol* 2001; **96**: 3142-3146

35 **Giannini E**, Risso D, Botta F, Chiarbonello B, Fasoli A, Malfatti F, Romagnoli P, Testa E, Ceppa P, Testa R. Validity and clinical utility of the aspartate aminotransferase-alanine aminotransferase ratio in assessing disease severity and prognosis in patients with hepatitis C virus-related chronic liver disease.*Arch Intern Med* 2003; **163**: 218-224

36 **Wong VS**, Hughes V, Trull A, Wight DG, Petrik J, Alexander GJ. Serum hyaluronic acid is a useful marker of liver fibrosis in chronic hepatitis C virus infection. *J Viral Hepat* 1998; **5**: 187-192

37 **Zheng M**, Cai WM, Weng HL, Liu RH. ROC curves in evaluation of serum fibrosis indices for hepatic fibrosis. *World J Gastroenterol* 2002; **8**: 1073-1076

38 **Chen YP**, Feng XR, Dai L, Ding HB, Zhang L. Screening and evaluation of non-invasive diagnosis markers for compensated liver cirrhosis in patients with chronic hepatitis B. *Zhonghua Ganzangbing Zazhi* 2003; **11**: 225-227

Edited by Xu JY and Wang XL

P.O.Box 2345, Beijing 100023,China
Fax: +86-10-85381893
E-mail: wjg@wjgnet.com www.wjgnet.com

World J Gastroenterol 2003;9(11):2579-2582
World Journal of Gastroenterology
 ISSN 1007-9327

• CLINICAL RESEARCH •

Expression of Bcl-2 and Bax in extrahepatic biliary tract carcinoma and dysplasia

Sheng-Mian Li, Shu-Kun Yao, Nobuyoshi Yamamura, Toshitsugu Nakamura

Sheng-Mian Li, Shu-Kun Yao, Department of Internal Medicine, the Fourth Hospital of Hebei Medical University, Shijiazhuang 050011, Hebei Province, China
Nobuyoshi Yamamura, Department of Internal Medicine, Suwa Red Cross Hospital, 5-11-50 Kogan-dori, Suwa 392-8510, Japan
Toshitsugu Nakamura, Department of Pathology, Suwa Red Cross Hospital, 5-11-50 Kogan-dori, Suwa 392-8510, Japan
Correspondence to: Dr. Sheng-Mian Li, Department of Internal Medicine, the Fourth Hospital of Hebei Medical University, Shijiazhuang 050011, China. kyc@hbmu.edu
Telephone: +86-311-6033946 Ext 302
Received: 2003-05-12 **Accepted:** 2003-06-12

Abstract

AIM: To compare the difference of expression of Bcl-2 and Bax in extrahepatic biliary tract carcinoma and dysplasia, and to analyze the role of Bcl-2 and Bax proteins in the progression from dysplasia to carcinoma and to evaluate the correlation of Bcl-2/Bax protein expression with the biological behaviors.

METHODS: Expressions of Bcl-2 and Bax were examined immunohistochemically in 27 cases of extrahepatic biliary tract carcinomas (bile duct carcinoma: n=21, carcinoma of ampulla of Vater: n=6), and 10 cases of atypical dysplasia. Five cases of normal biliary epithelial tissues were used as controls. A semiquantitative scoring system was used to assess the Bcl-2 and Bax reactivity.

RESULTS: The expression of Bcl-2 was observed in 10 out of 27 (37.0 %) invasive carcinomas, 1 out of 10 dysplasias, none out of 5 normal epithelial tissues. Bax expression rate was 74.1 % (20/27) in invasive carcinoma, 30 % (3/10) in dysplasia, and 40 % (2/5) in normal biliary epithelium. Bcl-2 and Bax activities were more intense in carcinoma than in dysplasia, with no significant difference in Bcl-2 expression (P=0.110), and significant difference in Bax expression (P=0.038). Level of Bax expression was higher in invasive carcinoma than in dysplasia and normal tissue (P=0.012). Bcl-2 expression was correlated to Bax expression (P=0.0059). However, Bcl-2/Bax expression had no correlation with histological subtype, grade of differentiation, or level of invasion.

CONCLUSION: Increased Bcl-2/Bax expression from dysplasia to invasive tumors supports the view that this is the usual route for the development of extrahepatic biliary tract carcinoma. Bcl-2/Bax may be involved, at least in part, in the apoptotic activity in extrahepatic biliary carcinoma.

Li SM, Yao SK, Yamamura N, Nakamura T. Expression of Bcl-2 and Bax in extrahepatic biliary tract carcinoma and dysplasia. *World J Gastroenterol* 2003; 9(11): 2579-2582
http://www.wjgnet.com/1007-9327/9/2579.asp

INTRODUCTION

Extrahepatic biliary tract carcinoma is a relatively rare disease[1], and its mortality is 5 % of all deaths from malignant neoplasms in Japan[2] and its prognosis is poor[3,4]. Its pathogenic mechanisms remain unknown. Genetic and some risk factors contribute to its pathogenesis[1]. It has been suggested that invasive carcinoma of extrahepatic biliary tract is preceded by dysplasia[1,5], which provides a good model for the study of genetic abnormalities and neoplastic progression.

Genetic control of cell death (apoptosis or programmed cell death) and cell survival play a crucial role in tumor growth[6]. Among the molecules related to the apoptotic process, Bcl-2 family proteins are important and critical regulators in a variety of physiological and pathological contexts[6-10]. Bcl-2 and Bax are members of the Bcl-2 family. Bcl-2 prevents cells from death through a variety of mechanisms, whereas overexpression of Bax protein increases the susceptibility of cells to apoptosis[11]. Although Bax and Bcl-2 have different functions, they share similar structures. Bax is a homologue protein of Bcl-2 and possesses two conserved regions, BH1 and BH2 that appear to be important for Bax/Bcl-2 binding[10]. Bax and Bcl-2 may form homodimers (Bax/Bax, or Bcl-2/Bcl-2) or heterodimers (Bax/Bcl-2). The balance of Bcl-2 and Bax determines survival or death of cells exposed to apoptotic stimuli[12] and relates with chemotherapeutic response and prognosis in some diseases[11].

Expressions of Bcl-2 and Bax in intrahepatic bile duct have been studied extensively by immunohistochemical methods[12-18], but little is known about extrahepatic biliary tract carcinoma and dysplasia. In this study, we attempted to clarify the difference of Bcl-2/Bax protein expression between extrahepatic biliary tract carcinoma and dysplasia, to analyze the role of Bcl-2/Bax proteins in the progression from dysplasia to carcinoma, and to evaluate the correlation of Bcl-2/Bax protein expression and biological behaviors.

MATERIALS AND METHODS

Specimens

Pathological slides of surgically removed extrahepatic biliary tract carcinoma were retrieved from a database file at Department of Pathology, Suwa Red Cross Hospital, Nagano, Japan, from 1993 to 2000. The slides stained with hemaloxylin and eosin (H&E) were reviewed, and slides in 27 cases were selected for this study. These 27 cases composed of 21 biliary duct carcinomas and 6 carcinomas of ampulla of Vater. Histological criteria for diagnosis of dysplasia have been described[1], that is, dysplasia is characterized by cuboidal or columnar cells showing mild to moderate nuclear dysplasia, with or without pseudostratification, loss of polarity, and occasional mitotic figures. Slides in 3 cases had both dysplasia and carcinoma, and other 7 dysplasia lesions were obtained from the margins of malignant tissue. In all, dysplasia (Figure A) was observed in 10 (37.1 %) of invasive carcinomas. As non-neoplastic controls, 5 cases of normal epithelial tissue adjacent to the lesions were used. The histopathological diagnosis was made according to literature[1] using the specimens stained with H&E. There were 17 cases of well-differentiated adenocarcinoma (17/27, 63.0 %), 7 moderately differentiated (7/27, 25.9 %), and 3 poorly differentiated (3/

27, 11.1 %). Clinical stages were determined according to Union International Centre le Cancer (UICC) classification[19]. The numbers of cases in stages I, II, III and IV were 4, 9, 10 and 4, respectively.

Immunohistochemistry

All specimens were fixed in 10 % buffered formalin and embedded in paraffin. The deparaffinized sections were treated in 0.3 % hydrogen peroxide in methanol for 30 minutes to eliminate endogenous peroxidase activity. Retrieval of antigenecity was performed by microwave. Slides were placed in 10 mmol/l citrate buffer (pH 6.0), boiled for 15 min in a microwave oven, cooled for 15 min, and rinsed in distilled water. Anti-Bcl-2 antibody (Clone 124, DAKO Corporation, Glostrup, Denmark, 1:40 dilution) or anti-Bax antibody (Clone 4F11, Immunotech, Marseille, France, pre-diluted) was applied and incubated for 1 hour at room temperature. Each antigen was detected by LSAB-2 kit (DAKO) with 3, 3-diaminobenzidine and hydrogen peroxide and the sections were finally counterstained with hematoxylin. For positive controls, mature lymphocytes in the sections were stained positively for Bcl-2 and neutrophils for Bax.

The results of Bcl-2 and Bax immunostains were scored as described previously[20]. The percentage of positive tumor cells was graded as follows: 0: 0 %, 1: 1-25 %, 2: 26-50 %, 3: more than 50 %. Immunostaining intensity was rated as follows, 0: none, 1: weak, 2: moderate, 3: intense. When a score of intensity multiplying percentage of positive cells is equal to or more than 1, the specimen was considered as immunopositive. Only cytoplasmic staining was evaluated and nuclear reaction was interpreted to be nonspecific staining.

Statistical analyses

Fisher' s exact test was used for statistical analysis. Spearman relation analysis was used for comparison of Bcl-2 and Bax expression. All statistical analyses were performed using STATA software (STATA Inc, Texas, USA). $P<0.05$ was considered as significant.

RESULTS

Bcl-2 and Bax protein expression

The results of immunostaining are shown in Table 1.

Significant Bcl-2 protein expression was observed in 9 out of 21 (42.9 %) bile duct carcinomas and 1 out of 6 (16.7 %) carcinomas of ampulla of Vater. The immunoreactive cases showed diffuse cytoplasmic staining (Figure 1 B). There was no significant difference according to the primary site of carcinoma (P=0.363). On the other hand, only one case out of 10 dysplasia was stained (Figure 1 C). Although there was an increasing tendency of Bcl-2 positive cases from normal to dysplasia and carcinoma, no statistical significance was observed among these three groups (P=0.110).

For Bax expression, the positive cases showed a granular cytoplasmic staining pattern. The positive rate of Bax expression was 17 out of 21 (81.0 %) cases of bile duct carcinoma (Figure 1D) and 3 out of 6 (50.0 %) carcinomas of ampulla of Vater, without statistical significance (P=0.290). Bax was positively stained in 3 out of 10 cases of dysplasia, and 2 out of 5 normal epithelia. There was a significant difference among these three groups (P=0.038), the Bax expression in invasive carcinoma was more obvious than that in dysplasia and normal group when further compared (P=0.012).

Table 1 Expression of Bcl-2 and Bax in biliary tract carcinoma and dysplasia lesions

Lesions	Bcl-2 expression			Bax expression		
	No. positive/tested	%	*P*	No. positive/tested	%	*P*
Invasive carcinoma	10/27	37.0		20/27	74.1	
Bile duct	9/21	42.9		7/21	81.0	
Ampulla of Vater	1/6	16.7	0.363	3/6	50.0	0.290
Dysplasia	1/10	10.0		3/10	30.0	
Normal	0/5	0	0.110	2/5	40.0	0.038[a]

a: Further compared, it was shown that the difference of Bax expression between dysplasia and normal epithelium was not significant (P=1.00), but Bax expression of carcinoma differed from that in dysplasia and normal tissues significantly (P=0.012).

Table 2 Comparison of Bcl-2/Bax protein expression with histological features or clinical stages in biliary tract carcinoma

Histological features	Bcl-2 expression			Bax expression		
	No.positive/tested	%	*P*	No.positive/tested	%	*P*
Differentiation grade						
Well	7/17	41.18		13/17	76.48	
Moderately	2/7	28.57		5/7	71.43	
Poorly	1/3	33.33	0.846	2/3	66.67	1.000
Perineural invasion						
No	4/9	44.44		7/9	77.78	
Yes	6/18	33.33	0.236	13/18	72.22	0.209
Vascular invasion						
No	8/19	42.11		15/19	78.95	
Yes	2/8	25.00	0.666	5/8	62.50	0.633
Lymph node metastasis						
No	7/14	50.00		12/14	85.71	
Yes	3/13	23.08	0.683	8/13	61.54	1.000
Stages						
I+II	5/13	38.46		10/13	76.92	
III+IV	5/14	35.70	1.000	10/14	71.431	1.000

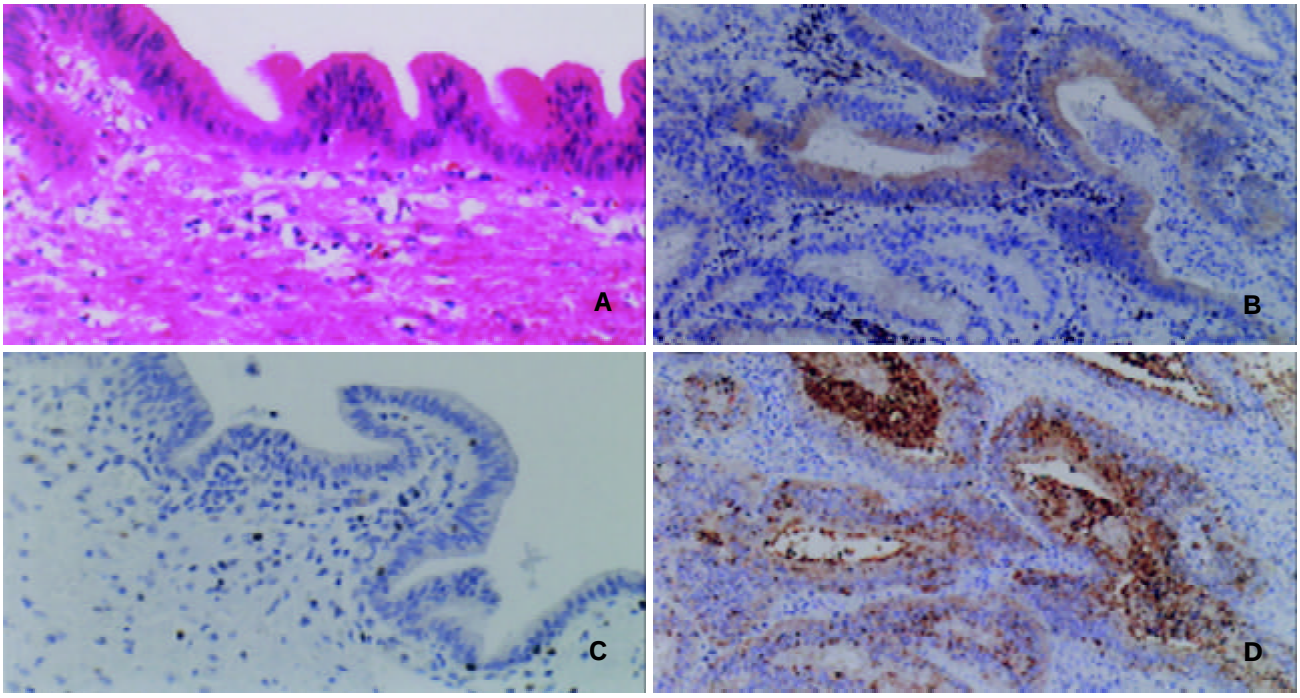

Figure 1 A: Cytological features of dysplasia (Hematoxylin-eosin stain, original ×100 magnification). B: Cytoplasmic expression of Bcl-2 in 1 % to 25 % cells in carcinoma (original magnification ×100). C: Bcl-2 expression in dysplasia with weak staining (original magnification ×100). D: Cytoplasmic expression of Bax in more than 50 % cells in carcinoma stained as intense granular patterns (original magnification ×100. B, D: serial sections).

Comparison between positive expression of Bcl-2/Bax protein and histological characteristics in carcinoma tissue

The results are shown in Table 2.

Out of 27 specimens with invasive carcinoma, the positive rate of Bcl-2/Bax expression was higher in well differentiated type than in poorly differentiated one, and higher in cases without invasion of vessels and lymph nodes than in those with tumor invasion with statistical significance, and higher in cases at stages I and II than in those at stages III and IV without statistical significance.

Correlation of Bcl-2 and Bax protein expression

Expression of Bcl-2 had a significant correlation with that of Bax in malignant tissues, dysplasia and normal epithelium (P=0.0059). Six invasive carcinomas expressed both Bcl-2 and Bax, 5 cases expressed only Bcl-2 protein, 10 cases expressed only Bax protein, 6 cases expressed neither Bcl-2 nor Bax.

DISCUSSION

Dysplasia-carcinoma sequence was regarded as a usual pathway in the development of invasive carcinoma of extrahepatic biliary tract[1]. The foci of dysplasia are multicentric in most cases, which probably explain the high incidence of local recurrence. Laitio [21] and Davis *et al*[22]. noted dysplasia in 45 % and 30 % of extrahepatic bile duct carcinomas, respectively. Suzuki *et al*[23]. found high grade dysplasia in 75 % of invasive carcinoma. In our study, dysplasia accounted for 37 % (10/27) of invasive carcinomas in extrahepatic bile duct and ampulla of Vater, which could be interpreted as an evidence for the theory that dysplasia is a precursor lesion of invasive carcinoma of biliary tract.

Apoptosis has caused great interest in many fields in recent years. Apoptosis-related genes such as p53, bcl-2, bax, c-myc, and bcl-x influence the susceptibility of normal and neoplastic cells to apoptosis[11]. High expression of Bcl-2 protein inhibited apoptosis of cells subjected to chemotherapy, irradiation, and nutritional withdrawal, whereas overexpression of Bax protein facilitated cell death[11]. In this study, we investigated the expression of Bcl-2 and Bax protein in 27 cases of biliary tract carcinoma and found that Bcl-2 protein was expressed in 37 % cases. Previous study showed that varying amounts of Bcl-2 protein were expressed in intrahepatic bile duct[24], while Okaro [14] and Arora[25] reported none of cholangiocarcinoma samples examined expressed Bcl-2 protein. For extrahepatic bile duct carcinoma, Ito *et al*[26]. reported Bcl-2 expression in 17 out of 38 (44.7 %) cases, which was similar to our result (10/27, 37.0 %). On the other hand, Bax was diffusely expressed along the intrahepatic biliary tree[15]. In biliary epithelial cells of rats the expression of Bax protein was visualized by immunohistochemistry and quantified stereologically[12], but in human extrahepatic biliary epithelium, Bax protein expression has not been reported. We observed Bax expression in 74 % cases of extrahepatic biliary carcinoma. Moreover, intensity of Bax staining was generally stronger than that of Bcl-2. Although further studies should be performed, our results suggest that both Bcl-2 and Bax play a role in regulating apoptosis in extrahepatic biliary tract carcinoma. Whether there is a difference of expression of Bcl-2 and Bax between carcinomas of intrahepatic and extrahepatic biliary tract should be clarified in the future.

Our study also showed that Bcl-2 protein expressed in 10 % biliary dysplasia, and no expression of Bcl-2 in 5 normal biliary epithelial cells. These findings were consistent with the results described by Okaro *et al*[14]. Bax protein expression rate was 30 % in dysplasia and 40 % in normal biliary epithelium. Incidence of Bcl-2 and Bax expression in invasive carcinoma was higher than that in dysplasia and normal tissue. Expression of Bax but not Bcl-2 showed a statistically significant difference among the malignant tissue, peri-cancerous tissue and normal one. Previously we demonstrated that Bcl-2 expression in premalignant lesions was an early event in the carcinogenesis of colorectal, gastric and cervix glandular tumors[27]. However, this was not true for biliary tract tumors. Bcl-2 and Bax might play some roles in the development from dysplasia to carcinoma. As the number of cases in each group was too small for statistical analysis, further studies are needed.

The ratio of anti-apoptotic to pro-apoptotic Bcl-2 family proteins appeared to control the relative sensitivity or resistance of many types of cells to apoptotic stimuli[15]. In our study, Bcl-2 expression was related to Bax protein expression in malignant, dysplasia and normal lesions. This finding was consistent with the conclusion of Harada *et al*[28], and supported that Bcl-2 and Bax were involved in the apoptotic activity in the development of extrahepatic biliary tract carcinomas as a couple of contrary functions.

There was a tendency that the low expression of Bcl-2/Bax was found in less differentiated and more advanced cases with metastasis of lymph node and perineural and vascular invasion, although statistical analysis revealed no significance. The impact of Bcl-2 expression on clinical outcome was demonstrated by Ito *et al*[29], who showed that Bcl-2 expression was inversely related to the incidence of apoptosis, and that Bcl-2 expression was more frequently absent in cases of advanced stages, lymph node metastasis, and perineural invasion (inverse relationship). On the other hand, previous study showed that Bax expression might be involved in tumor differentiation/histological types and metastatic progression in colorectal cancer[30], no reports on Bax expression/Bcl-2 in extrahepatic biliary tract tumor has been published yet. The study could not show any distinct correlation between Bcl-2/Bax expression and clinical stage or aggression, and a larger number of cases may be required to clarify this issue.

In conclusion, the increased incidence of Bcl-2/Bax expression observed from dysplasia to invasive tumor supports that this is the usual route for the development of extrahepatic biliary carcinoma. Bcl-2/Bax may be involved in the pathogenesis of extrahepatic biliary carcinoma and there is a correlation between Bcl-2 and Bax protein expression, suggesting that Bcl-2 and Bax regulate the apoptotic activity in extrahepatic biliary carcinoma as a couple of opposite functions.

ACKNOWLEDGMENT

The authors thank Mr. M.Yajima, Mr. M. Shimomura, Ms. H. Yabusaki, and Ms. R. Komatsu for their excellent technical assistance, and Ms. LM. Tang for her help with statistical analysis.

REFERENCES

1 **Albores-saavedra J**, Henson DE, Klimstra DS. Tumors of the gallbladder, extrahepatic bile ducts, and ampulla of Vater. Atlas of tumor pathology, third series, fascicle 27. *Washington, DC: Armed Forces Institute of Pathology* 2000: 181-191
2 **Yamamoto M,** Nakadaira H, Nakamura K. Biliary tract cancer. *Gan To Kagaku Ryoho* 2001; **28**: 155-158
3 **Ichikawa K,** Imura J, Kawamata H, Takeda J, Fujimori T. Down-regulated p16 expression predicts poor prognosis in patients with extrahepatic biliary tract carcinomas. *Int J Oncol* 2002; **20**: 453-461
4 **Niiyama H,** Mizumoto K, Kusumoto M, Ogawa T, Suehara N, Shimura H, Tanaka M. Activation of telomerase and its diagnostic application in biopsy specimenes from biliary tract neoplasms. *Cancer* 1999; **85**: 2138-2143
5 **Hoang MP,** Murakata LA, Padilla-Rodriguez AL, Albores-Saavedra J. Metaplastic lesions of the extrahepatic bile ducts: a morphologic and immunohistochemical study. *Mod Pathol* 2001; **14**: 1119-1123
6 **Adams J,** Cory S. The Bcl-2 protein family: Arbiters of cell survival. *Science* 1998; **281**: 1322-1326
7 **Kluck RM,** Bossy-Wetzed E, Green DR, Newmeyer DD. The release of cytochrome C from mitochondria: a primary site for Bcl-2 regulation of apoptosis. *Science* 1997; **275**: 1132-1136
8 **Yang J,** Liu X, Bhalla K, Kim CN, Ibrado AM, Cai J, Peng TI, Jones DP, Wang X. Prevention of apoptosis by Bcl-2: release of cytochrome c from mitochondria blocked. *Science* 1997; **275**: 1129-1132
9 **Boise LH,** Gonzalez-Garcia M, Postema CE, Ding L, Lindsten T, Turka LA, Mao X, Nunez G, Thompson CB. bcl-x, a bcl-2-related gene that functions as a dominant regulator of apoptotic cell death. *Cell* 1993; **74**: 597-608
10 **Yang E,** Zha J, Jockel J, Boise LH, Thompson CB, Korsmeyer SJ. Bad, a heterodimeric parter for Bcl-X_L and Bcl-2, displaces Bax and promotes cell death. *Cell* 1995; **80**: 285-291
11 **Wheaton S,** Netser J, Guinee D, Rahn M, Perkins S. Bcl-2 and Bax protein expression in indolent versus aggressive B-cell non-Hodgkins lymphomas. *Hum Pathol* 1998; **29**: 820-825
12 **Stahelin BJ,** Marti U, Zimmermann H, Reichen J. The interaction of Bcl-2 and Bax regulates apoptosis in biliary epithelial cells of rats with obstructive jaundice. *Virchows Arch* 1999; **434**: 333-339
13 **Korsmeyer SJ.** Bcl-2 initiates a new category of oncogenes: regulators of cell death. *Blood* 1992; **80**: 879-886
14 **Okaro AC,** Deery AR, Hutchins RR, Davidson BR. The expression of antiapoptotic proteins Bcl-2, Bcl-X(L), and Mcl-1 in benign , dysplastic and malignant biliary epithelium. *J Clin Pathol* 2001; **54**: 927-932
15 **Iwata M,** Harada K, Kono N, Kaneko S, Kobayashi K, Nakanuma Y. Expression of Bcl-2 familial proteins is reduced in small bile duct lesions of primary biliary cirrhosis. *Hum Pathol* 2000; **31**: 179-184
16 **Bergquist A,** Glaumann H, Stal P, Wang GS, Broome U. Biliary dysplasia, cell proliferation and nuclear DNA-fragmentation in primary sclerosing cholangitis with and without cholangiocarcinoma. *J Intern Med* 2001; **249**: 69-75
17 **Harnois DM,** Que FG, Celli A, LaRusso NF, Gores GJ. Bcl-2 is overexpressed and alters the threshold for apoptosis in a cholangiocarcinoma cell line. *Hepatology* 1997; **26**: 884-890
18 **Nakopoulou L,** Stefanaki K, Vourlakou C, Manolaki N, Gakiopoulou H, Michalopoulos G. Bcl-2 protein expression in acute and chronic hepatitis, cirrhosis and hepatocellular carcinoma. *Pathol Res Pract* 1999; **195**: 19-24
19 **Sobin LH,** Fleming ID. TNM classification of malignant tumors, fifth edition (1997). Union internationale contre le cancer and the american joint committee on cancer. *Cancer* 1997; **80**: 1803-1804
20 **Krajewska M,** Krajewski S, Epstein JI, Shabaik A, Sauvageot J, Song K, Kitada S, Reed JC. Immunohistochemical analysis of bcl-2, bax, bcl-X and mcl-1 expression in prostate cancers. *Am J Pathol* 1996; **48**: 1567-1576
21 **Laitio M.** Carcinoma of extrahepatic bile duct: a histopathologic study. *Pathol Res Pract* 1983; **178**: 67-72
22 **Davis RI,** Sloan JM, Hood JM, Maxwell P. Carcinoma of the extrahepatic biliary tract: a clinicopathological and immunohistochemical study. *Histopathology* 1988; **12**: 623-631
23 **Suzuki M,** Takahashi T, Ouchi K, Matsuno S. The development and extension of hepatohilar bile duct carcinoma. A three-dimensional tumor mapping in the intrahepatic biliary tree visualized with the aid of a graphic computer system. *Cancer* 1989; **64**: 658-666
24 **Skopelitou A,** Hadjiyannakis M, Alexopoulou V, Krikoni O, Kamina S, Agnantis N. Topographical immunohistochemical expression of bcl-2 protein in human liver lesions. *Anticancer Res* 1996; **16**: 975-978
25 **Arora DS,** Ramsdale J, Lodge JP, Wyatt JI. p53 but bcl-2 is expressed by most cholangiocarcinomas: a study of 28 cases. *Histopathology* 1999; **34**: 497-501
26 **Ito Y,** Takeda T, Sakon M, Tsujimoto M, Matsuura N. Expression and clinical implications of bcl-2 in extrahepatic bile duct carcinoma: its relationship with biological features. *Anticancer Res* 2000; **20**: 3891-3895
27 **Nakamura T,** Nomura S, Sakai T, Nariya S. Expression of Bcl-2 oncoprotein in gastrointestinal and uterine carcinomas and their premalignant lesion. *Hum Pathol* 1997; 28: 309-315
28 **Harada K,** Iwata M, Kono N, Koda W, Shimonishi T, Nakanuma Y. Distribution of apoptotic cells and expression of apoptosis–related proteins along the intrahepatic biliary tree in normal and non-biliary disease liver. *Histopathology* 2000; **37**: 347-354
29 **Ito Y,** Takeda T, Sasaki Y, Sakon M, Monden M, Yamada T, Ishiguro S, Imaoka S, Tsujimoto M, Matsuura N. Bcl-2 expression in cholangiocellular carcinoma is inversely correlated with biologically aggressive phenotypes. *Oncology* 2000; **59**: 63-67
30 **Jansson A,** Sun XF. Bax expression decreases significantly from primary tumor to metastasis in colorectal cancer. *J Clin Oncol* 2002; **20**: 811-816

Edited by Ren SY and Wang XL

P.O.Box 2345, Beijing 100023,China
Fax: +86-10-85381893
E-mail: wjg@wjgnet.com www.wjgnet.com

World J Gastroenterol 2003;9(11):2583-2586
World Journal of Gastroenterology
 ISSN 1007-9327

• CLINICAL RESEARCH •

Effect of a single oral dose of rabeprazole on nocturnal acid breakthrough and nocturnal alkaline amplitude

Jin-Yan Luo, Chun-Yan Niu, Xue-Qin Wang, You-Ling Zhu, Jun Gong

Jin-Yan Luo, Chun-Yan Niu, Xue-Qin Wang, You-Ling Zhu, Jun Gong, Department of Gastroenterology, The Second Hospital of Xi' an Jiaotong Uuniversity, Xi' an 710004, Shanxi Province, China
Correspondence to: Dr. Jin-Yan Luo, The Second Hospital of Xi' an Jiaotong University, Xi' an 710004, Shanxi Province, China. ljy18272@163.com
Telephone: +86-29-7678758 **Fax:** +86-29-7678758
Received: 2002-10-05 **Accepted:** 2003-04-05

Abstract

AIM: To study the effect of rabeprazole (RAB) on nocturnal acid breakthrough (NAB) and nocturnal alkaline amplitude (NAKA) and to compare it with omeprazole (OME) and pantoprazole (PAN).

METHODS: By an open comparative study, forty patients with active peptic ulcer were randomly assigned to receive one of the three PPIs (proton pump inhibitor) with a single oral dose. They were divided into RAB group (10 mg), OME group(20 mg) and PAN group (40 mg). Twenty healthy volunteers were enrolled to the control group (without taking any drug). Intragastric pH monitoring was then performed 1 hour before and 24 hours after the dose was given.

RESULTS: No clinically undesirable signs and symptoms possibly attributed to the administration of RAB or OME and PAN were recognizable throughout the study period. All subjects completed the study according to the protocol. All data were processed by a computer using the Student *t* test or *t* ' test followed by an analysis of covariance. $P<0.05$ was considered to have statistical significance. The intragastric pH of NAB was significantly higher in RAB group (1.84±0.55) than in either OME group (1.15±0.31) or PAN group (1.10±0.30) (both $P<0.01$). RAB produced a longer sustaining time (4.65±1.22 h) on NAKA than OME (3.22±1.89 h) ($P<0.05$), PAN (3.15±1.92 h) ($P<0.05$), and the sustaining time of NAKA in RAB group was longer than that in the healthy control group ($P<0.01$) too. In addition, RAB produced a much higher pH on NAKA (6.41±0.45) in comparison with PAN (6.01±0.92) ($P<0.05$).

CONCLUSION: A single oral dose of 10 mg RAB may increase the pH of NAB and shorten the sustaining time of NAB, and it may increase the pH of NAKA as well as prolong the sustaining time of NAKA.

Luo JY, Niu CY, Wang XQ, Zhu YL, Gong J. Effect of a single oral dose of rabeprazole on nocturnal acid breakthrough and nocturnal alkaline amplitude. *World J Gastroenterol* 2003; 9 (11): 2583-2586
http://www.wjgnet.com/1007-9327/9/2583.asp

INTRODUCTION

The first-generation proton pump inhibitors (PPIs) (such as omeprazole, lansoprazole and pantoprazole) have been considered to be the most primary and potent treatments of acid-related diseases since they were put into clinical application, and their efficacy and safety have been well-documented and widely recognized. However, researches during the last 10 years have shown that, despite the multiple treatment modalities such as modifying administer methods, increasing the dosages or adding H_2 receptor antagonist, the first-generation PPIs can not suppress the nocturnal acid secretion successfully especially NAB[1,2]. The objective in designing this trial was to observe the effect of the newer-generation of PPI rabeprazole on NAB (nocturnal acid breakthrough) and NAKA (nocturnal alkaline amplitude).

MATERIALS AND METHODS

Subjects and grouping

Forty patients with endoscopically proven active gastric or duodenal ulcer at our hospital from June, 2001 to May, 2002 entered into the study. They were randomly assigned to three groups: RAB group (n=15), OME group (n=15) and PAN group (n=10). The male/female ratio of patients was 9:6, 8:7, 6:4 in the three groups respectively. Their age (mean) was 20-61 (34.5±7.8)years, 22-60(30.6±6.7)years and 25-59(29.3±6.5) years respectively. Twenty healthy volunteers (10 men and 10 women) were enrolled as the control group, aged from 18 to 60 years (mean 25.7±9.5).

Methods

Administering method This study was an open comparative trial. With a single oral dose, every one was administered 10 mg RAB, 20 mg OME or 40 mg PAN respectively, ambulatory intragastric pH measurements were then performed. All subjects ceased the drugs that might affect acid secretion and gastrointestinal motility 2 weeks before the study.

Instruments and processes[3] Portable pH recorder (DIGITRAPPER MKIII, CTD Co., Sweden). After fasted for 12 hours, an electrode was placed via a nostril into the stomach at 8 am, to record the baseline pH for an hour, a dose of drug was given to one patient at 9 am, pH was recorded continuously for hours. All participants kept their normal daily activities and consumed their customary diet, except to abstain from drinking acid and alkali beverages during the test period. The pH electrode was withdrawn at the following morning 9 am, pH data were downloaded onto a computer for analysis.

Measuring indicator The impact of the three agents on NAB (identifying criterion[4]: Intragastric pH dropped to <4 and remained below that level for at least 1 hour during the 12 hours of night sleeping period after the dose of PPI). The impact of the three agents on NAKA (identifying criterion[5]: The time that intragastric pH remained >4 lasted for>1 hour from 0:00 to 8 am).

Statistical analysis

All data were processed by a computer. Data were presented as the mean ±SD. Comparisons between two groups and among three groups were made using the Student *t* test or *t*' test followed an analysis of covariance. $P<0.05$ was considered to have statistical significance.

Table 1 Effect of single dose of PPI on NAB

PPI group	*n*	Occurring cases(%)	Time range	pH($\bar{x}$±s)	Persisting time ($\bar{x}$±s)(h)
RAB10 mg	15	9(60 %)	0:00-4:0	1.84±0.55[ac]	4.10±2.38
OME20 mg	15	9(60 %)	20:00-2:0	1.15±0.31	5.40±2.73
PAN40 mg	10	8(80 %)	20:00-6:0	1.10±0.30	5.71±2.60

[a]*P*<0.05 *vs* OME, [c]*P*<0.05 *vs* PAN.

Table 2 Effect of single dose of PPI on NAKA

PPI group	*n*	Occurring cases (%)	Time range	pH($\bar{x}$±s)	Persisting time ($\bar{x}$±s) (h)
RAB10 mg	15	9(60 %)	2.0-7.0	6.41±0.45[cb]	4.65±1.22[acb]
OME20 mg	15	8(53.3 %)	1.0-7.0	6.51±0.82[b]	3.22±1.89
PAN40 mg	10	5(50 %)	2.0-6.0	6.01±0.92	3.15±1.92
Control group	20	9(45 %)	1.0-6.0	5.30±0.47	2.25±1.23

[a]*P*<0.05 *vs* OME, [c]*P*<0.05 *vs* PAN, [c]*P*<0.05 *vs* healthy control group.

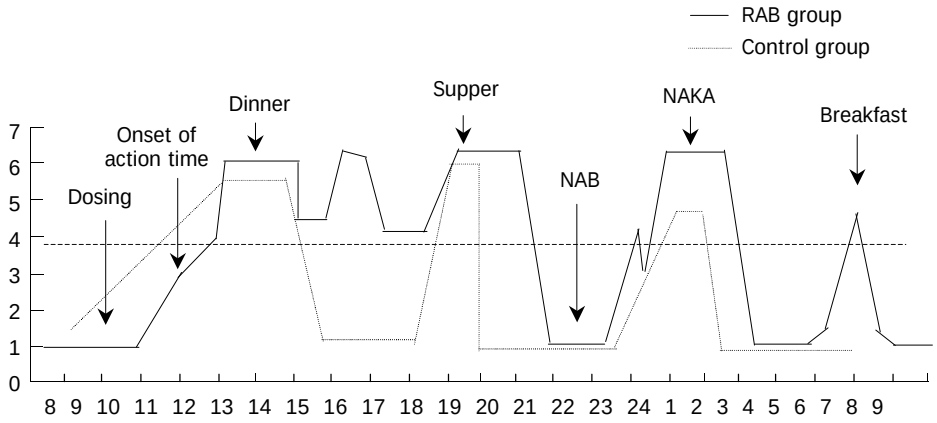

Figure 1 Simulating figure of NAB and NAKA. NAB and NAKA all occurred after midnight, and NAKA always appeared after NAB. Compared with the control group (didn't receive either PPI or placebo), RAB increased the pH of NAKA as well as prolonged the persisting time of NAKA.

RESULTS

Impacts of RAB, OME and PAN on NAB (Table 1)

NAB often occurs after 8 pm. Of the 40 patients, 26 (65 %) exhibited NAB, which occurred mostly from 8 pm to 4-6 am next morning. The results showed that RAB increased pH of NAB significantly (1.84±0.55) than OME and PAN (*P*<0.05), it also shortened persisting time of NAB. NAB occurred frequently in PAN group.

Impacts of RAB, OME and PAN on NAKA (Table 2)

Compared with the healthy group, all three PPIs could increase pH of NAKA and prolong the sustaining time of NAKA. The persisting time that pH>4 of NAKA in RAB group was longer than that in the other three groups (*P*<0.05, <0.05, <0.01), intragastric pHs in RAB group and OME group were all higher than that in the healthy control group (*P*<0.01) (Table 2).

DISCUSSION

NAB and NAKA are two common clinical phenomena, but the developing mechanisms are remain unclear. Our attention was to investigated the effects of PPIs on NAB and NAKA.

NAB was defined as the occurrence of intragastric pH dropped to below 4 and remained below that level for at least 1 hour during the 12 hours of night sleeping period (typically the second 6-hours) after the dose of PPI[1,4]. This study showed that the pH(1.84±0.55) of NAB was significantly higher in RAB group than in OME group and PAN group (*P*<0.05), the persisting time of NAB was shortened. Additionally, the occurrence of NAB was lower in RAB group than in PAN group. The above results suggested that RAB had an advantage over OME and PAN on suppressing NAB, which was consistent with other reports[6,7]. It might contribute to the pharmacological features of RAB such as longer half-life, rapid onset of action, acid-stability, no influences on foods, dosing time or patterns[8-10]. NAB had a high occurrence after midnight and typically in the second 6-hours during night sleeping[1,4,11]. NAB after taking PPIs was first reported by Peghini and Katz[4]. Peghini *et al.* considered that NAB could be explained by food-related factors (for example, the absence of the buffering effect of meals after midnight) which resulted in weakened acid-inhibiting efficacy of PPIs and increased night acid production. This might help to explain why the acid-suppressing effect of PPIs during daytime was greater than that during nighttime[12]. According to the fact that adding a dose of H_2RA at bed time could produce a much better controllable action than that of PPIs on NAB. Peghini *et al*. suggested that histamine played a major role in nocturnal acid secretion[4,13,14]. A study revealed that 70 % of patients with gastro-oesophageal reflux disease (GERD) receiving PPIs had NAB which was often accompanied by esophageal acid exposure. The prevalence of ineffective esophageal motility and low LES pressure was significantly higher in refluxers than in non-refluxers[15], so GERD was considered to correlate with NAB closely. This might be the result of gastric acid secretion following a circadian profile

which was characterized by an increase in the evening , with a peak at about midnight[16]. This might explain why only some refluxers developed esophagitis. There was another opinion that eradication of *H pylori* appeared to be closely related to the occurrence of nocturnal NAB when a dose of PPI was given[17]. There were important clinical implications of NAB, because there existed a close relationship between night acid-control and GERD as well as peptic ulcer. Esophageal protective mechanism was decreased during this time and it was unbeneficial for ulceric mucosa to restore[18,19]. It was thought that NAB might be particularly injurious to the esophageal mucosa and might arise lasting nocturnal heartburn or acid regurgitation and even respiratory complaints. Hence, there was a clinical rationale and greater importance for reducing or abolishing nocturnal acid secretion and increasing intragastric pH or intra-esopgageal pH in treatment of acid-related disorders to promote the healing of peptic ulcer, severe GER and Barrett' s esophagus in order to improve the quality of life[20]. But NAB was also reckoned to prove reversely the safety of PPI (i.e it was extremely difficult to render achlorhydric)[11]. Many studies supported that the addition of a low dose of H_2RA did enhance the control effect on NAB of PPIs because H_2RAs reduced basal gastric acid secretion, H_2RA nizatidine has been known to stimulate gastric emptying and elevate LES pressure and therefore decrease NAB as well as nightly reflux[21], low dose of H_2RA following a provocative dinner or a large fatty meal might effectively reduce esophageal acid exposure. Being prone to produce a tolerance to H_2RA due to its long-term intaking, an intermittent dosing fashion might be an optimal approach[22].

NAKA was also termed as "spontaneous nocturnal gastric alkalinization" (SNGAK), "spontaneous nocturnal alkalinization" (SNA), "nocturnal anhydrochloric wave" and "inversion of gastric pH"[23-25], which was defined as a phenomenon that an abrupt physiological or pathological raise of intragastric pH to above 4 to 6 after sleeping (mostly in the early morning). The prevalence of NAKA ranged between 40-80 % in normal populations, mostly beginning in the latter part of the night. Bianco *et al*[25] found that SNA lasted for 87.82±12.47min/time in normal volunteers and for 3.27±1.62 min/time in patients with duodenal ulcer. Ke *et al*[26]. reported that NAKA presented in 67 % of normal group, lasting for 169.7±40.2 min (total), and raised in 70 % of patients with duodenal ulcer, lasting for 57.6±12.0 min (total). In this study, NAKA presented in 45 %(9/20) of normal subjects, which sustained for 135.0±73.8 min (total), and in 55 %(22/40) of patients with duodenal ulcer. The results were lower than the above, the mean sustaining time of NAKA was 220.4±100.6 min (total) in patients with duodenal ulcer after a single administration of PPI. These findings indicated that RAB might increase the pH of NAKA and prolong persisting time of NAKA. We have previously conducted a simultaneous monitoring of intragastric pH and bile in normal subjects and patients with duodenal gastric reflux (DGR), and found that the pH and cholerythrin exhibited 2 models and 4 types[27]. The 2 models were simultaneous and non-simultaneous raise of pH and cholerythrin, and the 4 types were simultaneouse raise and drop of pH and cholerythrin. pH raised alone and cholerythrin raised alone. The test of neutralizing bile with gastric juice *in vitro* showed that until the absorbency had already raised to 0.900 when bile concentration was 20 %, while pH remained at 1 or so. Furthermore, only when bile concentration raised to >60 %, did gastric pH begin to raise to >4, suggesting that it was not until bile reached to a considerable level when it had an influence on intragastric pH. As bile is nocuous to esophageal mucosa, so only a solitary pH raise produces a protective action. NAKA was proposed by Bianco *et al*. at first in 1970s, there were several opinions about its pathophysiological mechanism. NAKA appeared to be a kind of self-protective mechanism for gastric mucosa against the damages of acid and mucosa-injuring agents, and helping expulse H^+ to gastric cavity continuously so as to relieve clinical symptoms[28]. In this trial, all 3 PPIs increased peak value and persisting time of NAKA(there was a significant difference in comparison with the control). The increase was more prominent for RAB than for OME and PAN, one likely explanation was that H^+-K^+ATPase was inhibited much more. Further investigation is needed. Based on earlier studies[23,27,29], we hypothesed that NAKA was related to DGR, this hypothesis was supported by conclusions of other countries[30,31]. Alkali reflux mostly occurred during MMC phase II and phase III, suggesting that NAKA together with duodenal uncoordinated motor activity could lead to the reflux of duodenal juice (not always bile) into gastric cavity and hence antrum "alkalinization" state at the end of phase III. NAKA was thought to be strongly related to sleeping and interrupted by waking up[31]. Some investigators deduced that NAKA correlated with reduced vagal tension and chlecystectomy as well as modulation of gastric secretions[24,32]. There were evidences that ulcer patients did not show SNA phenomenon before treatment, but the therapy led it to recurrence, and the lack of SNA in duodenal ulcer patients was so frequent that its absence might be a diagnostic sign of peptic ulcer (positively predictive value 82 %)[25,33]. In addition, we had an interesting observation that NAKA always appeared following NAB (Figure 1). There have been no findings concerning this phenomenon yet, and its etiology needs to be identified.

NAB is the most notable limitation of PPIs used at present. By comparison we can understand that available PPIs are unable to resolve the problem of NAB, including rabeprazole. In summary, we have shown that a single dose of 10 mg rabeprazole can achieve a much superior acid-suppressing efficacy as compared to omeprazole and pantoprazole. It can elevate pH of NAB, shorten persisting time of NAB, increase pH as well as sustaining time of NAKA. These findings show that rabeprazole may provide a profound control on nocturnal gastric acid secretion. However, there remain problems demanding further evaluations. For example, whether it is beneficial by increasing the dose or administering time of rabeprazole (i.e twice daily) or an on-demand treatment[19] should be given to enhance the acid-inhibiting efficacy of rabeprazole, whether the onset of NAKA correlates with more effective inhibiting on H^+-K^+ATPase of rabeprazole, etiology and clinical implications of NAB and NAKA, and why NAKA is always present after NAB.

REFERENCES

1 **Tytgat GNJ.** Shortcomings of the first-generation proton pump inhibitors. *Eur J Gastroenterol Hepatol* 2001; **13**(Suppl 1): S29-S33

2 **Sachs G.** Improving on PPI-based therapy of GORD. *Eur J Gastroenterol Hepatol* 2001; **13**(Suppl 1): S35-S41

3 **Gong J,** Zhu YL, Luo JY, Wang XQ. The acid-inhibiting effect of famotidine with a single dose by injection in musle. *Zhonghua Yixue Zazhi* 1998; **37**: 762-765

4 **Peghini PL,** Katz PO, Bracy NA, Castell DO. Nocturnal recovery of gastric acid secretion with twice-daily dosing of proton pump inhibitors. *Am J Gastroenterol* 1998; **93**: 763-767

5 **Bianco A,** Cagossi M, Piraccini R, Castrucci G, Greco AV. The nightly spontaneous alkalinization of the stomach. *Riv Eur Sci Med Farmacol* 1993; **15**: 17-27

6 **Robinson M**. New-generation proton pump inhibitors:overcoming the limitations of early-generation agents. *Eur J Gastroenterol Hepatol* 2001; **13**(Suppl 1): S43-S47

7 **Katz PO,** Frissora C. The pharmacology and clinical relevance of proton pump inhibitors. *Curr Gastroenterol Rep* 2002; **4**: 459-462

8 **Williams MP**, Pounder RE. Review article: the pharmacology of rabeprazole. *Aliment Pharmacol Ther* 1999; **13**(Suppl 3): 3-10

9 **Williams MP,** Sercombe J, Hamilton MI, Pounder RE. A placebo-controlled trial to assess the effects of 8 days of dosing with rabeprazole versus omeprazole on 24-h intragastric acidity and plasma gastrin concentrations in young healthy male subjects. *Aliment Pharmacol Ther* 1998; **12**: 1079-1089

10 **Skoczylas T,** Sarosiek I, Sostarich S, McElhinney C, Durham S, Sarosiek J. Significant enhancement of gastric mucin content after rabeprazole administration: its potential clinical significance in acid-related disorders. *Dig Dis Sci* 2003; **48**: 322-328

11 **Fackler WK,** Ours TM, Vaezi MF, Richter JE. Long-term effect of H_2RA therapy on nocturnal gastric acid breakthrough. *Gastroenterology* 2002; **122**: 625-632

12 **Chiverton SG,** Howden CW, Burget DW, Hunt RH. Omeprazole (20mg) daily given in the morning or evening: a comparison of effects on gastric acidity, and plasma gastrin and omeprazole concentration. *Aliment Pharmacol Ther* 1992; **6:** 103-111

13 **Peghini PL,** Katz PO, Castell DO. Ranitidine controls nocturnal gastric acid breakthrough on omeprazole: a controlled study in normal subjects. *Gastroenterology* 1998; **115**: 1335-1339

14 **Xue S,** Katz PO, Banerjee P, Tutuian R, Castell DO. Bedtime H2 blockers improve nocturnal gastric acid control in GERD patients on proton pump inhibitors. *Aliment Pharmacol Ther* 2001; **15**: 1351-1356

15 **Fouad YM,** Katz PO, Castell DO. Oesophageal motility defects associated with nocturnal gastro-oesophageal reflux on proton pump inhibitors. *Aliment Pharmacol Ther* 1999; **13**: 1467-1471

16 **Wolfe MM,** Soll AH. The physiology of gastric acid secretion. *N Engl J Med* 1988; **319**: 1707-1715

17 **Katsube T,** Adachi K, Kawamura A, Amano K, Uchida Y, Watanabe M, Kinoshita Y. *Helicobacter pylori* infection influences nocturnal gastric acid breakthrough Aliment. *Pharmacol Ther* 2000; **14**: 1049-1056

18 **Katz PO,** Anderson C, Khoury R, Castell DO. Gastro-oesophageal reflux associated with nocturnal gastric acid breakthrough on proton pump inhibitors *Aliment Pharmacol Ther* 1998; **12**: 1231-1234

19 **Holtmann G.** Reflux disease: the disorder of the third millennium. *Eur J Gastroenterol Hepatol* 2001; **13**(Suppl 1): S5-S11

20 **Galmiche JP,** Blum A. Editorial. *Eur J Gastroenterol Hepatol* 2001; **13**(Suppl 1): S1-S13

21 **Kurosawa S.** Maintenance therapy of mild form of GERD by H2 receptor antagonists. *Nippon Rinsho* 2000; **58**: 1859-1864

22 **Orr WC,** Harnish MJ. Sleep-related gastro-oesophageal reflux: provocation with a late evening meal and treatment with acid suppression. *Aliment Pharmacol Ther* 1998; **12**: 1033-1038

23 **Gong J,** Zhang Q, Zhang Y, Zhu YL, Wang XQ, Luo JY. The study of rhythm of 24h gastric pH. *Xi'an Yike Daxue Xuebao* 1999; **20**: 326-328

24 **Brown TH,** Walton G, Cheadle WG, Larson GM. The alkaline shift in gastric pH after cholecystectomy. *Am J Surg* 1989; **157**: 58-65

25 **Bianco A,** Cagossi M, Piraccini R, Greco AV. Human duodenogastric reflux, retroperistalsis, and MMC. *Riv Eur Sci Med Farmacol* 1992; **14**: 281-291

26 **Ke MY**, Lan Y, Wang ZF, Xing JH. Character of 24-hour intragastric pH change in patients with functional dyspepsia. *Linchuang Xiao huabing Zazhi* 1995; **7**: 97

27 **Gong J,** Zhang R, Luo JY, Zhu YL, Wang XQ. The effect of bile reflux on the intragastric pH. *Xi'an Yike Daxue Xuebao* 2001; **22**: 25-27

28 **Dalenback J,** Abrahamson H, Bjornson E, Fandriks L, Mattsson A, Olbe L, Svennerholm A, Sjovall H. Human duodenogastric reflux, retroperistalsis and MMC. *Am J Physiol* 1998; **275**(3Pt2): R762-769

29 **Gong J,** Zhang R, Luo JY, Zhu YL, Wang XQ. A study on the etiology of the spontaneous nocturnal gastric alkalinization. *Xi'an Yike Daxue Xuebao* 2001; **22**: 230-232

30 **Bjornsson ES,** Abrahamsson H. Nocturnal antral pH rises are related to duodenal phase III retroperistalsis. *Dig Dis Sci* 1997; **42:**2432-2438

31 **Dai F,** Gong J, Zhang R, Luo JY, Zhu YL, Wang XQ. Assessment of duodenogastric reflux by combined continuous intragastric pH and bilirubin monitoring. *World J Gastroenterol* 2002; **8**: 382-384

32 **Bianco A,** Cagossi M, Piraccini R, Castrucci G, Greco AV. The nightly spontaneous alkalinization of the stomach. *Riv Eur Sci Med Farmacol* 1993; **15**: 17-27

33 **Bianco A,** Cagossi M, Piraccini R, Greco AV. Twenty-four-hour intragastric pH-metry: H_2-receptor antagonist restoration of nightly gastric spontaneous alkalinization in duodenal ulcer healing. *Riv Eur Sci Med Farmacol* 1992; **14**: 281-291

Edited by Zhao M and Wang XL

P.O.Box 2345, Beijing 100023,China
Fax: +86-10-85381893
E-mail: wjg@wjgnet.com www.wjgnet.com

World J Gastroenterol 2003;9(11):2587-2591
World Journal of Gastroenterology
 ISSN 1007-9327

• CLINICAL RESEARCH •

Long-term effect of stent placement in 115 patients with Budd-Chiari syndrome

Chun-Qing Zhang, Li-Na Fu, Lin Xu, Guo-Quan Zhang, Tao Jia, Ji-Yong Liu, Cheng-Yong Qin, Ju-Ren Zhu

Chun-Qing Zhang, Li-Na Fu, Lin Xu, Ji-Yong Liu, Cheng-Yong Qin, Ju-Ren Zhu, Department of Gastroenterology, Shandong Provincial Hospital, Jinan 250021, Shandong Province, China
Guo-Quan Zhang, Tao Jia, Department of Ultrasound, Shandong Provincial Hospital, Jinan 250021, Shandong Province, China
Correspondence to: Chun-Qing Zhang, M.D, Department of Gastroenterology, Shandong Provincial Hospital, Jinan 250021, Shandong Province, China. chunqing9@hotmail.com
Telephone: +86-531-7938911-2350
Received: 2002-11-06 **Accepted:** 2002-12-16

Abstract

AIM: To report the long-term effect of stent placement in 115 patients with Budd-Chiari syndrome (BCS).

METHODS: One hundred and fifteen patients with BCS were treated by percutaneous stent placement. One hundred and two patients had IVC stent placement, 30 patients had HV stent placement, 17 of them underwent both IVC stent and HV stent. All the procedures were performed with guidance of ultrasound.

RESULTS: The successful rates in placing IVC stent and HV stent were 94 % (96/102) and 87 % (26/30), respectively. Ninety-seven patients with 112 stents (90 IVC stents, 22 HV stents) were followed up. 96.7 %(87/90) IVC stents and 90.9 %(20/22) HV stents remained patent during follow up periods (mean 49 months, 45 months, respectively). Five of 112 stents in the 97 patients developed occlusion. Absence of anticoagulants after the procedure and types of obstruction (segmental and occlusive) before the procedure were related to a higher incidence of stent occlusion.

CONCLUSION: Patients with BCS caused by short length obstruction can be treated by IVC stent placement, HV stent placement or both IVC and HV stent placement depending on the sites of obstruction. The long-term effect is satisfactory. Anticoagulants are strongly recommended after the procedure especially for BCS patients caused by segmental occlusion.

Zhang CQ, Fu LN, Xu L, Zhang GQ, Jia T, Liu JY, Qin CY, Zhu JR. Long-term effect of stent placement in 115 patients with Budd-Chiari syndrome. *World J Gastroenterol* 2003; 9(11): 2587-2591
http://www.wjgnet.com/1007-9327/9/2587.asp

INTRODUCTION

Budd-Chiari syndrome (BCS) is characterized by obstruction of outflow in hepatic vein (HV) and inferior vena cava (IVC) leading to hepatomegaly, portal hypertension, impaired liver function, formation of communicating channel, and edema in lower extremities. Various patterns of vascular obstruction can be seen in BCS. The most common type in the orient is short length obstruction (membranous and segmental) in IVC and/or in the ostium of main hepatic vein (HV), and most of them are chronic and idiopathic[1-3]; whereas thrombotic obstruction is the the most common cause in Western country[4,5].

The optimal management of BCS is difficulty, surgical shunting has been recommended as the most appropriate choice to relieve symptoms in most instances[6,7]. But the long-term patency of these shunts varied with high morbidity and mortality[7-9]. Orthotopic liver transplantation has been used to treat BCS cases, but it was mainly for patients with fulminant hepatic failure caused by acute BCS and those with end stage of cirrhosis[10,11]. Recently, the transjugular intrahepatic portosystemic shunt (TIPS) has been reported as an effective therapeutic method for BCS[12,13]. But primary TIPS shunt dysfunction occurred in 60 % of patients with TIPS stent modifications, and angioplasties were required to keep a long-term patency[13,14].

With the development of percutaneous transluminal angioplasty (PTA) and stent placement in the 1990's, a pseudosurgical technique has been employed as an alternative to the major portosystemic shunts[15]. This procedure, applied by Furuil for the first time in a case of BCS in 1990[16], has shown beneficial results. Up to now, almost all of the reports were based on small numbers of patients without long-term follow-up. PTA and stent placement were limited to case report especially for patients with hepatic vein occlusion[17,18]. The role of these therapies in the overall management of BCS has not been clearly established.

From 1994, we have performed percutaneous IVC stent placement in 102 patients and HV stent placement in 30 patients with BCS, 17 out of 102 were treated with combined IVC and HV stent placement. Different from the other reports, all procedures were performed under ultrasound guidance instead of x-ray guidance. Our previous reports demonstrated the safety and advantages of IVC and/or HV stent placement under ultrasound guidance[19,20]. In this study, the long-term effects of stent placement in BCS were reported. The large series of patients enabled us to evaluate the outcome of stent placement and to establish protocol for management of BCS.

MATERIALS AND METHODS

Patients

From April 1994 to June 2001, 115 patients with BCS underwent stent placement in our hospital (All were performed by Dr. Chunqing). There were 65 males and 50 females. The average age was 37.3±12.7 years (SD, range 17-67). The duration of the illness ranged from 3 months to 17 years. Underlying etiological factors for BCS were identified in 5 patients. Two patients had a history of tuberculosis infection, 2 patients took oral contraceptives, 1 patient was pregnant. No patients were examined for the levels of antithrombin-III, protein C and protein S. The main clinical features are listed in Table 1 according to the site of obstruction (see below). Patients manifested mainly as abdominal fullness, weakness, hepato-splenomegaly and ascites.

All patients underwent gray-scal sonography and colour Doppler sonography prior to the stent placement. Ultrasound scanning could identify the site, degree and extent of obstruction of hepatic IVC and hepatic veins, while colour

Doppler could demonstrate the altered hemodynamic within the IVC and HV. In our early study only 11 patients underwent venography.

Based on the findings by ultrasound, colour Doppler and the subsequent probing of the lesions with a guide wire or a 5F-cathetor during the interventional procedure, the patients were divided into obstruction of inferior vena cava with at least one patent hepatic vein (IVC group, *n*=85 patients), obstruction of three main hepatic veins (HV group, *n*=13 patients), obstruction of both inferior vena cava and three main hepatic veins (Combined group, *n*=17 patients). IVC stent were placed in both IVC group and combined group (102 patients). HV stent placement were performed in both HV group and combined group (30 patients). Of the102 patients who underwent IVC stent placement, 49 patients had membranous obstruction, and 53 patients had IVC segmental obstruction (range 1.0-7.6 cm, Table 2). While in 30 patients who underwent HV stent placement, 17 patients had membranous obstruction in HV and 13 patients had segmental obstruction in HV(range 1-4 cm, Table 2).

During the same period, sonography did not reveal hepatic IVC and the main hepatic vein in 30 patients, patients with thrombosis below the obstruction were excluded from this study.

Table 1 Clinical features and choice of management in 115 patients with Budd-Chiari Syndrome

	Site of obstruction		
	IVC (*n*=85)	HV (*n*=13)	Combined (*n*=17)
Symptoms			
Abdominal fullness	79	13	17
Weakness	71	13	17
Abdominal pain	58	13	15
Low extremities edema	53	3	13
Gastrointestinal bleeding	9	4	8
Jaundice	5	4	7
Hepatic encephalopathy	3	2	3
Signs			
Hepatomegaly	80	13	17
Splenomegaly	77	13	17
Ascites	36	10	12
Distended abdominal veins	55	3	5
Leg ulcer	21	0	3
Management	IVC stent	HV stent	IVC and HV stent

Table 2 Types of obstruction in the IVC and HV in 115 patients

	Membraneous	Segmental (extent, cm)
IVC Stenosis (*n*=54)	30	24 (1-7.6)
Occlusion (*n*=48)	19	29 (1-7.2)
HV Stenosis (*n*=11)	6	5 (1-4.5)
Occlusion (*n*=19)	11	8 (1-4.0)

IVC=IVC group + combined group, HV=HV group + combined group.

Methods

All the procedures were performed under ultrasound guidance[19,20]. Before the procedure, all the patients were given cisapride 10 mg and pipemidic acid 0.5 three times daily for 3 days. They were fasted and asked to have bed rest for 12 hours to reduce intestinal tympanites and to keep a clear image of ultrasound. In patients with massive ascites, before the procedure a therapeutic paracentesis was performed followed by intravenous administration of albumin. The methods were approved by the ethic committee of our hospital.

IVC stent placements: Briefly, the transducer of ultrasound unit was positioned in the infrasternal angle to show the longitudinal axis of hepatic IVC, the lesion and interventional devices. Though the right femoral vein, a 14F sheath was advanced over a guide wire into the IVC. Echo contrast in 5-10 ml normal saline was injected through the sheath. The soft end of a guide wire or a 5F-catheter was then introduced to probe the lesion under US guidance. If the obstruction was incompletely, the guide wire could easily cross the narrowed part of IVC into the right atrium. For complete obstruction, an 8-F Teflon catheter and its appropriate metal cannula were inserted through the sheath and were pushed carefully into the occluded IVC. If necessary, a Brockenbrough needle was inserted to cut through the lesion. Once the catheter or the needle was placed into right atrium, its strong rebound echo could be shown on US and blood return could be obtained. Then, a balloon catheter with a 1.8-2.4 cm diameter was inserted to dilate the IVC. At the end, under US guidance, the stent (Gianturco stent, Jayu Medical Equipment, Shenyang, China) was pushed into the obstructive part of IVC where it could completely support the obstructive portion after deployment.

HV stent placement: The procedures were performed by percutaneous and transhepatic route. Under ultrasound guidance, a 16-gauge needle was inserted into the hepatic vein via either an intracostal (for right HV) or infrasternal (for middle and left HV) approach. Then over a guide wire, a 10F sheath was put into HV, and all other operations were done thought the sheath to prevent damage of hepatic parenchyma. In patients with partially obstructed HV, the guide wire could cross the entrance of hepatic vein into IVC and finally into the right atrium. Otherwise, a Brockenbrough needle was used to make a tract from the hepatic vein into IVC. Then, the obstructive hepatic vein was dilated by a 1.0-1.2 cm diameter balloon catheter, and a metallic stent (Giantureco Z stent or Wallstent, Jayu Medical Equipment, Shenyang, China) was placed through the 10F catheter to support the hepatic vein. At the end, the 10-F sheath was withdrawn under guidance of ultrasound, and pieces of gelatin sponge were placed over the sheath to plug the tract.

After the procedure, antibiotics were given to all patients. Intravenous heparin was given for for 1 week and followed by aspirin (75-100 mg per day) at least for 6 months to prevent stent thrombosis.

Follow-up

During the follow-up period, manifestations of BCS were evaluated and the liver function was valued, and Doppler duplex ultrasonography was obtained to assess patency of the stent and the hemodynamics in HV and IVC. All patients underwent these examinations before discharge, and then they were seen at 3-6 month intervals, or when they had recurrence of symptoms of BCS.

Statistical analysis

Results were expressed as mean ± SD, range or absolute numbers. Chi-square test, Wilcoxon' s, or Student' s *t* test was used. $P<0.05$ was considered statistically significant.

RESULTS

IVC stent placement

IVC stent was placed successfully in 94 %(95 /102) of patients (IVC group and HV group). The procedure failed in 6 patients (all in IVC group) with segmental occluded IVC (3-4 cm). Pericardial effusion occurred in 3 patients and inferior infarction in 1 patient during dilatation of the occluded IVC with balloon, the Brockenbrough needle failed to cut through

the hard occlusive segment of IVC in 2 patients. Stent migrated into right atrium in one patient who had mesoatrial shunt with the stent fixed to the wall of right atrium and no procedural death occurred.

Hemodynamic features in patients with successful stent placement improved significantly, the inferior vena cava pressure below the obstruction decreased from 29±12.7 cm H_2O to 11.5±7.3 cm H_2O (P<0.05), and satisfactory antegrade flow in IVC was observed with a normal flow spectrum in colour Doppler ultrasound. All patients in IVC group improved clinically. Ascites, hepatomegaly, lower extremity edema, and distended abdominal veins disappeared or diminished at discharge.

Seventy-nine patients in IVC group were followed for 12-84 months (mean 58 months). Four patients were lost in follow-up. Of the remaining 75 patients, 48 had no symptoms, 24 improved clinically, but they still had mild weakness or abdominal swelling on physical examination. On the latest follow up, 68 patients were employed or engaged in full house keeping (Table 3). Of the 17 patients in combined group, 2 were lost to follow-up, the other 15 patients had no symptoms of IVC obstruction.

Thirty-four of the 90 patients (75 in IVC group and 15 in combined group) were followed up for 5 years, 31 patients for 3 years, 25 patients for 1 year. Doppler ultrasonography showed that IVC stent was patent and worked effectively in 87 patients. The overall IVC stent patency rate was 96.6 % (87/90). Stent occlusion occurred in 3 patients at 12-24 months (mean 19 months) following stent placement, these 3 patients had recurrence of abdominal fullness and edema of lower extremity, and 1 patient had ascites. Two patients underwent caval-portal shunt and the others were treated with diuretics and anticoagulants.

Table 3 Long term results of Stent placement in 97 follow up patients

	IVC group	HV group	Combined group
Number of patients	75	7	15
Follow-up (months)			
Mean	49	45	45
Range	7-84	9-78	9-78
Ascites			
Before procedure	29	7	11
Disappeared	21	5	8
improved	7	2	3
Hepatomegaly			
Before procedure	73	7	15
Disappeared	38	3	6
Improved	33	3	7
Splenomegaly			
Before procedure	67	7	15
Disappeared	9	1	3
Improved	46	3	8
Abnormal liver function test			
Before procedure	53	7	15
Disappeared	21	3	4
Improved	29	3	9
Employed or housekeeping	68	6	14
Stent occlusion	3	1	1

HV stent placement

Hepatic vein stent was placed in 30 patients, including 13 patients in HV group and 17 in combined group. In HV group, the patients had hepatic vein stent placement alone, although some patients had narrowed IVC pressed by enlarged caudate lobe. In combined group, successful IVC stent placement resulted in disappearance of all symptoms of IVC obstruction. However, ascites, and hepatosplenomegaly were not alleviated. Therefore, hepatic vein stent was placed 1 week after IVC stent placement.

HV stent were successfully placed in 86.6 % (26/30) patients. Four patients in HV group failed due to a long occluded hepatic vein (3.0-3.5 cm), which was difficult to cut through. All but one of the 26 successful patients had hemodynamic improvement immediately after the procedure. HV pressure dropped from 36.5±16.4 cm H_2O to 12.7±9.5 cm H_2O and satisfactory antegrade flow was noted with a normal phasic flow spectrum in the stented HV. At the time of discharge, 10 patients were free of ascites, the massive ascites decreased without diuretics, and hepato-splenomegaly disappeared or diminished obviously in 25 patients.

Early stent occlusion occurred in one patient of HV group on the third day after the procedure, because the stent immigrated into the hepatic vein and the ostium of hepatic vein was not support by the stent. The patient was treated with repeated paracentesis, intravenous albumin, and a portocaval shunt. Severe haemorrhage from the unplugged transhepatic access occurred in one patient in our early study. Emergent surgical haemostasis was performed, and the patient survived well with a patent hepatic vein stent. One patient with peritonitis and ascitis was treated with paracentesis and parenteral antibiotics. Two patients experienced pleural effusion resolved within 2 weeks. No other major complications occurred.

During a mean follow-up period of 53 months (range 15-78 months), three patients missed the follow-up (1 in HV group, 2 in combined group). Of the 22 follow-up patients (7 in HV group, 15 in combined group), 7 patients were followed up for 5 years, 11 for 3 years, 4 for 1 year. Clinical symptoms and signs of BCS patients improved (Table 3). In these patients, ascites disappeared or decreased, hepatomegaly and splenomegaly were greatly alleviated or dissapeared. Periodic liver function tests were consistent normal or improved. Colour Doppler ultrasonography examinations demonstrated patency of the stents in hepatic vein in 20 patients. The overall HV stent patency rate was 90.9 % (20/22). All were gainfully employed and leading productive lives of good quality. One woman married, pregnant and delivered a healthy baby.

Ascites recurred in 1 patient in combined group at 6 months after the procedure, varices bleeding occurred in 1 patient in HV group at 12 months after the stent placement. Doppler ultrasonography confirmed the stent occlusion and dysfunction in 2 patients. One patient underwent mesocaval shunt, the other was treated with diuretics.

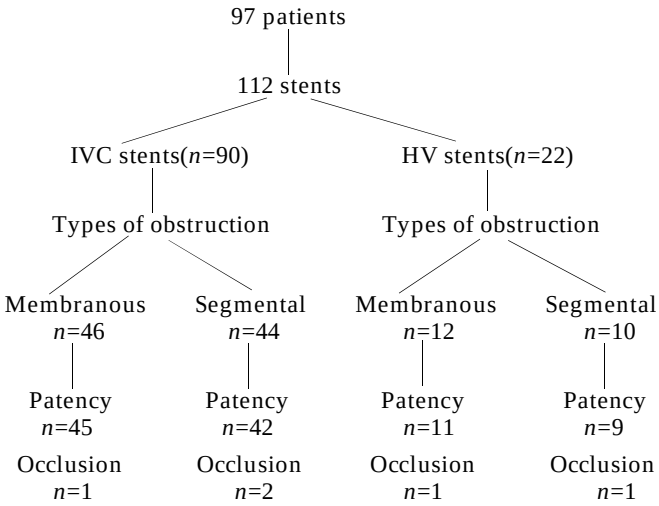

Table 4 The results of 112 stents in 97 follow patients.

Evaluation of risk of stent reocclusion

Of the 112 stents in 97 follow-up patients, occlusion was observed in 5 (4.5 %) stents (3 in IVC stents, 2 in HV stents) (Table 4). Risks of stent occlusion were evaluated (Table 5), and stent occlusion in HV stents (9.1 %) was more common than that in IVC stents (3.3 %) ($P<0.05$). Absence of long-term anticoagulants was related to stent occlusion, stent occlusion was observed in 3 out of 25 (12 %) stents in patients without anticoagulant therapy *versus* 2 of 87 (2.3 %) stents in patients with at least 6 months of anticoagulants for.

No significant difference was found between stent occlusion and severity of obstruction (Table 5). Stent occlusion occurred in 11 % (3/27) patients with segmental obstruction and occlusion *versus* 2.9 % (1/34) patients without them, the difference was significant ($P<0.05$).

Table 5 Analysis of factors influencing stent occlusion in 112 stents of 97 patients

	Number of stents	Number of occlusion	*P* valve
Total	112	5	
Site of stents			
IVC	90	3	
HV	22	2	<0.05
Degrees of obstruction			
Stenosis	60	2	
Occlusion	52	3	>0.05
Types of obstructon			
Membraneous	58	2	
Segmental	54	3	>0.05
Anticoagulants at least 6 months			
Yes	87	2	
No	25	3	<0.05

DISCUSSION

Since the location, extent and rapidity of venous obstruction are highly variable, a range of clinical presentations necessitates an individualized therapeutic strategy. The management of BCS has traditionally been classified as medical, surgical and radical. Conventional medical therapy with diuretics and anticoagulation has been reported to be of limited value in relieving hepatic venous outflow obstruction[21]. The use of fibrinolytic therapy might be of benefit for patients at early stage of acute thrombosis[23]. Surgical treatment was the most frequently reported approach for BCS[6,7]. When venous obstruction is limited to the main HV without serious involvement of IVC, a portacaval shunt or a mesocaval shunt is proposed. In cases of BCS complicated with obstruction of IVC, the mesoatrial shunt may be used to allow the portal flow to drain directly into the right atrium. Liver transplantation as the second surgical option for BCS was indicated for BCS in acute or chronic liver failure in the Western world[23,24]. Radiological interventions including balloon angioplasty, stent insertion and transjugular intrahepatic portosystemic shunts have been shown to be effective for selected patients with BCS during the past 10 years[11,25], but these results were confined to small series of patients with short term follow up.

In this series, all BCS patients were caused by short length obstruction of the hepatic IVC and/or of the main HV. Most patients were chronic and idiopathic. Our series was the largest report to date for the use of stent placement in BCS. The results demonstrated the long-term efficacy of stent placement for BCS.

In this series, stent placement was performed based on the locations of vascular obstruction.

IVC obstruction with short length lesion was a common cause for BCS in the Eastern countries including China[2,3,26]. Although balloon angioplasty has been regarded as the first choice for patients with IVC obstruction, restenosis and redilitation was reported[2,27], even in patients with membranous obstruction[28]. In our study, the residual membrane in most cases was often pushed back into the lumen of IVC once the balloon catheter moved back. This might be a cause of reccurrence of BCS. Therefore, stents were placed in the restricted part in all patients whether the lesion was a membraneous or a segmental obstruction. During a period of 12-84 months follow-up, 87 out of 90 (96.7 %) IVC stents remained patent and functioned well, the manifestions of BCS disappeared or improved in all the patients. The results demonstrate that IVC stent placement is effective and reliable in management of BCS and has a satisfactory long-term patency.

HV obstructon was one of the main causes of BCS, both in Eastern and in Western countries[2,29]. However, treatment of HV obstruction has been challenging. Usually the hepatic vein angioplasty or stent were performed under x-ray guidance via the jugular vein or both transhepatic and jugular veins. Under this condition, the ostium of hepatic vein could not be revealed directly. Thus, it was very difficult to cut through the occluded orifice of the hepatic vein from the vena cava, cardiac perforation or IVC rupture was reported during the procedure[30,31]. Up to now, reports on treatment on HV obstruction were limited with a small number of patients, and its successful rate was low[2,25]. We performed percutanous hepatic vein recanalization, dilation and stent placement in 26 out of 30 patients with a success rate of 86.7 %. This was a report involving the treatment of BCS with short length hepatic vein obstruction. All the patients had three obstructed hepatic veins, we chose to place stent in one of them. By intrahepatic communicating channels of hepatic veins, the stent was sufficient to drain the entire liver. During a period of 15-78 months follow-up, 90.9 % (20/22) patients had patent stents, the clinical manifestations of BCS improved obviously or disappeared. The long term stent patency was rather good compared with PTA of hepatic vein that had a high incidence of restenosis[31]. In our study, percutanous trashepatic hepatic vein stent placement was the first choice in the treatment of BCS caused by short length hepatic vein obstruction.

For the treatment of HV obstruction, percutanous transhepatic route was safe if the tract was plugged with gelatin sponge before removal of the sheath. Patients with short length HV obstruction should be treated by stent placement instead of simple angioplasty, because hepatic vein webs were more likely to restenose compared with caval webs following angioplasty[31]. Performance under ultrasound guidance contributed to a high success rate and low morbidity, reducing intestinal tympanites and ascites before the procedure was necessary for a clean image of ultrasound.

Combined IVC and HV obstruction was a special kind of BCS consisting of 15 % of our patients. Management of these patients was usually difficult[2,6,7]. When the procedures were divided into 2 steps, the treatment became simple. In 17 patients, the IVC stent were placed first, and the HV stent was placed one week later. During a long-term follow-up, only one patient developed HV stent occlusion, and all IVC stents worked well. The results showed that the combined procedure was an advisable choice for BCS patients with both IVC and HV obstruction.

The total stent occlusion rate was 4.5 % during the follow-up. The long term results were satisfactory. The stent occlusion was more likely to occurred in BCS patients with segmental and occluded obstruction than in patients with membraneous and stenosis obstruction, the stent occlusion rate was higher in patients without anticoagulants after operation than that in

patients with anticoagulants at least for 6 months. Stent occlusion occurred more likely at HV (9.1 %) than at IVC (3.3 %). Therefore, we suggest that anticoagulants should be used routinely after the procedure, especially for patients with segmental and occluded obstruction, and for patients having HV stent placement.

In conclusion, IVC and HV stents or combined IVC and HV stent can be applied to BCS patients with short length obstruction depending on the sites of obstruction. The stents can be placed under ultrasound guidance with a high successful rate and a low morbidity. Excellent long-term results can be obtained in IVC and HV stents as well as in combined stents. Anticoagulants are strongly recommended for at least 6 months after the procedure.

REFERENCES

1 **Okuda H**, Yamagata H, Obata H, Iwata H, Sasaki R, Imai F, Okudaira M, Ohbu M, Okuda K. Epidemiological and clinical features of Budd-Chiari syndrome in Japan. *J Hepatol* 1995; **22**: 1-9

2 **Kohli V**, Pande GK, Dev V, Reddy KS, Kaul U, Nundy S. Management of hepatic venous outflow obstruction. *Lancet* 1993; **18**: 718-722

3 **Dilawari JB**, Bambery P, Chawla Y, Kaur U, Bhusnurmath SR, Malhotra HS, Sood GK, Mitra SK, Khanna SK, Walia BS. Hepatic outflow obstruction (Budd-Chiari syndrome). Experience with 177 patients and a review of the literature. *Medicine (Baltimore)* 1994; **73**: 21-36

4 **Mahmoud AE**, Mendoza A, Meshikhes AN, Olliff S, West R, Neuberger J, Buckels J, Wilde J, Elias E. Clinical spectrum, investigations and treatment of Budd-Chiari syndrome. *QJM* 1996; **89**: 37-43

5 **Mitchell MC**, Boitnott JK, Kaufman S, Cameron JL, Maddrey WC. Budd-Chiari syndrome: etiology, diagnosis and management. *Medicine (Baltimore)* 1982; **61**: 199-218

6 **Slakey DP**, Klein AS, Venbrux AC, Cameron JL. Budd-Chiari syndrome: current management options. *Ann Surg* 2001; **233**: 522-527

7 **Orloff MJ**, Daily PO, Orloff SL, Girard B, Orloff MS. A 27-year experience with surgical treatment of Budd-Chiari syndrome. *Ann Surg* 2000; **232**: 340-352

8 **Panis Y**, Belghiti J, Valla D, Benhamou JP, Fekete F. Portosystemic shunt in Budd-Chiari syndrome: long-term survival and factors affecting shunt patency in 25 patients in Western countries. *Surgery* 1994; **115**: 276-281

9 **Bismuth H**, Sherlock DJ. Portasystemic shunting versus liver transplantation for the Budd-Chiari syndrome. *Ann Surg* 1991; **214**: 581-589

10 **Klein AS**, Sitzmann JV, Coleman J, Herlong FH, Cameron JL. Current management of the Budd-Chiari syndrome. *Ann Surg* 1990; **212**: 144-149

11 **Tilanus HW**. Budd-Chiari syndrome. *Br J Surg* 1995; **82**: 1023-1030

12 **Ganger DR**, Klapman JB, McDonald V, Matalon TA, Kaur S, Rosenblate H, Kane R, Saker M, Jensen DM. Transjugular intrahepatic portosystemic shunt (TIPS) for Budd-Chiari syndrome or portal vein thrombosis: review of indications and problems. *Am J Gastroenterol* 1999; **94**: 603-608

13 **Perello A**, Garcia-Pagan JC, Gilabert R, Suarez Y, Moitinho E, Cervantes F, Reverter JC, Escorsell A, Bosch J, Rodes J. TIPS is a useful long-term derivative therapy for patients with Budd-Chiari syndrome uncontrolled by medical therapy. *Hepatology* 2002; **35**: 132-139

14 **Cejna M**, Peck-Radosavljevic M, Schoder M, Thurnher S, Bassalamah A, Angermayr B, Kaserer K, Pokrajac B, Lammer J. Repeat interventions for maintenance of transjugular intrahepatic portosystemic shunt function in patients with budd-Chiari syndrome. *J Vasc Interv Radiol* 2002; **13**: 193-199

15 **Carrasco CH**, Charnsangavej C, Wright KC, Wallace S, Gianturco C. Use of the Gianturco self-expanding stent in stenoses of the superior and inferior venae cavae. *J Vasc Interv Radiol* 1992; **3**: 409-419

16 **Furui S**, Sawada S, Irie T, Makita K, Yamauchi T, Kusano S, Ibukuro K, Nakamura H, Takenaka E. Hepatic inferior vena cava obstruction: treatment of two types with Gianturco expandable metallic stents. *Radiology* 1990; **176**: 665-670

17 **Weernink EE**, Huisman AB, ten Napel CH. Treatment of Budd-Chiari syndrome by insertion of wall-stent in hepatic vein. *Lancet* 1991; **338**: 644

18 **Dolmatch BL**, Cooper BS, Chang PP, Gray RJ, Horton KM. Percutaneous hepatic venous reanastomosis in a patient with Budd-Chiari syndrome. *Cardiovasc Intervent Radiol* 1995; **18**: 46-49

19 **Zhang C**, Fu L, Zhang G, Xu L, Shun H, Wang Z, Zhu J. Ultrasonically guided inferior vena cava stent placement: experience in 83 cases. *J Vasc Interv Radiol* 1999; **10**: 85-91

20 **Chunqing Z**, Lina F, Guoquan Z, Lin X, Zhaohai W, Tao J, Chengyong Q, Juzhen Z. Ultrasonically guided percutaneous transhepatic hepatic vein stent placement for Budd-Chiari syndrome. *J Vasc Interv Radiol* 1999; **10**: 933-940

21 **McCarthy PM**, van Heerden JA, Adson MA, Schafer LW, Wiesner RH. The Budd-Chiari syndrome. Medical and surgical management of 30 patients. *Arch Surg* 1985; **120**: 657-662

22 **Mitchell MC**, Boitnott JK, Kaufman S, Cameron JL, Maddrey WC. Budd-Chiari syndrome: etiology, diagnosis and management. *Medicine (Baltimore)* 1982; **61**: 199-218

23 **Hemming AW**, Langer B, Greig P, Taylor BR, Adams R, Heathcote EJ. Treatment of Budd-Chiari syndrome with portosystemic shunt or liver transplantation. *Am J Surg* 1996; **171**: 176-180

24 **Rao AR**, Chui AK, Gurkhan A, Shi LW, Al-Harbi I, Waugh R, Verran DJ, McCaughan GW, Koorey D, Sheil AG. Orthotopic liver transplantation for treatment of patients with Budd-Chiari syndrome: a Singe-center experience. *Transplant Proc* 2000; **32**: 2206-2207

25 **Pisani-Ceretti A**, Intra M, Prestipino F, Ballarini C, Cordovana A, Santambrogio R, Spina GP. Surgical and radiologic treatment of primary Budd-Chiari syndrome. *World J Surg* 1998; **22**: 48-53

26 **Singh V**, Sinha SK, Nain CK, Bambery P, Kaur U, Verma S, Chawla YK, Singh K. Budd-Chiari syndrome: our experience of 71 patients. *J Gastroenterol Hepatol* 2000; **15**: 550-554

27 **De BK**, Biswas PK, Sen S, Das D, De KK, Das U, Mandal SK, Majumdar D. Management of the Budd-Chiari syndrome by balloon cavoplasty. *Indian J Gastroenterol* 2001; **20**: 151-154

28 **Hung WC**, Fang CY, Wu CJ, Lo PH, Hung JS. Successful metallic stent placement for recurrent stenosis after balloon angioplasty of membranous obstruction of inferior vena cava. *Jpn Heart J* 2001; **42**: 519-523

29 **Valla D**, Hadengue A, el Younsi M, Azar N, Zeitoun G, Boudet MJ, Molas G, Belghiti J, Erlinger S, Hay JM, Benhamou JP. Hepatic venous outflow block caused by short-length hepatic vein stenoses. *Hepatology* 1997; **25**: 814-819

30 **Lois JF**, Hartzman S, McGlade CT, Gomes AS, Grant EC, Berquist W, Perrella RR, Busuttil RW. Budd-Chiari syndrome: treatment with percutaneous transhepatic recanalization and dilation. *Radiology* 1989; **170**: 791-793

31 **Fisher NC**, McCafferty I, Dolapci M, Wali M, Buckels JA, Olliff SP, Elias E. Managing Budd-Chiari syndrome: a retrospective review of percutaneous hepatic vein angioplasty and surgical shunting. *Gut* 1999; **44**: 568-574

Edited by Ren SL and Wang XL

P.O.Box 2345, Beijing 100023,China
Fax: +86-10-85381893
E-mail: wjg@wjgnet.com www.wjgnet.com

World J Gastroenterol 2003;9(11):2592-2595
World Journal of Gastroenterology
 ISSN 1007-9327

• CLINICAL RESEARCH •

Detection of type IV collagenase activity in malignant ascites

Xiao-Min Sun, Wei-Guo Dong, Bao-Ping Yu, He-Sheng Luo, Jie-Ping Yu

Xiao-Min Sun, Wei-Guo Dong, Bao-Ping Yu, He-Sheng Luo, Jie-Ping Yu, Department of Gastroenterology, Renmin Hospital, Wuhan University, Wuhan 430060, Hubei Province, China
Supported by the Natural Science Foundation of Hubei Province, No. 99J163
Correspondence to: Dr. Wei-Guo Dong, Department of Gastroenterology, Renmin Hospital, Wuhan University, Wuhan 430060, Hubei Province, China. dongwg@public.wh.hb.cn
Telephone: +86-27-88041911 **Fax:** +86-27-88042292
Received: 2003-05-11 **Accepted:** 2003-06-02

Abstract

AIM: Type IV collagenase participates in invasion and metastasis of cancer cells. Malignant ascites is a manifestation of advanced malignant disease that is associated with invasion and metastasis of the peritoneal cavity. Thus, it is reasonable to hypothesize that type IV collagenase is linked to malignant ascites. The purpose of our study was to detect type IV collagenase activity in malignant ascites so as to provide the scientific basis for clinic diagnosis and treatment of malignant ascites.

METHODS: Cirrhotic ascites (n=36), tuberculous ascites (n=8) and malignant ascites (n=23) from patients with gastric cancer (n=6), colon cancer (n=5), ovarian cancer (n=8) and other cancers (n=4), including 2 hepatocellular cancers, 1 pancreatic cancer, 1 primary peritoneal carcinoma were collected by paracentesis. The ascites were made cell-free by centrifugation and stored frozen at -70 ℃ before determination. Type IV collagenase activity was determined by gelatin zymography.

RESULTS: The activity of matrix metalloproteinases-2 and -9 could not be detected in ascites of hepatic cirrhosis and tuberculous peritonitis but could be detected in 20 and 18 out of 23 malignant ascites respectively. The positive rate of type IV collagenase (MMP-2, 87.0 % and MMP-9, 78.3 %) was higher than that by routine ascites tests (P<0.01) in malignant ascites. Furthermore, the activity of MMP-2 was higher than that of MMP-9 (P=0.022<0.05).

CONCLUSION: Type IV collagenase is positive in malignant ascites. Detection of type IV collagenase activity is useful in qualitative diagnosis of ascites. Type IV collagenase may play an important role in malignant ascites formation.

Sun XM, Dong WG, Yu BP, Luo HS, Yu JP. Detection of type IV collagenase activity in malignant ascites. *World J Gastroenterol* 2003; 9(11): 2592-2595
http://www.wjgnet.com/1007-9327/9/2592.asp

INTRODUCTION

Although tumor invasion and metastasis are considered to be a dynamic, complex and multi-step process, proteolytic degradation of the extracellular matrix (ECM) made of interstitial matrix and basement membrane is the essential step[1-4]. The basement membrane, a specialized ECM containing large amounts of type IV collagen and laminin, serves a barrier function separating epithelial cells from the underlying stroma. For the occurrence of metastasis, a tumor cell must repeatedly cross this basement membrane barrier, a process for which proteolysis of ECM components is required[5,6]. It is reasonable to hypothesize that proteolysis of ECM also plays a key role in intraperitoneal metastasis of tumor cells, such as in disruption of the mesothelial cell layer, during extension of the implanted tumor through the submesothelial basement membrane into the visceral organ stroma, and importantly, in gaining access to the host vascular supply, a necessary step in progression of the implant.

In disruption of the ECM, the contribution of matrix metalloproteinases (MMPs) of proteolytic enzymes is direct and important in that it catalyzes the hydrolysis of numerous ECM molecules[7-11]. While in the matrix metalloproteinase, type IV collagenase, one of the most important members of MPPs family, including a 72 kD enzyme resembling matrix metalloproteinase-2 (MMP-2), also named gelatinase A and a 92 kD enzyme resembling matrix metalloproteinase-9 (MMP-9), also named gelatinase B, has been demonstrated to be closely associated with several tumor systems and linked to invasive potential of tumor cells[12-16]. Type IV collagenase can degrade not only interstitial matrix, but also basement membrane, and malignant ascites is the direct and prominent manifestation of advanced malignant disease that is associated with invasion and metastasis of peritoneal cavity by tumor cells. Thus it is possible and feasible to detect type IV collagenase in malignant ascites. In the present study, we detected type IV collagenase activity in various kinds of ascites by gelatin zymography so as to explore the relationship between type IV collagenase and malignant ascites, and to provide the scientific basis for clinic diagnosis and treatment of malignant ascites.

MATERIALS AND METHODS

Reagents and instruments

The common reagents and principal apparatus used in SDS-PAGE were provided by the Biochemical Laboratory, Medical College, Wuhan University. Gelatin was purchased from Sigma Co. Type IV collagenase was the product of Invitrogen. Matrix metalloproteinase inhibitor, 1,10-phenanthroline, was purchased from Sangon, Shanghai, China.

Clinical specimems

Sixty-seven inpatients with ascites were recruited respectively at Renmin Hospital of Wuhan University, Zhongnan Hospital of Wuhan University and Tumor Hospital of Hubei Province from July 2002 to March 2003. The ascites were obtained by therapeutic or diagnostic paracentesis. In all cases, informed consent of the patient and approval of the hospital were obtained prior to collection of ascites and medical records. All the diagnoses were confirmed by cytologic examination of the ascites, biopsy for pathological examination, B-ultrasound and CT scan. Details of the patient data are shown in Table 1. The ascites were made cell-free by centrifugation at 3 000 rpm for 15 min and stored frozen at -70 ℃ before determination. At the same time, the protein content of the ascites was measured.

Table 1 Patient data

Characteristics	*n*
Number of patients	67
Male	38
Female	29
Median age (y)	
Male	50.68
Female	48.60
Disease categories	
Cirrhotic ascites	36
Tuberculous ascites	8
Malignant ascites	23
Ovarian cancer	8
Gastric cancer	6
Colon cancer	5
Hepatocellular cancer	2
Pancreatic cancer	1
Primary peritoneal carcinoma	1

Sodium dodecyl sulfate-polyacrylamide gel electrophoresis (SDS-PAGE) zymography

Samples were analyzed by SDS-PAGE zymography according to the method of Kleiner and settler-Stevenson[17] to determine the molecular weights and relative abundance of the gelatinases present. Samples containing 70 μg of protein were incubated for 40 min at 37 ℃ and electrophoresed without reduction (no DTT) on 8 % SDS polyacrylamide gels copolymerized with 0.1 % gelatin. Electrophoresis was performed at 4 ℃ at a constant current of 20 mA. When the tracking dye at the front reached the bottom of the gel, the gel was removed and shaken gently for 45 min in 2.5 % Triton x-100 to remove SDS. Then, the gel slabs were transferred to a bath (without Triton x-100) and washed for 20 min to remove Triton x-100. The above operation was repeated twice both at 4 ℃. Next, the gels were incubated and shaken for 60 h in 0.1 mol/L glycine, 50 mmol/L Tris-HCl, 5 mmol/L $CaCl_2$, 1 μmol/L $ZnCl_2$, 0.5 mol/L NaCl, pH 8.3 , at 37 ℃. At last, following staining with 0.075 % Coomassie blue for 3 h, regions of proteolytic activity were visualized as clear zones against a blue background. Gelatinolytic bands were assessed for semiquantitative analysis using an arbitrarily graded scale. Scale categories were defined as follows: +/-, faint band detected, <1.0 mm in width: 1+, clear band detected, 1.0-1.5 mm in width: 2+, intense band detected, 1.5-3.0 mm in width.

Matrix metalloproteinase inhibition test[18]

In order to verify that the clear zones resembled matrix metalloproteinase, 2.5 mmol/L 1,10- phenanthroline was added into the samples before electrophoresis to inhibit matrix metalloproteinase activities.

Detection of LDH, cytologic examination of ascites and serum complex index

Detection of LDH, cytologic examination of ascites and serum complex index were performed by the Department of Clinical Laboratory and Pathology.

Statistical analysis

Chi-square test and Fisher' s exact probabilities test were used for statistical analysis. Differences were considered significant when *P* value was less than 0.05.

RESULTS

Metalloproteinase inhibition test

Except that when 2.5 mmol/L 1,10-phenanthroline was added to the sample prior to electrophoresis, the result of electrophoresis for the identical samples was negative, indicating what we had detected was matrix metalloproteinase (Figure 1).

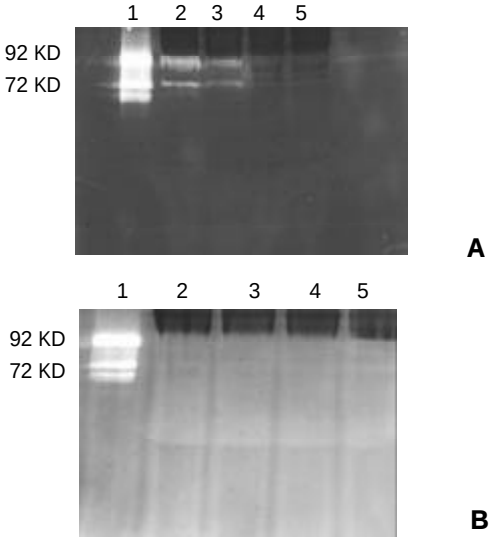

Figure 1 Results of SDS-PAGE zymography. A, Lane 1: type IV collagenase as marker, Lanes 2, 3: cancerous ascites, Lane 4: cirrhotic ascites (no bright bands), Lane 5: tuberculous ascites (no bright bands). B, Lane 1: Marker, Lanes 2-5: identical samples with A, except the addition of 2.5 mmol/L 1,10-phenanthroline. The result was negative.

Qualitative analysis of type IV collagenase activity in various kinds of ascites

Type IV collagenase activity could not be detected in ascites of hepatic cirrhosis and tuberculous peritonitis but could be detected in majority of malignant ascites (Table 2, Figure 1A).

Table 2 Qualitative analysis of type IV collagenase activity in various kinds of ascites

Ascites type	MMP-2 (Positive cases)	MMP-9 (Positive cases)
Cirrhotic ascites	0	0
Tuberculous ascites	0	0
Malignant ascites	20	18
Gastric cancer	5	5
Colon cancer	3	5
Hepatocellular cancer	2	1
Pancreatic cancer	1	0
Ovarian cancer	8	6
Primary peritoneal carcinoma	1	1

Table 3 Semi-quantitative analysis of MMP-2, MMP-9 activity in different kinds of malignant ascites

Type	Case (*n*)	MMP-2 activity (*n*)			MMP-9 activity (*n*)		
		+/-	1+	2+	+/-	1+	2+
Gastric cancer	6	1	4	0	3	2	0
Colon cancer	5	1	2	0	4	1	0
Hepatocellular cancer	2	1	1	0	0	1	0
Pancreatic cancer	1	0	1	0	0	0	0
Ovarian cancer	8	1	5	2	3	1	2
Primary peritoneal carcinoma	1	0	0	1	0	0	1

+/-, faint band detected, <1.0 mm in width; 1+, clear band detected, 1.0-1.5 mm in width; 2+, intense band detected, 1.5-3.0 mm in width.

Table 4 Comparison of detection of type IV collagenase and other indexes in malignant ascites

	Type IV collagenase		LDH in ascites / serum LDH (>1: positive)	Cytologic examination	Serum complex indexes (AFP, CEA, CA)
	MMP-2	MMP-9			
Positive numbers	20	18	10	11	13
Positive rates	87.0 %	78.3 %	43.4 %	47.8 %	56.5 %

Semi-quantitative analysis of type IV collagenase in different kind of cancerous ascites

Gelatinolytic bands were assessed for semiquantitative analysis using an arbitrary grade scale as described in Materials and Methods. The 72 kD MMP-2 was detected in 87.0 % of malignant ascites (n=23), with 80.0 % being scaled >1+; and the 92 kD MMP-9 was found in 78.3 %, with 44.4 % scaled >1+. The activity of MMP-2 was higher than that of MMP-9 ($0.01<P=0.022<0.05$). Additionally, three cases had the highest type IV collagenase activity (2+) for MMP-2 and MMP-9 respectively. Both included one primary peritoneal carcinoma, and two ovarian cancers (Table 3).

Comparison of detection of type IV collagenase and other indexes in malignant ascites

In 23 cases of carcinoma ascites, MMP-2 was found in 20 (87.0 %), significantly higher than that by routine ascites tests (including LDH, cytologic examination of ascites and complex indexes in serum) ($P<0.01$, respectively). MMP-9 was detected in 18 (78.3 %), higher than that by LDH and cytologic examination. However, compared with the two detection methods of type IV collagenase and serum complex indexes, there was no significant difference ($P>0.05$) (Table 4).

DISCUSSION

Type IV collagenase is closely linked with malignant ascites

Overexpression of type IV collagenase has been demonstrated in a variety of cancers, including colorectal cancer, gastric cancer, and breast cancer. Substantial evidences indicate that type IV collagenase activity or concentration was increased in plasma of patients with advanced carcinoma[19-24]. Recently, some researches found that type IV collagenase activity was increased in urine of patients with metastatic breast cancers[25,26] and in cerebrospinal fluid of patients with brain tumors[27]. However, few reports on type IV collagenase activity in ascites could be seen[18,21]. In the present study, we found that type IV collagenase activity could not be detected in ascites of hepatic cirrhosis and tuberculous peritonitis but could be detected in malignant ascites. At the same time, MMP-2 activity was higher than MMP-9 activity in malignant ascites, which might be attributed to the difference of expression of MMP-2 and MMP-9 in ascites of different kinds of tumor. Furthermore, the detection rate of type IV collagenase in ascites of malignant tumor was higher than that by routine ascites tests. Additionally, 2 out of 4 unidentified cases of ascites were identified by peritoneal biopsy. One was metastatic ovarian cancer, the other was primary peritoneal carcinoma. In these two cases, the activity of MMP-2 and MMP-9 was positive, and scale categories all exceeded 1+. Another 2 cases, gastric cancer and colon cancer, were identified by gastroscopy and colonoscopy respectively. The activity of MMP-2 and MMP-9 in these 2 cases was positive also. It was suggested that the peritoneal implants of tumors might secrete type IV collagenase (MMP-2 and/or MMP-9) into peritoneal cavity. Type IV collagenase activity in ascites reflects tumor biological behavior to some extent and is related with malignant ascites. So detection of type IV collagenase activity may probably provide a new approach with high sensitivity and specificity for differential diagnosis of benign and malignant ascites.

Type IV collagenase is correlated with malignant ascites formation

Some reports demonstrated that MMPs played a key role in intraperitoneal metastasis[21]. Others found metalloproteinase inhibitor could reduce ascites in patients with advanced malignant disease[28-30]. Our experiments indicated no expression of type IV collagenase in nonmalignant ascites. On the contrary, majority of malignant ascites showed higher activity of type IV collagenase. Thus, it is reasonable to infer that type IV collagenase is associated with malignant ascites formation to some extent. The probable mechanism of inducing malignant ascites formation by type IV collagenase may be explained as follows[31-37]: breakdown of apparent physical barriers to metastasis of peritoneal cavity, role of MMPs in angiogenesis, formation of new blood vessels which increases overall capillary membrane surface available for fluid filtration, inducing fluid accumulation. These new observations indicate that use of metalloproteinase inhibitors may offer a novel treatment of malignant ascites.

ACKNOWLEDGEMENTS

The authors are grateful to teachers of the Biochemical Laboratory, Medical College, Wuhan University, especially Xiao-Ming Li, Hong Yu and Chun-Yan He, and thank Dr. Hui-Lan Lu from the Department of Clinical Laboratory for their suggestions, advice, and cooperation in this study.

REFERENCES

1 **Meyer T**, Hart IR. Mechanisms of tumor metastasis. *Eur J Cancer* 1998; **34**: 214-221
2 **Kleiner DE**, Stetler-Stevenson WG. Matrix metalloproteinases and metastasis. *Cancer Chemother Pharmacol* 1999; **43**: S42-51
3 **Conway JG**, Trexler SJ, Wakefield JA, Marron BE, Emerson DL, Bickett DM, Deaton DN, Garrison D, Elder M, McElroy A, Willmott N, Dockerty AJ, McGeehan GM. Effect of matrix metalloproteinase inhibitors on tumor growth and spontaneous metastasis. *Clin Exp Metastasis* 1996; **14**: 115-124
4 **Heppner KJ**, Matrisian LM, Jensen RA, Rodaers WH. Expression of most matrix metalloproteinase family members in breast cancer represents a tumor-induced host response. *Am J Pathol* 1996; **149**: 273-282
5 **Ara T**, Fukuzawa M, Kusafuka T, Komoto Y, Oue T, Inoue M, Okada A. Immunohistochemical expression of MMP-2, MMP-9, and TIMP-2 in neuroblastoma: Association with tumor progression and clinical outcome. *J Pediatr Surg* 1998; **33**: 1272-1278
6 **Ellenrieder V**, Alber B, Lacher U, Hendler SF, Menke A, Boeck W, Wagner M, Wilda M, Friess H, Buchler M, Adler G, Gress TM. Role of MT-MMPs and MMP-2 in pancreatic cancer progression. *In J Cancer* 2000; **85**: 14-20
7 **Stracke JO**, Hutton M, Stewart M, Pendas AM, Smith B, Lopez-Otin C, Murophy G, Knauper V. Biochemical characterization of the catalytic domain of human matrix metalloproteinase 19. Evidence for a role as a potent basement membrane degrading enzyme. *J Biol Chem* 2000; **275**: 14809-14816
8 **Uria JA**, Lopez-Otin C. Matrilysin-2, a new matrix metalloproteinase expressed in human tumors and showing the minimal organization required for secretion, latency, and activity. *Cancer Res* 2000; **60**: 4745-4751
9 **Stock UA**, Wiederschain D, Kilroy SM, Shum-Tim D, Khalil PN,

Vacanti JP, Mayer Jr JE, Moses MA. Dynamics of extracellular matrix production and turnover in tissue engineered cardiovascular structures. *J Cell Biochem* 2001; **81**: 220-228

10 **Lauer-Fields JL**, Tuzinski KA, Shimokawa K, Nagase H, Fields GB. Hydrolysis of triple-helical collagen peptide models by matrix metalloproteinases. *J Biol Chem* 2000; **275**: 13282-13290

11 **Jiang ZS**, Gao Y. Biological feature of matrix metalloproteinase and its action in metastasis of liver cancer. *Shijie Huaren Xiaohua Zazhi* 2000; **8**: 1403-1404

12 **Wang ZN**, Xu HM. Relationship between collagen IV expression and biological behavior of gastric cancer. *World J Gastroenterol* 2000; **6**: 438-439

13 **Ji F**, Wang WL, Yang ZL, Li YM, Huang HD, Chen WD. Study on the expression of matrix metalloproteinase-2mrna in human gastric cancer. *World J Gastroenterol* 1999; **5**: 455-457

14 **He YD**, Zhao YW, Kong LF, Yin PZ. Activity alternating of matrix metalloproteinase-2 in hepatocellular carcinoma. *Shijie Huaren Xiaohua Zazhi* 2000; **8**: 952-953

15 **Tryggvason K**, Hoyhtya M, Pyke C. Type IV collagenases in invasive tumors. *Breast Cancer Res Treat* 1993; **24**: 209-218

16 **Zhu ZY**, Du Z, Wang YJ, Zhang W, Sun BC. Examination of E-cadherin and matrix metalloproteinases and its significance in primary HCC. *Shijie Huaren Xiaohua Zazhi* 2001; **9**: 839-840

17 **Kleiner DE**, Stetler-Stevenson WG. Quantitative zymography: detection of picogram quantities of gelatinases. *Anal Biochem* 1994; **218**: 325-329

18 **Young TN**, Rodriguze GC, Rinehart AR, Bast RC Jr, Pizzo SV, Stack MS. Characterization of gelatinases linked to extracellular matrix invasion in ovarian adenocarcinoma: purification of matrix metalloproteinase 2. *Gynecol Oncol* 1996; **62**: 89-99

19 **Sato H**, Takino T, Okada Y, Cao J, Shinagawa A, Yamamoto E, Seiki M. A matrix metalloproteinase expressed on the surface of invasive tumor cells. *Nature* 1994; **370**: 61-65

20 **Torii A**, Kodera Y, Uesaka K, Hirai T, Yasui K, Morimoto T, Yamamura Y, Kato T, Hayakawa T, Fujimoto N, Kito T. Plasma concentration of matrix metalloproteinase 9 in gastric cancer. *Br J Surg* 1997; **84**: 133-136

21 **Fishman DA**, Bafetti LM, Banionis S, Kearns AS, Chilukuri K, Stack MS. Production of extracellular matrix-degrading proteinases by primary cultures of human epithelial ovarian carcinoma cells. *Cancer* 1997; **80**: 1457-1463

22 **Ylisirnio S**, Hoyhtya M, Turpeenniemi-Hujanen T. Serum matrix metalloproteinase -2, -9 and tissue inhibitors of metalloproteinase -1, -2 in lung cancer-TIMP-1 as a prognostic marker. *Anticancer Res* 2000; **20**: 1311-1316

23 **Gohji K**, Fujimoto N, Hara I, Fujii A, Gotoh A, Okada H, Arakawa S, Kitazawa S, Miyake H, Kamidono S, Nakajima M. Serum matrix metalloproteinase –2 and its density in men with prostate cancer as a new predictor of disease extension. *Int J Cancer* 1998; **79**: 96-101

24 **Waas ET**, Lomme RM, DeGroot J, Wobbes T, Hendriks T. Tissue levels of active matrix metalloproteinase-2 and -9 in colorectal cancer. *Br J Cancer* 2002; **86**: 1876-1883

25 **Moses MA**, Wiederschain D, Loughlin KR, Zurakowski D, Lamb CC, Freeman MR. Increased incidence of matrix metalloproteinase in urine of cancer patient. *Cancer Res* 1998; **58**: 1395-1399

26 **Zhang Q**, Chen LB, Zang J, Chu XY. Detection of matrix metalloproteinases in urine of breast cancer patients with zymography. *Nanjing Daxue Xuebao* 2002; **38**: 192-195

27 Gao Y, Li XN, Li SY, Zong ZH, Wang XR, Yu BZ. Zymographic analysis of MMPs in human cerebrospinal fluid with brain tumor. *Zhongguo Yike Daxue Xuebao* 2000; **29**: 10-12

28 **Macaulay VM**, O'Byrne KJ, Saunders MP, Braybrooke JP, Long L, Gleeson F, Mason CS, Harris AL, Brown P, Talbot DC. Phase 1 study of intrapleural batimastat (BB-94), a matrix metalloproteinase inhibitor, in the treatment of malignant pleural effusions. *Clin Cancer Res* 1999; **5**: 513-520

29 **Beattie GJ**, Smyth JF. Phase I study of intraperitoneal metalloproteinase inhibitor BB94 in patients with malignant ascites. *Clin Cancer Res* 1998; **4**: 1899-1902

30 **Parsons SL**, Watson SA, Steele RJ. Phase I/II trial of batimastat, a matrix metalloproteinase inhibitor, in patients with malignant ascites. *Eur J Surg Oncol* 1997; **23**: 526-531

31 **Parsons SL**, Watson SA, Brown PD, Collins HM, Steele RJ. Matrix metalloproteinases. *Br J Surg* 1997; **84**: 160-166

32 **Ray JM**, Stetler-Stevenson WG. The role of matrix metalloproteinase and their inhibitors in tumor invasion, metastasis and angiogenesis. *Eur Respir J* 1994; **7**: 2062-2072

33 **O'Reilly MS**, Holmgren L, Shing Y, Chen C, Rosenthal RA, Moses M, Lane WS, Cao Y, Sage EH, Folkman J. A novel angiogenesis inhibitor that mediates the suppression of metastases by a Lewis lung carcinoma. *Cell* 1994; **79**: 315-328

34 **Giannelli G**, Falk-Marzillier J, Schiraldi O, Stetler-Stevenson WG, Quaranta V. Induction of cell migration by matrix metalloproteinase-2 cleavage of laminin-5. *Science* 1997; **277**: 225-228

35 **Chambers AF**, Matrisian LM. Changing views of the role of matrix metalloproteinases in metastasis. *J Natl Cancer Inst* 1997; **89**: 1260-1270

36 **Tamsma JT**, Keizer HJ, Meinders AE. Pathogenesis of malignant ascites: Starlings law of capillary hemodynamics revisited. *Ann Oncol* 2001; **12**: 1353-1357

37 **Aslam N**, Marino CR. Malignant ascites: new concepts in pathophysiology, diagnosis, and management. *Arch Intern Med* 2001; **161**: 2733-2737

Edited by Zhu LH and Wang XL

P.O.Box 2345, Beijing 100023,China
Fax: +86-10-85381893
E-mail: wjg@wjgnet.com www.wjgnet.com

World J Gastroenterol 2003;9(11):2596-2600
World Journal of Gastroenterology
 ISSN 1007-9327

• CLINICAL RESEARCH •

Role of VEGF and CD44v6 in differentiating benign from malignant ascites

Wei-Guo Dong, Xiao-Min Sun, Bao-Ping Yu, He-Sheng Luo, Jie-Ping Yu

Wei-Guo Dong, Xiao-Min Sun, Bao-Ping Yu, He-Sheng Luo, Jie-Ping Yu, Department of Gastroenterology, Renmin Hospital, Wuhan University, Wuhan 430060, Hubei Province, China
Supported by Natural Science Foundation of Hubei Province, No. 99J163
Correspondence to: Dr. Wei-Guo Dong, Department of Gastroenterology, Renmin Hospital, Wuhan University, Wuhan 430060, Hubei Province, China. dongwg@public.wh.hb.cn
Telephone: +86-27-88041911 **Fax:** +86-27-88042292
Received: 2003-06-05 **Accepted:** 2003-07-24

Abstract

AIM: To detect the vascular endothelial growth factor (VEGF) and soluble splice variant 6 of CD44 (sCD44v6) levels in ascites and to explore their role in differentiating benign from malignant ascites.

METHODS: Cirrhotic ascites (n=36), tuberculosis ascites (n=8) and malignant ascites (n=23) were collected and studied. Concentrations of soluble VEGF and sCD44v6 in various kinds of ascites (n=67) were measured using a sandwich enzyme-linked immunoadsorbent assay.

RESULTS: VEGF and sCD44v6 levels in malignant ascites were 640.74±264.81 pg/ml and 89.22±38.20 ng/ml, respectively, both of which were significantly higher than those in cirrhotic ascites and tuberculous ascites (q=18.98, 11.89 and q=8.92, 5.09; P<0.01). However, the levels of VEGF and sCD44v6 in cirrhotic and tuberculous ascites had no significant difference (q=0.48, 0.75; P>0.05). Furthermore, VEGF levels in malignant ascites in patients with ovarian cancer were higher than those with gastric and colon cancer (q=5.03, 6.79; P<0.01, respectively). But differences of VEGF levels between gastric and colon cancer were not significant (q=1.90, P>0.05). Whereas, sCD44v6 levels in malignant ascites from patients with ovarian, gastric and colon cancer had no significant difference (q=0.06, 0.91, 0.35; P>0.05, respectirely). In comparison with cirrhotic and tuberculous ascites, when the upper limit of its VEGF mean levels 119.44 pg/ml (70.90±48.54) and sCD44v6 mean levels 63.59 ng/ml (44.42±19.17) was taken as the minimum cutoff limit, the sensitivity and specificity of VEGF and sCD44v6 of this assay to the diagnos is of malignant ascites were 91.3 %, 90.9 % and 73.9 %, 88.7 % respectively.

CONCLUSION: Elevated levels of VEGF and sCD44v6 may be useful in differential diagnosis of benign and malignant ascites.

Dong WG, Sun XM, Yu BP, Luo HS, Yu JP. Role of VEGF and CD44v6 in differentiating benign from malignant ascites. *World J Gastroenterol* 2003; 9(11): 2596-2600
http://www.wjgnet.com/1007-9327/9/2596.asp

INTRODUCTION

Angiogenesis is an absolute requirement for neoplastic growth of solid tumors after tumors reach a critical size of 1-2 mm^3[1], and is also essential for tumor invasion and metastasis, facilitates the shedding of tumor cells into surrounding blood vessels. Tumor cells have been shown to secrete a variety of angiogenic factors and thereby induce local formation of new blood capillaries. Among these factors, vascular endothelial growth factor (VEGF), also called vascular permeability factor (VPF), is a bifunctional cytokine and has the role in enhancing vascular permeability and stimulating endothelial growth[2-5], and is recognized as one of the most important molecules in the growth, invasion, metastasis and recurrence of human tumors[6-9].

However, tumor invasion and metastasis are considered to be a complex and multi-step process. Since the initial observation that a splice variant of CD44 (CD44v) could endow non-metastasizing cells with metastasis potential[10]. Many studies have demonstrated that CD44v, especially splice variant 6 of CD44 (CD44v6), probably promoting cancer cells to adhere to vascular endothelium and base membranes and enhancing moving ability of cancer cells, is most likely responsible for the invasion and metastasis of several tumor systems[11-15].

Malignant ascites is the direct and prominent manifestation of advanced carcinoma metastasized to the peritoneum[16]. Thus it is reasonable to hypothesize that VEGF and CD44v6 can be detected in malignant ascites. In the present study, we measured the concentration of VEGF and soluble CD44v6 (sCD44v6) using an enzyme-linked immunoadsorbent assay (ELISA) in various kinds of ascites in order to assess the value of VEGF and CD44v6 in identifying benign and malignant ascites.

MATERIALS AND METHODS

Patients

A total of 67 inpatients with ascites were collected at Renmin Hospital of Wuhan University, Zhongnan Hospital of Wuhan University and Tumor Hospital in Hubei Province from July 2002 to March 2003(Table 1). Informed consent of the patient and approval of the hospital were provided prior to collection of samples and medical records. All the cases were confirmed by cytologic examination of ascites, pathological examination, B-ultrasound and CT scan, etc.

Table 1 Patient characteristics

Diagnosis	No. of Patients	Mean age (range)	Female / male
Ascite	67	47(19-86)	26 / 41
Cirrhotic ascites	36	48(30-86)	10 / 26
Tuberculous ascites	8	28(19-33)	4 / 4
Carcinoma ascites	23	66(35-76)	12 / 11
Ovarian cancer	8	60(35-70)	8 / 0
Gastric cancer	6	68(38-74)	1 / 5
Colon cancer	5	64(48-71)	2 / 3
Hepatocellular cancer	2	-	0 / 2
Pancreatic cancer	1	-	0 / 1
Primary peritoneal carcinoma	1	-	1 / 0

Sample processing

Ascites samples were collected during therapeutic or diagnostic paracentesis and centrifuged at 3 000 rpm for 15 minutes at 4 ℃. Cell free supernatants were collected and aliquots were stored at -70 ℃ before determination.

Experimental groups

Cirrhotic, tuberculous and malignant ascites were defined as groups 1, 2 and 3, respectively. Malignant ascites from patients with ovarian, gastric and colon cancer were grouped as groups A, B and C, respectively.

Immunoassay for human VEGF

Concentrations of VEGF in ascites were determined with an ELISA kit (R & D Systems) following the manufacturer' s guidelines. All samples were analyzed in the laboratory of the Department of Gastroenterology, Renmin Hospital, Wuhan University. For determination of VEGF, samples were analyzed in duplicate, human recombinant $VEGF_{165}$ was diluted in series and used as a standard. VEGF concentrations were measured according to the standard curve. Samples with VEGF values beyond the standard curve were diluted and reanalyzed.

ELISA for human sCD44v6

Levels of sCD44v6 in ascites were measured with a sCD44v6 ELISA kit (Bender MedSystems, Austria). Briefly, monoclonal antibody against CD44v6, VFF-7, was absorbed by microwells in 96-well microtiter plates. sCD44v6 in the sample or in the standard bound to antibodies was adsorbed by each microwell. Horseradish peroxidase-conjugated monoclonal antibody against CD44v6 was then added and bound to the sCD44v6 that had been captured by the first antibody. After incubation, unbound enzyme conjugated antibodies were removed by washing and a substrate solution was added to each well. A colorful reactive product was formed , the reaction was terminated by addition of acid, and absorbance was measured at 450 nanometers. A standard curve was prepared from six standard dilutions of sCD44v6, which allowed determination of the levels of sCD44v6 in our samples.

Statistical analysis

The data were presented as $\bar{x}\pm s$. One-way analysis of variance was used for statistical analysis. Differences were considered significant when P value was less than 0.05.

RESULTS

Concentrations of VEGF in ascites

Figure 1 shows VEGF levels in malignant ascites (640.74± 264.81 pg/ml), which were significantly higher than those in cirrhotic ascites (67.05±51.91 pg/ml), tuberculous ascites (88.25±24.12 pg/ml) (P<0.01). However, there was no significant difference of VEGF levels between cirrhotic and tuberculous ascites (P>0.05).

Levels of sCD44v6 in ascites

sCD44v6 levels in malignant ascites (89.22±38.20 ng/ml) were higher than those in cirrhotic ascites (44.79±18.02 ng/ml), tuberculous ascites (50.25±12.57 ng/ml) (P<0.01). But the difference of sCD44v6 levels in cirrhotic and tuberculous ascites was not statistically significant (P>0.05) (Figure 2). We found both VEGF and sCD44v6 levels were increased in malignant ascites.

Comparison of VEGF and sCD44v6 levels in different kinds of malignant ascites

Statistical comparison of VEGF and sCD44v6 levels in these kinds of malignant ascites was not performed due to the limited number of hepatocellular cancer (n=2), pancreatic cancer (n=1) and primary peritoneal carcinoma (n=1).

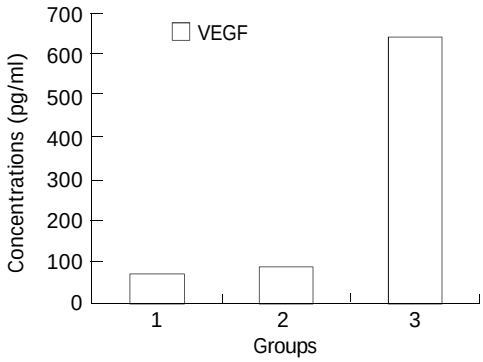

Figure 1 Comparison of VEGF concentrations in different kinds of ascites. Group 1: cirrhotic ascites, Group 2: tuberculous ascites, Group 3: malignant ascites.

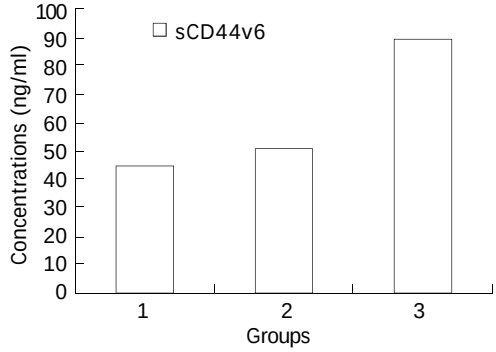

Figure 2 Comparison of sCD44v6 concentrations in different kinds of ascites. Group 1: cirrhotic ascites, Group 2: tuberculous ascites, Group 3: malignant ascites. Concentrations of sCD44v6 in group 3 were significantly higher than those in groups 1 and 2 (P<0.01).

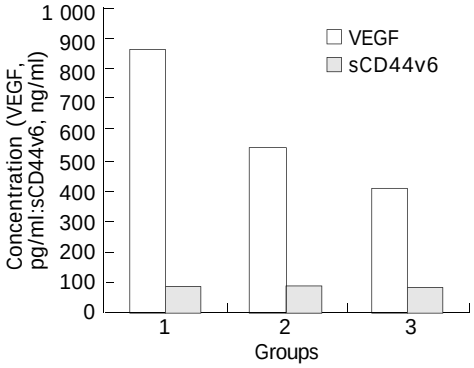

Figure 3 Concentrations of VEGF and sCD44v6 in different kinds of malignant ascites. Group A: ovarian cancer, Group B: gastric cancer, Group C: colon cancer. Concentrations of VEGF in group A were higher than those in groups B and C (P<0.01), while the difference of CD44v6 levels among groups A, B and C was not statistically significant (P>0.05).

Figure 3 shows VEGF levels in ascites from patients with ovarian cancer (866.25±208.46 pg/ml), which were higher than those with gastric cancer (541.30±123.17 pg/ml) and colon cancer (402.80±140.10 pg/ml), respectively (P<0.01). There was no significant difference of VEGF levels between gastric and colon cancer (P>0.05). Whereas, no statistical difference of sCD44v6 levels in ascites of patients with ovarian cancer

(89.42±25.70 ng/ml), gastric cancer (83.91±32.62 ng/ml) and colon cancer (80.10±9.97 ng/ml) was found (P>0.05).

Additionally, in our study, 2 out of 4 unidentified ascites cases were identified by peritoneum biopsy as metastatic ovarian cancer and primary peritoneal carcinoma. In these two cases, the levels of VEGF exceeded 1 200 pg/ml, and sCD44v6 levels exceeded 100 ng/ml. Another 2 cases of gastric and colon cancer, were identified by gastroscopy and colonoscopy, respectively. The concentration of VEGF and sCD44v6 in these 2 cases exceeded 650pg/ml and 80ng/ml respectively.

Sensitivity and specificity of VEGF and sCD44v6 levels to diagnosis of malignant ascites

Using benign ascites including cirrhotic and tuberculous ascites as control, and the upper limit of its VEGF mean levels, 119.44 pg/ml (70.90±48.54), as positive boundary value, 21 out of 23 malignant ascites cases and 4 out of 44 benign ascites cases exceeded the boundary line. So the sensitivity and specificity of this assay to the diagnosis of malignant ascites were 91.3 % (21/23) and 90.9 %(40/44), respectively, and calculated positive value, negative value and accurate rate were 84.0 %(21/25), 95.2 %(40/42) and 91.0 %(61/67), respectively. With same method, the sensitivity, specificity, positive value, negative value and accurate rate of sCD44v6 to the diagnosis of malignant ascites were 73.9 %(17/23), 88.7 % (39/44), 77.3 %(17/22), 86.4 %(39/45) and 83.4 % (56/67), respectively.

DISCUSSION

Human VEGF could be expressed in at least 5 isoforms, which have 206, 189, 165, 145 and 121 amine acids, respectively[17]. It is a multifunctional cytokine that has potent angiogenic activity and enhances microvascular permeability by direct action on vascular endothelium, promoting tumor growth and metastasis[18,19]. Strong VEGF expression has been demonstrated in various solid tumor types, including gastric[20-24], colorectal[25,26] and ovarian carcinomas[27,28]. Recently, substantial evidences indicated that serum concentration of VEGF was increased in cancerous patients[29-32]. Although some studies showed that VEGF levels were high in malignant ascites[30,33], its value to the diagnosis of malignant ascites has not been elucidated.

In the present study, we found that VEGF protein levels in malignant ascites were markedly higher than those in benign ascites, which were consistent with the previous results[30,33], and possessed a high sensitivity and specificity to the diagnosis of malignant ascites. Meanwhile, we also found that VEGF levels in malignant ascites in patients with ovarian cancer were higher than those in patients with gastric or colon cancer. No significant difference of VEGF levels was observed among those with gastric and colon cancer. Additionally, although the number of cases studied in our experiment was small, extremely increased VEGF levels in ascites of patients with ovarian cancer (n=8) and primary peritoneal carcinoma (n=1) could be measured. These data suggested that VEGF levels in ascites could reflect tumor biological behavior to a great extent, and cells of ovarian cancer and primary peritoneal carcinoma might secrete VEGF into peritoneal cavity directly[27]. Most importantly, detection of VEGF levels could provide a new approach for differential diagnosis of benign and malignant ascites, which remains a knotty problem all the time[34,35]. Moreover, detecting VEGF levels may contribute to the diagnosis of primary cancer that causes malignant ascites to a certain extent.

CD44 is an integral cell membrane glycoprotein, and is known to function in homing of lymphocytes, cell adhesion, activation of leukocytes and migration of cells. At least 20 variants (v) of CD44 have been reported due to the alternative splicing of 10 exons (v1-v10) that encode the membrane's proximal portion of the extracellular domain[36-38]. NH2-terminal function area of CD44 on the surface of cells could join the hyaluronate in the basement membrane to extracellular matrix, thus regulate the movement and function of cells. By this mechanism, neoplastic cells could adhere to the extracellular matrix and basement membrane of the host cell, resulting in invasion and metastasis of malignancy. On the other hand, the degraded products of hyaluronic acid could motivate the growth of local vessels, providing the basis for invasion and metastasis[39,40]. Many studies have reported that expression of CD44v, especially CD44v6, was correlated with invasion and metastasis of certain type of human cancer[11,40-47], including gastric cancer[48-50], colorectal cancer[51-53], ovarian cancer[54] and prostate cancer[55]. Furthermore, serum concentrations of sCD44v6 were found to be significantly increased in patients with advanced carcinoma[13,15,56]. To our knowledge, however, concentration of sCD44v6 has not been examined in malignant ascites, this might be the first study to document sCD44v6 in malignant ascites.

We found sCD44v6 levels were high in malignant ascites, and relatively low in nonmalignant ascites. It implies that elevated CD44v6 appears to be correlated to the invasion and metastasis of cancer cells into peritoneal cavity. But it is unclear why CD44v6 is closely associated with malignant ascites. The ability of CD44v6 to bind peritoneal mesothelial surfaces of abdominal cavity, and a subsequent cancer cell implantation may contribute to it. At the same time, our results showed a higher sensitivity and specificity of sCD44v6 to the diagnosis of malignant ascites. However, no evidence is available to show that detection of sCD44v6 could contribute to the determination of a potential primary cancer causing malignant ascites. It is reasonable to consider sCD44v6 may be a diagnostic index of malignant ascites.

In summary, VEGF and sCD44v6 are detectable in ascites and are significantly elevated in malignant ascites. Prospective monitoring of VEGF and sCD44v6 levels in ascites would be helpful in differential diagnosis of benign and malignant ascites.

REFERENCES

1 **Folkman J**, Watson K, Ingber D, Hanahan D. Induction of angiogenesis during the transition from hyperplasia to neoplasia. *Nature* 1989; **339**: 58-61

2 **Masood R**, Cai J, Zheng T, Smith DL, Hinton DR, Gill PS, Folkman J. Vascular endothelial growth factor (VEGF) is an autocrine growth factor for (VEGF) receptor-positive human tumors. *Blood* 2001; **98**: 1904-1913

3 **Leung DW**, Cachianes G, Kuang WJ, Goeddel DV, Ferrara N. Vascular endothelial growth factor is a secreted angiogenic mitogen. *Science* 1989; **246**: 1306-1309

4 **Senger DR**, Galli SJ, Dvorak AM, Perruzzi CA, Harvey VS, Dvorak HF. Tumor cells secreted a vascular permeability factor that promotes accumulation of ascitic fluid. *Science* 1983; **219**: 983-985

5 **Connolly DT**, Heuvelman DM, Nelson R, Olander JV, Eppley BL, Delfino JJ, Siegel NR, Leimgruber RM, Feder J. Tumor vascular permeability factor stimulates endothelial cell growth and angiogenesis. *J Clin Inves* 1989; **84**: 1470-1478

6 **Che X**, Hokita S, Natsugoe S, Tanabe G, Baba M, Takao S, Aikou T. Tumor angiogenesis related to growth pattern and lymph node metastasis in early gastric cancer. *Chin Med J* 1998; **111**: 1090-1093

7 **Erenoglu C**, Akin ML, Uluutku H, Tezcan L, Yildirim S, Batkin A, Erenogku C. Angiogenesis predicts poor prognosis in gastric carcinoma. *Dig Surg* 2000; **17**: 581-586

8 **Yoshikawa T**, Yanoma S, Tsuburaya A, Kobayashi O, Sairenji

M, Motohashi H, Noguchi Y. Angiogenesis inhibitor, TNP-470, suppresses growth of peritoneal disseminating foci. *Hepatogastroenterology* 2000; **47**: 298-302

9 **Xiangming C**, Hokita S, Natsugoe S, Tanabe G, Baba M, Takao S, Kuroshima K, Aikou T. Angiogenesis as an unfavorable factor related to lymph node metastasis in early gastric cancer. *Ann Surg Oncol* 1998; **5**: 585-589

10 **Gunthert U**, Hofmann M, Rudy W, Reber S, Zoller M, Haussmann I, Matzku S, Wenzel A, Ponta H, Herrlich P. A new variant of glycoprotein CD44 confers metastatic potential to rat carcinoma cells. *Cell* 1991; **65**: 13-24

11 **Sleeman J**, Moll J, Sherman L, Dall P, Pals ST, Ponta H, Herrlich P. The role of CD44 splice variants in human metastatic cancer. *Ciba Found Symp* 1995; **189**: 142-156

12 **Harn HJ**, Ho LI, Chang JY, Wu CW, Jing SY, Lee HS, Lee WH. Differential expression of the human metastasis adhesion molecule CD44V in normal and carcinomatous stomach mucosa of Chinese subjects. *Cancer* 1995; **75**: 1065-1071

13 **Harn HJ**, Ho Li, Shyu RY. Soluble CD44 isoforms in serum as potential markers of metastatic gastric carcinoma. *J Clin Gastroenterol* 1996; **22**: 107-110

14 **Fichtner I**, Dehmel A, Naundorf H, Finker LH. Expression of CD44 standard and isoforms in human breast cancer xenografts and shedding of soluble forms into serum of nude mice. *Anticancer Res* 1997; **17**: 3633-3645

15 **Zeimet AG**, Widschwendter M, Uhl-Steidl M, Muller-Holzner E, Daxenbichler G, Marth C, Dapunt O. High serum levels of soluble CD44 variant isoform are associated with favorable clinical outcome in ovarian cancer. *Br J Cancer* 1997; **76**: 1646-1651

16 **Enck RE**. Malignant ascites. *Am J Hosp Palliat Care* 2002; **19**: 7-8

17 **Neufeld G**, Cohen T, Gengrinovitch S, Poltorak Z. Vascular endothelial growth factor (VEGF) and its receptors. *FASEB J* 1999; **13**: 9-22

18 **Roussea S**, Houle F, Landry J, Huot J. P38MAP kinase activation by vascular endothelial growth factor mediates actin reorganization and cell migration in human endothelial cells. *Oncogene* 1997; **15**: 2169-2177

19 **Brock TA**, Dvorak HF, Senger DR. Tumor-secreted vascular permeability factor increased cytosolic Ca^{++} AND Von Willebrand factor release in human endothelial cells. *Am J Pathol* 1991; **138**: 213-221

20 **Tao HQ**, Lin YZ, Wang RN. Significance of vascular endothelial growth factor messenger RNA expression in gastric cancer. *World J Gastroenterol* 1998; **4**: 10-13

21 **Konno H**, Baba M, Tanaka T, Kamiya K, Ota M, Oba K, Shoji A, Kaneko T, Nakamura S. Overexpression of vascular endothelial growth factor is responsible for the hematogenous recurrence of early-stage gastric carcinoma. *Eur Surg Res* 2000; **32**: 177-181

22 **Ichikura T**, Tomimatsu S, Ohkura E, Mochizuki H. Prognostic significance of vascular endothelial growth factor (VEGF) and VEGF-C in gastric carcinoma. *J Surg Oncol* 2001; **78**: 132-137

23 **Kabashima A**, Maehara Y, Kakeji Y, Sugimachi K. Overexpression of vascular endothelial growth factor C is related to lymphogenous metastasis in early gastric carcinoma. *Oncology* 2001; **60**: 146-150

24 **Tian XJ**, Wu J, Meng L, Dong ZW, Shou CC. Expression of VEGF-121 in gastric carcinoma MGC803 cell line. *World J Gastroenterol* 2000; **6**: 281-283

25 **Zhao MF**, Mao H, Zhen JX, Yuan YW. Effect of vascular endothelial growth factor on adhesion of large intestine cancer cell HT-29. *Shijie Huaren Xiaohua Zazhi* 2000; **8**: 646-649

26 **Ishigami SI**, Arii S, Furutani M, Niwano M, Harada T, Mizumoto M, Mori A, Onodera H, Imamura M. Predictive value of vascular endothelial growth factor in metastasis and prognosis of human colorectal cancer. *Br J Cancer* 1998; **78**: 1379-1384

27 **Santin AD**, Hermonat PL, Ravaggi A, Cannon MJ, Pecorelli S, Parham GP. Secretion of vascular endothelial growth factor in ovarian cancer. *Eur J Gynaecol Oncol* 1999; **20**: 177-181

28 **Yamamoto S**, Konishi I, Mandai M, Kuroda H, Komatsu T, Nanbu K, Sakahara H, Mori T. Expression of vascular endothelial growth factor (VEGF) in epithelial ovarian neoplasms: correlation with clinicopathology and patient survival, and analysis of serum VEGF levels. *Br J Cancer* 1997; **75**: 1221-1227

29 **Dirix LY**, Vermeulen PB, Pawinski A, Prove A, Benoy I, De Pooter C, Martin M, Van Oosterom AT. Elevated levels of the angiogenic cytokines basic fibroblast growth factor and vascular endothelial growth factor in sera of cancer patients. *Br J Cancer* 1997; **78**: 238-243

30 **Kraft A**, Weindel K,Ochs A, Marth C, Zmija J, Schumacher P, Unger C, Marme D, Gastl G. Vascular endothelial growth factor in the sera and effusion of patients with malignant and nonmalignant disease. *Cancer* 1999; **85**: 178-187

31 **Zhang HT**, Hu S. Relationship between VEGF in the sera and invasion and metastasis of gastric cancer. *Shijie Huaren Xiaohua Zazhi* 2003; **11**: 344-345

32 **Mao ZB**, Xiao MB, Huang JF, Ni HB, Ni RZ, Wei Q, Zhang H. Expression of VEGF in the sera of patients with gastric cancer. *Shijie Huaren Xiaohua Zazhi* 2002; **10**: 1220-1221

33 **Zebrowski BK**, Liu W, Ramirez K, Akagi Y, Mills GB, Ellis LM. Markedly elevated levels of vascular endothelial growth factor in malignant ascites. *Ann Surg Oncol* 1999; **6**: 373-378

34 **Aslam N**, Marino CR. Malignant ascites: new concepts in pathophysiology, diagnosis, and management. *Arch Intern Med* 2001; **161**: 2733-2737

35 **Tamsma JT**, Keizer HJ, Meinders AE. Pathogenesis of malignant ascites: Starling's law of capillary hemodynamics revisited. *Ann Oncol* 2001; **12**: 1353-1357

36 **Screaton GR**, Bell MV, Jackson CG, Cornelis FB, Ferth U, Bell JI. Genomic structure of DNA encoding the lymphocyte homing receptor CD44 reveals at least 12 alternatively spliced exons. *Proc Natl Acad Sci U S A* 1992; **89**: 12160-12164

37 **Harn HJ**, Isola N, Cooper DL. The multispecific cell adhesion molecule CD44 is represented in reticulocyte cDNA. *Biochem Biophys Res Commun* 1991; **178**: 1127-1134

38 **Herrlich P**, Zoller M, Pals ST, Ponta H. CD44 splice variants: metastases meet lymphocytes. *Immunol Today* 1993; **14**: 395-399

39 **Strobel T**, Swanson L, Cannistra SA. *In vivo* inhibition of CD44 limits intra-abdominal spread of a human ovarian cancer xenograft in nude mice. *Cancer Res* 1997; **57**: 1228-1232

40 **Weber GF**, Bronson RT, Ilagan J, Cantor H, Schmits R, Mak TW. Absence of the CD44 gene prevents sarcoma metastasis. *Cancer Res* 2002; **62**: 2281-2286

41 **Chen GY**, Wang DR. The expression and clinical significance of CD44v in human gastric cancers. *World J Gastroenterol* 2000; **6**:125-127

42 **Xin Y**, Zhao FK, Zhang SM, Wu DY, Wang YP, Xu L. Relationship beteeen CD44v6 expression and prognosis in gastric carcinoma patients. *Shijie Huaren Xiaohua Zazhi* 1999; **7**: 210-214

43 **Gu HP**, Ni CR, Zhang RZ. Relationship of expressions of CD15, CD44v6 and nm23 H1 mRNA with metastasis and prognosis of colon carcinoma. *Shijie Huaren Xiaohua Zazhi* 2000; **8**: 887-891

44 **Mi JQ**, Zhang ZH, Sheng MC. Significance of CD44v6 protein expression in gastric carcinoma and precancerous lesions. *Shijie Huaren Xiaohua Zazhi* 2000; **8**: 156-158

45 **Liu YH**, Liu JZ, Xiao B, Wang SX. The clinical significance of CD44v6 abnormal expression in gastric cancer. *Shijie Huaren Xiaohua Zazhi* 2001; **9**: 89-90

46 **Wu LY**, Hao YD, Shi ML. Relationship between CD44v6 expression and biological behavior of gastric cancer. *Shijie Huaren Xiaohua Zazhi* 1999; **7**: 1034

47 **Xiao CZ**, Dai YM, Yu HY, Wang JJ, Ni CR. Relationship between expression of CD44v6 and nm23-H1 and tumor invasion and metastasis in hepatocellular carcinoma. *World J Gastroenterol* 1998; **4**: 412-414

48 **Yamaguchi A**, Coi T, Yu J, Hirono Y, Ishida M, Lida A, Kimura T, Takeuchi K, Katayama K, Hirose K. Expression of CD44v6 in advanced gastric cancer and its relationship to hematogenous metastasis and long-term prognosis. *J Surg Oncol* 2002; **79**: 230-235

49 **Sun XW**, Shen BZ, Shi MS, Dai XD. Relationship between CD44v6 expression and risk factors in gastric carcinoma patients. *Shijie Huaren Xiaohua Zazhi* 2002; **10**: 1129-1132

50 **Chen ZF**, Deng CS, Xia B, Zhu YQ, Zeng J, Gong LL. Expression of heat shock protein 60, CD44v6 splice variant in human gastric cancer. *Shijie Huaren Xiaohua Zazhi* 2001; **9**: 988-991

51 **Masaki T**, Goto A, Sugiyama M, Matsuoka H, Abe N, Sakamoto A, Atomi Y. Possible contribution of CD44 variant 6 and nuclear beta-catenin expression to the formation of budding tumor cells in patients with T1 colorectal carcinoma. *Cancer* 2001; **92**: 2539-2546

52 **Xu SH**, Feng JG, Li DC, Mou HZ, Lou RC. Relationship between CD44 in the peripheral blood of patients with colorectal cancer and clinicopathological features. *Shijie Huaren Xiaohua Zazhi* 2000; **8**: 432-435

53 **Cai Q**, Lu HF, Sun MJ, Du X, Fan YZ, Shi DR. Expression of CD44 v3 and v6 proteins in human colorectal carcinoma and its relevance with prognosis. *Shijie Huaren Xiaohua Zazhi* 2000; **8**: 1255-1258

54 **Schiffenbauer YS**, Meir G, Maoz M, Even-Ram SC, Bar-shavit R, Neeman M. Gonadotropin stimulation of MLS human epithelial ovarian carcinoma cells augments cell adhesion mediated by CD44 and by alpha (v)-integrin. *Gynecol Oncol* 2002; **84**: 296-302

55 **Ekici S**, Ayhan A, Kendi S, Ozen H. Determination of prognosis in patients with prostate cancer treated with radical prostatectomy: prognostic value of CD44v6 score. *J Urol* 2002; **167**: 2037-2041

56 **Saito H**, Tsujitani S, Katano K, Ikeguchi M, Maeta M, Kaibara N. Serum concentration of CD44 variant 6 and its relation to prognosis in patients with gastric carcinoma. *Cancer* 1998; **83**: 1095-1101

Edited by Ren SY and Wang XL

P.O.Box 2345, Beijing 100023,China
Fax: +86-10-85381893
E-mail: wjg@wjgnet.com www.wjgnet.com

World J Gastroenterol 2003;9(11):2601-2604
World Journal of Gastroenterology
 ISSN 1007-9327

• CLINICAL RESEARCH •

Effects of bowel rehabilitation and combined trophic therapy on intestinal adaptation in short bowel patients

Guo-Hao Wu, Zhao-Han Wu, Zhao-Guang Wu

Guo-Hao Wu, Zhao-Han Wu, Zhao-Guang Wu, Department of General Surgery, Zhongshan Hospital, Fu Dan University, Shanghai, 200032, China
Correspondence to: Guo-Hao Wu, Department of General Surgery, Zhongshan Hospital, Fu Dan University, Shanghai 200032, China. wugh@zshospital.net
Telephone: +86-21-64041990 Ext 2365 **Fax:** +86-21-64038472
Received: 2003-03-12 **Accepted:** 2003-05-11

Abstract

AIM: To evaluate the effects of bowel rehabilitation and combined trophic therapy on intestinal adaptation in short bowel patients.

METHODS: Thirty-eight patients with severe short-bowel syndrome (SBS) were employed in the present study, whose average length of jejunum-ileum was 35.8±21.2 cm. The TPN treatment was initiated early to attain positive nitrogen balance and prevent severe weight loss. The TPN composition was designated to be individualized and altered when necessary. Enteral feeding was given as soon as possible after resection and increased gradually. Meals were distributed throughout the day. Eight patients received treatment of growth hormone (0.14 mg/kg.day) and glutamine (0.3 g/kg.day) for 3 weeks. D-xylose test, ^{15}N-Gly trace test and ^{13}C-palmitic acid breath test were done to determine the patients' absorption capability.

RESULTS: Thirty-three patients maintained well body weight and serum albumin concentration. The average time of follow-up for 33 survival patients was 5.9±4.3 years. Twenty-two patients weaned from TPN with an average TPN time of 9.5±6.6 months. Two patients, whose whole small bowel, ascending and transverse colon were resected received home TPN. An other 9 patients received parenteral or enteral nutritional support partly as well as oral diet. Three week rhGH+GLN therapy increased nutrients absorption but the effects were transient.

CONCLUSION: By rehabilitation therapy, most short bowel patients could wean from parenteral nutrition. Dietary manipulation is an integral part of the treatment of SBS. Treatment with growth hormone and glutamine may increase nutrients absorption but the effects are not sustained beyond the treatment period.

Wu GH, Wu ZH, Wu ZG. Effects of bowel rehabilitation and combined trophic therapy on intestinal adaptation in short bowel patients. *World J Gastroenterol* 2003; 9(11): 2601-2604
http://www.wjgnet.com/1007-9327/9/2601.asp

INTRODUCTION

Short-bowel syndrome (SBS) is resulted from extensive small bowel resection due to infarction of the mesenteric vessels, intestinal volvulus, trauma, malignancy, or from complications of Crohn's disease, and is defined as the manifestations of signs, symptoms and complications associated with the inadequate absorptive surface area of functional bowel[1]. It is usually characterized by severe diarrhea, malabsorption, dehydration, electrolyte and metabolic disturbances, and progressive malnourishment.

The pathophysiological consequences following extensive intestinal resection depend on the length and site of resection and the extent of adaptation of the remaining intestine[2-4]. Patients often have to be supported with total parenteral nutrition (TPN) until maximal adaptation of the residual small bowel is complete. This process can take place for up to a year and sometimes longer. Certain patients may require lifelong TPN support depending on the length and health of the residual small bowel. TPN is associated with certain complications, which include catheter sepsis and liver failure[5-8]. It is therefore important for dietary management and pharmacological treatment in the short bowel patients hopefully to wean from TPN. Dietary management and some trophic factors are important in promoting intestinal adaptation after resection. The aim of the study was to define the role of bowel rehabilitation, trophic factors in intestinal adaptation in short bowel patients.

MATERIALS AND METHODS

Patients

Thirty-eight patients (28 men, 10 women; mean age 38.0±16.0 years, range 7-68 years) with severe short-bowel syndrome were eligible for this study. All patients had previously undergone extensive bowel resection for intestinal volvulus, mesenteric infarction or inflammatory bowel disease with or without colonic resection. The average length of jejunum-ileum, as determined from operative reports and confirmed by perioperative radiographs, was 35.8±21.2 cm (range, 0-110 cm) in all patients. Two patients had entire jejunum, ileum and right colon resected. The ileocecal valve and a portion of colon were resected in 13 patients, and 25 patients had intact colon (Table 1). The patients were clinically stable, and did not demonstrate evidence of infection, or extradigestive organ failure. In addition, they did not have a history of cancer. The protocol for the present study was approved by the Ethics Committee of Zhongshan Hospital.

Bowel rehabilitation

Clinical management Massive fluid and electrolyte losses were noted due to transient gastric hypersecretion and profound diarrhea during the initial postoperative periods. So, initial postoperative treatment was designed to maintain adequate fluid and electrolyte balance. TPN began early to attain positive nitrogen balance and to prevent severe weight loss. It should continue until the adaptive processes were complete or indefinitely, if clinically indicated. The composition of TPN was individualized and altered when necessary. Caloric requirements were delivered in accordance with the resting energy expenditure of patients, and it was reassessed often as the patient's clinical condition warranted. As the patient's oral

intake increased, the amount of TPN was reduced, the frequency of TPN was reduced to every other day in the first week, three times in the next week, and twice during the third week. If the patient lost 1 kg/week or more or if diarrhea exceeded 600 g/day or if laboratory abnormalities developed, then the patients were placed back on TPN. If the patient's eventual adaptation was insufficient to allow survival on oral/enteral feeding alone, the patients usually required lifelong TPN support.

Patients with SBS received at least some enteral feeding as soon as possible after resection. Usually this was administered for a postoperative period of 7-10 days. The ideal composition of enteral formulas for patients with SBS was also dependent upon the length of the small bowel and the presence of a colon. Originally, elemental and peptide based enteral formulas were favored for patients with SBS. Gradually, the diet with intact protein nutrient formulas and dietary fiber was given in accordance with the patients' need. Meals were distributed throughout the day.

Combined trophic therapy

Eight patients (4 males, 4 females, mean age 36±8 years) with severe SBS (mean jejunoileal length 44 cm, range 0 to 80 cm)

Table 1 Patient characteristics and status

Patient No.	Gender	Age(a)	Cause of resection	Jejunum-ileum(cm)	Colon	TPN(a)	Current status	Survival time(a)
1	F	28	Small bowel volvulus	0	ACR	17	HPN	17
2	M	7	Small bowel volvulus	0	ACR	7.6	HPN	7.6
3	M	41	Small bowel volvulus	35	All	0.8	Normal oral diet	13.5
4	M	61	SMA thrombosis	30	All	1.6	Died	2.2
5	M	62	SMA thrombosis	30	All	2.0	Died	2.6
6	M	33	Small bowel volvulus	28	All	1.2	Normal oral diet	14.4
7	M	24	Small bowel volvulus	18	All	1.8	PN+EN	1.8
8	M	35	Small bowel volvulus	45	All	0.5	Died	6.2
9	F	52	Small bowel volvulus	55	ICV(-)	0.3	Died	7.4
10	F	68	SMA thrombosis	70	ICV(-)	0.6	Normal oral diet	9.5
11	F	44	Small bowel obstruction	100	All	0.2	Normal oral diet	9.6
12	M	22	Crohn's disease	80	ICV(-)	0.5	Normal oral diet	12.2
13	M	15	Small bowel volvulus	20	ICV(-)	5.2	Died	5.4
14	M	50	Small bowel obstruction	60	ICV(-)	1.2	Normal oral diet	9.0
15	F	42	Small bowel volvulus	28	All	2.2	PN+oral diet	8.5
16	F	44	Small bowel volvulus	35	ICV(-)	1.0	Normal oral diet	10.8
17	M	59	Small bowel volvulus	30	All	1.2	Normal oral diet	6.4
18	F	50	SMA thrombosis	60	ICV(-)	0.4	Normal oral diet	5.4
19	M	55	SMA thrombosis	40	ICV(-)	1.0	Normal oral diet	7.6
20	M	56	Small bowel volvulus	30	All	0.8	PN+oral diet	4.5
21	M	26	Small bowel volvulus	30	All	1.0	Normal oral diet	8.8
22	M	40	Small bowel obstruction	50	ICV(-)	0.6	Normal oral diet	6.0
23	M	16	Small bowel volvulus	30	All	1.5	Normal oral diet	12.5
24	M	28	Small bowel volvulus	30	All	2.0	Normal oral diet	5.5
25	M	57	SMA thrombosis	45	All	0.3	Normal oral diet	6.5
26	M	34	Crohn's disease	60	All	0.5	Normal oral diet	4.0
27	M	41	Crohn's disease	70	All	0.4	Normal oral diet	2.0
28	M	30	Small bowel volvulus	40	All	0.2	Normal oral diet	1.8
29	M	62	SMA thrombosis	50	ICV(-)	0.8	EN+ oral diet	1.6
30	F	45	Small bowel volvulus	30	All	0.5	EN+ oral diet	1.5
31	M	18	Small bowel volvulus	30	All	0.4	Normal oral diet	2.0
32	M	20	Small bowel volvulus	30	All	0.5	Normal oral diet	2.0
33	M	16	Small bowel volvulus	20	All	1.0	EN+ oral diet	1.5
34	M	36	Small bowel volvulus	30	All	0.4	EN+ oral diet	1.2
35	M	18	Small bowel volvulus	18	All	0.6	HPN+ oral diet	2.6
36	F	46	SMA thrombosis	40	ICV(-)	0.5	EN+ oral diet	0.5
37	M	32	Small bowel volvulus	35	All	0.3	Normal oral diet	1.8
38	F	30	Small bowel volvulus	30	All	0.2	Normal oral diet	1.0
Mean		38±16		35.8±21.2		9.5±6.6		5.9±4.3

ACR=ascending colon resection, ICV(-)=without ileal cecal valve, HPN=home parenteral nutrition, PN=parenteral nutrition, EN=enteral nutrition, a=year.

Table 2 Absorption capability of patients before and after treatment with GH+GLN

	Baseline	End of therapy	One week after therapy
D-xylose test (%)	5.4±2.1	7.6±1.8[a]	6.0±2.0[b]
^{15}N-Gly trace test (%)	62.4±14.2	73.2±15.3[a]	58.4±11.8[b]
^{13}C-palmitic acid breath test (%)	55.3±8.8	64.5±11.2[a]	62.6±10.4[b]

Values are mean ±SEM, [a]$P<0.05$ *vs* baseline, [b]$P>0.05$ *vs* baseline.

who previously adapted to the provision of TPN and enteral feedings were admitted for 0.8±0.5 years in the study after surgical resection. The first week served as a control period when nutritional (parenteral and enteral) and medical managements were delivered as the routine therapy. Thereafter, the patients who received treatment of subcutaneous recombinant human growth hormone (rhGH) (0.14 mg/kg.day; Saizen, Serono Co., Switzerland) were divided into two daily injections, intravenous alanyl-glutamine solution (0.3 g/kg.day, Dipeptiven, Fresenius Co., Germany) was delivered daily for 3 weeks. D-xylose test, ^{15}N-Gly trace test and ^{13}C-palmitic acid breath test were done respectively before, at the end of therapy and one week after treatment to determine the patients' absorption capability.

Statistical analysis

Data were analyzed using standard statistical software (SPSS 10.0). For normally distributed data, a paired Student' s *t* test was used for statistical analysis. A probability value less than or equal to 0.05 was considered statistically significant. Data are expressed as mean ±SEM.

RESULTS

Thirty-eight patients were admitted and received nutritional support and rehabilitation therapy, among them 2 died of severe malnutrition 2 years after treatment because they failed to receive nutritional therapy, 2 died of accidental event, 1 died of liver failure 5 years later. Thirty-three patients maintained well body weight and serum albumin concentration. The average time of follow-up for 33 survival patients was 5.9±4.3 years (range, 0.5-17 years). Twenty-two patients weaned from TPN, their average TPN time was 9.5±6.6 months. They maintained their nutritional status well on normal oral diet. Two patients, whose whole small bowel, ascending and transverse colon were resected received home TPN. An other 9 patients received parenteral or enteral nutritional support partly as well as oral diet (Table 1). Eight patients developed gall bladder stones. Cholecystectomy was performed for three patients.

For the eight patients, the 3 week rhGH+GLN therapy resulted in weight gain, and stool output dramatically decreased. Three patients weaned from TPN completely after the treatment period, 3 patients reduced TPN requirements, and 2 patients failed the therapy. The absorption capability of D-xylose, ^{15}N-Gly and ^{13}C-palmitic acid in these SBS patients was much lower than normal level. After 3 week rhGH+GLN therapy, the absorption capability of D-xylose, ^{15}N-Gly and ^{13}C-palmitic acid improved. However, it dropped to the level of baseline at one week after treatment (Table 2).

DISCUSSION

After extensive resection of the small intestine, the remaining bowel, to some degree, had a significant adaptation response to resection. Bowel adaptation, characterized by epithelial hyperplasia and increase in villus diameter, height, and crypt depth, occurred weeks to months after resection[9-11]. Various nutritional and medical therapies can be tried to improve bowel absorptive capacity. TPN is the most important factor responsible for prolonging the lives of patients with SBS. In the initial stages after massive resection of bowel, TPN should begin early to attain positive nitrogen balance and to prevent severe weight loss[12,13]. TPN has been shown to greatly increase the chances of long-term survival. It should be delivered until the adaptive processes were complete or indefinitely, if clinically indicated[14]. This process can take place for up to a year and sometimes longer. Long-term TPN resulted in small bowel mucosa atrophy and was associated with certain complications, such as catheter sepsis and liver failure[15]. So, oral diet is encouraged, if there is any absorptive capacity of the remaining bowel, bowel adaptation should be promoted. An enteral tube feeding might be used to supplement the diet in an effort to wean patients from TPN[16]. At first, diluted solutions of chemically defined diets containing simple amino acids and short-chain peptides were offered. Gradually, the diet with intact protein nutrient formulas and dietary fiber was given in accordance with the patients' need. The parenteral supply had to be adjusted according to the oral intake. As the patient' s oral intake increased, the amount of TPN was reduced, the frequency of TPN was reduced to every other day for 1 week, three times in the next week, and twice during the third week or weaned from TPN at last[17]. If the patient lost or more 1 kg/week of body weight or more, if diarrhea exceeded 600 g/day or if laboratory abnormalities developed, then the patients were placed back on TPN[18]. In our group, 22 patients weaned from TPN among the 33 survived patients after receiving rehabilitation therapy. They maintained their nutritional status well on normal oral diet. It indicated that rehabilitation therapy for SBS played important roles in the intestinal adaptation.

Combination of glutamine, human recombinant growth hormone has been shown to influence bowel adaptation[19-24]. The study by Byrne *et al*[25,26] indicated that at one year of follow-up 40 % of treated patients were able to reduce or discontinue parenteral nutrition. Patients in the study were also receiving other medical therapy, including medications known to slow down intestinal motility and oral rehydration solutions. It is not clear whether glutamine, growth hormone, diet, or other factors contributed to the favorable outcome. It did not necessarily mean that fluid and nutrients absorption was increased because absorptive studies were not performed. Szkudlarek *et al*[27] reported in a randomized control study of eight short-bowel patients the combination of growth hormone and glutamine for 28 days did not result in a significant increase in fluid or nutrient absorption. In our clinical trial, we used D-xylose test, ^{15}N-Gly trace test and ^{13}C-palmitic acid breath test to determine the patients' nutrient absorption capability. The results showed that the absorption of carbohydrates (from 5.4 % to 7.6 %), protein (from 62.4 % to 73.2 %) and fat (from 55.3 % to 64.5 %) increased. Weight gain was observed and stool output dramatically decreased. Three patients weaned from TPN completely after the treatment period and 3 patients reduced TPN requirements. However, the absorption capability dropped to the level of baseline at one week after treatment. We found that the treatment with growth hormone and glutamine might increase absorption of nutrients but the effect seemed to be transient with no long term improvement in gut function when treatment was discontinued. This has been supported by recent clinical studies[28-30].

In conclusion, by rehabilitation therapy, most short bowel patients could wean from parenteral nutrition. Dietary manipulation is an integral part of the treatment of SBS. Treatment with growth hormone and glutamine may increase nutrients absorption but the effects are not sustained beyond the treatment period. Therapeutic efficacy can be achieved only when the treatment plan is tailored to meet individual need.

REFERENCES

1 **Thompson JS**. Comparison of massive vs. repeated resection leading to short bowel syndrome. *J Gastrointest Surg* 2000; **4**: 101-104

2 **Jeppesen PB**, Mortensen PB. Enhancing bowel adaptation in short bowel syndrome. *Curr Gastroenterol Rep* 2002; **4**: 338-347

3 **Welters CF**, Dejong CH, Deutz NE, Heineman E. Intestinal

adaptation in short bowel syndrome. *ANZ J Surg* 2002; **72**: 229-236
4 **Wasa M**, Takagi Y, Sando K, Harada T, Okada A. Intestinal adaptation in pediatric patients with short-bowel syndrome. *Eur J Pediatr Surg* 1999; **9**: 207-209
5 **Sondheimer JM**, Asturias E, Cadnapaphornchai M. Infection and cholestasis in neonates with intestinal resection and long-term parenteral nutrition. *J Pediatr Gastroenterol Nutr* 1998; **27**: 131-137
6 **Burstyne M**, Jensen GL. Abnormal liver functions as a result of total parenteral nutrition in a patient with short-bowel syndrome. *Nutrition* 2000; **16**: 1090-1092
7 **Terra RM**, Plopper C, Waitzberg DL, Cukier C, Santoro S, Martins JR, Song RJ, Gama-Rodrigues J. Remaining small bowel length: association with catheter sepsis in patients receiving home total parenteral nutrition: evidence of bacterial translocation. *World J Surg* 2000; **24**: 1537-1541
8 **Candusso M**, Faraguna D, Sperli D, Dodaro N. Outcome and quality of life in paediatric home parenteral nutrition. *Curr Opin Clin Nutr Metab Care* 2002; **5**: 309-314
9 **Schulzke JD**, Schmitz H, Fromm M, Bentzel CJ, Riecken EO. Clinical models of intestinal adaptation. *Ann N Y Acad Sci* 1998; **859**: 127-138
10 **Kvietys PR**. Intestinal physiology relevant to short-bowel syndrome. *Eur J Pediatr Surg* 1999; **9**: 196-199
11 **Welters CF**, Dejong CH, Deutz NE, Heineman E. Intestinal function and metabolism in the early adaptive phase after massive small bowel resection in the rat. *J Pediatr Surg* 2001; **36**: 1746-1751
12 **Platell CF**, Coster J, McCauley RD, Hall JC. The management of patients with the short bowel syndrome. *World J Gastroenterol* 2002; **8**: 13-20
13 **Sundaram A**, Koutkia P, Apovian CM. Nutritional management of short bowel syndrome in adults. *J Clin Gastroenterol* 2002; **34**: 207-220
14 **Messing B**, Crenn P, Beau P, Boutron-Ruault MC, Rambaud JC, Matuchansky C. Long-term survival and parenteral nutrition dependence in adult patients with the short bowel syndrome. *Gastroenterolog* 1999; **117**: 1043-1050
15 **Howard L**, Ashley C. Management of complications in patients receiving home parenteral nutrition. *Gastroenterology* 2003; **124**: 1651-1661
16 **Vanderhoof JA**, Matya SM. Enteral and parenteral nutrition in patients with short-bowel syndrome. *Eur J Pediatr Surg* 1999; **9**: 214-219
17 **Buchman AL**. The clinical management of short bowel syndrome: steps to avoid parenteral nutrition. *Nutrition* 1997; **13**: 907-913
18 **Gouttebel MC**, Saint Aubert B, Colette C, Astre C, Monnier LH, Joyeux H. Intestinal adaptation in patients with short bowel syndrome. Measurement by calcium absorption. *Dig Dis Sci* 1989; **34**: 709-715
19 **Gu Y**, Wu ZH. The anabolic effects of recombinant human growth hormone and glutamine on parenterally fed, short bowel rats. *World J Gastroenterol* 2002; **8**: 752-757
20 **Zhou X**, Li YX, Li N, Li JS. Effect of bowel rehabilitative therapy on structural adaptation of remnant small intestine: animal experiment. *World J Gastroenterol* 2001; **7**: 766-773
21 **Ukleja A**, Scolapio JS, Buchman AL. Nutritional management of short bowel syndrome. *Semin Gastrointest Dis* 2002; **13**: 161-168
22 **Seguy D**, Vahedi K, Kapel N, Souberbielle JC, Messing B. Low-dose growth hormone in adult home parenteral nutrition-dependent short bowel syndrome patients: a positive study. *Gastroenterolog* 2003; **124**: 293-302
23 **Li-Ling L**, Irving M. The effectiveness of growth hormone, glutamine and a low-fat diet containing high-carbohydrate on the enhancement of the function of remnant intestine among patients with short bowel syndrome: a review of published trials. *Clin Nutr* 2001; **20**: 199-204
24 **Scolapio JS**, Ukleja A. Short-bowel syndrome. *Curr Opin Clin Nutr Metab Care* 1998; **1**: 391-394
25 **Byrne TA**, Morrissey TB, Nattakom TV, Ziegler TR, Wilmore DW. Growth hormone, glutamine, and a modified diet enhance nutrient absorption in patients with severe short bowel syndrome. *J Parenter Enteral Nutr* 1995; **19**: 296-302
26 **Byrne TA**, Persinger RL, Young LS, Ziegler TR, Wilmore DW. A new treatment for patients with short- bowel syndrome. Growth hormone, glutamine, and a modified diet. *Ann Surg* 1995; **222**: 243-254
27 **Szkudlarek J**, Jeppesen PB, Mortensen PB. Effect of high dose growth hormone with glutamine and no change in diet on intestinal absorption in short bowel patients: a randomized, double blind, crossover, placebo controlled study. *Gut* 2000; **47**: 199-205
28 **Scolapio JS**, McGreevy K, Tennyson GS, Burnett OL. Effect of glutamine in short-bowel syndrome. *Clin Nutr* 2001; **20**: 319-323
29 **Jeppesen PB**, Szkudlarek J, Hoy CE, Mortensen PB. Effect of high-dose growth hormone and glutamine on body composition, urine creatinine excretion, fatty acid absorption, and essential fatty acids status in short bowel patients: a randomized, double-blind, crossover, placebo-controlled study. *Scand J Gastroenterol* 2001; **36**: 48-54
30 **Scolapio JS**. Effect of growth hormone, glutamine, and diet on body composition in short bowel syndrome: a randomized, controlled study. *J Parenter Enteral Nutr* 1999**; 23**: 309-312

Edited by Zhu LH and Wang XL

P.O.Box 2345, Beijing 100023,China
Fax: +86-10-85381893
E-mail: wjg@wjgnet.com www.wjgnet.com

World J Gastroenterol 2003;9(11):2605-2608
World Journal of Gastroenterology
 ISSN 1007-9327

• BRIEF REPORTS •

Restenosis following balloon dilation of benign esophageal stenosis

Ying-Sheng Cheng, Ming-Hua Li, Ren-Jie Yang, Hui-Zhen Zhang, Zai-Xian Ding, Qi-Xin Zhuang, Zhi-Ming Jiang, Ke-Zhong Shang

Ying-Sheng Cheng, Ming-Hua Li, Qi-Xin Zhuang, Ke-Zhong Shang, Department of Radiology, Sixth People' s Hospital, Shanghai Jiaotong University, Shanghai 200233, China
Ren-Jie Yang, Department of Interventional Diagnosis and Therapy, Clinical Oncology College of Beijing University, Beijing 100036, China
Hui-Zhen Zhang, Zhi-Ming Jiang, Department of Pathology, Sixth People' s Hospital, Shanghai Jiaotong University, Shanghai 200233, China
Zai-Xian Ding, Department of Animal Experiment, Sixth People' s Hospital, Shanghai Jiaotong University, Shanghai 200233, China
Supported by the National Key Technologies Research and Development Program of China During the 9th Five-Year Plan Period, No.96-907-03-04
Correspondence to: Dr. Ying-Sheng Cheng, Department of Radiology, Sixth People' s Hospital, Shanghai Jiaotong University, Shanghai 200233, China. chengys@sh163.net
Telephone: +86-21-64368920 **Fax:** +86-21-64701361
Received: 2003-05-13 **Accepted:** 2003-06-02

Abstract

AIM: To elucidate the mechanism of restenosis following balloon dilation of benign esophageal stenosis.

METHODS: A total of 49 rats with esophageal stenosis were induced in 70 rats using 5 ml of 50 % sodium hydroxide solution and the double-balloon method, and an esophageal restenosis (RS) model was developed by esophageal stenosis using dilation of a percutaneous transluminal coronary angioplasty (PTCA) balloon catheter. These 49 rats were divided into two groups: rats with benign esophageal stricture caused by chemical burn only (control group, *n*=21) and rats with their esophageal stricture treated with balloon catheter dilation (experimental group, *n*=28). Imaging analysis and immunohistochemistry were used for both quantitative and qualitative analyses of esophageal stenosis and RS formation in the rats, respectively.

RESULTS: Cross-sectional areas and perimeters of the esophageal mucosa layer, muscle layer, and the entire esophageal layers increased significantly in the experimental group compared with the control group. Proliferating cell nuclear antigen (PCNA) was expressed on the 5th day after dilation, and was still present at 1 month. Fibronectin (FN) was expressed on the 1st day after dilation, and was still present at 1 month.

CONCLUSION: Expression of PCNA and FN plays an important role in RS after balloon dilation of benign esophageal stenosis.

Cheng YS, Li MH, Yang RJ, Zhang HZ, Ding ZX, Zhuang QX, Jiang ZM, Shang KZ. Restenosis following balloon dilation of benign esophageal stenosis. *World J Gastroenterol* 2003; 9 (11): 2605-2608
http://www.wjgnet.com/1007-9327/9/2605.asp

INTRODUCTION

Balloon catheter dilation is a common nonsurgical treatment for benign esophageal stricture. Its short-term effect is good, but its long-term effect is not so good, because esophageal restenosis is a major complication. The underlying mechanism of esophageal restenosis has not been understood yet. To study this mechanism, we established a benign esophageal stricture model and restenosis model in Sprague-Dawley (SD) rats. We performed quantitative histopathological image analysis of sections of the rat esophagus, and qualitative immunohistochemical analysis of the related indicators of proliferation and restenosis of mucous and striated muscle layers of rat esophagus dilated by a balloon catheter at different time points. This provided us with an effective experimental model for investigation of the causes of restenosis.

MATERIALS AND METHODS

Materials

All protocols used for animal experiment and maintenance were approved by the Animal Ethics Committee in our university and conformed to the highest international standards of humane care.

70 male Sprague-Dawley (SD) rats weighing 305±50 g were obtained from the Shanghai Experimental Animal Center (Shanghai, China). The animals were weighed on day 0 and then 1 day before sacrifice. After anesthesia with 10 % ketamine (80 mg/kg) by abdominal injection, the animals were placed in a supine position and stabilized on an operating table. A 3F segmental epidural catheter was inserted into the mouth, and 10 ml of edible vinegar was injected into the stomach. The epidural catheter was then replaced by two 3F percutaneous transluminal coronary angioplasty (PTCA) balloon catheters at the mid-to-lower segment of the esophagus. The two balloons were at least 2 cm apart. These balloons were simultaneously inflated with air until they expanded to cling to the wall of the esophagus. Then 5 ml of a freshly prepared 50 % sodium hydroxide solution was injected through the orifice of the balloon catheter. After three minutes the air was released from the balloon. Distilled water was injected repeatedly through the same orifice for rinsing for 1 minute. The balloon catheters were removed and the animals returned to their cages for feeding. An esophageal barium-contrast examination was performed 2 and 4 weeks later to ascertain whether benign esophageal strictures had formed. We achieved 49 animal models from the 70 rats. These 49 rats were divided into two groups: rats with benign esophageal stricture caused by chemical burn only (control group, *n*=21) and rats with their esophageal stricture treated with balloon catheter dilation (experimental group, *n*=28).

Samples were collected at different times for immunohistochemical assay. We divided rats in both groups into seven subgroups according to the time after the dilation procedure when the samples were collected on day 1, 3, 5, 7, 14, 21 and 30. At the time of sacrifice, samples were fixed in 4 % buffered formaldehyde solution.

Table 1 Source of antigens and their effective concentrations

First antibody			Second antibody		
Goat antihuman PDGF	Promega	1:40	Biotinylated house antigoat IgG	Vector	1:200
Mouse antihuman FN	Life	1:20	Biotinylated house antimouse IgG	Vector	1:200
Mouse antihuman PCNA	Maxim	1:20	Biotinylated house antimouse IgG	Maxim	1:200

Statistical analysis: Data were expressed as the mean±SD. Statistical analysis was performed using the unpaired or paired *t*-test. A probability value less than 0.05 was considered significant.

Methods

Image analysis: Esophageal sections were stained with hematoxylin and eosin, and images were taken by a CCD camera (JVC, Osaka, Japan) and analyzed by a VIDAS imaging system (Carl Zeiss, Germany). The indicators used comprised the cross-sectional areas and perimeters of esophageal mucous layer, esophageal muscle layer, and the entire esophageal layers.

Immunohistochemical staining: ABC methods and SP methods were performed following the manufacturer's instructions using an ABC kit (Vector, USA) and an SP immunochemistry kit (Zymed Maxim, USA). The source of antibodies and their effective concentrations are listed in Table 1. The presence of platelet-derived growth factor (PDGF) and fibronectin (FN) was tested by the ABC method, and proliferating cell nuclear antigen (PCNA) was tested by the SP method.

RESULTS

Models of benign esophageal stricture and esophageal restenosis

Of the 49 model rats with benign esophageal stricture, 28 rats with esophageal restenosis were established.

Morphologic changes in benign esophageal stricture and esophageal restenosis

The control group showed chemical-burn lesions with an inflammatory reaction on the mucous layer of the esophagus, and comparatively slight thickening on the muscle layer of the esophagus. No broken regions were found in the muscle layer of the esophagus, and the esophageal wall was intact. Besides chemical-burn lesions, the experimental group showed mechanical damage in the mucosa of the esophagus. The muscle layer of the esophagus was thickened and broken, with accompanying inflammatory reactions (Figure 1). On the 5th day after the procedure, the broken section of the muscle layer of the esophagus became thickening, and 14 days later the degree of thickening was obvious. The changes in the cross-sectional areas and perimeters of mucosa, muscle layers, and the entire esophagus wall are listed in Table 2.

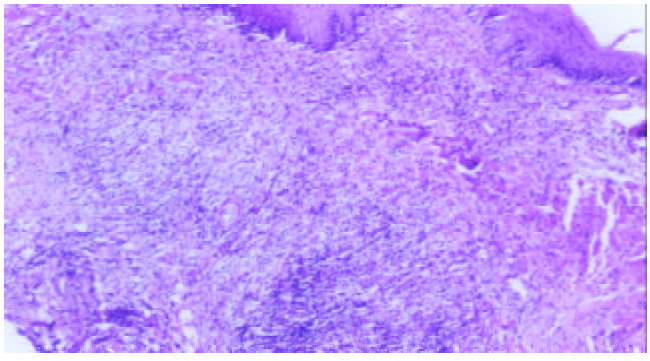

Figure 1 In the experimental group, on the 5th day after the procedure, muscle layers of the rat esophagus exhibited an inflammatory reaction. H&E stain, ×4.

Table 2 Morphologic changes in benign esophageal stricture and esophageal restenosis (area, mm^2; perimeter, mm)

	Control group	Experimental group
A1	0.49±0.14	0.75±0.18[b]
A2	1.70±0.42	1.97±0.33[a]
A3	2.20±0.45	2.72±0.46[a]
P1	4.83±1.52	6.65±1.22[b]
P2	6.89±1.96	8.80±1.67[b]
P3	9.86±2.25	14.19±2.89[b]

[b]$P<0.01$, [a]$P<0.05$ *vs* control group and experimental group. Abbreviations: A1: cross-sectional area of mucosa of esophagus, A2: cross-sectional area of muscle layer of esophagus, A3: cross-sectional area of entire esophagus wall, P1: perimeter of mucosa of esophagus, P2: perimeter of muscle layer of esophagus, P3: perimeter of entire esophagus wall.

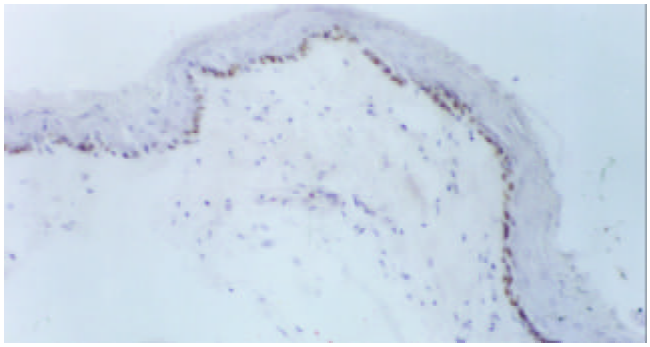

Figure 2 In the experimental group, on the 5th day after the procedure, the basal cells of the squamous epithelium in rat esophagus exhibited strong PCNA expression. Immunostaining, ×4.

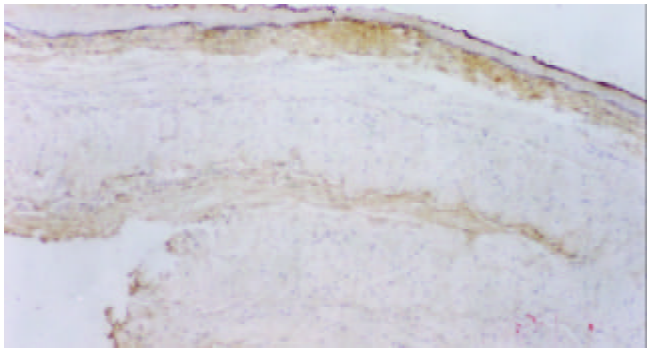

Figure 3 In the experimental group, on the 30th day after the procedure, the substratum of the rat esophageal mucosa and muscle layers exhibited strong FN expression. H&E stain, ×4.

Immunohistochemical staining of benign esophageal stricture and esophageal restenosis: In the control group, basal cells of the squamous epithelium and striated-muscle cells of the esophagus exhibited no PCNA expression. Five days after the dilation procedure, PCNA expression became obvious in

basal cells of the squamous epithelium, and this positive expression lasted for 30 days (Figure 2). In the control group, 3-7 days after the dilation procedure, the basal layer of the esophagus exhibited weak positive expression. Fourteen days later there was no FN expression in the basal layer. In the experimental group, on the 1st day after the procedure, the collagen fibers in submucosa and in the striated-muscle layer of esophagus were positive for FN, and this was still the case on the 14th day. After 1 month, FN positive expression was still reasonably strong (Figure 3). PDGF was not expressed at all in striated-muscle cells from the 1st to the 30th day in both control and experimental groups.

DISCUSSION

Models of benign esophageal stricture and esophageal restenosis

The causes of benign esophageal stricture are numerous and complicated, and hence the models thereof are difficult to reproduce consistently. However, benign esophageal stricture eventually manifests as thickened scars and reduced luminal sizes. We used chemical burns to develop the model of benign esophageal stricture because it allowed timing to be controlled and exhibited a high rate of success. Early in the 1970s, Przymanowski *et al*[1] used sodium hydroxide to establish a model of benign esophageal stricture. Their method was to perform an abdominal midsection on rats, thereby exposing the lower segment of the esophagus. They used surgical thread to tightly tie the region 2-cm either side of the lower segment of the esophagus. They then inserted a stomach tube via the mouth until it reached the tied point. Sodium hydroxide solution was injected, and then rinsed out three times for 3 minutes with distilled water later. Then they withdrew the tube, cut the threads, and closed the abdomen. Based on their procedure, we developed a nonsurgical method to establish a model of benign esophageal stricture. Since our method did not involve surgery, it was simpler and faster. Our experimental observations demonstrated that the model was satisfactorily established. Our use of two balloon catheters made manipulation somewhat difficult. We intended to make a single catheter with two balloons, but this was found to be too difficult since the rats had a narrow esophagus that demanded fine catheters and balloons. In contrast, a double-balloon catheter with a larger caliber was easy to be constructed. Therefore, the double-balloon method was used to establish the model of benign esophageal stricture.

The technique used to establish the model of esophageal restenosis is easier. After ascertaining the stricture position by esophageal visualization, we performed balloon catheter dilation under X-ray. In this way, the esophageal restenosis model was established. In a very few cases of severe stricture, the restenosis model could not be produced due to the catheters being unable to pass through.

Morphological changes in benign esophageal stricture and esophageal restenosis

After the benign esophageal stricture formed, its morphology was relatively stable. It manifested as thickened muscle layers, reduced luminal sizes, and inelastic lumens. Thus it caused dysphagia. The esophageal morphology was altered by balloon catheter dilation. The esophageal mucosa exhibited not only chemical-burn lesions, but also lesions caused by mechanical damage. The thickened muscle layer of the esophagus was torn or broken, causing the areas of mucosal and muscle layers of the esophagus to increase siginficantly in the experimental group. Significant differences were also observed in the perimeters of the mucosal and muscle layers of the esophagus and in the perimeter of the entire esophagus wall. Within the same group, after the dilation procedure the areas of each layer increased rather than decreased, whilst the perimeters also increased. This indicated that dysphagia improvement was due to an enlargement of the lumen of the esophagus after dilation. Up to a certain time, these new scar tissues would further contract and cicatrize. As a result, the duct lumen was further reduced and lacked elasticity. This was one of the key factors in esophageal restenosis. This also illustrated that if there was no treatment plan after balloon dilation in benign esophageal stricture, esophageal restenosis could not be resolved[2-28].

Immunohistochemical observation of benign estophageal stricture and estophageal restenosis

PCNA is a type of nuclear protein equivalent to the binding protein of DNA polymerase. It coordinates the synthesis of DNA up and down strands. The quantity of PCNA is minimal in normal cells at the G_0, whereas at the M stage the quantity of PCNA in transforming cells changes dramatically. The quantity of PCNA mostly declines at stage G_0/G_1. This quantative change coincides with DNA synthesis. Therefore, PCNA is used as an indicator to assess cell proliferation. There were a number of reports on the application of immunohistochemical methods to the study of tumor-cell proliferation[29]. In our study, we used the new method involving PCNA to investigate the basal-cell proliferation of the squamous epithelium in benign esophageal stricture by the procedure of balloon dilation. We found that there was no PCNA expression in the control group in basal cells of the squamous epithelium of the esophagus. However, in the experimental group, PCNA was expressed strongly from day 5 onwards 30 days later, PCNA expression was still positive. This consistently high proliferation of basal cells illustrated their importance in the development of esophageal restenosis.

FN was a glucoprotein with multiple functions[30]. As a noncollagenous substance in the extracellular matrix, it participates in various reactions between cells as well as between cells and the extracellular matrix, including adhesion, migration, injury, restoration, and tumor metasis. FN has two forms: a soluble dimerization in humor and a barely soluble polymerization in the extracellular matrix. After combining with its receptor through a tripeptide sequence Arg-Gug-(RGD), FN transmits cellular signals and facilitates cells' interfacing and kinetics. The study of FN expression in the lesion of benign estophageal stricture caused by balloon dilation is therefore helpful to elucidate the mechanism of proliferation and migration of cells. In the control group, we noticed that the expression of FN in the basal mucosa of the esophagus was weak, which indicates that FN expression after a chemical burn is related to the esophageal stricture. In the experimental group, soon after the procedure the squamous epithelium and striated-muscle cells expressed a large amount of FN. This reaction might be related to regulated cellular proliferation and chemotaxis. Previous studies have shown that FN has the similar function to growth factor in fibroblast cells. Even in small doses it can accelerate proliferation. An *in vitro* study has also shown that fibroblasts could adhere directly to the FN matrix or adhere to collagen through FN. FN can also facilitate unfolding of cells that adhere to the matrix. We also noticed that in the experimental group, FN was strongly expressed at both early and later stages after the procedure. This illustrates that FN is one of the key factors in the production of esophageal restenosis, especially at the late stage.

PDGF could stimulate the proliferation of fibroblasts *in vitro*[31-38]. Initially it was found in platelet granules, and afterwards its secretion was also found in normal cells and transformed cells. It exists in three biologically active isoforms: PDGF-AB, PDGF-AA, and PDGF-BB; comprising PDGF-A and PDGF-B polypeptide chains. It acts on target cells through receptors consisting of two subunits, α and β. PDGF-AB

combines αα and ββ functions. In our experiment, PDGF was not expressed in striated muscle cells of the esophagus, which indicates that PDGF is not a key factor in esophageal restenosis produced by balloon dilated esophageal stricture. However, the enhanced expression of PDGF was involved in the proliferation of smooth-muscle cells. In the study of restenosis, PDGF was regarded as a strong split promoter and chemotactic factor, playing an important role in the formation of blood vessel restenosis. The full length of the esophagus in SD rats (as used in our experiments) comprised striated muscle, and hence PDGF and its function could not be shown in esophageal restenosis in these rats. Besides, in clinical settings, relatively severe chemical burns of the esophagus are usually located at the middle and lower segments of the esophagus, while the upper segment is rarely involved. The middle and lower segments of the esophagus comprise smooth muscle, while the upper segment is striated muscle. This indirectly demonstrates that PDGF expressed in smooth-muscle cells plays a greater role than that in striated-muscle cells in the formation of benign esophageal stricture and restenosis.

REFERENCES

1 **Przymanowski Z.** Dilatational treatment of the esophageal constriction after burning in the light of experimental investigations and clinical observations (author's transl). *Acta Biol Med* 1970; **15**: 55-116
2 **London RL**, Trotman BW, DiMarino AJ Jr, Oleaga JA, Freiman DB, Ring EJ, Rosato EF. Dilatation of severe esophageal strictures by an inflatable balloon catheter. *Gastroenterology* 1981; **80**: 173-175
3 **Chang TS**, Wang W, Huang OL. One-stage reconstruction of esophageal defect by free transfer of jejunum: treatment and complications. *Ann Plast Surg* 1985; **15**: 492-496
4 **Kochhar R,** Nagi B, Mehta SK. Balloon catheter dilatation of esophageal strictures. *Indian J Gastroenterol* 1988; **7**: 97-98
5 **Othersen HB Jr**, Parker EF, Smith CD. The surgical management of esophageal stricture in children. A century of progress. *Ann Surg* 1988; **207**: 590-597
6 **Shemesh E**, Czerniak A. Comparison between Savary-Gilliard and balloon dilatation of benign esophageal strictures. *World J Surg* 1990; **14**: 518-522
7 **Wang C,** Wang CL, Chen CX. Four-year experience in the treatment of upper gastrointestinal strictures with balloon dilatation. *Chin Med J* 1991; **104**: 114-118
8 **Strautman PR,** Dorfman GS. Use of metallic stents to salvage and maintain patency in surgically created esophagocutaneous fistulas. *J Vasc Interv Radiol* 1992; **3**: 131-133
9 **Davies RP,** Linke RJ, Davey RB. Retrograde esophageal balloon dilatation: salvage treatment of caustic-induced stricture. *Cardiovasc Intervent Radiol* 1992; **15**: 186-188
10 **Song HY,** Han YM, Kim HN, Kim CS, Choi KC. Corrosive esophageal stricture: safety and effectiveness of balloon dilation. *Radiology* 1992; **184**: 373-378
11 **Chen PC.** Endoscopic balloon dilation of esophageal strictures following surgical anastomoses, endoscopic variceal sclerotherapy, and corrosive ingestion. *Gastrointest Endosc* 1992; **38**: 586-589
12 **Broor SL,** Lahoti D. Balloon dilation of corrosive esophageal strictures. *Gastrointest Endosc* 1993; **39**: 597-598
13 **De Wilde I,** Pieper CH, Moore SW, Hoffman B. Oesophageal stricture caused by washing powder ingestion. *S Afr Med J* 1995; **85**: 121
14 **Sinha KN**. Foley catheter self dilatation for strictures of the upper end of oesophagus. *Indian J Chest Dis Allied Sci* 1996; **38**: 91-93
15 **Hwang TL,** Chen MF. Surgical treatment of gastric outlet obstruction after corrosive injury-can early definitive operation be used instead of staged operation? *Int Surg* 1996; **81**: 119-121
16 **Panieri E,** Millar AJ, Rode H, Brown RA, Cywes S. Iatrogenic esophageal perforation in children: patterns of injury, presentation, management, and outcome. *J Pediatr Surg* 1996; **31**: 890-895
17 **Fan S,** Jiang Y, Li Z. Intraluminal stent and balloon of intraluminal stent for prevention of esophageal stenosis due to alkali corrosive injury: experimental and clinical studies. *Zhonghua Waike Zazhi* 1996; **34**: 170-172
18 **Cheng YS,** Shang KZ, Zhuang QX, Li MH, Xu JR, Yang SX. Interventional therapy and cause of restenosis of esophageal benign stricture. *Huaren Xiaohua Zazhi* 1998; **6**: 791-794
19 **Kadakia SC,** Wong RKH. Graded pneumatic dilation using Rigiflex achalasia dilators in patents with primary esophageal achalasia. *Am J Gastroenterol* 1993; **88**: 34-38
20 **Misra SP,** Dwivedi M. Entrapment of guide-wire during oesophageal dilation. *Trop Gastroenterol* 1997; **18**: 117-118
21 **De Peppo F,** Zaccara A, Dall'Oglio L, Federici di Abriola G, Ponticelli A, Marchetti P, Lucchetti MC, Rivosecchi M. Stenting for caustic strictures: esophageal replacement replaced. *J Pediatr Surg* 1998; **33**: 54-57
22 **Karnak I,** Tanyel FC, Buyukpamukcu N, Hicsonmez A. Esophageal perforations encountered during the dilation of caustic esophageal strictures. *J Cardiovasc Surg* 1998; **39**: 373-377
23 **Al-Jadaan S,** Bass J. Retrograde esophageal balloon dilatation for caustic stricture in an outpatient clinic setting. *Can J Surg* 1999; **42**: 48-50
24 **Hunt DR,** Wills VL, Weis B, Jorgensen JO, DeCarle DJ, Coo IJ. Management of esophageal perforation after pneumatic dilation for achalasia. *J Gastrointest Surg* 2000; **4**: 411-415
25 **Huang YC,** Chen SJ, Hsu WM, Li YW, Ni YH. Balloon dilation of double strictures after corrosive esophagitis. *J Pediatr Gastroenterol Nutr* 2001; **32**: 496-498
26 **Wilsey MJ Jr,** Scheimann AO, Gilger MA. The role of upper gastrointestinal endoscopy in the diagnosis and treatment of caustic ingestion, esophageal strictures, and achalasia in children. *Gastrointest Endosc Clin N Am* 2001; **11**: 767-787
27 **Gehanno P,** Guedon C. Inhibition of experimental esophageal lye strictures by penicillamine. *Arch Otolaryngol* 1981; **107**: 145-147
28 **Rivera EA,** Maves MD. Effects of neutralizing agents on esophageal burns caused by disc batteries. *Ann Otol Rhinol Laryngol* 1987; **96**: 362-366
29 **Alexandrov VA,** Novikov AI, Zabezhinsky MA, Stolyarov VI, Petrov AS. The stimulating effect of acetic acid, alcohol and thermal burn injury on esophagus and forestomach carcinogenesis induced by N-nitrososarcosin ethyl ester in rats. *Cancer Lett* 1989; **47**: 179-185
30 **Demirbilek S,** Bernay F, Rizalar R, Baris S, Gurses N. Effects of estradiol and progesterone on the synthesis of collagen in corrosive esophageal burns in rats. *J Pediatr Surg* 1994; **29**: 1425-1428
31 **Takagi K,** Tashiro T, Yamamori H, Mashima Y, Nakajima N, Sunaga K. Recombinant human growth hormone and protein metabolism of burned rats and esophagectomized patients. *Nutrition* 1995; **11**: 22-26
32 **Yoshikawa T**, Asai S, Takekawa Y, Kida A, Ishikawa K. Experimental investigation of battery-induced esophageal burn injury in rabbits. *Crit Care Med* 1997; **25**: 2039-2044
33 **Bingol-Kologlu M,** Tanyel FC, Muftuoglu S, Renda N, Cakar N, Buyukpamukcu N, Hicsonmez A. The preventive effect of heparin on stricture formation after caustic esophageal burns. *J Pediatr Surg* 1999; **34**: 291-294
34 **Kaygusuz I**, Celik O, Ozkaya OO, Yalcin S, Keles E, Cetinkaya T. Effects of interferon-alpha-2b and octreotide on healing of esophageal corrosive burns. *Laryngoscope* 2001; **111**(11 Pt1): 1999-2004
35 **Wornat MJ,** Ledesma EB, Sandrowitz AK, Roth MJ, Dawsey SM, Qiao YL, Chen W. Polycyclic aromatic hydrocarbons identified in soot extracts from domestic coal-burning stoves of Henan Province, China. *Environ Sci Technol* 2001; **35**: 1943-1952
36 **Arzbaecher R,** Jenkins JM. A review of the theoretical and experimental bases of transesophageal atrial pacing. *J Electrocardiol* 2002; **35**(Suppl): 137-141
37 **Trevisani M,** Smart D, Gunthorpe MJ, Tognetto M, Barbieri M, Campi B, Amadesi S, Gray J, Jerman JC, Brough SJ, Owen D, Smith GD, Randall AD, Harrison S, Bianchi A, Davis JB, Geppetti P. Ethanol elicits and potentiates nociceptor responses via the vanilloid receptor-1. *Nat Neurosci* 2002; **5**: 546-551
38 **Demirbilek S**, Aydin G, Yucesan S, Vural H, Bitiren M. Polyunsaturated phosphatidylcholine lowers collagen deposition in a rat model of corrosive esophageal burn. *Eur J Pediatr Surg* 2002;**12**: 8-12

Edited by Zhang JZ and Wang XL

P.O.Box 2345, Beijing 100023,China
Fax: +86-10-85381893
E-mail: wjg@wjgnet.com www.wjgnet.com

World J Gastroenterol 2003;9(11):2609-2611
World Journal of Gastroenterology
 ISSN 1007-9327

• BRIEF REPORTS •

Follow-up evaluation for benign stricture of upper gastrointestinal tract with stent insertion

Ying-Sheng Cheng, Ming-Hua Li, Wei-Xiong Chen, Qi-Xin Zhuang, Ni-Wei Chen, Ke-Zhong Shang

Ying-Sheng Cheng, Ming-Hua Li, Qi-Xin Zhuang, Ke-Zhong Shang, Department of Radiology, Sixth People' s Hospital, Shanghai Jiaotong University, Shanghai 200233, China
Wei-Xiong Chen, Ni-Wei Chen, Department of Gastroenterology, Sixth People' s Hospital, Shanghai Jiaotong University, Shanghai 200233, China
Supported by National Key Technologies Research and Development Program of China during 9th Five-Year Plan Period, No.96-907-03-04; Shanghai Nature Science Funds, No.02Z1314073; Shanghai Medical Development Funds, No.00419
Correspondence to: Dr. Ying-Sheng Cheng, Department of Radiology, Sixth People' s Hospital, Shanghai Jiaotong University, Shanghai 200233, China. chengys@sh163.net
Telephone: +86-21-64368920 **Fax.:** +86-21-64701361
Received: 2003-05-13 **Accepted:** 2003-06-02

Abstract

AIM: To determine the best mothod for benign stricture of the upper gastrointestinal tract (UGIT) with stent insertion by follow-up evaluation.

METHODS: A total of 110 stents insertions were performed in 110 cases of benign stricture of the UGIT. Permanent (group A) and temporary (group B) placement of an expandable metal stent in 30 cases and 80 cases respectively. All cases were completed under fluoroscopy.

RESULTS: In group A, 30 uncovered or antireflux covered or partially covered expandable metal stents were placed permanently. In group A, 5 cases (16.7 %) in 3-months, 5 cases (20.0 %) in 6-months, 6 cases (25 %) in the 1st year, 6 cases (50 %) in the 3rd year, and 4 cases (80 %) in the 5th year exhibited dysphagia relapse. In group B, a partially-covered expandable metal stent was temporarily placed in each patient and removed after 3-7 days via gastroscopy. Follow-up data in this group showed that 8 cases (7.5 %) in 3-months, 9 cases (12.0 %) in 6-months,10 cases (15.4 %) in the 1st year, 6 cases (20 %) in the 3rd year, and 3 cases (25 %) in the 5th year exhibited dysphagia relapse. The placement and withdrawal of all stents were all performed successfully. The follow-up of all cases lasted for 3-99 months (mean 41.6±19.7 months).

CONCLUSION: The best mothod for benign stricture of UGIT with stent insertion is temporary placement of a partially-covered expandable metal stent.

Cheng YS, Li MH, Chen WX, Zhuang QX, Chen NW, Shang KZ. Follow-up evaluation for benign stricture of upper gastrointestinal tract with stent insertion. *World J Gastroenterol* 2003; 9(11): 2609-2611
http://www.wjgnet.com/1007-9327/9/2609.asp

INTRODUCTION

Benign stricture of the upper gastrointestinal tract (UGIT) refers to stenosis caused by benign pathological changes in the pharynx, esophagus, stomach, and duodenum. Such stenosis includes marginal stricture after surgery, chemical-burn-related stricture, simple scar-related stricture after radiation therapy for tumor, digestive stricture, and functional stricture (achalasia). Since July 1994 , 110 cases with benign stricture of the UGIT have been treated with stent insertion and followed-up. We herein report our experiences.

MATERIALS AND METHODS

Materials

Our subjects were 110 patients with benign stricture of the UGIT (61 males, 49 females; age 18-84 years, mean 53.9 years). Sequential trials were adopted for these cases who were nonrandomly divided into the following two groups according to the method of stent insertion: 30 cases with permanent uncovered or antireflux covered or partially covered metal stent dilation (group A), and 80 cases with temporary partially covered metal stent dilation (group B). In group A there were 6 cases of simple cicatricial stricture after radiation therapy for esophageal carcinoma, 8 cases of achalasia, 13 cases of esophageal and esophagogastric marginal stricture, 2 cases of gastroduodenal marginal stricture, and 1 case of esophageal chemical-burn-related stricture. The mean diameter of the strictured UGIT was 3.2±2.3 mm before stent placement and 17.8±2.4 mm after stent placement. In group B there were 2 cases of simple scar-related stricture after radiation therapy for esphageal carcinoma, 67 cases of achalasia, 9 cases of esophageal and esophagogastric marginal stricture,and 2 cases of esophageal chemical burn. The mean diameter of the strictured UGIT was 3.3±2.1 mm before stent placement and 22.3±2.7 mm after stent placement. All cases had dysphagia grades 2-4 before stent insertion and dysphagia grades 0-2 after stent insertion. All casess were examined by barium-meal radiography of the UGIT and gastroscopy.

Methods

It involved an empty stomach for at least 4 h and examination of the normal bleeding and clotting time. Two types of metal stent were used: covered stainless steel wire Z-stent (COOK, USA), and partially covered or uncovered or antireflux covered nitinol stent (Zhiye Medical Equipment Research Institute, Changzhou, China; and Youyan Yijin Advanced Materials Co. Ltd, Beijing, China). The COOK stents were constructed from multiple fragments, each fragment was typically 2-cm long. The stent was completely coated on the outer layer and mounted with a metal barb. The diameter of the stent body was 18 mm and that of the horn was 25 mm. The body of the partially covered metal stents was coated with intracavity silica gel. The areas within 2 cm of both ends of the stents were not covered. Stents were 4-14 cm in length and 16-30 mm in diameter. They had single or double horns, the horn diameter was 20-35 mm.

The different types of metal stents were placed differently. For example, placement of the partially-covered nitinol internal stent used in groups B and C firstly involved spraying the

pharynx with 1% lidocaine (as a mist) for anesthesia. When a stent was a placed, the patients were placed in a sitting position or lying on the side, and where applicable with their false teeth removed and a teeth bracket mounted. A 260-cm-long guidewire was first led into the distal end of the benign stricture. The stent was mounted on the propeller whose front end was coated with sterilized liquid paraffin. Guided by the wire, the propeller on which the stent was mounted was moved through the strictured section. Under fluoroscopic control, the outer sheath was slowly withdrawn and the stent expanded under its own tension. After the stent was placed, radiography was performed to observe the patency of the UGIT. In group B, 500-1 000 ml of ice-cold water was injected 3-7 days after stent placement via a bioptic hole under gastroscopy, which caused the stent to reduce its diameter. Bioptic pliers were then used to withdraw the stent using a gastroscope. Gastroscopy was performed again in the UGIT to detect complications, such as bleeding, mucosal tearing, or perforation of the UGIT. The patients returned to the ward and consumed cold drinks and snacks for 2 days before resuming a normal diet. It was preferable for patients to eat solid food since the natural expansion caused by ingesting food reduced the retraction of the UGIT.

Criteria for therapeutic efficacy included diameter of the most-strictured section of the UGIT before and after dilation, and dysphagia score before and after dilation.

After stent placement barium-meal radiography was performed to observe patency of the UGIT. The patients ate semifluid food on the day after surgery, and were treated with antibiotics, antacids, and antireflux drugs. One week after stent removal, barium-meal radiography of the UGIT was performed to observe patency of the UGIT. The patients went to a clinic or were followed-up by telephone at the 3rd, 6th months, 1st, 3rd and 5th year.

RESULTS

In group A, 30 uncovered or antireflux covered or partially-covered stents were placed. Stent placement was successful in all the cases. In group B, 80 partially- covered stents were placed and removed under gastroscopy guidance 3-7 days after stent insertion. The successful rate of stent placement and extraction was 100 %. Relapse rate of dysphagia treated with stent insertion during follow-up is shown in Table 1.

DISCUSSION

Since Domschke *et al*[1] reported the first successful treatment of malignant esophageal strictures with an uncovered expandable metal stent in 1990, placement of covered or uncovered or antireflux covered expandable UGIT metal stents has been shown to be a safe, easy, and effective treatment for malignant UGIT strictures. Cwikiel *et al*[2] reported the first successful treatment of benign esophageal strictures in 1993. Cheng *et al*[3] reported the first successful treatment of benign esophageal strictures with temporary partially covered stent in 1999. Many patients with benign UGIT strictures have received treatment with uncovered or covered or temporary partially covered metal stents[4-26]. Permanent uncovered metal stent insertion for benign functional stricture in the UGIT had poor mid-term and long-term therapeutic efficiency, mainly due to frequent severe gastroesophageal reflux and restenosis (hyperplasia of granulation tissue). After a 12-month follow-up, three uncovered metal stents could not be removed in three cases of achalasia, and we had to resect and reconstruct the esophageal cardia. Therefore, permanent uncovered metal stent dilation is not suitable for cases of functional stricture of the UGIT. Permanent partially covered metal stent dilation had poor mid-term and long-term therapeutic efficiency, mainly due to reflux and stent migration[27-37].

Temporary partially-covered metal stent dilation was used for benign stricture of the UGIT with both excellent immediate and mid- and long-term therapeutic efficacy. Firstly, the design of the stent coincided with the specific anatomy of the UGIT and pathological manifestations of benign stricture. If a stent was not well designed, it did not exhibit therapeutic efficacy, and was also associated with a higher frequency of complications such as stent migration. With the aim of solving these problems, we designed a special stent for benign stricture of the UGIT. The stent was partially covered. A membrane covered the inner wall of the stent, with the area within 2 cm of the stent orifice not covered. The upper orifice of the stent was a large horn, which increased the stability of the stent but made it difficult to withdraw. Secondly, the diameter of the stents used in this group was 16-30 mm. By dilating the stent, the stricture could almost be returned to the maximum diameter of a normal strictured UGIT. What the diameter of a stent is most appropriate is that the stent should expand the strictured part without complications. We found that the bigger the diameter of stents was, the better the mid- and long-term therapeutic efficacy was ,but the ideal size still needs to be further investigated.

The further development of biologically degraded stents for the gastrointestinal tract would provide advantages of a very long retention time without the necessity to remove the stent[38]. This would provide potentially superior stent insertion for cases of benign stricture of the UGIT. In the treatment of UGIT benign stricture with stent insertion, temporary partially-covered metal stent dilation will gradually replace others and become the preferred method for the nonsurgical treatment of

Table 1 Relapse rate of dysphagia treated with stent insertion

Group	Follow-up >3 months (*n*)	Dysphagia relapse (*n*)	Dysphagia relapse rate (%)	Follow-up >6 months year (*n*)	Dysphagia relapse (*n*)	Dysphagia relapse rate (%)
A	30	5	16.7%	25	5	20.0%
B	80	8	7.5%	75	9	12.0%

Group	Follow-up>1st year (*n*)	Dysphagia relapse (*n*)	Dysphagia relapse rate (%)
A	24	6	25.0 %
B	65	10	15.4 %

Group	Follow-up >3rd year (*n*)	Dysphagia relapse (*n*)	Dysphagia relapse rate (%)	Follow-up >5th year (*n*)	Dysphagia relapse (*n*)	Dysphagia relapse rate (%)
A	12	6	50.0 %	5	4	80.0%
B	30	6	20.0 %	12	3	25.0%

benign stricture in gastrointestinal tract due to its superior mid-term and long-term therapeutic efficacy[39,40].

According to our experiences in the treatment of 110 casess of benign stricture of the UGIT with stent insertion, we consider that the method chosen for an individual case should be based on the nature of the stricture, course of disease, and complications. Moreover, long-term therapeutic efficacy and medical expense need to be comprehensively assessed. Finally, other combined therapies should be carried out concurrently both before and after the treatment in order to achieve a high therapeutic efficacy.

REFERENCES

1 **Domschke W,** Foerster EC, Matek W, Rodl W. Self-expanding mesh stent for esophageal cancer stenosis. *Endoscopy* 1990; **22**: 134-136
2 **Cwikiel W,** Willen R, Stridbeck H, Liool -Cil R, Von Holstein CS. Self-expanding stent in the treatment of benign esophageal stricture:experimental study in pigs and presentation of clinical cases. *Radiology* 1993; **187**: 667-671
3 **Cheng YS,** Yang RJ, Shang KZ, Li MH, Chen WX, Zhuang QX, Xu JR, Chen NW, Yang SX. Esophageal benign structure with temporary stent insertion. *Jieru Fangshexue Zazhi* 1999; **8**: 32-34
4 **Song HY,** Choi KC, Kwon HC, Yang DH, Cho BH, Lee ST. Esophageal strictures: treatment with a new design of modified Gianturco stent. Work in progress. *Radiology* 1992; **184**: 729-734
5 **Cwikiel W,** Willen R, Stridbeck H, Lillo-Gil R, von Holstein CS. Self-expanding stent in the treatment of benign esophageal strictures: experimental study in pigs and presentation of clinical cases. *Radiology* 1993; **187**: 667-671
6 **Song HY,** Do YS, Han YM, Sung KB, Choi EK, Sohn KH, Kim HR, Kim SH, Min YI. Covered, expandable esophageal metallic stent tubes: experiences in 119 patients. *Radiology* 1994; **193**: 689-695
7 **Foster DR.** Use of a Strecker oesophageal stent in the treatment of benign oesophageal stricture. *Australas Radiol* 1995; **39**: 399-400
8 **Profili S,** Bifulco V, Demelas P, Migaleddu V, Meloni GB. Possibility of using self-expanding uncoated stents in benign esophageal stenosis. Experience in a case of post-irradiation stenosis. *Radiol Med* 1995; **89**: 171-173
9 **Strecker EP,** Boos I, Vetter S, Strohm M, Domschke S. Nitinol esophageal stents: new designs and clinical indications. *Cardiovasc Intervent Radiol* 1996; **19**: 15-20
10 **De Gregorio BT,** Kinsman K, Katon RM, Morrison K, Saxon RR, Barton RE, Keller FS, Rosch J. Treatment of esophageal obstruction from mediastinal compressive tumor with covered, self-expanding metallic Z-stents. *Gastrointest Endosc* 1996; **43**: 483-489
11 **Moores DW,** Ilves R. Treatment of esophageal obstruction with covered, self-expanding esophageal Wallstents. *Ann Thorac Surg* 1996; **62**: 963-967
12 **Song HY,** Park SI, Do YS, Yoon HK, Sung KB, Sohn KH, Min YI. Expandable metallic stent placement in patients with benign esophageal strictures: results of long-term follow-up. *Radiology* 1997; **203**: 131-136
13 **Foster DR.** Self-expandable oesophageal stents in the management of benign peptic oesophageal strictures in the elderly. *Br J Clin Pract* 1997; **51**: 199
14 **Tan BS,** Kennedy C, Morgan R, Owen W, Adam A. Using uncovered metallic endoprostheses to treat recurrent benign esophageal strictures. *Am J Roentgenol* 1997; **169**: 1281-1284
15 **Sheikh RA,** Trudeau WL. Expandable metallic stent placement in patients with benign esophageal strictures: results of long-term follow-up. *Gastrointest Endosc* 1998; **48**: 227-229
16 **Neuhaus H,** Schumacher B. Use of metal stents in gastroenterology. *Z Gastroenterol* 1998; **36**: 121-134
17 **Sheikh RA,** Trudeau WL. Expandable metallic stent placement in patients with benign esophageal strictures: results of long-term follow-up. *Gastrointest Endosc* 1998; **48**: 227-229
18 **Wengrower D,** Fiorini A, Valero J, Waldbaum C, Chopita N, Landoni N, Judchack S, Goldin E. EsophaCoil: Long-term results in 81 patients. *Gastrointest Endosc* 1998; **48**: 376-382
19 **Sandha GS,** Marcon NE. Expandable metal stents for benign esophageal obstruction.*Gastrointest Endosc Clin N Am* 1999; **9**: 437-446
20 **Boulis NM,** Armstrong WS, Chandler WF, Orringer MB. Epidural abscess: a delayed complication of esophageal stenting for benign stricture. *Ann Thorac Surg* 1999; **68**: 568-570
21 **Fiorini A,** Fleischer D, Valero J, Israeli E, Wengrower D, Goldin E. Self-expandable metal coil stents in the treatment of benign esophageal strictures refractory to conventional therapy: a case series. *Gastrointest Endosc* 2000; **52**: 259-262
22 **Macdonald S,** Edwards RD, Moss JG. Patient tolerance of cervical esophageal metallic stents. *J Vasc Interv Radiol* 2000; **11**: 891-898
23 **Lee JG,** Hsu R, Leung JW. Are self-expanding metal mesh stents useful in the treatment of benign esophageal stenoses and fistulas? An experience of four cases. *Am J Gastroenterol* 2000; **95**: 1920-1925
24 **Song HY,** Jung HY, Park SI, Kim SB, Lee DH, Kang SG, Min Y. Covered retrievable expandable nitinol stents in patients with benign esophageal strictures: initial experience. *Radiology* 2000; **217**: 551-557
25 **Cordero JA Jr,** Moores DW. Self-expanding esophageal metallic stents in the treatment of esophageal obstruction. *Am Surg* 2000; **66**: 956-959
26 **Ackroyd R,** Watson DI, Devitt PG, Jamieson GG. Expandable metallic stents should not be used in the treatment of benign esophageal strictures. *J Gastroenterol Hepatol* 2001; **16**: 484-487
27 **Dormann AJ,** Deppe H, Wigginghaus B. Self-expanding metallic stents for continuous dilatation of benign stenoses in gastrointestinal tract - first results of long-term follow-up in interim stent application in pyloric and colonic obstructions. *Z Gastroenterol* 2001; **39**: 957-960
28 **Profili S,** Meloni GB, Feo CF, Pischedda A, Bozzo C, Ginesu GC, Canalis GC. Self-expandable metal stents in the management of cervical oesophageal and/or hypopharyngeal strictures. *Clin Radiol* 2002; **57**: 1028-1033
29 **Yates MR 3rd,** Morgan DE, Baron TH. Palliation of malignant gastric and small intestinal strictures with self-expandable metal stents. *Endoscopy* 1998; **30**: 266-272
30 **Mauro MA,** Koehler RE, Baron TH. Advances in gastrointestinal intervention: the treatment of gastroduodenal and colorectal obstructions with metallic stents. *Radiology* 2000; **215**: 659-669
31 **DePalma GD,** Catanzano C. Removable self-expanding metal stents: a pilot study for treatment of achalasia of the esophagus. *Endoscopy* 1998; **30**: S95-96
32 **Ell C,** May A, Hahn EG. Self-expanding metal endoprosthesis in palliation of stenosing tumors of the upper gastrointestinal tract. Comparison of experience with three stent types in 82 implantations. *Dtsch Med Wochensch* 1995; **120**: 1343-1348
33 **Smout AJ.** Back to the Whale bone? *Gut* 1999; **44**: 149-150
34 **Mumtaz H,** Barone GW, Ketel BL, Ozdemir A. Successful management of a nonmalignant esophageal perforation with a coated stent. *Ann Thorac Surg* 2002; **74**: 1233-1235
35 **Acunas B,** Poyanli A, Rozanes I. Intervention in gastrointestinal tract: the treatment of esophageal, gastroduodenal and colorectal obstructions with metallic stents. *Eur J Radiol* 2002; **42**: 240-248
36 **Petruzziello L,** Costamagna G. Stenting in esophageal strictures. *Dig Dis* 2002; **20**: 154-166
37 **Catnach S,** Barrison I. Self-expanding metal stents for the treatment of benign esophageal strictures. *Gastrointest Endosc* 2001; **54**: 140
38 **Fry SW,** Fleischer DE. Management of a refractory benign esophageal stricture with a new biodegradable stent. *Gastrointest Endosc* 1997; **45**: 179-182
39 **Catnach S,** Barrison I. Self-expanding metal stents for the treatment of benign esophageal strictures. *Gastrointest Endosc* 2001; **54**: 140
40 **Therasse E,** Oliva VL, Lafontaine E, Perreault P, Giroux MF, Soulez G. Balloon dilation and stent placement for esophageal lesions: indications, methods, and results. *Radiographics* 2003; **23**: 89-105

Edited by Zhang JZ and Wang XL

P.O.Box 2345, Beijing 100023,China
Fax: +86-10-85381893
E-mail: wjg@wjgnet.com www.wjgnet.com

World J Gastroenterol 2003;9(11):2612-2615
World Journal of Gastroenterology
 ISSN 1007-9327

• BRIEF REPORTS •

Relationship between genetic polymorphism of cytochrome P450IIE1 and fatty liver

Yun-Feng Piao, Jing-Tao Li, Yang Shi

Yun-Feng Piao, Jing-Tao Li, Yang Shi, Department of Gastroenterology, First Hospital, Jilin University, Changchun 130021, Jilin Province, China
Correspondence to: Dr. Yang Shi, Department of Gastroenterology, First Hospital, Jilin University, 1 Xinmin Road, Changchun 130021, Jilin Province, China. shiyangwhy@163.com
Telephone: +86-431-5612242 **Fax:** +86-431-5612542
Received: 2003-03-29 **Accepted:** 2003-05-17

Abstract

AIM: To study the correlation between genetic polymorphism of cytochrome P450IIE1 (CYPIIE1) and fatty liver.

METHODS: Peripheral blood mononuclear cells were collected in 56 patients with fatty liver, 26 patients without fatty liver and 20 normal controls. Then PCR-RFLP was used to analyze genetic polymorphism of CYPIIE1 in monocytes on the region of Pst I and Rsa I.

RESULTS: The frequency of homozygotic C1 gene in patients with alcoholic fatty liver (28.6 %), obese fatty liver (38.5 %), or diabetic fatty liver (33.3 %) was significantly lower than that of the corresponding patients without fatty liver (100 %, 100 % and 80 % respectively), while the frequency of C2 genes, including C1/C2 and C2/C2, was significantly higher (71.4 %/0 %, 61.5 %/0 %, and 66.7 %/20 %) (P<0.01). The frequency distribution of the above genes of non-fatty liver patients (100 %/0, 100 %/0, and 80 %/20 %) was not significantly different from that of the normal controls (85 %/15 %) (P>0.05).

CONCLUSION: The genetic polymorphism of CYPIIE1 on the position of Pst I and Rsa I is related to the susceptibility of fatty liver. Besides, C2 gene may play a key role in the pathogenesis of fatty liver.

Piao YF, Li JT, Shi Y. Relationship between genetic polymorphism of cytochrome P450IIE1 and fatty liver. *World J Gastroenterol* 2003; 9(11): 2612-2615

http://www.wjgnet.com/1007-9327/9/2612.asp

INTRODUCTION

Cytochrome P450 (CYP) is a group of isoenzymes encoded by genes with similar structure and function, whose molecular weight is 40-60KD. CYP is a kind of monooxygenase, located in the smooth endoplasmic reticulum of cells. According to the similarity of amino acid sequence, CYP is divided into CYPI, CYPII, CYPIII, and CYPIV gene families. The subfamily is named alphabetically, and every enzyme is named in number order. Cytochrome P450IIE1 (CYPIIE1) is a N-nitrosodimethylamine demethylase, which is mainly expressed in the liver with an evident racial and individual difference in activity. It not only takes part in the metabolism of drugs, but also activates a lot of precarcinogens and prepoison[1-4]. Human CYPIIE1 is located in 10q2403-qter. It is 1104Kb consisting of 9 extrons and 8 introns, encoding a 493-amino acid protein[5]. The polymorphism of CYPIIE1 gene is significantly different among races and individuals. It may be related to some genetic factors. CYPIIE1 has 6 restriction fragment length polymorphisms (RFLP), among which 5' -flanking region of Pst I and Rsa I affects CYPIIE1 expression at the transcription level. C2 allelic gene can enhance the transcription, which causes the different activities of CYPIIE1[6-11].

Fatty liver is common and is resulted frequently from alcohol excess, obesity, diabetes or drugs[12-17]. Its pathogenesis remains unclear. Studies on the relationship between genetic polymorphisms of CYPIIE1 and the development of alcoholic fatty liver has been reported, but the results are disputable[17-21]. In this study, we used PCR-RFLP to study the relationship between genetic polymorphisms of CYPIIE1 and alcoholic or non-alcoholic fatty liver.

MATERIALS AND METHODS

Reagents

Heparin and lymphocyte separation medium were purchased from Tianjin Hematologic Institution of Chinese Academy of Medical Sciences. The primers of CYPIIE1, PCR buffer, dNTP, and Taq enzyme were obtained from Roche (America). Restriction endonucleases (PstIand RsaI), their buffer, and pUC19-DNA marker were obtained from MBI Ferments.

Patients and controls

From October 1998 to January 2001, 82 patients from several hospitals in Jilin Province were studied, among them 28 cases had alcoholic fatty liver, 8 cases had alcoholism but no liver disease, 13 cases had obese fatty liver, 8 cases had obesity but no fatty liver, 15 cases had diabetic fatty liver, and 10 cases had diabetes but no fatty liver. Twenty health blood donors were used as normal controls. The standard of alcoholism for female was drinking alcohol >40 g/d, for male drinking alcohol >80 g/d, for at least 5 years. The age and sex distribution of the two groups were similar. Five ml venous blood was taken from every person and anticoagulated with heparin.

PCR-RFLP

Peripheral blood mononuclear cells (PBMC) were separated by density gradient centrifugation. Then DNA was extracted. The two primers of CYPIIE1 were 5' -ccagtcgagtctacattgtca-3' (1 370-1 349) and 5' -ttcattctgtcttctaactgg-3' (999-978) respectively. PCR was conducted for 40 cycles with denaturing at 94 ℃ for 1 min, annealing at 50 ℃ for 1 min, extending at 72 ℃ for 1 min, and then designed to extend at 72 ℃ for 10 min. The PCR products were digested with Pst I or Rsa I at 37 ℃ for 2 hours, then loaded onto a 20 g/L agarose gel for electrophoresis. At last, the DNA fragments were observed under ultraviolet lamp.

Statistical analysis

Analysis of data was performed using χ^2 test. P<0.05 was considered to be statistically significant.

RESULTS

Genetic polymorphism of CYPIIE1

The PCR products were fragments of 410 bp (Figure 1). After digestion with restriction enzyme Pst I or Rsa I, CYPIIE1 was divided wild type homozygote group (C1/C1, type A), heterozygote group (C1/C2, type B) and mutant homozygote group (C2/C2, type C) (Figure 2). C1 referred to wild type gene (PstI+, RsaI-), and C2 referred to mutant gene (PstI-,RsaI+).

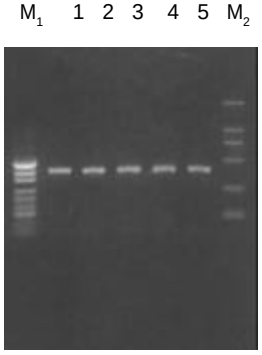

Figure 1 Electrophoregram of PCR products (Lanes 1-5). The signals of pUC19-DNA marker (M_1) present 489 bp, 404 bp, 331 bp, 242 bp, 190 bp, 147 bp and 110 bp from up to bottom. The signals of DL2000-DNA marker (M_2) present 2 000 bp, 1 000 bp, 750 bp, 500 bp, 250 bp and 100 bp from up to bottom.

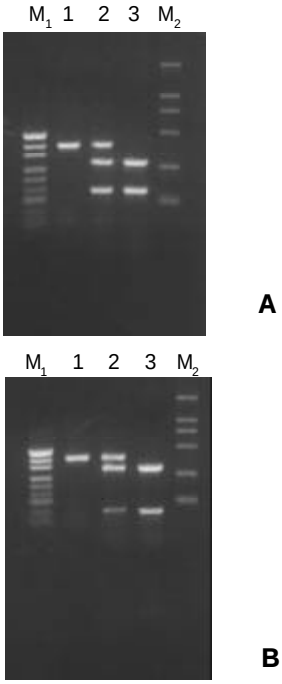

Figure 2 After digested with restriction enzyme PstI(A) or RsaI (B), CYPIIE1 was divided into three types, namely wild type homozygote (C1/C1) (Lane 1), heterozygote (C1/C2)(Lane 2) and mutant homozygote (C2/C2)(Lane 3). C1 means wild type gene (PstI+, RsaI-), and C2 mutant gene (PstI-, RsaI+). pUC19-DNA marker (M_1) and DL2000-DNA marker (M_2).

Genotype distribution

The genotype distribution of each group of patients and controls are presented in Table 1.

Comparison of gene frequency

The frequency of homozygotic C1 gene in patients with alcoholic, obese, or diabetic fatty liver was significantly lower than that of patients with corresponding diseases but without fatty liver, while the frequency of C2 genes, including C1/C2 and C2/C2, was significantly higher (P<0.01) (Table 2). Compared with healthy controls, the frequency of homozygotic C1 gene of the patients with alcoholic, obese, or diabetic fatty liver was apparently lower and the frequency of C2 gene was apparently higher (P<0.01). At the same time, there was no obvious difference in homozygotic C1 gene or C2 gene between healthy controls and patients with alcoholism, obesity or diabetes but without fatty liver (P>0.05).

Table 1 Genotype distribution of each group of patients and controls

Group	*n*	A (C1/C1)	B (C1/C2)	C (C2/C2)
Patients with alcoholic fatty liver	28	8	14	6
Patients with alcoholism but without liver diseases	8	8	0	0
Patients with obese fatty liver	13	5	6	2
Patients with obese but without fatty liver	8	8	0	0
Patients with diabetic fatty liver	15	5	8	2
Patients with diabetes but without fatty liver	10	8	2	0
Healthy controls	20	17	3	0

Table 2 Comparison of gene frequency of each group (%)

Group	A	B	C	C2 frequency
Patients with alcoholic fatty liver	28.6	50.0	21.4	71.4
Patients with alcoholism but without liver diseases	100	0	0	0
Patients with obese fatty liver	38.5	46.1	15.4	61.5
Patients with obese but without fatty liver	100	0	0	0
Patients with diabetic fatty liver	33.3	53.4	13.3	66.7
Patients with diabetes but without fatty liver	80	20	0	20
Healthy controls	85	15	0	15

DISCUSSION

There are three metabolic pathways of ethanol in the liver, alcohol dehydrogenase (ADH) in cytoplasm, microsomal ethanol oxidazing system (MEOS) in smooth endoplasmic reticulum, and catalase in peroxidase. The major component of MEOS is CYPIIE1[22,23]. When concentration of ethanol in blood and liver tissue is low, most of ethanol is oxidized by ADH. While for the alcoholism or the people in whose liver tissue the concentration of ethanol is higher than 10 mmol/L, the activation of MESO plays a key role in metabolism of ethanol. In the pathogenesis of alcoholic fatty liver, the function of CYPIIE1 was mainly to take part in lipid peroxidation (LOP) reaction and to increase the contents of microsomal oxygen and carbonyl free radical[16,24,25]. It has been proved in rat models that generation of microsomal oxygen and carbonyl free radical formed from oxidated ethanol was related to CYPIIE1[26,27]. It was presumed that these oxygen-derived free radicals might impair the liver by directly damaging liver cells, affecting the sensititity of the liver to LPO, and inducing antibody-dependent cytotoxic effect through combination with CYPIIE1 on the cell membrane[28-30]. Not every alcoholic abuser could inevitably induce liver injury. Iwahashi K and colleagues[31] reported that in the people who had C2 allele, CYPIIE1 activity was much

higher, and metabolic ability on ethanol was much stronger. Our results showed that homozygotic C1 gene frequency of the patients with alcoholic fatty liver was significantly lower than that of the controls or the patients with alcoholism but without fatty liver, while C2 gene frequency was much higher. It suggested that C2 gene might induce the expression of CYPIIE1 and facilitate genesis of alcoholic fatty liver.

LPO also took part in the pathogenesis of non-alcoholic fatty liver induced by obese or diabetes[32,33]. Now the precise stimulator of LPO reaction is unclear. The expression of CYPIIE1 in the animal models and patients with nonalcoholic fatty liver might be related to the induction of acetone and fatty acid[34,35]. It has been proved that the level of CYPIIE1 in the rats with obesity was four times as high as that of the rats without obesity[36]. The rising concentration of fatty acid and pyruvic acid in the liver might be a risk factor in pathogenesis of nonalcoholic fatty liver. When the increased fatty acid concentration in blood of patients with obesity could not be oxidated by mitochondria completely, CYPIIE1 would have the ability to oxidize fatty acid and in turn is activated by it so as to strengthen the oxidation ability. During oxidation of fatty acid, high reactivity carbonyl free radicals would be produced, which then stimulated the production of LPO, at last injured the liver[37]. In patients with diabetes, the ketone bodies produced by the liver could not be totally utilized by extrahepatic tissues, and the level of acetone would rise in the liver. The acetone could not only induce CYPIIE1 activation, but also be resolved by it. A great many of free radicals were produced, thus injuring the liver[38]. Not all patients with obesity or diabetes suffer from fatty liver. Our results showed that C2 gene frequency in patients with obese fatty liver or diabetic fatty liver was obviously higher than that of the patients without fatty liver. In conclusion, C2 gene frequency in patients with alcoholic or nonalcoholic fatty liver is much higher than that of controls. So C2 gene may be important for the pathogenesis of fatty liver.

REFERENCES

1 **Koop DR.** Oxidative and reductive metabolism by cytochrome P4502E1. *FASEB J* 1992; **6**: 724-730
2 **Gonzalez FJ**, Gelboin HV. Transcriptional and posttranscriptional regulation of CYP 2E1, an N-nitrosodimethylamine demethylase. *Princess Takamatsu Symp* 1990; **21**: 157-164
3 **Ramaiah SK**, Apte U, Mehendale HM. Cytochrome P450 2E1 induction increases thioacetamide liver injury in diet-restricted rats. *Drug Metab Dispos* 2001; **29**: 1088-1095
4 **Zangar RC**, Benson JM, Burnett VL, Springer DL. Cytochrome P450 2E1 is the primary enzyme responsible for low-dose carbon tetrachloride metabolism in human liver microsomes. *Chem Biol Interact* 2000; **15**: 233-243
5 **Umeno M**, McBride OW, Yang CS, Gelboin HV, Gonzalez FJ. Human ethanol-inducible P450IIE1: complete gene sequence, promoter characterization, chromosome mapping, and cDNA-directed expression. *Biochemistry* 1988; **27**: 9006-9013
6 **Han XM**, Zhou HH. Polymorphism of CYP450 and cancer susceptibility. *Acta Pharmacol Sin* 2000; **21**: 673-679
7 **Snawder JE**, Lipscomb JC. Interindividual variance of cytochrome P450 forms in human hepatic microsomes: correlation of individual forms with xenobiotic metalolism and implications in risk assessment. *Regul Toxical Pharmacol* 2000; **32**: 200-209
8 **Stephens EA**, Taylor JA, Kaplan N, Yang CH, Hsieh LL, Lucier GW, Bell DA. Ethnic variation in the CYPE1 gene polymorphism analysis of 695 African-Americans, European-Americans and Taiwanese. *Pharmacogenetics* 1994; **4**: 185-192
9 **Watanabe J**, Hayashi S, Kawajiri K. Different regulation and expression of the human CYP2E1 gene due to the Ras I polymrophim in the 5'-flanking region. *J Biochem* 1994; **116**: 321-326
10 **Hu Y**, Hakkola J, Oscarson M, Ingelman-Sundberg M. Structural and functional characterization of the 5'-flanking region of the rat and human cytochrome P4502E1 genes: indentification of a polymorphic repeat in the human gene. *Biochem Biophys Res Commun* 1999; **263**: 286-293
11 **Hayashi SI**, Watanabe J, Kawajiri K. Genetic polymorphisms in the 5'-flanking region change transcriptional regulation of human cytochrome P450IIE1. *J Biochem* 1991; **110**: 559-565
12 **Farrell GC**. Drugs and steatohepatitis. *Semin Liver Dis* 2002; **22**: 185-194
13 **Niemela O**, Parkkila S, Juvonen RO, Viitala K, Gelboin HV, Pasanen M. Cytochromes P450 2A6, 2E1, and 3A and production of protein-aldehyde adducts in the liver of patients with alcoholic and non-alcoholic liver diseases. *J Hepatol* 2000; **33**: 893-901
14 **Pirttiaho HI**, Salmela PI, Sotaniemi EA, Pelkonen RO, Pitkanen U, Luoma PV. Drug metabolism in diabetic subjects with fatty livers. *Br J Clin Pharmacol* 1984; **18**: 895-899
15 **Karvonen I**, Stengard JH, Huupponen R, Stenback FG, Sotaniemi EA. Effects of enzyme induction therapy on glucose and drug metabolism in obese mice model of non-insulin dependent diabetes mellitus. *Diabetes Res* 1989; **10**: 85-92
16 **Yang S**, Zhu H, Li Y, Lin H, Gabrielson K, Trush MA, Diehl AM. Mitochondrial adaptations to obesity-related oxidant stress. *Arch Biochem Biophys* 2000; **378**: 259-268
17 **Vidali M**, Stewart SF, Rolla R, Daly AK, Chen Y, Mottaran E, Jones DE, Leathart JB, Day CP, Albano E. Genetic and epigenetic factors in autoimmune reactions toward cytochrome P4502E1 in alcoholic liver disease. *Hepatology* 2003; **37**: 410-419
18 **Robertson G**, Leclercq I, Farrell GC. Nonalcoholic steatosis and steatohepatitis. II. Cytochrome P-450 enzymes and oxidative stress. *Am J Physiol Gastrointest Liver Physiol* 2001; **281**: 1135-1139
19 **Sinclair JF**, Szakacs JG, Wood SG, Walton HS, Bement JL, Gonzalez FJ, Jeffery EH, Wrighton SA, Bement WJ, Sinclair PR. Short-term treatment with alcohols causes hepatic steatosis and enhances acetaminophen hepatotoxicity in Cyp2e1 (-/-) mice. *Toxicol Appl Pharmacol* 2000; **168**: 114-122
20 **Jarvelainen HA**, Fang C, Ingelman-Sundberg M, Lukkari TA, Sippel H, Lindros KO. Kupffer cell inactivation alleviates ethanol-induced steatosis and CYP2E1 induction but not inflammatory responses in rat liver. *J Hepatol* 2000; **32**: 900-910
21 **Agundez J**, Ladero J, Diaz-Rubio M, Benitez J. Rsa I polymorphism at the cytochrome P4502E1 locus is not related to the risk of alcohol-related severe liver disease. *Liver* 1996; **16**: 380-383
22 **Donohue TM Jr**, Clemens DL, Galli A, Crabb D, Nieto N, Kato J, Barve SS. Use of cultured cells in assessing ethanol toxicity and ethanol-related metabolism. *Alcohol Clin Exp Res* 2001; **25**: 87S-93S
23 **Kunitoh S**, Imaoka S, Hiroi T, Yabusaki Y, Monna T, Funae Y. Acetaldehyde as well as ethanol is metabolized by human CYPIIE1 . *J Pharmacol Exp Ther* 1997; **280**: 527-532
24 **Ingelman-Sundberg M**, Ronis MJ, Lindros KO, Eliasson E, Zhukov A. Ethanol-inducible cytochrome P4502E1: regulation, enzymology and molecular biology. *Alcohol Alcohol Supl* 1994; **2**: 131-139
25 **Maher J**. The CYP2E1 knockout delivers another punch: first ASH, now NASH. Alcoholic steatohepatitis. Nonalcoholic steatohepatitis. *Hepatology* 2001; **33**: 311-312
26 **Ekstrom G**, Ingelman-Sundberg M. Rat liver nicrosomal NADPH-supported oxidase activity and peroxidation dependent on ethanol-inducible cytochrom P450. *Biochem Pharmacol* 1989; **38**: 1313-1319
27 **Albano E**, Clot P, Morimoto M, Tomasi A, Ingelman-Sundberg M, French SW. Role of cytochrome-P4502E1-dependent formation of hydroxyethyl free radical in the development of liver damage in rats intragstrically fed with ethanol. *Hepatology* 1996; **23**: 155-163
28 **Clot P**, Albano E, Eliasson E, Tabone M, Arico S, Israel Y, Moncada C, Ingelman-Sundberg M. Cytochrome P4502E1 hydroxyethyl radical adducts as the major antigen in autoantibody formation among alcoholics. *Gastroenterology* 1996; **111**: 206-216
29 **Albano E**, French SW, Ingelman-Sundberg M. Hydroxyethyl radical in ethanol hepatotoxicity. *Front Biosci* 1999; **4**: 533-540
30 **Britton RS**, Bacon BR. Role of free radical in liver diseases and hepatic fibrosis. *Hepatogastroenterology* 1994; **41**: 343-348

31 **Iwahashi K**, Miyatake R, Suwaki H, Kinoshita H, Ameno K, Ijiri I, Ishikawa Y, Matsuo Y. Blood ethanol levels and CYPIIE1 allele. *Arukoru Kenkyuto Yakubutsu Ison* 1994; **29**: 190-194
32 **Leclercq IA**, Farrell GC, Field J, Bell DR, Gonzalez FJ, Robertson GR. CYP2E1 and CYP4A as microsomal catalysts of lipid peroxides in murine nonalcoholic steatohepatitis. *J Clin Invest* 2000; **105**: 1067-1075
33 **Letteron P**, Fromenty B, Terris B, Degott C, Pessayre D. Acute and chronic hepatic steatosis lead to in vivo lipid peroxidation in mice. *J Hepatol* 1996; **24**: 200-208
34 **Weltman MD**, Farrell GC, Hall P, Ingelman-Sundberg M, Liddle C. Hepatic cytochrome P4502E1 is increased in patients with non-alcoholic steatohepatitis. *Hepatolygy* 1998; **27**: 128-133
35 **Weltman MD**, Farrell GC, Liddle C. Increased CYP2E1 expression in a rat nutritional model of hepatic steatosis with inflammation. *Gastroenterology* 1996; **111**: 1645-1653
36 **Raucy JL**, Lasker JM, Kraner JC, Salazar DE, Lieber CS, Corcoran GB. Introduction of cytochrome P450IIE1 in the obese overfed rat. *Mol Pharmacol* 1991; **39**: 275-280
37 **Osmundsen H**, Bremer J, Pedersen JI. Metabolic aspects of peroxisomal-oxidation. *Biochim Biophys Acta* 1991; **1085**: 141-158
38 **Zangar RC**, Novak RF. Effects of fatty acids and ketone bodies on cytochromes P450 2B, 4A and 2E1 expression in primary cultured rat hepatocytes. *Arch Biochem Biophys* 1997; **337**: 217-224

Edited by Zhang JZ and Wang XL

P.O.Box 2345, Beijing 100023,China
Fax: +86-10-85381893
E-mail: wjg@wjgnet.com www.wjgnet.com

World J Gastroenterol 2003;9(11):2616-2618
World Journal of Gastroenterology
 ISSN 1007-9327

• BRIEF REPORTS •

Significance of expression of heat shock protein90α in human gastric cancer

Dong-Sheng Zuo, Jie Dai, Ai-Hua Bo, Jie Fan, Xiu-Ying Xiao

Dong-Sheng Zuo, Ai-Hua Bo, Jie Fan, Xiu-Ying Xiao, Department of Pathology, Zhangjiakou Medical College, Zhangjiakou 075029, Hebei Province, China
Jie Dai, Capital University of Medical Sciences, Beijing 100054, China
Supported by the Natural Science Fundation of Hebei Province, No. 301427
Correspondence to: Dong-Sheng Zuo, Department of Pathology, Zhangjiakou Medical College, Zhangjiakou 075029, Hebei Province, China. dshz2003@yahoo.com.cn
Telephone: +86-313-8041652 **Fax:** +86-313-8041652
Received: 2003-04-08 **Accepted:** 2003-05-19

Abstract

AIM: To evaluate the significance of hsp90α expression in human gastric cancer tissues.

METHODS: Immunohistochemical staining was used in clinical specimens from 33 cases of gastric cancer and 33 cases of gastritis with rabbit anti-human hsp90α multi-clonal antibody in order to explore the relationship between the expression of hsp90α in gastric carcinoma tissue and gastritis tissue as well as in mucous membrane adjacent to cancer and lymph node metastasis.

RESULTS: Hsp90α was detected in 88 % of gastric carcinoma cases and 55 % of gastritis cases. The hsp90α positive rate in gastric cancer group was significantly higher than that in gastritis group ($P<0.01$, $P=0.005$). The hsp90α positive rate in gastric cancer and in mucous membrane adjacent to cancer was 88 % and 55 % respectively ($P<0.01$,$P=0.005$). The hsp90α positive rate in lymph node metastasis group and non-lymph node metastasis group was 100 % and 60 % respectively, and a significant correlation between hsp90α expression and lymph node metastasis was shown ($P<0.01$, $P=0.005$).

CONCLUSION: The hsp90α expression rate in gastric cancer group was significantly higher than that in gastritis group as well as that in the group of mucous membrane adjacent to cancer. The hsp90α expression in lymphatic node metastasis group was higher than that in non-lymphatic node metastasis group. The results indicate that increased hsp90α expression has a close relationship with occurrence and lymph node metastasis of gastric cancer.

Zuo DS, Dai J, Bo AH, Fan J, Xiao XY. Significance of expression of heat shock protein90α in human gastric cancer. *World J Gastroenterol* 2003; 9(11): 2616-2618
http://www.wjgnet.com/1007-9327/9/2616.asp

INTRODUCTION

Heat shock protein90α, commonly known as heat stress protein, is a highly conserved cytosolic protein during the evolution of living things. It extensively exists in the living organisms and has many important biological functions such as enhancing cellular tolerance to stress and maintaining cellular homeostasis, etc. There are two forms of hsp90 in the advanced organisms, i.e. α form and β form. Under stress, the synthesis of hsp90 increases. For example, high temperature and infection can induce increase of hsp90 synthesis. However, different inducers play different roles in inducing hsp90 synthesis. hsp90α is more sensitive to heat induction, hsp90β is more sensitive to mitosis induction[1]. Recent studies showed that hsp90 had a close relationship with carcinoma. It was highly expressed in cancer tissue[2]. hsp90 combines with many transformed proteins to form complexes that are transported into intracellular special sites and correlated with cancer cell proliferation and differentiation[3,4]. There is a close relationship between the occurrence of gastric cancer and the synthesis of heat shock protein. At present there have been few reports on the study of hsp90 expression during the genesis of gastric cancer. In our study, we used immunohistochemical staining SP method to detect the expression of hsp90α in gastric cancer, gastritis, mucous membrane adjacent to cancer and gastric cancer tissue with or without lymph node metastasis in order to explore the relationships among them and their clinical significances,as well as the roles of hsp90α expression in the genesis and development of gastric cancer. Our study showed that the hsp90α expression rate in gastric cancer group was significantly higher than that in gastritis group, and in group of mucous membrance adjacent to cancer, hsp90α expression in the lymphatic node metastasis group was higher than that in the non-lymphatic node metastasis group.

MATERIALS AND METHODS

Samples collection

A total of 66 samples were collected from our hospital which were cut off from the stomach after operation, including 33 cases of gastric cancer and 33 cases of gastritis. Twenty-three of the 33 cases of gastric cancer had lymph nodes metastases and 10 cases had no lymph node metastasis. The samples were fixed in 10 % formaldehyde, dehydrated and embedded in paraffin. Five μm-thick sections were sliced. All samples were confirmed by pathological diagnosis.

Immunohistochemistry reagents

Rabbit anti-human hsp90α multi-clonal antibody (650-871-1919 CA, U.S.A), immunohistochemical staining S-P kit and DAB were purchased from Maixin LTD.

Methods

Immunohistochemical SP staining method was used in our experiment. The conventional staining procedures were carried out. The main procedures were as follows. The tissue sections were routinely dewaxed and hydrated, then treated with 3 % peroxide for 10 minutes. Antigen restoration was carried out by heating in citrate buffer, blocked with normal goat serum, incubated overnight with anti-human hsp90α multi-clonal antibody at 4 ℃, washed three times with PBS, treated with antibody II for 30 minutes at 37 ℃ and then with antibody III

for 30 minutes at 37 ℃. Color was displayed with DAB. Negative control was designed with PBS instead of antibody I. The known positive tissue sections were used as positive control.

Statistic analysis

SPSS10.0 software was used for statistical analysis.

RESULTS

Evaluation standard

Under light-microscope the hsp90α immunoreactive products showed as granules with brown color. These granules were mainly located in cytoplasm, only a few in nuclei. According to the amount and color density of granules, the staining was divided into three grades: +: few granules, canary color; ++: lots of granules filled cytoplasm, brown color ; +++: cytoplasm was filled with brown-black granules. The granules were also found in nucleoli. Detailed expressions of hsp90α in tissues of gastric cancer, gastritis and lymph nodes are shown in Tables 1, 2 and 3.

Table 1 Hsp90α expression in tissues of gastric cancer and gastritis

Pathologic types	*n*	Grade of hsp90α expression				Positive rate (%)
		-	+	++	+++	
Gastric cancer	33	4	23	4	2	88
Gastritis	33	15	13	4	1	55

[b]$P<0.01$ *vs* group of Gastritis, $\chi^2=8.943$.

Table 2 Hsp90α expression in gastric cancer tissues and tissues adjacent to cancer

Pathologic types	*n*	Grade of hsp90α expression				Positive rate (%)
		-	+	++	+++	
Gastric cancer	33	4	23	4	2	88
Tissues adjacent to cancer	33	15	17	1	0	55

[b]$P<0.01$ *vs* group of tissue adjacent to cancer, $\chi^2=8.943$.

Table 3 Hsp90α expression in tissues of gastric cancer with and without lymph node metastasis

Pathologic types	*n*	Grade of hsp90α expression				Positive rate (%)
		-	+	++	+++	
With lymph node metastasis	23	0	17	4	2	100
Without lymph node metastasis	10	4	5	1	0	60

[b]$P<0.01$ *vs* group without ymph node metastasis, $\chi^2=10.469$.

The hsp90α immunoreactive signals in gastric cancer were mostly strong or very strong. The positive rate was 88 %. However, in gastritis samples, the positive rate of hsp90α immunoreactive signals was 55 %, most of which were weakly positive. There was a significant difference between gastric cancer and gastritis ($P<0.01$). The hsp90α immunoreactive positive rates in gastric cancer or in mucous membrane adjacent to cancer were 88 % and 55 % respectively. There was also a significant difference between them ($P<0.01$). A significant difference also existed between gastric cancer with lymph node metastasis (100 %) and that without lymph node metastasis (62.5 %) ($P<0.01$).

DISCUSSION

The expression of hsp90α in normal cells is controlled by cell cycle[5], but it can continuously express at high level in tumor cells without heat stimulation. The existence of mutant or abnormal proteins also stimulates HSPs synthesis[6-9]. Heat shock proteins can maintain oncogene products in inactive state[10]. On the other hand, it has the functions of transportation and transfer. In tumor cells, the expression of hsp90α is higher than that in normal cells. An increasing trend of hsp90α expression was seen in virus-transformed and chemical-induced tumor cells[11,12]. In pancreatic cancer, hsp90α showed a selective expression at high level. Jamell[13] found that hsp90α expressed in all human breast cancers and hsp90α expression was higher in malignant breast tissue[14]. An increased expression of hsp90α mRNA was also found in ovary cancer and the more serious the disease was, the higher the expression of hsp90α mRNA was[1]. It was also found that hsp90α showed a high expression in 29 % of endometrium cancer. Yano' s research[1] showed that the hsp90α mRNA level in breast cancer was higher than that in non-cancer tissues[14,15]. The expression of hsp90α mRNA has a close correlation with proliferating cell nuclear antigen labeling index (PCNA LI), indicating that high expression of hsp90α mRNA should have an important role in cell proliferation. It was identified in our study that the expression of hsp90α in gastric cancer was obviously higher than that in gastritis and mucous membrane adjacent to cancer.

HSPs take part in cell growth and proliferation by several means such as signal transduction and cell cycle regulation. HSPs express highly in germ cells and embryonic cells, but express lowly in aging cells. This suggests that the increase of protein synthesis in proliferating cells needs much more HSPs to take part in the formation of protein activities. Because tumor cells are a group of high proliferation heteromorphic cells, they may need much more HSPs to sustain their proliferation[16,17]. Our results also showed that the expression of hsp90α in gastric cancer with lymph node metastasis was higher than that without lymph node metastasis. All of these were consistent with the results from Jamell' s report that the higher the breast cancer malignancy is, the higher the hsp90α expresses. This indicats increase of hsp90α expression probably has some relationship with genesis, development, invasion and lymph node metastasis of gastric cancer.

Under various stimulations, gastric mucous membrane can transcript and translate high levels of HSPs that can change the metabolism and functions of cells in order to alleviate the damage caused by deleterious factors including exogenous stimulants such as heat, chemicals and ethanol, and endogenous stimulants such as acid, local ischemia, hypoxia. In this case, gastric mucous membrane should synthesize HSP rapidly to exert the protecting role for gastric mucous cells[1]. The genesis of gastric cancer is a gradual process under the long-term influence of various stimulants as well as other factors. During the process, HSPs synthesis increases gradually[16]. This viewpoint was confirmed by our results that hsp90α positive rate in gastric cancer was higher than that in gastritis and gastric tissues adjacent to cancer. The discovery of our study may provide some useful clues for early detection and clinical diagnosis of gastric cancer.

REFERENCES

1 **Yano M**, Naito Z, Tanaka S, Asano G. Expression and roles of heat shock proteins in human breast cancer. *Jpn J Cancer Res* 1996; **87**: 908-915

2 **Gress TM**, Muller-Pillasch F, Weber C, Lerch MM, Friess H, Buchler M, Beger HG, Adler G. Differential expression of heat shock proteins in pancreatic carcinoma. *Cancer Res* 1994; **54**: 547-551

3 **Pratt WB**. The hsp90-based chaperone system: involvement in

signal transduction from a variety of hormone and growth factor receptors. *Proc Soc Exp Biol Med* 1998; **217**: 420-434

4 **Whitesell L,** Mimnaugh EG, De Costa B, Myers CE, Neckers LM. Inhibition of heat shock Protein HSP90-PP60v-src heteroprotein complex formation by benzoquinone ansamycins: essential role for stress proteins in oncogenic transformation. *Proc Natl Acad Sci U S A* 1994**; 91**: 8324-8328

5 **Liu XL,** Xiao B, Yu ZC, Guo JC, Zhao QC, Xu L, Shi YQ, Fan DM. Down-regulation of HSP90 could change cell cycle distribution and increase drug sensitivity of tumor cells. *World J Gastroenterol* 1999; **5**: 199-208

6 **Maloney A**, Workman P. HSP90 as a new therapeutic target for cancer therapy: the story unfolds. *Expert Opin Biol Ther* 2002; **2**: 3-24

7 **Neckers L,** Mimnaugh E, Schulte TW. HSP90 as an anti-cancer target. *Drug Resist Updat* 1999; **2**: 165-172

8 **Darimont BD.** The Hsp90 chaperone complex-A potential target for cancer therapy? *World J Gastroenterol* 1999; **5**: 195-198

9 **Neckers L**. Hsp90 inhibitors as novel cancer chemotherapeutic agents. *Trends Mol Med* 2002; **8**(4 Suppl): S55-61

10 **Nagata Y,** Anan T, Yoshida T, Mizukami T, Taya Y, Fujiwara T, Kato H, Saya H, Nakao M. The stabilization mechanism of mutant-type p53 by impaired ubiquitination: the loss of wild-type p53 function and the HSP90 association. *Oncogene* 1999; **18**: 6037-6049

11 **Srivastava PK,** Vdono H. Heat shock protein-peptide complexes in cancer immunotherapy. *Curr Opin Immunol* 1994**; 6**: 728-732

12 **Cho G,** Park SG, Jung G. Localization of HSP90 binding sites in the human hepatitis B virus polymerase. *Biochem Biophys Res Commun* 2000**; 269**: 191-196

13 **Jameel A**, Skilton RA, Campbell TA. Clinical and biological significance of HSP89α in human breast cancer. *Int J Cancer* 1992; **50**: 409-415

14 **Munster PN,** Basso A, Solit D, Norton L, Rosen N. Modulation of HSP90 function by ansamycins sensitizes breast cancer cells to chemotherapy-induced apoptosis in an RB- and schedule-dependent manner. See: E. A. Sausville, Combining cytotoxics and 17-allylamino, 17-demethoxygeldanamycin: sequence and tumor biology matters, Clin. Cancer Res., **7**: 2155-2158, 2001. *Clin Cancer Res* 2001; **7**: 2228-2236

15 **Sausville EA**. Combining cytotoxics and 17-allylamino, 17-demethoxygeldanamycin: sequence and tumor biology matters. Commentary re: P. Munster *et al*, Modulation of HSP90 function by ansamycins sensitizes breast cancer cells to chemotherapy-induced apoptosis in an RB- and schedule-dependent manner. Clin. Cancer Res., **7**: 2228-2236,2001. *Clin Cancer Res* 2001; **7**: 2155-2158

16 **Zhang XY.** The basic research and clinic of gastric cancer. *Beijing Scientific Press* 1996: 32

17 **Kazlauskas A,** Sundstrom S, Poellinger L, Pongratz I. The hsp90 chaperone complex regulates intracellular localization of the dioxin receptor. *Mol Cell Biol* 2001; **21**: 2594-2607

Edited by Zhu LH and Wang XL

P.O.Box 2345, Beijing 100023,China
Fax: +86-10-85381893
E-mail: wjg@wjgnet.com www.wjgnet.com

World J Gastroenterol 2003;9(11):2619-2621
World Journal of Gastroenterology
 ISSN 1007-9327

• BRIEF REPORTS •

Prevention and therapy of fungal infection in severe acute pancreatitis: A prospective clinical study

Yue-Ming He, Xin-Sheng Lv, Zhong-Li Ai, Zhi-Su Liu, Qun Qian, Quan Sun, Ji-Wei Chen, Dao-Xiong Lei, Cong-Qing Jiang, Yu-Fong Yuan

Yue-Ming He, Xin-Sheng Lv, Department of General Surgery, Xiangya Hospital, Central South University, Changsha 410008, Hunan Province, China
Zhong-Li Ai, Zhi-Su Liu, Qun Qian, Quan Sun, Ji-Wei Chen, Dao-Xiong Lei, Cong-Qing Jiang, Yu-Fong Yuan, Department of General Surgery, Zhongnan Hospital, Wuhan University, Wuhan 430071, Hubei Province, China
Correspondence to: Dr. Yue-Ming He, Department of General Surgery, Zhongnan Hospital, Wuhan University, 169 Donghu Road, Wuhan 430071, Hubei Province, China. heym@medmail.com.cn
Telephone: +86-27-67813297 **Fax:** +86-27-87330795
Received: 2003-05-10 **Accepted:** 2003-06-02

Abstract

AIM: To investigate the prevention and therapy of fungal infection in patients with severe acute pancreatitis (SAP).

METHODS: Seventy patients with SAP admitted from Jan. 1998 to Dec. 2002 were randomly divided into garlicin prevention group, fluconazole (low dosage) prevention group and control group. The incidence of fungal infection, the fungal clearance and mortality after treatment were compared.

RESULTS: The incidence of fungal infection in garlicin group and fluconazole group was lower than that in control group (16 % *vs* 30 %, $P<0.05$ and 9 % *vs* 30 %, $P<0.01$, respectively). Amphotericin B or therapy-dose fluconazole had effects on patients with fungal infection in garlicin group and control group, but had no effects on patients with fungal infection in fluconzole group.

CONCLUSION: Prophylactic dosage of antifungal agents (garlicin or low dosage fluconazole) can reduce the incidence of fungal infection in patients with SAP. But once fungal infection occurs, amphotericin B should be used as early as possible if fluconazole is not effective.

He YM, Lv XS, Ai ZL, Liu ZS, Qian Q, Sun Q, Chen JW, Lei DX, Jiang CQ, Yuan YF. Prevention and therapy of fungal infection in severe acute pancreatitis: A prospective clinical study. *World J Gastroenterol* 2003; 9(11): 2619-2621
http://www.wjgnet.com/1007-9327/9/2619.asp

INTRODUCTION

Severe acute pancreatitis (SAP) accounts for about 20 % of acute pancreatitis. With understanding of the natural course of SAP and advances in critical care medicine, most SAP patients can survive systemic inflammatory response syndrome and accompanying dysfunction of important organs such as the heart, lung, kidney, etc[1]. The major complication in the middle and later phases of SAP is infection, its incidence is 40-50 % and its mortality is 10-20 %. About 80 % of mortality at the later phase of SAP is caused by infection[2]. For the time being, drug resistant bacteria infection, especially fungal infection is obviously increasing, and has become one of the major difficulties in the treatment of SAP[3]. In order to prevent and treat the deep fungal infection of SAP, this clinical research was conducted on fungal infection prevention and treatment by adopting garlicin, fluconazole and amphotericin B for SAP patients admitted from Jan. 1998 to Dec. 2002.

MATERIALS AND METHODS

Selection of cases

The selected cases accorded with the clinical diagnosis criteria proposed by the Pancreas Surgery Group of the Chinese Medical Association in 1997[4], and were complicated with one of the following predisposing factors of deep fungal infections[5-8], such as gerontism, history of diabetes, dysfunction of one or more organs, non-iatrogenic fasting hyperglycemia ($\geqslant$9 mmol/L), central venous catheter, TPN, retaining urethral catheterization, operation, gastrointestinal fistula, ICU, breathing machine supported$\geqslant$5d, user of glucocorticoid$\geqslant$5d, administration of broad spectrum antibiotics$\geqslant$5d or super broad spectrum antibiotics (such as Tienam, etc.)$\geqslant$3d.

Groups and methods

A total of 70 cases conforming to the above criteria were randomly divided into 3 groups. The garlicin group (25 patients) was given venous instillation of 120 mg garlicin one time per day plus routine treatment. The fluconazole group (22 patients) was given venous instillation of 100 mg fluconazole one time per day plus routine treatment. The control group (23 patients) received routine treatment only. The prophylactic medication for the garlicin and fluconazole groups was applied until relief of the predisposing factors (except gerontism and history of diabetes). The fungal infection treatment protocol was applied when the patients showed signs of deep fungal infection. The clinical data of these three groups are shown in Table 1.

Monitoring

Smears from peritoneal permeated liquid, pus of the infected wounds, throat specimen, sputum, urine and stool were prepared for fungus detection or/and fungal cultivation 2 times per week. If there was fungal infection, smears from the above sources were prepared for fungal identification 3 times per week. If the central venous catheter was suspected as the infection source, it was removed and cultured for fungi. Incidence and mortality of the patients with SAP complicated with deep fungal infection were observed.

Statistics analysis

All data were analyzed with SPSS11.0 software package, and a P value <0.05 was considered statistically significant. The average age, hospitalization duration, APACHE II grading etc, were displayed by $\bar{x}\pm s$, and differences were analysed using analysis of viariance and F test. Sex, etiological factor, death, fungal infection and number of cleared fungi and other data were analyzed using χ^2 or Fisher' s exact test.

Table 1 General clinical data of three groups

Group	Cases		Age	Etiological factor				APACHII
	Male:	Female		Biliary	Alcoholemia	Injury	Others	
Garlicin	12:	13	51.4±15.2	14	6	1	4	11.8±3.8
Fluconazole	12:	10	48.7±17.3	11	6	-	5	13.2±2.5
Control	13:	10	50.5±20.1	11	7	1	4	11.6±4.7

There were no statistically significant differences in three groups.

RESULTS

Incidence rate of fungal infection

Diagnostic criteria for SAP deep fungal infection[5,6] Doubtful clinical manifestations were fever after the broad spectrum antibiotics treatment with no drug resistant bacteria infection, cough, glue-like mucus or blood streak sputum, pseudo-membrane of the oral cavity or oral ulceration and symptoms of urinary tract stimulation, diarrhea with brown or/and jam-like feces, consciousness changes with unknown reasons, or bleedings irrelevant to pancreatitis such as fistula bleeding of the biliary and digestive tracts.Pathogenic evidences of fungi included positive fungal cultivation of blood, central venous catheter, smears of the fine-needle aspiration before operation, aspiration ascites or necrotic pancreas tissue during the operation, and drained bile, samples of sputum, peritoneal permeated fluid, pus of the infected wounds, throat specimen, sputum, urine and stool. Deep fungal infection could be diagnosed according to the suspicious clinical manifestations together with the same fungi existed in two or more systems.

Incidence rate of fungal infection The SAP patients infected with fungi in the garlicin and fluconazole groups were obviously less than those in the control group, and the number infected by fungi was the fewest in the fluconazole group (Table 2).

Table 2 Incidence rate of fungal infection in 3 groups

Group	Cases	Rate of fungal infection	Times of fungal infection after SAP(d)
Garlicin	25	4(16%)[a]	39-57
Fluconazole	22	2(9 %)[b]	35-62
Control	23	7(30 %)	24-183

[a]$P<0.05$, [b]$P<0.01$ *vs* control.

Treatment results of fungal infection

Protocol of treatment For highly suspicious pathogenic proofs of fungi or those with fungal infection, fluconazole was intravenous used to treat fungal infection, 200 mg (double dosage for the initial injection) once per day until the fungi were cleared. Amphotericin B was used for those with fungal infection in the fluconazole group. The dosage was started from 0.1 $mg.kg^{-1}$, and increased by 5 mg daily according to the patient's tolerance, and the treatment was continued till the dosage reached to 0.6 $mg.kg^{-1}$, the total accumulated amount reached 1.5-2 g. If the patients in garlicin and control groups were not sensitive to fluconazole, amphotericin B was then used.

Treatment results The fluconazole group had the lowest incidence of fungal infection, and the shortest hospital stay, but amphotericin B could not clear the fungi in fluconazole group, in which the patients were once complicated with fungal infection, they would inevitably died. When fungal infection occurred, the garlicin group had the highest clearance rate of fungi after treatment, and its mortality and average hospital stay were obviously lower or shorter than those in the control group. In the garlicin and control groups, each had one patient infected with fungi who was not cured by fluconazole therapy for 3 days, and their fungi were cleared when they changed to receive amphotericin B and they finally recuperated (Table 3).

Table 3 Treatment results of fungal infection in 3 groups

Group	Rate of fungal clearance	Mortality[#]	Times of Hospitalization
Garlicin	3(75 %)[a]	1(25 %)[a]	48.1±30.7[a]
Fluconazole	-	2(100 %)	43.3±26.9[b]
Contrast	4(57%)	3(43 %)	57.4±27.3

Note: # Mortality is the percentage (%) of patients who died of fungal septicemia. [a]$P<0.05$, [a]$P<0.01$ *vs* control.

DISCUSSION

Deep fungal infection often occurs in patients with impaired immunity, e.g. diabetes, AIDS, malignant tumor and organ transplantation, etc. In recent years, the incidence of SAP deep fungal infection has obviously increased. Before routine administration of prophylactic antibiotics for SAP, the proportion of fungi was 7 % in the bacteria spectrum of SAP infection[9]. After that, the incidence of fungal infection in SAP has increased to 12-41 %[2,3,5,6,8,10-14], which has become an important cause for death and mutilation by SAP[3,5,6,8,10-14]. Since lack of specific manifestations, unrecongizability of symptoms, a long time for fungal cultivation, and apparent relevance between the fungal infection and prognosis, active and effective measures to prevent SAP deep fungal infection will contribute to further decreasing the mortality of SAP.

It has been reported[7] that prophylactic application of fluconazole in patients after bone marrow transplantation or chemotherapy could reduce the incidence of fungal infection. But there was not any systematic or prospective study in preventing SAP fungal infection. This study initially showed that prophylactic application of anti-fungi garlicin or fluconazole could significantly reduce the incidence of deep fungal infection of SAP patients who had some predisposing factors. Garlicin is cheap but good in quality, which not only has anti-fungi effects, but also anti-bacteria and anti-viral effects. The normal prophylactic dosage of garlicin is 1-2 $mg.kg^{-1}.d^{-1}$. With respect to prevention alone, fluconazole is better than garlicin, but we have noticed that once those who used fluconazole to prevent infection were indeed infected by fungi, their treatment might become more difficult and the prognosis was much worse. Once fungal infection occurred, an in-time use of fluconazole could quickly clear fungi, and significantly improve prognosis. Low dosage (100-150 mg/d) of fluconazole is often used in prevention while high dosage (200-600 mg/d) is often used in treatment.

About 80 % of the fungal strains in SAP fungal infection are candida[3,5,6,10-14]. Once fungal infection has been ascertained, anti-fungal drugs should be applied in time. Besides direct application of amphotericin B for mucor infection, fluconazole has be the priority for other fungal infections. Like maphotericin B[15], fluconazole has a good permeability in pancreas. If

fluconazole is not effective, it should change for amphotericin B in time or combined medication. In this research, two patients with fungal infection died in fluconazole group possibly due to delayed treatment besides drug resistance.

Deep fungal infection is different from shallow one, sometimes its diagnosis depends on biopsy, because it is hard to differentiate "passenger" bacterial parasites from real infection under many circumstances. As shown by autopsy statistics, only less than 20 % of the patients with fungal infection received anti-fungal treatment[16]. It is believed that for SAP patients, even "passenger" bacterial parasites may probably develop into infection, the finding of fungi in extra-peritoneal positions has provided clues to fungal infection within abdominal cavity, especially when fungi have been cultured from the peritoneal draining liquid. Hoerauf *et al*[12] reported that anti-fungi chemotherapy could increase survival rate. Aloia *et al*[11] suggested small dosage and short course amphotericin B treatment. Grewe *et al*[10] and Gotzinger *et al*[13] reported that although amphotericin B could quickly clear fungi, it could not improve prognosis. This might be related to the fact that anti-fungi treatment was only started when the blood cultivation became positive. The authors agree with Keiser' s viewpoint[17] that the failure of treatment was unable to be realized in time because the fungi were the pathogenic bacteria, instead they were often regarded as pollution and "passenger" in the infection course of surgery, therefore treatment was delayed.

SAP complicated with fungal infection could be classified into primary infection (fungus found in samples of fine-needle aspiration before operation or the first operation) and secondary infection (no fungus found in samples of fine-needle aspiration before operation or the first operation, and fungal infection happens later)[10,13]. In time clearing and draining of the necrotic tissues should be done for primary fungal infection, conservative treatment is mainly for the secondary infection, operation should be done actively if there is a fungal abscess formation. There is no special clinical manifestation in fungal infection, and repeated fungal cultivation on sputum, urine, stool and peritoneal permeated liquid and blood sample can contribute to in-time diagnosis and treatment. Zhang[18] reported that it was helpful to rapid diagnosis of fungal infection in patients with severe acute pancreatitis by PCR using universal primers targeting the 18s rRNA gene of fungus.

REFERENCES

1 **Beger HG,** Rau B, Mayer J, Pralle U. Natural course of acute pancreatitis. *World J Surg* 1997; **21**: 130-135

2 **Ho HS,** Frey CF. The role of antibiotic prophylaxis in severe acute pancreatitis. *Arch Surg* 1997; **132**: 487-493

3 **Gloor B**, Muller CA, Worni M, Stahel PF, Redaelli C, Uhl W, Buchler MW. Pancreatic infection in severe pancreatitis: the role of fungus and multiresistant organisms. *Arch Surg* 2001; **136**: 592-596

4 **Pancreas Surgery Group of China Medical Association**. Clinical diagnosis and classify standard of acute pancreatitis. *Zhonghua Waike Zazhi* 1997; **35**: 773-775

5 **Lei RQ**, Liu W, Qu HP, Tang YQ, Yuan ZR, Han TQ, Zhang SD. Diagnosis and prophylaxis of fungi infection in severe acute pancreatitis. *Zongguo Shiyong Waike Zazhi* 1999; **19**: 544-545

6 **He YM**, Lu XS, Huang JH, Ai ZL, Liu ZS, Lei DX, Qian Q, Sun Q, Wang BY, Jiang CQ, Yuan YF. Fungal infection in severe acute pancreatitis (a report of 40 cases). *Zhongguo Putong Waike Zazhi* 2002; **11**: 135-138

7 **Edwards JE Jr**, Bodey GP, Bowden RA, Buchner T, de Pauw BE, Filler SG, Ghannoum MA, Glauser M, Herbrecht R, Kauffman CA, Kohno S, Martino P, Meunier F, Mori T, Pfaller MA, Rex JH, Rogers TR, Rubin RH, Solomkin J, Viscoli C, Walsh TJ, White M. International conference for the development of a consensus on the management and prevention of severe candidal infections. *Clin Infect Dis* 1997; **25**: 43-59

8 **Qin S**, Tang YQ, Qu HP, Liu W, Mao EQ. Study on the risk factors of fungal infection in severe acute pancreatitis. *Waike LiLun yu Shijian* 2001; **6**: 96-99

9 **Beger HG,** Bittner R, Block S, Buchler M. Bacterial contamination of pancreatic necrosis: A prospective clinical study. *Gastroenterology* 1986; **91**: 433-438

10 **Grewe M,** Tsiotos GG, Luque de-Leon E, Sarr MG. Fungal infection in acute necrotizing pancreatitis. *J Am Coll Surg* 1999; **188**: 408-414

11 **Aloia T**, Solomkin J, Fink AS, Nussbaum MS, Bjornson S, Bell RH, Sewak L, Mc Fadden DW. Candida in pancreatic infection: a clinical experience. *Am Surg* 1994; **60**: 793-796

12 **Hoerauf A,** Hammer S, Muller-Myhsok B, Rupprecht H. Intra-abdominal Candida infection during acute necrotizing pancreatitis has a high prevalence and is associated with increased mortality. *Crit Care Med* 1998; **26**: 2010-2015

13 **Gotzinger P**, Wamser P, Barian M, Sautner T, Jakesz R, Fugger R. Candida infection of local necrosis in severe acute pancreatitis is associated with increased mortality. *Shock* 2000; **14**: 320-324

14 **Isenmann R**, Schwarz M, Rau B, Trautmann M, Schober W, Beger HG. Characteristics of infection with Candida species in patients with necrotizing pancreatitis. *World J Surg* 2002; **26**: 372-376

15 **Shrikhande S**, Friess H, Issenegger C, Martignoni ME, Yong H, Gloor B, Yeates R, Kleeff J, Buchler MW. Fluconazole penetration into the pancreas. *Antimicrob Agents Chemother* 2000; **44**: 2569-2571

16 **Du B**, Zhang H, Chen D. Invasive fungal infection in 3447 autopsy cases. *Zhonghua Yixue Zazhi* 1996; **76**: 352-354

17 **Keiser P,** Keay S. Candidal pancreatic abscesses: report of two cases and review. *Clin Infect Dis* 1992; **14**: 884-888

18 **Zhang WZ**, Han TQ, Tang YQ, Zhang SD. Rapid diagnosis of fungal infection in patients with acute necrotizing pancreatitis by polymerase chain reaction. *Asian J Surg* 2002; **25**: 209-213

Edited by Zhang JZ and Wang XL

P.O.Box 2345, Beijing 100023,China
Fax: +86-10-85381893
E-mail: wjg@wjgnet.com www.wjgnet.com

World J Gastroenterol 2003;9(11):2622-2626
World Journal of Gastroenterology
 ISSN 1007-9327

• BRIEF REPORTS •

Formalized therapeutic guideline for hyperlipidemic severe acute pancreatitis

En-Qiang Mao, Yao-Qing Tang, Sheng-Dao Zhang

En-Qiang Mao, Yao-Qing Tang, Sheng-Dao Zhang, Department of Surgery, Ruijin Hospital, Shanghai Second Medical University, Shanghai 200025, China
Correspondence to: Dr. En-Qiang Mao, Department of Surgery, Ruijin Hospital, Shanghai Second Medical University, Shanghai 200025, China. maoeq@yeah.net
Telephone: +86-21-64370045 Ext 666014
Received: 2003-06-10 **Accepted:** 2003-08-16

Abstract

AIM: To investigate a formalized therapeutic guideline for hyperlipidemic severe acute pancreatitis (HL-SAP).

METHODS: Thirty-two consecutive patients with severe acute pancreatitis were included in the clinical trial. All of them met the following five criteria for admission to the study, namely the Atlanta classification and stratification system for the clinical diagnosis of SAP, APACHEII score more than 8, time interval for therapeutic intervention less than 72 hours after onset of the disease, serum triglyceride (TG) level 6.8 mmol/l or over, and exclusion of other etiologies. They were divided into severe acute pancreatitis group (SAP, 22 patients) and fulminant severe acute pancreatitis group (FSAP, 10 patients). Besides the conventional therapeutic measures, *Penta-association therapy* was also applied in the two groups, which consisted of blood purification (adsorption of triglyceride and hemofiltration), antihyperlipidemic agents (fluvastatin or lipanthyl), low molecular weight heparin (fragmin), insulin, topical application of Pixiao (a traditional Chinese medicine) over the whole abdomen. Serum triglyceride, pro-inflammatory cytokines and anti-inflammatory cytokines were determined before blood purification (PF), at the end of blood purification (AFE) and on the 7th day after onset of the disease (AF7) respectively. Simultaneously, severity of the diseases was assessed by the APACHE II system. Prognosis was evaluated by non-operation cure rate, absorption rate of pseudocyst, time interval pseudocyst absorption, hospital stay and survival rate.

RESULTS: Serum triglyceride level (mmol/L), TNFα (U/ml) concentration and APACHE II score were significantly decreased ($P<0.05$) at AFE and AF7, as compared with PF. However, serum IL-10 concentration (pg/ml) was increased significantly ($P<0.001$) at AFE, and decreased significantly ($P<0.05$) at AF7 when compared with PF. Operations: The First surgical intervention time was 55.8±42.6 days in SAP group (5 patients) and 12.2±6.6 days in FSAP group (7 patients), there was a significant difference between the two groups ($P=0.02$). The number of operations in the two groups was 1.33±0.5 *vs* 3.5±1.2 ($P=0.0037$), respectively. Prognosis: Non-operation cure rate, absorption rate of pseudocyst, hospital stay and survival rate in SAP group and FSAP group were 100 % (22/22) *vs* 11.1 % (1/9), 77.3 % (17/22) *vs* 11.1 % (1/9), 54.2±35.9 *vs* 99.1±49.5 days ($P=0.008$) and 100 % (22/22) *vs* 66.7 % (6/9) ($P=0.0044$). The time for absorption of pseudocyst was 135.1±137.5 days in SAP group.

CONCLUSION: *Penta-association therapy* is an effective guideline in the treatment of hyperlipidemic severe acute pancreatitis at its early stage (within 72 hours).

Mao EQ, Tang YQ, Zhang SD. Formalized therapeutic guideline for hyperlipidemic severe acute pancreatitis. *World J Gastroenterol* 2003; 9(11): 2622-2626
http://www.wjgnet.com/1007-9327/9/2622.asp

INTRODUCTION

Currently, cholilithiasis, alcohol abuse, hyperlipidemia and other specific factors, are the main causues of acute pancreatitis. The morbidity of severe acute pancreatitis secondary to hyperlipidemia (HL) has been apparently increased in recent years, acute pancreatitis occurred in 12-38 % of hyperlipidemic patients[1,2]. Hypertriglyceridemia (HTG) was the second cause of acute pancreatitis in our specialty center. However, this is in contrast with Yadav' s views point[3] that it was a rare cause of severe acute pancreatitis, obviously different from our situation.

Serum triglyceride (TG) level more than 10 to 20 mmol/l in patients with types I, IV, or V hyperlipidemia (Fredrickson' s classification) might lead to acute pancreatitis, so it has been considered as an identifiable risk factor[3]. It was reported that the mechanism leading to severe acute pancreatitis was that combining capacity of albumin surpassed by over production of free fatty acid would cause tissue toxicity. Thus, pancreatic acinar cells and microvessels were injured[4-8]. The main treatment for hyperlipidemic severe acute pancreatitis (HL-SAP) is to decrease serum triglyceride level and to prevent systemic inflammatory response. Although serum triglyceride could be decreased by plasmapheresis[9], there has been no formal therapeutic strategy to treat HL-SAP at present. We retrieved references about the treatment of HL-SAP from MEDLINE during 1966-2003 using severe acute pancreatitis and hyperlipidemia as the key words, and found that reports were all case reports of single treatment measure[10-12]. No formalized therapeutic strategy was found. Therefore, we prospectively treated patients with HL-SAP by *Pent-association therapy* which consisted of purification, antihyperlipidemic agents, insulin, heparin and topical application of Pixiao (a traditional Chinese medicine) over the whole abdomen to observe its therapeutic effects and influence on prognosis.

MATERIALS AND METHODS

Patients and groups

Patient Thirty-two consecutive patients with SAP admitted to Department of Surgical Intensive Care Unit, Ruijin Hospital, Shanghai, China, from April 2000 to March 2003 were included in the clinical trial. Therapeutic strategies to all patients were determined by a group of doctors from SICU and Department of Surgery.

Groups Five entry criteria for admission to the study were the Atalanta classification system to stratify patients with acute

pancreatitis (1992)[13], APACHEII score more than 8, within 72 hours after onset of the disease, serum triglyceride level more than 6.8 mmol/L, and exclusion of other etiologies.

The diagnosis of fulminant severe acute pancreatitis (FSAP) was made according to the following criteria.

FSAP was diagnosed by meeting one or more of the following indices within 72 hours after onset of the disease with adequate fluid resuscitation such as APACHEII score 20 or more, acute renal failure, ARDS, DIC, and Glasgow score less than 8.

According to the aforementioned criteria, 32 patients were divided into SAP group (22 patients) and FSAP group (10 patients). Of the FSAP group, one patient was excluded from the clinical trial due to giving up of the therapy. The patient did not undergo triglyceride adsorption and hemofiltration, and thus developed ARDS and acute renal failure within 48 hours. According to theoretical speculation and references, the *Penta-association therapy* might have some positive effects on patients. Therefore, we did not set control group in the present study. In addition, patients and/or their family were told about the trial in details. We were thus authorized to perform the study.

Etiology This included uncontrolled diabetes mellitus, long period alcohol abuse, heredity, pregnancy, obesity, *etc*. Among them, 23 men aged 45±9.4 years, 9 women aged 41.9±14.9 years.

Methods

Thearpy Conventional therapy: It included appropriate fluid resuscitation, fasting, gastrointestinal decompression, use of pancreatic enzyme inhibitors, prophylactic antibiotics, decoction of raw rhubarb poured into stomach via gastric tube, enteral nutrition and operation if necessary.

Specific therapy (Penta-association therapy) This included blood purification (adsorption of triglyceride and hemofiltration), triglyceride decreasing antihyperlipidemic agents (fluvastatin sodium capsules 40 mg, qn, P.O; lipanthyl, 200 mg qn, P.O), low molecular weight heparin (fragmin 5 000 IU, subcutaneous injection, qd, for 3 days), insulin by intravenous infusion (blood sugar controlled to less than 200 mg/dl), topical application of Pixiao over the whole abdomen.

Adsorption of triglyceride and hemofiltration Blood purification was performed using Diapact CRRT machine (B. Braun Co., Germeny). Polysulfone filters were used (Cut-off-point 30 000 Dalton, AV 600S, Fresenius Medical Care). Systemic anticoagulation was undergone with low molecular weight heparin (fragmin, 5 000 IU/ampule) at a dose of 100-140 IU/kg for bolus injection. Ultrafiltrate was replaced with substitutes made according to patient' s electrolyte and blood glucose. Pre-dilution mode was used. Extracoporeal blood flow ranged from 250 to 360 ml/min. Ultrafiltrating rate was controlled within 50-500 ml/h. In order to remove triglyceride rapidly, we changed the filter every 4 hours.

Indications for stopping blood purification Short veno-venous hemofiltration was stopped when the abdominal symptoms and signs disappeared, or the heart rate was less than 90 beats/min and the respiration rate was 20 times/min, respectively. Continuous veno-venous hemofiltration was stopped if the renal function was recovered and/or heart rate was less than 90 beats/min and the respiration rate was 20 times/min respectively.

Determination of Indices Serum levels of triglyceride, TNFα and IL-10 were determined before blood purification (PF), at the end of therapy (AFE) and on the 7th day (AF7) after onset of the disease. APACHE II scores were evaluated simultaneously. Activity of TNFα was assessed in the L929 cell line. IL-10 was tested using a commercially available ELISA kit (From Endogen Company, USA.).

Follow-up Enhanced CT scan of abdomen was performed every month for the patients with successful conservative treatment, and intra- and extra-pancreatic radiological changes were observed.

Prognosis Non-operation curative rate, survival rate, hospital stay, absorption rate of pseudocyst, time of first operation and total operation time were calculated and compared between the two groups.

Statistics

Data were reported as mean ± standard deviation, and analyzed using Student' s *t* and or chi square test.

RESULTS

Serum level of triglyceride, cytokine and APACHEII score

Serum concentrations of triglyceride and TNFα, and APACHE II scores were significantly decreased at AFE (t=5.687, P<0.001; t=6.342, P<0.001; t=12.12, P<0.001) and AF7 (t=7.576, P<0.001; t=10.19, P<0.001; t=15.09, P<0.001) compared with PF. Serum triglyceride level was decreased to safe range within 10 hours after the beginning of blood purification, and to normal range at AF7 when triglyceride was decreased as well as heparin and insulin were used continuously. But serum level of IL-10 at AFE was significantly increased compared with PF (t=19.21, P<0.001). However, it was significantly decreased (t=9. 87, P<0.001) at AF7 compared to PF.

Thus, serum triglyceride and pro-inflammatory cytokines were decreased, and anti-inflammatory cytokine was increased through blood purification (hemofiltration and adsorption of triglyceride), and severity of the disease was significantly decreased (Table 1).

Table 1 Levels of serum triglyceride, cytokines and APACHE II score

	PF	AFE	AF7
Serum triglyceride (mmol/L)	13.1±8.1	4.5±2.3	2.02±0.83
APACHE II score	18.4±4.4	7.38±2.5	5.8±1.5
TNFα (u/ml)	43.1±12.7	26.3±7.5	17.7±5.6
IL-10 (pg/ml)	72.1±20.0	179.6±23.9	31.2±11.5

Time duration for blood purification and number of filters used

Systemic inflammatory response syndrome (SIRS) was prevented through adsorption of triglyceride and short veno-venous hemofiltration in SAP group, but long time blood purification and/or drainage of large amounts of exudates from abdominal cavity and retroperitoneal space were needed in FSAP group. The number of filters used and time duration for blood purification in SAP group and FSAP group were 2.6±1.3 *vs* 2.9±1.5 h, 6.5 ±2.7 *vs* 48±62 h, respectively.

Surgical intervention

Time interval from onset of the disease to the first operation was significantly longer in SAP group (5 patients) than in FSAP group (7 patients) (t=2.715, P=0.02). Debridement of pancreatic necrosis and internal drainage of pseudocyst were performed in SAP group. Only debridement of pancreatic necrosis was performed in FSAP group, but operation number was more than that in SAP group (t=3.775, P=0.0037). This indicated that *Penta-association therapy* had better results in hyperlipidemic SAP than in FSAP group (Table 2).

Prognosis

We compared the results from this clinical trial with 283 patients treated with conventional therapy in our hospital, and found that non-operation cure rate was 100 %(22/22) in the present

SAP group, and was 43.5 % in our previous group (123/283) (χ^2=26.16, P=3.3×10^{-7}). The survival rate was 100 %(22/22) and was 84.1 % in our previous group (238/283) (χ^2=4.104, P=0.043). In SAP group, pancreatic pseudocysts were resolved spontaneously in 17 patients, with an absorption rate of 77.3 % (17/22), and surgical intervention was thus avoided. Absorption time was 135.1±137.5 days with a variation constant of 102 %.

In FSAP group, only one patient was cured through conservative treatment, its time interval for absorption of pseudocyst was 96 days. Another patient died without operation. Surgical drainage and debridement of pancreatic necrosis were done for the rest of 7 patients within 2 weeks after onset of the disease. The survival rate of 66.7 %(6/9) was slightly higher than 58 % (27/47) from Beger' s report[14] [χ^2=0.2653, P=0.61] without significant difference.

Absorption rate of pseudocyst, non-operation cure rate and survival rate in SAP group were higher than those in FSAP group. Hospital stay was also shortened compared to FSAP group (P=0.008, Table 3).

Table 2 Surgical intervention

	SAP	FSAP
Number of cases	5	7
Time of first operating (days)	55.8±42.6	12.2±6.6
Surgical procedures	Debridement and gastro-or jejuno-pancreatic anastomosis for pseudocyst	Debridement with drainage and nutritional jejunostomy
Number of operation	1.33±0.5	3.5±1.2

Table 3 Prognosis of SAP and FSAP

	SAP group	FSAP group
Number of cases	22	9
Rate of adsorption of pseudocyst	77.3 %(17 / 22)	11.1 %(1 / 9)
Time interval for absorption of pseudocyst	135.1±137.5	96
Non-operation cure rate	100 %(22 / 22)	11.1 %(1 / 9)
Hospital stay (days)	54.2±35.9	99.1±49.5
Survival rate	100 %(22 / 22)	66.7 %(6 / 9)

DISCUSSION

With an increased incidence of hyperlipidemia and its complication, acute pancreatitis also increased accordingly. SAP secondary to hypertriglyceridemia (HTG), presented typically as an episode of SAP, rarely as chronic pancreatitis. A level of serum triglyceride (TG) more than 6.8 mmol/L in patients with types I, IV, or V hyperlipidemia (Fredrickson' s classification) is an identifiable risk factor. The typical clinical profiles of hyperlipidemic pancreatitis were a patient with a preexisting lipid abnormality along with the presence of a secondary factor (e.g., poorly controlled diabetes, alcohol abuse or a medication) that could induce HTG[15]. Patients with isolated hyperlipidemia (type V or I) without a precipitating factor would rarely have pancreatitis. Interestingly, serum pancreatic enzymes might be normal or only minimally elevated even in the presence of SAP as diagnosed by imaging studies. The clinical course of HL-SAP was not different from severe acute pancreatitis caused by other causes. Although conventional management of SAP caused by hyperlipidemia is similar to that by other causes, but it still needs some specific management. So we did this clinical trial to investigate systematically how to manage HL-SAP within 72 hours after onset of the disease.

Formation of therapeutic regimen and its mechanism

At present, there have no formalized therapeutic strategies for the treatment of HL-SAP in the literature, besides single case report or the use of certain measures. In 2000, our Pancreatic Disease Therapy Center considered a therapeutic strategy aiming at HL-SAP that was based on the concepts that hyper-triglyceride, fatty acid and inflammatory mediators were the pathological mechanism of deterioration of HL-SAP[8,16-19]. A prospective investigation was thus carried out. Principles of the strategy included r*apid lowering serum triglyceride, blocking of induction pancreatic damage by pro-inflammatory mediators, preventing recurrence by the use of antihyperlipidemic agents, promoting self- absorption of pancreatic pseudocyst.* Concrete measures could be found in the details of *Penta-association therapy*, which included blood purification (adsorption of triglyceride and hemofiltration), fluvastatin (40 mg, qn, P.O) or lipanthyl (200 mg, qn, P.O), low molecular weight heparin (fragmin, 5 000 IU subcutaneous injection, qd, for three days.), insulin (intravenous infusion, blood sugar level controlled well below 200 mg/dl), and topical application of Pixiao (Chinese traditional medicine) over the whole abdomen. Hyperchylomicronemia caused by hyperlipidemia could lead to not only pulmonary edema[20] and systemic microcirculatory dysfunction, but also release of fatty acids, which would play an important role in causing pancreatic injury[8,17]. Thus, the first item of the therapeutic regimen was adsorption of serum triglyceride, and it was essential to lower blood triglyceride level within the safe range. Simultaneously, heparin could stimulate lipoprotein-lipase activity and accelerate chylomicron degradation[9]. It could also contribute to the decrease of serum triglyceride level. Besides this effect on blood triglyceride, it could also improve microcirculation and prevent activation of neutrophils activity[21]. Polymorphonuclear cells (PMN) could play an important role in the deterioration of severe acute pancreatitis, especially release of elastase (PMNE), which would lead to persistent pancreatic necrosis and acute lung injury[22]. Insulin could not only decrease blood sugar, but also accelerate degradation of chylomicrons[9]. Therefore insulin was given to control blood sugar well below 200 mg/dL. Simultaneously, fluvastatin sodium or lipanthyl was given to decrease blood lipid in order to avoid recurrence of acute pancreatitis.

Though the etiologies of patients with acute pancreatitis could be different, but their pathophysiological changes were just the same[23]. Activated enzymes and oxygen free radicals injured the acinar cells and caused release of cytokines and vasoactive mediators, attracted inflammatory cells and activated vascular endothelium as well as the expression of adhesion molecules. The disturbance of pancreatic microcirculation could induce progression from edematous to necrotizing pancreatitis independent of the early intracellular events, including protease activation. Specific therapy must be directed towards microperfusion failure as the secondary pathogenetic step, since the initial enzyme activation and cytokine release were irreversible by the time of clinical presentation. In experiments comparable to the clinical situation, following therapeutic principles have been proven to be beneficial: increase of blood fluidity, inhibition of leukocyte-endothelium interaction and blockade of systemic inflammatory response. As we know, Short time veno-venous hemofiltration could significantly decrease circulatory TNFα level and increase circulatory IL-10 level[24]. This could block systemic inflammatory response and pancreatic necrosis. Due to dynamic balance of pro-inflammatory and anti-inflammatory cytokines, long time hemofiltration was prohibited to avoid creation of new imbalance in SAP[25]. However, FSAP usually resulted in Ultra-SIRS (systemic inflammatory response syndrome), thus continuous veno-venous hemofiltration and

drainage of abdominal, retroperitoneal toxic exudates were essential to prevent recurrence of Ultra-SIRS. Based on this concept, hemofiltration could be used as a specific measure to treat HL-SAP.

After acute response phase, emphasis should be put on the prevention of infection, rapid subsidence of fluid accumulation in the third space as well as promotion absorption of pancreatic pseudocyst. Topical application of Pixiao (Chinese traditional medicine) over the whole abdomen could ameliorate tissue edema including that of abdominal wall, peritoneum and intestinal wall, and accelerate absorption of pancreatic pseudocyst. Therefore, Pixiao was used through out the whole course of the disease in order to relieve tissue edema and resolve pancreatic pseudocyst spontaneously. When patients were discharged with pancreatic pseudocyst, application of Pixiao was continued until it no longer absorbed fluid and became dry. Though the effect of this measure was slow, but it played an important role in decreasing operation rate.

Efficacy and prognosis

Although *Penta-association therapy* is far from perfect, especially for the prevention of recurrence of the disease, but good clinical efficacy has been obtained by these specific measures in the acute response phase of the episode.

In acute pancreatitis, medications, such as heparin and insulin *etc*. decreased trigylceride levels to less than 10 mmol/L within 2.8 days (1 to 6), the amylase and lipase levels returned to normal after 3 and 4 days respectively, and the abdominal pain was resolved[9,10]. Also, it was reported that plasmapheresis removed blood triglyceride[26-31] and got good results. Clinically, this method could not be propagated to wider use due to the problems of equipments and the need for large amounts of plasma. So we adopted the present measure to adsorb triglyceride. Within 72 hours after onset of the disease, serum triglyceride concentration was decreased to 6.8 mmol/l within 10 hours. At this time, abdominal pain was resolved in 31 patients. So adsorption of triglyceride can not only decrease triglyceride level rapidly, but also resolve abdominal pain and prevent deterioration of the disease. This has been regarded as a necessary measure in the treatment of HL-SAP at its early stage. As to the safe range of blood triglyceride level, it was reported that the level should be decreased to 5.65 mmol/L[32], but in our series when it was below 6.8 mmol/l, abdominal pain in 31 patients was resolved. This discrepancy might be due to different etiologies of hypertriglyceridemia or different preexisting factors. All the patients received insulin, heparin and antilipidemic agents to prevent deterioration of the disease by controlling serum triglyceride level at normal range 7 days after onset of the disease. Even though etiologies resulting in each SAP patients might be different, but pathophysiological lesions were just the same, such as overproduction of cytokines, microcirculation failure and over-activated neutrophils. Therefore, hemofiltration was continued after lipid adsorption to regulate the balance between proinflammatory and anti-inflammatory cytokines. This caused decrease of proinflammatory cytokines as well as temporary increase of anti-inflammatory cytokines with APACHEII score decreased. Our results were in accordance with the report in the literature[24]. Thus, hemofiltration used in the early treatment of HL-SAP was of important clinical significance.

Five patients with SAP underwent the first operation on the 56th day after onset of the disease. Surgical modalities used coincided with literature reports[31]. The major methods were debridement and drainage of pancreatic necrosis as well as internal drainage of pancreatic pseudocyst. But FSAP group underwent the first operation on the 12th day after onset of the disease. The first operation time was earlier than that of SAP group (P<0.01). Surgical methods in FSAP group were mainly debridement and drainage. Furthermore, the number of operations was also increased (P<0.01).

Non-operation cure rate and survival rate were both 100 % in SAP group, they were increased significantly compared with non-operation rate of 43.5 % and survival rate of 84.1 % in 283 patients with SAP in our hospital in the past. Meanwhile, the survival rate of 100 % was higher than that of 62 % (8/13) in literature report[31] [χ^2=9.872, P=0.002]. Incidence of pseudocyst in SAP group was 81.8 % (18/22) which was significantly higher than that of 37 % in literature report of[33]. Pseudocysts in 17 patients resolved spontaneously without operation. The reason why the morbidity and absorption rate of pseudocyst were very high was that the full-blown summit of SAP was at 72 hours, so pancreatic microcirculation was compromised, and ischemia occurred in the pancreas within 72 hours. Thirty-one patients were treated on time within 72 hours, thus pancreatic necrosis was prevented. After onset of the disease, the whole abdomen was covered with Pixiao (rough-wrought Glauber' s salt) until it could not be moistened. This treatment could accelerate absorption of pseudocyst. Ischemia occurred in the major component of Pixiao (rough-wrought Glauber' s salt) is Glauber' s salt, additionally, it contains magnesium sulfate, calcium chloride, magnesium chloride *etc*. and acts on inflammatory mass by the effect of shrinkage, anti-inflammation, dehydration and others. Based on the aforementioned results, we think that *Penta-association therapy* has quite good clinical efficacy, and should be regarded as a specific measure in the treatment of HL-SAP.

HL-FSAP is a sub-type of HL-SAP. Although we applied the same conservative therapeutic measures as those of SAP, but the efficacy was not the same. Only one patient recovered through conservative treatment. It took 96 days for the pseudocyst to resolve spontaneously. Another patient died. If conservative treatment could not control the disease, it was taken as the indication for operation in FSAP. Seven of them underwent debridement and drainage of abdominal and/or retroperitoneal exudates through laparotomy within 2 weeks after onset of the disease. Although its cure rate was 66.7 %, it was still higher than Beger' s 58 %[14] and Bosscha' s 61 %[34], the percentage of mortality was still 33 %. According to our data and literature data[34], survival rate has not been improved through early enthusiastic operation and surgical drainage. This demonstrated that conventional treatment and *Penta-association therapy*, optimal surgical indication, proper timing of operation and choice of drainage method, such as laparoscopy, drainage through single lumen catheter puncture guided by ultrasound, play an important role on survival rate in the treatment of HL-FSAP. Although the viewpoint that conservative treatment should be applied to treat FSAP during it' s early stage (within 2 weeks)[35] was controversial, it is advisable to apply cautiously drainage through laparotomy in the treatment of FSAP during its early stage, and this could achieve curing rate. Some authors suggested that management and clinical surveillance required specific expertise, and management of these patients was best undertaken in specialized centers.

It is thus evident that *Penta-association therapy* upon the basis of conventional therapy for HL-SAP can give good clinical results, but its efficacy in treating FSAP needs to be further improved.

Recommendation of formalized therapeutic regimen

Efforts has been made by the pancreatic disease specialists all over the world in the past hundred years, the therapy of acute pancreatitis has been basically formalized, and therapeutic principles were also basically established. Thus, the cure rate of SAP has reached 80 %. But there were still 20 % of patients who could not be cured. Among them, 15 % were still SAP,

5 % were another subtype - FSAP. Regardless of the etiologies of SAP, their pathophysiological changes were identical, and this determined the accordance of their management. But why there were still 15 % of these patients who could not be cured? Based upon our experimental results, we think some of them were not treated appropriately with regard to their etiologies during early stage (within 72 hours). Although pancreatic lesions could not be prevented from progression even after the etiologies were resolved, continuing existence of the etiological factors would aggravate the disease, such as choledocholithiasis and hyperlipidemia. At present, there are a lot of measures to treat biliary acute pancreatitis, such as EST, ENBD or surgical operation. Nevertheless, there is no formalized regimen to manage HL-SAP. On account of this, our Pancreatic Disease Therapy Center has suggested a formulated specific regimen to treat HL-SAP in order to save some of the 15 % patients. In the present study, from the standpoint of cure rate, almost all the patients were recovered from the disease. Based upon our results, we suggest that it is important to determine whether hyperlipidemia is existent or not by history and laboratory examinations or simply by the presence of chylous blood. Once the diagnosis of HL-SAP is established, besides the conventional therapy, *Penta-association therapy* should be given immediately to mange HL-SAP.

Additionally, 5 % of the patients belonged to FSAP. Although the therapeutic efficacy of HL-FSAP in the present group was somewhat improved, but it was not significant. This should be further investigated.

In summary, HL-SAP has not only the general characteristics of severe acute pancreatitis, but also some specific characteristics. So, besides conventional therapy of SAP, specific strategy should be taken into consideration. *Penta-association therapy* is not a perfect regimen, further refinement, especially to treatment for FSAP, is urgently required.

REFERENCES

1 **Toskes PP.** Hyperlipidemic pancreatitis. *Gastroenterol Clin North Am* 1990; **19:** 783-791
2 **Searles GE,** Ooi TC. Underrecognition of chylomicronemia as a cause of acute pancreatitis. *CMAJ* 1992; **147:** 1806-1808
3 **Yadav D,** Pitchumoni CS. Issues in hyperlipidemic pancreatitis. *J Clin Gastroenterol* 2003; **36:** 54-62
4 **Thompson GR.** Primary hyperlipidaemia. *Br Med Bull* 1990; **46:** 986-1004
5 **Havel RJ.** Pathogenesis, differentiation and management of hypertriglyceridemia. *Adv Intern Med* 1969; **15:** 117-154
6 **Nagai H,** Henrich H, Wunsch PH, Fischbach W, Mossner J. Role of pancreatic enzymes and their substrates in autodigestion of the pancreas. *In vitro* studies with isolated rat pancreatic acini. *Gastroenterol* 1989; **96:** 838-847
7 **Kimura W,** Mossner J. Role of hypertriglyceridemia in the pathogenesis of experimental acute pancreatitis in rats. *Int J Pancreatol* 1996; **20:** 177-184
8 **Domschke S,** Malfertheiner P, Uhl W, Buchler M, Domschke W. Free fatty acids in serum of patients with acute necrotizing or edematous pancreatitis. *Int J Pancreatol* 1993; **13:** 105-110
9 **Berger Z,** Quera R, Poniachik J, Oksenberg D, Guerrero J. Heparin and insulin treatment of acute pancreatitis caused by hypertriglyceridemia. Experience of 5 cases. *Rev Med Chil* 2001; **129:** 1373-1378
10 **Henzen C,** Rock M, Schnieper C, Heer K. Heparin and insulin in the treatment of acute hypertriglyceridemia-induced pancreatitis. *Schweiz Med Wochenschr* 1999; **129:** 1242-1248
11 **Routy JP,** Smith GH, Blank DW, Gilfix BM. Plasmapheresis in the treatment of an acute pancreatitis due to protease inhibitor-induced hypertriglyceridemia. *J Clin Apheresis* 2001; **16:** 157-159
12 **Lechleitner M,** Ladner E, Seyr M, Hoppichler F, Foger B, Hackl JM. Hypertriglyceridemia and acute pancreatitis. *Acta Med Austriaca* 1994; **21:** 125-128
13 **Bradley EL 3rd.** A clinically based classification system for acute pancreatitis. Summary of the international symposium on acute pancreatitis. Atlanta, Ga, September 11 through 13, 1992. *Arch Surg* 1993; **128:** 586-590
14 **Isenmann R,** Rau B, Beger HG. Early severe acute pancreatitis: characteristics of a new subgroup. *Pancreas* 2001; **22:** 274-278
15 **Pfau J.** Acute pancreatitis and hypertriglyceridemia. *Rev Med Chil* 1989; **117:** 907-909
16 **Saharia P,** Margolis S, Zuidema GD, Cameron JL. Acute pancreatitis with hyperlipemia: studies with an isolated perfused canine pancreas. *Surgery* 1977; **82:** 60-67
17 **Hofbauer B,** Friess H, Weber A, Baczako K, Kisling P, Schilling M, Uhl W, Dervenis C, Buchler MW. Hyperlipaemia intensifies the course of acute oedematous and acute necrotising pancreatitis in the rat. *Gut* 1996; **38:** 753-758
18 **Norman J.** The role of cytokines in the pathogenesis of acute pancreatitis. *Am J Surg* 1998; **175:** 76-83
19 **Van Laethem JL,** Eskinazi R, Louis H, Rickaert F, Robberecht P, Deviere J. Multisystemic production of interleukin 10 limits the severity of acute pancreatitis in mice. *Gut* 1998; **43:** 408-413
20 **Warshaw AL,** Lesser PB, Rie M, Cullen DJ. The pathogenesis of pulmonary edema in acute pancreatitis. *Ann Surg* 1975; **182:** 505-510
21 **Capecchi PL,** Ceccatelli L, Laghi Pasini F, Di Perri T. Inhibition of neutrophil function in vitro by heparan sulfate. *Int J Tissue React* 1993; **15:** 71-76
22 **Mao EQ,** Han TQ, Tang YQ, Zhang SD, Zhang SD. Polymorphonuclear elastase is the major causative factor in acute lung injury complicating severe acute pancreatitis in rats. *Zhonghua Xiaohua Zazhi* 1998; **18:** 207-209
23 **Klar E,** Werner J. New pathophysiologic knowledge about acute pancreatitis. *Chirurg* 2000; **71:** 253-264
24 **Mao E,** Tang Y, Han T, Zhai H, Yuan Z, Yin H, Zhang S. Effects of short veno-venous hemofiltration on severe acute pancreatitis. *Zhonghua Waike Zazhi* 1999; **37:** 141-143
25 **Mao EQ,** Tang YQ, Zhang SD. Effects of time interval for hemofiltration on the prognosis of severe acute pancreatitis. *World J Gastroenterol* 2003; **9:** 373-376
26 **Perrone G,** Critelli C. Severe hypertriglyceridemia in pregnancy. A clinical case report. *Minerva Ginecol* 1996; **48:** 573-576
27 **Mayan H,** Gurevitz O, Mouallem M, Farfel Z. Multiple spurious laboratory results in a patient with hyperlipemic pancreatitis treated by plasmapheresis. *Isr J Med Sci* 1996; **32:** 762-766
28 **Majlis S,** Anguita T, Weishaupt R, Socias M. Plasmapheresis in acute pancreatitis secondary to familial hyperlipidemia in a pregnant woman. *Rev Med Chil* 1989; **117:** 1275-1278
29 **Schranz W,** Bartels O. Early plasma exchange in acute pancreatitis. A successful therapeutic principle in extreme hyperlipidemia. *Fortschr Med* 1986; **104:** 530-532
30 **Sunamura M,** Yamauchi H, Takeda K, Suzuki T, Abe R, Oikawa S, Sano R. A case of acute pancreatitis associated with hyperlipidemia and pregnancy with reference to plasma exchange as a therapeutic intervention. *Nippon Shokakibyo Gakkai Zasshi* 1985; **82:** 2139-2143
31 **Ohmoto K,** Neishi Y, Miyake I, Yamamoto S. Severe acute pancreatitis associated with hyperlipidemia: report of two cases and review of the literature in Japan. *Hepatogastroenterology* 1999; **46:** 2986-2990
32 **Nair S,** Yadav D, Pitchumoni CS. Association of diabetic ketoacidosis and acute pancreatitis: observations in 100 consecutive episodes of DKA. *Am J Gastroentero l* 2000; **95:** 2795-2800
33 **Fortson MR,** Freedman SN, Webster PD 3rd. Clinical assessment of hyperlipidemic pancreatitis. *Am J Gastroenterol* 1995; **90:** 2134-2139
34 **Bosscha K,** Hulstaert PF, Hennipman A, Visser MR, Gooszen HG, van Vroonhoven TJ, vd Werken C. Fulminant acute pancreatitis and infected necrosis: results of open management of the abdomen and "planned" reoperations. *J Am Coll Surg* 1998; **187:** 255-262
35 **Gronroos JM,** Nylamo EI. Mortality in acute pancreatitis in Turku University Central Hospital 1971-1995. *Hepatogastroenterology* 1999; **46:** 2572-2574

Edited by Xu JY and Wang XL

P.O.Box 2345, Beijing 100023,China
Fax: +86-10-85381893
E-mail: wjg@wjgnet.com www.wjgnet.com

World J Gastroenterol 2003;9(11):2627-2631
World Journal of Gastroenterology
 ISSN 1007-9327

• BRIEF REPORTS •

Correlation between metastatic potential and variants from colorectal tumor cell line HT-29

Min Wang, Ilka Vogel, Holger Kalthoff

Min Wang, Department of Surgical Oncology, First Affiliated Hospital of Medical College, Zhejiang University, Hangzhou 310003, Zhejiang Province, China
Ilka Vogel, Holger Kalthoff, Molecular Oncology Research Laboratory, Clinic for General and Thoracic Surgery, Christian-Albrechts-University, 24105 Kiel, Germany
Supported by the Scientific Research Foundation for Returned Overseas Chinese Scholars, Personnel Affairs Bureau of Zhejiang Province
Correspondence to: Dr. Min Wang, Department of Surgical Oncology, First Affiliated Hospital of Medical College, Zhejiang University, 79 Qingchun Road, Hangzhou 310003, Zhejiang Province, China. pfeng@mail.hz.zj.cn
Telephone: +86-571-7236880 **Fax:** +86-571-7236628
Received: 2003-04-12 **Accepted:** 2003-05-19

Abstract

AIM: To evaluate the relationship between uPA, PAI-1, CEA, PI3K and metastatic potential in three colorectal tumor cell lines.

METHODS: Metastatic model in nude rats was established by variants HT-29c and HT-29d cell lines and the metastatic potential of two tumor cell variants was compared. Urokinase-type plasminogen activator (uPA) and plasminogen activator inhibitor type 1 (PAI-1) were determined using ELISA in colorectal carcinoma WiDr, HT-29 and HT-29d cell lines with different metastatic potentials. Expression of carcinoembryonic antigen (CEA) and phosphoinositide 3-kinase (PI3-Kinase) was analyzed using immunohistochemistry (IHC) in these cell lines *in vitro* and *in vivo*. CEA expression was compared using fluorescence activated cell sorter (FACS) *in vitro*.

RESULTS: The number of HT-29d cells arrested in liver dramatically decreased within the initial 24 hours after injection. The taking rate of liver metastases in the variant HT-29d increased as compared with parental HT-29 cells (70 % versus 50 %) and a variant HT-29b cells (70 % versus 60 %), and extensive organs were synchronously involved in metastases. The uPA concentration of variant HT-29d cell line was significantly higher than that of the non-metastatic WiDr and the low metastatic HT-29 cell lines. The variant HT-29d cells produced stronger PI3-kinase expression as compared with the non-metastatic WiDr cells and the low metastatic HT-29 cells *in vivo*.

CONCLUSION: The selected variant HT-29d cell exhibited an enhanced metastatic potential. The level of uPA and PAI-1 is positively correlated with the metastatic capacity of tumor cells. The expression of PI3-kinase correlates with tumor development and metastasis.

Wang M, Vogel I, Kalthoff H. Correlation between metastatic potential and variants from colorectal tumor cell line HT-29. *World J Gastroenterol* 2003; 9(11): 2627-2631
http://www.wjgnet.com/1007-9327/9/2627.asp

INTRODUCTION

The malignancy of a solid tumor is due to its ability to invade and metastasize. Metastasis is a major cause of cancer death. Cancer metastasis consists of multiple sequential and selective steps. The aggressiveness of a tumor is primarily dependent on its ability to invade adjacent tissues and to metastasize to distant sites. In recent years special attention has been paid to tumor-associated protease systems, such as urokinase-type plasminogen activator (uPA)[1]. A role of uPA in regulating tumor cell invasiveness has been proposed on the basis of generally increased uPA activity in several metastatic tumors[2,3]. For many malignant tumors, there is a significant correlation between the production of uPA and tumor invasion[4,5]. The activation of uPA is controlled by well-characterized plasminogen activator inhibitors: type 1 (PAI-1). Numerous studies have shown that PAI-1 antigen levels in primary tumor with lymph node involvement were significantly higher than those in cancers without lymph node involvement[6,7], and in metastatic lymph nodes their levels were also increased compared to primary tumors[8].

Carcinoembryonic antigen (CEA) is one of the most common tumor-associated substances produced by colorectal carcinoma, and it has been used in numerous studies as a tumor marker. Although the functional role of CEA in liver metastasis from colorectal carcinomas has been assumed to be an adhesion factor or receptor binding to Kupffer cells[9,10], a conclusive evidence *in vivo* has not been clarified yet.

Phosphoinositide 3-kinase (PI3-kinase) is a key signaling enzyme implicated in a variety of receptor-stimulated cell responses[11]. This lipid product is believed to act as the second messenger in a variety of signaling processes including cell survival and migration[12,13]. Numerous studies have implicated PI3K in signal transduction pathways correlated with cell proliferation, cell cycle progression, cell apoptosis, tumorigenesis, tumor angiogenesis and tumor invasiveness[14,15].

In this study, uPA, PAI-I, CEA and PI3K were determined in three colorectal cancer cell lines with different metastatic capacities *in vitro* and *in vivo*, and the relationship between metastatic potential and these biological factors in colorectal tumor was investigated.

MATERIALS AND METHODS

Experimental animals

Three-week old male athymic Rowett nude rats (Hsd:RH-nu/nu) were obtained from Harlan/Winkelmann (Borchen, Germany). All rats were housed under special pathogen-free conditions in a laminar flow cabinet (EHRET, DIPL.-ING. W. EHRET GmbH, Germany) with constant temperature (24-26 ℃), humidity (40-50 %) and 12-hour light/12-hour dark cycle. The rats were fed with standard rat food and water. All cages, bedding and operative equipments were autoclaved at 121 ℃ for 30 minutes. The nude rats were stabilized for one week in the laboratory before the experiments were started.

Cell lines and cell culture

Human colonic adenocarcinoma cell lines WiDr and HT-29

as well as their variants HT-29c and HT-29d were used in the present study. WiDr cell line was established from a moderately differentiated human primary rectosigmoid adenocarcinoma with non-distasnt metastatic capability and obtained from American Type Culture Collection (ATCC, Rockville, MD, USA). HT-29 cell line was established from a moderately differentiated human colon adenocarcinoma and was a gift of Dr. Dippold (Mainz, Germany). HT-29c and HT-29d cell lines were two variant cell lines after three and four cycles of selection of liver metastases from parental HT-29 cells[16].

All the cell lines were grown in RPMI-1640 medium (Life Technologies, Eggenstein, Germany) plus 10 % fetal bovine serum (FCS, Life Technologies) supplemented with 2 mM L-glutamine and 1 mM sodium pyruvate (Life Technologies) and maintained in a 37 ℃ incubator (Heraeus, Germany) with 100 % relative humidity and 5 % CO_2. Cells were seeded and grown as monolayers in 75 cm^2 culture flasks (Falcon, England).

Establishment of metastatic model

Cells were harvested from exponential growth phase by brief trypsinization. The number of cell concentration was determined using a hemocytometer (Marienfeld, Germany). The cell suspensions were resuspended in HBSS at a final concentration of 4×10^7 cells/ml. A toal of 12 rats were anesthetized, an abdominal incision about 2 cm long was made in midline and the portal vein and mesenteric vein were isolated and exposed. Single-cell suspension of 0.5 ml containing 2×10^7 cells of HT-29c or HT-29d was injected into the mesenteric vein of 2 or 10 rats, respectively. The rats were explored for the first time about 4 weeks after injection and killed and autopsied at 6-10 weeks or when moribund after injection. The liver, lung and other organs were removed and frozen in liquid nitrogen, then stored at -80 ℃ for IHC.

To investigate the distribution and fate of tumor cells in the liver at the initial 48 hours after injection, 3-4 rats were killed at 1, 24, 48 hours after injection, respectively. The livers were removed, frozen in liquid nitrogen immediately, then the liver tissues were sliced at 5 μm cryosections and analysed for tumor cells by IHC with anti-CK mAb KL-1.

Quantitative detection of uPA and PAI-1

Six-well tissue culture plates were used. The single cell suspension of WiDr cells, HT-29 cells and HT-29d cells containing 3×10^5 tumor cells in supplemented RPMI-1640 was seeded into each well, respectively, and incubated at 37 ℃ in a humidified 5 % CO_2 incubator. After incubation for 24 hours, the medium of each well was sucked away and freshly supplemented RPMI-1640 medium (1.5 ml/per well) was added. The cells were incubated under the same conditions as above for 24 and 48 hours, respectively. Then the medium of each well was removed into Eppendorf tubes and centrifuged at 10 000 rpm for 15 minutes at 4 ℃. The supernatant was for detection of uPA and PAI-1. To measure the concentration of uPA and PAI-1 antigen in tumor cell culture supernatants, the uPA and PAI-1 ELISA kits (Imubind, American Diagnostica, Greenwich, CT, USA) were used. The sample value was multiplied by the dilution factor to determine the uPA and PAI-1 concentration of the cell culture supernatant. Meanwhile, the cells in six-well tissue culture plates were harvested by brief trypsinization and cell number was determined using a hemocytometer.

Determination of PI3-kinase expression

Tumor cells were seeded on 10-well mask slides at a density of 2×10^5 cells/ml supplemented medium and incubated at 37 ℃ in an incubator with 100 % relative humidity and 5 % CO_2 as described above. 48 hours later, the slides were washed twice with PBS and fixed in cold acetone for 5 minutes. Tumor tissue samples were cut into 5 μm cryosections and placed on microscope slides. The 10-well mask cell slides or tissue cryosections were fixed in cold acetone (4 ℃) for 5 minutes. The rabbit polyclonal antibody against PI3-kinase p85α and P110α (Santa Cruz Biotechnology) was used for immunohistochemical evaluation. The standard ABC immunostaining method was employed as immunohistochemical staining with ABC kit (Vector Laboratories, CA, USA). A semiquantitated score of 5 categories based on color intensity was assigned as -: no reaction, +: weak positive reaction, ++: moderate positive reaction, +++: strong positive reaction. The percentage of positive tumor cells was determined by calculating 1 000 tumor cells in 5 random areas of one section.

CEA determination

FACS analysis of cell lines WiDr, HT-29 and HT-29d cells were harvested from exponential growth phase with 0.002 % EDTA in PBS and inactivated with supplemented medium, then centrifuged at 1 410 rpm for 5 minutes. The pellet was washed in Na-azide-PBS (7.5 mM) at 4 ℃, and cells were counted with 5×10^5 cells removed to each FACS tube. The cells were washed in 1 ml Na-azide-PBS and centrifuged again. The supernatant was sucked away, primary mAb to human CD66e (clone 85A12, 100 μg/ml, Cymbus Biotechnology, Chandlers Ford, Hants, UK) was diluted (2:3) with 3 % BSA in azide-PBS and added to each tube. The tube was vortexed and incubated on ice at 4 ℃ for 1 hour. One ml azide-PBS was added for inactivation and the cells were centrifuged. The supernatant was sucked away, the second antibody of dichlorotriazinyl amino fluorescein (DTAF)-conjugated affinipure goat anti-mouse IgG+IgM (1.3 mg/ml, Dianova, Hamburg, Germary) diluted (1:100) with 3 % BSA in azide-PBS was added to each tube. The tube was vortexed and incubated on ice in the dark at 4 ℃ for 30 minutes. One ml azide-PBS was added for inactivation and the cells were centrifuged. The supernatant was sucked away, 300 μl of azide-PBS was added to each tube and vortexed, then 100 μl of 4 % paraformaldehyde was added. The samples were stored at 4 ℃ in the dark for FACS analysis. The primary antibody and secondary antibody were replaced by 3 % BSA in azide-PBS as negative controls, the primary antibody was replaced by 3 % BSA in azide-PBS as the second antibody control.

Immunohistochemistry analysis To investigate the CEA expression of different cell lines, s.c tumor and liver metastasis tumor, mouse monoclonal antibody to human CD66e were used for immunohistochemical evaluation. The standard ABC immunostaining method and a semiquantitated score were performed as described above.

Statistical analysis

The data were presented as mean ± standard deviation. Statistical analyses were performed using the F test and χ^2 test. Differences were considered significant if the P-values were <0.05.

RESULTS

Phenotype of HT-29 variants with enhanced tumorigenicity in vivo

The distribution and fate of tumor cells HT-29d in the liver at the initial phase after inoculation were observed in the rats of each group at different time intervals, respectively. The number of HT-29d cells arrested in the liver was dramatically decreased within the initial 48 hours after injection. By 1 hour after mesenteric vein injection, many tumor cells could be found in

Table 1 Macroscopical pattern of HT-29c/d cell metastases

Cell	Hepatic metastasis				Lung metastasis			Other organs
	No of metast[a]	I	II	III	No of metast[a]	I	II	
HT-29c	1/2	0/2	0/2	1/2	1/2	1/2	0/2	2/2
HT-29d	7/10	2/10	3/10	2/10	3/10	1/10	2/10	9/10

a: metastasis.

the livers, with a mean of 14.7 tumor cells/mm^2, and the single and clustered cells in the liver were located surrounding portal vein and in hepatic sinusoids. By 24 hours, however, the number of tumor cells surviving in the liver was significantly decreased. Only a few cells were found, with a mean of 2.3 tumor cells/mm^2 (range, 0-9 tumor cells/mm^2), and the cells were located mostly in parenchyma of the liver. At 48 hours after injection, a similar tumor cell distribution was found.

Metastatic potential of HT-29c and HT-29d cells was studied by injecting tumor cells into the mesenteric vein of nude rats. All rats survived the surgery and tumor-cell injection. Exploration was performed at the fourth week after injection. The rats were killed 8 to 10 weeks after injection or when moribund. The metastases were determined either by macroscopy or by microscopy. Liver tumor burden was evaluated based on the number of lesions as Class I: histological evidence of tumor growth, Class II: <10 tumor foci (macroscopically), Class III: >10 tumor foci (macroscopically). Lung metastasis was evaluated as Class I: histological evidence of tumor growth, Class II: macroscopically positive. The results are shown in Table 1. One of the two rats injected HT-29c cells developed extensive hepatic metastases, in which 60 % of the right liver was occupied by tumor tissue. The other developed micrometastases in the lung, diaphragm, left kidney with hemorrhagic ascites. The two rats developed mesenteric metastases. Seven of the ten rats (70 %) injected HT-29d cells had either liver macrometastases or micrometastases. Still three of the ten rats (30 %) had lung metastasis, of which two developed extensively dispersed metastatic nodules in their lungs. Three of the ten rats (30 %) developed metastatic tumors in their thoracic cavity. Five developed metastatic tumors in the diaphragm. Two produced hemorrhagic ascites. Nine developed extensive mesenteric metastases within 8 to 10 weeks after injection of HT-29d. One suffered from hindlegs paralysis at day 30 after injection.

Level of uPA and PAI-1

The concentrations of uPA and PAI-I in cell supernatants were statistically significantly different among WiDr, HT-29 and HT-29d cells. The uPA and PAI-I concentrations of variant HT-29d cell line were significantly higher than those of HT-29 and WiDr cell lines at 24 hours (F value was 17.4, P=0.03) and at 48 hours (F value was 98.3, P=0.001). The uPA and PAI-I concentration of variant HT-29 cell line was also higher than that of WiDr cell line (Table 2).

Expression of CEA in cell lines and tumor tissues

The results by FACS showed that mAb CD66e could react with CEA on the surface of cells *in vitro*, but no differences were observed between WiDr, HT-29 and HT-29d cell lines. Their fluorescence intensities were 212, 215 and 207, respectively, (F value was 0.07, P=0.93).

CEA expressions among WiDr, HT-29 and HT-29d cell lines *in vitro* by IHC were not significantly different (χ^2 value was 2.311, P=0.315). However, HT-29d showed a slightly higher ratio of positive cells and stronger staining compared with WiDr and HT-29 in s.c. tumor, without significant difference (χ^2 value was 4.397, P=0.111). The ratio of positive cells and staining intensity showed no significant difference in liver metastases between HT-29 and HT-29d (χ^2 value was 0.823, P=0.364) (Table 3).

Expression of PI3-kinase

For detection of expression of PI3-kinase, we stained PI3-kinase with Abs against p85α and p110α subunits of PI3-kinase in WiDr, HT-29 and HT-29d cell lines. Immunochemical reactivity with polycolonal antibodies p85α and p110α subunits of PI3-kinase was present among all tumor cell lines *in vitro*. No significant difference was observed in positive cell ratio and staining intensity among WiDr, HT-29 and HT-29d cell lines (χ^2 value was 2.041, P=0.360).

PI3-kinase expression of HT-29d showed stronger staining intensity compared to WiDr and HT-29 in s.c tumor, and the ratio of positive cells of HT-29 and HT-29d was significantly higher than that of WiDr (χ^2 value was 6.161, P=0.046). HT-29d cells exhibited stronger staining and a slightly higher ratio than that of the parental HT-29 in liver metastatic tumor using mAb p85α and p110α (Table 3).

Table 2 uPA and PAI-1 level of different cell lines at 24 h

Cell	Level(pg/10^5 ell)	
	uPA($\bar{x}\pm s$)	PAI-1($\bar{x}\pm s$)
WiDr	16.7±5.8	1 613±90
HT-29	80.01±8.1[a]	2 650±1154[a]
HT-29d	87.0±20.8[b]	9 707±2450[b]

[a]P<0.05 *vs* WiDr, [b]P<0.05 *vs* HT-29.

Table 3 Expression of CEA and PI3-Kinase *in vitro* and *in vivo*

Cell lines and tumor	CEA		PI3-Kinase	
	Positive cell(%)	Intensity	Positive cell (%)	Intensity
WiDr	93±4.4	+++	99±0.8	++
HT-29	90±2.1	+++	98±1.6	++
HT-29d	94±3.0	+++	97±3.6	++
WiDr s.c[a].	29±2.6	++	14±0.8	+
HT-29 s.c.	31±4.6	++	22±0.8	+
HT-29d s.c.	40±6.0	+++	23±2.2	++
HT-29 Lm[b]	71±7.9	+++	28±0.8	+
HT-29d Lm	66±7.0	+++	34±0.8	++

a: s.c.: s.c. tumor, b: Lm: liver metastases.

DISCUSSION

Tumor metastasis in the liver is a complex process of tumor-cell invasion into normal tissue on the one hand and the anti-invasive mechanisms of host defense system on the other hand. Lodgment of tumor cells in a blood vessel is an important step of tumor cell invasion. The survival of cancer cells after they enter the circulation depends upon their abilities to successfully reach the microcirculation, invade the capillary endothelium, establish a microenvironment for subsequent vascularization and growth. In the present study the capacity of arrested tumor

cells in the liver was observed in HT-29d cell line. One hour after tumor cell injection via the mesenteric vein, the number of tumor cells arrested in the liver was very high. Most tumor cells were located in the portal vein and its surrounding hepatic sinusoids. Furthermore, at 24 hours, the number of tumor cells surviving in the liver was significantly decreased, most tumor cells had been removed from the liver, the survived cells were located mostly in parenchyma of the liver. The remaining tumor cells were likely to be able to proliferate and to develop metastatic colonies. The results suggested that not all cells that entered the liver via hematogenous dissemination produced metastasis, the majority of circulating tumor cells died and only a minority of the cells escaped from host defense systems (e.g. NK cell activity in nude rats), arrested and survived in the liver could develop metastasis.

Neoplasms are heterogeneous with regard to invasion and metastasis, they contain a variety of subpopulations of cells with different metastatic potentials[17]. The outcome of metastasis is to a large extent dependent on a selection process that favors the survival and growth of a special subpopulation of cells. Isolation of clonal populations of cells that differed from the parent neoplasm in their metastatic capacity supported the hypothesis that not all the cells in a primary tumor could successfully disseminate[18]. The liver is the first and primary site affected by the hematogenous spread in colorectal carcinoma. In the present study, although only two rats were injected variant HT-29c cells with three selections *in vivo* into the mesenteric vein, still they showed a higher metastatic potential. One of the two rats developed extensive hepatic metastases, and the other developed synchronous multiple organ metastases. Both rats developed mesenteric metastases. The variant HT-29d with four-cycle selections had a higher metastatic efficiency in nude rats. The taking rate of liver metastases was increased as compared with parental HT-29 cells (70 % versus 50 %), and variant HT-29b cells with two-cycles selections (70 % versus 60 %)[16]. Three of the ten rats developed lung metastasis, and extensive organs were synchronously involved in metastases. The results showed that HT-29d cells had more extensive metastatic potential than parental HT-29, variant HT-29b and HT-29c. The present study supported the hypothesis of metastatic heterogeneity. Pre-existing tumor cell subpopulations with heterogeneous metastatic capacity could be isolated from their parental neoplasms by means of cycles of selection *in vivo*. The availability of selected human colorectal cell lines and the *in vivo* model of metastasis in rats allows to search for the molecular determinants of human colorectal cancer metastases and for the establishment of relevant models to test novel therapeutic agents against colorectal cancer metastasis.

uPA is a serine protease with multiple actions that could enable it to play a role in cellular migration, tissue remodeling, and cancer spread[19]. Some investigators reported that patients with a high uPA or high PAI-1 level had a poorer prognosis for relapse than those with a low uPA or low PAI-1 antigen level. It was concluded that uPA and PAI-1 antigen levels in tumor tissue were an independent and useful prognostic marker in a variety of malignancies[20,21], especially breast cancer[22,23]. However, there have been no studies concerning the relation between uPA as well as PAI-1 level of high-metastatic cells and low-metastatic cells or non-metastatic cells. We analyzed the difference of uPA and PAI-1 level produced by WiDr (non-metastatic), HT-29 (low metastatic) and variant HT-29d cells (highly metastatic) in their supernatants by ELISA. It showed that variant HT-29d cells produced higher a levels of uPA and PAI-1 as compared with non-metastatic WiDr cells and low metastatic HT-29 cells. HT-29 cells produced higher levels of uPA and PAI-1 as compared with WiDr cells. uPA might act as an offensive mechanism for tumor cell invasion and metastasis. Although the functional role of PAI-1 in tumor biology has been unknown, PAI-1 might play a role in enhancing tumor spread by mechanisms involving in angiogenesis or promote tumor cell division[24]. Since PAI-1 is present in endothelial cells and platelets of normal tissues, increased PAI-1 levels may reflect a high degree of angiogenesis, which offers the possibility of tumor spread and metastasis. Our results showed that levels of uPA and PAI-1 in variant HT-29d cells were higher than that in HT-29 cells, suggesting that the process of metastasis might depend on the selection of tumor cell clones with increased expression of plasminogen activator, which was positively correlated with the metastatic potential of colorectal carcinoma cells in this study.

CEA has been implicated in the development of hepatic metastases from colorectal cancers, and has been described as an adhesion molecule either by Ca^{2+}-independent homophilic binding or heterophilic binding. The present results showed that CEA levels on cell surfaces *in vitro* were not different among WiDr, HT-29 and HT-29d cells. In CEA immunostaining, no difference was observed among the cell lines, s.c. tumor and liver metastases of WiDr, HT-29 and HT-29d cells, repectively. These results showed that CEA surface expression might not be correlated with the metastastic potential in this model. However, the secretion of CEA was significantly altered in metastatic cells. Moreover, other members of the CEA family might also be differently expressed in metastatic cells.

PI3-kinase is a heterodimer consisting of an 85-kDa regulatory subunit (p85), and a 110-kDa catalytic subunit (p110). The role of PI3-kinase in growth factor signaling pathways has been studied intensively[25]. Several reports have shown PI3-kinase was involved in signal transduction pathways associated with cell growth regulation, cell cycle progression, and cell survival[26]. Some studies showed increased cellular content of PI3-kinase products and also physical association of the enzyme with transmembrane receptor tyrosine kinases following stimulation by various growth factors, including hepatocyte growth factor[27,28] and insulin-like growth factor[29]. A recent research indicated the importance of PI3-kinase in increased cell motility stimulated by growth factors such as PDGF and hepatocyte growth factor[30]. However, these data do not indicate whether expression of PI3-kinase is associated with the metastatic potential of colorectal carcinoma cells. In this study, we investigated the PI3-kinase expression in colorectal carcinoma cell lines WiDr, HT-29 and HT-29d *in vitro* and in s.c. tumors and liver metastases of rats immunohistochemically. *In vitro*, non-metastatic WiDr cells, metastatic HT-29 cells and highly-metastatic vairant HT-29d cells all expressed PI3-kinase. No significant differences were found in positive cell ratio and staining intensity. In s.c. tumors, highly metastatic vairant HT-29d cells showed a stronger PI3-kinase expression in staining intensity and a higher ratio of positive cells compared to WiDr and HT-29 cells. In liver metastases, vairant HT-29d cells showed a stronger staining intensity and a higher positive ratio than that of parental HT-29 cells. These results suggest metastatic potential may positively correlate with synthesis of PI3-kinase in this *in vivo* model. The highly-metastatic HT-29d variant highly expresses PI3-kinase. The expression of PI3-kinase correlates with tumor development and metastasis, and it may be a late event of tumor development of colorectal carcinoma and may correlate with an invasive stage of cancer.

REFERENCES

1 **Schmitt M,** Wilhelm O, Janicke F, Magdolen V, Reuning U, Ohi H, Moniwa N, Kobayashi H, Weidle U, Graeff H. Urokinase-type plasminogen activator (uPA) and its receptor (CD87): a new target in tumor invasion and metastasis. *J Obstet Gynaecol* 1995; **21**: 151-165

2 **Gershtein ES,** Kushlinskii NE. Urokinase and tissue plasminogen activators and their inhibitor PAI-1 in human tumors. *Bull Exp Biol Med* 2001; **131**: 67-72

3 **Yamamoto M,** Ueno Y, Hayashi S, Fukushima T. The role of proteolysis in tumor invasiveness in glioblastoma and metastatic brain tumors. *Anticancer Res* 2002; **22**: 4265-4268

4 **Cho JY,** Chung HC, Noh SH, Roh JK, Min JS, Kim BS. High level of urokinase-type plasminogen activator is a new prognostic marker in patients with gastric carcinoma. *Cancer* 1997; **79**: 878-883

5 **Qin LX,** Tang ZY. The prognostic molecular markers in hepatocellular carcinoma. *World J Gastroenterol* 2002; **8**: 385-392

6 **Duffy MJ.** Urokinase plasminogen activator and its inhibitor, PAI-1, as prognostic markers in breast cancer: from pilot to level 1 evidence studies. *Clin Chem* 2002; **48**: 1194-1197

7 **Bouchet C,** Hacene K, Martin PM, Becette V, Tubiana-Hulin M, Lasry S, Oglobine J, Spyratos F. Breast cancer: Prognostic value of a dissemination index based on 4 components of the urokinase-type plasminogen activator system. *Pathol Biol (Paris)* 2000; **48**: 825-831

8 **Schmalfeldt B,** Kuhn W, Reuning U, Pache L, Dettmar P, Schmitt M,Janicke F, Hofler H, Graeff H. Primary tumor and metastasis in ovarian cancer differ in their content of urokinase-type plasminogen activator, its receptor, and inhibitors types 1 and 2. *Cancer Res* 1995; **55**: 3958-3963

9 **Minami S,** Furui J, Kanematsu T. Role of carcinoembryonic antigen in the progression of colon cancer cells that express carbohydrate antigen. *Cancer Res* 2001; **61**: 2732-2735

10 **Duffy MJ.** Carcinoembryonic antigen as a marker for colorectal cancer: is it clinically useful? *Clin Chem* 2001; **47**: 624-630

11 **Katada T,** Kurosu H, Okada T, Suzuki T, Tsujimoto N, Takasuga S, Kontani K, Hazeki O, Ui M. Synergistic activation of a family of phosphoinositide 3-kinase via G-protein coupled and tyrosine kinase-related receptors. *Chem Phys Lipids* 1999; **98**: 79-86

12 **Krasilnikov MA.** Phosphatidylinositol-3 kinase dependent pathways: the role in control of cell growth, survival, and malignant transformation. *Biochemistry (Mosc)* 2000; **65**: 59-67

13 **Khwaja A,** Lehmann K, Marte BM, Downward J. Phosphoinositide 3-kinase induces scattering and tubulogenesis in epithelial cells through a novel pathway. *J Biol Chem* 1998; **273**: 18793-18801

14 **Besson A,** Robbins SM, Yong VW. PTEN / MMAC1 / TEP1 in signal transduction and tumorigenesis. *Eur J Biochem* 1999; **263**: 605-611

15 **Keely PJ**, Westwick JK, Whitehead IP, Der CJ, Parise LV. Cdc42 and Rac 1 induce integrin- mediated cell motility and invasiveness through PI(3)K. *Nature* 1997; **390**: 632-636

16 **Vogel I**, Shen Y, Soeth E, Juhl H, Kremer B, Kalthoff H, Henne-Bruns D. A human carcinoma model in athymic rats reflecting solid and disseminated colorectal metastases. *Langenbecks Arch Surg* 1998; **383**: 466-473

17 **Morikawa K,** Walker SM, Nakajima M, Pathak S, Jessup JM, Fidler IJ. Influence of organ environment on the growth, selection, and metastasis of human colon carcinoma cells in nude mice. *Cancer Res* 1988; **48**: 6863-6871

18 **Dinney CP**, Fishbeck R, Singh RK, Eve B, Pathak S, Brown N, Xie B, Fan D, Bucana CD, Fidler IJ. Isolation and characterization of metastatic variants from human transitional cell carcinoma passaged by orthotopic implantation in athymic nude mice. *J Urol* 1995; **154**: 1532-1538

19 **Yamamoto M,** Ueno Y, Hayashi S, Fukushima T. The role of proteolysis in tumor invasiveness in glioblastoma and metastatic brain tumors. *Anticancer Res* 2002; **22**: 4165-4268

20 **Duffy MJ,** Maguire TM, McDermott EW, O'Higgins N. Urokinase plasminogen activator: a prognostic marker in multiple types of cancer. *J Surg Oncol* 1999; **71**: 130-135

21 **Duffy MJ.** Urokinase-type plasminogen activator: a potent marker of metastatic potential in human cancers. *Biochem Soc Trans* 2002; **30**: 207-210

22 **Gandolfo GM,** Conti L, Vercillo M. Fibrinolysis components as prognostic markers in breast cancer and colorectal carcinoma. *Anticancer Res* 1996; **16**: 2155-2159

23 **Janicke F,** Prechtl A, Thomssen C, Harbeck N, Meisner C, Untch M, Sweep CG, Selbmann HK, Graeff H, Schmitt M. Randomized adjuvant chemotherapy trial in high-risk, lymph node-negative breast cancer patients indentified by urokinase-type plasminogen activator and plasminogen activator inhibitor type 1. *J Natl Cancer Inst* 2001; **93**: 913-920

24 **Kaneko T,** Konno H, Baba M, Tanaka T, Nakamura S. Urokinase-type plasminogen activator expression correlates with tumor angiogenesis and poor outcome in gastric cancer. *Cancer Sci* 2003; **94**: 43-49

25 **Varticovski L,** Harrison-Findik D, Keeler ML, Susa M. Role of PI 3-kinase in mitogenesis. *Biochim Biophys Acta* 1994; **1226**: 1-11

26 **Divecha N,** Irvine RF. Phospholipid signaling. *Cell* 1995; **80**: 269-278

27 **Qiao H,** Saulnier R, Patryzkat A, Rahimi N, Raptis L, Rossiter J, Tremblay E, Elliott B. Cooperative effect of hepatocyte growth factor and fibronectin in anchorage-independent survival of mammary carcinoma cells: requirement for phosphatidylinositol 3-kinase activity. *Cell Growth Differ* 2000; **11**: 123-133

28 **Fan S,** Ma YX, Wang JA, Yuan RQ, Meng Q, Cao Y, Laterra JJ, Goldberg ID, Rosen EM. The cytokine hepatocyte growth factor / scatter factor inhibits apoptosis and enhances DNA repair by a common mechanism involving signaling through phosphatidyl inositol 3' kinase. *Oncogene* 2000; **19**: 2212-2223

29 **Gentilini A,** Marra F, Gentilini P, Pinzani M. Phosphatidylinositol-3 kinase and extracellular signal-regulated kinase mediate the chemotactic and mitogenic effects of insulin-like growth factor-I in human hepatic stellate cells. *J Hepatol* 2000; **32**: 227-234

30 **Yao J,** Morioka T, Oite T. PDGF regulates gap junction communication and connexin43 phosphorylation by PI 3-kinase in mesangial cells. *Kidney Int* 2000; **57**: 1915-1926

Edited by Zhu LH and Wang XL

P.O.Box 2345, Beijing 100023,China
Fax: +86-10-85381893
E-mail: wjg@wjgnet.com www.wjgnet.com

World J Gastroenterol 2003;9(11):2632-2634
World Journal of Gastroenterology
 ISSN 1007-9327

• CASE REPORT •

A case report of localized gastric amyloidosis

Dan Wu, Jian-Ying Lou, Jian Chen, Lun Fei, Gui-Jie Liu, Xiao-Yu Shi, Han-Ting Lin

Dan Wu, Jian-Ying Lou, Jian Chen, Lun Fei, Gui-Jie Liu, Xiao-Yu Shi, Han-Ting Lin, Department of General Surgery, Second Affiliated Hospital, Medical College of Zhejiang University, Hangzhou 310009, Zhejiang Province, China
Correspondence to: Dr. Dan Wu, Department of General Surgery, Second Affiliated Hospital, Medical College of Zhejiang University, Hangzhou 310009, Zhejiang Province, China. loujianying@163.com
Telephone: +86-571-87783580
Received: 2003-06-17 **Accepted:** 2003-07-15

Abstract

AIM: To elucidate the clinical and laboratory features of localized gastric amyloidosis via a rare report along with a review of related literatures.

METHODS: The clinical manifestations, laboratory results and surgical treatment of a female patient with localized gastric amyloidosis in our hospital were summarized. The relevant literatures were reviewed on the etiology, clinical features, diagnosis, treatment and prognosis of this disease.

RESULTS: The patient was lack of specific clinical manifestations and positive laboratory results. Prior to the treatment, she was suspected to be of malignization from gastric ulcer by both gastroscopy and endoscopic ultrasonography, which was denied by the gastric biopsy. The patient was treated with subtotal gastrectomy and clearance of perigastric lymph nodes. The postoperative pathological diagnosis determined the lesion to be the deposition of amyloid materials in the gastric mucosa, submucosa and blood vessel walls with intestinal metaplasia and atrophy of the gastric glands, in which no malignant tumor was found. Congo red staining with prior potassium permanganate incubation confirmed the AA type of amyloid in this case. Multiple biopsies from esophagus, remnant stomach, duodenum, colon and bone marrow in the follow-up survey showed no amyloidal deposition in these tissues and organs. Up to the present, no signs of recurrence have been found in this patient.

CONCLUSION: Localized gastric amyloidosis, being rare in incidence, should be considered in the differentiation of gastric tumors, in which biopsy is the only means to confirm the diagnosis. Currently, surgical resection of pathological tissue and circumambient lymph nodes may be a preferable therapeutic strategy for the localized amyloidosis to prevent possible complications. Although with a benign prognosis, gastric amyloidosis possesses a recurrent tendency as suggested by the literatures.

Wu D, Lou JY, Chen J, Fei L, Liu GJ, Shi XY, Lin HT. A case report of localized gastric amyloidosis. *World J Gastroenterol* 2003; 9(11): 2632-2634
http://www.wjgnet.com/1007-9327/9/2632.asp

INTRODUCTION

Amyloidosis is an abnormal intercellular deposition of insoluble proteins that share a remarkably similar and stable core structure of β sheets[1]. It may be resulted from a heterogeneous group of disorders and result in impairment or even dysfunction of involved organs. Generally, amyloidosis is more commonly manifested as a systemic involvement of multiple tissues and organs including the heart, liver, spleen, kidneys, lymph nodes, adrenals, thyroid, as well as many others. In contrast, the clinical implication of a single organ or tissue is relatively rare in this pathological condition[2-6], in which the amyloidal deposit confined to the stomach is extremely scarce in the previous literatures[7-9]. Recently, we have experienced and cured a case of localized gastric amyloidosis and now report it as follows.

CASE REPORT

A 50-year-old female was admitted to our hospital on Aug 23, 2002, with chief complaints of recurrent epigastric discomfort for 10 years and a newly-appeared dull pain in the upper abdomen for 4 months. The Inpatient No of this patient was 370655. Ever since being diagnosed as gastric ulcer and erosive gastritis with intestinal metaplasia 10 years ago by gastroscopy, she has not received any normal treatment except for long-term administration of metronidazole and omeprazole tablets herself. Prior to hospitalization, she was suggested to be of cancerization from gastric ulcer by gastroscopy at another medical institution. On admission, the patient displayed a good general condition and no positive signs including enlargement of superficial lymph node were revealed by physical check-up. Laboratory data showed negative results in the detection of serum anti-streptolysin O, rheumatoid factor and urine Bence-Jones protein. No abnormal signs were found on the chest radiograph. An upper gastrointestinal endoscopy revealed a gastric ulcer of 3 cm×1 cm in size that was located at the posterior wall of small curvature at the inferior part of gastric corpus. The margin of the ulcer was heaped up and rugged, the ambient mucosa was erosive, friable and prone to bleeding. The base of the ulcer was shaggy and covered with fibrinous layers. The malignization of this ulcer was suggested by endoscopic ultrasonography with low echo findings that the sick part of gastric wall was markedly and unevenly thickened, and some parts of the submucosa were infiltrated. On the contrary, a diagnosis of gastric amyloidosis, along with chronic gastritis with intestinal metaplasia, proliferation of lymphatic tissue and negative finding of *Helicobacter pylori*, was made by the biopsy of gastric mucosa. Exploratory laparotomy was carried out on Sep 3, 2002, in which no abnormal signs including enlargement of lymph node were found except that part of tumor-like, stiff and diffusely-thickened gastric wall was recognized at the inferior part of gastric corpus. Subtotal gastrectomy and clearance of perigastric lymph nodes were performed. Final pathological diagnosis determined the lesion to be the deposition of amyloidal materials in the gastric mucosa, submucosa and blood vessel walls with intestinal metaplasia and atrophy of the gastric glands, and no malignancies or other tumors were found. When stained with hematoxylin-eosin (Figure 1) and Congo red (Figure 2) respectively, the amyloidal deposits displayed as amorphous, homogeneous, translucent and acidophilic material under light microscope. The amyloidal protein was further proved to be

the AA type by the fact that it exhibited green birefrigence with Congo red staining under polarized light, which was disappeared when the specimens were pretreated with potassium permanganate. The patient got recovered and no complications occurred after operation. Multiple biopsies from esophagus, remnant stomach, duodenum, colon and bone marrow in the follow-up survey of 5 months post operation showed no amyloidal deposition in these tissues and organs. Up to the present, no signs of recurrence have been found in this patient.

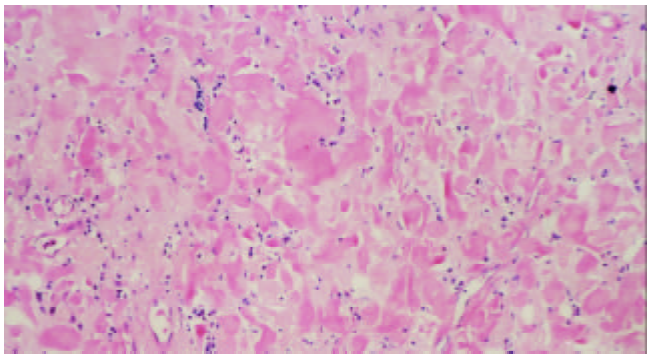

Figure 1 Stained with hematoxylin-eosin, amyloidal deposits in gastric mucosa and submucosa display amorphous, homogeneous, translucent and acidophilic materials under light microscope. (Magnification ×100).

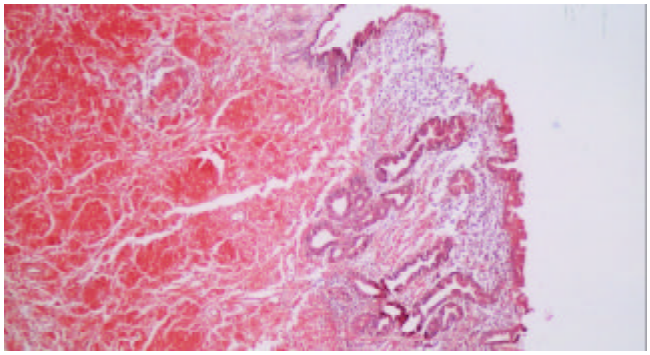

Figure 2 Stained with Congo red, deposition of amyloid could also be observed extending from gastric mucosa to submucosal layer. (Magnification ×50).

DISCUSSION

Amyloidosis, a disorder marked by the deposition of amyloid in various organs and tissues of the body, is usually associated with a variety of chronic diseases such as rheumatoid arthritis, tuberculosis, multiple myeloma and many others. Its classifications have been notoriously unsatisfactory for donkey' s years because the definition of this disorder was initially based on the morphological features, in which the amyloidosis was categorized according to the tissue distribution of amyloid (e.g. systemic versus localized amyloidosis) and the presence or absence of the identifiable predisposing factors (e. g. secondary versus primary amyloidosis). As the unique feature of amyloidal substance was, the component of the precursor protein that forms the fibrillar deposit has been now accepted as the basis for the classification of amyloidosis[10]. Up to the present, several types of the precursor proteins such as serum amyloid A (SAA), amyloid immunoglobulin light chains (AL), abnormal transthyretin (ATTR), β_2 microglobulin (β_2-M), amyloid precursor protein *etc* have been identified in amyloidosis.

Gastrointestinal tract is one of the regions to be commonly involved in the systemic amyloidosis. However, amyloidosis confined to the stomach is a rare occurrence. Although the detailed mechanism for the deposition of amyloidal materials in a specific tissue or organ remains unclear, the excessive accumulation of proteinaceous metabolites in local tissue might be a possible explanation[11]. The patient in our report suffered from gastric ulcer and gastritis for more than 10 years, which might cause a local disorder in protein metabolism and lead to localized deposition of amyloidal materials.

The clinical manifestations of amyloidosis were often uncharacteristic and varied with the involved organs. As for localized gastric amyloidosis, a variety of common gastrointestinal symptoms such as epigastric discomfort, poor appetite, hematemesis, hematochezia and gastric perforation might occur in the process of this disease because of involvement of local autonomic nervous system[7] and gastric wall structure damage[8]. Although localized gastric amyloidosis might associate with gastric malignancies in some cases[6,12,13], its non-tumorous form usually tended to be misdiagnosed as gastric tumors due to the likeness of gross appearance in endoscopic and imaging examinations. In this respect, biopsy has been suggested to be the only means to confirm the diagnosis[15]. The fact that pretreatment with potassium permanganate made biopsy specimens unstained by Congo red is helpful to determine the amyloidal component as AA type rather than AL protein. Scintigraphy with radiolabeled serum amyloid P (SAP) component could provide support for the diagnosis of amyloidosis in patients with negative histological studies[11] and distinguish localized lesion from systemic amyloidosis[14]. Besides, Immunohistochemical staining or immunofixation electrophoresis of biopsy specimens with the specific antibodies might guarantee the accurate classification of this disease[15-17].

The prognosis of amyloidosis depends on both the specific types of lesions and the involved organs. Systemic amyloidosis is usually with an unfavorable prognosis while the localized types of this disease such as the localized gastric amyloidosis have a relatively better outcome. Untreated AL amyloidosis often had the worst prognosis with a median survival time of one to two years[18], especially when cardiac involvement occurred. Patients with ATTR amyloidosis might survive up to 15 years from diagnosis but this time also varies with the specific mutation and the time of diagnosis - the younger the age of presentation the worse the outcome. However, the prognosis of patients with AA type was affected mainly by the underlying conditions[1,15]. Currently, there is no specific therapy for systemic amyloidosis. The treatment strategy has been directed both to support the affected organs and to deal with the underlying specific disease[19] in an attempt to reduce the deposition of amyloidal substances and improve prognosis, in which several supportive protocols and chemotherapeutic drugs including melphalan, iodinated anthracycline 4-iodo-4-deoxydoxorubicin, dimethylsulfoxide and colchicines have been widely used, although their effectiveness in ameliorating this disease has remained to be determined[15]. With the advances in molecular biology, some promising attempts have been made to reduce inflammatory response and amyloidal deposits by blocking the signal conduction of RAGE-NF-κB in monocytes/macrophages[20]. In patients with localized amyloidosis, thorough resection of the foci and their circumambient lymph nodes as performed in our case is probably the preferable therapeutic modality and the key measures to prevent postoperative recurrence. Up to the present, no signs of recurrence have been found in the follow-up survey of our patient.

REFERENCES

1 **Khan MF**, Falk RH. Amyloidosis. *Postgrad Med J* 2001; **77**: 686-693
2 **Kurokawa H**, Takuma C, Tokudome S, Yamashita Y, Kajiyama

M. Primary localization amyloidosis of the sublingual gland. *Fukuoka Igaku Zasshi* 1998; **89**: 216-220
3 **Aouda A**, Toyozaki T, Saito T, Yorimitsu K, Miyazaki A, Deguchi F, Inagaki Y. A case of primary cardiac amyloidosis with amyloid A protein. *Kokyu To Junkan* 1993; **41**: 89-92
4 **Matsui H**, Kato T, Inoue G, Onji M. Amyloidosis localized in the sigmoid colon. *J Gastroenterol* 1996; **31**: 607-611
5 **Hauben E**, Fierens H, Heylen H, Van Marck E. Localized amyloid tumour of the duodenum: a case report. *Acta Gastroenterol Belg* 1997; **60**: 304-305
6 **Aoyagi K**, Koufuji K, Yano S, Murakami N, Miyagi M, Koga A, Takeda J, Shirouzu K. Early gastric carcinoma associated with amyloidosis: a case report. *Kurume Med J* 2002; **49**: 153-156
7 **Zheng W**, Song S, Zhu Q, Tan H, Li P, Jiang Y. Local amyloidosis of stomach. *Zhonghua Waike Zazhi* 1998; **36**: 415-416
8 **Bjornsson S**, Johannsson JH, Sigurjonsson F. Localized primary amyloidosis of the stomach presenting with gastric hemorrhage. *Acta Med Scand* 1987; **221**: 115-119
9 **Macmanus Q**, Okies JE. Amyloidosis of the stomach: report of an unusual case and review of the literature. *Am Surg* 1976; **42**: 607-610
10 **Husby G**. A chemical classification of amyloid. Correlation with different clinical types of amyloidosis. *Scand J Rheumatol* 1980; **9**: 60-64
11 **Tan SY**, Pepys MB. Amyloidosis. *Histopathology* 1994; **25**: 403-414
12 **Goteri G**, Ranaldi R, Pileri SA, Bearzi I. Localized amyloidosis and gastrointestinal lymphoma: a rare association. *Histopathology* 1998; **32**: 348-355
13 **Hayashi I**, Muto Y, Fujii Y, Katsuda Y. Primary amyloidosis associated with early gastric carcinoma (IIb like IIa type) diagnosed by preoperative gastric biopsy-a case report. *Gan No Rinsho* 1983; **29**: 1686-1692
14 **Hachulla E**, Grateau G. Diagnostic tools for amyloidosis. *Joint Bone Spine* 2002; **69**: 538-545
15 **Falk RH**, Comenzo RL, Skinner M. The systemic amyloidoses. *N Engl J Med* 1997; **337**: 898-909
16 **Abraham RS**, Katzmann JA, Clark RJ, Bradwell AR, Kyle RA, Gertz MA. Quantitative analysis of serum free light chains. A new marker for the diagnostic evaluation of primary systemic amyloidosis. *Am J Clin Pathol* 2003; **119**: 274-278
17 **Linke RP**, Nathrath WBJ, Eulitz M. Classification of amyloid syndromes from tissue sections using antibodies against various amyloid fibril proteins: report of 142 cases. In: Glenner GG, Osserman EF, Benditt EP, Calkins E, Cohen AS, Zucker-Franklin D, eds. Amyloidosis, 1986. *New York: Plenum Publishers* 1986: 599-605
18 **Kyle RA**, Gertz MA. Primary systemic amyloidosis: clinical and laboratory features in 474 cases. *Semin Hematol* 1995; **32**: 45-59
19 **Skinner M**. Amyloidosis. In: Lichtenstein LM, Fauci AS, eds. Current therapy in allergy, immunology, and rheumatology. 5th ed. St. *Louis: Mosby-year Book* 1996: 235-240
20 **Yan SD**, Zhu H, Zhu A, Golabek A, Du H, Roher A, Yu J, Soto C, Schmidt AM, Stern D, Kindy M. Receptor-dependent cell stress and amyloid accumulation in systemic amyloidosis. *Nat Med* 2000; **6**: 643-651

Edited by Wang XL

P.O.Box 2345, Beijing 100023,China
Fax: +86-10-85381893
E-mail: wjg@wjgnet.com www.wjgnet.com

World J Gastroenterol 2003;9(12):2635-2641
World Journal of Gastroenterology
 ISSN 1007-9327

• REVIEW •

Reg gene family and human diseases

Yu-Wei Zhang, Liu-Song Ding, Mao-De Lai

Yu-Wei Zhang, Department of Pathology, School of Medicine, Zhejiang University, Hangzhou 310006, Zhejiang Province, China and Department of Pathology, School of Basic Medical Sciences, Southeast University, Nanjing 210009, Jiangsu Province, China
Mao-De Lai, Department of Pathology, School of Medicine, Zhejiang University, Hangzhou 310006, Zhejiang Province, China
Liu-Song Ding, Zhejiang University Libraries, Hangzhou 310006, Zhejiang Province, China
Supported by National Natural Science Foundation of China, No. 30200333 and No.30371605
Correspondence to: Dr. Yu-Wei Zhang, Department of Pathology, School of Basic Medical Sciences, Southeast University, Nanjing 210009, Jiangsu Province, China. yuwei123@seu.edu.cn
Telephone: +86-571-87217134 **Fax:** +86-571-87951358
Received: 2003-05-10 **Accepted:** 2003-06-02

Abstract

Regenerating gene (Reg or REG) family, within the superfamily of C-type lectin, is mainly involved in the liver, pancreatic, gastric and intestinal cell proliferation or differentiation. Considerable attention has focused on Reg family and its structurally related molecules. Over the last 15 years, 17 members of the Reg family have been cloned and sequenced. They have been considered as members of a conserved protein family sharing structural and some functional properties being involved in injury, inflammation, diabetes and carcinogenesis. We previously identified Reg IV as a strong candidate for a gene that was highly expressed in colorectal adenoma when compared to normal mucosa based on suppression subtractive hybridization (SSH), reverse Northern blot, semi-quantitative reverse transcriptase PCR (RT-PCR) and Northern blot. *In situ* hybridization results further support that overexpression of Reg IV may be an early event in colorectal carcinogenesis. We suggest that detection of Reg IV overexpression might be useful in the early diagnosis of carcinomatous transformation of adenoma. This review summarizes the roles of Reg family in diseases in the literature as well as our recent results of Reg IV in colorectal cancer. The biological properties of Reg family and its possible roles in human diseases are discussed. We particularly focus on the roles of Reg family as sensitive reactants of tissue injury, prognostic indicators of tumor survival and early biomarkers of carcinogenesis. In addition to our current understanding of Reg gene functions, we postulate that there might be relationships between Reg family and microsatellite instability, apoptosis and cancer with a poor prognosis. Investigation of the correlation between tumor Reg expression and survival rate, and analysis of the Reg gene status in human maliganancies, are required to elucidate the biologic consequences of Reg gene expression, the implications for Reg gene regulation of cell growth, tumorigenesis, and the progression of cancer. It needs to be further attested whether Reg gene family is applicable in early detection of cancer and whether Reg and Reg-related molecules can offer novel molecular targets for anticancer therapeutics. This has implications with regard to prognosis, such as in monitoring cancer initiation, progression and recurrence, as well as the design of chemotherapeutic drugs.

Zhang YW, Ding LS, Lai MD. Reg gene family and human diseases. *World J Gastroenterol* 2003; 9(12): 2635-2641
http://www.wjgnet.com/1007-9327/9/2635.asp

INTRODUCTION

Reg and Reg-related genes constitute a family belonging to calcium dependent lectin (C-type lectin) gene superfamily[1-4]. It represents a group of small secretory proteins, which can function as acute phase reactants, lectins, antiapoptotic factors or growth factors for pancreatic β-cells, neural cells and epithelial cells in the digestive system[5,6]. They play a wide range of roles in researching mammal physiology and human diseases. Ever since Reg (regenerating gene) I was discovered, special attentions have been paid to the regeneration of pancreatic β-cells and administration of Reg I protein and/or activation of the Reg I gene to be used as a potential therapeutic approach for diabetes[7]. Successively, the potential role of Reg family in tumors especially in digestive tract has drawn more attention[8-14]. We here focus on the members of Reg family, their functions and possible mechanisms.

REG FAMILY

Discovered members

In 1984, Yamanoto *et al*. found that administration of nicotinamide accelerated the regeneration of pancreatic islets in partially pancreatectomized rats. Subsequently, Terazono *et al.* screened a rat regenerating islet-derived cDNA library and isolated a novel gene encoding a 165 amino acid protein with a 21 amino acid signal peptide[15,16], which was called Reg gene. It was not termed Reg I until 1997. They also cloned human Reg I cDNA encoding a 166 amino acid protein with a 22 amino acid signal peptide. Reg I has other synonyms such as PTP (pancreatic thread protein), PSP (pancreatic stone protein) and lithostathine[17]. Human Reg I gene is a single copy gene spanning 3.0 kb, and is composed of six exons and five introns. The gene mRNA was detected predominantly in the pancreas, and at lower levels in gastric mucosa and kidneys[18]. Later they isolated two genes, one of which was a mouse homologue to rat and human Reg gene, the other a novel type of Reg gene. The two genes were designated as Reg I and Reg II, respectively.

In 1999, Okamoto grouped the members of the family, Reg and Reg-related genes from human, rat and mouse, into three subclasses, types I, II, and III[19]. Stephanova *et al.* determined that the three rat PAP genes and the related Reg gene (REGL, regenerating islet-derived-like/ pancreatic stone protein-like/ pancreatic thread protein-like) were all located at 4q33-q34[20]. The mouse Reg family genes were mapped to a contiguous 75 kb region in chromosome 6, including Reg I, Reg II, Reg III alpha, Reg III beta, Reg III gamma, and Reg III delta[21]. Reg III delta was expressed predominantly in exocrine pancreas, whereas both Reg I and Reg II were expressed in hyperplastic islets and Reg III alpha, Reg III beta and Reg III gamma were expressed strongly in the intestinal tract and weakly in pancreas.

Although Reg IV (1q12-q21), identified by Hartupee *et*

al, has not been found in the same chromosome as other members of human Reg gene and Reg-related gene (2p12), it shares some common features with other members such as: sequence homology, tissue expression profiles, and exon-intron junction genomic organization[1]. Thus by 2001, four types of Reg gene family had been identified. Data of RT-PCR results in our laboratory were consistent with the hybridization result of Hartupee and colleagues, and Reg IV mRNAs level was higher in colon than in rectum. We compared the results with Reg I expression pattern. Kawanami *et al*. discovered that expression of Reg I mRNA was higher in the stomach than in any other region of the gastrointestinal tract[22], which also suggested that Reg mRNA was higher in proximate gastrointestinal tract.

Table 1 Members of Reg family, length of amino acids and chromosome localization

Superfamily memeber	Species	Length of amino aAcid	Chromosome localization
Reg I	Mouse Reg I	165	6
	Rat Reg	165	4q33-q34
	Human Reg / PSP / PTP	166	2p12
Reg II	Mouse Reg II	173	6
Reg III	Rat PAP	175	4q33-q34
	Rat peptide 23	175	4q33-q34
	Human HIP	175	2p12
	Bovine PTP	175	
Reg IV	Human Reg IV	158	1q12-q21

So far, 17 members have been identified in mammals across human, pig, mouse, bovine and rat species. Table 1 lists some most important members of Reg family[23,24]. Among the mammalian members of this family, there is only mouse Reg II in type II and human Reg IV in type IV. Hartupee *et al*. also reported that a mouse homologue of Reg IV was likely existed[1], but up to now, there are no reports and also no investigations on mouse Reg IV.

Structure and function

Most members of Reg family have similar organization with respect to exon number and chromosome location. The most interesting characteristic is its common domain of lectin. Data have revealed a significant similarity of the sequences of Reg family with the C-type (Calcium-dependent) lectin superfamily. This domain of lectin could account for complex events such as human malignancy and other diseases[25,26].

Studies on Reg I protein receptor (Reg-R) revealed that regenerating protein might act not only as a regulator of gastric epithelial cell proliferation but also as a modifier of many other multiple physiologic functions[27,28]. Reg-R gene was isolated from a rat islet cDNA library[27] encoding a cell surface 919-amino acid protein. Its expression was detected mainly in chief cells and parietal cells of the deep layers and faintly in surface epithelial cells and mucous neck cells of the proliferating zone[29]. Reg I protein could induce β-cell proliferation via the Reg I receptor and ameliorate experimental diabetes[30].

Under physiological conditions, Reg I protein is not expressed in pancreatic β-cells, although Reg-R is expressed. In the regenerative process of pancreatic islets, Reg I gene expression is induced. Therefore, activation of Reg I gene is thought to be one of the important events in β-cell regeneration.

REG FAMILY AND HUMAN DISEASES

Injury response and inflammation

Regenerating gene family members are expressed in tissue injury. As tissue injury is concerned, pancreatitis is most frequently studied. Experimental induction of acute pancreatitis caused a coordinate increase both in PSP/reg (Reg I) and in PAP (Reg III). Since the regulation of this protein family was affected even under mild stress, they were defined as secretory stress proteins[31-33]. Reg levels are sensitive markers for pancreatic injury and early stage of the disease, which might be useful prognostic indicators for disease severity[34]. The expression level of PSP/Reg I protein varies with different degrees of injury. Mild to moderate injury to pancreatic tissue might stimulate the synthesis of PSP/reg-protein, whereas more severe injury tended to depress it[32,34].

There are other evidences supporting Reg' s roles in the healing of gastrointestinal mucosal lesions. Miyaura *et al*. measured Reg expression after implantation or resection of a solid insulinoma in rats and found that the diminution in pancreatic β-cell mass caused by subcutaneous implantation of insulinoma tissues was associated with reduced Reg I gene expression and increase of β-cell proliferation after resection of the tumor was preceded by return of Reg I gene expression toward normal[35]. In an injured state following indomethacin treatment, Reg I gene expression was sharply increased, accompanied by an overexpression of c-fos and healing of mucosal lesions[22]. In addition, Reg I mRNA was detected predominantly in the deepest mucosal layer. It was expressed almost exclusively in cells that were less than 11 μm in diameter, which suggested a role of Reg I in the healing.

This also may be one of reasons why Reg genes have been frequently screened as differentially expressed genes[8,10,36-38]. Shinozaki *et al*. isolated seven candidate genes that were presumed to be up-regulated in inflammatory colonic epithelia and Reg I was among them. Expression of Reg I alpha was confined to the crypt epithelia[36] and its selective expression in the crypt epithelia of inflammatory colonic mucosa might suggest its important regulatory functions.

Another interesting change was the length of Reg mRNA. The elongated mRNA of PAP II/Reg III was strongly induced in the early phase after acute pancreatitis. The elongated mRNA might affect the function of PAP II/Reg III protein because the elongated mRNA with long 3' untranslated regions (3' UTR) was involved in the translation efficiency and thus played an important role in the progression of pancreatitis[39].

Diabetes

Islet cells originate from the epithelial cells of primitive pancreatic ducts during embryogenesis, and can regenerate in response to the loss of islet cells even in adult pancreas. The ability of islet cells to regenerate could increase the possibility, which could restore the impaired and decreased islets of diabetic patients[40]. On the other hand, aging may be associated with selective dysfunction of β-cells, which may involve the expression of Reg I gene. Reg I gene could play an important role in β-cell growth/regeneration[41,42] and its expression could parallel to islet physiology, thus Reg I gene may become one of the targets of genetic engineering for diabetic β-cells.

In early 1980s, Takasawa *et al.* proposed a unifying model for β-cell damage (the okamoto model). In 1984, they demonstrated Reg I protein could induce β-cell proliferation and ameliorate experimental diabetes. Later, they showed that combined addition of IL-6 and dexamethasone could induce Reg I gene expression in β-cells and that inhibitors could enhance the expression[43]. In 2002, they reported that PARP and its inhibitors had key roles in inducing β-cell regeneration, maintenance of insulin secretion, and prevention of β-cell death[28].

The expression of Reg is a defense mechanism of the exocrine pancreas that is conserved in evolution. Sanchez *et al*. demonstrated that pancreatic Reg I and Reg II genes were overexpressed in non-obese diabetic (NOD) mice during active diabetogenesis[44,45]. They suggested that overexpression of the Reg gene(s) might represent a defense of acinar cells against pancreatic aggression. Although some results were opposite to their hypothesis[46,47], they further confirmed their previous findings by conducting the same protocol as Fu did.

Studies on differentially expressed genes have added proof to reveal Reg' s potential application in treatment. As we know, genes overexpressed in pancreatic islets of patients with diabetes are potential candidates for novel disease-related autoantigens. Subtractive hybridization was used on islets from a patient who died at the onset of type I diabetes, and a type I diabetes-related cDNA encoding hepatocarcinoma-intestine-pancreas/pancreatic-associated protein (HIP/PAP, Reg III) was identified[48]. In addition, treatment aimed at abrogation of autoimmunity combined with expansion of β-cell mass has become a potential therapeutic approach for the treatment of insulin-dependent diabetes[49]. Therefore, diabetes might be ameliorated with Reg protein treatment.

Tumors

Watanabe *et al*. firstly studied the relationship between cancer and Reg[16]. Reg I mRNA was detected at various levels in gastric cancer and colorectal cancer, but was not in esophageal cancers and nontumoral mucosae of the colon, rectum and esophagus. Reg gene family has been found to be up-regulated in human colorectal cancer cell lines during differentiation[50], this was reflected at the protein level by Western blotting in a small series of human colorectal cancers[14]. Macadam *et al*. later analyzed 142 cases of primary colorectal adenocarcinoma and demonstrated that 53 % tumors expressed Reg I mRNA, which was only detected in 16 out of 88 (18.1 %) paired normal mucosae[12]. PAP was also over-expressed in colorectal cancer[14]. Reg genes were expressed in a portion of cancers, whereas no expression was found in paired normal mucosae. The mechanisms altering the transcriptional control of Reg genes might be of interest from a therapeutic standpoint[12].

Even though there is a long history of observations related to up-regulated Reg expression in cancer. Only in the last five years, there have been experimental evidences directly supporting a role of these proteins in neoplastic transformation and tumor progression. Bernard-Perrone *et al*. localized Reg I protein in Paneth cells and immature columnar cells of human small intestinal crypts[50], which appeared to be associated with cell growth. Reg I protein may be down-regulated when growth is achieved and differentiation is induced.

Our study on Reg IV suggested that Reg IV might play an important role in initiating colorectal adenoma, and its detection might be useful in the early diagnosis of colorectal adenoma formation[8]. Reg IV has been screened 13 times in a subtracted cDNA library of human colon adenoma/normal mucosa by using suppression subtractive hybridization (SSH) method[8, 38]. The overexpression of Reg IV in colorectal adenomas was testified by reverse Northern blot. Our recent results showed that Reg IV was up-regulated in colorectal adenoma and carcinoma. Violette *et al*. also found its overexpression in colorectal cancer[10], and pointed out the potential role of Reg IV in colorectal tumors and its subsequent interest as a prognostic indicator.

Another interesting topic is involved in Reg I and gastric cancer. Reg I could be expressed in gastric enterochromaffin-like (ECL) cells[51,52]. Mutations of Reg I that inhibit secretion are associated with ECL cell carcinoids, suggesting that Reg I functions as an autocrine or paracrine tumor suppressor. Chiba suggested that Reg I might normally function as a negative regulator of ECL cell growth to restrain the stimulatory effect of gastrin in humans[53]. Abolition of Reg I protein secretion might result in an enhanced proliferation of ECL cells, and eventually lead to the development of ECL carcinoid tumors.

In addition to the study on relationships between diseases of gastrointestinal tract and Reg expression, there are many reports dealing with Reg and other digestive organs. Harada *et al*. examined the expression of Reg I in intrahepatic cholangiocarcinoma (ICC) and its precursor lesion (biliary dysplasia) and showed that the expression of Reg I protein was significantly dependent on the histologic differentiation[54]. HIP at a transcriptional level was elevated in liver tumors while it was not detected in nontumorous adjacent areas or in normal adult and fetal liver, suggesting that HIP could be involved in liver cell proliferation or differentiation. HIP mRNA expression is tissue specific, since it is expressed in the normal small intestine and pancreas, while it could not be evidenced in colon, brain, kidney, or lung[37]. HIP gene shows several potential regulatory elements, which might account for the enhanced expression of the gene during pancreatic inflammation and liver carcinogenesis[55]. Both Reg I mRNA and its product were localized in acinar cells of the pancreas, but neither was found in ductal or islet cells. Reg I protein has been considered as a useful marker for acinar cell differentiation[56] and immunohistochemical application of reg I protein may help to show histogenesis and differential diagnosis of pancreatic tumors.

Few reports are available on the association of Reg and tumors outside the digestive system. Bartoli *et al*. showed a weak expression of PAP/HIP gene in the pituitary gland, Reg I expression was not observed in tested adenomas or in pituitary gland[57], whereas REGL gene was observed in pituitary gland and in some subtypes of adenomas. Reg gene was expressed only in fetal pancreas and in some adult tissues. In contrast, REGL transcript was expressed not only in fetal pancreas but also in fetal colon and brain as well as in some adult tissues. In our results, we firstly reported Reg IV' s potential role in prostate cancer[8]. From the original results of bioinformatics analysis based on public databases (serial analysis of gene expression, SAGE), we could state that Reg IV was expressed in normal colon mucosa, colon adenocarcinoma, pancreatic cancer, gastric adenocarcinoma and prostate adenocarcinoma. Since Reg family was associated with different kinds of tumors in the digestive system, this was the report of Reg IV expression in prostate adenocarcinoma although its transcript level was rather low. On the other hand, if Reg is expressed in most cancers independent of their origins and is only expressed in limited normal tissues, it is of clinical significance that Reg expression is applied to early detection and treatment of cancer. But the most important point is to make sure whether its expression is tumor-specific.

ASPECTS TO BE FURTHER STUDIED

Reg family and microsatellite instability

Microsatellite instability (MSI) has been reported to be an important feature of solid malignancies[58]. Inactivation of the mismatch repair system (MMR) would lead to MSI that can profoundly affect cellular behaviors, since many genes playing important roles in inducing signal transduction, apoptosis, DNA repair and cell cycle control could be altered in tumors with MSI[59].

From the report of Akiyama *et al*.[30], we can hypothesize the possible relationship between Reg and DNA repair. Although it cannot supply strong evidences for the relationship between Reg and microsatellite instability, but other reports may further reveal its potential relationship. Cancers with MSI have a unique histological appearance and an altered response

to chemotherapy and radiotherapy. It has been more frequently seen in mucoid cancer with poor differentiation[60-64] and the subtype with MSI also has a characteristic of drug resistance. Interestingly, Violette *et al*. discovered that Reg IV mRNA-positive tumor cells displayed unique phenotypes such as: mucus-secreting, enterocyte-like or undifferentiated ones. What is more, it was overexpressed in HT-29 drug-resistant cells[10].

Possible early biomarkers of carcinogenesis

Zenilman *et al*. observed a phenomenon of Reg I protein expression changed in colorectal cancer[9] and postulated that colorectal production of Reg I might either be a marker for the presence of cancer or a risk of mucosa for development of neoplasia based on the fact that Reg I protein was ectopically expressed in colorectal mucosa at the transitional zone of colorectal cancer, and occasionally within the tumor itself[9].

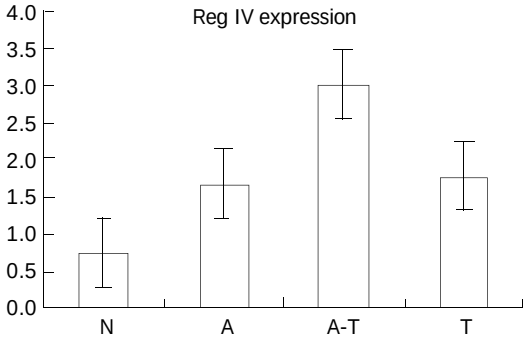

Figure 1 *In situ* hybridization results of 12 cases of colorectal adenoma with carcinomatous change. (N=normal mucosa, A=residual adenoma, A-T=adenoma with carcinomatous change, T=invasive cancer)[13].

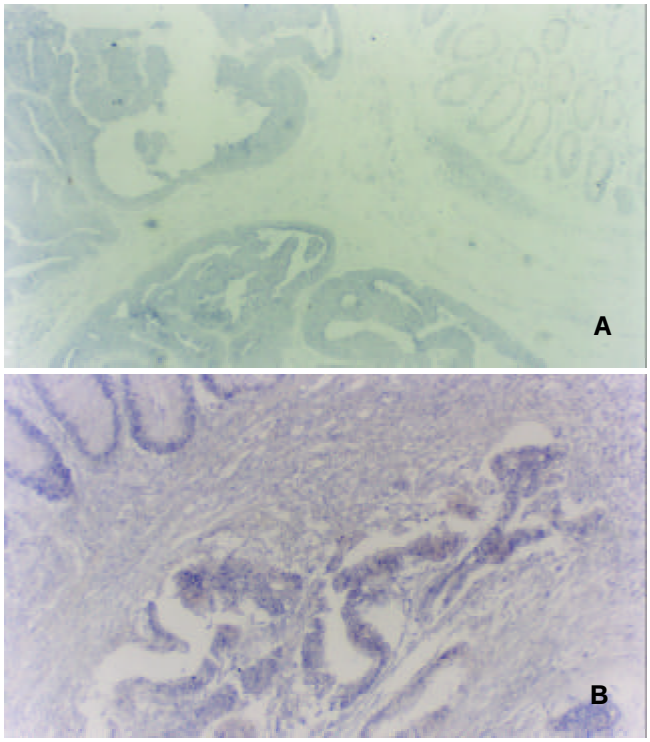

Figure 2 *In situ* hybridization of Reg IV. A: Reg IV is up-regulated in colorectal cancer, B: Reg IV is up-regulated in normal mucosa adjacent to adenoma and adenocarcinoma.

Other reports on Reg family can add some evidences to the confirmation of Reg family' s role as a predicator of early cancer. Harada *et al*. suggested that expression of Reg I was a good marker for biliary mucosa at risk for development of ICC, and that Reg I played a role in the early stages of biliary carcinogenesis, probably via a cell-proliferative effect[54]. Our results of *in situ* hybridization showed that Reg IV was up-regulated in colorectal adenoma and carcinoma and the greatest Reg IV positivity was typically observed at regions with carcinomatous change (Figures 1, 2). Another interesting phenomenon was that at some regions near adenoma or adenocarcinoma (Figure 2b), Reg IV was also up-regulated as it was in colorectal adenoma and carcinoma, and the expression became weaker with increasing distance away from the tumor border in the direction of normal epithelia. Thus Reg IV may be thought as the biomarker of early transformations such as *in situ* carcinoma. This further presented evidences that overexpression of Reg IV might be an early event in colorectal adenoma-carcinoma sequence and carcinogenesis. Our present data also show that Reg IV is more frequently overexpressed in poorly differentiated colorectal carcinomas and carcinomas with metastasis.

The tumor-promoting activity of Reg protein should be considered for its possible clinical applications[43]. Moreover, its sensitivity to carcinogenesis might be used for early diagnosis.

Antiapoptotic factors

Reg I might reduce epithelial apoptosis in inflammation[65,66]. In addition, tumor necrosis factor (TNF) pathway also reflects Reg' s potential role as an antiapoptotic factor. TNF-alpha contributes to the development of acute pancreatitis. Because TNF-alpha was involved in the control of apoptosis, Malka *et al*. studied its interaction with the pancreatic apoptotic pathway[65,66]. The antiapoptotic pancreatitis-associated protein (PAP) I is a candidate for mediating TNF-alpha activity. Its expression is induced by TNF-alpha, and cells overexpressing PAP I show significantly less apoptosis on exposure to TNF-alpha. Therefore, PAP I is one of the effectors of apoptosis inhibition.

Reg gene product may regulate a series of regeneration. This regenerative response may switch off apoptotic signals. Thus, those cells, which exhibit both a regenerative response and genetic mutations in some growth promoting or metastasis inducing genes, would have a survival advantage[12].

Up to now, we cannot confirm whether Reg I directly take part in apoptotic inhibition. But it is of interest to clarify the relationship between Reg I expression and inhibitors of apoptosis.

Predictions of poor prognosis

Expression of Reg might reflect the degree of tissue injury. Thus overexpression degree of Reg might be a useful marker to judge whether the tumor has a poor prognosis. The expression of Reg I alone and co-expression of Reg I with PAP have a significantly adverse effect on survival. Thus the expression of Reg I might provide a valuable selective indicator of adjuvant therapy in patients with early-stage colorectal cancer which would recur after curative surgery[12].

Reports also revealed that a role of Reg gene in the healing of gastrointestinal mucosal lesions. Up-regulation of Reg I expression in ulcerative colitis might reflect the activation of mucosal injury followed by down-regulation when the injury was healed. Interestingly, a similar feature was also appeared in Reg IV. Our results showed that higher levels of Reg IV mRNA were consistently scored in regions with more severe dysplasia in the same adenoma sample displaying a varying degree of dysplasia. We postulate that Reg IV overexpression may reflect the degree of body injuries. However, when two tumors coexisted in a single case, Reg IV transcript was usually

higher in adenomas compared with paired carcinomas. The mechanism is not clear.

In addition to these mechanisms, Reg family has been found to be implicated in other physiological processes. Reg II has a distinctive role in injury response[67] and its expression is a crucial step in ciliary neurotrophic factor (CNTF) survival pathway. Reg II has been found to be a neurotrophic factor and also an intermediate in the survival signalling pathway of CNTF-related cytokines[68].

In conclusion, we have characterized the structure and expression of Reg genes. Their possible functions and mechanisms were also discussed. These studies have led to a better understanding of the essential functions of these Reg family genes in mammalian physiological processes and human diseases. In addition to its potential application in diabetes, future studies on Reg family and human malignancy will shed lights on Reg' s unusual features on cancer. As we know, expression of Reg I inversely correlated with the level of cell differentiation, and it could be modulated via the glucocorticoid receptor, and has been found to be a potential marker of gastrointestinal epithelial differentiation[69]. Rechreche *et al*. suggested that inhibition of PAP/reg expression in normal colon cells by silencing their gene promoters could be relieved during colon carcinogenesis, allowing their up-regulation by mediators such as cytokines. Reg' s role in human malignancy especially in the digestive system should be further studied[11,14]. More recently, Kamarainen *et al*. identified and characterized a gene encoding a regenerating protein (REG)-like protein called RELP[70], and found there were several transcripts of RELP and the predicted protein product of the major transcript was annotated Reg IV.

All these encourage us to further study the potential roles of Reg family, especially Reg IV in human tumors. Are they sensitive reactants of tissue injury? Do they play oncogenic roles in colorectal cancers? Is there any potential if they are used as early biomarkers of carcinogenesis? Could they be used as prognostic indicators of tumor survival and disease severity? Before these conclusions can be drawn, further investigations are needed. Thus, detection of the expression level of Reg in cancers with different histological features and survival rates, and analysis of Reg gene status in human tumors at different stages or sites, are required to elucidate the pathophysiologic roles of Reg family.

REFERENCES

1 **Hartupee JC**, Zhang H, Bonaldo MF, Soares MB, Dieckgraefe BK. Isolation and characterization of a cDNA encoding a novel member of the human regenerating protein family: Reg IV. *Biochim Biophys Acta* 2001; **1518**: 287-293

2 **Lasserre C**, Simon MT, Ishikawa H, Diriong S, Nguyen VC, Christa L, Vernier P, Brechot C. Structural organization and chromosomal localization of a human gene (HIP/PAP) encoding a C-type lectin overexpressed in primary liver cancer. *Eur J Biochem* 1994; **224**: 29-38

3 **Chakraborty C**, Katsumata N, Myal Y, Schroedter IC, Brazeau P, Murphy LJ, Shiu RP, Friesen HG. Age-related changes in peptide-23/pancreatitis-associated protein and pancreatic stone protein/reg gene expression in the rat and regulation by growth hormone-releasing hormone. *Endocrinology* 1995; **136**: 1843-1849

4 **Katsumata N**, Chakraborty C, Myal Y, Schroedter IC, Murphy LJ, Shiu RP, Friesen HG. Molecular cloning and expression of peptide 23, a growth hormone-releasing hormone-inducible pituitary protein. *Endocrinology* 1995; **136**: 1332-1339

5 **Broekaert D**, Eyckerman S, Lavens D, Verhee A, Waelput W, Vandekerckhove J, Tavernier J. Comparison of leptin- and interleukin-6-regulated expression of the rPAP gene family: evidence for differential co-regulatory signals. *Eur Cytokine Netw* 2002; **13**: 78-85

6 **Dusetti NJ**, Frigerio JM, Fox MF, Swallow DM, Dagorn JC, Iovanna JL. Molecular cloning, genomic organization, and chromosomal localization of the human pancreatitis-associated protein (PAP) gene. *Genomics* 1994; **19**: 108-114

7 **Okamoto H**. The Reg gene family and Reg proteins: with special attention to the regeneration of pancreatic â-cells. *J Hepatobiliary Pancreat Surg* 1999; **6**: 254-262

8 **Zhang YW**, Lai MD, Gu XM. Reg IV, a differentially expressed gene in colorectal adenoma. *Chinese Medical Journal* 2003; **116**: 918-922

9 **Zenilman ME**, Kim S, Levine BA, Lee C, Steinberg JJ. Ectopic Expression of reg Protein: A Marker of Colorectal Mucosa at Risk for Neoplasia. *J Gastrointest Surg* 1997; **1**: 194-202

10 **Violette S**, Festor E, Pandrea-Vasile I, Mitchell V, Adida C, Dussaulx E, Lacorte JM, Chambaz J, Lacasa M, Lesuffleur T. Reg IV, a new member of the regenerating gene family, is overexpressed in colorectal carcinomas. *Int J Cancer* 2003; **103**:185-193

11 **Kadowaki Y**, Ishihara S, Miyaoka Y, Rumi MA, Sato H, Kazumori H, Adachi K, Takasawa S, Okamoto H, Chiba T, Kinoshita Y. Reg protein is overexpressed in gastric cancer cells, where it activates a signal transduction pathway that converges on ERK1/2 to stimulate growth. *FEBS Lett* 2002; **530**: 59-64

12 **Macadam RC**, Sarela AI, Farmery SM , Robinson PA, Markham AF, Guillou PJ. Death from early colorectal cancer is predicted by the presence of transcripts of the REG gene family. *Br J Cancer* 2000; **83**: 188-195

13 **Zhang Y,** Lai M, Lv B, Gu X, Wang H, Zhu Y, Zhu Y, Shao L, Wang G. Overexpression of Reg IV in colorectal adenoma. *Cancer Letters* 2003; **200**: 69-76

14 **Rechreche H**, Montalto G, Mallo GV, Vasseur S, Marasa L, Soubeyran P, Dagorn JC, Iovanna JL. pap, reg Ialpha and reg Ibeta mRNAs are concomitantly up-regulated during human colorectal carcinogenesis. *Int J Cancer* 1999; **81**: 688-694

15 **Terazono K**, Yamamoto H, Takasawa S , Shiga K, Yonemura Y, Tochino Y, Okamoto H. A novel gene activated in regenerating islets. *J Biol Chem* 1988; **263**: 2111-2114

16 **Watanabe T**, Yonekura H, Terazono K, Yamamoto H, Okamoto H. Complete nucleotide sequence of human reg gene and its expression in normal and tumoral tissues. The reg protein, pancreatic stone protein, and pancreatic thread protein are one and the same product of the gene. *J Biol Chem* 1990; **265**: 7432-7439

17 **De Reggi M**, Gharib B. Protein-X, Pancreatic Stone-, Pancreatic thread-, reg-protein, P19, lithostathine, and now what? Characterization, structural analysis and putative function(s) of the major non-enzymatic protein of pancreatic secretions. *Curr Protein Pept Sci* 2001; **2**: 19-42

18 **Unno M**, Yonekura H, Nakagawara K, Watanabe T, Miyashita H, Moriizumi S, Okamoto H, Itoh T, Teraoka H. Structure, chromosomal localization, and expression of mouse reg genes, reg I and reg II. A novel type of reg gene, reg II, exists in the mouse genome. *J Biol Chem* 1993; **268**: 15974-15982

19 **Okamoto H**. The Reg gene family and Reg proteins: with special attention to the regeneration of pancreatic β-cells. *J Hepatobiliary Pancreat Surg* 1999; **6**: 254-262

20 **Stephanova E,** Tissir F, Dusetti N , Iovanna J, Szpirer J, Szpirer C. The rat genes encoding the pancreatitis-associated proteins I, II and III (Pap1, Pap2, Pap3), and the lithostathin/pancreatic stone protein/regeneration protein (Reg) colocalize at 4q33–>q34. *Cytogenet Cell Genet* 1996; **72**: 83-85

21 **Abe M**, Nata K, Akiyama T, Shervani NJ, Kobayashi S, Tomioka-Kumagai T, Ito S, Takasawa S, Okamoto H. Identification of a novel Reg family gene, Reg IIIdelta, and mapping of all three types of Reg family gene in a 75 kilobase mouse genomic region. *Gene* 2000; **246**: 111-122

22 **Kawanami C**, Fukui H, Kinoshita Y, Nakata H, Asahara M, Matsushima Y, Kishi K, Chiba T. Regenerating gene expression in normal gastric mucosa and indomethacin-induced mucosal lesions of the rat. *J Gastroenterol* 1997; **32**: 12-18

23 **Schiesser M**, Bimmler D, Frick TW, Graf R. Conformational changes of pancreatitis-associated protein (PAP) activated by trypsin lead to insoluble protein aggregates. *Pancreas* 2001; **22**: 186-192

24 **Zenilman ME**, Magnuson TH, Swinson K, Egan J, Perfetti R, Shuldiner AR. Pancreatic thread protein is mitogenic to pancre-

atic-derived cells in culture. *Gastroenterology* 1996; **110**: 1208-1214
25 **Weis WI**, Kahn R, Fourme R, Drickamer K, Hendrickson WA. Structure of the calcium-dependent lectin domain from a rat mannose-binding protein determined by MAD phasing. *Science* 1991; **254**: 1608-1615
26 **Kishore U**, Eggleton P, Reid KB. Modular organization of carbohydrate recognition domains in animal lectins. *Matrix Biol* 1997; **15**: 583-592
27 **Kobayashi S**, Akiyama T, Nata K, Abe M, Tajima M, Shervani NJ, Unno M, Matsuno S, Sasaki H, Takasawa S, Okamoto H. Identification of a receptor for reg (regenerating gene) protein, a pancreatic β-cell regeneration factor. *J Biol Chem* 2000; **275**: 10723-10726
28 **Okamoto H**, Takasawa S. Recent advances in the Okamoto model: the CD38-cyclic ADP-ribose signal system and the regenerating gene protein (Reg)-Reg receptor system in β-cells. *Diabetes* 2002; **51** (Suppl 3): S462-473
29 **Kazumori H**, Ishihara S, Fukuda R , Kinoshita Y. Localization of Reg receptor in rat fundic mucosa. *J Lab Clin Med* 2002; **139**: 101-108
30 **Akiyama T**, Takasawa S, Nata K , Kobayashi S, Abe M, Shervani NJ, Ikeda T, Nakagawa K, Unno M, Matsuno S, Okamoto H. Activation of Reg gene, a gene for insulin-producing β-cell regeneration: poly(ADP-ribose) polymerase binds Reg promoter and regulates the transcription by autopoly(ADP-ribosyl)ation. *Proc Natl Acad Sci U S A* 2001; **98**: 48-53
31 **Graf R**, Schiesser M, Lussi A, Went P, Scheele GA, Bimmler D. Coordinate regulation of secretory stress proteins (PSP / reg, PAP I, PAP II, and PAP III) in the rat exocrine pancreas during experimental acute pancreatitis. *J Surg Res* 2002; **105**: 136-144
32 **Cavallini G**, Bovo P, Bianchini E , Carsana A, Costanzo C, Merola M, Sgarbi D, Frulloni L, Di Francesco V, Libonati M, Palmieri M. Lithostathine messenger RNA expression in different types of chronic pancreatitis. *Mol Cell Biochem* 1998; **185**: 147-152
33 **Meili S,** Graf R, Perren A, Schiesser M, Bimmler D. Secretory apparatus assessed by analysis of pancreatic secretory stress protein expression in a rat model of chronic pancreatitis. *Cell Tissue Res* 2003; **312:** 291-299
34 **Satomura Y**, Sawabu N, Ohta H, Watanabe H, Yamakawa O, Motoo Y, Okai T, Toya D, Makino H, Okamoto H. The immunohistochemical evaluation of PSP / reg-protein in normal and diseased human pancreatic tissues. *Int J Pancreatol* 1993; **13**: 59-67
35 **Miyaura C**, Chen L, Appel M, Alam T, Inman L, Hughes SD, Milburn JL, Unger RH, Newgard CB. Expression of reg / PSP, a pancreatic exocrine gene: relationship to changes in islet β-cell mass. *Mol Endocrinol* 1991; **5**: 226-234
36 **Shinozaki S,** Nakamura T, Iimura M , Kato Y, Iizuka B, Kobayashi M, Hayashi N. Upregulation of Reg 1alpha and GW112 in the epithelia of inflamed colonic mucosa. *Gut* 2001; **48**: 623-629
37 **Lasserre C**, Christa L, Simon MT , Vernier P, Brechot C. A novel gene (HIP) activated in human primary liver cancer. *Cancer Res* 1992; **52**: 5089-5095
38 **Luo MJ**, Lai MD. Identification of differentially expressed genes in normal mucosa, adenoma and adenocarcinoma of colon by SSH. *World J Gastroenterol* 2001; **7**: 726-731
39 **Honda H**, Nakamura H, Otsuki M. The elongated PAP II / Reg III mRNA is upregulated in rat pancreas during acute experimental pancreatitis. *Pancreas* 2002; **25**: 192-197
40 **Yamaoka T**, Itakura M. Development of pancreatic islets. *Int J Mol Med* 1999; **3**: 247-261
41 **Okamoto H**. Cyclic ADP-ribose-mediated insulin secretion and Reg, regenerating gene. *J Mol Med* 1999; **77**: 74-78
42 **Unno M**, Nata K, Noguchi N, Narushima Y, Akiyama T, Ikeda T, Nakagawa K, Takasawa S, Okamoto H. Production and characterization of Reg knockout mice: reduced proliferation of pancreatic β-cells in Reg knockout mice. *Diabetes* 2002; **51**(Suppl 3): S478-483
43 **Takasawa S**, Okamoto H. Pancreatic β-cell death, regeneration and insulin secretion: roles of poly(ADP-ribose) polymerase and cyclic ADP-ribose. *Int J Exp Diabetes Res* 2002; **3**: 79-96
44 **Sanchez D**, Baeza N, Blouin R, Devaux C, Grondin G, Mabrouk K, Guy-Crotte O, Figarella C. Overexpression of the reg gene in non-obese diabetic mouse pancreas during active diabetogenesis is restricted to exocrine tissue. *J Histochem Cytochem* 2000; **48**: 1401-1410
45 **Baeza N**, Sanchez D, Christa L, Guy-Crotte O, Guy-Crotte O, Vialettes B, Figarella C. Pancreatitis-associated protein (HIP / PAP) gene expression is upregulated in NOD mice pancreas and localized in exocrine tissue during diabetes. *Digestion* 2001; **64**: 233-239
46 **Ortiz EM**, Dusetti NJ, Vasseur S, Malka D, Bodeker H, Dagorn JC, Iovanna JL. The pancreatitis-associated protein is induced by free radicals in AR4-2 J cells and confers cell resistance to apoptosis. *Gastroenterology* 1998; **114**: 808-816
47 **Fu K**, Sarras MP Jr, De Lisle RC, Andrews GK. Regulation of mouse pancreatitis-associated protein-I gene expression during caerulein-induced acute pancreatitis. *Digestion* 1996; **57**: 333-340
48 **Gurr W**, Yavari R, Wen L , Shaw M, Mora C, Christa L, Sherwin RS. A Reg family protein is overexpressed in islets from a patient with new-onset type 1 diabetes and acts as T-cell autoantigen in NOD mice. *Diabetes* 2002; **51**: 339-346
49 **Gross DJ,** Weiss L, Reibstein I, van den Brand J, Okamoto H, Clark A, Slavin S. Amelioration of diabetes in nonobese diabetic mice with advanced disease by linomide-induced immunoregulation combined with Reg protein treatment. *Endocrinology* 1998; **139**: 2369-2374
50 **Bernard Perrone FR**, Renaud WP, Guy Crotte OM , Bernard P, Figarella CG, Okamoto H, Balas DC, Senegas-Balas FO. Expression of REG protein during cell growth and differentiation of two human colon carcinoma cell lines. *J Histochem Cytochem* 1999; **47:** 863-870
51 **Fukui H**, Kinoshita Y, Maekawa T, Okada A, Waki S, Hassan S, Okamoto H, Chiba T. Regenerating gene protein may mediate gastric mucosal proliferation induced by hypergastrinemia in rats. *Gastroenterology* 1998; **115**: 1483-1493
52 **Higham AD**, Bishop LA, Dimaline R. Mutations of RegIalpha are associated with enterochromaffin-like cell tumor development in patients with hypergastrinemia. *Gastroenterology* 1999; **116**: 1310-1318
53 **Chiba T**. Is reg gene mutation involved in the development of enterochromaffin-like cell carcinoid tumors? *Gastroenterology* 1999; **116**: 1489-1491
54 **Harada K**, Zen Y, Kanemori Y, Chen TC, Chen MF, Yeh TS, Jan YY, Masuda S, Nimura Y, Takasawa S, Okamoto H, Nakanuma Y. Human REG I gene is up-regulated in intrahepatic cholangiocarcinoma and its precursor lesions. *Hepatology* 2001; **33**: 1036-1042
55 **Lasserre C**, Simon MT, Ishikawa H, Diriong S, Nguyen VC, Christa L, Vernier P, Brechot C. Structural organization and chromosomal localization of a human gene (HIP / PAP) encoding a C-type lectin overexpressed in primary liver cancer. *Eur J Biochem* 1994; **224**: 29-38
56 **Kimura N,** Yonekura H, Okamoto H, Nagura H. Expression of human regenerating gene mRNA and its product in normal and neoplastic human pancreas. *Cancer* 1992; **70**: 1857-1863
57 **Bartoli C**, Baeza N, Figarella C, Pellegrini I, Figarella-Branger D. Expression of peptide-23 / pancreatitis-associated protein and Reg genes in human pituitary and adenomas: comparison with other fetal and adult human tissues. *J Clin Endocrinol Metab* 1998; **83**: 4041-4046
58 **Mao L**, Lee DJ, Tockman MS, Erozan YS, Askin F, Sidransky D. Microsatellite alterations as clonal markers for the detection of human cancer. *Proc Natl Acad Sci U S A* 1994; **91**: 9871-9875
59 **Polato F**, Broggini M. Microsatellite instability and genetic alterations in ovarian cancer. *Minerva Ginecol* 2003; **55**: 129-138
60 **Zhang YW**, Lai MD. Microsatellite alterations on chromosome 9p21-22 in sporadic colorectal cancer. *Zhonghua Binglixue Zazhi* 1999; **28**: 418-421
61 **Chao A**, Gilliland F, Willman C, Joste N, Chen IM, Stone N, Ruschulte J, Viswanatha D, Duncan P, Ming R, Hoffman R, Foucar E, Key C. Patient and tumor characteristics of colon cancers with microsatellite instability: a population-based study. *Cancer Epidemiol Biomarkers Prev* 2000; **9**: 539-544
62 **Alexander J**, Watanabe T, Wu TT , Rashid A, Li S, Hamilton SR. Histopathological identification of colon cancer with microsatellite instability. *Am J Pathol* 2001; **158**: 527-535
63 **Samowitz WS**, Curtin K, Ma KN, Schaffer D, Coleman LW,

Leppert M, Slattery ML. Microsatellite instability in sporadic colon cancer is associated with an improved prognosis at the population level. *Cancer Epidemiol Biomarkers Prev* 2001; **10**: 917-923

64 **Greenson JK**, Bonner JD, Ben-Yzhak O, Cohen HI, Miselevich I, Resnick MB, Trougouboff P, Tomsho LD, Kim E, Low M, Almog R, Rennert G, Gruber SB. Phenotype of microsatellite unstable colorectal carcinomas: Well-differentiated and focally mucinous tumors and the absence of dirty necrosis correlate with microsatellite instability. *Am J Surg Pathol* 2003; **27**: 563-570

65 **Malka D**, Vasseur S, Bodeker H, Ortiz EM, Dusetti NJ, Verrando P, Dagorn JC, Iovanna JL. Tumor necrosis factor alpha triggers antiapoptotic mechanisms in rat pancreatic cells through pancreatitis-associated protein I activation. *Gastroenterology* 2000; **119**: 816-828

66 **Dieckgraefe BK**, Crimmins DL, Landt V, Houchen C, Anant S, Porche-Sorbet R, Ladenson JH. Expression of the regenerating gene family in inflammatory bowel disease mucosa: Reg Ialpha upregulation, processing, and antiapoptotic activity. *J Investig Med* 2002; **50**: 421-434

67 **Averill S,** Davis DR, Shortland PJ, Priestley JV, Hunt SP. Dynamic pattern of reg-2 expression in rat sensory neurons after peripheral nerve injury. *J Neurosci* 2002; **22**: 7493-7501

68 **Nishimune H,** Vasseur S, Wiese S, Birling MC, Holtmann B, Sendtner M, Iovanna JL, Henderson CE. Reg-2 is a motoneuron neurotrophic factor and a signalling intermediate in the CNTF survival pathway. *Nat Cell Biol* 2000; **2**: 906-914

69 **Zenilman ME**, Magnuson TH, Perfetti R, Chen J, Shuldiner AR. Pancreatic reg gene expression is inhibited during cellular differentiation. *Ann Surg* 1997; **225**: 327-332

70 **Kamarainen M**, Heiskala K, Knuutila S, Heiskala M, Winqvist O, Andersson LC. RELP, a Novel Human Reg-Like Protein with Up-Regulated Expression in Inflammatory and Metaplastic Gastrointestinal Mucosa. *Am J Pathol* 2003; **163**: 11-20

Edited by Zhang JZ and Wang XL

P.O.Box 2345, Beijing 100023,China
Fax: +86-10-85381893
E-mail: wjg@wjgnet.com www.wjgnet.com

World J Gastroenterol 2003;9(12):2642-2649
World Journal of Gastroenterology
 ISSN 1007-9327

• REVIEW •

Aberrant crypt foci as microscopic precursors of colorectal cancer

Lei Cheng, Mao-De Lai

Lei Cheng, Mao-De Lai, Department of pathology, School of Medical Sciences, Zhejiang University, Hangzhou, 310006, Zhejiang Province, China
Correspondence to: Mao-De Lai, M.D., Professor of pathology, Department of Pathology, School of Medical Sciences, Zhejiang University, Hangzhou, 310006, Zhejiang Province, China. lmd@sun.zju.edu.cn
Telephone: +86-571-87217134 **Fax:** +86-571-87951358
Received: 2003-05-12 **Accepted:** 2003-06-02

Abstract

Since the first detection of aberrant crypt foci (ACF) in carcinogen-treated mice, there have been numerous studies focusing on these microscopically visible lesions both in rodents and in humans. ACF have been generally accepted as precancerous lesions in regard to histopathological characteristics, biochemical and immunohistochemical alterations, and genetic and epigenetic alterations. ACF show variable histological features, ranging from hyperplasia to dysplasia. ACF in human colon are more frequently located in the distal parts than in the proximal parts, which is in accordance with those in colorectal cancer (CRC). The immunohistochemical expressions of carcinoembryonic antigen (CEA), β-catenin, placental cadherin (P-cadherin), epithelial cadherin (E-cadherin), inducible nitric oxide synthase (iNOS), cyclooxygenase (COX-2), and $P16^{INK4a}$ are found to be altered. Genetic mutations of K-ras, APC and p53, and the epigenetic alterations of CpG island methylation of ACF have also been demonstrated. Genomic instabilities due to the defect of mismatch repair (MMR) system are detectable in ACF. Two hypotheses have been proposed. One is the "dysplasia ACF-adenoma-carcinoma sequence", the other is "heteroplastic ACF-adenoma-carcinoma sequence". The malignant potential of ACF, especially dysplastic ACF, makes it necessary to reveal the nature of these lesions, and to prevent CRC from the earliest possible stage. The technique of magnifying chromoscope makes it possible to detect "*in vivo*" ACF, which is beneficial to colon cancer research, identifying high-risk populations for CRC, and developing preventive procedures.

Cheng L, Lai MD. Aberrant crypt foci as microscopic precursors of colorectal cancer. *World J Gastroenterol* 2003; 9(12): 2642-2649
http://www.wjgnet.com/1007-9327/9/2642.asp

INTRODUCTION

Genetic changes in the malignant transformation process of colorectal mucosa include deletions, rearrangements, and mutations leading to either inactivation or activation of specific target genes[1-3]. A number of biomarkers associated with genetic changes have been identified for early detection of CRC. Two major classes of genes, oncogenes and suppressor genes, are involved in addition to mismatch repair (MMR) genes[4-6], which are associated with genomic instability. The major advances in understanding CRC include identification of the involvement of APC, p53, K-ras and MMR genes, as well as epigenetic alterations, such as CpG island methylation, in the formation and progression of the disease. Identification of ACF as an early preinvasive lesion and its relationship to the development of cancer have aroused an increasing interest in recent years.

Since the first detection of ACF in carcinogen-treated mice by Bird in 1987 and the hypothesis of ACF as the earliest precursors of CRC, there have been numerous studies focusing on these microscopically visible lesions both in rodents and in humans. The following table (Table 1) shows some highlights of studies on human ACF.

Table 1 Highlights of human ACF in recent years (from NCBI)

Major fields	Magazines and authors	Year
Histopathology	Kristt D, *et al.* Hum Pathol.	1999
	Nascimbeni R, *et al.* Am J Surg Pathol.	1999
	Shipitz B, *et al.* Hum Pathol.	1998
	Siu IM, *et al.* Am J Pathol.	1997
	Di Gregorio C, *et al.* Histopathology.	
	Roncucci L, *et al.* Cancer Epidemiol	1997
	Biomarkers Prev.	1991
	Roncucci L, *et al.* Hum Pathol.	1991
Gene mutations	Yuan P, *et al.* World J Gastroenterol.	2001
	Takayama T, *et al.* Gastroenterology.	2001
	Otori K, *et al.* Cancer.	1998
	Bjerknes M, *et al.* Am J Pathol.	1997
	Losi L, *et al.* J Pathol.	1996
	Zaidi NH, *et al.* Carcinogenesis.	1995
	Smith AJ, *et al.* Cancer Res.	1994
Epigenetic/phenotype alterations of genes		
CpG island methylation	Chan AO, *et al.* Am J Pathol.	2002
	Sakurazawa N, *et al.* Cancer Res.	2000
Microsatellite instability	Pedroni M, *et al.* Cancer Res.	2001
	Heinen CD, *et al.* Cancer Res.	1996
	Augenlicht LH, *et al.* Oncogene.	1996
Cell dynamics and proliferation	Roncucci L, *et al.* Cell Prolif.	2000
	Kristt D, *et al.* Pathol Oncol Res.	1999
	Otori K, *et al.* Cancer Res.	1995
	Roncucci L, *et al.* Cancer Res.	1993
Oncoproteins	Dong M, *et al.* Carcinogenesis.	2003
	Hao XP, *et al.* Cancer Res.	2001
	Shpitz B, *et al.* Anticancer Res.	1999
	Pretlow TP, *et al.* Gastroenterology.	1994
Dietary agents	Nascimbeni R, *et al.* Cancer Epidemiol Biomarkers Prev.	2002
	Johnson IT, *et al.* Food Chem Toxicol.	2002
	Alabaster O, *et al.* Mutat Res.	1996
Magnifying/chromoscopic colonoscopy	Hurlstone DP, *et al.* Br J Surg.	2002
	Matsumoto T, *et al.* Am J Gastroenterol.[a]	1999
	Takayama T, *et al.* N Engl J Med.	1998
	Yokota T, *et al.* Gastrointest Endosc.	1997
	Dolara P, *et al.* Cancer Detect Prev.	1997
Chemoprevention	Murillo G, *et al.* Int J Cancer.	2003
	Osawa E, *et al.* Gastroenterology.	2003
	Kassie F, *et al.* Carcinogenesis.	2003
	Osawa E, *et al.* Life Sci.	2002
	Mori H, *et al.* Biofactors.	2000
	Chung FL, *et al.* Carcinogenesis.	2000
Signal transduction pathways	Boon EM, *et al.* Cancer Res.[b]	2002

a: ileal microadenoma; b: in colorectal cell lines.

Identification of ACF both in carcinogen-treated rodents and in human colon makes the study of CRC at precancerous stages possible. The growth, morphological and molecular features of ACF support the contention that ACF are putative preneoplastic lesions. The traditional "adenoma-carcinoma" sequence of colorectal carcinogenesis has been extended to "ACF-adenoma-carcinoma" sequence. A better understanding of the underlying cellular and molecular events affected by cancer preventive or promoting agents will provide more insights into colorectal carcinogenesis and lead to the development of different cancer preventive strategies for high-risk individuals and the general population.

DEFINITION OF ACF

ACF was first reported by Bird in 1987[7] in the colons of carcinogen-treated C57BL/6J or CF1 female mice, and the assumption of ACF as potential preneoplastic lesions in murine colon was put forward one year later, coming up with the methodological approach to detect ACF[8]. Under microscope, aberrant crypts appeared larger and had a thicker epithelial lining compared to normal crypts, and usually gathered into a focus, consisting of aberrant crypts from one to hundreds[9,10]. These aberrant crypts sometimes were slightly elevated from the surrounding normal mucosa and often had oval or slit-like lumens[9,11-13]. It has been described as single or clusters of abnormally large crypts of the colon mucosal surface after stained with methylene blue. On colonoscopy, ACF were defined as being deeper with methylene blue staining than normal surrounding mucosa, and as a cluster of two or more crypts with dilated or slit-like openings rising above the surrounding mucosa[14,15].

ACF with a single crypt met the following criteria by McLellan[16]. The size of the crypt was at least twice that of the normal surrounding ones, the luminal opening was more elliptical than circular, and the epithelial lining was thicker than that of the normal surrounding crypts. ACF consisting of more than one crypt were defined as crypts to form a distinct focus. Individual crypts within the focus had a thicker epithelial lining and an elliptical luminal opening, and the total area occupied by the crypts of ACF was greater than that occupied by an equivalent number of surrounding morphologically normal crypts.

In humans, ACF were described and partially characterized for the first time in 1991[9,11], and in 1994, Pretlow first detected altered enzymatic activity, crypt dynamics and proliferation. ACF in human colon closely resembled aberrant crypts seen in rodents treated with carcinogens[7]. Some lines of evidences supported the view that ACF or at least some of them, might be precursors of CRC. In particular, ACF in human colon were more often located in the distal parts than in the proximal parts[17], which was verified in animal model[18]. Aberrant crypts had a hyperproliferative epithelium[19-21]. The size of ACF could increase with time, and it was evident that the nuclear atypia noted in some ACF was similar to those seen in the crypts of adenocarcinomas in rat colons[16]. In ACF, the immunohistochemical expressions of carcinoembryonic antigen[22] and β-catenin[23-25] were increased. K-ras, APC and P53 mutations, have been shown to be important genetic alterations in the development of CRC[26,27], have been demonstrated in ACF[28-33]. Identification of dysplasia and monoclonality in a putative precursor lesion would strongly link this lesion to neoplastic progression. ACF have been confirmed to arise from independent initiation events[28-30,34], and when examined histologically, ACF showed variable features, ranging from mild hyperplasia to dysplasia[12,22,35,36] as "nondysplasia", "dysplasia" and "mixed type"[10,12,16,17,35-40].

HISTOPATHOLOGICAL CHARACTERISTICS OF ACF

The final histological criteria for ACF are generally accepted

ACF without dysplasia

ACF with normal mucosa: lacking significant modifications of the epithelium lining the crypts, enlarged crypts (at least 1.5 times larger than normal) with only slightly enlarged and elongated nuclei, but no crowding or stratification, and no mucin depletion. Crypt cells with positive staining of PCNA and Ki-67 remain at the lower part of the crypts.

ACF with hyperplasia: analogous to the manifestations of hyperplastic polyps of colon. The crypts are larger or longer than normal crypts sometimes showing apical branching. The luminal opening is serrated and slightly elevated from the surrounding normal mucosa, but without dysplasia. Goblet cells are mixed with absorbing cells, with partial mucin depletion. Nuclei are enlarged or sometimes crowded without stratification. Cells with positive staining of PCNA and Ki-67 remain at the lower and middle parts of the crypts.

ACF with dysplasia (microadenoma)

Both crypts and cells have different degree abnormalities, with enlarged, elongated and sometimes stratified and depolarized nuclei. The number of goblet cells is decreased obviously and mucin is depleted. The major site of positive staining cells of PCNA and Ki-67 is extended to the upper part of the crypts. Serrated adenomatous ACF[41] could also be found to have similar histopathological manifestations of serrated adenomas[42].

Dysplastic ACF were common in FAP patients, and also occurred in sporadic patients at a low frequency[12,31,35]. Sporadic ACF had the characteristics similar to those of dysplastic ACF in FAP patients with less frequent APC mutations[10,43] and more frequent methylation[44].

Investigations showed the possibility of ACF transition from one pathological type to another. ACF have also been found to contain carcinoma *in situ*, or severe dysplasia in focal areas of human colon[36,40,41], and invasive carcinoma in the rat model[13], showing evidences of ACF as precancerous lesions[10,21,30,38,43,45].

ACF with mixed type of hyperplasia and dysplasia

ACF with mixed hyperplastic and adenomatous components histologically showed the combination of various proportions of pure adenomatous pattern with dysplasia and pure hyperplastic pattern without dysplasia[41].

The WHO classifications of ACF are simplified as hyperplastic ACF and dysplastic ACF.

ACF EVALUATION

The density of ACF is the number of ACF per square centimeter of mucosa surface, which was higher in diseases at a high risk of malignancy such as familial adenomatous polyposis (FAP) and in CRC, and was lower in patients with benign diseases of the colon such as diverticulosis[11,37]. ACF density is also significantly and progressively higher from proximal colon toward distal, being the highest in sigmoid and rectum, which was in accordance with the location of CRC[19,37]. It has been found that the density of FAP ACF was significantly higher than that of sporadic CRC and benign large bowel diseases[9]. In a comparative research of sporadic CRC, Gardner' s syndrome, and benign diseases such as diverticulosis, ACF density in Gardner' s syndrome was more common and ACF occupied a larger area of mucosa as compared to sporadic CRC[11]. All these findings showed that hereditary diseases prone to colon cancer had a higher density and crypt multiplicity of ACF than CRC, which shed lights on the differences between hereditary ACF and sporadic ACF, and helped to reveal the neoplastic nature of ACF.

The mechanism by which ACF increase in size seems to be a process of crypt division, which begins at the base of the crypt and proceeds upwards until two crypts are generated. Thus, the number of crypts per ACF, also termed "crypt multiplicity", would be an important parameter for evaluating ACF progression. It has been demonstrated that crypt multiplicity was significantly lower from proximal toward distal colon, which was opposite to that of ACF density, and was significantly larger when it was associated with carcinoma or adenoma than with nonneoplastic diseases[39]. Also no gradient in ACF density and crypt multiplicity was observed according to the distance from the tumor[11,37,39].

Increased mitotic activity, which has been proposed as a biomarker of colon cancer at early stages, was observed in a majority of ACF. Most of the crypts showed a mitotic pattern similar to that of normal adjacent crypts[19,46]. In some of the dysplastic foci, mitotic activity was seen to distribute throughout the crypts, as reported in adenomas. The above findings may be consistent with the assumption that ACF were preneoplastic lesions[47].

Protein kinase C (PKC) is a family of twelve distinct serine/ threonine kinases that participate in signaling pathways involved in cell proliferation, differentiation, and apoptosis. Alterations in PKC isozyme levels also played a role in colon carcinogenesis[48-50]. Elevated expression of PKC β_{II} was associated with neoplastic transformation both in rat and in human colonic epithelia[48,50]. It has been demonstrated that overexpression of protein kinase C β_{II} (PKC β_{II}) made transgenic mice more susceptible to carcinogen-induced colonic hyperproliferation and ACF formation[47], and the level of PKC β_{II} protein expression was strikingly increased in ACF compared with that in normal colonic epithelium[51].

The study of ACF and their relationships to growth factors, such as TGF-α, TGF-β, EGFR, TGFβRII, phosphorylated cellular tyrosine (P-tyr) revealed a strong correlation between altered expression of TGFs in all ACF that have been examined and the degree of dysplasia and crypt multiplicity[52]. TGF-α was undetectable in ACF[52,53], which had a high incidence of apoptosis (AI). The result was similar to that both in adenomas and in carcinomas[53]. Apoptosis provides a protective mechanism against neoplasia by moving genetically damaged stem cells from the epithelium before they can undergo clonal expansion. Manifestations are indicative of a high level of apoptosis in human ACF and carcinogen-treated animal ACF, in which apoptosis was said to eliminate cells damaged by carcinogen administration[54].

DIFFERENCES OF FAP AND SPORADIC ACF

Most FAP ACF are histopathologically, phenotypically and genetically different from sporadic ACF. Apart from the differences in ACF density between FAP ACF and sporadic ACF, there are significant differences in regard to dysplasia. Most FAP ACF were dysplastic, whereas sporadic ACF had the histopathological features of hyperplastic polyps with little or no dysplasia[38]. The degree of dysplasia in FAP ACF was severer than that of sporadic ACF[9]. Most ACF from FAP patients have phenotypic characteristics of adenomas, which are vital to carcinogenesis, and lack ras gene mutations, while sporadic ACF and a subset of FAP ACF closely resemble hyperplastic polyps, which are benign, but usually have ras gene mutations. There are also evidences identified in the colon of Min/+ mice after azoxymethane (AOM) treatment. Germline mutations in murine Apc homologous to human APC, caused multiple intestinal neoplasia in mice (Min/+ mice)[55]. ACF_{Min} resemble dysplastic ACF, which were described previously as potential precursors of adenomas in rodent and human colon carcinogenesis[35,36,39,52], and more severe in FAP ACF than in sporadic ACF. ACF_{Min} followed a continuous development from a single crypt to adenoma with fast crypt multiplication and altered expression of β-catenin, while classical ACF homologous to hyperplastic human ACF showed slow-growing crypts with normal β-catenin expression, and were probably not related to tumorigenesis[56]. In carcinogen-treated rodents and patients with sporadic CRC, only a very small fraction of ACF progressed to tumor[38]. This was consistent with the observation that a large fraction of ACF was hyperplastic whereas only a small fraction of ACF showed dysplasia, a hallmark of malignant potential[38,55]. In contrast, most ACF in FAP patients were dysplastic, resembling that of adenomas[38]. It has been proposed that only dysplastic ACF progressed to adenomas and carcinomas[35]. In non-FAP cases, K-ras mutations were detected in 82 % (89/106) of nondysplastic ACF and 63 % (17/27) of dysplastic ACF. FAP patients showed K-ras mutations in only 13 % (1/8) of dysplastic ACF, which was the predominant form of ACF found in FAP. In FAP patients, somatic APC mutations were found in 100 % of dysplastic ACF, as they were in adenomas[41]. A previous study showed an association between CpG island methylation in cancer and K-ras mutations[55]. It was found that CpG island methylation was present in more ACF from sporadic cancer than in FAP ACF, implying that FAP ACF usually lacked methylation or K-ras mutations and were frequently dysplastic, while sporadic ACF usually had methylation and/or K-ras mutations and lacked dysplasia[57].

BIOCHEMICAL AND IMMUNOHISTOCHEMICAL ALTERATIONS OF ACF

What we have discussed above is concerned about the determination of ACF under a microscope, and the histopathological characteristics of ACF. Yamada reported another kind of crypts with normal appearance harboring altered β-catenin expression, which was regarded as lesions different from ACF, and might occur earlier than ACF in rat models[58-60]. Previous studies explored phenotype alterations of ACF by means of biochemical and immunohistochemical methods. Pretlow reported enzyme-altered foci with normal morphology in colon and decreased expression of hexosaminidase in these lesions for the first time[61]. By using serial glycolmethacrylate-embedded sections of grossly normal colons from F344 rats treated with colon carcinogen, Pretlow' s group was able to detect multiple lesions with altered enzyme activities in the distal colon and rectum of those rats, and found that histochemically decreased demonstrable hexosaminidase activity could observed in more than 95 % of ACF in rats[22,29,61], and was also able to demonstrate two groups of lesions with decreased hexosaminidase activity: one with aberrant morphology resembling ACF, the other with normal appearance[29]. A decrease in hexosaminidase activity was also seen in colon tumors developed in those animals[13]. Hexosaminidase provided a marker of colon epithelial cells throughout the carcinogenesis progression[62]. Human ACF clearly resembled those seen in animals in morphology and histological appearance[11,12,22,36,63], but hexosaminidase activity was not a useful marker of human ACF because human colonic neoplasia was accompanied by a number of phenotypic changes that frequently included increased expressions of a variety of tumor-associated glycoproteins[64]. Carcinoembryonic antigen (CEA), a member of the immunoglobulin superfamily, was first isolated from human colon cancers, and seems to function as an intracellular adhesion molecule. The immunohistochemical expression of CEA was altered in as many as 93 % (39/42) of ACF in 15 patients, and was related to the size of the foci, but not to the presence or degree of dysplasia in Pretlow' s study[22]. The immunohistochemical localization of CEA in the

cytoplasms and on the basolateral membranes in ACF was similar to that of carcinomas. The finding that CEA appeared to be a marker of human ACF by means of immunohistochemistry should facilitate the identification and characterization of these lesions in human.

The other two members of the cadherin family of cell adhesion molecules were placental cadherin (P-cadherin) and epithelial cadherin (E-cadherin). It has been shown that striking membranous and/or cytoplasmic P-cadherin up-regulation and its co-expression with E-cadherin usually represented a pre-invasive dysplastic transformation[65,66]. P-cadherin was expressed from ACF to hyperplastic and adenomatous polyps, and was prior to and independent of disturbance in E-cadherin and β-catenin expression in ACF. P-cadherin was aberrantly expressed at the earliest stage of aberrant crypt formation, before the disturbance in E-cadherin and β-catenin[67].

β-catenin, which was originally discovered as a cadherin-binding protein, has been proved to function as a transcriptional activator[68]. Inactivation of β-catenin with the product of adenomatous polyposis coli (APC) gene highlighted a role of catenins in epithelial tumorigenesis. Target genes of the β-catenin-Tcf pathway were determined to be growth-promoting genes, such as c-myc and cyclin D1[69,70], suggesting β-catenin-Tcf pathway was oncogenic. Excessive β-catenin protein has been shown in colon cancers of rats and humans[71,72], and the aberrant expression of β-catenin in ACF was also seen. It was reported that in most ACF, namely ACF with hyperplasia, β-catenin was localized at the cell membrane like normal colon epithelium[25], and in ACF with dysplasia, reduced membranous expression of β-catenin was associated with increased nuclear and cytoplasmic expression. The membranous expression of β-catenin was reduced, and cytoplasmic and nuclear expression increased in ACF according to their degrees of dysplasia. Likewise, membranous expression of β-catenin was reduced, and the nuclear expression increased from ACF to adenoma and carcinoma[24], strongly suggesting that ACF and their aberrant expression of β-catenin played an important role in colorectal carcinogenesis, and the immunohistochemical staining of ACF for β-catenin could evaluate the malignant potential of ACF[25].

In carcinogen-treated animal carcinomas, it has been reported frequent mutation and altered cellular localization of β-catenin, and inducible nitric oxide synthase (iNOS) and cyclooxygenase (COX-2) were also found to be expressed in these carcinomas[72]. In carcinogen-treated animal colon, an altered cellular localization of β-catenin in all dysplastic ACF, adenomas and adenocarcinomas was shown, and iNOS expression was also observed in all but one of the lesions in which β-catenin alterations were observed. Neither iNOS expression nor β-catenin alterations were observed in any hyperplastic ACF. Nitric oxide (NO) was known to cause DNA damage and nitrosylation of proteins[73,74], and increased production in tumor cells would be expected to facilitate accumulation of sequential mutations. Since altered localization of β-catenin was apparent in all lesions expressing iNOS, it might be possible that β-catenin alteration was related to induction of iNOS expression. The positive expression of iNOS in dysplasia, but not hyperplastic ACF suggested that iNOS, like β-catenin, could be important at the early stages of tumor formation, and the cause of dysplastic changes[68]. There was also an overexpression of COX-2 detected in ACF, adenomas and carcinomas[68], which has been demonstrated to render tumor cells resistant to apoptosis[75] and to enhance neovascularization[76], thus conferring a survival advantage. The overexpression of COX-2 may contribute to ACF growth and sequential tumor growth.

P16^{INK4a} expression was seldom seen in epithelial cells at the base of normal colonic crypts. But at all the stages of tumor progression, including ACF, a higher fraction of epithelial cells was seen to express p16^{INK4a}. The staining of p16^{INK4a} correlated inversely with that of Ki67, cyclin A, and the retinoblastoma protein in ACF, adenomas and carcinomas, suggesting that cell cycle progression was inhibited. Thus, p16^{INK4a} appeared to constrain the proliferation of subsets of cells throughout intestinal tumorigenesis, however, the exact mechanisms remain unclear[77].

GENETIC AND EPIGENETIC ALTERATIONS OF ACF

Further development of ACF described by Gregorio had two pathways. One was headed for dysplastic ACF, which were to progress to adenomas, and the other was headed for hyperplastic polyps, which had little malignant potentials[40]. The investigation of ACF by using 25 different genetic markers, such as microsatellite instabilities and mutations of APC, H-ras, k-ras, p53, DCC, and DNA repair genes hMLH1, hMSH2, showed no difference between hyperplastic ACF and normal mucosa[78], which was in accordance with the latter hypothesis. Dysplastic ACF have been further identified to be precancerous lesions of CRC. However, an alternative pathway to the general adenoma-carcinoma sequence was also proposed as a hyperplastic polyp/serrated adenoma-carcinoma one[79-83]. Nucci' s study showed genetic differences between hyperplastic ACF and hyperplastic polyps in that the former had more frequent K-ras mutations. Therefore hyperplastic ACF should be named as "heteroplasia ACF" ("hetero' meaning "other", and "plasia" meaning "form") to avoid potential misleading as to their relationships[38]. Though the role of heteroplastic ACF in colorectal carcinogenesis remains controversial because of the lack of dysplasia in spite of the high frequency of K-ras mutations, there have been still lines of evidences supporting heteroplastic ACF as a precursor to a subset of CRC. They were clonal[84] and had genetic alterations of K-ras mutations[10,29,35,38,41], chromosome 1p loss[44], and CpG island methylation[44], hence the heteroplastic ACF-adenoma-carcinoma sequence, in which K-ras mutations preceded APC mutations in rodents and humans[41,85].

Stopera identified K-ras point mutation in carcinogen-induced colonic aberrant crypts in Sprague-Dawley rats in 1992 for the first time[86], and numerous studies have proved K-ras mutation as one of the major events in ACF formation since then. The mutation rate of K-ras in ACF was similar to that of small adenomas[28,29,35], and was found to be even significantly higher than that identified in CRC[86]. K-ras 12 codon mutation was most frequently observed, and in Losi' s study, different mutational types of GTT, TGT, GAT, *etc*, occurred in ACF of the same patient[31]. There were also different mutational types between carcinomas and ACF, the former had predominant GTT mutation, while the latter had GAT mutations almost as frequently as GTT in codon 12 of K-ras[30]. Therefore each ACF might originate independently from different clones[28-30,34]. Identification of monoclonality in a putative precursor lesion would strongly link this lesion to neoplastic progression. The monoclonality of various degrees of dysplastic ACF was determined by studying the differential methylation of a highly polymorphic site in the first exon of the androgen receptor gene to determine the pattern of X chromosome inactivation[34]. Controversial results were produced also by using the same method of clonality analysis based on X chromosome inactivation of the polymorphically X-linked human androgen receptor (HUMARA) gene, in addition to K-ras mutation detection. It was observed that a significant fraction of individual aberrant crypts that made up an ACF to be polyclonal, although by K-ras mutation genotyping, all ACF appeared to be monoclonal[84].

Other oncogenes as COX and c-myc were also found to

have an increased mRNA or protein expression in carcinogen-induced rats[18,88]. The immunoreactivity of oncoproteins of c-fos, ras, bcl-2 and p53 was evaluated in ACF, and abnormal expression and coexpression of oncoproteins could be identified in colorectal tumorigenesis at the earliest stages[89].

APC gene is considered to be "gatekeeper gene", maintaining the stability of colon epithelium. In carcinogen-treated rats, a decreased mRNA expression of APC was observed[18]. APC mutations could be detected in human ACF, but the mutation rates of APC in ACF were lower or undetectable compared to those in adenomas and carcinomas[28,41,90], which were the same as in animal models[85], suggesting that APC mutation was unlikely to initiate ACF. If a ras gene mutation occurred first, ACF would be nondysplasia, and if an APC mutation was the first to occur, it would result in a dysplastic ACF, whose progression was driven by subsequent K-ras and other gene mutations[35]. It has been proposed that in sporadic colorectal carcinogenesis, assuming the biological potential of ACF as a precursor of adenomas, there was a route where K-ras mutations mainly occurred during the formation of ACF. Some ACF then became adenomas in which APC mutations occurred. In FAP, however, somatic mutations of APC predominantly occurred during ACF formation, followed by K-ras mutations[35].

Apart from oncogene and tumor suppressor gene alterations in ACF, there is some other kind of genes concerning DNA repair. Inactivation of the mismatch repair (MMR) system can result in instability of the whole genome and an increased rate of spontaneous mutations of other vital genes to carcinogenesis. In addition to the cause of genomic instability, DNA mismatch repair proteins have several other functions that are highly relevant to cancer progression. Some MMR components have been found to be involved in cell-cycle regulation, and p53-dependent apoptotic response to a variety of DNA damages[91-97]. Germline mutations of any of them, especially hMSH2 and hMLH1, gave rise to hereditary nonpolyposis of colorectal cancer (HNPCC)[6,98]. There was also a link between hMSH6 mutations and a high incidence of endometrial cancer[99], and prevalence of colon cancer with TGFβRII gene and Tcf-4 gene[100,101]. hMSH2 deficiency resulted in the development of many ACF in mice colons, as well as reduced survival of the mice[102].

Epigenetic alterations such as CpG island methylation, and genetic phenotype alterations such as microsatellite instability (MSI) as a result of MMR defect, also play important roles as in ACF. Inactivation of genes might occur not by mutation or loss, but through silencing mediated by CpG island methylation of the gene' s promoter region. hMLH1 and MGMT are examples of DNA repair genes that were silenced by methylation. It has been demonstrated[103-105] that hMLH1 gene promoter had aberrant methylation in sporadic CRC. A novel pathway characterized by methylation of multiple CpG islands in colorectal carcinomas and adenomas, including genes known to be vital in tumorigenesis, such as p16 tumor suppressor gene and hMLH1 mismatch repair gene, was proposed as a CpG island methylator phenotype (CIMP)[57,106]. Ahuja questioned whether hMLH1 methylation preceded or was a consequence of the MSI phenotype[107]. The answer was presented by Chan that methylation of hMLH1 mismatch repair gene in ACF was not associated with the development of MSI, suggesting that hMLH1 methylation preceded MSI[44]. The frequency of CpG island methylation in ACF was related to the type of patients, as was concluded in Chan' s research, that methylation was detected in 53 % of ACF from sporadic colorectal carcinomas but only in 11 % of ACF from FAP patients[44], and methylation was more frequent in dysplastic sporadic ACF than in dysplastic FAP ACF. The epigenetic differences of CpG island methylation in ACF were similar to those in colorectal carcinomas.

Extensive genomic instabilities due to the defect of MMR system could be detected as MSI both in animal model and in human ACF[108,109]. MSI could occur either in dysplastic or hyperplastic (or "heteroplastic" as mentioned before) ACF from HNPCC patients, suggesting no association of MSI with histological features, being present even in small ACF. MSI in sporadic ACF also seemed to be independent of ACF size[110]. Heinen *et al*[45] detected MSI status in ACF, and found two ACFs from the same patient with different MSI status. One showed MSI-positive, while the other was MSI-negative, indicating independent initiation of individual ACF, as has been verified by sequential studies with different methods[28-30,34,84]. The role of ACF as precursors of some CRCs was verified by the presence of MSI in ACF from HNPCC patients, in whom carcinoma with high levels of MSI was the hallmark, and in ACF from sporadic CRC as well[44,108].

SUMMARY

The malignant potential of ACF, especially dysplastic ACF, makes it necessary to reveal the nature of these lesions. Many researches nowadays are focused on the mechanisms of ACF initiation, their genetic and environmental backgrounds, methods of early detection, dietary and chemoprevention. In spite of the increasing evidences of ACF as precancerous lesions of colorectal carcinomas, a lot remain to be clarified so as to reduce the incidence of CRC at the earliest stages.

First reported by Yokota in 1997[14], the application of endoscopy, either magnifying or dye/chromoscopic colonoscopy, made it possible to detect "*in vivo*" ACF. It is of great advantage over the detection of surgical specimens from with CRC. It may offer much benefit to colon cancer researches and identify high-risk populations for colorectal tumors. Recent studies have proved the validity of chromoendoscopy, or dye colonoscopy, which allows easy detection of mucosal lesions in the colon and facilitates visualization of the margins of flat lesions[111,112].

In summary, ACF, especially dysplastic ACF, are widely accepted as precursors of colon cancer morphologically, histologically, biologically, and genetically. They have an aberrant appearance of crypts, and display both hyperplasia and dysplasia. They are supposed to have alterations of enzymology and cell dynamics. They also harbor gene mutations that are vital to tumor formation and progression. By studying these lesions both grossly and genetically, it may be possible to learn more about the causes of colon carcinogenesis. By testing new compounds through ACF assay, it is possible to discover not only potentially new chemopreventive drugs, but also the mechanisms behind them. In addition, by developing available methods for "*in vivo*" ACF examination, it may be possible to evaluate high-risk individuals at the earliest possible stages, as well as the preventive procedures.

REFERENCES

1 **Fearon ER**, Vogelstein B. A genetic model for colorectal tumorigenesis. *Cell* 1990; **61**: 759-767
2 **Boland CR**. The biology of colorectal cancer. *Cancer Suppl* 1993; **71**: 4180-4186
3 **Kinzler KW**, Vogelstein B. Lessons from hereditary colorectal cancer. *Cell* 1996; **87**: 159-170
4 **Leach FS**, Nicolaides NC, Papadopoulos N, Liu B, Jen J, Parson R, Peltomaki P, Sistonen P. Mutation of a mutS homolog in hereditary nonpolyposis colorectal cancer. *Cell* 1993; **75**: 1215-1235
5 **Honchel R**, Halling KC, Schaid DJ, Pittelkow M, Thibodeau SN. Microsatellite instability in Muir-Torre syndrome. *Cancer Res* 1994; **54**: 1159-1163
6 **Jacob S**, Praz F. DNA mismatch repair defects: role in colorectal carcinogenesis. *Biochimie* 2002; **84**: 27-47
7 **Bird RP**. Observation and quantification of aberrant crypts in

the murine colon treated with a colon carcinogen: preliminary findings. *Cancer Lett* 1987; **30**: 147-151

8 **McLellan EA**, Bird RP. Aberrant crypts: potential preneoplastic lesions in the murine colon. *Cancer Res* 1988; **48**: 6187-6192

9 **Roncucci L**, Stamp D, Medline A, Cullen JB, Bruce WR. Identification and qualification of aberrant crypt foci and adenoma in the human colon. *Hum Pathol* 1991; **22**: 287-294

10 **Otori K**, Sugiyama K, Hasebe T, Fukushima S, Esumi H. Emergence of adenomatous aberrant crypt foci (ACF) from hyperplastic ACF with concomitant increase in cell proliferation. *Cancer Res* 1995; **55**: 4743-4746

11 **Pretlow TP**, Barrow BJ, Ashton WS, O'Riordan MA, Pretlow TG, Jurcisek JA, Stellato TA. Aberrant crypt foci: Putative preneoplastic foci in human colonic mucosa. *Cancer Res* 1991; **51**: 1564-1567

12 **Roncucci L**, Medline A, Bruce WR. Classification of aberrant crypt foci and microadenomas in human colon. *Cancer Epidemiol Biomarkers Prev* 1991; **1**: 57-60

13 **Pretlow TP**, O'Riordan MA, Pretlow TG, Stellato TA. Aberrant crypts in human colonic mucosa: putative preneoplastic lesions. *J Cell Biochem Suppl* 1992; **16G**: 55-62

14 **Yokota T**, Sugano K, Kondo H, Saito D, Sugihara K, Fukayama N, Ohkura H, Ochiai A, Yoshida S. Detection of aberrant crypt foci by magnifying colonoscopy. *Gastrointest Endosc* 1997; **46**: 61-65

15 **Adler DG**, Gostout CJ, Sorbi D, Burgart LJ, Wang L, Harmsen WS. Endoscopic identification and quantification of aberrant crypt foci in the human colon. *Gastrointest Endosc* 2002; **56**: 657-662

16 **McLellan EA**, Medline A, Bird RP. Dose response and proliferative characteristics of aberrant cyrpt foci: putative preneoplastic lesions in rat colon. *Carcinogenesis* 1991; **12**: 2093-2098

17 **Shpitz B**, Bomstein Y, Mekori Y, Cohen R, Kaufman Z, Neufeld D, Galkin M, Bernheim J. Aberrant crypt foci in human colons: distribution and histomorphologic characteristics. *Hum Pathol* 1998; **29**: 469-475

18 **Furukawa F**, Nishikawa A, Kitahori Y, Tanakamaru Z, Hirose M. Spontaneous development of aberrant crypt foci in F344 rats. *J Exp Clin Cancer* 2002; **21**: 197-201

19 **Roncucci L**, Pedroni M, Fante R, Di Gregorio C, Ponz de Leon M. Cell kinetic evaluation of human colonic aberrant crypts. *Cancer Res* 1993; **53**: 3726-3729

20 **Dashwood RH**, Xu M, Orner GA, Horio DT. Colonic cell proliferation, apoptosis and aberrant crypt foci development in rats given 2-amino-3-methylimidaz. *Eur J Cancer Prev* 2001; **10**: 139-145

21 **Nakagama H**, Ochiai M, Ubagai T, Tajima R, Fujiwara K, Sugimura T, Nagao M. A rat colon cancer model induced by 2-amino-1-methyl-6-phenylimidazo[4,5-b]pyridine, PhIP. *Mutat Res* 2002; **506-507**: 137-144

22 **Pretlow TP**, Roukhadze EV, O'Riordan MA, Chan JC, Amini SB, Stellato TA. Carcinoembryonic antigen in human colonic aberrant crypt foci. *Gastroenterology* 1994; **107**: 1719-1725

23 **Sparks AB**, Morin PJ, Vogelstein B, Kinzler KW. Mutational analysis of the APC/beta-catenin/Tcf pathway in colorectal cancer. *Cancer Res* 1998; **58**: 1130-1134

24 **Hao XP**, Pretlow TG, Rao JS, Pretlow TP. β-catenin expression is altered in human colonic aberrant crypt foci. *Cancer Res* 2001; **61**: 8085-8088

25 **Furihata T**, Kawamata H, Kubota K, Fujimori T. Evaluation of the malignant potential of aberrant crypt foci by immunohistochemical staining for beta-catenin in inflammation-induced rat colon carcinogenesis. *Int J Mol Med* 2002; **9**: 353-358

26 **Vogelstein B**, Fearon ER, Hamilton SR, Kern SE, Preidinger AC, Leppert M, Nakamura Y, White R, Smits AMM, Bos JL. Genetic alterations during colorectal-tumor development. *N Engl J Med* 1988; **319**: 525-532

27 **Powell SM**, Zilz N, Beazer-Barclay Y, Bryan TM, Hamilton SR, Thibodeau SN, Vogelstein B, Kinzler KW. APC mutations occur early during colorectal tumorigenesis. *Nature* 1992; **359**: 235-237

28 **Smith AJ**, Stern HS, Penner M, Hay K, Mitri A, Bapat BV, Gallinger S. Somatic APC and K-ras codon 12 mutations in aberrant crypt foci from human colons. *Cancer Res* 1994; **54**: 5527-5530

29 **Pretlow TP**, Brasitus TA, Fulton NC, Cheyer C, Kaplan EL. K-ras mutations in putative preneoplastic lesions in human colon. *J Natl Cancer Inst* 1993; **85**: 2004-2007

30 **Minamoto T**, Yamashita N, Ochiai A, Mai M, Sugimura T, Ronai Z, Esumi H. Mutant K-ras in apparently normal mucosa of colorectal cancer patients. Its potential as a biomarker of colorectal tumorigenesis. *Cancer* 1995; **75**: 1520-1526

31 **Losi L**, Roncucci L, di Gregorio C, de Leon MP, Benhattar J. K-ras and p53 mutations in human colorectal aberrant crypt foci. *J Pathol* 1996; **178**: 259-263

32 **Shivapurkar N**, Huang L, Ruggeri B, Swalsky PA, Bakker A, Finkelstein S, Frost A, Silverberg S. K-ras and p53 mutations in aberrant crypt foci and colonic tumors from colon cancer patients. *Cancer Lett* 1997; **115**: 39-46

33 **Janssen KP**, el-Marjou F, Pinto D, Sastre X, Rouillard D, Fouquet C, Soussi T, Louvard D, Robine S. Targeted expression of oncogenic K-ras in intestinal epithelium causes spontaneous tumorigenesis in mice. *Gastroenterology* 2002; **123**: 492-504

34 **Siu IM**, Robinson DR, Schwartz S, Kung HJ, Pretlow TG, Petersen RB, Pretlow TP. The identification of monoclonality in human aberrant crypt foci. *Cancer Res* 1999; **59**: 63-66

35 **Jen J**, Powell SM, Papadopoulos N, Smith KJ, Hamilton SR, Vogelstein B, Kinzler KW. Molecular determinants of dysplasia in colorectal lesions. *Cancer Res* 1994; **54**: 5523-5526

36 **Siu IM**, Pretlow TG, Amini SB, Pretlow TP. Identification of dysplasia in human colonic aberrant crypt foci. *Am J Pathol* 1997; **150**: 1805-1813

37 **Roncucci L**, Modica S, Pedroni M, Tamassia MG, Ghidoni M, Losi L, Fante R, Di Gregorio C, Manenti A, Gafa L, Ponz de Leon M. Aberrant crypt foci in patients with colorectal cancer. *Br J Cancer* 1998; **77**: 2343-2348

38 **Nucci MR**, Robinson CR, Longo P, Campbell P, Hamilton SR. Phenotypic and genotypic characteristics of aberrant crypt foci in human colorectal mucosa. *Hum Pathol* 1997; **28**: 1396-1407

39 **Bouzourene H**, Chaubert P, Seelentag W, Bosman FT, Saraga E. Aberrant crypt foci in patients with neoplastic and nonneoplastic colonic disease. *Hum Pathol* 1999; **30**: 66-71

40 **Di Gregorio C**, Losi L, Fante R, Modica S, Ghidoni M, Pedroni M, Tamassia MG, Gafa L, Ponz de Leon M, Roncucci L. Histology of aberrant crypt foci in the human colon. *Histopathology* 1997; **30**: 328-334

41 **Nascimbeni R**, Villanacci V, Mariani PP, Betta ED, Ghirardi M, Donato F, Salerni B. Aberrant crypt foci in the human colon: frequency and histologic patterns in patients with colorectal cancer or diverticular disease. *Am J Surg Pathol* 1999; **23**: 1256-1263

42 **Longacre TA**, Fenoglio-Preiser CM. Mixed hyperplastic adenomatous polyps/serrated adenoma. A distinct form of colorectal neoplasia. *Am J Surg Pathol* 1990; **14**: 524-537

43 **Takayama T**, Ohi M, Hayashi T, Miyanishi K, Nobuoka A, Nakajima T, Satoh T, Takimoto R, Kato J, Sakamaki S, Niitsu Y. Analysis of K-ras, APC, and beta-catenin in aberrant crypt foci in sporadic adenoma, cancer, and familial adenomatous polyposis. *Gastroenterology* 2001; **121**: 599-611

44 **Chan AO**, Broaddus RR, Houlihan PS, Issa JP, Hamilton SR, Rashid A. CpG island methylation in aberrant crypt foci of the colorectum. *Am J Pathol* 2002; **160**: 1823-1830

45 **Heinen CD**, Shivapurkar N, Tang Z, Groden J, Alabaster O. Microsatellite instability in aberrant crypt foci from human colons. *Cancer Res* 1996; **56**: 5339-5341

46 **Kishimoto Y**, Morisawa T, Hosoda A, Shiota G, Kawasaki H, Hasegawa J. Molecular changes in the early stage of colon carcinogenesis in rats treated with azoxymethane. *J Exp Clin Cancer Res* 2002; **21**: 203-211

47 **Murray NR**, Davidson LA, Chapkin RS, Clay Gustafson W, Schattenberg DG, Fields AP. Overexpression of protein kinase C betaII induces colonic hyperproliferation and increased sensitivity to colon carcinogenesis. *J Cell Biol* 1999; **145**: 699-711

48 **Craven PA**, DcRubertis FR. Alterations in protein kinase C in 1, 2-dimethylhydrazine induced colonic carcinogenesis. *Cancer Res* 1992; **52**: 2216-2221

49 **Chapkin RS**, Gao J, Lee DY, Lupton JR. Dietary fibers and fats alter rat colon protein kinase C activity: correlation to cell proliferation. *J Nutr* 1993; **123**: 649-655

50 **Kahl-Rainer P**, Karner-Hanusch J, Weiss W, Marian B. Five of six protein kinase C isoenzymes present in normal mucosa show reduced protein levels during tumor development in the human colon. *Carcinogenesis* 1994; **15**: 779-782

51 **Gokmen-Polar Y**, Murray NR, Velasco MA, Gatalica Z, Fields AP. Elevated protein kinase C betaII is an early promotive event

in colon carcinogenesis. *Cancer Res* 2001; **61**: 1375-1381
52 **Thorup I**. Histomorphological and immunohistochemical characterization of colonic aberrant crypt foci in rats: relationship to growth factor expression. *Carcinogenesis* 1997; **18**: 465-472
53 **Habel O**, Bertario L, Andreola S, Sirizzotti G, Marian B. Tissue localization of TGFalpha and apoptosis are inversely related in colorectal tumors. *Histochem Cell Biol* 2002; **117**: 235-241
54 **Pretlow TP**, Cheyer C, O'Riordan MA. Aberrant crypt foci and colon tumors in F344 rats have similar increases in proliferative activity. *Int J Cancer* 1994; **56**: 599-602
55 **Paulsen JE.** Modulation by dietary factors in murine FAP models. *Toxicol Lett* 2000; **112-113**: 403-409
56 **Paulsen JE,** Steffensen IL, Loberg EM, Husoy T, Namork E, Alexander J. Qualitative and quantitative relationship between dysplastic aberrant crypt foci and tumorigenesis in the Min/+ mouse colon. *Cancer Res* 2001; **61**: 5010-5015
57 **Toyota M**, Ohe-Toyota M, Ahuja N, Issa JP. Distinct genetic profiles in colorectal tumors with or without the CpG island methylator phenotype. *Proc Natl Acad Sci U S A* 2000; **97**: 710-715
58 **Yamada Y**, Yoshimi N, Hirose Y, Matsunaga K, Katayama M, Sakata K, Shimizu M, Kuno T, Mori H. Sequential analysis of morphological and biological properties of beta-catenin-accumulated crypts, provable premalignant lesions independent of aberrant crypt foci in rat colon carcinogenesis. *Cancer Res* 2001; **61**: 1874-1878
59 **Yamada Y**, Yoshimi N, Hirose Y, Kawabata K, Matsunaga K, Shimizu M, Hara A, Mori H. Frequent beta-catenin gene mutations and accumulations of the protein in the putative preneoplastic lesions lacking macroscopic aberrant crypt foci appearance, in rat colon carcinogenesis. *Cancer Res* 2000; **60**: 3323-3327
60 **Yamada Y**, Yoshimi N, Hirose Y, Hara A, Shimizu M, Kuno T, Katayama M, Qiao Z, Mori H. Suppression of occurrence and advancement of beta-catenin-accumulated crypts, possible premalignant lesions of colon cancer, by selective cyclooxygenase-2 inhibitor, celecoxib. *Jpn J Cancer Res* 2001; **92**: 617-623
61 **Pretlow TP**, O'Riordan MA, Kolman MF, Jurcisek JA. Colonic aberrant crypts in azoxymethane-treated F344 rats have decreased hexosaminidase activity. *Am J Pathol* 1990; **136**: 13-16
62 **Pretlow TP**, Pretlow TG. Putative preneoplastic changes identified by enzyme histochemical and immunohistochemical techniques. *J Histochem Cytochem* 1998; **46**: 577-583
63 **Konstantakos AK**, Siu IM, Pretlow TG, Stellato TA, Pretlow TP. Human aberrant crypt foci with carcinoma in situ from a patient with sporadic colon cancer. *Gastroenterology* 1996; **111**: 772-777
64 **Boland CR**, Martin MA, Goldstein IJ. Lectin reactivities as intermediate biomarkers in premalignant colorectal epithelium. *J Cell Biochem Suppl* 1992; **16G**: 103-109
65 **Williams HK**, Sanders DS, Jankowski JA, Landini G, Brown AM. Expression of cadherins and catenins in oral epithelial dysplasia and squamous cell carcinoma. *J Oral Pathol Med* 1998; **27**: 308-317
66 **Sanders DS**, Bruton R, Darnton SJ, Casson AG, Hanson I, Williams HK, Jankowski J. Sequential changes in cadherin-catenin expression associated with the progression and heterogeneity of primary oesophageal squamous carcinoma. *Int J Cancer* 1998; **79**: 573-579
67 **Hardy RG**, Tselepis C, Hoyland J, Wallis Y, Pretlow TP, Talbot I, Sanders DS, Matthews G, Morton D, Jankowski JA. Aberrant P-cadherin expression is an early event in hyperplastic and dysplastic transformation in the colon. *Gut* 2002; **50**: 513-519
68 **Takahashi M**, Mutoh M, Kawamori T, Sugimura T, Wakabayashi K. Altered expression of â-catenin, inducible nitric oxide synthase and cyclooxygenase-2 in azoxymethane-induced rat colon carcinogenesis. *Carcinogenesis* 2000; **21**: 1319-1327
69 **He TC**, Sparks AB, Rago C, Hermeking H, Zawel L, da Costa LT, Morin PJ, Vogelstein B, Kinzler KW. Identification of c-MYC as a target of the APC pathway. *Science* 1998; **281**: 1509-1512
70 **Tetsu O**, McCormick F. Beta-catenin regulates expression of cyclin D1 in colon carcinoma cells. *Nature* 1999; **398**: 422-426
71 **Morin PJ**, Sparks AB, Korinek V, Barker N, Clevers H, Vogelstein B, Kinzler KW. Activation of beta-catenin-Tcf signaling in colon cancer by mutations in beta-catenin or APC. *Science* 1997; **275**: 1787-1790
72 **Takahashi M**, Fukuda K, Sugimura T, Wakabayashi K. β-catenin is frequently mutated and demonstrates altered cellular location in azoxymethane-induced rat colon tumors. *Cancer Res* 1998; **58**: 42-46
73 **Wink DA**, Vodovotz Y, Laval J, Laval F, Dewhirst MW, Mitchell JB. The multifaceted roles of nitric oxide in cancer. *Carcinogenesis* 1998; **19**: 711-721
74 **Stamler JS**, Simon DI, Jaraki O, Osborne JA, Francis S, Mullins M, Singel D, Loscalzo J. S-nitrosylation of tissue-type plasminogen activator confers vasodilatory and antiplatelet properties on the enzyme. *Proc Natl Acad Sci U S A* 1992; **89**: 8087-8091
75 **Tsujii M**, DuBois RN. Alterations in cellular adhesion and apoptosis in epithelial cells overexpressing prostaglandin endoperoxide synthase 2. *Cell* 1995; **83**: 493-501
76 **Tsujii M**, Kawano S, Tsuji S, Sawaoka H, Hori M, DuBois RN. Cyclooxygenase regulates angiogenesis induced by colon cancer cells. *Cell* 1998; **93**: 705-716
77 **Dai CY**, Furth EE, Mick R, Koh J, Takayama T, Niitsu Y, Enders GH. p16 (INK4a) expression begins early in human colon neoplasia and correlates inversely with markers of cell proliferation. *Gastroenterology* 2000; **119**: 929-942
78 **Sedivy R**, Wolf B, Kalipciyan M, Steger GG, Karner-Hanusch J, Mader RM. Genetic analysis of multiple synchronous lesions of the colon adenoma-carcinoma sequence. *Br J Cancer* 2000; **82**: 1276-1282
79 **Jass JR**, Cottier DS, Pokos V, Parry S, Winship IM. Mixed epithelial polyps in association with hereditary non-polyposis colorectal cancer providing an alternative pathway of cancer histogenesis. *Pathology* 1997; **29**: 28-33
80 **Iino H**, Jass JR, Simms LA, Young J, Leggett B, Ajioka Y, Watanabe H. DNA microsatellite instability in hyperplastic polyps, serrated adenomas, and mixed polyps: a mild mutator pathway for colorectal cancer? *J Clin Pathol* 1999; **52**: 5-9
81 **Rashid A**, Houlihan PS, Booker S, Petersen GM, Giardiello FM, Hamilton SR. Phenotypic and molecular characteristics of hyperplastic polyposis. *Gastroenterology* 2000; **119**: 323-332
82 **Jass JR**, Iino H, Ruszkiewicz A, Painter D, Solomon MJ, Koorey DJ, Cohn D, Furlong KL, Walsh MD, Palazzo J, Edmonston TB, Fishel R, Young J, Leggett BA. Neoplastic progression occurs through mutator pathways in hyperplastic polyposis of the colorectum. *Gut* 2000; **47**: 43-49
83 **Jass JR**. Serrated route to colorectal cancer: back street or super highway? *J Pathol* 2001; **193**: 283-285
84 **Sakurazawa N**, Tanaka N, Onda M, Esumi H. Instability of X chromosome methylation in aberrant crypt foci of the human colon. *Cancer Res* 2000; **60**: 3165-3169
85 **De Filippo C**, Caderni G, Bazzicalupo M, Briani C, Giannini A, Fazi M, Dolara P. Mutations of the Apc gene in experimental colorectal carcinogenesis induced by azomymethane in F344 rats. *Br J Cancer* 1998; **77**: 2148-2151
86 **Stopera SA**, Murphy LC, Bird RP. Evidence for a ras gene mutation in azoxymethane-induced colonic aberrant crypts in Sprague-Dawley rats: earliest recognizable precursor lesions of experimental colon cancer. *Carcinogenesis* 1992; **13**: 2081-2085
87 **Benhattar J**, Losi L, Chaubert P, Givel JC, Costa J. Prognostic significance of K-ras mutations in colorectal carcinoma. *Gastroenterology* 1993; **104**: 1044-1048
88 **Kitamura T**, Kawamori T, Uchiya N, Itoh M, Noda T, Matsuura M, Sugimura T, Wakabayashi K. Inhibitory effects of mofezolac, a cyclooxygenase-1 selective inhibitor, on intestinal carcinogenesis. *Carcinogenesis* 2002; **23**: 1463-1466
89 **Otori K**, Sugiyama K, Fukushima S, Esumi H. Expression of the cyclin D1 gene in rat colorectal aberrant crypt foci and tumors induced by azoxymethane. *Cancer Lett* 1999; **140**: 99-104
90 **Yuan P**, Sun MH, Zhang JS, Zhu XZ, Shi DR. APC and K-ras gene mutation in aberrant crypt foci of human colon. *World J Gastroenterol* 2001; **7**: 352-356
91 **Davis TW**, Wilson-Van Patten C, Meyers M, Kunugi KA, Cuthill S, Reznikoff C, Garces C, Boland CR, Kinsella TJ, Fishel R, Boothman DA. Defective expression of the DNA mismatch repair protein, MLH1, alters G2-M cell cycle checkpoint arrest following ionizing radiation. *Cancer Res* 1998; **58**: 767-778
92 **Duckett DR**, Bronstein SM, Taya Y, Modrich P. hMutSα- and hMutLα-dependent phosphorylation of p53 in response to DNA methylator damage. *Proc Natl Acad Sci U S A* 1999; **96**: 12384-12388
93 **Hickman MJ**, Samson LD. Role of DNA mismatch repair and p53 in signaling induction of apoptosis by alkylating agents. *Proc Natl Acad Sci U S A* 1999; **96**: 10764-10769

94 **Li GM.** The role of mismatch repair in DNA damage-induced apoptosis. *Oncol Res* 1999; **11**: 393-400
95 **Toft NJ**, Winton DJ, Kelly J, Howard LA, Dekker M, te Riele H, Arends MJ, Wyllie AH, Margison GP, Clarke AR. Msh2 status modulates both apoptosis and mutation frequency in the murine small intestine. *Proc Natl Acad Sci U S A* 1999; **96**: 3911-3915
96 **Wu J**, Gu L, Wang H, Geacintov NE, Li GM. Mismatch repair processing of carcinogen-DNA adducts triggers apoptosis. *Mol Cell Biol* 1999; **19**: 8292-8301
97 **Zhang H**, Richards B, Wilson T, Lloyd M, Cranston A, Thorburn A, Fishel R, Meuth M. Apoptosis induced by overexpression of hMSH2 or hMLH1. *Cancer Res* 1999; **59**: 3021-3027
98 **Peltomaki P**. DNA mismatch repair and cancer. *Mutat Re* 2001; **488**: 77-85
99 **Wijnen J,** de Leeuw W, Vasen H, van der Klift H, Moller P, Stormorken A, Meijers-Heijboer H, Lindhout D, Menko F, Vossen S, Moslein G, Tops C, Brocker-Vriends A, Wu Y, Hofstra R, Sijmons R, Cornelisse C, Morreau H, Fodde R. Familial endometrial cancer in female carriers of MSH6 germline mutations. *Nat Genet* 1999; **23**: 142-144
100 **Myeroff LL**, Parsons R, Kim SJ, Hedrick L, Cho KR, Orth K, Mathis M, Kinzler KW, Lutterbaugh J, Park K, Bang YJ, Lee HY, Park JG, Lynch HT, Roberts AB, Vogelstein B, Markowitz SD. A transforming growth factor beta receptor type II gene mutation common in colon and gastric but rare in endometrial cancers with microsatellite instability. *Cancer Res* 1995; **55**: 5545-5547
101 **Duval A**, Iacopetta B, Ranzani GN, Lothe RA, Thomas G, Hamelin R. Variable mutation frequencies in coding repeats of TCF-4 and other target genes in colon, gastric and endometrial carcinoma showing microsatellite instability. *Oncogene* 1999; **18**: 6806-6809
102 **Reitmair AH**, Cai JC, Bjerknes M, Redston M, Cheng H, Pind MT, Hay K, Mitri A, Bapat BV, Mak TW, Gallinger S. MSH2 deficiency contributes to accelerated APC-mediated intestinal tumorigenesis. *Cancer Res* 1996; **56**: 2922-2926
103 **Kane MF**, Loda M, Gaida GM, Lipman J, Mishra R, Goldman H, Jessup JM, Kolodner R. Methylation of the hMLH1 promoter correlates with lack of expression of hMLH1 in sporadic colon tumors and mismatch repair-defective human tumor cell lines. *Cancer Res* 1997; **57**: 808-811
104 **Veigl ML**, Kasturi L, Olechnowicz J, Ma AH, Lutterbaugh JD, Periyasamy S, Li GM, Drummond J, Modrich PL, Sedwick WD, Markowitz SD. Biallelic inactivation of hMLH1 by epigenetic gene silencing, a novel mechanism causing human MSI cancers. *Proc Natl Acad Sci U S A* 1998; **95**: 8698-8702
105 **Herman JG**, Umar A, Polyak K, Graff JR, Ahuja N, Issa JP, Markowitz S, Willson JK, Hamilton SR, Kinzler KW, Kane MF, Kolodner RD, Vogelstein B, Kunkel TA, Baylin SB. Incidence and functional consequences of hMLH1 promoter hypermethylation in colorectal carcinoma. *Proc Natl Acad Sci U S A* 1998; **95**: 6870-6875
106 **Rashid A**, Shen L, Morris JS, Issa JP, Hamilton SR. CpG island methylation in colorectal adenomas. *Am J Pathol* 2001; **159**: 1129-1135
107 **Ahuja N**, Mohan AL, Li Q, Stolker JM, Herman JG, Hamilton SR, Baylin SB, Issa JP. Association between CpG island methylation and microsatellite instability in colorectal cancer. *Cancer Res* 1997; **57**: 3370-3374
108 **Augenlicht LH**, Richards C, Corner G, Pretlow TP. Evidence for genomic instability in human colonic aberrant crypt foci. *Oncogene* 1996; **12**: 1767-1772
109 **Luceri C**, De Filippo C, Caderni G, Gambacciani L, Salvadori M, Giannini A, Dolara P. Detection of somatic DNA alterations in azoxymethane-induced F344 rat colon tumors by random amplified polymorphic DNA analysis. *Carcinogenesis* 2000; **21**: 1753-1756
110 **Pedroni M**, Sala E, Scarselli A, Borghi F, Menigatti M, Benatti P, Percesepe A, Rossi G, Foroni M, Losi L, Di Gregorio C, De Pol A, Nascimbeni R, Di Betta E, Salerni B, de Leon MP, Roncucci L. Microsatellite instability and mismatch-repair protein expression in hereditary and sporadic colorectal carcinogenesis. *Cancer Res* 2001; **61**: 896-899
111 **Kiesslich R**, von Bergh M, Hahn M, Hermann G, Jung M. Chromoendoscopy with indigocarmine improves the detection of adenomatous and nonadenomatous lesions in the colon. *Endoscopy* 2001; **33**: 1001-1006
112 **Hurlstone DP**, Fujii T, Lobo AJ. Early detection of colorectal cancer using high-magnification chromoscopic colonoscopy. *Br J Surg* 2002; **89**: 272-282

Edited by Zhu LH and Wang XL

P.O.Box 2345, Beijing 100023,China
Fax: +86-10-85381893
E-mail: wjg@wjgnet.com www.wjgnet.com

World J Gastroenterol 2003;9(12):2650-2653
World Journal of Gastroenterology
 ISSN 1007-9327

• ESOPHAGEAL CANCER •

Expression properties of recombinant pEgr-P16 plasmid in esophageal squamous cell carcinoma induced by ionizing irradiation

Cong-Mei Wu, Tian-Hua Huang, Qing-Dong Xie, De-Sheng Wu, Xiao-Hu Xu

Cong-Mei Wu, Tian-Hua Huang, Qing-Dong Xie, Research Center of Reproductive Medicine, Shantou University Medical College, Shantou 515041, Guangdong Province, China
Xiao-Hu Xu, Department of Forensic Medicine, Shantou University Medical College, Shantou 515041, Guangdong Province, China
De-Sheng Wu, Lanzhou Medical College, Lanzhou 730000, Gansu Province, China
Supported by the National Natural Science Foundation of China, No.30210103904 and the Science and Technology Program of Guangdong Province, No.2003C30304
Correspondence to: Dr. Tian-Hua Huang, Research Center of Reproductive Medicine, Shantou University Medical College, Shantou 515041, Guangdong Province, China. thhuang@stu.edu.cn
Telephone: +86-754-8900442 **Fax:** +86-754-8557562
Received: 2003-06-21 **Accepted:** 2003-07-24

Abstract

AIM: To construct the recombinant pEgr-P16 plasmid for the investigation of its expression properties in esophageal squamous cell carcinoma induced by ionizing irradiation and the feasibility of gene-radiotherapy for esophageal carcinoma.

METHODS: The recombinant pEgr-P16 plasmid was constructed and transfected into EC9706 cells with lipofectamine. Western blot, quantitative RT-PCR and flow cytometry were performed to study the expression of pEgr-P16 in EC9706 cells and the biological characteristics of EC9706 cell line after transfection induced by ionizing irradiation.

RESULTS: The eukaryotic expression vector pEgr-P16 was successfully constructed and transfected into EC9706 cells. The expression of P16 was significantly increased in the transfected cells after irradiation while the transfected cells were not induced by ionizing irradiation. The induction of apoptosis in transfection plus irradiation group was higher than that in plasmid alone or irradiation alone.

CONCLUSION: The combination of pEgr-P16 and irradiation could significantly enhance the P16 expression property and markedly induce apoptosis in EC9706 cells. These results may lay an important experimental basis for gene radiotherapy for esophageal carcinoma.

Wu CM, Huang TH, Xie QD, Wu DS, Xu XH. Expression properties of recombinant pEgr-P16 plasmid in esophageal squamous cell carcinoma induced by ionizing irradiation. *World J Gastroenterol* 2003; 9(12): 2650-2653
http://www.wjgnet.com/1007-9327/9/2650.asp

INTRODUCTION

Early growth response gene-1 (Egr-1), also known as zif/268, NGFI-A, Krox-24 and TIS-8, encodes a nuclear phosphoprotein with a cysteine/hystidine zinc finger structure, which is partially homologous to the corresponding domain of the Wilm's tumor susceptibility gene[1-4] Zinc fingers are a protein structural motif that serves as DNA-binding domains in several transcriptional regulatory proteins. It was reported that Egr-1 was transcriptionally induced following exposure to irradiation. Promoter deletion analysis of Egr-1 promoter elements linked to the CAT reporter gene demonstrated that the first 5' CArG boxes (CC $(A/T)_6$GG elements) were of paramount importance for the induction of Egr-1 by irradiation or free radicals[5-7].

In this study, the pEgr-P16 plasmid was constructed and transfected into the human esophageal cancer cell line EC9706. The expression of P16 in the transfected cells exposed to different doses of γ-ray irradiation and its bioactivities were detected to explore the feasibility of gene- radiotherapy for esophageal carcinoma.

MATERIALS AND METHODS

Cell line and vectors

The EC9706 was maintained in Dulbecco's modified Eagle's medium (DMEM), high glucose media (Life Technologies) and generously supplemented with 100 ml· L^{-1} fetal bovine serum (Hyclone Laboratories), penicillin, streptomycin and nonessential amino acids (Life Technologies). The pcDNA3.1$^+$ vector was purchased from Invitrogen and pGL3-enhancer vector from Promega-Biotec.

Construction of pEgr-P16 plasmid

The expression vector for P16 was constructed as shown in Figure 1.

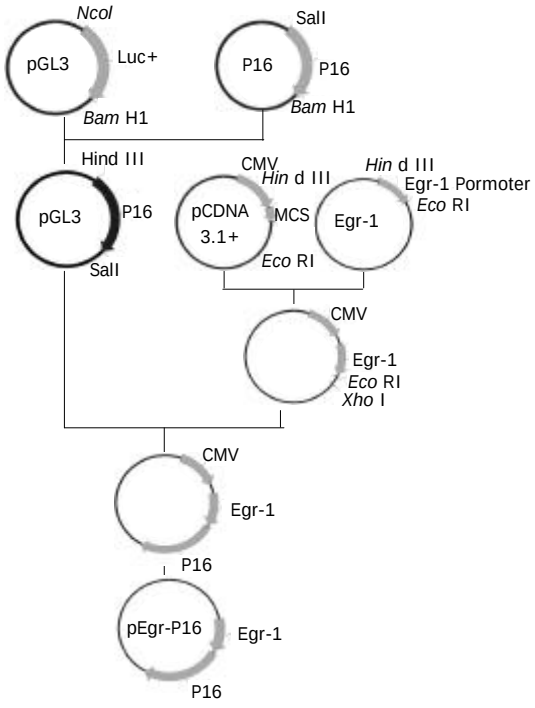

Figure 1 Diagram of the construction of the plasmid pEgr-P16.

Transfection

The transfection of EC9706 cells was carried out in a 6-well

plate. The transfection procedure began when the cells reached 70 % confluence on the surface of plate wells. Solution A was prepared by separate addition of 10 μg of pEgr-P16 and pcDNA3.1$^+$ to 100 μl serum-free medium (SFM), and solution B by addition of 10 μl Lipofectimine 2000 (Life Technologies) to 100 μl SFM. The two solutions were combined for 30 min at room temperature, 0.8 ml SFM was added to the tube containing the above solutions, and the mixture was added to the rinsed cells. The medium was replaced with fresh and complete one after 18 h in transfection. The cells were exposed to irradiation after 36 h in transfection.

Ionizing irradiation

The dose rate was 0.784 Gy/min for 0, 2, 4, 8, 10 and 20 Gy Co^{60} γ-ray irradiation, respectively.

Quantitative RT-PCR

Total RNAs of the transfection of EC9706 cells and control were obtained by extracting cells in Trizol (Invitrogen) and treated with heat-inactivated DNase I (Invitrogen). RNA quality and quantity were evaluated by UV spectrophotometry. Two μg total RNA was used for cDNA synthesis (25 μl) using M-MLV reverse transcriptase and random primers (Invitrogen).

A standard curve was constructed separately by the serial dilutions of PCR purified products of p16 and glyceraldehyde-3-phosphate-dehydrogenase (GAPDH). Template concentrations for reactions in the relative standard were 10^8, 10^7, 10^6 and 10^2 copies/μl. The cDNA (1:5 dilution) from the sample was analyzed as unknown. Real-time PCR was performed containing SYBRgreen I (1:20 000 QIAGEN), forward and reverse primers (50 nmol each), sample cDNA (1 μl) or standard sample (1 μl) under the following condition: denaturation at 95 ℃ (3 min); 40 cycles at 95 ℃ (45 s), at 59 ℃ (45 s), at 72 ℃ (40 s), at 80 ℃ (5 s). GAPDH was used as an internal reference in each PCR reaction. Primers were as follows: GAPDH, forward primer 5' -TGCACCACCAACTGCTTAGC-3' and reverse one 5' -GGCATGGACTGTGGTCATGAG-3' . P16, forward primer: 5' -GAATAGTTACGGTCGGAG-3' and reverse one 5' -CGGTGACTGATGATCTAA-3' . Amplification was followed by melting curve analysis using the program run at the step acquisition mode to verify the presence of a single amplification product in DNA contamination-free. For each set of primers, a non-cDNA template control was included to assess the overall specificity. Accumulation of PCR products was monitored and determined using the Icycler (Bio-Rad), and the crossing threshold (Ct) was determined using the Icycler software.

Flow cytometry analysis

Approximately 5×10^6 of centrifugally sedimented cells were immediately fixed in 700 ml· L^{-1} ethanol and stored at 4 ℃ in PBS in preparation for fluorescent-activated cell sorting. Flow cytometry analysis was performed on a FACStar flow cytometer (Becton Dicikinson). Histograms of cell number logarithmic fluorescence intensity were recorded for 10 000 cells per sample. The apoptotic cell rate was calculated.

Statistical analysis

Student' s *t* and correlation tests were used to determine the comparability of groups. Statistically significant *P* value was defined as <0.05.

RESULTS

Expression of P16 in EC9706 cells transfected with pEgr-P16 followed by different doses of γ-irradiation

EC9706 cells transfected with pEgr-P16 were irradiated by different doses of γ-rays. The cells of control group were transfected with pcDNA3.1$^+$. Eight hours after irradiation, the protein was extracted and the expression of P16 was detected by Western-blot. The results showed no P16 expression in the control and higher p16 expression in 2, 4, 8, 10 and 20 Gy groups than in 0Gy one.

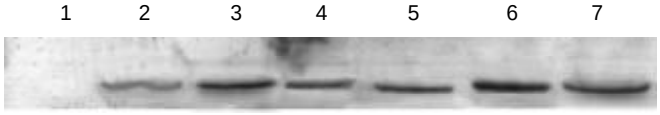

Figure 2 Expression of P16 in EC9706 cells after γ-irradiation. Lane 1: control; Lane 2: 0Gy; Lane 3: 2Gy; Lane 4: 4Gy; Lane 5: 8Gy; Lane 6: 10Gy; Lane 7: 20Gy.

P16 expression in EC9706 cells transfected with pEgr-P16 at different time points after 2Gy irradiation

EC9706 cells transfected with pEgr-P16 were irradiated by 2Gy irradiation. Total RNA was isolated at different time points after irradiation and the mRNA levels were detected by quantitative RT-PCR.

The results showed that P16 levels after 2Gy irradiation increased with time from 0 to 24 h. It reached the highest level at the 24th h and was about 4 times of that at the 2nd h (P<0.01).

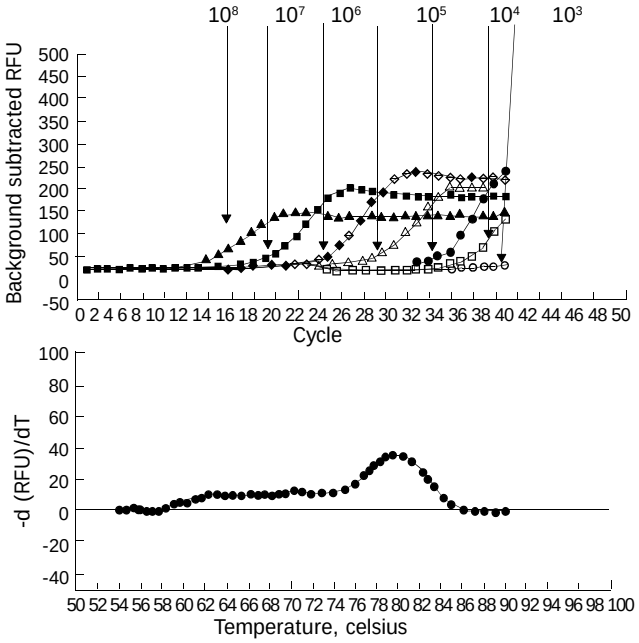

Figure 3 Amplification curves and post-amplification dissociation curves for P16 in EC9706 cells.

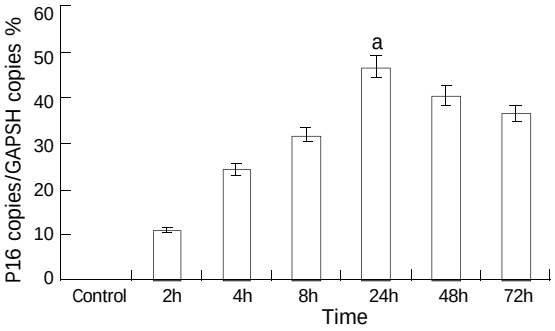

Figure 4 Expression of P16 in EC9706 cells at different time points after 2Gy γ-irradiation, ^aP<0.01 *vs.* 2 h group.

Apoptotic changes of transfected EC9706 cells after 2Gy g-irradiation

In P16 transfected EC9706 cells the apoptosis rate was 25.00, being higher than that of pcDNA3.1+ group (18.03, $P<0.05$). When exposed to 2Gy irradiation, the apoptosis rate was 33.23, higher than that in pcDNA3.1+ group (18.03, $P<0.01$) and P16 group (25.00). The differences were not significant between P16 and P16 plus irradiation groups.

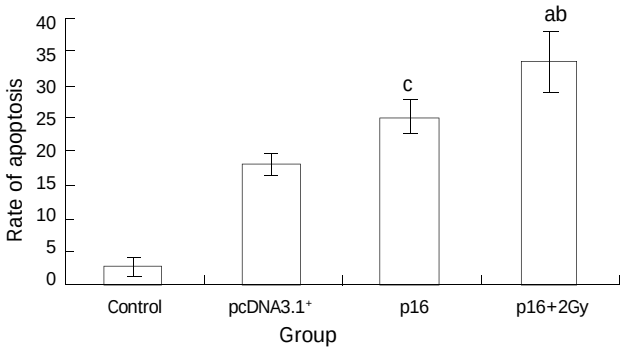

Figure 5 Apoptotic changes of transfected EC9706 cells. [a]$P<0.01$ *vs* pcDNA3.1$^+$group, [b]$P<0.001$ *vs* control group, [c]$P<0.05$ *vs* pcDNA3.1$^+$ group.

DISCUSSION

Radiotherapy is one of most important choices of the treatment for human tumors. Tumor destruction by radiation depends more on physical restriction of the radiation to a high-dose volume containing the tumor rather than a strict difference in radiosensitivity between tumor and normal cells. In fact, many tumor cells have lost the capacity for programmed cell death, resulting in radioresistance when compared with normal tissues. Vital structures are frequent within the radiotherapy volume restricting the amount of therapeutic radiation that can be safely delivered, thereby limiting tumor curability.

With the rapid development of molecular biology, gene radiotherapy has been considered as an effective way of cancer treatment. According to the mechanism that ionizing radiation could activate early Egr-1 gene promoter and induce the expression of downstream genes, Weichselbaum *et al* were the forerunners in tumor gene radiotherapy. They linked DNA sequences from the promotor region of Egr-1 with a cDNA sequence that encodes human tumor necrosis factor (TNF) alpha. The Egr-TNF construct was transfected into a human cell line of hematopoietic origin, HL525 (clone 2). The latter was injected into human xenografts of the radioresistant human squamous cell carcinoma cell line SQ-20B. Animals treated with radiation and clone 2 demonstrated an increase in tumor cures compared with animals treated with radiation alone or unirradiated animals given injections of clone 2 alone[6]. Thereafter, a variety of downstream genes were introduced to Egr-1 promoter to treat different tumors, and similar results were obtained[9-11].

The division cycle of eukaryotic cells is regulated by a family of protein kinases known as the cyclin-dependent kinases (CDKs). P16 is a tumor suppressor gene product. Serrano *et al* demonstrated that p16 could bind to CDK4 and inhibit the catalytic activity of the CDK4/cyclin D enzymes. P16 seemed to act in a regulatory feedback circuit with CDK4, D-type cyclins and retinoblastoma protein[12]. Overexpression of P16 gene could block cell cycle progression through the G_1-to-S phase boundary in a pRB-dependent manner[13-14]. Many P16 mutants identified from human tumors have been shown to have defects in this activity[15-17]. These data suggest that the CDK4-inhibitory activity of p16 is involved in regulating cell cycle progression through the G_1/S boundary.

On the basis of the antiangiogenic action of P16, we constructed pEgr-P16 plasmid and transfected EC9706 cells to study the expression properties of the plasmid induced by ionizing irradiation. The results revealed that no P16 expression in EC9706 cells transfected with pcDNA3.1$^+$ was detected and that the P16 expression in cells transfected with pEgr-P16 induced by irradiation was higher than that of sham-irradiation group. Time-course studies revealed that the P16 expression reached its peak at the 24th h after 2Gy irradiation, and the highest level was 4 times of that at the 2nd h ($P<0.01$). The combination of pEgr-P16 and radiation could induce markedly apoptosis of EC9706 cells although pEgr-P16 alone might induce transfected cells to undergo apoptosis. Our results suggested that pEgr-P16 could enhance expression property induced by radiation in EC9706 cells.

Esophageal carcinoma is still common in the world, especially in China[18-24], and the treatment remains a big problem up to date[25-31]. Gene radiotherapy may be of potential significance in the treatment of esophageal cancer. Our work will be a ground of further studies on esophageal cancer gene radiotherapy.

ACKNOWLEDGEMENT

We especially thank Prof. Ming Rong Wang for providing us the EC9706 cells line and Dr. Di Wu for providing the P16 gene.

REFERENCES

1 **Christy B**, Nathans D. DNA binding site of the growth factor-inducible protein Zif268. *Proc Natl Acad Sci U S A* 1989; **86**: 8737-8741
2 **Seyfert VL**, Sukhatme VP, Monroe JG. Differential expression of a zinc finger-encoding gene in response to positive versus negative signaling through receptor immunoglobulin in murine B-lymphocytes. *Mol Cell Biol* 1989; **9**: 2083-2088
3 **Joseph LJ**, Le-Beau MM, Jamieson GA Jr, Acharya S, Shows TB, Rowley JD, Sukhatme VP. Molecular cloning, sequencing, and mapping of EGR2, a human early growth response gene encoding a protein with "zinc-binding finger" structure. *Proc Natl Acad Sci U S A* 1988; **85**: 7164-7168
4 **Sukhatme VP**. Early transcriptional events in cell growth: The Egr family. *J Am Soc Nephro* 1990; **1**: 859-866
5 **Cao XM**, Koski RA, Gashler A, McKiernan M, Morris CF, GaffneyR, Hay RV, Sukhatme VP. Identification and characterization of the Egr-1gene product, a DNA-binding zinc finger protein induced by differentiation and growth signal. *Mol Cell Biol* 1990; **10**: 1931-1939
6 **Tsai-Morris CH**, Cao XM, Sukhatme VP. 5' flanking sequence and genomic structure of Egr-1, a murine mitogen inducible zinc finger encoding gene. *Nucleic Acids Res* 1988; **16**: 8835-8846
7 **Datta R**, Taneja N, Sukhatme VP, Qureshi SA, Weichselbaum R, Kufe DW. Reactive oxygen intermediates target CC(A/T)6GG sequences to mediate activation of the early growth response 1 transcription factor gene by ionizing radiation. *Proc Natl Acad Sci U S A* 1993; **90**: 2419-2422
8 **Weichselbaum RR**, Hallahan DE, Beckett MA, Mauceri HJ, Lee H, Sukhatme VP, Kufe DW. Gene therapy targeted by radiation preferentially radiosensitizes tumor cells. *Cancer Res* 1994; **54**: 4266-4269
9 **Hanna NN**, Seetharam S, Mauceri HJ, Beckett MA, Jaskowiak NT, Salloum RM, Hari D, Dahanabal M, Ramchandran R, Kalluri R, Sukhatme VP, Kufe DW, Weichselbaum RR. Antitumor interaction of short-course endostatin and ionizing radiation. *Cancer J* 2000; **6**: 287-293
10 **Takahashi T**, Namiki Y, Ohno T. Induction of the suicide HSV-TK gene by activation of the Egr-1 promoter with radioisotopes. *Hum Gene Ther* 1997; **8**: 827-833
11 **Griscelli F**, Li H, Cheong C, Opolon P, Bennaceur-Griscelli A, Vassal G, Soria J, Soria C, Lu H, Perricaudet M, Yeh P. Combined effects of radiotherapy and angiostatin gene therapy in glioma

tumor model. *Proc Natl Acad Sci U S A* 2000; **97**: 6698-6703
12 **Serrano M**, Hannon GJ, Beach D. A new regulatory motif in cell-cycle control causing specific inhibition of cyclin D / CDK4. *Nature* 1993; **366**: 704-707
13 **Koh J**, Enders GH, Dynlacht BD, Harlow E. Tumour-derived p16 alleles encoding proteins defective in cell-cycle inhibition. *Nature* 1995; **375**: 506-510
14 **Lukas J**, Parry D, Aagaard L, Mann DJ, Bartkova J, Strauss M, Peters G, Bartek J. Retinoblastoma-protein-dependent cell-cycle inhibition by the tumour suppressor p16. *Nature* 1995; **375**: 503-506
15 **Monzon J**, Liu L, Brill H, Goldstein AM, Tucker MA, From L, McLaughlin J, Hogg D, Lassam NJ. CDKN2A mutations in multiple primary melanomas. *N Engl J Med* 1998; **338**: 879-887
16 **Nobori T**, Miura K, Wu DJ, Lois A, Takabayashi K, Carson DA. Deletions of the cyclin-dependent kinase-4 inhibitor gene in multiple human cancers. *Nature* 1994; **368**: 753-756
17 **Soufir N**, Avril MF, Chompret A, Demenais F, Bombled J, Spatz A, Stoppa-Lyonnet D, Benard J, Bressac-de-Paillerets B. Prevalence of p16 and CDK4 germline mutations in 48 melanoma-prone families in France. The French Familial Melanoma Study Group. *Hum Mol Genet* 1998; **7**: 209-216
18 **Zhao XJ**, Li H, Chen H, Liu YX, Zhang LH, Liu SX, Feng QL. Expression of e-cadherin and beta-catenin in human esophageal squamous cell carcinoma: relationships with prognosis. *World J Gastroenterol* 2003; **9**: 225-232
19 **Li X**, Lu JY, Zhao LQ, Wang XQ, Liu GL, Liu Z, Zhou CN, Wu M, Liu ZH. Overexpression of ETS2 in human esophageal squamous cell carcinoma. *World J Gastroenterol* 2003; **9**: 205-208
20 **He YT**, Hou J, Qiao CY, Chen ZF, Song GH, Li SS, Meng FS, Jin HX, Chen C. An analysis of esophageal cancer incidence in Cixian county from 1974 to 1996. *World J Gastroenterol* 2003; **9**: 209-213
21 **Zhou HB**, Yan Y, Sun YN, Zhu JR. Resveratrol induces apoptosis in human esophageal carcinoma cells. *World J Gastroenterol* 2003; **9**: 408-411
22 **Song ZB**, Gao SS, Yi XN, Li YJ, Wang QM, Zhuang ZH, Wang LD. Expression of MUC1 in esophageal squamous-cell carcinoma and its relationship with prognosis of patients from Linzhou city, a high incidence area of northern China. *World J Gastroenterol* 2003; **9**: 404-407
23 **Heidecke CD**, Weighardt H, Feith M, Fink U, Zimmermann F, Stein HJ, Siewert JR, Holzmann B. Neoadjuvant treatment of esophageal cancer: Immunosuppression following combined radiochemotherapy. *Surgery* 2002; **132**: 495-501
24 **Tsunoo** H, Komura S, Ohishi N, Yajima H, Akiyama S, Kasai Y, Ito K, Nakao A, Yagi K. Effect of transfection with human interferon-beta gene entrapped in cationic multilamellar liposomes in combination with 5-fluorouracil on the growth of human esophageal cancer cells *in vitro*. *Anticancer Res* 2002; **22**: 1537-1543
25 **Nemoto K**, Zhao HJ, Goto T, Ogawa Y, Takai Y, Matsushita H, Takeda K, Takahashi C, Saito H, Yamada S. Radiation therapy for limited-stage small-cell esophageal cancer. *Am J Clin Oncol* 2002; **25**: 404-407
26 **Tachibana M**, Dhar DK, Kinugasa S, Yoshimura H, Fujii T, Shibakita M, Ohno S, Ueda S, Kohno H, Nagasue N. Esophageal cancer patients surviving 6 years after esophagectomy. *Langinbecks Arch Surg* 2002; **387**: 77-83
27 **Wilson KS**, Wilson AG, Dewar GJ. Curative treatment for esophageal cancer: Vancouver Island Cancer Centre experience from 1993 to 1998. *Can J Gastroenterol* 2002; **16**: 361-368
28 **Liu HH**, Yoshida M, Momma K, Oohashi K, Funada N. Detection and treatment of an asymptomatic case of early esophageal cancer using chromoendoscopy and endoscopic mucosal resection. *J Formos Med Assoc* 2002; **101**: 219-222
29 **Hou J**, Lin PZ, Chen ZF, Ding ZW, Li SS, Men FS, Gou LP, He YI, Qiao CY, Gou CL, Duan JP, Wen DG. Field population-based blocking treatment of esophageal epithelia dysplasia. *World J Gastroenterol* 2002; **8**: 418-422
30 **Wang AH**, Sun CS, Li LS, Huang JY, Chen QS. Relationship of tobacco smoking CYP1A1 GSTM1 gene polymorphism and esophageal cancer in Xi'an. *World J Gastroenterol* 2002; **8**: 49-53
31 **Shen ZY,** Shen WY, Chen MH, Shen J, Cai WJ, Yi Z. Nitric oxide and calcium ions in apoptotic esophageal carcinoma cells induced by arsenite. *World J Gastroenterol* 2002; **8**: 40-43

Edited by Ma JY

P.O.Box 2345, Beijing 100023,China
Fax: +86-10-85381893
E-mail: wjg@wjgnet.com www.wjgnet.com

World J Gastroenterol 2003;9(12):2654-2657
World Journal of Gastroenterology
 ISSN 1007-9327

• ESOPHAGEAL CANCER •

Epoxide hydrolase *Tyr*113*His* polymorphism is not associated with susceptibility to esophageal squamous cell carcinoma in population of North China

Jian-Hui Zhang, Xia Jin, Yan Li, Rui Wang, Wei Guo, Na Wang, Deng-Gui Wen, Zhi-Feng Chen, Gang Kuang, Li-Zhen Wei, Shi-Jie Wang

Jian-Hui Zhang, Xia Jin, Yan Li, Wei Guo, Na Wang, Deng-Gui Wen, Zhi-Feng Chen, Gang Kuang, Li-Zhen Wei, Shi-Jie Wang, Hebei Cancer Institute, Hebei Medical University, Shijiazhuang 050011, Hebei Province, China
Rui Wang, Shi-Jie Wang, The Fourth Affiliated Hospital, Hebei Medical University, Shijiazhuang 050011, Hebei Province, China
Supported by the Scientific Grant of Educational Department of Hebei Province, China, No. 2001150
Correspondence to: Professor Shi-Jie Wang, The Fourth Affiliated Hospital, Hebei Medical University, Jiankanglu 12, Shijiazhuang 050011, China. wang.sj@hbmu.edu
Telephone: +86-311-6085231 **Fax:** +86-311-6077634
Received: 2003-06-16 **Accepted:** 2003-08-25

Abstract

AIM: To investigate the possible association of *microsomal epoxide hydrolase* (*mEH*) *Tyr*113*His* polymorphism with susceptibility to esophageal squamous cell carcinoma (ESCC) in a population of North China.

METHODS: The *mEH Tyr*113*His* genotypes were determined by polymerase-chain reaction (PCR)-restriction fragment length polymorphism (RFLP) analysis in 257 patients with esophageal squamous cell carcinoma (ESCC) and 252 healthy subjects as a control group.

RESULTS: The frequencies for *Tyr* and *His* alleles were 44.2 %, 55.8 % in ESCC patients, and 44.0 % and 56.0 % in healthy subjects, respectively. No statistic difference in allele distribution was observed between ESCC patients and controls (χ^2=0.008, *P*=0.929). The overall genotype distribution difference was not observed between cancer cases and controls (χ^2=2.116, *P*=0.347). Compared with *Tyr/Tyr* genotype, neither *His/His* genotype nor in combination with *Tyr/His* genotype significantly modified the risk of the development of ESCC, the adjusted odds ratio was 1.076 (95 % CI=0.850-1.361) and 0.756 (95 % CI=0.493-1.157), respectively. When stratified for sex, age, smoking status and family history of upper gastrointestinal cancer, *His/His* genotype alone or in combination with *Tyr/His* genotype also did not show any significant influence on the risk of developing ESCC.

CONCLUSION: *MEH Tyr113His* polymorphism may not be used as a stratification marker in screening individuals at a high risk of ESCC.

Zhang JH, Jin X, Li Y, Wang R, Guo W, Wang N, Wen DG, Chen ZF, Kuang G, Wei LZ, Wang SJ. Epoxide hydrolase *Tyr*113*His* polymorphism is not associated with susceptibility to esophageal squamous cell carcinoma in population of North China. *World J Gastroenterol* 2003; 9(12): 2654-2657
http://www.wjgnet.com/1007-9327/9/2654.asp

INTRODUCTION

China is one of the prevalent areas of esophageal squamous cell cancer (ESCC). Exposure to environmental carcinogens is considered as the main risk factors of ESCC[1,2]. Among them, chemical carcinogens such as polycyclic aromatic hydrocarbons (PAHs) in consumed tobacco or ingested food may contribute to the high incidence of ESCC in China[3,4]. Metabolization of PAHs involves a complex enzymatic mechanism. Microsomal epoxide hydrolase (mEH) is an enzyme that hydrolyzes epoxides such as PHA, yielding corresponding *trans*-dihydrodiols. Usually, this hydrolysis acts as a detoxifying step, although in some instances, *trans*-dihydrodiols generated from PAHs are highly toxic and mutagenic. Therefore, mEH plays a dual role in the detoxification and activation of procarcinogens, and its role in carcinogenesis may depend on exposures to different environmental substrates[5].

There are two polymorphic sites that affect the enzyme activity in human *mEH* gene. One variant is characterized by substitution of histidine for tyrosine at the amino acid position 113, the other is characterized by substitution of arginine for histidine at the position 139. The proteins encoded by polymorphic alleles demonstrated different enzyme activities *in vitro*[6]. *MEH* polymorphism has been associated with chemical carcinogen-induced cancers occurring in lung[7,8], ovary[9], colorectum[10] and liver[11]. The correlation of *mEH* polymorphism with susceptibility to ESCC has not been reported so far. Therefore, the current study investigated the *Tyr*113*His* polymorphism in *mEH* exon 3 in ESCC patients and healthy individuals from North China.

MATERIALS AND METHODS

Subjects

This study included 257 patients with histologically confirmed esophageal squamous cell carcinomas and 252 healthy individuals without overt cancer. The cancer patients were hospitalized for surgery in the Fourth Affiliated hospital, Hebei Medical University between 2001 and 2003. The healthy subjects were from the same hospital for physical examination in the same period. All of the patients and control subjects were from Shijiazhuang city or its surrounding regions. Information of sex, age, smoking habits and family history was obtained from cancer patients and healthy controls by interview following sampling. The smokers were defined as former or current smoking 5 cigarettes per day for at least two years. The individuals with at least one first-degree relative or at least two second-degree relatives having esophageal/cardiac/gastric cancer were defined as having family history of upper gastrointestinal cancers (UGIC). The smoking status and family history were available from some of the cases and controls. Informed consent was obtained from all the recruited subjects. The study was approved by the Ethics Committee of Hebei Cancer Institute.

DNA extraction

Five ml of venous blood from each subject was drawn in Vacutainer tubes containing EDTA and stored at 4 ℃. Genomic DNA was extracted within one week after sampling by using proteinase K digestion followed by a salting out procedure.

MEH genotyping by PCR and restriction fragment analysis

The exon 3 T to C variant in *mEH* gene, changing tyrosine 113 to histidine, creates an *Eco*R restriction site (GATATC), which can be exploited for genotyping by PCR and subsequent RFLP analysis[12]. PCR was performed in a 25 μl volume containing 100 ng of DNA template, 2.5 μl of 10×buffer, 1 U of *Taq*-DNA-polymerase (BioDev-Tech., Beijing, China), 200 μmol of dNTPs and 200 nmol of sense primer (5'-GATCGATAAGTTCCGTTTCACC-3') and antisense primer (5'-ATCCTTAGTCTTGAAGTGAGGAT-3'). Initial denaturation at 94 ℃ for 5 min was followed by 35 cycles at 94 ℃ for 30 sec, at 56 ℃ for 30 sec and at 72 ℃ for 1 min. Subsequently, the PCR products were digested with 10 units of *Eco*R V (TakaRa Biotechnology Co., Ltd, Dalian, China) overnight at 37 ℃ and separated on a 3 % agarose gel. RFLP bands were visualized through ethidium bromide staining under UV light. *Tyr*113 wild-type homozygote was characterized by two bands at the position of 140 bp and 22 bp, while *His*113 homozygotes were identified by a single band (162 bp) and the heterozygotes by three bands (162 bp, 140 bp and 22 bp). For a negative control, each PCR reaction used distilled water instead of DNA in the reaction system. For 10 % of the samples, the reaction was repeated once.

Statistical analysis

Statistical analysis was performed using the SPSS10.0 software package (SPSS Company, Chicago, Illinois, USA). Comparison of *mEH* genotype distribution in the study groups was performed by means of two-sided contingency tables using Chi-square test. A probability level of 5 % was considered significant. The odds ratio (OR) and 95 % confidence interval (CI) were calculated using an unconditional logistic regression model and adjusted by age and sex accordingly.

RESULTS

The mean age of all ESCC cases was 58.5±9.39 years (range 32-85) and that of controls was 49.4±8.56 years (range 29-79 years). The gender distribution in ESCC patients (66.5 % men) was comparable to that in healthy controls (58.3 % men). Moreover, the proportion of smokers in ESCC patients (52.0 %) was also not significantly different from that in healthy controls (49.5 %) (χ^2=0.283, P=0.595). In addition, the frequency of the positive family history of UGIC in ESCC patients (44.1 %) was significantly higher than that in healthy controls (14.0 %) (χ^2=49.87, P<0.0001). Thus, the positive family history of UGIC significantly increased the relative risk to develop ESCC in this population, with an age and sex adjusted odds ratio of 4.06 (95 % CI=2.46-6.69). The demographic distribution of ESCC patients and healthy controls is shown in Table 1.

MEH Tyr113His genotyping was successfully performed in all study subjects. The *mEH* genotype distribution was not

Table 2 Influence of *mEH Tyr113His* polymorphism on ESCC development

	Tyr/Tyr	Tyr/His+His/His	His/His	aOR(95%CI)[c]	aOR (95%CI)[d]
Overall					
Normal	76 (30.2)	176 (69.8)	105 (41.7)		
ESCC	84 (32.7)	173 (67.3)	115 (44.7)	0.756 (0.493~1.157)	1.076 (0.850~1.361)
Male					
Normal	44 (30.6)	100 (69.4)	60 (41.7)		
ESCC	61 (35.7)	110 (64.3)	73 (42.7)	0.724 (0.427~1.225)	1.087 (0.811~1.458)
Female					
Normal	32 (29.6)	76 (70.4)	45 (41.7)		
ESCC	23 (26.8)	63 (73.2)	42 (48.8)	0.825 (0.398~1.710)	1.047 (0.704~1.558)
Age≤50					
Normal	46 (32.6)	95 (67.4)	60 (42.6)		
ESCC	19 (33.9)	37 (66.1)	22 (39.3)	0.867 (0.450~1.671)	1.064 (0.738~1.534)
Age>50					
Normal	30 (27.0)	81 (73.0)	45 (40.6)		
ESCC	65 (32.3)	136 (67.7)	93 (46.3)	0.790 (0.472~1.323)	1.018 (0.768~1.348)
Nonsmoker[a]					
Normal	31 (27.7)	81 (72.3)	49 (43.7)		
ESCC	34 (28.3)	86 (71.7)	60 (50.0)	0.659 (0.338~1.286)	1.135 (0.790~1.631)
Smoker					
Normal	35 (31.8)	75 (68.2)	41 (37.3)		
ESCC	46 (35.4)	84 (64.6)	52 (40.0)	0.901 (0.494~1.644)	1.022 (0.728~1.433)
Negative family history[b]					
Normal	59 (30.9)	132 (69.1)	80 (41.9)		
ESCC	49 (37.1)	83 (62.9)	51 (38.7)	0.660 (0.385~1.134)	1.237 (0.912~1.678)
Positive family history					
Normal	7 (22.6)	24 (77.4)	10 (32.2)		
ESCC	29 (27.9)	75 (72.1)	52 (50.0)	0.638 (0.241~1.689)	0.946 (0.546~1.639)

ESCC: esophageal squamous cell carcinoma. a,b. information of smoking status and family history was available from some of subjects. c,d. the age and sex adjusted odds ratio of Tyr/His+His/His (c) and His/His genotype (d) against Tyr/Tyr genotype.

correlated with gender, age and smoking status both in ESCC patients and in healthy controls (data not shown). The *Tyr* and *His* allele frequencies were 44.0 %, 56.0 % in ESCC patients and 44.2 %, 55.8 % in healthy controls, respectively. There was no statistic difference in allele distribution between ESCC patients and controls (χ^2=0.008, *P*=0.929). The frequencies of *Tyr/Tyr*, *Tyr/His* and *His/His* genotype were 30.2 %, 28.2 % and 41.6 % in healthy controls, respectively. The overall *mEH* genotype distribution in ESCC patients was not significantly different from that in healthy controls (χ^2=2.116, *P*=0.347) (Table 1).

Table 1 Demographic characteristics and *mEH Tyr113His* polymorphism in ESCC patients and healthy individuals

Groups	Control *n* (%)	ESCC *n* (%)
Sex		
Male	147 (58.3)	171 (66.5)
Female	105 (41.7)	86 (33.5)
Age (mean±SD)	49.4±8.56	58.5±9.39
Smoking status[a]		
Ex-or current smoker	110 (49.5)	130 (52.0)
Non-smoker	112 (50.5)	120 (48.0)
Family history of UGIC[b]		
Positive	31 (14.0)	104 (44.1)
Negative	191 (86.0)	132 (55.9)
Genotype		
Tyr/Tyr	76 (30.2)	49 (37.1)
Tyr/His	71 (28.2)	32 (24.2)
His/His	105 (41.6)	51 (38.7)
Allele type		
T	223 (44.2)	226 (44.0)
C	281 (55.8)	288 (56.0)

ESCC: esophageal squamous cell carcinoma, UGIC: upper gastrointestinal cancer. a. Information of smoking status was available from some of subjects, b. Positive family history of UGIC significantly increased the risk to develop ESCC. Age and sex adjusted OR=4.06 (95 % CI=2.46-6.69), χ^2=49.87, *P*<0.0001.

By using *Tyr/Tyr* as the reference genotype, neither *His/His* genotype alone nor in combination with *Tyr/His* genotype significantly modified the risk of ESCC, the adjusted odds ratio was 1.076 (95 % CI=0.850-1.361) and 0.756 (95 % CI=0.493-1.157), respectively. When stratified for sex, age, smoking status and family history of upper gastrointestinal cancer, the frequency of *His/His* and *Tyr/His* genotype in ESCC patients was not significantly different from healthy controls. Consistently, *His/His* alone, or in combination with *Tyr/His* genotype, did not show any significant influence on the risk of ESCC (Table 2).

DISCUSSION

Chemical carcinogens in consumed alcohol and tobacco, polluted water, ingested food, are in general considered as the main risk factors of ESCC in China. However, not all individuals exposed to the above exogenous risk factors will develop ESCC, indicating that the host susceptibility factors may play an important role in cancer development. In recent years, many polymorphic carcinogen metabolic enzymes, such as aldehyde dehydrogenase-2 (ALDH2)[13], cytochrome P450(CYP)[14,15], glutathione S-transferase(GST)[15,16], methylenetetrahydrofolate reductase (MTHFR)[17], NAD(P)H, quinone oxidoreductase 1 (NQO1)[18,19] have been found to be able to modify the susceptibility to chemically induced cancers including esophageal and gastric cancer. Therefore, these polymorphic genes, alone or in combination with each other or with other newly developed genetic markers, may be used as predicative parameters for screening individuals at a high risk of ESCC.

MEH is involved in the metabolism of environmental carcinogens. Polymorphisms in *mEH* gene might affect the enzyme expression and lead to different phenotypes, probably by the alteration of protein stability[6]. *Tyr113His* substitution in exon 3 could reduce the enzyme expression by about 40 %, producing a slow phenotype with a low epoxide hydrolase activity. In contrast, *Arg139 His* in exon 4 could increase the expression by about 25 %, producing a fast phenotype with an increased enzyme activity[6]. The relationship between *mEH* gene polymorphisms and susceptibility to cancers studied had inconsistent conclusions due to different cancer types and populations. The *Tyr* allele in exon 3 was reported to increase the risk of several cancer types including ovarian cancer[9], oropharyngeal carcer[20] and acute leukaemia[21], whereas the *His* allele was associated with increased susceptibility to cancers occurring in colon[10], liver[11] and cervix[22]. In addition, gene-environment interaction was strongly suggested by some investigations, thus, cumulative cigarette smoking might play a pivotal role in association of *His* homozygous genotype with lung cancer development, altering the direction of risk from a risk factor in nonsmokers to a relatively protective factor in heavy smokers[8].

Recently, a slight decrease in *mEH Tyr*113 frequency was observed in esophageal adenocarcinoma (42 %) compared to controls (53 %, *P*=0.05)[23]. In the present study, the frequencies of *Tyr/Tyr*, *Tyr/His* and *His/His* genotype in healthy controls were in consistent with a recent report from a Chinese group[24]. The genotype distribution difference was not found in ESCC patients and healthy controls, as well as in stratification comparison according to the sex, age (>50 or ⩽50), smoking status (never smoking or current and ever smoking), and family history of UGIC. The result suggests that although *mEH Tyr113His* polymorphism is correlated with some cancer types, this genetic alteration may not be associated with susceptibility to ESCC in population of North China.

ACKNOWLEDGEMENTS

We greatly acknowledge Mr. Baoshan Zhao and Mr. Fanshu Meng for their assistance in recruiting study subjects.

REFERENCES

1 **Yokokawa Y,** Ohta S, Hou J, Zhang XL, Li SS, Ping YM, Nakajima T. Ecological study on the risks of esophageal cancer in Ci-Xian, China: the importance of nutritional status and the use of well water. *Int J Cancer* 1999; **83**: 620-624

2 **Launoy G,** Milan CH, Faivre J, Pienkowski P, Milan CI, Gignoux M. Alcohol, tobacco and oesophageal cancer: effects of the duration of consumption, mean intake and current and former consumption. *Br J Cancer* 1997; **75**: 1389-1396

3 **van Gijssel HE,** Divi RL, Olivero OA, Roth MJ, Wang GQ, Dawsey SM, Albert PS, Qiao YL, Taylor PR, Dong ZW, Schrager JA, Kleiner DE, Poirier MC. Semiquantitation of polycyclic aromatic hydrocarbon-DNA adducts in human esophagus by immunohistochemistry and the automated cellular imaging system. *Cancer Epidemiol Biomarkers Prev* 2002; **11**: 1622-1629

4 **Roth MJ,** Dawsey SM, Wang G, Tangrea JA, Zhou B, Ratnasinghe D, Woodson KG, Olivero OA, Poirier MC, Frye BL, Taylor PR, Weston A. Association between GSTM1*0 and squamous dysplasia of the esophagus in the high risk region of Linxian, China. *Cancer Lett* 2000; **156**: 73-81

5 **Omiecinski CJ,** Aicher L, Swenson L. Developmental expression of human microsomal epoxide hydrolase. *J Pharmacol Exp Ther* 1994; **269**: 417-423

6 **Hassett C,** Aicher L, Sidhu JS, Omiecinski CJ. Human microso-

mal epoxide hydrolase: genetic polymorphism and functional expression *in vitro* of amino acid variants. *Hum Mol Genet* 1994; **3**: 421-428

7 **Lee WJ,** Brennan P, Boffetta P, London SJ, Benhamou S, Rannug A, To-Figueras J, Ingelman-Sundberg M, Shields P, Gaspari L, Taioli E. Microsomal epoxide hydrolase polymorphisms and lung cancer risk: a quantitative review. *Biomarkers* 2002; **7**: 230-241

8 **Zhou W,** Thurston SW, Liu G, Xu LL, Miller DP, Wain JC, Lynch TJ, Su L, Christiani DC. The interaction between microsomal epoxide hydrolase polymorphisms and cumulative cigarette smoking in different histological subtypes of lung cancer. *Cancer Epidemiol Biomarkers Prev* 2001; **10**: 461-466

9 **Lancaster JM,** Brownlee HA, Bell DA, Futreal PA, Marks JR, Berchuck A, Wiseman RW, Taylor JA. Microsomal epoxide hydrolase polymorphism as a risk factor for ovarian cancer. *Mol Carcinog* 1996; **17**: 160-162

10 **Harrison DJ,** Hubbard AL, MacMillan J, Wyllie AH, Smith CA. Microsomal epoxide hydrolase gene polymorphism and susceptibility to colon cancer. *Br J Cancer* 1999; **79**: 168-171

11 **Tiemersma EW,** Omer RE, Bunschoten A, van't Veer P, Kok FJ, Idris MO, Kadaru AM, Fedail SS, Kampman E. Role of genetic polymorphism of glutathione-S-transferase T1 and microsomal epoxide hydrolase in aflatoxin-associated hepatocellular carcinoma. *Cancer Epidemiol Biomarkers Prev* 2001; **10**: 785-791

12 **Cortessis V,** Siegmund K, Chen Q, Zhou N, Diep A, Frankl H, Lee E, Zhu QS, Haile R, Levy D. A case-control study of microsomal epoxide hydrolase, smoking, meat consumption, glutathione S-transferase M3, and risk of colorectal adenomas. *Cancer Res* 2001; **61**: 2381-2385

13 **Matsuo K,** Hamajima N, Shinoda M, Hatooka S, Inoue M, Takezaki T, Tajima K. Gene-environment interaction between an aldehyde dehydrogenase-2 (ALDH2) polymorphism and alcohol consumption for the risk of esophageal cancer. *Carcinogenesis* 2001; **22**: 913-916

14 **Tan W,** Song N, Wang GQ, Liu Q, Tang HJ, Kadlubar FF, Lin DX. Impact of genetic polymorphisms in cytochrome P450 2E1 and glutathione S-transferases M1, T1, and P1 on susceptibility to esophageal cancer among high-risk individuals in China. *Cancer Epidemiol Biomarkers Prev* 2000; **9**: 551-556

15 **Cai L,** Yu SZ, Zhang ZF. Glutathione S-transferases M1, T1 genotypes and the risk of gastric cancer: a case-control study. *World J Gastroenterol* 2001; **7**: 506-509

16 **Cai L,** Yu SZ, Zhang ZF. Cytochrome P450 2E1 genetic polymorphism and gastric cancer in Changle, Fujian Province. *World J Gastroenterol* 2001; **7**: 792-795

17 **Song C,** Xing D, Tan W, Wei Q, Lin D. Methylenetetrahydrofolate reductase polymorphisms increase risk of esophageal squamous cell carcinoma in a Chinese population. *Cancer Res* 2001; **61**: 3272-3275

18 **Zhang JH,** Li Y, Wang R, Geddert H, Guo W, Wen DG, Chen ZF, Wei LZ, Kuang G, He M, Zhang LW, Wu ML, Wang SJ. NQO1 C609T polymorphism associated with esophageal cancer and gastric cardiac carcinoma in North China. *World J Gastroenterol* 2003; **9**: 1390-1393

19 **Zhang J,** Schulz WA, Li Y, Wang R, Zotz R, Wen D, Siegel D, Ross D, Gabbert HE, Sarbia M. Association of NAD(P)H: quinone oxidoreductase 1 (NQO1) C609T polymorphism with esophageal squamous cell carcinoma in a German Caucasian and a northern Chinese population. *Carcinogenesis* 2003; **24**: 905-909

20 **Amador AG,** Righi PD, Radpour S, Everett ET, Weisberger E, Langer M, Eckert GJ, Christen AG, Campbell S Jr, Summerlin DJ, Reynolds N, Hartsfield JK Jr. Polymorphisms of xenobiotic metabolizing genes in oropharyngeal carcinoma. *Oral Surg Oral Med Oral Pathol Oral Radiol Endod* 2002; **93**: 440-445

21 **Lebailly P,** Willett EV, Moorman AV, Roman E, Cartwright R, Morgan GJ, Wild CP. Genetic polymorphisms in microsomal epoxide hydrolase and susceptibility to adult acute myeloid leukaemia with defined cytogenetic abnormalities. *Br J Haematol* 2002; **116**: 587-594

22 **Sierra-Torres CH,** Au WW, Arrastia CD, Cajas-Salazar N, Robazetti SC, Payne DA, Tyring SK. Polymorphisms for chemical metabolizing genes and risk for cervical neoplasia. *Environ Mol Mutagen* 2003; **41**: 69-76

23 **Casson AG,** Zheng Z, Chiasson D, MacDonald K, Riddell DC, Guernsey JR, Guernsey DL, McLaughlin J. Associations between genetic polymorphisms of Phase I and II metabolizing enzymes, p53 and susceptibility to esophageal adenocarcinoma. *Cancer Detect Prev* 2003; **27**: 139-146

24 **Yin L,** Pu Y, Liu TY, Tung YH, Chen KW, Lin P. Genetic polymorphisms of NAD(P)H quinone oxidoreductase, CYP1A1 and microsomal epoxide hydrolase and lung cancer risk in Nanjing, China. *Lung Cancer* 2001; **33**: 133-141

Edited by Su Q and Wang XL

P.O.Box 2345, Beijing 100023,China
Fax: +86-10-85381893
E-mail: wjg@wjgnet.com www.wjgnet.com

World J Gastroenterol 2003;9(12):2658-2661
World Journal of Gastroenterology
 ISSN 1007-9327

• GASTRIC CANCER •

Effect of body mass index on adenocarcinoma of gastric cardia

Ji Zhang, Xiang-Qian Su, Xiao-Jiang Wu, Ya-Hang Liu, Hua Wang, Xiang-Nong Zong, Yi Wang, Jia-Fu Ji

Ji Zhang, Xiang-Qian Su, Xiao-Jiang Wu, Xiang-Long Zong, Yi Wang, Jia-Fu Ji, Department of Surgery, Beijing Cancer Hospital, Beijing Institute of Cancer Research, School of Oncology, Peking University, Beijing 100036, China
Ya-Hang Liu, Hua Wang, Department of Surgery, 1st Teaching Hospital, Inner Mongolian Medical School, Hohhot 010005, Inner Mongolia Autonomous Region, China
Supported by the National High Technology Research and Development Program of China (863 Program), No.2001AA227101
Correspondence to: Professor Jia-Fu Ji, Department of Surgery, Beijing Cancer Hospital, Beijing Institute of Cancer Research, School of Oncology, Peking University, Beijing 100036, China. jiafuj@hotmail.com
Telephone: +86-10-88121122-2048 **Fax:** +86-10-88121122-2049
Received: 2003-07-12 **Accepted:** 2003-07-30

Abstract

AIM: Obesity has been proved as one of the main risk factors for gastric cardia adenocarcinoma (GCA) in the West. The objective of our research was to evaluate the relationship between obesity and the risk of GCA in people from North China.

METHODS: A total of 300 patients who had been diagnosed as GCA and had accepted surgical operation at Beijing Cancer Hospital from 1995 to 2002 were enrolled. Data were collected from pathology materials and hospital records. Two hundred and fifty-eight healthy people who had accepted health examination at the same hospital during the same period were enrolled as controls. Height, weight and gender of them at the time of examination were also collected. Obesity was estimated by body mass index (BMI), computed as weight in kilograms per square surface area (Kg/m^2). The degree of obesity was determined by using BMI$\leqslant$18.5, 24-27.9 and $\geqslant$28 (Kg/m^2) as the cut-off points for underweight/normal, overweight and obesity, respectively. Associations with obesity were estimated by odds ratios (ORs) and 95 % confidence intervals (CIs). All ORs were adjusted for age and sex.

RESULTS: The mean level of BMI was significantly lower in the patient group than that in the control group. The ORs for obesity in age groups 30-59 and 60-79 were 1.15 (95 % CI=0.37-3.65) and 0.16 (95 % CI=0.05-0.44) for males and 0.78 (95 % CI=0.26-2.36) and 0.28 (95 % CI=0.04-2.05) for females, respectively. The ORs for underweight were 2.42 (95 % CI=0.56-10.53) and 4.68 (95 % CI=1.13-19.40) for males in age subgroups 30-59 and 60-79 and 40.7 (95 % CI=9.32-177.92) for females older than 60 yrs. BMI was significantly associated with GCA ($P<0.01$). Underweight people were at high risk for GCA.

CONCLUSION: BMI is an independent risk factor for GCA. Underweight is positively associated with GCA.

Zhang J, Su XQ, Wu XJ, Liu YH, Wang H, Zong XN, Wang Y, Ji JF. Effect of body mass index on adenocarcinoma of gastric cardia. *World J Gastroenterol* 2003; 9(12): 2658-2661
http://www.wjgnet.com/1007-9327/9/2658.asp

INTRODUCTION

The incidence of gastric cardia adenocarcinoma (GCA) has been rising steadily over the past two decades in the United States and Western Europe[1-6]. Extensive studies have been conducted, trying to find its etiological reasons. Some studies showed that the risk for GCA was higher in obese people than that in normal counterparts. It has been generally accepted that obesity is one of the main risk factors for GCA[7-9]. Of all the hypotheses explaining the association between obesity and GCA, reflux theory is the widely accepted one[10-17]. Based on this theory, obesity can promote gastroesophageal reflux disease by increasing intra-abdominal pressure. Gastroesophageal reflux predisposes to Barrett' s esophagus which is a metaplastic precursor state for GCA[18-23]. But the reflux theory cannot explain every aspect of the manifestations of GCA. The real mechanism underlying the disease is still unclear.

We are still unaware if the incidence of GCA has the same pattern in China as in Western world. Based on previous studies, we know that GCA is not rare in China[24]. Great differences exist in life styles and diet habits between Chinese and the Westerners. Elucidating the association between obesity and GCA among Chinese people will be very helpful for prevention and early diagnosis of the disease. The objectives of our study were to investigate whether obesity was more prevalent in patients with GCA than in healthy people, whether the risk for GCA was greater in obese people than in non-obese counterparts, and whether obesity was a dependent/independent risk factor for GCA.

We used body mass index (BMI) to evaluate the degree of obesity. In Western world, the cut-off points of BMI for overweight and obesity are 25 kg/m^2 and 30 mg/m^2. The Chinese people are relatively lean. It is not appropriate to use the same criteria. Recently, a population-based investigation was conducted[25,26] by Zhou *et al* in China. Their results suggested that the cut-off points of BMI for underweight, overweight and obesity of the Chinese people were 18.5 kg/m^2, 24 kg/m^2 and 28 kg/m^2. We used the later criteria in our study.

MATERIALS AND METHODS

Materials

Three hundred patients were enrolled to receive radical operation for GCA in the Department of Surgery at Beijing Cancer Hospital from January 1, 1995 to December 31, 2002. All the hospital records and pathologic materials of these patients were reviewed. The inclusion criteria were listed as follows: The patients were 30 years old or older and the diagnosis of GCA was confirmed by pathologic examinations (reviewed by two independent pathologists). Classification was based on Dr. Siewert' s criteria for gastric cardia carcinoma[27].

The exclusion criteria were stipulated as follows: (1) The patients had a history of malignancies other than GCA; (2) The patients had a history of wasting disease before the diagnosis of the studied malignancy; (3) Adenocarcinoma was not diagnosed as the only histological type of the original malignancy; (4) The patients had a history of gastric cancer and received radical partial gastrectomy. The GCA arose from his/her gastric remnant.

Two hundred and fifty-eight residents who received health examination at Beijing Cancer Hospital from January 1, 2000 to December 31, 2002 were enrolled as healthy control subjects. All the healthy subjects were 30 years old or older, and had no history of any wasting disease. Pregnant women were not included in this study.

Methods

Data, including age, gender, height, weight of the patients and control subjects, were collected. For all patients who experienced weight loss during the disease, their usual height and weight before the disease were also collected. Patients whose hospital records could not provide all the information were not included in this study.

Obesity was measured by BMI, and computed as weight in kilograms per square surface area in square meters (kg/m^2). The height and weight before the disease were used to compute the BMI for patients who had experienced weight loss before the diagnosis was confirmed. The patients and control subjects of the same gender were compared with their mean values of BMI. The patients and control subjects were subdivided into five 10-year age subgroups (age 30-39, 40-49, 50-59, *etc.*). All the subjects were also divided into 2 age subgroups, age $\leqslant$60 yrs or age >60 yrs. Mean values of BMI were compared between patients and control subjects in the same age subgroup.

According to their value of BMI, all the subjects were subdivided into four subgroups (underweight, normal, overweight and obesity) using 18.5, 24 and 28 as the cut-off points of BMI for underweight, overweight and obesity. Relative risks of each group were estimated by odds ratios (ORs) and 95 % confidence intervals (CIs).

Statistic analysis of the data was performed using Chi-square test, with a level of significance at $P\leqslant0.05$. Monte Carlo estimate was used to balance the differences in age and sex structure between the two groups. Lastly, we used logistic regression to evaluate whether obesity was an independent risk factor for GCA.

RESULTS

A total of 300 patients, including 51 women and 249 men, aged 34-80 yrs (median 61.9 yrs), and 258 healthy control subjects (144 women and 114 men) aged 31-78 yrs (median 53.57 yrs), were finally enrolled. The age and sex structure of the patient group differed significantly from those of the control group ($P<0.01$).

The mean value of BMI was 22.90 kg/m^2 in the patient group and 24.85 kg/m^2 in the control group. In each coordinated sex or age subgroup, patients tended to have a low level of BMI than healthy control subjects (Table 1 and Table 2). After sex and age structures were balanced, the mean value of BMI was significantly lower in the patients group than that in the healthy control group ($P<0.01$).

Table 1 Mean levels of BMI in each age group of patients and healthy control subjects

Age	Patient group		Control group	
	Number of cases	Median level of BMI	Number of cases	Median level of BMI
30-39	8	21.94	50	24.26
40-49	27	22.37	69	25.54
50-59	84	22.64	55	24.71
60-69	134	23.46	54	24.93
70-79	47	22.25	30	24.38
Total	300	22.90	258	24.85

Table 2 Mean levels of BMI in each sex group of patients and healthy control subjects

Gender	Patient group		Control group	
	Number of cases	Median level of BMI	Number of cases	Median level of BMI
Male	249	22.88	115	24.75
Female	51	23.02	143	24.94
Total	300	22.90	258	24.85

After all the subjects were labeled as underweight, normal, overweight or obesity based on their BMI, the odds ratios and 95 % confidence intervals in each BMI subgroup were calculated. We used Monte Carlo estimate to balance the differences in age and sex between the two groups, 60 yrs as the cut-off point for age subdivision. In each coordinated subgroup, high BMI people did not show any elevated risk for GCA compared with low BMI ones. On the contrary, the relative risk for GCA rose significantly when the BMI of the subject reached the underweight criteria, especially in women older than 60 yrs ($P<0.05$ by Fisher' s exact test). The risk did not show significant differences only in men of 60 yrs old and younger (Table 3 and Table 4).

Table 3 Odds ratios (ORs) and 95 % confidence intervals (CIs) with body mass index (BMI) by age and sex

Age	Sex	BMI group	Studied group		Total	ORs	95 %	CIs
			Control	Patient				
1[a]	Male	UW[c]	2	16	18	2.42	0.56	10.53
		NM[d]	19	84	103	1.55	0.80	3.03
		OW[e]	20	42	62	0.45	0.23	0.89
		OB[f]	4	16	20	1.15	0.37	3.65
		TOTAL	45	158	203			
	Female	UW	0	5	5	-	-	-
		NM	18	12	30	1.01	0.40	2.55
		OW	18	8	26	0.56	0.21	1.49
		OB	11	6	17	0.78	0.26	2.36
		TOTAL	47	31	78			
2[b]	Male	UW	2	11	13	4.68	1.13	19.40
		NM	26	45	71	1.66	0.88	3.13
		OW	26	31	57	0.87	0.46	1.68
		OB	16	4	20	0.16	0.05	0.44
		TOTAL	70	91	161			
	Female	UW	1	6	7	40.7	9.32	177.92
		NM	45	7	52	0.61	0.22	1.66
		OW	35	6	41	0.75	0.26	2.12
		OB	15	1	16	0.28	0.04	2.05
		TOTAL	96	20	116			

a. Age group 1: $\leqslant$60 yrs, b. Age group 2: >60 yrs, c. UW=underweight (BMI<18.5 kg/m^2), d. NM=Normal (18.5$\leqslant$ BMI<24 kg/m^2), e. OW=Overweight (24$\leqslant$BMI<28 kg/m^2), f. OB=Obesity (BMI$\geqslant$28 kg/m^2).

Table 4 Fisher's exact test for evaluation of significance of association between underweight and high relative risk for GCA

Age	Sex	χ^2 value	*P*	Monte carlo sig. (2-sided) 99 % confidence interval	
				Lower bound	Upper bound
1[a]	Male	5.357	0.136	0.127	0.144
	Female	8.161	0.036	0.031	0.041
2[b]	Male	16.438	0.001	0.000	0.002
	Female	17.196	0.001	0.000	0.001

a. Age Group 1: $\leqslant$60 yrs, b. Age Group 2: >60 yrs.

Compared with age, sex, previous gastrointestinal disease history and family history of gastric cancer, MBI showed itself to be an independent risk factor for GCA (Table 5, Table 6) (P<0.01).

Table 5 Logistic regression analysis of sex, BMI and age group 1

	B	SE[a]	*P*	OR	95%	CIs
Sex	-1.714	0.210	<0.01	0.180	0.119	0.272
BMI	-0.152	0.028	<0.01	0.859	0.813	0.907
Age group1[b]	1.082	0.198	<0.01	2.952	2.002	4.351
Constant	4.473	0.777	<0.01	87.589		

a. SE=standard error, b. Age group1: The subjects were divided into two age subgroup: age ⩽60 yrs and age >60 yrs.

Table 6 Logistic regression analysis of sex, BMI and age group 2

	B	SE[a]	*P*	OR	95%	CIs
Sex	-1.668	0.214	<0.01	0.189	0.124	0.287
BMI	-0.156	0.029	<0.01	0.856	0.809	0.905
Age group2[b]	0.609	0.090	<0.01	1.838	1.541	2.193
Constant	4.105	0.790	<0.01	60.662		

a. SE=standard error, b. Age group 2: The subjects were divided into 5 10-year age subgroups (30-39 yrs, 40-49 yrs, 50-59 yrs, 60-69 yrs, 70-79 yrs, *etc.*).

DISCUSSION

Firstly, we wanted to elucidate whether obesity was more prevalent in patients with GCA than in healthy people. After calculating BMI of all the subjects, using the height and weight before the disease for patients who had experienced weight loss before the diagnosis was confirmed, we found that obesity did not tend to be more prevalent in patients with GCA than in healthy control subjects. The mean value of BMI in each group was 22.90 kg/m^2 and 24.85 kg/m^2 (P<0.01). Within each coordinated sex or age subgroup, the patients always had a lower level of BMI (Table 1 and Table 2). The trend did not show any change after sex and age were balanced between the two groups.

We divided all the subjects into four subgroups according to the criteria of BMI for underweight, overweight and obesity proposed by Zhou *et al*[25,26]. After we calculated the relative risk in each group, we found that it did not rise with the elevation of BMI. The ORs for obesity in age groups of 30-59 and 60-79 years were 1.15 (95 % CI=0.37-3.65) and 0.16 (95 % CI=0.05-0.44) for males and 0.78 (95 % CI=0.26-2.36) and 0.28 (95 % CI=0.04-2.05) for females, respectively. On the contrary, underweight people had the greatest risk, ORs for underweight were 2.42 (95 % CI=0.56-10.53) and 4.68 (95 % CI=1.13-19.40) for males in age subgroup 30-59 and 60-79 and 40.7 (95 % CI=9.32-177.92) for females older than 60 yrs. No underweight subject was found in healthy female subjects of 60 yrs old or younger. So the ORs for underweight in this subgroup could not be calculated. After performing Fisher' s exact test, we found that the underweight people were more likely to get GCA (P<0.05) except for men under 60 yrs old (Table 4).

Sex and age might be the influence factors for BMI. Logistic regression was performed to investigate the relationship between BMI and GCA. As shown in Table 5 and Table 6, the association between risk of GCA and BMI was significant (P<0.01). Underweight people showed a high possibility of GCA.

Our results differed greatly from not only those in the Western countries but also those of Chow *et al*. in Shanghai, China[7,8,9,28]. The reasons behind the difference might be the genetic background, life style and cut-off points for BMI. The genetic background of the Chinese people differs greatly from those of the Westerners. It even differs in different parts of China. It has been proved that life styles, including smoking, alcohol consumption, and dietary habits could influence the incidence and prognosis of GCA[29]. Even in China, people in different areas have their particular life styles. For example, citizens of Shanghai take more fresh fruits and vegetables than residents of Beijing. Results of the correlative researches conducted in Shanghai were similar to those of the Westerners. The patients enrolled in our research were mainly from North China, which may cause the difference. Secondly, the cut-off points for underweight, overweight and obesity used in our study were different from those used in previous researches. Our study suggests that obesity should not be a risk factor for the North Chinese people.

According to Siewert' s classification, GCA is classified into three types based on its anatomy location. Yasuhiro *et al* noticed a striking difference between the East and the West in the proportion of patients who fell into each type of GCA[30]. Type I cancer, or adenocarcinoma of the lower esophagus was reported to be more prevalent in the Western countries[31] while type III cancer, or adenocarcinoma of the proximal stomach was predominant in Japan. By reviewing pathologic materials of GCA patients, we found that the distribution of GCA types in our patient group was very similar to that of Japanese (data not shown). Obesity might be a risk factor for type I cancer. GCA might have a particular mechanism in the Eastern countries[32].

GCA tended to be more prevalent in aged people[33]. In our study, the median age of the patient group was significantly higher than that of the control group. Epidemiological evidences showed that the proportion of obese people rose with increase of age. It must be clarified that whether a high proportion of aged people can lead to a high prevalence of obesity in the patients group or obesity really predisposes to GCA. Evidences that were opposed to the reflux theory have been also available[34,35]. Besides, one important precondition of the obesity-reflux-carcinogenesis theory is that reflux is the real risk factor. Our next research will be focused on how reflux influences cells at the gastric cardia.

REFERENCES

1 **Blot WJ**, Devesa SS, Kneller RW, Fraumeni JF Jr. Rising incidence of adenocarcinoma of the esophagus and gastric cardia. *JAMA* 1991; **265**: 1287-1289

2 **Armstrong RW**, Borman B. Trends in incidence rates of adeno-carcinoma of the oesophagus and gastric cardia in New Zealand, 1978-1992. *Int J Epidemiol* 1996; **25**: 941-947

3 **Zheng T**, Mayne ST, Holford TR, Boyle P, Liu W, Chen Y, Mador M, Flannery J. The time trend and age–period-cohort effects on incidence of adenocarcinoma of the stomach in Connecticut from 1955-1989. *Cancer* 1993; **72**: 330-340

4 **Pera M**, Cameron AJ, Trastek VF, Carpenter HA, Zinsmeister AR. Increasing incidence of adenocarcinoma of the esophagus and esophagogastric junction. *Gastroenterology* 1993; **104**: 510-513

5 **Walther C**, Zilling T, Perfekt R, Moller T. Increasing prevalence of adenocarcinoma of the oesophagus and gastro-oesophageal junction: a study of the Swedish population between 1970 and 1997. *Eur J Surg* 2001; **167**: 748-757

6 **Posner MC**, Vokes EE, Weichselbaum RR. Cancer of the upper gastrointestinal tract. *Hamilton:BC Decker* 2002: 86-87

7 **Chow WH**, Blot WJ, Vaughan TL, Risch HA, Gammon MD, Stanford JL, Dubrow R, Schoenberg JB, Mayne ST, Farrow DC, Ahsan H, West AB, Rotterdam H, Niwa S, Fraumeni JF Jr. Body mass index and risk of adenocarcinomas of the esophagus and gastric cardia. *J Natl Cancer Inst* 1998; **90**: 150-155

8 **Vaughan TL**, Davis S, Kristal A, Thomas DB. Obesity, alcohol,

and tobacco as risk factors for cancers of the esophagus and gastric cardia: adenocarcinoma versus squamous cell carcinoma. *Cancer Epidemiol Biomarkers Prev* 1995; **4**: 85-92

9 **Lagergren J**, Bergstrom R, Nyren O. Association between body mass and adenocarcinoma of the esophagus and gastric cardia. *Ann Intern Med* 1999; **130**: 883-890

10 **Bremner CG**, Lynch VP, Ellis FH Jr. Barrett's esophagus: congenital or acquired? An experimental study of esophageal mucosal regeneration in the dog. *Surgery* 1970; **68**: 209-216

11 **Fisher BL**, Pennathur A, Mutnick JL, Little AG. Obesity correlates with gastroesophageal reflux. *Dig Dis Sci* 1999; **44**: 2290-2294

12 **Fraser-Moodie** CA, Norton B, Gornall C, Magnago S, Weale AR, Holmes GK. Weight loss has an independent beneficial effect on symptoms of gastro-oesophageal reflux in patients who are overweight. *Scand J Gastroenterol* 1999; **34**: 337-340

13 **Terry P**, Lagergren J, Wolk A, Nyren O. Reflux-inducing dietary factors and risk of adenocarcinoma of the esophagus and gastric cardia. *Nutr Cancer* 2000; **38**: 186-191

14 **Oberg S**, DeMeester TR, Peters JH, Hagen JA, Nigro JJ, DeMeester SR, Theisen J, Campos GM, Crookes PF. The extent of Barrett's esophagus depends on the status of the lower esophageal sphincter and the degree of esophageal acid exposure. *J Thorac Cardiovasc Surg* 1999; **117**: 572-580

15 **Attwood SE**, DeMeester TR, Bremner CG, Barlow AP, Hinder RA. Alkaline gastroesophageal reflux: implications in the development of complications in Barrett's columnar-lined lower esophagus. *Surgery* 1989; **106**: 764-770

16 **Oritz-Hidalgo C**, De La Vega G, Aguirre-Garcia J. The histopathology and biologic prognostic factors of Barrett's esophagus: a review. *J Clin Gastroenterol* 1998; **26**: 324-333

17 **Stein HJ**, Kauer WK, Feussner H, Siewert JR. Bile reflux in benign and malignant Barrett's esophagus: effect of medical acid suppression and nissen fundoplication. *J Gastrointest Surg* 1998; **2**: 333-341

18 **Sampliner RE**. Practice guidelines on the diagnosis, surveillance, and therapy of Barrett's esophagus. The practice parameters committee of the American college of gastroenterology. *Am J Gastroenterol* 1998; **93**: 1028-1032

19 **Cameron AJ**, Lomboy CT, Pera M, Carpenter HA. Adenocarcinoma of the esophagogastric junction and Barrett's esophagus. *Gastroenterology* 1995; **109**: 1541-1546

20 **Spechler SJ**, Goyal RK. The columnar-lined esophagus, intestinal metaplasia, and Norman Barrett. *Gastroenterology* 1996; **110**: 614-621

21 **DeMeester SR**, DeMeester TR. Columnar mucosa and intestinal metaplasia of the esophagus: fifty years of controversy. *Ann Surg* 2000; **231**: 303-321

22 **Clark GW**, Smyrk TC, Burdiles P, Hoeft SF, Peters JH, Kiyabu M, Hinder RA, Bremner CG, DeMeester TR. Is Barrett's metaplasia the source of adenocarcinomas of the cardia? *Arch Surg* 1994; **129**: 609-614

23 **Ishaq S**, Jankowski JA. Barrett's metaplasia:clinical implications. *World J Gastroenterol* 2001; **7**: 563-565

24 **Wang LD**, Zheng S, Zheng ZY, Casson AG. Primary adenocarcinomas of lower esophagus, esophagogastric junction and gastric cardia: In special reference to China. *World J Gastroenterol* 2003; **9**: 1156-1164

25 **Zhou BF**. Predictive values of body mass index and waist circumference for risk factors of certain related diseases in Chinese adults-study on optimal cut-off points of body mass index and waist circumference in Chinese adults. *Biomed Environ Sci* 2002; **15**: 83-96

26 **Zhou BF**. Effect of body mass index on all-cause mortality and incidence of cardiovascular diseases–report for meta-analysis of prospective studies open optimal cut-off points of body mass index in Chinese adults. *Biomed Environ Sci* 2002; **15**: 245-252

27 **Siewert JR**, Stein HJ. Classification of adenocarcinoma of the oesophagogastric junction. *Br J Surg* 1998; **85**: 1457-1479

28 **Ji BT**, Chow WH, Yang G, McLaughlin JK, Gao RN, Zheng W, Shu XO, Jin F, Fraumeni JF Jr, Gao YT. Body mass index and the risk of cancers of the gastric cardia and distal stomach in Shanghai, China. *Cancer Epidemiol Biomarkers Prev* 1997; **6**: 481-485

29 **Cai L**, Zheng ZL, Zhang ZF. Risk factors for the gastric cardia cancer: a case-control study in Fujian Province. *World J Gastroenterol* 2003; **9**: 214-218

30 **Kodera Y**, Yamamura Y, Shimizu Y, Torii A, Hirai T, Yasui K, Morimoto T, Kato T. Adenocarcinoma of the gastroesophageal junction in Japan: relevance of Siewert's classification applied to 177 cases resected at a single institution. *J Am Coll Surg* 1999; **189**: 594-601

31 **Wijnhoven BP**, Siersema PD, Hop WC, van Dekken H, Tilanus HW. Adenocarcinomas of the distal oesophagus and gastric cardia are one clinical entity. Rotterdam oesophageal tumour study group. *Br J Surg* 1999; **86**: 529-535

32 **Gao SS**, Zhou Q, Li YX, Bai YM, Zheng ZY, Zou JX, Liu G, Fan ZM, Qi YJ, Zhao X, Wang LD. Comparative studies on epithelial lesions at gastric cardia and pyloric antrum in subjects from a high incidence area for esophageal cancer in Henan, China. *World J Gastroenterol* 1998; **4**: 332-333

33 **Daly JM**, Karnell LH, Menck HR. National cancer Data Base report on esophageal carcinoma. *Cancer* 1996; **78**: 1820-1828

34 **Lagergren J**, Bergstrom R, Lindgren A, Nyren O. Symptomatic gastroesophageal reflux as a risk factor for esophageal adenocarcinoma. *N Engl J Med* 1999; **340**: 825-831

35 **Farrow DC**, Vaughan TL, Sweeney C, Gammon MD, Chow WH, Risch HA, Stanford JL, Hansten PD, Mayne ST, Schoenberg JB, Rotterdam H, Ahsan H, West AB, Dubrow R, Fraumeni JF Jr, Blot WJ. Gastroesophageal reflux disease, use of H2 receptor antagonists, and risk of esophageal and gastric cancer. *Cancer Causes Control* 2000; **11**: 231-238

Edited by Zhang JZ and Wang XL

P.O.Box 2345, Beijing 100023,China
Fax: +86-10-85381893
E-mail: wjg@wjgnet.com www.wjgnet.com

World J Gastroenterol 2003;9(12):2662-2665
World Journal of Gastroenterology
 ISSN 1007-9327

• GASTRIC CANCER •

Somatic mutation analysis of p53 and ST7 tumor suppressor genes in gastric carcinoma by DHPLC

Chong Lu, Hui-Mian Xu, Qun Ren, Yang Ao, Zhen-Ning Wang, Xue Ao, Li Jiang, Yang Luo, Xue Zhang

Chong Lu, Hui-Mian Xu, Zhen-Ning Wang, Laboratory of Medical Genomics, Oncology Department, the First Affiliated Clinical College, China Medical University, Shenyang, 110001, Liaoning Province, China
Qun Ren, Yang Ao, Xue Ao, Li Jiang, Yang Luo, Laboratory of Medical Genomics, China Medical University, Shenyang, 110001, Liaoning Province, China
Xue Zhang, Laboratory of Medical Genomics, China Medical University, Shenyang, 110001, Liaoning Province, China. Laboratory of Genetics, Peking Union Medical College, Chinese Academy of Medical Sciences, Beijing, 100021, China
Supported by National Science Fund for Distinguished Young Scholars, No. 30125017, and the Major State Basic Research Development Program of China (973 Program), No. G1998051203
Correspondence to: Xue Zhang, Laboratory of Medical Genomics, China Medical University, No. 92, Bei Er Road, Heping District, Shenyang, 110001, Liaoning Province, China. xzhang@mail.cmu.edu.cn
Telephone: +86-24-23256666-5532
Received: 2003-04-04 **Accepted:** 2003-06-07

Abstract

AIM: To verify the effectiveness of denaturing high-performance liquid chromatography (DHPLC) in detecting somatic mutation of p53 gene in gastric carcinoma tissues. The superiority of this method has been proved in the detection of germline mutations, but it was not very affirmative with respect to somatic mutations in tumor specimens. ST7 gene, a candidate tumor suppressor gene identified recently at human chromosome 7q31.1, was also detected because LOH at this site has also been widely reported in stomach cancer.

METHODS: DNA was extracted from 39 cases of surgical gastric carcinoma specimen and their correspondent normal mucosa. Seven fragments spanning the 11 exons were used to detect the mutation of p53 gene and the four exons reported to have mutations in ST7 gene were amplified by PCR and directly analyzed by DHPLC without mixing with wild-type allele.

RESULTS: In the analysis of p53 gene mutation, 9 aberrant DHPLC chromatographies were found in tumor tissues, while their normal-adjacent counterparts running in parallel showed a normal shape. Subsequent sequencing revealed nine sequence variations, 1 polymorphism and 8 mutations including 3 mutations not reported before. The mutation rate of p53 gene (21 %) was consistent with that previously reported. Furthermore, no additional aberrant chromatography was found when wild-type DNA was added into the DNA of other 30 tumor samples that showed normal shapes previously. The positivity of p53 mutations was significantly higher in intestinal-type carcinomas (40 %) than that in diffuse-type (8.33 %) carcinomas of the stomach. No mutation of ST7 gene was found.

CONCLUSION: DHPLC is a very convenient method for the detection of somatic mutations in gastric carcinoma. The amount of wild type alleles supplied by the non-tumorous cells in gastric tumor specimens is enough to form heteroduplex with mutant alleles for DHPLC detection. ST7 gene may not be the target gene of inactivation at 7q31 site in gastric carcinoma.

Lu C, Xu HM, Ren Q, Ao Y, Wang ZN, Ao X, Jiang L, Luo Y, Zhang X. Somatic mutation analysis of p53 and ST7 tumor suppressor genes in gastric carcinoma by DHPLC. *World J Gastroenterol* 2003; 9(12): 2662-2665
http://www.wjgnet.com/1007-9327/9/2662.asp

INTRODUCTION

Denaturing high performance liquid chromatography (DHPLC) is a relatively new technique with a high degree of sensitivity in the analysis of germline mutations in various inherited diseases[1-3]. It is known that equal amounts of wild-type and mutant DNA are required to form heteroduplexes for ideal DHPLC analysis. The pure mutant DNA could be available easily from germline mutations or tumor cell lines, but it is often not the case in actual tumor specimens because non-tumorous cells may be present in various amounts. Even using other methods, such as LCM, would not guarantee the gain of pure tumor DNA. So, there are few reports with respect to the analysis of somatic mutations in tumors. Fortunately, in more recent reports[4-6], it was proved that DHPLC had the ability to detect the heteroduplexes formed by mixing wild type alleles with homogenous mutant alleles of cell lines over a broad range of mutant allele concentrations, differing from 5 % to 95 %, which suggested that DHPLC may be well suited for the analysis of somatic mutations in tumor tissue samples in which the proportion of mutant and wild-type alleles is variable.

In our investigation about the somatic mutation of 2 genes by DHPLC, PCR amplification of DNA extracted from surgical tumor specimen was directly conducted without mixing with wild-type DNA, only if the existence of both tumor and normal cells was confirmed by pathology in a certain proportion but not strictly in equal amount. One gene we detected was p53 gene, which was reported to have a relatively high frequency of mutation in gastric carcinoma[7-10]. The other one was ST7 gene, which was cloned and mapped to chromosome 7q31.1-7q31.2, a region suspected of containing a tumor suppressor gene involved in a variety of human cancers[11-13]. Strong evidences to support ST7 as the key TSG at this locus have recently been reported by Zenklusen *et al*.[13]. LOH 7q31 in stomach cancer has also been widely reported[14-16], so we detected four exons of ST7 gene that was reported[13,17] to have mutations to clarify the role of ST7 gene in stomach cancer.

MATERIALS AND METHODS

Tissue samples and preparation of DNA

Thirty-nine cases of gastric cancer tissue and corresponding adjacent non-tumorous gastric tissue were obtained by surgical excision from patients at the Oncology Department of the First Affiliated Hospital of China Medical University, including 15

Table 1 Primer sequences used in PCR reactions (shown in the 5' to 3' direction)

Primer name		Forward sequence	Reverse sequence	Size (bp)	Annealing temp. (°C)
P53	Exon2+3	ccaggtgacccagggttg	gcaaggggactgtagatgg	402	62
	Exon4	acctggtcctctgactgctc	gccaggcattgaagtctcat	363	60
	Exon5+6	ccgtgttccagttgctttat	ttaacccctcctcccaga	488	58
	Exon7	tgcttgccacaggtctcc	ccggaaatgtgatgagaggt	301	60
	Exon8+9	ttccttactgcctcttgctt	agaaaacggcattttgagtg	411	57
	Exon10	ctcaggtactgtgtatatac	ctatggctttccaacctagga	218	55
	Exon11	tcatctctcctccctgcttc	ccacaacaaaacaccagtgc	300	60
ST7	Exon3	gtagtgtcactgaacttacgc	gctctctgaaccagaccca	154	55
	Exon4	aggtcttgcttttctctctca	caaaaagccctcccattcag	213	55
	Exon5	tgtcctctactgagtctacc	gtatcctatcaatggcaactg	223	55
	Exon12	gtgtagatgcttccgggttg	taacgagttcctgggggat	187	55

Table 2 p53 mutations in sporadic gastric carcinomas

Specimen No.	Pathology	Exon	Codon	Mutation	Effect	DHPLC (temp)	DHPLC gradient (B% in 4.5 min)
H3	Poorly diff.	6	188	CTG>CCG	Leu188Pro	63	60-66
54	Tubular	7	246	Del 24bp[a]	8 amino acid deletion	57,59,61	54-63
57	Tubular	6	215	AGT>GGT	Ser215Gly	62	57-66
64	Tubular	5	167	Ins 3bp[a]	Gln insertion	60	57-66
77	Tubular	7	235	Del 1bp(C)[a]	Framshift (246stop)	61	53-62
79	Papillary	8	301	CCA>CTA	Pro301Leu	60	54-63
86	Poorly diff.	5	161	GCC>GGC	Ala161Gly	61	53-62
133	Papillary	5	135	TGC>TGG	Cys135Trp	62	57-66
36		Intron 7		C>T, T>G		57	54-63

[a]Mutation that hasn't been reported previously.

cases of intestinal type (4 cases of papillary type and 11 cases of tubular type) and 24 cases of diffuse type (18 cases of poorly differentiated type, 4 cases of mucinous type and 2 cases of signet-ring cell type). Their average age was 58.5 years(from 42 to 79 years), male/female was 27/12. A portion of tissue was frozen and stored at -80 ℃ for DNA extraction, and the remaining tissue was fixed in 10 % buffered formalin for histological examination. DNA was isolated by a standard proteinase K digestion and phenol-chloroform extraction procedure.

PCR conditions

Primer pairs for the amplification are listed in Table 1. Oligonucleotide primers for exons of p53 were published before[18]. The underlying sequence was based on the NCBI database. The average fragment length ranged from 150 to 500 bp. Fragment amplification was accomplished with the UNO II PCR system (Biometra, Germany). PCR reactions were performed in a volume of 20-50 μl with 35 cycles consisting of a denaturation step at 94 ℃ for 45 s, primer annealing for 30 s and an elongation step at 72 ℃ for 1 min. The final step was extended at 72 ℃ for 5 min.

DHPLC analysis and DNA sequencing

Prior to DHPLC analysis, heteroduplex formation of the PCR products was carried out by heating for 5 min at 94 ℃ followed by cooling to 25 ℃ at a rate of 0.03 ℃ S^{-1}. DHPLC was performed using the transgenomic WAVE DNA fragment analysis system (transgenomic, Ohama, USA). Four μl of the PCR products was loaded on the DNASep column and DNA was eluted at a flow rate of 0.9 ml/min within a linear acetonitrile gradient consisiting of buffer A (0.1 M triethylammonium acetate, TEAA) and buffer B (0.1 M TEAA, 25 % acetonitrile). Elution of DNA from column was detected by absorbing at 260 nm. The optimal melting temperature for each fragment was selected by using WaveMaker 4.1 software (transgenomic) or by a software described before which is available freely at http:// insertion.Stanford.edu/melt.html. PCR amplification of the DNA extracted from surgical tumor specimen was directly conducted without mixing with wild-type DNA. The original PCR products of any tumor sample showing an aberrant DHPLC elution profile and its corresponding normal tissue sample were purified using a PCR fragment purification kit (Takara, Dalian), then sequenced directly. Sequence analysis was conducted with the same primers as those used in the original PCR using an ABI 377 automated DNA sequencer. The PCR products of those tumor samples that showed normal DHPLC chromatography were mixed with wile-type at the ratio of 2:1 prior to the reannealing step, and run again.

PCR reaction and DHPLC analysis of all the samples with positive results were repeated at least 2 times and a double direction sequencing was used.

RESULTS

p53 mutations

The results of DHPLC analysis are summarized in Table 2. Mutations of the p53 gene were investigated in 39 surgical specimens of primary gastric cancer by DHPLC. Altogether, 9 aberrant DHPLC chromatographies were found and all of them were from tumor tissues, while their normal-adjacent counterparts running in parallel showed a normal shape. Subsequent sequencing revealed nine sequence variations of 8 mutations and 1 polymorphism. The 8 mutations were localized at exons 5, 6, 7 and 8, including 5 missense mutations, 1 frameshift deletion of 1 bp, 1 in frame insertion of 3 bp and 1 in frame deletion of 24 bp (one example is shown in Figure 1). The latter 3 base pairs changes were not reported previously. Through the European Bioinformatics Institute (EBI) available

at ftp://ftp.ebi.ac.uk/pub/databases/p53/, one polymorphism was localized in intron 7. The positivity for p53 mutations was significantly higher in intestinal-type carcinoma (40 %, 6/15) than that in diffuse-type (8.33 %, 2/24) carcinoma of the stomach ($P<0.01$, χ^2 test).

ST7 mutations

All of the DHPLC chromatographies from 39 tumor tissues showed a normal single peak shape, just the same as with those from their corresponding normal adjacent tissues.

DISCUSSION

Some prescreening methods, such as single strand conformation polymorphism (SSCP) or denaturing gradient gel electrophoresis (DGGE), have been widely used for mutation analysis[19-35], but they were characterized by their lower sensitivity and more labor intensity[1,36,37]. A relatively new technique, DHPLC, is believed to be a superior method for its economic, automatic, time-saving features and higher sensitivities ranging from 95 % to 100 % for germline mutation detection[2,3,38-40]. However, with respect to somatic mutation in actual tumor specimens, one potential drawback that should be considered was that heteroduplexes formed by normal and mutant alleles were necessary for DHPLC detection. Such heteroduplexes were usually got by mixing tumor DNA with an normal equal amount of wild-type DNA when germline mutation was detected. Excitingly, some more recent reports[4-6] showed that heteroduplexes could still be detected by DHPLC when they changed the concentration of homogenous mutant alleles of cell lines from 5 % to 95 %. Their results indicated that DHPLC might also be well suitable for the analysis of somatic mutations in tumor tissue samples in which the proportion of mutants and wild-type alleles was variable. It has been demonstrated that many gastric cancers contained abundant non-neoplastic stromal cells[9]. So when somatic mutations in gastric cancer tissues were detected, it might not only be unnecessary but also laborious to mix normal wild-type alleles with tumor alleles. Further more it might yield a pseudo-negative result if the tumor cell concentration was relatively low in specimens.

In our study, the PCR products, which were amplified from the extracted DNA of surgical tumor specimens without mixing with extra wild type alleles, were directly analyzed by DHPLC. In the analysis of p53 gene mutations, 9 aberrant DHPLC chromatographies were found and all of them were from tumor tissues, while their normal-adjacent counterparts running in parallel showed a normal shape. Subsequent sequencing revealed nine sequence variations of 8 mutations and 1 polymorphism. The mutation rate (21 %, 8/39) was similar to the previously reported frequency of 20 % to 50 %[7-10]. Furthermore, no additional aberrant chromatography was found when wild-type DNA was added into the DNA of other 30 tumor samples that showed a normal shape previously. These results indicate that the amount of wild type alleles supplied by non-tumorous cells in actual gastric tumor specimens is enough to form heteroduplex with mutant alleles for the detection by DHPLC. So, DHPLC is a very convenient method for the detection of somatic mutations in gastric carcinomas.

In contrast to previous studies, p53 mutations did not follow a random distribution among different subtypes. The positivity for p53 mutations was significantly higher in intestinal-type carcinomas (40 %) than in diffuse-type carcinomas (8.33 %). This phenomenon was also observed in other reports[9,41]. Two hot spots for p53 gene mutations in gastric cancer at codon 251 and codon 173[42] were not observed in our study. Interestingly, we found three new mutations that have not been reported in the database of p53 mutations. Considering that all the patients in our study were from the northeast area of China, the above differences might be due to the different etiologies of gastric cancer in different geographical areas.

Evidence of LOH 7q31 has been found in many kinds of malignant tumors and also in gastric carcinomas[14-16], indicating that a putative tumor suppressor gene at this locus may be involved in the pathogenesis of many neoplasms. Strong evidences to support ST7 as the key TSG at this locus were recently reported by Zenklusen *et al*.[13]. Using a prostate cancer-derived cell line they showed that ST7 could suppress *in vivo* tumorigenicity. In addition, they described protein-truncating mutations of ST7 in three out of seven breast cancer derived cell lines and in four out of 10 primary colon carcinomas. But in our investigation on 39 cases of gastric carcinoma, no mutation was found. This could be due to the fact that in the previous study all the tumors were pre-screened for LOH at 7q31, thus increasing the likelihood of detecting a mutation. Other mechanisms of inactivation such as promoter hypermethylation, homozygous deletion, or genomic rearrangement that were not explored in our study were the common mechanisms of ST7 inactivation in stomach cancer. Our results were coincident with a few other recent reports[17,43-45] supporting the absence of ST7 alterations. In these studies, the researchers also failed to detect any further coding mutations in all exons of ST7 in a wide-range of carcinomas and cell lines, including that of ovarian, colon, breast, esophagus, head and neck, pancreatic and prostate. Our results extend the spectrum of malignant tumor types examined for ST7 somatic alterations, and suggest that one of the other tumor suppressor genes, or an undiscovered gene at 7q31 is the target involved in carcinogenesis of gastric carcinoma at this locus.

REFERENCES

1 **Gross E**, Arnold N, Goette J, Schwarz-Boeger U, Kiechle M. A comparison of BRCA1 mutation analysis by direct sequencing, SSCP and DHPLC. *Hum Genet* 1999; **105**: 72-78

2 **Holinski-Feder E**, Muller-Koch Y, Friedl W, Moeslein G, Keller G, Plaschke J, Ballhausen W, Gross M, Baldwin-Jedele K, Jungck M, Mangold E, Vogelsang H, Schackert H, Lohsea P, Murken J, Meitinger T. DHPLC mutation analysis of the hereditary nonpolyposis colon cancer (HNPCC) genes hMLH1 and hMSH2. *J Biochem Biophys Methods* 2001; **47**: 21-32

3 **O'Donovan MC**, Oefner PJ, Roberts SC, Austin J, Hoogendorn B, Guy C, Speight G, Upadhyaya M, Sommer SS, McGuffin P. Blind analysis of denaturing high-performance liquid chromatography as a tool for mutation detection. *Genomics* 1998; **52**: 44-49

4 **Wolford JK**, Blunt D, Ballecer C, Prochazka M. High-throughput SNP detection by using DNA pooling and denaturing high performance liquid chromatography (DHPLC). *Hum Genet* 2000; **107**: 483-487

5 **Keller G**, Hartmann A, Mueller J, Hofler H. Denaturing high pressure liquid chromatography (DHPLC) for the analysis of somatic p53 mutations. *Lab Invest* 2001; **81**: 1735-1737

6 **Liu MR**, Pan KF, Li ZF, Wang Y, Deng DJ, Zhang L, Lu YY. Rapid screening mitochondrial DNA mutation by using denaturing high-performance liquid chromatography. *World J Gastroenterol* 2002; **8**: 426-430

7 **Greenblatt MS**, Bennett WP, Hollstein M, Harris CC. Mutations in the p53 tumor suppressor gene: clues to cancer etiology and molecular pathogenesis. *Cancer Res* 1994; **54**: 4855-4878

8 **Hongyo T**, Buzard GS, Palli D, Weghorst CM, Amorosi A, Galli M, Caporaso NE, Fraumeni JF Jr, Rice JM. Mutations of the K-ras and p53 genes in gastric adenocarcinomas from a high-incidence region around Florence, Italy. *Cancer Res* 1995; **55**: 2665-2672

9 **Hsieh LL**, Hsieh JT, Wang LY, Fang CY, Chang SH, Chen TC. P53 mutations in gastric cancers from Taiwan. *Cancer Lett* 1996; **100**: 107-113

10 **Wu MS**, Lee CW, Shun CT, Wang HP, Lee WJ, Chang MC, Shen JC, Lin JT. Distinct clinicopathologic and genetic profiles in spo-

radic gastric cancer with different mutator phenotypes. *Genes Chromosomes Cancer* 2000; **27**: 403-411
11 **Zenklusen JC**, Thompson JC, Klein-Szanto AJ, Conti CJ. Frequent loss of heterozygosity in human primary squamous cell and colon carcinomas at 7q31.1: evidence for a broad range tumor suppressor gene. *Cancer Res* 1995; **55**: 1347-1350
12 **Matsuura K**, Shiga K, Yokoyama J, Saijo S, Miyagi T, Takasaka T. Loss of heterozygosity of chromosome 9p21 and 7q31 is correlated with high incidence of recurrent tumor in head and neck squamous cell carcinoma. *Anticancer Res* 1998; **18**: 453-458
13 **Zenklusen JC**, Conti CJ, Green ED. Mutational and functional analyses reveal that ST7 is a highly conserved tumor-suppressor gene on human chromosome 7q31. *Nat Genet* 2001; **27**: 392-398
14 **Kuniyasu H**, Yasui W, Yokozaki H, Akagi M, Akama Y, Kitahara K, Fujii K, Tahara E. Frequent loss of heterozygosity of the long arm of chromosome 7 is closely associated with progression of human gastric carcinomas. *Int J Cancer* 1994; **59**: 597-600
15 **Nishizuka S**, Tamura G, Terashima M, Satodate R. Commonly deleted region on the long arm of chromosome 7 in differentiated adenocarcinoma of the stomach. *Br J Cancer* 1997; **76**: 1567-1571
16 **Nishizuka S**, Tamura G, Terashima M, Satodate R. Loss of heterozygosity during the development and progression of differentiated adenocarcinoma of the stomach. *J Pathol* 1998; **185**: 38-43
17 **Brown VL**, Proby CM, Barnes DM, Kelsell DP. Lack of mutations within ST7 gene in tumor-derived cell lines and primary epithelial tumours. *Br J Cancer* 2002; **87**: 208-211
18 **Gross E**, Kiechle M, Arnold N. Mutation analysis of p53 in ovarian tumors by DHPLC. *J Biochem Biophys Methods* 2001; **47**: 73-81
19 **Deng ZL**, Ma Y. Aflatoxin sufferer and p53 gene mutation in hepatocellular carcinoma. *World J Gastroenterol* 1998; **4**: 28-29
20 **Luo D**, Liu QF, Gove C, Naomov NV, Su JJ, Williams R. Analysis of N-ras gene mutation and p53 gene expression in human hepatocellular carcinomas. *World J Gastroenterol* 1998; **4**: 97-99
21 **Peng XM**, Peng WW, Yao JL. Codon 249 mutations of p53 gene in development of hepatocellular carcinoma. *World J Gastroenterol* 1998; **4**: 125-127
22 **Berx G,** Nollet F, Strumane K, van Roy F. An efficient and reliable multiplex PCR-SSCP mutation analysis test applied to the human E-cadherin gene. *Hum Mutat* 1997; **9**: 567-574
23 **Peng XM**, Yao CL, Chen XJ, Peng WW, Gao ZL. Codon 249 mutations of p53 gene in non-neoplastic liver tissues. *World J Gastroenterol* 1999; **5**: 324-326
24 **Weng ML**, Li JG, Gao F, Zhang XY, Wang PS, Jiang XC. The mutation induced by space conditions in Escherichia coli. *World J Gastroenterol* 1999; **5**: 445-447
25 **Elledge RM,** Fuqua SA, Clark GM, Pujol P, Allred DC, William L. McGuire Memorial Symposium. The role and prognostic significance of p53 gene alterations in breast cancer. *Breast Cancer Res Treat* 1993; **27**: 95-102
26 **Yamada K,** Mori A, Seki M, Kimura J, Yuasa S, Matsuura Y, Miyamura T. Critical point mutations for hepatitis C virus NS3 proteinase. *Virology* 1998; **246**: 104-112
27 **Qin Y**, Li B, Tan YS, Sun ZL, Zuo FQ, Sun ZF. Polymorphism of p16INK4a gene and rare mutation of p15INK4b gene exon2 in primary hepatocarcinoma. *World J Gastroenterol* 2000; **6**: 411-414
28 **Wang Y**, Liu H, Zhou Q, Li X. Analysis of point mutation in site 1896 of HBV precore and its detection in the tissues and serum of HCC patients. *World J Gastroenterol* 2000; **6**: 395-397
29 **Wang XJ**, Yuan SL, Li CP, Iida N, Oda H, Aiso S, Ishikawa T. Infrequent p53 gene mutation and expression of the cardia adenocarcinomas from a high-incidence area of Southwest China. *World J Gastroenterol* 2000; **6**: 750-753
30 **He XS**, Su Q, Chen ZC, He XT, Long ZF, Ling H, Zhang LR. Expression, deletion and mutation of p16 gene in human gastric cancer. *World J Gastroenterol* 2001; **7**: 515-521
31 **Yuan P**, Sun MH, Zhang JS, Zhu XZ, Shi DR. APC and K-ras gene mutation in aberrant crypt foci of human colon. *World J Gastroenterol* 2001; **7**: 352-356
32 **Fang DC**, Luo YH, Yang SM, Li XA, Ling XL, Fang L. Mutation analysis of APC gene in gastric cancer with microsatellite instability. *World J Gastroenterol* 2002; **8**: 787-791
33 **Liu H**, Wang Y, Zhou Q, Gui SY, Li X. The point mutation of p53 gene exon7 in hepatocellular carcinoma from Anhui Province, a non HCC prevalent area in China.*World J Gastroenterol* 2002; **8**: 480-482
34 **Liao C**, Zhao MJ, Zhao J, Song H, Pineau P, Marchio A, Dejean A, Tiollais P, Wang HY, Li TP. Mutation analysis of novel human liver-related putative tumor suppressor gene in hepatocellular carcinoma. *World J Gastroenterol* 2003; **9**: 89-93
35 **Zheng M**, Liu LX, Zhu AL, Qi SY, Jiang HC, Xiao ZY. K-ras gene mutation in the diagnosis of ultrasound guided fine-needle biopsy of pancreatic masses. *World J Gastroenterol* 2003; **9**: 188-191
36 **Klein B**, Weirich G, Brauch H. DHPLC-based germline mutation screening in the analysis of the VHL tumor suppressor gene: usefulness and limitations. *Hum Genet* 2001; **108**: 376-384
37 **Xiao W**, Oefner PJ. Denaturing high-performance liquid chromatography: A review. *Hum Mutat* 2001; **17**: 439-474
38 **Arnold N**, Gross E, Schwarz-Boeger U, Pfisterer J, Jonat W, Kiechle M. A highly sensitive, fast, and economical technique for mutation analysis in hereditary breast and ovarian cancers. *Hum Mutat* 1999; **14**: 333-339
39 **Jones AC**, Austin J, Hansen N, Hoogendorn B, Oefner PJ, Cheadle JP, O'Donovan MC. Optimal temperature selection for mutation detection by denaturing HPLC and comparison to single-stranded conformation polymorphism and heteroduplex analysis. *Clin Chem* 1999; **45**(8 Pt 1): 1133-1140
40 **Roberts PS**, Jozwiak S, Kwiatkowski DJ, Dabora SL. Denaturing high-performance liquid chromatography (DHPLC) is a highly sensitive, semi-automated method for identifying mutations in the TSC1 gene. *J Biochem Biophys Methods* 2001; **47**: 33-37
41 **Fukunaga M**, Monden T, Nakanishi H, Ohue M, Fukuda K, Tomita N, Shimano T, Mori T. Immunohistochemical study of p53 in gastric carcinoma. *Am J Clin Pathol* 1994; **101**: 177-180
42 **Tamura G**, Kihana T, Nomura K, Terada M, Sugimura T, Hirohashi S. Detection of frequent p53 gene mutations in primary gastric cancer by cell sorting and polymerse chain single-strand conformation polymorhism analysis. *Cancer Res* 1991; **51**: 3056-3058
43 **Dong SM**, Sidransky D. Absence of ST7 gene alterations in human cancer. *Clin Cancer Res* 2002; **8**: 2939-2941
44 **Hughes KA**, Hurlstone AF, Tobias ES, McFarlane R, Black DM. Absence of ST7 mutations in tumor-derived cell lines and tumors. *Nat Genet* 2001; **29**: 380-381
45 **Thomas NA,** Choong DY, Jokubaitis VJ, Neville PJ, Campbell IG. Mutation of the ST7 tumor suppressor gene on 7q31.1 is rare in breast, ovarian and colorectal cancers. *Nat Genet* 2001; **29**: 379-380

Edited by Xu JY and Wang XL

P.O.Box 2345, Beijing 100023,China
Fax: +86-10-85381893
E-mail: wjg@wjgnet.com www.wjgnet.com

World J Gastroenterol 2003;9(12):2666-2670
World Journal of Gastroenterology
 ISSN 1007-9327

• LIVER CANCER •

Hepatic arterial infusion chemotherapy for hepatocellular carcinoma with tumor thrombosis of the portal vein

Yung-Chih Lai, Cheng-Yen Shih, Chin-Ming Jeng, Sien-Sing Yang, Jui-Ting Hu, Yung-Chuan Sung, Han-Ting Liu, Shaw-Min Hou, Chi-Hwa Wu, Tzen-Kwan Chen

Yung-Chih Lai, Cheng-Yen Shih, Sien-Sing Yang, Jui-Ting Hu, Yung-Chuan Sung, Han-Ting Liu, Chi-Hwa Wu, Tzen-Kwan Chen, Department of Internal Medicine, Cathay General Hospital, Taipei, Taiwan, China
Chin-Ming Jeng, Department of Radiology, Cathay General Hospital, Taipei, Taiwan, China
Shaw-Min Hou, Department of Surgery, Cathay General Hospital, Taipei, Taiwan, China
Correspondence to: Dr. Yung-Chih Lai, Department of Internal Medicine, Cathay General Hospital, 280, Jen-Ai Road, Section 4, Taipei 106, Taiwan, China. yungchihlai@hotmail.com
Telephone: +86-2-27082121 Ext.3120 **Fax:** +86-2-27074949
Received: 2003-09-06 **Accepted:** 2003-10-12

Abstract

AIM: Hepatocellular carcinoma (HCC) with portal vein tumor thrombosis (PVTT) is associated with poor prognosis. The aim of this prospective study was to evaluate the efficacy of hepatic arterial infusion chemotherapy (HAIC) for patients with this disease.

METHODS: Eighteen HCC patients with PVTT were treated with HAIC via a subcutaneously implanted injection port. A course of chemotherapy consisted of daily cisplatin (10 mg for one hour) followed by 5-fluorouracil (250 mg for five hours) for five continuous days within a given week. The patients were scheduled to receive four consecutive courses of HAIC. Responders were defined in whom either a complete or partial response was achieved, while non-responders were defined based on stable or progressive disease status. The prognostic factors associated with survival after treatment were analyzed.

RESULTS: Six patients exhibited partial response to this form of HAIC (response rate = 33 %). The 3, 6, 9, 12 and 18-month cumulative survival rates for the 18 patients were 83 %, 72 %, 50 %, 28 %, and 7 %, respectively. Median survival times for the six responders and 12 non-responders were 15.0 (range, 11-18) and 7.5 (range, 1-13) months, respectively. It was demonstrated by both univariate and multivariate analyses that the therapeutic response and hepatic reserve function were significant prognostic factors.

CONCLUSION: HAIC using low-dose cisplatin and 5-fluorouracil may be a useful alternative for the treatment of patients with advanced HCC complicated with PVTT. There may also be survival-related benefits associated with HAIC.

Lai YC, Shih CY, Jeng CM, Yang SS, Hu JT, Sung YC, Lin HT, Hou SM, Wu CH, Chen TK. Hepatic arterial infusion chemotherapy for hepatocellular carcinoma with tumor thrombosis of the portal vein. *World J Gastroenterol* 2003; 9(12): 2666-2670
http://www.wjgnet.com/1007-9327/9/2666.asp

INTRODUCTION

Hepatocellular carcinoma (HCC) is one of the most common malignancies worldwide, especially in Asia and South Africa[1]. The incidence of HCC has increased over the past decade, and it has become the leading cause of death among patients with cirrhosis[2]. Despite the marked progress in diagnostic techniques and therapeutic procedures, the prognosis for HCC patients remains discouraging. Surgical resection or liver transplantation for these individuals is frequently not feasible due to poor hepatic reserve function, advanced HCC stage, and/or lack of suitable donor livers[3,4]. In past studies, the median survival period for unresectable HCC cases has been only a few months. The survival rate for patients with advanced HCC with portal vein tumor thrombosis (PVTT) was even worse[5-8]. It has been reported that patients with diffuse HCC complicated with PVTT survived only 1-2 months if effective treatment could not be delivered[9]. Transcatheter arterial embolization (TAE), microwave coagulation therapy (MCT), radiofrequency ablation (RFA), and percutaneous ethanol injection (PEI) were all of limited value for such patients[10,11]. Systemic chemotherapy has also been trialed in cases of this type, but without any appreciable survival benefit[12].

Recent advances in implantable drug delivery systems have made it possible to administer repeated arterial infusion of chemotherapy agents[13,14]. Hepatic arterial infusion chemotherapy (HAIC) has the advantages of increased local drug concentrations and a reduction in systemic side effects, making it appropriate, therefore, as a palliative treatment for patients with advanced, unresectable HCC complicated with PVTT. Several authors in this field have reported the efficacy of HAIC[15], with favorable results achieved by a regimen consisting of cisplatin and 5-fluorouracil (5-FU)[16-18]. Based on these considerations, the aim of our prospective study was to evaluate the efficacy of low-dose cisplatin and 5-FU chemotherapy for cases of advanced HCC with PVTT, and analyze the clinical results.

MATERIALS AND METHODS

Patients

From June 1, 2000 to May 31, 2003, twenty patients with unresectable HCC complicated with PVTT received HAIC at the Department of Internal Medicine, Cathay General Hospital. The treatment consisted of low-dose cisplatin and 5-FU delivered via a subcutaneously implanted injection port. Given the severity of HCC or coexisting liver cirrhosis, these patients were not suitable for either surgical resection[4] or nonsurgical treatments such as MCT[19], RFA[20], PEI[21], or TAE[22]. Of the initial 20 subjects, two withdrew due to technical difficulties associated with the indwelling catheter. These were related to the excessive size of the tumor, which hindered insertion of the catheter in one case; and stenosis of the hepatic artery in the other. In total, 18 patients were enrolled in the current study. Informed consent was obtained from all the subjects before the start of the investigation. The diagnosis of HCC was made by histopathology and/or imaging study. Of the 18 diagnoses, six were proven by histopathology and 12 were confirmed clinically using imaging studies, including ultrasonography

(US), computed tomography (CT), angiography, and magnetic resonance imaging, and/or based on a high plasma level of α-fetoprotein (AFP). There were no distant metastases at the time of commencement of the interventional therapy. Patients with any evidence of cardiac disease (congestive heart failure or history of myocardial infarction within the previous three months), severe vascular disease or uncontrolled concomitant infection were excluded. The exlusion criteria also included hepatic encephalopathy, hepatorenal syndrome, gastrointestinal bleeding, refractory ascites, serum bilirubin >5 mg/dl, serum creatinine >1.8 mg/dl, WBC count <3 000/mm^3, and platelet count <30 000/mm^3. The presence of PVTT was confirmed in all the cases by demonstration of one of the following: an intraluminal mass in the portal vein or portal branch from US or enhanced CT scan[23]; the "thread-and streaks" sign or arterioportal shunts on hepatic angiography[24]; or filling defects in the portal vein or in the portal branch as noted in an indirect portogram obtained from a venous phase angiogram of the superior mesenteric artery.

The clinical characteristics for the 18 HAIC-treated HCC patients with PVTT are shown in Table 1. The average age of the 16 male and two female patients was 56.9 (range, 43-75) years. Thirteen individuals were infected with hepatitis B virus (HBV) and five with hepatitis C virus (HCV). The Child-Pugh' s staging classification was used to estimate the degree of hepatic reserve function[25]. Ten patients had a past history of HCC treatment using surgery and/or TAE. The PVTT grading and tumor-extent rating were evaluated using the criteria of the Liver Cancer Study Group of Japan[26]. The PVTT grading was based on the location of the tumor thrombus in the portal vein as follows: Vp1, tumor thrombus in a third or more of the peripheral branch of the portal vein; Vp2, tumor thrombus in a second branch of the portal vein; and, Vp3, tumor thrombus in the first branch or trunk of the portal vein. Tumor-extent rating was estimated from imaging study. The rating system was based on the tumor-extent percentage (E): E1, less than 20 % of the whole liver; E2, 20-40 % of the whole liver; E3, 40-60 % of the whole liver; and, E4, greater than 60 % of the whole liver.

Catheter-implantation technique

The hepatic artery was catheterized using a femoral approach. The tip of the catheter was placed in the proper hepatic artery after HCC localization. The other end of the catheter was connected to the injection port which was implanted in a subcutaneous pocket in the right lower abdominal quadrant[16]. The gastroduodenal artery was occluded using steel coils to prevent injury to the gastrointestinal tract from exposure to the chemotherapy agents[15,16]. Heparin solution was infused regularly via the injection port to keep the catheter from occluding.

Chemotherapeutic regimen

After the set up of drug delivery system, the patients began to receive repeated arterial infusions of chemotherapy agents via the injection port. One course of chemotherapy consisted of cisplatin (10 mg per day) followed by 5-FU (250 mg per day) for five continuous days, with the patients resting on days 6 and 7. Both the cisplatin and 5-FU were administered by a mechanical infusion pump set at a rate of 10 mg for 1 hour and 250 mg for 5 hours, respectively[16]. Basically, the patients were expected to undergo four consecutive courses of chemotherapy, and then they were deemed to have completed HAIC. HAIC was considered incomplete for patients whose chemotherapy was suspended before the completion of the four consecutive courses because of adverse reactions or complications. Maintenance therapy based on the above regimen (cisplatin 10 mg and 5-FU 250 mg for one day) was continued every two weeks after the completion of the initial four courses of the HAIC, with duration depending on tumor response, hepatic function, adverse reactions, and complications.

Assessment of therapeutic response

Abdominal US and CT were performed regularly (every 2-3 and 4-6 months, respectively) to measure the size of the tumor. Local response to treatment was classified according to World Health Organization criteria[27]. Complete response (CR) was defined as the complete disappearance of all known disease, and no new lesions, as determined from two observations no less than four weeks apart. Partial response (PR) was deemed to have occurred where there was a greater than 50 % reduction in total tumor load for all measurable lesions, as determined by two observations no less than four weeks apart. Stable disease (ST) did not qualify for CR/PR or progressive disease (PD) status, with the latter defined as a greater than 25 % increase in the size of one or more measurable lesions or the appearance of new lesions.

Statistical analysis

The Kaplan and Meier method was used to plot the estimated survival curves from the first day of treatment to the last day of follow-up. The results of the univariate analysis were compared to those from the log-rank test to identify predictors of survival. The results of the multivariate analysis were then investigated using Cox' s proportional hazards model. A *P* value less than 0.05 was considered to be statistically significant.

RESULTS

Therapeutic response and patient survival

The salient clinical characteristics for the patients are presented in Table 1. Fifteen patients completed HAIC, while three did not complete the initial four courses series because of deteriorating liver function, sepsis, and gastric ulcer bleeding, respectively. Overall the CR, PR, ST, and PD in response to chemotherapy were zero (0 %), six (33 %), seven (39 %), and five (28 %) in the 18 patients respectively. The response rate (CR and PR/all patients) was 33 %.

Table 1 Clinical characteristics of the 18 patients with hepatocellular carcinoma

Characteristics	*n*
Gender (male / female)	16 / 2
Age (younger than 60 yrs / 60 yrs and older)	9 / 9
HBV / HCV	13 / 5
Child-Pugh's stage (A / B / C)	7 / 7 / 4
Previous treatment (yes / no)	10 / 8
Serum AFP (<1 000 ng.ml^{-1} / ⩾1 000 ng.ml^{-1})	6 / 12
Tumor location (unilobe / bilobe)	10 / 8
Tumor type (nodular / massive / diffuse)	7 / 6 / 5
Maximum tumor size (<5 cm / ⩾5 cm)	13 / 5
Tumor extent (E1 / E2 / E3 / E4)[a]	1 / 6 / 7 / 4
Grade of portal vein invasion (Vp1 / Vp2 / Vp3)[bc]	0 / 5 / 13
Completion of protocol (yes / no)	15 / 3
Therapeutic response (CR / PR / ST / PD)	0 / 6 / 7 / 5

HBV: hepatitis B virus; HCV: hepatitis C virus; AFP: α-fetoprotein; Vp: portal vein tumor thrombosis; CR: complete response; PR: partial response; ST: stable disease; PD: progressive disease. [a]Tumor extent. Tumor replacement of liver parenchyma: E1, <20 %; E2, 20-40 %; E3, 40-60 %; E4,>60 %. [bc]Portal vein invasion. Vp1: in a third or more of the peripheral branch; Vp2: in the second branch; Vp3: in the first branch or trunk.

The cumulative survival for the 18 patients is shown in Figure 1. The 3, 6, 9, 12, 15 and 18-month cumulative survival rates for all the 18 patients were 83 %. 72 %, 50 %, 28 %, 14 %, and 7 %, respectively. While for the six responders (CR and PR), the 3, 6, 9, 12, 15 and 18-month cumulative survival rates were 100 %, 100 %, 100 %, 67 %, 44 %, and 22 %, respectively. The median survival time for the 18 HAIC-treated patients was 9.5 (range, 1-18) months.

The median survival times for the six responders (CR and PR) and the 12 non-responders (ST and PD) were 15.0 (range, 11-18) and 7.5 (range, 1-13) months, respectively. Based on hepatic reserve function, the median survival times for Child-Pugh' s stages A, B, and C were 13.0 (range, 11-18), 8.0 (range, 2-15), and 3.5 (range, 1-9) months, respectively.

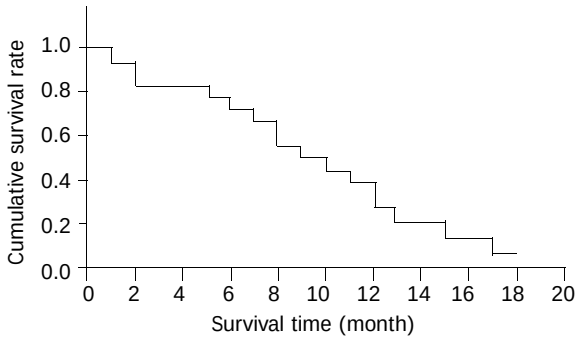

Figure 1 Cumulative survival for 18 hepatocellular carcinoma patients with portal vein tumor thrombosis undergoing hepatic arterial infusion chemotherapy. The 3, 6, 9, 12, 15 and 18-month cumulative survival rates for the 18 patients were 83 %, 72 %, 50 %, 28 %, 14 %, and 7 %, respectively.

Prognostic factors related to survival

Two of the 13 factors was demonstrated to have prognostic significance using univariate analysis: Child-Pugh' s stage (P=0.001) and therapeutic response (P<0.001; Table 2). Multivariate analysis also confirmed these two variables as independent predictors of survival (P=0.005 and 0.001, respectively). None of the other factors were significantly related to patient survival.

Serial computed tomography (CT) revealed progressive improvement in a 55-year-old male patient with HCC complicated with PVTT who presented with a good partial response to HAIC (Figure 2). The huge tumor was decreased markedly from 14×10×9 cm initially to 5×5×3 cm after four months of HAIC.

Table 2 Factors associated with cumulative survival of patients by univariate analysis (log-rank test)

	P value*
Gender (male / female)	0.950
Age (younger than 60 yrs / 60 yrs and older)	0.948
HBV / HCV	0.825
Child-Pugh's stage (A / B / C)	0.001
Previous treatment (yes / no)	0.753
Serum AFP (<1 000 ng.ml^{-1} / ⩾1 000 ng.ml^{-1})	0.994
Tumor location (unilobe / bilobe)	0.938
Tumor type (nodular / massive / diffuse)	0.541
Maximum tumor size (<5 cm / ⩾5 cm)	0.761
Tumor extent (E1 / E2 / E3 / E4)[ac]	0.429
Grade of portal vein invasion (Vp1 / Vp2 / Vp3)[bd]	0.309
Completion of protocol (yes / no)	0.155
Therapeutic response (CR / PR / ST / PD)	<0.001

HBV: hepatitis B virus; HCV: hepatitis C virus; AFP: α-fetoprotein; Vp: portal vein tumor thrombosis; CR: complete response; PR: partial response; ST: stable disease; PD: progressive disease. [ac]Tumor extent. Tumor replacement of liver parenchyma: E1,<20 %; E2, 20-40 %; E3, 40-60 %; E4,>60 %. [bd]Portal vein invasion. Vp1: in a third or more of the peripheral branch; Vp2: in the second branch; Vp3: in the first branch or trunk.

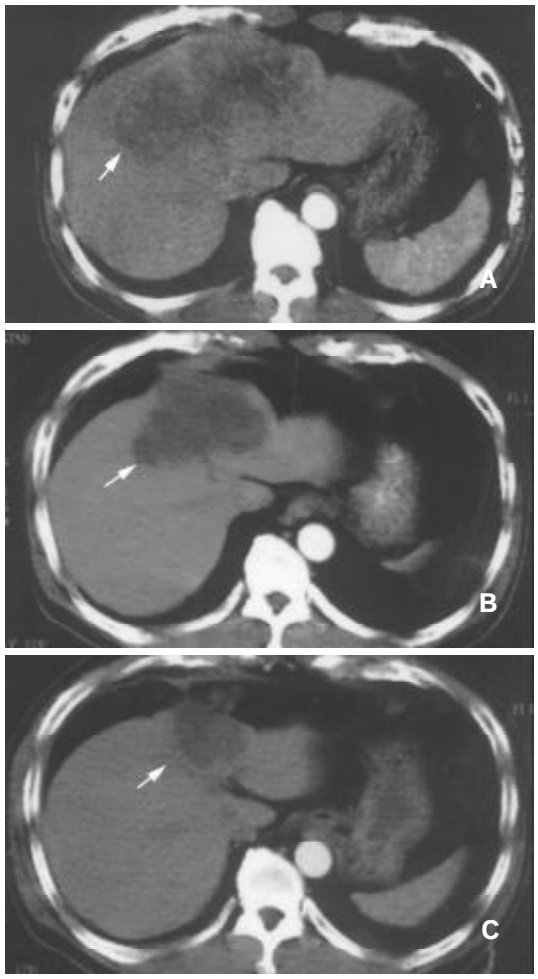

Figure 2 Image study using abdominal computed tomography (hepatic artery phase) of an HCC patient with good partial response to hepatic arterial infusion chemotherapy (HAIC) shows a marked decrease in tumor size from 14×10×9 cm (A: before HAIC) to 9×8×7 cm (B: 1.5 months after initiation of HAIC) and 5×5×3 cm (C: 4 months after initiation of HAIC).

Side effects and complications

The most common adverse reactions to HAIC were nausea and loss of appetite (five cases, 28 %). Two patients (11 %) experienced leukopenia and thrombocytopenia, with one of them unable to continue the chemotherapy due to severe leukopenia. Peptic ulcer was a complication in one case and renal damage in another. Deterioration of liver function occurred in two individuals, causing one of them to quit therapy. Most of these side effects were managed using medical treatment and were not considered serious.

Complications associated with the indwelling catheter were obstruction (n=2), infection (n=2), dislocation of the catheter tip (n=1), and hematoma around the injection port (n=1). All these technical problems were overcome by medical treatment, infusion of heparin solution, or implantation of a new catheter.

Causes of death

Two patients survived the follow-up period. The remaining 16 patients expired, ten (63 %) due to cancer-related causes.

Of these, seven were as a result of tumor extension and three due to tumor rupture. Three individuals (19 %) died of gastrointestinal bleeding; of the rest, three (19 %) died of sepsis related to pneumonia (*n*=2) or urinary tract infection (*n*=1).

DISCUSSION

A standard optimal therapy for advanced unresectable HCC is still lacking[28] . HCC has a high predilection for portal vein invasion, which has been shown to be a poor prognostic factor[5-8]. Although surgery may be considered for some HCC patients with PVTT[6], most are not suitable for this invasive treatment because of dissemination of the tumor throughout the liver, or the coexistence of cirrhotic change. The presence of tumoral portal invasion precludes most potential curative interventions such as TAE, PEI, MCT, and RFA[7]. Further, liver transplantation is not indicated for such patients. Additionally, systemic chemotherapy, hormonal therapy, and IFN therapy are all reported to be of limited value[1,11].

Most of the blood supply to HCC is derived from the hepatic artery, whereas the portal vein supplies the normal liver parenchyma. It is reasonable to assume, therefore, that intra-arterial administration of cytotoxic agents may facilitate delivery of a higher therapeutic concentration to the tumor tissue[29]. Both cisplatin and 5-FU have an anti-tumor effect[30]. In addition, cisplatin plays a synergistic role as a modulator of 5-FU, inhibiting the transport of neutral amino acids, including L-methionine, into tumor cells, and resulting in enhancement of its antitumor effects[31]. Additionally, the combination of cisplatin and 5-FU allows low-dose administration with an associated reduction in adverse reactions. Hepatic extraction of chemotherapeutic agents can result in minimal systemic concentrations of these agents and, thus, minimize systemic toxicity[32] .

In comparison to analogous research, more patients were enrolled in the study of Ando *et al*., (2002), with an HAIC response rate and median survival duration of 48 % and 10.2 (range, 1.7-76.9) months, respectively for their 48 patients with PVTT[18] . By comparison, our response rate and median survival time was 33.3 % and 9.5 (range, 1-18) months, respectively. Moreover, the median survival time for our six responders and 12 non-responders were 15.0 (range, 11-18) and 7.5 (range, 1-13) months, respectively. In the above larger study, the median survival times for the 23 responders and 25 non-responders were 31.6 (range, 9.3-76.9) and 5.4 (range, 1.9-29.0) months, respectively[18]. The longest follow-up for a survivor in their study was 76.9 months, whereas it was only 18 months in our investigation. This variation in the follow-up period may account for the difference in the results outlined above. More cases are needed to continue this study and deliver a more comprehensive and accurate result. Even in our non-responder group, however, the median survival time was 7.5 months, which is still longer than analogous reports[5,7]. The reason that some tumors responded to HAIC, and others not, was not determined in the current study, however. This critical piece of information awaits further investigations, including immunological and/or molecular biological study of tumor cells, to reveal the underlying causes.

In an evaluation of HCC prognosis conducted by the Liver Cancer Study Group of Japan, the severity of any associated cirrhosis, and the size and number of lesions were independent predictive factors[33]. In our study, however, only hepatic reserve function and the patient' s therapeutic response were associated with survival. This difference may result from variations in the patient-enrollment criteria. Our subjects were confined to cases of unresectable HCC with PVTT. In such advanced-stage patients, the influence of lesion size and number on survival is no longer significant. Cirrhosis-related complications (e.g. hepatic failure, variceal bleeding, and spontaneous bacterial peritonitis) were known to play key roles in HCC mortality[34]. The patients with more-favorable Child-Pugh' s classifications have fewer complications and may thus have better and more-favorable outcomes.

Kupffer cells and polymorphonuclear cell function are depressed in liver cirrhosis. The serum also shows a reduction in factors such as fibronectin, opsonins and chemo-attractants, including members of the complement system[35,36]. The hepatic cellular-immune responses, which involve natural killer cells, cytotoxic T lymphocytes and macrophages (Kupffer cells), and their cytotoxic reactions against tumor cells are important as a defense mechanism against hepatocarcinogenesis[37]. In cases of poor residual liver function, the complex molecular and cellular mechanisms, which prevent tumor formation and further development and spread of established tumors, are impaired[38]. Therefore, the prognosis for advanced HCC occurring in such patients is inevitably bleak and dismal.

Chemotherapeutic toxicity was infrequent in our study. Myelosuppression was noted in two cases, and deterioration of liver function also diagnosed in two individuals. The most common adverse reaction, nausea or loss of appetite, was related to the gastrointestinal tract.

Although the survival of HCC patients with PVTT can be improved using HAIC, the results remain unsatisfactory. Further research and investigation is still necessary. Combined therapy, consisting of an intra-arterial infusion of a cytotoxic agent and systemic administration of interferon-α was reportedly useful as a palliative treatment for HCC patients with major vascular involvement[1]. Additional therapy following HAIC, including surgery, MCT, PEI, and extra chemotherapy, might be another option for the prolongation of survival in advanced HCC patients[18,39]. Moreover, the identification of tumors which are more sensitive to cytotoxic agents, and the reason for this are also important areas for future research.

In conclusion, the use of HAIC improves the survival of HCC patients with PVTT. Further, most of the side effects are transient and well tolerated. Hepatic reserve function and therapeutic response are the most important survival-related prognostic factors. Based on our findings, therefore, it seems reasonable to suggest that HAIC is a safe and effective alternative for the treatment of advanced HCC.

REFERENCES

1 **Chung YH**, Song H, Song BC, Lee GC, Koh MS, Yoon HK, Lee YS, Sung KB, Suh DJ. Combined therapy consisting of intraarterial cisplatin infusion and systemic interferon-α for hepatocellular carcinoma patients with major poral vein thrombosis or distant metastasis. *Cancer* 2000; **88**: 1986-1991

2 **EI-Serag HB**, Mason AC. Rising incidence of hepatocellular carcinoma in United States. *N Engl J Med* 1999; **340**: 745-750

3 **Bismuth H**, Chiche L, Adam R, Castaing D, Diamond T, Dennison A. Liver resection versus transplantation for hepatocellular carcinoma in cirrhotic patients. *Ann Surg* 1993; **218**: 145-151

4 **Nagasue N**, Uchida M, Makino Y, Takemoto Y, Yamanoi A, Hayashi T, Chang YC, Kohno H, Nakamura T, Yukaya H. Incidence and factors associated with intrahepatic recurrence following resection of hepatocellular carcinoma. *Gastroenterology* 1993; **105**: 488-494

5 **Okuda K**, Ohtsuki T, Obata H, Tomimatsu M, Okazaki N, Hasegawa H, Nakajima Y, Ohnishi K. Natural history of hepatocellular carcinoma and prognosis in relation to treatment. Study of 850 patients. *Cancer* 1985; **56**: 918-928

6 **Fujii T**, Takayasu K, Muramatsu Y Moriyama N, Wakao F, Kosuge T, Takayama T, Makuuchi M, Yamasaki S, Okazaki N. Hepatocellular carcinoma with portal tumor thrombus: analysis of factors determining prognosis. *Jpn J Clin Oncol* 1993; **23**: 105-109

7 **Llovet JM**, Bustamante J, Castells A, Vilana R, Ayuso Mdej C, Sala M, Bru C, Rodes J, Bruix J. Natural history of untreated nonsurgical hepatocellular carcinoma: rationale for the design and evaluation of therapeutic trials. *Hepatology* 1999; **29**: 62-67

8 **Fan J**, Wu ZQ, Tang ZY, Zhou J, Qiu SJ, Ma ZC, Zhou XD, Ye SL. Multimodality treatment in hepatocellular carcinoma patients with tumor thrombi in portal vein. *World J Gastroenterol* 2001; **7**: 28-32

9 **Cady B**. Natural history of primary and secondary tumors of the liver. *Semin Oncol* 1983; **10**: 127-134

10 **Sakurai M**, Okamura J, Kuroda C. Transcatheter chemo-embolization effective for treating hepatocellular carcinoma: A histopathologic study. *Cancer* 1984; **54**: 387-392

11 **Bruix J**. Treatment of hepatocellular carcinoma. *Hepatology* 1997; **25**: 259-262

12 **Friedman M**. Primary hepatocellular cancer-present results and future prospects. *Int J Radiat Oncol Biol Phys* 1983; **9**: 1841-1850

13 **Iwamiya T**, Sawada S, Ohta Y. Repeated arterial infusion chemotherapy for inoperable hepatocellular carcinoma using an implantable drug delivery system. *Cancer Chemother Pharmacol* 1994; **33**(Suppl): S134-138

14 **Une Y**, Uchino J, Yasuhara M, Misawa K, Kamiyama T, Shimamura T, Sato N, Nakajima Y, Hata Y. Intra-arterial infusion chemotherapy on unresectable hepatocellular carcinoma under occlusion of hepatic arterial flow. *Clin Ther* 1993; **15**: 347-354

15 **Toyoda H**, Nakano S, Kumada T, Takeda I, Sugiyama K, Osada T, Kiriyama S, Suga T, Takahashi M. The efficacy of continuous local arterial infusion of 5-fluorouracil and cisplatin through an implanted reservoir for severe advanced hepatocellular carcinoma. *Oncology* 1995; **52**: 295-299

16 **Ando E**, Yamashita F, Tanaka M, Tanigawa K. A novel chemotherapy for advanced hepatocellular carcinoma with tumor thrombosis of the main trunk of the poral vein. *Cancer* 1997; **79**: 1890-1896

17 **Itamoto T**, Nakahara H, Tashiro H, Haruta N, Asahara T, Naito A, Ito K. Hepatic arterial infusion of 5-fluorouracil and cisplatin for unresectable or recurrent hepatocellular carcinoma with tumor thrombosis of the poral vein. *J Surg Oncol* 2002; **80**: 143-148

18 **Ando E**, Tanaka M, Yamashita F, Kuromatsu R, Yatani S, Fukumori K, Sumie S, Yano Y, Okuda K, Sata M. Hepatic arterial infusion chemotherapy for advanced hepatocellular carcinoma with portal vein tumor thrombosis: analysis of 18 cases. *Cancer* 2002; **95**: 588-595

19 **Sato M**, Watanabe Y, Ueda S, Iseki S, Abe Y, Sato N, Kimura S, Okubo K, Onji M. Microwave coagulation therapy for hepatocellular carcinoma. *Gastroenterology* 1996; **110**: 1507-1514

20 **Livraghi T**, Goldberg SN, Lazzaroni S, Meloni F, Solbiati L, Gazelle GS. Small hepatocellular carcinoma: treatment with radiofrequency ablation versus ethanol injection. *Radiology* 1999; **210**: 655-661

21 **Shiina S**, Tagawa K, Unuma T, Terano A. Percutaneous ethanol injection therapy for treatment of the hepatocellular carcinoma. *Am J Roentgenol* 1990; **154**: 947-951

22 **Nakamura H**, Hashimoto T, Oi H, Sawada S. Transcatheter oily chemoembolization of hepatocellular carcinoma. *Radiology* 1989; **170**(3 Pt1): 783-786

23 **Mathieu D**, Grenier P, Larde D, Vasile N. Portal vein involvement in hepatocellular carcinoma: dynamic CT features. *Radiology* 1984; **152**: 127-132

24 **Okuda K**, Musha H, Yamasaki T, Jinnouchi S, Nakasaki Y, Kubo Y, Shimokawa Y, Nakayama T, Kojiro M, Sakamoto K, Nakashima T. Angiographic demonstration of intrahepatic arterio-portal anastomoses in hepatocellular carcinoma. *Radiology* 1977; **122**: 53-58

25 **Pugh RN**, Murray-Lyon IM, Dawson JL, Pietroni MC, Williams R. Transection of the oesophagus for bleeding oesophageal varices. *Br J Surg* 1973; **60**: 646-649

26 **The Liver Cancer Study Group of Japan**. Classification of primary liver cancer. 1st Engl edi Tokyo: *Kanehara Shuppan Co* 1997: 14

27 **Tang ZY**, Uy YQ, Zhou XD, Ma ZC, Lu JZ, Lin ZY, Liu KD, Ye SL, Yang BH, Wang HW. Cytoreduction and sequential resection for surgically verified unresectable hepatocellular carcinoma: evaluation with analysis of 72 patients. *World J Surg* 1995; **19**: 784-789

28 **Llovet JM**, Beaugrand M. Hepatocellular carcinoma: present status and future prospects. *J Hepatol* 2003; **38**: S136-149

29 **Sangro B**, Rios R, Bilbao I, Beloqui O, Herrero JI, Quiroga J, Prieto J. Efficacy and toxicity of intra-arterial cisplatin and etoposide for advanced hepatocellular carcinoma. *Oncology* 2002; **62**: 293-298

30 **Scanlon KJ**, Newman EW, Lu Y, Priest DG. Biochemical basis for cisplatin and 5-fluorouracil synergism in human ovarian carcinoma cells. *Proc Natl Acad Sci U S A* 1986; **83**(Suppl): 8923-8925

31 **Shirasaki T**, Shimamoto Y, Ohshimo H, Saito H, Fukushima M. Metabolic basis of the synergistic antitumor activities of 5-fluorouracil and cisplatin in rodent tumor models *in vivo*. *Cancer Chemother Pharmacol* 1993; **32**: 167-172

32 **Ensminger WD**, Gyves JW. Clinical pharmacology of hepatic artery chemotherapy. *Semin Oncol* 1983; **10**: 176-182

33 **The Liver Cancer Study Group of Japan**. Predictive factors for longterm prognosis after partial hepatectomy for patients with hepatocellular carcinoma. *Cancer* 1994; **74**: 2772-2780

34 **Li YH**, Wang CS, Liao LY, Wang CK, Shih LS, Chen RC, Chen PH. Long-term survival of Taiwanese patients with hepatocellular carcinoma after combination therapy with transcatheter arterial chemoembolization and percutaneous ethanol injection. *J Formos Med Assoc* 2003; **102**: 141-146

35 **Imawari M**, Hughes RD, Gove CD, Williams R. Fibronectin and Kupffer cell function in fulminant hepatic failure. *Dig Dis Sci* 1985; **30**: 1028-1033

36 **Rajkovic IA**, Williams R. Abnormalities of neutrophil phagocytosis, intracellular killing, and metabolic activity in alcoholic cirrhosis and hepatitis. *Hepatology* 1986; **6**: 252-262

37 **Wisse E**, Luo D, Vermijlen D, Kanellopoulou C, De Zanger R, Braet F. On the function of pit cells, the liver–specific natural killer cells. *Semin Liver Dis* 1997; **17**: 265-286

38 **Tabor E**. Liver tumors and host defense. *Semin Liver Dis* 1997; **17**: 351-355

39 **Meric F**, Patt YZ, Curley SA, Chase J, Roh MS, Vanthey JN, Ellis LM. Surgery after downstaging of unresectable hepatic tumors with intra-arterial chemotherapy. *Ann Surg Oncol* 2000; **7**: 490-495

Edited by Zhu LH

P.O.Box 2345, Beijing 100023,China
Fax: +86-10-85381893
E-mail: wjg@wjgnet.com www.wjgnet.com

World J Gastroenterol 2003;9(12):2671-2675
World Journal of Gastroenterology
 ISSN 1007-9327

• LIVER CANCER •

Overexpression of HBxAg in hepatocellular carcinoma and its relationship with Fas/FasL system

Xiao-Zhong Wang, Xiao-Chun Chen, Yun-Xin Chen, Li-Juan Zhang, Dan Li, Feng-Lin Chen, Zhi-Xin Chen, Hong-Ying Chen, Qi-Ming Tao

Xiao-Zhong Wang, Xiao-Chun Chen, Yun-Xin Chen, Li-Juan Zhang, Dan Li, Feng-Lin Chen, Zhi-Xin Chen, Hong-Ying Chen, Department of Gastroenterology, Affiliated Union Hospital, Fujian Medical University, Fuzhou 350001, Fujian Province, China
Qi-Ming Tao, Research Institute of Hepatology, Beijing University, Beijing 100044, China
Supported by the Science Foundation of Fujian Province, No.99-Z-162
Correspondence to: Xiao-Zhong Wang, Department of Gastroenterology, Affiliated Union Hospital, Fujian Medical University, Fuzhou 350001, Fujian Province, China. drwangxz@pub6.fz.fj.cn
Telephone: +86-591-3322384
Received: 2003-06-04 **Accepted:** 2003-09-28

Abstract

AIM: To study the expression and serum level of HBxAg, Fas and FasL in tissues of HCC patients, and to assess the relationship between HBxAg and Fas/FasL system.

METHODS: Tissues from 50 patients with HCC were tested for the expression of HBxAg, Fas and FasL by S-P immunohistochemistry. Serum levels of sFas/sFasL and HBsAg/HBeAg were measured by ELISA assay. HBV X gene was detected by PCR in serum and confirmed by automatic sequencing. Fifty cases of liver cirrhosis and 30 normal controls were involved in serum analysis.

RESULTS: The expression of HBxAg, Fas and FasL in carcinoma tissues was 96 %, 84 % and 98 %, respectively. Staining of HBxAg, Fas and FasL was observed predominately in cytoplasms, no significant difference was found in intensity between HBxAg, Fas and FasL ($P>0.05$). HBxAg, Fas and FasL might express in the same area of carcinoma tissues and this co-expression could be found in most patients with HCC. The mean levels of sFas in serum from HCC, cirrhosis and normal controls were 762.29±391.56 $\mu g \cdot L^{-1}$, 835.36±407.33 $\mu g \cdot L^{-1}$ and 238.27±135.29 $\mu g \cdot L^{-1}$. The mean levels of sFasL in serum from HCC, cirrhosis and normal controls were 156.36±9.61 $\mu g \cdot L^{-1}$, 173.63±18.74 $\mu g \cdot L^{-1}$ and 121.96±7.83 $\mu g \cdot L^{-1}$. Statistical analysis showed that both sFas and sFasL in HCC and cirrhosis patients were significantly higher than those in normal controls ($P<0.01$). Serum HBV X gene was found in 32 % of HCC patients and 46 % of cirrhotic patients. There was no significant relationship between serum level of sFas/sFasL and serum X gene detection ($P>0.05$). Eight percent of HCC patients with negative HBsAg and HBeAg in serum might have X gene in serum and HBxAg expression in carcinoma tissues.

CONCLUSION: Our data suggest that HBxAg and Fas/FasL system plays an important role in the development of human HCC. Expression of HBxAg can leads to expression of Fas/FasL system which and reverse apoptosis of hepatocellular carcinoma induced by FasL.

Wang XZ, Chen XC, Chen YX, Zhang LJ, Li D, Chen FL, Chen ZX, Chen HY, Tao QM. Overexpression of HBxAg in hepatocellular carcinoma and its relationship with Fas/FasL system. *World J Gastroenterol* 2003; 9(12): 2671-2675
http://www.wjgnet.com/1007-9327/9/2671.asp

INTRODUCTION

Chronic infection with hepatitis B virus (HBV) is a major risk factor for the development of hepatocellular carcinoma (HCC). The pathogenesis of HBV-induced malignant transformation is incompletely understood[1-3]. HBV X gene encodes a 154 amino acid protein called HBV X protein (HBxAg)[4]. This protein is suspected as an oncogenic molecule responsible for hepatocarcinogenesis because of its multifunctional activities affecting gene transcription, intracellular signal transmission, cell proliferation and apoptotic cell death[5-7]. Of these activities, the best known is its promiscuous transactivation activity[8], which is subjected to complex mechanisms such as protein-protein interaction, regulation of phosphorylation, mRNA stablization and alteration of nucleocytoplasmic translocation[9-11]. Several transgenic mice experiments indicate that mice harboring HBV X gene either develop liver cancer or have accelerated development of neoplasms when they are exposed to other carcinogens[12,13]. HBxAg inhibits the function of tumor suppressor protein P^{53}, which is thought to be an early event in hepatocyte transformation before the later accumulation of inactivating P^{53} point mutations[14]. HBxAg inhibits apoptosis but also exerts pro-apoptotic effects[15,16]. In addition, HBxAg activates cell signaling cascades involving mitogen-activated protein kinase (MAPK) and Janus family tyrosine kinase (JAK) signal transducer and activators of transcription (STAT) pathways[17,18].

The signaling pathway mediated by "death factors" including TNFR1, Fas and TRAILR1 and their cognate ligands is an important mechanism to regulate apoptosis[19]. Fas is the first identified member of "death receptors" and the crosslinking of Fas by its ligand FasL binding leads to conformational changes of Fas, which result in formation of DISC (death induced signaling complex) followed by activation of Caspase-8 and finally induce apoptosis by cleaving their substrates. The Fas/FasL system is likely to play an important role in the regulation of apoptosis including apoptosis of tumor cells[20]. Up-regulation of Fas in the liver has been demonstrated in active viral hepatitis[21]. Human HCC cell lines have been shown to be resistant to Fas-mediated apoptosis[22], but very limited data are available on FasL expression in HCC tissue and its relationship with HBxAg. We investigated the immunohistochemical expression of HBxAg, Fas and FasL in specimens of HCC. The serum level of sFas, sFasL and HBV X gene was also determined.

MATERIALS AND METHODS

Tissue and blood samples

Tumor samples were randomly collected from 50 patients undergoing hepatic resection at the Affiliated Union Hospital

of Fujian Medical University from 1999-2001. Formalin-fixed and paraffin embedded tissues from these samples were used for immunohistochemical analysis. The diagnosis of each tumor was confirmed by pathologists. Blood samples of the tumor patients were taken from the cubital vein on day 3 of hospital admission before the tumor resection. Serum was separated within 30 minutes in a refrigerated centrifuge at 4 ℃, centrifuged at 1 000 g for 5 minutes and stored at –70 ℃ until analysis of sFas/sFasL and HBsAg/HBeAg. Anti- HCV analysis was also performed in order to exclude HCV-positive HCC. The sera of 50 patients with hepatic cirrhosis and 30 normal controls from the blood donators were enrolled in this study. Diagnosis of cirrhotic patients was made on the basis of clinical history, clinical examinations, laboratory findings, gastroscopy and ultrasonography. All the patients had decompensated cirrhosis complicated with ascites, variceal bleeding, or hepatic encephalopathy without infection. All the cirrhotic patients had no HCV infection and alcoholic cirrhosis.

Immunohistochemical analysis

Immunohistochemical staining of HBxAg, Fas and FasL was performed by S-P method. Paraffin embedded sections of 4 μm thickness were cut from the resected tumor samples and transferred onto glass slides. The slides were dewaxed and re-hydrated through a graded descending alcohol series (100 %, 90 %, and 70 %). The slides' endogenous peroxidase activity was blocked by covering the sections with freshly prepared 0.5 % H_2O_2 in methanol, the slides were incubated with horse serum (Vector Laboratories) to block non-specific binding of antibodies. Then, the slides were incubated with a 1:100 dilution of mouse anti-HBx monoclonal antibody, a 1:100 dilution of rabbit polyclonal anti-Fas and anti-FasL antibodies (Maixin-Bio) respectively, washed and incubated with secondary antibody. The slides were subsequently incubated with a freshly prepared 0.1 % v/v diaminobenzidine/TBS solution and counter-stained with haematoxylin. Stained slides were differentiated in acid alcohol prior to blueing in Scott' s solution (Sigma), followed by a wash in running tap water. Finally, the sections were dehydrated through a graded ascending (70 %, 90 %, and 100 %) alcohol series and mixed xylenes on the resulting slides, the sites of immunoperoxidase activity were stained brown and nuclei were blue. As a negative control for HBxAg immunohistochemistry, we used nonimmune mouse serum instead of HBxAg antibody. As negative controls of Fas and FasL, we used nonimmune sera of rabbits. The reaction for immunohistochemistry was evaluated as strong (3+), moderate (2+), weak (+) or negative (-).

DNA extraction and PCR amplification

DNA was extracted from the serum by using phenol-chloroform extracting method. In brief, the serum was mixed with phenol-chloroform-iso-pentanol (volume fraction 25:24:1). After centrifugation at 10 000 g for 10 minutes at 4 ℃. The supernatant was stored in 0.1 M sodium citrate and 100 % ethanol for 30 mintues at -20 ℃. The resulting pellet was dissolved in sterilized water. The sequences of oligonucleotide primers optimized to X region were 5' -ACGGAATTCATGGCTGCTAGGCTGTG-3', 3' -ATCCTGCAGAGGTGAAAAAGTTGCAT-5', respectively. PCR was carried in a final volume of 50 μl containing 5 μl of DNA solution, 20 pmol of each primer, 50 mM of each dNTP, PCR buffer (10 mmol· L^{-1} Tris-HCl, 50 mmol· L^{-1} KCl, 1.5 mmol· L^{-1} $MgCl_2$, 0.001 % gelatin), and 2.5 units of Taq DNA polymerase. Each PCR was as follows: 35 cycles of at 93 ℃ for 30 seconds, at 55 ℃ for 1 minute and at 72 ℃ for 1 minute. The resulting PCR products were separated in a 1 % agarose gel. Assessment of the positive results of PCR was essentially performed on ethidium bromide-stained gel. To confirm the results, PCR products of a positive sample were analyzed by automatic sequencing (Shanghai Shenggong).

Enzyme-linked immunosorbent assay

Serum level of sFas, sFasL, HBsAg and HBeAg was measured using a sandwich enzyme-linked immunosorbent assay (ELISA). Commercially available ELISA kits of sFas, sFasL, HBsAg and HBeAg (MBL) were used. ELISA was performed according to the manufacturer' s instructions. Briefly, diluted serum samples were added in duplicate to 96-well plates coated with antibody and incubated at 37 ℃ for 2 hours. After each well was washed five times with washing buffer (saline containing 0.05 % Tween20), peroxidase-labeled secondary antibody was added to each well and the plate was incubated at 37 ℃ for 1 hour. After each well was washed in a similar manner, the plate was incubated with tetramethylbenzine at room temperature for 20 minutes. The reaction was stopped by adding 1 N sulfuric acid. Optical density was measured at 450 nm using a spectrophotometric microtiter plate reader. The concentration of sample was determined from a standard curve.

Statistical analysis

The expression of HBxAg, Fas and FasL was analyzed using Redit analysis. The sFas and sFasL levels were expressed as mean ±SD, and analyzed using *t*-test. *P* value less than 0.05 was regarded as significant.

RESULTS

Expression of HBxAg and Fas/FasL system

HBxAg, Fas and FasL were detected in the majority of specimens from HCC patients. The results are summarized in Table 1. In most specimens HBxAg, Fas and FasL were detectable in a large number of carcinoma cells(Figures 1-3). No significant differences were found in the expression degrees of HBxAg whether the HCC patients were sero-positive in HBsAg/HBeAg or not ($P>0.05$). Staining of HBxAg, Fas and FasL was observed predominantly in cytoplasms, but no significant difference was found in intensity between HBxAg and Fas/FasL system ($P>0.05$). HBxAg could also express in membrane of carcinoma cells. Surprisingly, we found that HBxAg, Fas and FasL might express in the same area of HCC tissues and this co-expression could be found in most patients with HCC.

Table 1 Expression of HBxAg, Fas and FasL in HCC (n=50)

Expression	HBxAg (%)	Fas(%)	FasL(%)
-	2 (4)	8 (16)	1 (2)
+	5 (10)	9 (18)	4 (8)
++	11 (22)	9 (18)	12 (24)
+++	32 (64)	24 (48)	33 (66)

Table 2 Serum levels of sFas and sFasL in patients with HCC and Cirrhosis (μg· L^{-1})

Group	n	sFas	sFasL
HCC	50	762.29±391.56[a]	158.36±9.67[a]
Cirrhosis	50	835.63±407.33[a]	173.63±18.74[a]
Control	30	238.27±135.29	121.96±7.83

[a]$P<0.01$, *vs* control.

Serum level of sFas and sFasL

Concentrations of sFas and sFasL in HCC, cirrhotic patients and normal controls are shown in Table 2. The serum levels of

sFas and sFasL in both HCC and cirrhotic patients were significantly higher than those of normal controls ($P<0.01$), but there was no significant difference between cirrhosis and HCC patients in serum level of sFas and sFasL ($P>0.05$). In addition, we did not find a correlation between sFas/sFasL concentrations and serum HBV X gene detection ($P>0.05$).

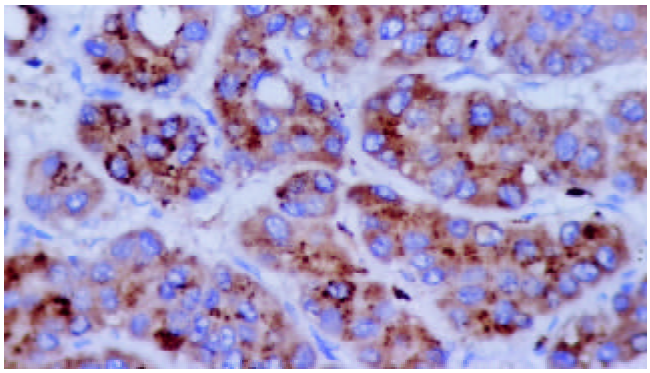

Figure 1 Positive expression of HBxAg in plasma of hepatocellular carcinoma (S-P stain, ×400).

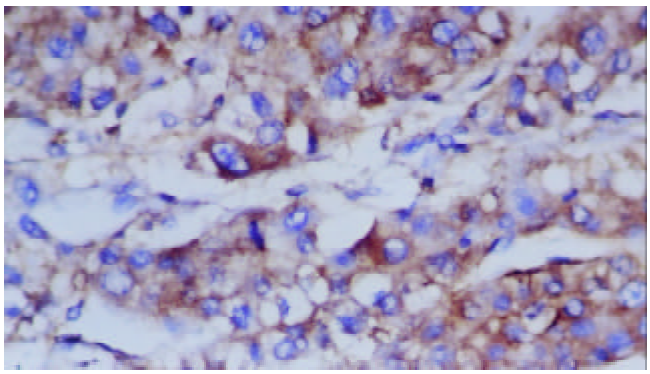

Figure 2 Positive expression of Fas in plasma of hepatocellular carcinoma (S-P stain, ×400).

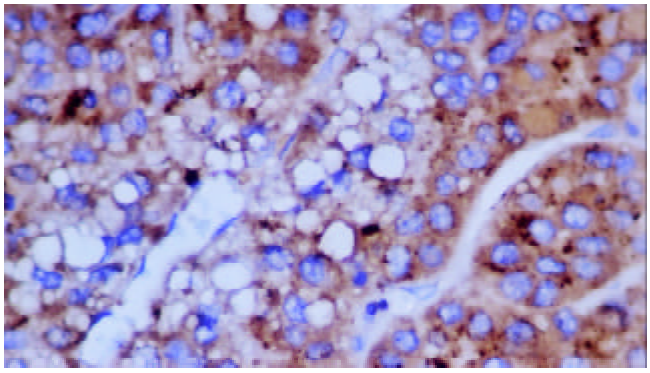

Figure 3 Positive expression of FasL in plasma of hepatocellular carcinoma (S-P stain, ×400).

Table 3 Positive rates of HBV X gene, HBsAg and HBeAg in HCC and cirrhotic patients (%)

Group	HBV X gene	HBsAg	HBeAg
HCC	32	86	34
Cirrhosis	46	82	38

Determination of X gene and HBsAg/HBeAg

The positive rates of HBV X gene, HBsAg and HBeAg in HCC and cirrhotic patients are shown in Table 3. Serum HBV X gene was found in 32 % of HCC patients and 46 % of cirrhotic patients. Eight percent of HCC patients with negative HBsAg and HBeAg in serum might have X gene in serum and HBxAg expression in carcinoma tissues.

The PCR products of X gene positive samples were analyzed by automatic sequencing and the resulting sequence was proved by Genebank.

DISCUSSION

HBV is one of the several agents causing infectious hepatitis, such as acute and chronic viral hepatitis. A strong association was found between chronic HBV infection and the development of HCC in our study. Multiple factors including damage caused by inflammatory cytokines, integration of viral DNA into host cell genomes, host genomic instability, activation of cellular oncogenes, and induction of cell survival pathways have been implicated as causes leading to HCC. However, HBV X gene and HBxAg play a major role in viral infection and carcinogenesis. X gene was the most frequently integrated protein of HBV DNA found in hepatocyte chromosomes during the development of HCC[23]. HBxAg was expressed in these integrated fragments, although no other viral proteins were present in most tumor cells. Recent studies using cDNA microarray analysis revealed that HBxAg expression in HepG2 cells could up- or down-regulate the expression of 39 genes[24]. These genes have a variety of cellular functions including oncogenesis, cell cycle regulation and cell adhesion. Our results demonstrated high levels of HBxAg expression in cirrhotic and HCC cells. Intracellular localization showed that HBxAg was predominant in cytoplasms. Serum levels of sFas and sFasL in both HCC and cirrhotic patients were significantly higher than those in controls. This could be explained by previous observations that X gene was greatly correlated with the development of cirrhosis and integrated into host chromosomes during chronic infection. It seems likely that HBxAg contributes to the initiation of tumor formation in the liver during the process of chronic active hepatitis and cirrhosis. However, whether this process is induced by Fas/FasL system remains to be elucidated.

With PCR detection, we found that some HBsAg and HBeAg negative HCC patients were X gene positive. These results were consistent with a previous report that circulating HBV X gene was detectable in a high proportion of Japanese HCC patients without HBsAg[25]. It could be explained as follows: First, a low level of viremia might exist and hardly result in expression[26]. Second, variant HBV clones might predominantly emerge, the variant HBV might have lost its common "A" determinant of HBsAg and result in loss of HBsAg[27]. Third, disrupted form of HBV was integrated into cellular chromosomes, resulting in failure to produce viral protein translated from deleted DNA[23]. Our results suggested that negative HBsAg and HBeAg HCC patients were required to examine HBV DNA in serum or in liver tissues in order to better understand HBV involvement in the etiology.

Our results indicated that HCC cells could strongly express both Fas and FasL in the same area of carcinoma. What is the target of this ligand? There are some hypotheses. First, because HCC cells can co-express Fas and FasL, they may undergo apoptosis induced not only by activated FasL-positive lymphocytes but also by their own FasL in an autocrine or paracrine manner. Such a fratricide mechanism may be involved in chemotherapeutic drug-induced death of HCC cells, as evidenced by the observations that bleomycin upregulated the expression of Fas and FasL in $HepG_2$ cells, and that apoptosis induced by this drug was almost completely inhibited by antibodies that interfere with Fas/FasL interaction[28]. Second, FasL expressed on HCC cells might be important in their

infiltration as well as dissemination into the liver[29], as has been demonstrated in the hepatic metastasis of colon cancer cells[30]. The third possibility is the so-called "counterattack" hypothesis. FasL expressed on tumor cells may be engaged with Fas receptors expressed on the surfaces of antitumor immune cells, causing them to undergo apoptosis. Strand *et al*[31] reported that HepG2 cells, expressing FasL after treatment with cytostatic drugs, could kill Fas-positive Jurkat lymphocytes, providing the first evidence that FasL is functional on HCC. Although the idea that tumor cells counterattack immune cells and escape from antitumor immunity has attracted popular attention, several investigators reported that the presence of surface FasL might be only an inflammatory response. The presence and function of FasL on HCC cells have become the subject of hot debate[32,33]. But why this happened only in HCC? Ito *et al*[34] examined the expression of Fas/FasL system in human HCC tissues and found that FasL expressing HCCs were moderately or poorly differentiated carcinomas. But FasL expression was not a critical factor in determining intrahepatic tumor spread. Fukuzawa *et al*[35] reported some conflicting results. They examined the expression of Fas and FasL in human HCC tissues, and found that Fas/FasL expression decreased in proportion to the malignancy of tumor cells. According to the concept that tumor cells become resistant to apoptosis during disease progression, their observation implies that FasL expressed on HCC may be involved in a self-regulatory mechanism of apoptosis, rather than being involved in a counterattack against immune cells or infiltration into the liver. Indeed, so far, HCC cells have often been found to be resistant to Fas-mediated apoptosis, despite their expression of Fas receptors[36]. Thus, there is no clinical evidence to directly support the idea that FasL expressed on HCCs was involved in their immune escape or infiltration into the liver. Because the mitochondrial death pathway was predominantly involved in Fas-mediated apoptosis in liver cells[37], overexpression of HBxAg might contribute to FasL-resistance in HCC. We found that Fas, FasL and HBxAg might express in the same area of HCC tissues. The precise mechanism of the co-expression of HBxAg and Fas/FasL system remains to be established. Recently Terradillos *et al*[38] reported that the proapoptotic activity of HBxAg could overcome or bypass the inhibitory effect of Bcl-2 against Fas cytotoxicity. The inability of Bcl-2 to protect HBxAg-expressing hepatocytes against Fas cytotoxicity might be resulted either from inactivation of Bcl-2 or from execution of a Bcl-2-independent death pathway. These indicate that the dominant function of HBxAg upon Bcl-2-regulated apoptosis might play an important role in carcinogenesis. It is known that HBxAg could activate various cellular transcription factors such as AP-1 and NF-kB[39]. In addition, HBxAg may induce FasL expression through activation of cellular transcription factors. Although there is no confirmative report of transcription factors regulating FasL expression, it has been found that the enhancer region of FasL gene has a putative binding site of NF-kB[40] and the important role of NF-kB has been reported in FasL gene activation. Because HBxAg could activate NF-kB, it is possible that HBxAg might induce FasL expression through NF-kB activation[41,42]. Our results also suggest that the expression of HBxAg can lead to expression of Fas/FasL system, which might not reflex apoptosis of hepatocellular carcinoma induced by FasL. This implies that Fas/FasL expression by itself, cannot be used as a reliable marker of apoptosis in HCC.

REFERENCES

1 **Koike K,** Tsutsumi T, Fujie H, Shintani Y, Moriya K. Molecular mechanism of viral hepatocarcinogenesis. *Oncology* 2002; **62** (Suppl 1): 29-37

2 **Tang ZY.** Hepatocellular carcinoma-cause, treatment and metastasis. *World J Gastroenterol* 2001; **7**: 445-454

3 **Wang WL,** Gu GY, Hu M. Expression and significance of HBV genes and their antigens in human primary intrahepatic cholangiocarcinoma. *World J Gastroenterol* 1998; **4**: 392-396

4 **Yeh CT.** Hepatitis B virus X protein: searching for a role in hepatocarcinogenesis. *J Gastroenterol Hepatol* 2000; **15**: 339-341

5 **Lian ZR,** Liu J, Pan JB, Tufan NLS, Zhu MH, Arbuthnot P, Kew M, Clayton MM, Feitelson MA. A cellular gene up-regulated by hepatitis B virus-encoded X antigen promotes hepatocellular growth and survival. *Hepatol* 2001; **34**: 146-157

6 **Qin LX,** Tang ZY. The prognostic molecular markers in hepatocellular carcinoma. *World J Gastroenterol* 2002; **8**: 385-392

7 **Qin LL,** Su JJ, Li Y, Yang C, Ban KC, Yian RQ. Expression of IGF-II, p53, p21 and HBxAg in precancerous events of hepatocarcinogenesis induced by AFB1 and/or HBV in tree shrews. *World J Gastroenterol* 2000; **6**: 138-139

8 **Murakami S.** Hepatitis B virus X protein: a multifunctional viral regulator. *J Gastroenterol* 2001; **36**: 651-660

9 **Diao J,** Garces R, Richardson CD. X protein of hepatitis B virus modulates cytokine and growth factor related signal transduction pathways during the course of viral infections and hepatocarcinogenesis. *Cytokine Growth Factor Rev* 2001; **12**:189-205

10 **Wang XZ,** Jiang XR, Chen XC, Chen ZX, Li D, Lin JY, Tao QM. Seek protein which can interact with hepatitis B virus X protein from human liver cDNA library by yeast two-hybrid system. *World J Gastroenterol* 2002; **8**: 95-98

11 **Kong HJ,** Hong SH, Lee MY, Kim HD, Lee JW, Cheong JH. Direct binding of hepatitis B virus X protein and retinoid X receptor contributes to phosphoenolpyruvate carboxykinase gene transactivation. *FEBS Lett* 2000; **483**: 114-118

12 **Kim CM,** Koike K, Saito I, Miyamura T, Jay G. HBx gene of hepatitis B virus induces liver cancer in transgenic mice. *Nature* 1991; **351**: 317-320

13 **Slagle BL,** Lee TH, Medina D, Finegold MJ, Butel JS. Increased sensitivity to the hepatocarcinogen diethylnitrosamine in transgenic mice carrying the hepatitis B virus X gene. *Mol Carcinog* 1996; **15**: 261-269

14 **Staib F,** Perwez Hussain S, Hofseth LJ, Wang XW, Harris CC. TP53 and liver carcinogenesis. *Hum Mutat* 2003; **21**: 201-216

15 **Pollicino T,** Terradillos O, Lecoeur H, Gougeon ML, Buendia MA. Pro-apoptotic effect of the hepatitis B virus X gene. *Biomed Pharmacother* 1998; **52**: 363-368

16 **Xu ZH,** Zhao MJ, Li TP. P73 beta inhibits transcriptional activities of enhancer I and X promoter in hepatitis B virus more efficiently than p73alpha. *World J Gastroenterol* 2002; **8**:1094-1097

17 **Kang-Park S,** Lee JH, Shin JH, Lee YI. Activation of the IGFII gene by HBV-X protein requires PKC and p44/p42 map kinase signalings. *Biochem Biophys Res Commun* 2001; **283**: 303-307

18 **Arbuthnot P,** Capovilla A, Kew M. Putative role of hepatitis B virus X protein in hepatocarcinogenesis: effects on apoptosis, DNA repair, mitogen-activated protein kinase and JAK/STAT pathways. *J Gastroenterol Hepatol* 2000; **15**: 357-368

19 **Nagata S.** Apoptosis by death factor. *Cell* 1997; **88**: 355-365

20 **Takehara T,** Hayashi N. Fas and Fas ligand in hunan hepatocellular carcinoma. *J Gastroenterol* 2001; **36**: 727-728

21 **Ibuki N,** Yamamoto K, Yabushita K, Okano N, Okamoto R, Shimada N, Hakoda T, Mizuno M, Higashi T, Tsuji T. *In situ* expression of Granzyme B and Fas-ligand in the liver of viral hepatitis. *Liver* 2002; **22**: 198-204

22 **Natoli G,** Ianni A, Costanzo A, De Petrillo G, Ilari I, Chirillo P, Balsano C, Levrero M. Resistance to Fas-mediated apoptosis in human hepatoma cells. *Oncogene* 1995; **11**: 1157-1164

23 **Paterlini P,** Poussin K, Kew M, Franco D, Brechot C. Selective accumulation of the X transcript of hepatitis B virus in patients negative for hepatitis B surface antigen with hepatocellular carcinoma. *Hepatol* 1995; **21**: 313-321

24 **Han J,** Yoo HY, Choi BH, Rho HM. Selective transcriptional regulations in the human liver cell by hepatitis B viral X protein. *Biochem Biophys Res Commun* 2000; **272**: 525-530

25 **Shiota G,** Oyama K, Udagawa A, Tanaka K, Nomi T, Kitamura A, Tsutsumi A, Noguchi N, Takano Y, Yashima K, Kishimoto Y, Suou T, Kawasaki H. Occult hepatitis B virus infection in HBs antigen-negative hepatocellular carcinoma in a Japanese

population: involvement of HBx and p53. *J Med Virol* 2000; **62**: 151-158
26 **Niitsuma H,** Ishii M, Miura M, Kobayashi K, Toyota T. Low level hepatitis B viremia detected by polymerase chain reaction accompanies the absence of the HBe antigenemia and hepatitis in hepatitis B virus carriers. *Am J Gastroenterol* 1997; **92**: 119-123
27 **Carman WF.** S gene variation of HBV. *Acta Gastroenterol Belg* 2000; **63**: 182-184
28 **Muller M,** Strand S, Hug H, Heinemann EM, Walczak H, Hofmann WJ, Stremmel W, Krammer PH, Galle PR. Drug -induced apoptosis in hepatoma cells is mediated by the CD95 (APO-1/Fas) receptor/ligand system and involves activation of wild-type p53. *J Clin Invest* 1997; **99**: 403-413
29 **Roskams T,** Libbrecht L, Damme BV, Desmet V. Fas and Fas ligand: strong co-expression in human hepatocellular carcinoma; can cancer induce suicide in peritumoural cells? *J Pathol* 2000; **191**: 150-153
30 **Shiraki K,** Tsuji N, Shioda T, Isselbacher KJ, Takahashi H. Expression of Fas ligand in liver metastases of human colonic adenocarcinoma. *Proc Natl Acad Sci U S A* 1997; **94**: 6420-6425
31 **Strand S,** Hofmann WJ, Hug H, Muller M, Otto G, Strand D, Mariani SM, Stremmel W, Krammer PH, Galle PR. Lyphocyte apoptosis induced by CD95(APO-1/Fas) ligand- expressing tumor cells-a mechanism of immune evasion? *Nat Med* 1996; **2**: 1361-1366
32 **O'Connell J,** Houston A, Bennett MW, O'Sullivan GC, Shanahan F. Immune privilege or inflammation? Insights into the Fas ligand enigma. *Nat Med* 2001; **7**: 271-274
33 **Restifo NP.** Countering the 'counterattack' hypothesis. *Nat Med* 2001; **7**: 259
34 **Ito Y,** Monden M, Takeda T, Eguchi H, Umeshita K, Nagano H, Nakamori S, Dono K, Sakon M, Nakamura M, Tsujimoto M, Nakahara M, Nakao K, Yokosaki Y, Matsuura N. The status of Fas and Fas ligand expression can predict recurrence of hepatocellular carcinoma. *Br J Canner* 2000; **82**: 1211-1217
35 **Fukuzawa K,** Takahashi K, Furuta K, Tagaya T, Ishikawa T, Wada K, Omoto Y, Koji T, Kakumu S. Expression of fas/fas ligand(fasL) and its involvement in infiltrating lymphocytes in hepatocellular carcinoma (HCC). *J Gastroenterol* 2001; **36**: 727-728
36 **Shin EC,** Shin JS, Park JH, Kim H, Kim SJ. Expression of Fas ligand in human hepatoma cell lines: role of hepatitis-B virus X (HBX) in induction of Fas ligand. *Int J Canner* 1999; **82**: 587-591
37 **Yin XM,** Wang K, Cross A, Zhao Y, Zinkel S, Klocke B, Roth KA, Korsmeyer SJ. Bid-deficient mice are resistant to Fas-induced hepatocellular apoptosis. *Nature* 1999; **400**: 886-891
38 **Terradillos O,** Coste ADL, Pollicino T, Neuveut C, Sitterlin D, Lecoeur H, Gougeon ML, Kahn A, Buendia MA. The hepatitis B virus X protein abrogates Bcl-2-mediated protection against Fas apoptosis in the liver. *Oncogene* 2002; **21**: 377-386
39 **Li J,** Xu ZM, Zheng YY, Johnson DL, Ou JH. Regulation of hepatocyte nuclear factor 1 activity by wild-type and mutant hepatitis B virus X proteins. *J Virol* 2002; **76**: 5875-5881
40 **Lu B,** Wang L, Medan D, Toledo D, Huang C, Chen F, Shi X, Rojanasakul Y. Regulation of Fas (CD95)-induced apoptosis by nuclear factor-kappaB and tumor necrosis factor-alpha in macrophages. *Am J Physiol Cell Physiol* 2002; **283**: C831-838
41 **Kasibhatla S,** Genestier L, Green DR. Regulation of fas-ligand expression during activation-induced cell death in T lymphocytes via nuclear factor kappaB. *J Biol Chem* 1999; **274**: 987-992
42 **Guo SP,** Wang WL, Zhai YQ, Zhao YL. Expression of nuclear factor-kappa B in hepatocellular carcinoma and its relation with the X protein of hepatitis B virus. *World J Gastroenterol* 2001; **7**:340-344

Edited by Wang XL

P.O.Box 2345, Beijing 100023,China
Fax: +86-10-85381893
E-mail: wjg@wjgnet.com www.wjgnet.com

World J Gastroenterol 2003;9(12):2676-2680
World Journal of Gastroenterology
 ISSN 1007-9327

• LIVER CANCER •

Combined transarterial chemoembolization and arterial administration of *Bletilla striata* in treatment of liver tumor in rats

Jun Qian, Daryusch Vossoughi, Dirk Woitaschek, Elsie Oppermann, Wolf O. Bechstein, Wei-Yong Li, Gan-Sheng Feng, Thomas Vogl

Jun Qian, Gan-Sheng Feng, Department of Radiology, Xiehe Hospital, Tongji Medical College, Huazhong University of Science and Technology, Wuhan 430022, China
Wei-Yong Li, Department of Pharmacology, Xiehe Hospital, Tongji Medical College, Huazhong University of Science and Technology, Wuhan 430022, China
Daryusch Vossoughi, Dirk Woitaschek, Thomas Vogl, Department of Diagnostic and Interventional Radiology, University Hospital Frankfurt, J. W. Goethe University of Frankfurt, Theodor-Stern-Kai 7, 60590 Frankfurt, Germany
Elsie Oppermann, Wolf O. Bechstein, Department of Surgery, University Hospital Frankfurt, J. W. Goethe University of Frankfurt, Theodor-Stern-Kai 7, 60590 Frankfurt, Germany
Correspondence to: Professor Dr. Thomas Vogl, Department of Diagnostic and Interventional Radiology, University Hospital Frankfurt, Johann Wolfgang Goethe-University, Theodor-Stern-Kai 7, D-60590 Frankfurt/Main, Germany. t.vogl@em.uni.frankfurt.de
Telephone: +49-69-63017277 **Fax:** +49-69-63017258
Received: 2003-08-23 **Accepted:** 2003-09-25

Abstract

AIM: To evaluate and compare the effect of combined transarterial chemoembolization (TACE) and arterial administration of *Bletilla striata* (a Chinese traditional medicine against liver tumor) *versus* TACE alone for the treatment of hepatocellular carcinoma (HCC) in ACI rats.

METHODS: Subcapsular implantation of a solid Morris hepatoma 3 924A (2 mm^3) in the liver was carried out in 30 male ACI rats. Tumor volume (V1) was measured by magnetic resonance imaging (MRI) on day 13 after implantation. The following different agents of interventional treatment were injected after retrograde catheterization via gastroduodenal artery (on day 14), namely, (A) TACE (0.1 mg mitomycin + 0.1 ml Lipiodol) + *Bletilla striata* (1.0 mg) (n=10); (B) TACE + *Bletilla striata* (1.0 mg) + ligation of hepatic artery (n=10), (C) TACE alone (control group, n=10). Tumor volume (V2) was assessed by MRI (on day 13 after treatment) and the tumor growth ratio (V2/V1) was calculated.

RESULTS: The mean tumor volume before (V1) and after (V2) treatment was 0.0355 cm^3 and 0.2248 cm^3 in group A, 0.0374 cm^3 and 0.0573 cm^3 in group B, 0.0380 cm^3 and 0.3674 cm^3 in group C, respectively. The mean ratio (V2/V1) was 6.2791 in group A, 1.5324 in group B and 9.1382 in group C. Compared with the control group (group C), group B showed significant inhibition of tumor growth (P<0.01), while group A did not (P>0.05). None of the animals died during implantation or in the postoperative period.

CONCLUSION: Combination of TACE and arterial administration of *Bletilla striata* plus ligation of hepatic artery is more effective than TACE alone in the treatment of HCC in rats.

Qian J, Vossoughi D, Woitaschek D, Oppermann E, Bechstein WO, Li WY, Feng GS, Vogl T. Combined transarterial chemoembolization and arterial administration of *Bletilla striata* in treatment of liver tumor in rats. *World J Gastroenterol* 2003; 9(12): 2676-2680
http://www.wjgnet.com/1007-9327/9/2676.asp

INTRODUCTION

HCC is a highly malignant tumor with a very high morbidity and mortality rate worldwide, carrying a poor prognosis due to its rapid infiltrating growth and complicating liver cirrhosis[1,2].

Surgical resection, liver transplantation and cryosurgery are regarded as potentially curative treatment for HCC[3-5], but most patients are not suitable candidates[6-9]. Thus, the local interventional therapy of liver tumor has been rapidly evolving currently, which includes transarterial chemoembolization (TACE), percutaneous ethanol injection (PEI), radiofrequency ablation (RFA), laser-induced thermotherapy (LITT) and microwave coagulation therapy (MCT)[10-19]. TACE is one of the most common forms of interventional therapies and seems most effective against encapsulated small HCCs without extracapsular invasion, whereas in large HCCs, viable residual tumor cells remain and the tumor frequently recurs[20-22]. Moreover, in patients with large lesions, multiple TACE sessions are necessary to control tumor growth but may increase the risk of worsening hepatic function through damage to noncancerous liver parenchyma[8,21,23].

In the past years, locoregional Chinese medicinal therapy for treating unresectable HCC has been reported with encouraging results, especially for inhibiting arterial collaterals of liver tumor and recurrence of HCC[24,25]. Such an adjuvant treatment in conjunction with TACE has the potential to enhance the therapeutic effect of TACE alone in experimental and clinical studies. However, no experimental study to assess the value and efficacy of this combined therapy in an animal model of HCC has been performed.

The current prospective randomized study was designed to compare the effect of combined TACE and arterial administration of *Bletilla striata* (a Chinese traditional medicine against liver tumor) *versus* TACE alone for the treatment of HCC in ACI rats.

MATERIALS AND METHODS

Tumor

The hepatoma cell line (Morris hepatoma 3924A), a rapidly growing, poorly differentiated hepatocellular carcinoma[26], was used in ACI rats in this study. The hepatoma specimens were obtained from the German Cancer Research Center (DKFZ; Heidelberg, Germany).

Animal

Thirty inbred male ACI-rats (Harlan Winkelmann; Borchen, Germany) weighing 220-260 g were used. The animals were kept under conventional conditions with a temperature of 22±2 ℃, a relative humidity of 55±10 %, a dark-light rhythm

of 12 hr, and had free access to laboratory chow and tap water. All of the experiments on animals were approved by the German government.

Agents

The original material of *Bletilla striata* microspheres is the stem tubers of *Bletilla striata*. *Bletilla striata* microspheres were kindly provided by Tongji Medical College (Wuhan, China). A dose of 1.0 mg *Bletilla striata* microspheres (50 μm) was suspended in 0.5 ml 0.9 % NaCl for 10 minutes before administration.

Anesthesia

The animals were anesthetized with intraperitoneal injection of ketamine hydrochloride (Ketanest, Parke-Davis, Germany; 100 mg/kg), Xylazinhydrochloride (Rompun, Bayer, Germany; 15 mg/kg) and atropine sulfate (Atropinsulfat Braun, Braun, Germany; 0.1 mg/kg) in all interventional and imaging procedures.

Tumor implantation (on day 1)

The technique for tumor implantation was basically similar to that described by Yang *et al*[26] with minor modifications[27-29]. The Morris hepatoma 3924A tumor tissue, recovered from the passaged animals 2 weeks after subcutaneous implantation (corresponding to 5×10^6 tumor cells), was cut into small cubes about 2 mm^3.

A small subcapsular incision on the left lateral lobe of the liver was made in the recipient ACI-rats under anesthesia. The tumor fragment was gently placed into the pocket with a small cotton swab on the liver surface and the abdominal wall was then closed.

Interventional therapy (on day 14)

For interventional studies a second laparotomy was performed. By using a binocular operative microscope (M651, Leica; Wetzler, Germany), a PE-10 polyethylene microcatheter (inner diameter 0.28 mm, outer diameter 0.61 mm; Wenzel; Heidelberg, Germany) was retrogradely inserted into the gastroduodenal artery. Different agents were then injected (20 minutes a duration time) through the microcatheter via hepatic artery using sandwich technique. Administration was as follows:

Group A (*n*=10): Mitomycin (0.1 mg) + Lipiodol (0.1 ml) + *Bletilla striata* (1.0 mg)
Group B (*n*=10): Mitomycin (0.1 mg) + Lipiodol (0.1 ml) + *Bletilla striata* (1.0 mg)+ligation of A. hepatica propria
Group C (*n*=10): Mitomycin (0.1 mg) + Lipiodol (0.1 ml) (*control group*).

MR imaging and analysis (on day 13 and 27)

A 1.5 Tesla Sonata (Siemens; Erlangen, Germany) supplemented by a wrist coil (Small field of view) was used for MRI before and after therapy (on day 13 and 27). T1-weighted (SE: TR/TE, 460/15 ms) and T2-weighted (TSE: TR/TE, 3170/99 ms) transverse images with a section thickness of 2 mm and 184×256 matrix were acquired. There was no gap between sections and no contrast medium was administered. The tumor volume was determined and evaluated in T2-weighted image according to the formula[30]:

$$\text{Tumor volume } (mm^3) = \frac{\text{Largest diameter (mm)} \times [\text{smallest diameter (mm)}]^2}{2}$$

The mean tumor growth ratio (V2/V1) was analyzed by using *t* test for comparing the effect of each therapeutic group with control group respectively. A *P*-value less than 0.05 was considered to indicate a significant difference.

RESULTS

The rate of tumor implantation reached 100 % in all the rats receiving tumor implantation with Morris hepatoma 3924A. None of the animals died during implantation or interventional therapy. A total of 30 individual HCC tumors were seen with unenhanced MR imaging in the livers of 30 rats (100 %) before treatment. The tumors showed homogeneously hypointense on the T1-weighted images and hyperintense on the T2-weighted images. T2-weighted sequences provided significantly higher tumor-liver contrast than T1-weighted sequences, and improved the detectability of intrahepatic metastasis. Intrahepatic metastasis occurred in two of 10 rats (20 %) in group C.

The mean tumor volume before (V1) and after (V2) therapy was 0.0355 cm^3 and 0.2248 cm^3 in group A, 0.0374 cm^3 and 0.0573 cm^3 in group B, 0.0380 cm^3 and 0.3674 cm^3 in group C, respectively. The mean ratio of V2/V1 was 6.2791 in group A, 1.5324 in group B and 9.1382 in group C. Compared with the control group (group C, TACE alone), group B (TACE + *Bletilla striata* + ligation of hepatic artery) showed significant inhibition of tumor growth ($P<0.01$), while group A (TACE + *Bletilla striata*) did not ($P>0.05$).

The tumor volume ratio (V2/V1) in different groups (*n*=30) is shown in Table 1.

Table 1 Tumor volume rate (V2/V1) in different groups (*n*=30)

Rat No.	Group A (BS)	Group B (BS+Lig.)	Group C (control)
1	6.4810	0.8556	5.6284
2	5.7038	1.4565	9.5091
3	6.2490	1.6469	10.5063
4	7.8920	1.3920	7.7416
5	7.8023	1.6577	8.6378
6	7.4781	1.6911	8.2029
7	5.5685	0.9025	8.3670
8	6.8346	1.9530	8.5399*
9	5.5800	1.9636	11.5310
10	3.2015	1.8054	12.7182*

BS: *Bletilla striata*. Lig.: Ligation of hepatic artery; *: tumor with intrahepatic metastasis.

In group B (TACE + *Bletilla striata* + ligation), relative small tumors with the size of 0.52×0.37 mm^2 and 0.44×0.38 mm^2 in diameter were shown in two treated rats, respectively, indicating a minimal response but no tumor growth after therapy compared with that before therapy (Figure 1).

In group C (control group), the tumor volume was generally markedly increased in treated rats compared to untreated. Two rats appeared to be accompanied with intrahepatic metastasis (Figure 2).

DISCUSSION

Since TACE was introduced as a palliative treatment in patients with unresectable HCC, it has become one of the most common forms of interventional therapies[11,31]. TACE with iodized oil has been shown to result in regression of HCC and reduction of systemic toxicity, thus improving the therapeutic effects[21,32,33]. However, prolongation of the overall survival of patients remains questionable[34]. TACE might ablate a significant portion of the tumor but had a high rate of recurrence[35]. In patients with focal HCC, TACE was well tolerated and provided a survival benefit. However, no apparent benefit of it has been found for patients with diffuse HCC[36,37]. TACE using various embolizers has been well documented to include

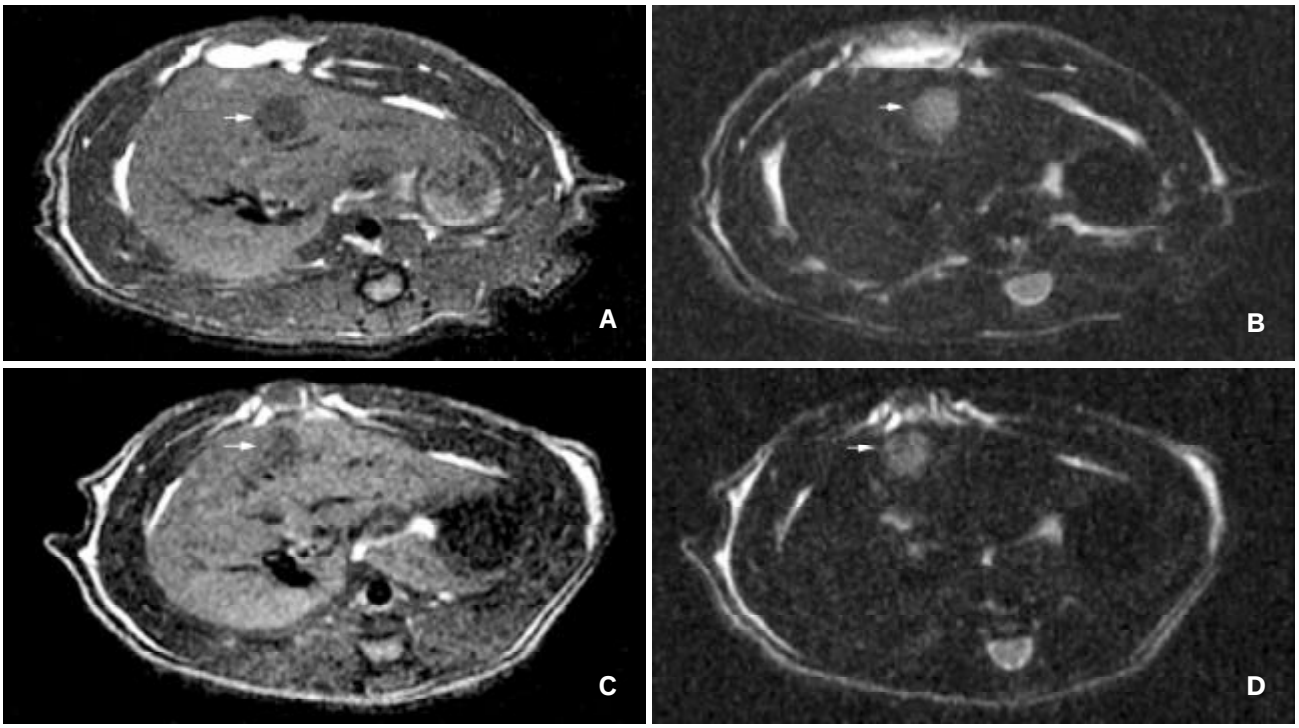

Figure 1 A: Images in a ACI rat with a solid HCC in group B. (a) Pretherapy did not enhance T1-weighted MR imaging with SE sequence (460/15). It shows a small hypointense tumor (arrow) in the left lateral lobe of liver; B: Pretherapeutic unenhanced T2-weighted MR imaging with TSE sequence (3170/99). The hyperintense lesion with a size of 0.44×0.40 mm^2 (arrow) is well discernible from the surrounding liver tissue. C: Images in a ACI rat with a solid HCC in group B. (a) Posttherapy did not enhance T1-weighted MR imaging with SE sequence (460/15). It shows a small hypointense tumor (arrow) in the left lateral lobe of liver. D: Unenhanced T2-weighted MR imaging with TSE sequence (3170/99) after therapy. It shows the inhomogeneous hyperintense lesion with a size of 0.44×0.38 mm^2 (arrow) and demonstrates that there is no difference between the tumor volume before and after therapy.

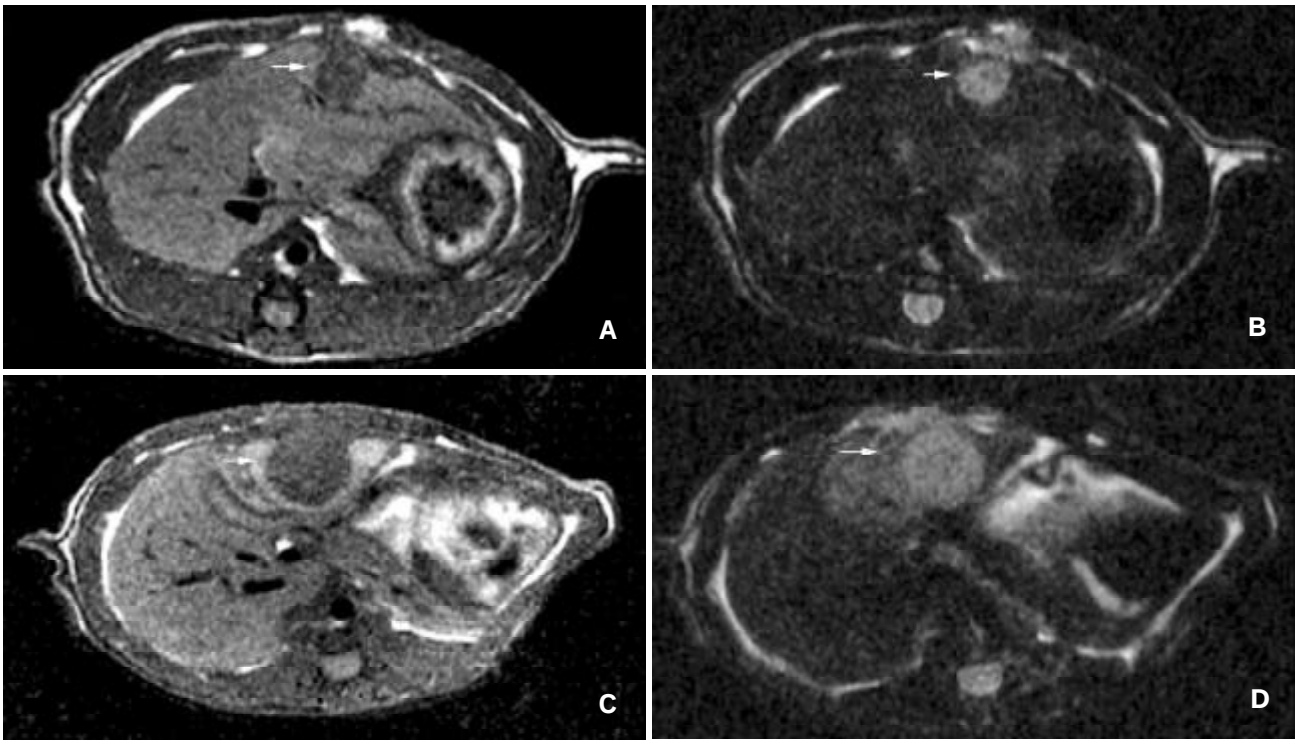

Figure 2 A: Images in a ACI rat with a solid HCC in group C. (a) Pretherapy did not enhance T1-weighted MR imaging with SE sequence (460/15). It shows a small hypointense tumor (arrow) in the left lateral lobe of liver. B: Unenhanced T2-weighted MR imaging with TSE sequence (3170/99) after therapy. The hyperintense lesion with a size of 0.49×0.46 mm^2 (arrow) is well discernible from the surrounding liver tissues. C: Images in a ACI rat with a solid HCC in group C. (a) Posttherapy did not enhance T1-weighted MR imaging with SE sequence (460/15). It shows a large hypointense tumor (arrow) in the left lateral lobe of liver. The lesion is surrounded by an iregular hypointense area. D: Unenhanced T2-weighted MR imaging with TSE sequence (3170/99) after therapy. The tumor with a size of 0.96×0.96 mm^2 had a rapid growth compared with that before therapy. It also shows the unhomogeneous hyperintense area (arrow) corresponding to the intrahepatic metastasis.

controlled studies. However, it is not indicated for patients with thrombosed main portal veins. Its therapeutic effect was also doubtful when the tumor was infiltrative in nature or hypovascular, too large or too small[38,39]. The rapid development of arterial collaterals after these treatments might reduce this therapeutic effect and thus, inhibition of the development of arterial collaterals might be important in enhancing the therapeutic efficacy of these treatments[40]. In addition, in patients with large lesions, multiple TACE sessions were necessary to control tumor growth but might increase the risk of worsening hepatic function through damage to noncancerous liver parenchyma[23]. Moreover, the types and doses of embolic agents have been extremely variable in several reported studies. The major problem with embolic agents were twofold[41]. First, they could often completely obstruct the hepatic artery, leading to difficulties in administration of subsequent courses of hepatic artery chemotherapy. With a relative short half-life of embolic agents, the effectiveness of TACE was not significantly improved. Second, it was easy to aggravate the liver cirrhosis and lead to hepatic failure after repeated TACE. The optimal treatment modality of TACE is still unknown[42].

Today, it is well known that improvement of the overall therapeutic effect of liver malignancies depends on the combined therapies. In the past years, locoregional Chinese medicinal therapy has gained wide acceptance as a safe, palliative and effective treatment even in patients with large HCC and liver cirrhosis in China. *Bletilla striata* (BS) is a common Chinese traditional medicinal herb and is usually used as an embolic material in TACE for HCC. Its compositions are mucilage, starch, and a little volatile oil. In a previous study, Zheng *et al*[24] used BS to embolize the hepatic artery in order to induce ischemic necrosis and shrinkage of tumor. It mainly blocked the trunk of the blood-supplying artery of tumor with a "vascular cast-like appearance". The embolization was extensive and lasted longer, hence a better therapeutic effect[24]. The mechanisms of embolization by BS are attributable to the following factors: non-absorbent property, total mechanical obstruction, no influence on coagulative and anticoagulative systems and secondary obstruction due to injury of the wall of blood vessels[43, 44]. Zheng *et al*[25] have confirmed that BS has an adherent function and can expand slowly in blood flow, leading to mechanical blockade of vessels. It was also hypothesized that BS could slowly diffuse into the liver parenchyma around the tumor as a colloidal form, leading to prolonged anticancer effect and inhibition of collateralisation and metastasis of tumor[25]. Compared with gelfoam embolus, BS had the following characteristics. It could produce extensive and permanent vascular embolization, while it could not be absorbed by body tissue. After embolization, tumor necrosis and shrinkage were significant with less collateral circulation that formed later. The mucilage component of BS is a wide-spectrum anticancer element that might inhibit tumor occurrence and development[45]. The 1, 2 and 3 year survival rates were 44.9 %, 33.6 % and 33.6 % in BS group while the rates were 48.9 %, 31.1 % and 16.0 % in gelfoam group, suggesting that BS is superior to gelfoam as an embolic agent, and transarterial administration of BS might provide a beneficial therapeutic modality for HCC[45]. In our experimental study, the best therapeutic effect was the combined therapy of BS+TACE+ligation of hepatic artery. There was almost no significant difference between the tumor volume before and after therapy (Figure 1). No intrahepatic metastasis was observed in this group. This approach of central- and peripheral chemoembolization is able to increase the inhibition of tumor growth more completely, resulting in local control of tumor growth in rats and has a promising prospect for treating patients with HCC in the future.

In summary, by combining TACE and arterial administration of *Bletilla striata* plus ligation of hepatic artery for treating HCC in ACI rats, an encouraging result can be obtained compared with TACE alone. However, the detailed therapeutic mechanisms, therapeutic indications, optimal strategy for the use, monitoring, and validation of these combined therapies remain unclear and more randomized experimental and clinical studies are required.

REFERENCES

1 **Cha C**, DeMatteo RP, Blumgart LH. Surgery and ablative therapy for hepatocellular carcinoma. *J Clin Gastroenterol* 2002; **35**(5 Suppl 2): S130-S137
2 **Yuen MF**, Cheng CC, Lauder IJ, Lam SK, Ooi CG, Lai CL. Early detection of hepatocellular carcinoma increases the chance of treatment: Hong Kong experience. *Hepatology* 2000; **31**: 330-335
3 **Tang ZY**. Treatment of hepatocellular carcinoma. *Digestion* 1998; **59**: 556-562
4 **Franco D**, Usatoff V. Resection of hepatocellular carcinoma. *Hepatogastroenterology* 2001; **48**: 33-36
5 **Durand F**, Belghiti J. Liver transplantation for hepatocellular carcinoma. *Hepatogastroenterology* 2002; **49**: 47-52
6 **Alsowmely AM**, Hodgson HJ. Non-surgical treatment of hepatocellular carcinoma. *Aliment Pharmacol Ther* 2002; **16**: 1-15
7 **Durand F**, Belghiti J. Liver transplantation for hepatocellular carcinoma. *Hepatogastroenterology* 2002; **49**: 47-52
8 **Poon RT**, Fan ST, Tsang FH, Wong J. Locoregional therapies for hepatocellular carcinoma: a critical review from the surgeon's perspective. *Ann Surg* 2002; **235**: 466-486
9 **Sturm JW**, Keese MA, Bonninghoff RG, Wustner M, Post S. Locally ablative therapies of hepatocellular carcinoma. *Onkologie* 2001; **24**(Suppl 5): 35-45
10 **Chen MS**, Li JQ, Zhang YQ, Lu LX, Zhang WZ, Yuan YF, Guo YP, Lin XJ, Li GH. High-dose iodized oil transcatheter arterial chemoembolization for patients with large hepatocellular carcinoma. *World J Gastroenterol* 2002; **8**: 74-78
11 **Li L**, Wu PH, Li JQ, Zhang WZ, Lin HG, Zhang YQ. Segmental transcatheter arterial embolization for primary hepatocellular carcinoma. *World J Gastroenterol* 1998; **4**: 511-512
12 **Huo TI**, Huang YH, Wu JC, Lee PC, Chang FY, Lee SD. Survival benefit of cirrhotic patients with hepatocellular carcinoma treated by percutaneous ethanol injection as a salvage therapy. *Scand J Gastroenterol* 2002; **37**: 350-355
13 **Teratani T**, Ishikawa T, Shiratori Y, Shiina S, Yoshida H, Imamura M, Obi S, Sato S, Hamamura K, Omata M. Hepatocellular carcinoma in elderly patients: beneficial therapeutic efficacy using percutaneous ethanol injection therapy. *Cancer* 2002; **95**: 816-823
14 **Jiang HC**, Liu LX, Piao DX, Xu J, Zheng M, Zhu AL, Qi SY, Zhang WH, Wu LF. Clinical short-term results of radiofrequency ablation in liver cancers. *World J Gastroenterol* 2002; **8**: 624-630
15 **Allgaier HP**, Galandi D, Zuber I, Blum HE. Radiofrequency thermal ablation of hepatocellular carcinoma. *Dig Dis* 2001; **19**: 301-310
16 **Vogl TJ**, Mack MG, Roggan A, Straub R, Eichler KC, Muller PK, Knappe V, Felix R. Internally cooled power laser for MR-guided interstitial laser-induced thermotherapy of liver lesions: initial clinical results. *Radiology* 1998; **209**: 381-385
17 **Pacella CM**, Bizzarri G, Cecconi P, Caspani B, Magnolfi F, Bianchini A, Anelli V, Pacella S, Rossi Z. Hepatocellular carcinoma: long-term results of combined treatment with laser thermal ablation and transcatheter arterial chemoembolization. *Radiology* 2001; **219**: 669-678
18 **Itamoto T**, Katayama K, Fukuda S, Fukuda T, Yano M, Nakahara H, Okamoto Y, Sugino K, Marubayashi S, Asahara T. Percutaneous microwave coagulation therapy for primary or recurrent hepatocellular carcinoma: long-term results. *Hepatogastroenterology* 2001; **48**: 1401-1405
19 **Seki T**, Tamai T, Nakagawa T, Imamura M, Nishimura A, Yamashiki N, Ikeda K, Inoue K. Combination therapy with transcatheter arterial chemoembolization and percutaneous microwave coagulation therapy for hepatocellular carcinoma. *Cancer* 2000; **89**: 1245-1251
20 **Liad inverted question marko L,** Virgili J, Figueras J, Valls C, Dominguez J, Rafecas A, Torras J, Fabregat J, Guardiola J, Jaurrieta

E. A prognostic index of the survival of patients with unresectable hepatocellular carcinoma after transcatheter arterial chemoembolization. *Cancer* 2000; **88**: 50-57

21 **Llovet JM**, Real MI, Montana X, Planas R, Coll S, Aponte J, Ayuso C, Sala M, Muchart J, Sola R, Rodes J, Bruix J. Arterial embolisation or chemoembolisation versus symptomatic treatment in patients with unresectable hepatocellular carcinoma: a randomised controlled trial. *Lancet* 2002;**359**: 1734-1739

22 **Vogl TJ**, Trapp M, Schroeder H, Mack M, Schuster A, Schmitt J, Neuhaus P, Felix R. Transarterial chemoembolization for hepatocellular carcinoma: volumetric and morphologic CT criteria for assessment of prognosis and therapeutic success-results from a liver transplantation center. *Radiology* 2000; **214**: 349-357

23 **Bartolozzi C**, Lencioni R, Caramella D, Vignali C, Cioni R, Mazzeo S, Carrai M, Maltinti G, Capria A, Conte PF. Treatment of large HCC: transcatheter arterial chemoembolization combined with percutaneous ethanol injection versus repeated transcatheter arterial chemoembolization. *Radiology* 1995; **197**: 812-818

24 **Zheng C**, Feng G, Liang H. *Bletilla striata* as a vascular embolizing agent in interventional treatment of primary hepatic carcinoma. *Chin Med J* 1998; **111**: 1060-1063

25 **Zheng C**, Feng G, Zhou R. New use of *Bletilla striata* as embolizing agent in the intervention treatment of hepatic carcinoma. *Zhonghua Zhongliu Zazhi* 1996; **18**: 305-307

26 **Yang R**, Rescorla FJ, Reilly CR, Faught PR, Sanghvi NT, Lumeng L, Franklin TD Jr, Grosfeld JL. A reproducible rat liver cancer model for experimental therapy: introducing a technique of intrahepatic tumor implantation. *J Surg Res* 1992; **52**: 193-198

27 **Qian J**, Truebenbach J, Graepler F, Pereira P, Huppert P, Eul T, Wiemann G, Claussen C. Application of poly-lactide-co-glycolide-microspheres in the transarterial chemoembolization in an animal model of hepatocellular carcinoma. *World J Gastroenterol* 2003; **9**: 94-98

28 **Trubenbach J**, Pereira PL, Graepler F, Huppert PE, Eul T, Konig CW, Duda SH, Claussen CD. Animal experiment studies on the effectiveness of permanent occlusion of the hepatic artery in transarterial chemoembolization. *Rofo Fortschr Geb Rontgenstr Neuen Bildgeb Verfahr* 2000; **172**: 274-277

29 **Trubenbach J**, Graepler F, Pereira PL, Ruck P, Lauer U, Gregor M, Claussen CD, Huppert PE. Growth characteristics and imaging properties of the morris hepatoma 3924A in ACI rats: a suitable model for transarterial chemoembolization. *Cardiovasc Intervent Radiol* 2000; **23**: 211-217

30 **Carlsson G**, Gullberg B, Hafstrom L. Estimation of liver tumor volume using different formulas-an experimental study in rats. *J Cancer Res Clin Oncol* 1983; **105**: 20-23

31 **Achenbach T**, Seifert JK, Pitton MB, Schunk K, Junginger T. Chemoembolization for primary liver cancer. *Eur J Surg Oncol* 2002; **28**: 37-41

32 **Yan FH**, Zhou KR, Cheng JM, Wang JH, Yan ZP, Da RR, Fan J, Ji Y. Role and limitation of FMPSPGR dynamic contrast scanning in the follow-up of patients with hepatocellular carcinoma treated by TACE. *World J Gastroenterol* 2002; **8**: 658-662

33 **Fan J**, Ten GJ, He SC, Guo JH, Yang DP, Weng GY. Arterial chemoembolization for hepatocellular carcinoma. *World J Gastroenterol* 1998; **4**: 33-37

34 **Choi BI**, Kim HC, Han JK, Park JH, Kim YI, Kim ST, Lee HS, Kim CY, Han MC. Therapeutic effect of transcatheter oily chemoembolization therapy for encapsulated nodular hepatocellular carcinoma: CT and pathologic findings. *Radiology* 1992; **182**: 709-713

35 **Clavien PA**, Kang KJ, Selzner N, Morse MA, Suhocki PV. Cryosurgery after chemoembolization for hepatocellular carcinoma in patients with cirrhosis. *J Gastrointest Surg* 2002; **6**: 95-101

36 **Lee HS**, Kim JS, Choi IJ, Chung JW, Park JH, Kim CY. The safety and efficacy of transcatheter arterial chemoembolization in the treatment of patients with hepatocellular carcinoma and main portal vein obstruction. A prospective controlled study. *Cancer* 1997; **79**: 2087-2094

37 **Lopez RR Jr,** Pan SH, Hoffman AL, Ramirez C, Rojter SE, Ramos H, McMonigle M, Lois J. Comparison of transarterial chemoembolization in patients with unresectable, diffuse vs focal hepatocellular carcinoma. *Arch Surg* 2002; **137**: 653-657

38 **Lin DY**, Lin SM, Liaw YF. Non-surgical treatment of hepatocellular carcinoma. *J Gastroenterol Hepatol* 1997; **12**: S319-S328

39 **Raoul JL**. Is chemoembolisation of value in inoperable primary hepatocellular carcinoma. *HPB Surg* 1998; **10**: 406-408

40 **Qian J**, Feng GS, Vogl TJ. Combined interventional therapies of hepatocellular carcinoma. *World J Gastroenterol* 2003; **9**:

41 **Iwai K**, Maeda H, Konno T. Use of oily contrast medium for selective drug targeting to tumor: Enhanced therapeutic effect and X-ray image. *Cancer Res* 1984; **44**: 2115-2121

42 **Camma C**, Schepis F, Orlando A, Albanese M, Shahied L, Trevisani F, Andreone P, Craxi A, Cottone M. Transarterial chemoembolization for unresectable hepatocellular carcinoma: meta-analysis of randomized controlled trials. *Radiology* 2002; **224**: 47-54

43 **Feng XS**, Qiu FZ, Xu Z. Experimental studies of embolization of different hepatotropic blood vessels using *Bletilla striata* in dogs. *J Tongji Med Univ* 1995; **15**: 454-459

44 **Qian J**, Feng G, Liang H. Action of DDPH in the interventional treatment of portal hypertension induced by liver cirrhosis in rabbits. *J Tongji Med Univ* 1998; **18**: 108-112

45 **Feng G**, Kramann B, Zheng C, Zhou R. Comparative study on the long-term effect of permanent embolization of hepatic artery with *Bletilla striata* in patients with primary liver cancer. *J Tongji Med Univ* 1996; **16**: 111-116

Edited by Wang XL

P.O.Box 2345, Beijing 100023,China
Fax: +86-10-85381893
E-mail: wjg@wjgnet.com www.wjgnet.com

World J Gastroenterol 2003;9(12):2681-2685
World Journal of Gastroenterology
 ISSN 1007-9327

• LIVER CANCER •

Side effects of budesonide in liver cirrhosis due to chronic autoimmune hepatitis: effect of hepatic metabolism versus portosystemic shunts on a patient complicated with HCC

Andreas Geier, Carsten Gartung, Christoph G. Dietrich, Hermann E. Wasmuth, Patrick Reinartz, Siegfried Matern

Andreas Geier, Carsten Gartung, Christoph G. Dietrich, Hermann E. Wasmuth, Siegfried Matern, Department of Internal Medicine III, University of Technology (RWTH) Aachen, Aachen, Germany
Patrick Reinartz, Nuclear Medicine, University of Technology (RWTH) Aachen, Aachen, Germany
Supported by Falk Pharma, Freiburgi. Br., Germany
Correspondence to: Andreas Geier, MD, Department of Internal Medicine III, University of Technology Aachen, Pauwelsstrasse 30, D-52074 Aachen, Germany. ageier@ukaachen.de
Telephone: +49-241-8088634 **Fax:** +49-241-8082455
Received: 2003-07-12 **Accepted:** 2003-09-13

Abstract

AIM: To investigate the systemic availability of budesonide in a patient with Child A cirrhosis due to autoimmune hepatitis (AIH) and primary hepatocellular carcinoma, who developed serious side effects.

METHODS: Serum levels of budesonide, 6β-OH-budesonide and 16α-OH-prednisolon were measured by HPLC/MS/MS; portosystemic shunt-index (SI) was determined by 99mTc nuclear imaging. All values were compared with a matched control patient without side effects.

RESULTS: Serum levels of budesonide were 13-fold increased in the index patient. The ratio between serum levels of the metabolites 6β-OH-budesonide and 16α-OH-prednisolone, respectively, and serum levels of budesonide was diminished (1.0 *vs*. 4.0 for 6β-OH-budesonide, 4.2 *vs*. 10.7 for 16α-OH-prednisolone). Both patients had portosystemic SI (5.7 % and 3.1 %) within the range of healthy subjects.

CONCLUSION: Serum levels of budesonide vary up to 13-fold in AIH patients with Child A cirrhosis in the absence of relevant portosystemic shunting. Reduced hepatic metabolism, as indicated by reduced metabolite-to-drug ratio, rather than portosystemic shunting may explain systemic side effects of this drug in cirrhosis.

Geier A, Gartung C, Dietrich CG, Wasmuth HE, Reinartz P, Matern S. Side effects of budesonide in liver cirrhosis due to chronic autoimmune hepatitis: effect of hepatic metabolism versus portosystemic shunts on a patient complicated with HCC. *World J Gastroenterol* 2003; 9(12): 2681-2685
http://www.wjgnet.com/1007-9327/9/2681.asp

INTRODUCTION

Autoimmune hepatitis is a chronic necroinflammatory liver disorder of unknown etiology associated with interface hepatitis, hypergammaglobulinemia and circulating autoantibodies, which was first described by Waldenström in 1950[1] and termed "autoimmune hepatitis" by the International Autoimmune Hepatitis Group in 1992[2]. The identification and characterization of serum autoantibodies led to differentiation of three different types characterized by antinuclear antibodies (type I), liver-kidney microsomal antibodies (type II) and soluble liver antigen (type III)[3,4]. The distinction between autoimmune hepatitis and other autoimmune liver diseases like primary biliary cirrhosis (PBC) and primary sclerosing cholangitis (PSC) is based on characteristic clinical, histological, biochemical and immunological features but overlap and variant syndromes may occur[5].

Primary hepatocellular carcinoma (HCC) is thought to be a consequence of the progression from chronic hepatitis to cirrhosis, although this sequence appears to be rare in autoimmune hepatitis[6]. In many patients who develop HCC hepatitis C virus infection has been found to be a complicating condition[7]. However, HCC also occurs in the absence of risk factors like hepatitis C infection and corticosteroid therapy[8].

Autoimmune hepatitis is generally responsive to corticosteroid therapy despite its striking heterogeneity[1]. Corticosteroids alone or in combination with azathioprine are the treatment of choice and result in remission induction in over 80 % of patients[9,10]. Early clinical trials with prednisolone documented improvement of liver function tests, amelioration of symptoms and prolonged survival, thereby establishing corticosteroids as the "standard therapy"[11-13]. Azathioprine has no role in inducing remission but may be used for maintenance of remission induced by initial corticosteroid therapy or their dose reduction in combination therapy[9]. The potential usefullness of other immunosuppressives like cyclosporine and tacrolimus has been shown but has not yet been clinically established[9]. Since about 70 % of patients with AIH require lifelong immunosuppressive therapy, long-term use of corticosteroids is often accompanied by numerous systemic side effects, such as osteoporosis, diabetes mellitus, systemic hypertension, psychiatric disorders and altered steroid metabolism[14].

The search for new corticosteroids with a more favourable risk-to-benefit ratio led to the discovery of a new class of corticosteroids with high receptor affinity and particularly high first-pass effect in the liver resulting in lower systemic side effects. Budesonide, a nonhalogenated glucocorticoid derivative of the second generation exhibits a receptor affinity 15-20 times that of prednisolone and a 90 % first-pass metabolism in healthy liver[9]. Two major metabolites, 6β-OH-budesonide and 16α-OH-prednisolone, have been identified which lack glucocorticoid activity making the original compound virtually devoid of systemic side effects[15]. Budesonide has been evaluated in patients with primary biliary cirrhosis (PBC) and primary sclerosing cholangitis (PSC) at a dose of 9 mg/day with contradicting results concerning additional benefit to the standard therapy with ursodeoxycholic acid (UDCA)[16-19]. In autoimmune hepatitis only two small uncontrolled trials with a limited number of patients and rather disappointing results have been published[20,21]. In one study including 10 patients who were dependent on continuous

treatment to prevent exacerbation budesonide failed to induce clinical and biochemical remission in 7 patients who either deteriorated or became drug intolerant[21]. In a second study with 13 patients budesonide has been found to lower transaminase levels significantly while causing a low frequency of systemic side effects and only a marginal reduction in plasma cortisol in noncirrhotic patients[20]. However, the majority of patients did not reach full biochemical remission defined as normal ALT values. Patients with cirrhosis experienced higher serum cortisol levels and a partial suppression of the hypothalamic-pituitary-adrenal (HPA) axis suggestive for at least a latent systemic activity of budesonide[20].

An explanation for a variable and so far unpredictable extent of systemic side effects in patients with early liver disease treated with budesonide may be either a reduced metabolic function or the presence of latent portosystemic shunts bypassing the liver. However, no data are presently available on the metabolism of budesonide in cirrhotic livers and the incidence of side effects in these patients. Thus, there are no recommendations for therapy with budesonide in cirrhotic patients with AIH to date.

To our knowledge, treatment of patients with coexisting HCC or other malignancies has so far not been reported in literature. Systemic immunosuppression exposes such patients to an increased risk of tumor recurrance after curative surgical treatment of the malignant disorder. A risk stratification for systemic effects of budesonide by assessment of the portosystemic shunt-index (SI) and the metabolic activity of the cirrhotic liver is of major importance in these patients. We report the first case of successfull treatment of a patient with AIH after resection of a HCC and show a predominance of hepatic metabolism over portosystemic shunting on sytemic availability and side effects of budesonide in this patient with Child A cirrhosis.

MATERIALS AND METHODS

Clinical data

A 65-year-old caucasian woman (patient 1) with a 27-year history of unclassified chronic hepatitis was referred to our liver unit with a newly diagnosed liver mass during regular ultrasound screening. She experienced icteric episodes 27 and 14 years ago and a known asymptomatic cholecystolithiasis. Physical examination of the anicteric patient was unremarkable despite liver enlargement without a palpable mass. Clinical chemistry on admission showed mild signs of hepatic inflammation (AST 24 U/L, GGT 53 U/L) without elevation of further liver function tests or pancreatic enzymes. Biochemical tests revealed type I autoimmune hepatitis with antinuclear (titer 1:320), anticytoplasmatic (titer 1:320) and anti-smooth muscle antibodies (titer 1:640) as well as elevated gamma-globulins (29 % of total proteins, IgG 25.7 g/L). Quantification of alpha-1-antitrypsin, ceruloplasmin, serum iron, ferritin, transferrin saturation, serum copper and urinary copper excretion were within normal limits, and serologic tests for anti-HAV, anti-HBs, anti-HBc, HBs-antigen and anti-HCV were all negative. On ultrasound the liver appeared cirrhotic with a 4.5×3.9 cm mass in the right lobe. Computed tomography (CT) depicted a 4 cm mass in segment VI of the right lobe of the liver with contrast enhancement. Alpha-1-fetoprotein (AFP) was not elevated. A CT-guided Tru-cut biopsy confirmed the diagnosis of a primary HCC in a cirrhotic liver. Tumor staging revealed no signs of metastasis in thoracic CT, ^{19}fluor deoxyglucose positron emission tomography. Preoperative staging of the liver disease led to a grade A cirrhosis according to the Child-Pugh classification. Endoscopy of the upper GI tract did not detect obvious varices of the esophagus and gastric fundus.

The patient underwent atypical resection of segment VI liver without further complications. Follow-up in our liver outpatient clinic showed functional liver tests at the preoperative level with mild AST and GGT elevation. Three months after resection of the HCC, transaminase levels sharply increased over a period of 4 months with peak transaminases of ALT 247 U/L and AST 312 U/L. No signs of tumor recurrance were detectable by abdominal CT and AFP levels. In order to prevent further progression of the Child A cirrhosis, we initiated a therapy with budesonide which was favoured over systemic immunosuppressive treatment with respect to the antecipated lower risk of tumor recurrance. Transaminase levels dropped rapidly to the normal range during a daily dose of 9 mg budesonide. Remission was achieved within two months after starting budesonide, but systemic side effects such as facial swelling, leg edemas and weight gain occurred. To minimize these adverse effects and systemic immunosuppression, we tapered the dose to 6 mg/day for maintenance therapy. Follow-up for potential tumor recurrance with corticosteroid therapy revealed normal CT-scans and AFP levels so far. Almost four years after tumor resection, the patient is still in remission in regard to AIH at a daily dose of 6 mg budesonide. In this index patient we assessed the determinants of systemic effects of budesonide in comparison with another AIH patient matched for age, sex and functional Child-Pugh stage (patient 2, caucasian female, 67 years of age, Child A cirrhosis diagnosed by liver biopsy) with steroid dependency, no apparent varices) and historic healthy controls.

Budesonide and its metabolites

Levels of budesonide, 6β-OH-budesonide and 16α-OH-prednisolone were determined in serum 3 hours (allowance ± 60 minutes) after intake by a validated HPLC/MS/MS assay. Serum was extracted by solid phase extraction and the reconstituted extract was analyzed by HPLC/MS/MS on a Micromass Quatro LC using reversed phase chromatography and the negative electrospray ionization mode. The limit of detection was defined as 100 pg/ml for all analytes. All determinations have been performed by H.W. Moellmann (Medical Clinic Bergmannsheil, Bochum, Germany) and funded by Falk Pharma (Freiburg i.B., Germany). Falk Pharma had no involvement in analysis, interpretation and publication of the data.

Cortisol levels

Basal cortisol levels and cortisol levels in response to 100 μg corticotropine releasing hormone (CRH) were measured with routine clinical chemistry. Both tests were performed at 8 A. M. and stimulated cortisol levels were determined over 90 minutes after intravenous application of CRH.

Portosystemic shunt-index (SI)

Portosystemic SI was determined by nuclear imaging after rectal application of ^{99m}Technetium pertechnetate (Tc) as described[22]. Briefly, the rectum was emptied by administration of a laxative and a polyethylene tube was inserted. After positioning of a large-field scintillation camera over the patient 340 MBq of ^{99m}Tc pertechnetate was given over the tube and time-activity curves for the areas of the liver and heart were obtained. After normalization portosystemic SI was calculated from the activity of the liver and heart.

Cortisol and portosystemic shunt-index was measured at the time of the first serum analysis on budesonide and metabolites. All measurements were determined with informed consent by both patients.

RESULTS

Serum levels of budesonide and its metabolites

Serum budesonide levels were determined 3 h after intake of 6 mg at 4 different time points during five months (Figure 1). At all time points serum budesonide levels were markedly elevated in the index case (mean 1.9 ng/ml) when compared with the control patient (mean budesonide level 0.15 ng/ml) and historic healthy controls without liver disease (0.4-0.7 ng/ml)[23]. Systemic availability in patient 2 was remarkably lower even with a higher dose of 9 mg budesonide. However, serum levels of this control patient was in close comparison with the historic healthy controls, further supporting a potential clinical relevance of the elevated serum budesonide levels in the index patient. To determine whether elevated serum budesonide levels resulted from impaired hepatic metabolism, 6β-OH-budesonide and 16α-OH-prednisolone as its major inactive metabolites were measured in both patients (Figure 2). Although both metabolites were detectable in both the index and control patient, the mean ratio of metabolites to drug serum levels were significantly lower for both 6β-OH-budesonide (1.0- *vs*. 4.0-fold) and 16α-OH-prednisolone (4.2- *vs*. 10.7-fold) in the index compared with the control patient (Figure 2).

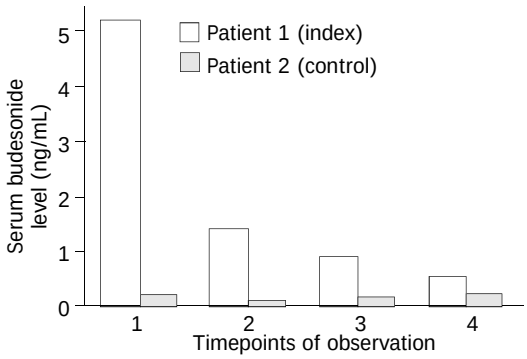

Figure 1 Serum concentration of budesonide. Serum levels of budesonide were analyzed 3 hours after intake of 6 mg 4 times during a 5-month period of follow-up. Budesonide levels were largely elevated in the index case compared to the control patient 2 with average drug levels of 1.9±2.1 ng/mL and 0.15±0.07 ng/mL, respectively. The dashed line indicates serum levels of heathy controls.

Effect of budesonide on cortisol levels

To further determine the potential systemic effects of budesonide, serum cortisol levels were measured at baseline and after stimulation by 100 μg corticotropine releasing hormone (CRH). Whereas basal and stimulated serum cortisol levels were within the normal range in the control patient, the index patient showed marked suppression of serum cortisol [<6 nmol/L (normal range 119-618 nmol/l)] and no significant stimulation by CRH within 90 min after application (maximum level 63 nmol/L at 60 min).

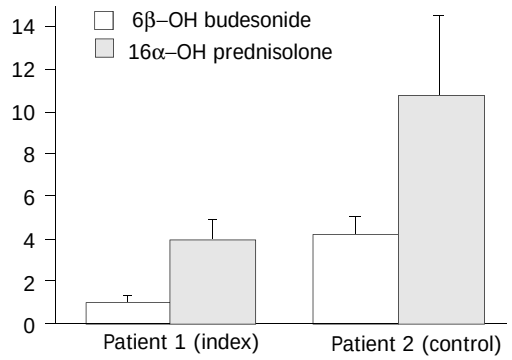

Figure 2 Ratio of metabolites to budesonide. 6β-OH-budesonide and 16α-OH-prednisolone serum levels were determined at the same time points as given in Figure 1. Metabolite-to-drug ratios were calculated and data are given as average ± SEM.

Portosystemic shunt index

To differentiate whether elevated serum budesonide levels were caused by increased portosystemic shunting due to liver cirrhosis, portal hemodynamics were assessed by per-rectal portal scintigraphy with ^{99m}Tc pertechnetate in both patients. In both the index and the control patient measurement of the portosystemic shunt index was 5.7 % and 3.1 %, respectively, which was in the range of healthy subjects (median 4.1 %; 25th percentile 2.8; 75th percentile 6.3 %)[22]. Thus, these data confirmed that no significant portosystemic shunting occurred in both patients (Figure 3).

DISCUSSION

Autoimmune hepatitis is currently treated with systemic administration of prednisolone, which has been shown to improve liver function tests and prolong survival[11-13]. These first-generation glucocorticoids may cause marked side effects in long-term therapy. In order to minimize the systemic bioavailability, a new class of corticosteroids with greater topical anti-inflammatory activity and particularly high first-pass effect in healthy liver was synthesized[24]. Budesonide, a member of this second generation, has a 90 % first pass metabolism in the healthy liver and its metabolites are virtually devoid of systemic side effects[9]. Therefore, it does not reduce peripheral cortisol levels as a measure of systemic effect on adrenal function to the same extent as prednisolone in

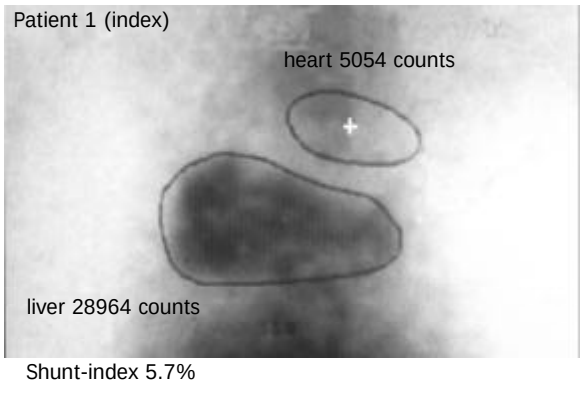

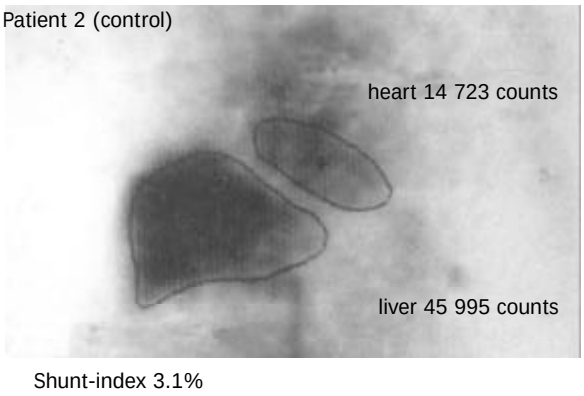

Figure 3 Portosystemic shunt index. Summed images with regions of interest over heart and liver of patients 1 (A) and 2 (B) after per rectal scintigraphy using 340MBq Tc-99m petechnetate.

noncirrhotic patients[24]. However, in a double-blind crossover study in healthy volunteers ileal release budesonide had a greater effect on plasma cortisol levels compared with placebo[25]. In patients with Crohn's disease budesonide reduced the median plasma cortisol concentrations at doses of 9-15 mg/day, whereas median cortisol values in the group given 3 mg/day were not different from placebo[26].

In patients with liver disease, systemic side effects are variable. In patients with primary biliary cirrhosis treated with 9 mg budesonide per day (in addition to UDCA) changes in bone mineral density were not significantly different as compared with pretreatment data and placebo over 2 years in the study by Leuschner *et al*.[16], whereas Angulo and coworkers found a significant loss of bone mass with the same treatment regimen over one year[17]. This difference may be related to the number of patients with PBC stage IV of disease who experienced a significantly greater loss of bone mass in the Angulo study compared with non-cirrhotic patients. Leuschner and coworkers enrolled only patients of PBC stages I to III in this study. Similar findings were obtained in patients with primary sclerosing cholangitis in whom budesonide appears to be of minimal if any benefit and is associated with a significant worsening of osteoporosis[18,19]. Although the drug is considered to be a promising candidate for treatment, only two small uncontrolled studies on budesonide in patients with autoimmune hepatitis have been published to date[20,21]. In parallel with findings in PBC and PSC therapeutic efficacy of budesonide on AIH appeared to be limitied and systemic side effects shown as decreased plasma cortisol levels were noted predominantly in those patients with cirrhosis[15,20]. Although there are no published data on a possible decrease in first pass hepatic metabolism in patients with cirrhosis and consecutive higher incidence of systemic adverse effects, indirect findings such as increased osteoporosis in budesonide-treated patients with more advanced liver disease support this hypothesis[17]. This could be due to reduced hepatic metabolism in the cirrhotic liver or, alternatively, due to increased spontaneous portosystemic shunting in these patients who may have a substantial bypass of the liver.

Portosystemic collaterals develop as chronic hepatitis and cirrhosis progress. Several methods for measurement of portosystemic shunting have been established, of which radio-isotopic imaging after per-rectal ^{99m}Tc administration with determination of the heart-liver ratio (shunt index) is most common[22,27-30]. A cross sectional study using this method has shown an increasing portal shunt index (SI) with progression of various liver diseases[22]. In this study, healthy controls and patients with chronic hepatitis showed shunt indices with medians between 5.9 % and 10 %, respectively. Patients with cirrhosis without esophageal varices had only moderatly increased portosystemic shunt indices with a median of 15 % (25^{th} percentile 9 %, 75^{th} percentile 28 %) whereas those cirrhotics with varices appeared to have dramatically increased shunting with a median SI of 70 % (25^{th} percentile 52 %, 75^{th} percentile 82 %).

Hepatic metabolism and the extent of the portosystemic shunting largely affects the bioavailability of drugs with high first-pass metabolism such as budesonide. To date, there are no data about systemic availability of the drug and its determinants in patients with advanced liver disease. To address this question and to distinguish between reduced hepatic metabolism and portosystemic shunting as the cause of higher bioavailability, we determined the serum levels of budesonide, its two major metabolites and the portal shunt index in two patients. The index patient 1 was compared with an age and sex matched AIH-patient with the same stage of cirrhosis but absent systemic effects as control. Serum levels of budesonide were largely elevated in the index case (1.9±2.1 ng/mL, n=4) compared with the control patient 2 (0.15±0.07 ng/mL, n=4) and historically healthy controls without liver disease (0.4-0.7 ng/mL)[23] (Figure 1). Although 6β-OH-budesonide and 16α-OH-prednisolone serum levels were also elevated 3-fold and 4.4-fold in the index patient as against patient 2, we detected 4-fold decreased metabolite-to-drug ratios for both 6β-OH-budesonide and 16α-OH-prednisolone in the index patient 1 compared with the control patient 2 (Figure 2). Both patients had similar shunt indices which were in the range of healthy subjects (Figure 3). These data demonstrate that an increased systemic bioavailability of budesonide may be rather due to a reduced hepatic metabolizing capacity in patients with early stages of liver disease than portosystemic shunting of an undetectable volume.

In these patients with coexisting malignancies, there is major concern about corticosteroid-related systemic immunosuppression which imposes a substantial risk of recurrance or progression of malignancy on these patients. To our knowledge, there is no report available on steroid therapy in a patient with autoimmune hepatitis and coexisting hepatic malignancy. The present case is the first reported patient with successfull treatment of AIH complicated by HCC. The substantial inflammatory activity in this patient, who had already developed liver cirrhosis, made an anti-inflammatory therapy unevitable to halt progression. In this complex situation between progression to end stage cirrhosis and recurrance of the carcinoma, budesonide seems to be the only therapeutic alternative to minimize both risks. Although low bioavailability and high first pass metabolism of budesonide are observed in healthy volunteers, systemic availability in patients with liver cirrhosis seems to be associated with decreased hepatic metabolism after exclusion of significant portosystemic shunting (Figure 3). In order to minimize systemic immunosuppression with a concommitant risk of recurrant malignancy, we tapered the daily dose from 9 mg to 6 mg per day after systemic side effects appeared. Our present study identified increased systemic budesonide levels due to reduced hepatic metabolism as a risk factor of tumor recurrance in this patient. Therefore, we closely monitored the recurrance of the HCC in short intervals by ultrasound, computed tomography and AFP levels without any signs of recurrant malignancy under budesonide for 36 months.

Whether budesonide becomes standard therapy in autoimmune hepatitis remains to be determined in larger clinical trials. In patients with concommitant malignant disorders, this drug may have the best benefit-to-risk ratio of all immunosuppressants and may be helpful even in patients with reduced hepatic metabolism due to liver cirrhosis. However, these patients have a substantial risk of systemic side effects even in the absence of detectable portosystemic shunting and need to be monitored carefully.

REFERENCES

1 **Krawitt EL**. Autoimmune hepatitis. *N Engl J Med* 1996; **334**: 897-903

2 **Johnson PJ**, McFarlane IG. Meeting report: International Autoimmune Hepatitis Group. *Hepatology* 1993; **18**: 998-1005

3 **Manns MP**, Strassburg CP. Autoimmune hepatitis: clinical challenges. *Gastroenterology* 2001; **120**: 1502-1517

4 **Strassburg CP**, Manns MP. Autoantibodies and autoantigens in autoimmune hepatitis. *Semin Liver Dis* 2002; **22**: 339-352

5 **Alvarez F**, Berg PA, Bianchi FB, Bianchi L, Burroughs AK, Cancado EL, Chapman RW, Cooksley WG, Czaja AJ, Desmet VJ, Donaldson PT, Eddleston AL, Fainboim L, Heathcote J, Homberg JC, Hoofnagle JH, Kakumu S, Krawitt EL, Mackay IR, MacSween RN, Maddrey WC, Manns MP, McFarlane IG, Meyer ZBK, Zeniya M. International Autoimmune Hepatitis Group Report: review of criteria for diagnosis of autoimmune hepatitis. *J Hepatol* 1999; **31**: 929-938

6 **Wang KK**, Czaja AJ. Hepatocellular carcinoma in corticosteroid-treated severe autoimmune chronic active hepatitis. *Hepatology* 1988; **8**: 1679-1683

7 **Ryder SD**, Koskinas J, Rizzi PM, McFarlane IG, Portmann BC, Naoumov NV, Williams R. Hepatocellular carcinoma complicating autoimmune hepatitis: role of hepatitis C virus. *Hepatology* 1995; **22**: 718-722

8 **Watanabe M**, Moritani M, Hamamoto S, Uchida Y, Ishihara S, Adachi K, Kinoshita Y. Hepatocellular carcinoma complicating HCV-negative autoimmune hepatitis without corticosteroid therapy. *J Clin Gastroenterol* 2000; **30**: 445-446

9 **Heneghan MA**, McFarlane IG. Current and novel immunosuppressive therapy for autoimmune hepatitis. *Hepatology* 2002; **35**: 7-13

10 **Czaja AJ**. Treatment of autoimmune hepatitis. *Semin Liver Dis* 2002; **22**: 365-378

11 **Soloway RD**, Summerskill WH, Baggenstoss AH, Geall MG, Gitnick GL, Elveback IR, Schoenfield LJ. Clinical, biochemical, and histological remission of severe chronic active liver disease: a controlled study of treatments and early prognosis. *Gastroenterology* 1972; **63**: 820-833

12 **Cook GC**, Mulligan R, Sherlock S. Controlled prospective trial of corticosteroid therapy in active chronic hepatitis. *Q J Med* 1971; **40**: 159-185

13 **Murray-Lyon IM**, Stern RB, Williams R. Controlled trial of prednisone and azathioprine in active chronic hepatitis. *Lancet* 1973; **1**: 735-737

14 **Obermayer-Straub P**, Strassburg CP, Manns MP. Autoimmune hepatitis. *J Hepatol* 2000; **32 (1 Suppl)**: 181-197

15 **Ryrfeldt A**, Andersson P, Edsbacker S, Tonnesson M, Davies D, Pauwels R. Pharmacokinetics and metabolism of budesonide, a selective glucocorticoid. *Eur J Respir Dis Suppl* 1982; **122**: 86-95

16 **Leuschner M**, Maier KP, Schlichting J, Strahl S, Herrmann G, Dahm HH, Ackermann H, Happ J, Leuschner U. Oral budesonide and ursodeoxycholic acid for treatment of primary biliary cirrhosis: results of a prospective double-blind trial. *Gastroenterology* 1999; **117**: 918-925

17 **Angulo P**, Jorgensen RA, Keach JC, Dickson ER, Smith C, Lindor KD. Oral budesonide in the treatment of patients with primary biliary cirrhosis with a suboptimal response to ursodeoxycholic acid. *Hepatology* 2000; **31**: 318-323

18 **Van Hoogstraten HJ**, Vleggaar FP, Boland GJ, van Steenbergen W, Griffioen P, Hop WC, van Hattum J, van Berge H, Schalm SW, van Buuren HR. Budesonide or prednisone in combination with ursodeoxycholic acid in primary sclerosing cholangitis: a randomized double-blind pilot study. Belgian-Dutch PSC Study Group. *Am J Gastroenterol* 2000; **95**: 2015 -2022

19 **Angulo P**, Batts KP, Jorgensen RA, LaRusso NA, Lindor KD. Oral budesonide in the treatment of primary sclerosing cholangitis. *Am J Gastroenterol* 2000; **95**: 2333 -2337

20 **Danielsson A**, Prytz H. Oral budesonide for treatment of autoimmune chronic active hepatitis. *Aliment Pharmacol Ther* 1994; **8**: 585-590

21 **Czaja AJ**. Drug therapy in the management of type 1 autoimmune hepatitis. *Drugs* 1999; **57**: 49-68

22 **Shiomi S**, Sasaki N, Habu D, Takeda T, Nishiguchi S, Kuroki T, Tanaka T, Ochi H. Natural course of portal hemodynamics in patients with chronic liver diseases, evaluated by per-rectal portal scintigraphy with Tc-99m pertechnetate. *J Gastroenterol* 1998; **33**: 517-522

23 **Mollmann HW**, Hochhaus G, Tromm A, Froehlich P, Mollmann AC, Krieg M, Weiser H, Derendorf H, Barth J. Pharmacokinetics and pharmacodynamics of budesonide pH-modified release capsules. In: Mollmann HW, May B, eds. Glucocorticoid therapy in chronic inflammatory bowel disease - from basic principles to rational therapy. Dordrecht, Boston, London: *Kluwer Academic Publishers* 1996: 107-120

24 **Spencer CM**, McTavish D. Budesonide. A review of its pharmacological properties and therapeutic efficacy in inflammatory bowel disease. *Drugs* 1995; **50**: 854-872

25 **Edsbacker S**, Nilsson M, Larsson P. A cortisol suppression dose-response comparison of budesonide in controlled ileal release capsules with prednisolone. *Aliment Pharmacol Ther* 1999; **13**: 219-224

26 **Greenberg GR**, Feagan BG, Martin F, Sutherland LR, Thomson AB, Williams CN, Nilsson LG, Persson T. Oral budesonide for active Crohn's disease. Canadian Inflammatory Bowel Disease Study Group. *N Engl J Med* 1994; **331**: 836-841

27 **Shiomi S**, Kuroki T, Kurai O, Kobayashi K, Ikeoka N, Monna T, Ochi H. Portal circulation by technetium-99m pertechnetate per-rectal portal scintigraphy. *J Nucl Med* 1988; **29**: 460-465

28 **Shiomi S**, Kuroki T, Ueda T, Takeda T, Ikeoka N, Nishiguchi S, Nakajima S, Kobayashi K, Ochi H. Clinical usefulness of evaluation of portal circulation by per rectal portal scintigraphy with technetium-99m pertechnetate. *Am J Gastroenterol* 1995; **90**: 460-465

29 **D'Arienzo A**, Celentano L, Cimino L, Panarese A, Lancia C, Vergara E, Castaldo G, Oriani G, Squame G, Budillon G. Per-rectal portal scintigraphy with technetium-99m pertechnetate for the early diagnosis of cirrhosis in patients with chronic hepatitis. *J Hepatol* 1992; **14**: 188-193

30 **Wang JY**, Chen SL, Chen FZ, Xu WG, Hu DC, Chen XF, Jin G, Liu HY. A non-invasive method for evaluating cirrhotic portal hypertension by administration of 99mTc-MIBI per rectum. *J Gastroenterol Hepatol* 1995; **10**: 169-173

Edited by Ma JY

P.O.Box 2345, Beijing 100023,China
Fax: +86-10-85381893
E-mail: wjg@wjgnet.com www.wjgnet.com

World J Gastroenterol 2003;9(12):2686-2689
World Journal of Gastroenterology
 ISSN 1007-9327

• LIVER CANCER •

Percutaneous cryoablation in combination with ethanol injection for unresectable hepatocellular carcinoma

Ke-Cheng Xu, Li-Zhi Niu, Wei-Bin He, Zi-Qian Guo, Yi-Ze Hu, Jian-Sheng Zuo

Ke-Cheng Xu, Li-Zhi Niu, Wei-bin He, Zi-Qian Guo,Yi-Ze Hu, Jian-Sheng Zuo, Fuda Cancer Hospital of Guangzhou,Guangzhou 510300, Guangdong Province, China
Correspondence to: Dr. Ke-Cheng Xu, Fuda Cancer Hospital of Guangzhou, Guangzhou 510300, Guangdong Province, China. xukc1818@sina.com
Telephone: +86-20-84196175 **Fax:** +86-20-84195515
Received: 2003-03-10 **Accepted:** 2003-05-16

Abstract

AIM: To evaluate the effectiveness and safety of percutaneous hepatic cryoablation in combination with percutaneous ethanol injection (PEI) in patients with unresectable hepaocellular carcinoma (HCC).

METHODS: A total of 105 masses in 65 HCC patients underwent percutaneous hepatic cryoablation. The cryoablation was performed with the Cryocare system (Endocare, Irvine, CA, USA) using argon gas as a cryogen. Two freeze-thaw cycles were performed, each reaching a temperature of -180 ℃ at the tip of the probe. PEI was given in 36 patients with tumor masses larger than 6 cm in diameter 1-2 weeks after cryoablation and then once per week for 4 to 6 sessions. The efficacy was evaluated with survival, change of tumor size and alpha-fetoprotein (AFP) levels.

RESULTS: During a follow-up duration of 14 months in average with a range of 5 to 21 months, 33 patients (50.8 %) were free of tumors, 22 patients (33.8 %) alive with tumor recurrence: two had bone metastases, three were found to have lung metastases, and the remaining 17 recurrences occurred in the liver, of whom only 3 developed a cryosite recurrence. Among the 41 patients who were followed up for more than one year, 32(78 %) were alive despite of tumor recurrence. Seven patients (10.8 %) died due to disease recurrence. Three patients (4.6 %) died due to some noncancer-related causes. Among the 43 patients who had a CT scan available for review, 38 (88.4 %) had a shrinkage of tumor mass. Among the 22 patients who received biopsies of cryoablated tumor mass, all biopsies except one, showed only dead or scar tissues. Of the patients who had an increased AFP preablatively, 91.3 % had a decrease of AFP to normal or nearly normal levels during postablative 3-6 months. Complications of cryoablation included liver capsular cracking in one patient,transient thrombocytopenia in 4 patients and asymptomatic right-sided pleural effusions in 2 patients. Two patients developed liver abscess at the previous cryoablation site at 2 and 4 months, respectively, following cryoablation, and was recovered after treated with antibiotics and drainage.

CONCLUSION: Percutaneous cryoablation offers a safe and possibly curative treatment option for patients with HCC that cannot be surgically removed, and its integration with PEI, may serve as an alternative to partial liver resection in selective patients.

Xu KC, Niu LZ, He WB, Guo ZQ, Hu YZ, Zuo JS. Percutaneous cryoablation in combination with ethanol injection for unresectable hepatocellular carcinoma. *World J Gastroenterol* 2003; 9(12): 2686-2689
http://www.wjgnet.com/1007-9327/9/2686.asp

INTRODUCTION

Hepatocellular carcinoma (HCC) is one of the most common and lethal cancers. Curative surgical resection of HCC is considered to be the optimal treatment. Unfortunately, only about 10 % of newly diagnosed HCC patients are eligible candidates for resection[1]. Therefore, alternative treatment modalities have been developed, including localized ablative techniques involving either freezing (cryoablation) or chemical desiccation (ethanol ablation)[2].

Cryoablation uses extremely low temperature to destroy tumor tissues, and has been shown to be as effective as surgical resection for treatment of primary or metastatic liver cancer[3]. Percutaneous ethanol injection (PEI) has been reported to be effective against small HCC, but is not eligible for advanced HCC[4]. We employed percutaneous cryoablation in combination with ethanol injection following cryoablation for treatment of unresectable HCC and yielded better results. This paper reports our experience using the combined therapy in 65 HCC patients and evaluates the effectiveness and safety.

MATERIALS AND METHODS

Subjects

Between March 2001 and January 2003, 65 HCC patients underwent combined treatment of percutaneous hepatic cryoablation and PEI. There were 47 men and 18 women. Their ages ranged from 32 to 78 years, with a mean age of 51 years. Sixty patients had histories of heapatitis B infection, and 4 had hepatitis C infection. Informed consents were obtained from all patients undergoing combined therapy.

The diagnosis of HCC in 43 patients was proven by liver pathology, and the remaining cases had HCC diagnosed by classical imagings, including computed tomography (CT), magnetic resonance and ultrasonography, and biochemical markers, such as increased alpha-fetoprotein (AFP). Forty-four patients had only one mass in the liver, being 4.8 cm to 15 cm in diameter with an average of 7.3 cm. Twenty-one patients had 2-4 masses from 6 cm to 14 cm in diameter. There were a total of 105 masses in 65 patients and the average number of masses per patient was 2.6.No patient had evidence of extrahepatic metastases.

All except 2 cases had cirrhosis. Using Child-Pugh' s score in assessing the severity of cirrhosis, 39 patients were classified as class A, and 25 as class B.

Cryoablation procedure

The cryoablation was performed with the Cryocare system (Endocare, Irvine, CA, USA) using argon gas as a cryogen.

Cryoprobes (3, 5 or 8 mm) were inserted into the center of tumor mass under ultrasonographic guidance, and two freeze-thaw cycles were performed, each reaching a temperature of -180 ℃ at the tip of the probe. The time of freezing was dependent on the achievement of an "ice ball", visible as a hypoechoic region by ultrasonography. Generally, the tumor was frozen at a maximum flow rate for about 15 minutes, thawed for 5 minutes and then refrozen for another 15 minutes. A margin of at least 1 cm normal hepatic tissue was frozen circumferentially around the tumor. For the mass larger than 5 cm in diameter, two or three cryoprobes were placed within the center and periphery of tumor respectively, to insure freezing of the entire tumor. Finally, the cryoprobe was removed when the tip temperature reached above 0 ℃, and the tract formed was sealed off with fibrin glue immediately after removal of the cryoprobe to ensure haemostasis.

Alcohol ablation

PEI was administered in 36 patients with tumor masses larger than 6 cm in diameter and was given 1-2 weeks after cryoablation and then once a week for up to 4-6 sessions. Absolute alcohol (100 %) was slowly injected into the peripheral zone of cancerous tissues in liver through a 20-gauge needle under ultrasonographic guidance. The goal of this procedure was to achieve a "black stain" shown by ultrasonography in the tumor tissues. A maximum of 5 ml alcohol was injected per site, with a maximum of 20 ml per session.

Postoperative follow-up

All patients were followed up at monthly intervals. The serum α-fetoprotein (AFP) levels were assayed during each visit. The first CT scanning was performed within one month after cryoablation to detect residual tumor, and then CT scan study was done every 3 months in the initial six months and every 6 months subsequently to detect recurrence.

RESULTS

Disease status and survival

All patients were followed up for a median duration of 14 months with a range of 5-21 months. The disease status of the patients is shown in Table 1. Thirty-three patients (50.8 %) were currently free of tumor with an average follow-up of 13.8 months. Twenty-two patients (33.8 %) were alive with disease recurrence: two had bone metastases, three were found to have lung metastases, and the remaining 17 had recurrences in the liver, of whom only 3 developed a cryosite recurrence. Among the 41 patients who were followed up for more than one year, 32 (78 %) were alive despite of tumor recurrence. Seven patients (10.8 %) died from their tumors, and had recurrence of tumor in the liver remnant at a mean of 7.8 months with an overall survival of 13.2 months. Three patients (4.6 %) died of noncancer-related causes. One died of myocardial infarction,1 died of pneumonia, and 1 died of liver failure,respectively.

Table 1 Disease status

	Number of patients	Percent of patients	Follow-up (months)
Alive free of tumor	33	50.8	16.8
Alive with tumor recurrence	22	33.8	17.2
Died of tumor recurrence	7	10.8	13
Died of noncancer-related diseases	3	4.6	4

Tumor size

Among the forty-three patients who had a CT scan available for review, 38 (88.4 %) had a shrinkage of tumor mass, with an average size of the dominant tumor changing from a preablative size of 7.9 cm (3.7-13.2 cm) to a 3-month postablative size of 5.6 cm (2.1-8 cm). Twenty-two received biopsies of their cryoablated tumor mass under ultrasonography guidance. All biopsies except one, showed only dead or scar tissues.

Serum AFP levels

An increased serum AFP, with a median level of 367 ng/L, ranging from 68 to 1 210 ng/L, was detected in 46 patients preablatively. The AFP levels were lowered to normal or nearly normal range in 42 patients (91.3%) during postablative 3-6 months, and the median AFP level was 59 ng/L with a range of 12-365 ng/L.

Complications

Complications of cryoablation included liver capsular cracking in one patient and recovered after blood transfusion. Transient thrombocytopenia occurred in 4 patients within 1 week following cryoablation, 2 of whom received platelet transfusion. Two patients developed asymptomatic right-sided pleural effusions, both had cancer in the right lobe which was close to the dome of the diaphragm. The pleural effusions disappeared spontaneously within 2-3 weeks. Two patients developed liver abscess at the previous cryoablation site 2 and 4 months respectively following cryoablation, and were recovered after antibiotics and drainage treatment.

The majority of patients receiving PEI had pain at injection site, fever and a feeling of alcohol intoxication, which were transient and subsided with conservative management. No patient experienced an appreciable risk.

DISCUSSION

Prognosis of unresectable HCC is very poor. In Japan, the median survival for 229 patients receiving no specific treatment was 1.6 months[5]. Although chemoembolization is associated with good objective responses in the tumor, a recent controlled trial showed that by itself, chemoembolization offered no improvement in survival compared with supportive therapy alone[6]. During the past years, great efforts have been made to improve the survival of patients with this disease[7]. In this trial, percutaneous cryoablation in combination with PEI showed more satisfactory therapeutic efficacy. Among the 65 HCC patients receiving this combined therapy and followed up for a median duration of 14 months, 50.8 % of the patients are currently free of tumor and 33.8 % are alive with tumor recurrences. Among the 41 patients who were followed up for more than one year, 78 % are alive despite of tumor recurrence. Only 10.8 % died from tumor recurrence with an overall survival for 13.2 months. Of the patients who had CT scan available for review, 88.4 % had a shrinkage of tumor masses. Of the 22 patients who received biopsies of their cryoablated tumor masses, all but one showed only dead tumor cells or scar. Of the patients who had an increased AFP preablatively, 91.3 % had a decrease of AFP to normal or nearly normal levels during postablative 3-6 months.

The present result is comparable with those by other authors. Crews *et al*[8] reported that forty patients with hepatic malignancy underwent cryoablation and the estimated 18-month survival was 60 % and 30 % for patients with HCC and with colorectal metastasis, respectively. Lam *et al*[9] treated 4 patients with recurrent HCC after previous curative hepatectomy with cryoablation. All their patients are still alive with a survival after cryoablation ranging from 12 to 23 months. Sheen *et al*[10] have demonstrated that the median survival for HCC patients after cryoablation was 36 months. Zhou *et al*[11,12]

reported 1-, 3- and 5-year survival rates of 78 %, 54 % and 40 %, respectively in 235 HCC patients who received cryoablation. It should be noted that the cryoablation reported by these authors was mainly performed through intraoperative approach with a large invasion, while in the present trial, cryoablation was performed percutaneously, being minimally invasive and allowing for a rapid recovery.

Cryoablation is a method of *in situ* tumor ablation. A circulated cryogen is used to target tumors to induce irreversible tissue destruction at a temperature below 40 ℃. Tumor cell death is caused by both direct and indirect mechanisms. The direct cellular damage is a result of intra- and extra-cellular ice crystal formation and solute-solvent shifts, which induce cell dehydration and rupture. The indirect effect was found to be resulted from the vessel obliteration which would result in ischemic hypoxia[13,14].

As a local therapy, cryoablation has been found to carry certain advantages over other forms of HCC treatment[15]. First, it is able to destroy only the tumor tissue in liver sparing more noninvolved tissues, which is of important significance to HCC patients, because the majority of these patients would been found to have cirrhosis and decreased reserve of liver function[16]. Second, because of the warming effect of flowing blood, large blood vessels, such as inferior vena cava and portal vein, are somewhat imperious to the effect of freezing. Therefore, tumors close to these venous systems could safely undergo cryoablation, whereas resection of tumors close to large vascular structures would be very difficult[17].Third, it is known that liver cirrhosis is a basis of HCC development, if the entire liver is cirrhotic, any part of the liver can develop new tumors. Liver cryoablation has been found to be more effective than surgical resection in treating multiple new tumors[13]. Forth,in contrast with other local ablations, such as radiofrequency, which are difficult to reliably destroy tumors greater than 5 cm in diameter, cryoablation would be a promising means for the treatment of this larger form of tumor[2]. Lastly, the rapid freeze-thaw process could enhance necrosis and help induce an immune response against the surviving tumor cells[18].

During cryoablation, freezing would occur in three main areas: (1) The center of iceball near the cryoprobe, where freezing would be rapid and the temperature would be lowest. (2) The middle of the iceball, where the tissue experienced intermediate cooling rate. (3) The periphery of the iceball, where slow rates of cooling would occur[18]. The cytotoxic effect from rapid cooling was the greatest in the center of the iceball, while cells at the periphery of the iceball might survive, particularly if the tumor abutted a large intrahepatic blood vessel that abrogated the effects of tissue cooling. The surviving tumor cells would result in recurrence of the disease. PEI has been used extensively for treatment of HCC. Ethanol could diffuse into the tumor cells and cause nonselective protein denaturation and cellular dehydration, leading to coagulated necrosis. Subsequent fibrosis and small vessel thrombosis would also contribute to cellular death. Therefore, after cryoablation which could destroy the majority of tumors, PEI used at periphery of tumor could destroy residue tumor tissues. It is obvious that cryoablation in combination with PEI had a complementary effects on preventing recurrence[18]. In this series, PEI was given to 36 patients with tumor masses larger than 6 cm in diameter 1-2 weeks after cryoablation, that might be contributory to a better outcome. Moreover, among the 17 patients who had recurrent tumors, only 3 had recurrence at the original cryosite, suggesting that the effectiveness of this combined therapy was good.

Cryoablation has been considered as a safe modality[10]. Transient intra-ablative hypothermia is the most common side effects. The use of warming blankets and fluid warmers has been proven beneficial. Transient thrombocytopenia and hypoglycemia have been observed. Patients should be observed for possible coagulopathy when large tumor (greater than 5 cm) has been frozen. Pleural effusions may occur in tumor mass treated close to the dome of the diaphragm. Cracking of the hepatic capsule might occur during the thawing process[13,17,19], which was seen in one patient in this series. It is one of the most serious complications of hepatic cryoablation, and could be controlled with conservative therapies for most of the cases. Cryoshock manifested as varying degrees of acute renal failure, disseminated intravascular coagulation and adult respiratory distress syndrome, was reported[15]. It has been shown that cryoshock occurred in greater than 40 % of the volume of tissue treated, and lesions over 6 cm were associated with a greater risk[17]. However, lesions up to 10 cm in size were treated safely in the present series. This complication might be related more to the total duration of cryoablation than to the volume of tumor tissue treated[10]. Nevertheless, it is necessary to prevent the disastrous complication. Diuresis with mannitol and alkalinization of urine should be used in all patients to avoid myoglobinuria and subsequent renal damage[8]. PEI has been proven safe, and no significant complication was associated with this modality in the present series.

In conclusion, this technique offers the curative treatment option for HCC that cannot be surgically removed due to the anatomic location of the tumor, and the presence of other comorbid conditions that would otherwise preclude a major liver resection. Percutaneous approach has the advantage of a minimal invasion and allows for a rapid recovery and does not produce appreciable complications. The integration of this technique with other adjuvant regional modalities, especially PEI, may be used as an alternative to resection, so as to improve a long-term disease-free survival in selected patients.

REFERENCES

1 **Staley CA.** Surgical therapy of hepatic tumors. In: Zakim D and Boyer TD, eds. Hepatology. A Textbook of Liver Disease. *Philadelphia: Saunders* 2003: 1371-1381

2 **Adam R**, Hagopian EJ, Linhares M, Krissat J, Savier E, Azoulay D, Kunstlinger F, Castaing D, Bismuth H. A comparison of percutaneous cryosurgery and percutaneous radiofrequency for unresectable hepatic malignancies. *Arch Surg* 2002; **137**: 1332-1339

3 **Onik GM**, Atkinson D, Zemel R, Weaver ML. Cryosurgery of liver cancer. *Semin Surg Oncol* 1993; **9**: 309-317

4 **Gournay J**, Tchuenbou J, Richou C, Masliah C, Lerat F, Dupas B, Martin T, Nouel JF, Schnee M, Montigny P, D'Alincourt A, Hamy A, Paineau J, Le Neel JC, Le Borgne J, Galmiche JP. Percutaneous ethanol injection vs. resection in patients with small single hepatocellular carcinoma: a retrospective case-control study with cost analysis. *Aliment Pharmacol Ther* 2002; **16**: 1529-1538

5 **Okuda K**, Ohtsuki T, Obata H, Tomimatsu M, Okazaki N, Hasegawa H, Nakajima Y, Ohnishi K. Natural history of hepatocellular carcinoma and prognosis in relation to treatment. Study of 850 patients. *Cancer* 1985; **56**: 918-928

6 **Groupe d'Etude et de Traitement du Carcimome Hepatocelltaire**. A comparison of lipiodol, chemoembolization and conservative treatment for unresectable hepatocellular carcinoma. *N Engl J Med* 1995; **332**: 1256-1261

7 **Lau WY,** Leung TW, Yu SC, Ho SK. Percutaneous local ablative therapy for hepatocellular carcinoma: a review and look into the future. *Ann Surg* 2003; **237**: 171-179

8 **Crews KA**, Kuhn JA, McCarty TM, Fisher TL, Goldstein RM, Preskitt JT. Cryosurgical ablation of hepatic tumors. *Am J Surg* 1997; **174**: 614-618

9 **Lam CM**, Yuen WK, Fan ST. Hepatic cryoablation for recurrent hepatocellular carcinoma after hepatectomy:a preliminary report.

J Surg Oncol 1998; **68**: 104-106
10 **Sheen AJ**, Poston GJ, Sherlock DJ. Cryotherapeutic ablation of liver tumours. *Br J Surg* 2002; **89**: 1396-1401
11 **Zhou XD**, Tang ZY, Yu YQ, Ma ZC. Clinical evaluation of cryosurgery in the treatment of primary liver cancer. Report of 60 cases. *Cancer* 1988; **61**: 1889-1892
12 **Zhou XD**, Tang ZY, Yu YQ, Weng JW, Ma ZC, Zhang BH, Zheng YX. The role of cryosurgery in the treatment of hepatic cancer: areport of 113 cases. *J Cancer Res Clin Oncol* 1993; **120**: 100-102
13 **Ross WB**, Horton M, Bertolino P, Morris DL. Cryotherapy of liver tumours-a practical guide. *HPB Surg* 1995; **8**: 167-173
14 **Erce C**, Parks RW. Interstitial ablative techniques for hepatic tumours. *Br J Surg* 2003; **90**: 272-289
15 **Shafir M**, Shapiro R, Sung M, Warner R, Sicular A, Klipfel A. Cryoablation of unresectable malignant liver tumors. *Am J Surg* 1996; **171**: 27-31
16 **Bilchik AJ**, Sarantou T, Wardlaw JC, Ramming KP. Cryosurgery causes a profound reduction in tumor markers in hepatoma and noncolorectal hepatic metastases. *Am Surg* 1997; **63**: 796-800
17 **Seifert JK**, Morris DL. Indicators of recurrence following cryotherapy for hepatic metastases from colorectal cancer.*Br J Surg* 1999; **86**: 234-240
18 **Wong WS**, Patel SC, Cruz FS, Gala KV, Turner AF. Cryosurgery as a treatment for advanced stage hepatocellular carcinoma: results, complication, and alcohol ablation. *Cancer* 1998; **82**: 1268-1278
19 **Dwerryhouse SJ**, Seifert JK, McCall JL, Iqbal J, Ross WB, Morris DL. Hepatic resection with cryotherapy to involved or inadequate resection margin (edge freeze) for metastases from colorectal cancer. *Br J Surg* 1998; **85**: 185-187

Edited by Ma JY and Wang XL

P.O.Box 2345, Beijing 100023,China
Fax: +86-10-85381893
E-mail: wjg@wjgnet.com www.wjgnet.com

World J Gastroenterol 2003;9(12):2690-2694
World Journal of Gastroenterology
 ISSN 1007-9327

• COLORECTAL CANCER •

Comparative evaluation of immune response after laparoscopical and open total mesorectal excisions with anal sphincter preservation in patients with rectal cancer

Jian-Kun Hu, Zong-Guang Zhou, Zhi-Xin Chen, Lan-Lan Wang, Yong-Yang Yu, Jin Liu, Bo Zhang, Li Li, Ye Shu, Jia-Ping Chen

Jian-Kun Hu, Zong-Guang Zhou, Zhi-Xin Chen, Yong-Yang Yu, Bo Zhang, Li Li, Ye Shu, Jia-Ping Chen, Department of General Surgery and Institute of Digestive Surgery, West China Hospital, Sichuan University, Chengdu 610041, Sichuan Province, China
Lan-Lan Wang, Jin Liu, Laboratory of Clinical Immunology, West China Hospital, Sichuan University, Chengdu 610041, Sichuan Province, China
Supported by the Key Project of National Outstanding Youth Foundation of China, No. 39925032
Correspondence to: Zong-Guang Zhou, Department of General Surgery and Institute of Digestive Surgery, West China Hospital, Sichuan University, Chengdu 610041, Sichuan Province, China. zhou767@21cn.com
Telephone: +86-28-85422479 **Fax:** +86-28-85422484
Received: 2003-05-12 **Accepted:** 2003-06-02

Abstract

AIM: The study of immune response of open *versus* laparoscopical total mesorectal excision with anal sphincter preservation in patients with rectal cancer has not been reported yet. The dissected retroperitoneal area that contacts directly with carbon dioxide is extensive in laparoscopic total mesorectal excision with anal sphincter preservation surgery. It is important to clarify whether the immune response of laparoscopic total mesorectal excision with anal sphincter preservation (LTME with ASP) in patients with rectal cancer is suppressed more severely than that of open surgery (OTME with ASP). This study was designed to compare the immune functions after laparoscopic and open total mesorectal excision with anal sphincter preservation for rectal cancer.

METHODS: This study involved 45 patients undergoing laparoscopic (n=20) and open (n=25) total mesorectal excisions with anal sphincter preservation for rectal cancer. Serum interleukin-2 (IL-2), interleukin-6 (IL-6), tumor necrosis factor α (TNF_α) were assayed preoperatively and on days 1 and 5 postoperatively. $CD3^+$ and $CD56^+$ T lymphocyte count, $CD3^-$ and $CD56^+$ natural killer cell (NK) count and immunoglobulin (IgG/IgM/IgA) were assayed preoperatively and on day 5 postoperatively. The numbers of $CD3^+$ and $CD56^+$ T lymphocytes and $CD3^-$ and $CD56^+$ NK cells were counted using flow cytometry. An enzyme-linked immunosorbent assay (ELISA) was used for IL-2, IL-6 and TNF_α determination. And IgG, IgM, and IgA were assayed using immunonephelometry.

RESULTS: The demographic data of the two groups had no difference. The preoperative levels of $CD3^+$ and $CD56^+$ T lymphocyte count, $CD3^-$ and $CD56^+$ NK count, serum IgG, IgM, IgA, IL-2, IL-6 and TNF_α also had no significant difference in the two groups (P>0.05). The $CD3^+$ and $CD56^+$ T lymphocyte counts had no obvious changes after surgery in laparoscopic (d=-0.79±3.83 %) and open (d=0.42±2.09 %) groups. The $CD3^-$ and $CD56^+$ NK counts were decreased postoperatively in both laparoscopic (d=-7.23±11.33 %) and open (d=-9.21±13.93 %) groups. The differences of the determined values of serum IgG, IgM and IgA on the fifth day after operation subtracted those before operation were -2.56±2.14 g/L, -252.35±392.94 mg/L, -506.15±912.24 mg/L in laparoscopic group, and -1.81±2.10 g/L, -282.72±356.75 mg/L, -252.20±396.28 mg/L in open group, respectively. The levels of IL-2 were decreased after operation in both groups. However, the levels of IL-6 were decreased after laparoscopic surgery (d_1=-23.14±263.97 ng/L and d_5=-40.08±272.03 ng/L), and increased after open surgery (d_1=27.38±129.14 ng/L and d_5=21.67±234.31 ng/L). The TNF_α levels were not elevated after surgery in both groups. There were no significant differences in the numbers of $CD3^+$ and $CD56^+$ T lymphocytes and $CD3^-$ and $CD56^+$ NK cells, the levels of IgG, IgM, IgA, IL-2, IL-6 and TNF_α between the two groups (P>0.05).

CONCLUSION: There are no differences in immune responses between the patients having laparoscopic total mesorectal excision with anal sphincter preservation and those undergone open surgery for rectal cancer.

Hu JK, Zhou ZG, Chen ZX, Wang LL, Yu YY, Liu J, Zhang B, Li L, Shu Y, Chen JP. Comparative evaluation of immune response after laparoscopical and open total mesorectal excisions with anal sphincter preservation in patients with rectal cancer. *World J Gastroenterol* 2003; 9(12): 2690-2694
http://www.wjgnet.com/1007-9327/9/2690.asp

INTRODUCTION

General anesthesia, major surgery, and severe trauma are all known to cause significant inhibition of the immune response[1]. The immunosuppression associated with major surgery is believed to contribute to the increased risk of metastasis and sepsis in the postoperative period[1]. In order to improve the immune response of postoperative patients, minimally invasive surgery has been performed. Reduced hospital stay, less wound pain, earlier resumption of diet and recovery of bowel function are recognized as benefits of laparoscopic cholecystectomy or colectomy[2]. The effects of laparoscopic colorectal surgery on the immune system varied from study to study. Meanwhile, study on immune response of open *versus* laparoscopical total mesorectal excision with anal sphincter preservation in patients with rectal cancer has not been reported yet. The dissected retroperitoneal area that contacts directly with carbon dioxide is extensive in laparoscopic total mesorectal excision with anal sphincter preservation surgery. It is important to clarify whether the immune response of laparoscopic total mesorectal excision with anal sphincter preservation (LTME with ASP) in patients with rectal cancer is suppressed more severely than that of open surgery (OTME with ASP). The aim of this nonrandomized prospective study was to compare the effects of LTME and OTME on immune response.

MATERIALS AND METHODS

Patients selection

From October 2001 to July 2002, 49 patients admitted to the General Surgery Department of West China Hospital with the diagnosis of rectal cancer confirmed by pathology were prospectively evaluated. The criterion for inclusion in the study was patients diagnosed with biopsy as adenocarcinoma of the rectum localized below 15 cm from the anal margin. The criteria for exclusion included age older than 80 years and younger than 18 years, presence of a fixed palpable mass or cancer infiltrating adjacent organs, evidence of metastatic disease, neoadjuvant chemoradiotherapy, severe cardiovascular (New York Heart Association class 3 or more) or respiratory dysfunction, patients with previous abdominal operation, acute intestinal obstruction or perforation, any malignancy within the recent 5 years, synchronous multiple adenocarcinomas and pregnancy, any contraindication to pneumoperitoneum, and patients with unresectable tumor.

Preoperative examinations including flexible endoscopy as well as biopsy, ultrasonography, computed tomography scan, radiography of the chest, etc. were routinely performed. All patients underwent preoperative bowel preparation (1L 10 % mannite electrolyte solution). Prophylactic antibiotics of ciprofloxacin and metronidazole were routinely given orally for three days before operation. A urinary catheter and a nasogastric tube were routinely used.

Data collection

The parameters measured were demographic data, operating time, distance of the tumor from the anal margin, time of first passing flatus, time removing urinary catheter, duration of hospital stay, postoperative complications and death. Demographic data included age, sex, serum total protein (TP), albumin (Alb), hemoglobulin (Hb), weight, and underlying diseases.

Operation techniques

All patients were administrated general anesthesia and operations were carried out in lithotomy position with 15° head-down tilt. Premedication and anesthetic techniques were standardized. Induction was made by intravenous injection of 3-5 mg/kg thiopentone together with fentanyl. Anesthesia was maintained by ventilation with an O_2/N_2O mixture and isoflurane. Operations were performed by surgeons experienced in both laparoscopic and conventional surgeries. The rectal surgery was performed according to the principle of total mesorectal excision (TME)[3,4]. Our laparoscopic techniques were reported previously[5].

Pneumoperitoneum was introduced through subumbilical incision to maintain the pressure at 12-14 mmHg (1 mmHg= 0.133 kPa). Camera port with subumbilical trocar was first created, then one operative port in the right midclavicular line at the level of umbilicus, and other two operative ports in the left and right McBurney point were also created respectively under the guidance of laparoscopic view to facilitate dissection. A laparoscope with 25 or 30 curvy degree was inserted into the abdominal cavity via a subumbilical trocar, following the no-touch technique. Routine exploration was performed to ascertain whether the tumor metastasized to the organs in the abdominal cavity and infiltrated the serosa or implanted in the abdominal cavity. With the operation proceeding of total mesorectal excision, division was moved downward into the pelvis along the anatomic space between visceral and parietal endopelvic fascia. In order to extract the bowel loop of the tumor, the port at the left McBurney' s point was extended to about 3.5 cm long, the tumor was routinely isolated by inserting it into a sheath-shaped bacteria-free plastic bag through the incision, and the tumor as well as the proximal colon were extracted through the bag, and then the bowel was transected at the level of 10-15 cm above upper margin of the tumor. After the anvil of a 29 mm-sized circular stapler was inserted into the end of the proximal bowel and secured with 2/0 prolene purse-string suture, the proximal bowel was internalized and the extended incision was closed. Pneumoperitoneum was then induced again, and laparoscopic colo-anal or colo-rectal anastomosis was performed using a CDH 29 circular stapler.

Immunological studies

Seven milliliters of venous blood were taken by peripheral venipuncture before surgery and on days 1 and 5 after surgery into one plain vacutainer and one heparin vacutainer. The specimens were centrifuged and the collected serum was stored at -20 ℃ for the assay of interleukin-2 (IL-2), interleukin-6 (IL-6) and tumor necrosis factor α (TNF_α). IL-2, IL-6 and TNF_α were assayed preoperatively and on days 1 and 5 postoperatively. $CD3^+$ and $CD56^+$ T lymphocyte count, $CD3^-$ and $CD56^+$ natural killer cell (NK) count and immunoglobulin (IgG/IgM/IgA) were determined preoperatively and on day 5 postoperatively. The numbers of $CD3^+$ and $CD56^+$ T lymphocytes and $CD3^-$ and $CD56^+$ NK cells were counted using flow cytometry (Elite-Esp, Beckman-Coulter, USA). An enzyme-linked immunosorbent assay (ELISA) was used for IL-2, IL-6 and TNF_α determination (Bio-Rad system, Immune Company, France), and immunoglobulin (Ig) G, IgM, and IgA were assayed using immunonephelometry (Immage analyzer, Beckman-Coulter, USA).

Statistics analysis

All the data were collected on designed forms, and analyzed with SPSS version 10.0 software. The differences of the determinated values on fifth or first postoperative day subtracted those before operation were compared between laparoscopic and open groups. Student' s *t* test was used for quantitative variables and chi-square test for qualitative variables. All *P* values were two sided. Statistical significance was established as $P<0.05$. The data were expressed as mean ± standard deviation (SD).

RESULTS

A total of 49 patients were entered into the study. Four patients did not meet the eligibility criteria for the trial (three in laparoscopic group and one in open). Three were found to have hepatic metastasis and one did not receive resection because the cancer infiltrated several adjacent organs.

Patient characteristics

The demographic features of the patients are shown in Table 1. The two groups had no differences with respect to age, gender, TP, Alb, Hb, weight and Duke' s classification ($P>0.05$).

Surgical treatment

Table 2 shows the results of the two treatments. All the 45 patients received the curative anterior resection with total mesorectal excision, and the low/ultralow/colo-anal anastomosis was performed by laparoscopic or open surgery. In laparoscopic group, no one required conversion to open surgery.

There was no surgical death in both groups. Operation time was significantly longer in the laparoscopic group than that in the open group (226.75±46.15 min *versus* 146.40±38.09 min, $P<0.05$). The time of first passing flatus in laparoscopic group was significantly shorter than that in the open group (3.15±1.14 min *versus* 4.36±1.19 min, $P<0.05$). There were

no differences in time of removing urinary catheter, duration of hospital stay and distance of tumor from anal margin between the two groups (P>0.05).

The two groups of patients had comparable preoperative underlying diseases. As for the postoperative complications, one patient in the open group had anastomotic leakage and one in the same group experienced wound infection, both of them were successfully treated conservatively. There was no postoperative complication in the laparoscopic group. There were no local recurrence, port site recurrence, and mortality in any patients observed during follow-up ranged from 8 to 17 months.

Table 1 Demographic and clinical characteristics of patients (mean ±SD)

	LTME n=20	OTME n=25	P value
Age (year)	61.60±8.44	57.96±10.70	0.213
Sex (n)			>0.05
M	9	16	
F	11	9	
TP (g/L)	69.36±5.14	71.55±8.23	0.298
Alb (g/L)	41.70±4.16	43.36±4.49	0.199
Hb (g/L)	123.05±14.43	125.18±15.14	0.627
Weight (kg)	58.45±7.86	59.88±10.85	0.619
Duke's classification (n)			>0.05
A	10	6	
B	4	7	
C_1	3	7	
C_2	3	5	
Underlying diseases (n)			>0.05
Diabetes mellitus	1	0	
Hypertension	1	1	
Anemia	0	2	

Table 2 Surgical treatment of patients

	LTME n=20	OTME n=25	P value
Operating time (min)	226.75±46.15	146.40±38.09	0.000[b]
Time of first passing flatus (day)	3.15±1.14	4.36±1.19	0.001[b]
Time of removing urinary catheter (day)	7.35±2.18	6.28±1.59	0.065
Duration of hospital stay (day)	18.30±4.28	18.04±5.47	0.863
Distance of tumor from anal margin (cm)	8.35±3.72	7.00±3.93	0.247

[b]P<0.01 *vs* open group.

Immune response

As expected, the preoperative levels of $CD3^+$ and $CD56^+$ T lymphocyte count, $CD3^-$ and $CD56^+$ NK count, serum IgG, IgM, IgA, IL-2, IL-6 and TNF_α had no difference in the two groups (Table 3, P>0.05).

Table 3 Preoperative immune indicators of two groups (mean ±SD)

	LTME n=20	OTME n=25	P value
$CD3^+$ $CD56^+$ T (%)	4.56±5.08	3.74±4.19	0.556
$CD3^-$ $CD56^+$ NK (%)	20.87±13.76	25.41±16.79	0.335
IgG (g/L)	11.50±2.41	12.61±2.90	0.178
IgM (mg/L)	1 407.40±420.27	1 582.40±735.41	0.350
IgA (mg/L)	2 726.40±2 048.28	2 380.16±928.99	0.454
IL-2 (ng/L)	85.20±303.81	128.30±387.12	0.686
IL-6 (ng/L)	88.70±231.52	49.06±81.63	0.429
TNFα(ng/L)	7.69±5.71	12.99±26.61	0.387

Table 4 shows the differences of the values of IL-2, IL-6 and TNF_α on the fifth or first postoperative day subtracted those before operation, respectively. The TNF_α levels were not elevated after surgery, and there were no significant differences between the two groups (P>0.05). However, the levels of IL-6 were decreased after laparoscopic surgery (d_1=-23.14±263.97 ng/L and d_5=-40.08±272.03 ng/L), but there were no significant differences between the laparoscopic and open groups (P>0.05). The levels of IL-2 were decreased after operation in both groups, the differences were no significant in postoperative days between the two groups (P>0.05).

Table 4 Changes of IL-2, IL-6 and TNF_α after surgery in two groups (mean ±SD)

		LTME n=20	OTME n=25	P value
IL-2(ng/L)	d_1	-80.54±304.30	-98.82±412.38	0.869
	d_5	-27.55±344.29	-33.59±560.20	0.967
IL-6(ng/L)	d_1	-23.14±263.97	27.38±129.14	0.405
	d_5	-40.08±272.03	21.67±234.31	0.418
TNFα (ng/L)	d_1	2.23±12.78	-1.01±7.82	0.301
	d_5	1.84±12.84	0.56±9.86	0.705

(d_1=the differences of the values of IL-2, IL-6 and TNF_α on the first postoperative day subtracted those before operation, respectively. d_5= the differences of the values of IL-2, IL-6 and TNF_α on the fifth postoperative day subtracted those before operation, respectively).

Table 5 shows the differences of the values of $CD3^+$ and $CD56^+$ T lymphocyte count, $CD3^-$ and $CD56^+$ NK count, and serum IgG, IgM, and IgA on the fifth postoperative day from those before operation, respectively. There were no significant differences of $CD3^+$ and $CD56^+$ T lymphocyte count, $CD3^-$ and $CD56^+$ NK count, and serum IgG, IgM, and IgA levels after surgery between the two groups (P>0.05).

Table 5 Changes of $CD3^+$ $CD56^+$ T lymphocyte count, $CD3^-$ $CD56^+$ NK count, and serum immunoglobulin after surgery in two groups (mean ±SD)

	LTME n=20	OTME n=25	P value
$CD3^+$ $CD56^+$ T lymphocyte (%)	-0.79±3.83	0.42±2.09	0.214
$CD3^-$ $CD56^+$ NK (%)	-7.23±11.33	-9.21±13.93	0.609
IgG (g/L)	-2.56±2.14	-1.81±2.10	0.248
IgM (mg/L)	-252.35±392.94	-282.72±356.75	0.787
IgA (mg/L)	-506.15±912.24	-252.20±396.28	0.216

Numbers listed were the differences of the values of $CD3^+$ $CD56^+$ T lymphocyte count, $CD3^-$ $CD56^+$ NK count, and serum IgG, IgM, IgA on the fifth postoperative day subtracted those before operation, respectively.

DISCUSSION

Rectal cancer is the common malignance in our country. Studies on rectal cancer have made great progresses both in clinical practice[6-15] and in theoretical basis[16-26] during the latest years. Multiple clinical studies have demonstrated the correlation of high pelvic recurrence with the degree of mesorectal excision[27]. Residual mesorectum, especially inadequate excision of distal mesorectum (DMR), contributed to poor oncologic outcomes. In order to reduce the rate of local recurrence in the pelvis of rectal carcinoma, total mesorectal excision (TME) has been performed in many colorectal surgery centers. TME has been applied in clinical practice, and the local recurrence rate has decreased dramatically to 5-7.1 %[28,29],

while the mean local recurrence rate of conventional operative procedure for treatment of rectal cancer remained 18.5 %. TME has been claimed to improve not only local recurrence rate, but also long term survival[30-34]. With the improvement of laparoscopic technique, laparoscopic colorectal surgery has been attempted in many countries[4,35-39]. The laparoscopic colorectal surgery has been proposed to be less traumatic than open surgery. It has been demonstrated that laparoscopic-assisted colectomy has many advantages during immediate postoperative period over the open colectomy with regard to the disappearance of postoperative ileus, fewer analgesia, early ambulation, less postoperative complications, and shorter hospital stay[4,35-39]. In this study, the time of first flatus in the laparoscopic group was significantly shorter than that in the open group.

Some randomised clinical trials of open versus laparoscopically assisted colectomy on systematic immunity in patients with colorectal cancer have been performed. Delgado *et al*[40] found that the plasma levels of cortisol and prolactin were higher in postoperative period, but no significant differences were observed between both groups of the patients. The level of interleukin-6 was higher with significant differences at 4, 12 and 24 hours in the patients undergone open colectomy than that in laparoscopic group. The plasma level of C-reactive protein (CRP) was significantly lower at 72 hours in patients receiving laparoscopic-assisted colectomy than that in patients receiving open one. They suggested that acute phase systematic response was attenuated in patients undergone laparoscopic-assisted colectomy in comparison with those undergone open colectomy. Leung *et al*[41] clarified tissue trauma as reflected by systematic cytokine response, such as interleukin-1β, interleukin-6 and CRP, was less after laparoscopic resection than after open resection of rectosigmoid carcinoma. Nishiguchi *et al*[42] showed that interleukin-6 and CRP levels were significantly higher in the open group than those in the laparoscopic group one day and two days after surgery, respectively. Lymphocyte counts were significantly higher in the laparoscopic group than those in the open group two days after surgery. They concluded that laparoscopic surgery for colorectal carcinoma led to less postoperative stress than conventional open surgery. Some researchers verified that the levels of serum IL-2, CRP, and TNF_α were significantly lower after surgery in the laparoscopic group than those in the open group[43-45]. Braga *et al*[46] also found that laparoscopic colorectal surgery was associated with less pronounced immunosuppression and inflammatory response and lower consumption of analgesic drugs than open surgery. But Tang *et al*[47] and Mehigan *et al*[48] showed that there was no difference in the systematic immune response in patients having laparoscopically assisted colectomy compared with those undergone conventional open surgery for colorectal cancer. Sandoval *et al*[49] also revealed that the laparoscopic surgery did not affect natural antitumoral cellular immunity in an animal model. Moreover, Fukushima *et al*[50] found that serum IL-6 after surgery was significantly higher in laparoscopic sigmoid colectomy than in the open group. They proposed that early IL-6 response after surgery be associated with operation time.

Previous immune response studies were only performed in colorectal surgery. However, the study on immune response of open *versus* laparoscopical total mesorectal excision with anal sphincter preservation in patients with rectal cancer has not been reported yet. The dissected retroperitoneal area that contacted directly with carbon dioxide was extensive in laparoscopic total mesorectal excision with anal sphincter preservation surgery. It is important to clarify whether the immune response of laparoscopic total mesorectal excision with anal sphincter preservation in patients with rectal cancer is suppressed more severely than that of open surgery or not. In this study, TNF_α levels were not elevated after surgery, and there were no significant differences between the two groups (P>0.05). However, the levels of IL-6 were decreased after laparoscopic surgery (d_1=-23.14±263.97 ng/L and d_5=-40.08±272.03 ng/L), but there were no significant differences between the laparoscopic and open groups (P>0.05). The levels of IL-2 were decreased after operation in both groups, and the differences were not significant in postoperative days between the two groups (P>0.05). There were no significant differences in $CD3^+$ and $CD56^+$ T lymphocyte count, $CD3^-$ and $CD56^+$ NK count, and serum IgG, IgM, and IgA levels after surgery between the two groups (P>0.05). Based on the results of our study, it is concluded that there is difference in immune responses in patients having laparoscopic total mesorectal excision with anal sphincter preservation compared with those undergone open surgery for rectal cancer.

REFERENCES

1 **Walker CB**, Bruce DM, Heys SD, Gough DB, Binnie NR, Eremin O. Minimal modulation of lymphocyte and natural killer cell subsets following minimal access surgery. *Am J Surg* 1999; **177**: 48-54

2 **Vittimberga FJ Jr**, Foley DP, Meyers WC, Callery MP. Laparoscopic surgery and the systemic immune response. *Ann Surg* 1998; **227**: 326-334

3 **Heald RJ**, Husband EM, Ryall RD. The mesorectum in rectal cancer surgery -the clue to pelvic recurrence? *Br J Surg* 1982; **69**: 613-616

4 **Hartley JE**, Mehigan BJ, Qureshi AE, Duthie GS, Lee PW, Monson JR. Total mesorectal excision: assessment of the laparoscopic approach. *Dis Colon Rectum* 2001; **44**: 315-321

5 **Zhou ZG**, Wang Z, Yu YY, Shu Y, Cheng Z, Li L, Lei WZ, Wang TC. Laparoscopic total mesorectal excision of low rectal cancer with preservation of anal sphincter: A report of 82 cases. *World J Gastroenterol* 2003; **9**: 1477-1481

6 **Sun XN**, Yang QC, Hu JB. Pre-operative radiochemotherapy of locally advanced rectal cancer. *World J Gastroenterol* 2003; **9**: 717-720

7 **Gu J**, Ma ZL, Li Y, Li M, Xu GW. Angiography for diagnosis and treatment of colorectal cancer. *World J Gastroenterol* 2003; **9**: 288-290

8 **Cai SJ**, Xu Y, Cai GX, Lian P, Guan ZQ, Mo SJ, Sun MH, Cai Q, Shi DR. Clinical characteristics and diagnosis of patients with hereditary nonpolyposis colorectal cancer. *World J Gastroenterol* 2003; **9**: 284-287

9 **Liu LX**, Zhang WH, Jiang HC. Current treatment for liver metastases from colorectal cancer. *World J Gastroenterol* 2003; **9**: 193-200

10 **Chen K**, Cai J, Liu XY, Ma XY, Yao KY, Zheng S. Nested case-control study on the risk factors of colorectal cancer. *World J Gastroenterol* 2003; **9**: 99-103

11 **Liu LX**, Zhang WH, Jiang HC, Zhu AL, Wu LF, Qi SY, Piao DX. Arterial chemotherapy of 5-fluorouracil and mitomycin C in the treatment of liver metastases of colorectal cancer. *World J Gastroenterol* 2002; **8**: 663-667

12 **Zheng S**, Liu XY, Ding KF, Wang LB, Qiu PL, Ding XF, Shen YZ, Shen GF, Sun QR, Li WD, Dong Q, Zhang SZ. Reduction of the incidence and mortality of rectal cancer by polypectomy: a prospective cohort study in Haining County. *World J Gastroenterol* 2002; **8**: 488-492

13 **Wan J**, Zhang ZQ, Zhu C, Wang MW, Zhao DH, Fu YH, Zhang JP, Wang YH, Wu BY. Colonoscopic screening and follow-up for colorectal cancer in the elderly. *World J Gastroenterol* 2002; **8**: 267-269

14 **Zhang YL**, Zhang ZS, Wu BP, Zhou DY. Early diagnosis for colorectal cancer in China. *World J Gastroenterol* 2002; **8**: 21-25

15 **Qing SH**, Rao KY, Jiang HY, Wexner SD. Racial differences in the anatomical distribution of colorectal cancer: a study of differences between American and Chinese patients. *World J Gastroenterol* 2003; **9**: 721-725

16 **Fang J**, Jin HB, Song JD. Construction, expression and tumor tar-

geting of a single-chain Fv against human colorectal carcinoma. *World J Gastroenterol* 2003; **9**: 726-730
17 **Hu HY**, Liu XX, Jiang CY, Zhang Y, Bian JF, Lu Y, Geng Z, Liu SL, Liu CH, Wang XM, Wang W. Cloning and expression of ornithine decarboxylase gene from human colorectal carcinoma. *World J Gastroenterol* 2003; **9**: 714-716
18 **Jiang YA**, Fan LF, Jiang CQ, Zhang YY, Luo HS, Tang ZJ, Xia D, Wang M. Expression and significance of PTEN, hypoxia-inducible factor-1 alpha in colorectal adenoma and adenocarcinoma. *World J Gastroenterol* 2003; **9**: 491-494
19 **Ma L**, Tai H, Li C, Zhang Y, Wang ZH, Ji WZ. Photodynamic inhibitory effects of three perylenequinones on human colorectal carcinoma cell line and primate embryonic stem cell line. *World J Gastroenterol* 2003; **9**: 485-490
20 **Huang ZH**, Fan YF, Xia H, Feng HM, Tang FX. Effects of TNP-470 on proliferation and apoptosis in human colon cancer xenografts in nude mice. *World J Gastroenterol* 2003; **9**: 281-283
21 **Chen XX**, Lai MD, Zhang YL, Huang Q. Less cytotoxicity to combination therapy of 5-fluorouracil and cisplatin than 5-fluorouracil alone in human colon cancer cell lines. *World J Gastroenterol* 2002; **8**: 841-846
22 **Xiong B**, Yuan HY, Hu MB, Zhang F, Wei ZZ, Gong LL, Yang GL. Transforming growth factor-beta1 in invasion and metastasis in colorectal cancer. *World J Gastroenterol* 2002; **8**: 674-678
23 **Zhou CZ**, Peng ZH, Zhang F, Qiu GQ, He L. Loss of heterozygosity on long arm of chromosome 22 in sporadic colorectal carcinoma. *World J Gastroenterol* 2002; **8**: 668-673
24 **Xiong B**, Gong LL, Zhang F, Hu MB, Yuan HY. TGF beta1 expression and angiogenesis in colorectal cancer tissue. *World J Gastroenterol* 2002; **8**: 496-498
25 **Li J**, Guo WJ, Yang QY. Effects of ursolic acid and oleanolic acid on human colon carcinoma cell line HCT15. *World J Gastroenterol* 2002; **8**: 493-495
26 **Wang X**, Lan M, Wu HP, Shi YQ, Lu J, Ding J, Wu KC, Jin JP, Fan DM. Direct effect of croton oil on intestinal epithelial cells and colonic smooth muscle cells. *World J Gastroenterol* 2002; **8**: 103-107
27 **Wexner SD**, Rotholtz NA. Surgeon influenced variables in resectional rectal cancer surgery. *Dis Colon Rectum* 2000; **43**: 1606-1627
28 **Killingback M**, Barron P, Dent OF. Local recurrence after curative resection of cancer of the rectum without total mesorectal excision. *Dis Colon Rectum* 2001; **44**: 473-483
29 **McCall JL**, Cox MR, Wattchow DA. Analysis of local recurrence rates after surgery alone for rectal cancer. *Int J Colorectal Dis* 1995; **10**: 126-132
30 **Law WL**, Chu KW. Impact of total mesorectal excision on the results of surgery of distal rectal cancer. *Br J Surg* 2001; **88**: 1607-1612
31 **Dahlberg M**, Pahlman L, Bergstrom R, Glimelius B. Improved survival in patients with rectal cancer: a population-based register study. *Br J Surg* 1998; **85**: 515-520
32 **Dahlberg M**, Glimelius B, Pahlman L. Changing strategy for rectal cancer is associated with improved outcome. *Br J Surg* 1999; **86**: 379-384
33 **Arenas RB**, Fichera A, Mhoon D, Michelassi F. Total mesenteric excision in the surgical treatment of rectal cancer: a prospective study. *Arch Surg* 1998;**133**: 608-612
34 **Heald RJ**, Moran BJ, Ryall RD, Sexton R, MacFarlane JK. Rectal cancer: the Basingstoke experience of total mesorectal excision, 1978-1997. *Arch Surg* 1998; **133**: 894-899
35 **Chapman AE**, Levitt MD, Hewett P, Woods R, Sheiner H, Maddern GJ. Laparoscopic-assisted resection of colorectal malignancies: a systematic review. *Ann Surg* 2001; **234**: 590-606
36 **Feliciotti F**, Paganini AM, Guerrieri M, Sanctis A, Campagnacci R, Lezoche E. Results of laparoscopic *vs* open resections for colon cancer in patients with a minimum follow-up of 3 years. *Surg Endosc* 2002; **16**: 1158-1161
37 **Hong D**, Tabet J, Anvari M. Laparoscopic vs open resection for colorectal adenocarcinoma. *Dis Colon Rectum* 2001; **44**: 10-18
38 **Lezoche E**, Feliciotti F, Paganini AM, Guerrieri M, De Sanctis A, Minervini S, Campagnacci R. Laparoscopic vs open hemicolectomy for colon cancer. *Surg Endosc* 2002; **16**: 596-602
39 **Maxwell-Armstrong CA**, Robinson MH, Scholefield JH. Laparoscopic colorectal cancer surgery. *Am J Surg* 2000; **179**: 500-507
40 **Delgado S**, Lacy AM, Filella X, Castells A, Garcia-Valdecasas JC, Pique JM, Momblan D, Visa J. Acute phase response in laparoscopic and open colectomy in colon cancer: randomized study. *Dis Colon Rectum* 2001; **44**: 638-646
41 **Leung KL**, Lai PB, Ho RL, Meng WC, Yiu RY, Lee JF, Lau WY. Systemic cytokine response after laparoscopic-assisted resection of rectosigmoid carcinoma: A prospective randomized trial. *Ann Surg* 2000; **231**: 506-511
42 **Nishiguchi K**, Okuda J, Toyoda M, Tanaka K, Tanigawa N. Comparative evaluation of surgical stress of laparoscopic and open surgeries for colorectal carcinoma. *Dis Colon Rectum* 2001; **44**: 223-230
43 **Ordemann J**, Jacobi CA, Schwenk W, Stosslein R, Muller JM. Cellular and humoral inflammatory response after laparoscopic and conventional colorectal resections. *Surg Endosc* 2001; **15**: 600-608
44 **Schwenk W**, Jacobi C, Mansmann U, Bohm B, Muller JM. Inflammatory response after laparoscopic and conventional colorectal resections-results of a prospective randomized trial. *Langenbecks Arch Surg* 2000; **385**: 2-9
45 **Kuntz C**, Wunsch A, Bay F, Windeler J, Glaser F, Herfarth C. Prospective randomized study of stress and immune response after laparoscopic vs conventional colonic resection. *Surg Endosc* 1998; **12**: 963-967
46 **Braga M**, Vignali A, Zuliani W, Radaelli G, Gianotti L, Martani C, Toussoun G, Di Carlo V. Metabolic and functional results after laparoscopic colorectal surgery: a randomized, controlled trial. *Dis Colon Rectum* 2002; **45**: 1070-1077
47 **Tang CL**, Eu KW, Tai BC, Soh JG, Machin D, Seow-Choen F. Randomized clinical trial of the effect of open versus laparoscopically assisted colectomy on systemic immunity in patients with colorectal cancer. *Br J Surg* 2001; **88**: 801-807
48 **Mehigan BJ**, Hartley JE, Drew PJ, Saleh A, Dore PC, Lee PW, Monson JR. Changes in T cell subsets, interleukin-6 and C-reactive protein after laparoscopic and open colorectal resection for malignancy. *Surg Endosc* 2001; **15**: 1289-1293
49 **Sandoval BA**, Robinson AV, Sulaiman TT, Shenk RR, Stellato TA. Open versus laparoscopic surgery: a comparison of natural antitumoral cellular immunity in a small animal model. *Am Surg* 1996; **62**: 625-630
50 **Fukushima R**, Kawamura YJ, Saito H, Saito Y, Hashiguchi Y, Sawada T, Muto T. Interleukin-6 and stress hormone responses after uncomplicated gasless laparoscopic-assisted and open sigmoid colectomy. *Dis Colon Rectum* 1996; **39**(10 Suppl): S29-S34

Edited by Zhang JZ and Wang XL

P.O.Box 2345, Beijing 100023,China
Fax: +86-10-85381893
E-mail: wjg@wjgnet.com www.wjgnet.com

World J Gastroenterol 2003;9(12):2695-2697
World Journal of Gastroenterology
 ISSN 1007-9327

• VIRAL HEPATITIS •

Hepatitis B virus genotype has no impact on hepatitis B e antigen seroconversion after lamivudine treatment

Henry Lik-Yuen Chan, May-Ling Wong, Alex Yui Hui, Angel Mei-Ling Chim, Ada Mei-Ling Tse, Lawrence Cheung-Tsui Hung, Francis Ka-Leung Chan, Joseph Jao-Yiu Sung

Henry Lik-Yuen Chan, May-Ling Wong, Alex Yui Hui, Angel Mei-Ling Chim, Ada Mei-Ling Tse, Lawrence Cheung-Tsui Hung, Francis Ka-Leung Chan, Joseph Jao-Yiu Sung, Department of Medicine and Therapeutics, Chinese University of Hong Kong, Hong Kong
Correspondence to: Dr. Henry Lik-Yuen Chan, Department of Medicine and Therapeutics, 9/F Prince of Wales Hospital, Shatin, Hong Kong. hlychan@cuhk.edu.hk
Telephone: +852-26323594 **Fax:** +852-26373852
Received: 2003-07-04 **Accepted:** 2003-10-08

Abstract

AIM: To investigate the association of hepatitis B virus (HBV) genotype and HBeAg seroconversion after nucleotide analogue treatment.

METHODS: Chronic hepatitis B patients receiving lamivudine followed up for at least 6 months post-treatment were studied. Consecutive treatment-naïve patients who were prospectively followed up in the clinic for at least 18 months were studied as controls. HBeAg seroconversion was defined as loss of HBeAg, appearance of anti-HBe and normalization of alanine aminotransferase for at least 6 months.

RESULTS: Thirty-five patients on lamivudine and 96 control patients followed up for 39 (18-49) months were studied. Lamivudine was given for 12 (10-18) months, and patients were followed up for 15 (6-34) months after drug cessation. Genotype B and C HBV were found in 43 and 88 patients and HBeAg seroconversion occurred in 12 (28 %) and 16 (18 %) patients, respectively (P=0.30). There was no difference in HBeAg seroconversion between patients infected by genotype B and C HBV in the control (35 % *vs* 21 %, P=0.25) and lamivudine-treated (14 % *vs* 10 %, P=1.00) groups.

CONCLUSION: HBeAg seroconversion after treatment by lamivudine was not influenced by the HBV genotype.

Chan HLY, Wong ML, Hui AY, Chim AML, Tse AML, Hung LCT, Chan FKL, Sung JJY. Hepatitis B virus genotype has no impact on hepatitis B e antigen seroconversion after lamivudine treatment. *World J Gastroenterol* 2003; 9(12): 2695-2697
http://www.wjgnet.com/1007-9327/9/2695.asp

INTRODUCTION

Hepatitis B virus (HBV) has 7 different genotypes (A-G) according to the homogeneity of the viral sequence[1,2]. In Southeast Asia including Hong Kong, genotype B and C HBV are the predominant species[3-6]. There are increasing evidences showing that genotype C HBV is associated with a more aggressive disease as compared with genotype B HBV[3,7-10]. A recent Japanese study suggests that HBV genotype is not associated with the development of lamivudine resistance after a median of 1.8 years of treatment[11]. However, data on the association of HBV genotype and HBeAg seroconversion response to anti-viral treatment is scanty. This information is potentially important in the selection of patients for anti-viral treatment and development of future therapeutic regimens as in the case of chronic hepatitis C.

Previous studies suggest that genotype B HBV is associated with a higher rate of HBeAg seroconversion versus genotype C HBV among patients receiving interferon treatment[12,13]. This finding, however, cannot be extrapolated to nucleos(t)ide analogues which have completely different mechanisms of action as compared with interferon. A study including 31 Taiwanese HBeAg-positive chronic hepatitis B patients treated by lamivudine does not show any difference in HBeAg seroconversion between patients infected by genotype B and C HBV[14]. This study is limited by the small number of patients and the absence of control group. Phase III, multi-centered studies on adefovir dipivoxil reveal no difference in viral load reduction among patients infected by different HBV genotypes, but both HBeAg-positive and HBeAg-negative patients are included and HBeAg seroconversion has not been studied[15]. In this study, we aimed to investigate the association of HBV genotype and HBeAg seroconversion after treatment by lamivudine, and a control group of untreated HBeAg-positive chronic hepatitis B patients was included for comparison.

MATERIALS AND METHODS

Patients on anti-viral treatment

Clinical data and stored serum samples of patients on lamivudine treated in Prince of Wales Hospital from 1998 to 2000 were included for analysis. These patients had positive hepatitis B surface antigen (HBsAg) for at least 6 months and positive hepatitis B e antigen (HBeAg), HBV DNA >1 000 000 copies/ml by DNA cross-linking assay (NAXCOR XLnt™, NAXCOR, Menlo Park, CA) or branched DNA assay (bDNA, Chiron Diagnostic, Emeryville, CA) before treatment[16]. None of these patients had evidence of liver cirrhosis complications, hepatocellular carcinoma (HCC) or co-infection by hepatitis C or human immunodeficiency viruses. All patients received lamivudine 100 mg daily. HBeAg seroconversion was defined as loss of HBeAg, appearance of antibodies to HBeAg (anti-HBe) and normalization of ALT at the end of anti-viral treatment and the response sustained for at least 6 months after cessation of treatment till the last follow-up visit.

Control patients

Consecutive chronic hepatitis B patients with positive HBeAg at the initial clinic visit recruited since 1997 in our hospital were studied as controls[3,17]. Patients who had previously received interferon or anti-viral treatment, liver cirrhosis complications and HCC were excluded from the study. To match the follow-up duration of patients treated by nucleoside analogues, patients who were followed up for less than 18 months were also excluded. All patients were followed up every 6 months, or more frequently as clinically indicated, with monitoring of HBeAg status and liver biochemistry. HBeAg

seroconversion was defined as sustained loss of HBeAg, appearance of anti-HBe and normalization of ALT during the follow-up period lasting for at least 6 months till the last visit.

HBV genotyping

The baseline samples of patients in clinical trial before starting anti-viral treatment and the serum samples at the first clinic visits of control patients were studied for HBV genotyping by restriction fragment length polymorphism as described previously[7,18]. In short, extracted HBV DNA was amplified by polymerase chain reaction (PCR) using primers flanking the HBV genome between nucleotide 256 to 796 (sense primer 5' -GTGGTGGACTTCTCTCAATTTTC and anti-sense primer 5' -CGGTA(A/T)AAAGGGACTCA(A/C)GAT). PCR product was then mixed and incubated with restriction enzymes *Tsp 5091* (New England Biolabs, Beverly, MA) and *HinfI* (Boehringer Mannheim, Mannheim, Germany) respectively. The samples were run on agarose gel and DNA was visualized by ethidium bromide staining. The restriction pattern was read accordingly.

Statistical analysis

Results were expressed as median (range). Data were analyzed using SPSS version 11.0 software package. Categorical variables were compared by Chi-square test and continuous variables were compared by Mann-Whitney U test. Proportion of patients developing HBeAg seroconversion in different HBV genotypes were also compared after adjustment of potential confounding variables with P value <0.1 by logistic regression analysis. All tests were two-tailed. Statistical significance was taken as $P<0.05$.

RESULTS

Thirty-five patients on lamivudine and 96 control patients were identified. The clinical data and viral genotype of the studied patients of two groups of patients are shown in Table 1. Lamivudine was given for 12 (10-18) months and the treated patients were followed up for 15 (6-34) months after the cessation of lamivudine. Only 1 of 35 lamivudine-treated patients had been treated for 10 months whereas the remaining patients had treatment for at least 12 months. All patients who did not achieve HBeAg seroconversion after lamivudine treatment developed biochemical relapse with ALT elevation after cessation of lamivudine. The 24 control patients who achieved sustained HBeAg seroconversion were followed up for 24.5 (8-40) months after the development of HBeAg seroconversion. Patients on lamivudine were significantly older with higher initial ALT levels and shorter follow-up duration as compared with the controls. There was no difference in the distribution of HBV genotypes and the percentage of HBeAg seroconversion between the treated and control patients.

Table 1 Clinical characteristics of patients on anti-viral treatments and controls

	Overall (n=131)	Controls (n=96)	Lamivudine (n=35)	P value
Age	30 (12-68)	29 (12-68)	38 (22-47)	0.007
Male gender (n, %)	75 (57 %)	50 (52 %)	25 (71 %)	0.074
Initial ALT (IU/l)	73 (17-1122)	57.5 (17-753)	135 (36-1122)	<0.001
Follow-up (months)	39 (18-49)	39 (19-49)	27 (18-46)	0.009
Genotype				0.40
B (n, %)	43 (33 %)	29 (30 %)	14 (40 %)	
C (n, %)	88 (67 %)	67 (70 %)	21 (60 %)	
HBeAg seroconversion (n, %)	28 (21 %)	24 (25 %)	4 (11 %)	0.15

Forty-three (33 %) and 88 (67 %) patients were infected by genotype B and C respectively. The clinical characteristics of patients infected by genotype B and C HBV are shown in Table 2. There was no difference in the age, gender ratio, initial ALT levels, follow-up duration and drug treatment between patients infected by the two HBV genotypes. There was no difference in HBeAg seroconversion among patients infected by the 2 HBV genotypes, and the overall trend was confirmed after adjusted for age, gender ratio, initial ALT level and the follow-up duration (Table 3).

Table 2 Clinical characteristics of patients infected by genotype B and C HBV

	Genotype B (n=43)	Genotype C (n=88)	P value
Age	34 (13-67)	29 (12-68)	0.14
Male gender (n, %)	28 (65 %)	47 (53 %)	0.28
Initial ALT (IU/l)	70 (17-1094)	77 (18-1122)	0.60
Follow-up (months)	38 (18-49)	39 (18-49)	0.49
Treatment (n, %)			0.40
Nil	29 (67 %)	67 (76 %)	
Lamivudine	14 (33 %)	21 (24 %)	

Table 3 Comparison of HBeAg seroconversion among patients infected by genotype B and C HBV

HBeAg seroconversion	Genotype B	Genotype C	P value 1	P value 2
Control	10/29 (35 %)	14/67 (21 %)	0.25	0.41
Lamivudine	2/14 (14 %)	2/21 (10 %)	1.00	0.51

P value 1: unadjusted comparison of genotype B versus genotype C; P value 2: comparison of genotype B versus genotype C after adjustment for age, gender, initial ALT levels and follow-up duration.

DISCUSSION

The results of this study concurred with previous data that HBV genotype could not predict HBeAg seroconversion after 1 year treatment of lamivudine. The percentages of patients infected by genotype B and C HBV undergoing HBeAg seroconversion were similar among the treatment and control groups.

In the previous study in Taiwan, the proportion of patients achieving HBeAg seroconversion after lamivudine treatment was similar between genotype B and C HBV[14]. However, genotype B HBV was reported to associate with earlier spontaneous HBeAg seroconversion by several series[9,10]. It was therefore uncertain whether there was really no difference in lamivudine response between the 2 HBV genotypes or the improved response of genotype C HBV has closed up the existing difference. In this study, a control group of untreated patients was included in the analysis. As the control group was not recruited together with the treated patients in a randomized manner, it was not surprising that untreated patients were generally younger and had lower ALT levels than the treated ones. In this study, the absence of association between HBV genotypes and HBeAg seroconversion among patients treated by nucleotide analogues was confirmed as there was no difference in HBeAg seroconversion between the 2 HBV genotypes in both the treated groups and the control group after adjustment for all the differences between the two groups.

The earlier age of spontaneous HBeAg seroconversion associated with genotype B HBV reported by recent longitudinal studies was not shown in this study[9,10]. Patient recruitment in the previous studies may be biased as one of them was a retrospective study and the other included only

patients who have consented for liver biopsy. The consecutive patient recruitment and prospective follow-up in our series has minimized the bias of sampling. Although the age of spontaneous HBeAg seroconversion did not differ between the 2 HBV genotypes, our previous studies agreed with others that genotype C HBV is associated with a more aggressive disease course than genotype B HBV[3,7].

In this study, the rate of HBeAg seroconversion was comparable between the treated and untreated patients. The rate of HBeAg seroconversion after 1 year of lamivudine treatment was comparable to that reported in the previous multicenter Asian lamivudine trial[19]. The rate of spontaneous HBeAg seroconversion (25 % in 3 years) was also comparable to previous reported Asian series after taken into consideration the young age and relatively lower ALT level of the control patients in this study[20,21]. As patients in the control group were followed up for longer duration and some of these patients might have milder disease as compared with the treated patients, the effect of treatment could not be concluded by the results of this study. This study was also not designed to assess the predictive factor of treatment response to the nucleoside analogues.

In conclusion, the results of this study did not support a role of HBV genotype in response to lamivudine among HBeAg-positive patients. Further studies are required to probe into the association of HBV genotypes and treatment response in other geographical locations where other HBV genotypes prevail.

REFERENCES

1 **Norder H,** Courouce AM, Magnius LO. Complete genomes, phylogenetic relatedness, and structural proteins of six strains of the hepatitis B virus, four of which represent two new genotypes. *Virology* 1994; **198**: 489-503

2 **Stuyver L,** De Gendt S, Van Geyt C, Zoulim F, Fried M, Schinazi RF, Rossau R. A new genotype of hepatitis B virus: complete genome and phylogenetic relatedness. *J Gen Virol* 2000; **81**: 67-74

3 **Chan HLY,** Wong ML, Hui AY, Hung LCT, Chan FKL, Sung JJY. Hepatitis B virus genotype C takes a more aggressive disease course than hepatitis B virus genotype B in hepatitis B e antigen-positive patients. *J Clin Microbiol* 2003; **41**: 1277-1279

4 **Sung JJY,** Chan HLY, Wong ML, Tse CH, Yuen SCH, Tam JSL, Leung NWY. Relationship of clinical and virological factors with hepatitis activity in hepatitis B e antigen-negative chronic hepatitis B virus-infected patients. *J Viral Hepat* 2002; **9**: 229-223

5 **Orito E,** Ichida T, Sakugawa H, Sata M, Horiike N, Hino K, Okita K, Okanoue T, Iino S, Tanada E, Suzuki K, Watanabe H, Huge S, Mizokami M. Geographic distribution of hepatitis B virus (HBV) genotype in patients with chronic HBV infection in Japan. *Hepatology* 2001; **34**: 590-594

6 **Kao JH,** Chen PJ, Lai MY, Chen DS. Hepatitis B genotypes correlate with clinical outcome in patients with chronic hepatitis B. *Gastroenterology* 2000; **118**: 554-559

7 **Chan HLY,** Tsang SWC, Liew CT, Tse CH, Wong ML, Ching JYL, Leung NWY, Tam JSL, Sung JJY. Viral genotype and hepatitis B virus DNA levels are correlated with histological liver damage in HBeAg-negative chronic hepatitis B virus infection. *Am J Gastroenterol* 2002; **97**: 406-412

8 **Kao JH,** Chen PJ, Lai MY, Chen DS. Genotypes and clinical phenotypes of hepatitis B virus in patients with chronic hepatitis B virus infection. *J Clin Microbiol* 2002; **40**: 1207-1209

9 **Chu CJ,** Hussain M, Lok ASF. Hepatitis B virus genotype B is associated with earlier HBeAg seroconversion compared with hepatitis B virus genotype C. *Gastroenterology* 2002; **122**: 1756-1762

10 **Sumi H,** Yokosuka O, Seki N, Arai M, Imazeki F, Kurihara T, Kanda T, Fukai K, Kato M, Saisho H. Influence of hepatitis B virus genotypes on the progression of chronic type B liver disease. *Hepatology* 2003; **37**: 19-26

11 **Akuta N,** Suzuki F, Kobayashi M, Tsubota A, Suzuki Y, Hosaka T, Someya T, Kobayashi M, Saitoh S, Arase Y, Ikeda K, Kumada H. The influence of hepatitis B virus genotype on the development of lamivudine resistance during long-term treatment. *J Hepatol* 2003; **38**: 315-321

12 **Kao JH,** Wu NH, Chen PJ, Lai MY, Chen DS. Hepatitis B genotypes and the response to interferon therapy. *J Hepatol* 2000; **33**: 998-1002

13 **Wai CT,** Chu CJ, Hussain M, Lok ASF. HBV genotype B is associated with better response in interferon therapy in HBeAg(+) chronic hepatitis than genotype C. *Hepatology* 2002; **36**: 1425-1430

14 **Kao JH,** Liu CJ, Chen DS. Hepatitis B viral genotypes and lamivudine resistance. *J Hepatol* 2002; **36**: 303-305

15 **Westland C,** Delaney W, Yang HL, Fry J, Brosgart C, Gibbs C, Miller M, Xiong S. Distribution and clinical response of HBV genotypes in phase III studies of adefovir dipivoxil. *J Hepatol* 2002; **36**(Supp1): 105

16 **Chan HLY,** Leung NWY, Lau TCM, Wong ML, Sung JJY. Comparison of three different sensitive assays for hepatitis B virus DNA in monitoring of responses to anti-viral therapy. *J Clin Microbiol* 2000; **38**: 3205-3208

17 **Chan HLY,** Leung NWY, Hussain M, Wong ML, Lok ASF. Hepatitis B e antigen negative chronic hepatitis B in Hong Kong. *Hepatology* 2000; **31**: 763-768

18 **Lindh M,** Andersson AS, Gusdal A. Genotypes, nt 1858 variants, and geographical origin of hepatitis B virus – large-scaled analysis using a new genotyping method. *J Infect Dis* 1997; **175**: 1285-1293

19 **Lai CL,** Chien RN, Leung NW, Chang TT, Guan R, Tai DI, Ng KY, Wu PC, Dent JC, Barber J, Stephenson SL, Gray DF. A one-year trial of lamivudine for chronic hepatitis B. *N Engl J Med* 1998; **339**: 61-68

20 **Lok ASF,** Lai CL. Acute exacerbation in Chinese patients with chronic hepatitis B virus (HBV) infection. *J Hepatol* 1990; **10**: 29-34

21 **Yuen MF,** Yuan HJ, Hui CK, Wong DK, Wong WM, Chan AO, Wong BC, Lai CL. A large population study of spontaneous HBeAg seroconversion and acute exacerbation of chronic hepatitis B infection: implications for antiviral therapy. *Gut* 2003; **52**: 416-419

Edited by Ma JY

P.O.Box 2345, Beijing 100023,China
Fax: +86-10-85381893
E-mail: wjg@wjgnet.com www.wjgnet.com

World J Gastroenterol 2003;9(12):2698-2700
World Journal of Gastroenterology
 ISSN 1007-9327

• VIRAL HEPATITIS •

N-acetyl cysteine therapy in acute viral hepatitis

Huseyin Gunduz, Oguz Karabay, Ali Tamer, Resat Özaras, Ali Mert, Ömer Fehmi Tabak

Huseyin Gunduz, Department of Internal Medicine and Gastroenterology, Izzet Baysal Medical Faculty, Izzet Baysal University/Bolu, Turkey
Oguz Karabay, Department of Infectious Diseases and Clinical Microbiology, Izzet Baysal Medical Faculty, Izzet Baysal University/ Bolu, Turkey
Ali Tamer, Department of Internal Medicine, Izzet Baysal Medical Faculty, Izzet Baysal University/Bolu, Turkey
Resat Özaras, Ali Mert, Ömer Fehmi Tabak, Department of Infectious Diseases and Clinical Microbiology, Cerrahpasa Medical Faculty, Istanbul University, Findikzade/Ýstanbul, Turkey
Correspondence to: Huseyin Gunduz, (MD, asistant professor) Department of Internal Medicine and Gastroenterology, Izzet Baysal Medical Faculty, Izzet Baysal University/Bolu, 14100 Turkey. drhuseyingunduz@yahoo.com
Telephone: +903742534656 **Fax**: +903742534559
Received: 2003-07-17 **Accepted:** 2003-09-02

Abstract

AIM: To investigate the effect of N-acetyl cysteine (NAC) on acute viral hepatitis (AVH).

METHODS: We administered 200 mg oral NAC three times daily (600 mg/day) to the study group and placebo capsules to the control group. All patients were hospitalized and diagnosed as AVH. Blood total and direct bilirubin, ALT, AST, alkaline phosphatese, albumin and globulin levels of each patient were measured twice weekly until total bilirubin level dropped under 2 mg/dl, ALT level under 100 U/L, follow up was continued and then the patients were discharged.

RESULTS: A total of 41(13 female and 28 male) AVH patients were included in our study. The period for normalization of ALT and total bilirubin in the study group was 19.7±6.9 days and 13.7±8.5 days respectively. In the control group it was 20.4±6.5 days and 16.9±7.8 days respectively ($P>0.05$).

CONCLUSION: NAC administration effected neither the time necessary for normalization of ALT and total bilirubin values nor duration of hospitalization, so we could not suggest NAC for the treatment of icteric AVH cases. However, our results have shown that this drug is not harmful to patients with AVH.

Gunduz H, Karabay O, Tamer A, Özaras R, Mert A, Tabak ÖF. N-acetyl cysteine therapy in acute viral hepatitis. *World J Gastroenterol* 2003; 9(12): 2698-2700
http://www.wjgnet.com/1007-9327/9/2698.asp

INTRODUCTION

Acute viral hepatitis (AVH) is an infectious disease that occurs as liver cell necrosis and inflammation as a result of the infection of liver cells by various viruses[1,2]. Its significant symptoms and alterations occur in the liver and its functions[3,4]. It is accepted that AVH is a liver disease with the highest incidence in the world and that it is a major cause of jaundice[5]. It is a public health problem in developing countries which include our country as well. Moreover, hepatitis B and C may lead to chronic hepatitis, cirrhosis and cancer, and also constitute an endemic health problem for the society and is a cause of serious economic loss[6,7]. Various medications have been tried in the treatment of acute viral hepatitis, but no superiorities to placebo was demonstrated in most of these medications and they were not recommended for routine use[8-9].

NAC (N-acetyl cysteine) is frequently used as a mucolitic and as an antidote in paracetamol intoxication[10-11]. NAC may maintain cell integrity by increasing the amount of glutathione within the cell or coming into direct reaction with spontaneous conjugation and/or reduction[12]. Recently, some studies have shown good results and absence of side effects in patients treated with interferon and NAS in chronic hepatitis C patients[13-15]. In addition, treatment of HBV-producing cell lines with NAC resulted in an at least 50-fold reduction of viral DNA in the tissue culture supernatant within 48 hours[16]. The need for a treatment to shorten duration of AVH is obvious, but it has not been found yet. We thought this problem might be solved with NAC which protects the cellular architecture by increasing the amount of intracellular glutathione that reacts with toxic free oxygen radicals[17].

We could not find any study that focused on the effects of NAC on acute viral hepatitis. For this reason, we aimed to determine the effect of NAC on acute hepatitis in this study.

MATERIALS AND METHODS

In this study, 41 acute viral hepatitis A or B cases were included. These cases were hospitalized and monitored in the Infectious Diseases Department Cerrahpasa Faculty of Medicine, Istanbul University.

Those aged 14-60 years, with transaminase values more than 10 times of the upper limit of the normal value (>400 U/L), total bilirubin values above 3 mg/dl and positive antiHBc-IgM or antiHAV-IgM detected in serological examinations and negative serologic tests for hepatitis C virus, hepatitis D virus and HIV were included. Serological tests were done for HBsAg, HBcIgM, antibody to Hepatitis C virus (Abbott Lab.) and antibody to hepatitis delta virus (Anti-HDV, Wellcozyme, Wellcome Diagnostic, England) using the EIA method.

The cases who were hospitalized and monitored in the clinic were randomized into study group (20 patients) and control group (21 patients). Randomization was carried out according to age, gender and etiological agents. In the study group, 200 mg NAC was given orally 3 times a day (600 mg/day). In the control group, placebo was given orally 3 times a day.

The study protocol was approved by the local ethics committee. All patients were informed to participate in by an inscription form in the study.

Levels of the biochemical parameters [total and direct bilirubin, alanine aminotransferase (ALT), aspartate aminotransferase (AST), alkaline phosphatase, albumin and globulin levels and prothrombine activities] were monitored in both drug and control groups. This monitoring process continued until the level of total serum bilirubin reached 2 mg/dl and the ALT level fell below 100 U/L. Then the patients were discharged from the hospital. All patients were followed up for six months after discharge.

In evaluating the results of the study, Student' s *t* test was used for average age, gender, values concerning the etiologic agents and covariate analysis tests were used for biochemical

parameters, averages of hyperbilirubinemia, ALT, and time needed before they reached normal values.

RESULTS

A total of 41 patients (28 female /13 male) were included in the study. The median age was 24 (range: 15-52). The median age of hepatitis A patients was 17 (range: 16-28) and that of hepatitis B patients was 26 (range: 15-52).

The median age was 23 (range: 15-48) in the study group and was 24 (range: 16-52) in the control group (P>0.05). Patients with HAV infection were younger than those with HBV infection. In the serological distinction of the cases, type A was detected in 9 (22 %) and type B in 32 (78 %). In study group type A was detected in 4, type B was detected in 16. In control group type A was detected in 5 (23 %) and B in 16 (76 %).

In our study, the most important finding was the time needed for ALT and total bilirubin to reach normal. The criteria used to include a case in our study was ALT value that was ten times higher than the normal and the criteria used to end the surveillance of a case was its falling below 100 U/L. Jaundice was defined as the situation in which the serum total bilirubin level was higher than 3 mg/dl. Period of jaundice was defined as the duration that ended when the increasing bilirubin decreased to 2 mg/dl.

The period for normalization of ALT in study group was 19.7±6.9 days (type A 11.2±6.1 days, type B 21.8±6.1 days), while in the control group it was 20.4±6.5 days (type A 16±7.4 days, type B 21.8±6.7 days). The period for normalization of total bilirubin in the study group was 13.7±8.5 days (type A 7.9±4.9 days, type B 15.2±8.6 days), in control group was 16.9±7.8 days (type A 7.9±4.9 days, type B 18.4±8.1 days). No significant difference could be found between the two groups (P>0.05). These data are summarized in Table 1.

As a conclusion, the hospitalization duration and time to normalization of ALT and total bilirubin of the patients did not get shorter or longer (as an adverse effect) with the use of NAC.

Table 1 Comparison of study and control groups

	Study group	Control group
Case number	20	21
Median Age (min -max) (year)	23 (15-48)	24 (16-52)
Genus (M / F)	12 / 8	16 / 5
ALT (U / L)	1 730±628	2 129±1 278
AST (U / L)	987±545	1 397±1 002
ALP (U / L)	488±201	410±149
Total bilirubin (mg / dL)	7.75±4.36	10.1±3.04
Direct bilirubin (mg / dL)	5.29±3.14	7.17±3.26
Activity of prothrombin (%)	72.6±22.7	74.1±18.9
Albumin (g / dL)	3.95±0.54	3.98±0.40
Type of hepatitis (A / B)	4 / 16	5 / 16
Time consumption for ALT <100 U / L	19.7±6.9	20.4±6.5
Time consumption for total bilirubin <2 mg / dl	13.7±8.5	16.9±7.8

DISCUSSION

Virus hepatitis is an important health problem in the world. Hepatitis A is a common infection in our country, so is in the world and 50 % of the population aged up to 15 and 90 % of the adults are exposed to this disease[18]. Annual disease reporting was approximately 25 000 according to the data of the Ministry of Health in Turkey[19]. However it was believed that the real number of the cases was at least 250 000-500 000 per year, when the unreported cases and anicteric and subclinical cases were added[20,21].

When AVH displays a symptomatic presentation, it is generally cured at the end but after a long course. It is a public health problem in developing countries which include our country as well. Hepatitis B, C, D viruses causing AVH may lead to cirrhosis and cancer, and also constitute an endemic health problem for the society and are the cause for serious economic losses[22,23]. Various medications including steroids, interferon, vidarabine, levamizol, ursodeoxicolic acids, *ribavarine* have been tried in the treatment of acute viral hepatitis, but advantages over placebo offered by most of these medications were not found to be good enough to be recommended for routine use[24,25]. Thus the gap in the treatment of AVH has not been filled yet. We thought that this gap could be filled by NAC.

NAC is frequently used as mucolitic and as an antidote for paracetamol intoxication. It was used in paracetamol intoxication as it could fill the mitochondrial and cytosolic glutathione stocks consumed by N acetyl benzoquinoneimine, which is a paracetamol metabolite, by stimulating glutathione synthesis[26]. Under physiological conditions, there is basal glutathione outrun from the liver into the blood. It has been observed that intracellular glutathione participated in some critical physiological activities such as provision of membrane and cell skeleton unity, arrangement of enzyme activities and biosynthesis of protein and nucleic acids[8,13]. It might also lead to serious decreases in the intracellular and tissue glutathione and heavy pathological transformations in this tissue[9,10].

Recently, some studies have shown good results and absence of side effects in patients treated with NAC in hepatitis B and chronic hepatitis C patients[13]. Addition of NAC which is a glutathione precursor, to 14 patients with chronic hepatitis C and high ALT level, caused a regular decrease of ALT in all patients and after a combined treatment it helped 41 % of the cases to heal completely after 5- 6 months. Consequently, it was reported that NAC increased interferon response in patients with hepatitis C[14]. Recently Neri *et al*. reported the presence of oxidative stress in patients with chronic hepatitis C, earlier relapse in patients treated with interferon alone. They obtained significant results in patients treated with interferon plus NAC compared to those with interferon alone[13]. Weiss *et al*. showed that NAC was able to inhibit hepatitis B virus (HBV) replication, by a mechanism independent of the intracellular level of reactive oxygen intermediates. Treatment of HBV-producing cell lines with NAC resulted in an at least 50-fold reduction of viral DNA in the tissue culture supernatant within 48 h. This decrease of viral DNA and thus of virions in the tissue culture supernatant was caused by a disturbance of the virus assembly, rather than by a reduction of viral transcripts. Their data strongly suggested a potential use of this well-established, non-toxic drug for the treatment of HBV infection. They found that NAC, in contrast to interferon, exerted its anti-HBV activity at a posttranscriptional level, a combination of NAC with the established interferon therapy could also be suggested.

We conducted a comparative study to examine the effects of NAC on the functions of liver in AVH. Taking the disease period as the period in which the ALT value came back to normal, we measured the duration of this period in the study group and control group. We also examined the effect of NAC on the period of jaundice. AST, ALT and serum bilirubin measurements were among the tests that were not specific in the diagnosis of AVH, and these were parameters in harmony with the hepatocellular injury. In AVHs, transaminases had diagnostic value, rather than prognostic value. It was accepted that in AVH, these enzymes increased 10 times, ALT maintained to be higher than AST and then it decreased in an evident way in the first week, then it came back to normal in 2- 4 weeks.

In AVH infections, the value of total serum bilirubin increased up to 3-20 mg/dl in 1-2 weeks under normal conditions and although serum aminotransferases levels started to fall, bilirubin levels might continue to increase, then they gradually decreased. In the study and control groups, total bilirubin levels were 7.75±4.36 mg/dl and 10.1±3.04 mg/dl respectively. The average period of jaundice was 13.7±8.5 days in the study group, and 16.9±7.8 days in the control group (P>0.05).

During ALT, AST, bilirubin values came back to normal in the study and control groups, the patients with hepatitis A and B infection were evaluated separately, the difference was not statistically meaningful. The curves of AST and ALT in the study and control groups were not statistically different (Figures 1 and 2). Thus it became obvious that NAC did not change the liver enzyme activities in the patients with AVH.

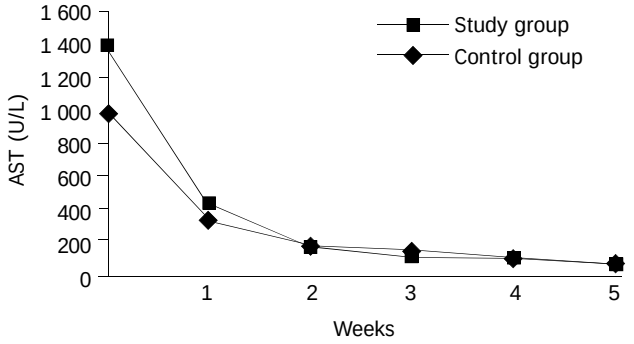

Figure 1 Changes in averages of ALT values in the study and control groups in time.

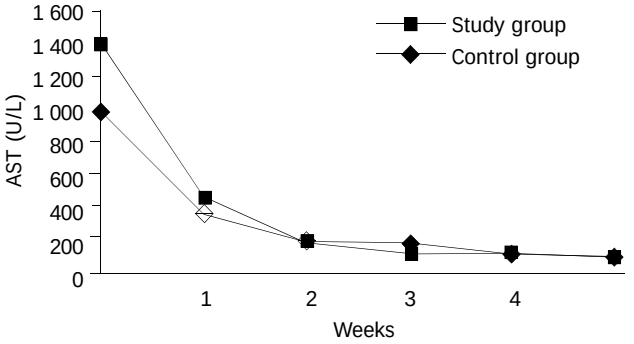

Figure 2 Changes in averages of AST values in the study and control groups in time.

This was the first study investigating the effect of NAC on AVH. In this study, it was determined that NAC had no effect on the jaundice duration in AVH infection and the period in which the ALT value came back to normal and accordingly hospitalization duration of AVH patients and the prognosis of biochemical parameters.

In conclusion, the use of NAC in acute viral hepatitis complicated by jaundice is no more effective than placebo. However, the use of NAC in AVH cases is not harmful.

REFERENCES

1 **Banker DD.** Viral hepatitis. *Indian J Med Sci* 2003; **57**: 363-368
2 **Mathur P**, Arora NK. Considerations for HAV vaccine in India. *Indian J Pediatr* 2001; **68**(Suppl 1): 23-30
3 **Batra Y**, Bhatkal B, Ojha B, Kaur K, Saraya A, Panda SK, Acharya SK. Vaccination against hepatitis A virus may not be required for schoolchildren in northern India: results of a seroepidemiological survey. *Bull World Health Organ* 2002; **80**: 728-731
4 **Alter MJ**, Mast EE. The epidemiology of viral hepatitis in the United States. *Gastroenterol Clin North Am* 1994; **23**: 437-455
5 **Ertekin V**, Selimoglu MA, Altinkaynak S. Sero-epidemiology of hepatitis B infection in an urban paediatric population in Turkey. *Public Health* 2003; **117**: 49-53
6 **Khan WI**, Sultana R, Rahman M, Akhter H, Haq JA, Ali L, Mohsin MA, Khan AK. Viral hepatitis: recent experiences from serological studies in Bangladesh. *Asian Pac J Allergy Immunol* 2000; **18**: 99-103
7 **Centers for Disease Control and Prevention (CDC)**. Transmission of hepatitis B and C viruses in outpatient settings–New York, Oklahoma, and Nebraska, 2000-2002. *MMWR Morb Mortal Wkly Rep* 2003; **52**: 901-906
8 **Gregory PB**, Knauer CM, Kempson RL, Miller R. Steroid therapy in severe viral hepatitis, a double blind, randomized trial of methylprednisolone versus placebo. *N Eng J Med* 1976; **294**: 681-687
9 **Mackenzie AR**, Molyneaux PJ, Cadwgan AM, Laing RB, Douglas JG, Smith CC. Increasing incidence of acute hepatitis B virus infection referrals to the Aberdeen Infection Unit: a matter for concern. *Scott Med J* 2003; **48**: 73-75
10 **Kucukardali** Y, Cinan U, Acar HV, Ozkan S, Top C, Nalbant S, Cermik H, Cankir Z, Danaci M. Comparison of the therapeutic efficacy of 4-methylpyrazole and N-acetylcysteine on acetaminophen (paracetamol) hepatotoxicity in rats. *Curr Med Res Opin* 2002; **18**: 78-81
11 **Zhao C**, Sheryl D, Zhou YX. Effects of combined use of diallyl disulfide and Nacetyl-cysteine on acetaminophen hepatotoxicity in β-naphthoflavone-pretreated mice. *World J Gastroenterol* 1998; **4**: 112-116
12 **Flanagan RJ**, Meredith TJ. Use of N-acetylcysteine in clinical toxicology. *Am J Med* 1991; **91**(Suppl 3C): 131-139
13 **Neri S**, Ierna D, Antoci S, Campanile E, D'Amico RA, Noto R. Association of alpha-interferon and acetyl cysteine in patients with chronic C hepatitis. *Panminerva Med* 2000; **423**: 187-192
14 **Beloqui O**, Prieto J, Suarez M, Gil B, Qian CH, Garcia N, Civeira MP. N-acetyl cysteine enhances the response to interferon-alpha in chronic hepatitis C: a pilot study. *J Interferon Res* 1993; **13**: 279-282
15 **Grand PR**, Black A, Garcia N, Prieto J, Garson JA. Combination therapy with interferon-alpha plus N-acetyl cysteine for chronic hepatitis C: a placebo controlled double-blind multicentre study. *J Med Virol* 2000; **61**: 439-442
16 **Weiss L**, Hildt E, Hofschneider PH. Anti hepatitis B virus activity of N acetylcysteine, new aspect a well estabilished drug. *Antiviral Res* 1996; **32**: 43-53
17 **Mandal AK**, Sinha J, Mandal S, Mukhopadhyay S, Das N. Targeting of liposomal flavonoid to liver in combating hepatocellular oxidative damage. *Drug Deliv* 2002; **9**: 181-185
18 **Wie J**, Wang YQ, Lu ZM, Li GD, Wang Y, Zhang ZC. Detection of anti-preS1 antibodies for recovery of hepatitis B patients by immunoassay. *World J Gastroenterol* 2002; **8**: 276-281
19 T.C Government Statically Instuty. *Stastical annual of Turkey Republic* 1993: 151-154
20 **Ozturk R**. Laboratuary Diagnosis of Viral Hepatitis. Yucel A, Tabak F (Eds): Currently Viral Hepatitis. *Istanbul Infectious Diseases Association's publications* 1998; **11**: 53-54
21 **Ozdemir O**, Arda K, Soylu M, Alyan O, Demir AD, Kutuk E. Seroprevalence of hepatitis B and C in subjects admitted to a cardiology clinics in Turkey. *Eur J Epidemiol* 2003; **18**: 255-258
22 **Shiell A**, Law MG. The cost of hepatitis C and the cost-effectiveness of its prevention. *Health Policy* 2001; **58**: 121-131
23 **Jacobs RJ**, Saab S, Meyerhoff AS, Koff RS. An economic assessment of pre-vaccination screening for hepatitis A and B. *Public Health Rep* 2003; **118**: 550-558
24 **Maier I**, Wu GY. Hepatitis C and HIV co-infection: a review. *World J Gastroenterol* 2002; **8**: 577-579
25 **Ryder SD**, Beckingham IJ. ABC of diseases of liver, pancreas, and biliary system: Acute hepatitis. *BMJ* 2001; **322**: 151-153
26 **MacNee W**, Bridgeman MME, Marsden M. Effects of N-acetylcysteine and glutathione on smoke induced changes in lung phagocytes and epithelial cells. *Am J Med* 1991; **91**(Suppl 3C): 60-71
27 **Taylor ER**, Hurrell F, Shannon RJ, Lin TK, Hirst J, Murphy MP. Reversible glutathionylation of complex I increases mitochondrial superoxide formation. *J Biol Chem* 2003; **278**: 19603-19610

Edited by Wang XL

P.O.Box 2345, Beijing 100023,China
Fax: +86-10-85381893
E-mail: wjg@wjgnet.com www.wjgnet.com

World J Gastroenterol 2003;9(12):2701-2705
World Journal of Gastroenterology
 ISSN 1007-9327

Expression of mucosal addressin cell adhesion molecule 1 on vessel endothelium of gastric mucosa in patients with nodular gastritis

Hiroshi Ohara, Hajime Isomoto, Chun-Yang Wen, Chieko Ejima, Masahiro Murata, Masanobu Miyazaki, Fuminao Takeshima, Yohei Mizuta, Ikuo Murata, Takehiko Koji, Hiroshi Nagura, Shigeru Kohno

Hiroshi Ohara, Hajime Isomoto, Masanobu Miyazaki, Fuminao Takeshima, Yohei Mizuta, Ikuo Murata, Shigeru Kohno, Second Department of Internal Medicine, 1-7-1 Sakamoto, Nagasaki, Japan
Chun-Yang Wen, Department of Molecular Pathology, Atomic Bomb Disease Institute, 1-12-4 Sakamoto, Nagasaki, Japan
Takehiko Koji, Department of Histology and Cell Biology, Nagasaki University School of Medicine, Nagasaki, 1-12-4 Sakamoto, Nagasaki, Japan
Chieko Ejima, Masahiro Murata, Hiroshi Nagura, Department of Pathology, Tohoku University School of Medicine, Aobaku, Sendai, Japan
Correspondence to: Dr. Hajime Isomoto, Second Department of Internal Medicine, Nagasaki University School of Medicine, 1-7-1 Sakamoto, Nagasaki, Japan. hajimei2002@yahoo.co.jp
Telephone: +81-95-849-7567 **Fax:** +81-95-849-7568
Received: 2003-09-06 **Accepted:** 2003-10-23

Abstract

AIM: The interaction of mucosal addressin cell adhesion molecule 1 (MAdCAM-1) with integrin α4β7 mediates lymphocyte recruitment into mucosa-associated lymphoid tissue (MALT). Nodular gastritis is characterized by a unique military pattern on endoscopy representing increased numbers of lymphoid follicles with germinal center, strongly associated with *H pylori* infection. The purpose of this study was to address the implication of the MAdCAM-1/integrin β7 pathway in NG.

METHODS: We studied 17 patients with NG and *H pylori* infection and 19 *H pylori*-positive and 14 *H pylori*-negative controls. A biopsy sample was taken from the antrum and snap-frozen for immunohistochemical analysis of MAdCAM-1 and integrin β7. In simultaneous viewing of serial sections, the percentage of MAdCAM-1-positive to von Willebrand factor-positive vessels was calculated. We also performed immunostaining with anti-CD20, CD4, CD8 and CD68 antibodies to determine the lymphocyte subsets co-expressing integrin β7.

RESULTS: Vascular endothelial MAdCAM-1 expression was more enhanced in gastric mucosa with than without *H pylori* infection. Of note, the percentages of MAdCAM-1-positive vessels were significantly higher in the lamina propria of NG patients than in *H pylori*-positive controls. Strong expression of MAdCAM-1 was identified adjacent to lymphoid follicles and dense lymphoid aggregates. Integrin β7-expressing mononuclear cells, mainly composed of CD20 and CD4 lymphocytes, were associated with vessels lined with MAdCAM-1-expressing endothelium.

CONCLUSION: Our results suggest that the MAdCAM-1/integrin α4β7 homing system may participate in gastric inflammation in response to *H pylori*-infection and contributes to MALT formation, typically leading to the development of NG.

Ohara H, Isomoto H, Wen CY, Ejima C, Murata M, Miyazaki M, Takeshima F, Mizuta Y, Murata I, Koji T, Nagura H, Kohno S. Expression of mucosal addressin cell adhesion molecule 1 on vessel endothelium of gastric mucosa in patients with nodular gastritis. *World J Gastroenterol* 2003; 9(12): 2701-2705
http://www.wjgnet.com/1007-9327/9/2701.asp

INTRODUCTION

Lymphocyte recruitment to inflammatory sites is regulated by differential expression of cell surface homing receptors and their interactions with relevant vascular adhesion molecules[1]. An immunoglobulin super family, single-chain 60-kDa glycoprotein, mucosal addressin cell adhesion molecule 1 (MAdCAM-1) is selectively expressed on the endothelium of high endothelial venules in gut-associated lymphoid tissues and vascular endothelial cells in the lamina propria of the small and large intestine[2]. Engagement of MAdCAM-1 to its exclusive ligand, integrin α4β7, on lymphocytes represents a tissue-specific homing mechanism for the intestine and gut-associated lymphoid tissue[2].

Helicobacter pylori causes one of the most common chronic infections in humans[3]. Although *H pylori* is a noninvasive pathogen[4], persistent infection causes chronic gastritis, which predisposes the mucosa to peptic ulceration, and is thought to be eventually linked to gastric cancer and primary gastric lymphoma, especially the lymphoma of mucosa-associated lymphoid tissue (MALT) type[5,6]. The histopathological features of *H pylori*-associated gastritis include intense infiltration of granulocytes and lymphocytes[7] and the formation of organized lymphoid follicles[8]. In this regard, nodular gastritis (NG), which is a unique military pattern resembling "goose flesh" on endoscopy[9], is characterized by increased numbers of lymphoid follicles with germinal center[10], in close association with *H pylori* infection[9, 10]. Although NG frequently occurs in children, there are ample evidences at present suggesting that NG is not so uncommon in adults, especially in pre-menopausal women[9,10].

Recently, Hatanaka *et al*[11] reported that expression of vascular endothelial MAdCAM-1 was enhanced in murine chronic gastritis induced by *H pylori*. Furthermore, Dogan *et al*[12] demonstrated strong expression of MAdCAM-1 protein on the vasculature in patients with *H pylori*-associated MALT type lymphoma. However, little is known about the implication of such adhesion molecules in the pathogenesis of NG. In this study, we investigated MAdCAM-1 expression on vessel endothelium in gastric mucosa of patients with NG by immunohistochemistry, along with the interaction with integrin α4β7. This could shed light on the mechanism of MALT organization in gastric mucosa in response to *H pylori* infection.

MATERIALS AND METHODS

Subjects and samples

We studied 17 patients who underwent upper gastrointestinal

endoscopy for dyspepsia and were diagnosed as having NG between April 1999 and March 2002. They included 2 men and 15 women, ranging 24 to 58 years old (mean, 43 years). As a control, age- and sex- matched 33 subjects with non-ulcer dyspepsia during the same period were recruited in the study. They consisted of 19 *H pylori*-infected patients without nodular gastritis (*H pylori*-positive controls) and 14 *H pylori*-negative ones. None of the control subjects had been treated with non-steroidal anti-inflammatory drugs, proton pump inhibitors, antibiotics, or bismuth compounds during the 4-week period prior to the present study. There were no differences in baseline characteristics such as alcohol intake, current tobacco use and body mass index among the three groups.

At endoscopy, one biopsy specimen was obtained from the antrum within 2 cm of the pyloric ring along the greater curvature. The sample was snap-frozen in OCT compound (Tissue-tek; Miles Inc., Elkhart, IN) in ethanol-dry ice bath and stored at -80 ℃ until use.

Detection of Helicobacter pylori infection

H pylori status was assessed by serology (anti-*H pylori* immunoglobulin G antibody, HEL-p TEST, AMRAD Co., Melbourne, Australia), rapid urease test (CLO test; Delta West Co., Bentley, Australia) using additional biopsy specimens obtained during endoscopy from the antrum within 2 cm of the pyloric ring and the corpus along the greater curvature. Patients were considered positive for *H pylori* infection when at least one examination yielded positive results. On the other hand, patients were defined as *H pylori*-negative if all test results were negative.

Immunohistochemical analysis

MAdCAM-1 protein expression on vascular endothelial cells was studied *in situ* by immunohistochemistry with the streptavidin-biotin-peroxidase-complex method (Histofine SAB-PO kit, Nichirei Co., Tokyo), as described previously[13]. In brief, frozen tissues were cut into 4-μm thick sections and placed on glass slides coated with 3-aminopropyltriethoxysilane (Dako Co., Glostrup, Denmark). The following steps were performed at room temperature unless otherwise specified. Sections were fixed in 4 % paraformaldehyde (Merck Co., Darmstadt, Germany) in phosphate-buffered saline (PBS, pH 7.4) for 20 minutes. After a brief washing in PBS, endogenous peroxidase activity was inhibited for 30 min with methanol containing 0.3 % H_2O_2. Sections were reacted for 20 min with 10 % normal rabbit serum (Nichirei Co.) to prevent non-specific binding, and incubated with anti-MAdCAM-1 mouse monoclonal antibody (clone 1G2)[14] at a concentration of 1:100 in PBS overnight at 4 ℃. On the next day, the sections were washed three times (10 min each) in PBS and incubated for 20 min with 10 mg/ml biotinylated rabbit anti-mouse immunoglobulins (Nichirei). After washed three times (10 min each) in PBS, the sections were re-incubated for 20 min with 100 μg/ml HRP-conjugated streptavidin (Nichirei). After washed three times (10 min each) in PBS, a color reaction was performed with 0.05 M Tris-HCl (pH 7.6) containing 3, 3' -diaminobendizine tetrahydrochloride (Dojin Chemical Co., Kumamoto, Japan) and H_2O_2. Sections were counterstained with Mayer' s hematoxylin and then dehydrated, cleared and mounted by standard procedures.

In each serial section of the same tissue specimen, vessels were immunostained with anti-von Willebrand factor monoclonal antibody (Dako Co.) in the same fashion described above, in order to assess quantitatively the difference in the extent of expression of endothelial adhesion molecules, based on the method reported by Hatz *et al*[15]. Briefly, two independent observers who were blind to the diagnosis and experimental results, counted the number of von Willebrand factor-positive vessels and then the number of MAdCAM-1-positive vessels on the section serial to that stained for von Willebrand factor. Percentage of the ratio of MAdCAM-1-positive to von Willebrand factor-positive vessels was calculated. As a negative control, each non-specific isotype antibody was used instead of the primary antibodies, or the primary antibodies were omitted. When the interobserver variability exceeded 10 %, the areas were simultaneously re-evaluated by the two investigators to reach a consensus.

Furthermore, immunoreactivity for integrin β7 on inflammatory cells infiltrating the gastric mucosa was similarly analyzed using a specific monoclonal antibody (Pharmingen Co., San Diego, CA) at a concentration of 1:10. On the section serial to that stained for β7, we also performed immunohistochemistry using anti-CD20, -CD4, -CD8 and -CD68 monoclonal antibodies (purchased from Dako Co.).

Reverse transcriptase polymerase chain reaction (RT-PCR)

Total RNA from biopsy samples that were also collected from the same location was extracted using a commercial kit according to the instructions provided by the supplier (ISOGEN, Nippon Gene Co., Toyama, Japan). Equivalent amounts of RNA were monitored by absorption at 260 nm and by monitoring the density of 28S and 18S RNA detected after electrophoresis. After 1 μg of total RNA was reverse transcribed to complementary DNA, the target sequence of MAdCAM-1 was amplified in 35 cycles, each consisting of 1 min at 94 ℃ for denaturation, 1 min at 60 ℃ for annealing and 1 min at 72 ℃ for extension, followed by a final extension for 5 min at 72 ℃ with specific primers[16], using a RT-PCR kit (Takara Shuzo Co., Otsu, Japan). Two primers designed to nucleotide positions 978-999 (TGC GGT GCT GGG ACT GCT GCT C, sense) and 1 344-1 364 (TCA GGG AGG GGC TTC AGG TCA, antisense) of human MAdCAM-1 cDNA sequence were used for amplification of a 387 bp product[16]. A 10 μl aliquot of each PCR product was analyzed by electrophoresis on 2 % agarose gel containing ethidium bromide, and the bands were examined under ultraviolet light for the presence of amplified DNA. Glyceraldehyde-3-phosphate dehydrogenase (G3PDH) gene transcript was routinely amplified as described previously[17] and used as an internal control of the processed RNA for each preparation.

All samples were obtained with informed consent in accordance with the Helsinki Declaration.

Statistical analysis

Statistical analyses were performed using Fisher' s exact, χ^2, Student' s *t*, and Mann-Whitney *U* tests, whichever appropriate. A *P* value less than 0.05 was accepted as statistically significant. Data were expressed as mean ± standard deviation (SD).

RESULTS

Clinicopathological features of NG

All 17 patients with NG were *H pylori*-positive. Among the 17 patients, no less than 9 (52.9 %) had endoscopic evidence of peptic ulcer (duodenal ulcer in 7 and gastric ulcer in 2). All except one specimen from the NG patients showed lymphoid follicle formation and/or dense lymphoid aggregates.

MAdCAM-1 expression on vessel endothelium

The MAdCAM-1antigen, recognized by the 1G2 antibody, was seen on vascular endothelial cells in gastric mucosa. In *H pylori*-negative group, MAdCAM-1 was rarely or occasionally localized in vascular endothelial cells in the lamina propria (Figure 1A). However, the relative endothelial area expressing MAdCAM-1 increased in inflammatory settings induced by *H pylori* infection (Figure 1B), particularly in association with

dense lymphocytic infiltration (Figure 1C). High endothelial venule-like vessels adjacent to the lymphoid follicle were intensely immunoreactive (Figure 1D). There was a significant difference in the percentages of MAdCAM-l-positive vessels between *H pylori*-positive and –negative controls ($P<0.001$, Figure 2). In addition, the expression of vascular MAdCAM-1 was more enhanced in patients with NG than that in *H pylori*-negative controls ($P<0.0001$, Figure 2). Of note, MAdCAM-1-positive vessels were more abundant in the antral mucosa of patients with NG, compared with *H pylori*-positive controls ($P<0.05$, Figure 2). The percentages of MAdCAM-1-positive vessels detected by the two observers were almost identical. When each non-specific isotype serum was used or primary antibodies were omitted, the specimens showed no immunoreactivity.

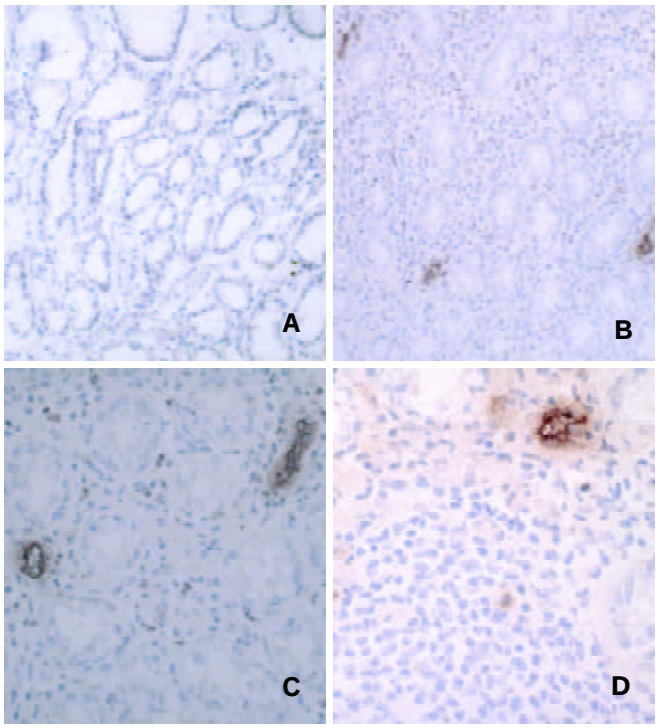

Figure 1 (A): *H pylori*-negative gastric mucosa showed little immunoreactivity for mucosal addressin cell adhesion molecule 1 (MAdCAM-1). MAdCAM-1 was expressed on the endothelium of numerous vessels within the lamina propria with *H pylori* infection (B), particularly in association with dense mononuclear infiltration (C). Strong endothelial expression of MAdCAM-1 was localized on high endothelial venule-like vessels adjacent to the lymphoid follicles D.

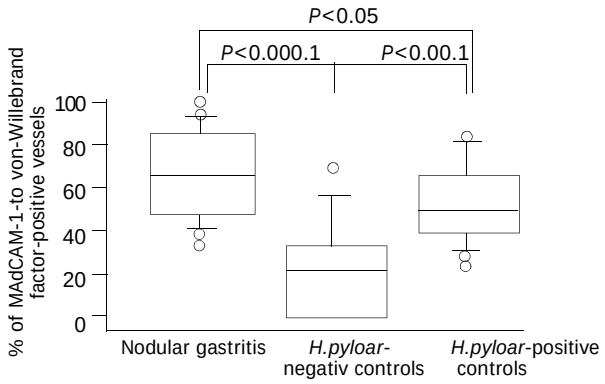

Figure 2 MAdCAM-1 immunoreactivity on mucosal vasculature of antral biopsy specimens from patients with nodular gastritis and *H pylori*-positive and –negative controls. Results were expressed as the percentage of von-Willebrand factor-positive vessels immunoreactive for MAdCAM -1 in serial sections.

Integrin β7 was expressed on increased number of mononuclear cells in the lamina propria of patients with *H pylori* infection, whereas there were few integrin β7-positive cells in the mucosa of *H pylori*-negative controls. Analysis of serial sections showed lymphocytes co-expressing anti-CD4 antibody and integrin β7 (Figure 3). Also, some CD20-positive cells also expressed integrin β7. However, the integrin β7-positive infiltrating cells showed little immunoreactivity for CD8 and CD68. The vessels lined with endothelial cells positive for MAdCAM-1 correlated well with the infiltration of integrin β7-expressing lymphocytes (Figure 4).

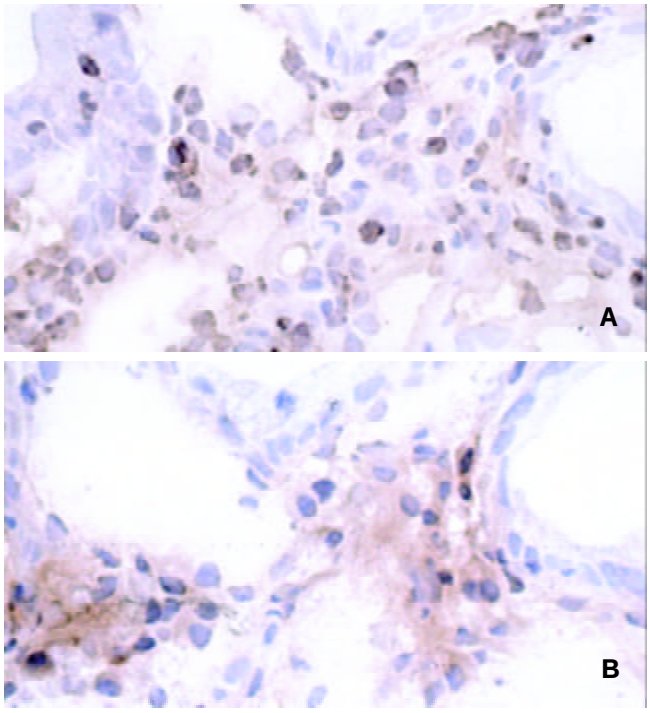

Figure 3 In simultaneous viewing of serial sections, integrin β7-expressing cells (A) consisted of CD-4-positive T lymphocytes (B).

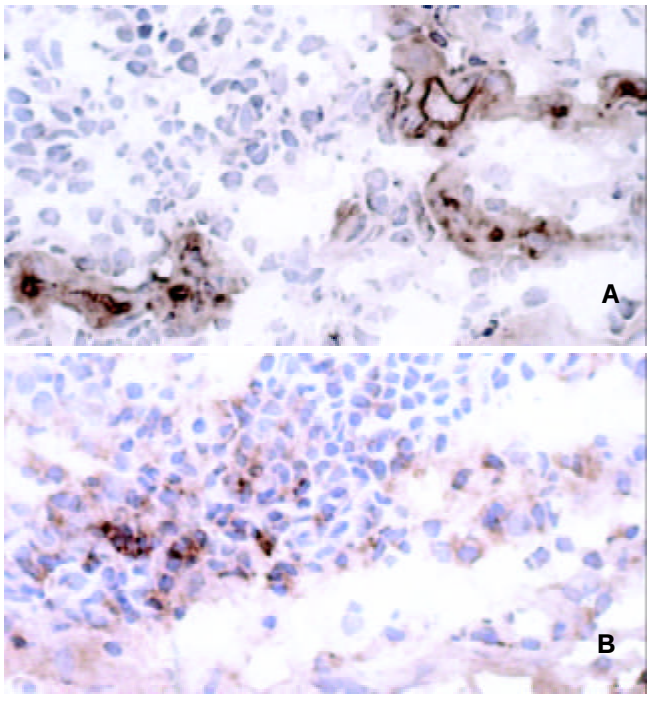

Figure 4 Vessels lined with MAdCAM-1-positive endothelium (A) were associated with infiltration of lymphocytes immunoreactive for integrin β7 (B).

Expression of MAdCAM-1 gene in antral biopsy specimens

We identified the *MAdCAM-1* gene-specific product as a 387-bp band by RT-PCR both in patients with NG and in *H pylori*-positive controls, but not in *H pylori*-negative controls despite the constitutive *G3PDH* housekeeping gene expression (Figure 5).

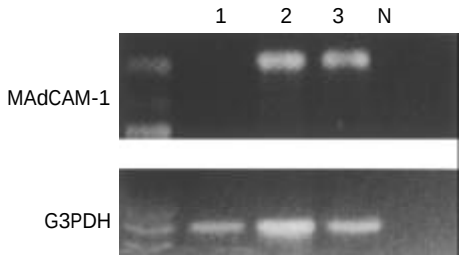

Figure 5 MAdCAM-1 and glyceraldehyde-3-phosphate dehydrogenase (G3PDH) mRNA transcripts were detected as 387 and 983 base pair-bands with reverse transcriptase-polymerase chain reaction, respectively. Lane N: negative control, lane 1: *H pylori*-negative control, lane 2: *H pylori*-positive control, lane 3: patients with nodular gastritis.

DISCUSSION

In the present study, vascular expression of MAdCAM-1 protein assessed by immunohistochemistry was more enhanced in gastric mucosa of *H pylori*-positive than in *H pylori*–negative subjects. On RT-PCR analysis, the mRNA for MAdCAM-l was detected only in *H pylori*-infected gastric mucosa, but not in the mucosa negative for the organism. In the previous *in vitro* study, MAdCAM-1 was induced on a murine endothelial cell line, by proinflammatory cytokines including interleukin 1 and tumor necrosis factor α[18], which were much more increased in human gastric mucosa with than without *H pylori* infection[19]. Considered together, these results indicate that MAdCAM-1 is selectively upregulated in the infected gastric mucosa. Integrin β7-expressing mononuclear cells were found surrounding blood vessels lined with MadCAM-1-postive endothelium, suggesting that the MAdCAM-1/integrin α4β7 pathway directs lymphocytes to the inflamed sites of *H pylori* infection, as shown in the murine model[11]. Together with other endothelially expressed adhesion molecules such as intercellular cell adhesion molecule 1 and vascular cell adhesion molecule 1[15], though more specifically, MAdCAM-1 could play a role in chronic inflammation induced by *H pylori*.

The striking finding of this study was that the percentages of MAdCAM-1-positive to von Willebrand factor-positive vessels in the lamina propria was significantly higher in patients with NG than in *H pylori*-positive controls. In addition to the prominent development of lymphoid follicles, intense mucosal inflammatory cell infiltration consisting mainly of lymphocytes was characteristic of NG[10]. The recruitment and emigration of circulating lymphocytes, on which integrin α4β7 is certainly expressed[20], may be accelerated in the gastric mucosa of NG, through, in part, the substantially enhanced expression of this vascular addressin.

MAdCAM-1 protein was strongly expressed on high endothelial venule-like vessels adjacent to lymphoid follicles and dense lymphoid aggregates within gastric mucosa. In the gut-associated lymphoid tissues such as Peyer' s patches and mesenteric lymph nodes, the homing of their constituent lymphocytes has been found to be largely dependent on the interaction of MAdCAM-1 on high endothelial venules with integrin α4β7[2]. Similarly, the vascular MAdCAM-1 localized near the lymphoid follicles may be a principal ligand for circulating lymphocytes to the specialized lymphoid sites and may contribute to the formation of MALT in *H pylori*-induced gastric inflammation, typically leading to the development of NG. This is a topic that warrants further studies, with special attention to the relationship between NG and MALT lymphoma[21], as a recent report documented the strong expression of MAdCAM-1 on the vasculature of patients with this type of lymphoma[12].

In the present study, simultaneous viewing of serial sections revealed the presence of integrin β7-expressing mononuclear cells in the infected gastric mucosa. These cells were mainly CD4-positive T and CD20-positive B cell populations, as described previously[12,20,22]. Several *in vitro* studies showed that *H pylori* antigen could induce the expression of integrin α4β7 on the surface of these cells[20,22]. In addition, employing immunomagnetic cell sorting, *H pylori* reactive circulating T lymphocytes were mainly found in the α4β7-positive cell fraction[20]. Accordingly, we believe that mucosally activated lymphocytes in response to *H pylori* infection can migrate from the inductive sites via circulation to their effector sites in the gastric mucosa, using this exclusive homing receptor as a ligand for MAdCAM-1.

In conclusion, our study demonstrated enhanced expression of MAdCAM-1 on the vascular endothelium and increased number of integrin β7-expressing T and B cells in *H pylori*-positive gastric mucosa. In NG, the proportion of MAdCAM-1-positive vessels was higher than that even in *H pylori*-positive controls. The selective MAdCAM-1/integrin α4β7 homing system is thought to play a significant role in gastric mucosal immunity in response to *H pylori* infection, especially in lymphoid follicle formation.

REFERENCES

1 **Springer TA**. Traffic signals for lymphocyte recirculation and leukocyte emigration: the multistep paradigm. *Cell* 1994; **76**: 301-314
2 **Briskin M**, Winsor-Hines D, Shyjan A, Cochran N, Bloom S, Wilson J, McEvoy LM, Butcher EC, Kassam N, Mackay CR, Newman W, Ringler DJ. Human mucosal addressin cell adhesion molecule-1 is preferentially expressed in intestinal tract and associated lymphoid tissue. *Am J Pathol* 1997; **151**: 97-110
3 **Dytoc M**, Gold B, Louie M, Huesca M, Fedorko L, Crowe S, Lingwood C, Brunton J, Sherman P. Comparison of *Helicobacter pylori* and attaching-effacing *Escherichia coli* adhesion to eukaryotic cells. *Infect Immun* 1993; **61**: 448-456
4 **Kuipers EJ**. *Helicobacter pylori* and the risk and management of associated diseases: gastritis, ulcer disease, atrophic gastritis and gastric cancer. *Aliment Pharmacol Ther* 1997; **11 (Suppl 1)**: 71-88
5 **Weber DM**, Dimopoulos MA, Anandu DP, Pugh WC, Steinbach G. Regression of gastric lymphoma of mucosa-associated lymphoid tissue with antibiotic therapy for *Helicobacter pylori*. *Gastroenterology* 1994; **107**: 1835-1838
6 **Blaser MJ**. *Helicobacter pylori* and the pathogenesis of gastroduodenal inflammation. *J Infect Dis* 1990; **161**: 626-633
7 **Meining A**, Stolte M, Hatz R, Lehn N, Miehlke S, Morgner A, Bayerdorffer E. Differing degree and distribution of gastritis in *Helicobacter pylori*-associated diseases. *Virchows Arch* 1997; **431**: 11-15
8 **Genta RM**, Hamner HW, Graham DY. Gastric lymphoid follicles in *Helicobacter pylori* infection: frequency, distribution, and response to triple therapy. *Hum Pathol* 1993; **24**: 577-583
9 **Miyamoto M**, Haruma K, Yoshihara M, Hiyama T, Sumioka M, Nishisaka T, Tanaka S, Chayama K. Nodular gastritis in adults is caused by *Helicobacter pylori* infection. *Dig Dis Sci* 2003; **48**: 968-975
10 **De Giacomo C**, Fiocca R, Villani L, Lisato L, Licardi G, Diegoli N, Donadini A, Maggiore G**.** *Helicobacter pylori* infection and chronic gastritis: clinical, serological, and histologic correlations in children treated with amoxicillin and colloidal bismuth subcitrate. *J Pediatr Gastroenterol Nutr* 1990; **111**: 310-316
11 **Hatanaka K**, Hokari R, Matsuzaki K, Kato S, Kawaguchi A, Nagao S, Suzuki H, Miyazaki K, Sekizuka E, Nagata H, Ishii H,

Miura S. Increased expression of mucosal addressin cell adhesion molecule-1 (MAdCAM-1) and lymphocyte recruitment in murine gastritis induced by *Helicobacter pylori*. *Clin Exp Immunol* 2002; **130**: 183-189

12 **Dogan A**, Du M, Koulis A, Briskin MJ, Isaacson PG. Expression of lymphocyte homing receptors and vascular addressins in low-grade gastric B-cell lymphomas of mucosa-associated lymphoid tissue. *Am J Pathol* 1997; **151**: 1361-1369

13 **Isomoto H**, Furusu H, Shin M, Ohnita K, Miyazaki M, Omagari K, Mizuta Y, Murase K, Inoue K, Murata I, Koji T, Kohno S. Enhanced expression of transcription factor E2F in *Helicobacter pylori*-infected gastric mucosa. *Helicobacter* 2002; **7**: 152-162

14 **Arihiro S**, Ohtani H, Suzuki M, Murata M, Ejima C, Oki M, Kinouchi Y, Fukushima K, Sasaki I, Nakamura S, Matsumoto T, Torii A, Toda G, Nagura H. Differential expression of mucosal addressin cell adhesion molecule-1 (MAdCAM-1) in ulcerative colitis and Crohn's disease. *Pathol Int* 2002; **52**: 367-374

15 **Hatz RA**, Rieder G, Stolte M, Bayerdorffer E, Meimarakis G, Schildberg FW, Enders G. Pattern of adhesion molecule expression on vascular endothelium in *Helicobacter pylori*-associated antral gastritis. *Gastroenterology* 1997; **112**: 1908-1919

16 **Leung E**, Berg RW, Langley R, Greene J, Raymond LA, Augustus M, Ni J, Carter KC, Spurr N, Choo KH, Krissansen GW. Genomic organization, chromosomal mapping, and analysis of the 5' promoter region of the human MAdCAM-1 gene. *Immunogenetics* 1997; **46**: 111-119

17 **Ikeda K**, Oka M, Yamada Y, Soda H, Fukuda M, Kinoshita A, Tsukamoto K, Noguchi Y, Isomoto H, Takeshima F, Murase K, Kamihira S, Tomonaga M, Kohno S. Adult T-cell leukemia cells over-express the multidrug-resistance-protein (MRP) and lung-resistance-protein (LRP) genes. *Int J Cancer* 1999; **82**: 599-604

18 **Takeuchi M**, Baichwal VR. Induction of the gene encoding mucosal vascular addressin cell adhesion molecule 1 by tumor necrosis factor alpha is mediated by NF-kappa B proteins. *Proc Natl Acad Sci U S A* 1995; **92**: 3561-3565

19 **Yamaoka Y**, Kita M, Kodama T, Sawai N, Kashima K, Imanishi J. Induction of various cytokines and development of severe mucosal inflammation by cagA gene positive *Helicobacter pylori* strains. *Gut* 1995; **41**: 442-451

20 **Quiding-Jarbrink M**, Ahlstedt I, Lindholm C, Johansson EL, Lonroth H. Homing commitment of lymphocytes activated in the human gastric and intestinal mucosa. *Gut* 2001; **49**: 519-525

21 **Miyamoto M**, Haruma K, Hiyama T, Kamada T, Masuda H, Shimamoto F, Inoue K, Chayama K. High incidence of B-cell monoclonality in follicular gastritis: a possible association between follicular gastritis and MALT lymphoma. *Virchows Arch* 2002; **440**: 376-380

22 **Barrett SP**, Riordon A, Toh BH, Gleeson PA, van Driel IR. Homing and adhesion molecules in autoimmune gastritis. *J Leukoc Biol* 2000; **67**: 169-178

Edited by Wang XL

P.O.Box 2345, Beijing 100023,China
Fax: +86-10-85381893
E-mail: wjg@wjgnet.com www.wjgnet.com

World J Gastroenterol 2003;9(12):2706-2710
World Journal of Gastroenterology
 ISSN 1007-9327

Epithelial cell proliferation and glandular atrophy in lymphocytic gastritis: Effect of *H pylori* treatment

Johanna M. Mäkinen, Seppo Niemelä, Tuomo Kerola, Juhani Lehtola, Tuomo J. Karttunen

Johanna M. Mäkinen, Tuomo J. Karttunen, Department of Pathology, University of Oulu, Oulu, Finland
Seppo Niemelä, Juhani Lehtola, Department of Internal Medicine, Oulu University Hospital, Oulu, Finland
Tuomo Kerola, Department of Pathology, Länsi-Pohja Central Hospital, Kemi, Finland
Correspondence to: Tuomo J. Karttunen, Department of Pathology, P.O. Box 5000 (Aapistie 5), FIN-90014 University of Oulu, Finland. tuomo.karttunen@oulu.fi
Telephone: +358-8-537-5951 **Fax:** +358-8-537-5953
Received: 2003-08-11 **Accepted:** 2003-10-12

Abstract

AIM: Lymphocytic gastritis is commonly associated with *Helicobacter pylori* infection. The presence of glandular atrophy and foveolar hyperplasia in lymphocytic gastritis suggests abnormalities in cell proliferation and differentiation, forming a potential link with the suspected association with gastric cancer. Our aim was to compare epithelial proliferation and morphology in *H pylori* associated lymphocytic gastritis and *H pylori* gastritis without features of lymphocytic gastritis, and to evaluate the effect of *H pylori* treatment.

METHODS: We studied 14 lymphocytic gastritis patients with *H pylori* infection. For controls, we selected 14 matched dyspeptic patients participating in another treatment trial *whose H pylori* infection had successfully been eradicated. Both groups were treated with a triple therapy and followed up with biopsies for 6-18 months (patients) or 3 months (controls). Blinded evaluation for histopathological features was carried out. To determine the cell proliferation index, the sections were labeled with Ki-67 antibody.

RESULTS: Before treatment, lymphocytic gastritis was characterized by foveolar hyperplasia (P=0.001) and glandular atrophy in the body (P=0.008), and increased proliferation in both the body (P=0.001) and antrum (P=0. 002). Proliferation correlated with foveolar hyperplasia and inflammation activity. After eradication, the number of intraepithelial lymphocytes decreased in the body (P=0.004) and antrum (P=0.065), remaining higher than in controls (P<0.001). Simultaneously, the proliferation index decreased in the body from 0.38 to 0.15 (P=0.043), and in the antrum from 0.34 to 0.20 (P=0.069), the antral index still being higher in lymphocytic gastritis than in controls (P=0.010). Foveolar hyperplasia and glandular atrophy in the body improved (P=0.021), reaching the non-LG level.

CONCLUSION: In lymphocytic gastritis, excessive epithelial proliferation is predominantly present in the body, where it associates with foveolar hyperplasia and glandular atrophy. These characteristic changes of lymphocytic gastritis are largely related to *H pylori* infection, as shown by their improvement after eradication. However, some residual deviation was still seen in lymphocytic gastritis, indicating either an abnormally slow improvement or the presence of some persistent abnormality.

Mäkinen JM, Niemelä S, Kerola T, Lehtola J, Karttunen TJ. Epithelial cell proliferation and glandular atrophy in lymphocytic gastritis: Effect of *H pylori* treatment. *World J Gastroenterol* 2003; 9(12): 2706-2710
http://www.wjgnet.com/1007-9327/9/2706.asp

INTRODUCTION

Lymphocytic gastritis (LG) is an inflammatory disorder first described by Haot and his group in 1985[1]. This histopathological entity is characterized by a marked increase in the number of intraepithelial lymphocytes (IELs), most being CD8+ or CD3+ cytotoxic T-cells[2]. The amount of 25 IELs per 100 epithelial cells is usually considered diagnostic[3]. The reported prevalence of LG among patients with dyspepsia varies between 1-8 %[4,5]. Most dyspeptic patients with LG are seropositive for *Helicobacter pylori*, indicating that LG may represent an atypical host immune response to the infection[6]. Cases associated with *H pylori* infection have been reported to respond to *H pylori* eradication treatment[7-9]. Gluten is one of the other suspected trigger factors in particular cases, and the prevalence of LG is high in patients with celiac disease, reaching levels up to 45 % in some series[10,11].

LG is common in patients with gastric carcinoma and gastric MALT lymphoma, suggesting that it may be pathogenetically related to gastric malignancies[12,13]. However, mechanisms linking LG with malignancy are not known. Atrophic changes and foveolar hyperplasia in the body mucosa are common in LG, suggesting that abnormal epithelial proliferation and differentiation may be present. Without treatment these abnormalities are usually considered to be persistent[5]. Furthermore, our previous follow-up study has shown that LG is linked to a tendency of more severe progression of intestinal metaplasia than in *H pylori* gastritis without LG[5].

Since foveolar hyperplasia is a characteristic of lymphocytic gastritis, we hypothesized that this might be associated with abnormal proliferation rate. In addition to testing this hypothesis by comparing the proliferation rate with non-LG *H pylori* gastritis, we evaluated the effect of *H pylori* treatment on epithelial cell proliferation and other histopathological features of LG, including glandular atrophy, to find out whether the abnormalities are related to *H pylori* infection and whether they are irreversible.

MATERIALS AND METHODS

Subjects

Two separate series of patients were studied with some differences in the treatment and follow-up protocol. Patients with LG were collected from among the out-patients referred to one endoscopist (SN) for upper abdominal complaints. Patients with histologically proven LG and either histologically or serologically confirmed *H pylori* infection were subsequently included in the open study, in which their *H pylori* infection was treated and they were invited to take part in the post-treatment examinations to document the effects of *H pylori* eradication. An informed consent was obtained from all the

patients according to the usual clinical practice. A total of 14 patients (six men, eight women; mean age 55.2 years, range 41-70 years) who fulfilled the criteria were included. Originally all of them were seropositive for *H pylori*, while only three patients (21 %) could be confirmed as positive on histology. All of the patients had normal findings in duodenal biopsy; no subjects with celiac disease were included. Follow-up gastroscopies with gastric biopsies were performed on all the patients after the eradication. The mean follow-up time was 12 months, ranging from six to 18 months. The effect of treatment on intraepithelial lymphocyte counts in a subset of these patients has been previously reported[9].

For the control group, a series of age and gender matched *H pylori* positive subjects were selected from another treatment trial: Prospective Phase IV clinical multicenter study aiming at testing the effects of sucralfate as an adjuvant to *H pylori* eradication therapy in non-ulcer dyspepsia (F-SUC-CL-0191-FIN; Orion Corporation, Orion Pharma, Finland). Inclusion criteria included the following: age over 18 years, dyspeptic symptoms not explained by any other disease, normal upper abdominal ultrasound, no active peptic ulcer or a history of ulcer, no endoscopic esophagitis, no other severe illness, no need for continuous use of NSAID or steroids. The patients were not allowed to use any anti-ulcer drugs including antacids or H2-antagonists during the two weeks before the trial. The study was approved by the ethical committees in the participating hospitals in Northern Finland. Only subjects with a successful eradication result based on histology were selected. The control group consisted of 14 patients (seven men, seven women, mean age 53.8 years, range 38-67 years) all presenting with *H pylori* positive gastritis without either LG, celiac disease or malignancy. Biopsies taken before the treatment and three months after the eradication therapy were studied.

Histopathology

A minimum of two biopsies was taken from both the antrum and the body at the initial and follow-up gastroscopy. In addition, routine biopsies from the descending part of the duodenum were taken during the primary endoscopy. The biopsies were fixed in formalin, embedded in paraffin and stained with hematoxylin and eosin. During the collection of the patient series one pathologist (TKa) made a preliminary diagnosis of LG. The diagnosis was based on the presence of intraepithelial lymphocytes at a ratio of 30 per 100 epithelial cells, or greater, in the areas of their maximal density.

After the follow-up of the whole series was completed, the slides were coded and evaluated for IEL counts by a second pathologist (TKe), blinded for any clinical data including treatment status and the results of preliminary histopathological evaluation. The IEL number was counted at three randomly selected fields of surface and foveolar epithelium separately in the antral and body mucosa. In addition, IEL number was counted in the area of the maximal IEL density in antral and body mucosa. Around 100 to 150 cells in epithelium were counted in each field. The grade of gastritis, quantity of different types of inflammatory cells, grade of atrophy, foveolar hyperplasia and intestinal metaplasia were similarly analyzed by a blinded investigator (TKa) according to the histological criteria of the updated Sydney system. The presence and quantity of *H pylori* was evaluated from sections stained with a modified Giemsa stain.

Immunohistochemistry and determination of the Ki-67 labeling index

Sections from each gastric biopsy specimen were treated with 10 mM citrate buffer, pH 6.0, for 2 x 5 minutes for antigen retrieval. The sections were incubated with Ki-67 monoclonal antibody (clone 7B11, Zymed, South San Francisco, CA, USA; 1:50 dilution) for 60 minutes at 37 ℃. Bound antigen was detected with labeled streptavidin-biotin method using AEC as a chromogen (Histostain™ –plus, Zymed, South San Francisco, CA, USA). Hematoxylin was used as a counterstain.

Labeled and unlabeled epithelial cells were counted under a high-power microscope (×100) in the optimal, longitudinally orientated and complete foveolae. The proportion of positive cells among foveolar epithelial cells indicated the proliferation (labeling) index (LI %). The mean LI % for each biopsy was calculated as an average from several foveolae. The counting was performed by a single person (JM) blinded for all previous clinical and histopathological data.

Serology

The serological diagnosis of *H pylori* was made by testing the specific IgG antibodies with an enzyme linked immunosorbent assay (ELISA, Pyloriset®, Orion Diagnostica, Finland). Titers of 1:500 or higher were considered positive.

Eradication treatment

In the LG group, *H pylori* eradication therapy consisted of a ten day course of bismuth subsitrate (240 mg twice daily) and metronidazole (400 mg three times daily) or amoxycillin (1 g twice daily). The controls were treated for two weeks with metronidazole (400 mg three times daily) and tetracycline (500 mg three times daily). In addition they got sucralfate (2 g twice daily for 6 weeks followed by 1 g once daily for 6 weeks). No proton inhibitors were allowed in the control group.

Statistics

LG patients and controls were compared by using the nonparametric Mann-Whitney test. Temporal changes in the results were evaluated by using the Wilcoxon signed ranks test. Spearman' s two-tailed rank correlation test was used to assess the correlations between the variables. A probability of *P* less than 0.05 in two-tailed tests was considered statistically significant. Analyses were made with the Statistical Package for Social Sciences (SPSS 10.0, Chicago, IL, USA).

RESULTS

Histopathological features and cell proliferation in H pylori related lymphocytic gastritis and controls before eradication

In all the patients with LG the maximal number IELs was 30 IEL/100 epithelia in either the body or antral mucosa. The histopathological features including the IEL density (per 100 epithelial cells) in random fields. (Table 1; Figure 1) and epithelial cell proliferation (Figure 2) before eradication treatment were compared between LG and non-LG *H pylori* gastritis. The density of *H pylori* organisms was higher in the control group in the body (P=0.009) and antral mucosa (P=0.001), and showed a significant negative correlation with age in LG (body mucosa; c=-0.633, P=0.002). The pre-treatment levels of specific IgG antibody titers were lower in the control group (median 1:1 575, range 1:140-1:5 600) than in LG (1:6 000, range 1:1 000-1:17 000; P= 0.011).

In the antral mucosa the degree of atrophy did not show any significant differences between LG and non-LG *H pylori* gastritis, but the body mucosa showed significantly more severe atrophy in LG (Table 1; P=0.008). Of LG subjects 50 % (n=7) showed mild and 14 % (n=2) moderate atrophy of the body mucosa (Figure 1), while 36 % (n=5) showed no sign of atrophy. No cases with severe atrophy were found. The severity of atrophy in the body showed a trend towards a positive association with IEL count (c=0.542, P=0.069). In the control group, only 17 % (n=2) of the cases showed atrophy of the body

mucosa prior to eradication. In the antrum, gastritis was more active in the controls (P=0.034), but no significant difference was seen in the body. The eosinophilic leukocytes score in the body mucosa was higher in LG (Table 1; P=0.001), while in the antral mucosa the score tended to be higher in the control group (P=0.062). The extent of intestinal metaplasia in the body mucosa tended to be greater in LG (Table 1; P=0.095). Elongation of the foveolae was more often seen in LG (Table 1; Figure 1; body mucosa P= 0.001; antral mucosa P= 0.074.)

Due to tangential sectioning, the proliferation index based on the number of cells with nuclear expression of Ki-67 could be determined in only about 80 % of the specimen slides. The pre-treatment epithelial cell proliferation rate was higher in LG in both the body (P=0.001) and antral mucosa (P=0.002) compared to the controls (Figure 1). In LG, the proliferation index of the body mucosa showed correlation with the degree of foveolar hyperplasia (c=0.798, P=0.010), but did not correlate with atrophy or any other histologic feature, except for a trend towards correlation with the activity of gastritis (c=0.655, P=0.078). In the antral mucosa the proliferation index correlated negatively with the patient' s age (c=-0.707, P=0.050). In the controls, proliferation showed no significant correlation with any of the histological markers or age.

Table 1 Antrum and body gastritis in subjects with lymphocytic gastritis (LG) and controls (non-LG) before and after *H pylori* eradication

Antrum	LG	Non-LG
H pylori score	0 (0-2)[f]	2 (0-3)[bf]
After treatment	0 (0-0)	0 (0-0)[b]
Atrophy	2 (1-2)	2 (0-3)
After treatment	1 (1-2)	2 (0-3)
Metaplasia	0 (0-2)	0 (0-1)
After treatment	0 (0-1)	0 (0-1)
Foveolar length (μm)	340 (290-650)[a]	300 (260-370)
After treatment	300 (250-330)[a]	320 (220-480)
IEL count (mean)	9.5 (1.0-30.7)[f]	1.7 (1.0-4.0)[f]
After treatment	5.7 (0.7-11.0)	1.3 (0.3-3.7)
Activity	1 (0-2)[ad]	2 (0-3)[ad]
After treatment	0 (0-0)[ad]	0 (0-2)[ad]
Eosinophils	1 (0-2)	1 (0-2)
After treatment	0 (0-1)[d]	1.5 (0-3)[d]
Body	**LG**	**Non-LG**
H pylori score	0 (0-3)[d]	2 (0-3)[bd]
After treatment	0 (0-0)	0 (0-0)[b]
Atrophy	2 (1-3)[ad]	1 (0-2)[d]
After treatment	1 (1-2)[a]	1 (0-2)
Metaplasia	0 (0-2)[d]	0 (0-0)[d]
After treatment	0 (0-1)	0 (0-0)
Foveolar length (μm)	310 (250-800)[bf]	170 (130-210)
After treatment	210 (140-290)[b]	200 (150-320)
IEL count (mean)	26.3 (3.7-56.7)[bf]	1.7 (0.3-2.7)[f]
After treatment	5.7 (1.0-41.7)[bf]	2.0 (0.3-3.7)[f]
Activity	1 (0-2)[a]	0.5 (0-2)[a]
After treatment	0 (0-2)[a]	0 (0-1)[a]
Eosinophils	1 (1-2)[af]	1 (0-1)[f]
After treatment	1 (0-2)[ad]	0 (0-1)[d]

Note: Median score and range are indicated except for IEL count, where mean is used. The significance of temporal changes was evaluated by Wilcoxon signed ranks test (a). LG patients and controls were compared with the Mann-Whitney test (d). c, f: P=<0.001; b, e: P=<0.005; a, d: P=<0.05 (two-tailed significance).

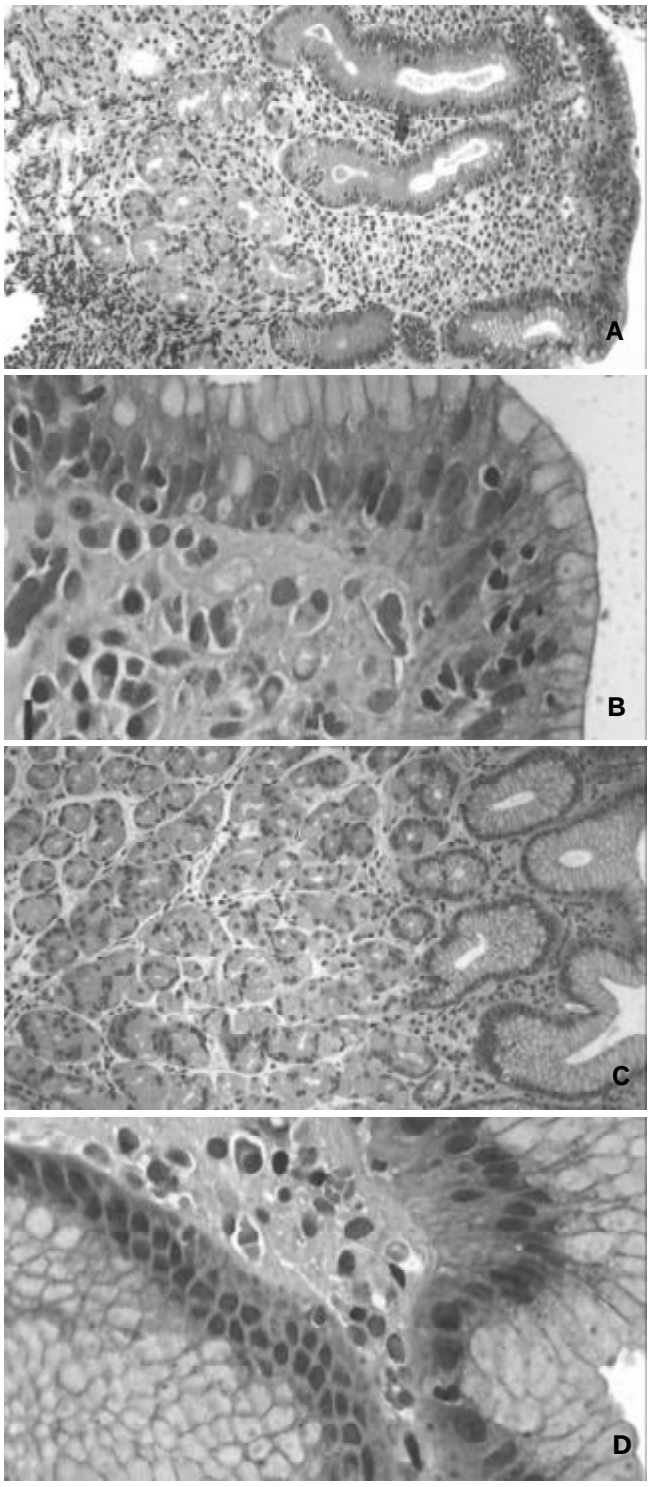

Figure 1 A,B,C,D. Hematoxylin-Eosin stained sections from gastric body mucosa in a case of lymphocytic gastritis before and after eradication treatment. Before treatment (A,B) there was a sharp increase of intraepithelial lymphocytes, moderate glandular atrophy and foveolar hyperplasia. After treatment (C,D) there were only occasional intraepithelial lymhocytes and no signs of glandular atrophy or foveolar hyperplasia. A,C, Bar=25 μm. B,D, Bar=10 μm.

Effect of eradication treatment

We then analyzed what kind of impact the eradication treatment had on cell proliferation and gastritis in LG patients and controls. In LG, successful eradication could be verified in 12 out of 14 patients. All the three patients initially positive on histology were now found to be *H pylori* negative, and showed a decrease of 50 % or more in titer of specific IgG antibodies. Nine cases initially negative on histology showed a similar

decrease in their antibody titers, thus indicating a successful eradication. In two patients, both negative on histology, the decrease in the IgG titers did not quite reach 50 %. However, on histological evaluation of the inflammation, these two patients showed a similar shift towards normal mucosal morphology as the other LG patients. In the control group, all cases were successfully eradicated and turned histologically negative. Yet on serology, only five non-LG patients showed a decrease of the IgG titer of 50 % or more.

In LG, the proliferation index decreased significantly after the eradication in the body mucosa (Figure 2; median from 0.38 to 0.15, *P*=0.043), and showed a similar trend in the antrum (from 0.34 to 0.20, *P*=0.069). In controls, no significant changes were seen (Figure 2). The post-eradication proliferation index in the antrum was nonetheless significantly higher in LG patients (*P*=0.010).

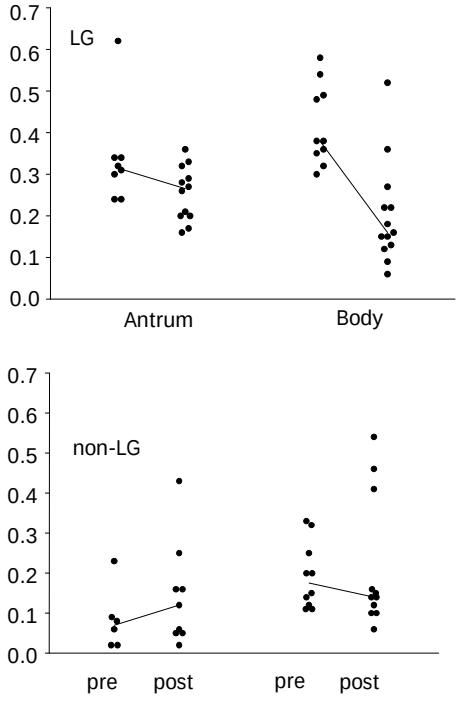

Figure 2 A scatterplot showing epithelial cell proliferation indexes in antral and body mucosa in patients with LG and non-LG *H pylori* gastritis before (pre) and after (post) treatment. The median is indicated with a solid line.

The IEL number decreased significantly in LG (Figure 1) both in areas of maximal density (data not shown) and in random fields (Table 1; body, *P*=0.004), but no change was seen among controls. The post-eradication IEL counts were still significantly higher in LG compared to the controls (Table 1; *P*<0.001). The overall score of inflammatory cells in the lamina propria decreased significantly in both groups (Table 1). In LG, glandular atrophy of the body mucosa improved significantly (*P*=0.021; Figure 1), and after the treatment most subjects (83 %) showed no atrophy at all. Two cases had mild atrophic changes at this stage. However, such a change could not be observed in the antrum. In the control group, eradication did not have any effect on the degree of atrophy in the body (Table 1; *P*=0.564) or in the antrum (*P*=0.783). In LG, a significant shallowing of the gastric pits was seen, as evidence of reduction in the foveolar hyperplasia (body, *P*=0.005; antrum, *P*=0.050). No significant changes were observed in controls.

Since both the IEL counts and proliferation remained significantly increased in LG, we searched for any correlation with inflammatory cell scores to see whether these features were related to residual inflammation, or possibly inherently abnormal. No significant correlations were seen in either antral or body mucosa between neutrophil, eosinophil or mononuclear inflammatory cell scores, but in the body the proliferation index showed a significant correlation with the IEL count (c=0.779, *P*=0.005). In controls, the proliferation index correlated similarly with the IEL number in the body mucosa (c=0.654, *P*= 0.040).

DISCUSSION

In the present study we have shown that gastric epithelial cell proliferation rate, as measured by the Ki-67 labeling index, was increased in LG associated with *H pylori* infection as compared to *H pylori* gastritis without significant increase of intraepithelial lymphocytes. Increased proliferation was predominantly present in the body mucosa, where it was correlated with foveolar hyperplasia and inflammation activity. In addition, our results suggest that in LG, the characteristic increase of IELs, abnormal proliferation, and atrophic changes of the body mucosa are all largely related to *H pylori* infection, as shown by their improvement after eradication therapy.

Increased proliferation induced by the chronic inflammation has been observed in *H pylori* associated gastritis, and the proliferation rate seems in principal to normalize after eradication therapy[14], although the antral mucosa may retain a somewhat abnormal proliferation pattern[15]. In LG, according to our findings, neither the IEL counts nor cell proliferation fell to the level observed in controls after successful treatment, even though the follow-up time was longer in LG patients (minimum six months, mean 12 months) than in controls (three months). This slow rate of normalization is likely to be related to the more pronounced initial abnormality in LG, possibly necessitating a longer period of time for full recovery. A more extended follow-up might be needed to see if these subjects show any permanent abnormality in the proliferation rate. Some intrinsic malfunction causing either a constant abnormal epithelial lymphocyte response or proliferation, or both, is also possible, but no such defects have been reported in LG. A further possible explanation is that there is some other environmental factor in addition to *H pylori* inducing these changes, the effect of which continues after eradication. In some cases, LG is associated with celiac disease[10,11]. The present study included no patients with this disorder. Other nutritional factors could be involved, as in the duodenal mucosa where an increase of IELs has been described in food allergy[16]. No such antigen related changes in the gastric mucosa are yet known.

The controversy between the negative histology and positive serology for *H pylori* in LG in the present and previous studies[5,6,13] might be explained by the fact that the bacteria are present in very small numbers, which could make them impossible to detect. In the present study, even the patients histologically positive for *H pylori* showed only a small amount of bacteria. This is likely to be related to decreased acid secretion associated with the atrophic changes in the body mucosa, which have been shown to associate with a low number of bacteria and a shift of bacteria to the body mucosa[17] in a way similar to the effect of proton pump inhibitors[18]. A significant decrease of the specific antibodies after treatment, along with the improvement of the inflammatory changes, indicates that even the cases negative on histology represent a true *H pylori* infection. It is of interest that the levels of *H pylori* specific IgG antibodies were significantly higher in LG than in non-LG *H pylori* positive gastritis. This has been noted previously[5]. Whether the intensive serological response is related to a certain bacterial strain, amount of antigen, or a matter of a genetically determined pattern of immune response, is not known.

The mechanisms behind the processes of body glandular atrophy and foveolar hyperplasia in LG are unknown. The question of whether atrophy is based on an autoimmune reaction, metaplasia, fibrosis, or on a disturbance in cell regeneration or differentiation in connection with foveolar hyperplasia, needs further study, but the last alternative is most likely the correct one. We could not see any significant change in the extent of intestinal metaplasia after eradication. No autoantibodies targeted against the gastric parietal cells have been found in LG patients (Niemelä *et al*, unpublished observation), suggesting that autoimmune mechanisms are not important in the pathogenesis of body atrophy in LG. The gastric epithelial stem cells situated in the proliferation zone are capable of differentiating into the direction of either gastric glandular cells or foveolar epithelial cells[19]. It is unknown which mechanisms are involved in the actual regulation of the direction of differentiation. We speculate that in untreated LG, the cells in the foveolar border area have a greater stimulus for differentiation towards foveolar epithelial cells than towards glandular cells, this pressure eventually leading to glandular atrophy and foveolar hyperplasia. Thus LG might provide a model for studying the mechanisms of selection of epithelial cell differentiation.

A longstanding *H pylori* infection has been shown to be associated with an increased risk of gastric malignancies[20,21], and successful eradication of this pathogen resulted in the disappearance of histologically malignant lymphomatous proliferation[22]. Mechanisms of the suggested increased risk of malignancy in LG[12,13] are unknown. The increased epithelial cell proliferation rate, as detected in the present study, might play an important part by increasing the potential for the accumulation of genetic changes. Glandular atrophy as seen in the present study, and reported previously[5,13], forms another potential link for gastric cancer, since an increased cancer risk has been documented with body atrophy[23]. Without any treatment, atrophy and foveolar hyperplasia seen in LG are generally considered to be persistent, and even to progress at a faster rate than in subjects with a non-LG *H pylori* gastritis[5], supporting the idea that LG has pre-malignant potential. However, more studies are required to find out whether patients with LG are indeed at an increased risk of a gastric malignancy, and whether *H pylori* eradication reduces the risk of gastric neoplasia in these patients.

In conclusion, we have shown that the highly increased epithelial cell proliferation, predominantly in the body mucosa, is a characteristic feature of LG. Abnormal proliferation together with atrophic changes in the body mucosa in LG provide a potential mechanism for the observed association with gastric malignancy. Furthermore, these changes in LG are largely caused by *H pylori* infection as shown by their normalization by eradication therapy.

REFERENCES

1 **Haot J**, Hamichi L, Wallez L, Mainguet P. Lymphocytic gastritis: a newly described entity: a retrospective endoscopic and histological study. *Gut* 1988; **29**: 1258-1264

2 **Oberhuber G**, Bodingbauer M, Mosberger I, Stolte M, Vogelsang H. High proportion of granzyme B-positive (activated) intraepithelial and lamina propria lymphocytes in lymphocytic gastritis. *Am J Surg Pathol* 1998; **22**: 450-458

3 **Lynch DA**, Dixon MF, Axon AT. Diagnostic criteria in lymphocytic gastritis. *Gastroenterology* 1997; **112**: 1426-1429

4 **Lynch DA**, Sobala GM, Dixon MF, Gledhill A, Jackson P, Crabtree JE. Lymphocytic gastritis and associated small bowel disease: a diffuse lymphocytic gastroenteropathy? *J Clin Pathol* 1995; **48**: 939-945

5 **Niemelä S**, Karttunen T, Kerola T, Karttunen R. Ten year follow up study of lymphocytic gastritis: further evidence on *Helicobacter pylori* as a cause of lymphocytic gastritis and corpus gastritis. *J Clin Pathol* 1995; **48**: 1111-1116

6 **Dixon MF**, Wyatt JI, Burke DA, Rathbone BJ. Lymphocytic gastritis: relationship to *Campylobacter pylori* infection. *J Pathol* 1988; **154**: 125-132

7 **Hayat M**, Arora DS, Dixon MF, Clark B, O'Mahony S. Effects of *Helicobacter pylori* eradication on the natural history of lymphocytic gastritis. *Gut* 1999; **45**: 495-498

8 **Müller H**, Volkholz H, Stolte M. Healing of lymphocytic gastritis by eradication of *Helicobacter pylori*. *Digestion* 2001; **63**: 14-19

9 **Niemelä S**, Karttunen TJ, Kerola T. Treatment of *Helicobacter pylori* in patients with lymphocytic gastritis. *Hepatogastroenterology* 2001; **48**: 1176-1178

10 **Karttunen TJ**, Niemelä S. Lymphocytic gastritis and coeliac disease. *J Clin Pathol* 1990; **43**: 436-437

11 **Wolber R**, Owen D, DelBuono L, Appelman H, Freeman H. Lymphocytic gastritis in patients with celiac sprue or spruelike intestinal disease. *Gastroenterology* 1990; **98**: 310-315

12 **Griffiths AP**, Wyatt J, Jack AS, Dixon MF. Lymphocytic gastritis, gastric adenocarcinoma, and primary gastric lymphoma. *J Clin Pathol* 1994; **47**: 1123-1124

13 **Miettinen A**, Karttunen T, Alavaikko M. Lymphocytic gastritis and *Helicobacter pylori* infection in gastric lymphoma. *Gut* 1995; **37**: 471-476

14 **Brenes F**, Ruiz B, Correa P, Hunter F, Rhamakrishnan T, Fontham E. *Helicobacter pylori* causes hyperproliferation of the gastric epithelium: pre- and post-eradication indices of proliferating cell nuclear antigen. *Am J Gastroenterol* 1993; **88**: 1870-1875

15 **El-Zimaity HM**, Graham DY, Genta RM, Lechago J. Sustained increase in gastric antral epithelial cell proliferation despite cure of *Helicobacter pylori* infection. *Am J Gastroenterol* 2000; **95**: 930-935

16 **Augustin M**, Karttunen TJ, Kokkonen J. TIA1 and mast cell tryptase in food allergy of children: increase of intraepithelial lymphocytes expressing TIA1 associates with allergy. *J Pediatr Gastroenterol Nutr* 2001; **32**: 11-18

17 **Karttunen T**, Niemelä S, Lehtola J. *Helicobacter pylori* in dyspeptic patients. Quantitative association with severity of gastritis, intragastric pH, and serum gastrin concentration. *Scand J Gastroenterol Suppl* 1991; **186**: 124

18 **Kuipers EJ**, Lundell L, Klinkenberg-Knol EC, Havu N, Festen HP, Liedman B. Atrophic gastritis and *Helicobacter pylori* infection in patients with reflux esophagitis treated with omeprazole or fundoplication. *N Engl J Med* 1996; **334**: 1018-1022

19 **Brittan M**, Wright NA. Gastrointestinal stem cells. *J Pathol* 2002; **197**: 492-509

20 **Nomura A**, Stemmermann GN, Chyou PH, Kato I, Perez-Perez GI, Blaser MJ. *Helicobacter pylori* infection and gastric carcinoma among Japanese Americans in Hawaii. *N Engl J Med* 1991; **325**: 1132-1136

21 **Parsonnet J**, Friedman GD, Vandersteen DP, Chang Y, Vogelman JH, Orentreich N. *Helicobacter pylori* infection and the risk of gastric carcinoma. *N Engl J Med* 1991; **325**: 1127-1131

22 **Wotherspoon AC**, Doglioni C, Diss TC, Pan L, Moschini A, de Boni M. Regression of primary low-grade B-cell gastric lymphoma of mucosa-associated lymphoid tissue type after eradication of *Helicobacter pylori*. *Lancet* 1993; **342**: 575-577

23 **Sipponen P**, Kekki M, Haapakoski J, Ihamäki T, Siurala M. 1985. Gastric cancer risk in chronic atrophic gastritis: statistical calculations of cross-sectional data. *Int J Cancer* 1985; **35**: 173-177

Edited by Zhu LH

P.O.Box 2345, Beijing 100023,China
Fax: +86-10-85381893
E-mail: wjg@wjgnet.com www.wjgnet.com

World J Gastroenterol 2003;9(12):2711-2714
World Journal of Gastroenterology
 ISSN 1007-9327

Expression of *Helicobacter pylori* Hsp60 protein and its immunogenicity

Yang Bai, Liang-Ren Li, Ji-De Wang, Ye Chen, Jian-Feng Jin, Zhao-Shan Zhang, Dian-Yuan Zhou, Ya-Li Zhang

Yang Bai, Liang-Ren Li, Ji-De Wang, Ye Chen, Dian-Yuan Zhou, Ya-Li Zhang, PLA Institute for Digestive Medicine, Nanfang Hospital, First Military Medical University, Guangzhou 510515, Guangdong Province, China
Jian-Feng Jin, Chemistry University of Beijing, Beijing 100071, China
Zhao-Shan Zhang, Institute of Biotechnology, Academy of Military Medical Science, Beijing 100071, China
Supported by the National Natural Science Foundation of China, No.30270078
Correspondence to: Dr. Ya-Li Zhang, PLA Institute for Digestive Medicine, Nanfang Hospital, First Military Medical University, Guangzhou 510515, Guangdong Province, China. baiyang1030@hotmail.com
Telephone: +86-20-61641532
Received: 2003-03-12 **Accepted:** 2003-05-16

Abstract

AIM: To express Hsp60 protein of *H pylori* by a constructed vector and to evaluate its immunogenicity.

METHODS: Hsp60 DNA was amplified by PCR and inserted into the prokaryotie expression vector pET-22b (+), which was transformed into BL21 (DE3) *E.coli* strain to express recombinant protein. Immunogenicity of expressed Hsp60 protein was evaluated with animal experiments.

RESULTS: DNA sequence analysis showed Hsp60 DNA was the same as GenBank's research. Hsp60 recombinant protein accounted for 27.2 % of the total bacterial protein, and could be recognized by the serum from *H pylori* infected patients and Balb/c mice immunized with Hsp60 itself.

CONCLUSION: Hsp60 recombinant protein might become a potential vaccine for controlling and treating *H pylori* infection.

Bai Y, Li LR, Wang JD, Chen Y, Jin JF, Zhang ZS, Zhou DY, Zhang YL. Expression of *Helicobacter pylori* Hsp60 protein and its immunogenicity. *World J Gastroenterol* 2003; 9(12): 2711-2714
http://www.wjgnet.com/1007-9327/9/2711.asp

INTRODUCTION

Helicobacter pylori (*H pylori*) infection is the major cause of chronic active gastritis and most peptic ulcer diseases[1-11], and is also closely related with gastric cancers such as adenocarcinoma, mucosa-associated lymphoid tissue (MALT) lymphoma and primary gastric non-Hodgkin's lymphoma[12-18]. This organism has been categorized as a class I carcinoma by the World Health Organization, and direct evidences of its carcinogenesis was recently demonstrated both in an animal model and in retrospective cohort and nested case-control studies in China[19-21]. In addition, seroprevalence studies indicated that *H pylori* infection was also associated with cardiovascular, respiratory, extra-gastroduodenal digestive, autoimmune diseases[22-24]. Successful eradication of *H pylori* is thus an important goal. Currently, its treatment involves antibiotic therapy, but this has some associated problems such as low patient compliance and increase of resistant strains[25-27]. An alternative approach is to develop a vaccine, which would not only clear the organism, but also prevent its reinfection[28-31].

Selection of antigenic targets and adjuvants is critical in developing *H pylori* vaccine. So far this area has achieved only a limited success. With most studies focusing on urease enzyme combined with cholera toxin (CT) or heat-labile toxin of *Escherichia coli* (LT), this antigen/adjuvant combination has been proved to be effective in many animal models, but some problems still exist such as toxicity of LT or CT and inadequate protection of urease enzyme, so new antigens and adjuvants should be looked for[32]. Some studies have proved that heat shock protein 60 (Hsp60) of mycobacteria was a kind of adjuvants, and could cause immune responses of priority in mouse and mankind models, so some researchers suspected *H pylori* Hsp60 might be an excellent antigen candidate[33,34]. In this study, recombinant plasmid of *H pylori* Hsp60 gene was constructed and expressed for the development of *H pylori* vaccine.

MATERIALS AND METHODS

Materials

Bacterial strain BL21(DE3) and plasmid pET-22b(+) were provided by the Institute of Biotechnology, Academy of Military Medical Sciences. *H pylori* SS1 was preserved in this research institute. Restriction enzyme Not I, Nco I and T4 DNA ligase, Vent DNA polymerase, isopropyl-β-D-thiogalactopyranoside (IPTG) were purchased from New England Biolabs Company. Goat anti-mouse and goat anti-human IgG-HRP were purchased from Huamei Bioengineering Company, China and His-Tag precolumn from Invitrogen Company. Specific-pathogen-free, female BALB/c mice were housed according to Health Research Council of China guidelines with free access to food and water. Eight *H pylori* positive sera (which were positive by urease test, pathological dying and germ culture) and three *H pylori* negative sera (which were detected negative by the above-mentioned three examinations) were from patients treated in the Endoscope Center of this institute. Other reagents were analytically pure reagents produced in China.

Recombinant DNA techniques

All restriction enzyme digestions, ligations and other common DNA manipulations, unless otherwise stated, were performed by standard procedures[31,35]. The genome of *H pylori* was prepared from cells collected from colonies on a agar plate. The gene of *H pylori* Hsp60 was amplified from the genome of *H pylori* by PCR (Techne PROGENE) using the primers Hsp601 (5' -TG GCC ATG GAT GGG CCA AGA GGC AGG AAT-3') as upstream primer and Hsp602 (5' -AG TGC GGC CGC CAT CAT GCC GCC CAT G -3') as downstream primer as described in the literature[36]. Hsp601 and Hsp602 contained *Nco* I and *Not* I sites, respectively. PCR was performed with the hot start method. PCR condition was that after initial denaturing at 95 ℃ for 30 s, each cycle of amplification consisted of denaturing at 95 ℃for 30 s, annealing at 55 ℃ for

30 s and polymerization at 72 ℃ for 60 sec and further polymerization for 10 min after 35 PCR cycles. PCR product was harvested from agarose gel, digested with *Nco* I and *Not* I, and inserted into *Nco* I and *Not* I restriction fragments of the expression vector pET-22b(+) using T4 DNA ligase. The resulting plasmid pET- Hsp60 was transformed into competent *E.coli* BL21 (DE3) cells using ampicillin resistance for selection. The alkaline lysis method was chosen for large-scale preparations of recombinant plasmid and the plasmids were identified by restriction enzymes. DNA sequence was performed with a DNA automatic sequencer.

Induced expression, purification and SDS-polyacrylamide gel electrophoresis

The recombinant strains were incubated overnight at 37 ℃ while shaking in 5 ml LB with 100 μg/mL ampicilline, 50 mL LB were inoculated and the cells grew until the optical density at 600 nm reached 0.4-0.6. Isopropyl-β-D-thiogalactopyranoside (IPTG) was added to a final concentration of 0.1, 0.2, 0.4, 0.6, 0.8, 1.0 mM, respectively.*E.coli* cells growing in 50 mL LB 3 h or 5 h after induction were harvested by centrifugation at 12 000 g for 10 min and the pellet was resuspended in 1 ml 30 mM Tris buffer (pH8.0) containing 1 mmol/L EDTA (pH8.0), 20 % sucrose. The suspension was put on ice for 10 min, and then centrifuged for 10 min at 12 000 g, and the resulting suspernatant contained proteins from periplasms. The resulting pellet was resuspended in 5 mL 50 mM Tris buffer (pH8.0) containing 2 mM EDTA, 0.1 mg/mL lysozyme and 1 % Triton X-100. The suspension was incubated at 30 ℃ for 20 min and then sonicated on ice until it became clarified. The lysate was centrifuged at 12 000 g for 15 min at 4 ℃, and then the resulting supernatant containing proteins from cytoplasms was purified with Ni-NTA column. Whole-cell lysates, sonicated supernatant, osmotic shock liquid of recombinant strains expressing *H pylori* Hsp60 genes and the purified rHsp60 were analyzed by electrophoretical analysis in a 10 % polyacrylamide gel.

Immunization of mice

Six to eight week old mice were immunized four times by hypodermic injection in the back of mice at weekly intervals. Each dose consisted of 20 μg of *H pylori* rHsp60 protein and 200 μg of adjuvant aluminum hydroxide gel. Age-matched control mice were not immunized. Four weeks after the last immunization, blood samples were taken from the retro-orbital sinus to measure anti Hsp60 systemic immune responses and stored at -20 ℃ until assay.

Serum antibody responses

Indirect ELISA as described evaluated serum samples from mice and patients for Hsp60-specific IgG previously[35]. Purified *H pylori* rHsp60 was used as the coating antigen in ELISA immunoassays.

RESULTS

PCR amplification of H pylori Hsp60 gene

According to the literature, the gene encoding Hsp60 protein was amplified by PCR with chromosomal DNA of *H pylori* Sydeny strain (ss1) as templates. The cloning products were electrophoresed and visualized on 8 g·L^{-1} agarose gel (Figure 1). It revealed that Hsp60 DNA fragment amplified by PCR contained a gene with approximately 1 548 nucleotides, which was compatible with previous reports[36].

Construction of recombinant plasmid and restriction enzyme confirmation

After PCR products and pET-22b(+) plasmid were cut by Not I and Nco I, directional cloning was performed, resulting in a recombinant plasmid named pET-22b(+)/Hsp60. The recombinant plasmids pET-22b(+)/Hsp60 were all digested by Not I or Nco I, and by Not I and Nco I simultaneously, then digestive products were visualized on 8 g·L^{-1} agarose gel eletrophoreses (Figure 2). It demonstrated that recombinant plasmid contained the objective gene.

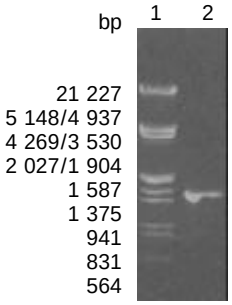

Figure 1 Eight g·L^{-1} agarose gels electrophoreses of Hsp60 DNA fragment amplified by PCR from *H pylori*. Lane1: Nucleotide marker, Lane2: PCR products.

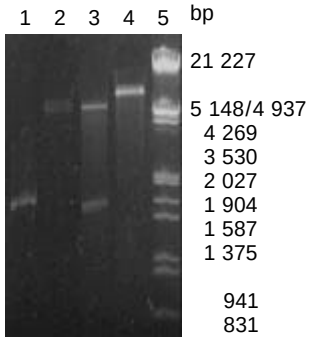

Figure 2 Identification of recombinant plasmid by restriction enzyme digestion. Lane1: PCR products, Lane2: pET22b (+)/ Not I, Lane3: Recombinant plasmid / Not I and Nco I, Lane4: Recombinant plasmid / Not I, Lane5: Nucleotide marker.

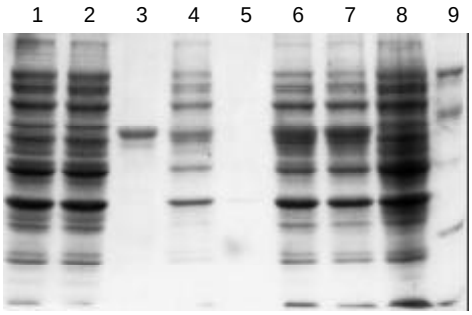

Figure 3 100 g·L^{-1} SDS-PAGE analysis of the fusion protein expressed in BL21(DE3). Lane1: control strain BL21(pET) before induction, Lane2: control strain BL21(pET) after 3 h induction with IPTG, Lane3: purified recombinant protein Hsp60, Lane4: sonicated supernatant of BL21(pET-Hsp60) cells after 3 h induction with IPTG, Lane5: BL21(pET-Hsp60) cell periplasm protein after 3 h induction with IPTG, Lane6: BL21 (pET- Hsp60) cells after 5 h induction with IPTG, Lane7: BL21 (pET- Hsp60) cells after 3 h induction with IPTG, Lane8: BL21 (pET-Hsp60) cells before induction, Lane9: molecular weight marker (20,30,43,67,94)×10^3

Sequence analysis of cloned Hsp60 nucleotide

The nucleotide sequence of cloned genes inserted in pET22b (+) was analyzed by automatic sequencing across the cloning

junction, using the universal primer T7. The results were as follows the cloned genes contained 1 548 nucleotides with a promoter and a start codon coding a putative protein of 516 amino acid residues with a calculated molecular mass of Hsp60. As compared with previous reports, the homogeneity was 100 % between them[36].

Expression and purification of Hsp60 gene in Escherichia coli

Whole-cell lysates, sonicated supernatant, osmotic shock liquid of recombinant strains expressing *H pylori* Hsp60 genes and the purified rHsp60 were analyzed by electrophoretical analysis in a 10 % polyacrylamide gel for detection of fusion proteins (Figure 3). The results showed that the clearly identifiable band was 60 000 Dalton highly expressed fusion proteins, which was similar to that predicted. Gel automatic scan analysis showed that it was 0.6 at D value and the final concentration of IPTG was 0.1 mmol/L and induction for 5 hours, the expression of Hsp60 rose remarkably, which accounted for 27.2 % of total bacterial proteins. Among them, soluble substance accounted for 14.7 % of supernatant. Hsp60 was further purified with Ni-NTA column; its final purity was 80 %.

Antigenicity study of recombinant fusion protein

The positive results by ELISA had colors, but the negative results had no colors, or weak colors. The results showed that the eight mice sera immunized with rHsp60 showed positive results. In contrast, the eight mice sera in control group showed negative results. At the same time, sera from patients also showed the same results. Eight *H pylori* positive sera from patients showed positive results and three *H pylori* negative sera from patients showed negative results, it showed that anti-Hsp60 antibody existed in sera of infected patients, indicating that rHsp60 could enable the organism to generate specific humoral immunity.

DISCUSSION

Hsps exists widely in nature and is one of the most conservative proteins of biosphere. For a long time, people have researched low Hsps as a molecular partner took part in physiological activities of cells. However, their results indicate that Hsps from microorganisms are the most important protective antigens when people and animals are infected with microorganisms. The protective immune response to 20 kinds of infectious diseases, such as tuberculosis and lepra was directly aimed at Hsps as far as reported[33,34]. Especially in the model of mice infected with tubercle bacillus, specific anti-Hsp60 only produced immunoreaction with Hsp60 of tubercle bacillus, not with mice Hsp60 themselves[37]. This resolved the autoimmune problems because of high conservation, which was perplexed. Furthermore, in models of mice and monkeys infected with plasmodium, immunoreactions did not depend on adjuvants when polypeptides were combined with Hsp60[38]. It showed that Hsp60 had similar functions of adjuvants. So under the uncertainty of *H pylori* urease preventing *H pylori* infection, *H pylori* Hsp60 as a *H pylori* vaccine component is not only used to combine urease to constitute multivalence vaccine, but also used as adjuvants to resolve the disadvantages of CT or LT.

In fact, *H pylori* Hsp60 immune protection function has been confirmed by experiments *in vitro* and *in vivo*. Yamaguchi *et al* reported *H pylori* Hsp60 monoclonal antibody could significantly inhibite adhesion of *H pylori* to human gastric epithelial MKN45 cells and gastric cancer cells[39]. Yamaguchi *et al* also evaluated the protective effect of immunization with amino acids 189 to 203 (VEGMQFDRGYLSPYF) on *H pylori* Hsp60 molecules[40]. The results suggested that the immune response to the epitope (VEGMQFDRGYLSPYF) was unique and could prevent *H pylori* infection in animal models. In this study, specific antibody to Hsp60 was detected in sera from the mice immunized with purified recombinant protein Hsp60, but not in sera from the mice in control group. Sera from patients also showed the same results. These results suggest that Hsp60 of *H pylori* may be a good candidate for a vaccine. However, whether it can be used as an adjuvant and antigen needs to be further researched.

REFERENCES

1 **Bai Y**, Zhang YL, Wang JD, Lin HJ, Zhang ZS, Zhou DY. Conservative region of the genes encoding four adhesins of *Helicobacter pylori*: cloning, sequence analysis and biological information analysis. *Diyi Junyi Daxue Xuebao* 2002; **22**: 869-871

2 **Vandenplas Y**. *Helicobacter pylori* infection. *World J Gastroenterol* 2000; **6**: 20-31

3 **Bai Y,** Chang SH, Wang JD, Chen Y, Zhang ZS, Zhang YL. Construction of the *E.coli* clone expressing adhesin BabA of *Helicobacter pylori* and evaluation of the adherence activity of BabA. *Diyi Junyi Daxue Xuebao* 2003; **23**: 293-295

4 **Hobsley M**, Tovey FI. *Helicobacter pylori*: the primary cause of duodenal ulceration or a secondary infection? *World J Gastroenterol* 2001; **7**: 149-151

5 **Huang XQ**. *Helicobacter pylori* infection and gastrointestinal hormones: a review. *World J Gastroenterol* 2000; **6**: 783-788

6 **Olbe L**, Fandriks L, Hamlet A, Svennerholm AM, Thoreson AC. Mechanisms involved in *Helicobacter pylori* induced duodenal ulcer disease:an overview. *World J Gastroenterol* 2000; **6**: 619-623

7 **Hou P**, Tu ZX, Xu GM, Gong YF, Ji XH, Li ZS. *Helicobacter pylori* vacA genotypes and cagA status and their relationship to associated diseases. *World J Gastroenterol* 2000; **6**: 605-607

8 **Bai Y**, Dan HL, Wang JD, Zhang ZS, Odenbreit S, Zhou DY, Zhang YL. Cloning, expression, purification and identification of conservative region of four *Helicobacter pylori* adhesin genes in AlpA gene. *Prog Biochen Biophys* 2002; **29**: 922-926

9 **Bai Y**, Zhany YL, Chen Y, Wang JD, Zhou DY. Study of Immunogenicity and safety and adherence of conservative region of four *Helicobacter pylori* adhesin *in vitro*. *Prog Biochen Biophys* 2003; **30**: 422-426

10 **Chi J**, Lu M, Fu BY, Nakajima S, Hattori T. The effect of mast cell on the induction of *Helicobacter pylori* infection in Mongolian gerbils. *World J Gastroenterol* 2000; **6**: 440-441

11 **Pena A**. Genetic factors determining the host response to *Helicobacter pylori*. *World J Gastroenterol* 2000; **6**: 624-625

12 **Morgner A**, Miehlke S, Stolte M, Neubauer A, Alpen B, Thiede C, Klann H, Hierlmeier FX, Ell C, Ehninger G, Bayerdorffer E. Development of early gastric cancer 4 and 5 years after complete remission of *Helicobacter pylori* associated gastric low grade marginal zone B cell lymphoma of MALT type. *World J Gastroenterol* 2001; **7**: 248-253

13 **Miehlke S**, Kirsch C, Dragosics B, Gschwantler M, Oberhuber G, Antos D, Dite P, Lauter J, Labenz J, Leodolter A, Malfertheiner P, Neubauer A, Ehninger G, Stolte M, Bayerdorffer E. *Helicobacter pylori* and gastric cancer:current status of the Austrain Czech German gastric cancer prevention trial (PRISMA Study). *World J Gastroenterol* 2001; **7**: 243-247

14 **Gao H**, Wang JY, Shen XZ, Liu JJ. Effect of *Helicobacter pylori* infection on gastric epithelial cell proliferation. *World J Gastroenterol* 2000; **6**: 442-444

15 **Zhuang XQ**, Lin SR. Research of *Helicobacter pylori* infection in precancerous gastric lesions. *World J Gastroenterol* 2000; **6**: 428-429

16 **Cai L**, Yu SZ, Zhang ZF. *Helicobacter pylori* infection and risk of gastric cancer in Changle County,Fujian Province,China. *World J Gastroenterol* 2000; **6**: 374-376

17 **Liu WZ**, Zheng X, Shi Y, Dong QJ, Xiao SD. Effect of *Helicobacter pylori* infection on gastric epithelial proliferation in progression from normal mucosa to gastric carcinoma. *World J Gastroenterol* 1998; **4**: 246-248

18 **Harry XH**. Association between *Helicobacter pylori* and gastric cancer: current knowledge and future research. *World J Gastroenterol* 1998; **4**: 93-96

19 **Lan J**, Xiong YY, Lin YX, Wang BC, Gong LL, Xu HS, Guo GS. *Helicobacter pylori* infection generated gastric cancer through p53-

Rb tumor-suppressor system mutation and telomerase reactivation. *World J Gastroenterol* 2003; **9**: 54-58

20 **Wang RT**, Wang T, Chen K, Wang JY, Zhang JP, Lin SR, Zhu YM, Zhang WM, Cao YX, Zhu CW, Yu H, Cong YJ, Zheng S, Wu BQ. *Helicobacter pylori* infection and gastric cancer: evidence from a retrospective cohort study and nested case-control study in China. *World J Gastroenterol* 2002; **8**: 1103-1107

21 **Yao YL**, Xu B, Song YG, Zhang WD. Overexpression of cyclin E in Mongolian gerbil with *Helicobacter pylori*-induced gastric precancerosis. *World J Gastroenterol* 2002; **8**: 60-63

22 **Bulajic M**, Stimec B, Milicevic M, Loehr M, Mueller P, Boricic I, Kovacevic N, Bulajic M. Modalities of testing *Helicobacter pylori* in patients with nonmalignant bile duct diseases. *World J Gastroenterol* 2002; **8**: 301-304

23 **Xu CD**, Chen SN, Jiang SH, Xu JY. Seroepidemiology of *Helicobacter pylori* infection among asymptomatic Chinese children. *World J Gastroenterol* 2000; **6**: 759-761

24 **Pace F**, Porro GB. Gastroesophageal reflux and *Helicobacter pylori*: a review. *World J Gastroenterol* 2000; **6**: 311-314

25 **Harris A**. Treatment of *Helicobacter pylori*. *World J Gastroenterol* 2001; **7**: 303-307

26 **She FF**, Su DH, Lin JY, Zhou LY. Virulence and potential pathogenicity of coccoid *Helicobacter pylori* induced by antibiotics. *World J Gastroenterol* 2001; **7**: 254-258

27 **Hua JS**, Bow H, Zheng PY, Khay-Guan Y. Prevalence of primary *Helicobacter pylori* resistance to metronidazole and clarithromycin in Singapore. *World J Gastroenterol* 2000; **6**: 119-121

28 **Bai Y**, Wang JD, Zhang ZS, Zhang YL. Construction of the Attenuated Salmonella typhimurium Strain Expressing *Helicobacter pylori* Conservative Region of Adhesin Antigen. *Chin J Biotech* 2003; **19**: 77-82

29 **Bai Y**, Zhang YL, Wang JD, Zhang ZS, Zhou DY. Cloning and immunogenicity of conservative region of adhesin gene of *Helicobacter pylori* [Article in Chinese]. *Zhonghua Yixue Zazhi* 2003; **83**: 736-739

30 **Bai Y**, Zhang YL, Wang JD, Zhang ZS, Zhou DY. Construction of the non-resistant attenuated Salmonella typhimurium strain expressing *Helicobacter pylori* catalase. *Diyi Junyi Daxue Xuebao* 2003; **23**: 101-105

31 **Bai Y**, Zhang YL, Jin JF, Wang JD, Zhang ZS, Zhou DY. Recombinant *Helicobacter pylori* catalase. *World J Gastroenterol* 2003; **9**: 1119-1122

32 **Solnick JV**, Canfield DR, Hansen LM, Torabian SZ. Immunization with recombinant *Helicobacter pylori* urease in specific-pathogen-free rhesus monkeys (Macaca mulatta). *Infect Immun* 2000; **68**: 2560-2565

33 **Zugel U**, Schoel B, Yamamoto S, Hengel H, Morein B, Kaufmann SH. Crossrecognition by CD8 T cell receptor alpha beta cytotoxic T lymphocytes of peptides in the self and the mycobacterial hsp60 which share intermediate sequence homology. *Eur J Immunol* 1995; **25**: 451-458

34 **Zugel U**, Kaufmann SH. Activation of CD8 T cells with specificity for mycobacterial heat shock protein 60 in Mycobacterium bovis bacillus Calmette-Guerin-vaccinated mice. *Infect Immun* 1997; **65**: 3947-3950

35 **Sambrook J**, Fritsch EF, Maniatis T. Molecular cloning:a laboratory manual.2nd ed. New York: *Cold Spring Harbor Laboratory Press* 1989: 35-400

36 **Macchia G**, Massone A, Burroni D, Covacci A, Censini S, Rappuoli R. The Hsp60 protein of *Helicobacter pylori*: structure and immune response in patients with gastroduodenal diseases. *Mol Microbiol* 1993; **9**: 645-652

37 **Lowrie DB**, Silva CL, Colston MJ, Ragno S, Tascon RE. Protection against tuberculosis by a plasmid DNA vaccine. *Vaccine* 1997; **15**: 834-838

38 **Del Giudice G**. Stress proteins in medicine. *New York:Marcel Dekker Inc* 1996: 533-545

39 **Yamaguchi H**, Osaki T, Kurihara N, Taguchi H, Hanawa T, Yamamoto T, Kamiya S. Heat-shock protein 60 homologue of *Helicobacter pylori* is associated with adhesion of *H pylori* to human gastric epithelial cells. *J Med Microbiol* 1997; **46**: 825-831

40 **Yamaguchi H**, Osaki T, Kai M, Taguchi H, Kamiya S. Immune response against a cross-reactive epitope on the heat shock protein 60 homologue of *Helicobacter pylori*. *Infect Immun* 2000; **68**: 3448-3454

Edited by Xia HHX and Wang XL

P.O.Box 2345, Beijing 100023,China
Fax: +86-10-85381893
E-mail: wjg@wjgnet.com www.wjgnet.com

World J Gastroenterol 2003;9(12):2715-2719
World Journal of Gastroenterology
 ISSN 1007-9327

• BASIC RESEARCH •

Distribution and expression of non-muscle myosin light chain kinase in rabbit livers

Hua-Qing Zhu, Yuan Wang, Ruo-Lei Hu, Bin Ren, Qing Zhou, Zhi-Kui Jiang, Shu-Yu Gui

Hua-Qing Zhu, Yuan Wang, Ruo-Lei Hu, Qing Zhou, Laboratory of Molecular Biology and Department of Biochemistry, Anhui Medical University, Hefei 230032, Anhui Province, China
Hua-Qing Zhu, Yuan Wang, Ruo-Lei Hu, Qing Zhou, Shu-Yu Gui, Anhui Province Key Laboratory of Genomic Research, Hefei 230032, Anhui Province, China
Bin Ren, Department of Pathology, BIDMC and Harvard Medical School, 99 Brookline, MA 02215 , Boston, U S A
Shu-yu Gui, Department of Respiratory Disease, the First Affiliated Hospital of Anhui Medical University, Hefei 230032, Anhui Province, China
Zhi-Kui Jiang, 105 Hospital of PLA, Hefei 230031, Anhui Province, China
Supported by National Natural Science Foundation of China, No. 39870324, Grant for Excellent Young Teachers of Ministry of education of China, No.39870324, National Science Foundation of AnHui Province, No.9904312
Correspondence to: Professor Yuan Wang, Laboratory of Molecular Biology and Department of Biochemistry, Anhui Medical University, Hefei 230032, Anhui Provience, China. wangyuan@mail.hf.ah.cn
Telephone: +86-551-5161140
Received: 2003-05-10 **Accepted:** 2003-06-02

Abstract

AIM: To study the distribution and expression of non-muscle myosin light chain kinase (nmMLCK) in rabbit livers.

METHODS: Human nmMLCK N-terminal cDNA was amplified by polymerase chain reaction (PCR) and was inserted into pBKcmv to construct expression vectors. The recombinant plasmid was transformed into XL1-blue. Expression protein was induced by IPTG and then purified by SDS-PAGE and electroelution, which was used to prepare the polycolonal antibody to detect the distribution and expression of nmMLCK in rabbit livers with immunofluorescene techniques.

RESULTS: The polyclonal antibody was prepared, by which nmMLCK expression was detected and distributed mainly in peripheral hepatocytes.

CONCLUSION: nmMLCK can express in hepatocytes peripherally, and may play certain roles in the regulation of hepatic functions.

Zhu HQ, Wang Y, Hu RL, Ren B, Zhou Q, Jiang ZK, Gui SY. Distribution and expression of non-muscle myosin light chain kinase in rabbit livers. *World J Gastroenterol* 2003; 9(12): 2715-2719
http://www.wjgnet.com/1007-9327/9/2715.asp

INTRODUCTION

Protein kinase plays an important regulatory role in response to both intracellular and extracellular signals[1]. Specific protein kinase is thought to control various cellular functions including glycogen metabolism, muscle contraction and growth, etc. Myosin light chain kinase (MLCK) is a Ca^{2+}/calmodulin activated enzyme in the kinase family which catalyses the phosphorylation of the 20-ku myosin light chain (MLC-20)[2]. In skeletal muscle, the phosphorylation of MLC-20 correlates with potentiated twitch tension after repetitive stimulation. In smooth muscle cells, this phosphorylation leads to an increase in actomyosin ATPase activity and contraction which appears to be required for initiation of contraction. Phosphorylation of MLC-20 by smooth muscle MLCK is a key event initiating smooth muscle contraction. Although the roles of MLCK in non-muscle cells have not been well defined, a variety of morphological changes such as cellular motility and organelle movement occur concurrently with the increased cytoplasmic Ca^{2+} levels, light chain phosphorylation and activation of MLCK. Intracellular localization studies performed in mammalian fibroblast cells have colocalized MLCK to the spindle apparatus and midbody of mitotic cells. These observations have led to the suggestion that the phosphorylation of MLC-20 by MLCK in non-muscle cells might have a role in cell division and cell motility[3]. There are at least two different stress fiber systems in fibroblasts including central stress fiber system and periphery stress fiber system and the latter system depends on MLCK[4]. And at least two distinct classes of MLCK (short and long) phosphorylate the MLC-20 of myosin in thick filaments but bind with high affinity to actin in thin filaments[5]. But which form of MLCK exists in hepatocytes? How is MLCK involved in cellular functions in hepatocytes? In order to investigate the roles of MLCK in the maintenance of liver functions and its association with some liver diseases in the future study, we prepared polyclonal antibody through expressed MLCK protein in *E. Coli* system, and the antibody was used to detect the distribution and expression of MLCK in hepatocytes with immunofluorescence microscopy. Our research provides the basis for further investigation MLCK functions of in the liver and its relation with the pathology of some hepatic diseases such as hepatocellular carcinoma and hyperlipoproteinmia.

MATERIALS AND METHODS

Reagents and instruments

Plasmid pBKcmv and *E. coli* XL1-blue were from STRATAGENE (La Jolla, CA, USA). The human-non-muscle-MLCK cDNA was a gift from Dr. Stull at University of Texas Southwestern Medical Center, USA. Concept rapid PCR purification system kit was purchased from Life Techology, GibcoBRL. pGEM-T vector system I was purchased from Promega (Madison WI, USA). Restriction endoenzyme, T_4DNA ligase, dNTPs, amplitaqe DNA polymerase, mounting media were obtained from Sigma Chemical Company. PCR primers were synthesized by BioAsia Biotechnology Co., Ltd (Shanghai, China). Other reagents were made in China and were of analytical purity. DYY-III type-2 electrophoresis and transfer system were made by Beijing Instrument Factory. UV-754 spectrophometer was made by The Third Factory of Analytical Instrument of Shanghai. Nikon eclipse E800 microscope was from Japan.

PCR of hnmMLCK DNA

The primers were designed according to human MLCK cDNA,

prime 1: 5' TGG AAT TCC ATG GGG GAC GTG AA3' containing *Eco*RI restriction site and prime 2: 5' CCA CTG CTG AAG AAG CTT AAA ATC3' containing *Hind*III restriction site. The PCR parameters were pre-denaturation at 94 ℃ for 5 min before amplification was done for 35 cycles at 94 ℃ for 1 min, annealing at 55 ℃ for 1 min and extension at 72 ℃ for 1 min, and final extension for 10 min at 72 ℃ after the last cycle. The PCR products were examined by 20 $g.L^{-1}$ agarose gel electrophoresis with TAE buffer at 80V for 40 min, visualized with ethidium bromide, and photographed under UV light.

Ligation, transformation and sequence of hnmMLCK DNA[6]

The PCR products were purified by concept rapid PCR purification system kit and inserted into the T-vector, the resulting ligation products were transferred into XL1-blue *E.coli* competent cells. The positive clone was picked up and the plasmids were prepared. The plasmid and pBKcmv vector were digested with *Eco*RI and *Hind* III and ligated before transferred into XL1-blue E *coli* competent cells. Individual recombinant white clones were picked up and recombinant DNA was prepared before digested with restrictive endonuclease. The recombinant plasmid sequence was detected with ABI377 auto analytical instrument.

Expression and purification of hnmMLCK in E. coli[7]

The positive recombinant plasmids were transformed into XL-1blue *E. coli*, the single clone was picked up and cultured overnight at 37 ℃ with shaking at 250 rpm. The media were diluted (1:100) with Luria-bertani liquid medium and isoploprl-h-D-thiogalactoside (IPTG) was added into the medium to induce protein expression when OD_{600}=0.6-0.8, and cultured for 4 h. The bacteria were harvested by centrifugation at 5 000 rpm for 10 min and the expressed protein was analyzed by SDS-PAGE. The expressed band was cut from SDS-PAGE gel and electroeluted in transfer buffer for isolation and purification.

Anti-myosin light chain kinase polyclonal antibody preparation

Polyclonal antibody to human MLCK was prepared according to the previously described method[8].

Immunofluorescence detection of MLCK in rabbit livers

The New Zealand rabbit liver tissues were embedded with O.C.T and frozen sections were prepared. The slices were incubated in 100 % acetone for 10 min at -20 ℃ and dried in air, then blocked in 5 % non-fat milk in PBS (pH7.4) overnight. The blocking solution was removed and anti-MLCK polyclonal antibody was added, and then incubated in a wet box for 2-3 h. The reactions were incubated with FITC-labeled secondary antibody for 1 h. Finally, the reactions were covered with mounting media before observation with a Nicon fluorescent microscope[9,10].

RESULTS

Amplification of human MLCK cDNA

The PCR products were detected by 20 $g\cdot L^{-1}$ agrose gel. The results showed that there was a 450 bp band in the gel (Figure 1), corresponding to the fragment of human MLCK cDNA N-terminate.

Enzymatic and sequence analysis of recombinant plasimid and cloned DNA

The recombinant plasmid was digested with *Eco*RI and *Hind*III and then run in 20 $g\cdot L^{-1}$ agrose gel, which showed that the PCR products were inserted into the pBKcmv vector (Figure 2). The DNA sequences of pBK-hnmMLCK were detected by ABI377 auto analytical instrument (Figure 3), and compared with Genbank (Figure 4).

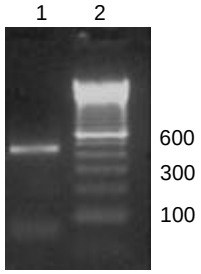

Figure 1 Amplification of hnmMLCK cDNA by PCR . 1. products of PCR amplification, 2. the 100 bp ladder.

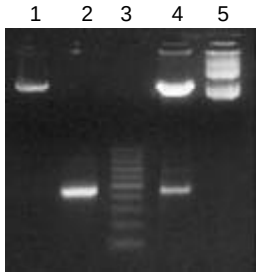

Figure 2 Analysis of human MLCK recombinant plasmids with restriction endonucleases mapping. 1. pBKcmv/*Eco*RI-*Hind*III, 2. PCR products/*Eco*RI-*Hind*III, 3. the 100 bp DNA ladder, 4. pBK-hnmMLCK/*Eco*RI-*Hind*III, 5. pBK-hnmMLCK.

Protein expression and purification

The expressed protein hnmMLCK in *E. coli* was induced with IPTG and bacteria were centrifuged at 5 000 rpm for 10 min. The pellet was resuspended with PBS, and an equal volume of 2×protein loading buffer was added, boiled at 100 ℃ for 5 min and analyzed by SDS-PAGE. The percentage of the expressed protein was about 21 % by scanning analysis (Figure 5).

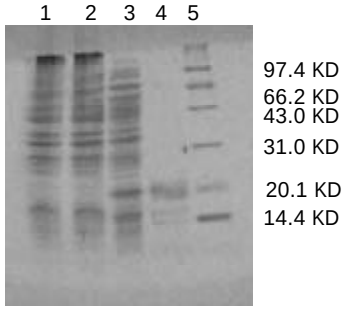

Figure 5 Analysis of pBK-hnmMLCK with SDS-PADE. 1. pBKcmv in XL1-blue, 2. pBK-hnmMLCK in XL1-blue before induced, 3. pBK-hnmMLCK in XL1-blue after induced, 4. purified expression protein, 5. protein markers.

Antiserum detection by immune double-diffusion

The ratio of antigen to antibody was at least 1:16 (Figure 6), suggesting that the polyclonal antibody could be used for immunoflouresence analysis.

Distribution of MLCK in rabbit livers

MLCK was mainly distributed peripherally in hepatocytes (Figure 7), and was hardly detected cytoplasms by immunofluorescence.

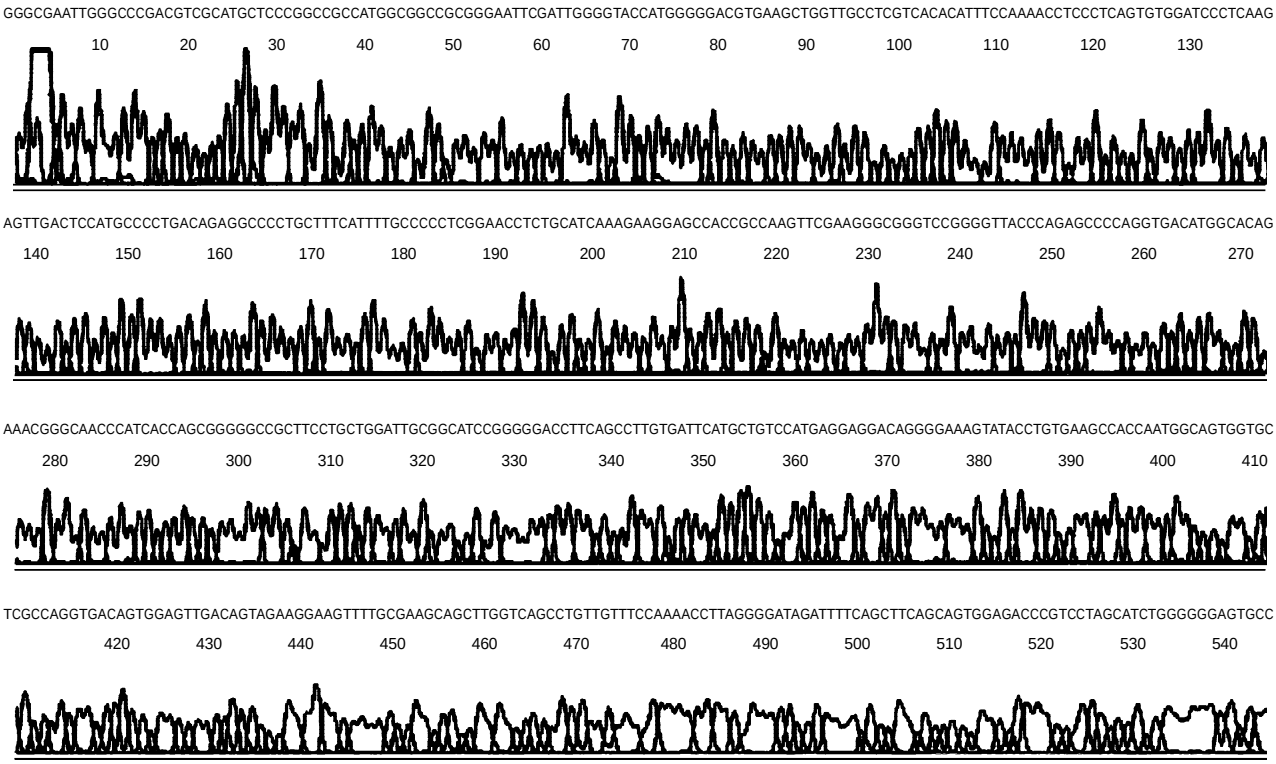

Figure 3 DNA sequences of pBK-hnmMLCK were detected by ABI377 auto analytical instrument.

>gi|7239697|gb|AF069601.2|AF069601 pBKcmv-hMLCK85-144
Homo sapiens myosin light chain kinase isoform 2 (MLCK) mRNA, complete cds
Length = 5719 Score = 852 bits (430), Expect = 0.0
Identities = 439/442 (99%) Strand = Plus / Plus
Query: 39 ccatgggggacgtgaagctggttgcctcgtcacacatttccaaaacctccctcagtgtgg 98
||||||||| ||||||||||||||||||||||||||||||||||||||||||||
Sbjct:118 ccatgggggatgtgaagctggttgcctcgtcacacatttccaaaacctccctcagtgtgg 177
Query: 99 atccctcaagagttgactccatgcccctgacagaggcccctgctttcattttgccccctc 158
||||||||||||||||||||||||||||||||||||||||||||||||||||||
Sbjct:178 atccctcaagagttgactccatgcccctgacagaggcccctgctttcattttgccccctc 237
Query:159 ggaacctctgcatcaaagaaggagccaccgccaagttcgaagggcgggtccggggttacc 218
||||||||||||||||||||||||||||||||||||||||||||||||||||||
Sbjct:238 ggaacctctgcatcaaagaaggagccaccgccaagttcgaagggcgggtccggggttacc 297
Query:219 cagagccccaggtgacatggcacagaaacgggcaacccatcaccagcgggggccgcttcc 278
||||||||||||||||||||||||||||||||||||||||||||||||||||||
Sbjct:298 cagagccccaggtgacatggcacagaaacgggcaacccatcaccagcgggggccgcttcc 357
Query:279 tgctggattgcggcatccgggggaccttcagccttgtgattcatgctgtccatgaggagg 338
|||||||||||||||||||| ||||||||||||||||||||||||||
Sbjct:358 tgctggattgcggcatccgggggactttcagccttgtgattcatgctgtccatgaggagg 417
Query:339 acaggggaaagtatacctgtgaagccaccaatggcagtggtgctcgccaggtgacagtgg 398
||||||||||||||||||||||||||||||||||||||||||||||||||||||
Sbjct:418 acaggggaaagtatacctgtgaagccaccaatggcagtggtgctcgccaggtgacagtgg 477
Query:399 agttgacagtagaaggaagttttgcgaagcagcttggtcagcctgttgtttccaaaacct 458
||||||||||||||||||||||||||||||||||||||||||||||||||||||
Sbjct:478 agttgacagtagaaggaagttttgcgaagcagcttggtcagcctgttgtttccaaaacct 537
Query:459 taggggatagattttaagcttc 480
|||||||||||||| |||||
Sbjct:538 taggggatagattttcagcttc 559

Figure 4 Comparison between sequencing results of hnmMLCK DNA and those published by Genbank.

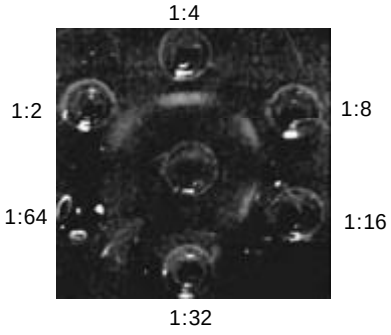

Figure 6 Antiserum titer detected by immuno-double-diffusion.

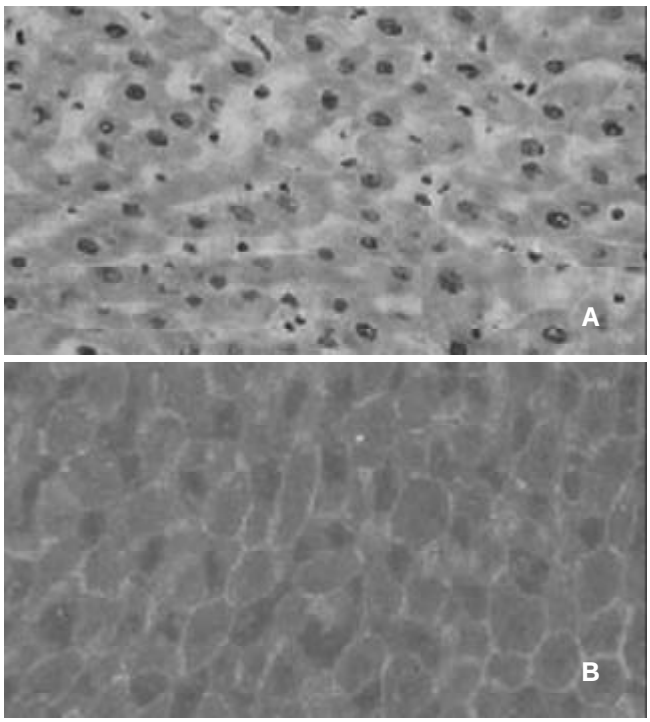

Figure 7 MLCK distribution in hepatocytes of New Zealand rabbits. A: H and E staining, B: MLCK distribution.

DISCUSSION

MLCK is the key regulator of cell motility and smooth muscle contraction in higher vertebrates[11-13]. MLCK expression shows a complex pattern. In undifferentiated myoblasts, 220-ku long or non-muscle form of MLCK is expressed during differentiation of skeletal muscle. During myoblast differentiation, the expression of 220-ku MLCK declines and expression of this long-term is replaced by 103-ku smooth muscle MLCK and a skeletal muscle-specific MLCK. The two isoforms are products of a single gene[14], and both short and long MLCKs are expressed in embryonic and adult non-muscle as well as smooth muscle cells[15,16]. Recently, some study showed the existence of a 208-ku protein, named embryonic MLCK because its expression could be detected in early embryonic tissue stem cells and in proliferating culture cells[17]. MLCK has several well characterized domains, and they are comprised of an amino-terminal "tail" of unknown function and a central catalytic core that is homologous to the catalytic core of other protein kinases, carboxy-terminal to the catalytic core and calmodulin binding domains, which are involved in the activation of the kinase in responses to increased Ca^{2+}[18]. In this study we constructed the expression vector which could express N-terminal MLCK, and used this protein to prepare polyclonal antibody. The results showed that the antibody could react with hepatic cells and MLCK was distributed in the peripheral region of hepatic cells. In rabbit portal vein myocytes, MLCK could mediate noradrenaline-evoked non-selective cation current[19]. In the liver, agents that elevated intercellular free Ca^{2+} concentration could increase tight junctional permeability and stimulate bile canalicular contraction. Myosin phosphorylation is might be responsible for the tight junctional permeability caused by elevation of intercellular Ca^{2+} in hepatocytes. Moreover, the integrity of the phosphorylation systems of myosin is essential for normal bile flow. In addition, hepatic sinusoidal Ito cells play a regulatory role on hepatic blood flow through their contraction, while the integrity of MLCK is essential for Ito cell contractions and normal sinusoidal blood flow. However, the role of myosin phosphorylation by MLCK in non-muscle tissues has not been well characterized but correlated with important activities such as cell division, receptor capping[20,21], *etc*. It has been found that MLCK was closely associated with non-muscle cells[16,19,20]. Phosphorylation of myosin light chain by MLCK in non-muscle cells and tissues demonstrated an important physiological function[22]. For example, myosin light chain phosphorylation has been implicated in secretory vesicle movement, cellular locomotion and changes in cellular morphology[23]. MLCK activation was a critical step in cytoskeletal changes causing pseudopod formation during polymorphonuclear leukocyte phagocytosis[24]. MLCK was also associated with the gap formations and endothelial hyperpermeability of coronary venular endothelial cell monolayers[25]. The preliminary studies showed that the light chain was obviously phosphorylated when CaM was added into the reaction buffer at a suitable concentration of Ca^{2+}. The activity of MLCK in rabbit livers increased markedly when CaM was added, and the activity changed with a substrate concentration or the concentration of light chain kinase[26]. MLCK immunoreactivity was found to be colocalized with the insulin granules, suggesting that it increased insulin granules in the ready-releasable pool by acting on different steps in the secretary cascade[27]. In this study, the expressed vector was successfully constructed and MLCK was expressed in *E coli* system, which lays a good basis for the manufacture and clinical application of the enzyme. The anti-MLCK polyclonal antibody was prepared and used to detect the distribution of MLCK in the cells of rabbit liver. MLCK may play an important role in maintaining the normal functions of tissues. But in the liver, which form of MLCK was expressed, long or short? If there are both forms, which form expresses more? What are their roles in the liver? What roles will it play in liver regeneration, injury or hepatic carcinoma? And what is the mechanim of MLCK activity in the liver? All these remain to be investigated and elucidated in future studies.

REFERENCES

1 **Kishi H**, Mikawa T, Seto M, Sasaki Y, Kanayasu-Toyoda T, Yamaguchi T, Imamura M, Ito M, Karaki H, Bao J, Nakamura A, Ishikawa R, Kohama K. Stable transfectants of smooth muscle cell line lacking the expression of myosin light chain kinase and their characterization with respect to the actomyosin system. *J Biol Chem* 2000; **275**: 1414-1420

2 **Deng JT**, Van Lierop JE, Sutherland C, Walsh MP. Ca2+-independent smooth muscle contraction. a novel function for integrin-linked kinase. *J Biol Chem* 2001; **276**: 16365-16373

3 **Goeckeler ZM**, Masaracchia RA, Zeng Q, Chew TL, Gallagher P, Wysolmerski RB. Phosphorylation of myosin light chain kinase by p21-activated kinase PAK2. *J Biol Chem* 2000; **275**: 18366-18374

4 **Katoh K**, Kano Y, Amano M, Kaibuchi K, Fujiwara K. Stress fiber organization regulated by MLCK and Rho-kinase in cultured human fibroblasts. *Am J Physiol Cell Physiol* 2001; **280**: C1669-1679

5 **Smith L**, Parizi-Robinson M, Zhu MS, Zhi G, Fukui R, Kamm KE, Stull JT. Properties of long myosin light chain kinase binding to F-actin *in vitro* and *in vivo*. *J Biol Chem* 2002; **277**: 35597-35604

6 **Xu CS**, Li YC, Lin JT, Zhang HY, Zhang YH. Cloning and analysing the up-regulated expression of transthyretin-related gene (LR1) in rat liver regeneration following short interval successive partial hepatectomy. *World J Gastroenterol* 2003; **9**: 148-151

7 **Hu RL**, Zhu HQ, Zhou Q, Gui SY, Wang Y. Construction of pBK-human non-muscle MLCK N-terminal and its expression in *E. coli* XL1-blue. *Anhui Yike Daxue Xuebao* 2002; **37**: 11-13

8 **Nunnally MH**, Stull JT. Mammalian skeletal muscle myosin light chain kinases. A comparison by antiserum cross-reactivity. *J Biol Chem* 1984; 259: 1776-1780

9 **Huang ZS**, Wang ZW, Liu MP, Zhong SQ, Li QM, Rong XL. Protective effects of polydatin against CCl(4)-induced injury to primarily cultured rat hepatocytes. *World J Gastroenterol* 1999; **5**: 41-44

10 **Chen YM**, Qian ZM, Zhang J, Chang YZ, Duan XL. Distribution of constitutive nitric oxide synthase in the jejunum of adult rat. *World J Gastroenterol* 2002; **8**: 537-539

11 **Jin Y**, Atkinson SJ, Marrs JA, Gallagher PJ. Myosin ii light chain phosphorylation regulates membrane localization and apoptotic signaling of tumor necrosis factor receptor-1. *J Biol Chem* 2001; **276**: 30342-30349

12 **Schmidt JT**, Morgan P, Dowell N, Leu B. Myosin light chain phosphorylation and growth cone motility. *J Neurobiol* 2002; **52**: 175-188

13 **Dudek SM**, Birukov KG, Zhan X, Garcia JG. Novel interaction of cortactin with endothelial cell myosin light chain kinase. *Biochem Biophys Res Commun* 2002; **298**: 511-519

14 **Birukov KG**, Schavocky JP, Shirinsky VP, Chibalina MV, Van Eldik LJ, Watterson DM. Organization of the genetic locus for chicken myosin light chain kinase is complex: multiple proteins are encoded and exhibit differential expression and localization. *J Cell Biochem* 1998; **70**: 402-413

15 **Blue EK**, Goeckeler ZM, Jin Y, Hou L, Dixon SA, Herring BP, Wysolmerski RB, Gallagher PJ. 220- and 130-kDa MLCKs have distinct tissue distributions and intracellular localization patterns. *Am J Physiol Cell Physiol* 2002; **282**: C451-460

16 **Davis JS**, Hassanzadeh S, Winitsky S, Lin H, Satorius C, Vemuri R, Aletras AH, Wen H, Epstein ND. The overall pattern of cardiac contraction depends on a spatial gradient of myosin regulatory light chain phosphorylation. *Cell* 2001; **107**: 631-641

17 **Murata-Hori M**, Suizu F, Iwasaki T, Kikuchi A, Hosoya H. ZIP kinase identified as a novel myosin regulatory light chain kinase in HeLa cells. *FEBS Lett* 1999; **451**: 81-84

18 **Gallagher PJ**, Herring BP. The carboxyl terminus of the smooth muscle myosin light chain kinase is expressed as an independent protein, telokin. *J Biol Chem* 1991; **266**: 23945-23952

19 **Aromolaran AS**, Albert AP, Large WA. Evidence for myosin light chain kinase mediating noradrenaline-evoked cation current in rabbit portal vein myocytes. *J Physiol* 2000; **524**(Pt 3): 853-863

20 **Watanabe H**, Tran QK, Takeuchi K, Fukao M, Liu MY, Kanno M, Hayashi T, Iguchi A, Seto M, Ohashi K. Myosin light-chain kinase regulates endothelial calcium entry and endothelium-dependent vasodilation. *FASEB J* 2001; **15**: 282-284

21 **Tran QK**, Watanabe H, Le HY, Pan L, Seto M, Takeuchi K, Ohashi K. Myosin light chain kinase regulates capacitative ca(2+) entry in human monocytes / macrophages. *Arterioscler Thromb Vasc Biol* 2001; **21**: 509-515

22 **Wadgaonkar R**, Nurmukhambetova S, Zaiman AL, Garcia JG. Mutation analysis of the non-muscle myosin light chain kinase (MLCK) deletion constructs on CV1 fibroblast contractile activity and proliferation. *J Cell Biochem* 2003; **88**: 623-634

23 **Iida Y**, Senda T, Matsukawa Y, Onoda K, Miyazaki JI, Sakaguchi H, Nimura Y, Hidaka H, Niki I. Myosin light-chain phosphorylation controls insulin secretion at a proximal step in the secretory cascade. *Am J Physiol* 1997; **273**(4 Pt 1): E782-789

24 **Mansfield PJ**, Shayman JA, Boxer LA. Regulation of polymorphonuclear leukocyte phagocytosis by myosin light chain kinase after activation of mitogen-activated protein kinase. *Blood* 2000; **95**: 2407-2412

25 **Tinsley JH**, De Lanerolle P, Wilson E, Ma W, Yuan SY. Myosin light chain kinase transference induces myosin light chain activation and endothelial hyperpermeability. *Am J Physiol Cell Physiol* 2000; **279**: C1285-1289

26 **Ren B**, Zhu HQ, Lou ZF, Zhou Q, Wang Y, Wang YZ. Preliminary research on myosin light chain kinase in rabbit liver. *World J Gastroenterol* 2001; **7**: 868-871

27 **Yu W**, Niwa T, Fukasawa T, Hidaka H, Senda T, Sasaki Y, Niki I. Synergism of protein kinase A, protein kinase C, and myosin light-chain kinase in the secretory cascade of the pancreatic beta-cell. *Diabetes* 2000; **49**: 945-952

Edited by Zhang JZ and Wang XL

P.O.Box 2345, Beijing 100023,China
Fax: +86-10-85381893
E-mail: wjg@wjgnet.com www.wjgnet.com

World J Gastroenterol 2003;9(12):2720-2725
World Journal of Gastroenterology
 ISSN 1007-9327

• BASIC RESEARCH •

Identification of *alkA* gene related to virulence of *Shigella flexneri 2a* by mutational analysis

Zhao-Xing Shi, Heng-Liang Wang, Kun Hu, Er-Ling Feng, Xiao Yao, Guo-Fu Su, Pei-Tang Huang, Liu-Yu Huang

Zhao-Xing Shi, Heng-Liang Wang, Kun Hu, Er-Ling Feng, Guo-Fu Su, Pei-Tang Huang, Liu-Yu Huang, Beijing Institute of Biotechnology, Beijing 100071, China
Xiao Yao, College of Environmental and Chemical Engineering, Xi' an Jiaotong University, Xi' an 710049, Shaanxi Province, China
Supported by the Major State Basic Research Development Program of China (973 Program), No. G1999054103; National High-technology Research and Development Program of China (863 Program), No. 2001AA215211; and Capital "248" Key Innovation Program of China, No. H010210360119
Correspondence to: Liu-Yu Huang, Beijing Institute of Biotechnology, 20 East Fengtai Street, Beijing 100071, China. huangly@nic.bmi.ac.cn
Telephone: +86-10-66948805 **Fax:** +86-10-63833521
Received: 2003-07-17 **Accepted:** 2003-07-30

Abstract

AIM: *In vivo* induced genes are thought to play an important role during infection of host. *AlkA* was identified as an *in vivo*-induced gene by *in vivo* expression technology (IVET), but its virulence in *Shigella flexneri* was not reported. The purpose of this study was to identify the role of *alkA* gene in the pathogenesis of *S. flexneri*.

METHODS: PCR was used to amplify *alkA* gene of *S. flexneri 2a* and fragment 028pKm. The fragment was then transformed into 2457T05 strain, a *S flexneri 2a* strain containing Red recombination system, which was constructed with a recombinant suicide plasmid pXLkd46. By *in vivo* homologous recombination, alkA mutants were obtained and verified by PCR and sequencing. Intracellular survival assay and virulence assay were used to test the intracellular survival ability in HeLa cell model and the virulence in mice lung infection model respectively.

RESULTS: Deletion mutant of *S. flexneri 2a alkA* was successfully constructed by λ Red recombination system. The mutant exhibited significant survival defects and much significant virulence defects in mice infection assay.

CONCLUSION: *AlkA* gene plays an important role in the infection of epithelial cells and is a virulent gene of *Shigella spp*.

Shi ZX, Wang HL, Hu K, Feng EL, Yao X, Su GF, Huang PT, Huang LY. Identification of *alkA* gene related to virulence of *Shigella flexneri 2a* by mutational analysis. *World J Gastroenterol* 2003; 9(12): 2720-2725

http://www.wjgnet.com/1007-9327/9/2720.asp

INTRODUCTION

Shigella spp. is a Gram-negative facultative pathogen, which causes bacillary dysentery, a world endemic bloody diarrhea, particularly in developing countries. The disease is caused by invasion of the colorectal mucosa by *Shigella spp.*, replicating within epithelial cells and moving between cells. The interaction between epithelial cells and *Shigella spp.* plays an important role in the pathogenicity of *Shigella spp.*[1-3]. During infection of epithelial cells, genes with inducible expression are important for *Shigella spp.* to replicate and survive in the cells. Hereby, these genes are generally thought to be related to the virulence of *Shigella spp.*. Many methods could be used to isolate *in vivo* expressed genes[4].Using *in vivo* expression technology (IVET) to identify the virulence-related genes of pathogens is a flourishing field in the world[5-11]. We have employed *in vivo* expression technology with *asd* gene as a reporter to screen *S. flexneri 2a* fusion gene library. The result indicated that *alkA* gene is an *in vivo*-induced gene for *Shigella flexneri 2a*.

AlkA gene or its homologous genes have been cloned from many organisms, such as *Escherichia coli*, *Helicobacter pylori*, *Bacillus subtilis*, *Saccharomyces cerevisiae*, human, etc[12-14]. They encode 3-methyladenine DNA glycosylase, whose function is excising hypoxanthine, demethylating, and mainly taking part in the repair of damaged DNA[15,16]. Up to now researches on *alkA* have mainly focused on regulation of its expression and its role in inducing repair after DNA alkylation damage. As for its relation to bacterial pathogenesis, it is a noteworthy issue. In this experiment, based on the sequence of *E.coli alkA*, *alkA* gene of *S. flexneri 2a* 2457T was cloned. Its mutant was constructed, and its role in pathogenesis was analyzed by a HeLa cell model and a mice infection model. This study perhaps would provide insights into the pathogenicity of this pathogen.

MATERIALS AND METHODS

Materials

The strains and plasmids used in this study are listed in Table 1.

HeLa cell line was maintained in our laboratory. BALB/c mice were bought from the Laboratory Animal Center in the Academy of Military Medical Sciences, Beijing. All mice used in this study were female, specific pathogen free animals, with an age of 7-8 weeks and weight of 18-22 g. DNA endonucleases, DNA marker, T4 DNA ligase, T4 DNA polymerase, Ex *Taq* DNA polymerase, and CIAP were purchased from Takara Company. Newborn calf sera and RPMI1640 media were from HyClone, and deoxycholate sodium from Sigma. Primers (P1, P2, P3, and P4) were synthesized in our laboratory.

Methods

Culture and maintenance of strains and HeLa cells Luria-Bertani (LB) broth and agar plate were used for the growth of *S. flexneri* and *Escherichia coli* strains at 37 ℃. SOC culture medium was applied to the restoration of bacteria after electroporation. When appropriate, antibiotics were added in media as follows: 100 μg ampicillin (Ap), 100 μg streptomycin (Sm), 50 μg kanamycin (Km), 25 μg chloramphenicol (Cm), and 25 μg naladixic acid (Nal) per ml. HeLa cells were maintained in the RPMI-1640 medium supplemented with 10 % fetal bovine serum, 200 mM L-glutamine, 2 mg sodium hydrogen carbonate per ml and 100 μg penicillin-streptomycin per ml. The cells were cultured in 37.5 cm^2 or 10 cm^2 flasks at 37 ℃ in a humidified atmosphere of 5% CO_2. Confluent monolayers were split by treatment with sterile phosphate-buffered saline (PBS) and trypsin-EDTA.

Table 1 Strains and plasmids

Strains and plasmids	Characteristics	Source (reference)
Strains		
DH5α	endA1 hsdR17($r_k^-m_k^+$) supE44 thi-1 recA1 gyrA(Nal^r) RelA1 △ lacIZYA-argF) U169 deoR (ϕ80dlac △ (lacZ)M15)	Our lab
S_{17-1}λpir	thi-1 thr leu tonA lacY supE recA::RP4-2-Tc::Mu, Sm^r, λpir	Guzman CA
MC1061	hsdR2 mcrB araD139 △ (ara ABC-leu)7679 △ lacX74 galU galK rpsL thi, Sm^r	Our lab
2457T	*S. flexneri 2a* wild type, Nal^r	Maurelli AT
2457T05	a derivative strain of 2457T, contained araBp-gam-bet-exo, Nal^r	This study
2457T028D	△ alkA, derivative strain of 2457T, Nal^r, Km^r	This study
Plasmids		
pMD18-T	a derivative constructed from pUC18, Ap^r	TaKaRa
pXL275	a mobile and suicide plasmid, ori R6K, mob RK2, sacBR, Cm^r	Rui *et al*.[17]
pKD46	oriR101, repA101(ts), araBp-gam-bet-exo, Ap^r	CGSC[a]
pXLkd46	pXL275 derivative, inserted a fragment containing araBp-gam-bet-exo, Cm^r	This study
pMDKm05	pMD18-T derivative, inserted Km^r gene, Km^r, Ap^r	Our lab
pMD028	pMD18-T derivative, inserted *alkA* gene, Ap^r	This study
pMD028pKm	pMD18-T derivative, inserted a cassette (5' *alkA* end-Km^r-3' *alkA* end), Km^r, Ap^r	This study

[a]CGSC: *E. coli* Genetic Stock Center.

Genetic techniques Plasmid DNA extraction was carried out using a Qiagen plasmid kit. Digestion, ligation, transformation, and other conventional methods of molecular biology were performed as previously described[18].

DNA amplifications For the amplification of *S. flexneri 2a alkA* gene, PCR was performed in a standard 100 μl reaction volume containing 2.5 mM Mg Cl_2, 0.25 mM of each dNTP, 100 pmol of P1 and P2 primers, 10 μl boiled *S. flexneri 2a* 2457T, and 5 U Taq DNA polymerase. Reactions were allowed to proceed in a Perkin-Elmer 2400 thermal cycler programmed for 10 min at 94 ℃, 30 cycles (for 45 s at 94 ℃, for 40 s at 55 ℃, for 3 min at 72 ℃) and an additional extension reaction for 10 min at 72 ℃. For the amplification of fragment 028pKm, PCR was carried out in 100 μl reaction volume containing 2.5 mM $MgCl_2$, 0.25 mM of each dNTP, 100 pmol of P3 and P4 primers, 2 μl plasmid pMD028pKm (about 10 ng), and 5 U Taq DNA polymerase. The program of this PCR was at 94 ℃ for 10 min, 30 cycles (for 30 s at 94 ℃, for 40 s at 58 ℃, for 1.5 min at 72 ℃) and for 10 min at 72 ℃.

Bacterial mating The donor and recipient strains were grown in LB medium containing appropriate antibiotics overnight. The liquid cultures were then washed in PBS, mixed at 1:1 ratio, and spreaded on LB agar plates. The plates were incubated at 37 ℃ for 6-8 h. After incubation, the conjugation mixture was washed in PBS and spread onto LB agar plates containing chloramphenicol (25 μg· mL^{-1}) and naladixic acid (25 μg· mL^{-1}). The plates were incubated at 37 ℃ until transconjugants were visible.

Disruption of *S. flexneri 2a alkA* gene *S. flexneri 2a* 2457T05 was grown in 5 ml LB cultures with chloramphenicol, naladixic acid and L-arabinose to an OD_{600}=0.45 and then made electrocompetent by concentrating 100-fold and washing three times with ice-cold 10 % glycerol. The gel-purified *028pKm* PCR products were digested with *DpnI*, repurified, and suspended in elution buffer (10 mM Tris, pH 8.0). Electroporation was done using a gene pulser® II with a pulse controller plus and 0.1 cm chambers according to the manufacturer's instructions (Bio-RAD) using 40 μl of competent cells and 100 ng of 028pKm fragments. The parameters for electro- transformation were resistance 200Ω, capacitance 25 μF, and voltage 2 500 V. Shocked cells were added to 1 ml SOC culture, incubated for 1 h at 37 ℃, and then one-half was spread onto agar to select Km^r and Nal^r transformants. If none grew within 24 h, the remainder was spread after standing overnight at room temperature.

Intracellular survival assay HeLa cell infection assay was routinely used to detect the intracellular replication or survival ability of the mutant[19-21]. *S. flexneri 2a* 2457T, 2457T05, mutant strain and *E. coli* MC1061 (noninvasive control) were grown in an appropriate medium overnight. The liquid cultures were then washed in PBS and resuspended in antibiotic-free medium. Approximately 10^6 HeLa cells were cultured in a 10 cm^2 flask. HeLa cells were washed three times in PBS prior to incubation with about 10^8 CFU bacteria at 37 ℃ for 3 h. The medium was removed from infected cells after 2.5 h, and the cells were washed three times in PBS. Fresh medium containing gentamicin (20 μg· mL^{-1}) was added and the flasks were incubated for 5 h to eliminate extracellular bacteria. After that, the medium was replaced by RPMI1640 containing gentamicin (20 μg· mL^{-1}) and the infected cells were cultured for another 40 h. The supernatants of culture were tested for extracellular surviving bacteria by plating them on LB agar plates. The monolayers were then washed three times in PBS and lysed by addition of 0.1 % deoxycholate sodium to liberate the intracellular bacteria. Dilutions of the lysates of HeLa cells infected with bacteria were plated on LB agar plates and cultured at 37 ℃ overnight. The CFU of the bacteria was then counted.

Competition assay To test the mutant strains for alterations in virulence relative to the wild type, a competition assay was carried out by using a murine intranasal infection model[22-24] with some modifications. The mutant or MC1061 (negative control) or 2457T (positive control) and 2457T05 grown overnight were mixed at 1:1 (v/v) ratio and washed in PBS. After concentration of the mixture was adjusted by dilutions, 20 μl mixtures containing about 10^6 CFU in PBS was used to introduce droplets into the nares of BALB/c mice that was anesthetized. The number of bacteria in each inoculum was determined by plating serial dilutions of the inoculum. After 24 h, the recovered bacteria from the lungs of mice were counted, and then the number of mutant strains and 2457T was counted. According to the method of Camilli *et al*.[25], the competitive index of each mutant was obtained.

Bioinformatics analysis The sequence of *S. flexneri 2a alkA* gene was analyzed by BLAST (http://www.ncbi.nlm.nih.gov/BLAST/). The identity and gene function were also analyzed by NCBI.

Statistical analysis

Data from the intracellular survival assay were analyzed by Dunnett *t* test, and *P* value less than 0.05 was considered as statistically significant. Data from the competition assay were analyzed by the sign test, and *P* value less than 0.0078 was

considered as statistically significant. The Dunnet *t* test and the sign test were performed using the SAS (Statistical Analysis Systems Inc., USA) program.

RESULTS

Cloning and homologous analysis of S. flexneri 2a alkA gene

In our previous work, we identified *S. flexneri 2a alkA* as an *in vivo*-induced gene, and obtained the partial sequence of *S. flexneri 2a alkA* gene which had an alignment with other bacteria. Based on the sequence of *E. coli alkA*, the primers, P1 (CGAGGAACGATTTTGGTGAT) and P2 (CTCGCT-GAAAGCGAATATGG) (Figure 3 B) were designed. Using *S. flexneri 2a* 2457T chromosome DNA as a template, PCR was performed and the PCR products were purified by agarose gel electrophoresis, and ligated into plasmid pMD18-T to produce plasmid pMD028 after the confirmation of *EcoRV* and *HindIII* digestion analysis. The recombinant plasmid pMD028 was subjected to DNA sequencing to obtain the whole length DNA sequence of *alkA*. Its open read frame was 849 bp. In the upstream there was a promoter sequence (AGCAAAGCGTAACGTCTGAATAACGTTTATGCT) and the binding site (AAAGCAAA) of Ada protein which was a regulator of *alkA* gene expression in *E. coli*. Based on the sequence of *S. flexneri 2a alkA*, homologous analysis was carried out on the NCBI website. The results are listed in Table 2. Interestingly, the sequence alignment revealed a Helix-hairpin-Helix (HhH) motif common to DNA glycosylases. *E. coli* alkA was identified as the helix-hairpin-helix DNA glycosylase[26]. Very possibly, alkA protein from *S. flexneri 2a* belonged to an HhH-GPD super family. Its hallmark was Helix-hairpin-Helix and Gly/Pro rich loop followed by a conserved aspartate and its function was presumably involved in DNA replication and repair.

Construction of S. flexneri 2a engineering strain

To delete *alkA* gene of *S. flexneri 2a*, construction of *S. flexneri 2a* engineering strain expressing *gam*, *bet*, and *exo* genes, was required. The fragment (about 4 kb) containing *gam*, *bet*, and *exo* genes was obtained by digestion of pKD46 plasmid with *Pvu I* and *Bstx I* and ligated into the *Sal I* site of suicide plasmid pXL275. Then the ligation products were then transformed into $S_{17\text{-}1}\lambda$pir. The recombinant plasmid was confirmed by *BamHI* digestion and known as pXLkd46. After bacterial mating of the donor ($S_{17\text{-}1}\lambda$pir/pXLkd46) and recipient (2457T), pXLkd46 plasmid was integrated into chromosome of *S. flexneri 2a* by homologous recombination. The process of pXLkd46 plasmid construction and chromosomal integration is showed in Figure 1. The resulting strain was verified with antibiotic selection and serum agglutination and designated as 2457T05.

Construction of deletion mutant of S. flexneri alkA gene

After 2457T05 was successfully constructed, the linear targeting DNA, *028pKm*, was required for disruption of *S.*

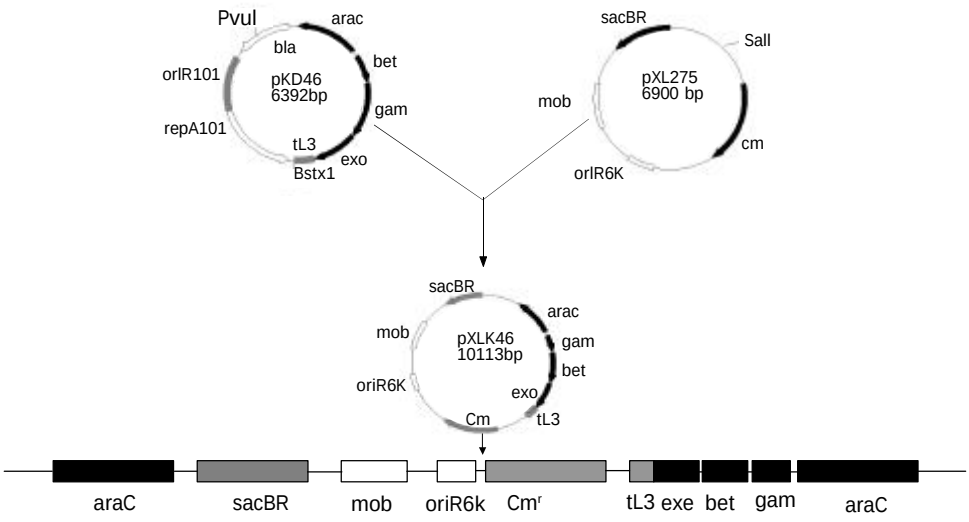

Figure 1 Construction and chromosomal integration of pXLkd46 plasmid.

Table 2 BLAST analysis of *S. flexneri 2a alkA* gene

Bacteria	Gene product	Gene function	Identities (%)
Escherichia coli K12	3-methyl-adenine DNA glycosylase II	DNA - replication, repair, restriction / modification	97 %
Escherichia coli O157:H7	3-methyl-adenine DNA glycosylase II	Macromolecule synthesis, modification: DNA-replication, repair, restriction / modification	97 %
Salmonella typhimurium	3-methyl-adenine DNA glycosylase II	Unknown	74 %
Ralstonia solanacearum	putative transcription regulator protein	Miscellaneous; not classified regulator	38 %
Pseudomonas aeruginosa	DNA-3-methyladenine glycosidase II	Unknown	37 %
Xanthomonas axonopodis	DNA methylation and regulatory protein	Unknown	35 %
Mycobacterium bovis	Methylated-DNA–protein-cysteine methyltransferase	Adaptative response	34 %
Mycobacterium tuberculosis	alkA protein	Unknown	34 %
Vibrio cholerae	ada regulatory protein	Unknown	32 %
Bacillus anthracis	DNA-3-methyladenine glycosidase	Unknown	32 %
Archaeoglobus fulgidus	3-methyladenine DNA glycosylase	DNA repair at suboptimal and maybe even mesophilic temperatures	30 %

flexneri 2a alkA gene with λ Red recombination system. To obtain the fragment *028pKm*, recombinant plasmid pMD028pKm was firstly to be constructed. Km^r gene fragment was obtained from plasmid pMDKm05 digested by *HincI I* and *Sma I* and inserted into the *alkA* gene of plasmid pMD028 digested by *EcoRV* and *StuI* and dephosphorized by CIAP. The ligation products were then transformed into *E. coli* DH5α. The recombinant plasmids were isolated from the transformants, confirmed by *EcoR I* digestion, and designated as pMD028pKm (Figure 2). Using pMD028pKm as a PCR template, P3 (TGTGCCAGTGAGGAAAGACC) and P4 (GAGAGAGCGT TTGCCCATTG) (Figure 3A) as primers, PCR was carried out. In order to reduce the interference of plasmid pMD028pKm, the second PCR was carried out at the same experimental condition except that the template was the first PCR products diluted by 1 000 times. The second PCR products (*028pKm*) did not contain the template plasmid pMD028pKm that would lead to false positive colonies in the latter electroporation experiment. The *028pKm* fragment was a cassette, 5' *alkA* end-Km^r-3' *alkA* end (Figure 3A). The concentrated *028pKm* was electroporated into *S. flexneri 2a* engineering strain 2457T05. The *alkA* gene was then replaced by kanamycin resistance gene through homologous recombination mediated by λ Red system. The positive transformants were selected on LB agar plates containing Km and Nal.

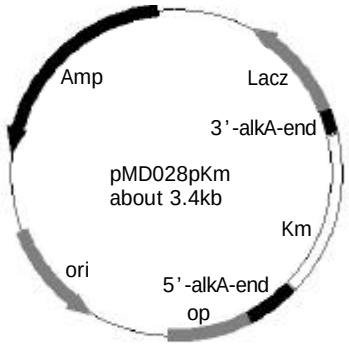

Figure 2 Construction of recombinant plasmid pMD028pkm.

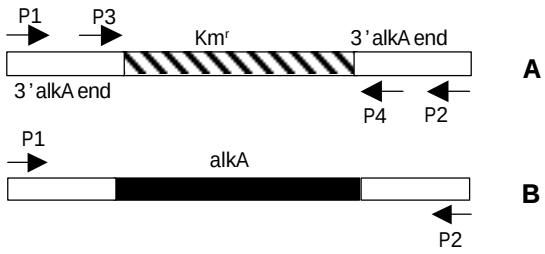

Figure 3 Location of primers P1, P2, P3 and P4 in PCR products of *alkA* and *028pKm*. A: *028pKm* (about 1.4 kb); B: *alkA* (about 1.7 kb).

To verify the replacement of *S. flexneri 2a alkA* gene, PCR and sequencing were used. PCR was performed in which 2457T05 (negative control), the transformant and pMD028pKm plasmid (positive control) were used as templates. The reaction conditions were the same as the amplification of *S. flexneri alkA* gene, and the primers were also P1 and P2. The PCR products from the transformant and pMD028pKm plasmid were about 1.4 kb and 1.7 kb from 2457T05 respectively (Figure 3, 4). Then the PCR products were sequenced and analyzed by BLAST (data not shown). The result indicated that *alkA* gene of *S. flexneri 2a* was replaced by Km^r gene. Hereby, the deletion mutant of *alkA* gene was successfully constructed and designated as 2457T028D.

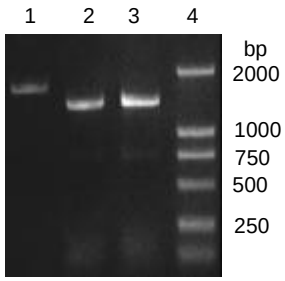

Figure 4 Verification of *alkA* gene deletion of 2457T028D mutant by PCR. 1: *alkA* PCR product (amplified from 2457T05), 2: *028pKm* PCR product (amplified from 2457T028D), 3: *028Kkm* PCR product (amplified from pMD028pKm), 4: DL2000 Marker.

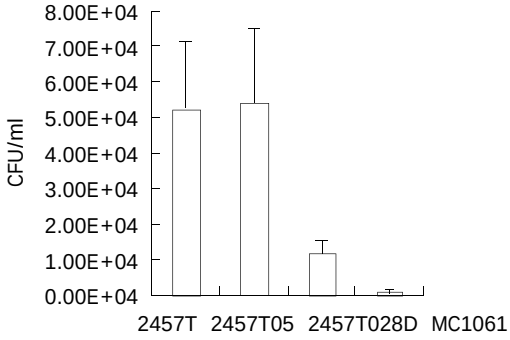

Figure 5 Comparison of HeLa cells infected by 2457T, 2457T05, 2457T028D and MC1061.

Functional analysis of deletion mutant of S. flexneri 2a alkA gene

In order to detect the role of *alkA* in the pathogenesis of *S. flexneri*, intracellular survival assay and virulence assay were respectively carried out in HeLa cells and BALB/c mice.

Mutant 2457T028D was tested for its survival ability in HeLa cells relative to the wild-type strain. Equal volume of each strain (2457T, 2457T05, 2457T028D and MC1061) was respectively used to infect the HeLa cell monolayer. Within 48 h, the integrity of the infected HeLa cell monolayer was good and the configuration of HeLa cells had no significant alterations relative to normal cells. But the growth rate of the infected cells became slow. After 48 h, CFU of bacteria recovered from HeLa cells was counted. The results of the infection assay are summarized in Figure 5. Noticeably, CFU levels of the mutant recovered from HeLa cells were five-fold lower than that of the wild type (P<0.01), indicating that the mutant had a lower capability of survival or replication. The survival probability of 2457T and 2457T05 showed no significant difference (Figure 5). In order to further confirm the survival probability of the mutant, competition assay was carried out with the HeLa cell infection model. A 1:1 (v/v) mixture of *S. flexneri 2a* 2457T05 and the mutant or 2457T or MC1061 was used to infect HeLa cells. The number of bacteria in each inoculum was determined by plating serial dilutions of the inoculum. After 48 h, recovered bacteria from HeLa cells were counted, and the number of bacteria was counted respectively. The experiment was separately repeated 3 times. Therefore, the competitive index of each strain obtained is shown in Table 3. The mutant 2457T028D whose survival probability was significantly lower in the infection assay, exhibited significant survival defects in this experiment (P<0.0078). The data strongly indicated that the mutant was much less able to survive in HeLa cells.

The mutant was also tested in a mice lung infection model for alterations in virulence relative to the wild-type parental strain. Mice that were challenged only with *S. flexneri* 2457T

showed early acute bronchiolitis at 24 h, followed by severe pneumonia at 48 h. Five mice were used for each group in the murine lung infection model. After 24 h, recovered bacteria from the lungs of mice were counted, and the number of each strain was counted. Then the competitive index of each strain obtained is summarized in Table 3. The mutant also exhibited significant colonization defects ($P<0.0078$). The data further indicated that *alkA* gene was potentially related to the virulence of *S. flexneri 2a* 2457T.

Table 3 Competitive analysis of different strains of *S. flexneri 2a*

Strains	Competitive index (CI)[a]	
	BALB/c mouse infection	HeLa cells infection
2457T05	0.96±0.27	1.07±0.35
2457T028D	0.21±0.09[b]	0.25±0.11[b]
MC1061	0.03±0.02[b]	0.02±0.01[b]

[a]Competitive index (CI) is the ratio of mutant CFU to wild-type CFU after correcting the ratios for deviations of the inoculum ratio from a value of 1. [b]$P<0.0078$.

DISCUSSION

It has been reported that *in vivo*-induced gene played an important role in the process of interaction between pathogen and host[27]. *In vivo*-induced genes are those whose expression is induced when pathogens infect their hosts. Their inducible expression is a molecular-level genetic adaptive response to special environments of host. Many virulent genes have been identified by mutational analysis of *in vivo*-induced genes. Heithoff *et al.*[28] used *purA-lacZY* as a reporter to identify *in vivo*-induced genes of *Salmonella typhimurim* utilizing macrophages or BALB/c mice as a model. They discovered some *in vivo*-induced genes, including regulatory genes (*phoP, pmrB, cadC*, etc.) and metabolic genes (*recD, hemA, mgtA, entF*, etc.). Furthermore, insertion mutants of these genes were constructed, and their virulence was detected. Seven of them exhibited significant virulence defects. In an another research on *Pseudomonas aeruginosa*, 22 genes were *in vivo*-induced during infecting BALB/c mice, including *np20*, which has been proved to be a virulence gene, and known as virulent factor FptA[29]. In our previous study, we identified *alkA* as an *in vivo*-induced gene. However, it is unknown if *alkA* gene is related to the virulence of *S. flexneri*.

In order to detect the role of *alkA* gene in the virulence of *S. flexneri 2a*, it is required to construct the deletion mutant of *alkA* gene. The mutant is conventionally constructed by twice homologous recombination mediated by suicide plasmid. Although the *asd* gene of *S. flexneri 2a* was successfully disrupted in our previous study[30], the efficiency of this method is very low and the experimental period is quite long. Recently, a new method, which depends on Red recombination system of λ phage, has been successfully established and used to speed up the knockout of genes[31,32]. However, its application was limited to *E. coli*[33-35]. It was not reported in other bacteria except that the *asd* gene was deleted with λ Red system in our laboratory[36]. In this study, the deletion mutant of *S. flexneri 2a alkA* gene was successfully constructed also with λ Red system. Importantly, an engineering strain 2457T05 of *S. flexneri 2a* was constructed, and it was confirmed that the strain could be used to study the function of *S. flexneri 2a* genes.

After the mutant of *S. flexneri 2a alkA* gene was constructed, intracellular survival and competition assays were carried out. The results showed that *alkA* mutant of *S. flexneri* could exhibit a low intracellular survival ability and a significant virulence defect, indicating that *alkA* was a virulence-related gene in *S. flexneri 2a*. However, it has not been reported before whether *alkA* was associated with the virulence of pathogens. *AlkA* is an expression-induced gene and its product, 3-methyladenine DNA glycosylase II, is involved in the SOS-dependent adaptive response. Expression of *alkA* is regulated by Ada protein. When alkylation damages bacterial DNA, *ada* gene would be induced by alkyl-DNA. The produced Ada finishes directly-repairing damage of alkyl-DNA by transferring the methyl group from alkyl-DNA to its cysteine residues. At the same time Ada loses its activity. The methyl-Ada turns into a positive regulator of *alkA, aidB, alkB*, and itself as well. Methyl-Ada could recognize and bind onto the special region (AAAGCAAA) of *alkA* promoter, start transcription of *alkA*, and further complete repairing damage of other type alkylation, avoiding bacterial death due to damage of DNA alkylation[37-40]. The base excision repair could protect against the deleterious effects of DNA alkyl lesions. However, the activities of *alkA* gene must be balanced for optimal protection against the biological consequences of damaged DNA bases because inappropriate expression of this activity might have a detrimental consequence[41]. During infection of host, *Shigella spp.* probably suffers strong damage of alkyl in host. But alkylated DNA activates the adaptive response of *Shigella spp.* to host. Expression of *alkA* effectively repairs damage of DNA alkylation so that the killing-effect resulted from DNA damage could not carry out. Therefore, from this point of view, *in vivo*-induced-expression of *alkA* provides a significant safeguard for infection of *Shigella spp.* and is an essential gene for exhibiting *Shigella spp.* virulence.

Although there has been no report about the relationship between *alkA* and virulence of pathogens, it is known that a close relation lies between DNA methylation and bacterial virulence. Heithoff *et al.*[42] discovered that DNA adenine methylase (Dam) could regulate expression of at least 20 *in vivo*-induced genes and that Dam$^-$ *S. typhimurium* as a live vaccine had a protective role with no side-effect. *S. typhimurium* with over-expressing Dam also exhibited a significant virulence defect and a protective effect as an oral vaccine[43]. Similar results have also been obtained in *Yersinia pseudotuberculosis* and *Vibrio cholerae*[44]. Hereby, during infection expression of Dam could induce the expression of *in vivo*-induced genes, but its over-expression could also lead to damage of methylation and attenuation of pathogens. Thus a suitable level of DNA methylation might play a key role for pathogens to keep the virulence. From this point of view, *alkA* may be a virulence-related gene of pathogens. The hypothesis illustrating the relationship between DNA methylation damage and *alkA* gene is shown in Figure 6. Whether a regulatory relation exists between *alkA* and *dam* remains to be further confirmed. However, we believe that *alkA* is a new target for studying on molecular pathogenesis mechanism of *Shigella spp.* and construction of attenuated live vaccines.

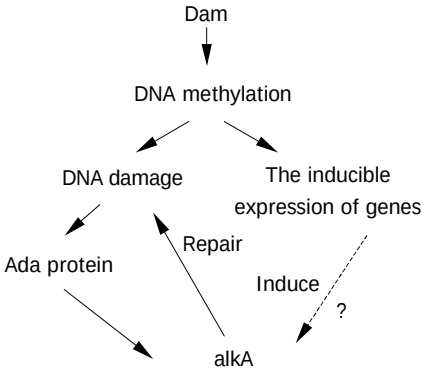

Figure 6 Hypothesis illustrating the relationship between *alkA* and damage of DNA methylation.

ACKNOWLEDGEMENTS

We thank Prof. Qi-Nong Ye and Dr Bao-Chang Fan for critical review of this manuscript. We also thank Miss Run-Yan Liu and Miss Hui-Ping Zhang for their help with experiments.

REFERENCES

1 **Sansonetti PJ**. Rupture, invasion and inflammatory destruction of the intestinal barrier by *Shigella*, making sense of prokaryote-eukaryote cross-talks. *FEMS Microbiol Rev* 2001; **25:** 3-14
2 **Fernandez MI**, Sansonetti PJ. *Shigella* interaction with intestinal epithelial cells determines the innate immune response in shigellosis. *Int J Med Microbiol* 2003; **293:** 55-67
3 **Yao X**, Wang HL, Shi ZX, Yan XY, Feng E, Yang BL, Huang LY. Identification of RanBMP interacting with *Shigella flexneri* IpaC invasion by two-hybrid system of yeast. *World J Gastroenterol* 2003; **9:** 1347-1351
4 **Handfield M**, Levesque RC. Strategies for isolation of *in vivo* expressed genes from bacteria. *FEMS Microbiol Rev* 1999; **23:** 69-91
5 **Mahan MJ**, Slauch JM, Mekalanos JJ. Selection of bacterial virulence genes that are specifically induced in host tissues. *Science* 1993; **259:** 686-688
6 **Young GM**, Miller VL. Identification of novel chromosomal loci affecting *Yersinia enterocolitica* pathogenesis. *Mol Microbiol* 1997; **25:** 319-328
7 **Staib P**, Kretschmar M, Nichterlein T, Kohler G, Michel S, Hof H, Hacker J, Morschhauser J. Host-induced, stage-specific virulence gene activation in *Candida albicans* during infection. *Mol Microbiol* 1999; **32:** 533-546
8 **Gahan CG**, Hill C. The use of listeriolysin to identify *in vivo* induced genes in the gram-positive intracellular pathogen *Listeria monocytogenes*. *Mol Microbiol* 2000; **36:** 498-507
9 **Lai YC**, Peng HL, Chang HY. Identification of genes induced *in vivo* during *Klebsiella pneumoniae* CG43 infection. *Infect Immun* 2001; **69:** 7140-7145
10 **Wu Y**, Lee SW, Hillman JD, Progulske-Fox A. Identification and testing of *Porphyromonas gingivalis* virulence genes with a pPGIVET system. *Infect Immun* 2002; **70:** 928-937
11 **Bartoleschi C,** Pardini MC, Scaringi C, Martino MC, Pazzani C, Bernardini ML. Selection of *Shigella flexneri* candidate virulence genes specifically induced in bacteria resident in host cell cytoplasm. *Cell Microbiol* 2002; **4:** 613-626
12 **Morohoshi F**, Hayashi K, Munkata N. *Bacillus subtilis alkA* gene encoding inducible 3-methyladenine DNA glycosylase is adjacent to the ada operon. *J Bacteriol* 1993; **175:** 6010-6017
13 **O'Rourke EJ**, Chevalier C, Boiteux S, Labigne A, Ielpi L, Radicella JP. A novel 3-methyladenine DNA glycosylase from *Helicobacter pylori* defines a new class within the endonuclease III family of base excision repair glycosylases. *J Biol Chem* 2000; **275:** 20077-20083
14 **Saparbaev M**, Mani JC, Laval J. Interactions of the human, rat, *Saccharomyces cerevisiae* and *Escherichia coli* 3-methyladenine-DNA glycosylases with DNA containing dIMP residues. *Nucleic Acids Res* 2000; **28:** 1332-1339
15 **Privezentzev CV**, Saparbaev M, Sambandam A, Greenberg MM, Laval J. AlkA protein is the third *Escherichia coli* DNA repair protein excising a ring fragmentation product of thymine. *Biochemistry* 2000; **39:** 14263-14268
16 **Mansfield C**, Kerins SM, McCarthy TV. Characterisation of Archaeglobus fulgidus AIKA hypoxanthine DNA glycosylase activity. *FEBS Lett* 2003; **540:** 171-175
17 **Rui X**, Xu Y, Wan H, Su G, Huang C. Construction of a stable and non-resistant bivalent vaccine candidate strain against *Shigella flexneri 2a* and *Shigella sonnei*. *Chin J Biotechnol* 1996; **12:** 89-97
18 **Sambrook J**, Friston E F, Maniatis T. Molecular Cloning: a Laboratory Manual. The 2end edition. New York: *Cold Spring Harbor Laboratory Press* 1989: 34-56, 237-261
19 **Roy S**, Biswas T. Murine splenocyte proliferation by porin of *Shigella dysenteriae type 1* and inhibition of bacterial invasion of HeLa cell by anti-porin antibody. *FEMS Microbiol lett* 1996; **141:** 25-29
20 **Niesel DW**, Chambers CE, Stockman SL. Quantitation of HeLa cell monolayer invasion by *Shigella* and *Salmonella* species. *J Clin Microbiol* 1985; **22:** 897-902
21 **Zhong QP**. Pathogenic effects of Opolysaccharide from *Shigella flexneri* strain. *World J Gastroenterol* 1999; **5:** 245-248
22 **Mallett CP**, VanDeVerg L, Collins HH, Hale TL. Evaluation of *Shigella* vaccine safety and efficacy in an intranasally challenged mouse model. *Vaccine* 1993; **11:** 190-196
23 **Van de Verg LL**, Mallett CP, Collins HH, Larsen T, Hammack C, Hale TL. Antibody and cytokine responses in a mouse pulmonary model of *Shigella flexneri* serotype 2a infection. *Infect Immun* 1995; **63:** 1947-1954
24 **Way SS**, Borczuk AC, Dominitz R, Goldberg MB. An essential role for gamma interferon in innate resistance to *Shigella flexneri* infection. *Infect Immun* 1998; **66:** 1342-1348
25 **Camilli A**, Mekalanos JJ. Use of recombinase gene fusions to identify *Vibrio cholerae* genes induced during infection. *Mol Microbiol* 1995; **18:** 671-683
26 **Hollis T**, Ichikawa Y, Ellenberger T. DNA bending and a flip-out mechanism for base excision by the helix-hairpin-helix DNA glycosylase, *Escherichia coli* AlkA. *EMBO J* 2000; **19:** 758-766
27 **Chiang SL**, Mekalanos JJ, Holden DW. *In vivo* genetic analysis of bacterial virulence. *Annu Rev Microbiol* 1999; **53:** 129-154
28 **Heithoff DM**, Conner CP, Hanna PC, Julio SM, Hentschel U, Mahan MJ. Bacterial infection as assessed by *in vivo* gene expression. *Proc Natl Acad Sci U S A* 1997; **94:** 934-939
29 **Wang J**, Mushegian A, Lory S, Jin S. Large-scale isolation of candidate virulence genes of *Pseudomonas aeruginosa* by *in vivo* selection. *Proc Natl Acad Sci U S A* 1996; **93:** 10434-10439
30 **Wang HL**, Feng EL, Lin Y, Liao X, Su GF. Construction of Δasd mutant of *Shigella flexneri* 2a strain T32. *Bull Acad Mil Med Sci* 2000; **24:** 81-87
31 **Murphy KC**. Use of bacteriophage lambda recombination functions to promote gene replacement in *Escherichia coli*. *J Bacteriol* 1998; **180:** 2063-2071
32 **Yu D**, Ellis HM, Lee EC, Jenkins NA, Copeland NG, Court DL. An efficient recombination system for chromosome engineering in *Escherichia coli*. *Proc Natl Acad Sci U S A* 2000; **97:** 5978-5983
33 **Hou S,** Chen X, Wang H, Tao M, Hu Z. Efficient method to generate homologous recombinant baculovirus genomes in *E. coli*. *Biotechniques* 2002; **32:** 783-784, 786, 788
34 **Murphy KC**, Campellone KG, Poteete AR. PCR-mediated gene replacement in *Escherichia coli*. *Gene* 2000; **246:** 321-330
35 **Loh T**, Murphy KC, Marinus MG. Mutational analysis of the MutH Protein from *Escherichia coli*. *J Biol Chem* 2001; **276:** 12113-12119
36 **Wang HL**, Feng EL, Shi ZX, Yao X, Su GF, Huang LY. Quick knockout of *Shigella flexneri* asd gene with Red system. *Bull Acad Mil Med Sci* 2002; **26:** 172-175
37 **Furuichi M**, Yu CG, Anai M, Sakumi K, Sekiguchi M. Regulatory elements for expression of the *alkA* gene in response to alkylating agents. *Mol Gen Genet* 1992; **236:** 25-32
38 **Landini P**, Busby SJ. Expression of the *Escherichia coli* ada regulon in stationary phase: evidence for rpoS-dependent negative regulation of *alkA* transcription. *J Bacteriol* 1999; **181:** 6836-6839
39 **Landini P**, Busby SJ. The *Escherichia coli* Ada protein can interact with two distinct determinants in the sigma70 subunit of RNA polymerase according to promoter architecture: identification of the target of Ada activation at the *alkA* promoter. *J Bacteriol* 1999; **181:** 1524-1529
40 **Saget BM**, Walker GC. The Ada protein acts as both a positive and a negative modulator of *Escherichia coli*'s response to methylating agents. *Proc Natl Acad Sci U S A* 1994; **91:** 9730-9734
41 **Wyatt MD**, Allan JM, Lau AY, Ellenberger TE, Samson LD. 3-methyladenine DNA glycosylases: structure, function, and biological importance. *BioEssays* 1999; **21:** 668-676
42 **Heithoff DM**, Sinsheimer RL, Low DA, Mahan MJ. An essential role for DNA adenine methylation in bacterial virulence. *Science* 1999; **284:** 967-970
43 **Dueger EL**, House JK, Heithoff DM, Mahan MJ. *Salmonella* DNA adenine methylase mutants elicit protective immune responses to homologous and heterologous serovars in chickens. *Infect Immun* 2001; **69:** 7950-7954
44 **Julio SM**, Heithoff DM, Provenzano D, Klose KE, Sinsheimer RL, Low DA, Mahan MJ. DNA adenine methylase is essential for viability and plays a role in the pathogenesis of *Yersinia pseudotuberculosis* and *Vibrio cholerae*. *Infect Immun* 2001; **69:** 7610-7615

Edited by Zhang JZ and Wang XL

P.O.Box 2345, Beijing 100023,China
Fax: +86-10-85381893
E-mail: wjg@wjgnet.com www.wjgnet.com

World J Gastroenterol 2003;9(12):2726-2731
World Journal of Gastroenterology
 ISSN 1007-9327

• BASIC RESEARCH •

Differentially expressed proteins of gamma-ray irradiated mouse intestinal epithelial cells by two-dimensional electrophoresis and MALDI-TOF mass spectrometry

Bo Zhang, Yong-Ping Su, Guo-Ping Ai, Xiao-Hong Liu, Feng-Chao Wang, Tian-Min Cheng

Bo Zhang, Yong-Ping Su, Guo-Ping Ai, Xiao-Hong Liu, Feng-Chao Wang, Tian-Min Cheng, Institute of Combined Injury of PLA, Third Military Medical University, Chongqing 400038, China
Supported by the National Natural Science Foundation of China, No.30230360
Correspondence to: Professor Yong-Ping Su, Institute of Combined Injury of PLA, Third Military Medical University, Gaotanyan Street 30, Chongqing 400038, China. mouse@mail.tmmu.com.cn
Telephone: +86-23-68752355 **Fax:** +86-23-68752279
Received: 2003-05-13 **Accepted:** 2003-06-12

Abstract

AIM: To identify the differentially expressed proteins involved in ionizing radiation in mice and to explore new ways for studying radiation-related proteins.

METHODS: Bal B/c mice grouped as sham-irradiation, 3 h and 72 h irradiation were exposed to 9.0Gy single dose of γ-irradiation. Intestinal epithelia were isolated from mice, and total proteins were extracted with urea containing solution. A series of methods were used, including two-dimensional electrophoresis, PDQuest 2-DE software analysis, peptide mass fingerprinting based on matrix-assisted laser desorption/ionization time of flight mass spectrometry (MALDI-TOF-MS) and SWISS-PROT database searching, to separate and identify the differential proteins. Western blotting and RT-PCR were used to validate the differentially expressed proteins.

RESULTS: Mouse intestine was severely damaged by 9.0 Gy γ-irradiation. Image analysis of two-dimensional gels revealed that averages of 638±39, 566±32 and 591±29 protein spots were detected in 3 groups, respectively, and the majority of these protein spots were matched. About 360 protein spots were matched between normal group and 3 h irradiation group, and the correlation coefficient was 0.78 by correlation analysis of gels. Also 312 protein spots matched between normal group and 72 h irradiation group, and 282 protein spots between 3 h and 72 h irradiation groups. Twenty-eight differential protein spots were isolated from gels, digested with trypsin, and measured with MALDI-TOF-MS. A total of 25 spots yielded good spectra, and 19 spots matched known proteins after database searching. These proteins were mainly involved in anti-oxidation, metabolism, signal transduction, and protein post-translational processes. Western-blotting confirmed that enolase was up-regulated by γ-irradiation. Up-regulation of peroxiredoxin I was verified by applying RT-PCR technique, but no change occurred in Q8VC72.

CONCLUSION: These differentially expressed proteins might play important roles when mouse intestine was severely injured by γ-irradiation. It is suggested that differential proteomic analysis may be a useful tool to study the proteins involved in radiation damage of mouse intestinal epithelia.

Zhang B, Su YP, Ai GP, Liu XH, Wang FC, Cheng TM. Differentially expressed proteins of gamma-ray irradiated mouse intestinal epithelial cells by two-dimensional electrophoresis and MALDI-TOF mass spectrometry. *World J Gastroenterol* 2003; 9(12): 2726-2731
http://www.wjgnet.com/1007-9327/9/2726.asp

INTRODUCTION

Since Wilkins and Williams first proposed the concept of "Proteome" in 1994[1], advances in the studies on proteome have made it possible to compare the total proteins of cells under different conditions on large scale. The proteomic strategy based on two-dimensional electrophoresis (2-DE) and mass spectrometry has been applied in a variety of studies[2,3].

Ionizing radiation is one of the main treatment modalities used in the management of pelvic cancer. Selective internal radiation therapy is a new method that can be used for patients given other routine therapies but without effects, and preoperative radiotherapy is effective and safe[4,5]. Although great success has been documented in cancer patients, certain side effects and complications have limited its applications in cancer radiotherapy. One of the major side effects of ionizing radiation is the depletion of normal cells along with cancer cells. For patients with pelvic cancer, a serious complication of radiotherapy is the radiation injury to small intestinal epithelium[6].

Small intestinal epithelium contains four major cell types: columnar cells, goblet cells, stem cells, and Paneth cells[7]. Intestinal stem cells, which are most sensitive to ionizing radiation, are located in the crypt portion of the intestine. The impact of ionizing radiation on intestinal stem cells can be detected at a dose as low as 0.05 Gy[8]. One of the early morphological changes that occur in mouse crypt cells upon treatment with ionizing radiation is the occurrence of apoptosis within 2-3 h after administration of the treatment. This apoptotic death can be visualized under both light and electron microscopy. Because of the emigration of crypt cells from the villi and the decreased proliferation of intestinal stem cells, the crypts become noticeably smaller 14-15 h after radiation[9]. The villous epithelial cells begin to decline from about the second day post radiation, and the villi become shorter. If a crypt contains viable clonogenic cells, the crypt begins to replenish its cellular population in the next few days.

Ionizing radiation can generate a series of biochemical events inside the cell. Free radicals produced from intercellular water interact with DNA and proteins, thus inducing inactivation of these macromolecules. It has been demonstrated that ionizing radiation can induce gene expression of intestinal epithelia[10,11]. As genes encode proteins, we can deduce that proteins of intestinal epithelia can be induced by ionizing radiation[12]. These proteins are associated with many important cellular processes including DNA repair, apoptosis, cell cycle control, and oxidative stress response[13,14]. With accumulating evidences in the literature that new proteins are implicated in

radiation response, the molecular mechanism underlying radiation response of the small intestine remains unknown. Our aim was to identify these proteins in the early stage of radiation injury. To achieve this purpose, we adopted comparative proteome approach to identify the mouse proteins whose expression was regulated by ionizing radiation. The proteomes of sham-irradiated mice were compared with those of irradiated mice 3 h and 72 h post-irradiation. The differentially displayed proteins were subjected to MALDI-TOF-MS to establish the identity. We also confirmed some differential proteins by Western blot and RT-PCR technique.

MATERIALS AND METHODS

Animal model and irradiation

A total of 15 male Bal b/c mice, 58-62 days of age, weighing 20-24 g, at the time of irradiation, were housed in conventional cages with free access to drinking water and standard chow. A pathogen-free environment with controlled humidity and temperature was maintained. These mice were randomly divided into 3 groups: one group received sham-irradiation (n=5), the other two groups received single dose of 9.0 Gy (n=5). The dose was chosen based on the data from our previous experiments. Whole-body irradiation was performed with a ^{60}Co-source at a dose rate of 0.78 Gy/min. The irradiated mice were killed 3 h and 72 h post-radiation, and intestines were removed and histological sections were made according to reference[15].

Isolation of mouse intestinal epithelia

Mouse intestinal epithelial cells were isolated according to the method described by Bjerknes[16] with slight modifications. In brief, animals were sacrificed, and the small intestine was removed and perfused with 30 ml of cold PBS. Then it was gently everted using a glass rod and flushed by PBS with its two ends enveloped. The swollen intestine was transferred to a flask, and immersed into warm PBSE solution (PBS containing EDTA 1 mmol/L), and shaken at 150 cycles per min. After shaken for 5 min, the intestine was transferred to another clean flask with warm PBSE solution, and vibrated for another 5 min. The shed intestinal epithelial cells were centrifuged at 500×g for 10 min, and prepared for protein extraction.

Protein extraction

The cell pellet harvested as described above was then washed in ice-cold PBS 3 times. Cells were resuspended in cold PBS, and counted. Total proteins were extracted from 10^7 cells with an appropriate volume (200 μl) of lysis buffer containing 7 mol/L urea, 2 mol/L thiourea, 65 mmol/L DTT, 2 % CHAPS, 2 mmol/L PMSF, 0.5 % IPG buffer, and protease inhibitor mixture. The extraction mixture was sonicated using a MSE 100 ultrasonic probe, and then centrifuged at 12 000×g for 20 min. After transferred to a clean tube, the supernatant was stored at -70 ℃ as aliquots. The protein concentration was determined using Bradford dye-binding assay with bovine serum albumin as the standard.

Two-dimensional electrophoresis

Two-dimensional electrophoresis was carried out by using the Mini-PROTEIN 2-D apparatus (Bio-Rad). For isoelectric focusing (IEF), precast IPG strips (Immobiline DryStrips, Amersham Pharmacia Biotech, Uppsala, Sweden) were used. Samples were applied via rehydration of IPG strips in sample solution for more than 12 h. Before application, the samples were diluted to a total volume of 350 μl with rehydration buffer (8 mol/L urea, 2 % CHAPS, 0.5 % IPG buffer, 0.3 % DTT, and a trace of bromophenol blue). Protein sample (1 000 μg) was loaded onto an 18 cm IPG strip (pH3-10, linear), and isoelectric focusing was run for 45 KVh at 20 ℃. To improve the sample entry, low voltage (100V) was applied for 2 h at the beginning. After IEF separation, the IPG strips were immediately equilibrated for 2×15 min with buffer (50 mmol/L Tris-HCl, pH6.8, 6 mol/L urea, 30 % glycerol, 2 % SDS, and a trace of bromophenol blue). DTT (2 %) was added in the first step, and iodoacetamide in the second step. For the second dimensional separation, the concentration of homogeneous SDS-polyacrylamide gels was 13 %. The proteins in the equilibrated strips were run at a current of 30 mA/strip for about 5 h until the bromophenol dye reached the bottom of the gels. Molecular mass marker was run on the same gel to determine the relative molecular masses of the proteins.

Image processing and analysis

After electrophoresis, the resolved proteins in 2-DE gels were fixed in ethanol/acetic acid/water (4/1/5) for at least 1 h, and then visualized by Coomassie blue R-250. The gels were scanned (Gel Doc 2000, Bio-Rad), and the images were processed with PDQuest software (Ver 7.0, Bio-Rad). To determine the variation, three gels were prepared for each sample. The computer analysis allowed automatic detection and quantification of protein spots, as well as matching between control gel and treatment. Protein spots that were new, absent, up- and down-regulated, were simultaneously displayed on the same image using the gels of sham-irradiated sample as the reference.

Protein identification by MALDI-TOF-MS

The differential protein spots were exactly excised from the gels. Gel pieces were destained with 50 % acetonitrile for several times until Coomassie blue was invisible. Then gel pieces were dried in a vacuum centrifuge. The shrinking gel pieces were re-swollen with 5 μl of protease solution (trypsin at 0.05 μg/μl in digestion buffer of 25 mmol/L NH4HCO3). Additional 50 μl of digestion buffer was added into the gel piece. Digestion was performed overnight at 37 ℃. Next, 50 μl of 5 % TFA solution was added to the gel piece, followed by incubation for 60 min at 42 ℃. The supernatant was collected and concentrated using ZipTip pipette tips (Millipore) according to the manufacturer' s instructions. The samples were mixed on the MALDI target with matrix DBA solution. Peptide mass maps were generated by applying Biosystems Voyager 6192 MALDI-TOF-Mass Spectrometry (ABI, USA). Database searching was performed using monoisotopic peptide masses obtained from MALDI-TOF-MS. The SWISS-PROT and TrEMBL database was searched with PeptIdent software (http://www.expasy.org/tools/pep-tident.html). Peptide masses were assumed to be monoisotopic masses and cystines were assumed to be iodoacetamided. The peptide mass tolerance was set to 0.2Da, and the maximum of missed cleavage site was set to 1. Species was set as mouse.

Immunoblotting

Total proteins were separated on 12 % SDS-polyacrylamide gel, and then transferred to nitrocellulose membranes. After blocked for 1 h in the Tris/NaCl (50 mmol/L Tris-HCl, 200 mmol/L NaCl, 0.05 % Tween-20, pH7.4) containing 2 % BSA, membranes were probed with the goat anti-mouse Enolase polyclonal antibody (Santa Cruz, USA). Immunoreactive bands were visualized with a solution containing 1 mg/ml DAB and 0.01 % H_2O_2.

Semi-quantitative RT-PCR

Total RNAs were isolated from mouse intestinal epithelia with

TriPure isolation reagent (Roche, USA) according to the manufacturer' s descriptions. Peroxiredoxin I, Q72VC8, and GAPDH transcripts were determined by reverse transcriptase-polymerase chain reaction (RT-PCR) with RNA PCR kit (Takara, China). The primers for peroxiredoxin I are 5' GTTCTCACGGCTCTTTCTGTTT-3' and 5' CTTCTGGCTGCTCAATGCTG-3', Q8VC72 5' TGGACAAAGCCTTCATAGCA-3' and 5' CCTGGCAGAAACCACAGTAGA-3', GAPDH 5' ACCACAGTCCATGCCATCAC-3' and 5' TCCACCACCCTGTTGCTGTA-3'. The amplification was performed with one denaturing cycle at 94 ℃ for 5 min, then 25-27 cycles at 94 ℃ for 40 s, at 55 ℃ for 40 s, at 72 ℃ for 40 s, and one final extension at 72 ℃ for 5 min. RT-PCR products were run on 1.2 % agarose gel.

RESULTS

Histological changes of mouse intestine after radiation

Mice after 9.0 Gy irradiation died within 4-6 days post-radiation, with the intestines severely injured. As shown in Figure 1, the histological changes after irradiation were in agreement with our previous experiments. Though the height of villi and crypts remained unchanged 3 h post-radiation, cell division of intestinal epithelia ceased, and the intestines were severely injured morphologically. Moreover, the height of intestinal crypts was obviously increased 72 h post-radiation, with villi decreased. This indicated that many survival epithelial cells proliferated.

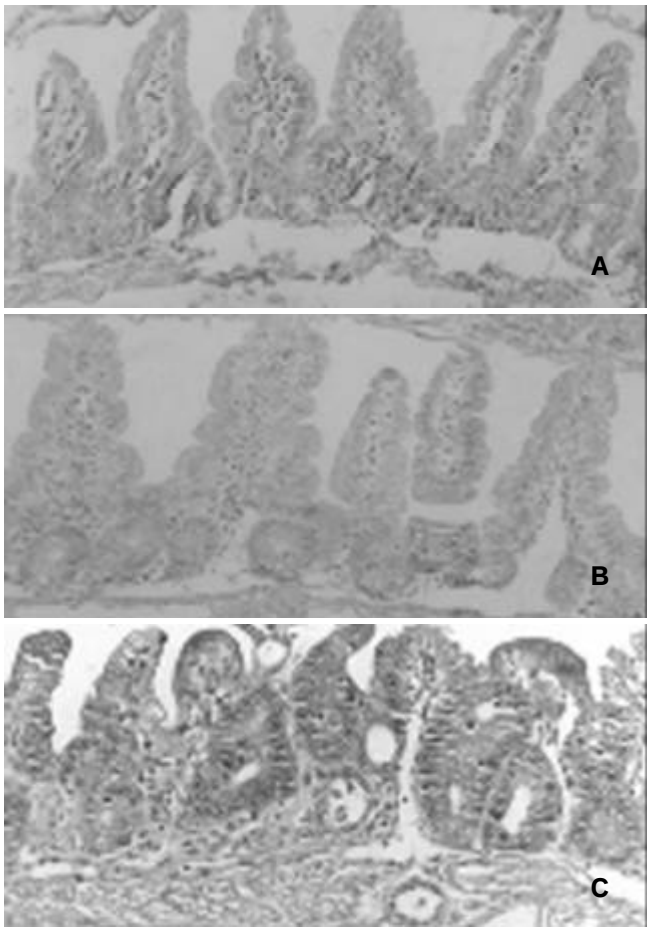

Figure 1 Histological changes in crypts following irradiation. A: Unirradiated controls (×100). B: 3 hours after a single dose of 9.0 Gy (×100). Villi and crypts remained unchanged, but cell division of intestinal epithelia ceased. C: 3 days after a single dose of 9.0 Gy (×100).

Two-dimensional electrophoresis and image analysis of mouse intestinal epithelia

To study the different proteins involved in ionizing radiation, we applied 2-DE to analyze the proteomic alteration of mouse intestinal epithelia. The 2-D patterns were highly reproducible since each experiment was performed in triplicate and produced similar results. Figure 2 showed the representative 2-D maps of the mouse intestinal epithelia. Image analysis of 2-D gels revealed that averages of 638±39, 566±32 and 591±29 protein spots were detected in 3 groups respectively, and the majority of these protein spots were matched. About 360 protein spots were matched between normal group and 3 h irradiation group, and the correlation coefficient was 0.78 by correlation analysis of gels. Three hundred and twelve protein spots were matched between normal group and 72 h irradiation group, and 282 protein spots between 3 h and 72 h irradiation groups. The unmatched spots represented those induced by irradiation as new or absent proteins, which were the main alteration of proteome.

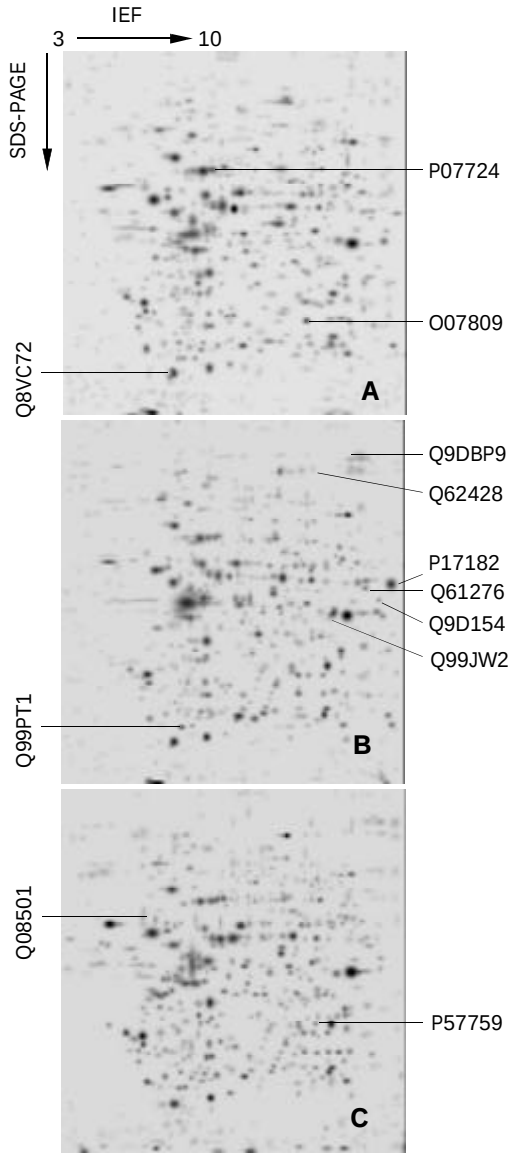

Figure 2 Two-dimensional electrophoresis maps. A: normal intestinal epithelial cells, B: 3 h irradiated epithelial cells, C: 72 h post-radiation. Number indicated proteins were summarized in Table 2.

Identification of proteins from 2-D gel spots

Out of a total of 28 spots excised from the gels, 25 spots yielded

nearly perfect MALDI spectra. A total of 19 spots were preliminarily identified by peptide mass fingerprinting. Figure 3 showed the typical peptide mass fingerprinting of Spot No. 11, whose peptides matched the mouse peroxiredoxin I. This spot was up-regulated by ionizing radiation. The identified proteins were summarized in Table 1. These proteins were involved in cellular process of anti-oxidation, metabolism, and protein post-translational processes. Other proteins, such as cellular structural proteins and hypothetic proteins derived from nucleic acid sequences, were also altered after irradiation. We also found, 6 spots with good MALDI spectra were returned with inconclusive match results, suggesting that they might be unknown proteins.

Induction of enolase by radiation

A protein spot was preliminarily identified as Enolase by

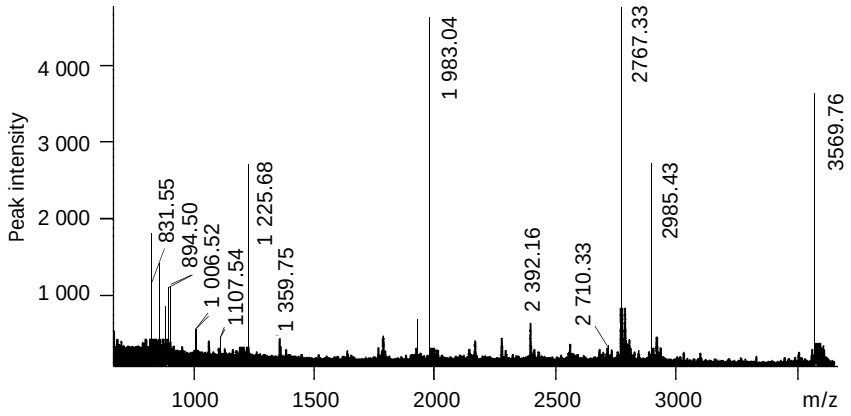

Figure 3 MALDI-TOF-MS spectrum of spot P35700 in 2-DE map. MS spectrum of peptide mixture was obtained from a typical in-gel digestion of the 2-DE separated protein.

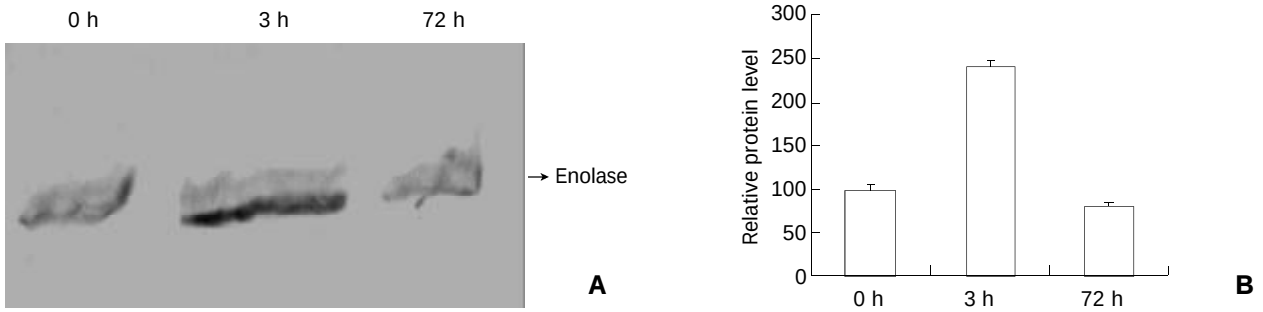

Figure 4 Western blot analysis of Enolase after radiation. A: Protein samples, obtained at indicated time after radiation, were separated by SDS-PAGE, and immunoblotted with corresponding antibody. Equal amounts of total proteins were applied to each lane. B: Relative protein level of Enolase was determined by quantitating the intensity of Enolase bands with a densitometer.

Table 1 Result of PeptIdent search of differential protein spots derived from BALB/c mice

Spot No.	Swiss-prot accession	Match rate	Theoretical pI/Mw	Sequence covered(%)	Protein name
N1	O08709	7/23	5.70/24871	28	Antioxidant protein 2
N2	P07724	17/39	5.53/65892	37.2	Serum albumin.
N3	Q8VC72	8/13	5.19/18573	58.9	Hypothetical 18.6 kDa protein
R1	Q9D154	8/28	5.85/42574	24.8	Serine protease inhibitor EIA
R2	Q99PT1	6/26	5.12/23391	27.0	Rho GDP-dissociation inhibitor 1
R3	Q61276	6/29	6.0/41693	26.0	A-X actin
R4	Q99JW2	9/31	5.9/45781	25.0	RIKEN cDNA 1110014J22 gene
R5	Q62428	15/27	5.72/92669	29.2	Villin 1
R6	Q9DBP9	12/38	6.2/105834	15.0	homolog to LON protease
R7	P17182	12/52	6.36/47009	36.7	Alpha enolase
R8	Q08501	5/20	5.00/68241	15.0	Prolactin receptor precursor
R9	P57759	5/17	5.74/25721	27.6	ERP29
R10	P19157	9/22	7.70/23609	48.8	Glutathione S-transferase P2
R11	Q9R0V2	6/40	4.86/21927	32.7	Truncated annexin IV.
R12	P35700	13/26	8.3/22177	33.0	Peroxiredoxin I
R13	P09041	5/33	6.6/44912	27.0	Phosphoglycerate kinase, testis specific
R14	P14701	5/15	4.80/19462	25.6	Translationally controlled tumor protein (TCTP)
R15	12847100[a]	8/14	6.9/28869	33.0	Aldo-keto reductase family 1, member A4
R16	P17182	13/35	6.36/47009	50.4	Alpha enolase

a: This protein was recorded in NCBI database.

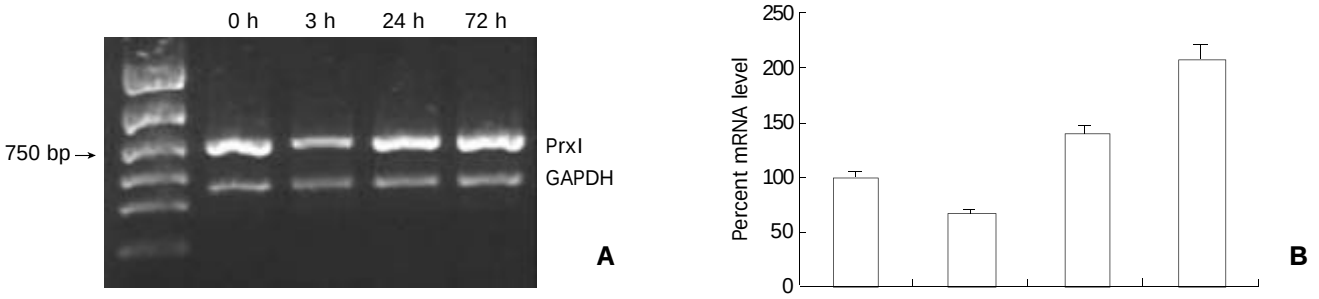

Figure 5 Semi-quantitative RT-PCR analysis of peroxiredoxin I. A: PCR product run on an agarose gel. The upper band represented peroxiredoxin I (750 bp), and the lower band represented GAPDH (450 bp). B: Relative abundance of the mRNA of peroxiredoxin I was normalized by GAPDH.

Figure 6 Semi-quantitative RT-PCR analysis of Q8VC72. RNA samples were prepared from mouse intestinal epithelia at indicated time. Left: The band represents Q8VC72 (461 bp). Right: The band represents GAPDH (450 bp). The expression of Q8VC72 remained unchanged after radiation.

MALDI-TOF-MS (Table 1), which was significantly increased in 3 h radiation group. Immunoblotting showed that Enolase was significantly up-regulated (2.1 fold more than the normal control, $P<0.01$, Figure 4). This confirmed our data of 2-D electrophoresis.

Induction of peroxiredoxin I and Q8VC72 by radiation

Semi-quantitative RT-PCR was used to detect the gene expression of peroxiredoxin I and Q8VC72. Total RNAs were isolated from normal and irradiated mouse intestine. The expression of peroxiredoxin I was markedly induced by radiation (Figure 5), using GAPDH as standard. However, the expression of Q8VC72 remained unchanged after radiation (Figure 6). This indicated that Q8VC72 might be a false-positive result.

DISCUSSION

A variety of techniques, including differential hybridization, differential display PCR, serial analysis of gene expression (SAGE), and gene array, have been used to identify the genes whose expression is selectively altered after radiation[17-19]. Recently, a new method termed gene trap strategy has also been used to predict radiation responsive genes[20]. All these methods are used to analyze the mRNA expression levels of radiation responsive genes. As mRNAs are easy to be degraded after transcription, and some are selectively translated, the quality and quantity of proteins do not correlate with that of mRNAs. Here, we applied 2-D electrophoresis to analyze the proteins involved in radiation response at protein level. As a large-scale screening of proteins, proteomics has been driven forward by the advent of the genome era[21], and it has become advantageous in analyzing total proteins of cells or tissues.

Many proteins have been demonstrated to be involved in radiation response among mammalians[22,23]. These proteins are associated with many important cellular processes such as DNA repair, apoptosis, signal transduction, and oxidative stress. Among the 19 preliminarily identified proteins, three spots belong to oxidative stress response proteins, i.e., peroxiredoxin I, glutathione S-transferase P2, and antioxidant protein 2. Radiation injuries are manifested as a result of increased production of reactive oxygen species (ROS), such as O_2, OH^-, and H_2O_2. These substances can induce the cellular antioxidant defense enzymes such as superoxide dismutase and glutathione peroxidase. In this study, peroxiredoxin I and glutathione S-transferase P2 were up-regulated by ionizing radiation, while antioxidant protein 2 was down-regulated. These proteins have been demonstrated to be involved in radiation[24-26]. Peroxiredoxin I is involved in the redox regulation of cells, such as reducing peroxides with reducing equivalents through the thioredoxin system but not from glutaredoxin. The function of glutathione S-transferase P2 has been found in conjugation of reduced glutathione to a large number of exogenous and endogenous hydrophobic electrophiles[27]. Antioxidant protein 2, also named 1-Cys peroxiredoxin, reduces H_2O_2 and phospholipid hydroperoxides. Our data confirmed the alteration of oxidative stress proteins with the exception of antioxidant protein 2. However, further studies will be performed to determine the mechanism as to why antixoxidant protein 2 does not play a critical role in ionizing radiation of small intestinal epithelial cells.

Using the proteomic strategy, we detected an interesting protein of ERP29 involved in ionizing radiation. ERP29 was first cloned from rat enamel cells, which had limited homology with protein disulfide isomerase and its cognate[28]. In this work, it was upregulated with ionizing radiation *in vivo*. ERP29 played an important role in the process of secretory proteins in the ER. Some researchers found that it played a role as a chaperone in protein folding[29,30]. The relationship between ERP29 and ionizing radiation has not yet been clarified, so it is worthy of further studying. In addition, some metabolic enzymes and hypothetical proteins, which were derived from nucleic acid sequences, were also found in this differential system. Their roles in ionizing radiation are unclear. Further researches are needed to draw precise conclusions. These data of hypothetical proteins suggest that these hypothetical proteins are expressed in intestinal epithelium indeed.

In brief, we compared the proteomics of mouse intestinal

epithelial cells with its irradiated counterparts *in vivo*. This strategy provides an efficient resolution to analyze radiation related proteins directly at protein level. The preliminarily identified proteins will be further studied in order to determine the cell signaling and molecular mechanisms of gene expression in radiation responses. This proteomic technique may contribute to the elucidation of the molecular mechanism of radiation damage, and can be applied in other research work as a useful tool.

REFERENCES

1 **Swinbanks D**. Government backs proteome proposal. *Nature* 1995; **378**: 653

2 **Xiong XD**, Xu LY, Shen ZY, Cai WJ, Luo JM, Han YL, Li EM. Identification of differentially expressed proteins between human esophageal immortalized and carcinomatous cell lines by two-dimensional electrophoresis and MALDI-TOF-mass spectrometry. *World J Gastroenterol* 2002; **8**: 777-781

3 **Fang DC**, Wang RQ, Yang SM, Yang JM, Liu HF, Peng GY, Xiao TL, Luo YH. Mutation and methylation of hMLH1 in gastric carcinomas with microsatellite instability. *World J Gastroenterol* 2003; **9**: 655-659

4 **Liu LX**, Zhang WH, Jiang HC. Current treatment for liver metastases from colorectal cancer. *World J Gastroenterol* 2003; **9**: 193-200

5 **Sun XN**, Yang QC, Hu JB. Pre-operative radiochemotherapy of locally advanced rectal cancer. *World J Gastroenterol* 2003; **9**: 717-720

6 **Smith DH**, DeCosse JJ. Radiation damage to the small intestine. *World J Surg* 1986; **10**: 189-194

7 **MacNaughton WK**. Review article: new insights into the pathogenesis of radiation- induced intestinal dysfunction. *Aliment Pharmacol Ther* 2000; **14**: 523-528

8 **Potten CS**, Owen G, Roberts SA. The temporal and spatial changes in cell proliferation within the irradiated crypts of the murine small intestine. *Int J Radiat Biol* 1990; **57**: 185-199

9 **Potten CS**. A comprehensive study of the radiobiological response of the murine (BDF1) small intestine. *Int J Radiat Biol* 1990; **58**: 925-973

10 **Somosy Z**, Horvath G, Telbisz A, Rez G, Palfia Z. Morphological aspects of ionizing radiation response of small intestine. *Micron* 2002; **33**: 167-178

11 **Hauer-Jensen M**, Richter KK, Wang J, Abe E, Sung CC, Hardin JW. Changes in transforming growth factor beta1 gene expression and immunoreactivity levels during development of chronic radiation enteropathy. *Radiat Res* 1998; **150**: 673-680

12 **Subramanian V**, Meyer B, Evans GS. The murine Cdx1 gene product localises to the proliferative compartment in the developing and regenerating intestinal epithelium. *Differentiation* 1998; **64**: 11-18

13 **Picard C**, Wysocki J, Fioramonti J, Griffiths NM. Intestinal and colonic motor alterations associated with irradiation-induced diarrhoea in rats. *Neurogastroenterol Motil* 2001; **13**: 19-26

14 **Dorr W**, Hendry JH. Consequential late effects in normal tissues. *Radiother Oncol* 2001; **61**: 223-231

15 **Jensen MH**, Sauer T, Devik F, Nygaard K. Late changes following single dose roentgen irradiation of rat small intestine. *Acta Radiol Oncol* 1983; **22**: 299-303

16 **Bjerknes M**, Cheng H. Methods for the isolation of intact epithelium from the mouse intestine. *Anat Rec* 1981; **199**: 565-574

17 **Hartmann KA**, Modlich O, Prisack HB, Gerlach B, Bojar H. Gene expression profiling of advanced head and neck squamous cell carcinomas and two squamous cell carcinoma cell lines under radio / chemotherapy using cDNA arrays. *Radiother Oncol* 2002; **63**: 309-320

18 **Amundson SA**, Bittner M, Meltzer P, Trent J, Fornace AJ Jr. Induction of gene expression as a monitor of exposure to ionizing radiation. *Radiat Res* 2001; **156**(5 Pt 2): 657-661

19 **Liu LX**, Jiang HC, Liu ZH, Zhou J, Zhang WH, Zhu AL, Wang XQ, Wu M. Integrin gene expression profiles of human hepatocellular carcinoma. *World J Gastroenterol* 2002; **8**: 631-637

20 **Vallis KA**, Chen Z, Stanford WL, Yu M, Hill RP, Bernstein A. Identification of radiation- responsive genes *in vitro* using a gene trap strategy predicts for modulation of expression by radiation *in vivo*. *Radiat Res* 2002; **157**: 8-18

21 **Yanagida M**. Functional proteomics; current achievements. *J Chromatogr B Analyt Technol Biomed Life Sci* 2002; **771**: 89-106

22 **Potten CS**, Booth C. The role of radiation-induced and spontaneous apoptosis in the homeostasis of the gastrointestinal epithelium: a brief review. *Comp Biochem Physiol B Biochem Mol Biol* 1997; **118**: 473-478

23 **Johnston MJ**, Robertson GM, Frizelle FA. Management of late complications of pelvic radiation in the rectum and anus: a review. *Dis Colon Rectum* 2003; **46**: 247-259

24 **Lee K**, Park JS, Kim YJ, Soo Lee YS, Sook Hwang TS, Kim DJ, Park EM, Park YM. Differential expression of Prx I and II in mouse testis and their up-regulation by radiation. *Biochem Biophys Res Commun* 2002; **296**: 337-342

25 **Mittal A**, Pathania V, Agrawala PK, Prasad J, Singh S, Goel HC. Influence of Podophyllum hexandrum on endogenous antioxidant defence system in mice: possible role in radioprotection. *J Ethnopharmacol* 2001; **76**: 253-262

26 **Lee YS**, Lee MJ, Lee M, Jang J. Susceptibility to the induction of glutathione S-transferase positive hepatic foci in offspring rats after gamma-ray exposure during gestation. *Oncol Rep* 2000; **7**: 387-390

27 **Strange RC**, Spiteri MA, Ramachandran S, Fryer AA. Glutathione-S-transferase family of enzymes. *Mutat Res* 2001; **482**: 21-26

28 **Hubbard MJ**, McHugh NJ, Carne DL. Isolation of ERp29, a novel endoplasmic reticulum protein, from rat enamel cells evidence for a unique role in secretory-protein synthesis. *Eur J Biochem* 2000; **267**: 1945-1957

29 **Sargsyan E**, Baryshev M, Szekely L, Sharipo A, Mkrtchian S. Identification of ERp29, an endoplasmic reticulum lumenal protein, as a new member of the thyroglobulin folding complex. *J Biol Chem* 2002; **277**: 17009-17015

30 **Kwon OY**, Park S, Lee W, You KH, Kim H, Shong M. TSH regulates a gene expression encoding ERp29, an endoplasmic reticulum stress protein, in the thyrocytes of FRTL-5 cells. *FEBS Lett* 2000; **475**: 27-30

Edited by Ma JY

P.O.Box 2345, Beijing 100023,China
Fax: +86-10-85381893
E-mail: wjg@wjgnet.com www.wjgnet.com

World J Gastroenterol 2003;9(12):2732-2736
World Journal of Gastroenterology
 ISSN 1007-9327

• BASIC RESEARCH •

Heterologous expression of human cytochrome P450 2E1 in HepG2 cell line

Jian Zhuge, Ye Luo, Ying-Nian Yu

Jian Zhuge, Ye Luo, Ying-Nian Yu, Department of Pathophysiology, School of Medicine, Zhejiang University, Hangzhou 310031, Zhejiang Province, China
Supported by National Natural Science Foundation of China, No. 39670801 and Natural Science Foundation of Zhejiang Province, No. 396467
Correspondence to: Professor Ying-Nian Yu, Department of Pathophysiology, School of Medicine, Zhejiang University, Hangzhou 310031, Zhejiang Province, China. ynyu@mail.hz.zj.cn
Telephone: +86-571-87217149 **Fax:** +86-571-87217149
Received: 2003-06-05 **Accepted:** 2003-07-24

Abstract

AIM: Human cytochrome P-450 2E1 (CYP2E1) takes part in the biotransformation of ethanol, acetone, many small-molecule substrates and volatile anesthetics. CYP2E1 is involved in chemical activation of many carcinogens, procarcinogens, and toxicants. To assess the metabolic and toxicological characteristics of CYP2E1, we cloned *CYP2E1* cDNA and established a HepG2 cell line stably expressing recombinant CYP 2E1.

METHODS: Human *CYP2E1* cDNA was amplified with reverse transcription-polymerase chain reaction (RT-PCR) from total RNAs extracted from human liver and cloned into pGEM-T vector. The cDNA segment was identified by DNA sequencing and subcloned into a mammalian expression vector pREP9. A transgenic cell line was established by transfecting the recombinant plasmid of pREP9-CYP2E1 to HepG2 cells. The expression of CYP2E1 mRNA was validated by RT-PCR. The enzyme activity of CYP2E1 catalyzing oxidation of 4-nitrophenol in postmitochondrial supernate (S9) fraction of the cells was determined by spectrophotometry. The metabolic activation of HepG2-CYP2E1 cells was assayed by *N*-nitrosodiethylamine (NDEA) cytotoxicity and micronucleus test.

RESULTS: The cloned *CYP2E1* cDNA segment was identical to that reported by Umeno *et al* (GenBank access No. J02843). HepG2-CYP2E1 cells expressed CYP2E1 mRNA and had 4-nitrophenol hydroxylase activity (0.162±0.025 $nmol \cdot min^{-1} \cdot mg^{-1}$ S9 protein), which were undetectable in parent HepG2 cells. HepG2-CYP2E1 cells increased the cytotoxicity and micronucleus rate of NDEA in comparison with those of HepG2 cells.

CONCLUSION: The cDNA of human *CYP2E1* can be successfully cloned, and a cell line, HepG2-CYP2E1, which can efficiently express mRNA and has CYP2E1 activity, is established. The cell line is useful for testing the cytotoxicity, mutagenicity and metabolism of xenobiotics, which may possibly be activated or metabolized by CYP2E1.

Zhuge J, Luo Y, Yu YN. Heterologous expression of human cytochrome P450 2E1 in HepG2 cell line. *World J Gastroenterol* 2003; 9(12): 2732-2736
http://www.wjgnet.com/1007-9327/9/2732.asp

INTRODUCTION

Cytochrome P450 2E1 (CYP2E1) is the only member of the CYP2E subfamily in humans. Approximately 7 % of the liver CYP content consists of CYP2E1, although individual variation of the level of hepatic CYP2E1 expression can be existed by an order of magnitude. CYP2E1 is also expressed in a number of extrahepatic tissues including the lungs[1] and brain[2]. CYP2E1 takes part in the biotransformation of ethanol, acetone, and many small-molecule substrates such as halogenated hydrocarbons (1,1,1-trichlorethane, 1,2-dichloropropane, carbon tetrachloride, chloroform, ethylene dibromide, ethylene dichloride, halothane, methylchloride, methylene dichloride, vinylchloride and trichloroethylene, most of which are hepatotoxic), acetaldehyde, benzene, and styrene. It is known for its ability to metabolize volatile anesthetics such as halothane, enflurane, isoflurane, and sevoflurane, acetaminophen, phenacetin and chlorzoxazone. Another group of CYP2E1 substrates are nitrosamines. CYP2E1 is involved in chemical activation of many carcinogens, procarcinogens, and toxicants[3-5].

Genetically engineered mammalian cells expressing CYP subtypes have provided new tools for investigations of the metabolism and CYP-mediated metabolic activation of chemicals. The stable expression system of CYP in cells has made it possible to evaluate the relative risk of a chemical in toxicological testing *in vitro*[6,7]. Human CYP1A1[8], CYP2B6[8], CYP2A6[9], CYP3A4[10], CYP2C9[11], CYP2C18[12] and a phase II metabolism enzyme UDP-glucuronosyltransferase, UGT1A9[13] have been stably expressed in Chinese hamster lung CHL cells in our laboratory. Among the human hepatic cell lines, HepG2 derived from a human liver tumor has been characterized to retain many xenobiotic-metabolizing activities as compared to fibroblasts. Therefore, HepG2 cell is useful in prediction of the metabolism and cytotoxicity of chemicals in human liver[14]. But it does not produce significant amounts of CYP[15,16]. Yoshitomi *et al*[17] have established in HepG2 cells stable expression of a series of human CYP subtypes, such as CYP1A1, CYP1A2, CYP2A6, CYP2B6, CYP2C8, CYP2C9, CYP2C19, CYP2D6, CYP2E1 and CYP3A4.

In this study, human *CYP2E1* cDNA was amplified by reverse transcription-polymerase chain reaction (RT-PCR), and a transgenic cell line HepG2-CYP2E1 stably expressing CYP2E1 was established to assess the metabolic and toxicological characteristics of CYP2E1.

MATERIALS AND METHODS

Materials

Restriction endonucleases, Moloney murine leukemia virus (M-MuLV) reverse transcriptase were supplied by MBI Fermentas AB, Lithuania. PCR primers, DNA sequence primers, random hexamer primers, and dNTPs were synthesized or supplied by Shanghai Sangon Biotechnology Corp. Expand fidelity PCR system and NADPH were from Roche Molecular Biochemicals. DNA sequencing kit was purchased from Perkin-Elmer Co. The TRIzol reagent, G418, Dulbecco' s modified Eagle' s medium (DMEM) and newborn

bovine calf sera were from Gibco. Diethyl pyrocarbonate (DEPC), MTT, and *N*-nitrosodiethylamine (NDEA) were purchased from Sigma Chemical Co. T4 DNA ligase and pGEM-T vector system were from Promega. 4-nitrophenol and *p*-nitrocatechol were from Tokyo Kasei Kogyo Co. Ltd, Japan. Other chemical reagents used were of analytical purity from the commercial sources.

Methods

Cloning of human CYP2E1 cDNA from human liver Total RNA was extracted from a surgical specimen of human liver with TRIzol reagent according to the manufacture' s instructions. RT-PCR amplifications were described before, using Expand fidelity PCR system[11]. Two specific 27 mer oligonucleotide PCR primers were designed according to the mRNA sequence of CYP2E1 reported by Song *et al*[18] (GenBank access No. J02625). The sense primer corresponding to base position -8 to 19 was 5' -AGGGTACCATGTCTGCCCTCGGAGTGA-3' , with a restriction site of *Kpn* I (underlined). The anti-sense primer, corresponding to the base position from 1 507 to 1 534, was 5' -ACAATTTGAAAGCTTGTTTGAAAGCGG-3' , with a restriction site of *Hin*d III (underlined). The anticipated PCR product was 1 542 bp in length. PCR was performed at 94 ℃ for 2 min, then 35 cycles at 94 ℃ for 60 s, at 62 ℃ for 60 s, at 72 ℃ for 2 min, and extension at 72 ℃ for 10 min. An aliquot (10 μL) from PCR was subjected to electrophoresis in a 1 % agarose gel stained with ethidium bromide.

Construction of recombinant pGEM-CYP2E1 and sequencing of CYP2E1 cDNA The PCR products were ligated with a pGEM-T vector, and transformed to *E. coli* DH5α. *CYP2E1* cDNA cloned in pGEM-T was sequenced by Perkin-Elmer-ABI Prism 310 automated DNA sequencer with primers of T7 and SP6 promoters and two specific primers of 2E1 m1 5' -GCATCTCTTGCCTATCCTT-3' (1 042-1 024), and 2E1 m2 5' -ATGGACCTACCTGGAAGGACAT-3' (353-374).

Construction of pREP9 based expression plasmid for CYP2E1 *Kpn* I/*Hin*d III fragment having the total span of human *CYP2E1* cDNA and correctly deduced amino acids sequence in pGEM-CYP2E1 were subcloned to a mammalian expression vector pREP9 (Invitrogen). The recombinant was transformed to *E. coli* Top 10, screened by ampicillin resistant, and identified by restriction mapping.

Transfection and selection[11, 19] HepG2 cells grown in DMEM containing 10 %(V/V) new born calf sera were transfected with the resultant recombinant plasmid, pREP9-CYP2E1, using a modified calcium phosphate method. The culture was split and then selected in the culture medium containing the neomycin analogue G418 (400 mg· L^{-1}). A transgenic cell line named HepG2-CYP2E1 was established.

Detection of CYP2E1 mRNA expression by RT-PCR Total RNA was prepared from G-418-resistant clones by TRIzol reagent. RT-PCR was performed as described before[11], using two primers 2E1 m1 and 2E1 m2 (200 nmol· L^{-1}), their sequence was described in above, with 20 nmol· L^{-1} primers of beta-actin as an internal control. The sense and anti-sense primers used for PCR amplification of beta-actin (GenBank access No. NM_001101) were 5' -TCCCTGGAGAAGAGCTACGA-3' (776-795) and 5' -CAAGAAAGGGTGTAACGCAAC-3' (1 217-1 237), respectively. PCR was performed at 94 ℃ for 2 min, then 35 cycles at 94 ℃ for 30 s, at 62 ℃ for 30 s, at 72 ℃ for 30 s, and extension at 72 ℃ for 7 min. The anticipated beta-actin PCR product was 462 bp in length and that of CYP2E1 was 690 bp in length. An aliquot (10 μL) from PCR was subjected to electrophoresis in a 1.5 % agarose gel stained with ethidium bromide.

Preparation of postmitochondrial supernate (S9) of HepG2-CYP2E1 The procedure of preparation of S9 fraction was described before[11]. The protein in S9 was determined by the Lowry' s method, with bovine serum albumin as standard.

4-nitrophenol hydroxylase assays[20-22] CYP2E1 4-nitrophenol hydroxylase activity of S9 was determined by spectrophotometry, 0.5 mL incubations contained 0.25 mg S9 protein, 0.2 mmol· L^{-1} 4-nitrophenol in 0.1 mmol· L^{-1} potassium phosphate buffer (pH 6.8), reactions were initiated with 1 mmol· L^{-1} NADPH and carried out in air at 37 ℃ for 60 min. Reactions were terminated by adding 0.25 mL of 0.6 mmol· L^{-1} perchloric acid and centrifuged at 10 000×g for 5 min to remove protein. The supernatant was mixed with 1/10 volume of 10 mol· L^{-1} NaOH. The absorbance of clarified supernatants was measured at 510 nm, and the amount of product was quantitated using a standard curve generated by adding known amounts of *p*-nitrocatechol to incubations without NADPH.

Cytotoxicity assay[23, 24] HepG2 and HepG2-CYP2E1 cells were seeded in 96 well cell culture plates at a density of 1×10^4 cells each well and incubated overnight. The medium was discarded, and a new medium containing NDEA 0, 1, 10, 100 mmol· L^{-1} was added to respective wells, with 6 duplications at each concentration. 72 h later, the medium was discarded and 20 μL of 50 g· L^{-1} MTT in PBS was added to each well. The MTT was discarded 4 h later and 100 μL dimethylsulfoxide was added. After formazan was dissolved, the absorbance was read at 570 nm with 630 nm as reference on the microtiter plate reader. Relative survival was represented as the relative toxicity to the control culture without NDEA. The significance of difference of relative survival between HepG2-CYP2E1 and HepG2 cells was analyzed by Student' s *t* test.

Micronucleus test[25-28] 1×10^5 HepG2 and HepG2-CYP2E1 cells were seeded in each 100 mL culture bottle and cultured overnight. The medium was discarded and 0, 5, 10, 20 mol· L^{-1} NDEA in 4 mL serum-free medium was applied to respective bottles and incubated for 4 h. Subsequently the cells were washed twice in PBS and incubated for 20 h with 4 mL completed medium containing 3 mg· L^{-1} of cytochalasin B. Then the cells were washed twice in PBS and harvested in 2 mL PBS and fixed with 0.4 mL fixed solution (methanol: acetic acid 3:1) for 30 min. The cells were centrifugated, the PBS was discarded and pelleted cells were refixed with 2 mL of fixed solution for 30 min. The cells were centrifugated, refixed and centrifugated again, and then dropped onto slides, dried in the air and stained with 10 % Giemsa solution. The scoring criteria for binucleated cells and micronucleus (MN) were based on a report of HUman MicronNucleus project[27]. The frequency of MN formation was expressed as per thousand of binucleated cells with MN. The significance of difference of MN rate between HepG2-CYP2E1 and HepG2 cells was analyzed by checking the tables for determining the statistical significance of mutation frequencies[28].

RESULTS

Construction of recombinants of pGEM-CYP2E1

The recombinant of pGEM-CYP2E1 was constructed with the human *CYP2E1* cDNA inserted into the cloning site of pGEM-T vector. Selection and identification of the recombinant were carried out by *Kpn* I/*Hin*d III endonuclease digestion and agarose gel electrophoresis (Figure 1). The cloned cDNA segment was sequenced completely. In comparison with the cDNA sequence reported by Song *et al* (GenBank access No. J02625), there was only one base difference in cloned cDNA, 105 T→C, while the encoding amino acid was 35G. But there was no sequence difference as compared with that reported by Umeno *et al*[29] (GenBank access No. J02843).

Construction of recombinants of pREP9-CYP2E1

The *Kpn* I/*Hin*d III fragment (1.54 kb) containing complete *CYP2E1* cDNA was subcloned into the *Kpn* I/*Hin*d III site

of mammalian expression vector pREP9. Selection and identification of the recombinant were carried out by *Kpn* I/ *Hin*d III endonuclease digestion and agarose gel electrophoresis (Figure 2). The resulting plasmid was designated as pREP9-CYP2E1 and contained the entire coding region, along with 8 bp of the 5' and 52 bp of the 3' untranslation region of *CYP2E1* cDNA, respectively.

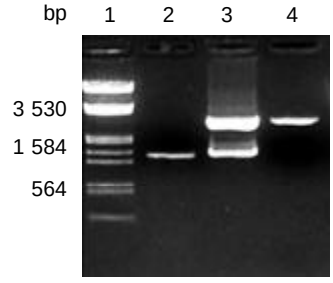

Figure 1 Electrophoretic identification of recombinant of pGEM-CYP2E1. Lane 1: Markers (λ / *Eco*R I and *Hin*d III), 2: PCR products of *CYP2E1* (1.54 kb), 3: Recombinant of pGEM-CYP2E1 digested by *Kpn* I and *Hin*d III, 4: pGEM-T vector.

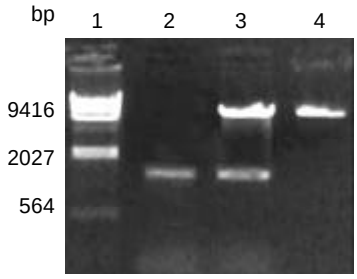

Figure 2 Electrophoretic identification of recombinant of pREP9-*CYP2E1*. Lane 1: λDNA / *Hin*d III Markers, 2: PCR products of *CYP2E1* (1.54 kb), 3: Recombinant of pREP9-*CYP2E1* digested by *Kpn* I and *Hin*d III, 4: pREP9 vector.

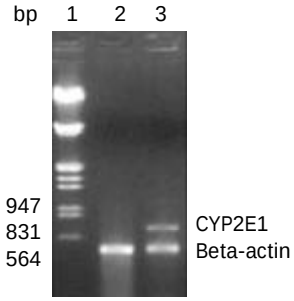

Figure 3 Identification of CYP2E1 mRNA expression in HepG2-CYP2E1 and HepG2 cells by RT-PCR with beta-actin as internal control. Lane 1: Markers (λ / *Eco*R I and *Hin*d III), 2: RT-PCR products of HepG2 cells showing only beta-actin 462 bp, 3: RT-PCR products of HepG2-CYP2E1 cells showing 462 bp of beta-actin and 690 bp of CYP2E1.

Establishment of transgenic cell line with CYP2E1 mRNA expression and 4-nitrophenol hydroxylase activity

HepG2 cells were transfected with pREP9-CYP2E1, and selected with G418. The surviving clones were propagated and a cell line termed HepG2-CYP2E1 was established. The expression of CYP2E1 mRNA could be detected in HepG2-CYP2E1 cells but not in HepG2 cells by RT-PCR (Figure 3). The 4-nitrophenol hydroxylase activity in S9 of HepG2-CYP2E1 cells was found 0.162±0.025 nmol· min^{-1}· mg^{-1} S9 protein (n=3), but not detectable in parent HepG2 cells.

HepG2-CYP2E1 cells increased cytotoxicity and MN rate by NDEA

Cells were exposed to various concentrations of NDEA. The relative survival rate of HepG2-CYP2E1 cells was lower than that of HepG2 cells in 10 and 100 mmol· L^{-1} NDEA (P<0.05 and P<0.01, respectively), as shown in Figure 4. The MN rate of HepG2-CYP2E1 was higher than that of HepG2 cells in 10 and 20 mmol· L^{-1} NDEA (P<0.05 and P<0.01 respectively) as shown in Figure 5.

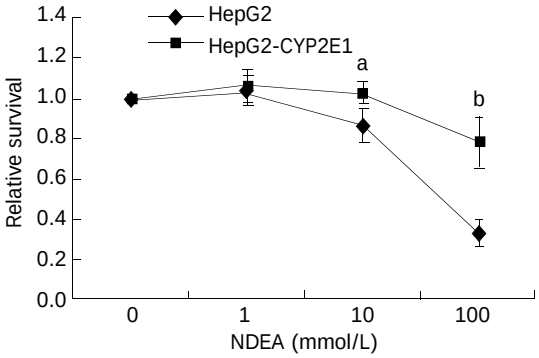

Figure 4 Cytotoxicity of NDEA against HepG2-CYP2E1 and HepG2 cells. Cells were exposed to various concentrations of NDEA. Relative survival rate was represented as the relative toxicity to the control culture without NDEA. The results presented were the average of six duplications ($\bar{x}$±s). ^aP<0.05, ^bP<0.01 *vs* HepG2 cells.

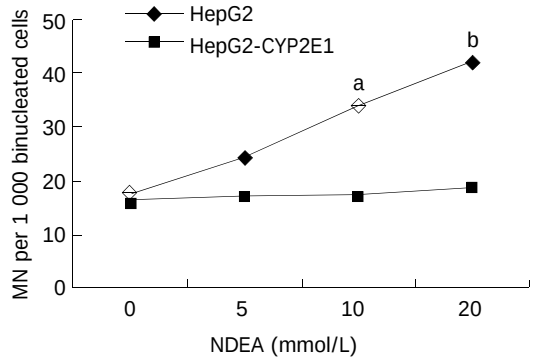

Figure 5 MN rates in HepG2-CYP2E1 and HepG2 cells induced by NDEA. Cells were exposed to various concentrations of NDEA. The data were expressed as per thousand of binucleated cells with MN. ^aP<0.05, ^bP<0.01 *vs* HepG2 cells.

DISCUSSION

Human *CYP2E1* gene is located on the chromosome 10q24.3-qter. Up to date, seven *CYP2E1* alleles have been identified (see: *CYP2E1* alleles nomenclature at: http://www.imm.ki.se/CYPalleles/cyp2e1.htm). Only 3 alleles have nucleotide substitute, resulting in amino acid change. *CYP2E1*1* is the wild type of human *CYP2E1*. *CYP2E1*2* has a 1 168 G→A point mutation in exon 2 causing an R76H amino acid substitution, and *CYP2E1*3* has a 10 059 G→A base substitution in exon 8 yielding a V389I amino acid exchange. The corresponding *CYP2E1* cDNAs were expressed in COS-1 cells by Hu *et al*[30]. The cellular levels of CYP2E1 mRNA, protein, and the rate of chlorzoxazone hydroxylation were monitored. *CYP2E1*3* cDNA variant was indistinguishable from the wild type cDNA on all variables investigated, whereas *CYP2E1*2* cDNA, although yielding similar amounts of mRNA, only caused 37 % of the protein expression and 36 % of the catalytic activity compared with the wild type cDNA. Complete screening by single-stranded conformation polymorphism of the three

populations revealed that these variant alleles were rare. Human *CYP2E1* gene was functionally well conserved compared with other CYP enzymes active in drug metabolism, which suggested an important endogenous function in humans[30]. *CYP2E1*4* has a 4 804 G→A point mutation in exon 4, resulting in V179I amino acid exchange. No significant difference in kinetic constants for chlorzoxazone hydroxylation between mutant and wild type was observed by expression of the wild type and mutated full length cDNAs in lymphoblastoid cells[31]. Our laboratory has once cloned a *CYP2E1* cDNA (GenBank access No. AF182276), which has two point mutations, i.e. 105 T→C, no amino change 35G, and 704G→T, and can result in V235A amino acid exchange. This cDNA was expressed in Chinese hamster lung CHL cells. We could not detect the *N*-nitrosodimethylamine demethylase activity in transgenic cells (data not shown). According to the homology modelling of human CYP2E1 based on the CYP2C5 crystal structure, the substrate recognition site (SRS) 1 was located at codon 100-118, SRS 2 at 200-211, SRS3 at 236-241, SRS4 at 291-305, SRS5 at 361-370, SRS6 at 470-480. The point mutations of CYP2E1*2, *3, *4 were not located on the SRS. The V235A amino acid exchange in our formerly cloned CYP2E1 was just at the front of SRS3. This might influence SRS3 and reduce the enzyme activity. Fortunately, this time we cloned a wild type CYP2E1.

It has been found that polymorphism of *CYP2E1* gene is significant for inter-individual differences in toxicity of its substrates[33], and has some effect on the development of gastric cancer[34] and colorectal cancer[35].

The expression of CYP2E1 mRNA in HepG2 cells was validated by RT-PCR. The commonly used CYP2E1 probe substrates were chlorzoxazone[36, 37] and 4-nitrophenol[38]. In this research, we used 4-nitrophenol 2-hydroxylase activity to evaluate the expression of CYP2E1, and the 4-nitrophenol hydroxylase activity of HepG2-CYP2E1 cells was found to be 0.162±0.025 nmol· min^{-1}· mg^{-1} S9 protein, a little lower than those of HepG2-CYP2E1 E43 and E47 cells (0.19 and 0.34 nmol· min^{-1}· mg^{-1} of microsome, respectively)[39], much lower than that of human liver (1.91±0.28 nmol· min^{-1}· $mg^{-1}$of microsome)[40].

The most frequently used genotoxicity test in mammals is the micronucleus test, which provides a simple and rapid indirect measure of induced structural and numerical chromosome aberrations and is a scientific and regulatory assay accepted by supranational authorities such as the Organization for Economic Cooperation and Development (OECD), International Conference on Harmonization (ICH) and European Union (EU). NDEA could induce early experimental hepatocellular carcinomas[41] and esophageal neoplasms[42]. The metabolic activation of NDEA was mediated mainly by CYP2A6 and CYP2E1[43]. This study has shown that NDEA can decrease the relative survival rate of HepG2-CYP2E1 cells and increase the MN rate in binucleated cells as compared with HepG2 cells.

cDNA of human *CYP2E1* was successfully cloned and a cell line, HepG2-CYP2E1, efficiently expressing mRNA and having the CYP2E1 enzymatic activities, was established. The cell line is useful for testing the cytotoxicity, mutagenicity and metabolism of xenobiotics and drugs, which may possibly be activated by CYP2E1.

REFERENCES

1 **Hukkanen J**, Pelkonen O, Hakkola J, Raunio H. Expression and regulation of xenobiotic-metabolizing cytochrome P450 (CYP) enzymes in human lung. *Crit Rev Toxicol* 2002; **32**: 391-411

2 **Upadhya SC**, Tirumalai PS, Boyd MR, Mori T, Ravindranath V. Cytochrome P4502E (CYP2E) in brain: constitutive expression, induction by ethanol and localization by fluorescence *in situ* hybridization. *Arch Biochem Biophys* 2000; **373**: 23-34

3 **Lieber CS**. Cytochrome P-4502E1: its physiological and pathological role. *Physiol Rev* 1997; **77**: 517-544

4 **Tanaka** E, Terada M, Misawa S. Cytochrome P450 2E1: its clinical and toxicological role. *J Clin Pharm Ther* 2000; **25**: 165-175

5 **Anzenbacher P**, Anzenbacherova E. Cytochromes P450 and metabolism of xenobiotics. *Cell Mol Life Sci* 2001; **58**: 737-747

6 **Sawada M**, Kamataki T. Genetically engineered cells stably expressing cytochrome P450 and their application to mutagen assays. *Mutat Res* 1998; **411**: 19-43

7 **Crespi CL**, Miller VP. The use of heterologously expressed drug metabolizing enzymes--state of the art and prospects for the future. *Pharmacol Ther* 1999; **84**: 121-131

8 **Wu J**, Dong H, Cai Z, Yu Y. Stable expression of human cytochrome CYP2B6 and CYP1A1 in Chinese hamster CHL cells: their use in micronucleus assays. *Chin Med Sci J* 1997; **12**: 148-155

9 **Yan LQ**, Yu YN, Zhuge J, Xie HY. Cloning of human cytochrome P450 2A6 cDNA and its expression in mammalian cells. *Zhongguo Yaolixue Yu Dulixue Zazhi* 2000; **14**: 31-35

10 **Chen Q**, Wu J, Yu Y. Establishment of transgenic cell line CHL-3A4 and its metabolic activation. *Zhonghua Yufang Yixue Zazhi* 1998; **32**: 281-284

11 **Zhuge J**, Yu YN, Li X, Qian YL. Cloning of cytochrome P-450 2C9 cDNA from human liver and its expression in CHL cells. *World J Gastroenterol* 2002; **8**: 318-322

12 **Zhuge J**, Yu YN, Qian YL, Li X. Establishment of a transgenic cell line stably expressing human cytochrome P450 2C18 and identification of a CYP2C18 clone with exon 5 missing. *World J Gastroenterol* 2002; **8**: 888-892

13 **Li X**, Yu YN, Zhu GJ, Qian YL. Cloning of UGT1A9 cDNA from liver tissues and its expression in CHL cells. *World J Gastroenterol* 2001; **7**: 841-845

14 **Rueff J**, Chiapella C, Chipman JK, Darroudi F, Silva ID, Duverger-van Bogaert M, Fonti E, Glatt HR, Isern P, Laires A, Leonard A, Llagostera M, Mossesso P, Natarajan AT, Palitti F, Rodrigues AS, Schinoppi A, Turchi G, Werle-Schneider G. Development and validation of alternative metabolic systems for mutagenicity testing in short-term assays. *Mutat Res* 1996; **353**: 151-176

15 **Rodriguez-Antona C**, Donato MT, Boobis A, Edwards RJ, Watts PS, Castell JV, Gomez-Lechon MJ. Cytochrome P450 expression in human hepatocytes and hepatoma cell lines: molecular mechanisms that determine lower expression in cultured cells. *Xenobiotica* 2002; **32**: 505-520

16 **Jover R**, Bort R, Gomez-Lechon MJ, Castell JV. Cytochrome P450 regulation by hepatocyte nuclear factor 4 in human hepatocytes: a study using adenovirus-mediated antisense targeting. *Hepatology* 2001; **33**: 668-675

17 **Yoshitomi S**, Ikemoto K, Takahashi J, Miki H, Namba M, Asahi S. Establishment of the transformants expressing human cytochrome P450 subtypes in HepG2, and their applications on drug metabolism and toxicology. *Toxicol In Vitro* 2001; **15**: 245-256

18 **Song BJ**, Gelboin HV, Park SS, Yang CS, Gonzalez FJ. Complementary DNA and protein sequences of ethanol-inducible rat and human cytochrome P-450s. Transcriptional and post-transcriptional regulation of the rat enzyme. *J Biol Chem* 1986; **261**: 16689-16697

19 **Sambrook J**, Fritsch EF, Maniatis T. Molecular Cloning, A Laboratory Manual. 2nd ed. New York: *Cold Spring Harbor Laboratory Press* 1989: 6.28-6.29

20 **Lin HL**, Roberts ES, Hollenberg PF. Heterologous expression of rat P450 2E1 in a mammalian cell line: in situ metabolism and cytotoxicity of *N*-nitrosodimethylamine. *Carcinogenesis* 1998; **19**: 321-329

21 **Koop DR**. Hydroxylation of *p*-nitrophenol by rabbit ethanol-inducible cytochrome P-450 isozyme 3a. *Mol Pharmacol* 1986; **29**: 399-404

22 **Tassaneeyakul W**, Veronese ME, Birkett DJ, Gonzalez FJ, Miners JO. Validation of 4-nitrophenol as an *in vitro* substrate probe for human liver CYP2E1 using cDNA expression and microsomal kinetic techniques. *Biochem Pharmacol* 1993; **46**: 1975-1981

23 **Zhuge J**, Wang LR, Bi AH, Liu GH. Investigation of the role of Interleukin-2 and soluble Interleukin-2 receptor in the pathogenesis of asthma. *Mianyixue Zazhi* 1994; **10**: 242-244

24 **Moskatelo D**, Benjak A, Laketa V, Polanc S, Kosmrlj J, Osmak M. Cytotoxic effects of diazenes on tumor cells *in vitro*. *Chemotherapy* 2002; **48**: 36-41

25 **Garriott ML**, Phelps JB, Hoffman WP. A protocol for the *in vitro* micronucleus test. I. Contributions to the development of a protocol suitable for regulatory submissions from an examination of 16 chemicals with different mechanisms of action and different levels of activity. *Mutat Res* 2002; **517**: 123-134

26 **Erexson GL**, Periago MV, Spicer CS. Differential sensitivity of Chinese hamster V79 and Chinese hamster ovary (CHO) cells in the *in vitro* micronucleus screening assay. *Mutat Res* 2001; **495**: 75-80

27 **Fenech M**, Chang WP, Kirsch-Volders M, Holland N, Bonassi S, Zeiger E. HUMN project: detailed description of the scoring criteria for the cytokinesis-block micronucleus assay using isolated human lymphocyte cultures. *Mutat Res* 2003; **534**: 65-75

28 **Kastenbaum MA**, Bowman KO. Tables for determining the statistical significance of mutation frequencies. *Mutat Res* 1970; **9**: 527-549

29 **Umeno M**, McBride OW, Yang CS, Gelboin HV, Gonzalez FJ. Human ethanol-inducible P450IIE1: complete gene sequence, promoter characterization, chromosome mapping, and cDNA-directed expression. *Biochemistry* 1988; **27**: 9006-9013

30 **Hu Y**, Oscarson M, Johansson I, Yue QY, Dahl ML, Tabone M, Arinco S, Albano E, Ingelman-Sundberg M. Genetic polymorphism of human CYP2E1: characterization of two variant alleles. *Mol Pharmacol* 1997; **51**: 370-376

31 **Fairbrother KS**, Grove J, de Waziers I, Steimel DT, Day CP, Crespi CL, Daly AK. Detection and characterization of novel polymorphisms in the CYP2E1 gene. *Pharmacogenetics* 1998; **8**: 543-552

32 **Lewis DF**, Lake BG, Bird MG, Loizou GD, Dickins M, Goldfarb PS. Homology modelling of human CYP2E1 based on the CYP2C5 crystal structure: investigation of enzyme-substrate and enzyme-inhibitor interactions. *Toxicol In Vitro* 2003; **17**: 93-105

33 **Bolt HM**, Roos PH, Thier R. The cytochrome P-450 isoenzyme CYP2E1 in the biological processing of industrial chemicals: consequences for occupational and environmental medicine. *Int Arch Occup Environ Health* 2003; **76**: 174-185

34 **Cai L**, Yu SZ, Zhan ZF. Cytochrome P450 2E1 genetic polymorphism and gastric cancer in Changle, Fujian Province. *World J Gastroenterol* 2001; **7**: 792-795

35 **Le Marchand L**, Donlon T, Seifried A, Wilkens LR. Red meat intake, CYP2E1 genetic polymorphisms, and colorectal cancer risk. *Cancer Epidemiol Biomarkers Prev* 2002; **11**(10 Pt 1): 1019-1024

36 **Lucas D**, Ferrara R, Gonzalez E, Bodenez P, Albores A, Manno M, Berthou F. Chlorzoxazone, a selective probe for phenotyping CYP2E1 in humans. *Pharmacogenetics* 1999; **9**: 377-388

37 **Yuan R**, Madani S, Wei XX, Reynolds K, Huang SM. Evaluation of cytochrome p450 probe substrates commonly used by the pharmaceutical industry to study *in vitro* drug interactions. *Drug Metab Dispos* 2002; **30**: 1311-1319

38 **Spatzenegger M**, Liu H, Wang Q, Debarber A, Koop DR, Halpert JR. Analysis of differential substrate selectivities of CYP2B6 and CYP2E1 by site-directed mutagenesis and molecular modeling. *J Pharmacol Exp Ther* 2003; **304**: 477-487

39 **Chen Q**, Cederbaum AI. Cytotoxicity and apoptosis produced by cytochrome P450 2E1 in Hep G2 cells. *Mol Pharmacol* 1998; **53**: 638-648

40 **Adas F**, Berthou F, Salaun JP, Dreano Y, Amet Y. Interspecies variations in fatty acid hydroxylations involving cytochromes P450 2E1 and 4A. *Toxicol Lett* 1999; **110**: 43-55

41 **Wang Z**, Ruan YB, Guan Y, Liu SH. Expression of IGF-II in early experimental hepatocellular carcinomas and its significance in early diagnosis. *World J Gastroenterol* 2003; **9**: 267-270

42 **Waddell WJ**. Threshold for carcinogenicity of *N*-nitrosodiethylamine for esophageal tumors in rats. *Food Chem Toxicol* 2003; **41**: 739-741

43 **Fujita K**, Kamataki T. Predicting the mutagenicity of tobacco-related *N*-nitrosamines in humans using 11 strains of Salmonella typhimurium YG7108, each coexpressing a form of human cytochrome P450 along with NADPH-cytochrome P450 reductase. *Environ Mol Mutagen* 2001; **38**: 339-346

Edited by Zhang JZ and Wang XL

P.O.Box 2345, Beijing 100023,China
Fax: +86-10-85381893
E-mail: wjg@wjgnet.com www.wjgnet.com

World J Gastroenterol 2003;9(12):2737-2741
World Journal of Gastroenterology
 ISSN 1007-9327

• BASIC RESEARCH •

Hepatocellular apoptosis after hepatectomy in obstructive jaundice in rats

De-Sheng Wang, Ke-Feng Dou, Kai-Zong Li, Zhi-Qing Gao, Zhen-Shun Song, Zheng-Cai Liu

De-Sheng Wang, Ke-Feng Dou, Kai-Zong Li, Zhi-Qing Gao, Zhen-Shun Song, Zheng-Cai Liu, Department of Hepatobiliary Surgery, Xijing Hospital, the Fourth Military Medical University, Xi' an 710032, Shannxi Province, China
Supported in part by a Grant-in-aid for Cancer Research and Scientific Research From the Osaka University of Japan
Correspondence to: De-Sheng Wang, MD, Department of Hepatobiliary Surgery, Xijing Hospital, the Fourth Military Medical University, Xi' an 710032, Shannxi Province, China. wangdesh@163.com
Telephone: +86-29-3375259 **Fax:** +86-29-3375255
Received: 2003-05-11 **Accepted:** 2003-06-04

Abstract

AIM: To investigate the hepatocellular apoptosis after hepatectomy in obstructive jaundice and biliary decompression rats.

METHODS: After bile duct ligation for 7 days, rats were randomly divided into OB group in which the rats underwent 70 % hepatectomy, OB-CD group in which the rats underwent hepatectomy accompanied by choledochoduodenostomy, CD-Hx group in which the rats underwent choledochoduodenostomy and then received 70 % hepatectomy on the fifth day after biliary decompression. The control group (Hx group) only underwent hepatectomy.

RESULTS: The level of total serum bilirubin and serum enzymes was significantly lower in CD-Hx group than in OB-CD and OB groups on day 1, 3 and 5 after hepatectomy. The apoptotic index was significantly lower in CD-Hx group than in OB-CD and OB groups on day 3 and 5. The oligonucleosomal DNA fragments and Caspase-3 activity were also lower in CD-Hx group than in OB-CD and OB groups 3 days after hepatectomy, without differences between CD-Hx and Hx groups.

CONCLUSION: Hepatocellular apoptosis plays vital roles in jaundice rats, and biliary decompression is more effective in treatment of patients with severe jaundice before operation.

Wang DS, Dou KF, Li KZ, Gao ZQ, Song ZS, Liu ZC. Hepatocellular apoptosis after hepatectomy in obstructive jaundice in rats. *World J Gastroenterol* 2003; 9(12): 2737-2741
http://www.wjgnet.com/1007-9327/9/2737.asp

INTRODUCTION

Obstructive jaundice is often a clinical manifestation of the disease of extrahepatic biliary system or pancreas. In jaundiced patients with hilar bile duct carcinoma or gallbladder carcinoma, hepatectomy is one of the surgical regimens, but surgical procedures are associated with increases of morbidity and mortality rates, mainly due to postoperative complications such as hepatic failure, sepsis, bleeding and renal failure[1,2]. The significance of biliary drainage before surgery is controversial. Preoperative biliary drainage decreased the mortality and morbidity rates in patients with obstructive jaundice in some studies but not in others[3-5]. Experimental and clinical studies have identified several etiological factors including hypotension, impaired nutritional status, depressed immune function, hepatic dysfunction and the presence of toxic bile salts in circulation[6-8]. A high serum bilirubin concentration in jaundiced patients undergoing operation has been recognized as a predictor of mortality[3].

Hepatocyte injury and progression of liver disease are due to direct chemical damage to hepatocytes by toxic hydrophobic bile salts[9]. Although toxic bile salts are known to cause hepatocyte toxicity by inducing apoptosis, the precise mechanisms responsible for bile salt-mediated apoptosis remain to be established. This information is important because it could help provide rational strategies for the treatment of cholestatic liver disorders and decreasing postoperative complications. The aim of this study was to investigate the hepatocellular apoptosis after hepatectomy in obstructive jaundice and biliary decompression rats.

MATERIALS AND METHODS

Animals and experimental design

Male Wistar rats (Shionogi Aburabi Laboratory, Shiga, Japan) weighing 190-240 g were used for this study. Animals were housed in a controlled environment with a 12 h light/dark cycle. Rats had free access to normal rat chow and water before surgery. The care and handling of the animals were made in accordance with the National Institutes of Health Guidelines for the Care and Use of Laboratory Animals. The rats were divided into four groups each containing 6 animals. Hx group in which normal rats underwent 70 % hepatectomy, OB group in which the rats underwent 70 % hepatectomy after bile duct ligation for 7 days, OB-CD group in which the rats underwent 70 % hepatectomy accompanied by choledochoduodenostomy after bile duct ligation for 7 days, CD-Hx group in which the rats underwent choledochoduodenostomy after bile duct ligation for 7 days and then received 70 % hepatectomy on the fifth day after biliary decompression, as described below.

Surgical procedures

All surgical procedures were carried out under ether anesthesia. All rats were weighed before surgery and at the end of the study.

Laparotomy was performed through an upper midline incision. After ligation of the proximal and distal bile ducts, the common bile duct was divided to prevent recanalization[10]. The ligatures were placed in the same position in all rats. The 70 % hepatectomy was done according to the method of Higgins and Anderson[11] on the seventh day after biliary obstruction in OB and OB-CD groups and on the fifth days after the biliary decompression in CD-Hx group.

Choledochoduodenostomy was performed according to the method of Ryan *et al* with minor modifications[12]. After biliary obstruction for 7 days, the abdomen was reopened through the previous incision. The dilated common hepatic bile duct was freed from its surrounding tissues and the contents were aspirated. A small incision was made in the bile duct and a silicone tube with an outer diameter of 0.9 mm was inserted and secured in position with a 7-0 silk suture. The free end of

the tube was inserted into duodenum approximately 1.5 cm from the pylorus, and then tied in position with a 6-0 PDS purse-string suture. Then the suture was carried out between the bile duct and the duodenal wall to protect the separation of the anastomosis.

Measurement of bilirubin and enzymes in blood

Blood samples were collected from the tail vein with a 27-gauge needle. Serum total bilirubin, activities of alkaline phosphatase (ALP) and aspartate aminotransferase (AST) levels were measured enzymatically using a commercial kit (Spotchem Co., Kyoto, Japan).

Quantification of oligonucleosomal (histone-associated) DNA fragments

An aliquot from the liver homogenate was centrifuged at 13 000×*g*. The supernatant was diluted 1 000-fold and subjected to a sandwich ELISA designed to detect DNA/histone fragments using a test kit from Boehringer Mannheim, according to the manufacturer' s instructions. Briefly, a 96-well microtiter plate was coated with antibody against histones. Diluted samples were then applied to the wells for 90 min, followed by incubation with peroxidase-conjugated anti-DNA antibody for 90 min. Color substrate was added and absorbance was measured at 405 nm at 5, 10, and 15 min using a 96-well microtiter plate reader.

In situ TdT-UTP nick-end labeling (TUNEL staining)

On the third and fifth day after hepatectomy, a section of liver tissue measuring approximately 5 mm in thickness was cut from the right lateral lobe and fixed in 10 % buffered formalin, processed by standard techniques and embedded in paraffin. Apoptotic change in the liver was analyzed by *in situ* TUNEL method using an apoptosis detection kit (ApopTag, Oncor S7100, Gaithersburg, MD) according to the manufacturer' s instructions. Briefly, after deparaffinization and rehydration, 4 μm thick tissue sections were incubated in PBS, and then preincubated with equilibration buffer for 15 min, and digoxigenin-labelled dUTP and dATP in TdT buffer were added to cover the section, which was then incubated in a humidified chamber at 37 ℃ for 60 min. The reaction was stopped by immersing the slides in a stop/wash buffer. Following washing in PBS, the sections were incubated in anti-digoxigenin-peroxidase for 30 min at room temperature. The slides were incubated with DAB and hydrogen peroxide and counterstained with hematoxylin. Apoptotic cells were counted from at least 10 randomly chosen high-power fields at ×400 magnification. Cells with clear brown nuclear labelling were defined as TUNEL-positive. Apoptotic index was defined as the total number of apoptotic cells seen in every ten high-power field sections.

Caspase-3-like protease activity assay

Liver tissues were immediately frozen by liquid nitrogen and stored at -80 ℃ on the third and fifth days after hepatectomy. The Caspase 3-like activity was measured using a commercially available kit (Clontech Laboratories, Palo Alto, CA) according to the manufacturer' s instructions. Caspase enzymatically cleaved the substrate and released free 7-amino-4-trifluoromethyl coumarin (AFC) that produced a blue-green fluorescence, which was measured fluorometrically. Liver samples were homogenized in 500 μl of lysis buffer. Samples were centrifuged at 16 000×g in a microfuge for 10 min at 4 ℃ and normalized to protein using the Bradford assay (Bio-Rad). Fluorescent substrate, DEVD- AFC was incubated with 50 μl supernatants for liver extracts at 37 ℃ for 60 min. The fluorescence of cleaved substrates was measured using a fluorometer (Molecular Dynamics Inc.) at an excitation wavelength of 400 nm and an emission wavelength of 505 nm. An AFC calibration curve was established by serial dilution of a pure AFC solution provided in the kit.

Statistical analysis

All data were expressed as mean ±SEM. Statistical analysis was done by statistical package of SPSS for Window release 9.0. Differences between mean were tested with the Mann-Whitney test. A probability value less than 0.05 was considered statistically significant.

RESULTS

Bilirubin and enzymes in blood

The level of total serum bilirubin reached more than 7 mg/dl after 7 days' biliary obstruction, and the high bilirubin level rapidly decreased to 0.8 mg/dl only on day 1 after biliary decompression. We therefore thought that our models functioned well for biliary decompression. The total serum bilirubin concentration on the first day after hepatectomy in OB-CD group was 1.6 mg/dl, which was higher than that in CD-Hx group. The level of bilirubin in OB group was increased, while there was no statistically significant differences among other three groups on day 5 after hepatectomy (Figure 1).

The ALP concentration of OB group was significantly higher than that of other groups, but no differences of serum ALP level were found among the other groups after hepatectomy (Figure 2).

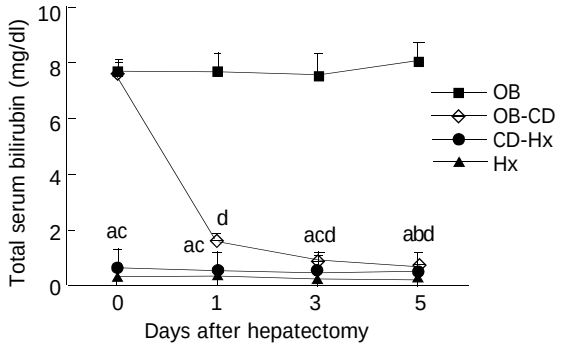

Figure 1 Changes of total serum bilirubin after hepatectomy. Blood was withdrawn from the tail vein while each rat was under ether anesthesia, and serum was obtained by means of centrifugation. Each point represents the mean ± SEM for six animals. [a]*P*<0.01 CD-Hx group *vs* OB group, [b]*P*<0.05 CD-Hx group *vs* OB-CD group, [c]*P*<0.01 CD-Hx group *vs* OB-CD group, [d]*P*<0.01 OB-CD group *vs* OB group.

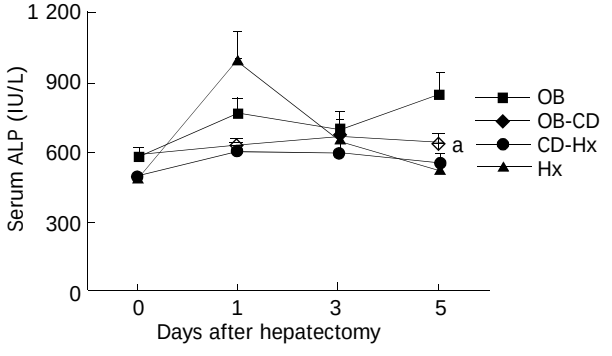

Figure 2 Changes of serum ALP after hepatectomy. Six rats were used for each group. Results were the mean ±SEM. [a]*P*<0.05 CD-Hx group *vs* OB group.

The level of serum AST peaked on the first day after hepatectomy and decreased gradually (Figure 3). There was no difference of AST concentration between CD-Hx and Hx groups on the third and fifth days after hepatectomy. The serum AST concentration in OB group on the fifth day was nearly 6 times that of the concentration in CD-Hx group.

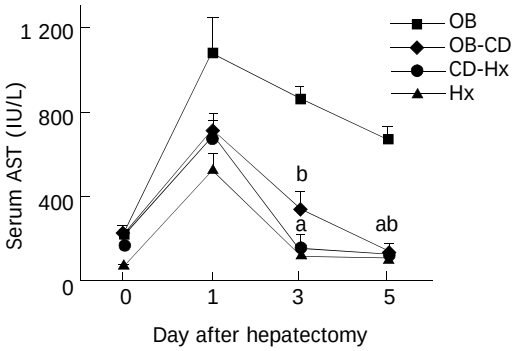

Figure 3 Changes of serum AST after hepatectomy. Six rats were used for each group. Results were the mean ±SEM. [a]*P*<0.01 CD-Hx group *vs* OB group, [b]*P*<0.01 OB-CD group *vs* OB group.

Accumulation of oligonucleosomal fragments

The cytoplasmic levels of DNA (histone-associated) oligonucleosomal fragments in hepatocytes after hepatectomy were determined. The presence of these fragments in the cytoplasm reflected the extent of DNA fragmentation and nuclear disruption that are characteristic of apoptosis. The level of DNA fragments in CD-Hx group was significantly lower than that in OB and OB-CD groups on the third day after hepatectomy (Figure 4). There was no significant difference between CD-Hx and OB groups.

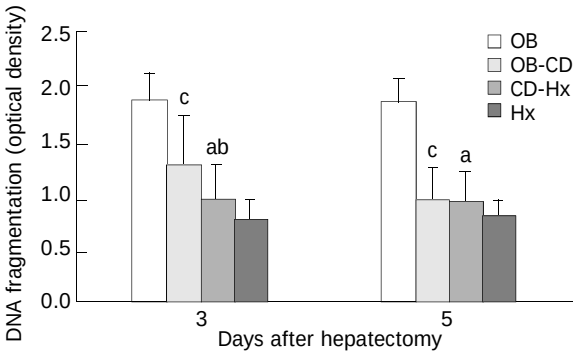

Figure 4 Quantification of oligonucleosomal DNA fragments. The supernatant from the liver homogenate was subjected to a sandwich ELISA designed to detect DNA / histone fragments. Each group consisted of 6 rats. Values were expressed as mean ±SEM. [a]*P*<0.01 CD-Hx group *vs* OB group, [b]*P*<0.05 CD-Hx group *vs* OB-CD group, [c]*P*<0.01 OB-CD group *vs* OB group.

Hepatocellular apoptosis index

TUNEL signal was defined by distinct nuclear staining. The number of hepatocellular apoptosis was high on day 3 and decreased on day 5 when the liver was harvested on days 3 and 5 from rats after hepatectomy. The data shown in Figure 5 indicate that apoptosis positive cells were significantly higher in OB group than in other groups. A very low rate of apoptosis was found in CD-Hx group, with no difference between CD-Hx and Hx groups.

Caspase-3-like protease activity

Cleavage of peptide substrate DEVD-AFC was used as an indicator of Caspase-3-like protease activity. The level of Caspase-3 activity in CD-Hx group was significantly lower than that in OB and OB-CD groups on the third day after hepatectomy. But on day 5, the level of Caspase-3 activity in OB-CD group decreased rapidly, without differences between OB-CD and CD-Hx groups (Figure 6).

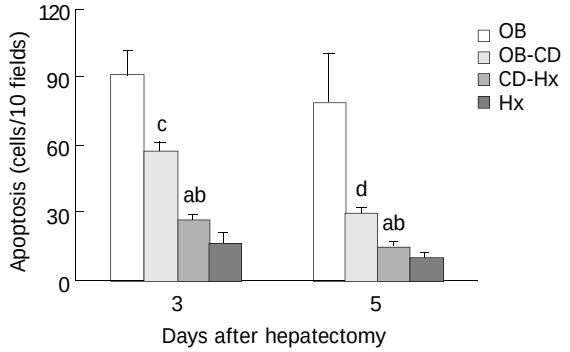

Figure 5 Changes of hepatocellular apoptotic index after hepatectomy. Morphometric analysis of the positive cells in tissue stained by TUNEL method was performed under high power magnification (×400) in a blinded fashion. Each group consisted of 6 rats. The number of positive cells was counted and expressed as the total number of apoptotic cells seen in every ten high-power fields sections. Values were expressed as mean ±SEM. [a]*P*<0.01 CD-Hx group *vs* OB group, [b]*P*<0.01 CD-Hx group *vs* OB-CD group, [c]*P*<0.05 OB-CD group *vs* OB group, [d]*P*<0.01 OB-CD group *vs* OB group.

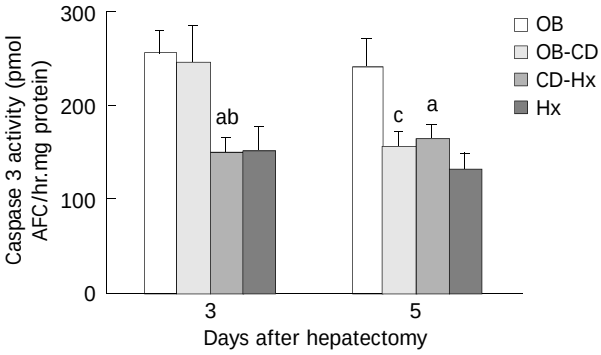

Figure 6 Changes of Caspase-3-like protease activity after hepatectomy. 50 μM DEVD-AFC was added to whole cell lysates (50 μg of total protein) for 1 h. The activity of *Caspase-3-like protease* was measured by determining the cleaved fluorogenic substrates using a spectrofluorometer at 400 / 505 nm. Each group consisted of 6 rats. Values shown represented mean ±SEM. [a]*P*<0.05 CD-Hx group *vs* OB group, [b]*P*<0.05 CD-Hx group *vs* OB-CD group, [c]*P*<0.05 OB-CD group *vs* OB group.

DISCUSSION

The perioperative mortality rate in patients with obstructive jaundice was reported to be 8 % to 28 %[13]. Perioperative complications in patients with obstructive jaundice included infections, endotoxemia, renal failure, stress ulceration, disseminated intravascular coagulation, and wound dehiscence[14,15]. Numerous reports suggested that in obstructive jaundice there was not only impairment of hepatocellular function but also depression of Kupffer cell activity and ultimately hepatic structural damage, leading to the development of portal hypertension[16,17]. In addition, it could result in depressed wound healing, significant portal and systemic endotoxaemia, decreased reticuloendothelial cell function, reduced T cell responses, depressed non-specific cell-mediated immunity, decreased bacterial clearance and increased bacterial translocation[18,19].

This animal model was designed to simulate the clinical treatment procedures used for patients with obstructive jaundice undergoing hepatectomy. Choledochoduodenal drainage was performed before or at the same time as 70 % hepatectomy. Obstruction at the choledochoduodenostomy occurred in about 2 % rats. These rats were excluded from further studies. The mortality rate was about 20 % following choledochoduodenostomy or hepatectomy in jaundice rats. No rats died during the procedure and all deaths occurred in the first 3 days postoperatively, usually secondary to bleeding.

During obstructive jaundice, the retention of biliary constituents and high biliary pressure caused hepatocellular injury[20]. This is supported by the fact that serum AST and ALP levels increased during obstructive jaundice and decreased after choledochoduodenostomy (data not shown). Kanno[21] reported that biliary obstruction for even 5 days suppressed rat liver function, as assessed with aminopyrine breath test and galactose tolerance test. These results suggested that obstructive jaundice could cause serious impairment of pivotal liver functions, consequently resulting in poor prognosis after partial hepatectomy. The present study clearly showed that biliary drainage before hepatectomy significantly improved liver functions and decreased hepatocellular apoptosis. Serum liver function tests showed that choledochoduodenal drainage was effective in both OB-CD and CD-Hx groups. Furthermore, serum enzyme levels, apoptotic index, DNA fragments and Caspase-3 activity were significantly lower in CD-Hx group than in other groups. These data suggested that biliary drainage before hepatectomy had beneficial effects in severe jaundice patients.

Accumulation of these toxic bile salts within hepatocytes has been thought to play a key role in liver injury during obstructive jaundice. Indeed, hepatic levels of toxic bile salts chenodeoxycholate and deoxycholate correlated with the degree of liver damage[22]. Because widespread necrosis was not prominent in most cholestatic liver diseases, it has become apparent that the occurrence of hepatocyte death during cholestasis was rather due to apoptosis than due to necrosis[23]. The mechanisms of apoptosis by toxic bile salts could been partially elucidated in recent years. Toxic bile salts could directly cause apoptosis in cultured rodent hepatocytes[24]. Bile acid-induced toxicity is typically characterized by hepatocyte swelling, disruption of plasma membrane integrity, and release of intracellular constituents. The apoptotic pathway in hepatocytes could be initiated by a ligand-independent activation of Fas by bile salt[25]. Apoptosis was triggered by the Fas pathway, at least in part, by the activation of intracellular enzymes called Caspases. Caspases have been found to be cysteine-containing, aspartic acid-specific proteases which exist as zymogens in the soluble cytoplasm, mitochondrial intermembrane space, and nuclear matrix of virtually all cells[26]. Upon activation of the apoptotic pathway, initiator Caspases (i.e., Caspases 8 and 9) were converted to their active forms, which in turn activated downstream Caspase 3, which could activate other Caspases and ultimately cleave various substrates[27]. One of these substrates has been found to be a Caspase-dependent endonuclease that is freed from its inhibitor by Caspase-3 in the cytoplasm, and subsequently enters the nucleus, where it cuts DNA into oligonuclesomal (180 bp) fragments[28]. Additionally, Bid, a protein responsible for the release of mitochondrial cytochrome C and amplification of the apoptotic cascade, could also be activated by Caspases[29]. Ultimately, this pathway would ensure the self-destruction of cells with the characteristic morphological features of apoptosis, including nuclear fragmentation, cellular shrinkage, and acidophilic staining of the cytoplasm[30]. Bile acid induced apoptosis also appeared to require an activation and translocation of protein kinase C, which then could lead to an increase of intracellular magnesium[31,32]. This would cause an activation of Mg^{2+}-dependent endonucleases, leading to DNA cleavage.

In conclusion, hepatocellular apoptosis plays a vital role in jaundice rats. Biliary drainage is preferable, as evidenced in rats by significantly better liver function and decrease of hepatocellular apoptosis. Biliary decompression is an effective preoperative treatment for patients with severe jaundice.

ACKNOWLEDGEMENTS

We would express our sincere thanks to Prof. Monden and Dr. Umeshita for their technical and financial support.

REFERENCES

1 **Su CH,** Tsay SH, Wu CC, Shyr YM, King KL, Lee CH, Lui WY, Liu TJ, P'eng FK. Factors influencing postoperative morbidity, mortality, and survival after resection for hilar cholangiocarcinoma. *Ann Surg* 1996; **223**: 384-394

2 **Qin LX**, Tang ZY. Hepatocellular carcinoma with obstructive jaundice: diagnosis, treatment and prognosis. *World J Gastroenterol* 2003; **9**: 385-391

3 **Dixon JM**, Armstrong CP, Duffy SW, Davies GC. Factors affecting morbidity and mortality after surgery for obstructive jaundice: a review of 373 patients. *Gut* 1983; **24**: 845-852

4 **Cherqui D**, Benoist S, Malassagne B, Humeres R, Rodriguez V, Fagniez PL. Major liver resection for carcinoma in jaundiced patients without preoperative biliary drainage. *Arch Surg* 2000; **135**: 302-308

5 **McPherson GA**, Benjamin IS, Hodgson HJ, Bowley NB, Allison DJ, Blumgart LH. Pre-operative percutaneous transhepatic biliary drainage: the results of a controlled trial. *Br J Surg* 1984; **71**: 371-375

6 **Greve JW,** Gouma DJ, Soeters PB, Buurman WA. Suppression of cellular immunity in obstructive jaundice is caused by endotoxins: a study with germ-free rats. *Gastroenterology* 1990; **98**: 478-485

7 **Ito Y**, Machen NW, Urbaschek R, McCuskey RS. Biliary obstruction exacerbates the hepatic microvascular inflammatory response to endotoxin. *Shock* 2000; **14**: 599-604

8 **Yerushalmi B**, Dahl R, Devereaux MW, Gumpricht E, Sokol RJ. Bile acid-induced rat hepatocyte apoptosis is inhibited by antioxidants and blockers of the mitochondrial permeability transition. *Hepatology* 2001; **33**: 616-626

9 **Rodrigues CM**, Steer CJ. Mitochondrial membrane perturbations in cholestasis. *J Hepatol* 2000; **32**: 135-141

10 **Lee E**. The effect of obstructive jaundice on the migration of reticulo-endothelial cells and fibroblasts into early experimental granulomata. *Br J Surg* 1972; **59**: 875-877

11 **Fukuhara Y**, Hirasawa A, Li XK, Kawasaki M, Fujino M, Funeshima N, Katsuma S, Shiojima S, Yamada M, Okuyama T, Suzuki S, Tsujimoto G. Gene expression profile in the regenerating rat liver after partial hepatectomy. *J Hepatol* 2003; **38**: 784-792

12 **Ryan CJ**, Than T, Blumgart LH. Choledochoduodenostomy in the rat with obstructive jaundice. *J Surg Res* 1977; **23**: 321-331

13 **Friedman LS**. The risk of surgery in patients with liver disease. *Hepatology* 1999; **29**: 1617-1623

14 **Gong JP**, Wu CX, Liu CA, Li SW, Shi YJ, Li XH, Peng Y. Liver sinusoidal endothelial cell injury by neutrophils in rats with acute obstructive cholangitis. *World J Gastroenterol* 2002; **8**: 342-345

15 **Plusa S**, Webster N, Primrose J. Obstructive jaundice causes reduced expression of polymorphonuclear leucocyte adhesion molecules and a depressed response to bacterial wall products *in vitro*. *Gut* 1996; **38**: 784-787

16 **Daglar GO**, Kama NA, Atli M, Yuksek YN, Reis E, Doganay M, Dolapci M, Kologlu M. Effect of 5-lipoxygenase inhibition on Kupffer cell clearance capacity in obstructive jaundiced rats. *J Surg Res* 2001; **96**: 158-162

17 **Zimmermann H**, Reichen J, Zimmermann A, Sagesser H, Thenisch B, Hoflin F. Reversibility of secondary biliary fibrosis by biliodigestive anastomosis in the rat. *Gastroenterology* 1992; **103**: 579-589

18 **Kimmings AN**, van Deventer SJ, Obertop H, Rauws EA, Huibregtse K, Gouma DJ. Endotoxin, cytokines, and endotoxin

binding proteins in obstructive jaundice and after preoperative biliary drainage. *Gut* 2000; **46**: 725-731
19 **Megison SM**, Dunn CW, Horton JW, Chao H. Effects of relief of biliary obstruction on mononuclear phagocyte system function and cell mediated immunity. *Br J Surg* 1991; **78**: 568-571
20 **Trauner M**, Meier PJ, Boyer JL. Molecular regulation of hepatocellular transport systems in cholestasis. *J Hepatol* 1999; **31**: 165-178
21 **Kanno Y**, Miyazaki M, Udagawa I, Koshikawa H, Ito H, Teramoto O, Okui K. Relation of hepatic protein synthesis and hepatic functional mass in obstructive jaundiced rats. *Nippon Geka Gakkai Zasshi* 1991; **92**: 160-166
22 **Schmucker DL**, Ohta M, Kanai S, Sato Y, Kitani K. Hepatic injury induced by bile salts: correlation between biochemical and morphological events. *Hepatology* 1990; **12**: 1216-1221
23 **Patel T**, Gores GJ. Apoptosis and hepatobiliary disease. *Hepatology* 1995; **21**: 1725-1741
24 **Takikawa Y**, Miyoshi H, Rust C, Roberts P, Siegel R, Mandal PK, Millikan RE, Gores GJ. The bile acid-activated phosphatidylinositol 3-kinase pathway inhibits fas apoptosis upstream of bid in rodent hepatocytes. *Gastroenterology* 2001; **120**: 1810-1817
25 **Faubion WA**, Guicciardi ME, Miyoshi H, Bronk SF, Roberts PJ, Svingen PA, Kaufmann SH, Gores GJ. Toxic bile salts induce rodent hepatocyte apoptosis via direct activation of Fas. *J Clin Invest* 1999; **103**: 137-145
26 **Hatano E,** Bennett BL, Manning AM, Qian T, Lemasters JJ, Brenner DA. NF-kappaB stimulates inducible nitric oxide synthase to protect mouse hepatocytes from TNF-alpha- and Fas-mediated apoptosis. *Gastroenterology* 2001; **120**: 1251-1262
27 **Cong B**, Li SJ, Yao YX, Zhu GJ, Ling YL. Effect of cholecystokinin octapeptide on tumor necrosis factor alpha transcription and nuclear factor-kappaB activity induced by lipopolysaccharide in rat pulmonary interstitial macrophages. *World J Gastroenterol* 2002; **8**: 718-723
28 **Sakahira H**, Enari M, Nagata S. Cleavage of CAD inhibitor in CAD activation and DNA degradation during apoptosis. *Nature* 1998; **391**: 96-99
29 **Luo X**, Budihardjo I, Zou H, Slaughter C, Wang X. Bid, a Bcl2 interacting protein, mediates cytochrome c release from mitochondria in response to activation of cell surface death receptors. *Cell* 1998; **94**: 481-490
30 **Hoglen NC**, Hirakawa BP, Fisher CD, Weeks S, Srinivasan A, Wong AM, Valentino KL, Tomaselli KJ, Bai X, Karanewsky DS, Contreras PC. Characterization of the caspase inhibitor IDN-1965 in a model of apoptosis-associated liver injury. *J Pharmacol Exp Ther* 2001; **297**: 811-818
31 **Liu XJ**, Yang L, Wu HB, Qiang O, Huang MH, Wang YP. Apoptosis of rat hepatic stellate cells induced by anti-focal adhesion kinase antibody. *World J Gastroenterol* 2002; **8**: 734-738
32 **Jones BA**, Rao YP, Stravitz RT, Gores GJ. Bile salt-induced apoptosis of hepatocytes involves activation of protein kinase C. *Am J Physiol* 1997; **272**: G1109-G1115

Edited by Ma JY and Wang XL

P.O.Box 2345, Beijing 100023,China
Fax: +86-10-85381893
E-mail: wjg@wjgnet.com www.wjgnet.com

World J Gastroenterol 2003;9(12):2742-2744
World Journal of Gastroenterology
 ISSN 1007-9327

• BASIC RESEARCH •

Effects of long-term tea polyphenols consumption on hepatic microsomal drug-metabolizing enzymes and liver function in Wistar rats

Tao-Tao Liu, Ning-Sheng Liang, Yan Li, Fan Yang, Yi Lu, Zi-Qing Meng, Li-Sheng Zhang

Tao-Tao Liu, Department of Pharmacy, First Affiliated Hospital, Guangxi Medical University, Nanning 530021, Guangxi Zhuang Autonomous Region, China
Ning-Sheng Liang, Yan Li, Fan Yang, Yi Lu, Zi-Qing Meng, Li-Sheng Zhang, Department of Pharmacology, Guangxi Cancer Institute, Nanning 530021, Guangxi Zhuang Autonomous Region, China
Supported by the National Natural Science Foundation of China, No. 39869001 and Guangxi Natural Science Foundation, No.9912038
Correspondence to: Professor Ning-Sheng Liang, Department of Pharmacology, Guangxi Cancer Institute, Nanning 530021, Guangxi Zhuang Autonomous Region, China. liangn01@163.net
Telephone: +86-771-5310576
Received: 2002-07-26 **Accepted:** 2002-09-25

Abstract

AIM: To investigate the effects of long-term tea polyphenols (TPs) consumption on hepatic microsomal drug-metabolizing enzymes and liver function in rats.

METHODS: TPs were administered intragastrically to rats at the doses of 833 mg· kg^{-1}· d^{-1} (n=20) and 83.3 mg· kg^{-1}· d^{-1} (n=20) respectively for six months. Controlled group (n=20) was given same volume of saline solution. Then the contents of cytochrome P450, b5, enzyme activities of aminopyrine N-demethylase (ADM), glutathione S-trasferase (GST) and the biochemical liver function of serum were determined.

RESULTS: The contents of cytochrome P450 and b_5 in the livers of male rats in high dose groups (respectively 2.66±0.55, 10.43±2.78 nmol· mg MS pro^{-1}) were significantly increased compared with the control group (1.08±1.04, 5.51±2.98 nmol· mg MS pro^{-1}; P<0.01, respectively). The enzymatic activities of ADM in the livers of female rats in high dose groups (0.91±0.08 mmol· mg MS $pro^{-1}min^{-1}$) were increased compared with the control group (0.82±0.08 mmol· mg MS pro^{-1}· min^{-1}; P<0.05). The GST activity was unchanged in all treated groups, and the function of liver was not obviously changed.

CONCLUSION: The antidotal capability of rats' livers can be significantly improved after long-term consumption of TPs. There are differences in changes of drug-metabolizing enzymes between the sexes induced by TPs and normal condition.

Liu TT, Liang NS, Li Y, Yang F, Lu Y, Meng ZQ, Zhang LS. Effects of long-term tea polyphenols consumption on hepatic microsomal drug-metabolizing enzymes and liver function in Wistar rats. *World J Gastroenterol* 2003; 9(12): 2742-2744
http://www.wjgnet.com/1007-9327/9/2742.asp

INTRODUCTION

Tea polyphenols (TPs) are a large and diverse class of compounds extracted from tea. These polyphenolic compounds, specifically catechins epigallocatechin-3-gallate (EGCG), epigallocatechin (EGC), and epicatechin-3-gallate (ECG), account for 30-40 % of the extractable solids in green tea leaves[1]. Many health benefits are associated with consumption of tea and such effects are mainly attributed to the polyphenolic constitutes of tea[2-8]. We are more concerned about the beneficial effect of TPs on cancer[9-13].

Primary liver cancer (PLC) is a very prevalent form of cancer in the world. The incidence of PLC in China is high. Guangxi Zhuang Autonomous Region is a high mortality and morbidity region of PLC. Unfortunately, its curative effect is disappointed no matter what therapy is used. How to improve the prevention and treatment of PLC is a long-term goal of our research work. There are some evidences indicating that TPs may play a positive role in PLC prevention and treatment[14-16]. However, the mechanism of the action is not fully understood. It is known that the risk factors of PLC are intake of AFB_1, pollution of drinking water and HBV infection[17-20]. The factors are closely related to the activity of hepatic microsomal drug metabolizing enzymes and function of the liver. Because bioactivation of precarcinorgens and detoxification of ultimate carcinogens are mainly carried out by drug metabolizing enzymes in the liver, to explore the effects of TPs on these enzymes and the liver function will be helpful to understanding the mechanism of TPs in prevention and treatment of PLC, and the safety of TPs. Further more, this work will provide some useful information for the application of TPs in PLC chemoprevention and chemotherapy.

MATERIALS AND METHODS

Chemicals and reagents

TPs were purchased from Shili Natural Food Co. Ltd (Guilin, China), NADPH from Lizhudongfang Biological Technology Co. (Shanghai, China), aminopyrine from Shanghai Chemical Co., glutathione S-transferase (GST) and protein assay kits from Jiancheng Biological Technology Institude (Nanjing, China), serum biochemical tests of liver function kits from Shenneng Co. (Shanghai, China).

Animals

Five-week-old Wistar rats weighing from 80 to 130 g provided by Experimental Animal Center of Guangxi Medical University were used in the study. The rats were randomly divided into high dose, low dose, and control groups, 20 each group. The animals in high dose and low dose groups were administered intragastrically with TPs at doses of 833 mg· kg^{-1}· d^{-1} and 83.3 mg· kg^{-1}· d^{-1} respectively six times each week for six months. Same procedures were also performed in the control rats except feeding equal amount of normal saline (1.0 ml· 100 g^{-1}· day^{-1}) instead of TPs. The animals were housed in a temperature-controlled room at 22 ℃-24 ℃ and fed with standard rat chow. At the end of six months experimental period, all the rats were anesthetized with intramuscular injection of sodium pentobarbital (30 mg/kg) before sacrificed. Blood was collected

from the heart and serum obtained through centrifugation to measure liver function. The livers were removed immediately, perfused with cold 0.15M KCl and homogenized in 4 volumes of 0.15M KCl solution containing 10 mM EDTA using a Potter-type Teflon glass homogenizer. The homogenate was centrifuged, 10 000×g for 15 min at 4 ℃ in a refrigerated centrifuge (OM 3593 IEC Co. Ltd.USA). The supernatant was then centrifuged 105 000×g for 60 min at 4 ℃ in a preparative ultracentrifuge (20PR-52D; Hitachi, Tokyo). The pellet of microsomes was suspended in the homogenization solution in the homogenizer and centrifuged again as described above. The resulting pellet was suspended in 20 mM potassium phosphate buffer (PH7.4) containing 15 % glycerol until analysis.

Microsomal enzyme assays

The content of cytochrome P450 was determined by the method of Omura and Sato[21,22]. The content of cytochrome b5 was assayed as described by Omura and Takesue[23]. The activities of ADM were determined as described by Imai *et al*[24]. The content of liver microsomal protein and the activities of GST were measured as described in the booklet of kits. All the microsomal enzymes were assayed by using a spectrophotometer (DU-64; Beckman, Fullerton, CA, USA).

Biochemical liver function tests

Biochemical liver function tests (ALT, AST, TP, and ALB) were performed by using an automatic biochemical analyzer (7170A, Hitachi, Tokyo).

Statistical analyses

Data were counted separately in male and female rats and expressed as $\bar{x}\pm s$. Statistical significances were analyzed by *t*-test. The difference was considered significant in case of a two-tailed *P* value less than 0.05, and $P<0.01$ as very significant.

RESULTS

Effects of TPs on contents of P450, b5 and activities of ADM and GST

In high dose group, the contents of P450 and b5 were significantly increased in male rats (respectively 2.66±0.55, 10.43±2.78 nmol· mg MS pro^{-1}) compared with those in the control group (1.08±1.04, 5.51±2.98 nmol· mg MS pro^{-1}; $P<0.01$, respectively). The enzymatic activities of ADM in female rats (0.91±0.08 mmol· mg MS $pro^{-1}min^{-1}$) were higher than those in the control group (0.82±0.08 mmol· mg MS $pro^{-1}\cdot min^{-1}$; $P<0.05$). But the activities of GST were unchanged in all treated groups. In control group, the contents of b5 and the activities of ADM in male and female rats were significantly different (5.51±2.98, 13.42±1.85 nmol· mg MS pro^{-1}; 0.92±0.11, 0.82±0.08 mmol· mg MS $pro^{-1}min^{-1}$, respectively, $P<0.05$). The results indicated that there was a difference of hepatic microsomal drug-metabolizing enzymes under normal conditions in different sex rats (Table 1).

Effects of TPs on biochemical liver functions

TPs did not damage rat liver function after used for a long-term, and it indicated that TPs were a quite safe agent, even at a high dose of 833.3 mg· $kg^{-1}\cdot d^{-1}$, for six months (Table 2).

DISCUSSION

Hepatic drug metabolizing enzyme is called mixed-function oxidase or monooxygenase containing many enzymes including phase I enzymes such as cytochrome P450, cytochrome b5 and NADPH-cytochrome P450 reductase and phase II enzymes such as GST, sulfatase and UDP-glucuronyl transferase[25]. AFB1, one of the risk factors of PLC, damages DNA after conversion to the reactive compound AFB1-epoxide, by the action of cytochrome P450-dependent enzymes[26]. Sufficient evidences have shown that tea and TPs possessed anticarcinogenic effects[27-32]. Some works have been done in the field of TPs modulated or interacted with drug metabolizing enzymes. Maliakal *et al* reported that treating with green tea from different sources could markedly increase cytochrome P450 1A2 activity in rats, and green tea from certain sources could increase cytochrome P450 1A1 and cytosolic GST activities[33]. However, *in vitro* experiment, Mukhtar *et al* and Wang *et al* reported that TPs had an inhibitory effect on microsomal cytochrome P450 enzyme system[34,35]. Until now, no one could give a clear explanation of the different results. We tried to make clear what would happen in these enzyme activities in rats treated with TPs. Considering PLC chemopreventive and chemotherapic effects could not be achieved in a short term of TPs administration, and a long-term experiment has not been carried out in this aspect, so the rats were treated for 6 months. At the end of treatment, we determined the contents of cytochrome P450 and b5, the activities of ADM and GST, and the liver function in the rats. The results showed that the contents and activities

Table 1 Effects of long-term TPs consumption on microsomal enzymes

	Group	P450 nmol / mg MS pro	b5 nmol / mg MS pro	ADM mmol / mg MS pro / min	GST U / mgpro
♂	High dose (n=10)	2.66±0.55[a]	10.43±2.78[a]	0.90±0.12	24.66±4.06
	Low dose (n=10)	1.94±0.90	7.82±1.66	0.94±0.11	27.05±4.59
	Control (n=10)	1.08±1.04	5.51±2.98[c]	0.92±0.11[c]	25.88±4.02
♀	High dose (n=10)	0.66±0.42	11.74±2.31	0.91±0.08[b]	29.48±4.16
	Low dose (n=10)	0.66±0.38	11.34±3.17	0.73±0.09	26.44±4.54
	Control (n=10)	0.36±0.18	13.42±1.85	0.82±0.08	29.40±4.19

[a]$P<0.01$ *vs* ♂ control, [b]$P<0.05$ *vs* ♀ control, [c]$P<0.05$ *vs* ♀ control.

Table 2 Effects of long-term TPs consumption on major biochemical parameters of rat liver

	Group	ALT U / L	AST U / L	TP g / L	ALB g / L
♂	High dose (n=10)	76.31±32.0	294.69±68.8	75.26±3.44	32.96±1.39
	Low dose (n=10)	74.75±11.62	285.4±54.95	78.75±1.83	32.71±1.34
	Control (n=10)	65.5±9.89	271.5±37.32	80.97±3.43	32.42±1.90
♀	High dose (n=10)	59.15±9.14	247.3±61.03	81.43±3.87	34.64±1.11
	Low dose (n=10)	50.31±22.32	213.15±75.92	78.76±5.31	34.86±2.30
	Control (n=10)	56.92±7.62	236.08±51.94	79.56±2.35	35.63±1.06

ALT: serum alanine transaminase, AST: serum asparate transaminase, TP: total protein, ALB: albumin.

of drug metabolizing enzymes and the antidotal capability of liver were significantly improved in the high dose group. It shortened the time of carcinogen staying in the body and reduced DNA damages. Therefore, TPs could protect human against the risk of chemically induced PLC and other cancers.

Gender differences in drug metabolism in rats have been known for more than 60 years since it was reported that the much shorter duration of drug action in the male was due to the effects of testicular androgens[36]. The activities of hepatic drug-metabolizing enzymes, especially cytochrome P450 and sulfotransferase, were regulated through the sex-related secretion pattern of growth hormone[37]. Some studies reported the sex-related effect on drug -metabolizing enzymes[38,39]. In our study, a marked sex difference in the effects of long-term treatment with TPs on hepatic drug-metabolizing enzymes in rats was observed. In control groups, there were differences between male and female rats. The results indicated that there was a sex difference in activities of hepatic drug-metabolizing enzymes and ability of liver detoxification in normal rats. Epidemiological studies of PLC showed that there was a sex difference in human (male>female). But it is not known whether this difference is related to the difference of hepatic drug-metabolizing enzymes.

ACKNOWLEDGMENTS

We appreciate the assistance of Drs Ren-Bin Huang, Xiao-Qun Duan and Yang Jiao from Gunagxi Medical University.

REFERENCES

1 **Brown MD**. Green tea (Camellia sinensis) extract and its possible role in the prevention of cancer. *Altern Med Rev* 1999; **4**: 360-370
2 **Ho CT**, Chen Q, Shi H, Zhang KQ, Rosen RT. Antioxidative effect of polyphenol extract prepared from various Chinese teas. *Prev Med* 1992; **21**: 520-525
3 **Wang ZY**, Cheng SJ, Zhou ZC, Athar M, Khan WA, Bickers DR, Mukhtar H. Antimutagenic activity of green tea polyphenols. *Mutat Res* 1989; **223**: 273-285
4 **Mukhtar H,** Wang ZY, Katiyar SK, Agarwal R. Tea components: antimutagenic and anticarcinogenic effects. *Prev Med* 1992; **21**: 351-360
5 **Zhang G,** Miura Y, Yagasaki K. Suppression of adhesion and invasion of hepatoma cells in culture by tea compounds through antioxidative activity. *Cancer Lett* 2000; **159**: 169-173
6 **Mcs KS**, Kuttan R. Anti-diabetic activity of green tea polyphenols and their role in reducing oxidative stress in experimental diabetes. *J Ethnopharmacol* 2002; **83**: 109-116
7 **Nie G,** Cao Y, Zhao B. Protective effects of green tea polyphenols and their major component,(-)-epigallocatechin-3-gallate (EGCG), on 6-hydroxydopamine-induced apoptosis inPC12 cells. *Rebox Ren* 2002; **7**: 171-177
8 **Shi S**, Zheng S, Jia C, Zhu Y, Xie H. The effect of an antioxidant tea polyphenols on cell apoptosis in rat model of cyclosporine-induced chronic nephrotoxicity. *Zhonghua Waike Zazhi* 2002; **40**:709-712
9 **Yang CS,** Wang ZY. Tea and cancer**.** *J Natl Cancer Inst* 1993; **85**: 1038-1049
10 **Bushman JL.** Green tea and cancer in humans: a review of the literature. *Nutr Cancer* 1998; **31**: 151-159
11 **Gong Y,** Han C, Chen J**.** Effect of tea polyphenols and tea pigments on the inhibition of precancerous liver lesions in rats. *Nutr Cancer* 2000; **38**: 81-86
12 **Hammons GJ,** Fletcher JV, Stepps KR, Smith EA, Balentine DA, Harbowy ME, Kadlubar FF. Effects of chemoprotective agents on the metabolic activation of the carcinogenic arylamines PhIP and 4-aminobiphenyl in human and rat liver microsomes. *Nutr Cancer* 1999; **33**: 46-52
13 **Jung YD**, Ellis LM. Inhibition of tumour invasion and angiogenesis by epigallocatechin gallate (EGCG), a major component of green tea**.** *Int J Exp Pathol* 2001; **82**: 309-316
14 **Lambert JD,** Yang CS. Cancer chemopreventive activity and bioavailability of tea and tea polyphenols. *Mutat Res* 2003; **523-524**: 201-208
15 **Hsu S,** Lewis J, Singh B, Schoenlein P, Osaki T, Athar M, Porter AG, Schuster G. Green tea polyphenol targets the mitochondria in tumor cells inducing caspase 3-dependent apoptosis. *Anticancer Res* 2003; **23**: 1533-1539
16 **Roy M,** Siddiqi M, Bhattacharya RK. Cancer chemoprevention: tea polyphenol induced cellular and molecular responses. *Asian Pac J Cancer Prev* 2001; **2**: 109-116
17 **Wogan GN**. Aflatoxins as risk factors for hepatocellular carcinoma in humans. *Cancer Res* 1992; **52**(7 Suppl): 2114s-2118s
18 **Lu P**, Kuang S, Wang J. Hepatitis B virus infection and aflatoxin exposure in the development of primary liver cancer. *Zhonghua Yixue Zazhi* 1998; **78**: 340-342
19 **Yen FS**, Shen KN. Epidemiology and early diagnosis of primary liver cancer in China. *Adv Cancer Res* 1986; **47**: 297-329
20 **Yu SZ.** Primary prevention of hepatocellular carcinoma. *J Gastroenterol Hepatol* 1995; **10**: 674-682
21 **Heffernan LM,** Winston GW. Distribution of microsomal CO-binding chromophores and EROD activity in sea anemone tissues. *Mar Environ Res* 2000; **50**: 23-27
22 **Bhamre S,** Anandatheerthavarada HK, Shankar SK, Ravindranath V. Microsomal cytochrome P450 in human brain regions. *Biochem Pharmacol* 1992; **44**: 1223-1225
23 **Omura T**, Takesue S. A new method for simultaneous purification of cytochrome b5 and NADPH-cytochrome c reductase from rat liver microsomes. *J Biochem* 1970; **67**: 249-257
24 **Imai Y**, Ito A, Sato R. Evidence for biochemically different types of vesicles in the hepatic microsomal fraction. *J Biochem* 1966; **60**: 417-428
25 **Sheweita SA**. Drug-metabolizing enzymes: mechanisms and functions. *Curr Drug Metab* 2000; **1**: 107-132
26 **De Oliveira CA**, Germano PM. Aflatoxins: current concepts on mechanisms of toxicity and their involvement in the etiology of hepatocellular carcinoma. *Rev Saude Publica* 1997; **31**: 417-424
27 **Ferguson** LR. Role of plant polyphenols in genomic stability. *Mutat Res* 2001; **475**: 89-111
28 **Suganuma M,** Okabe S, Kai Y, Sueoka N, Sueoka E, Fujiki H. Synergistic effects of (–)-epigallocatechin gallate with (–)-epicatechin, sulindac, or tamoxifen on cancer-preventive activity in the human lung cancer cell line PC-9. *Cancer Res* 1999; **59**: 44-47
29 **Isemura M,** Saeki K, Kimura T, Hayakawa S, Minami T, Sazuka M. Tea catechins and related polyphenols as anti-cancer agents. *Biofactors* 2000; **13**: 81-85
30 **Qi L,** Han C. Induction of NAD(P)H: quinone reductase by anticarcinogenic ingredients of tea. *Weisheng Yanjiu* 1998; **27**: 323-326
31 **Wei D,** Mei Y, Liu J. Quantification of doxorubicin and validation of reversal effect of tea polyphenols on multidrug resistance in human carcinoma cells. *Biotechnol Lett* 2003; **25**: 291-294
32 **Mei Y,** Wei D, Liu J. Reversal of cancer multidrug resistance by tea polyphenol in KB cells. *J Chemother* 2003; **15**: 260-265
33 **Maliakal PP**, Coville PF, Wanwimolruk S. Tea consumption modulates hepatic drug metabolizing enzymes in Wistar rats. *J Pharm Pharmacol* 2001; **53**: 569-577
34 **Mukhtar H,** Wang ZY, Katiyar SK, Agarwal R. Tea components: antimutagenic and anticarcinogenic effects. *Prev Med* 1992; **21**: 351-360
35 **Wang ZY**, Das M, Bickers DR, Mukhtar H. Interaction of epicatechins derived from green tea with rat hepatic cytochrome P-450. *Drug Metab Dispos* 1988; **16**: 98-103
36 **Shapiro BH,** Agrawal AK, Pampori NA. Gender differences in drug metabolism regulated by growth hormone. *Int J Biochem Cell Biol* 1995; **27**: 9-20
37 **Kato R**. Molecular pharmacological and toxicological studies of drug-metabolizing enzymes. *Yakugaku Zasshi* 1995; **115**: 661-680
38 **Finnen MJ**, Hassall KA. Effects of hypophysectomy on sex differences in the induction and depression of hepatic drug-metabolizing enzymes in the rat. *J Pharmacol Exp Ther* 1984**; 229**: 250-254
39 **Kobayashi Y**, Ohshiro N, Suzuki M, Sasaki T, Tokuyama S, Yoshida T, Yamamoto T. Sex-related effect of hemin on cytochrome P450 and drug-metabolizing enzymes in rat liver. *J Toxicol Sci* 2000; **25**: 213-222

Edited by Zhang JZ and Wang XL

P.O.Box 2345, Beijing 100023,China
Fax: +86-10-85381893
E-mail: wjg@wjgnet.com www.wjgnet.com

World J Gastroenterol 2003;9(12):2745-2750
World Journal of Gastroenterology
 ISSN 1007-9327

• BASIC RESEARCH •

Oil A induces apoptosis of pancreatic cancer cells via caspase activation, redistribution of cell cycle and GADD expression

Mi-Lian Dong, Yue-Chun Zhu, John V. Hopkins

Mi-Lian Dong, Affiliated Taizhou Hospital, Wenzhou Medical College, Linhai 317000, Zhejiang, Provice China
Yue-Chun Zhu, John V. Hopkins, Northwestern University Medical School, Chicago, IL60611-3008, U.S.A
Supported by the National Cancer Institute of USA, No. CA72712, and Special Funds for Zhejiang 151 Talent Project of China, No. 98-2095
Correspondence to: Dr Mi-Lian Dong, Taizhou Hospital of Wenzhou Medical College, 150 Ximen Street, Linhai 317000, Zhejiang, Provice China. mdong2@hotmail.com
Telephone: +86-576-5315829 **Fax:** +86-576-5315829
Received: 2003-08-23 **Accepted:** 2003-09-10

Abstract

AIM: To explore the mechanisms of effects of oil A on apoptosis of human pancreatic cancer cells.

METHODS: Cellular DNA content was analyzed by flow cytometry. Western blotting was used for caspase-3 and PARP, caspase-7, caspase-9, cytochrome c, Bcl-2, Bax, Mcl-1, cyclinA, cyclin B1, cyclin D1, cyclin E, CDK2, CDK4, CDK6, P21, P27,GADD45, GADD153.

RESULTS: The caspase-3, caspase-7, and caspase-9 activities were significantly increased as well as the cleavage of caspase-3, downstream substrate poly-ADP ribose polymerase (PARP) was induced. The amount of cytochrome c in the cytosolic fraction was increased, while the amount of cytochrome c in the mitochondrial fraction was decreased after oil A treatment. The anti-apoptosis proteins Bcl-2 and Mcl-1 were decreased in parallel and Bax increased, indicating that Bcl-2 family proteins-mitochondria-caspase cascade was responsible for oil-induced apoptosis. The proportion of cells in the G0/G1 decreased in MiaPaCa-2 and AsPC-1 cells after the treatment of oil A for 24 hours. The number of cells in S phase was increased in two cancer cell lines at 24 hours. Therefore, cells were significantly accumulated in G2/M phase. The cells with a sub-G0/G1 DNA content, a hallmark of apoptosis, were seen at 24 hours both in MiaPaCa-2 and AsPC-1 cells following exposure to oil A. The expression of cyclin A and cyclin B1 was slightly decreased and cyclin D1 levels were markedly lowered in MiaPaCa-2 cells. The expression of cyclin A and cyclin B1 was markedly decreased and cyclin D1 levels were slightly lowered in AsPC-1 cells, while cyclin E was not affected and the levels of CDK2, CDK4, and CDK6 were unchanged in MiaPaCa-2 and AsPC-1 cells. In response to oil A, P21 expression was increased, but P27 expression was not affected. The expression of both GADD45 and GADD153 was increased in two cell lines following oil A treatment.

CONCLUSION: Oil A induces apoptosis of pancreatic cancer cells via activating caspase cascade, modifying cell cycle progress and changing cell cycle-regulating proteins and GADD expression.

Dong ML, Zhu YC, Hopkins JV. Oil A induces apoptosis of pancreatic cancer cells via caspase activation, redistribution of cell cycle and GADD expression. *World J Gastroenterol* 2003; 9 (12): 2745-2750
http://www.wjgnet.com/1007-9327/9/2745.asp

INTRODUCTION

It is reported that oil A appears to exert anti-cancer effect by activating apoptosis. It should be speculated that oil A may be broadly active against pancreatic cancer cells. However, whether the use of oil A can be extended to pancreatic tumors is still uncertain. The alternative mechanisms of oil A effect need to be further studied. Our previous experiments showed the inhibition of proliferation and the induction of apoptotic effect by treatment of oil A in pancreatic cancer cells[1]. However, to date, no further information is available regarding the mechanism of effects of oil A on pancreatic cancer cells. In the present study, the mechanism of oil A effect on induction of apoptosis was investigated through activating caspase cascade, inducing cytochrome c release from the mitochondria, Bax, Bcl-2, and Mcl-1 expression, the distribution of cell cycle, changes of cycle-regulating proteins, P21 and P27 expression, and GADD expression in pancreatic cancer cells.

MATERIALS AND METHODS

Reagents

The human pancreatic cancer cell lines, MiaPaCa-2 and AsPC-1 were purchased from the American Type Culture Collection (Rockville, MD, USA). Oil A (Coastside Research Chemical Co., USA) was dissolved in 1:2 DMEM as a stock solution. The stock solution was diluted to appropriate concentrations in serum-free medium prior to experiments. Mitochondria/ Cytosol Fractionation Kit was purchased from BioVision (Mountain View, CA, USA). Enhanced chemiluminescence system (ECL) was obtained from Santa Cruz Biotechnology, Inc. (Santa Cruz, CA, USA). Mouse monoclonal antibodies against PARP, Bcl-2, Bax, Mcl-1, cyclin B1, cyclin D1, cyclin E, CDK2, CDK4, CDK6, P21, P27, GADD45, GADD153 and rabbit polyclonal antibodies against caspase-3, caspase-7, caspase-9, cytochrome c and cyclin A were purchased from Santa Cruz Biotechnology, Inc. (Santa Cruz, CA, USA). All other chemicals were purchased from Sigma (St Louis, MO, USA).

Cell culture

Cells were cultured in DMEM medium supplemented with penicillin G (100 U/mL), streptomycin (100 U/mL) and 10 % FBS at 37 ℃ in humidified air with 5 % CO_2. The cells were harvested by incubation in trypsin-EDTA solution for 10-15 minutes. Then cells were centrifuged at 300×g for 5 minutes and cell pellets suspended in fresh culture medium prior to seeding into culture flasks or plates[1].

Analysis of cellular DNA content by flow cytometry

The cells were grown to 50-60 % confluence in T75 flasks, serum-starved for 24 hours and then treated with or without 1:32 000 oil A for 24 hours. At the end of treatment, the cells were harvested with trypsin-EDTA solution to produce a single

cell suspension. The cells were then pelleted by centrifugation and washed twice with PBS. Cell pellets were then suspended in 0.5 ml PBS and fixed in 5 mL ice-cold 70 % ethanol at 4 ℃. The fixed cells were centrifuged at 300×g for 10 minutes and the pellets were washed with PBS. After resuspension with 1 ml PBS, the cells were incubated with 10 μL of RNase I (10 g/L) and 100 μL of propidium iodide (400 mg/L; Sigma) and shaken for 1 hour at 37 ℃ in the dark. Samples were analyzed by flow cytometry. The red fluorescence of the single events was recorded using a laser beam at 488 nm excitation λ with 610 nm as emission λ to measure the DNA index.

Preparation of cytosolic and mitochondrial extract

Collect cells (5×10^7) were centrifuged at 600×g for 5 minutes at 4 ℃ from control and oil A-treated MiaPaCa-2 and AsPC-1 cells. Wash cells with ice-cold PBS twice, and centrifuge at 600×g for 5 minutes at 4 ℃. Remove supernatant. Resuspend cells with 1.0 mL of 1×cytosol extraction buffer mix containing DTT and protease inhibitors. Incubate on ice for 10 minutes. Homogenize cells in an ice-cold dounce tissue grinder (45 strokes) until 70-80 % of the nuclei did not have the shiny ring. Transfer homogenate to a 1.5 mL microcentrifuge tube, and centrifuge at 700×g for 10 minutes at 4 ℃. Transfer the supernatant to a fresh 1.5 mL tube, and centrifuge at 10 000×g for 30 minutes at 4 ℃. Collect the supernanant as cytosolin fraction. Resuspend the pellet in 0.1 mL mitochondrial extraction buffer mix containing DTT and protease inhibitors, vertex for 10 seconds and save as mitochondrial fraction. Both cytosolic fraction and mitochondrial fraction were stored at -80 ℃ until ready for Western blotting.

Preparation of proteins

Cells were seeded into flasks and grown to 50-60 % confluence, then seeded in serum-free medium for 24 hours. Cells were then placed in serum-free medium with or without 1:32 000 oil A for a period of 24 hours. In the end, proteins were extracted from attached and floating cells in lysis buffer [20 mM Tris-HCl (pH 7.4), 2 mM sodium vanadate, 1.0 mM sodium fluoride, 100 mM NaCl, 2.0 mM phosphate substrate, 1 % NP40, 0.5 % sodium deoxycholate, 20 mg/L each aprotinin and leupeptin, 25 mg/L pepstatin, and 2.0 mM each EDTA and EGTA] for further analysis. Protein concentrations were determined using the bicinchoninic acid assay with BSA as standard.

Western blotting

Western blotting was carried out using standard techniques. In brief, equal amounts of proteins in the cell lysates were separated on SDS-PAGE and the proteins then transferred onto nitrocellulose membranes. After blocking non-specific sites with fat free dried milk, membranes were incubated with the appropriate dilution of primary antibody. Then, membranes were incubated with a horseradish peroxidase conjugated secondary antibody. Proteins were detected using an enhanced chemiluminescence detection system, and light emission was captured on Kodak X-ray films.

RESULTS

Effect of oil A on activation of caspase 3 and cleavage of PARP, caspase 7 and caspase 9

The expression and activation of caspase 3 by cleavage as well as the specific cleavage of its downstream substrate, PARP during apoptosis were observed by Western blotting. The 32 kDa procaspase 3 was cleaved into products of lower molecular weight, including a band corresponding to the 17 kDa active form. The uncleaved 116 kDa pro-form of PARP was only seen in untreated controls while in oil A treatment resulted in appearance of the active 85 kDa cleaved fragments. Caspase 7 and 9 degradation activation were also induced, and coincident with the induction of apoptosis (Figure 1).

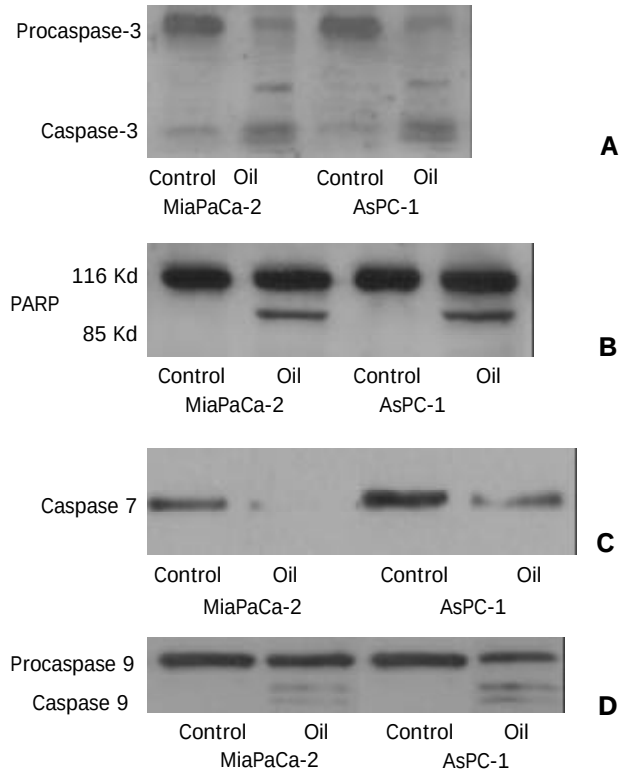

Figure 1 (A, B, C, D) Western blotting of the caspase-3, poly-ADP ribose polymerase (PARP), caspase 7 and caspase 9 in MiaPaCa-2 and AsPC-1 cells treated with 1:32 000 oil A for 24 hours. Proteins in whole cellular lysates were electrophoresed in SDS-PAGE gels and transferred to nitrocellulose membranes. Caspase-3, PARP, caspase 7 and caspase 9 were identified using specific antibodies.

Oil A induces cytochrome c release

Cytochrome c is a mitochondrial protein released from the mitochondria to cytosol during apoptosis when mitochondrial membrane permeability is disrupted. An increase in the amount of cytochrome c in the cytosolic fraction was seen in both cell lines after oil A treatment. Meanwhile, the amount of cytochrome c in the mitochondrial fraction was decreased also in both cell lines after oil A treatment (Figure 2).

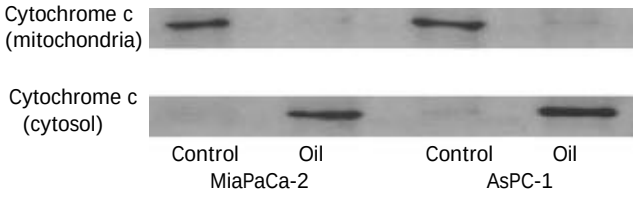

Figure 2 Western blotting of the cytochrome c protein in MiaPaCa-2 and AsPC-1 cells treated with 1:32 000 oil A for 24 hours. Proteins in cytosolic fraction and in mitochondria fraction were extracted. Proteins extracted from each sample were electrophoresed on an SDS-PAGE gel and transferred to nitrocellulose membrane. Cytochrome c was identified using a monoclonal cytochrome c antibody.

Effect of oil A on expression of Bax, Bcl-2, and Mcl-1 proteins

Expression of the anti-apoptosis proteins Bcl-2 and Mcl-1 was decreased and Bax increased following oil A treatment (Figure 3).

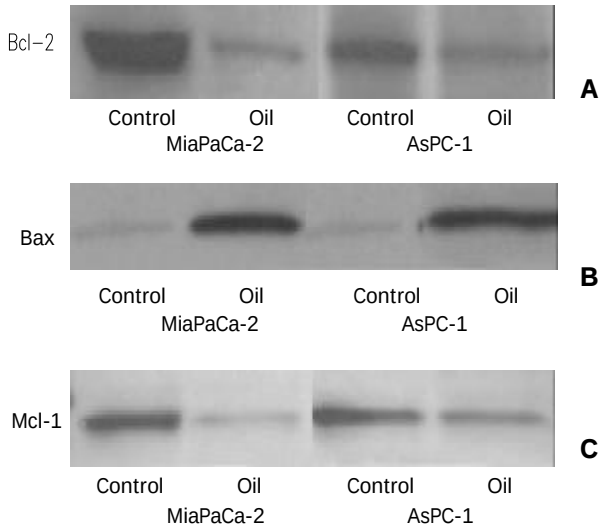

Figure 3 (A, B, C) Western blotting of the Bcl-2, Bax and Mcl-1 proteins in MiaPaCa-2 and AsPC-1 cells treated with 1:32 000 oil A for 24 hours. Whole cellular lysates were electrophoresed in SDS-PAGE gels and proteins were transferred to nitrocellulose membranes. Bcl-2, Bax and Mcl-1 were identified using specific antibodies.

Effect of oil A on cell cycle phase distribution

To understand the mechanism of induction of cell apoptosis, the redistribution of cell cycle phases were analyzed after the treatment with 1:32 000 oil A for 24 hours. The proportion of cells in the G0/G1 phase decreased in MiaPaCa-2 and AsPC-1 cell lines. Therefore, cells were significantly accumulated in the G2/M-phase in these two cancer cell lines. The number of cells in S-phase was increased also in both cell lines when compared with control. The cells with a sub-G0/G1 DNA content, a hallmark of apoptosis, were seen following 24-hour exposure to oil A in both cell lines (Figure 4).

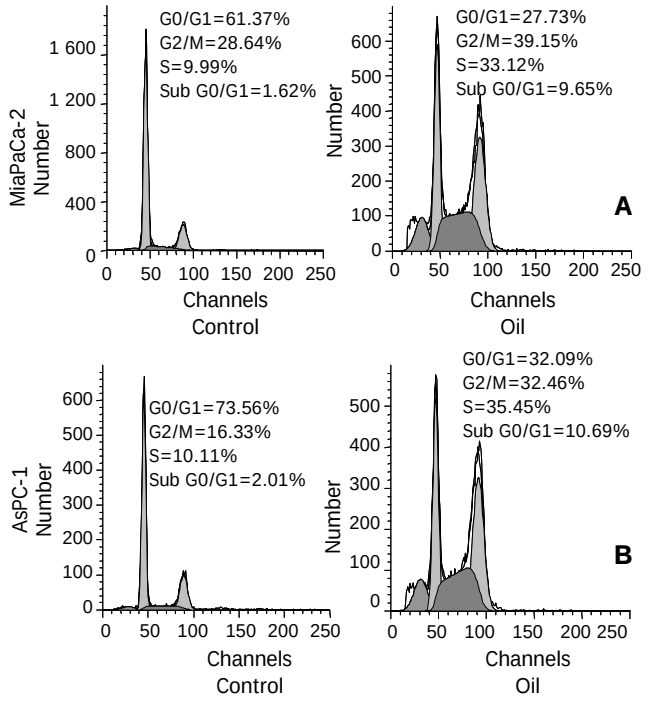

Figure 4 (A, B) Flow-cytometric analysis of cellular DNA content in control and oil A-treated MiaPaCa-2 and AsPC-1 cells, stained with propidium iodide. The cells were treated with 1:32 000 oil A in serum-free conditions for 24 hours. The distribution of cell cycle phases is expressed as % of total cells.

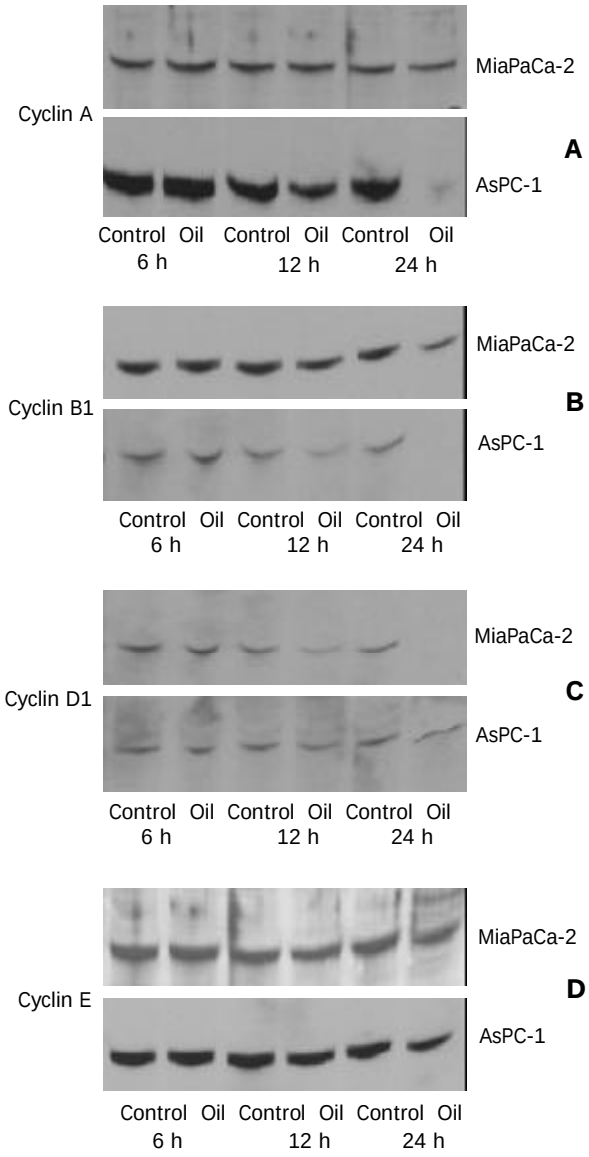

Figure 5 (A, B, C, D) Western blotting of the cyclin A, cyclin B1, cyclin D1 and cyclin E proteins in MiaPaCa-2 and AsPC-1 cells treated with 1:32 000 oil A for 24 hours. Whole cellular lysates were electrophoresed in SDS-PAGE gels and proteins were transferred to nitrocellulose membranes.

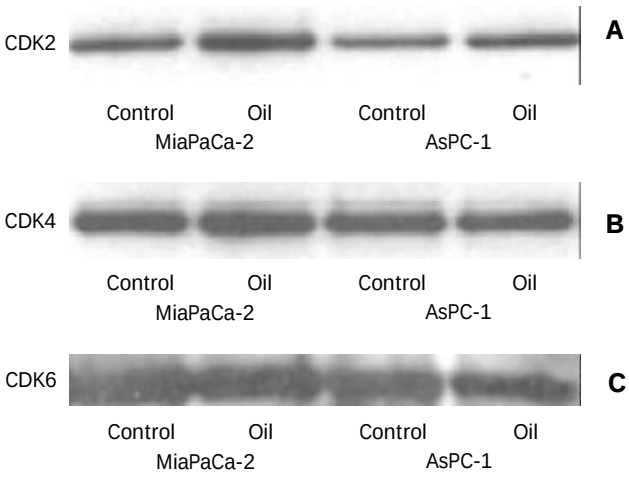

Figure 6 (A, B, C) Western blotting of the CDK2, CDK4 and CDK6 proteins in MiaPaCa-2 and AsPC-1 cells treated with 1:32 000 oil A for 24 hours. Whole cellular lysates were electrophoresed in SDS-PAGE gels and proteins were transferred to nitrocellulose membranes.

Effect of oil A on expression of cyclin proteins

The expression of cyclin A and cyclin B1was slightly decreased and cyclin D1 levels were markedly decreased in MiaPaCa-2 cell line. The expression of cyclin A and cyclin B1 was markedly decreased and cyclin D1 levels were slightly decreased in AsPC-1 cell line, while cyclin E was unaffected and the levels of CDK2, CDK4, and CDK6 remained unchanged in MiaPaCa-2 and AsPC-1 cell lines (Figures 5 and 6).

Effect of oil A on expression of P21 and P27 proteins

In response to red oil A, P21 expression was increased, but P27 expression was not affected (Figure 7).

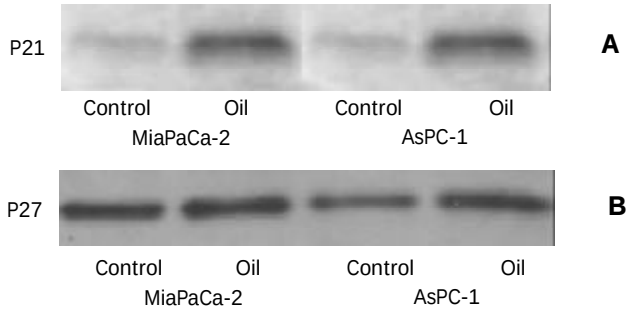

Figure 7 (A, B) Western blotting of the P21 and P27 proteins in MiaPaCa-2 and AsPC-1 cells treated with 1:32 000 oil A for 24 hours. Whole cellular lysates were electrophoresed in SDS-PAGE gels and proteins were transferred to nitrocellulose membranes. P21 and P27 were identified using specific antibodies.

Effect of oil A on expression of GADD

The expression of GADD 45 and GADD153 was enhanced in both pancreatic cancer cell lines following oil A treatment (Figure 8).

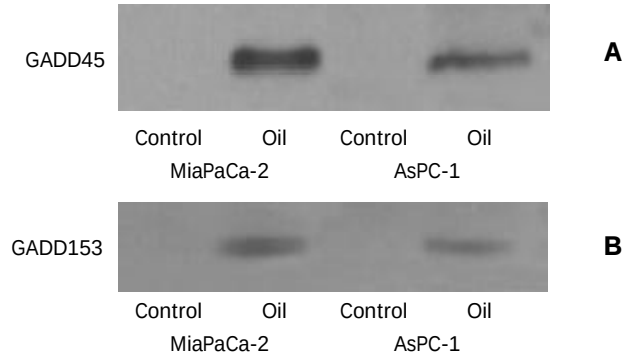

Figure 8 (A, B) Western blotting of GADD45 and GADD153 proteins in MiaPaCa-2 and AsPC-1 cells treated with 1:32 000 oil A for 24 hours. Whole cellular lysates were electrophoresed in SDS-PAGE gels and proteins were transferred to nitrocellulose membranes. GADD was identified using specific monoclonal antibodies.

DISCUSSION

Because of its significant medical properties, fish oil has been used for many years.

Recent studies indicate that diets containing a high proportion of long-chain n-3 polyunsaturated fatty acids were associated with inhibition of the growth and metastasis of human cancer including pancreatic cancer[1-3]. Diets rich in linoleic acid (LA), an n-6 fatty acid, stimulate the progression of human cancer cell in athymic nude mice, whereas supplement of fish oil components, docosahexaenoic acid (DHA) and eicosapentaenoic acid (EPA) exerts suppressive effects. Fish oil has been shown to reduce the induction of different cancer in animal models by a mechanism which may involve suppression of mitosis, increased apoptosis through long-chain n-3 polyunsaturated fatty acid EPA[1,2,4-6]. In parallel, dietary supplementation with DHA is accompanied by reduced levels of 12- and 15-hydroxyeicosatetraenoic acids (12- and 15-HETE), suggesting that changes in eicosanoid biosynthesis may have been responsible for the observed decrease in tumor growth[2,7-9]. Previous studies also have shown that the anti-cancer effect of fish oil is accompanied by a decreased production of cyclooxygenase and lipoxygenase metabolites[10-13]. The efficacy of fish oil which we have found exhibits particularly potent anticancer effects that appear to be related to its content of lipoxygenase inhibitors rather than its EPA or DHA contents.

Oil A is lipid isolates from the epithelial layer of the echinoderm. Little attention of the mechanism of apoptosis induced by oil A has been paid to pancreatic cancer, which is a major cause of cancer death. The results from the present study indicate that oil A induces apoptosis on pancreatic cancer cells via caspase activities, release of cytochrome c from mitochondria, decreased expression of Bcl-2 and Mcl-1 proteins, increased expression of Bax, redistribution of cell cycle phases, increased expression of P21, GADD45 and GADD153, in association with different expression of cyclins[14-21].

Caspases are cysteine proteases produced as inactive forms and activated during apoptosis. Caspase 3 is a major executioner protease, responsible for initiating in the apoptotic program[22-24]. Caspase 3 plays an important role in the apoptotic program of cells[22-28]. As a result, the caspase 3 and caspase 9 were activated, caspase 7 was decreased following oil A treatment. As a major executioner protease, the sequence alignment among caspase 3, 7 and 9 reveals the different structural basis of functions of caspase 3, 7 and 9. Caspase 3 and caspase 7 share the same sequence by 54 % and the backbone structures are nearly identical[29]. The activation of an effector, caspase 3, is performed by an initiator, caspase 9 through proteolytic cleavage at specific internal asp residues and caspase 3 is responsible for initiating the apoptotic program[22-24,30,31].

PARP cleavage could serve as a sensitive parameter for identification of early apoptosis[32,33]. In parallel, PARP provided further evidence that this apoptotic pathway is activated.

Oil A induced cytochrome c release from the mitochondria to cytosol. Once cytochrome c is released from the mitochondria, it complexes with apoptotic protease-activating factor 1 to activate caspase 3[34-37].

Also, the increase of Bax and the decrease of Bcl-2 and Mcl-1 indicate that Bcl proteins-mitochondria-caspase cascade play an important role in oil-induced apoptosis. To better understand the effect of oil A on apoptosis of pancreatic cancer cells, flow cytometric analysis of propidium iodide-stained cells was carried out. Cytometric analysis showed significant changes of cell cycle distribution in MiaPaCa-2 and AsPC-1 cells following oil treatment for 24 hours. At first (control), the proportion of cells was arrested in the G0/G1. The G2/M phase and S phase of cell cycle were accumulated after oil treatment. In the present study, we demonstrated that the distribution of cell cycle underwent changes from G0/G1 phase arrest to G2/M phase and S phase arrest following oil A treatment. The changes of cell cycle distribution suggest that apoptosis of pancreatic cancer cells may be related to some underlying mechanism, which may trigger an apoptosis signal. Thereafter, the cells with a sub-G0/G1 DNA content, a hallmark of apoptosis, were accumulated in both cell lines MiaPaCa-2 and AsPC-1 at 24 hours following exposure to oil A. The effects

of oil A persist throughout the course of cell growth, cells with DNA damage increase progressively and develop apoptosis successively. The typical peak of a sub-G0/G1 population of cells indicates oil-induced apoptosis of pancreatic cancer cells.

The cyclins and cyclin-dependent kinases (CDKs) are key components of the cell cycle machinery that is responsible for the progression through the G1/S and G2/M phases[38]. In our experiments, the differential expression of cyclins and CDKs were observed in pancreatic cancer cells. During oil A treatment, no detectable changes of CDK2, 4, 6 were observed. When the cell cycle procession was arrested in G0/G1 phase at 24 hours of treatment, the expression of cyclins remained unchanged. Thereafter, when the cell cycle procession was arrested in G2/M phase at 24 hours of treatment, expression of cyclins was different between MiaPaCa-2 and AsPC-1 cells. Cyclin A and cyclin B1 levels were slightly decreased and cyclin D1 was markedly decreased in MiaPaCa-2 cells, whereas cyclin A and cyclin B1 levels were markedly decreased and cyclin D1 was slightly decreased in AsPC-1 cells. At the same time, expression of cyclin E was still constantly expressed. These changes of cyclins suggested underlying mechanism of cell cycle distribution in pancreatic cancer cells response to oil stress. How the cyclins are regulated remains unclear.

It has been reported that P21 mediated a significant response to DNA-damaging agents[39,40]. The results show that oil induced an increased expression of P21, whereas the expression of P27 protein was not changed following oil treatment in the present work. These results suggested that P21 protein may play a key role in G0/G1 to G2/M phase arrest leading to apoptosis of pancreatic cancer cells.

The cell cycle is regulated by inhibitory proteins, such as GADDs, which are responsible for the maintenance of the cell cycle checkpoint that prevents inappropriate mitosis[41-44]. GADDs expression played an important role in signal transduction pathway in response to DNA damage[34,42-45]. Pancreatic cancer cells might respond to oil stress by activating signal transduction leading to cell cycle arrest. As an extracellullar stress signal, oil A induced expression of GADDs in pancreatic cancer cells, which may be related to cell cycle arrest through G0/G1 to G2/M phases. The experimental findings suggest that GADD expression may modulate the sensitivity to oil-induced DNA damage leading to apoptosis. The GADD45 is considered to be functionally p53-dependent or p53-independent and GADD153 to be p53-independent. The increase in GADD45 and GADD153 along with a decrease in Bcl-2 and Mcl-1 were seen in pancreatic cancer cells that underwent growth arrest and apoptosis, which may provide clues concerning the mechanism of the effects of oil A. Although GADD expression with cell cycle redistributions are responsive to oil stress, the underlying mechanisms remain obscure. Further studies are required to elucidate how oil modulates the GADD proteins expression.

REFERENCES

1 **Fay MP**, Freedman LS, Clifford CK, Midthune DN. Effect of different types and amounts of fat on the development of mammary tumors in rodents: a review. *Cancer Res* 1997; **57**: 3979-3988

2 **Hawkins RA**, Sangster K, Arends MJ. Apoptotic death of pancreatic cancer cells induced by polyunsaturated fatty acids varies with double bond number and involves an oxidative mechanism. *J Pathol* 1998; **185**: 61-70

3 **Huang PL**, Zhu SN, Lu SL, Dai ZS, Jin YL. Inhibitor of fatty acid synthase induced apoptosis in human colonic cancer cells. *World J Gastroenterol* 2000; **6**: 295-297

4 **Calviello G**, Palozza P, Franceschelli P, Frattucci A, Piccioni E, Tessitore L, Bartoli GM. Eicosapentaenoic acid inhibits the growth of liver preneoplastic lesions and alters membrane phospholipid composition and peroxisomal beta-oxidation. *Nutr Cancer* 1999; **34**: 206-212

5 **Bartsch H**, Nair J, Owen RW. Dietary polyunsaturated fatty acids and cancers of the breast and colorectum: emerging evidence for their role as risk modifiers. *Carcinogenesis* 1999; **20**: 2209-2218

6 **Lai PB**, Ross JA, Fearon KC, Anderson JD, Carter DC. Cell cycle arrest and induction of apoptosis in pancreatic cancer cells exposed to eicosapentaenoic acid *in vitro*. *Br J Cancer* 1996; **74**: 1375-1383

7 **Falconer JS**, Ross JA, Fearon KC, Hawkins RA, O`Riordain MG, Carter DC. Effect of eicosapentaenoic acid and other fatty acids on the growth *in vitro* of human pancreatic cancer cell lines. *Br J Cancer* 1994; **69**: 826-832

8 **Karmali RA**, Donner A, Gobel S, Shimamura T. Effect of n-3 and n-6 fatty acids on 7, 12 dimethylbenz (a) anthracene-induced mammary tumorigenesis. *Anticancer Res* 1989; **9**: 1161-1167

9 **Rose DP**, Connolly JM. Antiangiogenicity of docosahexaenoic acid and its role in the suppression of breast cancer cell growth in nude mice. *Int J Oncol* 1999; **15**: 1011-1015

10 **Ding XZ**, Tong WG, Adrian TE. Cyclooxygenases and lipoxygenases as potential targets for treatment of pancreatic cancer. *Pancreatology* 2001; **1**: 291-299

11 **Larsen LN**, Hovik K, Bremer J, Holm KH, Myhren F, Borretzen B. Heneicosapentaenoate (21: 5n-3): its incorporation into lipids and its effects on arachidonic acid and eicosanoid synthesis. *Lipids* 1997; **32**: 707-714

12 **Noguchi M**, Earashi M, Minami M, Kinoshita K, Miyazaki I. Effects of eicosapentaenoic and docosahexaenoic acid on cell growth and prostaglandin E and Leukotriene B production by a human breast cancer cell line (MDA-MB-231). *Oncology* 1995; **52**: 458-464

13 **Eibl G**, Reber HA, Wente MN, Hines OJ. The selective cyclooxygenase-2 inhibitor nimesulide induces apoptosis in pancreatic cancer cells independent of COX-2. *Pancreas* 2003; **26**: 33-41

14 **Katz MH**, Spivack DE, Takimoto S, Fang B, Burton DW, Moossa AR, Hoffman RM, Bouvet M. Gene therapy of pancreatic cancer with green fluorescent protein and tumor necrosis factor-related apoptosis-inducing ligand fusion gene expression driven by a human telomerase reverse transcriptase promoter. *Ann Surg Oncol* 2003; **10**: 762-772

15 **Tassone P**, Tagliaferri P, Viscomi C, Palmieri C, Caraglia M, D'Alessandro A, Galea E, Goel A, Abbruzzese A, Boland CR, Venuta S. Zoledronic acid induces antiproliferative and apoptotic effects in human pancreatic cancer cells *in vitro*. *Br J Cancer* 2003; **88**: 1971-1978

16 **Buchler P**, Gukovskaya AS, Mouria M, Buchler MC, Buchler MW, Friess H, Pandol SJ, Reber HA, Hines OJ. Prevention of metastatic pancreatic cancer growth *in vivo* by induction of apoptosis with genistein, a naturally occurring isoflavonoid. *Pancreas* 2003; **26**: 264-273

17 **Saldeen J**, Tillmar L, Karlsson E, Welsh N. Nicotinamide- and caspase-mediated inhibition of poly(ADP-ribose) polymerase are associated with p53-independent cell cycle (G2) arrest and apoptosis. *Mol Cell Biochem* 2003; **243**: 113-122

18 **Shibayama-Imazu T**, Sakairi S, Watanabe A, Aiuchi T, Nakajo S, Nakaya K. Vitamin K(2) selectively induced apoptosis in ovarian TYK-nu and pancreatic MIA PaCa-2 cells out of eight solid tumor cell lines through a mechanism different from geranylgeraniol. *J Cancer Res Clin Oncol* 2003; **129**: 1-11

19 **Irawaty W**, Kay TW, Thomas HE. Transmembrane TNF and IFNgamma induce caspase-independent death of primary mouse pancreatic beta cells. *Autoimmunity* 2002; **35**: 369-375

20 **Marriott JB**, Clarke IA, Czajka A, Dredge K, Childs K, Man HW, Schafer P, Govinda S, Muller GW, Stirling DI, Dalgleish AG. A novel subclass of thalidomide analogue with anti-solid tumor activity in which caspase-dependent apoptosis is associated with altered expression of bcl-2 family proteins. *Cancer Res* 2003; **63**: 593-599

21 **Thomas RP**, Farrow BJ, Kim S, May MJ, Hellmich MR, Evers BM. Selective targeting of the nuclear factor-kappaB pathway enhances tumor necrosis factor-related apoptosis-inducing ligand-mediated pancreatic cancer cell death. *Surgery* 2002; **132**: 127-134

22 **Thornberry NA**, Lazebnik Y. Caspase: enemies within. *Science* 1998; **281**: 1312-1316

23 **Mancini M**, Nicholson DW, Roy S, Thornberry NA, Peterson EP, Casciola-Rosen LA, Rosen A. The caspase-3 precursor has a cy-

tosolic and mitochondrial distribution: implications for apoptotic signaling. *J Cell Biol* 1998; **140**: 1485-1495

24 **Kothakota S**, Azuma T, Reinhard C, Klippel A, Tang J, Chu K, McGarry TJ, Kirschner MW, Koths K, Kwiatkowski DJ, Williams L. Caspase-3-generated fragment of gelsolin: effector of morphological change in apoptosis. *Science* 1997; **278**: 294-298

25 **Kobayashi D**, Sasaki M, Watanabe N. Caspase-3 activation downstream from reactive oxygen species in heat-induced apoptosis of pancreatic carcinoma cells carrying a mutant p53 gene. *Pancreas* 2001; **22**: 255-260

26 **Virkajarvi N**, Paakko P, Soini Y. Apoptotic index and apoptosis influencing proteins bcl-2, mcl-1, bax and caspases 3, 6 and 8 in pancreatic carcinoma. *Histopathology* 1998; **33**: 432-439

27 **Pirocanac EC**, Nassirpour R, Yang M, Wang J, Nardin SR, Gu J, Fang B, Moossa AR, Hoffman RM, Bouvet M. Bax-induction gene therapy of pancreatic cancer. *J Surg Res* 2002; **106**: 346-351

28 **Kirsch DG**, Doseff A, Chau BN, Lim DS, de Souza-Pinto NC, Hansford R, Kastan MB, Lazebnik YA, Hardwick JM. Caspase-3-dependent cleavage of Bcl-2 promotes release of cytochrome c. *J Biol Chem* 1999; **274**: 21155-21161

29 **Chai J**, Shiozaki E, Srinivasula SM, Wu Q, Datta P, Alnemri ES, Shi Y, Dataa P. Structure basis of caspase-7 inhibition by XIAP. *Cell* 2001; **104**: 769-780

30 **Akao Y**, Nakagawa Y, Akiyama K. Arsenic trioxide induces apoptosis in neuroblastoma cell lines through the activation of caspase-3 *in vitro*. *FEBS Lett* 1999; **455**: 59-62

31 **Jiang XH,** Wong BC, Yuen ST, Jiang SH, Cho CH, Lai KC, Lin MC, Kung HF, Lam SK, Chun YU, Wong B. Arsenic trioxide induces apoptosis in human gastric cancer cells through up-regulation of p53 and activation of caspase-3. *Int J Cancer* 2001; **91**: 173-179

32 **Decker P**, Isenberg D, Muller S. Inhibition of caspase-3-mediated poly (ADP-ribose) polymerase (PARP) apoptotic cleavage by human PARP autoantibodies and effect on cells undergoing apoptosis. *J Biol Chem* 2000; **275**: 9043-9046

33 **Sellers WR**, Fisher DE. Apoptosis and cancer drug targeting. *J Clin Invest* 1999; **104**: 1655-1661

34 **Tong WG**, Ding XZ, Witt RC, Adrian TE. Lipoxygenase inhibitors attenuate growth of human pancreatic cancer xenografts and induce apoptosis through the mitochondrial pathway. *Mol Cancer Ther* 2002; **1**: 929-935

35 **Gerhard MC**, Schmid RM, Hacker G. Analysis of the cytochrome c-dependent apoptosis apparatus in cells from human pancreatic carcinoma. *Br J Cancer* 2002; **86**: 893-898

36 **Mouria M**, Gukovskaya AS, Jung Y, Buechler P, Hines OJ, Reber HA, Pandol SJ. Food-derived polyphenols inhibit pancreatic cancer growth through mitochondrial cytochrome C release and apoptosis. *Int J Cancer* 2002; **10**: 761-769

37 **Kluck RM**, Bossy-Wetzel E, Green DR, Newmeyer DD. The release of cytochrome c from mitochondria: a primary site for Bcl-2 regulation of apoptosis. *Science* 1997; **275**: 1132-1136

38 **Sherr CJ**. G1 phase progression: cycling on cue. *Cell* 1994; **79**: 551-555

39 **Waldman T**, Kinzler KW, Vogelstein B. p21 is necessary for the p53-mediated G1 arrest in human cancer cells. *Cancer Res* 1995; **55**: 5187-5190

40 **Waga S**, Hannon GJ, Beach D, Stillman B. The P21 inhibitor of cyclin-dependent kinases controls DNA replication by interaction with PCNA. *Nature* 1994; **369**: 574-578

41 **Takahashi S**, Saito S, Ohtani N, Sakai T. Involvement of the Oct-1 regulator element of the GADD45 promoter in the P53-independent response to ultraviolet irradiation. *Cancer Res* 2001; **61**: 1187-1195

42 **Patton GW**, Paciga JE, Shelley SA. NR8383 alveolar macrophage toxic growth arrest by hydrogen peroxide is associated with induction of growth-arrest and DNA damage-inducible genes GADD45 and GADD153. *Toxicol Appl Pharmacol* 1997; **147**: 126-134

43 **Ou YC**, Thompson SA, Kirchner SC, Kavanagh TJ, Faustman EM. Induction of growth arrest and DNA damage-inducible genes Gadd45 and Gadd153 in primary rodent embryonic cells following exposure to methymercury. *Toxicol Appl Pharmacol* 1997; **147**: 31-38

44 **Carrier F**, Zhan Q, Alamo I, Hanaoka F, Fornace AJ Jr. Evidence for distinct kinase-mediated pathways in GADD gene responses. *Biochem Pharmacol* 1998; **55**: 853-861

45 **Zhan Q**, Fan S, Smith ML, Bae I, Yu K, Alamo I Jr, O'Connor PM, Fornace AJ Jr. Abrogation of p53 function affects Gadd gene responses to DNA base-damaging agents and starvation. *DNA Cell Biol* 1996; **15**: 805-815

Edited by Ma JY

P.O.Box 2345, Beijing 100023,China
Fax: +86-10-85381893
E-mail: wjg@wjgnet.com www.wjgnet.com

World J Gastroenterol 2003;9(12):2751-2758
World Journal of Gastroenterology
 ISSN 1007-9327

• BASIC RESEARCH •

Establishment and characterization of a rat pancreatic stellate cell line by spontaneous immortalization

Atsushi Masamune, Masahiro Satoh, Kazuhiro Kikuta, Noriaki Suzuki, Tooru Shimosegawa

Atsushi Masamune, Masahiro Satoh, Kazuhiro Kikuta, Noriaki Suzuki, Tooru Shimosegawa, Division of Gastroenterology, Tohoku University Graduate School of Medicine, Sendai, Japan
A.M. and M.S. equally contributed to this work
Supported by Grant-in-Aid for Encouragement of Young Scientists from Japan Society for the Promotion of Science (to A.M.), and Pancreas Research Foundation of Japan (to A.M.)
Correspondence to: Dr. Atsushi Masamune, Division of Gastroenterology, Tohoku University Graduate School of Medicine, 1-1 Seiryo-cho, Aoba-ku, Sendai 980-8574 Japan. amasamune@int3.med.tohoku.ac.jp
Telephone: +81-22-717-7171 **Fax:** +81-22-717-7177
Received: 2003-08-26 **Accepted:** 2003-09-15

Abstract

AIM: Activated pancreatic stellate cells (PSCs) have been implicated in the pathogenesis of pancreatic fibrosis and inflammation. Primary PSCs can be subcultured only several times because of their limited growth potential. A continuous cell line may therefore be valuable in studying molecular mechanisms of these pancreatic disorders. The aim of this study was to establish a cell line of rat PSCs by spontaneous immortalization.

METHODS: PSCs were isolated from the pancreas of male Wistar rats, and conventional subcultivation was performed repeatedly. Telomerase activity was measured using the telomere repeat amplification protocol. Activation of transcription factors was assessed by electrophoretic mobility shift assay. Activation of mitogen-activated protein (MAP) kinases was examined by Western blotting using anti-phosphospecific antibodies. Expression of cytokine-induced neutrophil chemoattractant-1 was determined by enzyme immunoassay.

RESULTS: Conventional subcultivation yielded actively growing cells. One clone was obtained after limiting dilution, and designated as SIPS. This cell line has been passaged repeatedly more than 2 years, and is thus likely immortalized. SIPS cells retained morphological characteristics of primary, culture-activated PSCs. SIPS expressed α-smooth muscle actin, glial acidic fibrillary protein, vimentin, desmin, type I collagen, fibronectin, and prolyl hydroxylases. Telomerase activity and p53 expression were negative. Proliferation of SIPS cells was serum-dependent, and stimulated with platelet-derived growth factor-BB through the activation of extracellular signal-regulated kinase. Interleukin-1β activated nuclear factor-κB, activator protein-1, and MAP kinases. Interleukin-1β induced cytokine-induced neutrophil chemoattractant-1 expression through the activation of nuclear factor-κB and MAP kinases.

CONCLUSION: SIPS cells can be useful for *in vitro* studies of cell biology and signal transduction of PSCs.

Masamune A, Satoh M, Kikuta K, Suzuki N, Shimosegawa T. Establishment and characterization of a rat pancreatic stellate cell line by spontaneous immortalization. *World J Gastroenterol* 2003; 9(12): 2751-2758
http://www.wjgnet.com/1007-9327/9/2751.asp

INTRODUCTION

Chronic pancreatitis as well as pancreatic cancer are accompanied by progressive fibrosis that is characterized by loss of functional tissue and its replacement by extracellular matrix rich connective tissues[1,2]. In contrast to liver fibrosis, the molecular mechanisms of pancreatic fibrogenesis remain to be elucidated. In 1998, star-shaped cells in the pancreas, namely pancreatic stellate cells (PSCs), were identified and characterized[3,4]. They are morphologically very similar to the hepatic stellate cells that play a central role in fibrosis of the liver[5]. In normal pancreas, stellate cells are quiescent and can be identified by the presence of vitamin A-containing lipid droplets in the cytoplasm. In response to pancreatic injury or inflammation, they are transformed ("activated") from quiescent phenotype into highly proliferative myofibroblast-like cells which express the cytoskeletal protein α-smooth muscle actin (α-SMA), and produce type I collagen and other extracellular matrix components. Many of the morphological and metabolic changes associated with the activation of PSCs in animal models of fibrosis also occur when these cells are grown in culture on plastics in serum-containing medium. Therefore, culture of primary PSCs on plastics has been accepted as an established model that mimics the phenotypic changes that occur during the process of PSC activation following pancreatic injury. There is accumulating evidence that PSCs, like hepatic stellate cells, are responsible for the development of pancreatic fibrosis[3,4,6]. Furthermore, PSCs might participate in the pathogenesis of acute pancreatitis through the expression of monocyte chemoattractant protein-1 and intercellular adhesion molecule-1[7,8]. The activation of signaling pathways such as p38 mitogen-activated protein (MAP) kinase[9] is likely to play a key role in PSC activation. However, the precise intracellular signaling pathways in PSCs are largely unknown.

Although primary stellate cell culture is a useful tool for studying molecular mechanisms of pancreatic fibrosis and inflammation *in vitro*, their isolation is time-consuming, yields are relatively low, and there is considerable heterogeneity between preparations. Several weeks in culture are required to obtain sufficient cells to perform experiments. In addition, primary cells can be subcultured only several times because of their limited life span *in vitro*. Because rat cells are known to be immortalized by spontaneous transformation, this study aimed to establish a rat PSC line by spontaneous immortalization.

MATERIALS AND METHODS

Materials

[γ-^{32}P]ATP was obtained from Amersham Biosciences UK, Ltd. (Buckinghamshire, England). Rat recombinant platelet-derived growth factor (PDGF)-BB was from R&D Systems (Minneapolis, MN). Recombinant human interleukin (IL)-1β was from Roche Applied Science (Mannheim, Germany). Rabbit antibodies against phosphorylated MAP kinases, total MAP kinases, and inhibitor of nuclear factor κB (NF-κB)-α (IκB-α) were purchased from Cell Technologies, Inc. (Beverly,

MA). Rabbit polyclonal antibody against p53 was from Santa Cruz Biotechnology (Santa Cruz, CA). Rabbit antibodies against rat type I collagen and prolyl hydroxylases (α, β) were from LSL Cosmo Bio (Tokyo, Japan). Rabbit anti-rat fibronectin antibody was from Chemicon International (Temecula, CA). Rabbit antibody against glyceraldehyde-3-phosphate dehydrogenase (G3PDH) was from Trevigen (Gaithersburg, MD). SP600125, U0126 and SB202190 were from Calbiochem (La Jolla, CA). All other reagents were products of Sigma-Aldrich (St. Louis, MO) unless specifically described.

Cell culture and immortalization

All animal procedures were performed in accordance with the National Institutes of Health Animal Care and Use Guidelines. Rat PSCs were prepared from the pancreas tissues of male Wistar rats (Japan SLC Inc., Hamamatsu, Japan) weighing 200-250 g as previously described[3]. Isolated stellate cells were cultured in Ham' s F-12 containing 10 % heat-inactivated fetal bovine serum (FBS; ICN Biomedicals, Aurora, OH), penicillin sodium, and streptomycin sulfate. When reaching confluent, the cells were trypsinized with 0.05 % trypsin/0.01 % EDTA. Initially, cells were passaged at a ratio of 1:3. After the 10th passage, cells were split at 1:5. A homogeneous population of cells, designated as SIPS, was cloned by limiting dilution, and expanded. SAM-K is another rat PSC line established by retrovirus-mediated introduction of simian virus 40 large T antigen[10]. SAM-K cells and primary PSCs were maintained in Ham' s F-12 containing 10 % FBS, penicillin sodium, and streptomycin sulfate.

Immunostaining

SIPS cells were grown directly on slides, serum-starved for 24 hours, and immunostaining for α-SMA was performed using a streptavidin-biotin-peroxidase complex detection kit (Histofine Kit; Nichirei, Tokyo, Japan) as previously described[11]. Briefly, cells were fixed in 100 % methanol at -20 ℃, and then endogenous peroxidase activity was blocked by incubation with hydrogen peroxide in methanol for 5 minutes. After immersion in normal rabbit serum, the slides were incubated with mouse anti-α-SMA antibody (at 1:200 dilution) at 4 ℃ overnight. The slides were incubated with biotinylated anti-mouse immunoglobulin antibody, and peroxidase-conjugated streptavidin. Finally, color was developed by incubating the slides with diaminobenzidine (Dojindo, Kumamoto, Japan). Expression of glial acidic fibrillary protein, vimentin, desmin, type I collagen, fibronectin, and prolyl hydroxylases (α, β) was examined in a similar manner.

Western blotting

The levels of activated, phosphorylated MAP kinases were determined by Western blotting as previously described[12]. Briefly, cells were lysed in sodium dodecyl sulfate buffer (62.5 mM Tris-HCl at pH 6.8, 2 % sodium dodecyl sulfate, 10 % glycerol, 50 mM dithiothreitol, 0.1 % bromphenol blue) for 15 minutes on ice. The samples were then sonicated for 2 seconds, heated for 5 minutes, and centrifuged at 12 000×g for 5 minutes to remove insoluble cell debris. Cellular proteins (approximately 100 μg) were fractionated on a 10 % sodium dodecyl sulfate-polyacrylamide gel. They were transferred to a nitrocellulose membrane (Bio-Rad, Hercules, CA), and the membrane was incubated overnight at 4 ℃ with rabbit anti-phosphospecific MAP kinase antibodies (at 1:1 000 dilution). After incubation with peroxidase-conjugated goat anti-rabbit secondary antibody for 1 hour, proteins were visualized using an ECL kit (Amersham Biosciences UK, Ltd.). Levels of total MAP kinases, p53, G3PDH, and IκB-α were determined in a similar manner.

Telomerase activity

Telomerase activity was measured using the telomere repeat amplification protocol (TRAP) with the Telo TAGGG Telomerase PCR ELISAkit (Roche Applied Science). Briefly, SIPS, SAM-K, and primary PSCs (passage 3) were harvested separately, and the cell number was counted. The cell extracts were prepared from an equal number of cells, and used in telomerase-mediated elongation, adding the telomeric repeats to the 3' end of the biotin-labeled synthetic P1-TS-primer. These elongation products were amplified by PCR using the primers P1-TS and P2, generating PCR products with the telomerase-specific 6-nucleotide increments. An aliquot of the resulting PCR product was denatured, hybridized to a digoxigenin-labeled, telomeric repeat-specific detection probe, and immobilized to a streptavidin-coated microtiter plate. Then, peroxidase-conjugated anti-digoxigenin antibody was added to detect the immobilized PCR product, and the telomerase activity was determined, after the addition of 3,3', 5,5' -tetramethylbenzidine (substrate), as O.D.450-O.D.690. Ribonuclease A-treated cell extracts were used as negative controls. The mean of the absorbance readings of the negative control was subtracted from those of the samples, and the samples were regarded as telomerase positive if the O.D. difference was higher than 0.2.

Senescence-associated *b*-galactosidase (SA-*b*-Gal) staining

Senescence of SIPS, SAM-K, and primary PSCs (passage 20) was examined by SA-β-Gal staining[13]. Cells were grown directly on slides, fixed, and stained with β-Gal staining solution (β-galactosidase staining kit; Mirus, Madison, WI), pH adjusted to 6.0, for 16 hours at 37 ℃. After washed with phosphate-buffered saline, the slides were viewed under light microscope.

Cell proliferation assay

Serum-starved SIPS cells (approximately 80 % density) were treated with FBS at various concentrations or PDGF-BB (at 25 ng/ml). Cell proliferation was assessed using a commercial kit (Cell proliferation ELISA, BrdU; Roche Applied Science) according to the manufacturer' s instructions. This is a colorimetric immunoassay based on the measurement of 5-bromo-2' -deoxyuridine (BrdU) incorporation during DNA synthesis[14]. After 24-hour incubation with experimental reagents, cells were labeled with BrdU for 3 hours at 37 ℃. Cells were then fixed, and incubated with peroxidase-conjugated anti-BrdU antibody. The peroxidase substrate 3,3' ,5,5' -tetramethylbenzidine was added, and BrdU incorporation was quantitated by O.D.370-O.D.492.

Electrophoretic mobility shift assay

Following 1-hour-incubation, approximately 5×10^6 cells were harvested and nuclear extracts were prepared, and electrophoretic mobility shift assay was performed as previously described[15]. Double-stranded oligonucleotide probes for NF-κB (5' -AGTTGAGGGGACTTTCCCAGGC-3'), and activator protein-1 (AP-1) (5' -CGCTTGATGAGTCAGCCGGAA-3') were end-labeled with [γ-^{32}P]ATP. Nuclear extracts (approximately 5 μg) were incubated with the labeled oligonucleotide probe for 20 minutes at 22 ℃, and electrophoresed through a 4 % polyacrylamide gel. Gels were dried and autoradiographed at -80 ℃ overnight. A 100-fold excess of unlabelled oligonucleotide was incubated with nuclear extracts for 10 minutes prior to the addition of the radiolabeled probe in the competition assays.

Enzyme immunoassay

After a 24 hour-incubation, cell culture supernatants were

harvested and stored at -80 ℃. CINC-1 levels in the culture supernatants were measured by enzyme immunoassay (Panapharm Laboratories, Udo, Japan) according to the manufacturer's instructions.

Statistical analysis

The results were expressed as mean ± standard deviation (mean ± SD). Luminograms and autoradiograms are representative of at least three experiments. Differences between experimental groups were evaluated by two-tailed unpaired Student' s *t* test. A *P* value of less than 0.05 was considered statistically significant.

RESULTS

Establishment of an immortalized rat PSC line

PSCs were isolated from the pancreas of male Wistar rats, and conventional subcultivation was performed repeatedly. This procedure yielded actively growing cells. After limited dilution, one clone was obtained and designated as SIPS. SIPS cells were myofibroblast-like shaped, and morphologically very similar to primary, culture-activated PSCs. The characteristic fiber-like pattern of positive α-SMA staining was observed throughout the cytoplasm in SIPS cells (Figure 1A). In addition, SIPS cells showed positive staining for cytoskeletal proteins glial acidic fibrillary protein (Figure 1B), vimentin

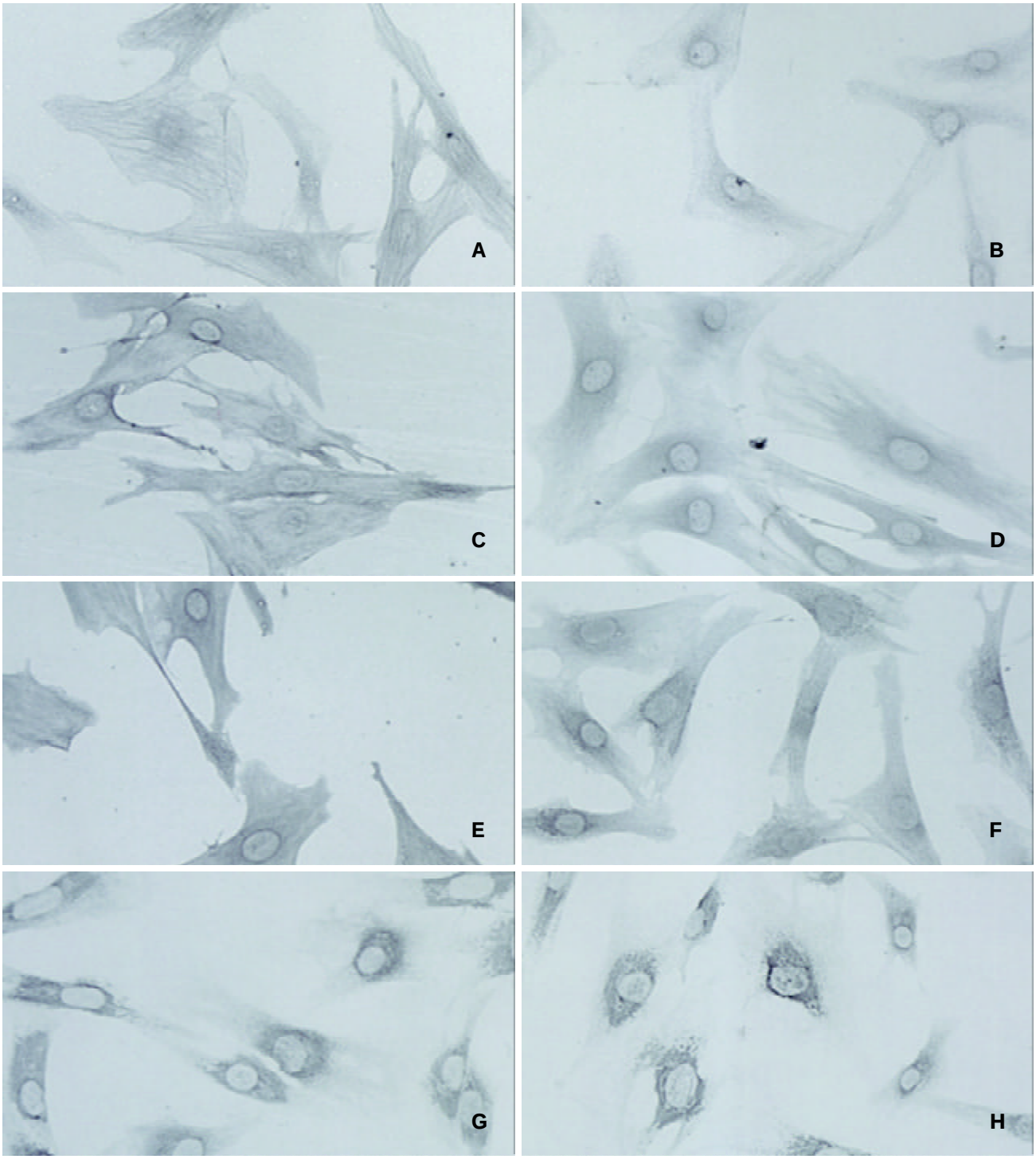

Figure 1 SIPS expressed cytoskeletal proteins and extracellular matrix proteins. Cells were grown directly on slides. Immunostaining for α-SMA (A), glial fibrillary acidic protein (B), vimentin (C), desmin (D), type I collagen (E), fibronectin (F), and prolyl hydroxylases (α) (G) and (β) (H) was performed using a streptavidin-biotin-peroxidase complex detection kit. Original magnification: ×20 objective.

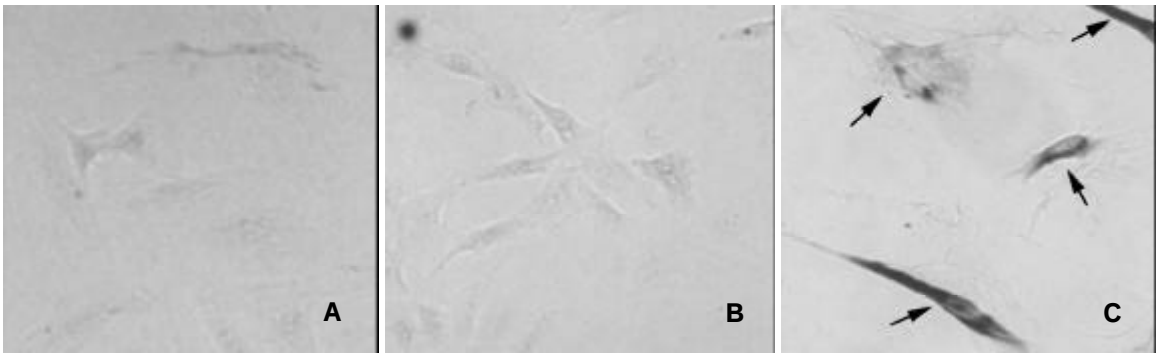

Figure 2 SIPS cells were negative for SA-β-Gal. SIPS cells (A), SAM-K cells (B), and late-passage (passage 20) PSCs (C) were grown directly on slides, fixed, and stained with β-Gal staining solution, adjusted to pH 6.0, for 16 hours at 37 ℃. After washed, the slides were viewed under light microscope. SA-β-Gal was not detected in SIPS and in SAM-K cells, but was detected in late-passage PSCs (arrows). Original magnification: ×20 objective.

(Figure 1C), and desmin (Figure 1D). SIPS cells also expressed extracellular matrix proteins type I collagen (Figure 1E) and fibronectin (Figure 1F). SIPS cells expressed prolyl hydroxylases (α, β) (Figure 1G, H), that are key enzymes in the hydroxylation of the proline residues in procollagen and are useful markers of collagen synthesis[7]. These results suggest that SIPS cells shared many phenotypical and functional characteristics with primary, culture-activated PSCs. During the two years of culture, SIPS cells have been passaged repeatedly over 100 population doublings without showing any evidence of senescence. Indeed, SA-β-Gal, a biomarker of senescent cells[13], was not detected in SIPS and in SAM-K cells (Figure 2A, B). In contrast, SA-β-Gal was detected in late-passage (passage 20) primary PSCs (Figure 2C). The phenotypic characteristics of SIPS remained unaltered, suggesting that they have acquired an immortalized phenotype. SIPS cells have conserved the characteristics of non-transformed cells since they did not form foci, and did not grow on soft agar (data not shown).

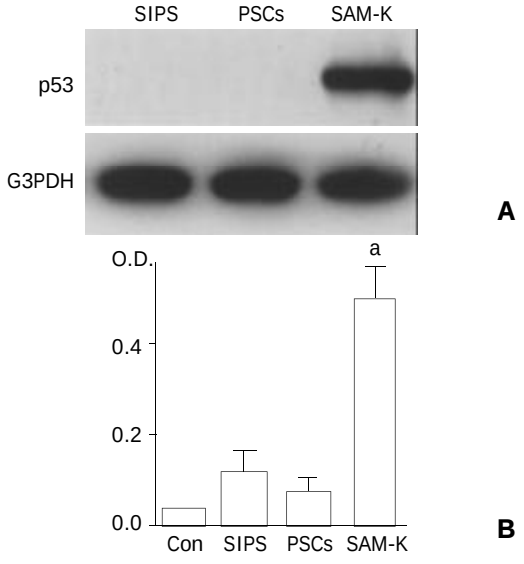

Figure 3 p53 expression and telomerase activity were negative in SIPS cells. (A) Total cell lysates (approximately 100 μg) were prepared from SIPS, primary PSCs (passage 3), and SAM-K cells. The level of p53 was determined by Western blotting. The level of G3PDH was also determined as a loading control. (B) Telomerase activity was measured utilizing the TRAP by enzyme-linked immunosorbent assay. The telomerase activity was determined by differences in absorbance at O.D.450-O.D. 690. Negative control was prepared by incubating the total cell extracts with ribonuclease A. The mean of the absorbance in negative control was subtracted from those of the samples, and the samples were regarded as telomerase positive ("**a**") if the difference in absorbance was higher than 0.2. Data are shown as mean ± SD (n=6).

Negative p53 expression and telomerase activity in SIPS cells

We next examined telomerase activity and p53 expression, potentially important factors in cellular immortalization[16,17]. p53 expression was not detected in SIPS cells and primary PSCs (passage 3), whereas the p53 level was very high in SAM-K cells (Figure 3A). As measured by the TRAP assay, SIPS cells and primary PSCs were negative for telomerase activity, whereas SAM-K cells were positive (Figure 3B).

Proliferation of SIPS stimulated by serum and PDGF

Previous studies have shown that proliferation of primary PSCs was stimulated by growth factors such as serum and PDGF-BB[18-20]. Especially, PDGF-BB has been shown to be the most potent mitogen for PSCs, and is likely to be an important mediator of the increased proliferation of the cells both *in vivo* and *in vitro*[18,19]. We examined whether proliferation of SIPS cells were also stimulated by serum and PDGF-BB. Treatment of the cells with FBS stimulated proliferation in a dose-dependent manner; serum-induced proliferation was significant at as low as 1 % (P<0.05) (Figure 4). In addition, PDGF-BB stimulated proliferation of SIPS cells; PDGF-BB (at 25 ng/ml) induced proliferation by approximately three fold in serum-free medium (Figure 4).

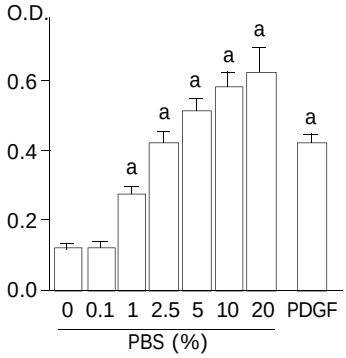

Figure 4 Proliferation of SIPS cells was serum-dependent and stimulated with PDGF-BB. SIPS cells were treated with FBS (at the indicated concentrations) or PDGF-BB (at 25 ng / ml. After 24-hour-incubation, cells were labeled with BrdU for 3 hours. Cells were then fixed, and incubated with peroxidase-conjugated anti-BrdU antibody. Then the peroxidase substrate 3,3', 5,5'-tetramethylbenzidine was added, and BrdU incorporation was quantitated by differences in absorbance at wavelength 370 minus 492 nm ("O.D."). Data are shown as mean ± SD (n=6). [a]P<0.01 *vs.* serum-free medium only. O.D.: optical density.

IL-1b activated NF-kB and AP-1

We have previously shown that proinflammatory cytokines IL-1β and tumor necrosis factor-α activated transcription factors NF-κB and AP-1 in primary PSCs[7, 8]. We examined whether IL-1β activated these transcription factors in SIPS cells. Nuclear extracts were prepared from SIPS cells treated with IL-1β for 1 hour, and specific binding activities of NF-κB and AP-1 were assessed by electrophoretic mobility shift assay. IL-1β increased NF-κB and AP-1 binding activities (Figure 5A, B). The specificity of these binding activities was confirmed by competition assays using 100-fold excess of unlabeled oligonucleotides (data not shown). Phosphorylation and degradation of IκB-α is necessary for the activation of NF-κB[21]. We examined the effects of IL-1β on the cellular IκB-α levels by Western blotting. IL-1β induced transient degradation of IκB-α, further supporting that IL-1β activated NF-κB (Figure 5C).

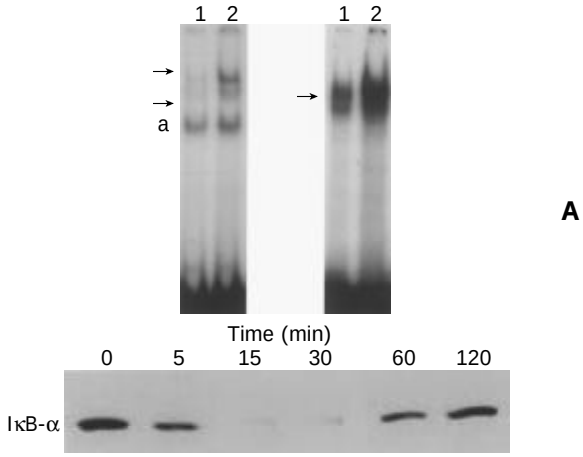

Figure 5 IL-1β activated NF-κB and AP-1 in SIPS cells. (A, B) SIPS cells were treated with IL-1β (at 2 ng / ml, lane 2) for 1 hour. Nuclear extracts were prepared, and specific binding activities of NF-κB (panel A) and AP-1 (panel B) were assessed by electrophoretic mobility shift assay. Arrows denote specific inducible complexes competitive with cold double-stranded oligonucleotide probes. Lane 1: control (medium only). a: non-specific band. (C) SIPS cells were treated with IL-1β for indicated times. Total cell lysates (approximately 100 μg) were prepared, and the level of IκB-α was determined by Western blotting.

IL-1b activated MAP kinases

Induction of the expression of AP-1 components c-Fos and c-Jun by a variety of stimuli such as growth factors and cytokines was mediated by the activation of three distinct MAP kinases: extracellular signal-regulated kinase (ERK) 1/2, c-Jun N-terminal kinase (JNK), p38 MAP kinase[22]. Because the activation of these kinases occurred through phosphorylation, we examined whether IL-1β activated these MAP kinases in SIPS cells by Western blotting using anti-phosphospecific MAP kinase antibodies. These antibodies recognized only phosphorylated form of MAP kinases, thus allowing the assessment of activation of these kinases. IL-1β activated these three classes of MAP kinases in a time-dependent manner, peaking from 5 to 15 minutes (Figure 6). The levels of total MAP kinases were unaffected by the treatment, indicating that the lanes had been equally loaded.

PDGF-BB induced proliferation of SIPS cells through ERK pathway

We and others have shown that activation of ERK plays key roles in the PDGF-induced proliferation of PSCs[20,23]. We examined whether PDGF-BB activated ERK in PSCs. PDGF-BB activated ERK1/2 in a time-dependent manner (Figure 7A). U0126, a specific MAP kinase kinase inhibitor[24], inhibited PDGF-induced proliferation in a dose-dependent manner (Figure 7B). Thus, activation of ERK plays a central role in the proliferation of SIPS, as is the case for primary PSCs.

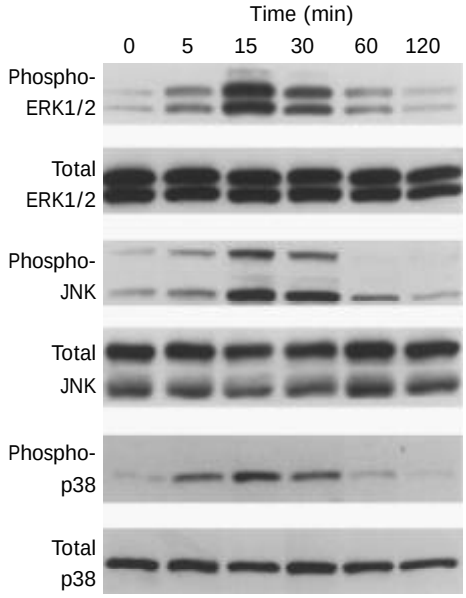

Figure 6 IL-1β activated MAP kinases. SIPS cells were treated with IL-1β (at 2 ng / ml) for the indicated time. Total cell lysates (approximately 100 μg) were prepared, and the levels of activated, phosphorylated MAP kinases were determined by Western blotting. The levels of total MAP kinases were also determined.

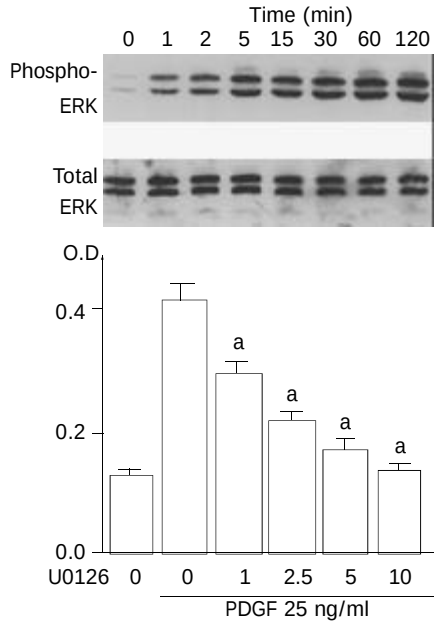

Figure 7 PDGF-BB induced proliferation of SIPS cells through ERK pathway. (A) SIPS cells were treated with PDGF-BB (at 25 ng / ml) for the indicated time. Total cell lysates (approximately 100 μg) were prepared, and the level of activated, phosphorylated ERK was determined by Western blotting. The level of total ERK was also determined. (B) SIPS cells were treated with PDGF-BB (at 25 ng / ml) in the presence of U0126 at the indicated concentrations (at μM). After 24-hour-incubation, cells were labeled with BrdU for 3 hours. Cells were fixed, and incubated with peroxidase-conjugated anti-BrdU antibody. Then the peroxidase substrate 3,3',5,5'-tetramethylbenzidine was added, and BrdU incorporation was

quantitated by differences in absorbance at O.D.370-O.D.492. Data are shown as mean ± SD (n=6). [a]P<0.01 versus PDGF only. O.D.: optical density.

IL-1b induced CINC-1 expression

Activated PSCs acquire the proinflammatory phenotype; they may modulate the recruitment and activation of inflammatory cells through the expression of monocyte chemoattractant protein-1[7] and intercellular adhesion molecule-1[8]. Monocyte chemoattractant protein-1 is a C-C chemokine and potent mononuclear cell chemoattractant. CINC-1, a C-X-C chemokine, is a rat homologue of IL-8, and a potent neutrophil attractant[25]. It remained unknown whether primary PSCs expressed CINC-1. We examined whether SIPS cells express CINC-1 in response to IL-1β by enzyme immunoassay. SIPS cells constitutively produced CINC-1 at very low levels. IL-1β significantly induced the production of CINC-1 (Figure 8). Ethanol and acetaldehyde at clinically relevant concentrations failed to induce CINC-1 production. To elucidate the roles of NF-κB and MAP kinases for the expression of CINC-1 in SIPS cells, we used specific inhibitors to block these pathways. First, we treated SIPS cells with IL-1β in the presence of pyrrolidine dithiocarbamate (PDTC), a specific inhibitor of NF-κB activation[26]. As shown in Figure 8, PDTC decreased the IL-1β-induced CINC-1 production to near the basal levels. SP600125 is a reversible ATP-competitive inhibitor of JNK that inhibits c-jun phosphorylation and the expression of proinflammatory genes such as IL-2, and tumor necrosis factor-α[27]. SP600125 at 10 μM decreased the IL-1β-induced CINC-1 production approximately by 75 %. We next examined the effects of U0126[24], a specific inhibitor of MAP kinase kinase activation, which prevents the activation of ERK1/2. U0126 at 10 μM partially inhibited inducible CINC-1 expression. A selective p38 MAP kinase inhibitor, SB202190[28], at 25 μM also partially inhibited inducible CINC-1 production. Similar results were obtained with tumor necrosis factor-α-induced CINC-1 expression (data not shown). In these experiments, the inhibitors at the indicated concentrations did not affect the cell viability during the incubation as assessed by trypan blue exclusion test (data not shown). However, at higher concentrations, some cytotoxic effects were observed during the incubation. These results suggested that activation of NF-κB and JNK plays a key role in inducible CINC-1 expression in SIPS cells. Activation of ERK and p38 MAP kinase pathways is partially required for optimal CINC-1 expression.

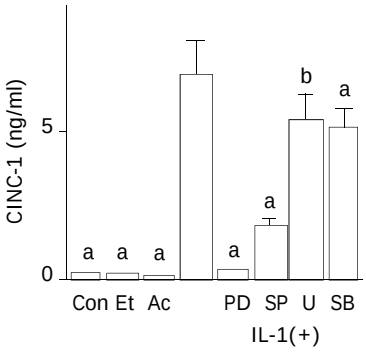

Figure 8 IL-1β induced CINC-1 expression. SIPS cells were left untreated, or treated with IL-1β (IL; at 2 ng/ml) in the absence or presence of PDTC ("PD" at 10 μM), SP600125 ("SP" at 10 μM), U0126 ("U" at 5 μM), or SB202190 ("SB" at 25 μM). After 24 hours, CINC-1 levels in the culture supernatant were determined by enzyme immunoassay. The effects of ethanol ("Et" at 50 mM) and acetaldehyde ("Ac" at 200 μM) were also examined. Con: control (medium only). Data shown are expressed as means ± SD (n=6). [a]P<0.01, [b]P<0.05 versus IL-1β only.

DISCUSSION

In response to pancreatic injury or inflammation, PSCs undergo a transformation from quiescent cells to activated, proliferating myofibroblast-like cells, which produce cytokines and extracellular matrix proteins. It has been established that activated PSCs play an important role in the pathogenesis of pancreatic fibrosis and inflammation[3,4,8]. Although primary stellate cell culture is a useful tool for studying molecular mechanisms of pancreatic fibrosis and inflammation *in vitro*, their isolation is time-consuming, yields are relatively low, and there is considerable heterogeneity between preparations. In addition, primary cells can be subcultured only several times because of their limited growth potential. To circumvent these problems, we have established and validated a new rat PSC line, named SIPS. This SIPS cell line has been developed through spontaneous immortalization, and can be passaged indefinitely compared with the limited number of passages for primary PSCs. SIPS cells have been passaged repeatedly without showing any evidence of senescence. Indeed, SA-β-Gal, a biomarker of senescent cells[13], was not detected in SIPS cells. SIPS cells retained the morphologic characteristics of primary PSCs as well as the expression of the cytoskeletal proteins α-SMA and glial acidic fibrillary protein. SIPS cells maintained the functional characteristics of primary PSCs; SIPS cells showed positive staining for type I collagen, fibronectin, and prolyl hydroxylases. Proliferation of PSCs was stimulated by FBS and PDGF-BB. SIPS cells responded to IL-1β, resulting in the activation of NF-κB, AP-1, and MAP kinases. In addition, SIPS cells exhibited proinflammatory response; SIPS cells expressed CINC-1 in response to IL-1β. Thus, SIPS cells retain several aspects of the primary and culture-activated PSCs.

We have previously established an immortalized cell line of rat PSCs, named SAM-K, by the introduction of the simian virus 40 T antigen[10]. Although SAM-K cells were found to be useful for establishment of stable transfectants, it was also shown that large T antigen led to the alternation of genome such as p53 expression[10]. The resulting genetic manipulations might limit the use of SAM-K cells for studies like defining genetic changes that occur during cell differentiation and transformation. In this study, we examined the expression of p53 and telomerase activity, both of which are shown to be associated with immortalization of mammalian cells[16,17]. We found that p53 expression and telomerase activity was negative in SIPS cells as is the case for primary PSCs. This is in striking contrast to SAM-K cells, where p53 expression and telomerase activity were high. These results suggest that different mechanisms involved for immortalization of SIPS and SAM-K cells, and that SIPS cells have more similar phenotype to primary PSCs than SAM-K cells do. Obviously, further studies are necessary to clarify the molecular mechanisms responsible for immortalization of SIPS cells.

To our knowledge, this is the first report describing the establishment of stellate cell line of the pancreas by spontaneous immortalization. In culture, PSCs are morphologically very similar to the hepatic stellate cells. To date, several hepatic stellate cell lines have been established by spontaneous immortalization. Greenwel *et al*[29] reported the characterization of two rat hepatic stellate cell lines, one from normal and the other from cirrhotic liver. Although both cell lines resembled primary cultures of hepatic stellate cells, significant differences in cell proliferation and IL-6 production between the two cell lines were found. Sauvant *et al*[30] reported that immortalized rat hepatic stellate cells were able to convert retinol into retinoic acid. Rodent cells are known to undergo spontaneous immortalization with a frequency of 10^{-5}–10^{-6} that makes isolation of immortal cell lines from rodent populations experimentally practical even without transfer of an oncogene, whereas the spontaneous immortalization of human cells is a

very rare event; the frequency is thought to be less than 10^{-12}[31]. Schnabl *et al*. reported immortal activated human hepatic stellate cells generated by ectopic telomerase expression[32]. They showed that activated human hepatic stellate cells had little, if any, detectable telomerase activity. Telomerase-induced hepatic stellate cells did not undergo oncogenic transformation and showed morphologic characteristics of activated stellate cells. In addition, mRNA expression in telomerase-positive cells and -negative cells were very similar. It would be of particular interest to see if human PSC line could be established by the introduction of ectopic telomerase expression.

Proliferation of PSCs is a fundamental feature of pancreatic fibrosis. PDGF has been shown to be the most potent mitogen for PSCs *in vitro*[18,19]. PDGF-BB stimulated proliferation of SIPS, and the stimulation was abolished in the presence of U126, a MAP kinase kinase inhibitor[24]. This is in agreement with the previous studies showing that ERK is a key mediator of mitogenic signals in rat PSCs[20,23].

Activated PSCs acquire the proinflammatory phenotype; they may modulate the recruitment and activation of inflammatory cells. We have shown that proinflammatory cytokines such as IL-1β and tumor necrosis factor-α induced expression of monocyte chemoattractant protein-1 and intercellular adhesion molecule-1 in primary PSCs[7,8]. In addition, we here showed for the first time that IL-1β induced CINC-1 expression in SIPS cells. CINC-1 production in response to IL-1β was also observed in primary PSCs (Satoh *et al*. manuscript in preparation). Although it has been shown that hepatic stellate cells express CINC-1 both *in vivo* and *in vitro*[33], whether PSCs expressed CINC-1 and its regulatory mechanisms remained unknown. In this study, inducible CINC-1 production was abolished by PDTC, a specific inhibitor of NF-κB activation, and strongly decreased by SP600125, an inhibitor of JNK. Inhibition of ERK pathway by U0126 and of p38 MAP kinase by SB202190 partially inhibited IL-1β-induced CINC-1 production. Collectively, activation of NF-κB and JNK plays a key role, and that of ERK and p38 MAP kinase plays a partial role for optimal CINC-1 expression in SIPS cells. This is in agreement with the regulatory mechanisms of IL-8, a human homologue of CINC-1[34]. Maximal IL-8 amounts are generated by a combination of three different mechanisms: first, de-repression of the gene promoter; second, transcriptional activation of the gene by NF-κB and JNK pathways; and third, stabilization of the mRNA by the p38 MAP kinase pathway. In addition, activation of ERK pathway contributes to IL-8 expression[34]. Similar to PSCs[35], ethanol and acetaldehyde at clinically relevant concentrations activated ERK, JNK and p38 MAP kinase (data not shown), but failed to induce CINC-1 expression in SIPS cells. Thus, activation of MAP kinases is required, but not sufficient for optimal CINC-1 expression in SIPS cells. We have previously shown that ethanol and acetaldehyde induced type I collagen gene expression through p38 MAP kinase in primary PSCs[35]. Further studies are necessary to clarify whether ethanol and acetaldehyde induce the collagen gene expression in a similar manner.

In summary, SIPS cells are a newly established PSC line morphologically, phenotypically and functionally similar to primary, activated PSCs. Unlike SAM-K cells, immortalization was not associated with elevated p53 expression or telomerase activity. SIPS cells can be used for both transient and stable transections (Masamune *et al*. unpublished observation), facilitating the overexpression of ectopic genes. Its phenotypic characteristics as well as its responsiveness to proinflammatory cytokines and growth factors make it a useful tool for investigation of the pathogenesis of pancreatic inflammation and fibrosis and thereby for future therapeutic development.

REFERENCES

1 **Etemad B**, Whitcomb DC. Chronic pancreatitis: diagnosis, classification, and new genetic developments. *Gastroenterology* 2001; **120**: 682-707

2 **Lankisch PG**. Natural course of chronic pancreatitis. *Pancreatology* 2001; **1**: 3-14

3 **Apte MV**, Haber PS, Applegate TL, Norton ID, McCaughan GW, Korsten MA, Pirola RC, Wilson JS. Periacinar stellate-shaped cells in rat pancreas: identification, isolation and culture. *Gut* 1998; **43**: 128-133

4 **Bachem MG**, Schneider E, Gross H, Weidenbach H, Schmid RM, Menke A, Siech M, Beger H, Grunert A, Adler G. Identification, culture, and characterization of pancreatic stellate cells in rats and humans. *Gastroenterology* 1998; **115**: 421-432

5 **Friedman SL**. Molecular regulation of hepatic fibrosis, an integrated cellular response to tissue injury. *J Biol Chem* 2000; **275**: 2247-2250

6 **Haber PS**, Keogh GW, Apte MV, Moran CS, Stewart NL, Crawford DH, Pirola RC, McCaughan GW, Ramm GA, Wilson JS. Activation of pancreatic stellate cells in human and experimental pancreatic fibrosis. *Am J Pathol* 1999; **155**: 1087-1095

7 **Masamune A**, Kikuta K, Satoh M, Sakai Y, Satoh A, Shimosegawa T. Ligands of peroxisome proliferator-activated receptor-g block activation of pancreatic stellate cells. *J Biol Chem* 2002; **277**: 141-147

8 **Masamune A**, Sakai Y, Kikuta K, Satoh M, Satoh A, Shimosegawa T. Activated rat pancreatic stellate cells express intercellular adhesion molecule-1 (1CAM-1) *in vitro*. *Pancreas* 2002; **25**: 78-85

9 **Masamune A**, Satoh M, Kikuta K, Sakai Y, Satoh A, Shimosegawa T. Inhibition of p38 mitogen-activated protein kinase blocks activation of rat pancreatic stellate cells. *J Pharmacol Exp Ther* 2003; **304**: 8-14

10 **Satoh M**, Masamune A, Sakai Y, Kikuta K, Hamada H, Shimosegawa T. Establishment and characterization of a simian virus 40-immortalized rat pancreatic stellate cell line. *Tohoku J Exp Med* 2002; **198**: 55-69

11 **Masamune A**, Shimosegawa T, Kimura K, Fujita M, Sato A, Koizumi M, Toyota T. Specific induction of adhesion molecules in human vascular endothelial cells by rat experimental pancreatitis-associated ascitic fluids. *Pancreas* 1999; **18**: 141-150

12 **Masamune A**, Satoh K, Sakai Y, Yoshida M, Satoh A, Shimosegawa T. Ligands of peroxisome proliferator-activated receptor-g induce apoptosis in AR42J cells. *Pancreas* 2002; **24**: 130-138

13 **Dimri GP**, Lee X, Basile G, Acosta M, Scott G, Roskelley C, Medrano EE, Linskens M, Rubelj I, Pereira-Smith O, Peacocke M, Campisi J. A biomarker that identifies senescent human cells in culture and in aging skin *in vivo*. *Proc Natl Acad Sci U S A* 1995; **92**: 9363-9367

14 **Porstmann T**, Ternynck T, Avrameas S. Quantitation of 5-bromo-2-deoxyuridine incorporation into DNA: an enzyme immunoassay for the assessment of the lymphoid cell proliferative response. *J Immunol Methods* 1985; **82**: 169-179

15 **Masamune A**, Igarashi Y, Hakomori S. Regulatory role of ceramide in interleukin (IL)-1 β-induced E-selectin expression in human umbilical vein endothelial cells. Ceramide enhances IL-1 beta action, but is not sufficient for E-selectin expression. *J Biol Chem* 1996; **271**: 9368-9375

16 **Banerjee A**, Srivatsan E, Hashimoto T, Takahashi R, Xu HJ, Hu SX, Benedict WF. Immortalization of fibroblasts from two patients with hereditary retinoblastoma. *Anticancer Res* 1992; **12**: 1347-1354

17 **Liu JP**. Studies of the molecular mechanisms in the regulation of telomerase activity. *FASEB J* 1999; **13**: 2091-2104

18 **Apte MV**, Haber PS, Darby SJ, Rodgers SC, McCaughan GW, Korsten MA, Pirola RC, Wilson JS. Pancreatic stellate cells are activated by proinflammatory cytokines: implications for pancreatic fibrogenesis. *Gut* 1999; **44**: 534-541

19 **Luttenberger T**, Schmid-Kotsas A, Menke A, Siech M, Beger H, Adler G, Grunert A, Bachem MG. Platelet-derived growth factors stimulate proliferation and extracellular matrix synthesis of pancreatic stellate cells: implications in pathogenesis of pancreas fibrosis. *Lab Invest* 2000; **80**: 47-55

20 **Masamune A**, Kikuta K, Satoh M, Kume K, Shimosegawa T. Dif-

ferential roles of signaling pathways for proliferation and migration of rat pancreatic stellate cells. *Tohoku J Exp Med* 2003; **199**: 69-84

21 **Grilli M**, Chiu JJ, Lenardo MJ. NF-κB and Rel: participants in a multiform transcriptional regulatory system. *Int Rev Cytol* 1993; **143**: 1-62

22 **Karin M**, Liu Z, Zandi E. AP-1 function and regulation. *Curr Opin Cell Biol* 1997; **9**: 240-246

23 **Jaster R**, Sparmann G, Emmrich J, Liebe S. Extracellular signal regulated kinases are key mediators of mitogenic signals in rat pancreatic stellate cells. *Gut* 2002; **51**: 579-584

24 **Favata MF**, Horiuchi KY, Manos EJ, Daulerio AJ, Stradley DA, Feeser WS, Van Dyk DE, Pitts WJ, Earl RA, Hobbs F, Copeland RA, Magolda RL, Scherle PA, Trzaskos JM. Identification of a novel inhibitor of mitogen-activated protein kinase. *J Biol Chem* 1998; **273**: 18623-18632

25 **Watanabe K**, Koizumi F, Kurashige Y, Tsurufuji S, Nakagawa H. Rat CINC, a member of the interleukin-8 family, is a neutrophil-specific chemoattractant *in vivo*. *Exp Mol Pathol* 1991; **55**: 30-37

26 **Schreck R**, Meier B, Mannel DN, Droge W, Baeuerle PA. Dithiocarbamates as potent inhibitors of nuclear factor kappa B activation in intact cells. *J Exp Med* 1992; **175**: 1181-1194

27 **Bennett BL**, Sasaki DT, Murray BW, O'Leary EC, Sakata ST, Xu W, Leisten JC, Motiwala A, Pierce S, Satoh Y, Bhagwat SS, Manning AM, Anderson DW. SP600125, an anthrapyrazolone inhibitor of Jun N-terminal kinase. *Proc Natl Acad Sci U S A* 2001; **98**: 13681-13686

28 **Lee JC**, Laydon JT, McDonnell PC, Gallagher TF, Kumar S, Green D, McNulty D, Blumenthal MJ, Heys JR, Landvatter SW, Strickler JE, McLaughlin MM, Siemens IR, Fisher SM, Livi GP, White JR, Adams JL, Young PR. A protein kinase involved in the regulation of inflammatory cytokine biosynthesis. *Nature* 1994; **372**: 739-746

29 **Greenwel P**, Schwartz M, Rosas M, Peyrol S, Grimaud JA, Rojkind M. Characterization of fat-storing cell lines derived from normal and CCl4-cirrhotic livers. Differences in the production of interleukin-6. *Lab Invest* 1991; **65**: 644-653

30 **Sauvant P**, Sapin V, Abergel A, Schmidt CK, Blanchon L, Alexandre-Gouabau MC, Rosenbaum J, Bommelaer G, Rock E, Dastugue B, Nau H, Azais-Braesco V. PAV-1, a new rat hepatic stellate cell line converts retinol into retinoic acid, a process altered by ethanol. *Int J Biochem Cell Biol* 2002; **34**: 1017-1029

31 **Hopfer U**, Jacobberger JW, Gruenert DC, Eckert RL, Jat PS, Whitsett JA. Immortalization of epithelial cells. *Am J Physiol* 1996; **270**(1 Pt 1): C1-C11

32 **Schnabl B**, Choi YH, Olsen JC, Hagedorn CH, Brenner DA. Immortal activated human hepatic stellate cells generated by ectopic telomerase expression. *Lab Invest* 2002; **82**: 323-333

33 **Maher JJ**, Lozier JS, Scott MK. Rat hepatic stellate cells produce cytokine-induced neutrophil chemoattractant in culture and *in vivo*. *Am J Physiol* 1998; **275**(4 Pt 1): G847-G853

34 **Hoffmann E**, Dittrich-Breiholz O, Holtmann H, Kracht M. Multiple control of interleukin-8 gene expression. *J Leukoc Biol* 2002; **72**: 847-855

35 **Masamune A**, Kikuta K, Satoh M, Satoh A, Shimosegawa T. Alcohol activates activator protein-1 and mitogen-activated protein kinases in rat pancreatic stellate cells. *J Pharmacol Exp Ther* 2002; **302**: 36-42

Edited by Ma JY

P.O.Box 2345, Beijing 100023,China
Fax: +86-10-85381893
E-mail: wjg@wjgnet.com www.wjgnet.com

World J Gastroenterol 2003;9(12):2759-2763
World Journal of Gastroenterology
 ISSN 1007-9327

• BASIC RESEARCH •

Effects of bile acids on proliferation and ultrastructural alteration of pancreatic cancer cell lines

Zheng Wu, Yi Lü, Bo Wang, Chang Liu, Zuo-Ren Wang

Zheng Wu, Yi Lü, Bo Wang, Chang Liu, Zuo-Ren Wang, Department of Hepatobiliary Surgery, The First Hospital of Xi' an Jiaotong University, Xi' an 710061, Shaanxi Province, China
Correspondence to: Yi Lü, Department of Hepatobiliary Surgery, The First Hospital of Xi' an Jiaotong University, 1 Jiankang Road, Xi' an 710061, Shaanxi Province, China. lvyi@newliver.net
Telephone: +86-29-5324009 **Fax:** +86-29-5323626
Received: 2003-03-02 **Accepted:** 2003-03-28

Abstract

AIM: Pancreatic cancer in the head is frequently accompanied by jaundice and high bile acid level in serum. This study focused on the direct effects of bile acids on proliferation and ultrastructural alteration of pancreatic cancer.

METHODS: Pancreatic cancer cell lines PANC-1, MIA PaCa-2 and PGHAM-1 were explored in this study. The cell lines were cultured in media supplemented with certain bile acids, CA, DCA, LCA, TCDC, TDCA and GCA. Their influence on cell growth was measured with MTT assay after 72 h of incubation. Cell cycles of PANC-1 cells in 40 μM of bile acids media were analyzed by flow cytometry. Ultrastructural alteration of PANC-1 cells induced by DCA was observed using scanning and transmission electron microscope (SEM and TEM).

RESULTS: At various concentrations of bile acids and incubation time, no enhanced effects of bile acids on cell proliferation were observed. Significant inhibitory effects were obtained in almost all media with bile acids. DCA and CA increased the percentage of G_0+G_1 phase cells, while GCA and TDCA elevated the S phase cell number. After 48 h of incubation in DCA medium, PANC-1 cells showed some structural damages such as loss of their microvilli and vacuolization of organelles in cytoplasm.

CONCLUSION: Bile acids can reduce proliferation of pancreatic cancer cells due to their direct cytotoxicity. This result implies that elevation of bile acids in jaundiced serum may inhibit pancreatic cancer progression.

Wu Z, Lü Y, Wang B, Liu C, Wang ZR. Effects of bile acids on proliferation and ultrastructural alteration of pancreatic cancer cell lines. *World J Gastroenterol* 2003; 9(12): 2759-2763
http://www.wjgnet.com/1007-9327/9/2759.asp

INTRODUCTION

Pancreatic cancer is the fourth leading malignancy in terms of incidence in Western countries. Chemotherapy and radiotherapy could only produce minimal benefit. Extensive surgery is not boundless, either[1]. Pancreatic cancer has been investigated in many institutes[2-5], a great improvement of prognosis will only depend on clarifying molecular-biology of this grim tumor[6]. Obstructive jaundice is the most common symptom of pancreatic cancer, especially in developing countries and regions. Pancreatic cancer patients are always complicated with profound jaundice. About 70 % of pancreatic cancer patients already have obstructive jaundice at the time of diagnosis. Obstructive jaundice is a very life threatening pathophysiological disorder because elevation of bile acids in serum may attack many vital organs. Only two days after bile duct ligation, bile acids in serum have been reported to increase 30 fold compared to that of sham operated animals[7]. Bile acids are amphiphilic compounds that behave as detergents in aqueous solution. The hydrophobicity-hydrophibicity determine the cytotoxicity of bile acids by destroying bio-membrane specifically. No specific cytotoxicities of bile acids have been proved in hepatocytes, erythrocytes[8] and intestinal mucous epithelium[9] culture systems. However, proliferation of colonic epithelium stimulated by bile acids has been reported to occur with or without obvious cell surface damage[10,11]. TUDC has been reported recently to enhance intrahepatic bile duct carcinogenesis in the hamster model. Although obstructive jaundice is very closely related to pancreatic cancer and both the pathophysiology of obstructive jaundice and biology of pancreatic cancer have already been investigated respectively, we know little of interaction between bile acids and biology of pancreatic cancer. In treatment of pancreatic cancer, the main purpose of surgery is to eliminate jaundice, and sometimes it is also a way to access extensive resection. If the biological effect of bile acids in serum on pancreatic cancer is clarified, it will be very helpful for treating pancreatic cancer with jaundice. In this study, three typical pancreatic cancer cell lines and six kinds of common bile acids were used to explore the direct effects of bile acids on proliferation and morphological changes of pancreatic cancer cells.

MATERIALS AND METHODS

Cell culture and treatment

Human pancreatic cancer cell lines PANC-1, MIA PaCa-2 (purchased from American Type Culture Collection) and hamster pancreatic cancer cell line PGHAM-1(induced by BOP in the laboratory of First Department of Surgery, Nippon Medical School[12]) were used in this study. PANC-1, MIA PaCa-2 were primarily cultured in a 75 cm^2 flask with the cell concentration of about 2.0×10^3/ml in RPMI 1640 (GIBCO BRL, New York) medium. PGHAM-1 was incubated in Dulbeccon' s modified eagle medium (MEM: GIBCO BRL, New York) in the same way. Both media were supplemented with 10 % fetal bovine serum (FBS), 100 u/ml penicillin-streptomycin and 100 g/ml kanamycin and 100 g/ml amphotericin B (GIBCO, New York). Four days later, PANC-1, MIA PaCa-2 and PGHAM-1 cells were harvested and re-suspended in media supplemented with or without certain concentrations of bile acids including cholic acid (CA), deoxycholic acid (DCA), lithocholic acid (LCA), taurochenodeoxycholic acid (TCDC), taurodeoxycholic acid (TDCA) and glycocholic acid (GCA) (Sigma Chemical Co. USA). PANC-1, MIA PaCa-2 and PGHAM-1 cells in each group were treated and continuously cultured according to the protocols that the concentration of bile acid in each medium ranged from 10 μmol/L to 60 μmol/L. Cell density in the

suspension was adjusted to 6.0×10^3/ml. In the 96-well plates, 100 μl of cell suspension was added to each well, 6 wells for each group. The cells were incubated for 72 h and the viability of cells was measured by MTT assay. In another 96-well plate, PANC-1 cell suspension at very low concentration of bile acids (from 2 μmol/L to 8 μmol/L) was incubated for 144 h and tested by MTT assay. The medium was changed every 2 days at the same concentration of bile acids. PANC-1 cell suspension was incubated in normal or 40 μmol/L of bile acids (DCA, CA, GCA and TDCA) media in 25 cm^2 flasks for 72 h for cell cycle analysis. For scanning and transmission electron microscopic (SEM and TEM) investigations, 4 ml of PANC-1 cell suspension was incubated in normal or 20 μmol/L or 40 μmol/L DCA modified media in 25 cm^2 flasks for 48 h.

MTT assay

After 48 h or 96 h incubation, the viability of cells in each group was measured by 3-(4, 5-dimethylthiazol-2-yl)-2, 5-diphenyltetrazolium bromide (MTT) (Chemicon International Inc. Temecula, CA, USA) assay[13]. Each group had six samples. With this method, 10 μl of (5 mg/ml) MTT was added to each cell suspension and the cells were incubated for 4 h. The purple formazan product formed by the action of mitochondrial enzymes in living cells was solubilized by the addition of acidic isopropanol. The absorbency of each cell suspension was measured using a microplate reader (Model 3550, Bio-Rad, CA, USA) at a test wavelength of 560 nm and a reference wavelength of 655 nm. The inhibitory rates were calculated according to the following formula: inhibitory rate=(1-tested MTT viability/mean of control MTT viability)×100 %.

Flow cytometry

The cell cycles of PANC-1 cells incubated in 40 μM of bile acids added media for 24 h were measured by the following method. Cells were washed, permeabilised and exposed for 30 min at 4 ℃ to 800 μl of DNA-staining solution in 0.1 % Nonidet P-40 (Sigma-milan, Italy) and 25 ug/ml propidium iodide (Sigma-Aldrich). The cellular DNA content was analysed by fluorescent activated cell sorter (FACS) can (Bencton Dickinson Immunocytometry Systems, San Jose, CA, USA) using cell Quest software system for histograms of cell frequency *versus* propidium iodide fluorescence intensity.

SEM and TEM

PANC-1 cells in 25 cm^2 flasks were harvested by trypsinization after 24 h and 48 h of incubation. The cells were fixed with 2.5 % glutaraldehyde and 1 % osmium tetroxide (TAAB Laboratories Equipment Ltd. Berkshire, UK). The dehydration was carried out with an ethanol series. SEM specimens were dried using a critical point dryer (Hitachi Hcp-2), and the sputter was coated with Pt+Cd using an ion sputtering device (Hitachi Oie-102). The cell surface alteration was observed under a SEM device (Hitachi S-570). The dehydrated TEM samples were mixed with proplylene oxide and Epok 812, which were embedded and proymerilizated. The semithin sections were stained with touluidine blue. Ultrathin sections were made using the ultra-microtome (Porter-Blum MTZ-B) and then were stained with uranyl acetate and lead critrate. The inner ultrastructure of the cells was investigated using the TEM Device (Hitachi H-500).

Statistical analyses

The digital data in this study were represented by $\bar{x}\pm s$ and assessed by the analysis of variance (ANOVA). Student' s *t*-test (SPSS/PC7.5) was also used for cross comparison between different groups and different incubation times. Probabilities of less than 0.05 were considered as significant.

RESULTS

Inhibitory effects of bile acids on cultured pancreatic cancer cell lines

PANC-1 cell growth in 50 μmol/L-1 000 μmol/L of bile acids added RPMI-1640 medium was significantly inhibited in only 24 h compared with control (data not shown). When PANC-1 cells were cultured in 0.05 mmol/L to 1.0 mmol/L bile acid modified medium for 48 h, including unconjugated bile acids CA, DCA over the concentration of 0.5 mmol/L, LCA over 1.0 mmol/L and conjugated bile acids GCA over 1.0 mmol/L greater than 50 % growth inhibition was obtained (Figure 1). While PANC-1 treated with very low bile acid concentration of 2 μmol/L to 8 μmol/L for 96 h also produced certain inhibitory effect, but only exceeding 6 μmol/L did DCA show significant effect (Figure 2). All of three cell lines: PANC-1, MIA PaCa-2 and PGHAM-1 were incubated in 10 μmol/L-60 μmol/L bile acid supplemented media for 72 h, cell proliferation was inhibited to a certain degree. But the unconjugated bile acids CA, DCA and LCA showed powerful inhibitive capacity (Figures 3, 4, 5).

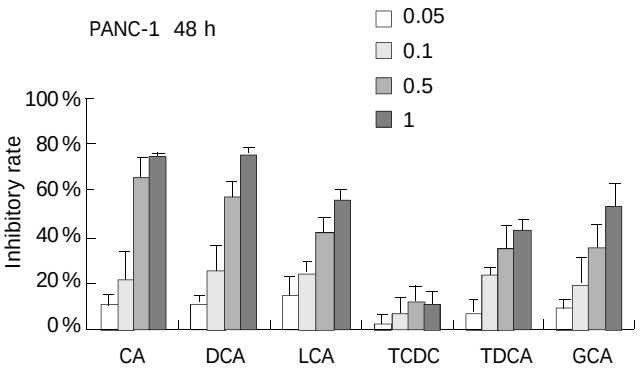

Figure 1 Bile acids (mmol/L) on PANC-1 for 48 h.

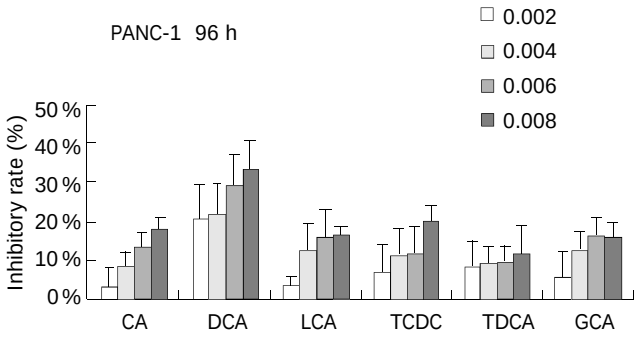

Figure 2 Bile acids (mmol/L) on PANC-1 for 96 h.

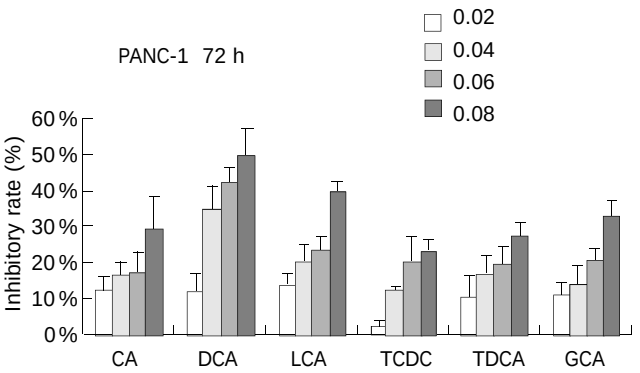

Figure 3 Bile acids (mmol/L) on PANC-1 for 72 h.

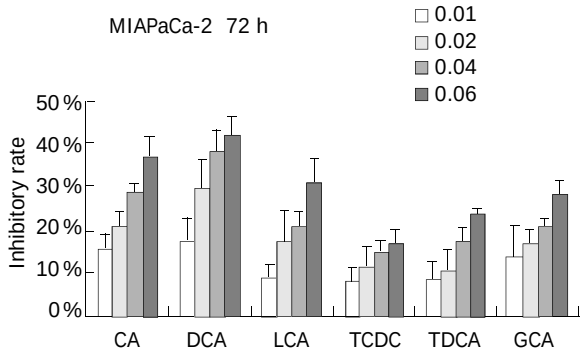

Figure 4 Bile acids (mmol/L) on MIA PaCa-2-1 for 72 h.

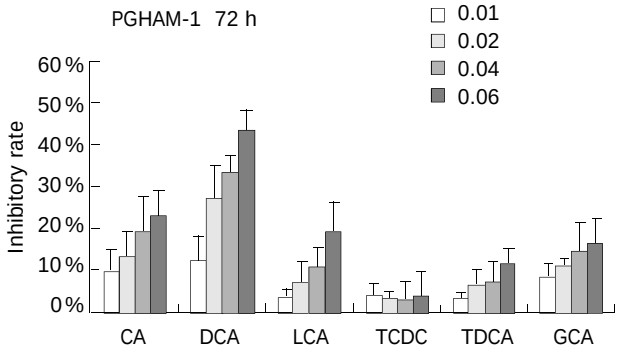

Figure 5 Bile acids (mmol/L) on PGHAM-1 for 72 h.

The inhibitive effects of all six bile acids were ranked in the following order: DCA>CA>LCA> GCA>TDCA>TCDC. Bile acid inhibition on the growth of three pancreatic cancer cells all showed a dosage dependent pattern. Among these bile acids, DCA produced the most powerful and obvious dosage-dependent inhibitory effect. Meanwhile PANC-1 cells were incubated in DCA (10-60 μmol/L) added medium supplemented with dexamethasone (50 μg per well), DCA' s inhibitive effects could not be reversed by supplement of membrane stabilizer dexamethasone (data not shown).

Ultrastructural alteration of PANC-1 cells incubated in DCA added medium

The untreated PANC-1 cells, as viewed by SEM, were characteristic of spherical in shape with plentiful microvilli which could be described as floss, spherical and leaf like microvilli (Figure 6A×7 500). When PANC-1 cells were cultured in 20 μmol/L DCA modified medium for 48 h, the majority of microvilli turned into spherical villi and the density of microvilli decreased obviously (Figure 6B×13 000). When PANC-1 cells were kept in 40 μmol/L DCA treated medium for 48 h, some cell surfaces were dotted with huge leaf-like microvilli or big microhills. Most cells lost their microvilli, becoming a bear ball with only some microvilli remnants, micro-trench and prominences (Figure 6C×20 000).

Observation of intracellular ultrastructure with TEM showed the cells in control group had normal distribution of organelles, with the integrity of mitochondria and other organelles preserved. The nuclei were surrounded by double

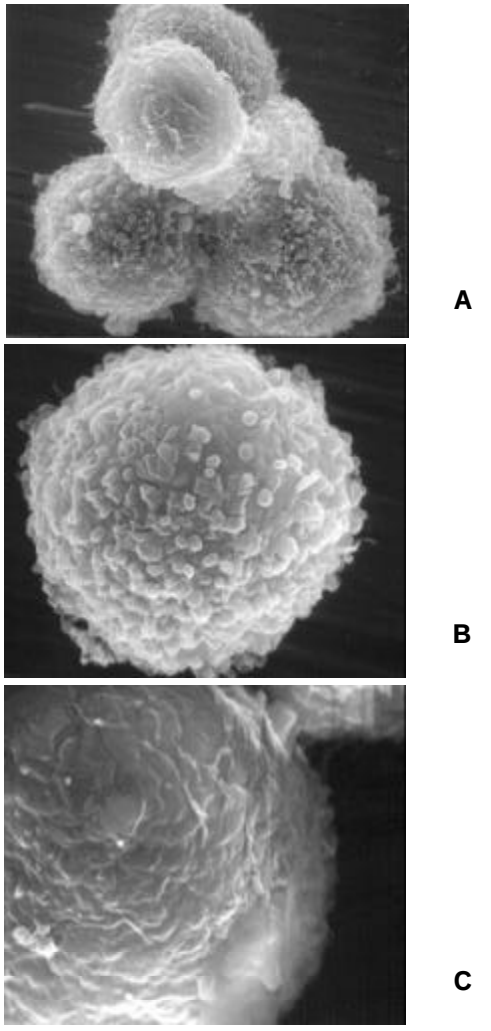

Figure 6 Ultrastructural alteration of PANC-1 viewed by SEM.

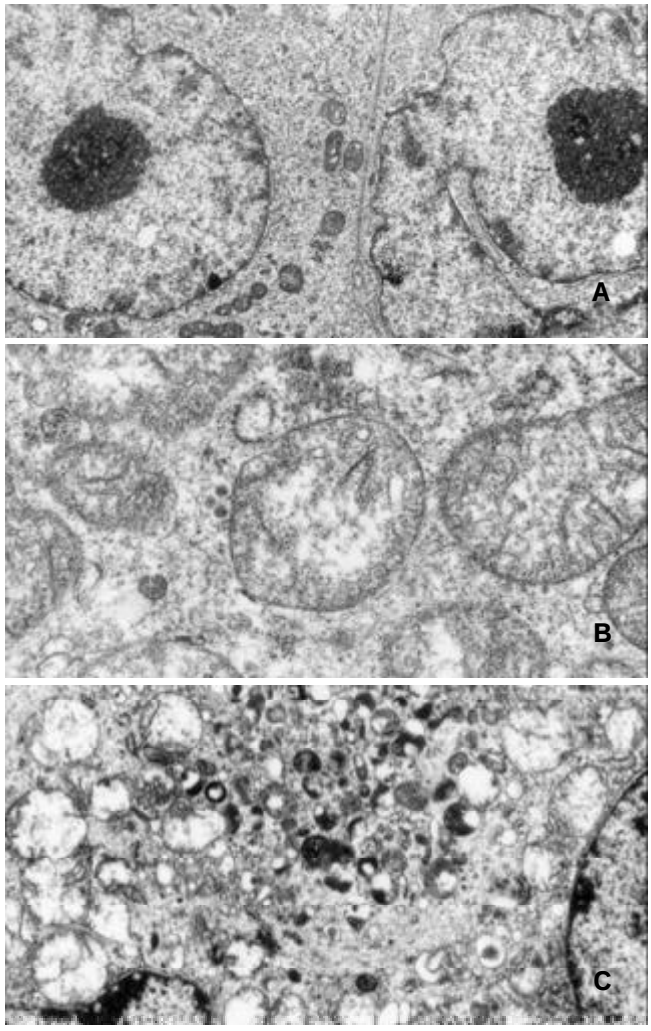

Figure 7 Ultrastructural alteration of PANC-1 viewed by TEM.

membrane envelope (Figure 7A×9 600). The cells growing in 20 μmol/L DCA modified medium for 48 h exhibited greatly extended mitochondria and dilated rough endoplasmic reticulum. All the organelles located in cells disorderly and the obviously dilated mitochondria contained twisted and broken cristae. Injured organelles were frequently seen in plasm (Figure 7B×30 000). When DCA concentration was increased to 40 μmol/L and incubated with cells for 48 h, exceedingly dilated mitochondria and vesicles formed by endoplasmic reticulum could be observed, some mitochondria lysed in cytoplasm were also seen. The lysosomes were also damaged and broken, which caused other surrounding organelles lysed in cytoplasm. The major portion of cytoplasm was occupied by vacuoles. The nuclear membrane double layer structure turned into indistinct and disconnected envelope. Rough granular masses against the inner surface of nuclear membrane could easily be observed (Figure 7C×12 000).

Cell cycles of PANC-1

The cell cycles of PANC-1 cells incubated in 40 μM of bile acids added media for 24 h were shown as follows. DCA and CA increased the percentage of G_0+G_1 phases cells, while GCA and TDCA elevated the S phase cell number compared with the control ($P<0.05$) (Figure 8).

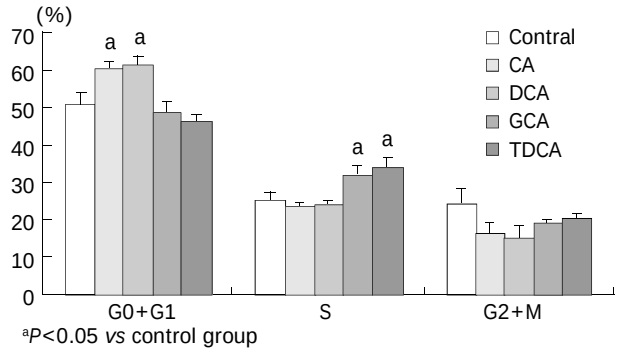

Figure 8 Cell cycles of PANC-1 cells incubated in 40 μM of bile acids added media for 24 h.

DISCUSSION

Pancreatic cancer frequently causes obstructive jaundice and elevates bile acid level in serum. For example, in non-pruritic jaundiced serum GCA concentration was 33.44±16.90 μmol/L[14]. Bile acids are steroid metabolites of cholesterol functioning as trophic factors for gut epithelium and as detergents for absorption of cholesterol and fat-soluble vitamins. The cytotoxicity of bile acids on various normal human cells[15,16] and a few malignant cells[17,18] has been demonstrated. It has been previously confirmed that bile acids could stimulate the growth of colonic epithelial cells but not that of colonic cancer cell lines[19]. While Debruyne *et al*. found recently that bile acids such as CA, chenodeoxycholic acid (CDCA), DCA, LCA could stimulate the invasion of HCT-8/E11 and PCmsrc human colorectal cancer cells into collagen type I gels[20]. Is there any interaction of elevated bile acids on human pancreatic cancer progression? However, how bile acids influence pancreatic cancer remains a subject of controversy. In order to investigate the direct effects of bile acids on pancreatic cancer, three typical pancreatic cancer cell lines(PANC-1, MIA PaCa-2 and PGHAM-1) and six common bile acids were selected and used in this study. Cultured pancreatic cancer cells have provided a model of pancreatic cancer free of other probable influencing factors such as immunoreaction and serum albumin in combination with bile acids in the body. MTT colorimetric assay is a very useful method for evaluating cell survival and proliferation. The reliability and sensitivity of MTT assay have been demonstrated to be comparable to that of tritiated thymidine incorporation in cell proliferation and cytotoxicity assays[21]. To a certain extent, the results of MTT reflect the final effects of cell proliferation or cytotoxicity instead of only earlier events detected by tritiated thymidine incorporation.

In this study, PANC-1 cells were incubated in 50 μmol/L to 1.0 mmol/L bile acid supplemented medium for 48 h, cell growth was inhibited to some extent at low concentration of bile acids and was also significantly inhibited by the higher concentration of bile acids. When bile acids concentration was reduced to only 2-8 μmol/L and the incubation time was prolonged to 96 h, cell proliferation was also observed. In 6-8 μmol/L of DCA supplemented medium significant inhibition could be obtained. Cell proliferation of PANC-1, MIA PaCa-2 and PGHAM-1 was significantly inhibited by bile acids supplemented media at certain concentrations for 72 h. The inhibitive effects of all six bile acids were ranked in the following order: DCA>CA>LCA> GCA>TDCA> TCDC. The inhibition exhibited a dosage-dependent manner, especially for DCA. Among these three cell lines, MIA PaCa-2 seemed to show the most sensitive response to all of the bile acids. The concentrations of bile acids resembled the elevation of some bile acids in jaundiced serum. Our investigation indicated that free bile acids in jaundiced serum might inhibit pancreatic cell growth and proliferation. Furthermore, we found that when PANC-1 cells were incubated in 40 μM of DCA or CA added media for 24 h, the percentage of G0+G1 phase cells was significantly increased compared with the control group ($P<0.05$). This implied that DCA and CA could induce cell cycle arrest, resulting in reduced proliferation and apoptosis of PANC-1 cells. Concerning its mechanism, Martinez *et al*. believed that cytotoxicity of DCA might be produced through induction of apoptosis via a protein kinase C-dependent signaling pathway[22].

According to our ultrastructural findings, the membrane and organelles were definitely damaged by supplement of bile acid DCA in medium, the inhibitory effects of bile acids on these pancreatic cancer cell lines might mainly depend on their cytotoxicity. Usually, cytotoxicity of bile acid is resulted from its hydrophobic features and hydrophobic-hydrophilic balance in serum. Lipophilic unconjugated bile acids have been shown to flip-flap rapidly across artificial lipid bilayers, so that unconjugated bile acids might enter the cytosol of every kind of cells even at a low concentration[23]. It has also been demonstrated that DCA or CDCA administration in rat colon could enhance cell membrane phospholipid turnover[24]. Hydrophobic bile acids, such as DCA, could damage cells by lysing membranes[25] and impairing mitochondrial function as well as increasing the generation of reactive oxygen radicals which can cause membrane lipid peroxidation and attack nucleic acids[26]. Velardi *et al* have demonstrated that the cytotoxicity of bile acids is partially dependent on the cell membrane composition. Because cell membrane components such as glycolipids, receptors, and transport proteins vary in different cell lines depending on cell origin and differentiation, cell lines may also differ in regard to their response to bile acids. The over susceptibility of MIA PaCa-2 to bile acids might be due to their unique membrane lipid components. Under SEM, we also found that DCA could reduce microvilli density of PANC-1 cells. The microvilli on the surface of malignant cells could contribute to movement, attachment and invasion of malignant cells[27]. Reduction of microvilli might potentially inhibit PANC-1 cell invasion.

Biliary drainage has been shown to be an appropriate, definitive therapy for biliary obstruction due to unresectable pancreatic and peripancreatic malignancies. Some surgeons preferred to choose billiary drainage as a preoperative treatment

to reduce the level of jaundice. They expected patients to get a better operation tolerance before the radical cure. However, patients with jaundice had a higher risk of bleeding complications while those with preoperative biliary drainage (PBD) had more infective complications[28]. Some researchers demonstrated that preoperative biliary drainage increased the risk of developing intraoperative infectious morbidity and postoperative infectious morbidity and mortality following pancreaticoduodenectomy. Preoperative biliary drainage should be avoided whenever possible in patients with potentially resectable lesions. Consequently, the effect of bile acids on pancreatic cancer should be evaluated. It is concluded that bile acids could inhibit proliferation of PANC-1, MIA PaCa-2 and PGHAM-1 cell lines *in vitro*[29]. This may imply that bile acid can inhibit the growth of pancreatic cancer. Although the observation that bile acids inhibited proliferation of cultured cell lines could not completely reflect the complex pathophysiology of pancreatic cancer patients accompanied with obstructive jaundice, this study, at least, provides a clue that bile acids in jaundiced serum may have potentially inhibitory effects on pancreatic cancer progression. However, our investigation is an *in vitro* one, further studies are needed.

ACKNOWLEDGEMENT

We would like to express our thanks to Mr. Masahiko Onda and Mr. Eiji Uchida, from the First Department of Surgery, Nippon Medical School, Tokyo, Japan, for their valuable help in the work.

REFERENCES

1 **Yao GY**, Zhou JL, Lai MD, Chen XQ, Chen PH. Neuroendocrine markers in adenocarcinomas: an invesigation of 356 cases. *World J Gastroenterol* 2003; **9**: 858-861
2 **Tan ZJ**, Hu XG, Cao GS, Tang Y. Analysis of gene expression profile of pancreatic carcinoma using cDNA microarray. *World J Gastroenterol* 2003; **9**: 818-823
3 **Rocha Lima CM**, Centeno B. Update on pancreatic cancer. *Curr Opin Oncol* 2002; **14**: 424-430
4 **Martignoni ME**, Wagner M, Krahenbuhl L, Redaelli CA, Friess H, Buchler MW. Effect of preoperative biliary drainage on surgical outcome after pancreatoduodenectomy. *Am J Surg* 2001; **181**: 52-59
5 **Sewnath ME**, Birjmohun RS, Rauws EA, Huibregtse K, Obertop H, Gouma DJ. The effect of preoperative biliary drainage on postoperative complications after pancreaticoduodenectomy. *J Am Coll Surg* 2001; **192**: 726-734
6 **McGrath PC**, Sloan DA, Kenady DE. Surgical management of pancreatic carcinoma. *Semin Oncol* 1996; **23**: 200-212
7 **Matsuzaki Y**, Bouscarel B, Le M, Ceryak S, Gettys TW, Shoda J, Fromm H. Effect of cholestasis on regulation of cAMP synthesis by glucagon and bile acids in isolated hepatocytes. *Am J Physiol* 1997; **273**(1 Pt 1): G164-G174
8 **Heuman DM**, Pandak WM, Hylemon PB, Vlahcevic ZR. Conjugates of ursodeoxycholate protect against cytotoxicity of more hydrophobic bile salts: *in vitro* studies in rat hepatocytes and human erythrocytes. *Hepatology* 1991; **14**: 920-926
9 **Velardi AL**, Groen AK, Elferink RP, Van Der Meer R, Palasciano G, Tytgat GN. Cell type-dependent effect of phospholipid and cholesterol on bile salt cytotoxicity. *Gastroenterology* 1991; **101**: 457-464
10 **Deschner E**, Cohen BI, Raicht RF. Acute and chronic effect of dietary cholic acid on colonic epithelial cell proliferation. *Digestion* 1981; **21**: 290-296
11 **Graven PA**, Pfanstiel J, Saito R, Derubertis FR. Relationship between loss of rat colonic surface epithelium induced by deoxycholate and initiation of the subsequent proliferative response. *Cancer Res* 1986; **46**: 5754-5759
12 **Yamamura S**, Onda M, Uchida E. Two types of peritoneal dissemination of pancreatic cancer cells in a hamster model. *Nippon Ika Daigaku Zasshi* 1999; **66**: 253-261
13 **Yoshida T**, Ohki S, Kanazawa M, Mizunuma H, Kikuchi Y, Satoh H, Andoh Y, Tsuchiya A, Abe R. Inhibitory effects of prostaglandin D2 against the proliferation of human colon cancer cell lines and hepatic metastasis from colorectal cancer. *Surg Today* 1998; **28**: 740-745
14 **Cabral DJ**, Small DM, Lilly HS, Hamilton JA. Transbilayer movement of bile acids in model membranes. *Biochemistry* 1987; **26**: 1801-1804
15 **Garner CM**, Mills CO, Elias E, Neuberger JM. The effect of bile salts on human vascular endothelial cells. *Biochim Biophys Acta* 1991; **1091**: 41-45
16 **Araki Y**, Fujiyama Y, Andoh A, Nakamura F, Shimada M, Takaya H, Bamba T. Hydrophilic and hydrophobic bile acids exhibit different cytotoxicities through cytolysis, interleukin-8 synthesis and apoptosis in the intestinal epithelial cell lines. IEC-6 and Caco-2 cells. *Scand J Gastroenterol* 2001; **36**: 533-539
17 **Lechner S**, Muller-Ladner U, Schlottmann K, Jung B, McClelland M, Ruschoff J, Welsh J, Scholmerich J, Kullmann F. Bile acids mimic oxidative stress induced upregulation of thioredoxin reductase in colon cancer cell lines. *Carcinogenesis* 2002; **23**: 1281-1288
18 **Shekels LL**, Lyftogt CT, Ho SB. Bile acid-induced alterations of mucin production in differentiated human colon cancer cell lines. *Int J Biochem Cell Biol* 1996; **28**: 193-201
19 **Shekels LL**, Beste JE, Ho SB. Tauroursodeoxycholic acid protects *in vitro* models of human colonic cancer cells from cytotoxic effects of hydrophobic bile acids. *J Lab Clin Med* 1996; **127**: 57-66
20 **Debruyne PR**, Bruyneel EA, Li X, Zimber A, Gespach C, Mareel MM. The role of bile acids in carcinogenesis. *Mutat Res* 2001; **1**: 480-481: 359-369
21 **Denizot F**, Lang R. Rapid colorimetric assay for cell growth and survival: Modifications to the tetrazolium dye procedure giving improved sensitivity and reliability. *J Immunol Methods* 1986; **89**: 271-277
22 **Martinez JD**, Stratagoules ED, LaRue JM, Powell AA, Gause PR, Craven MT, Payne CM, Powell MB, Gerner EW, Earnest DL. Different bile acids exhibit distinct biological effects: the tumor promoter deoxycholic acid induces apoptosis and the chemopreventive agent ursodeoxycholic acid inhibits cell proliferation. *Nutr Cancer* 1998; **31**: 111-118
23 **Cabral DJ**, Small DM, Lilly HS, Hamilton JA. Transbilayer movement of bile acids in model membranes. *Biochemistry* 1987; **26**: 1801-1804
24 **Craven PA**, Pfanstiel J, DeRubertis FR. Role of activation of protein kinase C in the stimulation of colonic epithelial proliferation and reactive oxygen formation by bile acids. *J Clin Invest* 1987; **79**: 532-541
25 **Lichtenberg D**, Robson RJ, Dennis EA. Solubilization of phospholipids by detergents. Structural and kinetic aspects. *Biochim Biophys Acta* 1983; **737**: 285-304
26 **Ljubuncic P**, Fuhrman B, Oiknine J, Aviram M, Bomzon A. Effect of deoxycholic acid and ursodeoxycholic acid on lipid peroxidation in cultured macrophages. *Gut* 1996; **39**: 475-478
27 **Knyrim K**, Paweletz N. Cell interactions in a "bilayer" of tumor cells. A scanning electron microscope study. *Virchows Arch B Cell Pathol* 1977; **25**: 309-325
28 **Srivastava S**, Sikora SS, Kumar A, Saxena R, Kapoor VK. Outcome following pancreaticoduodenectomy in patients undergoing preoperative biliary drainage. *Dig Surg* 2001; **18**: 381-387
29 **Lu Y,** Onda M, Uchida E, Yamamura S, Yanagi K, Matsushita A, Kobayashi T, Fukuhara M, Aida K, Tajiri T. The cytotoxic effects of bile acids in crude bile on human pancreatic cancer cell lines. *Surg Today* 2000; **30**: 903-909

Edited by Zhu LH and Wang XL

P.O.Box 2345, Beijing 100023,China
Fax: +86-10-85381893
E-mail: wjg@wjgnet.com www.wjgnet.com

World J Gastroenterol 2003;9(12):2764-2767
World Journal of Gastroenterology
 ISSN 1007-9327

• BASIC RESEARCH •

Loss of DPC4 expression and its correlation with clinicopathological parameters in pancreatic carcinoma

Zhan Hua, Yuan-Chun Zhang, Xiao-Ming Hu, Zhen-Geng Jia

Zhan Hua, Peking Union Medical College, China-Japan Friendship Institute of Clinical Medical Sciences, Beijing 100029, China
Yuan-Chun Zhang, Zhen-Geng Jia, Department of General Surgery, China-Japan Friendship Hospital, Beijing 100029, China
Xiao-Ming Hu, Department of Immunology, China-Japan Friendship Hospital, Beijing 100029, China
Correspondence to: Dr. Zhan Hua, Peking Union Medical College, China-Japan Friendship Institute of Clinical Medical Sciences, Beijing 100029, China. huazhan@hotmail.com
Telephone: +86-10-64221122-2353 **Fax:** +86-10-64278791
Received: 2003-05-10 **Accepted:** 2003-06-12

Abstract

AIM: DPC4 is a tumor suppressor gene on chromosome 18q21.1 that has high mutant frequencies in pancreatic carcinogenesis. The purpose of this study was to investigate the role of DPC4 alterations in tumorigenesis and progression of pancreatic carcinomas.

METHODS: We studied the immunohistochemical markers of DPC4 in 34 adenocarcinomas and 16 nonmalignant specimens from the pancreas. The 16 nonmalignant specimens from the pancreas included 8 non-neoplastic cysts and 8 normal pancreatic tissues. The relationship between DPC4 alterations and various clinicopathological parameters was evaluated by chi-square test or Fisher's exact test. Survivals were calculated using Kaplan-Meier method (by a log-rank test).

RESULTS: All the 16 nonmalignant cases of the pancreas showed expression of DPC4 gene. Loss of DPC4 expression was seen in 8 of 34(23.5 %) pancreatic adenocarcinomas. The frequency of loss of DPC4 expression was higher in poorly differentiated adenocarcinoma (G3) than in well and moderately differentiated adenocarcinoma (G1 and G2) histologically (P=0.037). Loss of DPC4 expression of the patients at TNM stage IV was also higher than that of the patients at TNM stages I, II and III (60.0 % at stage IV, *versus* 14.3 % at stage I, 18.2 % at stage II, and 18.2 % at stage III) (P=0.223). The mean and median survival in patients with DPC4 expression was longer than those in patients with loss of DPC4 expression. Kaplan-Meier survival analysis demonstrated patients with DPC4 expression had a higher survival rate than patients with loss of DPC4 expression, but the difference did not reach statistical significance (P =0.879).

CONCLUSION: This study suggests that DPC4 is involved in the development of pancreatic carcinoma and is a late event in pancreatic carcinogenesis, DPC4 expression may be a molecular prognostic marker for pancreatic carcinoma.

Hua Z, Zhang YC, Hu XM, Jia ZG. Loss of DPC4 expression and its correlation with clinicopathological parameters in pancreatic carcinoma. *World J Gastroenterol* 2003; 9(12): 2764-2767
http://www.wjgnet.com/1007-9327/9/2764.asp

INTRODUCTION

The incidence of pancreatic carcinoma has increased in recent decades in the world, and this cancer has the lowest five-year survival rate among all cancers. The dismal survival of patients with pancreatic carcinomas is caused by the late diagnosis and low resection rates[1,2]. However, understanding the molecular pathogenesis of pancreatic carcinomas may be the foundation upon which to develop novel strategies for identifying genetic markers useful for the early diagnosis and treatment. An association has been demonstrated between pancreatic carcinomas and various genetic alterations including genes K-ras[3,4], Her-2/neu[5], p16[6], and p53[7]. Recently, DPC4 (deleted in pancreatic carcinoma, locus 4; Smad4) located on chromosome 18q21.1, has received special attention as its alterations may play a role in activation of pancreatic carcinogenesis[8].

DPC4 gene is a tumor suppressor gene, which has been shown to mediate the downstream effects of TGF-β superfamily signaling, resulting in growth inhibition[9]. Inactivation of DPC4 tumor-suppressor gene is relatively specific for pancreatic carcinoma, although it has been shown to occur in a small percentage of primary carcinomas of the esophagus[10,11], stomach[11,12], head and neck[13], breast, ovary[14], colon[15], and biliary tract[16]. DPC4 can be inactivated by one of the two identified mechanisms: intragenic mutation of one allele coupled with loss of the other allele, or deletion of both alleles (homozygous deletions). Both mutations and homozygous deletions of DPC4 gene have been observed in a high proportion of pancreatic carcinomas[8]. In contrast, the role of DPC4 in human pancreatic carcinoma remains less well defined. Recently, immunohistochemical labeling for the DPC4 gene product has become an extremely sensitive and specific marker for DPC4 gene alterations in pancreatic carcinomas, and has been shown to mirror the DPC4 genetic status of pancreatic carcinomas, because most mutations of DPC4 could result in a loss of the protein. Therefore, immunolabeling for DPC4 could provide a useful tool to examine genetic status in pancreatic adenocarcinomas[17,18].

In the present study, we examined DPC4 expression in 34 adenocarcinomas and 16 nonmalignant specimens from the pancreas using a monoclonal antibody to human DPC4 protein by means of immunohistochemistry and studied the relation between expression of DPC4 and various clinicopathological parameters in order to elucidate whether altered DPC4 expression played a role in the tumorigenesis and progression of pancreatic carcinomas.

MATERIALS AND METHODS

Patients and samples

Thirty-four specimens of pancreatic adenocarcinomas were retrieved from the pathology archives of China-Japan Friendship Hospital between 1984 and 2000. There were 22 males and 12 females with pancreatic carcinomas, and the average age of the patients was 55.18±11.29 years (mean±SD), with a range of 30-75 years. Twenty-eight patients were followed up until death or until the time of this study.

Histopathological grade and clinical staging were evaluated according to the criteria by Klöppel for pancreatic tumors[19] and the International Union Against Cancer (UICC) TNM classification[20]. Histopathologic examination revealed well differentiated adenocarcinoma in 10 patients, moderately differentiated adenocarcinoma in 15 patients, and poorly differentiated adenocarcinoma in 9 patients. Seven patients were at UICC stages I, 11 at stages II, 11 at stage III, and 5 at stage IV. In addition, 16 nonmalignant specimens from the pancreas including 8 non-neoplastic cysts and 8 normal pancreatic tissues were used as controls.

Immunohistochemistry

Tissues were routinely fixed in neutral formalin, embedded in paraffin, and 5 μm thick consecutive sections were cut. After deparaffinized, the slides were placed in a solution of 3 % hydrogen peroxide (1:1) for 10 minutes to block the activity of endogenous peroxidase, and then heated in a microwave for 5 minutes at 100 ℃. After the slides were cooled for 30 minutes, nonspecific binding was blocked with a protein solution for 10 minutes, and then each slide was labeled with a 1:100 dilution of monoclonal antibody to DPC4 (clone B8, Santa Cruz, CA). Anti-DPC4 antibody was detected by adding biotinylated secondary antibodies, avidin-biotin complex, and 3,3' -diaminobenzidine. The sections were counterstained with hematoxylin. Positive cells were stained dark brown in the nuclei and/or cytoplasms, and the staining was graded into four categories: 0, no staining, 1+, weak staining, 2+, moderate staining, 3+, heavy staining. Positive staining was considered as expression of DPC4. Normal pancreatic ducts, islets of Langerhans, acini, lymphocytes, and stromal fibroblasts showing moderate to strong expression of DPC4 gene, served as positive internal controls for each section. For negative controls, the primary antibody was replaced with phosphate buffered solution (PBS).

Statistical analysis

The data were analyzed with chi-square test or Fisher' s exact test to compare the differences between the two subgroups of patients based on the results of DPC4 staining. All of the tests were two-tailed. Survivals were calculated using Kaplan-Meier method (by a log-rank test).

RESULTS

The results of DPC4 protein immunohistochemistry are summarized in Table 1, and typical examples of the positive and negative groups are shown in Figure 1 (A-E). It was observed that pancreatic carcinoma showed loss of DPC4 expression, whereas the adjacent normal pancreatic tissue had DPC4 expression (Figures 1B and C).

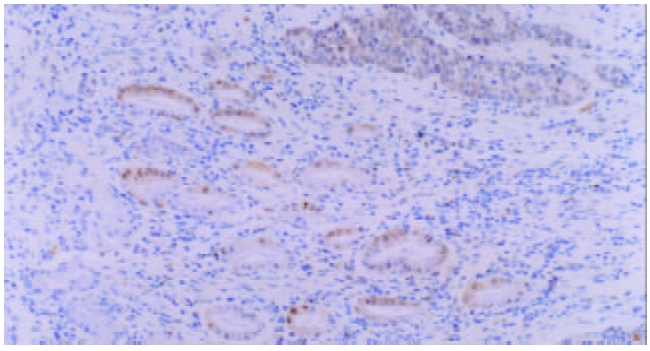

A: Well-differentiated pancreatic carcinoma showed DPC4 expression. hematoxylin counterstain. original magnification, ×100.

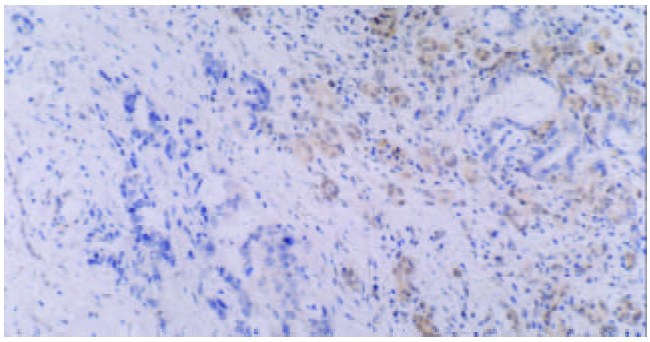

B: Well-differentiated pancreatic carcinoma showed loss of DPC4 expression (left), whereas the adjacent normal pancreatic tissue had DPC4 expression (right). hematoxylin counterstain. original magnification, ×200.

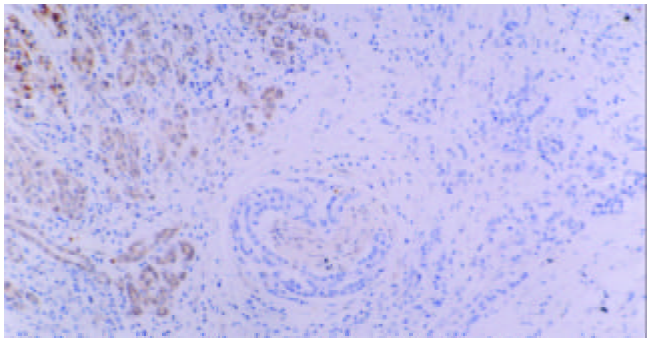

C: Moderately-differentiated pancreatic carcinoma showed loss of DPC4 expression (right), whereas the adjacent normal pancreatic tissue had DPC4 expression (left). Vortex in the middle shows invasion of pancreatic nerve. hematoxylin counterstain. original magnification, ×160.

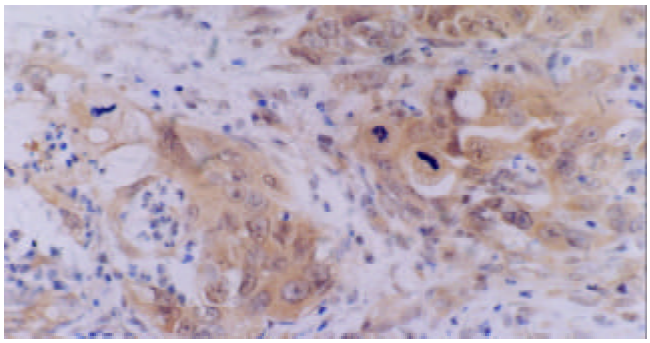

D: Poorly-differentiated pancreatic carcinoma showed DPC4 expression. Hematoxylin counterstain. original magnification, ×400.

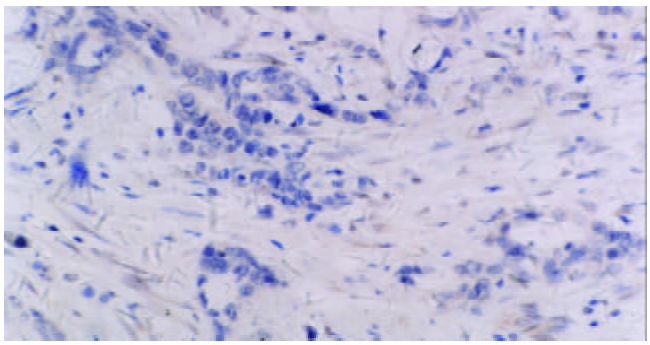

E: Poorly-differentiated pancreatic carcinoma showed loss of DPC4 expression. hematoxylin counterstain. original magnification, ×400.

Figure 1 Representative immunostaining results of DPC4 in pancreatic carcinoma (A-E). Positive cells were stained dark brown in the nuclei and/or cytoplasms (A-D).

All the 16 nonmalignant cases of the pancreas showed expression of DPC4 gene products. Loss of DPC4 expression was seen in 8 of 34 (23.5 %) pancreatic adenocarcinomas. The results of immunostaining of DPC4 expression in 34 pancreatic carcinomas and the correlation with various clinicopathological parameters are shown in Table 2. A significant difference was found in the frequency of loss of DPC4 expression between well and moderately differentiated adenocarcinomas (G1 and G2) and poorly differentiated adenocarcinoma (G3) histologically (P =0.037). Although loss of DPC4 expression in the patients at TNM staging IV was higher than that in those at stages I, II and III (60.0 % at stage IV, versus 14.3 % at stage I, 18.2 % at stage II, and 18.2 % at stage III), the difference did not reach any statistical significance (P=0.223). In addition, a higher frequency of loss of DPC4 expression in patients with lymph node-metastasis was also revealed, however the difference was not significant (P=0.228). The mean and median survival in patients with DPC4 expression was longer than that in patients with loss of DPC4 expression (Table 3). Kaplan-Meier survival analysis demonstrated patients with DPC4 expression had a higher survival rate than those with loss of DPC4 expression, but the difference did not reach any statistical significance (P=0.879) (Figure 2).

Table 1 Loss of DPC4 expression in pancreatic tissues (%)

Tissues	*n*	Loss expression of DPC4 (%)
Normal pancreas	8	0 (0)
Non-neoplastic cysts	8	0 (0)
Pancreatic carcinoma	34	8 (23.5)

Table 2 Correlations between loss expression of DPC4 and clinicopathological parameters in pancreatic carcinoma

Parameters	*n*	Loss expression of DPC4 (%)	*P*
Age (y)			
≥60	17	2 (11.8)	0.268
45≤x<60	11	4 (36.4)	
<45	6	2 (33.3)	
Sex			
Male	22	6 (27.3)	0.681
Female	12	2 (16.7)	
Pathological grade			
G1+G2	27	4 (14.8)	0.037
G3	7	4 (57.1)	
Tumor diameter			
≤4.5 cm	19	4 (21.2)	1.000
>4.5 cm	15	4 (26.7)	
Tumor location			
Head	24	6 (25.0)	0.842
Body and tail	10	2 (20.0)	
Lymph node			
Negative	20	3 (15.0)	0.228
Positive	14	5 (35.7)	
TNM staging			
I	7	1 (14.3)	0.223
II	11	2 (18.2)	
III	11	2 (18.2)	
IV	5	3 (60.00)	

G1, well differentiated; G2, moderately differentiated; G3, poorly differentiated.

Table 3 Mean and median survivals in pancreatic carcinomas

	Mean survival (days)	Median survival (days)
DPC4 expression	329.94±41.54	319.00±30.32
Loss of DPC4 expression	300.00±61.88	206.00±88.39

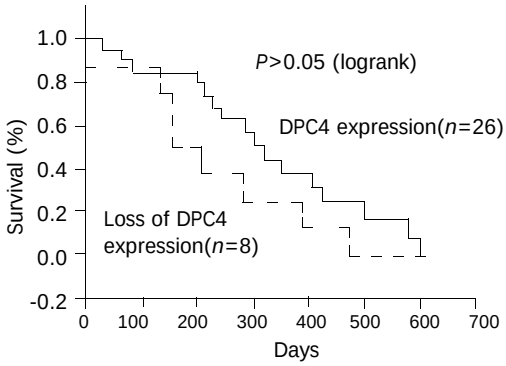

Figure 2 Kaplan-Meier survival curves comparing patients with DPC4 expression and patients with loss of DPC4 expression. Although patients with DPC4 expression had a higher survival rate than those with loss of DPC4 expression, the difference did not reach ang statistical significance.

DISCUSSION

This study aimed to clarify the role of DPC4 in the development of pancreatic carcinoma. The product of DPC4 gene belongs to the evolutionally conserved family of Smad proteins which are linked to TGF-β superfamily of cytokines. Smad proteins are involved in the regulation of cell differentiation as well as the inhibition of cell proliferation, and their alterations could confer resistance to TGF-β and thereby contribute to tumorigenesis[21,22]. DPC4 gene produces a 64-KD protein that influences gene transcription and growth arrest. In fact, DPC4 protein has three distinguishable domains, and mutations in each of these domains could lead to the loss of DPC4 function[8,23,24].

There were different findings about the frequency of DPC4 alterations in pancreatic carcinomas in previous reports (9 %-55 %)[8,25]. The discrepancies between studies might be due to differences in the study populations, techniques, or the statistical method. In our study, eight of the 34-pancreatic carcinoma specimens were immunohistochemically labeled for the loss of DPC4 protein (23.5 %). However, DPC4 immunohistochemical staining was found in all of the 16 nonmalignant specimens from the pancreas. This finding suggested that DPC4 might be involved in the tumorigenesis and development of pancreatic carcinoma.

Our study showed loss of DPC4 expression was correlated with the histological grade in patients with pancreatic carcinoma. Loss of DPC4 expression in those with poorly differentiated adenocarcinomas was significantly higher than that in those with well and moderately differentiated adenocarcinomas, which implied that DPC4 gene might preserve phenotypic characteristics under normal conditions and control the malignant progression of pancreatic carcinomas.

There was a trend toward a higher frequency of loss of DPC4 expression in patients at TNM staging IV in this study. When stratified by stage, the highest percentage of loss of DPC4 reactivity was found in carcinomas at stage IV (60.0 %), compared with 14.3 % at stage I, 18.2 % at stage II, and 18.2 % at stage III carcinomas. A higher frequency of loss of DPC4 expression in patients with lymph node-metastasis was also revealed. Survival analysis demonstrated patients with DPC4 expression had a higher survival rate than those with loss of DPC4 expression.

The data in our study were correlated fairly well with what has been reported. The results from Wilentz *et al* showed that DPC4 expression in duct lesions with a histologically low-grade (PanIN-1 and -2) was significantly higher than that in those with a histologically high-grade (PanIN-3)[26]. Another study showed that DPC4 expression in PanIN could be

predictive of DPC4 expression in the subsequent invasive ductal adenocarcinoma. Additionally, DPC4 expression could be used to differentiate recurrent or persistent adenocarcinomas from a second primary adenocarcinoma. A recent study found that survival of patients whose tumors expressed DPC4 protein was significantly longer (19.2 months) as compared with 14.7 months of those without DPC4 protein expression, and DPC4 expression was correlated with a better prognosis of pancreatic carcinomas[18]. Biankin *et al* also found DPC4/Smad4 expression had a potential as a prognostic indicator in patients with pancreatic carcinoma, and loss of DPC4 expression was associated with improved survival after resection, whereas resection did not improve the survival in patients whose tumor expressed DPC4.

These findings suggest that loss of DPC4 expression occurs biologically late in the neoplastic progression leading to the development of infiltrating pancreatic carcinoma, and indicates a poor prognosis for patients. It is reasonable to postulate that DPC4 plays a pivotal role in regulating all TGF-β superfamily signal pathways. Abrogation of DPC4 function might cause a breakdown in this signaling pathway and loss of transcription of genes critical to cell-cycle control. Cells might therefore become TGF-β resistant and escape from TGF-β-mediated growth control and apoptosis. Experimental evidences indicated that DPC4 could regulate an angiogenic switch by decreasing the expression of vascular endothelial growth factor (VEGF) and increasing the levels of angiogenesis inhibitor thrombospondin-1 (TSP-1).

In conclusion, our study shows that loss of DPC4 expression is involved in the carcinogenesis and development of pancreatic carcinoma and is a late event in pancreatic carcinogenesis. DPC4 expression may be a molecular prognostic marker for pancreatic carcinoma.

ACKNOWLEDGEMENTS

We thank Dr. Gonghua Zhao for her critical suggestions regarding this work and Mr. Jing Zhang for helping perform the immunohistochemical staining.

REFERENCES

1 **Bramhall SR**, Allum WH, Jones AG, Allwood A, Cummins C, Neoptolemos JP. Treatment and survival in 13,560 patients with pancreatic cancer, and incidence of the disease, in the West Midlands: an epidemiological study. *Br J Surg* 1995; **82**: 111-115

2 **Yeo CJ**, Cameron JL. Prognostic factors in ductal pancreatic cancer. *Langenbecks Arch Surg* 1998; **383**: 129-133

3 **Hruban RH**, van Mansfeld AD, Offerhaus GJ, van Weering DH, Allison DC, Goodman SN, Kensler TW, Bose KK, Cameron JL, Bos JL. K-ras oncogene activation in adenocarcinoma of the human pancreas. A study of 82 carcinomas using a combination of mutant-enriched polymerase chain reaction analysis and allele-specific oligonucleotide hybridization. *Am J Pathol* 1993; **143**: 545-554

4 **Robinson RA.** K-ras mutations and the diagnosis of pancreatic carcinoma. *Am J Clin Pathol* 1996; **105**: 257-259

5 **Safran H**, Steinhoff M, Mangray S, Rathore R, King TC, Chai L, Berzein K, Moore T, Iannitti D, Reiss P, Pasquariello T, Akerman P, Quirk D, Mass R, Goldstein L, Tantravahi U. Overexpression of the HER-2/neu oncogene in pancreatic adenocarcinoma. *Am J Clin Oncol* 2001; **24**: 496-499

6 **Hu YX**, Watanabe H, Ohtsubo K, Yamaguchi Y, Ha A, Okai T, Sawabu N. Frequent loss of p16 expression and its correlation with clinicopathological parameters in pancreatic carcinoma. *Clin Cancer Res* 1997; **3**: 1473-1477

7 **Li Y**, Bhuiyan M, Vaitkevicius VK, Sarkar FH. Molecular analysis of the p53 gene in pancreatic adenocarcinoma. *Diagn Mol Pathol* 1998; **7**: 4-9

8 **Hahn SA**, Schutte M, Hoque AT, Moskaluk CA, da Costa LT, Rozenblum E, Weinstein CL, Fischer A, Yeo CJ, Hruban RH, Kern SE. DPC4, a candidate tumor suppressor gene at human chromosome 18q21.1. *Science* 1996; **271**: 350-353

9 **Dai JL**, Turnacioglu KK, Schutte M, Sugar AY, Kern SE. Dpc4 transcriptional activation and dysfunction in cancer cells. *Cancer Res* 1998; **58**: 4592-4597

10 **Maesawa C**, Tamura G, Nishizuka S, Iwaya T, Ogasawara S, Ishida K, Sakata K, Sato N, Ikeda K, Kimura Y, Saito K, Satodate R. MAD-related genes on 18q21.1, Smad2 and Smad4, are altered infrequently in esophageal squamous cell carcinoma. *Jpn J Cancer Res* 1997; **88**: 340-343

11 **Lei J**, Zou TT, Shi YQ, Zhou X, Smolinski KN, Yin J, Souza RF, Appel R, Wang S, Cymes K, Chan O, Abraham JM, Harpaz N, Meltzer SJ. Infrequent DPC4 gene mutation in esophageal cancer, gastric cancer and ulcerative colitis-associated neoplasms. *Oncogene* 1996; **13**: 2459-2462

12 **Nishizuka S**, Tamura G, Maesawa C, Sakata K, Suzuki Y, Iwaya T, Terashima M, Saito K, Satodate R. Analysis of the DPC4 gene in gastric carcinoma. *Jpn J Cancer Res* 1997; **88**: 335-339

13 **Kim SK**, Fan Y, Papadimitrakopoulou V, Clayman G, Hittelman WN, Hong WK, Lotan R, Mao L. DPC4, a candidate tumor suppressor gene, is altered infrequently in head and neck squamous cell carcinoma. *Cancer Res* 1996; **56**: 2519-2521

14 **Schutte M**, Hruban RH, Hedrick L, Cho KR, Nadasdy GM, Weinstein CL, Bova GS, Isaacs WB, Cairns P, Nawroz H, Sidransky D, Casero RA Jr, Meltzer PS, Hahn SA, Kern SE. DPC4 gene in various tumor types. *Cancer Res* 1996; **56**: 2527-2530

15 **Takagi Y**, Kohmura H, Futamura M, Kida H, Tanemura H, Shimokawa K, Saji S. Somatic alterations of the DPC4 gene in human colorectal cancers *in vivo*. *Gastroenterology* 1996; **111**: 1369-1372

16 **Hahn SA**, Bartsch D, Schroers A, Galehdari H, Becker M, Ramaswamy A, Schwarte-Waldhoff I, Maschek H, Schmiegel W. Mutations of the DPC4/Smad4 gene in biliary tract carcinoma. *Cancer Res* 1998; **58**: 1124-1126

17 **Wilentz RE**, Su GH, Dai JL, Sparks AB, Argani P, Sohn TA, Yeo CJ, Kern SE, Hruban RH. Immunohistochemical labeling for dpc4 mirrors genetic status in pancreatic adenocarcinomas: a new marker of DPC4 inactivation. *Am J Pathol* 2000; **156**: 37-43

18 **Tascilar M**, Skinner HG, Rosty C, Sohn T, Wilentz RE, Offerhaus GJ, Adsay V, Abrams RA, Cameron JL, Kern SE, Yeo CJ, Hruban RH, Goggins M. The SMAD4 protein and prognosis of pancreatic ductal adenocarcinoma. *Clin Cancer Res* 2001; **7**: 4115-4121

19 **Klöppel G**. Pancreatic non-endocrine tumors. In: Klöppel G, Heitz PU ed. Pancreatic pathology. *Edinburg:Churchill Livingstone* 1984: 79-113

20 **Hermanek P**, Sobin LH. UICC TNM classification of malignant tumors. 4th ed. 2nd revision. *Berlin: Springer-Verlag* 1992: 71-73

21 **Zhang Y**, Feng X, We R, Derynck R. Receptor-associated Mad homologues synergize as effectors of the TGF-β response. *Nature* 1996; **383**: 168-172

22 **Chiao PJ**, Hunt KK, Grau AM, Abramian A, Fleming J, Zhang W, Breslin T, Abbruzzese JL, Evans DB. Tumor suppressor gene Smad4/DPC4, its downstream target genes, and regulation of cell cycle. *Ann N Y Acad Sci* 1999; **880**: 31-37

23 **Shi Y**, Hata A, Lo RS, Massague J, Pavletich NP. A structural basis for mutational inactivation of the tumour suppressor Smad4. *Nature* 1997; **388**: 87-93

24 **De Caestecker MP**, Hemmati P, Larisch-Bloch S, Ajmera R, Roberts AB, Lechleider RJ. Characterization of functional domains within Smad4/DPC4. *J Biol Chem* 1997; **272**: 13690-13696

25 **Moore PS**, Orlandini S, Zamboni G, Capelli P, Rigaud G, Falconi M, Bassi C, Lemoine NR, Scarpa A. Pancreatic tumours: molecular pathways implicated in ductal cancer are involved in ampullary but not in exocrine nonductal or endocrine tumorigenesis. *Br J Cancer* 2001; **84**: 253-262

26 **Wilentz RE**, Iacobuzio-Donahue CA, Argani P, McCarthy DM, Parsons JL, Yeo CJ, Kern SE, Hruban RH. Loss of expression of Dpc4 in pancreatic intraepithelial neoplasia: evidence that DPC4 inactivation occurs late in neoplastic progression. *Cancer Res* 2000; **60**: 2002-2006

Edited by Zhu LH and Wang XL

P.O.Box 2345, Beijing 100023,China
Fax: +86-10-85381893
E-mail: wjg@wjgnet.com www.wjgnet.com

World J Gastroenterol 2003;9(12):2768-2771
World Journal of Gastroenterology
 ISSN 1007-9327

• BASIC RESEARCH •

G and D cells in rat antral mucosa: An immunoelectron microscopic study

Feng-Peng Sun, Yu-Gang Song

Feng-Peng Sun, Yu-Gang Song, Department of Gastroenterology, Nanfang Hospital, First Military Medical University, Guangzhou 510515, Guangdong Province, China
Supported by Natural Science Foundation of Guangdong Province, No. 010578; Technological and Social Development Project of Guangdong Province, No. 2002C31210; the Key Scientific Research Project of Guangzhou City, No. 2002Z3-E0131
Correspondence to: Feng-Peng Sun, Department of Gastroenterology, Nanfang Hospital, First Military Medical University, Guangzhou 510515, Guangdong Province, China. sci@china.com
Telephone: +86-20-85140114-87101
Received: 2002-10-08 **Accepted:** 2003-03-10

Abstract

AIM: To investigate the gastrin secreting cells (G cells) and the somatostatin secreting cells (D cells) of antral mucosa in rats at the ultrastructural level.

METHODS: Revised immunoelectron microscopic technique was used to detect the G cells and D cells in rat antral mucosa through gastrin and somatostatin antibodies labeled by colloidal gold. Also the relevant quantitative analysis regarding the granular number of colloidal gold in G cells and in D cells was conducted.

RESULTS: Immunological granules of colloidal gold were distributed in G cells and D cells. Gastrin labeled golden granules or somatostatin labeled ones presented mainly as lobation-like or island-like congeries. Most of the golden congeries were observed dissociated in cytoplasms of G cells or D cells, near the basement membrane. A few golden congeries were located in nuclei. The number of golden granules in one G cell was around 107.04±19.68 and was 83.36±17.58 in one D cell.

CONCLUSION: Gastrin secreting granules are located in cytoplasms and nuclei of G cells, and somatostatin secreting granules both in cytoplasms and in nuclei of D cells. The number of golden granules can be quantitatively analyzed to determine the relative amount of gastrin secreting granules or somatostatin secreting granules.

Sun FP, Song YG. G and D cells in rat antral mucosa: An immunoelectron microscopic study. *World J Gastroenterol* 2003; 9(12): 2768-2771
http://www.wjgnet.com/1007-9327/9/2768.asp

INTRODUCTION

Gastrointestinal hormones such as gastrin and somatostatin, regulate the secretion, motility, absorption, blood flow and cell nutrition of the digestive tract. Abnormality of their secretion often affects the normal functions of digestive tract, even cause clinical symptoms or syndromes. Pathological impairment of gastrointestinal tract could also result in changes of the level of gastrointestinal hormones. Gastrin is mainly secreted from gastrin secreting cells (G cells) in antrum mucosa or upper small intestine. Medulla oblongata and dorsal nuclei of vagus nerve in central nervous system also have gastrin. Somatostatin is distributed in the body, hypothalamus and at other sites of the brain, peripheral nerve and gastrointestinal tract. In digestive system, for example, somatostatin is secreted from somatostatin secreting cells (D cells). D cells are distributed mainly in intestinal nerve plexus, stomach and pancreas[1-4].

Although there are some methods to observe the shape of G cells and D cells, microscope or electron microscope could not decide G cells or D cells alone. Immunohistochemical method could not demonstrate G cells or D cells at ultrastructural levels. Thus investigations at the ultrastructural level by immunoelectron microscopy are effective[5-8]. This study was to demonstrate G cells and D cells at the ultrastructural level by colloidal gold labeled immunoelectron microscopy technique.

MATERIALS AND METHODS

Guinea pigs and antral tissue processing

Seven healthy male Wistar rats weighing 230-250 g from the Center of Experimental Animals in Sun Yat-sen University of Medical Sciences (Guangzhou, China) were used. All rats received no special treatment before sacrificed. The rats were fasted overnight with free access to water. Four days later, the rat' s abdomen, anesthetized with 3 % of sodium pentobarbital intraperitoneally at a dosage of 30 mg/kg, was cut open and its stomach was split from the greater curvature. The antral tissue of about 0.5 mm×0.5 mm was separated using ophthalmic scissors. Then the specimens were immersed into a mixture of 0.1 % glutaraldehyde and 3 % paraformaldehyde in 0.1M PBS, pH7.4, for 2 hr at room temperature for fixation.

Specimen preparation for immunoelectron microscopy

Two hours after fixation, the antral tissue specimens were washed four times for 15 min in 0.1M PBS, pH7.4, and then postfixed for 1 hr in solution of 1 % osmium tetroxide (1 % potassium dichromate, pH 7.2, 1 % osmium tetroxide, 0.85 % NaC1) at room temperature. The specimens were washed three times for 10 min in 0.1M PBS, pH7.4, and dehydrated at room temperature in 50 % acetone (15 min), 70 % acetone (15 min), 90 % acetone (15 min), and 100 % acetone (three times for 15 min each). The specimens were then infused in an open desiccator containing 50 % acetone: 50 % Spurr resin (1 hr), 33 % acetone: 67 % Spurr resin (2 hr), and 100 % Spurr resin overnight. When the resin was infused in the specimens, it was polymerized at 40 ℃ for 4 days. To orientate the samples, 1 μm thick sections were cut, put on an objective glass, and stained with 0.1 % teluidin blue. Appropriate regions were chosen, and the pyramids were further trimmed, cut on a Leica Rechert ultramicrotome into 60-80 nm ultrathin sections, put onto 300 nickle mesh grids. All ultrathin sections were divided into G cells group, D cells group, and control group.

Postembedded antibody incubation and immunoelectron microscopy

All the ultrathin sections were oxidized in H_2O_2 for 10 min,

washed three times for 5 min in water. Osmium tetroxide was removed in 1 % sodium periodate, washed three times for 5 min in 0.05 M TBS, pH7.4. The ultrathin sections were incubated for 30 min at room temperature in 1.5 % BSA (Sigma, USA) in PBS for blocking. The sections of G cells group were then incubated with rabbit anti-gastrin polyclonal antibody (Sigma, USA) at a concentration of 1:80 in PBS, the sections of D cells group were incubated with rabbit anti-somatostatin polyclonal antibody (ZYMED, USA) at a concentration of 1:80 in PBS, and the sections of control group were incubated with PBS only. All sections were incubated in a wet box at 4 ℃ overnight and then at 37 ℃ for 1 hr. The sections were washed three times for 10 min in 0.05M TBS, pH7.4, then one time for 10 min in 0.02 M TBS, pH7.4. The sections were again incubated for 30 min at room temperature in 1.5 % BSA in PBS for blocking and then incubated with a gold-conjugated secondary antibody, colloidal-gold/staphylococcic-protein-A 1:80 (10 nm, Boster Biological Technology Co, Wuhan, China) in PBS, for 1 hr at 37 ℃. The sections were washed three times for 5 min in water and stained with 5 % uranyl acetate (in water) at room temperature for 60 min, and with lead citrate for 60 min. At last the specimens were examined and photographed under an electron microscope (Philips CM10).

Image analysis of colloidal gold granules

A total of 50 cells in either G cells group or D cells group were randomly photographed from sections of their photos. They were input into the Quantimet-500 image analysis system (Leica Co. German) for calculation of the average number of colloidal gold granules. The data thus obtained were expressed in $x \pm s$.

RESULTS

Immunoelectron microscopy of G cells

No immunological granules of colloidal gold in most antral mucosa cells were found, except those in G cells. Immunological granules of colloidal gold were well distributed in G cells, with the cells' ultrastructure clearly fixed. While the membrane of G cells was intact, rough endoplasmic reticules were increased, and mitochondria decreased. The nuclei of G cells were normal, and the chromatin was equally distributed. The gastrin labeled golden granules in G cells were clear, either round-shaped or oval-shaped, with a high electro-density. The granules presented mainly as lobation-like or island-like congeries, which were dispersed in cytoplasms of G cells, directing toward the basement membrane. A few golden congeries in the nuclei of G cells were mainly located in euchromatin area. No golden congeries were observed in heterochromatin area. There were immunological granules of colloidal gold in the nuclei of G cells as island-like congeries and penetrating nuclear pore in cytoplasms (Figure 1). The number of golden granules in a G cell was 107.04±19.68.

Immunoelectron microscopy of D cells

No immunological granules of colloidal gold were found in most antral mucosa cells, except those in D cells. Immunological granules of colloidal gold were found well distributed in D cells, with the ultrastructure clearly fixed. The membrane of D cells was intact, rough endoplasmic reticules were increased, and mitochondria decreased. The nuclei of D cells were normal, with their chromatin well distributed. The somatostatin labeled golden granules in D cells were clear, either round-shaped or olive-shaped, with a high electro-density. The granules presented mainly as lobation-like or island-like congeries, a few of them were dispersed in D cells while most of them were dissociated in cytoplasms of D cells, directing toward the basement membrane. Again, a few golden congeries in the nuclei of D cells were mainly located in euchromatin area (Figure 2). No golden congeries were found in heterochromatin area. The number of golden granules in a D cell was 83.36±17.58. No colloidal gold-labeled cell was observed in control group.

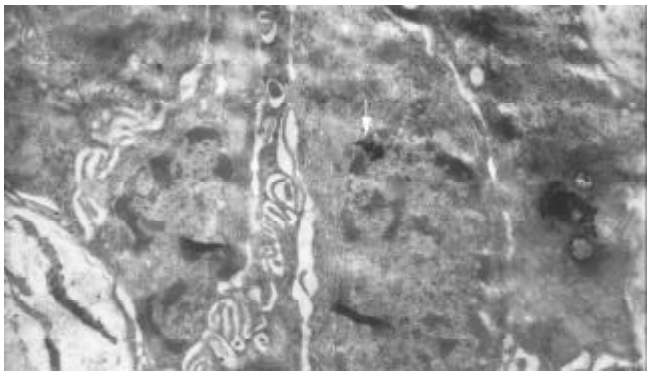

Figure 1 Immunological granules of colloidal gold located in nuclei of G cell as island-like congeries (↑), and penetrating nuclear pores into cytoplasms. ×21000.

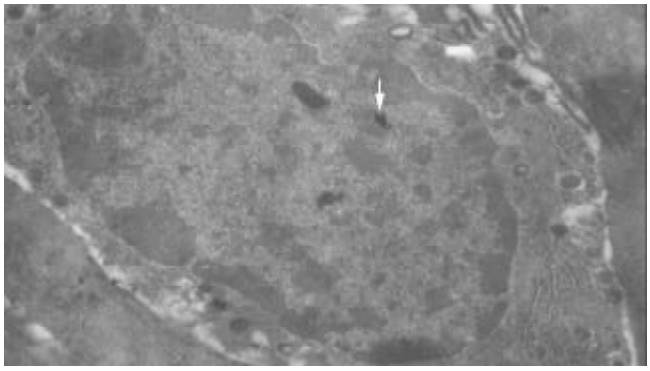

Figure 2 Immunological granules of colloidal gold locate in nuclei of D cell as island-like congeries (↑). ×8900.

DISCUSSION

Gastric mucosa consists of highly organic multi-functional glands. In a single gastric gland there are at least five kinds of cells. They are the parietal cell, chief cell, endocrine cell, superficial epithelial cell and mucous cell. The stem cells of all these kinds of cells are in the neck area near the surface of the gland. When migrating upward to the surface of gland, they changed into the surface mucous cells. When migrating downward deeper into the gland, the proliferative stem cells changed into cells in forms of parietal cells, chief cells, and endocrine cells[9-11].

The features of gastrin can be briefly summarized as follows. There are gastrin receptors both in parietal cells and in ECL cells. As the main regulating hormone of gastric acid secretion, gastrin stimulates parietal cells to secrete gastric acid directly via the gastrin receptors in parietal cells and also stimulates ECL cells to secrete histamine via the gastric receptors in the cells. Then histamine stimulates parietal cells to secrete gastric acid via H_2 receptors in parietal cells in a paracrine style. While accelerating the secretion of pepsin, secretin, pancreatic juice, and the secretion of water and salt in bile, gastrin also speeds up the releasing of insulin and calcitonin. It has both nutritional and accelerating effects on gastric mucosa. It also has a growth factor producing the similar effect. In the same way, the increase of gastrin would lead to the increasing number of both parietal cells and ECL cells.

Apart from all these, gastrin is also closely related with the occurrence of carcinoid tumor. Gastrin enhances the motion of gastrointestinal tract, thus increasing the contraction effect of the stomach, intestine and gall bladder. In addition, there are reports that G cells should be taken as the fourth histamine source in stomach besides chief cells, ECL cells, and intestinal nerve plexus. Increase of pH, intake of meal, increase of pressure in the stomach, and excitation introduced by vagus nerve or mucosa nerve plexus could make G cells secrete more gastrin. Decrease of pH stimulated by somatostatin or other gastrointestinal hormones, and excitation of sympathetic nerve could inhibit the secretion of gastrin[12-17].

What characterizes somatostatin is presented as follows. The main physiological effect produced by somatostatin on digestive system is inhibition. Somatostatin could inhibit peristalsis of stomach, intestine, gall bladder and proliferation of mucosal cells, reduce blood flow of gastrointestinal tract and small intestine to absorb water, electrolyte, glucose, amino acid, and triglycerides, depress the secretion of gastric acid, pepsin, hepatic bile, small intestinal juice, and secretion of gastrin and other gastrointestinal hormones. Excitation of sympathetic nerve could inhibit D cells to secrete somatostatin, but that of vagus nerve could stimulate D cells to do so. Gastrin has a unique regional regulatory effect on secretion of somatostatin in stomach. Gastrin could directly stimulate D cells to secrete somatostatin. In some species, gastrin receptors have been detected in D cells of stomach. As shown in some investigations, endogenous histamine inhibited the secretion of somatostatin via paracrine effect on H_3 receptor. Others showed that endothelins inhibited the secretion of somatostatin via endothelin receptors[18-23].

In histocyte, there are often different granules that are important symbols of classification. This includes neurosecretory granule of 80-600 nm with an electron-densed core, highly electron-densed zymogen granule of 1-2 μm, large and light mucus granules and endocrine secretory granules. Although some endocrine secretory granules in endocrine cells had definite characteristics and are somewhat significant to evaluate the type of such endocrine cells, it was difficult to differentiate the features of endocrine simply according to endocrine cells and their secretory granules[24-28].

Colloidal gold immunoelectron microscopic technique is the advanced method for microcosmic morphology. The colloidal gold probe is of high specification, high resolution, accurate localization and accurate quantity. The significance of colloidal gold immunoelectron microscopy is similar to common immunohistochemistry in testing specific antigens expressed in target cells. But it could not be more useful for immunoelectron microscopy to study the localization or the quantitative analysis of antigens at the ultrastructural level. There are many intervening factors in immunoelectron microscopy, the most important one is to protect the activity of antigen. In this aspect, improvement has been made in manipulating the integrating of samples, the fixative and embedding medium, the time of fixation, the temperature of aggregation, the purity and diluting ratio of antibody and colloidal gold, as well as the time of incubation[29-32].

On the whole, the result was satisfactory. The ultrastructure of G cells and D cells was well protected. The ultrastructures of secretory granules of both gastrin and somatostatin were definitely localized. The secretory granules of gastrin in cytoplasms of G cells were also found in the nuclei of G cells. The secretory granules of somatostatin in cytoplasms of D cells were also found in the nuclei of D cells. Therefore, the conclusion is thus made that there are secretory granules of gastrin or somatostatin in nuclei of G cells or D cells. After they are gradually matured, the secretory granules penetrate the nuclear pores into cytoplasms. At last, gastrin or somatostatin is secreted through the basement membrane into intercellular substances, playing their physiological roles. The lobe-like or island-like congeries of colloidal gold observed in G cells and D cells are in coincidence with the existing patterns of the secretory granules of gastrin or somatostatin. In our opinion, the size of secretory granules in congeries of colloidal gold could be subjected to quantitative analysis, though the quantitative scale of each piece of colloidal gold to bind gastrin or somatostatin has not been exactly decided. In this sense, the specific significance of colloidal gold number in congeries of G cells or D cells remains to be precisely interpreted.

REFERENCES

1 **Larsson LI**. Developmental biology of gastrin and somatostatin cells in the antropyloric mucosa of the stomach. *Microsc Res Tech* 2000; **48**: 272-281

2 **Portela-Gomes GM**, Albuquerque JP, Ferra MA. Serotonin and gastrin cells in rat gastrointestinal tract after thyroparathyroidectomy and induced hyperthyroidism. *Dig Dis Sci* 2000; **45**: 730-735

3 **Sun FP**, Song YG, Cheng W, Zhao T, Yao YL. Gastrin, somatostatin, G and D cells of gastric ulcer in rats. *World J Gastroenterol* 2002; **8**: 375-378

4 **Yao YL**, Xu B, Zhang WD, Song YG. Gastrin, somatostatin, and experimental disturbance of the gastrointestinal tract in rats. *World J Gastroenterol* 2001; **7**: 399-402

5 **Caplin ME**, Clarke P, Grimes S, Dhillon AP, Khan K, Savage K, Lewin J, Michaeli D, Pounder RE, Watson SA. Demonstration of new sites of expression of the CCK-B/gastrin receptor in pancreatic acinar AR42J cells using immunoelectron microscopy. *Regul Pept* 1999; **84**: 81-89

6 **Sereti E**, Gavriil A, Agnantis N, Golematis VC, Voloudakis-Baltatzis IE. Immunoelectron study of somatostatin, gastrin and glucagon in human colorectal adenocarcinomas and liver metastases. *Anticancer Res* 2002; **22**: 2117-2123

7 **Takahashi M**, Hoshii Y, Kawano H, Setoguchi M, Gondo T, Yamashita Y, Nakayasu K, Kamei T, Ishihara T. Multihormone-producing islet cell tumor of the pancreas associated with somatostatin-immunoreactive amyloid: immunohistochemical and immunoelectron microscopic studies. *Am J Surg Pathol* 1998; **22**: 360-367

8 **Stahlman MT**, Gray ME. Immunogold EM localization of neurochemicals in human pulmonary neuroendocrine cells. *Microsc Res Tech* 1997; **37**: 77-91

9 **Bakke I**, Qvigstad G, Sandvik AK, Waldum HL. The CCK-2 receptor is located on the ECL cell, but not on the parietal cell. *Scand J Gastroenterol* 2001; **36**: 1128-1133

10 **Karam SM**, Alexander G. Blocking of histamine H2 receptors enhances parietal cell degeneration in the mouse stomach. *Histol Histopathol* 2001; **16**: 469-480

11 **Okamoto CT**, Forte JG. Vesicular trafficking machinery, the actin cytoskeleton, and H+-K+-ATPase recycling in the gastric parietal cell. *J Physiol* 2001; **532**(Pt 2): 287-296

12 **Buchan AM**, Squires PE, Ring M, Meloche RM. Mechanism of action of the calcium-sensing receptor in human antral gastrin cells. *Gastroenterology* 2001; **120**: 1128-1139

13 **Koh TJ**, Chen D. Gastrin as a growth factor in the gastrointestinal tract. *Regul Pept* 2000; **93**: 37-44

14 **Cui GL**, Sandvik AK, Munkvold B, Waldum HL. Effects of anaesthetic agents on gastrin-stimulated and histamine-stimulated gastric acid secretion in the totally isolated vascularly perfused rat stomach. *Scand J Gastroenterol* 2002; **37**: 750-753

15 **Kirton CM**, Wang T, Dockray GJ. Regulation of parietal cell migration by gastrin in the mouse. *Am J Physiol Gastrointest Liver Physiol* 2002; **283**: G787-793

16 **Cobb S**, Wood T, Tessarollo L, Velasco M, Given R, Varro A, Tarasova N, Singh P. Deletion of functional gastrin gene markedly increases colon carcinogenesis in response to azoxymethane in mice. *Gastroenterology* 2002; **123**: 516-530

17 **Pagliocca A**, Wroblewski LE, Ashcroft FJ, Noble PJ, Dockray GJ, Varro A. Stimulation of the gastrin-cholecystokinin(B) receptor promotes branching morphogenesis in gastric AGS cells. *Am J Physiol Gastrointest Liver Physiol* 2002; **283**: G292-299

18 **Zavros Y**, Paterson A, Lambert J, Shulkes A. Expression of progastrin-derived peptides and somatostatin in fundus and antrum of nonulcer dyspepsia subjects with and without *Helicobacter pylori* infection. *Dig Dis Sci* 2000; **45**: 2058-2064
19 **Iyo T**, Kaneko H, Konagaya T, Mori S, Kotera H, Uruma M, Rhue N, Shimizu T, Imada A, Kusugami K, Mitsuma T. Effect of intragastric ammonia on gastrin-, somatostatin-and somatostatin receptor subtype 2 positive-cells in rat antral mucosa. *Life Sci* 1999; **64**: 2497-2504
20 **Zhang QX**, Dou YL, Shi XY, Ding Y. Expression of somatostatin mRNA in various differentiated types of gastric carcinoma. *World J Gastroenterol* 1998; **4**: 48-51
21 **Arebi N**, Healey ZV, Bliss PW, Ghatei M, Van Noorden S, Playford RJ, Calam J. Nitric oxide regulates the release of somatostatin from cultured gastric rabbit primary D-cells. *Gastroenterology* 2002; **123**: 566-576
22 **Raderer M**, Traub T, Formanek M, Virgolini I, Osterreicher C, Fiebiger W, Penz M, Jager U, Pont J, Chott A, Kurtaran A. Somatostatin-receptor scintigraphy for staging and follow-up of patients with extraintestinal marginal zone B-cell lymphoma of the mucosa associated lymphoid tissue (MALT)-type. *Br J Cancer* 2001; **85**: 1462-1466
23 **Lippl F**, Schusdziarra V, Allescher HD. Effect of endomorphin on somatostatin secretion in the isolated perfused rat stomach. *Neuropeptides* 2001; **35**: 303-309
24 **Varro A**, Dockray GJ. Post-translational processing of progastrin: inhibition of cleavage, phosphorylation and sulphation by brefeldin A. *Biochem J* 1993; **295**(**Pt 3**): 813-819
25 **Gromada J**, Hoy M, Buschard K, Salehi A, Rorsman P. Somatostatin inhibits exocytosis in rat pancreatic alpha-cells by G(i2)-dependent activation of calcineurin and depriming of secretory granules. *J Physiol* 2001; **535**(Pt 2): 519-532
26 **Patel YC**, Galanopoulou AS, Rabbani SN, Liu JL, Ravazzola M, Amherdt M. Somatostatin-14, somatostatin-28, and prosomatostatin [1-10] are independently and efficiently processed from prosomatostatin in the constitutive secretory pathway in islet somatostatin tumor cells (1027B2). *Mol Cell Endocrinol* 1997; **131**: 183-194
27 **Konda Y**, Kamimura H, Yokota H, Hayashi N, Sugano K, Takeuchi T. Gastrin stimulates the growth of gastric pit with less-differentiated features. *Am J Physiol* 1999; **277**(4 Pt 1): G773-784
28 **Bakke I**, Qvigstad G, Brenna E, Sandvik AK, Waldum HL. Gastrin has a specific proliferative effect on the rat enterochromaffin-like cell, but not on the parietal cell: a study by elutriation centrifugation. *Acta Physiol Scand* 2000; **169**: 29-37
29 **Sierralta WD**. Immunoelectron microscopy in embryos. *Methods* 2001; **24**: 61-69
30 **Renno WM**. Post-embedding double-gold labeling immunoelectron microscopic co-localization of neurotransmitters in the rat brain. *Neurobiology* 2001; **9**: 91-106
31 **Dolapchieva S**, Eggers R, Kuhnel W. N- and R-cadherins expression in the rat sciatic nerve demonstrated by postembedding immunogold method on semi-thin sections. *Ann Anat* 2001; **183**: 405-411
32 **Ishida S**, Kaito M, Kohara M, Tsukiyama-Kohora K, Fujita N, Ikoma J, Adachi Y, Watanabe S. Hepatitis C virus core particle detected by immunoelectron microscopy and optical rotation technique. *Hepatol Res* 2001; **20**: 335-347

Edited by Wang XL

P.O.Box 2345, Beijing 100023,China
Fax: +86-10-85381893
E-mail: wjg@wjgnet.com www.wjgnet.com

World J Gastroenterol 2003;9(12):2772-2775
World Journal of Gastroenterology
 ISSN 1007-9327

• BASIC RESEARCH •

Effect of complex amino acid imbalance on growth of tumor in tumor-bearing rats

Yin-Cheng He, Yuan-Hong Wang, Jun Cao, Ji-Wei Chen, Ding-Yu Pan, Ya-Kui Zhou

Yin-Cheng He, Jun Cao, Ji-Wei Chen, Ding-Yu Pan, Ya-Kui Zhou, Department of General Surgery, Zhongnan Hospital, Wuhan University, Wuhan 430071, Hubei Province, China
Yuan-Hong Wang, Wuhan Centre for Disease Prevention and Control, Wuhan 430022, Hubei Province, China
Supported by grants from Hubei Provincial Health Bureau, No. W98016 and the Education Committee of Hubei Province, No. 2001A14005
Correspondence to: Dr. Yin-Cheng He, Department of General Surgery, Zhongnan Hospital, Wuhan University, Wuhan 430071, Hubei Province, China. w030508h@public.wh.hb.cn
Telephone: +86-27-67812963
Received: 2003-06-05 **Accepted:** 2003-08-16

Abstract

AIM: To investigate the effect of complex amino acid imbalance on the growth of tumor in tumor-bearing (TB) rats.

METHODS: Sprague-Dawlley (SD) rats underwent jejunostomy for nutritional support. A suspension of Walker-256 carcinosarcoma cells was subcutaneously inoculated. TB rats were randomly divided into groups A, B, C and D according to the formula of amino acids in enteral nutritional solutions, respectively. TB rats received jejunal feedings supplemented with balanced amino acids (group A), methionine-depleted amino acids (group B), valine-depleted amino acids (group C) and methionine- and valine-depleted complex amino acid imbalance (group D) for 10 days. Tumor volume, inhibitory rates of tumor, cell cycle and life span of TB rats were investigated.

RESULTS: The G_0/G_1 ratio of tumor cells in group D (80.5±9.0) % was higher than that in groups A, B and C which was 67.0±5.1 %, 78.9±8.5 %, 69.2±6.2 %, respectively ($P<0.05$). The ratio of S/G_2M and PI in group D were lower than those in groups A, B and C. The inhibitory rate of tumor in groups B, C and D was 37.2 %, 33.3 % and 43.9 %, respectively ($P<0.05$). The life span of TB rats in group D was significantly longer than that in groups B, C, and A.

CONCLUSION: Methionine/valine-depleted amino acid imbalance can inhibit tumor growth. Complex amino acids of methionine and valine depleted imbalance have stronger inhibitory effects on tumor growth.

He YC, Wang YH, Cao J, Chen JW, Pan DY, Zhou YK. Effect of complex amino acid imbalance on growth of tumor in tumor-bearing rats. *World J Gastroenterol* 2003; 9(12): 2772-2775
http://www.wjgnet.com/1007-9327/9/2772.asp

INTRODUCTION

Malnutrition is encountered everyday in cancer patients and is associated with severe protein-amino acid metabolic disorder, uncorrectable negative nitrogen balance and low immune function[1-6]. Enteral nutrition (EN) and parenteral nutrition (PN) are both safe and effective methods of administering nutrients in cancer patients[7-9]. But PN with amino acid balanced solutions may prompt tumor growth[10-12]. Based on Harper's concept of amino acid imbalance, EN/TPN preparations with depleted or enriched specific amino acids produce tumor growth inhibition[13-18]. Previously, we found methionine/valine-depleted (0), low tyrosine (0.5 g/L) and arginine-enriched (6 g/L) complex amino acid imbalance solutions were the most rational formula in tumor-bearing (TB) rats[19]. In this study, we aimed to investigate the effect of complex amino acid imbalance on the growth of tumor.

MATERIALS AND METHODS

Animals

SD rats weighing 170±20 g were purchased from the Experimental Animal Center of Wuhan University (Wuhan, China) and fed with a stock rat diet *ad libitum*. The animals were maintained on a 12-hour light/12-hour dark cycle at ambient temperature of (23±2) ℃ and housed for 7 days before the experiment.

Catheterization of jejunostomy

After fasted for 12 hours, the rats (n=60) were anesthetized by intraperitoneal administration of 40 mg· kg^{-1} pentobarbital. They were then undergone catheterization during jejunostomy (day 0). A silicone rubber catheter with an internal diameter of 2 mm and an external diameter of 3 mm was inserted into the proximal jejunum. The catheter passed through a subcutaneous tunnel and emerged between the scapulae. The catheter was then mounted on a harness, passed through a protective coil, and connected to a swivel so that the animals could move without any restrictions in individual metabolic cages. The cannulation system consisted of a microinfusion pump, a swivel, rat-harness and a silicone-tube-jejunostomy. The rats were fasted for 48 hours after operation but were provided with water *ad libitum*, and then given normal rat diet.

Preparation of TB rats

Walker-256 carcinosarcoma cells were purchased from Chinese Center of Culture Preservation. On day 0, the rats were subcutaneously inoculated in the right flank with 10^7 tumor cells of approximately 0.1 ml of cell suspension.

Tumor weights and inhibitory rates of tumor

Tumors were palpable 7 days after transplantation. Measurements were made at the tumor site. The lengths of the major, minor axes and depth were measured with calipers. Growth of the tumor was evaluated every 3 days. Tumor volumes during experiments were calculated according to the following equation: $V=LWDp/6$. Where V is the tumor volume (mm^3), L is the length, W is the width and D is the depth of a solid tumor (mm). Inhibitory rates of tumor = (tumor volume of control group- tumor volume of experimental group)/tumor volume of control group×100 %.

Experimental groups and jejunal feeding

On day 8, 48 TB rats were randomly divided into four groups

(12 rats per group) according to the solutions administered: an amino acid balance solution (group A), methionine-depleted amino acid solution (group B), valine-depleted amino acid solution (group C), and methionine and valine-depleted complex amino acid solution (group D). They were administered enteral nutritional solutions (jejunal feeding) for 10 days. During EN, the rats were individually housed in metabolic cages. The compositions of EN solution infused to each rat are summarized in Table 1.

Administration methods

TB rats received continuous jejunal tube infusion for nutritional support at a daily dose of 330 ml· kg^{-1}, by means of a microinfusion pump (Sino-Swed Pharmaceutical Corp. Ltd. China). Non-protein calorie per day was approximately 1 104 K J· kg^{-1}. TB rats were not fed during the entire infusion experiment, however, they had free access to water.

Compositions of amino acid solutions

Table 1 lists the components of amino acid solution in four groups.

Table 1 Compositions of amino acid solution ($g \cdot L^{-1}$)

Amino acids	Group A	Group B	Group C	Group D
Isoleucine	5.5	5.5	5.5	5.5
Leucine	7.5	7.5	7.5	7.5
Lysine	7.0	7.0	7.0	7.0
Methionine	6.0	–	6.0	–
Phenylalanine	4.0	4.0	4.0	4.0
Threonine	5.0	5.0	5.0	5.0
Tryptophan	1.5	1.5	1.5	1.5
Valine	6.0	6.0	–	–
Arginine	6.0	6.0	6.0	6.0
Histidine	3.0	3.0	3.0	3.0
Proline	4.0	4.0	4.0	4.0
Tyrosine	1.0	1.0	1.0	1.0
Alanine	20.0	20.0	20.0	20.0
Glycine	7.5	7.5	7.5	7.5
Aspartic acid	4.0	4.0	4.0	4.0
Total amino acid	88.0	82.0	82.0	76.0
Total nitrogen	14.1	13.1	13.1	12.2

Compositions of EN solution

1 000 ml EN solution was composed of 350 ml of amino acid preparation (Table 1) supplemented with 300 ml of 50 % glucose, 100 ml of 20 % Intralipid (Sino-Swed Pharmaceutical Corp. Ltd. China), 20 ml of Soluvit, 20 ml of Vitalipid, 20 ml of Addamel and 190 ml of 0.9 % saline.

Specimen sampling

At the end of an administration period, 6 rats per group were respectively killed by cervical dislocation. The whole tumor was dissected and examined.

Cell cycle position measurement

Sections about 50 μm thick were cut from tumor tissues and washed 3 times in phosphate-buffered saline. Cell kinetics were measured by flow cytometry (FCM, PASIII, Partec Company, Germany).

Life span of TB rats

The remaining 6 rats per group were given solid food (Experimental Animal Center of Wuhan University, Wuhan, China) and water *ad libitum* according to their body weight until they died of advanced cancer. The life span of each rat in terms of median survival time (MST) was observed.

Statistical analysis

All results were presented as mean ±SD. Comparisons of the four groups were made using Uni-variate ANOVA test. The difference was considered significant when *P* value was less than 0.05.

RESULTS

Animals

Two rats in groups A, C and two rats in group D died of intestinal fistula, diarrhea, infection of abdominal cavity during enteral nutrition, respectively.

Changes in tumor cell cycle

Tumor-selective cell cycle arrest occurred in the S-G_2 phase during methionine depleted enteral nutrition. The distribution of cancer cell cycle was not obviously affected during valine starvation. The percentages of tumor cells in G_0G_1 phase in groups B and D were significantly higher than that in group A while the percentages of S phase cells in groups B and D were obviously lower than that in group A ($P<0.05$). There was no statistical difference between the percentages of G_2M cells in groups B and D and that in group A ($P>0.05$, Table 2).

Table 2 Distribution of cancer cell cycle after EN treatment (%)

Phase	Group A	Group B	Group C	Group D
G_0G_1	67.0±5.1	78.9±8.5[ac]	69.2±6.2[b]	80.5±9.0[ac]
S	20.1±1.8	11.8±2.9[ac]	19.9±3.0[b]	10.2±2.1[ac]
G_2+M	12.9±3.2	9.2±3.1	10.9±2.5	9.4±3.8
PI(S+G_2+M)	33.0±4.3	21.0±5.0[ac]	30.8±5.6[b]	20. 5±2.8[ac]

[a]$P<0.05$, *vs* group A, [b]$P<0.05$, *vs* group B, [c]$P<0.05$, *vs* group C.

Tumor volumes and inhibitory rates of tumor

Tumor volume had no statistical difference among each group before treatment. On day 10 of enteral nutrition, tumor growth in amino acid imbalance groups (groups B, C and D) was significantly lower than that in control group. The most remarkable inhibitory effect on tumor growth was found in complex amino acid imbalance group (group D) ($P<0.05$). The inhibitory rate of tumor (IRT) in groups B, C and D was respectively 37.2 %, 33.3 % and 43.9 % (Table 3).

Table 3 Changes in tumor volumes, IRT and MST before and after treatment

Group	Tumor volumes		IRT(%)	MST(d)
	Before	After		
Group A	0.028±0.015	2.85±0.43	...	26.8±1.5
Group B	0.039±0.010	1.79±0.56[a]	37.2	32.0±2.6[a]
Group C	0.033±0.020	1.90±0.30[ab]	33.3	35.6±3.2[a]
Group D	0.031±0.011	1.60±0.40[abc]	43.9	39.4±3.0[abc]

[a]$P<0.05$, *vs* group A, [b]$P<0.05$, *vs* group B, [c]$P<0.05$, *vs* group C.

Life span of TB rats

The median survival time (MST) in complex amino acid imbalance group was (39.4±3.0) days, as compared with (32.0±2.6) days in methionine-depleted group and (35.6±3.2) days in valine-depleted group (Table 3).

DISCUSSION

Influence of balanced amino acids on tumor growth

Compared with normal cells, the metabolism of tumor cells is significantly accelerated. *In vivo*, cancer cells have been known to have higher levels of protein synthesis, accompanied by a more active uptake of glucose and amino acids (nitrogen trap), and undergo more rapid differentiation and proliferation than healthy cells[20]. Amino acids are important materials of protein synthesis, Supplement of balanced amino acids results in the greatest increase of tumor cell cycles, thus tumor tissues compete with host tissues for nitrogen substrates. Nucleic acid and protein synthesis are increased, and tumor growth is accelerated. Table 3 indicates the experimental results of the anticancer effects of various amino acid imbalance solutions. As clearly shown in this table, tumor volume was especially large, and the median survival time was short after TB rats were administrated with balanced amino acid solutions (group A).

Influence of methionine/valine-depleted amino acid imbalance on tumor growth

Methionine dependency of many malignant tumor cells has been demonstrated in previous studies. That is to say, these cells were arrested in late S/G_2 phase in methionine free cell culture media, and tumor cellular proliferation was inhibited, and normal cells were methionine independent after methionine was replaced by hemocysteine[21-26]. Methionine is the principal biological methyl donor via S-adenosyl-L-methionine (SAM). SAM can easily transfer its methyl group to a large variety of acceptor substrates including rRNA, tRNA, mRNA, DNA, proteins, phospholipides, biological amines, and a long list of small molecules. Methionine dependency might be due to overutilization of methionine for transmethylation reactions resulting in a low free methionine pool and a low S-adenosylmethionie/S-adenosylhomocysteine ratio[27-31]. This directly inhibits the activity of transmethylase, thereby methionine depleted enteral nutrition can decrease methylation reaction of tumor tissues and lead to further reduction in nucleic acid synthesis and inhibition of cancer growth at molecular levels.

Our study demonstrated that tumor growth in group B was significantly slower than that in control group, the liver and peritoneum metastasis of cancer was much less in group B. It suggested that the invasive ability for metastasis be suppressed during methionine starvation. Breillout *et al* considered that methionine depletion disturbed the membrane lipids of tumor cells and inhibited their metastatic ability[32].

It was also found that valine depleted imbalance solution (group C) had a great inhibitory effect on Walker-256 carcinosarcoma cells. One possible mechanism was the alterations of intracellular protein synthesis due to deprivation of essential amino acids (Valine)[33-35]. Another possible mechanism seemed to be the inhibitory effect on the production of prolactin, which was likely to participate in tumor growth[20].

Influence of complex amino acid imbalance on tumor growth

As shown in Table 3, the most remarkable inhibitory effect on cancer growth was seen in the methionine/valine depleted complex amino acid imbalance group, followed by the methionine depleted imbalance group and then the valine depleted group. It suggested that complex amino acid imbalance solutions had the most strong anticancer effects. However, are we able to prevent the development of side effects of complex imbalance due to starvation of essential amino acids? This still needs further studies.

REFERENCES

1 **Nitenberg G,** Raynard B. Nutritional support of the cancer patient: issues and dilemmas. *Crit Rev Oncol Hematol* 2000; **34**: 137-168

2 **Xiao HB,** Cao WX, Yin HR, Lin YZ, Ye SH. Influence of L-methionine-deprived total parenteral nutrition with 5-fluorouracil on gastric cancer and host metabolism. *World J Gastroenterol* 2001; **7:** 698-701

3 **Karayiannakis AJ,** Syrigos KN, Polychronidis A, Pitiakoudis M, Bounovas A, Simopoulos K. Serum levels of tumor necrosis factor-alpha and nutritional status in pancreatic cancer patients. *Anticancer Res* 2001; **21**: 1355-1358

4 **Federico A,** Iodice P, Federico P, Del Rio A, Mellone MC, Catalano G, Federico P. Effects of selenium and zinc supplementation on nutritional status in patients with cancer of digestive tract. *Eur J Cin Nutr* 2001; **55:** 293-297

5 **Hatada T,** Miki C. Nutritional status and postoperative cytokine response in colorectal cancer patients. *Cytokine* 2000; **12:** 1331-1336

6 **Jagoe RT,** Goodship TH, Gibson GJ. Nutritional status of patients undergoing lung cancer operations. *Ann Thorac Surg* 2001; **71:** 929-935

7 **Buchman AL.** Must every cancer patient die with a central venous catheter? *Clin Nutr* 2002; **21:** 269-271

8 **Bozzetti F,** Cozzaglio L, Biganzoli E, Chiavenna G, de Cicco M, Donati D, Gilli G, Percolla S, Pironi L. Quality of life and length of survival in advanced cancer patients on home parenteral nutrition. *Clin Nutr* 2002; **21:** 281-288

9 **Buchman AL.** Enteral versus parenteral nutrition following resection in malnourished patients with gastrointestinal cancer. *Curr Gastroenterol Rep* 2002; **4:** 322-323

10 **Bozzetti F,** Gavazzi C, Cozzaglio L, Costa A, Spinelli P, Viola G. Total parenteral nutrition and tumor growth in malnourished patients with gastric cancer. *Tumori* 1999; **85**: 163-166

11 **Sasamura T,** Matsuda A, Kokuba Y. Tumor growth inhibition and nutritional effect of d-amino acid solution in AH109A hepatoma-bearing rats. *J Nutr Sci Vitaminol* 1998; **44:** 79-87

12 **Forchielli ML,** Paolucci G, Lo CW. Total parenteral nutrition and home parenteral nutrition: an effective combination to sustain malnourished children with cancer. *Nutr Rev* 1999; **57:** 15-20

13 **Komatsu H,** Nishihira T, Chin M, Doi H, Shineha R, Mori S, Satomi S. Effect of valine depleted total parenteral nutrition on fatty liver development in tumor-bearing rats. *Nutrition* 1998; **14:** 276-281

14 **Cao WX,** Cheng QM, Fei XF, Li SF, Yin HR, Lin YZ. A study of preoperative methionine-depleting parenteral nutrition plus chemotherapy in gastric cancer patients. *World J Gastroenterol* 2000; **6:** 255-258

15 **Nagahama T,** Goseki N, Endo M. Doxorubicin and vincristine with methionine depletion contributed to survival in the Yoshida sarcoma bearing rats. *Anticancer Res* 1998; **18:** 25-31

16 **Tang B,** Li YN, Kruger WD. Defects in methylthioadenosine phosphorylase are associated with but not responsible for methionine-dependent tumor cell growth. *Cancer Res* 2000; **60:** 5543 –5547

17 **Komatsu H,** Nishihira T, Chin M, Doi H, Shineha R, Mori S, Satomi S. Effects of caloric intake on anticancer therapy in rats with valine-depleted amino acid imbalance. *Nutr Cancer* 1997; **28:** 107-112

18 **Yoshida S,** Ohta J, Shirouzu Y, Ishibashi N, Harada Y, Yamana H, Shirouzu K. Effect of methionine-free total parenteral nutrition and insulin-like growth factor I on tumor growth in rats. *Am J Physiol* 1997; **273**(1 Pt 1): E10-16

19 **Chen JW,** He YC, Wang YH, Zhou YK, Liu QY, Shi HA. Rational formula of amino acids for nutritional supports in tumor-bearing rats. *Zhonghua Shiyan Waike Zazhi* 2001; **18:** 378

20 **Nishihira T,** Takagi T, Kawarabayashi Y, Izumi U, Ohkuma S, Koike N, Toyoda T, Mori S. Anti-cancer therapy with valine-depleted amino acid imbalance solution. *Tohoku J Exp Med* 1988; **156:** 259-270

21 **Sasamura T,** Matsuda A, Kokuba Y. Nutritional effects of a D-methionine-containing solution on AH109A hepatoma-bearing rats. *Biosci Biotechnol Biochem* 1998; **62:** 2418-2420

22 **Hoshiya Y,** Kubota T, Inada T, Kitajima M, Hoffman RM. Methionine-depletion modulates the efficacy of 5-fluorouracil in human gastric cancer in nude mice. *Anticancer Res* 1997; **17:** 4371-4375

23 **Poirson-Bichat F,** Goncalves RA, Miccoli L, Dutrillaux B, Poupon MF. Methionine depletion enhances the antitumoral efficacy of cytotoxic agents in drug-resistant human tumor xenografts. *Clin Cancer Res* 2000; **6:** 643-653
24 **Poirson-Bichat F,** Lopez R, Bras Goncalves RA, Miccoli L, Bourgeois Y, Demerseman P, Poisson M, Dutrillaux B, Poupon MF. Methionine deprivation and methionine analogs inhibit cell proliferation and growth of human xenografted gliomas. *Life Sci* 1997; **60:** 919-931
25 **Sasamura T,** Matsuda A, Kokuba Y. Effects of D-methionine-containing solution on tumor cell growth *in vitro*. *Arzneimittel Forschung* 1999; **49:** 541-543
26 **Cao WX,** Ou JM, Fei XF, Zhu ZG, Yin HR, Yan M, Lin YZ. Methionine-dependence and combination chemotherapy on human gastric cancer cells *in vitro*. *World J Gastroenterol* 2002; **8:** 230-232
27 **Lu SC.** Methionine adenosyltransferase and liver disease: It's all about SMA. *Gastroenterology* 1998; **114:** 403-407
28 **Zhu SS,** Xiao SD, Chen ZP, Shi Y, Fang JY, Li RR, Mason JB. DNA methylation and folate metabolism in gastric cancer. *World J Gastroenterol* 2000; **6**(Suppl 3): 18
29 **Avila MA,** Carretero MV, Rodriguez EN, Mato JM. Regulation by hypoxia of methionine adenosyltransferase activity and gene expression in rat hepatocytes. *Gastroenterology* 1998; **114:** 364-371
30 **Wang XY,** Li N, Gu J, Li WQ, Li JS. The effects of the formula of amino acids enriched BCAA on nutritional support in traumatic patients. *World J Gastroenterol* 2003; **9:** 599-602
31 **Yoshioka T,** Wada T, Uchida N, Maki H, Yoshida H, Ide N, Kasai H, Hojo K, Shono K, Maekawa R, Yagi S, Hoffman RM, Sugita K. Anticancer efficacy *in vivo* and *in vitro*, synergy with 5-fluorouracil, and safety of recombinant methioninase. *Cancer Res* 1998; **58:** 2583-2587
32 **Breillout F,** Antoine E, Poupon MF. Methionine dependency of malignant tumors: a possible approach for therapy. *J Natl Cancer Inst* 1990; **82:** 1628-1632
33 **Samuels SE,** Knowles AL, Tilignac T, Debiton E, Madelmont JC, Attaix D. Protein metabolism in the small intestine during cancer cachexia and chemotherapy in mice. *Cancer Res* 2000; **60:** 4968-4974
34 **Poirson-Bichat F,** Gonfalone G, Bras-Goncalves RA, Dutrillaux B, Poupon MF. Growth of methionine-dependent human prostate cancer (PC-3) is inhibited by ethionine combined with methionine starvation. *Br J Cancer* 1997; **75:** 1605-1612
35 **He YC,** Cao J, Chen JW, Pan DY, Zhou YK. Influence of methionine / valine-depleted enteral nutrition on nucleic acid and protein metabolism in tumor-bearing rats. *World J Gastroenterol* 2003; **9:** 771-774

Edited by Zhu LH and Wang XL

P.O.Box 2345, Beijing 100023,China
Fax: +86-10-85381893
E-mail: wjg@wjgnet.com www.wjgnet.com

World J Gastroenterol 2003;9(12):2776-2781
World Journal of Gastroenterology
 ISSN 1007-9327

• BASIC RESEARCH •

Alterations of intestinal mucosa structure and barrier function following traumatic brain injury in rats

Chun-Hua Hang, Ji-Xin Shi, Jie-Shou Li, Wei Wu, Hong-Xia Yin

Chun-Hua Hang, Ji-Xin Shi, Wei Wu, Hong-Xia Yin, Medical College of Nanjing University; Department of Neurosurgery, Jinling Hospital, Nanjing 210002, Jiangsu Province, China
Jie-Shou Li, Research Institute of General Surgery, Jinling Hospital, Clinical School of Medicine, Nanjing University, Nanjing 210002, Jiangsu Province, China
Supported by the Scientific Research Foundation of the Chinese PLA Key Medical Programs during the 10th Five-Year Plan Period, No. 01Z011
Correspondence to: Chun-Hua Hang, Department of Neurosurgery, Jinling Hospital, 305 East Zhongshan Road, Nanjing 210002, Jiangsu Province, China. hang1965@public1.ptt.js.cn
Telephone: +86-25-4597342 **Fax:** +86-25-4810987
Received: 2003-07-12 **Accepted:** 2003-07-30

Abstract

AIM: Gastrointestinal dysfunction is a common complication in patients with traumatic brain injury (TBI). However, the effect of traumatic brain injury on intestinal mucosa has not been studied previously. The aim of the current study was to explore the alterations of intestinal mucosa morphology and barrier function, and to determine how rapidly the impairment of gut barrier function occurs and how long it persists following traumatic brain injury.

METHODS: Male Wistar rats were randomly divided into six groups (6 rats each group) including controls without brain injury and traumatic brain injury groups at hours 3, 12, 24, and 72, and on day 7. The intestinal mucosa structure was detected by histopathological examination and electron microscopy. Gut barrier dysfunction was evaluated by detecting serum endotoxin and intestinal permeability. The level of serum endotoxin and intestinal permeability was measured by using chromogenic limulus amebocyte lysate and lactulose/mannitol (L/M) ratio, respectively.

RESULTS: After traumatic brain injury, the histopathological alterations of gut mucosa occurred rapidly as early as 3 hours and progressed to a serious state, including shedding of epithelial cells, fracture of villi, focal ulcer, fusion of adjacent villi, dilation of central chyle duct, mucosal atrophy, and vascular dilation, congestion and edema in the villous interstitium and lamina propria. Apoptosis of epithelial cells, fracture and sparseness of microvilli, loss of tight junction between enterocytes, damage of mitochondria and endoplasm, were found by electron microscopy. The villous height, crypt depth and surface area in jejunum decreased progressively with the time of brain injury. As compared with that of control group (183.7±41.8 EU/L), serum endotoxin level was significantly increased at 3, 12, and 24 hours following TBI (434.8±54.9 EU/L, 324.2±61.7 EU/L and 303.3±60.2 EU/L, respectively), and peaked at 72 hours (560.5±76.2 EU/L), then declined on day 7 (306.7±62.4 EU/L, $P<0.01$). Two peaks of serum endotoxin level were found at hours 3 and 72 following TBI. L/M ratio was also significantly higher in TBI groups than that in control group (control, 0.0172±0.0009; 12 h, 0.0303±0.0013; 24 h, 0.0354±0.0025; 72 h, 0.0736±0.0105; 7 d, 0.0588±0.0083; $P<0.01$).

CONCLUSION: Traumatic brain injury can induce significant damages of gut structure and impairment of barrier function which occur rapidly as early as 3 hours following brain injury and lasts for more than 7 days with marked mucosal atrophy.

Hang CH, Shi JX, Li JS, Wu W, Yin HX. Alterations of intestinal mucosa structure and barrier function following traumatic brain injury in rats. *World J Gastroenterol* 2003; 9(12): 2776-2781
http://www.wjgnet.com/1007-9327/9/2776.asp

INTRODUCTION

Gastrointestinal dysfunction occurs frequently in patients with traumatic brain injury (TBI)[1]. Dysfunction of the different segments of gastrointestinal tract leads to corresponding symptoms such as gastrointestinal bleeding[2-4], gastric reflux[5,6] and decreased intestinal peristalsis[7,8], mainly due to mucosal damage and alteration of gastrointestinal motility[9]. Studies on gastrointestinal dysfunction associated with head injury in the literature concentrated on the gastric mucosa, gastric emptying and lower esophageal sphincter tone[2-8]. However, the effect of TBI on intestinal mucosa has not been studied to date. Therefore, the alterations of intestinal mucosa morphology and barrier function following TBI remain unclear.

It is generally accepted that the intestine may serve as an important organ in the development of severe complications under critically ill conditions, including trauma, burns, shock, *etc*.[10-12]. Major trauma and shock may initiate a cascade of intestinal events such as intestinal cytokine response[13], increased intestinal permeability[14,15], translocation of intestinal bacteria and endotoxin[10,16], leading to systemic inflammatory response syndrome (SIRS) and sepsis with subsequent multiple organ failure[12]. TBI is a severe pathological stress and critically ill condition usually complicated with gastric stress ulcer[17]. Therefore, we hypothesized that TBI could also lead to significant gut structural alterations and barrier dysfunction as mentioned above in the same mechanism as trauma, hemorrhagic shock and burns. Additionally, brain-gut axis[18,19] and hypothalamic-pituitary adrenal axis[20] may also play a certain role in the development of gut dysfunction following TBI, but the potential mechanism underlying this action is not clear.

Studies have shown that cerebral inflammation following TBI occurs frequently and is associated with adverse outcomes[21,22]. Bacterial endotoxin (lipopolysaccharide, LPS) may exacerbate the inflammatory response of injured brain, leading to invasion of granulocytes into the brain and breakdown of the blood-brain barrier[23-26]. Severe extracerebral trauma can induce the expression of TNF-α mRNA in the brain of mice[27]. Therefore, we suggest that intestinal cytokine, translocation of bacteria and endotoxin secondary to gut barrier dysfunction into the injured brain through blood circulation should activate the cerebral inflammatory response. Because enteral nutrition and enterogenous sepsis are two of the important factors affecting the outcomes of comatose patients with TBI, the maintenance of normal gut integrity is

believed to be beneficial in improving the outcomes of head-injured patients[28,29].

Considering the important role of intestinal function in the rehabilitation of patients with TBI and no study reported previously on the intestinal aspects following TBI, additional studies need to be carried out to clarify the degree of mucosal damage and gut barrier dysfunction induced by TBI, and if possible, to explore the potential mechanisms that have not been interpreted yet. Therefore, we performed a series of studies on intestines of TBI rats. The purpose of this study was to explore the alterations of intestinal mucosa morphology and barrier function, and to determine how rapidly impairment of gut barrier function occurred and how long it persisted following TBI.

MATERIALS AND METHODS

Rat models of TBI

Male Wistar rats, weighing 220 g to 250 g, were purchased from Animal Center of Chinese Academy of Sciences, Shanghai, China. The rats were fed on rodent chow with free access to tap water and housed in temperature- and humidity-controlled animal quarters with a 12 hour light/dark cycle. All procedures were approved by the Institutional Animal Care Committee.

The rats were randomly divided into six groups (6 rats each group) including control group with right parietal bone window alone and no brain injury, and traumatic brain injury groups at hours 3, 12, 24, and 72, and on day 7, respectively. Following intraperitoneal anesthesia with urethane (1 000 mg.kg^{-1}), animal head was fixed in the stereotactic device. A right parietal bone window of 5 mm diameter was made under aseptic conditions with dental drill just behind the cranial coronal suture and beside midline. The dura was kept intact. Right parietal brain contusion was adopted using the impact method described by Feeney *et al*.[30] and severe traumatic brain injury was made by dropping weight with a 4 mm impact diameter, a 5 mm depth and total impact energy of 1 000 g.cm. The control animals were killed for sample collection at 72 hours, and TBI group rats were decapitated at corresponding time points. Blood samples were obtained by right ventricle puncture and centrifuged with the plasma stored at -40 ℃ before the animals were sacrificed at each time point. A 3 cm segment of the jejunum 12 cm distal to Treitz ligament was taken for histopathological studies and 1 mm^3 mucosa for ultrastructural observations.

Histopathological and ultrastructural examination

The 10 % buffered formalin-fixed jejunum was embedded in paraffin, sectioned at 4 μm thickness with a microtome and stained with hematoxylin and eosin. The sections were examined under light microscope. Villous height, diameter of middle villous segment and crypt depth in all tissues were determined using the HPIAS-1000 colorful image analysis system (Champion Image Engineering Company, Wuhan, China). Villous surface area was calculated according to the following formula: surface area=πdh, (d: diameter, h: villous height). At least 10 well-oriented crypt-villous units per small intestinal sample were measured and averaged by a pathologist who was blind to animal groups.

Samples for electron microscopy were fixed in phosphate-buffered glutaradehyde (2.5 %) and osmium tetroxide (1 %). Dehydration of the mucosa was accomplished in acetone solutions at increasing concentrations. The tissue was embedded in an epoxy resin. Semithin (1 μm) sections through the mucosa were then made and stained with toluidine blue. Then 600 angstrom-thin sections were made from a selected area of tissue defined by the semithin section, and these sections were stained with lead citrate and uranyl acetate. Ultrastructures of mucosa were observed under a transmission electron microscope (JEM-1200X).

Plasma endotoxin determination

The endotoxin content in plasma samples was assayed by the chromogenic limulus amebocyte lysate (LAL) test with a kinetic modification according to the test kit procedure.

Intestinal permeability

Intestinal permeability was quantified using the lactulose/mannitol (L/M) test as previously described[19]. Six hours before the animals were sacrificed at each time point, the rats with their bladders emptied were given the test solution of 2.5 ml by gastric tube feeding, containing 60 mg lactulose and 30 mg mannitol. All urine was collected for 5 hours through the metabolic cage and stored at -40 ℃ for further analysis. Urinary lactulose and mannitol were measured using high-performance liquid chromatography (Waters Co., USA). Results were expressed as a ratio of percentage of the administered dose of the two molecules excreted.

Statistical analysis

Software SPSS 11.0 was used in the statistical analysis. Each parameter was expressed as mean ± SD, and compared using one-way ANOVA analysis of variance, followed by Tukey test. The level of significance was $P<0.05$.

RESULTS

Histopathology

Histopathological examination showed that the morphology of jejunal mucosa was approximately normal in control rats. After TBI, mucosal damage occurred as early as 3 hours and was maximal at 72 hours, then progressed to mucosal atrophy on day 7. The type of jejunal mucosa damages induced by TBI is shown in Table 1. Representative histopathologic sections of jejunal mucosa are shown in Figures 1-4.

Table 1 Main histopathological changes of jejunal mucosa after traumatic brain injury

Type of mucosal damages	Group of TBI
Shedding of epithelial cells from the top of villi	3 and 12 hours
Epithelial cell necrosis and disarrangement of villi	24 and 72 hours
Focal mucosa ulcer with exposure of submucosal interstitium	72 hours
Fusion of adjacent villi into piece	72 hours and 7 days
Dilation of central chyle duct	72 hours and 7 days
Inflammatory cell infiltration in intestinal wall	72 hours and 7 days
Mucosal atrophy	7 days
Vascular dilation, congestion and edema in villous interstitium and lamina propria	3 hours throughout 7 days

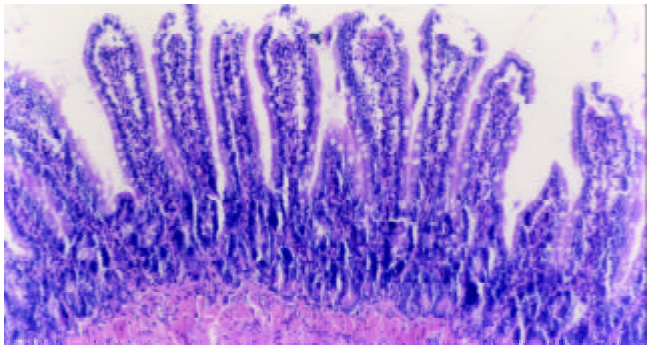

Figure 1 Epithelial cells shed from the top of villi with almost normal villous height and well defined arrangement of villi at 3 hours following TBI. H-E, magnification ×100.

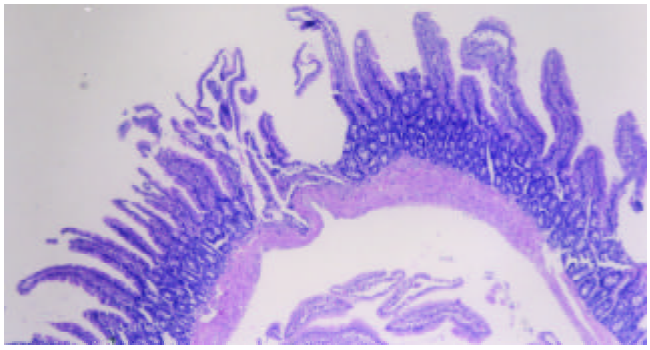

Figure 2 Markedly altered villous morphology and decreased height at 72 hours following TBI. Note the focal mucosa ulcer with exposure of submucosal interstitium and disarrangement of villi. H-E, magnification ×100.

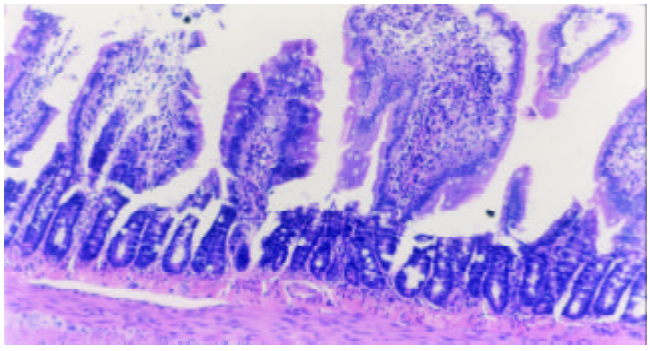

Figure 3 Marked alterations of villous morphology occurred 7 days following TBI, including mucosal atrophy, fusion of adjacent villi, inflammatory cell infiltration, and vascular dilation, congestion and edema in the villous interstitium and lamina propria. H-E, magnification ×100.

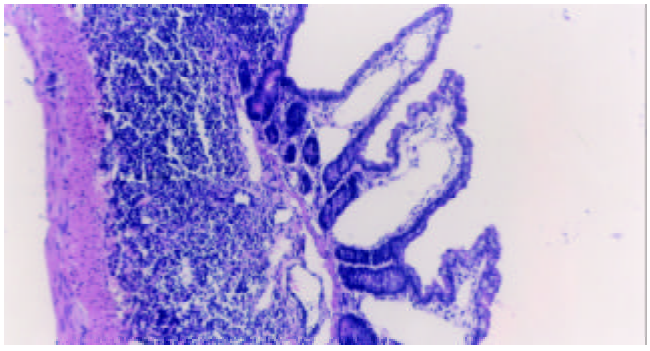

Figure 4 Dilation of central chyle duct of jejunal mucosa. H-E, magnification ×100.

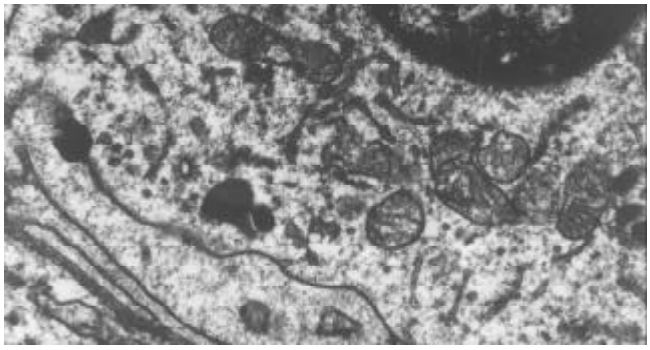

Figure 5 Reduction of mitochondrial matrix and disruption of its cristae at 72 hours following TBI. TEM, magnification ×15 k.

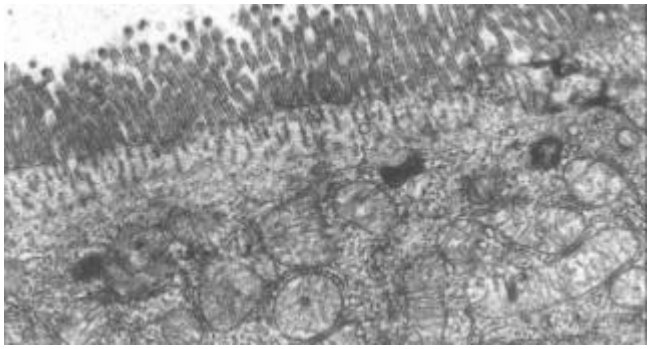

Figure 6 Ruptured, distorted and sparse microvilli at 24 hours following TBI. TEM, magnification ×10 k.

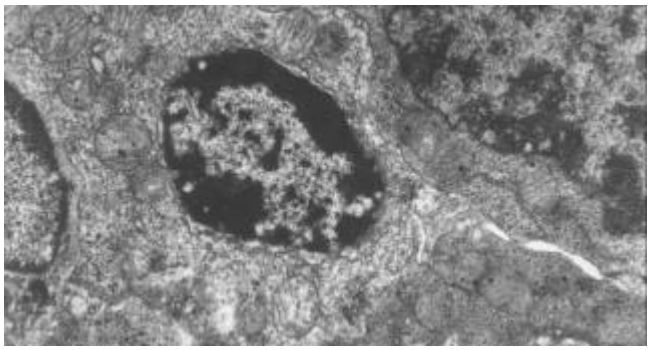

Figure 7 Apoptosis bodies in epithelial cytoplasms of jejunum following TBI. TEM, magnification ×8000.

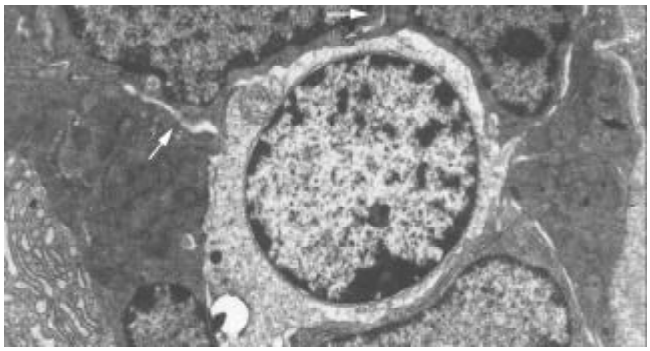

Figure 8 Disrupted and wider tight junction between epithelial cells at 72 hours and 7 days following TBI, shown as blank arrow. TEM, magnification ×5000.

Histomorphometric studies

Villous height, crypt depth and villous surface area were determined as specific indices for the evaluation of mucosal

Table 2 Changes in villous height, diameter, crypt depth and surface area of mucosa

Groups	Villous height (μm)	Villous diameter (μm)	Crypt depth (μm)	Surface area (mm^2)
Control	229.2±18.1	37.4±5.5	79.3±9.6	0.0259±0.0048
TBI 3 hours	219.5±21.2	37.6±6.1	78.9±9.4	0.0258±0.0035
TBI 12 hours	214.5±22.5	35.6±3.1	74.0±6.9	0.0241±0.0037
TBI 24 hours	189.2±13.6[b]	32.7±3.2	67.0±7.6[bc]	0.0195±0.0012[bc]
TBI 72 hours	150.8±10.4[bc]	32.1±4.2	34.8±5.6[bc]	0.0151±0.0010[bc]
TBI 7 days	136.7±15.7[bc]	30.8±5.8	38.3±6.1[bc]	0.0130±0.0015[bc]

Note: Values were expressed as mean ±SD. [b]P<0.01 *vs* control, [c]P<0.01 *vs* group of 3 hour TBI.

damages. The alterations of these parameters following TBI are shown in Table 2. Qualitative analyses of the villi demonstrated that the villous height, crypt depth and surface area were significantly decreased at 24 hours after TBI as compared with control group and further declined to the degree of mucosal atrophy on day 7 following TBI.

Ultrastructural observations

Within 24 hours of TBI, the nuclei of epithelial cells appeared irregular, but their membranes were still intact. At 72 hours and on day 7 following TBI, obvious ultrastructural alterations were found, including reduction of matrix of mitochondria and disruption of their cristae (Figure 5), ruptured, distorted and sparse microvilli (Figure 6), apoptosis bodies in cytoplasms (Figure 7), disrupted and wider tight junction between epithelial cells (Figure 8), swollen and degenerated vascular endothelial cells.

Changes in plasma endotoxin concentration

As shown in Figure 9, plasma endotoxin was significantly increased at 3 hours following TBI, and peaked at 72 hours, then declined on day 7, but was still significantly higher than that of controls (P<0.01). A marked correlation was noted between the changes in plasma level of endotoxin and intestinal permeability throughout 12 hours and 7 days following TBI (r=0.765, P<0.01).

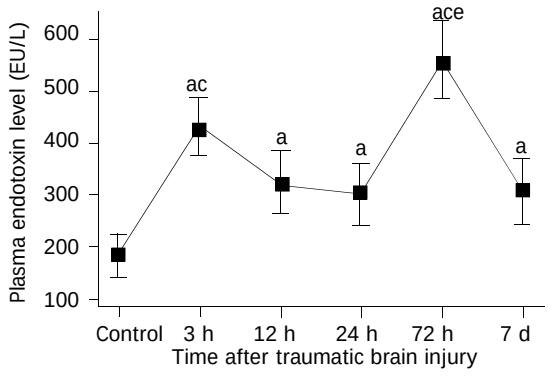

Figure 9 Significant increase of level of plasma endotoxin following TBI compared with control. Two peaks of plasma endotoxin existed at 3 h and 72 h postinjury, respectively. [a]P<0.05 *vs* control; [c]P<0.05 *vs* 12 h, 24 h and 72 h following TBI, [e]P<0.05 *vs* 3 h following TBI. Mean ± SD of six animals, control: 183.7±41.8 EU/L, 3 h: 434.8±54.9 EU/L, 12 h: 324.2±61.7 EU/L, 24 h: 303.3±60.2 EU/L, 72 h: 560.5±76.2 EU/L, 7 d: 306.7±62.4 EU/L.

Intestinal permeability and L/M ratio

As shown in Figure 10, intestinal permeability was significantly increased at 12 hours after TBI, peaked at 72 hours, and declined gradually afterward, but was still higher on day 7 following TBI than that of control group.

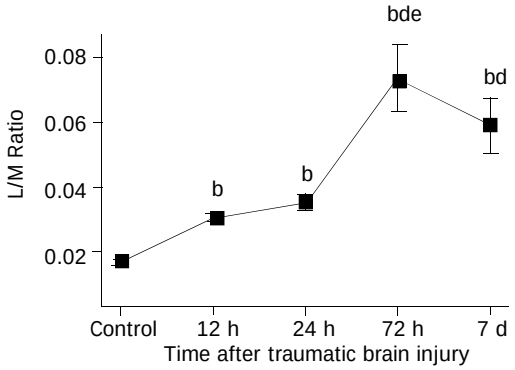

Figure 10 Significant increase of L/M ratio at 12 h, 24 h and 72 h following TBI compared with control and significant decline on day 7 compared with group at 72 h. The L/M ratio on day 7 was still significantly higher than that at 12 h and 24 h. [b]P<0.01 *vs* control, [d]P<0.01 *vs* 12 h and 24 h, [e]P<0.01 *vs* 7 d. Mean ± SD of six animals, control: 0.0172±0.0009, 12 h: 0.0303±0.0013, 24 h: 0.0354±0.0025,72 h: 0.0736±0.0105, 7 d: 0.0588±0.0083.

DISCUSSION

Major changes of gastrointestinal function following traumatic brain injury could be summarized in four aspects. The first was gastrointestinal mucosa ischemia, which usually resulted in stress ulcer and gastrointestinal bleeding[3,4]. The second was motility dysfunction, which manifested as abdominal distention, diarrhea, gastric retention, and even toxic intestinal paralysis[5-7,31]. The third was disruption of gut barrier, which led to bacterial and endotoxin translocation contributing to the development of SIRS and sepsis. The fourth was alteration of intestinal mucosal absorption of nutrients, which played an important role in malnutrition. Studies on stress ulcer and gastrointestinal bleeding after brain injury have been reported extensively[2]. Stress ulcer was one of the most common gastrointestinal complications following head trauma with a reported incidence of 74-100 %[3,4]. Endoscopic evidences of gastric mucosal lesions could appear within 24 hours, and 17 % of these erosions would progress to clinically significant gastrointestinal bleeding after severe brain injury.

Studies on intestinal mucosa structure and barrier function following TBI have not been found to date. In this study, we found that severe damage of intestinal mucosa occurred following TBI. The morphologic alterations of gut mucosa included shedding of epithelial cells, fracture of villi, focal ulcer, fusion of adjacent villi, dilation of central chyle duct, mucosal atrophy, and edema in the villous interstitium and lamina propria. Apoptosis of epithelial cells, fracture and sparseness of microvilli, disruption of tight junction between enterocytes, damage of mitochondria and endoplasm, were found by electron microscopy. These lesions occurred rapidly as early as 3 hours following TBI and lasted for more than 7 days. At the early stage (within 72 hours following TBI), it manifested as acute damages of intestinal epithelium, such as

epithelial necrosis and focal mucosa ulcer. On day 7 after TBI, the intestinal lesions were dominated by mucosal atrophy and edema of villous interstitium and lamina propria. Inflammatory cell infiltration in the small intestine was found 24 hours after TBI. Mucosal atrophy was considered to be associated with the necrosis and apoptosis of gut epithelium, which were induced by relative hypoperfusion (ischemia-reperfusion injury) and interaction of inflammatory mediators with their receptors located on the gut epithelial cells[13].

Intestinal mucosal injury could also be assessed by measuring the permeability of mucosal barrier to small or large solutes. Lactulose and mannitol have previously been used to assess intestinal mucosal permeability in burn and critically ill patients[12,14,15]. Mannitol, a smaller sugar, passes through aqueous pores in the cell membranes. Lactulose, a larger molecule, is absorbed paracelluarly through tight junctions. Increased absorption of lactulose can reflect mucosal leakiness, and decreased absorption of mannitol can reflect decreased functional absorptive area. The current study demonstrated that the L/M ratio was significantly greater at 3 hours following TBI, and reached its peak at 72 hours, then declined on day 7 with the value still markedly higher than that of control group and 24 hour TBI group. Additionally, the results showed that increased intestinal permeability might persist for 7 days in rats with TBI, which conformed highly to the histopathological alterations, i.e. mucosal atrophy and disruption of tight junction between epithelial cells.

The level of plasma endotoxin was positively related to L/M ratio, and manifested as two peaks at 3 hours and 72 hours after TBI, respectively. The first peak might be the result of acute gut mucosal damage mainly induced by splanchic ischemia due to the excited sympathetic nerve. With the resumption of liver anti-toxic function and the advent of specific antibodies to lipopolysaccharide, the plasma level of endotoxin was declined to some extent[34]. The second peak of plasma endotoxin might be related to severe mucosal damages such as focal ulcer and epithelial necrosis which usually occurred at 72 hours following TBI. High L/M ratio and plasma level of endotoxin following TBI implied that the gut barrier function was disrupted.

The potential mechanism underlying the alterations of gut structure and impairment of barrier function following TBI might be related to several factors, including ischemia-reperfusion, intramucosal acidosis[32], cytokines and inflammatory mediators[13,33]. Splanchnic hypoperfusion is a common finding in trauma. In systemic pathological stresses such as TBI, an adaptive response mediated by neuro-endocrine exists, which leads to selective splanchic vascular spasm in order to maintain the normal supply of vital organs such as the heart, lung and brain. The gut is highly susceptible to the consequent reduction in oxygenation, particularly mucosa of the stomach and intestine. This might induce increased gut permeability, alteration of enteral immune function, mucosal edema, epithelial necrosis and apoptosis, and even focal mucosa ulcer, which would contribute to bacterial and endotoxin translocation[13,14,20]. Brain-gut axis and hypothalamus-pituitary-adrenal axis might play a potential role in gut mucosal damages[18-20]. It may arise from the actions of parasympathetic centers of the hypothalamus with their connections to vagal nuclei in the medulla. Cytokines and inflammatory mediators such as TNF-α, IL-1, oxygen free radicals and nitric oxide could induce damages of microvilli, tight junction between enterocytes and paracelluar junction, which would lead to increased intestinal permeability[33].

Increased intestinal permeability has been implicated in the pathogenesis of both SIRS and progression to MODS[10,11,14,15]. The gut origin hypothesis suggests that a failure of gut barrier function as a result of a major stress insult permits bacterial and endotoxin translocation, which triggers systemic immunoinflammatory response to release cytokines and inflammatory mediators. These cytokines and mediators might exacerbate SIRS, sepsis and multiple organ failure[10-13]. This concept was supported by the data from animal studies in experimental models, including surgical trauma[14], malnutrition, jaundice, pancreatitis, hemorrhagic shock, and thermal injury[28]. Results of the current study showed that gut barrier dysfunction occurred with high plasma level of endotoxin and increased intestinal permeability following TBI. Therefore, we suggest that SIRS and MODS secondary to traumatic brain injury be possibly related to the disruption of gut barrier. Otherwise, translocated endotoxin and gut-derived cytokines may enter the injured brain with circulating blood, which was assumed to activate or exacerbate the inflammation of brain, and cause "two-hit" insult[22-26]. Circulating lipopolysaccharide and cytokines may stimulate the hypothalamic-pituitary-adrenal axis and sympathetic nervous system to affect the function of multiple organs. MODS is one of the common fatal complications following severe TBI.

ACKNOWLEDGEMENT

We would like to thank Dr. Genbao Feng, Fangnan Liu and Bo Wu for their technical assistance.

REFERENCES

1 **Pilitsis JG**, Rengachary SS. Complications of head injury. *Neurol Res* 2001; **23**: 227-236
2 **Lu WY**, Rhoney DH, Boling WB, Johnson JD, Smith TC. A review of stress ulcer prophylaxis in the neurosurgical intensive care unit. *Neurosurgery* 1997; **41**: 416-426
3 **Brown TH**, Davidson PF, Larson GM. Acute gastritis occurring within 24 hours of severe head injury. *Gastrointest Endosc* 1989; **35**: 37-40
4 **Kamada T**, Fusamoto H, Kawano S, Noguchi M, Hiramatsu K. Gastrointestinal bleeding following head injury: a clinical study of 433 cases. *J Trauma* 1977; **17**: 44-47
5 **Kao CH**, ChangLai SP, Chieng PU, Yen TC. Gastric emptying in head-injured patients. *Am J Gastroenterol* 1998; **93**: 1108-1112
6 **Saxe JM**, Ledgerwood AM, Lucas CE, Lucas WF. Lower esophageal sphincter dysfunction precludes safe gastric feeding after head injury. *J Trauma* 1994; **37**: 581-586
7 **Pedoto MJ**, O'Dell MW, Thrun M, Hollifield D. Superior mesenteric artery syndrome in traumatic brain injury: two cases. *Arch Phys Med Rehabil* 1995; **76**: 871-875
8 **Philip PA**. Superior mesenteric artery syndrome: an unusual cause of intestinal obstruction in brain-injured children. *Brain Inj* 1992; **6**: 351-358
9 **Jackson MD**, Davidoff G. Gastroparesis following traumatic brain injury and response to metoclopramide therapy. *Arch Phys Med Rehabil* 1989; **70**: 553-555
10 **Swank GM**, Deitch EA. Role of the gut in multiple organ failure: bacterial translocation and permeability changes. *World J Surg* 1996; **20**: 411-417
11 **Moore FA**. The role of the gastrointestinal tract in postinjury multiple organ failure. *Am J Surg* 1999; **178**: 449-453
12 **Doig CJ**, Sutherland LR, Sandham JD, Fick GH, Verhoef M, Meddings JB. Increased intestinal permeability is associated with the development of multiple organ dysfunction syndrome in critically ill ICU patients. *Am J Respir Crit Care Med* 1998; **158**: 444-451
13 **Grotz MR**, Deitch EA, Ding J, Xu D, Huang Q, Regel G. Intestinal cytokine response after gut ischemia: role of gut barrier failure. *Ann Surg* 1999; **229**: 478-486
14 **Langkamp-Henken B**, Donovan TB, Pate LM, Maull CD, Kudsk KA. Increased intestinal permeability following blunt and penetrating trauma. *Crit Care Med* 1995; **23**: 660-664
15 **Faries PL**, Simon RJ, Martella AT, Lee MJ, Machiedo GW. Intestinal permeability correlates with severity of injury in trauma patients. *J Trauma* 1998; **44**: 1031-1036

16 **Wang XD**, Soltesz V, Andersson R. Cisapride prevents enteric bacterial overgrowth and translocation by improvement of intestinal motility in rats with acute liver failure. *Eur Surg Res* 1996; **28**: 402-412
17 **Pepe JL**, Barba CA. The metabolic response to acute traumatic brain injury and implications for nutritional support. *J Head Trauma Rehabil* 1999; **14**: 462-474
18 **Glavin GB**, Hall AM. Brain-gut relationships: gastric mucosal defense is also important. *Acta Physiol Hung* 1992; **80**: 107-115
19 **Shanahan F**. Brain-gut axis and mucosal immunity: a perspective on mucosal psychoneuroimmunology. *Semin Gastrointest Dis* 1999; **10**: 8-13
20 **Grundy PL**, Harbuz MS, Jessop DS, Lightman SL, Sharples PM. The hypothalamo-pituitary-adrenal axis response to experimental traumatic brain injury. *J Neurotrauma* 2001; **18**: 1373-1381
21 **Morganti-Kossmann MC**, Rancan M, Otto VI, Stahel PF, Kossmann T. Role of cerebral inflammation after traumatic brain injury: a revisited concept. *Shock* 2001; **16**: 165-177
22 **Ghirnikar RS**, Lee YL, Eng LF. Inflammation in traumatic brain injury: role of cytokines and chemokines. *Neurochem Res* 1998; **23**: 329-340
23 **Bohatschek M**, Werner A, Raivich G. Systemic LPS injection leads to granulocyte influx into normal and injured brain: effects of ICAM-1 deficiency. *Exp Neurol* 2001; **172**: 137-152
24 **Ahmed SH**, He YY, Nassief A, Xu J, Xu XM, Hsu CY, Faraci FM. Effects of lipopolysaccharide priming on acute ischemic brain injury. *Stroke* 2000; **31**: 193-199
25 **Montero-Menei CN**, Sindji L, Garcion E, Mege M, Couez D, Gamelin E, Darcy F. Early events of the inflammatory reaction induced in rat brain by lipopolysaccharide intracerebral injection: relative contribution of peripheral monocytes and activated microglia. *Brain Res* 1996; **724**: 55-66
26 **Morganti-Kossmann MC**, Rancan M, Stahel PF, Kossmann T. Inflammatory response in acute traumatic brain injury: a double-edged sword. *Curr Opin Crit Care* 2002; **8**: 101-105
27 **Kamei H**, Yoshida S, Yamasaki K, Tajiri T, Ozaki K, Shirouzu K. Severity of trauma changes expression of TNF-alpha mRNA in the brain of mice. *J Surg Res* 2000; **89**: 20-25
28 **Zhu L**, Yang ZC, Li A, Cheng DC. Protective effect of early enteral feeding on postburn impairment of liver function and its mechanism in rats. *World J Gastroenterol* 2000; **6**: 79-83
29 **Suchner U**, Senftleben U, Eckart T, Scholz MR, Beck K, Murr R, Enzenbach R, Peter K. Enteral versus parenteral nutrition: effects on gastrointestinal function and metabolism. *Nutrition* 1996; **12**: 13-22
30 **Feeney DM**, Boyeson MG, Linn RT, Murray HM, Dail WG. Responses to cortical injury: I. Methodology and local effects of contusions in the rat. *Brain Res* 1981; **211**: 67-77
31 **Mackay LE**, Morgan AS, Bernstein BA. Factors affecting oral feeding with severe traumatic brain injury. *J Head Trauma Rehabil* 1999; **14**: 435-447
32 **Salzman AL**, Wang H, Wollert PS, Vandermeer TJ, Compton CC, Denenberg AG, Fink MP. Endotoxin-induced ileal mucosal hyperpermeability in pigs: role of tissue acidosis. *Am J Physiol* 1994; **266**(4 Pt 1): G633-646
33 **Gong JP**, Wu CX, Liu CA, Li SW, Shi YJ, Yang K, Li Y, Li XH. Intestinal damage mediated by Kupffer cells in rats with endotoxemia. *World J Gastroenterol* 2002; **8**: 923-927
34 **Buttenschoen K**, Berger D, Strecker W, Buttenschoen DC, Stenzel K, Pieper T, Beger HG. Association of endotoxemia and production of antibodies against endotoxins after multiple injuries. *J Trauma* 2000; **48**: 918-923

Edited by Zhang JZ and Wang XL

P.O.Box 2345, Beijing 100023,China
Fax: +86-10-85381893
E-mail: wjg@wjgnet.com www.wjgnet.com

World J Gastroenterol 2003;9(12):2782-2785
World Journal of Gastroenterology
 ISSN 1007-9327

• BASIC RESEARCH •

Changes of biological functions of dipeptide transporter (PepT1) and hormonal regulation in severe scald rats

Bing-Wei Sun, Xiao-Chen Zhao, Guang-Ji Wang, Ning Li, Jie-Shou Li

Bing-Wei Sun, Ning Li, Jie-Shou Li, Department of General Surgery, School of Medicine, Nanjing University, Nanjing 210093, Jiangsu Province, China
Bing-Wei Sun, Ning Li, Jie-Shou Li, Research Institute of General Hospital, Chinese PLA General Hospital of Nanjing Military Command, Nanjing 210002, Jiangsu Province, China
Xiao-Chen Zhao, Guang-Ji Wang , Center of Drug Metabolism and Pharmacokinetics, China Pharmaceutical University, Nanjing 210009, Jiangsu Province, China
Supported by National Natural Science Foundation of China, No. 39970862
Correspondence to: Bing-Wei Sun, Research Institute of General Surgery, Chinese PLA General Hospital of Nanjing Military Command, 305 East Zhongshan Road, Nanjing 210002, Jiangsu Province, China. sunbinwe@hotmail.com
Telephone: +86-25-3387871 Ext 58088 **Fax:** +86-25-4803956
Received: 2003-06-10 **Accepted:** 2003-08-16

Abstract

AIM: To determine the regulatory effects of recombinant human growth hormone (rhGH) on dipeptide transport (PepT1) in normal and severe scald rats.

METHODS: Male Sprague-Dawley rats with 30 % total body surface area (TBSA)IIIdegree scald were employed as the model. In this study rhGH was used at the dose of 2 IU.kg^{-1}d^{-1}. An everted sleeve of intestine 4 cm long obtained from mid-jejunum was securely incubated in Kreb's solution with radioactive dipeptide (^{3}H-glycylsarcosine, ^{3}H-Gly-Sar, 10 μCi/ml) at 37 ℃ for 15 min to measure the effects of uptake and transport of PepT1 of small intestinal epithelial cells in normal and severe scald rats.

RESULTS: Abundant blood supply to intestine and mesentery was observed in normal and scald rats administered rhGH, while less supply of blood to intestine and mesentery was observed in rats without rhGH. Compared with controls, the transport of dipeptide in normal rats with injection of rhGH was not significantly increased (P=0.1926), while the uptake was significantly increased (P=0.0253). The effects of transport and uptake of PepT1 in scald rats with injection of rhGH were significantly increased (P=0.0082, 0.0391).

CONCLUSION: Blood supply to intestine and mesentery of rats was increased following injection of rhGH. The effects of uptake and transport of dipeptide transporters in small intestinal epithelial cells of rats with severe scald were markedly up-regulated by rhGH.

Sun BW, Zhao XC, Wang GJ, Li N, Li JS. Changes of biological functions of dipeptide transporter (PepT1) and hormonal regulation in severe scald rats. *World J Gastroenterol* 2003; 9 (12): 2782-2785
http://www.wjgnet.com/1007-9327/9/2782.asp

INTRODUCTION

Small intestine is the major site of dietary protein absorption, the main route of absorption protein is transport of protein in the form of small peptides (di/tripeptide) across the small intestinal wall. H^+-coupled dipeptide transporter, PepT 1, is known to be located in the intestine and kidney, and plays an important role in the absorption of di/tripeptide. In addition, it mediates the intestinal absorption of β-lactam antibiotics, angiotension–converting enzyme inhibitors, and other peptide–like drugs[1].

Knowledge about the regulation of PepT 1 activity is limited. A number of studies have shown that dietary protein load causes an increase in di/tripeptide transport in small intestine of rats and mice[2,3]. Recent studies have shown that PepT1 in rat intestine is upregulated after a short period of fast via an increase in gene expression[4-6]. Another interesting regulation of PepT 1 expression is that PepT1 in rat' s small intestine is resistant to tissue damage induced by 5-flourouracil, whereas other markers such as sucrase activity, D-glucose uptake are significantly decreased[7]. This suggests that expression of PepT 1 is robust towards cellular damage.

Studies showed that some hormones metabolically regulated the expression of intestinal dipeptide transporter[8,9]. For example, insulin could increase the membrane population of PepT 1 by increasing its translocation from a preformed cytoplasmic pool[9]. Our previous study[10] showed that rhGH markedly stimulated the uptake and transport of cephalexin in Caco-2 cells with normal or anoxia/reoxygenation management. These results indicate that rhGH greatly upregulates the physiological functions of dipeptide transporters (PepT1) of human cell line. Although rhGH has been shown to be a major regulator of peptide transport activity[10], little is known about rhGH in regulation of peptide absorption *in vivo*, especially in rats with severe scald.

In this study, we determined whether rhGH could stimulate uptake and transport of small intestinal epithelial cells in normal or severe scald rats. We also investigated the *in vivo* application of 3H-glycylsarcosine (3H-Gly-Sar) as an ideal substrate for PepT1.

MATERIALS AND METHODS

Materials

[3H]-glycysarcosine (special activity of 1Ci (37GBq)/mmol, radiochemical purity >=97 %, work concentration in this study: 10 μCi/ml) was purchased from Moravek Biochemicals,USA. Recombinant human growth hormone (rhGH, 2 IU.kg^{-1}d^{-1}) was from Serono, Switzerland, Temperature-controlled surge culture device from Taicang Medical Instrument Co. Ltd, China. All other reagents were of analytical grade at least.

Animals

Adult male Sprague–Dawley (SD) rats (weighing 200±20 g) were housed in individual stainless steel cages in an air–conditioned room at 23±2 ℃ with a 12: 12-h light schedule and were fed normally. The weight of rats was measured daily during an experiment. The animals were treated in accordance with European Community Standards concerning the care and use of laboratory animals (INSERM and Ministere de 1' Agriculture et de la Foret, Paris, France).

Experimental groups

Rats were randomly divided into groups A, B, C and D. Group A(control group): normal feed rats, Group B: normal feed + injection of rhGH (2 IU.kg^{-1}d^{-1}) rats, Group C: scald rats and Group D: scald + injection of rhGH (2 IU.kg^{-1} d^{-1}) rats. The indices were observed on postburn days (PBDs) 0, 1, 3, 5 and 7 (n=4), respectively. Rats were killed by decapitation at every time point.

Scald injury models

Rats were anaesthetized with 2 % pentoburbite (30 mg.kg^{-1} body weight) and scald on the back to 30 % total body surface area (TBSA) III degree, and 30 min later, they were resuscitated with Ringer' s solution (2 ml.kg^{-1} per 1 % body surface area).

Preparation of everted sleeve of rat small intestine

The rats were fasted overnight and water was available ad libitum throughout the study. The rat was killed by decapitation, a laparotomy was performed. We defined the region approximately 6 cm below the ligament of Treitz, then a 4-cm long segment of small intestine (mid-jejunum) was removed, ringed immediately with Kreb' s buffer. One end of the intestinal fragment was ligated, an everted process was securely made by small tweezers, then an intact everted sleeve was formed after another terminal ligation. Each sleeve was weighed.

Uptake and transport measurement

We measured 3H-Gly-Sar taken up into intestinal epithelial cells of the everted sleeve across the brush–border membrane. The everted sleeve was rinsed with Kreb' s buffer, 0.2 ml Kreb' s buffer was injected slowly into the lumen of the everted intestinal sleeve. The whole segment was then immersed into a 50 ml flask containing dipeptide (3H-Gly-Sar) solution (10 μCi) while 5 % CO_2 and 95 % O_2 were filled into the flask. The uptake and transport experiments were performed when the device was surged continually with a frequency of 100 r/min at 37 ℃ for 15 min, then the everted sleeve was rinsed immediately with cold (4 ℃) Kreb' s buffer to stop subsequent transport and uptake of PepT1 in epithelial cells. The transport sample was harvested from the lumen of the sleeve, a 0.5 cm×0.5 cm segment was removed from the middle of the sleeve, weighed and digested with HCl_4 to obtain the uptake sample. All samples were mixed with 10 ml of scintillation cocktail and the radioactivity was determined by liquid scintillation counter.

Statistical analysis

Data were expressed as mean ±SD. Differences between groups were assessed by analysis of variance. Values less than 0.05 were considered statistically significant.

RESULTS

Blood Supply in bowel of rats

After killed by decapitation, a laparotomy was performed immediately at the different time point (0, 1, 3, 5 and 7 days) in rats (normal or scald) with or without injection of rhGH. Direct appearance of blood supply was observed in mesentery and the wall of intestine of rats. Abundant blood supply was shown in rats after injection of rhGH, while less blood supply was observed in rats without injection of rhGH (Figure 1, 2).

Uptake and transport in everted sleeve of normal rats after injection of rhGh

In comparison with the control, the transport of dipeptide (3H-Gly-Sar) in normal rats after injection of rhGH was not significantly increased (P=0.1923) while the uptake were markedly increased (P=0.0253) (Figure 3, 4).

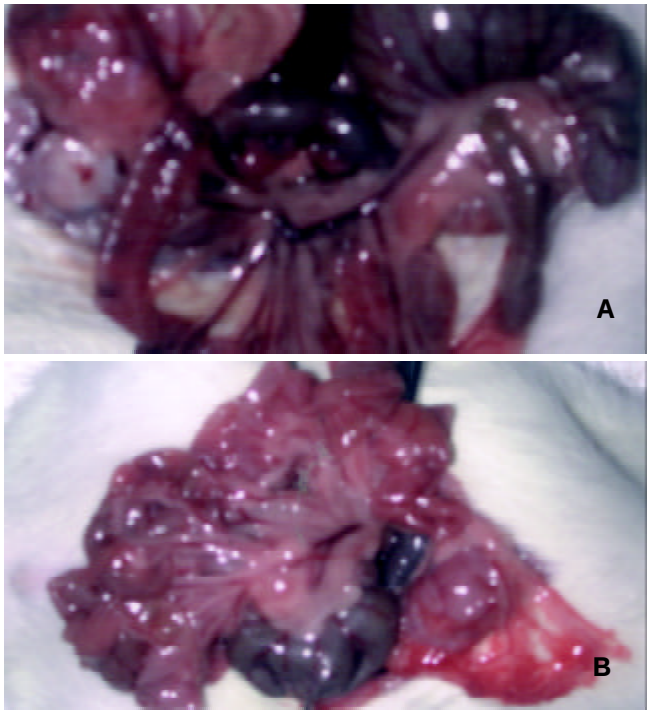

Figure 1 Blood supply to intestine and mesentery of rats 7 days after injection of rhGH was significantly abundant compared with controls. (A: rhGH group, B: control).

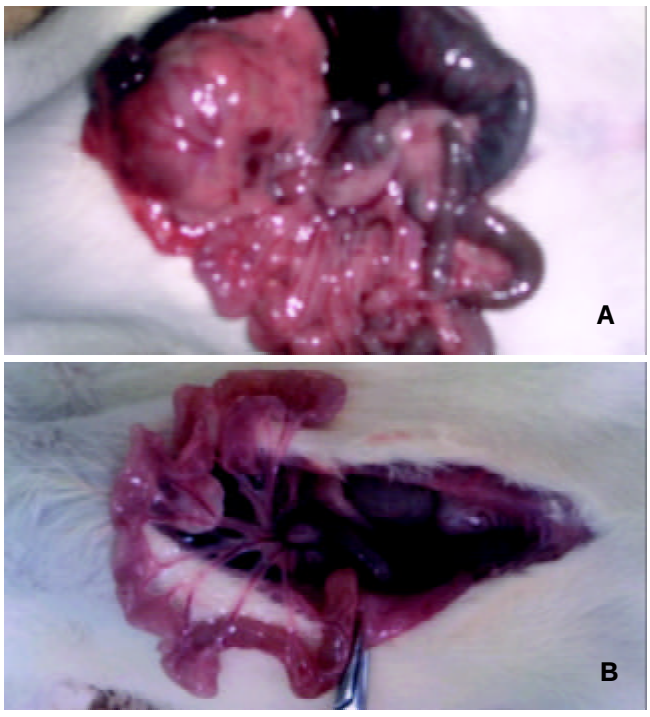

Figure 2 Blood supply to intestine and mesentery of rats with severe scald 7 days after injection of rhGH was significantly abundant compared with controls. (A: rhGH group, B: control).

Uptake and transport in everted sleeve of severe scald rats after injection of rhGH

The effects of transport and uptake of PepT1 in everted sleeve of severe scald rats after injection of rhGH were greatly increased compared with controls (P=0.0082, 0.0391) (Figure 5, 6).

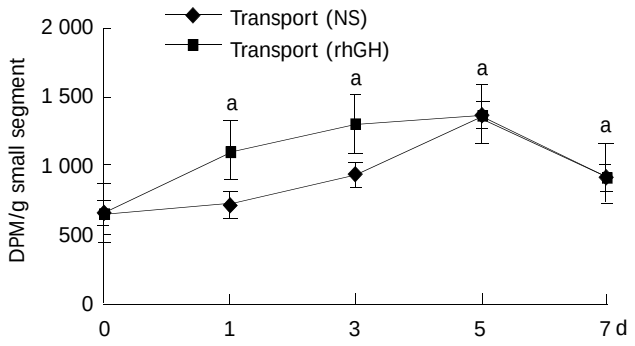

Figure 3 Transport of PepT1 in normal rats administered rhGH. Each point represents mean ±s, n=4, ^aP>0.05 *vs* control.

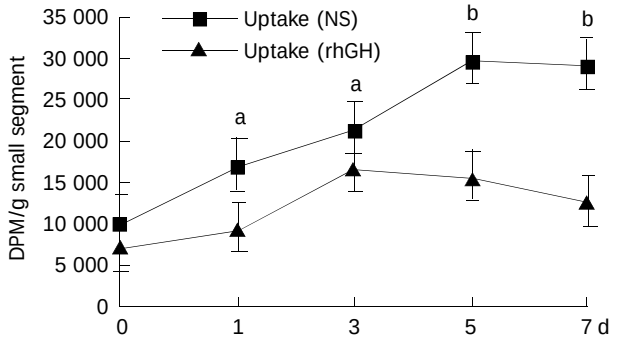

Figure 4 Uptake of PepT1 in normal rats administered rhGH. Each point represents mean ±s, n=4, ^aP<0.05, ^bP<0.01 *vs* control.

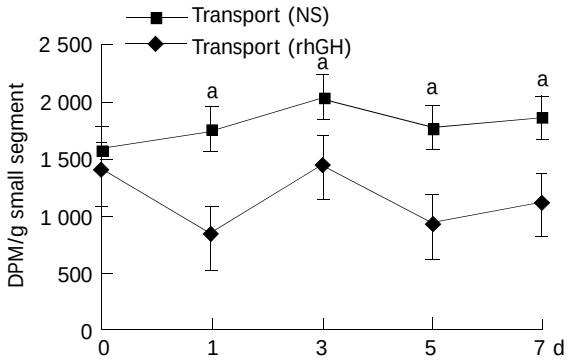

Figure 5 Transport of PepT1 in scald rats administered rhGH. Each point represents mean ±s, n=4, ^aP<0.05 *vs* control.

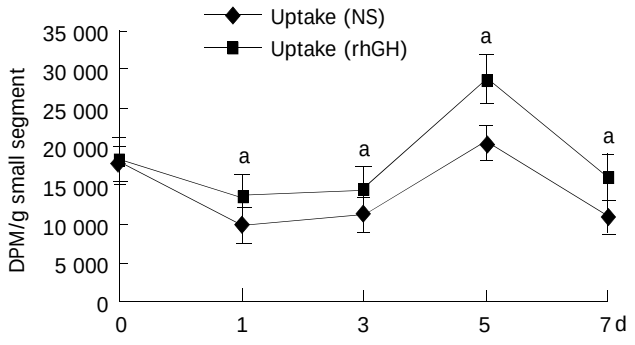

Figure 6 Uptake of PepT1 in scald rats administered rhGH. Each point represents mean ±s, n=4, ^aP<0.05 *vs* control.

DISCUSSION

We found in this study that rhGH could significantly increase the transport and uptake of peptides across intestinal epithelial barrier via proton–dependent transporter PepT1, suggesting that rhGH might be an important parameter in hormonal regulation of this transporter. It is well known that dietary proteins are absorbed as di – and tripeptides rather than free amino acids[11-14]. This absorption process is carried out by intestinal brush board transporter PepT1, which transfers peptides from a region with low dipeptidase activity (intestinal lumen) to a region with high dipeptidase activity (enterocyte cytoplasm)[15]. As a member of a family of transport proteins, PepT1 is located at the brush-border membranes of absorptive epithelial cells along the small intestine but absent in crypt and goblet cells[16,17]. PepT1 allows the use of small peptides as a source of nitrogen for enteral feeding and the route for delivery of peptidomimetic drugs such as β-lactam antibiotics. Therefore, PepT1 appears to be essential for the efficient absorption of dietary proteins[18]. Most studies on PepT1 have focused on its fundamental kinetic properties and its functional and structural characterization[19-21].

Previous studies have shown that the functions of intestine (including PepT1) were changed under the influence of many factors[22,23]. However, few reports have dealt with the hormonal regulation of PepT1. Insulin could stimulate dipeptide transport by increasing membrane insertion of PepT1 from a preformed cytoplasmic pool[9], and choleratoxin could decrease dipeptide transport by inhibiting the activity of PepT1 through an increase in intracellular concentration of adenosine 3', 5'-cyclic monophosphate[24]. Strong evidences have demonstrated that growth hormone (GH) was an important growth factor for intestine[25]. Complete GH depletion due to hypophysectomy could cause pronounced hypoplasia of small intestinal mucosa with decreased villus height and reduced crypt cell proliferation[26]. Simple replacement of GH could restore mucosal proliferative activity[27], rhGH could promote normal growth and development in the body by changing chemical activity in cells. It activates protein production in muscle cells and release of energy from fats. rhGH could significantly improve anabolism in parenteral feeding[28]. It has been typically used to stimulate growth of children with hormone deficiency, or to treat people with severe illness, burns or sepsis where destruction of human tissues and muscle occurs[29-31]. It remains unclear, however, whether the key hormone, human growth hormone (hGH) also shows some significant importance in transport and uptake of PepT1. To examine the functional changes of PepT1, everted sleeves of small intestine were used as *in vivo* intestinal model, and severe scald (30 % TBSA III degree) rats with or without injection of rhGH were employed as animal model. The results in this study indicated that the blood supply in mesentery and the wall of rat's intestine (normal or severe scald) with injection of rhGH was abundant compared with the controls. It was suggested that rhGH could increase blood supply of animal bowel, therefore, upregulate directly the physiological functions of PepT1 of small intestine.

The data in this study confirmed that both transport and uptake of PepT1 in everted sleeves of severe scald rats administered rhGH were significantly increased compared with controls. It indicated that rhGH upregulated the biological functions of PepT1. This result was in accordance with our previous research[10]. In our study, however, the transport of dipeptide in normal rats treated with rhGH was not markedly increased, while the uptake was greatly increased compared with controls. It might be due to the cytoplasmic level of dipeptidases, or a short period of experiment.

In conjunction with previous results[10], the present study further testified the enhancement effect of peptide transport by rhGH. The biological mechanism might involve increased translocation of the cytoplasmic pool of PepT1 to the apical membrance, or increased level of PepT1 mRNA. Clearly,

further study on physiology and biology of PepT1 is required to clarify the mechanism of rhGH in upregulating the functions of PepT1.

REFERENCES

1 **Hsu CP**, Walter E, Merkle HP, Rothen-Rutishauser B, Wunderli-Allenspach H, Hilfinger JM, Amidon GL. Function and immunolocalization of overexpressed human intestinal H^+/peptide cotransporter in adenovirus-transduced Caco-2 cells. *AAPS Pharm Sci* 1999; **1**: E12

2 **Erickson RH**, Gum JR Jr, Lindstrom MM, Mckean D, Kim YS. Regional expression and dietary regulation of rat small intestinal peptide and amino acid transporter mRNAs. *Biochem Biophys Res Commun* 1995; **216**: 249-257

3 **Ferraris RP**, Diamond J, Kwan WW. Dietary regulation of intestinal transport of the dipeptide carnosine. *Am J Physiol* 1998; **255** (2 Pt 1): G143-150

4 **Ihara T**, Tsuji Kawa T, Fujiyama Y, Bamba T. Regulation of PepT1 peptide transporter expression in the rat small intestine under malnourished conditions. *Digestion* 2000; **61**: 59-67

5 **Ogihara H**, Suzuki T, Nagamachi Y, Inui K, Takate K. Peptide transporter in the rat small intestine: ultrastructural localization and the effect of starvation and administration of amino acids. *Histochem J* 1999; **31**: 169-174

6 **Thamotharan M**, Bawani SZ, Zhou X, Adibi SA. Functional and molecular expression of intestinal oligopeptide transporter (Pept-1) after a brief fast. *Metabolism* 1999; **48**: 681-684

7 **Tanaka H**, Miyamoto KI, Morita K, Haga H, Segawa H, Shiraga T, Fujioka A, Kouda T, Taketani Y, Hisano S, Fukui Y, Kitagawa K, Takeda E. Regulation of the PepT1 peptide transporter in the rat small intestine in response to 5-fluorouracil-induced injury. *Grastroenterology* 1998; **114**: 714-723

8 **Thamotharan M**, Bawani SZ, Zhou X, Adibi SA. Hormonal regulation of oligopeptide transporter Pept-1 in a human intestinal cell line. *Am J Physiol* 1999; **276**(4 Pt 1): C821-826

9 **Nielsen CU**, Amstrup J, Steffansen B, Frokjaer S, Brodin B. Epidermal growth factor inhibits glycylsarcosine transport and hPepT1 expression in a human intestinal cell line. *Am J Physiol Gastrointest Liver Physiol* 2001; **281**: G191-199

10 **Sun BW**, Zhao XC, Wang GJ, Lin N, Li JS. Hormonal regulation of dipeptide transporter (PepT1) in Caco-2 cells with normal and anoxial/reoxygenation management. *World J Gastroenterol* 2003; **9**: 808-812

11 **Adibi SA**. The oligopeptide transporter Pept-1 in human intestine: biology and function. *Gastroenterology* 1997; **113**: 332-340

12 **Adibi SA**. Intestinal transport of dipeptides in man: relative importance of hydrolysis and intact absorption. *J Clin Invest* 1997; **50**: 2266-2275

13 **Hellier MD**, Holdsworth CD, McColl I, Perrett D. Dipeptide absorption in man. *Gut* 1972; **13**: 965-969

14 **Cook GC**. Comparison of intestinal absorption rates of glycine and glycylglycine in man and the effect of glucose in the perfusing fluid. *Clin Sci* 1972; **43**: 443-453

15 **Brodin B**, Nielsen CU, Steffansen B, Frekjaer S. Transport of peptidomimetic drugs by the intestinal Di/tri-peptide transporter, $PepT_1$. *Pharmacol Toxicol* 2002; **90**: 285-296

16 **Ogihara H**, Saito H, Shin BC, Terada T, Takenoshita S, Nagamachi Y, Inui K, Takata K. Immuno-localization of H^+/peptide cotransporter in rat digestive tract. *Biochem Biophys Res Commun* 1996; **220**: 848-852

17 **Adibi SA**. The oligopeptide transporter (PepT1) in human intestine. *Biol Funct Gastroenterol* 1997; **113**: 332-340

18 **Buyse M**, Berliozl F, Guilmeaul S, Tsocas A, Voisin T, Peranzi G, Merlin D, Laburthe M, Lewin MJ, Roze C, Bado A. $PepT_1$-mediated epithelial transport of dipeptides and cephalexin is enhanced by luminal leptin in the small intestine. *J Clin Invest* 2001; **108**: 1483-1494

19 **Mackenzie B**, Fei YJ, Ganapathy V, Leibach FH. The human intestinal H^+/oligopeptide cotransporter hPEPT1 transports differently- charged dipeptides with identical electrogenic properties. *Biochem Biophys Acta* 1996; **1284**: 125-128

20 **Chen XZ**, Steel A, Hediger MA. Functional roles of histidine and tyrosine residues in the H(+)-peptide transporter $PepT_1$. *Biochem Biophys Res Cormmun* 2000; **272**: 726-730

21 **Bolger MB**, Haworth IS, Yeung AK, Ann D, Von Grafenstein H, Hamm-Alvarez S, Okamoto CT, Kim KJ, Basu SK, Wu S, Lee VH. Structure, function, and molecular modeling approaches to the study of the intestinal dipeptide transporter $PepT_1$. *J Pharm Sci* 1998; **87**: 1286-1291

22 **Li YS**, Li JS, Li N, Jiang ZW, Zhao YZ, Li NY, Liu FN. Evaluation of various solutions for small bowel graft preservation. *World J Gastroenterol* 1998; **4**: 140-143

23 **Liang LJ**, Yin XY, Luo SM, Zheng JF, Lu MD, Huang JF. A study of the ameliorating effects of carnitine on hepatic steatosis induced by total parenteral nutrition in rats. *World J Gastroenterol* 1999; **5**: 312-315

24 **Ferraris RP**, Diamond J, Kwan WW. Dietary regulation of intestional transport of the dipeptide carnosine. *Am J Physiol* 1988; **255**(2 Pt 1): G143-150

25 **Zhou X**, Li YX, Li N, Li JS. Effect of bowel rehabilitative therapy on structural adaptation of remnant small intestine: animal experiment. *World J Gastroenterol* 2001; **7**: 66-73

26 **Bastie MJ**, Balas D, Laval J, Senegas-Balas F, Bertrand C, Frexinos J, Ribet A. Histological variations of jejunal and ileal mucosa on days 8 and 15 after hypophysectomy in rat: morphometrical analysis on light and electron microscopy. *Acta Anat* 1982; **112**: 321-337

27 **Scow RO**, Hagan SN. Effect of testosterone Propionate and growth hormone on growth and chemical composition of muscle and other tissues in hypophysectomized male rats. *Endocrinology* 1965; **77**: 852-858

28 **Gu Y**, Wu ZH. The anabolic effects of recombinant human growth hormone and glutamine on parenterally fed, short bowel rats. *World J Gastroenterol* 2002; **8**: 752-757

29 **Jeschke MG,** Herndon DN, Wolf SE, Debroy MA, Rai J, Lichtenbelt BJ, Barrow RE. Recombinant human growth hormone alters acute phase reactant proteins, cytokine expression, and liver morphology in burned rats. *J Surg Res* 1999; **83**: 122-129

30 **Roth E,** Valentini L, Semsroth M, Holzenbei T, Winkler S, Blum WF, Ranke MB, Schemper M, Hammerle A, Karner J. Resistance of nitrogen metabolism to growth hormone treatment in the early phase after injury of patient with multiple injuries. *J Trauma* 1995; **38**: 136-141

31 **Postel-Vinay MC**, Finidori J, Sotiropoulos A, Dinerstein H, Martini JF, Kelly PA. Growth hormone receptor: structure and signal transduction. *Ann Endocrinol* 1995; **56**: 209-212

Edited by Ren SY and Wang XL

P.O.Box 2345, Beijing 100023,China
Fax: +86-10-85381893
E-mail: wjg@wjgnet.com www.wjgnet.com

World J Gastroenterol 2003;9(12):2786-2790
World Journal of Gastroenterology
 ISSN 1007-9327

• BASIC RESEARCH •

Protective effect of *angelica sinensis* polysaccharide on experimental immunological colon injury in rats

Shao-Ping Liu, Wei-Guo Dong, Dong-Fang Wu, He-Sheng Luo, Jie-Ping Yu

Shao-Ping Liu, Wei-Guo Dong, He-Sheng Luo, Jie-Ping Yu, Department of Gastroenterology, Renmin Hospital of Wuhan University, 238 Jiefang Road, Wuhan 430060, Hubei Province, China
Dong-Fang Wu, Department of Pharmacy, Renmin Hospital of Wuhan University, 238 Jiefang Road, Wuhan 430060, Hubei Province, China
Supported by key Project in Scientific and Technological Researches of Hubei Province, No. 2001AA308B
Correspondence to: Professor Wei-Guo Dong, Renmin Hospital of Wuhan University, 238 Jiefang Road, Wuhan 430060, Hubei Province, China. dongwg@public.wh.hb.cn
Telephone: +86-27-88054511
Received: 2003-06-05 **Accepted:** 2003-09-18

Abstract

AIM: To study the effect of angelica sinensis polysaccharide (ASP) on immunological colon injury and its mechanisms in rats.

METHODS: Immunological colitis model of rats was induced by intracolon enema with 2, 4, 6-trinitrobenzene sulfonic acid (TNBS) and ethanol. The experimental animals were randomly divided into normal control, model control, 5-aminosalicylic acid therapy groups and three doses of ASP therapy groups. The 6 groups were treated intracolonically with normal saline, normal saline, 5-aminosalicylic acid (100 mg·kg^{-1}), and ASP daily (8: 00 am) at the doses of 200, 400 and 800 mg·kg^{-1} respectively for 21 days 7 d following induction of colitis. The rat colon mucosa damage index (CMDI), the histopathological score (HS), the score of occult blood test (OBT), and the colonic MPO activity were evaluated. The levels of SOD, MDA, NO, TNF-α, IL-2 and IL-10 in colonic tissues were detected biochemically and immunoradiometrically. The expressions of TGF-β and EGF in colonic tissues were also determined immunochemically.

RESULTS: Enhanced colonic mucosal injury, inflammatory response and oxidative stress were observed in colitis rats, which manifested as significant increases of CMDI, HS, OBT, MPO activity, MDA and NO contents, as well as the levels of TNF-α and IL-2 in colonic tissues, although colonic TGF-β protein expression, SOD activity and IL-10 content were significantly decreased compared with the normal control (P<0.01). However, these parameters were found to be significantly ameliorated in colitis rats treated intracolicly with ASP at the doses of 400 and 800 mg·kg^{-1} (P<0.05-0.01). Meantime, colonic EGF protein expression in colitis rats was remarkably up-regulated.

CONCLUSION: ASP has a protective effect on immunological colon injury induced by TNBS and ethanol enema in rats, which was propably due to the mechanism of antioxidation, immunomodulation and promotion of wound repair.

Liu SP, Dong WG, Wu DF, Luo HS, Yu JP. Protective effect of *angelica sinensis* polysaccharide on experimental immunological colon injury in rats. *World J Gastroenterol* 2003; 9(12): 2786-2790
http://www.wjgnet.com/1007-9327/9/2786.asp

INTRODUCTION

Angelica sinensis polysaccharide (ASP) possesses a variety of pharmacological effects including immunoregulation, anti-oxidation, anti-tumor, anti-irradiation injury, promotion of hematopoiesis[1-6]. ASP not only has regulatory effects on cytokines, complements, immunocompetent cells such as lymphocyte, macrophage but also shows manifold immunoregulation according to different organism immunological status, drug dose and drug administration surroundings; In addition, ASP has been recently found to be effective in preventing gastrointestinal injury induced by a neutrophil-dependent lesion model in rats, to promote gastrointestinal wound healing in rats *in vitro* and *vivo*[7-9].

Immunoregulation dysfunction plays a central role in the pathogenesis of inflammatory bowel disease (IBD) including Crohn' s disease and ulcerative colitis, although their etiology and pathophysiology remain to be elucidated. Immunoregulation dysfunction is mainly manifested as increased pro-inflammatory cytokines and decreased anti-inflammatory cytokines, which introduce the generation of "inflammation cascade", result in overproduction of oxygen and nitrogen reactive species, thus leading to intestinal and/or colonic injury[10-15]. Numerous studies have demonstrated that modulation of immunological disorders is an effective target for the treatment of IBD[15-19].

Based on ASP' s immunomodulatory feature with manifold efficacies, anti-oxidation property, promotion of gastrointestinal wound healing and safety in use, we therefore assumed that ASP might contribute to the treatment of IBD. To the best of our knowledge, there has been no report so far concerning the effect of ASP on IBD. The present study was to observe the effect of ASP on immunological colon injury in experimental colitis rats to test the hypothesis.

MATERIALS AND METHODS

Animals and reagents

Healthy Sprague-Dawley rats of both sexes, weighing 250±30 g, and C57BL/6J mice, weighing 20±2 g, supplied by the Animal Center of the Academy of Hubei Preventive Medical Sciences. The rats were allowed to take food and tap water *ad libitum*. ASP was isolated from angelica sinensis from Minxian County of China by water extraction and ethanol precipitation as described in the literature[4,10] and dissolved in normal saline, sanitized by high pressure before use. TNBS (Lot. 51K5001), ConA, MTT were all purchased from Sigma Co (USA). 5-aminosalicylic acid (5-ASA) was provided by Guoyi Pharmaceutical Ltd (Lot. 20029477, China). Occult blood test paper was provided by Tonyar Biotech Co (USA). Bovine serum and RPMI-1640 medium were purchased from Gibco Co (USA). Recombinant human TNF-α was provided by BangDing Biotech Co (China). Actinomycin D was provided by HuaMei Biotech Co (China). L929 cells were provided by Biological Classic Culture Store Centre of Wuhan University in China. IL-10 radioimmunoassay kits were provided by Radio-immunity Institute of PLA General Hospital in Beijing. Polyclonal rabbit anti-rat-TGF-β and EGF were purchased

from Santa Cruz Co. and Zymed Co., respectively. S-P kits were supplied by Zhongshan Biological Technology CO. Ltd in Beijng. MPO, SOD, MDA, NO detection kits were purchased from Nanjing Jiancheng Bioengineering Institute. Other reagents used in the present study were all of analytical grade.

Experimental protocol

According to the references[19,20], the rats were anesthetized with ether, then a flexible plastic rubber catheter with an outside diameter of 2 mm was inserted rectally into the colon, its tip was 8 cm proximal to the anus. TNBS (100 mg· kg^{-1}) dissolved in 50 % ethanol (v/v) was instilled into the colon lumen through the rubber cather (the final volume was 0.25 mL), saline was instilled as control. The experimental animals were randomly divided into 6 groups: normal group, model group, 5-ASA therapy group and three doses of ASP therapy groups. The 6 groups were treated intracolicly with normal saline, normal saline, 5-ASA (100 mg· kg^{-1}), and ASP daily (8:00 am) at the doses of 200, 400 and 800 mg· kg^{-1} respectively for 21 days 7 d following induction of colitis in rats. Then the colon mucosa damage index (CMDI) and the histopathological score (HS) were evaluated and the colonic tissue was sampled for a variety of determinations after the animals were sacrificed by decapitation.

Assessment of CMDI, HS and OBT

The tissue of colon 10 cm proximal to anus of the sacrificed rats was excised, opened longitudinally, washed in saline buffer, and pinned out on a wax block. The colonic tissue samples for HS were prepared according to the reference[19]. CMDI and HS in each colon were evaluated respectively by two independent observers. The assessment criteria of CMDI and HS were reported in previous literature[19]. CMID was as following: 0: normal mucosa, no damage on mucosal surface; 1: mild hyperemia and edema, no erosion or ulcer on mucosal surface; 2: moderate hyperemia and edema with erosion on mucosal surface; 3: severe hyperemia and edema with necrosis and ulcer on mucosal surface, the major ulcerative area extended less than 1 cm; 4: severe hyperemia and edema with necrosis and ulcer on mucosal surface, the major ulcerative area extended more than 1 cm. HS: (1) Infiltration of acute inflammatory cells: 0, without; 1, mild; 2, severe. (2) Infiltration of chronic inflammatory cells: 0, without; 1, mild; 2, severe. (3) Fibrin deposition: 0, negative; 1, positive. (4) Submucosal edema: 0, without; 1, focal; 2, diffuse. (5) Necrosis of epithelial cells: 0, without; 1, focal; 2, diffuse. (6) Mucosal ulcer: 0, negative; 1, positive. At the end of experiment, rat feces was collected for occult blood test (OBT) according to the instructions.

Determination of MPO, SOD activities and MDA and NO contents

The colon tissue samples taken for MPO detection were homogenized (50 g· L^{-1}) in ice-cold potassium phosphate buffer 50 mmol· L^{-1} (pH 6.0) containing 0.5 % hexadecyltrimethyl-ammoninm bromide. The homogenates were frozen and thawed three times, then centrifuged at 4 000 rpm for 20 min at 4 ℃. The level of MPO in supernatant was measured using a commercial kit according to its instructions. Other colon tissue samples were homogenized (50 g· L^{-1}) in ice-cold PBS (pH 7.4). The homogenates were centrifuged at 3 000 rpm for 10 min at 4 ℃, and the supernatant was stored at -20 ℃ until determination for SOD, MDA and NO using corresponding commercial kits according to the instructions.

Measurement of TNF-α, IL-2, IL-10 levels

The colon tissue samples were homogenized (100 g· L^{-1}) in ice-cold phosphate buffer saline (pH 7.4) containing penicillin 100 u· ml^{-1} and streptomycin 100 ug· ml^{-1}. The homogenates were centrifuged at 40 000 rpm for 10 min at 4 ℃, and the supernatant was stored at - 80 ℃ until determination for TNF-α, IL-2 and IL-10. The activity of TNF-α and IL-2 were measured by L929 cell cytotoxicity and C57BL/6J mice splenocytes using MTT colorimetry respectively as described in the literatue[19,21]. The content of IL-10 was detected by using a radioimmunoassay kit following the manufacturer's instructions.

Detection of colonic TGF-β and EGF expression

Immunohistochemical detection was performed using S-P technique. The experiment procedures were performed following the manufacturer's recommendations. Polyclonal rabbit anti-rat-TGF-β and EGF were diluted in PBS to 1:100, 1:150, and used as primary antibodies respectively. The dewaxed sections were incubated with polyclonal primary antibodies overnight at 4 ℃ after antigen repair. Biotinylated goat-anti-rabbit IgG was added as second antibody. Horseradish peroxidase labeled streptomycin-avidin complex was used to detect second antibody. Sections were stained with diaminobenzidine. Negative control sections were prepared by substituting primary antibodies with PBS. The bluely stained nucleus was considered as negative while the brown or dark brown stained cytoplasm and/or cell membrane were considered as positive. Expressions of these target proteins were semiquantitated respectively with an automatic image analyzer (Nikon, Japan) and HPIAS-2000 image analyzing program, in which the average value of positive cell's absorbance (A) in ten randomly selected high power fields (400×) for each section was used to compare the target protein expression.

Statistical analysis

Experimental results were analyzed by ANOVA and *t*-test for multiple comparisons between the groups. Data were finally expressed as mean ±SD. *P* value less than 0.05 was considered statistically significant.

RESULTS

Protective effect of ASP on colon injury

Results are shown in Table 1. CMDI, HS, OBT and MPO activity were regarded as main parameters that reflected the degree of colon injury and inflammation in inflammatory gut tissue. Compared with normal group, these parameters were significantly increased in model group ($P<0.01$). Both ASP (400, 800 mg· kg^{-1}) and 5-ASA (100 mg· kg^{-1}) could remarkably decrease these elevated parameters ($P<0.05$-0.01). Furthermore, the therapeutic effect of 800 mg· kg^{-1} ASP was as effective as that of 5-ASA (100 mg· kg^{-1}).

Table 1 Effect of ASP on CMDI, HS, OBT and MPO activity in colonic tissue of colitis rats (n=8, $\bar{x}\pm s$)

Group	Dose (mg·kg^{-1})	CMDI	HS	OBT	MPO (U·g^{-1})
Control	-	0.0±0.0	0.7±1.1	0.0±0.0	29±18
Model	-	3.1±1.1[d]	5.6±0.8[d]	2.2±0.8[d]	194±32[d]
5-ASA	100	1.7±0.6[b]	4.7±0.7[a]	1.0±0.9[a]	117±15[b]
ASP	200	2.1±0.5[a]	4.5±1.3	1.4±0.9	172±16
ASP	400	1.8±0.7[a]	4.3±1.1[a]	1.1±0.8[a]	158±19[a]
ASP	800	1.5±0.5[b]	4.1±0.9[b]	0.8±0.7[b]	133±17[b]

[a]$P<0.05$, [b]$P<0.01$, *vs* model group; [d]$P<0.01$ *vs* normal group.

Effect of ASP on colonic oxidation of colitis rats

Compared with normal group, the contents of MDA and NO

were significantly elevated while SOD activity was significantly decreased in model group (P<0.01). ASP (400, 800 mg· kg^{-1}) not only obviously decreased MDA content but also evidently increased SOD activity (P<0.05-0.01). Furthermore, ASP (200, 400, 800 mg· kg^{-1}) remarkably reduced the elevated NO content in a dose-dependent manner (P<0.05-0.01) (Table 2).

Table 2 Effect of ASP on activity of SOD and contents of MDA and NO in colonic tissue of colitis rats (n=8, $\bar{x}\pm s$)

Group	Dose (mg·kg^{-1})	SOD (kU·g^{-1})	MDA (nmol·g^{-1})	NO (nmol·g^{-1})
Control	-	23.16±5.13	27.41±9.66	294±73
Model	-	8.41±3.17^{d}	83.47±22.53^{d}	568±65^{d}
5-ASA	100	15.26±2.14^{b}	55.32±8.61^{b}	367±26^{b}
ASP	200	11.95±3.22^{a}	67.31±13.84	496±52^{a}
ASP	400	14.84±2.45^{b}	58.52±14.36^{a}	445±47^{b}
ASP	800	16.27±1.96^{b}	49.14±10.73^{b}	381±34^{b}

^{a}P<0.05, ^{b}P<0.01, *vs* model group; ^{d}P<0.01 *vs* normal group.

Effect of ASP on colonic TNF-α, IL-2 and IL-10 levels

Compared with normal group, the levels of TNF-α, IL-2 were significantly increased while the content of IL-10 was obviously reduced in model group (P<0.01). ASP (400, 800 mg· kg^{-1}) not only obviously decreased the levels of TNF-α, IL-2 but also significantly increased the content of IL-10 in model group (P<0.05-0.01) (Table 3).

Table 3 Effect of ASP on levels of TNF-α, IL-2, IL-10 in colonic tissue of colitis rats (n=8, $\bar{x}\pm s$)

Group	Dose (mg·kg^{-1})	TNF-α (kU·g^{-1})	IL-2 (A)	IL-10 (ng·g^{-1})
Control	-	30.6±12.6	0.176±0.028	43±8
Model	-	82.8±18.6^{d}	0.381±0.069^{d}	15±5^{d}
5-ASA	100	45.3±21.9^{b}	0.264±0.042^{b}	22±10
ASP	200	61.9±25.6	0.318±0.032^{a}	23±11
ASP	400	57.4±20.8^{a}	0.303±0.036^{a}	23±8^{a}
ASP	800	51.7±21.5^{b}	0.285±0.031^{b}	26±10^{a}

^{a}P<0.05, ^{b}P<0.01, *vs* model group; ^{d}P<0.01 *vs* normal group.

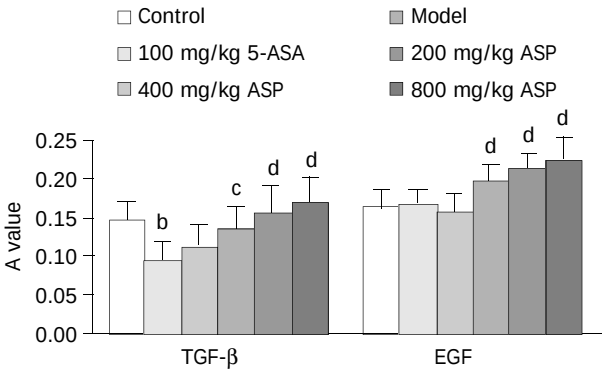

Figure 1 Effect of ASP on expressions of TGF-β and EGF in colonic tissue of colitis rats. n=8, $\bar{x}\pm s$, ^{b}P<0.01, *vs* normal control; ^{c}P<0.05, ^{d}P<0.01, *vs* model control.

Effect of ASP on colonic TGF-b and EGF expressions

As shown in Figures 1, 2 and 3, compared with normal group, TGF-β expression in model group was significantly decreased (0.096±0.021 *vs* 0.145±0.025, P<0.01) and EGF expression was hardly changed. ASP (200, 400, 800 mg· kg^{-1}) remarkably up-regulated the expressions of TGF-β and EGF in a dose - dependent manner (TGF-β: 0.132±0.031, 0.154±0.036, 0.169±0.032 *vs* 0.096±0.021; EGF: 0.197±0.021, 0.212±0.023, 0.225±0.029 *vs* 0.166±0.024, P<0.05-0.01), whereas 5-ASA (100 mg· kg^{-1}) had no obvious effect on the expressions of TGF-β and EGF.

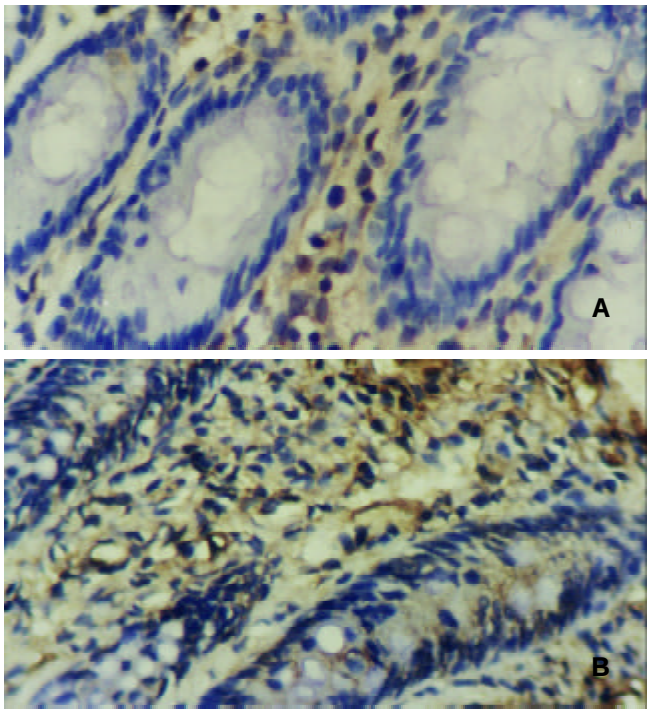

Figure 2 Expressions of TGF-β (A) and EGF (B) in inflammatory areas of colonic tissue from rats with colitis induced by TNBS and ethanol, respectively. Weakly positive signals were found. SP stain ×400.

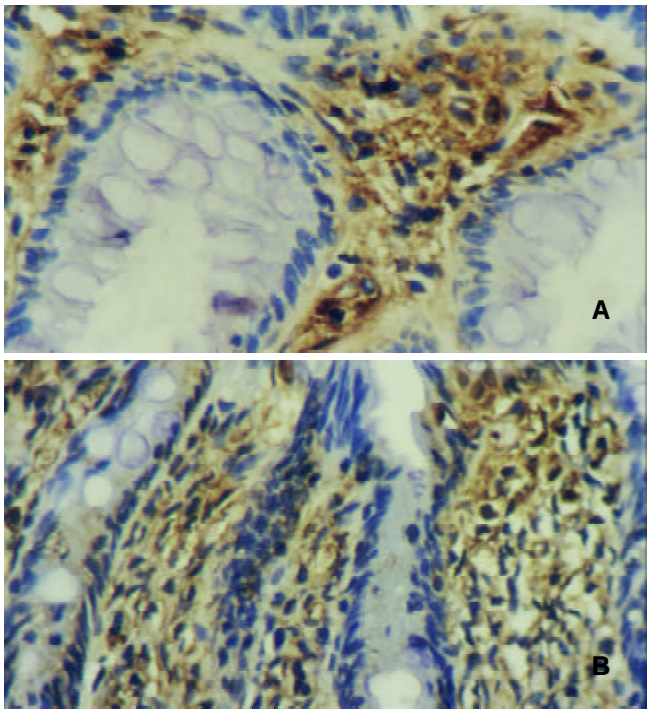

Figure 3 Significantly increaed expressions of TGF-β (A) and EGF (B) were in colonic tissue from rats with colitis induced by TNBS and ethanol after treated with 800 mg·kg^{-1} ASP. Strongly positive staining could be found. SP stain ×400.

DISCUSSION

TNBS-induced rats colitis model established by Morris *et al*

was regarded as a classic model for immunological colon injury which shares many of the histopathological and clinical features and pathogenesis of human IBD. The whole process was summarized as following: after destruction of mucosa integrity by ethanol, hapten TNBS was bound to colon tissue proteins, and changed into a modified protein compound, which was recognized by macrophages as an abnormal antigen and presented quickly to the sensitized T lymphocytes. So a series of immunoresponsiveness and severe colon inflammation were initiated subsequently[19,20]. In this study, an IBD model was successfully established, and intracolon enema with ASP showed obviously protective effects on immunological colon injury, which might be related with ASP's antioxidation property and function of balancing cytokine generation and modulating immune.

Many studies have revealed that reactive metabolites of oxygen and nitrogen were a notable characteristic of IBD, which led to the pathological aggravation of a series of free radicals chain reactions and strongly attack DNA, proteins, enzymes, biological membrances as well as disruption of the integrity and function of intestinal mucosa barrier, activaton of inflammatory mediators[22-25]. Besides direct and severe impairment of the function of intestinal barrier, excessive NO participated in complicated web system between inflammatory cells and immunocytes in IBD[12,15,22-25]. Our study showed that ASP, an anti-oxidant agent which can directly scavenge oxygen-derived free radicals, could not only remarkably decrease the elevated contents of MDA and NO, but also evidently increase the reduced SOD activity in colonic tissues of colitis rats. Reduction of NO by ASP might be related with its inhibition of nitric oxide synthase activity, which was proven by recent researches[3,4].

As the most important cytokine in "inflammation cascade" of IBD, TNF-α could directly impair gut mucosa, promote production of inflammatory mediators and oxygen free radicals, up-regulate the expression of adhesive factors. Moreover, TNF-α is also a main activator for NF-κB, a critical transcription factor, thus up-regulating many genes involved in proinflammatory and immune responses[12,15,16,26]. In this article, ASP, an immunomodulatory reagent, obviously decreased the elevated colonic TNF-α level in colitis rats. As it is known, TNF-α and NO mainly came from activated macrophages in inflammatory gut[12,19,26]. It deserves further investigation that whether inhibition of TNF-α and NO by ASP is related with its regulation of macrophage activation through the polysaccharide receptors on the surface of macrophages such as β-glucan receptor and mannose receptor[27,28].

As it is known, imbalance of type 1 helper T lymphocyte (Th1) and Th2 in IBD could promote excretion of important pro-inflammatory cytokines including TNF-α, INF-γ, and activate macrophages, which mediate inflammatory and immunological injury. Moderate IL-2 level is important for keeping the dynamic balance of Th1 and Th2 in normal gut mucosa, whereas excessive IL-2 could up-regulate the activity of Th1[29-31]. As a major anti-inflammatory cytokine mainly secreted by Th2, IL-10 could suppress inflammation by decreasing Th1 activation, reducing HLA class II expression, and diminishing production of pro-inflammatory cytokines from activated macrophages such as IL-1α, IL-1β, TNF-α and IL-8[12,32-34]. Data obtained in this study indicated that ASP could not only significantly reduce the markedly elevated IL-2 level but also increase the reduced IL-10 level in colonic tissue of colitis rats, thus partly correcting the aberrant immunological status, which might be related with the marked induction of TGF-β by ASP. As a strong immunosuppressant and anti-inflammation cytokine mainly secreted by macrophages, TGF-β plays an important role in gut local immunity in IBD. TGF-β could not only suppress the immunoresponse of Th1 in intestine, depress the activity of activated macrophages but also induce production of IL-10[12,18,34]. Investigations have demonstrated that deficiency of TGF-β in the intestine contributed to the development of IBD, whereas maintenance of TGF-β might be important in regulating immune homeostasis in the intestine[18, 35].

Besides modulating immune response, TGF-β could control cell growth, differentiation and migration, stimulate synthesis of extracellular matrix proteins, and promote angiogenesis, thus promoting wound repair and tissue reconstruction. Its functions are similar to those of cytokine EGF[36-41]. In addition, EGF could induce production of TGF-β and they showed cooperative effects[40-42]. Reseaches have proven that TGF-β and EGF were crucial for maintaining the integrity and functions of intestine mucosa barrier, and could effectively prevent and ameliorate its injury and dysfunction induced by oxidants, thus contributing to the treatment of intestinal inflammation[42-45]. Our study showed that ASP significantly increased the levels of EGF and markedly reduced TGF-β in colon tissue of colitis rats, thus accelerating repair of colon lesions, which agreed with investigations of Ye *et al*[8,9]. The underlying mechanism might be that ASP has pharmacological properties similar to heparin which can interacts with a variety of proinflammatory chemokines and growth factors, thus promoting production of many growth factors[7-9,42,47,48].

To sum up, the results of this study showed that intracolonic treatment with ASP at the doses of 400 mg·kg^{-1} and 800 mg·kg^{-1} could obviously attenuate experimental immunological colon injury in rats, suggesting that ASP in combination with well-established drugs, may contribute to the optimal therapy of IBD.

REFERENCES

1 **Xie L,** Yang LH, Li XH. Resarch on the pharmacologic effects of Angelica Sinensis. *Zhongyiyao Yanjiu* 2000; **16:** 56-58

2 **Ling XM,** Ding H, Luo SD, Zhang XJ, Zhang LH. Study on the pharmacological mehanism of angelica polysaccharide on the immunocompetence and the effects of its anti-oxidation. *Zhongguo Yiyuan Yaoxue Zazhi* 2002; **22:** 584-586

3 **Ye YN,** Liu ES, Li Y, So HL, Cho CC, Sheng HP, Le SS, Cho CH. Protective effect of polysaccharides-enriched fraction from Angelica sinensis on hepatic injury. *Life Sci* 2001; **69:** 637-646

4 **Ding H,** Peng R, Yu J. Modulation of angelica sinensis polysaccharides on the expression of nitric oxide synthase and Bax, Bcl-2 in liver of immunological liver-injured mice. *Zhonghua Ganzangbing Zazhi* 2001; **9**(Suppl): 50-52

5 **Yang TH,** Lu BH, Jia SM, Mei QB. Immunoregulation effect of Angelica polysaccharide isolated from Angelica sinensis on mice. *Zhongguo Yaolixue Tongbao* 2003; **19:** 448-451

6 **Xia XY,** Peng RX, Wang ZY. The effect of angelica sinensis polysaccharide and its ingredients on mice's immunocompetence. *Wuhan Daxue Xuebao(Medicine Edition)* 2001; **22:** 199-201

7 **Cho CH,** Mei QB, Shang P, Lee SS, So HL, Guo X, Li Y. Study of the gastrointestinal protective effects of polysaccharides from Angelica sinensis in rats. *Plant Med* 2000; **66:** 348-351

8 **Ye YN,** Koo MW, Li Y, Matsui H, Cho CH. Angelica sinensis modulates migration and proliferation of gastric epithelial cells. *Life Sci* 2001; **68:** 961-968

9 **Ye YN,** So HL, Liu ES, Shin VY, Cho CH. Effect of polysaccharides from Angelica sinensis on gastric ulcer healing. *Life Sci* 2003; **72:** 925-932

10 **Xia B.** Etiology and pathogenesis of inflammatory bowel disease. *Shijie Huaren Xiaohua Zazhi* 2001; **9:** 245-250

11 **Kirsner JB.** Historical origins of current IBD concepts. *World J Gastroenterol* 2001; **7:** 175-184

12 **Papadakis KA,** Targan SR. Role of cytokines in the pathogenesis of inflammatory bowel disease. *Annu Rev Med* 2000; **51:** 289-298

13 **Xia B,** Guo HJ, Crusius JBA, Deng CS, Meuwissen SGM, Pena A. *In vitro* production of TNF-alpha, IL-6 and sIL-2R in Chinese patients with ulcerative colitis. *World J Gastroenterol* 1998; **4:** 252-255

14 **Indaram AVK,** Nandi S, Weissman S, Lam S, Bailey B, Blumstein M, Greenberg R, Bank S. Elevated basal intestinal mucosal cytokine levels in asymptomatic first-degree relatives of patients with Crohn's disease. *World J Gastroenterol* 2000; **6:** 49-52

15 **Momeleone G,** Macdonald TT. Manipulation of cytokines in the management of patients with inflammatory bowel disease. *Ann Med* 2000; **32:** 552-560

16 **Blam ME,** Stein RB, Lichtenstein GR. Integrating anti-tumor necrosis factor therapy in inflammatory bowel disease: current and future perspectives. *Am J Gastroenterol* 2001; **96:** 1977-1997

17 **Das KM,** Farag SA. Current medical therapy of inflammatory bowel disease. *World J Gastroenterol* 2000; **6:** 483-489

18 **Fiocchi C.** TGF-beta / Smad signaling defects in inflammatory bowel disease: mechanisms and possible novel therapies for chronic inflammation. *J Clin Invest* 2001; **108:** 523-526

19 **Mei Q,** Yu JP, Xu JM, Wei W, Xiang L, Yue L. Melatonin reduces colon immunological injury in rats by regulating activity of macrophages. *Acta Pharmacol Sin* 2002; **23:** 882-886

20 **Morris GP,** Beck PL, Herridge MS, Depew WT, Szewczuk MR, Wallace JL. Hapten-induced model of chronic inflammation and ulceration in the rat colon. *Gastroenterology* 1989; **96:** 795-803

21 **Zhang JT.** Modern experimental methods in pharmacology. 1st ed. Beijing: *Beijing Medical College Xiehe Medical College Pub* 1997: 726-762

22 **Pavlick KP,** Laroux FS, Fuseler J, Wolf RE, Gray L, Hoffman J, Grisham MB. Role of reactive metabolites of oxygen and nitrogen in inflammatory bowel disease. *Free Radic Biol Med* 2002; **33:** 311-322

23 **Krieglstein CF,** Cerwinka WH, Laroux FS, Salter JW, Russell JM, Schuermann G, Grisham MB, Ross CR, Granger DN. Regulation of murine intestinal inflammation by reactive metabolites of oxygen and nitrogen: divergent roles of superoxide and nitric oxide. *J Exp Med* 2001; **194:** 1207-1218

24 **Huang J,** Luo HS, Yang JX. Therapeutic effects of butyrate on nitric oxide abnormity in experimental ulcerative colitis in rats. *Shijie Huaren Xiaohua Zazhi* 2001; **9:** 967-969

25 **Bai AP,** Shen ZX, Yu JP, Yu BP, Luo Y. Nitric oxide and the acute injury in colitis model. *Shijie Huaren Xiaohua Zazhi* 1999; **7:** 900-901

26 **Li JH,** Yu JP, He XF, Xu XM. Expression of NF-κB in rats with TNBS-induced ulcerative colitis. *Shijie Huaren Xiaohua Zazhi* 2003; **11:** 214-218

27 **Brown GD,** Taylor PR, Reid DM, Willment JA, Williams DL, Martinez-Pomares L, Wong SY, Gordon S. Dectin-1 is a major beta-glucan receptor on macrophages. *J Exp Med* 2002; **196:** 407-412

28 **Linehan SA,** Martinez-Pomares L, da Silva RP, Gordon S. Endogenous ligands of carbohydrate recognition domains of the mannose receptor in murine macrophages, endothelial cells and secretory cells; potential relevance to inflammation and immunity. *Eur J Immunol* 2001; **31:** 1857-1866

29 **Romagnani S.** Th1 / Th2 cells. *Inflamm Bowel Dis* 1999; **5:** 285-294

30 **Van Damme N,** De Keyser F, Demetter P, Baeten D, Mielants H, Verbruggen G, Cuvelier C, Veys EM, De Vos M. The proportion of Th1 cells, which prevail in gut mucosa, is decreased in inflammatory bowel syndrome. *Clin Exp Immunol* 2001; **125:** 383-390

31 **Bemiss CJ,** Mahon BD, Henry A, Weaver V, Cantorna MT. Interleukin-2 is one of the targets of 1,25-dihydroxyvitamin D3 in the immune system. *Arch Biochem Biophys* 2002; **402:** 249-254

32 **Dejaco C,** Reinisch W, Lichtenberger C, Waldhoer T, Kuhn I, Tilg H, Gasche C. *In vivo* effects of recombinant human interleukin-10 on lymphocyte phenotypes and leukocyte activation markers in inflammatory bowel disease. *J Investig Med* 2000; **48:** 449-456

33 **Asseman C,** Mauze S, Leach MW, Coffman RL, Powrie F. An essential role for interleukin 10 in the function of regulatory T cells that inhibit intestinal inflammation. *J Exp Med* 1999; **190:** 995-1004

34 **Kitani A,** Fuss IJ, Nakamura K, Schwartz OM, Usui T, Strober W. Treatment of experimental (Trinitrobenzene sulfonic acid) colitis by intranasal administration of transforming growth factor (TGF)-β_1 plasmid: TGF-β_1-mediated suppression of T helper cell type 1 response occous by intereukin (IL)-10 induction and IL-12 receptor beta2 chain downregulation. *J Exp Med* 2000; **192:** 41-52

35 **Hahm KB,** Im YH, Parks TW, Park SH, Markowitz S, Jung HY, Green J, Kim SJ. Loss of transforming growth factor beta signalling in the intestine contributes to tisse injury in inflammatory bowel disease. *Gut* 2001; **49:** 190-198

36 **Wiercinska-Drapalo A,** Flisiak R, Prokopowicz D. The role of transforming growth factors beta in pathogenesis of ulcerative colitis. *Pol Merkuriusz Lek* 2001; **10:** 177-179

37 **Fu XB,** Yang YH, Sun TZ, Gu XM, Jiang LX, Sun XQ, Sheng ZY. Effect of intestinal ischemia-reperfusion on expressions of endogenous basic fibroblast growth factor and transforming growth factor β in lung and its relation with lung repair. *World J Gastroenterol* 2000; **6:** 353-355

38 **Yuan YZ,** Lou KX, Gong ZH, Tu SP, Zhai ZK, Xu JY. Effects and mechanisms of emodin on pancreatic tissue EGF expression in acute pancreatitis in rats. *Shijie Huaren Xiaohua Zazhi* 2001; **9:** 128-130

39 **Xia L,** Yuan YZ, Xu CD, Zhang YP, Qiao MM, Xu JX. Effects of epidermal growth factor on the growth of human gastric cancer cell and the implanted tumor of nude mice. *World J Gastroenterol* 2002; **8:** 455-458

40 **Wu BW,** Wu Y, Wang JL, Lin JS, Yuan SY, Li A, Cui WR. Study on the mechanism of epidermal growth factor-induced proliferation of hepatoma cells. *World J Gastroenterol* 2003; **9:** 271-275

41 **Beck PL,** Podolsky DK. Growth factors in inflammatory bowel disease. *Inflamm Bowel Dis* 1999; **5:** 44-60

42 **Higasshiyama S,** Abraham JA, Miller J, Fiddes JC, Klagsbrun M. A heparin-binding growth factor secreted by macrophage-like cells that is related to EGF. *Science* 1991; **251:** 936-939

43 **Chen DL,** Wang WZ, Wang JY. Epidermal growth factor prevents gut atrophy and maintains intestinal integrity in rats with acute pancreatitis. *World J Gastroenterol* 2000; **6:** 762-765

44 **Banan A,** Zhang Y, Losurdo J, Keshavarzian A. Carbonylation and disassembly of the F-actin cytoskeleton in oxidant induced barrier dysfunction and its prevention by epidermal growth factor and transforming growth factor alpha in a human colonic cell line. *Gut* 2000; **46:** 830-837

45 **Banan A,** Fields JZ, Talmage DA, Zhang L, Keshavarzian A. PKC-zeta is required in EGF protection of microtubules and intestinal barrier integrity against oxidant injury. *Am J Physiol Gastrointest Liver Physiol* 2002; **282:** G794-808

46 **Sandborn WJ,** Targan SR. Biologic therapy of inflammatory bowel disease. *Gastroenterology* 2002; **122:** 1592-1608

47 **Miller MD,** Krangel MS. Biology and biochemistry of the chemokines: a family of chemotactic and inflammatory cytokines. *Crit Rev Immunol* 1992; **12:** 7-46

48 **Li Y,** Wang HY, Cho CH. Association of heparin with basic fibroblast growth factor, epidermal growth factor, and constitutive nitric oxide synthase on healing of gastric ulcer in rats. *The J Pharmacol Exp Ther* 1999; **290:** 789-796

Edited by Wang XL

P.O.Box 2345, Beijing 100023,China
Fax: +86-10-85381893
E-mail: wjg@wjgnet.com www.wjgnet.com

World J Gastroenterol 2003;9(12):2791-2795
World Journal of Gastroenterology
 ISSN 1007-9327

• BASIC RESEARCH •

Visceral hypersensitivity and altered colonic motility after subsidence of inflammation in a rat model of colitis

Jun-Ho La, Tae-Wan Kim, Tae-Sik Sung, Jeoung-Woo Kang, Hyun-Ju Kim, Il-Suk Yang

Jun-Ho La, Tae-Wan Kim, Tae-Sik Sung, Jeoung-Woo Kang, Hyun-Ju Kim, Il-Suk Yang, Department of Physiology, College of Veterinary Medicine, Seoul National University, Seoul, Republic of Korea
Correspondence to: Il-Suk Yang, Department of Physiology, College of Veterinary Medicine, Seoul National University, San 56-1 Sillim-Dong, Kwanak-Gu, Seoul, 151-742, Republic of Korea. isyang@snu.ac.kr
Telephone: +82-2-880-1261 **Fax:** +82-2-885-2732
Received: 2003-08-05 **Accepted:** 2003-09-17

Abstract

AIM: Irritable bowel syndrome (IBS) is a functional bowel disorder characterized by visceral hypersensitivity and altered bowel motility. There is increasing evidence suggesting the role of inflammation in the pathogenesis of IBS, which addresses the possibility that formerly established rat model of colitis could be used as an IBS model after the inflammation subsided.

METHODS: Colitis was induced by intracolonic instillation of 4 % acetic acid in male Sprague-Dawley rats. The extent of inflammation was assessed by histological examination and myeloperoxidase (MPO) activity assay. After subsidence of colitis, the rats were subjected to rectal distension and restraint stress, then the abdominal withdrawal reflex and the number of stress-induced fecal output were measured, respectively.

RESULTS: At 2 days post-induction of colitis, the colon showed characteristic inflammatory changes in histology and 8-fold increase in MPO activity. At 7 days post-induction of colitis, the histological features and MPO activity returned to normal. The rats at 7 days post-induction of colitis showed hypersensitive response to rectal distension without an accompaning change in rectal compliance, and defecated more stools than control animals when under stress.

CONCLUSION: These results concur largely with the characteristic features of IBS, visceral hypersensitivity and altered defecation pattern in the absence of detectable disease, suggesting that this animal model is a methodologically convenient and useful model for studying a subset of IBS.

La JH, Kim TW, Sung TS, Kang JW, Kim HJ, Yang IS. Visceral hypersensitivity and altered colonic motility after subsidence of inflammation in a rat model of colitis. *World J Gastroenterol* 2003; 9(12): 2791-2795
http://www.wjgnet.com/1007-9327/9/2791.asp

INTRODUCTION

Irritable bowel syndrome (IBS) is defined as a group of functional bowel disorders in which abdominal discomfort or pain is associated with defecation or a change in bowel habit in the absence of an identifiable disease process[1]. Clinical observations have revealed that patients with IBS show a disturbed colonic motor function and hypersensitivity to luminal distension, and these symptoms are generally accepted as cardinal features of IBS[2].

Although IBS is known as one of the most common disorder encountered in clinical practice[3], progress in the study of IBS in the basic scientific research fields has been hindered largely due to the lack of useful animal models that mimic the features of IBS[4]. Since the pathophysiological processes involved in IBS are multifactorial, researchers have employed various kinds of symptom-generating stimulus to establish animal models of IBS. These include a stressful event in adult animals[5], a chemical or mechanical irritation of colon in early life[4], and neonatal maternal separation[6].

Recently, attention has been directed to the role of inflammation in the pathogenesis of IBS[3,7], and IBS after enteric infection, namely post-infectious IBS has begun to be studied using rodent models experimentally infected with *Nippostrongylus brasilensis*[8] or *Trichinella spiralis*[9]. The infected animals underwent jejunitis and showed altered intestinal motor function or hypersensitivity to luminal distension even after the pathogens were eliminated. These inspiring reports addressed the possibility that the well-characterized rodent models of colitis could also exhibit some features of post-infectious IBS after resolution of colitis or, at least, in a certain period of time during the recovery course.

In the present study, we examined this possibility using one of the extensively studied rodent models of acute colitis, the rat model of acetic acid-induced colitis. Specifically, we aimed to find out whether the animal could show visceral hypersensitivity to rectal distension and altered defecation pattern under stress after the subsidence of colitis.

MATERIALS AND METHODS

Animals

Male Sprague-Dawley rats (270-310 g) were housed individually in an access-restricted room with controlled temperature (23 ℃) and light-dark cycles (12:12 h). All the experimental protocols in this study were reviewed and approved by the Animal Care and Use Committee of Seoul National University.

Induction of colitis

After an overnight fast, the rats were lightly anesthetized with ether, and colitis was induced by intracolonic instillation of 1 ml 4 % acetic acid (Fluka, Buchs SG, Switzerland) at 8 cm proximal to the anus for 30 s. Then, 1 ml phosphate buffered saline was instilled to dilute the acetic acid and flush the colon. Control animals were handled identically except that 1 ml saline was instilled instead of 4 % acetic acid.

Myeloperoxidase (MPO) activity assay

MPO activity assay was performed to quantify the inflammation in distal colon according to the procedure described previously[10]. Sixteen rats (4 animals at 2 and 7 days post-

enema in each group) were used for this study. These two time-points were selected according to previous reports[10,11] to represent the overt inflammatory phase and the subsiding phase, respectively. Briefly, an 8 cm segment of distal colon was collected via laparotomy, minced in 1 ml of 50 mM potassium phosphate buffer (pH 6.0) containing 14 mM hexadecyltrimethylammonium bromide (Fluka), homogenized and sonicated. The lysates were frozen and thawed three-times, then centrifuged for 2 min in cold at 15 000 g. Aliquots of the supernatants were mixed with potassium phosphate buffer containing *o*-dianisidine-HCl (Sigma-Aldrich, St. Louis, MO, USA) and 0.0005 % H_2O_2. The change in absorbance at 460 nm was spectrophotometrically measured. MPO activity was expressed as units/g of wet tissue. The enzyme unit was defined as the conversion of 1 μmol of H_2O_2 per min at 25 ℃.

Histological examination of inflammation

To examine the extent of colonic inflammation, histological samples were collected at the selected time points. Sections with a thickness of 5 μm were cut and processed for hematoxylin-eosin staining. The coded slides were analyzed by a pathologist blinded with regard to the treatment group and the time points.

Rectal distension procedure

At 7 days post-enema, eight rats from each group were used for studying visceral sensitivity to rectal distension. A disposable silicon balloon-urethral catheter for pediatric use (6 Fr, Sewoon Medical Co., Seoul, Korea) was used for this purpose. The maximal inflation volume for the balloon was 1.0 ml and the length of the maximally inflated balloon was 1.2 cm. After an overnight fast, the animals were lightly anesthetized with ether, and the balloon was carefully inserted into the rectum until the pre-marked line on the catheter (2 cm distal from the end of the balloon) was positioned to the anus, then the catheter was taped to the base of the tail to prevent displacement. After this procedure, the rats were placed in a transparent cubicle (20 cm×8 cm×8 cm) on a mirror-based elevated platform while still sedated, and were allowed to recover and acclimate for a minimum of 30 min before testing. The catheter was connected to a pressure transducer (RP-1500, Narco Bio-systems Inc., USA) via a 3-way connector, and a non-invasive pulse transducer (MLT125R, AD Instruments, Castle Hill, Australia) was attached so that the active site of the transducer was located on the ventral surface of the tail, directly below the caudal artery. The signals from both transducers were processed through PowerLab/400 (AD Instruments) and recorded on an IBM-compatible computer.

After the animals were fully awaken and acclimatized, ascending-limit phasic distension (0.1, 0.2, 0.3, 0.4, 0.6, 0.8 and 1 ml) was applied for 30 s every 4 min. The balloon was distended with pre-warmed (37 ℃) water. We chose this protocol as hypersensitivity was reported to be best elicited by rapid phasic distension[2]. In this experiment, the abdominal withdrawal reflex (AWR) was semiquantitatively scored as previously described[4] and the concomitant change in arterial pulse rate was measured. The AWR score was assigned as follows: 0=no behavioral response to distension, 1=brief head movements followed by immobility, 2=contraction of abdominal muscle without lifting of abdomen, 3=lifting of abdomen, 4=body arching and lifting of pelvic structure.

After the experiments, the balloon was withdrawn and immersed in 37 ℃ tap water. Since the compliance of balloon was not infinite, we measured intraballoon pressure at each distension volume in 37 ℃ water, and digitally subtracted the value from that recorded during the rectal distension experiment to calculate the intrarectal pressure.

Restraint stress procedure

Fifteen animals of each group were used for this experiment. The rats were housed individually with no restrictions on food intake before testing. At 7 days post-enema, ten rats of each group were placed in restraint cages (5 cm×5 cm×20 cm) for 1 hr at room temperature. The feces excreted during restraint stress were divided into three types: hard pellet, soft pellet and formless stool, and counted separately. In another experiment, five rats of each group were left to be unrestrained for 1 hr and served as unstressed control. All the experiments were performed between 1 000 and 1 200 h.

Statistical analyses

Data were expressed as mean ± SD. Significant difference between the two groups in MPO activity at the selected time-points and in the values (AWR score and the pulse rate change) at each distension volume was statistically analyzed using Mann-Whitney U-test with P value set at <0.05 significance level. The relationship between AWR score and the extent of pulse rate change was determined by linear regression analysis, and the estimated slope coefficients and intercepts were compared between groups using Student' s t-test at 2N-4 (N=the number of data points) degrees of freedom (*d.f.*). The intraballoon volume-intrarectal pressure relationship of each group was also analyzed as above. The number of fecal output was compared using ANOVA and further analyzed using Newman-Keuls multiple comparison test, and considered significantly different from others when $P<0.05$.

RESULTS

Histological features and MPO activity

Figure 1 represents the histology of the distal colon in control (A), at 2 days (B) and at 7 days (C) post-induction of colitis (PIC). At 2 days PIC, mucosal hemorrhage with an inflammatory infiltrate in lamina propria and the edematous submucosa was observed. On the other hand, there was no remarkable inflammatory feature at 7 days PIC. Similar result was obtained from the MPO activity assay of colonic tissue. As shown in Figure 2, the enzyme activity was dramatically increased (8-fold) at 2 days PIC (P=0.0015, n=4), however it was not significantly different from the control value at 7 days PIC ($P>0.5$, n=4). These results indicated that at 7 days PIC, acute colonic inflammation was in subsiding phase.

Rectal distension-induced visceral nociception

Animals awaken in the cubicle showed regular arterial pulse after about 30 min acclimation. The pulse rate was 345.6±6.2 beat per minute (BPM) in control group (n=8) and 329.7±7.3 BPM in the 7 days PIC group (n=8), and the resting pulse rates of the two groups were not significantly different from each other. Pulse rate was instantly increased as the balloon inflated in the rectum and returned to nearly the resting level as it deflated. Animals at 7 days PIC showed hypersensitive response to the ascending-limit phasic rectal distension. The nociceptive threshold (distension volume that produced the AWR of score 2, i.e., abdominal contraction) was about 0.6 ml in the control group, and it was lowered to around 0.3 ml in the 7 days PIC group. The AWR score in rats at 7 days PIC was generally higher than that in control animals, which shifted the distension volume-response curve to left (Figure 3A). In addition, the extent of rectal distension-induced tachycardia was also significantly increased in the 7 days PIC group (Figure 3B).

We further analyzed these results by determining the relationship between the AWR score and the extent of pulse rate change (D pulse rate). The mean value with its standard error of D pulse rate at a given AWR score was plotted in

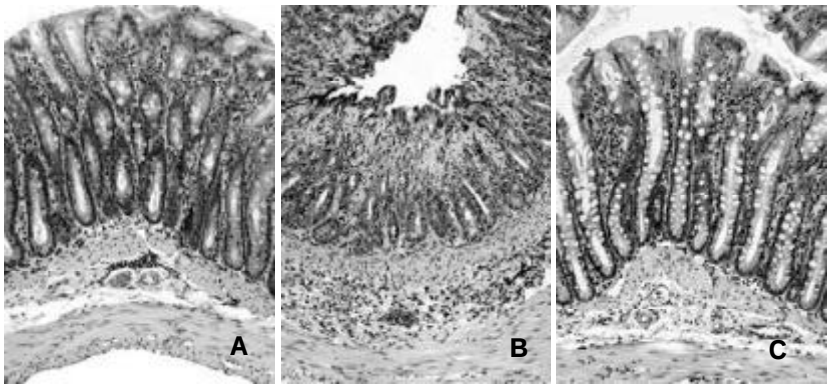

Figure 1 Photomicrographs of distal colons from control (A), at 2 days (B) and at 7 days (C) post-induction of colitis (PIC). At 2 days PIC, histological inflammatory features including mucosal hemorrhage, submucosal edema, and inflammatory infiltration in the lamina propria and the submucosa were observed. At 7 days PIC, there was no remarkable inflammatory feature compared with control.

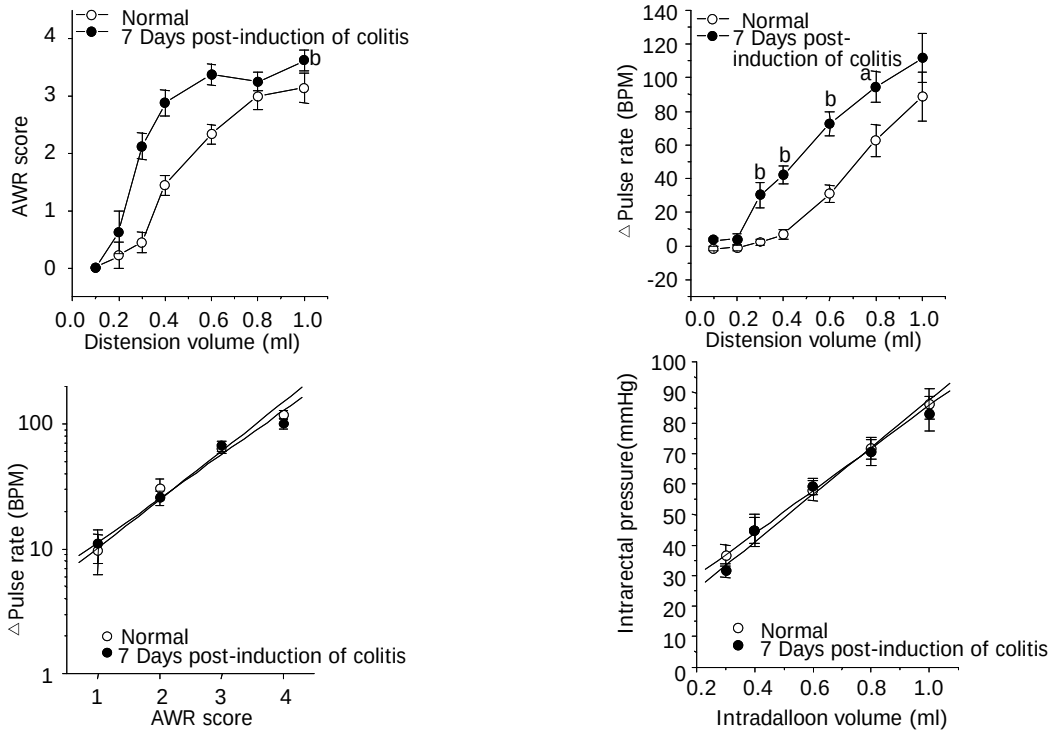

Figure 3 Summarized plots representing the rectal distension-induced AWR (A) and concomitant pulse rate change (B), the relationship between the AWR score and the extent of pulse rate change (C), and the relationship between intraballoon volume and intrarectal pressure (D) in each group. At 7 days PIC, AWR and tachycardia were exaggerated in response to rectal distension. Note the good linear correlation between the AWR score and the logarithmic D pulse rate, which was not significantly different between groups. Intrarectal pressure was linearly increased as the balloon inflated, and the fitted functions of two groups were not significantly different from each other. ($^aP<0.05$, $^bP<0.01$).

logarithmic scale for a linear fit. As shown in Figure 3C, there was a good linear correlation between the AWR score and the logarithmic D pulse rate (r=0.99, P<0.008 in control; r=0.99, P<0.007 in the 7 days PIC group). The fitted functions of two groups were not significantly different from each other (slope coefficient: 0.39±0.03 in control *vs*. 0.35±0.01 in the 7 days PIC group (P>0.45, *d.f.*=4), intercept: 0.62±0.07 in control *vs*. 0.69±0.06 in the 7 days PIC group (P>0.43, *d.f.*=4)). This implied that scoring the AWR in the present study was a reliable method to quantify the animal' s nociceptive response to rectal distension.

In order to examine whether the visceral hypersensitivity in rats at 7 days PIC was related to changes in rectal compliance, we compared the intraballoon volume-intrarectal pressure relationship of the two groups. The distension volume from 0.3 ml to 1.0 ml and the corresponding value of calculated intrarectal pressure (refer MATERIALS AND METHODS) were plotted for regression analysis (Figure 3D). Intrarectal pressure was linearly increased as the balloon inflated (r>0.99, P<0.0001 in control; r=0.99, P=0.0015 in the 7 days PIC group). The fitted functions of the two groups were not significantly different from each other (slope coefficient: 69. 83±0.99 in control *vs*. 77.46±6.81 in the 7 days PIC group (P>0. 3, *d.f.*=6), intercept: 15.94±0.64 in control *vs*. 10.15±3.67 in the 7 days PIC group (P>0.17, *d.f.*=6)).

Restrain stress-induced defecation

As shown in Figure 4, the number of fecal pellet output for 1 hr was negligible in unrestrained animals regardless of the treatment. However, restraint stress significantly increased defecation. The restrained control rats defecated 2.1±0.9 hard pellets, 1.9±0.4 soft pellets, 1.2±0.4 formless stool and a total

of 5.2±0.5 feces in 1 hr (n=10). Comparatively, animals at 7 days PIC group defected 4±0.9 hard pellets, 3±0.6 soft pellets, 2.7±0.6 formless stool and 9.7±0.8 feces in total during the 1 hr restraint stress (n=10). The number of formless stool and the total number of fecal output during 1 hr restraint stress in the 7 days PIC group were significantly larger than the corresponding values in control rats, which implied that the stress-induced increase in colonic motor function was enhanced in rats at 7 days PIC group.

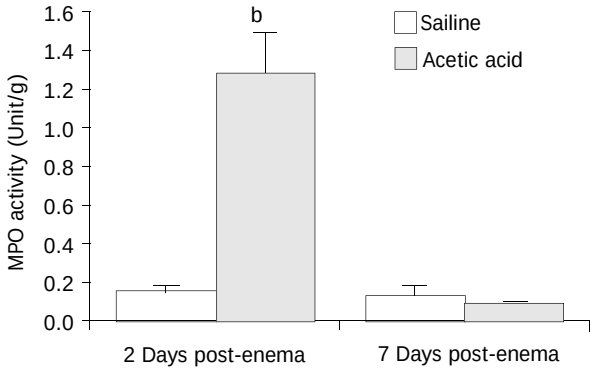

Figure 2 Tissue MPO activity at 2 and 7 days post-induction of colitis (PIC). MPO activity was increased about 8-fold at 2 days PIC. No statistically significant difference was detected between the saline-instilled and the acetic acid-instilled groups at day 7. (^bP<0.01).

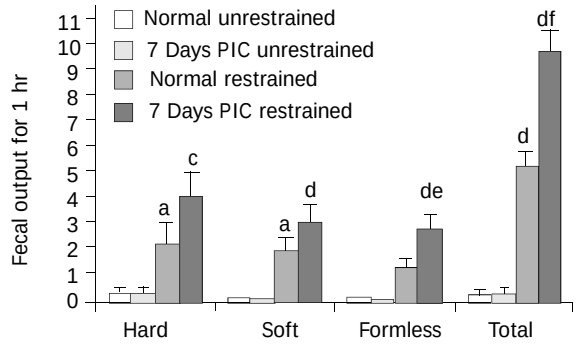

Figure 4 Restraint stress-induced defecation. The number of formless stool and the total number of defecation during 1 h restraint stress in the 7 days PIC group were significantly larger than the corresponding values in control rats. (^aP<0.05 restrained *vs*. unrestrained in control; ^bP<0.01; ^cP<0.05 restrained *vs*. unrestrained in 7 days PIC group; ^dP<0.01; ^eP<0.05 restrained 7 days PIC group *vs*. restrained control group; ^fP<0.01).

DISCUSSION

In human study, patients with ulcerative colitis were reported to show visceral hypersensitivity even when their disease was in quiescent state[12]. In the present study, we found that 7 days after the acetic acid-induced colitis subsided, the rats still showed visceral hypersensitivity, a generally accepted common feature of patients with IBS. Moreover, the rats at 7 days PIC defecated more stools in response to restraint stress than control animals, which was in good accordance with the clinical observations reporting the higher incidence of urgency to defecate and altered stool pattern under stress in IBS patients[13]. These results suggested that along with the previously reported parasite-infected rat models, acetic acid-induced colitis model could be used for the study of a subset of IBS that developed from intestinal inflammation (post-inflammatory IBS).

Indeed, it was well documented that colitis caused motility alteration and visceral hypersensitivity in various models. For instance, trinitronbenzene sulfonic acid (TNBS)/ethanol-induced colitis lowered the threshold for colorectal distension-induced visceromotor reflex at 3 days post-enema[14], and progressively altered colonic muscle function[15]. Similarly, acetic acid-induced colitis increased visceromotor response to colorectal distension at 6 and 24 h post-enema[16], and decreased colonic circular muscle contractility[17]. However, these studies mainly dealt with the alterations in acute or overt inflammatory phase, and few studies focused on the response of the animals with ‘ once’ inflamed colon.

Advantages of our model as a post-inflammatory IBS model include not only a relatively short period required for the subsidence of inflammation but also an easy access to the affected sites, i.e., rectum and colon, which make it possible to measure behavioral and pseudoaffective responses in the awake animals. In the nematode-infected IBS models, the affected site is jejunum to which anesthesia and surgical procedures are required to access for experiments. Another potential advantage is a large body of literatures reporting the pathophysiological mechanisms of alterations occurred during active colitis. Scrutinizing those reports might help to find the pivotal inflammatory changes that induce the IBS symptoms.

The reasons for the exaggerated responses to rectal distension and restraint stress in our model have been unclear, but at least, it seemed not related to changes in rectal compliance since the intraballoon volume-intrarectal pressure relationship was not different between the groups. It was noteworthy that mast cells were found to be increased in a group of IBS patients[3], and partially mediate functional disorder in the *N. brasiliensis*-infected rat model of post-infectious IBS[8]. We are currently investigating whether mast cell also plays a role in the post-colitis IBS features in rat.

In summary, we found that the rat model of acetic acid-induced colitis showed major features of IBS after subsidence of the acute inflammation in colon. The results suggest that this model has several advantages as a useful model of post-inflammatory IBS.

ACKNOWLEDGEMENTS

This work was supported by the Research Institute of Veterinary Science, College of Veterinary Medicine, Seoul National University.

REFERENCES

1 **Camilleri M**, Heading RC, Thompson WG. Clinical perspectives, mechanisms, diagnosis and management of irritable bowel syndrome. *Aliment Pharmacol Ther* 2002; **16**: 1407-1430
2 **Delvaux M**. Role of visceral sensitivity in the pathophysiology of irritable bowel syndrome. *Gut* 2002; **51** (Suppl 1): i67-i71
3 **Barbara G**, De Giorgio R, Stanghellini V, Cremon C, Corinaldesi R. A role for inflammation in irritable bowel syndrome? *Gut* 2002; **51 (Suppl 1)**: i41-i44
4 **Al-Chaer ED**, Kawasaki M, Pasricha PJ. A new model of chronic visceral hypersensitivity in adult rats induced by colon irritation during postnatal development. *Gastroenterology* 2000; **119**: 1276-1285
5 **Bradesi S**, Eutamene H, Garcia-Villar R, Fioramonti J, Bueno L. Acute and chronic stress differently affect visceral sensitivity to rectal distension in female rats. *Neurogastroenterol Motil* 2002; **14**: 75-82
6 **Coutinho SV**, Plotsky PM, Sablad M, Miller JC, Zhou H, Bayati AI, McRoberts JA, Mayer EA. Neonatal maternal separation alters stress-induced responses to viscerosomatic nociceptive stimuli in rat. *Am J Physiol Gastrointest Liver Physiol* 2002; **282**: G307-G316
7 **Tornblom H**, Lindberg G, Nyberg B, Veress B. Full-thickness biopsy of the jejunum reveals inflammation and enteric neuropathy in irritable bowel syndrome. *Gastroenterology* 2002; **123**: 1972-1979

8 **Gay J**, Fioramonti J, Garcia-Villar R, Bueno L. Alterations of intestinal motor responses to various stimuli after Nippostrongylus brasiliensis infection in rats: role of mast cells. *Neurogastroenterol Motil* 2000; **12**: 207-214
9 **Barbara G**, Vallance BA, Collins SM. Persistent intestinal neuromuscular dysfunction after acute nematode infection in mice. *Gastroenterology* 1997; **113**: 1224-1232
10 **Al-Awadi FM**, Khan I. Studies on purine enzymes in experimental colitis. *Mol Cell Biochem* 1999; **194**: 17-22
11 **Conner EM**, Grisham MB. Animal models of colitis. In: Gaginella TS, eds. Experimental models of mucosal inflammation. *New York: CRC press* 1996: 97-109
12 **Rao SS**, Read NW, Davison PA, Bannister JJ, Holdsworth CD. Anorectal sensitivity and responses to rectal distention in patients with ulcerative colitis. *Gastroenterology* 1987; **93**: 1270-1275
13 **Drossman DA**, Sandler RS, McKee DC, Lovitz AJ. Bowel patterns among subjects not seeking health care. Use of a questionnaire to identify a population with bowel dysfunction. *Gastroenterology* 1982; **83**: 529-534
14 **Morteau O**, Hachet T, Caussette M, Bueno L. Experimental colitis alters visceromotor response to colorectal distension in awake rats. *Dig Dis Sci* 1994; **39**: 1239-1248
15 **Hosseini JM**, Goldhill JM, Bossone C, Pineiro-Carrero V, Shea-Donohue T. Progressive alterations in circular smooth muscle contractility in TNBS-induced colitis in rats. *Neurogastroenterol Motil* 1999; **11**: 347-356
16 **Burton MB**, Gebhart GF. Effects of intracolonic acetic acid on responses to colorectal distension in the rat. *Brain Res* 1995; **672**: 77-82
17 **Myers BS**, Martin JS, Dempsey DT, Parkman HP, Thomas RM, Ryan JP. Acute experimental colitis decreases colonic circular smooth muscle contractility in rats. *Am J Physiol* 1997; **273**: G928-G936

Edited by Zhu LH

P.O.Box 2345, Beijing 100023,China
Fax: +86-10-85381893
E-mail: wjg@wjgnet.com www.wjgnet.com

World J Gastroenterol 2003;9(12):2796-2800
World Journal of Gastroenterology
 ISSN 1007-9327

• CLINICAL RESEARCH •

Relationship between clinical and pathologic findings in patients with chronic liver diseases

Lun-Gen Lu, Min-De Zeng, Yi-Min Mao, Ji-Qiang Li, De-Kai Qiu, Jing-Yuan Fang, Ai-Ping Cao, Mo-Bin Wan, Cheng-Zhong Li, Jun Ye, Xiong Cai, Cheng-Wei Chen, Ji-Yao Wang, Shan-Ming Wu, Jin-Shui Zhu, Xia-Qiu Zhou

Lun-Gen Lu, Min-De Zeng, Yi-Min Mao, Ji-Qiang Li, De-Kai Qiu, Jing-Yuan Fang, Ai-Ping Cao, Shanghai Institute of Digestive Disease, Renji Hospital, Shanghai Second Medical University, Shanghai 200001, China
Mo-Bin Wan, Cheng-Zhong Li, Department of Infectious Diseases, Changhai Hospital, Shanghai 200433, China
Jun Ye, Department of Infectious Diseases, Putuo District Central Hospital, Shanghai 200062, China
Xiong Cai, Department of Infectious Diseases, Changzheng Hospital, Shanghai 200003, China
Cheng-Wei Chen, Shanghai Liver Diseases Research Center of Nanjing Military Command, Shanghai 200233, China
Ji-Yao Wang, Department of Gastroenterology, Zhongshan Hospital, Shanghai 200032, China
Shan-Ming Wu, Shanghai Infectious Disease Hospital, Shanghai 200085, China
Jin-Shui Zhu, Department of Gastroenterology, Shanghai No.6 People' s Hospital, Shanghai 200233, China
Xia-Qiu Zhou, Department of Infectious Diseases, Ruijin Hospital, Shanghai 200025, China
Supported by grants from the Key Project of Shanghai Medical Development Foundation, No.99ZDI001
Correspondence to: Dr. Lun-Gen Lu, MD, Shanghai Institute of Digestive Disease, Renji Hospital, Shanghai Second Medical University, Shanghai 200001, China. lulungen@online.sh.cn
Telephone: +86-21-33070824 **Fax:** +86-21-63364118
Received: 2003-03-28 **Accepted:** 2003-05-11

Abstract

AIM: To explore the relationship between clinical findings of patients with chronic liver diseases and the pathologic grading and staging of liver tissues.

METHODS: The inflammatory activity and fibrosis of consecutive liver biopsies from 200 patients were determined according to the diagnosis criteria of chronic hepatitis in China established in 1995. A comparative analysis was carried out for 200 patients with chronic liver diseases by comparing their clinical manifestations, serum biochemical markers with the grading and staging of liver tissues.

RESULTS: It was revealed that age, index of clinical symptoms and physical signs were obviously relevant to the pathologic grading and staging of liver tissues ($P<0.05$). Blood platelet, red blood cells, aspartate aminotransferase (AST), N-terminal procollagen III (PIII NP) were apparently correlated with the degree of inflammation. PGA (prothrombin time, GGT, apoprotein A1) index, PGAA (PGA+△2-macroglobublin) index, albumin and albumin/globulin were relevant to both inflammation and fibrosis. Hyaluronic acid (HA) was an accurate variable for the severity of hepatic inflammation and fibrosis. The combination of serum markers for fibrosis could increase the diagnostic accuracy. It was notable that viral replication markers were not relevant to the degree of inflammation and fibrosis.

CONCLUSION: There is a good correlation between clinical findings and the pathologic grading and staging of liver tissues, which may give aid to the noninvasive diagnosis of liver fibrosis.

Lu LG, Zeng MD, Mao YM, Li JQ, Qiu DK, Fang JY, Cao AP, Wan MB, Li CZ, Ye J, Cai X, Chen CW, Wang JY, Wu SM, Zhu JS, Zhou XQ. Relationship between clinical and pathologic findings in patients with chronic liver diseases. *World J Gastroenterol* 2003; 9(12): 2796-2800
http://www.wjgnet.com/1007-9327/9/2796.asp

INTRODUCTION

Liver fibrosis is a common sequel to diverse liver injuries. It is characterized by an accumulation of interstitial collagens and other matrix components[1-4]. Chronic liver diseases usually develop into liver cirrhosis through the phase of liver fibrosis[5-8]. In recent years, researchers have been making efforts to study the noninvasive diagnostic methods of liver fibrosis[9-15]. Through a multi-center study, we carried out a comparative analysis of 200 patients with chronic liver diseases by comparing their clinical manifestations, serum biochemical markers with histopathological findings in liver biopsy, in order to appraise the relationship between clinical findings of patients with chronic liver diseases and the grading and staging of liver tissues, and to provide clues and basis for the noninvasive diagnosis of liver fibrosis.

MATERIALS AND METHODS

Patients recruitment

The study was organized and carried out by Shanghai Cooperative Group of Hepatic Fibrosis Project. The Cooperative Group was led by Renji Hospital and Changhai Hospital in Shanghai. Cases provided by the Cooperative Group were as follows: 37 from Changhai Hospital, 36 from Renji hospital, 30 from Putuo District Central Hospital, 22 from Shanghai Hepatic Disease Center of Nanjing Military Command, 20 from Changzheng Hospital, 14 from Zhongshan Hospital, 11 from Huashan Hospital, 9 from Shibei Hospital, 8 from Shanghai No. 6 People' s Hospital, 6 from Shanghai Infectious Diseases Hospital, 3 from Ruijin Hospital, 3 from Shanghai No. 9 People' s Hospital, 1 from Shanghai No. 1 People' s Hospital. A total of 200 patients between July and October 1999 were recruited, including 156 male and 44 female patients. The average age of the patients was 34 years (range 15-60 years).

Histological examination

Within 1 week after admission, all the patients received liver puncture biopsy under the guidance of B ultrasound with the 14G quick-cut needle (8-light Company, Japan) or Menghini needle. The length of liver specimens was just 1 cm or longer. The samples were fixed with 10 % formaldehyde, embedded in paraffin and sliced, stained with hematoxylin-eosin, reticular fibers and collagenous fibers. According to the prevention and

treatment program for virus hepatitis set up in 1995[16], all the patients were graded and staged for liver fibrosis and inflammatory activity. Three pathologists read the slides, respectively. The results were statistically analyzed with Kappa test. It was revealed that the consistency of the grading and staging by the pathologists was excellent. All the pathologic diagnoses of liver biopsy were performed by Department of Pathology, Medical College of Fudan University.

Clinical data

General data The general data included age (-25, 25-35, 35-), course of disease (from the time when hepatic symptoms or abnormal laboratory parameters appeared for the first time to the present study) and gender.

Degree of hepatitis The degree of hepatitis was clinically evaluated according to the criteria recommended at the meeting of prevention and treatment of viral hepatitis held in 1995.

Clinical symptoms According to the severity of clinical symptoms such as fatigue, inappetence, swelling, nausea, ache in hepatic region and gingival bleeding, it was scored as 0: no symptom, 1:with one kind of mild symptoms, 2: with one kind of symptoms between mild and severe, 3: with one kind of serious symptoms. It was further divided into 3 grades according to the totaled score: mild: 0-1, moderate: 2-3, severe: $\geqslant$4.

Physical signs According to the degree of hepatomegaly and splenomegaly, it was scored as 0: no hyperplasia (maximal oblique diameter of the right liver <14 cm, thickness of the spleen <4.0 cm); 1: with hepatomegaly (maximal oblique diameter of the right liver >14 cm); 1.5: with mild splenomegaly (thickness of the spleen was between 4-6 cm); 3: with splenomegaly above moderate degree (thickness of the spleen $\geqslant$6.0 cm). It was further divided into 4 grades according to the totaled score: 0: no hyperplasia, 1:hepatomegaly, 1.5: mild splenomegaly, and $\geqslant$2.5: splenomegaly above moderate degree or both splenomegaly and hepatomegaly.

Laboratory parameters

Routine blood test Red blood cells (RBC), white blood cells (WBC) and platelets (PLT) were counted.

Biochemical blood test Total serum bilirubin, AST, ALT, AST/ALT, GGT, albumin (A), albumin (A)/globulin (G), γ-globulin, prothrombin time (PT), apoprotein A1(ApoA1), α2-macroglobulin and α-fetoprotein(AFP) were detected. Among them, PT, GGT and Apo-A1 were integrated as PGA index. PGA and α2-macroglobulin were integrated as PGAA index.

Serum viral markers HBsAg, HBeAg, anti-HBe, anti-HBc, HBV-DNA, anti-HCV and HCV-RNA were detected.

Serum fibrosis parameters Hyaluronic acid (HA), lamilin (LN), N-terminal procollagen III(PIII NP), 7S collagen IV(7S-IV) were included.

Statistical analysis

Analysis of variance was carried out for all the data with SAS software. $P<0.05$ was considered statistically significant.

RESULTS

Relationship between general data and pathological grading and staging of liver tissues

It was revealed that there was a significant difference in inflammatory activity and fibrosis among different age groups (-25, 25-35, 35-) ($P<0.05$). With the increase of age, the degree of fibrosis became more severe. However, there was no significant difference in inflammatory activity and fibrosis between different courses of disease (-1 year, 1-5 years, 5-years) and sexes ($P>0.05$).

Relationship between clinical manifestations and pathological staging of liver fibrosis

The statistical results indicated that there was a significant difference between the severity of hepatitis and inflammatory grading, and fibrosis staging of liver tissues ($P<0.01$) (Table 1).

The symptom accumulation score at different stages of liver fibrosis was significantly different ($P<0.05$). With the increase of score, liver fibrosis tended to be more serious. However, there was no difference between symptom score and inflammatory grading. Statistical analysis of single symptom indicated that only nausea and gingival bleeding had a significant differnce at different stages of liver fibrosis ($P<0.05$ and $P<0.01$, respectively).

Among different groups of inflammatory grading and fibrosis staging, the score of physical signs differed significantly ($P<0.05$), with the increase of score, inflammatory and fibrosis became more serious.

When symptom score and physical signs were combined for a further analysis, all the subjects were divided into 6 groups (Table 1). There were correlations between the inflammatory activity and fibrosis staging, and the differences among different groups were significant ($P<0.01$).

Relationship between biochemical parameters and inflammatory grading and fibrosis staging

The relationship between each single parameter and inflammatory grading and fibrosis staging is shown in Table 2.

From Table 2 we could find that the main biochemical parameters related only to inflammatory grading were RBC, PLT, AST, and PIIINP. With inflammation becoming serious, RBC and PLT tended to decrease, while the level of AST and PIIINP tended to increase. GGT, A, A/G, HA, 7S-IV and AFP were correlated with both inflammation grading and fibrosis staging, with the inflammation and fibrosis becoming more serious. A and A/G tended to decrease, while GGT and AFP tended to increase. There was no significant difference in PT at different stages and grades.

Table 1 Relationship between clinical manifestations and pathological grading and staging of liver tissues

Groups	Symptom score+physical signs	*n*	Inflammatory grading (G) (%)				Fibrosis staging (s) (%)				
			1	2	3	4	0	1	2	3	4
1	0~1+ no hepatomegaly and splenomegaly	15	46.7	40	13.3	0	33.3	26.7	40	0	0
2	0~1+ hepatomegaly and splenomegaly	14	28.6	28.6	28.6	14.3	7.1	35.7	28.6	14.3	14.3
3	~3+no hepatomegaly and splenomegaly	28	42.9	53.6	3.5	0	14.3	50	35.7	0	0
4	2~3 +hepatomegaly and splenomegaly	42	30.9	26.2	28.5	16.7	9.5	23.8	40.5	16.7	9.5
5	$\geqslant$4+ no hepatomegaly and splenomegaly	32	43.7	25	15.6	15.6	12.5	34.3	25	15.6	12.5
6	$\geqslant$4+ hepatomegaly and splenomegaly	69	23.3	21.7	34.8	15.9	2.9	29	29	15.9	23.2
				$P<0.01$					$P<0.01$		

Table 2 Relationship between biochemical parameters and inflammatory grading and fibrosis staging

Parameters	Inflammatory (G) (%)						Fibrosis staging (s) (%)									
	1~2	1~3	1~4	2~3	2~4	3~4	0~1	0~2	0~3	0~4	1~2	1~3	1~4	2~3	2~4	3~4
RBC			b		b	b				a			a		a	a
PLT			b		b	b										
AST		b	b	a	b											
ALT																
AST/ALT																
GGTa	a	b	b	b			b	b	b	b	b	b				
A				b		b				b			b		b	b
A/G				b		b				b			b		b	b
HA	b	b	b	b	b	b			b	b	b	b	b		b	b
LN																
7S-IV		a	b	a	b					a			a		a	
PIIINP			b		b											
AFP	b	b	b	b	b	b		b	b		b	b			b	
PT																

$^{a}P<0.05$, $^{b}P<0.01$.

Table 3 Serologic parameters for diagnosing liver fibrosis and cirrhosis

Parameters	Fibrosis (S0/S1~4)			Cirrhosis (S1~3/S4)		
	Specificity(%)	Sensitivity(%)	Accuracy(%)	Specificity(%)	Sensitivity(%)	Accuracy(%)
HA	94.44	38.26	43.50	90.0	60.0	85.71
PIIINP	16.67	77.71	72.0	78.0	24.0	70.28
LN	55.26	50.29	50.10	54.0	52.0	53.71
7S-IV	50.22	24.67	51.0	93.29	24.0	89.08

Table 4 Serologic parameters for diagnosing liver fibrosis and cirrhosis

Parameters	Fibrosis (S0/S1~4)			Cirrhosis (S1~3/S4)		
	Specificity(%)	Sensitivity(%)	Accuracy(%)	Specificity(%)	Sensitivity(%)	Accuracy(%)
HA+7S-IV	88.89	37.93	42.50	89.93	60.0	85.63
HA+PIIINP	88.89	42.86	47.10	90.0	60.0	85.71
HA+7S-IV+ PIIINP+LN	88.89	47.13	51.04	89.93	64.0	86.21
HA+TIMP	92.86	38.28	43.67	90.27	60.0	86.72
PGA+HA	60.0	60.44	60.40	89.41	66.67	87.91
PGAA+HA	70.0	62.64	63.67	89.41	66.67	87.91
PGA+7S-IV	61.12	50.22	50.31	90.59	33.33	86.80
PGAA+7S-IV	60.0	48.22	50.67	92.94	33.33	89.0

Relationship between PGA, PGAA index and pathological staging and grading

PGA score had a relationship with inflammation and fibrosis ($P<0.01$, $P<0.05$ respectively). Its sensitivity and accuracy for the diagnosis of liver fibrosis were 70.33 % and 67.33 %, respectively, both of which were higher than those for early liver cirrhosis (50.00 % and 57.14 %, respectively). PGAA also correlated with inflammation and fibrosis ($P<0.05$), the sensitivity and accuracy for the diagnosis of liver fibrosis were 63.74 % and 63.37 %, respectively, both of which were higher than those for early liver cirrhosis (33.33 % and 61.64 %, respectively).

Relationship between serum parameters of liver fibrosis and pathological grading and staging

With discriminatory analysis method, we evaluated the significance of assaying single or combined serum parameters of liver fibrosis, in the diagnosis of liver fibrosis and cirrhosis (Tables 3 and 4).

Relationship between viral markers and pathological staging and grading

The statistical results revealed that there was no relationship between viral replication parameters and degrees of inflammation and fibrosis.

DISCUSSION

This study suggested that age was correlated with inflammatory activity, but the course of disease did not. Maybe it is because most of the patients were unaware of the disease, but the course of disease was always calculated from the time when symptoms appeared or people saw a doctor. It could not reflect the course accurately. So it was difficult to discover the relationship between fibrosis severity and the course of the disease[9,13,15].

With the integral method, we scored the severity of symptoms quantitatively, classified the total score, which could reflect the symptom severity comprehensively. The results indicated that there was no correlation between symptom score

and inflammatory activity (P>0.05), but the score correlated with fibrosis stage significantly (P=0.0106). With the symptoms becoming more prominent, fibrosis became more serious. At the same time, it was found that the score of physical signs had a strong relationship with inflammatory activity and fibrosis severity (P<0.05). The higher the physical sign score was, the more serious the inflammatory activity and fibrosis were. When the difference became more significant, the symptoms and signs were combined (P<0.01).

This study indicated that at different fibrosis stage and inflammatory grade of liver tissues, the serum level of HA differed remarkably (P<0.01), which could serve as a sensitive and accurate parameter to identify the severity of hepatic inflammation and fibrosis[17-20]. In addition, HA was a specific and accurate parameter for the diagnosis of early liver cirrhosis, the specificity and accuracy were 90 % and 85 %, respectively. It was also found that PIIINP differed at the different inflammatory grades significantly (P<0.01), but not significantly at different fibrosis stages (P<0.05), indicating that its correlation with inflammatory severity was closer than that with fibrosis. Thus it might be of significance in determining the inflammatory severity.

One conclusion that differs from others is that this study did not agree with the significance of LN in the diagnosis of liver fibrosis. It has been claimed that the diagnostic efficiency would increase when HA was assayed in combination with other parameters, yet it needs to be proved[21-28].

Based on the relationship between a single biochemical parameter and inflammation and fibrosis, we found that PLT, RBC and AST were important in identifying inflammatory severity rather than fibrosis. They differed significantly at grades 1, 2, 3 and 4, so they could help estimate the severity of inflammation. With the inflammation becoming serious, RBC and PLT tended to decrease. Both A and A/G ratio correlated with inflammation and fibrosis, and could be used to identify the severity. Additionally, our study proved that the level of AFP differed significantly at different inflammatory grades and fibrosis stages (P<0.01), indicating that it correlated with inflammation and fibrosis closely, and could be used as an adjuvant parameter[29-32].

PGA (PT, GGT, and ApoA1) and PGAA(PGA+α2-macroglobulin) index were mainly used as liver function indicators put forward in the early 1990' s by some experts to reflect the liver function of patients with alcoholic liver disease, and to screen or diagnose liver cirrhosis[9,33-38].

In recent years, researchers in China have probed into applying PGA index or combining it with other serum parameters to the diagnosis of liver cirrhosis. To some extent, the results of our study are in accordance with the conclusion that both PGAA and PGA correlated with inflammation and fibrosis significantly. However, when the foreign criteria were used, the score of ApoA1 in most normal samples were 4, which were too high, resulting in the increase of total PGA and PGAA scores. Therefore, we considered it abnormal when PGA score was above 6. This difference might be due to the following reasons. First, there was an ethnic difference in the normal range of ApoA1, so it is necessary to set up PGA and PGAA criteria applicable in China. Second, the two parameters were mainly used in alcoholic liver diseases, but most of the patients in our study were viral hepatitis[13-15,17,35,36,39,40].

Our study indicates that, viral replication parameters such as HBeAg and HBV DNA have no correlation with the severity of inflammation and fibrosis. We compared the inflammatory and fibrotic severity in patients with positive markers of hepatitis B only (141 cases) and in those with positive markers of both hepatitis B and C (10 cases), but no statistical difference was found between them. However, as the patients suffering from co-infection of hepatitis B and C were very few in the study, the conclusion needs to be verified by larger sample studies.

REFERENCES

1 **Albanis E**, Friedman SL. Hepatic fibrosis. Pathogenesis and principles of therapy. *Clin Liver Dis* 2001; **5**: 315-334
2 **Brenner DA**, Waterboer T, Choi SK, Lindquist JN, Stefanovic B, Burchardt E, Yamauchi M, Gillan A, Rippe RA. New aspects of hepatic fibrosis. *J Hepatol* 2000; **32**(1Suppl): 32-38
3 **Albanis E**, Safadi R, Friedman SL. Treatment of hepatic fibrosis: almost there. *Curr Gastroenterol Rep* 2003; **5**: 48-56
4 **Rockey DC**. The cell and molecular biology of hepatic fibrogenesis. Clinical and therapeutic implications. *Clin Liver Dis* 2000; **4**: 319-355
5 **Li D**, Friedman SL. Liver fibrogenesis and the role of hepatic stellate cells: new insights and prospects for therapy. *J Gastroenterol Hepatol* 1999; **14**: 618-633
6 **Friedman SL**. Molecular mechanisms of hepatic fibrosis and principles of therapy. *J Gastroenterol* 1997; **32**: 424-430
7 **Musca A**, Paoletti V, De Matteis A, Mammarella A, Labbadia G, Grassi M, Paradiso M. Liver fibrosis: what's the beginning of autonomic deficit? *Scand J Gastroenterol* 2002; **37**: 1235-1236
8 **Dai WJ**, Jiang HC. Advances in gene therapy of liver cirrhosis: a review. *World J Gastroenterol* 2001; **7**: 1-8
9 **Oberti F**, Valsesia E, Pilette C, Rousselet MC, Bedossa P, Aube C, Gallois Y, Rifflet H, Maiga MY, Penneau-Fontbonne D, Cales P. Noninvasive diagnosis of hepatic fibrosis or cirrhosis. *Gastroenterology* 1997; **113**: 1609-1616
10 **Tsutsumi M**, Takase S, Urashima S, Ueshima Y, Kawahara H, Takada A. Serum markers for hepatic fibrosis in alcoholic liver disease: which is the best marker, type III procollagen, type IV collagen, laminin, tissue inhibitor of metalloproteinase, or prolyl hydroxylase? *Alcohol Clin Exp Res* 1996; **20**: 1512-1517
11 **Aube C**, Oberti F, Korali N, Namour MA, Loisel D, Tanguy JY, Valsesia E, Pilette C, Rousselet MC, Bedossa P, Rifflet H, Maiga MY, Penneau-Fontbonne D, Caron C, Cales P. Ultrasonographic diagnosis of hepatic fibrosis or cirrhosis. *J Hepatol* 1999; **30**: 472-478
12 **Zaitoun AM**, Al Mardini H, Awad S, Ukabam S, Makadisi S, Record CO. Quantitative assessment of fibrosis and steatosis in liver biopsies from patients with chronic hepatitis C. *J Clin Pathol* 2001; **54**: 461-465
13 **Fontana RJ**, Lok AS. Noninvasive monitoring of patients with chronic hepatitis C. *Hepatology* 2002; **36**(5 Suppl 1): S57-S64
14 **Thabut D**, Simon M, Myers RP, Messous D, Thibault V, Imbert-Bismut F, Poynard T. Noninvasive prediction of fibrosis in patients with chronic hepatitis C. *Hepatology* 2003; **37**: 1220-1221
15 **Tran A**, Hastier P, Barjoan EM, Demuth N, Pradier C, Saint-Paul MC, Guzman-Granier E, Chevallier P, Tran C, Longo F, Schneider S, Piche T, Hebuterne X, Benzaken S, Rampal P. Non invasive prediction of severe fibrosis in patients with alcoholic liver disease. *Gastroenterol Clin Biol* 2000; **24**: 626-630
16 Prevention and treatment projects of virus hepatitis (tryout). *Zhonghua Neike Zazhi* 1995; **34**: 788-791
17 **Stickel F**, Urbaschek R, Schuppan D, Poeschl G, Oesterling C, Conradt C, McCuskey RS, Simanowski UA, Seitz HK. Serum collagen type VI and XIV and hyaluronic acid as early indicators for altered connective tissue turnover in alcoholic liver disease. *Dig Dis Sci* 2001; **46**: 2025-2032
18 **Guechot J**, Laudat A, Loria A, Serfaty L, Poupon R, Giboudeau J. Diagnostic accuracy of hyaluronan and type III procollagen amino-terminal peptide serum assays as markers of liver fibrosis in chronic viral hepatitis C evaluated by ROC curve analysis. *Clin Chem* 1996; **42**: 558-563
19 **Murawaki Y**, Ikuta Y, Okamoto K, Koda M, Kawasaki H. Diagnostic value of serum markers of connective tissue turnover for predicting histological staging and grading in patients with chronic hepatitis C. *J Gastroenterol* 2001; **36**: 399-406
20 **Pares A**, Deulofeu R, Gimenez A, Caballeria L, Bruguera M, Caballeria J, Ballesta AM, Rodes J. Serum hyaluronate reflects hepatic fibrogenesis in alcoholic liver disease and is useful as a marker of fibrosis. *Hepatology* 1996; **24**: 1399-1403
21 **Zheng M**, Cai WM, Weng HL, Liu RH. ROC curves in evaluation of serum fibrosis indices for hepatic fibrosis. *World J Gastroenterol* 2002; **8**: 1073-1076
22 **Zheng M**, Cai W, Weng H, Liu R. Determination of serum fibrosis indexes in patients with chronic hepatitis and its significance. *Chin Med J* 2003; **116**: 346-349

23 **Shahin M**, Schuppan D, Waldherr R, Risteli J, Risteli L, Savolainen ER, Oesterling C, Abdel Rahman HM, el Sahly AM, Abdel Razek SM. Serum procollagen peptides and collagen type VI for the assessment of activity and degree of hepatic fibrosis in schistosomiasis and alcoholic liver disease. *Hepatologl* 1992; **15**: 637-644

24 **Ramadori G**, Zohrens G, Manns M, Rieder H, Dienes HP, Hess G, Meyer KH, Buschenfelde Z. Serum hyaluronate and type III procollagen aminoterminal propeptide concentration in chronic liver disease. Relationship to cirrhosis and disease activity. *Eur J Clin Invest* 1991; **21**: 323-330

25 **Hirayama C**, Suzuki H, Takada A, Fujisawa K, Tanikawa K, Igarashi S. Serum type IV collagen in various liver diseases in comparison with serum 7S collagen, laminin, and type III procollagen peptide. *J Gastroenterol* 1996; **31**: 242-248

26 **Fabris C**, Falleti E, Federico E, Toniutto P, Pirisi M. A comparison of four serum markers of fibrosis in the diagnosis of cirrhosis. *Ann Clin Biochem* 1997; **34**(Pt 2): 151-155

27 **Walsh KM**, Fletcher A, MacSween RN, Morris AJ. Comparison of assays for N-amino terminal propeptide of type III procollagen in chronic hepatitis C by using receiver operating characteristic analysis. *Eur J Gastroenterol Hepatol* 1999; **11**: 827-831

28 **Castera L**, Hartmann DJ, Chapel F, Guettier C, Mall F, Lons T, Richardet JP, Grimbert S, Morassi O, Beaugrand M, Trinchet JC. Serum laminin and type IV collagen are accurate markers of histologically severe alcoholic hepatitis in patients with cirrhosis. *J Hepatol* 2000; **32**: 412-418

29 **Lin DY**, Chu CM, Sheen IS, Liaw YF. Serum carboxy terminal propeptide of type I procollagen to amino terminal propeptide of type III procollagen ratio is a better indicator than each single propeptide and 7S domain type IV collagen for progressive fibrogenesis in chronic viral liver diseases. *Dig Dis Sci* 1995; **40**: 21-27

30 **Myers RP**, De Torres M, Imbert-Bismut F, Ratziu V, Charlotte F, Poynard T. Biochemical markers of fibrosis in patients with chronic hepatitis C: a comparison with prothrombin time, platelet count, and age-platelet index. *Dig Dis Sci* 2003; **48**: 146-153

31 **Imbert-Bismut F**, Ratziu V, Pieroni L, Charlotte F, Benhamou Y, Poynard T. Biochemical markers of liver fibrosis in patients with hepatitis C virus infection: a prospective study. *Lancet* 2001; **357**: 1069-1075

32 **Naveau S**, Montembault S, Balian A, Giraud V, Aubert A, Abella A, Capron F, Chaput JC. Biological diagnosis of the type of liver disease in alcoholic patients with abnormal liver function tests. *Gastroenterol Clin Biol* 1999; **23**: 1215-1224

33 **Myers RP**, Ratziu V, Imbert-Bismut F, Charlotte F, Poynard T. Biochemical markers of liver fibrosis: a comparison with historical features in patients with chronic hepatitis C. *Am J Gastroenterol* 2002; **97**: 2419-2425

34 **Pilette C**, Rousselet MC, Bedossa P, Chappard D, Oberti F, Rifflet H, Maiga MY, Gallois Y, Cales P. Histopathological evaluation of liver fibrosis: quantitative image analysis vs semi-quantitative scores. Comparison with serum markers. *J Hepatol* 1998; **28**: 439-446

35 **Naveau S**, Poynard T, Benattar C, Bedossa P, Chaput JC. Alpha-2-macroglobulin and hepatic fibrosis. Diagnostic interest. *Dig Dis Sci* 1994; **39**: 2426-2432

36 **Jiang JJ**, Salvucci M, Thepot V, Pol S, Ekindjian OG, Nalpas B. PGA score in diagnosis of alcoholic fibrosis. *Lancet* 1994; **343**: 803

37 **Teare JP**, Sherman D, Greenfield SM, Simpson J, Bray G, Catterall AP, Murray-Lyon IM, Peters TJ, Williams R, Thompson RP. Comparison of serum procollagen III peptide concentrations and PGA index for assessment of hepatic fibrosis. *Lancet* 1993; **342**: 895-898

38 **Croquet V**, Vuillemin E, Ternisien C, Pilette C, Oberti F, Gallois Y, Trossaert M, Rousselet MC, Chappard D, Cales P. Prothrombin index is an indirect marker of severe liver fibrosis. *Eur J Gastroenterol Hepatol* 2002; **14**: 1133-1141

39 **Cadranel JF**, Mathurin P. Prothrombin index decrease: a useful and reliable marker of extensive fibrosis? *Eur J Gastroenterol Hepatol* 2002; **14**: 1057-1059

40 **Lu LG**, Zeng MD, Wan MB, Li CZ, Mao YM, Li JQ, Qiu DK, Cao AP, Ye J, Cai X, Chen CW, Wang JY, Wu SM, Zhu JS, Zhou XQ. Grading and staging of hepatic fibrosis, and its relationship with noninvasive diagnostic parameters. *World J Gastroenterol* 2003; **9**: 2574-2578

Edited by Zhu LH and Wang XL

P.O.Box 2345, Beijing 100023,China
Fax: +86-10-85381893
E-mail: wjg@wjgnet.com www.wjgnet.com

World J Gastroenterol 2003;9(12):2801-2804
World Journal of Gastroenterology
 ISSN 1007-9327

• CLINICAL RESEARCH •

Impact of endoscopically minimal involvement on IL-8 mRNA expression in esophageal mucosa of patients with non-erosive reflux disease

Yusei Kanazawa, Hajime Isomoto, Chun Yang Wen, Ai-Ping Wang, Vladimir A Saenko, Akira Ohtsuru, Fuminao Takeshima, Katsuhisa Omagari, Yohei Mizuta, Ikuo Murata, Shunichi Yamashita, Shigeru Kohno

Yusei Kanazawa, Hajime Isomoto, Ai-Ping Wang, Fuminao Takeshima, Katsuhisa Omagari, Yohei Mizuta, Shigeru Kohno, Second Department of Internal Medicine, Atomic Bomb Disease Institute, Nagasaki University School of Medicine, Nagasaki, Japan
Chun Yang Wen, Department of Molecular Pathology, Atomic Bomb Disease Institute, Nagasaki University School of Medicine, Nagasaki, Japan
Vladimir A Saenko, Akira Ohtsuru, Shunichi Yamashita, Department of Molecular Medicine, Atomic Bomb Disease Institute, Nagasaki University School of Medicine, Nagasaki, Japan
Ikuo Murata, Department of Pharmacotherapeutics, Nagasaki University Graduate School of Biomedical Sciences, Nagasaki, Japan
Correspondence to: Hajime Isomoto, M.D., Second Department of Internal Medicine, Nagasaki University School of Medicine, 1-7-1 Sakamoto, Nagasaki 852-8501, Japan. hajimei2002@yahoo.co.jp
Telephone: +81-95-849-7567 **Fax:** +81-95-849-7568
Received: 2003-08-05 **Accepted:** 2003-10-12

Abstract

AIM: Little has been known about the pathogenesis of non-erosive reflux disease (NERD). Recent studies have implicated interleukin 8 (IL-8) in the development and progression of gastroesophgeal reflux disease (GERD). The purpose of this study was to determine IL-8 RNA expression levels in NERD patients with or without subtle mucosal changes.

METHODS: We studied 26 patients with NERD and 13 asymptomatic controls. Biopsy sample was taken from the esophagus 3 cm above the gastroesophageal junction and snap frozen for measurement of IL-8 mRNA levels by real-time quantitative polymerase chain reaction (PCR). We also examined mRNA expression of IL-8 receptors, CXCR-1 and -2 by reverse transcriptase PCR. The patients were endoscopically classified into grade M (mucosal color changes without visible mucosal break) and N (neither minimal involvement nor mucosal break) of the modified Los Angeles classification.

RESULTS: The relative IL-8 mRNA expression levels were significantly higher in esophageal mucosa of NERD patients than those of the controls. There was a significant difference in IL-8 mRNA levels between grade M and N. The CXCR-1 and -2 mRNAs were constitutively expressed in esophageal mucosa.

CONCLUSION: Our results suggest that high IL-8 levels in esophageal mucosa may be involved in the pathogenesis of NERD through interaction with its receptors. NERD seems to be composed of a heterogeneous population in terms of not only endoscopically minimal involvement but also immune and inflammatory processes.

Kanazawa Y, Isomoto H, Wen CY, Wang AP, Saenko VA, Ohtsuru A, Takeshima F, Omagari K, Mizuta Y, Murata I, Yamashita S, Kohno S. Impact of endoscopically minimal involvement on IL-8 mRNA expression in esophageal mucosa of patients with non-erosive reflux disease. *World J Gastroenterol* 2003; 9(12): 2801-2804
http://www.wjgnet.com/1007-9327/9/2801.asp

INTRODUCTION

Gastroesophageal reflux disease (GERD) is one of the most common chronic disorders in modern humans. In the United States, 44 % of the adult populations reported experiencing heartburn at least once a month, 14 % on a weekly basis, and 7 % daily[1]. Esophageal erosions are the characteristic lesions of GERD seen on endoscopy[2]. A small number of GERD patients develop stricture, Barrett's esophagus and adenocarcinoma of the esophagus. In fact, the majority of GERD patients have endoscopically normal-appearing esophageal mucosa; this group is termed non-erosive reflux disease (NERD) or endoscopy-negative reflux disease[2,3].

The Los Angeles (LA) classification is widely used for endoscopic assessment of GERD[4]. The slightest degree of esophagitis, i.e., grade A, is defined as one or more mucosal breaks confined to the mucosal folds, each no longer than 5 mm. Accordingly, this classification scheme ignores subtle mucosal damage in the absence of mucosal breaks. In this regard, Hoshihara *et al*.[5,6] have proposed a modified LA system, in which grade O was subdivided into M and N, based on the concept of mucosal color changes. Thus, NERD patients can be classified into two subgroups (grade M and N) based on minimal esophageal involvement during endoscopy.

Recently, several studies have shown that mucosal immune and inflammatory responses, characterized by specific cytokine and chemokine profiles, may determine the diversity of esophageal phenotypes of GERD[7-9]. Of note, Fitzgerald *et al*.[7] reported significantly higher expression levels of interleukin 8 (IL-8) messenger ribonucleic acid (mRNA) in patients with reflux esophagitis (RE), assessed by competitive reverse transcriptase polymerase chain reaction (RT-PCR), compared with subjects with non-inflamed or Barrett's esophagus. Studies from our laboratories have also demonstrated high IL-8 protein levels in esophageal biopsy samples of patients with erosive esophagitis by enzyme linked immunosorbent assay (ELISA)[8]. Furthermore, we also showed significantly high mucosal IL-8 production, which paralleled the endoscopic severity of RE[8]. However, little has been known about the role of IL-8 in NERD.

The aim of the present study was to assess esophageal expression levels of IL-8 mRNA in NERD patients by quantitative real-time PCR procedure, with special reference to the difference between grade M and N subgroups of the modified LA scheme.

MATERIALS AND METHODS

Subjects and samples

We studied 26 patients with NERD and endoscopically confirmed normal-appearing esophageal mucosa who visited

the Outpatient Department between August 2002 and July 2003. They included 19 men and 7 women, aged between 28 and 80 years (mean, 62.0 years). The diagnosis of GERD was made with more than 6 points in the questionnaire for the diagnosis of reflux disease (QUEST) described by Carlsson *et al*[10]. None of these patients had been treated with non-steroidal anti-inflammatory drugs, proton pump inhibitors, histamine H_2-receptor antagonists, anti-cholinergic agents or antibiotics within 4 weeks prior to the present study. Furthermore, patients with severe concomitant diseases, prior esophageal or gastric surgery, peptic ulcer diseases and comorbid conditions that might interfere with esophageal or gastric motility including diabetes mellitus, systemic sclerosis and neurological disorders were excluded. As a control group, we recruited 13 asymptomatic subjects with no hiatal hernia or any lesions in the esophagus, stomach and duodenum at endoscopy for a health check-up.

In each case, a biopsy specimen was obtained from the esophageal mucosa, 3 cm above the gastroesophageal junction[8], snap-frozen in an ethanol-dry ice mixture for quantitative analysis of IL-8 mRNA expression and stored at -80 ℃ until use.

Endoscopic assessment of NERD

NERD was endoscopically classified into grade M and N in accordance with the modified Los Angeles (LA) classification system proposed by Hoshihara *et al*[5,6]. The criteria were: grade M represents minimal changes (irregular redness or whiteness) without any mucosal breaks and grade N represents esophageal mucosa with neither the minimal changes nor mucosal injury. In addition, we also evaluated the presence of hiatal hernia by endoscopy[11].

Real-time quantitative PCR

Total RNA from the biopsy samples was extracted using a commercial kit according to the instructions provided by the supplier (Isogen, Nippon Gene Co., Toyama, Japan). One μg of total RNA was reversely transcribed into complementary DNA (cDNA) in a volume of 25 μl with MuLV reverse transcriptase and random hexamers (both from PE Applied Biosystems, Warrington, UK).

Real-time PCR measurement of IL-8 cDNA was performed in the ABI PRISM 7700 sequence detector (PE Applied Biosystems) with TaqMan assay. The primers and probe sequences for IL-8 were synthesized (PE Applied Biosystems) as described previously[12]: IL-8 forward primer, 5' -CTCTTGGCAGCCTTCCTGATT-3' , reverse primer, 5' -TATGCACTGACATCTAAGTTCTTTAGCA-3' and probe, 5' -CTTGGCAAAACTGCACCTTCACACAGA-3' , labeled with the reporter dye 6-carboxyfluorescein at the 5' end and quencher dye 6-carboxytetramethylrhodamine at the 3' end. PCR was performed in a total volume of 50 μl of each amplification mixture containing 1 μl of each RT product, 25 μl of 2×Universal Master Mix (PE Applied Biosystems), 200 nM IL-8 forward and reverse primers, 100 nM fluorogenic probe. Thermal cycling was initiated with at 50 ℃ for 2 min, followed by a first denaturation step at 95 ℃ for 10 min, and followed by 50 cycles of at 95 ℃ for 15 s and at 60 ℃ for 1 min.

The *tubulin alpha 3* gene cDNA (internal control) was quantified in the same machinery using SYBR Green PCR Core reagents kit (PE Applied Biosystems). The primers used were: forward, 5' -AGATCATTGACCTCGTGTTGGA-3' and reverse, 5' -ACCAGTTCCCCCACCAAAG-3' , which correspond to nucleotides 437-458 and 537-519, respectively (*TUBA3*, GenBank accession number 17986282). PCR was performed in a total volume of 25 μl of each amplification mixture containing 1 μl of each RT product, 3 μl of 25 mM $MgCl_2$, 2.5 μl of 10×SYBR Green buffer, 2 μl of dNTP Mix (5 mM adenosine, deoxycytosine and deoxyguanosine triphosphate and 2.5 mM deoxyuridine triphosphate), 0.625 U AmpliTaq Gold polymerase, 0.125 U AmpErase and 100 nM tubulin alpha 3 forward and reverse primers. Thermal cycling was initiated at 50 ℃ for 2 min, followed by a first denaturation step at 95 ℃ for 10 min, and continued with 40 cycles of at 95 ℃ for 15 s and at 59 ℃ for 1 min.

Each assay included a standard curve, a no-template control and cDNA samples in triplicate. The standard curve was generated by serial 5-fold dilutions of pooled cDNA obtained from gastric tissues that were found to contain high levels of mRNAs of both genes. Contents of the tubulin alpha 3 and IL-8 cDNAs were expressed in arbitrary units calculated according to the standard curve. The relative expression level of IL-8 was expressed as the ratio of IL-8/tubulin alpha 3 in arbitrary units[13].

RT-PCR

Based on the technique described previously[14] with slight modification, the target sequence of CXCR-1 mRNA was amplified through 35 cycles, each consisting of denaturation at 94 ℃ for 30 sec, annealing at 53 ℃ for 30 sec and extension at 72 ℃ for 30 min, followed by a final extension at 72 ℃ for 5 min with specific primers (forward, 5' -CAGATCCACAGA-TGTGGGAT-3' and reverse, 5' -TCCAGCCATTCACCTTG-GAG-3') using an RT-PCR kit (Takara Shuzo Co., Otsu, Japan). Similarly, CXCR-2 mRNA expression was detected under the following conditions: amplification through 35 cycles, each consisting of denaturation at 94 ℃ for30 sec, annealing at 60 ℃ for 30 sec and extension at 72 ℃ for 30 min, followed by a final extension at 72 ℃ for 5 min with specific primers (forward, 5' -AGCTGCTCTTCTGGAGGTGT-3' and reverse, 5' -TTAGAGAGTAGTGGAAGTGTGC-3')[14]. A 10-μl aliquot of each PCR product was analyzed by electrophoresis on 2 % agarose gel containing ethidium bromide, and the bands were examined under ultraviolet light for the presence of amplified DNA. Glyceraldehyde-3-phosphate dehydrogenase (G3PDH) gene transcript was also amplified as described previously[15], and used as an internal control of the processed RNA for each preparation.

Detection of Helicobacter pylori infection

H pylori status was assessed by serology (anti-*H pylori* Immunoglobulin G antibody, HEL-p TEST, Amrad Co., Melbourne, Australia), rapid urease test (Helicocheck, Otsuka Pharmaceutical Co., Tokushima, Japan) and histopathology (hematoxylin-eosin and Giemsa staining) using additional biopsy specimens obtained during endoscopy from the antrum within 2 cm of the pyloric ring and the corpus along the greater curvature. Patients were considered positive for *H pylori* infection when at least two of these examinations yielded positive results. On the other hand, patients were defined as *H pylori*-negative if all the test results were negative[16].

All the samples were obtained with written informed consent of the patients prior to their inclusion in this study, in accordance with the Helsinki Declaration.

Statistical analysis

Statistical analyses were performed using Fisher' s exact, χ^2, Student' s *t*, Mann-Whitney U, and Kruskal-Wallis tests, whenever appropriate. A *P* value of less than 0.05 was accepted as statistically significant. Data are expressed as mean ± standard deviation (SD).

RESULTS

Patient demographics

According to the modified LA system, 14 patients were classified as grade M and 12 as grade N. There were no

significant differences in age, gender, current tobacco use, alcohol intake, body mass index, the presence of hiatus hernia and *H pylori* status among the patients with grade M and N and the controls (Table 1). None had such complications as stricture, bleeding and columnar-lined esophagus. The overall incidence of *H pylori* infection in our series was 51.3 %.

Table 1 Baseline characterisitics of the enrolled subjects

	Control group *n*=13	Nonerosive reflux disease group	
		Grade M[a] *n*=14	Grade N[a] *n*=12
Mean age, yr, (range)	61.6(39-80)	58.7(28-75)	62.5 (33-75)
Male / female	8 / 5	11 / 3	8 / 4
Smoker	53.8 %(7 / 13)	28.6 %(4 / 14)	33.3 %(4 / 12)
Alcohol drinker	46.2 %(6 / 13)	57.1 %(8 / 14)	33.3 %(4 / 12)
Hiatal hernia	0 %(0 / 13)	35.7 %(5 / 14)	50.0 %(6 / 12)
H pylori infection	53.8 %(7 / 13)	57.1 %(8 / 14)	41.7 %(5 / 12)

According to the modified Los Angeles system.

Relative expression levels of IL-8

We confirmed that both RT-PCR procedures for IL-8 and tubulin alpha 3 yielded 87- and 101-base pair (bp) specific bands, respectively (data not shown). As a whole, NERD patients had significantly higher expression levels of IL-8 than the controls (Figure 1, $P<0.05$). The expression levels of IL-8 in esophageal mucosa of grade M patients with NERD were significantly higher than those of grade N patients ($P<0.05$, Figure 2). In addition, the expression levels of IL-8 were higher in grade M than control group ($P<0.01$, Figure 2), but not significantly different between NERD-grade N and control group.

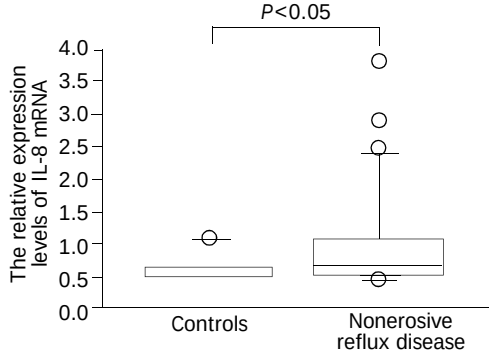

Figure 1 Relative interleukin 8 (IL-8) mRNA expression levels assessed by real-time quantitative polymerase chain reaction in patients with non-erosive reflux disease (NERD) and asymptomatic controls.

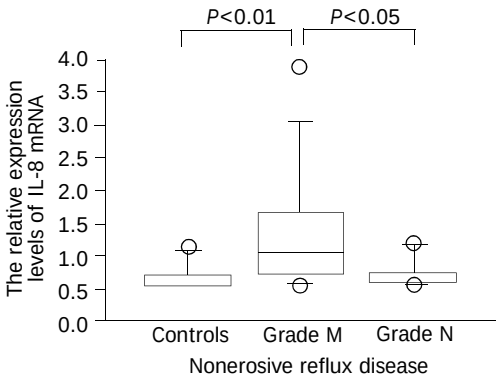

Figure 2 The expression levels of IL-8 assessed by real-time quantitative polymerase chain reaction in patients with non-erosive reflux disease (NERD) of grade M and N and asymptomatic controls.

Expression of CXCR-1 and CXCR-2 genes in esophageal mucosa

We identified the *CXCR-1* and *-2* gene-specific products as 257- and 1 154-bp bands, respectively, by RT-PCR (Figure 3). These mRNAs were constitutively expressed in each subject examined, irrespective of the presence of GERD-related symptoms or endoscopic grading. We confirmed that RT-PCR procedures for *G3PDH* housekeeping gene expression yielded 983 bp specific bands (data not shown).

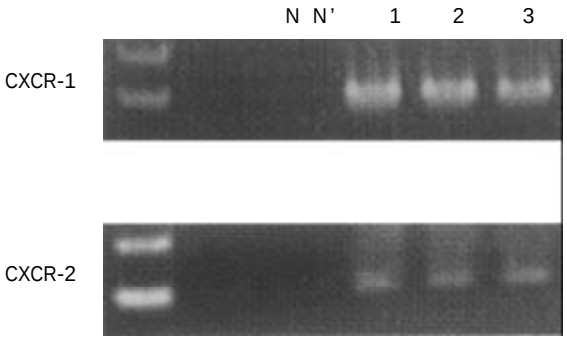

Figure 3 CXCR-1 and -2 mRNA transcripts were detected as 257 and 1 154 base pair (bp) bands with reverse transcription-polymerase chain reaction, respectively. Lane N; negative control, lane N'; RT (-) negative control, lane 1; asymptomatic normal control, lane 2; patient with NERD grade M, lane 3; patient with NERD grade N.

DISCUSSION

Several lines of evidence indicated that a prototype of CXC chemokine, IL-8, played a crucial role in the development and progression of erosive esophagitis[7,8]. In the present study, we focused on the implication of this potent inflammatory mediator in NERD. We found significantly higher expression levels of IL-8 mRNA in esophageal mucosa of patients with NERD than those in asymptomatic controls, suggesting that IL-8 is implicated in the pathogenesis of this incipient form of GERD.

The striking finding of this study was that NERD patients classified as grade M subgroup based on the modified LA system had significantly higher expression levels of IL-8 mRNA compared to those of grade N. IL-8 mediated the recruitment of neutrophils into sites of inflammation[17]. In addition, this potent chemoattractant acted on neutrophils to respiratory burst and release of a variety of reactive oxygen species (ROS), leading to tissue damage[18]. In our previous work employing ELISA, we found a significant association between the presence of intraepithelial neutrophils and increased IL-8 levels in esophageal mucosa of patients with RE[13]. Although we did not perform histopathological evaluation in the current study, elevated mucosal IL-8 expression may be involved even in such subtle mucosal changes as seen in the grade M subcategory, probably through its action on neutrophils, thus triggering chemotaxis and generating harmful ROS. This result also highlighted the possibility that NERD patients could encompass diverse subpopulations in terms of immune and inflammatory reactions. Further studies on the implication of other members of chemokines and proinflammatory cytokines can shed light on our understanding of the mechanisms underlying this poorly studied disorder.

In the present study, we demonstrated constitutive mRNA expression of CXCR-1 and -2 in esophageal biopsy samples by RT-PCR procedure. To date, CXCR-1 and -2 are two distinct receptors for IL-8[19]. It is suggested that the increased IL-8 may facilitate trafficking of neutrophils into the mucosa

affected by GERD process through the interaction with these receptors. Again, recent data from our laboratories showed a significant correlation between IL-8 protein levels and basal layer hyperplasia as well as papillary elongation in patients with RE[13]. IL-8 also exerted mitogenic actions directly or by binding to its receptors on epithelial cells[20,21]. Taken together, it is possible that IL-8, together with other cytokines as well as growth factors[14,22], could contribute to epithelial cell proliferation even in NERD, and could be eventually linked to carcinogenesis. Again, unlike CXCR-1, CXCR-2 is not specific for IL-8 and can bind to other chemokines such as growth related oncogene α, but it has 2- to 5-fold higher affinity for IL-8 than CXCR-1[19]. Further studies on the distribution of diverse IL-8 receptors and the receptor-mediated signaling pathway may help to elucidate the pathogenesis of GERD via IL-8 action.

In conclusion, our study demonstrated significantly enhanced expression of IL-8 mRNA level in NERD by real-time PCR technology. The interaction of IL-8 with CXCR-1 and -2 is likely to be involved in the pathogenesis of NERD. We also showed a significant difference in IL-8 mRNA levels between grade M and N subgroups of the modified LA classification, indicating the heterogeneity of NERD patients both immunologically and endoscopically.

REFERENCES

1 **Fass R**, Ofman JJ. Gastroesophageal reflux disease-Should we adopt a new conceptual framework? *Am J Gastroenterol* 2002; **97**: 1901-1909

2 **Frierson HF Jr**. Histology in the diagnosis of reflux esophagitis. *Gastroenterol Clin N Am* 1990; **19**: 631-644

3 **Quigley EMM**. Factors that influence therapeutic outcomes in symptomatic gastroesophageal reflux disease. *Am J Gastroenterol* 2003; **98**(Suppl): S24-S30

4 **Armstrong D**, Bennett JR, Blum AL, Dent J, De Dombal FT, Galmiche JP, Lundell L, Margulies M, Richter JE, Spechler SJ, Tytgat GN, Wallin L. The endoscopic assessment of oesophagitis: a progress report on observer agreement. *Gastroenterology* 1996; **111**: 85-92

5 **Hoshihara Y**, Hashimoto M. Endoscopic classification of reflux esophagitis. *Nippon Rinsho* 2000; **58**: 1808-1812

6 **Nishiyama Y**, Koyama S, Andoh A, Moritani S, Kushima R, Fujiyama Y, Hattori T, Bamba T. Immunohistochemical analysis of cell cycle-regulating-protein (p21, p27, and Ki-67) expression in gastroesophageal reflux disease. *J Gastroenterol* 2002; **37**: 905-911

7 **Fitzgerald RC**, Onwuegbusi BA, Bajaj-Elliott M, Saeed IT, Burnham WR, Farthing MJ. Diversity in the oesophageal phenotypic response to gastro-oesophageal reflux: immunological determinants. *Gut* 2002; **50**: 451-459

8 **Isomoto H**, Wang A, Mizuta Y, Akazawa Y, Ohba K, Omagari K, Miyazaki M, Murase K, Hayashi T, Inoue K, Murata I, Kohno S. Elevated levels of chemokines in esophageal mucosa of patients with reflux esophagitis. *Am J Gastroenterol* 2003; **98**: 551-556

9 **Fitzgerald RC**, Abdalla S, Onwuegbusi BA, Sirieix P, Saeed IT, Burnham WR, Farthing MJ. Inflammatory gradient in Barrett's oesophagus: implications for disease complications. *Gut* 2002; **51**: 316-322

10 **Carlsson R**, Dent J, Bolling-Sternevald E, Johnsson F, Junghard O, Lauritsen K, Riley S, Lundell L**.** The usefulness of a structured questionnaire in the assessment of symptomatic gastroesophageal reflux disease. *Scand J Gastroenterol* 1998; **33**: 1023-1029

11 **Jones MP**, Sloan SS, Rabine JC, Ebert CC, Huang CF, Kahrilas PJ. Hiatal hernia size is the dominant determinant of esophagitis presence and severity in gastroesophageal reflux disease. *Am J Gastroenterol* 2001; **96**: 1711-1717

12 **Yuan A**, Yang PC, Yu CJ, Chen WJ, Lin FY, Kuo SH, Luh KT. Interleukin-8 messenger ribonucleic acid expression correlates with tumor progression, tumor angiogenesis, patient survival, and timing of relapse in non-small-cell lung cancer. *Am J Respir Crit Care Med* 2000; **162**: 1957-1963

13 **Rogounovitch TI**, Saenko VA, Shimizu-Yoshida Y, Abrosimov AY, Lushnikov EF, Roumiantsev PO, Ohtsuru A, Namba H, Tsyb AF, Yamashita S. Large deletions in mitochondrial DNA in radiation-associated human thyroid tumors. *Cancer Res* 2002; **62**: 7031-7041

14 **Kondo S**, Yoneta A, Yazawa H, Kamada A, Jimbow K. Downregulation of CXCR-2 but not CXCR-1 expression by human keratinocytes by UVB. *J Cell Physiol* 2000; **182**: 366-370

15 **Ohnita K**, Isomoto H, Mizuta Y, Maeda T, Haraguchi M, Miyazaki M, Murase K, Murata I, Tomonaga M, Kohno S. *Helicobacter pylori* infection in patients with gastric involvement by adult T-cell leukemia/lymphoma. *Cancer* 2002; **94**: 1507-1516

16 **Isomoto H**, Furusu H, Morikawa T, Mizuta Y, Nishiyama T, Omagari K, Murase K, Inoue K, Murata I, Kohno S. 5-day vs. 7-day triple therapy with rabeprazole, clarithromycin and amoxicillin for *Helicobacter pylori* eradication. *Aliment Pharmacol Ther* 2000; **14**: 1619-1623

17 **Mukaida N**. Interleukin-8: An expanding universe beyond neutrophil chemotaxis and activation. *Int J Hematol* 2000; **72**: 391-398

18 **Graca-Souza AV**, Arruda MA, de Freitas MS, Barja-Fidalgo C, Oliveira PL. Neutrophil activation by heme: implications for inflammatory processes. *Blood* 2002; **99**: 4160-4165

19 **Chuntharapai A**, Kim KJ. Regulation of the expression of IL-8 receptor A/B by IL-8: possible functions of each receptor. *J Immunol* 1995; **155**: 2587-2594

20 **Metzner B**, Hofmann C, Heinemann C Zimpfer U, Schraufstatter I, Schopf E, Norgauer J. Overexpression of CXC-chemokines and CXC-chemokine receptor type 2 constitute an autocrine growth mechanism in the epidermoid carcinoma cells KB and A431. *Oncol Rep* 1999; **6**: 1405-1410

21 **Zachrisson K**, Neopikhanov V, Samali A, Uribe A. Interleukin-1, interleukin-8, tumour necrosis factor alpha and interferon gamma stimulate DNA synthesis but have no effect on apoptosis in small intestinal cell lines. *Eur J Gastroenterol Hepatol* 2001; **13**: 551-559

22 **Sfakianakis A**, Barr CE, Kreutzer DL. Localization of the chemokine interleukin-8 receptors in human gingival and cultured gingival keratinocytes. *J Periodont Res* 2002; **87**: 154-160

Edited by Zhu LH

P.O.Box 2345, Beijing 100023,China
Fax: +86-10-85381893
E-mail: wjg@wjgnet.com www.wjgnet.com

World J Gastroenterol 2003;9(12):2805-2808
World Journal of Gastroenterology
 ISSN 1007-9327

• CLINICAL RESEARCH •

Endoscopic banding ligation can effectively resect hyperplastic polyps of the stomach

Ching-Chu Lo, Ping-I Hsu, Gin-Ho Lo, Hui-Hwa Tseng, Hui-Chun Chen, Ping-Ning Hsu, Chiun-Ku Lin, Hoi-Hung Chan, Wei-Lun Tsai, Wen-Chi Chen, E-Ming Wang, Kwok-Hung Lai

Ching-Chu Lo, Ping-I Hsu, Gin-Ho Lo, Hui-Hwa Tseng, Hui-Chun Chen, Ping-Ning Hsu, Chiun-Ku Lin, Hoi-Hung Chan, Wei-Lun Tsai, Wen-Chi Chen, E-Ming Wang, Kwok-Hung Lai, Division of Gastroenterology, Department of Internal Medicine, Pathology, Kaohsiung Veterans General Hospital and National Yang-Ming University, Taipei, Taiwan, China
Hui-Hwa Tseng, Division of Pathology, Kaohsiung Veterans General Hospital and National Yang-Ming University, Taipei, Taiwan, China
Hui-Chun Chen, Department of Radiation Oncology, Kaohsiung Chang-Gang Memorial Hospital, Chang-Gang University, Taoyuan, Taiwan, China
Ping-Ning Hsu, Graduate Institute of Immunology, National Taiwan University, Taipei, Taiwan, China
Supported by the research grant NSC-90-2314-B-075B-003 from the National Science Council and VGHKS-91-35 from Kaohsiung Veterans General Hospital, Taiwan
Correspondence to: Ping-I Hsu, MD. Division of Gastroenterology, Department of Internal Medicine, Kaohsiung Veterans General Hospital, 386, Ta-Chung 1st Road, Kaohsiung, Taiwan 813, China. williamhsup@yahoo.com.tw
Telephone: +86-7-3422121 Ext 2075 **Fax:** +86-7-3468237
Received: 2003-08-28 **Accepted:** 2003-10-12

Abstract

AIM: Bleeding and perforation are major and serious complications associated with endoscopic polypectomy. To develop a safe and effective method to resect hyperplastic polyps of the stomach, we employed rubber bands to strangulate hyperplastic polyps and to determine the possibility of inducing avascular necrosis in these lesions.

METHODS: Forty-seven patients with 72 hyperplastic polyps were treated with endoscopic banding ligation (EBL). At 14 days after endoscopic ligation, follow-up endoscopies were performed to assess the outcomes of the strangulated polyps.

RESULTS: After being strangulated by the rubber bands, all of the polyps immediately became congested (100 %), and then developed cyanotic changes (100 %) approximately 4 minutes later. On follow-up endoscopy 2 weeks later, all the polyps except one had dropped off. The only one residual polyp shrank with a rubber band in its base, and it also dropped off spontaneously during subsequent follow-up. No complications occurred during or following the ligation procedures.

CONCLUSION: Gastric polyps develop avascular necrosis following ligation by rubber bands. Employing suction equipment, EBL can easily capture sessile polyps. It is an easy, safe and effective method to eradicate hyperplastic polyps of the stomach.

Lo CC, Hsu PI, Lo GH, Tseng HH, Chen HC, Hsu PN, Lin CK, Chan HH, Tsai WL, Chen WC, Wang EM, Lai KH. Endoscopic banding ligation can effectively resect hyperplastic polyps of the stomach. *World J Gastroenterol* 2003; 9(12): 2805-2808
http://www.wjgnet.com/1007-9327/9/2805.asp

INTRODUCTION

Bleeding is the most common complication of electrocautery snare polypectomy for upper gastrointestinal polyps, with an incidence ranging from 6.0 to 7.2 % in prospective studies[1-3]. To prevent polypectomy-elicited bleeding, epinephrine injection into the stalk[2] or placement of a metallic clip[4,5] before resection has been employed. Hachisu *et al*.[6] also reported favorable results of preventive ligation during polypectomy with placement of detachable snares at the bases of polyps. However, it is difficult to place detachable snares on sessile polyps or on polyps situated in technically difficult areas.

Endoscopic ligation using suction equipment and rubber bands or detachable snare[7-12] have been extensively applied in the management of bleeding esophageal and gastric varices. The varices are automatically eradicated through the use of ligation. In our pilot studies[13,14], we used detachable snares to strangulate gastric polyps, and demonstrated that most gastric polyps (89 %) developed avascular necrosis following ligation. Those results implied that a strangulating technique alone can achieve the bloodless transection of gastrointestinal neoplasm. However, it is important to note that a significant portion of gastric polyps (11 %) remain alive following detachable snare ligation. The aim of this study was to assess the safety and efficacy of endoscopic banding ligation (EBL) for removal of hyperplastic polyps of the stomach.

MATERIALS AND METHODS

Patients

From June 2000 to October 2001, forty-five patients (30 men and 15 women) who had 70 hyperplastic polyps documented in previous endoscopic biopsies were electively treated with EBL. Another two male patients received emergent EBL to treat bleeding gastric polyps. The mean patient age was 59.9 years (range 14 to 75 years). Written informed consent was obtained from all the subjects. The characteristics of their polyps are analyzed and illustrated in Table 1. The mean diameter of the head of polyps was 9.3 mm (range 5 to 25 mm).

EBL procedure

EBL was carried out with a GIF XQ200 endoscope (Olympus Optical Co., Tokyo, Japan) and a 19 cm flexible overtube (Sumitomo Bakelite Co., Tokyo, Japan). We set a transparent hood at the end of a scope that was equipped with a pneumoactivated esophageal variceal ligation (EVL) device set (Sumitomo Bakelite Co., Tokyo, Japan). The EVL device set consisted of an air feeding tube, a sliding tube, an inner cylinder, and a rubber band (O-ring). Pumping through an air feeding tube made a sliding tube slide on an inner cylinder and, as a result, the rubber band slipped off, thus ligating a lesion aspirated into the hood.

As premedication, 20 mg of hyoscine-N-butylbromide was given intramuscularly 5 minutes before performing EBL. The endoscope with a flexible overtube attached to its base was inserted and the overtube was inserted gently over the

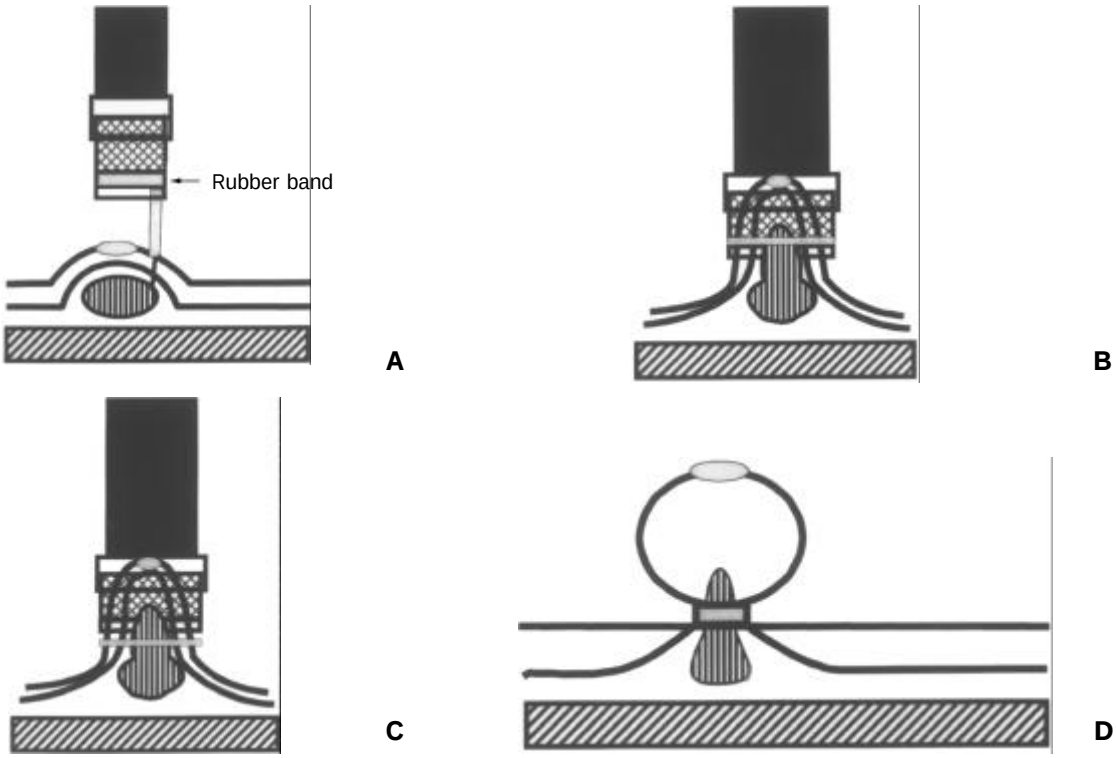

Figure 1 A: One to 4 ml of distilled water was injected locally into the submucosa adjacent to the polyp to lift the lesion from the muscle layer. B: The raised lesion was aspirated into the hood. C: The polyp was ligated by a rubber band after the air was pumped through the air feeding tube. D: The pneumoactivated EVL device set was removed.

endoscope to avoid mechanical injury to the thorax, larynx, and cervical esophagus. Before banding ligation, one to 4 ml of distilled water was injected into the submucosal layer near the lesion to tear and lift it off the muscle layer (Figure 1A). The endoscope was removed, and the pneumoactivated EVL device set was assembled on the instrument, which was then reinserted through the overtube. The raised lesion was aspirated into the hood (Figure 1B) and ligated with the rubber band after air was pumped through the air feeding tube (Figure 1C). Also, the polyp was observed for 5 minutes to investigate the sequential macroscopic changes of the strangulated lesion after EBL and biopsies were conducted later.

After the procedure, the patient was allowed to consume a liquid meal for a 24 hour period, and then issued a regular diet. An H2-receptor antagonist was administered orally for 4 weeks. A follow-up endoscopy was performed 14 days after initial endoscopic ligation to assess the outcome of the strangulated polyp.

RESULTS

Table 1 summarizes the results of 47 patients treated with EBL. EBL was performed easily and safely in each case. Following strangulation with detachable snares, all of the polyps immediately became congested (100 %), and then developed cyanotic change (100 %) approximately 4 minutes later. Figure 2 displays the typical sequential changes of a strangulated polyp. Following ligation, biopsies were conducted, and almost no bleeding was induced by biopsy procedures from the strangulated polyps. Pathological examination revealed severe venous congestion in the lamina propria of the lesions (Figure 2F). In the case of the two patients with bleeding gastric polyps above the antrum, EBL achieved successful hemostasis. The biopsies of polyps following EBL disclosed that they were hyperplastic lesions.

The follow-up endoscopy 2 weeks later revealed that all the polyps except one had dropped off, and EBL-related ulcers were found at the sites of the original lesions. The only one residual polyp shrank with a rubber band at its base. An additional follow-up endoscopy was performed for this lesion 1 month later, revealing that both the ligated polyp and rubber band had disappeared. No complications, such as bleeding or perforation, occurred during or after EBL and biopsies.

Table 1 Clinical characteristics and treatment results of endoscopic banding ligation in patients with hyperplastic gastric polyps

Variables	Number
Number of cases (M/F)	47 (32/15)
Age (years±SD)	59.9±15.1
Number of polyps	72
Mean size of polyps	9.3 mm (5-25 mm)
Morphology of polyps	
Sessile	70 (97.2 %)
Pedunculated	2 (2.8 %)
Location of polyps	
Cardia (superior, inferior, anterior, posterior)	(0, 1, 0, 2)
Fundus (superior, inferior, anterior, posterior)	(1, 4, 4, 1)
Antrum (superior, inferior, anterior, posterior)	(4, 5, 9, 7)
Body (superior, inferior, anterior, posterior)	(5, 10, 4, 15)
Initial endoscopic findings after ligation	
Congestion	72 (100 %)
Cyanosis	72 (100 %)
Endoscopic findings at second look	
Shrunken polyps	1 (1.4 %)[a]
Ligation-related ulcer	71 (98.6 %)

[a]The polyp dropped off spontaneously in subsequent follow-up.

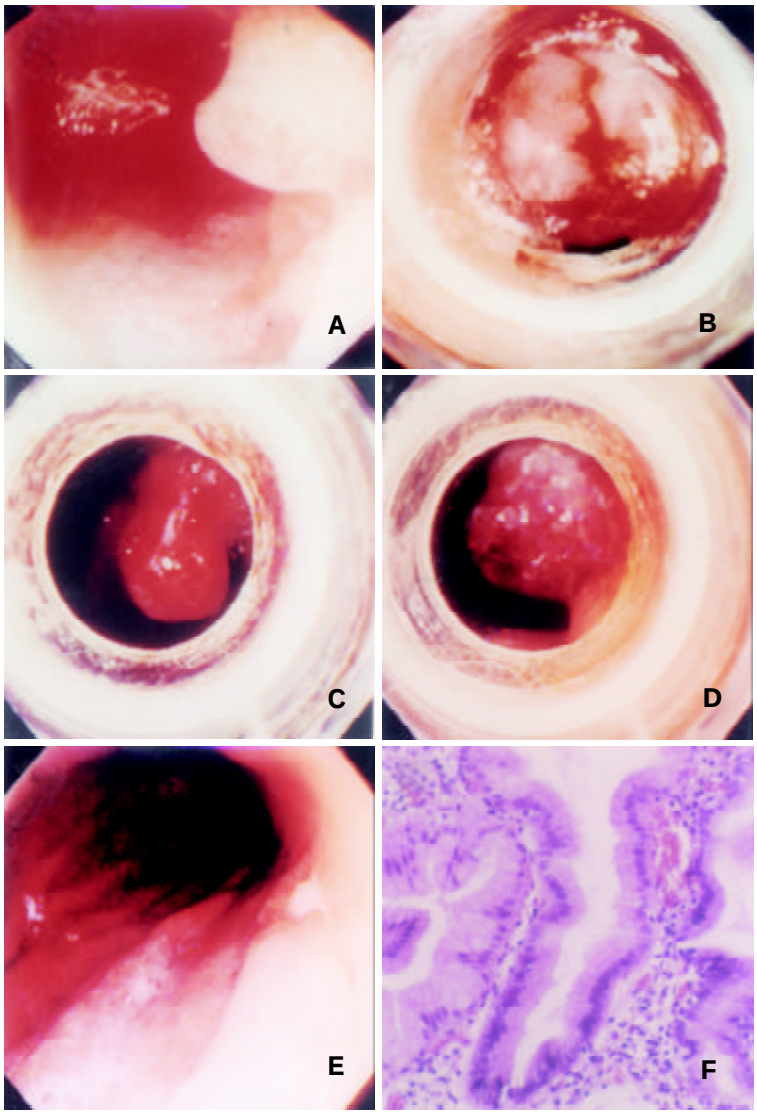

Figure 2 EBL for a hyperplastic polyp. A: A polyp over the posterior wall of corpus. B: The polyp was aspirated into the hood and ligated with a rubber band after local injection of distilled water into the submucosa. C: The polyp congested immediately after ligation. D: The polyp developed cyanotic change about 4 minutes later. E: An artificial ulcer presented at the previous ligation site. F: Pathological examination of the strangulated polyp revealed both foveolar hyperplasia of the gastric mucosa and severe venous congestion in the lamina propria.

DISCUSSION

The current study has confirmed that gastric hyperplastic polyps developED avascular necrosis following EBL. A strangulated polyp became congested immediately after ligation, and developed cyanotic changes within a few minutes. These important findings herein have not been documented before. Our study also reveals that EBL can be applied not only in the elective treatment of asymptomatic hyperplastic polyps, but also in the management of bleeding lesions. A strangulated polyp was bloodlessly transected without complications following the banding ligation.

Hyperplastic polyp is the most common polyp in the stomach, comprising 75 to 90 % of gastric polyps[15-17]. Most of the hyperplastic gastric polyps are asymptomatic. However, malignant transformation of hyperplastic polyps has been reported in several long-term follow-up studies[18,19]. They therefore should be resected when incidentally detected. Bleeding is a common complication of electrocautery snare polypectomy for gastric polyps. In a well-conducted prospective study[2], bleeding was observed in 16 of 222 snare polypectomies (7.2 %). Recently, various endoscopic mucosal resection (EMR) techniques have been developed. They included strip biopsy[20], double snare polypectomy[21] and cap-fitted panendoscopy[22]. However, complications (bleeding and perforation) of these new techniques were also high with an incidence ranging from 2.7 % to 23.9 %[23-25]. These studies underscored the importance of proficiency in endoscopic hemostatic techniques by the endoscopic team as a prerequisite for performing polypectomy in the stomach.

To prevent hemorrhage following polypectomy, preventive ligation could be conducted before the procedure[6]. However, bleeding can be encountered if a polyp is resected by electrocautery in cases where the distance above the detachable snare or rubber band is inadequate. According to our results, single ligation could effectively remove all the gastric polyps without requiring further electrocautery. No complications occurred during or after ligation. The low bleeding rate associated with EBL seemed to be attributed mainly to both a ligation of the vessels at the polyp bases and the avoidance of resecting polyps with a high-frequency electrocautery. Additionally, perforation was prevented by lifting the lesion from the muscle layer.

Our results further demonstrated that the ligating method could be employed to treat actively bleeding polyps. In the two patients with bleeding gastric polyps, EBL successfully achieved hemostasis for their bleeding polyps. Furthermore,

the strangulated polyps were bloodlessly transected without complications following the banding.

Conventional snare polypectomy or EMR methods encounter difficulties in effectively managing lesions located in the lesser curvature side, posterior wall and cardia of the stomach. Employing the EBL method allowed a lesion to be easily captured into the transparent hood, even in cases where it was situated tangentially.

Sessile polyps pose another dilemma for traditional electrocautery polypectomy, and it is difficult for snare to capture these polyps. EMR with cap-fitted panendoscopy[22] may solve this problem, but bleeding and perforation remain very problematic. Employing the proposed EBL procedure allowed theses polyps to be easily captured after submucosal injection with distilled water followed by suction. However, our EBL technique is not suitable for treating gastric adenoma, which has a high risk of carcinomatous conversion[16,17]. In managing such lesions, additional electrocautery is still required to assess the possibility of malignant transformation of polyps.

Previously, we also employed the endoscopic detachable snare ligation method to treat hyperplastic gastric polyps[13], and found that cyanotic change was an important predictor of the outcome of strangulated polyps. All the polyps with cyanotic changes developed avascular necrosis, but those without cyanotic changes remained alive following ligation by detachable snares. This study demonstrated that all the polyps became cyanotic following ligation by rubber bands, and that all the cyanotic polyps then developed avascular necrosis.

In conclusion, gastric polyps congest immediately following strangulation by rubber bands, and then develop cyanotic change within a few minutes. Avascular necrosis occurs in all the gastric polyps following banding ligation. Employing suction equipment, EBL can easily capture sessile polyps. It is an easy, safe and effective method to eradicate gastric hyperplastic polyps. Additionally, the new technique may be the choice of therapy for bleeding gastrointestinal polyps.

ACKNOWLEDGEMENTS

The authors would like to express their deep appreciation to Dr. Chang-Bih Shie, Jeng-Jie Pzeng, Miss Yu-San Chen, and Hsuan-Chun Huang for their invaluable support to this study.

REFERENCES

1 **Lanza FL**, Graham DY, Nelson RS, Godines R, Mckechnie JC. Endoscopic upper gastrointestinal polypectomy. Report of 73 polypectomies in 63 patients. *Am J Gastroenterol* 1981; **75**: 345-348
2 **Muehldorfer SM**, Stole M, Hahn EG, Ell C. Diagnostic accuracy of forceps biopsy versus polypectomy for gastric polyps: a prospective multicentre study. *Gut* 2002; 50: 465-470
3 **Hsieh YH**, Lin HJ, Tseng GY, Perng CL, Li AF, Chang FY, Lee SD. Is submucosal epinephrine injection necessary before polypectomy? A prospective comparative study. *Hepatogastroenterology* 2001; **48**: 1379-1382
4 **Chang FY**. Endoscopic ligation for removal of stomach hyperplastic polyp: less risk or saving money? *Chin Med J* 2001; **64**: 615-616
5 **Sobrino-Faya M**, Martinez S, Gomez Balado M, Lorenzo A, Iglesias-Garcia J, Iglesias-Canle J, Dominquez Munoz JE. Clip for the prevention and treatment of polypectomy bleeding. *Res Esp Enferm Dig* 2002; 94: 457-462
6 **Hachisu T**. A new detachable snare for hemostasis in the removal of large polyps or other elevated lesions. *Surg Endosc* 1991; **5**: 70-74
7 **Cipolletta L**, Bianco MA, Rotondano G, Piscopo R, Prisco A, Garofano ML. Emergency endoscopic ligation of actively bleeding gastric varices with a detachable snare. *Gastrointest Endosc* 1998; **47**: 400-403
8 **Lo GH**, Lai KH, Cheng JS, Chen MH, Huang HC, Hsu PI. Endoscopic variceal ligation plus nadolol and sucrafate compared with ligation alone for the prevention of variceal rebleeding: a prospective, randomized trial. *Hepatology* 2000; **32**: 461-465
9 **Lo GH**, Lai KH, Cheng JS, Lin CK, Hsu PI, Chiang HT. Prophylactic banding ligation of high-risk esophageal varices in patients with cirrhosis: a prospective randomized trial. *J Hepatol* 1999; **31**: 451-456
10 Lo GH, Chen WC, Chen MH, Hsu PI, Lin CK, Tai WL, Lai KH. Banding ligation versus nadolol and isosorbide mononitrate for the prevention of esophageal variceal rebleeding. *Gastroenterology* 2002; **123**: 728-734
11 **Hou MC**, Chen WC, Lin HC, Lee FY, Chang FY, Lee SD. A new "sandwich" method of combined endoscopic variceal ligation and sclerotherapy versus ligation alone in the treatment of esophageal variceal bleeding: a randomized trial. *Gastrointest Endosc* 2001; **53**: 572-578
12 **Deschenes M**, Barkun AN. Comparison of endoscopic ligation and propranolol for the primary prevention of variceal bleeding. *Gastrointest Endosc* 2000; **51**: 630-633
13 **Hsu PI**, Lai KH, Lo GH, Lin CK, Lo CC, Wang EM, Wang YY, Tsai WL, Lin CP, Tseng HH, Chen HC, Chen JL. Sequential changes of gastric hyperplastic polyps following endoscopic ligation. *Chin Med J* 2001; **64**: 609-614
14 **Hsu PI**, Lai KH, Lo GH, Lin CK, Lo CC, Wang EM, Wang YY, Tsai WL, Lin CP, Tseng HH, Chen HC, Chen JL. Sequential changes of gastric polyps following endoscopic ligation. *Gastrointest Endosc* 2001; **53**(Suppl): AB218
15 **Koch HK**, Lesch R, Cremer M, Oehlert W. Polyp and polypoid foveolar hyperplasia in gastric biopsy specimens and the precancerous prevalence. *Front Gastrointest Res* 1979; **4**: 183-191
16 **Laxen F**, Sipponen P, Ihamaki T, Hakkiluoto A, Dortscheva Z. Gastric polyps; their morphological and endoscopical characteristics and relation to gastric carcinoma. *Acta Pathol Microbiol Scand* 1982; **90**: 221-228
17 **Rosch W**. Epidemiology, pathogenesis, diagnosis, treatment of benign gastric tumors. *Front Gastrointest Res* 1980; **6**: 167-184
18 **Daibo M**, Itabashi M, Hirota T. Malignant transformation of gastric hyperplastic polyps. *Am J Gastroenterol* 1987; **82**: 1016-1025
19 **Kamiya T**, Morishita T, Asakura H. Histoclinical long-standing follow-up study of hyperplastic polyps of the stomach. *Am J Gastroenterol* 1981; **75**: 275-281
20 **Karta M**, Tada M, Okita K. The successive strip biopsy partial resection technique for large early gastric and colon cancers. *Gastrointest Endosc* 1992; **38**: 174-178
21 **Takekoshi T**, Takagi K, Kato Y. Radical endoscopic treatment of early gastric cancer. *Gann Monogr Cancer Res* 1990; **37**: 111-126
22 **Inoue H**, Takeshita K, Hori H, Muraoka Y, Yoneshima H, Endo M. Endoscopic mucosal resection with a cap-fitted panendoscopy for esophagus, stomach and colon mucosal lesions. *Gastrointest Endosc* 1993; **39**: 58-62
23 **Hirao M**, Asanuma T, Masuda K. Endoscopic resection of early gastric cancer following locally injecting hypertonic saline-epinephrine. *Stomach Intest* 1988; **23**: 399-409
24 **Yokota K**, Tanabe Y, Komatsu H. Safety and risk in the endoscopic mucosal resection of gastric disease: the strip biopsy method. *Endoscopia Digestiva* 1996; **8**: 465-471
25 **Ahmad NA**, Kochman ML, Long WB, Furth EE, Ginsberg GG. Efficacy, safety, and clinical outcomes of endoscopic mucosal resection: a study of 101 cases. *Gastrointest Endosc* 2002; **55**: 390-396

Edited by Zhu LH

P.O.Box 2345, Beijing 100023,China
Fax: +86-10-85381893
E-mail: wjg@wjgnet.com www.wjgnet.com

World J Gastroenterol 2003;9(12):2809-2812
World Journal of Gastroenterology
 ISSN 1007-9327

• CLINICAL RESEARCH •

Clinical manifestations and prognostic factors in patients with gastrointestinal stromal tumors

Shee-Chan Lin, Ming-Jer Huang, Chen-Yuan Zeng, Tzang-In Wang, Zen-Liang Liu, Ray-Kuan Shiay

Shee-Chan Lin, Tzang-In Wang, Division of Gastroenterology, Department of Internal Medicine, Mackay Memorial Hospital, Taipei, Taiwan and Mackay Junior College of Nursing, Taipei, Taiwan, China
Ming-Jer Huang, Ray-Kuan Shiay, Division of Hematology-Oncology, Department of Internal Medicine, Mackay Memorial Hospital, Taipei, Taiwan, China
Chen-Yuan Zeng, Department of Pathology, Mackay Memorial Hospital, Taipei, Taiwan, China
Zen-Liang Liu, Department of Surgery, Mackay Memorial Hospital, Taipei, Taiwan and Mackay Junior College of Nursing, Taipei, Taiwan, China
Correspondence to: Dr. Shee-Chan Lin, Chief of Division of Gastroenterology, Department of Internal Medicine, Mackay Memorial Hospital, 92, Sec. 2, Chung San North Road, Taipei, Taiwan, China. sheechan@ms2.mmh.org.tw
Telephone: +86-2-25433535 **Fax:** +86-2-25433642
Received: 2003-08-11 **Accepted:** 2003-10-12

Abstract

AIM: To investigate the incidence of CD117-positive immunohistochemical staining in previously diagnosed GI tract stromal tumors (GIST) and to analyze the tumors' clinical manifestations and prognostic factors.

METHODS: We retrospectively reviewed 91 cases with a previous diagnosis of GI stromal tumor, leiomyoma, or leiomyosarcoma. Tissue samples were assessed with CD117, CD34, SMA and S100 immunohistochemical staining. Clinical and pathological characteristics were analyzed for prognostic factors.

RESULTS: CD117 was positive in 81 (89 %) of 91 tissue samples. There were 59 cases (72.8 %) positive for CD34, 13 (16 %) positive for SMA, and 12 (14.8 %) positive for S100. There was no gender difference in patients with CD117-positive GIST. Their mean age was 65 years. There were 44 (54 %) tumors located in the stomach and 29 (36 %) in the small intestine. The most frequent presenting symptoms were abdominal pain and GI bleeding. The mean tumor size was 7.5±5.7 cm. There were 35 cases (43.2 %) with tumors >5 cm. The tumor size correlated significantly with tumor mitotic count and resectability. Tumor size, mitotic count, and resectability correlated significantly with tumor recurrence and survival. There was recurrent disease in 39 % of our patients, and their mean survival after recurrence was 16.6 months. Most recurrences were at the primary site or metastatic to the liver. Twenty-six percent of our patients died of their disease.

CONCLUSION: Traditional histologic criteria are not specific enough to diagnose GIST. This diagnosis must be confirmed with CD117 immunohistochemical staining. Prognosis is dependent on tumor size, mitotic count, and resectability.

Lin SC, Huang MJ, Zeng CY, Wang TI, Liu ZL, Shiay RK. Clinical manifestations and prognostic factors in patients with gastrointestinal stromal tumors. *World J Gastroenterol* 2003; 9 (12): 2809-2812
http://www.wjgnet.com/1007-9327/9/2809.asp

INTRODUCTION

Leiomyoma of the gastrointestinal (GI) tract has a typical pathologic picture with parallel spindle cells arranged in a fascicular pattern[1,2]. However, a number of tumors have atypical findings, with epithelioid cells or pleomorphic cells instead of spindle cells or even characteristics of neurons that stain for neuron-specific enolase. Therefore, pathologists used the umbrella term "stromal tumor" to refer to such atypical mesenchymal tumors. It has been thought that these tumors might originate from mesenchymal or stromal cells within the muscle layer of the GI tract[3-5]. Molecular biochemical studies have revealed expression of kit protein (CD117) in the primitive mesenchymal cells. CD117 can be demonstrated by immunohistochemical staining using anti-kit antibodies[6]. It has been found that most mesenchymal or stromal cell tumors of the GI tract are positive for CD117[7]. Leiomyoma or leiomyosarcoma of the GI tract with typical pathologic features also stain positive for CD117. There is therefore now a consensus that these tumors originate from a common cell and that the term gastrointestinal stromal tumors (GIST) be reserved for CD117-positive neoplasms[8].

These tumors arise from primitive cells with dual characteristics of muscle and neural cells, similar to interstitial cell of Cajal[9]. Cytogenetic analysis shows that most of these tumors have a mutation of the c-kit gene. Oncogenic mutations enable the kit protein, a transmembrane tyrosine kinase receptor, to phosphorylate various substrate proteins, leading to activation of signal transduction cascades which regulate cell proliferation, apoptosis, chemotaxis, and adhesion[9]. Additional chromosomal derangements in 22q or 24q may promote GIST development[10,11]. C-kit gene mutation and kit protein over-expression appear to be essential for the pathogenesis of GIST. Imatinib is a tyrosine kinase inhibitor that has resulted in remarkable myxoid degeneration and fibrosis of GIST in clinical trials[12]. Since specifically targeted therapy is thus becoming available, it is important to know if tumors with histology consistent with GIST in fact express the kit protein[13]. We retrospectively reviewed cases in our hospital in the past 13 years with a tissue diagnosis of leiomyoma, leiomyosarcoma, or GIST to assess their immunohistochemical staining patterns, clinical manifestations, and prognostic factors.

MATERIALS AND METHODS

Patients

Using our hospital database, we collected records with a pathologic diagnosis of leiomyoma or leiomyosarcoma or stromal cell tumor of the GI tract from 1988 until 2001. There were 91 such cases. All the patients had undergone surgical resection of their tumor. We recorded the patients' age, gender, clinical manifestations, tumor site, maximal tumor diameter, duration of surgery, resectability of the tumor, the presence and date of local recurrence or distance metastasis, and the outcome, including date of death. The data of patients who were still alive in January 2002 were censored.

Immunohistochemistry

The tumor samples from all the 91 cases were examined for

various markers by using immunohistochemistry with commercially available antibodies against CD117 (1:50 dilution), S-100 protein (1:1 500), desmin (1:50), and SMA (1:100) (Dako, Carpinteria, CA). Immunoreaction was detected according to the manufacturer' s instructions (Ventana Medical Systems, Tucson, AZ). The risk of aggressive behavior of the tumors was calculated according to the NIH consensus statement of 2001[13]. Briefly, a tumor size <2 cm and mitotic count <5/50 high power fields (HPF) was graded as very low risk, a tumor between 2 and 5 cm and a mitotic count <5/50 HPF as low risk, a tumor <5 cm and mitotic count between 5/50 HPF and 10/50 HPF or a tumor between 5 and 10 cm and a mitotic count less than 5/50 HPF as intermediate risk, and a tumor >10 cm or mitotic count >10/50 HPF or a tumor >5 cm and mitotic count >5/50 HPF as high risk.

Statistic analysis

Statistic analysis was performed with SPSS software (SPSS for Window 9.0). Student' s *t* test was used to compare continuous variables. And a χ^2 test was used for dichotomous variables. Survival was calculated from the day of diagnosis until death or the last day of a patient' s visit to the outpatient clinic. The disease-free survival was calculated from the first diagnosis until tumor recurrence or distant metastases were found. Kaplan Meier analysis with a log rank test was used to compare survival and disease-free survival. The Cox proportional hazard method was used to evaluate prognostic factors.

RESULTS

Of the 91 tissue samples tested, 81 (89 %) were positive for CD117 staining. There were no significant differences in the distribution of previous pathologic diagnoses between CD117-positive and –negative samples. The highest incidence of CD117 positivity was in samples previously diagnosed as malignant GIST (Table 1). Of the 10 cases negative for CD117, 6 tumors were located in the stomach, 2 in the small bowel, and 1 each in the colon and retroperitoneum. Three of these tumors were positive for CD34, 3 for SMA, and 3 S100 (Table 2). These 10 cases were excluded from further analysis.

Table 1 Immunohistochemical staining for CD117 in tumors with a previous pathologic diagnosis of leiomyoma, leiomyosarcoma or GIST

Previous pathologic diagnosis	CD117-positive (*n*)	CD117-negative (*n*)
Leiomyoma	6 (86 %)	1 (14 %)
Leiomyosarcoma	14 (78 %)	4 (22 %)
Benign GIST	10 (77 %)	3 (23 %)
Malignant GIST	51 (96 %)	2 (4 %)
Total	81 (89 %)	10 (11 %)

Table 2 Previous pathologic diagnoses, tumor site, and other immunohistochemical markers in CD117-negative patients

Previous pathologic diagnosis	*n*	Site	CD34	SMA	S100
Leiomyoma	1	Stomach	+	-	-
Leiomyosarcoma	1	Stomach	-	-	-
	1	Small bowel	-	-	+
	1	Colon	-	-	-
	1	Other	-	+	-
Benign GIST	2	Stomach	-	-	+
	1	Stomach	+	+	+
Malignant GIST	1	Stomach	+	-	-
	1	Small bowel	-	+	-

Of the 81 patients with CD117-positive tumors, there were 42 males and 39 females. Their ages ranged from 21 to 91 years (mean 65.2±13.6 years), with over half (44/81, 54 %) between 60 and 79 years of age (Table 3). Additional immunohistochemical staining showed that the tissue samples were positive for CD34 in 59 cases (73 %), for SMA in 13 (16 %), and for S100 in 12 cases (15 %).

Table 3 Age distribution of patients with CD117-positive GIST

Age range	No. of cases (*n*)	Percentage (%)
<30	1	1
30-39	2	3
40-49	7	9
50-59	15	19
60-69	19	24
70-79	26	32
80-89	10	12
>90	1	1
Total	81	100

The tumors were located in the stomach in 44 cases (54 %), the small intestine in 29 (36 %), the colon in 5 (6 %), and the retroperitoneum or mesentery in 3 (4 %). The most frequent presenting symptoms were GI tract bleeding and abdominal pain in 27 cases (33 %) each, abdominal fullness and discomfort in 14 (17 %). Four patients had anemia on presentation, 7 had a palpable abdominal mass, and 1 presented with vaginal bleeding due to a rectal GIST involving the uterus. One patient was asymptomatic and was incidentally found to have a 3.5 cm GIST in her stomach on routine physical examination.

On pathology of the resected tumors, the mean size was 7.5±5.7 cm, 10 (12 %) were <2 cm, 25 (31 %) between 2 and 5 cm, 27 (33 %) between 5 and 10 cm, and 19 (24 %) >10 cm. Mitotic counts were <5/50 HPF in 38 cases (47 %), between 5 and 10/50 HPF in 21 (26 %), and >10/50 HPF in 22 (27 %). There was a significant correlation between tumor size and mitotic count (Pearson correlation coefficient = 0.541, $P<0.001$, Table 4). There was ulceration of the tumor in 47 % (38/81), hemorrhage in 53 % (43), tumor necrosis in 54 % (44), and tumor perforation in 25 % (20). Sixty-two (77 %) of the tumors were completely resected. There was a significant correlation between tumor size and resectability (Pearson correlation coefficient = 0.505, $P<0.001$, Table 5).

Table 4 Correlation between tumor size and mitotic count in CD117-positive GIST

Tumor size	Mitotic counts/50 HPF[a]		
	<5	5-10	>10
≤2 cm	10 (100 %)	0	0
2 to 5 cm	14 (56 %)	8 (32 %)	3 (12 %)
5 to 10 cm	12 (44 %)	8 (30 %)	7 (26 %)
>10 cm	2 (11 %)	5 (26 %)	12 (63 %)

Pearson correlation = 0.541, $P<0.001$, [a]HPF=High power fields.

Table 5 Correlation between tumor size and resectability in CD117-positive GIST

Tumor sizes	Complete resection	Incomplete resection
≤2 cm	10 (100 %)	0
2 to 5 cm	25 (100 %)	0
5 to 10 cm	18 (69 %)	8 (30.8 %)
>10 cm	9 (47 %)	10 (52.6 %)

Pearson correlation = 0.505, $P<0.001$.

There were 31 patients (39 %) with local recurrence or distant metastasis, which was statistically associated with tumor size (P<0.001, Figure 1). The 31 included 3 of 25 (12 %) whose primary tumor had been between 2 and 5 cm, 13 of 27 (48 %) whose tumor had been between 5 and 10 cm, and 15 of 19 (79 %) whose tumor had been greater than 10 cm. Recurrence was also significantly associated with mitotic count, occurring in 5 of 38 (13 %) with counts <5/50HPF, 10 of 21 (48 %) with counts between 5 and 10/50HPF, 16 of 22 (73 %) with counts >10/50HPF (P<0.001, Figure 2).

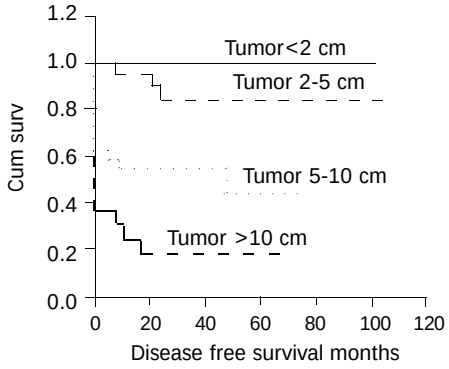

Figure 1 Cumulative disease-free survival for patients with CD117-positive GIST based on tumor size.

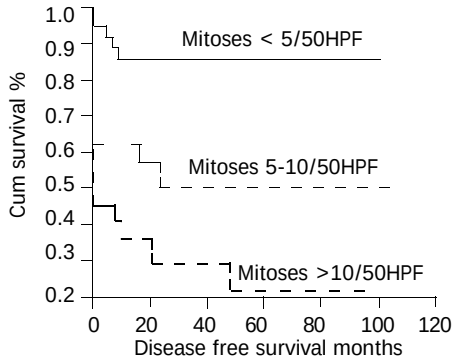

Figure 2 Cumulative disease-free survival for patients with CD117-positive GIST based on mitotic count.

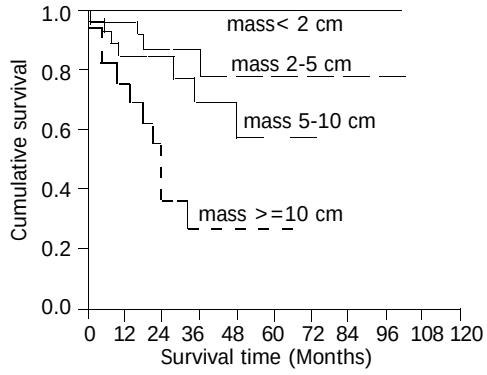

Figure 3 Cumulative survival for patients with CD117-positive GIST based on tumor size.

Twenty-one patients (26 %) died during follow up. The mean survival time after recurrence was 16.6±14.5 months. Tumor size, mitotic count, and resectability were significantly associated with survival (Figures 3,4,5). The 5-year survival was 78 % (mean survival 85.5±8.13 months) for patients with tumors between 2 and 5 cm, 57 % (mean survival 53.8±6.09 months) for those with tumors between 5 and 10 cm, and 27 % (mean survival 30.0±6.41 months) for those with tumors larger than 10 cm (Figure 3, log rank test, P<0.001). The 5-year survival was 76 % (mean survival 80.7±6.77 months) for patients with mitotic counts <5/50HPF, 73 % (mean survival 80.9±10.5 months) for those with counts between 5 and 10/50HPF, and 31 % (mean survival time 44.2±9.53 months) for those with counts >10/50HPF (Figure 4, P<0.02). Patients whose tumors were completely resected had a 5-year survival of 73 % (mean survival 82.0±5.78 months) while those without complete resection had a 5-year survival of 26 % (mean survival 27.0±5.23 months) (Figure 5, P<0.05).

The survival was also significantly correlated with the score for risk of aggressive behaviors (Figure 6, P<0.0001).

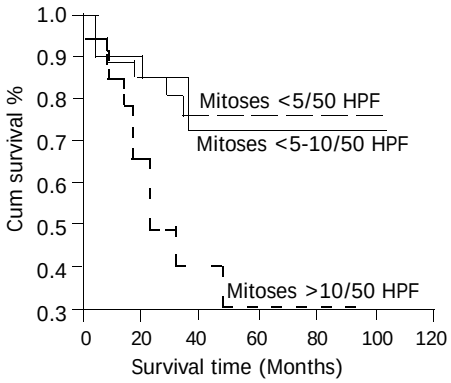

Figure 4 Cumulative survival for patients with CD117-positive GIST based on mitotic count.

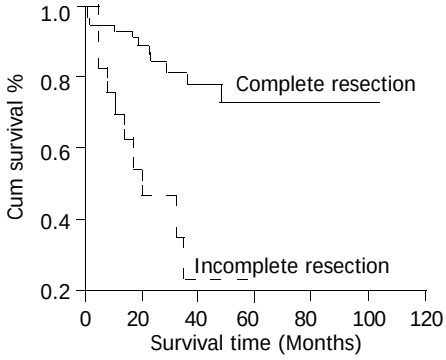

Figure 5 Cumulative survival for patients with CD117-positive GIST based on resectability.

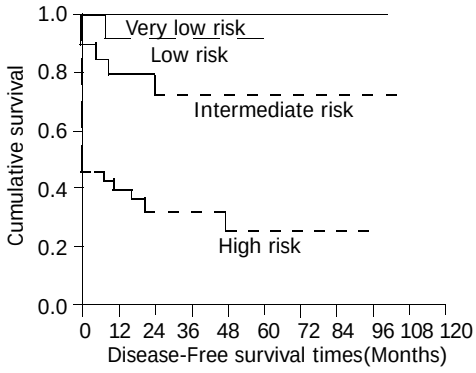

Figure 6 Cumulative disease-free survival for patients with CD117-positive GIST based on risk of aggressive behaviors.

DISCUSSION

Before the development of imatinib, surgical resection was the only treatment for tumors classified pathologically as GIST[14,15]. Tumor size was an independent prognostic factor, with tumors >10 cm having a disease-specific 5-year survival

of only 20 % after resection[16]. The tumors are often soft and fragile and prone to rupture or intraperitoneal dissemination during resection. The primary goal of surgery is complete resection of the disease, because rupture at surgery is another poor prognostic factor[17]. A number of other pathologic features have also been correlated with survival, including mitotic index, aneuploidy, cellular morphometry, proliferative index, and percent S-phase fraction[18]. Most patients with malignant stromal tumor or leiomyosarcoma have had either local recurrence or metastasis to the liver[14]. Locally recurrent tumors were usually not amenable to complete resection because of peritoneal implantation[19], nor has chemotherapy been very effective[20]. Solitary liver metastasis could be surgically resected[21], but multiple liver metastases are difficult to manage. Transcatheter arterial embolization has been used, but the partial response rate was low.

Our study confirms the contention that pathology alone is inadequate to confirm GIST by the current diagnostic criterion of CD117 immunohistochemical staining. Of the 91 tissue samples in our series, only 81 (89 %) were CD117-positive. Of the 10 negative samples, 2 were positive for SMA but negative for CD34 and S100 and therefore may be leiomyosarcomas. Another 3 were positive for S100 but negative for CD34 and SMA and therefore may be schwannomas. One case was positive and 2 were negative for all the 3 markers (that is, CD34, SMA and S100). The diagnosis in these cases is still unclear. A search for a gene mutation other than in the C-kit gene, for example PDGFR, might be helpful to clarify the diagnosis.

Among the 81cases positive for CD117, 73 % were also positive for CD34, 16 % for SMA, and 15 % for S100. These data are similar to that of previous reports.

Esophagogastroduodenoscopy is usually performed in Taiwan for any patient complaining of abdominal discomfort. As a result, we can, on occasion, find small submucosal tumors in the stomach. Most of our cases with a tumor less than 5 cm were located in the stomach. This accounted for 43 % of our patients with tumors less than 5 cm in size, all of whom had completely resectable lesions. None of our patients with tumors less than 4 cm in size died (data not shown). Our findings confired that complete resection of the tumor is one of the most important factors related to survival[16]. In our analysis, tumor size was significantly correlated with mitotic count and resectability, with larger tumors usually having higher mitotic counts and being more likely to be unresectable. Most of our patients with small intestinal GIST had lesions larger than 5 cm and a poorer outcome than those with gastric tumors. At the present time it is probably unwise to characterize any GIST benign[13]. This diagnosis mandates treatment.

Tumor grade was correlated, as expected, with mortality. No patients with very low grade tumors died, but the mortality increased as tumor grade increased, 14 % for low grade tumor, 30 % for moderate grade, and 35 % for high grade. Thirty-nine percent of our patients had recurrence, with a mean survival of 16.6 months after recurrence. Twenty-six percent of our patients died of their diseases.

We have done a clinical trial using imatinib 800 mg daily for 3 months in 11 patients with recurrent GIST. There was partial response in 3 cases and stable disease in 6 cases (unpublished data).

In conclusion, two recent developments are important with regard to GIST. The first is the ability to diagnose the tumor based on immunohistochemical staining. Our study confirms that traditional histologic criteria alone are not specific enough. The second is the development of imatinib, which specifically targets CD117, providing us a new tool to combat GIST. Early diagnosis and complete resection remain the ideal, as surgical removal provides the best prognosis. However, specific molecular diagnosis and treatment are expanding our ability to manage this disease.

REFERENCES

1 **Ranchod M**, Kempson RL. Smooth muscle tumors of the gastrointestinal tract and retroperitoneum. *Cancer* 1977; **39**: 255-262
2 **Akwari OE**, Dozois RR, Weiland LH, Beahrs OH. Leiomyosarcoma of the small and large bowel. *Cancer* 1978; **42**: 1375-1384
3 **Casper ES**. Gastrointestinal stromal tumors. *Curr Treat Options Oncol* 2000; **1**: 267-273
4 **Schaldenbrand JD**, Appelman HD. Solitary solid stromal gastrointestinal tumors in von Recklinghausen's disease with minimal smooth muscle differentiation. *Hum Pathol* 1984; **15**: 229-232
5 **Mazur MT**, Clark HB. Gastric stromal tumors: Reappraisal of histogenesis. *Am J Surg Pathol* 1983; **7**: 507-519
6 **Huizinga JD**, Thuneberg L, Kluppel M, Malysz J, Mikkelsen HB, Bernstein A. W/kit gene required for interstitial cells of Cajal and for intestinal pacemaker activity. *Nature* 1995; **373**: 347-349
7 **Corless CL**, McGreevey L, Haley A, Town A, Heinrich MC. KIT mutations are common in incidental gastrointestinal stromal tumors one centimeter or less in size. *Am J Pathol* 2002; **160**: 1567-1572
8 **Miettinen M**, Majidi M, Lasota J. Pathology and diagnostic criteria of gastrointestinal stromal tumors (GISTs): a review. *Eur J Cancer* 2002; **38**(Suppl 5): S39-51
9 **Heinrich MC**, Rubin BP, Longley BJ, Fletcher JA. Biology and genetic aspects of gastrointestinal stromal tumors: KIT activation and cytogenetic alterations. *Hum Pathol* 2002; **33**: 484-495
10 **Andersson J**, Sjogren H, Meis-Kindblom JM, Stenman G, Aman P, Kindblom LG. The complexity of KIT gene mutations and chromosome rearrangements and their clinical correlation in gastrointestinal stromal (pacemaker cell) tumors. *Am J Pathol* 2002; **160**: 15-22
11 **Gunawan B**, Bergmann F, Hoer J, Langer C. Schumpelick V, Becker H, Fuzesi L. Biological and clinical significance of cytogenetic abnormalities in low-risk and high-risk gastrointestinal stromal tumors. *Hum Pathol* 2002; **33**: 316-321
12 **Croom KF**, Perry CM. Imatinib mesylate: in the treatment of gastrointestinal stromal tumours. *Drugs* 2003; **63**: 513-522
13 **Fletcher CD**, Berman JJ, Corless C, Gorstein F, Lasota J, Longley BJ, Miettinen M, O'Leary TJ, Remotti H, Rubin BP, Shmookler B, Sobin LH, Weiss SW. Diagnosis of gastrointestinal stromal tumors: a consensus approach. *Int J Surg Pathol* 2002; **10**: 81-89
14 **Blanke CD**, Eisenberg BL, Heinrich MC. Gastrointestinal stromal tumors. *Curr Treat Options Oncol* 2001; **2**: 485-491
15 **Shiu MH**, Farr GH, Papachristou DN, Hajdu SI. Myosarcomas of the stomach: natural history, prognostic factors and management. *Cancer* 1982; **49**: 177-187
16 **DeMatteo RP**, Lewis JJ, Leung D, Mudan SS, Woodruff JM, Brennan MF. Two hundred gastrointestinal stromal tumors: Recurrence patterns and prognostic factors for survival. *Ann Surg* 2000; **231**: 51-57
17 **Ng EH**, Pollock RE, Munsell MF, Atkinson EN, Romsdahl MM. Prognostic factors influencing survival in gastrointestinal leiomyosarcomas. Implications for surgical management and staging. *Ann Surg* 1992; **215**: 68-77
18 **Miettinen M**, Sarlomo-Rikala M, Lasota J. Gastrointestinal stromal tumors: recent advances in understanding of their biology. *Hum Pathol* 1999; **30**: 1213-1220
19 **Dematteo RP**, Heinrich MC, El-Rifai WM, Demetri G. Clinical management of gastrointestinal stromal tumors: before and after STI-571. *Hum Pathol* 2002; **33**: 466-477
20 **Plaat BE**, Hollema H, Molenaar WM, Torn Broers GH, Pijpe J, Mastik MF, Hoekstra HJ, van den Berg E, Scheper RJ, van der Graaf WT. Soft tissue leiomyosarcomas and malignant gastrointestinal stromal tumors: Differences in clinical outcome and expression of multidrug resistance proteins. *J Clin Oncol* 2000; **18**: 3211-3220
21 **DeMatteo RP**, Shah A, Fong Y, Jarnagin WR, Blumgart LH, Brennan MF. Results of hepatic resection for sarcoma metastatic to liver. *Ann Surg* 2001; **234**: 540-548

Edited by Zhu LH

P.O.Box 2345, Beijing 100023,China
Fax: +86-10-85381893
E-mail: wjg@wjgnet.com www.wjgnet.com

World J Gastroenterol 2003;9(12):2813-2816
World Journal of Gastroenterology
 ISSN 1007-9327

• CLINICAL RESEARCH •

Eosinophilic gastroenteritis: Clinical experience with 15 patients

Ming-Jen Chen, Cheng-Hsin Chu, Shee-Chan Lin, Shou-Chuan Shih, Tsang-En Wang

Ming-Jen Chen, Cheng-Hsin Chu, Shee-Chan Lin, Shou-Chuan Shih, Tsang-En Wang, Division of Gastroenterology, Department of Internal Medicine, Mackay Memorial Hospital, Taipei, Taiwan, China
Correspondence to: Dr. Cheng-Hsin Chu, Division of Gastroenterology, Department of Internal Medicine, Mackay Memorial Hospital, 92, Section 2, Chungshan North Road, Taipei, Taiwan, China. jessierc@ms28.hinet.net
Telephone: +86-225433535 Ext 2260
Received: 2003-08-05 **Accepted:** 2003-10-12

Abstract

AIM: To evaluate the clinic features of eosinophilic gastroenteritis and examine the diagnosis, treatment, long-term outcome of this disease.

METHODS: Charts with a diagnosis of eosinophilic gastroenteritis from 1984 to 2002 at Mackay Memorial Hospital were reviewed retrospectively. There were 15 patients diagnosed with eosinophilic gastroenteritis. The diagnosis was established in 13 by histologic evaluation of endoscopic biopsy or operative specimen and in 2 by radiologic imaging and the presence of eosinophilic ascites.

RESULTS: All the patients had gastrointestinal symptoms and 12 (80 %) had hypereosinophilia (absolute eosinophil count 1 008 to 31 360/cm^3). The most common symptoms were abdominal pain and diarrhea. Five of the 15 patients had a history of allergy. Seven patients had involvement of the mucosa, 2 of muscularis, and 6 of subserosa. One with a history of seafood allergy was successfully treated with an elimination diet. Another patient improved spontaneously after fasting for several days. The remaining 13 patients were treated with oral prednisolone, 10 to 40 mg/day initially, which was then tapered. The symptoms in all the patients subsided within two weeks. Eleven of the 15 patients were followed up for more than 12 months (12 to 104 months, mean 48.7), of whom 5 had relapses after discontinuing steroids (13 episodes). Two of these patients required long-term maintenance oral prednisolone (5 to 10 mg/day).

CONCLUSION: Eosinophilic gastroenteritis is a rare condition of unclear etiology characterized by relapses and remissions. Short courses of corticosteroids are the mainstay of treatment, although some patients with relapsing disease require long-term low-dose steroids.

Chen MJ, Chu CH, Lin SC, Shih SC, Wang TE. Eosinophilic gastroenteritis: Clinical experience with 15 patients. *World J Gastroenterol* 2003; 9(12): 2813-2816
http://www.wjgnet.com/1007-9327/9/2813.asp

INTRODUCTION

Eosinophilic gastroenteritis is a rare disease characterized by eosinophilic infiltration into one or more layers of the gastrointestinal (GI) tract. It affects adults as well as children. The pathogenesis is poorly understood. Up to 40 % of cases were reported to have an underlying allergic basis[1]. It might involve any area of the gastrointestinal tract from the esophagus to the rectum[2,3], although the stomach and proximal small bowel were most commonly affected. Klein *et al*.[4] suggested a classification, based on the histology of the lesion: mucosal, muscularis, and subserosal disease. Clinical features depend on which layer and site are involved. Mucosal involvement leads to protein-losing enteropathy, fecal blood loss, and mal-absorption, muscularis disease often causes gastric outlet or small bowel obstruction, and subserosal involvement manifests as eosinophilic ascites. The disease often waxes and wanes in severity. Only a few studies have described the long-term outcome[5] and none have evaluated risk factors for relapse. In this study, we described the clinical manifestations of 15 patients with eosinophilic gastroenteritis.

MATERIALS AND METHODS

Charts with a diagnosis of eosinophilic gastroenteritis from 1984 to 2002 at Mackay Memorial Hospital were reviewed retrospectively. The diagnostic criteria included 1) the presence of gastrointestinal symptoms, 2) an eosinophilic infiltrate on a biopsy or operative specimen from the GI tract or else a high eosinophil count in ascitic fluid, 3) absence of parasite infestation, 4) no eosinophilic disease outside the GI tract, and 5) exclusion of intestinal lymphoma, Crohn' s disease or other tumors. As peripheral blood hypereosinophilia was not a universal finding in eosinophilic gastroenteritis, hypereosinophilia was not required for the diagnosis. Data collected from the charts included age, sex, presenting symptoms, allergy history (drug or food allergy, atopy, asthma, hay fever, etc), absolute eosinophil count, endoscopic, sonographic and radiological findings, operative records, histology of biopsies or operative specimens, response to medication, length of follow-up, and number of relapses.

An eosinophilic infiltrate was defined as at least 20 eosinophils per high power field. Klein' s criteria were followed: 1) mucosal disease was defined as infiltration of the mucosa without involvement of the muscularis or serosa, 2) muscular disease was defined as complete or incomplete intestinal obstruction and eosinophilic infiltration of the muscularis without eosinophilic ascites, and 3) subserosal disease was defined as eosinophilic infiltration of the GI tract with eosinophilic ascites.

RESULTS

Fifteen patients (6 men, 9 women), with a mean age of 38.4±14.2 (3 to 58) years, were diagnosed as eosinophilic gastroenteritis according to the above criteria. The patients are listed in Table 1 according to Klein' s classification. Hypereosinophilia (1 008 to 31 360/cm^3) in peripheral blood was noted in 12 (80 %) cases. The most common symptoms and signs in our series are shown in Table 2.

Endoscopic biopsies were performed in 12 patients from 30 different sites in the gastric antrum, duodenum, and colon. Sixteen specimens were positive, yielding the diagnosis in 12. Another 20-year-old female underwent endoscopic laparotomy for refractory ascites and was diagnosed as subserosal eosinophilic gastroenteritis based on a biopsy. The other two patients had general bowel wall thickening on CT scan and

eosinophils in their ascitic fluid. Although eosinophilic ascites might also be seen in parasitic disease and abdominal lymphoma, these entities were excluded by the clinical findings and response to treatment.

Table 1 General characteristics of patients with eosinophilic gastroenteritis according to histologic classification

Group / Patient		Sex	Age	WBC / cm^3	Eos count	% of Eos
I	1	M	43	13 800	1 380	13
	2	F	65	12 720	2 540	18
	3	F	38	11 220	4 704	41
	4	F	57	33 010	19 475	59
	5	F	34	7 900	2 291	27
	6	M	45	10 400	3 340	34
	7	F	64	13 700	3 973	29
II	8	M	31	14 500	6 960	43
	9	F	58	9 900	396	5
III	10	M	17	24 800	11 016	42
	11	F	38	13 400	1 008	12
	12	F	20	11 720	3 984	36
	13	M	35	5 650	621	10
	14	M	53	31 360	14 500	68
	15	F	3	8 800	264	3

Group I: mucosal, group II: muscular and group III: subserosal disease. Eos=eosinophil.

Table 2 Presenting symptoms and signs of the 15 patients

Symptoms and signs	*n*=15
Abdominal pain	12
Diarrhea	11
Bloating / fullness	10
Nausea / vomiting	9
Hypoalbuminemia (<3.5 g / dL)	11
Fecal blood loss	6

Table 3 Characteristics of patients with and without relapse

No.	Sex	Age	Klein classification	Followed up >12 m	Allergy
			Relapsing (number of episodes)		
4	F	57	Mucosal (3)	+	+
9	F	58	Muscular (4)	+	+
10	M	17	Subserosal (1)		+
12	F	20	Subserosal (3)		+
15	F	3	Subserosal (4)		+
			Non-relapsing		
1	M	43	Mucosal	+	
2	F	65	Mucosal	+	
3	F	38	Mucosal	+	+
5	F	34	Mucosal		
6	M	45	Muscular	+	
7	F	64	Muscular		
8	M	31	Muscular		+
11	F	38	Subserosal	+	+
13	M	35	Subserosal		
14	M	53	Subserosal	+	

The endoscopic findings were nonspecific, with most patients having only hyperemic mucosa, although 2 patients had ulcers in the antrum and duodenum. A barium study of the small intestine showed thickening of the duodenal wall in 1 patient with subserosal disease and ischemic changes in the proximal ileum in 1 patient with muscular disease. CT scan or sonography were performed on all the patients with muscular and subserosal diseases (Figures 1 and 2). Intestinal wall thickening was noted in the 2 with muscular disease and in 3 of 6 with subserosal disease. Ascites was present in all the 6 who had subserosal disease.

Figure 1 Abdominal computed tomography with intravenous contrast medium showing general thickening in the small bowel wall (white arrows), characteristic of the distribution of eosinophilic gastroenteritis.

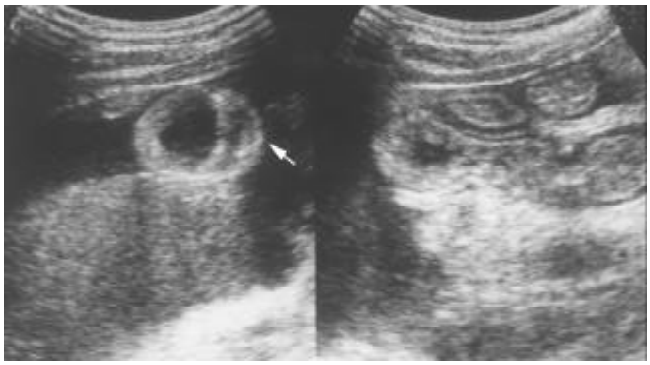

Figure 2 Transverse sonography of the proximal small bowel in the right subcostal area showing general thickening of the wall (white arrow) and ascites.

A history of allergy was noted in 5 of the 15 (34 %) patients (1 mucosal, 1 muscular, and 3 subserosal). One patient with mild mucosal disease and allergy to shellfish was successfully treated with an elimination diet. The mucosal disease in another patient (who had no history of allergy) remitted spontaneously after a fast of several days. Symptoms in both of these patients resolved within one week, and neither patient had a relapse over more than three years of follow up. Thirteen patients were treated with prednisolone, 10 to 40 mg/day initially, which was then gradually tapered over 4 to 6 weeks. Of these 13, 11 had relief of symptoms within one week, while 2 patients with subserosal disease improved within two weeks. The average hospital stay was 14.8 days (5 to 27 days).

Eleven of our patients have been followed up for more than one year (12 to 102 months). Of them, 5 (1 with mucosal, 1 with muscular and 3 with subserosal disease) had a total of 13 relapses after discontinuing steroids. A 58-year-old female with muscular disease had a relapse after discontinuing steroids and had an ileal perforation associated with ischemia. She underwent ileal resection. In general, an additional short course of steroids resulted in resolution, although 2 patients maintained on low-dose prednisolone (5 to 10 mg/day) to prevent relapses. Patients with and without relapse are compared in Table 3.

DISCUSSION

The pathogenesis of eosinophilic gastroenteritis is still unknown, but speculation has focused on the selective release

of eosinophil major proteins leading to intestinal epithelial damage. Keshavarzian *et al* demonstrated that the number of activated degranulated eosinophils in the mucosa correlated with the severity of eosinophilic gastroenteritis[6]. The disease was reportedly more prevalent in patients with seasonal allergies, food sensitivities[7], eczema, allergic rhinitis, and asthma[8]. There have been a few cases related to exposure to medications[9,10] The evidence of elevations in IgE suggested that atopy might be involved in the pathogenesis of the disease[11,12], however a history of allergy may be of little help in establishing the diagnosis. In our study 34 % of patients had a history of allergy, a proportion similar to that of other studies[1], but there was no correlation between an allergy history and the histologic type of disease.

Hypereosinophilia in the peripheral blood was absent in at least 20 % of the cases[1]. In our series, the results were similar. Therefore, the absence of hypereosinophilia should not exclude consideration of the diagnosis of eosinophilic gastroenteritis in patients with unexplained GI symptoms. Eleven of our patients had hypoalbuminemia (serum albumin <3.5 g/dl). Such a finding in patients with vague symptoms may be a hint to this disease, a chronic, organic rather than a transient, functional character.

Radiologically, the hallmark of eosinophilic gastroenteritis on CT is nodular and irregular thickening of the folds in the distal stomach and proximal small bowel[13,14]. However, similar thickening may also be seen in Menetrier' s disease, lymphoma, *scirrhous* carcinoma, Crohn' s disease, and granulomatous disease. It is thus not a specific sign of eosinophil gastroenteritis. Mesenteric inflammation as well as ascites are not uncommon but are still nonspecific. Sonography is a useful tool for detecting non-mucosal eosinophilic gastroenteritis in patients without peripheral hypereosinophilia. It may reveal generalized thickening of the intestinal wall as well as ascites, which prompted us to do cytological examination of ascitic fluid or endoscopic biopsy. Based on these sonographic abnormalities, we were able to diagnose eosinophilic gastroenteritis in 3 patients who had a normal serum eosinophil count (396 to 621/cm^3). In our series, all the 6 patients with subserosal disease had ascites on sonography, and 5 patients (3 with subserosal and 2 with muscular disease) had a thickened wall. Sonography could also evaluate the response to treatment by measuring the thickness of the affected layer[15].

The endoscopic appearance in eosinophilic gastroenteritis is nonspecific, including erythematous, friable, nodular, and occasional ulcerative changes. In our study, 10 patients had only nonspecific gastritis or colitis, while 2 had shallow gastric or duodenal ulcers. These were most likely peptic ulcers, because no eosinophilic infiltrate was found on biopsy.

Definitive diagnosis requires histological evidence of eosinophilic infiltration. Eosinophilic infiltrates are usually patchy in distribution and may be present in otherwise normal, non-inflamed bowel wall. Therefore, multiple biopsies may be required to avoid missing the diagnosis. In our study, the definitive diagnosis was established by endoscopic biopsy in 12 patients. Several different examinations, such as gastroduodenoscopy and colonoscopy, and multiple deep biopsies may be necessary to establish the diagnosis. Even then it may be difficult to evaluate accurately the degree and extent of disease in most patients, given the patchy distribution of the infiltrates. A new technique using Tc-99m HMPAO-labeled WBC SPECT may be useful in assessing the extent of disease and response to treatment. Lee *et al*, have proposed a grading system using this technology[16].

Eosinophilic gastroenteritis may present with symptoms suggesting an acute abdomen. There have been reports of the disease mimicking acute appendicitis, an obstructing cecal mass, pancreatitis, giant refractory duodenal ulcer, and intussusception[17-25]. If such patients have peripheral hypereosinophilia, the correct diagnosis of eosinophilic gastroenteritis might be suspected, avoiding an unnecessary operation. Surgery in eosinophilic gastroenteritis should be reserved for obstruction or perforation. One 53-year-old male with subserosal disease in our series underwent surgery twice, once for a refractory ulcer that had perforated, and again for an acute abdomen without definitive etiology, before the diagnosis of eosinophilic gastroenteritis. It is possible that the acute symptoms at the second time were a manifestation of eosinophilic gastroenteritis.

Once the diagnosis has been made, it is useful to look for specific food allergies, as an elimination diet may be successful if a limited number of food allergies are identified. One of our patients with mucosal disease had improvement after elimination of seafood. Katz *et al* reported that an elimination diet might fail to prevent recurrence[26], but our patient has remained well for more than 3 years. In general, patients responded quickly and well to steroids[27,28], as was true in our series. The appropriate duration of steroid treatment has been unknown, but short courses followed by a repeat course for a relapse have been described[29]. Patients with refractory relapsing disease are usually placed on long-term low-dose steroids or immunosuppressive therapy. Some authors have described the use of sodium cromoglycate (a stabilizer of mast cell membranes)[30] or montelukast (a selective, competitive leukotriene receptor antagonist)[31] as steroid-sparing agents.

We were able to follow 11 of our patients for more than one year and found that 5 of them had relapses. Three of the 5 relapse patients were all younger than 20 years old in our series. Our numbers are too small to draw firm conclusions, but this observation does raise the possibility that young age may be a risk factor for relapse. Larger series or a meta-analysis would be needed to investigate this possibility.

We found the incidence of subserosal disease (6/15=40 %) to be higher than in other studies, for example, 4.5 % to 9 % in Japan and 13 % in the USA[32,1]. Ascites as a manifestation of subserosal disease may be a more worrisome symptom, leading to a more aggressive approach to diagnosis. This in itself would not explain regional differences, but it might be that we under-diagnosed cases of mucosal and muscular disease, attributing vague symptoms to functional GI disease.

The diagnosis of eosinophilic gastroenteritis is problematic because the final diagnosis requires histological confirmation. However, this entity should be considered in the patient with unexplained chronic and relapsing gastrointestinal symptoms.

REFERENCES

1 **Talley NJ**, Shorter RG, Phillips SF, Zinsmeister AR. Eosinophilic gastroenteritis: a clinicopathological study of patients with disease of the mucosa, muscle layer, and subserosal tissues. *Gut* 1990; **31**: 54-58

2 **Matsushita M**, Hajiro K, Morita Y, Takakuwa H, Suzaki T. Eosinophilic gastroenteritis involving the entire digestive tract. *Am J Gastroenterol* 1995; **90**: 1868-1870

3 **Liacouras CA**, Markowitz JE. Eosinophilic esophagitis: A subset of eosinophilic gastroenteritis. *Curr Gastroenterol Rep* 1999; **1**: 253-258

4 **Klein NC**, Hargrove RL, Sleisenger MH, Jeffries GH. Eosinophilic gastroenteritis. *Medicine* 1970; **49**: 299-319

5 **Lee CM**, Changchien CS, Chen PC, Lin DY, Sheen IS, Wang CS, Tai DI, Sheen-Chen SM, Chen WJ, Wu CS. Eosinophilic gastroenteritis: 10 years experience. *Am J Gastroenterol* 1993; **88**: 70-74

6 **Keshavarzian A**, Saverymuttu S, Tai PC, Thompson M, Barter S, Spry C. Activated eosinophils in familial eosinophilic gastroenteritis. *Gastroenterology* 1985; **88**: 1041-1049

7 **Kelly KJ**. Eosinophilic gastroenteritis. *J Pediatr Gastroenterol Nutr*

2000; **30**: S28-35
8 **Von Wattenwyl F**, Zimmermann A, Netzer P. Synchronous first manifestation of an idiopathic eosinophilic gastroenteritis and bronchial asthma. *Eur J Gastroenterol Hepatol* 2001; **13**: 721-725
9 **Lee JY**, Medellin MV, Tumpkin C. Allergic reaction to gemfibrozil manifesting as eosinophilic gastroenteritis. *South Med J* 2000; **93**: 807-808
10 **Barak N**, Hart J, Sitrin MD. Enalapril-induced eosinophilic gastroenteritis. *J Clini Gastroenterol* 2001; **3**: 157-158
11 **Cello JP**. Eosinophilic gastroenteritis–a complex disease entity. *Am J Med* 1979; **67**: 1097-1104
12 **Von Wattenwyl F**, Zimmermann A, Netzer P. Synchronous first manifestation of an idiopathic eosinophilic gastroenteritis and bronchial asthma. *Eur J Gastroenterol Hepatol* 2001; **13**: 721-725
13 **Marco-Domenech SF**, Gil-Sanchez S, Jornet-Fayos J, Ambit-Capdevila S, Gonzalez-Anon M. Eosinophilic gastroenteritis: percutaneous biopsy under ultrasound guidance. *Abdom Imaging* 1998; **23**: 286-288
14 **Horton KM**, Corl FM, Fishman EK. CT of nonneoplastic diseases of the small bowel: spectrum of disease. *J Comput Assist Tomogr* 1999; **23**: 417-428
15 **Maroy B**. Nonmucosal eosinophilic gastroenteritis: sonographic appearance at presentation and during follow-up of response to prednisone therapy. *J Clin Ultrasound* 1998; **26**: 483-486
16 **Lee KJ**, Hahm KB, Kim YS, Kim JH, Cho SW, Jie H, Park CH, Yim H. The usefulness of Tc-99m HMPAO labeled WBC SPECT in eosinophilic gastroenteritis. *Clin Nucl Med* 1997; **22**: 536-541
17 **Box JC**, Tucker J, Watne AL, Lucas G. Eosinophilic colitis presenting as a left-sided colocolonic intussusception with secondary large bowel obstruction: an uncommon entity with a rare presentation. *Am Surg* 1997; **63**: 741-743
18 **Tran D**, Salloum L, Tshibaka C, Moser R. Eosinophilic gastroenteritis mimicking acute appendicitis. *Am Surg* 2000; **66**: 990-992
19 **Redondo Cerezo E**, Moreno Platero JJ, Garcia Dominguez E, Gonzalez Aranda Y, Cabello Tapia MJ, Martinez Tirado P, Lopez de Hierro Ruiz M, Gomez Garcia M. Comments to a report: eosinophilic gastroenteritis presenting as an obstructing cecal mass: review literature and our own experience. *Am J Gastroenterol* 2000; **95**: 3655-3657
20 **Tsai MJ**, Lai NS, Huang YF, Huang YH, Tseng HH. Allergic eosinophilic gastroenteritis in a boy with congenital duodenal obstruction. *J Microbiol Immunol Infect* 2000; **33**: 197-201
21 **Markowitz JE**, Russo P, Liacouras CA. Solitary duodenal ulcer: a new presentation of eosinophilic gastroenteritis. *Gastrointest Endosc* 2000; **52**: 673-676
22 **Shweiki E**, West JC, Klena JW, Kelley SE, Colley AT, Bross RJ, Tyler WB. Eosinophilic gastroenteritis presenting as an obstructing cecal mass–a case report and review of the literature. *Am J Gastroenterol* 1999; **94**: 3644-3645
23 **Kristopaitis T**, Neghme C, Yong SL, Chejfec G, Aranha G, Keshavarzian A. Giant antral ulcer: a rare presentation of eosinophilic gastroenteritis–case report and review of the literature. *Am J Gastroenterol* 1997; **92**: 1205-1208
24 **Scolapio JS**, DeVault K, Wolfe JT. Eosinophilic gastroenteritis presenting as a giant gastric ulcer. *Am J Gastroenterol* 1996; **91**: 804-805
25 **Siahanidou T**, Mandyla H, Dimitriadis D, Van-Vliet C, Anagnostakis D. Eosinophilic gastroenteritis complicated with perforation and intussusception in a neonate. *J Pediatr Gastroenterol Nutr* 2001; **32**: 335-337
26 **Katz AJ**, Twarog FJ, Zeiger RS, Fslshck ZM. Milk-sensitive and eosinophilic gastroenteropathy: similar clinical features with contrasting mechanisms and clinical course. *J Allergy Clin Immunol* 1984; **74:** 72-78
27 **Malaguarnera M**, Restuccia N, Pistone G, Panebianco MP, Giugno I, Grasso G, Seminara G. Eosinophilic gastroenteritis. *Eur J Gastroenterol Hepatol* 1997; **9**: 533-537
28 **Liacouras CA**, Wenner WJ, Brown K, Ruchelli E. Primary eosinophilic esophagitis in children: successful treatment with oral corticosteroids. *J Pediatr Gastroenterol Nutr* 1998; **26**: 380-385
29 **Naylor AR**. Eosinophilic gastroenteritis. *Scott Med J* 1990; **35**: 163-165
30 **Perez-Millan A**, Martin-Lorente JL, Lopez-Morante A, Yuguero L, Saez-Royuela F. Subserosal eosinophilic gastroenteritis treated efficaciously with sodium cromoglycate. *Dig Dis Sci* 1997; **42**: 342-344
31 **Schwartz DA**, Pardi DS, Murray JA. Use of montelukast as steroid-sparing agent for recurrent eosinophilic gastroenteritis. *Dig Dis Sci* 2001; **46**: 1787-1790
32 **Miyamoto T**, Shibata T, Matsuura S, Kagesawa M, Ishizawa Y, Tamiya K. Eosinophilic gastroenteritis with ileus and ascites. *Intern Med* 1996; **35**: 779-782

Edited by Zhu LH

P.O.Box 2345, Beijing 100023,China
Fax: +86-10-85381893
E-mail: wjg@wjgnet.com www.wjgnet.com

World J Gastroenterol 2003;9(12):2817-2820
World Journal of Gastroenterology
 ISSN 1007-9327

• CLINICAL RESEARCH •

Correlation of P-glycoprotein expression with poor vascularization in human gallbladder carcinomas

Yu Tian, Li-Li Zhu, Ren-Xuan Guo, Chui-Feng Fan

Yu Tian, **Ren-Xuan Guo**, Department of General Surgery, First Affiliated Hospital, China Medical University, Shenyang 110001, Liaoning Province, China
Li-Li Zhu, Department of General Surgery, Second Affiliated Hospital, China Medical University, Shenyang 110004, Liaoning Province, China
Chui-Feng Fan, Department of Pathology, China Medical University, Shenyang 110001, Liaoning Province, China
Correspondence to: Dr. Yu Tian, Department of General Surgery, First Affiliated Hospital, China Medical University, Shenyang 110001, Liaoning Province, China. tianyu5460@21cn.com
Telephone: +86-24-23256666-6237 **Fax:** +86-24-23896804
Received: 2003-06-05 **Accepted:** 2003-07-24

Abstract

AIM: To investigate the relationship between the expression of P-glycoprotein (P-gp) and the degree of vascularization in gallbladder carcinomas.

METHODS: P-gp was stained with streptavidin-peroxidase complex immunohistochemical method in routine paraffin-embedded sections of gallbladder carcinomas. Microvessel counts (MVC) were determined using factor-VIII-related antigens.

RESULTS: The average MVC in 32 cases of gallbladder carcinomas was (34±10)/HP. The value of MVC was closely correlated with Nevin staging and tumor differentiation ($P<0.01$ and $P<0.05$). The total expression rate of P-gp was 62.5 %. The P-gp expression rate in cases of Nevin staging S1-S3 (78.6 %) was higher than that of S4-S5 (50.0 %) with no statistical significance. The P-gp expression rate was not correlated with tumor differentiation or pathologic types. The value of MVC in P-gp (+) cases was markedly lower than that in P-gp (-) cases ($P<0.01$). The positive rate of P-gp was significantly higher in cases of smaller MVC than those of bigger MVC ($P<0.05$).

CONCLUSION: MVC may be used as one of the important parameters to reflect the biological behaviors of gallbladder carcinomas. As a major cause of drug resistance, the overexpression of P-gp is closely correlated with the poor vascularization in gallbladder carcinomas.

Tian Y, Zhu LL, Guo RX, Fan CF. Correlation of P-glycoprotein expression with poor vascularization in human gallbladder carcinomas. *World J Gastroenterol* 2003; 9(12): 2817-2820
http://www.wjgnet.com/1007-9327/9/2817.asp

INTRODUCTION

Because the rate of neovascularization (angiogenesis) frequently fails to keep pace with tumor growth, tumor vasculature is often insufficient in supplying the tumor mass, therefore many solid tumors contain subpopulation of hypoxic cells. Some researches showed that the drug resistance was partially due to the poor tumor vascularization in reducing the influx of cytotoxic agents. Additionally, the hypoxic environment due to poor vascularization could also inhibit tumor cell proliferation, yet noncycling cells would be expected to be less sensitive to many agents. In recent years, some biochemical mechanisms of drug resistance have been identified; one of them is the overexpression of transmembrane transport protein and P-glycoprotein. We therefore linked angiogenesis assessed by microvessel counts with the expression of P-gp in human gallbladder carcinomas. The aim of the present study was to investigate whether MVC could be used as an important parameter to reflect the biological behaviors of gallbladder carcinomas and to illustrate the relationship between P-gp expression and vascularization.

MATERIALS AND METHODS

Clinical materials

Thirty-two cases of gallbladder carcinomas were randomly selected and diagnosed histologically. All the patients were treated surgically in our hospital. No chemotherapy or anti-angiogenesis therapy was used prior to surgery. There were 17 males and 15 females with an average age of 56 years. Histological types included 4 cases of papillary adenocarcinoma (12.5 %), 25 cases of tubal adenocarcinoma (78.1 %) and 3 cases of mucous adenocarcinoma (9.4 %). Twelve cases had well-differentiated gallbladder carcinomas (37.5 %), 9 cases moderate-differentiated gallbladder carcinomas (28.1 %) and 11 cases poor-differentiated gallbladder carcinomas (34.4 %). The Nevin staging (Table 1) was determined based on clinical features: 14 cases at stages S1, S2 and S3, and 18 cases at stages S4 and S5. All available hematoxylin and eosin-stained sections in each case were reviewed.

Table 1 Nevin staging system for gallbladder cancer[1]

Stage	Definition
1	Tumor invades mucosa only
2	Tumor invades muscularis and mucosa
3	Tumor invades subserosa, muscularis and mucosa
4	Tumor invades all layers of gallbladder wall plus cystic lymph node
5	Tumor extends into liver bed or distant spread

Immunohistochemical stains

Four micrometer-thick sections from formalin-fixed and paraffin-embedded tissues were placed on poly-L-lysine-coated slides for immunohistochemistry study. The expression of P-gp was assessed by SP immunohistochemical method using a mouse-anti-human P-gp monoclonal antibody (JSB1) and a UltraSensitive™ S-P kit (kit 9710). Blood vessels were highlighted by staining endothelial cells for factor VIII-related antigens. The deparaffinized sections were boiled in citrate buffer at high temperature and high pressure for antigen retrieval for staining of P-gp, pepsin digestion for factor VIII-related antigen staining, and then incubated with each antibody

at 4 ℃ overnight. Immunohistochemical staining was then performed according to the UltraSensitive™ S-P kit manual. All reagents were supplied by Maixin-Bio Co, Fuzhou, China. The cells with brown-yellow granules in cytoplasms or on cytomembranes were considered as positive for P-gp expression.

Immunostaining

P-gp Stained slide was examined by two independent observers and scored semi-quantitatively. Staining intensity was assessed in comparison with positive slide of colon cancer, supplied by Maixin-Bio Co, Fuzhou, China. The staining intensity was scored as none (0), weak (1), moderate (2) and strong (3). The slides were classified as negative (0), positive (1), strong positive (2) and strongest positive (3) with corresponding rates of positive cells at <10 %, 10-20 %, 20-40 %, and >40 %, respectively. When the mean score in each group was 3 or more, the slide was considered as positive. Negative controls were stained without primary antibody.

Microvessel counts

MVCs were assessed according to Weidner *et al*[2]. The hot spots were selected under a microscope (40x), then individual counts were made under 200x field (Olympus BH-2 microscope,0.74 mm^2 per field). The average counts in 5 fields were recorded. Any single highlighted endothelial cell or endothelial cell cluster clearly separated from adjacent microvessel, and distinct clusters of brown-staining endothelial cells were counted as separate microvessels. Vessel lumens were not the sole criteria in identifying a microvessel.

Statistical analysis

Statistical analysis was performed using the Chi-square test and *t* test with SPSS software (Ver.10.0). $P<0.01$ or $P<0.05$ was considered as significant.

RESULTS

Expression of P-gp and MVC

The microvessels in malignant tissues were heterogeneously distributed. These highly neovascularized areas distributed within the tumor and dominated around the tumor margins (Figure 1). The P-gp was stained in cytoplasms and on the cytomembranes of gallbladder carcinoma cells (Figure 2).

Clinicopathologic characteristics of MVC and P-gp expressions

The average MVC in 32 cases of gallbladder carcinoma was (34±10)/HP. The number of MVC was markedly higher in cases of Nevin stages S4-S5 than in those of Nevin stages S1-S3 ($t=2.833$, $P=0.008$). MVC in moderately or poorly differentiated group was higher than that in well-differentiated group ($t=2.581$, $P=0.015$). The differences of MVC among the different pathologic types were not statistically significant ($P=0.313$, 0.822, 0.168) (Table 2).

The P-gp expression rate was 62.5 % in these 32 cases. The positive rate of P-gp was higher in cases of Nevin stages S1-S3 (78.6 %) than in those of Nevin stages S4-S5 (50.0 %) with no statistical significance ($\chi^2=2.743$, $P>0.05$). The expression rate of P-gp was not correlated with tumor differentiation or pathologic types ($P>0.05$) (Table 3).

Relationship between expression of P-gp and MVC

The value of MVC in P-gp (+) cases was 30±9/HP which was significantly lower than that in P-gp (-) cases (40±8/HP) ($t=2.987$, $P=0.006$). The P-gp expression rate was significantly higher in cases with less median MVC (33.6/HP) than in those with MVC over median MVC (81.3 % *vs* 43.8 %, $\chi^2=4.800$, $P<0.05$).

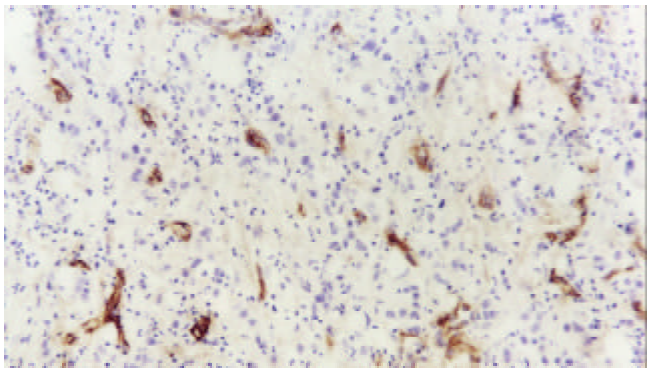

Figure 1 Distribution of microvessels in section of gallbladder carcinoma (S-P ×200).

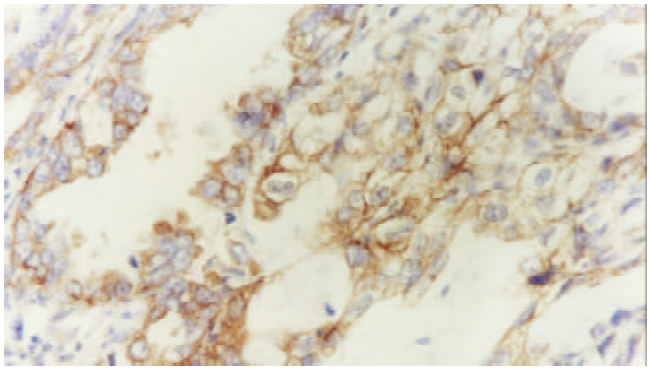

Figure 2 Expressed P-gp in gallbladder carcinoma (S-P ×400).

Table 2 Characteristics of MVC in gallbladder carcinoma

Characteristics	*n*	MVC
Pathologic types		
Papillary adenocacinoma	4	27±8[a]
Tubal adenocarcinoma	25	35±10[a]
Mucous adenocarcinoma	3	32±10[a]
Tumor differentiation		
Well	12	28±9[b]
Moderate-poor	20	37±9[b]
Nevin staging		
S1, S2, S3	14	28±10[c]
S4, S5	18	38±8[c]

[a]$P>0.05$, [b]$P<0.05$, [c]$P<0.01$.

Table 3 Characteristics of P-gp expression in gallbladder carcinoma

Characteristics	*n*	+	%
Pathologic types			
Papillary adenocacinoma	4	3	75.0[a]
Tubal adenocarcinoma	25	15	60.0[a]
Mucous adenocarcinoma	3	2	66.7[a]
Tumor differentiation			
Well	12	9	75.0[b]
Moderate-poor	20	11	55.0[b]
Nevin staging			
S1, S2, S3	14	11	78.6[c]
S4,S5	18	9	50.0[c]

[a]$P>0.05$, [b]$P>0.05$, [c]$P>0.05$.

DISCUSSION

In 1971, Folkman proposed that tumor growth be dependent on angiogenesis, and then considerable evidences showed that tumor growth was angiogenesis dependent, and the neovascularization was closely associated with the growth, invasion, metastasis, staging and prognosis of tumors[2-15]. Our study indicated that MVC was correlated to Nevin staging and tumor differentiation. The case at later stage and with poorer differentiation had higher level of MVC in gallbladder carcinomas. MVC might be one of the most important parameters in reflecting the biologic behaviors of gallbladder carcinomas.

Though tumor growth depends on the angiogenesis, its rate often fails to keep pace with tumor growth, as tumor vasculature is inadequate for the tumor mass. Therefore, many solid tumors have subpopulations of hypoxic cells. Studies showed that the hypoxic tumor cells were relatively resistant to certain cytotoxic drugs[16]. In the past, authors proposed that drug resistance be partly caused by poor tumor vascularization in reducing the influx of cytotoxic agents. Additionally, the hypoxic environment due to poor vascularization inhibited proliferation of tumor cells, yet noncycling cells would be expected to be less sensitive to many agents. In recent years, the identified biochemical mechanism of drug resistance was the overexpression of the transmembrane transport protein, P-glycoprotein (P-gp). P-gp is an ATP-binding-cassette transporter that is ubiquitously expressed, and often has high concentrations on plasma membrane of cancer cells, where it causes multidrug resistance by pumping lipophilic drugs out of the cell. The expression of P-gp influenced the efficacy of postoperative chemotherapy[17-24]. In our study, P-gp expression rate was 62.5 % which was similar to the result of another report on hepatocellular carcinoma[25]. Our result showed that overexpression of P-gp in gallbladder carcinoma tissue might be an important cause of drug resistance.

Recent studies showed that hypoxia-induced resistance to doxorubicin and methotrexate was attributed to an amplification of the P-gp gene and the dihydrofolate reductase gene[26-29]. Recently, it has also been shown that poor vascularization in lung carcinomas correlated with an up-regulation of drug-resistance enzymes, such as glutathione S-transferase-Ï, metallothionein and thymidylate synthase[30]. In another study on rectal cancer, poor angiogenesis was also linked to an expression of glutathione S-transferase and metallothionein[31]. Moreover, lung tumors with low vessel density and low VEGF expression have been found to be more frequently resistant to doxorubicin *in vitro* than tumors with high vessel counts and high expression of VEGF[32]. In our study, the value of MVC was markedly lower in P-gp (+) cases than in P-gp (-) cases. The positive rate of P-gp was significantly higher in cases with small MVC than in cases with big MVC.

In conclusion, the finding that poor vascularization links to overexpression of the most important multidrug resistance enzyme—P-gp provides us an additional insight into drug resistance in gallbladder carcinomas.

REFERENCES

1 **Nevin JE**, Moran TJ, Kay S, King R. Carcinoma of the gallbladder: staging, treatment and prognosis. *Cancer* 1976; **37**: 141-148

2 **Weidner N**, Semple JP, Welch WR, Folkman J. Tumor angiogenesis and metastasis-correlation in invasive breast carcinoma. *N Engl J Med* 1991; **324**: 1-8

3 **Macchiarini P**, Fontanini O, Hardin MJ, Squartini F, Angeletti CA. Relation of neovascularization to metastasis of non-small-cell lung cancer. *Lancet* 1992; **340**: 145-146

4 **Song ZJ,** Gong P, Wu YE. Relationship between the expression of iNOS, VEGF, tumor angiogenesis and gastric cancer. *World J Gastroenterol* 2002; **8**: 591-595

5 **Liu XP**, Song SB, Li G, Wang DJ, Zhao HL, Wei LX. Correlations of microvessel quantitation in colorectal tumors and clinicopathology. *Shijie Huaren Xiaohua Zazhi* 1999; **7**: 37-39

6 **Gao GL**, Yang Y, Yang SF, Ren CW. Relationship between proliferation of vascular andothelial cells and gastric cancer. *Shijie Huaren Xiaohua Zazhi* 2000; **8**: 282-284

7 **Jia L**, Chen TX, Sun JW, Na ZM, Zhang HH. Relationship between microvessel density and proliferating cell nuclear antigen and prognosis in colorectal cancer. *Shijie Huaren Xiaohua Zazhi* 2000; **8**: 74-76

8 **Liu H**, Wu JS, Li LH, Yao X. The expression of platelet-derived growth factor and angiogenesis in human coloreactal carcinoma. *Shijie Huaren Xiaohua Zazhi* 2000; **8**: 661-664

9 **Giatromanolaki A**, Sivridis E, Koukourakis MI, Polychronidis A, Simopoulos C. Prognostic role of angiogenesis in operable carcinoma of the gallbladder. *Am J Clin Oncol* 2002; **25**: 38-41

10 **Niedergethmann M**, Hildenbrand R, Wostbrock B, Hartel M, Sturm JW, Richter A, Post S. High expression of vascular endothelial growth factor predicts early recurrence and poor prognosis after curative resection for ductal adenocarcinoma of the pancreas. *Pancreas* 2002; **25**: 122-129

11 **Ng IO**, Poon RT, Lee JM, Fan ST, Ng M, Tso WK. Microvessel density, vascular endothelial growth factor and its receptors Flt-1and Flk-1/KDR in hepatocellular carcinoma. *Am J Clin Pathol* 2001; **116**: 838-845

12 **Niemoller K**, Jakob C, Heider U, Zavrski I, Eucker J, Kaufmann O, Possinger K, Sezer O. Bone marrow angiogenesis and its correlation with other disease characteristics in multiple myeloma in stage I versus stage II-III. *J Cancer Res Clin Oncol* 2003; **129**: 234-238

13 **Takahashi R**, Tanaka S, Kitadai Y, Sumii M, Yoshihara M, Haruma K, Chayama K. Expression of vascular endothelial growth factor and angiogenesis in gastrointestinal stromal tumor of the stomach. *Oncology* 2003; **64**: 266-274

14 **Onogawa S**, Tanaka S, Oka S, Morihara M, Kitadai Y, Sumii M, Yoshihara M, Shimamoto F, Haruma K, Chayama K. Clinical significance of angiogenesis in rectal carcinoid tumors. *Oncol Rep* 2002; **9**: 489-494

15 **Joo YE**, Sohn YH, Joo SY, Lee WS, Min SW, Park CH, Rew JS, Choi SK, Park CS, Kim YJ, Kim SJ. The role of vascular endothelial growth factor (VEGF) and p53 status for angiogenesis in gastric cancer. *Korean J Intern Med* 2002; **17**: 211-219

16 **Teicher BA**. Hypoxia and drug resistance. *Cancer Metastasis Rev* 1994; **13**: 139-168

17 **Chung HC**, Rha SY, Kim JH, Roh JK, Min JS, Lee KS, Kim BS, Lee KB. P-glycoprotein: the intermediate end point of drug response to induction chemotherapy in locally advanced breast cancer. *Breast Cancer Res Treat* 1997; **42**: 65-72

18 **Chen CY**, Zhu ZH. Relationship between expression of P-glycoprotein and efficacy of chemotherapy in gastric cancer. *Shijie Huaren Xiaohua Zazhi* 2003; **11**: 36-38

19 **Cao L**, Peng S, Duchrow M. Expression of P-glycoprotein in benign and malignant gallbladder neoplasms. *Zhonghua Zhongliu Zazhi* 1999; **21**: 119-121

20 **Cao L**, Duchrow M, Windhovel U, Kujath P, Bruch HP, Broll R. Expression of MDR1 mRNA and encoding P-glycoprotein in archival formalin-fixed paraffin-embedded gall bladder cancer tissues. *Eur J Cancer* 1998; **34**: 1612-1617

21 **Monden N**, Abe S, Hishikawa Y, Yoshimura H, Kinugasa S, Dhar DK, Tachibana M, Nagasue N. The role of P-glycoprotein in human gastric cancer xenografts in response to chemotherapy. *Int J Surg Investig* 1999; **1**: 3-10

22 **Yokoyama Y**, Sato S, Fukushi Y, Sakamoto T, Futagami M, Saito Y. Significance of multi-drug-resistant proteins in predicting chemotherapy response and prognosis in epithelial ovarian cancer. *J Obstet Gynaecol Res* 1999; **25**: 387-394

23 **Baekelandt MM**, Holm R, Nesland JM, Trope CG, Kristensen GB. P-glycoprotein expression is a marker for chemotherapy resistance and prognosis in advanced ovarian cancer. *Anticancer Res* 2000; **20**: 1061-1067

24 **Warnakulasuriya S**, Jia C, Johnson N, Houghton J. p53 and P-

glycoprotein expression are significant prognostic markers in advanced head and neck cancer treated with chemo / radiotherapy. *J Pathol* 2000; **191**: 33-38

25 **Kong XB**, Yang ZK, Liang LJ, Huang JF, Lin HL. Overexpression of P-glycoprotein in hepatocellular carcinoma and its clinical implication. *World J Gastroenterol* 2000; **6**: 134-135

26 **Rice GC**, Hoy C, Schimke RT. Transient hypoxia enhances the frequency of dihydrofolate reductase gene amplification in Chinese hamster ovary cells. *Proc Natl Acad Sci U S A* 1986;**83**: 5978-5982

27 **Rice GC**, Ling V, Schimke RT. Frequencies of independent and simultaneous selection of Chinese hamster cells for methotrexate and doxorubicin (adriamycin) resistance. *Proc Natl Acad Sci U S A* 1987; **84**: 9261-9264

28 **Kalra R**, Jones AM, Kirk J, Adams GE, Stratford IJ. The effect of hypoxia on acquired drug resistance and response to epidermal growth factor in Chinese hamster lung fibroblasts and human breast-cancer cells *in vitro*. *Int J Cancer* 1993; **54**: 650-655

29 **Luk CK**, Veinot-Drebot L, Tjan E, Tannock IF. Effect of transient hypoxia on sensitivity to doxorubicin in human and murine cell lines. *J Natl Cancer Inst* 1990; **82**: 684-692

30 **Koomagi R**, Mattern J, Volm M. Up-regulation of resistance-related proteins in human lung tumors with poor vascularization. *Carcinogenesis* 1995; **16**: 2129-2133

31 **Mattern J**, Kallinowski F, Herfarth C, Volm M. Association of resistance-related protein expression with poor vascularization and low levels of oxygen in human rectal cancer. *Int J Cancer* 1996; **67**: 20-23

32 **Volm M**, Koomagi R, Mattern J. Interrelationships between microvessel density, expression of VEGF and resistance to doxorubicin of non-small lung cell carcinoma. *Anticancer Res* 1996;**16**: 213-217

Edited by Ren SY and Wang XL

P.O.Box 2345, Beijing 100023,China
Fax: +86-10-85381893
E-mail: wjg@wjgnet.com www.wjgnet.com

World J Gastroenterol 2003;9(12):2821-2823
World Journal of Gastroenterology
 ISSN 1007-9327

• CLINICAL RESEARCH •

Clinical predictors of severe gallbladder complications in acute acalculous cholecystitis

Ay-Jiun Wang, Tsang-En Wang, Ching-Chung Lin, Shee-Chan Lin, Shou-Chuan Shih

Ay-Jiun Wang, Tsang-En Wang, Ching-Chung Lin, Shee-Chan Lin, Shou-Chuan Shih, Division of Gastroenterology, Department of Internal Medicine, Mackay Memorial Hospital, Taipei, Taiwan, China
Correspondence to: Dr. Ay-Jiun Wang, Division of Gastroenterology, Department of Internal Medicine, Mackay Memorial Hospital. 92, Sec. 2, Chung San North Road, Taipei, Taiwan, China. ajw@ms2.mmh.org.tw
Telephone: +86-2-25433535 **Fax:** +86-2-25574800
Received: 2003-08-26 **Accepted:** 2003-10-12

Abstract

AIM: To evaluate the relationship between clinical information (including age, laboratory data, and sonographic findings) and severe complications, such as gangrene, perforation, or abscess, in patients with acute acalculous cholecystitis (AAC).

METHODS: The medical records of patients hospitalized from January1997 to December 2002 with a diagnosis of acute cholecystitis were retrospectively reviewed to find those with AAC, confirmed at operation or by histologic examination. Data collected included age, sex, white blood cell count, AST, total bilirubin, alkaline phosphatase, bacteriology, mortality, and sonographic findings. The sonographic findings were recorded on a 3-point scale with 1 point each for gallbladder distention, gallbladder wall thickness >3.5 mm, and sludge. The patients were divided into 2 groups based on the presence (group A) or absence (group B) of severe gallbladder complications, defined as perforation, gangrene, or abscess.

RESULTS: There were 52 cases of AAC, accounting for 3.7 % of all cases of acute cholecystitis. Males predominated. Most patients were diagnosed by ultrasonography (48 of 52) or computed tomography (17 of 52). Severe gallbladder complications were present in 27 patients (52 %, group A) and absent in 25 (group B). Six patients died with a mortality of 12 %. Four of the 6 who died were in group A. Patients in group A were significantly older than those in group B (mean 60.88 y *vs*. 54.12 y, P=0.04) and had a significantly higher white blood cell count (mean 15 885.19 *vs*. 9 948.40, P=0.0005). All the 6 patients who died had normal white blood cell counts with an elevated percentage of band forms. The most commonly cultured bacteria in both blood and bile were *E. coli* and *Klebsiella pneumoniae*. The cumulative sonographic points did not reliably distinguish between groups A and B, even though group A tended to have more points.

CONCLUSION: Older patients with a high white cell count are more likely to have severe gallbladder complications. In these patients, earlier surgical intervention should be considered if the sonographic findings support the diagnosis of AAC.

Wang AJ, Wang TE, Lin CC, Lin SC, Shih SC. Clinical predictors of severe gallbladder complications in acute acalculous cholecystitis. *World J Gastroenterol* 2003; 9(12): 2821-2823
http://www.wjgnet.com/1007-9327/9/2821.asp

INTRODUCTION

Acute acalculous cholecystitis (AAC) is rare, occurring in only 5 % to 10 % of patients with acute cholecystitis[1]. It is more likely to be found in patients with recent severe trauma, critical illness, cardiovascular surgery[2,3] or severe burns. AAC has also been found in association with total parenteral nutrition[4], mechanical ventilation, and the use of narcotic analgesics. Major cardiovascular disorders, complicated diabetes mellitus, autoimmune disease[5-8], and AIDS[9] have all been recognized as possible inciting factors for AAC.

AAC is a surgical emergency. Without immediate treatment, there may be rapid progression to perforation or gangrenous cholecystitis, with a mortality as high as 65 %[10]. With early diagnosis and intervention, the mortality drops to 7 %[11]. Therefore, it is important to understand the clinical variables that may assist in making an early diagnosis of this condition. The aim of the present retrospective study was to assess what clinical information might accurately predict AAC.

MATERIALS AND METHODS

We retrospectively reviewed the charts of patients in a medical center from January1997 to December 2002 and found 1395 cases of acute cholecystitis. Gallstones were present in 1234 cases. We excluded patients with carcinoma of the gallbladder, pancreas, or biliary tract, common bile duct stones, intrahepatic stones, and patients who recovered without surgery, leaving 52 cases of AAC confirmed surgically or histologically. We divided the patients into two groups based on the presence (group A) or absence (group B) of severe complications involving the gallbladder, defined as perforation, gangrene, or abscess. We recorded the following data: age, sex, white blood cell count, AST, total bilirubin, alkaline phosphatase, sonographic findings, bacteriology, and mortality. The sonographic findings were scored, with 1 point each given for gallbladder distention, wall thickness greater than 3.5 mm, and sludge.

Student' s *t*-test was used to analyze differences in means between the two groups. Sonographic scores for the severity of gallbladder condition were analyzed using the χ^2 test. A P value <0.05 was considered significant.

RESULTS

The 52 cases of AAC in our study accounted for 3.7 % of the totally 1 359 cases of acute cholecystitis seen during the study period. Males predominated, with 37 cases. The mean age of males was 56.5 years and of females, 60.5 years (Table 2). Most of our cases were diagnosed by ultrasonography (48 of 52) or computed tomography (17 of 52), with 13 patients having both examinations. Severe complications of the gallbladder were encountered in 27 (52 %) patients (group A). Six patients (12 %), all men, died, of whom 4 were in group A. The underlying conditions in these 4 patients were major surgery in 2, sepsis in 1, and bacteremia caused by *Salmonella gr. D* in 1. Of the 2 patients in group B who died, 1 had severe burns and 1 had *Aeromonas* bacteremia. The predisposing conditions for all

the patients are shown in Table 1.

There were no significant differences between the two groups in terms of liver biochemistry, length of hospital stay, or thickness of the gallbladder wall. The white blood cell count and age were significantly higher in group A ($P<0.05$, Table 2). In 10 patients in both groups, the percentage of band forms was over 10 %, including the 6 patients who died. Blood cultures were positive in 24 % and bile cultures in 66 % (Table 3). *E. coli.* and *Klebsiella pneumoniae* were the most frequently cultivated organisms in both blood and bile (Tables 4 and 5).

Most patients had a score of at least 2 points for sonographic findings. There was a tendency for group A to have higher scores, but the difference was not statistically significant (Table 6).

Table 1 Predisposing factors in patients with acute acalculous cholecystitis

Predisposing factor	Total (*n*)
Shock	7
Trauma	2
Burn	1
Major surgery	2
Bacteremia	11
DM	8
HTN	13
Heart disease[a]	14
CVA	3
TPN	1
Hyperlipidemia	5

a: Heart disease includes atrial fibrillation, congestive heart failure, hypertensive cardiovascular disease, hypertrophic cardiomyopathy and dilated cardiomyopathy.

Table 2 Demographic and clinical data in patients with acute acalculous cholecystitis with and without severe complications

	Group A *n*=27	Group B *n*=25	*P*
Gender			
Female	8	7	0.28
Male	19	18	0.71
Age (years)	60.88	54.12	0.04
Hospital stay (days)	19.74	18.84	0.42
WBC / mm^3	15 885.19	9 948.40	0.0005
AST (u / l)	138.04	141.87	0.48
Bilirubin (mg / dl)	2.46	2.37	0.46
Alkaline phosphatase (u / l)	106.19	130.59	0.07
Gallbladder wall (mm)	8.8	8.55	0.38

Table 3 Results of blood and bile culture for bacteria in patients with acute acalculous cholecystitis

Culture	Blood (*n*)	Bile (*n*)
No growth	34 (76%)	14 (34%)
Bacteria(+)	11 (24%)	27 (66%)

Table 4 Bacteria cultured from blood in patients with acute acalculous cholecystitis

	Group A (*n*)	Group B (*n*)	Total (*n*)
E.coli	3	3	6
Klebsiella pneumoniae	1	2	3
Aeromonas sp	0	1	1
Salmonella gr.D	1	0	1
G(+) Bacilli	1	0	1

Table 5 Bacteria cultured from bile in patients with acute acalculous cholecystitis

	Group A (*n*)	Group B (*n*)	Total (*n*)
E.coli	12	1	13
Klebsiella pneumoniae	6	1	7
Aeromonas	0	1	1
Salmonella gr.D	1	1	2
Enterobacter sp.	2	0	2
Pseudomonas sp.	1	1	2
Burkholderia cepacia	1	0	1
Candida albican	0	1	1
Citro. Freundii	1	0	1
Enterococcus	1	0	1
Providencia	0	1	1
Stophy. Coagulase (-)	1	0	1

Table 6 Sonographic findings recorded including gallbladder thickening, distention, and sludge

Sonographic finding	1 point	2 points	3 points	Total
Group A	4	11	9	24
Group B	9	11	4	24
Subtotal	13	22	13	48
$\chi^2=3.85$	$P>0.05$			

DISCUSSION

Most of our patients had multiple conditions that probably predisposed them to AAC (Table 1). Bile stasis, gallbladder ischemia, cystic duct obstruction, and systemic infection have been considered to be the most important factors in the pathogenesis of AAC[12].

The bacteria we cultured from blood and bile were similar to those reported by others. Gastrointestinal flora such as *E. coli* and *Klebsiella pneumoniae* were most commonly cultured, as was true in our series. However, uncommon microorganisms have also been isolated from the bile, including *Leptospira spp*[13,14], *Salmonella spp*[15], *Vibrio cholerae*[16], or *Listeria monocytogenes*. We had two patients with *Salmonella group D* infection, one of whom died of gangrene of the gallbladder with sepsis.

Rapid and accurate diagnosis is essential because ischemia may progress rapidly to gangrene and perforation. If an operation was performed within 48 hours from the onset of symptoms, severe complications would be reduced[17]. AAC should be considered in every patient who is critically ill or injured and who has clinical findings of sepsis with no obvious source. Fever, right upper quadrant pain, and leukocytosis are common manifestations but are very nonspecific. However, our study revealed that a high white blood cell count and older age were associated with a higher incidence of gallbladder gangrene and perforation. More aggressive management should be considered in these patients. Patients with greater than 10 % band neutrophils might have an especially poor outcome.

Abdominal ultrasonography is the primary diagnostic modality for AAC. The most significant ultrasonographic findings are thickening of the gallbladder wall of more than 3.5 mm, gallbladder distention, a positive sonographic Murphy's sign, pericholecystic fluid, and a sonolucent intraluminal layer[18,19]. We did not find the 3 sonographic findings we used were adequate to predict those patients likely to have severe gallbladder complications, although there was a trend toward higher scores in the group with complications. It may be that a study with a larger sample might find this to be a useful criterion.

In a discussion of diagnostic strategies for AAC, Kalliafas *et al* reported that morphine cholescintigraphy had the highest sensitivity (9 of 10, 90 %), followed by computed tomography (8 of 12, 67 %) and ultrasonography (2 of 7, 29 %). They reported a mortality of 41 % and a morbidity (that is, gangrene, perforation, or abscess) of 82 %[20]. However, in our series, the mortality was only 11.5 % and morbidity 52 %. Why are the results so different? We diagnosed most of our cases by ultrasonography (48 of 52) or computed tomography (17 of 52), only two patients had cholescintigraphy. Further studies are needed to elucidate the relationship between the diagnostic modality and prediction of the morbidity and mortality of AAC.

The mainstay of therapy for AAC is cholecystectomy, which was traditionally performed by open laparotomy[21]. Recently, laparoscopic cholecystectomy was performed in a small study with no complications from the procedure[22]. Cholecystostomy has be come a potentially lifesaving alternative in patients too weak to undergo general anesthesia[23]. Percutaneous cholecystostomy by computed tomography or echo guidance is gaining acceptance as an alternative to an open procedure[24]. In the future, laparoscopy for early diagnosis and treatment may be further developed as a useful method to decrease the mortality of AAC.

Finally, early diagnosis and early operation are the key to managing acute acalculous cholecystitis. Older patients with a high white cell count are more likely to have severe gallbladder complications. In these patients, earlier surgical intervention should be considered if the sonographic findings support the diagnosis of AAC.

REFERENCES

1 **Howard R**. Acute acalculous cholecystitis. *Am J Surg* 1981; **141**: 194-198

2 **Saito A**, Shirai Y, Ohzeki H, Hoyashi J, Eguchi S. Acute acalculous cholecystitis after cardiovascular surgery. *Surg Today* 1997; **27**: 907-909

3 **Hagino RT**, Valentine RJ, Clagett GP. Acalculous cholecystitis after aortic reconstruction. *J Am Coll Surg* 1997; **184**: 245-248

4 **Hatada T**, Kobayashi H, Tanigawa A, Fujiwara Y, Hanada Y, Yamamura T. Acute acalculous cholecystitis in a patient on total parenteral nutrition: case report and review of the Japanese literature. *Hepato-Gastroenterology* 1999; **46**: 2208-2211

5 **Kamimura T**, Mimori A, Takeda A, Masuyama J, Yoshio T, Okazaki H, Kano S, Minota S. Acute acalculous cholecystitis in systemic lupus erythematous: a case report and review of the literature. *Lupus* 1998; **7**: 361-363

6 **Date K**, Shirai Y, Hatakeyama K. Antiphospholipid antibody syndrome presenting as acute acalculous cholecystitis. *Am J Gastroenterol* 1997: **92**: 2127-2128

7 **Parangi S**, Oz MC, Blume RS, Bixon R, Laffey KJ, Perzin KH, Buda JA, Markowitz AM, Nowygrod R. Hepatobiliary complications of polyarteritis nodosa. *Arch Surg* 1991; **126**: 909-912

8 **Imai H**, Nakamoto Y, Nakajima Y, Miura AB. Allergic granulomatosis and angiitis (Churg-Strauss syndrome) presenting as acalculous cholecystitis. *J Rheumatol* 1990; **17**: 247-249

9 **Jannuzzi C**, Belghiti J, Erlinger S, Menu Y, Fekete F. Cholangitis associated with cholecystitis in patients with acquired immunodeficiency syndrome. *Arch Surg* 1990; **125**: 1211-1213

10 **Flancbaum L**, Choban PS. Use of morphine cholescintigraphy in the diagnosis of acute cholecystitis in critically ill patients. *Intensive Care Med* 1995; **21**: 120-124

11 **Adam A**, Roddie ME. Acute cholecystitis: radiological management. *Baillieres Clin Gastroenterol* 1991; **5**: 787-816

12 **Barie PS**, Fischer E. Acute acalculous cholecystitis. *J Am Coll Surg* 1995; **180**: 232-244

13 **Vilaichone RK**, Mahachai V, Wilde H. Acute acalculous cholecystitis in leptospirosis. *J Clin Gastroenterol* 1999; **29**: 282-283

14 **Baelen E**, Roustan J. Leptospirosis associated with acute acalculous cholecystitis, Surgical or medical treatment. *J Clin Gastroenterol* 1997; **25**: 704-706

15 **McCarron B**, Love WC. Acalculous nontyphoidal salmonellal cholecystitis requiring surgical intervention despite ciprofloxacin therapy: report of three cases. *Clin Infect Dis* 1997; **24**: 707-709

16 **West BC**, Silberman R, Otterson WN. Acalculous cholecystitis and septicemia caused by non-O1 Vibrio cholerae: first reported case and review of biliary infections with Vibrio cholerae. *Diagn Microbial Infect Dis* 1998; **30**: 187-191

17 **Hsu JC**, Yang TL, Wang TC. Acute acalculous cholecystitis. *Chin Med J* 1993; **51**: 266-2704

18 **Deitch EA**, Engel JM. Acute acalculous cholecystitis: ultrasonic diagnosis. *Am J Surg* 1981; **142**: 290-292

19 **Becker CD**, Burckhardt B, Terrier F. Ultrasound in postoperative acalculous cholecystitis. *Gastrointest Radiol* 1986; **11**: 47-50

20 **Kalliafas S**, Ziegler DW, Flancbaum L, Choban PS. Acute acalculous cholecystitis: incidence, risk factors, diagnosis, and outcome. *Am Surg* 1998; **64**: 471-475

21 **Glenn F**, Becker CG. Acute acalculous cholecystitis: an increasing entity. *Ann Surg* 1982; **195**: 131-136

22 **McClain T**, Gilmore BT, Peetz M. Laparoscopic cholecystectomy in the treatment of acalculous cholecystitis in patients after thermal injury. *J Burn Care Rehabil* 1997; **18**: 141-146

23 **Glenn F**. Cholecystostomy in the high-risk patient with bililary tract disease. *Ann Surg* 1977; **185**: 185-191

24 **Vauthey JN**, Lerut J, Martini M, Becker C, Gertsch P, Blumgart LH. Indications and limitations of percutaneous cholecystostomy for acute cholecystitis. *Surg Gynecol Obstet* 1993; **176**: 49-54

Edited by Zhu LH

P.O.Box 2345, Beijing 100023,China
Fax: +86-10-85381893
E-mail: wjg@wjgnet.com www.wjgnet.com

World J Gastroenterol 2003;9(12):2824-2827
World Journal of Gastroenterology
 ISSN 1007-9327

• CLINICAL RESEARCH •

Imaging diagnosis of pancreato-biliary diseases: A control study

Liang Zhong, Qiu-Ying Yao, Lei Li, Jian-Rong Xu

Liang Zhong, Qiu-Ying Yao, Lei Li, Jian-Rong Xu, Department of Radiology, Renji Hospital, Shanghai Second Medical University, Shanghai 200001, China
Correspondence to: Dr. Liang Zhong, Department of Radiology, Renji Hospital, 145 Shandong Zhonglu, Shanghai 200001, China. zhong-liang@online.sh.cn
Telephone: +86-21-63260930 **Fax:** +86-21-63730455
Received: 2003-05-13 **Accepted:** 2003-06-04

Abstract

AIM: To evaluate the clinical value of various imageological methods in diagnosing the pancreato-biliary diseases and to seek the optimal procedure.

METHODS: Eighty-two cases of pancreato-biliary diseases confirmed by surgery and pathology were analyzed. There were 38 cases of cholelithiasis, 34 cases of pancreato-biliary tumors and 10 other cases. The imageological methods included B-US, CT, ERCP, PTC, cross-sectional MRI and MR cholangiopancreatography (MRCP).

RESULTS: The accuracy rate of MRCP in detecting the location of pancreato-biliary obstruction was 100 %. In differentiating malignant from benign obstruction, the sensitivity of the combination of MRCP and cross-sectional MRI was 82.3 %, the specificity was 93.8 %, and the accuracy rate was 89.0 %. The accuracy rate for determining the nature of obstruction was 87.8 %, which was superior to that of B-US (P=0.0000) and CT (P=0.0330), but there was no significant difference between direct cholangiopancreatography and the combination of MRCP and conventional MRI (P=0.6666).

CONCLUSION: In most cases, MRCP can substitute direct cholangiopancreatography for diagnosis. The combination of MRCP and cross-sectional MRI should be considered as an important means in diagnosing the pancreato-biliary diseases, pre-operative assessment and post-operative follow-ups.

Zhong L, Yao QY, Li L, Xu JR. Imaging diagnosis of pancreato-biliary diseases: A control study. *World J Gastroenterol* 2003; 9(12): 2824-2827
http://www.wjgnet.com/1007-9327/9/2824.asp

INTRODUCTION

Pancreato-biliary disorders are common diseases that often involve the biliary system to produce the symptom of obstructive jaundice. It is the precondition to investigate the obstructive location and causes of pancreato-biliary diseases. In this study, 82 cases of pancreato-biliary diseases confirmed by surgery and pathology were analyzed. The aims of the prospective study were to evaluate the clinical value of various imageological methods in diagnosing the pancreato-biliary diseases and to seek the optimal examination procedure.

MATERIALS AND METHODS

Patients

The study subjects included 82 patients (54 men and 28 women, mean age 60.0 years, range 11-82 years), 67 (81.7 %) cases had the symptom of obstructive jaundice. All patients underwent B-US, MR cholangiopancreatography (MRCP) and cross-sectional MRI examination. Fifty-seven patients underwent enhanced or un-enhanced CT scan. In addition, 48 patients had undergone direct cholangiopancreatography (41 ERCP and 7 PTC). However, direct cholangiopancreatography was unsuccessful in 4 cases due to difficult cannulation (2 ERCP), post-gastroenterostomy (1 ERCP) and sick patient (1 PTC). ERCP was incomplete in another 4 cases because only the pancreatic duct could be demonstrated and the biliary tree was not opacified. Therefore, 40 direct cholangiopancreatographies (34 ERCP and 6 PTC) were performed in all 82 cases, 1 patient had complication of acute pancreatitis after ERCP. All patients with pancreat-biliary diseases were confirmed by surgical findings and pathology, including 12 by laparoscopic cholecystectomy (LC), 6 by endoscopic sphincter tenotomy (EST) and 1 by PTC drainage (PTCD). Among the 82 cases, 38 were diagnosed as cholelithiasis, 34 as pancreato-biliary tumors and 10 as other diseases (Table 1).

Table 1 Pancreato-biliary diseases (n=82)

Pancreato-biliary diseases	No. of cases
Cholelithiasis[a]	38
Gallbladder stone	14
Intrahepatic bile duct stone	7
Choledocholithiasis	17
Pancreato-biliary tumor [b]	34
Gallbladder carcinoma	6
Cholangiocarcinoma	9
Ampullary carcinoma	3
Pancreatic head carcinoma	11
Bile papilla carcinoma	5
Other diseases	10
Bile duct injury	2
Choledochal cyst	2
Sclerosing cholangitis	2
Chronic pancreatitis	4

[a]Gallbladder stone mixed with intra-or extra-hepatic stone 15, Mirizzi syndrome 2; [b]Hepatic invasion or metastasis 5, lymphadenectasis 3.

Techniques

MR imaging was performed with a 1.0T superconductive unit (Philips Gyroscan T10-NT, software version 4.6.2) containing a body coil. The patients were examined in the supine position, quiet breathing and abdominal band compression. The routine upper abdominal axial T1WI, T2WI and coronal T2WI MR examinations with Turbo Spin-Echo (TSE) sequence were performed first, and followed by the additional axial T2WI and/or T1WI fat-suppressed sequence (spectral saturation

inversion recovery, SPIR). The routine axial images served as guides to locate the MR cholangiopancreatography (MRCP). MRCP was performed with coronal, multislices, heavily T2-weighted TSE sequence (TR=2 000 ms, TE=700 ms). A non-breath-hold, respiratory-triggering technique was used to decrease the respiratory motion artifact. The MRCP source images were three-dimensionally (3D) reconstructed using a maximum-intensity-projection (MIP) algorithm. The total imaging time was approximately 30 min.

Computed tomography (CT) used a whole body CT scan unit (Picker PQ-2000). All CT examinations were performed after the patients had fasted for 4-8 hours and took 5 00-1 000 ml oral contrast (0.5-1 % Meglumine Diatrizoate) before CT scanning. Enhanced CT examination used 80-100 ml non-ion intravenous contrast agents injected through anecubital vein in a bolus at the rate of 2-3 ml/s.

Direct cholangiopancreatography (ERCP and PTC) was performed with a digital imaging unit (Philips Diagnost 93).

Imaging analysis

All image data of 82 cases were carefully reviewed to observe the enlargement or stricture of pancreato-biliary tract. The study protocol included detecting the obstructive locations, distinguishing the malignant from benign causes and evaluating the clinical value of various imaging methods (including B-US, CT, MRCP, ERCP/PTC) in diagnosing the pancreato-biliary diseases. *SAS* software was used for all statistical analyses.

The diagnostic principles and evaluating criteria for direct cholangiopancreatography and MRCP were identical, but in MRCP it was more important to carefully review both the source images and the MIP reconstructed images. According to the findings of the dilatation or stricture of pancreato-biliary tree and gallbladder, the obstructive locations of pancreato-biliary duct were divided into three parts: intra-hepatic or extra-hepatic bile duct and main pancreatic duct. Normal gallbladder was 7-10 cm in length and 3-4 cm in width. Dilatation of the common bile duct was defined as larger than 8 mm in maximal diameter in patients without histories of cholecystectomy and 10 mm in patients with prior cholecystectomy. Dilatation of the intra-hepatic bile duct and main pancreatic duct was defined as larger than 3 mm in maximal diameter[1-4].

The cause of pancreato-biliary abnormality was evaluated using a five-point scale to assign a confidence level: 1. definitely benign, 2. probably benign, 3. indeterminate, 4. probably malignant, and 5. definitely malignant[5]. If the cause of pancreato-biliary abnormality was assumed to be malignant, the reasons were chosen from the following findings: visualization of tumor, double duct sign, abrupt obstruction of bile duct, irregularity of obstructed margin, or asymmetric obstruction of the distal margin of the dilated bile duct. Receiver operating characteristic (ROC) curve analysis was performed to compare the results of readings of MRCP images versus the results of readings of the combination of MRCP images and routine MR images and versus the results of readings of ERCP images. Binormal ROC curves were fitted using *ROCKIT 0.9B* software. The diagnostic capability was determined by calculating the area under the ROC curve (Az). Ratings of 1 or 2 indicated a reading of a benign lesion, ratings of 4 or 5 indicated a rating of a malignant lesion. Ratings of 3 were considered to indicate an indeterminate diagnosis. Sensitivity, specificity and accuracy of ERCP, MRCP and the combination of MRCP and routine MR imaging in differentiating malignant from benign causes of pancreato-biliary tract obstruction were calculated.

RESULTS

MRCP image quality

MR cholangiopancreatography was successfully performed in all 82 patients and the images of MRCP were similar to those of direct cholangiopancreatography. MRCP studies of diagnostic quality were obtained in 79 (96.3 %) subjects with fine contrast between the pancreato-biliary structure and the surrounding background. In the remaining 3 patients with pancreato-biliary tumor, the presence of ascitic fluid in the upper abdomen and the fluid-containing organs due to gastrointestinal obstruction obscured visualization of the pancreato-biliary tree and degraded the quality of the MRCP image. In 8 (16.7 %) patients in whom direct cholangiopancreatography was unsuccessful or incomplete, MRCP examinations all succeeded and the MRCP images were satisfactory.

Diagnosis of obstructive location

Among the 82 patients with pancreato-biliary diseases, 8, 60 and 21 cases had pancreato-biliary obstructive locations in intra-hepatic, extra-hepatic bile duct and main pancreatic duct, respectively (totally 89 locations). MRCP could clearly visualize the dilation of pancreato-biliary ducts above the obstructive level in their native state, thus being more suitable for demonstrating the extra-hepatic bile duct obstruction. The total accuracy of MRCP in detecting the location of pancreato-biliary obstruction was 100 %, which was superior to that of B-US (P=0.0002) and CT (P=0.0422), but there was no significant difference between MRCP and direct cholangiopancreatography (P=0.1487) (Table 2).

Table 2 Accuracy of pancreato-biliary obstruction level (%) by different imageological methods

Level	Intra-hepatic	Extra-hepatic	Main pancreatic	Total
B-US	100.0 (8/8)	81.7 (49/60)	90.5 (19/21)	85.4 (76/89)
CT	100.0 (4/4)	93.0 (40/43)	100.0 (19/19)	95.5 (63/66)
ERCP/PTC	100.0 (5/5)	96.7 (29/30)	100.0 (8/8)	97.7 (42/43)
MRCP	100.0 (8/8)	100.0 (60/60)	100.0 (21/21)	100.0 (89/89)

Differentiation of malignant from benign obstruction

The sensitivity, specificity and accuracy of MRCP in distinguishing malignant from benign causes of pancreato-biliary obstruction were 64.7 %, 81.2 % and 74.4 %, respectively, while those of ERCP/PTC were 77.8 %, 86.4 % and 82.5 %, respectively. The difference was not significant between MRCP and ERCP/PTC in Az area under the ROC curve (P=0.4590). The combination of MRCP and routine MR imaging could obviously improve the diagnostic capability of differentiating the causes of pancreato-biliary obstruction with a sensitivity of 82.3 %, a specificity of 93.8 % and an accuracy of 89.0 %. The difference was significant between MRCP and the combination of MRCP and routine MR imaging (P=0.0489) (Table 3 and Figure 1).

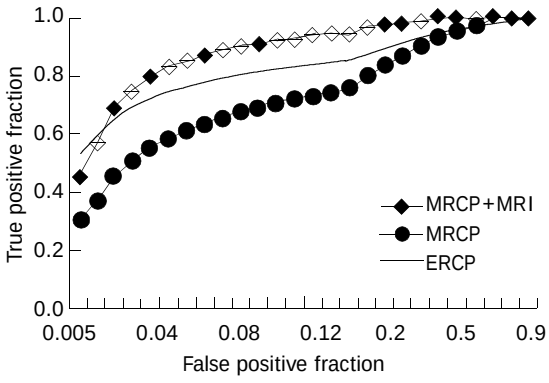

Figure 1 ROC curve analysis of differentiation between malignant and benign causes of pancreato-biliary obstruction.

Table 3 ROC analysis of pancreato-biliary obstruction

	ERCP / PTC (*n*=40)	MRCP (*n*=82)	MRCP+MRI (*n*=82)
True-positive	14	22	28
True-negative	19	39	45
False-positive	3	9	3
False-negative	4	12	6
Sensitivity (%)	77.8	64.7	82.3
Specificity (%)	86.4	81.2	93.8
Accuracy (%)	82.5	74.4	89.0
A_Z Values±SD	0.9281±0.0455	0.8833±0.0400	0.9687±0.0168

Diagnosis of obstructive causes

The total accuracy of MRCP in diagnosing the causes of pancreato-biliary obstruction was 75.6 %, which was similar to that of direct cholangiopancreatography (ERCP/PTC) (*P*=0.2345) and CT (*P*=0.7970), but superior to that of B-US (*P*=0.0131). The combination of MRCP and routine MR imaging significantly improved the clinical diagnostic ability with an accuracy of 87.8 %, which was superior to that of CT (*P*=0.0330) and US (*P*=0.0000).

The diagnostic rate by the combination of MRCP and routine MR imaging was 92.1 % and 94.1 %, for cholelithasis and choledocholithiasis respectively, which was superior to that of CT (*P*=0.0428) and US (*P*=0.0049). But the difference between ERCP/PTC and the combined MRCP and routine MR imaging was not significant (*P*=0.6445). The accuracy of CT, ERCP/PTC, MRCP and the combined MRCP and routine MR imaging in distinguishing the various pancreato-biliary tumors was significantly higher than that of US (*P*=0.0002) (Table 4).

Table 4 Accuracy of diagnosis of obstructive causes (%)

	B-US	CT	ERCP / PTC	MRCP	MRCP +MRI
Cholelithiasis					
Gallbladder stone	71.4	75.0	80.0	78.5	92.9
Intrahepatic bile duct stone	85.7	100.0	100.0	71.4	85.7
Choledocholithiasis	52.9	63.6	87.5	88.2	94.1
Pancreato-biliary tumor					
Gallbladder carcinoma	50.0	75.0	60.0	50.0	66.7
Cholangiocarcinoma	33.3	75.0	83.3	77.8	88.9
Ampullary carcinoma	33.3	50.0	100.0	66.7	66.7
Pancreatic head carcinoma	63.6	81.8	100.0	90.9	100.0
Bile papilla carcinoma	40.0	66.7	100.0	60.0	80.0
Other diseases					
Bile duct injury	50.0		100.0	100.0	100.0
Choledochal cyst	100.0	100.0	100.0	100.0	100.0
Sclerosing cholangitis	0	50.0	0	0	50.0
Chronic pancreatitis	75.0	75.0	100.0	50.0	75.0
Total	57.3	73.7	85.0	75.6	87.8

DISCUSSION

US or CT examination (including endoscopic US and spiral CT) has been the first choice in diagnosing the pancreato-biliary diseases[6-9]. Direct cholangiopancreatography obtained through ERCP or PTC has served as "golden standard" in pancreato-biliary imageology.

Magnetic resonance cholangiopancreatography (MRCP), advocated by German researcher Wallner BK and his group in 1991[10], has offered a new imaging modality for diagnosing pancreato-biliary system disorders[10-15]. In the present study, MRCP was successfully performed in all 82 patients and the images of MRCP were similar to those of direct cholangiopancreatography. MRCP studies of diagnostic quality were obtained in 79 cases (96.3 %), including 8 (16.7 %) in which direct cholangiopancreatography were unsuccessful or incomplete. Therefore, MRCP might provide an efficient alternative to direct cholangiopancreatography when diagnostic ERCP and PTC were unsuccessful or inadequate[1,16].

In our study, the accuracy of MRCP in detecting the location of pancreato-biliary obstruction was 100 %, which was superior to that of B-US and CT, but was not significantly different between MRCP and direct cholangiopancreatography. Compared with ERCP/PTC examination, the noninvasive MRCP could exhibit the whole pancreato-biliary duct system and demonstrate the level, degree and range of obstruction as well as morphological characteristics. In addition, MRCP could provide a plenty of valuable imageological information and help determine the best approach for palliative drainage and other interventional treatment for the patients with unresectable tumors[17,18].

In pancreato-biliary system imageology, it is very important in diagnosing and differentiating malignant from benign causes of pancreato-biliary obstruction. The combined MRCP and routine MR imaging could significantly improve the clinical diagnostic capability by exhibiting the pathological changes of the surrounding structures[19-22]. For pancreato-biliary tumors, MRCP could define the location and morphological characteristics of pancreato-biliary obstruction, and evaluate the range of tumors involvement and the surgical resectability. Furthermore, with the advantages of both CT and direct cholangiopancreatography examination, the combined routine MR imaging and MRCP might exhibit the pertinent surrounding structures and raise the clinical diagnostic accuracy[17,23,24].

US and CT techniques are most frequently used in the initial evaluation of patients with cholelithiasis and both have a high accuracy in diagnosing gallbladder and intrahepatic duct stones. The sensitivity of MRCP in diagnosing gallbladder and intrahepatic duct stones varied with the size, number and location of the stones and MRCP being more suitable for the diagnosis of choledocholithiasis. In summary, the MRCP could mainly detect the stones in common bile duct and exclude other pancreato-biliary obstructive diseases[25-27].

With the development of laparoscopic technique, laparoscopic cholecystectomy (LC) and endoscopic sphincter tenotomy (EST) have been widely used in the biliary surgery[28]. MRCP can depict the whole anatomic structure of biliary tree and help guarantee the success of laparoscopic cholecystectomy. Before surgical dissection, to identify the anatomic variants of the biliary tree with MRCP could result in a decreased risk of bile duct injury during laparoscopic cholecystectomy[29]. Now, ERCP is no longer the routine examination in patients with choledocholithiasis, and endoscopic sphincter tenotomy is chiefly used instead to remove stones in common bile duct.

As to the benign strictures, due to cholangitis, surgical injury or chronic pancreatitis, MRCP may have some difficulties in showing the mini-changes of pancreato-biliary duct. But the use of dynamic MRCP with secretin stimulation might be useful for diagnosing pancreatic papillary stenosis or dysfunction and for detecting reduced pancreatic exocrine reserve[30-32]. In addition, the literature indicates that MRCP could be used initially in evaluating choledochal cyst[33].

In conclusion, in recent optimal imageological procedures of diagnosing the pancreato-biliary diseases, B-US is still the first choice for evaluation. The combination of MRCP and routine MR imaging provides an efficient method to diagnose various pancreato-biliary obstructions, differentiate malignant from benign causes and carry out post-operative follow-ups. Cross-sectional MR imaging and CT are complementary modalities for pre-operative diagnosis and

assessment of pancreato-biliary tumors. Direct diagnostic cholangiopancreatography (ERCP/PTC) is chiefly used for difficult cases and combined with other interventional treatment, including EST or PTCD (Figure 2).

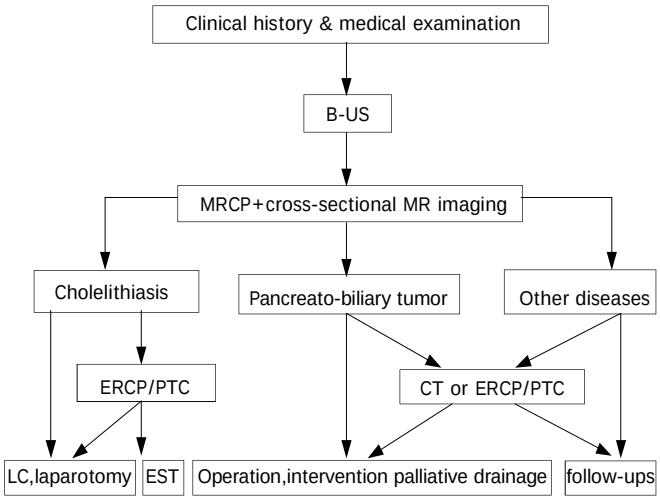

Figure 2 Optimal imageological examination procedure of pancreato-biliary diseases.

REFERENCES

1 **Soto JA**, Yucel EK, Barish MA, Chuttani R, Ferrucci JT. MR cholangiopancreatography after unsuccessful or incomplete ERCP. *Radiology* 1996; **199**: 91-98
2 **Guibaud L**, Bret PM, Reinhold C, Atri M, Barkun AN. Bile duct obstruction and choledocholithiasis: diagnosis with MR cholangiography. *Radiology* 1995; **197**: 109-115
3 **Reinhold C**, Bret PM. Current status of MR cholangiopancreatography. *AJR* 1996; **166**: 1285-1295
4 **Barish MA**, Soto JA. MR cholangiopancreatography: techniques and clinical applications. *AJR* 1997; **169**: 1295-1303
5 **Irie H**, Honda H, Tajima T, Kuroiwa T, Yoshimitsu K, masuda K. Optimal MR cholangiopancreatographic sequence and its clinical application. *Radiology* 1998; **206**: 379-387
6 **Kanemaki N**, Nakazawa S, Inui K, Yoshino J, Yamao J, Okushima K. Three-dimensional intraductal ultrasonography: preliminary results of a new technique for the diagnosis of disease of the pancreatobiliary system. *Endoscopy* 1997; **29**: 726-731
7 **de Ledinghen V**, Lecesne R, Raymond JM, Gense V, Amouretti M, Drouillard J, Couzigou P, Silvain C. Diagnosis of choledocholithiasis: EUS or magnetic resonance cholangiography? A prospective controlled study. *Gastrointest Endosc* 1999; **49**: 26-31
8 **Zeman RK**, Fox SH, Silverman PM, Davros WJ, Carter LM, Griego D, Weltman DI, Ascher SM, Cooper CJ. Helical (spiral) CT of the abdomen. *AJR* 1993; **160**: 719-725
9 **Stockberger SM**, Sherman S, Kopecky KK. Helical CT cholangiography. *Abdom Imaging* 1996; **21**: 98-104
10 **Wallner BK**, Schumacher KA, Weidenmaier W, Friedrich JM. Dilated biliary tract: evaluation with MR cholangiography with a T_2-weighted contrast-enhanced fast sequence. *Radiology* 1991; **181**: 805-808
11 **Takehara Y**. Fast MR imaging for evaluating the pancreaticobiliary system. *Eur J Radiol* 1999; **29**: 211-232
12 **Jara H**, Barish MA, Yucel EK, Melhem ER, Hussain S, Ferrucci JT. MR hydrography: theory and practice of static fluid imaging. *AJR* 1998; **170**: 873-882
13 **Hirohashi S**, Hirohashi R, Uchida H, kitano S, Ono W, Ohishi H, Makanishi S. MR cholangiopancreatography and MR urography: improved enhancement with a negative oral contrast agent. *Radiology* 1997; **203**: 281-285
14 **Papanikolaou N**, Karantanas A, Maris T, Gourtsoyiannis N. MR cholangiopancreatography before and after oralblueberry juice administration. *J Comput Assist Tomogr* 2000; **24**: 229-234
15 **Fulcher AS**, Turner MA. MR cholangiopancreatography. *Radiol Clin North Am* 2002; **40**: 1363-1376
16 **Owens GR**, Shutz SM. Value of magnetic resonance cholangiopancreatography (MRCP) after unsuccessful endoscopic retrograde cholangiopancreatography (ERCP). *Gastrointest Endosc* 1999; **49**: 265-266
17 **Bret PM**, Reinhold C. Magnetic resonance cholangiopancreatography. *Endoscopy* 1997; **29**: 472-486
18 **Macaulay SE**, Schulte SJ, Sekijima JH, Obregon RG, Simon HE, rohrmann CA Jr, Freeny PC, Schmiedl UP. Evaluation of a non-breath-hold MR cholangiography technique. *Radiology* 1995; **196**: 227-232
19 **Boraschi P**, Braccini G, Gigoni R, geloni M, Perri G. MR cholangiopancreatography: value of axial and coronal fast Spin-Echo fat-suppressed T2-weighted sequences. *Eur J Radiol* 1999; **32**: 171-181
20 **Lee MG**, Lee HJ, Kim MH, Kang EM, Kim YH, Lee SG, Kim PN, Ha HK, Auh YH. Extrahepatic biliary diseases: 3D MR cholangiopancreatography compared with endoscopic retrograde cholangiopancreatography. *Radiology* 1997; **202**: 663-669
21 **Kim MJ**, Mitchell DG, Ito K, Outwater EK. Biliary dilatation: differentiation of benign from malignant causes–value of adding conventional MR imaging to MR cholangiopancreatography. *Radiology* 2000; **214**: 173-181
22 **Qin LX,** Tang ZY. Hepatocellular carcinoma with obstructive jaundice: diagnosis, treatment and prognosis. *World J Gastroenterol* 2003; **9**: 385-391
23 **Pavone P**, Laghi A, Catalano C, Panebianco V, Fabiano S, Passariello R. MRI of the biliary and pancreatic ducts. *Eur Radiol* 1999; **9**: 1513-1522
24 **Pavone P**, Laghi A, Passariello R. MR cholangiopancreatography in malignant biliary obstruction. *Semin Ultrasound CT MR* 1999; **20**: 317-323
25 **Varghese JC**, Liddell RP, Farrell MA, Murray FE, Osborne DH, Lee MJ. Diagnostic accuracy of magnetic resonance cholangiopancreatography and ultrasound compared with direct cholangiography in the detection of choledocholithiasis. *Clin Radiol* 2000; **55**: 25-35
26 **Boraschi P**, Neri E, Braccini G, Gigoni R, Caramella D, Perri G, Bartolozzi C. Choledocholithiasis: diagnostic accuracy of MR cholangiopancreatography. Three-year experience. *Magn Reson Imaging* 1999; **17**: 1245-1253
27 **Chan YL**, Chan AC, Lam WW, Lee DW, Chung SS, Sung JJ, Cheung HS, Li AK, Metrewell C. Choledocholithiasis: comparison of MR cholangiography and endoscopic retrograde cholangiography. *Radiology* 1996; **200**: 85-89
28 **Fulcher AS**, Turner MA, Capps GW, Zfass AM, Baker KM. Half-Fourier RARE MR cholangiopancreatography: experience in 300 subjects. *Radiology* 1998; **207**: 21-32
29 **Yeh TS**, Jan YY, Tseng JH, Hwang TL, Jeng LB, Chen MP. Value of magnetic resonance cholangiopancreatography in demonstrating major bile duct injuries following laparoscopic cholecystectomy. *Br J Surg* 1999; **86**: 181-184
30 **Matos C**, Metens T, Deviere J, Nicaise N, Braude P, Van Yperen G, Cremer M, Struyven J. Pancreatic duct: morphologic and functional evaluation with dynamic MR pancreatography after secretin stimulation. *Radiology* 1997; **203**: 435-441
31 **Takehara Y**. MR pancreatography. *Semin Ultrasound CT MR* 1999; **20**: 324-339
32 **Manfredi R**, Costamagna G, Brizi MG, Maresca G, Vecchioli A, Colagrande C, Marano P. Severe chronic pancreatitis versus suspected pancreatic disease: dynamic MR cholangiopancreatography after secretin stimulation. *Radiology* 2000; **214**: 849-855
33 **Irie H**, Honda H, Jimi M, Yokohata K, Chijiiwa K, Kuroiwa T, Hanada K, Yoshimitsu K, Tajima T, Matsuo S, Suita S, Masuda K. Value of MR cholangiopancreatography in evaluating choledochal cysts. *AJR* 1998; **171**: 1381-1385

Edited by Ma JY

P.O.Box 2345, Beijing 100023,China
Fax: +86-10-85381893
E-mail: wjg@wjgnet.com www.wjgnet.com

World J Gastroenterol 2003;9(12):2828-2831
World Journal of Gastroenterology
 ISSN 1007-9327

• CLINICAL RESEARCH •

Overexpression of Caspase-1 in adenocarcinoma of pancreas and chronic pancreatitis

Yin-Mo Yang, Marco Ramadani, Yan-Ting Huang

Yin-Mo Yang, Yan-Ting Huang, Department of Surgery, The First Teaching Hospital, Health Science Center, Beijing University, Beijing 100034, China
Marco Ramadani, Department of General Surgery, University of Ulm, 89075 Ulm, Germany
Correspondence to: Professor Yin-Mo Yang, Department of Surgery, The First Teaching Hospital, Health Science Center, Beijing University, Beijing 100034, China. yangyinmo@263.net
Telephone: +86-10-66171122
Received: 2003-05-12 **Accepted:** 2003-06-12

Abstract

AIM: To identify the expression of Caspase-1(interleukin-1β converting enzyme) and its role in adenoma of the pancreas and chronic pancreatitis.

METHODS: The expression of Caspase-1 was assessed in 42 pancreatic cancer tissue samples, 38 chronic pancreatitis specimens, and 9 normal pancreatic tissues by immunohistochemistry and Western blot analysis.

RESULTS: Overexpression of Caspase-1 was observed in both disorders, but there were differences in the expression patterns in distinct morphologic compartments. Pancreatic cancer tissues showed a clear cytoplasmatic overexpression of Caspase-1 in tumor cells of 71 % of the tumors, whereas normal pancreatic tissues showed only occasional immunoreactivity. In chronic pancreatitis, overexpression of Caspase-1 was found in atrophic acinar cells (89 %), hyperplastic ducts (87 %), and dedifferentiating acinar cells (84 %). Although in atrophic cells a clear nuclear expression was found, hyperplastic ducts and dedifferentiating acinar cells showed clear cytoplasmic expression. Western blot analysis revealed a marked expression of the 45 kDa precursor of Caspase-1 in pancreatic cancer and chronic pancreatitis (80 % and 86 %, respectively). Clear bands at 30 kDa, which suggested the p10-p20 heterodimer of active Caspase-1, were found in 60 % of the cancer tissue and 14 % of the pancreatitis tissue specimens, but not in normal pancreatic tissues.

CONCLUSION: Overexpression of Caspase-1 is a frequent event in pancreatic disorders and its differential expression patterns may reflect two functions of the protease. One is its participation in the apoptotic pathway in atrophic acinar cells and tumor-surrounding pancreatitis tissue, the other is its possible role in proliferative processes in pancreatic cancer cells and hyperplastic duct cells and dedifferentiating acinar cells in chronic pancreatitis.

Yang YM, Ramadani M, Huang YT. Overexpression of Caspase-1 in adenocarcinoma of pancreas and chronic pancreatitis. *World J Gastroenterol* 2003; 9(12): 2828-2831
http://www.wjgnet.com/1007-9327/9/2828.asp

INTRODUCTION

Caspase-1 was the first described member of a group of cysteine proteases called Caspases. It was formerly designated as interleukin-1β converting enzyme, and was originally characterized by its ability to cleave the inactive precursor of interleukin-1β to generate the active 17.5 kDa proinflammatory cytokine IL-1β[1]. It has been found to express in many tissues as an inactive 45 kDa precursor protein (p45) from which the active enzyme is generated by an autocatalytic cleavage process[2]. Caspase-1 was first isolated from human monocytic cell line THP 1. Because of its similarity in sequence to the death gene product CED-3 of nematode Caenorhabditis elegans, it has been regarded as a key enzyme of the apoptotic pathway[3]. Today, more than 10 Caspases have been identified and their roles in apoptosis are well known[4-6].

Several new members of the group of Caspases have been identified and described. Similar to Caspase-1, overexpression of any of these enzymes would lead to apoptosis in a variety of cell types[7-9]. We investigated the expression of apoptosis-related enzyme Caspase-1 in pancreatic cancer and chronic pancreatitis. Interestingly, we found a clear overexpression of Caspase-1 in pancreatic cancer tissue as well as in chronic pancreatitis specimens.

MATERIALS AND METHODS

Tissue samples

Pancreatic tissue samples were obtained from 42 patients with pancreatic cancer and 38 patients with chronic pancreatitis who underwent surgery at the Department of General Surgery, University of Ulm. The median age of the patients with pancreatic cancer (20 women and 22 men) was 61.8 years (range 38 to 78 years). The group of patients with chronic pancreatitis was composed of 13 women and 25 men. The median age of this group was 52.2 years (range 22 to 73 years). The main indication for pancreatic head resection was long-lasting pain (36 of 38 patients) and obstruction of the common bile duct (19 of 38 patients). In all patients, duodenum-preserving pancreatic head resection was performed.

Tissues were collected after surgical removal, immediately snap-frozen in liquid nitrogen, and stored at -80 ℃, or fixed in 4 % formalin for 24 hours at room temperature, processed, and embedded in paraffin. All 42 pancreatic cancer tissue and 38 chronic pancreatitis tissue samples were used for immunohistochemical analysis. Five normal pancreatic tissue samples from organ donors and four normal pancreatic tissue samples from patients undergoing surgery for pancreatic cancer served as control specimens. Twenty pancreatic cancer tissues, 14 chronic pancreatitis tissues, and seven normal pancreatic tissues underwent Western blot analysis.

Immunohistochemistry

Paraffin-embedded tissues were cut into 5 μm-thick sections and adhered to silanized slides, deparaffinized, and hydrated. Endogenous peroxidase activity was blocked with 3 % hydrogen peroxide in methanol. The tissue sections were covered with 5 % normal goat serum (DAKO, Glostrup, Denmark) in Tris-buffered saline for 60 minutes and incubated overnight with polyclonal rabbit antihuman caspase-1 antibody (Upstate Biotechnology, Lake Placid, NY, USA.) in a dilution

of 1:100. For each case, a corresponding section was incubated in Tris-buffered saline without the primary antibody as a control for nonspecific staining. Further negative controls consisted of normal rabbit serum instead of specific antiserum. Biotinylated pig anti-rabbit secondary antibody was added for 45 minutes, followed by avidin-biotinylated peroxidase complex for an additional 45 minutes. Staining was achieved using 3,3' -diaminobenzidine. The sections were then counterstained with Mayer' s hemalum and mounted.

Grading of immunohistochemical findings

Immunohistochemical findings were scored depending on the extent and intensity of staining. Both intensity and extent were assessed in regions with hyperplastic ducts and atrophic acinar cells. All sections were graded by two experienced investigators who had no knowledge of the clinical data. At least 10 randomly selected high-power fields were scored. The intensity of staining was graded on a four points scale of 0=no staining, 1=weak, 2=moderate, and 3=strong. The extent of positive immunoreactivity was graded by the percentage of stained cells in the region of interest: 0 point=0 %, 1 point$\leqslant$20 %, 2 points=20-50 %, and 3 points$\geqslant$50 %. An overall score was obtained by the product of intensity and extent of positive staining. Cases with 0 points were considered to be negative, cases with a final score of 1-3 were considered to be weakly positive, cases with a score of 4-7 were considered to be moderately positive, and cases with a final score greater than 7 were considered to be strongly positive.

Western blot analysis

Frozen pancreatic samples were finely diced with a surgical blade and washed twice with ice-cold phosphate-buffered saline. After swelling on ice for 60 minutes, the samples were dissociated by sonication. The lysates were centrifuged and the protein fraction was aliquoted and stored at -80 ℃ until further analysis. For immunoblotting, the lysates were boiled in sodium dodecyl sulfate-gel sample buffer for 5 minutes. Thirty micrograms of protein were electrophoretically resolved on denaturing 15 % polyacrylamide gels with a 3 % stacking gel. Proteins were transferred to nitrocellulose membranes using a transblot apparatus (Phase, Lubeck, Germany). Nonspecific interactions were blocked by preincubation of the membranes with a milk powder suspension overnight at 4 ℃. After incubation of the membranes with monoclonal antibodies, the binding of antibodies was detected using the ECL-system (Amersham Pharmacia Biotech, Piscataway, NJ, USA). The autocleavage experiments of the monocytic cell line THP1 were performed as previously described[10].

RESULTS

Immunohistochemical findings

Staining of pancreatic tissue specimens with a polyclonal rabbit antiserum recognizing Caspase-1 revealed a marked overexpression of Caspase-1 in pancreatic cancer and chronic pancreatitis. Although normal pancreatic tissue showed only occasional slight staining (Figure 1A), we found predominantly cytoplasmic immunoreactivity of cancer cells in 71 % of the pancreatic tumors (Figure 1B). In primary chronic pancreatitis tissue samples, Caspase-1 overexpression was found in atrophic acinar cells, hyperplastic ducts, and acinar cells that appeared to dedifferentiate to form tubular structures. Hyperplastic ducts showed clear cytoplasmic staining in 87 % (Figure 1C). Atrophic acinar cells with pyknotic nuclei were stained positive in 89 % of the pancreatitis tissues, but the immunoreactivity was predominantly nuclear (Figure 1D). Dedifferentiating acinar cells showed positive cytoplasmic immunostaining with Caspase-1 antiserum in 84 %. In chronic pancreatitis tissues, which often surrounded pancreatic carcinoma because of tumor obstruction, we also found strong Caspase-1 expression, but immunoreactivity differed from that of chronic pancreatitis tissue specimens from patients without malignancy. The staining in tumor-surrounding pancreatitis tissues was generally stronger than that in non-tumor-related pancreatitis tissues, and the distinct distribution pattern found in primary chronic pancreatitis could not be observed. In addition to this tissue-specific staining, a positive immunoreactivity of tissue-infiltrating lymphocytes was found in 73 % of the tissues.

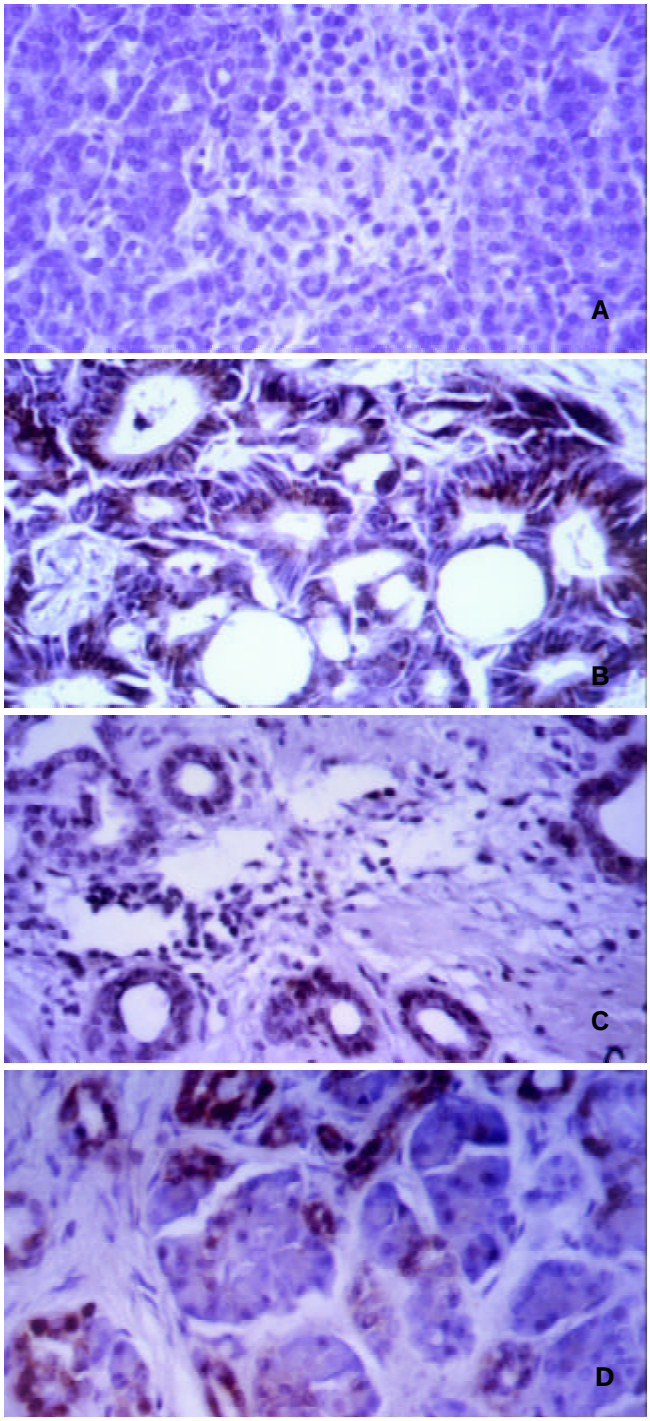

Figure 1 Immunohistochemical staining of pancreatic tissues using antiserum against human Caspase-1. A: Normal pancreas showed only occasional slight staining. B: Pancreatic cancer cells showed a clear cytoplasmatic immunoreactivity in 71 %. C: Hyperplastic ducts in chronic pancreatitis tissues also showed cytoplasmatic staining in 87 % of the tissues, whereas in atrophic acinar cells (D) a predominantly nuclear staining could be observed in 89 %.

Western blot analysis

To confirm the overexpression of Caspase-1 seen in immunohistochemical staining, Western blot analysis was performed with monoclonal antibody CAL against human Caspase-1. This antibody was developed to detect the 20 kDa subunit of active Caspase-1[11], but also detect the p45 precursor. Pancreatic cancer tissue as well as chronic pancreatitis tissue specimens showed specific bands migrating at 45 kDa (Figure 2) which suggested the p45 precursor protein of Caspase-1. This band was found in 80 % of cancer tissues and 86 % of chronic pancreatitis tissues.

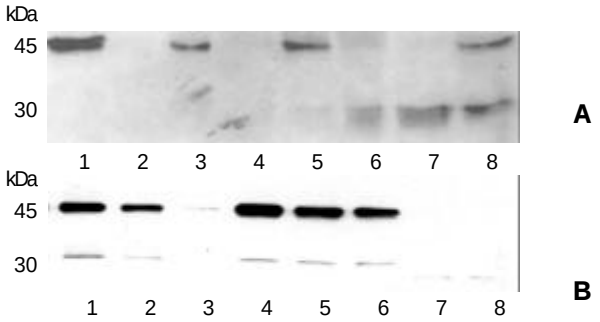

Figure 2 Western blot analysis of pancreatic tissues with anti-Caspase-1 antibody. The 45 kDa precursor of Caspase-1 was found in 86 % of chronic pancreatitis samples (A, Lanes 3-8) and 80 % of pancreatic cancer samples (B, Lanes 1-8). In 60 % of cancer specimens and 14 % of chronic pancreatitis tissue samples, the active 30 kDa p10-p20 heterodimer was found. In normal pancreatic tissues (A, lane 2), neither p45 precursor nor active Caspase-1 could be detected. Lane 1 (A) shows the positive control of THP 1 cells.

Lysates from THP-1 cells served as control specimens for active Caspase-1. In monocytic THP1 cells, p45 Caspase-1 precursor has been known to be cleaved by an autocatalytic process to the active Caspase-1 enzyme when kept at room temperature for 24 hours[11]. In 60 % of the cancer probes and 14 % of the pancreatitis lysates, and in lysates from the autocleavage experiments of THP1 cells, a further band at 30 kDa was detectable, which was suggested the active p10-p20 heterodimer of active Caspase-1. In pancreatic tissue of healthy organ donors, no signal was obtained using monoclonal antibody against human Caspase-1, suggesting an overexpression of Caspase-1 protein in pancreatic cancer and chronic pancreatitis. Since lysates from pancreatic cancer tissue and chronic pancreatitis specimens also showed the 30 kDa band, it was plausible that Caspase-1 was at least partly activated in these disorders.

Correlation with clinicopathological features

To assess the clinical importance of Caspase-1 overexpression in pancreatic cancer, we correlated the immunohistochemical findings with age, sex, tumor extent, lymph node metastasis, and grading. As a result, no correlation was found between Caspase-1 expression and any of these clinicopathologic features. In addition, no statistical difference was found with regard to postoperative survival. In patients with chronic pancreatitis, we correlated the expression of Caspase-1 with age, sex, onset of disease, need for analgesic drugs, and endocrine and exocrine pancreatic function. As in patients with pancreatic cancer, no correlation with any of the tested features could be found.

DISCUSSION

Caspases play an important role in the apoptotic pathway in a variety of cell types. However, little is known about the physiologic roles of different homologues during apoptosis. We assessed the expression of Caspase-1 in pancreatic cancer and chronic pancreatitis. Interestingly, immunohistochemical analysis revealed a clear overexpression of this enzyme in both disorders, but also differences in the expression patterns in distinct morphologic compartments. Furthermore, Western blot analysis of pancreatic cancer tissues and chronic pancreatitis tissues showed that Caspase-1 was at least partially activated in these diseases.

Caspase-1 is described as a cytosolic protein. However, in our experiments we found a clear nuclear staining with the antibody against human Caspase-1 in atrophic acinar cells in chronic pancreatitis specimens. Interestingly, most of the known substrates for Caspases in apoptosis were structural or catalytic nuclear proteins, the cleavage fragments of which were found in apoptotic bodies[12] . The nuclear immunoreactivity of atrophic acinar cells in chronic pancreatitis may, therefore, be an indication of ongoing apoptotic processes. In contrast, the marked cytoplasmatic overexpression of Caspase-1 in tumor cells could hardly be explained by apoptosis, since some tumors showed Caspase-1 overexpression in nearly all cancer cells. Furthermore, we found a clear correlation between Caspase-1 overexpression in pancreatic carcinoma and cyclin D1, which has been known to be involved in cellular proliferation and to contribute to an aggressive behavior in many tumors[13-16]. EGF and EGF-R have been shown to play a crucial role in autocrine stimulation of human pancreatic carcinoma[17]. In the pancreatic cancer tissues we investigated, the cytoplasmatic expression of Caspase-1 in pancreatic cancer cells also correlated significantly with the expression of EGF and EGF-R. Interestingly, it has recently been shown that EGF was also able to inhibit cell growth and induce apoptosis via Caspase-1 induction[18]. However, with regard to the fact that cyclin D1, EGF, and EGF-R overexpression was associated with poor prognosis in human pancreatic cancer[13,19], it is hard to believe that these factors could be an indication for the apoptotic state of these tumors.

Chronic pancreatitis is histologically characterized by the destruction of the pancreatic parenchyma, irregular sclerosis, and focal duct cell proliferation. Besides the predominantly nuclear staining with the antibody against Caspase-1 in atrophic acinar cells, we found a clear cytoplasmatic overexpression in two other distinct morphologic compartments in chronic pancreatitis—in hyperplastic ducts and in areas with tubularily dedifferentiating acinar cells. Cyclin D1, EGF, and EGF-R were also altered in chronic pancreatitis[20,21], which lend support to the hypothesis that chronic pancreatitis is a progressive process. Furthermore, we have recently found that positive nuclear MIB-1 (Ki67) expression in pancreatitis tissues might be an indication for proliferative processes[22,23]. Tumor surrounding pancreatitis tissues from patients with pancreatic cancer showed a strong positive immunoreactivity with antiserum against Caspase-1, but the differential expression pattern seen in primary chronic pancreatitis could not be observed. Nuclear and cytoplasmatic expression of Caspase-1 was found in atrophic acinar cells and in duct cells as well. One explanation for this overexpression might be the dramatic course of pancreatitis due to tumor obstruction. Another explanation might be that Caspase-1 was upregulated through paracrine stimulation with tumor-derived EGF in these cells. Nevertheless, destruction of pancreatic parenchyma due to tumor growth and invasion was likely to be associated with apoptosis of normal pancreatic cells.

In summary, Caspase-1 is overexpressed in atrophic acinar cells of chronic pancreatitis and tumor-surrounding pancreatitis tissues and is markedly expressed in cytoplasm of pancreatic cancer cells and hyperplastic duct cells and dedifferentiating acinar cells in chronic pancreatitis.

REFERENCES

1 **Kostura MJ**, Tocci MJ, Limjuco G, Chin J, Cameron P, Hillman AG, Chartrain NA, Schmidt JA. Identification of a monocyte specific pre-interleukin 1 beta convertase activity. *Proc Natl Acad Sci U S A* 1989; **86**: 5227-5231

2 **Thornberry NA,** Bull HG, Calaycay JR, Chapman KT, Howard AD, Kostura MJ, Miller DK, Molineaux SM, Weidner JR, Aunins J. A novel heterodimeric cysteine protease is required for interleukin-1 beta processing in monocytes. *Nature* 1992; **356**: 768-774

3 **Yuan J**, Shaham S, Ledoux S, Ellis HM, Horvitz HR. The C. elegans cell death gene ced-3 encodes a protein similar to mammalian interleukin-1 beta-converting enzyme. *Cell* 1993; **75**: 641-652

4 **Enari M**, Hug H, Nagata S. Involvement of an ICE-like protease in Fas-mediated apoptosis. *Nature* 1995; **375**: 78-81

5 **Zhu H**, Fearnhead HO, Cohen GM. An ICE-like protease is a common mediator of apoptosis induced by diverse stimuli in human monocytic THP. 1 cells. *FEBS Lett* 1995; **374**: 303-308

6 **Jacobsen MD**, Weil M, Raff MC. Role of Ced-3/ICE-family proteases in staurosporine-induced programmed cell death. *J Cell Biol* 1996; **133**: 1041-1051

7 **Duan H**, Chinnaiyan AM, Hudson PL, Wing JP, He WW, Dixit VM. ICE-LAP3, a noval mammalian homologue of the Caenorhabditis elegans cell death protein Ced-3 is activated during Fas- and tumor necrosis factor-induced apoptosis. *J Biol Chem* 1996; **271**: 1621-1625

8 **Faucheu C**, Diu A, Chan AW, Blanchet AM, Miossec C, Herve F, Collard Dutilleul V, Gu Y, Aldape RA, Lippke JA. A novel human protease similar to the interleukin-1 beta converting enzyme induces apoptosis in transfected cells. *Embo J* 1995; **14**: 1914-1922

9 **Kumar S**, Kinoshita M, Noda M, Copeland NG, Jenkins NA. Induction of apoptosis by the mouse Nedd2 gene, which encodes a protein similar to the product of the Caenorhabditis elegans cell death gene ced-3 and the mammalian IL-1 beta-converting enzyme. *Genes Dev* 1994; **8**: 1613-1626

10 **Miossec C**, Decoen MC, Durand L, Fassy F, Diu-Hercend A. Use of monoclonal antibodies to study interleukin-1 beta-converting enzyme expression: only precursor forms are detected in interleukin-1 beta-secreting cells. *Eur J Immunol* 1996; **26**: 1032-1042

11 **Gu Y**, Wu J, Faucheu C, Lalanne JL, Diu A, Livingston DJ, Su MS. Interleukin-1 beta converting enzyme requires oligomerization for activity of processed forms in vivo. *Embo J* 1995; **14**: 1923-1931

12 **Casciola Rosen LA**, Anhalt GJ, Rosen A. DNA-dependent protein kinase is one of a subset of autoantigens apecifically cleaved early during apoptosis. *J Exp Med* 1995; **182**: 1625-1634

13 **Gansauge S**, Gansauge F, Ramadani M, Stobbe H, Rau B, Harada N, Beger HG. Overexpression of cyclin D1 in human pancreatic carcinoma is associated with poor prognosis. *Cancer Res* 1997; **57**: 1634-1637

14 **Toyoda H**, Nakamura T, Shinoda M, Suzuki T, Hatooka S, Kobayashi S, Ohashi K, Seto M, Shiku H, Nakamura S. Cyclin D1 expression is useful as a prognostic indicator for advanced esophageal carcinomas, but not for superficial tumors. *Dig Dis Sci* 2000; **45**: 864-869

15 **Sallinen SL**, Sallinen PK, Kononen JT, Syrjakoski KM, Nupponen NN, Rantala IS, Helen PT, Helin HJ, Haapasalo HK. Cyclin D1 expression in astrocytomas is associated with cell proliferation activity and patient prognosis. *J Pathol* 1999; **188**: 289-293

16 **Keum JS**, Kong G, Yang SC, Shin DH, Park SS, Lee JH, Lee JD. Cylin D1 overexpression ia an indicator of poor prognosis in respectable non-small cell lung cancer. *Br J cancer* 1999; **81**: 127-132

17 **Korc M**, Chandrasekar B, Shah GN. Differential binding and biological activities of epidermal growth factor and transforming growth factor alpha in a human pancreatic cancer cell line. *Cancer Res* 1991; **51**(23 Pt 1): 6243-6249

18 **Chin YE**, Kitagawa M, Kuida K, Flavell RA, Fu XY. Activation of the STAT signaling pathway can cause expression of caspase1 and apoptosis. *Mol Cell Biol* 1997; **17**: 5328-5337

19 **Yamanaka Y**, Friess H, Kobrin MS, Buchler M, Beger HG, Korc M. Coexpression of epidermal growth factor receptor and ligands in human pancreatic cancer is associated with enhanced tumor aggressiveness. *Anticancer Res* 1993; **13**: 565-569

20 **Kornmann M**, Ishiwata T, Arber N, Beger HG, Korc M. Increased cyclin D1 expression in chronic pancreatitis. *Pancreas* 1998; **17**: 158-162

21 **Korc M**, Friess H, Yamanaka Y, Kobrin MS, Buchler M, Beger HG. Chronic pancreatitis is associated with increased concentrations of epidermal growth factor receptor, transforming growth factors alpha, and phospholipase C gamma. *Gut* 1994; **35**: 1468-1473

22 **Gansauge S**, Gansauge F, Yang Y, Muller J, Seufferlein T, Ramadani M, Beger HG. Interleukin 1 beta-converting enzyme (caspase-1) is overexpressed in adenocarcinoma of the pancreas. *Cancer Res* 1998; **58**: 2703-2706

23 **Ramadani M**, Yang Y, Gansauge F, Gansauge S, Beger HG. Overexpression of caspase-1 (interleukin-1β converting enzyme) in chronic pancreatitis and its participation in apoptosis and proliferation. *Pancreas* 2001; **22**: 383-387

Edited by Ma JY

P.O.Box 2345, Beijing 100023,China
Fax: +86-10-85381893
E-mail: wjg@wjgnet.com www.wjgnet.com

World J Gastroenterol 2003;9(12):2832-2835
World Journal of Gastroenterology
 ISSN 1007-9327

• CLINICAL RESEARCH •

Spider angiomas in patients with liver cirrhosis: Role of vascular endothelial growth factor and basic fibroblast growth factor

Chung-Pin Li, Fa-Yauh Lee, Shinn-Jang Hwang, Rei-Hwa Lu, Wei-Ping Lee, Yee Chao, Sung-Sang Wang, Full-Young Chang, Jacqueline Whang-Peng, Shou-Dong Lee

Chung-Pin Li, Fa-Yauh Lee, Shinn-Jang Hwang, Rei-Hwa Lu, Wei-Ping Lee, Sung-Sang Wang, Full-Young Chang, Shou-Dong Lee, Division of Gastroenterology, Department of Medicine, Taipei Veterans General Hospital and Institute of Clinical Medicine, National Yang-Ming University School of Medicine, Taipei, Taiwan, China
Yee Chao, Cancer Center, Taipei Veterans General Hospital and National Yang-Ming University School of Medicine, Taipei, Taiwan, China
Jacqueline Whang-Peng, Cancer Research Division, National Health Research Institutes and Institute of Clinical Medicine, National Yang-Ming University School of Medicine, Taipei, Taiwan, China
Correspondence to: Chung-Pin Li, Division of Gastroenterology, Department of Medicine, Taipei Veterans General Hospital, No. 201, Sec. 2, Shih-Pai Road, Taipei, 11217, Taiwan. cpli@vghtpe.gov.tw
Telephone: +886-2-28757308 **Fax:** +886-2-28739318
Received: 2003-08-23 **Accepted:** 2003-10-12

Abstract

AIM: To investigate whether vascular endothelial growth factor (VEGF) and basic fibroblastic growth factor (bFGF) are associated with spider angiomas in patients with liver cirrhosis.

METHODS: Eighty-six patients with liver cirrhosis were enrolled and the number and size of the spider angiomas were recorded. Fifty-three healthy subjects were selected as controls. Plasma levels of VEGF and bFGF were measured in both the cirrhotics and the controls.

RESULTS: Plasma VEGF and bFGF were increased in cirrhotics compared with controls (122±13 *vs*. 71±11 pg/mL, *P*=0.003 for VEGF; 5.1±0.5 *vs*. 3.4±0.5 pg/mL, *P*=0.022 for bFGF). In cirrhotics, plasma VEGF and bFGF were also higher in patients with spider angiomas compared with patients without spider angiomas (185±28 *vs*. 90±10 pg/mL, *P*=0.003 for VEGF; 6.8±1.0 *vs*. 4.1±0.5 pg/mL, *P*=0.017 for bFGF). Multivariate logistic regression showed that young age and increased plasma levels of VEGF and bFGF were the most significant predictors for the presence of spider angiomas in cirrhotic patients (odds ratio [OR]=6.64, 95 % confidence interval [CI]=2.02-21.79, *P*=0.002; OR=4.35, 95 % CI=1.35-14.01, *P*=0.014; OR=5.66, 95 % CI=1.72-18.63, *P*=0.004, respectively).

CONCLUSION: Plasma VEGF and bFGF are elevated in patients with liver cirrhosis. Age as well as plasma levels of VEGF and bFGF are significant predictors for spider angiomas in cirrhotic patients.

Li CP, Lee FY, Hwang SJ, Lu RH, Lee WP, Chao Y, Wang SS, Chang FY, Peng JW, Lee SD. Spider angiomas in patients with liver cirrhosis: Role of vascular endothelial growth factor and basic fibroblast growth factor. *World J Gastroenterol* 2003; 9 (12): 2832-2835

http://www.wjgnet.com/1007-9327/9/2832.asp

INTRODUCTION

Liver cirrhosis is a major disease in Asian countries and causes marked morbidity and mortality. Spider angioma is a common presentation of liver cirrhosis[1,2]. It appears frequently in alcoholic cirrhotics or when liver function deteriorates[2-4] and may be associated with esophageal variceal bleeding[5]. However, the exact pathogenesis has been unclear.

Angiogenesis is a possible mechanism in the pathogenesis of spider angiomas and has not been well investigated. Serum vascular growth factors, such as vascular endothelial growth factor (VEGF) and basic fibroblast growth factor (bFGF), have been found to be elevated in cirrhotic patients[6-9]. These vascular growth factors may play a role in the neovascularization and formation of spider angiomas in patients with liver cirrhosis.

The aim of this study was to evaluate the predictive value of plasma VEGF and bFGF for the presence of spider angiomas in patients with liver cirrhosis.

MATERIALS AND METHODS

Study patients

Eighty-six consecutive liver cirrhotic patients from Taipei Veterans General Hospital were enrolled into this study. Fifty-three age- and sex-matched subjects from apparently healthy adults who were admitted to our hospital for routine physical checkups were randomly selected as healthy controls. The etiologies of liver cirrhosis included hepatitis B in 37 patients (43 %), hepatitis C in 18 patients (21 %), alcoholism in 12 patients (14 %), primary biliary cirrhosis in 2 patients (2 %), hepatitis B and alcoholism in 7 patients (8 %), hepatitis C and alcoholism in 6 patients (7 %), and being cryptogenic in 4 patients (5 %). The diagnosis of cirrhosis was confirmed by liver biopsy or peritoneoscopy in 8 patients, and based on typical clinical findings (splenomegaly, ascites, and/or esophageal varices), imaging studies (abdominal sonography[10], computerized tomography, and/or angiography), and characteristic laboratory findings in the remaining 78 patients. The severity of cirrhosis was categorized according to the Child-Pugh classification[11]. Patients with hypertension, diabetes mellitus, atherosclerosis, uremia, and peripheral vascular occlusive diseases were excluded. None of these patients had received antibiotics or vasoactive drugs in the previous week before blood sampling. All the subjects gave informed consent to participate in this study, which was approved by the Hospital Ethics Committee. This study also conformed to the provisions of the World Medical Association Declarations of Helsinki.

All the patients received a complete physical examination to reveal the number and size of the spider angiomas. Serum albumin (reference range 3.7-5.3 g/dL), bilirubin (0.2-1.6 mg/dL), aspartate transaminase (AST, 5-45 U/L), alanine transaminase (ALT, 0-40 U/L), creatinine (0.7-1.5 mg/dl), and blood urea nitrogen (7-20 mg/dL) concentrations were measured in each patient using standard laboratory methods (Hitachi Model 736 automatic analyzer, Tokyo, Japan) on the same day the blood was sampled for assays of plasma vascular growth factors. Each cirrhotic patient underwent an upper GI endoscopy (Olympus GIF-XQ240; Olympus Corp., Taipei, Taiwan) to

document the presence of esophageal varices. The severity of varices was graded F1: small straight varices, F2: enlarged tortuous varices, and F3: largest-sized coil-shaped varices, as suggested by Beppu *et al*[12].

Determination of plasma levels of VEGF and bFGF

All the plasma samples were centrifuged at 3 000 rpm for 10 minutes at 4 ℃ and stored at -80 ℃ until tested. Samples from all the patients and controls were coded so that the technicians running the assays were blind to the sources of the samples. Plasma levels of VEGF and bFGF were measured by using commercially available enzyme-linked immunoabsorbent assay kits (R&D Systems Inc., Minneapolis, MN) according to the manufacturer's instructions. Standard curves were constructed using serial dilutions of recombinant VEGF and bFGF. Optical densities were determined using a micro-titer plate reader (Bio-Kinetics Reader, Bio-Tek Instruments, VT). Tests were performed in duplicate. The intra- and inter-assay variations of these assays were less than 10 %.

Statistical analysis

Results were expressed as mean ± SD. Unpaired Student *t*-test was used to analyze continuous variables between groups. Chi-square test or Fisher's exact test was used for comparison of categorical variables. Pearson correlation coefficient was used to determine the relationship between numerical variables, such as plasma levels of VEGF and the size of spider angiomas. Cut-off values were determined for each serum angiogenic factor according to the best discrimination between patients with or without spider angiomas regarding optimal values of sensitivity and specificity using the receiver operating characteristics (ROC) curve analysis. Logistic regression was used to assess the relationship of independent variables with the presence of spider angiomas in cirrhotic patients. Statistical analyses were performed using the SPSS software (SPSS 10. 0, SPSS Inc., Chicago, IL, USA). Results were considered statistically significant at $P<0.05$.

RESULTS

Plasma angiogenic factors in patients with liver cirrhosis

Plasma VEGF and bFGF levels in patients with liver cirrhosis are listed in Table 1. Plasma levels of VEGF and bFGF were increased in patients with liver cirrhosis compared with healthy controls ($P<0.05$). There was no difference in age, sex, and serum levels of creatinine between the two groups (data not shown).

Table 1 Plasma levels of VEGF and bFGF

Parameters	Healthy controls (n=53)	Cirrhotics (n=86)	P Value
VEGF (pg/mL)	71±11	122±13	0.003
bFGF (pg/mL)	3.4±0.5	5.1±0.5	0.022

VEGF=vascular endothelial growth factor, bFGF=basic fibroblast growth factor.

Patient characteristics

Characteristics of the 86 patients with liver cirrhosis are listed in Table 2. Plasma VEGF and bFGF were increased in the 31 cirrhotic patients with spider angiomas compared with the 55 patients without spider angiomas (185±28 pg/mL *vs*. 90±10 pg/mL, $P=0.003$ for VEGF; 6.8±1.0 pg/mL *vs*. 4.1±0.5 pg/mL, $P=0.017$ for bFGF). Plasma VEGF was also higher in the 26 patients with alcohol-related liver cirrhosis compared with the 60 patients with non-alcoholic liver cirrhosis (167±29 pg/mL *vs*. 103±13 pg/mL, $P=0.04$).

Table 2 Characteristics of patients'

	No. of patients	VEGF (pg/ml)	bFGF (pg/ml)
Sex			
Male	67	121±14	4.8±0.5
Female	19	123±27	6.1±1.5
Age			
≤60 years	36	149±24	5.2±0.8
>60 years	50	103±13	5.1±0.6
Etiology			
Alcohol-related	26	167±29*	4.6±0.7
Non-alcoholic	60	103±13	5.4±0.6
Albumin (g/dL)			
≤3.6	48	132±15	5.1±0.7
>3.6	38	109±21	5.2±0.7
Creatinine (mg/dL)			
≤1.5	83	122±13	5.2±0.5
>1.5	3	125±73	4.5±2.6
ALT (U/L)			
≤40	37	136±22	4.1±0.6
>40	49	111±15	5.9±0.7
Total bilirubin (mg/dL)			
≤1.6	54	115±16	5.2±0.6
> 1.6	32	133±20	5.0±0.9
Child-Pugh score			
A	47	98±19	5.5±0.7
B, C	39	141±16	4.8±0.7
Prothrombin time prolongation >4 s			
Yes	27	145±23	5.0±1.0
No	59	112±15	5.3±0.6
Platelet count (/μL)			
≤150 000	71	109±12†	6.8±1.5
> 150 000	15	204±41	4.7±0.5
Esophageal varices			
Yes	59	122±14	5.0±0.6
No	27	119±28	5.8±1.0
Spider angioma			
Yes	31	185±28[b]	6.8±1.0[a]
No	55	90±10	4.1±0.5

Data were presented as mean ±SD. [a]$P<0.05$, [b]$P<0.005$. VEGF=vascular endothelial growth factor, bFGF=basic fibroblast growth factor.

Plasma angiogenic factors and clinical features

Table 3 summarizes the clinical features of cirrhotic patients with spider angiomas and those without. Cirrhotic patients with spider angiomas were younger (54±2 years *vs*. 66±1 years, $P<0.001$) and had higher serum bilirubin (3.1±0.5 mg/dL *vs*. 1.7±0.2 mg/dL, $P=0.03$), longer prothrombin time (16.6±0.7 sec *vs*. 14.8±0.4 sec, $P=0.015$), and higher proportion of alcoholism (45 % *vs*. 20 %, $P=0.014$) than those without. Sex, serum albumin, creatinine, AST, ALT, platelet count, size of esophageal varices, and Child-Pugh score did not differ between the two groups.

In the cirrhotics, plasma VEGF was significantly correlated with the size of spider angiomas ($r=0.38$, $P<0.001$). Plasma VEGF level also showed correlation with serum bilirubin level ($r=0.3$, $P=0.006$) and platelet count ($r=0.5$, $P<0.001$).

Univariate analysis of predictive factors for spider angiomas

Univariate analysis of factors predicting the presence of spider angiomas in patients with liver cirrhosis by using logistic regression is shown in Table 4. The cut-off values of 134 pg/mL

for VEGF and 4.8 pg/mL for bFGF obtained by the ROC analysis were used in the univariate analysis. Young age, elevated serum AST and bilirubin, prolonged prothrombin time, elevated plasma VEGF and bFGF, and alcoholism were associated with the presence of spider angiomas in cirrhotic patients.

Table 3 Clinical features of cirrhotic patients with and without spider angiomas

Parameters	Spider (+) (n=31)	Spider (-) (n=55)	P Value
Age (years)	54±2	66±1	<0.001
Sex (male / female)	27 / 4	41 / 14	0.17
Albumin (g / dL)	3.4±0.1	3.5±0.1	0.69
Creatinine (mg / dL)	1.0±0.1	1.1±0.1	0.24
AST (U / L)	91±9	89±13	0.93
ALT (U / L)	59±9	72±11	0.36
Platelet count (/ uL)	108 097±12 379	94 762±7 541	0.33
Esophageal varices (nil / F1 / F2 / F3)	7 / 6 / 12 / 6	18 / 12 / 14 / 11	0.88
Child-Pugh score	8.2±0.5	7.3±0.3	0.99
Bilirubin (mg / dL)	3.1±0.5	1.7±0.2	0.03
Prothrombin time (s)	16.6±0.7	14.8±0.4	0.015
Alcoholism	14 (45 %)	11 (20 %)	0.014

AST=aspartate transaminase, ALT=alanine transaminase.

Table 4 Univariate analysis of predictive factors for spider angiomas

Parameters	Odds ratio	95 % Confidence interval	P Value
Age (≤60 years)	5.12	1.97-13.28	0.001
Albumin (≥3.7 g / dL)	0.66	0.27-1.64	0.369
Creatinine (>1.5 mg / dL)	0.58	0.06-5.81	0.642
AST (>45 U / L)	5.76	1.56-21.3	0.009
ALT (>40 U / L)	1.24	0.51-3.02	0.634
Bilirubin (>1.6 mg / dL)	2.71	1.09-6.74	0.031
Platelet count (>150 000 / uL)	1.41	0.44-4.52	0.563
Prothrombin time prolongation (>4 s)	2.96	1.15-7.58	0.024
Child-Pugh score C	1.64	0.59-4.53	0.344
VEGF (≥134 pg / mL)	5.33	1.93-14.74	0.001
bFGF (≥4.8 pg / mL)	4.38	1.67-11.5	0.003
Alcoholism	3.29	1.25-8.67	0.016

AST=aspartate transaminase, ALT=alanine transaminase, VEGF=vascular endothelial growth factor, bFGF=basic fibroblast growth factor.

Table 5 Multivariate analysis of predictive values of VEGF, bFGF, and age for spider angiomas

Parameters	Odds ratio	95% confidence interval	P Value
Age (≤60 years)	6.64	2.02-21.79	0.002
VEGF (≥134 pg / mL)	4.35	1.35-14.01	0.014
bFGF (≥4.8 pg / mL)	5.66	1.72-18.63	0.004

VEGF=vascular endothelial growth factor, bFGF=basic fibroblast growth factor.

Multivariate analysis of plasma VEGF and bFGF, age and their predictive values for spider angiomas

Multivariate analysis with logistic regression showed that young age and elevated plasma levels of VEGF and bFGF were the most independent predictive factors for spider angiomas in cirrhotic patients, as shown in Table 5. The predictive values of plasma VEGF for spider angiomas were the following: sensitivity, 53 %; specificity, 82 %; positive predictive value, 64 %; and negative predictive value, 75 %. The predictive values of plasma bFGF for spider angiomas were: sensitivity, 60 %; specificity, 75 %; positive predictive value, 58 %; and negative predictive value, 76 %.

DISCUSSION

Spider angioma has been commonly seen in patients with liver cirrhosis[1,2]. The pathogenesis is still unknown. Neovascularization is a likely mechanism, but has not been proved. In the current study, we found significantly elevated plasma levels of VEGF and bFGF in cirrhotic patients compared with healthy controls. Elevated plasma VEGF was correlated with the size of spider angiomas. To our knowledge, this is the first study to demonstrate that age and plasma VEGF and bFGF are the most significant independent predictors of spider angiomas in cirrhotic patients.

VEGF has been found to be a glycoprotein that selectively induces endothelial proliferation, angiogenesis, and capillary hyperpermeability[13-15]. VEGF gene was expressed in a wide variety of normal human tissues, including the liver[16,17]. Blood levels of VEGF in patients with cirrhosis remain controversial[6,18]. Our results showed that plasma VEGF was elevated in patients with liver cirrhosis. In addition, plasma VEGF levels were negatively correlated with liver function reserve in patients with liver cirrhosis. The elevated VEGF might be due to ischemic or damaged liver cells, which released cellular VEGF to facilitate damage repair by stimulating angiogenesis[19]. Increased production of VEGF by the cirrhotic liver has also been reported[20], and may subsequently lead to the formation of spider angiomas.

bFGF has also been found to be a potent stimulator of endothelial cell proliferation, migration, and angiogenesis[21]. Our results showed that plasma bFGF was elevated in patients with liver cirrhosis which was consistent with previous reports[7-9]. The elevated bFGF might be due to a release from damaged liver cells[22] or increased production by the cirrhotic liver[9]. bFGF could also stimulate the production of VEGF and enhance angiogenesis[23].

The presence of spider angiomas has been reported to be associated with esophageal variceal bleeding[5]. The pathophysiological mechanism has been unclarified. Spider angiomas originate from arterioles, while esophageal varices are one kind of veins. They are different in nature. In this study, there was no relationship between the presence of spider angiomas and the degree of esophageal varices. In addition, there was no association between esophageal varices and these angiogenic factors.

A positive correlation was also found between serum VEGF level and the platelet count. This result was in accordance with the findings reported by others[24]. Platelets release a variety of vasoactive substances, including VEGF, and promote angiogenesis, endothelial permeability, and endothelial growth[25]. Although there was a positive correlation between the serum VEGF level and platelet count, there was no significant association between platelet count and spider angioma in the present study. Serum VEGF level was an independent predictor of spider angioma.

Plasma VEGF was increased in alcoholic cirrhotics compared with non-alcoholic cirrhotics in our study. Ethanol could induce expression of vascular endothelial growth factor and stimulate angiogenesis[26]. This may lead to the high prevalence of spider angiomas in alcoholic cirrhotic patients.

Young age was a significant predictor for the presence of spider angiomas in cirrhotics in our study. This was in

conformity with previous reports[1]. The underlying mechanism is unknown. A decline in angiogenic capacity in the aged[27,28] may cause impaired neovascularization and formation of spider angiomas in cirrhotic patients.

In summary, plasma VEGF and bFGF are elevated in patients with liver cirrhosis, especially in those with spider angiomas. Age-related angiogenic capacity as well as VEGF and bFGF may play important roles in the formation of spider angiomas in cirrhotic patients.

ACKNOWLEDGMENT

This work was supported by grant NSC 89-2315-B-075-004 from the National Science Council, and grant VGH 90-070 from Taipei Veterans General Hospital, Taiwan.

REFERENCES

1 **Bean WB.** The cutaneous arterial spider: a survey. *Medicine* 1945; **24**: 243-331
2 **Sherlock S,** Dooley J. Hepato-cellular failure In: Sherlock S, Dooley J, eds. Diseases of the Liver and Biliary System. 11th ed. *Oxford: Blackwell Science* 2002: 81-92
3 **Schenker S,** Balint J, Schiff L. Differential diagnosis of jaundice: report of a prospective study of 61 proved cases. *Am J Dig Dis* 1962; **7**: 449-463
4 **Li CP,** Lee FY, Hwang SJ, Chang FY, Lin HC, Lu RH, Hou MC, Chu CJ, Chan CC, Luo JC, Lee SD. Spider angiomas in patients with liver cirrhosis: role of alcoholism and impaired liver function. *Scand J Gastroenterol* 1999; **34**: 520-523
5 **Foutch PG,** Sullivan JA, Gaines JA, Sanowski RA. Cutaneous vascular spiders in cirrhotic patients: correlation with hemorrhage from esophageal varices. *Am J Gastroenterol* 1988; **83**: 723-726
6 **Rosmorduc O,** Wendum D, Corpechot C, Galy B, Sebbagh N, Raleigh J, Housset C, Poupon R. Hepatocellular hypoxia-induced vascular endothelial growth factor expression and angiogenesis in experimental biliary cirrhosis. *Am J Pathol* 1999; **155**: 1065-1073
7 **Hsu PI,** Chow NH, Lai KH, Yang HB, Chan SH, Lin XZ, Cheng JS, Huang JS, Ger LP, Huang SM, Yen MY, Yang YF. Implications of serum basic fibroblast growth factor levels in chronic liver diseases and hepatocellular carcinoma. *Anticancer Res* 1997; **17**: 2803-2809
8 **Jin-no K,** Tanimizu M, Hyodo I, Kurimoto F, Yamashita T. Plasma level of basic fibroblast growth factor increases with progression of chronic liver disease. *J Gastroenterol* 1997; **32**: 119-121
9 **Napoli J,** Prentice D, Niinami C, Bishop GA, Desmond P, McCaughan GW. Sequential increases in the intrahepatic expression of epidermal growth factor, basic fibroblast growth factor, and transforming growth factor beta in a bile duct ligated rat model of cirrhosis. *Hepatology* 1997; **26**: 624-633
10 **Di Lelio A,** Cestari C, Lomazzi A, Beretta L. Cirrhosis: diagnosis with sonographic study of the liver surface. *Radiology* 1989; **172**: 389-392
11 **Pugh RN,** Murray-Lyon IM, Dawson JL, Pietroni MC, Williams R. Transection of the oesophagus for bleeding oesophageal varices. *Br J Surg* 1973; **60**: 646-649
12 **Beppu K,** Inokuchi K, Koyanagi N, Nakayama S, Sakata H, Kitano S, Kobayashi M. Prediction of variceal hemorrhage by esophageal endoscopy. *Gastrointest Endosc* 1981; **27**: 213-218
13 **Shweiki D,** Itin A, Soffer D, Keshet E. Vascular endothelial growth factor induced by hypoxia may mediate hypoxia-initiated angiogenesis. *Nature* 1992; **359**: 843-845
14 **Plate KH,** Breier G, Weich HA, Risau W. Vascular endothelial growth factor is a potential tumour angiogenesis factor in human gliomas *in vivo*. *Nature* 1992; **359**: 845-848
15 **Shi BM,** Wang XY, Mu QL, Wu TH, Liu HJ, Yang Z. Angiogenesis effect on rat liver after administration of expression vector encoding vascular endothelial growth factor D. *World J Gastroenterol* 2003; **9**: 312-315
16 **Berse B,** Brown LF, Van de Water L, Dvorak HF, Senger DR. Vascular permeability factor (vascular endothelial growth factor) gene is expressed differentially in normal tissues, macrophages, and tumors. *Mol Biol Cell* 1992; **3**: 211-220
17 **Warren RS,** Yuan H, Matli MR, Gillett NA, Ferrara N. Regulation by vascular endothelial growth factor of human colon cancer tumorigenesis in a mouse model of experimental liver metastasis. *J Clin Invest* 1995; **95**: 1789-1797
18 **Akiyoshi F,** Sata M, Suzuki H, Uchimura Y, Mitsuyama K, Matsuo K, Tanikawa K. Serum vascular endothelial growth factor levels in various liver diseases. *Dig Dis Sci* 1998; **43**: 41-45
19 **Klagsbrun M,** Dmore PA. Regulation of angiogenesis. *Annu Rev Physiol* 1991; **53**: 217-239
20 **El-Assal ON,** Yamanoi A, Soda Y, Yamaguchi M, Igarashi M, Yamamoto A, Nabika T, Nagasue N. Clinical significance of microvessel density and vascular endothelial growth factor expression in hepatocellular carcinoma and surrounding liver: possible involvement of vascular endothelial growth factor in the pathogenesis of cirrhotic liver. *Hepatology* 1998; **27**: 1554-1562
21 **Duthu GS,** Smith JR. *In vitro* proliferation and lifespan of bovine aorta endothelial cells: effect of culture conditions and fibroblast growth factor. *J Cell Physiol* 1980; **103**: 285-392
22 **Dmore PA.** Modes of FGF release *in vivo* and *in vitro*. *Cancer Metastasis Rev* 1991; **9**: 227-238
23 **Seghezzi G,** Patel S, Ren CJ, Gualandris A, Pintucci G, Robbins ES, Shapiro RL, Galloway AC, Rifkin DB, Mignatti P. Fibroblast growth factor-2 (FGF-2) induces vascular endothelial growth factor (VEGF) expression in the endothelial cells of forming capillaries: an autocrine mechanism contributing to angiogenesis. *J Cell Biol* 1998; **141**: 1659-1673
24 **Salgado R,** Vermeulen PB, Benoy I, Weytjens R, Huget P, Van Marck E, Dirix LY. Platelet number and interleukin-6 correlate with VEGF but not with bFGF serum levels of advanced cancer patients. *Br J Cancer* 1999; **80**: 892-897
25 **Maloney JP,** Silliman CC, Ambruso DR, Wang J, Tuder RM, Voelkel NF. *In vitro* release of vascular endothelial growth factor during platelet aggregation. *Am J Physiol* 1998; **275**: H1054-1061
26 **Gu JW,** Elam J, Sartin A, Li W, Roach R, Adair TH. Moderate levels of ethanol induce expression of vascular endothelial growth factor and stimulate angiogenesis. *Am J Physiol Regul Integr Comp Physiol* 2001; **281**: R365-372
27 **Rivard A,** Fabre JE, Silver M, Chen D, Murohara T, Kearney M, Magner M, Asahara T, Isner JM. Age-dependent impairment of angiogenesis. *Circulation* 1999; **99**: 111-120
28 **Reed MJ,** Corsa AC, Kudravi SA, McCormick RS, Arthur WT. A deficit in collagenase activity contributes to impaired migration of aged microvascular endothelial cells. *J Cell Biochem* 2000; **77**: 116-126

Edited by Zhu LH

P.O.Box 2345, Beijing 100023,China
Fax: +86-10-85381893
E-mail: wjg@wjgnet.com www.wjgnet.com

World J Gastroenterol 2003;9(12):2836-2838
World Journal of Gastroenterology
 ISSN 1007-9327

• CLINICAL RESEARCH •

Copper metabolism after living related liver transplantation for Wilson's disease

Xue-Hao Wang, Feng Cheng, Feng Zhang, Xiang-Cheng Li, Jian-Ming Qian, Lian-Bao Kong, Hao Zhang, Guo-Qiang Li

Xue-Hao Wang, Feng Cheng, Feng Zhang, Xiang-Cheng Li, Jian-Ming Qian, Lian-Bao Kong, Hao Zhang, Guo-Qiang Li, Liver Transplantation Center, First Affiliated Hospital of Nanjing Medical University, Nanjing 210029, Jiangsu Province, China
Supported by the Basic Research Program Foundation of Jiangsu Province, No.BJ98025
Correspondence to: Feng Cheng, Liver Transplantation Center, First Affiliated Hospital of Nanjing Medical University, Nanjing 210029, Jiangsu Province, China. docchengfeng@sohu.com
Telephone: +86-25-3718836-6476
Received: 2003-06-28 **Accepted:** 2003-08-16

Abstract

AIM: Liver transplantation is indicated for Wilson's disease (WD) patients with the fulminant form and end-stage liver failure. The aim of this study was to review our experience with living-related liver transplantation (LRLT) for WD.

METHODS: A retrospective review was made for WD undergoing LRLT at our hospital from January 2001 to Febuary 2003.

RESULTS: LRLT was carried out in 15 patients with WD, one of them had fulminant hepatic failure and the others had end-stage hepatic insufficiency. The mean age of the patients was 14.5±2.5 years (range 6 to 20 years). All the recipients had low serum ceruloplasmin levels with a mean value of 126.8±34.8 mg/L before transplantation. The serum ceruloplasmin levels increased to an average of 238.6±34.4 mg/L after LRLT at the latest evaluation, between 2 and 27 months after transplantation. A marked reduction in urinary copper excretion was observed in all the recipients after transplantation. Among the eight recipients with preoperative Kayser-Fleischer (K-F) rings, this abnormality resolved completely after LRLT in five patients and partially in three. All the recipients are alive and remain well, and none has developed signs of recurrent WD after a mean follow-up period of 15.4±9.3 months (range 2-27 months) except one who died of severe rejection. The donors were 14 mothers and 1 father. The serum ceruloplasmin levels were within normal limits in all the donors (mean: 220±22.4 mg/L). The mean donor age was 35.0±4.0 years (range, 30 to 45 years). Two donors had biliary leakage and required reoperation. Grafts were harvested as follows: four right lobe grafts without hepatic middle vein and eleven left lobe grafts with hepatic middle vein. The grafts were blood group-compatible in all recipents. Two patients had hepatic artery thrombosis and underwent retransplantation.

CONCLUSION: LRLT is a curative procedure in Wilson's disease manifested as fulminant hepatic failure and/or end-stage hepatic insufficiency. After liver transplantation, the serum ceruoplasmin level can increase to its normal range while urinary copper excretion decreases. Grafts chosen from heterozygote carriers do not appear to confer any risk of recurrence in recipients.

Wang XH, Cheng F, Zhang F, Li XC, Qian JM, Kong LB, Zhang H, Li GQ. Copper metabolism after living related liver transplantation for Wilson's disease. *World J Gastroenterol* 2003; 9(12): 2836-2838
http://www.wjgnet.com/1007-9327/9/2836.asp

INTRODUCTION

Wilson's disease (WD) is an autosomal recessive disease. Its clinical and pathological manifestations are the consequence of an excessive accumulation of copper in tissues, particularly in the liver, brain, cornea, and kidneys. Liver transplantation is indicated for fulminant form and end-stage liver disease of WD[1,2].Cadaveric liver transplantation has been reported to normalize copper metabolism in recipients[3,4]. Recently, LRLT has also been used for WD[5-14]. Asonuma *et al*[8] reported that LRLT from heterozygous carriers of the WD gene could also resolve clinical signs and symptoms of WD and correct the parameters of copper metabolism. In this study, we reported our experience with LRLT for hepatic complications of WD from January 2001 to February 2003.

MATERIALS AND METHODS

Clinical and laboratory data were obtained from a review of the files of patients from 2001 to 2003 at Liver Transplantation Center of Jiangsu Province. All treatments had an informed consent of the children' s parents and the approval of the Ethics Committee of Nanjing Medical University. Donors were selected based on blood type, liver function, negative serological test results(hepatitis B virus, hepatitis C,HIV),physical examination, psychosocial evaluation including alcohol abuse and liver volumes assessed by Doppler ultrasound equipment and computed tomography. The donors were 14 mothers and 1 father. The serum ceruloplasmin levels were within the normal limits in all donors (mean: 220±22.4 mg/L). The mean donor age was 35.0±4.0 years (range, 30 to 45 years). Serum ceruloplasmin and copper level were also normal in all donors who gave an informed consent.

The diagnosis of WD was maded on the basis of a combination of the findings, including hepatic and/or neurological clinical abnormalities ,the presence of Kayser-Fleischer rings (KFR), elevated 24-hr urine copper (>100 μg/24 hr), low cerulopasmin level (reference range 200-500 mg/L). The above mentioned routine laboratory data were obtained by using standard methods. No patient received any chelating agent and presented clinical signs of WD after LRLT.

Among the 15 patients with WD, one had fulminant hepatic failure and the others had end-stage hepatic insufficiency. Their mean age was 14.5±2.5years (range 6 to 20 years). Before transplantation, all recipients had a low serum ceruloplasmin level with a mean value of 126.8±34.8 mg/L and a high urinary copper excretion with a mean value of 1 825.6±187.4 μg/24 h. Eight recipients had preoperative Kayser-Fleischer (K-F) rings. Grafts were harvested as follows: four right lobe grafts without hepatic middle vein and eleven left lobe grafts with hepatic middle vein. The grafts were blood group-compatible in all recipents.

RESULTS

Donors

All the donors were discharged from the hospital after a mean hospital stay of 9-14 days, and then resumed their normal life without any significant adverse sequelae. Two complications of bile leaks occurred, and required reoperation.

Recipents

Two patients had hepatic artery thrombosis and underwent retransplantation. All the recipients enjoyed normal health with a good quality of life, and none had signs of recurrent WD after a mean follow-up period of 15.4±9.3 months (range 2-27 months). One patient died of severe rejection. Copper metabolism of the WD recipients and the presence of K-F rings were compared before and after transplantation. After LRLT, all the recipients had normal serum ceruloplasmin concentrations in the first month. Marked reduction of urinary copper excretion occurred in the first three months, which became normal 6-9 months after operation. Kayser-Fleischer (K-F) rings were resolved completely after LRLT in five patients and partially in three.

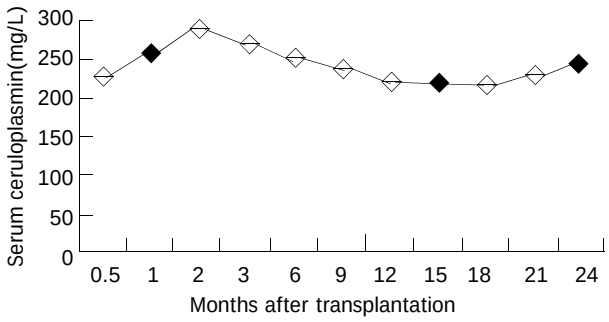

Figure 1 Changes in serum ceruloplasmin of postoperative recipients (Normal: 200-500 mg/L).

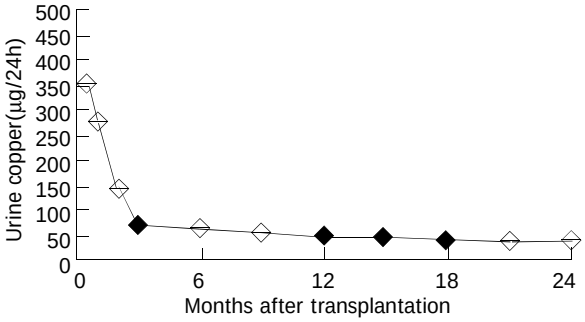

Figure 2 Changes in urine copper of postoperativ recipients (Normal: <50 μg/24 h).

DISCUSSION

Wilson's disease, first described by Kinnear Wilson in 1912, is an autosomal recessive condition with a prevalence in one of 30 000[15]. Its clinical and pathological manifestations are the consequence of an excessive accumulation of copper in tissues, particularly in the liver, brain, cornea, and kidneys. The WD gene is localized on the long arm of chromosome 13 and was recently cloned by several different research groups[16-19]. The gene product ATP7B is a copper transporting type ATPase. Establishing the diagnosis of Wilson's disease is usually straightforward if the major clinical and laboratory features are manifested as: typical hepatic and/or neurological symptoms and signs, Kayser-Fleischer rings, low serum caeruloplasmin concentrations, and increased urinary copper excretion.

It has been reported that the prognosis of fulminant WD is extremely poor and liver transplantation is currently the only available form of curative therapy when penicillamine therapy has failed or is no longer appropriate[20-22]. Cadaveric liver transplantation has been reported to normalize copper metabolism in recipients[3,4]. As scarcity of cadaveric donors is a serious problem in many countries, LRLT represents a critical form of rescue therapy in endstage liver disease. Recently, because of the shortage of donors for cadaveric liver transplantation, LRLT has also been indicated for WD[5-14]. Asonuma *et al*[8] reported that LRLT from heterozygous carriers of the WD gene could also resolve clinical signs and symptoms of WD and correct the parameters of copper metabolism.

The advantage of LRLT is that the donor liver can be obtained in an urgent situation when conservative therapy has failed. A successful transplantation of a liver from a living donor was performed in Australia in 1989 by Strong and colleagues[23], and the technique had been practised worldwide now, particularly in countries where cadaveric organs are not available. In general, the most important ethical dilemma with LRLT is that the process subjects a healthy person to a major operation. More than 1500 such surgeries in children have been performed throughout the world. Only two donors died. One died from pulmonary embolism, and the other died from an anesthetic accident. The patient with pulmonary embolisms was probably a poor surgical candidate. In neither case were there any technical complications related to the procedure. Both cases showed the importance of donor evaluation and selection in preventing living donor mortalities. In this study, 15 donors were discharged from the hospital and all resumed their normal life style without any significant adverse sequelae after a mean hospital stay of 15 days after the operation. Two complications of bile leakage occurred, and required a relaparotomy. The results, along with those from other centers, confirmed the general safety of the donor operation[24,25]. Hepatic arterial reconstruction is one of the most difficult procedures in living-donor liver transplantation (LDLT) because the artery used is generally small in diameter and has a short stalk. If hepatic artery thrombosis (HAT) occurred, the recipient clinical course would be unstable[26-30]. The introduction of microvascular hepatic arterial reconstruction has significantly decreased the incidence of HAT. In our group, HATs were recognized in 2 cases (13 %), retransplantations saved the patients. So surgeons who perform hepatic arterial reconstruction in LDLT should be well trained in microvascular techniques to decrease the incidence of HAT.

In this study, Copper metabolism in the WD recipients and the presence of K-F rings were compared before and after transplantation. After LRLT, all the recipients had a normal serum ceruloplasmin concentration and marked reduction in urinary copper excretion. All the donor ceruloplasmin levels were within the normal range, as were the post-transplant levels in the recipients. In addition to normal laboratory profiles of copper abnormalities, five out of eight patients with Kayser-Fleischer rings had a complete resolution and the remaining three showed improvement following transplantation. Despite these results, it is important to remember that about 10 % of WD heterozygotes would have low ceruloplasmin levels, so that they might be unsuitable as donors[31]. Based on the findings of this study, living related liver transplantation can be used safely in WD when appropriate cadaveric organs are unavailable. Despite the excellent results of the reported cases, there are some questions to be studied ,such as screening of potential WD heterozygote donors for uncommon abnormalities of copper metabolism, *etc*.

Furthermore, it is still unclear whether de-coppering after LRLT from heterozygote donors is slower than de-coppering after cadaveric transplantation from non-related donors. We

are reassured, however, by the fact that none of our transplanted recipients had persistent neurological abnormalities after LRLT, and K-F rings disappeared in most of the recipients, indicating that LRLT was indeed an effective and safe modality of therapy for patients with Wilsonian fulminant hepatic failure and end-stage hepatic insufficiency. After liver transplantation, serum ceruoplasmin level increased to normal range and urinary copper excretion decreased. Grafts chosen from heterozygote carriers did not appear to confer any risk of recurrence in the recipients, at least in the short term. Long-term follow-up should be continued to evaluate this specific therapy.

REFERENCES

1 **Bellary S**, Hassanein T, Van Thiel DH. Liver transplantation for Wilson's disease. *J Heptol* 1995; **23**: 373-381
2 **Sternlieb I.** Wilson's disease: indications for liver transplants. *Hepatology* 1984; **4**(Suppl): 15s-17s
3 **Emre S,** Atillasoy EO, Ozdemir S, Schilsky M, Rathna Varma CV, Thung SN, Sternlieb I, Guy SR, Sheiner PA, Schwartz ME, Miller CM. Orthotopic liver transplantation for Wilson's disease: a single-center experience. *Transplantation* 2001; **72**: 1232-1236
4 **Burdelski M,** Rogiers X. Liver transplantation in metabolic disorders. *Acta Gastroenterol Belg* 1999; **62**: 300-305
5 **Komatsu H,** Fujisawa T, Inui A, Sogo T, Sekine I, Kodama H, Uemoto S, Tanaka K. Hepatic copper concentration in children undergoing living related liver transplantation due to Wilsonian fulminant hepatic failure. *Clin Transplant* 2002; **16**: 227-232
6 **Tanaka K,** Uemoto S, Inomata Y, Tokunaga Y, Ueda M, Tokka A, Sato B, Yamaoka Y. Living-related liver transplantation for fulminant hepatic failure in children. *Transpl Int* 1994; **7**(Suppl 1): S108-110
7 **Tanaka K**, Uemoto S, Tokunaga Y, Fujita S, Sano K, Yamamoto E, Sugano M, Awane M, Yamaoka Y, Kumada K. Living related liver transplantation in children. *Am J Surg* 1994; **168**: 41-48
8 **Asonuma K,** Inomata Y, Kasahara M, Uemoto S, Egawa H, Fujita S, Kiuchi T, Hayashi M, Tanaka K. Living related liver transplantation from heterozygote genetic carriers to children with Wilson's disease. *Pediatr Transplant* 1999; **3:** 201-205
9 **Terajima H,** Tanaka K, Okajima K, Inomata Y, Yamaoka Y. Timing of transplantation and donor selection in living related liver transplantation for fulminant Wilson's disease. *Transplant Proc* 1995; **27**: 1177-1178
10 **Wang X,** Zhang F, Li X, Qian J, Kong L, Huang J, Huang Z, Zhang H, Li G, Cheng F, Wang K, Lu S. A clinical report of 12 case-times of living related liver transplantation. *Zhonghua Yixue Zazhi* 2002; **82**: 435-439
11 **Hattori H,** Higuchi Y, Tsuji M, Inomata Y, Uemoto S, Asonuma K, Egawa H, Kiuchi T, Furusho K, Yamaoka Y, Tanaka K. Living-related liver transplantation and neurological outcome in children with fulminant hepatic failure.*Transplantation* 1998; **65**: 686-692
12 **Wang X,** Li G, Li X, Zhang F, Qian J, Kong L, Zhang H, Sun B. Multimodal approach to clinical liver transplantation**.** *Zhonghua Waike Zazhi* 2002; **40**: 758-761
13 **Kobayashi S,** Ochiai T, Hori S, Suzuki T, Shimizu T, Gunji Y, Shimada H, Yamamoto S, Ogawa A, Kohno Y, Sunaga M, Shimazu M, Tanaka K. Copper metabolism after living donor liver transplantation for hepatic failure of Wilson's disease from a gene mutated donor. *Hepatogastroenterology* 2001**; 48**: 1259-1261
14 **Sakoguchi T,** Nishizaki T, Suehiro T, Nomoto K, Hashimoto K, Ohta R, Minagawa R, Hiroshige S, Terashi T, Ninomiya M, Nagata S, Shiotani S, Shimada M, Sugimachi K. Living donor liver transplantation in Kyushu University. *Fukuoka Igaku Zasshi* 2000; **91**: 198-202
15 **Schilsky ML.** Wilson's disease: genetic basis of copper toxicity and natural history. *Semin Liver Dis* 1996; **16**: 83-95
16 **Steindl P**, Ferenci P, Dienes HP, Grimm G, Pabinger I, Madl C, Maier-Dobersberger T, Herneth A, Dragosics B, Meryn S, Knoflach P, Granditsch G, Gangl A. Wilson's disease: in patients presenting with liver disease: a diag nostic challenge. *Gastroenterology* 1997; **113**: 212-218
17 **Tanzi RE**, Petrukhin K, Chernov I, Pellequer JL, Wasco W, Ross B, Romano DM, Parano E, Pavone L, Brzustowicz LM. The Wilson disease gene is a copper transporting ATPase with homology to the Menkes disease gene. *Nat Genet* 1993; **5**: 344-350
18 **Petrukhin K**, Fischer SG, Pirastu M, Tanzi RE, Chernov I, Devoto M, Brzustowicz LM, Cayanis E, Vitale E, Russo JJ. Mapping cloning and genetic characterization of the region containing the Wilson disease gene. *Nat Genet* 1993; **5**: 338-343
19 **Yamaguchi Y**, Heiny ME, Gitlin JD. Isolation and characterization of a human liver cDNA as a candidate gene for Wilson disease. *Biochem Biophys Res Commun* 1993; **197**: 271-277
20 **Nazer H,** Ede RJ, Mowat AP, Williams R. Wilson's disease: clinical presentation and use of prognostic index. *Gut* 1986; **27**: 1377-1381
21 **Rakela J,** Kurtz SB, McCarthy JT, Ludwig J, Ascher NL, Bloomer JR, Claus PL. Fulminant Wilson's disease treated with postdilution hemofiltration and orthotopic liver transplantation. *Gastroenterology* 1986; **90**: 2004-2007
22 **Stampfl DA,** Munoz SJ, Moritz MJ, Rubin R, Armenti VT, Jarrell BE, Maddrey WC. Heterotopic liver transplantation for fulminant Wilson's disease. *Gastroenterology* 1990; **99**: 1834-1836
23 **Strong RW**, Lynch SV, Ong TH, Matsunami H, Koido Y, Balderson GA. Successful liver transplantation from a living donor to her son. *N Engl J Med* 1990; **322**: 1505-1507
24 **Sugawara Y**, Makuuchi M, Takayama T, Imamura H, Kaneko J, Ohkubo T. Safe donor hepatectomy for living related liver transplantation. *Liver Transpl* 2002; **8**: 58-62
25 **Miller CM**, Gondolesi GE, Florman S, Matsumoto C, Munoz L, Yoshizumi T, Artis T, Fishbein TM, Sheiner PA, Kim-Schluger L, Schiano T, Shneider BL, Emre S, Schwartz ME. One hundred nine living donor liver transplants in adults and children: a single-center experience. *Ann Surg* 2001; **234**: 301-311
26 **Dalgic A**, Dalgic B, Demirogullari B, Ozbay F, Latifoglu O, Ersoy E, Mahli A, Ilgit E, Ozdemir H, Arac M, Akyol G, Tatlicioglu E. Clinical approach to graft hepatic artery thrombosis following living related liver transplantation. *Pediatr Transplant* 2003; **7**: 149-152
27 **Goldstein MJ**, Salame E, Kapur S, Kinkhabwala M, LaPointe-Rudow D, Harren NPP, Lobritto SJ, Russo M, Brown RS Jr, Cataldegirmen G, Weinberg A, Renz JF, Emond JC. Analysis of failure in living donor liver transplantation: differential outcomes in children and adults. *World J Surg* 2003; **27**: 356-364
28 **Uchiyama H**, Hashimoto K, Hiroshige S, Harada N, Soejima Y, Nishizaki T, Shimada M, Suehiro T. Hepatic artery reconstruction in living-donor liver transplantation: a review of its techniques and complications. *Surgery* 2002; **131**(1 Supp l): S200-S204
29 **Suehiro T**,Ninomiya M, Shiotani S, Hiroshige S, Harada N, Ryosuke M, Soejima Y, Shimada M, Sugimachi K. Hepatic artery reconstruction and biliary stricture formation after living donor adult liver transplantation using the left lobe. *Liver Transpl* 2002; **8**: 495-499
30 **Hatano E**, Terajima H, Yabe S, Asonuma K, Egawa H, Kiuchi T, Uemoto S, Inomata Y, Tanaka K, Yamaoka Y. Hepatic artery thrombosis in living related liver transplantation. *Transplantation* 1997; **64**: 1443-1446
31 **Gollan JL, Gollan TJ.** Wilson disease in 1998: genetic, diagnostic and therapeutic aspects. *J Hepatol* 1998; **28**(Suppl): 28-36

Edited by Xu JY and Wang XL

P.O.Box 2345, Beijing 100023,China
Fax: +86-10-85381893
E-mail: wjg@wjgnet.com www.wjgnet.com

World J Gastroenterol 2003;9(12):2839-2842
World Journal of Gastroenterology
 ISSN 1007-9327

• CLINICAL RESEARCH •

Clinical relationship between EDN-3 gene, EDNRB gene and Hirschsprung's disease

Xiang-Long Duan, Xian-Sheng Zhang, Guo-Wei Li

Xiang-Long Duan, Guo-Wei Li, Department of General Surgery, Second Hospital of Xi' an Jiaotong University, Xi' an 710004, Shaanxi Province, China
Xian-Sheng Zhang, Department of Pediatric Surgery, Second Hospital of Xi' an Jiaotong University, Xi' an 710004, Shaanxi Province, China
Supported by the Natural Science Foundation of Shaanxi Province, No. 2000SM58
Correspondence to: Dr. Duan-Xiang Long, Department of General Surgery, Second Hospital of Xi' an Jiaotong University, Xi' an 710004, Shaanxi Province, China. duanxl@21cn.com
Telephone: +86-29-8402350 **Fax:** +86-29-5535250
Received: 2003-05-11 **Accepted:** 2003-06-02

Abstract

AIM: To investigate the mutation of EDNRB gene and EDN-3 gene in sporadic Hirschsprung's disease (HD) in Chinese population.

METHODS: Genomic DNA was extracted from bowel tissues of 34 unrelated HD patients which were removed by surgery. Exon 3, 4, 6 of EDNRB gene and Exon 1, 2 of EDN-3 gene were amplified by polymerase chain reaction (PCR) and analyzed by single strand conformation polymorphism (SSCP).

RESULTS: EDNRB mutations were detected in 2 of the 13 short-segment HD. One mutant was in the exon 3, the other was in the exon 6. EDN-3 mutation was detected in one of the 13 short-segment HD and in the exon 2. Both EDNRB and EDN-3 mutations were detected in one short-segment HD. No mutations were detected in the ordinary or long-segment HD.

CONCLUSION: The mutations of EDNRB gene and EDN-3 gene are found in the short-segment HD of sporadic Hirschsprung's disease in Chinese population, which suggests that the EDNRB gene and EDN-3 gene play important roles in the pathogenesis of HD.

Duan XL, Zhang XS, Li GW. Clinical relationship between EDN-3 gene, EDNRB gene and Hirschsprung's disease. *World J Gastroenterol* 2003; 9(12): 2839-2842
http://www.wjgnet.com/1007-9327/9/2839.asp

INTRODUCTION

Hirschsprung' s disease (HD) is a congenital malformation with an incidence of one in 5 000 live newborns. The absence of intramural intestinal ganglia of Meissner and Auerbach results in poor coordination of propulsive movement, and hence functional intestinal obstruction. Patients were treated surgically with removal of the affected intestine[1-4]. In 1994, two major genes associated with HD were recognized. First, in the RET (receptor tyrosin kinase) gene, there are inactivating mutations in isolated HD. RET accounts for up to 20 % of sporadic and 50 % of familial cases[5-11]. The second major gene is the EDNRB (endothelin receptor B) gene. EDNRB accounts for 5-10 % of all HD cases. Heterozygous mutations in the EDNRB gene were reported in nonsyndromic HD[12-16]. The preferred ligand for the G-protein coupled transmembranous receptor EDNRB was EDN-3 (endothelin-3). The interaction between EDN-3 and EDNRB was reported to be essential for normal development of enteric ganglia. The importance of the EDN-3-EDNRB interaction in promoting the normal development of neural crest cells has been clearly demonstrated. Human mutations in the EDN-3 gene have been reported recently: heterozygous missense mutations in two cases of sporadic HD[17-19]. However, there are fewer reports about mutations of EDNRB gene and EDN-3 gene in HD in Chinese population. In order to further investigate the pathogenic mechanism of HD, we examined mutations on exon 3, 4, 6 of EDNRB gene and exon 1, 2 of EDN-3 gene in 34 sporadic HD cases with the single strand conformation ploymorphism analysis of polymerase chain reaction products (PCR-SSCP).

MATERIALS AND METHODS

Tissue preparation and extraction of DNA

Thirty-four specimens of sporadic HD cases were collected after operation in the Second Hospital of Xi' an Jiaotong University between 1999 and 2001, and the pathological statement was approved pathologically. There are four cases of long-segment HD, seventeen cases of common HD, and thirteen cases of short-segment HD based on Romen' s division. At the same time, normal recta and sigmoid flexure tissues were collected, serving as a control group. All specimens were put into liquid nitrogen to freeze quickly after cut off in 15 minutes, and stored at a temperature of -80 ℃. DNA was extracted according to the standard protocols.

PCR amplification

The designed primers were synthesized by Bioasia Company. The specific primer sequences of exon 3, 4, 6 of EDNRB gene and exon 1, 2 of EDN-3 gene are summarized in Table 1. The PCR mixture (total volume: 30 μL) contained 2 μL of template-DNA, 3 μL of 10×PCR buffer, 3 μL of 2.5 mmol/L $MgCl_2$, 3 μL of 2.5 mmol/L dNTPs, 1 μL each of two fragment-specific primers, 17 μL of triplex distilled water, and 1 unit of Taq DNA polymerase. Thirty-five PCR amplification cycles were performed with the following condition of temperature: 94 ℃ for 35 seconds, 55 ℃ for 50 seconds and 72 ℃ for 1 minute. Amplifications were performed with a final extension for 10 minutes at 72 ℃. The amplified fragments were run in 15 g/L agarose gel, and were confirmed to be in existence.

SSCP analysis

A conventional electrophoresis apparatus (PC-3000 Mini Electrophoresis Unit; Bio-Red Company, USA) was used with a constant temperature of 10 ℃ for SSCP. For SSCP, the PCR products were heated for 10 min at 94 ℃, transferred into an ice-cold water bath for 3 min, and then run on 60 g/L polyacrylamide gel for 3 hours. The gel was stained by ethidium bromide for 10 - 20 min to visualize DNA band patterns.

Table 1 EDNRB and EDN-3 primer sequences

Gene	Exon		Primer	bp
EDNRB	3	Forwoard	ATCTTCAGATATCGAGCTGTT	223 bp
		Reverse	TGAAATTTACCTGCATGAAAG	
	4	Forwoard	ATCCCTATAGTTTTACAAGACAGC	170 bp
		Reverse	ATTTTCTTACCTGCTTTAGGTG	
	6	Forwoard	ACAGAAGCTACAATGACTAC	240 bp
		Reverse	GAAAGGCTTATATTTGAGCC	
EDN-3	1	Forwoard	CAAGCGGCCGTCCTCCTGGTCCGGT	180 bp
		Reverse	CTTCTCCGCGCCTCGGTCC	
	2A	Forwoard	CCCTCCTCAGGTGTTTGGG	239 bp
		Reverse	TCGGCCGCCTGCTCCTGC	
	2B	Forwoard	TGGCGAGGAGACTGTGGCT	218 bp
		Reverse	TGGCGAGGAGACTGTGGCT	

RESULTS

Analysis of PCR products

EDNRB gene PCR products The increment of all DNA samples from HD patients was a single strand with a length of 223 bp, 170 bp and 240 bp and so was the normal control, which indicated that a large fragment insertion and deletion did not exist in the region of EDNRB gene exon 3, 4 and 6 among 34 HD patients.

EDN-3 gene PCR products The increment of all DNA samples from HD patients was a single strand with a length of 180 bp, 239 bp and 219 bp and so was the normal control, which indicated that a large fragment insertion and deletion did not exist in the region of EDN-3 gene exon 1, 2A and 2B among 34 HD patients.

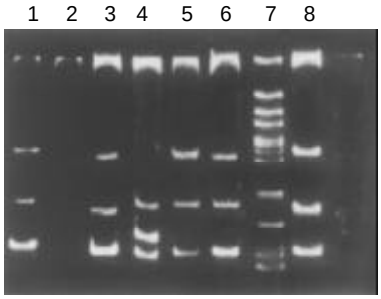

Figure 1 The abnormal shifted SSCP band in exon 3 of EDNRB. 1, 3, 5, 6: Normal shifted SSCP bands; 7: PGEM-3zf / *Hae* III marker; 8: Positive control; 2: Negative control; 4: Abnormal shifted SSCP band.

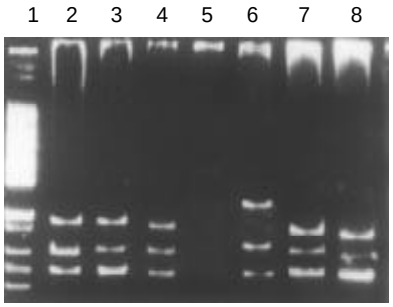

Figure 2 The abnormal shifted SSCP band in exon 6 of EDNRB. 1: PGEM-3zf / *Hae* III marker; 2: Positive control; 5: Negative control; 6: Abnormal shifted SSCP band. 3, 4, 7, 8: Normal shifted SSCP bands.

Results of SSCP

Among the 34 HD patients, abnormal SSCP migration patterns were found in 2 unrelated HD. EDNRB mutations were detected in 2 of the 17 short-segment HD. One mutant was in the exon 3 (Figure 1), the other was in the exon 6 (Figure 2). EDN-3 mutation was detected in 1 of the 17 short-segment HD and in the exon 2 (Figure 3). Both EDNRB mutation and EDN-3 mutation were detected in one short-segment HD (Figure 4). The mutation was absent in the ordinary, long-segment HD and normal control group samples.

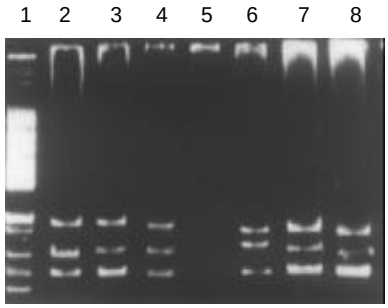

Figure 3 The abnormal shifted SSCP band in exon 2A of EDN-3. 1: PGEM-3zf / *Hae* III marker; 2: Positive control; 5: Negative control; 6: Abnormal shifted SSCP band. 3, 4, 7, 8: Normal shifted SSCP bands.

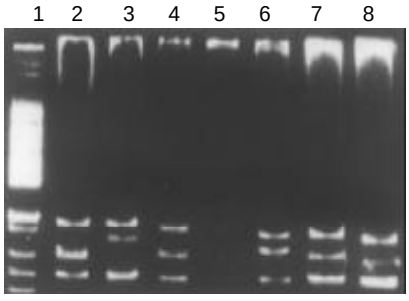

Figure 4 The abnormal shifted SSCP band in exon 2A of EDN-3 and exon 6 of EDNRB. 1: PGEM-3zf / *Hae* III marker; 2: Normal shifted SSCP band; 3: Abnormal shifted SSCP band; 4: Normal control; 5: Negative control; 6: Abnormal shifted SSCP band; 7: positive control; Lane 8: normal shifted SSCP band.

DISCUSSION

The endothelin peptide family of secreted peptides comprises four members to date: EDN-1, EDN-2, EDN-3, and VIP (vasoactive intestinal polypeptide)[20,21]. A diverse set of pharmacologic activities with different potencies are exerted by endothelin family peptides, suggesting the existence of

endothelin receptor subtypes.

The EDNRB gene encodes a heptahelical receptor that is involved in the G-protein-mediated intracellular signaling pathway. The human EDNRB gene lies on chromosome band 13q22 and comprises 7 exons, with a length of about 24 kb[22-27]. The predicted protein had 442 amino acids with a transmembrane topology similar to that of other G protein-coupled receptors which, when activated by a ligand, induce a calcium flux into the cells. Activation of EDNRB may result in upregulation of secretion of the endothelins, thereby amplifying their effects.

The EDN-3 gene encodes a large inactive preproendothelin-3 precursor which yields a biologically active 21 amino acid peptide containing four cysteines involved in two disulphide bonds. The human EDN-3 gene lies on chromosome band 20q13.3 and comprises 5 exons[28-30]. The EDN-3 is produced by a two-step proteolytic cleavage of a larger precursor molecule, preproendothelin. This molecule is enzymatically processed to an inactive progenitor (big endothelin) which is subsequently converted to the active peptide by a specific endothelin-converting enzyme 1. The mature peptide mediates its effect through two receptors, one of which is the EDNRB.

We have examined mutations on exon 3, 4, 6 of EDNRB gene and exon 1, 2 of EDN-3 gene in 34 sporadic Chinese HD patients with PCR-SSCP. The PCR result revealed that the increment of all DNA samples from HD patients was a single strand with a length of 223 bp, 170 bp and 240 bp and so was that from normal control, which indicated that a large fragment insertion and deletion did not exist in the region of EDNRB gene exon 3, 4 and 6 among 34 HD patients. And the increment of all DNA samples from HD patients was a single strand with a length of 180 bp, 239 bp and 219 bp and so was that from normal control, which indicated that a large fragment insertion and deletion did not exist in the region of EDN-3 gene exon 1, 2A and 2B among 34 HD patients. Among the 34 HD patients, we found abnormal SSCP migration patterns in 2 unrelated HD. EDNRB mutations were detected in 2 of the 17 short-segment HDs. One mutant was in the exon 3, the other in the exon 6. EDN-3 mutation was detected in 1 of the 17 short-segment HD and in the exon 2. Both EDNRB and EDN-3 mutations were detected in one short-segment HD. The mutation is absent in the ordinary, long-segment HD and normal control group samples. Due to the mutation of EDNRB, there would be no upregulation of secretion of the endothelins and amplification of endothelin effect, and the total amount of endothelin produced would be too small to initiate migration. Alteration of the structure of the preproendothelin by the mutation may conceivably result in a less efficient cleavage, or even a complete failure of cleavage of the preproendothelin, resulting in EDN-3 deficiency during development. This might lead to an incomplete colonization of the bowel by ganglion cells. We should bear in mind that EDNRB is the receptor for EDN-3, so it is reasonable to assume that the mutations of EDNRB and EDN-3 caused the maldevelopment of the enteric nervous system.

Similar to the receptor-ligand relationship between RET and GDNF observed in the etiology of some HD patients, in human fetuses, both EDNRB and EDN-3 have been demonstrated on enteric neurons and gut mesenchyme cells[31], suggesting that EDN-3 and EDNRB may regulate interactions between neural crest and gut mesenchyme cells, necessary for normal migration. There are reports on HSCR patients with GDNF-RET or NTN-RET gene mutation combinations, as well as a case with mutations in both RET and EDNRB[32-39]. So far, there has been no report on an EDN-3 mutation in combination with a mutation in other HSCR genes. In the present study, we found an EDN-3 mutation in combination with an EDNRB mutation in one short-segment HD patient.

To date, at least 16 different mutations or alterations of the EDNRB gene and 4 different mutations or alterations of the EDN-3 gene have been identified in HD patients. A variety of frameshift, nonsense, or missense mutations scattered along EDNRB gene and EDN-3 gene has been identified in HD patients[40, 41]. The combined results of our study for mutations in EDN3 and EDNRB may indicate the contributions of these genes to the HD phenotype. EDNRB and EDN3 mutations seem to account for a minority of cases. The majority of HSCR cases cannot be explained by mutations in any of the genes analysed so far, suggesting that other genes or additional factors may contribute to the occurrence of HD phenotype and that HD is a multifactorial disease.

REFERENCES

1 **Bates MD**. Development of the enteric nervous system. *Clin Perinatol* 2002; **29**: 97-114
2 **Amiel J**, Lyonnet S. Hirschsprung disease, associated syndromes, and genetics: a review. *J Med Genet* 2001; **38**: 729-739
3 **Meier-Ruge WA**, Brunner LA. Morphometric assessment of Hirschsprung's disease: associated hypoganglionosis of the colonic myenteric plexus. *Pediatr Dev Pathol* 2001; **4**: 53-61
4 **Li JC**, Mi KH, Zhou JL, Busch L, Kuhnel W. The development of colon innervation in trisomy 16 mice and Hirschsprung's disease. *World J Gastroenterol* 2001; **7**: 16-21
5 **Borrego S**, Wright FA, Fernandez RM, Williams N, Lopez-Alonso M, Davuluri R, Antinolo G, Eng C. A founding locus within the RET proto-oncogene may account for a large proportion of apparently sporadic Hirschsprung disease and a subset of cases of sporadic medullary thyroid carcinoma. *Am J Hum Genet* 2003; **72**: 88-100
6 **Griseri P**, Pesce B, Patrone G, Osinga J, Puppo F, Sancandi M, Hofstra R, Romeo G, Ravazzolo R, Devoto M, Ceccherini I. A rare haplotype of the RET proto-oncogene is a risk-modifying allele in hirschsprung disease. *Am J Hum Genet* 2002; **71**: 969-974
7 **Sancandi M**, Ceccherini I, Costa M, Fava M, Chen B, Wu Y, Hofstra R, Laurie T, Griffths M, Burge D, Tam PK. Incidence of RET mutations in patients with Hirschsprung's disease. *J Pediatr Surg* 2000; **35**: 139-143
8 **Fitze G**, Cramer J, Ziegler A, Schierz M, Schreiber M, Kuhlisch E, Roesner D, Schackert HK. Association between c135G/A genotype and RET proto-oncogene germline mutations and phenotype of Hirschsprung's disease. *Lancet* 2002; **359**: 1200-1205
9 **Pasini B**, Rossi R, Ambrosio MR, Zatelli MC, Gullo M, Gobbo M, Collini P, Aiello A, Pansini G, Trasforini G, degli Uberti EC. RET mutation profile and variable clinical manifestations in a family with multiple endocrine neoplasia type 2A and Hirschsprung's disease. *Surgery* 2002; **131**: 373-381
10 **Julies MG**, Moore SW, Kotze MJ, du Plessis L. Novel RET mutations in Hirschsprung's disease patients from the diverse South African population. *Eur J Hum Genet* 2001; **9**: 419-423
11 **Shimotake T**, Go S, Inoue K, Tomiyama H, Iwai N. A homozygous missense mutation in the tyrosine E kinase domain of the RET proto-oncogene in an infant with total intestinal aganglionosis. *Am J Gastroenterol* 2001; **96**: 1286-1291
12 **Newby DE**, Strachan FE, Webb DJ. Abnormal endothelin B receptor vasomotor responses in patients with Hirschsprung's disease. *Q J M* 2002; **95**: 159-163
13 **Von Boyen GB**, Krammer HJ, Suss A, Dembowski C, Ehrenreich H, Wedel T. Abnormalities of the enteric nervous system in heterozygous endothelin B receptor deficient (spotting lethal) rats resembling intestinal neuronal dysplasia. *Gut* 2002; **51**: 414-419
14 **Zaahl MG**, du Plessis L, Warnich L, Kotze MJ, Moore SW. Significance of novel endothelin-B receptor gene polymorphisms in Hirschsprung's disease: predominance of a novel variant (561C/T) in patients with co-existing Down's syndrome. *Mol Cell Probes* 2003; **17**: 49-54
15 **Fuchs S**, Amiel J, Claudel S, Lyonnet S, Corvol P, Pinet F. Functional characterization of three mutations of the endothelin B receptor gene in patients with Hirschsprung's disease: evidence for selective loss of Gi coupling. *Mol Med* 2001; **7**: 115-124
16 **Matsushima Y**, Shinkai Y, Kobayashi Y, Sakamoto M, Kunieda

T, Tachibana M. A mouse model of Waardenburg syndrome type 4 with a new spontaneous mutation of the endothelin-B receptor gene. *Mamm Genome* 2002; **13**: 30-35

17 **Bidaud C**, Salomon R, Van Camp G, Pelet A, Attie T, Eng C, Bonduelle M, Amiel J, Nihoul-Fekete C, Willems PJ, Munnich A, Lyonnet S. Endothelin-3 gene mutations in isolated and syndromic Hirschsprung disease. *Eur J Hum Genet* 1997; **5**: 247-251

18 **Pingault V**, Bondurand N, Lemort N, Sancandi M, Ceccherini I, Hugot JP, Jouk PS, Goossens M. A heterozygous endothelin 3 mutation in Waardenburg-Hirschsprung disease: is there a dosage effect of EDN3/EDNRB gene mutations on neurocristopathy phenotypes? *J Med Genet* 2001; **38**: 205-209

19 **Svensson PJ**, Von Tell D, Molander ML, Anvret M, Nordenskjold A. A heterozygous frameshift mutation in the endothelin-3 (EDN-3) gene in isolated Hirschsprung's disease. *Pediatr Res* 1999; **45**(5 Pt 1):714-717

20 **Goraca A**. New views on the role of endothelin (minireview). *Endocr Regul* 2002; **36**: 161-167

21 **Milla PJ**. Endothelins, pseudo-obstruction and Hirschsprung's disease. *Gut* 1999; **44**: 148-149

22 **Gariepy CE**, Williams SC, Richardson JA, Hammer RE, Yanagisawa M. Transgenic expression of the endothelin-B receptor prevents congenital intestinal aganglionosis in a rat model of Hirschsprung disease. *J Clin Invest* 1998; **102**: 1092-1101

23 **Shanske A**, Ferreira JC, Leonard JC, Fuller P, Marion RW. Hirschsprung disease in an infant with a contiguous gene syndrome of chromosome 13. *Am J Med Genet* 2001; **102**: 231-236

24 **Shin MK**, Levorse JM, Ingram RS, Tilghman SM. The temporal requirement for endothelin receptor-B signalling during neural crest development. *Nature* 1999; **402**: 496-501

25 **Tanoue A**, Koshimizu TA, Tsuchiya M, Ishii K, Osawa M, Saeki M, Tsujimoto G. Two novel transcripts for human endothelin B receptor produced by RNA editing/alternative splicing from a single gene. *J Biol Chem* 2002; **277**: 33205-33212

26 **Syrris P**, Carter ND, Patton MA. **N**ovel nonsense mutation of the endothelin-B receptor gene in a family with Waardenburg-Hirschsprung disease. *Am J Med Genet* 1999; **87**: 69-71

27 **Tanaka H**, Moroi K, Iwai J, Takahashi H, Ohnuma N, Hori S, Takimoto M, Nishiyama M, Masaki T, Yanagisawa M, Sekiya S, Kimura S. Novel mutations of the endothelin B receptor gene in patients with Hirschsprung's disease and their characterization. *J Biol Chem* 1998; **273**: 11378-11383

28 **Dupin E**, Glavieux C, Vaigot P, Le Douarin NM. Endothelin 3 induces the reversion of melanocytes to glia through a neural crest-derived glial-melanocytic progenitor. *Proc Nat Acad Sci U S A* 2000; **97**: 7882-7887

29 **Kenny SE**, Hofstra RM, Buys CH, Vaillant CR, Lloyd DA, Edgar DH. Reduced endothelin-3 expression in sporadic Hirschsprung disease. *Br J Surg* 2000; **87**: 580-585

30 **Woodward MN**, Kenny SE, Vaillant C, Lloyd DA, Edger DH. Time-dependent effects of endothelin-3 on enteric nervous system development in an organ culture model of Hirschsprung's disease. *J Pediatr Surg* 2000; **35**: 25-29

31 **McCallion AS**, Chakravarti A. EDNRB/EDN3 and Hirschsprung disease type II. *Pigment Cell Res* 2001; **14**: 161-169

32 **Angrist M**, Bolk S, Halushka M, Lapchak PA, Chakravarti A. Germline mutations in glial cell line-derived neurotrophic factor (GDNF) and RET in a Hirschsprung disease patient. *Nat Genet* 1996; **14**: 341-344

33 **Carrasquillo MM**, McCallion AS, Puffenberger EG, Kashuk CS, Nouri N, Chakravarti A. Genome-wide association study and mouse model identify interaction between RET and EDNRB pathways in Hirschsprung disease. *Nat Genet* 2002; **32**: 237-244

34 **Auricchio A**, Griseri P, Carpentieri ML, Betsos N, Staiano A, Tozzi A, Priolo M, Thompson H, Bocciardi R, Romeo G, Ballabio A, Ceccherini I. Double heterozygosity for a RET substitution interfering with splicing and an EDNRB missense mutation in Hirschsprung disease. *Am J Hum Genet* 1999; **64**: 1216-1221

35 **Tomiyama H**, Shimotake T, Ono S, Kimura O, Tokiwa K, Iwai N. Relationship between the type of RET/GDNF/NTN or SOX10 gene mutations and long-term results after surgery for total colonic aganglionosis with small bowel involvement. *J Pediatr Surg* 2001; **36**: 1685-1688

36 **Svensson PJ**, Anvret M, Molander ML, Nordenskjold A. Phenotypic variation in a family with mutations in two Hirschsprung-related genes (RET and endothelin receptor B). *Hum Genet* 1998; **103**: 145-148

37 **Inoue K**, Shimotake T, Tomiyama H, Iwai N. Mutational analysis of the RET and GDNF gene in children with hypoganglionosis. *Eur J Pediatr Surg* 2001; **11**: 120-123

38 **Ivanchuk SM**, Myers SM, Eng C, Mulligan LM. De novo mutation of GDNF, ligand for the RET/GDNFR-alpha receptor complex in Hirschsprung disease. *Hum Mol Genet* 1996; **5**: 2023-2026

39 **McCallion AS**, Stames E, Conlon RA, Chakravarti A. Phenotype variation in two-locus mouse models of Hirschsprung disease: tissue-specific interaction between Ret and Ednrb. *Proc Natl Acad Sci U S A* 2003; **100**: 1826-1831

40 **Parisi MA**, Kapur RP. Genetics of Hirschsprung disease. *Curr Opin Pediatr* 2000; **12**: 610-617

41 **Gath R**, Goessling A, Keller KM, Koletzko S, Coerdt W, Muntefering H, Wirth S, Hofstra RM, Mulligan L, Eng C, Von Deimling A. Analysis of the RET, GDNF, EDN3, and EDNRB genes in patients with intestinal neuronal dysplasia and Hirschsprung disease. *Gut* 2001; **48**: 671-675

Edited by Ma JY

P.O.Box 2345, Beijing 100023,China
Fax: +86-10-85381893
E-mail: wjg@wjgnet.com www.wjgnet.com

World J Gastroenterol 2003;9(12):2843-2845
World Journal of Gastroenterology
 ISSN 1007-9327

• CLINICAL RESEARCH •

Plasma matrix metalloproteinase-1 and tissue inhibitor of metalloproteinases-1 as biomarkers of ulcerative colitis activity

Alicja Wiercinska-Drapalo, Jerzy Jaroszewicz, Robert Flisiak, Danuta Prokopowicz

Alicja Wiercinska-Drapalo, Jerzy Jaroszewicz, Robert Flisiak, Danuta Prokopowicz, Department of Infectious Diseases, Intestinal Diseases Unit, Medical University of Bialystok, Poland
Correspondence to: Alicja Wiercinska-Drapalo MD., Department of Infectious Diseases, Medical University of Bialystok, 15-540 Bialystok, Zurawia str., 14, Poland. alicja@priv.onet.pl
Telephone: +48-85-7416921
Received: 2003-08-05 **Accepted:** 2003-10-12

Abstract

AIM: Overexpression of mucosal metalloproteinases (MMP) have been demonstrated recently in inflammatory bowel disease. Their activity can be counterbalanced by the tissue inhibitor of metalloproteinases (TIMP). The aim of this study was to evaluate the effect of ulcerative colitis (UC) on MMP-1 and TIMP-1 plasma concentrations, as two possible biomarkers of the disease activity.

METHODS: MMP-1 and TIMP-1 plasma concentrations were measured with an enzyme immunoassay in 16 patients with endoscopically confirmed active UC.

RESULTS: Plasma concentrations of both MMP-1 (13.7±0.2 ng/ml) and TIMP-1 (799±140 ng/ml) were significantly elevated in UC patients in comparison to healthy controls (11.9±0.9 ng/ml and 220±7 ng/ml respectively). There was no correlation between TIMP-1 and MMP-1 concentrations (r=-0.02). TIMP-1 levels revealed significant positive correlations with scored endoscopic degree of mucosal injury, disease activity index and clinical activity index values as well as C-reactive protein concentration. There was no correlation between MMP-1 and laboratory, clinical or endoscopic indices of the disease activity.

CONCLUSION: These results confirm the role of both MMP-1 and TIMP-1 in the pathogenesis of ulcerative colitis. However only TIMP-1 can be useful as a biomarker of the disease activity, demonstrating association with clinical and endoscopic pictures.

Wiercinska-Drapalo A, Jaroszewicz J, Flisiak R, Prokopowicz D. Plasma matrix metalloproteinase-1 and tissue inhibitor of metalloproteinases-1 as biomarkers of ulcerative colitis activity. *World J Gastroenterol* 2003; 9(12): 2843-2845
http://www.wjgnet.com/1007-9327/9/2843.asp

INTRODUCTION

Pathogenesis of ulcerative colitis (UC) is focused on abnormal immune response and diminished ability of mucosal protection and regeneration. These processes are controlled by signaling between epithelial cells involving complex network of cytokines, growth factors and other bioactive substances, responsible for cell proliferation and differentiation, as well as regulation of immune response[1-3]. Alterations in synthesis and breakdown of extracellular matrix components are known to play a crucial role in tissue remodeling during inflammation and wound healing. Inflammatory bowel disease (IBD) is sometimes complicated by stricture formation and muscle hypertrophy resulting from extracellular matrix (ECM) changes related to matrix metalloproteinases (MMPs) activity[4]. Overexpression of mucosal MMPs have been demonstrated recently in inflammatory bowel disease[5-7]. Effects of MMPs activity can be counterbalanced by the tissue inhibitor of metalloproteinases-1 (TIMP-1)[8]. The MMP/TIMP ratio imbalance plays an important role in many diseases including not only inflammatory bowel disease but also chronic liver injury[8] and carcinogenesis[9]. As we demonstrated recently, elevated plasma concentration of TGF-β_1, known as TIMP-1 stimulator, was related to inflammation activity and should be considered as a possible biomarker in UC patients[11,12]. According to Sch ppan and Hahn[10] blockade of certain MMPs could be a novel th rapeutic approach, and therefore some novel mucosa derived parameters, such as MMP-1 and TIMP-1, may prove useful to assess prognosis, disease activity, and treatment response in inflammatory bowel disease.

The aim of this study was to evaluate effect of ulcerative colitis on MMP-1 and TIMP-1 plasma concentrations, as two possible biomarkers of the disease activity.

MATERIALS AND METHODS

Patients

MMP-1 and TIMP-1 concentrations were measured in the plasma of 16 patients (6 females and 10 males) with active ulcerative colitis (UC), and age ranging from 25 to 68 years (mean: 42.5±3.8). All the patients had a history of diagnosed ulcerative colitis that required typical clinical and endoscopical signs of distal part of bowel involvement. MMP-1 and TIMP-1 plasma concentrations were compared with endoscopic picture scored according to Meyers *et al*.[13], the disease activity index (DAI) according to Schroeder *et al*.[14], clinical activity index (CAI) as previously described[11] and laboratory indices of UC activity such as C-reactive protein (CRP), sedimentation rate (SR), white blood count (WBC) and hemoglobin concentration. Plasma MMP-1 and TIMP-1 concentrations were also compared with those of 12 healthy controls (mean age: 40.8±2.7 years). The study was approved by the Bioethical Committee of the Medical University in Bialystok. Informed consent was obtained from each patient.

MMP-1 and TIMP-1 measurement

Venous blood was collected on ice using vacutainer tubes with EDTA as an anticoagulant and centrifuged at 1 000×g within 30 minutes of collection. Obtained plasma was additionally centrifuged at 10 000×g for 10 minutes at 2-8 ℃ for complete platelet removal and stored at -20 ℃. The samples were diluted 1:40 with 0.1M phosphate buffer before assay and then incubated in duplicate in microtitre wells precoated with anti-TIMP-1 or anti-MMP-1 antibodies (Amersham Pharmacia Biotech, Little Chalfont, Buckinghampshire, England). Any TIMP-1 or MMP-1 remained in the microtitre wells after four cycles of washing and aspiration were detected by peroxidase

labelled specific antibodies. The amount of peroxidase bound to each well was determined by the addition of tetramethylbenzidine substrate. The reaction was stopped by acidification and optical density was read with a microtitre plate photometer Stat Fax® 2100 (Alab/Poland) at 450 nm. The concentration of MMP-1 or TIMP-1 in the sample was determined by interpolation from a standard curve prepared with standard samples supplied by the manufacturer.

Statistical methods

Values were expressed by their mean and standard error of the mean (±SEM). The significance of the difference was calculated by two-tailed Student' s *t* test. Correlation analysis was calculated by the non-parametric Spearman rank order correlation test. Values of $P<0.05$ were considered to be significant.

RESULTS

Plasma mean concentration of MMP-1 measured in patients with active UC was significantly elevated (13.7±0.2 ng/ml) in comparison to that of healthy controls (11.9±0.9 ng/ml) (Figure 1). Mean TIMP-1 plasma concentration in UC patients (799±140 ng/ml) also exceeded normal values significantly (220±7 ng/ml), and the difference was much more apparent (Figure 2). Even the lowest TIMP-1 value (456 ng/ml) doubled the mean concentration from the controls. As demonstrated in Table 1, the majority of patients had CRP and SR values exceeding the upper limit of normal range. Moreover evaluation of the disease activity through CAI, DAI and endoscopic score demonstrated severe course of the present relapse (Table 1). There was no correlation between TIMP-1 and MMP-1 plasma concentrations (r=-0.02, P=0.95). As shown in Table 2 plasma TIMP-1 levels analyzed in UC patients revealed significant positive correlations with scored endoscopic degree of mucosal injury, DAI and CAI values as well as CRP concentration. There was no correlation between MMP-1 and laboratory, clinical or endoscopic indices of the disease activity (Table 2).

Table 1 Laboratory and clinical indices of ulcerative colitis activity in the patients

	Normal range	Mean	±SEM	Minimum	Maximum	Median
CRP (mg/dl)	0-5	17.7	4.6	6	62	6
SR (mm/h)	0-12	22.7	4.7	2	68	17
WBC (×10³/μl)	4-10	6.8	0.5	3.5	11.5	6.2
HGB (mg/dl)	12-16	13.3	0.3	10.5	14.9	13.4
CAI	0	10.6	0.75	7	15	9
DAI	0	6.4	0.7	3	10	5
Endoscopic score	0	11.6	0.8	8	16	10

CAI: clinical activity index, DAI: disease activity index.

Table 2 Correlation between plasma TIMP-1 or MMP-1 concentrations and values of selected laboratory indices, demonstrated through "r" values. Statistically significant correlation: [a]$P<0.05$; [b]$P<0.01$

	TIMP-1 (r)	MMP-1 (r)
CRP (mg/dl)	0.60[a]	0.05
SR (mm/h)	0.17	-0.07
WBC (x10³/ml)	0.24	-0.10
HGB (mg/dl)	-0.19	-0.10
CAI (clinical activity index)	0.55[a]	-0.18
DAI (disease activity index)	0.66[b]	-0.27
Score	0.66[b]	-0.11

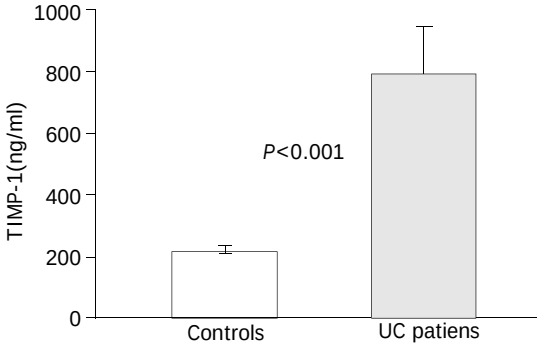

Figure 1 Comparison of mean (±SEM) TIMP-1 plasma concentrations in group of patients with ulcerative colitis and controls.

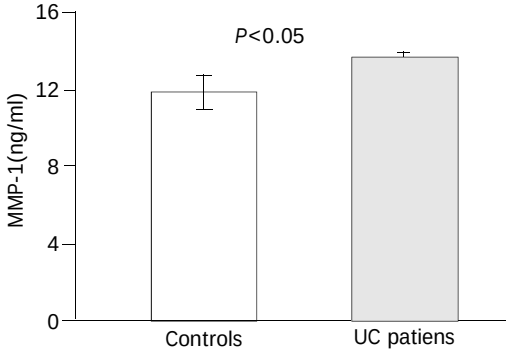

Figure 2 Comparison of mean (±SEM) MMP-1 plasma concentrations in group of patients with ulcerative colitis and controls.

DISCUSSION

Matrix metalloproteinases are involved in mucosal degradation causing tissue remodelling and ulcerations related to inflammatory bowel diseases. Enhanced expression of MMP-1, MMP-2 and MMP-3 has been demonstrated recently in inflammed mucosa from patients with UC and Crohn disease[5,6]. According to Arihiro *et al*.[15] in both UC and CD, MMP-1, MMP-9 and TIMP-1 were expressed by inflammatory cells, fibroblastic cells as well as by vascular smooth muscle cells most prominently in actively inflamed areas in ulcer bases. Stimulation of T lymphocytes in inflammatory lesions seemed to be responsible for activation of several MMPs[7,16,17]. TNF-α released by T lymphocytes was a powerful inducer of fibroblasts that were the prime source of MMPs[19,20]. This created link between mucosal inflammation and destruction of the subepithelial matrix, and MMP-1 expression in the mucosa might be related to the initial step of ulceration in UC[14]. According to Baugh *et al*.[20] the expression of matrix metalloproteinases 1, 2, 3 and 9 was significantly higher in inflamed areas of UC patients mucosa compared with noninvolved regions. In the study carried out by von Lampe *et al*.[5] MMP-1 and -3 correlated well with the histological degree of acute inflammation resulting in more than 15-fold increased levels in inflamed versus normal colon samples from patients with UC. In another study MMP-1 and -2 concentrations measured (using sandwich ELISA) in samples from pouchitis and active UC doubled the values obtained in samples of uninflamed mucosa. Mesenchymal cells were identified as major producers of MMP-1 and -2[6]. MMPs were implicated in the tissue destruction associated with inflammatory diseases and the role of MMPs in the pathogenesis of inflammatory bowel disease was also confirmed through improvement of experimentally induced colitis after treatment with a matrix metalloproteinase inhibitor[21].

Apart from protease-inhibitory action TIMP-1 serves

additional functions. Several investigators have demonstrated its growth-promoting properties and stimulation of tumor growth by inhibiting apoptosis indicating the role of TIMP-1 in cancer progression[22,23]. According to Holten-Andersen *et al*.[24] plasma TIMP-1 levels could be used to identify patients with colorectal cancer with a sensitivity of 63 % and a specificity of 98 %, so it was suggested as a marker for early identification of this cancer.

According to Heuschkel *et al*.[25] TIMP-1 measured in biopsies from patients with active IBD remained unchanged. In the study of Louis *et al*.[26] the production of TIMP-1 was undetectable in the majority of uninflamed biopsy samples from controls, UC and CD patients. However in inflamed mucosa, the production of TIMP-1 was increased significantly in both UC and CD. Its elevated plasma concentration, demonstrated in our study, can reflect situation in bowel mucosa. Enhanced expression of TIMP-1 can be a result of the stimulatory effect of transforming growth factor TGF-β_1. As we demonstrated recently, enhanced production of TGF-β_1 could be related to inflammation activity in UC patients[11]. This profibrogenic cytokine accelerated healing but during chronic inflammation might lead to excessive collagen deposition and eventually fibrosis[4]. In our recent study successful treatment of the disease resulted in decrease of its levels both in plasma and rectal mucosa, but better response has been achieved in patients with higher baseline TGF-β1 concentrations[12].

MMP-1 is the main enzyme responsible for degradation of fibrillar collagen and therefore we decided to use it as a possible biomarker in our study[6]. We demonstrated a significant increase of both MMP-1 and TIMP-1 plasma concentrations in UC patients, which could reflect their over-expression in the bowel mucosa. However significant correlation with clinical and endoscopical signs of UC activity was proved only for TIMP-1. Moreover the only laboratory parameter that showed any association with TIMP-1 was C-reactive protein.

In conclusion, our data confirm the role of both MMP-1 and TIMP-1 in the pathogenesis of ulcerative colitis. However only TIMP-1 may be useful as a biomarker of the disease activity, demonstrating association with clinical and endoscopic pictures.

REFERENCES

1 **Beck PL**, Podolsky DK. Growth factors in inflammatory bowel disease. *Inflamm Bowel Dis* 1999; **5**: 44-60
2 **Fiocchi C**. IBD: Etiology and Pathogenesis. *Gastroenterology* 1998; **115**: 182-205
3 **Zimmerman CM**, Padgett RW. Transforming growth factor b signaling mediators and modulators. *Gene* 2000; **249**: 17-30
4 **Mourelle M**, Salas A, Guarner F, Crespo E, Garcia-Lafuente A, Malagelada JR. Stimulation of transforming growth factor beta-1 by enteric bacteria in the pathogenesis of rat intestinal fibrosis. *Gastroenterology* 1998; **114**: 519-526
5 **von Lampe B**, Barthel B, Coupland SE, Riecken EO, Rosewicz S. Differential expression of matrix metalloproteinases and their tissue inhibitors in colon mucosa of patients with inflammatory bowel disease. *Gut* 2000; **47**: 63-73
6 **Stallmach A**, Chan CC, Ecker KW, Feifel G, Herbst H, Schuppan D, Zeitz M. Comparable expression of matrix metalloproteinases 1 and 2 in pouchitis and ulcerative colitis. *Gut* 2000; **47**: 415-422
7 **Salmela MT**, MacDonald TT, Black D, Irvine B, Zhuma T, Saarialho-Kere U, Pender SL. Upregulation of matrix metalloproteinases in a model of T cell mediated tissue injury in the gut: analysis by gene array and in situ hybridisation. *Gut* 2002; **51**: 540-547
8 **Nie** QH, Cheng YQ, Xie YM, Zhou YX, Bai XG, Cao YZ. Methodologic research on TIMP-1, TIMP-2 detection as a new diagnostic index for hepatic fibrosis and its significance. *World J Gastroenterol* 2002; **8**: 282-287
9 **Fan YZ**, Zhang JT, Yang HC, Yang YQ. Expression of MMP-2, TIMP-2 protein and the ratio of MMP-2/TIMP-2 in gallbladder carcinoma and their significance. *World J Gastroenterol* 2002; **8**: 1138-1143
10 **Schuppan D**, Hahn EG. MMPs in the gut: inflammation hits the matrix. *Gut* 2000; **47**: 12-14
11 **Wiercinska-Drapalo A**, Flisiak R, Prokopowicz D. Effect of ulcerative colitis activity on plasma concentration of transforming growth factor β_1. *Cytokine* 2001; **14**: 343-346
12 **Wiercinska-Drapalo A**, Flisiak R, Prokopowicz D. Effect of ulcerative colitis treatment on transforming growth factor β_1 in plasma and rectal mucosa. *Regul Pept* 2003: **113**: 57-61
13 **Meyers S**, Sachar DB, Present DH, Janowitz HD. Olsalazine in the treatment of ulcerative colitis among patients intolerant of sulphasalazine: a prospective, randomized, placebo controlled double blind, dose-ranging clinical trial. *Scand J Gastroenterol* 1988; **23** (Suppl 148): 29-35
14 **Schroeder KW**, Tremaine WJ, Ilstrup DM. Coated oral 5-aminosalicylic acid therapy for midly to moderately active ulcerative colitis. *N Engl J Med* 1987; **317**: 1625-1629
15 **Arihiro S**, Ohtani H, Hiwatashi N, Torii A, Sorsa T, Nagura H. Vascular smooth muscle cells and pericytes express MMP-1, MMP-9, TIMP-1 and type 1 procollagen in inflammatory bowel disease. *Histopathology* 2001; **39**: 50-59
16 **MacDonald TT**, Bajaj-Elliott M, Pender SL. T cells orchestrate intestinal mucosal shape and integrity. *Immunology Today* 1999; **20**: 505-510
17 **Pender SL**, Tickle SP, Docherty AJ, Howie D, Wathen NC, MacDonald TT. A major role of matrix metalloproteinases in T cell injury in the gut. *J Immunol* 1997; **158**: 1582-1590
18 **Pender SL**, Breese EJ, Gunther U, Howie D, Wathen NC, Schuppan D, MacDonald TT. Suppression of T cell mediated injury in human gut by interleukin-10: role of matrix metalloproteinases. *Gastroenterology* 1998; **115**: 573-583
19 **Daum S**, Bauer U, Foss HD, Schuppan D, Stein H, Riecken EO, Ullrich R. Increased expression of mRNA for matrix metalloproteinase -1 and -3 and tissue inhibitor of metalloproteinases-1 in intestinal biopsy specimens from patients with coeliac disease. *Gut* 1999; **44**: 17-25
20 **Baugh MD**, Perry MJ, Hollander AP, Davies DR, Cross SS, Lobo AJ, Taylor CJ, Evans GS. Matrix metalloproteinase levels are elevated in inflammatory bowel disease. *Gastroenterology* 1999; **117**: 814-822
21 **Sykes AP**, Bhogal R, Brampton C, Chander C, Whelan C, Parsons ME, Bird J. The effect of an inhibitor of matrix metalloproteinases on colonic inflammation in a trinitrobenzenesulphonic acid rat model of inflammatory bowel disease. *Aliment Pharmacol Ther* 1999; **13**: 1535-1542
22 **Li G**, Fridman R, Kim HR. Tissue inhibitor of metalloproteinase-1 inhibits apoptosis of human breast epithelial cells. *Cancer Res* 1999; **59**: 6267-6275
23 **Pellegrini P**, Contasta I, Berghella AM, Gargano E, Mammarella C, Adorno D. Simulatneous measurement of soluble carcinoembryogenic antigen and the tissue inhibitor of metalloproteinase TIMP-1 serum levels for use as markers of pre-invasive to invasive colorectal cancer. *Cancer Immunol Immunother* 2000; **49**: 388-394
24 **Holten-Andersen MN**, Christensen IJ, Nielsen HJ, Stephens RW, Jensen V, Nielsen OH, Sorensen S, Overgaard J, Lilja H, Harris A, Murphy G, Brunner N. Total levels of tissue inhibitor of metalloproteinases 1 in plasma yield high diagnostic sensitivity and specificity in patients with colon cancer. *Clin Cancer Res* 2002; **8**: 156-164
25 **Heuschkel RB**, MacDonald TT, Monteleone G, Bajaj-Elliott M, Smith JA, Pender SL. Imbalance of stromelysin-1 and TIMP-1 in the mucosal lesions in children with inflammatory bowel disease. *Gut* 2000; **47**: 57-62
26 **Louis E**, Ribbens C, Godon A, Franchimont D, De Groote D, Hardy N, Boniver J, Belaiche J, Malaise M. Increased production of matrix metalloproteinase-3 and tissue inhibitor of metalloproteinase-1 by inflamed mucosa in inflammatory bowel disease. *Clin Exp Immunol* 2000; **120**: 241-246

Edited by Zhu LH

P.O.Box 2345, Beijing 100023,China
Fax: +86-10-85381893
E-mail: wjg@wjgnet.com www.wjgnet.com

World J Gastroenterol 2003;9(12):2846-2848
World Journal of Gastroenterology
 ISSN 1007-9327

• BRIEF REPORTS •

Gastric pseudolipomatosis, usual or unusual? Re-evaluation of 909 endoscopic gastric biopsies

Murat Alper, Yusuf Akcan, Olcay K Belenli, Selma Çukur, Kamuran A Aksoy, Mazlume Suna

Murat Alper, Olcay K Belenli, Selma Çukur, Kamuran A Aksoy, Mazlume Suna, Department of Pathology, Medical School of Düzce, Abant Izzet Baysal University, Turkey
Yusuf Akcan, Department of Gastroenterology, Medical School of Düzce, Abant Izzet Baysal University, Turkey
Correspondence to: Assistant Professor. Dr. Murat Alper, Düzce T1p Fakültesi Patoloji ABD, Konuralp/Düzce 81650, Turkey. muratalper@tusdata.com
Fax: +90-212-5311616
Received: 2003-08-02 **Accepted:** 2003-10-22

Abstract

Microvesicular pneumatosis intestinalis, also called "pseudolipomatosis" for resembling fatty infiltration, is characterized by the presence of small gas voids in the gastrointestinal wall, especially in mucosa. These voids are not lined with epithelia. There are few reported cases about colon, duodenum and skin. Because there is only one case report about pseudolipomatosis in the stomach, we re-evaluated 909 endoscopic biopsies taken from gastric corpus to check the presence of pseudolipomatosis. We determined pseudolipomatosis foci in 3 percent (n=27) of biopsies. In two cases there were pseudolipomatosis foci in endoscopic biopsies having otherwise normal histologic findings, while there were pseudolipomatosis foci in endoscopic biopsies of 25 patients with gastritis. *Helicobacter pylori* was found in 85 % of biopsies having pseudolipomatosis foci. In this study, we presented some histopathologic characteristics of pseudolipomatosis seen in gastric mucosa.

Alper M, Akcan Y, Belenli OK, Çukur S, Aksoy KA, Suna M. Gastric pseudolipomatosis, usual or unusual? Re-evaluation of 909 endoscopic gastric biopsies. *World J Gastroenterol* 2003; 9(12): 2846-2848
http://www.wjgnet.com/1007-9327/9/2846.asp

INTRODUCTION

Microvesicular pneumatosis intestinalis which is also called "pseudolipomatosis" for resembling fatty infiltration, is characterized by the presence of small gas voids in the gastrointestinal wall, especially in mucosa[1]. These gas voids are not lined with epithelial cells. Since we came across only one letter about gastric mucosa while searching literature for our previous case report, in which we presented a case of pseudolipomatosis in the stomach, duodenum and colon, although recently in gastrointestinal system pseudolipomatosis was defined particularly in the colon, duodenum and skin, we investigated endoscopic biopsies with regard to pseudolipomatosis[1-8].

MATERIALS AND METHODS

In this study, 909 endoscopic gastric biopsies were investigated at the Department of Pathology of Düzce Medical Faculty Abant Ýzzet Baysal University, between December 1998 and June 2003. Biopsies taken from the corpus for various reasons other than cancer were included in this study. Biopsies were fixed in 10 % formaldehyde and subjected to automatic tissue follow-up procedures. We re-examined the 4-5 micron thick samples stained with hematoxylene eosin and modified Giemsa by a light microscope. When pseudolipomatosis was found, the presence and grade of inflammation, the presence of intestinal metaplasia, and the presence and concentration of *Helicobacter pylori* were determined. The absence of inflammation was designated as (0), and the presence of inflammation was classified as mild (1), moderate (2) and severe (3). The absence of *Helicobacter pylori* was designated as (0), and the presence was classified as scarce (1), moderate (2) and diffuse (3). Intestinal metaplasia was evaluated as present or absent, and atrophy as present or absent, if present as mild, moderate or severe. Three hundred and sixty-four (40 %) subjects were female and 545 (60 %) were male. The ages of patients ranged between 19 and 78 years with a mean of 46 years.

RESULTS

Pseudolipomatosis was found in 27 of 909 re-evaluated cases. Of these 27 patients, 15 were male and 12 were female. Male patients were between 28 and 56 years old, with a mean of 39 years, female patients were aged between 22 and 65 years, with a mean of 41 years. Mucosal vacuolation was characterized by empty spaces, 30-250 micron in diameter, associated with neither fibrosis/sclerosis nor a lymphocytic infiltrate. There was no evidence of true adipocyte differentiation, vascular markers, e.g. S-100 protein, F-VIII and F-XIII were negative. Vacuoles were found in different parts of the mucosa, although they could be seen beneath epithelia, in a few cases they were detected within muscularis mucosa as well (Figures 1-2). Twenty five of the patients with pseudolipomatosis had gastritis. Of these patients 23 were *Helicobacter pylori* positive. Among the *Helicobacter pylori* positive patients, five had scarce, ten had moderate, and eight had diffuse bacteria. Among the 25 patients with gastritis, 5 had mild, 13 had moderate, and 7 had severe chronic inflammation. In 8 cases with gastritis, intestinal metaplasia was encountered. In all the cases with metaplasia goblet cells and in 4 cases Paneth cells were noticed. Two cases of gastritis had severe atrophy, and one case had mild atrophy. Four patients with gastritis had prior endoscopy for gastric complaints. The previous biopsy results were *Helicobacter pylori* gastritis with severe inflammatory activity in three cases, and *Helicobacter pylori* gastritis with moderate inflammatory activity in one case. Pseudolipomatosis was not found in previous endoscopic gastric biopsies of these four patients. However, in one of these patients, pseudolipomatosis was detected in duodenal and colonic biopsies[8]. Two other patients had undergone colonoscopy while being searched for malignancy. In samples taken from the colon pseudolipomatosis was not detected.

The patients who were *Helicobacter pylori* positive were given a course of treatment for *Helicobacter pylori* eradication composed of lansoprazol 30 mg daily for 15 days, clarithromycin

bid 500 mg and amoxicilin bid 1 000 mg for 10 days. One month later control biopsies were performed for 5 patients whose complaints were not fully resolved. We found that in two of them pseudolipomatosis continued while in the other three biopsies pseudolipomatosis was not found. In those cases in which pseudolipomatosis continued, we noticed that although *Helicobacter pylori* was decreased, it was not completely eradicated, and in the other three patients we saw that *Helicobacter pylori* was eradicated and the gastritis continued though decreased. Control biopsies were not performed for the remaining patients. In two patients with pseudolipomatosis, a 45-year-old female and a 39-year-old man, biopsies taken for non-specific abdominal pain showed no *Helicobacter pylori*, inflammation or metaplasia. In these patients no pathologic finding except mild edema could be demonstrated. These patients had no previous endoscopies. Vacuoles were seen in small foci in lamina propria, and were considered as pseudolipomatosis.

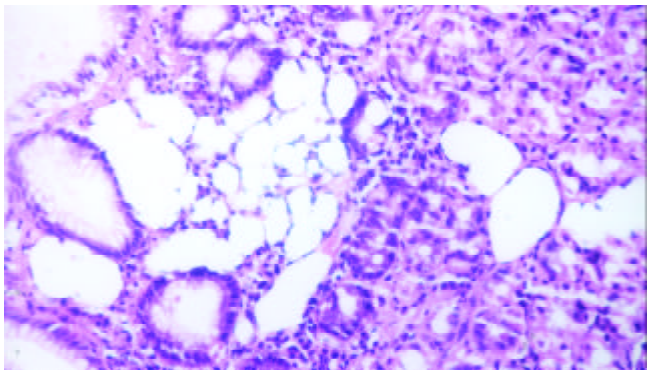

Figure 1 Presence of many vacuoles beneath epithelium in gastric mucosa (H & E ×200).

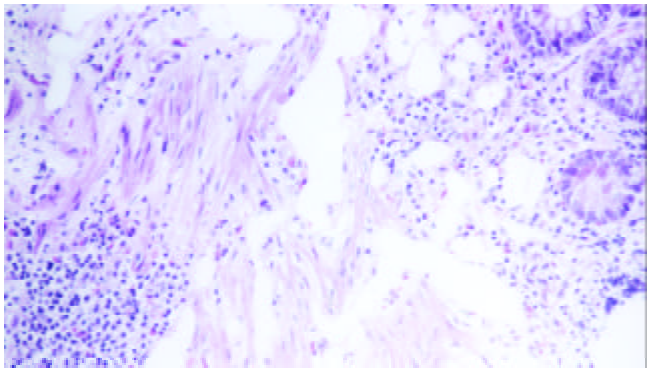

Figure 2 Presence of many vacuoles in muscularis mucosa and lamina propria as well (H & E ×200).

DISCUSSION

Mucosal pseudolipomatosis is a recently described endoscopic finding, most likely caused by intramucosal air. Because of their gross and microscopical similarity to fat, however, the term "pseudolipomatosis" is proposed. Although the etiopathogenesis of pseudolipomatosis is not so clear yet, some probable causes of it in the colon, duodenum and skin have been mentioned[1-8]. We could find only one case-report about gastric pseudolipomatosis except our one[6]. For this reason we searched how often pseudolipomatosis, yet its rate in colon increased contionusly, was found in gastric mucosa.

Pneumatosis coli is a rare condition characterized by multiple gas-filled cysts within the bowel wall. Mechanical, bacterial and biochemical theories have been availabe to explain the pathogenesis of pneumatosis in the colon[5]. Pneumatosis cyctoides intestinalis has been reported to be present together with other conditions such as pseudomembranous enterocolitis, necrotizing enterocolitis, bowel infarction, chronic obstructive pulmonary disease, intestinal obstruction, collagen vascular diseases (scleroderma, dermatomyositis, mixed connective tissue disease), systemic amyloidosis and iatrogenic conditions (after surgery or endoscopy), late-stage AIDS with cryptosporidial diarrhea, and Crohn' s disease[5]. Gagliardi *et al*. detected mucosal pseudolipomatosis foci in colon of 5 cases among 25 pneumatosis coli patients in their study[5]. Micropneumatosis was reported to be caused by disinfectant hydrogen peroxide solution[3]. It might also be a result of colonoscopy application and usually disappeared three weeks after the procedure[4]. Commercially available endoscope disinfecting hydrogen peroxide solution could cause the unique form of colitis referred as pseudolipomatosis[3]. It was also reported in asymptomatic patients as an air pressure- related colonoscopy complication[4]. Mucosal pseudolipomatosis of the colon is an infrequent condition that occurs mainly in elderly males, usually involves the left colon, and is manifested clinically by passage of blood per rectum. Colonoscopy showed solitary or multiple whitish-yellowish plaques, which were localized or involved several segments[1]. Superficial dermal vacuoles resembling fatty infiltration of the skin have also been reported as pseudolipomatosis cutis[2]. Dermal vacuoles likely represent an artifact of tissue fixation or processing and are unrelated to the underlying pathologic process. Trottor *et al*. suggested the name pseudolipomatosis cutis, analogous to insufflation-induced colonic vacuolation, to distinguish this phenomenon from true dermal fatty infiltration and to emphasize its incidental, likely artifactual nature[2]. As in colon and duodenum, histologic studies in the stomach demonstrated microscopic cavities in mucosa, measuring 20 to 300 micron in diameter. Histochemical stains showed that these cavities contained no lipids, suggesting that they were filled with gas. In the study of Gagliardi *et al*, 14 patients were treated with antidiarrhoeals and anti-inflammatory drugs, improvement was detected in 9 cases. There was a high recurrence rate, but with further courses of continued therapy remission was achieved in five patients. According to Gagliardi *et al*, the associations of pneumatosis coli with psychiatric disorders and mucosal pseudolipomatosis were new and of possible pathogenetic[5].

In our study, 23 out of 27 patients had *Helicobacter pylori*. In our previous case report, one patient was diagnosed as micropneumatosis on the first and second colonoscopy specimens at a four week interval[8]. After another four weeks during the first half of *Helicobacter pylori* gastritis treatment of the patient, colonoscopy was repeated for the third time, and micropneumatosis foci were not observed on pathological sections. In the present study, when control biopsy was performed one month later for 5 patients whose complaints were not resolved it was noticed that pseudolipomatosis continued in two of them while pseudolipomatosis was not seen in the other three in control biopsies. In those cases with persistent pseudolipomatosis, it was noticed that although *Helicobacter pylori* was decreased, it was not completely eradicated, and in the other three patients it was seen that *Helicobacter pylori* was eradicated and the gastritis findings were decreased. It is also possible that the control endoscopic biopsies may be taken from sites that are free of pseudolipomatosis. Since the conditions of some patients improved after the eradication therapy for *Helicobacter pylori*, this finding implicates that *Helicobacter pylori* may be one of the causative factors for micropneumatosis and pneumatosis cyctoides intestinalis. It can also be speculated that micropneumatosis grows with time and may lead to pneumatosis

cyctoides intestinalis. The fact that micropneumatosis foci are also reported in most pneumatosis cyctoides intestinalis cases is supportive for this suggestion. The pseudolipomatosis type changes seen in mucosal biopsies should not be ignored by just considering them as artifacts. We think that, in order to determine the etiopathogenesis and significance of gastric mucosal pseudolipomatosis, more case reports are required.

REFERENCES

1 **Ben Rejeb A**, Khedhiri F. Mucosal pseudo-lipomatosis of the colon. Apropos of a case with a review of the literature. *Arch Anat Cytol Pathol* 1989; **37**: 254-257

2 **Trotter MJ**, Crawford RI. Pseudolipomatosis cutis: superficial dermal vacuoles resembling fatty infiltration of the skin. *Am J Dermatopathol* 1998; **20**: 443-447

3 **Ryan CK**, Potter GD. Disinfectant colitis. Rinse as well as you wash. *J Clin Gastroenterol* 1995; **21**: 6-9

4 **Waring JP,** Manne RK, Wadas DD. Mucosal pseudolipomatosis: an air pressure-related colonoscopy complication. *Gastrointest Endosc* 1989; **35**: 93-94

5 **Gagliardi G**, Thompson IW, Hershman MJ. Pneumatosis coli: a proposed pathogenesis based on study of 25 cases and review of the literature. *Int J Colorectal Dis* 1996; **11**: 111-118

6 **Stebbing J**, Wyatt JI. Gastric 'pseudolipomatosis'. *Histopathology* 1998; **32**: 283-284

7 **Cook DS**, Williams GT. Duodenal 'pseudolipomatosis'. *Histopathology* 1998; **33**: 394-395

8 **Belenli OK**, Akcan Y, Alper M. Micropneumatosis (pseudolipomatosis) coexistent with *Helicobacter pylori* and its improvement. *Indian J Gastroenterol* 2003 (in press)

Edited by Wang XL

P.O.Box 2345, Beijing 100023,China
Fax: +86-10-85381893
E-mail: wjg@wjgnet.com www.wjgnet.com

World J Gastroenterol 2003;9(12):2849-2852
World Journal of Gastroenterology
 ISSN 1007-9327

• BRIEF REPORTS •

Oddi sphincter function after canine auto-pancreas transplantation with bladder drainage

Gui-Chen Li, Chun-Hui Yuan, Ying Cheng, Yong-Feng Liu

Gui-Chen Li, Chun-Hui Yuan, Ying Cheng, Yong-Feng Liu, Department of Surgery and Organ Transplant Unit, the First Affiliated Hospital, China Medical University, Shenyang 110001, Liaoning Province, China
Supported by programs foundation of Ministry of Education of Liaoning Province, No.202013146
Correspondence to: Dr. Gui-Chen Li, Department of Surgery and Organ Transplant Unit, the First Affiliated Hospital, China Medical University, Shenyang 110001, Liaoning Province, China. lgc763@sohu.com
Telephone: +86-24-23265284
Received: 2003-05-12 **Accepted:** 2003-06-02

Abstract

AIM: Several neural and hormonal factors are known to affect motility of sphincter of Oddi (SO). The major roles of SO are to regulate the flow of bile and pancreatic juice into the duodenum and to prevent the reflux of duodenal contents into the biliary and pancreatic duct. After pancreas transplantation, graft SO was denervated and graft pancreatitis might have relations to SO motility. The motility of SO after canine pancreas transplantation with bladder drainage was investigated.

METHODS: Normal canine SO manometry and pancreas graft SO manometry after pancreas transplantation with bladder drainage were performed in seven dogs respectively before and after cholecystokinin (CCK) administration. Data of SO basal pressure, contraction frequency, amplitude and motility index after transplantation and CCK administration were compared with that in controls and before CCK administration.

RESULTS: SO showed regular contractions with a certain basal pressure in control dogs. After transplantation, the graft SO basal pressure and contraction frequency were higher than that in controls, but the amplitude decreased ($P<0.01$). There was no great difference in SO motility index. CCK administration could relax normal SO but stimulate graft SO after pancreas transplantation with bladder drainage. After CCK administration, SO basal pressure, frequency and motility index were increased significantly ($P<0.05$), in comparison with that before administration. The amplitude remained unchanged ($P>0.05$), in comparison with that before CCK administration.

CONCLUSION: After auto-pancreas transplantation with bladder drainage, canine SO motility was inhibited. Basal pressure and frequency increased but amplitude decreased. CCK administration after transplantation had an inhibitory effect on canine SO instead of a relaxation effect observed in normal canine SO. This will increase the resistance of SO to the pancreatic juice flow and induce pancreatic juice stagnation and can not prevent reflux of urine and duodenal contents when the bladder pressure is increased to a certain extent, which may cause graft pancreatitis.

Li GC, Yuan CH, Cheng Y, Liu YF. Oddi sphincter function after canine auto-pancreas transplantation with bladder drainage. *World J Gastroenterol* 2003; 9(12): 2849-2852
http://www.wjgnet.com/1007-9327/9/2849.asp

INTRODUCTION

The major roles of the sphincter of Oddi (SO) are to regulate the flow of bile and pancreatic juice into the duodenum and to prevent the reflux of duodenal contents into the biliary and pancreatic duct. SO motility is composed of tonic contraction and phasic contraction. Neural factors, hormones and some drugs play important roles in the control of SO motility. SO motility is related to migrating motor complex (MMC) of the duodenum. Graft pancreatitis is one of the factors for graft dysfunction with bladder drainage. Reflux of urine and pancreatic juice can cause graft pancreatitis. After transplantation, the graft was denervated and graft duodenum lost its MMC. Little is known about the function of SO and its effect on the graft function after pancreas transplantation with bladder drainage. The aim of this paper was to study canine SO function after pancreas transplantation with bladder drainage and its effect on the graft.

MATERIALS AND METHODS

Preparation of animal

Fourteen healthy adult mongrel dogs, weighing 13-18 kg were anesthetized with 35 mg/kg intravenous pentobarbital sodium, and maintained under adequate anesthesia with 15 mg/kg intravenous pentobarbital sodium as required. System blood pressure was monitored through a catheter placed into the femoral artery. The femoral vein was cannulated and used for systemic administration of solutions and drugs.

Normal canine SO manometry

After an upper medium laparotomy using aseptic technique, the biliary tree was identified. A small longitudinal incision was made in the common bile duct. A triple lumen catheter was cannulated and tied in the bile duct to avoid any leakage and occlusion of the orifice of the catheters. The triple lumen catheter, measuring 1.7 mm of outer diameter and 0.5 mm of inner diameter, with three holes at 2-mm intervals, was perfused with sterile water at a rate of 0.25 ml/min per channel by means of a low-compliance pneumohydraulic pump, and connected via transducers to a computerized recording system. The catheter was sent into the duodenum. Intraduodenal pressure was taken as zero reference. By 1-mm station pull through technique, the catheter was placed just at the site of SO. After a stable basal recording for at least 2 min was obtained at the level of SO high pressure zone, 20 mg/kg cholecystokinin (CCK) diluted in 5 ml saline was injected intravenously and registration continued for a few more minutes until 2 min of stable recording was obtained during drug infusion. SO basal pressure above duodenal zero, amplitude above basal pressure, and frequency of phasic contractions before and after CCK

injection were calculated as well as the motility (amplitude per frequency).

Pancreas graft SO manometry

The dogs were fasted and anesthetized the same as the control group. After a midline celiotomy with aseptic techniques, the tail of the pancreas was mobilized by division of the veins which drain the distal pancreas into the spleen vein. The head of the pancreas was then mobilized without cutting the pancreaticoduodenal vessels. After the common bile duct at its entry into the duodenum was ligated and divided, the lessen omentum was opened. At least I cm of gastroduodenal artery and vein were dissected from the bifurcation. The proximal duodenum was cut 1 cm distal to pylorus and closed. After inferior pancreaticoduodenal vessels were cut out, the distal duodenum was divided at the end of the second part of duodenum. Thus the donor was skeletonized with intact vascular connections. Finally, the gastroduodenal artery was ligated and divided as far as possible from the bifurcation of proper hepatic arteries, and the gastroduodenal vein was removed with a cuff of portal venous wall. The graft was immediately immersed in and flushed with cold ringer solution while the portal vein wall was repaired. Reconstruction of vascular connections to the autograft was accomplished by an end-to-side anastomosis of the gastroduodenal vein to the right common iliac artery and end-to-end anastomosis of the accompanying artery to the internal iliac artery. After reperfusion, the distal pancreas was resected. Gastrointestinal continuity was restored by the Roux-en-Y technique with cholecystojejunal, gastrojejunal and graft-duodenal-host bladder anastomosis. Average graft ischemia time was 30-40 min. The bile duct residual of graft was placed under the skin. Fluid and antibiotics were given for 5 days. Oral alimentation was started on the second postoperative day. Serum and urinary amylase, free blood sugar and insulin were determined on days 1, 3, 5 postoperatively. Five days after operation, the same manometry procedure from the residual bile duct before and after CCK injection was performed as for the control dogs.

Statistical analysis

All values were expressed as mean ±SD. Comparison of values between the two groups was made with analysis of variance and paired *t* tests. Differences were regarded as significant when *P* value was less than 0.5.

RESULTS

1.Changes of SO activity before and after transplantation are shown in Table 1.

Table 1 SO activity in control and transplanted dogs

	Basal pressure (mmHg)	Amplitude (mmHg)	Frequency (min^{-1})	Motility index
Control	18.5±2.8	47.1±5.5	9.7±1.5	235.6±56.1
Transplant	27.8±2.8	7.2±1.4	13.1±1.9	211.3±33.2

SO showed regular contractions with a certain basal pressure in control dogs.

After transplantation, the graft SO basal pressure and contraction frequency increased as compared with that in controls, but the amplitude decreased (P<0.01). There was no great difference in SO motility index.

2.Changes of SO activity before and after administration of CCK in normal dogs are shown in Table 2.

Table 2 SO activity before and after CCK administration in normal dogs

	Basal pressure (mmHg)	Amplitude (mmHg)	Frequency (min^{-1})	Motility index
Before CCK	18.5±2.8	47.1±5.5	9.7±1.5	235.6±56.1
After CCK	10.2±2.2	18.7±5.3	5.0±1.2	49.6±16.9

CCK administration could relax SO motility. SO basal pressure, contraction frequency and amplitude decreased significantly after CCK administration in comparison with controls (P<0.01).

3.SO activity of grafts before and after CCKadministration is shown in Table 3.

Table 3 SO activity of grafts before and after CCK administration

	Basal pressure (mmHg)	Amplitude (mmHg)	Frequency (min^{-1})	Motility index
Before CCK	27.8±2.8	7.2±1.4	13.1±1.9	211.3±33.2
After CCK	35.5±5.1	9.7±2.1	18.9±1.9	515.4±42.3

CCK administration stimulated graft SO motility. After CCK administration, SO basal pressure, frequency and motility index increased significantly in comparison with those before administration (P<0.05),while the amplitude remained unchanged (P>0.05).

4.After transplantation, there was no great difference in serum amylase, blood sugar and blood insulin as compared with those on day 0 (P<0.05).Urine amylase that reflects graft function increased significantly. These data showed a good pancreas graft function (Table 4).

Table 4 Pancreas graft function after transplantation

	Day 0	Day 1	Day 3	Day 5
Serum amylase (IU/L)	22±5	30±11	26±7	24±4
Urine amylase (IU/L)	80±38	25 400±12 100	45 100±1 780	14 900±2 100
Blood sugar (mmol/L)	4.5±1.2	5.1±0.7	3.8±1.3	3.6±0.4
Blood insulin (IU/L)	8.5±2.2	7.3±3.2	7.0±2.4	5.5±1.0

DISCUSSION

Canine segmental pancreas auto-transplantation and pancreaticoduodenal allotransplantation were often carried out in other studies. In order to investigate the SO motility after pancreas transplantation, we excluded the effect of rejection on the graft and also the graft must have intact SO. So, we established a canine auto-pancreaticoduodenal transplantation model. The results of serum and urine amylase, free blood sugar and insulin level after transplantation showed that the endocrine and exocrine functions of the pancreas graft were both good enough for SO manometry. The transplantation model was stable and suitable for SO manometry.

Canine SO plays an important role in controlling the flow of bile and pancreatic juice into the duodenum and acts as a variable resister to prevent the reflux of duodenal contents[1-4]. SO is a complex neuromuscular structure located at the choledocho-pancreaticoduodenal junction. Canine SO exhibits regular phasic contractions superimposed on a low basal pressure under neurohormonal control. After pancreas transplantation with bladder drainage, the graft was denervated. Little was known about the SO motility after pancreas

transplantation. Several reports suggested that SO dysfunction played an important role in acute recurrent pancreatitis[5-7]. Graft pancreatitis was a serious complication after pancreas transplantation with bladder drainage. The late graft pancreatitis might be related to SO dysfunction caused by graft SO denervation. Our present study on canine SO motility after auto-pancreas transplantation with bladder drainage showed: (1)Canine SO exhibited regular contractions with a certain basal pressure. After transplantation, graft SO basal pressure and contraction frequency increased and amplitude decreased significantly. But there was no great difference in SO motility index. (2) CCK administration could relax normal canine SO, but stimulate graft SO after canine pancreas transplantation with bladder drainage. The denervated graft duodenum lost its normal migrating motor complex (MMC). These data suggested that the tonic contraction of SO remained and created a higher basal pressure than that before transplantation, and phasic contraction decreased significantly. This resulted in the obstruction of pancreatic juice flowing into the graft duodenum. Furthemore, when bladder pressure increased to a certain extent because of urine stasis, the urine would reflux into pancreatic duct and induce acute pancreatitis.

The role of extrinsic nerves in the control of SO motility has not been fully investigated. The SO was richly innervatd by cholinergic, adrenergic and peptidegic neurons[8]. Direct neural pathways couple the duodenum with the gallbladder and SO, and the SO with the gallbladder. Several surgical procedures,such as gastrectomy[9], vagotomy[10] and cholecystectomy[11,12] have been known to alter SO motility by disrupting certain aspects of the innervations. Numerous reports described SO motility after transection or electrical stimulation of extrinsic nerves,such as the vagal and splanchnic nerves[13-16]. Different effects of innervation on SO motility reflect the difference both in species and in experimental designs. Complete denervation using tetrodoxtoxin increased tonic pressure and amplitude of SO phasic contraction in the cats[10]. Ohtsuke reported increased biliary sphincter basal pressure and amplitude after neural isolation of the pancreatoduodenal region by surgical procedure in conscious dogs[17]. The present study showed that extrinsic innervation to the pancreatoduodenal region had an inhibitory effect on SO motility. The main role of extrinsic nerves was to regulate phasic contraction and relax SO. Under normal condition, the relaxing effect of extrinsic nerve on canine SO motility was better than the stimulation effect. But the amplitude decreased significantly after transplantation instead of increasing observed in Ohtsuke' s study. This is probably because the motility of graft SO was not affected by duodenum MMC. Furthermore, the effect of gastrointestinal hormone on SO motility may be different from that in normal canines because of its anastomosis to system vessels. Further investigations are needed to identify this guess.

CCK is the major physiological hormone regulating tone and motility of biliary system. It normally inhibited biliary sphincter motor activity in human and dogs but stimulated SO under various circumstances, which is known as a paradoxical response[18,19]. It is believed that these SO relaxant responses to CCK were induced via nonadrenergic, noncholinergic inhibitory neurons since cholenergic and adrenergic antagonists could not inhibit these relaxant responses[20]. Our present study showed that CCK could relax canine SO and lower SO basal pressure. But denervated SO after transplantation apparently produced paradoxical response of SO to CCK, which was likely caused by the direct effect of CCK on the smooth muscle of SO. Based on these data, we could consume that the paradoxical response of SO to CCK in SO dysfunctional patients might also be caused by the direct stimulation of CCK to SO smooth muscle because of injury of inhibitory nerves of SO.

Gancio reported that reflux pancreatitis was chemically induced by reflux of urine through SO into pancreatic duct during the voiding phase with high detrusor pressure (over 70 cmH_2O)[21]. Others hypothesized that this could be caused by an incompletent SO or by either pressure exerted on the pancreatic duct due to a large volume bladder or micturition narrowing the duodenocystostomy and obstructing it[22,23]. The current study showed that canine SO lost its normal contraction rhythm , increased basal pressure causing an obstruction of pancreatic juice into graft duodenum. When bladder pressure overrided the basal pressure, SO probably could not prevent the reflux of urine and duodenal contents into pancreatic duct. All these would contribute to graft pancreatitis.

In conclusion, after auto-pancreas transplantation with bladder drainage, canine SO motility was inhibited. Basal pressure and frequency increased but amplitude decreased. CCK administration after transplantation showed an inhibitory effect on canine SO instead of a relaxation effect to normal canine SO. This will increase the resistance of SO to the pancreatic juice flow and induce pancreatic juice stagnation and can not prevent reflux of urine and duodenal contents when the bladder pressure is increased to a certain extent, which may cause graft pancreatitis.

REFERENCES

1 **Torsoli A**, Corazziari E, Habib FI, De Masi E, Biliotti D, Mazzarella R, Giubilei D, Fegiz G. Frequencies and cyclical pattern of the human sphincter of Oddi phasic activity. *Gut* 1986; **27**: 363-369

2 **Liu YF**, Saccone GT, Thune A, Baker RA, Harvey JR, Toouli J. Sphincter of Oddi regulates flow by acting as a variable resister to flow. *Am J Physiol* 1992; **263**(5 Pt 1): G683-689

3 **Yokohata K**, Kimura H, Ogawa Y, Naritomi G, Tanaka M. Biliary motility. Changes in detailed characteristics correlated to duodenal migrating motor complex and effects of morphine and motilin in dogs. *Dig Dis Sci* 1994; **39**: 1294-1301

4 **Tanaka M**. Advances in research and clinical practice in motor disorders of the sphincter of Oddi. *J Hepatobiliary Pancreat Surg* 2002; **9**: 564-568

5 **Sakorafas GH**, Tsiotou AG. Etiology and pathogenesis of acute pancreatitis: current concepts. *J Clin Gastroenterol* 2000; **30**: 343-356

6 **Frulloni L**, Cavallini G. Acute recurrent pancreatitis and dysfunction of the sphincter of Oddi: Comparison between invasive and non-invasive techniques. *JOP* 2001; **2**: 406-413

7 **Lai KH**. Sphincter of Oddi and acute pancreatitis: A new treatment option. *JOP* 2002; **3**: 83-85

8 **Toouli J**, Baker RA. Innervation of the sphincter of Oddi: physiology and considerations of pharmacological intervention in biliary dyskinesia. *Pharmacol Ther* 1991; **49**: 268-281

9 **Odani K**, Nimura Y, Yasui A, Akita Y, Shionoya S. Paradoxical response to cerulein on sphincter of Oddi in the patients with gastrectomy. *Dig Dis Sci* 1992; **37**: 904-911

10 **Behar J**, Biancani P. Neural control of the sphincter of Oddi. Physiologic role of enkephalins on the regulation of basal sphincter of Oddi motor activity in the cat. *Gastroenterology* 1984; **86**: 134-141

11 **Grace PA**, Pitt HA. Cholecystectomy alters the hormonal response of the sphincter of Oddi. *Surgery* 1987; **102**: 186-194

12 **Wei JG**, Wang YC, Liang GM, Wang W, Chen BY, Xu JK, Song LJ. The study between the dynamics and the X-ray anatomy and regularizing effect of gallbladder on bile duct sphincter of the dog. *World J Gastroenterol* 2003; **9**: 1014-1019

13 **Shafik A**. Cholecysto-sphincter inhibitory reflex: identification of a reflex and its role in bile flow in a canine model. *J Invest Surg* 1998; **11**: 199-205

14 **Nabae T**, Yokohata K, Otsuka T, Inoue K, Yamaguchi K, Chijiiwa K, Tanaka M. Effect of truncal vagotomy on sphincter of Oddi cyclic motility in conscious dogs. *Ann Surg* 2002; **236**: 98-104

15 **Takahashi I**, Dodds WJ, Hogan WJ, Itoh Z, Baker K. Effect of vagotomy on biliary-tract motor activity in the opossum. *Dig*

Dis Sci 1988; **33**: 481-489

16 **Tansy MF**, Mackowiak RC, Chaffee RB. A vagosympathetic pathway capable of influencing common bile duct motility in the dog. *Surg Gynecol Obstet* 1971; **133**: 225-236

17 **Ohtsuka T**, Yokohata K, Inoue K, Nabae T, Takahata S, Tanabe Y, Sugitani A, Tanaka M. Biliary sphincter motility after neural isolation of the pancreatoduodenal region in conscious dogs. *Surgery* 2002; **131**: 139-148

18 **Toouli J**, Hogan WJ, Geenen JE, Dodds WJ, Arndorfer RC. Action of cholecystokinin-octapeptide on sphincter of Oddi basal pressure and phasic wave activity in humans. *Surgery* 1982; **92**: 497-503

19 **Toouli J**, Roberts-Thomson IC, Dent J, Lee J. Manometric disorders in patients with suspected sphincter of Oddi dysfunction. *Gastroenterology* 1985; **88**(5 Pt 1): 1243-1250

20 **Behar J**, Biancani P. Pharmacologic characterization of excitatory and inhibitory cholecystokinin receptors of the cat gallbladder and sphincter of Oddi. *Gastroenterology* 1987; **92**: 764-770

21 **Ciancio G**, Burke GW, Roth D, Luque CD, Coker D, Miller J. Reflux pancreatitis after simultaneous pancreas-kidney transplantation treated by α1-blocker. *Transplantation* 1995; **60**: 760-761

22 **Stephanian E**, Gruessner RW, Brayman KL, Gores P, Dunn DL, Najarian JS, Sutherland DE. Conversion of exocrine secretions from bladder to enteric drainage in recipients of whole pancreaticoduodenal transplants. *Ann Surg* 1992; **216**: 663-672

23 **Boudreaux JP**, Nealon WH, Carson RC, Fish JC. Pancreatitis necessitating urinary undiversion in a bladder-drained pancreas transplant. *Transplant Proc* 1990; **22**: 641-642

Edited by Ma JY and Wang XL

P.O.Box 2345, Beijing 100023,China
Fax: +86-10-85381893
E-mail: wjg@wjgnet.com www.wjgnet.com

World J Gastroenterol 2003;9(12):2853-2855
World Journal of Gastroenterology
 ISSN 1007-9327

• BRIEF REPORTS •

Incidence and treatment of hepatic artery complications after orthotopic liver transplantation

Ji-Chun Zhao, Shi-Chun Lu, Lu-Nan Yan, Bo Li, Tian-Fu Wen, Yong Zeng, Nan-Sheng Cheng, Jing Wang, Yan Luo, Yu-Lan Pen

Ji-Chun Zhao, Shi-Chun Lu, Lu-Nan Yan, Bo Li, Tian-Fu Wen, Yong Zeng, Nan-Sheng Cheng, Jing Wang, Department of General Surgery, West China Hospital, Sichuan University, Chengdu 610041, Sichuan Province, China
Yan Luo, Yu-Lan Pen, Department of Ultrasound Diagnosis, West China Hospital, Sichuan University, Chengdu 610041, Sichuan Province, China
Correspondence to: Dr. Ji-Chun Zhao, Department of General Surgery, West China Hospital, Sichuan University, Chengdu 610041, Sichuan Province, China. jichunzhao@hotmail.com
Telephone: +86-28-85422474
Received: 2003-03-19 **Accepted:** 2003-04-24

Abstract

AIM: To investigate the incidence and treatment of hepatic artery complications after orthotopic liver transplantation.

METHODS: From February 1999 to May 2002, orthotopic liver transplantations (OLT) were performed in 72 patients with end-stage liver diseases with an average age of 40.2±13.6 years (ranged from 11 to 68 years), 56 were males and 16 females. The preoperative evaluation for the 72 patients was performed using duplexsonography, abdominal CT scan, and angiography of the hepatic artery. All donor grafts were perfused and preserved in University of Wisconsin solution at 4 ℃. OLT was performed with standard techniques with or without a veno-venous bypass. Reconstructions of hepatic artery were performed between the branch patches of gastroduodenal/hepatic or splenic/common hepatic artery confluence of the donors and recipients, and an end-to-end anastomosis between other arterial vessels of the donors and recipients was done. Arterial anastomosis was performed with interrupted 7-0/8-0 monofilament polypropylene suture under 3.5 x loupe magnification. Diagnosis of the complications of hepatic artery after OLT was based on the clinical presentations, ultrasound findings and arterial angiography. All patients were followed up regularly for duplex ultrasound scan after discharge.

RESULTS: The overall incidence of arterial complications in 72 patients after OLTs was 1.4 % (1/72). One 3 cm pseudoaneurysm at the side of anastomotic site of hepatic artery was found by urgent arteriogram due to hemoperitoneum secondary to bile leakage after OLT. Subsequently the pseudoaneurysm was successfully embolized and the blood flow toward the donor liver in hepatic artery remained. The overall postoperative 30-day mortality rate was 8.33 %. The one-year survival rate was 83.72 % in 50 patients with benign diseases and was 71.43 % in 22 patients with malignant diseases following OLT. No death associated with complications of hepatic artery occurred.

CONCLUSION: Careful preoperative evaluations and intraoperative microsurgical technique for hepatic artery reconstructions are the keys in prevention of hepatic artery complications after OLT.

Zhao JC, Lu SC, Yan LN, Li B, Wen TF, Zeng Y, Cheng NS, Wang J, Luo Y, Pen YL. Incidence and treatment of hepatic artery complications after orthotopic liver transplantation. *World J Gastroenterol* 2003; 9(12): 2853-2855
http://www.wjgnet.com/1007-9327/9/2853.asp

INTRODUCTION

Vascular complications after orthotopic liver transplantation (OLT) ranges from 2 % to 25 % in most publications[1,2]. The most frequent complications involve the hepatic artery (2 % to 12 % in adults)[3-5], in which the hepatic artery thrombosis (HAT) is most common[6,7]. The complications of hepatic artery are usually associated with technical, hemodynamic, immunological and infectious factors[2,8,9], which may result in biliary tract complications or sepsis[10,11], and even a retransplantation may be required[12,13]. In the present study, we report the incidence and treatment of hepatic artery complications in 72 patients with end-stage liver diseases after OLT from February 1999 to May 2002.

MATERIALS AND METHODS

Patients

From February 1999 to May 2002, OLTs were performed in 72 patients with an average age of 40.2±13.6 years (range 11 to 68 years, and 56 males, 16 females). Indications for OLT included post-inflammatory liver cirrhosis complicated with hepatitis B and liver function failure (34 cases), primary hepatocellular carcinoma (19 cases), end-stage liver hydatid cyst disease complicated with liver function failure (4 cases), Caroli' s disease (3 cases), cholestatic liver cirrhosis complicated with hepatolithiasis (2 cases), polycystic liver disease complicated with liver function failure (2 cases), primary sclerosing cholangitis (2 cases), Budd-Chiari syndrome complicated with liver function failure (2 cases), cholangiocarcinoma (2 cases), alcoholic cirrhosis (one case) and secondary hepatic maligancy (gallbladder cancer) (one case).

Methods

The preoperative evaluation for the 72 patients was performed using duplexsonography, abdominal CT scan, and angiography of the hepatic artery. All donor grafts were perfused and preserved in University of Wisconsin solution at 4 ℃. OLT was performed with standard techniques and a veno-venous bypass was used in 61 patients, and no veno-venous bypass was used in 5 patients. Retro-hepatic vena cava was resected in 66 patients, and an end-end interposition of donor vena cava together with donor liver was performed. Hepatectomy was performed according to the classical technique with preservation of retrohepatic vena cava (piggy back) in the remaining 6 patients. Reconstruction of the portal vein was performed by an end-to-end veno-venous anastomosis. The reconstruction of hepatic artery was variable and dependent on hepatic artery anatomy of the donors and recipients. Arterial anastomosis was performed between the branch patches of gastroduodenal/hepatic or splenic/common hepatic artery

confluence of the donors and recipients in 22 out of the 72 cases. End-to-end anastomosis was done between the proper hepatic artery of the donors and recipients in 18 out of the 72 cases, and the remaining anastomosis was performed between the proper hepatic artery of the donors and the right hepatic artery or the common hepatic artery of the recipients respectively in 6 and 5 out of the 72 cases. Anastomoses were performed between the proper hepatic artery of the donors and the splenic artery, between the left gastric artery and the left hepatic artery of the recipients in one case each, and between the splenic artery of the donors and the proper hepatic artery, the common hepatic artery or the left hepatic artery of the recipients in 6, 4 and one case respectively, between the common hepatic artery of the donors and the proper hepatic artery or the left hepatic artery of the recipients in 3 and one case respectively, and between the coeliac trunk of the donors and the common hepatic artery of the recipients in 3 cases. Arterial reconstruction was performed by microsurgical techniques with interrupted 7-0/8-0 monofilament polypropylene suture under 3.5 x loupe magnification, interposition grafting with same donor' s part of common hepatic conduit was used selectively in one case with end-to-end anastomosis between the proper hepatic arteries of the donors and recipients when anastomotic thrombosis was suspected before closure of the abdominal incision[14,15]. Diagnosis of complications of hepatic artery after OLTs was based on the clinical presentations, ultrasound findings and arteriography of hepatic artery. The hepatic artery was detected with routine duplex sonography intraoperatively after completion of hepatic artery reconstruction and daily in the first week after OLTs[16,17]. When the patients had elevated hepatic enzymes, cholestasis, bile leakage and high fever in the absence of acute rejection and drug toxicity, spiral CT scan or angiography of hepatic artery should be considered. No anticoagulable pharmacotherapy to maintain arterial patency was used intraoperatively and postoperatively in this group, but laboratory examination of coagulation state should be done regularly. All the patients received immunosuppressive therapy including cyclosporine or FK506 regimens and were followed up from 3 to 34 months. Hepatic artery of liver transplant patients was detected regularly by duplex ultrasound scan three or six months after discharge.

Statistical methods

The Kaplan-Meier method was used to calculate survival rate, and statistical calculations for mean values and standard deviations were performed using the SPSS software package.

RESULTS

The overall incidence of arterial complications in the 72 patients after OLTs was 1.4 % (1/72) and no HAT and hepatic artery stenosis were found after OLTs. A 3 cm anastomotic pseudoaneurysm of hepatic artery was found in 1 case by urgent arteriogram due to hemoperitoneum secondary to bile leakage about one month after OLT. The pseudoaneurysm at the side of anastomotic site of hepatic artery was successfully embolized, and blood flow toward the donor liver in hepatic artery remained. This patient was fully recovered and discharged one month later when bile leakage was stopped. The patient was doing well 1 year after OLT. The overall postoperative 30-day mortality rate was 8.33 % (6 deaths in 72 patients). The one-year survival rate was 83.72 % in 50 patients with benign diseases and was 71.43 % in 22 patients with malignant diseases after OLTs. No death occurred due to complications of hepatic artery.

DISCUSSION

Vascular reconstructions are critical to a successful outcome in orthotopic liver transplantation (OLT), complications associated with hepatic artery reconstructions are one of the major causes of graft loss and mortality after OLT. Hepatic artery complications after OLT include HAT, hepatic artery stenosis, hepatic artery pseudoaneurysm (HAP) and hepatic artery fistula. The early complications of hepatic artery were usually caused by technical problems[1-3]. The late complications of hepatic artery were usually associated with hypercoagulable state, over transfusion of platelets and fresh-frozen plasma during the surgery, severe rejection and bile leakage[11,18,19]. The hepatic artery is relatively small (3 to 6 mm in diameter in adults) during the vascular reconstructions of OLT with a very fragile intima that requires highly careful atraumatic manipulating technique during the reconstruction of hepatic artery. The anatomical variations[20-22], diameter and length of hepatic artery, and injury to vessels including prolonged clamping of hepatic artery, kinking of a long artery, and hematoma of artery wall from improper flushing after clamping during operation, and the quality of recipient vessels and mismatch between donor and recipient arterial vessels should be carefully considered and managed preoperatively and intraoperatively[2,15]. The incidence of arterial complications after OLTs varied between 2 % and 25 % among the liver transplant patients[2], HAT was most common[6,7], and caused irreversible graft damage and often required immediate revascularization of hepatic artery, even retransplantation of the liver[12,13]. HAP occurred in less than 1 % patients after OLT[23,24]. The incidence of hepatic artery complications was low in this group. The technique of microsurgical hepatic artery reconstruction contributed greatly to the reduction of incidence of HAT and hepatic stenosis[6,15,25]. Current HAT rate reported after hepatic arterial reconstruction was 1.44 % via the branch patch technique using the hepatic-gastroduodenal bifurcation and interrupted suture of 7/0 monofilament polypropylene suture[6,20]. We found a single case of hepatic artery pseudoaneurysm whose openning was at the side of anastomotic site of hepatic artery as the complication following OLT and the pseudoaneurysm was embolized successfully. The reported incidence of pseudoaneurysm of hepatic artery was low, but this complication could be devastative with a high mortality rate due to massive bleeding that often required immediate revascularization[26,27], and even retransplantation[12,13]. Extrahepatic pseudoaneurysms of hepatic artery were associated with local infection, bile leakage while intrahepatic pseudoaneurysms were caused by liver punctures[2,5]. The most frequent presentations of hepatic artery pseudoaneurysm were hemorrhages including gastrointestinal hemorrhage, hemoperitoneum and hemobilia[5,19], which often occurred within the first two months after liver transplantation, and might lead to death due to massive bleeding or loss of the donor graft[5,28,29]. Although ultrasound and CT scanning were useful in the diagnosis of hepatic artery pseudoaneurysms[30-32], arteriography was more accurate[10,33], and might demonstrate clearly an anastomotic pseudoaneurysm of the hepatic artery with bleeding into peritoneum cavity or bile tract[23,29,33]. The treatment for hepatic artery pseudoaneurysm remains a challenging problem. The current treatment options include ligation or embolization, excision and immediate revascularization of hepatic arterial pseudoanurysm with or without a donor illiac artery or autogenous saphenous vein, and retransplantation. However, ligation resulted in an extremely high morbidity and mortality[12,26,34,35], especially at the early stage after liver transplantation. The excision and immediate revascularization of hepatic arterial pseudoanurysm appeared to be the best choice[26,27]. At the time of revascularization, bile leakage should be also repaired[26], and the donor iliac artery or autogenous saphenous vein was often used for arterial revascularization[34,35]. If an adequate donor

iliac artery or autogenous saphenous vein was not available, an autogenous radial artery could be used[36]. Embolization therapy of hepatic artery pseudoaneurysm after OLT was seldom reported. In our study, pseudoaneurysm at the side of the anastomotic site of hepatic artery was embolized successfully and the patency of the hepatic artery toward the donor liver remained, which salvaged the donor liver as well as the the recipient by the mini-invasive percutaneous endovascular techniques. This case provides a good example of safe and effective approach in the management of pseudoaneurysm of hepatic artery, but more experience is expected.

REFERENCES

1 **Turrion VS**, Alvira LG, Jimenez M, Lucena JL, Ardaiz J. Incidence and results of arterial complications in liver transplantation: experience in a series of 400 transplants. *Transplant Proc* 2002; **34**: 292-293

2 **Settmacher U**, Stange B, Haase R, Heise M, Steinmuller T, Bechstein WO, Neuhaus P. Arterial complications after liver transplantation. *Transpl Int* 2000; **13**: 372-378

3 **Sanchez-Bueno F**, Robles R, Acosta F, Ramirez P, Lujan J, Munitiz V, Rios A, Parrilla P. Hepatic artery complications in a series of 300 orthotopic liver transplants. *Transplant Proc* 2000; **32**: 2669-2670

4 **Stange B**, Settmacher U, Glanemann M, Nussler NC, Bechstein WO, Neuhaus P. Hepatic artery thrombosis after orthotopic liver transplantation. *Transplant Proc* 2001; **33**: 1408-1409

5 **Almogy G**, Bloom A, Verstandig A, Eid A. Hepatic artery pseudoaneurysm after liver transplantation. A result of transhepatic biliary drainage for primary sclerosing cholangitis. *Transpl Int* 2002; **15**: 53-55

6 **Proposito D**, Loinaz Segurola C, Garcia Garcia I, Jimenez C, Gonzalez Pinto I, Gomez Sanz R, De La Cruz J, Moreno Gonzalez E. Assessment of risk factors in the incidence of hepatic artery thrombosis in a consecutive series of 687 liver transplantations. *Ann Ital Chir* 2001; **72**: 187-205

7 **Abou Ella KA**, Al Sebayel MI, Ramirez CB, Rabea HM. Hepatic artery thrombosis after orthotopic liver transplantation. *Saudi Med J* 2001; **22**: 211-214

8 **Abou El-Ella K**, Al Sebayel M, Ramirez C, Hussien R. Outcome and risk factors of hepatic artery thrombosis after orthotopic liver transplantation in adults. *Transplant Proc* 2001; **33**: 2712-2713

9 **Pastacaldi S**, Teixeira R, Montalto P, Rolles K, Burroughs AK. Hepatic artery thrombosis after orthotopic liver transplantation: a review of nonsurgical causes. *Liver Transpl* 2001; **7**: 75-81

10 **Cavallari A**, Nardo B, Catena F, Montalti R, Cavallari G, Bellusci R, Golfieri R, Rossi C. Mini-invasive treatment of arterial and biliary complications after orthotopic liver transplantation. *Transplant Proc* 2001; **33**: 2001

11 **Leonardi LS**, Boin IF, Neto FC, de Oliveira GR, Leonardi MI. Biliary reconstructions in 150 orthotopic liver transplantations: an experience with three techniques. *Transplant Proc* 2002; **34**: 1211-1215

12 **Dudek K**, Nyckowski P, Zieniewicz K, Michalowicz B, Pawlak J, Malkowski P, Krawczyk M. Liver retransplantation: indications and results. *Transplant Proc* 2002; **34**: 638-639

13 **Bramhall SR**, Minford E, Gunson B, Buckels JA. Liver transplantation in the UK. *World J Gastroenterol* 2001; **7**: 602-611

14 **Zhao JC**, Lu SC, Huang FG, Yan LN, Li B, Jin LR, Wen TF, Wang J, Luo Y, Peng YL, Yuan ZX. Reconstruction of hepatic artery in orthotopic liver transplantation. *Zhongguo Xiandai Shoushuxue Zazhi* 2001; **5**: 24-26

15 **Zhao JC**, Huang FG, Lu SC, Yan LN, Li B, Jin LR, Wen TF, Wang J, Luo Y, Peng YL. Reconstructions of hepatic artery in orthotopic liver transplantation. *Zhonghua Qiguan Yizhi Zazhi* 2002; **23**: 37-39

16 **Lin M**, Crawford M, Fisher J, Hitos K, Verran D. Hepatic artery thrombosis and intraoperative hepatic artery flow rates in adult orthotopic liver transplantation. *ANZ J Surg* 2002; **72**: 798-800

17 **De Candia A**, Como G, Tedeschi L, Zanardi R, Vergendo M, Rositani P, Bazzocchi M. Color doppler sonography of hepatic artery reconstruction in liver transplantation. *J Clin Ultrasound* 2002; **30**: 12-17

18 **Bhattacharjya S**, Gunson BK, Mirza DF, Mayer DA, Buckels JA, McMaster P, Neuberger JM. Delayed hepatic artery thrombosis in adult orthotopic liver transplantation-a 12-year experience. *Transplantation* 2001; **71**: 1592-1596

19 **Hidalgo E**, Cantarell C, Charco R, Murio E, Lazaro JL, Bilbao I, Margarit C. Risk factors for late hepatic artery thrombosis in adult liver transplantation. *Transplant Proc* 1999; **31**: 2416-2417

20 **Proposito D**, Loinaz Segurola C, Garcia Garcia I, Jimenez C, Gonzales Pinto I, Gomez Sanz R, Moreno Gonzalez E. Role of anatomic variations and methods of hepatic artery reconstruction in the incidence of thrombosis following liver transplantation. *Ann Ital Chir* 2001; **72**: 303-314

21 **Gruttadauria S**, Foglieni CS, Doria C, Luca A, Lauro A, Marino IR. The hepatic artery in liver transplantation and surgery: vascular anomalies in 701 cases. *Clin Transplant* 2001; **15**: 359-363

22 **Jones RM, Hardy KJ**. The hepatic artery: a reminder of surgical anatomy. *J R Coll Surg Edinb* 2001; **46**: 168-170

23 **Marshall MM**, Muiesan P, Srinivasan P, Kane PA, Rela M, Heaton ND, Karani JB, Sidhu PS. Hepatic artery pseudoaneurysms following liver transplantation: incidence, presenting features and management. *Clin Radiol* 2001; **56**: 579-587

24 **Stange B**, Settmacher U, Glanemann M, Nuessler NC, Bechstein WO, Neuhaus P. Aneurysms of the hepatic artery after liver transplantation.*Transplant Proc* 2000; **32**: 533-534

25 **Egawa H**, Asonuma K, Sakamoto Y, Iwasaki M, Kim I, Tanaka K. Surgical techniques for vascular reconstruction of the portal vein and hepatic artery in living-donor liver transplantation. *Nippon Geka Gakkai Zasshi* 2001; **102**: 798-804

26 **Bonham CA**, Kapur S, Geller D, Fung JJ, Pinna A. Excision and immediate revascularization for hepatic artery pseudoaneurysm following liver transplantation. *Transplant Proc* 1999; **31**: 443

27 **Sellers MT**, Haustein SV, McGuire BM, Jones C, Bynon JS, Diethelm AG, Eckhoff DE. Use of preserved vascular homografts in liver transplantation: hepatic artery aneurysms and other complications. *Am J Transplant* 2002; **2**: 471-475

28 **Bussenius-Kammerer M**, Ott R, Wutke R, Grunewald M, Hohenberger W, Reck T. Pseudoaneurysm of the hepatic artery–a rare complication after orthotopic liver transplantation. *Chirurg* 2001; **72**: 78-81

29 **Glehen O**, Feugier P, Ducerf C, Chevalier JM, Baulieux J. Hepatic artery aneurysms. *Ann Chir* 2001; **126**: 26-33

30 **Garcia-Criado A**, Gilabert R, Nicolau C, Real I, Arguis P, Bianchi L, Vilana R, Salmeron JM, Garcia-Valdecasas JC, Bru C. Early detection of hepatic artery thrombosis after liver transplantation by Doppler ultrasonography: prognostic implications. *J Ultrasound Med* 2001; **20**: 51-58

31 **Quiroga S**, Sebastia MC, Margarit C, Castells L, Boye R, Alvarez-Castells A. Complications of orthotopic liver transplantation: spectrum of findings with helical CT. *Radiographics* 2001; **21**: 1085-1102

32 **Katyal S**, Oliver JH 3rd, Buck DG, Federle MP. Detection of vascular complications after liver transplantation: early experience in multislice CT angiography with volume rendering. *Am J Roentgenol* 2000; **175**: 1735-1739

33 **Cavallari A**, Vivarelli M, Bellusci R, Jovine E, Mazziotti A, Rossi C. Treatment of vascular complications following liver transplantation: multidisciplinary approach. *Hepatogastroenterology* 2001; **48**: 179-183

34 **Zamboni F**, Franchello A, Ricchiuti A, Fop F, Rizzetto M, Salizzoni M. Use of arterial conduit as an alternative technique in arterial revascularization during orthotopic liver transplantation. *Dig Liver Dis* 2002; **34**: 122-126

35 **Meyer C**, Riehm S, Perrot F, Cag M, Nizand G, Audet M, Veillon F, Jaeck D, Wolf P. Donor iliac artery used for arterial reconstruction in liver transplantation. *Transplant Proc* 2000; **32**: 2791

36 **Rogers J**, Chavin KD, Kratz JM, Mohamed HK, Lin A, Baillie GM, Shafizadeh SF, Baliga PK. Use of autologous radial artery for revascularization of hepatic artery thrombosis after orthotopic liver transplantation: case report and review of indications and options for urgent hepatic artery reconstruction. *Liver Transpl* 2001; **7**: 913-917

Edited by Zhang JZ and Wang XL

P.O.Box 2345, Beijing 100023,China
Fax: +86-10-85381893
E-mail: wjg@wjgnet.com www.wjgnet.com

World J Gastroenterol 2003;9(12):2856-2858
World Journal of Gastroenterology
 ISSN 1007-9327

• BRIEF REPORTS •

Management of choledocholithiasis: Comparison between laparoscopic common bile duct exploration and intraoperative endoscopic sphincterotomy

Qi Wei, Jian-Guo Wang, Li-Bo Li, Jun-Da Li

Qi Wei, Li-Bo Li, Jun-Da Li, Department of General Surgery, Sir Run Run Shaw Hospital, Zhejiang University, Hangzhou 310016, Zhejiang Province, China
Jian-Guo Wang, Department of Gastroenterology, Sir Run Run Shaw Hospital, Zhejiang University, Hangzhou 310016, Zhejiang Province, China
Correspondence to: Qi Wei, Department of General Surgery, Sir Run Run Shaw Hospital, Zhejiang University, Hangzhou 310016, Zhejiang Province, China. weiqi@hzcnc.com
Telephone: +86-571-86437761
Received: 2003-06-21 **Accepted:** 2003-07-24

Abstract

AIM: Choledocholithiasis is present in 5 to 10 percent of patients who have cholelithiasis. In the area of laparoscopic cholecystectomy (LC), laparoscopic common bile duct exploration (LCBDE) and intraoperative endoscopic sphincterotomy (IOES) have been used to treat choledocholithiasis. The purpose of this study was to compare the clinical outcomes and hospital costs of LCBDE with IOES.

METHODS: Between November 1999 and October 2002, patients with choledocholithiasis undergoing LC plus LCBDE (Group A, *n*=45) were retrospectively compared to those undergoing LC plus IOES (Group B, *n*=57) at a single institution.

RESULTS: Ductal stone clearance rates were equivalent for the two groups (88 % versus 89 %, *P*=0.436). The conversion rate was higher for Group B (8.8 % versus 4.4 %, *P*=0.381), as was the morbidity (12.3 % versus 6.7 %, *P*=0.336). There were no other significant differences between the two groups. The complications were mainly related to endoscopic sphincterotomy (ES), and the hospital costs were significantly increased in this subset of Group B (median, 23 910 versus 14 955 RMB yuan, *P*=0.03). Although hospital stay was longer in Group A (median, 7 versus 6 days, *P*=0.041), the patients in Group A had a significantly decreased cost of hospitalization compared with those in Group B (median, 11 362 versus 15 466 RMB yuan, *P*=0.000).

CONCLUSION: The results demonstrate equivalent ductal stone clearance rates for the two groups. LCBDE management appears safer, and is associated with a significantly decreased hospital cost. The findings suggest LCBDE for choledocholithiasis is a better option.

Wei Q, Wang JG, Li LB, Li JD. Management of choledocholithiasis: Comparison between laparoscopic common bile duct exploration and intraoperative endoscopic sphincterotomy. *World J Gastroenterol* 2003; 9(12): 2856-2858
http://www.wjgnet.com/1007-9327/9/2856.asp

INTRODUCTION

Laparoscopic cholecystectomy (LC) has become the standard method for cholecystectomy, but the same cannot be said of the management of choledocholithiasis. There is still no standard algorithm. Laparoscopic common bile duct exploration (LCBDE) and intraoperative endoscopic sphincterotomy (IOES) have been used to treat choledocholithiasis for many years in clinical practice[1-6]. The purpose of this study was to determine the most cost-effective approach for patients with choledocholithiasis.

MATERIALS AND METHODS

Between November 1999 and October 2002, patients with choledocholithiasis undergoing LC plus LCBDE (Group A, *n*=45) were retrospectively compared to those undergoing LC plus IOES (Group B, *n*=57) at a single institution.

The clinical demographic details and the pretreatment biochemical findings are shown in Table 1. There were no significant differences between the groups. Preoperative investigations included liver function tests and external ultrasound examination of the gallbladder and bile duct. Four patients in Group A underwent preoperative ERCP. Endoscopic sphincterotomy (ES) was unsuccessful in three patients, and another ERCP was performed but no stones were found. Five patients in Group B underwent preoperative ERCP. ES was not performed in two patients. The three other patients underwent ERCP but no stones were found.

Table 1 Clinical and demographic details in patients of groups A and B

	Group A	Group B
Total no.	45	57
Age range (yr)	29-79	18-75
Male patients	17	20
Female patients	28	37
Abnormal LFTa	40	38
Jaundice	18	19
Acute cholecystitis	19	12
Pancreatitis	11	6
Preoperative ERCP	4	5

a: Liver function test.

Laparoscopic ductal stone clearance was performed either by the transcystic duct route (*n*=10) or by direct CBDE with placement of T-tube (*n*=35). Intraoperative cholangiography (IOC) was done in all patients. Complete clearance of the ductal stones was determined by the end of IOC. The necessity to convert to a different technique or the presence of an unexpected retained stone was considered as a failure. LCBDE was performed at the same institution by experienced surgeons. Two experienced gastroenterologists performed IOES [5,6]. The exact technique was left up to the individual physician.

All hospital cost data were obtained from the hospital admission department. The cost of complications the patients

incurred was included in the cost data. If LCBDE or IOES failed and the patient required postoperative ES or chledochoscopy through the sinus tract, the cost of that intervention was included. The cost of additional anesthesia or IOC was also included.

Data and statistical analysis

Statistical analysis was performed using chi square test with a likelihood ratio and Mann-Whitney test for nonparametric data. Significance was set at the 5 % level.

RESULTS

Outcome of Group A (LCBDE)

Ductal stone clearance was successful in 40 out of 45 patients (88 %). There were two cases of conversions to open surgery (4.4 %)(Table 2). One patient had large impact stones, the other had multiple stones. Two patients (4.4 %) had unexpected retained stones, one requiring ES at readmission, the other choledochoscopy through the sinus tract.

Postoperative complications occurred in 3 patients (6.7 %) (Table 3). Two patients had infection around the T-tube, and the other had bile leak after the T-tube was removed.

The cost ranged from 6 979 to 23 813 RMB yuan with a median 11 362 RMB yuan (Table 2). Of the 42 patients having uncomplicated hospital stays, the median cost was 11210 RMB yuan compared with a cost of 15121 RMB yuan for the three patients with complications (Table 4). The hospital stay ranged from four to eighteen days with a median stay of seven days. The median postoperative stay was four days (range, 2-14) (Table 2).

Outcome of Group B (IOES)

Ductal stone clearance was successful in 51 out of 57 patients (89 %). There were five cases of conversions to open surgery (8.8 %) (Table 2). One had a microperforation of the duodenum, one had bleeding at the sphincterotomy, and the other three patients had unsuccessful ES. One patient (1.8 %) had an unrecognized retained stone and required ES at a second admission.

Seven cases had complications (12.3 %)(Table 3). Three patients developed pancreatitis, two of them had severe pancreatitis, and the other required open surgery for an abdominal abscess that resulted in a 51-day hospital stay with a cost of 133 239 RMB yuan. Two patients developed postoperative pneumonia.

The cost ranged from 8 823 to 133 239 RMB yuan with a median of 15 466 RMB yuan (Table 2). Of the 50 patients having uncomplicated hospital stays, the median cost was 14 955 RMB yuan compared with a cost of 23910 RMB yuan for the seven patients with complications (Table 4). The hospital stay ranged from 2 to 51 days with a median stay of six days. The median postoperative stay was three days (range, 1-51)(Table 2).

Table 3 Morbidity of two groups

	Group B	Group A
Patient no(%)	7 (12.3)	3 (6.7)
Bleeding	1	
Microperforation	1	
Pancreatitis	3	
Pneumonia	2	
Infection with t-tube		2
Bile leak		1

Comparison of clinical outcome and hospital costs of two groups

Statistical analysis and comparison between Groups A (LCBDE) and B (IOES) are presented in Table 2.

The ductal stone clearance rates were equivalent in the two groups (88 % versus 89 %, P=0.436). The conversion rate was higher in Group B (8.8 % versus 4.4 %, P=0.381), as was the morbidity (12.3 % versus 6.7 %, P=0.336). The operating time was shorter in Group B (median, 155 min versus 180 min, P=0.661). But there were no significant differences between the two groups. Although the hospital stay was longer in Group A(median,7 versus 6 days, P=0.041), the patients in Group A had a significantly decreased cost of hospitalization compared with those in Group B (median, 11 362 versus 15 466 RMB yuan, P=0.000), and the hospital costs significantly increased in complicated Group B (Table 4).

DISCUSSION

The presence of common bile duct stones (CBDS) significantly increases the morbidity, mortality, and cost of patients with gallstones. The potential complications of choledocholithiasis,

Table 2 Comparison of clinical outcome and cost between groups A and B

	Group A	Group B	χ^2(Z)	P value
Ductal stone clearance (%)	88	89	0.607	0.436[b]
Conversion to open surgery (%)	4.4	8.8	0.767	0.381[b]
Morbidity (%)	6.7	12.3	0.927	0.336[b]
Operative time(min)	180,130-220[a]	155,130-210[a]	(-0.439)	0.661[c]
Hospital stay(days)	7,6-9[a]	6,4.5-8[a]	(-2.046)	0.041[c]
Postoperative stay(days)	4,3-6[a]	3,2-5[a]	(-2.259)	0.024[c]
Cost (RMB)	11362,10196-14822[a]	15466,13555-17689[a]	(-4.822)	0.000[c]

a: Median, 25-75 % quartile range; b: Chi square test with a likelihood ratio; c: Mann-Whitney test.

Table 4 Comparison of cost with or without complication between two groups

	Without complication cost (RMB)	n	With complication cost (RMB)	n	P value
Group A	11210,10119-14380[a]	42	15121,11706-19895[a]	3	0.08[b]
Group B	14955,12650-16793[a]	50	23910,20746-111289[a]	7	0.03[b]
P value		0.000[b]		0.000[b]	

a: Median, 25-75 % quartile range; b: Mann-Whitney test.

cholangitis, and pancreatitis could be life-threatening[7,8]. The safest and most cost-effective approach for patients with CBDS could decrease suffering and disability and save millions of heath care us dollars each year[9,10].

ES was first described in 1974. Today, ES for choledocholithiasis remains the most difficult and dangerous procedure routinely performed by endoscopists. The application of ES to CBDS was advocated for patients with cholangitis, acute biliary pancreatitis, and for elderly high-risk patients[11]. Gong *et al* from China reported a ductal stone clearance rate of 91.7 % and a complication rate of 8.8 %[12]. In our experience, the ductal stone clearance rate was 89 %, the morbidity was 12.3 %. Although IOES was performed by experienced gastroenterologists, it still resulted in procedure-related complications that could be life-threatening[13-16]. The cost was significantly increased in complicated Group B (IOES) (median, 23 910 versus 14 955 RMB yuan, P=0.03)(Table 4), and the hospital stay was much longer.

Successful LCBDE has been reported in several large series in 57 to 98 percent of cases[17]. Our experience compared favorably with these results. LCBDE was used in our recent management of choledocholithiasis for the vast majority of patients, whereas early IOES was more commonly performed in the past two years. The clearance rate in Group A (LCBDE) was 88 %, and the complication rate was 6.7 %. With the experience and new instrumentation, the limiting factor in successful LCBDE was not the CBD access but the CBD pathologic alterations such as large impact stones or multiple stones[17].

On the other hand, Group A was associated with a significantly decreased cost of hospitalization compared with Group B (median, 11 362 versus 15 466 RMB yuan, P=0.000) (Table 2). The total hospital cost of Group B included two parts, and was higher even for uncomplicated patients (median, 14 955 versus 11 210 RMB yuan, P=0.000). The cost of complicated patients was significantly increased (Table 4). Therefore, a thorough evaluation and consideration of management options would reduce the risk of complications and the cost of CBDS management.

Although the hospital stay was longer in Group A (LCBDE), it was mainly related to postoperative stay (median, 4 versus 3 days, P=0.024) with placement of T-tube. Therefore, primary closure of CBD without T-tube would be more cost-effective.

The operation time was shorter in Group B (IOES) (median, 155 min versus 180 min, P=0.661). In most situations, we had to wait for gastroenterologists, and the waiting time was not included in the operation time. The actual procedure time was delayed, which partially contributed to an increased hospital cost[18].

The results demonstrate that the ductal stone clearance rate was equivalent in the two groups. The conversion rate and morbidity were higher in Group B (IOES), and mainly related to ES. The hospital cost was significantly increased in complicated Group B patients. LCBDE management appears safer, and has no life-threatening complications, and can significantly decrease the hospital cost. The findings suggest LCBDE for CBDS is a better option.

ACKNOWLEDGMENTS

We thank Dr. C.Welch for editorial assistance and helpful suggestions.

REFERENCES

1 **Paganini AM**, Feliciotti F, Guerrieri M, Tamburini A, De Sanctis A, Campagnacci R, Lezoche E. Laparoscopic common bile duct exploration. *J Laparoendosc Adv Surg Tech A* 2001; **11**: 391-400
2 **Lilly MC**, Arregui ME. A balanced approach to choledocholithiasis. *Surg Endosc* 2001; **15**: 467-472
3 **Moroni J**, Haurie JP, Judchak I, Fuster S. Single-stage laparoscopic and endoscopic treatment for choledocholithiasis: A novel approach. *J Laparoendosc Adv Surg Tech A* 1999; **9**: 69-74
4 **Sgourakis** G, Karaliotas K. Laparoscopic common bile duct exploration and cholecystectomy versus endoscopic stone extraction and laparoscopic cholecystectomy for choledocholithiasis. A prospective randomized study. *Minerva Chir* 2002; **57**: 467-474
5 **Wang YD,** Gao M, Zhang QY, Wang JG, yuan XM, Cai XJ, Wang XF. Single-stage laparoscopic cholecystectomy and endoscopic sphincterotomy for management of patients with cholecystocholedocholithiasis. *Zhonghua Putong Waike Zazhi* 2000; **15**: 108-109
6 **Hong DF**, Gao M, Bryner U, Cai XJ, Mou YP. Intraoperative endoscopic sphincterotomy for common bile duct stones during laparoscopic cholecystectomy. *World J Gastroenterol* 2000; **6**: 448-450
7 **Zhang WZ**, Chen YS, Wang JW, Chen XR. Early diagnosis and treatment of severe acute cholangitis. *World J Gastroenterol* 2002; **8**: 150-152
8 **Kohut M**, Nowak A, Nowakowska-Duiawa E, Marek T. Presence and density of common bile duct microlithiasis in acute biliary pancreatitis. *World J Gastroenterol* 2002; **8**: 558-561
9 **Liberman** MA, Phillips EH, Carroll BJ, Fallas MJ, Rosenthal R, Hiatt J. Cost-effective management of complicated choledocholithiasis: laparoscopic transcystic duct exploration or endoscopic sphincterotomy. *J Am Coll Surg* 1996; **182**: 488-494
10 **Urbach DR,** Khajanchee YS, Jobe BA, Standage BA, Hansen PD, Swanstrom LL. Cost-effective management of common bile duct stones: a decision analysis of the use of endoscopic retrograde cholangiopancreatography (ERCP), intraoperative cholangiography, and laparoscopic bile duct exploration. *Surg Endosc* 2001; **15**: 4-13
11 **Cuschieri A**, Lezoche E, Morino M, Croce E, Lacy A, Toouli J, Faggioni A, Ribeiro VM, Jakimowicz J, Visa J, Hanna GB. E.A.E.S. multicenter prospective randomized trial comparing two-stage *vs* single-stage management of patients with gallstone disease and ductal calculi. *Surg Endosc* 1999; **13**: 952-957
12 **Gong JP**, Zhou YB, Han BL, Li ZH. Endoscopic sphincterotomy in treatment of secondary common bile duct stones. *Shijie Huaren Xiaohua Zazhi* 1999; **7**: 320-322
13 **He GH**, Cai Y, Qian XY, Feng GH, Ying RC, Xu Q, Jia PH. Surgical management of the complications after endoscopic sphincterotomy. *Zhonghua Putong Waike Zazhi* 2002; **17**: 469-470
14 **Freeman ML**, DiSario JA, Nelson DB, Fennerty MB, Lee JG, Bjorkman DJ, Overby CS, Aas J, Ryan ME, Bochna GS, Shaw MJ, Snady HW, Erickson RV, Moore JP, Roel JP. Risk factors for post-ERCP pancreatitis: a prospective, multicenter study. *Gastrointest Endosc* 2001; **54**: 425-434
15 **Vandervoort J**, Soetikno RM, Tham TC, Wong RC, Ferrari AP Jr, Montes H, Roston AD, Slivka A, Lichtenstein DR, Ruymann FW, Van Dam J, Hughes M, Carr-Locke DL. Risk factors for complications after performance of ERCP. *Gastrointest Endosc* 2002; **56**: 652-656
16 **Masci E**, Toti G, Mariani A, Curioni S, Lomazzi A, Dinelli M, Minoli G, Crosta C, Comin U, Fertitta A, Prada A, Passoni GR, Testoni PA. Complications of diagnostic and therapeutic ERCP: a prospective multicenter study. *Am J Gastroenterol* 2001; **96**: 417-423
17 **Heili MJ,** Wintz NK, Fowler DL. Choledocholithiasis: endoscopic versus laparoscopic management. *Am Surg* 1999; **65**: 135-138
18 **Wright BE**, Freeman ML, Cumming JK, Quickel RR, Mandal AK. Current management of common bile duct stones: is there a role for laparoscopic cholecystectomy and intraoperative endoscopic retrograde cholangiopancreatography as a single-stage procedure? *Surgery* 2002; **132**: 729-735

Edited by Zhang JZ and Wang XL

P.O.Box 2345, Beijing 100023,China
Fax: +86-10-85381893
E-mail: wjg@wjgnet.com www.wjgnet.com

World J Gastroenterol 2003;9(12):2859-2862
World Journal of Gastroenterology
 ISSN 1007-9327

• BRIEF REPORTS •

Influence of liver nonparenchymal cell infusion combined with cyclosporin A on rejection of rat small bowel transplantation

Yan-Ling Yang, Ji-Peng Li, Ke-Feng Dou, Kai-Zong Li

Yan-Ling Yang, Ji-Peng Li, Ke-Feng Dou, Kai-Zong Li, Department of Hepatobiliary Surgery, Xijing Hospital, Fourth Military Medical University, Xi' an 710032, Shaanxi Province, China
Supported by the National Natural Science Fundation of China, No. 30070741
Correspondence to: Kai-Zong Li, Department of Hepatobiliary Surgery, Xijing Hospital, Fourth Military Medical University, Xi' an 710032, Shaanxi Province, China. gdwk@fmmu.edu.cn
Telephone: +86-29-3375259 **Fax:** +86-29-3375561
Received: 2003-06-06 **Accepted:** 2003-07-24

Abstract

AIM: To investigate the effect of liver nonparenchymal cell infusion combined with cyclosporin A (CsA) on rejection of heterostrain rat small bowel transplantation.

METHODS: The liver nonparenchymal cell suspension was prepared by density gradient centrifugation method with Percoll centrifugal solution. Heterotopic small bowel transplantation was performed. Then the rats were divided into four groups. Group one: homogenic transplantation (F344/N→F344/N), group two: allotransplantation (F344/N →Wistar), group three: allotransplantation (F344/N→Wistar) + CsA, with CsA 10 mg· kg^{-1}· d^{-1} after transplantation, group four: allotransplantation + CsA (F344/N→Wistar) + liver nonparenchymal cell infusion + CsA (F344/N→Wistar), in which recipient Wistar rats had been injected with 2×10^8 F344/N liver nonparenchymal cells 20 days before transplantation, and treated with CsA after transplantation. Finally, the survival time after small bowel transplantation, gross and histopathological examination, and IL-2 levels in serum were observed.

RESULTS: The survival time after small bowel transplantation was 7.14±0.33 d, 16.32±0.41 d and 31.41±0.74 d in group 2, 3, and 4, respectively. The survival time was significant longer (P<0.01) in group 4. The gross and histopathological examination showed that the rejection degree in group 4 was lower than those in groups 2 and 3. Serum IL-2 level in group 4 was also lower than those in groups 2 and 3 (P<0.01).

CONCLUSION: Liver nonparenchymal cell infusion combined with CsA can prolong the survival time of rat small bowel transplantation, and the anti-rejection effect is good.

Yang YL, Li JP, Dou KF, Li KZ. Influence of liver nonparenchymal cell infusion combined with cyclosporin A on rejection of rat small bowel transplantation. *World J Gastroenterol* 2003; 9 (12): 2859-2862

http://www.wjgnet.com/1007-9327/9/2859.asp

INTRODUCTION

In clinical practice, rejection responses induced by organ transplants necessitate the use of potent immunosuppressive drugs. It should be noted, however, that excessive dosage of immunosuppressive agents may result in severe side effects such as hypertension and hepatic and/or renal toxicity. Moreover, prolonged usage of immunosuppressants often leads to severe infection and increased susceptibility to malignant tumors, thus critically affecting the health of recipients[1-5]. It is therefore imperative to assess, as an alternative to immunosuppressants, the protective effect of induced immune tolerance on organ transplantation. The ideal strategy is to induce a immune tolerance state or a low reactive state toward donors' grafts in the recipients, while preserving normal immunological functions for the recognition of tumor antigens and prevention of infection. Thus immunosuppressive agents can be avoided or used at a dramatically reduced dosage. The key steps toward a successful transplantation therefore include either attenuated immune reactions or induced immune tolerance to grafts[6-10].

Small bowel transplantation is an ideal method to treat short bowel syndrome and other end stage small bowel dysfunctions, and thus can free the patients from total parenteral nutrition, returning to normal life pattern[11,12]. But because of the rich lymphatic tissue in small bowel and its mesentery, the mesenteric lymph nodes and lymphatic plexus are transplanted along with small bowel transplantation. So small bowel transplantation has more severe immune rejection compared with other organ transplantation, which is the main cause leading to failure of small bowel transplantation[13-16]. The liver is an immunologically privileged organ, and after liver transplantation, the incidence rate and degree of rejection are much lower than other solid organ transplantations. Liver transplantation can also induce tolerance in recipients to organs, such as the heart, kidneys, skin, etc, which are susceptible to be rejected[17-19]. Both in experimental study and in clinical practice of recent years, liver nonparenchymal cells (including lymphocytes, dendritic cells, Kupffer cells, *etc*) play an important role in immune tolerance induction[20-22]. In the present study, we took the advantage of liver nonparenchymal cell infusion combined with cyclosporin A (CsA) on rat small bowel transplantation. Some parameters were tested in order to confirm the anti-rejection effect of liver nonparenchymal cell infusion combined with CsA.

MATERIALS AND METHODS

Animals

Male FK344/N rats weighing 230-260 g as donors and male Wistar rats weighing 200-240 g as recipients were obtained from the Laboratory Animal Center of Beijing Medical University, and fed with standard rat chow.

Preparation of rat liver nonparenchymal cells from donor liver

Rats were anaesthetized with intraperitoneal pentobarbital and the abdomens were shaved and cleansed with betadine solution. The peritoneal cavity was widely exposed, with the inferior vena cava cannulated, the portal vein divided, and the suprahepatic vena cava ligated. The liver was perfused at a rate of 3-4 ml/min at 37 ℃ *in situ* with a Hank' s calcium-free solution for 5 min followed by perfusion with a 0.05 % collagenase (Sigma, type V) solution for 15 min. Hepatic

attachments were divided and the liver was transferred to a Petri dish, where the liver substance was gently minced and filtered (100 μm) to remove large aggregates, followed by incubation for 45 min in 50 ml of Hank's containing 0.05 % collagenase at 37 ℃ with continuous stirring. 0.5 mg DNAase in 1.0 ml of PBS was added 20 and 40 min after this incubation period. The cell suspension was filtered (40 μm) and nonparenchymal cells were separated by discontinuous density gradients of Percoll (Pharmacia Biotech) at 1.044 g/ml and 1.07 g/ml. The final cell suspension was prepared in PBS/15 % FCS at a concentration of 5×10^8/ml. Cell viability counting (usually greater than 95 %) was done using trypan blue exclusion test, the cell suspension was used for infusion within 4 hours of preparation[23,24].

Rat small bowel transplantation

Donor rats were fasted for 24 hours. All procedures were performed under inhalation anesthesia with ether. The entire small bowel from the ligament of Treitz to the ileocecal valve was isolated with the superior mesenteric artery on a segment of aorta and portal vein. After donor systemic heparinization (300 U), the graft was perfused with 20 ml of cold lactated Ringer's solution via the aorta. The lumen was also washed in 20 ml of the same solution. In the recipient, end-to-side vascular anastomoses were performed between the graft aorta and recipient infrarenal aorta and between the graft portal vein and recipient inferior vena cava with 10-0 sutures using the standard microsurgical technique. Superior extremity of transplanted small bowel was ligated and distal small bowel stoma was performed on left abdominal wall. Animals that died within 3 days were considered as technical failures and excluded from data collection[25-28].

Experimental groups and postoperative care

The rats were divided into the following four groups. Group 1: homogenic transplantation group (F344/N→F344/N), Group 2: allotransplantation group (F344/N→Wistar), Group 3: allotransplantation group +CsA group (F344/N→Wistar), in which recipient rats received CsA 10 $mg\cdot kg^{-1}\cdot d^{-1}$ after transplantation, Group 4: allotransplantation +CsA+ nonparenchymal cells infusion group (F344/N→Wistar), in which nonparenchymal cell infusion was performed 20 days prior to transplantation, and CsA applied after transplantation. Animals were fasted with access to water on the day of surgery, fed with only sugar water (7 g/day) on day 1, and rat chow and water on day 2 and thereafter. The rats' psyche status, appetite and ejection liquid of small bowel stoma were observed.

Graft histology

Rats' small bowel allografts were excised from stoma or by laparotomy and fixed in 10 % formalin. The fixed tissue was paraffin embedded, and tissue sections were stained with hematoxylin and eosin (H-E). Rejection was evaluated according to the following scoring system: grade 0, intact mucosa with complete villi; grade 1, mucosa with shortened villi and initial cellular infiltration; grade 2, mucosa with incomplete and damaged villi or complete loss of villi, usually with cryptitis and lymphocyte infiltration; grade 3, no mucosa with extensive necrosis and fibrosis[29-31].

Detection of interleukin-2 (IL-2)

The serum samples were collected on days 3, 5, and 7 after transplantation. Serum concentration of IL-2 was measured with ELISA kits (Beijing East Asia Immunological Technique Institute).

Graft survival

All recipients were followed by visual inspection, and submitted to autopsy as soon as they died. Graft survival time was defined as death of recipient due to acute rejection.

Statistics

All the data were analyzed by Student's *t* test and expressed as mean ± SD. The statistical difference $P<0.05$ was considered significant and $P<0.01$ as very significant.

RESULTS

Gross observation

The rats awaked soon after operation, then reactivated. In homogenic transplantation group (group 1), the psyche of rats was good with normal diet and activity. Mucosa of abdominal wall stoma was ruddy, and secretion was mucous. Exploratory laparotomy showed that intestinal graft was rubicund, mesentery blood vessel pulsated obviously, and the intestinal adhesion was seldom. In allotransplantation group (Group 2), the rats presented various degrees of lethargy, anorexia hair disorder, unresponsive to outside stimulation and body weight loss, until died. Exploratory laparotomy showed that intestinal graft was hoar, intestinal luminal amplificated with massive adhesion and gradually aggravated, accompanying mass purulent discharge, intestinal perforation occurred in some severe cases. In allotransplantation +CsA group (Group 3), the rats were vigorous, sensitive to outside stimulation, and low-grade adhesion occurred 7 days after transplantation. In allotransplantation +CsA+ nonparenchymal cell infusion group (Group 4), the manifestations were similar to those in Group 1.

Histopathologic examination

In group 1, the rats represented rejection of grade 0, with no rejection pathological finding but a few of lymphocytic infiltration in stroma. In group 2, rejection of grade 1 was found 3 days after transplantation, rejection of grade 2 was found 5 days after transplantation, and rejection of grade 3 was found 7 days after transplantation. In group 3, rejection of grade1was found 5 or 7 days after transplantation. In group 4, histopathologic examination showed similar results as in group 1.

Detection of IL-2

Expression level of IL-2 was low in group1, and increased in group2 on days 5 and 7 after transplantation. IL-2 level in group3 was mildly increased, but was lower than that in group 2 on days 3, 5 and 7 after transplantation. IL-2 level in group 4 was significantly lower than those in group 2 and group 3 ($P<0.01$), and was slightly increased on days 5 and 7 after transplantation.

Table 1 IL-2 level after small bowel transplantation in rats ($\bar{x}\pm s$, ng / ml)

Group	IL-2 level		
	3 d	5 d	7 d
Group 1	1.46±0.02	1.73±0.01	1.61±0.05
Group 2	2.44±0.07	5.15±0.31	5.83±0.52
Group 3	1.72±0.11	2.17±0.09	2.43±0.06
Group 4[b]	1.62±0.08	1.81±0.05	2.06±0.13

[b]$P<0.01$ *vs* group 2 and group 3

Survival time after transplantation

The survival time after small bowel transplantation was 7.14±0.33 d in group 2, 16.32±0.41 d in group 3, 31.41±0.74 d in group 4 which was significantly longer than that in other groups ($P<0.01$).

DISCUSSION

Small bowel transplantation is the ultimate therapy for patients with short-bowel syndrome or end stage intestinal function failure. But the small bowel is the maximal immunological organ in human body, the mesenteric lymph nodes and lymphatic plexus are transplanted along with the small bowel transplantation, thus the rejection of small bowel transplantation is much more fiercer than that of other organ transplantations. The failure of small bowel transplantation was more often due to severe rejection[32-34]. So rejection induced by small bowel transplantation necessitates the use of large potent immunosuppressive drugs. It should be noted, however, that excess dosage of immunosuppressive agents may result in severe side effects such as hypertension and hepatic and/or renal toxicity. Moreover, prolonged usage of immunosuppressants often leads to severe infection and increased susceptibility to malignancy, thus critically affecting the health of recipients. The ideal strategy is to induce a low responsiveness or irresponsiveness in recipients toward grafts from donors, while preserving normal immunological functions for the recognition of tumor antigens and prevention of infection. Thus immunosuppressive agents can be avoided or used at a dramatically reduced dosage. The key steps toward successful transplantation therefore should include either attenuated immune reactions or induced immune tolerance to grafts[35-38].

The liver is an immunologically privileged organ, the rejection incidence rate and degree of liver transplantation are much lower than other solid organs. Liver transplantation can also induce tolerance of other organ transplantations, such as the heart, kidneys, skin, *etc*. Experimental and clinical researches also showed that liver combined with small bowel transplantation could alleviate the rejection of small bowel transplantation. Investigations in recent years showed that liver nonparenchymal cells (including lymphocytes, dendritic cells, Kupffer cells, *etc*.) played an important role in inducing tolerance. Donor rat' s intrahepatic leucocytes were eliminated by rays before transplantation, acute rejection would happen after liver transplantation, and the recipients' survival time was shortened. Yet after intrahepatic leucocyte infusion to recipients with rays treated donor liver, the recipients' survival time was obviously prolonged[39-41]. So in our experiment, liver nonparenchymal cell transfusion combined with ciclosporin A was used to suppress the rejection of rat small bowel transplantation. It was observed that the rejection was effectively suppressed, indicating the feasibility of tolerance induction by this method. Compared with small bowel associated with liver transplantation, the method of donor liver nonparenchymal cell transfusion has the advantage of less demanding on manipulation and technique requirements. Its postoperative complications are relative less, yet the suppressive effect on rejection of small bowel transplantation is good. So the donor liver nonparenchymal cell transfusion is a simple and practical method, which has the prospect of becoming a new way to suppress rejection of small bowel transplantation in clinical practice. Further work is needed to reveal if chimerism is induced by liver nonparenchymal cells transfusion, and its possible influence on the immune system of graft recipients such as graft versus host reaction.

REFERENCES

1 **Yoo SJ**, Kahan BD. Combination treatment with sirolimus and ciclosporin in clinical renal transplantation: A comprehensive review. *Drugs Today* 2001; **37**: 385-400

2 **Qian YB**, Cheng GH, Huang JF. Multivariate regression analysis on early mortality after orthotopic liver transplantation. *World J Gastroenterol* 2002; **8**: 128-130

3 **Bramhall SR**, Minford E, Gunson B, Buckels JA. Liver transplantation in the UK. *World J Gastroenterol* 2001; **7**: 602-611

4 **Szabo A**, Muller V. Causes of late renal transplant dysfunction. *Orv Hetil* 2002; **143**: 2811-2819

5 **Becker BN**, Hullett DA, O'Herrin JK, Malin G, Sollinger HW, DeLuca H. Vitamin D as immunomodulatory therapy for kidney transplantation. *Transplantation* 2002; **74**: 1204-1206

6 **Yang YL**, Dou KF, Li KZ. Influence of intrauterine injection of rat fetal hepatocytes on rejection of rat liver transplantation. *World J Gastroenterol* 2003; **9**: 137-140

7 **Guo R**, Zou P, Fan HH, Gao F, Shang QX, Cao YL, Lu HZ. Repression of allo-cell transplant rejection through CIITA ribonuclease P(+) hepatocyte. *World J Gastroenterol* 2003; **9**: 1077-1081

8 **Zhang AB**, Zheng SS, Jia CK, Wang Y. Effect of 1,25-dihydroxyvitamin D3 on preventing allograft from acute rejection following rat orthotoic liver transplantation. *World J Gastroenterol* 2003; **9**: 1067-1071

9 **Jia CK**, Zheng SS, Li QY, Zhang AB. Immunotolerance of liver allotransplantation induced by intrathymic inoculation of donor soluble liver specific antigen. *World J Gastroenterol* 2003; **9**: 759-764

10 **Ding J**, Guo CC, Li CN, Sun AH, Guo XG, Miao JY, Pan BR. Postoperative endoscopic surveillance of human living-donor small bowel transplantations. *World J Gastroenterol* 2003; **9**: 595-598

11 **Platell CF**, Coster J, McCauley RD, Hall JC. The management of patients with the short bowel syndrome. *World J Gastroenterol* 2002; **8**: 13-20

12 **Westergaard H**. Short bowel syndrome. *Semin Gastrointest Dis* 2002; **13**: 210-220

13 **Nishida S**, Levi D, Kato T, Nery JR, Mittal N, Hadjis N, Madariaga J, Tzakis AG. Ninety-five cases of intestinal transplantation at the University of Miami. *J Gastrointest Surg* 2002; **6**: 233-239

14 **Kato T**, Ruiz P, Thompson JF, Eskind LB, Weppler D, Khan FA, Pinna AD, Nery JR, Tzakis AG. Intestinal and multivisceral transplantation. *World J Surg* 2002; **26**: 226-237

15 **Cicalese L**, Rastellini C, Sileri P, Abcarian H, Benedetti E. Segmental living related small bowel transplantation in adults. *J Gastrointest Surg* 2001; **5**: 168-172

16 **Reyes J**. Intestinal transplantation for children with short bowel syndrome. *Semin Pediatr Surg* 2001; **10**: 99-104

17 **Dresske B**, Lin X, Huang DS, Zhou X, Fandrich F. Spontaneous tolerance: experience with the rat liver transplant model. *Hum Immunol* 2002; **63**: 853-861

18 **Knolle PA**, Gerken G. Local control of the immune response in the liver. *Immunol Rev* 2000; **174**: 21-34

19 **Bishop GA**, Wang C, Sharland AF, McCaughan G. Spontaneous acceptance of liver transplants in rodents: evidence that liver leucocytes induce recipient T-cell death by neglect. *Immunol Cell Biol* 2002; **80**: 93-100

20 **Kreisel D**, Petrowsky H, Krasinskas AM, Krupnick AS, Szeto WY, McLean AD, Popma SH, Gelman AE, Traum MK, Furth EE, Moore JS, Rosengard BR. The role of passenger leukocyte genotype in rejection and acceptance of rat liver allografts. *Transplantation* 2002; **73**: 1501-1507

21 **Morelli AE**, O'Connell PJ, Khanna A, Logar AJ, Lu L, Thomson AW. Preferential induction of Th1 responses by functionally mature hepatic (CD8alpha- and CD8alpha+) dendritic cells: association with conversion from liver transplant tolerance to acute rejection. *Transplantation* 2000; **69**: 2647-2657

22 **Meyer D**, Loffeler S, Otto C, Czub S, Gassel HJ, Timmermann W, Thiede A, Ulrichs K. Donor-derived alloantigen-presenting cells persist in the liver allograft during tolerance induction. *Transpl Int* 2000; **13**: 12-20

23 **Vrochides D**, Papanikolaou V, Pertoft H, Antoniades AA, Heldin P. Biosynthesis and degradation of hyaluronan by nonparenchymal liver cells during liver regeneration. *Hepatology* 1996; **23**: 1650-1655

24 **Fiegel HC**, Park JJ, Lioznov MV, Martin A, Jaeschke-Melli S, Kaufmann PM, Fehse B, Zander AR, Kluth D. Characterization of cell types during rat liver development. *Hepatology* 2003; **37**: 148-154

25 **Nakao A**, Tahara K, Inoue S, Tanaka N, Kobayashi E. Experimental models of small intestinal transplantation in rats: orthotopic versus heterotopic model. *Acta Med Okayama* 2002; **56**: 69-74

26 **Motohashi H**, Masuda S, Katsura T, Saito H, Sakamoto S, Uemoto S, Tanaka K, Inui KI. Expression of peptide transporter following intestinal transplantation in the rat. *J Surg Res* 2001; **99**: 294-300

27 **Wu XT**, Li JS, Zhao XF, Zhuang W, Feng XL. Modified techniques of heterotopic total small intestinal transplantation in rats. *World J Gastroenterol* 2002; **8**: 758-762
28 **Nakao A**, Kobayashi E, Shen SD, Yoshino T, Tanaka N. Impact of tacrolimus and bone marrow augmentation on intestinal allograft survival and intragraft cytokine expression in rats. *J Med* 2001; **32**: 207-230
29 **Timmermann W**, Hoppe H, Otto C, Gasser M, Vowinkel T, Gassel AM, Meyer D, Gassel HJ, Ulrichs K, Thiede A. Videomicroscopic imaging of graft mucosa for monitoring immunosuppressive therapy after small intestinal transplantation in rats. *Transplantation* 1999; **67**: 1555-1561
30 **Hoppe H**, Gasser M, Gassel AM, Vowinkel T, Timmermann W, Otto C, Tykal K, Thiede A. Noninvasive videomicroscopic monitoring of rat small-bowel rejection. *Microsurgery* 1999; **19**: 89-94
31 **Furukawa T**, Kimura O, Go S, Iwai N. Small bowel allografts maintained by administration of Bombesin while under immunosuppression. *J Pediatr Surg* 2003; **38**: 83-87
32 **Veenendaal RA**, Ringers J, Baranski A, van Hoek B, Lamers CB. Clinical aspects of small-bowel transplantation. *Scand J Gastroenterol Suppl* 2000; **232**: 65-68
33 **Gilroy R**, Sudan D. Liver and small bowel transplantation: therapeutic alternatives for the treatment of liver disease and intestinal failure. *Semin Liver Dis* 2000; **20**: 437-450
34 **Goulet O**, Lacaille F, Jan D, Ricour C. Intestinal transplantation: indications, results and strategy. *Curr Opin Clin Nutr Metab Care* 2000; **3**: 329-338
35 **Xu MQ**, Yao ZX. Functional changes of dendritic cells derived from allogeneic partial liver graft undergoing acute rejection in rats. *World J Gastroenterol* 2003; **9**: 141-147
36 **Bagley J**, Iacomini J. Gene Therapy Progress and Prospects: Gene therapy in organ transplantation. *Gene Ther* 2003; **10**: 605-611
37 **Ohdan H**, Sykes M. B cell tolerance to xenoantigens. *Xenotransplantation* 2003; **10**: 98-106
38 **Diao TJ**, Yuan TY, Li YL. Immunologic role of nitric oxide in acute rejection of golden hamster to rat liver xenotransplantation. *World J Gastroenterol* 2002; **8**: 746-751
39 **Meyer D**, Otto C, Rummel C, Gassel HJ, Timmermann W, Ulrichs K, Thiede A. "Tolerogenic effect" of the liver for a small bowel allograft. *Transpl Int* 2000; **13**(Suppl): S123-126
40 **Meyer D**, Thorwarth WM, Otto C, Gassel HJ, Timmermann W, Ulrichs K, Thiede A. Orthotopic liver / small bowel transplantation in rats: a microsurgical model inducing tolerance. *Microsurgery* 2001; **21**: 156-162
41 **Otto C**, Kauczok J, Martens N, Steger U, Moller I, Meyer D, Timmermann W, Ulrichs K, Gassel HJ. Mechanisms of tolerance induction after rat liver transplantation: intrahepatic CD4(+) T cells produce different cytokines. *J Gastrointest Surg* 2002; **6**: 455-463

Edited by Zhang JZ and Wang XL

P.O.Box 2345, Beijing 100023,China
Fax: +86-10-85381893
E-mail: wjg@wjgnet.com www.wjgnet.com

World J Gastroenterol 2003;9(12):2863-2865
World Journal of Gastroenterology
 ISSN 1007-9327

• BRIEF REPORTS •

Expression of PCNA and CD44mRNA in colorectal cancer with venous invasion and its relationship to liver metastasis

Shu-Qiang Yue, Yan-Ling Yang, Ke-Feng Dou, Kai-Zong Li

Shu-Qiang Yue, Yan-Ling Yang, Ke-Feng Dou, Kai-Zong Li, Department of Hepatobiliary Surgery, Xijing Hospital, Fourth Military Medical University, Xi' an 710032, Shaanxi Province, China
Correspondence to: Kai-Zong Li, Department of Hepatobiliary Surgery, Xijing Hospital, Fourth Military Medical University, 710032 Xi' an, Shaanxi Province, China. gdwk@fmmu.edu.cn
Telephone: +86-29-3375259 **Fax:** +86-29-3375561
Received: 2003-05-13 **Accepted:** 2003-06-02

Abstract

AIM: To investigate the expression of proliferating cell nuclear antigen (PCNA) and CD44mRNA in colorectal cancer with venous invasion and its relationship with liver metastasis.

METHODS: Reverse transcriptase-polymerase chain reaction (RT-PCR) was used to detect the expression of PCNA and CD44mRNA in 31 cases of colorectal cancer with venous invasion.

RESULTS: Positive expression rates of PCNA and CD44mRNA in colorectal cancer were higher than those without liver metastasis ($P<0.05$ and $P<0.01$). In case of colorectal cancer with liver metastasis, strongly positive rates of PCNA and CD44mRNA were 94.1 % and 70.6 %, respectively, significantly higher than those without liver metastasis. There was a positive relationship between the expressions of PCNA and CD44mRNA ($r=0.67$, $P<0.05$).

CONCLUSION: Detection of PCNA and CD44mRNA expression in colorectal cancer may be useful for evaluating liver metastasis of cancer cells.

Yue SQ, Yang YL, Dou KF, Li KZ. Expression of PCNA and CD44mRNA in colorectal cancer with venous invasion and its relationship to liver metastasis. *World J Gastroenterol* 2003; 9 (12): 2863-2865
http://www.wjgnet.com/1007-9327/9/2863.asp

INTRODUCTION

Many mechanisms are involved in liver metastasis of colorectal cancer, of which venous invasion is considered to be the chief process[1-6]. Previous studies showed that the degree of venous invasion was positively related to the rate of liver metastasis. But it is unknown which factors participate in liver metastasis of colorectal cancer. PCNA is a chief marker reflecting the activity of cell proliferation, which is closely related to invasion and metastasis of malignant neoplasms and their prognosis[7-10]. Cell adhesion molecules (CAMs) correlate to the invasion and metastasis of tumor cells, and play an important role in occurrence, development and metastasis of neoplasms[11,12]. The goal of this study was to test the expression of PCNA and adhesion molecule CD44mRNA in colorectal cancer with venous invasion by RT-PCR and its relationships with liver metastasis.

MATERIALS AND METHODS

Materials

According to the pathological diagnosis standards, the severity of venous invasion was classified as V0- V3[13]. Thirty-one patients with severe venous invasion of colorectal cancer in V3 stage were chosen as study subjects (male 20, female 11), aged 44-82 years (average 66 years), of them 17 cases had liver metastasis. After operations, neoplasm samples were kept in liquid nitrogen. RNA extract reagent was purchased from Gibco Co., Taq enzyme from Takara Co., PCNA, CD44mRNA and β-actin primer were synthesized by BoYa Shanghai Co.. PCNA' s sequence of up-stream primer was 5' -GCCGAGATC-TCAGCCATATT-3' , that of down-stream primer was 5' -ATGTACTTAGAGGTACAAAT -3' . CD44' s sequence of up-stream primer was 5' -CTTCATCCCAGTGACC-3' , that of down-stream primer was 5' -TGCCACTGTTGATCAC-3' . β-actin' s sequence of up-stream primer was 5' -CACCATGTA-CCCTGGCATTG-3' , that of down-stream primer was 5' -TAACGCAACTAAGTCATAGT-3' . The size of anticipatively amplified products was 452 bp, 446 bp and 243 bp, respectively.

Methods

Using TRIzol reagent kit, total RNA was extracted according to the method previously described[14-20]. The purity and content of RNA were measured by a spectrophotometer, and kept at -80 ℃. Total RNA 5 μg, 5×reaction buffer 10 μl, 10 mmol· L^{-1} dNTPs 5 μl, RNasin 20 U, oligo$(dT)_{12-18}$ 0.25 μg, reverse transcriptase (M-MLV, Gibco) 200 U and 0.1 mol· L^{-1} DTT 0.5 μl were added to reaction volume of 50 μl, incubated at 37 ℃ for 1 h, then heated at 65 ℃ for 5 min to stop reaction. cDNA 0.1 μg, 10×PCR buffer 2.5 μl, 2 mmol· L^{-1} dNTPs 2.5 μl, 25 mmol· L^{-1} $MgCl_2$ 2.5 μl, PCR primer 20 pmol and Taq DNA polymerase (Takara) 5 U were added to reaction volume of 25 μl. Using PTC-100 equipment (MJ Research), PCR conditions were as follows: pre-denaturing at 93 ℃ for 1 min, then 35 cycles at 93 ℃ for 30 s, at 52 ℃ for 30 s and 72 ℃ for 1 min, followed by extension at 72 ℃ for 8 min. Each amplified product of 10 μl was detected via 3 g· L^{-1} sepharose electrophoresis, bromide staining, and analyzed by using a UVP gel imaging system and Labworks software. The ratio of density of positive PCNA and CD44 to that of β-actin was considered to be PCNA and CD44 relative expression quantity[21-28]. Expression intesity was classified into 3 grades: +: 1-30 % β-actin density, ++: 31-65 %, +++: 66-100 %.

Statistics

All the data were analyzed by χ^2-test, and a value of $P<0.05$ was considered significant and $P<0.01$ very significant.

RESULTS

Expression of PCNA and CD44mRNA in colorectal cancer tissue

PCNA, CD44 and β-actin gene expressions were detected in colorectal cancer tissues by RT-PCR, the size of amplified fragment was coincident with that of anticipation (Figure 1). All cases had expression of PCNA, the positive rate was 100 %,

but the expression levels were different among different cases (Figure 1A). Twenty cases had positive expression of CD44 mRNA, the positive rate was 64.5 %. The expression levels were different among different cases. As an inter-control, the expression level of β-actin was basically coincident among different cases (Figure 1C).

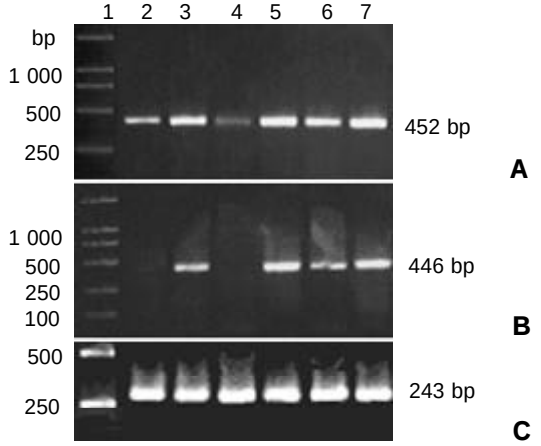

Figure 1 Expression of PCNA (A), CD44 (B) and β-actin (C) in colorectal cancer by PCR amplification. 1: DL2000 DNA marker (Takara), 2-7: Colorectal cancer tissues at various venous invasion stages.

Relationship between expression of PCNA and CD44mRNA and liver metastasis

In 17 cases of liver metastasis, 16 cases had strongly positive expression of PCNA mRNA (++, +++) (94.1 %), significantly higher than those without liver metastasis (28.6 %, $P<0.01$). There was a positive relationship between the expression of PCNA and colorectal cancer with liver metastasis ($r=0.82$, $P<0.01$). In 17 cases of liver metastasis, 12 cases had strongly positive expression of CD44mRNA (70.6 %), significantly higher than those without liver metastasis (21.4 %, $P<0.01$). There was a positive relationship between the expression of CD44mRNA and colorectal cancer with liver metastasis ($r=0.82$, $P<0.01$).

Relationship between expressions of PCNA and CD44mRNA in colorectal cancer

Of the 16 cases with strongly positive expression of CD44mRNA, 12 cases had strongly positive expression of PCNA (75.0 %). Of the 15 cases with weak or negative expression of CD44mRNA, 7 cases had strongly positive expression of PCNA (46.7 %), and there was a significant difference ($P<0.05$). There was a positive relationship between the expressions of PCNA and CD44mRNA ($r=0.67$, $P<0.05$).

DISCUSSION

Venous invasion of cancer cells was the first step of neoplasm' s liver metastasis[29]. However, in clinical cases, venous invasion by histological detection was not definitely related to liver metastasis. It implies that, besides venous invasion, other factors might also participate in the process of liver metastasis[30-32].

PCNA is a kind of non-histone nuclear polypeptide with 36 000 molecular weight, as an assistant protein to DNA polymerase, its content could reflect the degree of cell proliferation[33-37]. Previous studies showed that there was a significant relationship between PCNA labelling and degree of malignancy, vessel invasion, distant metastasis and prognosis[38-42]. In this study, we found that under the condition of venous invasion, the strong expression rate of PCNA mRNA in venous invasion of colorectal cancer with liver metastasis, was significantly higher than that without liver metastasis. This showed that there was a positive relationship between the strong expression of PCNA and colorectal cancer with liver metastasis. All these indicate that colorectal cancer cells with higher proliferating activity are much more easier to proceed liver metastasis.

CD44 is a kind of cell adhesion molecules. Under normal conditions, CD44 acts as the receptor of hyaluronic acid, and chiefly participates in infra-cells and cell-stroma specific adhesion[43-46]. Recent studies showed that CD44 could be expressed in different neoplasm tissues. Bhatavdekar *et al* found that over-expression of CD44 was associated with clinical staging of colorectal cancer. Furthermore, positive expression of CD44 is an important prognostic factor associated with colorectal cancer patients' relapse and total survival time. Further studies found that CD44 could make cancer cells be able to metastasize, adhere to vessel endothelium, accelerate cancer metastasis. We found that the strong expression rate of CD44 mRNA in colorectal cancer with liver metastasis was significantly higher than that without liver metastasis, further suggesting that CD44 might play an important role in colorectal cancer with liver metastasis. But it is still in argument whether CD44 can be taken as an independent marker for progress and metastasis of colorectal cancer.

We also found that under the condition of venous invasion in colorectal cancer patients with liver metastasis, the expression of PCNA and CD44mRNA was strong at the same time. All these indicate that there is a positive relationship between colorectal cancer with liver metastasis and expression of PCNA and CD44mRNA ($r=0.82$, $P<0.01$). Moreover, in colorectal cancer tissue with strong expression of CD44mRNA, PCNA mRNA was significantly higher than that with weak or negative expression, showing that there was a positive relationship between the expressions of CD44 and PCNA ($r=0.67$, $P<0.05$). Taken together, we conclude that detection of PCNA and CD44 expression in colorectal cancer may be useful for evaluating liver metastasis of cancer cells.

REFERENCES

1 **Gu J,** Ma ZL, Li Y, Li M, Xu GW. Angiography for diagnosis and treatment of colorectal cancer. *World J Gastroenterol* 2003; **9**: 288-290
2 **Liu LX**, Zhang WH, Jiang HC. Current treatment for liver metastases from colorectal cancer. *World J Gastroenterol* 2003; **9**: 193-200
3 **Cui JH**, Krueger U, Henne-Bruns D, Kremer B, Kalthoff H. Orthotopic transplantation model of human gastrointestinal cancer and detection of micrometastases. *World J Gastroenterol* 2001; **7**: 381-386
4 **Minagawa N**, Nakayama Y, Hirata K, Onitsuka K, Inoue Y, Nagata N, Itoh, H. Correlation of plasma level and immunohistochemical expression of vascular endothelial growth factor in patients with advanced colorectal cancer. *Anticancer Res* 2002; **22**: 2957-2963
5 **Berglund A**, Edler D, Molin D, Nordlinder H, Graf W, Glimelius B. Thymidylate synthase and p53 expression in primary tumor do not predict chemotherapy outcome in metastatic colorectal carcinoma. *Anticancer Res* 2002; **22**: 3653-3659
6 **Takashima T**, Onoda N, Ishikawa T, Ogawa Y, Kato Y, Fujimoto Y, Sowa M, Hirakawa-Y S Chung K. Proliferating cell nuclear antigen labeling index and p53 expression predict outcome for breast cancer patients with four or more lymph node metastases. *Int J Mol Med* 2001; **8**: 159-163
7 **Shen LJ**, Zhang HX, Zhang ZJ, Li JY, Chen MQ, Yang WB, Huang R. Detection of HBV, PCNA and GST-pi in hepatocellular carcinoma and chronic liver diseases. *World J Gastroenterol* 2003; **9**: 459-462
8 **Terada R**, Yasutake T, Nakamura S, Hisamatsu T, Nakagoe T, Ayabe H, Tagawa Y. Evaluation of metastatic potential of gastric tumors by staining for proliferating cell nuclear antigen and chromosome 17 numerical aberrations. *Ann Surg Oncol* 2001; **8**: 525-532

9 **Huang ZH,** Fan YF, Xia H, Feng HM, Tang FX. Effects of TNP-470 on proliferation and apoptosis in human colon cancer xenografts in nude mice. *World J Gastroenterol* 2003; **9**: 281-283

10 **Chen H**, Wang LD, Guo M, Gao SG, Guo HQ, Fan ZM, Li JL. Alterations of p53 and PCNA in cancer and adjacent tissues from concurrent carcinomas of the esophagus and gastric cardia in the same patient in Linzhou, a high incidence area for esophageal cancer in northern China. *World J Gastroenterol* 2003; **9**: 16-21

11 **Satyamoorthy K**, Herlyn M. Cellular and molecular biology of human melanoma. *Cancer Biol Ther* 2002; **1**: 14-17

12 **Gdor Y**, Timme TL, Miles BJ, Kadmon D, Thompson TC.Gene therapy for prostate cancer. *Expert Rev Anticancer Ther* 2002; **2**: 309-321

13 **Shirouzu K**, Isomoto H, Kakegawa T, Morimatsu M. A prospective clinicopathologic study of venous invasion in colorectal cancer. *Am J Surg* 1991; **162**: 216-222

14 **Zhang DL**, Li JS, Jiang ZW, Yu BJ, Tang XM, Zheng HM.Association of two polymorphisms of tumor necrosis factor gene with acute biliary pancreatitis. *World J Gastroenterol* 2003; **9**: 824-828

15 **Yang XL**, Zhang YL, Lai ZS, Xing FY, Liu YH. Pleckstrin homology domain of G protein-coupled receptor kinase-2 binds to PKC and affects the activity of PKC kinase. *World J Gastroenterol* 2003; **9**: 800-803

16 **Wen CY**, Ito M, Wang H, Chen LD, Xu ZM, Matsuu M, Shichijo K, Nakayama T, Nakashima M, Sekine I. IL-11 up-regulates Tie-2 expression during the healing of gastric ulcers in rats. *World J Gastroenterol* 2003; **9**: 788-790

17 **Wang HT**, Chen S, Wang J, Ou QJ, Liu C, Zheng SS, Deng MH, Liu XP. Expression of growth hormone receptor and its mRNA in hepatic cirrhosis. *World J Gastroenterol* 2003; **9**: 765-770

18 **Jeon MJ**, Shin JH, Suh SP, Lim YC, Ryang DW. TT virus and hepatitis G virus infections in Korean blood donors and patients with chronic liver disease. *World J Gastroenterol* 2003; **9**: 741-744

19 **Baptista M**, Kramvis A, Jammeh S, Naicker J, Galpin JS, Kew MC. Follow up of infection of chacma baboons with inoculum containing a and non-a genotypes of hepatitis B virus. *World J Gastroenterol* 2003; **9**: 731-735

20 **Fang J**, Jin HB, Song JD. Construction, expression and tumor targeting of a single-chain Fv against human colorectal carcinoma. *World J Gastroenterol* 2003; **9**: 726-730

21 **Hu HY,** Liu XX, Jiang CY, Zhang Y, Bian JF, Lu Y, Geng Z, Liu SL, Liu CH, Wang XM, Wang W. Cloning and expression of ornithine decarboxylase gene from human colorectal carcinoma. *World J Gastroenterol* 2003; **9**: 714-716

22 **Huang XH**, Sun LH, Lu DD, Sun Y, Ma LJ, Zhang XR, Huang J, Yu L. Codon 249 mutation in exon 7 of p53 gene in plasma DNA: maybe a new early diagnostic marker of hepatocellular carcinoma in Qidong risk area, China. *World J Gastroenterol* 2003; **9**: 692-695

23 **Ikeda O**, Egami H, Ishiko T, Ishikawa S, Kamohara H, Hidaka H, Mita S, Ogawa M. Expression of proteinase-activated receptor-2 in human pancreatic cancer: A possible relation to cancer invasion and induction of fibrosis. *Int J Oncol* 2003; **22**: 295-300

24 **Zhan J**, Tang XD. Expression of cyclooxygenase-2 in human transitional cell bladder carcinomas. *Ai Zheng* 2002; **21**: 1212-1216

25 **Tan Z**, Hu X, Ying K, Li Y, Tang R, Cao G, Tang Y, Jin G. cDNA microarray in the gene expression pattern in lymphatic metastasis of pancreatic carcinoma. *Zhonghua Zhongliu Zazhi* 2002; **24**: 243-246

26 **Diamond MP,** El-Hammady E, Wang R, Saed G. Metabolic regulation of collagen I in fibroblasts isolated from normal peritoneum and adhesions by dichloroacetic acid. *Am J Obstet Gynecol* 2002; **187:** 1456-1460

27 **Murphy N**, Ring M, Killalea AG, Uhlmann V, O'Donovan M, Mulcahy F, Turner M, McGuinness E, Griffin M, Martin C, Sheils O, O'Leary JJ. p16INK4A as a marker for cervical dyskaryosis: CIN and cGIN in cervical biopsies and ThinPrep smears. *J Clin Pathol* 2003; **56**: 56-63

28 **Schneider T**, Osl F, Friess T, Stockinger H, Scheuer WV. Quantification of human Alu sequences by real-time PCR–an improved method to measure therapeutic efficacy of anti-metastatic drugs in human xenotransplants. *Clin Exp Metastasis* 2002; **19**: 571-582

29 **Hanke B**, Wein A, Martus P, Riedel C, Voelker M, Hahn EG, Schuppan D. Serum markers of matrix turnover as predictors for the evolution of colorectal cancer metastasis under chemotherapy. *Br J Cancer* 2003; **88**: 1248-1250

30 **Yamauchi T**, Watanabe M, Hasegawa H, Nishibori H, Ishii Y, Tatematsu H, Yamamoto K, Kubota T, Kitajima M.The potential for a selective cyclooxygenase-2 inhibitor in the prevention of liver metastasis in human colorectal cancer. *Anticancer Res* 2003; **23**: 245-249

31 **Brenner AS**, Thebo JS, Senagore AJ, Duepree HJ, Gramlich T, Ormsby A, Lavery IC, Fazio VW. Analysis of both NM23-h1 and NM23-H2 expression identifies "at-risk" patients with colorectal cancer. *Am Surg* 2003; **69**: 203-208

32 **Kuwai T**, Kitadai Y, Tanaka S, Onogawa S, Matsutani N, Kaio E, Ito M, Chayama K. Expression of hypoxia-inducible factor-1alpha is associated with tumor vascularization in human colorectal carcinoma. *Int J Cancer* 2003; **105**: 176-181

33 **Sano B**, Sugiyama Y, Kunieda K, Sano J, Saji S. Antitumor effects induced by the combination of TNP-470 as an angiogenesis inhibitor and lentinan as a biological response modifier in a rabbit spontaneous liver metastasis model. *Surg Today* 2002; **32**: 503-509

34 **Farre L**, Casanova I, Guerrero S, Trias M, Capella G, Mangues R. Heterotopic implantation alters the regulation of apoptosis and the cell cycle and generates a new metastatic site in a human pancreatic tumor xenograft model. *FASEB J* 2002; **16**: 975-982

35 **Martins AC**, Faria SM, Cologna AJ, Suaid HJ, Tucci S Jr. Immunoexpression of p53 protein and proliferating cell nuclear antigen in penile carcinoma. *J Urol* 2002; **167**: 89-92

36 **Kawasaki G**, Kato Y, Mizuno A. Cathepsin expression in oral squamous cell carcinoma: relationship with clinicopathologic factors. *Oral Surg Oral Med Oral Pathol Oral Radiol Endod* 2002; **93**: 446-454

37 **Dong Y,** Sui L, Watanabe Y, Sugimoto K, Tokuda M. Aberrant expression of cyclin A in laryngeal squamous cell carcinoma. *Anticancer Res* 2002; **22**: 83-89

38 **Kouvaraki M**, Gorgoulis VG, Rassidakis GZ, Liodis P, Markopoulos C, Gogas J, Kittas C. High expression levels of p27 correlate with lymph node status in a subset of advanced invasive breast carcinomas: relation to E-cadherin alterations, proliferative activity, and ploidy of the tumors. *Cancer* 2002; **94**: 2454-2465

39 **Van Poznak C**, Tan L, Panageas KS, Arroyo CD, Hudis C, Norton L, Seidman AD. Assessment of molecular markers of clinical sensitivity to single-agent taxane therapy for metastatic breast cancer. *J Clin Oncol* 2002; **20**: 2319-2326

40 **Yue H**, Na YL, Feng XL, Ma SR, Song FL, Yang B. Expression of p57(kip2), Rb protein and PCNA and their relationships with clinicopathology in human pancreatic cancer. *World J Gastroenterol* 2003; **9**: 377-380

41 **Jiang YA**, Zhang YY, Luo HS, Xing SF. Mast cell density and the context of clinicopathological parameters and expression of p185, estrogen receptor, and proliferating cell nuclear antigen in gastric carcinoma. *World J Gastroenterol* 2002; **8**: 1005-1008

42 **Takashima T**, Onoda N, Ishikawa T, Ogawa Y, Kato Y, Fujimoto Y, Sowa M, Hirakawa K. Prognostic value of combined analysis of estrogen receptor status and cellular proliferative activity in breast cancer patients with extensive lymph node metastases. *Oncol Rep* 2002; **9**: 589-594

43 **Qin LX**, Tang ZY. The prognostic molecular markers in hepatocellular carcinoma. *World J Gastroenterol* 2002; **8**: 385-392

44 **Xin Y**, Li XL, Wang YP, Zhang SM, Zheng HC, Wu DY, Zhang YC. Relationship between phenotypes of cell-function differentiation and pathobiological behavior of gastric carcinomas. *World J Gastroenterol* 2001; **7**: 53-59

45 **Neumayer R**, Rosen HR, Reiner A, Sebesta C, Schmid A, Tuchler H, Schiessel R. CD44 expression in benign and malignant colorectal polyps. *Dis Colon Rectum* 1999; **42**: 50-55

46 **Nanashima A**, Yamaguchi H, Sawai T, Yasutake T, Tsuji T, Jibiki M, Yamaguchi E, Nakagoe T, Ayabe H. Expression of adhesion molecules in hepatic metastases of colorectal carcinoma: relationship to primary tumours and prognosis after hepatic resection. *J Gastroenterol Hepatol* 1999; **14**: 1004-1009

Edited by Zhang JZ and Wang XL

P.O.Box 2345, Beijing 100023,China
Fax: +86-10-85381893
E-mail: wjg@wjgnet.com www.wjgnet.com

World J Gastroenterol 2003;9(12):2866-2869
World Journal of Gastroenterology
 ISSN 1007-9327

• BRIEF REPORTS •

Relationship between expression of CD105 and growth factors in malignant tumors of gastrointestinal tract and its significance

Jian-Xian Yu, Xiao-Tun Zhang, Yong-Qiang Liao, Qi-Yi Zhang, Hua Chen, Mei Lin, Shant Kumar

Jian-Xian Yu, Xiao-Tun Zhang, Hua Chen, Department of Pathology, Qingdao Municipal Hospital, Qingdao 266011, Shandong Province, China
Qi-Yi Zhang, Department of Internal Medicine, Qingdao Municipal Hospital, Qingdao 266011,Shandong Province, China
Mei Lin, Shant Kumar, Department of Pathology, Manchester University, Manchester, United Kingdom
Yong-Qiang Liao, Department of Pathology, Xiamen People' s Hospital, Xiamen, Fujian Province, China
Correspondence to: Dr. Jian-Xian Yu, Department of Pathology, Qingdao Municipal Hospital, No.1 Jiaozhou Lu, Qingdao 266011, Shandong Province China. yujianxian@hotmail.com
Telephone: +86-532-2827971-4345 **Fax:** +86-532-2827971-4345
Received: 2003-04-04 **Accepted:** 2003-05-21

Abstract

AIM: Angiogenesis is an important step in the growth of solid malignant tumors. A number of angiogenic factors have been found such as transforming growth factorβ1 (TGF-β1) and vascular endothelial growth factor (VEGF). However, the roles of TGFβ1 and VEGF in gastrointestinal carcinogenesis are still unclear. This study was to investigate the expressions of TGF-β1 and VEGF in gastrointestinal tract malignant tumors, as well as their association with microvessel density (MVD). At the same time, we also observed the localization of TGF-β1 and its receptor CD105 in gastric malignant tumors.

METHODS: The expressions of TGF-β1 and CD105 were detected in 55 fresh specimens of gastric carcinoma and VEGF and CD105 in 44 fresh specimens of colorectal carcinoma by immunohistochemical staining (S-ABC). TGF-β1 and CD105 in 55 gastric carcinoma tissues on the same slide were detected by using double-stain Immunohistochemistry (DS-ABC).

RESULTS: Among the 55 cases of gastric carcinoma tissues, 30 were positive for TGF-β1 (54.55 %). The MVD of TGF-β1 strong positive group (++~+++ 23.22±5.8) was significantly higher than that of weak positive group (+17.56±7.2) and negative group (- 17.46±3.9) (q=4.5, q=5.3207, respectively, P<0.01). In the areas of high expression of TGF-β1, MVD and the expression of CD105 were also high. Among the 44 cases of colonic carcinoma tissues, 26 were positive for VEGF (59.1 %). The expressions of both VEGF and CD105 (MVD) were related with the depth of invasion (F=5.438, P<0.05; F=4.168, P=0.05), lymph node metastasis (F=10.311, P<0.01; F=20.282, P<0.01) and Dukes stage (F=6.196, P<0.01; F=10.274, P<0.01), but not with histological grade (F=0.487, P>0.05). There was a significant correlation between the expression of VEGF and CD105 (MVD) (r=0.720, P<0.01).

CONCLUSION: Over-expression of TGF-β1 and VEGF acts as stimulating factors of angiogenesis in gastrointestinal tumors. CD105, as a receptor of TGF-β1, can regulate the biological effect of TGF-β1 in tumor angiogenesis. MVD marked by CD105 is more suitable for detecting newborn blood vessels.

Yu JX, Zhang XT, Liao YQ, Zhang QY, Chen H, Lin M, Kumar S. Relationship between expression of CD105 and growth factors in malignant tumors of gastrointestinal tract and its significance. *World J Gastroenterol* 2003; 9(12): 2866-2869
http://www.wjgnet.com/1007-9327/9/2866.asp

INTRODUCTION

Angiogenesis occurs in diverse physiological and pathological situations and particularly in tumour growth. The development of a new blood vessel is a complex phenomenon and the result of a sequence of events, among which the release of growth factors of interstitial cells is the most important step. At present, many growth factors have been identified including transforming growth factor (TGF)-β1 and endothelial cell growth factor (VEGF). TGF-β1 is a potent inhibitor of endothelial cells (EC) proliferation and migration *in vitro* and an angiogenesis promoter *in vivo*. It has aroused much interests in study of the relationship between TGF-β1 and angiogenesis. In this research, we used CD105, a new EC marker, to count the intratumor microvessel density (MVD), and to detect the expression of TGF-β1 in 55 gastric carcinoma tissues. Because CD105 is one of the receptors of TGF-β1, we hoped to find out the biological effect of TGF-β1 by studying the relationship between the ligand and the receptor. We also detected the expression of VEGF and CD105 (MVD) in 44 colorectal carcinoma tissues and analyzed the effect of VEGF in angiogenesis of colorectal carcinoma tissues. Furthermore we demonstrated the confidence level and superiority of CD105 in studying tumor angiogenesis.

MATERIALS AND METHODS

Patients

Two groups of patients were chosen and examined. Group A: Fifty-five specimens of freshly resected malignant gastric tissues were collected from 55 patients with gastric carcinoma (median age 57.65±5.3 years, range 29-77 years) who were operated in Qingdao Municipal Hospital and the Affiliated Hospital of Medical College, Qingdao University (Shandong, China) from October 2000 to April 2001. Four cases were well-differentiated adenocarcinoma, nine moderately-differentiated adenocarcinoma and forty-two poorly-differentiated adenocarcinoma. Among the 55 cases, 36 cases had lymph node metastasis and five cases had distant metastasis. Normal tissue samples located at least 8 cm away from the margins of cancers, and 51 normal gastric tissue samples were frozen in liquid nitrogen. Group B: Forty-four freshly resected malignant intestinal tissue samples were collected from 44 patients with intestinal carcinoma (median age 62.5±6.2 years, range 31-79 years) who were operated in Qingdao Municipal Hospital and the Affiliated Hospital of Medical College, Qingdao University from July 2001 to March 2002. The group included one case of well-differentiated adenocarcinoma, thirty-eight cases of moderately-differentiated adenocarcinoma and five cases of poorly- differentiated adenocarcinoma. Among the 44 tumor patients, 20 cases had lymph node metastasis. 20 normal

intestinal tissue samples taken at least 8 cm away from the margins of cancers were frozen in liquid nitrogen.

None of the patients in groups A and B received any chemotherapy or radiation therapy prior to surgery. Fresh tissue samples were collected within 4 hours after resection. The pathological diagnosis was made on the basis of the size, infiltrating depth, histological grade, lymph node and distant metastasis. The grading standard was in accordance with "Practical and surgical pathology"(Chen-Zhong Nian, published by ShangHai Medical University, first edition). Written informed consent was obtained from each patient.

Methods

Immunohistochemistry Biopsy specimens were snap frozen in liquid nitrogen and serial cryostat sections were cut into 7 μm thick. Paraffin-embedded sections were cut into 4 μm thick. Immunohistochemical staining (S-ABC) and immunohistochemical double staining (DS-ABC) were performed in accordance with the introduction of the kit. PBS was used as the negative controls instead of Mab.

Identification of immunohistochemical staining results TGF-β1/VEGF staining was classified into four grades. +++, most carcinoma cells were stained with a very strong intensity, and distributed in clusters. ++, a large number of carcinoma cells were stained with a moderate intensity, and distributed in clusters occasionally. +, a few carcinoma cells were stained with a slight intensity. -, no staining of carcinoma cells.

Counting of MVD in carcinoma tissues was in accordance with Weidner' s standards with a minor modification. The slide was searched for the hot spots rich in vessels, which were located in or near the area of tumor tissues under a low power microscope (100×). MVD was counted under a high power (400×) or low power (100×) microscope according to the standards that any stained endothelial cell or cells were identified as an independent vessel. These vessels must be clearly separated from each other. However, apparent vasa or vasa with red blood cells could be regarded as vessels. Five different HP vision fields were chosen on each of the slides, and the stained vessels were counted simultaneously by two doctors under a multi-ocular len microscope. The results were averaged, which was the relative value of the amount of vessels per unit area.

Statistic analysis

The relation between MVD and expression of TGF-β1 was studied with analysis of variance and Q-test. The analysis of variance and χ^2-test were used for statistical analysis of the relation between MVD and expression of VEGF.

RESULTS

Results of TGF-b1 staining in gastric carcinoma tissues

Among the 55 specimens in group A, 30 were positively stained and 25 negatively stained, with a positive rate of 54.55 %. TGF-β1 was mainly existed in cytoplasms of carcinoma cells. In the 51 specimens of normal gastric tissues, TGF-β1 was mainly expressed in gastric mucosa epithelial cells.

Results of VEGF staining in colorectal carcinoma tissues

Among the 44 cases in group B, 26 were positively stained and 18 negatively stained, with a positive rate of 59.1 %. VEGF was mainly existed in cytoplasms of colorectal carcinoma cells.

Expression of CD105 and counting of MVD in carcinoma tissues

In both group A and group B CD105 was mainly expressed in cytoplasms and plasmalemma of newborn endothelial cells in cryostat section. CD105 was weakly expressed or absent in native blood vessels with thick walls and large lumina. MVD of gastric carcinoma tissues is listed in Figure 1.

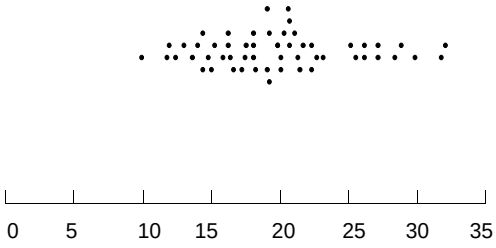

Figure 1 MVD marked by CD105 in 55 cases of gastric carcinoma tissues.

Table 1 Relations between MVD and TGF-β1 (under 400×)

Grade of TGF-β1 staining	*n*	%	MVD	*P* value
+++~++	21	38.18	23.22±5.8	<0.01[a]
+	9	16.36	17.56±7.2	>0.05[b]
-	25	45.46	17.46±3.9	<0.01[c]
Total	55	100		

[a]*P*<0.01, TGF-β1 +++ group *vs*. + group, [b]*P*>0.05, TGF-β1 + group *vs*. - group, [c]*P*<0.01, TGF-β1, group *vs*. +++ group.

Relation between TGF-b1 and MVD in gastric carcinoma tissues

When the gastric carcinoma tissues were double stained for CD105 and TGF-β1 in one cryostat section, TGF-β1 was highly

Table 2 Relations between VEGF / MVD and clinical pathological parameters in colorectal carcinoma (under 100×)

Clinical pathological parameters	Cases (*n*)	VEGF	P_x value	MVD (CD105)	*P* value
Histological grade					
Well differentiation	1	18.50		143.1	
Moderate differentiation	38	22.28±14.49	>0.05	144.8±31.9	>0.05
Poor differentiation	5	21.89±14.44		146.4±47.4	
Infiltrating depth					
Serous membrane (-)	5	9.37±4.79	<0.05	119.0±17.2	=0.05
Serous membrane (+)	39	22.55±12.32		150.0±32.7	
Lymph node metastasis					
(-)	24	14.76±9.62	<0.01	126.3±20.8	<0.01
(+)	20	27.31±12.17		167.7±30.3	
Dukes stage					
A	3	9.37±4.79	<0.01	119.0±17.2	<0.01
B	16	17.00±10.37		129.3±22.1	
C and D	25	27.31±12.16		167.7±30.3	

expressed and so was CD105 in the same area. It was also found that newborn vessels were present around carcinoma nests whereas TGF-β1 was observed mainly in cytoplasms of carcinoma cells. The relation between MVD and TGF-β1 is shown in Table 1. Analysis of variance and *Q*-test were used to analyze the difference of MVD counting among the three different TGF-β1 staining groups. It showed that MVD of TGF-β1 strong positive group was significantly higher than weak positive group and negative group, and the MVD between the two groups of TGF-β1 staining weak positive "+"and negative "-" had no significant difference.

Relation between VEGF/MVD and clinical pathological parameters in colorectal carcinoma

Analysis of variance showed the expression of VEGF was correlated with infiltrating depth (F=5.438, P<0.05), lymph node metastasis (F=10.311, P<0.01) and Duke' s staging (F=6.196, P<0.01), but had no relation with histological stage (F=0.487, P>0.05). MVD was correlated with infiltrating depth (F=4.168, P=0.05), lymph nodes metastasis (F=20.282, P<0.01) and Duke' s staging (F=10.274, P<0.01), but had no relation with histological stage (F=0.006, P>0.05), (Table 2).

DISCUSSION

Angiogenesis refers to the formation of new blood vessels from native blood vessels, which is essential for the unrestricted growth and metastasis of solid tumors[1]. Thus, highly hyperplastic microvessels are usually recognized as a marker of malignant tumor development. At present, many growth factors have been identified including TGF-β1 and VEGF. These factors could be paracrined by tumor cells[2]. However, the potential roles of these factors, especially TGF-β1, are not clearly known.

Human TGF-β is a large family consisting of 3 isomers: TGF-β1, TGF-β2 and TGF-β3. TGF-β1, the most widely studied protein of the three TGF-β isomers, derived from a 390-amino acid precursor cleaved to produce a 112-amino acid carboxy-terminal peptide, is the predominant form in humans. TGF-β1 influences the proliferation rate of many cell types, acting as a growth inhibitor in most but not all cases. In addition, TGF-β1 controls the processes of epithelial cell differentiation. In normal cells, TGF-β1 generally enhances adhesion through increased matrix production and decreased proteolysis. Resistance to the negative growth regulating properties of TGF-β1 has been observed in epithelial and mesenchymal tumors. In addition to a stimulator of angiogenesis, TGF-β1 also influences the growth of tumor cells directly or indirectly. Tumor cells can escape the inhibiting effect of TGF-β1 on normal cells at post- transcription level, receptor level or post-receptor level. When tumor cells are insensitive, TGF-β1 also can promote tumor metastasis through enhancing angiogenesis, adjusting the character of matrix, or adjusting the body' s immune response to tumor growth. TGF-β1 seems to affect tumor angiogenesis and play an important role in tumor progression in non-small cell lung carcinoma and lung adenocarcinoma. A significant correlation between TGF-β1 protein level and prognosis was detected by multivariate analysis[3]. Maehara[4] found that TGF-β1 was closely related to the invasion and metastasis of gastric cancer, and production of TGF-β1 in the tumor did not contribute to the total amount of TGF-β1 in the blood circulation. TGF-β1 might be associated with tumor progression by modulating angiogenesis in colorectal cancer and it could be used as a possible biomarker[5].

In the present study, 55 cases of gastric carcinoma tissues were stained for TGF-β1. 54.55 % of these tissues were positively stained including 21 strong positive cases "+++~++", 9 positive cases "+", 25 negative cases "-". MVD between the two groups of "+" and "-" staining had no significant difference (P>0.05), but MVD of the group of "+++~++" was significantly higher than the groups of "+" and "-" (P<0.01). Therefore, we propose that overexpression of TGF-β1 be positively correlated with MVD in tumors and one of the bio-effects of TGF-β1 act as a stimulating factor of angiogenesis *in vivo*. In our other studies, TGF-β1 was highly expressed in gastric carcinoma tissues with lymph node metastasis and distant metastasis.

TGF-β1 exerts its functions through binding its receptors. Receptors for TGF-β family include type I, type II, type III and CD105. CD105 could act as an auxiliary protein in the ligand-receptor compound and regulate the function of TGF-β1[6]. It has been found to mainly localize in vascular endothelial cells in normal or tumor tissues. Calabro[7] detected soluble TGF-β1 and CD105 (sCD105) in hematopoietic malignancies, and showed that high levels of sCD105 were present in myeloid malignancies characterized by a high cellular proliferation rate, and suggested that an altered balance between sCD105 and sTGF-β1 might favor disease progression and clinical complications.

In this study we used double staining to detect the expression of CD105 and TGF-β1 in one gastric carcinoma section, and found that CD105 was highly expressed around these cancer cells with more TGF-β1.

VEGF, also named vascular permeability factor, can specifically direct to endothelial cells and is one of the most important factors to induce, up-regulate and migrate angiogenesis. VEGF is a kind of dimer glycoproteins, with a molecular weight of 34-50 kD. VEGF specifically promotes the mitosis and proliferation of endothelial cells by paracrine. Furthermore, VEGF can induce angiogenesis, increase the permeability of vessels and stimulate endothelial cells to produce protease and other low molecule proteins. In addition, VEGF can significantly prolong the life span of endothelial cells, increasing the mitosis to 15-20 fold. Further studies showed VEGF could improve the function of vesicles in endothelial cells, thus increasing the permeability of vessels, which facilities tumor cells to invade the vessels and distant migration. Therefore, VEGF can effectively promote angiogenesis and maintain its existence.

Kaio[8] found that lymph node metastasis and VEGF expression were significant risk factors in advanced colorectal carcinoma patients. Song[9] noticed VEGF was closely related to gastric carcinoma angiogenesis, and involved in tumor progression and lymph node metastasis. Some other studies showed that high VEGF expression or high MVD would indicate a poor prognosis in breast carcinoma patients[10] or high VEGF could be a marker of metastasis and invasion in squamous cell carcinomas[11]. In our study, VEGF and MVD marked by CD105 were highly expressed in colorectal carcinoma tissues. The expression of VEGF and MVD in colorectal carcinoma tissues was closely related to infiltrating depth, lymph node metastasis and Duke' s staging but not related to histological staging. These observations suggested that the expression of VEGF and MVD in colorectal carcinoma tissues was important in monitoring tumor invasion, lymph node metastasis and Duke' s staging.

Our previous correlation analysis showed that the expression of VEGF was positively related to MVD, further proving the causality of VEGF and MVD, i.e., VEGF could stimulate angiogenesis through paracrine in colorectal carcinoma tissues and thus promoting the growth, infiltration and metastasis of tumors.

Newborn blood vessels have their own construction features. For example, the new vessels in tumor tissues do not further differentiate or rebuild corresponding arteries and veins, which means that newborn vessels have no smooth muscle and cannot contract. Newborn vessels in tumors are highly winded, sinusoid and slender. Functionally, blood stream in new vessels is irregular, tending to result in thrombosis or

hemorrhage spontaneously. In this case, tumor cells invade into new vessels and are carried to other organs, continuing to grow and become a metastasis. The more the newborn blood vessels are, the greater the possibilities of metastasis are. Because of the important effects of newborn vessels, great attention has been paid to the studies of angiogenesis.

While counting newborn blood vessels, most researchers selected several normal endothelial cell markers, such as CD31, CD34 and von Willerbrand (vWF). VWF, a factor VIII related antigen (VIII-RA), is a kind of EC marker that exists on EC of normal tissues. Many experiments showed that VIII-RA mainly existed in completely mature vessels, and the chapter restricts its utilization in angiogenesis of tumor tissues. CD31, a member of cell adhesion molecules, often participates in the adhesiveness of platelets in inflammation and wound. Parums pointed out that anti-CD31 monoclonal antibody could also bind normal blood vessels. CD34 is a transmembrane glycoprotein with a MW of 110 kD, and can express on endothelial cells. Ewoto[12] found that it was difficult to identify native or newborn vessels by using CD34. For this reason, CD34 is not an ideal marker of endothelial cells in the research of newborn vessels. Because of the heterogeneity of endothelial cells, the markers of normal endothelial cells are apparently unfit for the studies of angiogenesis in tumor tissues.

CD105, also called endoglin, is a new kind of cell adhesion molecules, first found by Quackenbush in pre-B cell line HOON[13]. CD105 mainly locates in EC and has become a new marker of EC[14]. CD105 is an endothelial homodimeric membrane antigen with 633 amino acid residues and its molecular mass is 180 kD. The gene of CD105 is located on 9q34, which is the target gene of HHT-I. Therefore, the expression of CD105 in EC showed it was highly related to the structure and function of EC[15]. Although CD105 can express in normal vessels, many studies showed CD105 could be detected more easily and reacted more strongly in tissues with angiogenesis.

Mab E9, a new murine anti-human monoclonal antibody, was produced by the Experimental Pathology Institute, Manchester University in early 1990's. It belongs to immunoglobulin G (IgG). Mab E9 does not react with large vessels but with microvessels in tumor tissues strongly. The series of responses of Mab E9 showed its uniqueness from other antibodies. Wang stained the vessels in breast carcinoma tissues with antibody Mab5.6E (anti-CD31) and Mab E9 (anti-CD105), and found blood vessels in or around tumor tissues stained intensely for Mab E9, whereas the same blood vessels were either weakly positive or did not stain at all for CD31. Furthermore, in most cases, unlike Mab 5.6E, Mab E9 failed to stain (a) some apparently normal blood vessels in tumor tissues and (b) a few apparently normal blood vessels in normal tissues were entrapped within a tumor mass. In several normal breast tissues, Mab E9 alone stained only a proportion of blood vessels (-20 %) that were positive for Mab 5.6E. Kumar stained CD34 and CD105 in series cryostat sections with Mab QBEND-10 and Mab E9, and found there was no relation between the two groups of MVD. The group of MVD marked with CD34 was only related to the size of tumors, while the group marked with CD105 could be the independent prognostic marker for patients with breast cancer. Further observation showed, in the same sites the native vessels were CD34 stained, and the newborn vessels were CD105 stained[16].

Because of the heterogeneity of endothelial cells, the markers of normal endothelial cells are apparently unfit for the studies of angiogenesis in tumor tissues. The growth of tumors includes not only the increase of blood vessels in number but also the change of protein molecules in structure of ECs. An ideal EC marker for angiogenesis should detect the newborn vessel quality as well as its quantity. Only in this way can we improve the sensitivity and credibility in detecting angiogenesis. From the above, it is reasonably believed that CD105 is a better marker of angiogenesis compared with CD34, CD31 and VIII-RA. Mab E9 increases the credibility in detecting angiogenesis. In our study, we used Mab E9 to stain MVD in malignant tumors of the gastrointestinal tract, so the credibility was high. We were able to prevent the possibility of mistaking native vessels for newborn vessels.

REFERENCES

1 **Griffioen AW**, Molema G. Angiogenesis: potentials for pharmacologic intervention in the treatment of cancer, cardiovascular diseases, and chronic inflammation. *Pharmacol Rev* 2000; **52**: 237-268

2 **De Jong JS**, van Diest PJ, van der Valk P, Baak JP**.** Expression of growth factors, growth-inhibiting factors, and their receptors in invasive breast cancer. II: Correlations with proliferation and angiogenesis. *J Pathol* 1998; **184**: 53-57

3 **Hasegawa Y**, Takanashi S, Kanehira Y, Tsushima T, Imai T, Okumura K. Transforming growth factor-beta1 level correlates with angiogenesis, tumor progression, and prognosis in patients with nonsmall cell lung carcinoma. *Cancer* 2001; **91**: 964-971

4 **Maehara Y**, Kakeji Y, Kabashima A, Emi Y, Watanabe A, Akazawa K, Baba H, Kohnoe S, Sugimachi K. Role of transforming growth factor-beta 1 in invasion and metastasis in gastric carcinoma. *J Clin Oncol* 1999; **17**: 607-614

5 **Xiong B**, Gong LL, Zhang F, Hu MB, Yuan HY. TGF beta1 expression and angiogenesis in colorectal cancer tissue. *World J Gastroenterol* 2002; **8**: 496-498

6 **Li C**, Hampson IN, Hampson L, Kumar P, Bernabeu C, Kumar S. CD105 antagonizes the inhibitory signaling of transforming growth factor beta1 on human vascular endothelial cells. *FASEB J* 2000; **14**: 55-64

7 **Calabro L**, Fonsatti E, Bellomo G, Alonci A, Colizzi F, Sigalotti L, Altomonte M, Musolino C, Maio M. Differential levels of soluble endoglin (CD105) in myeloid malignancies. *J Cell Physiol* 2003; **194**: 171-175

8 **Kaio E**, Tanaka S, Kitadai Y, Sumii M, Yoshihara M, Haruma K, Chayama K. Clinical significance of angiogenic factor expression at the deepest invasive site of advanced colorectal carcinoma. *Oncology* 2003; **64**: 61-73

9 **Song ZJ**, Gong P, Wu YE. Relationship between the expression of iNOS, VEGF, tumor angiogenesis and gastric cancer. *World J Gastroenterol* 2002; **8**: 591-595

10 **Li HJ**, Jing J, Zhao YB, Zhu JQ, Zhang SY, Shi ZD. Tumor angiogenesis in node-negative breast carcinoma. *Ai Zheng* 2002; **21**: 75-78

11 **Sauter ER**, Nesbit M, Watson JC, Klein-Szanto A, Litwin S, Herlyn M. Vascular endothelial growth factor is a marker of tumor invasion and metastasis in squamous cell carcinomas of the head and neck. *Clin Cancer Res* 1999; **5**: 775-782

12 **Emoto M**, Iwasaki H, Mimura K, Kawarabayashi T, Kikuchi M. Difference in the angiogenesis of benign and malignant ovarian tumors, demonstrated by analyses of solor Doppler ultrasound, immunohistochemistry, and microvesel density. *Cancer* 1997; **80**: 899-907

13 **Fonsatti E,** Del Vecchio L, Altomonte M, Sigalotti L, Nicotra MR, Coral S, Natali PG, Maio M. Endoglin: An accessory component of the TGF-β-binding receptor-complex with diagnostic, prognostic, and bioimmunotherapeutic potential in human malignancies. *J Cell Physiol* 2001; **188**: 1-7

14 **Miller DW,** Graulich W, Karges B, Stahl S, Ernst M, Ramaswamy A, Sedlacek HH, Muller R, Adamkiewicz J. Elevated expression of endoglin, a component of the TGF-beta-receptor complex, correlates with proliferation of tumor endothelial cells. *Int J Cancer* 1999; **81**: 568-572

15 **Bodey B**, Bodey B Jr, Siegel SE, Kaiser HE. Over-expression of endoglin (CD105): a marker of breast carcinoma-induced neovascularization. *Anticancer Res* 1998; **18**: 3621-3628

16 **Kumar S**, Ghellal A, Li C, Byrne G, Haboubi N, Wang JM, Bundred N. Breast carcinoma: vascular density determined using CD105 antibody correlates with tumor prognosis. *Cancer Res* 1999; **59**: 856-861

Edited by Zhu LH and Wang XL

P.O.Box 2345, Beijing 100023,China
Fax: +86-10-85381893
E-mail: wjg@wjgnet.com www.wjgnet.com

World J Gastroenterol 2003;9(12):2870-2872
World Journal of Gastroenterology
 ISSN 1007-9327

• CASE REPORT •

A case of pedunculated rectal carcinoid removed by endoscopic mucosal resection

Hisayuki Hamada, Saburo Shikuwa, Chun-Yang Wen, Hajime Isomoto, Kazuhiko Nakao, Kosei Miyashita, Manabu Daikoku, Koji Yano, Masahiro Ito, Yohei Mizuta, Long-Dian Chen, Zhao-Min Xu, Ikuo Murata, Shigeru Kohno

Hisayuki Hamada, Saburo Shikuwa, Kosei Miyashita, Manabu Daikoku, Koji Yano, Masahiro Ito, Institute for Clinical Research Center, WHO Collaborating Center for Reference and Research on Viral Hepatitis, National Nagasaki Medical Center, Nagasaki, Japan, Kubara 2-1001-1, Omura 852-8562, Nagasaki, Japan
Chun-Yang Wen, Department of Molecular Pathology, Atomic Bomb Disease Institute, Nagasaki University Graduate School of Biomedical Science, 1-12-4 Sakamoto, Nagasaki 852-8523, Japan
Chun-Yang Wen, Long-Dian Chen, Zhao-Min Xu, Department of Digestive Disease, Nanjing Drum Tower Hospital, Medical School of Nanjing University, Nanjing 210008, Jiangsu Province, China
Hajime Isomoto, Kazuhiko Nakao, Yohei Mizuta, Shigeru Kohno, Second Department of Internal Medicine, School of Medicine, Nagasaki University, 1-7-1 Sakamoto, Nagasaki, 852-8523 Japan
Ikuo Murata, Department of Pharmacotherapeutics, Nagasaki University, Graduate School of Biomedical Sciences, 1-14 Bunkyo-machi, Nagasaki 852-8521, Japan
Correspondence to: Chun-Yang Wen M.D Ph.D, Department of Molecular Pathology, Atomic Bomb Disease Institute, Nagasaki University Graduate School of Biomedical Science, 1-12-4 Sakamoto, Nagasaki 852-8523, Japan. cywen518@net.nagasaki-u.ac.jp
Telephone: +81-95-849-7107 **Fax:** +81-95-849-7108
Received: 2003-08-06 **Accepted:** 2003-10-23

Abstract

Carcinoid tumors generally appear as yellow/gray or tan submucosal nodules. We experienced a case of pedunculated rectal carcinoid showing a mushroom-like appearance. The case was a forty years old woman who was admitted to our hospital due to rectal bleeding. Colonoscopy revealed a pedunculated polyp presenting a mushroom-shaped appearance measuring 13 mm in diameter in the rectum. The histological diagnosis of specimens obtained by biopsy was adenocarcinoma and transanal ultrasonography revealed the tumor localization within the submucosal layer in the rectum. Endoscopic mucosal resection (EMR) was performed. Histopathological examination established the diagnosis of carcinoid tumor in the rectum. Frequencies of the pedunculated type in rectal carcinoids were reported to be 2.4 % to 7.1 % in the literature. Because of its rarity, pedunculated configuration may confuse the endoscopic diagnosis of carcinoids. Treatment for carcinoids of 1 to 1.5 cm in size remains controversial. Although such tumors are technically respectable by EMR, careful attention must be paid in dealing with these tumors because there may be unexpected behaviors of the tumors.

Hamada H, Shikuwa S, Wen CY, Isomoto H, Nakao K, Miyashita K, Daikoku M, Yano K, Ito M, Mizuta Y, Chen LD, Xu ZM, Murata I, Kohno S. A case of pedunculated rectal carcinoid removed by endoscopic mucosal resection. *World J Gastroenterol* 2003; 9 (12): 2870-2872
http://www.wjgnet.com/1007-9327/9/2870.asp

INTRODUCTION

Carcinoid tumors characteristically appear as yellow/gray or tan submucosal nodules, but they are occasionally polypoid or sessile. However, there have been few reports describing a pedunculated type of carcinoid. We presented here an extremely rare case with a pedunculated rectal carcinoid showing a mushroom-like appearance, and referred to the diagnosis and treatment of this rare tumor.

CASE REPORT

A 40 years old woman was admitted to our hospital due to rectal bleeding. Physical examination and laboratory data including serum tumor markers and hormones such as urinary 5-hydroxyindoleacetic acid (5-HIAA) were normal. Barium enema contrast examination showed a fungiform polyp in the rectum. Colonoscopy revealed a pedunculated polyp presenting a mushroom-shaped appearance in the rectum (Figures 1A, B). There was a hemispherical protrusion with a shallow central erosion in the top, surrounded by a marked mucosal bulge of the edge. Magnifying endoscopy (OLYMPUS CF-type XQ240ZI, Olympus, Tokyo, Japan) revealed no absence of the pit pattern in the center and enlarged pits at the edge, corresponding to the non-structure type of the pit pattern classification proposed by Kudo *et al*[1] (Figure 1C). Endoscopic ultrasonography (EUS), using a miniature probe (12-20 Hz) with a water-filling method, demonstrated a homogeneous hypoechoic mass, but the structure deeper than the third layer of the rectal wall was unclear (Figure 2). Therefore, we employed a soft-balloon technique using an ultrasonic probe with a balloon filled with deaerated water, which provided a clear ultrasonographic picture of the deeper part of the rectum. Judging from findings on EUS, abdominal computed tomography and chest roentgenography, there were no signs of metastasis in the regional lymph nodes or distant organs. Histology of the biopsy specimens suggested an adenocarcinoma, yielding a diagnosis of polypoid type of early rectal cancer. The depth of mural invasion was estimated to be limited to the submucosa by magnifying endoscopy and EUS. After an injection of saline in the submucosa, the lesion was excised by EMR. Macroscopically, the lesion was located in the submucosal layer. The mass was white-yellowish and solid, measuring 13 mm in diameter (Figure 3). Microscopically, the tumor was composed of small uniform cells, arranged in small nests and cords and with an anastomosing ribbon-like pattern in the submucosal layer (Figure 4). There were no atypical histopathologic features such as mitosis or nuclear atypism. Histochemically, the tumor cells possessed an argyrophil but not an argentaffin nature. Immunohistologically, the tumor cells were positive for neuron specific enolase (NSE) and chromogranin A, but were negative for p53 and Ki67. These findings established the diagnosis of carcinoid tumor in the rectum.

DISCUSSION

Carcinoid tumors are enigmatic slow growing malignancies

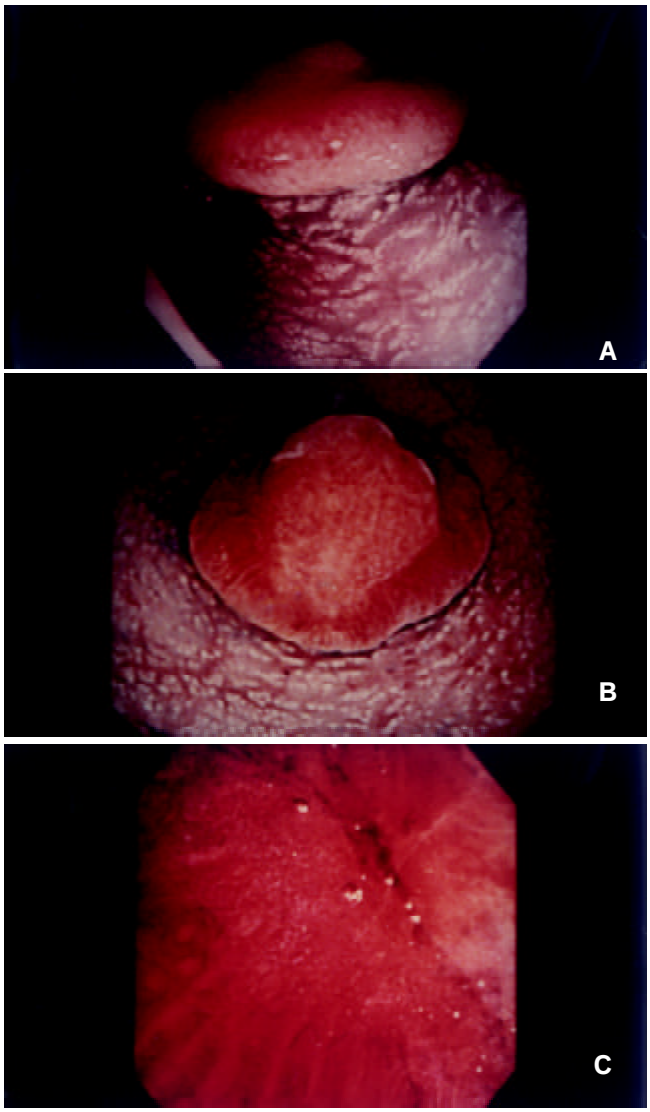

Figure 1 A: Pedunculated polypoid lesion presenting a mushroom appearance in the rectum; B: A round and shallow erosion in the center and a marked mucosal bulge at the edge of polyp; C: A non-structural pit pattern in the center with elongated pits at the edge revealed in magnifying endoscopy.

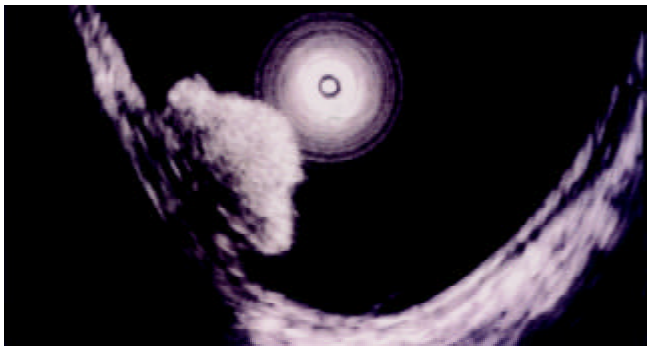

Figure 2 An endoscopic ultrasonography demonstrated homogeneous hypoechoic mass.

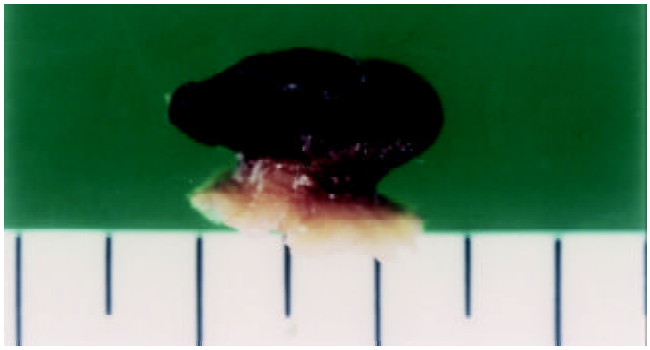

Figure 3 Gross appearance of excised polyp showing a white-yellowish and solid tumor, measuring 13×10 mm with a pedicle.

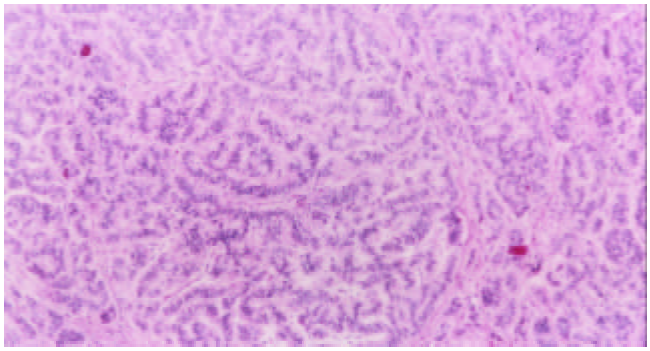

Figure 4 Histology of tumor showing small uniform cells arranged in small nests and cords with an anastomosing ribbon-like pattern in the submucosal layer.

and controversy remains as to their origin[2]. Gastrointestinal carcinoid is regarded as a tumor arising from subepithelial neuroendocrine cells or the totipotential crypt cells in the deep mucosa, usually presenting as a submucosal tumor. Therefore, endoscopic diagnosis is difficult unless biopsy provides a correct histological diagnosis. Macroscopically, a gastrointestinal carcinoid tumor appears as a yellow-gray tan nodule beneath the mucosa and develops a round or oval, sessile polyp as it grows[3]. A pedunculated polyp of carcinoid tumor is extremely rare in the rectum. To our knowledge, only nine cases of rectal carcinoid, including the present case, have been reported[4-9]. Frequencies of the pedunculated type in rectal carcinoids were reported to be 2.4 % to 7.1 % in the literature[5,6]. Because of its rarity, pedunculated configuration may confuse the endoscopic diagnosis of carcinoids.

Recently, Kudo *et al*. reported the usefulness of the pit pattern observation using magnifying endoscopy and stereomicroscopy in the diagnosis of epithelial neoplasms of the large intestine[1]. They classified the pit patterns into five types based on fine morphology of the surface, histology and size. Type V pit pattern showed an irregular or nonstructural surface, which was frequently seen in carcinomas[1]. In this case, we misdiagnosed this tumor as carcinoma because it showed the V pit pattern and pathological diagnosis of biopsy specimens was not correct. It was suggested that the carcinoid in the present case showed non-structural pit patterns because overlying mucosa of the tumor disappeared. It appears inappropriate, therefore, to use pit pattern analysis for evaluation of nature of the tumor in this case.

The size of carcinoid has been accepted as an important factor predicting its prognosis. Several surgical studies have shown that tumors less than 1 cm seldom metastasize, whereas tumors greater than 2 cm have a high incidence of metastasis[2,3,10]. As for the risk of metastasis from rectal carcinoid, Bates *et al*. reported an incidence of 1.7 % for tumors less than 9 mm in size, 10 % for tumor of 10 to 19 mm and 82 % for tumors larger than 20 mm[11]. It is uncertain whether gross appearance of the carcinoids is a predicting factor, although Haraguchi *et al*[12] reported that no metastasis was observed in pedunculated carcinoid in a review of 496 cases of rectal carcinoid.

These reports indicated that the most effective therapy for

rectal carcinoid was a complete surgical excision, particularly in tumors greater than 2 cm[3,13]. Recently, endoscopic treatment has been applied for gastrointestinal tumors including carcinoids. Ishikawa *et al.* suggested the following indications of conventional endoscopic polypectomy for rectal carcinoid tumors. They were tumors less than 15 mm in diameter, flat tumors with normal or yellow color, tumors consisting of nodular nests or trabecular or ribbon-like structures in histology[14]. This guideline of endoscopic treatment for rectal carcinoid may remain controversial. We do not recommend a conventional endoscopic polypectomy for common rectal carcinoid because there was a high incidence of tumor residue after treatment[15]. Recently, endoscopic mucosal resection (EMR) has been generally accepted as a choice of treatment for rectal carcinoid tumors less than 1 cm[9,14,16,17]. Treatment for carcinoids of 1 to 1.5 cm in size remains controversial. Although such tumors have been technically respectable by endoscopic aspiration mucosectomy using the hood technique or a ligating device[18], careful attention must be paid to these tumors because there may be unexpected behaviors of the tumors.

The carcinoid in the present case was negative for p53 and Ki-67. Hasegawa *et al*. reported that carcinoid tumors expressing p53 and Ki-67 had a high malignant potential and metastatic activity[4]. In future, the induction of molecular biology may be helpful in predicting the prognosis of carcinoid tumors[19, 20].

REFERENCES

1 **Kudo S**, Rubio CA, Teixeira CR, Kushida H, Kogure E. Pit pattern in colorectal neoplasia:endoscopic magnifying view. *Endoscopy* 2001; **33**: 367-373

2 **Koura AK**, Giacco GG, Curley SA, Skibber JM, Feig BW, Ellis LM. Carcinoid tumor of the rectum. *Cancer* 1997; **79**: 1294-1298

3 **Lauffer IM**, Zhang T, Modlin IM. Current status of gastrointestinal carcinoid. *Aliment Pharmacol Ther* 1999; **13**: 271-287

4 **Hasegawa O**, Iwashita A, Futami T, Kitamura K, Arima S. Pathological study of rectal carcinoid. *J the Japan society of colon Proctology* 1997; **50**: 163-176

5 **Ponka JL**, Walke L. Carcinoid tumor of rectum. *Dis Col Rect* 1971; **14**: 46-56

6 **Quan SHQ**, Bader G, Berg JW. Carcinoid of rectum. *Dis Col Rect* 1964; **7**: 197-206

7 **Masumori S**, Nogaki M, Ozeki T, Ktsuragi T, Koshimura Y, Higaki A, Hosoda S. The rectal carcinoid-clinicopathologic Study of five cases. *Jap J Cancer Clin* 1975; **21**: 1181-1188

8 **Kira J**, Fuchigami T, Murakami M, Koga A, Iwashita A. A case report of rectal carcinoid and an analysis of rectal carcinoids reported in Japan. *I to Cho(Stomach and Intestine)* 1980; **15**; 1105-1110

9 **Kobayashi K**, Katsumata T, Otani Y, Naka H. Diagnosis and treatment of rectal carcinoid. *Nippon Rinsho* 1991; **12**: 233-237

10 **Soga J**. Carcinoids of the rectum: An evaluation of 1271 reported cases. *Jpn J Surg* 1997; **27**: 112-119

11 **Bates HR Jr**. Carcinoid tumors of the rectum. A statistical review. Dis. *Colon Rectum* 1966; **9**: 90

12 **Haraguchi M**, Makiyama K, Yamakawa M, Yamasaki K, Iwanaga S, Mizuta Y, Ide T, Komori M, Tanaka T, Osabe M, Murata I, Imanishi T, Hara K. Six cases of rectal carcinoid treated by endoscopic polypectomy. *Gastroenterol Endosc* 1998; **30**: 2612-2620

13 **Kulke MH**, Mayer RJ. Carcinoid tumors. *N Engl J Med* 1999; **18**: 358-368

14 **Ishikawa H**, Imanishi K, Otani T, Okuda S, Tatsuta M, Ishiguro S. Effectiveness of endoscopic treatment of carcinoid tumors of the rectum. *Endscopy* 1998; **21**: 133-135

15 **Okamoto T**, Higaki K, Kawabata K. Autopsy case of malignant carcinoid tumor of the ascending colon. *Gan No Rinsho* 1983; **29**: 1361-1365

16 **Fujimura Y**, Mizuno M, Takeda M, Sato I, Hoshika K, Uchida J, Kihara T, Mure T, Sano K, Moriya T. A carcinoid tumor of the rectum removed by strip biopsy. *Endoscopy* 1993; **25**: 428-430

17 **Higaki S**, Nishiaki M, Mitani N, Yanai H, Tada M, Okita K. Effectiveness of local endoscopic resection of rectal carcinoid tumors. *Endoscopy* 1997; **29**: 171-175

18 **Shikuwa S**, Matsunaga K, Osabe M, Ofukuji M, Omagari K, Mizuta Y, Takeshima F, Murase K, Otani H, Ito M, Shimokawa I, Fujii M, Kohno S. Esophageal granular cell tumor treated by endoscopic mucosal resection using a ligating device. *Gastrointest Endosc* 1998; **47**: 529-532

19 **Lundqvist M**, Wilander E. Subepithelial neuroendocrine cells and carcinoid tumours of the human small intestine and appendix.A comparative immunohistochemical study with regard to serotonin, neuron-specific enolase and S-100 protein reactivity. *J Pathol* 1986; **148**: 141-147

20 **Moyana TN**, Satkunam N. Crypt cell proliferative micronests in rectal carcinoids. An immunohistochemical study. *Am J Surg Pathol* 1993; **17**: 350-356

Edited by Wang XL

P.O.Box 2345, Beijing 100023,China
Fax: +86-10-85381893
E-mail: wjg@wjgnet.com www.wjgnet.com

World J Gastroenterol 2003;9(12):2873-2875
World Journal of Gastroenterology
 ISSN 1007-9327

• CASE REPORT •

Bouveret's syndrome complicated by a distal gallstone Ileus

Rasim Gencosmanoglu, Resit Inceoglu, Caglar Baysal, Sertac Akansel, Nurdan Tozun

Rasim Gencosmanoglu, Unit of Surgery, Marmara University Institute of Gastroenterology, Istanbul, Turkey
Resit Inceoglu, Department of General Surgery, Marmara University School of Medicine, Istanbul, Turkey
Resit Inceoglu, Unit of General Surgery, Acibadem Hospital, Istanbul, Turkey
Caglar Baysal, Nurdan Tozun, Unit of Gastroenterology, Acibadem Hospital, Istanbul, Turkey
Sertac Akansel, Unit of Radiology, Acibadem Hospital, Istanbul, Turkey
Nurdan Tozun, Sub-department of Gastroenterology, Marmara University School of Medicine, Istanbul, Turkey
Correspondence to: Rasim Gencosmanoglu, M.D., Unit of Surgery, Marmara University Institute of Gastroenterology, Basibuyuk, Maltepe, PK: 53, TR-81532, Istanbul, Turkey. rgencosmanoglu@marmara.edu.tr
Telephone: +90-216-383-3057 **Fax:** +90-216-399-9912
Received: 2003-08-11 **Accepted:** 2003-10-12

Abstract

AIM: Gastric outlet obstruction caused by duodenal impaction of a large gallstone migrated through a cholecystoduodenal fistula has been referred as Bouveret's syndrome. Endoscopic lithotomy is the first-step treatment. However, surgery is indicated in case of failure or complication during this procedure.

METHODS: We report herein an 84-year-old woman presenting with features of gastric outlet obstruction due to impacted gallstone. She underwent an attempt of endoscopic retrieval which was unsuccessful and was further complicated by distal gallstone ileus. Physical examination was irrelevant.

RESULTS: Endoscopy revealed multiple erosions around the cardia, a large stone in the second part of the duodenum causing complete obstruction, and wide ulceration in the duodenal wall where the stone was impacted. Several attempts of endoscopic extraction by using foreign body forceps failed and surgical intervention was mandatory. Preoperative ultrasound evidenced pneumobilia whilst computerized tomography showed a large stone, 5×4×3 cm, logging at the proximal jejunum and another one, 2.5×2×2 cm, in the duodenal bulb causing closed-loop syndrome. She underwent laparotomy and the jejunal stone was removed by enterotomy. Another stone reported as located in the duodenum preoperatively was found to be present in the gallbladder by intraoperative ultrasound. Therefore, cholecystoduodenal fistula was broken down, the stone was retrieved and cholecystectomy with duodenal repair was carried out. She was discharged after an uneventful postoperative course.

CONCLUSION: As the simplest and the least morbid procedure, endoscopic stone retrieval should be attempted in the treatment of patients with Bouveret's syndrome. When it fails, surgical lithotomy consisting of simple enterotomy may solve the problem. Although cholecystectomy and cholecystoduodenal fistula breakdown is unnecessary in every case, conditions may urge the surgeon to perform such operations even though they carry high morbidity and mortality.

Gencosmanoglu R, Inceoglu R, Baysal C, Akansel S, Tozun N. Bouveret's syndrome complicated by a distal gallstone Ileus. *World J Gastroenterol* 2003; 9(12): 2873-2875
http://www.wjgnet.com/1007-9327/9/2873.asp

INTRODUCTION

Gallstones are completely asymptomatic in the majority of patients (60 %-80 %)[1]. When they become symptomatic, biliary colic is the most frequently encountered manifestation. Patients with mild symptoms have a higher risk of developing gallstone-related complications such as acute cholecystitis, choledocholithiasis with or without cholangitis, gallstone pancreatitis or gallstone ileus[2]. Biliary fistula occurs in 3 % to 5 % of the cases[3]. Gallstones can migrate into the terminal ileum through a cholecystoduodenal fistula and cause an intestinal obstruction at this level but they may also anchor at the duodenum and produce the symptoms of gastric outlet obstruction in rare cases as first described by Bouveret in 1893[4]. Since this syndrome is usually observed in older patients with poor medical status, a non-surgical approach such as endoscopic stone removal has been used as the first-line treatment. This may be performed by simple endoscopic lithotomy with snare or specific stone baskets designed for endoscopic retrograde cholangio-pancreatography. When feasible, stones are attempted to fragment into small pieces followed by endoscopic removal. Laser lithotripsy either with percutaneous or transendoscopic routes and extracorporeal shock-wave lithotripsy (ESWL) are the alternative treatment modalities[5-7]. In the case of unsuccessful stone removal or its distal migration resulting in mechanical intestinal obstruction, particularly with larger stones, these techniques may be ineffective and surgery may be needed. The main purpose of surgical intervention should be to remove the obstructing stone by enterotomy without cholecystectomy and cholecystoduodenal fistula breakdown to minimize the risks of surgery. However, when it is necessary as the case presented hereby, gallbladder excision can be performed successfully.

CASE REPORT

An 84-year-old woman presenting with 5 days of nausea and vomiting, hematemesis, loss of appetite, and a severe upper abdominal pain located to the periumbilical region was admitted to the emergency unit of the Marmara University Institute of Gastroenterology and referred to Acibadem Hospital according to her will. The physical examination did not show remarkable abdominal distention or any changes in bowel sounds. Abdominal ultrasound evidenced pneumobilia but the gallbladder was not visualized due to excess gas related to gastric and duodenal dilatation. Upper gastrointestinal endoscopy revealed multiple erosions around the cardia, ascribed to Mallory-Weiss syndrome, a large stone in the second part of the duodenum causing complete obstruction, and wide ulceration in the duodenal wall where the stone was

impacted (Figure 1). Although, no clear cholecystoduodenal fistula was demonstrated endoscopically, the typical appearance of the stone indicated its gallbladder origin. Attempts for mechanical fragmentation and retrieval of the stone at the same endoscopic session were unsuccessful. Computerized tomography of the abdomen showed pneumobilia, remarkable distention of stomach, and a 5 cm mass with a calcified rim in the jejunum (Figure 2A). Another mass of 2.5 cm in diameter, sharing similar radiologic features at the right upper abdominal quadrant (Figure 2B) was reported by radiologists as a second gallstone obstructing the duodenal lumen and resulting in a closed-loop syndrome.

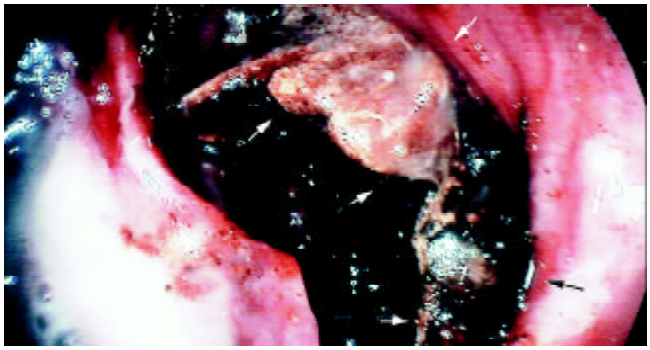

Figure 1 Endoscopic appearance of a large duodenal stone (black arrows) causing complete obstruction. Note the irregular edges of the stone (white arrows), which indicate its fragmentation.

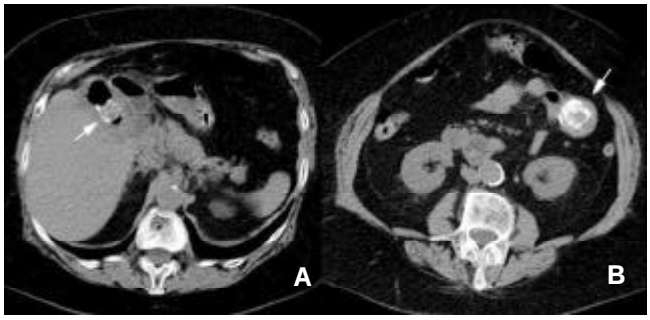

Figure 2 CT shows: A: A large, 5×3×3 cm, intraluminal stone (arrow) in the proximal jejunum, B: Another stone in the duodenal bulb (arrow).

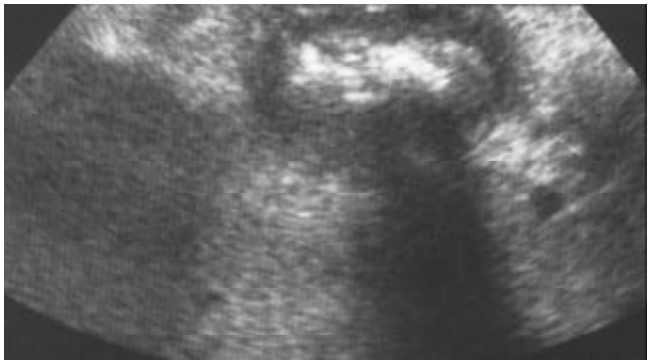

Figure 4 After the adhesions between the gallbladder (arrow) and the adjacent organs were dissected, cholecystoduodenal fistula (arrow head) was broken down and then the retained stone was removed.

The features of the stone, the failure of endoscopic retrieval and the general status of the patient urged to undertake a surgical lithotripsy by laparotomy and enterotomy. At laparotomy, the stone was palpated in the jejunum about 15 cm distal to the ligament of Treitz with a complete mechanical obstruction which was easily diagnosed with the presence of remarkable dilation of the proximal jejunal segment (Figure 3A). There were dense adhesions between the gallbladder and the duodenum, greater omentum, and right part of the transverse colon. The jejunum was opened and the large stone was removed (Figure 3B). Two small pieces of the stone were also removed from the proximal lumen (Figure 3C).

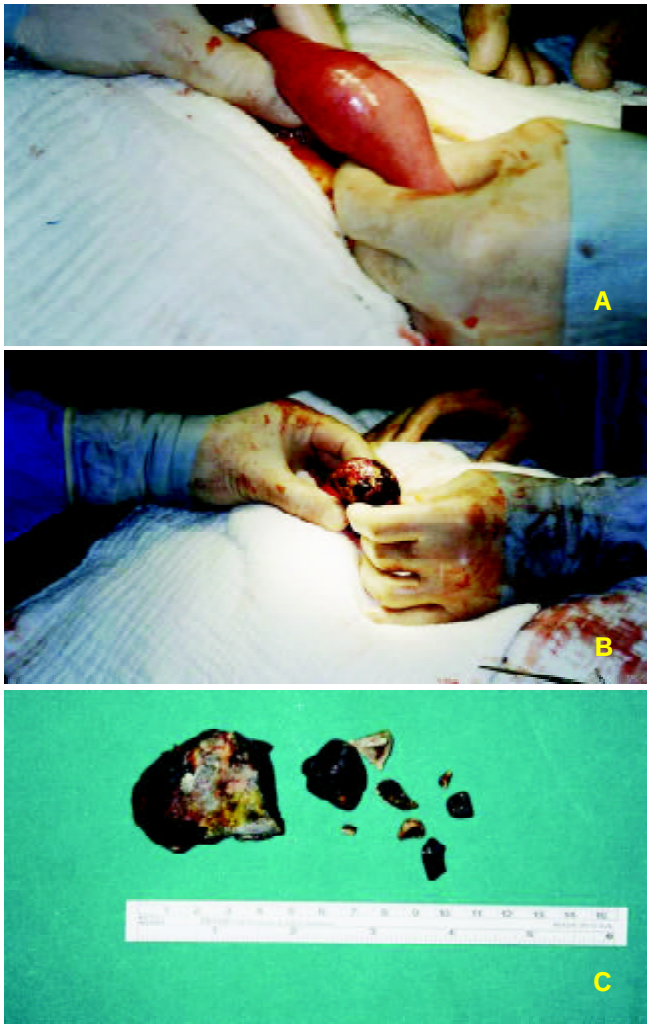

Figure 3 Intraoperative views: A: The obstructed proximal jejunal segment, note a large intraluminal stone causing complete intestinal obstruction at this level, B: Removal of the stone with enterotomy, C: Macroscopic view of the fragmented gallstone which had a very hard outer shell with a soft core.

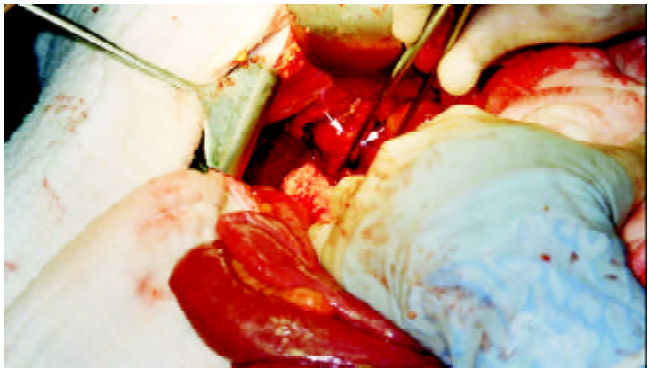

Figure 5 Intraoperative ultrasound revealed that the suspicious stone was in the gallbladder instead of the duodenal lumen.

Then the jejunum was primarily closed with double-layer running stitches of an absorbable material. Since the location of the other stone could not be detected by palpation and the subsequent operative strategy was dependent on its site, an intra-operative ultrasound was performed (Figure 4). Once the other stone was shown to be located in the gallbladder lumen, a cholecystectomy and a duodenal repair was undertaken to avoid further migration of the retained large fragment of the stone which would result in intestinal obstruction. Hence the gallbladder was opened, cholecystoduodenal fistula was broken down, and the stone was retrieved from the lumen followed by antegrade cholecystectomy (Figure 5). Duodenal lumen was also cleared from small stone fragments (Figure 3C) then the duodenal opening was closed by a transverse single-layer running stitch of an absorbable material. The post-operative period was uneventful and the patient was discharged on the eighth postoperative day. She has been symptom-free in the 3-month period of follow-up.

DISCUSSION

Bouveret' s syndrome as described by gastric outlet obstruction caused by a large gallstone passing into the duodenal bulb through a biliogastric or bilioduodenal fistula usually develops in older patients with poor medical conditions and surgical treatment consisting of cholecystectomy and duodenal repair following extraction of the stone through the broken-down cholecystoduodenal fistula or a separate duodenotomy results in considerable morbidity and mortality[8]. Developments in surgical techniques have reduced the reported mortality rate of 30 % before 1968 to 12 % in recent years. Accordingly, surgical aim has gradually shifted from a radical procedure in which the gallbladder is removed and the cholecystoduodenal fistula is repaired to a simple approach consisting of enterotomy and stone extraction. Alternatives to surgical lithotomy such as simple endoscopic lithotomy and laser or ESWL have been reported with successful outcomes in some cases[5].

Bouveret' s syndrome was reported to occur more frequently in females (65 %) with a median age of 69 years. Diagnosis is made usually during the upper GI endoscopy further supported by abdominal ultrasound findings. Computerized tomography is helpful in demonstrating the exact level of obstruction, the biliary site of duodenal fistula, and the status of gallbladder especially in cases of gallbladder rupture. Endoscopic lithotomy is the first line approach to treatment; however, it may be unsuccessful in some cases particularly with impacted large stones. Stones, usually larger than 2.5 cm in diameter, have been reported in cases with Bouveret' s syndrome[3]. Smaller stones generally pass through the duodenum and do not cause gastric outlet obstruction. Endoscopic extraction of stones up to 3 cm in size has been reported[3]. However, larger stones usually get impacted in the duodenum and cause an ischemic ulceration on its wall. On the other hand, large gallstones of mixed type tend to have a very hard outer shell, even though their core may be softer[5]. This feature may hamper their mechanical fragmentation with endoscopic forceps. Although these large stones can be broken down by ESWL, the irregular shape and the relatively large sizes of the fragments may hinder their passage to distal bowel, especially in the case of impacted stones. Percutaneous laser lithotripsy or Holmium: YAG laser via a flexible optic fiber through the working-channel of the endoscope, as recently reported by Alsolaiman *et al*.[5], do not always result in success. In addition, the non-availability of these expensive equipments in most centers restricts their wide-spread use.

Many cases have been reported with migration of the stone after unsuccessful attempts of endoscopic stone extraction or alternative lithotripsy methods. When un-fragmented stone migrates into the small bowel, its removal by a simple enterotomy is easily done. Enterotomy carries less morbidity rate when compared to duodenotomy particularly in patients with duodenal ulcer due to the erosion of duodenal wall by an impacted large stone. When the stone is broken down into several pieces by non-surgical methods and pieces are removed endoscopically, larger fragments which migrate distally can cause obstruction and require surgery. Intraoperative endoscopy may facilitate recognition and removal of remaining stones in the proximal gastrointestinal lumen. However, the presence of any remaining stone fragments in the gallbladder may critically raise the question whether the cholecystectomy is necessary or not. In the present case, the large piece of the gallstone was removed by enterotomy, but the presence of a remaining fragment, which was 2.5 cm in diameter in the gallbladder, necessitated cholecystectomy and cholecystoduodenal fistula breakdown in order to avoid any further attack as it has been reported in similar cases in the literature.

Intraoperative ultrasound is advised in cases where the surgeon is unable to localize exactly the site of the remaining stone fragments. In our case, although radiologists preoperatively reported the second stone fragment as situated in the duodenum causing closed-loop syndrome with a larger one located more distally, intraoperative ultrasound showed the remaining fragment still in the gallbladder. This finding changed our operative strategy from a simple enterotomy and stone extraction to a more complicated procedure such as cholecystectomy and duodenal wall repair.

In summary, endoscopic lithotripsy and stone extraction should be performed as a first-step treatment in patients with Bouveret' s syndrome. When it fails, surgical lithotomy consisting of simple enterotomy may solve the problem. Although cholecystectomy and cholecystoduodenal fistula breakdown is not recommended routinely, especially when the patient' s age and clinical status limit a more aggressive approach, they can be performed successfully when conditions force the surgeon to undertake such a decision.

REFERENCES

1 **Haris HW.** Biliary system. In: Norton JA, Bollinger RR, Chang AE, Lowry SF, Mulvihill SJ, Pass HI, Thompson RW, eds. Surgery Basic Science and Clinical Evidence. *New York: Springer-Verlag* 2001: 553-584

2 **Ahrendt SA,** Pitt HA. Biliary tract. In: Townsend CM Jr, Editor-in-Chief. Sabiston Textbook of Surgery, The Biological Basis of Modern Surgical Practice. Section X. Abdomen. 16th ed. *Philadelphia: W.B. Saunders Company* 2001: 1076-1111

3 **Salah-Eldin AA,** Ibrahim MA, Alapati R, Muslah S, Schubert TT, Schuman BM. The Bouveret syndrome: an unusual cause of hematemesis. *Henry Ford Hosp Med J* 1990; **38:** 52-54

4 **Nielsen SM,** Nielsen PT. Gastric retention caused by gallstones (Bouveret's syndrome). *Acta Chirurgica Scandinavica* 1983; **149:** 207-208

5 **Alsolaiman MM,** Reitz C, Nawras AT, Rodgers JB, Maliakkal BJ. Bouveret's syndrome complicated by distal gallstone ileus after laser lithotripsy using Holmium: YAG laser. *BMC Gastroenterol* 2002; **2:** 15

6 **Ondrejka P.** Bouveret's syndrome treated by a combination of extracorporeal shock-wave lithotripsy (ESWL) and surgical intervention. *Endoscopy* 1999; **31:** 834

7 **Maiss J,** Hochberger J, Muehldorfer S, Keymling J, Hahn EG, Schneider HT. Successful treatment of Bouveret's syndrome by endoscopic laser lithotripsy. *Endoscopy* 1999; **31:** S4-S5

8 **Malvaux P,** Degolla R, De Saint-Hubert M, Farchakh E, Hauters P. Laparoscopic treatment of a gastric outlet obstruction caused by a gallstone (Bouveret's syndrome). *Surg Endosc* 2002; **16:** 1108-1109

Edited by Zhu LH

P.O.Box 2345, Beijing 100023,China
Fax: +86-10-85381893
E-mail: wjg@wjgnet.com www.wjgnet.com

World J Gastroenterol 2003;9(12):2876-2877
World Journal of Gastroenterology
 ISSN 1007-9327

• CASE REPORT •

Icteric flare of chronic hepatitis B in a 95-year old patient

WS Wong, Wai Keung Leung, Henry L Y Chan

WS Wong, Wai Keung Leung, Henry L Y Chan, Department of Medicine and Therapeutics, the Prince of Wales Hospital, Hong Kong SAR, The Chinese University of Hong Kong
Correspondence to: Dr W K Leung, Department of Medicine and Therapeutics, 9/F, the Prince of Wales Hospital, 30-32 Ngan Shing Road, Shatin, N.T., Hong Kong. wkleung@cuhk.edu.hk
Telephone: +852-2632-3140 **Fax:** +852-2637-3852
Received: 2003-08-28 **Accepted:** 2003-10-23

Abstract

A 95-year old gentleman developed fatal icteric flare of chronic hepatitis B despite lamivudine treatment. This article highlights the atypical presentations of chronic hepatitis B in elderly patient and the need to consider this possibility for acute fulminant hepatitis in endemic areas.

Wong WS, Leung WK, Chan HLY. Icteric flare of chronic hepatitis B in a 95-year old patient. *World J Gastroenterol* 2003; 9(12): 2876-2877
http://www.wjgnet.com/1007-9327/9/2876.asp

CASE REPORT

A 95-year old gentleman was admitted in July 2003 for decreased appetite and reduced mobility. He enjoyed good past health and had no history of hepatitis or jaundice. Two weeks prior to admission, family members noted that he became drowsier and refused food. He was living at home with family and had no history of percutaneous exposure before admission. He had never had tattooing, blood transfusion, casual sex or illicit drug use. There was no traveling history for more than twenty years. The patient was not on any medication or herbs.

On admission, the patient was barely arousable. He could only answer simple questions. He was in deep jaundice and dehydrated. There was no stigma of chronic liver disease. Abdominal examination did not reveal any tenderness, organomegaly or ascites. Flapping tremor could not be demonstrated because the patient was in grade 3 hepatic encephalopathy.

Blood test results were compatible with the picture of severe hepatitis. The serum bilirubin level was 188 μmol/l, alkaline phosphatase was 76 IU/l (normal 40-100 IU/l), and alanine aminotransferase was 825 IU/l (normal <58 IU/l). The prothrombin time was prolonged at 18.1 seconds. Platelet count was 86×10^9/l. Renal function was normal. Urgent ultrasound scan showed normal liver echotexture and normal size spleen. The biliary trees were normal. There was no gallstone.

His hepatitis B surface antigen (HBsAg) was positive, IgM anti-hepatitis B core antigen (anti-HBc) was equivocal, hepatitis B e-antigen was negative, and antibodies to hepatitis B e-antigen (anti-HBe) was positive. Hepatitis B virus DNA was 97.9×10^6 copies/ml by TaqMan real-time polymerase chain reaction[1]. The serology tests for hepatitis A, C, D and E viruses were negative.

Lamivudine 100 mg daily was commenced on the fourth day of admission, and supportive treatment with vitamin K, lactulose and intravenous fluids replacement were prescribed. While the level of alanine aminotransferase was on decreasing trend, serum bilirubin and prothrombin time gradually increased (Figure 1). He developed progressive liver failure with worsening hepatic encephalopathy and eventually succumbed sixteen days after admission.

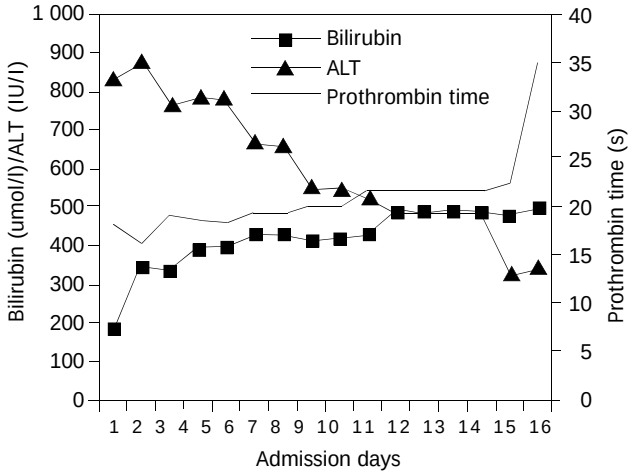

Figure 1 Serial blood results of the patient with acute flare of chronic hepatitis B. The serum bilirubin, alanine aminotransferase and prothrombin time are shown.

DISCUSSION

This case illustrates an unusual presentation of severe hepatitis B virus infection at an advanced age. Although liver biopsy has not been performed, other causes of acute hepatitis have been excluded by negative drug history and negative serology tests for other hepatitis viruses. The absence of risky percutaneous exposure renders the possibility of acute hepatitis B very unlikely. As a majority of chronic hepatitis B patients are asymptomatic and most people in Hong Kong do not have regular health check-up, it is most likely that this patient was suffering from chronic hepatitis B with HBsAg first discovered to be positive at this presentation. Equivocal IgM anti-HBc test is not diagnostic of acute hepatitis B but could also be detected in severe reactivation of chronic hepatitis B[2].

According to most prospective series, reactivation of chronic hepatitis B typically occurred at around the second and third decades[3-5]. Once a patient develops HBeAg seroconversion to anti-HBe, the durability reaches eighty percent. Patients often have quiescent disease afterwards, and the risks of complications, such as hepatocellular carcinoma and liver cirrhosis, are considerably reduced. Our patient probably has achieved sustained HBeAg seroconversion and disease remission several decades before this admission as he had negative HBeAg and no sign of liver cirrhosis at the age of 95. Reactivation of chronic hepatitis B causing jaundice and liver failure at this advanced age is uncommon. This case illustrates the importance to consider chronic hepatitis B as a cause of liver function derangement in endemic areas such as Asia.

Icteric reactivation of chronic hepatitis B carries a poor prognosis even with lamivudine treatment. In a series of 46

patients with severe reactivation of chronic hepatitis B with jaundice a quarter of patients died or required liver transplantation[6]. When both independent predictors of liver-related mortality including thrombocytopenia (platelet count below 143×10^9/l) and hyperbilirubinemia (serum bilirubin greater than 172 μmol/l) are present, as in our case, the mortality rate is up to 69.2 %.

In conclusion, despite atypical presentation and atypical age group, chronic hepatitis B should be considered in cases of acute fulminant hepatitis in endemic areas.

REFERENCES

1 **Chan HLY**, Chui AKK, Lau WY, Chan FKL, Wong ML, Tse CH, Rao ARN, Wong J, Sung JJY. Factors associated with viral breakthrough in lamivudine monoprophylaxis of hepatitis B virus recurrence after liver transplantation. *J Med Virol* 2002; **68**: 182-187

2 **Maruyama T**, Schodel F, Iino S. Distinguishing between acute and symptomatic chronic hepatitis B virus infection. *Gastroenterology* 1994; **106**: 1006-1015

3 **McMahon BJ**, Holck P, Bulkow L, Snowball M. Serologic and clinical outcomes of 1536 Alaska natives chronically infected with hepatitis B virus. *Ann Intern Med* 2001; **135**: 759-768

4 **Lok AS**, Lai CL, Wu PC, Leung EK, Lam TS. Spontaneous hepatitis B e antigen to antibody seroconversion and reversion in Chinese patients with chronic hepatitis B virus infection. *Gastroenterology* 1987; **92**: 1839-1843

5 **Liaw YF**, Chu CM, Lin DY, Sheen IS, Yang CY, Huang MJ. Age-specific prevalence and significance of hepatitis B e antigen and antibody in chronic hepatitis B virus infection in Taiwan: a comparison among asymptomatic carriers, chronic hepatitis, liver cirrhosis, and hepatocellular carcinoma. *J Med Virol* 1984; **13**: 385-391

6 **Chan HL**, Tsang SW, Hui Y, Leung NW, Chan FK, Sung JJ. The role of lamivudine and predictors of mortality in severe flare-up of chronic hepatitis B with jaundice. *J Viral Hepat* 2002; **9**: 424-428

Edited by Wang XL

P.O.Box 2345, Beijing 100023,China
Fax: +86-10-85381893
E-mail: wjg@wjgnet.com www.wjgnet.com

World J Gastroenterol 2003;9(12):2878-2879
World Journal of Gastroenterology
 ISSN 1007-9327

• CASE REPORT •

Pseudoaneurysm of gastroduodenal artery following radical gastrectomy for gastric carcinoma patients

Dong Yi Kim, Jae Kyoon Joo, Seong Yeob Ryu, Young Jin Kim, Shin Kon Kim, Yong Yeon Jung

Dong Yi Kim, Jae Kyoon Joo, Seong Yeob Ryu, Young Jin Kim, Shin Kon Kim, Division of Gatroenterologic Surgery, Department of Surgery, Chonnam National University Medical School, Gwangju, Korea
Yong Yeon Jung, Department of Radiology, Chonnam National University Medical School, Gwangju, Korea
Correspondence to: Dong Yi Kim, M.D. Division of Gatroenterologic Surgery, Department of Surgery, Chonnam National University Medical School, 8 Hakdong, Dongku, Gwangju 501-757, Korea. dockim@chonnam.ac.kr
Telephone: +82-62-220-6450 **Fax:** +82-62-227-1635
Received: 2003-08-28 **Accepted:** 2003-10-07

Abstract

We report a rare case of a postoperative pseudoaneurysm of the gastroduodenal artery following radical gastrectomy. Surgical trauma to the gastroduodenal artery during regional lymphadenectomy was considered the cause of the postoperative pseudoaneurysm. The pseudoaneurysm was successfully managed by ligating the bleeding vessel. We should consider the possibility of pseudoaneurysm formation in a patient with gastrointestinal bleeding in the postoperative period following radical gastrectomy with regional lymph node and perivascular lymphatic dissection.

Kim DY, Joo JK, Ryu SY, Kim YJ, Kim SK, Jung YY. Pseudoaneurysm of gastroduodenal artery following radical gastrectomy for gastric carcinoma patients. *World J Gastroenterol* 2003; 9(12): 2878-2879
http://www.wjgnet.com/1007-9327/9/2878.asp

INTRODUCTION

The causes of pseudoaneurysms include infection, trauma, and surgical procedures[1]. The development of pseudoaneurysms after upper abdominal surgery is rare, and most occur after biliary and pancreatic surgery[2-5]. There have been only a few reported cases of postoperative pseudoaneurysm of an artery following abdominal surgery. We recently encountered a patient with a ruptured pseudoaneurysm of the gastroduodenal artery following radical gastrectomy for gastric carcinoma.

CASE REPORT

A 73-year-old male was admitted with a two-month history of epigastric discomfort and weight loss. An upper gastrointestinal series, endoscopy, and abdominal CT scan suggested gastric carcinoma. The preoperative laboratory work-up was normal.

Laparotomy revealed an advanced gastric carcinoma involving the adjacent lymph nodes. No peritoneal dissemination or hepatic metastasis was found. The patient underwent a successful radical gastrectomy and the regional lymph nodes, and perivascular lymphatics surrounding the gastroduodenal artery were dissected.

Macroscopically, a curative resection was performed. Postoperative microscopic examination revealed poorly differentiated adenocarcinoma involving the serosal layer of the stomach, and metastasis in one of the twenty-eight lymph nodes dissected.

On postoperative day eight, a wound infection with moderate fever developed, and examination of the anastomotic site revealed no leakage. Twenty-five days after the operation, he suddenly developed abdominal distention with hypovolemic shock. A tentative diagnosis of hemoperitoneum was made and an emergency angiography was performed. An emergency celiac trunk arteriogram revealed a pseudoaneurysmal sac originating from the gastroduodenal artery (Figure 1). To obliterate the pseudoaneurysm transcatheter embolization with steel coils was attempted (Figure 2), but failed. We performed an emergent laparotomy. There was a large hematoma around the gastroduedenal artery. The gastroduodenal artery was allegedly ligated. The patient recovered and was discharged from the hospital two weeks later. He had no subsequent bleeding episodes and was doing well two months following discharge.

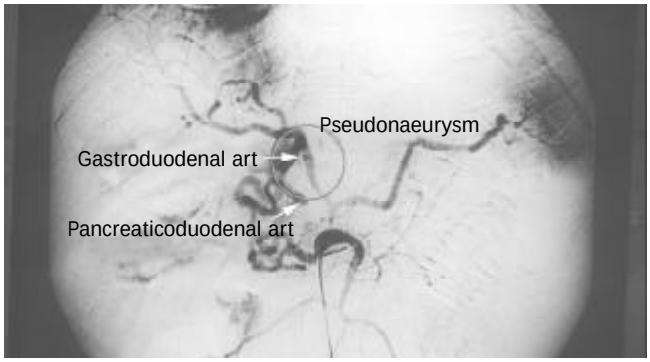

Figure 1 Anterior-posterior view of the superior mesenteric arteriogram showing a pseudoaneurysmal sac originating from the gastroduodenal artery.

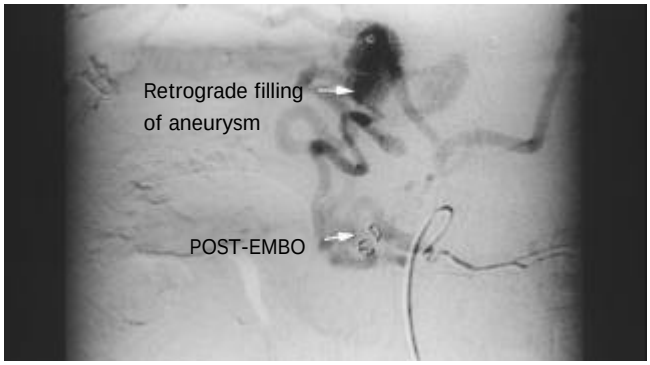

Figure 2 Superior mesenteric arteriogram after embolization shows the pseudoaneurysmal sac by retrograde filling.

DISCUSSION

Pseudoaneurysms result from a variety of mechanisms,

including infection, trauma, and surgical procedures[1]. All have in common disruption of arterial continuity with extravasation of blood into the surrounding tissues. This ultimately results in the formation of a fibrous tissue capsule that progressively enlarges due to the unrelenting arterial pressure[1]. Gastroduodenal artery aneurysms account for 1.5 % of all splanchnic artery aneurysms, but the true incidence of postoperative pseudoaneurysm of the gastroduodenal artery is unknown[6]. Postoperative pseudoaneurysm formation is uncommon, but can follow surgical trauma during gastrointestinal surgery or perioperative local infection[2,7,8]. There is usually a history of massive bleeding and perioperative local infection when the pseudoaneurysm develops[2]. Our patient had a local wound infection and massive intra-abdominal bleeding.

Our review of the literature revealed no reported cases of postoperative pseudoaneurysm of the gastroduodenal artery following radical gastrectomy. We assumed that the pseudoaneurysm formation had been caused by a weakness in the arterial wall according to skeletonization resulting from lymphadenectomy.

When an intra-abdominal pseudoaneurysm is suspected, angiography is useful for determining the exact location of the pseudoaneurysm. In addition, it can save time and prevent the danger of an emergency laparotomy to locate the source of bleeding without angiography[9]. In our case, emergent angiography was performed after the episode of massive intra-abdominal bleeding and demonstrated a pseudoaneurysm arising from the gastroduodenal artery. Many authors[4,6,9-11] have recommended transcatheter occlusion or selective embolization as a useful method in high-risk patients. Basile *et al*.[12], Bulut *et al*.[13] and Furukawa *et al*.[14], reported successful transcatheter arterial embolization in a patient who developed pseudoaneurysm after abdominal surgery. We tried transcatheter arterial embolization, but failed to control the bleeding.

Although it is impossible to know the true incidence of postoperative pseudoaneyrysm of the gastroduodenal artery, it may develop due to iatrogenic injury during surgery[4,15].

We should consider the possibility of pseudoaneurysm formation in a patient with inta-abdominal bleeding during the postoperative period following radical gastrectomy with regional lymph nodes and perivascular lymphatic dissection.

This report describes the successful management of a pseudoaneurysm of the gastroduodenal artery following radical gastrectomy, by ligation of the bleeding vessel.

REFERENCES

1 **Clark ET,** Gewertz BL. Pseudoaneurysms. In: Rutherford RB(ed): Vascular Surgery. 4th ed. Philadelphia: *W B Saunders* 1995: 1153-1161

2 **Iseki M,** Tada Y, Wada T, Nobori M. Hepatic artery aneurysm. Report of a case and review of the literature. *Jpn J Gastroenterol* 1983; **18:** 84-92

3 **Tan M,** Di Carlo A, Stein LA, Cantarovich M, Tchervenkov JI, Metrakos P. Pseudoaneurysm of the superior mesenteric artery after pancreas transplantation treated by endovascular stenting. *Transplantation* 2001; **72:** 336-338

4 **Sugimoto H,** Kaneko T, Ishiguchi T, Takai K, Ohta T, Yagi Y, Inoue S, Takeda S, Nakao A. Delayed rupture of a pseudoaneurysm following pancreatoduodenectomy: Report of a case. *Surg Today* 2001; **31:** 932-935

5 **Almogy G,** Bloom A, Verstandig A, Eid A. Hepatic artery pseudoaneurysm after liver transplantation. *Transpl Int* 2002; **15:** 53-55

6 **Eckhauser FE,** Stanley JC, Zelenock GB, Borlaza GS, Freier DT, Lindenauer SM. Gastroduodenal and pancreaticoduodenal artery aneurysms: A complication of pancreatitis causing spontaneous gastrointestinal hemorrhage. *Surgery* 1980; **88:** 335-344

7 **Kelley CJ,** Hemingway AP, Mcpherson GA, Allison DJ, Blumgart LH. Non-surgical management of post-cholecystectomy haemobilia. *Br J Surg* 1983; **70:** 502-504

8 **Aranha GV,** O' Neil S, Borge MA. Successful nonoperative management of bleeding hepatic artery pseudoaneurysm following pancreaticoduodenectomy. *Dig Surg* 1999; **16:** 528-530

9 **Stabile BE,** Wilson SE, Debas HT. Reduced mortality from bleeding pseudocysts and pseudoaneurysm caused by pancreatitis. *Arch Surg* 1983; **118:** 45-51

10 **Kuno RC,** Althaus SJ, Glickerman DJ. Direct percutaneous coil and ethanol embolization of a celiac artery pseudoaneurysm. *J Vasc Interv Radiol* 1995; **6:** 357-360

11 **Kitagawa T,** Iriyama K, Azuma T, Yamakado K. Nonoperative treatment for a ruptured pseudoaneurysm of the celiac trunk: report of a case. *Surg Today* 1997; **27:** 1069-1073

12 **Basile A,** Boullosa-Seoane E, Dominguez-Viguera L, Certo A, Casal-Rivas M. Percutaneous embolization of a gastroduodenal artery aneurysm secondary to antrectomy and Roux en Y reconstruction. *Radiol Med* 2002; **104:** 374-377

13 **Bulut T,** Yamaner S, Bugra D, Akyuz A, Acarli K, Poyanli A. False aneurysm of the hepatic artery after laparoscopic cholecystectomy. *Acta Chir Belg* 2002; **102:** 459-463

14 **Furukawa H,** Kosuge T, Shimada K, Yamamoto J, Ushino K. Helical CT of the abdomen after pancreaticoduodenectomy: Usefulness for detecting postoperative complications. *Hepatogastroenterology* 1997; **44:** 849-855

15 **Satoh H,** Morisaki T, Kishikawa H. A case of a postoperative aneurysm of the common hepatic artery which ruptured into the remnant stomach after a radical gastrectomy. *Jpn J Surg* 1989; **19:** 241-245

Edited by Zhu LH

P.O.Box 2345, Beijing 100023,China
Fax: +86-10-85381893
E-mail: wjg@wjgnet.com www.wjgnet.com

World J Gastroenterol 2003;9(12):2880-2882
World Journal of Gastroenterology
 ISSN 1007-9327

• CASE REPORT •

Surgical resection of duodenal lymphangiectasia: A case report

Chih-Ping Chen, Yee Chao, Chung-Pin Li, Wen-Ching Lo, Chew-Wun Wu, Shyh-Haw Tsay, Rheun-Chuan Lee, Full-Young Chang

Chih-Ping Chen, Chung-Pin Li, Wen-Ching Lo, Full-Young Chang, Division of Gastroenterology, Department of Medicine, Taipei Veterans General Hospital and Institute of Clinical Medicine, National Yang-Ming University School of Medicine, Taipei, Taiwan, China
Yee Chao, Cancer Center, Taipei Veterans General Hospital and National Yang-Ming University School of Medicine, Taipei, Taiwan, China
Chew-Wun Wu, Division of General Surgery, Department of Surgery, Taipei Veterans General Hospital and National Yang-Ming University School of Medicine, Taipei, Taiwan, China
Shyh-Haw Tsay, Department of Pathology, Taipei Veterans General Hospital and National Yang-Ming University School of Medicine, Taipei, Taiwan, China
Rheun-Chuan Lee, Department of Radiology, Taipei Veterans General Hospital and National Yang-Ming University School of Medicine, Taipei, Taiwan, China
Correspondence to: Chung-Pin Li, Division of Gastroenterology, Department of Medicine, Taipei Veterans General Hospital, No. 201, Sec. 2, Shih-Pai Road, Taipei, 11217, Taiwan, China. cpli@vghtpe.gov.tw
Telephone: +86-2-28757308 **Fax:** +86-2-28739318
Received: 2003-08-26 **Accepted:** 2003-10-12

Abstract

Intestinal lymphangiectasia, characterized by dilatation of intestinal lacteals, is rare. The major treatment for primary intestinal lymphangiectasia is dietary modification. Surgery to relieve symptoms and to clarify the etiology should be considered when medical treatment failed. This article reports a 49-year-old woman of solitary duodenal lymphangiectasia, who presented with epigastralgia and anemia. Her symptoms persisted with medical treatment. Surgery was finally performed to relieve the symptoms and to exclude the existence of underlying etiologies, with satisfactory effect. In conclusion, duodenal lymphangiectasia can present clinically as epigastralgia and chronic blood loss. Surgical resection may be resorted to relieve pain, control bleeding, and exclude underlying diseases in some patients.

Chen CP, Chao Y, Li CP, Lo WC, Wu CW, Tsay SH, Lee RC, Chang FY. Surgical resection of duodenal lymphangiectasia: A case report. *World J Gastroenterol* 2003; 9(12): 2880-2882
http://www.wjgnet.com/1007-9327/9/2880.asp

INTRODUCTION

Intestinal lymphangiectasia (IL) is a rare condition with widely variable symptoms and signs. Patients may be asymptomatic or present as vague abdominal pain, chronic diarrhea, steatorrhea, edema, chylous pleural effusion, ascites, hypoproteinemia, lymphocytopenia or protein-losing enteropathy[1,2]. IL usually occurs in children or young adults, and is suspected to be caused by a congenital abnormality in the lymphatic system[1-3]. Occasionally, IL can be seen in the aged people, which may be secondary to disorders causing lymphatic obstruction, such as lymphoma, carcinoma, tuberculosis, constrictive pericarditis, retroperitoneal fibrosis, post-radiation effects, and repeated parasite infestation[1,4-6]. Diagnosis depends on characteristic endoscopic findings and pathological features[7-9]. However, it is sometimes difficult to differentiate primary from secondary IL. Surgical intervention may be a final resort to make a definite diagnosis and to relieve symptoms. Herein, we present a case with a solitary duodenal lymphangiectasia presenting as epigastralgia and chronic blood loss. The patient finally received surgical intervention and the symptoms resolved.

CASE REPORT

A 49-year-old woman was admitted to our hospital in February 1999 with progressive epigastralgia and malaise for 2 months. She had been well in the past and denied family history of systemic disorders. Physical examination showed mild anemic conjunctivae and tarry stool. There was no evidence of significant enteric protein loss.

Complete blood count revealed mild normocytic normochromic anemia (hemoglobin 10.5 g/dL). Stool examination disclosed positive occult blood (+++). Serum biochemistries as well as serum concentrations of immunoglobulins and tumor markers, including α-fetoprotein, carcinoembryonic antigen, carbohydrate antigen 19-9, and carbohydrate antigen-125, were all within normal limits. Urinary excretion of 5-hydroxyindoleacetic acid (5-HIAA) was normal. Upper gastrointestinal endoscopy showed a 3 cm irregular elevation with bulging border, superficial whitish spots, as well as hemorrhagic and friable mucosa in the second portion of duodenum (Figure 1a). Histological examination showed prominent, dilated lymphatic vessels in the mucosal and submucosal layers (Figure 1b). Upper gastrointestinal barium radiography demonstrated a cluster of polypoid filling defects, 3×3 cm in size, in the second portion of duodenum (Figure 1c). Abdominal sonography and computerized tomography (CT) showed no obvious abnormalities. Small intestine series and barium enema did not disclose any lesion. Antacids and a low-fat, high-protein diet supplemented with medium-chain triglycerides were prescribed for one month with no obvious improvement.

For treating refractory epigastralgia and chronic bleeding and excluding underlying diseases, the modified Whipple's operation with pylorus preservation was carried out in March 1999. A polypoid lesion in the second portion of the duodenum, 3×3 cm in size, was found 1 cm lateral to the papilla of Vater (Figure 1d). Pathological examination confirmed it to be an idiopathic lymphangiectasia. No underlying etiologies could be identified. After operation, the patient recovered well. Epigastralgia resolved and the blood hemoglobin returned to normal after surgery and during the later four-years' follow-up.

DISCUSSION

Intestinal lymphangiectasia has been well recognized as a disorder characterized by dilated lymphatic vessels of the gastrointestinal tract, especially the small intestine[1-3]. It is a

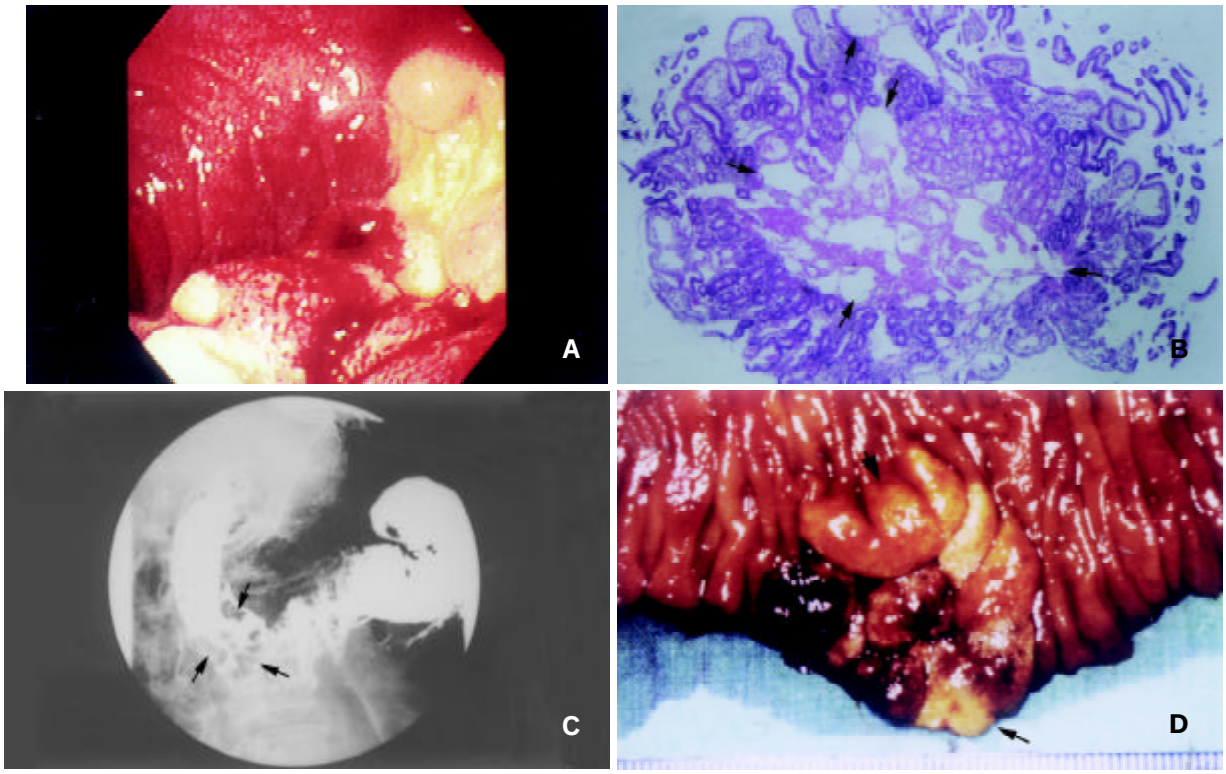

Figure 1 (a) Panendoscopy revealed a 3 cm irregular elevated lesion with whitish spots on the surface and a central crater with blood-coating in the second portion of duodenum. (b) Histology of the endoscopic biopsy showed prominent dilatation of intramucosal and submucosal lymphatic ducts (arrows), a picture of intestinal lymphangiectasia (Hematoxylin and eosin, ×40). (c) Upper gastrointestinal series demonstrated a cluster of polypoid filling defects, 3×3 cm in size, in the second portion of the duodenum (arrows). (d) Gross appearance of the surgical specimen revealed a sessile polypoid lesion, 3 cm in diameter, in the second portion of the duodenum (arrows).

rare condition related to fat malabsorption and protein-losing enteropathy. Distribution of IL can be segmented, multifocal or diffuse. The pathogenesis is believed to be due to obstruction of lymphatic drainage[1-3]. According to the etiologies, IL can be classified into primary and secondary forms[1,2]. Primary IL is usually associated with many genetic syndromes, such as Turner' s syndrome[2,10]. On the contrary, secondary IL is acquired, due to several kinds of gastrointestinal diseases and intra-abdominal or retroperitoneal pathologies, such as carcinoma, lymphoma, tuberculosis or constrictive pericarditis[1,4-6].

Clinical manifestations are similar in both forms of IL, but with variable severity according to the extent of involvement. Some patients can be completely asymptomatic, while at the other extreme, some may be associated with protein-losing enteropathy, growth retardation, or recurrent gastrointestinal tract bleeding[1,2,11]. The protein loss is suspected to be due to rupture of the dilated intramucosal or submucosal lacteals, or exudation from the epithelium[3]. The hemorrhage may be due to rupture of the dilated lacteals, which have potential communications with blood vessels[11].

Diagnosis depends on clinical suspicion. Specific endoscopic findings, accompanied by typical histological pictures can draw into the diagnosis[7]. These endoscopic findings include white-tipped villi, scattered white spots, white nodules, and submucosal elevations[7-9]. Typical histological pictures consist of dilated intramucosal and submucosal lacteals[7-9]. CT scan can help to find the underlying causes of secondary IL[12].

Treatment of IL depends on the severity and extent of involvement. For most patients with primary IL, due to generalized abnormalities and diffuse distribution, dietary modification with a low-fat, high-protein diet and supplementation of medium-chain triglycerides (MCT) is the mainstay of treatment[1, 2]. As MCT is absorbed from the portal venous system directly rather than via lymphatics, it may avoid engorgement of the lymphatics, and thus reduce the opportunity for rupture[2]. On the other hand, for patients with secondary IL, the underlying diseases should be treated. Surgical resection can be chosen when IL is confined to a segment of the intestine and has successfully treated protein-losing enteropathy, anemia or abdominal pain in intestine lymphangiectasia[2,13-15].

In this case, an irregularly elevated lesion in the second portion of the duodenum combined with epigastralgia and chronic blood loss was found. Biopsies showed a picture of IL, however, secondary IL could not be excluded. Due to segmental involvement and to rule out underlying causes, surgical resection was performed. The symptoms were relieved and a definite diagnosis of idiopathic duodenal IL was made. In conclusion, surgical resection may be chosen to relieve symptoms and exclude underlying diseases in patients with solitary duodenal IL.

REFERENCES

1 **Rubin DC.** Small intestine: anatomy and structural anomalies In: Yamada T, ed. Textbook of gastroenterology. 3rd ed. *Philadelphia: Lippincott Williams Wilkins* 1999: 1578-1579
2 **Vardy PA,** Lebenthal E, Shwachman H. Intestinal lymphagiectasia: a reappraisal. *Pediatrics* 1975; **55**: 842-851
3 **Waldmann TA,** Steinfeld JL, Dutcher TF, Davidson JD, Gordon RS Jr. The role of the gastrointestinal system in "idiopathic hypoproteinemia." *Gastroenterology* 1961; **41**: 197-207
4 **Nelson DL,** Blaese RM, Strober W, Bruce R, Waldmann TA. Constrictive pericarditis, intestinal lymphangiectasia, and reversible immunologic deficiency. *J Pediatr* 1975; **86**: 548-554
5 **Rao SS,** Dundas S, Holdsworth CD. Intestinal lymphangiectasia secondary to radiotherapy and chemotherapy. *Dig Dis Sci* 1987;

32: 939-942

6 **Oksuzoglu G,** Aygencel SG, Haznedaroglu IC, Arslan M, Bayraktar Y. Intestinal lymphangiectasia due to recurrent giardiasis. *Am J Gastroenterol* 1996; **91**: 409-410

7 **Abramowsky C,** Hupertz V, Kilbridge P, Czinn S. Intestinal lymphangiectasia in children: a study of upper gastrointestinal endoscopic biopsies. *Pediatr Pathol* 1989; **9**: 289-297

8 **Riemann JF,** Schmidt H. Synopsis of endoscopic and other morphological findings in intestinal lymphangiectasia. *Endoscopy* 1981; **13**: 60-63

9 **Aoyagi K,** Iida M, Yao T, Matsui T, Okada M, Oh K, Fujishima M. Characteristic endoscopic features of intestinal lymphangiectasia: correlation with histological findings. *Hepatogastroenterology* 1997; **44**: 133-138

10 **Rutlin E,** Wisloff F, Myren J, Serck-Hanssen A. Intestinal telangiectasia in Turner's syndrome. *Endoscopy* 1981; **13**: 86-87

11 **Perisic VN,** Kokai G. Bleeding from duodenal lymphangiectasia. *Arch Dis Child* 1991; **66**: 153-154

12 **Fakhri A,** Fishman EK, Jones B, Kuhajda F, Siegelman SS. Primary intestinal lymphangiectasia: clinical and CT findings. *J Comput Assist Tomogr* 1985; **9**: 767-770

13 **Kingham JG,** Moriarty KJ, Furness M, Levison DA. Lymphangiectasia of the colon and small intestine. *Br J Radiol* 1982; **55**: 774-777

14 **Jameson JS,** Boyle JR, Jones L, Rees Y, Kelly MJ. An unusual presentation of intestinal lymphangiectasia. *Int J Colorect Dis* 1996; **11**: 198-199

15 **Persic M,** Browse NL, Prpic I. Intestinal lymphangiectasia and protein losing enteropathy responding to small bowel resection. *Arch Dis Child* 1998; **78**: 194

Edited by Zhu LH

P.O.Box 2345, Beijing 100023,China
Fax: +86-10-85381893
E-mail: wjg@wjgnet.com www.wjgnet.com

World J Gastroenterol 2003;9(12):2883-2884
World Journal of Gastroenterology
 ISSN 1007-9327

• CASE REPORT •

Life-threatening hemobilia caused by hepatic artery pseudoaneurysm: A rare complication of chronic cholangitis

Tsu-Te Liu, Ming-Chih Hou, Han-Chieh Lin, Full-Young Chang, Shou-Dong Lee

Tsu-Te Liu, Ming-Chih Hou, Han-Chieh Lin, Full-Young Chang, Shou-Dong Lee, Division of Gastroenterology, Department of Medicine, Taipei-Veterans General Hospital, and School of Medicine, National Yang Ming University, Taipei, Taiwan
Supported by in part, grant VGH-91-A-17 from the Taipei-Veterans General Hospital
Correspondence to: Ming-Chih Hou, M.D., Division of Gastroenterology, Department of Medicine, Veterans General Hospital, No 201, Sec 2, Shih-Pai Road, Taipei 11217, Taiwan. mchou@vghtpe.gov.tw
Telephone: +86-2-2875-7308 **Fax:** +86-2-2873-9318
Received: 2003-06-04 **Accepted:** 2003-08-19

Abstract

Hemobilia is one of the causes of obscure gastrointestinal haemorrhage. Most cases of hemobilia are of iatrogenic or traumatic origin. Hemobilia caused by a hepatic artery pseudoaneurysm due to ascending cholangitis is very rare and its mechanism is unclear. We report a 74-year-old woman with a history of surgery for choledocholithiasis 30 years ago, suffering from a protracted course of life-threatening gastrointestinal bleeding. A small intestines series and endoscopic retrograde cholangiopancreatography revealed a chronic cholangitis with marked contrast reflux into the biliary tree. Angiography confirmed the bleeding from a pseudoaneurysm of the middle hepatic artery. Coil embolization achieved successful hemostasis. We discussed the mechanism and reviewed the literature.

Liu TT, Hou MC, Lin HC, Chang FY, Lee SD. Life-threatening hemobilia caused by hepatic artery pseudoaneurysm: A rare complication of chronic cholangitis. *World J Gastroenterol* 2003; 9(12): 2883-2884

http://www.wjgnet.com/1007-9327/9/2883.asp

INTRODUCTION

Hemobilia, a phenomenon of bleeding into the biliary tree, is an unusual cause of obscure upper gastrointestinal bleeding. Most of the etiologies of hemobilia are iatrogenic or traumatic in origin[1]. An hepatic artery aneurysm is a rare vascular lesion that accounts for nearly 10 % of hemobilia cases[2], and is mostly due to atherosclerosis or trauma[3,4]. A hepatic artery aneurysm due to biliary inflammation is less frequent and usually attributed to parasites or stone obstruction in the biliary tract[5]. Inflammatory causes of hemobilia in the Far East are mainly due to parasitic infections, such as ascariasis or clonorchiasis, which have the tendency to invade the bile ducts and induce bleeding. Impacted stones may also erode the biliary mucosa and lead to bleeding. Severe hemobilia is rare, but can occur when a large stone erodes vessels of the hepatoduodenal ligament or the cystic artery[6]. In contrast, hemobilia caused by reflux cholangitis without stones or parasitic infection, has not yet been reported and its mechanism is unclear. We present a case of life-threatening hemobilia from an hepatic pseudoaneurysm, complicated by reflux cholangitis due to previous biliary surgery.

CASE REPORT

A 74-year-old woman had a history of biliary stones and received a cholecystectomy, hepatic lateral segmentectomy and sphincterotomy over 30 years ago. In March 2001, she developed intermittent tarry stools and dizziness for one week and came to our hospital. At the emergency room, her blood pressure was 99/35 mmHg and her pulse rate was 93/minute. Physical examination showed a pale conjunctiva and mild epigastric tenderness. A hemogram showed microcytic hypochromic anemia with a hemoglobin level of 7.6 g/dl. An emergent gastro-duodenal endoscopy disclosed gastric ulcers near the angularis. Proton pump inhibitor therapy was started. On the third hospital day, massive hematemesis with hypovolemic shock occurred. An emergent endoscopy did not disclose any evidence of recent bleeding from the gastric ulcers, but a lot of fresh blood in the duodenal bulb and beyond was observed. An immediate angiography, Tc-99m-RBC scan, and colonoscopy all returned negative findings. An abdominal CT did not display any abnormal lesions. A small intestines series did not disclose any abnormal lesions, except an obvious contrast medium reflux from the duodenum into biliary tree (Figure 1).

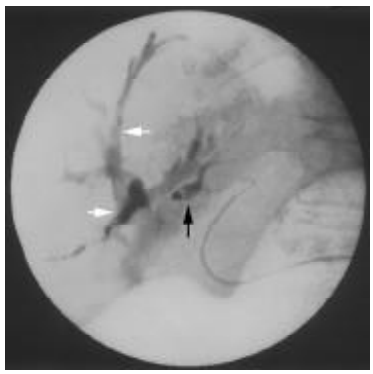

Figure 1 Small intestines series show chronic cholangitis with obvious contrast medium reflux into the biliary tree (arrow).

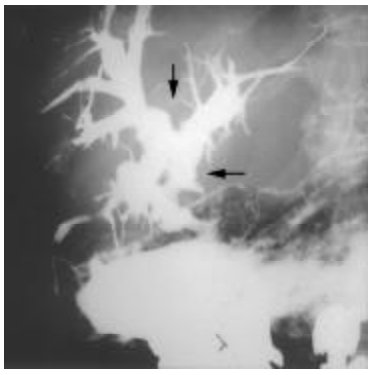

Figure 2 Angiography shows a small pseudoaneurysm (arrow) over the middle hepatic artery. Injecting the contrast medium into the middle hepatic artery opacified the intrahepatic biliary duct (arrowheads).

In the following days, intermittent tarry stools continued to pass. She suffered from upper abdominal pain before every bleeding episode. On the 16th day of admission, she had another massive hematochezia with hypovolemic shock. This time, the emergent endoscopy showed fresh blood flowing from the orifice of the ampulla of Vater. Endoscopic retrograde cholangiopancreatography found widening of the papillary orifice and amorphous filling defects of blood clots retained in the irregular and dilated biliary trees. An angiography showed a small pseudoaneurysm over the middle hepatic artery. Injection of a contrast medium into the middle hepatic artery also opacified the intrahepatic biliary ducts (Figure 2). A coil embolization was performed smoothly and no more event of hemobilia has been reported after this procedure.

DISCUSSION

There were many etiologies for hemobilia such as iatrogenic and accidental trauma, gallstones, inflammation, vascular malformations and tumours[1]. Because interventional procedures and laparoscopic cholecystectomy were used more to manage hepatobiliary disorders, iatrogenic origins were the more frequent etiology for hemobilia[1].

Hemobilia due to a hepatic artery aneurysm only accounted for 10 % of cases[2], and was mostly due to atherosclerosis or trauma[3,4]. Hepatic artery aneurysms due to biliary inflammation were usually attributed to parasites or stone obstruction in the biliary tract[5], and rarely due to non-obstructive inflammations, as in this case. After sphincterotomy, biliary reflux of the duodenal chyme was observed in most patients, aerobilia in half and bactibilia in all[7,8]. Infected bile may lead to cholangitis in more than 1 % of them[9]. Although such a reflux might not always produce clinical symptoms, the biochemical changes suggested that there might be some degree of continuing low-grade damage within the liver parenchyma. Twenty percent of asymptomatic patients undergoing an endoscopic sphincterotomy for biliary stones still had persistent subclinical injury to the biliary tract[10]. Liver biopsy showed periportal fibrosis and inflammation[10]. The bile ducts were richly supplied by the hepatic artery, which forms a peri-biliary vascular plexus[11]. As the inflammation proceeds and involves the collateral hepatic artery, a pseudoaneurysm forms and raises the risk of hemobilia.

The most common symptoms of hemobilia are upper gastrointestinal haemorrhage, upper abdominal pain, and jaundice. These occurred in 73 %, 52 %, and 30 % of cases, respectively, although the complete triad occurred in only 22 % of the them[1]. For patients with upper gastrointestinal bleeding, an endoscopy is the first step. If blood or clotting is seen at the ampulla of Vater, hemobilia is the likely cause of the haemorrhage. However, only 12 % of these endoscopies might be diagnostic[12]. The choice of subsequent investigations depends on the history and the level of suspicion. Abdominal sonography or computed tomography can detect common bile duct obstruction and identify intrahepatic lesions, such as stones or tumors. Endoscopic retrograde cholangiopancreatography may be helpful. Blood may be seen at the ampulla of Vater and contrast studies may show filling defects in the biliary tree. Angiography could detect significant hemobilia in over 90 % of patients[13], and allow the localization of vascular lesions and therapeutic embolization.

The management of hemobilia is aimed at stopping the bleeding and relieving biliary obstruction. Transarterial embolization is now the first line of intervention to stop the bleeding of hemobilia, which returned a high success rate of around 80 % to 100 %[1], and lower morbidity or mortality rates than surgery[14]. Surgical interventions, such as ligation of the bleeding vessel or excision of the aneurysm, should be considered if embolization fails or is contraindicated.

In conclusion, hemobilia is one of the causes of obscure gastrointestinal hemorrhage. Although iatrogenic cases have replaced traumatic ones as the major type of hemobilia, one should keep in mind that ascending cholangitis is a possibility and may sometimes be complicated by life-threatening hemobilia. In particular, the rupture of a hepatic artery aneurysm should be taken into consideration in patients with a remote history of endoscopic or surgical sphincterotomy.

REFERENCES

1 **Green MH**, Duell RM, Johnson CD, Jamieson NV. Haemobilia. *Brit J Surg* 2001; **88**: 773-786
2 **Harlaftis NN**, Akin JT. Hemobilia from ruptured hepatic artery aneurysm. Report of a case and review of the literature. *Am J Surg* 1977; **133**: 229-232
3 **Stauffer JT**, Weinman MD, Bynum TE. Hemobilia in a patient with multiple hepatic artery aneurysms: a case report and review of the literature. *Am J Gastroenterol* 1989; **84**: 59-62
4 **Baartz T**, Koveker G, Hehrmann R, Becker HD. Recurrent hematemesis and hemobilia in ruptured hepatic artery aneurysm - differential diagnostic aspects of acute, upper gastrointestinal hemorrhage. *Leber Magen Darm* 1996; **26**: 42-46
5 **Bloechle C**, Izbicki JR, Rashed MY, El-Sefi T, Hosch SB, Knoefel WT, Rogiers X, Broelsch CE. Hemobilia: presentation, diagnosis and management. *Am J Gastroenterol* 1994; **89**: 1537-1540
6 **Sandblom P**, Saegesser F, Mirkovitch V. Hepatic hemobilia: hemorrhage from the intrahepatic biliary tract, a review. *World J Surg* 1984; **8**: 41-50
7 **Seifert E**. Long-term follow-up after endoscopic sphincterotomy (EST). *Endoscopy* 1988; **20**(Suppl 1): 232-235
8 **Gregg JA**, De Girolami P, Carr-Locke DL. Effects of sphincteroplasty and endoscopic sphincterotomy on the bacteriologic characteristics of the common bile duct. *Am J Surg* 1985; **149**: 668-671
9 **Prat F**, Malak NA, Pelletier G, Buffet C, Fritsch J, Choury AD, Altman C, Liguory C, Etienne JP. Biliary symptoms and complications more than 8 years after endoscopic sphincterotomy for choledocholithiasis. *Gastroenterology* 1996; **110**: 894-899
10 **Greenfield C**, Cleland P, Dick R, Masters S, Summerfield JA, Sherlock S. Biliary sequelae of endoscopic sphincterotomy. *Postgrad Med J* 1985; **61**: 213-215
11 **Sherlock S**, Dooley K. Diseases of the liver and biliary system, 11th ed. *London, Blackwell Science* 2002: 255-265
12 **Yoshida J**, Donahue PE, Nyhus LM. Hemobilia: review of recent experience with a worldwide problem. *Am J Gastroenterol* 1987; **82**: 448-453
13 **Merrell SW**, Schneider PD. Hemobilia – evolution of current diagnosis and treatment. *West J Med* 1991; **155**: 621-625
14 **Lygidakis NJ**, Okazaki M, Damtsios G. Iatrogenic hemobilia: how to approach it. *Hepatogastroenterol* 1991; **38**: 454-457

Edited by Wang XL